

PAMPHLET BOX

# Physics Abstracts

Science Abstracts Series A  
July – December 1984

Subject Index (A – L)

U. T. C.

MAR 29 1985

LIBRARY

# inspec

The Institution of Electrical Engineers

## SIX-MONTHLY INDEXES TO PHYSICS ABSTRACTS

Twice a year as part of their subscription to Physics Abstracts subscribers receive cumulative indexes for the periods January-June and July-December. Each index is in two parts—a Subject Index, and an Author Index which comprises personal and corporate author indexes, and indexes to conferences, book titles, and bibliographies. The List of Journals and other Serial Sources abstracted by INSPEC in the particular year is also included with the July-December issue of the Author Index while the supplement to that List is included with the January-June issue. Cumulative indexes for earlier years are also available: for details please see the inside back cover.

### Subject index

The Subject index provides an alphabetical subject key to the articles included in the abstracts journal. Some general guidance on its use is given below:

1. Look in the index for the name of the specific subject in which you are interested. In most cases this name will be a heading in the index and you will find relevant articles listed under it. The majority of the subject headings fall into the following categories: property, phenomena, substance or named objects, instrument, device, theory, method, process, application, event.
2. Occasionally you will be directed from the subject heading chosen to a different heading under which the relevant or additional articles are listed.
3. If you do not find the subject heading you first chose, try a more general heading.
4. Each entry under the heading relates to an article appearing in the abstracts journal and gives the serial number of that article in the journal preceded by the last digit of the current year, e.g. 4-12345; i.e. Abstract number 12345 in the abstracts journal for 1984.

The language of the article, if it is not in English, is also indicated. e.g. Photo-induced CVD (Japanese) 4-40669.

Each entry starts with a Keyword or Keyphrase considered to be most relevant to the heading. On sorting these Keywords, the qualifying prefixes are usually ignored. (e.g.  $\alpha$ -brass, 5-sulphosalicylic, 31 Cygni, n-Ge are sorted under brass, sulphosalicylic, Cygni, Ge respectively).

There are three main Keyword lists: alphabetical A-Z, elementary particles, and chemical symbols (organic substances are written and not given as chemical formula). More than one Keyword list may be present under each subject heading.

For document on, say, 'photoemission of germanium' at least two access points 'photoemission' and 'germanium' are provided. Under the heading 'photoemission' the Keyword will be 'Ge' and under 'germanium' the Keyword will be 'photoemission'.

In a case like this, it is advisable and quicker to use the heading 'photoemission' and go straight to the chemical symbol list for 'Ge'.

Intermetallic compounds are indexed under the appropriate alloy headings. The chemical formula is used as Keyword. However, it is important to realise in searching the chemical symbol list that, at present, alloys and intermetallic compounds are sorted separately. For example FeCo is sorted at the end of the Fe- list e.g. Fe-Al,... Fe-Co,... Fe-Si,... Fe-Si-B,... FeCo,... FeSi and so on in this order.

PHYSICS ABSTRACTS is published twice monthly by the Institution of Electrical Engineers in association with the Institute of Electrical and Electronics Engineers Inc. 2nd Class postage paid at Piscataway, N.J. 08854, USA. POSTMASTER: Send address changes to INSPEC/IEEE SERVICE CENTER, 445 Hoes Lane, Piscataway, N.J. 08854.

Printed by Unwin Brothers Limited, The Gresham Press, Old Woking, Surrey.

©1985, THE INSTITUTION OF ELECTRICAL ENGINEERS. All rights reserved. No part of this publication may be reproduced, stored in a retrieval system, or transmitted, in any form or by any means, electronic, mechanical, photocopying, recording or otherwise without the prior permission of the Institution of Electrical Engineers.

Abbreviations and acronyms appeared in the modifiers in all INSPEC Compendex Plus subject indexes. Individual items should be readily understood in the context of the subject headings. Inorganic substances are usually given by their chemical formulae, and iron and aluminum garnets appear in the formulae as  $\text{Fe}_2\text{O}_3$  and  $\text{Al}_2\text{O}_3$  respectively. Inorganic elements, e.g. YIG and YAG:  $\text{Y}_3\text{Fe}_5\text{O}_{12}$  and  $\text{Y}_3\text{Al}_5\text{O}_{12}$ ;  $\text{ZnO}$ ,  $\text{PbO}$ ,  $\text{TiO}_2$ , and  $\text{Ca}_2\text{SiO}_4$  are also acceptable. In  $\text{FeCl}_3$ ,  $\text{Fe}$  and  $\text{Cl}$  are respectively. Organic substances are not given by formulae, but by names, and are used.

# Physics Abstracts

**Science Abstracts Series A**

## July – December 1984

## Subject Index (A – L)

## CONTENTS

Abbreviations and Acronyms	iii
Subject index (A-L)	S 1849

# Abstracts

## Science Abstracts Series A

July – December 1984

# Subject Index (A – L)

## CONTENTS

Abbreviations and Acronyms	iii
Subject index (A-L)	S 1849



# Abbreviations and Acronyms

Abbreviations and acronyms are used in the modifiers in all INSPEC Cumulative Subject Indexes. Individual terms should be readily understood in the context of the subject headings. **Inorganic substances** are usually given by their chemical formulae. Iron and aluminium garnets appear in the formulae lists as MIG and MAG (where M is metal element, e.g. YIG and YAG);  $(\text{Pb,Lu})(\text{Zr,Ti})\text{O}_3$ ,  $\text{Pb}(\text{Zr,Ti})\text{O}_3$  and  $\text{Ce}_2\text{Mg}_3(\text{NO}_3)_{12}$  appear as PLZT, PZT and CMN respectively. **Organic substances** including **liquid crystals** are not given as formulae but common abbreviations are used.

ABS resin	acrylonitrile-butadiene:styrene	CBOOA	cyanobenzylidene octyloxyaniline
AC	alternating current	CCBA	coupled channel Born approximation
ACV	air cushion vehicle	C-CD	charge-coupled device
A/D	analogue-to-digital	CCL	capacitor-coupled logic
ADC	analogue digital conversion	CDFR	commercial demonstration fast reactor
ADP	administrative data processing	CDI	collector diffusion isolation
AE	acoustic emission	CDM	code division multiplexing
AEC	atomic electron correlation(s)	CDW	charge-density wave
AES	Auger electron spectra(scopy)	CEM	channel electron multiplier
AF	audio frequency	CEPA	coupled electron pair approximation
AFC	automatic frequency control	CERN	Conseil Européen pour la Recherche Nucléaire
AFL	abstract family of languages	CESR	conduction electron spin resonance
AFMR	antiferromagnetic resonance	CGTO	contracted Gaussian-type orbital
AGC	automatic gain control	CHF	coupled Hartree-Fock
AGR	advanced gas-cooled reactor	CI	configuration interaction
ALARA	as low as reasonably achievable	CIDEP	chemically induced dynamical electron polarisation
ALU	arithmetic logic unit	CIDNP	chemically induced dynamical nuclear polarisation
AM	amplitude modulation	CIEH	charge iterated extended Huckel
APACHE	accelerator for physics and chemistry of heavy elements	CIHY	configuration interaction Hylleras
APR	acoustic paramagnetic resonance	CIM	constituent interchange model
APS	appearance potential spectra(scopy)	CMI	computer managed instruction
APW	augmented plane wave	CML	current-mode logic
ARMA	autoregressive moving average	CMOS	complementary metal-oxide-semiconductor
ASCII	American standard code for information exchange	CNC	computerised numerical control
ATC	air traffic control	CNDO	complete neglect of differential overlap
ATE	automatic test equipment	COC	cholesteryl oleyl carbonate
ATM	Axilrod-Teller-Moto	COM	computer output to microform (fiche or film)
ATR	attenuated total reflection	COOB	4,4'-cyano-octyloxy-biphenyl
ATWS	anticipated transients without scram	CP	charge, parity
AVC	automatic volume control	CPA	coherent potential approximation
BARITT	barrier injection transit time	CPA	critical path analysis
BBEA	4-butoxybenzal-4'-ethylaniline	CPM	critical path method
BBGKY	Bogoliubov-Born-Green-Kirkwood-Yvon	CPSK	coherent phase shift keying
BCC	body centred cubic	CPT	charge, parity, time
BCD	binary-code decimal	CPU	central processing unit
BCS	Bardeen-Cooper-Schrieffer	CRO	cathode ray oscilloscope
BFL	buffered FET logic	CRSR	coherent resonant Stokes rotation
BFO	beat-frequency oscillator	CRT	cathode ray tube
BH	buried heterostructure	CS	coupled states
BWO	backward wave oscillator	CSL	current-sinking logic
BWR	boiling water reactor	CSL	current-sourcing logic
BWT	backward wave tube	CSM	continuous slowing down models
C <sup>3</sup> L	complementary constant current logic	CSRS	coherent Stokes-Raman spectra(scopy)
CAD	computer aided design	CT	computerised tomography
CANDU	Canadian deuterium uranium	CTL	complementary-transistor logic
CAE	computer aided engineering	CTR	controlled thermonuclear reactor
CAI	computer assisted instruction	CVD	chemical vapour deposition
CAM	computer aided manufacturing	CW	continuous wave
CARS	coherent antiStokes Raman scattering (spectra)	D/A	digital-to-analogue
CATV	community antenna TV		
CB	citizen band		
CBI	computer based instruction		

DAC	digital analogue conversion	EDA	ethylene diamine
DBMS	database management system	EDP	electronic data processing
DBR	distributed Bragg reflector	EDTA	ethylene diamine tetra-acetic acid
DC	direct current	EEBAC	ethyl-4-(4'-ethoxy-benzylidene-amino) cinnamate
DCFL	direct-coupled FET logic	EEG	electroencephalography (-gram)
DCTL	direct-coupled transistor logic	EELS	electron energy loss spectra(scopy)
DDC	direct digital control	EEPROM	electrically erasable programmable read-only-memory
DDL	diode-diode logic	EFL	emitter-follower logic
DECENT	distribution of exact classical energy transfer	EFL	emitter-function logic
DESY	Deutsches Elektron Synchrotron	EFM	extended Flygare method
DF	Dirac-Fock	EFT	electronic funds transfer
DFB	distributed feedback	EHD	electrohydrodynamics
DH	double heterostructure	EHF	extremely high frequency
DIL	dual-in-line	EHP	electron-hole potential method
DIP	dual in-line package	EHT	extended Huckel theory
DITE	divertor in torus experiment	EHV	extra high voltage
DLTS	deep level transient spectra(scopy)	ELDOR	electron electron double resonance
DM	delta modulation	ELF	extremely low frequency
DMA	direct memory access	EM	electromagnetic
DMM	digital multimeter	EMC	electromagnetic compatibility
DMOS	double diffused metal-oxide-semiconductor	EMF	electromotive force
DMSO	dimethylsulphoxide	EMG	electromyography (-gram)
DNA	deoxyribonucleic acid	EMI	electromagnetic interference
DNMR	double nuclear magnetic resonance	EMP	electromagnetic pulse
DOBAMBC	p-decyloxybenzylidene p'-amino 2-methyl butyl cinnamate	ENDOR	electron nuclear double resonance
DOD	different orbitals for different spins	ENG	electronic newsgathering
DORIS	Dopple-Ring-Speicher	EOF	end of file
DOS	disc operating system	EPEN	empirical potential energy function based on interactions of electrons and nuclei
DOVETT	double velocity transit time	EPMA	electron probe microanalysis
DP	data processing	EPR	electron paramagnetic resonance
DPCM	differential pulse code modulation	EPRI	Electric Power Research Institute
DPPH	diphenylpicrylhydrazyl	EPROM	erasable programmable read-only-memory
DPSK	differential phase shift keying	ERG	electroretinography (-gram)
DSAM	Doppler shift attenuation method	ESCA	electron spectroscopy for chemical analysis
DSC	differential scanning calorimetry	ESCAR	experimental superconducting accelerating ring
DTA	differential thermal analysis	ESFJ	epitaxial silicon film on insulator
DTL	diode transistor logic	ESS	electronic switching system
DTU	dual topological unitarisation	EUV	extreme ultraviolet
DVM	digital voltmeter	EW	electronic warfare
DV-X $\alpha$	discrete variational X $\alpha$ method	EXAFS	extended X-ray absorption fine structure
DWBA	distorted wave Born approximation	EX-OR	exclusive-OR (logic)
DWIA	distorted wave impulse approximation	FAMOS	floating gate avalanche metal-oxide-semiconductor
E1,E2	electric dipole, quadrupole	FBR	fast breeder reactor
E <sup>2</sup> PROM	electronically erasable read-only-memory	FCC	face centred cubic
EAROM	electronically alterable read-only-memory	FDM	frequency division multiplex(ing)
EAS	extensive air shower	FDNC	frequency dependent negative conductance
EB	exponential Born	FDNR	frequency dependent negative resistance
EBBA	4-ethoxybenzylidene-4'-n-butylaniline	FECL	feedback ECL
EBIC	electron beam induced current(s)	FEM	field emission microscopy
EBR	experimental breeder reactor	FET	field effect transistor
EBT	Elmo Bumpy Torus	FFHR	fusion-fission hybrid reactor
ECCM	electronic counter-counter measures	FFT	fast Fourier transform
ECCS	emergency core cooling system		
ECELR	epithermal critical experiment laboratory reactor		
ECG	electrocardiography (-gram)		
ECL	emitter coupled logic		
ECM	electronic countermeasures		

FFTF	fast flux test facilities	HOBHA	p-n-heptyloxy-benzylidene-p-n-heptyl-aniline
FHNC	Fermi hypernetted chain	HOMO	highest occupied molecular orbitals
FIM	field ion microscopy	HTGR	high temperature gas-cooled reactor
FIMOS	floating gate ionisation injection metal-oxide-semiconductor	HV	high voltage
FIR	finite impulse response	HVDC	high voltage direct current
FM	frequency modulation	HVEM	high voltage electron microscopy
FMIT	fission materials irradiation test facility	HWR	heavy water reactor
FMR	ferromagnetic resonance	IAEA	International Atomic Energy Authority Agency
FMSR	fast mixed spectrum reactor	IAR	isobaric analogue resonance
FPT	finite perturbation theory	IAS	isobaric analogue state
FPLA	field programmable logic array	IBA	interacting boson approximation
FSK	frequency-shift keying	IBFA	interacting boson-fermion approximation
FSGO	floating spherical Gaussian orbitals	IBM	interacting boson model
FTR	fast test reactor	IBPBAC	isobutyl-4-(4'-phenylbenzylideneamino) cinnamate
GAMBIT	gate modulated bipolar transistor	IC	integrated circuit
GANIL	grand accélérateur national à ions Lourds	ICDF	intermediate coupling Dirac-Fock
GCFR	gas-cooled fast breeder reactor	ICF	inertial confinement fusion
GCM	generator coordinate method	IDT	interdigital transducer
GDR	giant dipole resonance	IEPA	independent electron pair approximation
GHF-NO-CI	generalised Hartree-Fock/natural orbital/configuration interactions	IETS	inelastic electron tunnelling spectroscopy
GIAO	gauge-invariant atomic orbitals	IF	intermediate frequency
GMR	giant monopole resonance	IFA	ionisation front accelerator
GO	Gaussian orbitals	IGFET	insulated gate field effect transistor
GOO	generalised Overhauser orbitals	IIR	infinite impulse response
GPM	ground potential model	IKO	Institute v. Kernph. Ouder Amsterdam
GQR	giant quadrupole resonance	I <sup>2</sup> L	integrated injection logic
GRIN	graded (gradient) refractive index	I <sup>3</sup> L	isoplanar I <sup>2</sup> L
GSPC	gas scintillation proportional chamber (or counter)	ILS	instrument landing system
GTO	Gaussian-type orbitals	IMPATT	impact avalanche transit time
GUT	grand unified theory	INDO	intermediate neglect of differential overlap
GVB	generalised valence bond	INDOR	internuclear double resonance
HAM	hydrogenic atoms in molecules	ING	intense neutron generator
HBAB	hexyloxybenzylidene-p'-aminobenzonitrile	INO	iterative natural orbital
HBT	N-(p-hexyloxybenzylidene)-p-toluidene	INTELSAT	international telecommunications satellite consortium
HCDA	hypothetical core disruptive accident	I/O	input/output
HCP	hexagonal close packed	IOC-6	inclusion of the overlap charges in the omega
HEED	high energy electron diffraction	IPSS	international packet switching service
HEMP	high altitude electromagnetic pulse	IR	infrared
HEMT	high electron mobility transistor	IRDO	intermediate retention of differential overlap
HF	high frequency or Hartree-Fock	IREB	intense relativistic electron beam
HFB	Hartree-Fock-Bogoliubov	IREL	infrared emitting diode
HFEF	hot fuel examination facility	IRS	information retrieval system
HFIR	high flux isotope reactor	ISABELLE	intersecting storage and acceleration
HFO	Hartree-Fock-Overhauser	ISDN	integrated services digital network
HFS	hyperfine structure	ISFET	ion-sensitive field effect transistor
HGMS	high gradient magnetic separation	ISL	integrated Schottky logic
HIXE	heavy ion induced X-ray emission	ISR	intersecting storage ring
HJFET	heterojunction field effect transistor	ISX	impurity study experiment
HLW	high level waste (radioactive)	ITC	ionic thermocurrents
HMO	Huckel molecular orbitals	ITEP	Institute of Theoretical and Experimental Physics
HMTSeF	hexamethylenetetraselenafulvalene (-inim)	ITR	ignition test reactor
HMTTF	hexamethyltetraethiofulvalene(-inim)	IU	Indiana University
HOAB	heptyloxyazoxybenzene		

IVO	improved virtual orbitals	MEDO	multipole expansion of diatomic overlap
JAERI	Japan Atomic Energy Research Institute	MESFET	metal-semiconductor field effect transistor
JET	Joint European torus	MF	medium frequency
JFET	junction field effect transistor	MFP	mean free path
JINR	Joint Institute for Nuclear Research	MHD	magnetohydrodynamics
KdV	Korteweg-de Vries	MIC	microwave integrated circuit
KEK	Japan National Laboratory for High Energy Physics	MID	magnetically insulated diode
KKR	Korringa-Kohn-Rostoker	MIDP	microwave induced delayed phosphorescence
LAMPF	Los Alamos meson physics facility	MIEHM	modified iterative extended Huckel method
LC	inductance-capacitance	MIM	metal-insulator-metal
LCAO	linear combination of atomic orbitals	MIMD	multiple input multiple data
LCBO	linear combinations of (semi-localised) band orbitals	MIS	metal-insulator-semiconductor or management information system
LCD	liquid crystal display/device	MIT	Massachusetts Institute of Technology
LCGO	linear combination of Gaussian orbitals	MM	millimetre
LCP	large coil program	MMF	magnetomotive force
LCRO	linear combination of Rydberg orbitals	MMIC	monolithic microwave integrated circuit
LEC	liquid encapsulated Czochralski	MNOS	metal-nitride-oxide-semiconductor
LED	light emitting diode	MO	molecular orbitals
LEED	low energy electron diffraction	MOCIC	molecular orbital constraint of interaction coordinates
LEP	large electron positron	MOCVD	metal-organic chemical vapour deposition
LET	linear energy transfer	MODPOT	model potential
LF	low frequency	MOS	metal-oxide-semiconductor
LMC	Large Magellanic Cloud	MOSFET	metal-oxide-semiconductor field effect transistor
LMFBR	liquid metal fast breeder reactor	MOST	metal-oxide-semiconductor transistor
LMTO	linear combination of muffin tin orbitals	MRD	multi-reference double excitation
LNG	liquified natural gas	MRINDO	modified Rydberg INDO
LOCA	loss of coolant accident	MS	management science
LOCE	loss of coolant experiment	MSI	medium scale integration
LOCOS	local oxidation of silicon	MSK	minimum shift keying
LOFT	loss of flow test facility	MSR	molten salt reactor
LPE	liquid phase epitaxy	MSU	Michigan State University
LPFL	low pinchoff-voltage FET logic	MSW	magnetostatic waves
LSA	limited space charge accumulation	MTBF	mean-time between failures
LSD	local spin density	MTF	modulation transfer function
LSI	large-scale integration	MTL	merged-transistor logic
LTE	local thermodynamic equilibrium	MTX $\alpha$	muffin-tin $X\alpha$
LUMO	lowest unoccupied molecular orbitals	MUF	maximum usable frequency
LV	low voltage	MWPC	multiwire proportional chamber
LWBR	light water breeder reactor	NAL	National Accelerator Laboratory
LWR	light water reactor	NAND	not-and(logic)
MADO	Mulliken approximation for differential overlap	NC	numerical control
M1,M2	magnetic dipole, quadrupole	NCMET	non-closed shell many electron theory
MBBA	4-methoxybenzylidene-4'-n-butylaniline	NDDO	neglect of diatomic differential overlap
MBE	molecular beam epitaxy	NDT	nondestructive testing
MBPT	many body perturbation theory	NEMO	non-empirical molecular orbitals
MCD	magnetic circular dichroism	NEVE	non-empirical valence-electron
MCP	microchannel plate	NHS	National Health Service
MCSCF	multiconfiguration self-consistent-field	NIC	negative impedance converter
MCPESCF	multiconfiguration paired excitation SCF	NMOS	N-channel metal-oxide-semiconductor
MCZDO	multi-centre zero differential overlap	NMR	nuclear magnetic resonance
MCX $\alpha$	multiconfiguration $X\alpha$	NMR-ON	NMR on oriented nuclei
MEC	molecular electron correlation(s)	NNDO	neglect of non-neighbour differential overlap
		NOR	not-or(logic)

NQR	nuclear quadrupole resonance	PMDR	phosphorescence microwave double resonance
NRC	nuclear regulatory committee	PMOS	P-channel metal-oxide-semiconductor
NRM	natural remanent magnetisation	PMR	proton magnetic resonance
NSSS	nuclear steam supply system	PND0	partial neglect of differential overlap
NTL	nonthreshold logic	PNO-CI	pair natural orbital configuration interaction
NTO	natural transition orbitals	POL	pair orthogonalised Lowdin
OCR	optical character recognition	POPAE	protons on protons and electrons
ODMR	optical detection of magnetic resonance	POPOP	phenyl-oxazolyI-phenyl-oxazolyI-phenyl
OEM	original equipment manufacture	POS	point of sale
OER	oxygen enhancement ratio	PPDP/S	Pariser-Parr-Del Bene-Pople/Segal calculations
OPHF	orbital polarised Hartree-Fock	PPI	plan position indicator
OPW	orthogonal plane wave	PPM	pulse position modulation or parts per million
OR	operations research	PPP	Pariser-Parr-Pople
ORELA	Oak Ridge electron linear accelerator	PRDDO	partial retention of diatomic differential overlap
ORNL	Oak Ridge National Laboratory	PRF	pulse recurrence (répétition) frequency
OS	operating system	PROM	programmable read-only-memory or Pockels readout optical modulator
OTEC	ocean thermal energy conversion	PS	proton synchrotron (CERN)
OTF	optical transfer function	PSK	phase shift keying
PAA	paraazoxyanisole	PTFE	polytetrafluoroethylene
PABX	private automatic branch exchange	PTM	pulse time modulation
PAC	perturbed angular correlation	PVC	polyvinyl chloride
PAHR	post accident heat removal	PWA	partial wave analysis
PAM	pulse amplitude modulation	PWB	printed wiring board
PAP	paraazoxyphenetole	PWBA	plane wave Born approximation
PBF	power bursts facility	PWIA	plane wave impulse approximation
PBR	pebble bed reactor	PWM	pulse width modulation
PBT	permeable base transistor	PWR	pressurised water reactor
PBX	private branch exchange	QAM	quadrature amplitude modulation
PC	printed circuit	QCD	quantum chromodynamics
PCAC	partially conserved axial currents	QDMBPT	quasi-degenerate many-body perturbation theory
PCB	printed circuit board	QED	quantum electrodynamics
PCES	phase change energy storage	QPM	quark-parton model
PCGVB	pairwise correlated generalised valence bond	QPSK	quaternary phase shift keying
PCILOCC	perturbative configuration interaction using localised orbitals for crystal calculation	RAM	random access memory
PCM	pulse code modulation	RBE	relative biological effectiveness
PCRv	prestressed concrete reactor vessel	RC	resistance-capacitance
PCX	plasma confinement experiment	RCNDO	Rydberg CNDO
PDX	poloidal divertor experiment	RCS	rapid cycling synchrotron
PEM	photoelectromagnetic	RCTL	resistor-capacitor-transistor logic
PEP	positron electron proton	R & D	research and development
PET	polyethylene terephthalate	RF	radio frequency
PETRA	positron electron tandem ringbeschleuniger anlage	RFI	radio frequency interference
PF	power factor	RG	renormalisation group
PFM	pulse frequency modulation	RHEED	reflection high energy electron diffraction
PFR	prototype fast reactor	RHF	restricted Hartree-Fock
PHWR	pressurised heavy water reactor	RINDO	Rydberg INDO
PID(PI,PD)	proportional+integral+differential (derivative)	RKKY	Rudermann-Kittel Kasuya-Yosida
PIXE	proton induced X-ray emission	RLC	resistance-inductance-capacitance
PLA	phase locked arrays or programmable logic array	RMS	root-mean-square
PLBR	prototype large breeder reactor	RNA	ribonucleic acid
PLC	programmable logic control	ROM	read-only memory
PLL	phase locked loops	RPA	random phase approximation
PLT	Princeton Large Torus		
PM	pulse modulation		
PMMA	polymethylmethacrylate		

RPAE	random phase approximation with exchange	SSFL	Schottky-barrier coupled Schottky-barrier gate FET logic
RPM	relaxation potential model or revolutions per minute	SSI	small scale integration
RPV	reactor pressure vessel	SST	supersonic transport
RTG	radioisotope thermoelectric generators	STD	salinity-temperature-depth or subscriber trunk dialling
RTL	resistor-transistor logic	STEC	solar thermal energy conversion
SACCI	symmetry adapted cluster configuration interaction	STEM	scanning transmission electron microscopy
SAMO	simulated ab initio molecular orbitals	STL	Schottky transistor logic
SAR	synthetic aperture radar	STO	Slater-type orbitals
SAW	surface acoustic waves	STOL	short take-off and landing
SCC	stress corrosion cracking	STP	Slater-transfer Preuss
SCF	self consistent field	SUSY GUT	supersymmetric grand unified theory
SCFL	source-coupled FET logic	SW	short wave
SCL	space charge limited	SWR	standing wave ratio
SCPT	self consistent perturbation theory	SXAPS	soft X-ray appearance potential spectrum
SCR	silicon controlled rectifier	TASI	time assignment speech interpolation
SDFL	Schottky-diode FET logic	TBBA	terephthal-butylaniline
SDM	space division multiplexing	TCNE	tetracyanoethylene
SDO	shielded diatomic orbitals	TCNQ	tetracyanoquinodimethane
SED	stochastic electrodynamics	TCR	temperature coefficient of resistance
SEHF	spin extended Hartree-Fock	TDHF	time dependent Hartree-Fock
SEM	scanning electron microscopy	TDM	time division multiplex(ing)
SFE	solar-flare effect	TDMA	time division multiple access
SFL	substrate fed logic	TDMF	time dependent mean field theory
SGEMP	system generated electromagnetic pulse	TDPAC	time differential perturbed angular correlation
SGHWR	steam generating heavy water reactor	TDS	thermal desorption spectra(oscopy)
SHF	superhigh frequency	TE	transverse electric
SHG	second harmonic generation	TEA	transversely excited atmosphere
SICOS	sidewall base contact structure	TEGFET	two-dimensional electron gas field effect transistor
SIMOS	stacked-gate injection metal-oxide-semiconductor	TEM	transverse electromagnetic or transmission electron microscopy
SIMS	secondary ion mass spectra(oscopy)	TEXT	Texas Experimental Tokamak
SIN	Swiss Institute of Nuclear Research	TFTR	Tokamak fusion test reactor
SINDO	scaled INDO	TGA	thermogravimetric analysis
SIS	semiconductor-insulator-semiconductor	TGFB	triglycine fluoroberyllate
SISAM	spectrometer with interference selective amplitude modulation	TGS	triglycine sulphate
SIT	static induction transistor	TGSe	triglycine selenate
SMC	Small Magellanic Cloud	TJS	transverse junction stripe
S/N	signal-to-noise	TLD	thermoluminescent dosimeter(-ry)
SOG	strongly orthogonal geminal	TM	transverse magnetic
SOS	silicon on sapphire	TMI	Three Mile Island
SPA	separated pair approximation	TMMC	tetramethylammonium manganese chloride
SPC	stored program control	TMTSeF	tetramethyltetraselenafulvalene(inium)
SPEAR	Stanford positron electron asymmetric ring	TMTTF	tetramethyltetraathiofulvalene
SPHF	spin polarised Hartree-Fock	TOP	transient overpower accident
SPIN-CIPSI	spin symmetry adapted generalisation of CIPSI	TNS	The Next Step
SPS	super proton synchrotron (CERN)	TPC	time projection chamber
SREMP	source region electromagnetic pulse	TRAPATT	trapped plasma avalanche triggered transit
SQUID	superconducting quantum interference device	TREAT	transient reactor test facility
SRMCASE	symmetry-restricted-multiconfiguration annihilation of single excitations	TRM	thermoremanent magnetisation
SSB	single sideband	TSC	thermally stimulated currents
SSBW	surface skimming bulk wave	TSEE	thermally stimulated exo-electron emission
SSC	sudden storm commencement	TSeF	tetraselenafulvalinium
		TSeT	tetraselenatetracene
		TTF	tetrathiofulvalinium

TTL	transistor transistor logic	VLBI	very long base line interferometry
TTT	tetrathiotetracene	VLF	very low frequency
TUCA	transient undercooling accident	VLSI	very large scale integration
TV	television	VMOS	vertical channel metal-oxide-semiconductor
TW	travelling wave	VOR	VHF omnidirectional range
TWT	travelling wave tube	VPE	vapour phase epitaxy
UART	universal asynchronous receiver/transmitter	VRC	visual record computer
UCHF	uncoupled Hartree-Fock	VRDDO	variable retention of diatomic differential
UCN	ultra cold neutrons	VS	virtual storage
UHF	ultra high frequency or unrestricted Hartree-Fock	VSF	vestigial sideband
UHPS	underground hydroelectric pumped storage	VSEPR	valence shell electron pair repulsion
UHV	ultra high voltage	VSWR	voltage standing wave ratio
UKAEA	United Kingdom Atomic Energy Authority	VTOL	vertical take-off and landing
ULA	uncommitted logic array	VTR	voltage transformation ratio or video tape recorder
ULF	ultra low frequency	VUV	vacuum ultraviolet
UMD	unitised microwave devices	VVER	water moderated water cooled reactors
UPS	ultraviolet photoelectron spectra	WARC	World Administrative Radio Conference
US	ultrasonic	WDM	wavelength division multiplex(ing)
UV	ultraviolet	WKB	Wentzel-Kramers-Brillouin
VAD	vapour phase axial deposition	WP	word processing
VB	valence bond	WWER	water moderated water cooled reactors
VCR	video cassette recorder	XPS	X-ray photoelectron spectra
VDM	vector dominance model	ZEBRA	zero energy breeder reactor assembly
VDU	visual display unit	ZGS	zero gradient synchrotron
VHF	very high frequency	ZPPR	zero power plutonium reactor
VHSIC	very high speed integrated circuit		



# Subject Index

1/f noise *see random noise*

## A-centres

- KBr:In,  $A^{2+}$ , F-centres formed by low-energy excitons, photoluminescence spectra (*Russian*) 4-113874  
KCl:Li, optically excited colour centres, relaxation dynamics 4-113896  
KCl:Li  $F_A(II)$  colour centre laser, optical pumping, improvement 4-107648  
Si, A-centre and thermal donor levels, Hall effect, DLTS meas., press. depend. 4-80529  
Si:H, grown by zone melting, A-centre distrib. study 4-76666  
Si:Li p-n junction solar cells, electron induced degradation, recovery under space conditions 4-105110  
ZnSe:I, vacancy-I complex hyperfine interactions, ESR study 4-70150

A/D conversion *see analogue-digital conversion*

## ab initio calculations

- 3d transition metals with adsorbed CO, electronic struct. and chemical reactivity of CO 4-93552  
 $A^{III}B^V$  semiconductors, ab initio band struct. calc. 4-75832  
acene oligomers, electronic struct., XPS, ab initio MO theory 4-68946  
acetaldehyde, ionised, keto-enol tautomerism mechanism and dissociation, ab initio MO study 4-91196  
acetylene conformers, relative stabilities, ab initio and CI calcs. 4-74145  
 $\alpha$ -acetylenic alcohols, Meyer-Schuster reaction, saddle points, transition-state struct. 4-114773  
acidic  $H_2O_2$  fuel cells, hydrogen-electrode processes investig. 4-105106  
actinide metals, light, cohesive energies calc. 4-75354  
adenine-water complexes, H bond, ab initio SCF CI STO-3G calcs. 4-64386  
aliphatic amines, unbranched primary, ab initio calc. on  $H^+$  affinity 4-91195  
alkali metal atoms, core polarisation pot., intershell correl. effects, ab initio SCF CI calcs. 4-68970  
alkali metal dimers, crossing states, pot. energy curves, ab initio calcs. 4-68995  
alkali metal dimers and cations, ground state props., effective core polarisation pots., SCF CI calcs. 4-68971  
alkaline earth metal atoms, core polarisation pot., intershell correl. effects, ab initio SCF CI calcs. 4-68970  
alkyl radicals, UV spectra, ab initio SCF and CI calcs. 4-96560  
n-alkylboronic acid binding to  $\alpha$ -chymotrypsin A substrate 4-89489  
allene, excited state, torsion and bending, full optimised reaction space MCSCF CI calcs. 4-59646  
allene, vertical excited states; mag. circ. dichroism spectra 4-78883  
allyl alcohol, conformational anal., ab initio MO study 4-64338  
allyl cations, monosubstituted, ab initio MO calcs., geometries, substituents stabilising and rot. barrier effects 4-112109  
allylamine, conformational anal., ab initio MO calcs. 4-102587  
atomic energy differences, electron correl. coeffs. approximate method 4-83304  
atoms, ab initio local-density pot., modified  $\bar{E}$  method 4-64371  
bacteriorhodopsin, conducting system, ab initio SCF calcs. 4-83288  
basis set error and geometry optimisation in ab initio calc. 4-64357  
benzene, reson. energies, ab initio calcs. 4-59617  
benzene dimer, interaction and dispersion effects, ab initio HF calcs. 4-102579  
benzene-s-tetrazine mixed dimer, interaction and dispersion effects, ab initio HF calcs. 4-102579  
benzenes, fluorinated, bond lengths, substituent effects, overtone spectra ab initio STO calcs. 4-107275  
benzoic acid,  $H^+$  transfer 4-93510  
benzoic acid, substituent effects, ab initio LCAO STO calcs. 4-96435  
biacetyl, vibr. spectra in the first singlet excited electronic states 4-74282  
bifurans, internal rotation barriers, ab initio MO STO calcs. 4-64337  
bis(trifluoromethyl)peroxide, struct. evaluated by ab initio gradient method at computational level 4-64355  
borabenzene, quantum chem. calcs. 4-96434  
1,3-butadiene, rot. isomerism, geometry optimisation and basis set size effect, ab initio study 4-87231  
butanal, conformational anal. and mol. struct., ab initio calcs. 4-102581  
n-butane, configs., rot. pot. surface, basis set and CI calcs. 4-96460  
butatriene, mol. struct., ab initio MO calcs. 4-64351  
butanal, photodissociation dynamics, ab initio and RRKM calcs. 4-109670  
carbonyl fluoride anion, struct. and vibr. spectrum, ab initio SCF MO theory 4-87038  
chloromethane, CI quadrupole coupling const., nonempirical calcs. 4-107281  
complex borohydrides of Be and Mg, bonding nature, ab initio calculations 4-59911  
composite surface,  $H^-$  and  $D^+$  ion generation rel. to surface/plasma ion source systems 4-93165  
conformational energy surfaces, MO STO calcs. 4-68954  
cycloalkanes, protonation, ab initio SCF MO calcs. 4-104982  
cyclobutadiene, reson. energies, ab initio calcs. 4-59617  
cyclohexane-1-d, isomers, IR and Raman spectra, vibr. anal., ab initio HF calcs. 4-59770  
cyclohexanol, H bonds, rot. barriers, INDO and ab initio STO-3G calcs. 4-112115  
cyclopropane-HCN, H bonded complex, ab initio SCF MO study 4-64343  
cyclopropyl anions,  $\alpha$ -substituted, ab initio MO study 4-64359  
cytosine, tautomerism, ab initio calcs. 4-112100  
diamond, cohesive and struct. props., ab initio LCAO calc. 4-60881  
diatomic hydrides, Hartree-Fock-Roothaan wavefunctions (*Chinese*) 4-96428

## ab initio calculations continued

- 2,4-diboramethylenecyclopropane, B=C double bond, ab initio SCF calcs. 4-112094  
difluorodimethoxymethane, conformation, pot. energy surfaces, ab initio SCF MO study 4-64341  
difluoromethanediol, conformation, pot. energy surfaces, ab initio SCF MO study 4-64341  
dimethyl anion, semiempirical and ab initio calcs. 4-64377  
dimethyl disulphide, rot. barrier about disulphide bridge, ab initio calc. 4-74138  
dimethyl peroxide, struct. evaluated by ab initio gradient method at computational level 4-64355  
dimethyl sulphoxide, basis set error and geometry optimisation in ab initio calc. 4-64357  
1,3-dioxan-5-ol, H bonds, rot. barriers, INDO and ab initio STO-3G calcs. 4-112115  
1,4-dithiane, conformational change from chair to boat upon ionisation, optical spectra, MO calcs. 4-89246  
dithioresorcinols, and derivatives, UPS, ab initio STO-3G calcs. 4-83421  
DNA, B and Z, interaction energies between purine and pyrimidine bases, ab initio SCF LCAO calcs. 4-66851  
DNA base components, electrostatic interactions, pot. derived point-charge model study 4-107271  
electron cloud displacement model in ab initio calcs., diatomic mol. case (*Chinese*) 4-74136  
electron cloud displacement model in ab initio calcs., polyatomic mol. case (*Chinese*) 4-74137  
enzyme action mechanism, quantum chemical study 4-71867  
epoxide-nucleophile reaction, effect on H bonding involving the nucleophile 4-76980  
ethanedinitrile, intermolecular dimer pot., ab initio calcs. 4-102758  
ethyl radical, direct adiabatic channel computation for excited state relax. to give H+ethylene 4-96433  
ethylamines, trans and gauche forms, vibr., force const., ab initio MO calcs. 4-59622  
ethylene, elastic electron scatt. cross section, ab initio SCF HF calcs. 4-112270  
ethylene+1 $_2$ , electrophilic addition reaction, ab initio MO calcs. 4-66566  
ethynyllithium, electron density superposition errors 4-113383  
EXAFS, struct. information, reliability of ab initio calcs. 4-66102  
fluorobenzene, mol. struct., ring distortion electron diff. study 4-112276  
5-fluorouracil, tautomerism, ab initio calcs. 4-112100  
formaldehyde, reaction energies, pot. energy surfaces, ab initio calcs. 4-114789  
formaldehyde+O(OH), H abstraction, pot. energy surface, ab initio HF CI calcs. 4-99770  
formaldehyde oxidation, H at. migration channel study 4-71897  
formaldoxime, photoelectron spectra, vibronic anal., ab initio SCF CI calcs. 4-112121  
formamide+glyoxals charge transfer, ab initio calcs., appl. electronic theory of cancer 4-87205  
formic acid dimer, struct., ab initio MO calcs. 4-102578  
formic acid H-bonded chains, struct. and stability, ab initio calcs. 4-102573  
glycine, aq. soln., conformational energy, ab initio LCAC-MO-SCF calcs. 4-96449  
glycine methyl ester, conformational anal., ab initio calc. 4-64358  
graphite intercalation compound with Li, LiC $_6$ , optical spectra, ab initio calc., origins of plasmons 4-88802  
group equivalents for converting ab initio energies to enthalpies of formation 4-102586  
guanidinium-carboxylate interaction, ab initio SCF HF calcs. 4-96436  
guanine-water complexes, H bond, ab initio SCF CI STO-3G calcs. 4-64386  
hexafluoroacetone, vibr. spectra and struct. 4-71372  
hydrides, first- and second-row, sp hybridisation, ab initio MO study 4-102575  
hyperconjugation, structural consequences 4-68951  
intermolecular interaction energy calc., first order, basis set development 4-64561  
isopropyl and ethyl formate, conformational anal., struct., ab initio gradient method appl. 4-102585  
isopropyl anions,  $\alpha$ -substituted, ab initio MO study 4-64359  
ketenimine, ab initio force field, scaling factors 4-87094  
macromolecular struct. determ. from X-ray data, multi-dimensional search method 4-74358  
magnesium malonate complexes, binding, STO-3G ab initio calcs. 4-64336  
main group cpds., sp hybridisation, substitution effect on orbital utilisation 4-102576  
malonic acid, intramol. H-bonding, ab initio study 4-87033  
malonic acid monoanion, intramol. H-bonding, ab initio study 4-87033  
metalloporphyrins, axial ligand conform preferences, ab initio SCF calcs. 4-96448  
methane, elastic electron scatt. 20-500 eV, cross sections, pots., quantum mechanical calcs. 4-96698  
methane, substituted, intermolecular pots., ab initio SCF calcs. 4-96640  
methanol, gaseous, high overtone C-H and O-H transitions 4-59620  
methyl chloride, anharmonic force field, ab initio MO calcs. 4-112125  
methyl derivatives, conformational preferences, ab initio SCF MO STO calcs. 4-68952  
methyl fluoride, anharmonic force field, ab initio MO calcs. 4-112125  
methyl propanoate, conformational anal., ab initio calc. 4-64358  
1-methyl-7-azaindole, struct. and props., ab initio MO calcs. 4-78782  
7-methyl-7H-pyrrolo(2, 3-b)pyridine, 1-methyl-7-azaindole, struct. and props., ab initio MO calcs. 4-78782

## ab initio calculations continued

methylenic, dipole moments, ab initio rot.-vibr. transition moments 4-59688  
 methylene, Renner-Teller pot. energy surfaces, analytic second derivatives 4-91250  
 methylenebis(oxo), H at. migration reaction channel, formed in formaldehyde oxidation 4-71897  
 methylglyoxal(-d<sub>3</sub>), vibr. spectra in the first singlet excited electronic states 4-74282  
 molecular solutes, absorpt. and emission transitions, ab initio calc. including solvent effects 4-64362  
 molecules, electric field depend. basis functions for elec. polarisability and moment calcs. 4-68956  
 molecules, internal motion, electron density dynamic anal., ab initio MO calcs. 4-87037  
 multiple bond molecules, nuclear spin-spin coupling consts., orbital diamag. contrib. 4-64388  
 nitromethane, electronic struct. calc. 4-87032  
 paraffin oligomers, electronic struct., XPS, ab initio MO theory 4-68946  
 polyacetylenes, ab initio Hartree-Fock calcs. 4-96728  
 polyethylene chains, torsional pot. ab initio cryst. orbital calcs. 4-69255  
 polyoxymethylene chain, struct. ab initio cryst. orbital calcs. 4-69256  
 polypeptides, transition dipole interaction, ab initio calcs. 4-89501  
 polypyrrole, band struct. calcs., ab initio HF study 4-84542  
 porphyrins, normal and hyperphosphorus electronic states, ab initio calcs. 4-96440  
 propanal, conformational anal. and mol. struct., ab initio calcs. 4-102581  
 propanal, struct. studied by electron diff., microwave and IR spectra, force field 4-64603  
 1-propanol in low temp. matrices, IR-induced rotamerisation, ab initio, calcs. 4-64634  
 propynal, photodissoc., pot. energy surfaces, ab initio and CI calcs. 4-66601  
 propynal, photodissociation dynamics, ab initio and RRKM calcs. 4-109670  
 pseudopotentials, ab initio norm-conserving, construction method 4-70619  
 pyrazoles, proton affinity, charge, ab initio STO-3G calcs. 4-64335  
 quantum chemical le Chatelier principle, general formulation 4-74127  
 rare earth oxyhalides, doped, crystal field, quadrupole moments, ab initio calc. 4-65650  
 reaction-path Hamiltonian, WKB approx., appl. to vibr. transition state theory, barrier heights and reson. calc. 4-99746  
 resorcinol and derivatives, UPS, ab initio STO-3G calcs. 4-83421  
 rotational spectra, quantum mech. calcs., ab initio MO method 4-69041  
 sodium hydrogen oxalate monohydrate, cryst., electron density, intermolecular interactions, ab initio LCAO-MO-SCF calcs. 4-88160  
 stability and electronic struct., ab initio calc. 4-68922  
 strained systems, electrostatic pots., reactive props., ab initio SCF-MO STO-5G calcs. 4-102580  
 substituent field parameters, theoretical scale 4-64350  
 tetramethylene diradical intermediate, singlet state, ab initio MC SCF geom. optimisation 4-96432  
 s-tetrazine dimer, interaction and dispersion effects, ab initio HF calcs. 4-102579  
 thioacetamide, cryst. struct., rotamers, neutron diff. study, ab initio MO CI calcs. 4-103734  
 thioketones, chiroptical props., circular dichroism spectra and ab initio RPA calcs. 4-78916  
 thymine, tautomerism, ab initio calcs. 4-112100  
 transition metal carbenes, nucleophiles and electrophiles, MO and CI calcs. 4-102605  
 transition metal sandwich metallocenes, correl. effects, ab initio HF calc. 4-68921  
 trichloromethane, CI quadrupole coupling consts., nonempirical calcs. 4-107281  
 trifluoromethoxide anion, struct. and vibr. spectrum, ab initio SCF MO theory 4-87038  
 uracil, tautomerism, ab initio calcs. 4-112100  
 Walden inversion reactions, solvent effect 4-66558  
 water clusters, neutral and protonated, struct. calc. with mol. graphics 4-96734  
 Al, charge densities, interionic pot., phonon freq., calcs. 4-113856  
 Al epitaxial growth on Ge (001), first principles calc. of energy 4-92580  
 Al<sub>2</sub>, electronic states, ab initio MO SCF and first-order CI calcs. 4-102604  
 AlF, vibr. struct., ionisation pot., PNO/CEPA calcs., photoelectron spectra 4-96613  
 AlF<sub>3</sub>, vibr. struct., ionisation pot., PNO/CEPA calcs., photoelectron spectra 4-96613  
 Ar<sub>2</sub> excimers, electronic struct., ab initio CI calc. (French) 4-78788  
 Au I, low-lying transitions, vol. isotope shifts 4-64409  
 B cluster surfaces, chemisorption of H<sub>2</sub> ab initio RHF calc. 4-92555  
 BCN, ground state, geometry, transition state, isomerisation reaction, ab initio calcs. 4-71908  
 BH<sub>2</sub>, Renner-Teller pot. energy surfaces, analytic second derivatives 4-91250  
 BH<sub>2</sub>NO<sub>2</sub>, electronic struct. calc. 4-87032  
 B<sub>2</sub>O<sub>3</sub>, geometrical struct., photoelectron spectra, ab initio MO calcs. 4-68932  
 B<sub>2</sub>O<sub>3</sub> vapour, struct., photoelectron spectra, ab initio STO calcs. 4-83414  
 Be, temp. and press. induced phase transitions 4-70369  
 Be<sub>18</sub> clusters, energy optimised configs., ab initio STO-3G SCF calcs. 4-69261  
 Be<sub>20</sub>, clusters, energy optimised configs., ab initio STO-3G SCF calcs. 4-69261  
 BeF, vibr. excitation of triplet core-ionised states 4-74175  
 BeO, A<sup>1</sup>Π-X<sup>1</sup>Σ<sup>+</sup> system perturbations, ab initio calcs. 4-59623  
 Br, ab initio calcs., spin-orbit coupling, kinetic energy operator, relativistic correction 4-102607  
 Br<sub>2</sub>, EXAFS, ab initio calcs. 4-64492  
 C- and O-containing cpds., oxidation number, electron distrib., ab initio MO wave functions 4-102726  
 C+NO(X<sup>2</sup>Π), collinear reaction pot. energy barrier, correl. diagram, ab initio calcs. 4-99766  
 CH bond length variations due to intramol. environment, isolated CH stretching freq. and ab initio calc. 4-68945  
 [C<sub>2</sub>H<sub>2</sub>O]<sup>+</sup>, isomerisation, ab initio SCF calc. in gas phase (French) 4-71880  
 C<sub>2</sub>NH<sub>5</sub>, isomers, struct., relative energies ab initio MO STO calcs. 4-102572

## ab initio calculations continued

C<sub>2</sub>NH<sub>5</sub><sup>+</sup>, isomers, struct., relative energies ab initio MO STO calcs. 4-102572  
 CO, electronic scatt., R-matrix method, ab initio calcs. 4-83484  
 CO, fine struct., K-shell EELS, ab initio methods 4-91346  
 CO, weakly chemisorbed, correl. between anomalous electronic and vibr. props. 4-78910  
 CO<sup>+</sup>, isolated ions, IR spectra quantitative prediction 4-69075  
 CO-H<sup>+</sup>(Li<sup>+</sup>)(Na<sup>+</sup>)(K<sup>+</sup>) struct., binding energies, ab initio HF calcs. 4-112096  
 CO<sub>2</sub>, intermolecular pots., ab initio SCF calcs. 4-96640  
 CO<sub>2</sub><sup>+</sup> isolated ions, IR spectra quantitative prediction 4-69075  
 C<sub>2</sub>O<sub>2</sub><sup>+</sup> cation radicals, matrix isolated, EPR and ab initio investig. 4-74273  
 CS<sub>2</sub>, jet-cooled, <sup>1</sup>B<sub>2</sub>(V)-Σ<sub>g</sub><sup>+</sup>(X) transition, excitation and dispersed fluorescence spectra 4-64527  
 CS<sub>2</sub><sup>+</sup> isolated ions, IR spectra quantitative prediction 4-69075  
 CSiF<sub>2</sub> isomers, lowest singlet and triplet surfaces, ab initio calcs. 4-107424  
 Ca, HFS, field isotope shift, multiconfigurational HF method 4-102594  
 Ca, hyperfine struct. of 4s4p and 4s3d configs., pair correl. effects, ab initio calcs. 4-64368  
 Cd ions in laser-prod. plasma, for UV spectra 4-68997  
 Cd(Hg)<sub>1-x</sub>Te, phonon states, far IR absorpt. spectra study (Chinese) 4-92312  
 CuH<sub>2</sub>, Renner-Teller pot. energy surfaces, analytic second derivatives 4-91250  
 CuO electronic valence states, energy level diagram 4-64394  
 FH<sub>2</sub> reaction energies, pot. energy surfaces, ab initio calcs. 4-114789  
 Fe, ab initio hyperfine struct. parameter calcs. 4-78981  
 Fe, BCC, interaction with H, ab initio/effective core pot. cluster calc. 4-108722  
 H-bonding systems, excited, electronic struct., ab initio MO-CI calcs., charge transfer 4-96461  
 H+D<sub>2</sub>→HD+D reaction, distorted wave calcs. at E<sub>trans</sub> (v=0) = 0.55 and 1.3 eV 4-99749  
 H+H<sub>2</sub>→H<sub>3</sub><sup>+</sup>→H<sub>2</sub>+H, H<sub>3</sub><sup>2+</sup> absorpt., transition state spectroscopy 4-69194  
 H<sub>2</sub>, electron elastic scatt. and rot. excitation at 10 to 100 eV, optical pot. model 4-96697  
 H<sub>2</sub>, electron scattering, ab initio nonadiabatic polarisation pots. 4-74347  
 H<sub>2</sub>, nonlinear optical props., ab initio calcs., freq. depend. dipole polarisabilities, susceptibilities 4-102608  
 H<sub>2</sub>, radiative lifetime, in nonadiabatically coupled J=1 state, ab initio calcs. 4-68976  
 H<sub>2</sub>+CO collisions, rigid-rotor pot. energy surface from ab initio calcs. and rot. inelastic scatt. data 4-78940  
 H<sub>2</sub>+methyl→H+methane, D isotope effect, ab initio pot. surface, transition state theory 4-81416  
 H<sub>3</sub><sup>+</sup>, vibr.-rot. levels, IR predissociation spectra 4-107344  
 H<sub>3</sub><sup>+</sup>+e<sub>2</sub>, dissociative recombination, reaction product channel anal. 4-74344  
 HCN, ground state, geometry, transition state, isomerisation reaction, ab initio calcs. 4-71908  
 HFPOH struct., bonding and internal rotation 4-68938  
 HN<sub>2</sub><sup>+</sup>, stretching vibr., pot. energy and electric dipole moment depend., ab initio calcs. 4-87105  
 HNO<sub>2</sub>, electronic struct. calc. 4-87032  
 (CHO<sub>2</sub>)<sup>-</sup>, struct., ab initio multiconfig. SCF gradient optimisation method 4-83290  
 H<sub>2</sub>O, fundamental freq., ab initio calc., geometries, vibr. energies, pot. surface 4-59624  
 H<sub>2</sub>O<sub>2</sub>, internal rot. effect on NMR params., ab initio SOS CI calcs. 4-91203  
 H<sub>2</sub>O<sup>+</sup>, linear and bifurcated complexation with electron donors, ab initio calc. 4-99752  
 HOC<sup>+</sup>, rot. vibr. spectrum, extended ab initio study 4-64395  
 HOF, neutral and cationic struct., ab initio calcs. 4-59616  
 H<sub>3</sub>PO, struct., bonding and internal rotation 4-68938  
 H<sub>2</sub>POH, struct., bonding and internal rotation 4-68938  
 H<sub>2</sub>PP, ab initio SCF and CI study of stability and electronic struct. 4-74164  
 HPPH, ab initio SCF and CI study of stability and electronic struct. 4-74164  
 HSNO, Ar low temp. matrix, photoinduced isomerisation, IR spectra 4-89249  
<sup>1</sup>H and <sup>13</sup>C chemical shifts, comparison between theory and expt. 4-74264  
 He, nonlinear optical props., ab initio calcs., freq. depend. dipole polarisabilities, susceptibilities 4-102608  
 He+H<sub>2</sub><sup>+</sup>, exchange reaction, ab initio pot. energy surface, quasiclassical trajectory study 4-76996  
 He+HF, energy transfer, differential cross sections, pot. energy surfaces 4-76992  
 HeH<sub>2</sub>, analytic ab initio pot. energy surfaces for ground and first singlet excited states 4-96456  
 He\*+He, pot. energy curves obtained by combining scatt., spectroscopy and ab initio theory 4-74177  
 Hg<sub>2</sub>, pot. energy curves, electronic states, ab initio CI calcs. 4-112124  
 Ions in laser-prod. plasma, for UV spectra 4-68997  
 KCN, ab initio dipole surfaces, vibr. averaged dipole moments and IR transition intensities 4-64461  
 Kr<sub>2</sub> excimers, electronic struct., ab initio CI calc. (French) 4-78788  
 Li clusters 4-98500  
 Li complexes, Li<sup>+</sup>/N-methylformamide-water, N-substitution effect on hydrogen bonds, ab initio calcs. 4-96716  
 Li complexes, Li<sup>+</sup>/formamide-water, N-substitution effect on hydrogen bonds, ab initio calcs. 4-96716  
 Li<sub>2</sub>, isotope separation, sequential two-photon ionisation 4-87167  
 Li<sub>2</sub>, isotope separation using different laser wavelengths for excitation and ionisation processes 4-69235  
 Li<sub>2</sub>, semiempirical parameters, bond length depend. correl. effective valence shell Hamiltonian appl. 4-64353  
 LiCN, ab initio dipole surfaces, vibr. averaged dipole moments and IR transition intensities 4-64461  
 LiH, electron scatt., R-matrix method, ab initio calcs. 4-83484  
 LiH+He rotationally inelastic collisions, quasi-classical dynamics of atom-rigid rotor trajectories 4-112260  
 LiH<sub>2</sub>, binding energy, ab initio calcs. 4-59615  
 LiNO<sub>3</sub>, force and vibr. spectrum, ab initio study 4-112110  
 MgD, nascent internal energy distrib. prod. in Mg+D<sub>2</sub> reaction 4-71872

**ab initio calculations continued**

- MgH, nascal internal energy distrib. prod. in Mg+H<sub>2</sub> reaction 4-71872  
 MgO (001), adsorption of CO and simple organic mols., ab initio MO calcs., lattice defect methods 4-81476  
 MgO, doped surfaces, {001} CO chemisorption 4-113805  
 Mo surfaces, {001}, {110} and {111}, electron states and atomic positions, ab initio calc. 4-65723  
 N<sub>2</sub>, accurate ab initio calcs. of radiative transition probabilities 4-112127  
 $\alpha$ -N<sub>2</sub>,  $\alpha$ - $\gamma$  phase transition, ab initio intermolecular pot. 4-88280  
 N<sub>2</sub>, Hopfield series, electronic autoionisation, multichannel quantum defect calcs. 4-83427  
 N<sub>2</sub>, symmetry restricted and unrestricted HF calc. at ab initio LCAO-MO-SCF level 4-87043  
 N<sub>2</sub>, weakly chemisorbed, correl. between anomalous electronic and vibr. props. 4-78910  
 N<sup>+</sup>, valence hole state, ab initio LCAO-MO-SCF level HF calcs. 4-68957  
 N<sub>2</sub>H<sup>+</sup>Li<sup>+</sup>(Na<sup>+</sup>)(K<sup>+</sup>) structs., binding energies, ab initio HF calcs. 4-112096  
 N<sub>2</sub>N<sub>2</sub>, intermol. pot. calc. using ab initio SCF, CI and many-body perturbation theory methods 4-102606  
 NH<sub>2</sub>, Renner-Teller pot. energy surfaces, analytic second derivatives 4-91250  
 NH<sub>3</sub>, <sup>6</sup>Ni(CO)<sub>4</sub>, geometry optimisation, relativistic corrections, HF approx. 4-78786  
 NH<sub>3</sub> dimer, effects of basis set and electron correlation on calculated props. 4-91205  
 N<sub>2</sub>H<sub>4</sub>, N magnetic-shielding tensors, conformational depend., ab initio calcs. 4-87056  
 NH<sub>3</sub>NH<sub>2</sub> 4-87032  
 NO<sup>+</sup>, stepwise hydration, struct., ab initio calcs. 4-81402  
 N<sub>2</sub>O, C<sub>2v</sub>/C<sub>s</sub> excitation spectra, ab initio MCSCF calcs. 4-68934  
 N<sub>2</sub>O, electron impact excited, K X-ray emission spectra 4-69100  
 N<sub>2</sub>O<sup>+</sup>, I<sup>2</sup>A(X<sup>2</sup>) state, isotopic scrambling, ab initio calcs. 4-91323  
 NOF, cubic force field determ. by vibr.-rot.  $\alpha$  const. 4-83491  
 NSCl, geometry, ab initio SCF force field calcs. 4-64344  
 NSCl, thiazyl chloride, nucl. quadrupole coupling consts. from microwave spectra and ab initio MO calc. 4-69103  
 N<sub>2</sub>-HF(HCl)(HBr), H bonded complexes, ab initio GO SCF MO calcs. 4-64369  
 NaCl, solvated adducts, ab initio MO calc. 4-68926  
 NaCl with U-centre, deep impurity states, cryst. cluster method 4-61324  
 Na<sup>+</sup>-HPO<sub>4</sub><sup>2-</sup>, tightly bound system, cation hydration, polarisation effects 4-69167  
 Nd(BrO<sub>3</sub>)<sub>3</sub>.9H<sub>2</sub>O, single cryst., mag. susceptibility, cryst. field effect and calcs. 4-71018  
 Ni (111) surface, adsorbed acetylene, ab initio MO study 4-92566  
 O+H<sub>2</sub>(D<sub>2</sub>) reaction dynamics, reduced dimensionality quantum and quasi-classical rate consts. 4-114784  
 O<sup>+</sup>+H<sub>2</sub>, ab initio pot. energy surface, CI calcs. 4-96470  
 O<sub>2</sub>, <sup>2</sup> $\Sigma_g^-$  ground state, electrostatic and exchange interactions 4-112249  
 O<sub>2</sub>, potential curves, quasidegenerate many-body perturbation theory calcs. 4-68994  
 O(D<sub>2</sub>) + HCl → OH + Cl reaction on a fitted ab initio surface 4-81414  
 OH (CO<sub>2</sub>)<sub>n</sub> clusters, (n=1, 2), ab initio investig. 4-96737  
 P<sub>2</sub>H<sub>4</sub>, P magnetic-shielding tensors, conformational depend., ab initio calcs. 4-87056  
 P<sub>2</sub>-HF(HCl)(HBr), H bonded complexes, ab initio GO SCF MO calcs. 4-64369  
 Pd<sub>2</sub>, electronic struct. and bonding, mass spectrosc. and ab initio HF-CI investig. 4-74167  
 S<sub>2</sub>H<sub>2</sub>, lone-pair interactions, rot. barriers, ab initio Gaussian basis set calcs. 4-64339  
 Si (100) with adsorbed O<sub>2</sub>, ab initio SCF calcs. 4-98440  
 Si oxy-hydroxide mols., ab initio SCF MO calcs. 4-96443  
 Si:H (100)(2×1), surface IR studies 4-99116  
 SiF<sub>4</sub>(NH<sub>3</sub>)<sub>n</sub> complexes, stability, ab initio STO-3G calcs. 4-59613  
 SiH<sub>3</sub> radical, pot. surface and rot. vib. energies, ab initio calc. 4-96457  
 Si<sub>2</sub>H<sub>2</sub> conformers, relative stabilities, ab initio and CI calcs. 4-74145  
 Si<sub>2</sub>H<sub>2+n</sub> defects, molecular cluster studies 4-84586  
 SiHCl<sub>3</sub>, Cl quadrupole coupling consts., nonempirical calcs. 4-107281  
 SiH<sub>3</sub>Cl, Cl quadrupole coupling consts., nonempirical calcs. 4-107281  
 SiO, dimerisation, ab initio quantum chemical study 4-76995  
 SiO protonated ions, ab initio calcs. appl. to interstellar detect. possibility 4-87051  
 SiO<sub>2</sub>, amorphous defects, ab initio MO calc. and Raman spectrum 4-96443  
 SiS protonated ions, ab initio calcs. appl. to interstellar detect. possibility 4-87051  
 Sr levels, config. mixing and isotope shifts 4-68978  
 TiH<sub>2</sub>, pot. energy curves, electronic states, ab initio CI calcs. 4-112124  
 W surfaces, {001}, {110} and {111}, electron states and atomic positions, ab initio calc. 4-65723

**abacs see nomograms****aberrations**

- aberrations in optics and particle optics only*  
*see also lenses; optical instrument testing; particle optics*  
 adaptive optics basis functions for obscured aperture, phase aberration correction 4-74427  
 adaptive primary mirror structural anal. 4-87422  
 aspherical surface testing with shearing interferometer using fringe scanning detection method 4-107909  
 aspherical surface testing with shearing interferometer using fringe scanning detection method 4-112592  
 astronomical large aperture mirror, assessment by Hartmann test (Korean) 4-115688  
 asymmetrical condenser-objective lenses, electron optical props. (Chinese) 4-96775  
 axisymmetric passive optical system without aberrations, MTF optimisation 4-87295  
 Baker-Meine-Bingham three-mirror telescope, aberration anal. 4-101155  
 biocular magnifiers for electro-optic displays, visual comfort assessment 4-97024  
 book, aberration and optical design theory 4-95086  
 Cassegrain-type spectrographic cameras, near axis ray tracing, aberrations and their correction (Japanese) 4-94617  
 catadioptric magnifiers, aberration corrected, for microfiche readers 4-69525  
 charged particle beams envelopes, distortion and spherical aberration 4-74405

**aberrations continued**

- chromatic aberration coefficient computation, power series weighted truncation 4-59993  
 chromatic aberration coefficients, weighted over doubling in computation 4-112352  
 Chromatic change in magnification and rotation for magnetic lenses, electron spectroscopy appl. 4-63820  
 chromatic coordinates in aberration theory 4-59992  
 cinematographic projector 5-element objective lens parameters, tolerances 4-90670  
 compensation plate, plane-parallel, aberration props. 4-60136  
 complicated optical system automated construction using a computer 4-74652  
 Couder telescope, optical quality of modified design 4-110530  
 cover sheet aberrations in optical recording 4-91408  
 diffraction gratings and optical aberrations 4-69302  
 DIFPD parameters influence on final image symmetry of optical systems 4-60130  
 electron holography, Fourier, aberrations elimination 4-69345  
 electron holography, Fourier, scatt. foil choice, resolution limitation 4-69346  
 electron lens aberration coeffs., dependence on object and aperture position 4-79025  
 electron micrograph astigmatism correction using joint transform 4-90694  
 electron Mollenstedt biprism interferometer interference pattern, effects of chromatic aberration and partial coherence 4-87265  
 electron-optical system, optimisation, spherical aberration minimisation, extended field lens (Chinese) 4-83535  
 electrostatic electron-optical systems with discontinuous fields 4-74408  
 field emission gun, paraxial rays and aberrations 4-106428  
 gain guided lasers with narrow stripe geometry, astigmatism, far-field pattern and spectral envelope 4-87326  
 gamma-ray imaging systems, aberrations 4-67084  
 gradient-index lens array, reduction/enlargement type 4-83665  
 gradient-index lens for laser-diode beam, focusing props. 4-87411  
 gradient-rod single radial lens, spherical aberration model 4-83545  
 holographic grating, stigmatic conditions for normal incidence mounts 4-83681  
 holographic lens, aberration-containing design for post-objective holographic deflector 4-102907  
 holographic lens for an optical correlator 4-107576  
 holographic lens imaging quality evaluation, use of classical OTF (Chinese) 4-87301  
 holographic microscope objective, small spherical aberration and coma 4-106379  
 holographic stereograms for three-dimens. imaging 4-74453  
 holography, general form for aberration coeffs. 4-87302  
 imaging quality limitations (German) 4-112346  
 interferograms, separating misalignment from misfigure on off-axis aspheres 4-112593  
 intracavity adaptive optics, theory and expt. comparison 4-74552  
 IR chopping secondary of Cass telescope, determ. of image aberration 4-107777  
 IR system optical quality assessment using 300 mm aperture high precision scanning interferometer 4-74765  
 large astronomical telescopes, optical system and aberrations 4-105877  
 laser TEM<sub>00</sub>-thermoinsensitive cavity with several thermoperturbing centres, mode aberration compensation 4-69457  
 lateral aberration measurements with a digital Talbot interferometer 4-87409  
 lateral chromatic aberration of the eye 4-100130  
 lens, test signal image appl. for computation of focal length and aberration (Russian) 4-107776  
 magnetic round lens and sextupole system, aberration theory (Chinese) 4-96774  
 mirror, segmented primary, testing, wavefront reconstruction, influence of higher order noise 4-107784  
 mirror mount design for cryogenic environments 4-87413  
 monochromator, stigmatic coma free grazing incidence 4-83678  
 monochromator with concave holographic diffr. grating, symm. scheme, aberration correction 4-107805  
 natural colour holographic stereograms by superimposing three rainbow holograms 4-112357  
 nonclassical concave gratings in fixed-slit monochromators, parameter calc. 4-74691  
 object reconstruction in nonisoplanatic devices from aberration coeffs. 4-79062  
 optical phase conjugation for removing dispersive self-phase-modulation effects 4-112523  
 optical propag., adaptive compensation for atmospheric turbulence effects (French, English) 4-67402  
 optical systems, anal. of foundations of Hartmann test 4-63076  
 opto-electronic coherent microscope based aberration studies 4-83548  
 phased array laser transmitter concept 4-106340  
 planar microlens, maximum and effective numerical apertures, Luneburg lens model 4-87410  
 planar waveguide optical channel multiplexers and demultiplexers, spectral and aberration characts. 4-107823  
 polynomials for computer anal. of interferograms 4-97148  
 prime focus corrector for f/3 true or quasi Ritchey-Chretien primaries 4-72879  
 prism charged-particle energy analysers, matrix calc. of aberrations 4-64670  
 RATAN-600 radio telescope, polarisation characts. for obs. at horizon with allowance for aberrations 4-63059  
 Seidel aberration effects on visual target discrimination 4-62491  
 single-mode fibre lens coupling to laser diodes, effect of aberrations 4-97064  
 spatial three-dimensional hologram and object projection system 4-74458  
 speckle processing, shift-and-add, instrum. aberration compensation 4-79031  
 spherical aberration coefficients, generic asymptotic form 4-112351  
 spherical aberration function singularities, generic behaviour of power series of geometrical optics 4-112350  
 starting system evaluation by Seidel correction with aspheric surfaces 4-69522  
 statistical size based description (German) 4-87293  
 structural mechanics of optical systems, conf. Cambridge, MA, USA (Nov. 1983) 4-86104  
 subaperture optical system testing 4-91556

**aberrations** continued

- surface error descriptors for near cylindrical optics 4-112551  
 synthetic aperture propag., point spread function, computer model 4-96813  
 Talbot and Lau effects, a parageometrical approach 4-69322  
 TEM, astigmatic, brightfield, image quality azimuthal development 4-106429  
 thermal-blooming-induced low-order aberrations 4-96807  
 third-order aberrations of electrostatic lenses by nonparaxial electron trajectories (*Chinese*) 4-83534  
 three-mirror anastigmat with main mirror and third mirror coincident, theory (*Russian*) 4-101168  
 truncated spherical mirror for energy anal. combined with direct meas. of ang. distrib. 4-64259  
 two-lens achromat, chromatic longit. aberration: convection, optical material struct. 4-97028  
 two-lens cemented objective calc. using a computer 4-74653  
 two-photon-resonant image upconverters using type I optical system, thickness aberrations (*Japanese*) 4-79336  
 two-photon-resonant image upconverters using Fourier mode optical systems, chromatic aberrations (*Japanese*) 4-60116  
 wave-front tomography by Zernike polynomial decomp. 4-91640  
 wavefront aberration description, structurally compatible surface vectors 4-87287  
 wavefront measurements from a knife edge test 4-112550  
 White cells, multiple refl. absorption type, minimisation of vol. and astigmatism 4-73522  
 X-ray telescope, two-channel three-mirror, design and analysis 4-110519  
 XUV grating contamination due to overlapping orders: a study through the electromagnetic theory 4-83682

**aberrations (visual)** *see* vision defects**abrasion**

- see also hardness; wear*  
 alkali borosilicate glass rods, partially leached, abraded and unabraded strength rel. to heat treatment 4-89144  
 Arctic offshore structures, lightweight concrete props. 4-114464  
 ball cratering, sample prep. technique for TEM 4-103620  
 cast iron, white, wear resist. meas. using abrasive wear testing machine (*Japanese*) 4-76874  
 flame-sprayed coatings, abrasive and erosion wear resist. 4-93428  
 glass and glass ceramic, brittle, disturbed surface layer parameters effect on struct. strength 4-99541  
 glass enamel used in heat energetics, abrasive wear 4-81291  
 magnetoabrasive powder polishing, optimum particle shape choice 4-89190  
 materials selection under erosive wear conditions (*German*) 4-62065  
 slag siltall used in heat energetics, abrasive wear 4-81291  
 steel, nitrided, abrasive and erosion wear resist. 4-93428  
 surface scratching in abrasive or erosive processes, effect of brittleness index and sliding speed 4-71741  
 Cu-Sn-Al<sub>2</sub>O<sub>3</sub>, abrasive composite, physicomach. props., effect of premoulding press. in elec. discharge sintering 4-89020  
 Fe, cast, white, high Cr, abrasion by quartz particles, carbide removal mechanism rel. to particle shape 4-85220  
 Fe, gray and nodular cast, laser surface hardening, erosion resist., near surface microstructure 4-66453  
 LiF single crystals, grinding, surface layer, strain hardening, dislocation density, microhardness 4-93312  
 SiO<sub>2</sub> thick films, prep. by vacuum evaporation, abrasive wear 4-104882  
 Ti-N, abrasion resistance, homogeneity region 4-114681

**abrasive wear** *see* abrasion**absolute gravity** *see* gravity**absolute pressure measurement** *see* pressure measurement**absolute temperature** *see* temperature**absorbers (surge)** *see* surge protection**absorption**

- for absorption of substances *see* sorption  
*see also* acoustic wave absorption; electromagnetic wave absorption  
 No entries

**absorption coefficients (optical)** *see* optical constants**absorption spectra** *see* spectra**abundance ratio** *see* element relative abundance; isotope relative abundance**a.c. network analysers** *see* network analysers**acceleration**

- see also* acceleration measurement; accelerometers

**acceleration measurement**

- fountain droplets, deceleration curve 4-78125  
 rotational inertia demonstration apparatus 4-95117  
 instrument for calibration of measured velocities of angular acceleration (*Russian*) 4-63703  
 MOS integrated sensors, electrochem. and charge-imaging effects 4-82786  
 SAW tensioned or flexured accelerometer 4-101816

**accelerators (particle)** *see* particle accelerators**accelerometers**

- see also* acceleration measurement

- acoustic background noise immunity, multisensor speech input 4-103131  
 DC monolithic accelerometer design and fabrication 4-111122  
 displacement measurement by double integration of accelerometer signals 4-73416  
 fiber optic accelerometer 4-106278  
 laser accelerometer of aviation gravimetric system (*Russian*) 4-96976  
 SAW tensioned or flexured accelerometer 4-101816

**acceptor levels** *see* impurity electron states**accidents**

- see also* explosions; safety  
 activation products impact on fusion reactor safety 4-111780  
 airborne radioactive releases from burning contaminated combustibles 4-106891  
 AVR, water ingress accident, whole facility behaviour, numerical simulation (*German*) 4-96215  
 boom effectiveness against oil ingress into estuary 4-109760  
 BWR, 1300 MW class, pipe fracture accident, thermal behaviour simulation 4-91087  
 BWR LOCA, instantaneous pipe rupture, void-fraction meas. with X-ray densitometer 4-74036  
 BWR LOCA, radiolytic gas generation in pressure suppression containment, calc. 4-111664

**accidents continued**

- CANDU-PHWR ECCS unavailability following small LOCA 4-64232  
 caustic waste tank, Pu build-up and recovery, nuclear criticality safety 4-106922  
 conference on multiphase processes in LMFBF safety analysis, Ispra, Italy (Mar.-Apr. 1982) 4-78042  
 core melt accidents, reactor safety goal compatibility using uncertain prob. risk anal. 4-111663  
 CRACOME code for reactor accidents, containment, meteorology and evacuation consequences 4-106886  
 criticality accidents review for European Community, Saclay, Mol and Windscale 4-106919  
 evacuation time estimate in nuclear accident using CLEAR code 4-107165  
 ferro-concrete structures for nuclear facilities, computer simulation for impact loadings 4-107006  
 fission reactor LWR, fission product transport anal., class 9 accident 4-106933  
 fusion reactor blanket structures, activation product release, safety research 4-111781  
 fusion reactors, activation product aerosol formation during accidents 4-111783  
 GERDA experimental facility for the investigation of PWR small break LOCAs 4-96228  
 Hanford Pulser, criticality accident in Pu scrap recovery building 4-106920  
 heterogeneous water moderated systems, criticality accident experience 4-106918  
 HTGR, spatial fission product behaviour within pebble bed, math. treatment (*German*) 4-68749  
 HTGR under hypothetical accident conditions, reactivity behaviour study 4-68780  
 HTR cooling breakdowns, temp. rises and safety margins 4-96241  
 HTR fuel elements, spherical, behaviour under accident conditions 4-83236  
 HTR irradiated spherical fuel elements with MOX-BISO particles, failure simulation at 1400-2500°C 4-96245  
 HTR modular fuel element, fission product release under accident conditions, calc. 4-96247  
 HTR under accident conditions, fission product retention in core and fuel (*German*) 4-64231  
 HTR-500, behaviour during failures leading to core heating, safety assessment 4-96244  
 hypothetical core-melt through in concrete foundations, core-concrete interactions 4-91088  
 KORI-1 PWR, very small LOCA, decay heat removal and operator intervention calcs. 4-102375  
 Livermore criticality accident, 1963, nuclear criticality safety aspects 4-106921  
 LMFBF, accident post-disassembly phase, event sequence and processes 4-78722  
 LMFBF, TOP and LOF accidents, post-clad failure phenomena 4-78721  
 LMFBF accident, core bubble/Na pool interface phenomena, SIMMER modification 4-78727  
 LMFBF accident, multiphase flow, heat and momentum transfer, phase change modelling 4-78724  
 LMFBF accident multiphase flow, hydrodynamical eqns., SIMMER-II code 4-78725  
 LMFBF accidents, upper struct. transient thermohydraulics, SIMMER-II anal. 4-78733  
 LMFBF HCDA, core expansion, UK expts. and calcs., review 4-78730  
 LMFBF HCDA, expansion phase phenomena, scale model expts., SIMMER-II and SOLA-VOF verification 4-78732  
 LMFBF HCDA and LOF accidents, core expansion phase models with Na entrainment 4-78728  
 LMFBF LOF accident, transition phase anal., recriticality, review 4-78731  
 LMFBF safety anal., core expansion studies, CARAVELLE expts. and IRIS code 4-78729  
 LMFBF safety anal., stability anal. and numerical procedures for SIMMER-II code 4-78726  
 LMFBFs, Na aerosols and puddles, fuel, fission products and Na release 4-91084  
 LOCA, hydrodynamic loading and structural response in PWR and HDR, STEALTH/WHAMSE anal. 4-68786  
 LWR containment, H<sub>2</sub> behaviour during accidents, production, mixing combustion 4-64221  
 LWR core-melt interaction with concrete foundations, crust form., long-time behaviour 4-96236  
 LWR LOCA, blowdown thrust force under pipe rupture accident, expt. eval., decompression 4-102379  
 LWR LOCA, blowdown thrust force under pipe rupture accident, partial and ramped opening breaks 4-102380  
 LWR overpower transients, fuel pellet-cladding interaction, safety analysis record review 4-96218  
 nuclear criticality safety research program at JAERI 4-68797  
 nuclear facility building concepts against aircraft crash, vibrs. effects 4-102381  
 nuclear facility design, impact of potential for criticality, safety, doses 4-106923  
 nuclear facility unplanned release, in situ noble gas radionuclide spectrometric meas. 4-106889  
 nuclear power plant buildings, stresses due to aircraft impact using 3-dimens. shell model 4-96230  
 nuclear power plant personnel nuclear safety, progress (*French*) 4-74033  
 nuclear power plants, emergency reactor core cooling system 4-97704  
 nuclear power stations, successes, failures and perspectives (*German*) 4-74026  
 nuclear reactor containment building, H<sub>2</sub> combustion and control 4-111666  
 nuclear reactor core melt-concrete foundations interaction, gas outflow 4-96237  
 nuclear reactor emergency evaluation program 4-107166  
 nuclear reactor in-plant post-accident radiation transport, computer model 4-83240  
 nuclear reactor primary coolant radioactivity monitoring under postaccident conditions 4-107169  
 nuclear reactors, electrical insulation degradation for chem. sprays during LOCA 4-68799  
 off-site dose rates estimation using BWR containment high range monitor after accident 4-106890

## accidents continued

- pebble bed HTGR spherical fuel elements, core heat-up simulation for accident conditions (*German*) 4-64230
- protective actions, off-site nuclear response considerations 4-107163
- PWR, cooling of core debris and impact on containment transient pressure during accident 4-64227
- PWR, heavy load drop consequences, critical and radiological anal., safety 4-106915
- PWR containment vessel mechanical behaviour during core-melt accidents and earthquakes ROTMEM code 4-96240
- PWR hypothetical core-melt accident, H<sub>2</sub> risks and containment 4-96239
- PWR LOCA, decay heat removal expts. in U-tube steam generator test facility 4-83239
- PWR pressurised thermal shock, eval. for B&W designed NSS plants 4-106924
- PWR small break LOCA, heat transfer, lower plenum break, parametric study 4-96195
- PWR small-break LOCA, ECC tests at GERDA expt. facility 4-96229
- RA-2 critical assembly, prompt critical excursion accident, causes and consequences 4-106916
- RA-2 criticality accident, yield and quench mech. anal. 4-106917
- radioactive waste repository geologic design study, probabilistic risk assessment 4-106744
- reactor accidents, off-site consequence modelling review, evacuation time significance 4-106888
- reactor accidents, off-site consequence modelling using Monte-Carlo method 4-106887
- reactor core heat transfer crisis, quasistationary method calcs. 4-74034
- reactor post-accident primary coolant sampling systems 4-96204
- real-time assessment system for reactor accidents 4-111671
- risk analysis method with fixed barrier models, radioactive leaks 4-91085
- severe reactor accident consequences, early evacuation, shelter and relocation effectiveness 4-106885
- severe reactor accident consequences, NRC modelling using CRAC code 4-106884
- SNR-300 prototype FBR, risk oriented anal., accident consequences 4-64219
- solid state track recorder neutron dosimetry, appl. to TMI-2 recovery 4-68878
- spontaneous evacuation during radiological emergency, planning 4-83229
- TMI-2 fuel debris location in cooling system, SSNTD neutron dosimetry appl. 4-96194
- TMI-2 reactor building polar crane repair procedures 4-59395
- TMI-2 special wastes from accident and cleanup, treatment 4-106787
- vehicular radiation monitoring system for emergency response 4-107168
- vibration isolation and large piles for nuclear building concepts, aircraft crashes 4-107007
- water layer stability over hot tin melt, core-melt accident simulation, ECC effects 4-96235
- <sup>241</sup>Am, medical course after accidental exposure 4-109890
- <sup>60</sup>Co  $\gamma$ -rays, fatal accidental exposure, dose estimation from watch jewels thermolum. 4-89754
- H<sub>2</sub> distribution in reactor containment following serious accidents, WAVCO anal. 4-96238
- <sup>131</sup>I, thyroid uptake blocking by RI, nuclear accidental appl., review 4-115232
- Li pool fires in fusion reactor safety anal., comp. with Na and Li-Pb, LITFIRE code 4-111787
- Na surface fires in reactor containment, convection current computation, KONVEC 4-91083
- Nb tubes internal protective coating, fuel pin accidental behaviour 4-68771
- V-Cr-Ti Path C alloy for fusion reactors, V volatility, safety anal. 4-111782

accommodation coefficient *see sorption*accretion disks *see circumstellar shells*

## accumulation layers

- quasi-2D electron systems, electron-phonon interaction and screening effects 4-98547
- Hg<sub>1-x</sub>Cd<sub>x</sub>Te surface accumulation layer, cyclotron resonance studies 4-98507
- Hg<sub>1-x</sub>Cd<sub>x</sub>Te zero gap MIS struct., size quantisation in accumulation layers 4-65753
- Si hole space charge layers, interaction between electronic and phonon Raman scatt. 4-98774
- Si MIS struct., magnetoresist. of inversion and accumulation layers 4-61461
- Te, dimensionally quantised accumulation layer, quantum kinetic phenomena 4-88555
- ZnO weak accumulation layers, electron transport and Hall effect 4-98686

accumulators *see secondary cells*acidity *see pH*acids, organic *see organic compounds*

## acoustic analysis

- nuclear power stations, monitoring and fault diagnosis system for early fault detection (*German*) 4-59384
- spectral-domain radial extrapolation of acoustic fields (*French*) 4-97228

## acoustic applications

- see also ultrasonic applications*
- communication system design, underwater acoustic channels characterisation and appl. 4-60201
- levitation, coating technology appl. 4-99306
- LMFBR, acoustic imaging of vapor bubbles through optically non-transparent media 4-59364
- ocean sounding, using multichannel meas. system 4-105741
- space experiments, containerless processing technologies using acoustic and electrostatic levitation 4-95397

## acoustic arrays

- adaptive arrays for signal separation (*Chinese*) 4-91691
- computer analysis using STARPAC package 4-107965
- digital split-beam array system, precise bearing method (*Chinese*) 4-107933
- hydrophone arrays, collinear, hybrid time-delay/phase-shift digital beam-forming 4-83777
- infrasonic impure, decomposition into: normal modes at acoustic array (*Chinese*) 4-107931
- near-field imaging, source reconstruction by acoustic field projection (*French*) 4-60194

## acoustic arrays continued

- noise-immune arrays, synthesis 4-103172
- oceanographic shallow water acoustics 4-64807
- piezoelectric array receivers using ceramics with high and low planar coupling, ang. response 4-97262
- pressure gain, Fresnel zone meas. 4-91710
- random acoustic arrays, freq.-wavenumber spectrum estimation using beampower pattern estimators 4-97208
- rectangular acoustic array elements, normal surface displacements, optical interferometry studies 4-112655
- sandwich transducers and arrays, practical design considerations, sonar appls. 4-69653
- single beam synthesis from thinned arrays 4-112642
- synthesis near reflecting surfaces 4-91705
- towed array response to acoustic field in shallow water 4-69618
- transducer arrays with nonuniform element spacing, radiation patterns 4-97263
- underwater source localisation, influence of unequal sub-array spacing configurations 4-112619
- unequal spaced array, optimisation, synthetic method (*Chinese*) 4-107964
- US beam, focusing by piezoelectric annular array 4-97219
- US transducer arrays, acoustic cross coupling, theory 4-74828
- vertical array in deep ocean, stochastic acoustic propagation, mutual coherence function 4-74796

## acoustic delay lines

- see also ultrasonic delay lines*
- modelling based on moving domain wall concept 4-98209
- pulsating fluid signal, transmission characteristics improvement, rarefied gas use (*Japanese*) 4-87762
- surface generated bulk waves, excitation and detection 4-91667

acoustic detectors *see acoustic transducers*

## acoustic devices

- see also acoustic delay lines; acoustic generators; acoustic microscopes; acoustic microwave devices; acoustic parametric devices; acoustic radiators; acoustic receivers; acoustic resonators; acoustic transducers; bells; surface acoustic wave devices; ultrasonic devices*
- acoustic telescope system using vane-type acoustic lenses, system construction 4-79404
- bulk-acoustic-wave-beam filters, effects of diffraction on freq. response 4-60232
- fibre-optic sensor, Sagnac interferometer based design 4-107967
- filters, optimum signal to noise enhancement of narrow band signals 4-112656
- lens, audio acoustic, vane type, and acoustic wavefront visualisation device (*Korean*) 4-112657

## acoustic dispersion

- see also ultrasonic dispersion*
- cylindrical shell in fluid, dispersion curves for normal modes 4-112610
- ferroelectric, acoustic-phonon dispersion at incommensurate phase transitions, Brillouin scatt. obs. 4-61724
- marine shallow seismic responses, dispersion compensation 4-110315
- porous media, fluid saturated, acoustic props., phenomenological description 4-69612
- <sup>3</sup>He, liquid, viscoelasticity and zero sound 4-98395

acoustic echoes *see echo*

## acoustic emission

- see also ultrasonic materials testing*
- adhesive bonded joint, strength tests using acoustic emission method 4-109614
- Betalloy, shape-memory alloy, stress-induced martensitic transformation, acoustic emission studies 4-81192
- brittle materials, fatigue testing, high-temp. device 4-66527
- capacitance transducer with a point-like probe for receiving acoustic emissions 4-112658
- ceramic materials, crack detection by acoustic emission 4-62155
- ceramics, heterogeneous, fracture, acoustic emission and sub-crit. events 4-62050
- ceramics, thermal shock resistance and fatigue, acoustic emission study 4-62054
- computerised burst-signals analysis using MPS 4944 microprocessor system (*German*) 4-79377
- crack resistance evaluation in steady loading 4-99699
- cracks, sound radiation by growing cracks 4-103258
- crystal in prefraction state, acoustic emission theory 4-80166
- ear, stimulated acoustic emissions in gerbil and man, suppressibility 4-109827
- energy flux density during transverse-shear crack propag. 4-109617
- ferroelectric, stochastic US signal emission on polarisation initiation (*French*) 4-109051
- ferromagnet, stochastic US signal emission on magnetisation initiation (*French*) 4-109051
- fibre reinforced composite laminates, onset of delamination, expt. and analytical study 4-76847
- fibre reinforced composites model, acoustic emission evaluation 4-81380
- fibre reinforced plastics, tensile tests, at-cryogenic temps., acoustic emission 4-76804
- fibre/matrix materials, acoustic emission waveforms in isotropic and orthotropic plates 4-97188
- gas, velocity-selective optical excitation, sound emission and Raman scatt. 4-113113
- glass, acoustic emission signal characteristics of Hertzian and unloading cracks 4-75617
- glass fibre reinforced plastics, filament wound pipes, acoustic emission under long-term loading 4-99457
- glass fibre reinforced polyamide, fracture mechanism, acoustic emission and microscopy obs. 4-66417
- glass-C hybrid reinforced plastics, mech. props. 4-93407
- granite from Oshima, Japan, acoustic, emission during creep (*Japanese*) 4-89910
- graphite, nuclear, fracture, acoustic emission and sub-crit. events 4-62050
- graphite fibre reinforced epoxy laminates, fatigue loading damage accumulation, acoustic emission monitoring 4-81265
- Hastelloy X, oxidation, thermal cycling, H permeation, acoustic emission 4-76905
- hollow objects in hydraulic immersion, acoustic emission test stand 4-71851
- hybrid composite, unidirectional fibre, amplitude distrib. A/E signatures 4-89198

**acoustic emission continued**

- Incoloy 800 H, oxidation, thermal cycling, H permeation, acoustic emission 4-76905  
 inspection tool, acoustic emission, techniques and appls. 4-93482  
 insulators, high tension, failure prediction, NDT methods comparison 4-62154  
 loaded structures, multiparameter acoustic emission prediction of strength, algorithm 4-71842  
 materials processing, review 4-99692  
 multichannel inspection device 4-109599  
 naval structures, underwater NDT methods 4-114759  
 nuclear reactors, relief valves, acoustic testing of operation 4-59377  
 optical glass fibres, acoustic location of fracture origin 4-112598  
 organic plastic, damage cumulation in quasistatic and cyclic loading 4-89090  
 PMMA, secondary cracks, form. mechanism, X-ray microanal. and acoustic emission 4-66421  
 polycrystalline materials, cumulative damage estimation 4-64894  
 pressure vessels, multiparameter acoustic emission prediction of strength, algorithm 4-71842  
 registration of continuous acoustic emission 4-76948  
 rocks, fracture mechanics and acoustic emission of anti-plane shear cracks 4-77507  
 salt rocks, acoustic emission props. during failure processes 4-77510  
 signals distortion by sensor temp. changes 4-87524  
 steam turbine rotor steel crack growth detection and monitoring by acoustic emissions meas. 4-76961  
 steel, Cr-Mo, nitrided cases, fracture process, acoustic emission obs. 4-99587  
 steel, CrMn, acoustic emission in H origin defects form. 4-99534  
 superconducting magnets, acoustic emission correlation with normal zone occurrence in epoxy-impregnated windings 4-70982  
 surface motion excited by acoustic emission from a buried penny-shaped crack 4-97423  
 tensile deformation, acoustic emission response and interpret. 4-114608  
 transition radiation by mass source moving over rough surface 4-91674  
 viscous vortex motion, axisymmetric, and acoustic emission 4-97578  
 weld heat affected zone, acoustic emission testing of cold crack initiation and growth (German) 4-99718  
 Al, high-purity polycrystals, acoustic emission during plastic deform. 4-71688  
 Al-Zn-Mg, 7075, heat-treated, acoustic emission during deform. 4-93343  
 Be, acoustic emission due to deform. (Russian) 4-92304  
 C fibre reinforced epoxy laminates, fatigue failure behaviour with edge notch 4-114669  
 Cu whiskers, sound emission 4-113839  
 Cu-based shape-memory alloy, mech. and elec. props., sonic studies 4-76773  
 Cu-Ga-V multifilamentary superconductors, brittle fracture, acoustic emission anal. 4-71715  
 Cu-Ti alloys, tensile deform., acoustic emission 4-66390  
 Fe-Cr-Ni(Si), acoustic emission and resist. variation during cyclic heating 4-81296  
 Fe-Ni(-C), martensitic transform., amplitude distrib. of acoustic emission 4-71651  
 Gd<sub>2</sub>(MoO<sub>4</sub>)<sub>3</sub>, ferroelectric-ferroelastic, acoustic emission and domain wall dynamics 4-84925  
 Nb-Ti superconductor, acoustic emission (Chinese) 4-92855  
 Ni base superalloys, diffusion coated, crack initiation, acoustic emission obs. (German) 4-62140  
 Ni-base superalloy, MAR-M002, cast, influence of prestress on yield surface at 750°C 4-93355  
 Ni-Cr-Mo superalloy, elastoplastic deform. and failure, acoustic emission obs. 4-66377  
 Tb<sub>2</sub>(MoO<sub>4</sub>)<sub>3</sub>, ferroelectric-ferroelastic, acoustic emission and domain wall dynamics 4-84925  
 W fibre reinforced Cu composite, fracture, acoustic emission obs. (Japanese) 4-62024
- acoustic equipment**  
 see also acoustic arrays; acoustic wave interferometers; ultrasonic equipment  
 acoustic telescope system using vane-type acoustic lenses, system construction 4-79404  
 flowmeter, long-wave, fluid flow meas. in pipe for single-phase 4-83965  
 oceanographic submerged buoy and ocean bottom station retrieval equipment 4-94271  
 penetrometer for sea bed sediment surveys 4-77668

**acoustic field**

- aerosols, acoustic wave dispersion and dissipation 4-97745  
 Arctic Ocean, dispersion and ranging of transient signals 4-105566  
 building facades, sound field reflection and transmission 4-87514  
 echosonde pattern synthesis study 4-112661  
 enclosure with diffusely and specularly reflecting boundaries, steady state sound field calcs. 4-60211  
 equatorial spherical band with pulsating surface, radiation field 4-107927  
 fluids, US field propag. calc. using finite difference techniques 4-98205  
 free liquids, fluid dynamical studies using acoustic levitation 4-97621  
 Gulf of Mexico, underwater sound from lightning strikes to water 4-105567  
 homogeneous isotropic turbulent medium light scatt. spectrum 4-59975  
 horns and baffles, exact acoustic field calc. 4-112605  
 linear source, transient acoustic pressure distribution, approximated closed form 4-83747  
 loudspeakers, sound-pressure responses effect of acoustic field in enclosure 4-64815  
 mechano-acoustic feedback between sound source and resonator system 4-97164  
 ocean, acoustic normal mode determ. method 4-103072  
 orifices, acoustic nonlinearities and power losses 4-112614  
 parametric focusing source, sound field calc. 4-74831  
 parametric sound radiator, gas bubble effects on sound field 4-91681  
 piezoelectric ceramic transducer, forward and backward projection of acoustic fields 4-87532  
 piezoelectric transducer, partially electroded, with ring electrodes, radiation pattern model 4-97246  
 radiation stress in solids 4-98210  
 reverberant room, sound absorbing coeffs. evaluation 4-107951  
 reverberation times of closed sound paths with low damping 4-91664  
 room sound press. level prediction using equivalent absorpt. coeff. 4-103101

**acoustic field continued**

- semicylindrical concave rigid wall, high-freq. acoustic press. fields excited by line source (Japanese) 4-112609  
 semifinite annular duct in subsonic mean flow, acoustic radiation 4-87496  
 single mode acoustic fiber waveguide 4-107928  
 sources located on walls of dihedral corners, sound fields 4-91670  
 spectral-domain radial extrapolation of acoustic fields (French) 4-97228  
 stratified fluid media, wave field calcs. 4-103071  
 transducer, large, nearfield, second harmonic and sum freq. radiation 4-74830  
 transducers, surface displacement, fibre optic meas. 4-97261  
 two-frequency spherical source, nonlinear sound field calc. 4-91677  
 US axisymmetric transducers, acoustical displacement reconstruction 4-97254  
 variable-width waveguide, acoustic field, 3D model (Ukrainian) 4-64805  
 vibroacoustic fields compensation by acoustic radiators, optimum distribution calc. 4-103055
- acoustic generators**  
 see also earphones; loudspeakers; photoacoustic effect  
 fluid-solid interface, acoustic wave generation and scatt. 4-87494  
 Hartmann generator of large amplitude sound, pipe acoustics appl. (Japanese) 4-91708  
 pulse discharge sound source for acoustic measurements (Japanese) 4-97243  
 pulsed discharge sound source for acoustic measurements, stability (Japanese) 4-112663  
 semifinite annular duct in subsonic mean flow, acoustic radiation 4-87496
- acoustic holography**  
 array imaging, complex holographic function anal. (Chinese) 4-60220  
 computer-aided, developments (Japanese) 4-74824  
 digital holographic reconstruction, sampling method 4-69630  
 Doppler effect influence (Chinese) 4-83779  
 electronic speckle pattern interferometry for vibr. anal. 4-87515  
 flaw sizing and characterisation, US holography and synthetic aperture focusing techniques 4-85274  
 liquid surface dynamics under the action of ultrasonic press., holography appl. 4-107955  
 multi-dimensional correlation function model (Russian) 4-60219  
 multifrequency acoustical holography using a narrow pulse 4-103124  
 position of object determ. (Chinese) 4-83780  
 review 4-107574  
 single beam synthesis from thinned arrays 4-112642  
 ultrasonic imaging, incoherent, technology review (Japanese) 4-87516  
 US NDT by acoustic holography (French) 4-76922
- acoustic imaging**  
 see also acoustic holography  
 A-mode speckle reduction with compound frequencies and compound bandwidths 4-105304  
 backward-projection reconstruction algorithm 4-103155  
 coating for tools and sliding elements, acoustic microscopy studies 4-104957  
 computer-aided, developments (Japanese) 4-74824  
 diagnosis by quantitative US backscatt. imaging 4-89666  
 echocardiograms, 2D, effective algorithm for extracting serial endocardial borders 4-85460  
 Fourier domain reconstruction of synthetic focus acoustic imaging system 4-97210  
 high resolution acoustic microscopy 4-60231  
 high resolution acousto-optic laser probe 4-97746  
 left ventricle, 3D reconstruction from 2D echocardiograms (Japanese) 4-100267  
 medical US imaging system for invasive appls. 4-89665  
 microwave thermoelastic tissue imaging—system design 4-115160  
 multisensor active system, two-dimensional image-reconstruction-using ARMA model 4-60218  
 near-field imaging, source reconstruction by acoustic field projection (French) 4-60194  
 phase difference technique 4-103125  
 polyvinylidene fluoride transducers for acoustic ranging and imaging in air 4-97251  
 pulse Doppler flow imaging using a SAW C/ZT processor 4-97728  
 pulsed fields used in diagnostic US, finite amplitude distortion 4-85465  
 room acoustics, image source computer model 4-79370  
 scanning electron acoustic microscopy imaging, depend. on chopping and detect. freq., appl. to Cu-Zn-Al 4-69639  
 scanning photoacoustic microscope, imaging and resolution, Fourier anal. 4-112654  
 sound-image quality, physical and psychological factors 4-79373  
 surface breaking cracks, location and sizing by synthetic aperture acoustic imaging system 4-85276  
 system using a Lamb wave device 4-97224  
 turbulent media, sound propag. and acoustic imaging (French) 4-97169  
 ultrasonic imaging, incoherent, technology review (Japanese) 4-87516  
 US imaging, lateral deconvolution of US beams 4-97211  
 US imaging, simultaneous algebraic reconstruction technique 4-97212  
 US imaging of tongue shape, characterisation from US image data by numerical methods 4-100271  
 US imaging through an inhomogeneous layer by least-mean-square error fitting 4-60234  
 US local critical angle measurements for the examination of materials, subsurface images 4-97236  
 Al welds, miniature, in composite structures, nondestructive inspection 4-66529  
 (Pb<sub>1-3x/4</sub>Sm<sub>x</sub>)(Ti<sub>1-y</sub>Mn<sub>y</sub>)O<sub>3</sub> ceramic ultrasonic probe 4-100341
- acoustic impedance**  
 see also acoustic wave velocity  
 borehole monitoring by US echography (French) 4-67444  
 frequency characts. for bulk element, determ. (Russian) 4-112652  
 liquid interfaces, acoustic impedance and Konstantinov effect 4-108550  
 liquid-solid phase transforming systems, acoustic absorpt. coeff. and specific acoustic impedance meas. method 4-97227  
 measurement using spark and steady state tubes 4-74821  
 microperforated panel, acoustic impedance meas. method (Chinese) 4-60230  
 pipe, acoustic plane wave propag. with mean flow 4-112608  
 polystyrene solutions, US studies and Rao formalism 4-103883  
 propellants, acoustic impedance meas. in impedance tube, gas-phase losses and propellant self-noise 4-60235

**acoustic impedance continued**

- sources located on walls of dihedral corners, sound fields 4-91670
- transversely isotropic plate, sound transmission and vibrs. 4-112613
- unidirectional piston in baffle, variable impedance, directivity patterns 4-112635
- <sup>3</sup>He, superfluid B-phase, collective modes, acoustic impedance investigation 4-98396

**acoustic insulating materials** *see noise abatement***acoustic intensity**

*see also acoustic noise; loudness*

- sound pressure level and acoustic intensity, misuse of terms 4-112600
- stratified random media, acoustic intensity 4-87495

**acoustic intensity measurement**

- condenser microphones, one inch, sound pressure meas. in open circuit (German) 4-91713
- impact sound loudness measurement by sound level meter, time constant meas. 4-87528
- jet, subsonic, near field, two-dimens. acoustic intensity probe measurements (French) 4-60227
- mean free path and acoustic power of sound source meas. in reverberation and anechoic chambers (French) 4-107962
- microphone arrangements for sound intensity meas. 4-87527
- noise source identification by acoustic intensity measurements (Japanese) 4-60210
- power determination using nine-point microphone array, intensity and mean square press. methods 4-103150
- selective two microphone techniques with dual channel analyzer 4-74823
- two-microphone cross-spectral method, introduction 4-103149
- two-microphone technique, scatt./diff. effects 4-103151
- wall constructions, sound transmission loss, intensity and two-room method meas. 4-103152

**acoustic magnetic resonance**

*see also acoustic nuclear magnetic resonance; acoustic paramagnetic resonance*

- MnZn spinels, acoustic mag. reson. obs. 4-61615
- YIG, acoustic mag. reson. obs. 4-61615

**acoustic measurements** *see acoustic variables measurement***acoustic microscopes**

- elastic discontinuities, acoustic microscopy 4-60237
- glass fibre reinforced polycarbonate composite, subsurface imaging of fibres by acoustic microscopy 4-76924
- high frequency, pulse compression method 4-103161
- high resolution acoustic microscopy 4-60231
- hyper sound in gigahertz region, application to investigation of solids (French) 4-64813
- materials testing, microscopy (German) 4-93492
- miniature lens scanner for acoustic microscopy 4-97230
- multiple leaky SAW, FFT vel. meas. by line focus-beam acoustic microscope 4-103164
- nonlinear scanning electron acoustic microscopy 4-74825
- operating principles and advances, SAM 4-91704
- phase information, appls. 4-97229
- photodisplacement microscopy, appl. to Si plate thick meas. and cross-section inhomogeneity visualisation 4-91702
- planar annular surface wave transducer 4-97232
- principles and appls. 4-112651
- pulsed reflection acoustic microscopy of materials and surface layers 4-64811
- reflection acoustic microscope, output volt., ray-optical evaluation 4-91703
- reflection acoustic microscopy, Rayleigh-wave suppression and filtering 4-103163
- reflection lens for acoustic microscopy 4-103165
- scanning, state-of-the-art and development trends (Chinese) 4-107966
- scanning acoustic microscope, reflection mode, nonlinear effects 4-107968
- scanning acoustic microscope in interference mode using frequency modulation method 4-97231
- scanning electron acoustic microscopy imaging, depend. on chopping and detect. freq., appl. to Cu-Zn-Al 4-69639
- scanning electron acoustic microscopy with subnanosecond time resolution 4-74826
- scanning laser acoustic microscopy and cryogenic scanning acoustic microscopy, review (Japanese) 4-64812
- scanning photoacoustic microscope, imaging and resolution, Fourier anal. 4-112654
- thermal wave imaging of GaAs material and devices 4-75711
- tomographic acoustic microscopy, data acquisition 4-103162
- He, liquid, microwave acoustics, high resolution microscopy and phonon dispersion meas. 4-61165

**acoustic microwave devices**

*see also acoustic transducers; surface acoustic wave devices*

No entries

**acoustic mode of crystals** *see lattice dynamics***acoustic noise**

- aerodynamic noise, multivariable analysis of the noise of an obstacle (French) 4-112630
- aerodynamic sound generation by turbulent boundary-layer flows along walls (German) 4-112637
- air jets from rectangular slits, noise meas. 4-60470
- aircraft noise, penetration into airport terminal buildings 4-114994
- aircraft noise, subjective responses of Chinese 4-72200
- aircraft noise impact parameters, variation with distance 4-103096
- amplified pop music and hearing level meas. 4-105254
- annoyance levels due to low level noise (Japanese) 4-105154
- audiometric data base for individual noise 4-109766
- auditory filter dynamic range and asymmetry 4-115065
- balanced vane pump pressure pulsation, fluidborne noise generation characts. 4-112843
- binaural anal., role of monaural freq. selectivity 4-115067
- binaural masking-level differences: effects of bandwidth, noise level and signal duration 4-93748
- binaural masking-level differences with tones masked by noises of various bandwidths and levels 4-93749
- body sensation of low freq. noise for deaf and normal hearing subjects 4-105262
- choked jet noise, screech spectra (Chinese) 4-83762
- circular cylinder, cavity/wake dynamics, noise spectra meas. 4-79631

**acoustic noise continued**

- cochlea, anatomical correlates of impulse noise-induced mech. damage 4-89592
- cochlear nerve and nucleus, single units, noise masking of tone responses and crit. ratios 4-93757
- concrete porous materials, improvement of sound-absorpt. props. 4-87513
- conference, acoustics, Paris, France (July 1983) 4-78035
- decibel calculation program for TI 59 calculator 4-83768
- discrimination of fundamental frequency of synthesized vowel sounds in a noise background 4-115066
- duct, circular, abrupt expansion, self-excited flow oscillation 4-103412
- ducts, regenerated noise due to closely spaced induct dampers 4-97199
- energy suppression of regular sound in intense random noise field (Chinese) 4-107929
- environmental noise, state prediction by generalized adaptive function model 4-62422
- environmental noise and vibr., random level distrib. prediction 4-103094
- environmental noise and vibration, effect on mental arithmetic tasks 4-114993
- environmental noise exposure in residential areas in Nagoya City (Japanese) 4-114996
- fan rotor blades, turbulent noise intensity and scale distrib. (Japanese) 4-97521
- filters, optimum signal to noise enhancement of narrow band signals 4-112656
- fish schools, detection against background interference 4-91685
- forge hammers, structural noise identification, multipole input models 4-60208
- forge hammers, structural noise source identification, multiple input models 4-60209
- German steel industry, measures for reduction of dust and noise (German) 4-91687
- hearing protection device effectiveness at industrial facility with 107 dB 4-112633
- highway traffic noise prediction accuracy 4-87510
- human behaviour patterns, noise sensitivity as function of task complexity 4-81707
- infrasound in the environment, review 4-105152
- internal oscillating flows, noise and vibr. in high press. gas valves 4-97519
- IR photoacoustic spectroscopy, acoustic isolation chamber effect on S/N ratio 4-101939
- Jeddah urban sites, environmental acoustic quality 4-79365
- layered ocean bottom, cross spectrum of radiated noise signal and reflected signal 4-115430
- loudness of complex noise consisting of impact sound and steady noise (Japanese) 4-83772
- machine elements, noise radiation, numerical calcs. (Japanese) 4-83767
- nonstationary random excitation processes, modelling 4-103093
- ocean surface-generated noise sensitivity to sonar and environmental parameters 4-110165
- passenger automobile, noise generated by studded snow tyres 4-79364
- personal noise exposure, database construction (Japanese) 4-93668
- pipe flow, acoustic radiation generation due to internal flow disturbances 4-75087
- plates, vibrating energy determ., points of meas. placement criteria 4-83760
- power determination using nine-point microphone array, intensity and mean square press. methods 4-103150
- psychometric tests, temporal averaging of subjective magnitude and proposed rating scale for fluctuating noise 4-83764
- pure tone noise generation by a system of open periodic cavities exposed to a flow (French) 4-112629
- quantised noisy systems and room acoustics, general state estimation algorithm 4-103092
- random noise and vibr., waveform acuity, statistical evaluation methods (Japanese) 4-97198
- reduction by scatt. in low velocity ducts 4-107948
- residential areas near chemical plants, noise complaints 4-109764
- retardation effect, fast moving sound source motion parameter estimation 4-103160
- road traffic noise, acoustic anal. for Southern France (French) 4-109765
- road traffic noise, statistical parameter identification method for sound propagation characts. (Japanese) 4-81603
- road traffic noise, subjective ratings (Japanese) 4-114995
- road traffic noise, time series prediction by adaptive functions (Japanese) 4-62425
- road traffic noise in Hiroshima 4-103095
- road traffic noise prediction for urban streets (Chinese) 4-85396
- road vehicles, noise emission, acoustic signature reconstitution 4-62423
- room window, unshielded and opened, acoustic performance 4-103099
- room with shielded open window, acoustic performance 4-103100
- roughly observed data with quantised levels, noise probability estimation 4-97195
- ship propeller cavitation noise power spectra (Chinese) 4-107949
- shipping noise, ambient low-frequency vertical directionality 4-115415
- ships, noise levels in accommodations, prediction 4-85395
- ships, noise radiation, autocorrelation function and rhythm patterns anal. (Chinese) 4-60207
- sleep disturbance by noise 4-105287
- solid body rotation, press. field (French) 4-112890
- speech, noisy, pitch estimation by autocorrelation method, spectral flattening effects 4-79379
- stereocilia on inner hair cells, fusion in various mammals after noise exposure 4-85437
- stochastic insulation effect of sound barrier, prediction method 4-79366
- supersonic propeller noise, wave eqn. soln. 4-103315
- thermal power stations, throttle type sound suppressors, acoustic efficiency improvement (Russian) 4-77166
- throttling valve noise, aerodynamic sound level calc. 4-74807
- traffic vibration, public nuisance, estimation formula 4-105153
- transient flow, acoustic noise emission 4-97193
- transient fluid instabilities, acoustic noise, natural monopoles 4-108067
- turbulence and acoustic noise relationship, recent experimental studies (German) 4-112844
- turbulent boundary layer, acoustic radiation anal. (French) 4-112632
- turbulent burner, thermal-acoustic efficiency spectrum 4-97518
- turbulent gas flame, sound radiation mechanism 4-71919
- turbulent jets, mixing process, noise, coherent struct. 4-64991
- turbulent shear flow, noise generation and propag. 4-60394
- turbulent shear flows, aeroacoustics 4-91805

- acoustic noise continued**  
 urban noise, dynamic state estimation 4-105151  
 warning sound perception and attention demand, hearing protector effects 4-105253  
 water flow, turbulent boundary layer with gas injection, press. fluctuations 4-103316  
 wedge, particle-vel. field of a signal and noise, spatial correlation function 4-91668  
 CdS, uniaxially deformed, current saturation and oscill. (*Russian*) 4-70818
- acoustic noise measurement**  
 acoustic power/intensity under water, measurement using dual-hydrophone system (*Chinese*) 4-103091  
 aeroacoustics, acoustic noise meas. and signal anal. (*French*) 4-60226  
 direct speech communication and ambient noise in restaurants and cafeterias, seating density criteria 4-79411  
 energy flux density measurement, using unidirectional reception system 4-103158  
 film camera acoustic noise characts. (*Russian*) 4-95549  
 impulse noise dosimetry 4-103159  
 ITTC foil-headform combination, cavitation noise experimental study (*Chinese*) 4-97223  
 nonlinear iterative technique for high-resolution spectral estimation 4-69649  
 nuclear power stations, monitoring and fault diagnosis system for early fault detection (*German*) 4-59384  
 personal noise dosimeter for hazard eval. in industry 4-91701  
 rail tractors, external noise reduction 4-74808  
 random noise and vibrations, nonstationary, multivariate probability evaluation from digital level measurements (*Japanese*) 4-103097  
 source identification by acoustic intensity measurements (*Japanese*) 4-60210  
 subsonic jets, high-speed, acoustic meas. 4-112649  
 UHF radio environment, man-made noise level meas. 4-107972
- acoustic nuclear magnetic resonance**  
 metals and alloys, nuclear acoustic resonance, review 4-76263  
 resonance with acoustic quasienergy levels in inhomogeneous broadening of NMR spectrum 4-71194  
 splitting of NMR lines by a quantizing acoustic field of resonance frequency 4-71195  
 transition metals, electron-phonon interactions, acoustic NMR meas. 4-70318
- acoustic paramagnetic resonance**  
 metals, acoustic excitation of spin waves due to conduction electrons (*Russian*) 4-98947  
 n-GaAs:Cr<sup>2+</sup>, acoustic paramagnetic resonance study 4-71171  
 Si:Li, phonon scatt., acoustic paramagnetic resonance study 4-71157
- acoustic parametric amplifiers**  
 No entries
- acoustic parametric devices**  
*see also acoustic parametric amplifiers; acoustic parametric oscillators*  
 broad-band signals, self-demodulation for signal transmission (*Japanese*) 4-103062  
 focusing source, sound field calc. 4-74831  
 radiator, second harmonic and sum freq. radiation 4-74830
- acoustic parametric oscillators**  
 No entries
- acoustic radiators**  
*see also acoustic generators; Doppler effect*  
 beams, vibrating, un baffled, sound radiation, thickness effects (*Japanese*) 4-103088  
 circular radiators at high freqs., surface acoustic field calc. 4-107943  
 equatorial spherical band with pulsating surface, radiation field 4-107927  
 Gaussian monochromatic source, acoustic radiation, nonlinear approx. solns. (*French*) 4-97177  
 liquids, cavitating, acoustic monopole and dipole radiation efficiency 4-91682  
 machine elements, noise radiation, numerical calcs. (*Japanese*) 4-83767  
 parametric generation of a low-frequency signal in guided-wave sound channels 4-107971  
 parametric sound radiator, gas bubble effects on sound field 4-91681  
 planar panels and rectangular beams, short wave acoustic radiation 4-112604  
 plate, circular, sound power for high freq. wave radiation 4-103084  
 sound field of arbitrary rigid radiator, synthesis by spherical sound fields (*German*) 4-79355  
 sources located on walls of dihedral corners, sound fields 4-91670  
 vibroacoustic fields compensation by acoustic radiators, optimum distribution calc. 4-103055
- acoustic reactance** *see acoustic impedance*
- acoustic receivers**  
*see also microphones*  
 induced polarisation infrasonic receiver (*Spanish*) 4-69640  
 piezoelectric array receivers using ceramics with high and low planar coupling, ang. response 4-97262
- acoustic resistance** *see acoustic impedance*
- acoustic resonators**  
 double mode resonators, acoustic coupling in thickness twist mode 4-97222  
 mechano-acoustic feedback between sound source and resonator system 4-97164  
 multilayered resonant systems, optimal energy absorption conditions 4-91669  
 partially coherent radiation from reverberant chambers 4-103052  
 sound column, resonance freq. and efficiency (*Chinese*) 4-107916  
 surface-skimming bulk wave reflection by system of periodic inhomogeneities, Bragg case 4-69642  
 LiTaO<sub>3</sub> temp. compensated bulk shear microwave resonators 4-112647
- acoustic signal processing**  
 acoustic arrays, digital signal processor module architecture, implementation using VLSIs 4-103122  
 acousto-optic signal processing 4-103102  
 acousto-optical signal processing systems, acoustic nonlinearity effects 4-103123  
 active low-pass RC-filter, design, for sharp bands-separation 4-112640  
 adaptive arrays for signal separation (*Chinese*) 4-91691  
 ADMF (average magnitude difference function) concept, pitch detection algorithm implementation 4-103137  
 aeroacoustics, acoustic noise meas. and signal anal. (*French*) 4-60226
- acoustic signal processing continued**  
 algorithm design for real-time audio signal processing 4-103111  
 alternate low-level primitive structures (ALPS), architectural approach 4-69629  
 audio signal enhancement, digital techniques appl. 4-103109  
 audio signal processing, digital, CMOS-VLSI rate conversion digital filter appl. 4-103121  
 auditory evoked brainstem responses, signal processing technique 4-85429  
 automatic glottal inverse filtering 4-103143  
 band-limited discrete-time signals interpolation, out-of-band energy minimisation 4-103110  
 beamformer preprocessing, high resolution method sensitivity reduction 4-103118  
 beamforming and spectral analysis, nonlinear approximation technique 4-60216  
 bearings-only tracking, recursive vs. batch processing algorithms 4-107942  
 Bragg cells, anisotropic bulk wave cells, design, fabrication and testing 4-103103  
 burst-signals analysis using MPS 4944 microprocessor system (*German*) 4-79377  
 cardiac tissue characterisation, stochastic approach to RF amplitude anal. 4-105302  
 conference, acoustics, Paris, France (July 1983) 4-78035  
 consonants recognition using ARMA model of speech signal 4-103120  
 correlation detection, optimally phase-fluctuation tolerant waveforms (*Japanese*) 4-103106  
 cue identification 4-81712  
 cues, acoustic and articulatory analysis 4-81710  
 digital audio technology, fundamentals and methods (*German*) 4-112641  
 digital holographic reconstruction, sampling method 4-69630  
 digital sound recorders, nonlinear distortion meas. (*Russian*) 4-60217  
 Doppler flow meas. and processing, signal-to-noise ratio enhancement 4-100286  
 ducts, acoustic transmission, impulse method using signal synthesis and averaging 4-74786  
 ear acoustic props., short-time power spectra parametric representation 4-103141  
 editing digital audio 4-103112  
 formant tracking and glottal inverse filtering, two channel (speech and EGG) anal. 4-103144  
 Fourier domain reconstruction of synthetic focus acoustic imaging system 4-97210  
 frequency stepping signal generator, digitally controlled (*Chinese*) 4-83776  
 GRASP sound separation system 4-103134  
 human classification of complex sounds 4-115078  
 hydrophone arrays, colinear, hybrid time-delay/phase-shift digital beamforming 4-83777  
 input/output and processing of acoustic signals with a minicomputer system 4-83778  
 interpolation scan conversion in pulse echo ultrasound 4-103108  
 inverse scattering solns. by sinc basis, multiple source, moment method 4-97213  
 jet, subsonic, near field, two-dimens. acoustic intensity probe measurements (*French*) 4-60227  
 laryngeal acoustic source modelling, labile nonlinear oscillations appl. 4-103142  
 laser light and SAW interaction appl. 4-74565  
 layered acoustic medium, inverse problem, appl. of Schur algorithm 4-103051  
 LMS spatial cancellation, interference extent effects 4-103081  
 medical US B scans, lateral filtering before image generation 4-105303  
 Monterey Fan expt., coherent recombination of sediment borne and water path acoustic signals 4-105770  
 neural auditory processing, computational models 4-103139  
 noise cancellation, adaptive, digital filter implementation using modified Widrow-Hoff algorithm 4-103114  
 noise reduction by nonlinear digital filtering, estimation method 4-91694  
 noise suppression using two-point receiving signals (*Japanese*) 4-91695  
 noise-alone reference AGC adaptive signal detection for random linear filtering deformations 4-91692  
 noisy speech, pitch extraction algorithms comparison 4-103138  
 nonstationary acoustic signals from moving sources, modelling and deconvolution using covariance equivalent formulation 4-103117  
 ocean for data inversion 4-74799  
 ocean sound channels, linearized travel time, intensity and waveform inversions 4-74800  
 OCEANS '83, utilisation of sea, conference, San Francisco, CA, USA (Aug.-Sept. 1983) 4-106113  
 parametric broad-band signals, self-demodulation for signal transmission (*Japanese*) 4-103062  
 personal computer based signal compression method for sound field meas. in pipes (*Japanese*) 4-97209  
 piezoelectric array receivers using ceramics with high and low planar coupling, ang. response 4-97262  
 piezoelectric multielement transducer, programmable pulse generator 4-87536  
 post-processing algorithm for time-domain pitch trackers 4-103136  
 postbeamformer interference canceller in presence of broadband directional signals 4-97207  
 Prony method for data processing with white or colored noise (*Chinese*) 4-91690  
 quartz matched filter block for phase-coded signals, expt. characts. 4-60240  
 random acoustic arrays, freq.-wavenumber spectrum estimation using beampower pattern estimators 4-97208  
 real-time, digital bandpass filters appl. 4-97206  
 recording and reproduction methods (*German*) 4-103104  
 reflection acoustic microscopy, Rayleigh wave suppression and filtering 4-103163  
 reflection coefficients and transfer functions meas. by cepstral techniques 4-60236  
 SAW finite amplitude waves, resonators, convolvers and correlators, appl. 4-74792  
 sea surface reverberation rejection 4-103119  
 shallow water multimodal sound transmission, signal processing and appl. to underwater acoustic communication 4-91693  
 single beam synthesis from thinned arrays 4-112642  
 sonar, CTFM, range accuracy improvement 4-69620

**acoustic signal processing continued**

- sonar echo fading in shallow water, rel. perform. of incoherent and coherent processing 4-69619
- sonar system performance measured by containment region 4-107939
- sound-image quality, physical and psychological factors 4-79373
- spectral analysis, uncertainty principle in frequency-time methods 4-74814
- speech, all-zero model for higher pole correction 4-103146
- speech, noisy, pitch estimation by autocorrelation method, spectral flattening effects 4-79379
- speech, pitch and spectral estimation, auditory synchrony model based 4-103140
- speech signals pitch determination, laryngograph appl. 4-103135
- statistical analysis of actual acoustical signals using high-order moments (French) 4-60215
- tomographic acoustic microscopy, data acquisition 4-103162
- TV sets, digital audio-signal processor appls. 4-103113
- two-channel FFT analysers 4-103107
- underwater acoustic telemetry error detection and correction codes 4-112624
- underwater acoustics, adaptive least squares lattice structure appls. 4-97205
- underwater transient signals, characterisation and recognition 4-103115
- US, quadratic-like complex residue number system arithmetic appls. 4-103116
- US, steel, stainless heat-treated samples, evaluation by split-spectrum processing 4-99721
- US attenuation and mean backscatter size meas. by digital signal processing 4-100269
- US diffraction tomography using beam waves: Z-average reconstruction 4-100274
- US imaging, lateral deconvolution of US beams 4-97211
- US imaging, simultaneous algebraic reconstruction technique 4-97212
- US imaging through an inhomogeneous layer by least-mean-square error fitting 4-60234
- US pulse echo systems, range resolution improvement by deconvolution 4-60199
- vowel duration, loudness in a CV syllable 4-81713
- wideband ocean noise and propagation loss, real-time digital signal processing algorithms 4-107938
- Wiener filtering and adaptive lattice filter, polynomial approx. (Chinese) 4-107954
- Wordfit, digital audio signal processing system, for automatic time alignment of post-synchronised dialogue 4-69628
- He speech, acoustic anal. of formant bandwidths and frequencies 4-103145
- LiNbO<sub>3</sub>, acoustoelec. coeffs. meas., appl. to signal processing devices 4-97214
- LiTaO<sub>3</sub>, acoustoelec. coeffs. meas., appl. to signal processing devices 4-97214

**acoustic streaming**

- molten metals, EM vibr. treatment under microgravity, hydrodynamic effects 4-97698

**acoustic superradiance**

- No entries

**acoustic surface wave devices** *see surface acoustic wave devices***acoustic surface waves** *see surface acoustic waves***acoustic transducers**

- see also acoustoelectric transducers; ultrasonic transducers*
- annular transducer accessories for mobility meas., prerequisites 4-103156
- arrays with nonuniform element spacing, radiation patterns 4-97263
- conference, acoustics, Paris, France (July 1983) 4-78035
- diffraction transducers, freq. props. and SAW emission 4-74834
- distortion of acoustic emission signals by sensor temp. variations 4-87524
- focused transducer with arbitrary surface velocity distrib., impulse response 4-87530
- Fresnel-phase-plate interdigital transducer for SAW vel. meas. 4-104060
- impedance-matched metallurgically sealed transducers, design and evaluation 4-91707
- interdigital transducer using piezoelectric thin film/amorphous substrate struct. 4-74835
- interdigital transducers, electrode withdrawal weighted, design method (Chinese) 4-107974
- Lamb wave frequency modulator with three IDTs using VCO 4-83794
- large transducer, nearfield, second harmonic and sum freq. radiation 4-74830
- NDT with acoustic flaw detector, appl. to fibre reinforced plastic (German) 4-76941
- parametric focusing source, sound field calc. 4-74831
- piezoelectric transducers, acoustic bonding materials anal. (Japanese) 4-60239
- piezoelectric transducers, crossed normal mode anal. 4-103173
- quartz matched filter block for phase-coded signals, expt. characts. 4-60240
- quasi free-field audiometry, modified transducer system 4-85462
- rectangular acoustic array elements, normal surface displacements, optical interferometry studies 4-112655
- sandwich transducers and arrays, practical design considerations, sonar appls. 4-69653
- SAW devices, transfer function scatt. due to technological defects (Russian) 4-69657
- SAW interdigital transducer pattern masks, computer aided fabrication 4-103168
- sonar ring-shell projectors, perform. and finite-element modelling 4-69652
- split-combined transducer, for impedance inspection unit, elec. simulation method 4-76945
- split-combined transducer, for impedance inspection unit, elec. simulation method 4-76946
- sub-bottom high-resolution multiple-freq. profiler 4-77672
- surface acoustic wave splayed interdigital transducer, radiation directivity 4-91712
- surface displacement, fibre optic meas. 4-97261
- surface generated bulk waves, excitation and detection 4-91667
- towed array response to acoustic field in shallow water 4-69618
- underwater sound detection using optical interference in optical fibers (Japanese) 4-112621
- He, superfluid vibrating superleak second-sound transducer 4-83795
- LiNbO<sub>3</sub>, weak periodic surface acoustic shock waves 4-61198

**acoustic variables measurement**

- see also acoustic intensity measurement; acoustic noise measurement; acoustic wave velocity measurement; Q-factor measurement; ultrasonic measurement*
- acoustic thermometry, research and commercial appls. 4-111133
- acoustics conference, Paris, France (July 1983) 4-78035
- ADMF (average magnitude difference function) concept, pitch detection algorithm implementation 4-103137
- amplified guitars, infinite sustain through controlled feedback 4-79402
- background noise immunity, multisensor speech input 4-103131
- bounded US waves, reflection expt., optical meas. 4-74822
- broadcasting studios, sound reflections, frequency anal. 4-107953
- Burghtheater electroacoustic system, modifications 4-79376
- fighter cockpit environment, adaptive noise cancellation 4-103132
- impedance measurement of propellants in an impedance tube, gas-phase losses and propellant self-noise 4-60235
- impedance measurement using spark and steady state tubes 4-74821
- impedance of microperforated panel, direct meas. method (Chinese) 4-60230
- liquid-solid phase transforming system, acoustic absorpt. coeff. and specific acoustic impedance meas. method 4-97227
- monitoring speakers for control rooms 4-79408
- near-field meas., toneburst techniques appl. 4-79410
- noisy speech, pitch extraction algorithms comparison 4-103138
- pitch of computer-generated complex tones, circularity, paired comparison expt. (Japanese) 4-100177
- pitch perception algorithm for speech 4-83782
- post-processing algorithm for time-domain pitch trackers 4-103136
- power levels of different acoustic sources, sound engineering influence 4-79407
- reflection coefficients and transfer functions meas. by cepstral techniques 4-60236
- reservation time of rooms, meas. using microprocessor audio analyzer 4-83792
- reverberation characts. improvement of enclosed space, with aid of computer (Slovak) 4-60213
- RF pulse method apparatus for US meas. in liqs. (Japanese) 4-95119
- room, sound power anal. (Hungarian) 4-74812
- sound reinforcement system, computer model and ray-tracing, speech transmission index prediction 4-79409
- sound reinforcement systems, comparison of real-time anal. and time-delay spectrometry 4-87526
- sound spectrograph appl., control methods 4-103154
- speech, noisy, pitch estimation by autocorrelation method, spectral flattening effects 4-79379
- speech signals pitch determination, laryngograph appl. 4-103135
- standard control room, proposal 4-79374
- studio, design, effects of glass 4-97201
- TECRON TEF System 10 acoustic analyser, appl. 4-97221
- US transducers for HF acoustic wave meas. in air 4-97252
- water, surface wave amplitude determ. by acoustic pulse method 4-79607

**acoustic velocity** *see acoustic wave velocity***acoustic wave absorption**

- see also noise abatement; ultrasonic absorption*
- %X CO<sub>2</sub>, optical generation and detection of acoustic pulse profiles for novel ultrasonic absorpt. spectroscopy 4-103460
- absorbent materials for noise and vibration control 4-83770
- aerosols, acoustic wave dispersion and dissipation 4-97745
- antiferromagnets, sound absorption and scattering by nuclear spin waves 4-88245
- Arctic Ocean, dispersion and ranging of transient signals 4-105566
- attenuative subsurface layered media parameter estimation, frequency-domain approach 4-107941
- barriers in enclosures, sound attenuation, ray-tracing computer model 4-69622
- chlorosilanes, liq., viscous flow, acoustic wave studies (Russian) 4-92402
- complex dielectric cryst. with impurities, acoustic wave absorption 4-80167
- concrete porous materials, improvement of sound-absorpt. props. 4-87513
- conical diffuser joined by two tubes, sound insulation (Russian) 4-79367
- duct, rectangular, acoustic attenuation of parabolic vel. profile (French) 4-112601
- duct with solid splitter, sound attenuation (Japanese) 4-74788
- expanding waveguide with gas flow, sound absorpt. and amplification 4-79401
- experimental study of transmission within an absorbing medium (French) 4-79358
- fibrous sound absorbing materials, struct. and acoustical props. 4-91688
- gases, optical generation and detection of acoustic pulse profiles for novel ultrasonic absorpt. spectroscopy 4-103460
- ground, wide barriers, sound attenuation 4-107947
- ice sheet, stress-strain state estimation by acoustic probe pulse 4-115428
- inhomogeneous, cryst., local phase transition points, fluctuation enhancement 4-65373
- linear transition wedges, sound absorpt. calc. (Chinese) 4-91666
- liquid interfaces, acoustic impedance and Konstantinov effect 4-108550
- liquid-solid phase transforming systems, acoustic absorpt. coeff. and specific acoustic impedance meas. method 4-97227
- liquids, highly viscous, sound absorption and propag. 4-92300
- multilayered resonant systems, optimal energy absorption conditions 4-91669
- noise reduction by scatt. in low velocity ducts 4-107948
- oceanic reverberation model 4-67226
- percolation lattices, acoustic wave absorpt. enhancement near a percolation threshold 4-69614
- perfluorobenzene, liq., acoustic relax. mechanism 4-92301
- periodically modulated nonlinear medium opacity to acoustic waves 4-91680
- reverberant room, sound absorbing coeffs. evaluation 4-107951
- rocks, sedimentary, elec. and acoustic props., theoretical description 4-72573
- room sound press. level prediction using equivalent absorpt. coeff. 4-103101
- sandstones, contact microphysics and viscous relax. 4-72575
- sea water, sound absorpt. due to low freq. chem. relaxations (Chinese) 4-87500
- seawater, low freq. acoustic absorpt., relaxation mechanisms (French) 4-107936
- seawater, sound absorpt. at low freqs., historical review (French) 4-107935

**acoustic wave absorption continued**

- sedimentary rocks, acoustic and elec. props., differential effective medium theory 4-67212
- semiconductor/piezoelec. layered struct., SAW vel. and attenuation 4-92503
- semiconductors, electroacoustic effects due to charged dislocations 4-65717
- sound absorpt. by turbulence and other hydrodynamic flows 4-60434
- stratifying solns., acoustic wave dispersion and absorption by conc., fluctuations 4-80164
- suspended sound absorbing plate, acoustical behaviour for random incidence 4-97194
- time filtering and fast Fourier transforms in acoustic scatt. and absorption meas. (French) 4-97166
- tube, turbulent flow, acoustic dissipation 4-87490
- CO<sub>2</sub>-H<sub>2</sub>O, optical generation and detection of acoustic pulse profiles for novel ultrasonic absorpt. spectroscopy 4-103460
- LiNbO<sub>3</sub> groove grating, bulk radiation by SAW propag. 4-92501
- Na<sub>2</sub>O-B<sub>2</sub>O<sub>3</sub> glass, undoped and Co<sup>2+</sup> doped, acoustic loss and optical absorpt. spectra, matrix analysis 4-84193
- Pd<sub>0.775</sub>Si<sub>0.165</sub>Cu<sub>0.06</sub> metallic glass, low-freq. elastic loss at low temp. 4-70289
- SiO<sub>2</sub>, vitreous, low-freq. elastic loss at low temp. 4-70289
- (Y<sub>1-x</sub>Lu<sub>x</sub>)<sub>2</sub>Al<sub>2</sub>O<sub>12</sub>, anharmonicity const., longit. acoustic wave absorpt. 4-88248

**acoustic wave amplification**

- see also *acoustoelectric effects*
- expanding waveguide with gas flow, sound absorpt. and amplification 4-79401
- CdS, piezoelec. semicond., stimulated Brillouin scatt. of electromagnetic wave, acoustic amplification 4-114291
- LiNbO<sub>3</sub>-Ge, parametric amplification of SAW 4-108697

**acoustic wave attenuation** see *acoustic dispersion; acoustic wave absorption; acoustic wave scattering; acoustic wave transmission; ultrasonic absorption***acoustic wave diffraction**

- see also *ultrasonic diffraction*
- bulk-acoustic-wave-beam filters, effects of diffraction on freq. response 4-60232
- circular acoustic rigid cylinders, acoustic backscattering 4-97165
- circular waveguide, acoustic normal mode diff. 4-107925
- cracks, acoustic wave diffraction anal. 4-74779
- cylinder, rigid, surrounded by inhomogeneous fluid layer, sound wave diff. 4-103057
- elastic wave diff. by subsurface crack 4-87492
- Fourier integral transforms appl. to theory 4-103048
- Fresnel diffraction by thin rigid disk, theory 4-60190
- ground effect, meteorology (French) 4-60196
- impulse diffraction, isochronous vol. and edge waves (French) 4-97176
- impulse response method of calc. 4-103049
- intensity meas. using two-microphone technique, scatt./diff. effects 4-103151
- interdigital transducers, electrode withdrawal weighted, design method (Chinese) 4-107974
- Lamb waves, mode conversion technique generation, directivity patterns 4-98417
- lateral waves, HF theory 4-73249
- layered media, spherical wave diff. anal. 4-83750
- liquids, laser-induced acoustic waves, diff. characts. 4-88239
- multiply scattered field of randomly distributed scatterers 4-87497
- nonplanar axisymmetric surfaces, impulse diff. response (French) 4-97175
- rigid baffle, random wave field suppression, adaptive system 4-112636
- rough sphere, spherical wave diff., small perturbation method anal. 4-112612
- SAW by acoustic grating 4-97185
- SAW diffraction by acoustic gratings (Chinese) 4-91665
- SAW filters, general diff. anal. 4-97184
- secondary source theorems, appls. to acoustic propag. and inverse problems (French) 4-97174
- stratified random media, acoustic intensity 4-87495
- tomography using arbitrary transmitter and receiver surfaces 4-103058

**acoustic wave diffusion** see *acoustic wave scattering***acoustic wave effects**

- see also *acoustic magnetic resonance; acousto-optical effects; acoustoelectric effects; biological effects of acoustic radiation; sonoluminescence; ultrasonic effects*
- laminar to turbulent flow transition under action of acoustic oscillations 4-103289
- local heat transport from heated cylinder, sound effect 4-112857
- membranes, streaming current and potential in a high-frequency acoustic field 4-109677
- shells, noncircular cylindrical, in fluid, radiation anal. 4-74787
- thermoacoustic heating at the closed end of an oscillating gas column 4-113101
- water, acoustic cavitation threshold, dil. polymer additives effect 4-103378
- Fe, cast, white, annealing, Fermi energy, thermoEMF obs. rel. to crystallisation in acoustic vibration field 4-76768

**acoustic wave interference**

- see also *acoustic wave interferometers; acoustic wave interferometry*
- layered ocean bottom, cross spectrum of radiated noise signal and reflected signal 4-115430
- multilayered resonant systems, optimal energy absorption conditions 4-91669

**acoustic wave interferometers**

- see also *acoustic wave interferometry*
- fibre-optic sensor, Sagnac interferometer based design 4-107967
- rock core samples, acoustoelastic consts., interferometric meas. using pulsed phase-locked US instrument 4-97237

**acoustic wave interferometry**

- see also *acoustic wave interferometers*
- axisymmetrical discontinuous flow, interference method study 4-60461
- impedance-freq. characts. for bulk element, determ. (Russian) 4-112652
- scanning acoustic microscope in interference mode using frequency modulation method 4-97231
- surface roughness measurement using acoustic speckle correlation (French) 4-60238
- US interferometric measurement of thickness 4-95379

**acoustic wave propagation**

- see also *acoustic dispersion; atmospheric acoustics; Doppler effect; liquid helium sound propagation; seismic waves; shock waves; surface acoustic waves; ultrasonic propagation; underwater sound*
- adiabatic sound wave propag. in grey radiative atmosphere, closed soln. 4-72929
- aerosols, acoustic wave dispersion and dissipation 4-97745
- annular pipes, sound propagation, rotational flow effects (French) 4-97520
- Arctic Ocean, dispersion and ranging of transient signals 4-105566
- branched pipes with small diameters appl. (Chinese) 4-83745
- caustics, geometrical acoustic expansion 4-60192
- cavities, acoustic wave propag., finite element techniques 4-83749
- communication system design, underwater acoustic channels characterisation 4-60201
- complex ocean environment, acoustic propagation loss calc. for simulator based training 4-60200
- concentric-tube resonator, gas flow and acoustic press. 4-113016
- conference, Strasbourg, France (June 1984) (French) 4-106111
- conference on acoustics and the sea-bed, Bath, England (April 1983) 4-90303
- conical diffusor joined by two tubes, sound insulation (Russian) 4-79367
- elastically inhomogeneous medium, acoustic wave propagation theory 4-107926
- Fermi liq., two-component, sound wave propag. 4-61311
- ferroelastic domain regular struct., bulk acoustic wave interaction 4-108551
- flanged circular finite duct with sources with varying wall admittances 4-74784
- flanged circular semi-infinite duct with varying wall admittance 4-74783
- fluid-saturated porous thermoelastic solid, acoustic perturbations (French) 4-79356
- fluid-solid interface, acoustic wave generation and scatt. 4-87494
- focused transducer with arbitrary surface velocity distrib., impulse response 4-87530
- gas mixture, acoustic waves driven by a radiation field 4-87835
- gases, sound propagation, boundary value problems 4-91860
- induced polarisation infrasonic receiver (Spanish) 4-69640
- inhomogeneous isotropic media, propagation by geometrical optics theory 4-83520
- integral equations, numerical methods 4-83748
- jets, sound propagation in nonuniform and nonstationary flows (French) 4-112842
- lateral waves, HF theory 4-73249
- layered acoustic medium, inverse problem, appl. of Schur algorithm 4-103051
- liquids, highly viscous, sound absorption and propag. 4-92300
- liquids, laser-induced acoustic waves, diff. characts. 4-88239
- nonuniform gas flows, acoustics, variational principles 4-91673
- null field method and modified Green functions 4-87498
- ocean, acoustic normal mode determ. method 4-103072
- parametricres, singularities, and high freq. asymptotics anal. 4-83753
- periodical inclusions, sound propag. anal. (French) 4-107923
- piezoelectric semiconductor, shear acoustic wave propagation study 4-108553
- pipe, acoustic plane wave propag. with mean flow 4-112608
- porous systems, acoustic properties microscopic description 4-69613
- quartz, X-cut, SAW temp. stability 4-108693
- quartz crystals, radiation induced transient acoustic loss 4-70279
- radiation stress in solids 4-98210
- range varying ocean, acoustic normal mode propag., asymptotic expansion anal. 4-112620
- ray bending in spherically symm. field, comparison with Sjödin's approach 4-97167
- ray equations in barycentric coordinates 4-91672
- ray theory, two-variable Taylor series 4-74798
- rectangular waveguide, acoustic wave propagation meas. (French) 4-83744
- resonantly excited elastic tube, acoustic spectrogram and complex-freq. poles 4-87491
- rubber, frequency-depend. elastic props. 4-103853
- seawater, nonlinearity parameter calcs. 4-103061
- secondary source theorems, appls. to acoustic propag. and inverse problems (French) 4-97174
- sediment/water plane interface, acoustic signal pulse transmission (French) 4-97181
- semiconductor-vacuum-ferrite struct., sound interaction with surface heli-con spin oscils. (Russian) 4-88713
- shallow water multimodal sound transmission, signal processing and appl. to underwater acoustic communication 4-91693
- shell, elastic spherical, interaction with plane acoustic wave 4-97382
- shells, noncircular cylindrical, in fluid, radiation anal. 4-74787
- single mode acoustic fiber waveguide 4-107928
- solid waveguide, resonant mode: reflection from periodic corrugations 4-91671
- solutions, concentration fluctuations, acoustic wave propag. and light scatt. 4-92302
- sonic detonation wave acceleration in perfect adiabatic fluids 4-112952
- sound propag. in nozzles of variable cross section containing low Mach number mean flows (German) 4-97596
- sound wave interaction with solid particles in viscous fluid 4-107930
- stochastic insulation effect of sound barrier, prediction method 4-79366
- stratified random media, acoustic intensity 4-87495
- stratifying solns., acoustic wave dispersion and absorption by conc., fluctuations 4-80164
- surface acoustic waves, propagation direction change by periodic corrugated system 4-92504
- surface sound propagation over curved boundary surfaces 4-112606
- three-dimensional wave equation computations on vector computers 4-60193
- transient sound radiation from a clamped circular plate 4-97192
- tubes, sound propagation, wall effects 4-74785
- tubes with irregular side holes, sound wave propag., filter props. (French) 4-97172
- turbulent media, sound propag. and acoustic imaging (French) 4-97169
- turbulent medium, spherical acoustic wave propag., mutual coherence function (French) 4-97170
- two-dimensional electron systems, sound propag. in strong mag. fields 4-65718
- type-II superconductors, flux pinning mechanism and fundamental theory of superconductors (Japanese) 4-65777

**acoustic wave propagation continued**  
underground structures, transient response to SH-waves 4-112607  
water, acoustic wave subharmonic obs. (Chinese) 4-75616  
H, spin-polarized film on <sup>4</sup>He substrate, superfluidity detection 4-70527  
BiSB, acoustical nonlinearity near electronic topological transition 4-113547  
LiNbO<sub>3</sub> rotated Y-cuts, SAW and SSBW propag. (Japanese) 4-61199  
LiTaO<sub>3</sub> rotated Y-cuts, SSBW and SAW propag. (Japanese) 4-61199  
N<sub>2</sub>, liq, acoustic wave subharmonic obs. (Chinese) 4-75616  
TeO<sub>2</sub> cryst., US wave reflection 4-75621  
TeO<sub>2</sub>, paratellurite, SAW and vol. acoustic wave propag. 4-70543  
ZnO channel waveguide formation on Si substrates 4-103012

**acoustic wave reflection**  
*see also echo; reverberation; ultrasonic reflection*  
broadcasting studios, sound reflections, frequency anal. 4-107953  
building facades, sound field reflection and transmission 4-87514  
circular acoustic rigid cylinders, acoustic backscattering 4-97165  
coefficients and transfer functions meas. by cepstral techniques 4-60236  
cylinder, immersed, insonification at large Ka (French) 4-107917  
elastic wave diff. by subsurface check 4-87492  
enclosure with diffusely and specularly reflecting boundaries, steady state sound field calcs. 4-60211  
fluid-solid interface, acoustic wave generation and scatt. 4-87494  
fluid-solid interface, loaded and stiffened, finite acoustic beam reflection 4-74780  
ideal interfaces, phonon transitions, reciprocity theorem with acoustic mismatch model 4-65539  
layered cpd., bulk wave energy reflection coeffs. 4-113545  
layered inhomogeneous half-space, plane wave reflection 4-91676  
linear transition wedges, sound absorpt. calc. (Chinese) 4-91666  
near-field meas., toneburst techniques appl. 4-79410  
obliquely incident plane wave reflection from layered half-space with periodic profile 4-103056  
oceanic reverberation model 4-67226  
oceanic sound, turn-around loss on bottom slope 4-89921  
parametric radiation, reflection from finite planar target 4-74789  
PZT piezoelectric ceramic transverse acoustoelectric wave refl. 4-83796  
ray bending in spherically symm. field, comparison with Sjödin's approach 4-97167  
reflection phase grating diffuser, design theory and appl. 4-64810  
rigid rectangular body with curved surfaces, sound reflection (Japanese) 4-97168  
rod, semiinfinite, cylindrical, connected to infinite elastic stratum longitud. wave reflection 4-87610  
rough boundary, acoustic signals reflection, time spread anal. 4-60191  
rough surface scattering via the smoothing method 4-87493  
shear surface electroacoustic waves, Bragg reflection 4-108698  
solid waveguide, resonant mode reflection from periodic corrugations 4-91671  
sound radiation from duct with circumferentially varying liner 4-112650  
subsonic passage above reflecting ground surface, expanding sound due to time-varying source 4-74795  
surface acoustic waves, propagation direction change by periodic corrugated system 4-92504  
surface generated bulk waves, excitation and detection 4-91667  
surface-skimming bulk wave reflection by system of periodic inhomogeneities, Bragg case 4-69642  
suspended sound absorbing plate, acoustical behaviour for random incidence 4-97194  
time filtering and fast Fourier transforms in acoustic scatt. and absorption meas. (French) 4-97166  
two-phase system, reflection of sound at an interface, taking into account mass and heat transport across it 4-97646  
Gd<sub>2</sub>(MoO<sub>4</sub>)<sub>3</sub>, acoustic wave reflection from ferroelastic domain walls 4-98209  
KCl, acoustic wave generation by electron beam, polarisation-optical recording method 4-109154  
LiNbO<sub>3</sub>, acoustoelec. coeffs. meas., appl. to signal processing devices 4-97214  
LiTaO<sub>3</sub>, acoustoelec. coeffs. meas., appl. to signal processing devices 4-97214  
NdP<sub>2</sub>O<sub>8</sub>, acoustic wave reflection from ferroelastic domain walls 4-98209

**acoustic wave refraction**  
*see also acoustic dispersion; ultrasonic refraction*  
Gulf Stream warm-core ring, acoustic velocity struct. from thermohaline obs. 4-115414  
ideal interfaces, phonon transitions, reciprocity theorem with acoustic mismatch model 4-65539  
layered inhomogeneous half-space, plane wave reflection 4-91676  
ray bending in spherically symm. field, comparison with Sjödin's approach 4-97167  
secondary source theorems, appls. to acoustic propag. and inverse problems (French) 4-97174  
shallow sea, sound wave horizontal refraction, perturbation calc. 4-112622

**acoustic wave scattering**  
*see also ultrasonic scattering*  
air-filled cylindrical shells in water, acoustic scatt. theory (French) 4-83756  
antiferromagnet, sound interaction with subsurface mag. inhomogeneities 4-114149  
antiferromagnets, sound absorption and scattering by nuclear spin waves 4-88245  
book, scattering theory for diff. gratings 4-86125  
boundary element methods and their asymptotic convergence 4-83751  
boundary value problems, pseudo-differential operators appl. 4-83752  
bubble layer, acoustic waves nonlinear backscattering 4-103060  
bubble size measurement using nonlinear freqs. of two acoustic freqs. 4-74790  
circular acoustic rigid cylinders, acoustic backscattering 4-97165  
complex shape targets, acoustic wave scatt., Helmholtz integral eqn. anal. 4-112603  
conference on acoustics and the sea-bed, Bath, England (April 1983) 4-90303  
conical diffuser joined by two tubes, sound insulation (Russian) 4-79367  
convection, perturbation theory 4-74794  
cracks, acoustic wave diffraction anal. 4-74779  
cylinder, elastic, immersed, acoustic backscatt., resonant response (French) 4-107918

**acoustic wave scattering continued**  
cylinder, immersed, insonification at large Ka (French) 4-107917  
cylindrical shell in fluid, dispersion curves for normal modes 4-112610  
elastic wave diff. by subsurface check 4-87492  
fish, acoustic scattering, two-parameter fit 4-60198  
infinitely long cylindrical shell under water, acoustic wave scatt. 4-87501  
intensity meas. using two-microphone technique, scatt./diff. effects 4-103151  
interfaces, acoustic and EM wave scattering anal. 4-83754  
inverse scattering in the first Born approximation 4-68057  
layered elastic obstacle in fluid, acoustic wave scatt., null field approach 4-112602  
liquid solutions, induced concentration scatt. of sound near segregation point 4-70274  
multiply scattered field of randomly distributed scatterers 4-87497  
noise reduction by scatt. in low velocity ducts 4-107948  
null field method and modified Green functions 4-87498  
oceanic reverberation model 4-67226  
plane waveguide, acoustic wave scatt. by small obstacles 4-91675  
plate, elastic, acoustic backscatt., resonance obs. (French) 4-107922  
resonantly excited elastic tube, acoustic spectrogram and complex-freq. poles 4-87491  
rough surface scattering, parabolic approx., PERUSE numerical method 4-74797  
rough surface scattering via the smoothing method 4-87493  
rubber, frequency-depend. elastic props. 4-103853  
sea ice surface backscatter strength meas. for sonar location of under-ice oil spills 4-109770  
seamounts, sound scatter and shadowing, hybrid physical soln. 4-77526  
secondary source theorems, appls. to acoustic propag. and inverse problems (French) 4-97174  
semiinfinite annular duct in subsonic mean flow, acoustic radiation 4-87496  
shell, spherical, immersed, low freq. scatt. (French) 4-107920  
shipping noise, ambient low-frequency vertical directionality 4-115415  
sine-wave burst, half-order derivative 4-103050  
solid waveguide, resonant mode reflection from periodic corrugations 4-91671  
sound radiation from duct with circumferentially varying liner 4-112650  
sphere, absorbing, acoustic scatt. (French) 4-107921  
spherical elastic shell in fluid, sound wave resonant scatt. 4-112611  
stratified random media, acoustic intensity 4-87495  
surface, locally reacting, Schroeder's diffusor 4-74781  
surface defect, defect, acoustic wave scatt., fibre optic detection 4-85275  
time filtering and fast Fourier transforms in acoustic scatt. and absorption meas. (French) 4-97166  
time harmonic waves, inverse scattering problem 4-103054  
Tollmien-Schlichting wave, excitation in boundary layer by acoustic and vortex disturbance scatt. 4-91792  
turbulent boundary layer on rigid surface, dipole acoustic radiation 4-112845  
two-dimensional acoustic medium, vel. and density from point source data 4-103053  
water, acoustic wave subharmonic obs. (Chinese) 4-75616  
LiNbO<sub>3</sub> groove grating, bulk radiation by SAW propag. 4-92501  
N<sub>2</sub>, liq., acoustic wave subharmonic obs. (Chinese) 4-75616

**acoustic wave transmission**  
*see also ultrasonic transmission*  
building facades, sound field reflection and transmission 4-87514  
ducts, acoustic transmission, impulse method using signal synthesis and averaging 4-74786  
experimental study of transmission within an absorbing medium (French) 4-79358  
glycerol/water model for water/sediment interface, acoustic props. (French) 4-97182  
impedance-matched metallurgically sealed transducers 4-91707  
parallelepiped-assembled structs., acoustic transmission 4-107946  
room acoustics, sound transmission through partitions 4-107952  
sediment/water plane interface, acoustic signal pulse transmission (French) 4-97181  
studio, design, effects of glass 4-97201  
suspended sound absorbing plate, acoustical behaviour for random incidence 4-97194  
time filtering and fast Fourier transforms in acoustic scatt. and absorption meas. (French) 4-97166  
transversely isotropic plate, sound transmission and vibrs. 4-112613  
wall constructions, sound transmission loss, intensity and two-room method meas. 4-103152

**acoustic wave velocity**  
*see also acoustic dispersion; liquid helium sound propagation; shock waves; ultrasonic velocity*  
acetonitrile, liq., sound vel. and thermodynamic props. 4-103886  
air, humid, sp. ht. and acoustic speed variation 4-113100  
alkali metals, liquid, influence of many-body interactions 4-98204  
Bose fluid, excitation spectrum, struct. factor and sound vel. 4-104014  
Brillouin scatt. width and line profile under acoustic instability conditions 4-61723  
chlorosilanes, liq., viscous flow, acoustic wave studies (Russian) 4-92402  
coating for tools and sliding elements, acoustic microscopy studies 4-104957  
dielectrics, amorphous, kinetic processes, multiphonon theory anal. 4-80186  
finite amplitude spherical waves in ideal gas, renormalisation calc. 4-83755  
fluid-solid interface, acoustic wave generation and scatt. 4-87494  
foams, acoustic properties of rigid closed-cell foams (Chinese) 4-85337  
focused transducer with arbitrary surface velocity distrib., impulse response 4-87530  
glass beads saturated with miscible liqs., sound vel. meas. (French) 4-98207  
Gulf Stream warm-core ring, acoustic velocity struct. from thermohaline obs. 4-115414  
ice sheet, stress-strain state estimation by acoustic probe pulse 4-115428  
liquid metals, acoustic nonlinearity parameter calc. 4-84346  
magnetic liquid in external mag. field, sound vel., field depend. with allowance for intermol. pot. changes 4-80808  
marine sediments, compaction model for compressional wave velocity 4-103067  
miscible fluid flows in porous medium, acoustic studies 4-97672

**acoustic wave velocity continued**

- molecular crystals, plasmon-phonon oscills. due to exciton-phonon interactions, sound vel. change 4-92646  
 perfluorobenzene, liq., acoustic relax. mechanism 4-92301  
 periodically modulated nonlinear medium opacity to acoustic waves 4-91680  
 piezoelectric, shear surface electroacoustic waves, Bragg reflection 4-108698  
 piezoelectric semiconductor, shear acoustic wave propagation study 4-108553  
 plane evanescent wave, vel. of energy transport (French) 4-97173  
 propyl alcohol, thermodynamic props. at atm. press. 4-80251  
 quartz, surface and bulk acoustic wave vel. 4-98425  
 quartz, X-cut, SAW temp. stability 4-108693  
 resonantly excited elastic tube, acoustic spectrogram and complex-freq. poles 4-87491  
 sedimentary rocks, acoustic and elec. props., differential effective medium theory 4-67212  
 semiconductor/piezoelec. layered struct., SAW vel. and attenuation 4-92503  
 solids, SAW prop. const. mapping using Fresnel-phase-plate interdigital transducer 4-104060  
 superlattice, SAW velocity, Brillouin spectra studies 4-108694  
 surfactant micelles in aq. soln., adiabatic compressibility 4-113516  
 p-terphenyl, improper ferroelastic transition, acoustic anomalies 4-65389  
 turbulent medium, spherical acoustic wave prop., mutual coherence function (French) 4-97170  
 two-dimensional acoustic medium, vel. and density from point source data 4-103053  
 two-dimensional electron systems, sound prop. in strong mag. fields 4-65718  
 wedge, particle-vel. field of a signal and noise, spatial correlation function 4-91668  
 Wigner cryst., two-dimensional, on He film, static and dynamical props. 4-98549  
 Al, sound velocity behind strong shock waves, optical technique anal. 4-108554  
 Ar, liquid, thermodynamic Grüneisen parameter, mol. compressibility and sound speed 4-60974  
 BaTiO<sub>3</sub>, centrosymmetric ceramics, elec. field induced acoustic anisotropy 4-60992  
 CdS, piezoelec. semicond., stimulated Brillouin scatt. of electromagnetic wave, acoustic amplification 4-114291  
 n-D<sub>2</sub>, liquid and liquid mixtures, intermolecular free length, acoustic study 4-88059  
 Fe<sub>2</sub>O<sub>3</sub>, external forces influence on sound velocity 4-70277  
 n-H<sub>2</sub>, liquid and liquid mixtures, intermolecular free length, acoustic study 4-88059  
 K<sub>2</sub>SeO<sub>4</sub>, acoustic phonon wavevector depend. near commensurate-incommensurate transition, Brillouin spectra 4-71313  
 LiNbO<sub>3</sub>, surface and bulk acoustic wave vel. 4-98425  
 NaNO<sub>3</sub>-KNO<sub>3</sub>, Brillouin scatt., sound wave attenuation and vel. meas., viscoelastic props. (French) 4-71396  
 Ne, liquid and liquid mixtures, intermolecular free length, acoustic study 4-88059  
 α-O<sub>2</sub>, solid, high press. props. 4-61066  
 SiO<sub>2</sub>, amorphous, polymorphism, optical study 4-88103  
 Ta, shocked, rarefaction velocities and high press. melting point 4-108524

**acoustic wave velocity measurement**

see also *ultrasonic velocity measurement*

- instrumented seabed penetrator system field tests 4-115637  
 multiple leaky SAW, FFT vel. meas. by line focus-beam acoustic microscope 4-103164  
 portable acoustic devices for divers, homing, surveying, navigation (French) 4-97220  
 retardation effect, fast moving sound source motion parameter estimation 4-103160  
 scanning acoustic microscope in interference mode using frequency modulation method 4-97231  
 US velocity, time of flight and sing around methods 4-83789

**acoustic waveguides**

- circular waveguide, acoustic normal mode diff. 4-107925  
 ferroelastic domain regular struct., bulk acoustic wave interaction 4-108551  
 infinite waveguide, septum vibr. modes 4-107924  
 metal strip waveguides with SAW convolvers, planar, for beam compression 4-103105  
 parametric generation of a low-frequency signal in guided-wave sound channels 4-107971  
 rectangular waveguide, acoustic wave propagation meas. (French) 4-83744  
 single mode acoustic fiber waveguide 4-107928  
 variable-width waveguide, acoustic field, 3D model (Ukrainian) 4-64805

**acoustic waves**

- see also *acoustic emission; magnetoacoustic effects; shock waves; surface acoustic waves; ultrasonic waves*  
 acoustic radiation force 4-67915  
 acoustic telescope system using vane-type acoustic lenses, system construction 4-79404  
 compressible fluid, transient elastocoustic problem 4-91686  
 distributed combustion effects on particle damping 4-79616  
 EM-acoustic excitation for radial resonances in metal rods 4-68213  
 flow and temperature profile independence of flow measurements using long acoustic waves 4-103445  
 gas vibrations, nonlinear, in closed pipe, rel. to thermoacoustic effects 4-69853  
 neutron anomalous transmission by crystals in Laue diff. case, reson. suppression 4-97975  
 optical and acoustic waves in solids; conf., Varna, Bulgaria (Sept. 1982) 4-58560  
 piezoelectric transducer, vibration and acoustic radiation, finite element method-equivalent circuit anal. 4-60241  
 sound wave visualisation technique 4-67930  
 time dependent inverse source problem 4-101659  
 Al cylinder, acoustic wave excitation by low energy electrons 4-80168  
 Na high-press. discharge, acoustic resonance obs. 4-65141  
 SiO<sub>2</sub> glass, rotary phonon echoes 4-70328

**acoustical laboratories**

see also *anechoic chambers; reverberation chambers*  
 No entries

**acoustics**

- see also *acoustic applications; acoustic devices; acoustic equipment; acoustic noise; anechoic chambers; architectural acoustics; atmospheric acoustics; audio acoustics; hearing; musical acoustics; photoacoustic effect; sound reproduction; ultrasonics; underwater sound; vibrations*  
 Acoustic Society of America conference, Minneapolis, MN, USA (Oct. 1984) 4-110804  
 bibliography of contemporary papers 4-95097  
 conference, Acoustical Society of America, Norfolk, VA, USA (May 1984) 4-58551  
 numerical techniques, book 4-82608  
 transient acoustics, boundary-element methods for transient response analysis, book contrib. 4-60298

**acousto-optical devices**

see also *acousto-optical effects*

- adaptive notch filtering using Bragg cells 4-74686  
 anisotropic acousto-optic interactions from bulk and surface acoustic waves 4-104570  
 anisotropic waveguide, acoustooptic and electrooptic guided wave conversion to leaky waves 4-91583  
 bistability, chaos onset, noise influence 4-97041  
 book, optical waves in crystals, laser radiation prop. and control 4-86135  
 Bragg cell, new concepts for efficiency improvement 4-97034  
 Bragg cells, anisotropic bulk wave cells, design, fabrication and testing 4-103103  
 Bragg cells, wide band, for radar warning and signal processing, design and performance 4-97032  
 bulk two-Bragg cell processor for continuous Fourier transforms 4-74428  
 crossed Bragg cell processors 4-87285  
 deflector, bichromatic nondispersive 4-91569  
 deflector MTF charact. (Chinese) 4-60138  
 directional couplers for an optical time-domain reflectometer 4-74703  
 fibre optics, acousto-optical parallel-to-serial converter for optical signals 4-64766  
 free electron IR laser, broadband optical cavities, acousto-optic output coupler 4-112479  
 gas lasers, picosecond pulse generation using acoustooptic modulator (Japanese) 4-74558  
 integrated acousto-optics, technology and competition 4-64674  
 light spatial coherence, acousto-optical diff. effect 4-74421  
 linear algebraic equations, direct and indirect optical solutions, error source modelling 4-96816  
 mode conversion of acoustooptic interaction in crossed channel waveguide 4-104568  
 modulator, design 4-107814  
 modulators, US waves divergence effect on spatial spectrum of pulse radio signal 4-74698  
 modulators for CO<sub>2</sub> chirp-modulated CW heterodyne laser rangefinder/velocimeter 4-96963  
 modulators with overlapping US beams in optical information processing systems 4-87296  
 multilayered thin film optical separators, tunable wavelength selection charact. 4-79275  
 notch filtering, optical transversal processor 4-91568  
 optical fibres, birefringent, acousto-optical freq. shifting 4-91600  
 output coupler for free electron lasers 4-83601  
 phased-array Bragg cells, acousto-optical generation of light 4-112556  
 processor architectures and techniques 4-87435  
 radiospectrometer for radio astronomy (Japanese) 4-90092  
 semiconductor lasers, acousto-optic synchronous mode locking by picosecond optoelectronic switch 4-96965  
 signal processing architectures 4-103102  
 signal processing systems, acoustic nonlinearity effects 4-103123  
 spectrographs, possible appls. in radio astronomy 4-63073  
 spectrometer, heterodyne receiver with open struct. mixer at 324 GHz and 693 GHz 4-86482  
 squared signal correlation and possible acoustooptic implementation 4-59988  
 stationary reference grating based optical detection method for SAW detect. 4-60180  
 tunable spectral filtering of spatially incoherent source using acousto-optic deflector 4-60137  
 underwater sound detection using optical interference in optical fibers (Japanese) 4-112621  
 Ar<sup>+</sup> ion lasers, acousto-optic mode locking, subnanosecond transient spectroscopy appl. (Japanese) 4-101923  
 HF 2-dimens. laser beam phase and intensity meas. technique using acousto-optic modulator, heterodyne detector and raster-scanning mirrors 4-74564  
 LiNbO<sub>3</sub> mirror-type optical switch and appls. 4-97043  
 LiNbO<sub>3</sub>, Ti diffused optical waveguide, effects of lossy thin plasma film 4-107818  
 LiNbO<sub>3</sub>:Ti integrated acousto-optic bistable device 4-107890  
 Nd:YAG CW laser, acoustooptic mode locking 4-69473  
 TeO<sub>2</sub> directional coupler, 130 km-long fault location, for single-mode optical fibre 4-91601  
 TeO<sub>2</sub>-crystal acousto-optical spectrograph, for RATAN-600 radio telescope 4-63074  
 XeCl laser, long pulse, generation of 300 psec pulse by direct mode locking using acousto-optic modulator and saturable absorber 4-112490  
 YAG lasers, pulse generation using US mode locker (Japanese) 4-74559
- acousto-optical effects**  
 see also *acousto-optical devices*  
 acousto-optic effect, in nonlocal optics regime 4-71346  
 acoustophotorefractive effect 4-104569  
 anisotropic media, light diff. by ultrasound 4-83542  
 anisotropic medium, light diff. from US wave, acousto-optic interaction 4-96798  
 bistability with fluctuations, nonlinear Fokker-Planck eqn. 4-83636  
 book, optical waves in crystals, laser radiation prop. and control 4-86135  
 bounded US waves, reflection coeff., optical meas. 4-74822  
 Bragg double diffraction of two laser beams by ultrasound 4-69308  
 Brillouin scatt. width and line profile under acoustic instability conditions 4-61723  
 crystals, ultrasound Bragg diff. SHG 4-79234

**acousto-optical effects continued**

- Gaussian laser beam intensity modification by acousto-optic effect (Chinese) 4-112491  
 high resolution acousto-optic laser probe 4-97746  
 integrated acousto-optics, technology and competition 4-64674  
 isotropic solid dielec., light diffraction from shear waves, theory 4-74417  
 laser active resonators, acousto-optic interaction, theory 4-79196  
 light diffraction by profiled ultrasound 4-79027  
 light spatial coherence, acousto-optical diffraction effect 4-74421  
 liquids, penetrating radiation absorpt. effect on sound generation 4-99089  
 methoxybenzylidenbutylaniline nematic liq. cryst., acousto-optical phenomena 4-112423  
 mode conversion of acoustooptic interaction in crossed channel waveguide 4-104568  
 noncentrosymmetric crystals, acoustophotorefractive memory 4-66007  
 photothermal laser probe, acoustic wave detection by collinear Bragg scatt. 4-86412  
 piezoelectric semiconductor with acoustic instability, threshold for controllable Franz-Keldysh stimulated scatt. 4-69507  
 semiconductor laser, direct FSK by acoustic waves 4-91507  
 three-wave noncollinear acoustooptic interaction at high light intensities 4-66006  
 US wave modulation of light wave, mutual coherence function (French) 4-107518  
 US waves, amplitude-time-modulation of diffracted laser beam 4-102876  
 CdS, piezoelec. semicond., stimulated Brillouin scatt. of electromagnetic wave, acoustic amplification 4-112421  
 Ga<sub>1-x</sub>Al<sub>x</sub>As superlattices, acoustic modes, Brillouin and Raman scatt. study 4-80928  
 LiNbO<sub>3</sub>, bulk acoustophotorefractive effects 4-93050  
 LiNbO<sub>3</sub>+Ti waveguide, acousto-optical conversion study 4-107827  
 NaCl F<sub>2</sub><sup>-</sup> centres, persistent spectral hole detection using ultrasonic modulation 4-83650  
 Pb<sub>3</sub>V<sub>2</sub>(1-x)P<sub>2</sub>O<sub>8</sub>, ferroelectric transition and acousto-optic props. 4-75660  
 Si plate, thick meas. and cross-section inhomogeneity visualisation using photodisplacement microscopy 4-91702  
 Te, second-order acoustooptical Bragg deflection and double-phonon light deflection 4-104571

**acoustoelasticity** *see elasticity***acoustoelectric devices**

- see also acoustoelectric transducers*  
 No entries

**acoustoelectric effects**

- ferroelectric, stochastic US signal emission on polarisation initiation (French) 4-109051  
 ferroelectric crystals, soliton propag. and electroacoustic interactions (French) 4-99047  
 ferroelectric domain layer surface wave, dispersion eqns. 4-88787  
 ferromagnetic material, EM-acoustic transform. by superimposed transducers 4-109613  
 microwave-induced thermoacoustic effect in dielectrics and its coupling to external medium—a thermodynamical formulation 4-115128  
 nonlinear scanning electron acoustic microscopy 4-74825  
 photoconducting piezoelectrics, opto-electric conversion during nonlinear optoacoustic interaction 4-109155  
 piezoelectric, shear surface electroacoustic waves, Bragg reflection 4-108698  
 piezoelectric powders, electroacoustic echoes, continuum approach 4-76343  
 piezoelectric powders, electroacoustic echoes 4-76342  
 piezoelectric semiconductors, transverse acoustoelectric effect characts. (Russian) 4-70878  
 piezoelectric-semiconductor multilayer structure, nonlinear self-contraction of acoustoelectric fluctuations spectrum 4-70877  
 PZT piezoelectric ceramic transverse acoustoelectric wave refl. 4-83796  
 review 4-76009  
 scanning electron acoustic microscopy with subnanosecond time resolution 4-74826  
 semiconducting piezoelectric plasma, parametric EM wave conversion into acoustic wave 4-65716  
 semiconductors, electroacoustic effects due to charged dislocations 4-65717  
 semiconductors, high resistivity, acoustoelectric interactions 4-104274  
 semiconductors, low-conductivity, carrier mobility using the travelling wave technique 4-92752  
 solids, transverse acoustic gap waves, parametric excitation by microwave elec. field 4-113774  
 volume acoustic wave excitation by electrostrictive effects 4-92767  
 Ag<sub>2</sub>As<sub>2</sub>S<sub>3</sub>, acoustoelectric interactions in electroacoustic echo 4-80631  
 Ag<sub>3</sub>SbS<sub>3</sub>, acoustoelectric interactions in electroacoustic echo 4-80631  
 Fe film and single cryst., microwave generation of 9.4 GHz phonons. 4-61422  
 Hg<sub>1-x</sub>Cd<sub>x</sub>Te, characterisation using transverse acoustoelectric volt. meas. 4-104275  
 InSb, magnetised plasma, parametric excitation of electron-acoustic waves 4-88545  
 KD<sub>2</sub>PO<sub>4</sub>, piezoelectrically induced acoustic waves, strain optic effect 4-66005  
 LiNbO<sub>3</sub>, acoustoelec. coeffs. meas., appl. to signal processing devices 4-97214  
 LiNbO<sub>3</sub>, complex elastoelectric effect 4-80629  
 LiNbO<sub>3</sub>-Ge multilayer structure, nonlinear self-contraction of acoustoelectric fluctuations spectrum 4-70877  
 LiTaO<sub>3</sub>, acoustoelec. coeffs. meas., appl. to signal processing devices 4-97214  
 LiTaO<sub>3</sub>, complex elastoelectric effect 4-80629  
 NH<sub>4</sub>D<sub>2</sub>PO<sub>4</sub>, piezoelectrically induced acoustic waves, strain optic effect 4-66005  
 Ni film and single cryst., microwave generation of 9.4 GHz phonons 4-61422  
 a-Si:H,P film, acoustoelectric effect, thickness depend. study 4-104273

**acoustoelectric transducers**

- see also earphones; headphones; hydrophones; loudspeakers; microphones*  
 asymmetrically radiating sectional bar transducer, elec. excitation synthesis 4-103171  
 auditory evaluation by equivalent scale methods 4-83793  
 vibration distrib. at diaphragms, quantitative determ. by holographic interferometry methods (German) 4-74829

**acoustoelectric transducers continued**

- <sup>4</sup>He, superfluid, temperature oscills., electroacoustic meas. by reciprocity method 4-98391  
 SiO<sub>2</sub> backplate electret transducer 4-69655  
**acoustomagnetic effects** *see magnetoacoustic effects*  
**acoustooptics** *see acousto-optical effects*  
**actinide alloys**  
*see also actinide compounds; neptunium alloys; plutonium alloys; thorium alloys; uranium alloys*  
 No entries  
**actinide compounds**  
*see also compounds of individual actinides, e.g. uranium compounds*  
*see also actinide alloys*  
 carbides, point defects and transport props. 4-98097  
 crystal field parameters in a modified point charge model 4-104176  
 magnetic and other props. of oxides and related epds., data collection 4-67886  
 oxides, highly radioactive, ESCA and AES apps. 4-73603  
 ternary carbide systems, actinides with 4th-8th group transition metals, phase relations (German) 4-85142  
**actinide metal compounds** *see actinide compounds*  
**actinide metals** *see actinides*  
**actinides**  
*see also individual actinides, e.g. uranium*  
 atomic and cryst. energy levels, f-shell config. parametric model, effective-operator Hamiltonian 4-74165  
 cohesive energies, calc. for light actinide metals 4-75354  
 electrodeposition method for alpha spectrometer source preparation 4-101969  
 fission processes, liquid-drop model, nuclear proximity energy, barrier heights 4-95999  
 ground state electron affinities 4-78983  
 highly radioactive materials, ESCA and AES apps. 4-73603  
 ions in aqueous solution, oxidation-state specific detect. by pulsed laser photoacoustic spectroscopy 4-99858  
 low-energy collective features of actinide region, IBA 4-95924  
 symmetry conserving mean field theory, alignment pattern in actinide nuclei 4-95932  
 transplutonium research, accomplishments and practical appl. 4-59661  
 transuranics, chemisorption from seawater, in-situ meas. technique 4-105057  
**actinium**  
*see also nuclei with .....*  
 superconducting transition temp. under high press., vol. depend. 4-84728  
<sup>227</sup>Ac excess in deep Pacific Ocean water 4-100627  
**actinium compounds**  
 No entries  
**actinometers** *see radiometers*  
**actinometry** *see radiometry*  
**activation analysis** *see chemical analysis by nuclear reactions and scattering*  
**active filters**  
 band-amplifier pulse shaper for nuclear radiation spectrometry 4-102544  
 RC-filter, low-pass, design, for sharp bands-separation 4-112640  
 time-variant filters for gamma spectrometry 4-64270  
**active nitrogen** *see nitrogen*  
**active oxygen** *see oxygen*  
**activity (thermodynamics)** *see thermodynamic properties*  
**actuators**  
 high technology electronics exhibition and conference, Detroit, MI, USA, (June, 1983) 4-95014  
**adaptive antenna arrays** *see antenna phased arrays*  
**adaptive control**  
*see also adaptive systems*  
 deployable optical systems, conf., Los Angeles, CA, USA (Jan. 1983) 4-73138  
 EMG, digital signal processor with adaptive decision boundaries 4-85543  
 heart, artificial and assist devices, adaptive control strategies 4-89838  
 left ventricular assist devices 4-89844  
 nuclear reactor digital control schemes, experimental evaluation 4-86932  
 vascular tree function optimisation by wall shear stress adaptive regulation 4-66980  
**adaptive optics**  
*see also optical phase conjugation*  
 control servo designs 4-87431  
 diffractive and refractive effects comparison in two-wavelength, adaptive transmission 4-87280  
 digital heterodyne interferometer for analysis and control of adaptive optics 4-111194  
 images, adaptive correction 4-107549  
 intracavity adaptive optics, theory and expt. comparison 4-74552  
 laser resonators with four-wave hypersonic reversing mirrors, self-excitation 4-60078  
 modal adaptive optics basis functions for obscured apertures 4-74427  
 notch filtering, optical transversal processor 4-91568  
 notch filtering using Bragg cells 4-74686  
 primary mirror structural anal. 4-87422  
 randomly inhomogeneous medium, ray description of waves reflected with wave front reversal 4-96804  
 spherical lens performance via elec. modulation of refr. index in tandem liq. cryst. cell arrangement 4-107782  
 stereograms, intermediate aspects, synthesis 4-91415  
 structural mechanics of optical systems, conf., Cambridge, MA, USA (Nov. 1983) 4-86104  
 thermal-blooming-induced low-order aberrations 4-96807  
 wavefront aberration description, structurally compatible surface vectors 4-87287  
 wavefront correction quality in adaptive systems 4-107550  
 AgCl in gelatin, adaptive optics studies 4-107735  
**adaptive systems**  
*see also adaptive control; adaptive optics; pattern recognition; self-adjusting systems*  
 acoustic noise cancellation, adaptive, digital filter implementation using modified Widrow-Hoff algorithm 4-103114  
 continuous speech recognition, adaptive anal., nonsteady-state speech 4-79388  
 fighter cockpit environment, adaptive noise cancellation 4-103132  
 noisy images, adaptive estimation procedure comparison 4-102902

**adaptive systems continued**

- spectral analysis of short-time biomedical data using adaptive filters 4-72453
- speech signal, frequency domain adaptive noise cancellation 4-69632

**adders**

- automatic telemetering range gauge, electronic logic circuit 4-110299
- parallel digital optical adder construction method 4-60001

**adding machines** *see calculating apparatus***adherence** *see adhesion***adhesion**

- acoustic emission method use in strength tests of adhesive bonded joints 4-109614
- antiplane shear in adhesively bonded semi-finite media with transverse cracks 4-60337
- bonded joints, model, thermal-moisture stresses 4-69677
- cavity formation by interaction between particles in a nonwetting liquid 4-61182
- cavity formation due to a contact between particles in a nonwetting liquid 4-61181
- cell interaction models based on differential adhesion 4-100103
- cells adhesivity to glass, change for unchanged density of surface charges 4-66904
- charged particle emission in failure of solids 4-99291
- charged particle emission in failure of solids 4-99292
- claddings, bond strength, multistep shear test 4-76925
- coating for tools and sliding elements, acoustic microscopy studies 4-104957
- composite layered structures, adhesion bond strength, US study (French) 4-62136
- cylinder, composite circular, perfectly bonded on end surfaces transient thermal stresses 4-112717
- detonation-deposited coatings on metals, contact zone structural characteristics 4-66502
- diffusion bonding, development of theoretical model 4-114762
- diffusion bonding, hot isostatic pressing 4-82239
- elastic and viscoelastic solids, metals, adherence phenomena (French) 4-71861
- elastomer-phenolformaldehyde oligomers, adhesion strength, diffusion and phase equilib. (Russian) 4-103906
- elastomers, spontaneous peeling, fracture mechanics concepts (French) 4-114761
- epoxy coated mild steel, polymer-metal adhesion, appl. of X-ray photoelectron spectroscopy 4-93485
- ethylene-vinyl acetate copolymer adhesion on grade 3 steel, surface modification effects 4-109623
- ethylene-vinyl acetate copolymers, crit. surface tension of wetting and adhesive strength 4-108676
- field emission deposition, high adherence coatings 4-81161
- joints, adhesively bonded, geometrically nonlinear anal. 4-99744
- joints, mode I and II fracture 4-93387
- metal films on SiO<sub>2</sub>, ion beam mixing 4-108732
- metal matrix composites, fabrication, book contrib. 4-66276
- metal-polymer bond, adhesion and durability, review 4-99743
- metallised layer formation under high pressures 4-66501
- orthotropic structures, adhesive bonded, with part through crack, stress intensity factors analysis 4-79494
- piezoceramic foil attached to Al membrane adhesive delamination, photothermal obs. 4-114732
- piezoelectric transducers, acoustic bonding materials anal. (Japanese) 4-60239
- plane cut in elastic medium with slip and adhesion of surfaces, 3D mixed problems 4-60326
- plane wave interaction with a cut in an elastic medium under transverse conditions 4-78152
- polyethylene coating, oxidised on catalytically inactive carrier, adhesive strength (Russian) 4-76913
- polyethylene terephthalate substrate surface condition, influence of adhesion layer components (Russian) 4-82850
- polyimide, cured, interfacial reaction during metallisation, XPS obs., chem. bond form. 4-88932
- polyimide, DUPONT 5878, adhesion on Si<sub>3</sub>N<sub>4</sub> wafers, polyimide thickness effect 4-71860
- polymer thin films, structure and morphology, investig. by integrated optical techniques 4-113835
- polymer-metal adhesion, appl. of X-ray photoelectron spectroscopy 4-93485
- polymer-metal adhesion compounds, spontaneous increase in strength 4-81396
- polymeric composites, phase transition between matrix and inclusions 4-114474
- scratch test for adhesion measurement (French) 4-71856
- shear strength test applicability to strength props. comparison of adhesives for metals (Polish) 4-66538
- silane coupling agents, adsorbed on Al<sub>2</sub>O<sub>3</sub>, IETS study 4-85336
- single-lap joint, strain meas. using embedded strain gauge 4-112779
- steel, diffusion bonding below A<sub>1</sub> transform. point, heat treatment effect on tensile strength (Japanese) 4-66547
- steel, friction and wear of hardened, nitrided and borided couples in air and vacuum 4-109523
- steel epoxy adhesive bond endurance under hydrothermal stress rel. to surface treatment 4-89238
- steel fibre reinforced cement, fibre debonding and pullout, adhesional interfacial shear strength 4-66388
- steel fibre reinforced mortar, polystyrene impregnated, interfacial failure 4-99571
- thin film adhesion meas. by scratch profile, SEM and X-ray analysis 4-99668
- thin film optical coatings, review 4-83671
- Zircaloy-4/VO<sub>2</sub> diffusion couple, interfacial energy and work of adhesion 4-83141
- Al alloy, surface preparation, adhesive bonding and corrosion developments 4-89173
- Al alloys, oxidised, charact. and adhesion of oxide films to epoxy resins 4-104925
- Al flame sprayed coating on CO, bonding, emission Mossbauer spectroscopy study 4-92979
- Al/Al adhesive bonds, US nondestructive testing 4-114740
- AlGaAs high power TJS laser diodes, mech. stress compensation 4-96914
- Al<sub>2</sub>O<sub>3</sub> sputtered coating, improved adhesion to Cu substrate 4-76967

**adhesion continued**

- Al<sub>2</sub>O<sub>3</sub>-Fe cermets, metal to ceramic bonding, Mossbauer studies 4-109622
- Au film, enhanced bonding by ion-assisted electron-beam deposition 4-109324
- BaFCl/Eu X-ray phosphor, transparent thin films prep. by evaporation 4-88874
- Be adherent film production by electron beam evaporation 4-66238
- C, amorphous hard films, growth from hydrocarbon RF plasma 4-85117
- C diamond-like thin film deposition on CaF<sub>2</sub> 4-74678
- C films, diamondlike, ion beam deposition and props. 4-85113
- Cu metallisation of polyimide, adhesion, nuclear scattering eval. 4-71749
- Fe-Ni amorphous alloys, flame spray quenching, coating on metal substrates 4-71797
- In vacuum condensates, adhesion to glass, effect of surface prep. of glass 4-81397
- LiNbO<sub>3</sub>, magnetron sputtered film, prep., crazing rel. to tensile stress 4-81130
- Ni metallisation of polyimide, adhesion, nuclear scattering eval. 4-71749
- Ni-Cu, vacuum arc-plasma deposition, on Pb(Zr,Ti)O<sub>3</sub> piezoceramic substrate 4-76691
- Si, metallic thin film adhesion enhancement by vacuum UV irradiation 4-93498
- Si<sub>3</sub>N<sub>4</sub> film deposition by plasma-enhanced CVD, appl. to GaAs LSI 4-71569
- SiO<sub>2</sub>-polymer film system, adhesion model and exptl. verification 4-75826
- Sn, electrodeposition on Al alloys (Russian) 4-88991
- Ti alloy, surface preparation, adhesive bonding and corrosion developments 4-89173
- Ti-N, abrasion resistance, homogeneity region 4-114681
- TiC deposited on cemented carbide or steel substrate, adhesion meas. using scratch test (French) 4-71857
- TiN deposited on cemented carbide or steel substrate, adhesion meas. using scratch test (French) 4-71857
- UO<sub>2</sub>/Zircaloy-4, diffusion couple, interfacial energy and work of adhesion 4-83141
- adiabatic compression, plasma** *see plasma heating*
- adiabatic demagnetisation** *see magnetic cooling*
- adion** *see adsorption*
- administrative data processing**
  - see also medical administrative data processing; word processing*
  - measurement instrument yard and metrology laboratory, administrative and technical management 4-106307
- admittance** *see electric admittance*
- admittance measurement** *see electric admittance measurement*
- ADP** *see administrative data processing*
- ADP (ammonium dihydrogen phosphate)** *see ammonium compounds*
- adsorbed layers**
  - see also monolayers*
  - 3d transition metals with adsorbed CO, electronic struct. and chemical reactivity of CO 4-93552
  - acetylene, adsorbed on Ni (III), K-edge X-ray absorpt. 4-85036
  - acetylene, on Pt (111), struct., NMR study 4-92526
  - acetylene, on Re (0001), vibrational electron energy loss spectroscopy (French) 4-75774
  - adamant dimer diffusion on (111) surface of Lennard-Jones face-centred crystal, molecular dynamics simulation 4-65557
  - adsorbed diatomic molecules, hindered and modulated rotations 4-70569
  - adsorbed on Ni (Cu), surface struct. determ. by photoelectron diffraction 4-85082
  - alcohol, adsorbed on Pt/TiO<sub>2</sub>, photocatalytic reaction mechanism, H<sub>2</sub> prod. 4-114820
  - alkali metal atoms, chemisorbed on W (110), NMR studies 4-98445
  - alkali metal atoms, nucl. spin polarised, chemisorbed on hot metal surfaces, NMR study 4-80374
  - alkali metal atoms, on Si (100) 2X1, surface plasmon dispersion, RPA calcs. 4-98447
  - n-alkanes, on WS<sub>2</sub>, gas chromatography 4-80371
  - alkylbenzenes, on WS<sub>2</sub>, gas chromatography 4-80371
  - aromatic and heteroaromatic hydrocarbons, adsorbed, inter-system-crossing rate, luminesc. spectra 4-59843
  - atoms and molcs., adsorbed, core-level binding energy shift anal. 4-61217
  - benzene adsorbed on Ag (111), angle-resolved surface Raman scattering 4-61677
  - benzene on graphite, orientation, Penning ionisation electron spectroscopy 4-87197
  - benzoic acid monolayers adsorbed on Al oxide inelastic electron tunnelling spectra studies 4-75782
  - 4-benzyl pyridine, on roughened Ag electrode, surface enhanced Raman bands, voltage induced intensity changes 4-93080
  - 4,4'-bipyridine, on Ag electrodes, redox behaviour, Raman and cyclic voltammetry study 4-75778
  - 2-bromonaphthalene, adsorbed on silica gel, quenching of pyrene fluoresc. 4-80369
  - 1,3-butadiene, adsorbed on silica surface, Fourier transform IR spectra 4-78843
  - butadiene iron tricarbonyl physisorbed layer, melting transition, optical spectroscopy study 4-80387
  - catalytic reactions on Cu surface, surface enhanced Raman scatt. 4-105018
  - charge transfer instability in optical absorpt. and photoelectron spectra 4-104552
  - chemisorbed and physisorbed systems, island growth kinetics, computer simulation studies 4-113813
  - commensurate phase, physisorbed on substrate of triangular lattice symm., melting transition 4-80386
  - covalent systems, models for desorption 4-61230
  - crystal/overlayer system, elastic surface waves, Green's function anal. 4-108695
  - 3,3'-diethyl-2,2'-benzthiatriethinecyanine, adsorbed on Ag colloidal particles, surface enhanced Raman scatt. 4-75779
  - dye molecule on metallic surface, distance dependence of surface enhanced luminescence 4-88877
  - dye molecules on Ag films, surface plasmon interactions, photoacoustic studies 4-104092
  - dyes adsorbed in Langmuir-Blodgett films, selectively laser excited, persistent spectral hole burning 4-88878
  - EELS technique for bulk and surface studies 4-61788

## adsorbed layers continued

- effective polarisability of atom near metal surface, Van der Waals and non-local effects 4-92559
- electronic structure 4-80651
- electronically excited states of adsorbates on metal surfaces, EELS 4-88917
- ethane monolayers adsorbed on graphite (0001) surfaces, collective excitations 4-104061
- ethene, on transition and noble metals, electronic struct. and conform. 4-92784
- ethylene, adsorbed on Ni (III), K-edge X-ray absorpt. 4-85036
- ethylene adsorbed on Pt or Pd, EELS and IR spectra studies 4-104065
- excitation of mols. and atoms on metal surface and their nonradiative relax. 4-81460
- formic acid monolayers adsorbed on Al oxide inelastic electron tunnelling spectra studies 4-75782
- gas-surface scattering from surfaces with imperfections, wavepacket approach 4-66176
- gelatin, interphase adsorptional layers, thickness meas. by internal reflection spectroscopy and ellipsometry (*Russian*) 4-104090
- graphite, adsorbed on Ni (III), geometrical struct., EELFS study 4-61789
- graphite with adsorbed ethylene film, thermodynamic props. study 4-104068
- graphite with adsorbed H<sub>2</sub>O, adsorption depend. on substrate struct. 4-92515
- graphite with adsorbed methane, commensurate-incommensurate transition model 4-70572
- graphite with adsorbed methane, orientational-transition calcs. 4-70573
- graphite with adsorbed N<sub>2</sub>, order-disorder herringbone transition kinetics 4-70570
- graphite with adsorbed noble gases, lateral variation of physisorption potential 4-92529
- graphite with surface adsorbed ethylene, molecular dynamics calcs. 4-104079
- graphite with surface adsorbed ethylene, surface diffusional and vibr. motion study 4-104078
- growth, AES investigations, scaling procedure 4-93153
- guanine adsorbed on small particles of colloidal Ag, surface enhanced Raman scatt. 4-87129
- heat capacities meas., using surface calorimeter 4-111136
- hexamethyl aluminium, surface adsorbed, laser photoreactions 4-81451
- incomplete wetting by adsorbed solid films 4-92530
- inert gas adsorbed films on graphite, incomplete wetting 4-92530
- inert gases, adsorbed on Li, conduction electron spin scatt. cross-sections 4-84663
- inert gases, on smooth solid substrates, wetting characts. at zero temp. 4-80388
- IR laser photoacoustic spectroscopy for surface studies 4-86490
- isotherms and adsorbed layers 4-113792
- Langmuir films on Ag film, surface plasmon enhanced Raman scatt. 4-76453
- layering transitions in solid films, renormalisation group anal. 4-104082
- lead phthalocyanine/Ni Schottky type solar cells, surface states, adsorbed gas effects 4-66695
- LEED angular profiles calc. for island size distributions meas. 4-88399
- liquids on Ag film, surface plasmon enhanced Raman scatt. 4-76453
- metal layer, adsorbed mols., surface polaritons, internal reflection spectrum 4-109150
- metal surface, adsorbed atom, intrinsic polarisability modification (*French*) 4-104064
- metallic films with adsorbed pyridine films, photocalorimetric spectroscopy and AC calorimetry 4-66629
- metallic thin films, crystal growth, initial steps, microscopic studies 4-98486
- metals, surface diffusion on non-metallic substrates 4-98415
- metals, vibrations of adsorbed atoms and molecules 4-113778
- metals, work functions, quantum size effects 4-92790
- metastable atom-surface interaction, electronic emission (*French*) 4-76623
- methane, on graphite, model of commensurate-incommensurate transitions 4-80394
- methane, on graphite, two-dimens. liq.-vapour crit. point exponent, sp. ht. study 4-92341
- methane adsorbed on graphite, intermol. pot. and lattice sums 4-80393
- methane submonolayer adsorbed on graphite, commensurate-incommensurate transition, neutron diff. study 4-65559
- mica with adsorbed methyl iodide, phenyl indogen and nitrobenzene 4-78922
- mixed valence compounds, vibrations of adsorbed atoms and molecules 4-113778
- molecular photoion production processes induced by surface laser irr. 4-81043
- molecular vibrations at surfaces, spectral studies, review 4-87098
- molecules, on metal surface, Raman spectra, intensity enhancement (*Polish*) 4-87128
- molecules, vibrational properties 4-80413
- molecules on metal surface, Raman scatt. enhancement 4-66040
- nickel tetraphenylporphyrine compounds on  $\gamma$ -Al<sub>2</sub>O<sub>3</sub> and SiO<sub>2</sub>, reson. Raman spectra 4-105012
- nonlinear optical detection of adsorbed monolayers 4-87398
- octopoles in planar surface field, mol. dynamics simulation 4-88402
- order-disorder phenomena, and surface struct. 4-80414
- oxide, exchange of O between gas and solid, electrochemical study 4-98357
- paramagnetic systems, two-dimens., nonlinear response theory for nearest-neighbour Ising model 4-80740
- phthalazine adsorbed on Ag electrode, surface enhanced Raman spectra and mol. orientation 4-104585
- polymer molecule, shear flow, bead-spring models 4-87830
- polystyrene spheres on Ag substrates, structural resonances observed in the fluoresc. emission 4-84984
- porous sample, optical props., adsorbed mols. effect 4-98454
- pyrene, adsorbed on silica gel, singlet quenching of fluoresc. 4-80369
- pyridine, adsorbed on LaMO<sub>3</sub> (M=Cr,Mn,Fe,Co), IR spectra 4-104071
- pyridine, on Ag, giant second harmonic photoactivation surface enhanced Raman scatt. 4-74612
- pyridine, on Cu and Ag, surface enhanced Raman scatt., effect of surface roughness, SEM obs. 4-76473
- pyridine adsorbed on Ag low-index faces, normal Raman scatt. 4-88838
- pyridine adsorbed on Cu or Ag, evidence of surface enhanced Raman scatt. active sites 4-88839

## adsorbed layers continued

- pyridine adsorbed on metal colloid, surface-enhanced Raman scatt. 4-88842
- $\alpha$ -quartz with adsorbed SnO<sub>2</sub>, interface struct., RHEED study 4-104043
- rare-gas atoms on alkali halides, neutral excited configurations 4-80390
- resonant tunnelling, secondary electron emission 4-71492
- rhodamine 6G adsorbed at Ag colloids, surface fluoresc. and surface Raman scatt. 4-108704
- rhodamine 6G dye molecules adsorbed on Ag island films, picosecond fluorescence decay 4-87156
- Rhodamine B, adsorbed on oxide semiconductors fluoresc. quenching, lifetime and intensity 4-102725
- rhodamine-590 physisorbed thin films, surface photoacoustic wave spectra 4-104693
- sapphire with surface adsorbed Na, laser irr., photostimulated desorption 4-113793
- semiconductor substrates, with adsorbed metallised atom submonolayers, cooperative phenomena 4-70556
- silane coupling agents on Al<sub>2</sub>O<sub>3</sub>, IETS study 4-85336
- surface electronic excitations and dynamic spectral properties 4-108708
- surface enhanced Raman scatt., adatom model, review 4-66037
- surface enhanced Raman scatt. of adsorbed mols., theory 4-114251
- surface free energy, contact angle meas., spreading press. effects 4-61173
- surface plasmon enhanced second harmonic generation on Ag electrodes 4-65617
- surface polarization induced by an adatom in a dielectric 4-70551
- surface structure determ. by XANES 4-99226
- TCNE, on Ag film, surface-enhanced Raman scatt., charge transfer effects 4-71358
- transition metal adsorbed mol. clusters, electronic struct., UPS, XPS studies 4-78995
- two-dimensional condensation, crit. temp. calc., lattice incompatibility effects 4-65561
- ultrahigh vacuum conditions, use of He gas flow-type cryostat 4-68224
- vibration spectroscopic studies of adsorbed species on metal surfaces 4-104065
- vibrational spectroscopy of adsorbed atoms and mols., overview 4-88837
- water, on Al and W, electron stimulated desorption, H<sup>+</sup> ion energy distrib. 4-92536
- water chemisorbed on Si (100)(2 $\times$ 1), multiple vibr. excitations, high resolution EELS study 4-109289
- wetting and thermodynamic pot. 4-98449
- Ag (001) with adsorbed Cl, inelastic He scatt. and surface phonons 4-99257
- Ag (110), adsorbed layers, vibr. props., He atom scatt. 4-65570
- Ag (111) with adsorbed NO, adsorption and decomposition study 4-98433
- Ag film with adsorbed O<sub>2</sub>, CO and ethylene, elec. cond., effect of adsorption 4-108950
- Ag, on Cu, electronic props., surface refl. spectroscopy study 4-85023
- Ag surfaces and halide layers protonation of pyridine by adsorbed H<sub>2</sub>O, Raman spectra 4-89322
- Al adatom-induced reconstruction on Si (111), pseudopotential calcs. 4-104076
- AlO with adsorbed TCNQ, CO<sub>2</sub>(CO)<sub>8</sub> and tetracyanethylene, glove box deposition system and study 4-101860
- Ar on Cu surface, He scatt., time depend. wavepacket calcs. 4-88918
- Ar on Mg and Al, optical spectra, configurational effects 4-80391
- BN with adsorbed ethylene film, thermodynamic props. study 4-104068
- Ba, on W (011), phase transitions, LEED study 4-92544
- Bi/Bi(0001) system, work function variation with surface coverage (*French*) 4-76019
- C, glassy with adsorbed H<sub>2</sub>O, adsorption depend. on substrate struct. 4-92515
- C on Mo (001), low energy alkali ion scatt. studies 4-76582
- C segregation to Ni (100) surface in presence of adsorbed S 4-61089
- CN adsorbed on Ag electrode, Fourier transform IR spectra studies 4-93067
- CN, chemisorbed on Ag island film, depolarisation effects in Raman scatt., classical microscopic local field 4-88832
- CO adsorbate vibrs., Stark effect 4-98453
- CO, adsorbed Cu {100}, 2 $\pi^*$  associated states, angle-resolved photoemission 4-65724
- CO, adsorbed on Ag (110), photoemission screening effects 4-66189
- CO adsorbed on K recovered Ru (001), EELS scatt. profiles of vibr. overtones and double losses 4-109287
- CO, adsorbed on LaMO<sub>3</sub> (M=Cr,Mn,Fe,Co), IR spectra 4-104071
- CO, adsorbed on metal surfaces, XPS satellite structures 4-114361
- CO, adsorbed on metals, bonding, EHT calcs. 4-113800
- CO, adsorbed on Ni (110), medium energy ion scatt. studies 4-88381
- CO adsorbed state over Pd/graphite catalyst, PES study of particle size effect 4-99274
- CO catalytic oxidation on Pt (100), MeV ion scatt. study 4-81069
- CO, chemisorbed, physisorbed, and free, high-resolution C 1s and O 1s core-excitation spectra 4-93125
- CO chemisorbed layer on Ru (001), electron-induced desorption 4-104075
- CO, chemisorbed on Pt (110), (111) and Ni (100), photoemission study 4-85055
- CO, coadsorbed with Na on Ru (001), mol. reorientations 4-108717
- CO, coadsorption with K on Ru (001), attractive interactions 4-65548
- CO, high coverage struct. on metal FCC (111) and HCP (0001) surfaces, LEED, HREELS and IR spectra study 4-65573
- CO, on metals, valence electronic excitations, EELS 4-81052
- CO, on Ni (100), Pt (111) and (110), photoelectron ang. distrib. patterns 4-109309
- CO, on Ni (100), stretching vibr., IR emission spectroscopy study 4-92508
- CO on Rh (001), photoemission, ion scatt. and secondary electron studies 4-75777
- CO, overlayer on Cu (111), band dispersion, multielectron effects 4-85056
- CO, oxidation on Ag catalyst, surface heterogeneity 4-105017
- CO, oxidation over Pt surface, kinetic oscils., Rutherford backscattering, LEED study 4-66611
- CO-covered Cu films, optical and elect. props. 4-80693
- Co<sub>2</sub>, adsorbed on LaMO<sub>3</sub> (M=Cr,Mn,Fe,Co), IR spectra 4-104071
- Co-Al<sub>2</sub>O<sub>3</sub> with adsorbed N<sub>2</sub>, FT-IR studies 4-113786
- Cr (110) with adsorbed O<sub>2</sub>, photon stimulated O<sup>+</sup> desorption 4-98438
- Cs evaporated layer on Ag surface, photoelectric emission stability 4-76637

## adsorbed layers continued

- Cs monolayer on Si (111), metal-insulator transition, Cs valence electron photoemission studies 4-84505  
 Cs on Si (111), inversion layers, positive and negative magnetoresist. 4-98645  
 Cu, on Ag, electronic props., surface refl. spectroscopy study 4-85023  
 Cu-Ti glasses, surface composition, composition profiles, Auger electron spectroscopy 4-113758  
 CuInSe<sub>2</sub>, sputtered surface characterisation using AES, O<sub>2</sub> adsorpt. 4-93147  
 D, on Ni (110) and (111), site location, surface channelling study 4-80375  
 D on W (111), diffusion, fluctuation method anal. 4-104088  
 D<sub>2</sub>O, chemisorbed on Si (100)(2×1), multiple vibr. excitations, high resolution EELS study 4-109289  
 Fe (100) with chemisorbed S, electronic struct. study 4-92779  
 GaAs (110) with adsorbed H, H<sub>2</sub>, temp. programmed desorption study 4-92528  
 Ge with adsorbed CaF<sub>2</sub>, layer thickness meas. by RBS (*Chinese*) 4-70968  
 H, on Ni, Pd and Pt vibr. spectra 4-104073  
 H, on Ni (110), dual path surface reconstruction study 4-108716  
 H on W (001), surface reconstruction, LEED and EELS study 4-92492  
 H, on W (100), surface reconstruction, symm. effects, refl. EELS study 4-80382  
 H on W (111), diffusion, fluctuation method anal. 4-104088  
 H-induced surface reconstruction on W (100), core level spectra studies 4-65527  
 H<sub>2</sub> adsorbed on Ni (111), phase diagram 4-104083  
 H<sub>2</sub> chemisorbed on Ni surface, quantum motion 4-80385  
 H<sub>2</sub>, electron-stimulated field desorption 4-92532  
 H<sub>3</sub>, electron-stimulated field desorption 4-92532  
 HCN adsorption on SiO<sub>2</sub> and Al<sub>2</sub>O<sub>3</sub> surfaces, far IR Fourier spectroscopy 4-104593  
 H<sub>2</sub>O, adsorbed on Pt/TiO<sub>2</sub>, photocatalytic reaction mechanism, H<sub>2</sub> prod. 4-114820  
 H<sub>2</sub>O, adsorbed on V<sub>2</sub>O<sub>3</sub>(Ti<sub>2</sub>O<sub>3</sub>)(α-Fe<sub>2</sub>O<sub>3</sub>), surface electronic struct. 4-84664  
<sup>3</sup>He adsorbed layer, spin-diffusion coeffs. 4-113742  
<sup>3</sup>He, adsorbed on fluorocarbon microspheres, dynamic polarisation effects, EPR study 4-80324  
<sup>4</sup>He, adsorbed layer on Y-zeolite, semiquantum liquid and ordered phases obs. 4-65515  
<sup>4</sup>He adsorbed on Grafoil, multilayer growth 4-104033  
<sup>4</sup>He monolayer film, effective pot. approx. (*Chinese*) 4-92471  
 In, adsorbed on Si (100), superlattice structures, RHEED study 4-113802  
 K, coadsorption with CO on Ru (001), attractive interactions 4-65548  
 K, on W (100) stepped surfaces, desorption kinetics and directional depend. of surface diffusion 4-92545  
 Kr monolayer, physisorbed on graphite, modulation of at. positions, anharmonicity 4-92531  
 Kr, on graphite, domain growth, Monte Carlo simulations 4-98444  
 Kr on Mg and Al, optical spectra, configurational effects 4-80391  
 MgO with adsorbed Kr, substrate preparation 4-104067  
 Mo (001), C, N, O overlayers, adsorbate ordering, low energy K<sup>+</sup>-ion scatt. 4-98448  
 MoO<sub>3</sub> with adsorbed methanol, desorption, oxidation to formaldehyde 4-92520  
 N covered Ti and Al surfaces, sputtered metal atoms, vel. distrib. 4-76608  
 N<sub>2</sub> chemisorbed on W (110), Ru (001), Ni (100), XPS lineshapes anal. 4-104723  
 N<sub>2</sub> on graphite, island growth kinetics, computer simulation studies 4-113813  
 N<sub>2</sub> on Ni (100), ang. depend. of N<sub>1s</sub> XPS peaks 4-93197  
 N<sub>2</sub> on Ru catalysts, temp. programmed desorption and isotopic study 4-93558  
 NH<sub>3</sub> adsorbed on Cu (100), time of flight mass spectra study on IR laser photodesorption 4-80384  
 NO adsorption on Pt (111) vibr. excitation and deexcitation rates 4-98443  
 N<sub>2</sub>O chemisorbed layer on Ru (001), electron-induced desorption 4-104075  
 Na, coadsorbed with CO on Ru (001), mol. reorientations 4-108717  
 NaCl with adsorbed methyl fluoride, IR laser-induced desorption, momentum distrib. study 4-80419  
 Nb (110)-Pd interface, electronic struct. 4-84674  
 Nb, adsorption of C, NbC formation and synchrotron radiation study of overlayers 4-108711  
 Ne on exfoliated graphite, 2-D press.-temp. phase diagram 4-92523  
 Ne solid with adsorbed <sup>4</sup>He liquid film, surface trapped two-dimensional electrons 4-98387  
 Ne, solid with adsorbed <sup>4</sup>He liquid film, normal density 4-98683  
 Ni (001) with adsorbed Se, S and O, electron photoelectron diffr. model 4-71516  
 Ni (100) surface with adsorbed O, surface phonons, EELS study 4-104086  
 Ni (100) with adsorbed N<sub>2</sub>, core level binding energy shift anal. 4-92517  
 Ni (100) with adsorbed N<sub>2</sub>, precursor state identification 4-93550  
 Ni (110) with adsorbed H<sub>2</sub>, O<sub>2</sub>, kinetics of adsorption and reaction 4-92519  
 Ni (111) with adsorbed graphite and C overlayers, electronic struct. study 4-61213  
 Ni (111) with surface adsorbed C and CO, thermal decomposition of ethylene 4-113782  
 Ni with adsorbed C and Se, Fourier transform anal. of PES, normal one beam model (*Chinese*) 4-75773  
 Ni with surface adsorbed S, O and CO, anharmonicity and adsorbate vibr. lifetimes 4-104084  
 O chemisorbed layer on W, island growth kinetics, computer simulation studies 4-113813  
 O chemisorbed on W, lattice gas-model, finite size scaling study 4-84513  
 O covered Ni, low energy neutral and ion scatt. studies 4-71494  
 O covered Ti and Al surfaces, sputtered metal atoms, vel. distrib. 4-76608  
 O on Al, secondary ion emission 4-76609  
 O, on Cu(110), azimuthal and polar angle depend. surface EXAFS 4-61770  
 O on Mo (001), low energy ion scatt. studies 4-76582  
 O on N (001), He atom diffraction study 4-80389  
 O, on Ni (100), surface vibr. dispersion, EELS study 4-109288

## adsorbed layers continued

- O<sub>2</sub> adsorbed layer on graphite, mag. and melting transitions 4-65576  
 O<sub>2</sub> adsorbed on Cu (110), surface reconstruction, angle-resolved UPS study 4-85083  
 O<sub>2</sub> adsorbed on Ni (100), surface-extended energy loss fine struct. study 4-61790  
 O<sub>2</sub> adsorbed on Ni (110), surface analysis by surface channeling using ion induced Auger electron emission 4-81068  
 O<sub>2</sub> adsorbed on V<sub>2</sub>O<sub>3</sub>(Ti<sub>2</sub>O<sub>3</sub>)(α-Fe<sub>2</sub>O<sub>3</sub>), surface electronic struct. 4-84664  
 O<sub>2</sub> adsorbed on W (110), vibrational modes, EELS study 4-80402  
 O<sub>2</sub> adsorbed p(2×2) layer on Ni (100), vibrational props., cluster anal. 4-113809  
 O<sub>2</sub> on Ti films, Ti gettingter, surface chem. 4-108707  
 O<sub>2</sub>, physisorbed on graphite, f phase struct., LEED determ. 4-108712  
 O<sub>2</sub>-Ar(N<sub>2</sub>) systems, adsorbed on Grafoil, mag. and thermal props., 3 to 70K 4-61214  
 OH, on oxygen dosed Ni (110), formation and orientation following H<sub>2</sub>O adsorption 4-66615  
 Pd (100) and (111) with adsorbed acetylene, decomposition, EELS evidence for CCH formation 4-99829  
 Pd (110) with adsorbed H<sub>2</sub>O, photon stimulated desorption of H<sup>+</sup> 4-98437  
 Pd on W, surface diffusion across steps, FEM study 4-92558  
 Pd with surface adsorbed Xe, finite size effect on critical temp. 4-104080  
 Pd-MOS struct. with adsorbed H<sub>2</sub>, use as H<sub>2</sub> sensor in catalytic reactions 4-93555  
 Pt (100) with adsorbed O<sub>2</sub>, interactions, XPS and work function 4-92521  
 Pt (110) with adsorbed H<sub>2</sub>O, photon stimulated desorption of H<sup>+</sup> 4-98437  
 Pt (111) surface with adsorbed I, core electron binding energies 4-104085  
 Re adsorbed on W (110), three-body interactions, field ion microscopy study 4-70564  
 Rh (111) with surface adsorbed HNCO, effects of preadsorbed O 4-113781  
 Rh, field evaporation, bonding distance and vibr. freq. determ. 4-93202  
 (Ru<sub>3</sub>S<sub>1-x</sub>)<sub>2</sub>O<sub>2</sub> with surface adsorbed pyridine, FT-IR study of surface acid sites 4-113783  
 (Ru<sub>3</sub>S<sub>1-x</sub>)<sub>2</sub>O<sub>2</sub> with surface adsorbed acetone, FT-IR study of surface acid sites 4-113783  
 S chemisorbed on Pt (110), effect on H adsorpt. (*French*) 4-84504  
 S covered Ni, low energy neutral and ion scatt. studies 4-71494  
 S, on Fe (110)p(2×2), surface ferromagnetism, chemisorption; adsorbate-induced substrate reconstruction effect, spin-polarised LEED calcs. 4-80395  
 S on Ni 100 and (111), angle resolved AES studies 4-80416  
 S on Ni (001), core-level azimuthal photoelectron diffr. 4-109306  
 S on Ni (001), intermediate energy azimuthal X-ray photoelectron diffr. 4-109307  
 Sb wedge-shaped films on Ag films, Raman scatt. 4-109172  
 Si (100) with adsorbed Cs, neutralisation of scattered He ions 4-109294  
 Si (100) with adsorbed O<sub>2</sub>, ab initio SCF calcs. 4-98440  
 Si with adsorbed Ag, growth and diffusion, SEM, study 4-80417  
 a-Si:H, Li, surface photovolt. and dark conductance, light-induced changes 4-70861  
 Si-polyacetylene interface, Auger spectra obs. of Si-C binding, peak shift depend. on adsorpt. level (*French*) 4-66141  
 Sn, adsorbed on Si (100), superlattice structures, RHEED study 4-113802  
 VO<sub>2</sub>-WO<sub>3</sub>-H, photoinjection of H into the heterostructure, semiconductor-metal transition studies 4-113478  
 W (100), oxidised and carbided, adsorbed ethylene and acetylene 4-93553  
 W (110) with adsorbed Au, work function meas. 4-98692  
 W (110) with surface adsorbed CO, electronic transitions, low-threshold neutral desorption, α-β conversion, calcs. 4-113785  
 Xe adsorbed multilayers on Pd, roughening transition study 4-61205  
 Xe disordered overlayers on W (110) self-diffusion, chem. diffusion consts., coverage depend. 4-80399  
 Xe monolayer, physisorbed on graphite, modulation of at. positions, anharmonicity 4-92531  
 Xe, on Pd, adsorptive bond, face specificity, s-resonance model 4-92540  
 ZnS:Li with adsorbed O<sub>2</sub>, surface states and LED props. 4-80643  
 Zr (0001), adsorbate-induced Auger attenuations 4-66137  
 Zr with surface adsorbed H, sticking coefficients, binding states, desorption studies 4-113784

## adsorption

- see also heat of adsorption  
 alkaline earth metal ions, permselectivities across cation exchange membrane (*Japanese*) 4-99842  
 alumina humidity sensor; moisture effect on dielectric props. analysis 4-95442  
 aniline, multilayer single solute adsorpt. from dilute sols. on C 4-65545  
 applied surface anal., conf., Dayton, USA (June 1983) 4-95016  
 blood, interfacial film, with vitreous body, struct., physicochemical props., in case of haemophthalmia 4-81610  
 Calgon BPL activated C adsorpt. of N<sub>2</sub>, CO<sub>2</sub>, methane and ethylene, Langmuir isotherm 4-104072  
 capillary porous bodies, transport processes, laser monitoring 4-112999  
 ceramics, porous, dielec. response, adsorbed water effects 4-65943  
 charcoal, activated, adsorpt. from binary sols. at high press. 4-104070  
 charcoal, activated, adsorption isotherms and heats of adsorption of H<sub>2</sub>(Ne)(N<sub>2</sub>) 4-114821  
 charcoal, activated, H<sub>2</sub> adsorption at low press. and at 20K 4-99844  
 charcoal, activated, organic liq. adsorpt. at high press. interfacial phase props. 4-104069  
 chlorophyll-a, surface cond. in various ambient gases 4-108921  
 colloidal suspensions, electric-field jump studies, negative second Wien effect theory 4-99850  
 copper phthalocyanine, chlorinated, mol. energetics of epitaxial growth on KCl 4-94880  
 critical wetting in systems with long-range forces 4-88374  
 crystalline sphere in fluid, thermodynamic equilibrium 4-98321  
 cyclohexanol, multilayer single solute adsorpt. from dilute sols. on C 4-65545  
 diamond (111), clean and adsorbed H<sub>2</sub>, photoemission studies 4-88939  
 diamond powders, synthetic, adsorpt. of organic compounds, IR spectroscopy (*Russian*) 4-75791

## adsorption continued

- dye adsorption on  $\text{SiO}_2$ , aq. soln.-solid diffusion model 4-65546  
 elastic substrate, transition to incommensurate phase 4-104089  
 energy and entropy 4-80412  
 epitaxial layer-by-layer two-dimensional random growth model, backscattered electron diff. beam profile 4-84535  
 FCC solid surfaces, memory function parameterisation in generalized Langevin eqn.-ghost atom function 4-92493  
 field adsorption kinetics of gas atoms of mols. 4-92541  
 film surfaces, isothermal coverage oscillations of charged species, kinetic model 4-92562  
 glass, porous with adsorbed rhodamine 6G, photostability study 4-99816  
 grain boundary model, impurity effects, cluster variation method calcs. 4-113465  
 graphite, ethylene adsorption, layering, prewetting and wetting 4-98450  
 graphite, of  $\text{N}_2$ , mol. dynamics simulation, herringbone orientational ordering 4-61211  
 graphite, physisorbed  $\text{O}_2$ , phase transitions, LEED studies 4-88396  
 graphite (0001), adsorption of hydrocarbons, polarisability anisotropy, mol. statistical theory 4-80379  
 graphite with adsorbed noble gases, lateral variation of physisorption potential 4-92529  
 heterogeneous adsorbents, gas adsorpt., Langmuir isotherms 4-104072  
 heterogeneous catalysts and catalytic surfaces characterisation 4-89335  
 heterogeneous microporous solids, single solute adsorption from dilute solns. 4-92513  
 heterogeneous surface, adsorpt. integral eqn. soln. 4-93546  
 heterogeneous surface characterization by photoemission of adsorbed Xe 4-88935  
 heterogeneous surfaces, phys. adsorpt. of gases 4-104074  
 Hill eqn. implementation 4-70562  
 hydrogenous species, adsorbed, vibr. spectrosc., inelastic incoherent neutron scatt. 4-70574  
 hydrophilic solid, of nonionic surfactant, fluoresc. decay obs 4-108679  
 insulating thin films, Auger electron spectra, electron and ion beam effects 4-109283  
 interface dynamics, conf., Lille, France (Sept. 1983) 4-78030  
 isotherm,  $\Gamma$  method modification for true monolayer capacity and surface area determ. 4-113814  
 isotherms and adsorbed layers 4-113792  
 kinetics, stochastic numerical simulation 4-75776  
 liquid films, Gibbs elasticity of multicomponent solutions 4-108681  
 liquid-liquid jet breakup, drops size, mass transfer and solute adsorpt. effects 4-64993  
 metal surfaces, anion and cation hydration, double layer simulation in ultrahigh vacuum 4-108703  
 metal surfaces, CO adsorption, SCF calcs. 4-88398  
 metallic thin films, etching with  $\text{CCl}_4$ , electron flux activation 4-93446  
 metallurgical thermodynamics, equilib. states and influencing factors, book contrib. 4-109375  
 metals, of anions, adsorpt. props. rel. to ions. pot. 4-61221  
 metals, surfaces, impurities and defects, embedded atom method 4-92590  
 methylmethacrylate-vinylferrocene copolymers adsorpt. at soln./solid interface, chromatography meas. 4-85332  
 mica surfaces in polyethylene oxide soln., long-range attractive forces 4-70563  
 mineral-water interfaces adsorption and elec. double layer phenomena 4-72576  
 molecular fluid mixture, adsorption and re-entrant wetting transition 4-108680  
 molecule-surface interactions and dynamics 4-99828  
 monolayers, adsorbed, spin-one Ising model 4-92534  
 Monte Carlo studies of adsorption phenomena 4-113816  
 multi-state models, interfacial adsorption, Monte Carlo studies 4-113812  
 multilayer solid adsorption and the roughening transition 4-113817  
 organic compounds, multilayer single-solute adsorption from dilute solutions on energetically heterogeneous solids 4-65545  
 organic dyes, photovoltaic cells, chem. props. 4-84998  
 photon stimulated desorption, surface characterization, instrumentation 4-90703  
 polydiacetylene,  $\text{O}_2$  absorpt. and adsorpt., Raman study 4-66612  
 polyethylene oxides, solution-gas interface, adsorption characts. 4-79921  
 polymer adsorption on colloidal particles 4-62250  
 polymer chain adsorption at crit. energy, random walk model 4-59923  
 polymer solutions, dil. interfacial props. 4-61180  
 polystyrene latex suspensions, in electrolyte solns., adsorpt. and elec. cond. props. (Russian) 4-114848  
 quartz, surface and vol. centres, optical and paramag. props. 4-66057  
 Raney Ni, of  $\text{H}_2$ , inelastic neutron scatt. spectrosc. obs. 4-113797  
 secondary electron multipliers, T adsorption and desorption, fusion reactor appl. 4-59413  
 SEM studies of surface processes, digital data acquisition and anal. system 4-78433  
 semiconductor, electron stimulated adsorption in presence of  $10^{-8}$  torr  $\text{H}_2\text{O}$  4-66150  
 small clusters stability, electronic struct. 4-74371  
 static polarisability modification by perfect metallic surface 4-113779  
 steel, mild, electrodes in  $\text{H}_2\text{SO}_4$ , adsorption of thiourea 4-88390  
 steel, use of surface behavior diagrams to study hydration/corrosion of aluminum and steel surfaces 4-89171  
 sticking probability, coverage depend., extended Kisliuk model 4-108719  
 substrates, of monatomic films, finite compressibility effects 4-61218  
 surface enhanced Raman scatt. from dielec. sphere 4-88843  
 surface enhanced Raman scattering 4-61672  
 surface structure anal. by low-energy ion scatt. 4-81077  
 surface study by resonant microwave cavity detuning, hysteresis effect obs. 4-70552  
 transition metals, of alkali metal atoms, electronic charge transfer 4-92554  
 transition metals, surface reactions and gas adsorption on alkali-promoted surfaces 4-85329  
 vacuum systems with adsorbing surfaces, adsorbed gas flows, iterative calc. 4-82801  
 n-valeric acid, multilayer single-solute adsorpt. from dilute solns. on C 4-65545  
 van der Waals induced dipole moment magnitude in physisorption 4-113791  
 vibrational, electronic and struct. props., book 4-78067  
 xanthene disordered dye monolayers on glass and on phenanthrene crystal surfaces, fluoresc. quenching 4-87150

## adsorption continued

- AG electrode, surface enhanced Raman scatt., contrib. of charge transfer complexes and photochemical effects 4-88841  
 Ag (110),  $\text{H}_2\text{O}$  and  $\text{O}_2$  adsorption and reaction, UPS study 4-80404  
 Ag (110),  $\text{O}_2$ , CO and  $\text{CO}_2$  interactions, AES, XPS, TDS and LEED studies 4-113810  
 Ag (111) surface, of  $\text{H}_2$ , EHT method studies 4-65544  
 Ag electrode, adsorpt. of KSCN, surfaced enhanced Raman spectra 4-80370  
 Ag electrode, of  $\text{NH}_3$ , surface enhanced Raman scatt., vibr. anal., charge transfer processes 4-93545  
 Ag electrodes, SERS and SHG from  $\text{CN}^-$  ( $\text{SO}_4^{2-}$ ) adsorbates during redox cycles 4-114282  
 Ag, of  $\text{SO}_4^{2-}$ , surface second harmonic generation 4-65547  
 Ag surface, (110), O adsorpt., model LEPS pot. 4-61204  
 Ag thin films, of O, photoelec. and elec. props. 4-92831  
 Al (111) surface, of  $\text{H}_2$ , EHT method studies 4-65544  
 Al, hydration/corrosion, surface behaviour diagrams, dissolution of adsorbed inhibitor 4-89171  
 Al, ion-induced Auger electron spectra,  $\text{O}_2$  adsorpt. effects 4-61795  
 Al, of H atoms, on (100) surface, CNDO/BW calcs. 4-61222  
 Al- $\text{Al}_2\text{O}_3$ -Pb(Ag) tunnelling junctions, interaction with 3-(trimethylsilyl)propanethiol, IETS study 4-92827  
 Al-insulator-Pb(Ag) tunnel junctions, doped with aromatic aldehydes, ring substituent effects, elastic tunnelling study 4-92828  
 $\gamma$ - $\text{Al}_2\text{O}_3$ , adsorption of alkanes and aromatic hydrocarbons, thermodynamic props., chromatography (Chinese) 4-61210  
 $\text{Al}_2\text{O}_3$ , of  $\text{N}_2$ , IR spectra 4-77030  
 $^{241}\text{Am}$  ultra-thin  $\alpha$ -source, preparation by adsorption 4-68853  
 Ar, on Ag film, adsorption process study using surface plasmons 4-80383  
 Au (110) and (111), of  $\text{O}_2$ , substrate impurity effects, EELS, AES, and XPS study 4-93160  
 Au adsorption and thermal decomposition of tricresylphosphate, XPS studies 4-98428  
 Au electrode, surface oxidation in  $\text{H}_2\text{SO}_4$  electrolyte, XPS study 4-93465  
 Au, of  $\text{O}_2$ , AES, XPS, and thermal desorption study 4-92556  
 Au, of  $\text{O}_2$ ,  $\text{Au}_2\text{O}_3$  prod. by DC reactive sputtering, EELS, AES, and XPS study 4-93161  
 Au- $\text{TiO}_2$ -Ti structures, RF sputtered, O adsorption effects on diode I-V characts. 4-98455  
 $\text{AuCl}_4^-$  complexes, adsorption on goethite 4-109678  
 Au(111), of Cu, is underpotential region, LEED and RHEED investig. 4-108702  
 $\text{BaSO}_4$ , of amphoteric 4-66619  
 C, active, ACS wheterites, porous struct. and adsorption 4-93547  
 C fluidised bed, continuous adsorpt. process 4-97651  
 C, graphitised, of sodium dodecyl sulphate (octyltetraethylene glycol), enthalpy determ. 4-70560  
 C powders,  $\text{Ar}(\text{N}_2)(\text{CO}_2)$  adsorption, second gas-solid virial coeffs., chromatographic determ. 4-114819  
 C surface, benzene adsorption equilibria 4-92512  
 CO, on Ag film, adsorption process study using surface plasmons 4-80383  
 CO oxidation over Pd deposited on  $\text{LiNbO}_3$  ferroelectrics, adsorptive and catalytic props., polarisation 4-99837  
 $\text{Ca}_{10}(\text{PO}_4)_6(\text{OH})_2$ , dissolution kinetics, effects of fluoride ions adsorption 4-98292  
 CdTe initial growth stages on (001) GaAs, AES and RHEED obs. 4-70580  
 $^{244}\text{Cm}$  ultra-thin  $\alpha$ -source, preparation by adsorption 4-68853  
 $^{57}\text{Co}$  ultra-thin  $\alpha$ -source, preparation by adsorption 4-68853  
 Cu (II) complexes, correl. of EPR parameters with thermodynamic stability 4-98937  
 Cu (100), of CO multilayers on (100) surface, epitaxial growth of new cryst. struct., LEED, IR spectra 4-113373  
 Cu (110), adsorption and chemisorption of water vapour, electron beam damage of adlayer 4-80397  
 Cu (110), clean and O covered, ethylene adsorption, UPS studies 4-70548  
 Cu (110), of  $\text{O}_2$ , influence of  $\text{Ne}^+$  ion bombard. 4-108723  
 Cu (110), of water vapour, electron beam damage to adlayer 4-80396  
 Cu single cryst., oxidation, electron microscopy and RHEED studies 4-85259  
 Cu surface, of S and O on cylindrical crystals. 4-61223  
 Cu surface, organic mol. adsorption 4-80409  
 Cu/Ru(001) bimetallic catalysts, static SIMS, XPS and TPD studies 4-80411  
 $\text{Cu}_2\text{S}$ , of ethyl xanthate, XPS study 4-85090  
 Fe (111), CO interaction, thermal desorpt. and LEED studies 4-65566  
 Fe, adsorption and thermal decomposition of tricresylphosphate, XPS studies 4-98428  
 Fe, annealed, stress enhanced  $\text{H}_2\text{S}$  adsorption, Auger spectra 4-75789  
 Fe films,  $\text{H}_2$  adsorption, surface pot. and thermal desorpt. spectra study 4-65555  
 Fe fine particles, prep. from goethite microcrysts., morphology and mag. props. 4-65835  
 Fe-Cr, surface segregation of S, annealing and  $\text{O}_2$  adsorption effect (Japanese) 4-61932  
 Fe-Si (3 wt.%) (100) surfaces, interaction with  $\text{O}_2$  and electron stimulated desorption 4-92560  
 GaAs (110),  $\text{H}_2\text{O}$  adsorption, TDS and LEED studies 4-65568  
 GaAs (110), of H, EHMO method calc. (Chinese) 4-113787  
 GaAs (111), of O, XPS study (Chinese) 4-85077  
 GaAs, ductile brittle transition in (001) surface layers in single crystals, effect of medium 4-70266  
 GaAs-Al contact, semicond. electron field emission props., metal adsorption effect 4-99289  
 Ge (111)-Pb interface form. dynamics and oxidation 4-84518  
 Ge(100)-(2x1), adsorption of Ag, HEED and photoemission study 4-75790  
 $^4\text{He}$ , solid, multilayer adsorption on graphite, two-dimensional crit. temp. increase. 4-88366  
 $^{131}\text{I}$ , gas adsorption on rocks 4-96147  
 $\text{LaCrO}_3$ , perovskite-type oxide, kinetics of CO adsorption 4-61208  
 $\text{La}_2(\text{MoO}_4)_3 \cdot x\text{H}_2\text{O}$ , solubility, Liesegang ring form., adsorpt. and salt effect 4-65410  
 Li film,  $\text{O}_2$  and water adsorption, XPS studies 4-98429  
 Li surface, interaction with acetylene electronic and geometric struct. of acetylide, AES and UPS study 4-92543  
 $\text{Li}_n$  cluster,  $\text{H}_2$  impact, Raman enhancement mechanism assoc. with Raman scatterer interaction 4-61675

## adsorption continued

- Li<sub>2</sub>O breeder blanket pellet, water vapour adsorption in He sweep gas stream 4-107032
- Mg, ion-induced Auger electron spectra, O<sub>2</sub> adsorpt. effects 4-61795
- MgO (001), of CO and simple organic mols., ab initio MO calcs., lattice defect methods 4-81476
- Mo (001), dissociative adsorption of O<sub>2</sub>, low energy ion scatt. study, adsorbate induced neutralisation effects 4-81078
- Mo (100) and MoS<sub>2</sub> (0001), CO coadsorption with S<sub>2</sub>, H<sub>2</sub>, and O<sub>2</sub>, LEED, AES and TDS studies 4-80407
- Mo, coadsorption of Cs monolayer and O on (100), electronic props., EELS, UPS, work function meas. 4-61787
- N<sub>2</sub>, chemisorption Al<sub>2</sub>O<sub>3</sub> supported Rh surfaces, IR spectra 4-81461
- NH<sub>3</sub>, on Ru (001) and Ru (1,1,10) surfaces 4-65572
- NO, on Ru (001) and Ru (1,1,10) surfaces 4-65572
- Na mordenite, of benzene, quasielastic neutron scatt. study 4-92537
- Na<sub>4</sub>(AlO<sub>2</sub>)<sub>8</sub>(SiO<sub>2</sub>)<sub>40</sub>·24H<sub>2</sub>O·Eu<sup>2+</sup>, adsorption of O<sub>2</sub>, fluorescence study 4-84511
- NaCl stepped surface, Au adatom, pot. energy calc. 4-80372
- Ni (001), of X, X-ray absorpt. near edge struct. results 4-66117
- Ni (100), adsorption of residual gases, electron impact effects 4-65543
- Ni (100), clean and with adsorbed O, surface vibr. dispersion curves, EELS study 4-80363
- Ni (100), coadsorption of CO and K, XPS, UPS, work function, and EELS meas. 4-92552
- Ni (100), Fe adsorption and growth, LEED and EELS studies 4-113808
- Ni (100), K-dosed, CO and D<sub>2</sub> adsorpt., XPS, UPS, TDS, EELS and work function studies 4-84509
- Ni (100), K-predosed, coadsorption of CD and D<sub>2</sub>, 4-92535
- Ni (100), N<sub>2</sub> adsorption, thermodynamic meas. 4-92563
- Ni (100), of K, coadsorption of K and D<sub>2</sub>, work function, TDS, XPS, UPS, AES studies 4-80398
- Ni (100), S-covered, adsorption of CO, vibr. spectroscopy study 4-108720
- Ni (100), surface electronic props. and poison/promotor effects for C adsorpt., AES study 4-85331
- Ni (110), adsorption of O<sub>2</sub>, AES study 4-98456
- Ni (110), H<sub>2</sub>(D<sub>2</sub>) adsorption, EELS study 4-65564
- Ni (110), molecular N<sub>2</sub> adsorpt., phase transitions obs. 4-88395
- Ni (110), of N<sub>2</sub> at low coverage, ion scatt. spectroscopy study 4-81080
- Ni (110), oxygen dosed, H<sub>2</sub>O adsorption, OH(ad) formation and orientation 4-66615
- Ni (111), adsorbed acetic acid and acetic anhydride, decomposition reactions, TPD and AES studies 4-114833
- Ni (111), adsorption and decomposition of NO, metastable quenching electron spectroscopy 4-92567
- Ni (111), dissociative adsorption and recomb. of CO, N<sub>2</sub>, SO, and O<sub>2</sub> 4-93559
- Ni (111), local adsorption site for S, angle-resolved AES study 4-92551
- Ni (111), of CO and CH<sub>3</sub>COCH<sub>3</sub>, UHV cell for Raman studies of gases adsorbed on metals 4-101947
- Ni, coadsorption of H<sub>2</sub> and CO, ion induced desorption study 4-92547
- Ni surface, of S and O on cylindrical crystals 4-61223
- Ni surface, polycryst., clean and S covered, low energy ion and neutral scatt. 4-81083
- Ni, surface segregation of S, annealing and O<sub>2</sub> adsorption effect (Japanese) 4-61932
- Ni-Fe, dissoln. and passivation, influence of S adsorpt. 4-71756
- Ni-Fe, dissoln. and passivation, influence of S adsorpt. 4-71757
- Ni<sub>14</sub> cluster, 14-atom, H atom interaction, MINDO/SR calc. 4-64647
- Ni<sub>60</sub>Fe<sub>40</sub> (100), O<sub>2</sub> and S<sub>2</sub> coadsorption, surface phases, LEED study 4-84506
- NiO-MgO solid solns., of CO, reactivity, spectrosc. obs. 4-113795
- NiO-MgO solid solns., of CO, reactivity, H<sub>2</sub> pretreatment effects, spectrosc. obs. 4-113796
- Ni(001) surface, dissc. adsorpt. of H<sub>2</sub>, London-Eyring-Polanyi-Sato model 4-62231
- O<sub>2</sub>, on Ag film, adsorption process study using surface plasmons 4-80383
- O<sub>2</sub>, adsorption and desorption, generation and feeding (German) 4-114822
- PD electrode of CO, IR refl. spectrosc. obs. 4-107348
- Pd (100), adsorpt. and catalytic reaction of H<sub>2</sub>O, O and H, EELS and LEED study 4-71969
- Pd (111), O<sub>2</sub> adsorption, AES, EELS, TDS, ESD and work function studies 4-80410
- Pd catalysts, monodisperse; adsorpt. and dissolution of H<sub>2</sub> 4-61220
- Pd thin overlayers on Nb (110) and Ta (110), CO adsorption 4-92533
- Pd-Al<sub>2</sub>O<sub>3</sub> catalyst plug of Pb/acid batteries, deterioration prevention 4-93613
- Pt (100) and (111), O<sub>2</sub> adsorption, XPS and TDS studies 4-80406
- Pt (110) chemisorbed S effect on H adsorpt. (French) 4-84504
- Pt (111), adsorption and decomp. of methyl isocyanide, EELS and thermal desorption study 4-108721
- Pt (111), cyclopentene adsorpt., cyclopentadienyl obs. by EELS and TDS 4-65558
- Pt (111), H<sub>2</sub> adsorption, vibr. props., EELS and inelastic neutron scatt. studies 4-113806
- Pt (111), H<sub>2</sub> adsorption location from corrugation anal. and He<sup>+</sup> diff. 4-65556
- Pt (111), of C<sub>2</sub>N<sub>2</sub>, coadsorption with H<sub>2</sub>, on (111), surface chem. 4-81478
- Pt electrode, of SO<sub>2</sub>, electrooxidation in conc. solns. 4-61219
- Pt electrodes, of tripeptide, AC admittance meas. 4-92538
- Pt electrodes, of tripeptide, kinetics and isotherms 4-92539
- Pt surface, K-promoted, NO adsorption 4-80403
- Pt surface, organic mol. adsorption 4-80409
- Ra, trace absorpt. and desorpt. on freshwater sediments and their mineral components 4-80376
- Re (0001), O<sub>2</sub> predosed, H<sub>2</sub>O adsorption, TDS study 4-113803
- Re (0001), of acetylene, vibrational electron energy loss spectroscopy (French) 4-75774
- Re (0001) and stepped surfaces, adsorption and dissc. of water, TDS, LEED, AES, ESD/AD studies 4-80401
- Rh (111), adsorption and decomposition of methanol, EELS and thermal desorption spectroscopy 4-92565
- Rh (111), Al+O<sub>2</sub> reactions, AES and LEED studies 4-89327
- Rh (111), CO and K coadsorption, HREELS, TPD, AES and LEED study 4-84508
- Rh (111) and (331), CO adsorption and desorption, XPS and SIMS study 4-65574
- Rh particles, adsorpt. of pyridine, Raman spectrosc. obs. 4-84954

## adsorption continued

- Rh surface, isotope exchange reaction of CO 4-81479
- Rh/Al<sub>2</sub>O<sub>3</sub> catalyst, highly dispersed, CO adsorption, EXAFS study 4-62243
- Ru (001) surface, coadsorption of K and CO, thermal desorption vibr. overtone spectroscopy 4-70565
- Ru (001) surface precovered with K, KOH form. and decomp. 4-93544
- Ru catalysts, adsorbed N<sub>2</sub>, temp. programmed desorption and isotopic study 4-93558
- Si (100), PH<sub>3</sub> and SiH<sub>4</sub> adsorption, saturation coverage 4-88392
- Si (100) 2×1, dissociative adsorption of water, IR spectra obs. 4-93557
- Si (100) with adsorbed O<sub>2</sub>, ab initio SCF calcs. 4-98440
- Si (111), annealed in high vac., electronic props., surface photovoltage study, effect of O<sub>2</sub> adsorption 4-80628
- Si (111), Cs adsorption, Cs valence electron photoemission studies 4-84505
- Si (111) (7×7), NO adsorption and reactions, EELS, LEED and AES studies 4-65562
- Si (111) surface, UPS rare gas titration for surface characteris. 4-88936
- Si (111)-Al(Ga)(In) abrupt interfaces, electronic props. 4-84696
- Si MBE layer, Sb adsorption, LEED, AES and TDS study 4-65560
- Si surface, H<sub>2</sub>O adsorpt. effect on charge exchange kinetics of slow electron states 4-84512
- Si/SiO<sub>2</sub>/Si<sub>3</sub>N<sub>4</sub>/electrolyte system, static and dynamic volt-ampere characs. (Russian) 4-65739
- SiO<sub>2</sub> powder, muonium hyperfine splitting, two freq. method anal. 4-65652
- SiO<sub>2</sub> suspension in polyacrylamide solns., rheological props., viscosity rel. to adsorpt. 4-74976
- SiO<sub>2</sub> thin films, chemical sputtering by Ar<sup>+</sup> ions and XeF<sub>2</sub>, adsorption F monolayer 4-93177
- SiO<sub>2</sub>, reactive film deposition, surface processes, planar magnetron sputtering 4-113798
- SnO<sub>2</sub>, of CO<sub>2</sub>, IR investigation 4-104603
- SnO<sub>2</sub> surface, chemical nature investig. 4-105019
- SnO<sub>2</sub>-PdO, of CO<sub>2</sub>, IR investigation 4-104603
- SnO<sub>2</sub>-PdO surface, chemical nature investig. 4-105019
- SnO<sub>2</sub>-SiO<sub>2</sub>, of CO<sub>2</sub>, IR investigation 4-104603
- SnO<sub>2</sub>-SiO<sub>2</sub> surface, chemical nature investig. 4-105019
- STiO<sub>2</sub>, of O<sub>2</sub>, photo-adsorption, ESR study 4-65550
- Ta (110), adsorption kinetics and absolute coverages of acetylene and ethylene, AES study 4-92546
- Ti, polycryst., O<sub>2</sub> adsorption, charact. and coadsorption with Pb 4-92568
- TiMn<sub>1.5</sub>, sorption of H<sub>2</sub> and D<sub>2</sub> at low press. (Japanese) 4-65552
- UO<sub>2</sub>, charact. of oxides formed by reaction with water IR and sorption anal. 4-74012
- W (001), reconstruction domains, finite size effects, adsorbed H<sub>2</sub> effects 4-88379
- W (001), surface reconstruction phase transition, model 4-88380
- W (100), EELS spectrum, effect of adsorption of gas mols. 4-93159
- W (100), H<sub>2</sub> and O<sub>2</sub> coadsorpt., temperature-programmed desorpt. study 4-84507
- W (110), activated N<sub>2</sub> adsorption, mol. beam studies 4-113811
- W (110), N<sub>2</sub> activated dissociative adsorpt., kinetic energy and angular dependence 4-113790
- W (110) film emitter, diffusion of H at low temp. 4-92549
- W (211), lattice steps and adatom binding, FIM study 4-108687
- W, clean and O covered, noble gas ion impact, adsorbate depend. ion neutralisation 4-81079
- W point cathodes, electron film emission instability, adsorption effects 4-61813
- W powders produced by plasma reduction, gas adsorpt., effect on electron work function and elec. cond. 4-70550
- W surface, absorption of Cu(Ag)(Be), work function changes 4-61202
- WC, electron stimulated desorption of O<sup>+</sup>, AES study 4-92569
- WS<sub>2</sub>, of n-alkanes and alkylbenzenes, gas chromatography 4-80371
- Zn anodic dissolution in alkaline electrolytes, three step model 4-103941
- ZnO (0001), interaction with methanol at low temp., XPS and UPS study 4-92542
- ZnO, adsorption sensitive elements, thermal characts. (Russian) 4-65549
- ZnO, of NO on (1010) surface, thermal desorpt. and photoelectron spectrosc. obs. 4-108705
- ZnO oriented crystal, cryst. violet dye adsorpt., press. effect 4-98442

## advertising

- Newport Button advertising premium item, large scale replication of combined three- and two-dimens. holographic images 4-112358
- optics in entertainment, conf., Los Angeles, CA, USA (Jan. 1984) 4-110802

## aerials see antennas

## aerodromes see airports

## aerodynamics

- see also hypersonic flow; jets; shock waves; supersonic flow; transonic flow; turbulence; wind tunnels
- aerodynamic characteristics of NACA 0012 airfoil in relation to wind generators 4-85355
- aeroelastic optimization of axisymmetric circular cylindrical shells for supersonic flow (German) 4-97607
- air quality improvement in open jet windtunnel 4-85393
- airfoil, lifting, Sears problem 4-75057
- annular flat-plate airfoil cascade, aerodynamic performance 4-64968
- application possibilities of wind energy systems 4-109722
- balloon flight dynamics 4-63436
- baseballs, aerodynamic drag crisis and its effect on flight 4-63440
- cine-camera optical accelerator rot. mirror aerodynamic drag determ. (Russian) 4-82845
- circular cylinder in crossflow, aerodynamic forces and press. meas., turbulence 4-103356
- circular rotating cylinder in crossflow, vibr. excitation mechanism 4-60437
- classification of different gas dynamic schemes by differential approx., two dimens. case 4-87748
- complex three-dimensional turbulent shear flows with longitudinal vorticity 4-69747
- computational method evolution 4-97595
- convective heat transfer coefficient in a highly circulating reheating furnace, aerodynamics props. 4-103318
- convergent-divergent expansion nozzles, ideal gas 2-dimens. flow (German) 4-83939
- cylinder, rot., in crossflow, aerodynamic forces 4-103337

## aerodynamics continued

- cylinder, rotating, in crossflow at two turbulence level, aerodynamic forces, separation 4-103357  
 fan, cross-flow, aerodynamics and performance 4-97597  
 finite triangular wing, hypersonic boundary layer flow 4-97606  
 floatation, basic aerodynamics 4-103355  
 flow round profile near rectilinear boundary, quasi theoretical profiles (Russian) 4-87749  
 fluid dynamics, numerical methods, book 4-110817  
 gas flow, 1-D, infinite Lie group of symmetry, entropy distributions 4-103358  
 gasdynamics with gravity allowance, operator-difference scheme stability 4-87753  
 heat transfer from heated wire at high subsonic gas velocities 4-83897  
 heat transfer in a corner flow with suction 4-112937  
 hovering flight, aerodynamic calc. 4-69780  
 hypersonic aerodynamics at low Mach numbers 4-60450  
 incompressible flows over infinite, swept wings, inverse mode boundary layer calcs. 4-112832  
 incompressible two dimens. pot. flow, compressor cascade, inverse boundary layer 4-97509  
 internal oscillating flows, noise and vibr. in high press. gas valves 4-97519  
 jet-aerodynamic surface interference effects, theoretical model 4-112970  
 jet-flap thrust recovery theory 4-75058  
 lateral aerodynamics of delta wings with leading-edge separation 4-79614  
 Laval nozzles, curved, two-phase flow, quasi-one dimens. method anal. 4-60476  
 lift airfoil, hypersonic flow, Navier-Stokes eqn. soln. 4-108088  
 lifting surfaces in unsteady flow, aerodynamic press., integral eqns. 4-64922  
 local solution existence to aerodynamics equations (Chinese) 4-112933  
 lunate-tail swimming propulsion, curved lifting line in unsteady flow, asymptotic theory 4-87750  
 natural gaseous inhomogeneities evolution 4-79619  
 nonequilibrium three-dimens. viscous shock-layer flows over complex geometries 4-112930  
 one-dimensional gas dynamics, infinite dimens. noncommutative Lie-Backlund algebra 4-75059  
 one-dimensional nonsteady gas flows 4-97593  
 packed spheres beds, heat transfer, local aerodynamics 4-97543  
 phenomena and paradoxes 4-113090  
 piecewise parabolic method in gas-dynamic simulations 4-69783  
 power characteristics and cavity formation in aerated agitations 4-112928  
 rarefied gases, subsonic flow, particle interaction at low Reynolds number 4-64969  
 road vehicles, drag, wake struct. flow visualisation study 4-97564  
 Shuttle Upper Atmosphere Mass Spectrometer experiment 4-82365  
 slender circular beam buffeting in axial turbulent flow 4-97495  
 sound generation by turbulent jets 4-69748  
 Space Shuttle heating analysis with variation in angle of attack and catalytic 4-82366  
 star shaped bodies, 3D, in rarefied gas, aerodynamic and thermal characteristics 4-69782  
 star-like body flight in rarefied hypersonic flow, aerodynamic and thermal characts. (Russian) 4-60458  
 subsonic flow past rectangular wings, discrete vortex scheme calcs. 4-64970  
 supercritical airfoil, self-sustained oscills. of a shock wave 4-103359  
 supercritical airfoil and wing design 4-91824  
 supersonic unsteady lifting surfaces, aerodynamic force, doublet point method 4-64975  
 swirl combustor flow meas. with and without combustion 4-103436  
 thin airfoil in subsonic flow, Dirichlet boundary-value problems, multiple scale soln. 4-97598  
 thin airfoil theory for planar inviscid shear flow 4-97594  
 three dimensional vortex flows, theoretical modelling 4-112889  
 throttling valve noise, aerodynamic sound level calc. 4-74807  
 time dependent aerodynamics, research review 4-87754  
 transonic straight cascade, unsteady aerodynamic press. coefficients computation 4-91823  
 turbulent shear flow, noise generation and propag. 4-60394  
 turbulent shear flows, aeroacoustics 4-91805  
 unsteady flow around airfoil 4-97567  
 viscous correction method for unsteady transonic flow about airfoils 4-112940  
 vortex chamber aerodynamics, flow pattern investigation 4-79601  
 water tunnel for aerodynamical studies 4-83920  
 windmills Betz optimum efficiency derivation 4-79617  
 wing aerodynamics in supersonic shear flow 4-97602  
 wing at large angle of attack, nonlinear hybrid vortex method 4-79615  
 XeCl excimer laser, aerodynamic device and elec. excitation system description (French) 4-102949

## aeroelasticity see elasticity

## aeronomy see meteorology; terrestrial atmosphere; upper atmosphere

## Aerosols see aerosols

## aerosols

## see also foams

- acoustic wave dispersion and dissipation 4-97745  
 Aitken nuclei evolution in urban area atmosphere (Spanish) 4-89476  
 aqueous aerosols, weakly absorbing, disruption and optical breakdown in intense light field 4-65108  
 Arctic haze, radiation absorption by combustion-generated C particles 4-105143  
 Arctic haze, vertical structure, net-flux radiometer meas. 4-105144  
 Arctic Haze during 1948-61 'Pirmarnig' weather reconnaissance flights, origin 4-77631  
 Arctic haze mapping by airborne LIDAR 4-110328  
 atmosphere; Arctic haze pollution measurement program (AGASP) 4-105722  
 atmosphere, 10  $\mu$ m cutpoint size selective inlet for hi-vol samplers 4-100049  
 atmosphere, aerosol conc. distrib. over Beijing city rel to synoptic pattern (Chinese) 4-66838  
 atmosphere, aerosol elemental composition in boundary layer at Boulder, Colorado, USA 4-67323  
 atmosphere, ambient aerosol composition determ. by PIXE 4-100031  
 atmosphere, Arctic haze microparticle size distrib. 4-105646  
 atmosphere, backscatt. determ. at 10.6  $\mu$ m 4-100728  
 aerosols continued  
 atmosphere, backscatter and attenuation meas. using CO<sub>2</sub> tunable coherent lidar 4-100763  
 atmosphere, backscattering at 10.6 microns, obs. made at Boulder, Colorado, USA 4-110246  
 atmosphere, characts. from bistatic lidar obs. of scatt. 4-77647  
 atmosphere, climate models using different aerosol types (Russian) 4-100723  
 atmosphere, composition temporal variations over Mauna Loa, Hawaii 4-77598  
 atmosphere, effects on IR imaging of sea surface temp. 4-67405  
 atmosphere, greenhouse effect 4-82228  
 atmosphere, ice nuclei rel. to cloud and microphysical struct. of mesoscale convective bands behind cold fronts 4-82199  
 atmosphere, industrial source complex dispersion model in rural setting, validation 4-77159  
 atmosphere; Lake Tahoe, USA, visibility and particle sources anal. 4-66828  
 atmosphere, latit. and seasonal effects in nuclear winter model 4-105674  
 atmosphere, light extinction model for aerosol meas. techniques 4-110251  
 atmosphere, marine boundary layer optical remote sensing method 4-100742  
 atmosphere, Mount St. Helens, volcanic plume disposal over USA and Atlantic 4-115482  
 atmosphere, optical depth and aerosol distrib. from sky brightness observations (Spanish) 4-115574  
 atmosphere, optical props. for mixed comp. aerosols 4-100726  
 atmosphere, particle size model for nitrate and sulphate aerosols 4-114981  
 atmosphere, pollutant characts. due to Space Shuttle launches 4-100022  
 atmosphere, pollutant transport, North America to North Atlantic Ocean 4-72197  
 atmosphere, props. of ice in anvil of winter maritime cumulonimbus cloud 4-62916  
 atmosphere, quartz content and elemental composition in US cities 4-100649  
 atmosphere, scatt. characts. of aerosol media with anisotropic particles, homogeneous spheres models use (Russian) 4-82235  
 atmosphere, temp. and radiation influenced by aerosol layer 4-67396  
 atmosphere, turbidity in India and atm. particulate matter 4-67395  
 atmosphere, visibility, suggested units 4-77629  
 atmosphere, volcanic aerosol from El Chichon, size and mass distrib. 4-115534  
 atmosphere at Barrow, Alaska, USA, giant particles 4-105644  
 atmosphere, El Chichon volcanic debris in Arctic atmosphere 4-105649  
 atmosphere, far IR backscatt., CO<sub>2</sub> lidar obs. at Pasadena, CA, USA 4-110247  
 atmosphere ice clouds, effects of crystals horizontal orientation on radiative props. (Chinese) 4-67397  
 atmosphere ice nuclei conc. in urban and rural environments 4-94223  
 atmosphere of Antarctica, aerosol content rel. to meteorological conditions 4-115547  
 atmosphere of Arabian Sea, heating due to radiation absorpt. by aerosol 4-94241  
 atmosphere of Arctic, particulate matter elemental composition observations 4-105647  
 atmosphere of Arctic, Western hemisphere, variations 4-62905  
 atmosphere of Arctic Ocean, origin of haze and giant particles 4-105645  
 atmosphere of Crimea coast, haze chem. composition (Russian) 4-100685  
 atmosphere of Grand Canyon, Arizona, USA, pollution, particulates, and visibility 4-115564  
 atmosphere transparency, long term variations derived from extinction meas. 4-110253  
 atmosphere-ocean system, radiative transfer, azimuthally depend. matrix-operator approach 4-72695  
 atmospheric, ice nucleus meas. using continuous flow chamber 4-62980  
 atmospheric, LAMMA and electron microprobe anal. 4-81501  
 atmospheric, microstruct. reconstruction from multifreq. sounding data 4-85769  
 atmospheric, wavelength depend. spectral extinction 4-72696  
 atmospheric heat plume characteristic parameter determ. by lidar (Spanish) 4-89483  
 atmospheric particle size meas. probe (French) 4-85761  
 atmospheric trajectories during AGASP 4-105655  
 Beijing, China, aerosol composition during summer, vertical, temporal and particle size distrib. 4-100041  
 benzo(a)pyrene tagged aerosol, generation and number conc. determ. 4-89351  
 binary gas mixture in nearly free mol. state, aerosol particles, thermophoresis 4-60483  
 bipolar diffusion charging of monodisperse particles 4-62254  
 blackness (light absorbing ability) rel. to filter blackening 4-62252  
 blood serum, analytical plasma spectrometry, dry aerosol dispersity 4-100215  
 Brownian coagulation in free-molecule regime, size distrib. 4-99847  
 buildings boundary-layer flows, near-wave parameters 4-79599  
 carbonaceous aerosol particles in lower stratosphere, discovery, origin, and implications 4-105659  
 cascade impactor samples collected over Pacific Ocean, PIXE anal. 4-100029  
 compressed gases in centrifugal precipitator, droplet removal 4-60482  
 computer study of clouds and aerosol vertical distribution 4-110330  
 conference on atm. radiation at Toronto, Canada (June 1981) 4-90300  
 conference on Mount St. Helens 1980 eruptions, at Washington, DC, United States (November 1980) 4-101575  
 deposition in human respiratory tract, PIXE investigation 4-105066  
 El Chichon volcanic dust cloud, twilight optical studies at Ahmedabad, India 4-89969  
 EDX systems in STEM, multielement salt standards, for calibration 4-72025  
 electrostatic precipitators, aerosol particle charging by free electrons, charge potential limit model 4-99853  
 elemental anal. of PIXE, FAST, LIPM and mass study 4-99896  
 ER-2 airborne LIDAR, NASA/CNES potential project 4-110326  
 Mt Etna, 1983 eruption, exchange of volatiles, radioactivity meas. (French) 4-115365  
 Faeroe Islands, marine and nonmarine transported aerosols anal. using PIXE 4-100034  
 fibrous aerosol particles, bipolar diffusion charging, elec. mobility and charge meas. 4-89348

**aerosols continued**

- fibrous filter, aerosol removal as function of particle size and vel. 4-105149
- fibrous particles, bipolar diffusion charging, theory 4-89347
- filters for nuclear process plants 4-64211
- flowing media, velocity distrib. meas. by laser beam, appls., aerosol introduction into fluid 4-97718
- fusion energy systems, potential aerosols characterisation 4-107016
- fusion reactors, activation product aerosol formation during accidents 4-111783
- gas-solid, Joule-Thomson effect statistical thermodynamics 4-65048
- Goteborg, Sweden, airborne particles distrib. determ. using EDXRF and PIXE methods 4-100033
- ice-forming nuclei in continental-maritime air 4-89971
- in-plant aerosols, PIXE anal. 4-105071
- in indoor air, aerosol size distrib. rel. to Rn daughters activity 4-93915
- interparticle forces and quasi-stationary equilibrium hypothesis 4-89346
- IR and optical propag., effects of meteorology on marine aerosol (*French, English*) 4-67400
- Lamb's Dust Veil Index, formulation 4-105699
- laser Doppler velocimeter using variable-fringe-spacing for particle number density meas. 4-108143
- laser modification of thermophoretic deposition of aerosol for optical fibre manufacture 4-60186
- liquid, instrument for meas. mass median diameter and total quantity in gas stream 4-60571
- LMFBR safety anal., core expansion studies, CARAVELLE expts. and IRIS code 4-78729
- LMFBRs, Na aerosols and puddles, fuel, fission products and Na release 4-91084
- marine aerosols in boundary layer, mixed-layer model appl. 4-115497
- marine atmosphere, spray field above wind-driven waves 4-67306
- marine atmosphere near Hawaii, sea salt conc., vertical distrib. 4-77591
- Mars, threshold wind velocity for particle entrainment 4-101222
- Mediterranean and Atlantic ocean, atmospheric aerosol particles transport determ. by PIXE 4-100035
- Mediterranean atmosphere, soil-sized particulates, ferrimagnetic minerals distrib. 4-100715
- metal body, electrification in an aerosol stream with dispersed particles 4-79651
- mica microfilter cascade fractionator for aerosol size distrib. 4-96394
- microparticles volatilisation and ionisation, laser-induced, mass spectroscopic analysis 4-105088
- migration displacement of particle, in turbulent flow with transverse shear 4-79640
- Milan aerosol monitoring by means of PIXE analysis 4-100040
- Mount St. Helens, 1980 May 18 eruption effect on tropopause region sulphate layer 4-105695
- Mount St. Helens, 1980 May 18 eruption plume dispersion 4-105691
- Mount St. Helens, 1980 May eruptions, atm. perspective 4-105513
- Mount St. Helens, aerosol props. of 1980 May eruptions, sunlight extinction anal. 4-105696
- Mount St. Helens, stratospheric aerosols due to 1980 eruptions, climatic implications 4-105706
- Mount St. Helens, stratospheric aerosols from 1980 May eruptions, scatt. sunlight obs. 4-105721
- Mount St. Helens, stratospheric clouds, physical and chem. processes modelling (May-June 1980) 4-105692
- Mount St. Helens 1980 eruptions, stratospheric aerosols, global distrib., lidar obs. 4-105689
- Mount St. Helens 1980 eruptions, stratospheric aerosols time var. 4-105685
- Mount St. Helens 1980 May eruptions, stratospheric tephra and aerosols, comp. and plume characts. 4-105687
- Mount St. Helens dust cloud (1980) over Wyoming, particles size and conc. evolution 4-105686
- Mount St. Helens eruption plumes (1980) at stratospheric altitudes, aerosol precursor gases anal. 4-105684
- Mount St. Helens stratospheric aerosol (1980), effect on sunlight transmission 4-105688
- Mount St. Helens stratospheric aerosols (1980), extinction meas. 4-105717
- nonpherical aerosol particles, light scatt. props. 4-96801
- nuclear war, climatic consequences, computational expt. (*Russian*) 4-67389
- optical aerosol breakdown producing extended plasma region, collective mode 4-113187
- optical breakdown, low-threshold; comprehensive diagnostics 4-65109
- particle, Brownian rotation, EM radiation absorpt. modulation 4-85341
- particle counting, multiple counting statistics 4-58929
- particle deposition from laminar boundary layer, wall suction and thermophoresis effect 4-97474
- particle deposition in straight tube with abrupt obstruction 4-89350
- particle impaction in the conducting airways of the lung 4-100213
- physico-chemical characteristics over Beijing 4-62906
- PIXE, conjunction with inertial spectrometer aerosol sampler, use in particle size meas. 4-99903
- PIXE's analytic appls., conference, Heidelberg, Germany (July 1983) 4-95034
- PIXE anal. in aerosol research 4-99901
- PIXE detection limits for some aerosol collection substrates by excitation with protons and  $^3\text{He}^{++}$  ions from a 3 MV tandem accelerator 4-99904
- PIXE spectra, least-squares fitting with digital filter 4-105062
- pollutant trajectories, aerosol conc. in Norwegian Arctic, sources 4-105140
- precipitation sampler intercomparison 4-100831
- production from aq. sols. using spinning top generator 4-62253
- radiant heat flux, effect of anisotropic scatt. 4-103182
- radioactive aerosol formation due to coolant leaks 4-106882
- radioactivity anal. using compressible flow capillary system 4-86975
- radioactivity registration stations, aerosol samples, elemental composition by PIXE 4-100030
- random fluctuations, effects on behaviour 4-82189
- Saharan dust in atmosphere, mobilisation, transport, and deposition, conference, Gothenburg, Sweden (1977 April 25 to 28) 4-90302
- Saharan dust incursion over the Tyrrhenian Sea 4-94180
- sea salt nuclei over ocean surf zone, size distrib. 4-115406
- single-breath deposition of jet-nebulized saline aerosol 4-100191
- size characteristics in nuclear research centre working areas, radiation protection appl. 4-96296
- size distrib. determ. from aureole around point source, theory 4-62961

**aerosols continued**

- size distrib. from aureole around point source, solar blind radiometer meas. 4-89991
- stratosphere, UV polarization inversion,  $\text{O}_3$  and aerosol profiling 4-62960
- stratosphere, extinction meas. by SAM II and SAGE 4-100805
- stratosphere, volcanic aerosols, effects on surface temp. 4-94238
- stratosphere at Davis, California, temporal var. effect on sunlight at ground 4-77599
- stratosphere  $\text{H}_2\text{SO}_4$  aerosols, contrib. of small-volume S-rich volcanic eruptions 4-105511
- stratosphere volcanic aerosols, optical depth and mass loading, SAGE and SAM II obs. 4-100692
- stratospheric aerosol and gas expt. instrument, satellite-based (SAGE II) 4-115587
- stratospheric aerosol layers, mid-latitude enhancement by El Chichon eruptions 4-94190
- stratospheric dust from El Chichon, optical sky polarimetry and photometry at Mauna Loa 4-62950
- Sweden, south, long range aerosol transport, multivariate statistical technique appl. to PIXE data 4-100037
- telecommunication exchange buildings, indoor and outdoor air, fine particle aerosols characterisation 4-100038
- trace element analysis, large scale intercomparison of different analytical methods 4-99897
- trimethylsilyl aerosol, thermodesorption of water (methanol), mass spectrometric investig. 4-62259
- tropospheric circulation patterns during AGASP 4-105654
- tropospheric trace species transport and conc. meas. using  $\text{CO}_2$  coherent IR laser mission, technology needs 4-100762
- turbulent dispersal of heavy particles 4-72680
- ultrafine, diffusion battery design and calibration 4-89349
- ultrafine chainlike or fibrous type particulate aerosols, Brownian coagulation and charge effect 4-99846
- W United States, atm. S conc., principal component anal. 4-100023
- Venus atmosphere,  $\text{SO}_2$  and submicron haze vars. as evidence for active volcanism 4-67660
- volcanic eruptions effect on climate 4-105514
- volcanic particles effect on sunlight extinction, climatic implications 4-105705
- water, nonselective preconcentration, PIXE anal. 4-100054
- water aerosol, polydisperse, laser-induced bleaching, microstruct. effects 4-79241
- water drop collisions, charge separation, contact-balloelectric mechanism 4-72676
- work environment aerosols, PIXE anal. 4-105070
- working environment aerosols in lead battery factory, toxicity monitoring by PIXE and AAS 4-105072
- Ag clusters, aerosols heating effects determ. 4-74389
- Ag clusters, aerosols, heating effects determ. 4-74389
- $^{210}\text{Bi}$ , aerosol radioactivity meas., Covasna mofette atmosphere (*Rumanian*) 4-72674
- $\text{H}_2\text{O}$  weakly absorbing aerosol, elevated-transmission zone form. upon initiation of laser discharge 4-77633
- $\text{H}_2\text{SO}_4$ , ambient aerosol, S losses, PIXE anal. 4-99876
- $\text{NH}_4\text{HSO}_4$ , ambient aerosol, S losses, PIXE anal. 4-99876
- $(\text{NH}_4)_2\text{SO}_4$ , ambient aerosol, S losses, PIXE anal. 4-99876
- Na surface fires in reactor containment, convection current computation, KONVEC 4-91083
- Pb particulate emission and dispersion from roadway, line-source models 4-66832
- $^{210}\text{Pb}$ , aerosol radioactivity meas., Covasna mofette atmosphere (*Rumanian*) 4-72674
- $^{210}\text{Pb}$ , aerosol radioactivity meas., Covasna mofette atmosphere (*Rumanian*) 4-72674
- Pu bearing, scanning transmission electron microscopy examination 4-73982
- Rn daughter attachment, indoor aerosol size distrib., automatic meas. system 4-93914
- Rn daughters, deposition rates on indoor surfaces 4-93917
- Rn daughters, turbulent plateau in rooms and mines 4-93920
- Rn daughters aerosol, activity size distrib. in buildings, cascade impactor meas. 4-93918
- Rn daughters in indoor air, aerosol particle conc. rel. to ventilation system 4-93922
- $^{220}\text{Rn}$ , A=220, 222, daughters in indoor aerosols, particle size distrib. 4-93921
- $^{99\text{m}}\text{Tc}$  Pseudogas for diagnostic studies in the lung 4-93861

**aerospace**

- see also aerospace computing; aerospace control; aerospace instrumentation; aerospace propulsion; aerospace simulation; aerospace test facilities; aircraft; space research; space vehicles; terrestrial atmosphere structures, conf., Boston, MA, USA (Nov. 1983) 4-73167
- Ni-Cd aerospace batteries, reliability determined from survival data 4-105104

**aerospace applications of computers see aerospace computing****aerospace biophysics**

- biodynamic test devices and methods, AGARD report 4-78058
- Biostack Experiments, HZE particles effects on biological systems 4-100334
- electrophoresis experiments on Salyut-7 orbiting space station, holographic interferometric obs. method 4-74468
- electrophoresis operations for pharmaceutical processing 4-72442
- linear accelerator system, microcomputer controlled, space flight induced vestibular changes appl. 4-89867
- military helicopter flight, disorientation, psychology of visual perception 4-85528
- military helicopter flight associated hearing loss, comparative tests on pilots 4-85529
- military helicopter operations, aeromedical support, conf., Soesterberg, Netherlands, (June 1984) 4-82597
- military helicopter operations, visual problems 4-85527
- red cells aggregation in space, meas., NASA Space Shuttle project 4-109970
- space environment, effect on man (*Japanese*) 4-89792
- Spacelab-1 mission, life sciences expt. packages 4-77408
- thermal strain measurement techniques, aircrew appl. 4-85526
- TLD for cosmic radiation dose meas. for orbital stations 4-105346

aerospace computer control

see also aerospace computing  
autonomous tracking of minor celestial body during spacecraft flyby, algorithm 4-105865

aerospace computing

see also aerospace computer control  
aerodynamics, computational method evolution 4-97595  
environmental and thermal control for space vehicles, conf. Toulouse, France (Oct. 1983) 4-73162  
gas-loaded variable conductance heat pipe performance uniaxial model, effects of vapour flow friction and inertia, use in spacecraft thermal modelling 4-74846  
Infrared Astronomical Satellite, computerised data processing 4-82421  
interplanetary trajectory design, optimum two-impulse transfers 4-115676  
weather radar simulator, for pilot training 4-85794

aerospace control

see also attitude control  
civil aircraft flight control data, appl. to wind meas. 4-105759  
conference on astrodynamics at Lake Placid, USA (August 1983) 4-78043  
deployable optical systems, conf., Los Angeles, CA, USA (Jan. 1983) 4-73138  
environmental and thermal control for space vehicles, conf. Toulouse, France (Oct. 1983) 4-73162  
Infrared Astronomical Satellite spacecraft thermal design and performance 4-77717  
interplanetary navigation 4-110493  
interplanetary trajectory optimisation (Japanese) 4-94548  
space station thermal control using heat pipes 4-74845  
spacecraft guidance and control techniques, conf., Florence, Italy (Sept. 1983) 4-73164  
Venus Orbiting Imaging Radar mission, aerobraking 4-82376

aerospace engines

jet engine turbines, ceramic technology for powerplant 4-104758

aerospace instrumentation

see also aircraft instrumentation; Langmuir probes  
autonomous satellite navigation using the stellar horizon atmospheric dispersion sensor 4-94555  
circular-scan photoconductor streak camera for spaceborne laser ranging applications 4-107725  
coded aperture  $\gamma$ -ray telescope, statistical anal. 4-67635  
CW diode laser instrumentation for geosynchronous orbits rendezvous and docking manoeuvres 4-107686  
grazing incidence telescope for X-ray astron. 4-67626  
groundbased transportable satellite laser ranging, space/airborne system complement 4-110324  
high dose MOS dosimeter for space use, design criteria 4-63026  
Infrared Astronomical Satellite spacecraft thermal design and performance 4-77717  
Landsat 4 onboard navigation using NAVSTAR GPS 4-72848  
LIDAR, spaceborne, atmospheric investigations 4-110325  
LIDAR, spaceborne, meteorology and environmental studies appl. 4-110321  
OTS-2 satellite in geostationary orbit, thermal testing experience 4-83656  
ROSAT X-ray telescope thermal design features 4-85879  
space based laser ranging systems, design 4-107726  
space telescope optical payloads accurate thermal control 4-85880  
spaceborne laser ranging transmitter, ultra-short pulses generation 4-107724  
Spacelab 2 telescopes with coded system, data processing of imperfectly coded images 4-67634  
wind meas. with coherent laser radar at 10 micron 4-107685

aerospace propulsion

see also aerospace engines  
interstellar travel using laser-pushed lightsails 4-82364  
nuclear electric propulsion missions 4-115675

aerospace simulation

see also aerospace test facilities  
cryopumping technique appl. 4-101861  
environmental and thermal control for space vehicles, conf. Toulouse, France (Oct. 1983) 4-73162

aerospace test facilities

see also wind tunnels  
biodynamic test devices and methods, AGARD report 4-78058  
environmental and thermal control for space vehicles, conf. Toulouse, France (Oct. 1983) 4-73162

a.f. amplifiers see audio-frequency amplifiers

AFMR see antiferromagnetic resonance

afterglows

active N, atm. press., emission spectrosc. anal. appls. 4-79855  
alkali halides solid in microwave-induced plasma afterglow, lattice atomisation, temp. depend. 4-79862  
inert gases,  $I_2^+$ ,  $A^+$ ,  $X^+$ ,  $T_2^+$  emission 4-112190  
recombination process in pulse discharge plasma, spectrosc. investig. 4-79782  
transparency of a laser plasma during afterglow 4-75166  
Ar afterglows, conversion reaction rate coeff. and ambipolar diffusion coeff. meas. 4-79877  
CO<sub>2</sub> TEA laser, electron density of afterglow of pulsed discharge and UV photoionisation, meas. using microwave interferometer (Chinese) 4-87315  
CuI laser with supraoptimal wall temp. metastable Cu atom conc. relax. in afterglow 4-60021  
H afterglow plasma, central struct. of H<sub>2</sub> line at low electron densities 4-59674  
HF laser mixtures, electron density of afterglow of pulsed discharge and UV photoionisation, meas. using microwave interferometer (Chinese) 4-87315  
He<sub>2</sub><sup>+</sup> afterglow, Rydberg dissociative recombination 4-81421  
Hg halides, electron impact and at. and mol. collisions in discharge, spectra (Chinese) 4-59830  
<sup>86</sup>Kr afterglow plasma, Kr <sup>2</sup>P<sub>2</sub> state at. binary collision ionisation rate const. determ. 4-91335  
Pb, metastable, relax. in decaying plasma 4-108236  
PbO<sub>2</sub> excitation luminescence under powerful laser excitation 4-109235  
SiBr<sub>4</sub><sup>+</sup>, rare gas flowing afterglows UV emission spectra 4-69095

age (Earth) see geochronology

age determination, radioactive see radioactive dating

age hardening see precipitation hardening

ageing

see also precipitation hardening; strain ageing  
accreting bodies subject to aging, nonlinear creep problems 4-79467  
acrylonitrile-butadiene copolymers,  $\alpha$  relax. kinetics near glass transition temp. 4-81231  
alloy single crystals, age-hardened, fatigue behaviour 4-99563  
basalt glass fibres, microhardness and microbrittleness 4-84342  
copolymer system, rubber plasticised, processing influence on morphology-prop. relationships (German) 4-85209  
cycloaliphatic epoxy resin,  $\gamma$ -irrad. under vacuum, phys. props., ageing 4-103800  
deformation kinetics of ageing materials 4-60278  
dielectric materials, measurements anal. appls., conf., Lancaster, England (Sept. 1984) 4-106120  
dielectrics, electrofracture mechanics and aging 4-93007  
electronics ageing mechanisms, neutron and  $\gamma$ -ray effects, nuclear power plant instrumentation 4-59363  
epoxy resins, crosslinking at interfaces, internal refl. spectrosc. obs. 4-104988  
epoxy resins, interaction with water, glass transition temp. depression 4-89157  
ferroelectric materials, electric aging, low freq. polarisation relaxation (Russian) 4-99010  
granular films, relax. phenomena 4-108747  
laser diodes, for undersea transmission systems, screening method 4-69477  
latent image stability, latensifying effect of temp. 4-78397  
lead acid batteries, electronic checking of charge state and ageing 4-114901  
low C, Al-killed, reversion and subsequent re-age-hardening 4-93308  
LV thermoplastic/thermosetting insulating materials for industrial use, laboratory tests (Italian) 4-99410  
nuclear plant electrical components, aging and seismic qualification correlation 4-59301  
nuclear power station cables, gamma radiation and thermal ageing of polyethylene insulation 4-75526  
nuclear reactor organic materials, accelerated ageing tests for radiation degradation prediction 4-83233  
optical fibres, hydrogen related degradation, system implications and practical solutions 4-103019  
phthalen films, amorphous vacuum deposited, crystn. and optical props. 4-71565  
polyacetylene/metal Schottky barrier diodes 4-65742  
polycarbonate, hot water ageing, form. of internal cracks and microvoids 4-81225  
polyethylene, crosslinked low density, morphology influence on treeing probability 4-113351  
polyethylene, elec. ageing effects, TSC and electroluminesc. meas. 4-109127  
polyethylene terephthalate films, photooxidation and ageing, ESCA and contact angle obs. 4-61806  
polymers, strength and deform. under artificial weathering (German) 4-89229  
polymers, thermal ageing kinetics, thermogravimetric testing 4-71859  
radiation aging of insulating resins, electrical effects, 4-111621  
reactor electrical equipment, qualification aging, German philosophy and practice 4-86961  
secondary cells, Ni sinter plates, electrochemical impregnation bath ageing of Ni(OH)<sub>2</sub> 4-72067  
slag glass fibres, microhardness and microbrittleness 4-84342  
space vehicle thermal central materials, effects of ultraviolet and oxygen plasma environments 4-85264  
steel, alloy, secondary hardening mechanisms 4-99396  
steel, austenitic stainless,  $\gamma'$  precip., influence on elastic limit (French) 4-81200  
steel, austenitic stainless, Alloy 800, low cycle fatigue at 600°C, influence of dislocation-precip. interaction 4-99529  
steel, austenitic stainless, containing Ti and Al, grain boundary precip. 4-99385  
steel, austenitic stainless, creep and plastic strains, under side steps of tension and torsion, at 593°C 4-76825  
steel, austenitic stainless, creep and plastic strains, under stress reversal in torsion, at 593°C 4-76826  
steel, austenitic stainless, dual-ion irrad., microstruct. evolution under various He injection schedules 4-98150  
steel, austenitic stainless, electron irrad.-induced struct. phase transformations 4-109418  
steel, austenitic stainless, precipitation kinetics, selective dissolution methods 4-114527  
steel, austenitic stainless, sensitised, Cr depletion in carbide vicinity rel. to heat treatment 4-71654  
steel, austenitic stainless, thermal and radiation-stimulated ageing, kinetics 4-66354  
steel, Cr-Mn austenitic, thermally aged, phase instability, precip. reactions 4-109410  
steel, Cr-Mo-V-W, ferritic, impact props., effect of specimen size and Ni content 4-104848  
steel, H embrittlement by cathodic charging 4-66420  
steel, high Cr, impurity redistrib. and mech. props. during 475°C ageing (Russian) 4-93317  
steel, low C, Al killed, decomp. of Mn-C dipoles during quench ageing, resist. obs. 4-71661  
steel, low C, carbide precip. during ageing treatments 4-114531  
steel, low C, deep drawing cold-rolled sheet prod. by continuous annealing, control of steel chem. 4-114565  
steel, low C, dual-phase, continuously annealed, effect of prior cold rolling 4-66350  
steel, low C, quenched, precip. kinetics 4-99394  
steel, maraging, Ni, fracture toughness, effect of treatment condition 4-76856  
steel, maraging, ultrahigh strength, delayed failure 4-93402  
steel, mild, SCC in NaH<sub>2</sub>PO<sub>4</sub> soln., effect of heat treatment and C 4-89167  
steel, Mn-Al, austenitic precipitation, fine structure after annealing (Russian) 4-104787  
steel sheet, continuous annealed cold-rolled, overaging treatment and ductility, interstitial atom supersaturation (French) 4-89096

## ageing continued

- steel sheet, plastic bending instability 4-99461  
 Ag-Mg(Cu), internal oxidation mechanism 4-93305  
 AgBr photographic model emulsion physical ageing (*Russian*) 4-82854  
 Ag,MnAl, Silmanal, magnetic phase growth (*Russian*) 4-109014  
 Al/Sn<sub>2</sub>O<sub>3</sub>/Al capacitor struct., dielec. props. and thermoluminescence 4-76047  
 Al-Cu (2 to 5 wt.%), precip. effects on thermopower 4-99384  
 Al-Cu (3.6 wt.%), aged, coarsening kinetics of rod shaped  $\theta$  particles, LSW theory 4-71652  
 Al-Cu (3.76 wt.%), Rheocast, ageing characts. rel. to incomplete homogenisation 4-109444  
 Al-Cu-Li-Cd, 2020, microstruct., fracture toughness and SCC 4-76851  
 Al-Cu-Mg alloy D16 plates, struct. strength, chem. comp. and heat treatment effects 4-61986  
 Al-Li, microcrystal evolution, DSC obs. 4-71659  
 Al-Li, nucleation, growth and coarsening of precipitates 4-81202  
 Al-Mg, ageing, metastable phases in early stages of precip., DSC and resist. obs. 4-71656  
 Al-Mg (10 wt.%), extrusion and mech. props. of compacts prep. from rapidly solidified powders 4-66395  
 Al-Mg-Si, creep life prediction, long-time, role of microstruct. instability 4-114622  
 Al-Mg-Si-Sn, ageing, clustering process rel. to Sn addition, elec. resist., TEM obs. 4-114529  
 Al-Sc (0.3 at.%) alloy, ageing, precipitation obs. (*Russian*) 4-104786  
 Al-Zn (3.5, 5.3 wt.%), GP zones, size distrib. 4-76779  
 Al-Zn alloy, quenched, dynamical scaling of struct. function 4-113659  
 Al-Zn dilute alloys,  $\alpha_2$ , Zn rich precipitate shape, small angle neutron scatt. studies 4-114547  
 Al-Zn-Mg, 7075-T651, fatigue crack growth, effect of short-term heating cycles 4-99484  
 Al-Zn-Mg, fatigue crack closure in 7475, microstruct. and ageing effect 4-62032  
 Al-Zn-Mg (4.25, 2.75 wt.%), SCC by slow strain-rate method 4-66495  
 Al-Zn-Mg alloy, quenched, dynamical scaling of struct. function 4-113659  
 Al-Zn-Mg alloys, struct. and mech. props., effect of low-temp. thermomech. treatment 4-66352  
 Al-Zn-Mg-Cu, precip. and quench sensitivity, effect of Cu additions 4-85155  
 Al<sub>2</sub>O<sub>3</sub> anodised films, breakdown statistics 4-109128  
 Al<sub>2</sub>O<sub>3</sub>.nH<sub>2</sub>O thin films, ageing, elec. struct. and moisture response characts., sensor apps. 4-86393  
 Au-Sn surface diffusion in air at room temp. 4-98459  
 BaTiO<sub>3</sub> crystals,  $\gamma$ -irradiated, with equilb. domain struct., polarisational state 4-76395  
 Be, acoustic emission due to deform. (*Russian*) 4-92304  
 Be, microplasticity, grain size and heat treatment effects (*Russian*) 4-104809  
 Cd,Hg<sub>1-x</sub>Te/In system, current noise in contact regions, defect influences 4-88595  
 CdSe photoelectrochemical solar cells, lifetime improvements 4-99969  
 CdSe-Al-Ni shape memory alloy, martensitic transform., effects of parent phase ageing 4-66334  
 $\beta$ -Cu-Al-Zn (8.7, 12.0 wt.%), with reversible martensite in struct., effect of ageing on damping capacity 4-109452  
 Cu-Al-Zn system, high damping  $\beta$  alloys, effect of ageing in martensite condition on mech. props. 4-114588  
 Cu-Be (1.0 wt.%), aged, twinned microstruct. 4-89070  
 Cu-Be alloy, struct. transform. mechanisms during ageing, internal friction and resist. obs. 4-114536  
 Cu-Co alloys, Co precipitate coarsening, electron microscope studies 4-114544  
 Cu-Fe (1.59 wt.%),  $\alpha$ - $\gamma$  martensitic transform: of Fe particles, magnetisation obs. 4-66335  
 Cu-In, precip. of  $\delta$ -phase on ageing 4-81201  
 Cu-Ni-Mn alloy, intergranular precipitation and ageing phenomena 4-114550  
 Cu-Ni-Si, cellular precip., effect of B and P additions 4-66342  
 Cu-Ni-Sn (9, 6 wt.%), ageing, internal friction, Young's modulus, modulated structure 4-66362  
 Cu-Ni-Sn alloys, spinodal decomposition, applied stress effects 4-114551  
 Cu-Ni-Sn spinodal alloys, deformation behaviour, ageing treatment effects 4-114628  
 Cu-Ni-Sn system, supersaturated solid soln. decomposition 4-81210  
 Cu-Sn (14.8%), austenitic and martensitic phase, thermally activated processes, kinetics 4-61963  
 Cu-Ti (3.5 wt.%), age hardening 4-76782  
 Cu-Ti-Cr (4, 0.5 wt.%), ageing, internal friction, Young's modulus, modulated structure 4-66362  
 Cu-Zn-Al, shape memory alloys, ageing and stabilisation of martensite 4-109441  
 Cu-Zn-Al (25, 6 wt.%), isothermal decomp. of  $\beta'$  phase 4-99387  
 CuAl<sub>2</sub>, second-phase particles, dissoln. rates in various microstruct. 4-89059  
 CuBe, age hardened, discontinuous flow studies, low temp. 4-113520  
 Cu<sub>2</sub>MnAl, Heusler alloy, decomposition during isochronal annealing 4-61916  
 Cu<sub>2</sub>O/CuO selective surface optical props. and surface composition 4-72170  
 $\beta$ -CuZn, martensite start temp., effect of Ti additions 4-61928  
 (Fe,Ni)<sub>3</sub>V alloy, long-range ordered, strain rate and ageing effect on mech. props. 4-109501  
 Fe-base metallic glasses, thermal embrittlement model 4-89098  
 Fe-Cr, spinodal decomposition, small angle neutron scatt. studies 4-114552  
 Fe-Cr-Al(-Y), precip., small-angle neutron scatt. study 4-93304  
 Fe-Cr-Co (12 wt.%) permanent magnet alloys, mag. props., effect of alloying 4-84771  
 Fe-Cr-Co alloys, spinodal decomposition, atom probe field ion microscopy studies 4-114553  
 Fe-Ni-Cr-C, Ti-modified, void swelling, pre-irrad. ageing effects 4-104798  
 Fe-Ni-V(-Mo) alloys, martensite ageing, positron annihilation studies (*Russian*) 4-104695  
 $\alpha$ -Fe(-C), H-induced grain boundary fracture, effect of C 4-93403  
 Fe(-C), SCC in NaH<sub>2</sub>PO<sub>4</sub> soln., effect of heat treatment and C 4-89167  
 FeCo based alloys, strength and mag. props. rel. to cold rolling and heat treatment 4-98918

## ageing continued

- Fe<sub>2</sub>Fe<sub>3</sub>Sn<sub>0.4</sub>N<sub>0.7</sub>C<sub>0.3</sub> ferromag. material for magnetic recording 4-104464  
 $\gamma$ -Fe<sub>2</sub>O<sub>3</sub>-Fe<sub>2</sub>O<sub>4</sub> thin films, coercivity study 4-114145  
 InGaAsP/InP 1.3  $\mu$ m buried crescent laser diode, degradation mechanism 4-96915  
 InGaAsP/InP buried crescent laser diode emitting at 1.3  $\mu$ m, high temp. CW operation 4-112427  
 InGaAsP/InP lasers, failure modes due to adhesives 4-107678  
 LiF crystals, annealed and aged, dislocation behaviour 4-103759  
 Li<sub>3-x</sub>Si<sub>2-x</sub>Y<sub>2-x</sub>O<sub>4</sub> solid electrolytes, ion trapping and conductivity 4-108648  
 Li<sub>3-x</sub>Zn<sub>1-x</sub>GeO<sub>4</sub> solid electrolytes, ion trapping and conductivity 4-108648  
 Mn-Cu, high-damping-capacity alloy, martensitic and mag. transitions after powder metallurgical prep. (*Russian*) 4-109403  
 NbN/Pb Josephson tunnel junctions with plasma oxidized barriers, annealing stability 4-84746  
 Ni-Al, recrystn. during rapid elec. heating 4-66347  
 Ni-Al thin foils, pre-martensitic phase, electron diff. study 4-114518  
 Ni-based superalloys,  $\gamma'$  particles, TEM and small angle neutron scatt. studies 4-93313  
 Ni-Cr base alloys, creep behaviour and microstruct. 4-71705  
 Ni-Cr-Al, recrystn. during rapid elec. heating 4-66347  
 Ni-Cu (22 at.%), annealed and quenched, creep behaviour and miscibility gap 4-66387  
 Ni-S, electrodes for alkaline electrolysis of water, microscopic and spectroscopic study 4-113766  
 Ni-Ti foils, electron irradi., precipitation characts. 4-108625  
 NiTi memory alloy, aging-induced precipitations, neutron diff. study 4-89055  
 PLZT, ageing and space charge arising in hot poling 4-76327  
 PLZT ceramics, poling strategy 4-76319  
 PLZT, ferroelec. ceramic, hot poling, polarisation, ageing rel. to space charge 4-99045  
 Pb/acid batteries for UPS and telephone system back-up power, acid ageing behaviour of polycarbonates 4-93612  
 Pb-In superconducting tunnel junctions, fabrication and cycling stability (*Chinese*) 4-104370  
 PbTe, sintered, elec. cond. and thermoelec. power, annealing effects 4-84621  
 Pb(Zr,Ti)O<sub>3</sub> ceramics, ageing and ferroelec. props., heterovalent substitution effects 4-99046  
 Pd<sub>75</sub>Au<sub>25</sub>Si<sub>18</sub>, amorphous alloy, crystn., SAXS study 4-65186  
 RbBr:Eu, optical study of Eu precipitation 4-80233  
 RbCl:Eu, optical study of Eu precipitation 4-80233  
 SbCl<sub>3</sub>-graphite intercalation cpd., de Haas-van Alphen effect meas. 4-88440  
 Se, amorphous, defect states and photoelec. behaviour 4-113903  
 Se, thin film solar, cell. 4-99966  
 Se:Te, As glassy films, pure and doped, deep level defects, xerographic spectra studies 4-61339  
 Se-Te-As, amorphous, defect states and photoelec. behaviour 4-113903  
 $\beta$ -Si<sub>3</sub>N<sub>4</sub>, Mossbauer spectra, effect of heat treatment and  $\gamma$ -irrad. 4-80846  
 SiO<sub>2</sub> core polymer coated waveguides low temp. gamma irradi. response 4-80100  
 SnO<sub>2</sub>, film, impurity phases, hydrolysis of SnCl<sub>4</sub> 4-113829  
 TbFe thin films, amorphous, ageing phenomena, hysteresis cycles 4-71134  
 Ti-Al-Mo-Sn-Si,  $\alpha/\beta$ , simulated flight fatigue 4-104838  
 Ti-Al-Mo-Sn-Si, TC9, microstruct. change during thermal exposure at 500°C (*Chinese*) 4-61959  
 Ti-Al-V (6, 4 wt.%), tensile props. and fracture mode, temp. depend. 4-109488  
 Ti-Cr(V)(Mn)(Fe)(Mo), influence of ageing on incommensurate struct. (*Russian*) 4-65218  
 TiC<sub>1-x</sub>, solubility of metals, microhardness, flow stress rel. to C content 4-61931  
 U-Nb (6 wt.%), microstruct., mech. props. and corrosion, effect of quench rate 4-114558  
 V, T charged, <sup>3</sup>He bubble formation, TEM obs. 4-103825  
 W-Ni-Fe (5, 5 wt.%) heavy alloy, precipitation hardening 4-114564  
 Zn-Al-Cu alloys, vol. change on ageing 4-114592  
 Zn-Al-Si alloys, quench-aged, phase transforms., rel. to hardness 4-114515  
 ZnO black surfaces as solar-selective absorber, optimisation and evaluation 4-81590  
 Zr tritides, ageing, TEM study 4-75503  
 Zr-Nb (20 wt.%),  $\beta$ -phase decomp. rel. to thermal treatment 4-109411  
 ZrO<sub>2</sub>, MgO partially stabilised, Weibull modulus 4-61972

aggregates (materials) see composite materials

aging see ageing

agriculture

see also farming

- aquatic organism cultivation and animal husbandry 4-115328  
 crop type discrimination with Landsat Thematic Mapper 4-82057  
 lined varieties,  $\gamma$ -ray effect on third generation 4-77349  
 W North America, 18.6-yr lunar nodal drought, agricultural implications 4-72665  
 onions, Egyptian, radiation inhibition of sprouting, economic evaluation 4-77350  
 ploughed field, microwave emissivity calc. for remote sensing application 4-100792  
 remote sensing of crop types with Landsat-4 MSS and TM instruments 4-82056  
 rice, radiation-induced mutation rel. to tolerance to salinity 4-77351  
 seaweed mariculture trials, critical pathway approach 4-114966  
 N fertilisers, effect on groundwater pollution in sandy soil 4-77156  
 Aharonov-Bohm effect see quantum theory
- air
- see also terrestrial atmosphere
- air-acetaldehyde mixture, two-stage ignition during rapid compression 4-71930  
 air-methane flame, CO detect. using two-photon absorpt. 4-62261  
 air-water bubbly flow, shear turbulence invest. for simple configs. 4-60489  
 air-water drop flow in subsonic nozzles (*French*) 4-60508  
 air-water gas transfer models 4-75754  
 air-water two-phase downward annular flow config. (*Japanese*) 4-97654

**air continued**  
air-water two-phase upward annular flow in near horizontal tube, flow configuration (*Japanese*) 4-97655  
air-water vapour mixture in greenhouse environment, thermal behaviour 4-87545  
alkaline storage battery aspects of air electrode research, appl. 4-66687  
arc column, expanding, current density determ., probe method 4-84067  
arcs and HF sparks, appl. to metals spectral anal. 4-79868  
atmospheric, DC arcs, ruby laser scattering diagnostics 4-103587  
avalanche breakdown, water vapour effects 4-65144  
breakdown plasma in air, induced by pulsed TEA-CO<sub>2</sub> laser radiation, evolution 4-79824  
cathode, <sup>60</sup>Al-air battery, rapidly refuellable, for electric vehicles, performance evaluation 4-72096  
compressed, with metal vapour and particles at high temp., elec. breakdown (*Japanese*) 4-103463  
cross flow, vel. fluctuations in space between tubes in bundles 4-83892  
discharge plasma, electron gas, transport coeff., binary collision rates 4-97759  
dry air, formative time lags calc. for crossed electric and magnetic fields 4-84096  
electron beam generated cond. 4-113131  
electron initiated EM showers, radiation dose distrib. close to shower axis 4-59020  
ethylene-air diffusion flames, N<sub>2</sub> CARS thermometry 4-77008  
fuel-air combustion in fluidised bed model 4-87787  
ionised, ionic cond. determ. using reson. cavity 4-60579  
jet impinging on inclined adjacent wall, flow characts. 4-87770  
laser increased breakdown thresholds by admixing electronegative gas 4-79708  
laser-produced breakdown interferograms, high-speed recording 4-75120  
methane-air flame, OH molecule photoacoustic detect. 4-77036  
methane-air premixed turbulent flames time resolved density meas. 4-99787  
microwave discharge with preexcitation of neutral mols. 4-103597  
plasma production, mirror electrode for laser initiated discharge channels 4-69932  
polar ice-trapped air age difference at Siple Station 4-115475  
positive corona breakdown, residual streamer channel 4-108233  
positive DC corona, breakdown parameters and current-voltage characts. 4-79887  
propane-air mixture, swirling flow in closed vessels, flame development 4-75029  
pulsed RF corona, ns. image intensifier investigation 4-84105  
Rayleigh scattering cross section, theoretical determ. 4-105714  
refrigeration, transient natural convection heat and mass transfer 4-75006  
RF corona discharge, pulsed, spatiotemporal spectrosc. obs. 4-79846  
sound vel. variation with temp., US meas. 4-86163  
spent fuel interim storage, storage medium selection 4-68762  
sphere-plane gaps in dry air, impulse breakdown, 0.25 to 2 atm. 4-79718  
steam-air mixture, air absorption during condensation in nuclear reactor 4-106874  
streamer inception field strength, area and time effect 4-79879  
supersonic jet, apparent mass calc. 4-79634  
temperature and density fluctuation meas. feasibility using laser-induced O<sub>2</sub> fluorescence 4-78311  
water-air mixture jet, quenching 4-97643  
Al-air batteries, electrochemical characteristics of air electrode with Fe phthalocyanine 4-93608  
H<sub>2</sub>-air mixtures, high-speed turbulent deflagration and transition to detonation 4-103432

**air bases** see *airports*  
**air bubbles** see *bubbles*  
**air compressors** see *compressors*  
**air conditioning**  
see also *ventilation*  
active solar air conditioning systems 4-81521  
energy conservation in buildings—the consequences for heat supply (*German*) 4-85383  
experimental solar house providing 960 W peak power in Saudi Arabia 4-77064  
ground source heat pumps for air conditioning, operation and characts. 4-114939  
hybrid desiccant air conditioning systems for commercial buildings, performance influencing factors 4-72166  
liquid desiccant heating and cooling system, operational experience in residential use 4-72167  
microcomputer simulation of thermal performance of a solar cooling system 4-93596  
single-family residences energy conservation and renewable options anal. 4-72051  
solar air conditioning system, with liquid desiccant, performance computer simulation 4-114944  
solar collectors, rooftop system for administrative building heating and hot water (*French*) 4-105122  
solar desiccant air-conditioner using heat exchangers and humidifiers 4-72164  
solar desiccant residential cooling system high performance dehumidifier 4-72165  
solar heating and cooling systems, Japan's research and development status 4-77065  
solar operated absorption air-conditioner for a Kufra house 4-77057

**air permeability** see *permeability*  
**air pollution**  
see also *air pollution detection and control; smoke*  
acetonitrile in atmosphere surface layer near Tucson, Arizona, USA 4-100676  
acid deposition, techniques for determ. of source-receptor relations 4-100025  
acid rain: questions and answers (*French*) 4-105138  
acid rain, meas. of mesoscale wetfall chemistry around Philadelphia during frontal storms 4-105145  
acid rain, US national R and D effort 4-100043  
acid rain information 4-90279  
acid rain spatial variability analysis using Kriging interpolation procedure 4-82251  
acidic pollution, soil chemistry response, tree-ring analysis 4-105068  
aerosol deposition in human respiratory tract, PIXE investigation 4-105066

**air pollution continued**  
aerosols, random fluctuations, effects on behaviour 4-82189  
aerosols of mixed composition, optical props. and visibility 4-100726  
North America, pollutant transport to North Atlantic Ocean 4-72197  
Arctic aerosol at Barrow, Alaska, USA, due to air pollution and El Chichon 4-105709  
Arctic aerosol front observations in Norwegian Arctic 4-105639  
Arctic atmosphere, acidic sulphate particles in winter 4-105648  
Arctic atmosphere, brominated organic gas content 4-105651  
Arctic atmosphere over Spitsbergen, organic gas composition obs. 4-105650  
Arctic haze, AGASP program and instrumentation for pollution monitoring 4-105722  
Arctic haze, airborne observations near Barrow, Alaska, USA 4-105643  
Arctic haze, microparticle size distrib. 4-105646  
Arctic haze, observations made at Alert, NWT, Canada 4-105642  
Arctic haze, radiation absorption by combustion-generated C particles 4-105143  
Arctic haze, vertical distrib. of particulate C, S, Br 4-105641  
Arctic haze, vertical structure, net-flux radiometer meas. 4-105144  
Arctic haze and giant particles, origins and air mass trajectories 4-105645  
Arctic Haze during 1948-61 'Ptarmigan' weather reconnaissance flights, origin 4-77631  
Arctic haze observations at Barrow, Alaska (AGASP program) 4-105640  
Arctic haze observations in March 1983 over Alaskan Arctic 4-105638  
Arctic haze optical properties 4-105710  
Arctic haze pollution, trace gas concs. and lifetimes in atmosphere 4-105653  
Arctic haze season, solar radiation absorption 4-105711  
Arctic Ocean, hydrography and pollution, conf., London, England (March 1980) 4-106117  
Arctic particulate matter elemental composition observations 4-105647  
Asian dust storm detection in Japan in April 1980, PIXE anal. 4-105661  
Athens, Greece, positive ion conc. and wind characts. 4-115492  
automobile studded tyres, environmental investigation using PIXE 4-105146  
Baden-Wuerttemberg power stations SO<sub>2</sub> emission reduction, cost/benefit anal. (*German*) 4-114988  
Barcelona, Spain, optical props. of turbid atmosphere (*Spanish*) 4-115575  
Beijing city, China, aerosol conc. distrib. in late autumn rel. to synoptic pattern (*Chinese*) 4-66838  
benz(a)pyrene in large Soviet industrial city 4-72198  
Bilbao, Spain, fumigation episode in industrialised estuary valley 4-72629  
biosphere, global C cycle, simulation anal., effects of human interference 4-93665  
Bombay, India, rain chem. composition in industrial area 4-85394  
book 4-90316  
Boulder, Colorado, USA, aerosol element composition 4-67323  
bromine containing gases in Arctic atmos., seasonal conc. variations 4-105652  
bromoform, in Arctic atmosphere 4-105651  
Calgary, Canada, air pollution hazard rel. to wind vel. and mixing depth 4-94193  
Chiba Prefecture, Japan, pollutants in residential areas 4-93662  
chlorofluoromethanes, conc. profile of winter stratosphere of Canada 4-115529  
Cleveland, Ohio, meteorological conditions during unfavourable pollutant dispersion conditions 4-77160  
climate, effects of air pollution via forests 4-94237  
coal fly ash, elemental particle size distrib. in thick samples, PIXE anal. 4-105069  
conference, Laxenburg, Austria (July 1982) 4-67848  
conference on acid deposition, in West Berlin (September 1982) 4-86116  
consumption, pollution and climate (book) 4-90310  
convective boundary layer, plume dispersion and vertical winds, Monte Carlo simulation 4-100019  
convective planetary boundary layer, vertical pollutant diffusion 4-94181  
cooling tower plume dispersion, advanced integral model 4-100016  
corrosion of C steel, influence of pollution, humidity, temp., solar rad. and rainfall 4-85244  
dense gas cloud dispersal in boundary layer 4-77574  
dust deposition in power plants catchment area 4-114984  
electric utilities, developments (*Dutch*) 4-89460  
energy systems and climate (book) 4-90311  
environmental/atmospheric pollution distribution, simulation using hydraulic analogy (*French*) 4-105150  
ethylene dibromide, in Arctic atmosphere 4-105651  
fallout from Pacific nuclear tests, Rongelap and Utrik Atolls experience 4-62611  
ferromagnetic minerals in Mediterranean atm. soil sized particles, distrib. 4-100715  
formic acid in upper troposphere, identification of 1105 cm<sup>-1</sup> band in solar absorpt. spectra 4-100679  
fusion energy systems, potential aerosols characterisation 4-107016  
German automobile industry, environmental protection, reduction of lead content in petrol (*German*) 4-93666  
German electricity supply industry, economic and environmentally safe fuel for energy generation, considerations (*German*) 4-93652  
German steel industry, measures for reduction of dust and noise (*German*) 4-91687  
West Germany, deposition patterns of acid components and heavy metals 4-72195  
Germany, Rn radioactivity and heavy metals from mining waste dumps 4-93906  
global environmental transport model review for <sup>3</sup>H, <sup>14</sup>C, <sup>85</sup>Kr and <sup>129</sup>I 4-83253  
greenhouse effect 4-82228  
ground source, contaminant cloud diffusion in boundary layer (*Russian*) 4-114990  
HCLB engine, air pollution remedy (*Dutch*) 4-114989  
heavy metals, historical record in pond sediments 4-100046  
hydrocarbons, from Brazil forest and grassland fires 4-67314  
India, turbidity and atm. particulate matter 4-67395  
indoor measurements of airborne natural radioactivity in Italy 4-93931  
indoors radiation surveys in the UK, rel. to <sup>222</sup>Rn decay prods. and terrestrial γ-rays 4-93883  
industrial cities, air pollutant and meteorological elements, statistical anal. 4-66834

**air pollution continued**

- industrial source complex dispersion model in rural setting, validation 4-77159
- Lake Tahoe, USA, visibility and particle sources anal. 4-66828
- LLW and ILW shallow land disposal site, radiological capacity and practical experience (*French*) 4-83191
- long-range transport modelling 4-72628
- Los Angeles, hydrocarbons and carbonyls meas. 4-100026
- Los Angeles smog and 1984 Olympic Games 4-109762
- low level exposure to radioactive pollutants, health risk assessment 4-109965
- Madrid, SO<sub>2</sub> pollution, stochastic models for real-time forecasts 4-81602
- Madrid, Spain, SO<sub>2</sub> pollution and assoc. meteorological conditions 4-81601
- Maritsa East 2 thermal power station SO<sub>2</sub> emissions reduction (*Bulgarian*) 4-100042
- medium range pollution transport, meteorological aspects 4-72626
- mesoscale dispersion modelling and application to Netherlands area 4-72627
- mesoscale flows, 3D model and pollutant convection-diffusion 4-100650
- mesoscale transport, appl. of atmospheric transport models for complex terrain 4-100668
- methane fueled engine performance and emissions characteristics [automobile engine] 4-66653
- methyl bromide, in Arctic atmosphere 4-105651
- methylene bromide, in Arctic atmosphere 4-105651
- MHD technology development, recent results, SO<sub>2</sub> and NO<sub>x</sub> emissions 4-72132
- SE Michigan, wet and dry deposition, local emissions effect 4-93664
- Misasa Spa, Japan, radioactivity of air and water, chromosome aberrations 4-93927
- modelling of pollution, cause and effect relationships 4-72196
- natural irradiation in dwelling places in France:  $\gamma$ -rays, Rn and Rn daughters obs. 4-93882
- Netherlands, SO<sub>2</sub> and NO<sub>x</sub> emission standards 4-72193
- New South Wales, Australia, SO<sub>2</sub> concs. due to Liddell power station emission 4-114979
- New York State, USA, sulphate aerosol transport from industrial Midwest 4-115481
- night-time measurements of NO<sub>2</sub> radicals and HONO, implications for atmospheric chemistry 4-105660
- nonmethane hydrocarbon in continental and marine atmos. 4-115526
- nonmethane hydrocarbons in urban and rural USA 4-114980
- Norwegian Arctic, S pollutants annual and seasonal variations 4-105637
- Norwegian Arctic, sources of Ni, Pb and Zn in aerosols 4-105140
- nuclear power industry radionuclide emissions, environmental aspects 4-83252
- nuclear war, climatic consequences, computational expt. (*Russian*) 4-67389
- nuclear war, climatic effects, global nuclear winter 4-105702
- ocean-atmosphere exchanges, two-phase flow aspects 4-62849
- open jet windtunnel for air quality improvement 4-85393
- plume dispersion calcs. using Boussinesq approx., strongly-buoyant case 4-82155
- plume equations, non-empirical closure 4-100015
- plume rise from sour gas flares 4-93658
- plume rise from stacks with scrubbers 4-66827
- point source, gaussian eqn. Basic computer program 4-66831
- pollutant distrib., 1-dimens. problem 4-62416
- pollutant distrib., 2-dimens., convection and diffusion 4-62417
- pollution hazards, evaluation using sedimentation methods (*Polish*) 4-105139
- polycyclic aromatic hydrocarbons in New Jersey, summertime vars. 4-100027
- precipitation water, effect of pollutants on extinction coeff. in 200 to 1100 nm region (*Russian*) 4-66836
- pseudo-lognormal distributions of air quality 4-77161
- puff diffusion model, skewed, in diabatic surface layer, parametric description, report 4-62941
- radioisotope atmospheric transport from notional nuclear plants, European doses, MESOS code 4-77612
- regional air quality modelling, use of precipitation data 4-66830
- Riser-Larsenisen Ice Shelf, Antarctica, snow chem. comp., marine and non-marine sources 4-100024
- rough terrain, air flow and dispersion Eurochem 173 report 4-82185
- Saharan dust incursion over the Tyrrhenian Sea 4-94180
- Santander and Torrelavega, Spain, urban SO<sub>2</sub> and particulate levels (*Spanish*) 4-114992
- Shanghai, China, pollutant influence on humidity and precipitation distrib. 4-94194
- smoke plume from steam power station chimney, trajectory calc., math. model (*Russian*) 4-81600
- sources pollutant release, optimisation 4-66837
- Space Shuttle, exhaust alumina, surface chloride salt form. 4-77163
- Space Shuttle launches, HCl and aerosol ground cloud characts. 4-100022
- Spitsbergen snow cores, pollutant analysis 4-105141
- steam power stations, fuel consumption, environmental problems (*Hungarian*) 4-109761
- steam power stations, high sulphur coal burning, strategies for compliance with SO<sub>2</sub> emission standards, economics 4-89480
- stratiform cloud photochemistry in remote marine locations 4-115524
- lower stratosphere, effects of pollution on radiative heating and O<sub>3</sub> distrib. 4-62920
- stratosphere, modified diabatic circulation model for tracer transport 4-62923
- stratosphere O<sub>3</sub> modification due to pollutants 4-77603
- Sudbury area, Ontario, INCO smelter impact 4-93663
- Sudbury Ni smelter, Ontario, Canada, air pollution observations 4-114982
- sulphate and nitrate aerosols, particle size model 4-114981
- sulphate pollution accumulation in sea-/land-breeze system 4-67321
- thermal power station boilers, air pollution compliance with USSR health standards 4-72199
- Tokyo Metropolitan Area, Japan, photochemical pollutants three-dimens. behaviour 4-100021
- trace elements in Europe, emission and long-range transport 4-114986
- trace metals in Bermuda rainwater, of continental origin 4-67320
- tracers transport and dispersion in nocturnal drainage flows 4-100648
- trajectories during AGASP 4-105655

**air pollution continued**

- transport and diffusion calcs. over uneven terrain, microcomputer model 4-66829
- transport models for complex terrain, three-dimensional theory 4-100667
- transport to Arctic 4-105142
- trichlorofluoromethane, for infrared spectra and composition of stratosphere and troposphere 4-72697
- tropospheric circulation patterns during AGASP 4-105654
- turbulent diffusion in environment, mathematical modelling, conference, Liverpool, England (1978 September 12 to 13) 4-101577
- turbulent dispersal of heavy particles 4-72680
- turbulent dispersion concentration patterns in boundary layer 4-67301
- NE United States, pollutant distrib. and mixing layer struct. during Sulphate Regional Experiment 4-100020
- E United States, rainfall duration and vol., freq. distrib. rel. to acidic precipitation 4-110235
- NE United States, rural area, organic matter in particulates 4-67315
- W United States, S conc., principal component anal. 4-100023
- SW USA, copper smelters and atmos. visibility 4-114985
- NE USA, regional photochemical air quality model 4-115485
- midwestern USA, visibility trends in air pollution in AD 1948 to 1951 period 4-115486
- NE USA-SE Canada region, acid precursor emissions and their airborne precipitation products 4-77158
- vapour dispersion, affect of molecular props. 4-114991
- vehicular pollution in city streets, numerical model of dispersion 4-89479
- vertical diffusion exchange between friction layer and free atmosphere 4-77589
- vertical dispersion of elevated releases in stable boundary layer, model 4-93659
- Vienna, Austria, particle composition indicative of traffic emissions 4-72194
- visibility in atm., suggested units 4-77629
- Westvaco Luke Mill, Maryland, pollutant dispersion and transport, complex terrain model 4-100018
- Be concentration and deposition in lower atmosphere over Kaohsiung City, Taiwan 4-62418
- Br<sub>2</sub> and Br compounds in stratosphere 4-115530
- CO conc. along urban roadsides, line-source model predictions 4-66833
- CO from Brazil forest and grassland fires 4-67314
- CO in Earth's atmosphere, increasing trend (1979 to 1983) 4-100045
- CO<sub>2</sub> effects on surface temperatures in long term 4-94238
- CO<sub>2</sub> in atmosphere, of Pacific, concentration variations and isotopic composition 4-115520
- CO<sub>2</sub> in atmosphere in AD 1860 to 2050 period, C cycle calcs. 4-67345
- CO<sub>2</sub> increase, sensitivity of climate models, influence of ocean heat transport 4-67386
- <sup>14</sup>C behaviour in atmosphere (*Russian*) 4-77162
- HNO<sub>3</sub>, conc. in southwestern USA atmosphere 4-115527
- HNO<sub>3</sub>, for infrared spectra and composition of stratosphere and troposphere 4-72697
- <sup>129</sup>I management from fuel reprocessing plants, air and water discharges 4-91115
- NH<sub>3</sub>, conc. in southwestern USA atmosphere 4-115527
- NO<sub>2</sub> radical, in nighttime atmosphere of S California, USA 4-100028
- NO<sub>x</sub> in atmosphere, photochemistry of troposphere with more than one steady state 4-77607
- NO<sub>x</sub> pollutants, conf. at Maastricht, Netherlands (May 1982) 4-101576
- O<sub>3</sub> destruction by pine forests 4-67303
- O<sub>3</sub> in boundary layer of Philadelphia, USA, transport by turbulence and clouds 4-115525
- O<sub>3</sub> in stratosphere, conc. trends from Umkehr O<sub>3</sub> profile data 4-115532
- Pb particulate emission and dispersion from roadway, line-source models 4-66832
- Pb pollution in Belgium, record held in pond sediments 4-114983
- Pb-acid accumulators and atmospheric pollution (*German*) 4-81537
- Pu isotopes in surface air, Japan (1979-82) 4-115239
- <sup>239</sup>Pu, A=238, 239, 240, content in tobacco crop near nuclear fuel separation facility 4-115237
- Rn and daughters conc. indoors, mathematical model 4-93916
- Rn and Rn daughter concs. in Swedish homes 4-93930
- Rn concentration in a basement, variation with barometric press. 4-67132
- Rn concentrations in residential buildings in Maryland and Pennsylvania, USA 4-93926
- Rn concentrations indoors, temporal variations 4-93924
- Rn, daughter activity concs. indoors, approx. meas. technique 4-93866
- Rn, daughter concentrations in northern part of Netherlands 4-93925
- Rn daughter dose: environmental vs. underground exposure 4-93887
- Rn daughter exposure at low doses, rel. to lung cancer in rats 4-93811
- Rn daughter product, passive detection rel. to plateau 4-93863
- Rn daughter products in indoor air 4-93912
- Rn daughters, deposition rates on indoor surfaces 4-93917
- Rn daughters, indoor concs., soil sources for Swedish houses 4-93903
- Rn daughters, indoor exposure, design and interpretation of large surveys 4-93879
- Rn daughters, indoor exposure, dosimetric approaches to risk assessment 4-93886
- Rn daughters, lung cancer risk for miners and atomic bomb survivors, rel. to indoor exposure 4-93812
- Rn daughters, respiratory tract deposition in humans 4-93932
- Rn daughters, turbulent plateau in rooms and mines 4-93920
- Rn daughters aerosol, activity size distrib. in buildings, cascade impactor meas. 4-93918
- Rn daughters exposure, possible cancer risk 4-93813
- Rn daughters in indoor air, aerosol and activity size distrib. 4-93915
- Rn daughters in indoor air, aerosol particle conc. rel. to ventilation system 4-93922
- Rn daughters rel. to lung tumours occurrence, rat. obs. 4-93810
- Rn daughters suspended in air, alpha activity, working level in U mines and houses 4-109966
- Rn detection in Finnish dwellings, film detectors calibration 4-93895
- Rn exhalation from concrete and alum shale bearing soil, moisture and temp. effect 4-93904
- Rn exhalation from Finnish building materials, room air ventilation rate 4-115236
- Rn, exhalation transients rel. to ventilation and atmospheric press. 4-93909
- Rn in dwellings, location and limiting 4-93933
- Rn in Finnish houses, geographical distrib. and temporal variation obs. 4-93929

## air pollution continued

- Rn, indoor concentration in Swiss dwellings rel. to weather-stripping, matched pair anal. 4-93928  
 Rn, indoor concs., sources and movement 4-93891  
 Rn, indoor exposure rel. to way of living: methodological study 4-93872  
 Rn, measurement in dwellings using activated charcoal 4-93897  
 Rn pollution inside houses, problems due to attachment to aerosols 4-93914  
 Rn, soil gas carrying, infiltration prevention in building constructions 4-93898  
 Rn transport into houses, theoretical evaluation 4-93923  
<sup>222</sup>Rn, A=220, 222, daughters in indoor aerosols, particle size distrib. 4-93921  
<sup>222</sup>Rn, A=220, 222, short-lived decay prods. and unattached fraction, meas. in air 4-105351  
<sup>222</sup>Rn and daughter product concs. in dwellings and open air; equil. factor 4-93919  
<sup>222</sup>Rn and daughters, short and long term techniques for meas.: inside houses 4-72441  
<sup>222</sup>Rn and daughters in indoor atm. of building contaminated with U ores, conc. meas. 4-72440  
<sup>222</sup>Rn and decay products, active and passive desimetry, international intercomparison 4-93864  
<sup>222</sup>Rn concs. in dwelling, seasonal variation 4-109968  
<sup>222</sup>Rn, indoor concs. in energy efficient homes, NY, USA 4-109963  
 SO<sub>2</sub>, conc. in southwestern USA atmosphere 4-115527  
 SO<sub>2</sub> distrib. over Norwegian Arctic Ocean during summer 4-114987  
 SO<sub>2</sub>, pollution conc. frequency distribution model 4-114979  
 SO<sub>2</sub>/sulphate, Eulerian transport/transformation/removal model 4-93660  
 SO<sub>2</sub> transport in E USA, Eulerian model calcs. 4-93661  
 T from CANDU nuclear power stations permeation through tube walls 4-111813  
 T<sub>2</sub>, airborne plume, oxidation rate rel. to release height and atmospheric stability 4-115241  
 Th daughter radioactivity released from burning gas lantern mantles 4-89787  
 Th, processing plant, airborne radioactivity monitoring 4-109964  
<sup>133</sup>Xe, released effluent, sector averaged plume, gamma dose rate from side sectors 4-115240

## air pollution detection and control

- acid deposition, techniques for determ. of source-receptor relations 4-100025  
 acid deposition decision framework modification for State-level application 4-62419  
 acid rain, Canadian research 4-105676  
 acid rain, US national R and D effort 4-100043  
 aerosol filters for nuclear process plants 4-64211  
 aerosol measurement, 10 µm cutpoint size selective inlet for hi-vol samplers 4-100049  
 aerosol physico-chemical characteristics over Beijing 4-62906  
 aerosols, LAMMA and electron microprobe anal. 4-81501  
 airborne LIDAR for Arctic haze anal. 4-110328  
 airborne radioactive releases from burning contaminated combustibles 4-106891  
 Aitken nuclei evolution in urban area atmosphere (Spanish) 4-89476  
 ambient aerosol composition determ. by PIXE 4-100031  
 Arctic haze, AGASP program and instrumentation for pollution monitoring 4-105722  
 area monitoring with high pulse repetition freq. coherent DIAL systems 4-100051  
 atmospheric radionuclide releases, CRRIS computerised system 4-64242  
 Beijing, China, aerosol composition during summer, vertical, temporal and particle size distrib. 4-100041  
 cascade impactor samples collected over Pacific Ocean; PIXE anal. 4-100029  
 coherent IR radar systems and appls., conf., Arlington, VA, USA (Apr. 1983) 4-95019  
 combustion products analysis, using dilution tunnel system 4-62266  
 cooling tower drift-measuring devices compared 4-62432  
 diesel exhaust particulate emissions, photoacoustic measurements 4-66842  
 diffusion denuder assembly for gas collection and determ. in air 4-89475  
 dust, chemical species identification by X-ray powder diffractometry 4-105164  
 dust measurements, solid phase sampling and deposition (German) 4-72202  
 electrostatic precipitator for the study of airborne radioactivity 4-89786  
 environmental pollution monitoring by NAA of hair of free-living mammals 4-105147  
 ethylene monitoring with high pulse repetition freq. coherent DIAL systems 4-100051  
 exhaust emission analysis, using electrohydraulic gas sampling valve 4-78305  
 exhaust gas from petrol engine, Pb compounds distrib. 4-89478  
 Faeroe Islands, marine and nonmarine transported aerosols anal. using PIXE 4-100034  
 fibrous filter, aerosol removal as function of particle size and vel. 4-105149  
 fine particles in environmental samples, characterization by transmission electron microscopy (French) 4-81502  
 flue gas desulphurisation processes and subsystems 4-62420  
 Göteborg, Sweden, airborne particles distrib. determ. using EDXRF and PIXE methods 4-100033  
 ground level air, radionuclide conc. in N Germany and N. Norway, 1980-3 4-77164  
 heat plume characteristic parameter determ. by lidar (Spanish) 4-89483  
 heterodyne detection SNR in turbulent atm., matrix formalism calcs. 4-72201  
 hydrazine monitoring with high pulse repetition freq. coherent DIAL systems 4-100051  
 I, radioiodide conc. from aqueous soln., sorbent materials and prep. 4-77023  
 India's requirements and priorities 4-105156  
 indoor exposure to natural radiation, conf., Anacapri, Italy (Oct. 1983) 4-90285  
 integrating nephelometers for air quality monitoring 4-109768  
 lasers in chemistry, appl. to analysis, vibr. relax. and mol.-surface interaction 4-66641  
 LIDAR registration of air pollutants (German) 4-96972  
 lidar remote sensing of atmosphere, book 4-82607
- air pollution detection and control continued  
 mass determination on lightly loaded membrane filters, gravimetric determ. 4-77168  
 Mediterranean and Atlantic ocean, atmospheric aerosol particles transport determ. by PIXE 4-100035  
 methyl iodide removal efficiency of charcoal bed in reactor 4-107171  
 microwave spectrometer, 140 GHz, for detect. of gaseous pollutants and other mol. species 4-106404  
 Milan aerosol monitoring by means of PIXE analysis 4-100040  
 mm-wave system for remote sensing acidic clouds and precursor gases in troposphere 4-77170  
 multicomponent gas analyser based on He-Ne laser (Russian) 4-89485  
 nuclear facility unplanned release, in situ noble gas radionuclide spectrometric meas. 4-106889  
 nuclear fuel reprocessing gaseous wastes management, <sup>3</sup>H, <sup>14</sup>C, <sup>85</sup>Kr and <sup>129</sup>I emissions 4-59438  
 off-site dose rates estimation using BWR containment high range monitor after accident 4-106890  
 open-loop fast response gas sampling valve with current control 4-62428  
 optical remote sensing, conf., Ispra, Italy (April 1983) 4-73168  
 Paks Nuclear Power Plant, air activity measurement computerised system, using basic (Hungarian) 4-96289  
 petrol engine, homogeneous combustion parameters and emissions control, computer simulation 4-77171  
 PIXE for power station particulate emission analysis 4-105163  
 pollutant long range transport, treatment using variable stepsize variable formula method 4-105148  
 power plant flue gas desulphurisation system evaluations and cost calculations 4-66839  
 power reactor plumes, noble gas radionuclide concs. determ., calibration procedures 4-86974  
 precipitation sampler intercomparison 4-100831  
 propane gas spillage monitoring, by 5 Km-long fibre optics method 4-105155  
 radioactive dispersion in atmosphere, specific effects review 4-66840  
 radioactive dispersion in atmosphere, specific effects review 4-66841  
 radioactive emissions from nuclear plants, permitted levels, ICRP-26 effects 4-91120  
 radioactive plumes from nuclear power plant, monitoring methods 4-107167  
 radionuclide air conc. near building, screening approach to estimations 4-109961  
 relative air quality merits 4-81605  
 Sao Paul PIXE system and its use on a national monitoring air quality program 4-100032  
 semiconductor gas sensor, environmental changes effect on sensitivity 4-62431  
 stack effluent monitoring for an operating four reactor unit CANDU nuclear station 4-59450  
 statistical errors in air pollution measurement systems 4-93670  
 stratospheric multispecies trace gas meas. using balloon borne tunable diode laser absorption spectrometer 4-115591  
 Sweden, south, long range aerosol transport, multivariate statistical technique appl. to PIXE data 4-100037  
 telecommunication exchange buildings, indoor and outdoor air, fine particle aerosols characterisation 4-100038  
 time integrated photographs for cooling tower visible plume rise anal. 4-100017  
 trace elements in air dust (Benghazi, Libya) NAA and AAS determ. 4-66835  
 transuranic on-line air monitor, alarm characteristics 4-74099  
 tropospheric air trace gas meas. using tunable diode laser absorpt. spectrometer 4-114998  
 western United States, anthropogenic pollutants, long range transport and transformation obs. by PIXE 4-100036  
 working environment aerosols in lead battery factory, toxicity monitoring by PIXE and AAS 4-105072  
 Zurich, ambient air, particulate matter sampling and anal. 4-100039  
 CO<sub>2</sub>-laser long-path absorption system for gaseous pollutant monitoring 4-62426  
 Cl<sub>2</sub>, determ. in air in presence of NH<sub>3</sub>, capillary GC method 4-114855  
 Cl<sub>2</sub> absorption coefficients at <sup>12</sup>C<sup>18</sup>O<sub>2</sub> and <sup>12</sup>C<sup>16</sup>O<sub>2</sub> laser wavelengths, appl. to remote monitoring 4-114997  
<sup>152</sup>Eu, atmospheric fallout samples collected in 1981 4-62891  
 HCl detection at sub-parts-per-billion level using tunable diode laser absorpt. 4-115176  
 Kr adsorption after separation from nuclear installation waste gases 4-100047  
 (NH<sub>4</sub>)<sub>2</sub>SO<sub>4</sub> conditioning of flue gas for electrostatic precipitator performance improvement 4-62421  
 NO<sub>2</sub>, atm. conc. determ. by differential absorpt. lidar 4-85392  
 NO<sub>2</sub> determ. using extractive spectrophotometric method 4-93669  
 NO<sub>2</sub> remote monitoring using DIAL based mobile lidar system 4-77167  
 Pb concentration at roadside, effects on human and animal health 4-100044  
 Pb concentrations in urban area (Spanish) 4-89477  
<sup>210</sup>Pb distribution in environmental samples by CR-39 α-detector 4-100053  
<sup>210</sup>Po distribution in environmental samples by CR-39 α-detector 4-100053  
 Rn and decay prods., equil. factor meas., method using passive track detectors 4-105352  
 Rn control programme in theory and practice 4-93936  
 Rn daughter, removal by filtration and elec. field 4-93934  
 Rn, daughter activities, meas. instrumentation 4-93867  
 Rn, daughter activity concs. indoors, approx. meas. technique 4-93866  
 Rn daughter collection and passive monitors calibration 4-93673  
 Rn daughter conc. in room air, continuous spectrometry by twin channel device 4-93672  
 Rn daughters, population exposure, annual dose assessment problems 4-93885  
 Rn detection in Finnish dwellings, film detectors calibration 4-93895  
 Rn, indoor meas. using activated C collectors 4-89771  
 Rn, measurement in dwellings using activated charcoal 4-93897  
 Rn progeny conc. indoors, cost evaluation of control measures 4-115229  
 Rn, soil gas carrying, infiltration prevention in building constructions 4-93898  
<sup>222</sup>Rn, A=220, 222, daughter energy concs. in air, simple field method for determ. 4-93674  
<sup>222</sup>Rn, A=220, 222, daughters in indoor aerosols, particle size distrib. 4-93921

**air pollution detection and control continued**

- <sup>222</sup>Rn and daughters, airborne, meas. with CR-39 track detectors, plated-out <sup>218</sup>Po, <sup>214</sup>Po calibration 4-66844  
<sup>222</sup>Rn and decay products, active and passive dosimetry, international intercomparison 4-93864  
<sup>222</sup>Rn exhalation rate from surface of building materials or soil, meas. apparatus 4-93896  
SO<sub>2</sub> emission by power stations in Baden-Wurtemberg, reduction measures, costs and efficiency 4-89481  
SO<sub>2</sub> pollution conc. measurement by far IR laser spectroscopy method 4-74246  
SO<sub>2</sub> pure rotational spectroscopy using fixed line far IR lasers 4-74246  
U mobilisation, obs. and decay products in Australian rain 4-105162  
<sup>88</sup>Y, atmospheric fallout samples collected in 1981 4-62891

**air pumps** *see compressors***air terminals** *see airports***air tightness detection** *see leak detection***aircraft**

- see also aerospace control; aerospace instrumentation; helicopters*  
eddy current equipment for aircraft maintenance 4-76943  
fighter cockpit environment, adaptive noise cancellation 4-103132  
jet engine turbines, ceramic technology for powerplant 4-104758  
noise, subjective responses of Chinese 4-72200  
retardation effect, fast moving sound source motion parameter estimation 4-103160

**aircraft instrumentation**

- ER-2 airborne LIDAR, NASA/CNES potential project 4-110326  
laser accelerometer of aviation gravimetric system (Russian) 4-96976  
LIDAR, Arctic haze mapping 4-110328

**airfields** *see airports***airglow**

- see also atmospheric spectra; aurora; nightglow; sky brightness; twilight*  
geocoronal He airglow obs., contamination by radiation belt particles and O II emissions 4-105787  
lower ionosphere, obs. of pulsating luminesc. synchronous with pulsed radio wave 4-82332  
upper mesosphere, tidal and solar cycle effects on O I 5577 Å, Na I D, and OH(8,3) airglow 4-110341  
UV dayglow and daylight aurora, imaging from space under full sunlight 4-100843  
He 1083 nm airglow at midlatitude, seasonal and solar zenith angle depend. 4-105786  
O I 557.7 nm emission, implications of meas. of O concs. in high latit. winter upper atmosphere 4-105784  
O layer and 5577 Å emissions, latitudinal and seasonal variations 4-72766  
OH airglow in polar cap, rot. temps. at mesopause during stratospheric warming event 4-110340

**airports**

- noise, penetration into airport terminal buildings 4-114994

**alarm systems**

- CCTV solid state storage system for nuclear material safeguards 4-106976  
diver physiological monitoring system 4-109984  
intruder detection using pulsed-Doppler ultrasonic motion detector for limited area surveillance in an unconfined region 4-64817  
motion detection for burglar and false alarm signals, developments in ultrasonic and IR detectors 4-64816  
nuclear safeguards, automatic identification in containment and surveillance 4-106972  
power plant alarm systems, procedure for reviewing and improving 4-68798  
synchrocyclotron monitoring, alarm system for VIK of Dubna (German) 4-111988  
toxic substance detector alarm using ion mobility spectrometry, developments 4-99907

**albedo**

- albedo changes due to dust fallout, laboratory expts. 4-115702  
asteroids, light curves, contrib. of shape of asteroid and albedo var. 4-94668  
atmospheric gamma-ray flux, E>30 MeV, characteristics in near-Earth cosmic space 4-101035  
charged particles telescope to observe proton albedos 4-101039  
clear sky planetary and surface albedos 4-72703  
cloud identification by NIMBUS 7 ERB, effect on albedo 4-100694  
concrete, photon backscattering, energy albedo meas. 4-61782  
cosmic ray neutron albedo at E<1 MeV 4-115664  
cosmic rays, albedo gamma-ray flux at balloon altitudes 4-100964  
133 Cyrene, asteroid lightcurve, phase relation, rot. period 4-115706  
Earth, numerically simulated climates, sensitivity to albedo 4-82221  
electrons, source under radiation belts 4-101040  
ice clouds, effects of horizontal orientation of crystals on radiative props. (Chinese) 4-67397  
Mars, south polar cap region during 1971 apparition, photometric props. 4-115705  
oceanic whitecaps, effective reflectance 4-89916  
Pade approximant calculations for number of scatterings during particle diffusion 4-101126  
Saturn's satellites, photometric obs. at large phase angle 4-101248  
Saturn ring system, properties from 3 mm observations 4-115709  
soil, albedo effect on surface temps., outdoor expt. 4-106153  
Al photon backscattering, energy albedo meas. 4-61782  
Fe, photon backscattering, energy albedo meas. 4-61782  
Pb, photon backscattering, energy albedo meas. 4-61782  
Sn, photon backscattering, energy albedo meas. 4-61782

**alclad** *see aluminium alloys***Alfvén waves** *see magnetohydrodynamic waves; solid-state plasma***algebra**

- see also Boolean algebra; linear algebra; matrix algebra*  
algebraic structure count, recursion rels. 4-107269  
Clifford algebras, exponential mapping 4-95131  
Clifford algebras and Cayley-Dickson algebras, construction 4-95132  
Clifford algebras and finite groups relationship 4-63538  
Delhi schools, class X students, evaluation of achievement in algebra 4-101604  
gauge algebra, operator canonical transformation 4-95218  
generalised function associative algebras, quantum mech. appl., Schrodinger eqn. free solns., review 4-95244  
Hirota-Satsuma system, prolongation algebra 4-63478

**algebra continued**

- Lie algebra Gsl(2), unified description of irreducible representations 4-78105  
Lie algebras, Kostant partition function 4-95134  
Lie algebras, semisimple subalgebras, generators 4-78104  
Lie algebras, structure constants in root space 4-78103  
quantum field theory, unbounded operator algebras, Wightman's theory 4-68389  
relativistic fields, Clifford algebra formalism, unifying description 4-86530  
sixteen vertex model, diagrammatic construction of algebraic invariants 4-78264  
spin algebras, diagrammatic approach 4-104384  
Steinrod algebra and stable homotopy, book 4-63433  
superalgebra representations, in extended supersymmetry 4-106495  
superconformal algebra, extended N=2 with central charges 4-58983  
tensor product of generalized sample spaces 4-106170  
thermo field dynamics of a quantum algebra 4-102022  
vector fields on straight line, Lie algebra, general position homologs (Russian) 4-68446  
Yang-Baxter eqn., solutions for simple superalgebras 4-102063

**algorithms (computer listings)** *see subroutines***aliphatic compounds** *see organic compounds***alkali metal alloys**

- see also caesium alloys; lithium alloys; potassium alloys; rubidium alloys; sodium alloys*  
alkali-group IV alloys, liq. and solid, electronic struct. and cluster form. 4-92601  
MAu (M=Li, Na, K, Rb, Cs), electronic props., self-consistent relativistic band struct. calcs. 4-92604

**alkali metal compounds**

- see also alkali metal alloys; alkali metal halides; caesium compounds; francium compounds; lithium compounds; potassium compounds; rubidium compounds; sodium compounds*  
alkali alkaline earth phosphate glasses, He migration, thermal expansion, glass transition temp. 4-108661  
alkali borate glass, thermal expansion, Gruneisen parameter 4-80272  
alkali borate glass melts, demixing, stable long-period comp. variations 4-84407  
alkali silicate glass, thermal expansion, Gruneisen parameter 4-80272  
borate mixed glasses containing Ni, induced optical absorpt. rel. to γ-ray exposure 4-76502  
chalcogenide, ionic crystals, index of refraction 4-61645  
cyanides, symmetry reduction in phase transitions 4-92344  
dimers and cations, ground state props., effective core polarisation pots., SCF CI calcs. 4-68971  
double molybdates and tungstates, cation-tetrahedral anion distance 4-113386  
halogenides with admixture halogenide anions, electron transitions in C<sub>4v</sub> symm. centres, formed from S<sup>2-</sup> ions 4-76404  
hexahydroaluminate, struct. chemistry 4-70119  
intercalation cpds. with graphite, intercalation compounds, theory of press-induced staging transitions 4-75696  
iodides, iodides, angle-resolved photoelectron spectroscopy 4-96617  
oxide glass, cond. polarization characts. and comparison with halide cryst. 4-99003  
oxide glasses, ionic elec. cond., temp. depend. 4-113703  
oxides, binary, high temp. vapourisation behaviour 4-98260  
oxides, effect on alkali resistance of Na<sub>2</sub>O-Al<sub>2</sub>O<sub>3</sub>-SiO<sub>2</sub> glass 4-81317  
phosphates, A'B<sup>II</sup>PO<sub>4</sub>, A=Na, K, B=Ca, Zn, Sr, Cd, Ba, Pb, ferroelec., phys. props. 4-65992  
pyrophosphates, M<sup>III</sup>P<sub>2</sub>O<sub>7</sub>, vibr. spectra and crystal struct. 4-65247  
rare earth fluorides, MR<sub>3</sub>F<sub>6</sub>·Eu<sup>2+</sup> (M=K, Rb, Cs; R=Y, Gd, Lu), Eu<sup>2+</sup> luminesc. 4-66073  
silicate glasses, ion bombard., alkali depletion, ion beam mixing 4-70239  
silicate glasses, ion irradi., glass comp. modification by alkali ion migration 4-70238  
silicate glasses, thermotransport, at. migration process under effect of temp. gradient 4-80283  
ternary molten salt systems, additive and reciprocal, phase diagrams, thermodynamic props. 4-84368  
MR<sub>2</sub>Cl<sub>2</sub> (M=alkali metal, R=rare earth), crystallographic characterisation and phase transitions 4-70077  
TiO<sub>2</sub>-P<sub>2</sub>O<sub>5</sub>-M<sub>2</sub>O (M=alkali metal), vitreous semiconductors, EPR and optical studies (Russian) 4-98939

**alkali metal halides**

- see also compounds of individual alkali metals, e.g. sodium compounds*  
activator light sum photorelease, photoluminescence (Russian) 4-114321  
addition, to dextran solns., effects on ordered conform. states (Russian) 4-59932  
alkali chloride: Cu<sup>+</sup>(Ag<sup>+</sup>), two-photon spectra, impurity states 4-109215  
alkali halide: BH<sub>4</sub><sup>-</sup>, IR and Raman spectra, Fermi resonances isotope shift 4-61695  
alkali halide: CN<sup>-</sup>, vibrational fluoresc., nonradiative luminesc. quenching 4-81005  
alkali halide: TI<sup>+</sup> cryst., optical props. and Jahn-Teller effects 4-61643  
bicyrystals, high-angle (001) twist grain boundaries 4-103768  
Born-Mayer parameters for next nearest neighbours 4-92127  
cleaved crystal surfaces, ledge struct., evaporation, electric field effect 4-66194  
clusters, secondary cluster ion distrib., SIMS 4-66166  
colour centre form. dynamics under ionising radiation 4-80085  
compression, theory 4-75604  
conduction polarization characts. and comparison with alkali glass 4-99003  
crack edge contact restoration phenomena 4-98191  
crystals, laser-produced damage in UV region and in crossed UV-IR beams 4-75514  
defect creation mechanisms 4-60915  
diffusion along grain boundaries and dislocations 4-92439  
dimers, electric dipole polarisabilities 4-69239  
dislocation etching, etch pits, crystal growth, review 4-70159  
dislocation vel., stress depend. 4-70167  
divalent alkaline earth metal impurity complex binding energies 4-60912  
doped with En<sup>2+</sup>(Pb<sup>2+</sup>)(Ca<sup>2+</sup>)(Sr<sup>2+</sup>), X-irrad. effect on impurity vacancy dipoles and aggregation precipitation state, F-centre production 4-70209  
elastic constants, multipole expansion 4-80139  
elastic const. and force const., bond deform. model 4-61034  
etch pit studies of dislocations, dissolution kinetics and impurity effects 4-70158

**alkali metal halides continued**

excitonic and impurity-excitonic mechanisms for F<sub>2</sub>H pair creating in alkali halides (*Russian*) 4-80034  
 F<sub>2</sub> centre, K band 4-60923  
 F-centre states, hybrid method with floating 1-s Gaussian basis 4-70709  
 F-centres, photoacoustic signals 4-80964  
 force field simulation of moving ions in multimolecular systems 4-79977  
 Frenkel defect accumulation, temp. and impurity conc. depend. 4-98093  
 gamma-irradiated, lyoluminescence characts. (*Chinese*) 4-76526  
 hole-induced thermo-exoemission 4-85092  
 hopping-type electronic processes in pre-breakdown elec. fields, effect of F-centres 4-108868  
 interstitial atomic H centers in mixed config., unrelaxed excited states, MCD optical absorpt. 4-70747  
 ionic crystals., index of refraction 4-61645  
 IR modulation spectroscopy 4-63790  
 lattice energies calc. from elastic constants 4-79971  
 localised phonon mode associated with dislocations 4-70321  
 longitudinal excitons and plasmons 4-84569  
 low temp. processes, reaction-rate theory 4-60925  
 matrix for ReO<sub>4</sub> molecules, anharmonic vibr. relax. dynamics 4-91311  
 microcrystalline powders, reduced stability of coloration, dislocation model 4-60926  
 microwave-induced plasma afterglow, lattice atomisation, temp. depend. 4-79862  
 mixed crystals, growth and characterisation, microhardness, colour centres, radiation hardening 4-70152  
 molecules, collisional dissoc. and chemical relax. at 2000-4200K 4-89269  
 molecules, empirical interionic pots. 4-87179  
 molten, Raman scatt. study 4-61711  
 nonlinear acoustic paraelectric resonance calcs. (*Russian*) 4-88788  
 optical const. calcs. 4-99084  
 phosphors, S<sup>2</sup> ion impurity centres with O<sub>h</sub>, D<sub>4h</sub>, C<sub>4v</sub> and C<sub>2v</sub> symm., cryst. field theory 4-61346  
 photoconductivity of colour centres, temp. depend. 4-98669  
 point defects, elastic dipole tensor 4-60924  
 polarisation energy by point defects, INDO cluster calc. 4-80861  
 radiolysis process 4-70194  
 short-range repulsive pot. anal. 4-75361  
 solid solutions, high conc., lattice dilatation 4-75410  
 solution enthalpies of divalent defects 4-98316  
 space charge elec. field form. during cleaving 4-76021  
 sputtering, contrib. of electronic processes 4-61803  
 sputtering by electrons 4-61791  
 stability and optical props. of self-trapped exciton 4-104129  
 surface, adsorbed rare gas atoms, neutral excited configurations 4-80390  
 surfaces, electronic desorption of excited alkali atoms 4-61236  
 NO<sub>3</sub><sup>-</sup> isolated in alkali halide systems, IR and Raman spectra 4-59761

**alkali metals**

*see also caesium; francium; lithium; potassium; rubidium; sodium*  
 adsorbed on Si (111) and (100), desorption kinetics and surface phase changes, surface ionisation studies 4-65571  
 adsorption on transition metal surfaces, electronic charge transfer 4-92554  
 alkyl halide+alkali metal, nonadiabatic processes, electron harpoon mechanism, vibronic excitation 4-102781  
 anharmonic effects and thermodynamic props., theory 4-61033  
 atom+SCl<sub>2</sub>, chemiluminesc., vibr. population inversion in B state of S<sub>2</sub> 4-89303  
 atoms, adsorbed on Si (100) 2X1, surface plasmon dispersion, RPA calcs. 4-98447  
 atoms, chemisorbed on W (110), NMR studies 4-98445  
 atoms, core polarisation pot., intershell correl. effects, ab initio SCF CI calcs. 4-68970  
 atoms, excited states, photoionisation, initial wave functions 4-83438  
 atoms, nucl. spin polarised, chemisorbed on hot metal surfaces, NMR study 4-80374  
 atoms, optically pumped, collision with inert gas atoms causing nuclear spin polarisation via spin exchange 4-78932  
 atoms, optically pumped, electron spin randomisation in spin temp. limit (*Chinese*) 4-112147  
 BCC, thermodynamic props. at high temps. 4-92392  
 closed shell ions, repulsive interactions with Ar, Kr and Xe, beam and transport meas. comparison 4-96653  
 clusters, thermodynamic props., ionis. pots. and binding energies 4-69266  
 combustion gas plasmas, atomic density meas. by near-resonant Rayleigh scatt. 4-113218  
 conjugated bonds, reson. energies and bond orders (*Chinese*) 4-84555  
 dimers, bonds, stability, nonorthogonal CI calcs. 4-64390  
 electron-phonon interaction, exchange effect (*Chinese*) 4-75872  
 equations of state, shock wave isotherms 4-108573  
 impurities in quartz crystals, effect on elec. cond. and dielec. loss 4-71271  
 ionic crystals, heat of vaporisation 4-113593  
 ions, impact-collision scatt. for surface reconstruction determ. 4-81100  
 ions, primary particles in low energy ion scatt. 4-81074  
 lattice props., Heisenberg Hamiltonian studies 4-108501  
 liquid, acoustic wave velocity, influence of many-body interactions 4-98204  
 liquid, longitudinal viscosity, classical one-component plasma model 4-61126  
 liquid, structure factor near freezing point, calcs. 4-113296  
 liquid, surface tension theory 4-84487  
 liquid, thermodynamic props. using classical plasma reference system 4-60810  
 melting, Lindemann coeff. rel. with temp. 4-108591  
 melting theory using pseudopotential calcs. 4-88268  
 molten, O<sub>2</sub> solubility study 4-113641  
 nuclear magnetic props. and solvation, review 4-74179  
 plasmas, elec. cond. and comp., nonideality effects 4-83984  
 vapour, reson. interaction of an atom with monochromatic field 4-109226  
 vapour+H ions, spin-depend. charge transfer 4-59890  
 CdF<sub>2</sub>, alkali metal doped, association and bound motion 4-80294

**alkaline earth alloys**

*see also barium alloys; beryllium alloys; calcium alloys; magnesium alloys; strontium alloys*  
 No entries

**alkaline earth compounds**

*see also barium compounds; beryllium compounds; calcium compounds; magnesium compounds; radium compounds; strontium compounds*  
 alkali alkaline earth phosphate glasses, He migration, thermal expansion, glass transition temp. 4-108661  
 chalcogenides, ionic crystals., index of refraction 4-61645  
 epitaxial growth on semiconductors, Rutherford backscatt./channelling studies 4-80438  
 fluoride, stress induced birefringence calcs. 4-109152  
 fluorides, IR modulation spectroscopy 4-63790  
 halides, ionic crystals., index of refraction 4-61645  
 niobates, electronic cond. rel. to complex perovskite structs. 4-70821  
 oxides, elastic const. and force const., bond deform. model 4-61034  
 pnictides, cryst. struct. and plastic phases 4-80018  
 Nd<sub>2</sub>O<sub>3</sub>-WO<sub>3</sub>-GeO<sub>2</sub> (MO; M-Ca, Sr, Ba, Mg, Zn), subsolidus phase equilib. and fluorescence activity 4-113597

**alkaline earth metals**

*see also barium; beryllium; calcium; magnesium; radium; strontium*  
 atoms, core polarisation pot., intershell correl. effects, ab initio SCF CI calcs. 4-68970  
 atoms, dynamic polarisabilities, semiempirical calc. methods 4-102599  
 crystal structure from first principles calcs. 4-70064  
 ions; permselectivities across cation exchange membrane (*Japanese*) 4-99842  
 neutral and ionized alkaline metal bombardment type heavy negative-ion source (NIABNIS) 4-86987  
 NMR props. 4-74180

**alkalinity *see pH*****allotropy *see polymorphism*****alloy steel**

*see also tool steel*  
 acoustoelastic coeffs. of Rayleigh waves, US obs. 4-114733  
 arc shaped specimens of pipe, errors in J-integral determ. 4-62142  
 bar sorting, two parametric eddy current method 4-71833  
 bearing, surface layers, effect of grinding (*Chinese*) 4-99628  
 carburisation, sintering, mech. props. rel. to Cu and P alloying 4-89069  
 carburised, fatigue of steels with internal oxides and non-martensitic microstruct. near surface 4-114655  
 cast, fatigue, const. and variable amplitude, room temp. and -45°C 4-99551  
 cast, fracture toughness, Charpy V notch test 4-99560  
 chemical reactor cooling coils, corrosion, X-ray radiographic test (*Chinese*) 4-62141  
 constructional, carburised case relax. props. influence on antigalling resist. 4-114684  
 constructional, fracture resist., method of stress raiser appl. influence 4-62037  
 corrosion, atmospheric, effect of Cu 4-89175  
 corrosion fatigue, Monte Carlo simulation model (*Japanese*) 4-99647  
 Cr-Ni-Mo-V, cyclic creep in complex stress state 4-99447  
 critical brittleness temperatures determined on specimens with different stress raisers 4-104937  
 damping capacity and residual life of 40 Kh steel, preliminary cyclic loading influence 4-99544  
 diffusion bonding below A<sub>1</sub> transform. point, heat treatment effect on tensile strength (*Japanese*) 4-66547  
 dual phase, fatigue crack growth rel. to prestrain and ageing 4-85213  
 dual-phase, cold-rolled sheet, recrystn. kinetics 4-93310  
 dual-phase, metallography and partitioning of alloying elements 4-93301  
 dual-phase, Mn segregation during intercrit. annealing 4-114535  
 dual-phase, Mn-Si, stabilisation of retained austenite, effect on mech. props. (*Korean*) 4-104818  
 dual-phase, work hardening at small plastic strains 4-114568  
 electrical, hysteresis losses, stress and induction depend. 4-61553  
 fatigue crack growth, surface strain hardening effect 4-66439  
 ferritic, corrosion behaviour in eutectic Pb-Li environment 4-107056  
 ferritic, Cr-Mo, welded joints, creep behaviour 4-93357  
 ferritic, Cr-Mo-V-Nb, microstruct. after irradi. to 36 dpa at elevated temps. in HFIR 4-98153  
 ferritic, exposed to static Pb-Li, corrosion reactions, surface analysis 4-107064  
 ferritic, for use in fusion reactor liq. metal blankets, compatibility, review 4-107054  
 ferritic, low alloy, carbide precip., Mo<sub>2</sub>C→M<sub>6</sub>C transform. 4-66344  
 ferritic, press. vessel, viscoplasticity at room temp., crit. uniaxial expt. 4-93336  
 ferritic transformable specific heat capacity (*German*) 4-80252  
 ferritic-austenitic specific heat capacity (*German*) 4-80252  
 fracture strain and characteristic fracture distance, microstruct. interpretation 4-85211  
 fracture toughness, quasi-state and impact, effect of different thermal treatments 4-99599  
 fracture toughness meas. using specimen strength ratio 4-81371  
 fusion reactor blanket structures, activation product release, safety research 4-111781  
 fusion reactor candidate first-wall materials 4-111799  
 heat resistant, fatigue resist., cycle asymmetry with long loading bases 4-99545  
 heat treated, retempering effect on strength props. 4-114587  
 heat treated, surface segregates, Auger and XPS studies 4-99856  
 heat-resistant, crack resist. characts., temp. and loading cycle asymmetry influence 4-99535  
 heat-resistant, static and dynamic fracture toughness, influence of microstruct. and temp. 4-99600  
 heat-resisting, surface layer fatigue failure, protective effect of alloy coatings 4-93470  
 high C, optimisation of heat treatment (*French*) 4-81224  
 high strength, fatigue crack prop., overload-induced 4-99482  
 high strength, fatigue fracture, X-ray fractography (*Japanese*) 4-89123  
 high strength, H cracking parameters for predicting safe welding conditions 4-66044  
 high strength, H embrittlement; Ni-Pd alloy plating method (*Japanese*) 4-104861  
 high strength, H embrittlement fracture morphology, (*Japanese*) 4-99511  
 high strength, high temp. sintering 4-89005  
 high strength, SCC, growth mechanisms 4-81333  
 high strength structural, stress relief cracking susceptibility 4-109509  
 high-alloy, quenched, residual austenite transformation, high temp. X-ray study (*Russian*) 4-104777  
 high-speed, W-Mo, sintered, heat treatment 4-66357

## alloy steel continued

- high-tension steel, corrosion fatigue crack growth in NaCl soln. 4-114711  
 HSLA, crack resist. of differently alloyed steels 4-104877  
 HSLA, Cu-bearing, hot shortness 4-89104  
 HSLA, deformation and fracture at isolated holes in plane-strain tension 4-61976  
 HSLA, fatigue fracture surface, X-ray obs. (Japanese) 4-114644  
 HSLA, fatigue threshold, effect of strength and surface asperities on closure 4-76852  
 HSLA, fatigue threshold, thermally activated behaviour of effective stress intensity 4-76853  
 HSLA, Mn, bearing, strengthening mechanisms rel. to treatment and microstruct. 4-81209  
 HSLA, rolled, impact toughness and transition temp., effect of delamination (Korean) 4-76848  
 HSLA, SCC initiation under vibratory stress (Japanese) 4-62111  
 HSLA, shear failure, development of fractographic features 4-76837  
 HSLA, sheet, press forming problems 4-99471  
 HSLA, solubility of niobium carbide and carbonitrides 4-61934  
 HSLA, strain meas. near growing fatigue crack tip 4-114651  
 HSLA, tensile strength and ductility, dependence on microstruct. 4-114603  
 hypereutectoid, Mode III fracture initiation toughness, depend. on strength and microstruct. 4-71720  
 intergranular corrosion of steels and alloys, book 4-95084  
 J-integral, method for determ. 4-66524  
 LMFBR fuel element materials, swelling resist. (German) 4-83148  
 low alloy, brittle fracture, fractographic characteristics, test temp. effects (Russian) 4-109495  
 low alloy, cast, thermal-mech. fatigue crack propag., effect of strain wave shape 4-66445  
 low alloy, cavity initiation criteria at inclusions 4-104874  
 low alloy, Cr, dislocation structure and phase composition during annealing (Russian) 4-108366  
 low alloy, Cr-Mo-V, high temp. low cycle fatigue rel. to softening and embrittlement (Japanese) 4-99519  
 low alloy, creep fatigue and environmental interactions 4-99593  
 low alloy, Cu role in radiation damage 4-108423  
 low alloy, cyclic creep, relationship with hysteresis loop energy 4-109456  
 low alloy, cyclic strength, effect of laser irradiation 4-71723  
 low alloy, fatigue crack propag. in viscous environment 4-99579  
 low alloy, fracture toughness studies 4-109491  
 low alloy, fracture under corrosive environment, high temp. creep, fatigue, creep-fatigue 4-99592  
 low alloy, high-temp. brittle fracture, review 4-99562  
 low alloy, HY-80, microstruct. after small plastic strains, TEM characterisation 4-93340  
 low alloy, irradiation embrittlement 4-93392  
 low alloy, low C weld metal, transform. behaviour and toughness 4-114670  
 low alloy, mech. props. rel. to second phase particle size 4-99591  
 low alloy, oxidation at 1200°C, scale morphology and growth rate 4-62118  
 low alloy, oxidation wear, origins and developments at low ambient temps. 4-81293  
 low alloy, quenched directly from hot deform. temp., influence of austenite substruct. on final struct. and props. 4-99439  
 low alloy, reheat cracking during stress relief annealing, numerical approach 4-93412  
 low alloy, reversible temper embrittlement, role of microstructure, scanning Auger microscopy study 4-81286  
 low alloy, small fatigue crack growth behaviour under two-stress level, multiple loading 4-66411  
 low alloy, small scale yielding, crack tip opening displacement determ. 4-81270  
 low alloy, sulphide stress cracking, role of H 4-89168  
 low alloy, wedge opening loaded specimens, applied crack tip stress intensity, effect of loadline shift 4-79530  
 low alloy cast, temper embrittlement, microstruct. obs. by Auger electron spectrosc. (Chinese) 4-71725  
 low alloy high strength steel, acoustic emission testing of cracks in heat affected zone of welds (German) 4-99718  
 low alloy mild, ductile fracture, rel. between J-integral and COD 4-104842  
 low alloys heat treated, grinding residual stress, hardness (Japanese) 4-89117  
 low and medium strength, crack resist. 4-62034  
 low temperature transformation products in microalloyed steels, charact. 4-103948  
 low-alloy, powder metallurgical, elec. cond., thermal cond. and thermal expansion, temp. depend. 4-65658  
 magnetostriction rel. to plane stressed state 4-71152  
 maraging, H embrittlement, notch tensile strength rel. to ion-plated Al coating 4-114671  
 maraging, Ni, fracture toughness, effect of treatment condition 4-76856  
 maraging, SCC in chloride soln. 4-66477  
 maraging, tensile strength and ductility, dependence on microstruct. 4-114603  
 maraging, ultrahigh strength, delayed failure 4-93402  
 mechanical props. rel. to US detectable discontinuities 4-71713  
 microalloyed, cast, microstruct. and mech. props., influence of phase charges (French) 4-81278  
 microalloyed, EXAFS invest. 4-109594  
 microalloyed, fracture micromechanics 4-99602  
 microalloyed, hot-rolled, isothermal decomp. of austenite 4-99409  
 microalloyed, rel. between microstruct. and H embrittlement 4-99605  
 microalloyed, structural, yield props., influence of dislocation density and precip. 4-114601  
 microalloyed eutectoid, austenite recrystn. and pearlite colony size, effect of Nb 4-114572  
 nitriding kinetics under electrolytic heating conditions of 40Kh steel (Russian) 4-85253  
 nuclear structural, A-203D, low temp. deform., effect of microstruct. 4-66386  
 phase identification and anal. using SIMS (French) 4-76936  
 plate, laser melted surface, microstruct., hardness, residual stress 4-71794  
 powder, rapidly solidified, shock consolidation 4-109353  
 pressure vessel, A 508 2 and A 533 B, comparison of stress relief cracking 4-109510  
 pressure vessel, explosively bonded stainless clad steel plate, fatigue crack growth (Japanese) 4-114643

## alloy steel continued

- pressure vessel, mech. props. and precip. hardening response 4-89107  
 pressure vessel, plated with anticorrosive claddings, fracture behaviour 4-99595  
 pressure vessel, unstable ductile fracture under combined load of thermal shock and tension (Japanese) 4-93380  
 pressure vessels, steel, corrosion fatigue, development of engineering codes 4-93406  
 radiation embrittlement of type 15Kh2NMFA steel, temper brittleness (Russian) 4-66407  
 reactor pressure vessel, A533B, environmentally-assisted cyclic crack growth 4-99627  
 reheat cracking, scanning Auger and electron microscopy study 4-71490  
 resulphurised, Ca treated, mech. props. and machinability, S and sulphide shape effect, report 4-62048  
 roll type 9Kh, small N and B additions effect on struct. and mech. props. 4-93342  
 rotor, mag. induction, cooling rate depend 4-76184  
 rotor forgings, unstable fracture, effect of small clustered flaws (Japanese) 4-93378  
 SCC, simulated cracks, current and pot. meas. 4-104904  
 sintered, Mn diffusion coatings 4-89186  
 solute redistribution at pearlite growth front, field emission STEM X-ray chem. microanalysis obs. 4-81191  
 steam turbine casing and rotor, mech. props. rel. to service life (Japanese) 4-89119  
 strengthening effects of Cu in steel 4-89062  
 structural, cast, strength toughness rel. to intercritical treatment (French) 4-81222  
 structural, deform. mechanisms using high temp. tests 4-109481  
 structural, fatigue fractured surfaces, residual stress, X-ray diffraction (Japanese) 4-99513  
 structural, fine-grained, low cycle fatigue, influence of cold forming 4-104841  
 structural, mech. props. and precip. hardening response 4-89107  
 surface hardening by laser, technological control of surface condition parameters 4-71779  
 surface plastic deformation, structural change in case-hardened layers 4-66484  
 tubes, autofrettage, fatigue strength, thermal shock, tempering, electropolishing 4-104865  
 tubes, autofrettaged, fatigue strength 4-104864  
 weathering, preetched, electrochemical and corrosion props. 4-62092  
 weathering performance, effect of Cu 4-89175  
 weld metal deposits, austenite decomposition products, influence of O-rich inclusions 4-114513  
 weldment, HT80, fracture toughness evaluation of heterogeneous bond region 4-99713  
 B, hardenability and B segregation (Chinese) 4-61945  
 Co eutectoid, mech. props. 4-114629  
 Cr, contact zone under friction, X-ray and Auger electron microanal. 4-75763  
 Cr, fatigue crack growth under rot., three-point bend loading, tempering temp. influence (Chinese) 4-114633  
 Cr, fracture toughness and mech. props., effect of tempering 4-76854  
 Cr, hardenability, effect of hot working 4-81211  
 Cr, impurity redistrib. and mech. props. during 475°C ageing (Russian) 4-93317  
 Cr, ledeburitic cold work, microstruct. and abrasive wear 4-114679  
 Cr,  $m = \delta$  superplasticity relation (Chinese) 4-81237  
 Cr, martensitic, impurity level rel. to fusion reactor first wall appl. 4-107013  
 Cr, tempered, residual stress meas. in near surface layers (German) 4-71818  
 Cr-Al-Y, FeCrAlloy, high temp. oxidation, protective scale microstruct. 4-89162  
 Cr-Mn, acoustic emission in H origin defects form. 4-99534  
 Cr-Mn, austenitic, phase stability and corrosion on exposure to pure Li 4-107061  
 Cr-Mn, diffusion reaction with Al coating, Si content effect 4-114723  
 Cr-Mn austenitic, thermally aged, phase instability, precip. reactions 4-109410  
 Cr-Mn-Ti, carburised, struct. and hardness rel. to cyclic heat treatment 4-66406  
 Cr-Mo, anal. of second phase particles; energy dispersive X-ray spectra, EELS obs. 4-81207  
 Cr-Mo, carbonitrided, crack initiation and propag. bending fatigue (Japanese) 4-99509  
 Cr-Mo, cast, corrosion fatigue strength in fresh water, freq. and inhibitor effect (Japanese) 4-99650  
 Cr-Mo, compatibility with flowing Li 4-107062  
 Cr-Mo, creep and plasticity, constitutive eqns. 4-93347  
 Cr-Mo, creep and precip. (German) 4-66375  
 Cr-Mo, creep failure, influence of state of stress 4-93419  
 Cr-Mo, ductile fracture and fracture toughness, effect of stress triaxiality and temp. (Japanese) 4-93379  
 Cr-Mo, fatigue crack growth at 525°C, effects of environment and dwell 4-99523  
 Cr-Mo, fatigue crack growth at 525°C, prediction of continuous cycling endurance 4-99524  
 Cr-Mo, fatigue crack growth at elevated temps., effect of hold periods 4-104867  
 Cr-Mo, fatigue props., effect of intermittent rest periods 4-99588  
 Cr-Mo, fatigue strength, statistical analysis of S-N data (Japanese) 4-99500  
 Cr-Mo, fatigue strength under varying stress amplitude at high temp. (Japanese) 4-114646  
 Cr-Mo, fracture toughness,  $J_{IC}$  test procedures in transition temp. region (Japanese) 4-93486  
 Cr-Mo, fracture toughness degradation after long-term service in petroleum refining (Japanese) 4-89126  
 Cr-Mo, fracture toughness in transition region, interpretation of scatter and thickness effect 4-99603  
 Cr-Mo, high strength, fatigue crack propag., microfractography (Chinese) 4-62006  
 Cr-Mo, intergranular H stress cracking rel. to grain boundary segregation of P 4-62112  
 Cr-Mo, nitrided cases, fracture process, acoustic emission obs. 4-99587  
 Cr-Mo, reduction of rust in high temp. liq. Na 4-104914  
 Cr-Mo, temper-embrittled, effects of grain size and hardness 4-99554  
 Cr-Mo (Japanese) 4-89124

## alloy steel continued

- Cr-Mo (2.25, 1 wt.%), annealed, creep-rupture props., heat-to-heat variations 4-76860  
 Cr-Mo-V, crack growth, influence of cyclic loading 4-93421  
 Cr-Mo-V, creep recovery by reheat treatment, carbide distrib., X-ray analysis 4-66392  
 Cr-Mo-V, fracture toughness for steam turbine rotor appl. 4-104868  
 Cr-Mo-V, hot work, powder metallurgically produced by hot isostatic pressing 4-93248  
 Cr-Mo-V, liq. metal induced embrittlement, dislocation emission from crack tips 4-85210  
 Cr-Mo-V, nonisothermal fatigue tests and analysis 4-93497  
 Cr-Mo-V, ultrahigh strength, H-induced delayed cracking of smooth torsional specimens 4-85203  
 Cr-Mo-V(W), reloading stress relax. behaviour with specified reloading time interval 4-81234  
 Cr-Ni, annealed,  $\phi$ -phase precipitation, potentiostatic etching (*German, English*) 4-71823  
 Cr-Ni, austenitic, reactor irradi. effect on refractory characts. 4-66398  
 Cr-Ni, precipitation and recrystn. processes (*Russian*) 4-93299  
 Cr-Ni, tribological characts. after complex thermochem. treatment 4-93427  
 Cr-Ni ferritic, rapidly solidified, struct. and mech. props. 4-109388  
 Cr-Ni stainless, electrochemical treatment of surface bearing photoresist layer (*Russian*) 4-71773  
 Cr-Ni-Mo, nonisothermal fatigue tests and analysis 4-93497  
 Cr-Ni-Mo-V, high-strength structural, fatigue fracture kinetics, endurance limit and crack resist. 4-99537  
 Cr-Ni-Mo-W-Nb, reloading stress relax. behaviour with specified reloading time interval 4-81234  
 Cr-Si-Mo-V, stamping tool, service life, low cycle fatigue, effect of surface roughness 4-114668  
 Cu, strain meas. near growing fatigue crack tip 4-114651  
 Cu-bearing, hot shortness in controlled rolling process 4-89105  
 Cu-bearing, precip. hardening, effect of austenitising temp. 4-89063  
 Cu-Ni-Cr, compact and surface-flawed specimens, fracture toughness meas. comp. 4-104858  
 Fe-Si laser scribed grain oriented steel, stacked transformer core appls. 4-61552  
 Fe-Si steel, magnetisation, thermodynamic pot. model 4-61557  
 Fe-Si steel, magnetostriction and magnetocrystalline energy anisotropy, texture effects 4-61532  
 Fe/Si strips, mag. props. and domain struct., laser scribing effects 4-61550  
 H corrosion, theory of void growth limited by C diffusion 4-81338  
 Mn, 13 to 19 wt.%, sinter-forged, mech. props. 4-81283  
 Mn, 13 wt.%, prod. by powder metallurgy method 4-81169  
 Mn, controlled hot rolling and intercrit. annealing, time-temp.-reaction diagrams 4-66351  
 Mn, pearlitic ferrite, fatigue dislocation structure (*Chinese*) 4-85201  
 Mn-Mo-Al, transform. of austenite and cryogenic mech. props., effect of intercrit. heat treatment (*Chinese*) 4-85152  
 Mn-Mo-Ni, creep fracture and rupture life (*Japanese*) 4-114647  
 Mn-Mo-Ni, for reactor pressure vessels, neutron irradiation effects on mech. props. 4-108467  
 Mn-Si-Cu, low-alloy, low-cycle surface cracks exam. under tensile loadings 4-89214  
 Mn-V-Cu, austenitic, microstructure rel. to heat treatment and alloying additions 4-89066  
 Mo, fracture toughness,  $J_{IC}$  test procedures in transition temp. region (*Japanese*) 4-93486  
 Mo, secondary hardening mechanisms 4-99396  
 Mo type, passivation mechanism in phosphoric acid solns. in  $P_2O_5$  (*French*) 4-62125  
 Nb, laser hardening 4-114563  
 Nb microalloyed, nonisothermal static softening after hot working 4-114578  
 Nb, solubility product of  $NbC_{0.87}$  in austenite, 950-1250°C 4-61933  
 Nb, strengthening mechanisms, influence of rolling variables 4-71666  
 Nb-V, low C, controlled-rolled, transform. textures 4-99405  
 Nb-V, Nb- and V-carbonitride precipitates, fine struct. (*Chinese*) 4-61929  
 Ni type, phase comp. effect on low-cycle impact fatigue resist. 4-93389  
 Ni-Co-Mo, ultrahigh strength maraging, H embrittlement enhancement by Ni or Cu coatings (*Japanese*) 4-89114  
 Ni-Co-Mo maraging, H embrittlement rel. to coating and heat treatment (*Japanese*) 4-89113  
 Ni-Co-Mo-Ti, controlled hot rolling and intercrit. annealing, time-temp.-reaction diagrams 4-66351  
 Ni-Cr, carburised case depth and hardness, electromag. obs. 4-71830  
 Ni-Cr-Mo, crack paths and H assisted crack growth in  $H_2$  and  $H_2S$ , temp. and press. depend. 4-66429  
 Ni-Cr-Mo, environmental crack growth, temp.-depend., specimen and expt. design 4-109575  
 Ni-Cr-Mo, H embrittlement susceptibility, delayed failure time, effect of specimen geometry 4-85204  
 Ni-Cr-Mo, high strength, stress corrosion cracking: loading history effect 4-109551  
 Ni-Cr-Mo, low alloy, crack branching 4-109490  
 Ni-Cr-Mo maraging, nitrogen effect on struct. and mech. props. 4-114532  
 Ni-Cr-Mo steel, high strength, stress corrosion cracking life, statistical anal. 4-60980  
 Ni-Cr-Mo-V, creep rupture and service properties improvement (*German*) 4-76862  
 Ni-Cr-Mo-V, fracture behaviour effect of S content 4-99601  
 Ni-Cr-Mo-V, fracture toughness, overheating, effect of S content (*Japanese*) 4-93377  
 Ni-Cr-Mo-V, free surface segregation, Mn content effect, Auger spectra 4-66345  
 Ni-Cr-Mu-Si, endurance limit, accelerated Locati method 4-99702  
 Ni-Cu-Mo, sintered Ancoloy SA powder, fracture toughness rel. to pore size and heat treatment 4-76843  
 Ni-Mo, A533B, fatigue crack growth in simulated PWR loop 4-104834  
 Ni-Mo, martensitic A533B pressure vessel, tempered, brittle fracture and fatigue crack growth, segregation effects, Auger obs. 4-66400  
 Ni-Mo-Cr, strain meas. near growing fatigue crack tip 4-114651  
 Ni-Mo-Si, 300M, occurrence of blocky martensite 4-114582  
 Ni-Mo-V, ferritic, low cycle fatigue, elevated temps., crack propag. and fracture modes (*Japanese*) 4-89125  
 Si, anisotropic, rot. magnetisation, tensorial permeability 4-76181

## alloy steel continued

- Si steel surface with oxide, silicate and phosphate coatings, Fourier transform IR spectra 4-104688  
 Si-Fe grain oriented sheets, transformer building factor, cryst. texture effects 4-61554  
 Si-Fe nonoriented semiprocessed steel, core loss and permeability, elec. resist. effects 4-61556  
 Si-Fe-Sn(Cu) high permeability, grain oriented steel, recrystallisation and grain sizes 4-61953  
 V, EELS of small particles 4-104795  
 V, secondary hardening mechanisms 4-99396
- alloying additions**  
 alloys, oxidation rel. to inert dispersoids and rare earth additions 4-114710  
 liquid metals, intrastructural distrib. of additions 4-113297  
 metallurgical systems, mechanisms and kinetics of dissolution 4-114530  
 pure, cold worked, annealing characts. rel. to trace element additions 4-109438  
 solid surface, chemical and electrochemical treatment, low energy electron induced X-ray spectra 4-76572  
 steel, alloy, solute redistribution at pearlite growth front, field emission STEM X-ray chem. microanalysis obs. 4-81191  
 steel, austenitic stainless, cavity formation during electron irradi., effect of pre-implanted He 4-108444  
 steel, austenitic stainless, containing Ti and Al, grain boundary precip. 4-99385  
 steel, austenitic stainless, electron irradiated, void swelling, effect of C and N 4-108445  
 steel, austenitic stainless, modified, void suppression, effect of segregation of minor alloying elements 4-104789  
 steel, austenitic stainless, repassivation kinetics, effect of Mo alloying 4-81331  
 steel, austenitic stainless, Ti-modified, irradi. response in specimens prep. by rapid solidification processing 4-103816  
 steel, austenitic stainless, weld metal, ferrite decomp., effect of Mo additions 4-99374  
 steel, austenitic stainless superalloy, as-cast, corrosion in molten sulphates, influence of Si and W additions 4-71759  
 steel, carburisation, sintering, mech. props. rel. to Cu and P alloying 4-89069  
 steel, Co eutectoid, mech. props. 4-114629  
 steel, Cr, martensitic, impurity level rel. to fusion reactor first wall appl. 4-107013  
 steel, Cr-Mo-V-W, ferritic, impact props., effect of specimen size and Ni content 4-104848  
 steel, Cu-bearing, conf., Luxembourg (May 1983) 4-86106  
 steel, Cu-bearing, precip. hardening, effect of austenitising temp. 4-89063  
 steel, electric spark alloying with TiN and ZrN (*Russian*) 4-76912  
 steel, eutectoid, mech. props., effect of Si additions 4-93365  
 steel, high speed, W-Mo-V, transform. in matrix during austenitising and quenching, influence of Mo 4-114516  
 steel, high strength, high temp. sintering 4-89005  
 steel, HSLA, crack resist. of differently alloyed steels 4-104877  
 steel, microalloyed eutectoid, austenite recrystn. and pearlite colony size, effect of Nb 4-114572  
 steel, Mn-V-Cu austenitic, microstructure rel. to heat treatment and alloying additions 4-89066  
 steel, normalised 04G2B, Y additions effects on mech. props. 4-93390  
 steel, roll type 9Kh, small N and B additions effect on struct. and mech. props. 4-93342  
 steel, stainless, Ni-free, alloyed with rare-earth metals and Ca, struct. and props. 4-62116  
 steel, strengthening effects of Cu 4-89062  
 steel, type G20, influence of V, Nb, Ti additions and phase transition (*Russian*) 4-66327  
 steel, weathering performance, effect of Cu 4-89175  
 steel, weld metal, heat-affected-zone toughness, influence of Cu 4-89106  
 steels, grain refinement by Ti inoculation during submerged arc welding 4-85138  
 Udimet 700, metalloid strengthening mechanism 4-61974  
 Al, with small Sn additions, microstruct. and corrosion behaviour 4-99630  
 Al-Cu-Cd, strengthening mechanism of Cd additions 4-61985  
 Al-Cu-Li alloys, mech. props., effect of minor alloying additions of Zr, Cd or Fe 4-99526  
 Al-Cu-Mg-Ag, precipitate struct. and orientation relationship, effect of Ag additions 4-93303  
 Al-Mg-Si alloy, effect of Fe on precipitation 4-104783  
 Al-Mg-Si-Sn, ageing, clustering process rel. to Sn addition, elec. resist., TEM obs. 4-114529  
 Al-Si, silumens, permanent modification with Sr and Sb (*Polish*) 4-85145  
 Al-Si alloy, cast, graphite additions influence on wear characts. 4-109520  
 Al-Si-Mg-Sr, hypoeutectic alloys, melting losses of Sr rel. to holding time 4-114498  
 Al-Si-Mg-Sr, struct. and props., comp. and Sr addition effects 4-61987  
 Al-Si-Sb, eutectic, struct. rel. to Sb addition, electron beam microanalysis (*German, English*) 4-66314  
 Al-Sn (0.1 wt.%), corrosion-resist, electrochemical props. rel. to alloying additions 4-81342  
 Al-Zn-Mg, SCC study, effect of various alloying additions (*German*) 4-71798  
 Al-Zn-Mg-Cu, precip. and quench sensitivity, effect of Cu additions 4-85155  
 $Al_2O_3$  fibre reinforced Mg alloys, tensile and fatigue behaviour, matrix alloying effects 4-114653  
 Cu alloy with Sn electroplate, diffusion reaction, effect of additional Fe and Sn 4-71755  
 Cu alloys, dil., chem. redistrib. under simulation irradi. 4-108478  
 $\beta$ -CuZn, martensite start temp., effect of Ti additions 4-61928  
 $\alpha$ -Fe binary alloys, BCC, fatigue, effect of alloying elements 4-66426  
 Fe, sintered compacts, alloying element effect on carburising response 4-99642  
 Fe-Al-Cr (Ni)(Mn), oxidation, effect of ternary alloying additions 4-85242  
 Fe-B metallic glass, transition elements effect on thermal stability, crystn. activation energy 4-108283  
 Fe-base austenitic alloys, high strength evaluation for generator retaining rings 4-99448  
 Fe-Cr-Al(-Y), precip., small-angle neutron scatt. study 4-93304

## alloying additions continued

- Fe-Cr-Co (12 wt.%) permanent magnet alloys, mag. props., effect of alloying 4-84771  
 Fe-Cr-Co alloy, Ti effect on rate of high-coercivity transform. 4-93296  
 Fe-Cu, strengthening effect of Cu 4-89062  
 Fe-Mn-Al-Si system alloys, phase comp., Al and Si additions effect 4-114481  
 Fe-Ni-Cr (16, 15 wt.%), void swelling, effect of C and Nb additions 4-103817  
 Fe-Ni-Cr-Al-(Y)(Zr)(Ti), high temp. oxidation resist. influence of Y, Zr or Ti additions 4-104899  
 Fe-Ni-Cr-B-C, swelling behaviour, influence of Li shell effect on microscopy determ. 4-109580  
 Fe-Ni-Cr-C, Ti-modified, void swelling, pre-irrad. ageing effects 4-104798  
 Fe-P-W(Mo)(Mn), grain boundary embrittlement, impurity-induced, influence of alloying elements 4-114654  
 Fe-Si (3 wt.%), texture development and final mag. props., effect of secondary cold-reduction ratios (*Korean*) 4-81215  
 FeCo based alloys, strength and mag. props. rel. to cold rolling and heat treatment 4-98918  
 FeNi(Cr,Mo), neutron irrad. effect on mag. props. 4-92907  
 Fe<sub>40</sub>Ni<sub>40</sub>B<sub>20</sub>, metallic glass, melt surface tension and embrittlement, effects of elemental additions and superheat 4-65184  
 Mn-Ge, Invar type, antiferromag., transition metal influence on props. (*Japanese*) 4-65826  
 Mo, ductility transition temp. rel. to alloying elements (*Japanese*) 4-61979  
 Mo-base alloys, welded joints, long-term strength characts. effect of alloying with N 4-109513  
 Mo-V(Zr)(Ti)(Nb)(Ru)(Cr), interstitial-free, workability and ductility, effect of alloying element 4-93345  
 Ni, O assisted intergranular H embrittlement, effects of B, P, Sn and Sb additions 4-62030  
 Ni-Cr-Co-B, melt spun superalloy, annealing, castability, ductility and microstruct. rel. to B additions 4-66323  
 Ni-Mo ordered alloys, phys. metallurgy, microstruct. and props., review 4-114556  
 Ni-Si-Cr (Mo)(Nb), microsegregation, influence of mutual interaction of alloying elements 4-66340  
 Sb, effect of addition to Fe-Si (3 wt.%) steel, textures 4-81216  
 Ti alloys, rapid solidification by melt spinning technique, alloy additives selection 4-89034  
 Ti-Fe-Ni, sintering processes, Ni effect 4-61889  
 Ti-Nb (5 to 20 wt.%), oxidation resist., 500-850°C, influence of Nb (*French*) 4-71788  
 TiAl intermetallic, ductility, strength and microstruct., Ag addition effect (*Japanese*) 4-66391  
 TiCr<sub>2</sub>, solubility of metals, microhardness, flow stress rel. to C content 4-61931  
 W alloys, dispersion and solid solution hardening of vacuum-melted W 4-66346  
 WC-Co-P, wear resist., P addition influence 4-66458  
 Zn-Al, review of commercial alloys 4-88954  
 Zr-Sn (0.1-1.5 wt.%), neutron irrad., effect of tin on growth of polycryst. Zr 4-75537

## alloys

- alloys such as Au-Cu, Au-Cu-Zn are indexed under components of the named elements i.e. gold alloys; copper alloys; zinc alloys in these examples  
 see also actinide alloys; alkali metal alloys; alkaline earth alloys; alloying additions; aluminium alloys; antimony alloys; arsenic alloys; bismuth alloys; boron alloys; cadmium alloys; dilute alloys; eutectic alloys; gallium alloys; germanium alloys; indium alloys; lead alloys; liquid alloys; mercury alloys; rare earth alloys; selenium alloys; silicon alloys; solid solutions; superalloys; tellurium alloys; thallium alloys; tin alloys; transition metal alloys; zinc alloys  
 advanced HTR systems, alloys eval., creep, fatigue, corrosion, neutron effects 4-78699  
 amorphous, atomic struct. model, computer simulation 4-103653  
 amorphous, compaction process, stability, DSC obs. 4-114448  
 amorphous, crystallisation, activation energies from elec. resist. meas., review 4-108285  
 amorphous, plastic deform. and failure, in situ electron microscopy 4-93481  
 amorphous, stress relief annealing, mag. props. 4-104797  
 amorphous, thermopower, electron-phonon enhancement 4-108839  
 amorphous alloys, zero-magnetostriuctive, struct. approach to permeability aftereffect 4-84832  
 amorphous alloys and metallurgy, EXAFS results 4-93135  
 amorphous and cryst., magnetisation, temp. and field depend. 4-76190  
 anisotropic superconducting, time depend. Ginzburg-Landau eqns. 4-88630  
 atmospheric corrosion monitoring using electrochemical sensors 4-109544  
 Auger spectra, partial long range order effects 4-99238  
 BCC binary, bulk decomposition, surface monolayer ordering 4-65383  
 BCC binary alloys, with first, second, third and fifth neighbour interactions, ordered structures 4-113577  
 bicomponent, liquid mixtures separation in a freezing-out process 4-103185  
 binary, BCC and FCC, test of statistical approximations, Monte Carlo simulation 4-113681  
 binary, cellular solidification theory 4-76764  
 binary, equilb. short-range order, effect of lattice geometry (*Russian*) 4-92142  
 binary, FCC, modelling of mag. and chemical ordering 4-104421  
 binary, free energy, high temp. calc. (*Russian*) 4-92389  
 binary, freezing, periodic growth rate effect on morphological stability 4-98039  
 binary, order-disorder transitions, critical surface scattering of X-rays at grazing angles 4-103603  
 binary, quadratic Padé approximant method for calculating densities of states 4-92594  
 binary, solidification model 4-89032  
 binary, sputtered material composition transients, oxide and segregation effects 4-76606  
 binary, transparent phase diagram model, succinonitrile-water, light scatt. obs. 4-104768  
 binary alloy surface segregation, modelling, low index planes, steps, kinks, and chemisorption 4-92495

## alloys continued

- binary alloy surfaces, irradiated, conc. profiles calc. 4-113509  
 binary alloys, charge transfer and energy of formation, CScI intermetallic cps. 4-77026  
 binary alloys, electronegativity in local density functional formalism 4-70061  
 binary alloys, hydride precipitation, two-level model 4-75688  
 binary alloys, kinetics of first order phase transition 4-75642  
 binary alloys, order-disorder transitions, electronic theory 4-113572  
 binary alloys, parabolic growth of oxide solid solutions 4-109563  
 binary alloys, press. influence on precipitation (*Russian*) 4-80232  
 binary alloys, short-range order, ordering transitions, determ. of pair interaction parameters, segregation 4-114512  
 binary alloys, surface comp. profiles, generalised free enthalpy 4-75761  
 binary solid solutions, high conc., lattice dilatation 4-75410  
 binary solutions, decomposition processes 4-109419  
 binary substitutional alloy, FCC struct., interstitial impurity effect on atomic ordering 4-60919  
 binary substitutional alloys, order-disorder transitions, appl. of grand canonical ensemble 4-113570  
 carbide precipitates, computer simulated dissoln. 4-109416  
 castings, light alloy, radioscope for inspection 4-99671  
 catalyst dispersed particles, stacking faults and struct., electron microdiff. studies 4-88178  
 chem. bonding and heat of form., core level shift calorimetry method 4-104714  
 chemical diffusion in binary FCC solid solutions 4-65434  
 close-packed ordered alloys lattice const., Pauling-Simon law 4-75365  
 concentrated, radiation-induced instability calc. 4-75505  
 concentrated alloys, quantitative anal. of diffuse scatt., phase transforms., review 4-113613  
 creep, determ. for long-service lives by multistage process 4-114624  
 creep, nonsteady, system of kinetic eqns. 4-65334  
 cubic alloy, vibr. entropy due to order-disorder transition 4-113668  
 damping alloys, noise and vibration control appl., service condition parameters (*German*) 4-66365  
 diffusion, book contrib. 4-113689  
 diffusion in metals and alloys, conf., Tibany, Hungary (Aug.-Sept. 1982) 4-63405  
 diffusionless phase transformations, book contrib. 4-109405  
 diffusive phase transformations in the solid state, book contrib. 4-109378  
 direct current comparator resistance bridge automation, alloy resistivity appl. 4-90613  
 dislocations, book contrib. 4-108361  
 dislocations and strength of metals at very low temperatures, book contrib. 4-99452  
 disordered, Auger spectra, core-valence-valence, CPA theory, disorder-induced vertex corrections role 4-71491  
 disordered, phonon states, data compilation 4-73178  
 disordered binary, role of excess vol. of form., virtual cryst. model 4-92133  
 disordered binary alloy, short-range order treatment 4-103655  
 disordered binary alloys, diffuse X-ray scatt., separation of thermal component 4-103704  
 DTA using cassette-type installation 4-66522  
 electric field gradient, charge shift model calc., validity regions 4-113915  
 electron theory of metals, book contrib. 4-108770  
 electronic energy calc., improved perturbation theory 4-65601  
 electronic structure of metals and alloys, conf., Johnsbach, Germany (May 1983) 4-67867  
 fatigue, book contrib. 4-109514  
 fatigue failure curves, centre portion anal. 4-92292  
 FCC, Suzuki segregation, TEM study 4-89054  
 FCC binary, ordering and phase separation, miscibility gap 4-113652  
 FCC random, atom transport, phenomenological coeffs. computer simulation 4-84444  
 friction and wear, appl. of dislocation concepts, book contrib. 4-98103  
 fusion reactor materials, radiation damage, pulse ion irrad. microstruct. 4-103821  
 fusion reactor structural materials, strategic planning issue for irrad. programme 4-107035  
 grain boundaries and cryst. defects, interatomic pots. 4-113464  
 heterogeneous, selective erosion, rel. to emission spectral anal. 4-81292  
 Heusler ternary alloys, cubic, order-disorder transitions, theory 4-61080  
 Heusler-type, X-ray spectra and electronic struct., mag. band struct. 4-71465  
 impurity atoms solubility, impurity-atom complexes formation (*Russian*) 4-103937  
 indirect exchange interaction, computer simulation for cryst. and amorphous metals 4-84779  
 inhomogeneity evaluation, thermo-EMF method 4-66521  
 inhomogeneous ordered binary alloys, stationary states, long-period superlattices 4-113399  
 inorganic cryst. struct. data, standardisation 4-75386  
 interfacial and surface microchemistry, book contrib. 4-109421  
 intergranular corrosion of steels and alloys, book 4-95084  
 intermetallic, recursion method calc. of density of states 4-70626  
 intermetallic compound structure, book contrib. 4-108309  
 intermetallic compound-H system, two-phase coexistence region, H chemical pot., interface rel. effect 4-104769  
 interstitial, phase transitions of interstitial atoms in voids (*Russian*) 4-103741  
 interstitial alloys, thermal expansion study (*Russian*) 4-103976  
 interstitial atom ordering, transition in variable volume model (*Russian*) 4-92124  
 interstitial distrib., variable-volume model (*Russian*) 4-84289  
 interstitial solid solutions, impurity solute atoms distribution, interactive interaction effects (*Russian*) 4-108405  
 ion implantation for materials processing, book 4-73184  
 irradiated, solute enhanced diffusion due to interstitials 4-88334  
 isomorphous precipitation, modulated struct. form. (*Russian*) 4-92369  
 Kondo problem soln. for orbital singlet 4-75960  
 magnetic properties, book contrib. 4-114093  
 magnetisation and phase decomposition, structural diagrams 4-76138  
 mechanical properties of solid solns. and intermetallics, book contrib. 4-109423  
 mechanisms and kinetics of dissolution 4-114530  
 metallic glasses, atomic size effect on formability 4-75300  
 metallic solid solns., microstruct., X-ray and neutron obs. 4-66341  
 metallurgical thermodynamics, equilb. states and influencing factors, book contrib. 4-109375

**alloys continued**

- metals, noncubic, elec. quadrupole interaction studies, review, book contrib. 4-70764  
 microsegregation model, dendritic struct., undercooling, temp. depend. diffusion 4-89056  
 microstructure, classification, overview 4-66309  
 monotectic solidification, microstruct. and phase spacings 4-93284  
 multiphase, mech. props., book contrib. 4-109424  
 NBS standard reference materials catalogue (1984-5) 4-78062  
 neutron irradiated, localised plastic flow characterisation with indentation hardness 4-109581  
 nonferrous alloys, surface modification of materials by laser treatment 4-109547  
 nonrandom, substitutionally. disordered, densities of states calcs. 4-113843  
 nonrandom substitutionally disordered alloys, cluster density of states 4-70737  
 nuclear acoustic resonance, in metals and alloys, review 4-76263  
 omega phase, struct. and X-ray diffuse scatt. (*Japanese*) 4-113390  
 one-dimensional disordered binary alloys, cluster mean-field theory 4-92599  
 one-dimensional long-period superstructural alloys, config. of antiphase domains 4-113663  
 optical techniques for investigation of props. 4-71858  
 ordered, two-dimensional antiphase structures, dark-field high resolution images 4-113662  
 ordering kinetics accompanying phase separation 4-113653  
 oxidation rel. to inert dispersoids and rare earth additions 4-114710  
 peritectic, solidification mechanism, microstruct. aspects 4-93273  
 phase diagrams, book contrib. 4-109376  
 phase transformations investigation with X-ray diffractometer 4-99669  
 PIXE for elemental analysis of thick target metal alloys 4-89359  
 plastic deformation, mech. props. and struct. (*Russian*) 4-109468  
 plastic eqn. of state rel. to scaling behaviour 4-109462  
 point defects, book contrib. 4-108357  
 polycrystalline and amorphous, anisotropic effects and mag. props. 4-84781  
 polycrystalline materials, creep at low stresses and intermediate temp., diffusion flow mechanism 4-71701  
 polycrystalline materials, grain boundaries model and effect on mech. props. 4-113458  
 powders, rapidly solidified, production using unidirectional atomiser 4-109338  
 precipitation rel. to elec. resist. 4-114546  
 preferred sputtering, segregation effects 4-81203  
 radiative properties at high temp. 4-84952  
 random substitutional alloys with environmental disorder, muffin-tin potentials, self-consistent approx. 4-61269  
 rapid solidification, research and appls., review 4-66322  
 rapid solidification by free jet melt spinning 4-89035  
 rapid solidification techniques, review 4-89033  
 rapidly quenched from melt, book contrib. 4-109356  
 recovery and recrystallization, book contrib. 4-109429  
 refractory, sintering, conf., Atlanta, GA, USA (Mar. 1983) 4-95042  
 refractory, thermal expansion meas. 4-75710  
 refractory metal base sintered materials, erosion resist. in stationary arc 4-62068  
 residual resist. changes due to clustering, t-matrix anal. 4-98591  
 scanning electron acoustic microscopy imaging, depend. on chopping and detect. freq., appl. to Cu-Zn-Al 4-69639  
 semiconductor detector, anomalous X-ray scattering, local structure of amorphous alloy 4-91174  
 sheet formability and plastic instability, effect of geometry and materials props. 4-93351  
 short fatigue crack behaviour and the concept of absolute and relative fatigue thresholds 4-84344  
 short-range order fluctuations and Fermi surface effects (*Japanese*) 4-113391  
 short-range ordered, elec. resist., tight-binding calcs. 4-70778  
 soft magnetic, domain wall motion modelling 4-76162  
 soldering alloys, PIXE anal. 4-99898  
 solid particle erosion 4-109518  
 solid soln., partial impurity volume and lattice deform. 4-108390  
 solid solutions, short range order or segregation, Monte Carlo simulation 4-108282  
 solidification, book contrib. 4-109393  
 solidification, theory of form. of closed shrinkage cavities 4-114506  
 solidification and cooling, dendritic segregation development (*Polish*) 4-85144  
 solidification mechanisms, microsegregation-free 4-89039  
 strain hardening, plastic deform., elastic-plastic problem soln. 4-114623  
 strain-hardening type, plastic deform, theory, defining eqns. and calcs. 4-79466  
 stress-rupture strength in complex stressed state, criteria development 4-99540  
 structural, mech. props. at low temps. rel. to stressed state and mode of loading 4-93350  
 superconducting materials, book contrib. 4-108959  
 superconducting transition temp. correlation with electronic struct. 4-88627  
 superdislocation traps in inhomogeneous glide plane (*Russian*) 4-92210  
 superlattice alloys, one-dimensional long-period, stability due to Madelung energy 4-60880  
 superplastic materials, elongation, grain growth and cavitation effects 4-71711  
 ternary, ion implantation prep., surface binding energy 4-79972  
 ternary alloy source material for rod-fed evaporation, fabrication process 4-114581  
 ternary alloys, short-range order, ordering transitions, determ. of pair interaction parameters, segregation 4-114512  
 Thermodynamics and entropy of mixing 4-109395  
 thin amorphous layer, produced by laser radiation 4-80089  
 three component solid soln., equilb. competitive segregation 4-66338  
 tracer diffusion in concentrated alloys 4-65442  
 tracer diffusion in intermetallic compounds 4-65443  
 two-dimensional phase fraction charts 4-76756  
 undercooled melts, dendritic growth 4-89042  
 virtual bound state, proximity effect tunnelling 4-114074  
 X-ray production and quantitative electron-probe micro anal., depth distrib. (*Chinese*) 4-99855  
 rapidly quenched, struct. and thermal props., review 4-109443

**alnico alloys see iron alloys****Al<sub>2</sub>O<sub>3</sub> see alumina****Al<sub>2</sub>O<sub>3</sub>-α see corundum****α-Al<sub>2</sub>O<sub>3</sub> see corundum****alpha-decay**

see also *alpha-decay theory; alpha-particle spectra*

- <sup>263</sup>108, identification by α-chains to daughter isotopes 4-86863  
 data sources and inconsistencies 4-73859  
<sup>12</sup>C(<sup>6</sup>Li,d)<sup>16</sup>O\*(α), α-d ang. correl. functions, optical pot. determ. 4-86859  
<sup>213</sup>Fr, in-beam α, e and γ-spectroscopy 4-68647  
<sup>7</sup>Li-αt, vertex const. determ., shell and cluster structure coexistence, generator ward. anal. 4-59212  
<sup>20</sup>Ne 2<sup>+</sup> level, γ and highly retarded α-decay partial widths from <sup>19</sup>F(<sup>3</sup>He,d) 4-59211  
<sup>18</sup>O-<sup>14</sup>Ca, sequential breakup in <sup>12</sup>C(<sup>18</sup>O,<sup>14</sup>Ca), DWBA anal. 4-83095  
<sup>212</sup>Po, spherical nuclei, α-clustering and absolute α-decay widths 4-68657  
<sup>238</sup>Pu α-activity fraction in NBS Pu standard reference materials 946 and 947, safeguards 4-107000  
<sup>224</sup>Ra α-decay, emission probability meas. 4-68656

**alpha-decay theory**

see also *alpha decay*

No entries

**alpha-particle absorption**

No entries

**alpha-particle angular distribution**

see also *alpha-particle spectra*

- Ag(<sup>40</sup>Ar,X), 285 MeV, α-particle form., cross-sections, energy and ang. distrib. 4-78650  
<sup>9</sup>Be(α,α), 23.1 MeV, elastic and inelastic, anomalous large angle scatt., Regge pole anal. (*Chinese*) 4-83080  
<sup>12</sup>C(<sup>18</sup>O,α), 10-15 MeV, resonances, excitation functions, ang. distrib. 4-106603

**alpha-particle attenuation see alpha-particle absorption****alpha-particle detection and measurement**

see also *alpha-particle spectrometers; radioactivity measurement*

- aluminised plastic track detectors, spot development around track- and electric tree-induced perforations 4-102474  
 blood, smokers and non-smokers, α-activity meas. by CR-39 SSNTDs 4-100371  
 CA8015 plastic detectors, pseudocolour techniques for nuclear track differentiation 4-96360  
 cellulose nitrate track detectors, α-track anal. using Interactive Image Analysis System 4-96348  
 chemical anal., emission count data anal. procedure 4-93580  
 CN-85 Kodak-Pathe track etch foil, Rn and daughters detection appl. 4-96405  
 conference, alpha-particle spectrometry techniques and appl., Geel, Belgium (Oct. 1981) 4-67853  
 conference on solid state nuclear track detectors, Acapulco, Mexico (Sept. 1983) 4-95027  
 counting rate to activity conversion on multichannel analysers 4-68868  
 CR-39, α-energy discrimination, pre-etched track length/electrochem. etching track spot size relation 4-96401  
 CR-39 detectors, α-particle registration props., temp. depend. 4-91180  
 CR-39 detectors, p and α electrochem. etched tracks, pre-etching effects 4-102470  
 CR-39 plastic detector, response to γ-radiation, effect on track registration 4-96346  
 CR-39 plastic track detector, α-track registration props., pre-irradiation annealing effect 4-59589  
 CR-39 plastic track detectors, light charged particle registration characts. 4-64306  
 CR-39 proton and alpha etch pits, automated assessment techniques 4-96354  
 CR-39 sheets, possible high resolution spectroscopy for particles at selected dip angles 4-102483  
 CR-39 solid state nucl. track detector for alpha induced reaction and scatt. at VEC 4-59588  
 CR-39 SSNTD, scanning by a sampling method, automated country 4-96357  
 CR-39 thin SSNTD, alpha track etch formation, variable etch rate ratio 4-96329  
 CR-39 track detector, automatic PEPR device for counting α-tracks 4-96349  
 CR-39 Track Profile Technique, alpha and fission fragment range and energy meas. 4-96336  
 DIGITRACK, CCD based system for automatic nuclear track counting and eval. 4-96358  
 electrostatic precipitator for the study of airborne radioactivity 4-89786  
 flight-time detector with KBr as the sensitive substance 4-74097  
 Fusion Neutronic Sources, absolute yield meas. using α-particle method 4-96321  
 gas-flow proportional counter for simultaneous α and β counting (*Spanish*) 4-87000  
 gridded ion chambers, particle counting method 4-102429  
 high resolution semiconductor detector, relative alpha intensities of several actinide nuclides 4-102432  
 human lung, α-active nuclides microdistrib. using CR-39 SSNTD 4-100370  
 ion beam image formation in gelatine and various polymers 4-96339  
 Karlsruhe Rn diffusion chamber sensitivity using electrochem. etched Makrofol detectors 4-96283  
 lineshape of alpha particle from natural source, ionisation loss formulae anal. 4-96413  
 low power radiation survey instruments 4-59440  
 LR115 SSNTD, bulk and α-track etch rates 4-96331  
 LR-115 with spark counter, detection efficiency for 1.24-3.3 MeV alpha-particles 4-96355  
 Makrofol E, neutron induced recoil- and α-tracks, temp. and humidity depend. fading 4-102486  
 microchannel plate detector appl. 4-74111  
 modified spark counter for α-spectroscopy 4-96397  
 multidetector alpha spectroscopy analysis system 4-59483  
 passive track detectors for Rn dosimetry, plate-out effects 4-96402  
 polycarbonate, α and recoil track electrochem. etching response, energy and track density effects 4-102471  
 polymer track detectors for alpha particles recording, atmospheric pressure influence 4-102530

**alpha-particle detection and measurement continued**

- SHIP position sensitive surface barrier detection system 4-102431  
solid state nuclear track detector use in radiation dosimetry, medicine and biology 4-72430  
spectra, computerised anal., resolution, distribution 4-68866  
spectra fitting method 4-102436  
spectrometers, radioactivity meas. development and applications 4-68870  
spectrometry, irradiation research and reprocessing appl. 4-68864  
spectrometry, nuclear applications, influencing factors 4-68863  
SSNTD, CR-39, CN-85; CA 80-15, LR 115 and Melinex O, high energy charged particle response 4-102484  
SSNTD, use of different Mexican commercial polymers, etching, dosimeters 4-102476  
SSNTD autoradiography appls. in nuclear industry, weld inspection, Pu distrib. 4-99665  
strong ionising events along medium energy  $\alpha$ -tracks in nuclear emulsions 4-96342  
superconductive thin strips as high-resolution vertex detectors 4-96326  
<sup>12</sup>C( $\alpha$ ,<sup>3</sup>Be), 2.4-6.4 MeV, subbarrier cross section meas. using plastic detectors 4-96048  
Am alpha-particle spectrometer, computerised system for low level actinides 4-68867  
Am alpha-spectrum anal., peak ratio's 4-68865  
Ar-N<sub>2</sub> gas proportional scintillation counter, alpha particle detection 4-59546  
Cm alpha-spectrum anal., peak ratio's 4-68865  
<sup>6</sup>Li( $\alpha$ ,<sup>3</sup>He), A=6,7,  $\alpha$  and <sup>3</sup>He detection using CR-39 SSNTD 4-96078  
<sup>210</sup>Pb distribution in environmental samples by CR-39  $\alpha$ -detector 4-100053  
<sup>210</sup>Po,  $\alpha$ -particle detection with Sn-SnO<sub>x</sub>-Sn tunnel junction detectors 4-74112  
<sup>210</sup>Po distribution in environmental samples by CR-39  $\alpha$ -detector 4-100053  
Pu alpha-particle spectrometer, computerised system for low level actinides 4-68867  
Pu alpha-spectrum anal., peak ratio's 4-68865  
<sup>238</sup>Pu alpha emission, absolute energy determ. using cellulose nitrate films 4-102433  
<sup>238</sup>Pu, decay  $\alpha$ -particle and  $\gamma$ -ray emission probabilities 4-102434  
Rn, daughter activities, meas. instrumentation 4-93867  
Rn daughter concn. in room air, continuous spectrometry by twin channel device 4-93672  
Rn daughter product, passive detection rel. to plateau 4-93863  
Rn daughters suspended in air, alpha activity, working level in U mines and houses 4-109966  
Rn detection in Finnish dwellings, film detectors calibration 4-93895  
Rn, thoron and Rn daughter meas. by multi-detector devices in caves and dwellings 4-96282  
<sup>220</sup>Rn, <sup>222</sup>Rn discrimination in soil gas using solid state nuclear track detectors 4-100767  
<sup>222</sup>Rn and daughters, short and long term techniques for meas. inside houses 4-72441  
<sup>222</sup>Rn exhalation rate from surface of building materials or soil, meas. apparatus 4-93896  
<sup>222</sup>Rn measurements inside household dwellings using LR-115 SSNTD 4-96279  
<sup>222</sup>Rn, use of silicon surface barrier detectors 4-68902  
<sup>222</sup>Rn-<sup>218</sup>Po, activity meas. using surface barrier detector (Chinese) 4-68872  
Si counter monitoring system for separation of transplutonium elements 4-102537  
Si surface barrier detector, review of  $\alpha$ -particle spectrometric meas. 4-68869  
Si surface barrier detector, asymmetrical response to light ions 4-102435  
p-Si:P surface-barrier detectors fabrication and appl. 4-87018  
Th alpha-particle spectrometer, computerised system for low level actinides 4-68867  
Th halide crystal cond. counters, appl. to  $\alpha$ -particle and  $\gamma$ -ray detection 4-59577  
U, alpha spectroscopy and ang. depend. for CR-39 SSNTD 4-96384  
U alpha-particle spectrometer, computerised system for low level actinides 4-68867  
U determination in mineral rocks by CR-39 SSNTD 4-100766

**alpha-particle effects**

- borosilicate waste glasses, ion bombard., fracture toughness and leaching behaviour 4-75545  
chromosome damage in Chinese hamster cells, flow cytometric determ., correl. with cell survival 4-105291  
fibroblasts, bone, mouse, effect of <sup>241</sup>Am  $\alpha$ -particles 4-77348  
fusion reactor material, irradi. damage simulation, induced radioactivity by 16 MeV, protons and 30 MeV  $\alpha$ -particles 4-107038  
graphite composites in reactors, influence of neutron and  $\alpha$ -particle bombardment 4-96141  
lipid multilayers, modifications induced by <sup>241</sup>Am  $\alpha$ -particles 4-115140  
molecular targets, proton and  $\alpha$ -particle irradiated,  $\delta$ -ray emission 4-81058  
mutagenicity of  $\alpha$ -particles in Ehrlich ascites tumour cells 4-105292  
nuclear emulsions, alpha particle tracks; strong ionising events 4-92270  
nuclear waste storage materials, radiation effects 4-73973  
Rutherford backscattering spectra of <sup>12</sup>C, <sup>1</sup>H and <sup>4</sup>He, low energy background 4-88921  
simulated nuclear waste glass, Cm doped, radiation damage, annealing, short term leach test 4-83149  
steel, austenitic stainless, TiC precipitation, influence on creep rupture strength, ductility and He embrittlement 4-99388  
stilbene, mol. cryst., triplet exciton  $\alpha$ -particle excitation, diffusion coeff. 4-104130  
zirconolite-based ceramic, self-irradiation damage 4-75546  
<sup>109</sup>Ag( $\alpha$ ,2n), induced radiation damage by TDPAC (Chinese) 4-70225  
Al, alpha-particle ang. blocking dips, multistrong Monte-Carlo simulation and analytical calcs. 4-92274  
Bi:Po, impurity atom location, channelling studies with point  $\alpha$  sources 4-113470  
Cu, polycrystalline, He porosity, profilometric investigations 4-103834  
GaAs, E3 centre accumulation, effect of defect charge state 4-60966  
n-GaAs:Si,  $\alpha$ -irrad., positron annihilation study 4-104696  
Ge single cryst.,  $\alpha$ -particle irrad., defects and photoelectromag. effects 4-84654

**alpha-particle effects continued**

- KBr,  $\alpha$ -particle ionisation, controlled secondary electron emission 4-76570  
Kr<sub>2</sub>, VUV-excimer radiation build-up and decay frequencies, excited by  $\alpha$ -particles 4-91437  
LiF,  $\alpha$ -particle ionisation, controlled secondary electron emission 4-76570  
MgO,  $\alpha$ -particle ionisation, controlled secondary electron emission 4-76570  
Mo, alpha-irrad., defect annealing, positron annihilation, Doppler broadening 4-70227  
NaPO<sub>3</sub> glass, alpha-particle induced damage, vibr. Raman spectra 4-70237  
SiO<sub>2</sub> glass, alpha-particle induced damage, vibr. Raman spectra 4-70237  
Ta, blister formation by 30 MeV alpha particles bombardment 4-113507  
Ti-Nb-Ta oxides, metamict, alpha-recoil damage study by EXAFS and XANES spectroscopy 4-76559  
Y(PO<sub>3</sub>)<sub>3</sub> glass, alpha-particle induced damage, vibr. Raman spectra 4-70237  
ZrSiO<sub>4</sub>, swelling induced by alpha and gamma irrad. 4-75543  
**alpha-particle interactions** *see alpha particle-nucleus reactions*  
**alpha-particle model** *see nuclear cluster model*  
**alpha particle-nucleus reactions**  
*for inelastic alpha particle-nucleus scattering, see "alpha particle-nucleus scattering"*  
cold breakup of spectator residues in nucleus-nucleus collisions at high energy 4-59577  
conference on nuclear physics at large tandem accelerators, Padova, Italy (March 1983) 4-86108  
resonating group method, equiv. local pots., Perey factors, orthogonality condition model 4-83008  
( $\alpha$ , $\alpha'$ ), actinide region, giant resonance fission decay, review 4-73942  
( $\alpha$ , $\alpha'$ ), 4.5 GeV/c/N, 4-102273  
( $\alpha$ , $\alpha'$ ), continuum spectra from medium energy reactions, cross sections, extended exciton model anal. 4-73898  
( $\alpha$ , $\alpha'$ ), nucleon emission deexcitation of highly excited states and giant resonances 4-73868  
( $\alpha$ ,d) reactions, D-state and nuclear struct. effects, DWBA calcs. 4-96041  
( $\alpha$ ,f), on A=255-258, fission fragments and mechanisms 4-106637  
( $\alpha$ ,He), inner and outer subshell investigation 4-73883  
( $\alpha$ ,He), 218 MeV, 2 nucleon strengths, inner and outer subshell investigation 4-73883  
( $\alpha$ ,p), pre-equilibrium light particle emission 4-73888  
( $\alpha$ ,t), inner and outer subshell investigation 4-73883  
( $\alpha$ ,X), 20-200 MeV, energy and momentum transfer processes 4-59241  
( $\alpha$ ,X), on A~60, 90, >160 MeV, particle spectra, excitation functions, model calcs. 4-86838  
( $\alpha$ ,X) on C, Cu, Pb, neutron energy spectra, anal. 4-73908  
( $\alpha$ ,X) on C, Fe, Cu, Pb, neutron and photon prod., expt., Monte Carlo calcs. 4-73907  
<sup>107</sup>Ag( $\alpha$ ,2n)<sup>111</sup>In, simultaneous prod. of <sup>96</sup>Tc and <sup>111</sup>In by stacked foil method 4-77385  
<sup>27</sup>Al( $\alpha$ ,He), <sup>27</sup>Al ang. distributions, DWBA calcs. 4-83086  
<sup>27</sup>Al( $\alpha$ ,t), <sup>27</sup>Al ang. distributions, DWBA calcs. 4-83086  
<sup>27</sup>Al( $\alpha$ ,t), 26.2-26.7 MeV, <sup>27</sup>Si states, spectroscopic amplitudes, DWBA and Hauser-Feshbach anal. 4-95898  
<sup>197</sup>Au( $\alpha$ ,2n), 26 MeV, <sup>199</sup>Tl rotational states, J<sup>π</sup> and transitions (Chinese) 4-82980  
( $\alpha$ ,X) cross-section oscillation damping in quasi-elastic processes (Ukrainian) 4-86837  
<sup>13</sup>B( $\alpha$ ,X), A=10.11, X=p,d,t, 31.2 MeV ang. distrib. and reaction mech. (Chinese) 4-73884  
<sup>13</sup>B( $\alpha$ ,2n), 20-27 MeV, <sup>14</sup>C positive and negative parity excited state above the 6<sup>+</sup> isomer 4-64036  
<sup>7</sup>Be( $\alpha$ , $\gamma$ ), reson. alpha capture study 4-68706  
<sup>12</sup>C( $\alpha$ ,H), 49-159 MeV, fragment mass, energy and ang. distrib. 4-73917  
<sup>12</sup>C( $\alpha$ ,H), fragment mass, energy and ang. distrib., intranuclear cascade, Fermi breakup 4-73909  
<sup>4</sup>Ca( $\alpha$ , $\alpha$ ), A=40, 42, 44, 48, local density approximation 4-83089  
<sup>108</sup>Cd( $\alpha$ ,n)<sup>111</sup>Sn, excited states, in-beam spectroscopic methods, shell model predictions 4-102221  
<sup>59</sup>Co( $\alpha$ ,X), excitation functions using exciton model 4-86840  
<sup>59</sup>Co( $\alpha$ ,n), 30 MeV, excitation function, non-compound effects 4-59257  
<sup>59</sup>Co( $\alpha$ ,p), 18 MeV, pre-equilib. emission, even-odd effect, exciton model anal. 4-64154  
<sup>52</sup>Cr( $\alpha$ , $\alpha$ ), 104 MeV,  $\alpha$ -particle optical pot. and nucl. matter densities, isotopic and isotonic differences 4-68707  
<sup>63</sup>Cu( $\alpha$ ,p), 18 MeV, pre-equilib. emission, even-odd effect, exciton model anal. 4-64154  
Cu( $\alpha$ ,p), 3.6 GeV/nucleon, inclusive proton spectra 4-78643  
<sup>162</sup>Dy( $\alpha$ ,2n $\gamma$ ), <sup>164</sup>Er rotational side-band study 4-86763  
<sup>2</sup>H( $\alpha$ , $\gamma$ )<sup>3</sup>Li capture cross-section, 0<sup>+</sup> T=1 parity violating decay 4-59252  
<sup>2</sup>H( $\alpha$ ,p)n resonating group Faddeev method, few cluster system anal. 4-59183  
<sup>3</sup>He( $\alpha$ , $\gamma$ )<sup>7</sup>Be, 165-1169 keV, cross section, low energy behaviour 4-68702  
<sup>3</sup>He( $\alpha$ , $\gamma$ )<sup>7</sup>Be, radiative capture study with resonating-group wave functions 4-68703  
<sup>4</sup>He( $\alpha$ ,X), high energy, collective quark tubes and multiplicity distrib. 4-82948  
<sup>4</sup>He( $\alpha$ ,X), 124 GeV, central region, anomalous nuclear enhancement of neutral energy spectrum 4-68701  
<sup>4</sup>He( $\alpha$ ,x), two-particle rapidity correl. at CERN ISR 4-59118  
<sup>165</sup>Ho( $\alpha$ ,x), x=n, 2n, 30 MeV, excitation function, non-compound effects 4-59257  
<sup>6</sup>Li( $\alpha$ , $\gamma$ ), vector polarised, parity mixing effect and 5.11 MeV state width in <sup>10</sup>B 4-59249  
<sup>7</sup>Li( $\alpha$ , $\gamma$ ), reson. alpha capture study 4-68706  
<sup>93</sup>Nb( $\alpha$ ,n)<sup>96</sup>Tc, simultaneous prod. of <sup>96</sup>Tc and <sup>111</sup>In by stacked foil method 4-77385  
<sup>93</sup>Nb( $\alpha$ ,x), x=n, 2n, 30 MeV, excitation function, non-compound effects 4-59257  
<sup>58</sup>Ni( $\alpha$ ,d), breakup-fusion description, continuum spectra fit, ( $\alpha$ ,p) comparison 4-102242  
<sup>58</sup>Ni( $\alpha$ ,n)<sup>61</sup>Zn, <sup>58</sup>Zn decay scheme and level props. 4-102223  
<sup>58</sup>Ni( $\alpha$ ,p), breakup-fusion description, continuum spectra fit, ( $\alpha$ ,d), ( $\alpha$ ,t) comparison 4-102242  
<sup>58</sup>Ni( $\alpha$ ,t), breakup-fusion description, continuum spectra fit, ( $\alpha$ ,p) comparison 4-102242

**alpha particle-nucleus reactions continued**

- <sup>69</sup>Ni( $\alpha$ ,p), 18 MeV, pre-equilib. emission, even-odd effect, exciton model anal. 4-64154
- <sup>237</sup>Np( $\alpha$ ,xn), E>45 MeV,  $x=1$  to 4; excitation function calc., precompound evaporation anal. 4-73918
- <sup>16</sup>O( $\alpha$ , $\gamma$ )<sup>20</sup>Ne direct capture reaction at low energies 4-102284
- <sup>206</sup>Pb( $\alpha$ ,d) <sup>208</sup>Pb excitation levels, DWBA calcs. 4-83087
- <sup>85</sup>Rb( $\alpha$ ,3n) 30-55 MeV, <sup>86</sup>Y high spin states,  $\gamma$ -transitions 4-73808
- <sup>187</sup>Re( $\alpha$ ,3n), 30-55 MeV, <sup>189</sup>Ir levels, J<sup>π</sup>, T<sub>1/2</sub>, transitions and ICC 4-111490
- <sup>99</sup>Ru( $\alpha$ ,2np), 30-55 MeV, <sup>100</sup>Rh high spin states; isomers, J<sup>π</sup>, T<sub>1/2</sub> and transitions 4-86762
- <sup>34</sup>S( $\alpha$ , $\alpha'$ ), 0-2.2 MeV, transition, neutron and proton transition matrix element sign determination 4-73828
- <sup>86</sup>Se( $\alpha$ ,2n), 21-27 MeV, <sup>87</sup>Kr levels, J<sup>π</sup>, T<sub>1/2</sub>, collectivity, bands, 2p and 2n excitations 4-111491
- <sup>4</sup>Sn( $\alpha$ ,He), A=116,118,120 high-lying neutron particle states 4-111546
- <sup>Sn</sup>( $\alpha$ ,p), 3.6 GeV/nucleon, inclusive proton spectra 4-78643
- <sup>181</sup>Ta( $\alpha$ ,2n), 16-30 MeV, <sup>183</sup>Re  $\gamma$ -decay spectrum 4-95952
- <sup>122</sup>Te( $\alpha$ ,Zn), <sup>124</sup>Xe band, superbands, J<sup>π</sup>, backbending and  $\gamma$ -transitions 4-102167
- <sup>230</sup>Th( $\alpha$ ,f), 50 MeV, total kinetic energy release, mass yield distrib. 4-59291
- <sup>232</sup>Th( $\alpha$ , fission) fission fragment ang. distribution, momentum transfer 4-86869
- <sup>A</sup>U( $\alpha$ ,f), A=235, 238, fissionable nuclei lifetime meas. 4-78654
- <sup>A</sup>U( $\alpha$ ,xn), A=233-235, E>45 MeV,  $x=1$  to 4, excitation function calc., precompound evaporation anal. 4-73918
- <sup>230</sup>U ( $\alpha$ , $\alpha'$ X), X=p or fission fragment, 172 MeV, direct N knockout, precompound emission 4-83084
- <sup>62</sup>Zn( $\alpha$ ,p), 18 MeV, pre-equilib. emission, even-odd effect, exciton model anal. 4-64154

**alpha particle-nucleus scattering**

- charged particle fusion cross sections, data status for reactor design 4-111772
- resonances and surface waves in complex ang. momentum plane 4-78648
- ( $\alpha$ , $\alpha$ ), 1p shell nuclei, generalised optical pots. 4-95982
- ( $\alpha$ , $\alpha'$ ), effective AN force density depend., isoscalar transition rates 4-64063
- <sup>27</sup>Al( $\alpha$ , $\alpha'$ ), 36 MeV, elastic scatt., ang. distrib. meas. 4-59254
- <sup>197</sup>Au( $\alpha$ , $\alpha'$ ), 36 MeV, elastic scatt., ang. distrib. meas. 4-59255
- ( $\alpha$ , $\alpha'$ ) on <sup>4</sup>He, <sup>9</sup>Be, <sup>12</sup>C, <sup>16</sup>O, <sup>24</sup>Mg, Glauber multiple scatt., total cross-section dependence 4-86835
- <sup>A</sup>Ba( $\alpha$ , $\gamma$ )<sup>A</sup>Ba, A=135,137, E=9.6-12.2 MeV, study of low-lying states 4-95904
- <sup>136</sup>Ba( $\alpha$ , $\alpha'$ ), first 2<sup>+</sup> state, quadrupole moment and Coulomb excitation probability, reorientation effect 4-73825
- <sup>9</sup>Be( $\alpha$ , $\alpha'$ ), 23.1 MeV, elastic and inelastic, anomalous large angle scatt., Regge pole anal. (Chinese) 4-83080
- <sup>12</sup>C( $\alpha$ , $\alpha'$ )<sup>12</sup>C channel coupling and distortion effects in O<sub>2</sub><sup>+</sup> excitation 4-68704
- <sup>12</sup>C( $\alpha$ , $\alpha'$ ), angular correlations, distortions in eikonal approx. 4-78644
- <sup>12</sup>C( $\alpha$ , $\alpha'$ )<sup>12</sup>C inelastic scatt., angular  $\alpha$ - $\gamma$  correlation meas. 4-91010
- <sup>12</sup>C( $\alpha$ , $\alpha'$ ), pot. inversion at fixed energy 4-68688
- <sup>12</sup>C( $\alpha$ , $\alpha'$ ), 35 MeV, isoscalar transition rates, stripping probabilities, and spectroscopic factors, DWBA anal. 4-111519
- <sup>A</sup>Ca( $\alpha$ , $\alpha'$ ), A=40, 42, 43, 44, 48, 104 MeV,  $\alpha$ -particle optical pot. and nucl. matter densities, isotopic and isotonic differences 4-68707
- <sup>40</sup>Ca( $\alpha$ , $\alpha'$ ), elastic and inelastic scatt., folding model, density-dependent force 4-102231
- <sup>40</sup>Ca( $\alpha$ , $\alpha'$ ), orbiting mechanism and background amplitude interference 4-68708
- <sup>40</sup>Ca( $\alpha$ , $\alpha'$ ) elastic scatt., statistical interpretation 4-73919
- <sup>40</sup>Ca( $\alpha$ , $\alpha'$ )<sup>40</sup>Ca, <sup>44</sup>Ti resonance spectroscopy 4-86841
- <sup>2</sup>Cr( $\alpha$ , $\alpha'$ ), 104 MeV,  $\alpha$ N force dynamic density depend., deformed folding model anal. 4-78597
- <sup>1</sup>H( $\alpha$ , $\alpha'$ ), 63 GeV, central rapidity region, quark-gluon plasma search, ISR results 4-68700
- <sup>1</sup>H( $\alpha$ , $\alpha'$ ), longitudinal analysing power, parity violation study 4-83069
- <sup>1</sup>H( $\alpha$ , $\alpha'$ ) A=1, 2, elastic diff. cross-sections, Glauber theory 4-68705
- <sup>4</sup>He( $\alpha$ , $\alpha'$ ), 63 GeV, central rapidity region, quark-gluon plasma search, ISR results 4-68700
- <sup>4</sup>He( $\alpha$ , $\alpha'$ ), pot. inversion at fixed energy 4-68688
- <sup>4</sup>He( $\alpha$ , $\alpha'$ ) A=3, 4, elastic diff. cross-sections, Glauber theory 4-68705
- <sup>24</sup>Mg( $\alpha$ , $\alpha'$ ), elastic scatt., quasi-molecular states obs. 4-59258
- <sup>4</sup>Ne( $\alpha$ , $\alpha'$ ), A=143, 145; Coulomb excitation of levels 4-68646
- <sup>58</sup>Ni( $\alpha$ , $\alpha'$ ), elastic and inelastic scatt., folding model, density-dependent force 4-102231
- <sup>58</sup>Ni( $\alpha$ , $\alpha'$ ) refractive phase relation for elastic and inelastic scatt. 4-78640
- <sup>16</sup>O( $\alpha$ , $\alpha'$ ), Orthogonality Condition Model study 4-78609
- <sup>16</sup>O( $\alpha$ , $\alpha'$ )<sup>16</sup>O, <sup>20</sup>Ne resonant energies, widths, strengths, spins, parities 4-83085
- <sup>208</sup>Pb( $\alpha$ , $\alpha'$ ), elastic and inelastic scatt., folding model, density-dependent force 4-102231
- <sup>32</sup>S( $\alpha$ , $\alpha'$ ), 2.6-3.0 MeV, elastic scatt. study 4-59151
- <sup>28</sup>Si( $\alpha$ , $\alpha'$ )<sup>28</sup>Si\*, 28 MeV, unnatural parity states excitation 4-59256
- <sup>A</sup>Ti( $\alpha$ , $\alpha'$ ) A=46, 48, 50, elastic and inelastic scatt., folding model, density-dependent force 4-102231
- <sup>50</sup>Ti( $\alpha$ , $\alpha'$ ), 104 MeV,  $\alpha$ N force dynamic density depend., deformed folding model anal. 4-78597
- <sup>50</sup>Ti( $\alpha$ , $\alpha'$ ), 104 MeV,  $\alpha$ -particle optical pot. and nucl. matter densities, isotopic and isotonic differences 4-68707
- <sup>51</sup>V( $\alpha$ , $\alpha'$ ), 104 MeV,  $\alpha$ -particle optical pot. and nucl. matter densities, isotopic and isotonic differences 4-68707
- <sup>90</sup>Zr( $\alpha$ , $\alpha'$ ),  $\alpha$ -clustering probe in statistical multistep direct theory 4-83082
- <sup>90</sup>Zr( $\alpha$ , $\alpha'$ ), elastic and inelastic scatt., folding model, density-dependent force 4-102231

**alpha-particle scattering** *see alpha particle-nucleus scattering***alpha-particle spectra***see also alpha-particle angular distribution*

- background in (n, p) and (n,  $\gamma$ ) spectrometry 4-73606
- computerised anal., resolution, distribution 4-68866
- counting rate to activity conversion on multichannel analysers 4-68868
- modified spark counter for  $\alpha$ -spectroscopy 4-96397
- spectra fitting method 4-102436
- <sup>27</sup>Al(<sup>32</sup>S, <sup>59</sup>Cu), ang. momentum induced deformations,  $\alpha$ -spectra, rot. liq. drop model 4-102175
- Am alpha-spectrum anal., peak ratio's 4-68865
- Cm alpha-spectrum anal., peak ratio's 4-68865

**alpha-particle spectra continued**

- <sup>59</sup>Co( $\alpha$ ,X), excitation functions using exciton model 4-86840
- Pu alpha-spectrum anal., peak ratio's 4-68865
- <sup>238</sup>Pu  $\alpha$ -activity fraction in NBS Pu standard reference materials 946 and 947, safeguards 4-107000
- Si surface barrier detector, review of  $\alpha$ -particle spectrometric meas. 4-68869
- SiB, implanted, impurity depth profiles,  $\alpha$ -particle spectra, Monte Carlo calc 4-80081
- SiO<sub>2</sub>B, implanted, impurity depth profiles,  $\alpha$ -particle spectra 4-80081
- alpha-particle spectrometers**  
*see also alpha-particle spectra*
- actinide determination by alpha spectrometry at Radiological and Environmental Sciences Lab. 4-105051
- actinide electrodeposition method for alpha spectrometer source preparation 4-101969
- alpha spectrometric sources, standardisation and practical aspects 4-101970
- application to superheavy element discoveries 4-102430
- band-amplifier pulse shaper for nuclear radiation spectrometry 4-102544
- chemical separation techniques for alpha spectrometric meas., review 4-105048
- combination filter-funnel-counting planchet for alpha spectrometry 4-102449
- computerised system for low level actinides 4-68867
- conference, alpha-particle spectrometry, low-level meas., Harwell, England, (May, 1983) 4-101565
- conference, alpha-particle spectrometry techniques and appl., Geel, Belgium (Oct. 1981) 4-67853
- CR-39 alpha particle autoradiography, trace element anal., activity micro-distribution 4-102446
- environmental U, Th, Pu levels in bone, solvent extraction and alpha spectrometry meas. 4-105350
- geometrical factor tables for source-detector configurations 4-102555
- gridded ion chambers, particle counting method 4-102429
- gridded ionisation chamber for alpha-particle spectroscopy 4-102427
- high resolution alpha-particle spectroscopy using CR-39 plastic track detector 4-102490
- high resolution semiconductor detector, relative alpha intensities of several actinide nuclides 4-102432
- HTR fuel, alpha spectrometric anal. 4-102444
- instrumental factors affecting observed spectrum 4-102426
- irradiation research and reprocessing appl. 4-68864
- large area Frisch grid chambers for low level alpha spectrometry 4-102428
- liquid scintillation alpha spectrometry techniques 4-102441
- low level radionuclide metrology, appl. review 4-102348
- natural radionuclides in marine environment, radiochemical anal. techniques 4-105055
- nuclear applications, influencing factors 4-68863
- nuclear data measurements appl. 4-102348
- radioactivity meas. development and applications 4-68870
- rapid radiochemical analysis method for transurans in nuclear facilities 4-105049
- scattering measurement in low geometry alpha counter 4-102440
- separation procedures for alpha spectrometric meas. of environmental and biological materials 4-105050
- SHIP position sensitive surface barrier detection system 4-102431
- source preparation in alpha spectrometry 4-101968
- spectra fitting method 4-102436
- stopping power measurement using thick alpha sources 4-102442
- transuranic speciation in geosphere, assessment using alpha spectrometry 4-105053
- twin filter detector for radon daughter spectra 4-93672
- <sup>241</sup>Am concentration in <sup>239</sup>Pu, alpha-spectrometry determ. 4-102438
- Ge detectors for Ra isotope meas. in natural water 4-102447
- <sup>210</sup>Pb, determ. in seawater and marine particulate matter 4-105059
- <sup>210</sup>Pb and heavy metal content in Finnish peat, alpha spectrometric meas. 4-102445
- <sup>210</sup>Po, determ. in seawater and marine particulate matter 4-105059
- Pu, alpha particle spectrometry 4-102347
- Pu drop deposited source for alpha spectrometric assay 4-101971
- <sup>A</sup>Pu, A=238-241, simultaneous determ. in low activity environmental samples 4-102443
- <sup>236</sup>Pu alpha emission, absolute energy determ. using cellulose nitrate films 4-102433
- <sup>238</sup>Pu concentration in <sup>239</sup>Pu, alpha-spectrometry determ. 4-102438
- <sup>238</sup>Pu, decay  $\alpha$ -particle and  $\gamma$ -ray emission probabilities 4-102434
- <sup>239</sup>Pu/<sup>240</sup>Pu isotopic ratio, high resolution alpha spectrometric determ. 4-102439
- <sup>224</sup>Ra, indirect meas. by high resolution alpha spectrometry 4-105061
- Si surface barrier detector, asymmetric response to light ions 4-102435
- p-SiP surface-barrier detectors fabrication and appl. 4-87018
- <sup>99</sup>Tc, alpha spectrometric determ. in environmental samples 4-105052
- Th, extraction from granite for alpha spectrometry 4-105060
- <sup>228</sup>Th, indirect meas. by high resolution alpha spectrometry 4-105061
- U extraction from granite for alpha spectrometry 4-105060
- U oxidation state determ. in natural waters 4-105054

**alpha-particles***see also cosmic ray alpha-particles and helium nuclei*

- distribution function and diffusion in DT fusion plasma 4-102394
- large tokamaks,  $\alpha$ -particle confinement, low hybrid wave heating effects 4-75170
- plasma edge conditions in Tokamak, effect of alpha drift and instabilities 4-97847
- solar wind, upstream particle events,  $\alpha$  particle/proton ratio 4-67592
- <sup>40</sup>Ar on Ag, two  $\alpha$ -particle correlations 4-91019
- ( $\alpha$ ,  $\alpha$ X) anomalous interaction mean free path of relativistic alpha-particles 4-96077

**alpha-radiation** *see alpha-particles***alpha-rays** *see alpha-particles***alpha-rhythm** *see bioelectric potentials***alpha-rhythm measurement** *see electroencephalography***alternators**

- 1 kW free-piston Stirling engine alternator unit, development 4-66782

**altimeters***see also radioaltimeters*

- ERS-1 radar altimeter, development 4-85864
- satellite-ocean remote sensing systems and their prospects 4-110164

altitude measurement *see* height measurement

## alumina

*see also* corundum

$\alpha$  phase, high-temperature thermal expansion standard, neutron diffraction meas. 4-103972

abrasive blasting of steel, improved corrosion resist. in water 4-62099

adhesion of sputtered coating to Cu substrate 4-76967

adsorbed silane coupling agents, IETS study 4-85336

adsorption on  $\text{Al}_2\text{O}_3$ , IR spectra 4-77030

$\gamma\text{-Al}_2\text{O}_3\text{-NiO}$  ( $\text{MoO}_3$ ), atomic distrib. studied by ion scatt., spectroscopy 4-71972

$\text{Al-Al}_2\text{O}_3\text{-H}_2\text{O}$ , two high-pressure  $\text{Al}(\text{OH})_3$  phases 4-85141

aluminosilicate refractories, compressive stress influence on thermal cond. 4-65506

aluminosilicate refractories, creep 4-81242

anodic porous films, piezo-electrocapillary effect 4-88774

anodised films, breakdown statistics 4-109128

anodised films, Ni-impregnated, selective coatings for photothermal conversion of solar energy 4-100000

anodised layer, spectrally selective, solar collector appl., ESCA studies 4-66789

bend specimens, crack resistance curves, influence of grain size 4-62058

catalysts, short range order, EXAFS studies 4-62246

ceramic, strength rel. to microstructure 4-62060

ceramic, thermal shock resist. 4-81289

ceramic materials for fusion reactor applications 4-111758

ceramic substrate for ZnO film, SAW study 4-104053

ceramic windows, neutron-induced RF loss meas. and thermal stress calcs. 4-113501

ceramics, interaction between polyvinyl butyral binder burn-out and sintering in reducing atm. 4-114460

ceramics, subcrit. crack propag., activation enthalpies and mechanisms (German) 4-62010

ceramics, surface topography rel. to ion beam sputtering, SEM obs. 4-76884

coatings from plasma spraying process, IR study 4-61681

compacts, homogeneously packed, intermediate-stage sintering 4-76702

compacts, second phase particle struct., high resolution TEM studies 4-108627

crack kinetics of bend specimens 4-62061

CVD on cemented carbide, non-equilib. conditions 4-71598

defect structure, electron emission meas. 4-93145

determination in geological samples, neutron activation method 4-66628

diamond dispersed alumina composite, very high press. sintered, fracture toughness, phase transform. 4-99372

differently produced powders, sintering behaviour, positron annihilation studies 4-114436

doped, mixed cond. and impurity electron states 4-92773

electrophoretic deposition kinetics, zetapotential meas. 4-114428

faceted grain boundaries 4-84301

fibre reinforced  $\text{Al}_2\text{O}_3$ , mech. aspects of failure (French) 4-81280

fibre reinforced FP alloy, orthotropic plate with circular hole, fatigue failure 4-74953

fibre reinforced Mg, tensile and fatigue behaviour, fibre fraction and orientation 4-114652

fibre reinforced Mg alloys, tensile and fatigue behaviour, matrix alloying effects 4-114653

fibres, polycryst., prod. 4-71618

films obtained by electron-beam evaporation 4-74669

films on Au, Al, and Si, vibr. props., IR refl. absorpt. spectroscopy study 4-71459

friction with superhard abrasive grains 4-109522

fusion reactor first wall coatings, gas release under electron impact 4-91097

gamma phase, spherical particles, cryst. struct. and surface morphology, electron microscopy study 4-92149

glass filled composite, hot isostatically pressed, macropore struct. 4-71629

glass/alumina composites, density, crystallisation, elec. cond. 4-113937

humidity sensor, moisture effect on dielectric props. analysis 4-95442

indirect plasma-enhanced CVD technique for  $\text{Al}_2\text{O}_3$  gate dielec. 4-104529

insulator for InP MOSFET structures, carrier channel mobility correl. with interface state meas. 4-88600

internal friction and Young's modulus under thermal shock conditions 4-62009

ion implantation, ion beam mixing, and annealing of metals 4-70229

jet engine turbines, ceramic technology for powerplant 4-104758

laser sputtering mechanism, SEM study 4-71484

membranes, prep. and microstruct. 4-66285

metastable phases, TEM, X-ray diffraction obs. 4-113661

mullite, solid solubility of  $\text{Na}_2\text{O}$  4-113645

mullite-cordierite composites, sintering, hot pressing, microstruct., mech. and thermal props. 4-89017

mullite-zirconia composites, microstruct. and mech. props 4-114672

multilayer UV reflectors, laser damage results under multiple-shot irradiation 4-74580

$\alpha$ -phase, (0001), high resolution EELS meas., surface phonons 4-99247

plasma, thermodynamic and transport props. in temp. range 5000-30000K 4-60584

polycrystalline, strength rel. to flow distrib. 4-109505

powder, shear strength up to 600°C and 4 GPa 4-104811

powder, shock induced densification and sinterability 4-109350

powder, shock loaded densification, X-ray study 4-114439

powder, surface area after shock treatment 4-109344

powders, granule compaction rel. to binder glass transition temp. 4-85129

powders, with bimodal particle size distrib., sintering 4-85127

protective coatings for in-vessel fusion devices 4-111751

PVC: $\text{Al}_2\text{O}_3$ , resist. to tracking study 4-69969

scales formed on Fe-based  $\text{Y}_2\text{O}_3$  dispersed alloys 4-89180

shock-modified powders, X-ray line-broadening 4-113539

single crystals, muonium decoupling in high transverse mag. field 4-92985

sintered, fracture strength, effect of surface condition 4-62057

sintered, humidity sensor appl., elec. resistivity rel. to surface area of oxides (Japanese) 4-63751

sintered, microstructure and optical props. 4-61649

slow crack growth at high temp., characterisation by double torsion method 4-62053

## alumina continued

solidification point determ. by specular reflection and centrifugal methods (Japanese) 4-76770

solubility in LiCl-KCl eutectic mixtures 4-75686

spray-dried, compaction behaviour 4-76714

steel, sulfidizing corrosion protection by  $\text{Al}_2\text{O}_3$ , diffusion model 4-93467

strength charact. using controlled flaws, microstruct. effects 4-85205

strongly coupled mag. ions, obs. by low temp. thermal expansion meas. 4-70419

substructure in vitreous  $\text{SiO}_2$ , elec. cond. 4-113341

support for Mo catalysts, Fourier transform IR spectroscopy of sulphidation 4-105014

supported Ni catalysts, particle size distrib., superparamagnetic meas. 4-104465

supported Rh catalyst, O interaction, EXAFS study 4-66097

surface, adsorbed nickel tetraphenylporphine compounds, reson. Raman spectra 4-105012

surface with adsorbed HCN, far IR Fourier spectroscopy 4-104593

surfaces Lewis acid sites on different modification 4-108919

synthesis by  $\text{O}_2^-$  ion implantation into Al 4-70174

thermal diffusivity in gaseous media and in vacuum of  $\text{Al}_2\text{O}_3$  containing 10 to 30%Ni 4-79704

thermal solidification of layers on W and Mo substrates in elec. field 4-80405

thermal shock resistance and fatigue, acoustic emission study 4-62054

thin film and powder,  $\gamma$  to  $\alpha$  transformation, TEM studies 4-108613

thin film deposition by UV laser photolysis 4-99337

thin films, interaction with W 4-70576

thin layers, dielec. breakdown, definition and charact. 4-109122

thin microporous layers, prep. and characterisation 4-70601

translucent sintered tubes, thermophysical stability rel. to impurities and dopants 4-61937

tubes, multiaxial loading fracture, Weibull statistical predictions 4-62017

tubes, multiaxial loading fracture 4-62016

$\beta''$ -type structural and transport props. 4-84458

VAD fibres, props. 4-103043

X-ray irradiated, F-centre glow peaks spectral emission 4-71452

Young's modulus and internal friction, temp. depend. 4-61965

$\text{Al}/\text{Al}_2\text{O}_3$ /chlorophyll *a*/Ag photovoltaic cell charact. and behaviour 4-85370

$\text{Al-Al}_2\text{O}_3$ -Ag tunnel junctions, surface plasmons and light emission 4-98553

$\text{Al-Al}_2\text{O}_3$ -Pb junction, effects of patterned laser illumination 4-70998

$\text{Al-Al}_2\text{O}_3$ -Pb(Ag) tunnelling junctions, interaction with 3-(trimethyloxy)silylpropanethiol, IETS study 4-92827

$\text{Al-Al}_2\text{O}_3$ -metal junctions, thermally shorted, point contact spectroscopy 4-80687

$\text{Al-Al}_2\text{O}_3$ -(Si), creep deform., stress and temp. depend. 4-81246

$\text{Al-Mg-Al}_2\text{O}_3$ , incorporation of  $\text{Al}_2\text{O}_3$  particles by stirring in melt 4-93252

$\gamma\text{-Al}_2\text{O}_3$ , adsorption of alkanes and aromatic hydrocarbons, thermodynamic props., chromatography (Chinese) 4-61210

$\eta\text{-Al}_2\text{O}_3$ , anodic film, microarc oxidation of Al in  $\text{H}_2\text{SO}_4$  4-76900

$\alpha\text{-Al}_2\text{O}_3$ , electronic energy levels from Al L-edge photoabsorption, small-cluster CNDO calcs. 4-81038

$\text{Al}_2\text{O}_3$  fibre reinforced Mg composite, off-axis fracture, critical stress intensity 4-66430

$\beta\text{-Al}_2\text{O}_3$   $\text{Na}_2\text{O}$  in Na/S secondary battery, electrolytic degradation 4-61141

$\text{Al}_2\text{O}_3$ -Co, thermoluminescence and trap parameters 4-76532

$\text{Al}_2\text{O}_3$ -Cr, grain boundary diffusion, anisotropy and doping effects 4-92443

$\text{Al}_2\text{O}_3$ -Cr, photoacoustically detected EPR (Korean) 4-114155

$\alpha\text{-Al}_2\text{O}_3$ - $\text{Cr}_2\text{O}_3$  ( $\text{Y}_2\text{O}_3$ ), ionic cond., doping effects 4-92417

$\text{Al}_2\text{O}_3$ - $\text{Cr}^{3+}$ ,  $\text{Cr}^{3+}$  electron spin resonance line ENDOR and saturation optical detect. 4-84873

$\text{Al}_2\text{O}_3$ - $\text{Cr}^{3+}$  ( $\text{V}^{4+}$ ), phonons, far IR ion. generation and detection 4-61005

$\beta\text{-Al}_2\text{O}_3$ - $\text{Li}^+$ , vibr. dynamics of Li ions 4-70441

$\beta''\text{-Al}_2\text{O}_3$ - $\text{MgO}$ , long-period polymorph, microtwins, selected-area electron diffraction obs. 4-103770

$\text{Al}_2\text{O}_3$ - $\text{MgO}$ - $\text{CaO}$ , translucent, fracture, influence of temp. and CaO 4-92290

$\text{Al}_2\text{O}_3$ - $\text{SiO}_2$ , struct. and surface comp. X-ray diffraction and SIMS investigation 4-113764

$\text{Al}_2\text{O}_3$ -Ti, sintering and densification, defect models 4-109364

$\text{Al}_2\text{O}_3$ -V, quasi-diffusive phonon propagation obs. 4-61012

$\text{Al}_2\text{O}_3$ - $\text{V}^{3+}$ , zero-field hyperfine splitting by Josephson phonon spectroscopy 4-61353

$\text{Al}_2\text{O}_3$ - $\text{V}(\text{Mn})$ , low-temp. thermal expansion meas. 4-61112

$\text{Al}_2\text{O}_3$ -Zr, sintering and densification, defect models 4-109364

$\text{Al}_2\text{O}_3/\text{Au}$  cermets, optical props. and dielec. const., quantum size effects 4-65941

$\text{Al}_2\text{O}_3/\text{Au}$  cermets, optical props. and dielec. const., quantum size effects 4-65942

$\gamma\text{-Al}_2\text{O}_3$ /Pt catalyst for HI decomposition in thermochemical  $\text{H}_2$  production 4-93647

$\text{Al}_2\text{O}_3$ -Al plasma coatings on graphite, oxidation resist., bonding strength and elec. cond. 4-66462

$\text{Al}_2\text{O}_3$ -AlN spinel, fabrication, thermomech. props. 4-89097

$\text{Al}_2\text{O}_3$ -AlN system, high temp. reactions and microstructs. 4-76763

$\text{Al}_2\text{O}_3$ -AlON composite ceramic, hot pressing reaction sintering, mech. props., high temp. appls. 4-62062

$\text{Al}_2\text{O}_3$ -BN( $\alpha$ -AlON) composite ceramics, mech. props. (French) 4-81177

$\beta''\text{-Al}_2\text{O}_3$ -BaO, short-range ordering in  $\text{Ba}^{2+}$  ion distrib. at 295K 4-84245

$\text{Al}_2\text{O}_3$ - $\text{Bi}_2\text{O}_3$ -CuO system, phase relations, thick film cond. appls. 4-104770

$\text{Al}_2\text{O}_3$ -Fe cermets, metal to ceramic bonding, Mossbauer studies 4-109622

$\text{Al}_2\text{O}_3$ -InP MIS struct., CVD growth and elec. props. 4-80680

$\beta\text{-Al}_2\text{O}_3$ - $\text{La}_2\text{O}_3$ - $\text{Eu}^{3+}$ , structure, laser excited fluorescence study 4-66071

$\text{Al}_2\text{O}_3$ - $\text{NH}_4^+$ ,  $\text{H}^+$  ( $\text{H}_2\text{O}$ ) $_m$   $\beta''$  and ion-rich  $\beta$  phases, protonic cond. 4-92412

$\beta\text{-Al}_2\text{O}_3$ -Na  $2\gamma$ - $\text{K}_2\text{O}$ , NMR imaging in solids appl. 4-76274

$\text{Al}_2\text{O}_3$ -Na  $\beta$  and  $\beta''$  phases, ion-rich, high temp. struct. and elec. cond. props. 4-70454

$\beta/\beta''\text{-Al}_2\text{O}_3$ - $\text{Na}_2\text{O}$ , struct. transform. during sintering and annealing 4-93292

$\beta''\text{-Al}_2\text{O}_3$ - $\text{Na}_2\text{O}$  electrolyte ceramic tubes, sintering, radial DC resist. 4-103994

## alumina continued

- $\beta''$ - $\text{Al}_2\text{O}_3$ - $\text{Na}_2\text{O}$ :Fe, decomposition processes, microscopic mechanisms 4-109415  
 $\beta''$ - $\text{Al}_2\text{O}_3$ - $\text{Na}_2\text{O}$ (Ag<sub>2</sub>O), electrode noise 4-98337  
 $\text{Al}_2\text{O}_3$ -PMMA (PBMA), composite biomaterials, fracture 4-76844  
 $\text{Al}_2\text{O}_3$ - $\text{SiO}_2$  fibres, cristobalite form. at elevated temp. (*German, English*) 4-81197  
 $\text{Al}_2\text{O}_3$ - $\text{SiO}_2$  gate dielectric ISFET ph sensor, surface and buried channel, characterisation 4-72033  
 $\text{Al}_2\text{O}_3$ - $\text{SiO}_2$  system, diphasic xerogel, prep., DTA and powder X-ray diff. 4-114846  
 $\text{Al}_2\text{O}_3$ - $\text{SiO}_2$ /InSb system, slow states, field effect studies 4-65752  
 $\text{Al}_2\text{O}_3$ - $\text{SiO}_2$ - $\text{TiO}_2$ - $\text{Cr}_2\text{O}_3$ , high alumina refractory brick, creep resist. rel. to  $\text{Cr}_2\text{O}_3$  addition 4-109457  
 $\beta''$ - $\text{Al}_2\text{O}_3$ - $\text{ZrO}_2$ , slip cast transform. toughened composites, mech. props., ionic cond. 4-103995  
 $\text{Al}_2\text{O}_3$ - $\text{ZrO}_2$ , transformation-toughened, fracture toughness, crack-size depend. 4-93373  
 $\text{Al}_2\text{O}_3$ - $\text{ZrO}_2$  ceramics, high press. sintered, fracture toughness rel. to phase transform. 4-76839  
 $\text{Al}_2\text{O}_3$ - $\text{ZrO}_2$  ceramics, strain around large inclusions, quantitative anal. 4-103621  
 $\text{Al}_2\text{O}_3$ - $\text{ZrO}_2$  composite tool bit, microstruct., toughening mechanisms, performance 4-61946  
 $\text{Al}_2\text{O}_3$ - $\text{ZrO}_2$  composites, grain growth hindrance by  $\text{ZrO}_2$  inclusions 4-76743  
 $\text{Al}_2\text{O}_3$ - $\text{ZrO}_2$  powder compacts, stresses induced by differential sintering 4-85135  
 $\text{Al}_2\text{O}_3$ - $\text{ZrO}_2$  powders, prep. by evaporative decomp. of sols. 4-85137  
 $\text{Al}_2\text{O}_3$ - $\text{ZrO}_2$ - $\text{SiO}_2$  refractory, corrosion by Pb glass 4-71753  
 $\text{Al}_2\text{O}_3$ - $\gamma$  anodic oxide films, paramagnetic centres and optical absorpt. spectra studies 4-104494  
 $\text{Al}_2\text{O}_3$ - $\text{H}_2\text{O}$ -glycine, mixtures, points of zero charge (*German*) 4-85314  
 $\alpha$ - $\text{Al}_2\text{O}_3$  growth from transition  $\text{Al}_2\text{O}_3$  matrix 4-84380  
 $\text{Ba}_{79}\text{Al}_{109}\text{O}_{1714}$ , hexaaluminate phase I, cryst. struct. and nonstoichiometry 4-70087  
 $\beta$ - $\text{Al}_2\text{O}_3$ , sintering, microstruct. and mech. props. 4-85136  
 $\text{CaO}$ - $\text{Al}_2\text{O}_3$  eutectic melt, interaction with  $\text{Al}_2\text{O}_3$  4-61924  
 $\text{CaO}$ - $\text{B}_2\text{O}_3$ - $\text{Al}_2\text{O}_3$ - $\text{Fe}_2\text{O}_3$  glass system, photoacoustic spectra of Fe 4-99130  
 $\text{Co}$ - $\text{Al}_2\text{O}_3$  coevaporated composite films, solar selectivity 4-72169  
 $\text{Co}$ - $\text{Al}_2\text{O}_3$  with adsorbed  $\text{N}_2$ , FT-IR studies 4-113786  
 $\text{CsO}$ - $\text{Al}_2\text{O}_3$ - $\text{TiO}_2$  system, phase stability, TGA and DTA obs. 4-71642  
 $\text{Cu}$ - $\text{Al}_2\text{O}_3$ , dispersion hardened, tensile failure, temp. depend., grain boundary fracture 4-66405  
 $\text{CuCl}$ ( $\text{Al}_2\text{O}_3$ ) composites, elec. cond., particle size effects 4-88548  
 $\text{Fe}$ - $\text{Cr}$ - $\text{Al}$  alloys, sulphidation protection by  $\text{Al}_2\text{O}_3$  scales 4-93468  
 $\text{Fe}_{818}\text{B}_{18}\text{Al}_2\text{O}_3$  granular system; XPS anal., surface composition study 4-81113  
 $\text{Li}_2\text{O}$ -( $\text{LiCl}$ )- $\text{B}_2\text{O}_3$ - $\text{Al}_2\text{O}_3$  system, Raman spectra of glasses (*Chinese*) 4-93065  
 $\text{Li}_2\text{O}$ - $\text{Al}_2\text{O}_3$ - $\text{B}_2\text{O}_3$  glass, form. and transition temp. 4-113634  
 $\beta$ - $\text{Li}_2\text{O}$ - $\text{Na}_2\text{O}$ - $\text{Al}_2\text{O}_3$ , water absorpt., TG, DSC and X-ray meas. 4-113794  
 $\text{MgO}$ - $\text{nAl}_2\text{O}_3$ :Cr(Mn), impurity ion distrib. in spinel lattice 4-84311  
 $(\text{MnO})$ -( $\text{Al}_2\text{O}_3$ )-( $\text{SiO}_2$ ), spin glass, amorphous, crit. behaviour, field expansion and scaling, susceptibility, magnetisation meas. 4-92920  
 $\text{Mo}$ - $\text{Al}_2\text{O}_3$ - $\text{Cr}_2\text{O}_3$  cermet emitter electrodes, directionally solidified, development and evaluation for thermionic energy converters 4-77126  
 $\text{Mo}$ - $\text{Al}_2\text{O}_3$ - $\text{Cr}_2\text{O}_3$  eutectic thermionic emitter 4-72141  
 $\text{Mo}$ - $\text{Al}_2\text{O}_3$  gasohermic coatings, wear resist. 4-66500  
 $\text{Mo}$ - $\text{Al}_2\text{O}_3$  solar highly absorbing coatings using graded refractive indices and textured surfaces 4-77146  
 $\text{Na}$ - $\text{Al}_2\text{O}_3$  system, ionic conducting phases, thermodynamic props., 800 to 1200K 4-92427  
 $\beta''$ - $\text{Na}_2\text{Al}_2\text{O}_3$  ceramic, spinel block doping and ionic cond. 4-84459  
 $\text{Na}_2\text{O}$ - $\text{Al}_2\text{O}_3$ , effect of  $\text{F}^-$ ,  $\text{Co}^{2+}$  and  $\text{Ti}^{4+}$  on synthesis and props. 4-114370  
 $\beta$ - $\text{Na}_2\text{O}$ - $\text{Al}_2\text{O}_3$  single cryst., thermal expansion and optical length variation 4-108636  
 $\beta''$ - $\text{Na}_2\text{O}$ - $\text{Al}_2\text{O}_3$  solid electrolyte, surface degradation in Na-S battery cells 4-65526  
 $\text{Na}_2\text{O}$ - $\text{Al}_2\text{O}_3$ - $\text{B}_2\text{O}_3$  glass, form. and transition temp. 4-113634  
 $\text{Na}_2\text{O}$ - $\text{Al}_2\text{O}_3$ - $\text{SiO}_2$ -S cluster cryst., Raman, ESR spectra and dielec. permittivity 4-61714  
 $\text{Na}_2\text{O}$ - $\text{Al}_2\text{O}_3$ - $\text{nSiO}_2$  (zeolite), charged particle induced short-wave radiation in natural hollow crystallographic channels (*Russian*) 4-81031  
 $\text{Na}_2\text{O}$ - $\text{K}_2\text{O}$ - $\text{Al}_2\text{O}_3$ - $\text{B}_2\text{O}_3$ - $\text{SiO}_2$  glasses, nucl. spin stimulated echoes, pulsed NMR meas. 4-92976  
 $\text{Na}_2\text{O}$ - $\text{Li}_2\text{O}$ - $\text{Al}_2\text{O}_3$  ternary system, phase relations 4-76760  
 $\text{Ni}$ - $\text{Al}_2\text{O}_3$  electron beam evaporated condensates, creep props. 4-93361  
 $\beta''$ - $\text{Nb}_2\text{O}_5$ - $\text{Al}_2\text{O}_3$ - $\text{ZnO}$  ceramics, ionic cond. and activation energy 4-113708  
 $\text{P}_2\text{O}_5$ - $\text{Al}_2\text{O}_3$ - $\text{MgO}$ - $\text{Nd}_2\text{O}_3$  glasses, low temp. dielec. props. in mag. field 4-61638  
 $\text{Pd}$ - $\text{Al}_2\text{O}_3$  catalyst plug of Pb/acid batteries, deterioration prevention 4-93613  
 $\text{Pd}$ - $\text{Al}_2\text{O}_3$ - $\text{SiO}_2$ -Si MIS struct., flat band voltage shift 4-108945  
 $\text{Pt}$ - $\text{Al}_2\text{O}_3$  graded cermet selective absorber coatings, sputter-deposited 4-72171  
 $\text{Pt}$ - $\text{Al}_2\text{O}_3$  graded-cermet selective absorbers, graded infinitesimal-lamellae model 4-114948  
 $\text{Pt}$ - $\text{Al}_2\text{O}_3$  solar highly absorbing coatings using graded refractive indices and textured surfaces 4-77146  
 $\text{Rh}$ / $\text{Al}_2\text{O}_3$  catalyst, highly dispersed, CO adsorption, EXAFS study 4-62243  
 $\text{SiO}_2$ - $\text{Al}_2\text{O}_3$ - $\text{P}_2\text{O}_5$  optical fibre, optimum doping level determ. 4-97097  
 $\text{SiO}_2$ - $\text{TiO}_2$ - $\text{Al}_2\text{O}_3$ , thin film deposition using sol-gel technology 4-76697  
 $\text{WO}_3$ - $\text{Al}_2\text{O}_3$ ,  $\text{O}_2$  and  $\text{H}_2\text{O}$ - $\text{D}_2\text{O}$  exposure cycles, surface struct., O exchange, spectra studies 4-114271  
 $\text{ZrO}_2$ - $\text{Al}_2\text{O}_3$  ceramic, grain boundaries, TEM studies 4-108382  
 $\text{ZrO}_2$ - $\text{Al}_2\text{O}_3$  powders, plasma sprayed, TEM and energy dispersive spectroscopy 4-104756  
 $\text{ZrO}_2$ - $\text{Al}_2\text{O}_3$ - $\text{SiO}_2$ - $\text{CaO}$  system, compatibility relations, microscopy, energy dispersive X-ray exam: 4-61925

## aluminium

- see also nuclei with ....  
 (001) surface electronic struct. calcs., embedding approach 4-61429  
 24.8 MeV electrons backscattering, energy spectra 4-88912  
 (110) surface, truncation-induced multilayer relax. 4-70534

## aluminium continued

- (200)-zone boundary collective mode, perturbation theory anal. 4-104139  
 $\beta$ -decay electrons and positrons energy distrib. parameters (*Russian*) 4-75592  
 absorptivity of 10.6  $\mu\text{m}$ , temp. depend., computed from Drude theory 4-76405  
 adatom-induced reconstruction on Si (111), pseudopotential calcs. 4-104076  
 adsorbed water, electron stimulated desorption,  $\text{H}^+$  ion energy distrib. 4-92536  
 adsorption of H atoms, on (100) surface, CNDO/BW calcs. 4-61222  
 adsorption and reaction with  $\text{O}_2$  on Rh (111), AES and LEED studies 4-89327  
 adsorption of  $\text{H}_2$  on (111) surface, EHT method studies 4-65544  
 $\text{Al}$ - $\text{Al}_2\text{O}_3$ - $\text{H}_2\text{O}$ , two high-pressure  $\text{Al}(\text{OH})_3$  phases 4-85141  
 $\text{Al}$ -Mn, commercial, homogenisation, stability of primary particles, resist. and TEM obs. 4-99408  
 alloy conductors, electromigration (*German*) 4-75737  
 alpha-particle ang. blocking dips, multistrating Monte-Carlo simulation and analytical calcs. 4-92274  
 anode,  $^6\text{Li}$ -Al-air battery, rapidly refuellable, for electric vehicles, performance evaluation 4-72096  
 anodes for dry and reserve batteries 4-62323  
 anodic films, pore filling, elec. breakdown characts. 4-81350  
 anodic layers, black Zn-coated, solar collector coatings, optimisation and microstruct. anal. 4-62397  
 anodic oxidation, film formation by microarc in  $\text{H}_2\text{SO}_4$  4-76900  
 anodic oxidation by spark discharge, process characts. and parameters 4-104893  
 anodised, permanent black coatings, corrosion resistant 4-104922  
 atom, angle dependent energy loss of 7-MeV protons, stopping powers meas., geometrical effect 4-96658  
 atom, multiplet transitions,  $\text{KL}^2\text{-L}^3$  X-ray emission spectra 4-83323  
 Auger electron emission in LVV peak region, continuous background struct.,  $\text{O}_2$  partial press. effect (*French*) 4-66140  
 Auger spectra induced by  $\text{Ne}^+$  and  $\text{Ar}^+$  impact 4-109292  
 band energies, elec. resist., thermolec. power, pseudopotential parameters determ. 4-98512  
 band struct., pseudopotential coeffs., deform. potentials, piezoreflectance meas. 4-98514  
 beam, dynamic contact law, expt. determ. method 4-69714  
 behaviour under microsecond pulsed TEA  $\text{CO}_2$  laser radiation 4-79815  
 biaxial creep behaviour, thermodynamic aspects (*French*) 4-85187  
 bicrystals, grain boundaries diffusivity 4-65485  
 cavitation erosion, decontamination of surfaces (*French*) 4-70222  
 cavity formation in samples irradiated with pulsating beam of 225 MeV electrons 4-108443  
 cavity nucleation and growth, relative role of gas generation and displacement rates 4-108473  
 charge densities, interionic pot., phonon freq., calcs. 4-113856  
 chemical colouring by conversion coating process 4-81349  
 chemisorption of noble gases, excited states and decay mechanisms 4-98436  
 chondrites, ordinary, Al-rich inclusions classification and description 4-77785  
 clad low C steel, reaction diffusion, intermetallic layer growth kinetics 4-114722  
 clusters, electronic struct. and props. 4-74374  
 coated optical fibre, optical, mechanical and radiation perform. at high temp. 4-97111  
 coating on Cr-Mn steel, diffusion reaction, Si content effect 4-114723  
 coating with Si, protective coatings for in-vessel fusion devices 4-111751  
 continuum X-rays produced by a few MeV proton bombardment 4-99215  
 core level binding energies, density functional calcs. 4-113861  
 corrosion behaviour and microstruct., effect of small Sn additions 4-99630  
 corrosion resistance of oxide layers rel. to impurity content 4-62102  
 crack growth under rolling contact, defect installing technique 4-85284  
 creep substructure effect on stress exponent following stress reductions 4-104820  
 creep velocity, high-energy ion irradiation effects 4-70243  
 crystallographic transitions and equilib. props., Gaussian-orbitals calcs. 4-92353  
 cyclic irradiation, void growth and swelling at low temp. 4-103795  
 cylinder, acoustic wave excitation by low energy electrons 4-80168  
 damage simulation in high velocity impact 4-108529  
 Debye-Waller factor for substitutional Mossbauer impurity 4-75633  
 degassing rate of materials, compensated meas. method (*Polish*) 4-111145  
 diffusion of  $^{63}\text{Zn}$ , effects of hydrostatic press. 4-63483  
 diffusion of H, desorption study 4-65489  
 diffusion of Mo and W in Al 4-65477  
 dislocation internal friction hysteresis 4-70165  
 doped, muon localisation, transverse  $\mu\text{SR}$  linewidth study 4-65906  
 doped, trapping of muons and protons, effect of substitutional impurities 4-65631  
 dynamic heterogeneous response to stress waves 4-108540  
 dynamic plastic response and press.-shear impact 4-109485  
 dynamic yield strength meas. 4-89110  
 electric field gradient in cryst. with vacancies, adjustable parameter free calc. 4-61347  
 electrical and thermal cond., 400 to 850K 4-75927  
 electrical contacts, fretting 4-92798  
 electrode material in vacuum spark discharge, electron temp. scaling 4-103592  
 electromigration at high current density, phenomenological obs. 4-84470  
 electron and positron slowing down 4-108486  
 electron backscatt., Monte Carlo calcs. 4-66157  
 electron backscattering from thick layers 4-99249  
 electron irradiation, incoherent tunnelling of positive muons and trapping by vacancies, muon spin relax. meas. 4-65909  
 electron scatt., X-ray intensity calc. by Monte Carlo simulation (*Chinese*) 4-71480  
 electron scattering processes, Monte Carlo simulation, rel. to AES 4-66145  
 electronic stopping power, excitation energy alpha-particle time of flight expt. 4-67916  
 epitaxial growth on Ge (001), first principles calc. of energy 4-92580  
 FCC crystal, force consts. between interstitial H atoms and host atoms 4-75629

## aluminium continued

- FCC crystals, plastic deform. in plane strain compression, theoretical and expt. study 4-70260  
 FCC metal lattice dynamics, nine-parameter model, specific heats 4-75625  
 FCC tilt boundary, vacancy migration, computer simulation studies 4-113694  
 Fermi surface, topological transitions under stress (*Russian*) 4-108761  
 film, clean and H<sub>2</sub> exposed, H<sub>2</sub> adsorption, electron stimulated desorption study 4-75792  
 film, effects on Ti diffused LiNbO<sub>3</sub> optical waveguide 4-107818  
 film, ion plating, using inexpensive rotating barrel 4-66494  
 film, quantum corrections to resistance above superconducting T<sub>c</sub> 4-84710  
 film deposition, using plasma evaporator design with heated needle cathode 4-88989  
 film on glass substrate, laser damage study 4-108433  
 film on LiNbO<sub>3</sub> substrate, elastic const. study 4-104052  
 film on Si, thickness determ. by Monte Carlo code with secondary fluorescence correction 4-63716  
 films, amorphous and polycryst., plural electron scatt., Monte Carlo calc. 4-66158  
 films, prep. by low press. MOCVD 4-81156  
 films, subsurface, in fused SiO<sub>2</sub>, ion beam mixing 4-88189  
 flame sprayed coating on CO, bonding, emission Mossbauer spectroscopy study 4-92979  
 flaming particles produced by rocket propellant in accel. field, high speed photography 4-111226  
 foil, H<sup>+</sup> ion energy loss ang. depend. 4-65313  
 foil, inelastic ion energy loss and scatt. angle in transmission expts. 4-92265  
 foil, laser shock press. and energy loss at 1.05  $\mu$ m wavelength 4-80159  
 foil irradiated with Nd:YAG laser pulses particle vel. meas. of laser-induced shock waves using ORVIS 4-113495  
 foil melting by laser-guided discharges 4-75219  
 forming by underwater Cu wire explosions, bulging expt. 4-75217  
 fracture form., shock wave exit angle effect on free surface 4-99498  
 galvanic corrosion kinetics in H<sub>2</sub>SO<sub>4</sub>, gas evolution role 4-114726  
 gap closure, cathode surface impurities 4-60777  
 Geiger tube planes, trigger for nucleon decay expt. 4-91151  
 grain boundary struct., computer simulation studies 4-113459  
 graphite fibre reinforced Al, interfacial strength meas. 4-99370  
 Hall coeff., size effect for single crystals 4-104183  
 hermetically coated optical fibre, transmission loss reduction 4-97112  
 high purity, polygonised, TEM, internal friction peak 4-113534  
 hot rolling control, IR thermometry 4-82796  
 impact by steel spheres, velocity propagation 4-108532  
 internal friction, time measurement technique with torsion pendulum 4-112778  
 internal friction originated by grain boundaries 4-103872  
 ion implantation of Fe, reduction of T permeation 4-88184  
 ion plated maraging steel, H embrittlement 4-114671  
 ion-excited Auger electron emission, angular distrib. 4-76592  
 ion-induced Auger electron spectra, O<sub>2</sub> adsorp. effects 4-61795  
 isoelectronic sequence, struct. calc. using multiconfig. optimised pot. model, oscillator strengths 4-102592  
 K $\alpha$  chem. shifts, MO calcs. 4-59638  
 laser diffusive reflectivity standard made of Al flame-sprayed coatings 4-107715  
 laser produced plasma, resonant absorpt., K $\alpha$  spectral line 4-69931  
 lattice dynamics, second-order perturbation theory 4-92320  
 liquid, and reaction bonded SiC, cast bonding, exchange diffusion phenomenon involving free Si 4-99741  
 liquid, band energies, elec. resist., thermoelec. power, pseudopotential parameters determ. 4-98512  
 liquid, chem. reaction with B fibres 4-61891  
 liquid, computer simulation of dynamic behaviour 4-60811  
 liquid, heterogeneous nucleation of TiB<sub>2</sub> 4-61096  
 liquid, radial distrib. functions calc. using Percus-Yevick and mean spherical model approx. 4-70020  
 liquid, struct. factor, influence of electron-gas response junction 4-75265  
 liquid, structural props., elec. resist., X-ray diff. 4-79925  
 liquid, surface tension theory 4-84487  
 liquid, thermal expansion 4-84425  
 local-field enhancement of rough surface 4-104047  
 longitudinal and transverse US wave pulses 4-92305  
 low energy heavy ion range parameters, Z<sub>1</sub> dependence 4-92248  
 many-electron systems, ground state energy and X-ray scatt. cross sections 4-114344  
 mechanoluminescence at low loading rates 4-81019  
 melt, wetting of graphitised C strip 4-92476  
 melting curve study at high press. 4-103911  
 metallic granular, three-dimensional, magnetoresist., localisation and electron-interaction contribs. 4-113923  
 microfractography, SEM study (*Polish*) 4-93363  
 mirrors, laser irradiated in air, damage study by electron microscopy 4-79203  
 mirrors, thin film deposited and dielectric overcoated, UV laser damage studies 4-74567  
 molecule, electronic states, at initio MO SCF and first-order CI calcs. 4-102604  
 muon motion appl. of quantum theory of diffusion 4-65892  
 muon trapping by dislocations, spin depolarisation rate meas. 4-65911  
 neutron irradi., trapping of muons by voids, muon spin rot. spectra 4-65912  
 nonlinear resonance interaction of ultrasonic waves 4-88242  
 normalised core-valence band Auger spectra 4-61783  
 optical const. meas. above melting point 4-88798  
 oxide formation in presence of CO<sub>2</sub> and electron irradi. 4-93441  
 P-V-T relation as press. and temp. scale under very high press. 4-75637  
 photodissociation lasers using metal hydrides 4-107616  
 photon backscattering, energy albedo meas. 4-61782  
 picosecond laser induced shock wave press. meas. 4-113259  
 pipe, yield stress determ. by proportional loading tests 4-112777  
 plane hypervelocity fluid impact effects 4-108534  
 plane target voltage meas. in laser plasmas (*Chinese*) 4-108211  
 plasma, electron and laser beam prod. and heating 4-84040  
 plasma, laser prod., gas press. depend., self-generated mag. fields meas. 4-113224  
 plasma, transfer processes of high energy electrons 4-79812  
 plasma etching, AlCl<sub>3</sub> management 4-81345

## aluminium continued

- plasma radiative recombination, electron-bremsstrahlung, VUV emission 4-83989  
 plastic deformation at high strain rates 4-84337  
 plastic deformation of high-purity polycrystals, acoustic emission 4-71688  
 plate, acoustoelastic stress meas., suppression of microstruct. influences 4-99729  
 plate, US waveforms using laser generation and interferometric detection 4-97265  
 plates, anticlastic curvature suppression 4-83832  
 plating bath system, <sup>27</sup>Al NMR spectroscopy studies 4-66245  
 trans-polyacetylene/Al photodiode, defect-related current transport 4-76002  
 polycrystalline, surface strain determ. using optical ellipsometry 4-74972  
 polycrystalline aggregates with transverse isotropy, US acoustoelastic response 4-62129  
 polycrystalline surface, oxidised, interaction with electron beams, AES study 4-93154  
 polycrystalline thin films, 1/f-type noise 4-104328  
 polycrystals, microform. anal. 4-65328  
 polyethylene-Al contact, elec. pot. distrib., SEM study 4-104314  
 polythiophene-carbon films containing Co(Al) clusters, plasma polymerisation 4-81433  
 positive muon diffusion theory, at low temps. 4-65898  
 positive muon pot., self-consistent cluster calc. 4-71236  
 positron experiments, computational anal. 4-76554  
 potential at al. boundaries in Thomas-Fermi model and eqns. of states (*Chinese*) 4-70333  
 powder, sintered, protective coatings for in-vessel fusion devices 4-111751  
 powders, rotating electrode process atomisation mechanisms 4-89001  
 proton small angle scatt. at grazing incidence 4-71499  
 proton stopping power, energy loss straggling, effective-charge fractions and straggling of heavy ions 4-103843  
 pure, 600 MeV proton irradi., H and He bubble form. at grain boundaries 4-108479  
 radiation shielding geometry, dose factors of  $\gamma$ -ray build up 4-102406  
 radiators, quality assurance by IR thermography 4-66531  
 rare gas bubble press. and density, EELS, TEM obs. 4-113508  
 recrystallisation annealing, twin boundaries misorientation (*Russian*) 4-108379  
 relative abundance, in metal-deficient stars (*French*) 4-115756  
 relativistic electron beam propag., energy absorpt. 4-70221  
 relaxation creep, computer model for high temp. 4-84340  
 rod, long, impulsively loaded, stress meas. using manganin stress transducers 4-97448  
 rods impactation on PMMA target, radial displacement meas. method 4-106280  
 rough surface, s-polarised surface polariton propagation 4-80510  
 SAW excitation and magnetoacoustic effects 4-70545  
 seawater and marine sediment Al content meas. by atomic laser photoionisation method 4-94263  
 secondary ion emission, O effects 4-76609  
 self-ion damage and comparison of ion damage rates with neutron damage rates 4-113506  
 self-ion sputtering yields 4-76628  
 shear bands, localised flow 4-99460  
 shear strength, measurement techniques, high temps. and pressures 4-81376  
 shear strength under torsional impact, strain rate depend. (*Japanese*) 4-99432  
 sheet, deep drawing, influence of temp. 4-66399  
 sheet, prod. by elec. bursting method, struct. 4-93250  
 sheet formability and plastic instability, effect of geometry and materials props. 4-93351  
 sheets, square cup drawing characts. 4-61941  
 shock compressibility in range 0.4 to 4 Gbar, reflection method 4-92294  
 shock impedance match expts., 0.1-2.5 TPa 4-108522  
 shock loaded, microstructure and hardness 4-109515  
 shock-compressed, vapourisation on expansion 4-61063  
 single crystal, under plane-strain compression, Bauschinger effect 4-89085  
 single crystal, supercond., penetration layers, microwave magnetoabsorption studies 4-104360  
 single crystal, cutting mechanism rel. to orientation, slip theory 4-80144  
 single crystal, dislocation multiplication during creep 4-98106  
 single crystals, close packed, dislocation drag 4-103762  
 solids, heavy ion charge states and charge transfer 4-76589  
 sound velocity behind strong shock waves, optical technique anal. 4-108554  
 sprayed coatings in cold regions, corrosion resistance 4-104906  
 sputtering techniques, semiconductors metallisation 4-81129  
 steel, austenitic stainless, aluminised, phase comp. and strength of coating 4-66487  
 strain hardening exponent 4-99406  
 strain softening, materials model with appl. in modelling strain localisation 4-99407  
 structure factors obtained from X-ray diff. meas., Debye-Waller factors 4-92158  
 subgrain growth during static annealing 4-114573  
 substrate with transparent film coating, inverting ratio of complex parallel and perpendicular refl. coeffs. 4-87271  
 superconducting film, charge imbalance induced by a temp. gradient 4-76070  
 superconducting film, polycryst., US attenuation of bulk shear waves below 4K 4-98811  
 superconducting films, antisymmetry, Fermi liq. and Pauli susceptibility renormalisation, spin polarised tunnelling meas. 4-70997  
 superconducting fluctuation regime of cylindrical films, quantum oscils. 4-114068  
 superconducting thin film, granular, current induced hotspot 4-76069  
 superconducting thin film, N ion implanted, critical temp. 4-61485  
 surface, adsorbed Ar and Kr optical spectra, configurational effects 4-80391  
 surface, chemisorption of O, cluster and slab model calcs. 4-70559  
 surface, ion bombarded, Auger emission anisotropies anal. 4-114355  
 surface, lattice relax., effect of strong elec. field 4-75766  
 surface, molten, laser wave power increases caused by reflections from workpiece surfaces 4-91519  
 surface, O and N covered, sputtered metal atoms, vel. distrib. 4-76608  
 surface (100), Ar chemisorption, dipole moment and interaction energy 4-98452  
 surface (111), low energy electronic excitations, EELS studies 4-99253

## aluminium continued

- surface (111), O chemisorption, LCAO-X $\alpha$  method anal. 4-113799  
 surface (111), pure textured polycrystalline, analytical SEM with JAMP-10 Auger microprobe 4-61785  
 surface acoustic waves and de Haas-van Alphen meas. 4-70540  
 surface damage from elec. pulse discharge 4-81343  
 surface layer thermal expansion, determ. using plasmon losses in EELS 4-88317  
 surface roughness effect on XPS and AES, Monte Carlo simulation 4-80352  
 surface struct. from low energy electron channelling 4-92482  
 surface with oxide, anodic oxide, phosphate and chromate coatings, Fourier transform IR spectra 4-104688  
 surface-A<sup>+</sup> collisions; L<sub>23</sub>Al Auger electrons, polar angular distrib. 4-76585  
 Taiwan Research Reactor, irradiated fuel rod testing 4-59326  
 target, laser interaction, time resolved K $\alpha$  spectra 4-66133  
 target, laser-driven shock wave evolution 4-113258  
 target for laser pulses, press. meas. 4-111097  
 tensile deformation, acoustic emission response and interpret. 4-114608  
 thermal diffusivity and sp. ht., 400-850K 4-75926  
 thick layers, penetration of 24.8 MeV electrons, energy spectra 4-66148  
 thin film, effect of vapour contaminants on props. 4-88435  
 thin film, electron transmission, electron NGR spectroscopy study 4-60971  
 thin film, laser induced melting, time resolved picosecond electron diff. study 4-88269  
 thin film with chemisorbed H, chemisorption effect an elec. cond. 4-88391  
 thin films, magnetoconductance and superconducting T<sub>c</sub> 4-70958  
 thin superconducting film, quantum effects at T>T<sub>c</sub> 4-80691  
 transverse thermal vibrations and strength 4-80178  
 trilayer with island metal film recording layer as optical data disc 4-91548  
 ultrafine particles, correlation between positron age and momentum of annihilating pairs 4-76555  
 ultrahigh-pressure laser-driven shock-wave experiments at 0.26  $\mu$ m wavelength 4-75180  
 use of surface behavior diagrams to study hydration/corrosion of aluminium and steel surfaces 4-89171  
 vacancy formation vol. calc. 4-70136  
 vacancy migration energy, exoelectron emission meas. 4-65456  
 vertical distribution in Arctic Ocean rel to Cd and Fe profiles and hydrography 4-82089  
 void and bubble form., 600 MeV proton irradi., temp. depend., 130-430°C 4-108482  
 welds, miniature, nondestructive inspection 4-66529  
 wires, low cycle fatigue, lattice defects, resist., temp. depend. (*Japanese*) 4-99508  
 X-ray generated ultrasonic signals 4-103889  
 yield surface, thermal loading effect, plastic strain 4-85178  
 yield surfaces in stress-temp. space generated by thermal loading 4-97357  
 $\alpha$ -particle stopping power, ang. distrib. 4-83276  
 (111)-Al abrupt interfaces, electronic props. 4-84696  
 Al, angular distribution of particle-induced X-ray emission 4-99213  
 Al IV, VUV spectrum, line wavelengths, relative intensities and transition identification 4-87065  
 Al, liquid, pair pots., Monte Carlo simulation 4-92047  
 Al, radioactive fuel cladding matrix materials, long-term disposal (*German*) 4-82410  
 Al VIII(IX)(X), intercombination lines in PLT tokamak 4-83322  
 Al XI, doubly excited states, fine struct. meas. by beam-foil spectra (*French*) 4-69236  
 Al XIII plasma, laser prod. high resol. k-shell dielectronic satellite lines 4-103571  
 Al<sup>+</sup> secondary ion emission, ionisation probability following Ar<sup>+</sup> bombardment 4-66177  
 Al:Ne target for soft X-ray laser investigations 4-97819  
 Al:P, etching chars. using magnetron plasma 4-81300  
 Al:Sb, ion implanted, hardness, friction and wear props. 4-66451  
 Al/a-C/Si MIS structures, DC sputter deposited, HF chars. 4-88601  
 Al/Ag system, react diffusion, effect of high press. 4-108666  
 Al/Al adhesive bonds, US nondestructive testing 4-114740  
 Al/Al<sub>2</sub>Cu bicrystal, two-phase, oriented, prod. by diffusion bonding technique 4-61244  
 Al/Al<sub>2</sub>O<sub>3</sub>/chlorophyll a/Ag photovoltaic cell charact. and behaviour 4-85370  
 Al/AlN/SiO<sub>2</sub>/Si struct., conduction mechanisms, shallow junction technique study 4-88599  
 Al/GaAs (110) interface, low temp. form. and structure, LEED, AES and work function meas. 4-80425  
 Al/MgF<sub>2</sub> Fabry-Perot coatings chars., in vacuum UV range 4-58886  
 Al/Mo thin films, reactions 4-61148  
 Al/n-Si planar Schottky diodes, changes in breakdown chars. 4-88594  
 Al/n<sup>+</sup>GaAs/n-GaAs Schottky contacts, MBE grown, field-enhanced tunnelling and barrier lowering study 4-114037  
 Al/NiSi(Pd<sub>3</sub>Si)(PtSi) Schottky barriers, Cr diffusion barrier 4-88352  
 Al/Si interface, atomic redistributions, XPS studies 4-80311  
 Al/Si:As interface, sintering and diffusion, As dopant effect 4-80427  
 Al/Si<sub>3</sub>N<sub>4</sub>/SiO<sub>2</sub>/Si capacitors, ion/atom beam milling, damage effects 4-70941  
 Al/SiC interface form., annealing and oxidation, AES studies 4-80420  
 Al/SiO<sub>2</sub>/Si capacitor struct., ion beam fluorination and interface state density 4-70176  
 Al/SiO<sub>2</sub>/Si capacitors, radiation-induced oxide defects, ESR study, bias effects 4-70205  
 Al/SiO<sub>2</sub>/Si capacitors, interface trap generation and H electromigration 4-70940  
 Al/Sm<sub>2</sub>O<sub>3</sub>/Al capacitor struct., dielec. props. and thermoluminescence 4-76047  
 Al-(SnO<sub>2</sub>+Sb<sub>2</sub>O<sub>3</sub>)-Al mixed thin films, dielec. studies 4-84719  
 Al-Ag(In)(Sn) systems, mixing behaviour study by Ar ion beam irradiation 4-65402  
 Al-air batteries, electrochemical characteristics of air electrode with Fe phthalocyanine 4-93608  
 Al-Al<sub>2</sub>O<sub>3</sub> composite anodised layer, spectrally selective, solar collector appl., ESCA studies 4-66789  
 Al-Al<sub>2</sub>O<sub>3</sub> film in plating, using inexpensive rotating barrel 4-66494  
 Al-Al<sub>2</sub>O<sub>3</sub>-Ag tunnel junctions, surface plasmons and light emission 4-98553

## aluminium continued

- Al-Al<sub>2</sub>O<sub>3</sub>-Pb junction, effects of patterned laser illumination 4-70998  
 Al-Al<sub>2</sub>O<sub>3</sub>-Pb(Ag) tunnelling junctions, interaction with 3-(trimethylsilyl)propanethiol, IETS study 4-92827  
 Al-Al<sub>2</sub>O<sub>3</sub>-metal junctions, thermally shorted, point contact spectroscopy 4-80687  
 Al-Al<sub>2</sub>O<sub>3</sub>-Pb junctions, ion irradi., defect vibr., supercond. tunnelling meas. 4-98826  
 Al-AlO<sub>2</sub>-Pb(Ag), barrier height and electric field induced barrier shifts 4-70946  
 Al-As<sub>2</sub>S<sub>3</sub>-Al MIM struct., bias voltage depend. of capacitance 4-104325  
 Al-Au(Cu) thin film bilayers, ion beam bombarded, interfacial phase formation 4-70241  
 Al-based dilute foils, conduction electron spin resonance linewidths 4-92961  
 Al-chalcogenide glass structures, cathode effect in electrostimulated chem. transformations 4-88804  
 Al-chalcogenide glass-Al sandwich struct., Schottky barrier form. 4-104291  
 Al-Cr thin film couple, diffusion barriers, Auger study 4-88407  
 Al-Cu couple, galvanic corrosion in uninhibited aq. glycol soln. 4-66480  
 Al-GaAs contact, semicond. electron field emission props., metal adsorption effect 4-99289  
 Al-GaAs Schottky diodes, barrier height modification using MBE 4-70937  
 Al-Ge films, granular, sp. ht., thermal cond. meas., supercond. transitions 4-98809  
 Al-glass composite, produced by powder metallurgy route, mech. props. 4-66275  
 Al-I-Au(Cu)(Ag) tunnel junction, fast light emission, plasmon polaritons (*French*) 4-80998  
 Al-insulator-Pb(Ag) tunnel junctions, doped with aromatic aldehydes, ring substituent effects, elastic tunnelling study 4-92828  
 Al-LiClO<sub>4</sub> shock compression, physicochemical transformations 4-70273  
 Al-plexiglass target, high speed water jet penetration simulation 4-108533  
 Al-poly-N-vinylcarbazole-Al struct., dark cond. meas. of cryst. polymer layer 4-76050  
 Al-Si interconnects, DC magnetron-sputtered, influence of residual gas composition on lifetime 4-71560  
 Al-SiO<sub>2</sub>-Si MIS structures, with plasma deposited SiO<sub>2</sub>, alkali ion motion, C-V chars. (*Russian*) 4-114042  
 Al-SiO<sub>2</sub>-Si MOS structure, X-ray induced interface traps, stress relax. effects 4-98755  
 Al-SiO<sub>2</sub>-Si struct., X-ray irradi., interface traps. 4-104281  
 Al-SiO<sub>2</sub>-Si structures, dipolar relax. effects, transient capacitance spectroscopy study 4-80683  
 Al-SiO<sub>2</sub>-Si<sub>3</sub>N<sub>4</sub>-Si struct. circuit, nonlinear reson. curve illuminated by light 4-84704  
 Al-steel interface, Al diffusion, mech. activation effects 4-61151  
 Al-Ti-C-Si contact system, thermal stability 4-84703  
 Al+Cu smoke particles, coalescence, electron microscopy study 4-81483  
 Al+H<sup>+</sup>(He<sup>+</sup>), KL vacancy production cross sections, projectile depend. 4-96676  
 AlGaAs semiconductor laser, frequency stabilization by thermal and current feedback control 4-60071  
 AlN/Al cermets, reactive DC planar magnetron sputtering prep., elec. transport props. 4-88607  
<sup>27</sup>Al, HFS and radiative lifetimes in 3s<sup>2</sup>np<sup>2</sup>P<sub>3/2</sub> sequence using time resolved laser spectroscopy 4-74198  
<sup>27</sup>Al, negative muon hyperfine transition rate 4-69248  
 Au/Al contacts, intermetallic bonds and contact resist. (*Russian*) 4-113819  
 Au-As<sub>2</sub>S<sub>3</sub>-Al MIM struct., bias voltage depend. of capacitance 4-104325  
 Au-GaAs Schottky barrier contacts, LEC grown, electron traps, DLTS signals, effect of metal 4-84691  
 Au-Sb<sub>2</sub>S<sub>3</sub>-Al MIM struct., bias voltage depend. of capacitance 4-104325  
 B fibre reinforced Al, fibre-matrix bond form. kinetics during rolling 4-71674  
 B fibre reinforced Al, fracture mode and shear strength rel. to interface strength 4-62022  
 B fibre reinforced Al, rolling in direction of reinforcement 4-66353  
 B fibre reinforced Al, stress-strain and failure behaviour 4-76831  
 Bi<sub>2</sub>SiO<sub>5</sub>/Al, optical absorp. spectra, photochromism (*Russian*) 4-114311  
 Bi<sub>2</sub>SiO<sub>5</sub>/Al, photocond., absorption spectra and TSC studies 4-65710  
 Cu/Al thin film interface reactions, X-ray diff. and Rutherford backscatt. studies 4-88409  
 Fe/Al cylinders, diffusion under high mech. stress and accelerations, AES studies (*German*) 4-103993  
 GaAs (110)-Al interface form. at low temp., electronic and struct. props. 4-84695  
 GaAs:Si, Al p-n structures, radiative recomb., electrolum. chars. (*Russian*) 4-109249  
 GaAs/nAlGaAs superlattice devices, high speed electrons and hot electron effects appls. (*Japanese*) 4-61449  
 GaAs-Al interface, IR surface second harmonic generation and chars. (*Chinese*) 4-74606  
 Ge:Al, implanted ion projected range distrib. 4-80079  
 Ge:Si(Sn)(Al), thermal cond. meas., impurity conc. effect, temp. depend. 4-80318  
 He blistering effect of stress state 4-60969  
 He bubble nucleation on dislocations during 600 MeV proton irradi. 4-113504  
 Li-Al electrode secondary cell, cycling behaviour in LiClO<sub>4</sub>-propylene carbonate solutions 4-72058  
 Li-Al electrode secondary cell at room temp., Li-Al alloy electrochemical formation kinetics 4-72059  
 Li-Al/FeS cell, FeS positive electrode effective conductivities in LiCl-KCl eutectic electrolyte 4-99958  
 MIM Mo-Si<sub>3</sub>N<sub>4</sub>-O<sub>2</sub>-Al structures, electrode surface relief effect on parameters 4-76048  
<sup>14</sup>N<sup>+</sup> stopping cross section in Al 4-107266  
 NiO:Al, elec. cond. and high temp. defect struct. 4-80617  
 Si:Al, electronically simulated defect migration 4-113730  
 Si:Al, third-period interstitials, electronic struct. calcs. 4-108808  
 Si:Al epitaxial film, packing defects, growth conditions 4-61255  
 Si:H, Al-covered, solid-state reaction between film and substrate 4-92498  
 Si-SiO<sub>2</sub>-phosphosilicate glass-Al struct., positive charge buildup 4-98777  
 SiC fibre reinforced Al alloy, squeeze cast, thermal expansion, elastic to plastic deformation, transition 4-108635  
 SiC:Al, B(Be), <sup>6</sup> interstitial diffusion studies 4-80302

## aluminium continued

- SiC:Al, linear photogalvanic effect 4-70869  
 SiC:Al, vapour deposition and doping for epitaxial p-n structures 4-76690  
 Sr(NO<sub>3</sub>)<sub>2</sub>:Al, d.c. ionic cond. meas. 4-84456  
 V/Al thin film couples, phase form. and diffusion in couples prep. under varying deposition conditions 4-75736  
 Xe atom implantation in Al, depth distribution obs. by Rutherford backscattering (*Japanese*) 4-104707  
 ZnO:Al films, RF magnetron sputtering, elec. and optical props. 4-85100  
 Zr-Al composite-cathode sputter-ion pump 4-78332
- aluminium alloys**  
 see also *aluminium compounds*  
 Al-Fe, cold worked, damping capacity, mech. props. rel. to heat treatment and comp. (*Japanese*) 4-61968  
 Al-Ni alloy, effects of morphology of Al<sub>3</sub>Ni whiskers on tensile strength 4-88133  
 Alnico magnets, microstruct., comp., atom probe field ion microscopy 4-71828  
 anisotropic material response on continuum damage, expt. evaluation 4-99565  
 cast two-component, distrib. of alloying elements between phase components 4-114482  
 collinear beam-mixing by amplitude modulated US wave 4-98211  
 corrosion behaviour in HCl, inhibitive effect of heterocyclic compounds 4-104919  
 crack growth under rolling contact, defect installing technique 4-85284  
 cracked specimens, elastic and plastic anal., use of laser holographic and speckle interferometry (*Chinese*) 4-83854  
 creep crack propag., DC pot. meas. of crack length (*Japanese*) 4-99688  
 D-16 sample, particle vel. distrib. in elastic precursor of compression wave 4-92296  
 degassing rate of materials, compensated meas. method (*Polish*) 4-111145  
 endurance limit, accelerated Locati method 4-99702  
 erosion morphology, solid particle impact and particle shape effect 4-114682  
 fatigue crack closure, dependence on fracture features 4-80149  
 fatigue crack growth, thermoactivation anal. 4-99597  
 fatigue crack propagation rate, correl. with J-integral or crack opening displacement (*Japanese*) 4-114649  
 fatigue life of duralumin PA6N, effect of programmed load spectrum parameters (*Polish*) 4-62028  
 fatigue strength, biaxial plastic prestrain effect 4-104833  
 fatigue tests, accelerated, methodology 4-66542  
 fatigue-crack growth in vacuum and gaseous media 4-93398  
 FeCrAlloy, Fe-Cr-Al, D permeation 4-11754  
 graphite fibre reinforced Al alloy, tensile strength rel. to gauge length 4-81239  
 heat-treatable, prep. of samples for DSC, punching vs. spark cutting 4-62150  
 Heusler alloys, band struct., mag. moments, hyperfine fields, local spin density method 4-108767  
 homogenising ingots, struct. changes 4-61961  
 laser treatment, strengthening and microstruct. (*Russian*) 4-71665  
 Magnox alloys, etched, surface anal. by secondary ion mass spectrometry and ion scatt. spectroscopy 4-93456  
 material aspects of crack tip yielding and subcrit. crack growth in eng. alloys 4-93408  
 mirror, IR MTF measurements, effect of surface textures on reliability 4-97027  
 multiaxial creep and creep recovery at 200°C of 2618 Al 4-104830  
 multiaxial creep under proportional loading steps of 2618-T61 Al 4-104831  
 OTEC heat exchanger biofouling, corrosion and heat resistive expts. 4-114935  
 oxidised, charact. and adhesion of oxide films to epoxy resins 4-104925  
 panels, cylindrical, integrated-stiffened, buckling test (*Chinese*) 4-79475  
 panels, surface damage due to projectile impact 4-76865  
 permanent black coatings, corrosion resistant 4-104922  
 plasma etching, AlCl<sub>3</sub> management 4-81345  
 plastic deformation, sliding contact with wedge, friction-wear relations 4-89139  
 plate having rectangular notches with rounded corners, under tension, stress conc. 4-97311  
 plates, flat, strains determ. by moiré displacement patterns 4-87642  
 positron annihilation determ. of Guinier-Preston zones (*Russian*) 4-114342  
 R-tokamak, first wall design from low activation Al alloy, cooling 4-111802  
 R-tokamak, low activation Al alloy vacuum vessel, EM forces, stress anal. 4-111801  
 rare earth alloys, AlAl<sub>3</sub>, paramagnets, spin correlations, muon spin resonance studies 4-65816  
 rare earth alloys, AlAl<sub>3</sub>, spin fluctuations and zero-field muon spin relax. 4-65817  
 scale removal, improved fatigue strength 4-85263  
 seamless bellows with thick ends (*Japanese*) 4-73444  
 shear strength under torsional impact, strain rate depend. (*Japanese*) 4-99432  
 sheet, flaw inspection, fatigue crack parameter selection in setting specimens 4-109605  
 solid surface, chemical and electrochemical treatment, low energy electron induced X-ray spectra 4-76572  
 solidification, grain refinement, pseudosurface nucleation mechanisms 4-114497  
 space vehicle thermal central materials, effects of ultraviolet and oxygen plasma environments 4-85264  
 steel fibre reinforced Al alloy, prep. by explosion techniques, mech. props. at low temp. 4-114634  
 steel wire reinforced Al alloy, KAS-1A composite, resources eval. 4-66442  
 surface characterisation, for vacuum chamber materials 4-88386  
 surface preparation, adhesive bonding and corrosion developments 4-89173  
 thermodynamics and struct., solvent-solute interaction 4-113670  
 thin-walled cross sections under pure torsion, elastoplastic stress conc. at reentrant corners 4-97345  
 transcrystalline SCC mechanism, cleavage-like fracture surfaces 4-71793

## aluminium alloys continued

- transition metal alloys, M<sub>2</sub>MnAl (M=Cu, Ni, Co, Pd, Pt) ternary alloys, cubic, atomic ordering, X-ray diff. study 4-61081  
 wear of Al alloy rubbing on low C steel 4-114688  
 Al-Sn(In), ion irradi., vacancy-solute atom complexes, channelling study 4-103836  
 Ag-Al (10 at.%), transient creep, effect of  $\mu$  phase precip. 4-114618  
 $\alpha$ -AgAl, short-range order parameter, determ. from resist. meas. 4-98287  
 Ag<sub>5</sub>MnAl, Silmanal, magnetic phase growth (*Russian*) 4-109014  
 Al-1100 alloys, in HCl, thiourea and derivative corrosion inhibitors 4-99643  
 Al bronze on steel, sliding friction break-in curves, effect of flat-on-ring sample alignment 4-81294  
 Al/Al<sub>2</sub>Cu bicrystal, two-phase, oriented, prod. by diffusion bonding technique 4-61244  
 Al-Ag, age hardened, persistent slip bands, energy dispersive spectra 4-104794  
 Al-Ag, dil., single cryst., doped, muon localisation, transverse  $\mu$ SR line-width study 4-65906  
 Al-Ag, solubility of Ag in Al, effect of high press. 4-81179  
 Al-Al<sub>2</sub>Cu, eutectic alloy thin films, growth 4-88995  
 Al-Al<sub>2</sub>Cu eutectic thin films, directionally solidified, interlamellar spacing 4-93285  
 Al-Al<sub>2</sub>O<sub>3</sub>-(Si), creep deform., stress and temp. depend. 4-81246  
 Al-Al<sub>3</sub>Ni eutectic composites, work hardening in stage II, 293-673K (*Japanese*) 4-89067  
 Al-Al<sub>3</sub>Ni eutectics, directionally solidified, interfacial microstructures, TEM obs. 4-81187  
 Al-Ca-Zn superplastic alloy, composite, fibre reinforced, hot pressing, tensile props. 4-99369  
 Al-Co, sputtering, surface comp., quantitative AES anal. 4-104045  
 Al-Co-Fe, Alcofer 122, magnetostrictive, piezomagnetic coeffs., annealing, mag. field depend. 4-76214  
 Al-Cr-Ni system, phase equilib. relations, review 4-114479  
 Al-Cu, and thermal cond., 400 to 850K 4-75927  
 Al-Cu, columnar crystals, unidirectionally solidified in flowing melt 4-81181  
 Al-Cu, dil., quenched, positive muon spin depolarisation 4-65910  
 Al-Cu, directional solidification, off-eutectic composite growth, segregation, convection effects 4-71647  
 Al-Cu, droplet solidification on chill block, predendrite form. rel. to supercooling 4-89037  
 Al-Cu, dynamic recovery and recryst. (*Korean*) 4-76785  
 Al-Cu, fatigue crack growth anal., cycle counting 4-104839  
 Al-Cu, implanted, disorder studied by ion channelling and Rutherford backscattering 4-98145  
 Al-Cu, liq., structural props., elec. resist., X-ray diff. 4-79925  
 Al-Cu, phase transform., thermoelec. power study 4-114473  
 Al-Cu, rapidly solidified, decomp. struct. 4-104775  
 Al-Cu, rheocasting, grain refinement rel. to stirrer rotation velocity (*Japanese*) 4-89036  
 Al-Cu, thermal diffusivity and sp. ht., 400-850K 4-75926  
 Al-Cu,  $\theta$  phase form., departures from Matthiessen's rule, elec. resist. obs. 4-71660  
 Al-Cu (10 wt.%), prod. by rheocasting, rel. between struct. and mech. props. 4-99467  
 Al-Cu (2 to 5 wt.%), precip. effects on thermopower 4-99384  
 Al-Cu (3.6 wt.%), aged, coarsening kinetics of rod shaped  $\theta$  particles, LSW theory 4-71652  
 Al-Cu (3.76 wt.%), Rheocast, ageing characts. rel. to incomplete homogenisation 4-109444  
 Al-Cu (4 wt.%), dissoln. kinetics of  $\theta$  phase using thermoelec. power meas. 4-114533  
 Al-Cu (4 wt.%), plastically deformed, stability of GP zones 4-61992  
 Al-Cu (4.3 wt.%), randomly nucleated two-dimens. grain struct., effect of grain growth anisotropy 4-104774  
 Al-Cu alloy, EELS for GP zones and precipitates 4-71886  
 Al-Cu alloys, Guinier-Preston zones and solute clusters, high resolution lattice images 4-114543  
 Al-Cu casting alloys, cold cracking mech., plasticity-elasticity transition (*Chinese*) 4-62026  
 Al-Cu eutectic, rapid solidification, with nonhomogeneous thermal contact 4-93276  
 Al-Cu films, microstructure and electromigration studies 4-88413  
 Al-Cu films deposited by sputtering techniques, microstruct. 4-108733  
 Al-Cu system, metastable states controlled by diffusion 4-65463  
 Al-Cu-Cd, strengthening mechanism of Cd additions 4-61985  
 Al-Cu-Fe(Mg), strain meas. near growing fatigue crack tip 4-114651  
 Al-Cu-Li, recrystallised 2024, mech. props. rel. to soln. heat treatment 4-76781  
 Al-Cu-Li alloys, mech. props., effect of minor alloying additions of Zr, Cd or Fe 4-99526  
 Al-Cu-Li-Cd, 2020, microstruct., fracture toughness and SCC 4-76851  
 Al-Cu-Li-Mg-Zr, splat-quenched, microstruct. and tensile props. 4-114620  
 Al-Cu-Li-Mn-Cd, Al 2020, fatigue crack growth behaviour 4-71728  
 Al-Cu-Mg, 2017, surface characterisation as vacuum vessel for nuclear fusion devices 4-96266  
 Al-Cu-Mg, 2024, plates, flow stress under quasi-static compression by steel punches 4-76827  
 Al-Cu-Mg, 2024 sheets, plastic energy dissipation and toughness, size effect 4-89102  
 Al-Cu-Mg, fatigue crack propag., overload-induced 4-99482  
 Al-Cu-Mg, fatigue crack propag., statistical characts. (*Japanese*) 4-99501  
 Al-Cu-Mg, low cycle fatigue, influence of cold forming 4-104841  
 Al-Cu-Mg, near threshold fatigue crack growth, stress intensity factors, crack closure 4-99583  
 Al-Cu-Mg, notch fatigue, limits to applicability of LEFM 4-71721  
 Al-Cu-Mg, RR-58, anelastic creep at 180°C 4-99472  
 Al-Cu-Mg, shot peening effect on fatigue crack initiation by fretting 4-66448  
 Al-Cu-Mg, thermomech. treatment, age hardening rel. to Mg/Cu ratio (*Japanese*) 4-89064  
 Al-Cu-Mg alloy D16 plates, struct. strength, chem. comp. and heat treatment effects 4-61986  
 Al-Cu-Mg wrought alloy 1163, props. 4-62038  
 Al-Cu-Mg-Ag, precipitate struct. and orientation relationship, effect of Ag additions 4-93303  
 Al-Cu-Si, Al 2014, punch-stretching behaviour, 250 to 500°C 4-76817  
 Al-Cu-Si, Al 2014, tensile props., 250 to 500°C 4-76816  
 Al-Cu-Si, low temp. deposition and SiO<sub>2</sub> film growth 4-71783

## aluminium alloys continued

- Al-Cu-Si sputtered thin film conductors electromigration resistance 4-88611
- Al-Cu-Al, lamellar eutectic composites, high temp. yield strength rel. to microstruct. 4-81247
- Al-Cu-Al, system, directionally solidified, faceting behaviour 4-76766
- Al-Cu (4 wt.%), polycrystals containing  $\theta'$  precipitates, cyclic deform., grain size depend. and correl. with single crystals, 4-66379
- Al-Fe alloys, Fe precipitation and dissolution, thermoelec. study 4-61938
- Al-Fe-Mg-Cu, periodic load serrations in tensile curve, occurrence conditions 4-85194
- Al-Fe-Mn system, Al-rich corner, phase equilib. and crystn. studies 4-11480
- Al-Fe-Ni-Co, prep. from atomised powder, prod. struct. and props. 4-114446
- Al-Fe-Si (0.31, 0.11 wt.%), recovery and recrystn., DSC study 4-85167
- Al-Fe-misch metal, rapidly solidified, microstruct. characterisation 4-114442
- Al-Fe(Cu),  $\text{Ar}^+$  ions impact in ultrahigh vacuum, secondary ion and Auger electron emission (French) 4-66170
- Al-Ga equilibrium diagrams, thermodynamic anal., appl. of modified sub-regular soln. model 4-92387
- Al-Ge, binary constitution diagrams at very high press. 4-104766
- Al-In, dil., He localised diffusion around In impurities, PAC obs. 4-65470
- Al-In (17.5 wt.%), monotectic alloy, unidirectional solidification struct. 4-109371
- Al-In (17.5 wt.%), unidirectional solidification, monotectic struct. 4-109392
- Al-In-Sn, irregular monotectic struct., effects of temp. gradient and growth vel. 4-66321
- Al-Li, microcrystal evolution, DSC obs. 4-71659
- Al-Li, nucleation, growth and coarsening of precipitates 4-81202
- Al-Li, precipitate-matrix interfacial energy 4-85160
- Al-Li (22 wt.%), dislocation dynamics, mean jump distance and activation length of moving dislocations 4-108364
- Al-Li-Cu-Mg-Zr, powder metallurgy produced, superplastic behaviour 4-76820
- Al-Li-Si system, liquidus surface, thermal and microstructural analysis 4-61921
- Al-Li-Zr (2.34, 1.07 wt.%), composite precipitates 4-85154
- Al-Mg, 5083 alloy plates, mech. props. and stress corrosion cracking, anisotropy effects (Japanese) 4-66496
- Al-Mg, ageing, metastable phases in early stages of precip., DSC and resist. obs. 4-71656
- Al-Mg, cold rolled strip, texture, X-ray diff. obs., defocusing corrections 4-92029
- Al-Mg, creep, stress range of Class I behaviour 4-81249
- Al-Mg, dil., muon spin relax. 4-65907
- Al-Mg, dil., neutron irradi., internal friction, elastic modulus, recovery stages studied by elec. resist. meas. 4-103876
- Al-Mg, dil., quenched, positive muon spin depolarisation 4-65910
- Al-Mg, kinetics of Mg loss during melting and holding 4-114499
- Al-Mg, neutron irradi., radiation damage 4-80112
- Al-Mg, oxidation, Mg diffusion and surface segregation, AES 4-98293
- Al-Mg (0.047 at.%), dil., positive muon spin relax. meas., diffusion, trapping and detrapping 4-65908
- Al-Mg (10 wt.%), extrusion and mech. props. of compacts prep. from rapidly solidified powders 4-66395
- Al-Mg (1.74 at.%), creep, strain transients in stress drop tests 4-85196
- Al-Mg (3 wt.%), shear bands, localised flow 4-99460
- Al-Mg (4 wt.%), corrosion in chloride containing electrolytes, inhibitor efficiency 4-109337
- Al-Mg (5 wt.%), direct hot extrusion of billet, pure Al-cladding effect 4-109355
- Al-Mg (5 wt.%), high temp. fatigue, squared-up grain struct. 4-81277
- Al-Mg alloy, welded joint, crack resistance limit determ. by the moment of crack displacement (Russian) 4-81275
- Al-Mg alloys, heat treated and cold rolled, oxidation, AES study 4-66474
- Al-Mg alloys, Mg diffusion coeff. and thermomodification 4-65462
- Al-Mg alloys, steady-state creep, stress components 4-85181
- Al-Mg class I high temp. creep alloys, internal and friction stresses 4-85185
- Al-Mg dilute alloys, oxidation behaviour, ESCA studies 4-76907
- Al-Mg solid solution alloys, high stress levels, breakdown in creep 4-113526
- Al-Mg solid solutions, ductility loss at high temps. 4-104857
- Al-Mg- $\text{Al}_2\text{O}_3$ , incorporation of  $\text{Al}_2\text{O}_3$  particles by stirring in melt 4-93252
- Al-Mg-Bi, Al-Mg-Li and Al-Li-Mg low-activation alloy development for fusion device 4-108460
- Al-Mg-Cu, tubes, biaxial yield and flow, evaluation of anisotropic effective stress-strain criteria 4-104826
- Al-Mg-La system, Al-rich corner, liquidus invest. (Chinese) 4-61917
- Al-Mg-Mn, hot deform. and dynamic recrystn. 4-109479
- Al-Mg-Sc, electron irradi., precipitation and struct. (Russian) 4-66339
- Al-Mg-Sc, He blistering effect of stress state 4-60969
- Al-Mg-Si, age hardened, fatigue crack propág. under two-step loading (Japanese) 4-99518
- Al-Mg-Si, creep life prediction, long-time, role of microstruct. instability 4-114622
- Al-Mg-Si, cyclic creep, relationship with hysteresis loop energy 4-109456
- Al-Mg-Si alloy, effect of Fe on precipitation 4-104783
- Al-Mg-Si alloys, transitional state formation by diffusion 4-61135
- Al-Mg-Si: Pb, Sn, Mossbauer and X-ray diff. obs. 4-65882
- Al-Mg-Si-Sn, ageing, clustering process rel. to Sn addition, elec. resist., TEM obs. 4-114529
- Al-Mg-V alloys for nonbreeding blanket in fusion reactor 4-111744
- Al-Mg(Ga)(In)(Si)(Ge)(Sn), distribution of electric field gradients around impurities, conduction electron screening lattice strain 4-113910
- Al-Mg (7 wt.%), hot-rolled, prep. from rapidly solidified powder, fracture mechanism 4-71731
- Al-Mn, commercial, quenched-in vacancy defects 4-108365
- Al-Mn, polyvalent films, elec. cond. anomaly 4-80688
- Al-Mn dilute alloys,  $^{65}\text{Zn}$  diffusion 4-65482
- Al-Mn-Zr, rapidly quenched from melt transform. behaviour 4-81185
- Al-Mo alloys, ion implanted, corrosion resist., AES studies 4-99626
- Al-Ni, vacancies obs. by positive muons trapping (Japanese) 4-104515
- Al-Sb system, phase diagram calc., Krupkowski's eqn. (Polish) 4-85139
- Al-Sc (0.3 at.%) alloy, ageing, precipitation obs. (Russian) 4-104786
- Al-Sc alloys, age hardening kinetics 4-61949

## aluminium alloys continued

- Al-Sc system, metastable state diagram 4-114485
- Al-Si, Al halo form, during directional solidification 4-99381
- Al-Si, binary constitution diagrams at very high press. 4-104766
- Al-Si, cast, graphite additions influence on user characts. 4-109520
- Al-Si, cold worked, damping capacity, mech. props. rel. to heat treatment 4-61967
- Al-Si, dil., quenched, positive muon spin depolarisation 4-65910
- Al-Si, directional solidification, eutectic fibrous struct. rel. to comp. and growth velocity 4-61927
- Al-Si, eutectic solidification 4-89045
- Al-Si, phase comp. and struct. rel. to electric field treatment of melt 4-93274
- Al-Si, silumins, permanent modification with Sr and Sb (Polish) 4-85145
- Al-Si (12.4 wt.%), near-eutectic, solid-liq. interface (German) 4-81184
- Al-Si (3 wt.%) ingots, quality and feedability during solidification 4-109389
- Al-Si eutectic, surface morphology, crack section morphology and metallographic struct. after laser irradi., SEM study (Chinese) 4-62106
- Al-Si eutectic alloy, U centre mechanism for superconductivity enhancement (Chinese) 4-92203
- Al-Si interdiffusion ohmic contact achieved by capacitance discharge (Chinese) 4-98752
- Al-Si melt, wetting of graphitised C strip 4-92476
- Al-Si system, enthalpies of form. of liq. alloys 4-113679
- Al-Si system, phase relations up to 5.5 GPa 4-104765
- Al-Si/n<sup>+</sup>-Si system, metallisation by fast heat pulse alloying, hillock elimination 4-114034
- Al-Si-Cu, reactive ion etching, rel. to film deposition characteristics 4-81357
- Al-Si-Cu-Mg, strengthening with continuous  $\text{CO}_2$  laser 4-62117
- Al-Si-Fe, Al-4, stress relax. resist., effect of plastic surface strain methods 4-109453
- Al-Si-Fe, Luders band deform., stress relax., load suppression effect 4-76801
- Al-Si-Fe-Mn, cast, quaternary Fe-containing phases 4-81204
- Al-Si-Ge, Si<sup>+</sup> ion implantation effects on supercond. temp. (Chinese) 4-76062
- Al-Si-Mg casting alloys, quality evaluation, thermal analysis, data acquisition system (French) 4-81365
- Al-Si-Mg-Mn eutectic, surface morphology, crack section morphology and metallographic struct. after laser irradi., SEM study (Chinese) 4-62106
- Al-Si-Mg-Sr, hypoeutectic alloys, melting losses of Sr rel. to holding time 4-114498
- Al-Si-Mg-Sr, struct. and props., comp. and Sr addition effects 4-61987
- Al-Si-Sb, eutectic, struct. rel. to Sb addition, electron beam microanalysis (German, English) 4-66314
- Al-Sn, dil., small Sn additions effect on microstruct. and corrosion behaviour 4-99630
- Al-Sn (0.1 wt.%), corrosion resist., electrochemical props. rel. to alloying additions 4-81342
- Al-Ti long-period one-dimensional antiphase structures, electron diff. and microscopy, X-ray diff. 4-113398
- Al-Ti-B alloys, Al-rich, nature and morphology of Ti- and B-rich crystals. (French) 4-61919
- Al-Ti(B), impurity distrib. 4-114538
- Al-Zn, cellular decomp., TEM, DSC obs. 4-114528
- Al-Zn, EXAFS in dispersive mode for fast microanalysis, use of synchrotron radiation plus photodiode array 4-72019
- Al-Zn, neutron irradi., radiation damage 4-80112
- Al-Zn, tunnelling relax. of mixed dumbbell 4-92406
- Al-Zn (Cu)(Mg), dendritic solidification and segregation in accordance with Krupkowski's formula (Polish) 4-85146
- Al-Zn (Cu)(5 wt.%), with and without Ti, stress corrosion cracking, electrochemical aspects 4-104920
- Al-Zn (3.5, 5.3 wt.%), GP zones, size distrib. 4-76779
- Al-Zn (40 wt.%), dendritic segregation and solidification (Polish) 4-85147
- Al-Zn alloy, quenched, dynamical scaling of struct. function 4-113659
- Al-Zn alloy coated sheet steel, composition of chromate passivation films, XPS anal. 4-93453
- Al-Zn alloys, Guinier-Preston zones, appl. of EXAFS in metallurgy, review 4-66104
- Al-Zn alloys, microsegregation, solidification effects 4-61940
- Al-Zn alloys, plastic deformation, precipitation and precipitate morphology 4-114548
- Al-Zn dilute alloys,  $\alpha_{\text{Zn}}$  rich precipitate shape, small angle neutron scatt. studies 4-114547
- Al-Zn film, ion plating using inexpensive rotating barrel 4-66494
- Al-Zn solid solns., creep and Zn self-diffusion 4-65461
- Al-Zn system, diffusion along grain boundaries and precipitation reactions 4-113697
- Al-Zn-Mg, 7075, heat-treated, acoustic emission during deform. 4-93343
- Al-Zn-Mg, 7075-T6, fatigue strength under combined axial loading and torsion 4-99483
- Al-Zn-Mg, 7075-T651, fatigue crack growth, effect of short-term heating cycles 4-99484
- Al-Zn-Mg, cyclic SCC, crack growth rate (Japanese) 4-99648
- Al-Zn-Mg, fatigue crack advance model, crack tip parameters 4-66401
- Al-Zn-Mg, fatigue crack closure in 7475, microstruct. and ageing effect 4-62032
- Al-Zn-Mg, SCC study, effect of various alloying additions (German) 4-71798
- Al-Zn-Mg, strain meas. near growing fatigue crack tip 4-114651
- Al-Zn-Mg (4.25, 2.75 wt.%), SCC by slow strain-rate method 4-66495
- Al-Zn-Mg alloy, quenched, dynamical scaling of struct. function 4-113659
- Al-Zn-Mg alloys, struct. and mech. props., effect of low-temp. thermomech. treatment 4-66352
- Al-Zn-Mg single crystals, environmentally-assisted cracking 4-71762
- Al-Zn-Mg-Cn, phase identification, X-ray analysis, sequential etching 4-104950
- Al-Zn-Mg-Cu, cold working, recovery and recrystn. (German) 4-71670
- Al-Zn-Mg-Cu, corrosion, effect of water-displacing corrosion preventives 4-114720
- Al-Zn-Mg-Cu, ERGAL 7075, plastic deformation at high strain rates 4-84337
- Al-Zn-Mg-Cu, precip. and quench sensitivity, effect of Cu additions 4-85155
- Al-Zn-Mg-Cu, SCC, nature of occluded cell 4-85248
- Al-Zn-Mg-Cu, V95, microstruct. at early stages of spalling 4-114665

## aluminium alloys continued

- Al-Zn-Mg-Cu (7.8, 2.6, 1.5 wt.%), 7049 notch sensitivity (*French*) 4-81251
- Al-Zn-Si phase diagram, vertical profile (*Bulgarian*) 4-93267
- Al-Zn-base alloys, tribological props. (*Polish*) 4-85216
- Al-Zr,  $2^{1/2}$ D imaging of precipitates 4-81206
- Al-Zr (9.4 wt.%), melt-quenched, decomp. study using TEM 4-93262
- Al-Zr alloys, precipitation reactions 4-114545
- Al-Zr-Mg-Cu-Mn, supersaturation of Mn solid soln. 4-61935
- AlCuZr, AlCu eutectic, fine grained superplastic alloys, anelastic strains, grain boundary cavity distrib., sintering 4-66359
- AlH<sub>2</sub>, electronic contrib. to elastic consts. 4-65326
- AlMg fracture form., shock wave exit angle effect on free surface 4-94948
- AlMnFeSi particles in Al alloys, STEM study 4-76920
- Al<sub>2</sub>O<sub>3</sub>-Al plasma coatings on graphite, oxidation resist., bonding strength and elec. cond. 4-66462
- AlSi high volume wafer metallisation, process parameters 4-88977
- AlZn, residual resist. of Guinier-Preston zones, pseudopot. approach 4-70779
- B fibre reinforced Al-Mg, interaction between B and matrix 4-70577
- B fibre reinforced Al-Mg alloy, fibre/matrix interface effect on fatigue, optimum processing parameters 4-114635
- B<sub>2</sub>C/B fibre reinforced Ti-Al-V, fatigue crack growth behaviour 4-93374
- Be fibres reinforced Al alloy, stress-strain and failure behaviour 4-76831
- Ca<sub>2</sub>CuAl<sub>7</sub> and CaCr<sub>2</sub>Al<sub>10</sub>, crystal structures (*German*) 4-75367
- CeAl, valence band photoemission at 3d absorption edges, reson. enhancement 4-81110
- CeAl<sub>3</sub>, bound state between phonons and crystalline electric field states 4-104175
- CeAl<sub>3</sub>, mixed valence system, high press. L<sub>III</sub> X-ray absorption spectra study 4-61342
- CeAl<sub>3</sub>, phonon softening, neutron scatt. studies 4-92318
- CeAl<sub>3</sub>, low-temp. specific heat meas. 4-75702
- CeAl<sub>100-x</sub>, amorphous, transport and mag. props. 4-108985
- Ce<sub>1-x</sub>Al<sub>1-x</sub>Al<sub>2</sub>, dense Kondo state, elec. resist., mag. susceptibility meas. 4-108984
- CeNi<sub>1-x</sub>Al<sub>x</sub> alloys, H<sub>2</sub> storage props. 4-61206
- Co-Al, directionally solidified eutectic, compressive yield stress rel. to lamellar termination density 4-81263
- Co-Al, long range 21R struct. during martensitic transform. (*Chinese*) 4-103699
- Co-Cr-Al(-Y), Si<sup>+</sup> implanted, 1050°C oxidation behaviour 4-62124
- CoCrAlY alloy surface protection coating, deposited by plasma spray, for gas turbine blades (*German*) 4-99639
- CoCrAlY, low temp. hot corrosion inhibition by ZnSO<sub>4</sub>-Na<sub>2</sub>SO<sub>4</sub> deposits 4-76903
- Co<sub>2</sub>MnAl, spin echo study of hyperfine interactions 4-71209
- CoTi<sub>1-x</sub>Al<sub>x</sub>, transition from nonmag.-ferromag. state, magnetisation and NMR meas. 4-76133
- Cr-Al BCC solid solns., valence band, XPS and X-ray emission spectra study 4-93194
- Cr-Al dilute alloys, thermal expansion, elastic consts. and mag. props. 4-80138
- Cu-Al, cold worked, recrystn., effect of stacking fault energy 4-81221
- Cu-Al, dendritic solidification and segregation in accordance with Krupkowski's formula (*Polish*) 4-85146
- Cu-Al, neutron irradiat., microhardness, resistivity, electron microscopy 4-103811
- Cu-Al, sliding wear induced residual stresses, X-ray diff. analysis methods 4-76927
- Cu-Al, strain hardening in microdeform., dislocation density, internal friction obs. 4-66397
- Cu-Al, vacancies obs. by positive muons trapping (*Japanese*) 4-104515
- Cu-Al (14 at.%), plastic flow instability boundaries at low temps. 4-99421
- Cu-Al (3 wt.%), surface chemistry of wear scars 4-99830
- Cu-Al system, dual-phase, deform. behaviour 4-61993
- Cu-Al-Co, with noncoherent particles, crit. shearing stresses, temp. depend. rel. to slip and twinning (*Russian*) 4-93333
- Cu-Al-Co (15.2 at.%), with non-coherent particles, superelasticity effects due to twinning 4-76795
- Cu-Al-Fe (10, 1 wt.%), corrosion and mech. props., effect of solidification struct. 4-85243
- Cu-Al-Fe alloys, laser surface melted, microstruct., X-ray diff. study 4-108628
- Cu-Al-Ni shape memory alloy, martensitic transform., effects of parent phase aging 4-66334
- Cu-Al-Ni single crystals, regions of thermoelastic phase stability, comp. depend. 4-66311
- Cu-Al-Ti, internal oxidation, dispersion hardening (*Japanese*) 4-89065
- Cu-Al-Zn,  $\beta$ -phase, damping capacity rel. to mech. props. and martensite morphology 4-99414
- $\beta$ -Cu-Al-Zn (8.7, 12.0 wt.%), with reversible martensite in struct., effect of ageing on damping capacity 4-109452
- Cu-Al-Zn system, high damping  $\beta$  alloys, effect of aging in martensite condition on mech. props. 4-114588
- Cu-Ni(Al)/(Zn) alloys, microsegregation, solidification effects 4-61940
- $\beta$ -Cu-Zn-Al,  $\gamma$ -brass-type precipitates, origin of incommensurate electron diff. pattern 4-76775
- Cu-Zn-Al, obs. using scanning electron acoustic microscopy imaging, depend. on chopping and detect. freq. 4-69639
- Cu-Zn-Al, shape memory alloys, ageing and stabilisation of martensite 4-109441
- Cu-Zn-Al, sliding contact with steel, micro-indentation hardness gradients of worn surface 4-76842
- Cu-Zn-Al (25, 6 wt.%), isothermal decomp. of  $\beta'$  phase 4-99387
- Cu-Zn-Al (26.3, 4 wt.%), shape memory alloy for wires and springs 4-114517
- Cu-Zn-Al alloy, shape-memory effect, practical appls. 4-104782
- Cu-Zn-Al alloys, martensitic transformations, positron annihilation studies 4-89053
- Cu-Zn-Al alloys, softened phonons, calorimetry, susceptibility and inelastic neutron scatt. study 4-75636
- Cu-Zn-Al single crystals, second martensitic transform., stress-induced 4-81195
- Cu-Zn-Al single crystals, tensile test, stress-strain curve anal. 4-81260
- CuAl, dil. disordered, diffuse size effect scatt. in high voltage electron diff. 4-113395
- CuAl<sub>3</sub>, second-phase particles, dissoln. rates in various microstruct. 4-89059

## aluminium alloys continued

- Cu<sub>2</sub>Al<sub>1-x</sub>, amorphous, elec. resist. and temp. coeff., pseudopot. theory 4-92692
- Cu<sub>2</sub>MnAl, Heusler alloy, decomposition during isochronal annealing 4-61916
- Cu<sub>2</sub>MnAl single crystals, Heusler alloy, compression, 77-367K, fracture slip, superlattice dislocation disloc. 4-66369
- DyAl<sub>3</sub>, ferromag., magnetisation, NMR studies 4-80787
- DyFe<sub>2</sub>Al<sub>2-x</sub>, Fe L<sub>III</sub> X-ray emission spectra, electron microprobe anal. 4-76563
- Dy<sub>2</sub>(Fe<sub>1-x</sub>Al<sub>x</sub>)<sub>3</sub>, pseudobinary intermetallic cpd., mag. props. 4-71032
- EuFe<sub>4</sub>Al<sub>2</sub>, X-ray absorpt. near edge struct. study 4-61769
- Fe-Al, anodic polarisation characteristics in 1N H<sub>2</sub>SO<sub>4</sub> 4-85247
- Fe-Al, at. correlations, Mossbauer spectra 4-61613
- Fe-Al, coercive field rel. to solid solubilities and nucleation behaviour 4-76185
- Fe-Al (10 to 50 at.%), quenched, shrinkage during annealing 4-89074
- Fe-Al (40 at.%), ion implantation, phase changes, TEM studies 4-108403
- Fe-Al (48 at.%), mag. props. rel. to heat treatment 4-109003
- Fe-Al alloys, Ar<sup>+</sup>-ion-sputtered, secondary ion and Auger electron emission 4-81101
- Fe-Al alloys, nitrided, interaction of Al and N atoms, mag. aftereffect study 4-84829
- Fe-Al alloys, segregation to static and migrating diffuse antiphase boundaries 4-114541
- Fe-Al rapidly quenched cryst. ribbons, mag., elec. and mech. props. 4-76174
- Fe-Al-Cr (Ni)(Mn), oxidation, effect of ternary alloying additions 4-85242
- Fe-Al-Mo, Mossbauer study of atomic struct. and mag. polarisation 4-80848
- Fe-Al-Ni-Mo (5.7, 2.5, 2.0 at.%), containing coherent precipitates, effect of plastic deformation on elevated temp. Ostwald ripening 4-85159
- Fe-Al-Si, anodic polarisation characteristics in 1N H<sub>2</sub>SO<sub>4</sub> 4-85247
- Fe-Al-Si, Sendust, brittleness, effect of solidification and heat treatment 4-81281
- Fe-Al-Si (20.5 at.%), DO<sub>3</sub>-ordered alloys, tensile behaviour 4-93337
- Fe-Al-Si (6, 9 at.%), ordering with phase separation, annealing, TEM, X-ray diff. study 4-114472
- Fe-Co-Ni-Al, Alnico 5, hot workability, microstruct. 4-114626
- Fe-Cr-Al, oxide dispersion strengthened MA 956, fatigue crack growth 4-62031
- Fe-Cr-Al, oxide films, characterisation by soft X-ray spectroscopy and microanal. 4-76909
- Fe-Cr-Al sulphidation in H<sub>2</sub>S, multilayered corrosion scales 4-71801
- Fe-Cr-Al alloys, sulphidation protection by Al<sub>2</sub>O<sub>3</sub> scales 4-93468
- Fe-Cr-Al-Ti alloy, Y<sub>2</sub>O<sub>3</sub> dispersed, characts. of Al<sub>2</sub>O<sub>3</sub> scales 4-89180
- Fe-Cr-Al-X, X=Cu, Ti, Ni, anodic polarisation in H<sub>2</sub>SO<sub>4</sub> 4-114719
- Fe-Cr-Al-Y plasma sprayed coatings, post-treated, mech. props. 4-93471
- Fe-Cr-Al(-Y), precip., small-angle neutron scatt. study 4-93304
- Fe-Mn-Al, high temp. oxidation, scale struct., metallography, SEM obs. 4-109562
- Fe-Mn-Al-C (15, 8, 2 wt.%), rapidly solidified, phase struct. and morphology 4-114504
- Fe-Mn-Al-Si, high-temp. oxidation resistant alloys 4-93461
- Fe-Mn-Al-Si, high-temp. oxidation, in situ SEM study 4-93462
- Fe-Mn-Al-Si system alloys, phase comp., Al and Si additions effect 4-114481
- Fe-Ni-Cr-Al(-Y)(Zr)(Ti), high temp. oxidation resist. influence of Y, Zr or Ti additions 4-104899
- Fe-Ni-Ti(Cr)(Al), nitrided layer, Mossbauer studies (*Russian*) 4-109555
- Fe-Si-Al, Sendust, hot rolling rel. to alloy comp. and mag. props. 4-93322
- Fe-Si-Al, Sendust, hot workability, microstruct. 4-114626
- FeAl, ordered, LMT0 approach to optical props. 4-71342
- FeAl-CoAl, length changes rel. to heat treatment, phase transform., vacancy annihilation 4-109442
- Fe<sub>2</sub>Al, neutron irradiat., at. ordering, Mossbauer spectra, X-ray diff. 4-65306
- Fe<sub>80-x</sub>Bi<sub>20-x</sub>Al<sub>x</sub>, crystallisation and mag. props. study 4-114137
- Fe<sub>80-x</sub>Hf<sub>20-x</sub>Bi<sub>20-x</sub>Al<sub>x</sub>, metallic glass, crystallisation and hyperfine fields 4-71030
- (Fe<sub>64</sub>Mn<sub>10</sub>Co<sub>26</sub>)<sub>75</sub>Pi<sub>6</sub>B<sub>6</sub>Al<sub>3</sub>, spin glass transition calcs. 4-88667
- Fe<sub>70-x</sub>Ni<sub>15-x</sub>Pi<sub>15-x</sub>B<sub>6</sub>Al<sub>3</sub>, metallic glass, Mossbauer study of high press. 4-84880
- Gd<sub>1-x</sub>La<sub>x</sub>Al<sub>3</sub>, loss of ferromagnetism 4-98885
- Gd<sub>1-x</sub>Th<sub>x</sub>Al<sub>3</sub>, loss of ferromagnetism 4-98885
- Gd<sub>1-x</sub>U<sub>x</sub>Al<sub>3</sub>, loss of ferromagnetism 4-98885
- GdAl<sub>3</sub>, ferromag., magnetisation, NMR studies 4-80787
- GdAl<sub>3</sub>,  $\mu$ SR spectroscopy 4-84894
- Gd<sub>2</sub>AuAl<sub>1-x</sub>, pseudobinary cpd., mag. behaviour 4-76136
- GdCo<sub>2-x</sub>Al<sub>x</sub>, magnetoelastic interactions (*Russian*) 4-65845
- Gd<sub>1-x</sub>Dy<sub>x</sub>Al<sub>3</sub>, NMR spectra, dipole field rot. 4-109084
- Gd<sub>2</sub>Ni<sub>2</sub>Al<sub>5</sub>, band struct. and ferrimag. moments, APW calc. 4-80487
- Ge-Al amorphous thin films, hopping cond. meas., 130 to 300K, localised state variations 4-92713
- HoAlGa, mag. transitions, mag. and cryst. structures, X-ray diff., thermal expansion meas. 4-114113
- La<sub>100-x</sub>Al<sub>x</sub>, amorphous, supercond., thermodynamic and transport props. 4-70986
- La<sub>90-x</sub>Al<sub>10-x</sub> metallic glass, elastic props. and thermal expansion 4-84335
- La(Fe<sub>1-x</sub>Al<sub>x</sub>)<sub>13</sub>, metamagnetic transitions and struct. aspects 4-92910
- LaNi<sub>4-x</sub>Al<sub>x</sub>, H<sub>2</sub> storage, appl. in H<sub>2</sub> masers 4-69352
- LaNi<sub>4-x</sub>Al<sub>x</sub>, stability of rechargeable hydriding alloys during extended cycling 4-72190
- LaNi<sub>5</sub>(Ni<sub>1-x</sub>Al<sub>x</sub>)<sub>3</sub> and misch metal analogues, H<sub>2</sub> desorption kinetics 4-75787
- Li-Al, T release on heating or NaOH dissolving rel. to Li conc. 4-75733
- LiAl, fast Li ion conductor, irreversible behaviour on elec. resist. 4-80634
- LiAl thin film electrodes for secondary batteries, overpotentials 4-109737
- Mg-Li-Al-Mn and Mg-Li-Al-Zn-Mn-Ce systems, mech. props. and corrosion resist. 4-93455
- Mn-Al hard magnets formed by rapid quenching 4-80794
- MnAlC permanent magnet, isotropic, mag. domain struct. 4-62070
- MnAlC permanent magnet, mag. anisotropy and rotational hysteresis 4-84784
- Mn<sub>1-x</sub>Al<sub>x</sub>-Fe<sub>x</sub>, thermal expansion, atomic order effects (*Russian*) 4-103971
- Mo-Al-B-C, welded joints, long-term strength characs. effect of alloying with N 4-109513

**aluminium alloys continued**

- Nb-Al multifilamentary superconductors for superconducting magnets, powder metallurgy processing 4-80731  
 Nb-Al-Ga, vacuum deposited films, struct. and supercond. transition temp. rel. to heat treatment 4-65764  
 Nb<sub>3</sub>Al based ternary phases, superconducting  $T_c$  volume depend. (*Russian*) 4-65765  
 Nb<sub>3</sub>Al, low temp. diffusion, supercond. and struct. props. 4-65498  
 Nb<sub>3</sub>Al, thermodynamic props. calc. 4-84741  
 Nb<sub>3</sub>Al-based ternary supercond. A-15 phases, vol. depend. of  $T_c$  4-92846  
 NdAl<sub>2</sub>, cryst. elec. fields, conduction electron screening effects 4-75906  
 Ni-(Al-Ti)-(Cr-Mo), pseudoternary phase diagram, phase relationship study using EPMA 4-76933  
 Ni-Al,  $\gamma$  precip. growth prediction 4-71658  
 Ni-Al, internal oxidation, O transport at high temps. 4-92442  
 Ni-Al, recrystn. during rapid elec. heating 4-66347  
 Ni-Al, soft X-ray emission spectra 4-93143  
 Ni-Al (13 at.%), HVEM irradi., void form. rel. to  $\gamma$  precipitation 4-108446  
 Ni-Al film growth, development of grain struct. 4-65580  
 Ni-Al plasma coatings from thermoreactive intermetallic powders, form. and props. 4-71556  
 Ni-Al thick films, grain struct. variation with temp. 4-88412  
 Ni-Al thin film, ion irradi., EELS study 4-88916  
 Ni-Al thin foils, pre-martensitic phase, electron diff. study 4-114518  
 Ni-Al-Hf superalloys, thermally activated deform., mech. 4-93327  
 Ni-Al-Hf system,  $\beta$  + (Ni,Al)-Hf<sub>2</sub> eutectic struct., cryst. morphology, struct., stacking faults, TEM, X-ray diff. obs. 4-81182  
 Ni-Al-Mo,  $\gamma$ - $\gamma'$ - $\alpha$  and  $\gamma$ - $\alpha$  eutectic alloys, yield stress and deform. struct., temp. depend. 4-93346  
 Ni-Al-Mo alloy, unidirectional solidification 4-76765  
 Ni-Al-Mo-Ta system, constitution of Ni-rich alloys at 1523K 4-66313  
 Ni-Al-Ta superalloys, thermally activated deform., mech. 4-93327  
 Ni-Al-Ti,  $\gamma$ - $\gamma'$  eutectic alloys, yield stress and deform. struct., temp. depend. 4-93346  
 Ni-base superalloy, single cryst., CMSX2, long-range order and phase comp. in  $\gamma$  phase, atom probe study 4-66337  
 Ni-Cr-Al,  $\gamma$  precip. growth prediction 4-71658  
 Ni-Cr-Al, recrystn. during rapid elec. heating 4-66347  
 Ni-Cr-Al (20, 4 wt.%), high temp., oxidation, tensile stress depend. 4-109572  
 Ni-Cr-Al films, highly disordered, temp. depend. resist. 4-80690  
 Ni-Cr-B-Al detonation deposited coatings, wear resist. 4-62123  
 Ni-Cr-Co-Al-Ti-Nb-W-Mo-V-Hf, cryst. lattice periods mismatch determ. 4-65219  
 Ni-Mn-P-B-Al alloys, amorphous, mag. props. studies 4-71086  
 Ni-Mo-Al eutectic alloy, unidirectionally solidified composite,  $\gamma$ / $\gamma'$  phases, microstruct. changes 4-114493  
 Ni-Mo-Al unidirectionally solidified eutectic, microstruct. instability 4-61926  
 Ni-Nb-Al  $\gamma$ - $\gamma'$  eutectic composite, prep. and morphology 4-114500  
 Ni-Ni<sub>3</sub>Al-Mo eutectic composite, crystallographic orientation of phases 4-114501  
 Ni-Ni<sub>3</sub>Al-NbC, eutectic, thermal cycling, calc. of residual stresses and strains 4-66380  
 NiAl, Ni-rich, extruded, deform. struct., TEM study 4-93341  
 NiAl on Ni, coatings struct. and morphology 4-70605  
 NiAl, vacancy dislocation loops, annealing effect, TEM obs. 4-103756  
 NiAl, vacancy dislocation loop growth, role of surface oxidation 4-103757  
 NiAl-Cr quasibinary eutectic, rapidly solidified, microstruct. and phase solubility extension 4-66319  
 Ni<sub>3</sub>Al, cold-rolled, recrystn. annealing 4-81213  
 Ni<sub>3</sub>Al, ordered alloy, flow stress and creep props. 4-114611  
 Ni<sub>3</sub>Al powders, rapidly solidified and annealed 4-93278  
 Ni<sub>3</sub>Al, weak itinerant ferromagnet, de Haas-van Alphen effect, Curie temp. 4-113848  
 NiCuAl alloys, spontaneous magnetisation, thermal variation 4-65796  
 Pb-Ag<sub>1-x</sub>Mn<sub>1-y</sub>Al<sub>1-y</sub>Pb, S-N-S junction, pair-breaking mechanism 4-98824  
 Pd-Al alloys, T mobility and permeability, influence of struct. of segregation overlayers 4-70472  
 PrAl<sub>2</sub>, elec. resist. dominated by quadrupole scatt., spin correl. effects 4-104191  
 Pt<sub>3</sub>Al single crystal, plastic flow, temp. range from liq. He to 1080K 4-76798  
 Re-Al alloys, phase relations and cryst. struct., X-ray diff. studies 4-70066  
 SiC fibre reinforced Al alloy, fabrication and mech. props. (*Korean*) 4-104755  
 SiC fibre reinforced Al alloy, composite strengthening, influence of microstruct. 4-99398  
 SiC fibre reinforced Al alloy, squeeze cast, thermal expansion, elastic to plastic deform. transition 4-108635  
 SiC fibre reinforced Ti-Al-V, fatigue crack growth behaviour 4-93374  
 SiC fibre/platelet reinforced Al-Mg-Si, magnitude and mechanism of strengthening 4-76710  
 SiC particle reinforced Al alloy, composite strengthening, influence of microstruct. 4-99398  
 SiC-Al, sintered composite interfacial reactions, joint bending strength rel. to microstruct. 4-66295  
 Sn, electrodeposition on Al alloys (*Russian*) 4-88991  
 Sr<sub>2</sub>Al<sub>2</sub>Sb<sub>2</sub>, Zn<sub>2</sub> phases with complex anions (*German*) 4-70067  
 ThNiAlH<sub>2</sub>, <sup>1</sup>H NMR and mag. susceptibility 4-71202  
 Ti-Al, sputtering and secondary ion yields under O<sub>2</sub><sup>+</sup> ion bombard. 4-93174  
 Ti-Al VT1-0, anodic soln. under potentiostatic conditions (*Russian*) 4-71778  
 Ti-Al-Fe, Mossbauer study of <sup>57</sup>Fe atom vibr. 4-84882  
 Ti-Al-Mo-Sn-Si,  $\alpha/\beta$ , simulated flight fatigue 4-104838  
 Ti-Al-Mo-Sn-Si, TC9, microstruct. change during thermal exposure at 500°C (*Chinese*) 4-61959  
 Ti-Al-Mo-Zr, VT9, nitriding after shock wave treatment 4-93444  
 Ti-Al-N ternary system, phase equilibria and solubility 4-99375  
 Ti-Al-Nb-Ta-Mo, welds and castings, impact roughness, segregation and influence of B 4-114658  
 Ti-Al-Nb-Ta-Mo, Widmanstatten struct., effect on deform. modes and mech. props. 4-99436  
 Ti-Al-Sn (5, 2.5 wt.%), internal stress, deform. at 300K 4-71700  
 Ti-Al-Sn (5, 2.5 wt.%), stressed at room temp., hydride precip., dislocation substruct. 4-71655

**aluminium alloys continued**

- Ti-Al-Sn-Zr-Mo-Si, H-enhanced fatigue crack growth 4-114640  
 Ti-Al-V, deformation and fracture at isolated holes in plane-strain tension 4-61976  
 Ti-Al-V, ion implantation effect on fretting fatigue 4-76916  
 Ti-Al-V (6, 4 wt.%), electron beam welding, mech. props., fusion reactor apps. 4-109471  
 Ti-Al-V (6, 4 wt.%), evolution of  $\alpha$  +  $\beta$  struct. rel. to thermomech. treatment 4-109431  
 Ti-Al-V (6, 4 wt.%), fatigue strength, effect of rest periods during monitoring 4-66414  
 Ti-Al-V (6, 4 wt.%), fatigue strength, influence of adiabatic shear bands 4-99485  
 Ti-Al-V (6, 4 wt.%), fatigue endurance, influence of rest period 4-99486  
 Ti-Al-V (6, 4 wt.%), powder metallurgical prod. 4-104750  
 Ti-Al-V (6, 4 wt.%), strongly textured, tensile props. after superplastic deform. 4-71703  
 Ti-Al-V (6, 4 wt.%), tensile props. and fracture mode, temp. depend. 4-109488  
 Ti-Al-V (6.4 wt.%), dynamic yield strength meas. 4-89110  
 Ti-Al-V (6.4 wt.%), erosion by spherical particles at 90° impact angles, effect of microstruct. 4-76876  
 Ti-Al-V (6.4 wt.%), laminated plate, damage tolerance life 4-104862  
 Ti-Al-V (6.4 wt.%), near-threshold fatigue crack growth, effect of corrosive environment 4-81269  
 Ti-Al-V (6.4 wt.%), strongly textured, superplastic deform. anisotropy 4-99427  
 Ti-Al-V (6.4 wt.%), superplastic, solid state bonding 4-61989  
 $\alpha$  +  $\beta$  Ti-Al-V and Ti-Al-Cr-Mo-V, annealed, struct. and mech. props. 4-61988  
 Ti-Al-V plate, residual stresses after localised heat treatment, US eval. 4-99728  
 Ti-Al-V (6, 4 wt.%), superplasticity rel. to grain struct. and deform. temp. 4-109459  
 Ti-Mo (V)(Al), stacking fault energies and dislocation structure (*Russian*) 4-108384  
 Ti-V-Fe-Al (10, 2, 3 wt.%), technique for revealing deformed and recrystallised structs. 4-114571  
 TiAl, cryst. struct. determ. 4-113401  
 TiAl intermetallic, ductility, strength and microstruct., Ag addition effect (*Japanese*) 4-66391  
 TiAl, intermetallic cpd., specimen prep., microcracks obs. on polished surfaces 4-81382  
 TiAl<sub>3</sub>, powdered, nitriding investig. 4-89189  
 TiAl<sub>3</sub>-Al, molten system, peritectic equilib., EM phase separation 4-89027  
 Ti<sub>3</sub>Al and TiAl, Young's modulus and Debye temp., 300 to 1300K (*Russian*) 4-92281  
 Ti(Fe,Al<sub>1-x</sub>)<sub>2</sub>, paramagnetic props. study (*Russian*) 4-71020  
 Ti<sub>87.8</sub>Ni<sub>12.2</sub>Al<sub>13.8</sub>, charge wave density transitions, electron microscopy study 4-98596  
 UNiAlH<sub>2</sub>, <sup>1</sup>H NMR and mag. susceptibility 4-71202  
 V-Al rapidly quenched alloys, struct. and supercond. props., alloying addition effects 4-70400  
 V<sub>2</sub>CrAl<sub>1-x</sub>B<sub>x</sub>, melt spinning and phase transforms 4-114450  
 V<sub>2</sub>Ge<sub>1-x</sub>Al<sub>x</sub>, superconductivity and electron-phonon parameter 4-114058  
 V<sub>2</sub>(Co, Al)<sub>17</sub>, single cryst. cpds., growth conditions and characterisation 4-66220  
 Y(Fe,Al<sub>1-x</sub>)<sub>2</sub> alloys, mag. behaviour 4-76116  
 Yb-Al interdiffusion cpds., dil., surface segregation and mixed valency, photoemission study 4-108688  
 Zn-Al, diecasting alloy, fracture 4-89128  
 Zn-Al, review of commercial alloys 4-88954  
 Zn-Al (21 wt.%), lamellar, superplastic and cast dendritic, water vapour corrosion 4-62097  
 Zn-Al (22wt.%), superplastic, closed die forging 4-104817  
 Zn-Al eutectoid, strain-enhanced grain growth during superplastic flow 4-71686  
 Zn-Al superplastic alloys, Al atoms redistribution, elec.-resist. and small angle X-ray scatt. study 4-62004  
 Zn-Al-Cu alloys, vol. change on ageing 4-114592  
 Zn-Al-Si (21, 2 at.%), frictional surface charact. under boundary lubrication 4-66452  
 Zn-Al-Si alloys, quench-aged, phase transforms., rel. to hardness 4-114515  
 Zr-Al alloys, inhomogeneous, X-ray fluoresc. intensities, Monte Carlo simulation 4-109246  
 Zr-Al and Zr-Al-Ni, amorphous, anodic electrochem. treatment 4-114716  
 Zr-Al getter pumps in ISX-B tokamak 4-108204  
 Zr<sub>3</sub>Al, electron damage, high resolution electron microscopy study 4-92241  
 Zr<sub>3</sub>Al, ordered alloy, flow and fracture, review 4-114639  
 Zr<sub>80</sub>Nb<sub>20</sub>Si<sub>2</sub>Al<sub>8</sub>, amorphous supercond. alloy, appl. in liq. He level indicator 4-86403  
 ZrAl eutectoid, fine grained superplastic alloys, anelastic strains, grain boundary cavity distrib., sintering 4-66359

**aluminium compounds**

- see also alumina; aluminium alloys  
 acetates, <sup>13</sup>C chemical shielding anisotropies 4-65871  
 AlSb/InAs/AlSb quantum wells, magneto-transport meas. 4-98745  
 aluminosilicates, correl. between SiO<sub>2</sub> angles and <sup>29</sup>Si NMR chemical shift 4-88730  
 bauxite brick, lower temp. firing, microanalyses and SEM fractographs, K<sub>2</sub>O content 4-61892  
 beryl, hexagonality to cubicity transition 4-60891  
 hydroxysulphate, crystallisation, high resol. NMR chem. shift 4-114174  
 III-V semiconductor, phys. data, compilation, book 4-63420  
 metal/AlGaAs/GaAs modulation-doped structs., physical correspondence with MOS struct. 4-76041  
 potash alum small crystals, decreasing number suspended in agitated supersaturated soln. 4-92117  
 PVC:Al(OH)<sub>3</sub>, resist. to tracking study 4-69969  
 sialon, fracture toughness, effect of deform. 4-76868  
 $\alpha$ -sialon ceramics, hot pressing, thermal expansion, 40°-1040°C 4-88315  
 sialon ceramics, liq. phase sintering, densification and transform. mechanisms 4-76724  
 sialon ceramics, thermal diffusivity, effect of crystn. of grain boundary phase 4-88355  
 sialon X-phase, Si<sub>3</sub>Al<sub>2</sub>O<sub>12</sub>N<sub>2</sub>, cryst. struct. 4-75427

## aluminium compounds continued

- sialon-metal oxide, oxynitride glasses, prep. and props. 4-76737  
sialons, hot-pressed and reaction-bonded, phase equilib. and props.  
4-76761  
 $\beta$ -sialons, microstruct. evaluation by TEM, correl. to mech. props.  
4-76732  
 $\beta$ -sialons, oxidation behaviour in  $O_2$  and  $CO_2$  4-76891  
sodalite frameworks, cubic, tetragonal tetrahedra distortions 4-84241  
 $\beta'$ -Mg-Si-Al-O-N system, X-ray and electron diff., rhombohedral struct.  
4-65246  
(Al,Ga)As heterojunctions, laser-induced defects, photochem. etching  
4-113439  
(Al,Ga)As, interrupted MBE growth, epitaxial InAs protection layer  
4-114400  
(Al,Ga)As, proton-bombarded, thermal annealing, elec. cond. recovery  
4-98146  
n-(Al,Ga)As/GaAs heterojunctions, hot-electron mobility study at moderate elec. fields 4-84678  
(Al,Ga)As/GaAs/Ge:Ga polar semicond. quantum well system, growth and optical props. 4-114314  
(Al,Ga)As-GaAs double heterostructure laser technology 4-74539  
Al hexacoordination complexes,  $^{19}F$  NMR, second coordination sphere  
4-81410  
Al/AlN/SiO<sub>2</sub>/Si struct., conduction mechanisms, shallow junction technique study 4-88599  
Al-AlO<sub>2</sub>-Pb(Ag), barrier height and electric field induced barrier shifts  
4-70946  
Al-based sputtered solar selective absorbing surfaces, props., effects of various antireflection coatings 4-114954  
AlAs, high-press. phase transition 4-88283  
AlAs, MOCVD growth 4-99329  
AlAs/GaAs heterojunctions, interface struct., TEM and STEM studies 4-108728  
AlAs-GaAs heterojunction barriers, inelastic tunnelling characts. 4-98710  
AlAs-GaAs semiconductor superlattices, MOCVD prep., interface struct. study 4-108726  
AlAs-GaAs superlattice, MBE growth and luminescence 4-114403  
Al<sub>10</sub>B<sub>3</sub>F<sub>3</sub>O<sub>12</sub>, Jeremejevitze, cryst. struct. refinement 4-92173  
AlBr<sub>3</sub>, in vapour phase, IR spectra, valence force fields 4-74244  
(AlBr<sub>3</sub>)<sub>n</sub>, clusters, (n=2, 4, 6), mass spectra, stability 4-74386  
Al<sub>2</sub>CO ligand-metal bonding, charge transfer and polarisation 4-69265  
AlCl<sub>3</sub>-SOCl<sub>2</sub>, based electrolytes, transport props. 4-88323  
AlCl<sub>3</sub>·6H<sub>2</sub>O·Cr<sup>3+</sup>, EPR study 4-84852  
AlF, vibr. struct., ionisation pot., PNO/CEPA calcs., photoelectron spectra 4-96613  
AlF<sub>3</sub> fluoride glass, optical props. 4-65189  
AlF<sub>3</sub>, vibr. struct., ionisation pot., PNO/CEPA calcs., photoelectron spectra 4-96613  
AlGaAs CSP high-power laser diodes under modulation, freq. stabilisation using short guides 4-79190  
AlGaAs CSP semiconductor laser, negative feedback stabilised for coherent FSK transmitter 4-107875  
AlGaAs CSP-type lasers, linewidth enhancement estimation method 4-83577  
AlGaAs, crystal growth by MOCVD (Japanese) 4-76684  
AlGaAs DH diode lasers fabricated on monolithic GaAs/Si substrate 4-112408  
AlGaAs DH semiconductor diode laser, passive mode locking, subpicosec. coherent pulse generation (Japanese) 4-60060  
AlGaAs, epitaxial short wavelength visible laser diodes 4-107628  
AlGaAs GaAs modulation doped heterostruct., persistent photocond. studies 4-98705  
(AlGa)As heterolasers with distrib. feedback, polarisation effects 4-64708  
AlGaAs heterostructure laser with distributed feedback 4-74538  
AlGaAs heterostructure, photoelectron luminescence study 4-99193  
(AlGa)As heterostructure laser diodes, psec. pulse generation 4-107632  
AlGaAs high power TJS laser diodes, mech. stress compensation 4-96914  
AlGaAs injection laser with external dispersion resonator using returning mirror 4-107641  
AlGaAs injection laser, dispersion of linewidth enhancement factor 4-112425  
AlGaAs LED, radiative and nonradiative, recombination rates, meas. 4-112434  
AlGaAs laser, 0.8  $\mu$ m, spectral width with 1/f noise 4-96892  
AlGaAs laser, modulation freq. characts. for FM direct modulation 4-69463  
AlGaAs laser amplifiers for fibre transmission, device characts. 4-69578  
n-AlGaAs, MBE grown, deep electron traps 4-98570  
AlGaAs, MBE growth on Si (100), optical props. 4-88975  
AlGaAs, MBE growth of high purity layers, photolum. charact. 4-98474  
AlGaAs mode locked laser, subpicosecond pulse generation 4-107697  
AlGaAs nonabsorbing mirror constricted DH large-optical-cavity diode lasers 4-83579  
AlGaAs p/n graded band-gap solar cells grown by organometallic VPE 4-99961  
AlGaAs phase-locked injection laser arrays with nonuniform stripe spacing 4-107672  
AlGaAs quantum well lasers, threshold currents 4-79136  
AlGaAs single- and multiple-stripe quantum-well heterostruct. laser diodes in external grating cavity 4-96902  
AlGaAs TJS external cavity laser for fibre optic laser Doppler velocimeter 4-97096  
AlGaAs:Si MBE layers, donor levels anal. 4-61316  
AlGaAs/GaAs, single quantum well heterostruct. on Al<sub>0.30</sub>Ga<sub>0.70</sub>As buffers, MBE grown, electron mobility study 4-114029  
AlGaAs/GaAs concentrator solar cells under high temp. and humidity conditions 4-66708  
AlGaAs/GaAs heterostruct., 2D magnetotransport, electron heating effects 4-98736  
(AlGa)As/GaAs modulation-doped heterostruct., optimisation for TEG-FET operation at room temp. 4-92804  
AlGaAs/GaAs modulation-doped heterostructures, anomalous photomagnetoresist. 4-98702  
AlGaAs/GaAs quantum wells, photoluminescence studies 4-93105  
n-AlGaAs/GaAs selectively doped heterojunctions, high mobility electron gas 4-80657  
AlGaAs/GaAs single quantum well structs., MBE grown, photoluminesc. props. 4-61863

## aluminium compounds continued

- AlGaAs/GaAs solar cell battery on Venera spacecraft, optical and metrological characts. 4-93615  
AlGaAs/GaAs/AlGaAs single quantum well transistor with 2-D electron gas, logic device appl. 4-61443  
p-AlGaAs/p-GaAs/n-GaAs solar cells, high efficiency 4-114910  
AlGaAs/Si cascade solar cells, sensitivity and efficiency 4-85375  
AlGaAs-GaAs heterojunction interfaces, deep levels, forward I-V and DLTS meas. 4-70915  
AlGaAs-GaAs CW DH long-lifetime laser operated at room temp. 4-69474  
AlGaAs-GaAs DH, photoluminescence efficiency 4-85006  
AlGaAs-GaAs DH LED, efficiency for optical communications (Spanish) 4-69586  
AlGaAs-GaAs heterojunction, two-dimens. electron gas gate control characts., optimum doping (Chinese) 4-114021  
AlGaAs-GaAs laser with external dispersive cavity multimode rate-eqn. soln. of mode selection and tuning props. (Chinese) 4-91462  
AlGaAs-GaAs modulation doped layers, 2-D electron gas, room temp. mobility, parallel conduction effects 4-76027  
AlGaAs-GaAs short-cavity laser and its monolithic integration using microcleaved facets process 4-60064  
AlGaAs-GaAs solar cells for space appls. 4-81543  
n-AlGaAs-GaAs structures, modulation doped, elec. props., effect of IR flashlamp annealing 4-98712  
AlGaAs-GaAs superlattice optical cavity multiple-quantum-well lasers, MBE grown, struct. and fabrication 4-64719  
AlGaAs-GaAs superlattices, magnetisation meas., de Haas-van Alphen oscills. 4-98734  
Al<sub>0.2</sub>Ga<sub>0.8</sub>As:Si MBE layers, electron trap conc., DLTS study 4-61317  
Al<sub>0.3</sub>Ga<sub>0.7</sub>As, encapsulated with Si<sub>3</sub>N<sub>4</sub> films, disorder-activated modes, Raman spectra 4-80916  
Al<sub>0.3</sub>Ga<sub>0.7</sub>As-GaAs distributed feedback surface emitting laser diode 4-112424  
Al<sub>0.3</sub>Ga<sub>0.7</sub>As-GaAs heterojunction, selectively doped, persistent photocond. effect 4-98717  
Al<sub>0.88</sub>Ga<sub>0.12</sub>As/GaAs:Zn diffused superlattice, X-ray rocking curve and backscatt. studies 4-113818  
Al<sub>0.9</sub>Ga<sub>0.1</sub>As avalanche diodes, heat and radiation-resistant, elec. props. 4-65728  
Al<sub>0.9</sub>Ga<sub>0.1</sub>As, cathodoluminescence study 4-71449  
Al<sub>0.9</sub>Ga<sub>0.1</sub>As, correlation of photoluminescence and deep trapping 4-80537  
n-Al<sub>0.9</sub>Ga<sub>0.1</sub>As epilayers, photoluminescence study 4-114316  
Al<sub>0.9</sub>Ga<sub>0.1</sub>As epitaxial film, XPS study 4-93189  
Al<sub>0.9</sub>Ga<sub>0.1</sub>As, Fourier anal. of optical spectra 4-99131  
Al<sub>0.9</sub>Ga<sub>0.1</sub>As, graded-gap, effective resistance, temp. dependence 4-113961  
Al<sub>0.9</sub>Ga<sub>0.1</sub>As heteroepitaxial struct. photoluminescence study 4-104673  
Al<sub>0.9</sub>Ga<sub>0.1</sub>As layers, Rutherford backscatt. using 30 MeV <sup>16</sup>O ions 4-93170  
Al<sub>0.9</sub>Ga<sub>0.1</sub>As, line broadening in photoluminescence spectra 4-109241  
n-Al<sub>0.9</sub>Ga<sub>0.1</sub>As, MBE grown, deep electron traps, growth conditions and alloy composition influence 4-98558  
Al<sub>0.9</sub>Ga<sub>0.1</sub>As MBE growth, Ga desorp., AES and photoluminesc. studies 4-93220  
Al<sub>0.9</sub>Ga<sub>0.1</sub>As MBE layers, free carrier conc., Raman scatt. study 4-84970  
Al<sub>0.9</sub>Ga<sub>0.1</sub>As MBE layers, persistent photocond. centre (Chinese) 4-88529  
Al<sub>0.9</sub>Ga<sub>0.1</sub>As p-n junctions, organometallic VPE, anomalous light sensitivity 4-92817  
Al<sub>0.9</sub>Ga<sub>0.1</sub>As pulsed DH laser, emission characts., influence of longit. mode carrier-depend. shifts and gain profile 4-87335  
Al<sub>0.9</sub>Ga<sub>0.1</sub>As, Si donor behaviour, effect of Al comp. 4-98709  
Al<sub>0.9</sub>Ga<sub>0.1</sub>As solar cell structs., photoluminescence and spectral response 4-89404  
Al<sub>0.9</sub>Ga<sub>0.1</sub>As:Be, conference, Charlotte, NC, USA (Nov. 1983) 4-73146  
Al<sub>0.9</sub>Ga<sub>0.1</sub>As:Be, radiative recombinations 4-76515  
Al<sub>0.9</sub>Ga<sub>0.1</sub>As:Si, grown by MBE, photoluminesc. composition depend. 4-84996  
Al<sub>0.9</sub>Ga<sub>0.1</sub>As:Si, grown by MBE, photoluminesc. spectra, defect-related emissions 4-84997  
Al<sub>0.9</sub>Ga<sub>0.1</sub>As:Si MOCVD layers, transport props. 4-92834  
Al<sub>0.9</sub>Ga<sub>0.1</sub>As:Te(Sn) epitaxial films, carrier density changes due to band struct. modifications 4-61381  
Al<sub>0.9</sub>Ga<sub>0.1</sub>As:Zn, CVD deposited, luminescence study 4-80985  
Al<sub>0.9</sub>Ga<sub>0.1</sub>As/GaAs heterostructure, selectively doped, transient photocond. obs. 4-70862  
Al<sub>0.9</sub>Ga<sub>0.1</sub>As/GaAs heterojunction FET, 2D electrons, cyclotron resonance studies 4-98743  
Al<sub>0.9</sub>Ga<sub>0.1</sub>As/GaAs heterojunction, subband struct. at low temp. 4-104298  
Al<sub>0.9</sub>Ga<sub>0.1</sub>As/GaAs single quantum well, exciton transport 4-88451  
Al<sub>0.9</sub>Ga<sub>0.1</sub>As-GaAs concentrator solar cells, efficient circular contact grid design 4-72113  
Al<sub>0.9</sub>Ga<sub>0.1</sub>As-GaAs double heterostructure optically pumped laser 4-96888  
Al<sub>0.9</sub>Ga<sub>0.1</sub>As-GaAs heterostructures, 2D electron gas, disorder, fractional quantum Hall effect 4-76033  
Al<sub>0.9</sub>Ga<sub>0.1</sub>As-GaAs heterostructures, electron mobility, temp. depend. from 1-10K 4-80669  
Al<sub>0.9</sub>Ga<sub>0.1</sub>As-GaAs heterostructures, 1/3 and 2/3 fractional quantum Hall effect, activation energies 4-92811  
Al<sub>0.9</sub>Ga<sub>0.1</sub>As-GaAs heterostruct. anal. of quantised Hall resist. at finite temps. 4-98727  
Al<sub>0.9</sub>Ga<sub>0.1</sub>As-GaAs heterostruct., thermopower meas. on 2D electron gas 4-98729  
Al<sub>0.9</sub>Ga<sub>0.1</sub>As-GaAs heterojunction, EMF due to dynamic deform. 4-98746  
Al<sub>0.9</sub>Ga<sub>0.1</sub>As-GaAs heterostruct., growth conditions effect in organometallic-AsH<sub>3</sub>-H<sub>2</sub> systems on solar cell param. 4-113838  
Al<sub>0.9</sub>Ga<sub>0.1</sub>As-GaAs injection lasers, longitudinal mode selection obs. 4-79153  
Al<sub>0.9</sub>Ga<sub>0.1</sub>As-GaAs injection laser self-modulation associated with external optical feedback 4-112440  
Al<sub>0.9</sub>Ga<sub>0.1</sub>As-GaAs multiple well quantum well lasers, wavelength modification 4-64705  
Al<sub>0.9</sub>Ga<sub>0.1</sub>As-GaAs multiple quantum well laser structures, MBE growth conditions 4-91465  
Al<sub>0.9</sub>Ga<sub>0.1</sub>As-GaAs twin-channel substrate mesa guide laser with antirefl. coatings, single longit. mode operation 4-83619  
p-Al<sub>0.9</sub>Ga<sub>0.1</sub>As-n-GaAs-p-GaAs:Si solar heterophotocells with increased p-n junction depth 4-77103

## aluminium compounds continued

- Al<sub>1-x</sub>Ga<sub>x</sub>-yAs laser waveguides, light absorpt. 4-103011  
 Al<sub>1-x</sub>Ga<sub>x</sub>-yAs<sub>1-y</sub>Sb<sub>y</sub>/GaSb heterostruct., conditions for LPE growth 4-114429  
 Al<sub>1-x</sub>Ga<sub>x</sub>-yAs<sub>1-y</sub>Sb<sub>y</sub> heterojunction photocells, LPE fabrication 4-81559  
 AlGaInP/GaInP DH visible light lasers, MOCVD grown, room temp. pulsed operation 4-69445  
 AlGaInPAs lattice matched to GaAs, LPE growth, photolum. obs. 4-70581  
 Al<sub>1-x</sub>Ga<sub>x</sub>In<sub>1-x-y</sub>Sb<sub>y</sub> epitaxial layers, luminescence studies 4-76505  
 AlGaSb, LPE, substrate treatment optimisation, carrier conc., Raman spectra, photoluminesc. 4-93235  
 Al<sub>0.17</sub>Ga<sub>0.83</sub>Sb/GaSb multi-quantum well lasers, room-temp. operation, MBE growth 4-60033  
 Al<sub>1-x</sub>Ga<sub>x</sub>-ySb multilayer heterostructures, coherent light polarisation props. 4-71460  
 Al<sub>1-x</sub>Ga<sub>x</sub>-ySb-InAs<sub>1-y</sub>Sb<sub>y</sub> heterostructures, LPE growth 4-104097  
 AlHe<sup>3+</sup>, bonding, dissociation energies, CASSCF calcs. 4-68948  
 Al<sub>13</sub>, in vapour phase, IR spectra, valence force fields 4-74244  
 AlInAs/GaInAs avalanche photodiodes and AlInAs electroabsorption p-i-n photodiodes grown by MBE 4-69591  
 AlInAs/GaInAs heterojunctions and superlattices, 2-D magnetophonon resonance 4-98740  
 Al<sub>0.48</sub>In<sub>0.52</sub>As/Ga<sub>0.47</sub>In<sub>0.53</sub>As avalanche photodiode for long wavelength fibre optic communication, MBE growth 4-79337  
 Al<sub>0.48</sub>In<sub>0.52</sub>As/n<sup>+</sup>-Ga<sub>0.49</sub>In<sub>0.51</sub>As, low resist. alloyed ohmic contacts 4-84692  
 Al<sub>1-x</sub>In<sub>x</sub>As, epitaxial growth on InP 4-104735  
 Al<sub>1-x</sub>In<sub>x</sub>As, nominally undoped, MBE growth and charact. 4-98472  
 AlN, CVD films, stability, surface morphology, CVD conditions 4-70604  
 AlN ceramic, thermal shock resist. 4-81289  
 AlN films, ion beam deposition technique 4-85114  
 AlN, oxyinitride bonded ceramics, sintering, microstruct., densification, flexural strength, oxide additions effect 4-76727  
 AlN piezoelectric films, charge injection and memory effect 4-99039  
 AlN powder, hot pressing kinetics, oxidation, mech. props. 4-76731  
 AlN powder, shock compression study 4-109349  
 AlN powder, shock effects, TEM study 4-109345  
 AlN, powder, surface area after shock treatment 4-109344  
 AlN, sputter deposited, electron binding energy Auger and XPS study 4-75820  
 AlN sputtered films, polycryst. and amorphous, optical phonons, Raman studies 4-80179  
 AlN transparent ceramics, powder and sintering characts. 4-81171  
 AlN/Al cermet, reactive DC planar magnetron sputtering prep., elec. transport props. 4-88607  
 Al<sub>13</sub>NH<sub>3</sub>, ligand-metal bonding, charge transfer and polarisation 4-69265  
 Al(NO<sub>3</sub>)<sub>3</sub>:Cr<sup>3+</sup>, exchange-coupled Cr<sup>3+</sup>-Cr<sup>3+</sup> pairs, EPR obs. 4-88717  
 Al<sub>3</sub>Ni whisker reinforced Al, effects of morphology of Al<sub>3</sub>Ni whiskers on tensile strength 4-88133  
 AlO, blue-green band, transition moment, Franck-Condon factors, perturbed simple harmonic model 4-59852  
 AlO with adsorbed TCNQ, Co<sub>2</sub>(CO)<sub>8</sub> and tetracyanethylene, glove box deposition system and study 4-101860  
 Al<sub>2</sub>O<sub>3</sub>-AlN spinel, fabrication, thermomech. props. 4-89097  
 Al<sub>2</sub>O<sub>3</sub>-AlN system, high temp. reactions and microstructs. 4-76763  
 Al<sub>2</sub>O<sub>3</sub>-AlON composite ceramic, hot pressing reaction sintering, mech. props., high temp. apps. 4-62062  
 Al(OH)<sub>3</sub>, high-pressure phases in Al-Al<sub>2</sub>O<sub>3</sub>-H<sub>2</sub>O 4-85141  
 Al<sub>2</sub>O(OH)<sub>3</sub>, bauxite, Mossbauer spectra with environmentally broadened spectral lines 4-105550  
 Al<sub>2</sub>O<sub>3</sub>.nH<sub>2</sub>O thin films, ageing, elec. struct. and moisture response characts., sensor apps. 4-86393  
 AlP, high-pressure phase transition 4-88283  
 AlPO<sub>4</sub>, berlinite, incommensurate phase, colorimetric and neutron scatt. studies 4-84277  
 α-AlPO<sub>4</sub>, berlinite, temp. depend. of SAW parameters 4-104054  
 AlPO<sub>4</sub>, cation ordering and struct. anal. based on Coulomb repulsion forces 4-98074  
 AlPO<sub>4</sub>, polymorphs, chem. shift, bond angles, <sup>27</sup>Al and <sup>31</sup>P NMR 4-109088  
 Al<sub>4</sub>(P<sub>2</sub>O<sub>7</sub>)<sub>3</sub>, chem. shift anisotropy, <sup>13</sup>P NMR 4-88731  
 Al(PO<sub>3</sub>)<sub>3</sub>, BaF<sub>2</sub>-AlF<sub>3</sub> glasses, nonlinearity of refractive index 4-80900  
 Al<sub>2</sub>(SO<sub>4</sub>)<sub>3</sub>-K<sub>2</sub>SO<sub>4</sub>-24H<sub>2</sub>O, potash alum small crystals, decreasing number suspended in agitated supersaturated soln. 4-92117  
 AlSb, high-pressure phase transition 4-88283  
 AlSb-GaSb superlattice, MBE growth and luminescence 4-114403  
 AlSb-InAs quantum wells, electron densities 4-98711  
 Al<sub>4</sub>SiC<sub>4</sub> mixed carbide, prep. and struct. studies 4-88144  
 Al<sub>2</sub>SiO<sub>5</sub>, sillimanite, absorption edge fine struct. study using electron channelling 4-80127  
 Al<sub>2</sub>SiO<sub>4</sub>(F.OH)<sub>2</sub>, topaz 4-94101  
 Al<sub>2</sub>TiO<sub>5</sub> ceramics, stabilisation by cation substitution, sintering and hot pressing 4-109362  
 Al<sub>2</sub>TiO<sub>5</sub> ceramics, synthesis and sintering characts. 4-109361  
 BaF<sub>2</sub>-LaF<sub>3</sub>-ZrF<sub>4</sub>-AlF<sub>3</sub> glass, crystallisation, devitrification on reheating 4-84194  
 Ba(PO<sub>3</sub>)<sub>2</sub>-AlF<sub>3</sub>-LiF, elec. cond. rel. to struct. 4-92771  
 CaAl<sub>2</sub>Si<sub>2</sub>O<sub>7</sub> glass, shock compressed, optical emission spectra 4-114305  
 Cs<sub>0.5</sub>Al<sub>0.5</sub>Si<sub>1.5</sub>O<sub>6</sub>, cryst. struct., X-ray diff. studies 4-92187  
 Fe-Al-O, γ-spinels, vacancy substituted, order-disorder, IR spectra (French) 4-76447  
 α-(Fe<sub>1-x</sub>Al<sub>x</sub>)<sub>2</sub>O<sub>3</sub> substituted hematite, Morin transition, <sup>57</sup>Fe Mossbauer study 4-71072  
 (Ga,Al)As/GaAs double heterostructures, LPE, struct. and lasing characts. rel. to As vapour press. 4-66249  
 Ga-Al-As system, MOVPE, current status for optoelectronic apps. 4-104737  
 Ga-Al-As/GaAs, hq. epitaxy capillary effect 4-98408  
 GaAlAs BH 100 Mbit/s laser diode terminal with optical gain for fibre-optic LANs 4-112586  
 GaAlAs BH window lasers, 11 GHz direct modulation bandwidth 4-112410  
 GaAlAs bright visible-range injection laser development 4-69441  
 GaAlAs buried multi-quantum-well laser fabricated by diffusion induced disordering 4-74547  
 GaAlAs buried multi-quantum well lasers fabricated by diffusion-induced disordering 4-91452  
 (GaAl)As cleaved coupled-cavity laser anal. 4-96900  
 (GaAl)As cleaved-coupled-cavity lasers, coupling strength study 4-91459  
 GaAlAs diode laser, picosecond gain meas. 4-107638

## aluminium compounds continued

- (GaAl)As diode lasers, spectral characteristics at 1.7K 4-112411  
 GaAlAs electroabsorption modulators, monolithically integrated array 4-103006  
 (GaAl)As heterojunction laser, optically controlled two-component 4-107640  
 GaAlAs laser, MESFET and photodiode, monolithic optoelectronic integration 4-74747  
 GaAlAs laser, picosecond pulse generation by optoelectronic feedback 4-96885  
 GaAlAs laser, simultaneous wavelength and power stabilisation using single detector scheme 4-91456  
 GaAlAs laser, wavelength stabilisation using integrated optic Fabry-Perot interferometer 4-91457  
 GaAlAs laser diode coupled to an external cavity intensity noise suppression and modulation characts. 4-79144  
 GaAlAs laser diode optical switches, isolation characteristics 4-107680  
 GaAlAs laser oscillating in single longit. mode, LF feedback noise 4-96909  
 GaAlAs laser picosecond pulse temporal coherence props., directly modulated and freq. stabilised optical communication system apps. 4-74509  
 GaAlAs lasers, catastrophic and latent damage due to elec. transients 4-79146  
 GaAlAs lasers, transverse-mode stabilised MOCVD grown, with embedded confining layer on optical waveguide 4-69443  
 GaAlAs light sources, radiative coeffs., carrier dependence 4-64703  
 GaAlAs, luminescence lineshapes of electron-hole plasma 4-109242  
 GaAlAs, MBE, thermodynamics of O incorporation 4-61253  
 GaAlAs material epitaxial growth, devices for optical communications 4-74746  
 GaAlAs, optical communication through low-visibility atmosphere using a CW diode laser 4-112589  
 GaAlAs, proton energy loss straggling meas. for nucl. profiling appl. 4-70246  
 GaAlAs semiconductor laser fabrication, integration with fibre V-groove alignment struct. 4-96948  
 GaAlAs single quantum well size effect modulation light sources 4-97014  
 (GaAl)As<sup>+</sup> transverse-mode stabilised laser diodes, MOCVD growth 4-96912  
 GaAlAs V-groove lasers, 4 ps light pulses generation 4-69407  
 GaAlAs very high speed lasers and detectors for integrated optoelectronic devices 4-96889  
 GaAlAs/GaAs quantum-well lasers, organometallic VPE and MBE grown, developments and expt. study 4-69442  
 GaAlAs/GaAs selectively doped heterojunction, electron conc., FET appl. 4-98703  
 GaAlAs/GaAs surface-emitting injection laser, pulsed oscill. 4-79175  
 GaAlAs/GaAs surface emitting injection laser, room-temp. pulsed operation 4-112416  
 GaAlAs/GaAs twin channel laser with high CW power and low beam divergence 4-74548  
 GaAlAs-GaAs 4-80664  
 (GaAl)As-GaAs DH lasers, D<sub>2</sub><sup>+</sup> bombardment isolated stripe geometry (Chinese) 4-112431  
 GaAlAs-GaAs DH lasers, narrow-channelled substrate stripe-type, characts. meas. and anal. (Chinese) 4-112433  
 GaAlAs-GaAs heterostructures, hot photoluminescence polarisation and spectrum 4-61743  
 GaAlAs-GaAs heterostructure, nuclear profiling of Al 4-98123  
 GaAlAs-GaAs heterostructures, interband scatt. in mobility 4-98732  
 GaAlAs-GaAs integrated optical repeater 4-97143  
 GaAlAs-GaAs interface, 2D electron gas, cyclotron reson. 4-109077  
 GaAlAs-GaAs modulation doped heterostruct., self-consistent variational calcs. and alloy scatt. 4-98733  
 GaAlAs-GaAs quantum well struct., optical props., review 4-104146  
 GaAlAs-GaAs quantum wells, reflectance of two-dimensional excitations 4-109211  
 Ga<sub>0.4</sub>Al<sub>0.6</sub>As-GaAs heterostructures, LPE growth, layer height profiles rel. to convection and cooling rates 4-66248  
 Ga<sub>1-x</sub>Al<sub>x</sub>As(Si/Se), dopant incorporation during MBE growth 4-99320  
 Ga<sub>1-x</sub>Al<sub>x</sub>As, carrier transport under impurity radiative recombination conditions 4-104211  
 Ga<sub>1-x</sub>Al<sub>x</sub>As, crystalline struct., two-phonon Raman spectra study 4-71385  
 Ga<sub>1-x</sub>Al<sub>x</sub>As, spatial dielec. functions, site and comp. depend. 4-104136  
 Ga<sub>1-x</sub>Al<sub>x</sub>As superlattices, acoustic modes, Brillouin and Raman scatt. study 4-80928  
 p-Ga<sub>1-x</sub>Al<sub>x</sub>As:Be-p-GaAs:Be-n-GaAs:Si heterojunction LPE growth for solar cells 4-109334  
 Ga<sub>1-x</sub>Al<sub>x</sub>As:Zn, (Se), doping in MOCVD growth, carrier conc. and cond. 4-88982  
 Ga<sub>1-x</sub>Al<sub>x</sub>As/GaAs solar cell with antiref. coating, LPE grown, design, fabrication and characts. (Polish) 4-114904  
 Ga<sub>1-x</sub>Al<sub>x</sub>As-GaAs, Raman scatt. theory 4-76460  
 Ga<sub>1-x</sub>Al<sub>x</sub>As-GaAs heterostructure, LPE grown, dislocation extension and density distrib. (Chinese) 4-113449  
 Ga<sub>1-x</sub>Al<sub>x</sub>As-GaAs interface, fractional quantum Hall effect in a two-dimensional hole system 4-108930  
 Ga<sub>1-x</sub>Al<sub>x</sub>As-GaAs/GaAs (001) superlattices, structural parameters, X-ray diff. 4-84257  
 Ga<sub>1-x</sub>Al<sub>x</sub>As/GaAs system, elastic surface waves, Green's function anal. 4-108695  
 Ga<sub>1-x</sub>Al<sub>x</sub>P, epitaxial struct., luminesc. study 4-85011  
 Ga<sub>1-x</sub>Al<sub>x</sub>P p-n structures, epitaxially grown, plastically and elastically deformed, quantum efficiency spectra 4-84651  
 Ga<sub>1-x</sub>Al<sub>x</sub>Sb, phonon dispersion calcs. 4-88252  
 GaAlSbAs-GaSb injection laser, operation and luminescence study 4-74508  
 Ga<sub>1-x</sub>Al<sub>x</sub>Sb<sub>1-x-y</sub>As<sub>y</sub>/GaSb epitaxial films As-segregation coeff. and distrib. over thickness 4-75692  
 Ga<sub>1-x</sub>Al<sub>x</sub>Sb<sub>1-x-y</sub>As<sub>y</sub>/GaSb, LPE, phase equilib. rel. to lattice mismatch strain 4-93236  
 GaAs/Si/AlGaAs DH TJS lasers grown by MBE 4-107671  
 GaAs/(GaAl)As two-dimens. electron gas, cyclotron reson. study 4-104297  
 GaAs/Al<sub>1-x</sub>Ga<sub>x</sub>As superlattices and heterojunctions, elec. props., numerical solns. 4-70924  
 GaAs/Al<sub>1-x</sub>Ga<sub>x</sub>As heterostructures, 2D electron localisation 4-98718  
 GaAs/Al<sub>1-x</sub>Ga<sub>x</sub>As heterostruct., photocond. studies 4-98744

## aluminium compounds continued

- GaAs/Al<sub>1-x</sub>Ga<sub>x</sub>As quantum well struct., low temp. electron mobility, alloy disorder scatt. contrib. 4-92808  
 GaAs/Al<sub>1-x</sub>Ga<sub>x</sub>As quantum wells, struct. and optical props. 4-99151  
 GaAs/Al<sub>1-x</sub>Ga<sub>x</sub>As quantum wells, Be doped, photoluminescence studies 4-104653  
 GaAs/AlAs multiple quantum well struct., electron-hole plasma, picosecond dynamics 4-92803  
 GaAs/AlAsGaAs superlattice/GaAs superlattice barrier capacitor: a structure for the investigation of heterojunction interfaces 4-84679  
 GaAs/AlGaAs, MOCVD growth and homogeneous nucleation 4-99340  
 GaAs/AlGaAs DH laser, LPE fabricated, design optimisation for entertainment electronics (*German*) 4-102948  
 GaAs/AlGaAs heterointerfaces, struct. evaluation, TEM studies 4-84516  
 GaAs/AlGaAs heterojunction, 2D electron gas, cyclotron resonance studies 4-76032  
 GaAs/AlGaAs heterostructures, 2D electron plasma, optical processes 4-76523  
 GaAs/AlGaAs heterostructures, carrier density, hydrostatic press. control 4-98735  
 GaAs/AlGaAs heterostruct., screening and polaron effects, cyclotron resonance studies 4-98741  
 GaAs/AlGaAs heterostruct., organometallic VPE growth and characterisation 4-99341  
 GaAs/AlGaAs inverted heterojunctions, photoluminescence studies 4-98460  
 GaAs/AlGaAs MQW heterostructure current-injection lasers, carrier-induced energy-gap shrinkage 4-112423  
 GaAs/AlGaAs multi-quantum-well lasers, polarization-dependent gain 4-112412  
 GaAs/AlGaAs multiple quantum well structures, room temp. excitonic nonlinear absorpt. and refract. 4-74590  
 GaAs/AlGaAs multiple quantum well structs., photoexcited carriers intraband relax., femtosecond studies 4-88565  
 GaAs/AlGaAs single quantum well struct., enhanced luminescence 4-99150  
 GaAs/AlGaAs three-dimensional optical waveguides, anal. of charact. (*Chinese*) 4-83689  
 GaAs/AlGaAsGaAs heterojunction barrier, MOCVD grown, electron transport 4-80661  
 GaAs/Ga<sub>1-x</sub>Al<sub>x</sub>As quantum well wires, hydrogenic impurity states 4-92815  
 GaAs/GaAlAs, antirefl. coated twin DH diode external cavity ring laser, optical bistability study 4-91460  
 GaAs/GaAlAs DH stripe geometry lasers, Be-implanted, MOCVD growth 4-107635  
 GaAs/GaAlAs integrated optoelectronics for optical interconnect applications 4-97140  
 GaAs/GaAlAs lasers, synchronous mode locking by picosecond optoelectronic switch 4-96965  
 GaAs/GaAlAs monolithically Peltier-cooled laser diodes 4-74540  
 GaAs/GaAlAs multiple-quantum-well semicond., optical bistability due to increasing absorpt. 4-74598  
 GaAs/GaAlAs quantum well self-electro-optic effect device as hybrid optically bistable switch 4-91522  
 GaAs/GaAlAs quantum well structs., oscillatory magnetoresist. studies 4-98738  
 GaAs/GaAlAs single mode laser diodes, free space optical. communication, design and system requirements 4-79176  
 GaAs/GaAlAs subthreshold DH twin stripe laser, interstripe coupling and current spreading 4-79139  
 GaAs/GaAlAs twin stripe lasers, current rise time effect on beam stability, expt. study 4-91510  
 GaAs/GaAlAs waveguide phase modulator, MBE grown heterostruct., design for PSK optical fibre systems 4-83685  
 GaAs/N-AlGaAs heterostructures, selectively doped, MBE grown, tungsten-halogen lamp annealing effects 4-61444  
 GaAs-(AlGa)As superlattices, MBE grown, growth temp. influence 4-81139  
 GaAs-(AlGa)As large optical cavity lasers 4-107631  
 GaAs-(AlGa)As lasers, passive waveguide coupled, mode behaviour 4-91499  
 GaAs-(AlGa)As modulation-doped heterostructures., reson. inelastic light scatt. studies 4-84973  
 GaAs-(AlGa)As strip geometry laser diodes, dynamical thermal props. 4-79206  
 GaAs-(AlGa)As twisted DH laser, composite cavity config., design and longit./transverse mode operation 4-69456  
 GaAs-(AlGa)As two-dimens. electron plasma, optical emission and excitation processes 4-104666  
 GaAs-(GaAl)As DH diode laser, pulse modulation by picosecond optoelectronic GaAs:Cr switches 4-107701  
 GaAs-Al<sub>0.5</sub>Ga<sub>0.5</sub>As, quantised Hall resistance and 2D electron gas behaviour 4-98724  
 GaAs-Al<sub>0.5</sub>Ga<sub>0.5</sub>As quantum wells, photoluminesc. from spike doped hydrogenic donors 4-104668  
 GaAs-Al<sub>0.5</sub>Ga<sub>0.5</sub>As DH laser with two sections in a common cavity (*Chinese*) 4-112466  
 GaAs-Al<sub>0.5</sub>Ga<sub>0.5</sub>As abrupt heterojunctions grown by MBE, Auger composition profiles 4-80429  
 GaAs-Al<sub>1-x</sub>Ga<sub>x</sub> quantum well structs., Raman scatt. study 4-93079  
 GaAs-Al<sub>1-x</sub>Ga<sub>x</sub>As heterostructure, low temp. fractional quantum Hall effect 4-98722  
 GaAs-Al<sub>1-x</sub>Ga<sub>x</sub>As heterostructure, quantum Hall resistance, temp. depend. 4-114028  
 GaAs-Al<sub>1-x</sub>Ga<sub>x</sub>As multiple quantum well struct., magneto-Raman characterisation 4-104577  
 GaAs-Al<sub>1-x</sub>Ga<sub>x</sub>As quantum well struct., exciton binding energy 4-75868  
 GaAs-Al<sub>1-x</sub>Ga<sub>x</sub>As quantum wells, energy-gap discontinuities and effective masses 4-92623  
 GaAs-Al<sub>1-x</sub>Ga<sub>x</sub>As superlattices, Raman probing of phonons and interfaces 4-80927  
 GaAs-Al<sub>1-x</sub>Ga<sub>x</sub>As stripe geometry lasers, spectral behaviour, lateral hole-burning effects, numerical investigation 4-87334  
 GaAs-Al<sub>1-x</sub>Ga<sub>x</sub>As tunnel junctions, sequential single-phonon emission obs. in electron transport 4-80667  
 GaAs-AlAs heterostructures, photoacoustic spectroscopy by piezoelec. transducers 4-61448  
 GaAs-AlAs multiple quantum well struct., Raman scatt. and luminescence study 4-99105  
 GaAs-AlAs:Zn superlattice, Zn impurity diffusion, X-ray study 4-75729

## aluminium compounds continued

- GaAs-AlGaAs, optical activity of plasma oscills. 4-84930  
 GaAs-AlGaAs GRIN-SCH lasers, MBE grown for optoelectronic integrated circuit appl. 4-96894  
 GaAs-AlGaAs heterojunction, phonon emission and electron heating 4-70927  
 GaAs-AlGaAs injection lasers (*Dutch*) 4-87329  
 GaAs-AlGaAs monolithically integrated optical circuit fabrication 4-69597  
 GaAs-AlGaAs multiple quantum well heterostruct., delocalised exciton state 4-92621  
 GaAs-AlGaAs superlattice and interface, acoustic props. 4-80366  
 GaAs-AlGaAs superlattices, MBE grown, direct obs. of lattice arrangement 4-84528  
 GaAs-AlGaAs superlattice grown by MBE, struct. and optical props. 4-84558  
 GaAs-AlGaAs transverse junction stripe laser, Si doped, MBE fabrication 4-96893  
 GaAs-AlGaAs window-stripe multi-quantum well heterostruct. laser fabrication 4-69436  
 GaAs-Ga<sub>1-x</sub>Al<sub>x</sub>As, lateral superlattice struct. 4-92816  
 GaAs-Ga<sub>1-x</sub>Al<sub>x</sub>As, binding energy of exciton in GaAs quantum well, magneto-optical determination 4-114027  
 GaAs-Ga<sub>1-x</sub>Al<sub>x</sub>As heterojunction, electron energy level calcs. 4-108915  
 GaAs-Ga<sub>1-x</sub>Al<sub>x</sub>As multilayer struct. masked and selective and thermal oxidation, technology for stripe-geometry DH lasers and integrated optics 4-69610  
 GaAs-Ga<sub>1-x</sub>Al<sub>x</sub>As multiple quantum well structs., Hall mobility, electron conc. and buffer width depend. 4-80668  
 GaAs-GaAlAs channelled-substrate lasers, single longit. mode, grown by MBE 4-69403  
 GaAs-GaAlAs double heterostructure, quantisation of excitonic polaritons 4-92634  
 GaAs-GaAlAs heterostructure, electron mobility limits 4-76030  
 GaAs-GaAlAs heterostructs., 2-D electron gas, electron mobility, temp. dependence 4-98704  
 GaAs-GaAlAs multiple-quantum-well structures, sharp line photolum. spectra 4-93110  
 GaAs-GaAlAs npn negative-resistance laser with low threshold current density 4-69448  
 GaAs-GaAlAs quantum well lasers tunable by long wavelength radiation 4-69404  
 GaAs-GaAlAs quantum wells, coupled, photoluminesc. and excitation spectroscopy 4-104667  
 GaAs-GaAlAs superlattices, third order nonlinear optical susceptibility 4-74586  
 GaAs-GaAlAs superlattice, Raman study of folded modes 4-80929  
 GaAs-GaAlAs system, superlattices, quantum wells, and heterostructs., review 4-80666  
 Ga<sub>1-x</sub>In<sub>x</sub>Al<sub>1-x</sub>As based materials, recrystallisation in temp. gradient 4-114390  
 GaInAs/AlInAs heterojunctions, cyclotron resonance and polaron effects 4-98742  
 Ga<sub>0.47</sub>In<sub>0.53</sub>As/Al<sub>0.48</sub>In<sub>0.52</sub>As heterojunction, conduction band discontinuity, photoluminescence study 4-76028  
 GaInP/AlGaAs double heterostructures, LPE, lasing, 77-230K 4-71606  
 GaSb-AlSb, superlattices, light and heavy valence subband reversal, lattice mismatch 4-114013  
 GaSb-AlGaAsSb injection heterolaser, emitted radiation charact. 4-79152  
 H<sub>2</sub>AlP<sub>2</sub>O<sub>10</sub>·2H<sub>2</sub>O, electrorheological suspensions, disperse phase, charge transport characteristics 4-103426  
 Hf-Al-N ternary system, phase equilib. invest. rel. to fusion reactor materials 4-76759  
 HfF<sub>2</sub>-BaF<sub>2</sub>-LaF<sub>3</sub>-AlF<sub>3</sub> glass, IR transparent, stability in humid air, AES study 4-109534  
 InGaAs/InGaAlAs/InAlAs/InP separate confinement heterostruct. multi-quantum-well laser diodes, MBE grown 4-83617  
 InGaP/InAlP quantum well structures for visible region, MBE growth 4-99314  
 InP-n-AlInAs heterostructure, magnetotransport study 4-88570  
 KAlF<sub>4</sub>, structural phase transition and cryst. struct. 4-80225  
 KAl(SO<sub>4</sub>)<sub>2</sub>·12H<sub>2</sub>O for laboratory scale saturated solar ponds 4-62396  
 α-KAl(SO<sub>4</sub>)<sub>2</sub>·12H<sub>2</sub>O alum, high pressure mag. resonance study of crystal fields 4-70757  
 LiAlCl<sub>4</sub> solutions conductivity in nitromethane containing SO<sub>2</sub>, concentration and temp. dependence, applicability assessment for Li/SO<sub>2</sub> cells 4-66596  
 LiF-AlF<sub>3</sub> cryolite melts, interdiffusion 4-88324  
 LiF-AlF<sub>3</sub> thin film, ionic cond. meas. 4-84450  
 Li<sub>0.5</sub>Fe<sub>1.5</sub>Al<sub>1.5</sub>O<sub>4</sub>, atomically ordered spinel, mag. struct., neutron diffraction 4-61513  
 Mg-Al spinel, microtwins, selected-area electron diffraction obs. 4-103770  
 NH<sub>4</sub>AlF<sub>6</sub>, structural phase transition and cryst. struct. 4-80225  
 α-NH<sub>4</sub>Al(SO<sub>4</sub>)<sub>2</sub>·12H<sub>2</sub>O alum, high pressure mag. resonance study of crystal fields 4-70757  
 NaAlH<sub>4</sub>, decomposition, Na single cryst. form., electron microscopic study 4-108296  
 NaAl(SO<sub>4</sub>)<sub>2</sub>·12H<sub>2</sub>O·Fe<sup>3+</sup>, single crystal EPR, resonance linewidths, crystal field splittings 4-84851  
 NaF-AlF<sub>3</sub>, natural cryolite, vaporisation and high temp. thermodynamics, mass spectra 4-77025  
 NaF-AlF<sub>3</sub>, melt, thermodynamic data for reactions from vapour pressure meas. 4-85325  
 NaF-AlF<sub>3</sub>, melt, vapour phase studies, activity data 4-84423  
 NaF-Al(P<sub>2</sub>O<sub>3</sub>)<sub>3</sub>-RF<sub>2</sub>-B<sub>2</sub>O<sub>3</sub>-BaO glass, moisture resistance and other props. 4-60126  
 Na<sub>1+x</sub>Mg<sub>1-x</sub>Al<sub>11-x</sub>O<sub>17</sub>:Nd<sup>3+</sup> platelet laser absorpt. spectra, fluoresc. lifetime, laser-pulse shape and peak emission wavelength 4-60044  
 Pb-Al<sub>2</sub>O<sub>3</sub>-Al junctions, ion irradi., defect vibrs., supercond. tunnelling meas. 4-98826  
 PbF<sub>2</sub>-GaF<sub>3</sub>-Al(P<sub>2</sub>O<sub>3</sub>)<sub>3</sub>-ErF<sub>3</sub>-based fluoride glasses, fluorescence studies 4-99170  
 RbAlF<sub>4</sub>, structural phase transition and cryst. struct. 4-80225  
 Si-Al-O-N oxynitride glasses, synthesis, stability and microstruct. 4-70042  
 Si-Al-O-N phases, struct. studies using magic-angle-spinning NMR 4-71198  
 Si-Al-O-N system, hot-pressed and reaction-bonded, phase equilib. and props. 4-76761  
 Si<sub>3</sub>Al<sub>6</sub>O<sub>12</sub>N<sub>2</sub>, sialon X-phase, cryst. struct. 4-75427

**aluminium compounds continued**

- $\text{Si}_3\text{Al}_2\text{O}_5\text{N}_{5.5}$ , oxidation behaviour in  $\text{O}_2$  and  $\text{CO}_2$  4-76891  
 $\text{Si}_3\text{AlON}$ , fracture toughness, effect of deform. 4-76868  
 $\text{Si}_{6-2}\text{Al}_2\text{O}_{8-2}\text{N}_{8-2}$ ,  $\beta$ -sialon, hot pressed; flexural strength, phase struct., comp. depend. (Japanese) 4-76828  
 $\text{Si}_{6-2}\text{Al}_2\text{O}_{8-2}\text{N}_{8-2}$ ,  $\beta$ -sialon synthesis from  $\text{Si}_3\text{N}_4$  and Al alkoxides (Japanese) 4-114461  
 $\text{SiC-AlN}$  solid solution,  $\text{Si}_3\text{Al}_4\text{N}_3\text{C}$  and  $\text{Si}_3\text{Al}_2\text{C}_3$  cpds. 4-66316  
 $\text{Si}_3\text{N}_4\text{-SiO}_2\text{-AlN-Al}_2\text{O}_3\text{-Y}_2\text{O}_3$  system; phase relations, solid-liq. reactions 4-76762  
 $(\text{ThF}_{0.2}\text{BaF}_{0.8})(\text{MnF}_{0.5})(\text{AlF}_{0.2})_{0.2}$  glass, low temp. ultrasonic behaviour 4-70285  
 $\text{TiAlF}_6$ , structural phase transition and cryst. struct. 4-80225  
 $\text{Y-Si-Al-O-N}$  glasses, viscosity, glass transition, microhardness rel. to comp. 4-70383  
 $\text{Zr-Ba-La-Al-F}$  glass, crystn. kinetics 4-70037  
 $\text{ZrF}_4\text{-BaF}_2\text{-LaF}_3\text{-AlF}_3$  glass, IR transparent, stability in humid air, AES study 4-109534  
 $\text{ZrO}_2\text{-Y}_2\text{O}_3\text{-Al}_2\text{TiO}_5$  refractory composites, props. 4-71626

**aluminosilicate glasses**

- crystallisation and properties of glasses prep. from Illinois coal fly ash 4-79940  
 decomposition under acidic conditions, glass-ionomer dental cement prep. 4-99373  
 E-glass fabric, vol. resist. depend. on temp. and leaching parameters 4-70880  
 nepheline glass-ceramic, microwave heating characts. 4-65294  
 $\text{Al}_2\text{O}_3\text{-Fe}_2\text{O}_3\text{-CaO-SiO}_2$  glass; crystallisation and mag. props. 4-65188  
 $\text{Al}_2\text{O}_3$ -glass composite, hot isostatically pressed, macropore struct. 4-71629  
 $\text{Al}_2\text{O}_3\text{-ZrO}_2\text{-SiO}_2$  glass refractory, fusion-cast high  $\text{ZrO}_2$ , corrosion resistance in soda lime glass 4-62080  
 $\text{BaO-Al}_2\text{O}_3\text{-SiO}_2$  thick film crossover dielec.-compositions, dielec. props. rel. to multiple refiring 4-109113  
 $\text{CaO-Al}_2\text{O}_3\text{-P}_2\text{O}_5\text{-SiO}_2\text{-Na}_2\text{O}(\text{K}_2\text{O})$  system glasses, opacification and crystn. 4-89021  
 $\text{CaO-Al}_2\text{O}_3\text{-SiO}_2$  glasses, struct. features, EXAFS and XANES studies 4-60850  
 $\text{CaO-Al}_2\text{O}_3\text{-SiO}_2$  glass powder, vitrification kinetics, effect of water vapour 4-92094  
 $\text{CoO-Al}_2\text{O}_3\text{-SiO}_2$  insulating spin glass, light-induced mag. effects 4-71085  
 $\text{Li}_2\text{O-Al}_2\text{O}_3\text{-SiO}_2$ , structural features, for gradient optical elements 4-79947  
 $\text{Li}_2\text{O-Al}_2\text{O}_3\text{-SiO}_2$  glass ceramic, effective radiative thermal cond./diffusivity, role of view factor 4-84473  
 $\text{Li}_2\text{O-Al}_2\text{O}_3\text{-SiO}_2$  glasses, Young's modulus, effect of vol. and struct. 4-85170  
 $\text{Li}_2\text{O-Al}_2\text{O}_3\text{-SiO}_2$  glass-ceramic; superplastic ductility, rel. to hydrostatic press. and humidity 4-109474  
 $\text{MnO-Al}_2\text{O}_3\text{-SiO}_2$  insulating spin-glass, spin freezing, expt. study 4-71096  
 $\text{Na}_2\text{O-Al}_2\text{O}_3\text{-SiO}_2$ , alkali resistance, effects of alkali metal and zinc oxide additions 4-81317  
 $\text{Na}_2\text{O-Al}_2\text{O}_3\text{-SiO}_2$ , structural features, for gradient optical elements 4-79947  
 $\text{Na}_2\text{O-Al}_2\text{O}_3\text{-SiO}_2$  glasses, Young's modulus, effect of vol. and struct. 4-85170  
 $\text{Na}_2\text{O-B}_2\text{O}_3\text{-Al}_2\text{O}_3\text{-SiO}_2$  transparent glazes; with enhanced chem. and thermal shock-resist. 4-81305  
 $\text{Na}_2\text{O-B}_2\text{O}_3\text{-SiO}_2\text{-CaO-Al}_2\text{O}_3$  glasses UV-transmissivity of a tempered sodium-borosilicate glass (German) 4-88856  
 $\text{Na}_2\text{O-MO-Al}_2\text{O}_3\text{-SiO}_2$  glass,  $\text{M}=\text{Ca, Mg, Zn}$ , leaching 4-84404  
 $\text{SiO}_2\text{-B}_2\text{O}_3\text{-Al}_2\text{O}_3\text{-Na}_2\text{O}$  glass, porous, precipitation of colloidal silica and pore size distrib. 4-109412  
 $\text{SiO}_2\text{-CaO-Al}_2\text{O}_3\text{-MgO}$ , elastic and strength props., effect of temp. 4-114597  
 $\text{TiO}_2\text{-Al}_2\text{O}_3\text{-SiO}_2$  glass system preparation using  $\text{CO}_2$  laser melting (Chinese) 4-114466  
 $\text{WO}_3\text{-Al}_2\text{O}_3\text{-SiO}_2$  glasses, insulating spin glass, field cooled magnetisation, cooling rate effect 4-71084  
 $\text{ZrO}_3\text{-Al}_2\text{O}_3\text{-SiO}_2$  glass system preparation using  $\text{CO}_2$  laser melting (Chinese) 4-114466

**a.m. (modulation) see amplitude modulation****ambient temperature see temperature****amblyopia see vision defects****americium**

see also nuclei with .....

- alpha-particle spectrometer, computerised system for low level actinides 4-68867  
 alpha-spectrum anal., peak ratio's 4-68865  
 Columbia River, Oregon, USA, radioactive pollution in sediments 4-66824  
 fission reactor fuel, burnup and isotopic composition determ. in VVER-440 4-102355  
 localisation of 5f electrons, XPS study 4-70892  
 TRU nuclides, in vivo meas. using high purity Ge detector,  $\gamma$  and X-ray meas. 4-115194  
 USA Transuranium Registry, human experience with Pu and Am 4-111972  
 Am III in aqueous solution, oxidation-state specific detect. by pulsed laser photoacoustic spectroscopy 4-99858  
<sup>241</sup>Am carcinogenic effect in rat expts. (Russian) 4-67008  
<sup>241</sup>Am in the beagle skeleton: microdistrib. and local dosimetry 4-77394  
<sup>241</sup>Am, L-Auger spectra meas. 4-96511  
<sup>241</sup>Am, long-term distrib. in skeletons of adult rats 4-77404  
<sup>241</sup>Am, medical course after accidental exposure 4-109890  
<sup>241</sup>Am, microdistrib. and localised dosimetry in bones of beagle dogs 4-115242  
<sup>241</sup>Am ultra-thin  $\alpha$ -source, preparation by adsorption 4-68853  
 $\text{NaI(Tl)}-\text{^{241}Am}$  light pulser, increased reliability in sealing 4-102506

**americium compounds**

No entries

**ammeters**

- clamp-on DC ammeter using Hall effect transducers 4-111120  
 NPL moving-coil ampere determination (Japanese) 4-101824

**anionia**

- absorption band lines near 645 nm in spectra of Saturn (Russian) 4-101241  
 adsorbed on Cu (100), time of flight mass spectra study on IR laser photodesorption 4-80384

**ammonia continued**

- adsorption and decomposition on Ru (001) and Ru (1,1,10) surfaces 4-65572  
 atmospheric concentration over southwestern USA 4-115527  
 chemisorbed on Ni (111), surface Penning ionisation study 4-65575  
 chemisorbed on transition metal surfaces, acceptor and donor functions 4-70568  
 diatomic-fragment data calc. for the diatomics in mols. method 4-78783  
 dimer, effects of basis set and electron correlation on calculated props. 4-91205  
 dimers, IR photodissoc., mass spectra detection 4-69158  
 existence of  $\text{Na}^-$  in liq.  $\text{NH}_3$ , thermodynamic properties 4-99825  
 fertilizers production using electrolytic  $\text{H}_2$  4-89474  
 gas, selectively IR emitting, radiative cooling 4-87834  
 gas backed by Al, materials for radiative cooling to low temperatures 4-112683  
 gaseous,  $\text{H}^+$  spin longitudinal relax. time 4-107367  
 intercalation cpd. with  $3\text{R-TaS}_2$ , proton NMR meas. 4-61598  
 interstellar  $\text{NH}_3$ , obs. in isolated dark globule (B335) 4-115794  
 interstellar  $\text{NH}_3$  obs. in Taurus dark cloud complex rel. to star counts and visual extinction 4-115791  
 ion implantation, low energy, in  $\text{Si}$ ,  $\text{Si}_3\text{N}_4$  formation 4-75484  
 laser, optically pumped, 10-W CW 12- $\mu\text{m}$  output 4-64697  
 laser, TEA  $\text{CO}_2$  laser pumped, high-power pulsed operation at 257/281  $\mu\text{m}$  transitions 4-79182  
 lasers, far IR, Lorenz instability obs. 4-107612  
 lasers, IR, dynamics, investigation using tunable diode lasers 4-112375  
 lasing lines 16 to 35  $\mu\text{m}$ , two-photon optical pumping in multipass cell 4-74495  
 liquid,  $\text{e}_a+\text{H}_2\text{O}$  reactions, kinetics 4-104966  
 methanol- $\text{NH}_3$  associated species, D isotope effect, vibr., Raman spectra, normal coordinate anal. 4-66035  
 molecular jet, expanding, rotational temp. and mol. density determ. by IR absorpt. 4-83490  
 molecule,  $^6\text{Ni}(\text{CO})_4$ , geometry optimisation, relativistic corrections, HF approx. 4-78786  
 molecule, absorpt. spectrum obtained using intracavity spectroscopy utilising  $\text{LiF F}_2$  colour centre lasers 4-59774  
 molecule,  $\text{C}^{13}\text{A}$ , state, predissoc. dynamics, multiphoton ionis. spectrosc. investig. 4-102752  
 molecule, chemisorbed on Ni (110), site selection by electron donor mechanism 4-70549  
 molecule, collisional relax., steady-state IR-IR double reson. 4-69188  
 molecule, electron and X-ray scatt., incoherent scatt. factors, Waller-Hartree calcs. 4-112271  
 molecule, electron density, fitting method 4-74143  
 molecule, electron impact dissc.,  $\text{H}^*$  energy distrib., Balmer emission 4-69226  
 molecule, inversion lines, self broadening 4-78914  
 molecule, IR multiple photon absorpt. spectra, optothermal detection 4-69059  
 molecule, light induced drift 4-74349  
 molecule, localised second-order elec. props., Hartree Fock calcs. 4-68947  
 molecule, lone pair ligand interaction with Cu, constrained space orbital variation method 4-114823  
 molecule, lowest triplet state detect. by electron impact excitation 4-102809  
 molecule, photolysis,  $\text{NH}_2(\text{X}^2\text{B}_1)$ , free radical detect. by CARS spectroscopy 4-62262  
 molecule, Q branch transition, diode laser IR spectra 4-59750  
 molecule, reson. rovibronic Raman scatt., Franck-Condon factors, line-shape anal. 4-96550  
 molecule, single-collision energy transfer and catalytic decomposition on Re at high temps. 4-71971  
 molecule, total energies calc. using electron cloud displacement model (Chinese) 4-74137  
 molecule isolated in solid gas matrices, far IR Fourier spectroscopy 4-102677  
 molecules, IR absorpt. spectroscopic data spectral slit width and blind deconvolution estimation by homomorphic filtering 4-73533  
 molecules, IR laser optogalvanic spectroscopy, Doppler free and double reson. effects 4-74230  
 molecules, sub-Doppler double reson. spectroscopy using tunable diode laser 4-111220  
 molecules, tunable diode laser optogalvanic spectroscopy 4-112168  
 neutral clusters, unimol. fragmentation pathways 4-81412  
 optical hysteresis obs. in all-optical passive ring cavity 4-64730  
 OTEC closed system optimisation with dual-zoned condenser and reverse osmosis desalination unit 4-66740  
 partitioning in atm. between gaseous and aqueous phases 4-77590  
 pollutant monitoring using  $\text{CO}_2$ -laser long-path absorption system 4-62426  
 production from  $\text{H}_2\text{O}+\text{N}_2^-$  in presence of  $\text{TiO}_2$  catalysts, effect of compounded metal on  $\text{NH}_3$  yield 4-62230  
 Raman laser emission, pure MW in superradiant mode,  $\text{CO}_2$  laser line pumping 4-69376  
 rotational structure of spectra, inversion effect, anomalous behaviour of spectroscopic parameters 4-83370  
 Sagittarius B2, mol. cloud,  $\text{NH}_3$  (5,2) transition detect. 4-94915  
 solid films, photon-stimulated ion desorption 4-61239  
 surface catalysed formation, field promoted on transition metals 4-66616  
 synthesis over Re single crystals, surface struct. sensitivity 4-109685  
 $\text{D}^{14}\text{N}_3$ ,  $\nu$  band, Raman and IR rot. vib. spectra 4-69087  
 $\text{H}_2$  produced from  $\text{NH}_3$ , cost comparisons of various processes 4-105128  
 $\text{H}_2^+(\text{NH}_3)_n$  clusters, photoionisation in pulsed supersonic nozzle beam by VUV rare-gas reson. lines 4-69258  
 $\text{Hg-NH}_3$  complex, excited, laser-induced luminesc. 4-107381  
 $\text{ND}_3$ ,  $\text{C}^{13}\text{A}$  state, predissoc. dynamics, multiphoton ionis. spectrosc. investig. 4-102752  
 $\text{ND}_3$  gas, DC breakdown strength, isotope depend. 4-79723  
 $\text{ND}_3$ , UV laser photodissoc. 4-69157  
 $(\text{ND}_3)_n$ , D-O, IR spectra and phase transitions between 100 and 15K 4-114258  
 $(\text{ND}_3)_n$ ,  $\text{H}_2\text{O}$ , IR spectra and phase transitions between 100 and 15K 4-114258  
 $\text{NH}_3$  icy solids, surface mol. photodetachment and photodissociation 4-66604  
 $\text{NH}_3$  laser, 16-21  $\mu\text{m}$  line, tunable, two-step optical pumping 4-112381  
 $\text{NH}_3$  on Ag electrode, surface enhanced Raman scatt., vibr. anal., charge transfer processes 4-93545

## ammonia continued

- $\text{NH}_3\text{-BH}_3$ , orbital interaction, charge transfer, bond form., CNDO/2 study 4-102597  
 $\text{NH}_3\text{-HCN}$ , rot., mol. beam elec. reson., microwave spectra 4-64505  
 $\text{NH}_3\text{-HCl}$ , H bonded complex, matrix isolated IR vibr. spectra 4-96543  
 $\text{NH}_3\text{-N}_2$  laser amplifier in 800-870  $\text{cm}^{-1}$  range 4-69440  
 $\text{NH}_3\text{-N}_2\text{O-Ar}$ , shock-heated, oxidation, conc. time profiles obtained by absorpt. and emission spectra 4-89298  
 $\text{NH}_3\text{-H}^+$ , differential cross sections 4-85295  
 $\text{NH}_3\text{-In}$ , intramultiplet mixing collisions 4-107393  
 $\text{NH}_3\text{-N}$  reaction, spectrophotometric studies 4-114793  
 $\text{NH}_3\text{-NH}_3$ , quenching, radiative lifetimes, transition moments 4-74292  
 $\text{NH}_3\text{-O}$ , absolute rate consts. 4-66557  
 $\text{NH}_3\text{-H}_2\text{S}$  reaction, depend. on translational and internal energy of  $\text{NH}_3$  4-71891  
 $(\text{NH}_3)_n$  cluster beams, differential scatt. anal. 4-74376  
 $(\text{NH}_3)_n$  clusters, multiphoton ionisation with tunable laser 4-74368  
 $(\text{NH}_3)_n$  clusters, photochemistry computationally based speculations 4-96741  
 $(\text{NH}_3)_n$  clusters, mass spectra 4-74382  
 $(\text{NH}_3)_n^+$  clusters, (n=2, 3, 4), photoionisation in pulsed supersonic nozzle beam by VUV rare-gas reson. lines 4-69258  
 $\text{NH}_2\text{D}$ , inverted Lamb dip for  $\text{CO}_2$  waveguide laser freq. stabilisation 4-79098  
 $(\text{NH}_3)_5\text{H}_2^{2+}$ , form. from electr. impact ionisation, H bonds 4-107480  
 $(\text{NH}_3)_2\text{D}_2\text{O}$ , IR spectra and phase transitions between 100 and 15K 4-114258  
 $(\text{NH}_3)_2\text{H}_2\text{O}$ , IR spectra and phase transitions between 100 and 15K 4-114258  
 $^{16}\text{NH}_3$ ,  $\nu_2=1$  inversional dependence of quadrupole coupling 4-87140  
 $\text{SiF}_4\text{-(NH}_3)_n$  complexes, stability, ab initio STO-3G calcs. 4-59613

## ammonia clocks see atomic clocks

## ammonium compounds

- halides, ionic compressibilities and static polarizabilities 4-88130  
 halides, struct. stability and static props. 4-98059  
 intercalation cpd. with graphite,  $\text{K}(\text{NH}_4)_2\text{C}_{24}$ , tuneable sandwich thickness, cryst. struct. 4-70101  
 UV-visible and IR spectra, radiative transition probabilities for fluoresc. level 4-114309  
 $\text{Al}_2\text{O}_3\text{-NH}_4^+$ ,  $\text{H}^+(\text{H}_2\text{O})_n$ ,  $\beta^+$  and ion-rich  $\beta^-$  phases, protonic cond. 4-92412  
 $\text{Ca}(\text{NH}_4)\text{PO}_4\cdot 7\text{H}_2\text{O}$ , cryst. struct., H bonds, X-ray diff. determ. 4-92150  
 $\text{Co}(\text{NH}_4)_2(\text{BeF}_4)_2\cdot 6\text{H}_2\text{O}$ , optical absorption spectrum 4-104588  
 $\text{Fe}(\text{NH}_4)\text{H}_2\text{PO}_4$ , unit cell parameters, anion packing 4-113410  
 $\text{Fe}(\text{NH}_4)_2(\text{SO}_4)_2\cdot 6\text{H}_2\text{O-Ni}(\text{NH}_4)_2(\text{SO}_4)_2$ , co-precipitated, thermal decomp. Mossbauer investig. 4-65883  
 $\text{H}(\text{NH}_4)_2\text{SbO}_3$ , proton cond. and cryst. struct. (French) 4-84451  
 $\text{HgCl}_2\text{-(NH}_4)_2\text{C}_2\text{O}_4$ , cryst. struct. determ. 4-75391  
 $\text{LiNH}_2\text{SO}_4\text{-Mn}^{2+}$ , impurity electronic absorpt. spectrum 4-66055  
 $\text{Mg}(\text{NH}_4)\text{PO}_4\cdot 6\text{H}_2\text{O}$ , synthetic struvite, complementary forms, correct polarity and surface features 4-84248  
 $(\text{ND}_4)_2(\text{SO}_4)_2$ , successive phase transitions studied by  $\text{VO}^{2+}$  ion and  $\text{SeO}_3$  radical EPR 4-76388  
 $\text{NH}_4^+$  charge redistrib. in mol. vibr. M-H bond moments 4-69047  
 $\text{NH}_4^+$  ion selective electrode, electrochem. props. 4-81445  
 $\text{NH}_4^+$ ,  $\nu_3$  band, vel. modulation IR laser spectra 4-69062  
 $(\text{NH}_4)_2\text{BeF}_4$ , dielectric hysteresis and anomalous temperature 4-93026  
 $\text{N}_2\text{H}_4$  intercalation cpd. with  $3\text{R-TaS}_2$ , proton NMR meas. 4-61598  
 $\text{NH}_4\text{AlF}_6$  clusters and critical slowing down near  $T_c$ , EPR study 4-65982  
 $\text{NH}_4\text{AlF}_6\text{-NH}_4^+$  ions rotation, and phase transition, nucl. spin relaxation study 4-71201  
 $\text{NH}_4\text{AlF}_6$ , structural phase transition and cryst. struct. 4-80225  
 $\alpha\text{-NH}_4\text{Al}(\text{SO}_4)_2\cdot 12\text{H}_2\text{O}$  alum, high pressure mag. resonance study of crystal fields 4-70757  
 $\text{NH}_4\text{B}_3\text{O}_6\cdot 4\text{H}_2\text{O}$ , stress optical behaviour under linear and hydrostatic stresses 4-80903  
 $\text{NH}_4\text{BF}_3$ , ferroelastic, successive phase transitions, sp. ht., thermal expansion meas. 4-108605  
 $\text{NH}_4\text{BF}_3$ , ferroelastic, domain struct., polarising microscope obs. 4-108629  
 $(\text{NH}_4)_2\text{BeF}_4$ , incommensurate phase, SHF Obs. 4-61635  
 $(\text{NH}_4)_2\text{BeF}_4$ , incommensurate phase, in applied elec. field 4-76376  
 $(\text{NH}_4)_2\text{BeF}_4$ , incommensurate phase, dielec. dispersion in microwave range 4-104524  
 $(\text{NH}_4)_2\text{BeF}_4$ , sp. ht. in region of incommensurate phase transition 4-61104  
 $\text{NH}_4\text{Br}$ , cohesion and thermodynamic props. calcs. 4-92126  
 $\text{NH}_4\text{Br}$ , continuous and discontinuous phase transitions, Raman modes 4-61070  
 $\text{NH}_4\text{Br}$ , model calcs. for phonons 4-84353  
 $\text{NH}_4\text{Br}$ , polymorphous transitions, pseudoharmonic theory 4-61078  
 $\text{NH}_4\text{Br}$ , third order elastic consts. near  $\lambda$ -point 4-88223  
 $\text{NH}_4\text{Cl}$ , cohesion and thermodynamic props. calcs. 4-92126  
 $\text{NH}_4\text{Cl}$ , continuous and discontinuous phase transitions, Raman modes 4-61070  
 $\text{NH}_4\text{Cl}$ , critical exponents, Pippard relations, Raman spectra 4-61694  
 $\text{NH}_4\text{Cl}$  crystal, Raman scatt. intensity from polaritons near a phase transition 4-84967  
 $\text{NH}_4\text{Cl}$ , hypersound attenuation and dispersion, back and forward Brillouin scatt. 4-76487  
 $\text{NH}_4\text{Cl}$ , librational motion of  $\text{NH}_4^+$  4-60865  
 $\text{NH}_4\text{Cl}$  metal-model unidirectional solidification in microgravity optical obs. 4-80194  
 $\text{NH}_4\text{Cl}$ , model calcs. for phonons 4-84353  
 $\text{NH}_4\text{Cl}$ , polymorphous transitions, pseudoharmonic theory 4-61078  
 $\text{NH}_4\text{Cl}$ , time of flight neutron spectrometer resolution improvement 4-86997  
 $\text{NH}_4\text{Cl-Co}^{2+}(\text{Ni}^{2+})$ , X-irrad. effects, optical absorpt. spectra, EPR 4-70206  
 $\text{NH}_4\text{Cl-H}_2\text{O}$ -decylammonium chloride, lyotropic liquid crystal, smectic-nematic transition 4-88289  
 $\text{NH}_4\text{Cl-NaCl-NH}_4\text{HCO}_3\text{-NaHCO}_3\text{-H}_2\text{O}$  ( $-(\text{NH}_4)_2\text{CO}_3\text{-Na}_2\text{CO}_3\text{-H}_2\text{O}$ ) systems, phase diagrams 4-104773  
 $\text{NH}_4\text{Cl-Br}_2$  solid solns., heat capacity near  $\gamma$ - $\beta$  transition 4-103958  
 $(\text{NH}_4)_2\text{CoCl}_4$ , commensurate-incommensurate phase transitions 4-75667  
 $(\text{NH}_4)_2\text{Cr}_2\text{O}_7$  crystals grown from aqueous soln., morphology and charact. 4-103679

## ammonium compounds continued

- $\alpha\text{-NH}_4\text{Cr}(\text{SO}_4)_2\cdot 12\text{H}_2\text{O}$  alum, high pressure mag. resonance study of crystal fields 4-70757  
 $\text{NH}_4\text{H}_2\text{PO}_4$ , piezoelectrically induced acoustic waves, strain optic effect 4-66005  
 $\text{NH}_4\text{F}$ , model calcs. for phonons 4-84353  
 $\text{NH}_4\text{F}$ , time of flight neutron spectrometer resolution improvement 4-86997  
 $\text{NH}_4\text{HCO}_3$ , augmentation of rural biogas digester yield 4-66734  
 $\text{NH}_4\text{HCO}_3$ , relations between crystallographic characts. and cryst. struct. (Chinese) 4-75378  
 $\text{NH}_4\text{H}_2\text{PO}_4$ , monoclinic, cryst. struct. 4-75389  
 $\text{NH}_4\text{H}_2\text{PO}_4$ , cryst. perfection, flow visualisation expts. 4-65042  
 $\text{NH}_4\text{H}_2\text{PO}_4$  crystals, high power CW sum-freq. generation near 243 nm using two intersecting enhancement cavities 4-79235  
 $\text{NH}_4\text{H}_2\text{PO}_4$ , crystallisation, supersaturation, soln. velocity, crystal habit and growth rate 4-114372  
 $\text{NH}_4\text{H}_2\text{PO}_4$ , electrooptic Kerr effect, electronic contrib. 4-109164  
 $\text{NH}_4\text{H}_2\text{PO}_4$ , microcrystal growth in aq. soln. under nonstationary conditions 4-71540  
 $\text{NH}_4\text{H}_2\text{PO}_4$ , oriented crystallisation, electron-microscope study 4-65202  
 $\text{NH}_4\text{HSO}_4$ , ambient aerosol, S losses, PIXE anal. 4-99876  
 $(\text{NH}_4)_2\text{H}(\text{SO}_4)_2$ , successive phase transitions studied by  $\text{VO}^{2+}$  ion and  $\text{SeO}_3$  radical EPR 4-76388  
 $\text{NH}_4\text{HSO}_4$ , deuterated, polymorphous transition, NMR study 4-114215  
 $\text{NH}_4\text{HSO}_4$ , dielec. nonlinearity, ferroelec. transition 4-76366  
 $\text{NH}_4\text{HSO}_4$ , dielectric, piezoelectric and elastic props. 4-80878  
 $\text{NH}_4\text{HSO}_4$ , ferroelec. phase transition mechanisms, NMR studies 4-93015  
 $\text{NH}_4\text{HSO}_4$ , ferroelec. transitions, Raman scatt. and vibr. props. 4-93066  
 $\text{NH}_4\text{HSO}_4$ , ferroelec., with varying D content, phase transitions, dielec. anomalies 4-99061  
 $\text{NH}_4\text{HSO}_4$ , high temp. phase transition, ionic motion 4-108651  
 $(\text{NH}_4)_2\text{H}(\text{SeO}_4)_2$ , thermal and dielec. studies, 90 to 357K, isotope effects 4-70365  
 $\text{NH}_4\text{I}$ , cohesion and thermodynamic props. calcs. 4-92126  
 $\text{NH}_4\text{I}$ , model calcs. for phonons 4-84353  
 $\text{NH}_4\text{I}$ , polymorphous transitions, pseudoharmonic theory 4-61078  
 $\text{NH}_4\text{I-Cu}^{2+}$ , anomalous positive g-shift 4-92952  
 $\text{NH}_4\text{I-Mn}^{2+}$ , Q-band EPR study 4-114154  
 $\text{NH}_4\text{IO}_4$ , Raman spectra and cryst. struct. (Russian) 4-84968  
 $\text{NH}_4\text{MgF}_3$ , phase transition, heat capacity and NMR study 4-70366  
 $\text{NH}_4\text{MnF}_3$ ,  $\text{NH}_4^+$  group libration and reorientation, struct. transitions 4-65198  
 $\text{NH}_4\text{MnFeF}_6$ , crystal structure and mag. props. 4-71038  
 $\text{NH}_4\text{NO}_3$ , single-cryst. disorder, diffuse X-ray scatt. 4-103711  
 $\text{NH}_4\text{NO}_3\cdot \text{Ti}^{3+}$  soln., optical absorpt. spectra 4-84957  
 $(\text{NH}_4)_2\text{NaFeF}_6$ , phase transition, X-ray diff. and  $^{57}\text{Fe}$  Mossbauer study 4-65398  
 $(\text{NH}_4)_2\text{PdCl}_4$ , press. depend. of rot. states 4-60999  
 $\text{NH}_4\text{ReO}_4$ ,  $\text{NH}_4^+$  ion reorientation, quasi-elastic neutron scatt., anomalous NQR freq. 4-65880  
 $\text{NH}_4\text{SCN-poly(ethylene oxide)}$  complex, amorphous and cryst., form., stoichiometry and cond. response 4-88303  
 $(\text{NH}_4)_2\text{SO}_4$ , ambient aerosol, S losses, PIXE anal. 4-99876  
 $(\text{NH}_4)_2\text{SO}_4$ , conditioning of flue gas for electrostatic precipitator performance improvement 4-62421  
 $(\text{NH}_4)_2\text{SO}_4$ , first order paraelectric-antiferroelec. transition, X-ray topography 4-65990  
 $(\text{NH}_4)_2\text{SO}_4$ , proton spin-lattice relax. time, effect of  $^{17}\text{O}$  natural abundance 4-109092  
 $(\text{NH}_4)_2\text{SO}_4\cdot \text{CrO}_3$ , phase transitions studied by EPR spectra 4-88723  
 $(\text{NH}_4)_2\text{SO}_4\cdot \text{K}_2\text{SO}_4\cdot \text{CrO}_3$ , phase transitions studied by EPR spectra 4-88723  
 $(\text{NH}_4)_2\text{SnCl}_6$ , quantum disorder and molecular rotation 4-103677  
 $(\text{NH}_4)_2\text{ZnBr}_4$ , ferroelec., Raman scatt. study of phase transitions 4-104589  
 $(\text{NH}_4)_2\text{ZnCl}_4$ , incommensurate phase transition, dielec. props., X-ray diff. study 4-93021  
 $(\text{NH}_4)_2\text{ZnCl}_4$ , X-ray irrad., photoluminescence and EPR studies 4-93108  
 $\text{NH}_4\text{Zr}_2\text{O}_7$ , X-ray diff., IR spectra 4-109175  
 $(\text{NY}_4)_2\text{SO}_4$ ,  $\gamma$ -ray interaction in energy range 30-660 KeV 4-80096  
 $(\text{NH}_4)_2\text{HPO}_4(\text{PO}_3\text{H}_2)\text{Te}(\text{OH})_6$ , NMR study of phase transition 4-80877  
 $\text{RB}_{1-x}(\text{NH}_4)_x\text{H}_2\text{PO}_4$ , mixed crystals, phase transitions in cluster approx., pseudospin model 4-80881  
 $\text{Rb}_{1-x}(\text{NH}_4)_x\text{H}_2\text{PO}_4$ , ferroelec. pseudo-spin glass state, NMR meas., dynamic cluster freeze-out model 4-65875  
 $\text{Rb}_{1-x}(\text{NH}_4)_x\text{H}_2\text{PO}_4$  single cryst. proton glasses, struct. and dielec. props. 4-76323  
 $\text{Rb}_{1-x}(\text{NH}_4)_x\text{H}_2\text{PO}_4$  glass, H-bonded, NMR relax. study 4-98974  
 $\text{Rb}_{1-x}(\text{NH}_4)_x\text{H}_2\text{PO}_4$ , dipole glass phase, dielec., thermal, elastic, and struct. props. (Japanese) 4-104525  
 $\text{Te}(\text{OH})_6\cdot 2\text{NH}_4\text{H}_2\text{AsO}_4\cdot (\text{NH}_4)_2\text{HAsO}_4$ , cryst. struct., X-ray diff. study 4-60888  
 $\text{Te}(\text{OH})_6\cdot 2\text{NH}_4\text{H}_2\text{PO}_4\cdot (\text{NH}_4)_2\text{HPO}_4$ , cryst. struct., X-ray diff. study 4-60888  
 $\text{Te}(\text{OH})_6\cdot 2\text{NH}_4\text{H}_2\text{PO}_4\cdot (\text{NH}_4)_2\text{HPO}_4$ , dielec., thermal and optical props. 4-61636  
 $\text{Te}(\text{OH})_6\cdot 2\text{NH}_4\text{H}_2\text{PO}_4\cdot (\text{NH}_4)_2\text{HPO}_4$ , single cryst. growth and morphology 4-61821  
 $\text{VNH}_4\text{H}_2\text{P}_2\text{O}_{10}$ , unit cell parameters 4-113410

## amorphisation

- depreciation by ion bombardment 4-99157  
 dielectric solids, thermal cond. theory, effect of radiation damage 4-70482  
 ferromagnetic Ising model, dilute crystalline, amorphisation and high-field magnetisation 4-98911  
 ice I, amorphous phase formed at 77K and 10 kbar 4-98016  
 Ising ferromagnet, amorphisation, high-field magnetisation 4-84762  
 Ising ferromagnet, diluted, amorphisation, effective field theory with correl. 4-80771  
 magnetic thin films, amorphisation of regular domain structures at second-order phase transitions, dislocation-disclination mechanism 4-98928  
 metals, light ion implantation, amorphisation, statistical aspect 4-80114  
 nonmetallic solids, amorphisability under heavy ion bombard., covalent-ion transition 4-80122  
 polyethylene, electron irrad., melting and crystallisation, calorimetric study (Russian) 4-84223

**amorphisation continued**

- polyethylene, high press. high temp. transition to amorphous phase 4-84381  
 semiconductors, amorphisation by ion implantation, modification to defect accumulation models 4-88210  
 SOS, ion implanted, elec. props., effect of heat treatment 4-98759  
 zirconolite-based ceramic, self-irradiation damage 4-75546  
 Au-Ge bilayers, ion beam mixing, amorphous and metastable phases formation 4-80113  
 Bi<sub>2</sub>FeO<sub>4</sub> glass, IR study 4-70381  
 GaAs, surface disordering by picosecond laser pulses 4-92233  
 Ge-Te, ion implanted, amorphisation phenomena, electron microscope and electron diff. studies 4-103656  
 Hf-Ni films, amorphisation by thin film solid state reaction 4-80428  
 MnB<sub>2</sub> alloy, spontaneous magnetisation changes due to amorphisation (*Russian*) 4-104407  
 Mo<sub>2</sub>Ge, fast neutron irradi., effects on struct. and supercond. props. (*Russian*) 4-92841  
 Pd-Si film, ion implanted, amorphisation, channelling anal. 4-92247  
 Si, CVD growth, solid state phase transformations 4-70598  
 Si, electron structure change during amorphisation, electrorefl. spectra (*Russian*) 4-98509  
 Si evaporated amorphous film, growth conditions by solid phase epitaxy 4-99307  
 Si, heavy-ion induced damage and annealing TEM and channelling studies 4-80115  
 Si, ion implanted, pyrometric temp. meas. during laser annealing 4-70203  
 Si polycrystalline films amorphised by ion implantation, solid phase epitaxial growth 4-108731  
 Si, pulse laser irradiated, surface morphology and phase transitions 4-88197  
 Si substrate, ion implanted and processed, interface characterisation 4-84304  
 Si, surface disordering by picosecond laser pulses 4-92233  
 Si:As(Sb)(In), ion implanted, pulsed electron beam annealing, impurity diffusion 4-103984  
 Si-Ge, implantation, pre-amorphisation/rapid thermal annealing procedure for shallow junction formation 4-88188  
 Ti/Ni bilayered thin films, amorphisation and ion beam mixing 4-88408  
 Ti-Au, amorphisation, pulsed ion beam annealing study 4-103831  
 TiNi-based alloy, radiation-induced amorphisation 4-103830  
 ZrSiO<sub>4</sub>, swelling induced by alpha and gamma irradi. 4-75543

**amorphous-crystalline transformations** *see crystallisation***amorphous magnetic materials** *see magnetic properties of amorphous substances***amorphous semiconductors**

- see also chalcogenide glasses; electrical conductivity of amorphous semiconductors and insulators; insulators*  
 amorphous, doped, IR and reson. Raman spectrosc. obs. 4-61707  
 CVD, low pressure, thin film growth rate, to reactor parameters 4-81143  
 DC electronic transport, long-range pot. influence 4-113947  
 deuterated amorphous hydrogenated, NMR obs. on fusion reactor first wall materials 4-91096  
 diamond, amorphous film deposition using generation/reaction of methylene species 4-104739  
 dispersive transport, multiple trapping model, effect of energy depend. capture cross section 4-70830  
 electron states, multielectron effects 4-98510  
 electron transport, Mott-CFO model anal. 4-113939  
 electronic states, transitions from localised states, rel. to density of states meas. 4-84547  
 generation-recombination noise calcs. (*Russian*) 4-114008  
 hopping cond., freq. and temp. depend., extended pair approx. 4-98615  
 Husimi cacti alloys, topological disorder 4-104119  
 II-IV-V<sub>2</sub> glassy semicond., synthesis, stability and microstruct. 4-70042  
 lone pair, intimate valence-alternation pair-originated two level systems 4-60834  
 long-range structural and electronic coherence in amorphous semiconductors 4-80485  
 low-conductivity, carrier mobility using the travelling wave technique 4-92752  
 non-equilibrium diffusive transport 4-70801  
 physico-chemical props., review 4-93038  
 picosecond electronic relaxations 4-108892  
 polyphenylacetylene, dye-sensitised amorphous films, semiconducting photoconductor 4-76001  
 Raman characterisation 4-99106  
 a-Si:H film, prep. by reactive sputtering, optical and elec. props. 4-71457  
 a-Si solar cells, shunt conductance and fill factor, incident light wavelength depend. 4-77090  
 Si solar photovoltaic cell technologies 4-72109  
 solar cells, amorphous, optical loss mechanisms 4-77108  
 solar cells, amorphous/crystalline tandem struct., conversion efficiency determ. using computer anal. 4-72116  
 spatially extended quasiparticles, disorder effects 4-98499  
 thin films, trapping and switching 4-113942  
 time-dependent geminate recombination for hopping site energy disorder 4-61395  
 transient photocond., effect of repeated carrier trapping 4-61420  
 Si amorphous or polycrystalline, epitaxial regrowth and bridging epitaxy by flash lamp irradiation 4-75813  
 AlN, sputter deposited, electron binding energy Auger and XPS study 4-75820  
 As<sub>2</sub>S<sub>3</sub> film based joint transform real time optical correlator 4-74461  
 Au-Ge-(H) interfaces on amorphous Ge, Schottky barrier and cpd. formation 4-84669  
 BaO-VO<sub>2.5</sub>-PO<sub>2.5</sub>, semiconductor glass, crystallisation rel. to composition, temp. and duration of heat treatment 4-92096  
 BaTiO<sub>3</sub>, semicond. glass/ceramics, oxidation, barrier layer form. 4-114699  
 Bi<sub>2</sub>O<sub>3</sub>-B<sub>2</sub>O<sub>3</sub> glasses, memory switching process, role of chem. reduction 4-114002  
 C, arc evaporated amorphous film, optical const. study 4-81026  
 a-C:H, low emittance coatings for high temperature solar collectors 4-114950  
 C:H amorphous coating for IR-optical elements, optical props., thickness, density, laser damage tests 4-76422  
 C:H amorphous coating material for passive IR materials 4-74668

**amorphous semiconductors continued**

- CdGe<sub>1-x</sub>Si<sub>x</sub>As<sub>2</sub> glasses, elec. props. and phase stability 4-104202  
 CdS amorphous films, optical absorption coeff. and gap state density 4-66088  
 CdS:Sb films, vacuum deposited, struct., elec. and optical props., impurity conc. effect 4-98607  
 Cu/a-Si:H/a-Si:H(n-type)/Cr Schottky diodes, RF magnetron sputtered 4-88557  
 GaAs, amorphous, high-defect-density, subpicosecond carrier trapping 4-80621  
 GaAs, amorphous, MBE grown, local struct., EPR and NMR studies 4-104492  
 GaAs amorphous thin films, transient annealing, Raman scatt. study 4-80926  
 GaAs, crystal and amorphous, pulsed laser irradi. under O<sub>2</sub> and silane atmospheres, O incorporation and losses 4-80091  
 GaAs:Se<sup>+</sup>, implanted, amorphous-cryst. interface, high resolution struct. charact. 4-70171  
 GaP amorphous film, local order study and electronic props. 4-70591  
 GaS, amorphous, short range order (*Russian*) 4-98015  
 GaSb amorphous film, local order study and electronic props. 4-70591  
 GaTe<sub>2</sub> amorphous films, elec. breakdown in pulsed fields 4-114209  
 Ge amorphous film, laser enhanced crystallisation, nucleation, growth velocity, recombination enhanced diffusion 4-65295  
 a-Ge films, laser-beam annealing time resolved TEM studies 4-65297  
 a-Ge, localised impurity states 4-104163  
 Ge, optical props. meas. 4-95496  
 a-Ge, phonon struct., inelastic electron tunnelling spectra obs. 4-61031  
 a-Ge, struct. disorder model, thermodynamic props. 4-75303  
 a-Ge, thermal cond. at low temp. 4-80319  
 a-Ge:Fe(Ni) films, cond. and localised states 4-104163  
 a-Ge:H, bond angle disorder and optical absorption edge 4-99083  
 a-Ge:H, photoinduced absorption spectra 4-109220  
 a-Ge:H,P, new paramagnetic centres and impurity states 4-109056  
 a-Ge:H films, planar magnetron sputtering, electronic props. 4-88972  
 Ge-Te, ion implanted, amorphisation phenomena, electron microscope and electron diff. studies 4-103656  
 Ge-Si, amorphous, RF sputtered, electronic props. 4-61370  
 Ge-Sn(Sb)(Al) amorphous thin films, hopping cond. meas., 130 to 300K, localised state variations 4-92713  
 GeS film, crystalline and amorphous, photoconductivity study (*Russian*) 4-70870  
 InP amorphous film, local order study and electronic props. 4-70591  
 InTe<sub>2</sub> amorphous films, elec. breakdown in pulsed fields 4-114209  
 KP<sub>15</sub> crystalline and amorphous, semiconductor props. 4-98603  
 a-Sb, elec. resist. and thermoelec. power meas. 4-108886  
 Sb<sub>2</sub>S<sub>3</sub>, amorphous thin films, struct. and crystn. 4-60842  
 Se, amorphous, DC conductivity thickness dependence 4-84620  
 Se, amorphous, defect states and photoelec. behaviour 4-113903  
 Se amorphous film, photo-EMF due to surface barriers 4-88541  
 Se, condensates, kinetics of crystallisation 4-109327  
 a-Se, electronic and vibr. struct., Raman spectra, cluster method 4-74387  
 a-Se:Bi films, crystallisation, dark cond. and activation energy 4-88104  
 Se-Te, As glassy films, pure and doped, deep level defects, xerographic spectra studies 4-61339  
 a-Si, AC field effect and density of gap states 4-92670  
 Si absorbing films, optical const. unambiguously determ. by reflectance and transmittance meas. 4-65997  
 Si alloy, recent developments in photovoltaic technology 4-99974  
 Si alloy thin film amorphous solar cells, roll-to-roll continuous prod. 4-114903  
 a-Si alloys, metastable defect states, X<sub>α</sub> scatt. wave calc. 4-113899  
 a-Si alloys, photocond., dark Fermi level position depend. 4-113987  
 Si, amorphous, from ion implantation, refractive index, thermal annealing effect 4-76417  
 Si, amorphous, high-defect-density, subpicosecond carrier trapping 4-80621  
 Si, amorphous, highly doped, MBE grown, epitaxial regrowth 4-98468  
 Si, amorphous, ion implanted, crystn. growth velocities, charged dangling bonds 4-88093  
 Si, amorphous, minority carrier diffusion length, intensity dependence 4-70829  
 Si, amorphous, photovoltaic detector for optical-optical guided-wave modulator 4-103004  
 Si, amorphous CVD films, H<sub>2</sub> plasma annealing localized state density 4-61337  
 Si amorphous film, laser enhanced crystallisation, nucleation, growth velocity, recombination enhanced diffusion 4-65295  
 Si, amorphous films as deep UV lithography masks 4-82837  
 a-Si, amorphous layer effect on lattice images of dislocations 4-79939  
 Si, atomic particle delocalisation effect in disordered media 4-92405  
 Si, CVD growth, solid state phase transformations 4-70598  
 a-Si, cond. and thermoelectric power below mobility edge 4-108888  
 Si, electron structure change during amorphisation, electrorefl. spectra (*Russian*) 4-98509  
 a-Si, electron transport, photocurrent transit time method 4-65679  
 a-Si, electronic struct., photoemission and optical props. 4-71522  
 a-Si, electronic struct. of defects, cluster Bethe lattice method 4-70739  
 Si, energy transfer during laser irradi. 4-76412  
 Si evaporated amorphous film, growth conditions by solid phase epitaxy 4-99307  
 a-Si, excess carrier lifetime and mobility studies 4-104219  
 Si, explosive crystallisation 4-98019  
 a-Si film, CVD CO<sub>2</sub> laser deposition process 4-114412  
 a-Si film, elastic and inelastic props. 4-88225  
 a-Si film, epitaxial crystallisation on GaP substrate 4-80452  
 a-Si, film, gap density of states determ. 4-80551  
 a-Si film, RF sputtered, optical absorpt., elec. cond., effect of thermal annealing 4-80583  
 a-Si films, localised density of states, electrophotography studies 4-113844  
 a-Si films, polarisability, refr. index meas. 4-93001  
 a-Si films, RF sputtered, photocond. meas. 4-61416  
 Si films, UHV deposited, crystn. temp. 4-88410  
 Si, highly undercooled, molten, nucleation and amorphous phase form. 4-70346  
 a-Si, hot carrier thermalisation, picosecond electronic relaxations 4-108892  
 a-Si, inert gas implantation and sputtering yield enhancement 4-76600  
 a-Si, ion implantation form. and optical state characterisation 4-88186  
 a-Si, ion implanted, etching in HF soln. and annealing effects 4-80063

**amorphous semiconductors continued**

- Si, ion implanted, explosive liq. phase crystallisation by double pulse laser irradiat. 4-84188
- Si, ion implanted, pyrometric temp. meas. during laser annealing 4-70203
- a-Si, localised electron state spectroscopy 4-70741
- a-Si, long-range structural and electronic coherence in amorphous semiconductors 4-80485
- Si, MBE, capabilities, materials prospects 4-81144
- a-Si, mobility edge, temp. depend. 4-92723
- Si noncrystalline thin films, struct. props. and impurity content 4-88434
- Si optically controlled amorphous photosensitive device 4-108896
- a-Si, phonon density of states calc., bond angle and length fluctuations 4-75631
- Si photovoltaic solar cells, future projections 4-89417
- a-Si photovoltaic technology, future speculations and forecasts 4-89431
- Si porous layers, electrophysical and optical props. 4-65680
- a-Si, pulsed laser irradiation, melting temp. and explosive crystallisation 4-88201
- Si, screening energy variations and Auger parameters, XPS studies 4-92975
- Si solar cells, efficiency improvement by optical confinement effect using  $\text{TiO}_2/\text{Ag}/\text{SUS}$  back-surface reflector 4-77106
- Si solar cells, Japanese Sunshine Project/solar photovoltaic program 4-66719
- a-Si solar cells with conversion efficiency >9% 4-85376
- Si, solar-grade, growth by Zn reduction of  $\text{SiCl}_4$ , morphology 4-66199
- a-Si, solid phase epitaxy, bond rearrangement process, quantitative anal. 4-84534
- a-Si, space charge limited current rel. to density of states 4-98637
- a-Si, space-charge limited currents and photocond. 4-61387
- a-Si, static charge fluctuations, band struct. calcs. 4-70636
- a-Si, struct. disorder model, thermodynamic props. 4-75303
- Si substrate for  $\text{RhSi}$ , struct. and growth kinetics 4-80446
- a-Si, vacuum deposited, solid-phase epitaxial growth anisotropy 4-75811
- Si vapour deposited cryst. and amorphous films, stresses, X-ray diff., studies 4-75824
- Si:As(Sb)(In), ion implanted, pulsed electron beam annealing, impurity diffusion 4-103984
- a-Si:B, pure and doped, ion implanted, recrystallisation studies 4-88422
- a-Si:B film, optical props. study 4-76540
- Si:B(As), low resistance ion implanted films 4-108398
- a-Si:Cl, H films, photocond. spectra (*Chinese*) 4-113989
- Si:F, amorphous, electronic struct. theory 4-92600
- Si:F, amorphous and cryst., ion implanted, elec. quadrupole hyperfine interaction at impurity sites 4-92675
- Si:F, As, ion implanted, defect struct. detection 4-103776
- Si:Ga sputtered amorphous alloys, thermopower and elec. cond. 4-61403
- a-Si:H, absorpt. edge, struct. disorder model for amorphous semiconductor 4-80483
- Si:H, amorphous, CVD growth by  $\text{Si}_2\text{H}_6$  pyrolysis in hot wall reactor 4-61864
- Si:H, amorphous, DC triode sputtered, electronic transport 4-61374
- Si:H, amorphous, electron mobility meas. using 4-terminal FET structures 4-75964
- Si:H, amorphous, electron-excited Coster-Kronig transitions 4-88908
- Si:H, amorphous,  $\text{Fe}_2\text{O}_3$ -coated semiconductor electrode by solar cell, XPS, AES and electrochem. meas. 4-66691
- Si:H, amorphous, glow discharge chemical vapour deposited, X-ray photoelectron spectroscopy 4-93201
- Si:H, amorphous, glow-discharge deposition, efficiency of gas usage, for solar cells 4-71602
- Si:H, amorphous, high-rate deposited annealing effects 4-61876
- Si:H, amorphous, light-induced defects, annealing 4-92762
- p-Si:H, amorphous, prepared by photo-CVD, electronic and optical props. 4-70959
- Si:H, amorphous films, glow discharge decomposition, Hg(Kr) effects 4-76687
- Si:H, amorphous films, optical storage technique 4-91547
- Si:H, amorphous solar cells, CVD growth 4-66694
- a-Si:H, As, dispersive transport, trap saturation, transient photocurrent meas. 4-76006
- a-Si:H, B, P, electron structure and density of states of B-P pairs, cluster calc. 4-65642
- Si:H, B(P), amorphous CVD layer, impurity doping 4-60941
- a-Si:H, broken bonds and electronic density of states, H effects 4-65178
- a-Si:H, conductivity, localisation and mobility edge 4-70819
- a-Si:H, DC elec. cond. Meyer-Neldel rule and Staebler-Wronski effect 4-113948
- a-Si:H, deep recombination centres, luminescence and EPR studies 4-104164
- a-Si:H, doping and gap states 4-70734
- a-Si:H, electronic density of states calcs. (*Russian*) 4-70740
- a-Si:H, electronic struct., theoretical models 4-70638
- a-Si:H, electronic struct. study using Auger electron spectroscopy (*French*) 4-75840
- a-Si:H, energy distrib. of light-induced gap states, photocond. meas. 4-76004
- a-Si:H, extended state mobility 4-104208
- a-Si:H, F, p-n junctions, generation; recombination currents, computer simulation 4-84683
- a-Si:H, geminate recombination and mobility 4-104223
- a-Si:H, glow discharge decomposition prep., electron drift mobility, photocurrent (*Chinese*) 4-84616
- a-Si:H,  $\text{H}_2$  chemisorption, AES and EELS meas. 4-108715
- a-Si:H, high-rate deposition from  $\text{SiH}_4$  using RF discharge technique, elec. and optical props. 4-85119
- a-Si:H, high-resolution PMR, high resolution of narrow spectral component 4-104498
- a-Si:H, homogeneous CVD growth, review 4-88984
- a-Si:H, IR absorpt., gaseous  $\text{H}_2$  and Si-H overtone spectra 4-93075
- a-Si:H, long-time drift mobility, photocurrent study 4-104221
- a-Si:H, MIS diode, glow discharge deposited, flat-band capacitance freq. depend. 4-76042
- a-Si:H, non-substitutional dopant states and carrier density statistics 4-113902
- a-Si:H, P(B), dark cond. and photocond., thickness depend. 4-84624
- a-Si:H, photoinduced absorption spectra 4-109220
- a-Si:H, plasma deposition, two layer struct., surface contribs. 4-70593
- Si:H, plasma-enhanced deposition 4-81160
- amorphous semiconductors continued**
- a-Si:H, prep. by glow discharge of  $\text{Si}_2\text{H}_6$ , optical and elec. props. 4-114237
- Si:H, RF sputtered amorphous film, dark cond. and photocond., annealing effects 4-70960
- a-Si:H, radiative combination at dangling bonds, quantitative model, expt. study 4-114326
- a-Si:H, resolution of DLTS energy scale controversy 4-104166
- a-Si:H, structural and vibr. spectra calcs. 4-98017
- a-Si:H, TSC meas., density of states behaviour 4-98636
- a-Si:H, time-resolved charge transport and photocond. 4-70871
- a-Si:H, transient photoinduced absorpt. 4-104634
- a-Si:H, undoped, carrier trapping; picosecond electronic relaxations 4-108892
- Si:H,B, amorphous, solar cells, deposition from  $\text{Si}_2\text{H}_6$  and B doping profiles 4-81540
- a-Si:H,B, doping effect on gap states 4-88488
- a-Si:H,B amorphous CVD films, optical props., B doping effects 4-99086
- a-Si:H,B film, optical props. study 4-76540
- a-Si:H,Cl films, glow discharge deposition from  $\text{SiCl}_4$ - $\text{SiH}_4$  mixtures, elec. and optical characts. 4-71580
- a-Si:H,F films, F incorporation during glow discharge deposition 4-114426
- a-Si:H,Li, surface photovolt. and dark conductance, light-induced changes 4-70861
- a-Si:H,N film, TSC and photoconductivity 4-104222
- a-Si:H,O(N) alloys, electron trapping states, tight binding formalism calcs. 4-113901
- a-Si:H,P, defect states and carrier capture processes 4-104165
- a-Si:H,P, new paramagnetic centres and impurity states 4-109056
- a-Si:H,P,B film, drift mobility, photoconductivity meas. 4-104259
- a-Si:H,P film, acoustoelectric effect, thickness depend. study 4-104273
- a-Si:H,P(B), ESR and optical props., thickness depend. 4-84853
- Si:H amorphous compensated films, xerographic discharge meas. 4-80603
- Si:H amorphous film, plasma polymerisation and deposition from RF and DC silane plasmas 4-85115
- Si:H amorphous film optical waveguides, propag. characts. 4-107821
- Si:H amorphous films, glow discharge deposited, electron drift mobility, substrate temp. dependence 4-61393
- Si:H amorphous films, glow discharge deposition in cascade reactors 4-76680
- Si:H amorphous films, laser CVD by ArF excimer laser photodissociation of  $\text{Si}_2\text{H}_6$  4-61859
- Si:H amorphous films, prep., characterisation absorpt. and laser-damage resistance 4-74676
- Si:H amorphous p-i-n solar cell, design, fabrication and characts. 4-114905
- a-Si:H film, annealing behaviour of  $g=2.0026$  ESR line 4-109057
- a-Si:H film, complex impedance meas. 4-76055
- a-Si:H film, deposition mechanism from plasma 4-114411
- a-Si:H film, drift mobility, xerographic determ. 4-104224
- a-Si:H film, high rate prep. by reactive evaporation method, photocond. and dark cond. meas. 4-61248
- a-Si:H film, hole mobility model 4-104220
- a-Si:H film, hyperfine interaction, ENDOR study 4-65881
- a-Si:H film, IR quenching of photoluminescence and photoconductivity 4-104656
- a-Si:H film, low freq. glow discharge prep. (*Japanese*) 4-76692
- a-Si:H film, optical props. meas. 4-76539
- a-Si:H film, produced by magnetron sputtering, ion beam anal. 4-92583
- a-Si:H film, sputtered, elemental anal., STEM study 4-104105
- a-Si:H film, Staebler-Wronski effect 4-108852
- a-Si:H film, time resolved photoluminescence and phonon transport 4-71445
- a-Si:H film, transient space charge limited cond. study 4-104215
- a-Si:H film for H passivation of implantation defects in Si-SiO<sub>2</sub> MOS struct. 4-71744
- a-Si:H films, anodic oxidation, elec. and optical props. of oxidised films 4-109527
- a-Si:H films, CVD growth, phys. props. 4-92715
- a-Si:H films, DC planar magnetron reactive sputtering and characterisation 4-93218
- a-Si:H films, doping effect, RF sputtering and p-n junction form. 4-88973
- a-Si:H films, electron drift mobility, xerographic determination 4-61377
- a-Si:H films, low defect grade, prep. by RF magnetron sputtering 4-114397
- a-Si:H films, luminescence fatigue and ODMR studies 4-85005
- a-Si:H films, planar magnetron sputtering, electronic props. 4-88972
- a-Si:H films, pot. barriers and photo-EMF 4-88561
- a-Si:H films, RF sputtering, substrate temp. calibration (*Japanese*) 4-76672
- a-Si:H films, reactive sputtering, elec. and optical props. 4-104203
- a-Si:H films, thickness effects on electrical and photoelectrical properties 4-98484
- a-Si:H films, transient photocond. meas. 4-88539
- a-Si:H films reactively RF sputtered, electrophotographic props. (*Japanese*) 4-81127
- a-Si:H glow discharge deposited films, morphology, temp. and substrate depend. 4-61260
- a-Si:H MIS Schottky barrier struct., dark currents 4-104322
- a-Si:H nip solar cells, B contamination and photoresponse 4-89407
- a-Si:H optical confinement type solar cell using milky tin oxide on glass 4-81556
- a-Si:H p-i-n devices, EBIC decay 4-92796
- a-Si:H p-i-n solar cells, performance, effect of prep. conditions (*Korean*) 4-114908
- a-Si:H p-i-n solar cells on  $\text{SnO}_2$  on glass, stability and efficiency 4-62354
- a-Si:H photocceptors, electrophotographic imaging process 4-73544
- a-Si:H pin devices, excess dark currents and diode quality factor 4-114016
- a-Si:H pin solar cells, LPCVD growth, transport props. 4-114907
- a-Si:H reactively sputtered films, H partial press. effects 4-93219
- a-Si:H Schottky barriers, photocurrent spectral sensitivity 4-65727
- a-Si:H Schottky barriers, sputtered, freq. depend. capacitance, admittance meas. 4-98693
- a-Si:H Schottky diodes and nip devices, single and double carrier injection 4-114015
- a-Si:H Schottky solar cells, gap state density 4-88438
- a-Si:H solar cells, EBIC microcharacterisation of fabrication defects 4-93629

**amorphous semiconductors continued**

- a-Si:H solar cells, photovoltage profiling 4-93617  
 a-Si:H sputtered films, steady-state photocond. and recombination processes 4-108902  
 a-Si:H surface barrier structs., photocurrent, freq. depend. 4-61418  
 a-Si:H thin films, glow discharge effects on electronic and optical props. 4-75977  
 a-Si:H thin films, O distrib. and modifications induced by heavy ion bombard. 4-70233  
 Si:H wide optical gap binary alloy films, elec. props. 4-113956  
 a-Si:H/Si p-n junction, optoelectronic props. 4-114020  
 Si:H/SiN<sub>x</sub>:H amorphous semiconductor superlattices, charge transfer doping 4-92219  
 a-Si:H/SiO<sub>2</sub>/Pd diodes, H induced Schottky barrier modulation detect. by photoemission 4-70905  
 a-Si:H/a-Ge:H/a-Si<sub>1-x</sub>C<sub>x</sub>/a-SiN<sub>x</sub>:H superlattices, CVD growth and struct. 4-114416  
 a-Si:H/a-Si<sub>1-x</sub>N<sub>x</sub>:H quantum well struct., luminescence and current transport 4-114024  
 a-Si:H/a-SiN<sub>x</sub>/a-SiO<sub>2</sub> multilayer films, struct., elec. and optical props. 4-114025  
 a-Si:H-Si n<sup>+</sup>-p amorphous-cryst. heterojunctions, elec. characts. 4-84688  
 a-Si:H-a-SiN<sub>x</sub>:H heterojunction, lattice mismatch, electroabsorption study 4-76029  
 a-Si:H(D) thin films, coupled local mode vibrs., IR absorpt. study 4-88259  
 a-SiO<sub>2</sub>H CVD films, struct. model 4-88427  
 a-Si:P, ion implanted, phonon scatt. study 4-70325  
 Si(P/B), substrate orientation depend. of enhanced epitaxial regrowth 4-108737  
 Si:Sn, amorphous vacuum deposited films, impurity states 4-84595  
 Si/a-Si:H/B/metal junctions, current-volt. characts. 4-114033  
 Si/a-Si/metal tunnel rectifier 4-88586  
 a-Si/a-SiC<sub>x</sub>/a-SiN<sub>x</sub> superlattices, optical bandgap and elec. resist. 4-114026  
 Si/SiO<sub>2</sub> interface, amorphous Si/cryst. Si facet form. during solid phase epitaxy 4-88423  
 a-Si-based alloy p-i-n solar cells, performance enhancement rel. to B profiling 4-77087  
 a-Si-based alloy p-i-n solar cells, elec. field distrib. and open circuit volt. 4-89405  
 a-Si-based alloys, vibr. props. and local modes 4-70323  
 a-Si-based field effect transistors, flat-band volt. and surface states 4-92825  
 Si-based solar absorber converters, SiO<sub>2</sub>N<sub>2</sub> reactively sputtered films for antireflection coatings 4-99998  
 a-Si-based solar cells, high conversion efficiency 4-93619  
 a-Si-Ge-B alloys, props. and electronic device appls. (*Japanese*) 4-92728  
 SiC sputtered films, preparation-phys. struct. relations 4-88414  
 p-SiC:H, amorphous, prepared by photo-CVD, electronic and optical props. 4-70959  
 SiC:H amorphous film, C diffusion into Si:H 4-80289  
 SiC:H amorphous films, plasma deposition from SiH<sub>4</sub>+methane (ethylene) 4-114410  
 a-SiC:H glow-discharge film, electronic and optical props. 4-84623  
 a-SiC/c-Si p<sup>+</sup>n heterostructure, plasma CVD growth and elec. props. 4-80660  
 Si-C<sub>1-x</sub>H<sub>x</sub>, amorphous, CVD prep. XPS and optical studies 4-70600  
 a-Si-C<sub>1-x</sub>H<sub>x</sub>:H, low emittance coatings for high temperature solar collectors 4-114950  
 a-Si-C<sub>1-x</sub>H<sub>x</sub>:H, luminescence from photo-generated carriers, polarisation memory 4-99186  
 a-Si-C<sub>1-x</sub>H<sub>x</sub>:H GD thin film, plasmon behaviour studied by XPS, chem. shifts 4-65627  
 a-Si-C<sub>1-x</sub>H<sub>x</sub>:H/a-Si:(H) heterojunctions, photoemission studies 4-65731  
 Si<sub>1-x</sub>Ge<sub>x</sub>:H, amorphous, gap state distrib., photoconductivity study 4-108820  
 Si<sub>1-x</sub>Ge<sub>x</sub>:H, amorphous, occupied gap state obs. 4-70637  
 Si<sub>1-x</sub>Ge<sub>x</sub>:H amorphous films, planar magnetron sputtered, optical and elec. props. 4-98671  
 Si<sub>1-x</sub>Ge<sub>x</sub>:H amorphous planar magnetron sputtered films, elec. and optical props. (*Japanese*) 4-99312  
 Si<sub>1-x</sub>Ge<sub>x</sub>:H amorphous sputtered films, optical absorpt. 4-93090  
 (SiH<sub>2</sub>)<sub>x</sub> films, thermal dehydrogenation, IR spectra study 4-99781  
 a-SiH<sub>2</sub> solar cell, on Lambertian reflector substrate, optical absorpt. 4-81020  
 a-SiN:H RF sputtered films, internal stress rel. to local H bonding 4-88437  
 a-SiN<sub>2</sub>H layers, prep. by glow discharge decomp. of N<sub>2</sub>/SiH<sub>4</sub> mixtures, optical and photoelectronic props., effects of doping 4-114001  
 Si<sub>3</sub>N<sub>4</sub>:H, amorphous, CVD growth 4-60941  
 Ta<sub>2</sub>O<sub>5</sub>, amorphous, conductivity changes study during degradation in strong elec. field 4-108872  
 Ta<sub>2</sub>O<sub>5</sub> amorphous semicond., space charge limited transient injection currents 4-65686  
 TiO<sub>2</sub>-P<sub>2</sub>O<sub>5</sub>-M<sub>2</sub>O (M=alkali metal), vitreous semiconductors, EPR and optical studies (*Russian*) 4-98939  
 V<sub>2</sub>O<sub>5</sub>-As<sub>2</sub>O<sub>3</sub> glasses, semicond. props. 4-80593  
 V<sub>2</sub>O<sub>5</sub>-GeO<sub>2</sub>, sp. heat, thermal cond. and diffusivity coeff. 4-92384  
 V<sub>2</sub>O<sub>5</sub>-P<sub>2</sub>O<sub>5</sub>-ZnO thin film glasses, space charge limited conduction 4-84627  
 (V<sub>2</sub>O<sub>5</sub>)<sub>x</sub>(P<sub>2</sub>O<sub>5</sub>)<sub>100-x</sub> glasses, V mixed valence state, X-ray absorpt. near edge struct. determ. 4-65645  
 WO<sub>3</sub>-xH<sub>2</sub>O amorphous films, elec. cond. and thermopower 4-61378  
 ZnGeAs<sub>2</sub>-CdGeAs<sub>2</sub>, semiconducting alloys, melt quenched, phase stability, glass form., TEM obs. 4-71641

**amorphous state**

- see also electrical conductivity of amorphous metals and alloys; electrical conductivity of amorphous semiconductors and insulators; electron energy states of amorphous solids; magnetic properties of amorphous substances; vitreous state  
 alloys, amorphous, compaction process, stability, DSC obs. 4-114448  
 alloys, amorphous, plastic deform. and failure, in situ electron microscopy 4-93481  
 alloys, rapidly quenched, struct. and thermal props., review 4-109443  
 alloys, thermopower, electron-phonon enhancement 4-108839  
 atomic system, quenched condensation, computer simulation 4-75295  
 book on amorphous materials 4-110819  
 ceramics, N-based, conf., Falmer, England (Aug. 1981) 4-67873

**amorphous state continued**

- condensed matter physics, Iberian Symposium, Lisbon, Portugal (Sept. 1983) 4-78036  
 covalent solid, 3-dimensional model, internal energy 4-103654  
 crystallisation of amorphous alloys effect of irradiat. particle mass 4-79936  
 diagrammatic approach to hopping transport 4-88496  
 dielectrics, kinetic processes, multiphonon theory anal. 4-80186  
 diffraction data normalisation (*Chinese*) 4-75234  
 dirty conductor, quantum corrections to thermoelectromotive force 4-113916  
 disordered binary alloy, short-range order treatment 4-103655  
 disordered binary harmonic chain, renormalisation group decimation technique 4-88489  
 disordered fermion system, interaction driven metal-insulator transition 4-104127  
 disordered solids, linear sp. ht. at low temps. 4-75701  
 disordered superconductor, T<sub>c</sub>(p) theory 4-84732  
 electronic states, theoretical models 4-70638  
 energy gap and electronic density of states calcs. 4-88485  
 ice I, amorphous phase formed at 77K and 10 kbar 4-98016  
 ion beam bombardment, SASAMAL computer code using liquid model (*Japanese*) 4-109295  
 melt-spun ribbons, form. control, thermal transport, momentum transport 4-114441  
 metals, amorphous, atomic struct. model, computer simulation 4-103653  
 metals, amorphous, one-component, vacancy self-diffusion (*Russian*) 4-103990  
 metals, amorphous non-transition, superconductivity and phonon spectra (*Chinese*) 4-98793  
 metals, energy spectrum and density of states calcs. (*Russian*) 4-113854  
 mixed valence compounds, phonon-induced virtual states 4-70750  
 one-dimensional chaotic atomic configurations, amorphicity 4-98018  
 one-dimensional disordered binary alloys, cluster mean-field theory 4-92599  
 phthalene films, amorphous vacuum deposited, crystn. and optical props. 4-71565  
 physics of amorphous solids, book 4-90312  
 poly(ethylene oxide)-ammonium trifluoromethylsulphate, complex, amorphous and cryst., form., stoichiometry and cond. response 4-88303  
 poly(ethylene oxide)-NH<sub>4</sub>SCN complex, amorphous and cryst., form., stoichiometry and cond. response 4-88303  
 polymer, amorphous, local orientational order (*Russian*) 4-75328  
 ribbons, amorphous, under torsion, elastic and magnetoclastic effects 4-103854  
 Rutherford backscatt. enhancement, two-atom scatt. model anal. 4-66180  
 semiconductor detector, anomalous X-ray scattering, local structure of amorphous alloy 4-91174  
 solar cells, photogenerated current improvement by optical parameter optimisation 4-81558  
 spinodal decomp., internal stress effect due to coherency strain 4-113646  
 thin amorphous layer of metal, produced by laser radiation 4-80089  
 transient photocurrent curve scaling 4-104269  
 transition metal alloys, amorphous, Hall coeff., temp. depend. 4-92698  
 As, amorphous, optic vibr. modes, Raman, IR and inelastic neutron spectra 4-76461  
 As, amorphous and polycryst., Compton profile studies 4-99218  
 As amorphous film, UV photoemission study 4-88942  
 Au<sub>1-x</sub>Si<sub>x</sub> liq. and amorphous, elec. resist., Ziman theory anal. 4-70774  
 B, amorphous, CVD diagrams, nucleus density 4-71583  
 BaFe<sub>2</sub>O<sub>9</sub> glassy ferrites, effects of mag. quenching 4-61898  
 Ba<sub>2</sub>O<sub>3</sub>-(Li<sub>2</sub>O)<sub>0.7</sub>-(LiClO<sub>4</sub>)<sub>0.7</sub>, amorphous, fast ionic cond. meas. (*Chinese*) 4-103996  
 BaTiO<sub>3</sub> amorphous film, elec. and struct. props. 4-80701  
 BaTiO<sub>3</sub> thin films, crystallisation from amorphous phase, electron microscopy study 4-113830  
 Bi, amorphous, supercond., upper critical fields 4-76089  
 Bi-Pb alloys, amorphous, supercond., upper critical fields 4-76089  
 Bi<sub>1-x</sub>Kr<sub>x</sub> mixtures, metal-insulator transition, elec. cond., supercond. transition temp. meas., scaling theories 4-75860  
 Bi<sub>10</sub>Te<sub>10</sub>, amorphous film, quantum corrections to resistance above superconducting T<sub>c</sub> 4-84710  
 C, amorphous, structural modelling and Raman spectra calcs. 4-108281  
 C amorphous film growth by CVD, methane plasma diagnostics and modelling 4-104979  
 C, amorphous hard films, growth from hydrocarbon RF plasma 4-85117  
 C amorphous thin film, low energy electron attenuation length studies 4-84323  
 C film, spectral momentum density obs. using (e,2e) spectrometer 4-111257  
 C films, amorphous and graphitic, growth by ion bombardment in RF plasma 4-85116  
 C overlayers on Nb, resonant photoemission and photon-induced Auger spectra 4-93182  
 C:H amorphous film, H<sub>2</sub> gas reactive RF sputtering prep. on low temp. substrates 4-76673  
 a-C:H hard thin films, RF plasma deposition 4-76681  
 a-C/Si MIS structures, DC sputter deposited, HF resist. 4-88601  
 C-Si<sub>1-x</sub> film, elec. and optical props. 4-113962  
 Cd<sub>2</sub>P<sub>2</sub>(As<sub>2</sub>)<sub>3</sub>(Sb<sub>2</sub>), disordered, Mott transitions and impurity scattering (*Russian*) 4-88450  
 Ce<sub>0.8</sub>La<sub>0.2</sub>Cu<sub>2</sub>Si<sub>2</sub> disordered, low-temp. specific heat meas. 4-75702  
 Ce<sub>0.9</sub>Y<sub>0.1</sub>Cu<sub>2</sub>Si<sub>2</sub> disordered, low-temp. specific heat meas. 4-75702  
 Co-Nb amorphous film, ion mixing and mag. props. 4-104471  
 Co-P, amorphous, microstruct., TEM and small angle X-ray scatt. study 4-113332  
 Co-P amorphous electrodeposits, elastic props. and struct. relax. 4-92282  
 Co<sub>1-x</sub>B<sub>x</sub>, amorphous alloy, electrolytical and chemical prep., struct. 4-70603  
 Co<sub>100-x</sub>B<sub>x</sub>, metallic glass, mag. and mechanical props. 4-84841  
 Co<sub>80</sub>B<sub>20</sub>, amorphous, high press. and temp. phase stability (*Chinese*) 4-103923  
 Co<sub>55</sub>Ni<sub>14</sub>Fe<sub>5</sub>B<sub>10</sub>Si<sub>6</sub> foil, thermal expansion coeff. and isothermal compressibility (*Russian*) 4-65421  
 Co<sub>90</sub>P<sub>10</sub>, galvanomagnetic characts. temp. depend. 4-84635  
 Cr<sub>1-x</sub>Mn<sub>x</sub>Ge, amorphous thin films, elec. resist., Hall resist. 4-114049  
 Cu-Ni, disordered, positron spatial struct. effects 4-104170  
 Cu-Zr, amorphous, local struct., EXAFS study 4-88101  
 Cu<sub>60</sub>Ti<sub>40</sub>, amorphous, crystallisation, quenching method effects 4-84185  
 β-CuZn, disordered, vibr. spectra study (*Russian*) 4-65366  
 Cu<sub>60</sub>Zr<sub>40</sub> alloy system, amorphous, crystallisation kinetics 4-108279  
 ErF<sub>3</sub> amorphous thin films, AC cond. meas. 4-76059

**amorphous state continued**

- Fe amorphous alloys, structural relaxation (*Russian*) 4-104801  
 Fe-B, amorphous alloys, mag. anisotropy, plastic deform., annealing, Mossbauer obs. 4-65803  
 Fe-B, crystalline and amorphous, cryst. struct., NMR study (*Russian*) 4-79982  
 Fe-Ni amorphous alloys, flame spray quenching, coating on metal substrates 4-71797  
 Fe-Ni-Cr-W amorphous alloys, corrosion resist. 4-99632  
 Fe-P amorphous electrodeposits, elastic props. and struct. relax. 4-92282  
 Fe-Si (6.5 wt.%) rapidly quenched ribbons, mag. props. and preparation 4-84819  
 Fe-Si(B) amorphous film, ion mixing and mag. props. 4-104471  
 Fe-Ti-C surface on Ti implanted steel, corrosion resist. 4-76917  
 Fe-Zr amorphous films, corrosion props. in 1N H<sub>2</sub>SO<sub>4</sub> 4-76904  
 Fe<sub>80</sub>B<sub>20</sub>, amorphous alloy, He ion irradiation, blister and bubble form., TEM obs. 4-108434  
 Fe<sub>84</sub>B<sub>16</sub>, amorphous, microcrystalline domain obs. 4-113333  
 Fe<sub>86</sub>B<sub>14</sub>, amorphous, thermoelectric power and elec. cond. (*Russian*) 4-65660  
 Fe<sub>78</sub>B<sub>22</sub>Si<sub>10</sub>, amorphous, isothermal crystallisation and mag. props. (*Russian*) 4-65384  
 Fe<sub>80</sub>B<sub>20</sub>Si<sub>8</sub>Al<sub>2</sub>, crystallisation and mag. props. study 4-114137  
 Fe<sub>81</sub>B<sub>19</sub>Si<sub>4</sub>C<sub>2</sub>, amorphous, mag. anisotropy meas. (*Russian*) 4-65804  
 (FeCoNi)SiB nonmagnetostriuctive amorphous ribbons for magnetic cores, DC and AC magnetic charact. 4-92939  
 (FeCo)SiB nonmagnetostriuctive amorphous ribbons for magnetic cores, DC and AC magnetic charact. 4-92939  
 Fe<sub>70</sub>Co<sub>30</sub>Si<sub>13</sub>B<sub>10</sub>, amorphous, mag. noise study (*Russian*) 4-65846  
 Fe<sub>90</sub>Ni<sub>10</sub>B<sub>20</sub> foil, thermal expansion coeff. and isothermal compressibility (*Russian*) 4-65421  
 Fe<sub>80-x</sub>Ni<sub>x</sub>B<sub>20</sub>, amorphous, mag. props. study 4-84840  
 Fe<sub>40</sub>Ni<sub>60</sub>P<sub>14</sub>B<sub>6</sub>, proton irradiation, crystallisation study 4-88099  
 Fe<sub>1-x</sub>P<sub>x</sub>, struct. determ. (*Russian*) 4-65177  
 Fe<sub>78</sub>P<sub>22</sub>, amorphous alloys, EXAFS contributions and near neighbour components 4-61774  
 Fe<sub>90</sub>Zr<sub>10</sub>, amorphous alloy, struct. and mech. props. rel. to heat treatment 4-75305  
 Ga thin films, optical props., elec. meas. 4-88800  
 Gd-Co amorphous films, spontaneous Hall effect in vicinity of the compensation composition 4-75929  
 Gd-Fe-Co amorphous film, struct. and mag. props. 4-80434  
 Gd-Fe-Ni amorphous film, struct. and mag. props. 4-80434  
 Gd-Ni-Co amorphous film, struct. and mag. props. 4-80434  
 GdTbFe amorphous sputtered films, mag. props. 4-65843  
 GeO<sub>2</sub> films, amorphous, elec. characterisation in MIS and MIM structs. 4-70816  
 Hf-Mo, amorphous, upper critical fields 4-98829  
 (In<sub>1-x</sub>Te<sub>x</sub>)<sub>1-x</sub>Sn<sub>1-x</sub>, obtained by splat cooling, Mossbauer study 4-109101  
 LiNbO<sub>3</sub> amorphous films, dielec. and elec. props. 4-104531  
 Li<sub>2</sub>WO<sub>3</sub> amorphous film, electrochromism colouring/bleaching processes, Li<sup>+</sup> ion transport 4-114244  
 Mo-Ge ultrathin supercond. films, localisation and interaction effects 4-65766  
 Mo-Ni, amorphous, contacts to Si, elec. charact. study 4-80653  
 MoGe<sub>1-x</sub>(Si<sub>1-x</sub>)<sub>2</sub> amorphous sputtered films, supercond. transition temp. (*Chinese*) 4-98794  
 MoS<sub>3</sub>, amorphous, local and intermediate range struct., X-ray diffr. meas. and computer calc. 4-70034  
 Na<sub>2</sub>WO<sub>3</sub> bronzes, rapidly quenched, DTA and X-ray diffr. study 4-93277  
 Nb<sub>2</sub>O<sub>5</sub> amorphous film, elec. behaviour study (*Russian*) 4-84722  
 Nb<sub>2</sub>O<sub>5</sub>, XPS and optical spectra, low-valence cations and electron props. 4-98623  
 Ni-based amorphous alloys, crystallisation processes, microstruct. anal. 4-84183  
 Ni-P, amorphous, microstruct., TEM and small angle X-ray scatt. study 4-113332  
 Ni-P amorphous, hexagonal metastable phase formed during crystallisation (*Chinese*) 4-103698  
 Ni-P amorphous alloys, crystn. phases, electron diffr. study (*Chinese*) 4-113331  
 Ni-P amorphous electrodeposits, IR reflectivity spectra 4-93078  
 NiFe-G amorphous and cryst. films, planar Hall effect and magnetisation reversal 4-75930  
 Ni<sub>36</sub>Fe<sub>32</sub>Cr<sub>14</sub>P<sub>12</sub>B<sub>6</sub>, metallic glass, surface oxidation comparison with crystalline state 4-89187  
 Ni<sub>80-x</sub>Fe<sub>x</sub>P<sub>20</sub>, amorphous film, composition study 4-76633  
 Ni<sub>80-x</sub>Fe<sub>x</sub>P<sub>20</sub>, amorphous, surface characterisation study 4-76634  
 NiNb metallic glass contacts on GaAs, TEM obs. 4-104094  
 Ni<sub>80</sub>P<sub>20</sub>, amorphous powder, warm pressing consolidation kinetics 4-81168  
 Ni<sub>32</sub>Zr<sub>65</sub>, proton irradiation, crystallisation study 4-88099  
 PZT, amorphous, ferroelec. phase transition 4-61637  
 PZT microparticle materials, amorphous state ferroelectricity 4-104542  
 Pb-acid batteries, positive plates cryst. and amorphous components, quantitative phase anal., elec. vehicle appl. 4-77068  
 PbF<sub>2</sub>-ZnF<sub>2</sub> system, amorphous phase form. by roller splat cooling 4-85122  
 PbTiO<sub>3</sub>, amorphous, Raman spectra, low wave-number response 4-104590  
 PbTiO<sub>3</sub> amorphous films, dielec. and elec. props. 4-104531  
 Pd<sub>1-x</sub>Si<sub>x</sub>, struct. determ. (*Russian*) 4-65177  
 Sb, amorphous film, vacuum deposited, isochronous annealing, crystallisation 4-61854  
 Sb amorphous film, UV photoemission study 4-88942  
 Sb amorphous films, obliquely vacuum deposited, growth and crystn. 4-98491  
 Se<sub>1-x</sub>Te<sub>x</sub> alloys, amorphous, elastic const., role of Te 4-84333  
 Si, explosive crystallisation 4-98019  
 Si<sub>1-x</sub>N<sub>x</sub>H amorphous film, photoinduced ESR study 4-114161  
 Si<sub>3</sub>N<sub>4</sub>, amorphous, controlled crystn. by Ti and Cl additions 4-113334  
 Si<sub>3</sub>N<sub>4</sub> amorphous films, impurities, IR investig. 4-80913  
 Si<sub>3</sub>N<sub>4</sub> films, hydrogenated and deuterated, prepared from plasma-enhanced CVD, IR absorpt. spectra 4-81021  
 SiO, amorphous, optical study of defects 4-88862  
 SiO, amorphous thin films, optical absorpt. edge 4-81023  
 SiO<sub>2</sub>, amorphous, photoinduced paramag. defects 4-92959  
 SiO<sub>2</sub>, amorphous, polymorphism, optical study 4-88103  
 SiO<sub>2</sub>, amorphous defects, ab initio MO calc. and Raman spectrum 4-96443

**amorphous state continued**

- SiO<sub>2</sub> amorphous matrix for Au particles, grain growth and twin formation 4-113340  
 SiO<sub>2</sub> amorphous rods, laser-induced deposition, optical studies 4-66235  
 SiO<sub>2</sub>H<sup>+</sup>, amorphous, O<sub>2</sub> vacancy annealing 4-103743  
 SiSnH, amorphous sputtered layer, structural props. 4-108739  
 Si<sub>1-x</sub>Sn<sub>x</sub>, (0≤x≤0.3), amorphous RF sputtered film, struct. and elec. props. 4-70956  
 Si<sub>1-x</sub>Sn<sub>x</sub>H, (0≤x≤0.3), amorphous RF sputtered film, struct. and elec. props. 4-70956  
 Sn-H system, superconductivity, <sup>119</sup>Sn Mossbauer effect study 4-92840  
 Sn<sub>1-x</sub>Cu<sub>x</sub> amorphous films, quench-condensed, low temp. sp. ht. 4-70403  
 (Sn<sub>1-x</sub>Cu<sub>x</sub>)<sub>1-x</sub>H<sub>x</sub>, superconductivity and cond. studies 4-92840  
 T<sub>2</sub>C film, superconducting T<sub>c</sub> and critical fields 4-104353  
 TaO<sub>2</sub>, amorphous film, electret state relax. 4-88765  
 Ta<sub>2</sub>O<sub>5</sub>, XPS and optical spectra, low-valence cations and electron props. 4-98623  
 TaSi<sub>2</sub> amorphous films, sputtering and electron gun co-deposition form. 4-108750  
 Ti-Au, amorphisation, pulsed ion beam annealing study 4-103831  
 Ti-Ni amorphous alloys, thermal stability, short-range order effects 4-88096  
 Ti-Pd(Mo), amorphous, upper critical fields 4-98829  
 Ti<sub>1-x</sub>Cu<sub>x</sub> alloys, electrochemical and thermal oxidation and electrochemical O<sub>2</sub> evolution 4-93452  
 TiO<sub>2</sub>-SiO<sub>2</sub>, RF sputtered amorphous films, density, refractive index, thermal expansion, X-ray spectra 4-61263  
 Ti<sub>80</sub>Si<sub>20</sub>, amorphous, crystallisation study (*Chinese*) 4-103922  
 WO<sub>3</sub> amorphous films, colour centres, EPR study 4-84291  
 Y<sub>3</sub>Ga<sub>2</sub>O<sub>12</sub>:Nd thin film waveguide, RF sputtering growth, fluoresc. spectrum, optical amplifier appl. 4-60146  
 Y<sub>3-x</sub>Gd<sub>x</sub>Fe<sub>2</sub>O<sub>12</sub> noncrystalline garnet films, electron transport and thermopower 4-108958  
 Zn<sub>3</sub>P<sub>2</sub>(As<sub>2</sub>)(Sb<sub>2</sub>), disordered, Mott transitions and impurity scattering (*Russian*) 4-88450  
 Zr-based amorphous alloys, supercond., two-level systems, sp. ht. meas. 4-108973  
 Zr-Cu, amorphous, sputtered, low-energy excitations, thermal cond., sp. ht. meas. 4-70987  
 Zr-Mo(Pd)(Rh), amorphous, upper critical fields 4-98829  
 Zr-Ni cryst. and amorphous alloys, electronic, lattice and sp. ht. props. 4-75700  
 Zr-Ni cryst. and amorphous alloys, enthalpies of form. and crystallisation 4-88097  
 Zr-Pd(Ni), amorphous, electronic density of states and superconducting props. 4-70738  
 Zr-Si, amorphous, upper critical field meas. 4-84754  
 Zr<sub>70</sub>Cu<sub>30</sub>, thermal cond., phonon-electron contrib., heat treatment effects 4-70988  
 Zr<sub>76</sub>Ni<sub>24</sub>, amorphous, low-energy excitations, thermal cond., sp. ht. meas. 4-70987  
 ZrO<sub>2</sub>, amorphous coatings, prep. from metal-organic solns. 4-76696  
 ZrO<sub>2</sub>, short-range struct., radial distrib. curve of atomic density 4-75801  
 ZrO<sub>2</sub>SiO<sub>2</sub> thin amorphous film prep. by electron-beam evaporation from multiple sources 4-74674
- amorphous state structure** see *noncrystalline state structure*
- amplification**  
 see also *acoustic wave amplification; amplifiers*  
 NRAO 300-foot telescope, gain curve from 5 GHz obs. 4-94981
- amplification measurement** see *gain measurement*
- amplifiers**  
 see also *amplification; audio-frequency amplifiers; d.c. amplifiers; fluidic amplifiers; microwave amplifiers; operational amplifiers; preamplifiers; pulse amplifiers; radiofrequency amplifiers; ring lasers; wide-band amplifiers*  
 electromyographic equipment provision for polyclinics 4-72448  
 feedback amplifier, phase transitions 4-90546  
 MM waves and IR, conf., Miami Beach, FL, USA (Dec. 1983) 4-73154  
 optical fibre communications receiver, circuit noise, theoretical anal. and computer calculation (*Chinese*) 4-79290  
 unguided wave Cherenkov amplifier 4-102913
- amplifying** see *amplification*
- amplitude modulation**  
 fibre optic gyroscope, phase-reading, using optical phase and amplitude modulation 4-97088  
 laser beam, CW Gaussian, harmonic-like and efficient AM by mech. chopper 4-69461  
 liquids, refr. indices determ. at submm. wavelengths, phase and amplitude modulation techniques 4-111186  
 projected interference fringes applied to nonoptical surface microscopic topography, pulsed illumination 4-111099  
 quasi-harmonic capillary-gravity waves, modulational instability, mag. field effect 4-91845  
 unimode fibre light guide, sound excitation and additional losses occurrence, when transmitting AM optical waves 4-69582
- analogue computer applications** see *analogue simulation*
- analogue computer methods** see *analogue simulation*
- analogue-digital conversion**  
 see also *digital-analogue conversion*  
 10-bit, nuclear spectrometry appl. 4-68909  
 AC potential drop system for steel crack length monitoring 4-114741  
 amplitude-digital convertor with impulsing cct., for scintillation detector 4-90571  
 binary Fourier transform holograms, quantisation and phase encoding errors reduction 4-107557  
 biological image processing, shading compensation, A/D convertor appl. (*Japanese*) 4-85595  
 continuous flow anal. system, microcomputer-controlled, matching colorimeter output to A/D convertor 4-97717  
 dead-time correction method, short-lived radioisotopes, gamma-ray spectrometry 4-102543  
 digital audio technology, fundamentals and methods (*German*) 4-112641  
 dispersive models for A-to-D and D-to-A conversion systems 4-79378  
 double-integrating DVM, A/D convertor interf. suppression and error considerations (*Bulgarian*) 4-86398  
 FASTBUS, ADC for pulse height data from EM calorimeter 4-59604  
 fibre and integrated optical devices for signal processing 4-64794  
 high-speed logarithmic ADC for Yale PDS 2020G microdensitometer 4-110538

**analogue-digital conversion continued**

- image vector quantization with perceptually-based cell classifier 4-102900  
 integrating IR detector, interface to A/D converter, readout electronics 4-90653  
 interface for D3-28 microcomputer 4-106288  
 interfacing 15VSM5 minicomputer and Elektronika D3-28 to expt. equipment, using TTL ICs 4-90569  
 linear colour-temp./freq. converter, design principles (*Russian*) 4-101847  
 logarithmic charge-digital converters for operation with proportional chambers 4-68910  
 medical image diagnostic processing and analysis 4-115199  
 multichannel A/D interface for ion beam phase volume meas., using Elektronika-1001 computer 4-91130  
 NODAPEC, online system for low temp. nuclear orientation expts. 4-102563  
 porous media, impregnated, serial sectioning and digitisation for two- and three-dimens. analysis 4-114744  
 radionuclide image quality, digitisation influence 4-115198  
 rare event recorder interface 4-91185  
 ratio-to-digital converter, linear discharge functions in memory condensers 4-102540  
 read-out system on 6-bit fast ADC for MWPC and drift chambers 4-91165  
 seismic data, digital processing of analogue high-freq. data 4-77673  
 speech digitization, real-time, evaluation methodology 4-79399  
 trigger rejection for scattering expts., fast readout ADC system 4-102562  
 video-bandwidth ADC using optical techniques for extended precision 4-69594  
 waveform display instrumentation, operation and sampling aspects (*German*) 4-82788  
 Wordfit, digital audio signal processing system, for automatic time alignment of post-synchronised dialogue 4-69628

**analogue simulation**

- cone retina, vertebrate, electronic simulation of cones, horizontal cells and bipolar cells 4-105231  
 cone retina, vertebrate, influence of amacrine cells on receptive field organisation of ganglion cells 4-105233  
 ganglion cells of generalised vertebrate cone retina, electronic simulation 4-105232  
 internal inverse heat conductivity problem, soln. using analogue computers (*Russian*) 4-82766  
 voltage clamp expts., simulation with FET analogue circuits 4-85591

**analysing power** see polarisation in nuclear reactions and scattering

**analytical chemistry** see chemical analysis

**anaphoresis** see electrophoresis

**Anderson model**

- asymmetric degenerate impurity model, spectral density, mag. susceptibility 4-104113  
 asymmetric single orbital Anderson model, localized magnetic moments, full rotational invariance 4-98856  
 charge exchange in HF approx. of time depend. Anderson model 4-107448  
 compounds with intermediate valency, polaron density waves (*Russian*) 4-84576  
 conductivity and dielectric constant, universal relations at Anderson transition 4-75857  
 degenerate, with strong correl., mag. susceptibility 4-92659  
 degenerate comparison of 1/N expansion and Bethe ansatz results 4-92587  
 dielectric constant near the Anderson transition 4-92992  
 dirty supercond. in weakly localised regime, transition temp., upper crit. field 4-108964  
 disordered systems, diagrammatic two-particle locator theory, Anderson Hamiltonian 4-70765  
 disordered systems, diagrammatic two-particle locator theory, Anderson transition and role of hopping processes 4-70766  
 disordered systems, field depend. charge carrier trapping process 4-104226  
 electron gas, Anderson localisation and elec. cond., self-consistent mode-coupling theory 4-61336  
 electron gas, cond. near mobility edge 4-98616  
 ethene, adsorbed on transition and noble metals, electronic struct. and conform. 4-92784  
 Fermi liquid descriptions of periodic Anderson Hamiltonian 4-75827  
 Friedel-Anderson model, dynamics and development 4-95128  
 Hamiltonian with cryst. field splitting and spin-orbit interactions, ground state props. 4-108821  
 heavy fermion superconductivity, renormalised perturbation theory anal. 4-104354  
 Kondo effect and magnetoresist. in weakly localised regime 4-108837  
 lattice in Kondo regime, one particle excitation spectrum 4-61270  
 localisation, rigorous approach 4-61267  
 localisation on basis of projection operator formalism, systematic treatment 4-70611  
 magnetocapacitance origin in Anderson-localised regime 4-61285  
 mathematical theory of Anderson localisation 4-75828  
 metal-insulator transition, renormalisation group theory (*Japanese*) 4-104128  
 N-fold degenerate magnetic impurity model, Bethe ansatz and 1/N expansion 4-80760  
 one-dimensional, Lyapunov exponent, weak disorder expansions 4-104111  
 perturbative approach and convergence 4-70618  
 positive ion-surface scatt., negative ion form., Anderson correl. energy 4-66577  
 random systems, electron localisation and diffusion 4-98572  
 rare earth mag. alloys, thermodynamics of degenerate Anderson model 4-71009  
 Schrodinger operator, random, absence of diffusion 4-67991  
 semiconductor, doped, uncompensated, thermodynamic props. 4-92391  
 semiconductors, deep levels, expt. and theoretical studies, review 4-84593  
 SU(N) Anderson impurity model, thermodynamic Bethe-ansatz eqns. 4-104110  
 symmetric Anderson lattice, ground states calcs. 4-70614  
 two- and three-dimensional, density of states, diagonal and off-diagonal disorder effects 4-113846  
 AgCl(Br)(I), anharmonic props., interionic pot. model 4-98056  
 Cd<sub>1-x</sub>Mn<sub>x</sub>Se, semimagnetic semiconductor with metallic conduction, anomalous magnetocapacitance 4-65692

**Anderson model continued**

- Ce ion in cubic environment, ground state, effects of cryst. fields 4-104403  
 Cr<sub>1.45</sub>Nb<sub>2.5</sub>Se<sub>10</sub>, cryst. struct., metal-insulator transition, resist., mag. susceptibility meas. 4-88448  
 Cs<sub>3</sub>Ti<sub>2</sub>Cl<sub>9</sub>, exchange interaction in orbitally degenerate binuclear units 4-71054  
 CuCl(Br)(I), anharmonic props., interionic pot. model 4-98056  
 Fe<sub>1+x</sub>Nb<sub>3-x</sub>Se<sub>10</sub>, cryst. struct., metal-insulator transition, resist., mag. susceptibility meas. 4-88448  
 In, liquid, mag. props. of transition metal solutes 4-76109  
 Na<sub>3</sub>Ta<sub>2</sub>W<sub>1-x</sub>O<sub>3</sub>, metal-nonmetal transition 4-70884  
 Sb, liquid, mag. props. of transition metal solutes 4-76109  
 Sn, liquid, mag. props. of transition metal solutes 4-76109  
 IT-TaS<sub>2</sub>(S<sub>1-x</sub>Se<sub>x</sub>)<sub>3</sub>, paramagnetic susceptibility in Anderson localised states 4-65786  
 Ta<sub>0.93</sub>Ti<sub>0.07</sub>S<sub>2</sub> 1T polytype, sp. ht. in Anderson localised states 4-75703  
 Te, liquid, mag. props. of transition metal solutes 4-76109  
 TiCl(Br)(I), anharmonic props., interionic pot. model 4-98056  
 WV<sub>2</sub>O<sub>6</sub>, exchange interaction in orbitally degenerate binuclear units 4-71054

**Anderson transition** see Anderson model; metal-insulator transition

**anechoic chambers**

- absorber-lined chamber, correlation of theoretical and measured site attenuation 4-69645  
 EMC meas., degraded absorber performance effect 4-69646  
 magnification factor for mode stirred chambers 4-69647  
 mean free path and acoustic power of sound source meas. in reverberation and anechoic chambers (*French*) 4-107962  
 microwave, optimal designs 4-69650  
 open field site, chamber factor for correlation 4-69644

**anelastic relaxation**

- see also Bordoni effect; creep; elastic aftereffect; internal friction; Snoek effect; stress relaxation; Zener relaxation  
 acrylonitrile-butadiene copolymers, a relax. kinetics near glass transition temp. 4-81231  
 adipic acid-hexanediols copolymers, mechanical relax. 4-80157  
 butadiene elastomers, relax. process assoc. with supermol. struct., creep meas. (*Russian*) 4-85175  
 butadiene-(methyl)styrene elastomers, relax. process assoc. with supermol. struct., creep meas. (*Russian*) 4-85175  
 butadiene-styrene block copolymer films, mech. and opt. props., temp. depend., superlattice fusion (*Russian*) 4-76547  
 cooperative model of relaxation behaviour, appl. to elastic and viscoelastic materials 4-65340  
 ethylene-propylene elastomers, relax. process assoc. with supermol. struct., creep meas. (*Russian*) 4-85175  
 Gorsky relaxation of light interstitials, linear response anal. 4-75613  
 nylon 66 and 6, mech. relax., elastic moduli, chain orientation, birefringence, wide angle X-ray obs. 4-93323  
 poly(2,6-dimethyl 1,4-phenylene oxide)-atactic polystyrene blends, orientation and relax. 4-79955  
 poly(pentamethylene pimelate), synthesis and characterisation by dilatometry and X ray diff. 4-79956  
 polyesters, aliphatic, dielec. relax. is oriented specimens 4-80158  
 polyethylene, linear,  $\gamma$ -irrad., NMR and mech. relax. In  $\gamma$ -loss band 4-80832  
 polyethylene, linear,  $\gamma$ -loss band, NMR and mech. relaxations after HNO<sub>3</sub> treatment 4-60986  
 polyethylene, thermally stimulated creep 4-84339  
 polyethylene-polypropylene copolymers and blends, thermally stimulated creep 4-84339  
 polypropylene, isotactic,  $\alpha$  and  $\beta$  relax. kinetics 4-81255  
 polypropylene, physical ageing by freezing-in of nonequilib. values of limiting compliances 4-81254  
 polypropylene, thermally stimulated creep 4-84339  
 steel, constructional, carburised case relax. props. influence on antigalling resist. 4-114684  
 steel 40 Kh, damping capacity and residual life, preliminary cyclic loading influence 4-99544  
 Al-Cu-Mg, RR-58, anelastic creep at 180°C 4-99472  
 Cu-Al-Zn alloy,  $\beta$ -phase, damping capacity rel. to mech. props. and martensite morphology 4-99414  
 Fe amorphous alloys, structural relaxation (*Russian*) 4-104801  
 $\alpha$ -PdH<sub>0.5</sub>, Gorsky effect and diffusion coeffs. 4-75614

**anelasticity**

see also anelastic relaxation

- block copolymers of styrene and vinyltrimethyl silane, optical and mech. props. (*Russian*) 4-81227  
 dynamic material response to shock wave propagation 4-108531  
 fibre reinforced composites, inelasticity, effect on strength in static loading 4-71678  
 graphite fibre enforced epoxy composites, thermomech. props., glass transition 4-92364  
 metals, anelastic interaction between moving kink and point defect pairs (*Chinese*) 4-103785  
 poly  $\alpha$ -olefins, spherulitic, dynamic tensile deform., X-ray diff. obs. 4-85173  
 $\alpha$ -quartz, natural, twinning dynamics, internal friction study 4-103766  
 rocks, porous, fluid saturated, viscoelastic model of anelasticity 4-72574  
 AlCuZr, AlCu eutectic, fine grained superplastic alloys, anelastic strains, grain boundary cavity distrib., sintering 4-66359  
 Cu<sub>60</sub>Zr<sub>40</sub> metallic glass, elastic props. and thermal expansion 4-84335  
 L<sub>80</sub>Al<sub>20</sub> metallic glass, elastic props. and thermal expansion 4-84335  
 Pd<sub>75</sub>Cu<sub>25</sub>Si<sub>16.5</sub> metallic glass, elastic props. and thermal expansion 4-84335  
 Sn-Bi elastic behaviour near melting point from sound vel. and attenuation meas. 4-75597  
 ZnAl eutectoid, fine grained superplastic alloys, anelastic strains, grain boundary cavity distrib., sintering 4-66359  
 ZnAl eutectoid, fine grained superplastic alloys, anelastic strains, grain boundary cavity distrib., sintering 4-66359

**anemometers**

see also laser velocimeters

- calibration of a three-element hot-wire anemometer 4-69842  
 detection bridge cct. appl., constant temp., frequency response optimisation 4-63735  
 differential laser Doppler anemometer with semiconductor laser (*Russian*) 4-69476  
 digital recording system for wind vel. meas. 4-86165

**anemometers continued**

- fibres optic laser Doppler anemometry device for gas/liquid flow and solid surface velocity meas. 4-108152
- heat transfer from heated wire at high subsonic gas velocities 4-83897
- hot-wire, boundary layer turbulent wake on rough surface meas. 4-87724
- laser anemometer gas streak vel. meas. electro-optical converter and photoelectric controller appl. (*Russian*) 4-60564
- laser Doppler, vel. meas. in free-jet, mixing process 4-87771
- laser Doppler anemometry, burst mode, flow related data processing (*German*) 4-103375
- laser Doppler anemometry, Mie scattering functions for milk fat globules 4-79682
- laser Doppler anemometry, signal processing requirements (*German*) 4-78294
- laser Doppler anemometry signal processing, using processor operated correlator 4-78299
- laser Doppler velocity meter signal processing using automatically controlled filter (*Russian*) 4-106277
- monolithic integrated ZnO on Si pyroelectric anemometer 4-69846
- Newtonian fluid steady laminar flows between ball and spherical cavity, expt. anal. using laser Doppler anemometry 4-97470
- particle transverse vel. meas. using laser Doppler-anemometers 4-97724
- pulsed-probe anemometer for meas. of vel. and flow direction in slowly moving air 4-100337
- supersonic laminar flow past flat plate, boundary layer separation 4-97603
- thermal, appls. (book contrib.) 4-79686
- thermistor, appl. to fluid vel. meas. in convection flows 4-97729
- two-phase turbulent round jet, laser Doppler anemometer meas. 4-97627
- ultrasonic anemometer, microprocessor-based 4-105778
- vortex shedding from circular cylinder with step 4-112892
- wind speed measurement (*French*) 4-75102

**angiography see radiography****angle measurement see angular measurement****angular correlation techniques**

- differential perturbed ang. correl. method for mag. moments meas. 4-64047
- muon scattering by nuclei meas., angular resolution determ. 4-87010
- ( $^{16}\text{O}$ , X), 2.1 GeV/A, in emulsion, evidence of dynamical correlation 4-96052

**angular measurement****see also angular velocity measurement**

- angle-to-code measurement transducers, high-precision, testing 4-90577
- gyroscopic sensor for motion parameters of pan-head meas. (*Russian*) 4-90678
- interferometers for laser scanners 4-82821
- ion-beam cross-section tilt angle monitoring 4-92223
- knee movement determ. for external orthotic linkage design 4-100228
- mirrors of X-ray satellite ROSAT, manufacture and testing, cone angle 4-115686
- moire method for small angles and ang. rots. 4-63780
- optical angle-measuring instrument having a quasi-ideal coordinate system 4-78295
- optical band extremely weak signals, tracking accuracy of moving targets 4-64760
- optical method of ang. displacement meas. when axis of rot. inclines 4-78356
- optical method of angular displacement meas. when axis of rot. inclines 4-68207
- optical-fibre end-cleave angle measurement device, simplification 4-83706
- orientation of small plane surfaces, high precision laser method 4-111098
- quartz doubly rotated crystals, angle of cut meas. using automated X-ray orientation system 4-58814
- rotating angle meter (*Japanese*) 4-111103
- telescope lens distortion effect reduction on ang. meas. error 4-79265
- theodolite readings, processing using HP-41 calculator (*French*) 4-90572
- windowing system for rotating equipment tests 4-86392

**angular momentum**

- asteroids, angular momentum drain by impact ejecta 4-82437
- binary protostars, ang. momentum transfer by gravit. torques rel. to evolution 4-110598
- contact and near-contact binary stars, location in total mass-total ang. momentum plane 4-110684
- galaxies and galaxy clusters, ang. momentum-mass relation rel. to origin of rot. 4-67804
- multivectors, use in physics 4-91384
- solar system, distrib. of ang. momentum vectors of comets, asteroids and meteor streams 4-101204

**angular momentum theory****see also quantum theory; Regge poles and trajectories**

- half orbital angular momentum and Lorentz invariance in an anisotropic space 4-68449
- nuclear multifragmentation, angular momentum partition' function 4-59218

**angular velocity measurement**

- instrument for calibration of measured velocities of angular acceleration (*Russian*) 4-63703
- motion-analysis photography, high-speed video with pulsed Cu lasers 4-112494
- retardation effect, fast moving sound source motion parameter estimation 4-103160
- tachometer calibration and checking equipment modernisation 4-58842

**anharmonic oscillators see harmonic oscillators****animal communication see biocommunications****anisotropy, magnetic see magnetic anisotropy****anisotropy, magnetocrystalline see magnetic anisotropy****annealing**

- see also graphitising; laser beam annealing; magnetic annealing; recrystallisation annealing; solution annealing; stress relaxation**
- alloys, amorphous, stress relief annealing, mag. props. 4-104797
- amorphous ribbons, power loss, annealing and surface roughness effects 4-76159
- anthracene crystals, reduction of grown-in dislocation density due to heat treatment and growth conditions 4-113450
- apatite, fission track annealing anisotropy using track-in-track length meas. 4-100485
- benzoic acid monolayers adsorbed on Al oxide inelastic electron tunnelling spectra studies 4-75782
- $\alpha$ -brass, anneal-hardening, change in mechs. props. 4-99397

**annealing continued**

- brass, Cu-Zn-Pb, precipitation and coarsening of Pb particles 4-109413
- cellulose acetate, water sorption and pore vol. 4-97067
- copolymers, thermotropic liq. cryst., X-ray diffr., studies 4-113302
- CR-39 plastic track detector,  $\alpha$ -track registration props., pre-irradiation annealing effect 4-59589
- CR-39 track detector, heavy ion latent damage trail annealing 4-96383
- creep voids, mechanism of sintering out during subsequent annealing 4-92213
- crystalline materials, characteristic deformation temperatures 4-70258
- cyclohexane, quenched plastic cryst. glass, Raman vibr. spectra studies 4-114280
- diffusion expts. using radioactive isotope method; mathematical anal. (*Russian*) 4-92431
- dimyristoyl phosphatidylcholine-water system, phase transitions, high press. study 4-113624
- FCC alloys, Suzuki segregation, TEM study 4-89054
- FCC crystals, annealing texture development by multiple twinning 4-98113
- fluorapatite, natural, high temperature fission track annealing, track dating 4-100486
- formic acid monolayers adsorbed on Al oxide inelastic electron tunnelling spectra studies 4-75782
- Frenkel defects, high concentrations, explosive annealing 4-108356
- garnet films, struct. props. 4-80805
- glass fibre filled polypropylene, injection molded bars, residual stress distrib., distortion, annealing temp. gradient 4-81256
- graphite, ion damaged, annealed, 2-D ordering, Raman study 4-70535
- II-VI compounds, irradiation-produced dislocation loops, HVEM study 4-75529
- Invar, atomic short range order, neutron scatt. study 4-113337
- ion implantation, dose control, annealing and gettering 4-84309
- Ising model, next-nearest neighbour, soliton pinning and annealing 4-82764
- liquid crystalline polymer, thermotropic, thin films, transform. of banded struct. on annealing 4-92357
- Makrofol Polycarbonate plastic track detector, calibration using heavy ions 4-64307
- metal, damaged, microprobe healing kinetics under isothermal heating conditions (*Russian*) 4-92196
- metals, deformed, shear bands 4-85191
- metals, mechanical instability of cellular dislocation structure 4-65268
- mica, muscovite, ion implanted, defect struct. thermal annealing 4-70177
- minerals, nuclear track formation models, etching and annealing, review 4-70235
- Muscovite mica track detector, heavy ion latent damage trail annealing 4-96383
- nuclear fuel particles, TRISO-coated, fission product release during post-irrad. annealing 4-111606
- optoelectronic materials fabrication using MBE and ion implantation 4-109325
- Permalloy, mag. domain struct., complex permeability meas. 4-76164
- Perminvar, mag. domain struct., complex permeability meas. 4-76164
- PET filaments, orientational stretching, intermolecular interaction energy (*Russian*) 4-109460
- PET film, amorphous, extrusion drawn, irreversible spontaneous elongation 4-109440
- PET films, uniaxially drawn, crystallisation kinetics, DSC obs. 4-92103
- PMMA, stress-orientation-strain relationships, glassy deform. model 4-76812
- poly(*p*-phenylene sulfide), oriented, acceptor doping, struct. changes on annealing 4-75325
- poly L-lactic acid, isothermal melting behaviour, hot stage microscopy, heat of fusion rel. to annealing time 4-65377
- poly *p*-phenylene terephthalamide films, extruded and drawn, tensile strength, void struct. rel. to heat treatment 4-81257
- poly *p*-xylylene, high temp. phase transform. and struct., EM obs. 4-66330
- poly-1,4-dimethylene-trans-cyclohexyl suberate, crack propag., morphology effects 4-114661
- trans-polyacetylene films, thermally isomerised and doped/dedoped 4-65196
- polyethylene, high-density, moulded sheets tear strength 4-104846
- polyethylene, low density, blow extended annealed films, relax. characts. (*Russian*) 4-109446
- polyethylene films, melt-drawn, microstruct., TEM and X-ray diffr. study 4-92102
- polyethylene single crystals, annealing, real time small angle X-ray scatt. 4-60859
- polyimide surface, chem. bonding characts., annealing and desorption effects 4-88933
- polyolefins, semicrystalline,  $^1\text{H}$  NMR spectra, spin-lattice relax. rel. to morphology 4-65877
- polyoxymethylene, cryst. modulus estimation using ultradrawn' tapes 4-76793
- polypropylene, isotactic, cold drawn, annealing, superstructure, SAXS obs. 4-61955
- polypropylene, mech. deform., Fourier transform IR obs. 4-66363
- polystyrene, injection molded bars, residual stress distrib., distortion, annealing temp. gradient 4-81256
- polystyrene film, atactic, liq-liq. transition, birefringence, temp. depend. 4-114241
- polyurethane elastomer, MDI/diol-based, hard-segment polymorphism 4-65195
- pulsed irradiation, theory of depleted zone annealing 4-108417
- pure, cold worked, annealing characts rel. to trace element additions 4-109438
- quartz, diffusional crack healing in aqueous environment 4-94098
- quartz, neutron irrad., point defects, EPR and optical absorpt. study 4-103742
- radiation defect clusters, annealing of divacancies 4-108351
- RF sputter-deposited Schottky barrier diodes 4-98691
- ribbons, amorphous, under torsion, elastic and magnetoelastic effects 4-103854
- scanning electron beam annealing of implanted semiconductors appl., using REM-200 electron microscope 4-93319
- Schottky metal-semiconductor contact, annealing (*Russian*) 4-98688
- semiconductors, by pulsed microwaves, power distribution effects (*French*) 4-61781
- n-Si, radiation defect formation, annealing, defect interactions 4-113499
- silicates, high energy U ion tracks, struct. and annealing 4-70236

annealing continued

simulated nuclear waste glass, Cm doped, radiation damage, annealing, short term leach test 4-83149  
 single mode optical fibre preform, thermally induced refractive index changes 4-97101  
 SOI structures, recryst. by electron beam annealing (*Japanese*) 4-88207  
 SOS, ion implanted, elec. props., effect of heat treatment 4-98759  
 SOS films, material improvement process by solid phase epitaxial growth 4-81124  
 SOS heteroepitaxial film, surface photovoltage characterisation 4-80697  
 spin glass, quenched and annealed free energies, 4-104428  
 stability of rechargeable hydriding alloys during extended cycling 4-72190  
 stainless steel, Cr-Ni-Nb (20, 25, 1%), C deposits, inhibition, prior selective oxidation 4-114708  
 steel, austenitic, AM-2, various properties and products of nonmagnetic steels 4-114590  
 steel, austenitic stainless, annealed, load relax. near 563K, thermally activated dislocation motion 4-99413  
 steel, austenitic stainless, creep exposure, influence of regenerative heat treatment on remaining life 4-114602  
 steel, austenitic stainless, metallographic revelation of  $\alpha$ -phase and  $\delta$ -ferrite, etching and mag. techniques (*German, English*) 4-66540  
 steel, austenitic stainless, Nb-stabilised, hot deformed, grain coarsening 4-93329  
 steel, austenitic stainless, sensitised, Cr depletion in carbide vicinity rel. to heat treatment 4-71654  
 steel, austenitic stainless, thermal and radiation-stimulated ageing, kinetics 4-66354  
 steel, austenitic stainless, vacuum annealed, duplex oxidation in CO<sub>2</sub>/CO gas mixtures between 500 and 700°C 4-104900  
 steel, C, cast and wrought, H induced ductility losses, annealing effects 4-85193  
 steel, Cr-Mo, fatigue crack growth at 525°C, effects of environment and dwell 4-99523  
 steel, Cr-Mo, fatigue crack growth at 525°C, prediction of continuous cycling endurance 4-99524  
 steel, Cr-Ni, annealed,  $\alpha$ -phase precipitation, potentiostatic etching (*German, English*) 4-71823  
 steel, dual-phase, Mn segregation during intercrit. annealing 4-114535  
 steel, dual-phase, Mn-Si, stabilisation of retained austenite, effect on mech. props. (*Korean*) 4-104818  
 steel, electric, effective grain growth inhibition 4-81218  
 steel, ferritic, impact testing, classification of absorbed energy-temperature curves 4-89230  
 steel, high-speed, W-Mo, sintered, heat treatment 4-66357  
 steel, HSLA, tensile strength and ductility, dependence on microstruct. 4-114603  
 steel, low alloy, Cr, dislocation structure and phase composition during annealing (*Russian*) 4-108366  
 steel, low alloy, reheat cracking during stress relief annealing, numerical approach 4-93412  
 steel, low C, deep drawing cold-rolled sheet prod. by continuous annealing, control of steel chem. 4-114565  
 steel, low C, deep-drawing, prod. by continuous annealing 4-114566  
 steel, low C, dual-phase, continuously annealed, effect of prior cold rolling 4-66350  
 steel, low C, fatigue crack initiation rel. to annealing and prestressing (*Japanese*) 4-99517  
 steel, low C, Mn, austenite form-mechanism during annealing 4-85151  
 steel, low C, nitrocarburising, annealing, positron annihilation, vacancy-impurity clusters in surface layer 4-66094  
 steel, maraging, tensile strength and ductility, dependence on microstruct. 4-114603  
 steel, mild, SCC in NaH<sub>2</sub>PO<sub>4</sub> soln., effect of heat treatment and C 4-89167  
 steel, Mn, controlled hot rolling and intercrit. annealing, time-temp.-reaction diagrams 4-66351  
 steel, Ni-Co-Mo-Ti, controlled hot rolling and intercrit. annealing, time-temp.-reaction diagrams 4-66351  
 steel, pressure vessels, radiation embrittlement and annealing 4-111626  
 steel, rimmed and killed, cavitation erosion resist. rel. to heat treatment and deoxidation (*Japanese*) 4-89138  
 steel, roll type 9Kh, small N and B additions effect on struct. and mech. props. 4-93342  
 steel, rotor, mag. induction, cooling rate depend 4-76184  
 steel, sheet, continuous heat treatment 4-114591  
 steel, stainless, Cr-Mn, ferritic-austenitic, superplasticity 4-61984  
 steel, stainless, Nb-stabilized, Cr-depleted, oxidation, Cr conc. for healing layer form. 4-81326  
 steel, stainless, type 316, with TiC coating, void form. near interface by diffusion annealing 4-109557  
 steel, structural, cast, strength toughness rel. to intercritical treatment (*French*) 4-81222  
 steel sheet, continuous annealed cold-rolled, overaging treatment and ductility, interstitial atom supersaturation (*French*) 4-89096  
 ternary alloy source material for rod-fed evaporation, fabrication process 4-114581  
 track annealing studies in glasses and minerals, SSNTD appl. 4-96381  
 transition metal silicides on Si, thermal oxidation and diffusion, review 4-66464  
 travelling salesman problem, optimization by simulated annealing 4-79433  
 TRISO coated fuel particles, irradi., failure during high temp. annealing 4-73979  
 vacuum furnaces AC power supply, temp. controller 4-106297  
 vinylidene chloride-methyl acrylate copolymers, thermal behaviour 4-113581  
 AL-Sn(In), ion irradi., vacancy-solute atom complexes, channelling study 4-103836  
 Ag halides, selective latent image distribution 4-78398  
 Ag, radiation damage, O deoeration and <sup>111</sup>In TDPAC studies 4-75555  
 Ag with surface adsorbed Ag deposits, roughening study 4-104087  
 Ag-Cu dilute alloys, defect production and annealing 4-75442  
 Ag-Zn, conc., electron irradi., elec. resist., recovery 4-104182  
 $\alpha$ -Al<sub>2</sub>O<sub>3</sub>, short-range order parameter, determ. from resist. meas. 4-98287  
 AgI-Ag<sub>2</sub>O-B<sub>2</sub>O<sub>3</sub> system, stable and metastable phases 4-113343  
 Al, corrosion resistance of oxide layers rel. to impurity content 4-62102  
 Al, internal friction originated by grain boundaries 4-103872  
 Al, subgrain growth during static annealing 4-114573  
 Al/Mo thin films, reactions 4-61148

annealing continued

Al/SiO<sub>2</sub>/Al capacitor struct., dielec. props. and thermoluminescence 4-76047  
 Al-Al<sub>2</sub>O<sub>3</sub>-metal junctions, thermally shorted, point contact spectroscopy 4-80687  
 Al-Co-Fe, Alcoa 122, magnetostrictive, piezomagnetic coeffs., annealing, mag. field depend 4-76214  
 Al-Cu-Si, Al 2014, punch-stretching behaviour, 250 to 500°C 4-76817  
 Al-Cu-Si, Al 2014, tensile props., 250 to 500°C 4-76816  
 Al-Fe-Si (0.31, 0.11 wt.%), recovery and recryst., DSC study 4-85167  
 Al-Mg, dil., neutron irradi., internal friction, elastic modulus, recovery stages studied by elec. resist. meas. 4-103876  
 Al-Mn alloy, commercial, quenched-in vacancy defects 4-108365  
 Al-Si/n<sup>+</sup>-Si system, metallisation by fast heat pulse alloying, hillock elimination 4-114034  
 Al-SiO<sub>2</sub>-Si MIS structures, with plasma deposited SiO<sub>2</sub>, alkali ion motion, C-V characs. (*Russian*) 4-114042  
 Al-Ti-C-Si contact system, thermal stability 4-84703  
 Al-Zn(Mg), neutron irradi., radiation damage 4-80112  
 Al-Zr (9.4 wt.%), melt-quenched, decomp. study using TEM 4-93262  
 Al<sub>3</sub>Ga<sub>1-x</sub>As p-n junctions, organometallic VPE, anomalous light sensitivity 4-92817  
 Al<sub>3</sub>Ga<sub>1-x</sub>As-GaAs multiple well quantum well lasers, wavelength modification 4-64705  
 Al<sub>2</sub>O<sub>3</sub>, ion implantation, ion beam mixing, and annealing of metals 4-70229  
 Al<sub>2</sub>O<sub>3</sub>/Co, thermoluminescence and trap parameters 4-76532  
 $\beta/\beta'$ -Al<sub>2</sub>O<sub>3</sub>-Na<sub>2</sub>O, struct. transform, during sintering and annealing 4-93292  
 $\beta'$ -Al<sub>2</sub>O<sub>3</sub>-Na<sub>2</sub>O:Fe, decomposition processes, microscopic mechanisms 4-109415  
 As<sub>2</sub>S<sub>3</sub> chalcogenide films, solvent-cast morphology and thermal props. 4-84530  
 Au clad Nb wire, Meissner effect in Au induced by Nb proximity effect 4-108970  
 Au films deposited by electron beam evaporation or sputtering, Si outdiffusion, annealing ambients effects 4-70459  
 Au on GaAs, alloying behaviour 4-80454  
 Au thin films 4-75814  
 Au-Ge-(Ni) on GaAs, alloying behaviour 4-80454  
 AuGa<sub>2</sub> (001), surface net characterisation and electronic struct. 4-80642  
 BaF<sub>2</sub>/Mn<sup>2+</sup>, annealed, EPR spectra 4-71169  
 BaO-B<sub>2</sub>O<sub>3</sub>-Fe<sub>2</sub>O<sub>3</sub> system, magnetic vitroceraamics, prep. and props. 4-93256  
 Be, acoustic emission due to deform. (*Russian*) 4-92304  
 Be, microplasticity, grain size and heat treatment effects (*Russian*) 4-104809  
 Be, neutron irradi. at various temps., compression props. and swelling 4-108458  
 Bi<sub>2</sub>SiO<sub>5</sub>/Al, photocond., absorption spectra and TSC studies 4-65710  
 Bi<sub>2</sub>Te<sub>3</sub>-Sb<sub>2</sub>Te<sub>3</sub>, n-type solid solution, effect of annealing in air on electro-physical props. 4-113945  
 C films, as-deposited and annealed, disorder and crystallite form., Raman scatt. study 4-61254  
 C materials, neutron irradiated, restoration of dynamic modulus of elasticity in annealing 4-63304  
 a-C:H, low emittance coatings for high temperature solar collectors 4-114950  
 C:H amorphous film, H<sub>2</sub> gas reactive RF sputtering prep. on low temp. substrates 4-76673  
 CaNi<sub>2</sub>, stability of rechargeable hydriding alloys during extended cycling 4-72190  
 Ca<sub>10</sub>(PO<sub>4</sub>)<sub>6</sub>F<sub>2</sub>, fluorapatite, radiation damage and annealing, optical studies 4-70192  
 CdCr<sub>2</sub>Se<sub>4</sub>In, static I-V characts. 4-70815  
 CdIn<sub>2</sub>S<sub>4</sub> single cryst., photocond., photoluminescence and non-equilib. carrier recombination 4-65706  
 CdS chemically deposited films, cubic phase, air annealing effects, XPS and XRD examination 4-99356  
 CdS, electron beam annealing, defects diffusion 4-103801  
 CdS sintered layers for solar cells, prep. and annealing effects on characts. 4-62369  
 CdS thin films prep. by spray deposition, vacuum annealing effect on elec., structural and optical props. 4-70966  
 CdS/CdTe solar cell, annealing, admittance spectroscopy 4-77101  
 CdS<sub>1-x</sub>Se<sub>x</sub> single cryst., elec. cond. and Hall effect studies 4-113974  
 n-CdTe, electron traps, DLTS study 4-80533  
 CdTe epitaxial films, OMCDV grown on sapphire, growth rates, mobilities, X-ray diff. 4-80444  
 CdTe, p-type, undoped, thin dielectric films deposition as protection against decomposition during annealing 4-92755  
 Co-P amorphous electrodeposited layers, Barkhausen effect, torsion effects 4-76198  
 Co-P amorphous electrodeposits, elastic props. and struct. relax. 4-92282  
 Co-Si-B (-Fe) metallic glasses, mag. props., annealing effects 4-109039  
 Co<sub>92</sub>Ni<sub>8</sub>Fe<sub>2</sub>B<sub>10</sub>Si<sub>16</sub>, amorphous, mag. aftereffects after field annealing 4-84823  
 CoP, amorphous alloy characterisation using SEM 4-76937  
 CoSi<sub>2</sub> films, solid-phase epitaxial growth, patterning effects 4-84537  
 CoSi<sub>2</sub>, formation and Schottky barrier heights 4-108922  
 CoSi<sub>2</sub>, formation from evaporated Si, kinetics 4-104099  
 Cr foil, influence of heat treatment on struct. and props. (*Russian*) 4-65412  
 Cr<sub>2</sub>O<sub>3</sub>, doped, hot pressing, annealing, elec. cond., density, grain size, XPS 4-113946  
 Cr<sub>2</sub>Si single cryst., <sup>51</sup>Cr self diffusion 4-65453  
 Cs<sub>2</sub>O-Na<sub>2</sub>O-SSiO<sub>2</sub> glass, vibr. spectra 4-109179  
 Cu, neutron cross sections for defect prod. by high energy displacement cascades 4-108462  
 Cu, positron lifetime after annealing and cooling (*Russian*) 4-109270  
 Cu, recrystallisation, effect of prior cold work on the influence of elec. current pulses 4-61957  
 Cu/Al thin film interface reactions, X-ray diff. and Rutherford backscatt. studies 4-88409  
 Cu-Ag (3.93 wt.%), electron-positron annihilation study (*Russian*) 4-99223  
 Cu-Fe, elastic distortion of  $\alpha$ -Fe particles by Orowan loops, moire fringes, TEM obs. 4-66358  
 Cu-H, electron irradi., elec. resist. meas., annealing behaviour 4-92240  
 Cu-In, dil., channelling effect of conversion electrons emitted from radioactive impurities 4-75569

## annealing continued

- Cu-In (0.1 at.%), vacancy trapping, PAC and ion channelling study 4-84876  
 Cu-Ni-Sn (9, 6 wt.%), ageing, internal friction, Young's modulus, modulated structure 4-66362  
 Cu-Sn-Cu-Nb composite, reaction annealing, Nb<sub>3</sub>Sn layer growth conditions 4-61886  
 Cu-Ti-Cr (4, 0.5 wt.%), ageing, internal friction, Young's modulus, modulated structure 4-66362  
 Cu-Zn-Al alloys, martensitic transformations, positron annihilation studies 4-89053  
 Cu-Zn-Ni, superplastic, post-deform. tensile props., effect of cavitation 4-114621  
 Cu-Zr, amorphous, local struct., EXAFS study 4-88101  
 Cu-(Al), cold-worked, recrystn., effect of stacking fault energy 4-81221  
 CuFe<sub>2</sub>O<sub>4</sub>, conduction mechanism, annealing effect, resist. and thermopower meas. 4-104206  
 Cu<sub>2</sub>MnAl, Heusler alloy, decomposition during isochronal annealing 4-61916  
 (CuZn)S-CuInSe<sub>2</sub>, heterojunction solar cell, interface props. 4-89401  
 Cu<sub>60</sub>Zr<sub>40</sub> alloy system, amorphous, crystallisation kinetics 4-108279  
 Fe amorphous alloys, structural relaxation (*Russian*) 4-104801  
 Fe, annealed, stress enhancing H<sub>2</sub>S adsorption, Auger spectra 4-75789  
 Fe, cast, white, annealing, Fermi energy, thermoEMF obs. rel. to crystallisation in acoustic vibration field 4-76768  
 Fe, cold rolled, defect annealing, alloying element effects, positron studies 4-76550  
 $\alpha$ -Fe, electron and neutron irradiated, low-temp., mag. relax. spectra 4-84831  
 Fe, electron irradi., internal friction (*Polish*) 4-92234  
 Fe, electronic struct., XPS studies 4-75838  
 Fe, pure, annealed, fatigue crack nucleation sites under reversed bending stress (*Japanese*) 4-99516  
 Fe, pure, carbonitride precipitation by successive ion implantation of C and N, XPS and Mossbauer obs. 4-76906  
 Fe, pure, irradi. in HVEM, void form. onset temp. 4-103804  
 Fe, pure and doped, muon trapping at vacancies 4-65901  
 Fe, sintered, crack propag. and processes near crack tip 4-66435  
 Fe/Ni system, interdiffusion, activation energy and freq. factor 4-65495  
 Fe-Al (10 to 50 at.%), quenched, shrinkage during annealing 4-89074  
 Fe-Al (40 at.%), ion implantation, phase changes, TEM studies 4-108403  
 Fe-Al (48 at.%), mag. props. rel. to heat treatment 4-109003  
 Fe-Al-Si (6, 9 at.%), ordering with phase separation, annealing, TEM, X-ray diffr. study 4-114472  
 Fe-B, amorphous alloys, mag. anisotropy, plastic deform., annealing, Mossbauer obs. 4-65803  
 Fe-base metallic glasses, thermal embrittlement model 4-89098  
 Fe-Cr, surface segregation of S, annealing and O<sub>2</sub> adsorption effect (*Japanese*) 4-61932  
 Fe-Ni, positron lifetime after annealing and cooling (*Russian*) 4-109270  
 Fe-Ni alloy,  $\alpha$ - $\gamma$  transformation, austenite grain growth (*Russian*) 4-109402  
 Fe-Ni dilute alloys, electron and neutron irradiated, low-temp., mag. relax. spectra 4-84831  
 Fe-Ni films, reverse  $\alpha$ - $\gamma$  transformation (*Russian*) 4-109401  
 Fe-Ni-Cr-Mo-N, weld metal, annealing, precipitation, metallographic analysis 4-109417  
 Fe-Ni-Mn-C alloys, martensitic transform. studies 4-99383  
 Fe-Ni-P-B amorphous alloys, mag. props., proton implantation effects 4-104416  
 Fe-Ni-based metallic glasses, fracture and annealing, ferromag. resonance studies 4-109078  
 Fe-P amorphous electrodeposited layers, Barkhausen effect, torsion effects 4-76198  
 Fe-P amorphous electrodeposits, elastic props. and struct. relax. 4-92282  
 Fe-P-C amorphous alloys, B impurity diffusion, SIMS studies 4-92435  
 Fe-Si (3 wt.%), electrical engineering steel, anisotropic, mag. losses, annealing and elongation effects (*Russian*) 4-104459  
 Fe-Si (6.5 wt.%) rapidly quenched ribbons, mag. props. and preparation 4-84819  
 Fe-Si (6.5 wt.%) rapidly quenched ribbon, texture and mag. props. 4-104455  
 Fe-Ta(Mn), neutron irradi. at 325K, defect annealing stages (*Russian*) 4-92242  
 Fe(-C), SCC in NaH<sub>2</sub>PO<sub>4</sub> soln., effect of heat treatment and C 4-89167  
 Fe<sub>1-x</sub>B<sub>x</sub> amorphous alloys, electronic struct., XPS studies 4-75838  
 FeCo based alloys, strength and mag. props. rel. to cold rolling and heat treatment 4-98918  
 Fe<sub>3</sub>Co<sub>7</sub>B<sub>20</sub>, amorphous, mag. aftereffects after field annealing 4-84823  
 Fe<sub>70</sub>Co<sub>18</sub>Si<sub>12</sub>B<sub>14</sub>, metallic glass, crystn. kinetics 4-65187  
 Fe<sub>2.96</sub>Mg<sub>0.04</sub>O<sub>4</sub>, magnetite, annealing and cryst. struct., X-ray diffr. studies 4-113402  
 Fe<sub>78</sub>Mo<sub>2</sub>B<sub>20</sub>, metallic glass, elec. resist., crystallisation and thermoelec. power, annealing effects 4-108831  
 Fe<sub>40</sub>Ni<sub>40</sub>B<sub>20</sub> amorphous alloy, ferromag. resonance and antiresonance studies 4-76256  
 Fe<sub>40</sub>Ni<sub>40</sub>B<sub>20</sub> metallic glass, amorphous-cryst. transition kinetics, elec. resist. meas. 4-70039  
 Fe<sub>40</sub>Ni<sub>40</sub>B<sub>14</sub>B<sub>6</sub> foil, amorphous-cryst. transition, elec. resist. variations 4-65182  
 Fe<sub>40</sub>Ni<sub>38</sub>Mo<sub>2</sub>B<sub>18</sub>, metallic glass, elec. resist., crystallisation and thermoelec. power, annealing effects 4-108831  
 Fe<sub>39</sub>Ni<sub>39</sub>Mo<sub>2</sub>Si<sub>12</sub>B<sub>12</sub>, metallic glass, elec. resist., crystallisation and thermoelec. power, annealing effects 4-108831  
 Fe<sub>40</sub>Ni<sub>40</sub>P<sub>14</sub>B<sub>6</sub> amorphous ribbons, mag. props. and struct., influence of laser annealing 4-88663  
 Fe<sub>40</sub>Ni<sub>40</sub>P<sub>14</sub>B<sub>6</sub>, Metglas 2826, struct. factor, influence of cold rolling 4-61954  
 (Fe<sub>0.9</sub>Ni<sub>0.1</sub>)<sub>78</sub>Si<sub>14</sub>B<sub>8</sub> metallic glass, short range ordering study 4-88108  
 FeO-Fe<sub>2</sub>O<sub>3</sub>, magnetite, magnetostriktion isotherms at low temps. 4-61582  
 Fe<sub>3.005</sub>O<sub>4</sub>, magnetite, annealing and cryst. struct., X-ray diffr. studies 4-113402  
 FeSi-Fe<sub>3</sub>Si<sub>2</sub>, eutectic alloy, sintered, annealing, FeSi<sub>2</sub> form., elec. props. 4-109414  
 Fe<sub>90</sub>Zr<sub>10</sub> glass, H induced mag. phase transform., Mossbauer spectroscopy study, annealing effect 4-61536  
 GaAlAs, proton-bombarded, thermal annealing, elec. cond. recovery 4-98146  
 GaAs (100), chemical etching and annealing 4-65722  
 GaAs (100), clean surface prep. using Ar<sup>+</sup> ion bombard. 4-104886

## annealing continued

- GaAs amorphous thin films, transient annealing, Raman scatt. study 4-80926  
 GaAs, dislocations and point-defect complex formations, thermal stability 4-103758  
 GaAs, encapsulated annealing in AsH<sub>3</sub>, surface protection 4-88378  
 GaAs flash annealing of Mg implants using incoherent radiation 4-84306  
 GaAs, implanted layers, elec. props., Si<sub>3</sub>N<sub>4</sub> encapsulation effects 4-98609  
 GaAs, ion implanted, ion implanted, diffusion of Be and Mn during damage recovery 4-104002  
 GaAs, ion implanted, transient capless annealing appl. to IC fabrication 4-103779  
 GaAs, LEC grown, improved elec. uniformity by high temp. annealing 4-65684  
 GaAs, proton-bombarded, thermal annealing, elec. cond. recovery 4-98146  
 GaAs Schottky diodes, transport mechanism, deep centre effects 4-88558  
 GaAs, semi-insulating, undoped and low Cr doped, LEC grown, photoluminescence props., whole ingot annealing effects 4-84994  
 GaAs semi-insulating substrate, inhomogeneity characterisation, expt. study 4-65759  
 GaAs, sputter etch induced electrically active defects, H passivation 4-108918  
 GaAs substrate, annealing as gettering technique prior to MBE growth 4-99615  
 GaAs:Be, ion implanted, reduced damage generation 4-113474  
 GaAs:Be, ion implanted, annealing behaviour, spectroscopic ellipsometry and Raman scatt. 4-113482  
 GaAs:Cr, ion implanted, Cr redistrib. 4-88194  
 GaAs:Cr, ion irradi. effect on defect thermal annealing 4-98156  
 GaAs:Mn, Mn redistribution, interstitial-substitutional model anal. 4-92433  
 GaAs:Se, deep acceptor, photoluminescence study 4-80534  
 GaAs:Si, (100), vacuum annealed, free carrier reduction 4-98610  
 n-GaAs:Si,  $\alpha$ -irrad., positron annihilation study 4-104696  
 GaAs:Si, implanted, radiation annealing with CW Xe arc lamp 4-75486  
 GaAs:Si, local vibr. modes and elec. activation, Raman study 4-84357  
 GaAs:Sn,Te, dual implanted damage and annealing, challenging studies 4-80116  
 GaAs:Te, H ion bombarded, free carrier density, EELS studies 4-98632  
 GaAs:V, semi-insulating, V redistribution during heat treatment 4-80070  
 p-GaAs:Zn, emission band, electron irradi. and annealing effects 4-88881  
 GaAs/Au interface struct., XPS, RHEED and ion scatt./channelling studies 4-80421  
 GaAs/AuGe ohmic contact, Ge and Au profiles, SIMS studies 4-103782  
 GaAs/N-AlGaAs heterostructures, selectively doped, MBE grown, tungsten-halogen lamp annealing effects 4-61444  
 GaAs/Ni film system, interfacial reactions, TEM and X-ray diffr. studies 4-108729  
 GaAs-AlGaAs transverse junction stripe laser, Si doped, MBE fabrication 4-96893  
 GaAs-Al(Au) Schottky barrier contacts, LEC grown, electron traps, DLTS signals, effect of metal 4-84691  
 GaAs-n-AlGaAs structures, modulation doped, elec. props., effect of IR flash lamp annealing 4-98712  
 Ga<sub>0.47</sub>In<sub>0.53</sub>As, ion implanted, annealing, TEM obs. 4-70228  
 n-GaP, electron irradi., defects, positron annihilation studies 4-109273  
 (GaSb)<sub>1-x</sub>(Ge)<sub>x</sub>, semicond. alloys, phase transforms. 4-92347  
 GaSe single cryst., luminescence spectra, isothermal annealing effects 4-81001  
 Ge bolometer, neutron-transmutation-doped, resist. meas. 4-106386  
 Ge, deep level impurities, low temp. passivation techniques 4-59561  
 Ge, electrically neutral impurities on muonium, low temp. meas. 4-65279  
 Ge, gamma-irradiated, hole traps 4-103799  
 Ge, high purity, coaxial detectors performance after fast neutron damage 4-59553  
 Ge, high-purity, purification, cryst. growth and annealing props. 4-61831  
 Ge, neutron transmutation doped, annealing, DLTS study 4-60942  
 Ge, radiation-induced rod-like defects 4-92238  
 Ge, sputter etch induced electrically active defects, H passivation 4-108918  
 Ge:Cu, impurity states, annealing effects 4-104148  
 Ge:Ga(Sb), film on GaAs, doping and elec. props. study (*Russian*) 4-70182  
 Ge-Se glasses, microstructure, electron microscopy obs. 4-88305  
 Ge<sub>20</sub>Se<sub>80-x</sub> thin films, optical properties determ., annealing effect on refractive index 4-114337  
 Hg<sub>1-x</sub>Cd<sub>x</sub>Te, annealing of radiation defects, electron irradiation 4-108442  
 Hg<sub>1-x</sub>Cd<sub>x</sub>Te, electron irradi., elec. props., heat treatment effects 4-65713  
 In, deformed, low-temp. recovery activation enthalpy, positron annihilation meas. 4-76556  
 InAs evaporated films, Hall mobility and carrier conc. 4-70961  
 InAs, struct. and electrical cond. behaviour under deposition conditions 4-98787  
 InP p<sup>+</sup>-n junctions,  $\gamma$ -ray irradi., electron trap annealing 4-98748  
 InP, semi-insulating, simulation of anomalous Be diffusion 4-88193  
 InP:Fe, semi-insulating, with phosphosilicate glass encapsulation heat treatment, photoluminesc. and Raman scatt. characterisation 4-84995  
 InP:Gd(Yb) epitaxial films, doping effects on low-temp. edge photoluminescence 4-85028  
 InP:Sn(Sn)(Ge), (100), vacuum annealed, free carrier reduction 4-98610  
 InP:Se, ion implanted, annealing and transport props. 4-108397  
 InP:Si MISFETs, post-implantation capless annealing 4-113472  
 InP:Zn, electron irradi. damage, carrier conc. effects, minority carrier diffusion length 4-80107  
 InP:Zn, grown-in defects, annealing effects, DLTS studies 4-84287  
 InP/Ta-Si sputtered film contacts, rectifying behaviour and barrier heights 4-70932  
 In<sub>2</sub>Se<sub>3</sub> films, flash and thermal evaporation growth, struct. and elec. characterisation 4-114409  
 In<sub>2</sub>Se<sub>3</sub> in Se vapour, physical props. 4-61414  
 In<sub>2</sub>-Sn<sub>2</sub>O<sub>3</sub>-y coating deposition, three-step process, low sheet resist. 4-81159  
 K halides, Ba-doped, impurity colour centres, absorpt. spectra 4-88865  
 KBr, H centres, low temp. pair associates 4-70149  
 KBr, IR spectra, elec. field influence 4-99122  
 KCl single-crystal, technique for increasing optical strength through temp. cycling 4-75516

# annealing continued

- KCl surface breakdown threshold, effect of treatment and ageing 4-75521
- KCl(Br)(I):Ag, surface-enhanced Raman scatt. from Ag colloids, optical absorpt. spectra 4-99117
- KH<sub>2</sub>PO<sub>4</sub> crystals, bulk laser-damage resistance improvement by baking and pulsed laser irradi. 4-75517
- LaNi<sub>5</sub>, stability of rechargeable hydriding alloys during extended cycling 4-72190
- LiF crystals, annealed and aged, dislocation behaviour 4-103759
- LiF, dislocation struct. evolution at premelting temp. (*Russian*) 4-88174
- LiF TLD, reproductive annealing procedure 4-99401
- LiNbO<sub>3</sub> amorphous films, dielec. and elec. props. 4-104531
- LiNbO<sub>3</sub>, electron irradi., point defects, ESR and IR spectra studies 4-70139
- LiNbO<sub>3</sub> grating, annealing effect on surface relief 4-107812
- Li<sub>2</sub>O-B<sub>2</sub>O<sub>3</sub>-Fe<sub>2</sub>O<sub>3</sub> system, magnetic vitroceraamics, prep. and props. 4-93256
- Li<sub>2</sub>O-Nb<sub>2</sub>O<sub>5</sub> amorphous dielectrics, crystallisation, elastic and dielec. props. 4-104518
- Li<sub>2</sub>SiO<sub>3</sub>, coloration of irradiated samples, during isothermal annealing (*Russian*) 4-98100
- (Mg,Fe)<sub>2</sub>Al<sub>2</sub>Si<sub>2</sub>O<sub>18</sub> cordierites, heating and radiation effects on optical absorpt. and Mossbauer spectra 4-89911
- Mg, hot rolled, texture, grain size and yield strength 4-114579
- Mg-Nd-Zr, cyclic strengthening and loss of strength in air and vacuum at 293 and 140K 4-93399
- Mg<sub>2</sub>Al<sub>2</sub>Si<sub>2</sub>O<sub>18</sub>, cordierite, Al-Si ordering, Raman studies 4-98073
- MgO single crystals, thermolum. kinetics rel. to Cr<sup>3+</sup> and Fe<sup>3+</sup> impurity conc. (*Japanese*) 4-9202
- MgO, vacancies and multiphonon IR-absorpt. spectra (*Russian*) 4-71420
- MgO:Ni, irradiated, thermolum. study 4-81018
- Mg<sub>2</sub>Si form., thin film reaction kinetics, AES and SIMS 4-81131
- Mn-Cu-Bi, thin film, RF sputtering prep., mag. and magneto-optical props. 4-61847
- Mn-Ni-Bi thin film, RF-sputtering prep., mag. and magneto-optical props. 4-61847
- Mn<sub>3</sub>B<sub>2</sub>O<sub>7</sub>Cl(Br)(I), cubic-orthorhombic ferroelec. transition, sp. ht. studies 4-104545
- Mo, alpha-irrad., defect annealing, positron annihilation, Doppler broadening 4-70227
- Mo, ductility transition temp. rel. to alloying elements (*Japanese*) 4-61979
- Mo electrodes, selective SiO<sub>2</sub> form. for MOS struct. 4-98467
- Mo, high temp. neutron irradi., annealing, void form., mech. props. 4-108456
- Mo, irradiation by fast neutrons, annealing, interstitial clusters, X-ray scatt. obs. 4-75538
- Mo, isochronal annealing study of neutron induced defects, positron annihilation obs. 4-65305
- Mo MOS structures, stabilisation using H<sub>2</sub> doping and high temp. forming gas annealing 4-98761
- Mo, pulse ion irradi., void nucleation 4-103826
- Mo, pulsed irradiation, theory of depleted zone annealing 4-108417
- Mo<sub>2</sub>O films, O depth profiles under high temp. annealing 4-98490
- Mo<sub>2</sub>Ge, fast neutron irradi., effects on struct. and supercond. props. (*Russian*) 4-92841
- MoO<sub>3</sub>, black solar selective absorbers, thermal stability and performance 4-114952
- NaCl, cryst., X-irrad., F-centre decay during photoannealing 4-80036
- NaCl,  $\gamma$ -irrad., interstitial dislocation loops (*Russian*) 4-113455
- NaCl single-crystal, technique for increasing optical strength through temp. cycling 4-75516
- NaCl:Ag, surface-enhanced Raman scatt. from Ag colloids, optical absorpt. spectra 4-99117
- NaCl:Gd, microhardness, influence of Gd impurity 4-103868
- Nb, electron-irradiated, muon diffusion and trapping by defects 4-65905
- Nb powder, high-purity, first stage sintering, influence of gas atm. 4-99367
- NbN/Pb Josephson tunnel junctions with plasma oxidized barriers, annealing stability 4-84746
- Nb<sub>2</sub>Sn, growth kinetics by bronze process 4-114451
- Nb<sub>2</sub>Zr<sub>2</sub>Si<sub>5</sub> amorphous alloy, supercond. props., effect of annealing 4-104345
- Ni alloy based thermocouples, hysteresis and short-term instabilities up to 1200°C 4-82793
- Ni, cold rolled, defect annealing, alloying element effects, positron studies 4-76549
- Ni, dislocation/obstacle interaction during low dose D irradi. creep 4-104813
- Ni foils, He injected, self-ion irradi., annealing, voids, TEM obs. 4-103827
- Ni, grain boundaries,  $\Sigma$  distrib., in polycryst. prep. by strain annealing 4-108377
- Ni, He<sup>+</sup> ion irradiated, bubble growth, microstruct. contrib. 4-108472
- Ni, ion implanted D trapping by vacancies, channelling studies 4-108409
- Ni, O assisted intergranular H embrittlement, effects of B, P, Sn and Sb additions 4-62030
- Ni O embrittlement, prevention and reversal 4-71733
- Ni powder, low-temp. diffusion, positron annihilation study 4-98365
- Ni superalloy, Mar-M 200 powder, shock induced compaction, mech. props. 4-109430
- Ni, surface segregation of S, annealing and O<sub>2</sub> adsorption effect (*Japanese*) 4-61932
- Ni-Al-Mo-Ta system, constitution of Ni-rich alloys at 1523K 4-66313
- Ni-B alloys, CVD deposited, microstruct. and mech. props. 4-71581
- Ni-Cr-Co-B, melt spun superalloy, annealing, castability, ductility and microstruct. rel. to B additions 4-66323
- Ni-Cu (22 at.%), annealed and quenched, creep behaviour and miscibility gap 4-66387
- Ni-Ge dilute alloys, defect reactions, diffuse X-ray scatt. studies 4-75440
- Ni-Si dilute alloys, defect reactions, diffuse X-ray scatt. studies 4-75439
- Ni-Si-B, amorphous, cryst. form. on annealing, TEM study 4-75304
- NiAl, vacancy dislocation loops, annealing effect, TEM obs. 4-103756
- NiAl, vacancy dislocation loop growth, role of surface oxidation 4-103757
- Ni<sub>3</sub>Al powders, rapidly solidified and annealed 4-93278
- NiCr thin films, Cr<sub>2</sub>O<sub>3</sub> phase appearance, electron microscopy and diff. study 4-81344
- Ni<sub>3</sub>Cr, ordered state, annealing, elec. resist., electron diff. obs. 4-109394
- NiP, amorphous alloy characterisation using SEM 4-76937

# annealing continued

- Ni<sub>3</sub>(Ti,V<sub>1-x</sub>) alloys, long period struct., electron diff. studies (*Chinese*) 4-98064
- NiZn ferrites, prod. by shock hot working, props. 4-61905
- PLZT ferroelec. films, prep., props. and appls. 4-66230
- Pb-Al<sub>2</sub>O<sub>3</sub>-Al junctions, ion irradi., defect vibrs., supercond. tunnelling meas. 4-98826
- Pb-Sn (7.6 wt.%) role of excess vacancies in discontinuous precipitation (*Russian*) 4-81199
- PbS thin films, laser and thermal annealing effects on elec. props. 4-65298
- PbTe, sintered, elec. cond. and thermoelec. power, annealing effects 4-84621
- PbTiO<sub>3</sub>, amorphous and cryst., bond lengths, annealing effect, Raman spectra, EXAFS study 4-79935
- PbTiO<sub>3</sub> amorphous films, dielec. and elec. props. 4-104531
- Pd-Fe, ion implanted, ferromagnetism study 4-71137
- Pd-Si (111), study by LEED, RHEED and AES 4-113765
- Pd<sub>2</sub>Be<sub>3</sub>, metallic glass, stale structure, X-ray methods study 4-113344
- Pd<sub>2</sub>Si<sub>2</sub>, amorphous and annealed, neutron irradi., elec. resist. meas., structural relax. 4-70772
- Rb halides, Ba-doped, impurity colour centres, absorpt. spectra 4-88865
- RbBr:Eu, optical study of Eu precipitation 4-80233
- RbCl:Eu, optical study of Eu precipitation 4-80233
- RbMgF<sub>2</sub>:Mn<sup>2+</sup>, electron irradi., vacancy-interstitial pair and F-centre-impurity ion pair form. 4-70215
- Sb, amorphous film, vacuum deposited, isochronous annealing, crystallisation 4-61854
- Se, amorphous, defect states and photoelec. behaviour 4-113903
- Se:Te, As glassy films, pure and doped, deep level defects, xerographic spectra studies 4-61339
- Se-Te:As, amorphous, defect states and photoelec. behaviour 4-113903
- Si (100), chemisorption of H, TDS study (*Chinese*) 4-92510
- Si (100) 2<sup>nd</sup>, pre-exposed to O in submonolayer range, chem. shifts of Si-H stretching freqs. 4-80368
- Si (111), annealed in high vac., electronic props., surface photovoltage study 4-80628
- Si, amorphous, from ion implantation, refractive index, thermal annealing effect 4-76417
- Si, amorphous CVD films, H<sub>2</sub> plasma annealing localized state density 4-61337
- Si, Czochralski growth, impurity clouds, microdefects, scatt. light intensity and etch pit density after annealing 4-84312
- Si, deep level impurities, low temp. passivation techniques 4-59561
- Si EFG ribbon solar cells, ion implantation and pulsed electron beam annealing fabrication 4-62364
- Si, electron beam annealing, pulsed, thermal model 4-60963
- a-Si film, elastic and inelastic props. 4-88225
- a-Si film, RF sputtered, optical absorpt., elec. cond., effect of thermal annealing 4-80583
- Si films, monocrystalline and polycrystalline, simultaneous epitaxial growth, struct., elec. props. 4-98488
- Si films, UHV deposited, cryst. temp. 4-88410
- n-Si, gamma and neutron irradi., radiation defect interactions 4-92227
- Si, heat treatment influence on dislocation motion kinetics (*Russian*) 4-88173
- Si, heavy-ion induced damage and annealing TEM and channelling studies 4-80115
- Si, implanted oxides, annealing, activation energy 4-75490
- a-Si, ion implantation form. and optical state characterisation 4-88186
- Si, ion implanted, beam annealing 4-75510
- a-Si, ion implanted, etching in HF soln. and annealing effects 4-80063
- Si, ion implanted, halogen lamp rapid annealing, p-n junction formation 4-88195
- Si, ion implanted, laser or electron beam annealing, electronically active defects, DLTS 4-80527
- Si, ion implanted, laser or electron beam annealing, minority carrier recomb., EBIC, photoluminescence meas. 4-80601
- Si, ion implanted, pulsed laser and thermal processing, defect anal. 4-70133
- Si, ion implanted, rapid thermal arc lamp and pulsed laser annealing, photoluminesc. study 4-93094
- Si, low pressure CVD growth and phys. props. 4-81150
- Si MOS struct., implantation-induced defects, RF annealing using H plasma 4-84308
- Si, neutron irradi., radiation defects and electrophys. parameters 4-84319
- Si, polycrystalline, implantation under thermal and laser annealing, sheet resist. and doping profiles 4-75487
- Si, polycrystalline, recrystallisation by combined CW laser and furnace heating 4-88199
- Si, proton irradi., acceptor level positions of divacancy 4-70725
- Si, proton irradi. induced defects interaction with surface 4-75564
- Si, radiation-induced rod-like defects 4-92238
- Si, recrystallized on SiO<sub>2</sub>, laterally seeded, implantation and annealing studies 4-98121
- Si solar cell fabrication by ion implantation and thermal annealing 4-77089
- Si solar cells, ion implantation and pulsing annealing processes 4-81563
- Si solar cells, low-dose ion implanted, optimum flashlamp annealing conditions for fabrication 4-85368
- Si solar cells, P ion implantation emitter tailoring and annealing 4-62366
- Si, sputter etch induced electrically active defects, H passivation 4-108918
- Si substrate, ion implanted and processed, interface characterisation 4-84304
- Si surface, paramag. centre form. during strong cooling 4-65861
- Si, surface properties after ion chem. etching 4-66463
- Si TaSi<sub>2</sub> struct., annealing and sheet resistivity 4-108741
- Si:Ar, carrier lifetime reduction by Ar ion implantation 4-80604
- Si:As, high current density implantation, dynamic self-annealing mechanism 4-65280
- Si:As, high dose ion implanted, As clustering, TEM and SIMS studies 4-70384
- Si:As, implanted (111), twin formation, effect of heating rate and annealing temp. 4-103765
- Si:As, ion implanted, carrier density profiles, elec. meas., annealing behaviour 4-70179
- Si:As, ion implanted, IR radiation annealing of extended defects 4-92228
- Si:As, ion implanted regions, 2-D shape, etching and EBIC studies 4-88187

## annealing continued

- Si:As, ion implanted through screen oxide, residual disorder after high temp. anneal 4-113511  
 Si:As, low-energy ion implantation 4-75466  
 Si:As, P, B, ion implanted, fast isothermal annealing and elec. props. 4-92224  
 Si:As thin films, As fast diffusion during rapid thermal annealing 4-113714  
 Si:As<sup>+</sup>(BF<sub>3</sub>), implanted, rapid thermal annealing 4-88181  
 Si:As(B), ion implanted and electron beam annealed, TEM and HREM studies 4-80058  
 Si:Au, effect of mobile dislocations on surface saturation (*Russian*) 4-98107  
 Si:B, implanted, elec. activation and damage annealing by flash lamp irradi. 4-70196  
 p-Si:B, ion implanted, electron beam annealing 4-60960  
 Si:B, ion implanted, flash-lamp annealing study 4-108395  
 Si:B, ion implanted shallow layers, electron beam annealing, expt. study using SIMS 4-98133  
 Si:B, P, compensated semiconductors, coalescence process, effect and rad. and heat treatment 4-65288  
 a-Si:B, pure and doped, ion implanted, recrystallisation studies 4-88422  
 Si:B-SiO<sub>2</sub> MIS struct., ion bombarded, defect annealing study 4-80685  
 Si:C, self-interstitial enhanced C diffusion 4-98358  
 Si:F, As, ion implanted, defect struct. detection 4-103776  
 n-Si:Fe, impurity bands of Fe clusters, ESR and elec. props. 4-109067  
 Si:Ge, implantation, pre-amorphisation/rapid thermal annealing procedure for shallow junction formation 4-88188  
 Si:H, Al-covered, solid-state reaction between film and substrate 4-92498  
 Si:H, amorphous, glow discharge chemical vapour deposited, X-ray photoelectron spectroscopy 4-93201  
 Si:H, amorphous, high-rate deposited annealing effects 4-61876  
 Si:H, amorphous, light-induced defects, annealing 4-92762  
 Si:H, RF sputtered amorphous film, dark cond. and photocond., annealing effects 4-70960  
 a-Si:H, radiative combination at dangling bonds, quantitative model, expt. study 4-114326  
 Si:H, study of H-induced defects (*Chinese*) 4-103736  
 a-Si:H film, annealing behaviour of g=2.0026 ESR line 4-109057  
 a-Si:H film, Staebler-Wronski effect 4-108852  
 a-Si:H film for H passivation of implantation defects in Si-SiO<sub>2</sub> MOS struct. 4-71744  
 Si:Li p-n junction solar cells, electron induced degradation, recovery under space conditions 4-105110  
 Si:Mg, implanted, doping behaviour, elec. props. 4-75485  
 Si:O, C, annealed, photoluminesc. of impurity complexes 4-88866  
 Si:O, Czochralski grown, annealed, impurity precipitates, induced defects, TEM obs. (*Chinese*) 4-92368  
 Si:O, Czochralski grown, thermally-induced microdefects, high resolution TEM studies 4-108626  
 Si:O, recombination centres induced by heat treatment at 600 to 800°C 4-104154  
 Si:O cryst., minority carrier lifetime, O precipitation effects, IR studies 4-113971  
 Si:O Czochralski crystals, O precipitation and microdefects 4-84411  
 Si:P, ion implanted, diffusion during rapid thermal annealing 4-113713  
 Si:P, ion implanted, Xe flash lamp annealing, Rutherford backscatt. study 4-88196  
 Si:P(B), substrate orientation depend. of enhanced epitaxial regrowth 4-108737  
 Si:P(Sb), ion implanted, flash lamp annealing 4-108735  
 Si:S, implanted, depth distrib. as function of ion energy, fluence and anneal temp., SIMS meas. 4-80078  
 Si:Sb, ion implanted, supersaturation, vitreous C strip heater annealing, Rutherford backscattering, elec. meas. 4-92375  
 Si:Sn, implanted, subthreshold energy electron beam annealing, Mossbauer effect 4-88205  
 Si/SiO<sub>2</sub> interface, Ar annealed, fixed oxide charge density 4-98756  
 Si/SiO<sub>2</sub> interface, atomic struct. and elec. props. 4-80677  
 Si/SiO<sub>2</sub> MOS struct., interface state density and atomic roughness 4-98684  
 Si/SiO<sub>2</sub>/Al capacitor struct., ion beam fluorination and interface state density 4-70176  
 Si/Ti:P(B)<sup>+</sup>(As<sup>+</sup>), ion implanted, doping effects on TiSi<sub>2</sub> formation 4-88183  
 Si/V-Ta(Ti), interaction of alloy films with Si, silicide formation 4-88436  
 Si-Mo contacts, ion beam sputter deposition, defects, DLTS and EBIC studies 4-61848  
 Si-on-insulator films, ion implanted, annealing using scanned graphite strip heater 4-80066  
 SiC fibres, tensile strength, struct. and phase comp., effect of isothermal annealing 4-66381  
 SiC, ion implantation, ion beam mixing, and annealing of metals 4-70229  
 SiC, sintered and siliconised, microstruct. of neutron irradi. induced defects 4-108459  
 SiC/Al(Pd) interface form., annealing and oxidation, AES studies 4-80420  
 a-Si<sub>1-x</sub>C<sub>x</sub>-H, low emittance coatings for high temperature solar collectors 4-114950  
 Si<sub>3</sub>N<sub>4</sub> film deposition by plasma-enhanced CVD, appl. to GaAs LSI 4-71569  
 Si<sub>3</sub>N<sub>4</sub>, ion implantation, ion beam mixing, and annealing of metals 4-70229  
 Si<sub>3</sub>N<sub>4</sub> layers, ion beam synthesised, dielec. breakdown, current density-voltage and capacitance-voltage characs. 4-80706  
 Si<sub>3</sub>N<sub>4</sub>, reaction bonded, flexural strength, oxidation resist, annealing effect 4-76832  
 Si<sub>3</sub>N<sub>4</sub>-SiO<sub>2</sub>-AlN-Al<sub>2</sub>O<sub>3</sub>-Y<sub>2</sub>O<sub>3</sub> system, phase relations, solid-liq. reactions 4-76762  
 SiO, amorphous thin films, optical absorpt. edge 4-81023  
 SiO<sub>2</sub> gate oxide breakdown, expt. study 4-114207  
 SiO<sub>2</sub>, ion implanted, damage recovery, EPR studies 4-92245  
 SiO<sub>2</sub>, ion implanted, E<sub>i</sub> defects, isothermal annealing studies 4-70146  
 SiO<sub>2</sub> MIS struct., electroluminescence emission studies 4-93114  
 SiO<sub>2</sub> synthesis using ion implantation into Si 4-70175  
 SiO<sub>2</sub> thin film, annealing in NH<sub>3</sub>+CF<sub>4</sub> plasma, nitride layer form. 4-93433  
 SiO<sub>2</sub>H<sup>+</sup>, amorphous, O<sub>2</sub> vacancy annealing 4-103743  
 5SiO<sub>2</sub>-M<sub>2</sub>O glass, (M=Li, Na, K, Rb, Cs), vibr. spectra 4-109179

## annealing continued

- Si-H, bonds and H-induced defects study 4-66058  
 Sn, single crystal, lattice defect kinetics (*Russian*) 4-80029  
 SnO<sub>2</sub>(Sb) films, resistivity and optical transmittance, annealing effects 4-70967  
 Ta, electron-irradiated, muon diffusion and trapping by defects 4-65905  
 Ta<sub>2</sub>O<sub>5</sub> amorphous films, leakage current suppression with micro-pinhole growth control 4-84723  
 TaSi, sputtered film on polycryst. Si, stress 4-70606  
 Tb, electrical cond. and magnetoresistance anomalies at 90K 4-84606  
 Te, neutron irradi. induced defects, optical props. near fundamental energy gap 4-84318  
 Ti, proton irradi., positron annihilation study (*Russian*) 4-85033  
 Ti-Al-Mo-Zr, VT9, nitriding after shock wave treatment 4-93444  
 α+βTi-Al-V and Ti-Al-Cr-Mo-V, annealed, struct. and mech. props. 4-61988  
 Ti-Au, amorphisation, pulsed ion beam annealing study 4-108331  
 Ti-Ni-Mo system, homogeneity ranges of MNi<sub>3</sub> phases 4-89025  
 Ti-R, R=Ce, Dy, Er, Gd, La, Nd or Y, rapidly solidified dispersion strengthened, struct. and props. 4-114561  
 Ti-Sn, proton irradi., positron annihilation study (*Russian*) 4-85033  
 TiAl, intermetallic cpd., specimen prep., microcracks obs. on polished surfaces 4-81382  
 TiC-stainless steel interface, reaction zone struct. produced by vacuum annealing 4-104918  
 Ti<sub>61</sub>Cu<sub>16</sub>Ni<sub>23</sub>, amorphous, X-ray diffr. pattern prepeak, temp. depend. 4-79942  
 Ti<sub>62.5</sub>Cu<sub>12.5</sub>Ni<sub>25</sub>, amorphous, X-ray diffr. pattern prepeak, temp. depend. 4-79942  
 TiN<sub>x</sub> sputtered films for diffusion barriers in metallisation of III-V cpds. 4-88968  
 TiNi, martensitic transform., mech. props., struct. rel. to thermomech. treatment 4-66376  
 TiO<sub>0.5</sub>, evaporated films, phase transformations by annealing 4-113615  
 TiO<sub>2</sub>, vacancies and multiphonon IR-absorpt. spectra (*Russian*) 4-71420  
 TiO<sub>2</sub> (047) surface, preparation by ion bombardment and annealing, XPS and UPS studies 4-65528  
 TiSi<sub>2</sub> films, sputter deposition at high substrate temps., elec. and struct. props. 4-114393  
 TiSi<sub>2</sub> formation, effect of O<sub>2</sub> distrib. 4-80447  
 VO<sub>x</sub> films, ion irradi. and thermal annealing 4-70244  
 V<sub>2</sub>O<sub>5</sub>-B<sub>2</sub>O<sub>3</sub> glasses, struct. study, IR spectra anal. 4-84961  
 VS<sub>2</sub> form., thin film reaction kinetics, AES and SIMS 4-81131  
 VSi, precursor effects of martensitic transformation, magnetoresist. studies 4-65659  
 W fibre reinforced Ni, mech. props. at elevated temps., diffusion barriers to improve struct. stability 4-93423  
 W, noble gas atom implanted, cascade annealing, computer simulation studies 4-75556  
 WC, indented, dislocation interactions, crack nucleation, TEM obs. 4-80039  
 WSi<sub>2</sub>-poly-Si-SiO<sub>2</sub>-Si MOS struct., interface reaction and resistivity 4-114040  
 Y film, substrate temp., deposition rate and annealing effect on elec. resist. 4-98779  
 YIG, Me<sup>+</sup> implanted, mag. props., annealing effects 4-71057  
 YIG:Ca epitaxial layers, elec. cond. meas. 4-80694  
 YIG:Ca films, charge compensation mechanism, annealing effects, behaviour on treatment with oxidising and reducing solns. 4-80799  
 YIG:Ca films, surface layer contraction, X-ray diffr. and magneto-optical studies 4-61262  
 Zn, strain history effects at low temperature deformation 4-71683  
 n-ZnIn<sub>2</sub>S<sub>4</sub>, single-crystals, annealing under high Mn pressure 4-114911  
 Zn,Mn<sub>1-x</sub>S single crystals, vapour phase grown, stacking faults, structural transform. 4-88278  
 ZnO crystallite growth during annealing, morphological anal. 4-61902  
 ZnS:Cu film, cathodoluminescence study of annealing 4-81008  
 Zn:Mn electroluminesc. thin layers, doping and cryst. struct. 4-75810  
 ZnS,Se<sub>x</sub>, deep impurity, trap embedding, luminesc. spectra 4-61321  
 ZnSe (110)-G interface, ordered and disordered, electronic struct. 4-84666  
 ZnSe, thin film, optical properties in the wavelength range 400 to 1500 nm, annealing in air 4-114336  
 Zr, fusion neutron irradi., damage prod. and recovery, resist. obs. 4-108461  
 Zr, grain boundaries, annealing structures 4-92215  
 Zr, pure, neutron irradi., annealing, point defect prod. and annihilation saturation resist. 4-108465  
 Zr-Cu, amorphous, sputtered, low-energy excitations, thermal cond., sp. ht. meas. 4-70987  
 Zr<sub>70</sub>Cu<sub>30</sub>, amorphous, thermal cond., phonon-electron contrib., heat treatment effects 4-70988  
 Zr<sub>76</sub>Cu<sub>24</sub>, amorphous, sputtered, structural relax. induced by annealing X-ray diffr. 4-84189  
 Zr<sub>7</sub>Cu<sub>1-x</sub> metallic glass, sp. ht., thermal cond. props. after structural relax. 4-70406  
 ZrO<sub>2</sub>, shock modified, energy release and phase transform. 4-108612  
 ZrO<sub>2</sub>, short-range struct., radial distrib. curve of atomic density 4-75801  
 Zr<sub>85</sub>Si<sub>15</sub> amorphous alloy, supercond. props., effect of annealing 4-104345

## annealing, magnetic see magnetic annealing

## anodes

- arc discharges, anode current density, jet generation, multiparameter anal. 4-87983  
 molten carbonate fuel cell isotropic porous anode model 4-66688  
 pyrrole black electrodes as battery positive electrodes 4-99801  
 resistive readout with MEPSICRON photon counter 4-94621  
 vacuum arc in anode vapours with non-sputter cathode 4-87971  
 Al anodes for dry and reserve batteries 4-62323  
 Al-air batteries, electrochemical characteristics of air electrode with Fe phthalocyanine 4-93608  
 Al-air battery, rapidly refuellable, for electric vehicles, performance evaluation 4-72096  
 Al-battery, rapidly refuellable, for electric vehicles, current development trends 4-72095  
 CaSOCl<sub>2</sub> cells with anodes made from Ca/Ca-Li alloys, electrochemical studies 4-72080  
 Fe<sub>2</sub>O<sub>3</sub> thin film photoanodes, carrier conc. determ. in MIS struct. 4-88505  
 Li anode batteries high watt-hour per unit weight, electrolytes 4-93601

# anodes continued

- Li/CrO<sub>2</sub> battery, performance characts. and safety tests, for electronic applications 4-93602
- Li-Al alloy anodes for solid state cells, fabrication and testing 4-77079
- Li-Al/FeS cell, FeS positive electrode effective conductivities in LiCl-KCl eutectic electrolyte 4-99958
- Mn anodes for dry and reserve batteries 4-62323
- Pb-acid batteries, with fibre reinforced Pb composites, corrosion behaviour analysis, obs. 4-72099
- Si:H, amorphous, Fe<sub>2</sub>O<sub>3</sub>-coated semiconductor electrode by solar cell, XPS, AES and photochem. meas. 4-66691
- TiO<sub>2</sub> thin film photoanodes, carrier conc. determ. in MIS struct. 4-88505
- TiO<sub>2</sub> thin films, plasma-enhanced CVD, photoelectrochemical props. 4-80627

# anodes, electrochemical *see electrochemical electrodes*

# anodic machining *see electrolytic machining*

# anodisation

- metals, anodisation and oxide film diffusion and transport numbers 4-104001
- spark discharge induced anodic oxidation, process characts. and parameters 4-104893
- Ag, polycrystalline, anodic oxidation in KOH solns. 4-93451
- Al alloys, oxidised, charact. and adhesion of oxide films to epoxy resins 4-104925
- Al, anodic oxidation, film formation by microarc in H<sub>2</sub>SO<sub>4</sub> 4-76900
- Al, anodic oxidation by spark discharge, process characts. and parameters 4-104893
- Al, anodised and its alloys, permanent black coatings, corrosion resistant 4-104922
- Fe, passive film form. in borate solns., electrochem. and ellipsometric studies 4-66490
- Fe-Cr, passive film form. and props. 4-81332
- GaAs solar cells, fabrication using plasma-deposited Si<sub>3</sub>N<sub>4</sub> as oxidation mask 4-89409
- InGaAsP/oxidised films interface, Auger/ion sputtering anal. 4-104884
- Si, anodic oxidation, XPS studies (*Chinese*) 4-85224
- Si, multiwafer plasma system for anodic nitridation and oxidation 4-85237
- a-Si:H films, anodic oxidation, elec. and optical props. of oxidised films 4-109527
- SiO<sub>2</sub> film, O<sub>2</sub> plasma anodised, IR absorpt. bands (*Chinese*) 4-109263
- Ta, anodic oxidation, electron injection and avalanche breakdown 4-89183
- Ti-Cu-x alloys, electrochemical and thermal oxidation and electrochemical O<sub>2</sub> evolution 4-93452
- Zn, black, selective solar absorber surfaces, produced by anodic oxidation, optimisation and evaluation 4-81590
- Zr alloy, amorphous, anodic electrochem. treatment 4-114716

# anodised coatings *see anodised layers*

# anodised layers

- Al, anodic films, pore filling, elec. breakdown characts. 4-81350
- Al film, black Zn-coated, solar collector coatings, optimisation and microstruct. anal. 4-62397
- Al-Al<sub>2</sub>O<sub>3</sub> composite anodised layer, spectrally selective, solar collector appl., ESCA studies 4-66789
- Al<sub>2</sub>O<sub>3</sub> anodic porous films, piezo-electrocapillary effect 4-88774
- Al<sub>2</sub>O<sub>3</sub> anodised films, breakdown statistics 4-109128
- Al<sub>2</sub>O<sub>3</sub> anodised films, Ni-impregnated, selective coatings for photothermal conversion of solar energy 4-100000
- Al<sub>2</sub>O<sub>3</sub>-x anodic oxide films, paramagnetic centres and optical absorpt. spectra studies 4-104494
- Fe, pure, anodic behaviour in high temp. and high press. aq. soln., straining electrode technique 4-109571
- GaAs MOS structures with anodic oxides, defect states, DLTS study 4-11043
- InSb, anodic oxide film, surface relief and struct. 4-109531
- NbO<sub>2</sub> anodic layer, contamination studies by emission angle dependent XPS with double-pass CMEs 4-99282
- Nb<sub>2</sub>O<sub>5</sub> anodic films, AES sputter profiling, contamination effects 4-99270
- Sb<sub>2</sub>S<sub>3</sub> anodic films on Sb electrodes, form. and reduction 4-93435
- SiO<sub>2</sub>/Cr thin films, cathodoluminescence and C-V characts. (*Russian*) 4-99173
- Ta<sub>2</sub>O<sub>5</sub> anodic films, AES sputter profiling, contamination effects 4-99270
- Ta<sub>2</sub>O<sub>5</sub> anodic films as reference materials for AES and XPS sputter depth profiles 4-99916
- Ta<sub>2</sub>O<sub>5</sub>, anodically growth on Ta, ultra-high resolution depth profiling 4-81098
- WO<sub>3</sub> anodic films, electrochromic, TEM, RHEED and Raman studies 4-99114

# anodised thin films *see anodised layers*

# anolytes *see electrolytes*

# anomalous skin effect

- ferromagnetic cylindrical conductor with weak nonlinearity in harmonic quasistationary regime, weak skin effect (*French*) 4-65698
- metal, anomalous skin effect and surface scatt. of electrons 4-70904
- metal, surface impedance temp. depend., effect of impurity dynamic disorder, rel. to anomalous skin effect 4-92788
- metal surface impedance calc. in IR domain 4-104251
- metallic thin slabs, EM field spikes under anomalous skin effect conditions 4-104250
- nonlocal theory of EM elastic solids, appl. to anomalous skin effect 4-80870
- Cu, temperature dependent absorpt., calorimetric meas. 4-76420

# antenna arrays

- see also antenna phased arrays; directional couplers; microwave antenna arrays*
- CW arc pluming at high-power aerials, pulsed RF plasmas obs. 4-69970
- CW arc pluming at high-power aerials, scale-model studies 4-69971
- microwave propagation and antenna characts. for solar power satellite (*Japanese*) 4-62932
- millimeter wave imaging lens antenna 4-91560
- near-MM wave IC imaging polarimeter antenna arrays 4-82827
- phase-stable multielement long-baseline interferometric system, use of reference object method 4-94608

# antenna feeders

- RATAN-600, zenith feed use for broadening observed sky region 4-94610

# antenna lobe patterns *see antenna radiation patterns*

# antenna patterns *see antenna radiation patterns*

# antenna phased arrays

- radar for mesosphere-stratosphere research, mobile SOUSY radar system 4-85791
- water-immersed microwave antenna array for medical imaging and therapy, local field study 4-115159

# antenna radiation patterns

- human head, absorbed power distrib. inside simulating sphere in near field of  $\lambda/2$  dipole antenna 4-89653
- ionosphere, multitrans loop VLF antenna, impedance measurements 4-85858
- ionospheric equipment, electron beam antenna expt. for satellites, EM wave excitation study 4-94281
- Onsala 20 m radiotelescope, test of phase-retrieval holography 4-110527
- RATAN-600, characts. with primary feed offset from focus 4-94607
- RATAN-600 radio telescope, parameters of antenna and radio spectrometer at 21 cm wavelength 4-63052
- RATAN-600 radio telescope, polarisation characts. for obs. at horizon with allowance for aberrations 4-63059
- RATAN-600 radio telescope, scattered background determ. from Sun obs. 4-63055
- variable profile antenna (VPA) of RATAN-600, surface-error scattered background of antenna directional pattern 4-63053

# antenna reflectors

- offset Cassegrain microwave antenna subreflector, numerical. anal. 4-102861
- RATAN-600 radiotelescope, radioholography use for refl. surfaces relative position adjustment 4-94611

# antenna theory

- cable radiation, evaluation model 4-107497
- dipole antennas appl. to electric field meas., geometric asymmetry effects determ. 4-58834
- EHF aplanatic zoned dielectric lens antenna, anal. 4-102998
- EM near-field sensor for simultaneous electric and magnetic field meas. 4-112317
- offset Cassegrain microwave antenna subreflector, numerical. anal. 4-102861
- radiation from planar aperture distributions by evanescent wave and complex ray analysis 4-74398
- RATAN-600 radio telescope, polarisation characts. for obs. at horizon with allowance for aberrations 4-63059
- receiving antenna theory, use in calc. voltage across load of TV antenna, circuit 4-82632
- space reflector antenna structure design concepts 4-77709
- variable profile antenna (VPA) of RATAN-600, surface-error scattered background of antenna directional pattern 4-63053
- variable-profile antenna, influence of field distrib. on periscope-system parameters 4-63057
- water-immersed microwave antenna array for medical imaging and therapy, local field study 4-115159

# antennas

- see also antenna radiation patterns; dipole antennas; directive antennas; microwave antennas; receiving antennas; reflector antennas; scanning antennas*
- ELF ground design and installation 4-115602
- EM wave phenomena Fourier synthesis approach 4-95106
- eyes, microwave radiation hazard, metal-framed spectacles effect 4-109877
- GOES satellite signal reception antenna, for time keeping in Canadian Arctic 4-82274
- gravitation, torsional type antenna for low temp. expts. 4-68119
- gravitational interferometric wave antennas, active vibration isolation 4-111012
- gravitational radiation antenna, coupling of oscillation modes 4-90479
- gravitational-wave antennas, resonance band width 4-86320
- inhomogeneous unmagnetised plasma with antenna, wave propag. 4-79801
- MM waves and IR, conf., Miami Beach, FL, USA (Dec. 1983) 4-73154
- open field site, chamber factor for correlation 4-69644
- RATAN-600 radio telescope, parameters of antenna and radio spectrometer at 21 cm wavelength 4-63052
- terrestrial gravitational noise on a gravitational wave antenna 4-111011
- variable-profile antenna, influence of field distrib. on periscope-system parameters 4-63057
- vehicular technology conf. Pittsburgh, PA, USA (May 1984) 4-106118
- warm carrier device with thin film antenna for CO<sub>2</sub> laser detection 4-73507

# anti-transmit-receive tubes *see gas-discharge tubes; radar equipment*

# antibaryons *see baryons*

# anticorrosion coatings *see corrosion protective coatings*

# anticrossing spectroscopy *see energy level crossing*

# antiferromagnetism

No entries

# antiferroelectric materials

- see also antiferroelectricity; ferroelectric materials*
- chiral triphenyl esters, columnar mesophases, structure and ferroelectric-antiferroelectric transition 4-60815
- cyanoadamantane, glassy cryst. phase and plastic phase, local mol. order, diffuse X-ray scatt. anal. 4-98022
- organic halides, [(CH<sub>3</sub>)<sub>4</sub>N]<sub>2</sub>MX<sub>4</sub>, ferroelectricity and antiferroelectricity 4-65957
- oxides, phys. props., phase transitions 4-65974
- squaric acid, Ising model, Monte Carlo calc. 4-71306
- squaric acid, layered antiferroelectric, Ising spin chain models 4-71285
- squaric acid, thermal expansion, high resolution meas. along b-axis 4-92393
- CsH<sub>2</sub>PO<sub>4</sub>, antiferroelec., fluctuations, Raman spectroscopy studies 4-71297
- CsH<sub>2</sub>(SeO<sub>3</sub>)<sub>2</sub>, antiferroelectric, elastic compliance consts., anomalies at transition point 4-108500
- KCN antiferroelectric phase III, lattice dynamic calcs. 4-103890
- KCN, electric dipole ordering 4-61633
- KNO<sub>3</sub> liq. cryst. mixtures, ferroelec. behaviour 4-109134
- NaCN, antiferroelectric phase III, lattice dynamic calcs. 4-103890
- NaCN, electric dipole ordering 4-61633

**antiferroelectric materials continued**

- NaNbO<sub>3</sub> antiferroelect. cryst., twinning, dipole motif and polar directivity pattern 4-60939  
 NaNbO<sub>3</sub>, bladed crystallisation in Na<sub>2</sub>O-Nb<sub>2</sub>O<sub>5</sub>-B<sub>2</sub>O<sub>3</sub> system 4-61061  
 Pb<sub>2</sub>InNbO<sub>6</sub>, single crystal, perovskite and pyrochlore modifications, prep. and props. 4-76662  
 PbZrO<sub>3</sub>, with O vacancies, phase transitions, dielec. props. 4-76391  
 PbZrO<sub>3</sub>, with vacancies, para, ferro and antiferroelectric phase transitions, influence of hydrostatic press. 4-76390  
 RB<sub>1-x</sub>(NH<sub>4</sub>)<sub>x</sub>H<sub>2</sub>PO<sub>4</sub> mixed crystals, phase transitions in cluster approx., pseudospin model 4-80881  
 Rb<sub>0.52</sub>(ND<sub>4</sub>)<sub>0.48</sub>D<sub>2</sub>PO<sub>4</sub> cryst., proton glass dielec. behaviour 4-114218  
 Rb<sub>1-x</sub>(NH<sub>4</sub>)<sub>x</sub>H<sub>2</sub>PO<sub>4</sub> glass, H-bonded, NMR relax. study 4-98974

**antiferroelectricity**

see also antiferroelectric materials

- betaine arsenate and phosphate, deuterated, ferroelectric props. 4-80876  
 order-disorder phase transitions, crit. anomalies of vibr. lineshape 4-103893

**antiferromagnetic Curie temperature** see Curie temperature**antiferromagnetic-ferromagnetic transitions** see ferromagnetic-antiferromagnetic transitions**antiferromagnetic-paramagnetic transitions** see paramagnetic-antiferromagnetic transitions**antiferromagnetic properties of substances**

see also antiferromagnetism; magnetic semiconductors

- <sup>1</sup>H NMR and mag. susceptibility 4-71202  
 \$X\$ VF<sub>2</sub>, antiferromagnetic spin structures on rutile-type lattice, statistical theory 4-65793  
 antiferromagnetic phase transition, muon spin relax. studies 4-65811  
 bis-ethylammonium copper tetrachloride, mag. phase diagram near Neel temp. 4-114112  
 bisethylammonium tetrachlorocuprate, AFMR line distortion by RF field power 4-104495  
 bis[1,2-bis(2-methoxyethoxy)ethane] sodium biphenylide, spin diffusion, mag. props. ESR study 4-71154  
 catena- $\mu$ -oxohemiporphyrinato iron (IV), mag. struct. study 4-71024  
 di(alkylammonium) ferrous chloride, birefringence and Brillouin scatt. at struct. phase transition 4-75661  
 di(ethylammonium) copper tetrachloride, mag. phase diagram (Russian) 4-92908  
 dielectric, hybrid excitations, anal. of mag. and optical props. 4-76233  
 diethyl ammonium copper tetrachloride, antiferromag.-paramag. first order transition 4-92913  
 graphite-FeCl<sub>3</sub> and CoCl<sub>2</sub> intercalation cpd., mag. order, neutron diff. studies 4-61511  
 hexyl diammonium iron cadmium chloride, (NH<sub>3</sub>)<sub>2</sub>(C<sub>6</sub>H<sub>13</sub>)<sub>2</sub>Fe<sub>2</sub>Cd<sub>1-x</sub>Cl<sub>4</sub>, dilute system, mag. susceptibility meas. 4-65795  
 hyperfine fields determ., using internal standard 4-114185  
 linear Ising model, crystal field effect, ferromag. and antiferromag. susceptibilities 4-98845  
 metals, anomalous antiferromag. structures, by isotropic indirect exchange 4-98860  
 one-dimensional antiferromagnet, energy migration, luminesc. 4-99149  
 polyenes, even and odd, molecular PPP correlations, optical excitations, Heisenberg antiferromagnet 4-74362  
 rare earth-Gd equiatomic cpds., struct. and mag. phase transitions 4-84795  
 rare earth alloys, RCo<sub>2</sub>B<sub>4</sub>, R=Gd-Tm, antiferromag. and paramag. states, NMR spectra 4-109089  
 rare earth alloys, RM<sub>2</sub>Si<sub>2</sub>, M=Ru, Rh, itinerant and local magnetism, supercond., mixed valence phenomena 4-76134  
 rare earth compound, RD<sub>2</sub> (R=Tb, Dy, Ho, Er), mag. struct., neutron diff. studies 4-98858  
 rare earth orthoferrites, muon site determ. 4-71227  
 rare earth-Y alloys, mag. ordering and local mag. moments 4-61524  
 TCNQ salt, MEM(TCNQ)<sub>2</sub>, spin-Peierls distorted phase, polarised neutron scatt. study 4-80745  
 TCNQ salt with quinolinium, mag. props. and electron-nuclear interaction 4-76126  
 tetramethylammonium manganese (iron) cyanide octahydrate, chain struct. and magnetism 4-71073  
 TMMC, EPR study of antiferromagnetic state 4-80811  
 TMNB, 1-D short range and 3-D long range mag. order, neutron scatt. study 4-108991  
 Ag<sub>0.59</sub>Cr<sub>0.59</sub>PS<sub>3</sub>, quasi-one-dimensional antiferromagnet, electron irradiation induced disorder 4-98866  
 BaMnF<sub>6</sub>, 2D antiferromag., optical magnon sidebands and exciton dynamics 4-98875  
 BaMnF<sub>6</sub>, antiferromagnets, hot magnon sidebands temp. depend. 4-76493  
 BaMnF<sub>6</sub>, magneto-electric, unsolved problems 4-76255  
 BaMnF<sub>6</sub>·H<sub>2</sub>O and Ba<sub>2</sub>Fe<sub>17</sub>·3H<sub>2</sub>O, hydrated fluorometallates (III), one-dimens. antiferromagnet 4-71035  
 Ba<sub>2</sub>NiF<sub>6</sub>(FeF<sub>6</sub>), 2-D antiferromagnet, mag. structure 4-71028  
 BaO-B<sub>2</sub>O<sub>3</sub>-Fe<sub>2</sub>O<sub>3</sub> glasses, sput cooled, mag. props. 4-71107  
 Bi<sub>2</sub>Fe<sub>2</sub>O<sub>7</sub>, amorphous, mag., optical and resonant props. 4-104424  
 Ca<sub>2</sub>Mn<sub>1-x</sub>Fe<sub>0.65</sub>O<sub>10</sub>, struct. and frustrated antiferromag. props. 4-108998  
 Cd<sub>1-x</sub>Mn<sub>x</sub>Se, Raman scatt., magnetisation and exchange energy 4-80940  
 Cd<sub>1-x</sub>Ni<sub>x</sub>Fe<sub>2</sub>O<sub>4</sub> system, nonlinear spin struct., magnetisation and Mossbauer obs., Yafet-Kittel angles 4-71022  
 CeB<sub>6</sub>, antiferromagnetic-quadrupole ordering 4-80763  
 CeBi, type-I antiferromag., hybridisation-mediated exchange, anisotropic excitation behaviour 4-71053  
 CeD<sub>2-x</sub>, mag. order and cryst. field effects 4-104408  
 CeMg, antiferromag. cpd., magnons and phonons 4-84777  
 Ce<sub>1-x</sub>Nd<sub>x</sub>Ag mixed crystals, mag. phase diagram 4-65812  
 Co complexes, mag. susceptibilities determ. in temp. region below 77K. 4-71029  
 Co II complexes, IR spectra, mag. susceptibility meas., antiferromag. interactions 4-80918  
 CoCl<sub>2</sub>-FeCl<sub>3</sub>-graphite intercalation cpds. mag. phase transitions; susceptibility meas. 4-98881  
 CoCl<sub>2</sub>·6H<sub>2</sub>O, paramagnetic phase boundary of antiferromagnet at low temp. 4-88668  
 CoCl<sub>2</sub>·6H<sub>2</sub>O, anisotropic antiferromagnet, temp. depend. of paramag. boundary 4-84786  
 CoF<sub>2</sub>, antiferromagnets, hyperfine fields, muon spin relax. 4-71253  
 CoF<sub>2</sub>, mag. props., localisation of implanted positive muons,  $\mu$ SR obs. 4-98994

**antiferromagnetic properties of substances continued**

- CoF<sub>2</sub>, sublattice magnetisation and phase transitions, muon probe studies 4-98864  
 Co<sub>2</sub>MoO<sub>8</sub>, crystal growth, mag. and elec. props. 4-71537  
 Co<sub>2</sub>Ni<sub>1-x</sub>Mn<sub>x</sub>O<sub>4</sub>, magnetic transforms., effect of external press. 4-104418  
 CoRh<sub>2</sub>Ga<sub>2-x</sub>O<sub>4</sub>, oxide spinel solid soln., cation distrib. study 4-80016  
 Co<sub>2</sub>Zn<sub>1-x</sub> complex, (C<sub>2</sub>H<sub>5</sub>NO)<sub>6</sub>(NO<sub>3</sub>)<sub>2</sub> Co<sub>1-x</sub>Zn<sub>x</sub>, ant. ferromag., AC susceptibility 4-61517  
 Co<sub>2</sub>Zn<sub>1-x</sub>Al<sub>x</sub>O<sub>4</sub>, oxide spinel solid soln., cation distrib. study 4-80016  
 Cr (110), electronic struct., PES study 4-85064  
 Cr, effect of mag. anisotropy on spin wave spectra (Russian) 4-80750  
 Cr, Neel transition, effect and uniaxial compressive stress, US attenuation and neutron scatt. meas. 4-76208  
 Cr-Al dilute alloys, thermal expansion, elastic consts. and mag. props. 4-80138  
 Cr-Fe, antiferromagnetic spin glass, HF characts. (Russian) 4-71105  
 CrCl<sub>3</sub>, optical spectra near mag. transition temp. 4-61729  
 Cr<sub>2</sub>Mn<sub>1-x</sub>As<sub>x</sub>, thermal and mag. props., 100 to 500K 4-92922  
 CrSb, mag. props., mol. field theory 4-108995  
 Cr<sub>2</sub>TeO<sub>6</sub>, antiferromag. insulator, MM wavelength mag. reson. study 4-80812  
 CrVNB<sub>6</sub>, semicond., elec. resist., mag. susceptibility meas. 4-109000  
 Cr<sub>2</sub>WO<sub>6</sub>, antiferromag. insulator, MM wavelength mag. reson. study 4-80812  
 CsFeS<sub>2</sub>, quasi 1-D alternating antiferromag., EPR study 4-109062  
 CsMnCl<sub>3</sub>, antiferromagnetic, optical absorpt. spectra, luminesc. studies 4-99133  
 CsMn<sub>1-x</sub>Co<sub>x</sub>Cl<sub>2</sub>·2H<sub>2</sub>O, random mixture with competing anisotropies, PMR meas. 4-88647  
 CsMnI<sub>2</sub>·Er<sup>3+</sup>, one-dimensional antiferromagnet, energy migration, luminesc. 4-99149  
 CsMn<sub>2</sub>Mg<sub>1-x</sub>Br<sub>3</sub>, biquadratic exchange 4-61531  
 CsNiF<sub>3</sub>, specific heat, sine-Gordon kinks and renormalisation 4-71100  
 CsVX<sub>2</sub> (X=Cl, Br, I) linear chain antiferromagnets, mag. excitations 4-65800  
 Cu complex, 2DMSO·CuCl<sub>2</sub>, 1D Heisenberg antiferromag., mag. susceptibility 4-61516  
 Cu II complexes, IR spectra, mag. susceptibility meas., antiferromag. interactions 4-80918  
 Cu-Mn, elec. resist. max. and thermo-EMF, short-range antiferromagnetism (Russian) 4-84608  
 CuCl<sub>2</sub>·2H<sub>2</sub>O, antiferromagnetic, magnon amplitude oscillations under parallel microwave pumping 4-65798  
 Cu<sub>2</sub>Mg<sub>1-x</sub>Al<sub>x</sub>O<sub>4</sub>, oxide spinel solid soln., cation distrib. study 4-80016  
 Cu<sub>2</sub>(diethylenetriamine)<sub>2</sub>Cl<sub>2</sub>(ClO<sub>4</sub>)<sub>2</sub>, cryst. and mol. struct. 4-75431  
 DyB<sub>6</sub>, antiferromagnet, elec. resist. and thermoelec. power studies 4-113982  
 DyB<sub>6</sub>, low temp. resistivity and mag. props. 4-108859  
 DyCu<sub>2</sub>Ge<sub>2</sub>, mag. and cryst. struct., neutron diff. studies 4-65794  
 DyMoS<sub>4</sub>, two-stage flux penetration 4-108971  
 ErCrO<sub>3</sub>, quadrupole splitting and NMR near Morin-type transition 4-80839  
 Er<sub>2</sub>O<sub>3</sub> and Er(OH)<sub>3</sub>, relative concs. in tunnelling barriers, XPS obs., antiferromag. transition 4-88934  
 Er<sub>2</sub>O<sub>3</sub>·SO<sub>4</sub>, magnetic phase diagram, magnetisation and susceptibility meas. 4-92912  
 ErRh<sub>2</sub>B<sub>4</sub>, coexistence of superconductivity and mag. order 4-104423  
 Eu, BCC, generalised susceptibility and joint density of states 4-76118  
 Eu oxide and chalcogenides, exchange interactions, LCAO calculations 4-109009  
 EvSb, collinear antiferromag. struct., neutron diff. studies 4-108993  
 Fe (III) solutions, magnetisation meas. for oligomer formation detection 4-98917  
 $\alpha$ -(Fe<sub>1-x</sub>Al<sub>x</sub>)<sub>2</sub>O<sub>3</sub>, substituted hematite, Morin transition, <sup>57</sup>Fe Mossbauer study 4-71072  
 FeBO<sub>3</sub>, single crystal, magneto-optic effects 4-114248  
 Fe<sub>2</sub>BO<sub>6</sub>, antiferromag., Raman scatt. from phonons and magnons 4-76471  
 Fe<sub>1-x</sub>Co<sub>x</sub>Br<sub>2</sub>, antiferromag., random mixture with competing spin anisotropies, uniform and localised mag. modes 4-109066  
 Fe<sub>1-x</sub>Co<sub>x</sub>Br<sub>2</sub>, randomly mixed antiferromag. with competing Ising and XY spin anisotropies, mag. transitions 4-104446  
 Fe<sub>0.72</sub>Co<sub>0.28</sub>Cl<sub>2</sub>, disordered spin-flip phase obs. 4-104420  
 Fe<sub>1-x</sub>Co<sub>x</sub>Cl<sub>2</sub>, competing anisotropy system, Fe<sup>2+</sup> spin orientation, Mossbauer spectra 4-92906  
 Fe<sub>1-x</sub>Co<sub>x</sub>Cl<sub>2</sub>, nondiluted random-field Ising system, neutron diff. study 4-108992  
 $\alpha$ -Fe<sub>2-x</sub>Co<sub>x</sub>Si<sub>2-x</sub>O<sub>7</sub>, hematite, resonant and static mag. props., Co<sup>2+</sup> doping effects 4-92938  
 FeF<sub>2</sub>, antiferromagnet, mag. polarizations, photothermal detection 4-61526  
 Fe<sup>II</sup>Fe<sup>III</sup>F<sub>8</sub>(H<sub>2</sub>O)<sub>2</sub>, cryst. struct. and idle spin behaviour 4-108321  
 FeMO<sub>2</sub>S<sub>2</sub>, Chevrel-phase cpd., struct. and mag. transitions 4-76139  
 Fe<sub>2</sub>(MoO<sub>4</sub>)<sub>3</sub>, antiferromagnetic, magnetic and Mossbauer studies 4-71034  
 Fe<sub>2</sub>MoO<sub>8</sub>, crystal growth, mag. and elec. props. 4-71537  
 Fe<sub>0.99</sub>Ni<sub>0.01</sub>Cr<sub>20</sub>, mag. phase diagram, neutron diff. study 4-71069  
 Fe<sub>2</sub>Ni<sub>0.99</sub>Mn<sub>0.01</sub>, specific heat determ. (Russian) 4-65414  
 (Fe<sub>1-x</sub>Ni<sub>x</sub>)<sub>1-x</sub>Sb, antiferromag., mag. props. 4-104422  
 $\alpha$ -Fe<sub>2</sub>O<sub>3</sub>, anisotropy of elec. props., mag. order depend. 4-108853  
 $\alpha$ -Fe<sub>2</sub>O<sub>3</sub>, topotactic conversion of  $\gamma$ -FeOOH and comparative transform. methods of iron oxide in mag. spinels 4-109632  
 $\beta$ -FeOOH, Neel temp., struct. depend. 4-88665  
 $\gamma$ -FeOOH powder, grinding, lepidocrocite to hematite transform., morphology and mag. props., Mossbauer obs. 4-66329  
 Fe<sub>2</sub>(PO<sub>4</sub>)<sub>3</sub>, mixed valent, prep., cryst. struct., mag. props., Mossbauer spectra (French) 4-88146  
 FeSb<sub>2</sub>S<sub>4</sub>, berthierite, antiferromag. phase transition 4-65813  
 Fe<sub>2</sub>TiSe<sub>4</sub>, intercalation cpd., cryst. struct., mag. ordering, susceptibility meas., X-ray diff. 4-76119  
 FeVSe<sub>4</sub>, Mossbauer spectra, 4.8 to 700K 4-80849  
 Fe<sub>2</sub>Zn<sub>1-x</sub>p complex, hexa(pyridine-N-oxide) (ClO<sub>4</sub>)<sub>2</sub>, randomly diluted mag., sp. ht. studies 4-98903  
 Fe<sub>0.007</sub>Co<sub>0.993</sub>Cl<sub>2</sub> magnetoelastic coupling at Fe<sup>2+</sup> ions Mossbauer spectrum 4-92948  
 GaCrSe<sub>3</sub>, antiferromag. semicond., mag. susceptibility, cond., EPR, IR reflection spectrum, Neel temp., energy gap meas. 4-61522  
 Gd<sub>2</sub>Au<sub>2</sub>Al<sub>1-x</sub>, pseudobinary cpd., mag. behaviour 4-76136  
 Gd<sub>2</sub>B<sub>6</sub>, antiferromagnet, elec. resist. and thermoelec. power studies 4-113982  
 Gd<sub>2</sub>B<sub>6</sub>, low temp. resistivity and mag. props. 4-108859  
 Gd<sub>2</sub>Co<sub>2</sub> crystn., cryst. struct. and mag. props. in microgravity 4-98915

**antiferromagnetic properties of substances continued**

GdFe<sub>2</sub>H<sub>2</sub> films, ferromag. resonance and mag. props. 4-61594  
GdIn<sub>2</sub>Sn<sub>3-x</sub>, elec. resist. below Neel temp. 4-75924  
(Gd<sub>0.2</sub>Tb<sub>0.8</sub>)<sub>3</sub> Co<sub>2</sub> crystn., cryst. struct. and mag. props. in microgravity 4-98915  
H, atomic phase, binding and cohesive energy 4-70518  
HoAlGa, mag. transitions, mag. and cryst. structures, X-ray diffr., thermal expansion meas. 4-114113  
K<sub>2</sub> CoF<sub>4</sub> 2D Ising model, critical fluctuations, neutron scatt. meas. 4-92927  
K<sub>2</sub>Co<sub>0.27</sub>Fe<sub>0.73</sub>F<sub>4</sub>, magnetic ordering, elastic neutron study 4-104404  
K<sub>2</sub>Co<sub>1-x</sub>Fe<sub>x</sub>F<sub>4</sub>, mag. struct., phase transition, excitations, neutron scatt. meas. 4-88648  
K<sub>2</sub>Co<sub>1-x</sub>Fe<sub>x</sub>F<sub>4</sub>, spin waves, obs. in planar and oblique antiferromag. phases, Raman and far IR absorpt. spectra 4-98869  
KMnCl<sub>3</sub>, canted antiferromagnet, mag. props. 4-88655  
K<sub>2</sub>Ni<sub>1-x</sub>Zn<sub>x</sub>F<sub>4</sub>, dil. weakly anisotropic antiferromag., random-field effects on order 4-114092  
La(Fe<sub>1-x</sub>Al<sub>x</sub>)<sub>2</sub>, metamagnetic transitions and struct. aspects 4-92910  
LaNi<sub>1-x</sub>Fe<sub>x</sub>O<sub>3</sub>, antiferromagnetic interactions, mag. susceptibility meas. 4-88662  
LiMnFeF<sub>6</sub>,  $\alpha$ - and  $\beta$ -phases, magnetisation, Mossbauer and neutron studies 4-88752  
LiMnMF<sub>6</sub> (M = Fe, V, Ti, Cr, Ga), cationic distribution and mag. behaviour 4-71026  
Mn complexes, mag. susceptibilities determ. in temp. region below 77K. 4-71029  
Mn-Ge, Invar type, antiferromag., transition metal influence on props. (Japanese) 4-65826  
Mn<sub>3</sub>B<sub>4</sub>, mag. props. under high mag. field 4-84799  
MnCO<sub>3</sub>, antiferromagnetic, elastic oscillations generated by parametric excitation of spin waves 4-65802  
MnF<sub>2</sub>, antiferromagnetic, photoinduced single-ion mag. anisotropy 4-65806  
MnF<sub>2</sub>, antiferromagnets, hyperfine fields, muon spin relax. 4-71253  
MnF<sub>2</sub>, antiferromagnets, hot magnon sidebands temp. depend. 4-76493  
Mn<sub>2</sub>, mag. props., localisation of implanted positive muons,  $\mu$ SR obs. 4-98994  
MnF<sub>2</sub>, sublattice magnetisation and phase transitions, muon probe studies 4-98864  
Mn<sub>1-x</sub>Fe<sub>x</sub>CO<sub>3</sub>, mixed antiferromag. system, competing anisotropy and random field effects 4-109019  
MnFe<sub>2</sub>F<sub>8</sub>(H<sub>2</sub>O)<sub>2</sub>, cryst. struct. and idle spin behaviour 4-108321  
Mn<sub>0.75</sub>Mg<sub>0.25</sub>(Cr<sub>1-x</sub>V<sub>x</sub>)<sub>2</sub>O<sub>4</sub> mixed spinel systems, spin-glass-like behaviour 4-109024  
MnO, muon spin precession obs., local fields and phase transition 4-65921  
MnS<sub>2</sub>, antiferromag. struct., antiferromag. phase transition, neutron diffr. obs. 4-76115  
MnSb<sub>2</sub>O<sub>4</sub>, antiferromagnetic, structural and vibr. studies, anisotropic effects 4-113561  
MnSeO<sub>4</sub>, antiferromag. ordering EPR study 4-92954  
MnTiO<sub>3</sub>, electron density distrib., cryst. struct. determ. 4-103709  
Mn<sub>2</sub>Zn<sub>1-x</sub>Cr<sub>2</sub>O<sub>4</sub> mixed spinel systems, spin-glass-like behaviour 4-109024  
NH<sub>4</sub>MnFeF<sub>6</sub>, crystal structure and mag. props. 4-71038  
NaCa<sub>2</sub>Cu<sub>2</sub>V<sub>2</sub>O<sub>12</sub> garnet, mag. props. study 4-61563  
NaFeP<sub>2</sub>O<sub>7</sub>, crystallographic, mag. and Mossbauer studies 4-108323  
Na<sub>3</sub>Fe<sub>2</sub>(PO<sub>4</sub>)<sub>3</sub>, antiferromagnetic, magnetic and Mossbauer studies 4-71034  
NdB<sub>6</sub>, low temp. resistivity and mag. props. 4-108859  
Ni-Mn antiferromag. alloys, sublattice moment, composition depend. 4-76120  
NiBr<sub>2</sub>, helimag. and antiferromag., mag. excitations, neutron scatt. studies 4-104409  
NiCl<sub>2</sub> (Br<sub>2</sub>), optical spectra near mag. transition temp. 4-61729  
NiCl<sub>2</sub>·6H<sub>2</sub>O(4H<sub>2</sub>O), paramagnetic phase boundary of antiferromagnet at low temp. 4-88668  
NiCl<sub>2</sub>·6H<sub>2</sub>O, anisotropic antiferromagnet, temp. depend. of paramag. boundary 4-84786  
NiO single cryst. and powder, mag. susceptibility and exchange const. 4-84775  
NiSb<sub>2</sub>O<sub>4</sub>, antiferromagnetic, structural and vibr. studies, anisotropic effects 4-113561  
O, solid, mag. ordering in  $\beta$ -phase and  $\alpha$ - $\beta$  transition, general mol. field approx. 4-92883  
O<sub>2</sub>, solid  $\alpha$ -phase, far IR spectra in high mag. fields, magnons 4-114260  
Pb(Fe<sub>0.5</sub>Nb<sub>0.5</sub>)O<sub>3</sub>, ferroelec., mag. and magnetoelec. props. 4-65847  
PbFe<sub>2</sub>Ta<sub>0.5</sub>O<sub>7</sub>, single cryst., ferroelec./antiferromag., spontaneous birefringence 4-71344  
Pd<sub>0.5</sub>Cu<sub>0.5</sub>Si<sub>1.5</sub>M<sub>0.5</sub> (M = Fe or Mn), glasses, ferro- and antiferromagnetism study 4-71063  
Pd<sub>2</sub>(Fe<sub>1-x</sub>Mn<sub>x</sub>)<sub>3</sub> alloys, ordered and disordered, average mag. moments (Russian) 4-104406  
PrB<sub>6</sub>, low temp. resistivity and mag. props. 4-108859  
PrD<sub>1.35</sub>, mag. order and cryst. field effects 4-104408  
Pt-Fe alloys, mag. props. 4-84842  
Pt<sub>2</sub>Fe<sub>1-x</sub>Mn<sub>x</sub>, elec. cond. and mag. props. 4-104180  
Rb<sub>2</sub>Co<sub>2</sub>Mg<sub>1-x</sub>F<sub>8</sub>, spin exchange-flips, order-disorder transformations, magnetisation meas. 4-109023  
 $\beta$ -Rb<sub>2</sub>FeF<sub>6</sub>·H<sub>2</sub>O, one-dimens. antiferromagnet, mag. studies 4-71037  
RbMnBr<sub>3</sub>Er<sub>3</sub>, one-dimensional antiferromagnet, energy migration, luminesc. 4-99149  
RbMnCl<sub>3</sub>, antiferromag. with alternating strong and weak coupling, absorpt. spectra, fluoresc. meas. 4-88659  
RbMnCl<sub>3</sub>, antiferromagnetic, optical absorpt. spectra, luminesc. studies 4-99133  
RbMnCl<sub>3</sub>, crystal and mag. structure heterogeneities 4-84276  
Rb<sub>2</sub>MnCl<sub>4</sub>, 2D antiferromag., optical absorption and luminesc. 4-80991  
Rb<sub>2</sub>MnCl<sub>4</sub>, mag. moment origins, magnon sidebands, excitons, optical absorpt. spectra, MCD meas. 4-99097  
Rb<sub>2</sub>MnCl<sub>4</sub>, two-dimensional antiferromagnet, IR absorpt., Raman spectra, MCD studies 4-61713  
Rb<sub>2</sub>Mn<sub>2</sub>Cl<sub>7</sub>, 2D antiferromag., optical absorption and luminesc. 4-80991  
Rb<sub>2</sub>Mn<sub>2</sub>Cl<sub>7</sub>, two-dimensional antiferromagnet, IR absorpt., Raman spectra, MCD studies 4-61713  
Rb<sub>2</sub>Mn<sub>1-x</sub>Cr<sub>x</sub>Cl<sub>3</sub> mixed insulating ferromag. and antiferromag., ferromag. resonance studies 4-65863  
RbMnFeF<sub>6</sub>, crystal structure and mag. props. 4-71038  
RhMnSi, mag. props., magnetometry, neutron diffr. studies 4-71025

**antiferromagnetic properties of substances continued**

Sc<sub>1-x</sub>Ti<sub>x</sub>Fe<sub>2</sub>, itinerant electron system, coexistence of ferro- and antiferromagnetism 4-98857  
Si (111)-(1 $\times$ 1)-total energy calcs. for 2 $\times$ 1 antiferromag. and 1 $\times$ 1 paramag. states 4-80809  
SmRh<sub>4</sub>B<sub>4</sub>, mag. supercond., muon spin relax. studies 4-65923  
SrMnF<sub>2</sub>·H<sub>2</sub>O, hydrated fluorometallates (III), one-dimens. antiferromagnet 4-71035  
Sr<sub>2</sub>YRuO<sub>6</sub>, cryst. and mag. struct., time of flight neutron diffr. studies 4-88141  
Tb, critical sp. ht. meas. 4-84804  
TbFe<sub>1-x</sub>Al<sub>x</sub>O<sub>3</sub>, magnetic props., influence of mag. vacancies 4-104414  
TbIr<sub>2</sub>Si<sub>2</sub>, polymorphic, antiferromag., Neel temp., paramag. Curie temp., mag. struct. 4-109017  
Tb<sub>2</sub>Ir<sub>2</sub>Si<sub>2</sub>, antiferromag., Neel temp., paramag. Curie temp. 4-109017  
Tb<sub>2</sub>O<sub>2</sub>SO<sub>4</sub>, magnetisation, AC susceptibility, spectroscopic Zeeman effect meas. 4-76121  
TbPO<sub>4</sub>, magnetically annealed, magnetoelectric: susceptibility and mag. symmetry 4-71149  
U dipnictides, mag. props., cryst. field interpretation 4-76146  
U mononitrides, antiferromagnetic transition theory 4-88672  
UAs<sub>1-x</sub>Se<sub>x</sub>, mag. phase diagram, mag. susceptibility meas. 4-88651  
UN, antiferromag. and paramag. phases, mag. excitations, neutron inelastic scatt. 4-98873  
UNiAlH<sub>3</sub>, <sup>1</sup>H NMR and mag. susceptibility 4-71202  
U<sub>1-x</sub>Np<sub>x</sub>O<sub>2</sub>, solid solns., <sup>235</sup>Np Mossbauer effect and magnetisation 4-76125  
U<sub>1-x</sub>Th<sub>x</sub>As<sub>2</sub>, mag. phase diagram, mag. susceptibility meas. 4-88651  
VBr<sub>2</sub>, 2-D triangular Heisenberg antiferromag., heat capacities 4-76156  
VBr<sub>2</sub>, triangular lattice antiferromag., spin struct., neutron pol. anal. 4-76112  
VCl<sub>2</sub>, 2-D triangular Heisenberg antiferromag., heat capacities 4-76156  
VCl<sub>2</sub>(Br<sub>2</sub>)<sub>1/2</sub>, triangular Heisenberg antiferromagnet in paramag. state, hyperfine field, <sup>51</sup>V nucl. relax., NMR 4-92973  
Vl<sub>2</sub>, 2-D triangular Heisenberg antiferromag., heat capacities 4-76156  
V<sub>2</sub>O<sub>3</sub>, metal-insulator transition and Neel temp. 4-70656  
V<sub>2</sub>O<sub>3</sub>, muon spin precession obs., local fields and phase transition 4-65921  
V<sub>2</sub>O<sub>3</sub>, NMR study of mag. props. 4-80835  
YFeO<sub>3</sub>, mag. spectrum meas. using submillimetre spectroscopy 4-109005  
(Y<sub>1-x</sub>Gd<sub>x</sub>)Ni<sub>3</sub>, mag. props. meas. 4-80785  
YMn<sub>2</sub>, electronic struct. and spontaneous volume magnetostriction 4-104395  
Y(Mn<sub>1-x</sub>Co<sub>x</sub>)<sub>2</sub>, mag. struct., neutron diffr. study (Chinese) 4-92892  
ZnCr<sub>1-x</sub>Ga<sub>x</sub>O<sub>4</sub> antiferromag. frustrated spinel, spin glass behaviour 4-114119  
ZnFe<sub>2</sub>O<sub>4</sub> ferrite, mag. struct. and Neel temp. 4-108986  
Zn<sub>1-x</sub>Ga<sub>2x</sub>Cr<sub>2</sub>Se<sub>4</sub>, magnetic semiconducting solid solutions study 4-109002

**antiferromagnetic resonance**

bisethylammonium tetrachlorocuprate, AFMR line distortion by RF field power 4-104495  
cyclohexylammonium copper trichloride and tribromide, exchange anisotropy study 4-80758  
BaMnF<sub>4</sub>, magneto-electric, unsolved problems 4-76255  
Fe<sub>1-x</sub>Co<sub>x</sub>Br<sub>2</sub>, antiferromag., random mixture with competing spin anisotropies, uniform and localised mag. modes 4-109066  
Fe<sub>1-x</sub>Co<sub>x</sub>Cl<sub>2</sub>, random mixture with competing spin anisotropies, AFMR, FMR obs. 4-76259  
 $\alpha$ -Fe<sub>2-x</sub>Co<sub>x</sub>/Si<sub>1-x</sub>O<sub>2</sub>, hematite, resonant and static mag. props., Co<sup>2+</sup> doping effects 4-92938  
FeF<sub>2</sub>, antiferromagnet, mag. polaritons, photothermal detection 4-61526  
O<sub>2</sub>, solid  $\alpha$ -phase, far IR spectra in high mag. fields, magnons 4-114260  
YFeO<sub>3</sub>, mag. spectrum meas. using submillimetre spectroscopy 4-109005

**antiferromagnetism**

see also antiferromagnetic properties of substances; exchange interactions (electron); metamagnetism

anisotropic antiferromagnet, temp. depend. of paramag. boundary 4-84786  
antiferromagnetic ferroelectric, equilibrium state of mag. subsystem 4-71150  
antiferromagnetic semiconductors, mag. polaron study (Russian) 4-70682  
antiferromagnetic spin glass, HF characts. (Russian) 4-71105  
conduction electrons, ground state, strong mag. field effect 4-108981  
dilute antiferromag. chain, critical dynamic response 4-71119  
dilute magnets, phase transitions, critical behaviour, percolation, random fields 4-88690  
disordered spin system with frustration, phase transitions (Russian) 4-104427  
easy plane, NQR linewidths, diagrammatic calcs. 4-109094  
extended Hubbard model with half-filled band, ground state beyond the HF approx. 4-76147  
first order phase, phase transitions of the order-disorder type 4-65814  
fluctuation driven first order transitions, possibility, review 4-71077  
frustrated Ising zigzag chains, dilution and boundary condition effects, 2 spin corrs. 4-71109  
fully frustrated Ising model on 2-dimens. lattice, Kosterlitz-Thouless phase transition 4-76152  
Heisenberg, antiferromagnet, susceptibility, spin-wave Hamiltonian 4-104393  
Heisenberg antiferromagnetic chain, anisotropic, degenerate ground states and excited states 4-61506  
Heisenberg antiferromagnetic: linear chain, spin-Peierls instabilities, antiferromag. transitions and phonon dynamics 4-65824  
Heisenberg classical chain with two anisotropies, low temp. thermodynamics and correlation functions 4-92929  
Heisenberg linear chain in mag. field, Green's function approach 4-114129  
Heisenberg model, 1-D isotropic, ground state props. 4-98851  
Heisenberg model, correlation theory, dimension, field and temp. depend. 4-114086  
Heisenberg model with planar anisotropy, ferromag. and antiferromag., ground state magnetisation transitions 4-71120  
Heisenberg quantum chains, axially anisotropic, ground state props. 4-61505  
Heisenberg two-dimensional classical isotropic model, phase diagram in mag. field 4-109031  
hexagonal lattice, simple, with competing interactions, modulated phases, Ising model 4-92925

**antiferromagnetism** continued  
 hierarchical Dyson models, ground states, devil's stair-type functions 4-95367  
 homogeneously random Ising antiferromagnet, Monte Carlo study 4-61501  
 incommensurate magnetic structures formation, exchange integrals 4-114088  
 Ising model, anisotropic, long-range order, quenched impurity effects 4-98848  
 Ising model, FCC, hysteresis and free energy, computer simulation 4-114127  
 Ising model, partially frustrated systems 4-104387  
 Ising model decorated hypercubic lattice with multiple transitions, transition point location 4-109034  
 lattice gases, antiferromag., generalised Bragg-Williams method 4-86369  
 linear Ising ferromagnet with antiferromagnetic impurities ground state 4-71118  
 longitudinally magnetized antiferromagnet, exchange-free spin waves 4-71047  
 magnetoacoustic effects, ferromagnets and antiferromagnets, symmetry breaking for mag. ordering 4-84844  
 magnetoacoustics of ferro- and antiferromagnets 4-76224  
 magnetocaloric effect near a spin-reorientation transition (*Russian*) 4-80764  
 magnon specific heat, temp. dependence 4-88658  
 metallic jellium and Wigner cryst., cooperative magnetism and transitions 4-76149  
 metals, antiferromagnetic, magnon relax. study (*Russian*) 4-80749  
 mixed valence d<sup>1</sup>-d<sup>2</sup> clusters, vibronic reduction effects 4-88490  
 NMR amplification coeff. for mag. wave-elastic wave superstrong coupling 4-8825  
 noncollinear antiferromagnet, spin-flip transitions 4-104425  
 one-dimensional classical Heisenberg antiferromagnetic, equivalence at low temp. between mag. field and anisotropy 4-98912  
 one-dimensional classical planar model with competing interactions 4-80767  
 percolating Heisenberg model, spin excitation waves, effective medium approx. anal. 4-114131  
 plane rotator model on triangular lattice, spin wave anal., symm. breaking in mag. field 4-109004  
 Potts model of magnetism, critical dimensionalities and props. 4-61499  
 Potts model on a closed Cayley tree 4-61497  
 Potts model partition function, location of the phase transition 4-86346  
 Potts models, ferromag. and antiferromag., phase transition, Bethe approx. 4-92918  
 quantum Heisenberg spin systems, Monte Carlo soln. 4-104453  
 s-f model in zero bandwidth limit, complete analytical soln. 4-76101  
 sound absorption and scattering by nuclear spin waves 4-88245  
 sound interaction with subsurface mag. inhomogeneities 4-114149  
 spin glasses, antiferromagnetic, spin waves and metastability 4-80768  
 spin waves in system with helical ordering (*Russian*) 4-71049  
 spin-1 antiferromagnetic chain, ground-state props. calcs. 4-71102  
 spin-1 antiferromagnetic Heisenberg-Ising chain 4-71101  
 stacked frustrated antiferromagnetic triangular Ising system, ordering study 4-71116  
 SU<sub>2</sub> magnet, excitation of anisotropic generalisation 4-65783  
 superconductivity-weak ferromagnetism coexistence phase, mag. structs. 4-92897  
 superconductor, antiferromag., theory of upper critical field 4-76090  
 superconductor, upper critical field theory 4-84755  
 superconductors, Cooper pairing in the presence of antiferromagnetism 4-88631  
 surface polaritons in conductive antiferromagnetic media (*Russian*) 4-92627  
 susceptibility, transfer matrix in plane-rotator model 4-114084  
 tetragonal antiferromagnet, refractive index 4-80907  
 TMMC, specific heat, sine-Gordon kinks and renormalisation 4-71100  
 two-dimensional, anisotropy and magnetisation 4-109010  
 two-dimensional antiferromagnetic plane rotator model on triangular lattice, phase transitions 4-65818  
 uniaxial, one and three dimensional dynamic solitons 4-80757  
 uniform magnetic chain with second-neighbour interactions at finite temperatures 4-61504  
 weakly anisotropic, phase diagram and critical lines (*Russian*) 4-71062  
 weakly ferromagnetic rhombohedral antiferromagnets, magneto-optic effects 4-114248  
 XY chain with impurities, local magnetisation, Green's function calc. 4-98846  
 Fe complex,  $\mu$ -oxo Fe (III) porphyrin dimers, antiferromag. coupling, <sup>13</sup>C NMR spectra 4-64508

**antihyperons** see hyperons

## antimony

see also nuclei with .....  
 adsorption on Si MBE layer 4-65560  
 amorphous, elec. resist. and thermoelec. power meas. 4-108886  
 amorphous films, obliquely vacuum deposited, growth and crystn. 4-98491  
 amorphous-crystalline transition, stability anal. 4-103686  
 biogeochemistry in Baltic Sea 4-77154  
 crystal growth rate of pure metals nucleated from undercooled melt 4-98042  
 effect of addition to Fe-Si (3 wt.%) steel, textures 4-81216  
 electro-oxidation and electro-reduction kinetics in alkaline solns. 4-66681  
 film on glass substrate, laser damage study 4-108433  
 L-shell X-ray prod. cross sections, H<sup>+</sup> induced, ratios 4-66131  
 layer coating on Fe, oxidation, Mossbauer spectra obs. 4-61609  
 liquid, self-diffusion coeffs., temp. depend. 4-65426  
 liquid, thermodynamics, pseudopotential theory 4-79924  
 phase transitions at hydrostatic press. up to 9 GPa 4-75666  
 Raman scatt. from wedge-shaped Sb films on Ag films 4-109172  
 single crystal, reaction diffusion, chemoeptaxial nucleation of In, Cd and S vapours 4-65583  
 speciation and content in Saanich Inlet water column and interstitial waters 4-82314  
 speciation in seawater 4-82313  
 Al-Sb, ion implanted, hardness, friction and wear props. 4-66451  
 amorphous film, UV photoemission study 4-88942  
 amorphous film, vacuum deposited, isochronous annealing, crystallisation 4-61854  
 BaTiO<sub>3</sub>/Sb, sintering, microstruct. 4-89012

## antimony continued

CdS/Sb films, vacuum deposited, struct., elec. and optical props., impurity conc. effect 4-98607  
 Ge:Ar(Sb), neutron-transmutation-doped, defects 4-60967  
 Ge:Sb, heavily doped, US attenuation, mag. field depend. 4-70283  
 Ge:Sb, impurity state breakdown under uniaxial compression 4-70715  
 Ge:Sb, intervalley neutral impurity scatt. (*Russian*) 4-104197  
 Ge:Sb, photoexcited, impurity breakdown and impact ionisation 4-92739  
 n-Ge:Sb, US attenuation, mag. field effects, impurity conc. depend. 4-75618  
 Ge:Sb, wave-function phase, relax. time, temp. depend. 4-88517  
 Ge:Sb film on GaAs, doping and elec. props. study (*Russian*) 4-70182  
 Ge:Zn, Sb, degree of compensation from optical absorption meas. 4-109221  
 InP:Ga/Sb crystals, dislocation density reduction by isoelectronic double doping 4-60940  
 Sb/SnTe superlattice, SAW velocity, Brillouin spectra studies 4-108694  
 Sb-Co multilayered films, cpd. form., interface magnetism, <sup>57</sup>Co NMR obs. 4-109095  
 Sb-KMnO<sub>4</sub> pyrotechnic composition, thermal conductivity meas., embedded Cu probe appl. 4-111128  
 Sb + <sup>4</sup>He<sup>+</sup>, L-shell X-ray prod. cross-sections 4-107305  
 Sb<sub>4</sub>, He I photoelectron spectra, high temp. 4-107399  
 Si:As(Sb)(In), ion implanted, pulsed electron beam annealing, impurity diffusion 4-103984  
 Si:Ga(Sb), amorphous, highly doped, MBE grown, epitaxial regrowth 4-98468  
 Si:Ge(Sb)(W), electron beam doping, SIMS and RBS studies (*Japanese*) 4-108401  
 Si:P, Sb, P diffusion, self-interstitial supersaturation and vacancy undersaturation 4-70457  
 Si:Sb, electrolytic Sb diffusion in MOS structures 4-80299  
 Si:Sb, implanted laser irradi., crystn. annealing, time-resolved reflectivity, TEM, Rutherford backscattering anal. 4-80093  
 Si:Sb, ion implanted, dopant site location and profiles, channelling studies 4-108393  
 Si:Sb, ion implanted, supersaturation, vitreous C strip heater annealing, Rutherford backscattering, elec. meas. 4-92375  
 Si:Sb, possible obs. of electronic phase transition, low temp. magnetoresist. study 4-80633  
 Si:Sb, shallow donor polarisability 4-92666  
 Si:Sb, shallow dopant profile production by low-angle ion implantation 4-108396  
 Si:Sb epilayer, ion implanted, annealing study 4-108735  
 Si:Sb single crystals, impurity atom localisation, Rutherford backscatt. yield in planar channelling 4-75489  
 Si:Sb<sup>+</sup>, ion implanted and laser annealed, defects, photoluminescence studies 4-75433  
 Si, Ge<sub>1-x</sub>P<sub>x</sub>(As)(Sb), paired donor impurities energy levels 4-61315  
 SnO<sub>2</sub>/Sb film deposition by sol-gel technique, optical and elec. characts. 4-71604  
 SnO<sub>2</sub>(Sb) films, resistivity and optical transmittance, annealing effects 4-70967

**antimony alloys**  
 see also antimony compounds  
 Heusler alloys, band struct., mag. moments, hyperfine fields, local spin density method 4-108767  
 liquid, mag. props. of transition metal solutes 4-76109  
 Al-Sb system, phase diagram calc., Krupkowski's eqn. (*Polish*) 4-85139  
 Al-Si-Sb, eutectic, struct. rel. to Sb addition, electron beam microanalysis (*German, English*) 4-66314  
 Au-Cu-Sb metallic glass, liq.-quenched, form. and low temp. electronic props. 4-75919  
 Bi-Sb, liq. alloys, activities and free energy of form., EMF obs. (*Japanese*) 4-61920  
 Bi-Sb, temp. effect on elastic props. 4-98171  
 Bi-Sb, US attenuation and quantum oscils. 4-92768  
 Bi-Sb single crystals, etching characts. of edge and screw dislocations on cleavage plane 4-80044  
 n-Bi<sub>1-x</sub>Sb<sub>x</sub>, electron scatt., low temp. 4-108835  
 Bi<sub>1-x</sub>Sb<sub>x</sub>, electronic density of states and its mass 4-88439  
 Bi<sub>100-x</sub>Sb<sub>x</sub>, mould grown cryst., component distrib., X-ray study 4-75694  
 Ce-Ni-Sb system, phase equilib. diagram, X-ray analysis 4-114491  
 Cu-Sb, free enthalpy of impurity-vacancy binding, solvent diffusion meas. 4-84465  
 Cu-Sb, liq., Sb activity meas. by Knudsen effusion method with electrobalance 4-66312  
 Cu-Sb (1 wt.%), creep rupture life, effects of pre-existing grain boundary cavities 4-62042  
 Cu-Sb alloys, grain boundary segregation and cracking, Monte Carlo studies 4-114542  
 EuPd<sub>2</sub>Sb<sub>3</sub>, cryst. struct. determ. 4-79985  
 EvSb, collinear antiferromag. struct., neutron diffr. studies 4-108993  
 Fe-Sb-Ce alloys, Ce state at cryst. boundaries, electron diffr. studies (*Chinese*) 4-98114  
 (GaSb)<sub>1-x</sub>(Ge<sub>2</sub>)<sub>x</sub>, semicond. alloys, phase transforms. 4-92347  
 Ge-Sb amorphous thin films, hopping cond. meas., 130 to 300K, localised state variations 4-92713  
 In-Ga-Sb alloys, liq., phase diagram calc., Krupkowski's eqn. (*Polish*) 4-85139  
 In-Sb system, high press. intermediate phases, form., struct., stability, supercond. props. 4-89029  
 InSb film, condensed at low temp., conductance, transition temp. meas. 4-61482  
 LaNi<sub>2</sub>Sb<sub>2</sub>, cryst. struct. determ. 4-79985  
 MnSb-based solid solns., recording media in optical memory appls. 4-61572  
 Mn<sub>2</sub>Sb, NMR of <sup>55</sup>Mn, <sup>121</sup>Sb and <sup>123</sup>Sb, hyperfine fields 4-114167  
 Nb<sub>3</sub>Sb, phonon dispersion curves and electron-phonon interaction calcs. 4-70313  
 Ni-Sb,  $\alpha$ -solid solution, interdiffusion (*Japanese*) 4-113700  
 Ni-Sb, retardation of grain boundary self-diffusion 4-84447  
 Ni<sub>2-x</sub>MnSb, chemical order and mec. props. 4-88666  
 Pb-Sb ingot casting, equiaxed zone form., dendritic solidification front 4-99379  
 PtMnSb, magneto-optical props. and electronic struct. 4-61662  
 Sb-Bi, muon spin rot. and muon Knight shift meas. 4-71235  
 Sb-Cd system, reaction diffusion, chemoeptaxial nucleation of Cd vapour 4-65583  
 Sb-Cu-Sb, eutectic alloys, melting mechanism 4-114507

# antimony alloys continued

- Sb-In system, reaction diffusion, chemoeptitaxial nucleation of In vapour 4-65583  
Sb-InSb, eutectic alloys, melting mechanism 4-114507  
Sb-S system, reaction diffusion, chemoeptitaxial nucleation of S vapour 4-65583  
SbZn liquid alloys, entropy of mixing, hard-sphere system calcs. 4-92371  
Sr<sub>2</sub>Al<sub>2</sub>Sb<sub>6</sub>, Zintl phases with complex anions (*German*) 4-70067  
V<sub>2</sub>Ge<sub>1-x</sub>Sb<sub>x</sub>, superconductivity and electron-phonon parameter 4-114058

# antimony compounds

- see also *antimony alloys*  
intercalation compound with graphite, SbCl<sub>3</sub>-graphite, ultrasonic velocity meas. 4-70284  
Ag<sub>2</sub>SbS<sub>3</sub>, absorpt. edge temp. depend. (*Russian*) 4-71410  
Ag<sub>2</sub>SbS<sub>3</sub>, acoustoelectric interactions in electroacoustic echo 4-80631  
Al-(SnO<sub>2</sub>+Sb<sub>2</sub>O<sub>3</sub>)-Al mixed thin films, dielec. studies 4-84719  
As-Sb-Sc system, glass-ceramic composites, varistor-like behaviour 4-114009  
Au-Sb-S<sub>3</sub>-Al MIM struct., bias voltage depend. of capacitance 4-104325  
Bi-Sb-Te, solid solutions, maximum figure of merit 4-113981  
Bi<sub>2</sub>-Sb<sub>2</sub>Se<sub>3</sub> single cryst., magnetoresist. in transverse quantising mag. fields 4-98643  
Bi<sub>2</sub>Sb<sub>2</sub>Te<sub>3</sub> films, strain-resist. effects, struct. effects 4-114052  
Bi<sub>2</sub>Te<sub>3</sub>-Sb<sub>2</sub>Te<sub>3</sub>, n-type solid solution, effect of annealing in air on electro-physical props. 4-113945  
Ge-Sb-Se, antireflection coatings for YAG crystals (*Russian*) 4-97012  
Ge-Sb-Se glasses, dilatometric studies 4-108634  
Ge-Sb-Se vitreous chalcogenide based multilayer reflecting sytems for IR lasers 4-69532  
GeO<sub>2</sub>-Sb<sub>2</sub>OP<sub>3</sub> optical fibres fabricated by vapour-phase axial deposition method 4-107855  
(GeSe<sub>3</sub>)<sub>100-x</sub>Sb<sub>x</sub>, struct. and resist. effect of dopants, high press. study 4-103660  
GeTe-Ag<sub>2</sub>Te-Sb<sub>2</sub>Te<sub>3</sub> system, solid soln., fabrication technology 4-75682  
KSbF<sub>4</sub>, structural phase transitions, NQR, specific heat, X-ray powder anal., permitt., elec. cond. 4-113605  
Sb chalcogenohalide based ACH-2 ferroelectric, soft microwave modes 4-84920  
Sb<sub>2</sub>Te<sub>3</sub> single cryst., weak field charge transport 4-108887  
SbCl<sub>3</sub>, <sup>55</sup>Cl NQR linewidths, dipolar second moments calc., degeneracy of  $\pm 3/2$  and  $\pm 1/2$  levels 4-71206  
SbCl<sub>3</sub>, ionic crystals growing from melts, morphology and kinetics 4-113370  
SbCl<sub>3</sub> intercalation compound with graphite, absolute spin susceptibility, orbital paramagnetism 4-76105  
SbCl<sub>3</sub>-C<sub>12</sub>SbCl<sub>3</sub> intercalation cpd. with graphite, resistivity and Hall effect (*Russian*) 4-113917  
SbCl<sub>3</sub>-graphite intercalation cpd., de Haas-van Alphen effect meas. 4-88440  
SbCl<sub>3</sub>-graphite intercalation cpd., lattice expansion, phase transition effects, X-ray diff. studies 4-98076  
SbCl<sub>6</sub><sup>3-</sup> in cryst. lattice, intervalence absorpt., IR study 4-61734  
SbF<sub>3</sub>+diaminotetrachlorotriphosphazenes, fluorinating reaction, <sup>19</sup>F and <sup>1</sup>H NMR study 4-66581  
SbF<sub>3</sub>Cl<sub>2</sub>, valence force field pot. consts., vibr. anal. 4-102661  
Sb(III) complexes, struct., <sup>121</sup>Sb Mossbauer spectral obs. 4-96583  
Sb<sub>2</sub>-Mo<sub>2</sub>O<sub>4</sub>, preparation, cryst. struct., elec. and optical props. 4-84266  
Sb<sub>2</sub>MoO<sub>4</sub>, cryst. struct., X-ray and powder neutron diff. studies 4-108334  
Sb<sub>2</sub>MoO<sub>6</sub>, band struct., transport props. 4-108773  
Sb<sub>2</sub>O<sub>3</sub>Cl<sub>2</sub>, onoratoite, pure and hydrated, cryst. structs. and twin planes 4-113407  
Sb<sub>2</sub>O<sub>3</sub>.nH<sub>2</sub>O, d.c. proton cond. and Nernst effect meas. 4-84462  
Sb<sub>2</sub>S<sub>3</sub>, amorphous thin films, struct. and crystn. 4-60842  
Sb<sub>2</sub>S<sub>3</sub>, anodic films on Sb electrodes, form. and reduction 4-93435  
Sb<sub>2</sub>S<sub>3</sub> glassy film, Schottky barrier form. at contact with metal 4-104291  
Sb<sub>2</sub>S<sub>3</sub>Se, spectrographic Se determination 4-109698  
SbSBr, ferroelec. phase transitions, elec. permittivity studies 4-65981  
SbSI, differential polarisability, optical reflectance ellipsometry study 4-88796  
SbSI ferroelec. semicond., energy band struct., X-ray spectral studies 4-65609  
SbSI ferroelectric, L<sub>III</sub> edge above transition temp., EXAFS study 4-61772  
SbSI, L absorption edges, EXAFS studies 4-71475  
SbSI, para-ferroelec. phase transition, photoacoustic spectra studies 4-65975  
SbSI, paraelectric and ferroelec. phases, L-edge XANES and EXAFS obs. 4-88904  
SbSI type cryst., soft modes, microwave dielec. studies 4-71293  
SbSI<sub>1-x</sub>Se<sub>x</sub>I cryst., soft mode in microwave dielec. spectrum 4-76361  
SbS<sub>2</sub>Se<sub>1-x</sub>, ferroelec. phase transition, dilatometric study 4-114222  
Sb<sub>2</sub>Se<sub>3</sub>-S system, liq. and amorphous, phase diagram and short range order 4-103905  
SbSeI, differential polarisability, optical reflectance ellipsometry study 4-88796  
Sb<sub>2</sub>Te<sub>3</sub> single cryst., band struct. and scatt. mechanisms, IR transmission studies 4-80934  
Sb<sub>2</sub>Te<sub>3</sub>, weak-field transport, thermoelec., galvano- and thermo-mag. coefficients 4-98613  
Sb<sub>2</sub>Te<sub>3</sub>-Pb(Ge), doping props., elec. cond. and Seebeck measurements 4-73467  
Sb<sub>2</sub>Te<sub>3</sub>-Bi<sub>2</sub>Te<sub>3</sub>-Bi<sub>2</sub>Se<sub>3</sub>-Se-Te, physicochemical equilibria and crystallisation 4-61053  
Sb<sub>2</sub>Te<sub>3</sub>-Bi<sub>2</sub>Te<sub>3</sub>-Te, physicochemical equilibria and crystallisation 4-61053  
SbTeI, cryst. struct., full matrix least squares refinement 4-92168  
Sb<sub>2</sub>/Zn<sub>1/3</sub>O<sub>4</sub> sintered spinel, elec. cond. and Seebeck coeff., 400-800°C 4-61368  
Se-Sb amorphous, DC conductivity thickness dependence 4-84620  
Sn<sub>2</sub>Sb<sub>2</sub>S<sub>6</sub>, cryst. struct., TEM, X-ray diff. 4-65238  
Sn<sub>2</sub>Sb<sub>2</sub>S<sub>6</sub>, cryst. struct. determ. 4-84263

# antineutrinos see neutrinos

# antineutrons see neutrons

# antinucleons see nucleons

# antiphas boundaries

- alloys, microstructure, classification, overview 4-66309  
alloys, ordered, two-dimensional antiphase structures, dark-field high resolution images 4-113662  
alloys, superdislocation traps in inhomogeneous glide plane (*Russian*) 4-92210

# antiphas boundaries continued

- alumina, metastable phases, TEM, X-ray diff. obs. 4-113661  
superlattice alloys, one-dimensional long-period, stability due to Madelung energy 4-60880  
Al-Ti long-period one-dimensional antiphase structures, electron diff. and microscopy, X-ray diff. 4-113398  
Au-Mn long-period ordered structures, electron microscopy study 4-113396  
Au<sub>2</sub>Mn crystal, antiphase boundaries, high resolution TEM image simulation 4-97985  
Au<sub>2</sub>Mn<sub>2</sub>, long period antiphase boundary struct., electron diff., electron microscopy obs. 4-103946  
Cu-Al-Ni shape memory alloy, martensitic transform., effects of parent phase aging 4-66334  
Cu-Zn-Au, ordered, two-dimensional antiphase struct., electron diff. study 4-113397  
CuAu, microstructure, field ion microscopy study 4-88177  
Cu<sub>2</sub>NiZn, superlattice dislocations, TEM microstruct. study 4-75450  
CuZn, antiphase boundary energy, superlattice dislocations, slip systems, weak-beam electron microscopy obs. 4-104792  
Fe-Al alloys, segregation to static and migrating diffuse antiphase boundaries 4-114541  
FeCo alloy, brittleness, purity and impurity segregation effects (*Russian*) 4-109496  
Ni (100), N<sub>2</sub> adsorption, thermodynamic meas. 4-92563  
Ni<sub>3</sub>Al, cold-rolled, recrystn. annealing 4-81213  
Ni<sub>3</sub>Fe, short range ordering, atomic configurations 4-113338  
Sc<sub>2</sub>S<sub>3</sub>, cryst. struct., electron irradi. induced disorder 4-103713  
Si, partial 90° dislocation, structural and elec. props. 4-108368
- antiphase domains  
see also *antiphase boundaries*  
alloys, ordered, two-dimensional antiphase structures, dark-field high resolution images 4-113662  
alloys, superdislocation traps in inhomogeneous glide plane (*Russian*) 4-92210  
one-dimensional long-period superstructural alloys, config. of antiphase domains 4-113663  
order-disorder transformations, order-wave description using continuum model 4-113574  
polar thermotropic liq. cryst. binary mixture, smectic A<sub>1</sub>-A<sub>2</sub> transition, X-ray diff. study 4-88293  
poly(vinylidene fluoride), struct. disorder and polymorphic transformations 4-98028  
Al-Ti long-period one-dimensional antiphase structures, electron diff. and microscopy, X-ray diff. 4-113398  
Au-Mn long-period ordered structures, electron microscopy study 4-113396  
Cu-Al-Ni shape memory alloy, martensitic transform., effects of parent phase aging 4-66334  
 $\beta$ -Cu-Zn-Al,  $\gamma$ -brass-type precipitates, origin of incommensurate electron diff. pattern 4-76775  
Cu-Zn-Au, ordered, two-dimensional antiphase struct., electron diff. study 4-113397  
Cu<sub>2</sub>NiZn, superlattice dislocations, TEM microstruct. study 4-75450  
Fe<sub>3</sub>Si<sub>10</sub>, defect struct., high resolution transmission electron microscopy studies 4-108388  
GaAs:Ge(001), MBE grown, TEM image contrast from antiphase domains 4-104098  
NiAl-Cr quasibinary eutectic, rapidly solidified, microstruct. and phase solubility extension 4-66319  
Tb,Pr<sub>1-x</sub>, x=0.803, 0.798, neutron diffuse scatt., profile anal. 4-61510  
Ti<sub>58.7</sub>Ni<sub>37.5</sub>Al<sub>3.8</sub>, charge wave density transitions, electron microscopy study 4-98596  
W (112) with chemisorbed O<sub>2</sub>, kinetics of antiphase domain coarsening 4-98435
- antiprotons see protons
- antireflection coatings  
broad double-band antirefl. coatings on glasses for 1.06  $\mu$ m, visible or UV radiation 4-69530  
dielectric coating refractive index meas. during deposition 4-74750  
diffuse reflection coatings, heat-resistant, for concentrating high-intensity sources radiation onto receiving surface 4-91566  
five-layer achromatic antirefl. coatings for high refr. index glasses, development and testing 4-79271  
Giotto spacecraft thermal design 4-74635  
glass, Na<sub>2</sub>O-CaO-SiO<sub>2</sub>, development of porous antireflective films 4-62083  
gradient-index antireflection layer props. on phase-separable glass 4-69533  
interface between isotropic media, monolayer coating thickness providing antirefl. coating at two wavelengths, thickness calc. 4-60132  
IR optics elements design, materials, coatings and fabrication, update 4-79250  
laser damage thresholds of thin film optical coatings at 248 nm 4-74579  
laser induced failure of antirefl.-coated LiNbO<sub>3</sub> surfaces 4-75524  
laser two-wavelength antireflection coating at 1.06 and 0.53  $\mu$ m (*Chinese*) 4-91485  
multilayer antireflection coatings, design and optimisation 4-69531  
multiple halfwave antireflection coating design 4-69529  
optical films and antirefl. coatings deposited from solns. mech. strength 4-74670  
optical films for solar energy applications 4-85356  
pyrene thin film coating for Si solar cells, energy transfer processes 4-77109  
reflectivity meas. using mirror reflectometer 4-78364  
scatter and residual reflectance in visible region from coated optical components, meas. 4-102999  
silica low-reflection coatings for collector covers, by a dip-coating process 4-62389  
single-layer antireflection coatings on InGaAsP laser facets, theoretical design 4-69409  
solar collectors, evacuated, all-glass, materials science progress 4-62391  
solar reflective control film, effectiveness in solar heat control and thermal insulation (*Japanese*) 4-99950  
thickness error influence during evaporation process, linear correction 4-69601  
thin film applications in optics, principles and design methods 4-74662  
thin film technology, industrial applications, review 4-95126  
two-film, stable optical props., CAD method (*Russian*) 4-109261

**antireflection coatings** continued

- ultrawide wave band optical materials and systems, multi-sensor appl. 4-11252
- undercoats and overcoats, effects on damage thresholds of 248 nm coatings 4-74671
- UV coatings, high-efficiency, materials research, design and prod. 4-69528
- vacuum deposition, coater modernisation using cryopump 4-71562
- wide spectrum coating for fused SiO<sub>2</sub> and other glasses 4-74661
- window and mirror components, coated, pulsed DF chain laser damage 4-74582
- Al-based sputtered solar selective absorbing surfaces, props., effects of various antireflection coatings 4-114954
- AlGaAs/GaAs concentrator solar cells under high temp. and humidity conditions 4-66708
- Al<sub>0.9</sub>Ga<sub>0.1</sub>As-GaAs twin-channel substrate mesa guide laser with antirefl. coatings, single longit. mode operation 4-83619
- a-C:H hard thin films, RF plasma deposition 4-76681
- CaF<sub>2</sub>, antireflection coatings for YAG crystals (*Russian*) 4-97012
- CdGa<sub>2</sub>Se<sub>4</sub>, antireflection coatings for YAG crystals (*Russian*) 4-97012
- Cu/CuO(N<sub>x</sub>) composites, reactive ion beam sputter deposited, optical recording appl. 4-79249
- Ga<sub>1-x</sub>Al<sub>x</sub>As/GaAs solar cell with antirefl. coating, LPE grown, design, fabrication and charact. (*Polish*) 4-114904
- GaAs/GaAlAs, antirefl. coated twin DH diode external cavity ring laser, optical bistability study 4-91460
- Ge microrelief surface, reflecting power and etching form. (*Russian*) 4-64757
- Ge-As(Sb)-S(Se), antireflection coatings for YAG crystals (*Russian*) 4-97012
- HfO<sub>2</sub> optical films and antirefl. coatings deposited from solns. mech. strength 4-74670
- In/InO<sub>x</sub>(N<sub>x</sub>) composites, reactive ion beam sputter deposited, optical recording appl. 4-79249
- MgF<sub>2</sub> antireflection coating for CuO/stainless steel- and CuO/stainless steel tandem solar absorber converters 4-99999
- MgF<sub>2</sub> film deposition process, form. and optimisation 4-61855
- Na<sub>2</sub>O-B<sub>2</sub>O<sub>3</sub>-SiO<sub>2</sub> graded-index coatings deposited by sol-gel process, high power laser appls. 4-74673
- Na<sub>2</sub>O-CaO glass, antireflection effects induced by Ar<sup>+</sup> implantation 4-60125
- Si microrelief surface, reflecting power and etching form. (*Russian*) 4-64757
- Si photocells, two-film antireflection coating, surface film resist. reduction (*Russian*) 4-109742
- Si solar cells with high energy conversion efficiencies 4-81550
- SiO<sub>2</sub> on Si p<sup>+</sup>-n-n<sup>+</sup> solar cells, all-implanted, charact. 4-62355
- SiO<sub>2</sub> optical films and antirefl. coatings deposited from solns. mech. strength 4-74670
- SiO<sub>2</sub> porous antireflection coating for use at 248, 266 nm 4-79268
- SiO<sub>2</sub>/TiO<sub>2</sub> multilayer films, reactively evaporated 4-99327
- SiO<sub>x</sub>N<sub>y</sub> reactively sputtered films for antireflection coatings, for a-Si solar absorber converters 4-99998
- Ta<sub>2</sub>O<sub>5</sub>/SiO<sub>2</sub> coatings, electron-beam deposited, 1064-nm damage tests, review 4-75525
- TiO<sub>2</sub> optical films and antirefl. coatings deposited from solns. mech. strength 4-74670
- ZnSe-CaF<sub>2</sub> deposited by laser-assisted evaporation, as broadband gradient-index antirefl. coating 4-107765
- ZrO<sub>2</sub>-SiO<sub>2</sub> thin amorphous film prep. by electron-beam evaporation from multiple sources 4-74674

**APD** *see avalanche photodiodes***aperture cards** *see microforms***API gravity** *see density***apodisation** *see acoustic imaging; optical images***apparatus** *see instrumentation; instruments***apparent porosity** *see porosity***appearance potential** *see ionisation potential***appearance potential spectra**

- extended fine structure in APS, pseudodipole selection rules 4-85040
- extended fine structure in APS 4-61780
- transition metals, core electron binding energies determ. by XPS, AEAPS and EELS 4-85081
- Co, polycrystalline, ferromagnetic, density of unoccupied states, SXAPS study 4-85039
- DyFe<sub>2</sub>, intermetallics, SXAPS studies 4-81039
- ErFe<sub>2</sub>, intermetallics, SXAPS studies 4-81039
- Fe, polycrystalline, ferromagnetic, density of unoccupied states, SXAPS study 4-85039
- NH<sub>3</sub>+Re surface, single-collision energy transfer and catalytic decomposition at high temps. 4-71971
- Na<sub>n</sub> (n≤7), cluster geom. calc. by Hellmann-Feynman forces 4-74372
- Ni, polycrystalline, ferromagnetic, density of unoccupied states, SXAPS study 4-85039
- Ti, SXAPS, DAPS and AEAPS studies of L<sub>3</sub> threshold 4-93141
- TiFe, bulk and surface two-particle spectra 4-84550

**appearance potential spectroscopy**

- Auger electron appearance potential spectroscopy 4-99230
- impregnated dispenser cathodes, appearance pot. spectroscopy, XPS and AES (*Chinese*) 4-106437
- stainless steel, surface composition, electron bombardment effects, SXAPS obs. 4-108683
- steel, stainless, Auger electron appearance potential spectroscopy 4-99230
- surface microanalysis, threshold spectroscopy study 4-69998
- Cr, appearance potential spectroscopy 4-99230

**Appleton layer** *see ionosphere***appliances, domestic** *see domestic appliances***applied mechanics** *see mechanics***approximation theory**

- see also function approximation; interpolation; least squares approximations*
- computer-extended series, bad behaviour and counter measures 4-67981
- EELS, parametric partial cross section 4-73602
- EELS, plural scattering removal techniques 4-73601
- finite element method, projection-mesh diagrams construction using soft-tened-mixed approxs. 4-63508
- Riemann solvers, the entropy condition, and difference approximations 4-68192

**approximation theory** continued

- ring laser, bidirectional homogeneously broadened, stability analysis 4-107690
  - tectonics, Signorini problem without friction in linear thermoelasticity 4-67199
  - underwater spark discharges, computer modelling using approx. relationships (*Russian*) 4-84093
- APR** *see acoustic paramagnetic resonance*
- APS** *see appearance potential spectra; appearance potential spectroscopy*
- APW calculations**
- III-V cpds., band struct., APW calc. method appl. 4-92608
  - linearised APW method using quadratic energy expansions 4-98504
  - total energy full potential linearised APW method 4-104143
  - transition metal, cubic, relativistic APW calcs. of nucl. spin-lattice relax. rates 4-71204
  - Ag-Fe (001), interface magnetism, self-consistent spin-polarised localised spin-density calcs. using APW method 4-98863
  - BN band struct., APW calc. method appl. 4-92608
  - BiS(Se)(Te), band-overlap metallisation, self-consistent augmented-spherical-wave calc. 4-80499
  - CaH<sub>2</sub>, bonding and electronic struct., APW calc. and photoemission studies 4-113384
  - Cu, linearised APW method using quadratic energy expansions 4-98504
  - Fe, BCC, Fermi surface and energy bands under press., APW calc. 4-80478
  - FeB BCC alloys, electronic struct., APW calcs. 4-108769
  - Gd<sub>2</sub>Ni<sub>2</sub>Al<sub>3</sub>, band struct. and ferrimag. moments, APW calc. 4-80487
  - LaH<sub>2</sub>, electron-phonon interaction and supercond. destruction by H absorption 4-65622
  - NbH<sub>2</sub>, electron-phonon interaction and supercond. destruction by H absorption 4-65622
  - Pd, band struct. approach to X-ray absorpt. and emission spectra 4-71479
  - Pd, X-ray emission spectra, anisotropy of cyclotron masses and many-body effects 4-104700
  - PdH<sub>x</sub>, electronic props. of dilute H 4-88472
  - Pr, band structure, Fermi surface and supercond. under high press. 4-98511
  - ScRu, band struct. calcs. 4-98515
  - ScRu, electron struct. and X-ray emission spectra, exchange and correl. effects 4-70697
  - Tc, superconducting props., energy band struct. calcs. 4-104343
  - TiC, electron density, density of states and chem. binding, APW calc. 4-75356
  - TiC, Fermi surface, const. energy KKR-GF calc. 4-84545
  - TiN, Fermi surface, const. energy KKR-GF calc. 4-84545
  - TiTe, band struct., elec. and mag. props. 4-92595
  - W (001), electronic struct., linear-augmented plane wave calc. 4-80649
  - W film (001), bonding of surface states, local density functional studies 4-80648
  - W, total energy full potential linearised APW method 4-104143
  - WC, hexagonal, surface and bulk electronic struct., density of states 4-113867
  - α-Zr, band structure, APW calcs., optical props., superconducting props. 4-113857
  - ZrN (100) surface, energy band struct. study 4-104285
- arbiters (computers)** *see computer interfaces*
- arc discharges** *see arcs (electric)*
- arc lamps**
- flow stabilised DC arc lamp for high radiation densities 4-88032
  - hollow cathode arc as optical line source 4-60129
  - types and charact. 4-103601
  - uniform illumination using water-cooled mirror 4-79264
- arc welding**
- metal, arc fusion welding, solidification microstruct. 4-89050
  - plasma jet welding and deposition, industrial applications (*French*) 4-114425
  - steel weld metal, globular silicates effect on ductility and microstruct. 4-114607
  - strip electrode deposited metal, controlling ease of slag removal 4-81325
- archaeoastronomy** *see astroarchaeology*
- archaeology**
- see also astroarchaeology*
  - age determination during second millennium BC, appl. of geomag. field intensity curve 4-100443
  - experimental archaeometry, use of PIXE 4-99898
  - external PIXE milliprobe at Davis cyclotron, laser alignment, calibration and quality assurance 4-105076
  - geomagnetic secular variation in W United States, AD 750 to 1450, congruent paleomag. and archaeomag. records 4-100446
  - microfluorescence X-ray spectroscopy, appl. to study of works of art (*French*) 4-85350
  - late Minoan civilisation, Crete, fired destruction levels archaeomagnetic dating 4-85647
  - Morocco, paleomagnetic data from archaeological sites 4-105405
  - New Zealand obsidian anal., provenance studies, PIXE and PIGE meas. 4-100573
  - potsherds from West Africa, PIXE anal. and provenance study 4-100571
  - pottery and glasses, 18th and 19th century, PIXE and PIPPS anal. 4-100572
  - pottery samples, powdered bound in organic matrix, quantitative PIXE anal. 4-99899
  - upper Thames basin, Holocene alluviation and hydrology, archaeological evidence 4-72618
  - Ag Celtic coins, surface compositions determ. by PIXE 4-99900
- archaeomagnetism** *see palaeomagnetism*
- archeomagnetism** *see palaeomagnetism*
- architectural acoustics**
- see also anechoic chambers; echo; noise abatement; reverberation*
  - auditoria, impulse testing techniques 4-69623
  - auditoria in Ljubljana, acoustic props., echographic study (*German*) 4-79369
  - auditorium acoustic simulation (*French*) 4-79375
  - BBC digital sound control vehicle for outside broadcasting, acoustic design 4-83774
  - broadcasting, studio acoustics for the eighties, design advice 4-69624
  - broadcasting studio, acoustical holes in multi-pane windows 4-79372
  - broadcasting studios, sound reflections, frequency anal. 4-107953
  - building facades, sound field reflection and transmission 4-87514

**architectural acoustics** continued  
buildings, transmission loss measurements using an impulse source (French) 4-60214  
Burghtheater electroacoustic system, modifications 4-79376  
concert hall, spectral estimation 4-69627  
concert hall acoustics and number theory, progress in architectural acoustics and artificial reverberation 4-64808  
concert halls, acoustic irradiation (German) 4-83773  
concert halls, image model appl. 4-83775  
concert halls, NC-15 acoustical environment 4-97204  
concrete porous materials, improvement of sound-absorpt. props. 4-87513  
conference, acoustics, Paris, France (July 1983) 4-78035  
direct speech communication and ambient noise in restaurants and cafeterias, seating density criteria 4-79411  
enclosure with diffusely and specularly reflecting boundaries, steady state sound field calcs. 4-60211  
enclosures, acoustics, free pathlengths, statistical distrib. 4-74810  
halls, public address systems, acoustic characteristic indices (Chinese) 4-91689  
horns, high-frequency, near and far coverage requirements in central array 4-79371  
Hungarian Broadcasting Company, programme problems 4-74813  
interaural crosscorrelation coefficient and related factors in music reproduction (German) 4-74809  
Jeddah urban sites, environmental acoustic quality 4-79365  
lateral sound meas. in small halls 4-107950  
LF sound reproduction system design using Thiele-Small driver parameters 4-87533  
loudspeaker arrays, coverage modelling for any room configuration 4-64809  
magnetic video recording, neighbouring control booths, sound level difference requirements (German) 4-79368  
measurements using periodic pseudorandom sequences and FFT 4-112638  
monitoring speakers for control rooms 4-79408  
music recording studio in St Luke's Church, Dresden, architectural acoustics shaping (German) 4-69626  
near-field meas., toneburst techniques appl. 4-79410  
noise reduction by scatt. in low velocity ducts 4-107948  
party walls and facade elements, laboratory and field sound insulation measurements 4-74811  
plates, vibrating energy determ., points of meas. placement criteria 4-83760  
power levels of different acoustic sources, sound engineering influence 4-79407  
quantised noisy systems and room acoustics, general state estimation algorithm 4-103092  
reflection phase grating diffuser, design theory and appl. 4-64810  
residential housing, acoustic insulation, angle of incidence effects 4-87511  
reverberant room, sound absorbing coeffs. evaluation 4-107951  
reverberation characts, improvement of enclosed space, with aid of computer (Slovak) 4-60213  
reverberation times of closed sound paths with low damping 4-91664  
room, sound power anal. (Hungarian) 4-74812  
room acoustics, image source computer model 4-79370  
room acoustics, sound transmission through partitions 4-107952  
room sound press. level prediction using equivalent absorpt. coeff. 4-103101  
room window, unshielded and opened, acoustic performance 4-103099  
room with shielded open window, acoustic performance 4-103100  
rooms, reverberation time measurements, instrument time constants elimination (Japanese) 4-112639  
semicylindrical concave rigid wall, high freq. acoustical fields (Japanese) 4-97203  
sound reinforcement system, computer model and ray-tracing, speech transmission index prediction 4-79409  
sound reinforcement system, intelligibility estimates 4-97200  
standard control room, proposal 4-79374  
studio, design, effects of glass 4-97201  
Virginia Center for Performing Arts, acoustical design 4-60212  
wall constructions, sound transmission loss, intensity and two-room method meas. 4-103152

**architectural CAD**  
auditorium acoustic simulation (French) 4-79375

**architectural computer aided design** see *architectural CAD*

**arcing** see *arcs (electric)*

**arcing, switches** see *circuit-breaking arcs*

**arcs (electric)**  
see also *arc lamps; arc welding; circuit-breaking arcs*  
ablation-stabilised arcs in cylindrical tubes 4-79867  
air, arcs and HF sparks, appl. to metals spectral anal. 4-79868  
air, atmospheric, DC arcs, ruby laser scattering diagnostics 4-103587  
air column, expanding, current density determ. probe method 4-84067  
alkali metal vapours arc discharges, optical and electrophysical characts. 4-113248  
anode current density, jet generation, multiparameter anal. 4-87983  
arc-shock interaction 4-88024  
axially blown quasi-steady arc 4-88020  
cascade arc, wall-stabilised, CW Ar<sup>+</sup> laser beam Thomson scatt. 4-84078  
cathode material properties, simulation studies, influence on discharges 4-97918  
cathode spot retrograde motion, ampere force compensation 4-87979  
characteristics and light source appl. 4-103601  
combustion, arc generated plasma 4-69984  
current distribution in quasisteady MPD arcjet, anode geometry effects 4-113132  
CW arc pluming at high-power aerials, pulsed RF plasmas obs. 4-69970  
CW arc pluming at high-power aerials, scale-model studies 4-69971  
DC arc, stabilisation by rot. mag. fields 4-113241  
double plasma arc in graphite tube (German) 4-79873  
drift in uniform mag. field 4-88023  
electrical and optical props., emission plasma tomograph study 4-88033  
electrode processes and engineering appl., review 4-113250  
electrode processes in an open-cycle MHD generator 4-114916  
electron beam production with grid plasma emitter, low-press. arc use 4-69966  
electron feed assembly for ORNL/MFTF-B 30-s ion sources, arc behaviour 4-58917

**arcs (electric)** continued  
erosion arc plasma flux expansion into vacuum 4-87986  
field free plasma expansion, induced wall arcing 4-87877  
flow investigation of constricted arc burning in longitudinal gas stream with a vortex 4-88026  
free burning arc, high current in air, two dimens. calc. 4-88025  
free-burning arcs, vapour flow patterns meas. 4-87961  
gases, corrosive, thermal conductivity meas. by holographic interferometry 4-87546  
high current, MHD flow study 4-113245  
hollow cathode arc, rotating, particle density and temp. distrib. 4-88005  
hollow cathode filled with dense inert gas plasma, arc discharges, temp. and density 4-65148  
hollow cathode in magnetised arc, ion source props. meas. 4-88007  
hollow cathode ion source, plasma invest. (German) 4-84102  
impulse arc processes in air, laser scatt. diagnostics development 4-87945  
interferometry of plasma in a stationary closed arc discharge 4-113219  
ion source, multiply charged, using heated gas discharge chamber 4-73578  
laser probe-molecular beam sampling plasma diagnostic technique 4-84071  
laser-plasma interaction, heating, unipolar arcing 4-103535  
low pressure plasma, probe characts, plotting and electron vel. distrib. measuring equipment (German) 4-84060  
low-current arcs on insulating surface, expt. investigation 4-75229  
low-density plasma, initial disequilib. in supersonic flow, engineering method 4-87962  
low-pressure constricted arc, unsustained, upper limit for discharge parameters 4-88009  
magnetic field distribution in high current vacuum arcs 4-88021  
metal, surface, contaminated, arc initiation on plasma exposure 4-65093  
metal-vapour arcs, cathode spot plasma, ion acceleration, Ohm's law 4-87975  
metallic surfaces selective cleaning by capacitor-discharged arcing, technique and cct. 4-103588  
MGD-vortexes generation in electrical arc 4-88027  
mineral raw materials, arc excitation, spectral anal. 4-81494  
multiarc plasma reactor, heat flux distrib. to calorimetric probe 4-79848  
multielement gas detectors, appls. to plasma diagnostics 4-84088  
neutral beam injectors, O<sub>2</sub> impurities reduction using gettering techniques 4-60712  
organic insulation, tracking discharges, light emission, corona, scintillation and arc discharges 4-84097  
pinched low pressure, transition to cascade arc 4-97928  
plasmatron, two-dimens. model of arc 4-65140  
pressure of plasma arc on metal 4-91938  
pulsed arc discharge ion source with pulsed gas feed 4-90688  
pulsed low-press. pinched arc, maximum current anal. 4-108244  
rail gun armature, current spatial distributions meas. 4-78346  
in soil, arc initiation characteristics, effect of ambient gas 4-62799  
stochastically disturbed, turbulent axial gas flow, simulation 4-113240  
turbulent axial gas flow, fluctuating local props. 4-113239  
unhomogeneous discharge, double layer characts. study 4-87882  
unipolar arcs, burning, erosion 4-79861  
vacuum and unipolar arcs, induced elec. field effects 4-87973  
vacuum arc, cathode spot region microparticle generation 4-87977  
vacuum arc, moving cathode spot theory 4-108241  
vacuum arc, stationary cathode spot 4-108240  
vacuum arc at threshold currents, nonstationary processes 4-87974  
vacuum arc channel in vacuum interrupters by axial mag. field appl. 4-88022  
vacuum arc in anode vapours with non-spent cathode 4-87971  
vacuum arcs, cathode spot lateral spread in transverse mag. field 4-87978  
vacuum arcs, current density at the cathode 4-103590  
vacuum arcs, rel. between electrode phenomena 4-92005  
vacuum-arc cathode spot, current density estimation 4-97902  
vacuum-arc discharge, integral cathode temp. effects 4-79859  
wall stabilised AC arc, nonequilibrium theory 4-88031  
Ar arc plasma, non-LTE diagnostics 4-113251  
Ar, arcs and HF sparks, appl. to metals spectral anal. 4-79868  
Ar cascade arc plasma pulsed with 2200 Amperes 4-88029  
Ar free-burning arc, temp. distrib. determ. 4-79866  
Ar, free-burning arcs, local thermodynamic equilibrium 4-92003  
Ar-F arc, spectroscopic anal. in case of two emitting layers 4-79856  
CO production from C and CO<sub>2</sub> in plasma arc reactor 4-76978  
Cu arc, in air, absolute spectral intensity meas. (Japanese) 4-97924  
Cu vapour diffusion in N<sub>2</sub> arc chamber 4-88019  
Cu-W electrodes, arcing phenomena, current density 4-87984  
H arc plasma, electron density, interferometric and spectrosc. investig. 4-84082  
H nonequilibrium positive columns, state transitions, two-temp. model 4-92007  
K, wall-stabilised arc, electron temp. and density, Stark broadening meas. 4-112140  
KrF\* electrodischarge, excimer laser plasmas, runaway electron current and form. of spatial struct. 4-97929  
Mo, vacuum-arc discharge, integral cathode temp. effects 4-79859  
N arc, wall stabilised, electron ambipolar diffusion flux determ. 4-88028  
N<sub>2</sub> arc, perturbed in turbulent axial flow, power balance, averaged props. 4-113233  
N<sub>2</sub>, dynamic arc, temp. distrib. in high-speed flow 4-69960  
N<sub>2</sub>, wall stabilised arc, thermal and electrical cond. calc. 4-79761  
NO synthesis in DC arc plasma, modelling, temps, vels., kinetic meas. 4-71914  
Na D-line reabsorption in high pressure Na arcs, wall temp. depend. 4-87955  
Na high-press. discharge, acoustic resonance obs. 4-65141  
Na-Hg-Xe high press., pulsed arc, spectrum meas. 4-87956  
SF<sub>6</sub> arc discharge, continuum emission investigation 4-88013  
SF<sub>6</sub> decomp. by arc discharge, product meas. at sub-p.p.m. level 4-114869  
SF<sub>6</sub> plasma, net radiation emission coeffs. 4-87845  
SF<sub>6</sub> transient arc plasma column, striation phenomena obs. 4-88015  
SF<sub>6</sub> wall-stabilised arcs, temp. distrib. meas. 4-88014  
Ti, vacuum-arc discharge, integral cathode temp. effects 4-79859  
Xe plasma, continuous radiation absorpt. determ. 4-87942

**area measurement**

microcomputer based system for area measurement 4-82781

## area measurement continued

- optical fibre endface angle, effect of meas. of mode spot size from far-field pattern 4-107856
- powders, surface area meas., permeametry and diffusion flow methods comparison 4-73419
- pulmonary nodules, CT images, problems of attenuation and area meas. 4-67074
- TV system, low-cost meas. device 4-73417

## argon

- see also nuclei with .....
- adsorbed layer on Ag film, adsorption process study using surface plasmons 4-80383
- adsorbed layer on Mg and Al, optical spectra, configurational effects 4-80391
- adsorbed on Cu surface, He scatt., time depend. wavepacket calcs. 4-88918
- adsorbed on Si (111), UPS rare gas titration for surface characteris. 4-88936
- adsorption on C powders, second gas-solid virial coeffs., chromatographic determ. 4-114819
- afterglows, conversion reaction rate coeff. and ambipolar diffusion coeff. meas. 4-79877
- Allende meteorite, presolar age indicated by Ar isotopes 4-105906
- Ar I and II systems, collisional radiative coeffs. of 4p groups 4-65059
- <sup>40</sup>Ar/<sup>39</sup>Ar dating of a basite from the Western Antarctic 4-85763
- arc plasma, non-LTE diagnostics 4-113251
- arcs and HF sparks, appl. to metals spectral anal. 4-79868
- atom, 2p orbital, electron impact ionisation differential cross sections 4-112282
- atom, 2p shell, photoionisation, excited electron wave functions 4-83350
- atom, (<sup>2</sup>P<sub>1/2</sub>) state, orientation by laser optical pumping 4-112148
- atom, alignment prod. in ionisation of 2p shell by specific momentum transfer 4-96701
- atom, branching ratios and absolute transition probabilities in 4s-4p transition array 4-87081
- atom, correlation satellites for K-shells, gas-phase photoemission with soft X-rays 4-96614
- atom, electron cloud size meas. in gas mixtures 4-59519
- atom, electron impact ionisation spectrum, CI calcs. 4-64615
- atom, excited state lifetimes, inelastic electron-photon delayed coincidence technique 4-102644
- atom, fast electron impact ionisation, differential cross section 4-74338
- atom, L<sub>1</sub>-L<sub>2,3</sub>M<sub>1</sub> Coster-Kronig spectrum, intermediate coupling calcs. 4-102619
- atom, near-threshold electron impact excitation functions 4-96702
- atom, outer shells, photoionisation cross sections calc. using relativistic local-density approx. 4-83352
- atom, photoionisation, electron source, collision processes 4-83338
- atom, relativistic electron beam excitation, fluoresc. and absorpt. 4-69220
- atom, self interaction corrected Compton profiles 4-96495
- atomic fluid, mol. dynamics simulation method in the canonical ensemble 4-75252
- atomic metastable densities in Ar-NH<sub>3</sub> glow discharge 4-87059
- atoms, ionisation coeff. and total excitation cross section 4-92011
- atoms, K<sub>α</sub> X-ray emission spectrum, CI calcs., radiative transition probabilities calc. 4-59668
- atoms, L<sub>1</sub>-L<sub>2,3</sub>M<sub>1</sub> Coster-Kronig spectrum, exchange, electron correl., and relax. effects 4-74172
- atoms, laser induced cascade ionisation, secondary ionisation processes 4-83355
- atoms, low energy positron scatt., critical points 4-74313
- atoms, single and multiple ionisation by low energy electron impact using crossed beam apparatus 4-69217
- bubble press. and density in Al, EELS, TEM obs. 4-113508
- chemisorption on Al (100), dipole moment and interaction energy 4-98452
- clathrate hydrate formation in struct. II modification 4-112251
- cluster ion formation in free jet expansion processes at low temperatures 4-74381
- clusters, electron diff. patterns 4-74367
- clusters, Penning, photo and electron impact ionisation 4-74366
- condensation in He studied using nozzle flow of cryogenic Ludwig tube 4-98251
- core electrons, Coulomb and exchange operators, matrix elements, valence electron only SCF calcs. 4-59630
- cryocrystals, high-energy excitations, hot luminesc. 4-99194
- cryogenic liquids flowing in tubes, heat transfer during boiling 4-69749
- crystals, low temp. internal friction 4-60987
- dimers, model pot. method, SCF and dispersion energy calcs. 4-107426
- electrical discharge, externally maintained, preionised, IR radiation generation, laser efficiency 4-64695
- electron collision frequency, resonant determ. method 4-69223
- emission source for line analysis, using hollow cathode arc 4-60129
- ethylene-Ar, van der Waals mols., hindered internal rotors, IR photodissociation spectra 4-74238
- excimers, electronic struct., ab initio CI calc. (French) 4-78788
- film, ion beam irradi., secondary electron, ion, and photon emission 4-76577
- films, structural order effects in low-energy electron transmission spectra 4-98520
- flow of a nonequilibrium recombining plasma in a magnetogasdynamic duct 4-60602
- fluid, electron energy bands 4-84645
- fluid, orthobaric props., internat. pot. effect 4-74310
- free-burning arc, temp. distrib. determ. 4-79866
- free-burning arcs, local thermodynamic equilibrium 4-92003
- gas, effective viscosity oscillatory depend. on Knudsen number 4-64983
- gas, high press. PVT meas. 4-97737
- gas, mag. birefr. meas. 4-103465
- gas, weak imploding shock waves, streak camera obs. 4-112950
- gas breakdown threshold near metal target by laser heating 4-69933
- gas drift chambers, spatial resolution 4-64308
- gas permeability in polymer microballoons, interferometric meas. 4-70469
- glow discharge, electrode treatment, afterdischarge electron emission 4-87987
- glow discharge plasma, diagnostics 4-87944
- HF and d.c. low press. discharges 4-79865
- HF discharge, anomalous plasma resistance in transverse mag. field 4-92023

## argon continued

- high resolution acousto-optic laser probe in Ar gas 4-97746
- high-voltage discharge in crossed inhomogeneous mag. field 4-88004
- highly ionised, VUV spectrum (Chinese) 4-91213
- inductively coupled plasma, lifetimes and collisions, laser fluoresc. investig. 4-60729
- inductively coupled plasma, vacuum UV emission spectra, 85 to 200 nm 4-90665
- ion, Na-like, dielectronic recombination rates 4-96696
- ion beam, optical pumping study 4-87072
- ion beam etching, SAW devices 4-81318
- ion etching, of Si, effect of ion species ion bombardment induced topography 4-81320
- ion impact on V, Cu, Nb, Ta and Pt, K and L X-ray prod. 4-99216
- ion laser, air cooled, design and appl. 4-64722
- ion laser, cavity dumped freq. doubled, sine-wave modulated UV radiation 4-69459
- ion laser, injection locking for high-power single-freq. emission 4-102960
- ionisation yield of low-energy electrons, statistical fluctuations 4-59899
- ions, charge exchange processes 4-96694
- laser amplifier system, mode synchronised, high-power pulse prod. at high repetition freq. (Russian) 4-69369
- light-induced detonation, thermodynamic props. 4-97796
- liquid, geminate recombination 4-69207
- liquid, pair pots., Monte Carlo simulation 4-92047
- liquid, short wavelength sound modes, neutron diff. 4-98231
- liquid, sound nonanalytic dispersion relations 4-103887
- liquid, surface tension, liq.-vapour phase interface, statistical mechs. 4-113755
- liquid, thermodynamic Gruneisen parameter, mol. compressibility and sound speed 4-60974
- liquid and gas, viscosity determ. 4-61125
- low-current discharge with two parallel plane cathodes, electron motion simulation 4-91981
- LX spectrum interpretation in terms of vacancies distrib. 4-99225
- neutral system, numerical collisional radiative model 4-91868
- octafluoropropane-Ar mixtures, nanosecond pulse discharges 4-108235
- particle excitation mechanisms F, Ar, O, N<sub>2</sub>, CO and perfluoromethyl radical in glow discharge 4-79860
- picosecond laser-induced breakdown study 4-103462
- pinched discharges, self-oscillation mode and dispersion of strata 4-65147
- plasma, Cs seeded, MHD channels, discharge struct., load change characts. 4-97912
- plasma, discharge column, low-press., nonlinear behaviour, density changes 4-60771
- plasma, elec. cond. meas. 4-79763
- plasma, prod. in microwave capillary discharge, spectral line intensities 4-88000
- plasma, sheath motion and related wave phenomena 4-91941
- plasma impurities, nonlinear screening in dense hot plasmas 4-113199
- plasma jet, thermal decomp. of CO<sub>2</sub> 4-109631
- plasma production, mirror electrode for laser initiated discharge channels 4-69932
- positive column, low press., stepwise ionisation effects modelling 4-92013
- Rayleigh wing spectrum, crit. effect 4-84971
- solid, cathodoluminescence excitation spectra 4-85013
- solid, cond. band struct., floating 1-s gaussian basis functions calcs. 4-92609
- solid, electron stimulated desorpt., luminesc. and exciton creation 4-80381
- solid, electronically excited, spitting and luminesc. 4-104708
- solid, excimer-like states, numerically optimised geometries 4-65624
- solid, shock induced lattice damage simulation 4-108542
- solid, vacancy formation vol. calc. 4-70136
- solid, volume and isothermal bulk modulus, press. depend. 4-92278
- solid and liq., excitons, reflection spectra study 4-84570
- sputter etching of YIG and Ta<sub>2</sub>O<sub>5</sub> for fabricating artificial anisotropic waveguide 4-83694
- submonolayer on graphite, melting transition, specific heat study 4-104077
- thermal plasma flow in water-cooled tube 4-108208
- third virial coefficient, nonadditive three-particle interactions effects 4-69857
- transient electron mobility in pulse irradiated gas under steady field 4-113106
- triple point, appl. to Pt resistance thermometer calibration 4-111135
- triplet and cold radical prod. with pulsed elec. discharge in pulsed supersonic flow 4-84090
- working fluid for closed-cycle diesel engines, effects on performance 4-66743
- Z-pinch high-current discharge current struct. diagnostics 4-91976
- Ar cascade arc plasma pulsed with 2200 Amperes 4-88029
- Ar I, 2p level lifetime determ. 4-107310
- Ar IV to Ar VIII ions, emission spectra, 100 to 900 Å 4-59664
- Ar<sup>+</sup> and Ar<sup>2+</sup> in Ar, transverse diffusion coeff. 4-83969
- Ar<sup>+</sup> and He-Ne laser low-freq. beat note (Chinese) 4-91511
- Ar<sup>+</sup> closed shell ions repulsive interaction, beam and transport meas. comparison 4-96653
- Ar<sup>+</sup> ion lasers, acousto-optic mode locking, subnanosecond transient spectroscopy appl. (Japanese) 4-101923
- Ar<sup>+</sup> passively mode-locked laser, output light energy characts. 4-64696
- Ar<sup>16+</sup> excited states in D Tokamak plasma, recombination population 4-87936
- Ar<sup>3+</sup> pulsed hollow cathode discharge laser, operational characteristics 4-83565
- Ar:Ag solid, EXAFS of Ag particles 4-104699
- Ar:Xe, fluid, extrinsic photocond., Wannier-Mott impurity exciton, binding energy and effective mass 4-65701
- Ar:Xe, photoconductivity in liq. and solid phase 4-84643
- Ar/Kr system, mutual diffusion coeff. D<sub>12</sub> det. by mol. dynamics method 4-103628
- Ar-C<sub>2</sub>H<sub>2</sub>-CH<sub>3</sub> gas mixture for multiwire proportional counters 4-59515
- Ar-C<sub>2</sub>H<sub>2</sub>-CH<sub>3</sub>-CH<sub>2</sub>OH, wire chamber gas mixture, breakdown processes 4-59539
- Ar-C<sub>2</sub>H<sub>2</sub> gas mixture for multiwire proportional counters 4-59515
- Ar-CH<sub>4</sub> gas mixture for multiwire proportional counters 4-59515
- Ar-F arc, spectroscopic anal. in case of two emitting layers 4-79856
- Ar-fluoromethane filled counters, radiation stability 4-59554
- Ar-HCN mixtures, thermal decomposition behind incident shock waves 4-89279

- argon continued  
 Ar-HCl(HF), intermolecular forces, HF plus damped dispersion calcs. 4-87039  
 Ar-HF-NF<sub>3</sub>, photolysis, HF multiquantum vib-rot. relax. rates 4-102775  
 Ar-He mixtures in microwave capillary discharges 4-87999  
 Ar-Hg interaction pots. calcs. from temp.-depend. absorpt. spectra 4-69170  
 Ar-isobenzene streamer gas, dead time evolution and after pulse development 4-59538  
 Ar-isotriethylamine streamer gas, dead time evolution and after pulse development 4-59538  
 Ar-methane gas mixture, appl. to resist. pattern reform. by reactive ion etching 4-81301  
 Ar-N<sub>2</sub> gas proportional scintillation counter, alpha particle detection 4-59546  
 Ar-N<sub>2</sub> gas scintillation proportional counters, X-ray response 4-91159  
 Ar-NO van der Waals complex, resonant multiphoton ionisation spectroscopy 4-107421  
 Ar-Ne mixture, ionisation coeff. and total excitation cross section 4-92011  
 Ar-Xe(Ne)(butane) filled proportional counters for practical appl. 4-64288  
 Ar+aniline, mode-to-mode energy transfer, fluoresc. 4-83450  
 Ar+Ar<sub>2</sub>, three-body exchange reactions, tunnelling process, WKB calcs. 4-64589  
 Ar+Ar<sup>4+</sup>, recoil ion charge state distrib., projectile charge state depend. 4-69204  
 Ar+Br<sub>2</sub>, collisional energy transfer, binary trajectory calcs. 4-96665  
 Ar+CH<sub>4</sub>(CD<sub>4</sub>)(CF<sub>4</sub>)(SiH<sub>4</sub>), energy transfer, model trajectory calcs. 4-102771  
 Ar+Cr, intramultiplet mixing collisions, fluoresc. 4-64588  
 Ar+CsF(CsBr), collision-induced dissociation, cross sections 4-76993  
 Ar+D<sub>2</sub>, rotationally inelastic cross sections, anisotropic interaction pot. determ. 4-83452  
 Ar+D<sub>2</sub><sup>+</sup>, collisional dissociation, correl. between channel probabilities 4-78933  
 Ar+Fe<sup>26+</sup>, near-symmetric collisions, K-K transfer cross-sections 4-64571  
 Ar+H<sub>2</sub><sup>+</sup>(O<sub>2</sub><sup>+</sup>)(NO<sup>+</sup>), charge transfer reactions 4-89272  
 Ar+H<sub>2</sub>, electron detachment and charge exchange to shape reson. 4-69203  
 Ar+H<sub>2</sub><sup>+</sup>(Li<sup>+</sup>)(Na<sup>+</sup>)(K<sup>+</sup>), electron detachment cross sections 4-78952  
 Ar+I<sub>2</sub>, state-to-state rot. transfer rates, induced fluoresc. 4-91333  
 Ar+K, fine-struct. transitions, interatomic pots. tests and coupling mechanism 4-87199  
 Ar+Kr atoms, ionisation processes for highly excited Ar atoms 4-87201  
 Ar+Li<sub>2</sub><sup>+</sup>, rot. inelastic collisions, vel. depend. 4-102764  
 Ar+Li<sub>2</sub><sup>+</sup>(A<sup>1</sup>Σ), rotationally inelastic collisions, rate consts., fitting laws 4-74319  
 Ar+methane, exchange interactions, crossed-beam expt. (German) 4-96670  
 Ar+N<sub>2</sub>, cross sections and rate consts. of rot. excitation 4-112264  
 Ar+N<sub>2</sub>, state-selected charge transfer cross sections 4-87206  
 Ar+N<sub>2</sub>O, mol. <sup>2</sup> mean square torques and rot. correl. functions of ν<sub>3</sub> vibr. perturbed by Ar 4-78838  
 Ar+N<sub>2</sub>O collisions, intermol. pot., electron gas model, comparison with mean square torques meas. 4-78923  
 Ar+N<sub>2</sub>(HF) rotationally inelastic cross-sections and fitting laws, energy depend. 4-102772  
 Ar+NH<sub>3</sub>, quenching, radiative lifetimes, transition moments 4-74292  
 Ar+NO<sub>2</sub>, fluoresc. quenching, cross sections, time resolved spectra 4-96603  
 Ar+Na, collisional redistribution and fine-structure transitions, collisional redistribution 4-83457  
 Ar+Na, emitted monochromatic light reson. scatt. 4-69022  
 Ar+Na<sub>2</sub> collisions, mol. rot. rainbow struct., vel. depend. 4-78938  
 Ar+Na<sup>+</sup>, excited Na states, collisional depopulation cross-sections 4-83456  
 Ar+Ne<sup>2+</sup>, low energy electron transfer collisions 4-87213  
 Ar+OCS, IR linewidth meas., rot. levels, intermol. pot. 4-59764  
 Ar+S<sup>15+</sup>, K vacancy transfer, interference effects 4-78961  
 Ar+SF<sub>6</sub>, rot. and vibr. excitation, time of flight spectra 4-107438  
 Ar+SO<sub>2</sub>, afterglow reaction, SO(A<sup>1</sup>Π) formation dynamics study 4-76968  
 Ar+Si<sup>13+</sup>, single and multiple electron capture, K X-ray production 4-102785  
 Ar+Ti, up-conversion using stimulated anti-Stokes Raman scatt. and stimulated collisional induced fluoresc. in Ti 4-69498  
 Ar+TlF, rotational excitation, ang. momentum transfer 4-102776  
 Ar+X<sub>2</sub> (X=halogen), metastable atom quenching cross-section calcs. 4-107304  
 Ar+Xe, correls. between charge-changing interactions and projectile K-alpha X-ray emission 4-64595  
 Ar<sup>+</sup>+CS(PN) radicals, emission spectra prod. from thermal energy charge transfer reactions 4-74325  
 Ar<sup>+</sup>+H<sup>+</sup>, electron detachment, energy spectra, Born approx. 4-83459  
 Ar<sup>+</sup>+organic mols., charge transfer, mass spectra 4-112267  
 Ar<sup>+</sup>+N<sub>2</sub>, energy depend. of reactions 4-69193  
 Ar<sup>+</sup>+CO(N<sub>2</sub>) collisions, integral cross section meas. 4-78929  
 Ar<sup>2+</sup>+Cu, two electron transfer collisions, Ar I VUV line intensity 4-83462  
 Ar<sup>2+</sup>+He, charge transfer processes studied by crossed-beam expt. 4-91339  
 Ar<sup>21+</sup>+Ar, recoil ion charge state distrib., projectile charge state depend. 4-69204  
 Ar<sup>21+</sup>+Li collisions, q=2 to 10, electron capture cross sections from slow projectiles 4-74328  
 Ar<sub>2</sub>, VIM theory of mol. thermodynamics, analytic eqn. of state 4-113282  
 Ar<sub>2</sub>, van der Waals pot. model 4-69166  
 Ar<sub>2</sub><sup>+</sup>, electron impact dissociation 4-102812  
 Ar<sub>2</sub><sup>+</sup>, photodissoc. angular distrib. in intense fields 4-62213  
 Ar<sub>2</sub>+Xe, three-body exchange reactions, tunnelling process, WKB calcs. 4-64589  
 Ar<sub>2</sub><sup>+</sup>+CS<sub>2</sub> charge transfer reaction in Ar afterglow, CS<sub>2</sub><sup>+</sup>(A<sup>~</sup>-X<sup>~</sup>) emission 4-96552  
 Ar<sub>4</sub> cluster, statistical behaviour 4-59939  
 Ar<sub>n</sub> cluster beams, differential scatt. anal. 4-74376  
 Ar<sub>n</sub>9,10-dichloroanthracene, van der Waals complexes, UV absorpt. and fluoresc. spectra meas. 4-96594
- argon continued  
 Ar, release rate from human subjects following intravenous injection, meas. on volunteers 4-100313  
<sup>40</sup>Ar/<sup>39</sup>Ar ages of L-chondrites 4-110578  
<sup>40</sup>Ar/<sup>39</sup>Ar dating of basalt containing incompletely degassed xenoliths 4-85764  
 Ar<sup>2+</sup>(\*)+He(Ne), electron capture reactions studied by means of double translational spectroscopy 4-96686  
 Ar<sup>3+</sup>(\*)+Ar, electron capture reactions studied by means of double translational spectroscopy 4-96686  
 Ar<sub>2</sub><sup>+</sup>, avoided crossings, use of effective Hamiltonians, nearly diabatic pot. curves 4-59858  
 Ar(4s<sup>2</sup>P<sub>20</sub>) beam, intracavity state selection using CW dye laser 4-60095  
 CH<sub>4</sub>-Ar gas proportional chamber, properties (Chinese) 4-68875  
 CO-Ar gas mixtures, thermal conductivity meas. 4-113102  
 CO<sub>2</sub>-Ar gas proportional chamber, properties (Chinese) 4-68875  
 HCl-Ar, ps. IR spectroscopy, nearly free induction decay obs. 4-96529  
 HF+Ar, finite duration of collisions and vibr. dephasing effect on broadened IR line shapes 4-69177  
 Hg-Ar VLF discharge, positive column, theory 4-103596  
 Li<sub>2</sub><sup>+</sup>/Ar, rotationally inelastic transfer, scaling of state multipoles 4-87198  
 N<sub>2</sub>-Ar gas mixture, investigation of viscomagnetic diffusion flux 4-112960  
 N<sub>2</sub>-Ar mixtures, viscous diffusion in mag. field 4-112959  
 NH<sub>3</sub>-N<sub>2</sub>O-Ar, shock-heated, oxidation, conc. time profiles obtained by absorpt. and emission spectra 4-89298  
 Ne-Ar, interatomic pot., dilute gas bulk and microscopic props. 4-96638  
 O<sub>2</sub>-Ar, adsorbed on Grafoil, mag. and thermal props., 3 to 70K 4-61214  
 Si-Ar, carrier lifetime reduction by Ar ion implantation 4-80604  
 Si-Ar Schottky barrier, ion implantation effects on elec. characts. 4-114014  
 Si-SiO<sub>2</sub>-Ar<sup>+</sup>, ion implanted layers, EPR study 4-84849  
 Xe-Ar collision induced absorpt. lineshape, Mori theory 4-64579
- argon compounds  
 Ar-aniline Van der Waals complexes, in supersonic jets, laser-induced fluoresc. spectra, rot. anal. 4-74280  
 ArF excimer amplifier, phase conjugation by four wave mixing 4-107613  
 ArF excimer laser, doubly preionised 4-112398  
 ArF, laser action using transverse discharge pumping scheme 4-69382  
 ArH, pot. energy curves of ground and excited states, MRD-CI calcs. 4-64393  
 ArHCl, IR spectrum, thermodynamic props. 4-74236
- arithmetic (digital) see digital arithmetic  
 Armco iron see iron  
 armouring (cables) see cable sheathing  
 aromatic compounds see organic compounds  
 ARPES see photoemission  
 arrays (antenna) see antenna arrays  
 arsenic  
 see also nuclei with .....  
 amorphous, optic vibr. modes, Raman, IR and inelastic neutron spectra 4-7461  
 amorphous and polycryst., Compton profile studies 4-99218  
 amorphous film, UV photoemission study 4-88942  
 Atlantic Ocean, As, Mn, Cd vertical profiles and correl. with phosphate 4-85712  
 biogeochemistry in Baltic Sea 4-77154  
 galvanomagnetic props. and current carriers energy spectrum (Russian) 4-98638  
 pollutant release, of soil and groundwater 4-66820  
 rhombohedral, electronic band struct., angle-resolved UPS and pseudopot. studies 4-113868  
 speciation in seawater 4-82313  
 As VII spectrum, 3d<sup>4</sup>s, 3d<sup>4</sup>p and 3p<sup>5</sup>3d<sup>10</sup> configs. 4-74190  
 As VIII, spectrum, 3d<sup>4</sup>, 3d<sup>4</sup>p and 3p<sup>5</sup>3d<sup>10</sup> configs. 4-69005  
 As<sub>4</sub>, low temp. phase states, IR spectra 4-61683  
 GaP:As, impurity influence on electron-hole plasma 4-75862  
 Ge:As(Sb), neutron-transmutation-doped, defects 4-60967  
 n-Ge:As, conductivity and magnetoresistance, effect of localised states 4-113950  
 n-Ge:As, growth on Si by MBE, charact. 4-98469  
 Ge:As, impurity state breakdown under uniaxial compression 4-70715  
 Se:Te, As glassy films, pure and doped, deep level defects, xerographic spectra studies 4-61339  
 Si:As, high current density implantation, dynamic self-annealing mechanism 4-65280  
 Si:As, high dose ion implanted, As clustering, TEM and SIMS studies 4-70384  
 Si:As, implanted (111), twin formation, effect of heating rate and annealing temp. 4-103765  
 Si:As, implanted under channelling conditions, impurity spatial distrib., localisation, defect form. characts. 4-84321  
 Si:As, ion implant in-depth error anal., mass interference effects in ion microprobe studies (Chinese) 4-111248  
 Si:As, ion implantation doses, ellipsometry and spectral reflectance meas. 4-113480  
 Si:As, ion implanted, carrier density profiles, elec. meas., annealing behaviour 4-70179  
 Si:As, ion implanted, IR radiation annealing of extended defects 4-92228  
 Si:As, ion implanted and electron beam annealed, TEM and HREM studies 4-80058  
 Si:As, ion implanted and laser annealed, struct. changes, X-ray diffr. study 4-75461  
 Si:As, ion implanted channelling Rutherford back-scatt. study (Chinese) 4-84324  
 Si:As, ion implanted film, elec. props. 4-61473  
 Si:As, ion implanted regions, 2-D shape, etching and EBIC studies 4-88187  
 Si:As, ion implanted through screen oxide, residual disorder after high temp. anneal 4-113511  
 Si:As, low energy implanted, laser-annealed, channelling and high-resolution backscatt. studies 4-75493  
 Si:As, low resistance ion implanted films 4-108398  
 Si:As, low-energy ion implantation 4-75466  
 Si:As, P, B, ion implanted, fast isothermal annealing and elec. props. 4-92224  
 Si:As, P, ion implanted, diffusion modelling 4-113729  
 Si:As, segregation to grain boundaries and surface plasmons 4-98289

## arsenic continued

- Si:As, shallow donor polarisability 4-92666  
 Si:As, shallow dopant profile production by low-angle ion implantation 4-108396  
 Si:As, shallow implants, depth profiling using SIMS 4-108408  
 Si:As, X-ray standing wave anal. with synchrotron radiation 4-103607  
 Si:As implanted layers, struct., total external reflection spectra studies 4-108330  
 Si:As thin films, As fast diffusion during rapid thermal annealing 4-113714  
 Si:As/Al interface, sintering and diffusion, As dopant effect 4-80427  
 Si:As/Ti interface, As implantation, As out-diffusion during  $\text{TiSi}_2$  formation 4-65493  
 Si:As<sup>+</sup>, ion implanted and laser annealed, defects, photoluminescence studies 4-75433  
 Si:As<sup>+</sup>(BF<sub>3</sub>-T<sub>+</sub>), implanted, rapid thermal annealing 4-88184  
 Si:As(Sb)(In), ion implanted, pulsed electron beam annealing, impurity diffusion 4-103984  
 Si:B(P)(As), dopant diffusion, numerical soln. by solving impurity, vacancy and self-interstitial continuity eqns. 4-80303  
 Si:F, As, ion implanted, defect struct. detection 4-103776  
 a-Si:H, As, dispersive transport, trap saturation, transient photocurrent meas. 4-76006  
 Si/Ti:As<sup>+</sup>, ion implanted, doping effects on  $\text{TiSi}_2$  formation 4-88183  
 Si-SiO<sub>2</sub> interface, As<sup>+</sup> implanted, defects, ESR study 4-61591  
 Si-SiO<sub>2</sub>:As<sup>+</sup>, ion implanted layers, EPR study 4-84849  
 Si<sub>2</sub>Ge<sub>1-x</sub>(P)(As)(Sb), paired donor impurities energy levels 4-61315  
 SiO<sub>2</sub>:As, shallow implants, depth profiling using SIMS 4-108408  
 V:As, ion implanted, plastic deformation, channelling studies 4-70178

## arsenic alloys

see also arsenic compounds

- As<sub>2</sub>Se<sub>3</sub>Ge<sub>2</sub> glassy semicond., photostructural transformations 4-61076  
 Ga-As-Sn system, phase diagram and LPE growth rates 4-93237  
 MnAs, electronic struct. and phase transitions, tight binding calc. 4-108768  
 MnAs, mag. struct. under high press., powder neutron diffr. studies 4-108988  
 MnRhAs, antiferromagnetic-ferromagnetic transition, mag. props., elec. resist. meas. 4-104417

## arsenic compounds

see also arsenic alloys

- iodate-arsenite systems, bistability and chemical waves form. 4-85303  
 As<sub>2</sub>S<sub>3</sub>, thin film, photostructural changes studied by photo-ESR 4-114162  
 Ag/As<sub>2</sub>S<sub>3</sub> evaporated layers, offset printing plates, prep. processing and sensitising 4-68297  
 Ag-As<sub>2</sub>S<sub>3</sub> multilayer struct., optical props. study 4-104563  
 Ag<sub>2</sub>As<sub>2</sub>S<sub>3</sub>, acoustoelectric interactions in electroacoustic echo 4-80631  
 Ag<sub>2</sub>As<sub>2</sub>S<sub>3</sub>, low temp. elec. cond. anisotropy 4-88509  
 Ag<sub>2</sub>S<sub>3</sub>-Ag multilayer structure, photosensitive props. (Russian) 4-97013  
 Al-As<sub>2</sub>S<sub>3</sub>-Al MIM struct., bias voltage depend. of capacitance 4-104325  
 As-Ge-Se, glass, small conc. of Se, elec. cond. rel. to temp. 4-92729  
 As-Ge-Se system, compound form., diagrams, DTA and X-ray investigation (Russian) 4-113587  
 As-S amorphous system, vibr. props. and network topology 4-109178  
 As-Sb-Se system, glass-ceramic composites, varistor-like behaviour 4-114009  
 As-Se, thermal cond., in solid and liq. states 4-108669  
 As-Se chalcogenide glass films, thermally-induced light scatt. (Russian) 4-109167  
 As<sub>2</sub>Se<sub>3</sub>, cryst. and amorphous, recomb. and excited-state absorption at photolum. centres 4-99182  
 As<sub>2</sub>S<sub>3</sub>, intercalated with graphite, X-ray absorpt. near edge struct. meas. 4-66115  
 As<sub>2</sub>S<sub>3</sub>-doped polyacetylene, millimeter-wave and far IR cond. 4-70850  
 As<sub>2</sub>F<sub>6</sub>, (n=3, 5, 6), cage molcs., K-edge excitonic fine struct. 4-83287  
 As<sub>2</sub>F<sub>6</sub>, electronic struct., variational Xalpha calc., electron affinity 4-87044  
 AsH<sub>3</sub>, ground state, far IR spectrum, spectrosc. consts. 4-59742  
 As<sub>2</sub>S<sub>3</sub> chalcogenide films, solvent-cast morphology and thermal props. 4-84530  
 As<sub>2</sub>S<sub>3</sub> chalcogenide glass films, photostruct. changes 4-104560  
 As<sub>2</sub>S<sub>3</sub> chalcogenide glass films, thermally-induced light scatt. (Russian) 4-109167  
 As<sub>2</sub>S<sub>3</sub> evap. photoresist., dissolution rate rel. to evap. conditions 4-68299  
 As<sub>2</sub>S<sub>3</sub> film based joint transform real time optical correlator 4-74461  
 As<sub>2</sub>S<sub>3</sub> glassy film, Schottky barrier form. at contact with metal 4-104291  
 As<sub>2</sub>S<sub>3</sub> planar waveguide, hologram recording and readout 4-83553  
 As<sub>2</sub>S<sub>3</sub>:Ag, photostimulated diffusion kinetics (Russian) 4-70471  
 As<sub>2</sub>S<sub>3</sub>-S system, liq. and amorphous, phase diagram and short range order 4-103905  
 (As<sub>2</sub>S<sub>3</sub>)<sub>x</sub>(AsI<sub>3</sub>)<sub>1-x</sub> glasses, Raman scatt., IR and depolarisation spectra 4-109182  
 As<sub>2</sub>S<sub>3-x</sub> glass, X-ray struct. factor, temp. depend. near glass transition 4-60847  
 AsSI, glassy, optical props. meas. (Russian) 4-71340  
 As<sub>2</sub>S<sub>3</sub>I<sub>2</sub>, Raman spectra and struct. 4-76455  
 As<sub>2</sub>S<sub>3</sub>-Se<sub>2</sub> glasses, geminate recomb., picosecond electronic relaxations 4-108892  
 AsSe chalcogenide glass films, photostruct. changes 4-104560  
 AsSe vitreous chalcogenide semiconductor films, optical data. storage 4-10775  
 AsSe:Sn chalcogenide glass, photostruct. transformations, Mossbauer studies 4-61075  
 AsSe-chiral-liquid-crystal struct., phase boundary effect on electrooptical props. 4-93057  
 As<sub>2</sub>Se<sub>3</sub>, amorphous, carrier diffusion, multiple-trapping limited 4-70831  
 As<sub>2</sub>Se<sub>3</sub> amorphous film, photo-EMF due to surface barriers 4-88541  
 As<sub>2</sub>Se<sub>3</sub>, crystallisation kinetics and viscosity 4-75298  
 As<sub>2</sub>Se<sub>3</sub> glass, photoluminescence fatigue and structural disorder 4-104672  
 As<sub>2</sub>Se<sub>3</sub> glass, X-ray struct. factor, temp. depend. near glass transition 4-60847  
 As<sub>2</sub>Se<sub>3</sub>, glassy and liq., thermally generated defects 4-113335  
 As<sub>2</sub>Se<sub>3</sub>:Ag, photodoping physics study 4-75464  
 As<sub>2</sub>Se<sub>3</sub>Ni(Cu)(Fe)(Bi)(Sn), extrinsic cond. and optical const. meas. 4-75971  
 As<sub>2</sub>Se<sub>3</sub>:Te film, transient photocurrent study 4-113991  
 As<sub>2</sub>Se<sub>3</sub>:As<sub>2</sub>S<sub>3</sub>:Ag, holographic diff. grating recording (Russian) 4-69341  
 As<sub>2</sub>Se<sub>3</sub>-Cu<sub>2</sub>Se:Mn, interaction of Mn with glass framework, mag. susceptibility, EPR spectra 4-60838

## arsenic compounds continued

- As<sub>2</sub>Se<sub>3</sub>-x thin films, photoinduced optical absorption, storage apps. 4-85026  
 As<sub>2</sub>Se<sub>3</sub>(S<sub>2</sub>) thin films, large scale domain struct. 4-88106  
 As<sub>2</sub>Se<sub>3</sub>Te<sub>2</sub>, amorphous, radiation and thermal induced defects, electrical cond. 4-75528  
 As<sub>2</sub>Se<sub>3</sub>Te<sub>2-x</sub> glasses, DC props., neutron and gamma-ray effects 4-103814  
 As<sub>2</sub>Te<sub>3</sub> amorphous films, electronic struct., field effect and time of flight studies 4-113852  
 As<sub>2</sub>Te<sub>3</sub>, cryst., semiconductor-metal transition, elec. resist., thermoelec. power meas. 4-98523  
 As<sub>2</sub>Te<sub>3</sub>-GaS, phase diagram, peritectic reaction 4-61046  
 Au-As<sub>2</sub>S<sub>3</sub>-Al MIM struct., bias voltage depend. of capacitance 4-104325  
 Ge-As-S-I glasses, chemical bonding and mag. susceptibility (Russian) 4-70041  
 Ge-As-S(Se), antireflection coatings for YAG crystals (Russian) 4-97012  
 Ge-As-S(Se) vitreous chalcogenide based multilayer reflecting systems for IR lasers 4-69532  
 graphite-AsF<sub>5</sub> intercalated foils and compacted flakes, elec. resist. studies 4-92683  
 Hg<sub>1-x</sub>AsF<sub>6</sub>, incommensurate, mag. breakdown 4-84543  
 PbO-K<sub>2</sub>O-Na<sub>2</sub>O-As<sub>2</sub>O<sub>3</sub>-SiO<sub>2</sub>, optical glass, effects of salt additions on specific surface and polishing 4-79257  
 Se-Te-As, amorphous, defect states and photoelec. behaviour 4-113903  
 Sn-Se-GeSe<sub>2</sub>-AsSe, glass formation, physicochemical props. 4-92365  
 UAs<sub>2</sub>Se<sub>3-x</sub>, electronic and mag. struct. determ. 4-61281  
 V<sub>2</sub>O<sub>5</sub>-As<sub>2</sub>O<sub>3</sub> glasses, semicond. props. 4-80593  
 V<sub>2</sub>O<sub>5</sub>As<sub>2</sub>O<sub>3</sub> glasses, IR study 4-104614

articulation (speech) see speech

artificial hearts see artificial organs

artificial intelligence

- see also adaptive systems; biocybernetics; brain models; heuristic programming; neural nets; self-adjusting systems  
 nuclear power plants, artificial intelligence based operator aid, NRC eval. 4-115166  
 OCEANS '83, utilisation of sea, conference, San Francisco, CA, USA (Aug.-Sept. 1983) 4-106113  
 organic cpds., substructure recognition, artificial intelligence method, IR spectra 4-59762  
 problem-solving, computer and human brain comparisons 4-62460  
 speech analysis, phonemic errors simulation 4-89603  
 triple quadrupole mass spectrometer, artificial intelligence appl. 4-58912  
 weather prediction, EXPERT-2 expert system 4-82148

artificial kidneys see artificial organs

artificial limbs

- above-knee prosthesis with knee joint torque generation mechanism adaptable to walking period (Japanese) 4-93966  
 arm, prosthetic/orthotic, end-point control via binary coded EMG signal 4-89839  
 arm control by EMG pattern recognition 4-77427  
 bioelectric control of powered prosthesis for amputees 4-93969  
 control interface strategies 4-100363  
 elbow, optimal site selection for prosthetic control 4-89840  
 electrohydraulic arm-prosthesis, design, construction and operation (Hungarian) 4-115268  
 EMG processing method for prosthesis control, walking period prediction (Japanese) 4-93967  
 gait analysis and alignment system for lower-limb prostheses 4-100362  
 myoelectrically-controlled prosthetic arms, multiple degree-of-freedom, control 4-85580  
 review of recent technology (Japanese) 4-110005  
 signal processing for proportional myoelectric control 4-62629

artificial organs

see also prosthetics

- assist pump applied to cardiovascular system, optimal driving conditions (Japanese) 4-93968  
 assisted circulation and ventricular assist devices, review (Japanese) 4-110003  
 cardiac surgery and artificial hearts 4-105374  
 glucose measurement, implantable bidirectional telemetry system, artificial pancreas appl. 4-89834  
 haemodialysis, K<sup>+</sup> transport through poly(2-hydroxyethylmethacrylate) membranes 4-77203  
 haemodialysis unit, microprocessor-controlled, for terminal renal patients 4-93963  
 heart, artificial and assist devices, adaptive control strategies 4-89838  
 heart, mag. actuated, ventricular kinetics 4-85579  
 heart, total artificial, development, pulsatile vs. nonpulsatile flow, control algorithm 4-93972  
 heart assist pump, motor-driven, with implanted compliance chamber: in vivo experience 4-89836  
 heart valve, Si alloyed pyrolytic C and SiC, characterization of treated surfaces 4-89830  
 hearts, design problems and solutions found at Utah University 4-62632  
 hearts, review (Japanese) 4-110004  
 kidneys, review (Japanese) 4-109998  
 left ventricular assist device, motor driven, digital vel. feedback control 4-89835  
 left ventricular assist devices, adaptive control 4-89844  
 lungs, review (Japanese) 4-109999  
 magnetically actuated left ventricular assist device 4-89837  
 mass transfer principles (Japanese) 4-109997  
 pneumatic artificial ventricle, haemodynamic models 4-93971  
 pneumatic total artificial heart, new driver, in vitro testing 4-67149  
 review of artificial organs and their materials (Japanese) 4-89831

artificial satellites

- 1967-104B, orbital anal. rel. to determ. of 29th-order geopotential coeffs. 4-105398  
 1982 launchings list (French) 4-94544  
 active microwave instrument (AMI), development 4-85863  
 adaptive satellite orbit estimation scheme 4-82373  
 advanced X-ray astrophysics facility technology mirror assembly epoxy shrinkage effects 4-86512  
 Arizona State University research related to thermionic energy conversion 4-59399  
 Astron UV telescope, characts. and preliminary obs. (Russian) 4-67630  
 astronomical telescope, design of multiple mirror system for very high resolution, COSMIC approach 4-101161  
 Atmosphere Explorer C satellite, auroral photometry 4-72778

**artificial satellites continued**

- attitude motion, effect of atm. superrotation 4-67594
- autonomous orbit computation, appl. of delta-rho perturbation method 4-90058
- autonomous satellite navigation using the stellar horizon atmospheric dispersion sensor 4-94555
- CERS communications engineering research satellite, spacecraft description 4-72855
- Chinese space programme 4-77690
- close approaches between pairs of satellites, times of approach prediction 4-82382
- closest approach and encounter duration for two satellites in circular non-coplanar orbits 4-82384
- communication satellite launching, operators perspective 4-90055
- communications satellites, ephemeris representations 4-94560
- conference on astrodynamics at Lake Placid, USA (August 1983) 4-78043
- COS-B, gamma-ray astronomy operation 4-67813
- Cosmic Background Explorer Satellite (COBE), potential constraints on cometary origins 4-101273
- cosmic ray access to satellites from large zenith angles 4-101027
- Cosmos 482 orbit anal. 4-72849
- differential absorption, LIDAR in space for atmospheric temperature and humidity profiles 4-110331
- Doppler remote sensing, removal of troposphere radiowave refr. effects 4-77649
- Doppler satellite system for Earth surface position meas. 4-63001
- earth radiation budget experiment design and development 4-72853
- ephemeris correction and radar altimeter data for ocean surface obs. 4-67488
- equilibrium stability in problems with double reson., appl. to artificial satellites 4-82395
- ERS-1, active microwave instrumentation for ocean area monitoring 4-82363
- ERS-1, benefits for UK 4-85862
- ERS-1, satellite for ocean and climate monitoring, status and future plans 4-82369
- ERS-1 radar altimeter, development 4-85864
- ERS-1 satellite, mission objectives 4-85861
- ERS-1 satellite for ocean remote sensing 4-72854
- Europe's solar power research program, development (*Japanese*) 4-63029
- European Space Agency, report to 25th COSPAR meeting, Graz, Austria (June 1984) 4-105868
- EXOSAT, mission and instrumentation 4-90054
- EXOSAT, X-ray astronomy satellite, appls. 4-105867
- EXOSAT imaging X-ray detectors, pre-flight and in-orbit performance 4-63066
- Exosat mission, satellite description and results 4-82368
- Extreme Ultraviolet Explorer, microchannel plate EUV detectors 4-63063
- first order short-periodic motion due to third body perturbations, numerical evaluation 4-94561
- Gamma Ray Observatory, imaging Compton telescope design 4-63061
- geodynamic satellites, drag in atm., neutral and elec. components 4-82370
- GEOS-2, de-orbiting of geosynchronous satellite to eliminate collision risk 4-90049
- geosynchronous satellites in inclined orbits, long-term motion 4-82372
- global Positioning System (GPS) appl. to geodesy, estimation and large-scale multiple hypothesis testing 4-77656
- GOES satellite signal used for timekeeping at high latitude field stations 4-82274
- GPS time data recording system using a multi-task minicomputer (*Japanese*) 4-90566
- HEAO-2, definitive orbit determ. 4-82381
- HF band radiowaves, ionospheric heating experiments (*Japanese*) 4-63011
- high energy satellite surveys 4-63089
- Hipparcos astrometry mission 4-63031
- HIPPARCOS mission, linking of reference systems from space 4-72856
- imaging radars overview 4-77694
- Indian remote sensing satellite, programme overview 4-115614
- Infrared Astronomical Satellite (IRAS), early results 4-101501
- Infrared Astronomical Satellite cryogenic system, use of superfluid Helium 4-77718
- Infrared Astronomical Satellite spacecraft thermal design and performance 4-77717
- Infrared Space Observatory 4-63069
- Infrared Space Observatory dual liquid H<sub>2</sub>/He superfluid He coding system thermal design 4-73441
- intersatellite links, future mission requirements and spacecraft limitations 4-110497
- ionosphere satellite, elec. field pot. distrib. at beginning of electron injection 4-110353
- ionospheric satellite charged particle beam expts., changes in satellite elec. pot. 4-72851
- IRAS fast-moving object search 4-77691
- IRAS infrared astronomical telescope in orbit, design and performance 4-77712
- IRAS mission, Monte Carlo simulation and proposed catalogue completeness 4-94559
- IRAS mission 4-85857
- IRAS mission operations experience at RAL 4-101116
- IRAS preliminary scientific results from the first six months 4-77692
- IUE SEC videocon detector as origin for 'interstellar' 280 nm feature 4-82538
- Japan's solar energy supply program, development (*Japanese*) 4-63030
- Japanese developments (*Japanese*) 4-94545
- Japanese scientific satellites (*Japanese*) 4-94549
- L-SAT Telecommunication Satellite thermal design 4-74844
- LAGEOS, laser ranging data during MERIT (*Russian*) 4-94551
- Lageos, orbit var. and lower mantle viscosity determ. 4-85641
- Landsat 4, orbit solns., ephemerides and Global Positioning System navigation results 4-94556
- Landsat 4 onboard navigation using NAVSTAR GPS 4-72848
- Landsat fourth geo-scanner, characts. (*German*) 4-110491
- Landsat Multispectral Scanner and Thematic Mapper effective bandwidths 4-82272
- Landsat satellite remote-sensing imagery, ground control points, automatic relocation 4-67511
- Landsat-4 imaging processing techniques and map making 4-82260

**artificial satellites continued**

- Landsat-4 MSS and Thematic Mapper data quality and information content 4-82261
- Landsat-4 MSS and Thematic Mapper image quality 4-82053
- Landsat-4 Thematic Mapper, radiometric calibration technique 4-82263
- Landsat-4 Thematic Mapper and Multispectral Scanner, information contents 4-82266
- Landsat-4 Thematic Mapper geometric accuracy 4-82268
- Landsat-4 Thematic Mapper radiometric and geometric correction methods 4-82262
- large spaceborne microwave radiometers, mission planning 4-94552
- laser ranging meas., system anal. and computer simulation 4-107723
- Long Duration Exposure Facility (LDEF) mission, micro-meteoroid capture-cell expt. 4-105876
- magnetised satellite in circular polar orbit plane, eqn. of motion 4-101113
- magnetosphere electric field measurement with spherical double probes on satellites 4-82367
- magnetospheric VLF emissions, wave normal directions meas. observed onboard satellites 4-110367
- METEOSAT system, appl. to hazard monitoring and assessment in Mediterranean region 4-94251
- microwave propagation and antenna characts. for solar power satellite (*Japanese*) 4-62932
- microwave transmission, ionospheric effects (*Japanese*) 4-63010
- microwave transmissions, neutral atmosphere effects (*Japanese*) 4-62931
- missions involving spectroscopy of celestial objects 4-90051
- motions, conf. at Embu, Brazil (December 1981) 4-78039
- NASA space programs in IR astronomy 4-110490
- Nimbus-7 Coastal Zone Colour Scanner 4-67456
- NOAA satellite data utilisation by oceanographers 4-115621
- NOAA satellite sea ice image analysis using ice-breaker Shirase's meteorological data processing systems 4-85762
- nuclear reactor space power systems, gas-cooled and liquid-metal-cooled, comparison 4-72149
- orbit errors effect on satellite altimetry meas. of tides in oceans 4-67487
- orbit estimation using atmospheric density models 4-72768
- orbit evolution of satellite in 12-hour orbit (*Russian*) 4-115678
- orbit prediction by vector techniques, SPIRAL program anal. 4-94642
- orbit theories based on elimination of parallax 4-82371
- orbit theory for LSI-11 microprocessor 4-94554
- orbital inclination and Love's constant for Earth models 4-77474
- orbital lifetime estimation method for near Earth satellites 4-82374
- orbital mechanics, use of empirical anal. density models 4-82320
- orbital perturbations due to vars. in Earth rotation, theory 4-101212
- orbits, coupled perturbations anal. appl. of Lagrange method 4-82375
- orbits, general anomaly and time elements 4-67596
- organic Rankine cycle power conversion systems for space applications 4-72150
- orientation at libration point in restricted three-body problem 4-90061
- OTS-2 satellite in geostationary orbit, thermal testing experience 4-83656
- perigee elimination in satellite problem 4-67605
- photographic satellites, orbits and positions determ. from statistical characts. of obs. (*Chinese*) 4-82242
- plasma interactions 4-82377
- plasma interactions (book) 4-67900
- POPSAT, center of mass correction and statistical confidence 4-110034
- power supplies using Si and GaAs solar cells 4-99972
- power system construction, environmental effects (*Japanese*) 4-62981
- power systems, laboratory and field experiments on atmospheric environmental effects (*Japanese*) 4-62982
- power systems for terrestrial electricity generation (*Japanese*) 4-63028
- precession dynamics in spin-orbit coupling, unified theory 4-110503
- quasiasymmetric satellite, periodic oscill. stability in elliptical orbit plane 4-82392
- radio beacons for use in star coords. determ. method 4-63034
- remote sensing, satellite imagery, ground control points selection, geometrical correction 4-67510
- remote sensing, space appl. 4-85860
- remote sensing and Landsat (*Japanese*) 4-94256
- remote sensing satellite, concept 4-72852
- ROSAT X-ray telescope thermal design features 4-85879
- satellite exploration, ground stations features (*German*) 4-110284
- satellite power systems, terrestrial EM environmental effects (*Japanese*) 4-62930
- satellite-ocean remote sensing systems and their prospects 4-110164
- SEASAT, instrumentation performance and mission overview 4-82281
- SEASAT—data acquisition and processing by the Royal Aircraft Establishment 4-82241
- Seasat mission, goals and accomplishments survey 4-67404
- SEASAT mission (book) 4-78054
- SEASAT satellite orbit determ. by laser ranging 4-82299
- SEASAT satellite orbit tracking over Europe 4-82298
- SEASAT-SASS instrument, validation and appl. in JASIN 4-82283
- SEASAT-SASS program, instrument characts. and wind vel. determ. 4-82282
- Shuttle imaging spectrometer experiment for the late 1980s 4-77695
- SIGMA, high resolution space observatory project for gamma-ray sources 4-105875
- Solar Maximum Mission, instrumentation and observatories (*French*) 4-101111
- Solar Maximum Mission, X-ray position sensitive detector system 4-63065
- Solar Mesosphere Explorer, stratospheric NO<sub>2</sub> meas. 4-72668
- solar photometric satellite for flux var. obs. 4-101191
- Solar Power Satellites as interstellar beacons, theoretical anal. 4-63027
- space operations and navigation, appl. 4-110496
- space power system using Fresnel lenses for solar power utilisation, thermal energy storage 4-72176
- Space Shuttle glow, N<sub>2</sub> spectral emission mechanism 4-110492
- Space Telescope, Wide Field/Planetary Camera, CCD use for faint planetary satellites 4-82423
- Space Telescope mission planning 4-94557
- space-based ocean remote sensing technology 4-105775
- space-nuclear-reactor ultralloys, thermionic-energy-conversion implications 4-9398
- spaceborne LIDAR for meas. from satellites, design 4-110327
- Starlette satellite, orbital perturbations by ocean tides (*Chinese*) 4-82362
- synchronous orbits, appl. of extended semianalytical Kalman filter 4-90057

**artificial satellites continued**

- synodic motion of satellites related to the Sun 4-82383  
 TDRSS satellite, navigation and orbit determ., use of dedicated VLBI system 4-82380  
 Tenma, instrumentation and preliminary results 4-110487  
 Thematic Mapper on Landsat-4, image quality study 4-82265  
 Thematic Mapper on Landsat-4, in-flight radiometric calibration 4-82264  
 three-body problem, restricted case, eccentricity effect on halo orbits, artificial satellite appl. 4-82404  
 Advanced TIROS-N, Windsat lidar equipment for wind meas. 4-110266  
 TOPEX satellite project, end-to-end ground data system 4-77657  
 two-body problem with drag, semi-analytic soln., appl. to artificial satellites 4-110505  
 US radioisotope thermoelectric generator space operating experience (June 1961-December 1982) 4-72135  
 US space nuclear reactors 4-59397  
 X-ray, ROSAT, manufacture and testing of mirrors 4-115686  
 zonal satellite, appl. of equations of motion regularisation in central force field 4-90062  
 Li-metal sulphide cell development for satellite batteries 4-72075  
 Na-S cells for high power satellite/spacecraft appls. 4-72076  
 Ni-H<sub>2</sub> cells for communications satellites, effect of geosynchronous altitude radiation 4-72071  
 Ni-H<sub>2</sub> satellite batteries, cell stack and pressure vessel in series, feasibility study 4-72072

**asbestos**

- charged particle induced short-wave radiation in natural hollow crystallographic channels (*Russian*) 4-81031  
 powdered or porous samples, low freq. photoacoustic spectra 4-88792

**asdic see sonar****aspherical lenses**

see also aberrations

- Bragg-grating optical-waveguide lenses, out-of-phase props. 4-87444  
 diamond machining applications and capabilities 4-107899  
 Fresnel lens design for low conc. photovoltaic conversion (*French*) 4-105107  
 geodesic optics 4-64756  
 interferograms, separating misalignment from misfigure on off-axis aspheres 4-112593  
 lathe for generation of aspherical surfaces of revolution 4-107898  
 micro-Fresnel high-performance lens fabricated by UV lithography 4-87408  
 multichannel optical system for target acquisition and ranging, use of aspheric surfaces 4-107794  
 oblate spheroidal surface null tests 4-79259  
 phase Fresnel lens realisation by multiple beam interferometry 4-87429  
 planar microlens, maximum and effective numerical apertures, Luneburg lens model 4-87410  
 planar microlens distributed-index form, process 4-87487  
 prime focus corrector for f/3 true or quasi Ritchey-Chretien primaries 4-72879  
 starting system evaluation by Seidel correction with aspheric surfaces 4-69522  
 surface testing with shearing interferometer using fringe scanning detect. method 4-107909  
 testing, optical, by lateral shearing interferogram analysis 4-112594  
 waveguide grating lenses for optical couplers 4-87443

**association**

see also association of liquids; associative ionisation

- acetic acid, dipole assoc. in nonpolar solvents (*German*) 4-109116  
 acetonitrile, autoassociation, supersonic mol. beam mass spectrometer study 4-81411  
 acetylene mol. affinity for Li<sup>+</sup>, STO calc. 4-62182  
 acridine dyes, assoc., thermally stimulated slow fluoresc. 4-78904  
 alkali metals, nuclear magnetic props. and solvation, review 4-74179  
 alkanethiol-tri-n-butylphosphine, H bonding, PMR investig. (*German*) 4-107369  
 amide complexes, ionic H bonds, intramol. and multiple bonds 4-66568  
 amino acid derivative complexes, ionic H bonds, intramol. and multiple bonds 4-66568  
 anthracene-TEA (DMA) complexes formed in supersonic jets, van der Waals and charge transfer states 4-112226  
 aromatic compounds, dipolar association as a function of molecular structure studied by nonlinear dielectric effect 4-89253  
 aromatic systems, liq., muonic radical form., relative rate consts. 4-71948  
 7-azaindole, H-bonded complexes, MPI PES and two-colour MPI threshold spectroscopy 4-91320  
 azole derivatives, H bonded complex form. with nitrophenols, IR and UV investig. 4-66562  
 benzothiazole cationic dyes, aggregation in water, equilibr. consts., thermodynamics props. 4-62181  
 t-butanol in aq. soln., Raman linewidth, hydration struct. 4-74252  
 n-butanol in soln., low temp., <sup>1</sup>H NMR spectra 4-89254  
 butyrophonones and related cpds., assoc. with I<sub>2</sub>, dielectric study 4-104971  
 carbon tetrachloride-methanol mixtures, thermal diffusion factors meas. 4-61119  
 chlorocoumarins, solid-state photodimerisation rel. to cryst. engineering 4-109669  
 α-chymotrypsin-dyes assoc., fluoresc. circular polarisation, Cotton effect 4-102838  
 composite ionberg-iceberg model of aqueous nonpolar solvation and water exchange reactions 4-91326  
 cryptand 222, aq. soln. mono- and diprotonation, heat capacities and vols. 4-85300  
 cryptands, halogen interactions, decomplexation, equilibr. consts., UV and NMR study 4-104975  
 p-cyanonitrobenzene anion radical, H bonding, kinetic parameters 4-102713  
 cyclic urethane-ZnCl<sub>2</sub> cluster complex form. 4-62187  
 cycloalkanes, protonation, ab initio SCF MO calcs. 4-104982  
 electrolyte solns., ion assoc. reactions, cluster approach 4-99755  
 2,3-epoxy-1-propanol, hydration to glycerine, multiple attractors, nonequilibrium phase transitions 4-71889  
 ethanol-tri-n-butylphosphine, H bonding, PMR investig. (*German*) 4-107369  
 ferene-Fe (II) complexation study 4-109626  
 formaldehyde-H<sub>2</sub>O addition, transition struct. determ. and characterisation 4-66576

**association continued**

- formyl radical+NO(O<sub>2</sub>) reaction, collision complex form. 4-71899  
 gas hydrates, form., distrib. and appls., review 4-71912  
 glass, stressed nuclear waste material, hydration in saturated water vapour 4-66554  
 glycine zwitterion protonation reactions, thermodynamic props. 4-93513  
 halide anion-organic acid (alcohol) complexes, binding energies, struct. effects, equilb. meas. 4-85293  
 hydrocarbons, unsaturated, PMR spectral shift induced by complex Ag-lanthanide shift reagents 4-99776  
 ion-molecule association reaction rates, endothermic reactivity correl. 4-99767  
 ligand exchange process, mathematical modelling 4-114769  
 lithium benzophenone-LiBr complex form., equilb. const. 4-71906  
 magnetic particle conglomerate form. and props. 4-109692  
 metal salts, complex form. with elec. neutral ligands grafted to surface, reaction model 4-109686  
 methane-keV proton irradiation interplanetary hydrocarbon generation 4-115711  
 7-methoxycoumarin, topochem. dimerisation in solid state 4-109628  
 methyl cation, termolecular association reactions, statistical phase space theory appl. 4-89266  
 methyl-d<sub>3</sub> cation, termolecular association reactions, statistical phase space theory appl. 4-89266  
 methylcoumarins, solid-state photodimerisation rel. to cryst. engineering 4-109669  
 methylnicotinate, protonation sites, H bonding, IR obs. 4-87118  
 N-methylthioacridone triplet +O<sub>2</sub>, photophysical behaviours and O<sub>2</sub> singlet generation efficiency 4-104999  
 microemulsions extractant anions, FTIR studies on hydration 4-99848  
 molecular ions, electron scatt., dissoci. recombination processes 4-74345  
 nucleic acid-base interactions, solvent effects, Monte Carlo simulation 4-64559  
 organic molecules, luminescence of excimers and exciplexes 4-104997  
 oxides, surface exchange reactions, oxygen transport characteristics 4-98355  
 paired macromolecules, form. kinetics and mechanism (*Russian*) 4-62202  
 perylene-TEA (DMA) complexes formed in supersonic jets, van der Waals and charge transfer states 4-112226  
 phenol, H-bonded complexes, MPI PES and two-colour MPI threshold spectroscopy 4-91320  
 poly(diphenylphosphinomethyl)benzene oxides, conform. anal. and complex form. 4-62186  
 poly-1,1,2-trichlorobuta-1,3-diene-polystyrene, paired polymer form. kinetics and mechanism (*Russian*) 4-62202  
 polyethers, macrocyclic, thiophosphonyl containing, complexation with Ag(I), NMR obs. 4-109642  
 propionitrile, autoassociation, supersonic mol. beam mass spectrometer study 4-81411  
 pyrene-sodium lauryl sulphate micellar system, caffeine effect on photo-induced reactions 4-104998  
 pyridine derivatives, H bonded complex form. with nitrophenols, IR and UV investig. 4-66562  
 reactive components, fluctuation thermodynamic props., species correl. function integrals 4-71965  
 semiquinones-Mn<sup>2+</sup>(Cu<sup>2+</sup>)(Gd<sup>3+</sup>) interaction in aq. solns. relax. and complex formation 4-99777  
 stream of recombining atoms, chemical reactions and relax. 4-108103  
 tetra(4-sulphonatophenyl)porphyrin dimers, ESR study of photoexcited triplets 4-64515  
 ter-molecular ion-molecule association reaction, rates and energy randomisation time 4-99765  
 1,1,2,2-tetrachloroethane binary systems, dielec. props. at 308.15K 4-104521  
 thermodynamic association const. and standard enthalpy of association 4-88047  
 three-atom reactions, Kramers' theory 4-109637  
 three-body ion+molecule association reaction rate consts., temp. variation constraints 4-85292  
 (TMTSF)<sub>x</sub> salts, anion size, structural props., intracolumnar effects, assoc. 4-98084  
 water vapour, self-deactivation, dimer effect 4-102773  
 Al, liq., chem. reaction with B fibres 4-61891  
 Ar, relativistic electron beam excitation, fluoresc. and absorpt. 4-69220  
 Au/Ru<sub>4</sub>(μ-H)(CO)<sub>2</sub>(PPh<sub>3</sub>)<sub>3</sub> synthesis, mol. and cryst. struct. 4-104969  
 B fibres, chem. reaction with liq. Al 4-61891  
 C neutral bases, H<sup>+</sup> and methyl- and ethyl-cation affinities, MNDO calcs. 4-64381  
 CN<sup>-</sup>e<sup>-</sup>, electronic/positronic struct. examined using Hartree-Fock-Roothaan theory 4-64352  
 Ca<sup>2+</sup> dielectronic recombination via 4s to 4p excitation 4-74341  
 Ca<sup>18+</sup>, electron scatt., collision strengths for inelastic transitions including fine struct. 4-96704  
 CaCO<sub>3</sub> crystallisation with chem. absorpt. 4-98038  
 CdF<sub>2</sub>, alkali metal doped, association and bound motion 4-80294  
 Cl<sub>2</sub>, photodissociation, termolecular recombination, photoacoustic detection 4-99809  
 Cu complex, bis(di-ethanol-dithiocarbamate) Cu(II), intermol. interactions, EPR obs. 4-64516  
 Fe (III) solutions, magnetisation meas. for oligomer formation detection 4-98917  
 Gd complexes, pyridoxine-Gd(III) in aq. soln., PMR study of struct. 4-114179  
 H<sub>2</sub>, evolution in liq. He chamber, recombination and burial 4-77003  
 (HF)<sub>n</sub>, in solid Ar matrix, FT IR spectra 4-69066  
 H<sub>2</sub>O+methyl cation (protonated formic acid), ternary association reaction in He buffer 4-93525  
 H<sub>3</sub>O<sup>+</sup> linear and bifurcated complexation with electron donors, ab initio calc. 4-99752  
 I<sup>-</sup> atoms in solns., geminate recombination, generalized Langevin treatment, inelastic transitions effect 4-62162  
 I, photolytic cage effect and atom recombination in compressed gases and liqs. 4-99807  
 Mg(H<sub>2</sub>PO<sub>4</sub>)<sub>2</sub> soln., complex form. and phosphate-H<sub>2</sub>O interactions 4-89256  
 N atom recombination at Pd surface, field ionization evidence of excited molecules 4-99288  
 N neutral bases, H<sup>+</sup> and methyl- and ethyl-cation affinities, MNDO calcs. 4-64381  
 N<sub>2</sub> internal subshells, rel. to bond form. and XPS struct. 4-59850

association continued

$N_2^+ + 2N_2$ , association reaction rate const. determ. in temp. range 20 to 160K by CRESU technique 4-76986  
 $N_2^+ + N_2 + M \rightarrow N_4^+ + M$ , ion-molecule association reaction for  $M = N_2$ , Ne and He 4-99764  
 $N_2^- - e^+$ , electronic/positronic struct. examined using Hartree-Fock-Roothaan theory 4-64352  
 $NO^+$ , three-body assoc. reactions with Kr and Ar at 80K 4-71883  
 $NO_2^-$ , cluster form, with HONO mols. mass spectrosc. investig. 4-69260  
 $NO_2$ , synthesis in low press. plasma, energy cost improvement 4-85305  
 $NO(B^2\Pi_u)$ , specific prod. from recombination of NO on Ni surface, chemilumesc. 4-89304  
 $N(S)$ , recombination kinetics Vegard-Kaplan chemiluminescence bands 4-109629  
Na, ion formation in vapour containing Rydberg atoms 4-91242  
 $Na^+ + Na$ , associative ionisation reaction, rate const. 4-89283  
 $Ne_2^+$  mol. ions in decaying plasma, dissociation, recombination, vibr. excitation 4-99783  
Ni (II) complexes with macrocyclic tetraaza ligands, form., XPS obs. 4-59851  
Ni (III), dissociative adsorption and recomb. of CO,  $N_2$ , SO, and  $O_2$  4-93559  
Ni complexes, dibromo( $N,N'$ -di-*tert*-butyldiazabutadiene) nickel, structural phase transform. 4-103717  
 $O$  neutral bases,  $H^+$  and methyl- and ethyl-cation affinities, MNDO calcs. 4-64381  
 $O_2^+$ , three-body assoc. reactions with Kr and Ar at 80K 4-71883  
 $O_2^+ + 2O_2$ , association reaction rate const. determ. in temp. range 20 to 160K by CRESU technique 4-76986  
 $OH^- - e^+$ , electronic/positronic struct. examined using Hartree-Fock-Roothaan theory 4-64352  
PaV extraction with 2-phenyltrifluoroacetone from strongly acidic solns. 4-72034  
Pd complexes, Pd(0,II,IV) states, synthesis, mol. spectrosc. obs. 4-64458  
 $SH^- - e^+$ , electronic/positronic struct. examined using Hartree-Fock-Roothaan theory 4-64352  
p-Si surface,  $^{14}N_2^+ (H_2^+)$  bombardment, Raman scatt. obs. 4-114283  
 $SiF_4$ , ion-molecule reactions, FT mass spectra 4-93518  
 $Xe + Br(P_{3/2})$ , laser photodissociation,  $XeBr(B)$  fluoresc. 4-114772  
 $XeCl$  mols., photoassociative laser-induced fluoresc., radiative lifetimes, quenching rate const. 4-87152  
Zn tetraphenylporphyrin, spectral-fluoresc. props., aggregate state and temp. effects 4-78906  
 $\alpha$ -Zr, hydride form., an  $\alpha$ -phase, pendulum technique investig. 4-70398

association factor (liquids) see association of liquids

association of gases see association

association of liquids

see also colloids  
binary associating mixtures, zero wavenumber struct. factors 4-92041  
t-butyl alcohol, aq. solns., conc. fluctuations, light scatt. study 4-76484  
p-cyano- $N,N$ -dialkylanilines in nonpolar solns., luminescence studies 4-99168  
dimethyl sulphoxide, self-association and dipolar interactions, Raman spectral study in  $H_2O$  and  $CCl_4$  solns. 4-71907  
excess Gibbs energy and vap. press. of associated systems 4-88048  
halogens quadrupolar nuclei, NMR spectroscopy 4-73476  
methanol-aqueous soln., hydrophobic interaction, Monte Carlo calc. 4-97994  
methanol-cyclohexane mixtures, self-assoc., NMR relax. investig. 4-80836  
6-methylpurine in aq. soln., relax. behaviour of self-association 4-114780  
molten salts, assoc. and mobility isotherms 4-75247  
thermodynamic association const. and standard enthalpy of association 4-88047  
thiopicvalic acid, solns., self-assoc., IR and PMR spectrosc. obs. 4-74241  
n-valeric acid, association study from dielec. props. 4-76998  
Au-Zn, liquid alloy, mixing thermodynamics 4-109420  
CoCl solns., US relax. mechanisms 4-92308  
Ga-Te, molten, at. arrangement of  $Ga_2Te_3$  associates, metallic-like bonding, neutron scatt. obs. 4-103639  
 $Mn(NO_3)_2$ , aq. solns. conc., hydration and ion-pairing, X-ray and Raman spectra 4-93512  
Se-Te, melt, near-order struct., X-ray diffraction study 4-60804

associative ionisation

laser optogalvanic effect for ats. and mols. in recomb.-limited plasmas 4-87091  
He capillary glow discharge, collisional radiative model with atomic collisions 4-60773

astatine

see also nuclei with .....

No entries

astatine compounds

astatobenzenes, substituted, C-At bond dissociation energy calcs. 4-114779

ASTERISK spectroscopy see Raman spectroscopy

asteroid satellites see planetary satellites

asteroids

1982 RA, Amor-type asteroid, precise positions, orbital elements, and ephemeris 4-101226  
1983 KD, Apollo asteroid, precise positions, visual magnitude estimates, and orbital elements 4-85887  
1983 SN, IRAS semicircular positions of Apollo object 4-82439  
1983 TB, orbital evolution rel. to future observability 4-77753  
1983 VA, ephemeris (1984 February 10 to April 30) 4-67668  
1984 AB, orbital elements and ephemeris (1984 February 10 to July 19) 4-67669  
1984 BC, fast-moving asteroid, precise positions, orbital elements, and ephemeris 4-63094  
1984 KB, Apollo asteroid, precise positions, orbital elements, and ephemeris 4-77752  
1984 KB, Apollo asteroid, precise positions orbital elements, and ephemeris 4-82438  
1984 KB, discovery and obs. (1984 May 27-29) 4-77751  
1984 KD, ephemeris (1984 July 9 to October 7 in five day intervals) 4-94667  
1984 KD, ephemeris (1984 June 19 to July 24) 4-85888  
1984 KD, new Apollo asteroid, precise positions, orbital elements, and ephemeris 4-85886  
1984 QA, fast-moving asteroid object, Aug. 1984 discovery 4-110557

asteroids continued

1984 QA, positions, orbital elements and ephemeris (1984 Aug.-Sep.) 4-115707  
ages of asteroid families 4-90105  
82 Alkeme, lightcurve and phase relation obs. 4-67665  
angular momenta in solar system, statistical distrib. for comets, asteroids and meteor streams 4-101204  
angular momentum drain by impact ejecta 4-82437  
astrometric observations, topocentric (1982-3) 4-110554  
astrometric positions of minor planets (1979 to 1983) 4-94666  
belt, gravitational perturbations on celestial bodies and spacecraft 4-90098  
binary nature from light curve studies 4-82435  
brightness opposition effect model 4-94565  
123 Brunhild, rotation period from V photometry 4-110556  
Cerro El Roble positions for 19 objects (1979-80) 4-110555  
2060 Chiron, stellar appulses and occultations during November 1984, predictions 4-77750  
classifications and mineralogy, implications for solar nebula characts. 4-101207  
collisional origin of asteroid families, effects of target's gravity 4-90104  
133 Cyrene, lightcurve and phase relation observations 4-115706  
discoveries, historical aspects (*Danish*) 4-72905  
dynamical motions and Fundamental Reference System systematic accuracy determ. 4-82386  
extinct comets in high-inclination orbits, steady state number 4-90118  
1224 Fantasia, tentative rotation period from V photometry 4-110556  
Galileo spacecraft for asteroid or comet rendezvous, trajectories 4-82378  
376 Geometria, rotation period from V photometry 4-110556  
444 Gysitis, lightcurve and phase relation obs. 4-67665  
Icarus, perihelion shift due to electric charge of Sun 4-110507  
impacts of large asteroids and comets on Earth, geological implications, conference, Snowbird, Utah (1981 October 19 to 22) 4-100577  
IRAS fast-mover program 4-101227  
IRAS fast-moving object search 4-77691  
Kiev astrometric obs. of 13 objects (*Russian*) 4-101225  
Kirkwood gaps depletion mechanism 4-90063  
light curves, contrib. of shape of asteroid and albedo var. 4-94668  
lightcurve inversion, convex profiles 4-82436  
low-velocity encounters with outer planets 4-90106  
main belt and IR cirrus, IRAS obs. 4-85892  
meteorite formation processes 4-67707  
Minor Planet Circulars, precise posns., elements, ephemerides, new nos. and names 4-77754  
Minor Planet Circulars 8579-8690, precise posns., elements, ephemerides, and new nos. 4-63095  
Minor Planet Circulars 8827-8946, precise posns., elements, ephemerides, new nos. and names 4-101228  
Minor Planet Circulars 8947-9036, precise posns., elements, ephemerides and new nos. 4-105900  
motion and evolution, obs. data base 4-101275  
orbital elements for stability regions 4-90099  
orbital stability 4-90100  
photoelectric photometry, advances for small telescopes, book 4-110816  
positions of four asteroids during 1982 August from GPO telescope at ESO, Chile 4-67664  
properties and classifications 4-77755  
resonant orbits stability 4-90101  
437 Rhodia, tentative rotation period from V photometry 4-110556  
rotational parameter statistics for small asteroids 4-67667  
rotational properties 4-94669  
satellite detection by occultations of stars (*French*) 4-67663  
search strategies for Earth-approaching objects 4-67666  
shapes rel. to fragments from hypervel. impact expts. 4-72906  
Spacewatch camera, use in asteroid research (*French*) 4-82418  
spherical shape attainment by viscous relaxation process 4-90096  
stability and capture anal., use of the Lyapunov Character. Numbers 4-82397  
stellar occultations during 1984, photographic search and ephemerides 4-101224  
thermal histories, rel. to multiple parent bodies of ordinary chondrites 4-67704  
Trojan asteroids, long periods in three-dimens. motion 4-90102  
Trojan asteroids, orbital evolution 4-90103  
375 Ursula, diameter determ. from occultation of star (AG+39°303) 4-82434

**astigmatism** see vision defects  
**astroarchaeology**  
native American astronomy 4-94653  
**astrobiology** see extraterrestrial life  
**astrobles** see meteorite craters  
**astrometry**  
1982 RA, Amor-type asteroid, precise positions, (1984 July 25 to 26) 4-101226  
1983 KD, Apollo asteroid, precise positions (1984 June 13 to 16) 4-85887  
1984 BC, fast-moving asteroid, precise positions (1984 January 30 to February 21) 4-63094  
1984 KB, Apollo asteroid, precise positions (1984 May 27 to 30) 4-77752  
1984 KB, Apollo asteroid, precise positions (1984 May 27 to June 3) 4-82438  
1984 KD, new Apollo asteroid, discovery and precise positions (1984 May 27 to June 13) 4-85886  
1984 QA, positions, orbital elements and ephemeris (1984 Aug.-Sep.) 4-115707  
(1984), recovery, precise position, and orbital elements 4-110568  
absolute stellar proper motions, error anal. for astrometric determ. via Monte Carlo simulation 4-94563  
AGK3 star catalogue declinations, comparison with results of latit. obs. (*Russian*) 4-101120  
Askania Transit Instrument at Graz, latitude determ. from stars astrometric obs. (*German*) 4-72590  
asteroids, astrometric observations, topocentric (1982-3) 4-110554  
asteroids, Cerro El Roble positions for 19 objects (1979-80) 4-110555  
asteroids, Kiev astrometric obs. of 13 objects (*Russian*) 4-101225  
astrolabe observations, apparent posns. calc. and IAU recommendations (*French*) 4-63032  
atmospheric dispersion coefficient, determ. and correction for its influence (*Russian*) 4-101121

## astrometry continued

- binary and proper-motion stars, photographic astrometry 4-115777  
 binary stars, interferometric meas. by combining light issuing from two telescopes (*French*) 4-105888  
 binary stars, speckle interferometric measurements during (1981) 4-94862  
 binary stars in Hyades, results from lunar occultation obs. 4-101407  
 4C 14.27, 74.16, 13.66, 51.40, bright radio sources, CCD position of optical counterpart 4-110761  
 3C 292, bright radio source, CCD position of optical counterpart 4-110761  
 $\beta$  Capricorni, orbital elements from lunar occultation obs. 4-101407  
 $\mu$  Cassiopeiae, astrometric binary, speckle interferometry and mass meas. 4-72977  
 $\mu$  Cassiopeiae, binary star orbit, parallax and proper motion 4-110688  
 Circinus X-1, precise radio position from VLBI obs. 4-94877  
 P/Comet Arend-Rigaux (1984k), precise position (August 1984) 4-110567  
 P/Comet Arend-Rigaux (1984k), recovery and accurate position (1984 August 9) 4-110571  
 P/Comet Arend-Rigaux (1984k), recovery positions and ephemeris 4-101269  
 Comet Austin (1984i), July 1984 comet observations and ephemeris 4-101264  
 Comet Austin (1984i), positions, magnitudes, orbital elements, ephemeris and coma diameters 4-94687  
 Comet Austin (1984i), positions, orbital elements, ephemeris, magnitudes and tail obs. 4-115725  
 P/Comet Bradfield (1984a), positions, magnitude estimates and orbital elements 4-85896  
 Comet Bradfield (1984a), precise positions, orbital elements and ephemeris 4-67687  
 P/Comet Gehrels 3 (1984i), recovery, precise position, and orbital elements 4-110568  
 P/Comet Gehrels 3 (1984i), recovery and precise positions (1984 August 7 and 8) 4-110568  
 P/Comet Giacobini-Zinner (1984e), recovery and precise positions (January to April 1984) 4-63100  
 P/Comet Halley (1982i), astrometry (1984 March 4) and flux 4-67700  
 P/Comet Halley (1982i), precise positions (1983 December 31 to 1984 January 30) 4-63105  
 Comet IRAS (1983k), positions, parabolic orbit elements, and ephemeris (1984 Feb.-Aug.) 4-67688  
 Comet Meier (1984o), precise positions (1984 September 18 to 21) 4-115726  
 P/Comet Neujmin 1 (1984c), recovery and precise positions (1984 February 26) 4-63107  
 P/Comet Russell 4 (1984d), discovery posns., orbital elements, and ephemeris 4-67689  
 P/Comet Russell 4 (1984d), positions, orbital elements and ephemeris 4-67696  
 P/Comet Russell 4 (1984d), precise positions (1984 March 12) 4-67691  
 Comet Shoemaker (1984f), astrometric obs., orbital elements and ephemeris (1984 May 30 to July 29) 4-82453  
 Comet Shoemaker (1984f), precise position (1984 May 31) 4-77778  
 P/Comet Takamizawa (1984j), orbital elements and ephemeris 4-110566  
 P/Comet Takamizawa (1984j), positions, elements and ephemeris (1984 June-Aug.) 4-110574  
 Comet Takamizawa (1984j), possible short period comet, astrometry, orbit and ephemeris 4-101267  
 P/Comet Takamizawa (1984j), precise positions (1984 July-August) 4-101271  
 Comet Takamizawa (1984j) 1984 July 29 to August 28 ephemeris 4-101267  
 Periodic Comet Wolf-Harrington, June 1984 rediscovery obs. 4-85894  
 computational spherical astronomy (book) 4-78071  
 Danjon prismatic astrolabe, var. control and zenith distance stability 4-94606  
 Fundamental Reference System, systematic accuracy from obs. of asteroids motions 4-82386  
 fundamental stars, apparent places (1984 onwards), computational procedure 4-77696  
 G34.3+0.2, H II region, precise positions of compact radio source and masers 4-63238  
 Galilean satellites, mutual phenomena in 1973 and 1979/80, astrometric obs. 4-63098  
 Galilean satellites, results of photographic positional observations (*Russian*) 4-101237  
 Hipparcos astrometry mission 4-63031  
 Hipparcos Input Catalogue, preliminary lists of stars 4-94647  
 Jupiter, results of photographic positional observations (*Russian*) 4-101237  
 KSZ catalogue stars, astrometric obs. in areas with galaxies using meridian instruments (*Russian*) 4-101119  
 M-type giant stars in Baade's Window, spectral classifications, positions and apparent I magnitudes 4-101325  
 M-type stars in galactic centre region, RI photometry, astrometry and spectral classification 4-101194  
 Markarian galaxies 1400 to 1500, accurate optical positions 4-73063  
 Minor Planet Circulars, precise posns. for asteroids and 19 comets 4-77754  
 Minor Planet Circulars 8579-8690, precise posns. for asteroids and 21 comets 4-63095  
 Minor Planet Circulars 8827-8946, precise posns. for asteroids and 16 comets 4-101228  
 Minor Planet Circulars 8947-9036, precise posns. for asteroids and 16 comets 4-105900  
 minor planets, astrometric positions (1979 to 1983) 4-94666  
 Neptune and Triton, topocentric positions (1978 to 1983) 4-110561  
 NGC 2264, young star cluster, positions of 195 atoms 4-110706  
 Nova Vulpeculae 1984, precise position and tentative identification of pre-nova 4-101365  
 Nova Vulpeculae 1984, precise position and visual magnitude estimates (1984 Aug.) 4-101366  
 occultations of stars by asteroids during 1984, photographic search and ephemerides 4-101224  
 outer planets, astrometric observations, topocentric (1982-3) 4-110554  
 planetary satellites, faint, use of CCD 4-82423  
 Pluto, astrometric positions (1980-1983) 4-110561  
 pulsars, interferometric and timing data use 4-110543

## astrometry continued

- PZT stars on international parallel, preliminary Right Ascension catalogue (*Russian*) 4-101201  
 R136a, supermassive star and visual binary, position angle and separation 4-85949  
 radio sources, extragalactic, in ecliptic region, VLBI obs. 4-73088  
 radio-emitting stars, optical positions and proper motions 4-94769  
 radio sources, DSN positions for 117 compact extragalactic sources 4-115829  
 reference systems, linking from space 4-72856  
 Sagittarius B2, precise positions and are second resolution maps of compact radio sources 4-63238  
 Saturn satellites, mutual phenomena in 1973 and 1979/80, astrometric obs. 4-63098  
 Second Cape Photographic Catalogue 1950.0, Cape zone  $-40^\circ$  to  $-52^\circ$ , positions provisional catalogue 4-85882  
 star coordinates determ. using extragalactic radio sources and satellite beacons 4-63034  
 star declinations, first obs. with Pulkovo horizontal meridian circle 4-63033  
 stars, proper motion as means of detecting planets 4-77727  
 stars in SRS, BS and FK4 catalogues, declinations determ. and catalogue corrections 4-94652  
 stars observed with Cagliari Danjon astrolabe, pre-MERIT results 4-110498  
 stellar appulses by asteroid 2060 Chiron, November 1984, predictions and precise positions of stars 4-77750  
 stellar equatorial coordinates, alternative derivation of influence of precession (*German*) 4-67597  
 stellar parallaxes and proper motions from McCormick Observatory, 45th list 4-82464  
 stellar proper motions calculation, rigorous formulae (*German*) 4-67715  
 stellar trigonometric parallaxes, determ. from obs. in hour angles (*Russian*) 4-101118  
 supernova in IC 121, astrometric observations of position 4-115771  
 supernova in NGC 3169, astrometry, spectra and magnitudes 4-67758  
 supernova in NGC 991, astrometric observations of position 4-115771  
 supernova in NGC 991, UVB photometry, astrometry and spectrometry 4-110637  
 Sydney Southern Star Catalogue, 26926 stars between  $-51^\circ$  and  $-63^\circ$  declination 4-63088  
 test of 2.12 m San Pedro Martir telescope 4-85878  
 Tokyo Astronomical Obs., Time and Latitude Bulletins (October-December 1983) 4-101122  
 Uranus, zenith distance residuals (1980-2) rel. to American Ephemeris from Danjon Astrolabe of Santiago 4-77761  
 Uranus and satellites, topocentric positions (1978 to 1983) 4-110561  
 variable stars in globular cluster M3, positions, space distrib. and number (*Russian*) 4-101202  
 visual binaries, orbital elements and masses 4-67764  
 visual binary stars, dynamical parallax and orbital inclination determ. from obs. of short arc (*Russian*) 4-101414  
 visual double and multiple stars, components equatorial coords. from Bordeaux Observatory obs. 4-101413  
 visual observations with zenith telescope, for simultaneous determ. of time and latit. (*German*) 4-67598  
 white dwarfs, trigonometric parallax determ. candidates 4-94768  
 OH masers, type II, 1612 MHz positions of optically invisible sources 4-73089

## astronautics see space research

## astronomical catalogues

## see also astrometry

- Abell clusters, catalogue of membership in superclusters, red shift anal. 4-77732  
 AGK3 star catalogue declinations, comparison with results of latit. obs. (*Russian*) 4-101120  
 Almagest star catalogue, stellar variability from 21 century perspective 4-110691  
 Asiatic Catalogue of Quasi-Stellar Objects 4-105892  
 Becklin-Neugebauer objects, catalogue of extremely young, massive and compact IR sources 4-94643  
 BV magnitudes of 1150 OBA stars in W3/W4 region (*Russian*) 4-101330  
 cataclysmic variables, UVB colours 4-101200  
 close double stars, catalogue of orbital elements, masses and luminosities 4-94648  
 compact extragalactic radio sources, DSN positions, for 117 objects 4-115829  
 computational spherical astronomy (book) 4-78071  
 P Cygni theoretical profiles for  $\zeta$  Aur and VV Cep stars, atlas 4-67644  
 disc galaxies, distance moduli from H I 21 cm line widths 4-101198  
 double and multiple stars, SDS identifications of IDS components 4-94873  
 double stars with IDS number error, approx. positions 4-94872  
 early type supergiants, spectra atlas, meas. and reduction procedure 4-94634  
 EIC-1 sources in AFGL catalogue, optical identification 4-82560  
 galactic supernova remnants 4-94931  
 galaxies with UV excess, Kiso survey 4-101196  
 galaxy supercluster catalog 4-63086  
 gamma ray source catalogue from SAS II data 4-101525  
 general catalogue of astronomical objects 4-94651  
 Hipparcos Input Catalogue, preliminary lists of stars 4-94647  
 IRAS mission, Monte Carlo simulation and proposed catalogue completeness 4-94559  
 Kiso Observatory (Japan) Schmidt plates, Nos. 1 to 4269, sorted catalogue 4-94646  
 KSZ catalogue stars, astrometric obs. in areas with galaxies using meridian instruments (*Russian*) 4-101119  
 Lunar Transient Phenomena List (1972 to 1973) 4-77730  
 Lund catalogue of open cluster parameters 4-63087  
 M-type stars in galactic centre region, RI photometry, astrometry and spectral classification 4-101194  
 metal-deficient F-M stars, new catalogues 4-94650  
 Mira variables in southern hemisphere, spectral classification 4-110628  
 nearby stars, photometric systems used 4-94766  
 Northern Luminous Stars catalogues, new list of suspected variables and named variables 4-72951  
 novae, galactic, catalogue and finding list 4-82424  
 open cluster stars, masses and ages 4-94649

## astronomical catalogues continued

- photometric star catalogues from UB<sub>V</sub> data and model atm. anal. 4-67645  
 PZT stars on international parallel, preliminary Right Ascension catalogue (*Russian*) 4-101201  
 QSO luminosity profiles, atlas 4-110544  
 quasar fields, catalogue of objects discovered in imaging survey 4-94644  
 radial velocities for stars in open NGC and IC clusters 4-94738  
 radio sources in  $\alpha=08^h 52^m 15^s$ ,  $\delta=+17^\circ 16'$  field, deep VLA survey 4-101192  
 radio sources near North Galactic Pole, deep 4.85 GHz survey of  $\zeta$  C 12 area 4-110545  
 Second Cape Photographic Catalogue 1950.0, Cape zone  $-40^\circ$  to  $-52^\circ$ , positions provisional catalogue 4-85882  
 solar-type stars of known age, sample 4-82471  
 southern A5-G0 stars brighter than 8.3 m, H $\beta$  photometry catalogue 4-77729  
 southern clusters of galaxies, survey 4-77731  
 stars in SRS, BS and FK4 catalogues, declinations determ. and catalogue corrections 4-94652  
 stars of high tangential velocity, catalogue 4-101193  
 stellar photometry, data compilation at Lausanne Institute of Astronomy 4-94636  
 stellar spectrophotometric catalogues, absolute energy distrib. 4-105976  
 supernova remnants in Magellanic Clouds 4-90210  
 Sydney Southern Star Catalogue, 26926 stars between  $-51^\circ$  and  $-63^\circ$  declination 4-63088  
 variable stars in globular cluster M3, positions, space distrib. and number (*Russian*) 4-101202  
 36W radioresource catalogue in M31 area 4-77915  
 X-ray sources, high-energy, HEAO 1 A-4 catalogue 4-94645  
 X-ray sources spectra observed with Ariel V proportional counter (Experiment C) 4-101199  
 Zwicky's near clusters of galaxies, red shifts list 4-101197  
 Th, spectral atlas (312.4 nm to 904.8 nm) 4-101195

## astronomical ephemerides

- 1982 RA, Amor-type asteroid, orbital elements and ephemeris (1984 July 29 to November 6) 4-101226  
 1983 KD, Apollo asteroid, orbital elements 4-85887  
 1983 VA, ephemeris (1984 February 10 to April 30) 4-67668  
 1984 AB, orbital elements and ephemeris (1984 February 10 to July 19) 4-67669  
 1984 Astronomical Almanac 4-63418  
 1984 BC, fast-moving asteroid, orbital elements and ephemeris (1984 February 10 to June 9) 4-63094  
 1984 ephemerides (*French*) 4-67646  
 1984 KB, Apollo asteroid, orbital elements and ephemerides (1984 May 20 to June 13) 4-77752  
 1984 KB, Apollo asteroid, orbital elements and ephemeris (1984 May 30 to August 8) 4-82438  
 1984 KD, ephemeris (1984 July 9 to October 7 in five day intervals) 4-94667  
 1984 KD, ephemeris (1984 June 19 to July 24) 4-85888  
 1984 KD, new Apollo asteroid, orbital elements and ephemeris (1984 June 13 to 24) 4-85886  
 1984 QA, positions, orbital elements and ephemeris (1984 Aug.-Sep.) 4-115707  
 (1984j), elliptical orbital elements and ephemeris (1984 August 18 to September 27) 4-101261  
 artificial satellites, orbit theory for LSI-11 microprocessor 4-94554  
 2060 Chiron, stellar apulses and occultations during November 1984, predictions 4-77750  
 P/Comet Arend-Rigaux (1984k), recovery positions and ephemeris 4-101269  
 Comet Austin (1984i), discovery, orbital elements and ephemeris (1984 July 21 to 31) 4-94684  
 Comet Austin (1984j), IR magnitudes and ephemeris (1984 August 28 to October 15) 4-101272  
 Comet Austin (1984i), July 1984 comet observations and ephemeris 4-101264  
 comet Austin (1984i), parabolic orbital elements and ephemeris (1984 August 28 to October 2) 4-101262  
 Comet Austin (1984i), positions, orbital elements, ephemeris, magnitudes and tail obs. 4-115725  
 Comet Austin (1984i) ephemeris for 1984 July 25 to September 7 and orbital elements 4-94687  
 Comet Bradfield (1984a), elliptical orbital elements and ephemeris (1984 March 21 to August 28) 4-63111  
 Comet Bradfield (1984a), ephemeris (1984 March 1 to June 29) 4-67684  
 Comet Bradfield (1984a), precise positions, orbital elements and ephemeris 4-67687  
 P/Comet Clark (1983w), ephemeris for 1984 April 30 to August 28 in 10 day intervals 4-77777  
 P/Comet Crommelin (1983n), ephemeris continuation (1984 April-June) 4-63112  
 P/Comet Encke, 1984 March visual magnitudes and 1984 April 10 to June 29 ephemeris 4-67699  
 P/Comet Encke, ephemeris (1984 February 10 to April 20) 4-63106  
 P/Comet Faye (1984h), recovery and ephemeris (1984 June 29 to September 17) 4-85897  
 P/Comet Gehrels 3 (1984l), recovery, precise position, and orbital elements 4-110568  
 P/Comet Hartley-IRAS (1983v), ephemeris (1984 April 10 to August 28) 4-67703  
 P/Comet Hartley-IRAS (1983v), ephemeris (1984 April 20 to June 19) 4-72910  
 Comet IRAS (1983k), positions, parabolic orbit elements, and ephemeris (1984 Feb.-Aug.) 4-67688  
 Comet IRAS (1983o), ephemeris for 1984 April 10 to August 28 in 10 day intervals 4-63103  
 P/Comet Kowal-Mrkos (1984n), discovery observations, orbit and ephemeris 4-115724  
 Comet Meier (1984o), parabolic orbital elements and ephemeris (1984 September 17 to October 17) 4-115726  
 P/Comet Russell 4 (1984d), discovery posns., orbital elements, and ephemeris 4-67689  
 P/Comet Russell 4 (1984d), positions, orbital elements and ephemeris 4-67696

## astronomical ephemerides continued

- P/Comet Schuamasse (1976XV, 1984m), orbital elements and ephemeris 4-115722  
 Comet Shoemaker (1984f), astrometric obs., orbital elements and ephemeris (1984 May 30 to July 29) 4-82453  
 Comet Shoemaker (1984f), ephemeris continuation (1984 July-October) 4-94688  
 P/Comet Takamizawa (1984j), positions, elements and ephemeris (1984 June-Aug.) 4-110574  
 communications satellites, ephemeris representations 4-94560  
 $\alpha$  Doradus, Si star, ephemeris (1983 to 1988) and orbit anal. 4-77852  
 Galilean satellites, eclipse timings rel. to ephemerides 4-110558  
 Galilean satellites, ephemerides comparison with obs. and mutual phenomena 4-82440  
 Galilean satellites, motion, analytic theory first approx. and ephemerides 4-82443  
 Galilean satellites, obs., ephemerides and residuals anal. 4-82441  
 geocentric zones of bright planets, limiting lines (3000 BC to 3000 AD) (*German*) 4-67654  
 HEAO-2, definitive orbit determ. 4-82381  
 EX Hydrae, dwarf nova, high speed photometry 4-101378  
 JPL ephemeris DE 102/LE 51, appl. 4-90059  
 Landsat 4, orbit solns., ephemerides and Global Positioning System navigation results 4-94556  
 Minor Planet Circulars, ephemerides for 65 asteroids and six comets 4-77754  
 Minor Planet Circulars 8579-8690, ephemerides for 17 asteroids and three comets 4-63095  
 Minor Planet Circulars 8827-8946, ephemerides for 96 asteroids and two comets 4-101228  
 Minor Planet Circulars 8947-9036, ephemerides for eight asteroids and two comets 4-105900  
 occultations of stars by asteroids during 1984, photographic search and ephemerides 4-101224  
 Phoebe, ephemeris including planetary perturbations (*French*) 4-82446  
 planetary and lunar coordinates, 1984-2000 (book) 4-101596  
 Uranus, zenith distance residuals (1980-2) rel. to American Ephemeris from Danjon Astrolabe of Santiago 4-77761
- astronomical instruments**  
*see also astronomical observations; astronomical techniques; astronomical telescopes; planetary; radiotelescopes*  
 acousto-optical radiospectrometer for radio astronomy (*Japanese*) 4-90092  
 ADC CR-39 detector module for Space Shuttle/Spacelab 3 cosmic ray expt. 4-101180  
 aligning on-line checking facility for satellite laser ranging system 4-63079  
 AZT-16 fast two-meniscus astrograph, photometric characts. (*Russian*) 4-101166  
 birefringent filter, development by Lockheed, solar appl. 4-97048  
 bolometer system, He-3 cooled, 1 mm continuum obs. appl. 4-105882  
 Bristol University cosmic ray detector for anomalous component comp. meas. 4-101185  
 BUGS-4 cosmic ray detector, design, charge and energy resolution 4-101184  
 camera for atmospheric Cherenkov light emission detect. in  $\gamma$ -ray astronomy 4-101176  
 CCD, use for imaging faint planetary satellites 4-82423  
 CCD characts. and future developments (*Japanese*) 4-115690  
 CCD device in cinematographic mode for enhanced resolution of telescope 4-94622  
 CCD/transit instrument, progress report 4-72886  
 CERGA two-telescope interferometer, appl. to meas. of stellar diameters (*French*) 4-105888  
 coded aperture cameras, performance of practical designs, computer simulations 4-67638  
 coded-mask imaging system for X-ray astronomy 4-67633  
 coelostat and heliostat alignment and use for eclipse and other field purposes 4-110521  
 combined telescope and spectrograph of high efficiency 4-77713  
 complex FFT processor for image synthesis in radio astronomy (*Japanese*) 4-94639  
 computing facilities and applications software at Kiso Observatory, Japan 4-94604  
 conference on astronomical instrumentation, at London, England (September 1983) 4-106099  
 cosmic ray detectors for ultraheavy particles 4-101183  
 Danjon prismatic astrolabe, var. control and zenith distance stability 4-94606  
 data collecting and processing system, for RATAN-600 radio surveys 4-63077  
 Deep Underwater Muon and Neutrino Detection (DUMAND) expt., instrumentation 4-101181  
 diffraction gratings, relative distrib. of efficiency over surface of blazed concave grating 4-105881  
 Duruy diffraction micrometer for double star work (*French*) 4-101157  
 epoxy mirrors, mechanical stability and usefulness (*Russian*) 4-101169  
 European Southern Observatory polarimeter 4-101172  
 EUV detectors onboard Extreme Ultraviolet Explorer astronomical satellite 4-63063  
 EXOSAT, mission and instrumentation 4-90054  
 EXOSAT, X-ray astronomy satellite, appls. 4-105867  
 Exosat mission, satellite description and results 4-82368  
 Fabry-Perot camera and digitized interferogram reduction 4-67631  
 Fabry-Perot interferometers for solar prominence characts. determ. 4-101165  
 Fabry-Perot visible region spectrometer for H II region line profiles 4-110536  
 fibre optics spectrograph for high resolution spectra of point sources (*French*) 4-82419  
 filters for vacuum UV and ultrasoft X-ray astronomy, structurally nonuniform design 4-94626  
 Fourier spectrometer, theory and use for astronomical obs. (*Japanese*) 4-94628  
 Fourier transform spectrometers, absolute radiometry 4-101944  
 Galileo Mission, near IR mapping spectrometer 4-94612  
 Galileo mission to Jupiter, CCD TV camera design 4-94615  
 gamma-ray balloon-borne detector, background  $\gamma$ -ray spectra origin 4-100720

## astronomical instruments continued

- gamma-ray imaging Compton telescope onboard Gamma Ray Observatory 4-63061  
 gamma-ray imaging device for telescope, using rotating coded mask 4-63062  
 gamma-ray spectrometer using n-type Ge detector 4-63060  
 gamma-ray telescopes, choice of astatic system for controlling DC motor speed for altazimuth mountings 4-105886  
 Giotto cometary mission, microchannel plate electron multiplier for mass spectrometer 4-63064  
 Giotto mission to Periodic Comet Halley (1982i), instrumentation 4-101274  
 grazing incidence relay optics design and evaluation 4-67627  
 image intensifier tube VARO 4215, testing for astronomical appls. 4-72889  
 infrared detector arrays for telescopes, using CCD and CID arrays 4-101159  
 infrared detectors using InSb, for ground based instruments 4-95517  
 infrared detectors using Si:P or Ge:Be for low photon background work 4-101160  
 infrared spectrometry, with 52-element InSb array 4-94625  
 far IR Michelson interferometer for GIRL telescope on Spacelab 4-77716  
 IR photometer for 0.9 to 2.5  $\mu\text{m}$  spectral region, design and construction (Russian) 4-101174  
 IR technology and appl., conf., San Diego, CA, USA (Aug. 1983) 4-110800  
 Irvine-Michigan-Brookhaven proton decay detector, appl. to cosmic ray muon detect. 4-96411  
 J.R. Frost Observatory, telescope and spectrometer for extrasolar planets detect. 4-82412  
 Kodak Precision Line Film (LPD7), copying appls. in astronomy 4-101178  
 Kodak Technical Pan Film 2415, hypersensitisation via bathing or baking 4-101177  
 liquid scintillator detector in Mount Blanc tunnel for cosmic neutrinos detect. 4-96410  
 Long Duration Exposure Facility (LDEF) mission, micro-meteoroid capture-cell expt. 4-105876  
 MEPSICRON photon counter for high dispersion spectrophotometry 4-94621  
 Michelson spatial interferometer, use in far IR astronomy 4-106367  
 micrometeoroid impact simulator, electrostatic prism for microparticle beam steering 4-64263  
 millimetre-wave detector for Italian IR Telescope on Gornegrat, appl. to millimetre-wave continuum photometry 4-72888  
 MM-wave superconducting tunnel junction receiver for 2.6 mm 4-77714  
 multichannel Pockels cell spectropolarimeter for Anglo-Australian Telescope 4-110533  
 NASA development of large deployable reflector astronomical facility, modular approach, feasibility study 4-115669  
 Near-IR Mapping Spectrometer, optical subsystem development and testing 4-110526  
 nuclear particle identification in space plasma research, review 4-100820  
 objective grating spectrometer aboard Einstein Observatory, high resolution soft X-ray spectra obs. 4-101170  
 OMA system of the Rozhen National Observatory 4-77720  
 optical instrumentation, observing possibilities for supernova in immediate solar neighbourhood 4-77711  
 photoelectric photometer for 200 mm Newtonian telescope, photometer head and electronics 4-105883  
 photoelectric photometers, computer controlled, three statistical tests 4-94630  
 photometer for submm continuum obs. 4-115692  
 Photometric Data System, appl. to anal. of astronomical pictures 4-105887  
 Pulkovo horizontal meridian circle, first stellar declination obs. 4-63033  
 pulse timing system, high-precision, for meas. of arrival time of ultrahigh-energy photons 4-105885  
 rocket-borne pure interferometric high-resolution (Japanese) 4-115687  
 S 520-3 controlled nosecone rocket-borne VUV instrumentation characts. (Japanese) 4-94620  
 SIGMA, high resolution space observatory project for gamma-ray sources 4-105875  
 solar disc sextant 4-82416  
 solar disc sextant concept evaluation 4-82414  
 solar disc sextant optical config. 4-82415  
 solar global oscills. meas. method and instruments 4-105918  
 solar magnetic and vel.-field meas., new instrum. concepts 4-82417  
 Solar Maximum Mission, instrumentation and observatories (French) 4-101111  
 solar total irradiance meas. by pyrhelimetric method, review 4-115738  
 spectrometer CCD detector, comparison of two commercially available chips 4-110534  
 spectrometer for use with McMath solar telescope for stellar work 4-85881  
 spectrophotometer, five-channel, expansion of dynamic range of data-gathering and measuring system 4-105880  
 SSNTD array for ultra-heavy cosmic ray nuclei aboard NASA LDEF 4-96389  
 stellar interferometer with fibre optic synthetic aperture 4-110524  
 stellar photometry, Pickering-Racine prism method for plate calibration 4-110535  
 sub-beam prism for photographic photometry of faint stars, calibration (Japanese) 4-94640  
 submillimetre heterodyne receiver for 584 and 803 GHz operation 4-77715  
 television speckle interferometer with real-time digital image processing 4-63072  
 Tenma, instrumentation and preliminary results 4-110487  
 two-dimensional photon counting system, appl. in astronomy (Japanese) 4-94627  
 underground cosmic ray detectors, characts. 4-101182  
 UV camera, S201 instrument operated by Apollo 16, results and implications for future instruments 4-110531  
 UV converter transients induced by electrons 4-110520  
 uvby  $H_\beta$  photometer using spectrograph exit slots 4-63075  
 variable profile antenna (VPA) of RATAN-600, surface-error scattered background of antenna directional pattern 4-63053  
 VATPOL, microcomputer-controlled photoelectric polarimeter 4-105884  
 windowless rare-gas ionisation chamber for EUV solar flux 4-101156

## astronomical instruments continued

- X-ray detectors onboard EXOSAT 4-63066  
 X-ray imaging proportional counter, Xe gas filled 4-68888  
 X-ray imaging system for Solar Max. Mission 4-63065  
 X-ray rotation modulation collimator for high energy imaging 4-72884  
 X-ray telescope design for broad band spectrophotometry 4-63025  
 Yale PDS 2020G microdensitometer, use of high speed photometer 4-110538  
 TeO<sub>2</sub>-crystal acousto-optical spectrograph, for RATAN-600 radio telescope 4-63074
- astronomical observations**  
 see also gamma-ray astronomical observations; infrared astronomical observations; radioastronomical observations; ultraviolet astronomical observations; visible astronomical observations; X-ray astronomical observations  
 Arp 91 (NGC 5953-4) 4-90230  
 Chinese observatories, evaluation of accuracy of time synchronisation via portable clock (Chinese) 4-82420  
 cosmic ray electrons, energy spectrum meas. rel. to cosmic ray confinement 4-94460  
 cosmic ray electrons, solar modulation meas. (1978 to 1983) 4-85851  
 cosmic ray protons, estimate of heliolat. gradient (1981-1982) 4-85849  
 Cygnus X-3,  $\gamma$ -ray emission var., small air showers arrival directions obs. 4-101529  
 galaxies, optical and IR photometry rel. to H I contents 4-90233  
 gamma-ray sources ( $E > 10^{15}$  eV), search in Kiel EAS data 4-94991  
 Hubble-Sandage variables in M31 and M33, IUE and ground-based obs. 4-85941  
 Io plasma torus, evidence for ion-cyclotron instability 4-101230  
 Kuffner Observatory in Vienna-Ottakring (German) 4-72878  
 BL Lacertae objects, continuum spectral energy distrib. of X-ray observed sample 4-82546  
 NGC 3448, interacting galaxy, combined optical, radio and UV investigation 4-73065  
 quasars, emission-line ratios rel. to X-ray heating in broad-line region 4-90254  
 Seyfert galaxies, emission-line ratios rel. to X-ray heating in broad-line region 4-90254  
 solar cosmic ray protons, absolute fluxes above  $E=100$  MeV from meas. in stratosphere and with neutron monitors 4-110397  
 solar cosmic ray protons, spectral and temporal characts. rel. to coronal mag. field struct. 4-110396  
 solar wind, ionisation temps. inferred from charge state comp. of diffuse particle events 4-85854  
 solar wind corotating interaction region proton events, Pioneer 11 obs. 4-67589  
 symbiotic stars, X-ray to radio obs. 4-82480  
 Venus, dayside ionosphere, Pioneer RPA obs. 4-82431  
 Venus dayside ionosphere conditions, effects of ionospheric mag. field and solar EUV flux 4-94661
- astronomical observatories**  
 Arecibo observatory, facilities 4-101163  
 Canary Islands, new observatories 4-63051  
 Haute-Provence Observatory, telescopes general description (French) 4-105874  
 Herstmonceux parallax programme, meas. for 28 stars 4-77819  
 IRAM observatories in France and Spain (French) 4-115684  
 J.R. Frost Observatory, telescope and spectrometer for extrasolar planets detect. 4-82412  
 Kiso Observatory, Japan, computing facilities and applications software 4-94604  
 Kiso Observatory, Japan, sorted catalogue of Schmidt plates (Nos.1 to 4269) 4-94646  
 Rozhen National Observatory, OMA system 4-77720  
 Rozhen Peak, extinction meas. at Bulgarian National Astronomical Observatory 4-77630
- astronomical spectra**  
 see also atmospheric spectra; stellar spectra  
 0215+015, BL Lac object, absorpt. struct. at 20  $\text{km s}^{-1}$  resolution 4-77941  
 0241+622, low-redshift quasar, spectrophotometry and image anal. of assoc. nebulosity 4-90253  
 758.1 nm predicted diffuse H<sup>-</sup> interstellar line, obs. 4-90212  
 2021+614, narrow-line radiogalaxy, dust content, core luminosity and visible spectra 4-86045  
 Abell 1795 cD galaxy, star form. characts. and UV spectral obs. 4-90236  
 Abell 30, planetary nebula and central star, UV spectra obs. and anal. 4-86011  
 Abell 576, galaxy cluster X-ray line emission, temp. and elemental abundances 4-86067  
 Abell galaxy clusters, X-ray spectrum of volume emissivity 4-86064  
 active galactic nuclei, emission spectra due to accretion onto massive black holes 4-106063  
 active galactic nuclei, observational props. and interpretation 4-63289  
 active galaxies nuclei, gamma-ray emission characts. due to cosmic ray interactions 4-101537  
 active galaxies nuclei, line continuum luminosity ratio 4-90226  
 AFGL 2688, bipolar nebula, visible spectra and spectrophotometry obs. 4-106054  
 AMD-1 automatic densitometer spectra, scanning and processing software 4-94635  
 Arp 91 (NGC 5953-4), spectroscopic obs. rel. to interaction and star form. in galaxy pair 4-90230  
 Asiago Catalogue of Quasi-Stellar Objects 4-105892  
 B335, isolated dark globule, obs. of NH<sub>3</sub> (1, 1) and (2, 2) lines 4-115794  
 background  $\gamma$ -ray spectrum, balloon-borne spectrometer meas. 4-59482  
 black holes, accreting, X-ray spectral signatures 4-72973  
 black holes, mass accretion and plasma processes,  $\gamma$ -ray emission model, 3C 273 appl. 4-101536  
 blue galaxies in distant clusters, nature from spectral obs. 4-77933  
 blue objects in field of BD+15°2469, nature and spectra 4-106071  
 Braccesi deep quasar survey, completeness anal., spectral obs. 4-90256  
 3C 109, broad-line radiogalaxy, dust characts. from visible and IR obs. 4-90223  
 3C 273, high-energy X-ray spectrum and luminosity 4-106076  
 3C 293, radio galaxy, extended optical line emission due to radio jets propagating through gaseous disc 4-63267  
 3C 371, N galaxy with BL Lac nucleus, multifrequency obs. 4-90222

## astronomical spectra continued

- 3C 391, supernova remnant, X-ray map and X-ray spectrum 4-86005  
 3C 411, distant radio galaxy, spectral indices and polarisation characters. from VLA obs. 4-73064  
 Cassiopeia A, SNR, high energy X-ray spectra, ionisation nonequilibrium model fitting 4-73008  
 CG 195+04,  $\gamma$ -ray line emission search 4-101521  
 channel-bank spectrometer data processing 4-86074  
 CI 1447+2619, blue galaxies spectral chars. and star form. anal. 4-94976  
 Cn 1-1, possible planetary nebula and F5 III-IV star as binary components, obs. 4-90196  
 Comet Austin (1982 VI), H I Balmer  $\alpha$  production rate in corona 4-94681  
 Comet Austin (1982 VI), spectrophotometry during post-perihelion period 4-77770  
 Comet Austin (1984i), photometric and spectroscopic obs. (1984 July 25 and 27) 4-101266  
 Comet Bowell (1982 I) optical filter photometry and optical and UV spectrophotometry 4-82451  
 Comet Cernis (1983), coma icy grains detect. in IR 4-101258  
 P/ Comet Crommelin (1983n), IUE spectrum features and total visible magnitude estimates 4-63102  
 P/Comet Crommelin (1983n), spectra, images and visual mag. estimates (1984 Feb.-March) 4-67692  
 P/Comet Crommelin (1983n), spectroscopic obs. and total visual magnitude estimates 4-63104  
 P/Comet Crommelin (1983n), UV and visible spectra, mag. estimates (1984 Feb.-March) 4-67686  
 Comet IRAS-Araki-Alcock (1983d), new molecules in visible spectrum 4-94691  
 Comet IRAS-Araki-Alcock (1983d), spectroscopic obs. and molecular identifications 4-67683  
 P/Comet Wild 2 (1983s), appearance, spectra and V photometry (1984 Jan.-March) 4-67693  
 comets, CN radiance/column density ratio, calc. from Swings effect 4-90117  
 comets, O I, 557.7 nm forbidden line detect. 4-77772  
 compact H II regions, He I 10830 Å line obs. 4-72998  
 compact planetary nebulae, expansion vels. from high dispersion spectra 4-101456  
 conference on QSOs, at Padova, Italy (March 1983) 4-101568  
 3 CR radio sources, optical redshifts 4-94982  
 Crab nebula, gamma radiation spectrum in  $10^{13}$  eV energy range 4-73006  
 Crab Nebula, search for  $\gamma$ -ray lines 4-101462  
 Crab Nebula filaments, visible and IR spectrophotometry 4-90200  
 CTB 1, spectrophotographic obs. of SNR candidate 4-86023  
 Cygnus A, multi-frequency radio study of spectral index distrib. 4-101492  
 Cygnus Loop, SNR, X-ray images and spectra 4-73035  
 Cygnus Loop, struct. in coronal lines and X-ray continuum rel. to evaporation around filamentary struct. 4-73000  
 DDM 1, halo planetary nebula, chem. comp. 4-90198  
 diffuse background radiation, soft X-ray and EUV spectra rel. to super-bubble model of local interstellar medium 4-94926  
 diffuse galactic  $\gamma$ -rays, bremsstrahlung component spectra and cosmic ray electrons energy spectra 4-100889  
 diffuse interstellar 578.0 and 579.6 nm bands towards NGC 7027, nature 4-106054  
 disc galaxies, distance moduli from H I 21 cm line widths 4-101198  
 disk galaxies, absolute (blue) luminosity/21 cm linewidth relation 4-63276  
 DR 4, spectrophotographic obs. of former SNR candidate 4-86023  
 1E 0102.2-7219, SMC SNR, nature and spectra 4-82545  
 1E 0102-7219, SMC, SNR, dynamical anal. 4-73024  
 1E 0104.2+3153, BAL QSO behind giant elliptical galaxy 4-63332  
 E and S0 galaxies (NGC 1052, 2749, 3998 and 4125), stellar and gaseous kinematics 4-73066  
 effective dielectric recomb. coeffs. of C, N, O ions 4-96477  
 electron-positron annihilation line emission from sources contributing to X-ray background 4-77976  
 elliptical galaxies, survey of forbidden O II emission 4-77927  
 emission nebulae, appl. of emission line intensities to photographic density-to-intensity conversion 4-101179  
 fibre optics spectrograph for high resolution spectra of point sources (French) 4-82419  
 G292.0+1.8, SNR, optical velocity field mapping 4-73023  
 G35.2-0.74, mol. cloud with bipolar and monopolar outflow, EHF obs. 4-106050  
 galactic corona, soft X-ray emission evidence 4-73103  
 galactic disc  $^{13}\text{C}$  emission in  $l=40^\circ$ - $60^\circ$  range 4-63313  
 galactic nuclei,  $\text{H}_2\text{O}$  maser emission obs. 4-101478  
 galactic nuclei, spectroscopic obs. of LINERS rel. to element abundances 4-67807  
 galactic radiosources,  $^{13}\text{CN}$  detect., EHF obs. 4-106072  
 galaxies, interacting spirals, induced nuclear emission-line activity 4-90242  
 galaxies, spectral emission of active nuclei, H-line ratios 4-110753  
 galaxies in Horologium 4-110757  
 galaxy clusters, hard X-ray spectra 4-86065  
 galaxy clusters, radial velocities, determ., using submm spectrophotometry (Russian) 4-86071  
 galaxy companions to low- $z$  quasars, CCD spectra 4-115828  
 gamma ray line obs., statistical reliability 4-101190  
 gamma-ray background, meas. at balloon altitudes above Beijing area (Chinese) 4-82355  
 gamma-ray burst sources, 1983 review 4-110780  
 gamma-ray burst sources, Franco-Soviet and Soviet results, obs. overview 4-110781  
 gamma-ray burst sources, obs. by Hakucho 4-110786  
 gamma-ray burst sources, spectral props. review 4-110782  
 gamma-ray emission lines, prospects for detection 4-106084  
 gamma-ray sources, absorpt. features, effects of emitted photons-interstellar photon interactions 4-101535  
 gamma-ray sources, MeV emission spectrum of steady mildly relativistic thermal plasmas 4-94582  
 giant planets, atm. struct. and comp., implications for solar nebular chars. 4-101207  
 globular clusters, metallicities and radial velocities, spectral obs. 4-106045

## astronomical spectra continued

- graphite detection, interstellar, spectroscopic method 4-101187  
 H 2155-304, BL Lac object, X-ray spectra and intensity var. 4-101483  
 HB 9, SNR, nearby small diameter radiosources, nature 4-73093  
 Herbig-Haro and related objects, spectrophotometry 4-67783  
 Herbig-Haro objects, spectrum model and shock wave interaction 4-115801  
 HH 32A, UV spectrum of reddened high-excitation H-H object 4-63243  
 hydrogenic ions excitation by electron impact, high energy collision strengths and excitation limits 4-77702  
 IC 2153, shock-induced star formation in colliding galaxy pair 4-110739  
 IC 5135, mini-Seyfert galaxy with starburst chars., UV spectral anal. 4-110734  
 interacting galaxies, star form. rates from spectrophotometric obs. 4-77926  
 interstellar 280 nm absorption feature 4-82539  
 interstellar 280 nm feature as artifact of IUE SEC videocon detectors 4-82538  
 interstellar C II regions, upper limits to mag. fields from C16 $\alpha$  lines obs. 4-86003  
 interstellar diffuse clouds, search for  $\text{H}_2\text{O}^+$  towards four stars 4-63240  
 interstellar dust, identification of 'unidentified' IR emission features 4-115790  
 interstellar emission lines, IR and visible 4-63257  
 interstellar extinction towards dusty WC8/9 Wolf-Rayet stars 4-77897  
 interstellar formaldehyde, 14.5 GHz and 4.8 GHz transition obs. 4-110723  
 interstellar formaldehyde in Orion molecular flow, evidence for gentle acceleration 4-63239  
 interstellar gas, ion composition and chem. reactions 4-101460  
 interstellar grains, spectroscopic identification 4-67780  
 interstellar HCN, radio spectra and hyperfine rot.-level splitting, isotopic modifications 4-94925  
 interstellar He flow in Solar System, obs. at 58.4 nm (by Prognos 6) 4-77767  
 interstellar IR extinction towards G333.6-0.2 H II region 4-94917  
 interstellar lines and matter distrib. around Sun 4-115789  
 interstellar matter diffuse component, radio obs. anal. 4-63252  
 interstellar medium, absorpt. line spectroscopy 4-63253  
 interstellar medium, conf. at Cargèse, France (September 1982) 4-58564  
 interstellar methanol maser, detect. at 23.121 GHz 4-77889  
 interstellar molecular cloud assoc. with multiple IR source (GL 437), CO obs. 4-85999  
 interstellar molecular clouds, fluctuation spectrum determ. form CO line profiles 4-115795  
 interstellar molecular clouds, meas spectrum and mean lifetime from  $^{13}\text{CO}$  obs. (Chinese) 4-82543  
 interstellar molecular clouds, ortho- $\text{H}_2$ /para- $\text{H}_2$  ratio rel. to collisional excitation processes 4-94927  
 interstellar molecules, effective straight-line trajectory approach to collisional excitation 4-101129  
 interstellar  $\text{NH}_3$  towards SNR Cassiopeia A, vel., temp. and densities 4-101453  
 interstellar  $\text{O}_2$ , abundance, excitation, and prospects for radio detect. of  $^{18}\text{O}$  4-90205  
 interstellar  $\text{O}_2$ , vacuum-UV oscillator strengths of Schumann-Runge lines rel. to prospects for Space Telescope obs. 4-90206  
 interstellar polarization, wavelength depend. towards stars 4-77896  
 interstellar proteins and 280 nm feature 4-82537  
 interstellar radio recomb. line obs. toward CT 123, upper limit to H I ionisation rates 4-101448  
 interstellar UV extinction and diffuse band strength correlations 4-63241  
 interstellar UV extinction curves, vars. from mean galactic extinction law 4-86004  
 IR sources, dust emission spectra from 1-millimetre continuum obs; 4-115834  
 IR sources, spectral features near 10  $\mu\text{m}$ , extinction estimation 4-86018  
 IUE high dispersion spectra, correction for echelle grating blaze function 4-110542  
 Jupiter, auroral emission, longitudinal and temporal vars., IUE obs. 4-90107  
 Jupiter, periodic intensity var. in [S III] 9531 Å emission from hot plasma torus 4-94671  
 Jupiter atmosphere, voyager far-IR spectra 4-105901  
 Kazaryan 163, new Seyfert galaxy, spectrophotometric obs. and direct photography 4-94938  
 Kleinmann-Low  $\text{H}_2\text{O}$  maser outburst chars. (Russian) 4-94933  
 BL Lacertae objects, continuum spectral energy distrib. of X-ray observed sample 4-82546  
 BL Lacertae objects, nuclei X-ray emission, origin and anal. 4-77940  
 BL Lacertae objects, UV and X-ray props. anal. 4-106060  
 BL Lacertae type objects, interpretation of optical spectrum 4-101469  
 line formation theory, accurate solns. to non-LTE problems using approximate lambda operators 4-94596  
 line formation theory, appl. of escape probability methods to non-LTE line transfer 4-94591  
 line formation theory, probabilistic radiative transfer method 4-94594  
 line source functions, accurate and approximate probabilistic eqns. 4-94593  
 LMC X-ray Balmer-dominated supernova remnants, optical obs. and radio emission 4-77907  
 M17 SW, giant mol. cloud, CO emission obs. 4-73002  
 M1-7, planetary nebula, plasma chars., element abundances and central star nature 4-115797  
 M33, nucleus stellar population from UV spectral obs. 4-115817  
 M33 globular clusters, ages and metallicities, spectral obs. 4-110695  
 M82, far IR forbidden O I and III emission 4-90241  
 M82, mol. halo, CO obs. 4-86047  
 M87, mass profile and gas content anal. 4-90224  
 M87, optical spectrophotometry of jet and environs 4-86037  
 Markarian 231, IR spectra, effects of silicate interstellar features 4-110744  
 Markarian 266, double Seyfert nucleus, UV spectra obs. and anal. 4-90239  
 Markaryan 201 (NGC 4194), spectroscopic investigation 4-94936  
 Mars atmosphere, 10 micron heterodyne spectroscopy 4-105896  
 massive black holes, 511 keV annihilation line, origin due to tidally disrupting stars 4-101405  
 methylene ( $\text{CH}_2$ ) in interstellar mol. clouds, Einstein A-coefficients for rot. transitions 4-67613

## astronomical spectra continued

- methylenimine,  $\nu_8$  band, high-resolution IR spectra in 10  $\mu\text{m}$  region 4-96534
- molecular clouds, formaldehyde ortho-para ratio 4-115799
- molecular clouds, gamma-ray line emission and cosmic ray interactions 4-101463
- molecular clouds near Monoceros OB1 and OB2, OH emission anal. 4-94916
- Monogem Ring, extended X-ray source, X-ray spectral energy distrib. from thermal bremsstrahlung model 4-94992
- N44, H II region in LMC, obs. of high-vel. component within small shell 4-115815
- narrow-line absorpt. systems, ionisation spectra 4-82557
- nebular emission coeffs., three-level atom approx. 4-77894
- NGC 1068, Seyfert 2 galaxy, IR spectrophotometry 4-106068
- NGC 1275, 20-year spectral evolution of radio nucleus (3C 84) 4-86029
- NGC 1275,  $\gamma$ -ray line emission search 4-101521
- NGC 1275, Seyfert galaxy, Lyman  $\alpha$  emission and intracluster gas inflow 4-73077
- NGC 1510, galaxy, centre condensations struct. and nature 4-63278
- NGC 1535 and 2022, planetary nebulae, expansion vel. fields 4-106047
- NGC 1667 and 5135, mini-Seyfert galaxies, H I Lyman  $\alpha$  anal. 4-110734
- NGC 1714, spectrophotometric observations of H II region 4-110719
- NGC 2024 IRS 2, interstellar CO absorpt. lines in IR spectrum 4-86000
- NGC 2403, H II region spectrophotometry and Cepheid extinction 4-63247
- NGC 253 edge-on spiral galaxy, spectral index of radio continuum emission 4-115814
- NGC 3448, interacting galaxy, combined optical, radio and UV investigation 4-73065
- NGC 3783, Seyfert galaxy, reddening and high-excitation emission lines 4-63286
- NGC 4151, Seyfert galaxy, HEAO 1 obs. from 2 keV to 2 MeV 4-86038
- NGC 4151 and 7469, IUE UV spectra of nuclei of Seyfert galaxies 4-63319
- NGC 4449, irregular galaxy, SNR models, age and obs. 4-77910
- NGC 4650A, spindle-like galaxy, rot. of diffuse stellar component 4-90232
- NGC 4736, spiral galaxy bulge dispersion velocity meas. (Spanish) 4-90244
- NGC 6166 and 7720, brightest cluster galaxies and their multiple nuclei, orbit anal. 4-86066
- NGC 6543, planetary nebulae, Ne III forbidden line at 36  $\mu\text{m}$ , detect. and abundance determ. 4-110718
- NGC 7027, Mg IV and V line obs. of planetary nebula 4-63242
- NGC 7027, planetary nebula, high spatial resolution obs. with 10-micron array camera 4-86002
- NGC 7172, obscured edge-on disc galaxy, nucleus activity obs. 4-73074
- NGC 7385, radio galaxy, optical properties of blue knots 4-90231
- North Polar Spur, SNR, X-ray spectrum 4-73103
- nuclear H II regions in galaxies with emission lines 4-110721
- $\rho$  Ophiuchi cloud core, turbulent velocity structure determ. from  $\text{C}^{18}\text{O}$  obs. 4-90204
- Ophiuchus complex, OH obs. 4-90211
- Orion A, mol. cloud temp. from methyl cyanide obs. 4-106049
- Orion Nebula, large-scale internal motions 4-115800
- Orion Nebula, Stark broadening in radio recomb. lines 4-90215
- PKS 0219-164, BL Lac. object, rapid optical variability and polarisation 4-82549
- PKS 0349-27, extended ionized gas, optical and radio obs. 4-77921
- PKS 0528-250, QSO, spectral obs. 4-73098
- PKS 0548-322, BL Lac. object, X-ray spectra and intensity var. 4-101483
- PKS 0634-20, radiogalaxy, O III forbidden line emission along radio axis 4-86059
- PKS 2155-304, BL Lacertae object, optical redshift and implications for X-ray absorpt. feature 4-86057
- PKS 2155-304, BL Lacertae object, sharp X-ray absorpt. feature obs. 4-86056
- planetary atmospheres, effective depth of line form 4-101213
- planetary nebula in SMC, discovery 4-94960
- planetary nebulae, electron density determ. using Si III UV emission line strengths 4-94583
- planetary nebulae, in Magellanic Clouds, UK Schmidt objective prism spectra 4-77899
- planetary nebulae, internal motion obs. 4-106048
- planetary nebulae, IRAS spectra of five objects 4-86013
- planetary nebulae, narrow-band photoelectric photometry, absolute H $\beta$  fluxes 4-86024
- planetary nebulae, spectrophotometric observations of four southern objects 4-110719
- planetary nebulae, visible spectra and spectrophotometry obs. 4-106054
- plasma diagnostics by transition probabilities and spin-changing lines meas. of at. ions 4-90088
- polymeric residues of astrophysical interest, IR spectra 4-72859
- PP 85, blue excess in cometary nebula spectrum 4-77902
- Puppis A, SNR, brightest knot plasma characts., X-ray obs. 4-73034
- Q1101-264, red shift systems anal., intervening galaxies or intergalactic clouds 4-90250
- QS 0630+180, identification of B III rel. to proton quasar model 4-90252
- QSO 2345+007A,B, gravit. lens characts. 4-110769
- QSOs, evolution and origin of sharp metal-rich absorpt. lines 4-73096
- QSOs absorption line spectra, rest wavelengths systematically 4-73095
- QSOs with complex, broad absorption lines, spectroscopy 4-63333
- quasar pairs, absorpt. lines anal. and nature of intervening objects 4-77966
- quasar pairs, absorption lines, origin 4-106081
- quasars, absolute spectrophotometry of 3000 Å bump 4-63334
- quasars, absorpt. lines due to intergalactic clouds and their evolution 4-77964
- quasars, absorption line spectra, origin in mol. clouds of intervening galaxies 4-77965
- quasars, C I line strengths rel. to background radiation temp. at epochs ( $z \geq 2$ ) 4-63343
- quasars, emission and absorpt. lines, red shifts 4-82556
- quasars, emission line redshifts distrib. 4-94985
- quasars, emission-line ratios rel. to X-ray heating in broad-line region 4-90254

## astronomical spectra continued

- quasars, form of broad emission lines 4-86085
- quasars, gamma-ray emission characts. due to cosmic ray interactions 4-101537
- quasars, Hubble diagrams for flat and steep spectrum radio sources from optical monitoring 4-110763
- quasars, radio-optical spectral indices from optical identifications of weak radio sources 4-86073
- quasars at high redshift, continuum energy distrib. and absorpt. by intervening material 4-110765
- quasistellar objects, reliability of identifications of absorption lines with small redshifts 4-94984
- radiative transfer methods, book 4-90304
- radio galaxies nuclei, time vars. of centimetre-wave spectra and radio brightness 4-63282
- radio source, extended, near Coma A, centimetre-wavelength spectrum 4-73091
- radio sources, extragalactic, low frequency spectral index distrib. of complete sample of sources 4-73087
- radio sources extragalactic, spectra from millimetre-wave obs. 4-106075
- radio sources near North Galactic Pole, spectral index distrib. from deep 4.85 GHz survey of SC 12 area 4-110545
- radio supernovae, radio light curves, spectral indices and models 4-72965
- radiogalaxies, SHF maps and polarisation spectra 4-110733
- radiosources, extragalactic, spectral index flux density relation 4-90249
- radiosources, visible-IR spectra cutoff due to cosmic ray electrons energy spectra evolution 4-106073
- RCW 103, SNR, optical emission, spectrophotometry 4-73033
- resonance lines, photon escape and scattering 4-94592
- Sagittarius B2, mol. cloud,  $\text{NH}_3$  (5,2) transition detect. 4-94915
- Saturn atmosphere, voyager far-IR spectra 4-105901
- Saturn  $\text{NH}_3$  absorption band near 645 nm, line obs. (Russian) 4-101241
- Sc I galaxies, distances and props., visible and IR anal. 4-90220
- separation of highly correlated bands of multispectral image 4-101189
- Seyfert and radio galaxies, catapult model for narrow-line region 4-101477
- Seyfert galaxies, emission-line ratios rel. to X-ray heating in broad-line region 4-90254
- Seyfert galaxies, H I redshifts and line profiles 4-63268
- Seyfert galaxies, line intensity ratios rel. to dynamics of narrow line regions 4-86034
- Seyfert galaxies, nuclei X-ray emission anal. 4-77940
- Seyfert galaxies, spectral characts., visible and UV anal. 4-63322
- Seyfert galaxies, variability of emission-line spectra and optical continua 4-86035
- Seyfert nuclei, envelopes cloud form. and line emission 4-101480
- Simeis 147, SNR, nearby small diameter radiosources, nature 4-73093
- SMC compact emission-line nebulae, discovery and spectra 4-94960
- SNR in irregular galaxy NGC 4449 H II region, UV spectra anal. 4-90195
- SO(3-2) mapping of the Orion KL cloud components 4-63244
- southern compact bright-nucleus galaxies, spectral obs. 4-110750
- southern galactic hemisphere line surveys 4-63297
- spectroscopy from space, review 4-90051
- spiral galaxies, discs luminosity-depend. line ratios 4-110745
- spiral galaxies, obs. of IR H I recomb. line emission 4-86039
- supernova remnants, coronal [Fe] lines for nonequilibrium ionisation models 4-94913
- supernova remnants, extragalactic, spectroscopy and galaxies interstellar matter chem. comp. determ. 4-77905
- supernova remnants, non-equilibrium ionisation X-ray emission 4-73014
- supernova remnants, non-radiative shock, struct. and emission, appl. to Cygnus Loop 4-73031
- supernova remnants, optical props. and elemental abundances 4-73027
- supernova remnants, shock wave struct. and spectra, non-equilib. modelling 4-73030
- supernova remnants, struct., effect on non-equilibrium X-ray spectra 4-73016
- supernova remnants, X-ray line emission and nonequilibrium ionisation models 4-73015
- supernova remnants, X-ray spectra anal. 4-73028
- supernova remnants in Galaxy and Magellanic Clouds, spectra 4-73032
- supernova remnants in LMC and the Galaxy, kinematics 4-73041
- suspected planetary nebulae in ESO-Uppsala survey, identifications 4-101454
- Taurus dark cloud complex,  $\text{NH}_3$  obs. and star counts 4-115791
- Taurus molecular clouds, implications of 3  $\mu\text{m}$  ice band for interstellar chemistry 4-101457
- TMC-1, dark dust cloud, methylidyne detect., SHF obs. 4-94915
- Tycho's SNR, high energy X-ray spectra, ionisation nonequilibrium model fitting 4-73008
- Tycho's supernova remnant, distance determ. from vel. components in foreground H I 21-cm line 4-72994
- UGC 6697 in Abell 1367, struct. visible, SHF and UHF obs. 4-115818
- UGC 7576, spindle-like galaxy, mapping in H I, UHF obs. 4-73076
- UV spectroscopic electron density diagnostics, multidensity plasma effects 4-94574
- variable radiosources, spectral evolution in UHF 4-115830
- Vela SNR, UV absorpt. lines anal. 4-90202
- Venus, IR spectrometry by Venera 15 and 16, first results (Russian) 4-85884
- Venus, upper atm. reson. lines scatt., Venera 11 and 12 data anal. 4-101219
- Voigt spectral line profile, mathematical props. 4-63043
- W28, spectrophotographic obs. of SNR candidate 4-86023
- W3 molecular clouds, formaldehyde mapping at 60 mm 4-73003
- W51 molecular cloud complex,  $^{13}\text{CO}$  J=1-0 obs., maps and cloud vels. 4-115806
- X-ray emission spectra from ionising plasmas, theory 4-67617
- X-ray emitting Seyfert I galaxy discovery in field of LMC; nature 4-63279
- X-ray sources, spectra observed with Ariel V proportional counter (Experiment C), catalogue 4-101199
- young southern compact IR sources, Brackett-alpha emission obs. 4-77904
- II Zw 73, spindle-like galaxy, mapping in H I, UHF obs. 4-73076
- $\gamma$ -ray diffuse spectra and positronium annihilation 4-63045
- AIO, blue-green band, transition moment, Franck-Condon factors, perturbed simple harmonic model 4-59852
- C II, IR and UV lines, fine struct. transitions and electron collision strengths, astron. appl. 4-77701

## astronomical spectra continued

- C II regions, heavy elements radio recomb. lines obs. 4-90197  
 $C^+$ , branching ratios of  $2s^3\ ^3P^o$  term, Fourier transform and VUV spectroscopy 4-87066  
 $C_2H$ , interstellar, millimetre-wave spectrum rel. to distrib. and abundance in mol. clouds 4-72999  
CO J=1-0 obs. of peculiar nebulosities and star formation regions 4-86022  
CO J=6-5 691 GHz transition, heterodyne detection 4-90218  
CO survey of Southern Hemisphere dark clouds, refl. nebulae and Herbig-Haro objects 4-101455  
Cl, abundance and chem. in Galaxy 4-86020  
CO III, transition probabilities for forbidden lines in  $3d^7$  ground configuration 4-63041  
Fe II spectrum, comparison between observed and predicted emission lines in different plasmas 4-87061  
FeO, laboratory millimetre-wave spectrum meas. 4-85867  
H I cloud in Pleiades, line profile obs. rel. to cloud-cluster collision 4-101449  
H I regions, 21 cm spectra rel. to latitude struct. of galactic H I on small ang. scales 4-94924  
HCN J=1-0 88 GHz transition in W3 IRS 4, aperture synthesis map 4-115804  
 $HCO^+$  high velocity flow in star-bearing mol. cloud NGC 2071, J=1-0 and J=3-2 lines obs. 4-85997  
HDO in Kleinmann Low Nebula and W 51 M, mapping 4-77891  
 $H_2O$  maser sources, obs. with acousto-optical 1008 channel radio spectrometer (Russian) 4-94934  
He I astrophysical lines, Stark broadening 4-102638  
 $Ne^{2+}$ , electron impact excitation, fine struct. level transitions 4-74336  
Ni IV, transition probabilities for forbidden lines in  $3d^7$  ground configuration 4-63041  
OH megamaser in peculiar galaxy IC 4553, VLA-A obs. 4-86036  
S III,  $3s^23p^2\ ^3P_{21}, 3s3p^3\ ^3S_2$  intersystem lines, astrophysical appl. 4-96476  
Si I, meas. of  $3\ ^3P_0-3\ ^3P_1$  fine-struct. interval and g<sub>J</sub>-factor by laser mag. reson. 4-85866  
Si III, UV emission line strengths in low density plasmas 4-94583  
SiO protonated ions, ab initio calcs. appl. to interstellar detect. possibility 4-87051  
SiS protonated ions, ab initio calcs. appl. to interstellar detect. possibility 4-87051  
Tm I spectrum, lifetime meas. using pulsed dye laser 4-72861

astronomical spectroscopy see astronomical spectra; spectroscopy

## astronomical techniques

- see also astrometry; radioastronomical techniques  
adaptive orbit estimation scheme for artificial satellites 4-82373  
advanced IR sensor technology, conf., Geneva, Switzerland (April 1983) 4-95018  
AMD-1 automatic densitometer spectra, scanning and processing software 4-94635  
Ap stars, mag. fields meas. via polarimetry of 5200 Å depression (German) 4-67738  
artificial satellites, times of close approach between satellite pairs, prediction method 4-82382  
ASPECT, area spectroscopy technique 4-105889  
asteroid light curve, method for determ. of components contrib. 4-94668  
asteroid lightcurve inversion using integral geometry 4-82436  
asteroid search strategies for Earth-approaching objects 4-67666  
asteroids, dynamical motions used for Fundamental Reference System systematic accuracy determ. 4-82386  
astrometric determ. of absolute stellar proper motions, error anal. via Monte Carlo simulation 4-94563  
astrometry, determ. of atmospheric dispersion coeff. and correction for its influence (Russian) 4-101121  
astrometry, linking of reference systems from space 4-72856  
astronomy with Schmidt-type telescopes, 78th IAU Colloquium, Asiago, Italy (1983 August 30 to September 2) 4-106115  
atomic spectroscopy, symposium, Berkeley, CA, USA (Sept. 1983) 4-67852  
automatic measurement and reduction procedure for spectra anal. 4-94634  
Baade-Wesselink method and distance to field RR Lyrae star VY Serpentis 4-90154  
binary stars, orbit determ. method (French) 4-67632  
CCD, use for imaging faint planetary satellites 4-82423  
CCD device in cinematographic mode for enhanced resolution of telescope 4-94622  
coded aperture  $\gamma$ -ray telescope, statistical anal. 4-67635  
coded aperture cameras, performance of practical designs, computer simulations 4-67638  
coded aperture imaging, advanced deconvolution techniques 4-67636  
coded masks telescopes, numerical method for virtual image recognition 4-67639  
comet orbit determ. by means of optimally selected observations 4-82385  
complex analysis, appl. to spherical coordinate geometry 4-105890  
computational procedure for apparent places of fundamental stars (1984 onwards) 4-77696  
computing facilities and applications software at Kiso Observatory, Japan 4-94604  
continuum imaging technique for planetary nebulae, appl. to determ. of apparent magnitudes and Zanstra temps. of central stars 4-115754  
cosmic ray variation studies, necessary geographic distrib. for meas. stations 4-110539  
curve of growth method, appl. to IR and radio spectrum of early-type stars with mass loss 4-101312  
data processing of imperfectly coded images 4-67634  
delta-rho perturbation method for autonomous orbit calc. 4-90058  
digital speckle interferometry of binary stars (Russian) 4-67641  
digitized interferogram reduction for Fabry-Perot camera system 4-67631  
Doppler imaging of rapidly rot. RS CVn stars spots 4-94641  
dust formation in stellar winds, rapid computation method rel. to graphite condensation 4-72927  
effective temp. and accel. of gravity determ. from Kurucz model H line contours 4-94632  
estimation method for small perturbations determ. in orbits 4-82403  
extrasolar planetary systems in Galaxy search methods and results 4-106043  
extrasolar planets, detect. methods 4-77727

## astronomical techniques continued

- extreme UV solar flux absolute meas. using windowless rare-gas ionisation chamber 4-101156  
faint object detection on photographic plates 4-94638  
galactic  $\gamma$ -ray emission characts. determ. 4-86049  
galactic orbit isolating integral determ. 4-110694  
galaxies intrinsic orientation determ., appl. to S0 galaxies with polar rings 4-101465  
galaxy classification, two dominant dimensions in objective classification scheme for spiral galaxies 4-86027  
gamma ray burst sources, optical counterparts detect. methods 4-101516  
Giotto spacecraft mission to Comet Halley, navigation problems 4-90048  
Giotto spacecraft mission to Comet Halley, terminal navigation problem 4-90091  
global star cluster stellar photometry by electrographic method, image reduction 4-94623  
Hartmann test, diff. struct. of Hartmann-pattern images 4-63076  
heterodyne detection of CO at 691 GHz 4-90218  
heterodyne spectroscopy for astrophysical applications using tunable laser sidebands at 10 microns 4-94637  
identification method for very remote galaxy clusters 4-77946  
image intensifier tube VARIO 4215, testing for astronomical appls. 4-72889  
image processing 4-82422  
image processing algorithms, appl. to coma morphology and dust-emission pattern of Periodic Comet Halley (1910 II) 4-82450  
image processing characts. for rocket UV filtergrams anal. 4-101186  
image restoration and processing methods 4-67637  
image sharpening techniques, maximum entropy method (German) 4-67640  
Infrared Astronomical Satellite, computerised data processing 4-82421  
infrared detectors using InSb, for ground based instruments 4-95517  
interferometry, meas. of stellar diameters by combining light issuing from two telescopes (French) 4-105888  
International Ultraviolet Explorer echelle grating, blaze function ripple correction 4-110542  
interstellar H I kinematics used to determine outer Galaxy gamma rays distrib. 4-63303  
IR interferometry for extrasolar planets detect. 4-77725  
IR photometry, comparison of SAAO, AAO and CTIO systems 4-77726  
IR photometry, one-channel instrument for 0.9 to 2.5  $\mu$ m spectral region (Russian) 4-101174  
IR technology and appl., conf., San Diego, CA, USA (Aug. 1983) 4-110800  
IUE SWP camera spectra, order overlap problem, correction algorithm 4-77723  
Lagrange method appl. to coupled perturbations on artificial satellites orbits anal. 4-82375  
light curve soln. method for shallow partial eclipses 4-63207  
long-baseline Michelson interferometry with large ground-based telescopes operating at optical wavelengths, general formalism 4-90094  
mathematical technique allowing comparison and contrasting of SNR models 4-73016  
mathematical technique for homogeneous cosmological models global anisotropy, effects on background radiation ang. distrib. 4-90093  
matrix methods for galactic cosmic ray propag. anal. 4-100927  
meteor observations analysis, allowance for astronomical selection 4-105904  
meteoroid capture cell technique for satellite deployment 4-77722  
micrometeoroid impact simulation, electrostatic prism for microparticle beam steering 4-64263  
millimetre-wave continuum photometry, using Italian IR Telescope on Gornegrat 4-72888  
molecular clouds, age determ., use of cyanopolynes 4-110541  
Multiple Mirror Telescope use as a phased array 4-110523  
multispectral imaging using IHS display mode, separation of highly correlated bands 4-101189  
NASA space programs in IR astronomy 4-110490  
numerical data and functional relationships, Landolt-Bornstein series 4-82603  
numerical integration procedure for Galilean satellites 4-82402  
numerical techniques for galaxies distrib. determ. 4-77950  
optical resonance spectrophotometry, appl. to obs. of large scale photospheric vel. structs. 4-115729  
orbit determination for spectroscopic binary stars, analytical method 4-101408  
orbital lifetime estimation method for near Earth satellites 4-82374  
photoelectric photometers, computer-controlled, three statistical tests 4-94630  
photoelectric photometry, advances for small telescopes, book 4-110816  
photographic copying appls. of Kodak Precision Line Film (LPD7) 4-101178  
photographic photometry for anal. of flare stars in assoc. 4-63083  
photographic photometry of faint stars, use of sub-beam prism, calibration (Japanese) 4-94640  
photography, hypersensitisation of Kodak Technical Pan Film 2415 via bathing or baking 4-101177  
photometry of Ap stars, meas. of 5200 Å depression rel. to galactic distrib. (German) 4-67738  
picture processing and analysis, appl. of Photometric Data System 4-105887  
planet photographs transmission to Earth (Afrikaans) 4-77724  
planetary nebulae central stars, temp. and radius determ. methods 4-101336  
planetary remote sensing, computer program package 4-101114  
polarimetric mapping of Moon, appl. of electronic analogue transform. of polarisation pictures 4-105893  
quasar search techniques for high red shift objects ( $>3.5$ ) 4-77963  
radiative transfer, difference eqns. and linearisation methods 4-94598  
radiative transfer, operator perturbation methods 4-94603  
radiative transfer eqn. soln. method for expanding spherical medium 4-85872  
radiative transfer methods, book 4-90304  
radiative transfer problems in spherical media, soln. using integral eqns. 4-94601  
radiative transfer problems with spherical symmetry, iterative soln. using single-ray approximation 4-94597  
radiative transfer theory, accurate solns. to non-LTE problems using approximate lambda operators 4-94596  
radiative transfer theory, appl. of escape probability methods 4-94591  
radiative transfer theory, approximate probabilistic transfer eqn. 4-94594

**astronomical techniques continued**

- radioluminescent light sources used to standardise astronomical photographs (*Russian*) 4-101188
- SETI, search strategy of signals with small duty cycle (*German*) 4-67648
- solar coelostat and heliostat alignment and use for eclipse and other field purposes 4-110521
- solar diameter meas. using solar disc sextant optical config. 4-82415
- solar disc sextant concept evaluation 4-82414
- solar global oscills. meas. method and instruments 4-105918
- solar magnetic and vel.-field meas., new instrum. concepts 4-82417
- solar photosphere granulation velocities, determ. from spectral line anal. 4-105891
- solar shape and size measurement using solar disc sextant 4-82416
- solar total irradiance meas. by pyrheliometric method, review 4-115738
- speckle imaging at low light levels, phase estimation 4-74430
- spectral classification of Mira variables, phenomenological and photometric procedures 4-82476
- spectral deconvolution, appl. to anal. of contact binary star AE Phoenicis 4-82513
- spectrophotometry, density-to-intensity conversion using emission line intensities 4-101179
- spectropolarimetry, multichannel Pockels cell spectropolarimeter for Anglo-Australian Telescope 4-110533
- spectroscopic method for detect. of circumstellar and interstellar graphite 4-101187
- spectroscopic techniques for chemical composition, using tunable diode laser heterodyne spectroscopy 4-115590
- spectroscopy, appl. of high efficiency combined telescope and spectrograph 4-77713
- spectroscopy, relative distrib. of efficiency over surface of blazed concave grating 4-105881
- star coordinates determ. using extragalactic radioresources and satellite beacons 4-63034
- statistical method for gamma-ray lines and sources obs. 4-101190
- stellar magnetic field photographic representations, effects of spectral line characts. 4-94633
- stellar mass loss determination methods for late type giants and supergiants 4-85938
- stellar photometry, CCD obs. of photoelectric standard stars 4-94740
- stellar photometry, meas. of four photoelectric UBVRI sequences near bright Virgo galaxies 4-94741
- stellar photometry, observing method using photoelectric photometer 4-105883
- stellar photometry, Pickering-Racine prism method for plate calibration 4-110535
- stellar photometry, possible appls. and photometric characts. of AZT-16 two-meniscus astrophotograph (*Russian*) 4-101166
- stellar photometry techniques and solar flux meas. 4-101191
- stellar proper motions calculation, rigorous formulae (*German*) 4-67715
- stellar spectrophotometry, calibration of augmented system of bright secondary standards 4-94736
- stellar spectroscopy, expansion of dynamic range of data-gathering and measuring system of five-channel spectrophotometer 4-105880
- stellar trigonometric parallaxes, determ. from obs. in hour angles (*Russian*) 4-101118
- submilliarcsecond speckle displacement meas. using cross spectrum anal. 4-94631
- sunspot motions used for solar torsional oscills. determ., differential rot. effects 4-90133
- supernova neutrinos detection, appl. of existing proton decay detector 4-101095
- supernovae detection in distant galaxies, automatic system developments 4-67642
- surface photometry of galaxies, digital processing techniques (*Russian*) 4-115695
- temperature models iterative fitting to spectral data 4-105926
- time measurement, accuracy of LF and TV synchronisation techniques (*Chinese*) 4-82420
- turbulent velocity structure determ. in interstellar clouds, appl. of mean vel. fluctuations meas. 4-90204
- two-dimensional imaging of atm. Cherenkov light, appl. to  $\gamma$ -ray astronomy 4-101176
- universal age determ. methods 4-73122
- UV photometry of late-type stars, comparison of different photometric systems 4-72928
- vector techniques for artificial satellites orbit prediction 4-94642
- visual binary stars, dynamical parallax and orbital inclination determ. from obs. of short arc (*Russian*) 4-101414
- VLBI system for TDRSS satellite navigation 4-82380
- Wessink's modified method appl. in RV Tau stars mean radii determ. 4-77839
- X-ray and  $\gamma$ -ray imaging techniques, Int. Workshop, Southampton, England (July 1983) 4-63386
- X-ray spectroscopy, high resolution obs. with objective grating spectrometer aboard Einstein Observatory 4-101170
- $^{14}\text{C}$  dating in tree rings, determ. of cosmic ray solar mod. cycle 4-94423
- $\text{H}^2/\text{He}$  ratios determ. in Jupiter and Saturn atm., determ. methods 4-77757
- He I forbidden lines used to determine solar flare plasma characts. 4-77798
- Ne III forbidden line at 36  $\mu\text{m}$ , use for planetary nebulae Ne abundance determ. 4-110718

**astronomical telescopes**

- see also radiotelescopes
- advanced X-ray astrophysics facility technology mirror assembly epoxy shrinkage effects 4-86512
- Anglo-Australian Telescope, multichannel Pockels cell spectropolarimeter 4-110533
- apochromatic two-element objectives, computerized design 4-102994
- Aries X-ray Telescope mirrors, metrology 4-67628
- Astron UV telescope, characts. and preliminary obs. (*Russian*) 4-67630
- astronomy with Schmidt-type telescopes, 78th IAU Colloquium, Asiago, Italy (1983 August 30 to September 2) 4-106115
- AZT-16 fast two-meniscus astrophotograph, photometric characts. (*Russian*) 4-101166
- Baker-Meine-Bingham three-mirror telescope, aberration anal. 4-101155
- balloon borne  $\gamma$ -ray telescope, background induced by neutron-payload interactions 4-101171
- balloon mounted  $\gamma$ -spectrometers,  $\gamma$ -ray background induced by atmospheric neutrons 4-67512

**astronomical telescopes continued**

- Cassegrain-type spectrographic cameras, near axis ray tracing, aberrations and their correction (*Japanese*) 4-94617
- CCD device in cinematographic mode for enhanced resolution of telescope 4-94622
- CCD/transit instrument, progress report 4-72886
- coded aperture  $\gamma$ -ray telescope, statistical anal. 4-67635
- coded masks telescopes, numerical method for virtual image recognition 4-67639
- combined telescope and spectrograph of high efficiency 4-77713
- conference on advance technology optical telescopes, at London, England (September 1983) 4-106098
- conference on astronomical instrumentation, at London, England (September 1983) 4-106099
- Couder telescope, modified design and optical quality 4-110530
- cryogenic IR radiance instrument for shuttle CIRRIS telescope 4-94614
- cryogenic telescope on IRAS 4-110525
- deployable optical systems, conf., Los Angeles, CA, USA (Jan. 1983) 4-73138
- deployable reflector configurations 4-77707
- deployable reflector segmented mirror system point spread function generation 4-74433
- deployable telescopes, alignment and phasing 4-77708
- double prism corrector for atmospheric dispersion in converging beam 4-101175
- environmental and thermal control for space vehicles, conf. Toulouse, France (Oct. 1983) 4-73162
- epoxy mirrors, mechanical stability and usefulness (*Russian*) 4-101169
- EUV detectors onboard Extreme Ultraviolet Explorer astronomical satellite 4-63063
- EXOSAT imaging X-ray detectors, pre-flight and in-orbit performance 4-63066
- fibre optics appl. (*Russian*) 4-110537
- Galileo Mission, near IR mapping spectrometer 4-94612
- Galileo mission to Jupiter, CCD TV camera design 4-94615
- gamma-ray imaging Compton telescope onboard Gamma Ray Observatory 4-63061
- gamma-ray imaging device for telescope, using rotating coded mask 4-63062
- gamma-ray imaging systems for low energy range 4-72881
- gamma-ray telescope with arc minute resolution, image reconstruction 4-72882
- gamma-ray telescopes, choice of astatic system for controlling DC motor speed for altazimuth mountings 4-105886
- grazing incidence telescope for X-ray astron. 4-67626
- Haute-Provence Observatory, telescopes general description (*French*) 4-105874
- horizontal solar telescope, instrumental polarisation assoc. with refl. from flat mirror (*Russian*) 4-101167
- HXR81 M Poker balloon borne hard X-ray telescope 4-101511
- hyperbolic primary telescope configuration 4-110518
- Infrared Astronomical Satellite cryogenic system, use of superfluid He dewar 4-77718
- Infrared Astronomical Satellite spacecraft thermal design and performance 4-77717
- infrared detector arrays for telescopes, using CCD and CID arrays 4-101159
- infrared detectors using Si:P or Ge:Be for low photon background work 4-101160
- infrared InSb detectors used at European Southern Observatory 4-94624
- Infrared Space Observatory dual liquid  $\text{H}^2/\text{He}$  superfluid He coding system thermal design 4-73441
- infrared spectrometry, with 52-element InSb array 4-94625
- Infrared Telescope in Space, mirror testing apparatus and cooling effects (*Japanese*) 4-91565
- Infrared Telescope in Space (IRTS), optical system and mirror physical characts. (*Japanese*) 4-94619
- IR contrast-mode radiometer for AMOS 1.6 m telescope 4-115691
- far IR Michelson interferometer for GIRL telescope on Spacelab 4-77716
- IR telescope design, fused- $\text{SiO}_2$  mirror cryogenic test implications 4-105878
- IR telescopes, purging flow protection 4-101158
- IRAS infrared astronomical telescope in orbit, design and performance 4-77712
- IRAS mission 4-85857
- Isaac Newton Telescope (2.54 metres), at new site on La Palma, Canary Islands 4-72885
- Italian IR Telescope on Gornergrat, appl. to millimetre-wave continuum photometry 4-72888
- Japanese solar eclipse expedition, telescopes and instrumentation description (*Japanese*) 4-94715
- J.R. Frost Observatory, telescope and spectrometer for extrasolar planets detect. 4-82412
- large aperture mirror, assessment by Hartmann test (*Korean*) 4-115688
- large Cassegrain telescopes, optical system 4-105877
- Large Cosmic X-ray Telescope, performance, operation 4-72880
- large telescope system testing using multiple subapertures 4-97021
- long-baseline Michelson interferometry with large ground-based telescopes operating at optical wavelengths, general formalism 4-90094
- McMath solar telescope, adaptation with spectrometer for stellar spectra obs. 4-85881
- mirror testing methods, astron. appl. (*Japanese*) 4-91642
- modulation collimator for X-ray astronomy at high energies 4-90050
- MOSAIC, Mosaicked Optical Self-Scanned Array Imaging Camera for space UV 4-110522
- multimirror telescope alignment systems using fan beams and translation insensitive interferometers 4-101162
- Multiple Mirror Telescope use as a phased array 4-110523
- NASA space programs in IR astronomy 4-110490
- NASA space telescope faint objects-camera active thermal control 4-77719
- Nordic Optical Telescope, case for 2.5 m instrument 4-63071
- Nordic Optical Telescope, galaxy observing projects 4-63321
- Nordic Optical Telescope, meeting in Oslo (August 1983) 4-58569
- Nordic Optical Telescope, planned obs. of interstellar medium 4-63265
- Nordic Optical Telescope, Solar System studies 4-63130
- Nordic Optical Telescope, star cluster obs. projects 4-63235
- Nordic Optical Telescope, stellar activity studies 4-63136
- Nordic Optical Telescope, stellar atmosphere studies, projects 4-63135
- Nordic Optical Telescope, stellar structure projects 4-63137

**astronomical telescopes continued**

- Nordic Optical Telescope obs. proposals rel. to galactic populations and kinematics 4-63320  
 Nordic Optical Telescope plans for interacting close binary star studies 4-63208  
 off-axis parabola fabrication at Kitt Peak National Observatory 4-103028  
 optical telescopes, observing possibilities for supernova in immediate solar neighbourhood 4-77711  
 Osaka City University Hard X-ray Telescope, description and obs. 4-101435  
 photographic zenith tube, timing mechanisms hysteresis (*Japanese*) 4-94618  
 pointing system beam jitter transmission and correction 4-87426  
 pointing system using IR multiplex encoding imager 4-94613  
 prime focus corrector for f/3 true or quasi Ritchey-Chretien primaries 4-72879  
 reflector antenna structure design concepts 4-77709  
 resolution concepts comparison, satellite telescope appl. 4-96809  
 ROSAT X-ray telescope thermal design features 4-85879  
 S 520-3 controlled nosecone rocket-borne VUV instrumentation, characts. and obs. (*Japanese*) 4-94620  
 San Pedro Martir 2.12 m telescope, astrometric test 4-85878  
 segmented primary mirror tilt and phase alignment using multiple-order radial-grating shearing interferometer 4-74642  
 shuttle infrared telescope facility, secondary mirror, microprocessor based position control system 4-85873  
 Shuttle IR telescope facility, system design parameter study 4-110489  
 Shuttle IR Telescope Facility, thermal modelling 4-110488  
 SIGMA, high resolution space observatory project for gamma-ray sources 4-105875  
 solar soft X-ray spectrograph-telescope performance 4-85874  
 sonine's Bessel identity applied to apodization 4-94605  
 space borne charged particle telescope calibration using 0.4-20 MeV protons 4-77710  
 Space Telescope, Wide Field/Planetary Camera, CCD use for faint planetary satellites 4-82423  
 space telescope design, multiple mirror system for very high resolution, COSMIC approach 4-101161  
 Space telescope design, ray tracing in finite element models 4-87425  
 Space Telescope mission planning 4-94557  
 space telescope optical payloads accurate thermal control 4-85880  
 Spacelab 2 telescopes with coded system, data processing of imperfectly coded images 4-67634  
 Spacewatch camera, use in asteroid research (*French*) 4-82418  
 spider diffraction, curved and straight leg comparison 4-91397  
 stellar interferometer with fibre optic synthetic aperture 4-110524  
 structural mechanics of optical systems, conf., Cambridge, MA, USA (Nov. 1983) 4-86104  
 synthetic aperture systems, conf., San Diego, CA, USA (Aug. 1983) 4-95020  
 synthetic aperture telescope, laser mirror positioning system 4-97016  
 three-mirror anastigmat with main mirror and third mirror coincident, theory (*Russian*) 4-101168  
 University of California 10 m telescope mirror support anal. 4-90090  
 UV camera, S201 instrument operated by Apollo 16, results and implications for future instruments 4-110531  
 X-ray coded mask telescope for Spacelab 2 mission 4-72883  
 X-ray mirror for ROSAT satellite, manufacture and testing 4-115686  
 X-ray telescope, two-channel three-mirror, design and analysis 4-110519  
 X-ray telescope design for broad band spectrophotometry 4-63025  
 ZEBRA,  $\gamma$ -ray telescope, evaluation of background introduced from coded aperture mask 4-67629  
 zenith telescope, visual obs. for simultaneous determ. of time and latit. (*German*) 4-67598  
 PtSi Schottky IR CCD evaluation for astron. appls. 4-64789

**astronomy** *see astronomy and astrophysics*

**astronomy and astrophysics**

- see also astroarchaeology; astronomical catalogues; astronomical instruments; astronomical observations; astronomical observatories; astronomical spectra; clusters of galaxies; cosmology; extraterrestrial life; galaxies; gamma-ray astronomy; infrared astronomy; intergalactic matter; interplanetary matter; interstellar magnetic fields; occultations; planetaria; radioastronomy; solar system; stars; ultraviolet astronomy; X-ray astronomy*  
 5th Gottingen-Jerusalem Symposium (October 1980) 4-58570  
 21st Goddard memorial symposium at Greenbelt, USA (March 1983) 4-63399  
 1984 Astronomical Almanac 4-63418  
 1984 ephemerides and physical data (*French*) 4-67646  
 American Astronomical Society, 164th meeting, Baltimore, Maryland (1984 June 10 to 13) 4-101560  
 astrometric reference systems, linking from space 4-72856  
 astrometry, determ. of atmospheric dispersion coeff. and correction for its influence (*Russian*) 4-101121  
 astronomical methods, constants and solar system, Landolt-Bornstein series 4-82603  
 Astronomical Science Group of Ireland, conf. at Armagh Observatory, N Ireland (May 1983) 4-95038  
 astronomy with Schmidt-type telescopes, 78th IAU Colloquium, Asiago, Italy (1983 August 30 to September 2) 4-106115  
 atmosphere-less cosmic bodies, brightness opposition effect model 4-94565  
 atomic data calculation for astrophysics at University College London 4-90089  
 atoms in astrophysics, book 4-106125  
 Bibliography of Astronomical Objects 4-94902  
 Cannon, Annie Jump (1863-1941), life and stellar spectra classification 4-78087  
 computational spherical astronomy (book) 4-78071  
 conference, neutrino phys. and astrophys., Erice, Sicily (June 1980) 4-90293  
 conference on star bursts in galaxies, at London, England (May 1983) 4-73148  
 conference on Universe early evolution and present struct., at Kolymbari, Crete (August-September 1982) 4-73160  
 continuous spectrum in differentially rotating perfect fluids, effect of gravit. radiation reaction 4-101149  
 convective flow in slip flow regime 4-101128

**astronomy and astrophysics continued**

- cosmic-ray-mediated shocks with variable compression ratio, theory 4-63021  
 creationism and astronomy 4-90344  
 data collection (book) 4-86127  
 dense matter in liq. metal phase, low-temp. quantum corrections to elec. and thermal conds. 4-63040  
 double stars, physical properties and generic relations, IAU Colloquium No.80, Lembang, Java (1983 June 3 to 7) 4-78020  
 Earth in the Universe, general discussion (book) 4-73180  
 eye characts. and vision in astronomy 4-62464  
 first-flight escape from spheres with  $R^{-2}$  density distribution 4-90085  
 flow past impulsively started infinite vertical plate, mass transfer effects 4-101130  
 fluid oscillations, analytic soln. for continuous spectrum in differentially rotating perfect fluids 4-94581  
 free-convection flow past exponentially accelerated vertical plate, theory 4-67610  
 gamma-ray astronomy, review 4-106084  
 gravitation, axisymmetric stationary vacuum fields in general scalar tensor theory 4-101135  
 gravitational interaction of bodies immersed in fluids, theory 4-101124  
 halo formation, mathematical soln. of MHD equations 4-101468  
 heat and mass transfer in flow through porous medium, effects of Hall current 4-101125  
 hydrogenic ions excitation by electron impact, high energy collision strengths and excitation limits 4-77702  
 hydromagnetic free convection with mass transfer in rotation fluid, effects of Hall current 4-101134  
 IAU recommendations and astrolabe observations, apparent posns. calc. (*French*) 4-63032  
 image-tube spectrograms, density-to-intensity conversion using emission line intensities 4-101179  
 interstellar molecular cloud chemistry, prod. mechanism for  $\text{CH}_3\text{CN}$  and  $\text{CH}_3\text{OH}$  4-94192  
 ionisation equilibrium in rarefied gas, effect of charge-exchange reactions 4-94577  
 Japanese research activity 4-78094  
 linear series and stability, catastrophe theory 4-63091  
 low-energy neutrinos in astrophysics, reviews 4-94535  
 meteor astronomy, allowance for astronomical selection 4-105904  
 MHD cylindrical shock propagation in self-gravitating gas, theory 4-101127  
 MHD free-convection flow near vertical oscillating plate, theory 4-67618  
 MHD free-convection oscillatory flow past porous limiting surface; effects of Joule heating and viscous dissipation 4-67616  
 MHD free-convective oscillatory flow past porous limiting surface, effects of Joule heating and viscous dissipation 4-67615  
 molecular excitation and ionisation by photons and electron impact 4-83481  
 neutrino mass upper limit astrophysical consequences 4-72874  
 nomenclature anomalies 4-67647  
 nonradial oscillations of stars, book 4-90141  
 Nordic Astronomy Meeting, Oslo (August 1983) 4-58568  
 plasma physics, processes and props. of steady mildly relativistic thermal plasmas 4-94582  
 propynol cation, potential interstellar molecule, geometry 4-102602  
 radiative transfer, accurate and approximate probabilistic eqns. for line source functions 4-94593  
 radiative transfer, difference eqns. and linearisation methods 4-94598  
 radiative transfer methods, book 4-90304  
 radiative transfer problems with spherical symmetry, iterative soln. using single-ray approximation 4-94597  
 radiative transfer theory, accurate solns. to non-LTE problems using approximate lambda operators 4-94596  
 radiative transfer theory, appl. of escape probability methods 4-94591  
 radiative transfer theory, approximate probabilistic transfer eqn. 4-94594  
 Rayleigh-Taylor instability in astrophysical fluids 4-77704  
 relativistic magnetoplasma, three-plasmon processes in electron-positron plasma 4-87924  
 restricted quantum-mechanical three-body problems, asymptotic eigenvalues and wave functions of electron 4-101132  
 rigidly rotating gaseous disks with mag. field, gravit. instability, dispersion relation 4-72866  
 Rutherford Appleton Laboratory 1983 4-73130  
 self-similar flow stability, Primakoff soln. 4-87668  
 space astronomy (book) 4-73181  
 Space Shuttle astronomy missions 4-77688  
 space warps (book) 4-67892  
 spherical coordinate geometry, complex anal. appl. 4-105890  
 stellar equatorial coordinates, alternative derivation of influence of precession (*German*) 4-67597  
 supersonic fluid jets, surface waves propag. and growth 4-63039  
 UV stellar synthesis calcs., spectroscopic data 4-90139  
 Voigt spectral line profile, mathematical props. 4-63043  
 X-ray emission spectra from ionising plasmas, theory 4-67617  
 n-pe $\beta$ ,  $\beta$ -decay role in astrophysics 4-67620  
 Co III, transition probabilities for forbidden lines in 3d<sup>7</sup> ground configuration 4-63041  
 He I, electron excitation rate coeffs. for transitions from ground state to excited states 4-94571  
 Ni IV, transition probabilities for forbidden lines in 3d<sup>7</sup> ground configuration 4-63041  
 O+H collisions, energy transfer rate coeff. 4-110517  
 OH astronomical maser, pump mechanism from OH+H<sub>2</sub> collisions 4-96652  
 Tm I spectrum, lifetime meas. using pulsed dye laser 4-72861

**astronomy computing**

- see also computerised instrumentation*  
 AMD-1 automatic densitometer spectra, scanning and processing software 4-94635  
 artificial satellites, autonomous orbit computation, appl. of delta-rho perturbation method 4-90058  
 artificial satellites, orbit theory for LSI-11 microprocessor 4-94554  
 ASPECT, area spectroscopy technique in astronomy 4-105889  
 Bibliography of Astronomical Objects 4-94902  
 CEDAG, clusters of galaxies data centre 4-94974  
 CLEAN, deconvolution algorithm enhancement 4-115694  
 cosmic ray automatic data collection system 4-72891

**astronomy computing continued**

- digital sign correlator for a very long baseline radiointerferometer 4-94609
- globular star cluster stellar photometry by electrographic method, image reduction 4-94623
- image processing 4-82422
- Kiso Observatory, Japan, computing facilities and applications software 4-94604
- photoelectric photometers, computer controlled, three statistical tests 4-94630
- planetary remote sensing, computer program package 4-101114
- radio sources detection against set-noise background, optimum filtering method 4-63080
- RATAN-600 radio surveys, data collecting and processing system 4-63077
- SIMBAD data base, astronomical contents 4-94901
- SIMBAD data base at CDS, 1984 software capabilities for stellar astronomy 4-94900
- SPIRAL program for artificial satellites orbit prediction 4-94642
- supernovae detection in distant galaxies; automatic system developments 4-67642
- surface photometry of galaxies, digital processing techniques (*Russian*) 4-115695
- television speckle interferometer with real-time digital image processing 4-63072

**astrophysics computing**

- see also computerised instrumentation
- IUE SWP camera spectra, order overlap problem, correction algorithm 4-77723

**ATM forces see intermolecular forces****atmosphere, solar see solar atmosphere****atmosphere, terrestrial see terrestrial atmosphere****atmosphere, upper see upper atmosphere****atmospheric acoustics**

- acoustic wave generation by low freq. gravity modes 4-82109
- bistatic sounding, refr. effects (*Russian*) 4-82259
- ground effect, meteorology (*French*) 4-60196
- infrasonic impure, decomposition into normal modes at acoustic array (*Chinese*) 4-107931
- land and sea breezes at La Spezia, Italy, sodar obs. 4-77582
- radioacoustic sounding, wind influence on limiting height (*Russian*) 4-82258
- sound field calc. for plane sound waves (*Chinese*) 4-89956
- subsonic passage above reflecting ground surface, expanding sound due to time-varying source 4-74795
- troposphere, sound waves due to meteors as cause of solar haloes ripple struct. 4-105715
- ultrasonic anemometer, microprocessor-based 4-105778
- wave in thermosphere, interaction with ionosphere, plasma characts. var. 4-90026

**atmospheric boundary layer**

- aerosol in coastal boundary layer, meas. technique of satellite optical imagery 4-100742
- AIDJEX air stress meas. 4-89986
- AIDJEX conf. at Seattle, United States (September 1977) 4-86121
- AIDJEX ice model testing, use of Landsat remote sensing 4-89927
- AIDJEX model response to axisymmetric loadings 4-89931
- AIDJEX planetary boundary layer models 4-89980
- air flow around thin closed fence, field study 4-105623
- air temperature in polar regions, cause of 'Fram' type seasonal change in diurnal amplitude 4-110192
- alpine valley in Switzerland, wind circulation and surface energy flux 4-110198
- Antarctic marginal ice zone, sea ice modification of onshore wind 4-67326
- Arabian Sea monsoon depression, air-sea interface conditions observations 4-110204
- Arctic Ice Dynamics Joint Expt., boundary layer wind and press. effects 4-89978
- Arctic ice pack drift, wind stress determ., use of Fleet Numerical Weather Central predictions 4-89979
- Arctic sea ice wind stress meas. 4-89984
- arthropods, minute wingless, active aerial dispersal, exploitation of boundary-layer vel. gradients 4-66987
- North Atlantic, sea-air heat transfer in energy-active zones 4-105581
- North Atlantic trade wind zone, ocean-atmosphere thermal interaction 4-72611
- barotropic flow over large-scale topography, stochastic perturbation of simple blocking models 4-82195
- Beaufort Sea, geostrophic wind and surface press. for AIDJEX 4-89981
- Beaufort Sea, nearshore winter ice dynamics, role of wind 4-89925
- Beaufort Sea, surface press. and geostrophic wind for AIDJEX 4-89982
- Beaufort Sea, surface stress meas. from wind and temp. anal. during AIDJEX 4-89983
- Bering Sea, longitudinal rolls and steam fog in boundary layer 4-72641
- Bilbao, Spain, pollution episode in industrialised estuary valley 4-72629
- Boulder, Colorado, USA, aerosol element composition 4-67323
- Boundary Layer Experiment-1983, characts. 4-110255
- Bowen's ratio over bare cotton soil, temp. and humidity anal., instrumentation 4-67335
- NE Brazil, coastal precipitation, surface roughness effects and boundary layer convergence 4-94195
- East China Sea, surface wind field and mesoscale convection 4-115495
- cloud-topped mixed layers, buoyant production of turbulence 4-82180
- coastal area mesoscale atmos. circulation during upwelling event 4-72633
- coastal surface temp. field, representation using statistical objective anal. techniques 4-105626
- comparative energy balance study for Arctic tundra, sea surface, glaciers and boreal forests 4-94197
- convective boundary layer, plume dispersion and vertical winds, Monte Carlo simulation 4-100019
- convective boundary layer, turbulent profiles, urban effects 4-72648
- convective planetary boundary layer, scalar top-down and bottom-up diffusion 4-72650
- convective planetary boundary layer, vertical pollutant diffusion 4-94181
- convective stability, influence on potential evaporation 4-100666
- convective boundary layer, spectral representation of vertical struct. of turbulence 4-62915
- Cyprus, surface wind flow pattern, wind-tunnel expts. 4-115549
- dense gas cloud dispersal after an instantaneous release 4-77574

**atmospheric boundary layer continued**

- diffusion in convective boundary layer, by turbulent energy model 4-115483
- downdrafts from tropical oceanic cumulus clouds 4-77575
- dusty atmosphere of Sahel, turbulence affected by dust radiative props. (*French*) 4-77576
- Ekman layer flow during spin-up of thermally stratified fluid 4-100680
- electric field during thunderstorms, reduced by corona discharge from grounded objects 4-67324
- electric potential measurement, Hy-wire measurement system 4-67437
- energy balance at land surface, daily variations and statistical struct. 4-89959
- NE England, 1983 July heatwave, sea breeze occurrence effects on temp. 4-100717
- evaporation from land surface, Turc and Ivanov formulae applicability (*German*) 4-77559
- evapotranspiration calculations 4-77617
- evapotranspiration potential in Belgium, estimation procedure 4-115476
- Florida, USA land use rel. to surface temp. fluctuations 4-115499
- deciduous forest canopy, obs. of microscale pressure fluctuations 4-67300
- frictional velocity dependence on height, time and actual velocity 4-100706
- frontal precipitation, boundary layer struct. anal. 4-72670
- frontal regions, convective and boundary layer parametrizations in diagnostic model 4-82198
- German coast of North Sea, wind speed change near coast (*German*) 4-82187
- global sea state and marine wind speed seasonal variations 4-67330
- Goddard general circulation model climatology, effects of sea ice var. 4-89990
- gradient distributions and flux profile relations above rough forest, implications for evapotranspiration 4-82204
- heat and moisture transport over terrain, 3-D modeling 4-72684
- heat flux densities from vegetation, uncoupled multi-layer model for sensible and latent heat transfer 4-105618
- heat fluxes (sensible and latent) above water surface, parameterization (*Russian*) 4-100684
- height during AIDJEX and air stress meas. 4-89985
- hill with gentle slopes in boundary layer flow, wind and turbulence study 4-115493
- hydraulic jumps, simulation in presence of rot. and mountains 4-62919
- ice accretion at mountain site in Czechoslovakia, air temp. influence 4-89960
- Indian Ocean, factors affecting boundary-layer wind shear during FGGE 4-105627
- inversion layer growth and importance of gravity waves 4-110202
- ion dispersion expts. in turbulent boundary layer 4-77578
- Japan, seasonal characts. of wind duration (*Japanese*) 4-82150
- Japan seas, cold winters and warm winters, wind over sea charact. (*Japanese*) 4-82149
- katabatic wind in opposing wind flow 4-115511
- lake wind speed calc. methods using observations of overland wind speeds 4-67305
- land and sea breezes at La Spezia, Italy, sodar obs. 4-77582
- land surface heat and moisture transfer at macroscale for GCM models 4-77619
- large-scale sea ice model, surface wind and currents effects 4-89937
- lee waves in Aegean Sea 4-105622
- longitudinal roll vortices over ice covered Bering Sea 4-72641
- low-level jet in planetary boundary layer, dynamical model 4-67299
- marine, turbulence in surface layer, wind-wave tank expts. 4-67231
- marine, wind from Scanning Multichannel Microwave Radiometer data Fourier anal. 4-67475
- marine aerosols in boundary layer, mixed-layer model appl. 4-115497
- marine atmosphere, surface temperature long term trends 4-100580
- marine atmosphere near Hawaii, sea salt conc., vertical distrib. 4-77591
- marine atmospheric, interannual moisture vars. near surface of tropical Pacific Ocean 4-82200
- marine boundary layer, spray field above wind-driven waves 4-67306
- marine boundary layer struct. at Sable Island, Nova Scotia 4-67329
- marine surface layer, thermal struct. (*Russian*) 4-115507
- marine surface layer, worldwide temp. fluctuations (1856 to 1981) 4-105569
- marine surface layer winds, determ. from sea surface microwave backscatter data 4-67376
- mixed layer dynamics, lidar obs. rel. to tests of parameterised entrainment models 4-100669
- Mizuho Station, Antarctica, snow mass flux under variable wind conditions (*Japanese*) 4-105669
- mm-wave scintillation caused by turbulence in clear air near ground 4-77615
- mountain areas, cold air drainage, thermal belt and cold air lake 4-94199
- flat mountain ranges causing channeling of air flow 4-105634
- mountain valley daytime boundary layer evolution 4-100658
- nighttime drainage winds, observational study of instability and turbulence 4-105620
- NIMBUS-7 SMMR observations and results summary 4-100592
- nocturnal boundary layer over rough terrain, wind and temp. profile obs. 4-77581
- nocturnal stratocumulus cloud, simultaneous meas. of turbulent and microphysical struct. 4-62914
- nonlinear surface layer model (including turbulence) 4-100705
- North Sea, high winds observed from West Sole oil rig 4-72689
- obstacles in boundary layer flow, study of wakes and net forces 4-67304
- ocean and atmosphere boundary layers, baroclinic effects 4-77569
- ocean coastal circulation models, the use of land or sea based wind data? 4-77545
- ocean heating at equatorial regions, influence of atmosphere 4-100598
- oceanic surface winds, SEASAT-A scatterometer meas., global data assimilation expts. 4-100660
- oppositely directed jets interacting near mountainous obstacle, spontaneous oscils. 4-108101
- orographic and thermal nonhomogeneities effects 4-77588
- outflow from convective storm clouds, numerical model 4-77579
- Pacific Ocean, atm. surface layer Hg conc., correl. with marine upwelling and biological prod. 4-105599
- Pacific Ocean, surface wind stress var., island data anal. 4-100579
- photochemical model of trace gases in marine surface layer 4-115528
- planetary boundary layer, parameterisation for use in forecasting models 4-110215

**atmospheric boundary layer continued**

- planetary boundary layer, unstable stratification, quasi-steady simulation 4-82163
- planetary boundary layer-ecosystem interaction; heat and moisture fluxes 4-94196
- plume dispersion calcs. using Boussinesq approx., strongly-buoyant case 4-82155
- pollutant diffusion from ground source (*Russian*) 4-114990
- pollutant transport and diffusion calcs. over uneven terrain, microcomputer model 4-66829
- radar coverage and anomalous propag. through inhomogeneous atmospheres (*French, English*) 4-67384
- radar technique for monitoring boundary layer structure 4-115594
- radioacoustic method for boundary layer temp. and wind sounding (*Russian*) 4-115599
- Ross Sea polynya in Terra Nova Bay, forced by katabatic wind 4-85692
- roughness length, meas. of vertical var. at Boulder Atmospheric Observatory 4-105621
- San Francisco Bay, USA, gas transfer across sediment-water-air interfaces 4-85707
- Sardinia, 3D airflow over island 4-62910
- sea ice air drag coeffs. meas. over Bering Sea 4-85691
- sea ice formation in turbulent Ekman layer, role of atm. boundary layer 4-67238
- sea surface, drag, heat and moisture transfer coeffs. 4-82164
- sea surface gas transfer, model for rough conditions 4-67283
- sea surface microwave emissivity depend. on friction vel. 4-67277
- sea-breeze-like wind over Gulf Stream due to water temp. front 4-67328
- shipboard deployment of meteorological instruments at end of horizontal boom 4-110302
- Sierras de Cordoba, Argentina, energy balance of surface boundary layer during rainy season 4-105671
- smoke plume from steam power station chimney, trajectory calc., math. model (*Russian*) 4-81600
- snow and ice covered ground, heat and moisture vertical fluxes 4-77618
- bare soil surface, vertical flux of heat and moisture 4-77567
- South Polar Plateau, surface temp. regime, energy balance etc. 4-115540
- Srinagar, India, space charge behaviour before rain 4-67312
- stationary planetary waves form. in Northern Hemisphere, role of Greenland Plateau (*Chinese*) 4-67364
- steam fog occurring in condensation nuclei free air 4-80200
- stratocumulus-topped marine boundary layer, mixed layer modeling 4-115516
- structure functions in atmospheric surface layer estimates of power-band exponents  $\mu$  and  $\mu_0$  4-105625
- sulphate pollution accumulation in sea-/land-breeze system 4-67321
- surface layer over crops,  $\text{CO}_2$ , wind, temp. and humidity fluctuations 4-77580
- surface layer wind and summer pack ice drift in AIDJEX 4-89926
- surface pressure and temp. rel. to sea ice extent predictability 4-89948
- surface temperatures, effects of  $\text{CO}_2$ , volcanic aerosols and solar radiation var. 4-94238
- surface torques, friction torque and mountain torque estimates from global atmospheric data 4-72654
- surface wind and sea ice motion, appl. to Beaufort Sea 4-90014
- surface wind stress and sea ice modelling 4-89936
- Taylor columns over Earth surface topography, temporal evolution 4-62843
- temperature of air and soil during nighttime for frosty conditions, model 4-115544
- temperature prediction for complex terrain area, statistical model 4-77577
- temperature profile from sunlight refr. anal. (*Russian*) 4-82167
- tracers transport and dispersion in nocturnal drainage flows, pollutant appl. 4-100648
- trade-wind boundary layer, thermodynamic structure, downstream vars. 4-62899
- transpiration and evaporation from weather moorland, meas. 4-105619
- transport models for complex terrain, appl. to mesoscale transport of pollutants 4-100668
- transport models for complex terrain, appl. to pollutant dispersion 4-100667
- tropical air-sea heat flux, usefulness of shipboard meas. for detect. of secular changes 4-100582
- tropospheric evaporation duct, height evaluation (*French*) 4-82215
- turbulence, parametrization of viscous dissipation and kinetic energy 4-72625
- turbulent diffusion equation with mean vertical wind 4-82212
- turbulent dispersion concentration patterns 4-67301
- turbulent exchange coeff. in convective planetary boundary layer 4-110193
- turbulent structures and turbulence meas. technique 4-115494
- two dimensional spatial deterministic model for prediction of wind characteristics 4-85729
- unsteady convective vortices model 4-67302
- vegetated land surface, heat and moisture vertical flux calc. 4-77617
- vehicular pollution in city streets, numerical model of dispersion 4-89479
- vertical diffusion exchange between friction layer and free atmosphere 4-77589
- vertical dispersion of elevated releases in stable boundary layer, model 4-93659
- vertical wind velocity changes meas. at Turbigo, Italy 4-67298
- Westaco Luke Mill, Maryland, pollutant dispersion and transport, complex terrain model 4-100018
- wind at ocean surface, remote sensing by satellite radar method 4-67469
- wind at ocean surface, remote sensing method using Seasat scatterometer 4-67470
- wind engineering, conf., Gold Coast, Australia (March 1983), and Auckland, New Zealand (April 1983) 4-63391
- wind field in marine surface layer, influenced by mesoscale convection 4-115495
- wind flow over complex terrain, variational-kinematical model 4-115488
- wind measurement by lidar, on-line data system for cw laser Doppler anemometer 4-110263
- wind oscillations at Edinburgh, Scotland, due to travelling gravity waves 4-67333
- wind profile measurement technique using CW Doppler radar 4-82253
- wind speed shears for frontal and undisturbed synoptic conditions, comparison 4-105624
- winds over ocean, meas. technique based on seafloor acoustic observations 4-85686

**atmospheric boundary layer continued**

- $\text{CO}_2$  and  $\text{H}_2\text{O}$  turbulent transport in boundary layer, observations and meas. technique 4-115583
  - $\text{O}_3$  destruction by pine forests 4-67303
  - $\text{O}_3$  in boundary layer of Philadelphia, USA, transport by turbulence and clouds 4-115525
- atmospheric chemistry**  
*see also atmospheric composition*
- Arctic haze pollution, trace gas concs. and lifetimes in atmosphere 4-105653
  - book 4-86130
  - cloudiness effects on photolysis and  $\text{O}_3$  formation in unpolluted troposphere 4-72669
  - conference on Mount St. Helens' 1980 eruptions, at Washington, DC, United States (November 1980) 4-101575
  - dimethyl sulphide chem. reaction with  $\text{NO}_3$  radical in nighttime atmosphere 4-89975
  - Dinosaur Park badlands, Alberta, Canada, rainfall chem., effect on solute and sediment on microcatchments 4-100636
  - electrical conductivity of thermosphere and low and middle atmosphere, solar activity effects 4-85826
  - F-region, recombination dynamics 4-110352
  - geochemistry (book) 4-73192
  - ionosphere depletion expts., snowplough effects or plasma recomb. model for depletion core form 4-100851
  - mesosphere, radiative-photochemical theory for  $\text{O}_3$  concs. 4-62924
  - monoterpenes chem. reaction with  $\text{NO}_3$  radical in nighttime atmosphere 4-89975
  - Mount St. Helens, 1980 May eruptions, atm. perspective 4-105513
  - Mount St. Helens, stratospheric clouds, physical and chem. processes modelling (May-June 1980) 4-105692
  - night-time chemistry of  $\text{NO}_3$  radicals and HONO, implications of simultaneous meas. 4-105660
  - red auroral arc, sunlight effects on chem. processes 4-100841
  - sea surface gas transfer, model for rough conditions 4-67283
  - snow  $\text{O}$  isotope composition prediction model for glacier core climate studies 4-115522
  - stratiform cloud photochemistry in remote marine locations 4-115524
  - stratosphere, common source for acetonitrile ( $\text{CH}_3\text{CN}$ ) and methanol ( $\text{CH}_3\text{OH}$ ) 4-94192
  - stratosphere, modified diabatic circulation model for tracer transport and photochemistry 4-62923
  - stratosphere, north-south asymmetries of solar particle events in stratospheric  $\text{O}_3$  4-110229
  - stratosphere photochemistry, implications of new  $\text{O}_2$  UV absorpt. spectra obs. 4-107357
  - surface layer over ocean, trace gas profile by photochemical model 4-115528
  - thermosphere, general circulation model with coupled dynamics and comp. 4-72769
  - thermosphere, neutral and ion chemistry 4-63003
  - thermosphere, NO conc. and IR emission assoc. with mag. storm heating 4-110333
  - thermosphere, O concentration, eddy diffusivity and circulation 4-72767
  - lower thermosphere and mesosphere photochemistry 4-72774
  - NE USA, regional photochemical air quality model 4-115485
  - volcanic eruption cloud from El Chichon, chemistry of  $\text{SO}_2$ ,  $\text{H}_2\text{S}$  and sulphate 4-115533
  - volcanic eruptions and climate 4-105514
  - water vapour, photodissociation in mesosphere 4-110230
  - $\text{CO}$  in Earth's atmosphere, effects of increasing trend on trace gases and  $\text{O}_3$  layer 4-100045
  - $\text{CO}_2$  in atmosphere in AD 1860 to 2050 period, C cycle calcs. 4-67345
  - Cl in stratospheric  $\text{O}_3$  layer and diurnal ClO var. 4-110234
  - Hg, air-sea exchange 4-82092
  - $\text{N}_2 + \text{O}(\text{O})$ , metastable mol. quenching reaction 4-87195
  - $\text{N}_2^+ + \text{O}_2$ , charge transfer study 4-87214
  - $\text{NH}_3$  partitioning between gaseous and aqueous phases 4-77590
  - NO in upper atmosphere, concs. influenced by planetary waves 4-82318
  - $\text{NO}^+$  ionospheric chemistry 4-67528
  - $\text{NO}^+$ , stepwise hydration, struct., ab initio calcs. 4-81402
  - $\text{NO}_2$  radical, in nighttime atmosphere of S California, USA 4-100028
  - $\text{NO}_2$  radical nighttime reactions with biogenic organic cpds. 4-89975
  - $\text{NO}_x$  releases and photochemistry of troposphere with more than one steady state 4-77607
  - $\text{N}_2\text{O}$  production by lightning 4-67319
  - O layer in lower thermosphere, latitudinal and seasonal variations 4-72766
  - $\text{O}_2$  seasonal var. in lower atmosphere 4-77678
  - $\text{O}^+ + \text{O}$  in thermosphere, control of auroral source of magnetospheric  $\text{O}^+$  ions 4-72786
  - $\text{O}_2$  photodissociation in mesosphere and thermosphere in Schumann-Runge bands 4-77679
  - $\text{O}_3$  conc. in urban Florida, USA, due to natural processes 4-115484
  - $\text{O}_3$  destruction by pine forests 4-67303
  - $\text{O}_3$  vertical profiles in mesosphere and thermosphere 4-115642
  - $\text{O}(\text{S})$  production in high latit. upper atmosphere, implications of 1302 Å absorpt. meas. of O concs. 4-105784
  - $\text{O}_2(\text{e}^-\Sigma_g^-)$ , nighttime, vibr. distrib. and relax., altitude depend., O ( $^1\text{S}$ ) form. 4-105785
  - Si geochemical processes (book) 4-78057
- atmospheric composition**  
*see also atmospheric chemistry; atmospheric structure*
- acetonitrile in atmosphere surface layer near Tucson, Arizona, USA 4-100676
  - acid deposition, techniques for determ. of source-receptor relations 4-100025
  - acid rain, meas. of mesoscale wetfall chemistry around Philadelphia during frontal storms 4-105145
  - aerosol content measurement, use of light extinction model 4-110251
  - aerosol in atmos., optical depth and aerosol distrib. from sky brightness observations (*Spanish*) 4-115574
  - aerosol in coastal boundary layer, meas. technique of satellite optical imagery 4-100742
  - aerosols, quartz content and elemental composition in US cities 4-100649
  - aerosols distrib. in stratospheric, determ. using satellite-based instrument, SAGE II expt. 4-115587
  - Antarctica, aerosol content rel. to meteorological conditions 4-115547
  - Arctic, Western Hemisphere, variations 4-62905
  - Arctic aerosol at Barrow, Alaska, USA, giant particles 4-105644

## atmospheric composition continued

- Arctic aerosol front observations in Norwegian Arctic 4-105639  
 Arctic atmosphere, acidic sulphate particles in winter 4-105648  
 Arctic atmosphere, brominated organic gas content 4-105651  
 Arctic atmosphere containing volcanic debris from El Chichon 4-105649  
 Arctic atmosphere over Spitsbergen, organic gas composition obs. 4-105650  
 Arctic haze, AGASP program and instrumentation for pollution monitoring 4-105722  
 Arctic haze, airborne observations near Barrow, Alaska, USA 4-105643  
 Arctic haze, microparticle size distrib. 4-105646  
 Arctic haze, observations made at Alert, NWT, Canada 4-105642  
 Arctic haze, vertical distrib. of particulate C, S, Br 4-105641  
 Arctic haze and giant particles, origins and air mass trajectories 4-105645  
 Arctic haze observations at Barrow, Alaska (AGASP program) 4-105640  
 Arctic haze observations in March 1983 over Alaskan Arctic 4-105638  
 Arctic haze pollution, trace gas concs. and lifetimes in atmosphere 4-105653  
 Arctic particulate matter elemental composition observations 4-105647  
 Athens, Greece, positive ion conc. and wind characts. 4-115492  
 Bahia State, Brazil, rain comp. and chem. weathering of rocks 4-100560  
 balloon mounted  $\gamma$ -spectrometers,  $\gamma$ -ray background induced by atmospheric neutrons 4-67512  
 Boulder, Colorado, USA, aerosol element composition 4-67323  
 Bratislava, Czechoslovakia, turbidity measurements 4-90002  
 bromine containing gases in Arctic atmos., seasonal conc. variations 4-105652  
 bromoform, in Arctic atmosphere 4-105651  
 bromomethanes in Arctic atmosphere (CBrCl<sub>2</sub> and CH<sub>2</sub>BrCl) 4-105652  
 carbonaceous aerosol particles in lower stratosphere, discovery, origin, and implications 4-105659  
 carbonyl compounds in Los Angeles air, concs. of individual compounds 4-100026  
 chlorofluoromethanes, conc. profile of winter stratosphere of Canada 4-115529  
 conference on atm. radiation at Toronto, Canada (June 1981) 4-90300  
 Crimea coast, chemical composition and optical props. of haze (*Russian*) 4-100685  
 dimethyl sulphide chem. reaction with NO<sub>3</sub> radical in nighttime atmosphere 4-89975  
 El Chichon eruption cloud influence on solar radiation in Michigan, USA 4-115572  
 electrical conductivity of thermosphere and low and middle atmosphere, solar activity effects 4-85826  
 ethylene bromide, in Arctic atmosphere 4-105652  
 ethylene dibromide, in Arctic atmosphere 4-105651  
 Mt Etna, 1983 eruption, exchange of volatiles, radioactivity meas. (*French*) 4-115365  
 formic acid in upper troposphere, identification of 1105 cm<sup>-1</sup> band in solar absorpt. spectra 4-100679  
 Grand Canyon, Arizona, USA, pollution, particulates and visibility 4-115564  
 haematite dust at 60 km altitude, spectra and particle size 4-94227  
 hydrocarbons, from Brazil forest and grassland fires 4-67314  
 hydrocarbons in Los Angeles air, concs. of individual compounds 4-100026  
 instrumentation for stratospheric composition, design of balloon borne laser instrument 4-115589  
 interplanetary dust collected from stratosphere, Bi content 4-115712  
 ionosphere, accelerated ions comp. and flux to magnetosphere 4-94292  
 ionosphere, Langmuir probe use 4-105731  
 ionosphere, obs. of hot heavy ions assoc. with Space Shuttle Orbiter 4-110495  
 isoprene chem. reaction with NO<sub>3</sub> radical in nighttime atmosphere 4-89975  
 Kara Sea, hydrocarbons in snow, ice and seawater 4-105600  
 laser for remote sensing, mini-TEA 1 kHz CO<sub>2</sub> laser design 4-107662  
 lidar remote sensing of atmosphere, signal processing problems (*Russian*) 4-72705  
 limb obs. by rocket at 4.3 microns wavelength 4-110195  
 magnetosphere, ion comp. meas. in magnetotail between 60 and 240 Earth radii 4-100881  
 Central Mediterranean, dust in atmosphere 4-72672  
 mesosphere O<sub>3</sub> concentrations, theory and obs. 4-62924  
 methane, NIMBUS 7 SAMS obs. rel. to in situ data and 2-D model calcs. 4-100690  
 methyl bromide, in Arctic atmosphere 4-105651  
 methyl bromide, in Arctic atmosphere 4-105652  
 methylene bromide, in Arctic atmosphere 4-105651  
 methylene bromide, in Arctic atmosphere 4-105652  
 monoterpenes chem. reaction with NO<sub>3</sub> radical in nighttime atmosphere 4-89975  
 Mount St. Helens, eruption loud (April 1980), chem. comp. and ash characts. 4-105515  
 Mount St. Helens 1980 May eruptions, stratospheric tephra and aerosols, comp. and plume characts. 4-105687  
 Mount St. Helens eruption plumes (1980) at stratospheric altitudes, aerosol precursor gases anal. 4-105684  
 neutron detection from lightning bolts using Pb-free monitors 4-100832  
 night-time measurements of NO<sub>2</sub> radicals and HONO, implications for atmospheric chemistry 4-105660  
 NIMBUS 7 SAMS data use for comp. retrieval 4-100691  
 nonmethane hydrocarbon in continental and marine atmos. 4-115526  
 nonmethane hydrocarbons in urban and rural USA 4-114980  
 Northern Ireland, Saharan dust washout in rain, Sept. 1983 obs. 4-82209  
 Norwegian Arctic, S pollutants annual and seasonal variations 4-105637  
 nuclear particle identification in space plasma research, review 4-100820  
 Pacific Ocean, atm. surface layer Hg conc., correl. with marine upwelling and biological prod. 4-105599  
 San Francisco Bay, USA, gas transfer across sediment-water-air interfaces 4-85707  
 Santander and Torrelavega, Spain, urban SO<sub>2</sub> and particulate levels (*Spanish*) 4-114992  
 stratiform clouds of S Carolina, USA, acidity and chem. composition 4-67322  
 stratosphere, BUV polarization inversion, O<sub>3</sub> and aerosol profiling 4-62960  
 stratosphere, common source for acetonitrile (CH<sub>3</sub>CN) and methanol (CH<sub>3</sub>OH) 4-94192

## atmospheric composition continued

- stratosphere, O<sub>3</sub> distrib. in modified diabatic circulation model for tracer transport 4-62923  
 lower stratosphere, radiative heating, rel. to O<sub>3</sub> distrib. in two-dimensional model 4-62920  
 stratosphere H<sub>2</sub>SO<sub>4</sub> aerosols, contrib. of small-volume S-rich volcanic eruptions 4-105511  
 stratosphere NO<sub>2</sub> conc., spectral obs. 4-115542  
 stratosphere O<sub>3</sub> depressions following solar particle events, north-south asymmetries 4-110229  
 stratosphere O<sub>3</sub> determ., SAGE and SBUV methods comparison 4-100801  
 stratosphere O<sub>3</sub> determ. by SAGE, comparison with other methods 4-100804  
 stratosphere temperature and chem. composition remote sensing by satellite IR limb scanning method 4-105753  
 stratospheric multispecies trace gas meas. using balloon borne tunable diode laser absorption spectrometer 4-115591  
 stratospheric O<sub>3</sub> effects of injected Cl and water vapour from Mount St. Helens 4-105692  
 stratospheric SO<sub>2</sub> and O<sub>3</sub> from Mount St. Helens 1980 May eruptions 4-105694  
 submillimetre FT spectrometer for stratosphere spectra and chem. composition 4-110268  
 sulphate and nitrate aerosols, particle size model 4-114981  
 sulphate layer near tropopause sampling after Mount St. Helens 1980 May 18 eruption 4-105695  
 sulphate pollution accumulation in sea-/land-breeze system 4-67321  
 surface layer over ocean, trace gas profile by photochemical model 4-115528  
 thermosphere, general circulation model with coupled dynamics and comp. 4-72769  
 thermosphere, NO conc. and IR emission assoc. with mag. storm heating 4-110333  
 thermosphere, O concentration, eddy diffusivity and circulation 4-72767  
 thermosphere, superrotation and struct. of atmosphere, model 4-110335  
 thermosphere, two-dimens. high resolution nested grid model, neutral response to elec. field spike 4-85807  
 topside ionosphere, light ions winter nighttime abundances 4-85815  
 trace gas measurements using airborne tunable diode laser system 4-115588  
 trace gas mixing ratios obtained from occultation spectra, effects of systematic errors 4-110186  
 trace metals in Bermuda rainwater, of continental origin 4-67320  
 trichlorofluoromethane, for infrared spectra and composition of stratosphere and troposphere 4-72697  
 tropospheric air trace gas meas. using tunable diode laser absorpt. spectrometer 4-114998  
 twin filter detector for radon daughter spectra 4-93672  
 NE United States, rural area, organic matter in particulates 4-67315  
 upper atmosphere circulation; temp. and composition model and geomag. activity influences 4-67515  
 volcanic aerosol from El Chichon, size and mass distrib. 4-115534  
 volcanic dust from El Chichon in atmos. of New England, USA, atmos. optical phenomena obs. 4-110249  
 Western Mediterranean Sea, ozone climatology, 1968-1976 4-105668  
<sup>210</sup>Bi, aerosol radioactivity meas., Covansa mofette atmosphere (*Rumanian*) 4-72674  
 Br<sub>2</sub> and Br compounds in stratosphere 4-115530  
 C, global cycle in atmosphere-ocean-biosphere system, models 4-72681  
 C isotope record in pinyon pine tree rings, variability within and between trees 4-115607  
 CO from Brazil forest and grassland fires 4-67314  
 CO in Earth's atmosphere, increasing trend (1979 to 1983) 4-100045  
 CO<sub>2</sub> and global C balance, climate interactions 4-94228  
 CO<sub>2</sub> and greenhouse effect 4-82228  
 CO<sub>2</sub> and H<sub>2</sub>O turbulent transport in boundary layer, observations and meas. technique 4-115583  
 CO<sub>2</sub> as an inverse greenhouse gas 4-110194  
 CO<sub>2</sub> changes in atmosphere due to marine biota at high latitude 4-115521  
 CO<sub>2</sub> conc. var. due to oceanic primary productivity fluctuation 4-94182  
 CO<sub>2</sub> concentration, new model for determining role of oceans 4-62908  
 CO<sub>2</sub> concentration, rapid vars. during ice age related to ocean circulation 4-62909  
 CO<sub>2</sub> effects on climate modelling 4-110243  
 CO<sub>2</sub> fluctuations over a crop surface 4-77580  
 CO<sub>2</sub> in atmosphere, of Pacific, concentration variations and isotopic composition 4-115520  
 CO<sub>2</sub> in atmosphere in AD 1860 to 2050 period, C cycle calcs. 4-67345  
 CO<sub>2</sub> induced climatic change and spectral vars. in outgoing IR radiation 4-115558  
 COS in stratosphere, meas. in El Chichon volcanic plume 4-105658  
<sup>14</sup>C behaviour in atmosphere (*Russian*) 4-77162  
<sup>14</sup>C exchange between atmosphere and oceans 4-72682  
<sup>14</sup>C prod. var. and solar modulation of galactic cosmic rays 4-94424  
 Cl and S from volcanic eruptions 4-115366  
 CO<sub>2</sub> diurnal var. in stratospheric O<sub>3</sub> layer and Cl chemistry 4-110234  
<sup>35</sup>Cl( $\alpha$ )<sup>32</sup>P, lithosphere reactions, neutron flow, radiation: chronology (*Russian*) 4-73897  
 D, optical detect. in upper atmosphere by Spacelab 1 mission 4-90016  
 HCl in stratosphere, trace meas. using tunable diode laser absorption 4-89997  
 HNO<sub>3</sub> conc. in southwestern USA atmosphere 4-115527  
 HNO<sub>3</sub> conc. profile of Canadian stratosphere in winter 4-115529  
 HNO<sub>3</sub>, for infrared spectra and composition of stratosphere and troposphere 4-72697  
 HNO<sub>3</sub> in middle atmosphere, conc. monitoring by IR Earth limb scanning from satellite 4-105757  
 HNO<sub>3</sub> in stratosphere, spectral obs. for comparison with NIMBUS-7 LIMS method 4-105666  
 H<sub>2</sub>O isotopic composition at Palisades, New York, USA 4-115539  
 H<sub>2</sub>O vapour in stratosphere, LIMS infrared monitoring method from NIMBUS-7 satellite 4-105752  
 H<sub>2</sub><sup>18</sup>O and HDO atmospheric cycles, general circulation model 4-115551  
 H<sub>2</sub>O<sub>2</sub> in Greenland ice core samples 4-115552  
 He<sup>+</sup> dominance regions in high-latit. topside ionosphere, role of plasma convection 4-110363  
 Hg, volcanogenic contrib. determ. from annual Hg flux at Kilauea main vent 4-72559  
 N and NO in upper atmosphere, global distrib. model 4-67516

## atmospheric composition continued

- NH<sub>3</sub>, conc. in southwestern USA atmosphere 4-115527  
 NH<sub>3</sub>, partitioning between gaseous and aqueous phases 4-77590  
 NO flux from thermosphere to mesosphere 4-100834  
 NO in upper atmosphere, concs. influence by planetary waves 4-82318  
 NO meas. using balloon-borne chemiluminescent sonde 4-115617  
 NO, stratospheric, in situ meas. using balloon-borne tunable diode laser spectrometer 4-72706  
 NO<sub>2</sub> in Antarctic springtime stratosphere 4-94189  
 NO<sub>2</sub> in atmosphere, meas. method using NIMBUS 7 satellite IR limb monitor 4-105751  
 NO<sub>2</sub> in stratosphere, mixing ratio, vertical profiles 4-77602  
 NO<sub>2</sub> in stratosphere, SMB results 4-72668  
 NO<sub>2</sub> in stratosphere, spectral obs. for comparison with NIMBUS-7 LIMS method 4-105666  
 NO<sub>2</sub>, nocturnal troposphere in rural New Zealand, long-path absorption meas. 4-94188  
 NO<sub>2</sub>, remote monitoring using DIAL based mobile lidar system 4-77167  
 NO<sub>2</sub>, radical, in nighttime atmosphere of S California, USA 4-100028  
 NO<sub>2</sub>, conc. profile of Canadian stratosphere in winter 4-115529  
 N<sub>2</sub>O, NIMBUS 7 SAMS obs. rel. to in situ data and 2-D model calcs. 4-100690  
<sup>14</sup>N( $\alpha$ )<sup>14</sup>C, lithosphere reactions, neutron flow, radiation chronology (Russian) 4-73897  
 Na clouds in lower thermosphere, prod. by meteoroid ablation 4-110336  
 O and N<sub>2</sub> changes in thermosphere rel. to topside ionisation depletion event 4-67514  
 O, conc. at lower ionosphere altitudes in auroral zone 4-100835  
 O concentrations in high latit. winter upper atmosphere, 1302 Å absorpt. meas. 4-105784  
 O II in upper atmosphere, UV emissions as contaminants of geocoronal He airglow obs. 4-105787  
 O<sub>2</sub> in lower thermosphere, two-photon differential absorpt. meas. technique 4-82243  
 O<sub>2</sub> layer in lower thermosphere, latitudinal and seasonal variations 4-72766  
 O<sub>2</sub>, seasonal var. in lower atmosphere 4-77678  
 O<sup>+</sup> density depressions in topside nighttime ionosphere, ISS-b satellite obs. 4-63009  
 O<sup>+</sup> ions in magnetosphere, thermospheric control of auroral O<sup>+</sup> source 4-72786  
 O<sub>2</sub> in early atmosphere, evidence from cosmic spherules in deep-sea sediments 4-85900  
 O<sub>3</sub> conc. in urban Florida, USA, due to natural processes 4-115484  
 O<sub>3</sub>, conc. profile of Canadian stratosphere in winter 4-115529  
 O<sub>3</sub> content of stratosphere influenced by solar activity cycle 4-67316  
 O<sub>3</sub> distrib. in stratosphere, determ. using satellite-based instrument, SAGE II expt. 4-115587  
 O<sub>3</sub> electrochemical sonde for meas. of tropo- and stratosphere profiles 4-67436  
 O<sub>3</sub>, height profile in upper atm. from occultation meas. of star (Russian) 4-82317  
 O<sub>3</sub> in Beijing area, China, basic state of ozonosphere and correl. with meteorological factors (Chinese) 4-67362  
 O<sub>3</sub> in boundary layer of Philadelphia, USA, transport by turbulence and clouds 4-115525  
 O<sub>3</sub> in high-latitude stratosphere during winter, spatial variability 4-94218  
 O<sub>3</sub> in middle atmosphere, profile remote sensing by satellite IR limb scanning method 4-105756  
 O<sub>3</sub> in stratosphere, conc. modifications, Bayesian probability calcs. 4-77603  
 O<sub>3</sub> in stratosphere, conc. trends from Umkehr O<sub>3</sub> profile data 4-115532  
 O<sub>3</sub> in stratosphere, concentration changes observed by NIMBUS 7 LIMS expt. 4-105667  
 O<sub>3</sub> in stratosphere, semiannual oscillation observations 4-110207  
 O<sub>3</sub> in stratosphere, spectral obs. for comparison with NIMBUS-7 LIMS method 4-105666  
 O<sub>3</sub>, meas. with NIMBUS 7 SBVU-TOMS instruments 4-100800  
 O<sub>3</sub> profile for 1979, NIMBUS-7 SBVU instrument obs. 4-100689  
 O<sub>3</sub> profiles determ., use of 290-305 nm wavelengths 4-100798  
 O<sub>3</sub> profiles determ., use of NIMBUS 7 SBVU instrument 4-100799  
 O<sub>3</sub>, total amount determ. from TIROS radiance meas. 4-100672  
 O<sub>3</sub>, vertical profiles in mesosphere and thermosphere 4-115642  
 OH conc. at ground level, optical absorption meas. 4-72666  
 O<sub>2</sub>(<sup>2</sup>Σ<sub>g</sub><sup>-</sup>), nightglow, vibr. distrib. and relax., altitude depend., O (<sup>1</sup>S) form. 4-105785  
<sup>212</sup>Pb, aerosol radioactivity meas., Covasna mofette atmosphere (Rumanian) 4-72674  
<sup>214</sup>Pb, aerosol radioactivity meas., Covasna mofette atmosphere (Rumanian) 4-72674  
 Rn and daughters conc. indoors, mathematical model 4-93916  
 Rn, daughter activities, meas. instrumentation 4-93867  
 Rn, daughter activity concs. indoors, approx. meas. technique 4-93866  
 Rn daughters, deposition rates on indoor surfaces 4-93917  
 Rn daughters, turbulent plateau in rooms and mines 4-93920  
 Rn daughters aerosol, activity size distrib. in buildings, cascade impactor meas. 4-93918  
 Rn daughters in indoor air, aerosol and activity size distrib. 4-93915  
 Rn daughters in indoor air, aerosol particle conc. rel. to ventilation system 4-93922  
 Rn detection in Finnish dwellings, film detectors calibration 4-93895  
 Rn emanometry in active volcanoes using LR-115 track detectors 4-100516  
 Rn, measurement in dwellings using activated charcoal 4-93897  
 Rn, methodology for meas. with passive instruments 4-93673  
<sup>222</sup>Rn and daughter product concs. in dwellings and open air, equilib. factor 4-93919  
<sup>222</sup>Rn and decay products, active and passive dosimetry, international intercomparison 4-93864  
<sup>222</sup>Rn exhalation rate from surface of building materials or soil, meas. apparatus 4-93896  
 SO<sub>2</sub> and particulates in Spanish towns (Spanish) 4-114992  
 SO<sub>2</sub>, conc. in southwestern USA atmosphere 4-115527  
 Xe and noble gases in shales, plastic bag expt. 4-94220

atmospheric density *see atmospheric pressure and density*

atmospheric disturbances *see atmospheric movements; thunderstorms*

atmospheric duct *see atmospheric electromagnetic wave propagation*

atmospheric dynamics *see atmospheric movements*

## atmospheric electricity

- see also atmospheric electromagnetic wave propagation; atmospheric ionisation; atmospheric; aurora; electrojets; ionosphere; lightning; thunderstorms*  
 air-earth current meas., design for eliminating displacement currents 4-90007  
 auroral electrojet, elec. field and plasma density meas. 4-72783  
 auroral F-region, convection elec. fields rel. to non-isotropic ion temp. distrib. 4-105793  
 bow shock, collisionless energy dissipation of plasma, mag. and elec. fields role 4-72800  
 clouds electrically charged water droplet production expts. 4-85734  
 conference at Manchester, England (July to August 1980) 4-101578  
 E-region, electron gas heating due to magnetosphere convection, effect on cond. 4-100847  
 electric field and air-Earth current responses to cond. profiles vars., global circuit model 4-89970  
 electrostatic H cyclotron waves on auroral field lines, ion-beam-driven 4-72826  
 fair weather atmospheric electric variability 4-67313  
 field aligned current transport from ionosphere to magnetosphere, role of ion beams 4-72780  
 field aligned currents rel. to Pi 1 in morning sector 4-67560  
 global electric circuit, anal. 4-77605  
 Hy-wire apparatus for meas. of boundary layer elec. potential 4-67437  
 ionosphere, aurora and electrojet configuration in early morning sector 4-72789  
 ionosphere, cond. vars. at high latits. rel. to correl. between optical and mag. pulsations 4-105789  
 ionosphere, convection electric field as manifestation of magnetosphere convection 4-72790  
 ionosphere, dynamo currents representing geomag. L variation 4-82341  
 ionosphere, elec. current during mag. storms, effect on VHF equatorial scintillation 4-90034  
 ionosphere, elec. current system rel. to induced mag. field at Peruvian dip equator 4-62668  
 ionosphere, elec. field pot. distrib. near electron-injection satellite 4-110353  
 ionosphere, elec. fields rel. to hemispherical Joule heating as function of AE indices 4-72788  
 ionosphere, energy principle for high-latitude electrodynamics 4-85812  
 ionosphere, field-aligned currents interaction with VLF waves 4-100852  
 ionosphere, generation of nonuniform elec. fields and currents assoc. with auroral arcs 4-110370  
 ionosphere, high latitude, electric fields and potential patterns for different situations in interplanetary space 4-110365  
 ionosphere, latit. profile of magnetosphere convection elec. field from mag. and radar data 4-72787  
 ionosphere, local time depend. of response of equatorial electrojet to DP2 and SI disturbances 4-105802  
 ionosphere, mid-latitude, ion vel., electric fields and neutral wind 4-100846  
 ionosphere, plasma drift instabilities and longitudinal currents, auroral rays mechanism 4-94286  
 ionosphere, S<sub>p</sub> current vars. assoc. with periodic VLF emissions rel. to short-period mag. pulsations 4-85836  
 ionosphere, SABRE obs. of morning sector convection reversal assoc. with DPY current system 4-110364  
 ionosphere, seasonal vars. of L equivalent current systems 4-72785  
 ionosphere conductivities, spatial distrib. rel. to control of magnetospheric convection 4-72807  
 ionosphere currents meas. from daily geomag. var., coastal effect at equatorial latits. 4-110044  
 ionosphere dynamo currents, anal. of variability 4-90021  
 ionosphere E and F-regions, nonthermal low energy electrons prod. by dynamo currents 4-63008  
 ionosphere E-region, elec. current-carrying props. of mid-latitude type E<sub>s</sub> 4-82330  
 ionosphere electric current global distrib. during substorm disturbances 4-67534  
 auroral ionosphere electrodynamic parameters, radar sound study 4-100850  
 lightning, optical and elec. field signal from return strokes 4-115536  
 magnetopause, evidence for MHD generator process in solar wind energy transfer regions 4-105814  
 magnetopause, MHD generator model for solar wind energy transfer regions 4-105813  
 magnetosphere, core-field aligned current assoc. with flux transfer events 4-94313  
 magnetosphere, elec. field evidence on viscous interaction at magnetopause 4-94314  
 magnetosphere, electric field pulsations 4-110381  
 magnetosphere, energy var. and elec. fields in collisionless ion-electron plasma 4-100868  
 magnetosphere, field-aligned currents as diagnostic tool for renovated model 4-72806  
 magnetosphere, generation of nonuniform elec. fields and currents assoc. with auroral arcs 4-110370  
 magnetosphere, ISEE 1 and 2 obs. of oscillating outward moving current sheet near midnight 4-85832  
 magnetosphere, penetration of solar wind electric field 4-94305  
 magnetosphere, rapidly moving current structures during substorms, short irregular pulsations origin 4-72812  
 magnetosphere, trans-polar pot. rel. to ring coupling model and magnetosphere ground state 4-72809  
 magnetosphere electric field measurement with spherical double probes on satellites 4-82367  
 magnetosphere field-aligned currents in polar cap 4-110372  
 magnetosphere longitudinal currents, effects on ionosphere electron density profiles 4-94289  
 magnetosphere ring current and convection, control by spatial distrib. of ionospheric conductivities 4-72807  
 mesosphere, ambipolar diffusion rel. to elec. fields and currents 4-72771  
 Mount St. Helens 1980 May 18 eruption, fine particles generation and electrification 4-105693  
 oblique double layers in auroral magnetosphere, effects on upgoing ion pitch angle and gyrophase 4-85841

**atmospheric electricity continued**

- plasma sheet, inner edge, energy dispersion rel. to dusk reactor radial elec. field 4-85843  
 plasmasphere, bulge location var. and convection elec. field (*Chinese*) 4-110347  
 polar cap currents, devel. rel. to auroral electrojets evolution during geomag. disturbances 4-77682  
 polar cap electric field and current distrib., Fourier anal. 4-72791  
 polar cap vertical currents associated with northward interplanetary magnetic field 4-94296  
 radio noise, global distrib. study using satellite obs. of thunderstorm activity (*Japanese*) 4-63015  
 raindrop shape affected by elec. charge and elec. field 4-85743  
 ring current, obs. during intense mag. storms rel. to dynamic variation of auroral oval 4-72776  
 ring current characts. from surface mag. field anal. 4-94306  
 ring current injection, assoc. geomag. field var., cosmic ray penetration use in anal. 4-94303  
 Sq current loop positions over Africa 4-82323  
 Srinagar, India, space charge behaviour before rain 4-67312  
 surf zone waves creating electric charge in atmosphere 4-110203  
 lower thermosphere, Hall conductivity rel. to quasi-two-day variation of wind vels. (*Russian*) 4-67513  
 thermosphere, two-dimens. high resolution nested grid model, neutral response to elec. field spike 4-85807  
 thermosphere and low and middle atmosphere, solar activity effects 4-85826  
 thunderstorm elec. field reduction by corona discharge from land surface 4-67324  
 water drop collisions, charge separation, contact-balloelectric mechanism 4-72676  
 westward travelling surge, mechanism involving magnetosphere Hall current blockage and ionosphere charge buildup 4-72781

**atmospheric electromagnetic wave propagation**

- see also Atmospheric light propagation; ionospheric electromagnetic wave propagation; magnetospheric electromagnetic wave propagation; tropospheric electromagnetic wave propagation*  
 1.140 micron solar radiation attenuation and water vapour content 4-94259  
 12 GHz rain attenuation meas. using Japanese BSE satellite 4-77608  
 144 MHz sporadic-E propag. modes 4-85730  
 Allan variances, calc. for rain attenuated microwave geostationary satellite beacon, and appl. to site diversity switching 4-89964  
 amplitude scintillations observations on low-elevation Earth-space path 4-62902  
 atmospheric coherent and incoherent X-ray scattering, photon counting investig. 4-82166  
 drop-size distribution: cross-polarization discrimination and attenuation for propagation through rain 4-100661  
 earth terminal-to-satellite link availability using new rain event duration statistics 4-67372  
 EHF attenuation in atmosphere due to water vapour 4-77614  
 electrical breakdown of upper atm. due to radiowaves, calc. of layer characts. 4-90017  
 Fairbanks, Alaska, solar IR and radio emission received, El Chichon dust cloud effects 4-67296  
 FM broadcast reception in coastal and mountainous areas in Norway, reduction of propag. problems 4-82206  
 FM broadcast reception quality in coastal and mountainous areas 4-82205  
 ground, sky and space wave propag. 4-110231  
 lighting generated ELF and VLF transverse reson. in Earth-ionosphere cavity 4-82345  
 microwave atmospheric attenuation, differential emission meas. at 20.3 and 31.4 GHz by radiometry 4-85751  
 microwave attenuation and temp. of atmosphere (*Czech*) 4-85792  
 microwave transmissions, neutral atmosphere effects (*Japanese*) 4-62931  
 millimeter wave advantages for satellite communications 4-67373  
 opacity, quasi-continuous record at 1.1 mm of Mauna Kea observatory 4-110250  
 radar attenuation, effect on satellite meas. of ocean wind 4-67479  
 radar signal scatt. and refl. from turbulent atmos., theory 4-85750  
 radiowave refraction effects in troposphere, removal from satellite Doppler remote sensing data 4-77649  
 radiowave scintillation intensity, meas. and modelling to estimate turbulence parameters in Earth-space path 4-89965  
 rain depolarisation evaluations for microwave satellite/Earth links 4-67371  
 raindrop size distribution, inference from attenuation and rain rate meas. 4-94201  
 refraction correction calc. 4-77611  
 satellite link frequency band choice, propag. factors (*Polish*) 4-85741  
 satellite power systems, laboratory and field experiments on atmospheric environmental effects (*Japanese*) 4-62982  
 satellite power systems, terrestrial EM environmental effects (*Japanese*) 4-62930  
 Sirio SHF experiment, results and appls. to satellite telecommunication systems 4-105700  
 skywave interference signals for 535 to 1605 kHz, pre-selection principles 4-105683  
 submillimeter (0.89 mm) attenuation observations in clear atmosphere 4-77616  
 Sun tracker attenuation meas. at 35 GHz 4-105636  
 transparency meas. using automated digital instrument 4-78358  
 UV occultation of stars through atm. and O<sub>3</sub> height profile determ. (*Russian*) 4-82317  
 water vapour continuum below 300 GHz 4-94202  
 wave propagation in random media, Rytov approximation 4-110236  
 wet air refraction at microwaves, prediction 4-89995

**atmospheric electron precipitation**

- see also aurora; radiation belts*  
 afternoon auroral oval, field-aligned currents, electron beams and density enhancements 4-82338  
 aurora excitation and energy dissipation processes, general description 4-72798  
 auroral double layers and ion conics production 4-67522  
 auroral electron generation process in magnetosphere 4-110375  
 auroral electron precip., correl. between VLF hiss and auroral pulsations 4-110346

**atmospheric electron precipitation continued**

- auroral electron precip., generation of EM ion cyclotron mode (ELF) waves in magnetosphere 4-85842  
 auroral electron precipitation, effects on spatial distrib. of ionospheric conds. and magnetospheric convection 4-72807  
 auroral electrons, generation of nonuniform elec. fields and currents assoc. with auroral arcs 4-110370  
 auroral electrons, intensity meas. rel. to photometry from Atmosphere Explorer C satellite 4-72778  
 auroral electrons, precip. patterns and visual aurora characts. during geomag. quiescence 4-85810  
 auroral electrons acceleration, wave-particle interaction model 4-100853  
 auroral plasma formation by magnetospheric convection and injection 4-110356  
 discrete aurora associated with energetic particle boundaries 4-67519  
 E-region, EISCAT data rel. to GEOS 2 electron flux vars. 4-100857  
 induced precipitation zones around ground-based VLF signal sources, dimensions 4-85813  
 intense low-energy electron flux above 85° geomag. latitude 4-94320  
 inverted-V precipitation, rel. to generation of auroral kilometric radiation by maser synchrotron instability 4-85840  
 inverted-V precipitation and assoc. plasma drift instability, auroral rays mechanism 4-94286  
 ionosphere, electron precip. induced by periodic VLF emissions rel. to short-period mag. pulsations 4-85836  
 ionosphere, spikelike electric field obs. at poleward edge of auroral zone 4-67535  
 ionospheric F-region, corpuscular ionisation, latitudinal depend. during Forbush decrease 4-101051  
 low-latitude auroral types and precipitation mechanisms 4-110344  
 magnetotail, processes in current sheet leading to precipitation 4-110379  
 mid-latitude ionospheric trough and ion densities, electron precipitation and 630 nm emission 4-100845  
 midday gap aurora, powered by low energy electron precipitation 4-100841  
 relativistic electron precipitation, X-ray bremsstrahlung and ELF emission 4-67530  
 thermal electron heating rate due to precipitation and photoelectrons 4-72793
- atmospheric elementary particle precipitation**  
*see also Atmospheric electron precipitation; atmospheric proton precipitation*  
 auroral particles, effects of oblique double layers on upgoing ion pitch angle and gyrophase 4-85841  
 magnetotail particle influx, rel. to onset time interval of geomag. disturbances in conjugate areas 4-110386  
 radiation belt particles, contamination of geocoronal He airglow obs. 4-105787  
 ring-current zone stimulated by ground based VLF transmitter, particle precip. obs. 4-72796
- atmospheric energetics** *see Atmospheric movements*
- atmospheric humidity**  
*see also hygrometers*  
 aerosols water content determ. 4-100726  
 anticyclonic stratocumulus, sympathetic fluctuations of cloud water content and cloud top height 4-62926  
 Arabian Sea, zonal and meridional eddy fluxes of dry and moist energy components 4-110217  
 Beijing, China, environment during thunderstorm season compared with Topeka, Kansas 4-100674  
 Belgium, AD 1983 weather conditions 4-115553  
 Bermuda area of North Atlantic, AD 1981 meteorological obs. 4-105682  
 Bombay, India, radar refractive index vertical var. 4-67342  
 boundary layer CO<sub>2</sub> and H<sub>2</sub>O turbulent transport, observations and meas. technique 4-115583  
 marine boundary layer struct. at Sable Island, Nova Scotia 4-67329  
 boundary layer uncoupled multi-layer model for latent heat flux density 4-105618  
 Bowen's ratio over bare cotton soil, temp. and humidity anal., instrumentation 4-67335  
 NE Brazil, humidity, rain and atmos. circulation 4-115501  
 Canary Islands, mountain site, atm. precipitable water, EHF/THF emission and attenuation anal. 4-89968  
 cloudless atmosphere integral humidity content from radio emission meas. (*Russian*) 4-115600  
 clouds, stability criterion for moist compressible atmosphere (*Russian*) 4-67310  
 clouds liquid water content meas., appl. of passive optical device 4-62978  
 convective boundary layer, turbulent profiles, urban effects 4-72648  
 corrosion of C steel, influence of pollution, humidity, temp., solar rad. and rainfall 4-85244  
 cumulus clouds, importance of cloud top lifetime in description of cloud characts. 4-100670  
 Dead Sea area during advective sharav condition 4-94184  
 differential absorption LIDAR in space for atmospheric temperature and humidity profiles 4-110331  
 direct insertion type zirconia oxygen analyzer hygrometer, Fuji Electric 4-111142  
 EHF attenuation in atmosphere due to water vapour 4-77614  
 forecasting methods 4-72683  
 global atmospheric water vapour maps, Nimbus 7 obs. 4-67411  
 gradient distributions and flux profile relations above rough forest, implications for evapotranspiration 4-82204  
 ice nuclei, meas. using continuous flow chamber 4-62980  
 IR hygrometer appl. to convective phenomena anal. 4-94259  
 IR sounder for moisture and temp. meas., design requirements 4-62959  
 isotopic composition of water vapour at Palisades, New York, USA 4-115539  
 Jilin province, China, water vapour supply for heavy rain events (*Chinese*) 4-67368  
 laboratory clouds, control of liq. water content and drop size distrib. 4-62927  
 laser remote sensing of humidity profile, lidar signal processing problems (*Russian*) 4-72705  
 lidar, quantitative 532 nm data for vertical extinction profiles, relative humidity effect 4-100755  
 lidar method for H<sub>2</sub>O vapour profile remote sensing 4-110267  
 marine atmospheric, interannual moisture vars. near surface of tropical Pacific Ocean 4-82200

**atmospheric humidity continued**

- mesosphere, photodissoc. of water vapour by solar UV radiation 4-110230
- microwave propagation, effects of water vapour, rain, humidity, temp. and press. 4-100716
- moist convective adjustment scheme, convergence 4-67356
- monsoon depressions, equivalent pot. temp., convection, cloud heights and humidity zones 4-110224
- NIMBUS-7 SMMR observations and results summary 4-100592
- planetary boundary layer-ecosystem interaction, heat and moisture fluxes 4-94196
- positive wire to plane coronas, atmospheric humidity effect on inception voltage 4-97937
- potential evaporation, influence of atmospheric stability 4-100666
- precipitable water over global oceans, NIMBUS 7 SMMR data anal. 4-100693
- precipitable water vapour determ., implications for sea surface temp. accuracy in remote sensing obs. 4-67406
- remote sensing of humidity and wind over sea by satellite microwave radiometry method 4-82302
- satellite observations, use for dewpoint anal. 4-115490
- Scanning Multichannel Microwave Radiometer data anal. and atm. water content 4-67475
- sea surface, drag, heat and moisture transfer coeffs. 4-82164
- SEASAT SMMR data quality for atm. water determ. 4-67474
- Shanghai, China, pollutant influence on humidity and precipitation distrib. 4-94194
- Sieras de Cordoba, Argentina, evapotranspiration and energy balance of surface boundary layer 4-105671
- steam fog occurring in condensation nuclei free air 4-80200
- lower stratosphere, aircraft meas. of humidity between 45°N and 65°N, (1977 to 1980) 4-82192
- stratosphere humidity remote sensing by satellite IR limb scanning 4-105752
- stratosphere water vapour distrib. determ. using satellite-based instrument 4-115587
- stratospheric humidity, NIMBUS 7 LIMS monitoring method 4-105666
- surface layer dynamics, three-dimensional heat and moisture transport modelling 4-72684
- surface layer over crops, CO<sub>2</sub>, wind, temp. and humidity fluctuations 4-77580
- Tokyo, Japan, temperature and humidity data (1976 to 1980) 4-105675
- Topeka, Kansas, environment during thunderstorm season compared with Beijing, China 4-100674
- transpiration and evaporation from weather moorland, meas. 4-105619
- tropospheric and stratospheric parameter meas. using ground-based coherent lidar 4-100662
- tropospheric evaporation duct, height evaluation (French) 4-82215
- vertical distribution in the Mediterranean, Red Sea and Indian Ocean 4-77600
- water vapour, radiowave propagation delays study 4-89966
- water vapour content, radiative effects 4-115496
- water vapour continuum below 300 GHz 4-94202
- water vapour profiles, IR radiation satellite meas. (Chinese) 4-115596
- water vapour totals and multichannel sea surface temp. retrieval 4-67407
- water vapour transport in stratosphere-troposphere general circulation model, fluxes 4-82193
- water vapour transport in stratosphere-troposphere general circulation model, trajectories 4-82194

**atmospheric ionisation**

- see also atmospheric radioactivity; ionosphere
- anisotropic ionisation in ionosphere (French) 4-77681
- electrical conductivity of thermosphere and low and middle atmosphere, solar activity effects 4-85826
- F<sub>2</sub>-layer, electron density modulation by 160-minute solar pulsations rel. to micropulsation amplitudes 4-105803
- F<sub>2</sub>-layer ionospheric electron content of Wuchang, China, VHF obs. 4-115659
- F-region, recombination dynamics 4-110352
- ionosphere, elec. field and plasma density meas. in auroral electrojet 4-72783
- ionosphere, field-aligned irregularities rel. to direct multiple path magnetospheric propag. for VLF waves 4-85839
- ionosphere, obs. of hot heavy ions assoc. with Space Shuttle Orbiter 4-110495
- ionosphere depletion expts., snowplough effects or plasma recomb. model for depletion core form 4-100851
- ionosphere photoionisation, inconsistency of EUV and photoelectron fluxes 4-110362
- mesosphere, ambipolar diffusion rel. to elec. fields and currents 4-72771
- meteor burst communications systems 4-63016
- meteors, physical phenomena (book) 4-58578
- negative ion zone at 88 km altitude 4-115647
- plasmaphere, plasma density model rel. to diurnal period var. of mid-latitude ULF pulsations 4-105812
- sporadic-E layers, vertical and horiz. struct. using HF Doppler technique 4-100867
- surf zone waves creating electric charge in atmosphere 4-110203
- X-ray and electron absorpt. in nighttime middle atmosphere 4-110361
- He<sup>+</sup> dominance regions in high-latit. topside ionosphere, role of plasma convection 4-110363
- NO<sup>+</sup>, stepwise hydration, struct., ab initio calcs. 4-81402
- O<sup>+</sup> density depressions in topside nighttime ionosphere, ISS-b satellite obs. 4-63009
- O<sup>+</sup> ions in magnetosphere, thermospheric control of auroral O<sup>+</sup> source 4-72786

**atmospheric light propagation**

- adaptive compensation for atmospheric turbulence effects (French, English) 4-67402
- adaptive systems, wavefront correction quality 4-107550
- adaptive transmission, two-wavelength, diffractive and refractive effects comparison 4-87280
- aerosol light extinction model 4-110251
- aerosols, atmospheric, wavelength depend. spectral extinction 4-72696
- aerosols from Mount St. Helens 1980 May eruptions, sunlight extinction anal. 4-105696
- aperture-averaged spectral correlations of beams in a turbulent atmosphere 4-100725
- Arctic haze optical properties 4-105710
- band transmittance, approx. of product error during calc. 4-72701

**atmospheric light propagation continued**

- bistatic lidar used for aerosol characts. determ. from scatt. 4-77647
- bleaching capacity of continuous laser beam in atmosphere 4-79243
- blue-green propagation through clouds (French, English) 4-67399
- Boulder, Colorado, atm. dust from Mount St. Helens 1980 May 18 eruption, optical effects 4-105719
- broken cloudiness, model, Poisson indicator field, optical radiation transfer 4-85756
- cloud shortwave spectral absorption, parameterization scheme improvement 4-94243
- cloudiness, Poisson indicator field model, stochastic props. 4-85755
- clouds, droplet scatt. rel. to optical device for liq. water content meas. 4-62978
- conference on Mount St. Helens 1980 eruptions, at Washington, DC, United States (November 1980) 4-101575
- discrete random media, comparison of diffusion theories for optical pulse waves 4-69312
- discrete random media, difference between Ishimaru and Furutsu theories on pulse propag. 4-69313
- dispersion coefficient, determ. and correction for influence on astrometric meas. (Russian) 4-101121
- dispersion in converging beam, double prism corrector for astronomical telescope 4-101175
- extinction due to Mount St. Helens 1980 eruptions stratospheric aerosols, climatic implications 4-105706
- extinction in stratosphere due to Mount St. Helens aerosols (1980) 4-105717
- fog monitoring using variable angular field-of-view transmissometer 4-100813
- haze influence on accuracy of multispectral remote sensing 4-100746
- heat plume characteristic parameter determ. by lidar (Spanish) 4-89483
- holography, appl. to investigation of spatial distrib. of fog droplets 4-62979
- ice clouds, effects of horizontal orientation of crystals on radiative props. (Chinese) 4-67397
- imaging through turbulence, Fried's parameter estimation from time series of arbitrary resolved imaged object 4-72698
- IR and optical propag., effects of meteorology on marine aerosol (French, English) 4-67400
- IR transmission in 8-14  $\mu$ m band, airborne meas. 4-115567
- IR transmission of atmosphere, fast computation method 4-94282
- laser discharge initiation in weakly absorbing H<sub>2</sub>O aerosol, elevated-transmission zone form. 4-77633
- lidar, quantitative 532 nm data for vertical extinction profiles, relative humidity effect 4-100755
- moments of irradiation fluctuations in atmospheric optical propagation, uniqueness of statistics 4-74425
- multiple scattering effect on propag. of light beams in dense homogeneous media (French, English) 4-67401
- optical communication through low-visibility atmosphere using a CW diode laser 4-112589
- optical propagation, effects of atmospheric turbulence (French, English) 4-67403
- outgoing thermal radiation, effect of antiscreening by cloudiness (Russian) 4-67392
- radiative fluxes computation, accuracy, of approximate method in presence of broken cloud (Russian) 4-67393
- radiative transfer in atm.-ocean system, azimuthally depend. matrix-operator approach 4-72695
- radiative transfer Pade approximant calcs. for number of scatts. during particle diffusion 4-101126
- radiometer for long-term monitoring of atmospheric transmittance in far infrared region 4-100730
- Rayleigh scattering cross section, theoretical determ. 4-105714
- scattering, computing aspects 4-67391
- scattering characteristics of aerosol media with anisotropic particles, homogeneous spheres models use (Russian) 4-82235
- speckle effects on pulsed CO<sub>2</sub> lidar signal returns from remote targets 4-77628
- specular reflection in turbulent atmosphere, intensity fluctuations 4-72702
- lower stratosphere, radiative heating, rel. to O<sub>3</sub> distrib. in two-dimensional model 4-62920
- stratosphere aerosols from Mount St. Helens 1980 May eruptions, scatt. sunlight obs. 4-105721
- stratus clouds, lidar determ. of extinction 4-94239
- submilliarcsecond speckle displacement meas. using cross spectrum anal. 4-94631
- sunlight refraction and boundary layer temp. profile determ. (Russian) 4-82167
- sunlight transmission, effect of Mount St. Helens stratospheric aerosol (1980) 4-105688
- transparency, long term variations derived from extinction meas. 4-110253
- tropospheric trace species transport and conc. meas. using CO<sub>2</sub> coherent IR lidar mission, technology needs 4-100762
- turbidity in India and atm. particulate matter 4-67395
- turbulence effect on focused laser beam propag., appl. to time-of-flight velocimeter 4-89994
- turbulent atmosphere, light polarisation change 4-105725
- volcanic particles effect on sunlight extinction, climatic implications 4-105705
- water vapour, reson. absorpt. study using line-tunable CO laser (Chinese) 4-67398
- water vapour profiles, IR radiation satellite meas. (Chinese) 4-115596
- D, in upper atmosphere, Spacelab 1 detect. of resonantly scattered Lyman- $\alpha$  emission 4-90016
- DF-HF chemical laser attenuation meas. (Chinese) 4-62951

**atmospheric measuring apparatus**

- see also air pollution detection and control; ionospheric measuring apparatus; meteorological instruments
- angular scintillation measurement, 116-173 GHz, quasi-optical MM-wave transmitter/receiver array system 4-82304
- Arctic haze, AGASP program and instrumentation for pollution monitoring 4-105722
- automatic DC measurement instrument 4-77641
- automatic weather station for mountain top deployment 4-82279
- balloon-borne chemiluminescent sonde for tropospheric and stratospheric NO meas. 4-115617

**atmospheric measuring apparatus continued**

- boundary layer CO<sub>2</sub> and H<sub>2</sub>O turbulent transport, measurement apparatus 4-115583
- Bowen's ratio over bare cotton soil, temp. and humidity anal., instrumentation 4-67335
- chemical composition of stratosphere, balloon borne laser instrumentation 4-115589
- coherent IR radar systems and appls., conf., Arlington, VA, USA (Apr. 1983) 4-95019
- continuous flow chamber for ice nucleus meas., design and appl. 4-62980
- digital meter for meas. of star jitter, appl. to turbulence evaluation 4-94254
- double focusing ion mass spectrometer of cylindrical symmetry 4-68318
- EISCAT facility for high latitude upper atmosphere research 4-100806
- electrostatic precipitator for the study of airborne radioactivity 4-89786
- European Southern Observatory polarimeter and sky background polarisation meas. 4-101172
- Fourier transform spectroscopy analysis method for atmospheric remote sensing 4-110269
- gravity waves measurement network 4-115582
- heterodyne spectrometer for 10 micron region 4-94255
- hi-vol aerosol samplers, 10  $\mu$ m cutpoint size selective inlet 4-100049
- infrared (2.6-5  $\mu$ m) mosaic detector mounted on a balloon, design of optical subsystem 4-77652
- infrared Earth limb scanning apparatus (LIMS) for middle atmos. props. 4-105753
- ionisation chamber system, for indoor gamma-ray exposure meas. 4-93894
- IR hygrometer appl. to convective phenomena anal. 4-94259
- IR sounder for moisture and temp. meas., design requirements 4-62959
- laser for remote sensing, mini-TEA 1 kHz CO<sub>2</sub> laser design 4-107662
- lidar remote sensing of atmospheric, signal processing problems (*Russian*) 4-72705
- lidar system for chem. composition monitoring, range resolved DIAL CO<sub>2</sub> laser 4-94245
- magnetosphere electric field measurement with spherical double probes on satellites 4-82367
- mm wave imaging radiometer for airborne applications 4-77665
- mm wave spectrometer for chem. composition measurement 4-77170
- neutron detection from lightning bolts using Pb-free monitors 4-100832
- NIMBUS 7 Stratospheric and Mesospheric Sounder, design, performance and calibration 4-100802
- nuclear particle identification in space plasma research, review 4-100820
- open-loop fast response gas sampling valve with current control 4-62428
- optical device, for meas. of clouds liquid water content 4-62978
- optical scanner on NIMBUS-7 satellite, calibration accuracy 4-105749
- particle size meas. probe (*French*) 4-85761
- passive Rn monitors, calibration and methodology for Rn meas. 4-93673
- precipitation sampler intercomparison 4-100831
- spectral pyranometers with filter domes, polarisation and anisotropy effects 4-105733
- radar for mesosphere-stratosphere research, mobile SOUSY radar system 4-85791
- radiation sensors on NIMBUS satellite ERB instrument package, performance 4-105747
- radiometers on NIMBUS satellites, inflight calibration adjustment of wide field of view instruments 4-105748
- shipboard deployment of meteorological instruments at end of horizontal boom 4-110302
- Shuttle Upper Atmosphere Mass Spectrometer experiment 4-82365
- solar radiometer for meas. horizontal global solar irradiance 4-82636
- spectrometer, balloon-borne tunable diode laser, for stratospheric NO in situ meas. 4-72706
- spectrometer, tunable diode laser absorpt., for trace gas meas. in tropospheric air 4-114998
- stratospheric aerosol and gas expt. instrument, satellite-based (SAGE II) 4-115587
- submillimetre FT spectrometer for stratosphere spectra and chem. composition 4-110268
- submillimetre spectroscopy of stratosphere with three-channel <sup>3</sup>He-cooled bolometer, balloon mounting 4-77663
- super-pressure balloons, use for stratosphere circulations determ. 4-77648
- telephotometer and integrating nephelometer, intercomparison of two atmospheric optics instruments 4-115581
- temperature remote sensing from satellite, TIROS-N infrared and microwave systems 4-115605
- tunable airborne diode laser system for trace gas meas. 4-115588
- turbulence measurement, MM-wave system design and operation 4-82305
- twin filter detector for radon daughter spectra 4-93672
- UV radiometer onboard NIMBUS 7 satellite, sensor degradation during separation 4-105746
- variable angular field-of-view transmissometer for fog monitoring 4-100813
- VHF-UHF radar instrumentation, plasma disturbance investigation (*Japanese*) 4-62983
- wind and atmospheric composition meas., mini-TEA 1 kHz CO<sub>2</sub> laser design 4-107662
- wind measurement by Doppler lidar, airborne instrumentation and observations 4-90001
- wind measurement by lidar, on-line data system for cw laser Doppler anemometer 4-110263
- wind remote sensing, Advanced TIROS-N Windsat lidar equipment 4-110266
- CO<sub>2</sub> tunable coherent lidar for atm. aerosol backscatter and attenuation meas. 4-100763
- O<sub>3</sub> electrochemical sonde for meas. of tropo- and stratosphere profiles 4-67436
- Pb salt tunable diode lasers for heterodyne appls. 4-96940
- Rn, daughter activities, meas. instrumentation 4-93867

**atmospheric measuring instruments** *see atmospheric measuring apparatus*

**atmospheric motion** *see atmospheric movements*

**atmospheric movements**

- see also atmospheric turbulence; wind*
- advection-diffusion equations, integration, time scheme 4-62892
- East Africa low-level jet diurnal cycle, model 4-89963
- W Africa monsoon circulation deduced from satellite and aircraft obs. 4-82158
- E African coast, low-level flow mesoscale struct. 4-72634

**atmospheric movements continued**

- alpine valley in Switzerland, wind circulation and surface energy flux 4-110198
- ambient aerosol composition determ. by PIXE 4-100031
- North America, pollutant transport to North Atlantic Ocean 4-72197
- analogues (recurrent flow fields) in wintertime 500 mbar height field, rel. to weather forecasting 4-72653
- annual eddy momentum flux cycle due to planetary-scale N hemisphere 500 mbar seasonally forced waves 4-72664
- anticyclonic stratosculum, vertical adiabatic displacements rel. to water content and height fluctuations 4-62926
- Arabian Sea, cyclonic storms and depressions of 1982 AD 4-85732
- Arabian Sea, zonal and meridional eddy fluxes of dry and moist energy components 4-110217
- auroral oval, dynamic var. during intense mag. storms 4-72776
- NW Australia, large-scale flow rel. to cloud clusters development and tropical cyclogenesis 4-62917
- baroclinic flow instabilities rel. to topographic forcing 4-94212
- baroclinic model and non-modal wave development, theory 4-94215
- barotropic  $\beta$ -plane flow, stochastic orographic forcing 4-62897
- barotropic flow over large-scale topography, stochastic perturbation of simple blocking models 4-82195
- barotropic instability of 2-D non-divergent atmos. flow 4-62903
- barotropic instability of zonal flow in a nondivergent atmosphere on rotating spherical coordinates 4-63004
- barotropic Kelvin and Poincaré waves, effect of variable rot. and depth 4-72645
- barotropic perturbations, general solns. (*Turkish*) 4-115504
- barotropic vorticity equation, forced coherent struts. and local multiple equilibria 4-72657
- Bay of Bengal, cyclonic storms and depressions of 1982 AD 4-85732
- Bay of Bengal, monsoon depression core struct. 4-72637
- Bay of Bengal, water thermal struct., effect of summer monsoon forcing 4-67254
- Bering Sea, longitudinal rolls and steam fog in boundary layer 4-72641
- blast wave in thermosphere due to ground weak explosion, perturbed atm. equilb. attainment (*Russian*) 4-115641
- Boundary Layer Experiment-1983, characts. 4-110255
- NE Brazil, barotropic instability possibility 4-62901
- NE Brazil, coastal precipitation, surface roughness effects and boundary layer convergence 4-94195
- buoyancy waves assoc. with thunderstorms, VHF Doppler radar obs. 4-72659
- China, long-range weather forecasts, geophysical factors, appl. 4-72671
- circulation in winter Northern Hemisphere, transient eddy forcing 4-82173
- Cleveland, Ohio, meteorological conditions during unfavourable pollutant dispersion conditions 4-77160
- climate model, sensitivity to atm. CO<sub>2</sub> increase, effect of ocean heat transport 4-67386
- climatology, thermohydrodynamic eqns. for three-component zonal model of climate 4-62948
- climatology time dependent models, variational formulation for diffusion 4-77623
- cloud clusters in tropical easterly wave, precipitation struct. 4-100657
- cloud dynamics, effects of turbulent mixing 4-72661
- cloud dynamics, observational study of winter maritime cumulonimbus cloud anvils 4-62916
- conditional instability of second kind (CISK), effect of vertical wind shear (*Chinese*) 4-67367
- conference on climate and offshore energy resources at London, England (October 1980) 4-78044
- conference on mesoscale meteorology at Melbourne, Australia (February 1984) 4-63402
- conference on Mount St. Helens 1980 eruptions, at Washington, DC, United States (November 1980) 4-101575
- convection, parameterization in diagnostic model of atmospheric 4-82198
- convection, stability criterion for moist compressible atmosphere and energy conditions for cloud development (*Russian*) 4-67310
- convection parameterisation scheme based on direct algorithm for dry convective adjustment 4-67357
- convection processes 4-105677
- convective boundary layer, plume dispersion and vertical winds, Monte Carlo simulation 4-10019
- convective draught cores, MONEX aircraft meas. 4-82183
- convective phenomena anal., use of IR hygrometer 4-94259
- convective planetary boundary layer, scalar top-down and bottom-up diffusion 4-72650
- convective planetary boundary layer, vertical pollutant diffusion 4-94181
- convective stability, influence on potential evaporation 4-100666
- cooling tower plume dispersion, advanced integral model 4-100016
- cooling tower visible plume rise anal., use of time integrated photographs 4-100017
- cumulus convection, anelastic and Boussinesq approx. comparison 4-82188
- cyclogenesis, theory of baroclinic wave development 4-94215
- cyclone-anticyclone system devel. through ocean-atm. interactions 4-100619
- Cyprus, trough-induced surface press. gradients and winds 4-110214
- deep convection, three-dimens. nonhydrostatic cloud model 4-94224
- dust storms over SE Australia and associated cold fronts 4-72685
- dynamical meteorology, non-hydrostatic eqns. in pressure and sigma coordinates 4-82202
- easterly jet with downstream variation, nonlinear and linear effects 4-94211
- easterly zonal flow generation in monsoon region, role of atmos. waves 4-85735
- Edinburgh, Scotland, wind oscillation due to travelling gravity waves 4-67333
- EHD stability in quasi-spherical geometry, model of atmospheric circulation 4-100719
- Ekman layer flow during spin-up of thermally stratified fluid 4-100680
- Elton, Louisiana, 1976 March 24 tornado, storm characts. 4-105665
- equatorial forcing of climate telecommunications, dynamical anal. 4-72652
- Europe, synoptic evolution of barometric systems rel. to snowfall in Athens 4-110189
- extratropical cyclones in Northern Hemisphere, primary and secondary tracks 4-110190
- extratropical cyclones within numerically simulated linear baroclinic waves, mass and ang. momentum 4-100653

atmospheric movements continued  
F-region, plasma flows during prolonged northward IMF, EISCAT obs. 4-100855  
F-region plasma enhancements, appl. of velocity shear stabilization of the current convective instability 4-85819  
Faeroe Islands, marine and nonmarine transported aerosols anal. using PIXE 4-100034  
Florida, USA, cumulus convection, radar echo study 4-72632  
flow field, predictability measures 4-60360  
flows, optimisation problems (*French*) 4-62928  
forced equatorial long waves, simple analytical solns. 4-62922  
form drag instability and multiple equilibria in barotropic case 4-62911  
Front Range, Colorado, USA, terrain height variance spectra and atmos. flow 4-115519  
frontal evolution model 4-67346  
frontogenesis, convective parameterization in quasigeostrophic diagnostic model 4-94217  
frontogenesis and predictability 4-62883  
frontogenesis associated with nondivergent vortex, kinematic analysis 4-115518  
general circulation, corrls. between large-scale meridional eddy momentum transport and zonal mean quantities 4-72656  
general circulation, zonally symmetric model for volcanic influence 4-100678  
general circulation by penetrative cumulus convection 4-105632  
general circulation climate models including hydrologic cycles 4-77626  
general circulation model, blocking events in winter 4-105631  
general circulation model of water isotope cycles 4-115551  
general circulation model response to Pacific sea surface temp. anomalies 4-100710  
general circulation models, multilevel prognostic schemes 4-72677  
general circulation models, use of surface albedo and emissivity data 4-77620  
general circulation models and atmospheric irregularities 4-62895  
general circulation models for climate simulations, sensitivity to land surface boundary conditions 4-82221  
general circulation models in climatology 4-82219  
general circulation models of climate, conf., Greenbelt, Maryland, USA (Jan. 1981) 4-73159  
general circulation models with cloud parameterizations, sensitivity study 4-105633  
geophysical fluid dynamics variational principle 4-62847  
geostrophic approximation, theory and appls. 4-62913  
quasi-geostrophic potential vorticity eqn., simplified forms 4-62900  
GFDL global spectral model for medium range prediction 4-100652  
Goddard general circulation model climatology, effects of sea ice var. 4-89990  
gravity wave excitation from free shear layer 4-94205  
gravity wave-turbulence interaction in presence of critical level 4-94214  
gravity waves, algorithm for nonlinear dispersion relation 4-72772  
gravity waves measurement network 4-115582  
Hadley circulation subject to climate perturbations, GCM model 4-94203  
Hanford, Washington, dust from Mount St. Helens 1980 May 18 eruption, conc. 4-105698  
hemispheric circulation, rel. to distrib. of fronts over central-southern Europe and Mediterranean 4-110188  
hurricane vortex, axisymmetric nonhydrostatic numerical model 4-115513  
hydraulic jumps, simulation in presence of rot. and mountains 4-62919  
hydromagnetic planetary-gravity waves in zonal wind-magnetic shears, instability 4-62940  
Indian summer monsoon region, divergent wind contrib. to kinetic energy budget 4-85733  
industrial source complex dispersion model in rural setting, validation 4-77159  
inertial-gravity waves and convective cloud echo bands, merging rel. to heavy rain prod. (*Chinese*) 4-67369  
inertial-internal gravity waves, hydrostatic and nonhydrostatic eqns. 4-100654  
internal gravity waves (*Russian*) 4-82170  
Intertropical Convergence Zone dynamics, GLAS climate model symm. version anal. 4-72643  
inversion layer growth and importance of gravity waves 4-110202  
ionosphere, auroral F-region, dynamic coupling with thermosphere 4-100864  
ionosphere, electron drift vel. in eastward electrojet rel. to auroral power spectra vars. 4-72777  
ionosphere, energy principle for high-latitude electrodynamics 4-85812  
topside ionosphere, high-latit., plasma convection rel. to He<sup>+</sup> dominance regions 4-110363  
ionosphere, outflowing energetic ions, magnitude and comp., mag. activity depend. 4-72779  
ionosphere, SABRE obs. of morning sector convection reversal 4-110364  
ionosphere, topside, nighttime, downward plasma flow rel. to O<sup>+</sup> density depressions 4-63009  
ionosphere dayside high-latitude correction, influence of interplanetary mag. field orientation 4-85811  
ionosphere electron content at mid-latitude in winter influenced by neutral winds 4-82336  
ionosphere travelling disturbances, dispersion relations rel. to determ. of thermospheric wind vectors 4-90015  
ionospheric convection at high latitudes, EISCAT obs. 4-100865  
ionospheric disturbances due to great earthquakes in Japan area 4-105801  
ionospheric velocities, EISCAT data errors 4-100860  
Jilin province, China, background circulation rel. to heavy rain events (*Chinese*) 4-67368  
land surface heat and moisture transfer at macroscale for GCM models 4-77619  
large-scale waves in thermosphere at approx. 260 km altitude 4-100838  
laser sounding of atmospheric dynamics 4-77640  
lee cyclogenesis, model of baroclinic waves due to mountains 4-115512  
lee waves in Aegean Sea 4-105622  
LIDAR, statistical accuracy of time variations in atmospheric dynamics 4-96971  
long nonlinear waves on the layers of large wind velocity gradient (*Russian*) 4-115506  
magnetosphere, convective motions assoc. with field-aligned currents in polar cap 4-110372  
magnetosphere, ion comp. and vel. meas. in magnetotail, between 60 and 240 Earth radii 4-100881

atmospheric movements continued  
magnetosphere, ISEE 1 and 2 obs. of oscillating outward moving current sheet near midnight 4-85832  
magnetosphere convection, average plasma flow between 70 and 220 Earth radii in geomag. 4-100880  
magnetosphere convection, control by spatial distrib. of ionospheric conductivities 4-72807  
magnetosphere convection, effect on ionosphere conductivities 4-100847  
magnetosphere convection, energy vars. and elec. fields in collisionless ion-electron plasma 4-100868  
magnetosphere convection, ionospheric signatures 4-72790  
magnetosphere convection; latit. profile of assoc. elec. field at ionospheric altitudes 4-72787  
magnetosphere convection, renovated model using field-aligned currents as diagnostic tool 4-72806  
magnetosphere large scale convection, role in ionospheric energy exchange processes 4-100844  
magnetosphere plasma global convection characts. var. and polar F<sub>2</sub>-layer modelling 4-94293  
magnetotail, energetic ion streaming reversal during substorm 4-67556  
Western Mediterranean, atm. press. oscills. and associated sea level oscills. (*Spanish*) 4-94166  
Mediterranean and Atlantic ocean, atmospheric aerosol particles transport determ. by PIXE 4-100035  
mesoscale meteorological phenomena, predictability 4-62887  
upper mesopause, wind changes during stratospheric warmings 4-115643  
mesoscale atmos. circulation during a coastal upwelling event 4-72633  
mesoscale atmospheric movements, vel. determ. 4-62893  
mesoscale circulation systems, appl. of statistical objective anal. techniques to coastal surface temp. field 4-105626  
mesoscale convective bands behind cold fronts, cloud and microphysical struct. 4-82199  
mesoscale convective bands behind cold fronts, mesoscale organisation 4-62918  
mesoscale flows, 3D model and pollutant convection-diffusion 4-100650  
mesoscale predictability, corrl. with initial state uncertainty 4-62888  
mesoscale processes, predictability problem 4-62889  
mesoscale stability of entrainment into cloud-topped mixed layers 4-72649  
mesosphere, ambipolar diffusion rel. to elec. fields and currents 4-72771  
mesosphere, wind determs. from P<sub>1</sub>(2)<sub>cg</sub> lines of X<sup>2</sup>Π OH (8-3) band 4-105781  
mid-latitude ionospheric trough and plasma convection 4-100845  
middle atmosphere, wave characts, simulation in general circulation model 4-62921  
mixed layer dynamics, lidar obs. rel. to tests of parameterised entrainment models 4-100669  
moist convective adjustment scheme, convergence 4-67356  
monsoon depression over Bay of Bengal of July 1979, quasi-geostrophic analysis 4-94206  
monsoon depressions, equivalent pot. temp., convection, cloud heights and humidity zones 4-110224  
monsoon depressions, mass, heat and moisture balances 4-100701  
monsoon of East Asia 4-62894  
southwest monsoon onset over W India, influence of S African and Indian Ocean frontal systems 4-100703  
Mount St. Helens, 1980 May 18 eruption plume dispersion 4-105691  
Mount St. Helens, dust cloud from 1980 May 18 eruption, downwind deposition and radiation doses 4-105697  
Mount St. Helens, dust distrib. and dispersion from 1980 May eruptions 4-105690  
Mount St. Helens, volcanic plume disposal over USA and Atlantic 4-115482  
Mount St. Helens, Washington, USA, pressure wave from 1980 eruption 4-115535  
Mount St. Helens 1980 May eruptions, stratospheric tephra and aerosols, comp. and plume characts. 4-105687  
mountain areas, cold air drainage, thermal belt and cold air lake 4-94199  
flat mountain ranges causing channeling of air flow 4-105634  
multi-dimensional flows, radiation boundary conditions 4-82203  
neutral winds in high latit. winter F-region, coordinated obs. from ground and space 4-100836  
New York State, USA, sulphate aerosol transport from industrial Midwest 4-115481  
nonlinear wave processes in quiescent winter stratosphere, importance for stratosphere circulation 4-82191  
nonlinear waves in barotropic atmosphere, second order approximations (*Chinese*) 4-67366  
nonzonal flows satisfying sufficient conditions for stability 4-77596  
North America, evidence for enhanced atmospheric circulation during Early Holocene 4-100712  
Northern Ireland, Saharan dust washout in rain, Sept. 1983 obs. 4-82209  
nuclear war, climatic consequences, computational expt. (*Russian*) 4-67389  
obstacles in boundary layer flow, study of wakes and net forces 4-67304  
oppositely directed jets interacting near mountainous obstacle, spontaneous oscills. 4-108101  
orographic and thermal nonhomogeneities effects 4-77588  
orographically induced Rossby wave instabilities 4-72646  
oscillations, quasi-2 day, anomalous atmospheric wave aspects 4-67517  
perturbations of atmosphere at different levels (*Spanish*) 4-94232  
planetary boundary layer, momentum flux and frictional vertical vel. 4-110215  
planetary-scale 200 mb divergent flow; evolution during, FGGE year 4-82197  
planetary-scale N hemisphere 500 mbar seasonally forced waves, annual eddy momentum flux cycle 4-72664  
planetary-scale traveling waves, theory and obs., review 4-110233  
plume dispersion calcs. using Boussinesq approx., strongly-buoyant case 4-82155  
plume equations, non-empirical closure 4-100015  
plume rise from sour gas flares 4-93658  
plume rise from stacks with scrubbers 4-66827  
polar cap, convection, interplanetary mag. field effects 4-72791  
polar cap convection, depend. on interplanetary mag. field direction 4-94305  
pollutant ground source, diffusion in boundary layer (*Russian*) 4-114990  
pollutant releases, optimisation, turbulence and diffusion 4-66837

**atmospheric movements continued**

- pollutant trajectories, aerosol conc. in: Norwegian Arctic, sources 4-105140
- pollution long-range transport modelling 4-72628
- pollution medium range transport, meteorological aspects 4-72626
- pollution transport to Arctic 4-105142
- potential vorticity, powers in hemispherical barotropic quasigeostrophic model 4-67352
- predictability of atmospheric low-freq. motions 4-62890
- proton diffusion in radiation belt, steady state transport eqn. soln. 4-67555
- Qinghai-Xizang Plateau, China, glaciers distrib. rel. to atm. circulation 4-62863
- quasi-biennial oscillation and large scale waves in equatorial stratosphere 4-100699
- quasi-biennial oscillation and stratosphere sudden warming 4-115531
- quasi-periodic oscillations in a symmetric general circulation model 4-72644
- quasigeostrophic uniform pot. vorticity, predictability and energy transfer props. 4-62879
- radioisotope atmospheric transport from notional nuclear plants, European doses, MESOS code 4-77612
- rocket probing of atmos. temp. and wind, comparison of French and Soviet methods 4-105763
- Rossby wave multiple non-linear interaction via zonal flow 4-110200
- rough terrain, air flow and dispersion Eurochem 173 report 4-82185
- Saharan dust in atmosphere, mobilisation, transport, and deposition, conference, Gothenburg, Sweden (1977 April 25 to 28) 4-90302
- Sardinia, 3D airflow over island 4-62910
- sea-breeze-like wind over Gulf Stream due to water temp. front 4-67328
- seasonal variation in atmospheric energy cycle, general circulation model study 4-94204
- short waves initial representation accuracy, effect on forecasting from spectral model 4-67353
- smoke plume from steam power station chimney, trajectory calc., math. model (*Russian*) 4-81600
- solar eclipse causing travelling press. waves, Feb. 1979 Canadian eclipse 4-115541
- southern hemisphere, blocking flow onset and cyclogenesis 4-115509
- Southern Hemisphere, circulation interannual variability 4-72635
- Southern Oscillation/El Nino, relation to interannual length-of-day variation 4-105396
- sporadic-E layers, HF Doppler traces rel. to models of moving sporadic-E clouds 4-100867
- squall line in E tropical Atlantic, air motion and rain struct. 4-94207
- stationary planetary waves form, in Northern Hemisphere, role of Greenland Plateau (*Chinese*) 4-67364
- stratified flow over mountain ridge on rotating Earth, theory 4-62898
- stratosphere, circulation at 200 mb level, monthly variations 4-110199
- stratosphere, effects of vertical mixing in COS concs. 4-105658
- stratosphere, evidence for equatorial Kelvin modes in Nimbus-7 LIMS 4-72655
- stratosphere, seasonal vars. rel. to north-south asymmetries of solar particle events in stratospheric O<sub>3</sub> 4-110229
- stratosphere, zonal mean flow rel. to equatorial Kelvin modes 4-72655
- mid-stratosphere circulation in Southern Hemisphere, use of super press. balloon trajectories 4-77648
- stratosphere tracer transport, modified diabatic circulation model 4-62923
- stratosphere winter circulation affected by orographic forcing and blocking 4-105630
- stratosphere-troposphere general circulation model, water vapour fluxes 4-82193
- stratosphere-troposphere general circulation model, water vapour trajectories 4-82194
- stratospheric aerosols from Mount St. Helens 1980 eruptions, global distrib., lidar obs. 4-105689
- stream function and velocity potential from wind field, calculation procedure 4-100700
- structure functions in atmospheric surface layer estimates of power-band exponents  $\mu$  and  $\mu_\theta$  4-105625
- summer general circulation over Asia southern hemisphere cross equatorial current effect 4-110211
- summer monsoon onset over E Asia, 1979, observational study (*Chinese*) 4-67360
- surface torques, friction torque and mountain torque estimates from global atmospheric data 4-72654
- Sweden, south, long range aerosol transport, multivariate statistical technique appl. to PIXE data 4-100037
- symmetric baroclinic instability for small Ekman numbers 4-101146
- synoptic atmospheric vortices with vertical motions 4-67350
- synoptic circulation over Beijing city in late autumn, relation to aerosol conc. distrib. (*Chinese*) 4-66838
- synoptic-scale vertical vels., MST radar detection 4-94185
- thermals with large density difference, turbulent thermal theory 4-112848
- thermosphere, general circulation model with coupled dynamics and comp. 4-72769
- thermosphere, generation of vertical winds and gravity waves at auroral latits. 4-105782
- thermosphere, internal gravity waves, parametric instabilities, Doppler spectra 4-100837
- thermosphere, midlatitude vertical motion and horizontal flow 4-94285
- thermosphere, numerical modelling of vertical winds and gravity waves generation at auroral latits. 4-105783
- thermosphere, O<sub>2</sub> concentration, eddy diffusivity and circulation 4-72767
- thermosphere, two-dimens. high resolution nested grid model, neutral response to elec. field spike 4-85807
- polar thermosphere, winds and general circulation observations 4-110334
- thermosphere super-rotation, meas. by Dynamics Explorer 2 satellite 4-105780
- thermospheric circulation over N Scandinavia rel. to ionosphere drift 4-100859
- three-dimensional asymmetric vortex, numerical stimulation 4-72660
- thunderstorms, wind distrib. rel. to storm struct. and lightning activity 4-105657
- time variation of atmos. energetics in FGGE winter 4-89961
- Tokyo Metropolitan Area, Japan, photochemical pollutants three-dimens. behaviour 4-100021
- topographically obstructed flow, long-wave theory for multiple obstructions 4-115515

**atmospheric movements continued**

- trace elements in Europe, emission and long-range transport 4-114986
- tracers transport and dispersion in nocturnal drainage flows, pollutant appl. 4-100648
- trajectories during AGASP 4-105655
- transient eddy forcing of time-mean flow 4-82173
- transport models for complex terrain, appl. to mesoscale transport of pollutants 4-100668
- transport models for complex terrain, appl. to pollutant dispersion 4-100667
- tropical cloud clusters mesoscale circulation, implications for large-scale dynamics and climate 4-72651
- tropical cyclone recurvature over Bay of Bengal 4-100704
- tropical cyclones, cumulus momentum transport effects 4-94208
- tropical general circulation, response to lateral forcing 4-115514
- tropical middle atmosphere in Indian region, vertical air motions 4-94210
- tropics, unstable air-sea interactions responsible for Southern Oscillation phenomena 4-94209
- troposphere, quasi-geostrophic pot. vorticity fluxes 4-115491
- troposphere, temporal evolution of Taylor columns over topography 4-62843
- troposphere, tidal fluctuations, correl. with ionosphere, perturbation effects 4-89967
- troposphere general circulation influenced by polar night jet 4-115510
- tropospheric circulation patterns during AGASP 4-105654
- tropospheric trace species transport and conc. meas. using CO<sub>2</sub> coherent IR lidar mission, technology needs 4-100762
- turbulent diffusion in environment, mathematical modelling, conference, Liverpool, England (1978 September 12 to 13) 4-101577
- ultralow wave baroclinic instability, nonlinear baroclinic outburst episodes 4-105629
- ultralow waves, baroclinic instability by low order model 4-105628
- United States, intensified meridional circulation rel. to cold Januaries of recent winters 4-100663
- NE United States, pollutant distrib. and mixing layer struct. during Sulphate Regional Experiment 4-100020
- upper atmosphere, dynamics and electrodynamics of thermosphere 4-72773
- upper atmosphere circulation, temp. and composition model and geomag. activity influences 4-67515
- upper atmosphere wind reversals 4-82319
- eastern USA, east coast secondary cyclogenesis models 4-72630
- USA East coast cyclone in Feb. 1979 synoptic overview and subtropical jet streak influence 4-72631
- vertical diffusion exchange between friction layer and free atmosphere 4-77589
- vertical wind variability at Poker Flat, Alaska, USA 4-115502
- volcanic eruption pressure wave from Mt. St. Helens 1980 eruption 4-115535
- wave disturbances due to large fires in USSR 4-72642
- wave interactions and baroclinic/barotropic predictability in geostrophic turbulence 4-62880
- wave interactions and blocking, predictability 4-62878
- wave-mean flow interaction in Southern Hemisphere 4-82175
- wave-wave interactions during quiet and active winter periods 4-82176
- Westwaco Luke Mill, Maryland, pollutant dispersion and transport, complex terrain model 4-100018
- westward travelling surge, mechanism involving convection patterns distortion in magnetosphere 4-72781
- wind waves, growth and equilib. in laboratory channel (*Russian*) 4-82172
- zonal circulation and climate anomalies (*Spanish*) 4-115563
- zonal circulation annual variation by small component spectral model (*Russian*) 4-100682
- zonal wind and temp. fields of troposphere, response to heat and momentum heat source changes 4-115508
- NO flux from thermosphere to mesosphere 4-100834
- NO<sub>x</sub> pollutants, conf. at Maastricht, Netherlands (May 1982) 4-101576
- atmospheric noise** see *atmospherics*
- atmospheric optics**
- see also *airglow; atmospheric light propagation; sky brightness; sunlight; twilight*
- adaptive optics basic functions for obscured aperture, phase aberration correction 4-74427
- aerosol backscatter determ. at 10.6  $\mu\text{m}$  4-100728
- aerosol backscattering at 10.6 microns, obs. made at Boulder, Colorado, USA 4-110246
- aerosol extinction in stratosphere, meas. by SAM II and SAGE 4-100805
- aerosol far IR backscatt., CO<sub>2</sub> lidar obs. at Pasadena, CA, USA 4-110247
- aerosol in atmos., optical depth and aerosol distrib. from sky brightness observations (*Spanish*) 4-115574
- aerosol layer in stratosphere and influence on atmospheric radiation and temp. 4-67396
- aerosol light scattering matrix, statistical characts. (*Russian*) 4-100732
- air pollution optical remote sensing, conf., Ispra, Italy (April 1983) 4-73168
- Arabian Sea area, atmospheric heating by radiation flux, due to aerosols 4-94241
- Arctic aerosol at Barrow, Alaska, USA, due to air pollution and El Chichon 4-105709
- Arctic haze optical properties 4-105710
- aureole around point source, aerosol size distrib. determ., theory 4-62961
- aureole around point source, solar blind radiometer meas. 4-89991
- band transmittance, approx. of product error during calc. 4-72701
- Barcelona, Spain, optical props. of turbid atmosphere (*Spanish*) 4-115575
- cirrus cloud, depolarisation, backscatt. and attenuation of IR laser radiation 4-110248
- broken cloud cover, calc. of mean photon path lengths (*Russian*) 4-100731
- cloud decoupling of surface and planetary radiative budgets 4-94242
- cloud shortwave spectral absorption, parameterization scheme improvement 4-94243
- cloudiness of atmosphere and influence on model diagnosed radiative fluxes 4-115523
- clutter modelling for down-looking satellite platform 4-115565
- Crimea coast, chemical composition and optical props. of haze (*Russian*) 4-100685

atmospheric optics continued

dispersion coefficient, determ. and correction for influence on astrometric meas. (*Russian*) 4-101121  
El Chichon volcanic dust cloud, twilight optical studies at Ahmedabad, India 4-89969  
Earth radiation budget, determ. from NIMBUS-7 satellite ERB expt. obs. 4-105712  
Earth radiation budget determ. by ERB expt. on NIMBUS satellite, overview 4-105745  
Earth radiation budget determ. by satellite, combining NIMBUS-6 and -7 data sets 4-105744  
Earth radiation budget measurement by NIMBUS 7 accuracy of ERB data set 4-105750  
Earth radiation budget measurement using NIMBUS 7 satellite ERB expt. 4-105713  
Earth radiation budget radiometers on NIMBUS satellite, inflight calibration 4-105748  
El Chichon eruption cloud influence on solar radiation in Michigan, USA 4-115572  
Elbrus region, Caucasus, astroclimatic characts. 4-62953  
Ne England, 1983 July heatwave, sea breeze occurrence effect on temp. 4-100717  
equilibrium-reflectance model for clear or cloudy atmosphere 4-100729  
Europe, solar radiation incident on land surface, estimated from METEO-SAT data 4-82159  
far infrared (0.89 mm) attenuation observations in clear atmosphere 4-77616  
fog, attenuation of IR radiation 4-115480  
fog, terminal velocity of droplets and optical extinction coeffs. in fog models 4-82151  
Grand Canyon, Arizona, USA, pollution, particulates and visibility 4-115564  
ground level illumination rapid variations due to aurora 4-110342  
halo phenomena, Monte Carlo simulation, sun ray path tracing through ice crystals 4-72699  
haze, spectral luminance calc. 4-82240  
haze influence on accuracy of multispectral remote sensing 4-100746  
heating of atmosphere due to direct solar radiation absorpt. 4-77570  
ice crystal optical display at South Pole, photographs and field notes 4-89993  
infrared imaging through atmosphere, image quality in various weather conditions 4-105708  
infrared radiation budget of Earth, LOWTRAN5 band model 4-82232  
infrared spectral monitoring method for stratosphere method for stratosphere temp. and composition, NIMBUS 7 LIMS expt. 4-105754  
IR Earth/atmosphere background meas. during sunrise, using radiometer and interferometer 4-115569  
Krakatau, 1883 eruption and effects (book) 4-101587  
Lake Tahoe, USA, visibility and particle sources anal. 4-66828  
land surface shortwave albedo and surface emissivity data for climate models 4-77620  
laser beam propagation, refractive turbulence influences on diffraction-limited lidar 4-110244  
lidar remote sensing, truncated beam propagation in turbulent atm. 4-110245  
lidar remote sensing of atmosphere, book 4-82607  
light absorption vol. coeff., determ. method (*Russian*) 4-82234  
lightning, optical and elec. field signal from return strokes 4-115536  
longwave (infrared) radiation balance variability at ocean surface, review 4-110252  
monthly average regional radiation balance, simulation using satellite data 4-115570  
morning glory formation, theory 4-105707  
night sky background polarisation, meas. with European Southern Observatory polarimeter 4-101172  
night sky brightness at USSR Academy of Sciences Special Astrophysical Observatory 4-94240  
noctilucent cloud phenomena, solar illumination screening by, troposphere 4-82236  
noctilucent clouds observed from Scotland, July 1979 obs. 4-82236  
nocturnal lights, auroras and lightning (book) 4-78060  
ocean suspended sediment satellite, remote sensing, atmospheric correction 4-100741  
spectral pyranometers with filter domes, polarisation and anisotropy effects 4-105733  
radiation budget of Earth, satellite measurement technique 4-82239  
radiation sensors on NIMBUS satellite ERB instrument packages, performance 4-105747  
radiative transfer theory, nonuniqueness of soln. for nonlinear integral eqns. 4-72864  
radiometer for long-term monitoring of atmospheric transmittance in far infrared region 4-100730  
receiving telescope focal plane light intensity fluctuations caused by round-trip propag. through turbulent atm. 4-62952  
refraction effects on EM distance meas. instruments 4-110313  
remote sensing by reflectance spectroscopy, quantitative analysis techniques 4-115604  
remote sensing of land surface, effects of land surface optical contrast 4-77632  
Rozhen Peak, extinction meas. at Bulgarian National Astronomical Observatory 4-77630  
Sapporo, Japan, snowfall intensity rel. to visibility (*Japanese*) 4-105670  
sea ice in Beaufort Sea, spectral albedo and incident irradiance 4-85693  
solar haloes, ripple struct. due to sound waves from meteors 4-105715  
global solar radiation absorption by land surface 4-89957  
specular reflection in turbulent atmosphere, intensity fluctuations 4-72702  
stellar image motion, atm. effects (*Russian*) 4-100727  
stratosphere volcanic aerosols, optical depth and mass loading, SAGE and SAM II obs. 4-100692  
stratospheric fountain region, radiative heating rate calcs. 4-67394  
stratus clouds in Arctic, solar radiation studies 4-82231  
sunsets, twilights and evening skies (book) 4-67887  
teletphotometer and integrating nephelometer, intercomparison of two atmospheric optics instruments 4-115581  
temperature profiling of atmosphere by satellite IR method 4-85804  
thermal radiation budget of Earth, comparison of diurnal models 4-82233  
thermal radiation from land surface, to clear night sky, teaching expt. 4-73200

atmospheric optics continued

turbidity measurement; extinction models for continental and rural aerosols 4-110251  
upper atmosphere, EUV nightglow and light scattering observations 4-110339  
SW USA, copper smelters and atmos. visibility 4-114985  
midwestern USA, visibility trends in air pollution in AD 1948 to 1951 period 4-115486  
UV radiation at Skalnaté Pleso, Czechoslovakia, influence of cloud and snow cover 4-89958  
UV radiometer onboard NIMBUS 7 satellite, sensor degradation during separation 4-105746  
UV sky brightness at 311.2 and 332.3 nm, Monte Carlo calc. 4-105716  
visibility, aerosol effects, suggested units 4-77629  
visibility, effects of aerosols of mixed composition 4-100726  
visibility at Hanford, Washington, effects of Mount St. Helens 1980 May eruptions 4-105718  
visibility over SW USA; effects of 1980 April Mount St. Helens dust incursion 4-105720  
volcanic dust from El Chichon in atmos. of New England, USA, atmos. optical phenomena obs. 4-110249  
wind meas. with laser Doppler anemometer, influence of fog and cloud 4-110262

atmospheric pollution *see air pollution*

atmospheric precipitation  
*see also ice; rain; snow*  
acid deposition, techniques for determ. of source-receptor relations 4-100025  
acid rain, Canadian research 4-105676  
annual series, search for periodicities 4-82125  
Beijing city, China, effect of precip. on aerosol conc. distrib. (*Chinese*) 4-66838  
Belgium, AD 1983 weather conditions 4-115553  
NE Brazil, coastal precipitation, surface roughness effects and boundary layer convergence 4-94195  
NE Brazil, humidity, rain and atmos. circulation 4-115501  
China, long-range weather forecasts, geophysical factors, appl. 4-72671  
cloud clusters in tropical easterly wave, precipitation struct. 4-100657  
cloud seeding with salt particles, numerical simulation for cumulus clouds (*Chinese*) 4-67365  
conference on acid deposition, in West Berlin (September 1982) 4-86116  
cumulus clouds, importance of cloud top lifetime in description of cloud characts. 4-100670  
cyclogenesis, latent heat induced energy transformations and precipitation 4-100659  
Czechoslovakia, precipitation statistics from 1881 to 1980 (*German*) 4-77573  
extinction coefficient of precipitation water in 200 to 1100 nm region, effects of pollutants (*Russian*) 4-66836  
frontal precipitation, boundary layer struct. anal. 4-72670  
frontal storms around Philadelphia, meas. of mesoscale wetfall chemistry 4-105145  
frost-free record reconstruction for E Massachusetts (1733 to 1980) 4-100673  
Greece, hail occurrence freq. 4-100718  
Greenland and Canadian Arctic Holocene precipitation rate from ice core obs. 4-110306  
hail and wet ice, radar differential reflectivity 4-85774  
hail detection radar, mismatched antenna beam pattern effects in dual wavelength radar 4-85779  
hail fall from two vaulted storms in NE Colorado, implications of radar obs. 4-72658  
hail growth in storm cloud over Westplains, Colorado, USA 4-82154  
hailfall incidence and azimuth angles meas. equipment and techniques (*Afrikaans*) 4-77646  
hydrometeor characteristics, radar backscattering anisotropy coeff. anal. (*Russian*) 4-115601  
hydrometeorology, average value of correlated time series 4-100665  
ionosphere, upward ion injection into magnetosphere and subsequent precipitation 4-67564  
Israel, Coastal Plain, precipitation probability algorithm 4-94183  
Japan, precipitation causing landslide (*Japanese*) 4-105635  
measurement of oceanic precipitation by monitoring of underwater sound 4-85687  
melting spherical ice particles greater than 500  $\mu$ m radius, expt. and theory 4-82178  
melting spherical ice particles less than 500  $\mu$ m radius, theory 4-82177  
ocean-atmosphere exchanges, two-phase flow aspects 4-62849  
S Ontario, cyclonic storm precipitation bands, deep 0°C isothermal layers and wind shear 4-77601  
Padova, Italy, AD 1725 to 1981 rainfall records analysis 4-62945  
palaeoclimate precipitation rate determ. by glacier ice core method 4-110306  
precipitation sampler intercomparison 4-100831  
radar for severe storm studies, circular polarisation radar 4-85786  
radar identification of precipitation type and other targets, dual-polarisation radar 4-85780  
radar measurement of precipitation, circular depolarization ratios and Doppler velocities 4-85781  
radar measurement of rain and graupel, hydrometeor size estimation 4-85783  
radar measurement using multiparameter techniques 4-85771  
radar method for precipitation type identification, using dual-polarisation radar 4-85778  
radar multi-parameter methods for precipitation meas., review 4-85772  
radar scattering properties of hydrometeors meas. by dual-polarisation radar 4-85782  
regional air quality modelling, use of precipitation data 4-66830  
river flows reconstruction from precipitation data in UK 4-77560  
Shanghai, China, pollutant influence on humidity and precipitation distrib. 4-94194  
West Siberia, long-range forecasting of temp. and precipitation 4-105679  
Sierras de Cordoba, Argentina, effect of precip. on energy balance of surface boundary layer 4-105671  
United States, climatological contingency anal. and seasonal forecasting skill 4-77586  
USSR, drought forecasting methods 4-105678  
USSR (European), long-range forecasting of temp. and precipitation 4-105679  
variations, correl. with tectonic stress and earthquake occurrence 4-81998

**atmospheric precipitation continued**

- World Ocean, estimation of mean manual precipitation 4-115500
- Xinjiang Reservoir, China, effects on precipitation 4-94198
- CO<sub>2</sub> global concentration influence on air temp. and precipitation 4-67388
- O<sup>+</sup>, mid-latitude precipitation from ring current, aurora evidence 4-110345

**atmospheric pressure** *see atmospheric pressure and density***atmospheric pressure and density**

- 200 mbar geopotential, corals. between large-scale meridional eddy momentum transport and zonal mean quantities 4-72656
- 500 mb. height anomalies, geographical locations and regional persistence charact. 4-62885
- 500 mbar geopotential height field annual cycle 4-72664
- ageostrophic geopotential, determ. for nonlinear waves in barotropic atmosphere (*Chinese*) 4-67366
- Alaska, north coast, long-range ice forecasting method and meteorological conditions 4-89947
- Arctic, Fleet Numerical Weather Central predictions use in Arctic ice pack drift anal. 4-89979
- Arctic Ice Dynamics Joint Expt., boundary layer wind and press. effects 4-89978
- baric field changes and seismic activity 4-115343
- barotropic instability of zonal flow in a nondivergent atmosphere on rotating spherical coordinates 4-63004
- Beaufort Sea, geostrophic wind and surface press. for AIDJEX 4-89981
- Beaufort Sea, surface press. and geostrophic wind for AIDJEX 4-89982
- Cyprus, trough-induced surface press. gradients and winds 4-110214
- density profiles and photographic fireball data interpretation 4-77781
- dynamical meteorology, non-hydrostatic eqns. in pressure and sigma coordinates 4-82202
- empirical upper atmosphere density models for artificial satellite orbits anal. 4-82320
- Europe, synoptic evolution of barometric systems rel. to snowfall in Athens 4-110189
- exosphere, drag on artificial satellites, coupling with Earth oblateness, effect on orbit 4-82375
- exosphere, orbital lifetime estimation method for near Earth satellites 4-82374
- geopotential field in Northern Hemisphere, long range control 4-67359
- global models for satellite orbit estimation 4-72768
- India, daily rainfall forecasting using atmos. press. anomaly patterns 4-85736
- Indian Ocean, surface press. var. rel. to SW Monsoon rainfall in India 4-110223
- polar ionosphere, UHF scintillation evidence for HF-produced electron density irregularities 4-105794
- ionosphere depletion expts., snowplough effects or plasma recomb. model for depletion core form 4-100851
- Japan, summer temperature low rel. to 100 mb height var. 4-110239
- magnetosphere, plasma distrib. model using field-aligned currents as diagnostic tool 4-72806
- marine surface pressure anal., use of SEASAT scatterometer data 4-67375
- measurement at balloon altitudes using Si detector and  $\alpha$ -source 4-115644
- Western Mediterranean, atm. press. oscills. and associated sea level oscills. (*Spanish*) 4-94166
- microwave propagation, effects of water vapour, rain, humidity, temp. and press. 4-100716
- monthly mean sea level press., rel. to long-range vars. of atmospheric centres of action (*Chinese*) 4-67361
- oceanic subtropical high pressure areas, comparative effect on thunderstorm climatology of Beijing and Topeka 4-100674
- N Pacific Ocean cyclones, central press. rel. to sea surface temp. and land coverage 4-110240
- plasmasphere, plasma density model rel. to diurnal period var. of mid-latitude ULF pulsations 4-105812
- pressure change corrections to borehole volume strainmeter data (*Japanese*) 4-72711
- sea-surface temperature seasonal variation in E Pacific, effect on 500 mb subtropical high 4-110153
- solar eclipse causing travelling press. waves, Feb. 1979 Canadian eclipse 4-115541
- Southern Hemisphere sea level pressure data set for use in climatic studies 4-77622
- Southern Oscillation, signal and noise 4-100722
- Southern Oscillation persistence rel. to seasonal var. of cloudiness 4-94226
- surface pressure and isobaric height data, rel. to atmosphere mountain torque estimates 4-72654
- surface pressure and temp. rel. to sea ice extent predictability 4-89948
- tropical depression in NW Australia, comparative study rel. to tropical cyclogenesis 4-62917
- United States, pressure spectral anal. as indicator of synoptic-scale activity climatic var. 4-100756
- upper atm., meridional wind, density scale heights and day-to-night variation in density determ. 4-72849
- upper atmosphere, drag on artificial satellites, neutral and elec. components 4-82370
- variations in pressure, effect on solar intensity oscills. meas. 4-105912
- vertical interpolation for relative geopotential 4-72727
- winter mean 700 mbar heights and Southern Oscillation Index, contrib. of warming episodes in tropical E Pacific 4-100664
- wintertime 500 mbar height field, recurrent flow patterns (analogues) rel. to weather forecasting 4-72653
- O<sup>+</sup> density depressions in topside nighttime ionosphere, ISS-b satellite obs. 4-63009
- Rn concentration in a basement, variation with barometric press. 4-67132

**atmospheric propagation** *see atmospheric electromagnetic wave propagation***atmospheric proton precipitation**

- see also aurora; radiation belts*
- discrete aurora associated with energetic particle boundaries 4-67519
- high-energy protons of inner radiation belt, stochastic instability at low altitudes 4-110368
- low-latitude aurorae types and precipitation mechanisms 4-110344
- magnetosphere, precipitation stimulated by artificial low-freq. radiation 4-115653

**atmospheric proton precipitation continued**

- proton aurorae, prediction of photon yields for N<sub>2</sub> atmos. 4-67521
- pulsed proton precipitation with E<sub>p</sub> > 500 MeV from the L=2 shell during a mag. storm 4-82333

**atmospheric radiation***see also aurora*

- aerosol layer in stratosphere and influence on atmospheric radiation and temp. 4-67396
- Arabian Sea area, atmospheric heating by radiation flux, due to aerosols 4-94241
- Arctic haze season, solar radiation absorption rel. to radiation balance 4-105711
- auroral kilometric and Z-mode radiation, generation by cyclotron maser mechanism 4-72815
- auroral kilometric radiation, appl. of loss cone driven cyclotron maser 4-87889
- auroral kilometric radiation, generation, theory 4-110387
- auroral kilometric radiation-aurora correlation, electron density anal. 4-90039
- auroral kilometric radiation generation, relativistic dispersion of extraordinary mode waves 4-94312
- auroral roar, characts. 4-90025
- auroral VLF hiss, correl. with television images of auroral pulsations 4-110346
- Barcelona, Spain, optical props. of turbid atmosphere (*Spanish*) 4-115575
- Beaufort Sea, sea ice spectral albedo and incident irradiance 4-85693
- Belgium, AD 1983 weather conditions 4-115553
- Cherenkov light emission due to small air showers in  $\gamma$ -ray astronomy 4-101176
- clear sky emissivity 4-62937
- cloud decoupling of surface and planetary radiative budgets 4-94242
- cloud identification by NIMBUS 7 ERB, effect on albedo 4-100694
- cloud shortwave spectral absorption, parameterization scheme improvement 4-94243
- cloud-radiation interactions, implications for climate 4-82220
- cloudiness of atmosphere and influence on model diagnosed radiative fluxes 4-115523
- clouds, radiative transport, Palm point fluxes anal. (*Russian*) 4-82171
- conference on atm. radiation at Toronto, Canada (June 1981) 4-90300
- Czechoslovakia, energy balance at land surface (*German*) 4-77572
- daily global solar irradiation diffuse component estimation at Corvallis, Oregon (USA), using regression anal. 4-62934
- daily shortwave energy budget over oceans, satellite obs. 4-67374
- darkness at midday in southern England, 6 August 1981 event 4-67334
- Davis, California, stratosphere aerosols, temporal var. effect on sunlight at ground 4-77599
- diffuse sky radiation models comparison 4-62938
- diffuse solar radiation determined from shade-ring meas., anisotropy of sky radiance 4-62925
- diffuse solar radiation measurement using ring method, corrective factor 4-62933
- diffuse sunlight meas., effects of Mount St. Helens stratospheric aerosol (1980) 4-105688
- Earth radiation budget, determ. from NIMBUS-7 satellite ERB expt. obs. 4-105712
- Earth radiation budget determ. by ERB expt. on NIMBUS satellite, overview 4-105745
- Earth radiation budget determ. by satellite, combining NIMBUS-6 and -7 data sets 4-105744
- Earth radiation budget measurement by NIMBUS 7 accuracy of ERB data set 4-105750
- Earth radiation budget measurement using NIMBUS 7 satellite ERB expt. 4-105713
- Earth radiation budget radiometers on NIMBUS satellite, inflight calibration 4-105748
- EHF/THF emission and attenuation from Canary Islands site 4-89968
- El Chichon eruption cloud influence on solar radiation in Michigan, USA 4-115572
- electrostatic bursts associated with chorus, generation theory 4-72818
- ELF emissions, relativistic electron precipitation and X-ray bremsstrahlung 4-67530
- ELF waves from ionosphere, produced during radiowave heating expt. 4-67538
- energy balance at land surface, daily variations and statistical struct. 4-89959
- equilibrium-reflectance model for clear or cloudy atmosphere 4-100729
- Europe, solar radiation incident on land surface, estimated from METEOSAT data 4-82159
- far infrared radiation budget of Earth 4-115571
- gamma rays in atmosphere, due to cosmic ray interactions 4-110400
- gamma-ray background, meas. at balloon altitudes above Beijing area (*Chinese*) 4-82355
- gamma-ray flux at balloon altitudes, approximate analytical representation 4-100964
- gamma-ray fluxes, improved ionisation chamber system for indoor exposure meas. 4-93894
- gamma-rays detected by balloon borne cosmic ray detector 4-100720
- Great Britain, daily global irradiation estimation from sunshine records 4-110213
- ground level illumination rapid variations due to aurora 4-110342
- auroral hiss emissions correl. with upward polar cusp. electron beams 4-72819
- hook-induced electrostatic bursts in magnetosphere, computer simulation 4-94319
- India, daily diffuse-global radiation correl. 4-77594
- India, diffuse and global radiation characts. 4-77593
- infrared radiation budget of Earth, LOWTRAN5 band model 4-82232
- ionosphere, plasma interaction with STS-3 DC and modulated electron beams, wave emissions 4-90023
- ionosphere, plasma-pulsed electron beam interaction, EM wave emission 4-87886
- ionosphere, spectrum of orbiting vehicle induced luminosities on Space Shuttle STS-8 mission 4-105866
- IR, cloud, radiance model, high-altitude sensor systems, appl. 4-115566
- IR emission, temp. and comp. retrieval via NIMBUS 7-SAMS data 4-100691
- IR emission meas. by NIMBUS 7 SAMS instrument, temp. profile determ. 4-100803
- IR imaging of sea surface temp., atm. effects 4-67405

# atmospheric radiation continued

- IR radiances from broken fields of cumulus, angular distrib. 4-72662  
 IR radiation from ice clouds, effects of crystals horizontal orientation (Chinese) 4-67397  
 IR water-vapour absorption in 8-14  $\mu\text{m}$  atmospheric window, temp. dependence 4-77613  
 Northern Ireland, daily global irradiation estimation from sunshine records 4-110213  
 land surface shortwave albedo and surface emissivity data for climate models 4-77620  
 lightning, optical and elec. field signal from return strokes 4-115536  
 limb obs. by rocket at 4.3 microns wavelength 4-110195  
 limb thermal emission meas., pointing error correction method 4-89996  
 long-wave spectral emissivities, calcs. for Bangkok, Songkhla and Ubon Ratchathane, Thailand 4-100733  
 longwave (infrared) radiation balance variability at ocean surface, review 4-110252  
 magnetosphere, auroral kilometric radiation due to a new plasma instability 4-67565  
 magnetosphere, electron-cyclotron maser emission, growth and damping 4-72816  
 magnetosphere, electrostatic emission bands between electron gyrofrequency harmonics 4-85844  
 magnetosphere, EM waves nonlinear generation 4-103481  
 magnetosphere, plasma-pulsed electron beam interaction, EM wave emission 4-87886  
 magnetosphere, VLF emissions triggering by variable freq. whistler mode waves 4-82354  
 magnetospheric VLF emissions, wave normal directions meas. observed onboard satellites 4-110367  
 magnetotail, broadband electrostatic noise generation by ion beam instabilities 4-94318  
 mesosphere and lower temperature, IR radiative transfer and temp. model 4-115573  
 mid-latitude ionospheric trough and ion densities, electron precipitation and 630 nm emission 4-100845  
 mm wave emissions from atmosphere, ground based obs. 4-77666  
 moments of irradiation fluctuations in atmospheric optical propagation, uniqueness of statistics 4-74425  
 monthly average regional radiation balance, simulation using satellite data 4-115570  
 multiple atmospheric-window techniques for satellite-derived sea surface temperatures 4-67454  
 Nimbus 7 SMMR obs. of atm. water content 4-67411  
 NIMBUS 7 Stratospheric and Mesospheric Sounder, design, performance and calibration 4-100802  
 NIMBUS-7 satellite optical scanner, calibration accuracy 4-105749  
 nocturnal lights, auroras and lightning (book) 4-78060  
 nonthermal continuum radiation, generation by upper hybrid turbulence 4-94315  
 oceanic whitecaps, effective reflectance 4-89916  
 opacity, quasi-continuous record at 1.1 mm of Mauna Kea observatory 4-110250  
 optical depth and aerosol distrib. from sky brightness observations (Spanish) 4-115574  
 outgoing IR spectral vars. and CO<sub>2</sub> induced climatic change 4-115558  
 outgoing thermal radiation, effect of antiscreening by cloudiness (Russian) 4-67392  
 polar winter stratosphere, four day oscill. in brightness temp. 4-72700  
 radiative effects of changing atmospheric water vapour 4-115496  
 radiative fluxes computation, accuracy, of approximate method in presence of broken cloud (Russian) 4-67393  
 radio emission use for cloudless atmosphere integral humidity content determ. (Russian) 4-115600  
 radio noise spectral characts., few hertz to 50 kHz., expt. data-review 4-89879  
 radiowave emission from ocean-atmos. system 4-105762  
 received ultraviolet radiation at the South Pole 4-62936  
 reflected solar radiance from broken cloud scenes 4-72663  
 Sahel region, global solar radiation estimation from satellite data 4-115546  
 satellite measurement of global radiation budget, sampling problems 4-82239  
 satellite remote sensing method for Sahel global solar radiation 4-115546  
 Scanning Multichannel Microwave Radiometer data anal. and atm. water content 4-67475  
 Schumann-Runge bands and O<sub>2</sub> photodissociation in thermosphere and magnetosphere 4-77679  
 SEASAT SMMR brightness temps. use for sea surface temp. 4-67477  
 sensors on NIMBUS satellite ERB instrument package, performance 4-105747  
 Sicily, high-cloud occurrence and influence on solar radiation 4-110226  
 Singapore, diffuse, global and extra-terrestrial, correlations 4-100651  
 solar energy irradiance on inclined surface, calc. for optimal utilisation 4-72049  
 global solar radiation absorption by land surface 4-89957  
 solar radiation attenuation in urban atmosphere (Spanish) 4-115575  
 solar radiation data anal. using cubic splines for Peninsular Malaysia 4-62935  
 direct solar radiation heating of lowest 5 km 4-77570  
 solar radiation long-term variability and climate, review 4-115739  
 solar radiation measurements in 330 to 1250 nm region, review 4-115737  
 solar radiation model using total cloud cover and percentage sunshine meas. 4-62942  
 solar spectral irradiance measurement at Tanashi, Tokyo (35°43' N.L.) (Japanese) 4-85731  
 solar total irradiance by pyrheliometric method, review 4-115738  
 South Polar Plateau, surface temp. regime, energy balance etc. 4-115540  
 N Spain, sunshine statistics, Markovian model study 4-100702  
 stratosphere limb radiance due to scatt. sunlight off aerosols from Mount St. Helens eruptions 4-105721  
 stratospheric fountain region, radiative heating rate calcs. 4-67394  
 stratus clouds in Arctic, solar radiation studies 4-82231  
 submillimetre FT spectrometer for stratosphere spectra and chem. composition 4-110268  
 summer energy budget simulation for latitudinal transect along America's east coast 4-77583  
 surface radiation budget measurement method using satellite platform 4-72717  
 surface radiation budget of USA, satellite obs. 4-72717  
 temperature at 3.2 cm, automated measurement 4-89972

# atmospheric radiation continued

- Thailand, new estimates of mean daily diffuse solar radiation 4-100697  
 Thailand, simple statistical model of daily global solar radiation 4-100698  
 thermal radiation budget of Earth, comparison of diurnal models 4-82233  
 thermal radiation from land surface, to clear night sky, teaching expt. 4-73200  
 thermal radiation upward flux, effects of three-layer cloudiness model (Russian) 4-82169  
 thermosphere, NO conc. and IR emission assoc. with mag. storm heating 4-110333  
 TIROS radiance measurements, appl. to determ. of total O<sub>3</sub> amount 4-100672  
 USA, severe winters rel. to global radiation and heating degree days 4-115498  
 solar UV flux and photoelectron fluxes showing inconsistency 4-110362  
 UV irradiance (290-305 nm) use for stratosphere O<sub>3</sub> determ. 4-100798  
 UV radiation at Pune (Poona), India 4-100707  
 UV radiation at Skalnat Pleso, Czechoslovakia, influence of cloud and snow cover 4-89958  
 UV radiometer onboard NIMBUS 7 satellite, sensor degradation during separation 4-105746  
 UV sky brightness at 311.2 and 332.3 nm, Monte Carlo calc. 4-105716  
 VHF radiation near to lightning return strokes 4-67318  
 VLF emissions from magnetosphere, R-X mode AKR 4-72824  
 VLF noise suppression induced by whistlers 4-72825  
 volcanic dust from El Chichon in atmos. of New England, USA, atmos. optical phenomena obs. 4-110249  
 X-ray and electron absorpt. in nighttime middle atmosphere 4-110361  
 X-ray bremsstrahlung due to relativistic electron precipitation 4-67530  
 X-ray images of auroral arcs, satellite observations 4-100842  
 H<sub>2</sub>O 16 micron band obs. use in remote sensing of sea surface temp. 4-67406  
 H<sub>2</sub>O emission, effect on multichannel sea surface temp. retrieval 4-67407  
 O<sub>2</sub> I<sub>1</sub>, UV emissions as contaminants of geocoronal He airglow obs. 4-105787  
 O<sub>3</sub> profile determ. from backscattered UV radiation meas. with NIMBUS 7 SBUV instrument 4-100799

# atmospheric radioactivity

- see also fallout  
 dispersion in atmosphere, specific effects review 4-66840  
 dispersion in atmosphere, specific effects review 4-66841  
 electrostatic precipitator for the study of airborne radioactivity 4-89786  
 Mt. Etna, 1983 eruption, exchange of volatiles, radioactivity meas. (French) 4-115365  
 I, radioiodide conc. from aqueous soln., sorbent materials and prep. 4-77023  
 indoor exposure to natural radiation, conf., Anacapri, Italy (Oct. 1983) 4-90285  
 low level exposure to radioactive pollutants; health risk assessment 4-109965  
 Mount St. Helens, dust cloud from 1980 May 18 eruption, downwind deposition and radiation doses 4-105697  
 power reactor plumes, noble gas radionuclide concs, determ., calibration procedures 4-86974  
 sources, dangers (French) 4-93667  
 twin filter detector for radon daughter spectra 4-93672  
<sup>214</sup>Bi, aerosol radioactivity meas., Covasna mofette atmosphere (Romanian) 4-72674  
<sup>14</sup>C, behaviour in atmosphere (Russian) 4-77162  
<sup>35</sup>Cl(n, $\alpha$ )<sup>32</sup>P, lithosphere reactions, neutron flow, radiation chronology (Russian) 4-73897  
<sup>155</sup>Eu, atmospheric fallout samples collected in 1981 4-62891  
<sup>14</sup>(n,p)<sup>14</sup>C, lithosphere reactions, neutron flow, radiation chronology (Russian) 4-73897  
<sup>212</sup>Pb, aerosol radioactivity meas., Covasna mofette atmosphere (Romanian) 4-72674  
<sup>214</sup>Pb, aerosol radioactivity meas., Covasna mofette atmosphere (Romanian) 4-72674  
 Pu isotopes in surface air, Japan (1979-82) 4-115239  
<sup>239</sup>Pu, A=238, 239, 240, content in tobacco crop near nuclear fuel separation facility 4-115237  
 Rn and daughters conc. indoors, mathematical model 4-93916  
 Rn, daughter activities, meas. instrumentation 4-93867  
 Rn, daughter activity concs. indoors, approx. meas. technique 4-93866  
 Rn daughters, deposition rates on indoor surfaces 4-93917  
 Rn daughters, turbulent plateout in rooms and mines 4-93920  
 Rn daughters aerosol, activity size distrib. in buildings, cascade impactor meas. 4-93918  
 Rn daughters in indoor air, aerosol and activity size distrib. 4-93915  
 Rn daughters suspended in air, alpha activity, working level in U mines and houses 4-109966  
 Rn detection in Finnish dwellings, film detectors calibration 4-93895  
 Rn emanometry in active volcanoes using LR-115 track detectors 4-100516  
 Rn, indoor meas. using activated C collectors 4-89771  
 Rn, measurement in dwellings using activated charcoal 4-93897  
 Rn, methodology for meas. with passive instruments 4-93673  
 Rn progeny conc. indoors, cost evaluation of control measures 4-115229  
<sup>222</sup>Rn and daughter product concs. in dwellings and open air, equilib. factor 4-93919  
<sup>222</sup>Rn and decay products, active and passive dosimetry, international intercomparison 4-93864  
<sup>222</sup>Rn concs. in dwelling, seasonal variation 4-109968  
<sup>222</sup>Rn exhalation rate from surface of building materials or soil, meas. apparatus 4-93896  
 T<sub>2</sub>, airborne plume, oxidation rate rel. to release height and atmospheric stability 4-115241  
 Th daughter radioactivity released from burning gas lantern mantles 4-89787  
 Th, processing plant, airborne radioactivity monitoring 4-109964  
<sup>133</sup>Xe, released effluent, sector averaged plume, gamma dose rate from side sectors 4-115240  
<sup>88</sup>Y, atmospheric fallout samples collected in 1981 4-62891

# atmospheric spectra

- see also atmospheric optics  
 airglow, tidal and solar cycle effects on O I 5577 Å, Na I D, and OH(8,3) emissions 4-110341

**atmospheric spectra continued**

- auroral  $N_2^+$  427.8 nm emission, photometry from Atmosphere Explorer C satellite 4-72778  
 cloud shortwave spectral absorption, parameterization scheme improvement 4-94243  
 clouds, spectrometry from Meteor-Priroda satellite 4-77587  
 D-region, ion line spectra, EISCAT meas. during CAMP 4-100840  
 EHF/THF emission and attenuation from Canary Islands site 4-89968  
 formic acid in upper troposphere, identification of  $1105\text{ cm}^{-1}$  band in solar absorpt. spectra 4-100679  
 Fourier transform spectroscopy analysis method for atmospheric remote sensing 4-110269  
 gamma rays detected by balloon borne cosmic ray detector 4-100720  
 haematite dust at 60 km altitude, spectra and particle size 4-94227  
 ionosphere, spectrum of orbiting, vehicle induced luminosities on Space Shuttle STS-8 mission 4-105866  
 IR Earth/atmosphere background meas. during sunrise, using radiometer and interferometer 4-115569  
 IR transmittance band model for atmospheric  $N_2O$  4-115568  
 limb obs. by rocket at 4.3 microns wavelength 4-110195  
 long-wave spectral emissivities, calcs. for Bangkok, Songkhla and Ubon Ratchathane, Thailand 4-100733  
 Rayleigh scattering cross section, theoretical determ. 4-105714  
 red auroral arc, O I enhancement and  $N_2^+$  First Negative bands enhancement 4-100841  
 submillimetre FT spectrometer for stratosphere spectra and chem. composition 4-110268  
 TIROS radiance measurements, appl. to determ. of total  $O_3$  amount 4-100672  
 trace gas mixing ratios obtained from occultation spectra, effects of systematic errors 4-110186  
 trichlorofluoromethane, for infrared spectra and composition of stratosphere and troposphere 4-72697  
 tropospheric air trace gas meas. using tunable diode laser absorpt. spectrometer 4-114998  
 upper atmosphere, EUV nightglow and light scattering observations 4-110339  
 UV absorpt. features and Mount St. Helens, 1980 May eruptions, stratospheric  $SO_2$  and  $O_3$  spectral obs. 4-105694  
 UV sky brightness at 311.2 and 332.3 nm, Monte Carlo calc. 4-105716  
 water vapour, reson. absorpt. study using line-tunable CO laser (Chinese) 4-67398  
 water-vapour IR absorption in 8-14  $\mu\text{m}$  atmospheric window, temp. dependence 4-77613  
 D, in upper atmosphere, Spacelab 1 detect. of resonantly scattered Lyman- $\alpha$  emission 4-90016  
 $HNO_3$ , for infrared spectra and composition of stratosphere and troposphere 4-72697  
 $HO_2$ , 265.8 GHz rotational emission lines obs. in stratosphere 4-72667  
 $H_2O$  vapour absorption in visible and near IR, field meas. 4-89992  
 $H_2O_2$ , absolute IR intensity calc. of binary overtone, combination and difference bands 4-69074  
 $N_2^+$  (B-X) 427.8 nm auroral obs. rel. to IR spatial structure 4-110343  
 NO in thermosphere, IR emission intensity during mag. storm heating 4-110333  
 NO, stratospheric, in situ meas. using balloon-borne tunable diode laser spectrometer 4-72706  
 NO, absorption in twilight sky spectra 4-115542  
 O concentration in lower thermosphere, two-photon differential absorpt. meas. technique 4-82243  
 O I 557.7 nm emission, implications of meas. of O concs. in high latit. winter upper atmosphere 4-105784  
 O I (D-p) 630 nm auroral obs. rel. to IR spatial structure 4-110343  
 O II, UV emissions as contaminants of geocoronal He airglow obs. 4-105787  
 $O_2$ , UV absorpt. spectra, Herzberg continuum pressure depend. 4-107357  
 OH airglow in polar cap, rot. temps. at mesopause during stratospheric warming event 4-110340  
 OH nightglow, wavelengths of  $P_1(2)_d$  lines rel. to mesospheric wind determs. 4-105781  
 OH, stratospheric, submm detect. and line assignments in emission spectrum 4-110209

**atmospheric structure**

- see also *atmospheric composition*  
 Arctic haze, vertical structure, net-flux radiometer meas. 4-105144  
 auroral oval, dynamic var. during intense mag. storms 4-72776  
 cold front simulation, radiation boundary condition for multi-dimensional flows 4-82203  
 cold fronts, cloud and microphysical struct. of mesoscale convective bands 4-82199  
 frontal regions, convective and boundary layer parametrizations in diagnostic model 4-82198  
 ionosphere, aurora and electrojet configuration in early morning sector 4-72789  
 topside ionosphere,  $He^+$  dominance regions at high latits. 4-110363  
 ionosphere, SABRE obs. of morning sector convection reversal 4-110364  
 ionosphere, test of International Reference Ionosphere using single-freq. AI absorpt. data 4-90020  
 magnetopause structure and particle accessibility 4-67553  
 magnetosphere, ISEE 1 and 2 obs. of oscillating outward moving current sheet near midnight 4-85832  
 magnetosphere ground state structure, implications of ring coupling model 4-72809  
 magnetosphere polar cusps, struct. determ. from satellite mag. field meas. 4-110373  
 plasma sheet-lobe boundary structure 4-67558  
 sporadic-E layers, vertical and horiz. struct. using HF Doppler technique 4-100867

**atmospheric techniques**

- see also *air pollution detection and control; geophysical equipment; ionospheric measuring apparatus; ionospheric techniques; meteorological instruments; weather forecasting*  
 8th Australasian Fluid Mechanics Conference, Newcastle, NSW, Australia (Nov.-Dec. 1983) 4-67858  
 acid rain spatial variability analysis using Kriging interpolation procedure 4-82251  
 acoustic bistatic sounding, ref. effects (Russian) 4-82259  
 aerosol backscatter and attenuation meas. using  $CO_2$  tunable coherent lidar 4-100763  
 aerosol content measurement, use of light extinction model 4-110251

**atmospheric techniques continued**

- aerosol extinction meas. by SAM II and SAGE 4-100805  
 aerosol in coastal boundary layer, meas. technique of satellite optical imagery 4-100742  
 aerosol measurement,  $10\text{ }\mu\text{m}$  cutpoint size selective inlet for hi-vol samplers 4-100049  
 aerosol size distrib. determ. from aureole around point source, theory 4-62961  
 aerosols, atmospheric, microstruct. reconstruction from multifreq. sounding data 4-85769  
 air pollution measurement methods, statistical errors 4-93670  
 air-earth current meas., design for eliminating displacement currents 4-90007  
 airborne LIDAR, Arctic haze mapping 4-110328  
 anelastic interactive grid nesting for windstorm calc. 4-82174  
 Arctic haze, AGASP program and instrumentation for pollution monitoring 4-105722  
 aurora imaging, UV obs. from space under full sunlight 4-100843  
 auroral arc X-ray imaging by satellite 4-100842  
 automatic weather station for mountain top deployment 4-82279  
 balloon measurements of troposphere and stratosphere wind, tracking errors 4-110293  
 baroclinic primitive equations, implicit scheme devel., use of exact soln. 4-100655  
 bistatic lidar used for aerosol characts. determ. from scatt. 4-77647  
 boundary layer  $CO_2$  and  $H_2O$  turbulent transport, measurement apparatus 4-115583  
 BUV polarization inversion, stratospheric  $O_3$  and aerosol profiling 4-62960  
 chemical composition meas., range-resolved lidar equipment 4-94245  
 chemical composition of stratosphere, accuracy of NIMBUS 7 limb scanning method 4-105666  
 chemical composition of stratosphere, balloon borne laser instrumentation 4-115589  
 chemical composition of stratosphere, satellite remote sensing by infrared limb spectra method 4-105754  
 chemical composition remote sensing using tunable diode laser heterodyne spectroscopy 4-115590  
 cirrus cloud, IR lidar remote sensing method 4-110248  
 climate record in Andean tropical glacier ice cores 4-115560  
 climatological network design for United Kingdom 4-67331  
 cloud characteristics description, importance of cloud top lifetime 4-100670  
 cloud height determ. technique, for optically thin ice clouds 4-105734  
 cloud seeding with salt particles, numerical simulation for cumulus clouds (Chinese) 4-67365  
 cloud shape recognition in satellite remote sensing, computer programming 4-72707  
 cloud spectrometry from Meteor-Priroda satellite 4-77587  
 cloud temperature and motion meas. technique, by mm wave remote sensing 4-100797  
 clouds and aerosol vertical distribution, computer study 4-110330  
 clouds liquid water content meas., appl. of passive optical device, 4-62978  
 clouds studied by stereo-pair photographic method 4-90000  
 coherent IR radar systems and appls., conf., Arlington, VA, USA (Apr. 1983) 4-95019  
 cold front simulation, radiation boundary condition for multi-dimensional flows 4-82203  
 conodonts,  $O$  isotopic comp., use for palaeoclimate and palaeoceanography anal. 4-110283  
 cooling tower drift-measuring devices compared 4-62432  
 correlated time series averaging, appls. in dendroclimatology and hydrometeorology 4-100665  
 crosswind measurement using photon-burst correl. techniques 4-62966  
 differential absorption LIDAR in space for atmospheric temperature and humidity profiles 4-110331  
 dispersion coefficient determination, correction for influence on astrometric meas. (Russian) 4-101121  
 drought forecasting in NE Brazil, monitoring and prediction method 4-82196  
 Earth, land and ocean interaction 4-77662  
 Earth radiation budget determ. by ERB expt. on NIMBUS satellite, overview 4-105745  
 Earth radiation budget determ. by satellite, combining NIMBUS-6 and -7 data sets 4-105744  
 electric potential of boundary layer, Hy-wire measurement system 4-67437  
 ER-2 airborne LIDAR, NASA/CNES potential project 4-110326  
 ERS-1, satellite for ocean and climate monitoring, status and future plans 4-82369  
 evapotranspiration potential in Belgium, estimation procedure 4-115476  
 fog remote sensing by satellite IR radiometry method (German) 4-82276  
 Fourier transform spectroscopy analysis method for atmospheric remote sensing 4-110269  
 geomagnetic micropulsations, data acquisition procedures used at L'Aquila, Italy 4-110301  
 hail detection by radar, differential reflectivities 4-85774  
 hail detection radar, mismatched antenna beam pattern effects in dual wavelength radar 4-85779  
 heat storage in oceans, design of temp. sampling survey for climatological purposes 4-100809  
 heterodyne detection SNR in turbulent atm., matrix formalism calcs. 4-72201  
 holography, appl. to investigation of spatial distrib. of fog droplets 4-62979  
 homogeneous monodisperse particle number density meas. using variable-fringe-spacing Doppler velocimeter 4-108143  
 humidity values meas. by satellite, use for dewpoint anal. 4-115490  
 ice nucleus meas., appl. of continuous flow chamber 4-62980  
 information volume content on combining time series differing in length with homogeneous dispersion 4-67448  
 ionosphere HF radar probing using pulse compression techniques 4-94278  
 IR hygrometer appl. to convective phenomena anal. 4-94259  
 IR transmission of atmosphere, fast computation method 4-94282  
 laboratory clouds production, steam injection technique 4-62927  
 lake wind speed calc. methods using observations of overland wind speeds 4-67305  
 land surface remote sensing for climate model application 4-77677  
 Landsat data, visual range determination 4-96822

**atmospheric techniques continued**

- laser remote sensing of humidity profile, lidar signal processing problems (*Russian*) 4-72705
- laser sounding of atmospheric dynamics 4-77640
- lasers for analytical and industrial chem., conf., Los Angeles, CA, USA (Jan. 1984) 4-106100
- lidar, quantitative 532 nm data for vertical extinction profiles, relative humidity effect 4-100755
- LIDAR, spaceborne, atmospheric investigations 4-110325
- LIDAR, spaceborne, meteorology and environmental studies appl. 4-110321
- LIDAR, statistical accuracy of time variations in atmospheric dynamics 4-96971
- lidar chemical composition profiling, signal processing problems (*Russian*) 4-72705
- lidar determinations of extinction in stratus clouds 4-94239
- lidar remote sensing, conf., Aspen, Colorado, USA (Aug. 1983) 4-106090
- lidar remote sensing, truncated beam propagation in turbulent atm. 4-110245
- lidar remote sensing of atmos., book 4-82607
- light absorption vol. coeff., determ. method (*Russian*) 4-82234
- limb thermal emission meas., pointing error correction method 4-89996
- magnetosphere cosmic rays penetration, use in ring current characts. determ. 4-94303
- magnetosphere electric field measurement with spherical double probes on satellites 4-82367
- magnetosphere electron temp. estimation method using whistler spectrograms 4-82353
- marine weather measurement system and data transmission equipment 4-115622
- mesoclimatic conditions determ. for mountainous regions 4-94253
- meteorological Doppler radars, pseudonoise phase modulation appl. 4-90013
- meteorological hazard monitoring and assessment in Mediterranean region, appl. of METEOSAT system 4-94251
- micropulsation data acquisition and primary processing at Adolf Schmidt Observatory (*German*) 4-72704
- microwave atmospheric attenuation, differential emission meas. at 20.3 and 31.4 GHz by radiometry 4-85751
- microwave attenuation by rain, prediction using dual-polarisation radar 4-85748
- microwave path attenuation prediction using rain data collected by radar 4-85746
- microwave radiometry of atmosphere and ocean parameters using 5-channel obs. 4-105762
- MST radar detection of synoptic-scale vertical vels. 4-94185
- multiple atmospheric-window techniques for satellite-derived sea surface temperatures 4-67454
- Naval Oceanographic Data Distribution System for atm. and ocean data 4-62986
- NIMBUS 7 SAMS data, use for temp. and comp. retrieval 4-100691
- NIMBUS 7 SAMS instrument use for temp. determ. from IR obs. 4-100803
- NIMBUS 7 SBUV instrument use for O<sub>3</sub> profiles determ. 4-100799
- NIMBUS 7 SBUV-TOMS instruments use for total O<sub>3</sub> meas. 4-100800
- Nimbus 7 SMMR obs. of atm. water content 4-67411
- Nimbus and SMMR data, evaluation in Norwegian Sea with surface and airborne obs. 4-67476
- nuclear particle identification in space plasma research, review 4-100820
- optical propag., adaptive compensation for atmospheric turbulence effects (*French, English*) 4-67402
- optical scanner on NIMBUS-7 satellite, calibration accuracy 4-105749
- paleo-climate from marine sediment core foraminifera method, choice of correct mesh size 4-72690
- paleoclimatic indicators for weathered cratons, use of tropical stone lines and podzolised sand plains 4-110275
- parameter ranking methods, comparison and appl. in weather forecasting 4-67358
- parameterisation method for planetary boundary layer use in forecasting models 4-110215
- passive microwave measurements for ocean and atm. remote sensing 4-67478
- passive microwave remote sensing of the atmosphere and ocean 4-110304
- pollution detection, techniques for determ. of source-receptor relations for acid deposition 4-100025
- pollution optical remote sensing, conf., Ispra, Italy (April 1983) 4-73168
- precipitation area size from rain gauge meas., inversion problem 4-82184
- precipitation meas. by radar, conf., Bournemouth, England (Aug. 1982) 4-82592
- precipitation measurement with multi-parameter radar, review 4-85772
- precipitation rates during Holocene, glacier ice core determination technique 4-110306
- precipitation type identification, using dual-polarisation radar 4-85778
- pressure spectral anal. as indicator of synoptic-scale activity climatic var. 4-100756
- propane gas spillage monitoring, by 5 Km long fibre optics method 4-105155
- proton injection region size determ. during substorm 4-94307
- pyranometer in solar energy research and development: a technique of radiation measurement 4-82306
- radar backscattering anisotropy coeff. anal. use for hydrometeor characts. determ. (*Russian*) 4-115601
- radar for hail and rain studies of severe storms, use of radar circular polarisation 4-85786
- radar for mesosphere-stratosphere research, mobile SOUSY radar system 4-85791
- radar identification of precipitation type and other targets, dual-polarisation radar 4-85780
- radar measurement of precipitation, circular depolarization ratios and Doppler velocities 4-85781
- radar measurement of rain, influence of elec. charge and field on drop shape 4-85743
- radar measurement of rain and graupel, hydrometeor size estimation 4-85783
- radar scattering properties of hydrometeors meas. by dual-polarisation radar 4-85782
- radar sounding of stratosphere, using quasi-complementary codes 4-85789
- radar technique for monitoring boundary layer structure 4-115594

**atmospheric techniques continued**

- radiation budget of Earth, determ. from NIMBUS-7 satellite ERB expt. obs. 4-105712
- radiation budget of Earth; measurement by NIMBUS 7 accuracy of ERB data set 4-105750
- radiation budget of Earth, measurement by NIMBUS-7 IR radiometry 4-105713
- radiation budget of Earth, satellite measurement technique 4-82239
- radiation sensors on NIMBUS satellite ERB instrument package, performance 4-105747
- radiative fluxes computation, accuracy, of approximate method in presence of broken cloud (*Russian*) 4-67393
- radio emission use for cloudless atmosphere integral humidity content determ. (*Russian*) 4-115600
- radioacoustic method for boundary layer temp. and wind sounding (*Russian*) 4-115599
- radioacoustic sounding, wind influence on limiting height (*Russian*) 4-82258
- radiometers on NIMBUS satellites, inflight calibration adjustment of wide field of view instruments 4-105748
- radiowave propagation, method for estimating atmos. path delay in VLBI radioastronomy 4-85877
- rain drop size meas. by vertically pointing Doppler radar 4-85745
- rain meas. by differential polarisation radar, influence of drop size distrib. 4-85773
- rain meas. by dual-polarisation radar, comparison with distrometer obs. 4-85784
- rain meas. by radar, backscatt. theory for dual-polarisation radar 4-85775
- rain meas. by radar, differential refl. method with multiple polarisation planes 4-85777
- rain meas. using coherent polarization-diversity radar 4-85776
- rain measurement using multiparameter radar, review 4-85771
- rain remote sensing by anal. of satellite IR images 4-82252
- raindrop size distrib. by mm wave attenuation and use of Mellin deconvolution 4-85803
- raindrop size meas. using vertically pointing radar 4-85785
- rainfall rate meas. technique using dual-polarisation radar 4-85787
- rainfall remote meas. by radar and other methods, review 4-85770
- rainfall remote sensing, by soil moisture microwave emission method 4-100796
- rainfall-rate measurement via FM radar, echo power estimation rel. to accuracy improvement (*Chinese*) 4-67450
- remote sensing, digital image processing techniques, book 4-86132
- remote sensing using airborne 92/183 GHz imaging radiometer 4-77520
- rocket probing of atmos. temp. and wind, comparison of French and Soviet methods 4-105763
- SAGE used to determine stratosphere O<sub>3</sub>, comparison with other methods 4-100804
- satellite Doppler remote sensing, removal of tropospheric refr. effects 4-77649
- satellite meteorology, survey 4-110232
- satellite power system construction, environmental effects (*Japanese*) 4-62981
- satellite power systems, laboratory and field experiments on environmental effects (*Japanese*) 4-62982
- satellite rainfall estimation techniques, thunderstorm cloud height-rainfall rate relations 4-100671
- satellite-borne cryogenic limb array etalon spectrometer for upper atmosphere research, performance analysis 4-115668
- Scanning Multichannel Microwave Radiometer data anal. and use 4-67475
- SEASAT scatterometer data use for marine surface press. anal. 4-67375
- SEASAT SMMR data quality for atm. water determ. 4-67474
- shipboard deployment of meteorological instruments at end of horizontal boom 4-110302
- shipboard measurements, usefulness for detect. of secular changes of tropical air-sea heat flux 4-100582
- solar radiation estimation for Sahel region, by METEOSAT satellite data method 4-115546
- spaceborne laser appl. 4-110320
- spaceborne LIDAR for meas. from satellites, design 4-110327
- species measurement using excimer lasers 4-110279
- statistical objective anal. techniques, appl. to representation of coastal surface temp. field 4-105626
- stochastic prediction technique for monsoon rainfall forecasting 4-110241
- stratosphere temperature and chem. composition remote sensing by satellite IR limb scanning method 4-105753
- stratospheric multispecies trace gas meas. using balloon borne tunable diode laser absorption spectrometer 4-115591
- stream function and velocity potential from wind field, calculation procedure 4-100700
- submillimetre spectroscopy of stratosphere with three-channel <sup>3</sup>He-cooled bolometer, balloon mounting 4-77663
- surface radiation budget measurement method using satellite platform 4-72717
- TEA and multiatmosphere CO<sub>2</sub> lasers, remote sensing appl. 4-110332
- temperature data from meteorological stations, statistical quality control method 4-77639
- temperature determination for microwave emitting region of atmos. during microwave transmission study (*Czech*) 4-85792
- temperature measurement by automatic techniques 4-90003
- temperature of stratosphere, monitoring from NIMBUS 7 satellite, LIMS infrared limb spectra method 4-105754
- temperature of surface air, remote sensing of seasonal variations 4-100743
- temperature profiles determ. from radiative-convective models, appl. of Newton-Raphson method 4-110228
- temperature profiling by satellite IR method 4-85804
- temperature remote sensing from satellite, TIROS-N infrared and microwave system 4-115605
- temperature remote sensing of stratosphere, NIMBUS 7 infrared limb scanning method 4-105755
- thermosphere, wind vel. vectors determ. from dispersion relations of TID's 4-90015
- trace gas measurements using airborne tunable diode laser system 4-115588
- trace gas mixing ratios obtained from occultation spectra, effects of systematic errors 4-110186
- transparency meas. using automated digital instrument 4-78358

**atmospheric techniques continued**

- tropospheric and stratospheric parameter meas. using ground-based coherent lidar 4-100662  
 turbidity measurement by photometric method 4-90002  
 turbulence evaluation, appl. of digital meter for meas. of star jitter 4-94254  
 turbulence in boundary layer, VITA meas. technique 4-115494  
 turbulence monitoring by laser-induced O<sub>2</sub> fluoresc. method 4-78311  
 turbulence structure remote sensing by Fourier spectroscopy method 4-110270  
 UV radiometer onboard NIMBUS 7 satellite, sensor degradation during separation 4-105746  
 vertical interpolation for relative geopotential and temp. recovery 4-72727  
 water vapour profiles from IR radiation satellite meas. (*Chinese*) 4-115596  
 weather forecasting method utilising satellite determined wind data 4-115538  
 weather map production methods utilizing satellite cloud photographs 4-115598  
 weather radar simulator, for pilot training 4-85794  
 weather station buoys to be deployed off West coast of Great Britain 4-72741  
 weather station using BBC microcomputer for online data acquisition 4-110256  
 wind and humidity remote sensing method using satellite microwave radiometry 4-82302  
 wind and precipitation meas. at sea by monitoring of underwater sound 4-85687  
 wind at ocean surface, remote sensing by satellite radar method 4-67469  
 wind at sea surface, remote sensing using L-band radar method 4-67468  
 wind flow over complex terrain, variational-kinematical model 4-115488  
 wind meas. with laser Doppler anemometer, influence of fog and cloud 4-110262  
 wind measurement, comparison of Poker Flat MST radar and meteorological rocketsonde wind profiles 4-105656  
 wind measurement by Doppler lidar, airborne instrumentation and observations 4-90001  
 wind measurement by lidar on satellite (Windsat) 4-110265  
 wind measurement by meteo-oceanographic spar buoy, static equilb. response 4-82249  
 wind measurement method using pulsed IR Doppler lidar 4-110264  
 wind measurement technique, radar tracked chaff method 4-105742  
 wind measurement via flight control data on board civil aeroplane 4-105759  
 wind profiling in boundary layer using CW Doppler lidar 4-82253  
 wind remote sensing, Advanced TIROS-N Windsat lidar equipment 4-110266  
 wind remote sensing at ocean surface using Seasat scatterometer 4-67470  
 wind remote sensing by laser, Nd:YAG lidar meas. technique 4-110261  
 wind remote sensing by satellite radar, study of ocean radar cross-sections 4-85767  
 wind speed anal. Weibull distribution 4-82156  
 extreme wind speed calculation from visual observations made on ships 4-72688  
 wind speed determ. by SEASAT radar, errors due to atmosphere and ocean conditions 4-100810  
 wind speed determ. from drifting vessel 4-72730  
 wind speed measurement using instruments on towers and chimneys 4-67445  
 wind speed measurement via time-of-flight velocimeter, effect of turbulence on focused laser beam 4-89994  
 mesoscale wind system meas. technique using radar wind profiler 4-115550  
 winds over ocean, meas. technique based on seafloor acoustic observations 4-85686  
 C isotope record in pinyon pine tree rings, variability within and between trees 4-115607  
 CO<sub>2</sub> coherent IR lidar mission for tropospheric trace species transport and conc. meas. 4-100762  
 HCl detection at sub-parts-per-billion level using tunable diode laser absorpt. 4-115176  
 HCl in stratosphere, trace meas. using tunable diode laser absorption 4-89997  
 HNO<sub>3</sub> in middle atmosphere, conc. monitoring by IR Earth limb scanning from satellite 4-105757  
 H<sub>2</sub>O vapour in stratosphere, LIMS infrared monitoring method from NIMBUS-7 satellite 4-105752  
 H<sub>2</sub>O vapour profile remote sensing by lidar method 4-110267  
 NO<sub>2</sub> in atmosphere, meas. method using NIMBUS 7 satellite IR limb monitor 4-105751  
 NO<sub>2</sub> remote monitoring using DIAL based mobile lidar system 4-77167  
 O determ. in lower thermosphere by lidar method 4-82243  
 O<sub>3</sub> determ. in stratosphere, SAGE and SBUV method comparison 4-100801  
 O<sub>3</sub> in middle atmosphere, profile remote sensing by satellite IR limb scanning method 4-105756  
 O<sub>3</sub> measurement, determ. of total O<sub>3</sub> from TIROS radiance meas. 4-100672  
 O<sub>3</sub> profiles determ., use of 290-305 nm wavelengths 4-100798  
 O<sub>3</sub> vertical distribution study using heterodyne spectrometer 4-94255  
 Rn, daughter activity concs. indoors, approx. meas. technique 4-93866  
 Rn daughters meas. in room air, appl. of continuous spectrometry via twin channel device 4-93672  
 Rn detection in Finnish dwellings, film detectors calibration 4-93895  
 Rn emanometry in active volcanoes using LR-115 track detectors 4-100516  
 Rn, indoor meas. using activated C collectors 4-89771  
 Rn measurement with passive instruments 4-93673  
 Rn and decay products, active and passive dosimetry, international intercomparison 4-93864  
 SO<sub>2</sub> pollution conc. measurement by far IR laser spectroscopy method 4-74246

**atmospheric temperature**

see also *atmospheric thermodynamics*

- acoustic bistatic sounding, refr. effects (*Russian*) 4-82259  
 aerosol layer in stratosphere and influence on atmospheric radiation and temp. 4-67396  
 AIDJEX air stress meas. 4-89986

**atmospheric temperature continued**

- Arabian Sea area, atmospheric heating by radiation flux, due to aerosols 4-94241  
 Arabian-Sea monsoon depression, air-sea interface conditions observations 4-110204  
 North Atlantic, sea-air heat transfer in energy-active zones 4-105581  
 auroral F-region, expt. evidence of non-isotropic ion temp. distrib. 4-105793  
 automated measurement of temperature at 3.2 cm 4-89972  
 Beaufort Sea, surface stress meas. from wind and temp. anal. during AIDJEX 4-89983  
 Belgium, AD 1983 weather conditions 4-115553  
 Bermuda area of North Atlantic, AD 1981 meteorological obs. 4-105682  
 Bombay Airport, India, max. and min. temp. rel. to wind levels 4-110219  
 Boulder Atmospheric Observatory, temp. meas. during nighttime drainage wind events 4-105620  
 boundary layer and soil temp. during nighttime for frosty conditions, model 4-115544  
 marine boundary layer struct. at Sable Island, Nova Scotia 4-67329  
 boundary layer temp. profile from sunlight refr. anal. (*Russian*) 4-82167  
 Bowen's ratio over bare cotton soil, temp. and humidity anal., instrumentation 4-67335  
 central Canada, temperature records from 1768 to 1910 AD 4-62944  
 Carpathian Mountains, Poland, orographic patterns refl. in meso- and microclimatic conditions 4-94236  
 China, long-range weather forecasts, geophysical factors, appl. 4-72671  
 climate variations, correl. with monsoon rainfall and sea surface temp. 4-82218  
 climatic effects of volcanic eruptions 4-105514  
 cloud temperature and motion meas. technique, by mm wave remote sensing 4-100797  
 coastal surface temp. field, representation using statistical objective anal. techniques 4-105626  
 conference on atm. radiation at Toronto, Canada (June 1981) 4-90300  
 Cretaceous climate model sensitivity, geographic variables effect 4-72692  
 Czechoslovakia, energy balance at land surface (*German*) 4-77572  
 D-region, auroral, heated patch effect on VLF propag. 4-85820  
 Dead Sea area during advective sharav condition 4-94184  
 differential absorption LIDAR in space for atmospheric temperature and humidity profiles 4-110331  
 diurnal amplitude of air temp. in polar regions, cause of 'Fram' type seasonal change 4-110192  
 E-region, electron temperature profile at high latitude 4-105800  
 Elton, Louisiana, 1976 March 24 tornado, storm characts. 4-105665  
 energy balance at land surface, daily variations and statistical struct. 4-89959  
 NE England, 1983 July heatwave, sunshine totals and temp. characts. 4-100717  
 central England, homogeneity of annual temp. (1659 to 1973) 4-110187  
 Eurasia, statistical prediction of seasonal surface air temp. 4-62896  
 F-region, ion temperatures, at high latitude 4-72794  
 Florida, USA land use rel. to surface temp. fluctuations 4-115499  
 forecasting of max. daily temperatures (*Spanish*) 4-94230  
 frost-free record reconstruction for E Massachusetts (1733 to 1980) 4-100673  
 global temperature field, long-term time evolution (*Chinese*) 4-67363  
 global warming influence on northern hemisphere meteorological variables 4-105704  
 Goddard general circulation model climatology, effects of sea ice var. 4-89990  
 gradient distributions and flux profile relations above rough forest, implications for evapotranspiration 4-82204  
 Great Britain and N Ireland, diurnal range of temperature 4-115548  
 greenhouse effect, role of CO<sub>2</sub>, minor gaseous components and aerosols 4-82228  
 heating of lowest 5 km of atmos. due to direct solar radiation 4-77570  
 Hunza region, Karakoram, rocks chem. weathering and temp. meas. 4-62816  
 Iceland, climate and sea-ice record (AD 870 to 1780) 4-94235  
 India, meteorological requirements on airconditioning rel. to human habit comfort 4-67336  
 India, SW monsoon activity, effect on upper troposphere thermal features 4-67337  
 India, tropical cyclones tropopause, height var. with temp. 4-67338  
 Indian Ocean temp. meas. during FGGE rel. to boundary-layer wind shear 4-105627  
 ionosphere, electron temperature empirical model for F<sub>2</sub>-layer 4-105795  
 ionosphere, obs. of hot heavy ions assoc. with Space Shuttle Orbiter 4-110495  
 ionosphere and thermosphere, particle heating 4-105790  
 ionosphere E and F-regions, nonthermal components of low energy electrons 4-63008  
 ionosphere heating, soliton vs. parametric instabilities params. 4-82334  
 ionosphere ion temps., non-isotropic ion vel. distrib. EISCAT meas. 4-105799  
 IR sounder for moisture and temp. meas., design requirements 4-62959  
 Northern Ireland, use of anomaly maps for local forecasting 4-110212  
 Japan, summer temperature low rel. to 100 mb height var. 4-110239  
 land distribution influence on global climate 4-105701  
 long term variations (*Russian*) 4-115505  
 Lower Beskid Range, Poland, mesoclimatic and thermal relations 4-94253  
 magnetosphere, electron temp. rel. to relativistic dispersion and generation of auroral kilometer radiation 4-94312  
 magnetosphere, evidence for heating of thermal electrons at magnetopause boundary layer 4-105810  
 marine atmosphere, surface temperature long term trends 4-100580  
 marine surface layer, thermal struct. (*Russian*) 4-115507  
 marine surface layer, worldwide temp. fluctuations (1856 to 1981) 4-105569  
 measurement of atmospheric temp. by automatic techniques 4-90003  
 mesopause, polar cap OH airglow rot. temps. during stratospheric warming event 4-110340  
 mesosphere, temp. profiles rel. to O<sub>3</sub> concs. 4-62924  
 mesosphere and lower temperature, IR radiative transfer and temp. model 4-115573  
 Mesozoic climate, significance of fossil flora on Alexander Island 4-82229  
 meteorological station temp. data, statistical quality control method 4-77639

**atmospheric temperature continued**

- microwave emitting region of atmos. during microwave transmission study, temp. determ. methods (*Czech*) 4-85792
- microwave propagation, effects of water vapour, rain, humidity, temp. and press. 4-100716
- monsoon depressions, equivalent pot. temp., convection, cloud heights and humidity zones 4-110224
- mountain areas, cold air drainage, thermal belt and cold air lake 4-94199
- mountain valley daytime boundary layer evolution 4-100658
- New Delhi, India, night minimum temp. forecasting 4-110221
- NIMBUS 7 SAMS data use for temp. retrieval 4-100691
- NIMBUS 7 SAMS instrument use for temp. determ. from IR obs. 4-100803
- nocturnal boundary layer over rough terrain, wind and temp. profile obs. 4-77581
- nocturnal stratocumulus cloud, simultaneous meas. of turbulent and micro-physical struct. 4-62914
- nuclear war, climatic consequences, computational expt. (*Russian*) 4-67389
- nuclear winter, prolongation by snow and ice feedbacks 4-105674
- S Ontario, cyclonic storm precipitation bands, deep 0°C isothermal layers and wind shear 4-77601
- polar winter stratosphere, four day oscill. in brightness temp. 4-72700
- Quebec, relation between dunes, fire and climate recorded in Holocene deposits 4-85753
- radiative budget of atmosphere, influence of clouds 4-94242
- radioacoustic method for boundary layer temp. and wind sounding (*Russian*) 4-115599
- remote sensing method for stratosphere temp., NIMBUS 7 infrared limb scanning method 4-105755
- remote sensing of air temp. and temp. of bare soil 4-100743
- rocket probing of atmos. temp. and wind, comparison of French and Soviet methods 4-105763
- satellite remote sensing, TIROS-N infrared and microwave systems 4-115605
- satellite temp. profiling method 4-85804
- Scott Base, Antarctica, temp. record, 1958-82 4-100711
- sea ice decay in Canada and Alaska, air temp. and sunlight effects 4-89943
- sea surface, drag, heat and moisture transfer coeffs. 4-82164
- West Siberia, long-range forecasting of temp. and precipitation 4-105679
- solar-terrestrial relationship in mesosphere and stratosphere temp. 4-85739
- South Polar Plateau, surface temp. regime, energy balance etc. 4-115540
- Southern Oscillation persistence, rel. to seasonal var. of cloudiness 4-94226
- stratosphere, equatorial Kelvin modes rel. to temp. variance in tropics 4-72655
- lower stratosphere, radiative heating, rel. to O<sub>3</sub> distrib. in two-dimensional model 4-62920
- stratosphere, search for depend. on 11 year solar activity cycle 4-100713
- stratosphere, temp. distrib. rel. to north-south asymmetries of solar particle events in stratospheric O<sub>3</sub> 4-110229
- stratosphere and mesosphere at Thumba, India, temp. perturbations in winter 4-105663
- stratosphere sudden warmings and quasi-biennial oscills. 4-115531
- stratosphere warming event, meas. of polar cap OH airglow rot. temps. at mesopause 4-110340
- stratospheric fountain region, radiative heating rate calcs. 4-67394
- surface layer over crops, CO<sub>2</sub>, wind, temp. and humidity fluctuations 4-77580
- surface potential temperature, prediction model for complex terrain area 4-77577
- surface pressure and temp. rel. to sea ice extent predictability 4-89948
- surface temperatures, effects of CO<sub>2</sub>, volcanic aerosols and solar radiation var. 4-94238
- Tanzania, temperature records and statistical method for data quality control 4-77639
- thermosphere, heating during mag. storms rel. to NO conc. and IR emission 4-110333
- thermosphere, night-time winds and temps. during solar cycle min. and max. 4-72770
- thermosphere, superrotation and struct. of atmosphere, model 4-110335
- thermosphere, two-dimens. high resolution nested grid model, neutral response to elec. field spike 4-85807
- thermosphere, vertical profiles from EISCAT and HF Doppler radar 4-100839
- thermosphere, wind vectors and temp. determ. from dispersion relations of TID's 4-90015
- Tokyo, Japan, temperature and humidity data (1976 to 1980) 4-105675
- troposphere, effects of volcanic eruptions on temp. distrib. and general circulation 4-100678
- United States, climatological contingency anal. and seasonal forecasting skill 4-77586
- United States, role of January in character of recent winters (1975 to 1982) 4-100663
- upper atmosphere circulation, temp. and composition model and geomag. activity influences 4-67515
- upper atmosphere temp. from cosmic ray meas. 4-100966
- USA, severe winters rel. to global, radiation and heating degree days 4-115498
- USSR (European), long-range forecasting of temp. and precipitation 4-105679
- USSR temp. and rain forecasts based on heat content of N Atlantic water 4-67351
- vertical interpolation for temp. recovery 4-72727
- vertical temperature profiles determ. from radiative-convective models, appl. of Newton-Raphson method 4-110228
- winter anomaly over European USSR, numerical simulation 4-72678
- zonal mean temperature, correl. with large-scale meridional eddy momentum transport 4-72656
- zonal temperature annual variation by small component spectral model (*Russian*) 4-100682
- zonal wind and temp. fields of troposphere, response to heat and momentum heat source changes 4-115508
- CO<sub>2</sub> global concentration influence on air temp. and precipitation 4-67388

**atmospheric thermodynamics**

see also atmospheric temperature

- Antarctic marginal ice zone, sea ice destruction due to heat transfer from atm. 4-67326
- Arabian Sea, zonal and meridional eddy fluxes of dry and moist energy components 4-110217
- Arabian Sea area, atmospheric heating by radiation flux, due to aerosols 4-94241
- North Atlantic, sea-air heat transfer in energy-active zones 4-105581
- North Atlantic trade wind zone, ocean-atmosphere thermal interaction 4-72611
- middle atmosphere; wave characts. simulation in general circulation model 4-62921
- boundary, layer, uncoupled multi-layer model for sensible and latent heat flux densities 4-105618
- Bowen's ratio over bare cotton soil, temp. and humidity anal., instrumentation 4-67335
- climate sensitivity, energy balance models and oscillatory climate models 4-72693
- climatology, thermohydrodynamic eqns. for three-component zonal model of climate 4-62948
- comparative energy balance study for Arctic tundra, sea surface, glaciers and boreal forests 4-94197
- continental thermal energy storage in a zonally averaged global thermodynamic model 4-110242
- convection, stability criterion for moist compressible atmosphere and energy conditions for cloud development (*Russian*) 4-67310
- convective boundary layer, turbulent profiles, urban effects 4-72648
- cyclogenesis, latent heat induced energy transformations and precipitation 4-100659
- Czechoslovakia, energy balance at land surface (*German*) 4-77572
- E-region, electron gas heating due to magnetosphere convection, effect on cond. 4-100847
- energy balance at land surface, daily variations and statistical struct. 4-89959
- energy balance climate model, snow and ice feedbacks prolong nuclear winter 4-105674
- energy balance models incorporating transport of thermal and latent energy 4-82181
- equatorial forcing of climate telecommunications, dynamical anal. 4-72652
- extratropical eddy heat flux and vertical shear on short time scales 4-82179
- F-region, polar, ohmic heating by HF pulses, effects on electron density and temp. 4-85814
- NW Florida continental shelf, cold air outbreaks, heat flux with ocean 4-67237
- forced equatorial long waves, simple analytical solns. 4-62922
- general circulation, zonally symmetric model for volcanic influence 4-100678
- Goddard general circulation model climatology, effects of sea ice var. 4-89900
- gradient distributions and flux profile relations above rough forest, implications for evapotranspiration 4-82204
- greenhouse effect, role of CO<sub>2</sub>, minor gaseous components and aerosols 4-82228
- heat fluxes (sensible and latent) above water surface, parameterization (*Russian*) 4-100684
- heat storage and poleward transport in ocean-atmos. system, interannual variability 4-110197
- ice edge latitude, sensitivity to finite amplitude baroclinic heat flux divergence 4-72691
- Intertropical Convergence Zone dynamics, GLAS climate model symm. version anal. 4-72643
- ionosphere, energy principle for high-latitude electrodynamics 4-85812
- ionosphere, hemispherical Joule heating as function of AE indices 4-72788
- ionosphere, latit. vars. of Joule heating due to auroral electrojets 4-72784
- ionosphere and thermosphere, particle heating 4-105790
- ionosphere E and F-regions, nonthermal low energy electrons prod. by dynamo currents 4-63008
- kinetic energy spectrum of large- and mesoscale atmospheric processes 4-94225
- long-wave spectral emissivities, calcs. for Bangkok, Songkhla and Ubon Ratchathani, Thailand 4-100733
- magnetosphere, energy var. and elec. fields in collisionless ion-electron plasma 4-100868
- magnetosphere, heavy ions turbulent heating on auroral field lines 4-72805
- magnetosphere, MHD generator process in solar wind energy transfer regions inside dayside magnetopause 4-105814
- magnetosphere, obs. of solar wind energy transfer regions inside dayside magnetopause 4-105813
- marine atmospheric, interannual moisture vars. near surface of tropical Pacific Ocean 4-82200
- mesosphere and lower thermosphere, IR radiative transfer and temp. model 4-115573
- multiplicity of thermal regimes (*Russian*) 4-115505
- planetary boundary layer-ecosystem interaction: heat and moisture fluxes 4-94196
- polar regions, surface energy balance rel. to seasonal change in diurnal amplitude of air temp. 4-110192
- potential evaporation, influence of atmospheric stability 4-100666
- quasigeostrophic uniform pot. vorticity, predictability and energy transfer props. 4-62879
- radiative flux balance, effect of antiscreening of outgoing thermal radiation by clouds (*Russian*) 4-67392
- radiative fluxes computation, accuracy, of approximate method in presence of broken cloud (*Russian*) 4-67393
- Sierras de Cordoba, Argentina, energy balance of surface boundary layer during rainy season 4-105671
- South Polar Plateau, surface temp. regime, energy balance etc. 4-115540
- stationary planetary waves form. in Northern Hemisphere, role of Greenland Plateau (*Chinese*) 4-67364
- stratosphere, equatorial Kelvin modes rel. to temp. variance in tropics 4-72655
- lower stratosphere, radiative heating, rel. to O<sub>3</sub> distrib. in two-dimensional model 4-62920
- stratosphere tracer transport, modified diabatic circulation model 4-62923
- stratospheric fountain region, radiative heating rate calcs. 4-67394

**atmospheric thermodynamics continued**

- summer energy budget simulation for latitudinal transect along America's east coast 4-77583
- temperature profiles determ. from radiative-convective models, appl. of Newton-Raphson method 4-110228
- thermal radiation budget of Earth, comparison of diurnal models 4-82233
- thermosphere, energy and momentum input at auroral latits, rel. to vertical winds and gravity waves generation 4-105783
- thermosphere, general circulation model with coupled dynamics and comp. 4-72769
- thermosphere, NO conc. and IR emission assoc. with mag. storm heating 4-110333
- thermosphere, tidal modes due to in situ heating rel. to variability of ionospheric dynamo currents 4-90021
- trade-wind boundary layer, thermodynamic structure, downstream vars. 4-62899
- transpiration and evaporation from weather moorland, meas. 4-105619
- tropical air-sea heat flux, usefulness of shipboard meas. for detect. of secular changes 4-100582
- tropical cloud clusters and diabatic heating of atm. 4-72651
- Uccle, Belgium, radiation balance (1972 to 1982) 4-110227
- winter temp. anomaly over European USSR, numerical simulation 4-72678

**atmospheric turbulence**

- adaptive optics basis functions for obscured aperture, phase aberration correction 4-74427
- adaptive systems, wavefront correction quality 4-107550
- adaptive transmission, two-wavelength, diffractive and refractive effects comparison 4-87280
- air vortex flow struct., operating and geometrical param. effects 4-82186
- aperture-averaged spectral correlations of beams in a turbulent atmosphere 4-100725
- Bering Sea, longitudinal rolls and steam fog in boundary layer 4-72641
- boundary layer, turbulent diffusion equation with mean vertical wind 4-82212
- boundary layer, turbulent dispersion concentration patterns 4-67301
- boundary layer CO<sub>2</sub> and H<sub>2</sub>O turbulent transport, measurement apparatus 4-115583
- Boundary Layer Experiment-1983, characts. 4-110255
- marine boundary layer struct. at Sable Island, Nova Scotia 4-67329
- boundary layer turbulence and VITA meas. technique 4-115494
- boundary layer vertical wind velocity changes 4-67298
- clear air turbulence generation 4-105681
- cloud-topped mixed layers, buoyant production of turbulence 4-82180
- clouds, effects of turbulent mixing 4-72661
- coherent IR radar systems and appls., conf., Arlington, VA, USA (Apr. 1983) 4-95019
- coherent structures in planetary flows as systems endowed with enhanced predictability 4-62886
- continuous systems, discrete simulation, implementation of noise 4-58758
- convective boundary layer, turbulent profiles, urban effects 4-72648
- convective planetary boundary layer turbulent exchange coeff. 4-110193
- convective boundary layer, spectral representation of vertical struct. of turbulence 4-62915
- crosswind measurement using photon-burst correl. techniques 4-62966
- diffusion in convective boundary layer, by turbulent energy model 4-115483
- dispersal of heavy particles 4-72680
- dusty atmosphere of Sahel, turbulence affected by dust radiative props. (French) 4-77576
- evaluation, appl. of digital meter for meas. of star jitter 4-94254
- extratropical eddy heat flux and vertical shear on short time scales 4-82179
- deciduous forest canopy, obs. of microscale pressure fluctuations 4-67300
- quasi-geostrophic potential vorticity eqn., simplified forms 4-62900
- geostrophic turbulence, baroclinic and barotropic predictability 4-62880
- gravity wave-turbulence interaction in presence of critical level 4-94214
- heterodyne detection SNR in turbulent atm., matrix formalism calcs. 4-72201
- hill with gentle slopes in boundary layer flow, wind and turbulence study 4-115493
- imaging through turbulence, Fried's parameter estimation from time series of arbitrary resolved imaged object 4-72698
- ion dispersion expts. in turbulent boundary layer 4-77578
- ionosphere, D-region, artificial periodic electron density inhomogeneities, turbulent spreading 4-115657
- ionosphere, plasma turbulence due to interaction with Space Shuttle Orbiter 4-110495
- ionosphere, VLF waves interaction with turbulence 4-100852
- isolated coherent vortices in turbulent flow 4-60433
- Lagrangian particle diffusion simulation with wind shear effects, Monte Carlo scheme 4-115487
- large-scale meridional eddy momentum transport, correls. with zonal mean quantities 4-72656
- large-scale turbulence and predictability, obs. aspects 4-62876
- laser beam propagation, turbulence effect, appl. to time-of-flight velocimeter 4-89994
- light polarisation change in turbulent atmosphere 4-107525
- magnetosphere, electron accel. by plasma turbulence (Chinese) 4-110366
- magnetosphere, electrostatic plasma turbulence rel. to auroral electrons accel. 4-100853
- magnetosphere, heavy ions turbulent heating on auroral field lines 4-72805
- magnetosphere, upper hybrid turbulence as source of nonthermal continuum radiation 4-94315
- marine boundary layer, baroclinic effects on wind and turbulence 4-77569
- measurement of temp. and density fluctuations by laser-induced O<sub>2</sub> fluoresc. method 4-78311
- mixing efficiency in stably-stratified decaying turbulence 4-112824
- mm-wave scintillation caused by turbulence in clear air near ground 4-77615
- moments of irradiation fluctuations in atmospheric optical propagation, uniqueness of statistics 4-74425
- nighttime drainage winds, observational study of instability and turbulence 4-105620
- nocturnal boundary layer over rough terrain, wind and temp. profile obs. 4-77581

**atmospheric turbulence continued**

- nocturnal stratocumulus cloud, simultaneous meas. of turbulent and microphysical struct. 4-62914
- optical propag., adaptive compensation for atmospheric turbulence effects (French, English) 4-67402
- optical propagation, effects of atmospheric turbulence (French, English) 4-67403
- parametrization of viscous dissipation and kinetic energy 4-72625
- puff diffusion model, skewed, in diabatic surface layer, parametric description, report 4-62941
- radar technique for monitoring boundary layer structure 4-115594
- radiowave scintillation intensity, meas. and modelling to estimate turbulence parameters in Earth-space path 4-89965
- receiving telescope focal plane light intensity fluctuations caused by round-trip propag. through turbulent atm. 4-62952
- remote sensing of turbulence struct., by Fourier spectroscopy method 4-110270
- rough terrain, air flow and dispersion Euromech 173 report 4-82185
- stably stratified atmosphere, internal mixing layers characteristic scale (Russian) 4-82168
- star image scintillation in Elbrus region, Caucasus 4-62953
- stratosphere thin turbulence layer, vertical eddy diffusivity calc. 4-100677
- structure functions in atmospheric surface layer estimates of power-band exponents  $\mu$  and  $\mu_g$  4-105625
- subtropical jet stream, water vapour transport by large-scale eddy motions 4-82193
- surface layer dynamics, three-dimensional heat and moisture transport modelling 4-72684
- surface layer of atmosphere, nonlinear model 4-100705
- thermosphere, O concentration, eddy diffusivity and circulation 4-72767
- transient eddy forcing of time-mean flow 4-82173
- tropospheric and stratospheric parameter meas. using ground-based coherent lidar 4-100662
- turbulent diffusion in environment, mathematical modelling, conference, Liverpool, England (1978 September 12 to 13) 4-101577
- two-dimensional isotropic turbulence, effect of finite Rossby radius 4-110210
- unsteady convective vortices model for boundary layer 4-67302
- vertical turbulent transport in mixed layer, model 4-94216
- water vapour transport and potential evaporation, influence of atmospheric stability 4-100666
- Rn daughters, turbulent plateout in rooms and mines 4-93920

**atmospheric wind** *see wind***atmospherics**

- see also atmospheric electromagnetic wave propagation; whistlers*
- auroral kilometer radiation, direct generation by maser synchrotron instability 4-85840
- auroral kilometer radiation, emission through new plasma 4-67565
- auroral kilometer radiation generation, relativistic dispersion of extraordinary mode waves 4-94312
- auroral VLF hiss, correl. with television images of auroral pulsations 4-110346
- Calcutta, India, cloudiness effects on atmospherics during SW monsoon season 4-67325
- Calcutta, VLF/LF records due to Indian Ocean-Bay of Bengal storm 4-77604
- chorus emissions, wave normal directions near equatorial source region 4-85837
- daily variation of 10 and 27 kHz atmospheric in Germany 4-110205
- daily variation of VLF atmospherics, depend. on meteorological conditions 4-110206
- EM ion cyclotron mode (ELF) waves generated by auroral electron precip., S3-3 satellite obs. 4-85842
- Gaighata tornado of 12 April 1983, case study 4-100686
- ionosphere, ELF noise assoc. with interaction between VLF waves and turbulence 4-100852
- lightning, space-time mapping of VHF sources rel. to severe storm struct. 4-105657
- magnetosphere, microwave atmospherics generation by mag. field line reconnection 4-84011
- magnetosphere chorus emissions observed by GEOS 2; wave normals determ. 4-85838
- nonthermal continuum radiation, generation by upper hybrid turbulence 4-94315
- periodic VLF emissions assoc. with short-period mag. pulsations, ISIS 2 and Syowa obs. 4-85836
- quasigeostrophic flows predictability 4-60376
- radio noise, global distrib. study using satellite obs. of thunderstorm activity (Japanese) 4-63015
- sudden ionospheric disturbances in VLF atmospheric noise, rel. to solar flares 4-77680
- VHF radiation near to lightning return strokes 4-67318

**atom-atom collisions**

- includes reactive collisions*
- inert gas atoms, metastable states, quenching by Cu atoms 4-96485
- inert gas atoms, nuclear spin polarisation by spin exchange with optically pumped alkali metal atoms 4-78932
- laser-assisted atom-atom collisions 4-96646
- multiple collisions, group theory approach 4-87176
- multiplet component alignment during collisions 4-107445
- shock-heated Ar plasma, collisional and radiative mechanism simulations 4-91965
- spectral line collisional broadening 4-87202
- Ag+He, collisional depolarisation cross section, Hanle effect meas. 4-64585
- Ar+Kr atoms, ionisation processes for highly excited Ar atoms 4-87201
- Ba<sup>+</sup> gas phase collisional quenching and intramultiplet mixing 4-87153
- Ba+Pb(L) collisions,  $\delta$ -electron spectra study 4-74321
- Cr+He(Ar), intramultiplet mixing collisions, fluoresc. 4-64588
- Cs resonance lines, low press. noble gas broadening 4-74186
- Cs+Cs(He), absolute polarisation meas., natural lifetime in Cs 7S<sub>1/2</sub> state 4-83448
- F-Xe, two-state collision problems for exponential coupling 4-74315
- H+He, rate const. meas. for orientation transfer 4-107435
- H+inert gas atoms, laser excitation, electron loss from H(sp) atoms, H(3p) beam prod. 4-87200
- H+O, electron capture, electron loss, excitation 4-64590
- He+H(D), H(D) 2s and 2p excitation, integral cross sections 4-102786

## atom-atom collisions continued

- He+He multiple polarisabilities, dispersion forces, many-body theory 4-87192  
 He+high-Rydberg atoms in circular states, collisional props. using free electron model 4-96654  
 He+inert gas atom, single and double electron loss cross sections of He metastable and ground states 4-59884  
 He+Xe, collision induced absorpt. coeff., quantum mech. and classical approach 4-91330  
 He<sup>+</sup>+He, pot. energy curves obtained by combining scatt., spectroscopy and ab initio theory 4-74177  
 He<sup>+</sup>+Ne, electronic energy transfer in nozzle-beam scatt. cell expt., visible emission, odd-J levels 4-64578  
 Hg, multiplet component alignment during collisions 4-107445  
 Hg vapour, laser assisted collisional effects in nonlinear optical phenomena 4-96996  
 I+Pb collisions,  $\delta$ -electron spectra study 4-74321  
 K+Na(3P), differential scatt. cross sections 4-112255  
 K+Ar, fine-struct. transitions, interatomic pots. tests and coupling mechanism 4-87199  
 Kr-Hg mixture, ionisation coeff. meas. 4-79707  
 Kr+Kr, metastable interaction, <sup>3</sup>P<sub>2</sub> state 4-91335  
 Kr+Kr (Xe), 4f<sub>7</sub> excitation, L-shell vacancy prod. 4-59883  
 Li, multiplet component alignment during collisions 4-107445  
 Li+He, Li(2s-3d) excitation, D state scatt. amplitudes 4-64570  
 Mg+He, fine struct. transitions, close coupled transitions 4-78951  
 Mg+He(S) interaction calcs. using SA-MCSCF ICF-CI wavefunctions 4-74314  
 Na, ion formation in vapour containing Rydberg atoms 4-91242  
 Na, virtually excited state, inelastic collisions 4-74316  
 Na+Ar, collisional redistribution and fine-structure transitions, collisional redistribution 4-83457  
 Na+Ar, emitted monochromatic light reson. scatt. 4-69022  
 Na+Ba, two-photon radiative collision, Ba<sup>+</sup> prod. 4-64587  
 Na+Br collisions, ion pair prod. 4-112266  
 Na+He, emitted monochromatic light reson. scatt. 4-69022  
 Na+He, two-state collision problems for exponential coupling 4-74315  
 Na+He(Ne), population transfer, mol. pot. curves, avoided crossings 4-96655  
 Na+inert gases, collisional relax., two-photon absorpt. spectra 4-78930  
 Na+Na, associative ionisation reaction, rate consts. 4-89283  
 Ne-Ar, interatomic pot., dilute gas bulk and microscopic props. 4-96638  
 Ne+Ne, interaction excimer pots., atomic beam study 4-64563  
 Ni+Ni collisions, isolated K MO transitions, emission anisotropy 4-69180  
 O+Cu(Zr)(Ag)(Pb) collisions, K-shell ionisation, angular depend. 4-74322  
 Rb, fine struct. mixing induced in collisions with atoms and mol's., fluoresc., 4-96659  
 Rb+Rb(Ss), Rb<sup>+</sup>+Rb<sup>-</sup> collisional reaction investig. 4-102769  
 Sr+Ca collisions, multistate coupled eqn., laser-induced transition process 4-74323  
 Ti+Ar, up-conversion using stimulated anti-Stokes Raman scatt. and stimulated collisional induced fluoresc. in Ti 4-69498  
 Ti+inert gases, adiabatic pots. and oscillator strengths, improved pseudopot. calc. 4-91228  
 Xe, collision using two-photon laser excitation, fluoresc., inelastic quenching 4-74184  
 Xe+Br(2P<sub>3/2</sub>), laser photoassociation, XeBr(B) fluoresc. 4-114772

## atom-ion collisions

- includes reactive collisions*  
*see also charge exchange*  
 alkali closed shell ions, repulsive interactions with Ar, Kr and Xe, beam and transport meas. comparison 4-96653  
 alkali metal vapour+H ions, spin-depend. charge transfer 4-59890  
 approximate electron- and proton-impact line widths within a spectral series 4-91237  
 asymmetric collisions, inner shell ionisation, binding effects 4-96674  
 asymmetric ion-atom collisions, charge transfer to a fast projectile in the presence of a nuclear resonance 4-96691  
 atoms with Z=64, H<sup>+</sup> impact, K-shell ionisation cross sections 4-96508  
 charge exchange processes 4-96694  
 charge exchange transitions to excited states 4-74332  
 charge transfer, laser assisted, coupled dressed quasimolecular states approach 4-96684  
 collisional dissociation, form. of H<sub>2</sub><sup>+</sup> 4-66555  
 coulomb effects in atomic reactions in the presence of a low-frequency laser field 4-66578  
 doubly alignment parameter A<sub>2</sub> for L<sub>3</sub> subshell ionisation by light-ion impact 4-96510  
 electron capture, symmetries eikonal-type approx. 4-83464  
 Electronic relativistic effect in inner-shell ionization cross section and electron momentum distribution 4-96509  
 elements, medium Z, H<sup>+</sup> impact, X-ray prod. cross sections 4-96648  
 foil-excited Rydberg states in atoms+ion collisions, elec. field ionisation 4-102784  
 halogen closed shell ions, repulsive interactions with Ar, Kr and Xe, beam and transport meas. comparison 4-96653  
 heavy target elements bombarded with protons in energy range 0.5 MeV to MeV, K-shell ionisation 4-96507  
 heavy targets, L subshell X-ray production by 1 to 3 MeV protons and He<sup>+</sup> ions 4-96651  
 inert gas atom+ion electron capture collisions, recoil charge distrib. 4-59892  
 inert gas atoms+H<sup>+</sup>(He<sup>+</sup>), charge transfer and direct ionisation channels, electron prod. 4-87191  
 inert gas ion+atom collisions, integral cross section meas. 4-78929  
 inner shell ionisation by light ions, conf., Linz, Austria (Aug. 1983) 4-95035  
 inner shell vacancy production in ion-atom collisions, review 4-69199  
 inner-shell ionisation, nonperturbative effects 4-99260  
 inner-shell ionization by light ions 4-64582  
 ionisation cross sections, numerical calcs. 4-96675  
 ionisation probabilities, charge scaling calcs. 4-107434  
 K-shell ionisation cross section expression derived using plane wave Born approx. 4-96647  
 light ion impact, K-shell ionisation cross sections 4-99258  
 low energy ion scatt. using alkalis 4-81074  
 metals, H<sup>+</sup> induced L shell X-ray production cross sections 4-96649

## atom-ion collisions continued

- metals, L-subshell ionisation cross section, projectile atomic number depend. 4-99267  
 metals, L-subshell ionisation cross sections by protons 4-99266  
 methylamine cation, mobilities in He at 293K 4-79706  
 monopole polarisation, time-depend. Schrodinger eqn. 4-87189  
 multiply charge ion-gas target collision, charge transfer cross sections 4-102789  
 negative ions, electron detachment in slow collisions with atoms 4-69198  
 polyatomic ion-neutral target collisions over 10 to 6000 eV, collision energy effect 4-93520  
 polyatomic ions, collision induced decomposition with He 4-93514  
 proton impact K-shell ionisation, binary encounter approx. 4-59887  
 quasis resonant collisions, Schrodinger eqn. modelling 4-87190  
 relativistic effect on L<sub>2</sub>-shell binding energy 4-96671  
 relativistic heavy ion-atom collisions, radiative capture obs. 4-96679  
 single electron capture 4-74327  
 target L-shell vacancy, probability, saturation rate calc. by coupled-channels calcs. 4-96650  
 Ag, angle dependent energy loss of 7-MeV protons, stopping powers meas., geometrical effect 4-96658  
 Al, angle dependent energy loss of 7-MeV protons, stopping powers meas., geometrical effect 4-96658  
 Al+H<sup>+</sup>(He<sup>+</sup>), KL vacancy production cross sections, projectile depend. 4-96676  
 Ar+Ar<sup>+</sup>, recoil ion charge state distrib., projectile charge state depend. 4-69204  
 Ar+H<sup>+</sup>(Li<sup>+</sup>)(Na<sup>+</sup>)(K<sup>+</sup>), electron detachment cross sections 4-78952  
 Ar+S<sup>15+</sup>, K vacancy transfer, interference effects 4-78961  
 Ar+Si<sup>13+</sup>, single and multiple electron capture, K X-ray production 4-102785  
 Ar+Xe, correls. between charge-changing interactions and projectile K-alpha X-ray emission 4-64595  
 Ar<sup>+</sup>+Cu, two electron transfer collisions, Ar I VUV line intensity 4-83462  
 Ar<sup>+</sup>+He, charge transfer processes studied by crossed-beam expt. 4-91339  
 Au, H<sup>+</sup> impact, K-shell ionisation cross sections 4-96508  
 Au, ion impact L-shell ionisation, higher order processes 4-99265  
 Au, L X-ray emission probabilities by 70 MeV Ar ion impact 4-78949  
 Au, L-shell ionisation by Si and S ions, cross sections and alignment 4-99263  
 Au, L-substate ionisation cross sections, projectile depend. 4-99264  
 Au<sup>+</sup>+He, electron capture, ionisation and transfer ionisation cross sections 4-78960  
 Ba, L-shell X-ray prod. cross sections for protons of energy 1-2 MeV 4-96656  
 Be, angle dependent energy loss of 7-MeV protons, stopping powers meas., geometrical effect 4-96658  
 Be+C(N)(O)(Ne) ions, single and double K-shell ionization cross-sections meas. 4-64583  
 Be<sup>+</sup>+H, charge transfer cross sections calc. using close coupling calc. 4-78959  
 B<sup>n+</sup>+Ne→B<sup>n+1</sup>+Ne<sup>q+</sup>, contribution of K-capture to Ne<sup>q+</sup> production 4-83466  
 C<sup>q+</sup>, (q=6, 5, 4), incident on inert gas atoms, K-Auger electron prod. 4-78818  
 C<sub>2</sub>H<sub>2</sub>N<sup>+</sup>, mobilities in He at 293K 4-79706  
 C<sub>2</sub>N<sup>+</sup>, mobilities in He at 293K 4-79706  
 C<sub>2</sub>N<sub>2</sub><sup>+</sup>, mobilities in He at 293K 4-79706  
 CO<sup>+</sup>+He, electronically excited CO<sup>+</sup> collisional deactivation 4-64580  
 Cl<sup>+</sup>+inert gas atoms, positive ion prod., double electron detachment cross sections 4-87187  
 Cs, L-shell X-ray prod. cross sections for protons of energy 1-2 MeV 4-96656  
 Cs+H<sup>+</sup>(D<sup>+</sup>), spin-depend. charge transfer 4-59890  
 Cs<sup>+</sup>+Cs<sup>+</sup> (deut. collisions, Cs<sup>2+</sup> prod., plasma target technique study 4-78954  
 Cu, angle dependent energy loss of 7-MeV protons, stopping powers meas., geometrical effect 4-96658  
 D<sup>+</sup>+H→D+H<sup>+</sup>, polarised ion sources using ring magnetron ioniser 4-107236  
 D<sub>2</sub><sup>+</sup>+Ar collisional dissociation, correl. between channel probabilities 4-78933  
 F<sup>q+</sup>, (q=9, 8, 7), incident on inert gas atoms, K-Auger electron prod. 4-78818  
 F+H<sup>+</sup>, two-state collision problems for exponential coupling 4-74315  
 Fe<sup>26+</sup>+Ar(Kr)(Zr)(Ag)(Sn) near-symmetric collisions, K-K transfer cross-sections 4-64571  
 Gd, L-shell X-ray prod. cross sections for protons of energy 1-2 MeV 4-96656  
 Gd, heavy charged particle impact, K-shell ionis. 4-69195  
 H<sup>+</sup> rare gas collisions, electron detachment 4-102766  
 H<sup>+</sup> in gases, vacuum UV radiation prod. cross sections 4-78931  
 H+Be<sup>+</sup>(B<sup>+</sup>)(C<sup>+</sup>)(N<sup>+</sup>)(O<sup>+</sup>) electron capture cross-sections calcs. 4-102791  
 H+C<sup>2+</sup>(C<sup>3+</sup>) ions, state-selective electron capture, translational energy spectroscopy 4-59891  
 H+C<sup>4+</sup>, electron transfer into C<sup>3+</sup>(nl) orbitals, at. basis calcs. 4-107450  
 H+C<sup>4+</sup>(N<sup>3+</sup>)(O<sup>6+</sup>) electron capture, 0.25-25 keV amu<sup>-1</sup> 4-69205  
 H+C<sup>q+</sup>(N<sup>q+</sup>)(O<sup>q+</sup>) ions, electron removal cross section 4-83460  
 H+formyl ion (acetyl ion), different activation energies 4-62161  
 H+fully stripped ion, final-states mixing following slow collision, electron capture 4-107451  
 H+H<sup>+</sup>, charge exchange and cross sections, symmetric orthogonalization of travelling molecular orbitals 4-64581  
 H+H<sup>+</sup>, elastic scatt., intermediate energies, model calcs. 4-107430  
 H+H<sup>+</sup>, collisions, reson. electron transfer from Rydberg atom 4-74329  
 H+H<sup>+</sup> reson. electron capture, T-matrix element calcs. 4-102792  
 H+He<sup>2+</sup>(Be<sup>+</sup>)(B<sup>+</sup>)(C<sup>+</sup>)(N<sup>+</sup>)(O<sup>+</sup>) collisions, electron transfer, at. orbital expansion description 4-78962  
 H+isofomyl ion, metastability and isomerisation, interstellar appl. 4-91327  
 H+Li<sup>+</sup>, charge exchange cross-sections, low-energy calcs. 4-64592  
 H+O<sup>+</sup>(CO<sup>+</sup>)(CH<sup>+</sup>), reaction rate coeffs. 4-81427  
 H+X<sup>2+</sup>, charge transfer collisions, long-range secondary couplings 4-102790  
 H+Ar(He), electron detachment, energy spectra, Born approx. 4-83459  
 H<sup>+</sup>→H<sup>+</sup>+H<sup>+</sup>, polarised ion sources using ring magnetron ioniser 4-107236

## atom-ion collisions continued

- $H^+ + He$ , electron detachment in slow collisions 4-69198  
 $H^+ + He(Ar)(H_2)(N_2)(O_2)(CO_2)$ , electron detachment and charge exchange to shape resonances, 4-69203  
 $H^+ +$  atom collisions, L-shell X-ray prod. and ionisation cross sections 4-67883  
 $H^+ + Au(U)(W)$ , K-shell ionisation cross sections 4-78953  
 $H^+ + C$  foil, 2p and 3p population, beam-foil excitation 4-64584  
 $H^+ + C(Ne)$ , charge transfer at large scattering angles in the strong-potential Born approximation 4-87210  
 $H^+ + Cu(Mo)(Ag)$  collisions, K-shell ionisation, angular depend. 4-74322  
 $H^+ + H$  collisions, triple-centre treatment of ionisation 4-78956  
 $H^+ + H(He)$ , electron capture, symmetries eikonal-type approx. 4-83464  
 $H^+ + H(He)$  Thomas peak in electron capture 4-96692  
 $H^+ + He$ , electron capture, coherent excitation, multiple scatt. approach 4-87212  
 $H^+ + He$  autoionising state excitation cross section 4-59886  
 $H^+$  + heavy atom, inelastic scatt. relativistic effects, Born approx. 4-83449  
 $H^+$  + inert gas atom, multiply ionising collisions,  $\delta$ -electron spectra 4-83458  
 $H^+ + Li^+(C^+)(N^+)$ , ionisation cross section, PWBA 4-83461  
 $H_2^+ + C$  foil, 2p and 3p population, beam-foil excitation 4-64584  
 $H_2^+ + H$ , excitation to  $n=2$  level, ang. differential and total cross sections 4-102782  
 $H_2^+ + C$  foil, 2p and 3p population, beam-foil excitation 4-64584  
 $HCN^+$ , mobilities in He at 293K 4-79706  
 $He$ , double ionisation by collisions with fast, fully stripped ions 4-112265  
 $He$  I, Stark broadening params., semiclassical calc. 4-91224  
 $He$  ion impacts, target ionisation, dissociation, excitation 4-96682  
 $He + C^{3+}(N^{3+})(O^{3+})(F^{3+})(Ne^{3+})(Kr^{3+})$ , one-electron capture at low energies, Landau-Zener model calcs. 4-96685  
 $He + C^{3+}(N^{3+})(O^{3+})$  ions, electron removal cross section 4-83460  
 $He + H_2^+$ , exchange reaction, ab initio pot. energy surface, quasiclassical trajectory study 4-76996  
 $He + H_2^+(D_3^+)(HD_2^+)$ , three body dissoc. absolute cross section meas. 4-104984  
 $He + H^-(Li^-(Na^-(K^-)))$ , electron detachment cross sections 4-78952  
 $He + H^+$ , autoionising reson. excited at small ejection angles 4-96681  
 $He + H^+$ , impact line widths 4-102638  
 $He + HCO^+(HCS^+)$ , collision cross sections and rate coeffs. for rot. excitation 4-110514  
 $He +$  isoformyl ion, metastability and isomerisation, interstellar appl. 4-91327  
 $He +$  methane ion, collision-induced dissoc., beam scatt. study 4-89263  
 $He^+ + H$ , excitation cross sections calc. using Vainshtein Presnyakov-Sobel'man approx. 4-64586  
 $He^+ + He$ , double excitation 4-96677  
 $He^+ + H$ , charge transfer, laser assisted, coupled dressed quasimolecular states approach 4-96684  
 $He^+ + He$  collisions, Coriolis coupling effect in time depend. HF calcs. 4-91342  
 $He^+ +$  neutral atoms, charge transfer in low-energy collisions 4-74326  
 $He^+ + Ag(Sn)(Sb)(Te)(Ho)(Ta)(W)(Pt)(Bi)$ , L-shell X-ray prod. cross-sections 4-107305  
 $Ho, H^+$  impact, K-shell ionisation cross sections 4-96508  
 $I^+ + He$ , kinetic energy loss, double-focussing mass spectrometer meas. 4-64567  
 $K + H^+$ , electron transfer collisions, at. basis calcs. 4-102793  
 $La$ , L-shell X-ray prod. cross sections for protons of energy 1-2 MeV 4-96656  
 $Li + Ar^{3+}(Ne^{3+})(Kr^{3+})(Xe^{3+})$  collisions,  $q=2$  to 10, electron capture cross sections from low projectiles 4-74328  
 $Li + C^{3+}$ , electron transfer into  $C^{3+}(nl)$  orbitals, at. basis calcs. 4-107450  
 $Li + Na^+$  collisions, semiclassical scatt. theory based on dynamical-state representation 4-78955  
 $Li^+ + Li$ , differential cross sections calc. using mol. bases, quantum effect 4-87211  
 $Li^+ + Li^+$  collision, charge transfer and ionis. cross-sections determ. 4-64593  
 $Li^+ + Na$  collisions, semiclassical scatt. theory based on dynamical-state representation 4-78955  
 $Li^{3+} +$  neutral ats., charge transfer in low-energy collisions 4-74326  
 $Li^{3+} + C^{2+}(N^{2+})(O^{2+})$  core-conserving electron capture ion excitation, metastable fraction meas. 4-83465  
 $N$  II +  $He^+(N_2)$  collisions, N II reson. line excitation in VUV region in cathode sheath of hollow cathode discharge 4-87203  
 $N^{q+}$ , ( $q=7, 6, 5$ ), incident on inert gas atoms, K-Auger electron prod. 4-78818  
 $N^{3+} + H$ , charge transfer cross sections, extreme UV radiation emission 4-64596  
 $N^{6+} + He$ , electron capture in autoionising configurations  $N^{4+}$  studied by electron spectroscopy 4-59889  
 $N^{6+} + He$ , transfer ionisation and two-electron capture processes at 3-34 keV energies 4-96688  
 $Na + H^+$ , electron transfer collisions, at. basis calcs. 4-102793  
 $Na + He^+$ , laser and ion beam excitation, autoionisation 4-69196  
 $Na + Na^+$ , differential scatt. 4-87208  
 $Na^+ + Ar(He)(Xe)$ , excited Na states, collisional depopulation cross-sections 4-83456  
 $Na^+ + Na^+$ , ang. differential cross section for p to d collision excitation 4-96678  
 $Ne^{2+}$ , H-like, 110 MeV, collisional quenching of np states 4-64418  
 $Ne +$  butene ion, collision-induced dissoc., beam scatt. study 4-89263  
 $Ne + H^-(Li^-(Na^-(K^-)))$ , electron detachment cross sections 4-78952  
 $Ne^{2+} + Ar(Kr)$ , low energy electron transfer collisions 4-87213  
 $O^{q+}$ , ( $q=8, 7, 6$ ), incident on inert gas atoms, K-Auger electron prod. 4-78818  
 $O + H^+(H)(H^-)$ , electron capture, electron loss, excitation 4-64590  
 $O + O^+$ , charge transfer calcs. 4-78958  
 $O^+ + He$ , charge transfer at thermal energies, cross sections and rate coeff. 4-76991  
 $Ta$ , angle dependent energy loss of 7-MeV protons, stopping powers meas., geometrical effect 4-96658  
 $^{90}Th$  heavy charged particle impact, K-shell ionis. 4-69195  
 $^{71}W$ , heavy charged particle impact, K-shell ionis. 4-69195  
 $Xe^+ + Xe$  collisions using decelerated heavy ions from GSI-UNILAC 4-87207

## atom-molecule collisions

- see also atom-molecule reactions; molecular rotational-vibrational energy transfer  
 angular momentum transfer in state-to-state reactive scattering 4-77001  
 atom-triatom collisions, quantisation, scaling behaviour, classical trajectory anal. 4-91328  
 CS method, kinematics 4-102778  
 ethene +  $He^+(He)$ , vibr. modes, relax. and excitation, rate consts., vibr.-translation energy transfer 4-59881  
 fluoromethane +  $H$ , vibr. excitation, IR emission study 4-69186  
 generalised reorientation cross section, scatt. frame transformations and propensity rules 4-69159  
 localized Gaussian wave packet methods for inelastic collisions involving anharmonic oscillators 4-64569  
 nonintegrable collision system, collision dynamics, classical scaling 4-91329  
 organic molecules, highly vibr. excited state, collisional energy exchange with inert gas, biased random walk model 4-78939  
 quantum mechanical coplanar scatt., action angle variables 4-69176  
 rotational excitation, ang. momentum transfer 4-102776  
 T-approximation, appls. to at. forces and scatt. 4-59868  
 Van der Waals rare gas dimers, three-body exchange reactions, tunnelling process, WKB calcs. 4-64589  
 $X_2Y_2 + A$  collinear collisions, quantum calc. of vibr. harmonic energy transfer 4-96664  
 $Ar + CH_4(CD_4)(CF_4)(SiH_4)$ , energy transfer, model trajectory calcs. 4-102771  
 $Ar + D_2$ , rotationally inelastic cross sections, anisotropic interaction pot. determ. 4-83452  
 $Ar +$  methane, exchange interactions, crossed-beam expt. (German) 4-96670  
 $Ar + N_2$ , cross sections and rate consts. of rot. excitation 4-112264  
 $Ar + N_2(HF)$  rotationally inelastic cross-sections and fitting laws, energy depend. 4-102772  
 $Ar + TIF$ , rotational excitation, ang. momentum transfer 4-102776  
 $Ar + X_2$  ( $X =$  halogen) metastable atom quenching cross-section calcs. 4-107304  
 $Ar_{cl}$  cluster beams, differential scatt. anal. 4-74376  
 $Br_{cl}$  gas phase collisional quenching and intramultiplet mixing 4-87153  
 $CO + H(D)$ , collisional excitation, cross sections, quasiclassical trajectory study 4-78950  
 $CO_2 + O$ , translational-to-vibrational energy transfer, quantum mechanical calcs., basis set effects 4-74317  
 $Cl +$  ethyl chloride- $d_3$  ( $-d_2$ ), ( $-d_1$ ), D abstraction from methyl- $d_3$  group 4-62163  
 $Cr + H_2(D_2)(N_2)(CO)(O_2)(N_2O)(NH_3)$  (ethylene), intramultiplet mixing collisions, fluorine 4-64588  
 $CsBr + Ar(Kr)(Xe)$ , collision-induced dissoc., cross sections 4-76993  
 $CsF + Ar(Kr)(Xe)$ , collision-induced dissoc., cross sections 4-76993  
 $Cu$ , oxidation, collision model for fume formation 4-62114  
 $D_3^+ + Ar$ , collisional dissoc., correl. between channel probabilities 4-78933  
 $Ga +$  ethylene, visible multiphoton dissoc., time-resolved multiphoton ionisation 4-87164  
 $H + D_2$ , nascent HD prod. quantum state distrbs., pulsed laser photolysis, Raman spectra 4-104977  
 $H + D_2$ , opacity analysis of steric requirements in elementary chemical reactions 4-62159  
 $H + H_2$ , laser excitation, electron loss from  $H(3p)$  atoms,  $H(3p)$  beam prod. 4-87200  
 $H + H_2$ , quantum mechanical coplanar scatt., action angle variables 4-69176  
 $H + H_2$ , reagent rot. effect, classical trajectory calcs. 4-93506  
 $H + H_2$  rearrangement collisions, resonances, and dynamics calcs. 4-71901  
 $H + H_2 - H_2^+ - H_2 + H, H_2^{2+}$  absorpt., transition state spectroscopy 4-69194  
 $H + HD - H_2 + D$  collinear reaction, competition between dissoc. and exchange processes, exact quantum results 4-81409  
 $H + HF$ , nonreactive scatt., quantum mechanical calcs. using localised rot. basis functions 4-59882  
 $H + NO$  chemiluminescence reactions,  $HNO(A^2A')$  internal energy distrib. 4-71871  
 $H_2$ , radiative lifetimes and collisional quenching cross sections of selectively excited rovibronic states 4-83422  
 $HCN$ , (101) level relax. by collisional energy transfer, time-resolved fluorescence, 4-107440  
 $HF + Ar$ , finite duration of collisions and vibr. dephasing effect on broadened IR line shapes 4-69177  
 $HF + F$ , vibr. level deactivation 4-96666  
 $HO_2 - He$ , collisional energy transfer in low-pressure limit unimol. dissoc. 4-83451  
 $He +$  aniline ( $S_0$ ), state to state vibr. excitation, kinetic energy depend. 4-69184  
 $He +$  cyclopropane, vibr. energy transfer rate consts. calcs. 4-78935  
 $He + H_2$ , energy sudden scaling relations, off-energy-shell effects incorporation method 4-69161  
 $He + HF$ , energy transfer, differential cross sections, pot. energy surfaces 4-76992  
 $He +$  methane, exchange interactions, crossed-beam expt. (German) 4-96670  
 $He + N_2$ , collision, rot. energy transfer 4-59879  
 $He + N_2$ , thermal charge transfer reaction,  $N_2^+$  predissoc. channel 4-91317  
 $He + HD$ , vibr. relax., mechanisms and rate consts. 4-96669  
 $Hg$ , CO matrix isolated, electronic to vibr. energy transfer, IR emission 4-107441  
 $Hg$  halides, electron impact and at. and mol. collisions in discharge, spectra (Chinese) 4-59830  
 $I_2 + ^3He(^4He)(Ne)(Ar)$ , state-to-state rot. transfer rates, induced fluorescence 4-91333  
 $I^+ + DF(HF)(HCl)$ , quenching, time resolved IR fluorescence used to determ. rate const. 4-102730  
 $In + CO(O_2)(NH_3)$  (methane) (ethane) (ethane), intramultiplet mixing collisions 4-107393  
 $Kr + X_2$  ( $X =$  halogen) metastable atom quenching cross-section calcs. 4-107304  
 $LiH + He$  rotationally inelastic collisions, quasi-classical dynamics of atom-rigid rotor trajectories 4-112260  
 $Li_2^+ + Ar(Ne)(Xe)$  4-74319  
 $Li_2^+ + Ne(Ar)(Xe)$ , rot. inelastic collisions, vel. depend. 4-102764  
 $(NH_3)_n$  cluster beams, differential scatt. anal. 4-74376

**atom-molecule collisions continued**

- NO<sup>+</sup>, (X,v>0), collisional quenching by neutrals at low energies 4-87196  
 NO+inert gas atoms, mol. beam expt. for rot. excitation, fluoresc., cross sections meas. (*German*) 4-78957  
 N<sub>2</sub>O+Ar, mol. mean square torques and rot. correl. functions of  $\nu_3$  vibr. perturbed by Ar 4-78838  
 N<sub>2</sub>O+Ar collisions, intermol. pot., electron gas model, comparison with mean square torques meas. 4-78923  
 Na+N<sub>2</sub>, electronic to vibr.-energy transfer collision, Na(3p) fluoresc. 4-74320  
 Na<sub>2</sub>+Ar collisions, mol. rot. rainbow struct., vel. depend. 4-78938  
 Ne+H<sub>2</sub>(O<sub>2</sub>), bimol. and three-body quenching 4-112139  
 Ne+methane, exchange interactions, crossed-beam expt. (*German*) 4-96670  
 O<sub>2</sub>+He, in Ar shock tube, O<sub>2</sub> vibr. relax. study 4-96668  
 OCS-He(Ar), rot. relax. rates for J=0-1 pure rot. transition 4-69185  
 OCS+He(Ar), IR linewidth meas., rot. levels, intermol. pot. 4-59764  
 Rb, fine struct. mixing induced in collisions with atoms and mols., fluoresc., 4-96639  
 Rb-Co, quenching cross sections, Rydberg electron-molecular dipole interaction 4-96604  
 Rb+N<sub>2</sub>, thermal energy collision, Rb total depopulation cross sections 4-102783  
 SF<sub>6</sub>+Ar, rot. and vibr., excitation, time of flight spectra 4-107438  
 SF<sub>6</sub>+He(Ne), multiproperty empirical anisotropic intermol. pots. 4-74308  
 Si+F<sub>2</sub>, collision, time-resolved at. reson. absorpt. spectrosc. investigation 4-102765  
 Si+H<sub>2</sub>, C<sub>2v</sub> surfaces, MC SCF calcs. 4-91192  
 Sr, electronically excited (5<sup>2</sup>P<sub>1/2</sub>) state, collisional quenching, time-resolved emission investigation 4-102635  
 Xe+iodomethane scattering, elastic and inelastic differential cross sections at superthermal collision energies 4-87186  
 Xe+Na<sub>2</sub><sup>+</sup>, rotationally inelastic cross-sections and fitting laws, energy depend. 4-102772  
 Xe+X<sub>2</sub> (X=halogen) metastable atom quenching cross-section calcs. 4-107304

**atom-molecule reactions**

- see also *atom-molecule collisions*  
 alkali atom+SCl<sub>2</sub>, chemiluminesc., vibr. population inversion in B state of S<sub>2</sub> 4-89303  
 angular momentum transfer in state-to-state reactive scattering 4-77001  
 atom-diatom collisions, vibrational transitions, rate constants and cross-sections 4-87193  
 bimolecular rate const., energetic reactant atoms effect 4-104976  
 ethene+<sup>3</sup>He(He), vibr. modes, relax. and excitation, rate const., vibr.-translation energy transfer 4-59881  
 polyatomic ion-neutral target collisions over 10 to 6000 eV, collision energy effect 4-93520  
 polyatomic ions, collision induced decomposition with He 4-93514  
 quantum mechanical coplanar scatt., action angle variables 4-69176  
 reaction cross section, collision energy depend., microcanonical transition state model anal. 4-104983  
 reactions, crossed laser mol. beam studies and CaF prod. mol. rot. polarisation 4-91364  
 Van der Waals rare gas dimers, three-body exchange reactions, tunnelling process, WKB calcs. 4-64589  
 Ar+SO<sub>2</sub>, afterglow reaction, SO(A<sup>3</sup>Π) formation dynamics study 4-76968  
 Ba+ICl(IBr), chemiluminescence broad emission study 4-114801  
 Ba+N<sub>2</sub>O chemiluminescent reaction obs., quadrupole mass filter appl. (*Chinese*) 4-104993  
 Be+H<sub>2</sub>, pot. surface walking and reaction paths 4-114790  
 Be+H<sub>2</sub>→BeH<sub>2</sub>, multireference CI gradients and MCSCF second derivatives 4-93522  
 Be+HF(v,J)→BeF(v',J')+H reaction, classical trajectory study in three dims. 4-99763  
 Br<sub>2</sub>+Ar(Br), collisional energy transfer, binary trajectory calcs. 4-96665  
 C+H<sub>2</sub>, CH radical prod. energetics, laser induced fluoresc. 4-114777  
 C+NO(X<sup>2</sup>Π), collisional reaction pot. energy barrier, correl. diagram, ab initio calcs. 4-99766  
 C+SO<sub>2</sub>, chemiluminesc. reaction dynamics, vibr. energy distrib. 4-93531  
 Ca+F<sub>2</sub> reactions, crossed laser mol. beam studies and CaF prod. mol. rot. polarisation 4-91364  
 Cl+alkyl iodide, differential reaction cross-sections, collision dynamics 4-85291  
 Cl+ethylene, ab initio MO studies, rot. barrier, dissociation energy 4-99773  
 Cl+N<sub>2</sub>Cl reactions, rate const. determ. at 295K 4-71863  
 Cl<sub>2</sub>+inert gases, spectroscopic and kinetic study with VUV synchrotron radiation excitation 4-85289  
 Cl<sub>2</sub>+H(D), oriented-averaged rot.-decoupled vibr. 4-99753  
 D+FD reactive reson., partial widths and isotope effects calc. by reaction path Hamiltonian model 4-71890  
 D+H<sub>2</sub>, initial and state to state cross sections, quantum chemical study, rate const. 4-62160  
 D+NO chemiluminescence reaction, DNO internal energy distrib. 4-71871  
 F+D<sub>2</sub>, reactive infinite order sudden approx. calc., cross-sections and vibr. branching ratios 4-66571  
 F+DBr, collinear H-transfer reactions, dominant reaction probabilities evaluation 4-89245  
 F+H<sub>2</sub>, reactive scatt. resonances 4-99780  
 F+H<sub>2</sub>, reaction, quantum dynamics; energy partitioning and entropy anal. of collision complex 4-114782  
 F+H<sub>2</sub>, reaction, quantum dynamics; scatt. wave function density and flux analysis 4-114783  
 F+H<sub>2</sub>, reactions, reson. periodic orbits, semiclassical theory 4-114788  
 F+H<sub>2</sub>O, HO<sub>2</sub> prod., vibr. band strength for  $\nu_3$  band meas. 4-74220  
 F+H<sub>2</sub>(HD)(D<sub>2</sub>), collinear exchange reactions, probability densities, stabilisation calcs. 4-81415  
 F+I<sub>2</sub>(HI)(ICN), exchange reaction, pot. surface, I(2P<sub>1/2</sub>) two photon laser induced fluoresc. 4-76982  
 H+2-chloroethyl radical, ab initio MO studies, rot. barrier, dissociation energy 4-99773  
 H+Cl<sub>2</sub>, quantum classical reaction path model 4-114764  
 H+D<sub>2</sub>, opacity analysis of steric requirements in elementary chemical reactions 4-62159  
 H+D<sub>2</sub>, vibr. and rot. energy disposal reaction at 1.3 eV, surprisal anal. 4-76973

**atom-molecule reactions continued**

- H+D<sub>2</sub>, reaction dynamics, product state distrib. determ. at collision energy of 1.3 eV 4-71896  
 H+D<sub>2</sub>→HD+D reaction, coupled state quantum calc. at E<sub>rel</sub>(v=0, i=0)=0.55 eV 4-99750  
 H+D<sub>2</sub>→HD+D reaction, distorted wave calcs. at E<sub>trans</sub> (v=0, i=0)=0.55 and 1.3 eV 4-99749  
 H+FH reactive reson., partial widths and isotope effects calc. by reaction path Hamiltonian model 4-71890  
 H+H<sub>2</sub>, quantum mechanical coplanar scatt., action angle variables 4-69176  
 H+H<sub>2</sub>, reagent rot. effect, classical trajectory calcs. 4-93506  
 H+H<sub>2</sub>, reaction, three dims., coupled channel distorted wave calcs. 4-99761  
 H+H<sub>2</sub>O reaction dynamics, state distrib. for OH product 4-71873  
 H+H<sub>2</sub>(MuH), H and Mu exchange, isotope effects, semiclassical techniques 4-71884  
 H+H<sub>2</sub>→H<sub>2</sub><sup>2+</sup>→H<sub>2</sub>+H, H<sub>3</sub><sup>2+</sup> absorpt., transition state spectroscopy 4-69194  
 H+XY and X+HY where X and Y are Cl, Br or I. 3D DIM-3C pot. energy surfaces 4-66572  
 H<sub>2</sub>+D(F), BKLT eqn. for reactive scatt. of collinear nonsymm. systems 4-114787  
 H<sub>2</sub>+H(D), reactive differential cross sections in rot. linear model, ang. distrib. 4-99775  
 H<sub>2</sub>+H(F) reactions, semiclassical adiabatic theory 4-114786  
 H<sub>2</sub>+O(F) reactions, MRD-CI pot. surfaces using balanced basis sets 4-93521  
 He+Li<sub>2</sub>, collision-induced dissociation, reaction mechanism, rate const. 4-76976  
 I+HI(MuI), H and Mu exchange, isotope effects, semiclassical techniques 4-71884  
 K+acetyl chloride, product translational energy 4-99771  
 Li+FH collinear reaction, quasi-classical versus quantum calcs. 4-66556  
 Mg+H<sub>2</sub>(D<sub>2</sub>) reactions, MgH(MgD) nascent internal energy distrib. 4-71872  
 N+HI(HBr), crossed beam reaction, chemiluminescence study 4-77012  
 N+NH<sub>3</sub> (H<sub>2</sub>S) (formaldehyde), spectrophotometric studies 4-114793  
 N<sub>2</sub>+O(O<sub>2</sub>), metastable mol. quenching reaction 4-87195  
 NH<sub>3</sub>+O, absolute rate const. 4-66557  
 Na+CCl<sub>4</sub> reaction, chemilum. spectra, quenching and vibr. relax. rates 4-66583  
 O+cyclic hydrocarbons, H abstraction reaction, OH prod. internal state distrib. study 4-77000  
 O+formaldehyde, H abstraction, pot.-energy surface, ab initio HF CI calcs. 4-99770  
 O+H<sub>2</sub>(D<sub>2</sub>) reaction dynamics, reduced dimensionality quantum and quasi-classical rate const. 4-114784  
 O+HCN reaction dynamics, laser fluoresc. spectroscopy 4-114785  
 O+(D<sub>2</sub>)+HCl→OH+Cl reaction on a fitted ab initio surface 4-81414  
 Pb+O<sub>2</sub> reaction, chemiluminesc. characterisation 4-99799  
 Xe+ClCN (BrCN), CN(B<sup>2</sup>Σ<sup>+</sup>) prod., vibr. and rot. state distrib. 4-89250  
 Xe+iodomethane scattering, elastic and inelastic differential cross sections at superthermal collision energies 4-87186  
 Xe\*+HCl, supersonic beam-gas conditions, chemiluminescence polarisation meas. 4-89305
- atom probe field ion microscopy**  
 Alnico magnets, microstruct., comp., atom probe field ion microscopy 4-71828  
 (μ-cyano)phthalocyaninatometal bridged macrocyclic metal complexes, synthesis and conductivity 4-75948  
 microrefrigerators appl. 4-95438  
 pulsed-laser atom probe, ionic masses and appearance energies meas. appl. 4-111256  
 spectral analysis of APFIM composition profile using Fourier techniques 4-89232  
 steel, ferritic, D and He trapping at TiC particles 4-98152  
 surface analysis, in situ, using field-ion microscope/imaging atom probe 4-79916  
 time of flight combined type, linear and energy compensated modes comparison 4-68319  
 Fe-Be system, B32 metastable precip., identification by APFIM and TEM 4-61922  
 Fe-Cr-Co, phase separation and coarsening 4-109407  
 Fe-Cr-Co alloys, spinodal decomposition, atom probe field ion microscopy studies 4-114553  
 Nb-Zr (1.5 at.%), oxidation, O distrib., field ion microscopy, mass spectrometry 4-66483  
 Ni base superalloys, Li<sub>2</sub> type precipitates, long range order study by atom probe field ion microscopy (*French*) 4-104788  
 Ni/Si interfaces, silicide form., atom-probe study 4-70475  
 Ni-base superalloy, single cryst., CMSX2, long-range order and phase comp. in γ phase, atom probe study 4-66337  
 W (011), field evaporated ions, charge states distrib., atom probe FIM study 4-81118  
 W:He, ion implanted, diffusivity study 4-104004  
 W-Re (10 at.%), neutron irradi., homogeneous rad.-induced precip., atomic resol. study 4-108449  
 W-Re (25 at.%), neutron irradi., rad.-induced precip. and solute segregation, atom resol. study 4-108450
- atom-surface impact**  
 see also *sputtering*  
 anharmonic crystal, response to localised initial impetus 4-88925  
 benzene adsorbed on graphite, orientation, Penning ionisation electron spectroscopy 4-87197  
 coalescent resonances 4-96660  
 coalescent resonances 4-96661  
 corrugated surface pot., at. beam scatt. semiclassical approach 4-93179  
 gas-surface scattering from surfaces with imperfections, wavepacket approach 4-66176  
 impact activation of chemical reactions 4-99843  
 metal, attractive interaction with atom, derivations from Van der Waals force 4-81086  
 metal surface, He atom sticking probabilities and electronic surface response 4-66175  
 metal surfaces, atom bombardment, electronic excitations, quantum wave packet theory 4-66173  
 metals, thermalised He atom-surface scatt., electronic Debye-Waller effect 4-93172

**atom-surface impact continued**

- metastable atom-surface interaction, electronic emission (*French*) 4-76623  
 metastable atoms and ions for surface studies 4-85050  
 polyacrylonitrile thin films; metastable at. deexcitation spectroscopy (*French*) 4-71506  
 potentials for atom-surface scatt., validity of Esbjerg-Norskov approach using atomic charge densities 4-93176  
 rough surface, atom scattering, non-Markovian effects 4-66172  
 stepped surfaces, electron and atom diff., anal. 4-65530  
 thermal attenuation in resonant atom-surface scattering 4-114353  
 Ag (001), inelastic He scatt. and surface phonons 4-99257  
 Ag (001) with adsorbed Cl, inelastic He scatt. and surface phonons 4-99257  
 Ag (110), adsorbed layers, vibr. props., He atom scatt. 4-65570  
 Ag (110) surface, diffraction of He atoms, anticorruating effect 4-104709  
 Ag (111), inelastic He scatt. from Rayleigh waves, atom-surface interaction 4-109299  
 Ag (111), phonon inelastic scatt. from He atom impact 4-98426  
<sup>111,113</sup>Cd<sup>+</sup> matrix isolated, fast atom bombardment, ESR investig. 4-74218  
<sup>111,113</sup>CdOH matrix isolated, fast atom bombardment, ESR investig. 4-74218  
 Cu (110), He atom scatt., validity of Esbjerg-Norskov approach to pots. 4-93176  
 Cu (110) surface diffraction of Ne atoms, surface states 4-104706  
 Cu, impact of He atoms, interaction potentials 4-99256  
 Cu surface, adsorbed Ar, He scatt. time depend. wavepacket calcs. 4-88918  
 Cu surface, diffraction of He atoms, anticorruating effect 4-104709  
 GaSe, phonon inelastic scatt. from He atom impact 4-98426  
 He+Cu surface, time-depend. wavepacket scatt. calcs., isolated impurities effect 4-61794  
 LiF (001), inelastic He scatt., eikonal approx., surface dynamics 4-108700  
 Li(2p) excitation by electron transfer in slow metal surface collisions 4-66179  
 NaCl (001) surface, He atom diffraction 4-114352  
 NaF (001), inelastic He scatt., eikonal approx., surface dynamics 4-109300  
 NaF, phonon inelastic scatt. from He atom impact 4-98426  
 Ni (110) with H(2X6), He diff., GR method study 4-99268  
 Ni, impact of He atoms, interaction potentials 4-99256  
 Ni surface, diffraction of He atoms, anticorruating effect 4-104709  
 Ni surface, polycryst., clean and S covered, low energy ion and neutral scatt. 4-81083  
 Pd surface, diffraction of He atoms, anticorruating effect 4-104709  
 Pt (111), adsorbed H, He scattering studies 4-88400  
 Si (100) surface, reconstructed, rainbow atom scattering 4-66174  
 W (100) surface, fast He atom scatt. 4-93178  
 W (110), inelastic scatt. of He and Ne, semiclassical perturbation approx. 4-85052  
 W surface, interstitial atom interactions, field-ion microscopy studies 4-61798

**atomic absorption spectroscopy**

- aerosol trace element analysis, large scale intercomparison of different analytical methods 4-99897  
 alkali halides solid in microwave-induced plasma afterglow, lattice atomisation, temp. depend. 4-79862  
 calibration algorithm 4-109708  
 double-beam atomic absorption spectrophotometer for atomic beam intensity monitoring 4-96722  
 electrothermal vaporisation sample introduction system for ICP ADS 4-106395  
 flame spectrophotometer, S-302, appl. as at. absorpt. spectrometer 4-82830  
 laser atomic absorption spectrometry, matrix interference 4-89369  
 metal organics pyrolyses, InP growth mechanism by MOCVD 4-99334  
 red blood cells, human, Cu determ., AAS 4-100364  
 seawater, trace metals determ. by Zeeman graphite furnace AAS 4-114857  
 working environment aerosols in lead battery factory, toxicity monitoring by PIXE and AAS 4-105072  
 Ba atomisation mechanisms in furnace AAS 4-114851  
 Cd, Cu, Pb determ. in hydrological samples by AAS and ICP-AES methods 4-62430  
 Pb, gas phase temperatures in Massmann furnaces equipped with L'vov platforms 4-105038  
 ZrO<sub>2</sub>-Cr<sub>2</sub>O<sub>3</sub>(ZrB<sub>2</sub>), sintering materials, rapid chem. anal. (*Japanese*) 4-109339

**atomic beam electric resonance**

- surface analysis by resonance ionisation of sputtered atoms 4-105080

**atomic beam magnetic resonance**

- In isotopes, nucl. spin meas. 4-106569  
 Mo, hyperfine struct., RF, at beam mag. reson. and laser spectroscopic investig. 4-64410  
<sup>195</sup>Pt, <sup>2</sup>D<sub>23</sub> states, magnetic dipole hyperfine interaction 4-102622  
 TI isotopes, nucl. spin meas. 4-106569

**atomic beams**

- see also atom-molecule reactions; atom-surface impact; atomic beam electric resonance; atomic beam magnetic resonance; particle velocity analysis; plasma-beam interactions  
 alkali closed shell ions, repulsive interactions with Ar, Kr and Xe, beam and transport meas. comparison 4-96653  
 atom-surface impact, coalescent resonances 4-96661  
 corrugated surface pot., at. beam scatt., semiclassical approach 4-93179  
 double-beam atomic absorption spectrophotometer for atomic beam intensity monitoring 4-96722  
 fast beam development for SIMS analysis of polymers and insulators 4-93576  
 halogen closed shell ions, repulsive interactions with Ar, Kr and Xe, beam and transport meas. comparison 4-96653  
 metal atom beam source, beam intensity monitoring (*Chinese*) 4-102821  
 precise high-intensity atomic and ionic beam production 4-73579  
 pulsed superthermal beam source for metastable atomic and molecular species 4-86504  
 slowing down and pumping using very long cavity laser 4-96723  
 Ar, (<sup>2</sup>P<sub>3/2</sub>) state, orientation by laser optical pumping 4-112148  
 Ar(4s<sup>2</sup>P<sub>2,0</sub>), intracavity state selection using CW dye laser 4-60095

**atomic beams continued**

- Ba I, 6sn<sup>2</sup>F<sub>3</sub>, <sup>2</sup>F<sub>2</sub>, <sup>3</sup>F<sub>2</sub> Rydberg state energies, laser at. beam spectroscopy 4-78794  
 CS optically pumped vapour, relax. depend. on detection beam radius 4-64432  
 Co, quartet states, electron impact excitation cross sections 4-78970  
 Cr+He(Ar)(H<sub>2</sub>)(D<sub>2</sub>)(N<sub>2</sub>)(CO)(O<sub>2</sub>)(N<sub>2</sub>O)(NH<sub>3</sub>), intramultiplet mixing collisions, fluoresc. 4-64588  
 Ga single atoms detection in atomic beams 4-107321  
 H, atomic beam polarized proton source 4-107464  
 H atomic beam source for ion production 4-107234  
 H polarised atomic beam source, feasibility study 4-107468  
 He in 2<sup>2</sup>S<sub>1/2</sub> state, polarised electron beam production 4-59468  
 K+acetyl chloride, product translational energy 4-99771  
 Kr(5s<sup>2</sup>P<sub>2</sub>), intracavity state selection using CW dye laser 4-60095  
 N+HI(HBr), crossed beam reaction, chemiluminescence study 4-77012  
 Na beam laser cooling by AC Stark effect 4-69017  
 Na atomic beam, polarisation by laser optical pumping 4-107467  
 Ne+Ne, interaction excimer pots., atomic beam study 4-64563  
<sup>20</sup>Ne metastable atomic fast beam, population trapping obs. in two-photon reson. three-level atom 4-74357  
 Ne(3s<sup>2</sup>P<sub>2,0</sub>), intracavity state selection using CW dye laser 4-60095  
 Pd I, Rydberg series in photoionization spectrum 4-83351  
 Zr surface, laser irradi., at. beam prod., fluoresc. investig. 4-108435

**atomic clocks**

- see also frequency measurement; time measurement  
 average atomic time determination (*Japanese*) 4-58824  
 history of at. and mol. time and freq. standards 4-63470  
 Loran C for atomic time announcement services (*Japanese*) 4-58825  
 standard frequency and time services, development (*Japanese*) 4-58829  
 Cs atomic clock characterisation in perturbed environment 4-95374  
 Cs atomic reference frequency and clock supply, freq. keeping algorithm 4-106275  
 H<sub>2</sub> maser frequency standards, limitations due to receiver noise 4-96854  
 Rb and H<sub>2</sub> maser time and frequency standards, status and appl. (*Italian*) 4-86389

**atomic clusters**

- helical, electron diff., patterns, computer simulation (*French*) 4-59940  
 inert gas clusters, ionisation effect on magic numbers 4-96735  
 melting behaviour Metropolis Monte Carlo simulations 4-113579  
 metallic atomic clusters, electronic props., photoionization and TOF mass spectroscopy studies 4-83509  
 microclusters, production and props. 4-74365  
 Raman spectroscopy, ion dip, Raman spectra meas. at 4X10<sup>-9</sup> bar 4-68285  
 Ag clusters, aerosols heating effects determ. 4-74389  
 Ag clusters isolated in glass, UV optical and ESR study 4-112315  
 Ag<sub>n</sub> clusters, equil. geom., binding energy and ionisation pots. 4-74373  
 Ag<sub>n</sub><sup>+</sup> clusters, equil. geom., binding energy and ionisation pots. 4-74373  
 Al<sub>2</sub>CO ligand-metal bonding, charge transfer and polarisation 4-69265  
 Al<sub>3</sub>NH<sub>3</sub>, ligand-metal bonding, charge transfer and polarisation 4-69265  
 Ar, cluster ion formation in free jet expansion processes at low temperatures 4-74381  
 Ar, clusters, electron diff. patterns 4-74367  
 Ar clusters, Penning, photo and electron impact ionisation 4-74366  
 Ar<sub>4</sub> cluster, statistical behaviour 4-59939  
 Ar<sub>n</sub> cluster beams, differential scatt. anal. 4-74376  
 Be<sub>18</sub> clusters, energy optimised configs., ab initio STO-3G SCF calcs. 4-69261  
 Be<sub>20</sub> clusters, energy optimised configs., ab initio STO-3G SCF calcs. 4-69261  
 Cu<sub>n</sub> clusters, equil. geom., binding energy and ionisation pots. 4-74373  
 Cu<sub>n</sub><sup>+</sup> clusters, equil. geom., binding energy and ionisation pots. 4-74373  
 Fe<sub>n</sub> clusters Ar, Kr and Xe matrices, mag. circular dichroism study 4-78799  
 H, cluster ion formation in free jet expansion processes at low temperatures 4-74381  
 Li-H systems, thermodynamic props., ionis. pots. and binding energies 4-69266  
 Li-O systems, thermodynamic props., ionis. pots. and binding energies 4-69266  
 Li<sub>3</sub> clusters, matrix isolated, g-value, HF coupling, EPR spectra 4-74266  
 Na clusters under equil. conditions with Knudsen cell; mass spectra study 4-74379  
 Na<sub>n</sub> (n≤7), cluster geom. calc. by Hellmann-Feynman forces 4-74372  
 Na<sub>n</sub> clusters, (N=4 to 100), electronic shell struct. 4-78994  
 Na<sub>n</sub> clusters, electronic structs., equil. geometry self-consistent LSD calcs. 4-102843  
 Ni<sub>14</sub> cluster, 14-atom, H atom interaction, MINDO/SR calc. 4-64647  
 Pb doubly charged cluster obs. by time of flight mass spectra 4-112316  
 Se clusters, electronic and vibr. struct., Raman spectra, cluster method 4-74387

**atomic collision processes** see atomic inelastic collisions; elastic scattering of atoms and molecules**atomic electric moment**

- atomic 4f and 5d shells, elec. quadrupole moment, semiempirical Sternheimer shielding factors 4-102615  
 light absorpt., semiclassical radiation theory 4-102651  
 transition probabilities calc. 4-87083  
 Be isoelectronic series, oscill. strengths and at. wavefunctions accuracy 4-87084  
 Bi II spectrum, electric quadrupole line λ=587.0 nm, hyperfine struct. 4-102627  
 Eu I spectrum, 4f<sup>6</sup>6s<sup>2</sup> configuration, isotope shift, parametric anal. of quadrupole moments 4-59678  
 Fe XV, lifetimes of low lying levels 4-107313  
 In, 5s<sup>2</sup>5p(<sup>2</sup>P<sub>1/2</sub>), static elec. dipole polarisability 4-78979  
 Ti XI, energy levels and oscillator strengths, at. struct. calc. 4-69016  
<sup>129</sup>Xe, spin exchange with Rb, permanent elec. dipole moment meas. 4-87086

**atomic electron configuration interactions** see atomic electron correlations**atomic electron correlations**

- 3s<sup>2</sup>3p<sup>4</sup> ground configurations, (ionised Cu to Mo), magnetic-dipole transition predicted wavelengths and transition rates 4-68969  
 actinide atomic and crystal. energy levels, f-shell config. parametric model, effective-operator Hamiltonian 4-74165  
 alkali metal cations, core polarisation pot., intershell correl. effects, ab initio SCF CI calcs. 4-68970

# atomic electron correlations continued

- alkaline earth metal atoms, core polarisation pot., intershell correl. effects, ab initio SCF CI calcs. 4-68970
- atom, photoionisation processes in 5d, 6s and 6p shells, electron correl. and relativistic effects 4-96502
- atoms, transition from collective to independent-particle motion within valence shell 4-96464
- avoided crossings, use of effective Hamiltonians, adiabatic pot. curves 4-59681
- CI comparison with group theoretical basis functions for two excited electrons 4-74168
- diagrammatic many-body perturbation theory 4-59611
- direct CI method for large CI expansion in small orbital space 4-112086
- effective electrostatic-spin-orbit and effective spin-orbit interactions in (n<sub>l</sub>)<sup>n</sup>l' configurations 4-74170
- energy differences, electron correl. effects, approximate method 4-83304
- first row atoms, relativistic and nonrelativistic g-Hartree calcs. of correl. energies 4-96463
- group theory applied to CI methods 4-59609
- lanthanide atomic and cryst. energy levels, f-shell config. parametric model, effective-operator Hamiltonian 4-74165
- lanthanide atoms and ions, average energy of config. and valence orbital ions, pots. (Chinese) 4-78785
- levels, config. mixing and isotope shifts 4-68978
- light atoms, density functional exchange correlation pots. and orbital eigenvalues 4-74169
- multipole polarisabilities, spectra sums and multipole-multipole two-body dispersion coeff. 4-83302
- neutral atoms, ns<sup>2</sup>np radiative transition rates, correl. and relax. effects 4-96492
- rates of convergence of variational calculations and of expectation values 4-91206
- spectra, superposition of configurations calc. 4-112128
- two-electron atoms, doubly excited states, collective mol. model 4-59656
- Al isoelectronic sequence, struct. calc. using multiconfig. optimised pot. model, oscillator strengths 4-102592
- Ar electron impact ionisation spectrum, CI calcs. 4-64615
- Ar, K<sub>β</sub> X-ray emission spectrum, CI calcs., radiative transition probabilities calc. 4-59668
- Ar, L<sub>1</sub>-L<sub>2,3</sub>M<sub>1</sub> Coster-Kronig spectrum, exchange, electron correl., and relax. effects 4-74172
- Ar, outer shells, photoionisation cross sections calc. using relativistic local-density approx. 4-83352
- As VIII, spectrum, 3d<sup>9</sup>, 3d<sup>4</sup>4p and 3p<sup>5</sup>3d<sup>9</sup> configs. 4-69005
- Be, 1s binding energy, core levels, state-specific many-electron theory 4-75887
- Be, atomic correlation energies with explicitly correlated Gaussian geminals 4-91204
- Be, doubly excited states, electron correls. 4-87052
- Be<sup>+</sup>, doublet states, transition wavelengths and fine struct. 4-74171
- Be<sup>+</sup>, quartet-states, transition wavelength and fine struct., relativistic corrections 4-64397
- Be-like atoms, two-electron correls. calcs. 4-64392
- Be-like ion, isoelectronic series, oscillator strengths, wavelengths, energy levels 4-67881
- Br, ab initio calcs., spin-orbit coupling, kinetic energy operator, relativistic correction 4-102607
- C-like ions, optically allowed transitions, oscillator strengths, CI calcs. 4-74196
- Ca<sup>+</sup>, 4s, 4p and 3d states, hyperfine struct., many-body perturbation theory 4-102610
- Cr, half-filled shells, photoionisation 4-83353
- Fe transition series atoms, s-d interconfig. energies, s-spin flip energies and ionisation pots. 4-83303
- He, atomic correlation energies with explicitly correlated Gaussian geminals 4-91204
- He doubly excited states, electron correls. 4-87052
- He, nonlinear optical props., ab initio calcs., freq. depend. dipole polarisabilities, susceptibilities 4-102608
- Hg, relativistic oscillator strengths, correl. effects, reson. transitions 4-96490
- Kr, outer shells, photoionisation cross sections calc. using relativistic local-density approx. 4-83352
- Li I, 1s2snl and 1s2pnl quartet levels, transition wavelengths, radiative lifetimes, fine struct. 4-96491
- Li<sup>+</sup>, doubly excited quintet states, fine and hyperfine struct., many-body calcs. 4-102609
- Mg, 4snp, 1<sup>3</sup>P<sup>0</sup> autoionising states; energies calc. using configuration interaction method 4-96500
- Mg, doubly excited states, electron correls. 4-87052
- Mg+He(S) interaction calcs. using SA-MSCF ICF-CI wavefunctions 4-74314
- Mn, half-filled shells, photoionisation 4-83353
- Mn, photoelectron asymmetries and two-electron satellites near 3p to 3d giant reson. region 4-102655
- Nb IV, two electron jump transitions Stark mixing, CI calcs. 4-87063
- Ne, outer shells, photoionisation cross sections calc. using relativistic local-density approx. 4-83352
- Pb, photoionisation processes in 5d, 6s and 6p shells, electron correl. and relativistic effects 4-96502
- Se IX, UV spectrum 100 to 140 Å, configuration interactions 4-59667
- Sr I, <sup>1</sup>P<sub>1</sub> and <sup>3</sup>F<sub>3</sub> sequences, natural radiative lifetimes 4-74197
- SrV, spectrum, struct. 4-107295
- Tc, half-filled shells, photoionisation 4-83353
- Ti IX, energy levels and oscillator strength 4-59649
- Ti XI, energy levels and oscillator strengths, at. struct. calc. 4-69016
- Xe, 5s<sup>2</sup>5p<sup>6</sup> and 5s<sup>2</sup>5p<sup>5</sup> configs., correl. effects, Auger-electron study 4-107286
- Xe, outer shells, photoionisation cross sections calc. using relativistic local-density approx. 4-83352
- Zr III, two electron jump transitions Stark mixing, CI calcs. 4-87063

# atomic electron impact excitation

- see also electron spectra
- approximate electron- and proton-impact line widths within a spectral series 4-91237
- bound electrons, bremsstrahlung in field, differential cross sections calcs. 4-69221
- coherence in inelastic low-energy electron scattering, review 4-74343
- coulomb effects in atomic reactions in the presence of a low-frequency laser field 4-66578

# atomic electron impact excitation continued

- coupled-channel scattering eqns., L<sup>2</sup> soln. 4-69208
- electron scatt., collision strengths for inelastic transitions including fine struct. 4-96704
- electron-photon ang. correl. parameters 4-64619
- electronic excitation of atoms and molecules by electron impact in a linear algebraic, separable potential approach 4-59897
- fine structure level excitation by polarized electrons, cross section algebraic form invariance 4-69237
- free-free scattering processes, inhomogeneous radiation fields effects 4-107455
- gas atom finite assemblies, positron annihilation 4-59896
- gas discharge resonant atomic state excitation rate const., depend. on plasma ionisation degree 4-69977
- hydrogenic ions, high energy collision strengths and excitation limits 4-77702
- inert gas atoms, metastable state, low energy electron inelastic scatt. 4-112279
- neutral system, numerical collisional radiative model 4-91868
- relative populations of excited states produced by sputtering and electron impact, similarities 4-61801
- stepwise electron and laser excitation, theory 4-64431
- stepwise electron and laser optical excitation theory 4-83477
- Al, multiplet transitions, KL<sup>2</sup>-L<sup>3</sup> X-ray emission spectra 4-83323
- Ar, collision frequency, resonant determ. method 4-69223
- Ar, near-threshold electron impact excitation functions 4-96702
- Ar, relativistic electron beam excitation, fluoresc. and absorpt. 4-69220
- Au, photon linear polarization in the elementary process of atomic-field bremsstrahlung 4-91354
- C II, IR and UV lines, fine struct. transitions and electron collision strengths, astron. appl. 4-77701
- C metastable state, low energy electron inelastic scatt. 4-112279
- C, photon linear polarization in the elementary process of electron-electron bremsstrahlung 4-91355
- Ca XIX, effective excitation and recomb. rate coeffs., appl. to Sun 4-87218
- Ca<sup>+</sup>, dielectronic recombination via 4s to 4p excitation 4-74341
- Co, quartet states, electron impact excitation cross sections 4-78970
- Co, two-electron, one-photon transitions 4-74340
- Cr, two-electron, one-photon transitions 4-74340
- Cs, electron impact excitation, light emission, Stokes' parameter 4-96703
- Cu, photon linear polarization in the elementary process of atomic-field bremsstrahlung 4-91354
- Cu, two-electron, one-photon transitions 4-74340
- Er<sup>3+</sup>, electron impact excitation, level population mechanism 4-74335
- Eu I, II, electron-impact excitation of 4f electrons 4-83478
- Fe, two-electron, one-photon transitions 4-74340
- Fe XI, electron collisional excitation rate coeffs. 4-91862
- H, electron impact excitation, linear algebraic separable pot. approach appl. 4-59897
- H, electron impact excitation, distorted wave approx. 4-91353
- H, electron scattering, pseudostate expansions convergence 4-102805
- H, electron scattering total and ionisation cross sections, simplified model 4-74337
- H I like ions, electron impact polarisation of Lyman-α radiation 4-67609
- H, muonic, e<sup>-</sup> scattering amplitude estimated below μ<sup>-</sup> excitation threshold 4-64611
- H, positron elastic scatt. and positronium form. cross sections 4-83471
- H-like ions, fine struct., spectral intensities, collisional-radiative calcs. 4-102643
- H<sub>2</sub>, positron scatt., coupled-state method calcs. 4-64616
- He, 2<sup>1</sup>P state, electron impact excitation, orbital angular momentum transfer 4-64614
- He, 2<sup>3</sup>S state, electron impact excitation, intermediate and high energies 4-69218
- He, collision frequency, resonant determ. method 4-69223
- He, electron impact 2S singlet state excitation, field theoretic approach 4-91350
- He electron impact in supersonic beam, resons. and metastable states (French) 4-78971
- He, electron scattering, 11-state r-matrix calcs. 4-69210
- He I, electron excitation rate coeffs. for transitions from ground state to excited states 4-94571
- He I, principal series spectral line excitation in electro-atom collisions 4-91352
- He I, Stark broadening params., semiclassical calc. 4-91224
- He I astrophysical lines, electron impact line widths 4-102638
- He II, principal series spectral line excitation in electro-atom collisions 4-91352
- He II, 2p level excitation by electron impact, resonance states (Russian) 4-112283
- He ion, dielectronic recombination study 4-107459
- He, metastable state electron impact excitation 4-102802
- He<sup>+</sup>, electron impact excitation, 1s-2p transition, modified Glauber approx. 4-112280
- He<sup>+</sup>, electron impact excitation in dense plasma 4-112281
- He<sup>+</sup>(<sup>2</sup>S), electron beam excited, transient absorpt. in UV and VUV 4-78796
- Hg halides, electron impact and at. and mol. collisions in discharge, spectra (Chinese) 4-59830
- Hg low press. discharge, 6<sup>1</sup>P<sub>1</sub>, state direct electron impact excitation cross section 4-102801
- Hg, metastable state electron impact excitation, resons. 4-64622
- Kr, near-threshold electron impact excitation functions 4-96702
- KrXe<sup>+</sup>, form. and decay in electron beam excited inert gas mixtures 4-83479
- Mg II, 3p<sup>2</sup>P level, electron impact excitation cross section, reson. struct. 4-91351
- Mg, multiplet transitions, KL<sup>2</sup>-L<sup>3</sup> X-ray emission spectra 4-83323
- Mg XI, effective excitation and recomb. rate coeffs., appl. to Sun 4-87218
- N, metastable state, low energy electron inelastic scatt. 4-112279
- Na, 3p electron impact excitation, electron exchange 4-69219
- Na, electron impact excitation, electron-photon ang. correl. parameters 4-64619
- Na, multiplet transitions, KL<sup>2</sup>-L<sup>3</sup> X-ray emission spectra 4-83323
- Ne, electron impact excitation cross sections, EELS 4-64620
- Ne, low-lying levels, electron impact excitation, many-body theory 4-64621
- Ne metastable states, electron-impact excitation cross sections 4-78972
- Ne<sup>2+</sup>, electron impact excitation, fine struct. level transitions 4-74336

**atomic electron impact excitation continued**

- Ni, single X-ray photon excitation of two and three electrons using X-ray absorpt. 4-74182  
 O, metastable state, low energy electron inelastic scatt. 4-112279  
 O VII, electron impact excitation to  $n=2$  and 3 states, collision strengths calc. 4-59898  
 Pd, free atoms,  $M_{4,5}N_{4,5}$  Auger-electron spectrum 4-74209  
 Rb, elastic and inelastic electron scatt. cross section meas. 4-83473  
 Rb I, II, III, electron impact excitation, excited state relative populations 4-61801  
 S V electron impact collision rates and strengths calcs. 4-107458  
 Xe, electroluminescence and electron resonance trapping 4-108158  
 Xe, near-threshold electron impact excitation functions 4-96702  
 XeI, lifetimes of 7p levels, electron-photon excitation 4-112132  
 Zr, electron-impact excitation cross sections meas. 4-78969

**atomic electron impact ionisation**

- see also electron spectra*  
 adiabatic ang. wave functions in atomic ionisation problem (Russian) 4-112289  
 electron ionization cross-sections for K, L and M shells 4-96705  
 electron scatt., collision strengths for inelastic transitions including fine struct. 4-96704  
 excited states; ionization/recombination kinetics 4-64613  
 inert gas ions, electron-impact double ionisation 4-64618  
 inert gases, ionisation yield of low-energy electrons, statistical fluctuations 4-59899  
 inner-shell ionisation, Auger electron lineshapes in coincidence with scattered electrons 4-107322  
 interstellar wind atoms ionisation, role of 'core' and 'halo' solar wind electrons 4-105863  
 scattering cross sections, electron microscopy aspects 4-64623  
 three-particle system, Coulomb break-up, Wannier threshold theory 4-83475  
 Ar, 2p orbital, electron impact ionisation differential cross sections 4-112282  
 Ar, alignment prod. in ionisation of 2p shell by specific momentum transfer 4-96701  
 Ar clusters, Penning, photo and electron impact ionisation 4-74366  
 Ar electron impact ionisation spectrum, CI calcs. 4-64615  
 Ar, fast electron impact ionisation, differential cross section 4-74338  
 Ar, single and multiple ionisation by low energy electron impact using crossed beam apparatus 4-69217  
 Ba<sup>+</sup>, electron impact ionisation, excitation-autoionisation contrib., distorted-wave approx. 4-102800  
 C, gaseous, stopping power, zero-energy density effect 4-80129  
 Ca, electron impact double ionisation modified binary encounter model 4-83476  
 Ca<sup>+</sup>, electron impact ionisation, excitation-autoionisation contrib., distorted-wave approx. 4-102800  
 Cd, electron impact ionisation cross-section, semi-empirical formula 4-74342  
 Fe<sup>+</sup>, electron impact ionis. cross-section meas. 4-69222  
 H, electron impact ionisation, cross sections DWBA and DWIA 4-102803  
 H, electron scattering total and ionisation cross sections, simplified model 4-74337  
 He, coincidence electron impact ionisation, absolute triplet differential cross sections 4-102799  
 He, electron impact ionisation, triple differential cross section 4-87220  
 He electron impact ionisation cross-section meas., by fast crossed beams 4-107457  
 He, fast electron impact ionisation, differential cross section 4-74338  
 He, positron impact electron capture, differential and total cross-sections calcs. 4-107447  
 He<sup>+</sup>, low energy electron impact, Schwinger's variational principle 4-74339  
 Kr, single and multiple ionisation by low energy electron impact using crossed beam apparatus 4-69217  
 Ne, fast electron impact ionisation, differential cross section 4-74338  
 Sr; electron impact double ionisation modified binary encounter model 4-83476  
 W<sup>+</sup>, electron impact ionisation cross section 4-87219  
 Xe<sup>+</sup>, electron impact, single-ionisation cross sections 4-59900  
 Xe<sup>+</sup> ions, electron impact multiple ionisation 4-59901  
 Xe<sup>+</sup>, ionuclear series, electron impact ionisation, distorted wave approx. 4-64617  
 Zn, electron impact ionisation cross-section, semi-empirical formula 4-74342

**atomic electron scattering** *see atomic electron impact excitation; atomic electron impact ionisation; elastic scattering of electrons by atoms and molecules*

**atomic emission spectroscopy**

- electrothermal atomic absorpt. spectrometry, using external sampling tube atomiser 4-99913  
 graphite, laser localised emission spectroscopic anal., discharge gas effects (German) 4-64206  
 ICP-AES, sequential multielement anal. system 4-90666  
 internal reference point in ICP atomic emission spectroscopy, determ. using emission spectral profiles 4-90664  
 nebuliser, cross-flow, for ICP at. emission spectrometry 4-90667  
 reactively-deposited compound thin film composition control, optical emission spectroscopy monitoring 4-85101  
 C furnace AES, automatic background correction by square wave wavelength modulation system 4-106393  
 Cd, Cu, Pb determ. in hydrological samples by AAS and ICP-AES methods 4-62430  
 Mo, resonant detector spatial-temporal characts. for intracavity spectroscopy 4-78798  
 N determ. in aq. soln. by ICP-AES with extended torch 4-106396  
 Pb, electrothermal atomic absorpt. spectrometry using external sampling tube atomiser 4-99913  
 Si, electronic and solar grade, anal. using atomic emission spectroscopy from inductively coupled plasma 4-60948  
 TIC limiter surface analysis exposed to JIPP-II stellarator/tokamak hybrid device 4-108177

**atomic energy** *see nuclear power*

**atomic excited states**

- see also atomic metastable states; atomic resonant states*  
 alkali metal atoms, excited states, photoionisation, initial wave functions 4-83438

**atomic excited states continued**

- atom-ion collisions, charge exchange transitions to excited states 4-74332  
 fast ions in solids, excited state populations and charge-exchange 4-80126  
 foil-excited Rydberg states in atoms+ion collisions, elec. field ionisation 4-102784  
 highly excited states, radiative transitions in presence of strong microwave field 4-83312  
 highly ionised, lifetime meas. using fast ion beam excitation method, review 4-87079  
 highly-excited atoms in the electromagnetic field, bound-bound and bound-free transitions 4-83311  
 hydrogenic atoms,  $n=2$  excited state, state multipoles, Rayleigh scatt. 4-83360  
 inert gases, ionisation coeff. and total excitation cross section 4-92011  
 inert gases, Rydberg at. states fine struct. 4-107290  
 lanthanide atoms and ions, average energy of config. and valence orbital ionis. pots. (Chinese) 4-78785  
 laser-induced collective binding in two-electron systems 4-91209  
 low-level atom, time-depend. cluster variation method calcs. (Turkish) 4-112082  
 pinpoint discharge diagnostic with two-step optogalvanic effect using intersecting laser beams 4-87964  
 radiative lifetime distribution relationships of highly excited at. and ionic states 4-91229  
 RF glow discharges, spectral line shapes, optical emission actinometry 4-87931  
 Rydberg atoms with large orbital ang. momentum, prod. 4-59655  
 Rydberg energy level shifts induced by blackbody radiation 4-96496  
 Rydberg series of doubly excited resons. near two-electron escape threshold 4-64402  
 spontaneous emission 4-63443  
 transitions  $n_l \rightarrow n_l'$  between the Rydberg states in the Born approximation 4-83313  
 two-dimensional highly excited atoms, Zeeman effect, Coulomb and harmonic pots. 4-59673  
 two-electron atoms, doubly excited states, collective mol. model 4-59656  
 two-level atoms, excited system cooperative spontaneous emission 4-64444  
 XUV spectra of solids as an atomic information source (Russian) 4-80962  
 Al XI, doubly excited states, fine struct. meas. by beam-foil spectra (French) 4-69236  
 Ar, excited state lifetimes, inelastic electron-photon delayed coincidence technique 4-102644  
 Ar, K $\alpha$  X-ray emission spectrum, CI calcs., radiative transition probabilities calc. 4-59668  
 Ar, laser induced cascade ionisation, secondary ionisation processes 4-83355  
 Ar<sup>16+</sup>, excited states in D Tokamak plasma, recombination population 4-87936  
 Ar+Kr atoms, ionisation processes for highly excited Ar atoms 4-87201  
 Ba, 7sn'd autoionisation states, two-photon spectroscopy 4-78822  
 Ba, excited states, inner and outer shell photoionisation 4-83340  
 Ba I, 6snf F<sub>3</sub>, <sup>3</sup>F<sub>2</sub>, <sup>3</sup>F<sub>3</sub> Rydberg state energies, laser at. beam spectroscopy 4-78794  
 Ba, multiplet excitation of autoionizing Rydberg states 4-74202  
 Ba, nonlinear ionisation, influence of self-ionisation states 4-107324  
 BaI, highly excited states, Stark effect, hyperfine struct., isotope shifts 4-64405  
 Be, doubly excited states, electron correls. 4-87052  
 Be isoelectronic sequence, transition energy calc. using multiconfig. Dirac Fock and RPA calcs. 4-64364  
 Be<sup>+</sup> doubly excited states, autoionisation widths calcs. 4-64403  
 Br, ab initio calcs., spin-orbit coupling, kinetic energy operator, relativistic correction 4-102607  
 Cr<sup>+</sup> ( $q=6, 5, 4$ ), incident on inert gas atoms, K-Auger electron prod. 4-78818  
 Ca II, reson. electron capture to high Rydberg states 4-112268  
 Ca XIX, effective excitation and recomb. rate coeffs., appl. to Sun 4-87218  
 CaI, highly excited states, Stark effect, hyperfine struct., isotope shifts 4-64405  
 Cd vapour, interatomic pots., UV absorpt. spectra 4-107297  
 Cl, electronic Raman spectra, ion laser excitation 4-102621  
 Cl3p<sup>2</sup>(<sup>3</sup>P<sub>2</sub>), collisional quenching time-resolved at. reson. VUV absorpt. 4-59665  
 Cs, excited 7S state, photoionisation cross section absolute meas. 4-78816  
 Cs, Rydberg series in autoionising continua 4-83337  
 Cs, ground and excited states, Zeeman effect, optical pumping 4-91208  
 Cu I, lifetimes of some excited levels, beam foil spectra 4-87082  
 Cu II, lifetimes of some excited levels, beam foil spectra 4-87082  
 D\*, electron impact dissociation of D<sub>2</sub>O, emission cross section 4-107462  
 F, 3p state radiation lifetimes 4-107311  
 Fe<sup>+</sup> ( $q=9, 8, 7$ ), incident on inert gas atoms, K-Auger electron prod. 4-78818  
 Fe<sup>+</sup>+He(Ne), K Auger-electron prod. cross sections, charge-state depend. 4-96693  
 Fe, scattered atom vel. and electronic state distrib. by laser-induced fluorescence spectroscopy 4-93168  
 Ga, photoionisation saturation by reson. ionisation 4-64434  
 H excited state, prod. by electron impact on methanol 4-112286  
 H, muonic, excited state, isotope exchange process influence on fusion 4-106653  
 H, radiative lifetimes of excited levels 4-107312  
 H spectrum transformation in crossed electric and mag. fields 4-59672  
 H, spherical quadratic Zeeman problem, factorised wavefunction approach 4-64425  
 H, Stark-mixed  $n=2$  states, excitation and decay obs. in electron-photon coincidence expt. 4-87073  
 H, three-dimensional, excited state, Zeeman effect 4-102640  
 H+fully stripped ion, final-states mixing following slow collision, electron capture 4-107451  
 H+H<sup>+</sup> collisions; reson. electron transfer from Rydberg atom 4-74329  
 H<sub>2</sub><sup>+</sup>+H, excitation to  $n=2$  level, ang. differential and total cross sections 4-102782  
 H\* electron impact dissociation of H<sub>2</sub>O, emission cross section 4-107462  
 He, <sup>1</sup>P Feshbach reson., line-shape parameters, autoionisation states 4-64433  
 He, 1s2p states, isotope shifts and energies 4-74199

**atomic excited states continued**

- He doubly excited states, electron correls. 4-87052  
 He, electron impact 2S singlet state excitation, field theoretic approach 4-91350  
 He, excited state lifetimes, inelastic electron-photon delayed coincidence technique 4-102644  
 He excited state radiative lifetimes, regularities (*Russian*) 4-112145  
 He, fourth-order quantum electrodynamic corrections of order  $\alpha^2 mc^2$  4-78769  
 He, HF discharge, param. investig. at intermediate press. by spectroscopic methods 4-84099  
 He I, electron excitation rate coeffs. for transitions from ground state to excited states 4-94571  
 He, laser induced cascade ionisation, secondary ionisation processes 4-83355  
 He, photoionisation in 'S' ground state, photoelectron and photon decay 4-59683  
 He+high-Rydberg atoms in circular states, collisional props. using free electron model 4-96654  
 He<sup>+</sup>+He, double excitation 4-96677  
 He<sup>2+</sup>+neutral at., charge transfer in low-energy collisions 4-74326  
<sup>4</sup>He I 1snl energy levels, ionisation energies and Lamb shift 4-64427  
 Hg low press. discharge, 6<sup>1</sup>P<sub>1</sub> state direct electron impact excitation cross section 4-102801  
 Hg, reson. multiphoton ionisation, polarisation depend. 4-78813  
 Hg vapour, interatomic pots., UV absorpt. spectra 4-107297  
 Hg-Ar(Ka) interaction pots. calcs. from temp.-depend. absorpt. spectra 4-69170  
 K, excited states, inner and outer shell photoionisation 4-83340  
 K<sup>+</sup>+K<sup>\*</sup> collisional ionis., spectral variation 4-69197  
 Li in inert gas matrices, mag. circular dichroism study of <sup>2</sup>S-<sup>2</sup>P transition 4-59670  
 Li isoelectronic series, Rydberg energy levels determ. by relativistic quantum defect interpretation 4-107278  
 Li, orbital relax. in Rydberg series, excited state SCF calc. 4-64361  
 Li<sup>+</sup>, P Feshbach reson., line-shape parameters, autoionisation states 4-64433  
 Li<sup>3+</sup>+neutral at., charge transfer in low-energy collisions 4-74326  
 Li(2p) excitation by electron transfer in slow metal surface collisions 4-66179  
 Mg, 3snf Rydberg states, Doppler-free three-photon spectroscopy 4-74210  
 Mg, doubly excited states, electron correls. 4-87052  
 Mg XI, effective excitation and recomb. rate coeffs., appl. to Sun 4-87218  
 Nq<sup>+</sup>, (q=7, 6, 5), incident on inert gas atoms, K-Auger electron prod. 4-78818  
 N+NH<sub>3</sub> (H<sub>2</sub>S) (formaldehyde), spectrophotometric studies 4-114793  
 Na, ion formation in vapour containing Rydberg atoms 4-91242  
 Na, nondegenerate two-photon emission meas. 4-102660  
 Na Rydberg atoms, in low-Q cavities, quantum theory 4-107583  
 Na, Rydberg levels, microwave field ionisation 4-96710  
 Na, virtually excited state, inelastic collisions 4-74316  
 Na+He<sup>+</sup>, laser and ion beam excitation, autoionisation 4-69196  
 Na+He(Ne), population transfer, mol. pot. curves, avoided crossings 4-96655  
 Na+Na, associative ionisation reaction, rate consts. 4-89283  
 Na<sup>+</sup>+Ar(He)(Xe), excited Na states, collisional depopulation cross-sections 4-83456  
 Na<sup>+</sup>+Na<sup>+</sup>, ang. differential cross section for p to d collision excitation 4-96678  
 Nd laser glass, fluorescence line narrowing study 4-64411  
 Ne, excited state lifetimes, inelastic electron-photon delayed coincidence technique 4-102644  
 Ne, high Rydberg states and autoionising resons., centrifugal 4-68989  
 Ne, resonant stimulation of atomic transitions by 3391 nm radiation 4-107289  
 Ne VII, 1s2s2p<sup>2</sup> <sup>5</sup>P<sub>123</sub>-1s2p<sup>3</sup> <sup>5</sup>S<sub>2</sub><sup>0</sup> VUV transition 4-107300  
 Ne<sup>\*</sup> recombination pumping in Ne-H<sub>2</sub> pulsed transverse elec. discharge (*Russian*) 4-112133  
 Ni low-lying electronic states, inert gas matrix, laser-induced fluoresc. 4-102630  
 Oq<sup>+</sup>, (q=8, 7, 6), incident on inert gas atoms, K-Auger electron prod. 4-78818  
<sup>195</sup>Pt, <sup>3</sup>D<sub>3,3</sub> states, magnetic dipole hyperfine interaction 4-102622  
 Rb, atom, two-photon resonant excitation of highly excited state, transient coherent effect 4-69032  
 Rb, excited states, photoionisation Stark spectra, spin-orbit interaction effect 4-64426  
 Rb, fine struct. mixing induced in collisions with atoms and mols., fluoresc., 4-96659  
 Rb I, II, III, electron impact excitation, excited state relative populations 4-61801  
<sup>85</sup>Rb, ground and excited states, Zeeman effect, optical pumping 4-91208  
 Sr, (<sup>5</sup>P<sub>1</sub>) state, time-resolved emission kinetics 4-68990  
 Sr, electronically excited (<sup>5</sup>P<sub>1</sub>) state, collisional quenching, time-resolved emission investigation 4-102635  
 Sr I, <sup>1</sup>P<sub>1</sub> and <sup>3</sup>F<sub>3</sub> sequences, natural radiative lifetimes 4-74197  
 Xe II, excited states, radiative lifetimes 4-78805  
 XeI, lifetimes of 7p levels, electron-photon excitation 4-112132  
 Yb, 6snp Rydberg states, diamagnetic shift and singlet-triplet mixing 4-102618  
 Yb I, interchannel interaction between single excitation from 4f<sup>14</sup> and double excitation from 6s<sup>2</sup> 4-96478  
 Zn vapour, interatomic pots., UV absorpt. spectra 4-107297

**atomic explosions see nuclear explosions****atomic fine structure**

- atomic electron impact excitation, electron-photon ang. correl. parameters 4-64619  
 excitation by polarized electrons, cross section algebraic form invariance 4-69237  
 fine struct. transitions, close coupled transitions 4-78951  
 first-row and second-row atoms, fine-struct. intervals, Breit-Pauli approx., relativistic calcs., relevance to mol. calcs. 4-96467  
 gases, atomic and molecular, intracavity state selection using CW dye laser 4-60095  
 high resol. spectroscopy, at. struct. studies 4-78795  
 hydrogenic fine struct. spectrum in space of const. negative curvature 4-102591  
 inert gases, Rydberg at. states fine struct. 4-107290

**atomic fine structure continued**

- lanthanum ethyl sulphate:Gd<sup>3+</sup>, zero field splitting of Gd<sup>3+</sup> 4-96713  
 light atoms, fine-struct. intervals, Breit-Pauli approx., relativistic calcs., relevance to mol. calcs. 4-96467  
 multicharged ions in alternating field, fine struct., two level approx. (*Russian*) 4-91207  
 space-curvature effects in atomic fine-and hyperfine-structure calculations 4-74352  
 vapour density meas. by least-squares fit to spectra 4-102825  
 Al XI, doubly excited states, fine struct. meas. by beam-foil spectra (*French*) 4-69236  
 Be<sup>+</sup>, doublet states, transition wavelengths and fine struct. 4-74171  
 Be<sup>+</sup>, quartet-states, transition wavelength and fine struct., relativistic corrections 4-64397  
 Be-like ions, fine struct. transitions between 2l<sub>a</sub>2l<sub>b</sub> and 2l<sub>a</sub>3l<sub>b</sub> configurations, collision and line strengths 4-95072  
 C I in quasars, ground state level populations rel. to background radiation temp. at epochs (z≥2) 4-63343  
 C II, IR and UV lines, fine struct. transitions and electron collision strengths, astron. appl. 4-77701  
 Ca<sup>18+</sup>, electron scatt., collision strengths for inelastic transitions including fine struct. 4-96704  
 Cl, H-like, is Lamb shift determ. by X-ray transitions meas. using beam-foil excitation 4-74195  
 Cs, 6S-7S transition, parity-violating E1-amplitude, relativistic many-body calc. 4-91230  
 F-Xe, two-state collision problems for exponential coupling 4-74315  
 F+H<sup>+</sup>, two-state collision problems for exponential coupling 4-74315  
 Fe, sputtered atom vel. and electronic state distrib. by laser-induced fluorescence spectroscopy 4-93168  
 Ga isoelectronic sequence from Rb<sup>6+</sup> to In<sup>18+</sup>, 4s<sup>2</sup>4p<sup>2</sup>P intervals, fine struct. splitting meas. 4-64400  
 H, fine-struct. intervals, Breit-Pauli approx., relativistic calcs., relevance to mol. calcs. 4-96467  
 H-like ions, fine struct., spectral intensities, collisional-radiative calcs. 4-102643  
 H-like ions plasma, Balmer α fine struct. relative intensities 4-84059  
<sup>4</sup>He I 1snl energy levels, ionisation energies and Lamb shift 4-64427  
 K+Ar, fine-struct. transitions, interatomic pots. tests and coupling mechanism 4-87199  
 Kr ion, H- and He-like, time of flight X-ray emission spectra 4-102629  
 Li I, 1s2snl and 1s2pnl quartet levels, transition wavelengths, radiative lifetimes, fine struct. 4-96491  
 Li<sup>+</sup>, doubly excited quintet states, fine and hyperfine struct., many-body calcs. 4-102609  
 Mg+He(<sup>1</sup>S) interaction calcs. using SA-MCSCF ICF-CI wavefunctions 4-74314  
 N, relative fine-structure intensities in two-photon excitation 4-112291  
 N<sub>2</sub>+B<sup>+</sup> fast beam excitation study 4-107294  
 Na, electron impact excitation, electron-photon ang. correl. parameters 4-64619  
 Na+Ar, collisional redistribution and fine-structure transitions, collisional redistribution 4-83457  
 Na+He, two-state collision problems for exponential coupling 4-74315  
 Ne, high-resolution spectra by means of opticalvacnic spectroscopy (*Chinese*) 4-112137  
 Ne I lifetime and absolute transition probabilities of 2p<sub>10</sub>(<sup>3</sup>S<sub>1</sub>) level 4-83334  
 Ne VII, 1s2s2p<sup>2</sup> <sup>5</sup>P<sub>123</sub>-1s2p<sup>3</sup> <sup>5</sup>S<sub>2</sub><sup>0</sup> VUV transition 4-107300  
 Ne<sup>2+</sup>, electron impact excitation, fine struct. level transitions 4-74336  
 O, relative fine-structure intensities in two-photon excitation 4-112291  
 Rb, fine struct. mixing induced in collisions with atoms and mols., fluoresc., 4-96659  
 Si I, meas. of 3 <sup>3</sup>P<sub>0</sub>-3 <sup>3</sup>P<sub>1</sub> fine-struct. interval and g<sub>J</sub>-factor by laser mag. reson. 4-85866  
 Zr surface, laser irradi., at. beam prod., fluoresc. investig. 4-108435

**atomic fluorescence**

- atom driven by standing-wave laser field, reson. fluoresc. 4-102633  
 autoionising state radiative decay in laser fields, photoemission spectra 4-74205  
 autoionising state radiative decay in laser fields 4-74204  
 dipole-dipole stability in cooperative resonance fluorescence 4-91220  
 dissipative systems in quantum optics, reson. fluoresc. optical bistability superfluoresc., book 4-63410  
 double ionization in inner shells two electrons-one photon radiative decay 4-64415  
 excited atom, spontaneous emission 4-63443  
 intensity-fluctuation spectroscopy of optical fields with non-Gaussian statistics 4-95530  
 light ion impact, K-shell ionisation cross sections 4-99258  
 light scattering and resonance fluorescence meas., optical system calibration 4-101887  
 nonMarkovian dephasing of two-level reson. fluoresc. in strong radiation field 4-64419  
 optical double resonance spectra under finite bandwidth excitations 4-96475  
 plasma impurities meas. in neutral beam by laser-induced fluoresc. 4-91985  
 pre-Gaussian noise in strong laser-atom interactions 4-83335  
 radiative two-electron single-photon n<sub>1</sub> l<sub>1</sub> n<sub>2</sub> l<sub>2</sub>-1 s<sup>2</sup> transitions 4-91218  
 resonance fluorescence, optical bistability and superfluoresc., introduction, book contrib. 4-64690  
 resonance fluorescence-lame atomic detection, polarisation rejection of scatt. laser light 4-109707  
 resonance fluorescence in strong monochromatic laser fields, book contrib. 4-64422  
 spectral technique for measuring hyperfine struct. of atoms 4-91219  
 transition metal ions, in alkali halide matrix, lifetimes, fluoresc. spectra 4-102631  
 two atom cooperative systems, fluoresc. dipole interaction, finite detuning 4-83326  
 two-atom interacting system, reson. fluoresc., photon antibunching and squeezing 4-64420  
 two-level atom, fluorescence spectrum 4-102636  
 two-level atom, resonance fluorescence, photon number statistics anal. 4-64417  
 two-level atom, squeezed states reson. fluoresc., photon-counting statistics 4-64421  
 two-level atom driven by smooth pulse, reson. fluoresc. 4-96487  
 two-photon resonance fluorescence, excitation spectrum 4-87070

**atomic fluorescence continued**

- vapour density meas. by least-squares fit to spectra 4-102825  
 X-ray emission, hadron and muon induced, imaging feasibility 4-68993  
 Al surface, O and N covered, sputtered metal atoms, vel. distrib. 4-76608  
 Ar inductively coupled plasma, lifetimes and collisions, laser fluoresc. investig. 4-60729  
 Ar, relativistic electron beam excitation, fluoresc. and absorpt. 4-69220  
 Ar<sup>+</sup> ion beam, optical pumping study 4-87072  
 Au, average M-shell fluorescence yield meas. 4-87071  
 Au in inert gas matrices, radiative lifetimes 4-102642  
 Au, L X-ray emission probabilities by 70 MeV Ar ion impact 4-78949  
 Be, 1s binding energy, core levels, state-specific many-electron theory 4-75887  
 Bi I, obs. of superfluorescence and stimulated emission after nonresonant two-photon pumping 4-107600  
 Bi-Ne discharge, difficulties associated with stimulated emission 4-96484  
 C, two photon induced VUV fluoresc. 4-83325  
 Ca target, ground and excited state sputtering obs. using laser-fluoresc. 4-93169  
 Co, two-electron, one-photon transitions 4-74340  
 Cr target, ground and excited state sputtering obs. using laser-fluoresc. 4-93169  
 Cr, two-electron, one-photon transitions 4-74340  
 Cr+He(Ar)(H<sub>2</sub>)(D<sub>2</sub>)(N<sub>2</sub>)(CO)(O<sub>2</sub>)(N<sub>2</sub>O)(NH<sub>3</sub>), intramultiplet mixing collisions, fluoresc. 4-64588  
 Cs, excited 7S state, photoionization cross section absolute meas. 4-78816  
 Cs, fluorescence spectrum, inter-Doppler resonances 4-107306  
 Cu in inert gas matrices, radiative lifetimes 4-102642  
 Cu, two-electron, one-photon transitions 4-74340  
 Eu (III) in silica gel glass, fluoresc., cation binding and cage symm. 4-114835  
 Fe atoms, sputtered, laser-induced fluoresc. investig. (German) 4-69008  
 Fe in solar flares, excitation mechanism 4-90128  
 Fe, sputtered atom vel. and electronic state distrib. by laser-induced fluoresc. spectroscopy 4-93168  
 Fe sputtered neutrals, ionisation length near wall in ISX-B using laser-induced fluoresc. 4-91971  
 Fe, two-electron, one-photon transitions 4-74340  
 Fe\* production from electron impact on Fe(CO)<sub>5</sub>, at. fluoresc. study 4-96709  
 H, emission line shapes in hollow-cathode discharge 4-102645  
 H three-photon-excited fluoresc. detect. in acetylene/O<sub>2</sub> atm.-press. flame 4-81440  
 H<sup>+</sup>, K X-ray prod. cross sections using fluoresc. yield 4-96483  
 He metastable atoms in plasma, density meas. by laser-induced fluoresc. method 4-60722  
 \*He<sup>+</sup> + Ag(Sn)(Sb)(Te)(Ho)(Ta)(W)(Pt)(Bi), L-shell X-ray prod. cross-sections 4-107305  
 Hg, effective lifetimes of 6<sup>3</sup>P<sub>1</sub> level in low press. discharges 4-91233  
 I laser degenerate mag. dipole transitions self-induced transparency 4-83653  
 I, two photon induced VUV fluoresc. 4-83325  
 I(P<sub>1/2</sub>), fluoresc. study as product of F+HI(I<sub>2</sub>)(ICN) reactions 4-76982  
 I\*+DF(HF)(HCl), quenching, time resolved IR fluoresc. used to determ. rate const. 4-102730  
 In, 410 nm line, perturbation by foreign gases, press. broadening and shift. 4-102634  
 K atomic D line fluoresc. from NaK photodissociation 4-69136  
 Li isoelectronic series, radiative decay following charge exchange on neutral gas targets 4-87069  
 Mg, metastable atoms, self-quenching, second-order rate coeff. 4-59669  
 Mo I, lifetimes, branching ratios and transition probabilities 4-112143  
 Mo, resonant detector spatial-temporal charact. for intracavity spectroscopy 4-78798  
 N, fluoresc. from N<sub>2</sub> photodissociative excitation 4-77021  
 N<sup>+</sup> ion beam surface interaction, fluorescence, Stark effect obs. 4-78948  
 Na, 3p electron impact excitation, electron exchange 4-69219  
 Na atomic D line fluoresc. from NaK photodissociation 4-69136  
 Na D<sub>2</sub> line, laser-induced fluoresc. line narrowing 4-69012  
 Na, virtually excited state, inelastic collisions 4-74316  
 Na+Ar, collisional redistribution and fine-structure transitions, collisional redistribution 4-83457  
 NaI, 3d level lifetime meas. using fast ion beam selective excitation by laser 4-91226  
 Na(3p), reson. lines, fluorescence of Na-N<sub>2</sub> collision complex 4-74320  
 Nd laser glass, fluorescence line narrowing study 4-64411  
 Ne RF discharge, plasma polarisation spectroscopy 4-87933  
 Ni low-lying electronic states, inert gas matrix, laser-induced fluoresc. 4-102630  
 Ni, matrix-isolated atoms, fluoresc. spectra 4-96481  
 Pb, average M-shell fluorescence yield meas. 4-87071  
 Rb, fine struct. mixing induced in collisions with atoms and molcs., fluoresc., 4-96659  
<sup>85</sup>Rb, 5<sup>2</sup>P<sub>1/2</sub> level, lifetime determ. using Hanle effect 4-64428  
 S, two photon induced VUV fluoresc. 4-83325  
 Sr, (5<sup>3</sup>P<sub>1</sub>) state, time-resolved emission kinetics 4-68990  
 Ta II, radiative lifetime and reemitted fluorescence 4-87076  
 Th, average M-shell fluorescence yield meas. 4-87071  
 Ti surface, O and N covered, sputtered metal atoms, vel. distrib. 4-76608  
 Ti, up-conversion using stimulated anti-Stokes, Raman scatt. and stimulated collisional induced fluoresc. 4-69498  
 U, average M-shell fluorescence yield meas. 4-87071  
 W II, radiative lifetime and reemitted fluorescence 4-87076  
 Xe, collision using two-photon laser excitation, fluoresc., inelastic quenching 4-74184  
 Zr, collision cascade anisotropy by light-ion irradiat., fluorescence studies 4-76607  
 Zr, sputtering, atomic vel. distrib. meas. by laser-induced fluorescence 4-61792  
 Zr surface, laser irradiat., at. beam prod., fluoresc. investig. 4-108435

**atomic fluorescence spectroscopy** see *atomic emission spectroscopy***atomic forces**

- atomic plasma physics in inertial fusion 4-102762  
 atoms in astrophysics, book 4-106125  
 effective electrostatic spin-orbit and effective spin-orbit interactions in (nl)<sup>n</sup> configurations 4-74170  
 intramolecular interactions, local electron pair model, test calcs. (German) 4-107428

**atomic forces continued**

- metals, interatomic forces near a defect, impurity-susceptibility method 4-113490  
 molecular systems, interatomic force, second energy gradient, momentum density approach 4-112250  
 spectral line collisional broadening 4-87202  
 T-approximation, appls. to at. forces and scatt. 4-59868  
 two-two-level atoms, driven, light absorpt. spectra, anal. solns. 4-64408  
 two-atom interacting system, reson. fluoresc., photon antibunching and squeezing 4-64420  
 Ag (111) and (100), surface at. vibrs., phonon dispersion, interatomic forces 4-92506  
 Au (111) and (100), surface at. vibrs., phonon dispersion, interatomic forces 4-92506  
 H<sub>2</sub>, interatomic force, second energy gradient, momentum density approach 4-112250  
 He, attractive forces at intermediate distances from metal surface, a matrix element effect 4-80707  
 He Coulomb and exchange interaction energy, HF calcs. 4-112245  
 He+He multipole polarisabilities, dispersion forces, many-body theory 4-87192  
 Hg-Ar(Ka) interaction pots. calcs. from temp.-depend. absorpt. spectra 4-69170  
 Ni (111) and (100), surface at. vibrs., phonon dispersion, interatomic forces 4-92506  
 Si, mol. type axial channelling radiation from MeV electrons 4-75582

**atomic hyperfine structure**see also *Lamb shift*

- atomic 4f and 5d shells, elec. quadrupole moment, semiempirical Sternheimer shielding factors 4-102615  
 atomic electron impact excitation, electron-photon ang. correl. parameters 4-64619  
 atomic spectroscopy, symposium, Berkeley, CA, USA (Sept. 1983) 4-67852  
 effective operators, review 4-64633  
 H, muonic, weak interactions connect. to hyperfine level splitting 4-83494  
 high resol. spectroscopy, at. struct. studies 4-78795  
 hyperfine interactions of excited nuclei, review, book contrib. 4-68950  
 lanthanum ethyl sulphate:Gd<sup>3+</sup>, zero field splitting of Gd<sup>3+</sup> 4-96713  
 many-body theory 4-78066  
 muonic atoms, hyperfine anomalies, Breit interaction calcs. 4-69246  
 muonic atoms, hyperfine splitting energy meas. 4-83496  
 muonic atoms, light neutral,  $\mu$  SR spectroscopy study 4-69244  
 muonic atoms, magnetic hyperfine anomalies 4-112135  
 muonium, hyperfine struct. for n=2 level 4-83495  
 muonium, radiative recoil corrections and hyperfine splitting 4-78987  
 muonium weak interactions connect. to hyperfine level splitting 4-83494  
 negative muon precession in nuclei with spin 4-69247  
 space-curvature effects in atomic fine- and hyperfine-structure calculations 4-74352  
 spectral technique for measuring hyperfine struct. of atoms 4-91219  
 transition metal atoms, Bauche-Arnoult hyperfine struct. parameters, discrete spectrum contributions 4-59652  
<sup>2</sup>Al, HFS and radiative lifetimes in 3s<sup>2</sup>np<sup>2</sup>P<sub>3/2</sub> sequence using time resolved laser spectroscopy 4-74198  
<sup>2</sup>Al, negative muon hyperfine transition rate 4-69248  
 Ba multichannel-quantum-defect theory wave functions tested or improved by laser measurements 4-68929  
 BaI, highly excited states, Stark effect, hyperfine struct., isotope shifts 4-64405  
 Bi I, 6p<sup>3</sup> S<sub>3/2</sub>-6p<sup>3</sup> D<sub>5/2</sub> 647.5 nm forbidden transition hyperfine struct. 4-74351  
 Bi II spectrum, electric quadrupole line  $\lambda$ =587.0 nm, hyperfine struct. 4-102627  
<sup>209</sup>Bi, muonic, magnetic hyperfine structure 4-91368  
 Ca, HFS, field isotope shift, multiconfigurational HF method 4-102594  
 Ca, hyperfine struct. of 4s4p and 4s3d configs., pair correl. effects, ab initio calcs. 4-64368  
 Ca<sup>+</sup>, 4s, 4p and 3d states, hyperfine struct., many-body perturbation theory 4-102610  
 CaI, highly excited states, Stark effect, hyperfine struct., isotope shifts 4-64405  
<sup>111</sup>Cd self-alignment in a discharge 4-87963  
 Co I oscillator strengths from Fraunhofer line equivalent widths 4-63125  
 Cs, 6S-7S transition, parity-violating E1-amplitude, relativistic many body calc. 4-91230  
 Cs hyperfine struct. intervals, relativistic many-body calcs. 4-68986  
 Cs, polarisation spectroscopy 4-74193  
<sup>133</sup>Cs atoms, optical pumping by monochromatic light, efficiency calc. 4-107317  
<sup>133</sup>Cs, ground and excited states, Zeeman effect, optical pumping 4-91208  
 D<sub>2</sub>, hyperfine transitions in liq. H-D mixture 4-59295  
 Eu I spectrum, 4f<sup>6</sup>6s<sup>2</sup> configuration, isotope shift, parametric anal. 4-59678  
 Eu II, hyperfine structure and isotope shifts 4-87085  
 F ion bombardment of ferromagnetic surface, polarization pick-up detection 4-81062  
<sup>19</sup>F, 197 keV <sup>3/2</sup>-state, g factor measurement from hyperfine frequencies 4-96712  
 Fe, ab initio hyperfine struct. parameter calcs. 4-78981  
 Fr hyperfine struct. intervals, relativistic many-body calcs. 4-68986  
 H and meso-H, quadrupole moment in the excited 2P<sub>1/2</sub> state 4-59906  
 H in He, collisional hyperfine line shifts calc. using exchange perturbation theories 4-64401  
 H-like heavy ions, energies calc. of 1s, 2s and 2p states 4-83307  
<sup>83</sup>Kr, 5p levels, hyperfine struct. const. meas. (French) 4-78980  
 Li<sup>+</sup>, doubly excited quintet states, fine and hyperfine struct., many-body calcs. 4-102609  
 Mg, 3snf Rydberg states, Doppler-free three-photon spectroscopy 4-74210  
 Mn I in sunspots spectral line hyperfine struct. and broadening 4-77795  
 Mo, hyperfine struct., RF, at beam mag. reson. and laser spectroscopic investig. 4-64410  
<sup>95</sup>Mo 4d<sup>5</sup> 5p 2<sup>7</sup>P<sub>3,4</sub> states, HFS investigation by levelcrossing spectroscopy 4-96499  
<sup>95</sup>Mo 4d<sup>5</sup> 5p 2<sup>7</sup>P<sub>3,4</sub> states, HFS investigation by levelcrossing spectroscopy 4-96499  
 Na atoms, synchronized-quantum-beat echoes obs. for Zeeman and hyperfine transitions 4-112527

**atomic hyperfine structure continued**

- Na collision induced coherence, high resol. four-wave light mixing 4-102767  
 Na, electron impact excitation, electron-photon ang. correl. parameters 4-64619  
<sup>16</sup>O, 6.13 MeV 3<sup>-</sup> state, g factor measurement from hyperfine frequencies 4-96712  
<sup>195</sup>Pt, <sup>3</sup>D<sub>3/2</sub> states, magnetic dipole hyperfine interaction 4-102622  
 Rb, polarisation spectroscopy 4-74193  
<sup>87</sup>Rb, ground state hyperfine transition, adiabatic rapid passage parameters 4-102616  
<sup>87</sup>Rb, ground and excited states, Zeeman effect, optical pumping 4-91208  
<sup>235</sup>U II hyperfine structures measured by collinear fast-beam-laser and RF-laser double-reson. spectroscopy 4-74178  
 W I, isotope and hyperfine splittings for two UV transitions, saturation and polarisation spectroscopy 4-87064  
<sup>135</sup>Xe, hyperfine struct. const. meas. (French) 4-78980  
 Yb, 6snp Rydberg states, diamagnetic shift and singlet-triplet mixing 4-102618

**atomic inelastic collisions**

- see also atom-atom collisions; atom-ion collisions; atom-molecule collisions; atom-molecule reactions; atomic electron impact excitation; atomic electron impact ionisation; beam foil spectra; ionisation of atoms atomic processes, rel. to fusion plasma diagnostics and modelling, conf., Nagoya, Japan (August 1982) 4-67866*  
 atoms in astrophysics, book 4-106125  
 Auger electrons, ang. distrib. and spin polarisation 4-59684  
 collision induced absorpt. lineshape, Mori theory 4-64579  
 Dalitz integral, three denominator, closed formula 4-87177  
 energy sudden scaling relations, off-energy-shell effects incorporation method 4-69161  
 inert gases, electrical discharge, externally maintained, preionised, IR radiation generation, laser efficiency 4-64695  
 interstellar diffuse component, excitation 4-63258  
 ion inelastic collisions, kinetic energy loss, double-focussing mass spectrometer meas. 4-64567  
 K-shell electrons, ionisation probability as function of impact parameter 4-96680  
 K-shell ionisation cross section expression derived using plane wave Born approx. 4-96647  
 line broadening, final state distrib. 4-102768  
 muonium solution kinetics, muon spin rot. study 4-71957  
 neutral atom lines, binary collisions and broadening, phase shift, trajectory effect calcs. 4-69179  
 radiatively-aided inelastic collisions, electronic-state coherences theory 4-83446  
 Rydberg atoms, binary-encounter form encounter and its use in calc. inelastic cross sections 4-96657  
 state multipoles meas. using level-crossing techniques 4-96498  
 symmetric orthogonalization of travelling molecular orbitals 4-64581  
 T-approximation, appls. to at. forces and scatt. 4-59868  
 two-angle dependent reactive infinite order sudden approximation 4-66551  
 two-atom coherence, laser-induced 4-64572  
 two-level atom, laser light interaction, decay induced coherence 4-78823  
 two-mode laser with coupled transitions, atomic coherence effects 4-107591  
 X-ray emission, hadron and muon induced, imaging feasibility 4-68993  
 Ar, electrical discharge, externally maintained, preionised, IR radiation generation, laser efficiency 4-64695  
 Ar, positive column, low press., stepwise ionisation effects modelling 4-92013  
 Be-like ions, fine struct. transitions between 2l<sub>a</sub>2l<sub>b</sub> and 2l'<sub>a</sub>3l'<sub>b</sub> configurations, collision and line strengths 4-95072  
 C<sup>+</sup> inelastic collisions, kinetic energy-loss spectra 4-64568  
 Ca, hypersatellite X-ray spectra, H<sup>+</sup> induced 4-107301  
 Cl3p<sup>2</sup>(<sup>2</sup>P<sub>1/2</sub>), collisional quenching time-resolved at. reson., VUV absorpt. 4-96635  
 H in He, collisional hyperfine line shifts calc. using exchange perturbation theories 4-64401  
 H, Stark-mixed n=2 states, excitation and decay obs. in electron-photon coincidence expt. 4-87073  
 I<sup>+</sup> atoms in solns., geminate recombination, generalized Langevin treatment, inelastic transitions effect 4-62162  
 In, 410 nm line, perturbation by foreign gases, press. broadening and shift. 4-102634  
 K+Rb impact broadening of first K reson. line 4-69013  
 K<sup>+</sup>+K<sup>+</sup> collisional ionis., spectral variation 4-69197  
 LiCs recombining plasma, optimisation of inverse population of Li levels (Russian) 4-69023  
 Na collision induced coherence, high resol. four-wave light mixing 4-102767  
 O+H collisions, energy transfer rate coeff. 4-110517  
 Ti, hypersatellite X-ray spectra, H<sup>+</sup> induced 4-107301  
 Xe-Ar collision induced absorpt. lineshape, Mori theory 4-64579  
 Yb optically inhibited collisional dephasing photon-echo expt. 4-102987

**atomic interaction potential** *see atomic forces***atomic magnetic moment**

- see also gyromagnetic ratio*  
 forbidden lines in hot plasmas 4-87937  
 laser, degenerate transition, self-induced transparency, coherent pulse propagation 4-96882  
<sup>27</sup>Al, HFS and radiative lifetimes in, 3s<sup>2</sup>n<sup>2</sup>p<sup>3/2</sup> sequence using time resolved laser spectroscopy 4-74198  
 Bi, effective dipole moment and polarisability (French) 4-76019  
 Fe XV, lifetimes of low lying levels 4-107313  
 Fe-Al (48 at.%), mag. props. rel. to heat treatment 4-109003  
 I, pulse reshaping in coherent interaction with resonant absorber, homogeneous relax. time meas. 4-69511  
<sup>195</sup>Pt, <sup>3</sup>D<sub>3/2</sub> states, magnetic dipole hyperfine interaction 4-102622  
<sup>235</sup>U II hyperfine structures measured by collinear fast-beam-laser and RF-laser double-reson. spectroscopy 4-74178

**atomic mass**

- see also isotopes; mass spectra; nuclear mass*  
<sup>A</sup>B (A=10,11) atomic mass meas. 4-91357  
<sup>124</sup>Sn mass determ. from spectroscopic mass differences 4-59138  
<sup>A</sup>Sr A=87, 86, high precision mass meas. using spectrometer 4-68317  
<sup>124</sup>Te mass determ. from spectroscopic mass differences 4-59138  
<sup>124</sup>Xe mass determ. from spectroscopic mass differences 4-59138

**atomic metastable states**

- alkalilike atoms and ions, quasi-metastable quartet levels 4-74201  
 forbidden lines in hot plasmas 4-87937  
 gases, atomic and molecular, intracavity state selection using CW dye laser 4-60095  
 inert gas atoms, metastable state, low energy electron inelastic scatt. 4-112279  
 inert gas atoms, metastable states, quenching by Cu atoms 4-96485  
 muonic He, 2S metastable state, lifetime and quenching rate meas. 4-83497  
 plasmas, particle transport, tracking by lasers 4-103564  
 Ar, (<sup>3</sup>P<sub>2</sub>) state, orientation by laser optical pumping 4-112148  
 Ar metastable densities in Ar-NH<sub>3</sub> glow discharge 4-87059  
 Ar+X<sub>2</sub> (X=halogen) metastable atom quenching cross-section calcs. 4-107304  
 Ar<sup>+</sup>+N<sub>2</sub>, energy depend. of reactions 4-69193  
 Ba, time-differential ground-state Hanle effect in fast-beam laser spectroscopy 4-78800  
 Bi-Ne discharge, difficulties associated with stimulated emission 4-96484  
 C metastable state, low energy electron inelastic scatt. 4-112279  
 Ca target, ground and excited state sputtering obs. using laser-fluoresc. 4-93169  
 CaI, doubly excited 4p<sup>2</sup> config. radiative lifetimes, stark shift parameters 4-91232  
<sup>113</sup>Cd self-alignment in a discharge 4-87963  
 Cr target, ground and excited state sputtering obs. using laser-fluoresc. 4-93169  
 Fe<sup>+</sup>, electron impact ionis. cross-section meas. 4-69222  
 H, radiative decay, final-state interferences 4-83333  
 H+C<sup>2+</sup> (C<sup>+</sup>) ions, state-selective electron capture, translational energy spectroscopy 4-59891  
 H+H<sub>2</sub> (inert gas atoms), laser excitation, electron loss from H(3p) atoms, H(3p) beam prod. 4-87200  
 H+Li<sup>2+</sup>, charge exchange cross-sections, low-energy calcs. 4-64592  
 He electron impact in supersonic beam, reions. and metastable states (French) 4-78971  
 He metastable atoms in plasma, density meas. by laser-induced fluoresc. method 4-60722  
 He, metastable state electron impact excitation 4-102802  
 He-H<sub>2</sub>O mixtures, gas discharges, metastable He atom density 4-97922  
 He+inert gas atom, single and double electron loss cross sections of He metastable and ground states 4-59884  
 He<sup>+</sup>+Ne, electronic energy transfer in nozzle-beam scatt. cell expt., visible emission, odd-J levels 4-64578  
 He\*(S), electron beam excited, transient absorpt. in UV and VUV 4-78796  
 Hg, effective lifetimes of 6<sup>3</sup>P<sub>1</sub> level in low press. discharges 4-91233  
 Hg, metastable state electron impact excitation, reions. 4-64622  
 Kr+Kr, metastable interaction, <sup>3</sup>P<sub>2</sub> state 4-91335  
 Kr+X<sub>2</sub> (X=halogen) metastable atom quenching cross-section calcs. 4-107304  
 Li<sup>+</sup>C<sup>2+</sup>(N<sup>2+</sup>)(N<sup>3+</sup>)(O<sup>4+</sup>) core-conserving electron capture ion excitation, metastable fraction meas. 4-83465  
 Li<sup>+</sup>(1s2s), excited metastable state prod. by laser-produced plasma soft X-rays 4-112131  
 Mg, metastable atoms, self-quenching, second-order rate coeff. 4-59669  
 Mo, hyperfine struct., RF, at beam mag. reson. and laser spectroscopic investig. 4-64410  
 N, metastable state, low energy electron inelastic scatt. 4-112279  
 N<sup>-</sup> existence investig., rel. to form. by electron capture 4-74331  
 Ne gas, weakly ionised, laser-induced perturbation spectrosc. investig. 4-83319  
 Ne<sup>2+</sup>+Ar(Kr), low energy electron transfer collisions 4-87213  
<sup>20</sup>Ne metastable atomic fast beam, population trapping obs. in two-photon reson. three-level atom 4-74357  
 O, metastable state, low energy electron inelastic scatt. 4-112279  
 O<sub>2</sub><sup>+</sup>, 166 nm intersystem line emission, <sup>3</sup>S<sub>2</sub><sup>0</sup> metastable level radiative lifetime 4-110512  
 O<sup>++</sup>+He, charge transfer at thermal energies, cross sections and rate coeff. 4-76991  
 Pb, metastable, relax. in decaying plasma 4-108236  
 Si<sup>13+</sup>, H-like, metastable 2S<sub>1/2</sub> state, Lamb-shift meas. 4-102649  
 W<sup>+</sup>, electron impact ionisation cross section 4-87219  
 Xe+X<sub>2</sub> (X=halogen) metastable atom quenching cross-section calcs. 4-107304

**atomic orbitals** *see atomic structure***atomic orbitals calculations**

- see also GO calculations; GTO calculations; STO calculations*  
 convolution theorems 4-78757  
 f-shell orthogonalised operators 4-74139  
 Fourier transforms of atomic orbitals, reduction to 4D harmonics and quadratic transformations 4-78756  
 interacting configuration determ. using computer code 4-78753  
 Lowdin's alpha-function calc. 4-68010  
 metalloporphyrins, axial ligand conform preferences, ab initio SCF calcs. 4-96448  
 orthogonal scalar operator complete set for config. <sup>3</sup> 4-74141  
 SCF calcs., convergence problems, inverse Fock operators 4-74135  
 Slater-type basis functions, iteration procedure 4-68920  
 transition metal atoms, fourth-row, Gaussian basis sets 4-96447  
 valence minimising orbitals, Roothaan-like matrix eqn. 4-68919  
 B<sup>4+</sup>, H-like, elastic positron scatt., polarised orbital method 4-102798  
 B<sup>3+</sup>, H-like, elastic positron scatt., polarised orbital method 4-102798  
 H-like atomic orbitals, bound-states 4-64366  
 H+He<sup>2+</sup>(Be<sup>4+</sup>)(B<sup>5+</sup>)(C<sup>6+</sup>)(N<sup>7+</sup>)(O<sup>8+</sup>) collisions, electron transfer, at. orbital expansion description 4-78962  
 He photoionisation cross sections, oscillator strengths, polarised orbital method 4-64438  
 He<sup>+</sup>, H-like, elastic positron scatt., polarised orbital method 4-102798  
 Li<sup>+</sup>, photoionisation cross sections, oscillator strengths, polarised orbital method 4-64438  
 Li<sup>2+</sup>, H-like, elastic positron scatt., polarised orbital method 4-102798

**atomic polarisability**

- adatom near metal surface, effective polarisability, Van der Waals and non-local effects 4-92559  
 alkali metal atoms, core polarisation pot., intershell correl. effects, ab initio SCF CI calcs. 4-68970  
 alkaline earth metal atoms, core polarisation pot., intershell correl. effects, ab initio SCF CI calcs. 4-68970

**atomic polarisability continued**

- alkaline earth metal atoms, dynamic polarisabilities, semiempirical calc. methods 4-102599  
 atom-ion collisions, monopole polarisation, time-depend. Schrodinger eqn. 4-87189  
 Cauchy moments for at. and mol. dynamic polarisabilities, coupled HF calc. 4-74147  
 dynamic response in elec. field, Born-Oppenheimer and Feynman-Hellmann approx. 4-102589  
 dynamic Stark effect in RF elec. field, possibility for at. polarisability meas. 4-102637  
 highly-excited atoms in the electromagnetic field, bound-bound and bound-free transitions 4-83311  
 inert gas atoms, nuclear spin polarisation by spin exchange with optically pumped alkali metal atoms 4-78932  
 linearly polarized nonreson. light irr. of at. system. orientation classical-oscillator model 4-83336  
 metal surface, adsorbed atom, intrinsic polarisability modification (French) 4-104064  
 multiple polarisabilities, spectra sums and multiple-multipole two-body dispersion coeff. 4-83302  
 N-electron atomic core, adiabatic polarisation pot. experienced by single valence electron 4-96444  
 neutral atoms, dipole polarisabilities,  $\chi_\alpha$  density matrix calcs. 4-64370  
 pentachlorophenol in soln., IR dispersion of H-bonded systems, dielec. function for weak complexes 4-102676  
 relativistic SCF calcs. for stationary states, optical response 4-87229  
 SCF calcs. in stationary states, optical response 4-87228  
 silicides, screening energy variations and Auger parameters, XPS studies 4-99275  
 Stark effect, higher-order, on atomic multiplets 4-59671  
 static polarisability modification by perfect metallic surface 4-113779  
 surface polarization induced by an adatom in a dielectric 4-70551  
 2,4,6-trimethylphenol in soln., IR dispersion of H-bonded systems, dielec. function for weak complexes 4-102676  
 Be<sup>+</sup>, doublet states, transition wavelengths and fine struct. 4-74171  
 Bi, effective dipole moment and polarisability (French) 4-76019  
 Cs electronic orientation after CsI photodissociation 4-93541  
 Cs + Cs(He), absolute polarisation meas., natural lifetime in Cs 7S<sub>1/2</sub> state 4-83448  
 Eu(II), relativistic mode-potential oscillator strengths and transition probabilities for 4f<sup>6</sup>s-4f<sup>6</sup>p transitions 4-112144  
 F<sup>-</sup>, dipole polarisability, electron affinity, many-body perturbation theory 4-64363  
 H, atomic beam polarized proton source 4-107464  
 H, dynamic response in elec. field, Born-Oppenheimer and Feynman-Hellmann approx. 4-102589  
 H, ground state, multiple moments, time derivative fields 4-69021  
 H, one-dimens.,  $\delta$  function interaction, polarisability 4-106149  
 H<sub>2</sub>, nonlinear optical props., ab initio calcs., freq. depend. dipole polarisabilities, susceptibilities 4-102608  
 He, multiple props., time depend. CHF method 4-87040  
 He, nonlinear optical props., ab initio calcs., freq. depend. dipole polarisabilities, susceptibilities 4-102608  
 He, photoionisation in 1S<sup>2</sup> ground state, photoelectron and photon decay 4-59683  
 He+He multipole polarisabilities, dispersion forces, many-body theory 4-87192  
 Hg, reson. multiphoton ionisation, polarisation depend. 4-78813  
 Hg vapour, ninth-order nonlinear polarisation and VUV generation 4-83642  
 Ho(II), relativistic mode-potential oscillator strengths and transition probabilities for 4f<sup>6</sup>s-4f<sup>6</sup>p transitions 4-112144  
 In, 5s<sup>2</sup>5p<sup>2</sup>(P<sub>1/2</sub>), static elec. dipole polarisability 4-78979  
 NH<sub>4</sub> halides, ionic compressibilities and static polarizabilities 4-88130  
 Nd laser glass, fluorescence line narrowing study 4-64411  
 Ne, multiple props., time depend. CHF method 4-87040  
 Si, screening energy variations and Auger parameters, XPS studies 4-99275  
 SiO<sub>2</sub>, screening energy variations and Auger parameters, XPS studies 4-99275  
 Tb(II), relativistic mode-potential oscillator strengths and transition probabilities for 4f<sup>6</sup>s-4f<sup>6</sup>p transitions 4-112144  
**atomic positron scattering** *see* **atomic electron impact excitation; atomic electron impact ionisation; elastic scattering of electrons by atoms and molecules**  
**atomic potentials** *see* **atomic forces**  
**atomic power** *see* **nuclear power**  
**atomic reactors** *see* **fission reactors**  
**atomic resonant states**  
 atom driven by standing-wave laser field, reson. fluoresc. 4-102633  
 atom-surface impact, coalescent resonances 4-96661  
 atom-surface scatt., coalescent resonances 4-96660  
 complex coord. method with Hermitian Hamiltonian, error estimates 4-68915  
 gas discharge resonant atomic state excitation rate const., depend. on plasma ionisation degree 4-69977  
 laser-induced collective binding in two-electron systems 4-91209  
 level degeneracy effects in resonant nonlinear phenomena 4-68913  
 multiphoton ionisation process, final-state interactions 4-96503  
 prydronium negative ions, doubly excited reson. 4-78986  
 Rydberg series of doubly excited reson. near two-electron escape threshold 4-64402  
 two-level atom, resonance fluorescence, photon number statistics anal. 4-64417  
 Ar, positive column, low press., stepwise ionisation effects modelling 4-92013  
 Ar+Xe, cor. between charge-changing interactions and projectile K $\alpha$ -X-ray emission 4-64595  
 Ca<sup>18+</sup>, electron scatt., collision strengths for inelastic transitions including fine struct. 4-96704  
 Cl, reson. struct., autoionisation, photoionisation spectra 4-83339  
 Cs, fluorescence spectrum, inter-Doppler resonances 4-107306  
 Cs resonance lines, high press. noble gas broadening 4-74187  
 Cs resonance lines, low press. noble gas broadening 4-74186  
 Ga XXX, X-ray spectra excited in low-inductance spark plasma 4-74181  
 Ge XXXI, X-ray spectra excited in low-inductance spark plasma 4-74181  
 H photoionisation in elec. field, reson. and interference effects 4-69028

**atomic resonant states continued**

- H photoionisation in elec. field, overlapping resons. and interference effects 4-69029  
 H, Rayleigh scatt. from n=3 resonance states, one-pole approx. 4-78824  
 H+H<sub>2</sub>, rearrangement collisions, resons. and dynamics calcs. 4-71901  
 He, <sup>3</sup>P Feshbach reson., line-shape parameters, autoionisation states 4-64433  
 He electron impact in supersonic beam, resons. and metastable states (French) 4-78971  
 He II 2p level excitation by electron impact, resonance states (Russian) 4-112283  
 He, photoionisation cross sections for photon energies 59-67 eV, autoionising reson., Rydberg series 4-64437  
 He<sup>+</sup>, (1s2s2s)<sup>2</sup>S reson., saddle-point complex-rot. method appl. 4-64404  
 He+H<sup>+</sup>, autoionising reson. excited at small ejection angles 4-96681  
 Hg, relativistic oscillator strengths, cor. effects, reson. transition 4-96490  
 Li in high mag. field, spacing between quasi-Landau reson. 4-87058  
 Li<sup>+</sup>, <sup>3</sup>P Feshbach reson., line-shape parameters, autoionisation states 4-64433  
 Mg II, 3p <sup>2</sup>P level, electron impact excitation cross section, reson. struct. 4-91351  
 Mn, photoelectron asymmetries and two-electron satellites near 3p to 3d giant reson. region 4-102655  
 Mo, hyperfine struct., RF, at beam mag. reson. and laser spectroscopic investig. 4-64410  
 Na collision induced coherence, high resol. four-wave light mixing 4-102767  
 Na(3p), reson. lines, fluorescence of Na-N<sub>2</sub> collision complex 4-74320  
 Ne, lowest 'two particles-two holes' reson. calc., diagonalisation approx. 4-83310  
 U, resonant pulsed laser excitation 4-102650  
**atomic scattering factors** *see* **crystal atomic structure; crystallography; lattice dynamics**  
**atomic spectra**  
*see also* **atomic fluorescence; atomic hyperfine structure; atomic spectral line breadth; atomic structure; beam-foil spectra; conversion electron spectra; radiative corrections; Russell-Saunders coupling; Stark effect; Zeeman effect  
 3s<sup>3</sup>p<sup>3</sup> ground configurations, (ionised Cu to Mo), magnetic-dipole transition predicted wavelengths and transition rates 4-68969  
 alkali-like atoms and ions, quasi-metastable quartet levels 4-74201  
 Ar I and II systems, collisional radiative coeffs. of 4p groups 4-65059  
 atomic spectra and oscillators, conf., Lund, Sweden, 17-19 Aug. (1983) 4-86109  
 atoms and ions, wavelengths, transition rates, relativistic struct. program 4-83283  
 atoms in astrophysics, book 4-106125  
 dipole tom, electric field commutation rel. 4-64445  
 energy level distributions, HF calc. 4-64333  
 forbidden lines in hot plasmas 4-87937  
 heavy atom X-ray spectra, spatial parity nonconservation 4-107303  
 high resol. spectroscopy, at. struct. studies 4-78795  
 highly excited states, radiative transitions in presence of strong microwave field 4-83312  
 highly ionised atoms, spectral classification for 1980-3 period 4-67875  
 highly-ionized atoms in fusion research plasmas, diagnostic techniques 4-87915  
 inert gases, flowing, in hollow cathode discharge, vac. UV radiation investig. 4-91988  
 interstellar atoms, resonance radiation pressure effects 4-63251  
 ions, solvation shifts of core electron binding energies, statistical model 4-91359  
 isoelectronic series from Cu to Mo, P sequence ion ground config. 4-74140  
 laser spectroscopy of mol. and atoms, review 4-63788  
 level degeneracy effects in resonant nonlinear phenomena 4-68913  
 line profile produced by emitter-perturber interactions, multiple interactions 4-87075  
 line resonance polarisation in non-magnetic collisionless regimes, appl. to solar spectra 4-101150  
 M-shell vacancies, radiative transition rates, X-ray emission, DF approx. 4-96445  
 multiple terms of atomic spectra, eigenfunction struct. 4-83318  
 multiply ionised atoms, np-1s transition intensity, semiempirical scaling law 4-64429  
 photofragment spectra of SO<sup>+</sup> 4-105000  
 relativistic heavy ion-atom collisions, radiative capture obs. 4-96679  
 resonance lines, low press. noble gas broadening 4-74186  
 resonance lines, photon escape and scattering 4-94592  
 Rydberg energy level shifts induced by blackbody radiation 4-96496  
 Rydberg giant atoms interacting with radiation 4-69018  
 sputtered atoms, inner shell vacancies and Auger spectra 4-74208  
 superposition of configurations calc. 4-112128  
 symposium, Berkeley, CA, USA (Sept. 1983) 4-67852  
 synchrotron radiation as probe for atomic physics 4-91217  
 three level at. ladder system, laser cross cor. effects, optical double reson. 4-83362  
 time-resolved FTS of molecular and atomic IR emission 4-96473  
 two two-level atoms, driven, light absorpt. spectra, anal. solns. 4-64408  
 two-level atom, interaction with time-symmetric pulse, transition probability 4-102647  
 two-level atom, transition probabilities, eigenvalue problem 4-64330  
 two-level system, degenerate four-wave mixing, extra resonances triggered by pressure-induced decay of lower state 4-112499  
 U, neutral, oscillator strengths 4-74192  
 vapour density meas. by least-squares fit to spectra 4-102825  
 VUV high resolution spectroscopy with and without mag. fields 4-91214  
 XUV spectra of solids as an atomic information source (Russian) 4-80962  
 Al IV, VUV spectrum, line wavelengths, relative intensities and transition identification 4-87065  
 Al, multiplet transitions, KL<sup>2</sup>L<sup>3</sup> X-ray emission spectra 4-83323  
 Al VIII(IX)(X), intercombination lines in PLT tokamak 4-83322  
 Al XI, doubly excited states, fine struct. meas. by beam-foil spectra (French) 4-69236  
 Al XIII plasma, laser prod. high resol. k-shell dielectronic satellite lines 4-103571  
 Ar, branching ratios and absolute transition probabilities in 4s-4p transition array 4-87081**

atomic spectra continued

Ar, excited state lifetimes, inelastic electron-photon delayed coincidence technique 4-102644  
Ar, highly ionised, VUV spectrum (*Chinese*) 4-91213  
Ar IV to Ar VIII ions, emission spectra, 100 to 900 Å 4-59664  
Ar,  $K_{\alpha}$  X-ray emission spectrum, CI calcs., radiative transition probabilities calc. 4-59668  
Ar,  $L_{1-2}M_1$  Coster-Kronig spectrum, exchange, electron correl., and relax. effects 4-74172  
Ar, relativistic electron beam excitation, fluoresc. and absorpt. 4-69220  
 $Ar^{16+}$ , excited states in D Tokamak plasma, recombination population 4-87936  
Ar+Xe, corrls. between charge-changing interactions and projectile K $\alpha$  X-ray emission 4-64595  
 $Ar^{22+}$ +Cu, two electron transfer collisions, Ar I VUV line intensity 4-83462  
As VII spectrum,  $3d^84s$ ,  $3d^84p$  and  $3p^33d^{10}$  configs. 4-74190  
As VIII, spectrum,  $3d^8$ ,  $3d^84p$  and  $3p^33d^9$  configs. 4-69005  
Au I, low-lying transitions, vol. isotope shifts 4-64409  
B ions, extreme UV absorption spectroscopy using two laser-produced plasmas 4-60728  
B ions, He- and Li-like, laser produced plasma, EUV spectra 4-83320  
Ba,  $7s/n d$  autoionisation states, two-photon spectroscopy 4-78822  
Ba I,  $6sn^2F_3$ ,  $^3F_2$ ,  $^3F_3$  Rydberg state energies, laser at. beam spectroscopy 4-78794  
Ba I, II, energy levels in optical spectrum, isotope shifts, specific mass effect 4-74200  
 $Ba^{2+}$ , discrete 4d photoabsorpt. spectrum 4-102624  
 $Ba^{2+}$  ions, 4d photoabsorption spectrum, potential-barrier effects 4-112138  
Be II autoionis. widths, optical emission spectrosc. investig. 4-69025  
Be ions, extreme UV absorption spectroscopy using two laser-produced plasmas 4-60728  
Be ions, He- and Li-like, laser produced plasma, EUV spectra 4-83320  
Be isoelectronic sequence, transition energy calc. using multiconfig. Dirac-Fock and RPA calcs. 4-64364  
Be-like ion, isoelectronic series, oscillator strengths, wavelengths, energy levels 4-67881  
Be-like isoelectronic series, oscillator strengths, transition wavelengths, HF relativistic calcs. 4-106127  
C I line strengths in quasars, rel. to background radiation temp. at epochs ( $z \geq 2$ ) 4-63343  
C II, IR and UV lines, fine struct. transitions and electron collision strengths, astron. appl. 4-77701  
C ions, effective dielectric recomb. coeffs., astrophysical appl. 4-96477  
C ions, He- and Li-like, laser produced plasma, EUV spectra 4-83320  
C, transition probability meas. for spectral lines of 3s-4p transition array 4-74194  
 $C^+$ , branching ratios of  $2s^23p$   $^2P^o$  term, Fourier transform and VUV spectroscopy 4-87066  
CA XVIII/CA XIX ionisation balance in solar flares, derivation from XRP solar X-ray data 4-72916  
Ca, hypersatellite X-ray spectra,  $H^+$  induced 4-107301  
Ca XIX, effective excitation and recomb. rate coeffs., appl. to Sun 4-87218  
Cd ions in laser-prod. plasma, for UV spectra 4-68997  
 $^{111}Cd$  vapour, coherent nonlinear phenomena in random fields 4-102980  
Cl, electronic Raman spectra, ion laser excitement 4-102621  
Cl, H-like, is Lamb shift determ. by X-ray transitions meas. using beam-foil excitation 4-74195  
Cl VII, Na-like, lifetimes, beam-foil excitation spectra 4-59677  
 $Cl3p^2(^2P_{1/2})$ , collisional quenching time-resolved at. reson. VUV absorpt. 4-59665  
Co III, transition probabilities for forbidden lines in  $3d^7$  ground configuration 4-63041  
Co, two-electron one-photon excitation, X-ray absorpt. spectra 4-83324  
Cr, laser-produced plasmas,  $2p^33s$ ,  $3p$  and  $3d$  configurations 4-102620  
Cr, spectral line intensities and transition probabilities (*French*) 4-78809  
Cs, plasma jet flowing into He, diagnostics 4-91993  
Cs resonance lines, high press. noble gas broadening 4-74187  
Cs, Rydberg series in autoionising continua 4-83337  
Cs vapour, nonsteady reson. induced electron Raman scatt., polarisation features 4-107293  
 $^{133}Cs$  atom ensemble, paramag. resonance line shift in narrow band noise fields 4-91212  
Cu, excited H reflection at grazing incidence, light emission 4-76587  
Cu I, lifetimes of some excited levels, beam foil spectra 4-87082  
Cu I lines, rel. oscil. strengths, hook and emission meas. 4-69000  
Cu II, lifetimes of some excited levels, beam foil spectra 4-87082  
Cu-like ions,  $Ge^{3+}$ - $Mo^{13+}$   $3d-4p$  transitions, anal. 4-69001  
 $D^*$  electron impact dissc. of  $D_2O$ , emission cross section 4-107462  
Eu I, II, electron-impact excitation of 4f electrons 4-83478  
Eu I, VUV absorpt. spectrum identification,  $4f^55d(^2D)np$  state calc. 4-91215  
Eu I spectrum,  $4f^6s6p$  configuration, isotope shift, parametric anal. 4-59678  
F, absolute transition probability of visible lines in Ar-F arc 4-79856  
Fe group atoms,  $3d^N4p$  configs., effective electrostatic interactions 4-83317  
Fe I, ionisation potential by multistep laser spectroscopy 4-74353  
Fe I oscillator strengths meas. 4-87080  
Fe II emission and excitation in stellar atm. and laboratory anal. 4-10516  
Fe II fluorescence in stellar atmospheres, UV triplet lines 4-63154  
Fe II spectrum, comparison between observed and predicted emission lines in different plasmas 4-87061  
Fe XVII, Ne-like, laser-produced plasmas,  $2p^53s$ ,  $3p$  and  $3d$  configurations 4-102620  
Fe XVII transitions identification in solar flares 4-72922  
Fe XVIII-XXIII 8-14 nm lines, plasma electron density meas. 4-87927  
Fe XXIV, spectral line strengths in laser plasma 4-107314  
 $Fe^{22+}$  and  $Fe^{23+}$ , X-ray spectra of inner-shell transitions 4-94707  
 $Fe^{24+}$ , high precision X-ray spectra 4-78797  
 $Fe_{\alpha}$  clusters Ar, Kr and Xe matrices, mag. circular dichroism study 4-78799  
 $FeSO_4 \cdot 7H_2O$  dosimeter,  $\epsilon(Fe^{3+})$  determ. (*Chinese*) 4-68833  
H, atomic beam polarized proton source 4-107464  
H, atomic spectroscopy and holography, laboratory expt. 4-67927  
H, electromag. transitions, wavelengths, dipole strengths, oscillator strengths and transition probabilities 4-59676  
H I like ions, electron impact polarisation of Lyman- $\alpha$  radiation 4-67609

atomic spectra continued

H, laser spectroscopy, resolution of tunable dye lasers 4-64412  
H, narrow-band VUV laser spectroscopy, two-photon spectra 4-83383  
H, optical spectra in strong mag. fields (*Japanese*) 4-107307  
H plasma, ion temps., spectral line broadening (*Chinese*) 4-87840  
H, spectra and struct. in strong mag. field, spherical basis (*French*) 4-68927  
H spectrum transformation in crossed electric and mag. fields 4-59672  
H, Stark-mixed  $n=2$  states, excitation and decay obs. in electron-photon coincidence expt. 4-87073  
 $H^+$  in gases, vacuum UV radiation prod. cross sections 4-78931  
H-like ions, fine struct., spectral intensities, collisional-radiative calcs. 4-102643  
H-like ions, reson. doublet spectrum in intense elec. field, laser plasma diagnostics appl. 4-84074  
H-like ions plasma, Balmer  $\alpha$  fine struct. relative intensities 4-84059  
 $H+N^{3+}$ , charge transfer cross sections, extreme UV radiation emission 4-64596  
 $H_2+C^{4+}$ , charge transfer, polarised light emission 4-83463  
 $H_2$  edge region line emission in PDX Tokamak 4-91970  
 $H^*$  electron impact dissc. of  $H_2O$ , emission cross section 4-107462  
He  $1s2p^1P_1-1s2p^1P_1$  transition energy, radiative correction 4-64399  
He, excited state lifetimes, inelastic electron-photon delayed coincidence technique 4-102644  
He I, broadening parameters of  $\lambda=447.15$  nm line in laser prod. plasma 4-78803  
He I, electron excitation rate coeffs. for transitions from ground state to excited states 4-94571  
He I, principal series spectral line excitation in electro-atom collisions 4-91352  
He I astrophysical lines, Stark broadening 4-102638  
He I autoionisation rate determ. by optical emission spectroscopy 4-78087  
He II, principal series spectral line excitation in electro-atom collisions 4-91352  
He parity-violating elec. dipole transitions, electron-electron neutral weak interaction 4-64407  
He principle series transition energies 4-83321  
He, spectra and struct. in strong mag. field, spherical basis (*French*) 4-68927  
He, Stark broadening, electron and  $H^+$  impact line width and shift 4-69009  
He+H(D), H(D) 2s and 2p excitation, integral cross sections 4-102786  
He+Xe, collision induced absorpt. coeff., quantum mech. and classical approach 4-91330  
He\*+He, pot. energy curves obtained by combining scatt., spectroscopy and ab initio theory 4-74177  
He\*+Ne, electronic energy transfer in nozzle-beam scatt. cell expt., visible emission, odd-J levels 4-64578  
He\*( $^3S$ ), electron beam excited, transient absorpt. in UV and VUV 4-78796  
Hg vapour, ninth-order nonlinear polarisation and VUV generation 4-83642  
Hg-Ar(Ka) interaction pots. calcs. from temp.-depend. absorpt. spectra 4-69170  
Ho (XXXIX), laser produced plasma, Cu-like lines in X-ray spectra 4-84053  
I laser degenerate mag. dipole transitions self-induced transparency 4-83653  
In ions in laser-prod. plasma, for UV spectra 4-68997  
K+Rb impact broadening of first K reson. line 4-69013  
Kr, highly ionised, unresolved transition arrays 4-87062  
Kr IV  $4s^24p^3$  and  $4s4p^4$  configs., VUV spectrosc. 4-69003  
Kr ion, H- and He-like, time of flight X-ray emission spectra 4-102629  
Kr, matrix isolated in solid Kr, Ar and  $N_2$ , EXAFS studies 4-64416  
Li I, autoionisation rate determ. by optical emission spectroscopy 4-87087  
Li I 670.7 nm resonance doublet in Ba stars, Li abundance 4-67746  
Li in high mag. field, spacing between quasi-Landau reson. 4-87058  
Li in inert gas matrices, mag. circular dichroism study of  $^2S \rightarrow ^2P$  transition 4-59670  
Li isoelectronic series, radiative decay following charge exchange on neutral gas targets 4-87069  
 $Li^{+}$ , doubly excited quintet states, fine and hyperfine struct., many-body calcs. 4-102609  
Li-like ion plasma, kinetics excitation spectral line intensities 4-91989  
LiCs recombining plasma, optimisation of inverse population of Li levels (*Russian*) 4-69023  
Mg I triplet lines, cool prominence plasma diagnostics 4-94698  
Mg, multiplet transitions,  $KL^2-L^3$  X-ray emission spectra 4-83323  
Mg, X-ray emission spectra meas. 4-87067  
Mg XI, effective excitation and recomb. rate coeffs., appl. to Sun 4-87218  
 $Mg^{3+4+}$  in IR spectra of NGC 7027 planetary nebula 4-63242  
Mn I, relative oscillator strengths,  $0eV-3eV$  4-69002  
Mn I lines in solar spectrum, anal. using accurate oscillator strengths 4-94710  
Mn, spectral line intensities and transition probabilities (*French*) 4-78809  
Mo, hyperfine struct., RF, at beam mag. reson. and laser spectroscopic investig. 4-64410  
Mo, inner-shell transitions, two-photon X-ray emission spectra 4-96515  
N II+He( $N_2$ ) collisions, N II reson. line excitation in VUV region in cathode sheath of hollow cathode discharge 4-87203  
N IV singlet lines, non-LTE calcs. of equivalent widths 4-63048  
N ions, effective dielectric recomb. coeffs., astrophysical appl. 4-96477  
 $N_2+B^+$  fast beam excitation study 4-107294  
Na absorption spectra recorded using freq. modulation spectroscopy with pulsed dye laser 4-73520  
Na atoms trapped in Ar and Xe solids, site form., computer simulation 4-96472  
Na D-line reabsorption in high pressure Na arcs, wall temp. depend. 4-87955  
Na, multiplet transitions,  $KL^2-L^3$  X-ray emission spectra 4-83323  
Na Rydberg states, linear Stark effect, near degeneracies between m sublevels 4-107308  
Nb IV, two electron jump transitions Stark mixing, CI calcs. 4-87063  
Nd laser glass, fluorescence line narrowing study 4-64411  
Ne, 585.2 nm line intensity variation due to return to gas phase from glass bulb 4-69006  
Ne, excited state lifetimes, inelastic electron-photon delayed coincidence technique 4-102644

## atomic spectra continued

- Ne gas, weakly ionised, laser-induced perturbation spectrosc. investig. 4-83319  
 Ne, high Rydberg states and autoionising reson., centrifugal 4-68989  
 Ne, high-resolution spectra by means of optogalvanic spectroscopy (Chinese) 4-112137  
 Ne I lifetime and absolute transition probabilities of  $2p_{10}(^2S_1)$  level 4-83334  
 Ne I lines, Stark effect 4-69011  
 Ne, level-crossing spectroscopy of atoms dressed by optical photons in degenerate four-wave mixing 4-107299  
 Ne VII,  $1s2s2p^3\ ^3P_{21}-1s2p^3\ ^3S_2$  VUV transition 4-107300  
 Ne\* recombination pumping in Ne-H<sub>2</sub> pulsed transverse elec. discharge (Russian) 4-112133  
 Ni atoms isolated in Kr and SF<sub>6</sub> matrices, electronic ground state, absorpt., and MCD spectra 4-64423  
 Ni IV, transition probabilities for forbidden lines in 3d<sup>7</sup> ground configuration 4-63041  
 Ni, matrix-isolated atoms, fluoresc. spectra 4-96481  
 Ni XIX transitions identification in solar flares 4-72922  
 Ni+Ni collisions, isolated K MO transitions, emission anisotropy 4-69180  
 O atom flame detection, multiphoton photochemical and collisional effects 4-109673  
 O I (<sup>1</sup>D-<sup>3</sup>P) 630 nm auroral obs. rel. to IR spatial structure 4-110343  
 O I and III forbidden line emission from M82 galactic nucleus, far IR obs. 4-90241  
 O ions effective dielectric recomb. coeffs., astrophysical appl. 4-96477  
 O<sup>2+</sup> 166 nm intersystem line emission, <sup>2</sup>S<sub>2</sub><sup>0</sup> metastable level radiative lifetime 4-110512  
 P-like ions, energy levels, transition probabilities, multiconfiguration DF study 4-106126  
 Pb, L<sub>2</sub>-L<sub>3</sub> Coster-Kronig transition probability meas. 4-96493  
 Pb, muonic even-A isotopes, L and M transition energies 4-107469  
 Rb, atom, two-photon resonant excitation of highly excited state, transient coherent effect 4-69032  
 Rb IX, spectrum and energy levels 4-102625  
 Rb saturated-vapour density meas. at 302-351 K 4-107298  
 Rb V 4s<sup>4</sup>p<sup>2</sup> and 4s4p<sup>2</sup> configs., VUV spectrosc. 4-69003  
 Rb XI ions, spectra meas. 4-112136  
 S III, 3s<sup>2</sup>3p<sup>2</sup> <sup>2</sup>P<sub>1/2</sub>-3s3p<sup>2</sup> <sup>2</sup>S<sub>2</sub> intersystem lines, astrophysical appl. 4-96476  
 S VII 3d-4f transition in laser-produced plasma 4-69004  
 Se, laser-produced plasmas, 2p<sup>3</sup>3s, 3p and 3d configurations 4-102620  
 Se IX, UV spectrum 100 to 140 Å, 3d<sup>4</sup>, 3d<sup>3</sup>4p and 3d3d<sup>2</sup> configurations 4-59667  
 Se VIII, configuration level revision 4-74189  
 Si I, meas. of 3 <sup>3</sup>P<sub>0</sub>-3 <sup>1</sup>P<sub>1</sub> fine-struct. interval and g<sub>F</sub>-factor by laser mag. reson. 4-85866  
 Si III, UV emission line strengths in low density plasmas 4-94583  
 Si+F<sub>2</sub> collision, time-resolved at. reson. absorpt. spectrosc. investigation 4-102765  
 Sr I, principal series, photoabsorpt. spectrum 4-68996  
 Sr levels, config. mixing and isotope shifts 4-68978  
 Sr VI 4s<sup>4</sup>p<sup>2</sup> and 4s4p<sup>2</sup> configs., VUV spectrosc. 4-69003  
 Sr XII ions, spectra meas. 4-112136  
 SrV, spectrum, struct. 4-107295  
 Th and U optogalvanic spectral reference lines, dye laser wave number calibration appls. 4-83628  
 Th, spectral atlas (312.4 nm to 904.8 nm) 4-101195  
 Ti, hypersatellite X-ray spectra, H<sup>+</sup> induced 4-107301  
 Ti XI, energy levels and oscillator strengths, at. struct. calc. 4-69016  
 Ti XIII, Ne-like, laser-produced plasmas, 2p<sup>3</sup>3s, 3p and 3d configurations 4-102620  
 Ti XX, spectral line strengths in laser plasma 4-107314  
 Ti, coinduced press. broadening and shift of 535 nm line 4-78801  
 Tm I spectrum, lifetime meas. using pulsed dye laser 4-72861  
 U and Th optogalvanic spectral reference lines, dye laser wave number calibration appls. 4-83628  
 U III, wavelength and energy level meas. using Fourier-transform spectrometer 4-102623  
 V (II), UV lines oscillator strengths in V-He plasma of wall stabilised arc 4-112142  
 V II spectrum 3d<sup>3</sup>(<sup>4</sup>F)4f config. 4-96479  
 V, laser-produced plasmas, 2p<sup>3</sup>3s, 3p and 3d configurations 4-102620  
 WI, isotope and hyperfine splittings for two UV transitions, saturation and polarisation spectroscopy 4-87064  
 Xe, 5s, 5p photoelectron satellite spectrum 4-102658  
 Xe, 5s, 5p satellite spectrum studied using synchrotron radiation in region of Cooper minimum 4-59663  
 Xe (III), Auger electron energies, surface effect 4-85045  
 Xe I, accurate wavelength of 731.6874 nm line 4-105781  
 Xe, optical processes study by 4-83661  
 Xe soft X-ray absorpt., dielec. screening and core hole relax. 4-64414  
 Xe, VUV oscillator strength, geometry-independ. phase-matched meas. 4-102646  
 Y V, 4f and 5p configs., transitions 4-68942  
 Yb, 555.6 nm absorption line, storage and phase conjugation of light pulses using stimulated proton echoes 4-112528  
 Yb, 6snp Rydberg states, diamagnetic shift and singlet-triplet mixing 4-102618  
 Yb (XLI), laser produced plasma, Cu-like lines in X-ray spectra 4-84053  
 Yb I, interchannel interaction between single excitation from 4f<sup>14</sup> and double excitation from 6s<sup>2</sup> 4-96478  
 Yb vapour, temporally programmed free-induction decay 4-112529  
 Zn IV, ionisation pot., UV spectra 4-59666  
 Zn-like ions from Ru<sup>14+</sup> to Dy<sup>36+</sup>, 4s<sup>2</sup> 1S-4s4p<sup>1</sup>P<sub>1</sub> transitions 4-102626  
 Zr III, two electron jump transitions Stark mixing, CI calcs. 4-87063

## atomic spectral line breadth

- absorption line profiles for 39 rapidly rotating stars 4-77825  
 approximate electron- and proton-impact line widths within a spectral series 4-91237  
 atomic collisions, line broadening, final state distrib. 4-102768  
 cathode glow, sputtered atom light emission, interferometry 4-87981  
 collision induced absorpt. lineshape, Mori theory 4-64579  
 collisional broadening 4-87202  
 P Cygni profiles, velocity law plateau effects 4-67713  
 fourth-row elements, Nb-Sb, L X-ray spectral linewidths meas. 4-68998  
 fourth-row elements, Nb-Sb, L X-ray spectral linewidths meas. 4-68999

## atomic spectral line breadth continued

- hot dense plasma, line and level broadening, Thomas-Fermi model 4-83331  
 hydrogenic ions, Stark profiles, ion dynamics effect in hot and dense plasmas 4-87077  
 inner-shell ionisation, Auger electron lineshapes in coincidence with scattered electrons 4-107322  
 intensity-fluctuation spectroscopy of optical fields with non-Gaussian statistics 4-95530  
 intermediate Voigt broadening, tables for direct determ. of spectral line parameters 4-112141  
 line profile produced by emitter-perturber interactions, multipole interactions 4-87075  
 multiphoton ionisation, electron spectra, strong-field effects 4-102654  
 neutral atom lines, binary collisions and broadening, phase shift, trajectory effect calcs. 4-69179  
 nonMarkovian dephasing of two-level reson. fluoresc. in strong radiation field 4-64419  
 optical properties of an isolated resonance line with high density self-broadening 4-113112  
 pulsed two-photon absorpt., laser linewidth and lineshape effect 4-78821  
 pump-probe studies of homogeneously broadened lines, spectral holes origin 4-64734  
 resonance light scattering, intensity depend., stationary homogeneously broadened atom driven by incident field, book contrib. 4-64430  
 RF glow discharges, spectral line shapes, optical emission actinometry 4-87931  
 Stark width and shift depend. on ionisation pot. 4-91221  
 Thomas-Fermi atoms, level and line broadening, finite temp. 4-74154  
 Thomas-Fermi line broadening at finite temp. 4-83330  
 two-level atom, fluorescence spectrum 4-102636  
 two-level atom driven by smooth pulse, reson. fluoresc. 4-96487  
 two-level system, degenerate four-wave mixing, extra resonances triggered by pressure-induced decay of lower state 4-112499  
 vapour density meas. by least-squares fit to spectra 4-102825  
 Ar, K<sub>α</sub> X-ray emission spectrum, CI calcs., radiative transition probabilities calc. 4-59668  
 As VII spectrum, 3d<sup>8</sup>4s, 3d<sup>8</sup>4p and 3p<sup>3</sup>3d<sup>10</sup> configs. 4-74190  
 Ba, oscillator strengths, rare gas-induced broadening of principal series lines 4-107309  
 C IV line broadening in dense plasmas 4-91235  
 Ca II H and K lines, teaching exercise for Wilson-Bappu effect in late-type stars 4-110841  
 Ca target, ground and excited state sputtering obs. using laser-fluoresc. 4-93169  
 Cd vapour, interatomic pots., UV absorpt. spectra 4-107297  
 Co I oscillator strengths from Fraunhofer line equivalent widths 4-63125  
 Cr target, ground and excited state sputtering obs. using laser-fluoresc. 4-93169  
 Cs, polarisation spectroscopy 4-74193  
 Cs resonance lines, high press. noble gas broadening 4-74187  
 Cs resonance lines, low press. noble gas broadening 4-74186  
 Eu I, VUV absorpt. spectrum: identification, 4f<sup>7</sup>5d(<sup>2</sup>D)np state calc. 4-91215  
 Fe I 557.61 nm line changes rel. to solar oscils. 4-63127  
 Fe, sputtered atom vel. and electronic state distrib. by laser-induced fluorescence spectroscopy 4-93168  
 Fe sputtered neutrals, ionisation length near wall in ISX-B using laser-induced fluoresc. 4-91971  
 Fe XXIV, spectral line strengths in laser plasma 4-107314  
 H afterglow plasma, central struct. of H<sub>β</sub> line at low electron densities 4-59674  
 H, emission line shapes in hollow-cathode discharge 4-102645  
 H, H<sub>α</sub> line Stark broadening at low densities, quantal and semiclassical calcs. 4-64424  
 H I Balmer lines broadened by plasma turbulence, Stark profiles 4-105871  
 H in He, collisional hyperfine line shifts calc. using exchange perturbation theories 4-64401  
 H ions in plasma, spectral line wing broadening theory (Russian) 4-69015  
 H, parity nonconservation, Zeeman and Stark effect, reson. line shapes 4-96489  
 H, radiative decay, final-state interferences 4-83333  
 H, Stark effect shape resonances in fields up to 3 MV/cm 4-102641  
 H<sub>β</sub> edge region line emission in PDX Tokamak 4-91970  
 He, <sup>1</sup>P Feshbach reson., line-shape parameters, autoionisation states 4-64433  
 He I, broadening parameters of λ=447.15 nm line in laser prod. plasma 4-78803  
 He I, principal series spectral line excitation in electro-atom collisions 4-91352  
 He I, Stark broadening params., semiclassical calc. 4-91224  
 He I astrophysical lines, Stark broadening 4-102638  
 He I D<sub>3</sub> line in G and K stars 4-67724  
 He II, principal series spectral line excitation in electro-atom collisions 4-91352  
 He, photoionisation cross sections for photon energies 59-67 eV, autoionising reson., Rydberg series 4-64437  
 He, Stark broadening, electron and H<sup>+</sup> impact line width and shift 4-69009  
 He<sup>-</sup>, (1s2s2s)<sup>2</sup>S reson., saddle-point complex-rot. method appl. 4-64404  
 Hg vapour, interatomic pots., UV absorpt. spectra 4-107297  
 Hg vapour, laser assisted collisional effects in nonlinear optical phenomena 4-96996  
 In, 410 nm line, perturbation by foreign gases, press. broadening and shift. 4-102634  
 K, wall-stabilised arc, electron temp. and density, Stark broadening meas. 4-112140  
 K+Rb impact broadening of first K reson. line 4-69013  
 Li in inert gas matrices, mag. circular dichroism study of <sup>2</sup>S-<sup>2</sup>P transition 4-59670  
 Li<sup>+</sup>, <sup>1</sup>P Feshbach reson., line-shape parameters, autoionisation states 4-64433  
 Li<sup>+</sup>, <sup>1</sup>P levels, beam-foil spectral line identification 4-74188  
 N IV singlet lines, non-LTE calcs. of equivalent widths 4-63048  
 Na beam laser cooling by AC Stark effect 4-69017  
 Na collision induced coherence, high resol. four-wave light mixing 4-102767  
 Na D<sub>1</sub> line, laser-induced fluoresc. line narrowing 4-69012  
 Na vapour, optical bistability with symmetry breaking 4-64733

atomic spectral line breadth continued

- Nd laser glass, fluorescence line narrowing study 4-64411
- Ne, high-resolution spectra by means of optogalvanic spectroscopy (Chinese) 4-112137
- Ne, level-crossing spectroscopy of atoms dressed by optical photons in degenerate four-wave mixing 4-107299
- Rb, polarisation spectroscopy 4-74193
- Se VIII, configuration level revision 4-74189
- Sr, two- and three-photon autoionisation under strong laser radiation 4-78812
- Ti XX, spectral line strengths in laser plasma 4-107314
- Tl, coinduced press. broadening and shift of 535 nm line 4-78801
- U II, wavelength and energy level meas. using Fourier-transform spectrometer 4-102623
- Xe II, Stark broadening, linewidth meas. 4-83328
- Xe, spectral line shift in high electron density plasmas 4-91236
- Xe-Ar collision induced absorpt. lineshape, Mori theory 4-64579
- Yb vapour, temporally programmed free-induction decay 4-112529
- <sup>174</sup>Yb 555.6 nm absorption line, field-inhibited optical dephasing and shape locking of photon echoes 4-79242
- Zn vapour, interatomic pots., UV absorpt. spectra 4-107297

atomic structure

- see also atomic electron correlations; atomic excited states; atomic fine structure; atomic orbitals calculations; atomic polarisability; atomic spectra; nuclear screening; Russell-Saunders coupling; triplet state
- 3s<sup>2</sup>3p<sup>2</sup> ground configurations, (ionised Cu to Mo), magnetic-dipole transition predicted wavelengths and transition rates 4-68969
- ab initio local-density pot., modified Z method 4-64371
- alkaline earth metal atoms, dynamic polarisabilities, semiempirical calc. methods 4-102599
- atomic 1/Z expansions, poorly convergent perturbation expansions via shifted origin series 4-112089
- atomic plasma physics in inertial fusion 4-102762
- atoms, transition from collective to independent-particle motion within valence shell 4-96464
- atoms and ions, wavelengths, transition rates, relativistic struct. program 4-83283
- atoms and ions with small Z, screening parameters, analytic wave functions 4-78792
- atoms in astrophysics, book 4-106125
- bound state, maximum number of electrons 4-112085
- Coulomb radial wave functions, JWKB approximations 4-96420
- Coulombic systems energy limits 4-106205
- coupled-channel equations, stabilisation of solns. and Green's function, at. and mol. appls. 4-101703
- dipole tom, electric field commutation rel. 4-64445
- dynamic response in elec. field, Born-Oppenheimer and Feynman-Hellmann approx. 4-102589
- dynamical relaxation energy shift of medium to high Z elements 4-102628
- effective electrostatic-spin-orbit and effective spin-orbit interactions in (n'l')n'l' configurations 4-74170
- electron atom shell influence on effective neutron charge value (Russian) 4-96505
- electronic and nucl. charges, Hellmann-Feynman and virial theorems 4-112083
- electronic density of the nucleus, bounds calcs. 4-68935
- energy density functional, four-dimens. density 4-64328
- energy differences, electron correl. effects, approximate method 4-83304
- energy formulas for atoms and molecules 4-74130
- energy level distributions, HF calc. 4-64333
- energy levels calc. using HF approx. 4-102570
- f-shell orthogonalised operators 4-74139
- Fermi atomic pseudopotential 4-106142
- forces in standing-wave laser field calcs. 4-96497
- gas phase XPS 4-59847
- H, muonic, weak interactions contrib. to hyperfine level splitting 4-83494
- halogen atoms, compact contracted Gaussian type basis sets 4-102583
- Hartree-Fock wavefunctions, reduced local energy using computer program 4-96421
- heavy atoms, electron struct., local density calc. 4-74173
- heavy atoms, ionisation pot., universal asymptotic limit in non-relativistic theory 4-112084
- heavy-ion induced satellite X-ray emission 4-99870
- high resol. spectroscopy, at. struct. studies 4-78795
- hot dense plasma, line and level broadening, Thomas-Fermi model 4-83331
- Hund's multiplicity rule, quantum mechanical explanation 4-96418
- information entropy and Thomas-Fermi theory 4-91201
- inner-shell transitions 4-68928
- ionised atoms, ionisation effects in inner electron shells, review 4-87068
- ions, electrostatic pot. at nucleus, rel. to chem. pot. 4-68916
- isoelectronic series, second differences in total electronic energies (German) 4-78761
- isoelectronic series atoms, electrostatic pot., total energy Z expansion 4-96637
- isoelectronic series from Cu to Mo, P sequence ion ground config. 4-74140
- K-shell ionisation cross section expression derived using plane wave Born approx. 4-96647
- kaonic hydrogen, atomic ground state interaction, model-independent formalism 4-96726
- laser-atom interactions, noise modelling by jump processes 4-69019
- laser-induced collective binding in two-electron systems 4-91209
- level degeneracy effects in resonant nonlinear phenomena 4-68913
- low-level atom, time-depend. cluster variation method calcs. (Turkish) 4-112082
- Lowdin spin-adapted wave functions, recurrent construction, matrix element evaluation 4-74134
- magnetic resonance in degenerate quasi-energy states 4-107296
- many-body theory 4-78066
- many-electron atomic systems, statistical representation, total binding energy 4-74126
- many-electron systems, quasiparticle energy density functional 4-64329
- momentum expectation values, gradient terms 4-78760
- multiply charged ion, shell correction, Thomas-Fermi model 4-102596
- multipole polarisabilities, spectra sums and multipole-multipole two-body dispersion coeff. 4-83302
- muonium weak interactions contrib. to hyperfine level splitting 4-83494
- N equivalent electron energies, orthogonal operator set 4-83281

atomic structure continued

- neutral atoms, energy levels, binding energies calcs. 4-64367
- neutral atoms, shell binding energies 4-83280
- one-electron ion, quasi-energy level width in electric field 4-68987
- orthogonal scalar operator complete set for config. f<sup>3</sup> 4-74141
- positive ions, chem. pot., density functional theory 4-96437
- quasi-degenerate atomic systems, response to self-radiation fields (Russian) 4-91190
- relativistic calculations 4-87041
- relativistic H atom, WKB semiclassical approx. 4-90407
- relativistic SCF calcs. for stationary states, optical response 4-87229
- resonance complex coord. method with Hermitian Hamiltonian, error estimates 4-68915
- Rydberg atoms, binary-encounter form-encounter and its use in calc. inelastic cross sections 4-96657
- Rydberg atoms with large orbital ang. momentum, prod. 4-59655
- Rydberg energy level shifts induced by blackbody radiation 4-96496
- Rydberg states, recent results 4-91189
- SCF calcs. in stationary states, optical response 4-87228
- screened Coulomb potential, critical screening parameters 4-102612
- semiconductor materials, theoretical anal. (Italian) 4-65721
- spin adapting many-body theory, use of spin graphs 4-78758
- sputtered atoms, inner shell vacancies and Auger spectra 4-74208
- statistical atom: handling the strongly bound electrons 4-74151
- statistical atom: some quantum improvements 4-74152
- statistical atom, numerical study 4-74153
- symposium, Berkeley, CA, USA (Sept. 1983) 4-67852
- synchrotron radiation as probe for atomic physics 4-91217
- theory, teaching approach using game board and rubber rings 4-90331
- third-row atoms, core electron Coulomb and exchange operators, matrix elements 4-96446
- Thomas-Fermi atom, asymptotic region 4-74131
- Thomas-Fermi atoms, level and line broadening, finite temp. 4-74154
- Thomas-Fermi eqn., variational-iterative approximate soln. 4-91191
- transplutonium research, accomplishments and practical appl. 4-59661
- two electron atom, ground state, lowest level energy in quantum mech. system, generalised convexity props. 4-73299
- two-electron atomic model 4-67921
- two-electron atoms, ground state calc., choice of internal co-ordinates 4-78772
- two-electron atoms, momentum-space integral Schrodinger equation 4-96426
- two-level system, degenerate four-wave mixing, extra resonances triggered by pressure-induced decay of lower state 4-112499
- two-level systems in arbitrarily strong alternating fields dynamic behaviour description, forgotten method 4-107316
- two-photon ionisation: interference and population trapping 4-74203
- variational calcs. extrapolation techniques, 4-83285
- virial and the independent particle models of the atom 4-74133
- $\sigma$  conjugation, chem. effects 4-74128
- Ar, highly ionised, VUV spectrum (Chinese) 4-91213
- Ar L<sub>1</sub>-L<sub>2,3</sub>M<sub>1</sub> Coster-Kronig spectrum, intermediate coupling calcs. 4-102619
- As VIII, spectrum, 3d<sup>8</sup>, 3d<sup>7</sup>4p and 3p<sup>3</sup>3d<sup>2</sup> configs. 4-69005
- Au, 4f binding energies, Auger effect 4-78817
- Au in inert gas matrices, radiative lifetimes 4-102642
- <sup>79</sup>Au, electron wavefunctions, momentum-space representation, relativistic effects calcs. 4-107288
- Ba multichannel-quantum-defect theory wave functions tested or improved by laser measurements 4-68929
- Be isoelectronic sequence, transition energy calc. using multiconfig. Dirac-Fock and RPA calcs. 4-64364
- Be<sup>+</sup>, doublet states, transition wavelengths and fine struct. 4-74171
- Be-like ion, isoelectronic series, oscillator strengths, wavelengths, energy levels 4-67881
- Be-like ions, fine struct. transitions between 2l<sub>a</sub>2<sub>b</sub> and 2l<sub>a</sub>3l<sub>b</sub> configurations, collision and line strengths 4-95072
- Cd I, d<sup>8</sup>s<sup>2</sup>p electron configs., empirical Slater-Condon parameters 4-68943
- CdBr<sub>2</sub>:Cu, photoionis., phosphoresc., at. states 4-102632
- CdCl<sub>2</sub>:Cu, photoionis., phosphoresc., at. states 4-102632
- Cs vapour, nonsteady reson. induced electron Raman scatt., polarisation features 4-107293
- Cu in inert gas matrices, radiative lifetimes 4-102642
- Fe atoms, sputtered, laser-induced fluoresc. investig. (German) 4-69008
- Fe group atoms, 3d<sup>4</sup>4p configs., effective electrostatic interactions 4-83317
- Fe I, II and III, atomic partition functions 4-107270
- Fe II spectrum, comparison between observed and predicted emission lines in different plasmas 4-87061
- Fe transition series atoms, s-d interconfig. energies, s-spin flip energies and ionisation pots. 4-83303
- Fe XV, energy levels, oscillator strengths 4-102617
- Ge<sup>IV</sup> ionic pseudopotentials, atomic number depend., general theory 4-83292
- H, 3-dimens. atom, rel. to harmonic oscillator, zero-energy case 4-74132
- H atom, wave function, analytic structure 4-83284
- H atoms in superstrong mag. fields 4-74148
- H, bound-state energies calc. using variational functional method 4-78765
- H, dynamic response in elec. field, Born-Oppenheimer and Feynman-Hellmann approx. 4-102589
- H, exact path integral treatment 4-59627
- H, ground state energy, quadratic Zeeman effect, Rayleigh-Schrodinger perturbation theory 4-102639
- H, one-dimens.,  $\delta$  function interaction, polarisability 4-106149
- H, phase-space, formulation, nonrelativistic quantum mechanics 4-102590
- H, spectra and struct. in strong mag. field, spherical basis (French) 4-68927
- H<sup>+</sup> level population in H II regions 4-101136
- H-like atoms, Dirac eqn. soln. within algebraic approx. 4-59621
- H-like heavy ions, energies calc. of 1s, 2s and 2p states 4-83307
- He atoms in superstrong mag. fields 4-74148
- He I, 3p<sup>1</sup>P and 4d<sup>1</sup>D levels alignment and orientation, foil tilt angle depend. 4-102780
- He isoelectronic series, poorly convergent perturbation expansions via shifted origin series: atomic 1/Z expansions 4-112089
- He, Schrodinger eqn. soln. 4-112112
- He, spectra and struct. in strong mag. field, spherical basis (French) 4-68927
- He, two-electron atomic model 4-67921

**atomic structure continued**

- He-like ions, asymptotic eigenvalues and wave functions for restricted quantum-mechanical three-body problems 4-101132  
 He-like ions, electronic density of the nucleus, bounds calcs. 4-68935  
 Hg I,  $d^9s^1p$  electron configs., empirical Slater-Condon parameters 4-68943  
 Hg-Ar(K $\alpha$ ) interaction: pots. calcs. from temp.-depend. absorpt. spectra 4-69170  
 Kr II, Stark broadening params. 4-91225  
 Kr IV  $4s^24p^3$  and  $4s4p^4$  configs., VUV spectrosc. 4-69003  
 Li in high mag. field, spacing between quasi-Landau reson. 4-87058  
 Li isoelectronic series, Rydberg energy levels determ. by relativistic quantum defect interpretation 4-107278  
 Li to Ar, core electrons, Coulomb and exchange operators, matrix elements, recombin. electron only SCF calcs. 4-59630  
 LiCs, recombining plasma, optimisation of inverse population of Li levels (*Russian*) 4-69023  
 N isoelectronic sequence, level values of  $n=2$  configurations 4-102593  
 Na, electron density, expectation values, gradient expansion correction effects 4-83295  
 Na Rydberg states, linear Stark effect, near degeneracies between  $m$  sublevels 4-107308  
 Ne,  $3s_2$  level lifetime determ. from Faraday rotation angle at resonance 4-91227  
 Ni atoms isolated in Kr and  $SF_6$  matrices, electronic ground state, absorpt., and MCD spectra 4-64423  
 Ni, matrix-isolated atoms, fluoresc. spectra 4-96481  
 P-like ions, energy levels, transition probabilities, multiconfiguration DF study 4-106126  
 Rb IX, spectrum and energy levels 4-102625  
 Rb V  $4s^24p^3$  and  $4s4p^4$  configs., VUV spectrosc. 4-69003  
 S VII  $3d^4$  transition in laser-produced plasma 4-69004  
 $Si^{4+}$  ionic pseudopotentials, atomic number depend., general theory 4-83292  
 $Si+F_2$  collision, time-resolved at. reson. absorpt. spectrosc. investigation 4-102765  
 $Sn^{4+}$  ionic pseudopotentials, atomic number depend., general theory 4-83292  
 Sr levels, config. mixing and isotope shifts 4-68978  
 Sr VI  $4s^24p^3$  and  $4s4p^4$  configs., VUV spectrosc. 4-69003  
 SrV, spectrum, struct. 4-107295  
 Ti IX, energy levels and oscillator strength 4-59649  
 Ti X, energy levels, oscillator strengths  $3s-3p$ ,  $3p-3d$  transition arrays 4-68955  
 Ti XI, energy levels and oscillator strengths, at. struct. calc. 4-69016  
 Xe,  $5s^25p^3$  and  $5s^15p^4$  configs., correl. effects, Auger-electron study 4-107286  
 Xe II, Stark broadening params. 4-91225  
 Y V,  $4f$  and  $5p$  configs., transitions 4-68942  
 Yb vapour, temporally programmed free-induction decay 4-112529  
 Zn I,  $d^9s^1p$  electron configs., empirical Slater-Condon parameters 4-68943

**atomic structure, crystals** *see crystal atomic structure***atomic weight** *see atomic mass***atoms**

- see also exotic atoms; helium atoms; hydrogen neutral atoms; positronium*  
 No entries

**ATR tubes** *see gas-discharge tubes; radar equipment***attaching** *see joining processes***attenuation** *see absorption; dispersion (wave); scattering; transmission***attenuation measurement**

- absorber-lined chamber, correlation of theoretical and measured site attenuation 4-69645  
 atmospheric attenuation determ. in microwave range, using temp. models (*Czech*) 4-85792  
 EMC, degraded absorber performance effect 4-69646  
 open field site, chamber factor for correlation 4-69644  
 plastic optical fibres, preparation 4-103047  
 submillimetre (0.89 mm) attenuation observations in clear atmosphere 4-77616  
 Sun tracker atmospheric attenuation meas. at 35 GHz 4-105636

**attenuators**

- see also waveguide attenuators*  
 optical-fibre attenuator, tension adjusted, in-line 4-112581

**attitude control**

- conference on astrodynamics at Lake Placid, USA (August 1983) 4-78043  
 environmental and thermal control for space vehicles, conf. Toulouse, France (Oct. 1983) 4-73162  
 Filtered Attitude Determination System for spacecraft measurement and control 4-73434  
 Galileo, dual-spin spacecraft, pointing performance 4-67595  
 hopping system, one-legged, performance evaluation, simulation 4-115102  
 spacecraft guidance and control techniques, conf., Florence, Italy (Sept. 1983) 4-73164

**audio acoustics**

- see also audio recording; audio systems; hearing; speech*  
 conference, acoustics, Paris, France (July 1983) 4-78035  
 headphone acoustics (*German*) 4-97202  
 recording disks, reproduced sound, A-weighted sound press. level distribution (*Japanese*) 4-87520  
 sound-image quality, physical and psychological factors 4-79373  
 theatre and cinema sound, standards improvement 4-69625

**audio amplifiers** *see audio-frequency amplifiers***audio discs** *see video and audio discs***audio equipment**

- see also audio-frequency amplifiers; gramophones; loudspeakers; microphones; pick-ups; video and audio discs*  
 editing digital audio 4-103112  
 filter design, appl. of simple hearing model 4-105260  
 subjective component of the fidelity of sound reproduction (*Italian*) 4-72268  
 Virginia Center for Performing Arts, acoustical design 4-60212

**audio-frequency amplifiers**

- guitars, infinite sustain through controlled feedback 4-79402

**audio recording***see also video and audio discs*

- 70 mm sound tracks, striping, recording and reproducing 4-73538  
 cinematography, video/sound tracks, time-advanced noise reduction system (*Russian*) 4-90679  
 Dallas Sound Lab, design 4-73537  
 digital sound recorders, nonlinear distortion meas. (*Russian*) 4-60217  
 electroacoustic recording and reproduction methods (*German*) 4-103104  
 motion picture optical sound tracks, worn-out, spatial filtering using white light (*Russian*) 4-73551  
 music recording studio in St Luke's Church, Dresden, architectural acoustics shaping (*German*) 4-69626  
 sound dubbing techniques for film and video: a comparison 4-78394  
 student introduction to psychophysics of high-fidelity sound 4-58612

**audio systems***see also acoustic devices; acoustic equipment*

- Burghtheater electroacoustic system, modifications 4-79376  
 computer model and ray-tracing, speech transmission index prediction 4-79409  
 Dallas Sound Lab, design 4-73537  
 GRASP sound separation system 4-103134  
 intelligibility estimates 4-97200  
 sound quality measurements of audio systems based on models of auditory perception 4-105258  
 sound reinforcement systems, comparison of real-time anal. and time-delay spectrometry 4-87526  
 theatre and cinema sound, standards improvement 4-69625  
 Virginia Center for Performing Arts, acoustical design 4-60212

**auditory activity** *see hearing***auditory evoked potentials** *see bioelectric potentials; hearing***auditory perception** *see hearing***Auger deexcitation** *see Penning ionisation***Auger effect**

- AES, crystalline effects 4-99243  
 AES, detection limits 4-81049  
 AES, N(E) Auger spectra, peak energies, rel. sensitivity factors 4-89371  
 AES, quantitative, instrumental effects 4-85352  
 AES, surface analysis by low energy SEM with a field emission gun 4-79915  
 Al (111), pure textured polycrystalline, analytical SEM with JAMP-10 Auger microprobe 4-61785  
 alloy, Auger spectra, core-valence-valence, CPA theory, disorder-induced vertex corrections role 4-71491  
 alloys, Auger spectra, partial long range order effects 4-99238  
 alloys, ternary, ion implantation prep., surface binding energy 4-79972  
 angular distribution and spin polarisation of Auger electrons 4-59684  
 appearance potential spectroscopy 4-99230  
 applied surface anal., conf., Dayton, USA (June 1983) 4-95016  
 background continuum effect in AES 4-66146  
 Boltzmann transport eqn. theory of electron scatt. 4-66159  
 brass, preferential sputtering studies by AES and XPS 4-93215  
 $\beta$ -brass, Sn alloyed, Auger/SEM obs. of corrosion 4-89172  
 brass 70/30, oxidised surface, Auger spectrometry and RHEED study 4-69994  
 conference, X-ray optics and microanalysis, Toulouse, France (Sept. 1983) 4-63389  
 core-level electron-electron coincidence spectroscopy 4-78420  
 cylindrical mirror analyser alignment technique for Auger spectroscopy 4-95561  
 diamond, Auger line shape 4-66138  
 dielectric system, mobility and surface recombination processes of primary electrons during AES 4-93151  
 EBIC technique using scanning Auger microprobe 4-97981  
 elastic backscattering effects on AES and XPS spectra of solids 4-109284  
 electron beam interactions with solids, rel. to microscopy, microanal., and microlithography 4-63394  
 electron energy analyser using a cylindrical mirror with ring-to-axis focusing 4-90696  
 electron spectroscopy, backscattering factors calc. (*Chinese*) 4-73597  
 electrostatic field emission microscope for Auger electrons spectroscopic microanalysis 4-72021  
 elemental intensity determination by pre-filtered least squares fitting 4-96512  
 energy analyser design for electron spectrometry (*French*) 4-63826  
 ferromagnetic metals, spin-polarised AES, theory 4-104703  
 field emission gun for high resolution Auger spectroscopy (*French*) 4-63825  
 forward scattering, Auger electron, tool for studying epitaxial growth and core-level binding-energy shifts 4-109304  
 free atoms, Auger transitions, kinetic energies calc. using multiconfig. Dirac-Fock method 4-107323  
 graphite, localised behaviour in Auger spectra 4-93148  
 graphite with adsorbed  $H_2O$ , adsorption depend. on substrate struct. 4-92515  
 high-temperature analysis techniques, surface characteristics 4-99927  
 highly radioactive materials, ESCA and AES appls. 4-73603  
 hybrid electron-ion gun, structural design electron optics and appl. 4-63807  
 II-VI semiconductors, crystal growth, optical and surface props. (*Japanese*) 4-88957  
 III-V semiconductor lasers, threshold current, temp. dependence 4-79132  
 impregnated dispenser cathodes, appearance pot. spectroscopy, XPS and AES (*Chinese*) 4-106437  
 IN-738 LC, Ni-base superalloy, creep fracture, effect of grain boundary chem. and segregation 4-81285  
 Inconel, aluminiumed, microstruct. characterisation of coating 4-76911  
 inelastic electron scatt. in solids, review 4-66151  
 inner-shell ionisation, Auger electron lineshapes in coincidence with scattered electrons 4-107322  
 insulating thin films, Auger electron spectra, electron and ion beam effects 4-109283  
 introduction to AES and appls. in materials science (*Afrikaans*) 4-73598  
 ion scattering spectrometry in a commercial scanning Auger microprobe 4-68336  
 ion-induced  $KL^1$  and  $K^2L^1$  multiple vacancy production 4-99262  
 laser materials, Auger recomb. and intervalence band absorpt. 4-80885  
 metal, ferromag., spin polarisation of Auger photoelectrons 4-71528  
 d-metal carbides, Auger C lines 4-93149

# Auger effect continued

metal overlayer/metal structures, sputtering, AES and EELS studies 4-76617  
metal-S cpds., quantitative AES, effects of chem. struct. 4-85046  
metal-semiconductor heterostructures, transition regions, exam. using electron microscopy and Auger spectroscopy 4-65579  
metallic thin films, crystal growth, initial steps, microscopic studies 4-98486  
metastable atoms and ions for surface studies; Auger neutralisation 4-85050  
mixtures, XPS and Auger spectra resolution by spectral ratioing 4-99856  
N(E) distribution curve, need for exact knowledge (French) 4-66144  
nitroaromatic explosives, C(KVV) Auger line shapes, intra- and intermol. H bond form. 4-71928  
nitroaromatic explosives, molecular electronic props., Auger study 4-93530  
nonideal system, poorly conducting, beam techniques for surface analysis 4-93575  
organometallic films, ion beam assisted deposition using focused ion beams, AES 4-85112  
organosilanes covalently bonded to metal oxide surfaces, SIMS and electron stimulated desorption obs. 4-89324  
polyacrylonitrile film, electropolymerisation on metal substrate, spectroscopic obs. of film attachment and growth mechanism (French) 4-66191  
polyethylene, Auger line shape 4-66138  
proportional electron detector for nuclear gamma-resonance spectroscopy 4-86448  
pulse counting interface for scanning Auger microscopy 4-78432  
quantitative Auger analysis, peak to background ratio use 4-66139  
quantitative Auger electron spectroscopy and microscopy, review 4-95578  
radiative Auger transitions and their consideration in deconvolution of energy dispersive X-ray spectra 4-99923  
refractory metal silicides, AES, principal component anal. 4-77041  
scanning Auger microscope, field emission gun, emission noise, anode cleanliness effect 4-78437  
scanning Auger microscope digital images, noisy and sparse, comparison of smoothing techniques 4-78434  
selected area stationary beam cratering for high sensitivity depth profiling with computerised Auger microprobe 4-97711  
semiconductor, HF relaxational oscils. in homogeneous electron-hole plasma heated by Auger recomb. 4-108891  
semiconductors, Auger and impact ionisation processes, calc. of commonly neglected terms in matrix element 4-99237  
semiconductors, multi-valley, Auger processes with energy transfer to bound charge carriers 4-80607  
semiconductors, small gap, intrinsic photocond., electron and hole heating effects 4-88542  
signal acquisition and processing system, ATD 16 (French) 4-66639  
silicides, screening energy variations and Auger parameters, XPS studies 4-99275  
single crystals, orientational effect in emission of Auger electrons of various energies 4-99239  
solid surface, Auger spectra data acquisition improvement (French) 4-71488  
solids, Auger CVV line shapes, dynamical screening effects 4-93152  
spectrometer for x-ray photoelectron microprobe analysis and related techniques 4-72018  
spectroscopy, anisotropic electron emission from localised and delocalised sources 4-99244  
sputtered atoms, inner shell vacancies and Auger spectra 4-74208  
stainless steel, Auger electron microscopic anal. 4-72027  
steel, alloy, heat treated, surface segregates, Auger and XPS studies 4-99856  
steel, alloy, reheat cracking, scanning Auger and electron microscopy study 4-71490  
steel, austenitic stainless, D permeation, plasma-driven, effect of surface comp. 4-113718  
steel, austenitic stainless, oxide layer structure, formed in simulated LWR conditions 4-76893  
steel, bearing, surface layers, effect of grinding (Chinese) 4-99628  
steel, C-Mn, grain boundary segregation of Cu, Sb and Sn at 900°C 4-93300  
steel, contact zone under friction, X-ray and Auger electron microanal. 4-75763  
steel, improved corrosion resist. in water after abrasive blasting with  $Al_2O_3$  4-62099  
steel, low alloy, reversible temper embrittlement, role of microstructure, scanning Auger microscopy study 4-81286  
steel, low alloy cast, temper embrittlement, microstruct. obs. by Auger electron spectrosc. (Chinese) 4-71725  
steel, mild, corrosion inhibition by molybdate 4-99635  
steel, Ni-Cr-Mo-V, free surface segregation, Mn content effect, Auger study 4-66345  
steel, Ni-Mo, martensitic A533B pressure vessel, tempered, brittle fracture and fatigue crack growth, segregation effects, Auger obs. 4-66400  
steel, stainless, Auger electron appearance potential spectroscopy 4-99230  
steel, stainless 4-109564  
steel, stainless and bearing, surface analysis, ion implantation and tribological processes 4-99607  
steel, tool, brittle fracture, dopants and impurities effects, AES study 4-62063  
Stellite, Co-based wear-resistant alloy, liq. phase sintered, carbide comp. 4-99365  
surface anal., background subtraction techniques 4-93577  
surface anal., determ. of intensities of known spectral components 4-93578  
surface analysis application of AES 4-71998  
surface and thin film analysis, review 4-81506  
surface band bending variation during thermal oxidation 4-70897  
surface microanalysis, threshold spectroscopy study 4-69998  
surface microscopic examination, Auger type emission 4-72022  
surface quantitative anal. by electron spectroscopy (French) 4-72023  
surface roughness effect on Auger electron spectroscopy 4-71487  
surface roughness effect on XPS and AES, Monte Carlo simulation 4-80352  
Synroc, hydrothermal attack, surface analysis 4-68760  
thin film thickness measurement by SEM or AES, appl. of low angle beveling 4-95380  
thin layer growth, AES investigations, scaling procedure 4-93153  
transition metals, 3d, autoionisation emission by electron impact 4-81051

# Auger effect continued

transition metals, core electron binding energies determ. by XPS, AEAPS and EELS 4-85081  
X-ray excited AES, hole-hole repulsion energy, expt. determ. 4-93198  
X-ray induced AES for microanalysis review 4-85351  
X-ray induced Auger electron effect in microanalysis 4-71489  
X-ray induced Auger electrons, influence in quantitative AES 4-99242  
Zircaloy-4, SAM determ. of O gradients, deform. modelling 4-88191  
Ag (110),  $O_2$ , CO and  $CO_2$  interactions, AES, XPS, TDS and LEED studies 4-113810  
Ag (110) surface catalysis of selective epoxidation of ethylene 4-93554  
Ag, Auger electron spectra 4-81050  
Ag clusters in Si matrix, Auger anal. using electrostatic field emission microscope 4-72021  
Ag electrodes, laser damage, surface-enhanced Raman scatt. and Auger emission spectrosc. obs. 4-60955  
Ag electroplated surfaces, dropwise condensation of steam 4-112694  
Ag epitaxial film on Cu (111), interfacial effects in electron transmission 4-114050  
Ag islands, microAuger anal. interpretation by backscatt. electrons 4-71486  
Ag-Pb (111) solid solns., Pb surface segregation and vapour deposition on Ag (111), LEED-AES study 4-113837  
AgPd, anomalous Auger spectrum theory 4-81047  
Al alloys, Type 6063, surface characterisation, for vacuum chamber materials 4-88386  
Al, Auger electron emission in LVV peak region, continuous background struct.,  $O_2$  partial press. effect (French) 4-66140  
Al, Auger spectra induced by  $Ne^+$  and  $Ar^+$  impact 4-109292  
Al, ion-excited Auger electron emission, angular distribns. 4-76592  
Al, ion-induced Auger electron spectra,  $O_2$  adsorpt. effects 4-61795  
Al, KV electron scatt. processes, Monte Carlo simulation, rel. to AES 4-66145  
Al, normalised core-valence band Auger spectra 4-61783  
Al, oxide formation in presence of  $CO_2$  and electron irradi. 4-93441  
Al polycrystalline surface, oxidised, interaction with electron beams, AES study 4-93154  
Al, secondary ion emission, O effects 4-76609  
Al surface, ion bombarded, Auger emission anisotropies anal. 4-114355  
Al, surface- $A^+$  collisions,  $L_{23}Al$  Auger electrons, polar angular distribns. 4-76585  
Al-Co, sputtering, surface comp., quantitative AES anal. 4-104045  
Al-Cr thin film comp., diffusion barriers, Auger study 4-88407  
Al-Cu films, microstructure and electromigration studies 4-88413  
Al-Fe(Cu),  $Ar^+$  ions impact in ultrahigh vacuum; secondary ion and Auger electron emission (French) 4-66170  
Al-Mg, oxidation, Mg diffusion and surface segregation, AES 4-98293  
Al-Mg alloys, heat treated and cold rolled, oxidation, AES study 4-66474  
Al-Mo alloys, ion implanted, corrosion resist., AES studies 4-99626  
Al-Ti-C-Si contact system, thermal stability 4-84703  
Al<sub>3</sub>Ga<sub>1-x</sub>As MBE growth, Ga desorpt., AES and photoluminesc. studies 4-93220  
Al<sub>1-x</sub>In<sub>x</sub>As, nominally undoped, MBE growth and charact. 4-98472  
AlN, sputter deposited, electron binding energy Auger and XPS study 4-75820  
Al<sub>2</sub>O<sub>3</sub> thin film deposition by UV laser photolysis 4-99337  
<sup>241</sup>Am, L-Auger spectra meas. 4-96511  
Ar, alignment prod. in ionisation of 2p shell by specific momentum transfer 4-96701  
Ar ion, Na-like, dielectronic recombination rates 4-96696  
Au, 4f binding energies, Auger effect 4-78817  
Au (110) and (111), adsorption of  $O_2$ , substrate impurity effects, EELS, AES, and XPS study 4-93160  
Au, adsorption of  $O_2$ , AES, XPS, and thermal desorption study 4-92556  
Au, adsorption of  $O_2$ ,  $Au_2O_3$  prod. by DC reactive sputtering, EELS, AES, and XPS study 4-93161  
Au, Auger electron spectra 4-81050  
Au deposition on H saturated Si (111) surfaces, AES and EELS study 4-108742  
Au films, growth on Ni as function of substrate temp., AES study (French) 4-65581  
Au/Cr bilayers on GaAs, interfacial chemical reactions and drive-out diffusion, AES study 4-80313  
Au-Ag thin film, grain boundary diffusion coeff. from Ag surface coverage, AES 4-92430  
Au-Ge/Au ohmic contact struct., grain boundary diffusion of Ge through Au, Auger anal. 4-88344  
Au-Sn surface diffusion in air at room temp. 4-98459  
AuGa<sub>2</sub> (001), surface net characterisation and electronic struct. 4-80642  
B compounds, low energy Auger transitions 4-88909  
BN gate insulators, CVD growth on InP, ellipsometry, XPS, AES, cond. meas. 4-80443  
BN:P film in InP, grown by CVD, elec. props. 4-99336  
Be, normalised core-valence band Auger spectra 4-61783  
Bi<sub>2</sub>Te<sub>3</sub> cryst., external shape, impurity complex effects 4-75347  
C, Auger electron spectra 4-81050  
C, glassy with adsorbed  $H_2O$ , adsorption depend. on substrate struct. 4-92515  
C overlayers on Nb, resonant photoemission and photon-induced Auger spectra 4-93182  
C segregation to Ni (100) surface in presence of adsorbed S 4-61089  
 $C^{+}$  ( $q=6, 5, 4$ ), incident on inert gas atoms, K-Auger electron prod. 4-78818  
CO, Auger spectra, Green's function calcs. 4-64389  
CO+N<sub>2</sub>, Auger and X-ray photoelectron spectra, reson. enhanced shakeup near-threshold core 4-96627  
Ca, electron impact double ionisation modified binary encounter model 4-83476  
Ca<sub>10</sub>(PO<sub>4</sub>)<sub>6</sub>(OH)<sub>2</sub>, coatings in Ti, comp. and struct., Auger spectroscopic analysis 4-109558  
CaTiSiO<sub>5</sub>, La sphere-based glass-ceramics, La partitioning, Auger studies 4-88112  
Cd,  $Mn_xTe$ , MBE growth, Auger depth profile anal. 4-71567  
CdTe films, MBE grown on (001) GaAs and (001) InSb, charact. 4-94711  
CdTe films in InSb, MBE growth, charact. 4-98470  
CdTe initial growth stages on (001) GaAs, AES and RHEED obs. 4-70580  
CdTe photoelectrodes, photoelectrochemical props., XPS and AES studies 4-88578

## Auger effect continued

- <sup>250</sup>Cf, L-Auger spectra meas. 4-96511  
 Co single crystals, spin polarised Auger electrons 4-85044  
 Co-Al<sub>2</sub>O<sub>3</sub> coevaporated composite films, solar selectivity, AES studies 4-72169  
 Co-base alloys, gaseous corrosion in H<sub>2</sub>O-HCl environment 4-89164  
 Co-Mo oxide film, immersion coated, for selective absorber 4-72173  
 Co-Ni-Zn ferrites, microstruct., mag. props., BaO additions effect 4-88302  
 Cr (110) with adsorbed O<sub>2</sub>, photon stimulated O<sup>+</sup> desorption 4-98438  
 Cr, appearance potential spectroscopy 4-99230  
 Cr, oxide film thickness and composition, AES decomposition 4-61193  
 Cr/Ni/Cu multilayer film system, laser mixed, AES and Rutherford backscatt. studies 4-98458  
 Cr/SiO<sub>2</sub> thin films, elec. transport props. 4-92830  
 Cr-SiO<sub>2</sub> cermet films, composition and sheet resistance effect on strain sensitivity obs. 4-111117  
 Cs evaporated layer on Ag surface, photoelectric emission stability 4-76637  
 CsBr, scatt. primary and recoiled surface neutrals and ions, TOF spectra 4-63800  
 Cu, Auger electron spectra 4-81050  
 Cu clusters on graphite, valence bands and core levels, XPS, Auger and EELS studies 4-113860  
 Cu electrodeposition on Pt (111), LEED and AES studies 4-66244  
 Cu, low energy N atom implantation, profiles, ranges and straggling 4-80062  
 Cu oxidised surface solar absorbers, thermal stability, AES and refl. meas. 4-114951  
 Cu surface, adsorpt. of S and O on cylindrical crystals 4-61223  
 Cu-Al (3 wt.%), surface chemistry of wear scars 4-99830  
 Cu-Pb engine bearings, multilayer diffusion barriers 4-98331  
 Cu-Pd binary alloys, quantitative AES anal., backscatt. factors and matrix corrections 4-99241  
 Cu-Ti glasses, surface composition, composition profiles, Auger electron spectroscopy 4-113758  
 CuInSe<sub>2</sub>, sputtered surface characterisation using AES, O<sub>2</sub> adsorpt. 4-93147  
 Cu<sub>2</sub>O, ESCA and Auger spectroscopy determ. of binding energy (*French*) 4-66638  
 Cu<sub>2</sub>O/CuO selective surface optical props. and surface composition 4-72170  
 epitaxial layers, plasma enhanced CVD growth of free-standing films, AES study 4-61866  
 F<sup>9F</sup> ( $q=9, 8, 7$ ), incident on inert gas atoms, K-Auger electron prod. 4-78818  
 F<sup>9F</sup>+He(Ne), K Auger-electron prod. cross sections, charge-state depend. 4-96693  
 Fe and alloys, N implanted, SIMS, Auger and nucl. reaction analysis 4-88185  
 Fe, annealed, stress enhanced H<sub>2</sub>S adsorption, Auger spectra 4-75789  
 Fe ion, Na-like, dielectronic recombination rates 4-96696  
 Fe, laser irradi., surface structural and electronic props. 4-60956  
 Fe single crystals, spin polarised Auger electrons 4-85044  
 Fe/Al cylinders, diffusion under high mech. stress and accelerations, AES studies (*German*) 4-103993  
 Fe-Al alloys, Ar<sup>+</sup>-ion-sputtered, secondary ion and Auger electron emission 4-81101  
 Fe-base alloy, gaseous corrosion in H<sub>2</sub>O-HCl environment 4-89164  
 Fe-Cr, passive film form. and props. 4-81332  
 Fe-Cr, surface segregation of S, annealing and O<sub>2</sub> adsorption effect (*Japanese*) 4-61932  
 Fe-Cr (30 wt.%), high temp. corrosion mechanism, XPS and AES studies 4-62098  
 Fe-P alloys, intergranular fracture planes, chemical states, Auger and electron energy loss spectra 4-93385  
 Fe-P-W(Mo)(Mn), grain boundary embrittlement, impurity-induced, influence of alloying elements 4-114654  
 Fe-Si (3 wt.%) alloy, surface segregation kinetics, Auger spectroscopic obs. (*French*) 4-66142  
 Fe-Zr amorphous films, corrosion props. in 1N H<sub>2</sub>SO<sub>4</sub>, XPS and AES studies 4-76904  
 Fe<sub>23</sub>B<sub>7</sub>, ferromag., spin polarised L<sub>23</sub>M<sub>23</sub>M<sub>23</sub> AES 4-104703  
 α-Fe<sub>2</sub>O<sub>3</sub> and Fe<sub>3</sub>O<sub>4</sub>, ESCA and Auger spectroscopy determ. of binding energy (*French*) 4-66638  
 Fe(OH)<sub>3</sub> and γ-FeOOH, ESCA and Auger spectroscopy determ. of binding energy (*French*) 4-66638  
 FeS<sub>2</sub> (Fe<sub>2</sub>S<sub>3</sub>)(FeS) surfaces, AES and EELS studies 4-114349  
<sup>254</sup>Fm, L-Auger spectra meas. 4-96511  
 GaAlSbAs-GaSb injection laser, operation and luminescence study 4-74508  
 GaAs (100), chemical etching and annealing, AES study 4-65722  
 GaAs (100), clean surface prep. using Ar<sup>+</sup> ion bombard. 4-104886  
 GaAs (100), laser irradi., photoemission of electrons 4-81116  
 GaAs (110), H<sub>2</sub>O chemisorption and Ga and As species-specific densities of states 4-80373  
 GaAs (110), O<sub>2</sub> chemisorption, photon simulation, AES and EELS studies 4-113804  
 GaAs (110)-ZnSe interface, LEED and AES characterisation 4-84517  
 GaAs (111), direct electron beam writing of oxide layer, AES studies 4-92235  
 GaAs (111) A surface, contact with In-Ga-As-P saturated liq., Auger anal. 4-104046  
 GaAs, implanted layers, elec. props., Si<sub>3</sub>N<sub>4</sub> encapsulation effects, AES study 4-98609  
 GaAs, ion bombarded heated specimens, surface comp., AES and SIMS anal. 4-113510  
 GaAs, photoenhanced oxidation, AES and work function meas. 4-81302  
 GaAs, reactive ion etching in CCl<sub>4</sub>/H<sub>2</sub> and CCl<sub>4</sub>/O<sub>2</sub>, AES, Raman spectra 4-81306  
 GaAs substrate, organo-metal CVD growth of Fe and FeAs<sub>2</sub> films, AES study 4-61868  
 GaAs/Al interface, low temp. form. and structure, LEED, AES and work function meas. 4-80425  
 GaAs/AlGaAs heterostruct., organometallic VPE growth and characterisation 4-93341  
 n-GaAs/Au Schottky contacts, elec. props. and interface chem., sputtering effects 4-80674  
 GaAs/Ni-Ta interfacial reactions, metallisation appl. 4-98367  
 GaAs-Al<sub>0.5</sub>Ga<sub>0.5</sub>As abrupt heterojunctions grown by MBE, Auger composition profiles 4-80429  
 Auger effect continued  
 GaInAsP, nonlinear carrier dynamics, optical bleaching study 4-74625  
 Ge (111)-Pb interface form. dynamics and oxidation 4-84518  
 Ge, clean and H<sub>2</sub>O adsorbed, scatt. primary and recoiled surface neutrals and ions, TOF spectra 4-63800  
 Ge, cyclotron resonance and radiative recombination for excitons, free carriers, electron-hole droplets 4-71183  
 Ge, exciton condensation, microwave methods using pulsed optical excitation, kinetics 4-70671  
 Ge exciton microwave breakdown, exciton and free carrier kinetics with electron-hole drops 4-70669  
 GeO<sub>2</sub>, scatt. primary and recoiled surface neutrals and ions, TOF spectra 4-63800  
 H<sub>2</sub>, vibrationally excited generation by H<sub>2</sub><sup>+</sup> wall collisions 4-76574  
 He, interchannel reson. coupling, photo- and Auger emission 4-83356  
 HfF<sub>2</sub>-BaF<sub>2</sub>-LaF<sub>3</sub>-AlF<sub>3</sub> glass, IR transparent, stability in humid air, AES study 4-109534  
 In, oxide film thickness and composition, AES decomposition 4-61193  
 InGaAs, 1.6 μm, radiative and nonradiative minority carrier lifetimes 4-70826  
 InGaAs epilayers, optical studies of carrier dynamics 4-98788  
 InGaAs-InP injection laser, operation and luminescence study 4-74508  
 InGaAs-InP superlattices, chloride VPE growth, struct. and optical props. 4-81158  
 In<sub>0.53</sub>Ga<sub>0.47</sub>As 1.6-μm lasers, temp. sensitive operation 4-96903  
 In<sub>0.53</sub>Ga<sub>0.47</sub>As, laser operation, thermal behaviour 4-87331  
 InGaAsP, 1.3 μm bandgap, photoexcited carrier lifetime and Auger recomb. 4-108893  
 InGaAsP epilayers, optical studies of carrier dynamics 4-98788  
 InGaAsP/GaAs, double heterojunctions, photoluminesc. studies 4-76504  
 InGaAsP/InP DH, luminescence and laser threshold charact. 4-85008  
 InGaAsP/InP double heterojunctions, photoluminesc. studies 4-76504  
 InGaAsP/InP lasers, 4-5 μm emissions and excitations in split-off valence band 4-96916  
 InGaAsP/oxidised films interface, Auger/ion sputtering anal. 4-104884  
 InGaP/InAlP quantum well structures for visible region; MBE growth, sputtering AES study 4-99314  
 InP (100), laser irradi., photoemission of electrons 4-81116  
 InP, absence of core exciton induced resonant photoemission 4-114360  
 InP, surface and interface states 4-92782  
 InP surface decomp. rel. to In<sub>0.45</sub>N<sub>0.55</sub> Auger spectrum fine struct. 4-81046  
 n-InSb, Auger recombination of holes via deep donors 4-104229  
 InSb, photoconductivity under picosecond illumination (*Russian*) 4-88543  
 InSb surface, Auger inverse sensitivity factors of In and Sb 4-81048  
 InSb, thermal oxidation method, XPS study, resistivity 4-114690  
 La, photoionisation, local density-based random phase approx. calc. 4-102656  
 La, scatt. primary and recoiled surface neutrals and ions, TOF spectra 4-63800  
 La, threshold electron excitation of Auger electron and X-ray emissions 4-93142  
 La-Ni, scanning Auger surface study 4-80356  
 Li, normalised core-valence band Auger spectra 4-61783  
 Li surface, interaction with acetylene electronic and geometric struct. of acetylide, AES and UPS study 4-92543  
 Mg, atom-metal XPS and Auger shifts, excited atom model using ΔSCF HF calcs. 4-93191  
 Mg, Auger spectra induced by Ne<sup>+</sup> and Ar<sup>+</sup> impact 4-109292  
 Mg, band struct. and screening effects on KVV and L<sub>23</sub>VV Auger spectra 4-80488  
 Mg, ion-excited Auger electron emission, angular distrib. 4-76592  
 Mg, ion-induced Auger electron spectra, O<sub>2</sub> adsorpt. effects 4-61795  
 Mg, many-body effects in CVV Auger spectra 4-99236  
 Mg, normalised core-valence band Auger spectra 4-61783  
 Mg-based binary alloys, Mg K<sub>L23</sub>V Auger spectra, hybridisation effects 4-81109  
 Mg<sub>2</sub>Si form., thin film reaction kinetics, AES and SIMS 4-81131  
 Mo (100) and MoS<sub>2</sub> (0001), CO coadsorption with S<sub>2</sub>, H<sub>2</sub>, and O<sub>2</sub>, LEED, AES and TDS studies 4-80407  
 Mo, FCC needle crystals, Auger and electron diff. studies 4-92584  
 Mo film on W substrate, electron backscattering Auger spectroscopy 4-99240  
 Mo ion, Na-like, dielectronic recombination rates 4-96696  
 Mo, polycryst., slow secondary electrons, energy analysis in cylindrical mirror 4-93155  
 Mo, purification by arc melting, mech. props. (*Japanese*) 4-89116  
 Mo surface, kinetics of N<sub>2</sub><sup>+</sup> and N<sup>+</sup> reactions, 7.5-100 eV impact energies 4-93560  
 MoSi<sub>2</sub>, surface comp., dynamic changes during sputtering 4-76625  
 N<sup>9F</sup> ( $q=7, 6, 5$ ), incident on inert gas atoms, K-Auger electron prod. 4-78818  
 Na halide mols., vapour-phase Auger electron spectra using electron impact excitation 4-102808  
 β<sup>0</sup>-Na<sub>2</sub>O-Al<sub>2</sub>O<sub>3</sub> solid electrolyte, surface degradation in Na-S battery cells 4-65526  
 Na<sub>2</sub>O-SiO<sub>2</sub> glass, electron irradiated, evidence of enhanced diffusion process 4-80108  
 Na<sub>2</sub>O-SiO<sub>2</sub> glass surface, electron stimulated desorption mechanisms 4-92514  
 Nb, adsorption of C, NbC formation and synchrotron radiation study of overlayers 4-108711  
 Nb barrier layers between Au and a-SiO<sub>2</sub> 4-88969  
 Nb/Si, metal-semiconductor heterostructures, exam. using electron microscopy and Auger spectroscopy 4-65579  
 Nb-Mo (7-27 at.%) oxidation studied using Auger electron electron and mass spectroscopy 4-71784  
 Nb<sub>2</sub>O<sub>5</sub>, anodic films, AES sputter profiling, contamination effects 4-99270  
 Ni (001) with chemisorbed pyridine, molecular orientation effects on electronic excitations 4-93551  
 Ni (100), adsorption of K, coadsorption of K and D<sub>2</sub>, work function, TDS, XPS, UPS, AES studies 4-80398  
 Ni (100), S-covered, adsorption of CO<sub>2</sub> vibr. spectroscopy study 4-108720  
 Ni (100), surface electronic props. and poison/promotor effects for C adsorpt., AES study 4-85331  
 Ni (100) and (111), clean and S covered, angle resolved AES studies 4-80416  
 Ni (110), adsorption of O<sub>2</sub>, AES study 4-98456

## Auger effect continued

- Ni (110), surface analysis by surface channeling using ion induced Auger electron emission 4-81068  
 Ni (110) with adsorbed  $H_2$ ,  $O_2$ , kinetics of adsorption and reaction 4-92519  
 Ni (111), adsorbed acetic acid and acetic anhydride, decomposition reactions, TPD and AES studies 4-114833  
 Ni (111), dissociative adsorption and recomb. of  $CO$ ,  $N_2$ ,  $SO$ , and  $O_2$  4-93559  
 Ni (111), local adsorption site for  $S$ , angle-resolved AES study 4-92551  
 Ni (111) with surface adsorbed  $C$  and  $CO$ , thermal decomposition of ethylene 4-113782  
 Ni exposed to ethylene, formation and oxidation of  $C$  4-93440  
 Ni,  $L_{2,3}VV$  Auger spectrum, satellite identification and interpretation 4-114347  
 Ni oxides on Ni, transpassive thin films, sputter profiling, AES, XPS studies 4-113823  
 Ni single crystals, spin polarised Auger electrons 4-85044  
 Ni surface, adsorpt. of  $S$  and  $O$  on cylindrical crysts. 4-61223  
 Ni, surface segregation of  $S$ , annealing and  $O_2$  adsorption effect (Japanese) 4-61932  
 Ni, X-ray photoelectron and Auger electron spectra 4-109310  
 Ni-base alloys, gaseous corrosion in  $H_2O$ - $HCl$  environment 4-89164  
 Ni-Si, electrodes for alkaline electrolysis of water, microscopic and spectroscopic study 4-113766  
 $Ni_{16}Fe_2Cr_{14}P_6$  metallic glass, surface oxidation in crystalline and amorphous states 4-89187  
 NiO, ESCA and Auger spectroscopy determ. of binding energy (French) 4-66638  
 NiO, interaction with  $O_2$ ,  $H_2S$  and  $SO_2$ , surface and vol. processes 4-98372  
 NiO, X-ray photoelectron and Auger electron spectra 4-109310  
 NiSe, surface-segregation anal. by Auger electron spectroscopy, surface composition 4-93150  
 NiSi, Ni-Si, thin films, metal silicide form., AES and SIMS study 4-75795  
 NiSi, surface comp., dynamic changes during sputtering 4-76625  
 NiSi<sub>2</sub> epilayers on Si (001), electronic struct. determ. 4-88549  
 $O^{+}$  ( $q=8, 7, 6$ ), incident on inert gas atoms, K-Auger electron prod. 4-78818  
 Pb, oxidation, XPS and EELS obs. 4-88913  
 PbSe<sub>0.9</sub> small gap semiconductor, second order Auger recombination 4-80606  
 PbTe cryst., external shape, impurity complex effects 4-75347  
 Pd (111),  $O_2$  adsorption, AES, EELS, TDS, ESD and work function studies 4-80410  
 Pd, free atoms,  $M_{4,5}N_{4,5}N_{4,5}$  Auger-electron spectrum 4-74209  
 Pd-Si (111), study by LEED, RHEED and AES 4-113765  
 Pt (100), electrodeposition of Ag, thermal desorption, Auger effect, LEED 4-80449  
 Pt surface, K-promoted, NO adsorption 4-80403  
 PtSi, Pt-Si, thin films, metal silicide form., AES and SIMS study 4-75795  
 PtSi, surface comp., dynamic changes during sputtering 4-76625  
<sup>239</sup>Pa, L-Auger spectra meas. 4-96511  
 Re (0001) and stepped surfaces, adsorption and dissoc. of water, TDS, LEED, AES, ESD/AD studies 4-80401  
 Rh (111), Al+ $O_2$  reactions, AES and LEED studies 4-89327  
 Rh (111), CO and K coadsorption, HREELS, TPD, AES and LEED study 4-84508  
 Rh (111), NO+CO reactions, AES, LEED, XPS, UPS and temp. programmed desorpt. study 4-89326  
 Rh (111), resonant valence-band photoemission and Auger transitions 4-114359  
 Rh (111) with surface adsorbed HNCO, effects of preadsorbed O 4-113781  
 S monolayer on Ni and Cu, substrate Auger signal attenuation and recovery rates determ. (French) 4-66143  
 Se, X-ray photoelectron and Auger electron spectra 4-109310  
 Se<sub>2</sub>O<sub>3</sub>, X-ray photoelectron and Auger electron spectra 4-109310  
 Se, MBE growth on cleaved Te, RHEED, AES and LEELS characterisation 4-99343  
 Si (100), surface cleaning, Ag deposition effects, SEM, AES and RHEED studies 4-66471  
 Si (111), laser irradi., photoemission of electrons 4-81116  
 Si (111), surface, far UV laser induced oxidation by bond rearrangement 4-81310  
 Si (111) (7X7), NO adsorption and reactions, EELS, LEED and AES studies 4-65562  
 Si (111) surface composition and band struct. 4-92778  
 Si (111)-Mo interfaces, electronic struct., XPS and X-ray excited AES study 4-85085  
 Si, Auger electron spectra 4-81050  
 Si, Auger spectra induced by  $Ne^+$  and  $Ar^+$  impact 4-109292  
 Si growth of insulating SiO<sub>2</sub> films by oxidation 4-98485  
 Si, ion-excited Auger electron emission, angular distribs. 4-76592  
 Si, ion-implanted, pulsed laser annealing, reflectivity studies 4-80087  
 Si MBE layer, Sb adsorption, LEED, AES and TDS study 4-65560  
 Si, native oxide form. initial phase, AES study 4-104891  
 Si, plasma anodic nitridation in  $N_2$ - $H_2$  system, struct. and optical props. 4-81307  
 Si reconstructed surface reordering on room temperature Ge deposition 4-98411  
 Si, screening energy variations and Auger parameters, XPS studies 4-99275  
 Si solar cells, limiting efficiency, extended detailed balance method 4-81554  
 Si solar cells, open-circuit voltage and efficiency, limits imposed by Auger recomb. processes 4-81549  
 Si wafer, lapped and polished, surface state evaluation 4-76883  
 Si with adsorbed Ag, growth and diffusion, SEM, study 4-80417  
 Si:As/Al interface, sintering and diffusion, As dopant effect 4-80427  
 Si:H, amorphous, electron-excited Coster-Kronig transitions 4-88908  
 Si:H, amorphous, Fe<sub>2</sub>O<sub>3</sub>-coated semiconductor electrode by solar cell, XPS, AES and electrochem. meas. 4-66691  
 a-Si:H, electronic struct. study using Auger electron spectroscopy (French) 4-75840  
 a-Si:H,  $H_2$  chemisorption, AES and EELS meas. 4-108715  
 a-Si:H, plasma deposition, two layer struct., surface contribs. 4-70593  
 Si:N, low energy implant depth profiles, surface peak, Auger studies 4-80074

## Auger effect continued

- Si:O, buried oxide layers formation by  $O^+$  implantation, AES studies 4-88180  
 Si/Pt interface, silicide form., Raman spectra studies 4-80423  
 Si/SiO<sub>2</sub>/Si<sub>3</sub>N<sub>4</sub>, N and O distrib. profiles, Auger studies (Russian) 4-65578  
 Si/V-Ta(Ti), interaction of alloy films with Si, silicide formation 4-88436  
 Si-polyacetylene interface, Auger spectra obs. of Si-C binding, peak shift depend. on adsorpt. level (French) 4-66141  
 Si-Pt interface, silicide formation and chemical reactions 4-92570  
 Si-SiO<sub>2</sub> interface, negative elec. effects produced by Gd and La impurities 4-108940  
 Si-SiO<sub>2</sub>:P interface, Auger study of P pile-up 4-103780  
 Si-Ti interface, TiSi<sub>2</sub> formation by fast radiative processing, AES study 4-113731  
 Si-Ti(Hf) 4-70906  
 SiC (3C), mol. and ion beam epitaxy 4-114398  
 SiC/Al(Pd) interface form., annealing and oxidation, AES studies 4-80420  
 Si<sub>3</sub>N<sub>4</sub>,  $Ar^+$  ion bombarded, electron irradiation effect on surface composition 4-80109  
 Si<sub>3</sub>N<sub>4</sub> films, plasma enhanced CVD, transient phenomena, AES study 4-93225  
 Si<sub>3</sub>N<sub>4</sub> thin film deposition by UV laser photolysis 4-99337  
 SiO<sub>2</sub> films, plasma enhanced MOCVD, MOSFET fabrication AES and SIMS anal. 4-81153  
 SiO<sub>2</sub> films, thermally nitrided, Si LW and N KLL Auger signals 4-88911  
 SiO<sub>2</sub> grown in  $O_2$ /HCl mixtures, Auger sputter profiling and SIMS study 4-88924  
 SiO<sub>2</sub>, reactive ion etching, contamination, AES study 4-89155  
 SiO<sub>2</sub>, screening energy variations and Auger parameters, XPS studies 4-99275  
 SiO<sub>2</sub>, synthesis using ion implantation into Si 4-70175  
 SiO<sub>2</sub> thin film, annealing in  $NH_3$ + $CF_4$  plasma, nitride layer form. 4-93433  
 SiO<sub>2</sub> thin film deposition by UV laser photolysis 4-99337  
 SiO<sub>2</sub> thin films, chemical sputtering by  $Ar^+$  ions and  $XeF_4$  4-93177  
 SiO<sub>2</sub> thin films, nitridation and elec. props. 4-61435  
 SiO<sub>2</sub> thin films, photon-induced O loss, ESR and Auger electron spectroscopy 4-80092  
 SiO<sub>2</sub>-MgO-CaO-Na<sub>2</sub>O( $K_2O$ ), glass, surface alkali metals Auger anal. (French) 4-76568  
 SiO<sub>2</sub>-Na<sub>2</sub>O( $K_2O$ ), glass, surface alkali metals Auger anal. (French) 4-76568  
 SiO<sub>2</sub>N<sub>2</sub>,  $Ar^+$  ion bombarded, electron irradiation effect on surface composition 4-80109  
 Sn-Pb sputtering alloy, effect of ion mass and energy on the surface composition 4-98493  
 Sr; electron impact double ionisation modified binary encounter model 4-83476  
 Ta (110), adsorption kinetics and absolute coverages of acetylene and ethylene, AES study 4-92546  
 Ta<sub>2</sub>O<sub>5</sub>, altered layer prod. by He ion sputtering, depth profiling 4-80075  
 Ta<sub>2</sub>O<sub>5</sub>, anodic films, AES sputter profiling, contamination effects 4-99270  
 Ta<sub>2</sub>O<sub>5</sub>, anodic films as reference materials for AES and XPS sputter depth profiles 4-99916  
 Ta<sub>2</sub>O<sub>5</sub>, anodically growth on Ta, ultra-high resolution depth profiling 4-81098  
 Ta<sub>2</sub>O<sub>5</sub> films, AES sputter profiling and angle resolved XPS 4-99283  
 TaSi<sub>2</sub> film, electronic transport props. and struct. 4-88610  
 Th, photoionisation, local density-based random phase approx. calc. 4-102656  
 Ti (0001), clean and oxidised, electron emission and ion desorption spectroscopy 4-92561  
 Ti film, adsorbed  $O_2$ , Ti gettering, surface chem. 4-108707  
 Ti film, characterisation in TMX-U 4-93579  
 Ti, many-body effects in CVV Auger spectra 4-99236  
 Ti oxidation, Auger and electron energy loss studies 4-109550  
 Ti, polycryst.,  $O_2$  adsorption, charact. and coadsorption with Pb 4-92568  
 Ti, polycryst., slow secondary electrons, energy analysis in cylindrical mirror 4-93155  
 Ti, SXPS, DAPS and AEAPS studies of  $L_3$  threshold 4-93141  
 Ti, X-ray photoelectron and Auger electron spectra 4-109310  
 Ti-base alloys, gaseous corrosion in  $H_2O$ -HCl environment 4-89164  
 Ti-Si interface, Ti-Si<sub>2</sub> formation by wide-area electron beam irradi., AES study 4-92236  
 TiC, C KVV and Ti  $L_{2,3}M_{2,3}V$  Auger spectra, discrete variational X<sub>a</sub> anal. 4-66136  
 TiC CVD coatings on cemented carbides, differences in appearance 4-71596  
 TiC<sub>x</sub>, Ti  $L_{2,3}M_{2,3}V$  Auger spectra 4-88910  
 TiFe, bulk and surface two-particle spectra 4-84550  
 TiFe, H uptake activation, Auger electron spectroscopy 4-70558  
 TiO<sub>2</sub> (110), surface defects, XPS, X-ray induced AES, EELS, study 4-80351  
 TiO<sub>2</sub>, X-ray photoelectron and Auger electron spectra 4-109310  
 TiSi<sub>2</sub> film, electronic transport props. and struct. 4-88610  
 TiW barrier layers between Au and a-SiO<sub>2</sub> 4-88969  
<sup>20</sup>Ti, local absorbed dose due to low energy electrons from Auger and Coster-Kronig transitions 4-72424  
 U, photoionisation, local density-based random phase approx. calc. 4-102656  
 V, Auger electron spectra 4-81050  
 V, X-ray photoelectron and Auger electron spectra 4-109310  
 V/Al thin film couples, phase form. and diffusion in couples prep. under varying deposition conditions 4-75736  
 V<sub>2</sub>O<sub>5</sub>, X-ray photoelectron and Auger electron spectra 4-109310  
 VSi<sub>2</sub> form., thin film reaction kinetics, AES and SIMS 4-81131  
 W (100), oxidised and carbided, adsorbed ethylene and acetylene 4-93553  
 W (100) with chemisorbed  $N_2$ , diffusion and evaporation study 4-98434  
 W, Auger electron spectra 4-81050  
 W bicrystals, oriented, brittle-ductile transition temp. rel. to O and C content, AFS 4-104859  
 W, brittle fracture, impurity effects, Auger electron and scanning electron spectroscopy (French) 4-70268  
 W CVD films, selectively deposited, elec. props. 4-88609  
 W impregnated cathodes, Ir coated, surface anal. by AES 4-76630

**Auger effect continued**

- W thermionic dispenser cathode, electronic activation by B and O, orientation dependence, AES study 4-66183  
 W/O surface, S surface diffusion, AES study 4-113789  
 W-Fe, dil., segregation of Fe to grain boundaries, elec. resist., thermo-power, AES meas. 4-103943  
 W-Ni-Fe(Cu), liq. phase sintered, interphase boundary precip. 4-99364  
 WC, electron stimulated desorption of O<sup>+</sup>, AES study 4-92569  
 WC/C system for X-ray dispersion, Auger depth profile, anal. and sputter deposition 4-98466  
 WS<sub>2</sub> film, electronic transport props. and struct. 4-88610  
 Xe, 5s<sup>2</sup>5p<sup>6</sup> and 5s<sup>1</sup>5p<sup>5</sup> configs., correl. effects, Auger-electron study 4-107286  
 Xe (111), Auger electron energies, surface effect 4-85045  
 Xe, interchannel reson. coupling, photo-and Auger emission 4-83356  
 Zn-Al-Si (21, 2 at.%), frictional surface charact. under boundary lubrication 4-66452  
 ZnO black surfaces as solar-selective absorber, optimisation and evaluation 4-81590  
 ZnS films, RF sputtering prep. and microstruct. props. 4-88417  
 Zr 702, gaseous corrosion in H<sub>2</sub>O-HCl environment 4-89164  
 Zr (0001), adsorbate-induced Auger attenuations 4-66137  
 Zr-Al composite-cathode sputter-ion pump, AES study 4-78332  
 ZrC<sub>x</sub> surface layers, electronic struct., chem. composition, Auger effect 4-72024  
 ZrC<sub>y</sub> surface layers, electronic struct., chem. composition, Auger effect 4-72024  
 ZrF<sub>4</sub>-BaF<sub>2</sub>-LaF<sub>3</sub>-AlF<sub>3</sub> glass, IR transparent, stability in humid air, AES study 4-109534  
 ZrO<sub>2</sub>-CaO, partially stabilized, grain boundary chem., Auger analysis 4-109409

**Auger electrons** *see Auger effect***Auger recombination** *see Auger effect; electron-hole recombination***Auger showers** *see cosmic ray showers and bursts***Auger spectra** *see Auger effect***Auger spectroscopy** *see Auger effect***augmented plane wave calculations** *see APW calculations***aural null direction finders** *see radio direction-finding***aurora**

- see also airglow; atmospheric electron precipitation; atmospheric proton precipitation; atmospheric spectra*  
 arcs, generation of assoc. nonuniform elec. fields and currents 4-110370  
 auroral kilometric radiation-aurora correlation, electron density anal. 4-90039  
 daylight aurora, UV imaging from space under full sunlight 4-100843  
 dayside auroral dynamics, colour and intensity observed at South Pole 4-67520  
 diameter of auroral oval, ring coupling model and implications for ground state of magnetosphere 4-72809  
 diffuse aurora, triggering, role of electron distrib. function in plasma sheet 4-72813  
 discrete aurora associated with energetic particle boundaries 4-67519  
 dynamic variation of auroral oval during intense mag. storms, satellite obs. 4-72776  
 electron density vars., power spectra rel. to electron drift vel. in eastward electrojet 4-72777  
 electrostatic ion cyclotron waves in diffuse aurora 4-67536  
 excitation and energy dissipation processes, general description 4-72798  
 F-region heating during intense aurora, EISCAT study 4-100863  
 ionosphere, aurora and electrojet configuration in early morning sector 4-72789  
 ionosphere electrical conductance, mapping technique using auroral spectroscopic method 4-67438  
 IR spatial structure from rocket-borne TV limb meas. 4-110343  
 kilometric radiation, generation, theory 4-110387  
 low-latitude aurorae types and spectral characts. 4-110344  
 micropulsations correl. with auroral pulsations 4-67518  
 occurrence freq. anal., existence of 88 yr cycle 4-85808  
 optical emission and related phenomena (book) 4-78060  
 photometric observations from Atmosphere Explorer C satellite, results and model anal. 4-72778  
 plasma instability, auroral kilometric radiation 4-67565  
 popular account, book 4-82619  
 proton aurorae, prediction of photon yields for N<sub>2</sub> atmos. 4-67521  
 pulsating aurora, correl. between television images and VLF hiss 4-110346  
 pulsating aurora, correl. with geomag. pulsations 4-105789  
 radar aurora, resonant echoes due to ion cyclotron waves 4-67531  
 radio aurora at medium latitude, diurnal, seasonal, solar cycle variations 4-115649  
 radiowave absorption, day/night absorpt. ratio in auroral and subauroral zone riometer meas. 4-90018  
 rapid ground level illumination variations due to aurora 4-110342  
 rays, form, mechanism 4-94286  
 red auroral arc, O I enhancement and N<sub>2</sub><sup>+</sup> First Negative bands enhancement 4-100841  
 stable auroral red arcs and spread-F, latitudinal distrib. 4-82325  
 visual aurora, characts. and electron precip. patterns during geomag. quiescence 4-85810  
 visual observations (1982) 4-105788  
 X-ray images of auroral arcs, satellite observations 4-100842  
 O, excited atom emissions at mid-latitude 4-110345  
 O I 557.7 nm emission, implications of meas. of O concs. in high latit. winter upper atmosphere 4-105784

**auroral ionisation** *see aurora***austempering** *see heat treatment***austenitic stainless steel**

- A-286, stress relax. in bending at 773K 4-81229  
 acoustoelastic coeffs. of Rayleigh waves, US obs. 4-114733  
 Alloy 800,  $\gamma$  precip., influence on elastic limit (French) 4-81200  
 Alloy 800, low cycle fatigue at 600°C, influence of dislocation-precip. interaction 4-99529  
 Alloy 800 H, surface crack form. and propag., effect of temp. reactor primary circuit He 4-114641  
 aluminised, phase comp. and strength of coating 4-66487  
 annealed, load relax. near 563K, thermally activated dislocation motion 4-99413  
 beam, edge-cracked, ductile fracture under EM bending force 4-91763  
 biaxial yield, time-dependence at room temp. 4-104827

**austenitic stainless steel continued**

- blanket materials, candidate, for fusion reactor appl. 4-91107  
 brittle fracture, environmentally induced, crystallographic charact. techniques 4-81383  
 butt joint, friction welded, fatigue strength and fractographic features (Japanese) 4-114648  
 BWR piping, induction heating stress improvement method (Japanese) 4-96137  
 BWRs, austenitic stainless steel piping systems, intergranular stress corrosion cracking, experience 4-96197  
 cavity formation during electron irradi., effect of pre-implanted He 4-108444  
 claddings, fatigue crack growth rate in air and vacuum at 300°C 4-66413  
 claddings, ring test of tubes oxidised in high temp. steam 4-104816  
 cold worked and irradiated, correl. of fracture toughness with tensile props. 4-93376  
 constitutive eqns. for large plastic deform. 4-104822  
 corrosion behaviour in eutectic Pb-Li environment, type 316 4-107056  
 corrosion by liq. Li using LALO-7 thermoconvection loop, type 316 4-107059  
 corrosion of pure Fe, Ni and Cr in formic acid soln., comparison with austenitic stainless steel 4-71763  
 corrosion products release rate in BWR primary system, radiotracer technique 4-91040  
 corrosion rate in liquid Na environment (Japanese) 4-96138  
 corrosion rate measurement, low, comparison of AC impedance and thin layer-activation methods 4-62139  
 crack growth under creep-fatigue interaction (Japanese) 4-99507  
 crack initiation and growth anal. by direct optical obs. during slow strain rate tests in high temp. water 4-71768  
 creep, applicability of creep J-integral to microscale propag. (Japanese) 4-93384  
 creep, high temp., biaxial expts., constitutive laws 4-93352  
 creep, kinetic damage and failure at sharp notch tip 4-66441  
 creep, Portevin-Le Chatelier effect and dynamic strain ageing 4-114617  
 creep and plastic strains, under side steps of tension and torsion, at 593°C 4-76825  
 creep and plastic strains, under stress reversal in torsion, at 593°C 4-76826  
 creep and plasticity, constitutive eqns. 4-93347  
 creep crack growth 4-104837  
 creep crack growth in damaged material, biaxial test facility 4-93490  
 creep crack initiation and growth 4-99584  
 creep crack propag., DC pot. meas. of crack length (Japanese) 4-99688  
 creep crack propag. after boiler service (Japanese) 4-99510  
 creep exposure, influence of regenerative heat treatment on remaining life 4-114602  
 creep of cylindrical specimens, dia. deviations (German) 4-99697  
 creep of tubular components, influence of multiaxiality of stress and environmental induced degradation 4-93360  
 creep-fatigue, in high temp. materials, constitutive relationships 4-93353  
 creep-fatigue studies under biaxial stress state at elevated temps. 4-66409  
 crevice corrosion and SCC, metallography 4-109566  
 crevice corrosion behaviour in seawater and related environments 4-99638  
 crystallographic contrast of polycrystals using channelling micrography technique (Chinese) 4-60789  
 cumulative damage strain controlled fatigue tests, 20°C 4-104863  
 cyclic creep and life 4-99445  
 deformation-rate law, classical rate-theory-based 4-99417  
 dislocation struct. during radiation creep (Russian) 4-80041  
 dual-ion irradiated, microstruct. evolution under various He injection schedules 4-98150  
 ductile fracture resistance, assessment based on engineering approach 4-104876  
 dynamic strain ageing, serrated flow rel. to strain rate, temp. and grain size 4-114604  
 electron irradi.-induced struct. phase transformations 4-109418  
 electron irradiated, void swelling, effect of C and N 4-108445  
 electropolishing (German) 4-71771  
 fast reactor fuel cladding, sigma phase form. rel. to liquid Na exposure 4-106672  
 fatigue, high temp., damage mechanics 4-93422  
 fatigue, high temp. low cycle, comparison between mech. props. and microstruct. 4-93410  
 fatigue, initial stage, morphometrical evaluation of surface roughness 4-104840  
 fatigue, low cycle, notch effect in creep-fatigue interaction at elevated temp. 4-66444  
 fatigue crack propag. threshold 4-99590  
 fatigue crack propagation by crack-tip plastic blunting 4-71719  
 fatigue crack propagation in specimens subjected to thermal shock 4-93413  
 fatigue damage, cumulative, at high temps., effect of cyclic strain 4-93414  
 fatigue props. rel. to 20 MeV proton irradi. 4-71737  
 fatigue strength under varying stress amplitude at high temp. (Japanese) 4-114646  
 fatigue-oxidation interaction, 550°C, microcrack propag. (Japanese) 4-99520  
 fibre reinforced refractories, fibre-matrix bonding rel. to brazing 4-109367  
 forming limit diagrams, comparison between expt. and theoretical 4-93348  
 fracture modes under He ion and neutron irradi., temp. depend. 4-104853  
 fusion reactor blanket structures, activation product release, safety research 4-111781  
 fusion reactor candidate first-wall materials 4-111799  
 fusion reactor first wall, crit. flaw size prediction methodology 4-96268  
 fusion reactor material, crack growth modelling 4-104851  
 fusion reactor materials, conf., Albuquerque, NM, USA (Sept. 1983) 4-90290  
 fusion reactor materials, material property uncertainty, projection, anal. approach 4-96267  
 gamma-ray induced short-range ordering, point defect influence 4-92123  
 grain boundary precipitation in specimens containing Ti and Al 4-99385  
 heat resistant, precip. and carbide transform. (German) 4-81196  
 heat-resistant, high Si content, oxidation resist. 4-114724  
 high Cr, surface hardening with  $\alpha$ -phase form., effect on wear resist. 4-62115

**austenitic stainless steel continued**

high temp. creep rel. to carbide precipitates 4-76802  
 Incoloy 800, tensile fracture charact. in liq. Hg 4-99558  
 Incoloy 800 H, oxidation, thermal cycling, H permeation, chemical emission 4-76905  
 interface with TiC, reaction zone struct. produced by vacuum annealing 4-104918  
 ion implanted with N, SIMS, Auger and nucl. reaction analysis 4-88185  
 ion irradi., pore formation in type 0Kh16N15M3B steel (*Russian*) 4-65308  
 ion irradiated, C or N 4-98147  
 ion-irradiated, depth-dependent microstruct. 4-98151  
 irradiated, dual-ion and/or electron in HVEM, in-situ obs. of cavity growth process 4-98134  
 irradiated, void swelling, He bubbles 4-103792  
 irradiation, fracture toughness, SEM obs. 4-104836  
 irradiation creep, light ion simulation 4-104815  
 Kh18N10Ti, tensile stresses behind spalling plane, meas. 4-89222  
 low cycle fatigue, elevated temps., crack propag. and fracture modes (*Japanese*) 4-89125  
 low cycle fatigue damage at high temp., X-ray obs. (*Japanese*) 4-114642  
 low temperature yield strength modelling 4-104825  
 mechanical properties, at room temp., effect of plastic strain at 77K 4-114625  
 melt layer form. under repetitive electron beam heating, simulation of plasma disruption 4-75535  
 metallographic revelation of  $\alpha$ -phase and  $\delta$ -ferrite, etching and mag. techniques (*German, English*) 4-66540  
 metastable, preliminary plastic deform. effect on mech. props. at low temp. 4-99443  
 microhardness changes under fast neutron irradiation and cold deformation for type 18-10 (*Russian*) 4-76861  
 microstructural evolution in PCA, dual ion irradi., effect of He 4-103819  
 microstructural image for improved He embrittlement resist. under HFIR irradi. 4-103790  
 microstructure and tensile props., rad.-induced changes, depend. on displacement rate 4-103808  
 modified, void suppression, effect of segregation of minor alloying elements 4-104789  
 modified PCA, mass transfer behaviour in Li 4-107063  
 neutron irradiated, comparison of tensile props. with high Mn austenitic steel 4-103807  
 neutron irradiated, swelling and creep 4-108452  
 neutron irradiated to high fluence, swelling resist. 4-98142  
 nitrided, microstructure, optical microscopy, TEM obs. 4-81359  
 nuclear power stations, single-loop, low-pressure, heater system 08Cr18Ni10Ti steel replacement by carbon steel feasibility 4-93469  
 nuclear reactor construction material CO release rates in oxidising and reducing water environments 4-66476  
 optical quality machining and polishing of type 304 and 316, specular mirror production 4-107903  
 oxidation nonprotective, alloys depletion profiles 4-62101  
 oxide layer structure, formed in simulated LWR conditions 4-76893  
 Path A-type alloys, neutron irradi., mech. props. 4-98139  
 PCA, unirrad., tensile props. from room temp. to 700°C 4-104812  
 pitting corrosion detection using double layer activation technique 4-81368  
 pitting corrosion in water-organic solvent mixtures 4-81348  
 plastic deformation by tensile straining, damage 4-81238  
 plastic deformation in symmetrical cyclic bending of different length specimens 4-99442  
 plasticity at elevated temps., effect of prior creep 4-104828  
 precipitation hardening (*Japanese*) 4-89122  
 precipitation kinetics, selective dissolution methods 4-114527  
 pressure vessel, explosively bonded stainless clad steel plate, fatigue crack growth (*Japanese*) 4-114643  
 pressurised tube, ion bombardment, fatigue life, simulated fusion first wall environment 4-104850  
 proton irradiation creep of thin foil specimens, thickness effects on mech. props. 4-103820  
 radiation damage, fusion reactor candidate material 4-98140  
 radioactive waste disposal container materials, corrosion in synthetic groundwater (*French*) 4-59338  
 radiographic crack detection in thick sections using linear accelerator source 4-89224  
 radiographs, diffraction patterns on steel welds 4-114735  
 recrystallisation, grain boundary diffusion and free energy 4-114569  
 repassivating in acid solutions, film growth and dissoln. kinetics 4-81330  
 repassivation kinetics, effect of Mo alloying 4-81331  
 SCC in MgCl<sub>2</sub> soln., fractography, grain struct., SEM obs. (*Japanese*) 4-99651  
 SCC in molten salts 4-71758  
 SCC propag. rate, fracture mechanics parameters (*Japanese*) 4-99649  
 SCC under compressive stress 4-99636  
 sensitised, Cr depletion in carbide vicinity rel. to heat treatment 4-71654  
 sheet, deep drawing, influence of temp. 4-66399  
 sintered, anodic behaviour in H<sub>2</sub>SO<sub>4</sub> soln. rel. to carburisation 4-62096  
 sorption of gaseous T<sub>2</sub>, etching obs. 4-75788  
 specific heat at low temps. (*Chinese*) 4-103956  
 specific heat capacity 4-92383  
 standard reference material for calibrating X-ray diff. equipment 4-62153  
 steel, austenitic stainless, BWR pipe cracks, weld overlay repair 4-111638  
 steel, austenitic stainless, Ti- and Si-modified, microstruct. evolution, effects of pulsed and/or dual ion irradi. 4-98154  
 strain hardening, hysteresis, constitutive eqns. 4-104805  
 strain rate effect on plastic props. (*Russian*) 4-89094  
 stress corrosion in boiling Na<sub>2</sub>S soln. 4-109539  
 stress relaxation in bending at 773K 4-81229  
 stress rupture in-reactor creep cavity form. model 4-104854  
 stress rupture strength, statistical prediction 4-99701  
 stress-rupture under increasing stress, time-temp. parameter 4-66447  
 structure and mech. props., casting environment effects 4-109433  
 superalloy, as-cast 4-71759  
 surface alloying with Ta using powerful monochromatic radiation 4-71782  
 surface reactions with light elements, EPMA, wavelength-dispersive spectrometry 4-81360  
 swelling and cavity microstruct. development, irradi. in EBR-II and HFIR 4-98131

**austenitic stainless steel continued**

swelling and precip. behaviour during irradi., effect of P 4-103818  
 swelling behaviour, neutron-induced 4-98141  
 swelling incubation, effect of microchem., microstruct. and environmental mechanisms 4-108413  
 swelling resistance in fusion reactors 4-107012  
 swelling resistance under HFIR irradi., improvement through microstruct. control 4-103791  
 texture development during annealing and rolling 4-76786  
 thermal and radiation-stimulated ageing, kinetics 4-66354  
 thermal creep and stress-affected precip. 4-99428  
 thermal passivation in controlled oxygen atoms 4-104902  
 thermal shock fatigue fracture, surface obs. (*Japanese*) 4-99547  
 tubular specimens, endurance and long-term ductility; effect of prior irradi. 4-92243  
 type 304, Cr diffusion coeff. meas. at low temps. 4-108644  
 type 304, stress relax. in bending at 773K 4-81229  
 type 316, chem. compatibility with Li<sub>2</sub>O fusion reactor breeder 4-107060  
 type 316, compatibility with flowing Li 4-107062  
 type 316, exposed to static Pb-Li, corrosion reactions, surface analysis 4-107064  
 type 316, flowing Li environment effect on fatigue and tensile props. 4-107055  
 type 316, transmutation and activation effects in fusion neutron spectrum 4-107040  
 type 316, with TiC coating, void form. near interface by diffusion annealing 4-109557  
 vacuum annealed, duplex oxidation in CO<sub>2</sub>/CO gas mixtures between 500 and 700°C 4-104900  
 viscoplasticity at room temp., crit. uniaxial expt. 4-93336  
 void swelling, effect of C and Nb additions 4-103817  
 void swelling, effects of C and N 4-98149  
 weld metal, ferrite decomp., effect of Mo additions 4-99374  
 weldments, US inspection, compression crack closure effect; 4-85277  
 work hardening rel. to grain size 4-81220  
 WWR steam generator tubes, hardening and intergranular corrosion cracking of type 08Cr18Ni10Ti (*Czech*) 4-85257  
 X-ray analysis of C in 316 steel 4-76931  
 yield point in low-temp. loading, previous deform. effect 4-99444  
<sup>60</sup>Co tracer diffusion 4-75731  
 Cr-Mn, ferritic-austenitic, superplasticity 4-61984  
 Cr-Mn austenitic stainless steels, props. for fusion reactor appls. 4-111746  
 D permeation, plasma-driven, effect of surface comp. 4-113718  
 Fe-Cr-Al-Y plasma sprayed coatings, post-treated, mech. props. 4-93471  
 H attack, TEM study 4-114657  
 H embrittlement by cathodic charging 4-66420  
 H induced slow crack growth rel. to  $\alpha'$  martensite form. 4-66428  
 H<sub>2</sub> permeation inhibition by corrosion oxide layers on Incoloy 800 (*German*) 4-66506  
 N ion implanted, wear and friction 4-66459  
 N-strengthened, high temp. phase chem. and solidification mode prediction 4-114503  
 Nb stabilised, oxide-scale cracking and spallation, initiation conditions 4-62100  
 Nb-bearing, creep props., effect of Fe<sub>2</sub>Nb precip. 4-114619  
 Nb-stabilised, Cr-depleted, oxidation, Cr conc. for healing layer form. 4-81326  
 Nb-stabilised, hot deformed, grain coarsening 4-93329  
 P segregation, radiation-induced 4-98148  
 T permeation barrier development 4-113717  
 Ti modified, prep. by rapid solidification processing, dual-ion irradi. 4-98155  
 Ti stabilised type DN 1.4970, irradiation, induced  $\gamma'$ -phase form. 4-98144  
 Ti- and Si-modified, microstruct. evolution, effects of pulsed and/or dual ion irradi. 4-98154  
 Ti-modified, irradi. response in specimens prep. by rapid solidification processing 4-103816  
 Ti-modified, prep. by rapid solidification processing, microstruct. response to neutron irradi. 4-98143  
 Ti-modified, void swelling, pre-irradi. ageing effects 4-104798  
 TiC precipitation, influence on creep rupture strength, ductility and He embrittlement 4-99388

**austenitic steel**

see also austenitic stainless steel  
 corrosion behaviour in eutectic Pb-Li environment 4-107056  
 explosion hardened high Mn, residual stress distribution (*Japanese*) 4-114645  
 fusion reactor liq. metal blankets use, compatibility, review 4-107054  
 high Mn, AM-2, various properties and products of nonmagnetic steels 4-114590  
 high Mn, neutron irradiated, comparison of tensile props. with 316 stainless steel 4-103807  
 LMFBR fuel element materials, swelling resist. (*German*) 4-83148  
 neutron irradiated, high temp. deform. behaviour (*German*) 4-81262  
 neutron irradiated, swelling and creep 4-108452  
 specific heat capacity 4-92383  
 specimens with flat ends, region of appl. of method of upsetting 4-109597  
 surface reactions with light elements, EPMA, wavelength-dispersive spectrometry 4-81360  
 welded joints, transverse wave US examination, optimal parameter selection 4-66544  
 Cr-Mn, phase stability and corrosion on exposure to pure Li 4-107061  
 Cr-Mn, thermally aged, phase instability, precip. reactions 4-109410  
 Cr-Mo, compatibility with flowing Li 4-107062  
 Cr-Ni type, reactor irradi. effect on refractory charact. 4-66398  
 H isotope permeation in structural alloys 4-113720  
 Mn, cast, shock wave loaded, struct. and residual props. 4-93369  
 Mn-Al, austenitic precipitation, fine structure after annealing (*Russian*) 4-104787  
 Mn-V-Cu, microstructure rel. to heat treatment and alloying additions 4-89066  
 VC nucleation and growth during diffusion vanadizing 4-93439

austenitising *see* heat treatment

Autler-Townes effect *see* Stark effect

autoalignment model *see* Hanle effect

## autoionisation

*see also* Auger effect

alkalilike atoms and ions, quasi-metastable quartet levels 4-74201

atoms, autoionising, finite interaction times and laser-bandwidth effects on photoemission 4-102652

atomic spectra and oscillators, conf., Lund, Sweden, 17-19 Aug. (1983) 4-86109

atoms, autoionisation state radiative decay in laser fields 4-74204

atoms, autoionising state radiative decay in laser fields, photoemission spectra 4-74205

atoms 4-102614

bromomethane, photoelectron spin polarisation, VUV spectra 4-83418

dielectronic recombination, complex-pot. model 4-96695

formaldehyde metastable cations, unimol. decay 4-68988

inert gas ions, electron-impact double ionisation 4-64618

laser optogalvanic effect for ats. and mols. in recomb.-limited plasmas 4-87091

lifetime calc., constrained variational procedure 4-96501

nonexponential decay in autoionization near threshold 4-91315

Rydberg series, autoionisation, multichannel quantum defect theory 4-64439

steady-state spectrum of radiation from autoionizing states 4-69026

transition metals, electron-stimulated autoionisation emission 4-88915

Ba, 7s<sup>n</sup>d autoionisation states, two-photon spectroscopy 4-78822

Ba, autoionisation rate enhancement of two-photon excited states near Ba<sup>+</sup>6d<sub>3/2</sub> limit 4-91239

Ba, multistep excitation of autoionizing Rydberg states 4-74202

Ba<sup>+</sup>, autoionisation in photoionisation 4-78811

Ba<sup>+</sup>, electron impact ionisation, excitation-autoionisation contrib., distorted-wave approx. 4-102800

Be II autoionis. widths, optical emission spectrosc. investig. 4-69025

Be<sup>+</sup> doubly excited states, autoionisation widths calcs. 4-64403

Br, relative photoionis. cross-section, autoionis. Rydberg series 4-64435

CO<sub>2</sub>, autoionisation, fluoresc. polarisation study 4-83402

CS<sub>2</sub>, autoionisation, fluoresc. polarisation study 4-83402

Ca<sup>+</sup>, electron impact ionisation, excitation-autoionisation contrib., distorted-wave approx. 4-102800

Ca<sup>18+</sup>, electron scatt., collision strengths for inelastic transitions including fine struct. 4-96704

Cd I, d<sup>9</sup>s<sup>2</sup>p electron configs., empirical Slater-Condon parameters 4-68943

Cl, reson. struct., autoionisation, photoionisation spectra 4-83339

Cr, half-filled shells, photoionisation 4-83353

CS, Rydberg series in autoionising continua 4-83337

F<sup>9+</sup>+He(Ne), K Auger-electron prod. cross sections, charge-state depend. 4-96693

Ga I, autoionising levels studied by photoionisation expts. 4-78810

H<sup>+</sup>, autoionisation states, single configuration approx., orthogonality conditions 4-107318

H<sup>+</sup>+He autoionising state excitation cross section 4-59886

H<sub>2</sub>, radiative excited level lifetimes, time resolved fluoresc. meas. 4-87160

HCN, photoelectron branching ratio and asymmetry parameters for two outermost MO 4-59849

He, <sup>1</sup>P Feshbach reson., line-shape parameters; autoionisation states 4-64433

He, <sup>1</sup>S autoionisation reson. by complex coordinate method with Hermitian Hamiltonian 4-102653

He, autoionisation states, single configuration approx., orthogonality conditions 4-107318

He I autoionisation rate determ. by optical emission spectroscopy 4-87087

He II 2p level excitation by electron impact, resonance states (Russian) 4-112283

He, interchannel reson. coupling, photo- and Auger emission 4-83356

He isoelectronic series, autoionis. states and widths 4-69024

He, photoionisation cross sections for photon energies 59-67 eV, autoionising reson., Rydberg series 4-64437

He, autoionisation states, single configuration approx., orthogonality conditions 4-107318

He+H<sup>+</sup>, autoionising reson. excited at small ejection angles 4-96681

HeH<sup>+</sup>, quasimolecules, autoionisation states 4-64550

Hg<sub>2</sub>, photoionisation, dissoci. energy, autoionisation peaks, bond distance 4-59859

In I, autoionising levels studied by photoionisation expts. 4-78810

Kr+Kr, metastable interaction, <sup>2</sup>P<sub>2</sub> state 4-91335

Li, autoionisation states, single configuration approx., orthogonality conditions 4-107318

Li I, 1s2snl and 1s2pnl quartet levels, transition wavelengths, radiative lifetimes, fine struct. 4-96491

Li I, autoionisation rate determ. by optical emission spectroscopy 4-87087

Li<sup>+</sup>, <sup>1</sup>P Feshbach reson., line-shape parameters, autoionisation states 4-64433

Mg, 4snp <sup>1</sup>3p<sup>0</sup> autoionising states, energies calc. using configuration interaction method 4-96500

Mn, half-filled shells, photoionisation 4-83353

N<sup>7+</sup>+He (H<sub>2</sub>), electron capture in autoionising configurations N<sup>4+</sup> studied by electron spectrometry 4-59889

N<sub>2</sub>, dissoci. photoionisation from threshold to 29 eV 4-96631

N<sub>2</sub>, dissociative photoionisation caused by autoionisation 4-83431

N<sub>2</sub>, Hopfield series, electronic autoionisation, multichannel quantum defect calcs. 4-83427

NO, partial photoionisation cross section excited by synchrotron radiation 4-87163

NO, supersonic free jets, high Rydberg states, two-colour excitation, autoionisation 4-107411

Na+He<sup>+</sup>, laser and ion-beam excitation, autoionisation 4-69196

Na<sub>2</sub>, excited Rydberg states, electronic and nucl. motion stroboscopic effect 4-68991

Ne, high Rydberg states and autoionising reson., centrifugal 4-68989

Ne<sub>2</sub>, photoionisation efficiency curve, autoionisation mechanism, dissoci. energy 4-87166

O<sub>2</sub>, dissociative photoionisation caused by autoionisation 4-83431

O<sub>2</sub>, partial photoionisation cross section excited by synchrotron radiation 4-87163

Pd I, Rydberg series in photoionization spectrum 4-83351

## autoionisation continued

Sr, two- and three-photon autoionisation under strong laser radiation 4-78812

Tc, half-filled shells, photoionisation 4-83353

Tl I, autoionising levels studied by photoionisation expts. 4-78810

Xe, interchannel reson. coupling, photo- and Auger emission 4-83356

Xe, VUV radiation, reson. enhanced tunable source 4-83661

Xe<sup>4+</sup>, isonuclear series, electron impact ionisation, distorted wave approx. 4-64617

Yb, autoionisation decay following strong 5p hole-5d electron interaction, photoemission study 4-76636

## automatic test equipment

30 MHz standard attenuator, design 4-73408

artificial human respiration, biosignals, microprocessor assisted meas. (Polish) 4-71283

cable inspection using electro-optical technique and microprocessing technology 4-106347

eddy current equipment for aircraft maintenance 4-76943

eddy current test lines, integration of microcomputers, review 4-62137

fatigue, high-cycle, strain-controlled loading regimes realisation 4-66543

goniophotometer, 7.5 m moving arm, performance for spatial distrib. of luminaire light 4-111181

hardness tester with electronic data processing (German) 4-66533

high-speed compression testing at constant true strain rates for hot working studies 4-76928

Jominy end-quench testing, computer-controlled hardness tester 4-99666

liquid chromatograph injection and sampling automation 4-72005

microprocessor-based thin film thickness meas. system 4-95388

microtome, instrumented for improved histological sections and fracture toughness meas. 4-62637

modular isotopic thermoelectric generator test facilities, software and hardware requirements 4-72138

MTF testing of IR and visible wavelength optics 4-97150

multimeters, digital type, config., operation and microprocessor control (German) 4-106300

optical fibre performance parameters measurement in prod. environments 4-83739

portable test instrumentation development, using CMOS LSI technology, flat displays and microprocessors 4-73429

radiography, TV fluoroscopy, automated inspection system 4-93476

reactor pressure vessels, thick walled components, US inspection, time of flight data evaluation, ALOK system 4-71804

secant stiffness meas. of composite materials, using peak valley detector 4-66514

semiconductor wafer surface defects, automated detection by laser scanning 4-113773

SL, lightweight submarine cable system sea trial, transmission tests 4-107842

thermoplastics impact strength determs. 4-104934

welded joints in pipes, automatic ultrasonic inspection apparatus characts. 4-66510

X-ray TV system for automatic flaw detection, interface unit and software 4-76950

Ni-Cd cell residual charge meas. using microprocessor-based unit 4-81535

## automatic testing

fatigue, high-cycle, strain-controlled loading regimes realisation 4-66543

microfractography of fibrous fracture, automatic image analyses appl. 4-89212

microtome, instrumented for improved histological sections and fracture toughness meas. 4-62637

optical fibre performance parameters measurement in prod. environments 4-83739

quality control of surfaces, automated interference meas. 4-81391

## automobile industry

German, environmental protection, reduction of lead content in petrol (German) 4-93666

## automobiles

automotive Stirling engine development program—overview and status report 4-66777

batteries for motor cars, research in Sweden (Swedish) 4-77066

high technology electronics exhibition and conference, Detroit, MI, USA, (June, 1983) 4-95014

metal hydride hydrogen storage in automobiles, technio-economic aspects 4-105130

methane fueled engine performance and emissions characteristics [automobile engine] 4-66653

MOD 1 automotive Stirling engine development 4-66776

passenger automobile, noise generated by studded snow tyres 4-79364

petrol engine, homogeneous combustion parameters and emissions control, computer simulation 4-77171

street lighting, car headlight disability glare mitigation using visibility model 4-93732

studded tyres, environmental investigation using PIXE 4-105146

vehicular technology conf. Pittsburgh, PA, USA (May 1984) 4-106118

Ni-Fe accumulators for automobiles, operating characts. and dimensions (French) 4-93604

ZnCl<sub>2</sub> battery technology, status 1983 4-77075

## autoradiography *see* radioisotope scanning and imaging

## autoresonant accelerators *see* collective accelerators

## avalanche diodes

*see also* avalanche photodiodes; IMPATT diodes

Al<sub>0.4</sub>Ga<sub>0.6</sub>As avalanche diodes, heat- and radiation-resistant, elec. props. 4-65728

## avalanche photodiodes

absorption, grading and multiplication, excess noise statistics meas. 4-112587

III-V semiconductors, MBE growth for optoelectronic appl. 4-81134

optical fibre communication, APD digital receiver, non-Gaussian design methods (Chinese) 4-97132

photon counting with avalanche photodiodes, OTDR long-range fibre-optic fault locator 4-73480

AlInAs/GaInAs avalanche photodiodes and AlInAs electroabsorption p-i-n photodiodes grown by MBE 4-69591

Al<sub>0.48</sub>In<sub>0.52</sub>As/Ga<sub>0.47</sub>In<sub>0.53</sub>As avalanche photodiode for long wavelength fibre optic communication, MBE growth 4-79337

Ge avalanche photodiode detectors for long-wavelength optical fibre communication systems 4-97134

# avalanche photodiodes continued

- Ge avalanche photodiodes for long-wavelength optical communication appls. 4-97135
- Ge receivers for long-wavelength optical communication systems 4-97133
- InGaAs avalanche photodiodes for long-wavelength optical communication appls. 4-97135
- InGaAs/InP receivers for long-wavelength optical communication systems 4-97133
- InP/InGaAs avalanche photodiode detectors for long-wavelength optical fibre communication systems 4-97134
- InP/InGaAs/InGaAs high-speed avalanche photodiodes 4-69590
- Si LV avalanche photodiode for optical fibre data transmission 4-107877
- Si large-area reach-through photodiodes in scintillation detector 4-64300

# avalanches, carrier *see impact ionisation*

# avalanches, electron *see electron avalanches*

# avalanches, electron-hole *see impact ionisation*

# avionic systems *see aircraft instrumentation*

# Avogadro's number *see constants*

# avoided crossing *see energy level crossing*

# axicons *see lenses*

# Axilrod-Teller-Moto dispersion forces *see intermolecular forces*

# axiomatic field theory

- $\lambda\phi^4$  theory, approx. technique for quenched master field eqns. 4-68354
- $\lambda\phi^4$  theory, physical mass calc. for small  $\lambda$  4-58938
- $\lambda\phi^4$  theory, (1+1) dimens. supersymmetric, kink mass and Witten-Olive bound 4-111309
- $\lambda\phi^4$  theory, nonequilib. thermodynamics, transport coeffs. 4-68347
- $\lambda\phi^4$  theory in 3+1 D; variational approach 4-95691
- $\lambda\phi^4$  theory in curved spacetime and varying background fields, effective Lagrangian, quasilocal approx. 4-111302
- $\lambda\phi^4$  theory in Robertson-Walker space-times, symmetry behaviour at finite temp. 4-63372
- $\lambda(\Phi^4 - \Phi^2)$ , lattice Hamiltonian field theory, bound state spectrum 4-90731
- $\sigma$  model, nonlinear, superspace formulation 4-73616
- $\phi^6$  O(N) symmetric theory, UV fixed point, scale invariance spontaneous breaking 4-58942
- $(\phi^2)^2$  theory, gap eqn. and effective action from inverse scatt. transformation 4-86568
- $(\phi^2)^2$  theory, instantons and 1/N series, vacuum decay rate, inverse scatt. transform. 4-86569
- $\phi^4$  effective pot., thermo-field theory and imaginary time formalism 4-86555
- $\phi^4$  field theories, random walk appls., survey 4-68391
- $\phi^4$  model, effective lattice actions for continuum theories, locality proof and construction 4-68364
- $\phi^4$  model, soln. depend. on initial condition 4-90719
- $\phi^4$  theory, Coleman-Weinberg symmetry breaking in an anisotropic spacetime 4-90270
- $\phi^4$  theory, skeleton inequalities and asymptotic nature of perturbation theory 4-68351
- $\phi^4$  theory in 4-D, renormalisation scheme in continuum limit 4-90715
- $\phi^4$ ,  $x=4n+2$ ,  $y=2+n^{-1}$ , non-perturbative breakdown of scale invariance 4-58944
- 't Hooft loop operator, perimeter law, U(N) and SU(N) lattice gauge theory 4-111291
- Abelian Higgs models, nontrivial fixed points, renormalisation group functions 4-95663
- aesthetic field theory, bounded systems, confluence type topological particles 4-95652
- aesthetic field theory, lattice of particles 4-68369
- Anderson transition and nonlinear  $\sigma$ -models 4-58960
- arbitrary lattices with arbitrary SU(N) actions, perturbation theory without Feynman diagrams, Wilson loops 4-68417
- baryon spectrum in quenched QCD on  $16^4$  lattice 4-68555
- Baxter type model, fermionisation, U(1) invariance emergence 4-68402
- Bogomolny-type equations, curved spacetime, Yang-Mills-Higgs system 4-95676
- book, gauge theories in construction QFT and stat. mechanics 4-63413
- book, lattice gauge theories and Monte Carlo simulations 4-63414
- boson formulation of fermion field theories 4-68414
- broken SU(N) massless Thirring models, soluble, two dimens. fermionic models 4-68401
- Coleman-Weinberg type  $\lambda\phi^4$  theory, Casimir energy of Higgs field configs. 4-68416
- collective field theory 4-68440
- conference, common trends in particle and condensed matter physics, Les Houches, France (Feb., 1983) 4-58554
- conference on quark matter in rel. nucleus-nucleus collisions, Long Island, NY, USA (Sept. 1983) 4-67855
- conservation laws, relation to algebra of space-time symmetry group 4-95703
- Coulomb interaction, string potential, static quarks on random lattice, strong coupling limit 4-111292
- $CP^N$  lattice model, topology in strong coupling 4-102031
- $CP^N$  model, 2-dimens., nonperturbative aspects, topological charge, mass gap 4-82873
- $CP^N$  models at large N, lattice to continuum transition 4-95646
- $CP^N$  supersymmetric model, 1/N expansion 4-102044
- $CP^N$  model, perturbative renormalisation 4-68357
- curved lattice models, continuum limit, induced gravitational action 4-90732
- dielectric lattice gauge theory 4-68365
- Drell-Yan process, lepton pair  $P_T$  distrib. is asymptotically free scalar field theory 4-59043
- duality and large N limit in non-abelian gauge theories 4-78466
- effective pot. convexity and finite temp. phase transitions 4-58967
- euclidean field theory stochastic quantization with fermions 4-68359
- Euclidean space, algebraic field description, spinor field, Minkowski double light cones 4-106462
- extended  $\phi^4$  model, square lattice, critical behaviour 4-86535
- fermion models, two-dimensional curved space-time, Thirring and Schwinger models 4-90734
- fermionic degrees of freedom on a lattice; particles and strings for Ising model 4-58948
- field theories without fundamental (gauge) symmetries 4-58981
- finite element approximation for quantum field theory 4-68388
- finite fermion density on the lattice 4-58961
- finite size scaling test of an SU(2) gauge-spin system 4-86550

# axiomatic field theory continued

- finite temperature QCD, strong coupling lattice model, chiral symmetry 4-86652
- finite-action fields, topological charges conservation 4-95636
- four-fermion operators, matrix elements, nonleptonic decays 4-86665
- free random surface simulation using Monte Carlo techniques 4-68403
- $g\phi^4$  spontaneously broken field theory, effective potential renormalisation 4-90708
- gauge field construction, Abelian Higgs model, UV cutoffs, (QED)<sub>2</sub> and lattice regularisation 4-68387
- glueball mass in mixed action SU(2) lattice gauge theory 4-111407
- glueball masses in SU(2) lattice gauge theory, Monte Carlo study 4-111409
- gluon thermodynamics near the continuum limit 4-78470
- hadron mass inequalities, extended form based on lattice QCD 4-95765
- hadron masses in lattice QCD 4-59061
- hadronic mass spectrum, computer calcs. in lattice QCD 4-59060
- Hamiltonian lattice gauge theories and the role of longitudinal modes 4-95667
- hamiltonian lattice models, iterative technique for strong coupling 4-63887
- hamiltonian SU(2) lattice gauge theory, mean field anal. 4-68362
- Hamiltonian XY model, Green's function Monte Carlo method appl. 4-68418
- higher derivative quantum gravity, unitarity, Euclidean lattice formulation 4-58710
- hot twisted Eguchi-Kawai model, deconfinement transition at large N, SU(5) 4-86558
- hybrid mesons with excited glue from SU(3) lattice gauge theory 4-102033
- ICL DAP parallel processor, Monte Carlo simulations in solid-state and elementary particle physics 4-59029
- infinite temperature limit, renormalisable 4-dimensional Euclidean QFT 4-90706
- instantons versus factorization in large-N field theories 4-86551
- Ising lattice gauge theory, successive screw approx. 4-68170
- Ising model, Euclidean lattice field theory, particle masses, perturbation theory 4-106473
- Ito's formula, integration of Schrodinger equation, quantum stochastic calculus 4-95225
- large-N chiral model reduction by dimensional reduction of gauge theories 4-95709
- large-N QCD, single point model, hot twists, twisted Eguchi-Kawai model 4-63956
- lattice action for Wilson fermions interacting with gauge fields 4-63862
- lattice degeneracies of fermions 4-102006
- lattice fermions, axial anomaly, Wilson and Kogut-Susskind actions, lattice QCDs 4-111267
- lattice field theories, review 4-102043
- lattice field theory, solitons with  $1/2$  integral charge in (1+1)D 4-78472
- lattice field theory, thermodynamics at finite density 4-73656
- lattice field theory, zero modes, boundary conditions and anomalies 4-86520
- lattice gauge QCD theories 4-95694
- lattice gauge system in 2-D with mixed action,  $1/N^2$  correction 4-95639
- lattice gauge theories, Bethe approx. 4-82882
- lattice gauge theories, confinement props. of coset pure gauge fields of nonabelian chiral group (Chinese) 4-73643
- lattice gauge theories, effective actions from block diagonalisation, renormalisation 4-68367
- lattice gauge theories, higher order mean field expansions 4-73655
- lattice gauge theories, Monte Carlo calcs., perturbative background 4-102002
- lattice gauge theories, monte Carlo calculation of renormalized coupling parameters 4-58941
- lattice gauge theories, propagators and renormalisation transformations 4-111266
- lattice gauge theories, SU(2) and SU(3), chiral symmetry breaking, deconfinement 4-82907
- lattice gauge theories with Susskind fermions, strong coupling expansion 4-95645
- lattice gauge theory, ang. momentum decomposition (Chinese) 4-68350
- lattice gauge theory, fermion integrations handling 4-58969
- lattice gauge theory, Manton and Wilson actions universality 4-63890
- lattice gauge theory, microcanonical ensemble simulation 4-68386
- lattice gauge theory, Monte Carlo studies of chiral phase transition 4-68385
- lattice gauge theory, QCD mass spectrum, numerical computations 4-68349
- lattice gauge theory, topological props. of one-plaquette action and phase transitions 4-58940
- lattice gauge theory Monte Carlo evaluation of hadron masses and decay consts. 4-68439
- lattice gauge theory with Higgs matter field in the adjoint representation 4-68573
- lattice Hamiltonian field theory, bound state spectrum of  $\lambda(\Phi^4 - \Phi^2)$  4-58978
- lattice nonlinear vector models in 1-D, continuum-limit 4-111280
- lattice O(3) nonlinear  $\sigma$ -model, scaling props., Monte Carlo with Symanzik's improved actions 4-68363
- lattice QCD, chiral symmetry breaking at finite temp. 4-86650
- lattice QCD, current normalisation 4-63856
- lattice QCD, hadron spectra, random walk approx. 4-63857
- lattice QCD, Monte Carlo calc. of hadron masses, light dynamical quarks 4-111392
- lattice QCD, Monte Carlo calc. with unquenched Wilson fermions 4-68507
- lattice QCD, quarks and hadron mass formulae 4-73716
- lattice QCD, renormalisation group behaviour, perturbative corrections, two-loop contrib. 4-86559
- lattice QCD at finite temp., dynamical light quark incorporation 4-86646
- lattice quantum gravity, correlation decay theorem at high temp. 4-78223
- lattice spin and gauge models, weak coupling phase for O(N),  $CP^{N-1}$  and chiral models 4-68366
- lattice strong coupling expansions, large order anal. in 1-D 4-106452
- lattice theories, reconstruction of dynamics from vacuum 4-95687
- lattice tubes for loop-loop correlation in lattice gauge theory, stat. mech. 4-111308
- lattice Yang-Mills theory, Wilson loops 4-58937

## axiomatic field theory continued

- light quark mass renormalisation in lattice gauge theory, strong coupling and crossover regions (*Chinese*) 4-73644  
 local and global Markov random fields 4-63677  
 mass gap of lattice  $O(3)$  non-linear  $\sigma$ -model with naive and improved actions 4-86553  
 massive Schwinger model, partition function  $N$ th order term bound, vacuum to vacuum amp. 4-86538  
 mean field theory and the  $SU(2)$  adjoint Higgs model 4-95649  
 mean-field theory for lattice gauge systems at finite temperature 4-95650  
 microcanonical renormalisation group, Monte Carlo techniques,  $SU(2)$  lattice gauge theory 4-111822  
 Monte Carlo method, appls. in condensed-matter physics, statistical mechanics and related fields, book 4-101584  
 Monte Carlo methods, lattice gauge theories, path integrals in quantum mechanical problems 4-95292  
 multicolour QCD in terms of random surfaces 4-63959  
 negative absolute press., axiomatic thermodynamics 4-73659  
 non-abelian bosonisation in operator language 4-68437  
 non-interacting random surfaces, large-scale props. 4-63883  
 nonAbelian systems, field strength formulation,  $SU_2$  gauge theory 4-95677  
 nonlinear Klein-Gordon field eqns., 2- and 3-dimens.,  $N$ -soliton solns. 4-73622  
 nontrivial weakly local massive Wightman field class with interpolating props. 4-95637  
 $O(2,1)$ - $\sigma$ -model solns. for Einstein and Einstein-Maxwell eqns. 4-110947  
 $O(2)$  and  $O(3)$  lattice systems, 2-dimens., exact  $\sqrt{2}$  scale transformation 4-86528  
 $O(3)$ - $\sigma$ -model, scaling and  $\theta$ -depend., Monte Carlo simulations 4-102027  
 $O(3)$  nonlinear  $\sigma$  model, conformally invariant, geometrical props. 4-102014  
 $O(3)$  supersymmetric  $\sigma$  model, instantons, exact Gell-Mann-Low function 4-78468  
 $O(N)$   $\sigma$ -model, 2-dimens., effective lattice actions for continuum theories, locality proof and construction 4-68364  
 $O(N)$  lattice  $\sigma$  models, zero modes, Feynman rules 4-86564  
 $O(N)$  lattice spin models,  $1/D$  expansion, two-loop effective action 4-102041  
 $O(n)$  nonlinear  $\sigma$  model, mass gap calc. 4-58962  
 $O(N)$  spin system in  $1+1$  dimens., Green's function method 4-68415  
 $O(N)$  two-dimensional chiral models, mass gap, perturbative eval. 4-58946  
 one-dimensional nonlinear lattice, critical props. and hadron phys. 4-59032  
 $P(\phi)_2$  models with variable coefficients 4-73609  
 phase transition in an Abelian gauge theory at finite temperature 4-78478  
 Polyakov correlation functions for  $SU(2)$  string tension, large distance exponentiation 4-78469  
 Potts gauge model, saddle-point approach 4-82877  
 Potts lattice gauge theory,  $n$ -depend. topological anomalies 4-68358  
 Potts model, plaquette percolation, Fortuin-Kasteleyn result extension 4-68149  
 QCD, finite temp., effective spin model, deconfining phase transition 4-63958  
 QCD, glueballs, hybrids and baryonia,  $\psi(1440)$ ,  $\theta(1700)$  and  $\xi(2220)$  exotic states 4-102084  
 QCD, lattice gauge theory, strong coupling expansion of  $SU(3)$  and  $U(3)$  4-73664  
 QCD, noncompact with stochastic gauge fixing, Monte Carlo simulation 4-78451  
 QCD, quark mass gauge-parameter independence,  $SU(6)$  model 4-106512  
 QCD lattice field theory, string tension 4-68408  
 QCD lattice gauge theory, statistical mechanical view 4-86540  
 QCD modelling with soliton bag model, nuclear matter and forces calcs. 4-63953  
 QCD on a random lattice 4-68527  
 QCD parameters on lattice and in continuum 4-86645  
 QCD  $SU(3)$  deconfining transition, with closed quark loops 4-86644  
 quantum few-body problem, Monte Carlo calc. 4-95293  
 quantum integrable systems,  $d \geq 2$ , Baxter model 4-86563  
 quark-gluon plasma, colour-singlet partition function, finite baryon density, lattice QCD 4-111381  
 quarkless QCD, Monte Carlo mass calculations, lattice gauge dynamics 4-68524  
 quenched, reduced,  $N = \infty$ , lattice QCD Wilson loops 4-78520  
 quenched QCD on  $16^4$  lattice, meson spectrum 4-63970  
 $r$ -particle irreducible kernels, asymptotic completeness, several particle collision amplitudes anal. props. 4-68390  
 random lattices, Monte Carlo study of  $U(1)$  and  $SU(2)$  gauge fields 4-82879  
 reduced finite  $N$  continuum chiral model 4-63882  
 reflection positivity and modified Migdal-Kadanoff procedure, lattice gauge theories 4-95675  
 scalar  $\phi^4$  model, imaginary coupling, high-order behaviour of critical exponents 4-86533  
 scalar field, self-cancellation of cosmological terms 4-63377  
 scalar field compactification, Kaluza-Klein theories, four dimensional gauge symm. 4-110967  
 scalars coupled to fermions in  $1+1$  dimensions 4-86584  
 scalar-covariant  $A_0(\phi^2)$  field theory, scaling parameter 4-86536  
 simple nonpolynomial lagrangian theories, finite Green's functions 4-86556  
 $SO(3)$  composite fermion model with lattice gauge theory scalars, chiral symmetry breaking 4-111426  
 spin-statistics theorem for fields with arbitrary high energy behavior 4-68344  
 spinor field quantisation, joint Bose-Fermi spectral problems 4-63869  
 static  $SU(2)$  gauge fields and chiral symm. breaking 4-68405  
 string formation in gas of Feynman diagrams 4-68545  
 $SU(2) \times U(1)$  electroweak theory, lattice gauge model using Wilson fermions 4-111356  
 $SU(2)$  euclidean lattice gauge theories, Rayleigh-Ritz variational techniques 4-95648  
 $SU(2)$  gauge theory,  $q$ -instanton solutions 4-106455  
 $SU(2)$  lattice gauge theories, chiral symmetry breaking absence at high temps. 4-78494  
 $SU(2)$  lattice gauge theories, variant action independence of phys. quantities 4-58968

## axiomatic field theory continued

- $SU(2)$  lattice gauge theory, 4-dimens., stochastic confinement and dimensional reduction 4-58979  
 $SU(2)$  lattice gauge theory, deconfinement, spontaneous global symm. breaking 4-111379  
 $SU(2)$  lattice gauge theory, Hamiltonian variational study 4-78497  
 $SU(2)$  lattice gauge theory, Monte Carlo renormalisation group,  $\beta$ -function 4-102029  
 $SU(2)$  lattice gauge theory, Monte Carlo renormalisation group improved action 4-102030  
 $SU(2)$  lattice gauge theory, stochastic confinement and dimensional reduction in 4-D 4-106458  
 $SU(2)$  lattice gauge theory, strings in 3-D 4-102038  
 $SU(2)$  lattice gauge theory, universality in 4-D 4-73671  
 $SU(2)$  lattice gauge theory in three dimens., obs. of string 4-58980  
 $SU(2)$  lattice gauge theory with disordered trial wave function, vacuum state estimate 4-68419  
 $SU(2)$  lattice theory, Monte Carlo calcs. with dynamical fermions 4-106453  
 $SU(2)$  mass gap with Symanzik's tree level improved action on  $8^4$  lattice 4-63889  
 $SU(2)$  string tension from large Wilson loops 4-63881  
 $SU(2)$  Yang-Mills theory, colour screening 4-78498  
 $SU(3)$  adjoint Higgs model, Monte Carlo study 4-63941  
 $SU(3)$  flux-tube quark model of hadrons 4-63951  
 $SU(3)$  gauge theory, on  $8^4$  lattice, correlation length 4-63888  
 $SU(3)$  gauge theory with next-to-nearest neighbour interactions on  $12^4$  lattice, Monte Carlo study 4-111288  
 $SU(3)$  lattice gauge Monte Carlo simulation results 4-58785  
 $SU(3)$  lattice gauge theory, computation by computer array 4-86544  
 $SU(3)$  lattice gauge theory, deconfinement phase transition, influence of quarks 4-68383  
 $SU(3)$  lattice gauge theory, finite temp. phase transition 4-102058  
 $SU(3)$  lattice gauge theory, hadron mass calcs. 4-106459  
 $SU(3)$  lattice gauge theory, heavy quark potential calcs. 4-86545  
 $SU(3)$  lattice gauge theory, phase transition of pure glue, Monte Carlo calcs. 4-68384  
 $SU(3)$  lattice gauge theory, QCD simulation using 1080 element subgroup 4-106456  
 $SU(3)$  lattice gauge theory, renormalisation group improved action, string tension, Wilson loops 4-111287  
 $SU(3)$  lattice gauge theory, status of deconfinement 4-58973  
 $SU(3)$  lattice gauge theory, string tension and glueball masses 4-58956  
 $SU(3)$  lattice gauge theory, string tension coeff., Monte Carlo calcs. 4-68503  
 $SU(3)$  lattice gauge theory, vectorised Monte Carlo code 4-86523  
 $SU(3)$  lattice gauge theory,  $Z(3)$  flux loop density in 4-D 4-58972  
 $SU(3)$  lattice gauge theory in  $3+1$ -D, Hamiltonian variational approach 4-78455  
 $SU(3)$  lattice gauge theory Monte Carlo calc., matrix multiplier/accumulator 4-90713  
 $SU(4)$  lattice gauge theory, deconfining transition at strong coupling, Monte Carlo study 4-86574  
 $SU(4)$  lattice gauge theory, finite temp. confinement phase transition 4-86543  
 $SU(4)$  lattice gauge theory, first order deconfinement phase transition, Monte Carlo calcs. 4-111294  
 $SU(N)$  lattice gauge theory, quark-gluon partition function 4-95712  
 $SU(N) \times SU(N)$  chiral model, improved lattice action, Symanzik improvement procedure 4-95708  
 $SU(N) \times SU(N)$  chiral model, mass gap by Green's function method, 2D lattice 4-95707  
 $SU(N)$  lattice gauge theories, deconfining transitions, mean field analysis 4-73613  
 $SU(N)$  lattice gauge theory,  $\Lambda$ -parameters for Yang-Mills actions 4-102037  
 $SU(N)$  lattice gauge theory, block mean field method 4-78463  
 $SU(N)$  lattice gauge theory, phase diagrams in 4-D 4-78456  
 $SU(N)$  lattice QCD, non-zero baryon density, hamiltonian formalism, Susskind fermions 4-102062  
 supersymmetric  $(1+1)$  dimens. models with restricted supersymmetry on lattice, hamiltonian Monte Carlo study 4-63880  
 supersymmetric field theory, stochastic quantisation, Parisi-Wu method 4-90742  
 supersymmetric four-fermion interactions, Gross-Neveu and Thirring models 4-106487  
 Susskind fermions, mass term symmetry properties 4-90816  
 symmetry operators for neutrino and Dirac fields on curved spacetime 4-90733  
 Toda lattice, generalized, translationally noninvariant quantisation, cyclic space coordinate 4-86557  
 twisted Eguchi-Kawai model, finite temp., deconfining phase transition 4-82876  
 twisted Eguchi-Kawai model, heat bath method 4-111289  
 twisted Eguchi-Kawai model, numerical study of Langevin eqn. 4-106451  
 two-loop corrections to the  $\Lambda$  parameters of one-plaquette actions 4-68360  
 $U(1)$  gauge-Higgs system with a radial degree of freedom 4-86552  
 $U(1)$  lattice, monopole-antimonopole potential, Monte Carlo simulation 4-111301  
 $U(1)$  lattice gauge theory, 2+1 dimens., string tension and glueball mass 4-86586  
 $U(1)$  lattice gauge theory, linked cluster expansions in 2+1 and 3+1-D 4-82881  
 $U(1)$  lattice gauge theory, mean field in Feynman gauge 4-82880  
 $U(1)$  lattice gauge theory, mean field perturbation 4-106457  
 $U(1)$  lattice gauge theory with long range gauge invariant interactions, Wilson parameter behaviour 4-102003  
 $U(2)$  four-dimensional simplicial lattice gauge theory, Monte Carlo simulations 4-111318  
 $U(N)$  invariant matrix  $\phi^4$  theories, exact solns. in zero dimens. 4-102005  
 $U(N)$  lattice gauge theories, gauge symmetry spontaneous breakdown at infinite  $N$  4-68399  
 $U(N)$  lattice gauge theories, loop dynamics, Monte Carlo calcs. 4-78450  
 universal combinations between thermodynamic crit. amplitudes for Ising-like systems 4-102023  
 universal Wightman field, commutativity axioms (*Russian*) 4-82904  
 universal Wightman field (*Russian*) 4-111314  
 vector algebra on a lattice 4-86570  
 vertex functions, non-perturbative renormalisation using dimensional regularisation 4-86534

# axiomatic field theory continued

- Wess-Zumino  $N=2$  model on lattice, 2-dimens., Dirac-Kähler approach 4-58947
- Wightman's theory, unbounded operator algebras 4-68389
- Wightman field relative identification operator struct., Haag-Ruelle scatt. theory 4-90716
- Wightman functional, integral representation, positive definiteness condition, Fourier transform 4-111270
- Wightman functions, Feynman rules and vacuum expectation values 4-90717
- $Z_N$  lattice gauge theories,  $D=1+2$  phase diagram, variational method 4-111317
- $Z_N$  spin systems identified with two component  $\phi^4$  field theory, continuum limit 4-111274
- $Z(2)$  Higgs model, vortex free energy in screening phase 4-68361
- $Z(2)$  Higgs model and lattice gauge theories, nonlocal order parameters for phase tests 4-82905
- $Z(4)$  model, phase diagrams for square lattice in whole parameter space 4-90521
- $Z(N)$  clock model, deconfinement transition 4-78471
- $\gamma e^- \gamma e^-$  cross-sections from QED on lattice 4-90849
- $(\phi^4)_A$  renormalisation scheme ambiguity and fixed point perturbation theory 4-68491

# axions see intermediate bosons

## backscatter

- see also particle backscattering
- air-sea interface remote sensing by microwave acoustics 4-110316
- atmospheric aerosol backscatter and attenuation meas. using  $CO_2$  tunable coherent lidar 4-100763
- atmospheric aerosol backscatter determ. at 10.6  $\mu m$  4-100728
- Auger electron spectroscopy, backscattering factors calc. (Chinese) 4-73597
- dielectric spheres, large, backscattering, reson. component 4-102859
- discrete scatterers, random, distrib., backscattering enhancement 4-102884
- interplanetary plasma, radio backscatter method for meas. of ion-acoustic turbulence and solar wind vel. 4-110480
- lidar, quantitative 532 nm data for vertical extinction profiles, relative humidity effect 4-100755
- ocean current profiling with 115 kHz shipboard Doppler acoustic backscatter system 4-110314
- ocean surface, microwave backscattering rel. to shipboard remote meas. of internal waves (Russian) 4-67225
- optical backscatter channel, point process estimation 4-79333
- optical fibre, single mode, 1.55  $\mu m$  time-domain-reflectometry, long fault location appl. 4-64797
- optical fibre multiple scattering effects, backscattering meas. method (Japanese) 4-60169
- optical fibres, multimode, graded-index, with differential mode attenuation, backscatt. signatures 4-74715
- optical fibres, single-mode, backscattering theory 4-74711
- perturbed sinusoidal surface, backscattering coeff., coherent model 4-69284
- radar backscatter from ocean surface, interpretation, use of optical meas. 4-82073
- raindrop axial and backscatter ratios, collisional probability model 4-94187
- sea ice surface backscatter strength meas. for sonar location of under-ice oil spills 4-109770
- sea surface microwave backscatter data and atm. surface layer wind determ. 4-67376
- spherical particles, dense distrib., retroreflectance 4-102883
- Thomson-scattering experiment to determine parallel vel. spread in intense relativistic electron beam 4-96776
- three-dimensional current and scattering strength distribution mapping system 4-105774
- time-of-flight Thomson backscattering technique for large fusion devices 4-69955
- two-frequency microwave scatterometer meas. of ocean gravity wave spectra from aircraft 4-67471
- velocimeter, backscatter-modulated Doppler, S/N ratio 4-91850
- Nd:glass laser with plasma mirror, mode locking due to stimulated Brillouin backscatt. 4-107704

# backward wave oscillations see backward wave tubes; electromagnetic oscillations

## backward wave tubes

- see also carcinotrons
- frequency measurement chain to 30 THz using FIR Schottky diodes and submm. backward wave oscillator 4-73414

## bacteriorhodopsin see proteins

## Badgers rule see bond lengths; molecular force constants

## bag models see quark confinement; quark models

## bagging see packaging

## bainitic steel see steel

## bainitic transformations see solid-state phase transformations

## balance (physiological) see mechanoreception

## balances

- see also weighing
  - automatic balance beam rest position determining microcomputer system (Slovak) 4-86383
  - electronic counting scales employing count-by-weight method 4-63722
  - industrial weighing and dosing (Spanish) 4-73423
  - nuclear fuel fabrication plant, weighing scales accuracy and precision for nuclear safeguards 4-111701
  - quartz crystal microbalance for thin film thickness monitoring 4-95378
  - weighing and measurement devices, tolerances, Handbook 44 4-67895
- Balescu-Lennard theory see plasma collision processes**
- ball lightning see lightning**
- ballistics**
- see also impact (mechanical); military equipment
  - flying object visualisation using high-resolution holography at a very long distance 4-74463
  - projectile motion measurement using laser interferometric techniques 4-111192
  - rail gun arc armature, current spatial distributions meas. 4-78346
  - railgun plasma profile expt. 4-84054
  - rigid-plastic missile impact force 4-101645
  - water droplet trajectory around air intake, calcs. (German) 4-113006

## balloons

- see also aircraft
- automatic portable balloon weather station 4-62984
- conference on nuclear track registration, Richland, WA, USA (Jül. 1982) 4-67851
- emulsion chamber design for cosmic ray expts. at balloon altitudes 4-72890
- Pointed InfraRed Observing Gondola, Swedish plans 4-63069
- stratospheric long flight-time balloons, possibilities offered for exploration (French) 4-100739
- super-pressure balloons, use for stratosphere circulations determ. 4-77648
- wind measurement by balloon tracking, errors 4-110293

## banana regime see plasma collision processes

## band gap see energy gap

## band model of magnetism

- see also Hubbard model
- antiferromagnet, conduction electrons, ground state, strong mag. field effect 4-108981
- disordered mag. chain, density of magnon states 4-71045
- extended Hubbard model with half-filled band, ground state beyond the HF approx. 4-76147
- ferromagnetic semiconductor, electron-phonon interaction, s-d model 4-92326
- ferromagnetic slab, power spectra and localised retarded modes 4-80736
- ferromagnets, local-band theory anal. of spin polarised, angle-resolved photoemission spectroscopy 4-92886
- helimagnetic ordering of weak itinerant magnets, theory (Russian) 4-98852
- Heusler-type alloy, X-ray spectra and electronic struct., mag. band struct. 4-71465
- Ising ferromagnet, polar states and charge ordering 4-71117
- linear Ising ferromagnet with antiferromagnetic impurities ground state 4-71118
- magnetic insulator, second quantisation and equivalent two-body operators 4-88642
- metal, electron theory, book contrib. 4-108770
- metallic glasses, itinerant magnetism 4-104438
- paramagnetic cryst., electron impurity centres (Russian) 4-88483
- s-f model in zero bandwidth limit, complete analytical soln. 4-76101
- spin-1 antiferromagnetic chain, ground-state props. calcs. 4-71102
- spin-1 antiferromagnetic Heisenberg-Ising chain 4-71101
- superconductivity under ferromagnetic mol. field, one-dimensional electron-band model, appl. to  $ErRh_4B_4$  4-98805
- transition metal, local spin fluctuations-CPA model of mag. 4-71016
- transition metals and cpds., weak band magnetism theory of paramag. susceptibility (Russian) 4-108980
- two-band itinerant ferromagnet, discontinuous transition to ferromagnetic phase, band model 4-104397
- two-dimensional mag. system, stationary states (Russian) 4-84765
- Wannier functions for magnetic sub-bands 4-71015
- CdSb, mag. band struct. in valence band 4-75849
- Cr and its alloys, SDW, kink lattice struct. 4-104480
- Cr-Mn-V, phase diagram, two-band models, influence of reservoir and Fermi surface 4-114107
- Fe epitaxial films, electronic and mag. states 4-80646
- Fe fully relativistic band struct. calcs. 4-113855
- $Fe_2B_{1-x}$ , itinerant magnetism in metallic glasses 4-104438
- MnSi itinerant ferromag., neutron scattering and muon spin rotation collaborations 4-65890
- Ni fully relativistic band struct. calcs. 4-113855
- $Sc_2Ti_2Fe_2$ , itinerant electron system, coexistence of ferro- and antiferromagnetism 4-98857
- $YCo_2$ , itinerant metamagnetism 4-84788
- $YMn_2$ , electronic struct. and spontaneous volume magnetostriction 4-104395

## band-pass filters

- see also crystal filters; vocoders
- cryogenic metal mesh bandpass filters for submm astronomy 4-110532
- modelling based on moving domain wall concept 4-98209
- real-time signal processing with digital bandpass filters 4-97206
- recursive digital filters, IIR design for velocity selection/rejection in seismic signals 4-115592
- X-ray bandpass filter from Ge solid state detector and  $GeO_2$  foil. 4-91176
- $In_2O_3$  film, transparent and electrically conductive, props. and appl. 4-107802

## band structure

- see also band structure of crystalline metals and alloys; band structure of crystalline semiconductors and insulators; band structure of semimetals; band theory models and calculation methods; Brillouin zones; conduction bands; degenerate semiconductors; electron energy states of amorphous solids; electron energy states of liquid metals; electron energy states of liquid semiconductors; energy gap; Fermi surface; many-valley semiconductors; valence bands
- beryllium hydride polymer, LCAO band struct. calcs. 4-70628
- biethylenedithiolyene-TTF compounds, cryst. struct. and elec. props. 4-75430
- bipolarons, energy bands, stability and thermodynamic props. (Chinese) 4-70675
- chromosomes, micro-Raman spectroscopy, protein and DNA contribs. 4-115033
- complex layer struct., normal mode dispersion and spectral density, band struct. 4-113554
- crystals, inhomogeneous electron damping and electron states 4-70615
- diatomic polymers, Green's function study 4-80552
- disordered systems with periodic lattice distortion, electronic structure 4-70733
- EELS microspectroscopy, characterisation of solids 4-66161
- FCC thin films, electronic struct., thickness depend., tight-binding approx. calc. (German) 4-108758
- graphite intercalation compounds, modification of material props. 4-60890
- ion stopping cross-section in solids, effects of electronic struct. 4-92273
- Jahn-Teller crystals, antiferrodistortive ordering in external mag. field 4-108608
- mixed valence compounds, phonon-induced virtual states 4-70750
- phthalocyaninato polymers,  $[Si(Pc)(OH)_2]_n$  electronic struct. of monomers, DV-X $\alpha$  calc. 4-65600
- poly(2,6-naphthylene), electronic props. calcs. 4-88441
- poly(4-phenylquinoline), electronic props. calcs. 4-88441

**band structure continued**

- polyacetylene and related cpds., anisotropy of small polaron narrowing of electron bands 4-61273  
 polydiacetylenes, charge-transfer exciton spectra, Green's function study 4-71405  
 polyene, finite linear chains, electronic struct. and spectra 4-75830  
 polymer donor-acceptor systems, one-dimens., band struct., INDO calcs. 4-113847  
 polypyrrole, band struct. calcs., ab initio HF study 4-84542  
 porphyrinolate, electronic props. calcs. 4-88441  
 porphyrinato-nickel(II) polymer, band struct., semiempirical INDO crystal-orbital approach 4-75829  
 quantum dissipative systems in crystallographic potentials 4-108757  
 quasi-1D solids, band struct. shapes 4-92592  
 RKKY interaction, band structure and matrix element effects 4-98877  
 space, groups band representations, localised orbitals in crystals 4-88124  
 space groups, band representations, appl. in theory of electronic states of crystalline solids 4-75833  
 symmetric Anderson lattice, ground states calcs. 4-70614  
 tetraza porphyrin nickel (II), one-dimensional, electronic struct., solid state props., SCF HF crystal-orbital approach based on semiempirical Hamiltonian 4-70627  
 thin films, anal. techniques, review 4-113832  
 (TMTSF)<sub>2</sub>X and related cpds., anisotropy of small polaron narrowing of electron bands 4-61273  
 two-dimensional strip, quantized Hall cond. and edge states 4-92591  
 VUV radiation physics, conf., Jerusalem, Israel, 8-12 Aug. (1983) 4-82583  
 Cu complexes, Cu-phthalocyanine single cryst., visible absorpt. band, temp. depend. 4-76489  
 H, metallic, ground state energy in Wigner-Seitz approx. 4-80469  
 K complex, K<sub>2</sub>Pt(CN)<sub>4</sub>·3H<sub>2</sub>O, electronic struct., multiple scatt. generalised partitioning mol. cluster model 4-70629  
 Ni(CN)<sub>4</sub><sup>2-</sup> system, symm. isolations in partially oxidised one dimens. transition metal polymers 4-98524  
 Rh<sub>2</sub>Si, Rh<sub>3</sub>Si and RhSi, electronic state distrib. in valence band, X-ray emission and photoelectron spectra 4-65599  
 TaS<sub>2</sub>-1T, thermoelectric power in CDW phase 4-80570  
 VS<sub>2</sub> (1T), reflectivity, CDW band struct., Kramers-Kronig anal. 4-71401

**band structure of crystalline metals and alloys**

- for band structure of semiconductor alloys see band structure of crystalline semiconductors and alloys or electronic energy states of amorphous solids  
 actinide metals, light, cohesive energies calc. 4-75354  
 alkali metal alloys, MAu (M=Li, Na, K, Rb, Cs), electronic props., self-consistent relativistic band struct. calcs. 4-92604  
 alkali-group IV alloys, liq. and solid, electronic struct. and cluster form. 4-92601  
 alkaline earth metal, cryst. struct. from first principles calcs. 4-70064  
 brass, momentum density of annihilation photons, one-dimens. Fourier transform method 4-70634  
 data compilation, electron states and Fermi surfaces of homogeneously strained metallic elements 4-73178  
 disordered alloy, Auger spectra, core-valence-valence, CPA theory, disorder-induced vertex corrections role 4-71491  
 electron theory of metals, book contrib. 4-108770  
 Heusler alloys, band struct., mag. moments, hyperfine fields, local spin density method 4-108767  
 Heusler-type alloy, X-ray spectra and electronic struct., mag. band struct. 4-71465  
 intermetallic compound structure, book contrib. 4-108309  
 layer metals, electron spectrum and structural transition 4-92605  
 martensite, elec. cond., thermoelectric power and electronic struct. (*Russian*) 4-65657  
 metals, electron spectrum, changes under press. (*Russian*) 4-108766  
 metals and alloys, superconducting transition temp. correlation with electronic struct. 4-88627  
 noble metals, unoccupied band critical point energies 4-61276  
 pure metal, electronic and cryst. struct., bonding, book contrib. 4-108304  
 rare earth metal, cryst. struct. from first principles calcs. 4-70064  
 superconducting transition temp. and energy gap, band struct. calcs. 4-92842  
 transition metal alloy, second-order perturbation treatment of corals and disorder 4-70645  
 transition metal alloys, binary alloys, multiautom interactions, relevance for determ. of stability of ordered structures and short range order 4-88444  
 transition metal alloys, electronic struct. and multiautom interaction calcs. 4-113863  
 transition metal alloys, electronic struct. and ordering calcs. 4-113864  
 transition metal alloys, electronic structure and surface comp., ion etching, X-ray photoelectron spectra 4-66187  
 transition metals, 3d, band struct. interpolation (*Rumanian*) 4-98513  
 transition metals, interstitial migration anomaly, vel. to band electron energy 4-98364  
 transition metals, magnetism and electronic struct., validity of simple alloy model 4-98865  
 transition metals, paramag. susceptibility, influence of density of states singularities (*Russian*) 4-92889  
 Ag, band struct., photoemission spectroscopy meas. 4-70643  
 Ag, band structure and direct transitions, ARUPS studies 4-75842  
 Ag, core level binding energies, density functional calcs. 4-113861  
 Ag film, dielectric function by ATR technique 4-88463  
 Ag<sub>2</sub>Pd<sub>1-x</sub>, elec. cond. and thermopower calcs. 4-70776  
 Ag<sub>2</sub>Pd<sub>1-x</sub>, Hall coeff. and band struct. calcs. 4-70780  
 Al, band energies, elec. resist., thermoelec. power, pseudopotential parameters determ. 4-98512  
 Al, band struct., pseudopotential coeffs., deform. potentials, piezoreflectance meas. 4-98514  
 Al, charge densities, interionic pot., phonon freq. calcs. 4-113856  
 Al, normalised core-valence band Auger spectra 4-61783  
 Au (111), band struct., synchrotron radiation study 4-85074  
 Au (111), electronic band struct., photoemission spectra determ., cryst. symm. effect 4-84549  
 Au, band struct., photoemission spectroscopy meas. 4-70643  
 Au, band structure and direct transitions, ARUPS studies 4-75842  
 Au<sub>2</sub>Pt<sub>1-x</sub>(Ni<sub>1-x</sub>), substitutionally disordered, electronic struct. calcs. 4-70644  
 α-B, electronic energy levels of icosahedron calcs. 4-113862  
 Be, normalised core-valence band Auger spectra 4-61783

**band structure of crystalline metals and alloys continued**

- Be, unoccupied band distortion due to electron-plasmon interaction 4-80486  
 Cd<sub>2</sub>Mg alloys, electron energy spectrum and de Haas-van Alphen effect (*Russian*) 4-70639  
 Cd<sub>2</sub>Mg, band struct. and stability (*Russian*) 4-84552  
 Ce, electronic struct., press induced 4f occupancy enhancement 4-75844  
 Ce<sub>1-x</sub>La<sub>x</sub>Ni<sub>2</sub>, mixed valence, thermopower and band struct. 4-113927  
 CeNi<sub>2</sub>, mixed valence, thermopower and band struct. 4-113927  
 Co, electronic struct., magnetism and Curie temps. 4-75843  
 Co-Ge eutectics, X-ray spectral investigation (*Russian*) 4-76564  
 Cr (001), photoemission spectra interpretation, effect of correlations 4-76635  
 Cr, paramag., angular correlation of position annihilation, radiation appl. of Lock-Crisp-West theorem 4-85031  
 Cr, valence band and 2p core lines, XPS obs. 4-99278  
 Cr-Al BCC solid solns., valence band, XPS and X-ray emission spectra study 4-93194  
 Cs, struct. above s-d transition, LMTO calc. 4-75669  
 Cu (100), band struct., synchrotron radiation study 4-85074  
 Cu (111), angle and energy synchronised photoemission spectrum 4-85065  
 Cu, band structure and direct transitions, ARUPS studies 4-75842  
 Cu, band structure SCF calc. by LMTO method 4-61277  
 Cu, electronic props. of 4d transition metal and sp impurities 4-70731  
 Cu, linearised APW method using quadratic energy expansions 4-98504  
 Cu, phonon anomalies on Fermi surface maps 4-70312  
 Cu, total Compton profile, nonlocal exchange-correlation effects 4-81032  
 Cu<sub>2</sub>Au, substitutionally disordered, electronic struct. calcs. 4-70644  
 CuZn, electronic struct. 4-61278  
 Er, electronic struct., press induced 4f occupancy enhancement 4-75844  
 Eu, BCC, generalised susceptibility and joint density of states 4-76118  
 Fe (001) ferromagnetic, spin- and angle-resolved photoemission spectra 4-85063  
 Fe (110), exchange split empty energy bands inverse photoemission studies 4-84551  
 Fe, BCC, Fermi surface and energy bands under press., APW calc. 4-80478  
 Fe, BCC, local density of states via recursion and equation of motion methods, comparative study 4-98505  
 Fe, electronic struct., exchange splitting, spin- and angle-resolved photoemission spectra 4-88944  
 Fe, electronic struct., magnetism and Curie temps. 4-75843  
 Fe, electronic struct., XPS studies 4-75838  
 Fe, ferromagnetic, wave-vector depend. temp. behaviour of empty bands 4-104123  
 Fe fully relativistic band struct. calcs. 4-113855  
 Fe small clusters, electronic struct., spin density functional theory anal. 4-113859  
 Fe-Ge eutectics, X-ray spectral investigation (*Russian*) 4-76564  
 FeB BCC alloys, electronic struct., APW calcs. 4-108769  
 Fe<sub>2</sub>B<sub>2</sub>Si<sub>6</sub>, amorphous and crystallised, UPS, XPS and EELS 4-104122  
 Gd<sub>2</sub>Ni<sub>2</sub>Al<sub>3</sub>, band struct. and ferrimag. moments, APW calc. 4-80487  
 Ir<sub>6</sub> clusters, electronic struct., Xα-SW and EHT calcs. 4-92603  
 K, anisotropic Hall coeff., induced-torque anomaly theory 4-104185  
 K, struct. above s-d transition, LMTO calc. 4-75669  
 La, pressure effects on band structure, Fermi surface and super conductivity 4-84553  
 Li, normalised core-valence band Auger spectra 4-61783  
 Mg, band struct. and screening effects on KVV and L<sub>2,3</sub>VV Auger spectra 4-80488  
 Mg, core level binding energies, density functional calcs. 4-113861  
 Mg, normalised core-valence band Auger spectra 4-61783  
 Mg-based binary alloys, Mg KL<sub>2,3</sub>V Auger spectra, hybridisation effects 4-81109  
 MnAs, electronic struct. and phase transitions, tight binding calc. 4-108768  
 MoPt, electronic struct. and stability 4-113865  
 Nb, thermomodulation optical spectrum and electronic struct. 4-66018  
 NbPt, electronic struct. and stability 4-113865  
 Nd-Pd, electronic struct. and stability 4-113865  
 Ni fully relativistic band struct. calcs. 4-113855  
 Ni, resonant photoemission, intensity and spin polarisation calc. 4-71526  
 Ni, X-ray absorpt. near edge struct. and band struct. 4-114346  
 Ni-Al, soft X-ray emission spectra 4-93143  
 Ni-Ge eutectics, X-ray spectral investigation (*Russian*) 4-76564  
 NiH<sub>0.85</sub>, X-ray absorpt. near edge struct. and band struct. 4-114346  
 Ni<sub>1-x</sub>Pt<sub>x</sub>, substitutionally disordered, electronic struct. calcs. 4-70644  
 Ni(111) films, electronic struct. and magnetism 4-70640  
 Pb (111), electronic energy bands, angle resolved photoemission and self-consistent field calcs. 4-113858  
 Pd, band struct. approach to X-ray absorpt. and emission spectra 4-71479  
 Pd, reflection electron energy loss study of electronic and struct. props. 4-70641  
 Pd, X-ray emission spectra, anisotropy of cyclotron masses and many-body effects 4-104700  
 Pd-H, electronic structure, cluster anal. using SW-Xα method, relativistic effects 4-65605  
 PdH<sub>2</sub>, electronic props. of dilute H 4-88472  
 PdMn, thermoelectric power, phonon drag effect 4-104187  
 Pr, band structure, Fermi surface and supercond. under high press. 4-98511  
 Pt, band struct., photoemission spectroscopy meas. 4-70643  
 Pt-H, electronic structure, cluster anal. using SW-Xα method, relativistic effects 4-65605  
 Pt<sub>6</sub> clusters, electronic struct., Xα-SW and EHT calcs. 4-92603  
 PtMnSb, magneto-optical props. and electronic struct. 4-61662  
 Rb, struct. above s-d transition, LMTO calc. 4-75669  
 Rh (111), resonant valence-band photoemission and Auger transitions 4-114359  
 ScRu, band struct. calcs. 4-98515  
 ScRu, electron struct. and X-ray emission spectra, exchange and correl. effects 4-70697  
 Sm, electronic struct., press induced 4f occupancy enhancement 4-75844  
 TaPd<sub>2</sub>, electronic struct. and stability 4-113865  
 Tc, superconducting props., energy band struct. calcs. 4-104343  
 TiNi, band struct., Slater-Koster parametrisation 4-75841  
 UBe<sub>13</sub>, electronic struct., XPS study 4-70642  
 V, angular correlation of position annihilation, radiation appl. of Lock-Crisp-West theorem 4-85031

**and structure of crystalline metals and alloys continued**

- V-Ni(Pt)(Pd), electronic struct. and stability 4-113865  
 W, total energy full potential linearised APW method 4-104143  
 W-Re, electronic and fine cryst. struct. (*Russian*) 4-75377  
 YM<sub>2</sub> (M=Mn, Fe, Co, Ni), electronic struct. and mag. props. 4-92602  
 Yb, autoionisation decay following strong 5p hole-5d electron interaction, photoemission study 4-76636  
 Yb, electronic struct., press induced 4f occupancy enhancement 4-75844  
 $\alpha$ -Zr, band structure, APW calcs., optical props., superconducting props. 4-113857  
 Zn, electron-positron pair momentum density distrib., independ. particle model anal. 4-66095  
 Zn-Nb, electronic and fine cryst. struct. (*Russian*) 4-75377  
 ZrZn<sub>2</sub>, optical props. from 0.6 to 3.8 eV 4-84934

**and structure of crystalline semiconductors and insulators**

see also conduction bands; energy gap; valence bands  
 alkali metal, conjugated bonds, reson. energies and bond orders (*Chinese*) 4-84555

- alkali metal alloys, MAu (M=Li, Na, K, Rb, Cs), electronic props., self-consistent relativistic band struct. calcs. 4-92604  
 amplification of total reflection mode surface phonons 4-70547  
 antiferromagnetic semiconductors, mag. polaron study (*Russian*) 4-70682  
 Auger and impact ionisation processes in semicond., calc. of commonly neglected terms in matrix element 4-9237  
 $\alpha$ -Bi<sub>2</sub>, band struct., energy gaps, bonding, cluster approx. 4-70646  
 band structure calculations in 1950s, effect on science 4-92597  
 bisglyoximate nickel(II), solid phase transitions and band struct. 4-88282  
 diamond, conduction band struct., core electron excitation spectra anal. 4-70647  
 diamond, energy bands, variational cellular method 4-92598  
 elemental semiconductors, band struct., semi-empirical tight binding calc. 4-70631  
 ferroelectric semicond., controllable variband structs., energy schemes 4-80871  
 fractional quantum Hall effect and mag. symm. 4-108881  
 graphite, conduction band struct., core electron excitation spectra anal. 4-70647  
 graphite, conjugated bonds, reson. energies and bond orders (*Chinese*) 4-84555  
 graphite, localised behaviour in Auger spectra 4-93148  
 Hubbard, ferromagnet, narrow-band, carriers in spin wave range of temps. 4-92887  
 II-IV semiconductor compounds and alloys, cluster-Bethe-lattice approach to electronic struct. 4-70625  
 III-V cpds., band struct., APW calc. method appl. 4-92608  
 III-V semiconductors, band struct., semi-empirical tight binding calc. 4-70631  
 III-VI layered semiconductors, electronic and vibrational spectra 4-71390  
 layer semiconductors, electron spectrum and structural transition 4-92605  
 n-p-i doping superlattices based on III-V and IV-VI semiconds., electronic props. 4-104300  
 porphyrinonickel (II) system, one dimens. tetrahedrally distorted, electronic struct. 4-75851  
 Raman characterisation 4-99106  
 rare earth monosulphide, RS, R=La, Ce, Pr, Nd, Sm, Gd, Eu, Er, Yb, energy band struct., X-ray study 4-84565  
 rare earth sesquisulphides, energy band struct., X-ray spectral anal. 4-80492  
 refractory compounds, phys. props. depend. on electronic struct. (*Russian*) 4-75423  
 refractory materials, recrystallisation physics, depend. on electronic struct. 4-76788  
 sapphire, single cryst., high temp. electronic struct., VUV reflectance spectra 4-84556  
 semiconductor complex structs., EMF due to dynamic deformation 4-65953  
 semiconductors, band struct. parameters and tetrahedral const. calcs. (*Russian*) 4-88446  
 semiconductors, conf., Cambridge, MA, USA (Nov. 1983) 4-95025  
 semiconductors, density of states for position-dependent band struct. 4-61271  
 semiconductors, electronic excitations, variational Green's function approach 4-108759  
 semiconductors, four-photon transitions 4-80894  
 semiconductors, undoped, Thomas-Fermi-Dirac statistics of dielectric screening 4-61314  
 semiconductors non-local density function theory for electronic and struct. props. 4-108760  
 tetracyanoplatinate, LCAO band struct. calcs. 4-70628  
 tetrahedrally bonded semicond., anisotropies of Compton profiles 4-99217  
 tetraza porphyrin polyglyoxane:halogen, band struct. studied by crystal orbital formalism and CNDO approx. 4-65606  
 tetraza porphyrin polysiloxane:halogen, band struct. studied by crystal orbital formalism and CNDO approx. 4-65606  
 transition metal carbide and carbonitride solid solns., mag., elec. transport, supercond. props., review 4-80590  
 transition metal carbides and nitrides, vacancy-ordered, electronic struct. and stability 4-113869  
 transition metal compounds, band struct. calcs., Mossbauer spectra 4-92611  
 transition metal compounds, electronic struct. and ordering calcs. 4-113864  
 transition metal halide, single cryst., permittivity, electronic states, UV reflectivity 4-84975  
 transition metal monoarsenides, struct. trends, tight binding model anal. 4-92160  
 transition metal nitrides, electronic struct. studies 4-84558  
 transition metal silicides, electronic density of states, XPS study 4-61272  
 zinc-blende semiconductors, localised lattice instability, microscopic model for large lattice relax. and high temp. anomalous diamagnetism 4-70718  
 $\alpha$ -Sn, semiconducting phase, band structure 4-80489  
 AlGaAs injection laser, dispersion of linewidth enhancement factor 4-112425  
 $\alpha$ -Al<sub>2</sub>O<sub>3</sub>, electronic energy levels from Al L-edge photoabsorption, small-cluster CNDO calcs. 4-81038  
 Ar films, structural order effects in low-energy electron transmission spectra 4-98520  
 Ar, solid, cond. band struct., floating 1-s gaussian basis functions calcs. 4-92609

**band structure of crystalline semiconductors and insulators continued**

- As, rhombohedral, electronic band struct., angle-resolved UPS and pseudopot. studies 4-113868  
 Bi<sub>2</sub>As<sub>2</sub>, band struct., energy gaps, bonding, cluster approx. 4-70646  
 BN band struct., APW calc. method appl. 4-92608  
 Bi<sub>2</sub>P<sub>2</sub>, band struct., energy gaps, bonding, cluster approx. 4-70646  
 BaS(Se)(Te),  $\pi$ -band-overlap metallisation, self-consistent augmented-spherical-wave calc. 4-80499  
 BaTiO<sub>3</sub>, band struct. and ferroelec. transition, two-photon spectra studies 4-93016  
 BaTiO<sub>3</sub>, cubic to tetragonal transition, covalency effects, band struct. calculations 4-70361  
 BaTiO<sub>3</sub>, oxygen-octahedral ferroelectrics, two-photon spectroscopy study 4-114300  
 Bi-Se-Te system, struct. and band gap, X-ray and IR absorpt. obs. 4-104124  
 BiSi ferroelec. semicond., energy band struct., X-ray spectral studies 4-65609  
 Bi<sub>1-x</sub>Sb<sub>x</sub>, composition influence on electron scatt. intensity 4-88518  
 C, glassy, conduction band struct., core electron excitation spectra anal. 4-70647  
 CO films, structural order effects in low-energy electron transmission spectra 4-98520  
 CaH<sub>2</sub>, bonding and electronic struct., APW calc. and photoemission studies 4-113384  
 Cd<sub>3</sub>As<sub>2</sub>, role of vacancies in band struct. 4-75853  
 Cd<sub>2</sub>Hg<sub>1-x</sub>Te, ellipsometric studies of interband transitions 4-92999  
 Cd<sub>2</sub>, optical functions and energy band parameters (*Russian*) 4-88793  
 CdIn<sub>2</sub>S<sub>4</sub>, conduction band anisotropy, piezoresistance studies 4-98614  
 Cd<sub>1-x</sub>Mn<sub>x</sub>Se, valence band, Mn 3D electron contrib. 4-75855  
 Cd<sub>1-x</sub>Mn<sub>x</sub>Te, piezomodulation study of absorpt. edge and Mn<sup>2+</sup> transition 4-114242  
 CdS, spin relax. of free carriers, Raman scatt. 4-104619  
 CdSb, mag. band struct. in valence band 4-75849  
 CdTe films, electrochem. deposited, optical props. 4-85022  
 CeO<sub>2</sub>, localised and extended f-symmetry states 4-92648  
 CoS<sub>2</sub>, electronic struct., reflectivity spectra, optical consts., meas. between 0.2-4.4 eV 4-80963  
 CrSi<sub>2</sub>, optical props. and electronic struct. 4-80935  
 CsMnBr<sub>2</sub>, with cryst. field of low symm., spectral splittings (*Chinese*) 4-70754  
 Cu chalcogenides, electronic struct., X-ray spectra and X-ray photoemission studies 4-61283  
 Cu compounds, chem. bonding and electronic struct., XPS studies 4-71524  
 Cu-III-V<sub>2</sub> chalcopyrites, valence bands study, photoemission and X-ray emission spectra, electronic structure calcs. 4-65608  
 CuCl (110), angle resolved photoemission 4-85071  
 CuCl, electronic struct., crystal. cluster model 4-61280  
 Cu<sub>2</sub>O, para-exciton luminesc. polarisation in mag. field 4-92624  
 Cu<sub>2</sub>S-Zn<sub>2</sub>Cd<sub>1-x</sub>S heterojunction, energy band diagrams 4-104296  
 Eu oxide and chalcogenides, exchange interactions, LCAO calculations 4-109009  
 EuEr<sub>2</sub>S<sub>4</sub>, band gap width, rel. to short-range environment of S atom 4-80493  
 EuGd<sub>2</sub>S<sub>4</sub>, band gap width, rel. to short-range environment of S atom 4-80493  
 EuHo<sub>2</sub>S<sub>4</sub>, band gap width, rel. to short-range environment of S atom 4-80493  
 EuLa<sub>2</sub>S<sub>4</sub>, band gap width, rel. to short-range environment of S atom 4-80493  
 EuPr<sub>2</sub>S<sub>4</sub>, band gap width, rel. to short-range environment of S atom 4-80493  
 FeAs<sub>2</sub> and related minerals, reinterpretation of electronic struct. 4-113866  
 Fe<sub>2</sub>O<sub>4</sub>, magnetite, Verwey transition 4-88447  
 FePS<sub>3</sub>, electronic struct., partial-yield synchrotron-radiation photoelectron spectra 4-61810  
 FeS<sub>2</sub>, electronic struct., reflectivity spectra, optical consts., meas. between 0.2-4.4 eV 4-80963  
 GaAs, conduction band splitting for  $\vec{k}$  along [110] 4-108777  
 n-GaAs, conduction band struct. in 2 and 3 valley band models 4-70649  
 GaAs, conduction bands, strain-induced splitting 4-75854  
 GaAs, electron irradi., surface electron energy spectrum, photoemission studies 4-88554  
 GaAs, electronic structure of (100) and (111) faces, angle resolved photoemission 4-84559  
 GaAs/AlGaAs multiple quantum well structures, room temp. excitonic nonlinear absorpt. and refract. 4-74590  
 GaAs-Ge(100) interfaces, Fermi level position and valence-band edge discontinuity study 4-61450  
 (GaAs)<sub>1-x</sub>Ge<sub>x</sub>, bond and struct. models 4-108772  
 GaInAsP lattice matched to InP, electronic struct., book contrib. 4-61284  
 Ga<sub>1-x</sub>In<sub>x</sub>Se single crystals, energy gap, temp. dependence 4-92610  
 GaP, donor wave functions and band struct. 4-98519  
 GaSb, conduction bands, strain-induced splitting 4-75854  
 GaTe, semicond., electronic struct. and bonding 4-84563  
 Ge (111)-(2 $\times$ 1), dangling bond states, HREELS and photoelectron spectra study 4-65725  
 Ge, band calcs., empirically adjusted zone variational method (*Chinese*) 4-75831  
 Ge, electronic and structural props., non-local density functional theory 4-108760  
 Ge, electroreflectance spectra, oscillations anal. for electron-hole Coulomb interactions 4-66011  
 Ge-Si alloys, band calcs., empirically adjusted zone variational method (*Chinese*) 4-75831  
 Ge-Sn alloy, semiconducting phase, band structure 4-80489  
 GeS single crystal, reflectance and thermoreflectance studies 4-71356  
 HfS<sub>2</sub>, electronic struct. by high resolved angular photoemission 4-84557  
 Hg<sub>1-x</sub>Cd<sub>x</sub>Te, CPA calcs., Green's function calcs., simplification through analytic continuation 4-61274  
 Hg<sub>1-x</sub>Cd<sub>x</sub>Te,  $\Gamma_6$ - $\Gamma_8$  band crossover under press., phase transform., thermoelec. power meas. 4-88524  
 HgCr<sub>2</sub>Se<sub>4</sub> ferromag. semiconductor, luminesc. study with quantum energy exceeding the forbidden band gap 4-80992  
 HgPS<sub>3</sub>, electronic struct., partial-yield synchrotron-radiation photoelectron spectra 4-61810  
 HgTe,  $\Gamma_6$ - $\Gamma_8$  band crossover under press., phase transform., thermoelec. power meas. 4-88524

**band structure of crystalline semiconductors and insulators continued**

- HgTe, zero-gap, intrinsic cond. theory 4-70813  
 HgTe-CdTe superlattice, far IR magneto-optics, band structure 4-99101  
 n-InAs, hybrid quantum oscills., temp. depend. 4-70839  
 InAs/GaSb superlattices, Landau levels and magneto-optical props. 4-98737  
 InGaAsP, linear electro-optic effects and nonlinear optical coeffs., device design appls. 4-88809  
 InSb, band struct., angular resolved photoemission studies 4-84554  
 InSb dielectric constant calc. using Kane's band model (*Spanish*) 4-70648  
 InSb, spin reson. of magnetoresist. and photo-EMF under stimulated Raman scatt. conditions 4-92962  
 KNO<sub>3</sub>, cubic to tetragonal transition, covalency effects, band struct. calculations 4-70361  
 K<sub>2</sub>SnTe<sub>6</sub> semicond., electronic struct. and bonding 4-84563  
 KTaO<sub>3</sub>, oxygen-octahedral ferroelectrics, two-photon spectroscopy study 4-114300  
 Kr films, structural order effects in low-energy electron transmission spectra 4-98520  
 LiCl crystal, electronic energy bands, density functional calcs., self-interaction-correction theory 4-70651  
 LiH, ground-state props., LCAO HF study using polarisable basis set 4-60882  
 Li<sub>3</sub>N, electronic struct., Hartree-Fock studies 4-98522  
 LiNbO<sub>3</sub>, ferroelec., band struct. and optical props. in fundamental absorption region 4-75845  
 LiTaO<sub>3</sub>, ferroelec., band struct. and optical props. in fundamental absorption region 4-75845  
 MgCO<sub>3</sub>·Fe (II), orbit-lattice interaction effect on Mossbauer studies 4-71222  
 MgSiP<sub>2</sub>, electronic struct. calcs. 4-108774  
 MnO, self-consistent Hartree energy band calcs. 4-92612  
 MnSb, electronic struct., density of states and mag. moments 4-75856  
 MoS<sub>2</sub>, electronic struct. and angle depend. X-ray S K-emission bands 4-98521  
 MoS<sub>2</sub>, poorly crystallised, electronic states, UPS study 4-92607  
 MoS<sub>2</sub> type layered compounds, valence band spectrum, crystal struct. rel. to electrophysical props. 4-75395  
 N<sub>2</sub> crystalline, exciton luminesc. and luminesc. spectrum struct. 4-104641  
 N<sub>2</sub> films, structural order effects in low-energy electron transmission spectra 4-98520  
 Na<sub>2</sub>CoO<sub>2-x</sub> electrode material, electronic processes during intercalation 4-76012  
 Ne, FCC, high press. eqn. of state, Gaussian orbital techniques 4-92332  
 Ne, solid, cond. band struct., floating 1-s gaussian basis functions calcs. 4-92609  
 Ni complex, porphyrinatonicel(II), band struct., tight binding semiempirical cryst. orbital calcs. 4-75846  
 Ni compounds, chem. bonding and electronic struct., XPS studies 4-71524  
 Ni compounds, multielectron satellites and spin polarisation in photoemission 4-71519  
 Ni, electronic struct., magnetism and Curie temps. 4-75843  
 NiCl<sub>2</sub>(Br<sub>2</sub>)(I<sub>2</sub>), UV reflectance and electronic states 4-71406  
 NiPS<sub>3</sub>, valence states, reson. and partial-yield synchrotron-radiation photoelectron spectra 4-61810  
 NiS<sub>2</sub>, electronic struct., reflectivity spectra, optical consts., meas. between 0.2-4.4 eV 4-80963  
 O<sub>2</sub> films, structural order effects in low-energy electron transmission spectra 4-98520  
 P, black, band struct. and optical props. 4-70650  
 P, black, electronic props. and elec. cond. (*Japanese*) 4-92606  
 P, black, electronic struct., polarised X-ray emission and absorption studies 4-108771  
 P, black, reson. photoemission study 4-85088  
 Pb<sub>1-x</sub>Ge<sub>x</sub>Te, In, elec. props., band edge struct., impurity effects 4-108880  
 Pb<sub>1-x</sub>Mn<sub>x</sub>Te, band struct., cyclotron reson. obs. 4-84546  
 PbSe epitaxial narrow-gap semicond. films, optical four-wave mixing 4-83640  
 Pb<sub>1-x</sub>Sn<sub>x</sub>Te, band struct. changes during struct. and band inversion transitions 4-65607  
 Pb<sub>1-x</sub>Sn<sub>x</sub>Te, longitudinal magnetoresist., magnetophonon oscills. 4-65694  
 Pb<sub>1-x</sub>Sn<sub>x</sub>Te, valence band struct. near phase transition 4-84564  
 PbTe epitaxial narrow-gap semicond. films, optical four-wave mixing 4-83640  
 PdH<sub>x</sub>, X-ray photoemission study of electronic struct. 4-84561  
 PdO cathodes, photoelectrolysis and electronic props. 4-85313  
 Rb<sub>2</sub>ZnBr<sub>4</sub>, incommensurate cryst. energy levels, optical transmission study 4-98518  
 Re<sub>2</sub>Te<sub>3</sub> semicond., electronic struct. and bonding 4-84563  
 Sb<sub>2</sub>Te<sub>3</sub> single cryst., weak field charge transport 4-108887  
 Sb<sub>2</sub>Mo<sub>2</sub>O<sub>6</sub>, band struct., transport props. 4-108773  
 SbSI ferroelec. semicond., energy band struct., X-ray spectral studies 4-65609  
 Sb<sub>2</sub>Te<sub>3</sub> single cryst., band struct. and scatt. mechanisms, IR transmission studies 4-80934  
 Si, band calcs., empirically adjusted zone variational method (*Chinese*) 4-75831  
 Si, channelling electrons, energy band structure, wave functions, calcs. 4-108493  
 Si, electronic and structural props., non-local density functional theory 4-108760  
 Si, energy bands, variational cellular method 4-92598  
 Si, heavily doped, band-gap narrowing study 4-80490  
 Si, heavily doped, intervalley mixing study 4-80491  
 Si, hole space-charge layers, lifting quasipin degeneracy by surface electric field 4-98516  
 Si overlayer on GaP, heterojunction band discontinuities, synchrotron radiation photoemission 4-81111  
 Si, self interstitials, electronic struct. and total energy migration barriers 4-108811  
 Si:P(B), heavy doping effect on band struct. and optical props. 4-92998  
 SiC-A<sup>III</sup>B<sup>V</sup> nitride solid soln. electrophys. parameter determ. 4-80241  
 Si<sub>3</sub>N<sub>4</sub>, amorphous, electronic struct., photoemission 4-108776  
 SiO/SnO<sub>2</sub> coevap. films in sandwich struct., high-field cond. and opt. absorpt. 4-108948  
 SiO<sub>2</sub>, properties of high-press. fluorite struct. phase 4-110135  
 α-Sn, band struct., angular resolved photoemission studies 4-84554

**band structure of crystalline semiconductors and insulators continued**

- SnS<sub>2</sub>, electronic struct. and angle depend. X-ray S K-emission bands 4-98521  
 SnSe, electroreflectance and thermoreflectance 4-71348  
 SnSe<sub>2</sub>-2H, band struct., X-ray photoemission study 4-84562  
 St<sub>2</sub>, low carrier conc., Fermi surface, Shubnikov-de Haas studies 4-98506  
 SrTiO<sub>3</sub>, band struct. and ferroelec. transition, two-photon spectra studies 4-93016  
 SrTiO<sub>3</sub>, oxygen-octahedral ferroelectrics, two-photon spectroscopy study 4-114300  
 n-SrTiO<sub>3</sub>/Nb, electronic struct., PES and IPES studies 4-108775  
 Te (0001), weak localisation under lifted spin degeneracy conditions 4-92781  
 TiC refractories, electronic struct., CNDO/2 calc. 4-75848  
 TiN<sub>1-x</sub>, electronic struct., PES study, stoichiometry effect 4-84560  
 TiSe<sub>2</sub>, electronic struct. by high resolved angular photoemission 4-84557  
 Ti<sub>2</sub>V<sub>1-x</sub>Se<sub>2</sub>, electronic struct. by high resolved angular photoemission 4-84557  
 TiInSe<sub>2</sub>, reflection spectrum and band struct. calcs. 4-104562  
 U chalcogenides, electronic struct. rel. to cryst. data 4-75850  
 UAs<sub>2</sub>Se<sub>2</sub>, electronic and mag. struct. determ. 4-61281  
 WC (0001), bulk band struct., photoemission studies 4-80496  
 WC, hexagonal, surface and bulk electronic struct., density of states 4-113867  
 WC refractories, electronic struct., CNDO/2 calc. 4-75848  
 Xe films, structural order effects in low-energy electron transmission spectra 4-98520  
 Yb<sub>2</sub>O<sub>3</sub>, 4f<sup>13</sup> config., strong intrasite interaction, pseudopot. model anal. 4-80495  
 ZnGeP<sub>2</sub>, electronic struct. calcs. 4-108774  
 ZnIn<sub>2</sub>S<sub>4</sub>, optical consts., ellipsometric determ. 4-76414  
 ZnSiAs<sub>2</sub>, optical props. 4-109212  
 ZnSiP<sub>2</sub>, valence band struct. and chem. binding 4-88445  
 ZnSiP<sub>2</sub>(As<sub>2</sub>), electronic struct. calcs. 4-108774  
 ZnSnP<sub>2</sub>, electronic struct. calcs. 4-108774  
 ZrN<sub>1-x</sub>, electronic struct., PES study, stoichiometry effect 4-84560  
 ZrN<sub>2</sub>, non-stoichiometric, electronic struct., XPS study 4-76638
- band structure of semimetals**  
 Bi<sub>1-x</sub>Sb<sub>x</sub>, electronic density of states and its mass 4-88439  
 TiTe<sub>2</sub>, band struct., elec. and mag. props. 4-92595
- band theory models and calculation methods**  
 see also APW calculations; band model of magnetism; band structure; cellular method; free-electron approximation; Hubbard model; KKR calculations; k-p calculations; Kronig-Penney model; muffin-tin potential; nearly-free-electron approximation; OPW calculations; pseudopotential methods; relativistic band structure calculations; tight-binding calculations  
 A<sup>III</sup>B<sup>V</sup> semiconductors, ab initio band struct. calc. 4-75832  
 alloys, electronic energy calc., improved perturbation theory 4-65601  
 Anderson model, one-dimensional, Lyapunov exponent, weak disorder expansions 4-104111  
 asymptotic medium concept and averaged Green function, optical consts. and electronic density of states 4-80472  
 Coulomb gap effects in 4f systems, one-body treatment 4-75834  
 deformation potentials and electron-phonon scatt. theorems 4-61306  
 disordered binary harmonic chain, renormalisation group decimation technique 4-88489  
 energy level spacings, irregular sequence as quantum chaos 4-104112  
 FCC lattice, k-space integration using correctly weighting tetrahedron method 4-80474  
 Heusler alloys, band struct., mag. moments, hyperfine fields, local spin density method 4-108767  
 linear interpolation used in analytical tetrahedron method, Fermi surface 4-70617  
 linearised APW method using quadratic energy expansions 4-98504  
 metals, surfaces, impurities and defects, embedded atom method 4-92590  
 nonspherical charge distrib. and electrostatic interactions 4-80475  
 one-dimensional disordered binary alloys, cluster mean-field theory 4-92599  
 one-dimensional Hubbard model, use of finite-cell-scaling method 4-70616  
 oxides, non-stoichiometric, segregation and chem. diffusion 4-98297  
 perturbation theory, band model for understanding of divergences 4-92586  
 recursion coeffs., linear prediction theory, appl. to electronic densities of states of Si and GaAs 4-98502  
 recursion method, analytic continuation in complex plane 4-70626  
 recursion method with plane wave basis, band struct. calc. appls. 4-80471  
 semiconductor band structure calculations in 1950s, effect on science 4-92597  
 semiconductors, electronic excitations, variational Green's function approach 4-108759  
 semiconductors, tetrahedrally bonded, anisotropies of Compton profiles 4-99217  
 semiconductors non-local density function theory for electronic and struct. props. 4-108760  
 space groups, band representations, appl. in theory of electronic states of crystalline solids 4-75833  
 total energy full potential linearised APW method 4-104143  
 two-band model, One-Particle Green's functions analytical props. 4-84541  
 Ag, core level binding energies, density functional calcs. 4-113861  
 Ar, solid, cond. band struct., floating 1-s gaussian basis functions calcs. 4-92609  
 CuCl, electronic struct., cryst. cluster model 4-61280  
 Ge, band calcs., empirically adjusted zone variational method (*Chinese*) 4-75831  
 Ge-Si alloys, band calcs., empirically adjusted zone variational method (*Chinese*) 4-75831  
 InSb dielectric constant calc. using Kane's band model (*Spanish*) 4-70648  
 Mg, core level binding energies, density functional calcs. 4-113861  
 MgSiP<sub>2</sub>, electronic struct. calcs. 4-108774  
 MnO, self-consistent Hartree energy band calcs. 4-92612  
 Ne, solid, cond. band struct., floating 1-s gaussian basis functions calcs. 4-92609  
 Ni<sub>2</sub>Al, weak itinerant ferromagnet, de Haas-van Alphen effect, Curie temp. 4-113848

and theory models and calculation methods continued. *see also* *barium compounds*  
 Si, band calcs., empirically adjusted zone variational method (Chinese) 4-75831  
 Si, channelling electrons, energy band structure, wave functions, calcs. 4-108493  
 ZnGeP<sub>2</sub>, electronic struct. calcs. 4-108774  
 ZnSiP<sub>2</sub>(As<sub>2</sub>), electronic struct. calcs. 4-108774  
 ZnSnP<sub>2</sub>, electronic struct. calcs. 4-108774  
*bands (kink) see kink bands*  
*bandwidth compression*  
*see also vocoders*  
 pacemaker cardiac spike detect. in ECG signal, encoding in digital ambulatory recorder 4-100353  
*band-pass control*  
 PWR spatial power oscillations, Xe-induced, time optimal control 4-111652  
*Bardeen-Cooper-Schrieffer theory see BCS theory*  
*barium*  
*see also nuclei with .....*  
 adsorbed on W (011), phase transitions, LEED study 4-92544  
 Amazon River system, Ra isotope activity and U, Th and Ba concs. 4-67193  
 atom, 7<sup>th</sup>d autoionisation states, two-photon spectroscopy 4-78822  
 atom, dynamic polarisabilities, semiempirical calc. methods 4-102599  
 atom, electric quadrupole transition probabilities, GTO and STO valence basis sets, CI calcs. 4-87053  
 atom, excited states, inner and outer shell photoionisation 4-83340  
 atom, L-shell X-ray prod. cross sections for protons of energy 1-2 MeV 4-96656  
 atom, multichannel-quantum-defect theory wave functions tested or improved by laser measurements 4-68929  
 atom, oscillator strengths, rare gas-induced broadening of principal series lines 4-107309  
 atom, three- and five-photon ionis. probabilities meas. 4-69031  
 atom, time-differential ground-state Hanle effect in fast-beam laser spectroscopy 4-78800  
 atomisation mechanisms in furnace AAS 4-114851  
 atoms, autoionisation rate enhancement of two-photon excited states near Ba<sup>+</sup> 6d<sub>3/2</sub> limit 4-91239  
 atoms, multistep excitation of autoionizing Rydberg states 4-74202  
 atoms, nonlinear ionisation, influence of self-ionisation states 4-107324  
 atoms, nonlinear ionisation by 0.53 mkm wavelength laser radiation 4-83354  
 crystal structure from first principles calcs. 4-70064  
 enhancement in atmospheres of red giant stars 4-63145  
 fluoride optical fibre, preparation 4-103045  
 metal at, and solid state effects, photoionisation processes 4-83346  
 metastable isomer prod. for analytical work using isotopic neutron sources, Sr, Cd, In, Ba detection 4-77037  
 Ba, H<sup>+</sup> impact, X-ray prod. cross sections 4-96648  
 Ba I, 6sn<sup>+</sup> F<sub>3</sub>, F<sub>2</sub>, F<sub>1</sub> Rydberg state energies, laser at. beam spectroscopy 4-78794  
 Ba I, II, energy levels in optical spectrum, isotope shifts, specific mass effect 4-74200  
 Ba<sup>+</sup>, autoionisation in photoionisation 4-78811  
 Ba<sup>+</sup>, critical double-well, many-body approach by g-Hartree method 4-59870  
 Ba<sup>+</sup>, electron impact ionisation, excitation-autoionisation contrib., distorted-wave approx. 4-102800  
 Ba<sup>+</sup>, gas phase collisional quenching and intramultiplet mixing 4-87153  
 Ba<sup>+</sup>, discrete 4d photoabsorpt. spectrum 4-102624  
 Ba<sup>+</sup>, formation via reson. nonlinear process 4-107320  
 Ba<sup>+</sup> ions, 4d photoabsorption spectrum, potential-barrier effects 4-112138  
 Ba+ICI(1Br), chemiluminescence broad emission study 4-114801  
 Ba+N<sub>2</sub>O chemiluminescent reaction obs., quadrupole mass filter appl. (Chinese) 4-104993  
 Ba+Na, two-photon radiative collision, Ba<sup>+</sup> prod. 4-64587  
 BaI, highly excited states, Stark effect, hyperfine struct., isotope shifts 4-64405  
<sup>137</sup>Ca, proton impact, K-shell ionisation cross sections 4-96507  
 K halides, Ba-doped, impurity colour centres, absorpt. spectra 4-88865  
 Na<sub>0.5</sub>Bi<sub>0.5</sub>TiO<sub>3</sub>, Ba, cryst. struct., ferroelec. props., neutron diff. 4-70102  
 NaCl:Ba, post γ-irradiation thermolum., effect of plastic deform. 4-104682  
 NaCl:Ba, thermoluminescence, pre- and post-irrad. deformation effects 4-66083  
 Rb halides, Ba-doped, impurity colour centres, absorpt. spectra 4-88865  
*barium alloys*  
*see also barium compounds*  
 No entries  
*barium compounds*  
*see also barium alloys*  
 atomic and solid state effects, photoionisation processes 4-83346  
 dicalcium barium propionate, symm. change at I-II phase transition, X-ray diff. study 4-108607  
 melting, solid-solid transitions at high pressures 4-80195  
 stearate, Langmuir films, structure 4-108734  
 β-Al<sub>2</sub>O<sub>3</sub>:BaO, short-range ordering in Ba<sup>2+</sup> ion distrib at 295K 4-84245  
 Al(PO<sub>3</sub>)<sub>2</sub>:BaF<sub>2</sub>-AlF<sub>3</sub>, glasses, nonlinearity of refractive index 4-80900  
 (Ba,Sr)TiO<sub>3</sub> heteroepitaxial ferroelec. films, domain struct. 4-65993  
 (Ba,Sr)TiO<sub>3</sub> polycryst. and heteroepitaxial ferroelec. films, phase transition 4-65977  
 Ba-ferrite films deposited using Targets-Facing sputtering method, ion substitution effects (Japanese) 4-61851  
 Ba-Sr-Cn carbonate suspension, rheological props. (Polish) 4-83870  
 BaABNb<sub>2</sub>O<sub>15</sub> (A=Ca or Sr; B=K or TI)-ferroelectric materials, synthesis and characteristics 4-104547  
 Ba<sub>0.75</sub>Al<sub>11</sub>O<sub>17.5</sub>, cryst. struct., X-ray diff. determ. 4-92155  
 Ba<sub>0.75</sub>Al<sub>11</sub>O<sub>17.5</sub>, elastic consts., press. and temp. derivatives, US resonance study 4-92284  
 Ba<sub>0.79</sub>Al<sub>10.9</sub>O<sub>17.14</sub>, hexaaluminate phase I, cryst. struct. and nonstoichiometry 4-70087  
 α-BaB<sub>2</sub>O<sub>4</sub>, low temp. phase, space group and refractive index 4-92165  
 Ba(Bi<sub>0.5</sub>Nb<sub>0.5</sub>)O<sub>3</sub>, dielec. props. and chem. inhomogeneity, effect of sintering 4-85128  
 BaBiO<sub>3</sub>-BaPbO<sub>3</sub>, dielec. and supercond. transitions, Mossbauer line isomer shift 4-65973  
 BaBiSe<sub>3</sub>, cryst. struct. determ. and preparation 4-80017

## barium compounds continued

Ba(Cd<sub>0.3</sub>Nb<sub>0.6</sub>)O<sub>3</sub>, dielec. props. and chem. inhomogeneity, effect of sintering 4-85128  
 BaCeO<sub>3</sub>:La(Nd)(Ho), mixed elec. cond., dopant effects 4-108910  
 BaCl<sub>2</sub>, hydrate and anhydrous, filler for reinforcement of polybutadiene 4-61914  
 BaClF ionic conductor, anharmonic thermal vibrs., X-ray diff. study 4-113560  
 BaClF:Sm<sup>2+</sup>, impurity states in mag. field, fluoresc. study 4-108805  
 BaClF:Sm<sup>2+</sup>, low-lying energy levels under mag. field 4-98564  
 Ba(ClO<sub>4</sub>)<sub>2</sub>·3H<sub>2</sub>O, γ-irrad., ClO<sub>4</sub> radical, ESR temp. depend. 4-98950  
 Ba(ClO<sub>4</sub>)<sub>2</sub>·H<sub>2</sub>O, broadband population inversion in solid state NMR 4-98959  
 BaCl<sub>2</sub>·2H<sub>2</sub>O, γ-ray interaction in energy range 30-660 KeV 4-80096  
 Ba<sub>2</sub>Cs<sub>2</sub>Al<sub>2x+1</sub>Ti<sub>8-2x</sub>O<sub>16</sub>, hollandite phase of SYNROC, struct., X-ray analysis 4-106675  
 Ba<sub>3</sub>Cs<sub>2</sub>Ti<sub>18</sub>O<sub>40</sub>, hollandite-related superstructures 4-70085  
 BaF<sub>2</sub>, ultrasonic transverse meas. 4-88241  
 BaF<sub>2</sub>He, interstitial diffusion, solubility of He, dissolution energy 4-113727  
 BaF<sub>2</sub>, binding energy, bulk modulus and press. derivatives, interionic pot. model 4-60884  
 BaF<sub>2</sub> detector efficiency for monoenergetic γ-rays and γ cascades 4-68896  
 BaF<sub>2</sub>, dielectric constant, temp. depend., polarisability 4-92995  
 BaF<sub>2</sub> epitaxial films, vacuum deposition on PbSe 4-99316  
 BaF<sub>2</sub>, filler for reinforcement of polybutadiene 4-61914  
 BaF<sub>2</sub>, fluorite struct., inner displacement, internal strain tensor, lattice dynamic models 4-92315  
 BaF<sub>2</sub> scintillator, light yield, energy resolution, time resolution (Chinese) 4-112041  
 BaF<sub>2</sub>:Mn<sup>2+</sup>, annealed, EPR spectra 4-71169  
 BaF<sub>2</sub>:Y<sup>3+</sup>(Pb<sup>2+</sup>) crystals, electronic excitation decay, impurity effect 4-109209  
 BaF<sub>2</sub>-LaF<sub>3</sub>-ZrF<sub>4</sub>-AlF<sub>3</sub> glass, crystallisation, devitrification on reheating 4-84194  
 BaF<sub>2</sub>-ZrF<sub>4</sub> glasses, Raman spectra interpretation 4-84960  
 BaFBr, Matlockite-type struct., lattice dynamics calcs. 4-108560  
 BaFCl, flux-grown crystals, thermoluminesc., effect of flux 4-104680  
 BaFCl, Matlockite-type struct., lattice dynamics calcs. 4-108560  
 BaFCl:Eu<sup>+</sup> X-ray phosphor, transparent thin films prep. by evaporation 4-88874  
 BaFCl:Eu<sup>2+</sup> + γ-ray irradi., thermoluminescence glow curves 4-76533  
 BaFCl:Gd flux grown cryst., thermoluminescence studies 4-66081  
 BaFCl:Na crystals, flux grown thermoluminesc. glow curves, emission spectra 4-99200  
 BaFCl(FBr)(Cl), far IR spectra 4-66047  
 Ba(Fe(CN)<sub>6</sub>NO)<sub>2</sub>·H<sub>2</sub>O, IR spectra, vibr. dipole-dipole coupling between nitrosyl groups, fine struct., force consts. 4-96540  
 BaFe<sub>2-x</sub>M<sub>x</sub>O<sub>19</sub> (M=Al, Ga, Sc) ferrites, anisotropy fields and FMR linewidths 4-71058  
 BaFe<sub>2-x</sub>M<sub>x</sub>O<sub>19</sub>, bipyramidal site occupancy, Mossbauer spectra 4-75420  
 BaFe<sub>2</sub>O<sub>19</sub> ferrite, M phase, superstruct. obs. 4-84275  
 BaFe<sub>2</sub>O<sub>19</sub> ferrite, prep., phase transition study (Chinese) 4-93254  
 BaFe<sub>2</sub>O<sub>19</sub> glassy ferrites, effects of mag. quenching 4-61898  
 BaFe<sub>2</sub>O<sub>19</sub>, magnetic vitroceraamics, prep. and props. 4-93256  
 BaFe<sub>2</sub>O<sub>19</sub> permanent magnets, sintering temp. effect on mag. props. and density (Afrikaans) 4-76170  
 Ba<sub>3</sub>Ga<sub>2</sub>Se<sub>6</sub>, prep., cryst. struct., X-ray diff. (German) 4-75415  
 Ba<sub>3</sub>Ga<sub>2</sub>S<sub>7</sub>, prep., cryst. struct., X-ray diff. (German) 4-75415  
 Ba<sub>2</sub>MgCrF<sub>9</sub> and Ba<sub>2</sub>MgFeF<sub>9</sub> (M=Ni, Co, Fe), crystal structure and mag. props. 4-71040  
 BaMnF<sub>4</sub> 2D antiferromag., optical magnon sidebands and exciton dynamics 4-98875  
 BaMnF<sub>4</sub>, acoustic-phonon dispersion at incommensurate phase transitions, Brillouin scatt. obs. 4-61724  
 BaMnF<sub>4</sub>, antiferromagnets, hot magnon sidebands temp. depend. 4-76493  
 BaMnF<sub>4</sub>, incommensurate phase, neutron scatt. study, press. effect 4-75654  
 BaMnF<sub>4</sub>, magneto-electric, unsolved problems 4-76255  
 BaMnF<sub>4</sub>, optical props. near incommensurate and mag. transitions 4-66004  
 BaMnF<sub>3</sub>·H<sub>2</sub>O and Ba<sub>2</sub>Fe<sub>3</sub>F<sub>17</sub>·3H<sub>2</sub>O, hydrated fluorometallates (III), one-dimens. antiferromagnet 4-71035  
 BaMnO<sub>3-x</sub>, system, electron irradi., phase transform., high resolution electron microscopy 4-65395  
 Ba(Mn<sub>1/3</sub>Ta<sub>2/3</sub>)O<sub>3</sub> ceramic, ultra-low dielec. loss at microwave freq. 4-84905  
 BaMoO<sub>4</sub> single cryst., flux evaporation growth and morphology 4-114369  
 Ba(NO<sub>3</sub>)<sub>2</sub>, cohesive energy, elastic const. and Gruneisen coeff. calcs. 4-84230  
 Ba(NO<sub>3</sub>)<sub>2</sub>, efficient reflection with phase conjugation in stimulated Raman scatt. 4-107754  
 Ba(NO<sub>3</sub>)<sub>2</sub>:K, d.c. ionic cond. meas. 4-84456  
 Ba(NO<sub>3</sub>)<sub>2</sub>·H<sub>2</sub>O, pure and doped single crystals, fluoresc. and phosphoresc. study 4-109227  
 Ba(NO<sub>3</sub>)<sub>2</sub>·xH<sub>2</sub>O, anisotropy of imaginary parts of N at. scatt. factors (German) 4-80004  
 Ba<sub>2</sub>NaNb<sub>2</sub>O<sub>12</sub>, acoustic-phonon dispersion at incommensurate phase transitions, Brillouin scatt. obs. 4-61724  
 Ba<sub>2</sub>NaNb<sub>2</sub>O<sub>15</sub>, elec. cond., oscillatory and chaotic states 4-98611  
 Ba<sub>2</sub>NaNb<sub>2</sub>O<sub>15</sub>, ferroelastic-incommensurate transition, Brillouin scatt. study 4-70362  
 Ba<sub>2</sub>NaNb<sub>2</sub>O<sub>15</sub>, ferroelec. transition, critical narrowing of central peak, Raman studies 4-71291  
 Ba<sub>2</sub>NaNb<sub>2</sub>O<sub>15</sub>, incommensurate, Brillouin spectra meas. 4-76482  
 Ba<sub>2</sub>NaNb<sub>2</sub>O<sub>15</sub>, incommensurate phase, superspace symmetry, Landau theory 4-103689  
 Ba<sub>2</sub>NaNb<sub>2</sub>O<sub>15</sub>, interaction of incommensurate modulation with mobile and fixed defects 4-75446  
 Ba<sub>2</sub>NaNb<sub>2</sub>O<sub>15</sub>, tetragonal bronze-like struct., modulated phases and domain struct. 4-113616  
 Ba<sub>2.11</sub>Na<sub>0.84</sub>Nb<sub>0.99</sub>O<sub>15</sub>, incommensurate system, thermal hysteresis in birefringence and permittivity 4-61656  
 Ba<sub>2</sub>NiF<sub>4</sub>(FeF<sub>6</sub>), 2-D antiferromagnet, mag. structure 4-71028  
 Ba<sub>2</sub>Ni(N<sub>3</sub>)<sub>6</sub>·3H<sub>2</sub>O, cryst. struct., X-ray diff. studies 4-92182  
 BaO, enthalpy and specific heat in high temp. region 1200 to 2200K 4-113672

## barium compounds continued

- BaO, microwave optical polarization spectroscopy of excited states 4-91294
- BaO-Al<sub>2</sub>O<sub>3</sub>-SiO<sub>2</sub> thick film crossover dielec.-compositions, dielec. props. rel. to multiple refining 4-109113
- BaO-B<sub>2</sub>O<sub>3</sub>-Fe<sub>2</sub>O<sub>3</sub> glasses, sput coated, mag. props. 4-71107
- BaO-B<sub>2</sub>O<sub>3</sub>-Fe<sub>2</sub>O<sub>3</sub> system, magnetic vitroceraamics, prep. and props. 4-93256
- BaO-Fe<sub>2</sub>O<sub>3</sub> glass, glass forming region and Fe<sup>3+</sup> coordination (*Japanese*) 4-113348
- BaO-Li<sub>2</sub>O-Nb<sub>2</sub>O<sub>5</sub>, phase equilibria in crystn. region, tetragonal phase 4-114495
- BaO-P<sub>2</sub>O<sub>5</sub> glass, internal friction, temp. depend. 4-61966
- BaO-PbO-Nd<sub>2</sub>O<sub>3</sub>-TiO<sub>2</sub> dielec. resonators, microwave characts 4-84908
- BaO-SiO<sub>2</sub> glasses, cryst. nucleation kinetics, effect of amorphous phase separation 4-65185
- BaO-TiO<sub>2</sub>-SiO<sub>2</sub> glass-ceramics, ferroelec., depolarisation currents, dielec. and electrooptical props. 4-76317
- BaO-VO<sub>2</sub>-PO<sub>2.5</sub> semiconductor glass, crystallisation rel. to composition, temp. and duration of heat treatment 4-92096
- BaO-Al<sub>2</sub>O<sub>3</sub>-B<sub>2</sub>O<sub>3</sub> photochromic optical fibres 4-79329
- BaO<sub>2</sub>-(Li<sub>2</sub>O)<sub>0.7</sub>-(LiCl)<sub>0.7</sub>, amorphous, fast ionic cond. meas. (*Chinese*) 4-103996
- BaO\* (A<sub>2</sub>), vibr. relaxation and electronic quenching in Ar and N 4-107442
- Ba(PO<sub>3</sub>)<sub>2</sub>-AlF<sub>3</sub>-LiF, elec. cond. rel. to struct. 4-92771
- Ba(PO<sub>3</sub>)<sub>2</sub>-CdF<sub>2</sub>, high refractive index glass, optical constants, density and atomic refraction rel. to struct. 4-93043
- BaP<sub>2</sub>O<sub>6</sub>(WO<sub>3</sub>)<sub>2m</sub>, X-ray diffr. and high-temperature electron microscopy study of struct. 4-84250
- Ba(PO<sub>3</sub>)<sub>2</sub>·Er<sup>3+</sup>(Yb<sup>3+</sup>)(Nd<sup>3+</sup>), quenching of Er luminesc., effect of Nd<sup>3+</sup> and OH 4-81006
- BaPb<sub>0.7</sub>Bi<sub>0.3</sub>O<sub>3</sub> superconducting films, current-voltage curves, discrete current behaviour 4-61492
- BaPb<sub>0.7</sub>Bi<sub>0.3</sub>O<sub>3</sub> films, two-dimensional Josephson tunnel junction arrays, EM coupling effects 4-61493
- BaPb<sub>0.7</sub>Bi<sub>0.3</sub>O<sub>3</sub> films, supercond. props., high press. study 4-84733
- BaPb<sub>0.7</sub>Bi<sub>0.3</sub>O<sub>3</sub> superconducting photodetector 4-71002
- BaPb<sub>0.7</sub>Bi<sub>0.3</sub>O<sub>3</sub> supercond. thin films for highly sensitive optical detector fabrication 4-82825
- BaPb<sub>0.7</sub>Bi<sub>0.3</sub>O<sub>3</sub> supercond. ceramics, heat capacity near transition temp. 4-114067
- BaPb<sub>1-x</sub>Bi<sub>x</sub>O<sub>3</sub> perovskite supercond., transition temp., substitution effects 4-104341
- BaPb<sub>1-x</sub>Bi<sub>x</sub>O<sub>3</sub>, sp. ht. and supercond. 4-108972
- Ba(Pb<sub>1-x</sub>Bi<sub>x</sub>)O<sub>3</sub>, supercond. transition temp. and Mossbauer line isomeric shift 4-61486
- BaPb<sub>1-x</sub>Bi<sub>x</sub>O<sub>3</sub>, superconducting cryst., crystal growth from solution 4-61825
- BaPb<sub>1-x</sub>Bi<sub>x</sub>O<sub>3</sub>:Sn supercond. transition temps., Mossbauer spectra, positron lifetime distrib. 4-76293
- BaPbO<sub>3</sub>-BaBiO<sub>3</sub> dielec. and supercond. transitions, Mossbauer line isomer shift 4-65973
- BaPbO<sub>3</sub>-BaBiO<sub>3</sub> system, supercond. and ferroelec. phase transitions 4-76061
- Ba<sub>2</sub>Pt<sub>2</sub>(H<sub>2</sub>P<sub>2</sub>O<sub>6</sub>)<sub>4</sub>, two-level phosphoresc., magneto-optical effect 4-93102
- Ba<sub>2</sub>(ReO<sub>4</sub>)<sub>2</sub>X (X=I, Br, Cl, F, NO<sub>3</sub>, CO<sub>3</sub>, O<sub>2</sub>), apatite like phases, structure and physical props. 4-70115
- BaRu<sub>1-x</sub>M<sub>x</sub>O<sub>3-y</sub>, M=Rh, Ir, Mn, Fe, Co, Ni, cryst. struct. and elec. cond. (*German*) 4-84265
- BaS, band-overlap metallisation, self-consistent augmented-spherical-wave calc. 4-80499
- BaS:R, phosphors, photoluminescence spectra 4-61747
- BaSO<sub>4</sub>, adsorpt. of amphoteric polymer, effect on colloid stability 4-66619
- BaSO<sub>4</sub>, barytes single crystals, γ irradi., optical absorpt., thermolum. 4-66080
- BaSO<sub>4</sub>, electrolyte crystals in supersaturated aqueous soln., crystal growth kinetics 4-114373
- BaSO<sub>4</sub> paint, refl. characts. compared with PTFE containing silicone paints 4-69516
- BaSO<sub>4</sub>:Dy, thermoluminesc. detectors response functions to γ-radiation 4-112037
- BaSO<sub>4</sub>:Eu thermoluminescent detectors, screening in cosmic ray expts. 4-102523
- BaSO<sub>4</sub>:MnO<sub>4</sub><sup>2-</sup>, absorpt. spectra, comparison with other host lattices 4-109217
- BaSb<sub>2</sub>S<sub>4</sub>, struct., SbS<sub>2</sub> strings 4-103724
- BaS, band-overlap metallisation, self-consistent augmented-spherical-wave calc. 4-80499
- BaSnF<sub>4</sub>, fluoride ionic cond. with α-PbSnF<sub>4</sub> struct., ionic cond. and Mossbauer study 4-92411
- BaSnFeO<sub>13</sub>, cryst. struct., neutron diffr., Mossbauer spectra, magnetisation meas. 4-75406
- BaSn<sub>1-x</sub>Hf<sub>x</sub>O<sub>3</sub>, solid solns., cryst. struct. determ. 4-70122
- BaSn<sub>1-x</sub>Ti<sub>x</sub>O<sub>3</sub>, solid solns., cryst. struct. determ. 4-70122
- BaSn<sub>1-x</sub>Zr<sub>x</sub>O<sub>3</sub>, solid solns., cryst. struct. determ. 4-70122
- Ba<sub>2-x</sub>Sr<sub>x</sub>D<sub>1-y</sub>Na<sub>1-y</sub>Nb<sub>0.5</sub>O<sub>15</sub>, ferroelec. props., dielec. const., piezoelec. and electromechanical coupling coeffs. 4-65958
- Ba<sub>2</sub>Sr<sub>1-x</sub>F<sub>2</sub>, lattice-matched single cryst. film growth on InP (001) by MBE 4-70582
- Ba<sub>2</sub>Sr<sub>1-x</sub>F<sub>2</sub> single cryst. dielec. films, MBE growth on InP (001) 4-81137
- BaSr<sub>1-x</sub>Nb<sub>x</sub>O<sub>3</sub>, defect struct., elec. and ionic cond. 4-98676
- Ba<sub>0.39</sub>Sr<sub>0.61</sub>Nb<sub>0.6</sub>O<sub>6</sub>, elastic compliances, temp. depend. 4-76336
- Ba<sub>0.4</sub>Sr<sub>0.6</sub>Nb<sub>0.6</sub>O<sub>6</sub> ferroelec. cryst., electrooptical coefficients 4-76434
- Ba<sub>0.5</sub>Sr<sub>0.46</sub>Nb<sub>0.6</sub>O<sub>6</sub>, pure and La(Ce) doped, thermally stimulated electron emission, dielec. characts., impurity effects (*Russian*) 4-114356
- Ba<sub>2</sub>Sr<sub>1-x</sub>Nb<sub>x</sub>O<sub>6</sub>, pyroelectric effect, ferroelectric transition 4-114214
- Ba<sub>1-x</sub>Sr<sub>x</sub>Pb<sub>1-2x</sub>Bi<sub>2x</sub>O<sub>3</sub> ceramic, composition depend. of superconductivity 4-114055
- Ba<sub>2</sub>SrRu<sub>2</sub>O<sub>9</sub>, cryst. struct., Rietveld refinement of neutron powder diffr. data 4-84256
- Ba<sub>0.9</sub>Sr<sub>0.1</sub>TiO<sub>3</sub>, soft mode behaviour, ferroelec. transition and IR reflectometry 4-80872
- BaTe, band-overlap metallisation, self-consistent augmented-spherical-wave calc. 4-80499
- BaTe, band-overlap metallisation, energy-dispersive X-ray diffr. 4-98526
- BaTiF<sub>6</sub>, crystal struct. and mag. props. 4-70084
- BaTi<sub>2</sub>Fe<sub>2</sub>O<sub>11</sub>, cryst. struct., neutron diffr., Mossbauer spectra, magnetisation meas. 4-75406

## barium compounds continued

- Ba<sub>2</sub>TiGe<sub>2</sub>O<sub>8</sub>, glass ceramics, grain oriented, hydrostatic piezoelec. props. and appls. 4-84913
- BaTiO<sub>3</sub> amorphous film, elec. and struct. props. 4-80701
- BaTiO<sub>3</sub>, anisotropic self diffraction 4-107762
- BaTiO<sub>3</sub>, band struct. and ferroelec. transition, two-photon spectra studies 4-93016
- BaTiO<sub>3</sub> based solid solns., ferroelec. transition temp. and electron spectra 4-93013
- BaTiO<sub>3</sub>, birefr., Kerr effect 4-88805
- BaTiO<sub>3</sub>, centrosymmetric ceramics, elec. field induced acoustic anisotropy 4-60992
- BaTiO<sub>3</sub> ceramics, lanthanide doped, EPR spectra 4-109072
- BaTiO<sub>3</sub>, combined doping, electron-conduction compensation 4-113475
- BaTiO<sub>3</sub>, conf., Alanya, France (June-July 1982) 4-95052
- BaTiO<sub>3</sub> cryst., ferroelec. domain struct., SEM and optical microscopy studies 4-71319
- BaTiO<sub>3</sub> crystal, phase conjugator for CW dye laser resonator cavity 4-107692
- BaTiO<sub>3</sub> crystals, γ-irradiated, with equil. domain struct., polarisation state 4-76395
- BaTiO<sub>3</sub>, cubic to tetragonal transition, covalency effects, band struct. calculations 4-70361
- BaTiO<sub>3</sub>, displacive type ferroelastic, lattice model 4-76394
- BaTiO<sub>3</sub>, displacive/order-disorder crossover, soft mode temp. depend., contribution to low freq. permittivity 4-65369
- BaTiO<sub>3</sub> doped single cryst., ferroelec. transition, substitutional defects influence 4-65984
- n-BaTiO<sub>3</sub> electrolyte redox systems, photoelectrochemistry 4-72124
- BaTiO<sub>3</sub>, electron energy struct. of cond. band, X-ray photoemission yield spectra 4-61282
- BaTiO<sub>3</sub>, ferroelec., permittivity, effect of grain size 4-76306
- BaTiO<sub>3</sub>, ferroelec., sp. ht. at low temps. 4-65416
- BaTiO<sub>3</sub>, ferroelec. cryst., photovoltaic current anal. 4-75994
- BaTiO<sub>3</sub>, ferroelec. crystal, electrostatic pot. at surface 4-76350
- BaTiO<sub>3</sub>, ferroelec. diffuse phase transition, exponent γ determ. 4-76384
- BaTiO<sub>3</sub>, ferroelec. phase transitions, stress effects 4-71315
- BaTiO<sub>3</sub>, ferroelec. phase transition microregion approach 4-76363
- BaTiO<sub>3</sub> films, vacuum deposited, struct. and elec. props. (*Japanese*) 4-94882
- BaTiO<sub>3</sub> form. by thermal decomposition of oxalate (*Japanese*) 4-76718
- BaTiO<sub>3</sub>, gamma irradi., influence on photovoltaic effects 4-84656
- BaTiO<sub>3</sub>, lattice deformation induced cryst. field variations, Mossbauer and EPR studies 4-71159
- BaTiO<sub>3</sub>, liquid phase sintering and composite ceramics with Pb<sub>2</sub>Ge<sub>2</sub>O<sub>7</sub> 4-104746
- BaTiO<sub>3</sub>, optimal properties of photorefractive materials for optical data processing 4-74640
- BaTiO<sub>3</sub> oxide perovskites, dielec. meas., surface layer effects 4-65962
- BaTiO<sub>3</sub>, oxygen-octahedral ferroelectrics, two-photon spectroscopy studies 4-114300
- BaTiO<sub>3</sub>, PTC ceramic, strength and fracture toughness 4-62051
- BaTiO<sub>3</sub> photorefractive crystal, asymmetric transmission studies 4-84927
- BaTiO<sub>3</sub>, photorefractive effect speed 4-99069
- BaTiO<sub>3</sub>, piezoceramic, dielec. props., influence of 90° domain structure 4-76396
- BaTiO<sub>3</sub>, point defects and thermodynamics 4-98098
- BaTiO<sub>3</sub> poly and single cryst. dielec. after-effects and domain wall 4-71267
- BaTiO<sub>3</sub> polycryst. and heteroepitaxial ferroelec. films, phase transition 4-65977
- BaTiO<sub>3</sub>, powder processing, grain size, ferroelec. props. 4-93253
- BaTiO<sub>3</sub>, pure and Nb-doped, elec. cond. 600-800°C, defect structure 4-98604
- BaTiO<sub>3</sub>, reverse switching effect 4-76393
- BaTiO<sub>3</sub>, reversed c-domain patterns and elastic wave velocity surface 4-84924
- BaTiO<sub>3</sub>, self-pumped phase conjugation, optical feedback, wavelength response and interf. effects 4-97004
- BaTiO<sub>3</sub>, semicond. glass ceramics, oxidation, barrier layer formation 4-114699
- BaTiO<sub>3</sub>, soliton physics and ferroelectric transitions 4-80875
- BaTiO<sub>3</sub>, substituted, ferroelec. phase transitions and phase diagram 4-65978
- BaTiO<sub>3</sub>, surface domains, double Laue pattern topography 4-104548
- BaTiO<sub>3</sub> synthesis, polycryst., nonstoichiometry rel. to solid-solid reaction mechanism 4-99305
- BaTiO<sub>3</sub> thick film, grain boundaries, TEM obs. 4-84300
- BaTiO<sub>3</sub> thin films, crystallisation from amorphous phase, electron microscopy study 4-113830
- BaTiO<sub>3</sub> type oxide fluoride growth at low temp. using LiF-BaF<sub>2</sub>-LiBO<sub>2</sub> mixture flux 4-92996
- BaTiO<sub>3</sub>:Ca, impurity site occupancy, channelling enhanced microanal. studies 4-108394
- BaTiO<sub>3</sub>:Co, impurity valence states, EPR 4-75901
- BaTiO<sub>3</sub>:Fe, electrochem., elec. field depend. 4-66077
- BaTiO<sub>3</sub>:Fe, soft mode behaviour, ferroelec. transition and IR reflectometry 4-80872
- BaTiO<sub>3</sub>:Fe(Nb), dielectric relax. meas. 4-80864
- BaTiO<sub>3</sub>:Nb(Al), donor doped, defect chem. 4-84307
- BaTiO<sub>3</sub>:Sb(Nb), sintering, microstruct. 4-89012
- BaTiO<sub>3</sub>:Yb, dielec. and X-ray diffr. study 4-84896
- BaTiO<sub>3</sub>-based materials, dielec. props. and chem. inhomogeneity, effect of sintering 4-85128
- BaTiO<sub>3</sub>:SrTiO<sub>3</sub>, high-temp. reactions, EPMA and SEM investigation 4-80292
- BaTiO<sub>3</sub> single cryst., struct. refinement, X-ray diffr. studies 4-113408
- BaTiO<sub>3</sub> type ceramics, dielectric characts., microwave freqs. 4-76311
- BaTiO<sub>3</sub> single cryst., struct. refinement, X-ray diffr. studies 4-113401
- BaTiSi<sub>2</sub>O<sub>8</sub>, glass ceramics, grain oriented, hydrostatic piezoelec. props. and appls. 4-84913
- BaTiSi<sub>2</sub>O<sub>8</sub> polar glass ceramics for sonar transducers 4-69651
- Ba<sub>1-x</sub>U<sub>x</sub>F<sub>2+2x</sub>, high temp. ionic cond. study 4-70450
- Ba<sub>1-x</sub>U<sub>x</sub>F<sub>2+2x</sub>, ionic conductivity, crit. temp. 4-92423
- Ba<sub>0.15</sub>WO<sub>3</sub>, pentagonal tunnel struct. bronze, cryst. data X-ray diffr., electron microscopy studies 4-75404
- Ba<sub>2</sub>Yr<sub>2</sub>O<sub>9</sub>, mixed valence, dimeric unit, electronic and vibronic coupling, mag. aspects 4-92674
- BaYb<sub>2</sub>Er lamp-pumped 2 μm range laser, energy characts. 4-69414
- Ba(Zn,Ta)O<sub>7</sub>-BaZrO<sub>3</sub>, complex perovskite struct., dielec. resonator with high microwave Q-value 4-84926

**iridium compounds continued**

- Ba<sub>2</sub>(Zn<sub>1-x</sub>Co<sub>2/3</sub>Fe<sub>1/3</sub>O<sub>22</sub>) ferrites, first-order magnetisation processes 4-76188  
 Ba(Zn<sub>1/3</sub>Nb<sub>2/3</sub>O<sub>3</sub>)<sub>2</sub>-Sr(Zn<sub>1/3</sub>Nb<sub>2/3</sub>O<sub>3</sub>)<sub>2</sub> solid soln., dielectric props. meas. 4-98996  
 BaZrO<sub>3</sub>-BaTiO<sub>3</sub> high-temp. reactions, EPMA and SEM investig. 4-80292  
 Ca<sub>0.25</sub>Ba<sub>0.75</sub>Tb<sub>0.05</sub>Mg<sub>1.05</sub>B<sub>2</sub>O<sub>5</sub> Kurchatovite struct., phosphor props. 4-66074  
 Co-Ni-Zn ferrites: BaO, microstruct., mag. props. 4-88302  
 HfF<sub>2</sub>-BaF<sub>2</sub>-LaF<sub>3</sub>-AlF<sub>3</sub> glass, IR transparent, stability in humid air, AES study 4-109534  
 KMg<sub>2</sub>Si<sub>3</sub>AlO<sub>10</sub>F<sub>2</sub>-Ba<sub>0.5</sub>Mg<sub>1.5</sub>Si<sub>3</sub>AlO<sub>10</sub>F<sub>2</sub> system, solid solns., lattice constns., melting temp. 4-109384  
 (K<sub>1</sub>Na<sub>1-x</sub>)<sub>0.4</sub>(Sr<sub>1-x</sub>)<sub>0.8</sub>Nb<sub>2</sub>O<sub>6</sub> ferroelec. single cryst. series, pyroelec. props. 4-76345  
 La<sub>2</sub>Ba<sub>2</sub>Cu<sub>0.4+y</sub>O<sub>14+y</sub> struct., electron transport and mag. props. 4-70110  
 La<sub>1-x</sub>Ba<sub>x</sub>F<sub>3-x</sub> solid solns., elec. props., small-signal AC response and TSDC meas. 4-70449  
 La<sub>1-x</sub>Ba<sub>x</sub>F<sub>3-x</sub> solid solutions, small signal AC response 4-92424  
 La<sub>1-x</sub>Ba<sub>x</sub>F<sub>3-x</sub> tysonite-type solid solns., ionic cond. 4-92410  
 LaF<sub>3</sub>-BaF<sub>2</sub>-ZrF<sub>4</sub> fluoride glass, surface crystals. formed by reaction with water 4-81298  
 La<sub>1-x</sub>Ba<sub>x</sub>F<sub>3-x</sub> crystals, fluoride ion cond., electronic cond. meas. 4-92772  
 LiF-BaF<sub>2</sub>-LiBO<sub>2</sub> mixture field for BaTiO<sub>3</sub> type oxide fluoride growth at low temp. 4-99296  
 Na<sub>2</sub>Nd<sub>2</sub>Ba<sub>1-x</sub>Ga<sub>2</sub>S<sub>4</sub> luminescent props. and electron transfer 4-109233  
 Na<sub>2</sub>O-BaO-SiO<sub>2</sub> glass system, glass transition temp. and devitrification behaviour 4-98285  
 Nd<sub>2-x</sub>Ba<sub>1-x</sub>Cu<sub>(1-y)/2</sub>O<sub>5-x</sub> cryst. struct., mag. susceptibility, elec. cond. (French) 4-75418  
 (Pb<sub>0.7</sub>Ba<sub>0.3</sub>)<sub>1-x</sub>La<sub>x</sub>Nb<sub>2</sub>O<sub>6</sub> ceramic, dielectric, piezoelectric and optical props. 4-98999  
 Pb<sub>1-x</sub>Ba<sub>x</sub>Nb<sub>2</sub>O<sub>6</sub> ceramics, hot pressed, dielec. and piezoelec. props. 4-104533  
 Pb<sub>1-x</sub>Ba<sub>x</sub>Nb<sub>2</sub>O<sub>6</sub> ferroelec. props., dielec. const., piezoelec. and electromechanical coupling coeffs. 4-65958  
 (Pb<sub>0.7</sub>Ba<sub>0.3</sub>)<sub>1-x</sub>Ti<sub>x</sub> ferroelec., phase-transition, high press. Raman study 4-76451  
 PbO-BaO-TiO<sub>2</sub>-B<sub>2</sub>O<sub>3</sub> glass ceramic system, crystal clamping, X-ray diffr., dilatometry 4-109386  
 Sr<sub>1-x</sub>Ba<sub>x</sub>Nb<sub>2</sub>O<sub>6</sub> ferroelec. diffuse phase transition, exponent  $\gamma$  determ. 4-76384  
 ThF-BaF<sub>2</sub> multispectral glass development and characts. 4-74639  
 (ThF<sub>0.2</sub>(BaF<sub>2</sub>)<sub>0.1</sub>(MnF<sub>2</sub>)<sub>0.5</sub>(AlF<sub>3</sub>)<sub>0.2</sub>)<sub>0.2</sub> glass, low temp., ultrasonic behaviour 4-70285  
 TiO-Ba<sub>x</sub>Nb<sub>2</sub>O<sub>5</sub> monosized powders, synthesis and characterisation 4-114453  
 W bronze tetragonal struct. non-stoichiometric phases, dielec., ferroelastic and nonlinear optical props. 4-65972  
 Zr-Ba-La-Al-F glass, crystn. kinetics 4-70037  
 ZrF-BaF<sub>2</sub> multispectral glass development and characts. 4-74639  
 ZrF<sub>2</sub>-BaF<sub>2</sub>-LaF<sub>3</sub>-AlF<sub>3</sub> glass, IR transparent, stability in humid air, AES study 4-109534  
 ZrF<sub>2</sub>-BaF<sub>2</sub>-based fluorozirconate glasses, crystallisation, X-ray diffr. and DSC studies 4-84197  
 ZrF<sub>0.575</sub>(BaF<sub>2</sub>)<sub>0.375</sub>(ThF<sub>4</sub>)<sub>0.75</sub> (V-52) glass, reson. interaction of acoustic waves with two-level systems 4-70290

**Barkhausen effect**

- laminations, location of Barkhausen jumps and moving domain walls 4-88700  
 magnetisation and eddy current losses, space-time correlation props. for fine wall spacing 4-88698  
 transition metal-Fe-B amorphous alloys, magnetisation reversal, mech. stress effects 4-76171  
 Co-P amorphous electrodeposited layers, Barkhausen effect, torsion effects 4-76198  
 Fe whisker, Barkhausen jump field distrib., temp. depend. 4-76182  
 Fe wires, Barkhausen jumps, deform. effects 4-76187  
 Fe-Ni wires, Barkhausen jumps, deform. effects 4-76187  
 Fe-P amorphous electrodeposited layers, Barkhausen effect, torsion effects 4-76198  
 Fe-Si sheets, magnetisation processes, grain boundary effects 4-76180  
 Ni wires, Barkhausen jumps, deform. effects 4-76187

**Barnett effect** see gyromagnetic effect; magnetisation

**barometers**

- solid state barometer with digital readout 4-94275

**barometric pressure** see atmospheric pressure and density

**barographs** see dams

**barrel distortion** see aberrations

**barretters** see thermistors

**baryon-baryon interactions**

- see also baryon-baryon scattering; hyperon-nucleon interactions; nucleon-nucleon interactions  
 initial state interactions, factorization, and the Drell-Yan process 4-63967  
 spin orbit and tensor interactions from quark exchange kernels 4-86688  
 spin orbit interaction in nonrelativistic quark model 4-86689

**baryon-baryon scattering**

- see also baryon-baryon interactions; hyperon-nucleon scattering; nucleon-nucleon scattering  
 No entries

**baryon decay**

- see also baryon hadronic decay; baryon leptonic decay; hyperon decay  
 atmospheric neutrinos, ang. distrib. and flux, nucleon decay expt. appl. 4-63023  
 atmospheric neutrinos and astrophysical neutrinos in proton decay experiments 4-63024  
 baryon number violating nucleon decay 4-68476  
 bottom hadrons, lifetimes, review 4-73751  
 charm particle lifetimes and production 4-68566  
 chiral Lagrangian for proton decay in SU(3) $\times$ SU(3) theory 4-73696  
 conference, particles and fields, Blacksburg, VA, USA (Sept. 1983) 4-73135  
 conference, unification and supergravity, La Jolla, CA, USA (1983) 4-110797  
 conference on grand unification, Philadelphia, PA, USA, (April 1983) 4-58573

**baryon decay continued**

- conference on low energy tests of conservation laws, Blacksburg, VA, USA (Sep. 1983) 4-90281  
 gravitationally induced in supersymmetric theories 4-111347  
 GUTs, minimal SU(5) Higgs scalar effects and supersymmetry, p decay 4-90763  
 HPW water Cherenkov proton decay detector, triggers and sensitivity 4-91147  
 KAMIOKANDE nucleon decay expt., status and performance 4-90875  
 KGF nucleon decay expt., exptl. details, anal. methods and results 4-59074  
 magnetic monopole catalysed, Rubakov interaction 4-95734  
 magnetic monopole flux determ. from baryon decay expt. 4-95735  
 minimal SU(5) model with canonical particle content, proton lifetime, fermion masses 4-73694  
 MIT bag model, confinement of non-Abelian monopoles, colour singlet bag size 4-86680  
 Monte Carlo code DECAY 4-78552  
 neutron, half-life meas. by in-beam method 4-64319  
 neutron properties, interactions, expt. data review 4-63997  
 nucleon branching ratios, chiral Lagrangian calc. in supersymmetry SU(5) model 4-58995  
 nucleon decay, future expts. review 4-59077  
 nucleon decay, Mont Blanc NUSEX expt. results 4-106500  
 nucleon decay detection expts., review 4-63994  
 nucleon decay detector calibration with cosmic ray neutrinos 4-91148  
 nucleon disintegration by monopole catalysis, gauge fields, anomalies 4-59014  
 nucleon three-lepton decays with fermion-number conservation 4-68570  
 nucleon two-body decay modes with vector mesons, chiral dynamics in SU(5) supersymmetric model 4-63995  
 proton, use of NUSEX (Nucleon Stability Experiment) 4-96410  
 proton decay, 1982 predictions in minimal SU(5) theory 4-68483  
 proton decay, GUT and supersymmetry, review 4-73687  
 proton decay, hadronic dynamics role 4-73701  
 proton decay, monopole catalysis S-matrix 4-111345  
 proton decay, next to leading corrections in SU(5) model 4-59072  
 proton decay, SU(5) grand unification, two-loop renormalisation group anal. 4-111353  
 proton decay and  $\Delta B=2$  processes, expt. limits at IMB detector 4-90874  
 proton decay experiments 4-90784  
 proton decay generation from Hopf instanton in SU(5) 4-86622  
 proton decay in SU<sub>3</sub> and its radiative corrections 4-95740  
 proton decay in SU(4)<sub>C</sub> $\times$ SU(2)<sub>L</sub> $\times$ SU(2)<sub>R</sub> model 4-59007  
 proton decay in SU(5) theory, monopole catalysts 4-78514  
 proton decay inside the nucleus 4-73753  
 proton decay results from Kolar Gold Field expt. 4-106499  
 proton decay search at Baksan underground telescope 4-107264  
 proton nonexponential decay and effective lifetime 4-78506  
 relativistic statistical model for proton decay, baryon wavefunctions 4-95717  
 s-wave monopole-fermion interactions, strong and weak effects, GUTs, p lifetime 4-63926  
 SU(5) GUTs, proton decay, electroweak mixing angle, gauge hierarchy problem 4-95737  
 SU(5) model, proton lifetime and weak angle predictions 4-86602  
 SU(7) model with improved proton lifetime value and embedded SU(4)<sub>C</sub> $\times$ SU(2)<sub>L</sub> $\times$ SU(1)<sub>Y</sub> intermediate symmetry and SU(N) unification series (Chinese) 4-111349  
 weak decays of charmed particles 4-95791  
 N decay, Soudan-I detector results 4-59075  
 N $\rightarrow$ e<sup>+</sup>h(nonstrange), nonstandard fermion mass matrices, branching ratios 4-90776  
 n $\rightarrow$ K<sup>0</sup><sub>S</sub> two-loop finite supersymm. SU(5) GUT, coloured Higgs triplet exchange 4-106497  
 N $\rightarrow$ IV (vector meson) in SU(5) model, supersymmetric 4-102074  
 N $\rightarrow$ III $\pi$  mesons within SU(4) of colour unifying quarks with leptons 4-59073  
 n $\rightarrow$ K<sup>0</sup> GUT predictions for strangeness yield 4-86624  
 n $\rightarrow$ pe $\pi$ ,  $\beta$ -decay asymmetry 4-63992  
 n $\rightarrow$ pe $\pi$ ,  $\beta$ -decay role in astrophysics 4-67620  
 n $\rightarrow$ pe $\pi$ , T invariance, triple correlation expt. 4-63993  
 n $\rightarrow$ e<sup>+</sup> $\pi$ <sup>+</sup> decay in minimal SU(5) GUT 4-102078  
 p decay rate, MIT bag model, zeroth order, smaller  $\alpha_s$ , Coulomb spike effect 4-59053  
 p decay theory in SU(5) GUT, lifetime uncertainties, Higgs scalar effects 4-59013  
 p $\rightarrow$ e<sup>+</sup> $\pi$ <sup>0</sup> $\pi$ <sup>+</sup> (e<sup>+</sup> $\pi$ <sup>0</sup>), constraints on decay and SU(16)<sub>C</sub> GUT 4-59003  
 p $\rightarrow$ e<sup>+</sup> $\pi$ <sup>+</sup>, baryon wave functions, currents uncertainties, GUTs, lifetime 4-82922  
 p $\rightarrow$ e<sup>+</sup> $\pi$ <sup>0</sup> lifetime calcs. in SU(5) with split fermion representations 4-102072  
 p $\rightarrow$ e<sup>+</sup> $\pi$ <sup>0</sup>, lifetime estimate, orthogonal unification theories 4-111355  
 p $\rightarrow$ e<sup>+</sup> $\pi$ <sup>+</sup>, meson field quenching in SU(5) GUT, barrier penetration factors 4-95720  
 p $\rightarrow$ K<sup>0</sup><sub>S</sub> $\pi$ <sup>+</sup> in locally supersymmetric GUT 4-73688  
 p $\rightarrow$ K<sup>0</sup><sub>S</sub> $\pi$ <sup>+</sup>, two-loop finite supersymm. SU(5) GUT, coloured Higgs triplet exchange 4-106497  
 p $\rightarrow$ K<sup>0</sup><sub>S</sub> $\pi$ <sup>+</sup>, two-loop finite supersymm. SU(5) GUT, coloured Higgs triplet exchange 4-106497  
 p $\rightarrow$  $\mu$ <sup>+</sup>K<sup>0</sup>(K<sup>0</sup><sub>S</sub>) GUT predictions for strangeness yield 4-86624  
 p $\rightarrow$  $\mu$ <sup>+</sup>K<sup>0</sup>, Higgs mediated in SU(5) theory, 5-D interactions, fermion masses 4-86703  
 p $\rightarrow$ K<sup>0</sup><sub>S</sub> gluino exchange in supersymmetric theories 4-86617  
 p $\rightarrow$  $\pi$ <sup>0</sup> $\pi$ <sup>0</sup> (e<sup>+</sup> $\pi$ <sup>0</sup>), single and double pion emission via 3-quark fusion 4-111448  
 p $\rightarrow$ e<sup>+</sup> $\pi$ <sup>+</sup> ( $\mu$ <sup>+</sup>K<sup>0</sup>), lifetime and monopole catalysis, IMB detector results 4-59076  
 p $\rightarrow$ e<sup>+</sup> decay in minimal SU(5) GUT 4-102078

**baryon hadronic decay**

- $\Delta I=1/2$  non-leptonic hyperon decays, S- and P-wave amplitudes 4-73752  
 hyperon nonleptonic s-wave amplitudes, negative parity excited baryons 4-86704  
 soft pion S-wave nonleptonic hyperon decay amplitudes, evidence for corrections 4-95793  
 $\Delta\rightarrow N\gamma$ , radiative decay, effect of quark-quark tensor and spin-spin force 4-64003  
 $\Delta\rightarrow N\pi$ ,  $\Delta T=3/2$  amplitudes, effective weak Hamiltonian, QCD short distance corrections 4-111449  
 $\Delta^*\rightarrow\pi\Delta$  pion decay widths using OPE potential 4-90878

**baryon hadronic decay continued**

- $\Delta$  nonleptonic decays, chiral bag model and weak interactions, s- and p-wave amplitudes 4-102119
- $\Lambda_c$ - $\Lambda$  inclusive nonleptonic decays, bag model, W-exchange contribs. 4-106529
- $\Lambda_c^+ \rightarrow K^0 p \pi^+$ , decay probabilities 4-64149
- $\Lambda_c^+ \rightarrow K^0 p \pi^+ \pi^-$  ( $\Lambda_c^+ \rightarrow \pi^+ \pi^- \pi^+$ ), branching ratios, mass 4-95830
- $\Lambda_c^+ \rightarrow \Lambda \pi^+ \pi^+ \pi^-$ , decay probabilities 4-64149
- N-strange particles,  $x_i$  distributions, cross-sections 4-111478
- $N^* \rightarrow \pi N$  pion decay widths using OPE potential 4-90878
- $\Omega^-$ , nonleptonic decay matrix elements in variable press. bag model 4-111418
- $\Omega^-$  hadronic and radiative decays, lifetime, branching ratios and decay asymmetry 4-86702
- $\pi N \rightarrow \pi N$ , second  $F_{35}$   $\pi N$  resonance near 2000 MeV,  $\rho N$  decay mode 4-78563
- $\Sigma^- \rightarrow N \pi$ ,  $\Delta T=3/2$  amplitudes, effective weak Hamiltonian, QCD short distance corrections 4-111449
- $\Xi^- \rightarrow \Lambda \pi$ ,  $\Delta T=3/2$  amplitudes, effective weak Hamiltonian, QCD short distance corrections 4-111449

**baryon interactions** *see baryon-baryon interactions; lepton-hadron interactions; meson-baryon interactions; photon-hadron interactions***baryon leptonic decay**

- $n \rightarrow \bar{\nu} K^0$ , lifetimes and branching ratios 4-73684
- $p \rightarrow e^+ \pi^0 (e^+ K^0)$  lifetimes and branching ratios 4-73684
- $p \rightarrow \mu^+ K^0$  4-73684

**baryon mass**

- see also hyperon mass*
- ground-state baryon mass splittings from unitarity in SU(6) 4-68556
- hadrons, quark rel. center-of-mass motion in bags, mass and mag. moment corrections 4-102091
- $J=1/2, 3/2$  baryons, masses in quark-diquark model based on Bethe-Salpeter eqn. 4-90844
- lattice QCD, Monte Carlo calc. of baryon mass, light dynamical quarks 4-111392
- light hadron masses in chiral and cloudy bag models, N- $\Delta$  and  $\Sigma$ - $\Lambda$  mass differences 4-90821
- neutron metrology with simple expt. arrangement 4-106656
- neutron properties, interactions, expt. data review 4-63997
- nucleon mass and pionic form factor 4-78554
- potential model masses of mesons and baryons 4-78542
- spectrum in quenched QCD on  $16^3$  lattice 4-68555
- SU(3) lattice gauge theory, hadron mass calcs. 4-106459
- supersymmetric hadrons,  $\bar{t}Q\bar{Q}$  and  $\bar{g}Q\bar{Q}$ , variational model, resonance wave functions 4-106493
- (bbb) Faddeev eqns., mass calcs. of  $J^P=3/2$  systems 4-90832
- (ccc) Faddeev eqns., mass calcs. of  $J^P=3/2$  systems 4-90832
- $dp \rightarrow \pi^+ \pi^-$  + missing mass, 3.3 GeV/c, structs. in nn and  $nn^+$  invariant mass spectra 4-59100
- $\Delta$  Faddeev eqns., mass calcs. of  $J^P=3/2$  systems 4-90832
- $N^*$  and  $\Delta^*$  negative parity states, masses in chiral bag model 4-68543
- p mass prediction from  $\pi\pi$  scatt. data, effective chiral Lagrangians 4-102107

**baryon photoproduction**

- see also hyperon production; neutron production; proton production*
- $\gamma\gamma$  - baryon + antibaryon, high  $p_T$  exclusive scatt., perturbative QCD appl. 4-90815
- $\gamma\gamma \rightarrow p\bar{p}\pi^+\pi^-$ , 16.95 GeV, cross section and resonance prod. limit 4-95868
- $\gamma p \rightarrow D^- \Sigma^{*++}$ , cross section threshold enhancement 4-106534
- $\gamma p \rightarrow \Delta^+ \pi^-$ , cross section threshold enhancement 4-106534

**baryon production**

- see also baryon photoproduction; hyperon production; neutron production; proton production*
- cosmological, baryon number origin and related problems 4-72875
- cosmological baryon generation at low temps., SU(3)  $\times$  SU(2)  $\times$  U(1) calcs., 1 TeV physics 4-90264
- particle in early Universe 4-72877
- SO(10) GUT with low mass  $W_R$  boson, baryon generation mechanism 4-95721
- SU(3)  $\times$  SU(2)<sub>L</sub>  $\times$  U(1) model, baryogenesis, CP breaking, GUT scale 4-111336
- $\gamma\gamma \rightarrow \Delta\bar{p} + \Delta p \rightarrow N\bar{N}\pi$ , contact terms, cross sections, hadron dynamics 4-111488
- $\gamma p \rightarrow$  charmed baryon + charmed meson, 5-10 GeV, cross section threshold enhancement search 4-64008
- $\bar{p}p \rightarrow$  baryon-antibaryon, spin structure, polarisation amplitudes in SU(6) 4-90909
- $pp \rightarrow \Delta^{*++} \pi^- p$ , diffractive dissociation in Deck model, slope-mass-cos  $\theta^{GJ}$  correlation 4-86725
- $pp \rightarrow A^0 K^+ p$ , partial wave anal., deck model, double Regge exchange 4-78564
- $\pi^- N \rightarrow N(\Sigma)(Z)$ ,  $x_i$  distributions, cross-sections 4-111478
- $\gamma p \rightarrow \pi N$ ,  $D_{13}(1520)$  resonance photoprod., bag model recoil corrections 4-102125

**baryon resonances**

- see also hyperon resonances*
- bottom hadrons, lifetimes, review 4-73751
- constituent quark model, rotational bands in baryon spectrum 4-90825
- dibaryon resonance signal, evidence in  $\pi d$  scatt. tensor polarisation meas. 4-82972
- dibaryon resonances, expt. anal. 4-59028
- dibaryon state formation in  ${}^4\text{He}(p,ppn){}^4\text{H}$  4-102272
- dibaryons, B=2, T=1 system evidence from missing mass in  $p({}^3\text{He}, d){}^4\text{He}$  4-78642
- dibaryons, SU(3) 27-plet 4-111327
- non-relativistic quark-potential model, nucleon and delta spectra, oscillator variational states 4-106515
- potential quark model with cloud, QCD, N and  $\Delta$  isobar appl. 4-73723
- QCD sum rules implications for nucleon and  $\Delta$  size 4-95773
- quark potential model, NN scatt. phase shifts, delta cross sections 4-106538
- skyrmin breathing mode, phase shifts, N(1440) and  $\Delta(1600)$  resonances 4-111283
- supersymmetric hadrons,  $\bar{t}Q\bar{Q}$  and  $\bar{g}Q\bar{Q}$ , variational model, resonance wave functions 4-106493
- (bbb) Faddeev eqns., mass calcs. of  $J^P=3/2$  systems 4-90832
- $dp \rightarrow \pi^+ \pi^-$  + missing mass, 3.3 GeV/c, structs. in nn and  $nn^+$  invariant mass spectra 4-59100
- $\Delta$ , free propagator in Rarita-Schwinger formalism 4-82898

**baryon resonances continued**

- $\Delta(1600) 1/2^-$ , rotational bands in the baryon spectrum 4-68544
- $\Delta \rightarrow N\gamma$ , radiative decay, effect of quark-quark tensor and spin-spin forces 4-64003
- $\Delta$ -isobar, spherical nature in Skyrme model 4-111296
- $\Delta^* \rightarrow \pi\Delta$  pion decay widths using OPE potential 4-90878
- $\gamma d \rightarrow pn$ , 0.4-0.8 GeV, cross-section asymmetry, dibaryon resonance 4-111464
- $\gamma\gamma \rightarrow p\bar{p}\pi^+\pi^-$ , 16.95 GeV, cross section and resonance prod. limit 4-95868
- $\gamma p \rightarrow \Delta^+ \pi^-$ , cross section threshold enhancement 4-106534
- N(1440)  $1/2^-$ , rotational bands in the baryon spectrum 4-68544
- N- $\Delta$  quadrupole transition amplitude in quark models, form factor 4-111405
- $N^*$  and  $\Delta^*$  negative parity states, masses in chiral bag model 4-68543
- $N \rightarrow \pi N$  pion decay widths using OPE potential 4-90878
- NN,  $J^P=1^-$  bound state production in  $p\bar{p} \rightarrow \pi^+ X^-$  4-106544
- NN scatt., description in OBE-NN dynamics 4-86723
- $\bar{p}A \rightarrow HX$ , doubly strange  $\bar{p}$  annihilation channels in complex nuclei 4-106614
- $\bar{p}p \rightarrow$  baryon-antibaryon, spin structure, polarisation amplitudes in SU(6) 4-90909
- $pp \rightarrow NN\pi$ , Deck model comparison, dibaryon resonance, total cross sections 4-111467
- $\pi d$  forward amplitude, dibaryon reson. contrib. 4-68739
- $\pi N \rightarrow \pi N$ , isobar model partial wave anal. 4-111470
- $\pi N \rightarrow \pi N$ , second  $F_{35}$   $\pi N$  resonance near 2000 MeV,  $\rho N$  decay mode 4-78563
- $R\Delta^{*+}$ , production of gluonic long-lived state 4-111481
- $\gamma p \rightarrow \pi N$ ,  $D_{13}(1520)$  resonance photoprod., bag model recoil correction 4-102125
- ${}^{16}\text{O}(\pi^+, \pi^-){}^{16}\text{Ne}(\text{g.s.})$ , double charge exchange,  $\Delta$ -hole formalism, non-analog states 4-106632

**baryon scattering** *see baryon-baryon scattering; lepton-hadron scattering; meson-baryon scattering; photon-hadron scattering***baryon spin and parity**

- see also hyperon spin and parity*
- antinucleon-nucleus inelastic scatt., spin dependence test of NN annihilation pot. 4-102127
- hyperon nonleptonic decay s-wave amplitudes, negative parity excited baryons 4-86704
- neutron properties, interactions, expt. data review 4-63997
- nucleon internal structure, spin-isospin excitation, sum rules 4-78594
- nucleon-nucleon scattering, total cross sections, spin effects, superhigh energies, quasipotential approach 4-95816
- (bbb) Faddeev eqns., mass calcs. of  $J^P=3/2$  systems 4-90832
- (ccc) Faddeev eqns., mass calcs. of  $J^P=3/2$  systems 4-90832
- $\Delta(1600) 1/2^-$ , rotational bands in the baryon spectrum 4-68544
- $\Delta$  Faddeev eqns., mass calcs. of  $J^P=3/2$  systems 4-90832
- N(1440)  $1/2^-$ , rotational bands in the baryon spectrum 4-68544

**baryons**

- see also baryon resonances; baryon spin and parity; hyperons; nucleons*
- asymmetry prod. in Universe by GUTs 4-77705
- charmed baryons mag. moments in MIT bag model, recoil corrections 4-111454
- cloudy bag model for baryonic and mesonic props. in nuclei 4-63977
- cosmology, baryon symm., nature depend. on CP violation type, obs. tests 4-78012
- dark matter in Universe, role in galaxy form. 4-67838
- early Universe, locally supersymmetric model, primordial inflation and supercosmology 4-67831
- galaxies, massive haloes, baryonic nature 4-67794
- magnetic moment, contribution of two-body interaction 4-82962
- magnetic moments, quark model anal. 4-86710
- nonrelativistic approach for describing props. in quark model 4-86657
- nontopological chiral soliton bag for hedgehog model 4-63954
- number violation in GUTs, suppression by supersymmetry 4-90780
- particle properties review, masses, decays and lifetimes 4-67885
- QCD in Veneziano limit, cfln theory, string model, baryon dynamics 4-59037
- relativistic heavy-ion collisions, baryon distribution 4-111396
- strong fine interactions and kinetic energy correction in baryons 4-63962
- SU(3) flux-tube quark model of hadrons 4-63951
- SU(3) Skyrme model, static props. of baryons 4-111338
- two-phase quark models, chiral Casimir effect 4-86661
- uncoupled fluids, gauge invariant cosmological fluctuations, early Universe axions 4-67819
- very early Universe, astrophysical scale, isotropy and baryonic and non-baryonic content 4-63355
- $n \rightarrow p e \bar{\nu}_e$ , lifetime, constraints imposed by  ${}^3\text{H}$  beta decay 4-90876

**barysphere** *see Earth core***BASIC**

- learning, course evaluation 4-101603
- GaAs-GaAlAs quantum wells, coupled, photoluminesc. and excitation spectroscopy 4-104667

**basicity** *see pH***batch processing (computers)**

- bearings-only tracking, recursive vs. batch processing algorithms 4-107942

**bathymetry**

- central Adriatic Sea, sediments near Tremiti Islands indicating uplift 4-82030
- NE Atlantic, seafloor topography of Orphan Knoll 4-62793
- Australia-New Zealand region, oceanic plateaus and basins 4-94053
- Australian Antarctic Territory, Davis-Mawson stations region, sedimentation anal. 4-82036
- E Black Sea coast, underwater canyon origin 4-105542
- coastal bathymetry, rel. to use of two-layer models of coastally trapped waves 4-82842
- conference on acoustics and the sea-bed, Bath, England (April 1983) 4-90303
- continental margin off Western Provence, France, morphology (anal. (French) 4-105540
- digital signal processing for precision wide-swath bathymetry 4-67432
- East Pacific Rise, submersible study of tectonics near 12°50'N 4-67207
- edge waves over a shelf, linearised shallow water eqns. soln. 4-82068
- English Channel, extent of hydrographic surveys 4-72569
- Farallon plate, Mesozoic aseismic ridges rel. to southward migration and shallow subduction during Laramide orogeny 4-94063

# bathymetry continued

- Galicia Bank, Northern wall, using 'sea beam' multichannel system (French) 4-115389
- Gorringe Ridge, North Atlantic Ocean, interpretation of geoid anomalies 4-67162
- Gulf of Aden, lithosphere flexure and isostatic compensation, bathymetry and gravity profiles anal. 4-105484
- E Indonesia collision zone, tectonic, bathymetric, seismic, volcanic and paleomagnetic features 4-82012
- Kingfisher charts of sea-bed, around British Isles, electronic chart display 4-72736
- Kuril-Kamchatka deep-sea trench, tectonics, magnetic anomalies, bathymetry and seismic struct. 4-82006
- laser system operating 50 m above bottom for seafloor imaging 4-82275
- Mediterranean, continental margin of Israel, bathymetry, crust struct., seafloor topography 4-72567
- Nakagusuku Bay of Okinawa-jima, sonic survey 4-82027
- North Sea, extent of hydrographic surveys 4-72569
- ocean bottom topography, numerical simulation of hydraulic jumps 4-62919
- ocean ridge-transform intersection, topography rel. to lithospheric stress field 4-94085
- ocean trench, effects on bathymetry of interaction with seamount 4-105526
- oceanic trenches, bathymetry of outer topographic rise rel. to stress and relaxation time of viscoelastic lithosphere 4-85654
- South Pacific geoid, and bottom topography, satellite altimetry 4-85606
- East Pacific Rise, structure and evolution of midocean ridge 4-115356
- Pratt-Welker seamount chain, Gulf of Alaska, flexure and subsidence, geoid obs. 4-105523
- Reykjanes Ridge, subsidence and basement topography of midocean ridge 4-81986
- ridge-transform-ridge plate boundaries, tectonic model rel. to struct. of oceanic lithosphere 4-94081
- Sea of Japan, submersibles use for bathymetry and sediment characts. determ. 4-100818
- seafloor topography, anal. of stability of oceanic lithosphere with variable viscosity 4-105492
- seamounts, sound scatter and shadowing, hybrid physical soln. 4-77526
- shallow sea areas, depth mapping using LANDSAT satellite data 4-110127
- side-looking phase sonar use 4-100817
- sonar bottom sounding processing, model 4-105769
- sonar method for seafloor irregularity, using amplitude modulated signal 4-115619
- sonar side-scan device for mapping sea-floor topography 4-72737
- submerged continental margin 4-100534
- surface effects of bathymetry, obs. with SEASAT-SAR 4-82292
- surface wave propagation over sinusoidally varying topography 4-103352
- Taylor columns over sea floor topography, temporal evolution 4-62843
- tidal current bedforms and sedimentary processes from SEASAT-SAR imagery anal. 4-82293
- TOPEX satellite project, end-to-end ground data system 4-77657
- trench depths and tectonic plate characts. in Pacific 4-82032
- undersea volcanoes 4-100521
- Vema fracture zone of mid-Atlantic ridge, faulting, seismicity and sediments 4-115377
- Yermak Plateau (Arctic Ocean), bathymetry rel. to form. at triple junction 4-85669

batteries see cells (electric); primary cells; secondary cells; solar cells

# Bauschinger effect

- elastic-plastic materials, isotropic, Bauschinger effect model for large computer codes 4-108504
- impact-tension compression test using split-Hopkinson bar 4-87639
- metal, plastic deform., book contrib. 4-109483
- metals, polycrystalline, finite elastic-plastic deformation 4-89093
- plastic flow theory, constitutive eqn. deform. anisotropy 4-92285
- shell, double-walled elastoplastic, with complex nonisothermal loading, stress/strain state 4-64865
- steel, dual-phase, work hardening at small plastic strains 4-114568
- steel, ferrite-martensite, dual phase, Bauschinger effect, coercivity meas. (Chinese) 4-93330
- steel, plastic properties, effect of nonlinear strain paths 4-99474
- steel, structural, fine-grained, low cycle fatigue, influence of cold forming 4-104841
- Al, single cryst., under plane-strain compression, Bauschinger effect 4-89085
- Al-Al<sub>3</sub>Ni eutectic composites, work hardening in stage II, 293-673K (Japanese) 4-89067
- Al-Cu-Mg, low cycle fatigue, influence of cold forming 4-104841
- Co-Cr-Mo, single-phase, low stacking fault energy, back stresses 4-76787
- Cu, Bauschinger effect, influence of surface removal 4-114616

Mayard-Alpert gauges see ionisation gauges

# Bayes methods

- seismic hazard modelling using Bayesian theory 4-85624

Bayes (magnetic) see geomagnetic variations

BGKY equation see integro differential equations

# BCS theory

see also many-body problems

- anisotropic superconductor with Kondo impurities, transition temp. 4-104352
- bipolarons and superconductivity 4-65620
- Cooper pairing, crit. temps. calc. 4-104359
- first-kind superconductors, paulion and boson picture 4-108969
- high temp. superconductors, theoretical model (German) 4-80716
- IBM, microscopic approach, angular momentum projection, large deformed nuclei 4-102198
- impurities with negative Hubbard energy; BCS theory 4-70981
- proximity effect between BCS superconductor and nonmetal metal with negative U centres 4-108975
- strong-coupling superconductors, non-BCS behaviour of gap edge near T<sub>c</sub> 4-70980
- superconducting film, optical irradiation, periodic excitation, relaxation processes and response time 4-61489
- superconductor, relaxational shift of EPR line (Russian) 4-92860
- superconductors, Cooper pairing in the presence of antiferromagnetism 4-88631
- superconductors, ground state wavefunction, BCS model 4-114064
- <sup>3</sup>He-B superfluids, vortex interactions, quasiclassical theory 4-98394

# beam choppers

- neutron chopper transmission function, monoenergetic beams, time-of-flight spectra 4-102456
- synchrotron radiation, UHV beam chopper design 4-95559

# beam-foil spectra

- alkali metal atoms, chemisorbed on W (110), NMR studies 4-98445
- electron capture, surface roughness effects on polarization 4-78942
- electron-stripping cross-sections for fast hydrogenic ions penetrating solids 4-78947
- grazing incidence monochromator, extended relative efficiency calibration, fast-beam spectroscopy appl. 4-87439
- L-shell populations of ions penetrating solids 4-78946
- polarisation by selective loss 4-78943
- solids, at. collisions, conf., Bad Iburg, Germany (July 1983) 4-73144
- three electron systems, (2p2p2p) <sup>4</sup>S<sup>o</sup> states, optical emission 4-87175
- three-electron systems, (2p2p2p) <sup>4</sup>S<sup>o</sup> states, optical emission 4-87175
- Al XI, doubly excited states, fine struct. meas. by beam-foil spectra (French) 4-69236
- Be II, (2p2p2p) <sup>4</sup>S<sup>o</sup> states, optical emission 4-87175
- C, beam-foil excitation spectra, investigation of mechanism (Chinese) 4-69192
- C foil, excitation by fast B<sup>+</sup> beam 4-107294
- C foil, heavy ion irradiated, charge distribution meas. 4-78945
- Cl, H-like, is Lamb shift determ. by X-ray transitions meas. using beam-foil excitation 4-74195
- Cl VII, Na-like, lifetimes, beam-foil excitation spectra 4-59677
- Cu I, lifetimes of some excited levels, beam foil spectra 4-87082
- Cu II, lifetimes of some excited levels, beam foil spectra 4-87082
- Fe<sup>2+</sup>, high precision X-ray spectra 4-78797
- Fe<sup>2+</sup>, He-, Li- and Be-like ions, radiative lifetimes and oscillator strengths 4-96494
- H atom, Stark quantum beats, use of density matrix neutral expansion beam foil excited 4-83327
- H<sup>+</sup>+C foil, 2p and 3p population, beam-foil excitation 4-64584
- H<sub>2</sub><sup>+</sup>+C foil, 2p and 3p population, beam-foil excitation 4-64584
- H<sub>2</sub><sup>+</sup>+C foil, 2p and 3p population, beam-foil excitation 4-64584
- He I, 3p <sup>1</sup>P and 4d <sup>3</sup>D levels alignment and orientation, foil tilt angle depend. 4-102780
- He I autoionisation rate determ. by optical emission spectroscopy 4-87087
- Li I, (2p2p2p) <sup>4</sup>S<sup>o</sup> states, optical emission 4-87175
- Li I, autoionisation rate determ. by optical emission spectroscopy 4-87087
- Li<sup>+</sup>, <sup>1</sup>P<sup>o</sup> levels, beam-foil spectral line identification 4-74188
- Li-like ions, (2p2p2p) <sup>4</sup>S<sup>o</sup> states, optical emission 4-87175
- Ne VII, 1s2s2p<sup>2</sup> <sup>1</sup>P<sub>12</sub>-1s2p<sup>2</sup> <sup>3</sup>S<sub>2</sub><sup>o</sup> VUV transition 4-107300

# beam-foil spectroscopy

- atomic spectroscopy, symposium, Berkeley, CA, USA (Sept. 1983) 4-67852
- grazing incidence monochromator, extended relative efficiency calibration, fast-beam spectroscopy appl. 4-87439

# beam handling equipment

see also particle beam diagnostics

- 2MV Van der Graaf dust accelerator, electrostatic prism for microparticle beam steering 4-64263
- acceleration column, laminar flow quadrupole-focused, design 4-107212
- ACHAT, a beam transport system with very high acceptance 4-83264
- beamline for light ion fusion demonstration reactor 4-102390
- charged particle beam focusing devices, quantum mech. anal. 4-59470
- conference, synchrotron radiation instrumentation, Upton, NY, USA (Sept. 1983) 4-95033
- distributed control system for photon factory 4-96312
- electron source based on a duoplasmatron 4-86503
- electrostatic switch used for 600 kV ion implanter 4-73594
- external PIXE milliprobe at Davis cyclotron, laser alignment, calibration and quality assurance 4-105076
- half-quadrupoles for SIN cyclotron beam lines 4-83263
- instrumentation at pulsed neutron sources 4-102422
- ion beam transmission by equipotential electrostatic lens (Czech) 4-83262
- light atom beams of neutralised neg. ions, fusion applications 4-107224
- linear induction accelerators for heavy ions 4-59459
- magnetic insulation time for coaxial diodes 4-73580
- mismatched intense charged particle beams in periodic focusing channels, envelope oscills, and instabilities 4-74079
- multiple electrostatic quadrupole array linear accelerator for negative ion beams 4-107179
- neutral beam injector system for MARS tandem mirror reactor 4-107221
- neutral beam lines, mech. installation for TFTR 4-111950
- neutral beam system, negative-ion based, design considerations 4-107220
- neutral beam systems, negative-ion-based, tokamak and mirror confinement device requirements 4-107219
- neutral beam test-bed cryopump appl. 4-95455
- neutron acceleration tube, flux and energy meas. 4-59467
- Oxford proton microprobe, wide area scanning system 4-101972
- Perfectron mol. beam scatt. apparatus (Japanese) 4-106425
- photodetachment neutraliser with laser resonator technology 4-107218
- pilot CW superconducting electron accelerator design, fabrication and test 4-102409
- polarised proton acceleration project at KEK 4-59475
- quadrupole lenses, three dims., made with permanent magnets 4-107251
- radio-frequency quadrupole accelerator at BNL 4-107187
- RIKEN heavy ion linear accelerator, variable freq., cavity mech. and thermal characts. (Japanese) 4-91122
- spin-flip switching system for neutron spectral modulation 4-74074
- splitting loaded resonant RF-cavity, postaccelerator sections for Van de Graaf generators 4-102415
- storage ring, 3 TeV, electrodynamic characteristics of accel. waveguide struct. 4-74070
- synchrotron beam line wiggler-undulator, modeling studies 4-95603
- synchrotron facility, beam line optical design at Hefei 4-96308
- synchrotron radiation, beam line monochromator for photoelectron spectroscopy 4-95604
- synchrotron radiation, toroidal grating monochromator, nonstigmatic optics 4-97052
- synchrotron radiation, X-ray beam lines, high flux, grain boundary diffusion of coolants 4-95626
- synchrotron radiation beam lines, high flux, thermal stresses 4-95611
- synchrotron radiation sources, SSRL Beam Line Winder 4-58928

**beam handling equipment continued**

- synchrotron radiation X-ray lithography, results 4-95590
- synchrotron X-ray beamlines for topography and spectroscopy 4-95618
- synchrotron X-ray lines, optical design wiggler beam 4-95609
- toroidal magnetic lens systems for intense ion beam focusing 4-112006
- two-stage electron energy analyzer for angle-resolved photoemission spectroscopy 4-101986
- variable emittance filter for electron laser facility 4-82859
- variable energy cyclotron at Calcutta, high power wideband RF system 4-59465
- X-ray imaging with UIS beamline 4-95598
- X-ray lithography, storage ring design 4-96303
- X-ray lithography and appls. of soft X-rays to technology, conf., Upton, NY, USA (Oct. 1983) 4-95023
- H<sup>-</sup> extraction and acceleration from mag. multipole source 4-107206
- H<sup>-</sup> injector for radio-frequency quadrupole accelerator 4-107188

**beam handling techniques**

see also mass spectroscopy; particle beam diagnostics; particle optics

- <sup>23</sup>Na beam prod., cold cathode PIG source for use with cyclotron 4-74072
- acceleration column, laminar flow quadrupole-focused, design 4-107212
- beam current integrator, single cup calorimeter 4-91129
- beam phase spaces with centro-symmetric config. in field region, transport theory (Chinese) 4-83259
- betatron injection scheme, simulation studies 4-111991
- charged particle beam focusing devices, quantum mech. anal. 4-59470
- charged particle beams envelopes, distortion and spherical aberration 4-74405
- charged particle slow extraction using nonlinear betatron oscill. resonance (Russian) 4-86993
- charged particles, RF bunching technique 4-73581
- conference, synchrotron radiation instrumentation, Upton, NY, USA (Sept. 1983) 4-95033
- crossed field injection into modified betatron, external transport scheme 4-68848
- cyclic beam bunchers and wave generators 4-112034
- direct-drive RF cavities for high power beams 4-112028
- EGP-10-1 tandem generator, heavy-ion accel., ion optical investigations 4-59456
- electron beams, picosecond current pulse formation method using micro-wave deflector 4-68857
- electron source of HV glow discharge, geometrical parameters control (Russian) 4-68320
- electron storage between cathode and anticathode in axial mag. field 4-107250
- electron-ion ring, transverse two-stream instability, kinetic treatment 4-74071
- EM pulses emission and shaping in systems with cylindrical symmetry 4-107249
- fast atom beam development for SIMS analysis of polymers and insulators 4-93576
- glow discharge laser amplifier, rel. to effect of quantum modulation of electron beams by lasers 4-96864
- heavy ion beams from GSI-UNILAC using acceleration-stripping deceleration method 4-87207
- Heidelberg proton microprobe, secondary electron imaging 4-101973
- imploding linear driven ring accelerators, stability 4-111980
- instrumentation at pulsed neutron sources 4-102422
- intense pulsed ion beams for fusion reactors, generation and transportation (Japanese) 4-74078
- ion beam transmission by equipotential electrostatic lens (Czech) 4-83262
- ion linac, effect of drift spaces on longitudinal motion 4-91128
- light atom beams of neutralised neg. ions, fusion applications 4-107224
- low-energy positive ions, microchannel plate gain characts. in reflection mode 4-78423
- negative ion beam acceleration by multiple electrostatic quadrupole array linear accelerator 4-107179
- negative ion neutralisation by plasma targets 4-107217
- neutral beam line ion beam raster scanning with a dipole magnet 4-86991
- neutral beam line of neg. ions stripped in photoneutraliser 4-107216
- neutral beams, high energy, stopping cross section increase with multistep collision processes 4-107222
- neutron spectrometer, inelastic scatt., quantum-mechanical effects on beam chopping 4-91134
- nuclear polarised ion beams production by grazing incidence surface interactions 4-81067
- PEP and PETRA, single beam stability, computer simulation 4-68843
- photodetachment neutraliser with laser resonator technology 4-107218
- PIXE anal. laboratory based on 4 MV Van der Graff accelerator 4-95566
- PIXE analysis, appl. of microprobes 4-105074
- polarised H target spin refrigerator as neutron polariser 4-68855
- power capacitive coupling of accelerating resonators with HF oscillator 4-107253
- production and neutralisation of negative ions and beams, conf. Brookhaven, NY, USA (Nov. 1983) 4-73134
- proton beam intensity meas. and slow beam extraction efficiency 4-59471
- pulsed superthermal beam source for metastable atomic and molecular species 4-86504
- quantum mech. effects on beam chopping 4-68013
- roughened neutron mirror as wavelength filter, spill-over suppression 4-64254
- slow wave cyclotron amplifier, nonlinear efficiency and bandwidth 4-96313
- space-time focused light plasma beams for ICF fusion 4-107147
- strip and axisymmetrical ion beams, mutual transformation (Chinese) 4-74081
- synchrotron facility, beam line optical design at Hefei 4-96308
- synchrotron radiation, polarisation characteristics of two undulator system 4-96309
- synchrotron radiation, transverse undulator spectra, polarisation profiles 4-96310
- synchrotron radiation, undulator trajectories, variational derivation 4-96311
- transfer lines and circular machines, theory and hardware 4-74083
- truncated spherical mirror for energy anal. combined with direct meas. of ang. distrib. 4-64259
- VEC, variable energy cyclotron, central region parameters study 4-59464

**beam handling techniques continued**

- X-ray exposure area enlargement possibility with X-ray mirror or by electron beam vertical motion 4-95593
- A beam at KEK, design and operation 4-64261
- Be single crystals, for neutron monochromators, prep. and props. 4-83533
- CaBr beam, elec. quadrupole refocusing, hyperfine levels and low-J lines 4-102824
- D<sup>-</sup> ribbon beams, focusing by transverse electric fields 4-107211
- H atomic beam, spin polarised, focusing and optics 4-107228
- H<sup>-</sup> extraction and acceleration from mag. multipole source 4-107206
- H<sup>+</sup> injector/buncher with grounded ion source 4-107252
- Si curved single crystal, 1 GeV proton beam focusing in channelling regime 4-91131

**beam splitters (optical) see optical elements****beam-trapping see self-trapping****bearings (machine) see machine bearings****BEBO method see bonds (chemical)****behavioural sciences computing see social and behavioural sciences computing****bells**

see also musical instruments

- elliptical cone bells, sound radiation, directional characteristics (Chinese) 4-83785

**Belousov-Zhabotinski reaction see chemical equilibrium; chemical reactions and reaction kinetics theory****bending**

see also bending strength; buckling; stress analysis; torsion

- anisotropic materials, generalisation of Mindlin's kinematic plate theory 4-91741
- bar, linear, elastic, isotropic, nonlinear bending, two fundamental cases 4-74895
- beam, infinitely long, contained in frictionless channel, flexural rigidity to axial compressive forces 4-74884
- beam, thermally restrained, nonlinear anal. 4-112732
- beam cross sections, optimal nonequal-strength shapes 4-112704
- beam theory, shear deformation, strain and stresses 4-112723
- beams, long, thin, open section, and corrugated panels, nonlinear bending and collapse 4-103221
- boundary function approximation, Lagrangian, spline and weighted finite difference methods 4-64848
- brittle materials, fatigue testing, high-temp. device 4-66527
- concrete beam, three point bending, cracking, dye penetrant obs., compliance calibration technique 4-89205
- cone-shaped bodies, plastic axisymm. flow 4-60300
- conical shells, stability under large deformation (German) 4-83840
- contact lenses, soft, toric, double-thin zone, flexure effects 4-109992
- Crack border-free surface intersection analysis 4-79515
- crack tip concordant displacement, finite element method employing singular element 4-69711
- curvilinear shallow elements of structures, optimal design problem 4-91729
- cyclic bending device in SEM (German, English) 4-71822
- cylindrical shell stresses due to penetration loads 4-91726
- elastic beam, dynamic flexural fracture, crack propag. path 4-97401
- fibres reinforced composite laminates, fracture toughness meas. using three-point bend and compact-tension specimen 4-99735
- fibres reinforced composites, laminated symmetric beams, damping and dynamic moduli 4-80154
- flat circular optical element support on 9-point Hindle mount in 1-g force, design anal. 4-87420
- fracture toughness, stress intensity factor formula of four point bending 4-62143
- frames with Timoshenko members, second order analysis 4-112712
- glass fibre reinforced plastic panel, three-layer, with cellular filler, deformation under static and shock loads 4-64880
- grids, triple-layer, stress and deform. 4-64861
- half-space, surface deflection due to crack presence 4-69703
- hardmetal, creation of stable cracks using bridge indentation 4-66434
- laminated cylindrical shells, contact rigidity 4-87635
- membranes, linear elastic circular, small deflections under lateral pressure 4-97319
- membranes, plane, subjected to lateral pressure, viscoelastic correspondence principle 4-97340
- membranes, plane, under lateral press., variation principles and bounds for approx. analysis 4-97320
- metals, fatigue test method for cyclic and pulsating torsional loads 4-66525
- moment measurement using invariant half-bridge ccts. 4-97446
- multiaperture speckle shearing arrangements for stress analysis 4-58888
- nonlinear bending of corrugated annular plates 4-110878
- nonlinear loading calcs., horizontal structure under bending (German) 4-83836
- orthotropic flat sandwich plates, thick faces theory 4-69692
- panels, corrugated and long thin open section beams, nonlinear bending and collapse 4-103221
- piezoceramic shell, reaction to concentrated effects 4-109129
- plane elastic arch, homogenisation 4-83814
- plane strain dynamic crack bifurcation 4-83857
- plate, freely supported, bending in presence of cracks 4-108026
- plate, homogeneous, cylindrical bending, asymptotic method 4-79458
- plate, orthotropic, bending stress intensity factors for Griffith crack (Chinese) 4-97397
- plate, orthotropic circular thin, nonlinear axisymmetric transient anal. 4-103208
- plate, rectangular, simply-supported, thermal deflection 4-112714
- plate, rhombic, finite element analyses, h- and p-versions 4-112701
- plate, round, mean flexure, appl. of method of successive approximation (Russian) 4-112736
- plate, thick circular, three dimens. elastic stress anal. 4-97309
- plate, thick circular in contact with isotropic elastic half-space, exam. using variational method 4-112775
- plate, transversely isotropic, circular, thick, initially stressed, vibrations 4-83849
- plate bending, comparative analysis of boundary methods and finite element methods 4-112727
- plate of finite width under bending, internal and edge cracks 4-74958
- plate problems using C<sup>0</sup> triangular plate element with one-point quadrature 4-78140

ending continued  
plate reinforced by symm. system of radial ribs, nonsymm. bending 4-108008  
plates, cantilevered, with bending-torsion coupling, freq. determ. techniques 4-79481  
plates, elastic, laminated, isotropic and anisotropic, mixed variational theorem and appls. 4-90374  
plates, elastic nonlinear theory, appl. to paper property characterisation 4-103201  
plates, elastoplastic, large deflection, incremental model (*French*) 4-74890  
plates, inelastic, fibre-reinforced, laminated, constitutive relations 4-103200  
plates, isotropic and composite, anticlastic curvature suppression 4-83832  
plates, laminated, anal. using mixed shear flexible finite element 4-103193  
plates, laminated, with free edge in edgewise bending and compression, buckling 4-79474  
plates, laminated composite, mixed finite element anal. 4-74904  
plates, normally stressed, orthotropic, right angle, bending, boundary disturbance ebbing (*German*) 4-83844  
plates, thin, isotropic, quadrilateral, subject to bending stresses, efficient anal. 4-64837  
plates, transversal-isotropic circular, elastic-plastic bending (*Russian*) 4-112735  
poked cylinder, nonlinear bending and collapse anal. 4-74881  
prismatic beams, finite deform., variational anal., warping stiffness - effects on buckling loads 4-79479  
propagation, double cantilever beam technique 4-103256  
rocks, fracture toughness under bending rel. to fatigue crack length (*Japanese*) 4-100557  
rod, rotating, max. deflection estimates 4-103217  
rod elements, damping capacity determ. in biharmonic oscillations 4-97447  
rod with eccentrically fixed mass, connected bending-torsional oscils. 4-108041  
rods, nonuniformly-heated, under creep conditions, combined extension and flexion (*Russian*) 4-79465  
sheet of constant-thickness, strain during reverse bending and folding (*Russian*) 4-64853  
shell, circular cylindrical, fluid filled beam-type, fluid filled, bending vs. membrane theory 4-87580  
shell, conoidal, shallow bending anal. (*Polish*) 4-60307  
shell, cylindrical, made of rings, equilib. problem (*Russian*) 4-91732  
shell, double-walled elastoplastic, with complex nonisothermal loading, stress/strain state 4-64865  
shell, explicit cubic representation, inextensional bending 4-112728  
shell, fluid-filled spherical, compression by rigid indenters 4-97441  
shell elements, bilinear, quadrilateral, bending, exact inextensional solns. 4-112730  
shells, deformable, in presence of EM effects, nonlinear theory 4-74864  
shells, plastic cylindrical, subjected to impulsive loading, additional support optimal location 4-97331  
single edge notched bend specimens, deflection meas. test setup 4-76929  
single mode fibre effective cutoff wavelength, bending effects 4-97103  
slab optical waveguide bending, radiation losses anal. (*Chinese*) 4-97059  
smooth pipe bends, flexibility factors, maximum stresses 4-76824  
solid, infinite, three dimens. crack, stress conditions 4-87627  
steel, austenitic stainless, edge-cracked beam, ductile fracture under EM bending force 4-91763  
steel, austenitic stainless, stress relax. in bending at 773K 4-81229  
steel, austenitic stainless, WWER steam generator tubes, hardening and intergranular corrosion cracking (*Czech*) 4-85257  
steel, butt-welded joint, welding stress and distortion (*Japanese*) 4-99424  
steel, Cr, fatigue crack growth under rot., three-point bend loading, tempering temp. influence (*Chinese*) 4-114631  
steel, IR emission of overloaded metals during fatigue process (*Chinese*) 4-114636  
steel, mild, plate with small circular hole, fatigue crack propag., fracture mechanisms (*Japanese*) 4-62025  
steel sheet, plastic bending instability 4-99461  
strain hardening materials, failure assessment diagram under cyclic and monotonic loading 4-93367  
stress intensity factors for slender surface cracks 4-60332  
strut, hinged, with initial curvature 4-91721  
thin plate flexure, Kirchhoff boundary-element theory 4-64847  
thin-walled cylinders, min. wt., of given torsional and flexural rigidity 4-97326  
three-point bend specimen, effect of inclusion or hole on approaching crack 4-91767  
three-point bending fracture toughness specimens, side groove effects, finite element anal. 4-113519  
Timoshenko beam, coupled thermoelastic vibr. and damping (*Japanese*) 4-74944  
transversely isotropic medium, stress conc. near a hyperboloid, notch in pure shear and bending 4-103210  
V-die bending, large elastic deflection of thin strips and onset of plasticity 4-79464  
Al<sub>2</sub>O<sub>3</sub>, bend specimens, crack resistance curves, influence of grain size 4-62058  
B fibres, elastic energy absorpt. mechanism 4-66366  
Fe, pure, annealed, fatigue crack nucleation sites under reversed bending stress (*Japanese*) 4-99516  
H induced delayed cracking in weldments (*Chinese*) 4-99478  
Na<sub>2</sub>O-CaO-SiO<sub>2</sub> glass, stress corrosion characts., bending test 4-109535  
Na<sub>1+x</sub>Zr<sub>2</sub>P<sub>3-2x</sub>-Si<sub>2</sub>O<sub>12</sub> ceramics, prep., ionic cond., durability and strength 4-113711  
Si<sub>3</sub>N<sub>4</sub>-MgO, hot pressed, fracture stress, temp. and strain rate depend. 4-85207  
WC-C, mechanical behaviour, room temp. to 1000°C 4-62002

bending of light see gravitation; light

## bending strength

ceramic-polymer composite biomaterials, fracture 4-76844  
ceramics, failure probability, Weibull modulus estimation 4-104928  
ceramics, flexure strength, Weibull fracture statistics 4-104954  
composite materials elastic moduli determ. using flexural tests 4-112784  
concrete beam, rectangular reinforced, behaviour and ultimate strength under combined torsion, bending and shear 4-62046  
epoxide composite, alumina particle filled, fractography (*Japanese*) 4-99512

## bending strength continued

ethylene-propylene elastomers, long-time dynamic compatibility with liq. N<sub>2</sub>H 4-114609  
fibre reinforced composite laminates, material design with required flexural stiffness 4-99391  
fibre reinforced plastics, stable crack growth, influence of fibre orientation 4-99570  
glass, soda-lime silicate, Vickers indented, delayed fracture in deionised water 4-81268  
glass, toughened, thin thermally polished, strength asymmetry 4-89103  
glass, type K108, bending strength 4-74637  
glass fibre, bending strength, static fatigue rel. to atmosphere 4-99490  
glass fibre reinforced epoxy, stable crack growth, influence of fibre orientation 4-99570  
glass fibre reinforced epoxy resins, amine cured, flexural props. and char yields 4-99425  
glass fibre reinforced epoxy resins, curing conditions effect on mech. props. 4-99487  
glass fibre reinforced polyester, creep behaviour of reinforced and non-reinforced resins 4-99456  
glass fibre reinforced polyester, laminated hybrid, crack growth resist., flexural strength 4-62012  
glass fibre reinforced polyurethane foam, flexural strength and modulus, thermal and photodegradation (*Japanese*) 4-99623  
graphite, neutron irradi., relationship between strength characts. 4-66443  
graphite, nuclear-grade, mech. and phys. props., influence of prehydrostatic loading 4-102353  
graphite fibre reinforced epoxy composites, buckling, hygrothermal and conditioning influence analysis 4-104810  
hybrid composite, unidirectional fibre, amplitude distrib. AE signatures 4-89198  
hybrid fibre reinforced epoxide composite, environmental response of flexural props. 4-76809  
Kevlar 29 braid, bending fatigue life rel. to resin impregnation 4-93394  
Kevlar fibre rope endurance obs. and selection guidelines 4-114676  
mullite-zirconia composites, microstruct. and mech. props. 4-114672  
nylon fibre rope endurance obs. and selection guidelines 4-114676  
orthotic knee joints, method for mech. characts. determ. 4-72463  
PMMA, dynamic fracture toughness, determ. by impact bending test (*Japanese*) 4-93488  
polyester fibre rope endurance obs. and selection guidelines 4-114676  
polyethylene fibres, strength and elasticity, electron microscopy (*Russian*) 4-85180  
polyethylene fibrillated tape reinforced cement, mech. props. 4-109493  
polypropylene fibre reinforced mortar, thin slabs, fracture toughness under flexural or impact loading 4-99576  
porcelain, high-alumina, for HV insulators, strength under dynamic and cyclic loads (*German, English*) 4-76836  
rig for testing specimens under static bending load in aggressive media at high temps. and press. 4-104941  
rock beams, combined bending and axial loading, distrib. damage approach 4-105553  
shortened test method for creep eval. during static bending fatigue tests (*German*) 4-71821  
silicon metalcutting tools, props. and appl. 4-66283  
silicons, hot-pressed and reaction-bonded, phase equilib. and props. 4-76761  
solar mirror glass, crack growth, strength, lifetime prediction 4-89194  
steel, austenitic stainless, Path A-type alloys, neutron irradi., mech. props. 4-98139  
steel, C, yield stress rel. to C content and pearlite morphology, tensile and Charpy obs. 4-81248  
steel, fracture toughness meas. using specimen strength ratio 4-81371  
steel, low C, notched fatigue strength rel. to pre-straining and nitriding 4-109489  
steel, mechanical props. rel. to US detectable discontinuities 4-71713  
steel, rotor forgings, unstable fracture, effect of small clustered flaws (*Japanese*) 4-93378  
steel, stainless, austenitic, plastic deform. symmetrical cyclic bending of different length specimens 4-99442  
steel fibre reinforced mortar, thin slabs, fracture toughness under flexural or impact loading 4-99576  
testing, defect position rel. to strength variance 4-99661  
AlN, oxynitride bonded ceramics, sintering, microstruct., densification, flexural strength, oxide additions effect 4-76727  
AlN powder, hot pressing kinetics, oxidation, mech. props. 4-76731  
Al<sub>2</sub>O<sub>3</sub>, crack kinetics of bend specimens 4-62061  
Al<sub>2</sub>O<sub>3</sub>, sintered, fracture strength, effect of surface condition 4-62057  
Al<sub>2</sub>O<sub>3</sub>:MgO:CaO, translucent, fracture, influence of temp. and CaO 4-92290  
Al<sub>2</sub>O<sub>3</sub>-AlN spinel, fabrication, thermomech. props. 4-89097  
Al<sub>2</sub>O<sub>3</sub>-AlON composite ceramic, hot pressing reaction sintering, mech. props., high temp. appls. 4-62062  
Al<sub>2</sub>O<sub>3</sub>-BN(-AlON) composite ceramics, mech. props. (*French*) 4-81177  
Al<sub>2</sub>O<sub>3</sub>-PMMA (PBMA), composite biomaterials, fracture 4-76844  
BaTiO<sub>3</sub>, PTC ceramic, strength and fracture toughness 4-62051  
C fibre reinforced plastics, unidirectional ultimate strength, influence of matrix resin 4-99455  
C fibre/glass fibre reinforced polyester, hybrid composites, flexural and fracture props. (*Japanese*) 4-99429  
Cu-Sn-Al<sub>2</sub>O<sub>3</sub>, abrasive composite, physicomech. props., effect of premoulding press. in elec. discharge sintering 4-89020  
(Fe,Ni)V, ordered alloy, irradi. in HFIR, microstruct. and bend ductility 4-108454  
Fe, nodular, cast, fatigue crack growth obs. using bonded-resistance gauges 4-93477  
MgO, resin-bonded, C-bearing magnesia, mech. props. 4-114673  
MgO-graphite, C-bearing magnesia, mech. props. 4-114673  
Mo, purification by arc melting, mech. props. (*Japanese*) 4-89116  
Mo single crystals, low temp. bend props., surface effect 4-99561  
Si<sub>6-7</sub>Al<sub>2</sub>O<sub>3</sub>N<sub>4-5</sub>, β-sialon, hot pressed, flexural strength, phase struct., comp. depend. (*Japanese*) 4-76828  
SiC, prod. methods and parameters, report (*German*) 4-61908  
α-SiC, sinterability, strength and oxidation 4-61899  
α-SiC, sintered, phenomenology of fracture 4-93372  
SiC-Al, sintered composite interfacial reactions, joint bending strength rel. to microstruct. 4-66295  
SiC-based ceramics, time-temp. effects 4-76963  
Si<sub>3</sub>N<sub>4</sub>, hot isostatic pressing, densification, bending strength rel. to additives (*Japanese*) 4-76721  
Si<sub>3</sub>N<sub>4</sub>, hot-pressed, strength rel. to high temp. oxidation 4-114697

**bending strength continued**

- $\text{Si}_3\text{N}_4$ , hot-pressed, transient creep parameters, determ. by dynamic bending tests 4-81381  
 $\text{Si}_3\text{N}_4$ , pressureless sintered, high temp. fatigue failure 4-76867  
 $\text{Si}_3\text{N}_4$ , reaction bonded, flexural strength, oxidation resist, annealing effect 4-76832  
 $\text{Si}_3\text{N}_4$ , reaction bonded, flexure strength, oxidation, microstruct. 4-76892  
 $\text{Si}_3\text{N}_4$ , reaction-bonded, flaw populations, effect of oxidation 4-62059  
 $\text{Si}_3\text{N}_4$ -based ceramics, time-temp. effects 4-76963  
 $\text{Si}_3\text{N}_4$ -based metalcutting tools, props. and appl. 4-66283  
 $\text{Si}_3\text{N}_4\text{-Y}_2\text{O}_3$ , isostatically hot pressed, strength and microstruct. rel. to sintering additives 4-85132  
 SiYON ceramics, mech. props. rel. to corrosion and microstruct. 4-76834  
 TiB<sub>2</sub> powder, pressureless sintered, mech. props. in liq. Al environment, impurity segregation 4-114700  
 TiB<sub>2</sub>, sintering and props. of samples made from powder synthesised in plasma-arc heater 4-76715  
 W, powder metallurgy rods, swaging process workability rel. to texture (Japanese) 4-89068  
 WC-Co cemented carbide, defect position in bending test rel. to strength variance 4-99661  
 Zn-Cu-Ti alloys, bendability, struct. aspects (French) 4-81252  
 ZrC-Co-base eutectic, mech. props. rel. to microstruct. 4-89135  
 ZrO<sub>2</sub>, MgO partially stabilised, Weibull modulus 4-61972

**berkelium**

see also nuclei with .....  
 No entries

**berkelium compounds**

No entries

**beryllium**

see also nuclei with .....

- $\beta$ -decay electrons and positrons energy distrib. parameters (Russian) 4-75592  
 acoustic emission due to deform. (Russian) 4-92304  
 adherent film production by electron beam evaporation 4-66238  
 adsorption on W, work function changes 4-61202  
 atom, angle dependent energy loss of 7-MeV protons, stopping powers meas., geometrical effect 4-96658  
 atom, doubly excited states, electron correls. 4-87052  
 atomic correlation energies with explicitly correlated Gaussian geminals 4-91204  
 atomic dynamic polarisability, Cauchy moments, coupled HF calc. 4-74147  
 atoms, relativistic SCF calc. with squared Dirac operator 4-78790  
 binding energy, core levels, state-specific many-electron theory 4-75887  
 coating for biological X-ray microanalysis 4-77431  
 cosmic radiation fossil record by <sup>10</sup>Be accelerator mass spectrometry 4-90047  
 crystal structure from first principles calcs. 4-70064  
 deformation of single crystals under compression parallel to basal plane 4-98187  
 diffusion in ion implanted GaAs during damage recovery 4-104002  
 electron density distrib., diff. study 4-84232  
 electron transport in sub-MeV region, Monte Carlo anal. (Chinese) 4-80560  
 fibre reinforced Al alloy, stress-strain and failure behaviour 4-76831  
 foil, stopping power of 7 MeV protons, geometrical effects 4-92264  
 fusion reactor use, advantages and limitations 4-107017  
 fusion reactor use, health risk implications 4-107015  
 high pressure phase transition, elec. resist. study 4-75663  
 ion implantation of (In,Ga)As/InP n-p-n heterojunction bipolar transistors grown by LPE with high gain 4-85097  
 ion-induced secondary electron emission projectile incident angle depend. 4-76596  
 ions, extreme UV absorption spectroscopy using two laser-produced plasmas 4-60728  
 isoelectronic sequence, optical pumped quasi-CW UV plasma lasers 4-102922  
 isoelectronic series, oscill. strengths and at. wavefunctions accuracy 4-87084  
 isoelectronic series, transition energy calc. using multiconfig. Dirac Fock and RPA calcs. 4-64364  
 limiters, heavy impurity contamination reductions in tokamak plasma 4-86969  
 many-electron systems, ground state energy and X-ray scatt. cross sections 4-114344  
 measurements in deep-sea sediments 4-110128  
 microplasticity, grain size and heat treatment effects (Russian) 4-104809  
 mirrors, advanced lightweight type 4-74649  
 molecules, electronic struct., bonding, lifetimes, laser induced fluoresc. 4-112220  
 monolayer, ground state energy and work function, local density functional anal. 4-92524  
 muon Knight shift, spin rot. meas. 4-65916  
 neutron irradiated at various temps., compression props. and swelling 4-108458  
 neutron wave propag., space and angle depend. study 4-73947  
 normalised core-valence band Auger spectra 4-61783  
 phase transitions, temp. and press. induced phase transitions 4-70369  
 polarised X-ray emission spectra and partial densities of states calc. 4-66132  
 single crystals, for neutron monochromators, prep. and props. 4-83533  
 soil <sup>10</sup>Be concentrations and possible <sup>10</sup>Be radioactive dating method 4-81880  
 sputtering, atomic excitation, projectile incidence angle depend. 4-76593  
 strength effect on determ. of high press 4-65344  
 surface tile material for fusion reactor DCT-8 pumped limiter design 4-96259  
 unoccupied band distortion due to electron-plasmon interaction 4-80486  
 X-ray refractive index meas. 4-104558  
 Al<sub>2</sub>Ga<sub>1-x</sub>As:Be, radiative recombinations 4-76515  
 Be<sub>2</sub>, <sup>12</sup>g ground state, pot. energy curve calcs. 4-68977  
 Be I, oscillator strengths, transition wavelengths, HF relativistic calcs. 4-106127  
 Be II, (2p<sup>2</sup>2p) <sup>4</sup>S<sup>o</sup> states, optical emission 4-87175  
 Be II autoions. widths, optical emission spectrosc. investig. 4-69025  
 Be II recombining plasma, lasing transitions 4-96878  
 Be ions, He- and Li-like, laser produced plasma, EUV spectra 4-83320  
 Be on Al target, laser irradi., lateral and axial transport charact. 4-79819  
 Be<sup>+</sup>, doublet states, transition wavelengths and fine struct. 4-74171
- beryllium continued**  
 Be<sup>+</sup> doubly excited states, autoionisation widths calcs. 4-64403  
 Be<sup>+</sup>, elec. and mag. field confined, strongly coupled, temp. and density, laser probe meas. 4-97757  
 Be<sup>+</sup>, quartet-states, transition wavelength and fine struct., relativistic corrections 4-64397  
 Be<sup>2+</sup>, photoionisation and double excitation spectrum 4-87089  
 Be<sup>3+</sup>, H-like, elastic positron scatt., polarised orbital method 4-102798  
 Be-D, retention and thermal release of implanted D 4-113477  
 Be-like atoms, two-electron correls. calcs. 4-64392  
 Be-like ions, fine struct. transitions between 2l<sub>2</sub>l<sub>2</sub> and 2l<sub>1</sub>3l<sub>1</sub> configurations, collision and line strengths 4-95072  
 Be-like ions in solar transition region diagnostics, electron vel. distrib. effects 4-101288  
 Be+C(N)(O)Ne ions, single and double K-shell ionization cross-sections meas. 4-60583  
 Be+H<sub>2</sub>, pot. surface walking and reaction paths 4-114790  
 Be+H<sub>2</sub>-BeH<sub>2</sub>, multireference CI gradients and MCSCF second derivatives 4-93522  
 Be+HF(v,J)-BeF(v',J')+H reaction, classical trajectory study in three dimensions 4-99763  
 Be<sup>4+</sup>+H, charge transfer cross sections calc. using close coupling calc. 4-78959  
 Be<sup>4+</sup>+H, electron capture cross-sections calcs. 4-102791  
 Be<sup>4+</sup>+H collisions, electron transfer, at. orbital expansion description 4-78962  
 Be<sub>18</sub> clusters, energy optimised configs., ab initio STO-3G SCF calc. 4-69261  
 Be<sub>20</sub>, clusters, energy optimised configs., ab initio STO-3G SCF calc. 4-69261  
 BeO, surface tile material for fusion reactor DCT-8 pumped limiter design 4-96259  
<sup>7</sup>Be concentration and deposition in lower atmosphere over Kaohsiung City, Taiwan 4-62418  
<sup>9</sup>Be<sup>+</sup> ions laser cooled, appl. in freq. standard 4-68204  
<sup>10</sup>Be detection and conc. meas. using tandem accelerator at 3 MeV 4-64632  
<sup>10</sup>Be detection using 2 MV tandem accelerator mass spectrometry 4-109702  
 p-Ga<sub>1-x</sub>Al<sub>x</sub>As:Be-p-GaAs:Si heterojunction LPE growth for solar cells 4-109334  
 GaAs:Be, ion implanted, reduced damage generation 4-113474  
 GaAs:Be, ion implanted, annealing behaviour, spectroscopic ellipsometry and Raman scatt. 4-113482  
 GaAs/GaAlAs DH stripe geometry lasers, Be-implanted, MOCVD grown 4-107635  
 GaAsP<sub>1-x</sub>GaP strained-layer superlattices, Be-implantation doping 4-80057  
 Ge:Be, site distortion of Be acceptor, IR spectra 4-92667  
 Ge:Be IR detectors for low-photon-background IR astronomy 4-101160  
 Ge:Be photoconductor, 30 to 50  $\mu\text{m}$  detector performance and material aspects 4-108899  
 InP:Be, semi-insulating, simulation of anomalous Be diffusion 4-88193  
 InP:Be(C<sub>2</sub>) acceptor levels, photoluminesc. study 4-80543  
 InSb:Be p<sup>+</sup>-n junction, ion implanted, insulated gate effects 4-61445  
 SiC:Al, Be, interstitial diffusion studies 4-80302
- beryllium alloys**  
 see also beryllium compounds  
 Magnox alloys, etched, surface anal. by secondary ion mass spectrometry and ion scatt. spectroscopy 4-93456  
 MoBe<sub>2</sub>, cryst. struct., X-ray diff. 4-84236  
 transition metal alloys, MBe (M=Fe, Co, Ni, Cu), coupled phase diagrams and thermochem. descriptions 4-104763  
 Be-HfO, Hf<sup>+</sup> implanted, O gettering 4-92218  
 Cu-Be, dil., chem. redistrib. under simulation irradi. 4-108478  
 Cu-Be, fusion materials, candidate materials for impurity control 4-91108  
 Cu-Be, struct. transform. mechanisms during ageing, internal friction and resist. obs. 4-114536  
 Cu-Be, work hardened thin sheets, determ. of plastic charact. 4-104938  
 Cu-Be (1.0 wt %), aged, twinned microstruct. 4-89070  
 Cu-Be (1.1, 1.5 wt %),  $\gamma$ -phase boundary 4-76754  
 Cu-Be (1.35 at %), undersaturated, irradiated, formation of precipitates 4-104791  
 Cu-Be alloys, Guinier-Preston zones and solute clusters, high resolution lattice images 4-114543  
 Cu-Be alloys, precipitation, elec. resist. and thermopower 4-114549  
 Cu-Be diffusion coating on Cu formed by surface berylliding 4-62127  
 Cu-Be/Fe systems, wear study 4-76875  
 Cu-Be-Co (2, 0.2 wt %), precip. hardening investigation by microhardness and elec. resist. meas. 4-61947  
 CuBe<sub>2</sub>, age hardened, discontinuous flow studies, low temp. 4-113520  
 Fe-Be system, B32 metastable precip., identification by APFIM and TEM 4-61922  
 Pd-Ni-Si-Be-B liquid metal ion source for maskless ion implantation 4-58913  
 Pd<sub>2</sub>Be<sub>28</sub>, metallic glass, stale structure, X-ray methods study 4-113344  
 Re<sub>95</sub>Be<sub>5</sub>, cryst. struct., X-ray diff. 4-84235  
 TiBe<sub>2</sub>-Cu, onset of ferromagnetism, neutron small angle scatt. study 4-84797  
 UBe<sub>3</sub>, electronic struct., XPS study 4-70642  
 UBe<sub>3</sub>, heavy-fermion supercond., valence band reson. photoelectron spectroscopy 4-104720  
 UBe<sub>3</sub>, p-wave supercond., sp. ht., spin fluctuation parameter 4-76073  
 UBe<sub>2.94</sub>Cu<sub>0.06</sub>, heavy fermion supercond., sp. ht. meas. 4-104363
- beryllium compounds**  
 see also beryllium alloys  
 beryl, hexagonality to cubicity transition 4-60891  
 beryllium hydride polymer, LCAO band struct. calcs. 4-70628  
 BeAl<sub>2</sub>O<sub>4</sub>, chrysoberyl, Czochralski grown, dislocation form. and distribution laws, X-ray diff. topography method 4-113453  
 BeAl<sub>2</sub>O<sub>4</sub>:Cr<sup>3+</sup>, alexandrite, resonant 40 cm<sup>-1</sup> phonons, lifetime and linewidth 4-65356  
 BeAl<sub>2</sub>O<sub>4</sub>:Cr<sup>3+</sup>, alexandrite, fluorescence of inversion site Cr<sup>3+</sup>, ion 4-107647  
 BeAl<sub>2</sub>O<sub>4</sub>:Cr<sup>3+</sup> laser technology for chem. apps. 4-107669  
 Be<sub>3</sub>Al<sub>2</sub>(SiO<sub>3</sub>)<sub>2</sub>:Cr<sup>3+</sup> (emerald) laser, CW Kr laser pumped, 728.8 to 809 nm tuning range 4-60041  
 BeB<sub>2</sub>H<sub>2</sub>, microcomputer-aided instruction and research in group theory 4-102584

**yttrium compounds continued**

- BeF, dissoc. energy; HF STO calcs. 4-112092  
 BeF, vibr. excitation of triplet core-ionised states 4-74175  
 Be $^{2+}$ , geometric struct., force field and vibr. spectrum, MO-LCAO-SCF calcs. 4-59629  
 BeH, pot. curves, spin-extend HF study 4-64383  
 BeH $^{+}$ , X $^{2+}$ , and A $^{2+}$  stats, pot. curves, adiabatic calcs. 4-68974  
 BeH $_{2}$ , multiconfigurational coupled-cluster calcs. for excited electronic states 4-78755  
 Be-H $_{2}^{+}$ , geometric struct., force field and vibr. spectrum, MO-LCAO-SCF calcs. 4-59629  
 BeO, A $^{1+}$ -X $^{1+}$  system perturbations, ab initio calcs. 4-59623  
 BeO ceramics, dielec. props. in near-mm wavelength range 4-99075  
 BeO dielectric props. in NMMW range, refract. index and absorpt. coeff. 4-73491  
 BeO, dissoc. energy; HF STO calcs. 4-112092  
 BeO films, laser evaporated, thermally and optically stimulated exoelectron emission 4-88949  
 BeO glass ion beam etching, optical waveguide appls. 4-62071  
 BeO powders, sintering, positron annihilation study 4-71469  
 BeO, structural and electronic props., phase transform., pseudopotential calcs. 4-70100  
 BeO, thermally stimulated spontaneous RF emission 4-99203  
 BeO used as transparent anvils in high-press. cell for Earth mantle studies 4-110291

**Bessel differential equation** *see Bessel functions***Bessel functions**

- elastic half space having spheroidal inhomogeneity under all-around tension, stress field 4-97321  
 Hankel transform of generalized Laguerre polynomial, special Bessel function convolution 4-101620  
 parabolic equation with Bessel operator, existence of periodic soln. 4-112673  
 sum rules, principle of analytic continuation 4-78110  
 synchrotron radiation, polarisation calcs., using modified Bessel functions 4-96766

**beta-decay***see also beta-decay theory; beta-ray spectra; nuclear electron capture*

- $^{40}\text{Ge}$  double beta decay, Batelle-Carolina expt. status 4-90976  
 axial-vector coupling const., model dependence, g-factor sensitivity 4-68621  
 conference on grand unification, Philadelphia, PA, USA, (April 1983) 4-58573  
 conference on low energy tests of conservation laws, Blacksburg, VA, USA (Sep. 1983) 4-90281  
 data sources and inconsistencies 4-73859  
 double beta decay, recent developments,  $\nu$  mass, review 4-59210  
 double beta decay half-lives 4-86800  
 double beta-decay and Ge detectors 4-59558  
 Gamow-Teller 1-forbidden transitions in H=39 nuclei 4-68644  
 Gamow-Teller strength dist. in exotic nuclei 4-68655  
 Gamow-Teller transitions, spin-isospin excitations and nuclear models 4-64091  
 hyperfine interactions of interstitial  $^{12}\text{B}$ , asymmetric  $\beta$  decay studies in Fe, V and Ta 4-65651  
 lepton conservation in weak interaction processes 4-90756  
 lepton generation puzzle, lepton universality and conservation, double  $\beta$ -decay 4-63944  
 light nuclei beta-decay half-lives, spectral distrib. methods 4-59171  
 modulation method for studying  $\beta$ -spectra 4-95965  
 neutrino mass mass from oscillations and double beta-decay expts. 4-73683  
 neutrinoless double  $\beta$ -decay, interference between light and heavy Majorana neutrinos 4-90973  
 nuclei far from stability, spectroscopy for model testing, hybrid model, excitation modes 4-86792  
 relative energy contribution effects in two-interaction transition 4-78608  
 SO(10) fermion mass matrix model, Majorana  $\nu$  masses and lepton mixing angle limits 4-68470  
 two-neutrino double beta-decay and related processes, rates estimation 4-64096  
 two-neutrino double positron decay rate estimate 4-86801  
 weak currents, supersymmetry,  $\beta$ -decay form factors, gluino exchange, scalar-quark masses 4-106505  
 $n$ -pe  $\bar{\nu}_e$  lifetime, constraints imposed by  $^3\text{H}$  beta decay 4-90876  
 $\nu$  mass from spectroscopic meas. and oscillations,  $\beta$ -decay, solar neutrinos 4-59016  
 $\nu$  mass matrix, oscillations and double beta-decay, review 4-90766  
 $^{106}\text{Ag}^{2+}$ , oriented in Fe and Ni, NMR, mag. movement,  $\beta^{+}$ -decay,  $^{106}\text{Pd}$  props. 4-106571  
 $^{117}\text{Ag}$ , quasiparticle-phonon coupling model 4-86804  
 $^{118}\text{Ag}$  decay,  $^{118}\text{Cd}$  0 $^{+}$  states, transitions, intruder state systematics 4-73805  
 $^{26}\text{Al}$ , half-life meas. 4-95972  
 $^{33}\text{Ar}$   $\beta$ -delayed proton spectra, cross sections, half-life, from  $^{24}\text{Mg}(^{12}\text{C},3n)$  (Chinese) 4-73858  
 $^{37}\text{Ar}$ , 1-forbidden Gamow-Teller decay 4-59206  
 $^{181}\text{Au}$ ,  $\beta^{+}$ /EC decay,  $\gamma$ -ray identification 4-95971  
 $^{143}\text{Ba}$ , mass-separated short-lived fission products, half-life meas. 4-59204  
 $^{251}\text{Bk}$   $\beta$ -decay, half-life, mass 4-64097  
 $^{15}\text{C}$ ,  $^{15}\text{N}$   $\beta$ -decay, matrix elements, branching ratios 4-83030  
 $^{123}\text{Ce}$ , mass and beta-delayed proton emission 4-64103  
 $^{39}\text{Ca}$ , 1-forbidden Gamow-Teller decay 4-59206  
 $^{143}\text{Ce}$ ,  $3/2^{-}$  to  $3/2^{+}$  beta transition to  $^{143}\text{Pr}$ , spectral shape 4-95970  
 $^{64}\text{Cu}$ , beta decay, search for massive neutrino branches 4-64095  
 $^{14}\text{Dy}$ , A=141, 143, mass and beta-delayed proton emission 4-64103  
 $^{147}\text{Dy}$  beta delayed proton activity, half-life from  $^{142}\text{Nd}(^{12}\text{C},7n)$  4-106594  
 $^{148}\text{Dy}$ ,  $\beta^{+}$  and EC decay energies 4-95963  
 $^{149}\text{Er}$  beta delayed proton activity, half-life from  $^{144}\text{Sm}(^{12}\text{C},7n)$  4-106594  
 $^{147}\text{Eu}$ , mass derivation from  $\beta^{+}$  decay and EC meas. 4-102169  
 $^{148}\text{Eu}$ ,  $^{148}\text{Sm}$ , nuclear orientation study 4-64090  
 $^{4}\text{Fe}$ , A=54, 56, Gamow-Teller strength functions with the Lanczos algorithm 4-64102  
 $^{49}\text{Fe}$   $\beta$ -delayed proton spectra, cross sections from  $^{40}\text{Ca}(^{12}\text{C},3n)$  (Chinese) 4-73858  
 $^{51}\text{Fe}$ , beta decay, half-life meas. 4-64100  
 $^{147}\text{Gd}$ , mass and beta-delayed proton emission 4-64103  
 $^{147}\text{Gd}$ , mass derivation from  $\beta^{+}$  decay and EC meas. 4-102169  
 $^{76}\text{Ge}$  double beta decay, neutrino mass upper limit 4-59208

**beta-decay continued**

- $^{76}\text{Ge}$  double  $\beta$ -decay, Guelph expt., preliminary tests using Ge crystal 4-90979  
 $^{76}\text{Ge}$  neutrinoless double  $\beta$ -decay, Mont-Blanc expt.,  $\nu$  mass effects 4-90974  
 $^{76}\text{Ge}$  neutrinoless double  $\beta$ -decay, CIT results, lepton number conservation,  $\nu$  mass 4-90975  
 $^{76}\text{Ge}$  neutrinoless double  $\beta$ -decay, half-life lower limit 4-90985  
 $^3\text{H}$ , atomic and molecular,  $\beta$ -decay expt., apparatus,  $\nu$  mass 4-90977  
 $^3\text{H}$ , beta decay, mag. field effects 4-90981  
 $^3\text{H}$ , beta decay, neutrino rest mass calcs. 4-95973  
 $^3\text{H}$ , beta decay and implications for neutron lifetime 4-90876  
 $^3\text{H}$   $\beta$ -decay, neutrino mass and end-point energy 4-90978  
 $^3\text{H}$  decay, relative biological effectiveness meas. in alanine radical formation 4-59437  
 $^3\text{H}$ - $^3\text{He}$ ,  $\nu$  mass bounds 4-90987  
 $^{166}\text{Ho}$ , 1.776 MeV first-forbidden beta transition, gamma-ray spectra 4-59205  
 $^{110}\text{In}^{m+g}$ - $^{110}\text{Cd}$ , A=106, 108,  $\beta^{+}$ /EC decay, levels study 4-68645  
 $^{38}\text{K}^{m+}$   $\beta^{+}$  decay, comparative half-life of superallowed transition 4-106593  
 $^{84}\text{K}^{m+}$ , inelastic neutron accel. in s-process nucleosynthesis 4-86824  
 $^{14}\text{La}$ , A=120, 122, mass and beta-delayed proton emission 4-64103  
 $^{180}\text{Lu}$ - $^{180}\text{Hf}$ ,  $\beta$ -decay branch meas. 4-102225  
 $^{26}\text{Mg}$ , Gamow-Teller strength functions with the Lanczos algorithm 4-64102  
 $^{100}\text{Mo}$  neutrinoless double  $\beta$ -decay, level diagrams 4-95964  
 $^{16}\text{N}$ - $^{16}\text{O}$   $\beta$ -decay, matrix elements, branching ratios 4-83030  
 $^{20}\text{Na}$ , superallowed  $\beta$ -decay  $2^{+} \rightarrow 2^{+}$  transition, weak interaction probe 4-64104  
 $^{98}\text{Nb}$ - $^{98}\text{Mo}$ , collective states, cross subshell excitation influence 4-73809  
 $^{147}\text{Nd}$   $\beta$ -decay,  $^{147}\text{Pm}$  level struct., transitions, J $^{\pi}$  4-59124  
 $^{4}\text{Ni}$ , A=58, 60, Gamow-Teller strength functions with the Lanczos algorithm 4-64102  
 $^{58}\text{Ni}$ , beta decay, half-life meas. 4-64100  
 $^{99}\text{Rb}$   $\beta$ -decay,  $^{99}\text{Sr}$  rotational bands meas., comparison with Nilsson RPA calcs. 4-82990  
 $^{187}\text{Re}$ ,  $\beta$ -decay calcs. in Thomas-Fermi potential with Dirac wavefunctions 4-110509  
 $^{108}\text{Rh}$  9 min. isomer,  $\beta$ -decay,  $^{108}\text{Pd}$  levels and EM transitions 4-73856  
 $^{75}\text{Sb}$ - $^{37}\text{Cl}$   $\beta$ -decay scheme 4-96031  
 $^{124}\text{Sb}$ - $^{124}\text{Te}$ , gamma transition following Beta decay 4-111523  
 $^{82}\text{Se}$ ,  $\beta\beta$  decay, He TPC meas. 4-59494  
 $^{51}\text{Sm}$ , s-process branching,  $\beta$  decay, neutron capture 4-86799  
 $^{111}\text{Sn}$  decay,  $^{111}\text{In}$  levels, J $^{\pi}$  and  $\gamma$ -transitions (Japanese) 4-95959  
 $^{4}\text{Sr}$ , A=93, 94, mass-separated short-lived fission products, half-life meas. 4-59204  
 $^{4}\text{Tb}$ , A=147, 148,  $\beta^{+}$  and EC decay energies 4-95963  
 $^{151}\text{Tb}$ , mass derivation from  $\beta^{+}$  decay and EC meas. 4-102169  
 $^{160}\text{Tb}$  decay,  $\gamma$ -rays and X-rays energies and relative intensities meas. 4-59197  
 $^{160}\text{Tb}$ - $^{160}\text{Dy}$ , beta-decay, gamma-gamma directional correl. coeffs. 4-106589  
 $^{97}\text{Tc}$  radionuclides, internal bremsstrahlung prod. probability from  $\beta$ -decay 4-83028  
 $^{4}\text{Xe}$   $\gamma$ -decay,  $\beta^{-}$  decay and electron capture 4-83032  
 $^{136}\text{Xe}$ ,  $\beta\beta$  decay, Xe TPC meas. 4-59495  
 $^{59}\text{Zn}$ , mirror transition, half-life,  $E_{\text{max}}$  meas. 4-83029

**beta-decay theory***see also beta-decay; beta-ray spectra*

- double  $\beta$ -decay, neutrinoless, CP violation 4-111528  
 electromagnetically enhanced beta-decay, no-go theorem 4-90984  
 electromagnetically induced nuclear beta decay calculated by a Green's function method 4-83031  
 electromagnetically induced nuclear beta decay in electric-field gauge 4-73857  
 forbidden  $\beta$ -decay, total probability, effect of intense EM wave 4-111524  
 laser field effect on beta decay 4-83035  
 probability in external EM field 4-90986  
 short-lived nuclides, decay data for JNDC FP Decay Data File 4-59209  
 two-neutrino double beta-decay and related processes, rates estimation 4-64096  
 $^{86}\text{As}$ ,  $\beta$ -decay, 2n emission probability, from half-life 4-95967  
 $^{48}\text{Ca}$  double  $\beta$ -decay, nuclear matrix element, closure approx. validity 4-111525  
 $^{76}\text{Ge}$ , double  $\beta$ -decay calcs. in GUT, B-L violation 4-102069  
 $^{4}\text{K}$ , A=50-52,  $\beta$ -decay, 2n emission probability, from half-life 4-95967  
 $^{131}\text{I}$ ,  $\beta$ -decay, 2n emission probability, from half-life 4-95967  
 $^{16}\text{O}(0^{+})$   $\beta^{+}$  decay, short range and medium polarisation effects 4-111526  
 $^{208}\text{Pb}$ , Gamow-Teller resonance, RPA calcs. 4-64098  
 $^{4}\text{Rb}$  (A=89-99), Gamow-Teller strength functions, RPA calcs. 4-64098  
 $^{4}\text{Rb}$  (A=93, 95, 97, 99)  $\beta^{-}$  strength function, GT transition probability 4-64099  
 $^{136}\text{Sb}$ ,  $\beta$ -decay, 2n emission probability, from half-life 4-95967  
 $^{82}\text{Se}$ , double  $\beta$ -decay calcs. in GUT, B-L violation 4-102069  
 $^{9}\text{Se}$ ,  $\beta$ -decay, 2n emission probability, from half-life 4-95967  
 $^{144}\text{Sm}$ , Gamow-Teller resonance, RPA calcs. 4-64098  
 T beta-decay two step probability amplitudes 4-83034  
 T  $\beta$ -decay and neutrinoless double  $\beta$ -decay, CP violation 4-111528  
 T  $\beta$ -spectrum, neutrino mass determ., model independent lower bound 4-111527  
 $^{17}\text{Te}$  A=128, 130 double  $\beta$ -decay calcs. in GUT, B-L violation 4-102069

**beta-particles** *see beta-rays***beta-radiation** *see beta-rays***beta-ray absorption***see also electron absorption*

No entries

**beta-ray angular distribution***see also beta-ray spectra*

No entries

**beta-ray detection and measurement***see also beta-ray spectrometers; radioactivity measurement*chemical anal., emission count data anal. procedure 4-93580  
 combined X-ray/beta sensor, nuclear gauging technology appl. 4-82790  
 film badge accuracy determ. 4-62591  
 gas proportional counter, detection of  $\beta$ -emitting gases 4-102500  
 gas sampling shower counter, energy resolution improvement (Chinese) 4-74115

**beta-ray detection and measurement continued**

- gas-flow proportional counter for simultaneous  $\alpha$  and  $\beta$  counting (Spanish) 4-87000  
 modulation method for studying  $\beta$ -spectra 4-95965  
 neutrinoless double-beta and electron decay, low-temperature calorimetry 4-102494  
 radioactivity standardisation using  $4\pi\beta(\text{PC})\gamma$  coincidence counting, systematic effects due to increasing self-absorpt. 4-87026  
 skin dose assessment, TLD response to beta radiation 4-89762  
 spectrometer-dosimeter, description 4-59442  
 spin polarisation meas. of ejectile in heavy ion reactions via beta-ray asymmetry 4-64318  
 terephthalate dosimeter for X,  $\gamma$  and  $\beta$ -radiation 4-74117  
 thermal neutron induced fission fragments of  $^{235}\text{U}$  and  $^{239}\text{Pu}$ , beta spectrum meas. 4-64320  
 two-lens spectrometer for  $\beta$  polarimetry 4-91143  
 Gd loaded scintillation detector systems for inverse beta decay reactions 4-68899  
 Ge detectors and double beta decay 4-59558  
 $^{85}\text{Kr}$  off-gas  $\beta$  monitor, for nuclear reprocessing plants 4-59447  
 Rn, daughter activity concs. indoors, approx. meas. technique 4-93866  
 T survey meter using windowless air proportional counter 4-74052  
 $^{204}\text{Tl}$  beta radiation source steam wetness meas. appl. 4-111653

**beta-ray effects**

- see also electron beam effects  
 aromatic hydrocarbons, polynuel., dil. solns.,  $\beta$ -induced fluoresc. spectra 4-88879  
 biological systems and tritiated water, review 4-81619  
 bone marrow and spleen cells, DNA struct. and catabolism, HTO and  $^{13}\text{Cs}$   $\gamma$ -ray effects (Russian) 4-115132  
 embryos, mouse, combined effects after exposure during the preimplantation period to X-rays or  $\beta$ -rays 4-67043  
 embryos, mouse, sensitivity during pronuclear and 2-cell stages 4-67040  
 generative cell death in mice, RBE of T low-level  $\beta$ -radiation (Russian) 4-67011  
 lymphocytes, human, chromosome aberrations induction by  $\beta$ -particles from HTO 4-67025  
 multi-component systems, beta-ray backscattering studies 4-60961  
 nuclear waste storage materials, radiation effects 4-73973  
 paint, cavitation erosion, decontamination of surfaces (French) 4-70222  
 perspex, cavitation erosion, decontamination of surfaces (French) 4-70222  
 phase  $\lambda$ , extracellular, lethal and mutagenic effects of  $^3\text{H}_2\text{O}$  and [ $^3\text{H}$ -methyl]-thymidine (Russian) 4-77313  
 quartz, natural, defects induced by vac. UV, X-ray and beta-ray irradiation 4-70191  
 steel, carbon, cavitation erosion, decontamination of surfaces (French) 4-70222  
 steel, stainless, cavitation erosion, decontamination of surfaces (French) 4-70222  
 Al, cavitation erosion, decontamination of surfaces (French) 4-70222  
 HTO ingestion, effects on mice, hexokinase isozymes in brain, liver and spleen 4-100259  
 $^3\text{H}$ , long-term effects in utero incorporation 4-67048  
 $^3\text{H}$  toxicity, multiple parameter evaluation 4-67047  
 T determ. by  $\beta$ -excited fluoresc. X-ray-counting 4-62265  
 ZnO-Gd(Pr), thermoluminesc. under UV,  $\beta$ - and  $\gamma$ -ray irradiations 4-93119

**beta-ray polarisation**

No entries

**beta-ray scattering** see beta-ray effects; collision processes; energy loss of particles; particle backscattering; potential scattering; transport processes

**beta-ray spectra**

- see also beta-decay theory  
 beta-ray spectra, data anal. using response function 4-59481  
 modulation method for studying  $\beta$ -spectra 4-95965  
 $\beta$ - $\gamma$  spectroscopic method for determ. of delayed neutron emission probability 4-59595

**beta-ray spectrometers**

- see also beta-ray spectra; electron spectrometers  
 beta-gamma coincidence spectrometer for low radioactivity measurements (Russian) 4-74093  
 scattering effects, Monte Carlo program 4-91138  
 solenoid field spectrometer, electron transport calcs. 4-91144  
 two-lens spectrometer, for  $\beta$  polarimetry 4-91143

**beta-rays**

see also electrons

No entries

**beta spectrometers** see beta-ray spectrometers

**betatrons**

- charged particle slow extraction using nonlinear betatron oscill. resonance (Russian) 4-86993  
 conventional and modified betatrons, beam focusing and trapping 4-112027  
 crossed field injection into modified betatron, external transport scheme 4-68848  
 current limitations due to instabilities 4-111996  
 electron beams, high current, formation in modified betatron fields 4-96305  
 electron ring acceleration 4-59463  
 emittance growth in a modified betatron crossing the orbital-turning-point transition 4-111997  
 high current, strongly focused, with toroidal mag. field 4-59462  
 high current betatron, beam behaviour 4-111995  
 high current betatron experiments and theory 4-111989  
 high current electron ring dynamics in conventional betatron accelerator 4-74069  
 injection scheme, simulation studies 4-111991  
 medical accelerator neutron survey, remmeter sensitivity to leakage X-rays 4-62568  
 mode coupling in the modified betatron, single particle eqns. of motion, electron orbits 4-74066  
 modified betatron anal. with adiabatic particle dynamics 4-111993  
 negative mass instability 4-111992  
 RECE-Christa, betatron acceleration in kiloampere electron rings 4-68847  
 self-consistent modified betatron equilibria and their adiabatic evolution 4-111998  
 stelltron accelerator 4-111990  
 stretched betatron 4-111994

**Bethe-Salpeter equation**

- indefinite metric and non-Feynman propagators for relativistic, two-body problem 4-102015  
 $J=1/2$ ,  $3/2$  baryons, masses in quark-diquark model based on Bethe-Salpeter eqn. 4-90844  
 $r$ -particle irreducible kernels, asymptotic completeness, several particle collision amplitudes anal. props. 4-68390  
 WKB quantisation, validity of approximations 4-78475  
 NN scattering relativistic calcs. with  $\Delta$  degrees of freedom 4-95806  
 qq bound states, Salpeter eqn. in position space, arbitrary confining potentials 4-106474  
 QQ mesons, mass spectra from Bethe-Salpeter confinement dynamics 4-68432  
 $^2\text{H}$ , Bethe-Salpeter amplitude, symmetry 4-106568

**Bethe-Uhlenbeck equations** see quantum statistical mechanics

**bevatrons** see synchrotrons

**BGO detector** see scintillation counters

**Bi-FET integrated circuits** see monolithic integrated circuits

**Bi-MOS integrated circuits** see monolithic integrated circuits

**bicrystals**

- alkali halides, high-angle (001) twist grain boundaries 4-103768  
 ceramics, bicrystal grain boundaries, orientational relationships 4-70579  
 grain boundaries, large angle type, detection of expansion, electron diffraction 4-84519  
 grain boundary migration during high temp. deform. 4-98115  
 grain boundary phase equilib., computer mol. dynamics simulation 4-113461  
 grain boundary slip at high temp., dislocation model (Russian) 4-92211  
 metallic bicrystal, galvanomagnetic props. 4-84675  
 semiconductor, elec. cond. for tunnel charge transport 4-88576  
 symmetry determ. using convergent beam electron diffraction 4-80431  
 symmetry var. due to relative displacements of components, analytical method 4-75794  
 two-phase, oriented, prod. by diffusion bonding technique 4-61244  
 Al bicrystals, grain boundaries diffusivity 4-65485  
 Al, FCC tilt boundary, vacancy migration, computer simulation studies 4-113694  
 $\text{Al}_2\text{O}_3/\text{Cr}$ , grain boundary diffusion, anisotropy and doping effects 4-92443  
 Au thin films 4-75814  
 Ge, anomalous magneto-transport props. of p-type inversion layers (Japanese) 4-70842  
 Ge bicrystal p-type inversion layers, anomalous magneto-transport properties 4-98719  
 InSb bicrystal, grain boundary barrier height and elec. cond. 4-92216  
 LiF bicrystals, fracture at plastic deform. 4-75609  
 $\text{MgAl}_2\text{O}_4$ , grain boundary diffusion, anisotropy and doping effects 4-92443  
 $\text{MgO}/\text{Cr}$ , grain boundary diffusion, anisotropy and doping effects 4-92443  
 Ni alloys, directional crystn. and grain boundary diffusion (Russian) 4-108643  
 W bicrystals, oriented, brittle-ductile transition temp. rel. to O and content, AFS 4-104859  
 W, dynamic fracture resist., effect of crack vel. 4-99528  
 W, grain boundaries of twist misorientation about (100), direct meas. of work of fracture 4-98116  
 W, intrinsic grain boundary brittleness (French) 4-99476  
 Zn, (1010)-tilt, grain boundary struct. transform. effect on sliding 4-103769  
 Zn, grain boundary sliding and cryst. slip relationship 4-80048

**biexcitons** see excitonic molecules

**big-bang theory** see cosmology

**Bildschirmtext** see viewdata

**bilinear systems** see linear systems; nonlinear systems

**bimetallic strips** see bimetals

**bimetallic wire** see bimetals

**bimetals**

claddings, bond strength, multistep shear test 4-76925

**binaries (stellar)** see binary stars

**binary adders** see adders

**binary stars**

- see also cataclysmic binary stars; eclipsing binary stars; X-ray binary stars  
 accretion discs, mag. field instabilities 4-63132  
 accretion discs in close binaries, MHD anal., use of three-dimens. pseudoparticle method 4-63209  
 active chromosphere stars, Ca II emission surface fluxes 4-77837  
 active dwarf stars, mag. fields and atm. characts. 4-94817  
 active red dwarfs, atm. emission, rot. and duplicity, X-ray and UV data anal. 4-94819  
 ADS 14396, radial vel. obs. of 1981 periastron passage 4-101416  
 $\lambda$  Andromedae, RS CVn star, starspot temp., differential rot. and spectrocycle evidence 4-85986  
 $\sigma$  Andromedae, shell star, spectroscopic binary, light curve and spectral characts. 4-77840  
 ET Andromedae (HD 219749), Ap star, photometric and spectroscopic study 4-94798  
 66 Arietis, radial vel. anal. and non-binary nature 4-77875  
 UX Arietis, RS CVn star, VLB1 obs. at 1.65 GHz 4-85973  
 atmospheres of binary stars, structural patterns and nonthermal phenomena 4-95071  
 CQ Aurigae, differential rotation and activity of RS Canum Venaticorum star 4-94859  
 $\alpha$  Aurigae (Capella), magnitude obs. for possible variability 4-94763  
 $\zeta$  Aurigae stars in Almagest star catalogue, stellar variability from 2000 year perspective 4-110691  
 BD+25°2511, spectroscopic binary star, discovery of light variability 4-82515  
 blue stragglers, mass transfer from evolved companion 4-94757  
 blue stragglers in NGC 7789, search for radial vel. vars. 4-85920  
 $\xi$  Bootis, visual binary star, spectrophotometric study, of Li star primary 4-105985  
 RU Cancri, differential rotation and activity of RS Canum Venaticorum star 4-94859  
 $\kappa$  Cancri, Hg Mn star, search for spectral line asymmetries 4-94752  
 RS Canum Venaticum stars, atm. UV line fluxes anal. and spot mode 4-94892

# binary stars continued

- RS Canum Venaticorum stars, chromospheric emission and rot. 4-94883  
RS Canum Venaticorum stars, interacting magnetospheres, coronal heating and flares, mag. models 4-94899  
RS Canum Venaticorum stars, obs. general anal. and trends 4-85985  
RS Canum Venaticorum stars, photometric behaviour, photospheric phenomena, rot. and orbital motion 4-94882  
RS Canum Venaticorum stars, photometric monitoring 4-101341  
RS Canum Venaticorum stars, photometric obs. by automatic photoelectric telescope (October to December 1983) 4-77816  
RS Canum Venaticorum stars, radio emission and flaring, five year survey 4-94891  
RS Canum Venaticorum stars, rot.-atm. activity relations 4-94896  
RS Canum Venaticorum stars, spot phenomena 4-94821  
RS Canum Venaticorum stars, starspots Doppler imaging 4-94641  
RS Canum Venaticorum stars, UVB photometry of five bright new variables 4-101361  
RS Canum Venaticorum stars, wave-like distortion features 4-94886  
RS Canum Venaticorum stars, X-ray luminosity, coronal activity, rot., binary period and spectra 4-94890  
RS Canum Venaticorum stars is soft X-ray sources 4-101507  
Capella HL, red dwarfs, X-ray and UV emission anal. 4-85932  
 $\beta$  Capricorni, orbital elements from lunar occultation obs. 4-101407  
Case 1, spectroscopic binary, white dwarf component model atm. anal., UV obs. 4-90147  
 $\mu$  Cassiopeiae, astrometric binary, speckle interferometry and mass meas. 4-72977  
 $\mu$  Cassiopeiae, binary star orbit, parallax and proper motion 4-110688  
Cepheid mass anomaly, duplicity and mass loss effects 4-67730  
 $\alpha$  Ceti, infalling matter characters, from inverse P Cyg profiles 4-72946  
close binary stars, evolution and accretion effects 4-110657  
close doubles, catalogue of orbital elements, masses and luminosities 4-94648  
FK Comae Berenices, binary star model involving mass transfer, UV spectral obs. 4-85964  
common-proper-motion pairs, nearby, UVRI photometric study 4-94876  
conference on red dwarf stars and related objects activity, of Catania, Italy (August 1982) 4-90295  
contact binaries at age zero, stability 4-72978  
contact F-type stars, magnetic activity 4-67714  
 $\sigma$  Coronae Borealis, IUE obs. of RS CVn-like binary 4-63205  
 $\sigma$  Coronae Borealis, RS CVn star, X-ray flare, detect. and spectra 4-101436  
detached close binary systems, fission candidates 4-82511  
digital speckle interferometry (Russian) 4-67641  
 $\alpha$  Doradus, Si star, ephemeris (1983 to 1988) and orbit anal. 4-77852  
double star positions, Duruy diffraction micrometer appl. (French) 4-101157  
double stars, micrometer obs. (1977 to 1981) 4-110655  
double stars, physical properties and generic relations, IAU Colloquium No.80, Lembang, Java (1983 June 3 to 7) 4-78020  
double stars with IDS number error, approx. positions 4-94872  
duplicity on main sequence, review 4-82509  
dynamical interaction with third body 4-67604  
early-type detached close binaries, orbital circularisation 4-94857  
encounters of pairs of binary stars 4-72982  
evolution and generic relations of binary systems, review 4-82507  
evolution of binary stars, implications of observational data 4-82517  
evolution to transient sources 4-110656  
formation, ang. momentum transfer by gravit. torques rel. to evolution of binary protostars 4-110598  
formation, fission sequence and equilib. models of rigidly rotating polytropes 4-82465  
formation through tidal capture in globular clusters and galactic bulge 4-101418  
 $\sigma$  Geminorum, RS CVn star containing red giant, UV lines anal. 4-85911  
TV Geminorum, SRc variable star with B-type companion, IUE obs. 4-77853  
giant stars in old open cluster M67, DDO and UVB photometry rel. to duplicity 4-82531  
globular clusters, close binaries form. and X-ray sources numbers 4-63219  
globular clusters evolution, effect of binary stars form. 4-63226  
hard binary-single star scattering cross sections for equal masses 4-110595  
hardening in globular clusters, effects on cluster after cluster collapse phase 4-101442  
HD 102010 and 102465, new spectroscopic orbits from radial vels. 4-110680  
HD 106225, UVB photometry and radial vels. of suspected RS CVn star 4-94864  
HD 155555, RS CVn star, UVB obs. 4-90185  
HD 193793 (WC7+O4-5), long-period orbit 4-63156  
HD 210647, high eccentricity spectroscopic binary, orbit 4-101417  
HD 218393, spectrophotometry of peculiar shell star revealing binary star nature 4-82491  
HD 224118, binary star nature and orbit 4-77876  
HD 35079, orbit of spectroscopic binary 4-85983  
HD 47129 (Plaskett's star), H $\alpha$  line profile vars. 4-82512  
HD 5303, RS Canum Venaticorum star, evidence for light vars. in comparison star (HD 5210) 4-94764  
HD 64704, radial vel. anal. and orbit 4-77875  
HD 81817, 'hybrid' K-type giant; discovery of white dwarf companion from IUE obs. 4-101326  
HD 8357, RS CVn star, X-ray emission anal. 4-85961  
HD 86590 short-period RS CVn star, recognition as triple system 4-101406  
HD 91948, new probable Be star, UVB photometry and spectrophotometric obs. 4-94803  
HDE 245770 (=A 0535+26), spectroscopic orbit 4-77879  
V652 Herculis, pulsating H-deficient star, possible binary system 4-77850  
horizontal branch binary stars in X-ray globular clusters, IUE obs. 4-101446  
hot components characteristics, obs. from Astron UV telescope (Russian) 4-67630  
HR 1099 (V711 Tauri), RS CVn star; G-band obs. rel. to transport model 4-77874  
HR 1099 (V711 Tauri), RS CVn star, VLBI obs. at 1.65 GHz 4-85973  
HR 2142, binary Be star photometric obs. 4-82492

# binary stars continued

- HR 3361, Bp star, orbital anal., spectra and masses 4-77851  
HR 5110, RS CVn star, radio source mechanism, SHF obs. 4-85975  
HR 7275, RS CVn star, starspot evolution, visible and IR photometry 4-85987  
Hyades binary stars, results from lunar occultation obs. 4-101407  
Hyades dwarf stars, X-ray flare activity, influence of duplicity 4-94906  
Hyades Supercluster, visual binaries membership, colour-luminosity relation and mass 4-110700  
interacting binaries, UV spectra of hot plasma 4-82522  
interacting close binaries, Nordic Optical Telescope plans for studies 4-63208  
interferometric binary stars, meas. by combining light issuing from two telescopes (French) 4-105888  
Kpr 75, rapid visual binary, orbit and magnitude 4-110689  
HK Lacertae, RS CVn star, light curve and starspot modelling 4-94887  
late type stars, coronal struct. and temp. from X-ray spectra anal. 4-101324  
LSS 2018, variable planetary nebula nucleus, spectroscopic obs. and radial vel. vars. 4-72940  
LSS 2018 in planetary nebula DS 1, UV continuum and spectra anal. 4-77824  
SZ Lyncis, binary dwarf Cepheid, pulsation characts. and radius, absolute magnitude, mass, BVJHK obs. 4-85954  
main sequence cool stars, coronal activity and X-ray emission rel. to rot. period and binarity 4-101351  
massive close binaries, late stages of evolution 4-82525  
O-type unevolved close binaries, absolute masses and luminosities 4-94852  
occultation binary stars, orbital elements and ang. dias. 4-101407  
open clusters, binaries and yellow giants behaviour and cluster evolutionary status 4-63223  
open clusters red giants and dwarfs, radial vel. anal. 4-63222  
orbit determination (French) 4-67632  
orbital periods freq. distrib. 4-110724  
orbits based on speckle interferometry of seven objects (Russian) 4-85982  
oscillations of gaseous spheres, effects of rotational and tidal distortions on periods 4-103339  
II Pegasi, RS CVn star, synoptic light curves, two spot modelling 4-94881  
photographic astrometry with 61 cm Sproul refractor 4-115777  
planetary orbits in binary star systems, periodic and quasiperiodic orbits (German) 4-67607  
Praesepe binaries, resolution by lunar occultations obs. from Mauna Kea 4-110698  
pre-main sequence stars, ang. momentum loss due to mag. controlled wind 4-101342  
protostellar formation in rot. interstellar clouds, nonisothermal collapse 4-94729  
PSR 0655+64, binary pulsar, orbital inclination and mass determ. from interstellar scintillation obs. 4-101389  
PSr 1913+16, binary pulsar, constraints on progenitor, pulse shape and proper motion anal. 4-90168  
PSR 1913+16, binary pulsar, neutron star component contraction, effect on period 4-77864  
PSR 1913+16, binary pulsar, post-Newtonian timing effects obs. 4-63192  
pulsar binary systems of two types, evolutionary histories 4-77860  
pulsars in binary systems, energy ejection and radio emission 4-67761  
R136a, supermassive star and visual binary, position angle and separation 4-85949  
radio binary pulsars, Ruderman-Sutherland model explanation 4-72968  
southern radio binary stars, emission mechanisms 4-85981  
radio-emitting stars, optical positions and proper motions 4-94769  
red giant-black dwarf system, dwarf inside giant envelope spiralling in 4-110685  
SDS identifications of IDS components 4-94873  
semi-detached binaries, mass loss 4-82526  
CV Serpentis, binary Wolf-Rayet star, double shell discovery, nature 4-94791  
speckle interferometric measurements during (1981) 4-94862  
speckle interferometry of 87 objects 4-110678  
spectroscopic binary stars, orbit determ. method 4-101408  
spectroscopic binary synchronous rotation and revolution 4-94860  
spectroscopic segregation 4-82521  
statistical properties, implications for star form. 4-82510  
in stellar systems, effect of cooling and heating by binary stars on dissipative evolution of system 4-63211  
in stellar systems, influence on dynamical evolution of globular clusters and galactic nuclei 4-63212  
structure of tidally distorted polytropes, numerical study 4-101310  
Sun, companion star rel. to periodic comet showers and terrestrial mass extinctions 4-72594  
Sun, distant companion star rel. to periodic mass extinctions on Earth 4-72593  
Sun, masses and positions of possible past companions 4-101307  
supernovae, Type I, as end products of evolution of moderate mass binary stars 4-94842  
 $\zeta$  Tauri, Be star, radial vel. and profile vars. of UV circumstellar lines 4-82482  
T Tauri, primary and infrared secondary nature (French) 4-82473  
V711 Tauri, RS CVn star, 1981-2 light curves and Ca II emission 4-94888  
thermodynamic equilibrium hard binary models for globular clusters 4-63236  
47 Tucanae, globular cluster, binary freq. and kinematic parameters 4-77884  
unevolved close binary systems, period distrib. 4-77870  
V 801 Arac, periodic light intensity of X-ray binary 4-85979  
 $\gamma^2$  Velorum, H $\alpha$  line profile vars. 4-82512  
visual binaries, orbital elements (French) 4-67765  
visual binaries, orbital elements and masses, astrometry 4-67764  
visual binaries, orbits for 16 objects 4-115776  
visual binaries with solar-type secondary stars, ages from Stromgren photometry 4-82471  
visual binary stars, dynamical parallax and orbital inclination determ. from obs. of short arc (Russian) 4-101414  
visual binary stars, obs. using television speckle interferometer with real-time digital image processing 4-63072

## binary stars continued

- visual double stars, components equatorial coords. from Bordeaux Observatory obs. 4-101413  
 PU Vulpeculae, photometry, spectra, spectrophotometry and polarization 4-63162  
 white dwarf binary systems, as progenitors of R Coronae Borealis stars and Type I supernovae 4-63144  
 white dwarfs, evolution and props. 4-105973  
 wide dwarfs stars with separations 0.002 pc to 0.08 pc, detect. 4-110677  
 wide visual binary and multiple systems, importance for stellar evolution and galactic dynamics 4-82508  
 Wolf-Rayet binary stars, evolutionary causes for distrib. in Galaxy 4-82484  
 Wolf-Rayet stars in clusters, binary evolution effects 4-105991  
 Ba stars, search for hot white dwarf companions 4-94784  
 RS Canum Venaticorum stars, IR excess obs. 4-85989  
 H-deficient binary stars, evidence for circumstellar shells, UBVRJHKL obs. 4-90158

## binding energy

- see also *lattice energy; nuclear binding energy; nuclear forces*  
 $\lambda_0^6 - 6\lambda_0^3$ , lattice Hamiltonian field theory, bound state spectrum 4-90731  
 adsorbed atoms and mols., adsorbed, core-level binding energy shift anal. 4-6217  
 alkali dimers and hydrides, binding energy calc. using Gaussian model 4-91193  
 alkali metal clusters thermodynamic props., ionis. pots. and binding energies 4-69266  
 alkali metal halides:  $Mg^{2+}(Ca^{2+})(Sr^{2+})$ , impurity complex binding energies 4-60912  
 alkali metal halides, short-range repulsive pot. anal. 4-75361  
 alkali metals, lattice props., Heisenberg Hamiltonian studies 4-108501  
 alkanes,  $C_9$  to  $C_{11}$ , enthalpies of vaporisation, cohesive energies 4-98257  
 alkyl carboxylate-alkyltrimethylammonium mixed amphiphilic system, alkali metal and halide ion binding 4-84143  
 alloys, chem. bonding and heat of form., core level shift calorimetry method 4-104714  
 alloys, disordered binary, role of excess vol. of form., virtual cryst. model 4-92133  
 alloys, ternary, ion implantation prep., surface binding energy 4-79972  
 amorphous covalent solid, 3-dimensional model, internal energy 4-103654  
 atomic inner-shell transitions 4-68928  
 atoms, maximum negative ionisation bound 4-78773  
 atoms and mols., electronic struct., gas phase XPS 4-59847  
 binary alloys, electronegativity in local density functional formalism 4-70061  
 carbonium ions, struct. bonding dipole moments, SINDO calcs. 4-87049  
 coherent mixtures, elastic energy, phase equilib. 4-84363  
 cohesive energy, elastic const. and Gruneisen coeff. calcs. 4-84230  
 core electron binding energy calcs., X-ray absorpt. edge chemical shifts 4-91216  
 cubic semiconductors, effect of spin-split valence band on exciton energy 4-88455  
 delocalised surface exciton-impurity states with low binding energy (*Russian*) 4-70900  
 density functional method (*German*) 4-103694  
 desorption, local density formalism 4-92548  
 diamond, cohesive and struct. props., ab initio LCAO calc. 4-60881  
 diatomic polar mols., dipole-bound anions, high excited states calcs. 4-83308  
 electron spectroscopy in solid-state physics, electronic energy levels interpret. (*French*) 4-66134  
 electron-phonon coupling in tight binding model 4-75628  
 ESCA core binding energies, inductive effects 4-78419  
 graphite, structural theory using pseudopotential local-density-functional approach 4-92135  
 guanidinium-carboxylate interaction, ab initio SCF HF calcs. 4-96436  
 halide anion-organic acid (alcohol) complexes, binding energies, struct. effects, equilib. meas. 4-85293  
 heavy atoms, in superstrong mag. fields, binding energies, statistical calcs. 4-78777  
 heterogeneous surface characterization by photoemission of adsorbed Xe 4-88935  
 ice Ih phase, multibody and nonadditive energy components 4-69263  
 III-V semiconductors, nonlinear absorpt., coherent radiation-exciton interaction model 4-99078  
 inert gas solids, self-trapped holes calcs. 4-84582  
 inner shell ionisation, wave function effects 4-99235  
 ionic crystals, diamagnetism and Van Vleck paramagnetism 4-71019  
 ionic crystals, rocksalt struct., homopolar and heteropolar energy gaps 4-92134  
 laser-induced collective binding in two-electron systems 4-91209  
 lattice sums, rapid convergence by use of Fourier transforms 4-79973  
 many-electron atomic systems, statistical representation, total binding energy 4-74126  
 metal surfaces, anion and cation hydration, double layer simulation in ultrahigh vacuum 4-108703  
 metals, cohesive energy and interionic interactions 4-79976  
 metals, dissoci. energies in interatomic pair potentials, relationship between thermal expansion coeffs. and sp. ht. 4-75357  
 metals, total energy gradient 4-70698  
 metals, vacancy-twin boundary interactions, computer simulation studies 4-113491  
 metals with adsorbed CO and  $N_2$ , anomalous electronic and vibr. props. 4-98441  
 micelles and vesicles, partition and binding constants. from fluoresc. quenching data 4-98845  
 molecules, ionisation pots., dipole moments geometries and binding energies calc. extended Huckel theories (*German*) 4-83299  
 molecules, maximum negative ionisation bound 4-78773  
 neutral atoms, energy levels, binding energies calcs. 4-64367  
 neutral atoms, shell binding energies 4-83280  
 nitroso cpds., closed and open forms, relative ionicity, XPS, NDO calcs. 4-107402  
 noble metals, lattice props., Heisenberg Hamiltonian studies 4-108501  
 PbTe:Bi, Hall study of self-compensation of donor effect 4-104242  
 phenylsilane plasma polymer films, XPS, binding energies, lineshapes and shake-up intensities 4-104717  
 polar cryst. plate, exciton state and binding energy, appl. to  $PbI_2$  4-70673  
 binding energy continued  
 proteins, ligand binding to receptor sites 4-69171  
 quantum well wire, hydrogenic impurity states 4-70708  
 rare gas, crystal binding energies, many-body pots. construction 4-70057  
 rare-earth compounds, XPS, binding energy 4-93193  
 semiconductor doping superlattice, hydrogenic donor, binding energy and wavefunction in effective pot. 4-75902  
 semiconductor superlattices, narrow, breakdown of three dimens. effective mass approx. 4-84681  
 semiconductors, diamagnetism and Van Vleck paramagnetism 4-71019  
 semiconductors, multihole binding energies in hydrogenic impurity centres variational calc. 4-61329  
 semiconductors, tetrahedral, core electron binding energy, tight-binding theory anal. 4-108800  
 toluene-He (methane) clusters, supersonic mol. jet, fluoresc., time of flight mass spectra 4-107387  
 total energy full potential linearised APW method 4-104143  
 transition metal alloys, binding energy, CPA calcs. (*Russian*) 4-98060  
 transition metal compounds, band struct. calcs., Mossbauer spectra 4-92611  
 transition metals, multi-ion interaction using empirical N-body pot. 4-103695  
 trimethyltin ion-Lewis bases, binding energy in gas phase, high press. mass spectra 4-96721  
 water clusters, neutral and protonated, struct. calc. with mol. graphics 4-96734  
 X-ray absorpt. edges, chemical shift calcs. 4-99228  
 XPS and Auger-electron forward scatt., tool for studying epitaxial growth and core-level binding-energy shifts 4-109304  
 zero-gap semiconductors, impurity states in mag. field 4-61332  
 Ag based binary alloys, effective vacancy formation energy and solute vacancy binding energy 4-65260  
 Ag, core level binding energies, density functional calcs. 4-113861  
 Ag, two-hole core-level satellite obs. 4-70896  
 Ag XPS, calibration problems (*Chinese*) 4-102822  
 $Ag_n$  clusters, equilib. geom., binding energy and ionisation pots. 4-74373  
 $Ag_n^+$  clusters, equilib. geom., binding energy and ionisation pots. 4-74373  
 Al (111), O chemisorption LCAO- $X\alpha$  method anal. 4-113799  
 Al, charge densities, interionic pot., phonon freq., calcs. 4-113856  
 AlP(As)(Sb), high-press. phase transition 4-88283  
 Ar:Xe, fluid, extrinsic photocond., Wannier-Mott impurity exciton, binding energy and effective mass 4-65701  
 $AsF_6^-$  ( $n=3, 5, 6$ ), cage mols., K-edge excitonic fine struct. 4-83287  
 Au, 4f binding energies, Auger effect 4-78817  
 Au (111), electronic band struct., photoemission spectra determ., crystal symm. effect 4-84549  
 Au electrode, surface oxidation in  $H_2SO_4$  electrolyte, XPS study 4-93465  
 Au, tilt boundary energy and segregation, computer simulation studies 4-114540  
 Au, two-hole core-level satellite obs. 4-70896  
 Au XPS, calibration problems (*Chinese*) 4-102822  
 Au(100), image pot. surface states identification, inverse photoemission 4-76015  
 $Be_2$ ,  $2\sigma_g^2$  ground state, pot. energy curve calcs. 4-68977  
 $BaF_2$ , binding energy, bulk modulus and press. derivatives, interionic pot. model 4-60884  
 $Ba(NO_3)_2$ , cohesive energy, elastic const. and Gruneisen coeff. calcs. 4-84230  
 Be, 1s binding energy, core levels, state-specific many-electron theory 4-75887  
 BeO, structural and electronic props., phase transform., pseudopotential calcs. 4-70100  
 Br+Pb(U) collisions,  $\delta$ -electron spectra study 4-74321  
 CO adsorbed state over Pd/graphite catalyst, PES study of particle size effect 4-99274  
 $CO-H^+(Li^+)(Na^+)(K^+)$  structs., binding energies, ab initio HF calcs. 4-112096  
 $CaF_2$ , binding energy, bulk modulus and press. derivatives, interionic pot. model 4-60884  
 $CaF_2$ - $SrF_2$  mixed crystals, cohesion, harmonic and anharmonic elastic props. 4-92132  
 $Cd_3Mg$ , band struct. and stability (*Russian*) 4-84552  
 $Ce_{1-x}Ca_xO_{2-x}$ , vacancy binding energy, polarisation contrib. 4-88165  
 $Ce_{1-x}Gd_xO_{2-x}$ , vacancy binding energy, polarisation contrib. 4-88165  
 $CeK_{2.5}(Pd)_3$ , 4f-derived photoemission study 4-81107  
 $Ce_{1-x}Y_xO_{2-x}$ , vacancy binding energy, polarisation contrib. 4-88165  
 $Cr_2$ , LCAO local spin density,  $X\alpha$  calcs. 4-87046  
 Cu (100), 2p core-level binding energy shifts, XPS 4-76016  
 Cu based binary alloys, effective vacancy formation energy and solute vacancy binding energy 4-65260  
 Cu, tilt boundary energy and segregation, computer simulation studies 4-114540  
 Cu, two-hole core-level satellite obs. 4-70896  
 Cu, vacancies and interstitials, energy and vol. characts. (*Russian*) 4-92199  
 Cu XPS, calibration problems (*Chinese*) 4-102822  
 $Cu_n$  clusters, equilib. geom., binding energy and ionisation pots. 4-74373  
 $Cu_n^+$  clusters, equilib. geom., binding energy and ionisation pots. 4-74373  
 $CuInSe_5$ , radiative recombination and shallow centres 4-109250  
 $Cu_2O$ , ESCA and Auger spectroscopy determ. of binding energy (*French*) 4-66638  
 Cu(100), image pot. surface states identification, inverse photoemission 4-76015  
 Fe (110) with chemisorbed Br, LEED and ARUPS study 4-92518  
 Fe-Cr(Mn), binding energy, CPA calcs. (*Russian*) 4-98060  
 $Fe_2$ , dissoci., CAS SCF and contracted CI calc. 4-81407  
 $\alpha$ - $Fe_2O_3$  and  $Fe_3O_4$ , ESCA and Auger spectroscopy determ. of binding energy (*French*) 4-66638  
 $Fe(OH)_3$  and  $\gamma$ - $FeOOH$ , ESCA and Auger spectroscopy determ. of binding energy (*French*) 4-66638  
 GaAs- $Al_xGa_{1-x}$ , As quantum well struct., exciton binding energy 4-75868  
 GaAs- $Ga_{1-x}Al_x$ , As, binding energy of exciton in GaAs quantum well magneto-optical determination 4-114027  
 GaAs- $P_xN_{1-x}$ , excitons and excitonic mols. bound to impurity, calcs. 4-108785  
 Ge (111)-Pb interface form. dynamics and oxidation 4-84518  
 Ge/Al interface, chemisorption and metallisation, electronic struct. 4-92527  
 H, atomic phase, binding and cohesive energy 4-70518

## binding energy continued

- H, metallic, ground state energy in Wigner-Seitz approx. 4-80469  
 H<sup>+</sup>, binding limit in Hartree approx. 4-102569  
 H<sub>2</sub><sup>+</sup>, ground state binding energy in intense mag. field 4-74354  
 He, binding limit in Hartree approx. 4-102569  
 He<sub>2</sub>, critical binding, pots., quantum parameters 4-69169  
<sup>4</sup>He films with <sup>3</sup>He, binding energy calcs. 4-70514  
<sup>4</sup>He, liq. binding energy, hypernetted chain method 4-61162  
 Hg<sub>1-x</sub>Mn<sub>x</sub>Te, transport meas. using the alternating current technique 4-92720  
 I+Pb collisions,  $\delta$ -electron spectra study 4-74321  
 In-pyrrole-N-methylpyrrole contact, XPS study of Schottky barrier 4-104289  
 In<sub>0.79</sub>Ga<sub>0.21</sub>As<sub>0.48</sub>P<sub>0.52</sub>, luminescence study of binding energy variation 4-71435  
 InP:Mg(Ca,Zn) crystals grown by synthesis solute diffusion, electrical and optical props. 4-85093  
 KCl, with and without F-centres, positive muon spin depolarisation rate 4-65915  
 Kr-Xe, fluid, extrinsic photocond., Wannier-Mott impurity exciton, binding energy and effective mass 4-65701  
 Li clusters 4-98500  
 Li, muon interactions with lattice defects, mol. cluster calcs. 4-65255  
 Li-H systems, thermodynamic props., ionis. pots. and binding energies 4-69266  
 Li-O systems, thermodynamic props., ionis. pots. and binding energies 4-69266  
 LiCl crystal, electronic energy bands, density functional calcs., self-interaction-correction theory 4-70651  
 LiH, ground-state props., LCAO HF study using polarisable basis set 4-60882  
 LiH<sub>2</sub>, binding energy, ab initio calcs. 4-59615  
 LuB<sub>12</sub>, XPS study 4-81112  
 Mg (0001), O chemisorption, LCAO-X $\alpha$  calcs. 4-113799  
 Mg, core level binding energies, density functional calcs. 4-113861  
 Mg(BO<sub>3</sub>), cryst. struct. refinement, X-ray diff. (German) 4-80003  
 MgO (001), adsorption of CO and simple organic mols., ab initio MO calcs., lattice defect methods 4-81476  
 Mo<sub>2</sub>, LCAO local spin density, X $\alpha$  calcs. 4-87046  
 N<sub>2</sub>H<sup>+</sup>(Li<sup>+</sup>)(Na<sup>+</sup>)(K<sup>+</sup>) struct., binding energies, ab initio HF calcs. 4-112096  
 NH<sub>4</sub>Br(Cl)(I), cohesion and thermodynamic props. calcs. 4-92126  
 Na<sub>2</sub>O, electron impact excited, K X-ray emission spectra 4-69100  
 Na nanoparticles, cohesive energy, density functional formalism 4-70060  
 Nb, adsorption of C, NBC formation and synchrotron radiation study of overlayers 4-108711  
 Nb, electronically induced trapping of H by impurities 4-108410  
 NdRu<sub>2</sub>(Pd<sub>2</sub>), 4f-derived photoemission study 4-81107  
 Ni (100), adsorption of K, coadsorption of K and D<sub>2</sub>, work function, TDS, XPS, UPS, AES studies 4-80398  
 Ni (100), coadsorption of CO and K, XPS, UPS, work function, and EELS meas. 4-92552  
 Ni (100) with adsorbed N<sub>2</sub>, core level binding energy shift anal. 4-92517  
 Ni (111) with adsorbed graphite and C overlayers, electronic struct. study 4-61213  
 Ni binding energy meas. using X-ray photoelectron spectrometers, calibration problems (Chinese) 4-102822  
 Ni, inner-shell photoelectron spectroscopy, many-body effects 4-88930  
 Ni, tilt boundary energy and segregation, computer simulation studies 4-114540  
 Ni<sub>80-x</sub>Fe<sub>20</sub>, amorphous, surface characterisation study 4-76634  
 NiN<sub>2</sub>, dissoci., CAS SCF and contracted CI calc. 4-81407  
 NiO, ESCA and Auger spectroscopy determ. of binding energy (French) 4-66638  
 P, black, reson. photoemission theory 4-85088  
 P, allotropes, bond energetics and mol. struct., MNDO calcs. 4-64374  
 P<sub>2</sub>H<sub>4</sub>, bond energetics and mol. struct., MNDO calcs. 4-64374  
 P<sub>2</sub>O<sub>5</sub>, bond energetics and mol. struct., MNDO calcs. 4-64374  
 P-PbF<sub>2</sub>, point defect stability, computer simulation 4-103744  
 Pbl<sub>2</sub>, binding energies of exciton-ionised donor complex and exciton line n=1 4-70666  
 n-Pb<sub>1-x</sub>Mn<sub>x</sub>Te, intraband magnetooptical transitions in epitaxial film 4-71355  
 Pd, free atoms, M<sub>45</sub>N<sub>45</sub>N<sub>45</sub>-Auger-electron spectrum 4-74209  
 PrRu<sub>2</sub>(Pd<sub>2</sub>), 4f-derived photoemission study 4-81107  
 Pt (111) surface with adsorbed I, core electron binding energies 4-104085  
 Si (100) surface with chemisorbed H, surface states, UVPS study 4-108709  
 Si (111) surface, UPS rare gas titration for surface characteris. 4-88936  
 Si, graphitic, structural theory using pseudopotential local-density-functional approach 4-92135  
 Si, molten, electronic and bonding props. 4-98503  
 Si, self interstitials, electronic struct. and total energy migration barriers 4-108811  
 Si, substitutional and interstitial donors, many electron effect 4-113895  
 Si:H, dislocated, impurity exodiffusion 4-103788  
 Si:Se<sub>2</sub>, ESR study 4-109071  
 Si-polyacetylene interface, Auger spectra obs. of Si-C binding, peak shift depend. on adsorpt. level (French) 4-66141  
 Si<sub>3</sub>Ge<sub>1-x</sub>, Frenkel core excitons, binding energy 4-75867  
 Sn-Pb sputtering alloy, effect of ion mass and energy on the surface composition 4-98493  
 SrF<sub>2</sub>, binding energy, bulk modulus and press. derivatives, interionic pot. model 4-60884  
 Sr(NO<sub>3</sub>)<sub>2</sub>, cohesive energy, elastic const. and Gruneisen coeff. calcs. 4-84230  
 TiN<sub>1-x</sub>, electronic struct., PES study, stoichiometry effect 4-84560  
 TiO<sub>2</sub> (110), surface defects, XPS, X-ray induced AES, EELS study 4-80351  
 TmB<sub>12</sub>, XPS study 4-81112  
 UF<sub>6</sub>, electron spectrum in gas phase 4-78907  
 $\beta$ -VH<sub>0.5</sub>(D<sub>0.5</sub>), stabilisation mechanism, elastic energy formulation 4-108303  
 W (211), lattice steps and adatom binding, FIM study 4-108687  
 W, interstitial atom interaction with grain boundaries (Russian) 4-65293  
 W, total energy full potential linearised APW method 4-104143  
 Xe, isoelectronic series, 3d photoabsorpt. in near-threshold region, HF approx. 4-83349

## binding energy continued

- Zn<sub>1-x</sub>Ga<sub>x</sub>Cr<sub>2</sub>Se<sub>4</sub>, magnetic semiconducting solid solutions study 4-109002  
 ZrN<sub>1-x</sub>, electronic struct., PES study, stoichiometry effect 4-84560
- Bingham plastics and solids** see *rheology*
- biacoustics**  
 see also *biological effects of acoustic radiation; biomedical ultrasonics; hearing; sonar*  
 bone, human tubular, struct. features rel. to ultrasound meas. 4-89650  
 breath sounds, anal. and automatic classification, diagnosis appl. 4-115147  
 breathing sounds anal. and classification 4-77356  
 cancellous, broadband US attenuation obs. 4-89648  
 eye, human, axially traversing US, ray tracing model 4-85458  
 fish, spatial sonic guidance (Russian) 4-72464  
 glottic cancer detection, throat microphone, pitch period and amplitude perturbation coeff. (Japanese) 4-85463  
 heart, second sound, spectral anal. in normal children by selective linear prediction coding 4-77353  
 heart sounds, spectral anal., phys. characts. rel. to freq. spectra in normals and hypertensives 4-62539  
 heart-sound processing, statistical approach 4-89664  
 heart-sound processing by average and variance calc., physiological basis and clinical implications 4-115148  
 liposomes, US absorption rel. to temp. 4-100239  
 muscle sounds 4-77355  
 phonocardiograms, pole-zero modelling and classification 4-85461  
 phonopneumogram, numerical methods for anal. 4-89667  
 prosthetic heart valves, instrum. for sound anal. 4-85582  
 semilunar valve vibr., math. study, rel. to 2nd heart sound prod. 4-115111  
 soft tissue, acoustic attenuation, minimum-phase digital filter model 4-100237  
 soft tissue, US attenuation, non-Gaussian spectra, spectra-shift procedures 4-100240  
 soft tissue characterisation, attenuation estimation, three-dimens. model 4-100242  
 tissue, broadband pulsed ultrasound appl., frequency-dependent attenuation meas. 4-100421  
 US frequency-dependent attenuation coeff. meas. in fresh tissue 4-100238  
 US pulse-echo attenuation meas. in tissue, diff. correction 4-100422
- biocommunications**  
 see also *biocybernetics; hearing; speech*  
 bullfrog, Rana catesbeiana, auditory system, nerve fibre responses, adaptation patterns 4-62502  
 crickets, ventral cord neurones, two-tone interactions and song coding 4-105240  
 monkey grunts, acoustic features 4-77264
- biocontrol**  
 see also *biocommunications; biocybernetics*  
 aquatic animals, temp. control of external coverings (Russian) 4-72214  
 arm, prosthetic/orthotic, end-point control via binary coded EMG signal 4-89839  
 arm motion, approach to control laws 4-115099  
 bioelectric control of powered prosthesis for amputees 4-93969  
 elbow, optimal site selection for prosthetic control 4-89840  
 electrocortical activity controlled by lateral hypothalamus, inference of stable dispersion relation 4-93713  
 electrocortical activity under lateral hypothalamic control, test for constant natural frequencies 4-93712  
 electrohydraulic arm-prosthesis, design, construction and operation (Hungarian) 4-115268  
 EMG processing method for prosthesis control, walking period prediction (Japanese) 4-93967  
 forearm blood flow control during exercise in the heat, effect of mild essential hypertension 4-100196  
 heart, total artificial, development, pulsatile vs. nonpulsatile flow, control algorithm 4-93972  
 homeothermic animal temp. regulation, five-dimensional dual butterfly catastrophe model 4-66884  
 hydrodynamic resistance, active control by skins of dolphins (Russian) 4-72278  
 inspiratory airflow in breathing, optimal control 4-89637  
 ligaments, control exerted in joint integrity maintenance 4-109860  
 maximal vertical jumps by humans, control strategies 4-93789  
 motor control and spring-like muscles, some problems 4-93788  
 muscle, elec. activated, input-output props. 4-89556  
 myoelectrically-controlled prosthetic arms, multiple degree-of-freedom, control 4-85580  
 neuroprostheses, controllers for electrically activated muscle 4-89843  
 synergistic control system for paralyzed extremity joint 4-100359  
 thermoregulation, cranial vasodilator control of lingual arteriovenous anastomoses 4-81630  
 upper extremity function restoration, elec. stimulation systems, open loop control 4-93973  
 vascular tree function optimisation by wall shear stress adaptive regulation 4-66980
- biocybernetics**  
 see also *artificial intelligence; brain models; man-machine systems; neural nets*  
 Hodgkin-Huxley model behaviour 4-81654  
 interspike interval of a cable model neuron with white noise input 4-81653  
 retinotopy and orientation columns in the monkey 4-81670
- bioidiffusion**  
 Artemia cysts, water diffusion, quasi-elastic neutron scatt. spectra 4-81649  
 blood-water diffusion barrier at secondary gill lamellae in Anabas Testudineus 4-100106  
 book, biophysical plant physiology and ecology 4-73191  
 cytoplasmic motions in growing pollen tube tips, laser Doppler microscopy obs. 4-89535  
 erythrocyte membrane elec. breakdown through diffusion pot. difference 4-66894  
 erythrocytes, anomalous diffusion in presence of polyvinylpyrrolidone 4-105203  
 hyaluronate gels, macromolecules, diffusion, methods and preliminary results 4-100366

**biodiffusion continued**

- ion diffusion at charged interfaces, Smoluchowski-Poisson-Boltzmann description 4-115038
- magnetosome dynamics in magnetotactic bacteria 4-105263
- membrane nonzero thickness effect on diffusion through membranes 4-72225
- membrane permeability properties, temp. depend., mass spectroscopic obs. 4-93698
- neuronal activity, inference for diffusion models 4-89545
- proton transport, protein-facilitated, evidence for rot. contrib. 4-85413
- rhodopsin lateral diffusion rel. to rod outer segment disk membrane axial position 4-66944
- rod outer segment disks, Necturus, barrier to lateral diffusion of porphyrins 4-66920
- O<sub>2</sub> consumption rates and diffusion coeffs. in multicellular spheroids, determ. method 4-115278
- O<sub>2</sub> diffusion in blood, translational model of shear-induced augmentation 4-105211

**bioelectric phenomena**

see also *bioelectric potentials; biomagnetism*

- anisotropic cardiac muscle, bidomain model 4-77222
- anisotropic two-dimensional cardiac tissue, propag. of excitation 4-89540
- auditory nuclei, hypersensitivity to elec. stimulation following hearing loss in cats 4-89593
- auditory primary fibres, discharge pattern with elec. stimulation of cochlea in cats 4-109829
- auditory system, electrically-evoked responses in animals with progressive spiral ganglion degeneration 4-109841
- bacteriology, use of a laser Doppler electrophoresis method 4-115288
- bacteriorhodopsin, direct meas. of ps charge separation 4-62523
- bilayer lipid membranes, ionic channels formed by polymyxin B 4-66895
- biomedical sensors and elec. props. of living bodies (Japanese) 4-89818
- body impedance data normalisation, rel. to diagnosis 4-77225
- bone, elec. and dielec. props. rel. to freq. 4-66940
- bone, fluid-saturated, dielec. props., immersion fluid cond. variation effect, rat expts. 4-81659
- bone composite material, elec. props. rel. to comp. 4-72232
- bronchi, excised, human, bioelec. props. and ion flow 4-100114
- cardiac cells, Na/K pump, book contrib. 4-93725
- cardiac electrical activity, implications of struct. and geometry 4-77219
- cardiac electrophysiological studies, software control of sensing and stimulation 4-85538
- cardiac muscle, elec. propag., discontinuous nature, quantitative model 4-73131
- cardiac muscle, elec. propag. modelling 4-89554
- cardiac muscle, intercalated discs as a cause for discontinuous propag. 4-77221
- cardiac Purkinje fibre, delayed rectification, rel. to intracellular Ca<sup>2+</sup> 4-66933
- cardiac Purkinje fibre, impulse functions of automaticity 4-66934
- cardiac rhythm, effects of short-duration transients 4-77224
- cell membranes, electroelastic effects 4-77206
- cell surface, concanavalin A receptors, migration in pulsed elec. fields 4-89532
- cells adhering to glass, change for unchanged density of surface charges 4-66904
- cerebellum in sheep fetus, elec. activity, acute hypoxia and sleep states effect 4-72239
- cerebrum, mouse, dielec. props. rel. to age 4-115049
- ciliary cells evolved for vision hyperpolarize 4-93741
- cochlea generated distortion, ear canal acoustic and round window elec. correlates 4-109828
- cochlear function in guinea pigs with long-term endolymphatic hydrops, electrophysiological meas. 4-93760
- conference, New Orleans, USA (April 1982) 4-73136
- current flow patterns in 2D anisotropic bismyocytia 4-89559
- dendritic spines with bulbous end terminals, elec. props. 4-105216
- denervated muscles; maintenance, training and functional use by elec. stimulation 4-100345
- ear, organ of Corti, elec. circuit props., anal. including reactive elements 4-100163
- eggs of marine polychaete, intrinsic gating of inward rectifier channels 4-89539
- electrical impedance imaging of the body with nonlinear reconstruction 4-89813
- electro-biorheology, piezoelec. in biopolymers 4-105267
- electrodes, intraneural, coiled wire, for chronic stimulation 4-100423
- electroneurography, modelling and anal. 4-89548
- electrophysiological meas., signal processing unit 4-100343
- electrostimulation system for paralysed muscles 4-93974
- EM fields, interaction with cells, microelectrophoretic effect on ligands and surface receptors 4-100231
- embryonic chick heart cells, channel currents during spontaneous action pots. 4-105219
- embryonic chick sensory neurons, low voltage-activated Ca<sup>2+</sup> cond. 4-115042
- embryonic heart cell aggregates, phase resetting of rhythmic activity 4-66908
- erythrocyte ghosts, human, microwave dielectric props. 4-85409
- erythrocyte plasma membrane surface, negative charge cluster detection using fluoresc. probes 4-66892
- erythrocyte suspensions, LF elec. resistance rel. to Fricke's formula 4-100096
- exercise conditioning system for paralysed leg muscle 4-100349
- fertilisation, time and voltage windows for reversing elec. block 4-77212
- fish erythrocytes, reaction of intracellular matter to detergent toxicity, dielec. studies 4-72230
- fluid distribution in human legs, extra- and intra-cellular fluid vol., elec. impedance meas. 4-77409
- focal peripheral nerve injuries, electrophysiological characterisation 4-89549
- forebrain neuron activity in cats during alternating movements 4-72235
- fucoxanthine layers, photocurrent action spectra 4-66863
- functional elec. stimulation for standing and forward progression 4-100348
- functional elec. stimulation system, portable 4-100357
- functional electrical stimulation, neural prostheses, natural and artificial sensors development 4-115275
- giant planar lipid bilayer, conductance and interfacial effect of inhalation anaesthetics 4-62451
- bioelectric phenomena continued**
- giant planar lipid bilayer capacitance and its biphasic response to inhalation anaesthetics 4-62450
- glycerylmonoeucin membranes, elec. pot. at amphotericin channel inlets 4-66917
- haemoglobin content of blood, conductimetric procedure for assay 4-85544
- haemorrheology, Copley-Scott Blair phenomenon rel. to elec. double layer 4-100185
- heart tissue, activation sequence effects simulation 4-81663
- horizontal cell bodies in tiger salamander retina, elec. coupling 4-89567
- intracellular recording, calibration pulse appl. device 4-115310
- intracellular stimulating electrodes, cylindrical coordinate Laplace's eqn., numerical soln. 4-89541
- ionic channels formed by haemocyanin in planar lipid bilayers, elec. props. 4-93699
- knee flexion contracture, electrostimulation, spina bifida 4-100347
- leaves, charge accumulation and photochem., thermoluminesc. and delayed light emission obs. 4-77211
- lipid bilayer, cation-anion selectivity and conductivity of venom formed channels 4-66891
- lipid bilayer membrane, cholesterol containing, reversible elec. breakdown 4-66890
- median nerve stimulation, time-dependent equiv. dipole source for response 4-85447
- microorganisms, enumeration by their dynamic AC conductance patterns, model and expt. method 4-62453
- multistate elec. stimulation for paretic gait, rehabilitation program 4-100360
- muscle, elec. activated, input-output props. 4-89556
- muscle-nerve ephaptic excitation in some repetitive after-discharges 4-105224
- nervous tissues, diffusely arranged, conductivities and anisotropies, determ. and importance in neurophysiological studies 4-93978
- neuronal response to stochastic stimulation 4-115045
- neurostimulation, elec. long-term, clinical tests of multiple sclerosis patients (German) 4-77423
- neurostimulation, elec. long-time: multiple sclerosis appl. (German) 4-62623
- paralysed limbs, elec. stimulation under feedback computer control 4-93958
- Paramaecium caudatum, voltage dependent inward current, voltage clamp expts. (German) 4-66927
- paraplegia, standing by functional elec. stimulation 4-89829
- paraplegics, electrical activation of muscles for open-loop walking 4-93962
- patch clamp studies of single ionic channels, book contrib. 4-93710
- perineurium of frog sciatic nerve, AC impedance 4-105217
- photocurrents of single retinal rods from Rana pipiens tadpoles 4-109809
- precipitation membranes, review 4-114827
- psychophysical response to electrocutaneous stimulation 4-115327
- purple membrane charged asymmetry, uranyl quenching of dansyl fluorosc. 4-89512
- reciprocal walking in paraplegic patients, internal functional elec. stimulation 4-100358
- rod outer segment disc membranes, bovine, attached to lecithin bilayers, photoelec. signals generation 4-105237
- Schwann cells, rabbit, neuronal-type Na<sup>+</sup> and K<sup>+</sup> channels 4-115040
- serum lipoprotein surface charge change at atherosclerosis early development stages 4-66848
- sickle red blood cells orientation in alternating elec. field, diagnosis appl. 4-93705
- skeletal muscle, impedance from 1 Hz to 1 MHz 4-85414
- skin conductance response analysis, microcomputer package 4-62635
- smooth muscle constants, anal. by pole-zero method 4-66941
- spinal biomechanics, transcutaneous elec. neuromuscular stimulation 4-100346
- spinal cord injured patients, assessment via epidural electrodes 4-89822
- spinal cord neurons, NMDA responses, voltage-dependent block by Mg<sup>2+</sup> 4-77226
- spinal nonunions, repair with a pulsed DC stimulator 4-93961
- stimulation of living body, spatial distrib. of current density in vol. conductor model (Japanese) 4-77230
- stimulation thresholds, effect of metal electrodes 4-85420
- subdermal stimulation implanted electrodes for electrocutaneous communication 4-100361
- synergistic control system for paralyzed extremity joint 4-100359
- thorax computerised electrical impedance imaging 4-77416
- time-domain dielectric spectroscopy, use with lossy dielectrics, precaution in use 4-85592
- tissue, normal and malignant, dielec. props. 4-72242
- urinary bladder fullness determ. by electrical impedance meas. 4-77411
- vascular thoracic impedance, meas. after complete obstruction of pulmonary artery (French) 4-66984
- venous occlusive RN plethysmography: comparison with electrical admittance plethysmography 4-62581
- vertebrate sensory neurons: low voltage-activated, fully inactivating Ca<sup>2+</sup> channel 4-100110
- visual cells of Limulus, sustained discharge, current pulse effect 4-89561
- voltage clamp expts., simulation with FET analogue circuits 4-85591
- wheat seeds, deuterium effect in dielectric losses 4-89544
- yeast cells, static and dynamic dielectrophoresis 4-100105
- Ca<sup>2+</sup> ion permeation mechanism through Ca channels, electrostatic repulsion 4-77215
- bioelectric potentials**
- see also *contact potential; electrocardiography; electroencephalography*
- action potential, circuit for max. rate of rise meas. 4-77432
- action potentials, propag. along nerve axons and cardiac strands, resistive barrier effects 4-89538
- artificial human respiration, microprocessor assisted automatic meas. (Polish) 4-77283
- audiometry, elec. response, theory and appl. of weighted averaging 4-105241
- auditory and visual evoked potentials in Huntington's disease 4-72244
- auditory brainstem response and temperature: relationship in guinea pig 4-77252
- auditory brainstem responses, averaged, quality estimation 4-115082
- auditory brainstem responses, effects of stimulus rise-time and polarity 4-85440

**bioelectric potentials continued**  
 auditory brainstem responses and behavioural thresholds, stimulus duration effects 4-115071  
 auditory brainstem responses recording, artifact rejection criteria efficiency comparison 4-85546  
 auditory compound action pot. recordings 4-100159  
 auditory evoked brainstem responses 4-85441  
 auditory evoked potentials, dissociation from perception by bilateral lesions 4-77251  
 auditory evoked potentials, objective response detect. 4-85559  
 auditory evoked potentials, simultaneous recording 4-85435  
 auditory evoked potentials in people with perfect pitch, tone processing without P300 prod. 4-81708  
 auditory evoked response in young children, middle components 4-85436  
 auditory evoked response of cat brain stem, hypothermia effects 4-72259  
 auditory nerve, elec. stimulated, single fibre recordings 4-100160  
 automatic glottal inverse filtering 4-103143  
 automatic recording of biological model variables (*German*) 4-77419  
 axon, squid giant, current generated by backward-running electrogenic Na pump 4-77228  
 axon, squid giant, Na threshold channels 4-77227  
 body surface multielectrode for inverse problem in electrocardiography and its application (*Japanese*) 4-62621  
 body surface potential mapping system development (*Japanese*) 4-72446  
 brain damage assessment in malnourished infants, use of visual and auditory evoked pots. 4-89821  
 brain stem auditory evoked potentials, lesions location, computer analysis 4-72258  
 brainstem auditory evoked pot. amplitude, latency and waveform: effects of high-pass filter freq. 4-105242  
 brainstem auditory evoked pots., human, 3-channel Lissajous' trajectory 4-67135  
 brainstem auditory evoked pots., latency rel. to click phase and rate 4-100158  
 brainstem auditory evoked responses, constituent components extraction 4-85433  
 brainstem auditory evoked responses and stapedius reflex in multiple sclerosis patients 4-85439  
 brainstem auditory evoked responses in chronic renal failure patients 4-100157  
 cardiac action potential generation, after the 1st ms 4-77220  
 cardiac action potential sequential processing 4-81829  
 cervical somatosensory evoked potential in man: far-field, conducted and segmental components 4-77267  
 cochlear microphonic responses prod. by noise exposure in guinea pigs, nonlinearity modifications 4-93756  
 cochlear potentials, gross, rel. to hair cell pathology in waltzing guinea pig 4-115060  
 compound action pots. and single unit responses to 1 kHz haversine 4-100164  
 cone retina, vertebrate, electronic simulation of cones, horizontal cells and bipolar cells 4-105231  
 cortical evoked potentials, interaction to electric and acoustic stimuli 4-115070  
 cortical evoked potentials using a microcomputer for stimulation and analysis 4-115277  
 differential evoked potential monitor 4-100344  
 ECG computerised processing, symptom pattern recognition 4-105372  
 electro-oculogram, gain calibration method using eye optical props. 4-115306  
 electro-oculography data acquisition system, microcomputer-based neurological diagnosis 4-89819  
 electrocardiology, oblique double layer potentials for direct and inverse problems 4-89546  
 electromyographic equipment provision for polyclinics 4-72448  
 EMG, bioelectric control of powered prosthesis for amputees 4-93969  
 EMG, decomposition, automatic signal processing method 4-93948  
 EMG, digital signal processor, theoretical results 4-81790  
 EMG, digital signal processor with adaptive decision boundaries 4-85543  
 EMG, freq. spectral measures during exercise 4-89558  
 EMG, intraluminal electrodes, evaluation for oesophagus and gastrointestinal tract studies 4-115313  
 EMG, mechanical impulse system for myotatic reflex investigation 4-115312  
 EMG, on-line signal processing system 4-62614  
 EMG, power spectral anal., rel. to muscle fatigue in myophosphorylase deficiency 4-93720  
 EMG, reference signal acquisition system 4-93944  
 EMG, rel. to localised muscular fatigue in humans 4-93729  
 EMG, respiratory muscle, fatigue anal., processing methods 4-77438  
 EMG, rhythmic slower wave, occurrence prior to a rapid voluntary movement 4-105225  
 EMG, signal characts., microcomputer anal. 4-89802  
 EMG, single-fibre, meas. unit based on a personal computer 4-77412  
 EMG, surface, median freq. monitor 4-81807  
 EMG, surface, rel. to distrib. of myoneural junctions 4-66939  
 EMG, surface, spectral characterisation, diagnostic classification appl. 4-115258  
 EMG algorithm, for sequential signal estimation and system identification 4-67141  
 EMG and EEG signals, data reduction technique 4-85561  
 EMG interference pattern, automatic anal. 4-67134  
 EMG noise reduction for high resolution ECG 4-85564  
 EMG of patients with pathological tremors, preferential freq. detect. and determ. 4-85542  
 EMG processing method for prosthesis control, walking period prediction (*Japanese*) 4-93967  
 EMG recorded with surface electrodes, artefacts suppression 4-115245  
 EMG signal, binary coded, end-point prosthetic/orthotic arm control 4-89839  
 EMG signal analysis rel. to upper extremity limb function discrimination 4-81661  
 EMG signal decomposition system 4-93943  
 EMG signal processing, algorithms comparison 4-93947  
 EMG signals in gait, interpretation 4-89810  
 EMG technique for muscle fibre cond. vel. meas. 4-105356  
 EMG-controlled electrical stimulation of paraplegics 4-93960  
 EMG/foot force anal., real time microprocessor system 4-85549  
 endocochlear potential and auditory nerve fibre tuning curves in cats 4-100165  
 epicardial potentials, determ. from body surface pots. 4-115044

**bioelectric potentials continued**  
 ERG, high fidelity extended duration obs. 4-62473  
 ERG, model and effect of vitreous haemorrhage 4-89571  
 ERG and visual evoked response, system for offline anal. and storage 4-85558  
 erythrocyte membrane elec. breakdown through diffusion pot. difference 4-66894  
 event-related brain pots., classification 4-85425  
 event-related potential concomitants of information processing dysfunction in schizophrenic children 4-77233  
 event-related potentials and functional assessment 4-89809  
 evoked potentials, computer reconstructed, high pass filters effect 4-72449  
 evoked potentials, digital signal processing 4-89808  
 evoked potentials recorded from scalp and spinous processes during spinal column surgery 4-66938  
 excitable cellular membranes, transient EM field effects, nonlinear anal. 4-100251  
 extracellular potentials, modelled, comparative anal. 4-115048  
 formant tracking and glottal inverse filtering, two channel (speech and EGG) anal. 4-103144  
 grating visual evoked pots., evaluation of bioeffects of 20 ns ruby laser foveal exposure 4-62476  
 hippocampal evoked potentials, amplitude changes during avoidance behaviour in cat 4-77218  
 human head, bone and air conducted impulse signals, phase relationships 4-100175  
 human movement biomechanics review, human locomotion study 4-62507  
 insect mechanosensory neuron, action pot. encoder dynamic props. 4-105261  
 interference EMG, characterisation 4-89803  
 leaf of higher plant, burning, damage signal characts. rel. to clamping the resting signal 4-89537  
 lipid bilayers, gramicidin channels, elec. potential difference effect 4-89527  
 lipid membrane, image potential of ion-pore system, symmetrical channel 4-89528  
 lipid membrane, image potential of ion-pore system, unsymmetrical channels 4-89529  
 lower-lip EMG and displacement during bilabial disfluencies in adult stutterers 4-115084  
 macro EMG, use of signal representation to identify abnormal motor unit pots. 4-62615  
 mammalian cochlea, sensitivity modulation by LF tones, inner hair cell receptor pots. 4-109825  
 membrane potential probe, use of lipophilic cation, critical assessment 4-77205  
 model acoustic fibre, end plate potentials, correction formulae 4-81652  
 motor disorders, EMG anal., spectral method 4-105358  
 motor unit action potentials, special-purpose orthonormal basis functions 4-81660  
 movement-related slow pots., contrast between finger and foot movements 4-100183  
 multichannel signal processing based on logic averaging, His-Purkinje system activity appl. 4-85534  
 multielectrode microprobe for extracellular biopotential recording 4-115320  
 multiple sclerosis diagnosis, significance of delayed long-loop responses, sensory evoked pots. obs. 4-93954  
 multivariate analysis of diaphragm EMG power spectral moments 4-62458  
 muscle, insect, resting pot., temp. effect 4-66929  
 neural compound action pots. models, anatomical and electrophysiological basis 4-89547  
 neuromuscular disease patients, elec. muscle activity during a gradual increase in force 4-93719  
 neuronal activity, inference for diffusion models 4-89545  
 octopus brain, ongoing compound field pots. obs. 4-105226  
 oosten streaming pots., anatomical model, bone electromech. effect characterisation 4-115046  
 pattern ERG of the cat 4-109803  
 pattern reversal visual evoked potential rel. to inspired N<sub>2</sub>O conc. 4-72245  
 photoreceptors, hyperpolarising, of giant clam *Tridacna*, UV sensitivity 4-77238  
 phrenic neurograms, computer algorithms for processing 4-100397  
 prosthetic arm control by EMG pattern recognition 4-77427  
 purple membrane, surface pot. and sidedness, resonance Raman dye probe method and obs. 4-67151  
 real-time optical imaging of naturally evoked electrical activity in intact frog brain 4-72470  
 retina, carp, L-type horiz. cell response, Ba<sup>2+</sup> ion effects (*Japanese*) 4-81671  
 saccade-related brain pots. in guessing tasks, late components 4-66946  
 sampled waveforms, high-resolution alignment 4-85533  
 scalp electrical activity analysis by computer 4-81662  
 sciatic nerve, frog, periodic and random evoked pots. 4-93766  
 sensory evoked responses, clinical appl. of dipole localisation method 4-93950  
 signal processing, time domain vs. spectral domain analysis, EMG 4-77437  
 single-fibre action potential, math. model 4-115047  
 skin potential, origin of stretch-caused motion artifacts under electrodes 4-85419  
 skin-surface recording electrodes, practical considerations in use 4-85557  
 somatosensory evoked pot. far field, stationary P9, unexpected latency shifts with shoulder position shift changes 4-66965  
 somatosensory evoked potentials from the human brain-stem: origins of short latency potentials 4-77266  
 somatosensory evoked potentials to posterior tibial nerve stimulation in humans 4-66966  
 somatosensory evoked pots., cortical and spinal, intraoperative monitoring 4-85576  
 somatosensory evoked pots., recording from spinal cord and brain 4-93949  
 somatosensory evoked pots., short latency, and central somatosensory cond. time in post-traumatic coma 4-66964  
 speech, cricothyroid muscle activity and voice fundamental freq., EMG meas. 4-77265  
 stem of higher plant, cond. system resist. meas. during variable signal propag. 4-66932

**bioelectric potentials continued**

- subdurally recorded pattern and luminance EPs in the alert rhesus monkey 4-93738
- surface electromyogram, spectral anal. as tool for studying rate modulation 4-93714
- surface motor unit action potentials, normal and myopathic propag., computerised EMG 4-72234
- swept visual evoked pot., spatiotemporal conditions rel. to oblique effect 4-81676
- tibia, rabbit, reference curve for axial bioelec. pots. 4-100112
- ventricular repolarisation assessment by pot. mapping 4-89806
- versatile simulator of evoked potentials 4-72237
- visual, evoked potentials, data archiving and analysis using electronic techniques (*Italian*) 4-62613
- visual electrically evoked potential, steady-state responses 4-77234
- visual evoked potential pattern generation, recording, and data analysis with a single microcomputer 4-67137
- visual evoked potentials, steady-state, foveal Xe flash disruption 4-81669
- visual evoked potentials, variability evaluation by two statistical tests 4-100135
- visual evoked potentials, visual acuity rel. to variable exposure times (*Italian*) 4-66942
- visual evoked potentials in patients with well-defined occipital lesions, hemispheric asymmetry 4-93737
- visual evoked potentials using single flashes in baboons, influence of intermittent light stimulation 4-105235
- visual evoked response, inhibiting effect of diplopia 4-100146
- visual evoked response, steady-state, factors contributing to amplitude variability 4-109797

**bioenergy conversion**

- alternative energy sources, 6th International Conference, Miami Beach, FL, USA (Dec. 1983) 4-63395
- biogas in agriculture and production of power and heat (*German*) 4-99980
- biogas installations using farm animal waste, design and costs (*Italian*) 4-77048
- biogas plant economics in developing countries 4-66651
- biogas production by solid fermentation in Chinese rural areas 4-66736
- biomass conversion to methane and fertiliser slurry 4-66733
- biomass energetic utilisation, possibilities and barriers (*Hungarian*) 4-99978
- biomass energetic utilisation (*Hungarian*) 4-99979
- biomass samples, involving wood, bark and foliage, definition 4-99977
- biomass to furan, by decarbonylation of furfural under mild conditions 4-99976
- biomass/MSW augmented OTEC systems 4-62373
- crop and forest residues utilisation, environmental risks 4-62374
- diesel engine fuel displacement by biomass producer gas 4-66652
- energy balance in Hungarian agriculture, present and future role (*Hungarian*) 4-109750
- energy from biomass by socio-economic groups—a case study of Bangladesh 4-77134
- energy generation economics, comparison of various sources (*German*) 4-66643
- ethyl alcohol production from waste bananas 4-66730
- food waste utilisation for biogas and fertilizer production 4-66735
- forestral biomass, importance as energy resource/raw material, utilisation possibilities (*Hungarian*) 4-99995
- fuels, conversion processes and economics 4-81518
- industrial cellulosic wastes conversion to diesel fuel 4-72143
- Jamaican biomass resource assessment, history and prospects 4-66674
- kelp culturing and utilisation for methane production 4-114887
- low-grade fuels—Swedish energy option 4-89376
- methane production, by fermentation of agricultural/organic waste, applications (*French*) 4-99981
- methanol fuel production from municipal solid waste 4-66732
- microcrystalline cellulose aqueous digestion process evaluation 4-66731
- Nepalese biogas developments and prospects 4-66650
- photosynthesis and bioconversion 4-81568
- reed culms as an energy resource in Sweden 4-77047
- renewable energy technologies, contribution to future energy requirements 4-99934
- solar energy option rating by Florida electric utilities 4-66662
- solar energy technology (*German*) 4-105096
- urban solid refuse treatment for fuel derivation, alternatives, processes, costs (*Italian*) 4-105091
- gasification of rice hulls and straw  $O_2$  4-66737
- $H_2$  production and technologies, today, tomorrow and beyond 4-93645
- $NH_4HCO_3$  augmentation of rural biogas digester yield 4-66734

**biographical dictionaries** *see biographies***biographies**

- Andrei Sakharov, American physical society meeting in Baltimore, 18-21 April 1983 4-67956
- Cannon, Annie Jump (1863-1941), life and stellar spectra classification 4-78087
- Lewis, G.N., research on triplet state 4-90341
- Moll, Gerrit, electromag. expts. 4-63466

**biological cybernetics** *see biocybernetics***biological effects of acoustic radiation**

- see also biomolecular effects of radiation; cellular effects of radiation*
- cell lysis, US-induced, nontrapped bubbles in rotating culture tube, kinetics 4-100277
- cochlea, anatomical correlates of impulse noise-induced mech. damage 4-89592
- colonial hydroid macrofouling, control by free-field US radiation 4-89866
- fish, acoustic scattering, two-parameter fit 4-60198
- gliucoma, thermal model for US treatment, rabbit obs. 4-89660
- guinea pigs, low freq. sound exposure effects on treadmill performance 4-105286
- hearing protectors, international standards 4-62424
- human behaviour patterns, noise sensitivity as function of task complexity 4-81707
- lymphocyte sister chromatic exchange, freq. to US beam exposure 4-100244
- lymphocytes, human, lack of US effect on sister chromatid exchange in vitro 4-89651
- noise, temporal averaging of subjective magnitude and proposed rating scale for fluctuating noise 4-83764
- non-ionising radiation dosimetry, lasers, UV, radiowaves, microwaves, ultrasound 4-105345

**biological effects of acoustic radiation continued**

- sleep disturbance by noise 4-105287
- stereocilia on inner hair cells, fusion in various mammals after noise exposure 4-85437
- swimbladder, carp, responses to sound stimulation, auditory appl. 4-93796
- thread-hair mechanoreceptors of *Acheta domesticus*, US induced responses 4-93762

**biological effects of gamma-rays**

- see also biomolecular effects of radiation; cellular effects of radiation*
- adenocarcinoma in mice,  $\gamma$ -ray effects, retention of incorporated radionuclides (*German*) 4-81748
- barley population, recurrently irradiated, radiosensitivity 4-62529
- barley seedlings, 1st leaf as a radiobiological test system 4-62532
- bone marrow and spleen cells, DNA struct. and catabolism, HTO and  $^{137}Cs$   $\gamma$ -ray effects (*Russian*) 4-115132
- chromatin degradation in rat thymus after irradiation with fast neutrons and  $\gamma$ -rays (*Russian*) 4-67005
- chromosome alterations in karyotype of Ceylonese type black rat born after  $\gamma$ -irrad. 4-77336
- clonogenic tumour cell release from NFSA2ALM1 tumours, radiation response 4-93823
- colo-rectal injury,  $^{137}Cs$   $\gamma$ -ray and neutron irradiation, RBE values and repair characts. 4-89654
- DNA, thymus, pyrimidine cluster changes after animal  $\gamma$ -irrad. with sublethal dose (*Russian*) 4-67004
- E. coli* chromosomes, double-strand breaks induction by  $\gamma$ -irrad., rel. to cell lethality 4-67017
- E. coli* K-12 radC102, radiation-sensitive mutant, characterisation 4-67031
- egg stage of *Trogoderma granarium*, sterilisation,  $\gamma$ -irrad. effects 4-72318
- electron donors and radiation protection, radiation effect modification by ascorbic acid 4-77194
- Euglena cells, X-ray induced single strand DNA breaks and their repair in chloroplasts 4-62531
- fibrosarcoma, murine, independent effect of a mixed-beam regimen of fast neutrons and  $\gamma$ -rays 4-66995
- fibrosis in gamma irradiated rat lung, D-penicillamine modification 4-77343
- foetal ovaries, effects of protracted external  $\gamma$ -irrad. rel. to internal  $^{90}Sr$  deposition 4-93803
- gene conversion in yeast as a function of LET for low LET radiation 4-89658
- gonads of adult *Ameba splendens*, effects of chronic  $\gamma$ -irrad. 4-100258
- granulocytic-macrophagal cell predecessors in mouse bone marrow,  $\gamma$  post-irrad. dynamics (*Russian*) 4-67010
- gum arabic, carbohydrate comp., microorganism growth and ESR spectra,  $\gamma$ -irrad. effects 4-72317
- imprinting of chickens irradiated during early embryogenesis, combined effect of microwaves and  $\gamma$ -rays (*Russian*) 4-77305
- intergeneric conjugants of *Vibrio cholerae* biotype proteus X Serratia marcescens,  $\gamma$ -radiation sensitivity (*Russian*) 4-77324
- intestinal uptake of bile acids, effect of external abdominal irradiation in rats 4-115139
- landfill leachate,  $\gamma$ -irrad. conditions required in combined radiation-microbial process 4-93677
- linseed varieties,  $\gamma$ -ray effect on third generation 4-77349
- liver cells, intact and regenerating rat, genome mutations yield after  $\gamma$ -irrad. (*Russian*) 4-67002
- lymphocytes, human, chromosome aberrations induction by  $^{60}Co$   $\gamma$ -rays, dose response relationship 4-89656
- lymphocytes, rat blood, influence of  $\gamma$ -rays on UV fluoresc. (*Russian*) 4-77322
- mammalian cells, DNA repair kinetics following split dose  $\gamma$ -irrad. 4-77338
- mammalian L5178Y cells, cultured, inhibition of  $\gamma$ -ray dose-rate effects 4-93819
- metaphase chromosome, damage and repair of active chromatin 4-93821
- multicellular spheroids, appl. as model system in NSD concept based studies (*Russian*) 4-77315
- nuclear DNA segregation in *Bacillus cereus* T, radiation induced failure 4-72231
- onions, Egyptian, radiation inhibition of sprouting, economic evaluation 4-77350
- peanut cells, cultured: age-dependent effects of  $\gamma$ -exposure on form, growth and peroxidase activity 4-62530
- peritoneal macrophages, mouse,  $\gamma$ -irrad. rel. to defect Fe-mediated phagocytosis 4-72310
- Peyer's patch lymphocytes, rat, effect of sublethal ionising radiation 4-105295
- pH changes in Chinese hamster cells after  $\gamma$ -irrad. 4-67020
- phage DNA, unpaired bases after  $\gamma$ -irrad. in-situ and in-vitro 4-77346
- phosphatidylcholine multilayer liposomes,  $\gamma$ -irrad. effects: calorimetric, NMR and spectrofluorimetric obs. 4-67037
- plethysmograph for respiration rate meas. of rats with lung damage 4-105394
- poly U in aq. soln., yields of radiation-induced main chain scission 4-66872
- potatoes, radiation-induced dormancy, biochem. mechanism, review 4-72313
- radiobiology research projects, AFRR1 annual report (1982) 4-73172
- radiosensitivity of three goldfish cell lines, comparison using short term endpoints 4-100257
- RBE for neutron source reactor beam, cyclotron neutron and  $^{60}Co$   $\gamma$ -ray 4-77301
- reproductive system of pond snail, gamma irradiation effect 4-77341
- review of radiation sources, effects and protection measures (*French*) 4-85525
- Rhodes grass seeds, mutagenic response to  $\gamma$ -rays 4-72307
- rice, radiation-induced mutation rel. to tolerance to salinity 4-77351
- seeds of sorghum grain, gamma irradiation, resist. to witchweed 4-72304
- small intestine, mouse, fibronectin content in basement membrane,  $^{137}Cs$   $\gamma$ -irrad. effect 4-81746
- small intestine irradiated at different times of day, S-phase cell distrib., recovery phase 4-81743
- stromal mechanocytes of human bone marrow and spleen, radiosensitivity (*Russian*) 4-93807
- testicular stem cells, mouse, strain differences in response to fractionated irradiation 4-67024

**biological effects of gamma-rays continued**

- tumours in dog liver, development at later times following long-term  $\gamma$ -irrad. (*Russian*) 4-77329  
 whole-body-irradiated mice, suppression of delayed-type hypersensitivity to oxazolone 4-93815  
 yeast DNA, S1 nuclease-sensitive sites, assay for radiation-induced base damage 4-72311

**biological effects of ionising particles**

*see also biomolecular effects of radiation; cellular effects of radiation*  
 Biostack Experiments, HZE particles effects on biological systems 4-100334

- bone, human, U and  $^{226}\text{Ra}$  contents in Russian samples 4-62607  
 boron neutron capture therapy, absorbed dose enhancement 4-109988  
 cancer risk, absolute and relative risk models 4-109885  
 cancer risks from ingested radionuclides 4-109886  
 chromosome damage in Chinese hamster cells, flow cytometric determ., correl. with cell survival 4-105291  
 cosmic ray exposure in space, doses and LET distrib. rel. to shielding 4-77393  
 DNA of Chinese hamster cells, effect of 70 GeV proton secondary radiation (*Russian*) 4-67001  
 dose mortality relationships for man after brief and protracted exposure to low LET radiation 4-77345  
 embryos, mouse, combined effects after exposure during the preimplantation period to X-rays or  $\beta$ -rays 4-67043  
 embryos, mouse, sensitivity during pronuclear and 2-cell stages 4-67040  
 eye lens, accelerated heavy particle irradiation, cataractogenic pot. 4-67036  
 eye lens alterations after chronic professional exposure to low LET ionising radiation (*Italian*) 4-81741  
 fibroblasts, bone, mouse, effect of  $^{241}\text{Am}$   $\alpha$ -particles 4-77348  
 generative cell death in mice, RBE of T low-level  $\beta$ -radiation (*Russian*) 4-67011  
 heavy ions, low-energy, photonuclear reactions used to study biological action (*Russian*) 4-67016  
 lipid multilayers, modifications induced by  $^{241}\text{Am}$   $\alpha$ -particles 4-115140  
 liver, animal, consumed by man, fallout nuclides conc. 4-62610  
 low level ionising radiation induced cancer, causal relation probabilities 4-109960  
 low level radiation, atmospheric ions and probable indirect biological effect 4-72315  
 lymphocyte radiosensitivity in vitro, age relation 4-62534  
 lymphocytes, human, chromosome aberrations induction by  $\beta$ -particles from HTO 4-67025  
 molecular desorption, fast heavy ion induced, mol. size effects 4-66880  
 mutagenicity of  $\alpha$ -particles in Ehrlich ascites tumour cells 4-105292  
 neutron radiobiology, radiation protection implications 4-109887  
 phage X, extracellular, lethal and mutagenic effects of  $^3\text{H}_2\text{O}$  and [ $^3\text{H}$ -methyl]-thymidine (*Russian*) 4-77313  
 radiation doses and biological effects of cosmic rays 4-100261  
 radiobiology research projects, AFRRI annual report (1982) 4-73172  
 radiocolloid therapy using  $^{211}\text{At}$ , mouse obs. and comparison with  $^{22}\text{P}$ ,  $^{165}\text{Dy}$  and  $^{90}\text{Y}$  4-81770  
 radiotherapy fraction size rel. to effects on human skin 4-115179  
 review of radiation sources, effects and protection measures (*French*) 4-85525  
 skin, mouse, repopulation kinetics during split course MFD or daily fractionated irradiation 4-77330  
 spore radiobiology, conf., Amsterdam, Netherlands (July 1983) 4-63388  
 Tradescantia, somatic mutations induction using T labeled thymidine and uridine 4-72306  
 tumour-related tissue samples, from mice, radioisotope induced X-ray fluoresc. anal. 4-105289  
 $^3\text{H}$ , long-term effects in utero incorporation 4-67048  
 $^3\text{H}$  toxicity, multiple parameter evaluation 4-67047  
 $^{129}\text{I}$ , in human thyroid tissues of Utah populations, 1947-54 4-109888  
 $\text{Pu}$  isotope concentration in human tissues of Northern Utah 4-109889  
 T concentrations in urine and hair use for dose estimation from chronic T exposure 4-62588  
 $^{99}\text{Tc}$ , relative radiation and chemical hazards when used as  $\text{NaTcO}_4$  4-62533
- biological effects of microwaves**  
*see also biomolecular effects of radiation; cellular effects of radiation*  
 915-MHz direct contact diathermy applicator, with reduced leakage, performance 4-72327  
 acetylcholinesterase, effect of exposure to 2450 MHz microwaves 4-100245  
 beetles, low-level microwave treatment of mountain pine beetle and darkling beetle 4-115125  
 blood-brain barrier, microwave energy effects, review 4-115127  
 cytoplasm of Chinese hamster cells, thermal action of 2.45 GHz microwaves 4-100248  
 diagnostic applications of microwave imagery methods 4-115170  
 dosimetry and EM energy deposition, RF and microwave exposure (*Japanese*) 4-62524  
 dosimetry in biomedical investigations, 4-115227  
 dual vital waveguide exposure facility for examining microwave effects in vitro 4-72467  
 erythrocyte, microwave bioeffects, temp. and  $\text{pO}_2$  dependence 4-100250  
 eye, crayfish, effects of X-band microwave 4-77309  
 eyes, microwave radiation hazard, metal-framed spectacles effect 4-109877  
 foetal rats, decreased body weight after 2450 MHz microwave irradiation 4-62522  
 fruit flies, effects on EMC 4-105288  
 giant algal cells exposed to X-band, absence of significant short-term EM bioeffects 4-115124  
 hearts, isolated, frog, microwave effects on beating rate 4-100249  
 high-power automatic network analyzer for measuring the RF power absorbed by biological samples in a TEM cell 4-115294  
 human mononuclear leukocytes exposure to pulse modulated microwaves 4-115126  
 hypothermia, ethanol-induced, and ethanol consumption in rats: rel. to low-level microwave irradiation 4-100247  
 hypothermia, pentobarbital-induced, effects of acute low-level microwaves in rats 4-100246  
 imprinting of chickens irradiated during early embryogenesis; combined effect of microwaves and  $\gamma$ -rays (*Russian*) 4-77305  
 insects, microwave power absorption characts. when exposed to standing-wave fields 4-89652

**biological effects of microwaves continued**

- localised microwave hyperthermia, waveguide applicator with convergent lens 4-81753  
 lymphocytes,  $\text{G}_0$ , human, in vitro microwave irradiation, lack of clastogenic effect 4-115130  
 multilayered material heating pattern exposed to microwaves 4-85482  
 non-ionising radiation dosimetry, lasers, UV, radiowaves, microwaves, ultrasound 4-105345  
 platelet aggregation induced in mice by whole-body hyperthermia 4-93800  
 pulsed microwave-induced post-exposure hyperthermia: involvement of endogenous opioids and serotonin 4-115129  
 TEM cells bandwidth limitations due to resonances 4-72300  
 thermoacoustic effect in dielectrics and coupling to external medium, thermodynamical formulation 4-115128  
 tissue permittivity, in vivo and in vitro expt. techniques and results 4-62640  
 tissue properties rel. to biomedical appls. of MM waves 4-77308

**biological effects of radiation**

- see also biological effects of acoustic radiation; biological effects of gamma-rays; biological effects of ionising particles; biological effects of microwaves; biological effects of ultraviolet radiation; biological effects of X-rays; biomolecular effects of radiation; cellular effects of radiation; dosimetry; radiation therapy*  
 450-MHz RF exposure of man, specific absorption rate average and distrib. 4-115119  
 AECL bibliography of biological effects on living systems 4-101602  
 air ionization and radiation hormesis 4-109883  
 ANSI C95.1-1982 standard, human exposure to RF EM fields, safe distances determination 4-109873  
 atomic bomb survivor data anal., effects of random dose meas. errors 4-93888  
 behavioural studies with mice exposed to DC and 60 Hz mag. fields 4-100230  
 bone marrow transplant patients receiving an increased mean dose rate of total irradiation, increased mortality 4-93843  
 bone tumours induction, rel. to radioisotopes incorporation 4-77347  
 breast carcinoma, ECG changes after radiation therapy 4-93845  
 carcinogenic effect of  $^{241}\text{Am}$  and  $^{244}\text{Cm}$ , rat expts. (*Russian*) 4-67008  
 ceramic electrodes for ELF bioeffects studies 4-115296  
 colo-rectal injury,  $^{137}\text{Cs}$   $\gamma$ -ray and neutron irradiation, RBE values and repair characts. 4-89654  
 conference, radiation protection in medicine, Jodhpur, Rajasthan, India (Feb. 1984) 4-73156  
 cortical bone, neutron irradiation effects on mech. props. (*Spanish*) 4-100234  
 electromagnetic field regulations and standards in connection with biomedical effects 4-69269  
 ELF naval communications facilities, health hazards assessment 4-115115  
 EM dosimetry and energy deposition, RF and microwave exposure (*Japanese*) 4-62524  
 EM field dosimetry in biomedical investigations, 4-115227  
 EM fields, cubical block model of man in specific absorption rate distrib. calc., limitations 4-115118  
 EM fields human exposure, energy deposition and thermal response models 4-115117  
 embryos, mouse, late, neutron irradiation in utero at 15-19 days 4-66994  
 epidemiology, methodologic assessment 4-86137  
 genetic effects of radiation 4-109872  
 growth inhibition in Vicia faba, OER and RBE of high energy neutron beams 4-93791  
 high energy electron beams, radiobiological and microdosimetric characts., radiotherapy appls. 4-72417  
 human EM hazard analysis, human body impedance in VLF to MF band 4-115120  
 human head, absorbed power distrib. inside simulating sphere in near field of  $\lambda/2$  dipole antenna 4-89653  
 hyperthermia, regional, mag. induction heating, beagle dog model, thermal dosimetry anal. 4-93697  
 industrial electric/magnetic fields, effects on health (*French, German*) 4-72299  
 ionising radiation appls., conf., Riyadh, Saudi Arabia (March 1982) 4-67859  
 ionising radiations, methodologies for predicting expected combined stochastic radiobiological effects 4-67039  
 laser low-level therapy, CW He-Ne laser use 4-77369  
 laser medicine, injurious effects and clinical appls. 4-72341  
 laser radiation hazards 4-77396  
 LD<sub>50</sub> for uniform low LET irradiation of man 4-72420  
 LF stray fields, EM smog (*German*) 4-59971  
 lossy dielectric bodies, EM wave specific absorption rate distrib., calc. using FFT method 4-85459  
 low level radiation, atmospheric ions and probable indirect biological effect 4-72315  
 lung cancer, possible risk from indoor exposure to Rn daughters 4-93813  
 lung cancer induction by Rn daughters inhalation, dose required 4-93809  
 lung cancer risk for miners and atomic bomb survivors, rel. to indoor exposure 4-93812  
 mammalian body mass and sensitivity to radiofrequency electromagnetic radiation, inverse relationship study 4-77307  
 mental retardation rel. to in utero exposure to A-bomb radiation 4-72303  
 methylcholanthrene carcinogenesis in mice, effect of a static uniform mag. field 4-77304  
 mouse skin, neutron RBEs at low doses per fraction 4-77303  
 multiple daily fractionation, treatment scheme, radiobiological evidence 4-72416  
 nuclear radiations, biomedical appls. 4-77352  
 ocular exposure to infrared radiation in the Swedish iron and steel industry 4-62603  
 ocular hazard from GaAs lasers and near IR radiation 4-93797  
 optical radiation hazards 4-100300  
 organ transformation calc. after radioactive aerosol inhalation 4-62593  
 organisms irradiated by weak electromagnetic fields, biological effects, panel discussion 4-93793  
 overhead power lines, 50 Hz elec. field, physiological effects 4-62520  
 penetration test on living body using low power He-Ne laser (*Chinese*) 4-93798  
 plasmoid MHD wave, impossibility of excitation in physiological aq. soln. 4-66968

**biological effects of radiation continued**

- power line, 3-phase, EM fields in vitro simulation 4-109874  
 prenatal exposure, human experience of radiation damage 4-67049  
 prenatal irradiation effects, conf., Bordeaux, France (July 1982) 4-63406  
 prostacyclin, rabbit aortic, long-lasting depression of form. by single-dose irradiat. 4-67027  
 pulmonary neoplasms, induction in rats by fission neutrons and Rn daughters 4-93818  
 radio stations, EM radiation meas. 4-106281  
 radiobiological analysis of the development of early and late radiation injuries (*Russian*) 4-62528  
 radiobiology publications growth, computer analysis (*Russian*) 4-109884  
 radiobiology research projects, AFRR annual report (1982) 4-73172  
 RF (28 MHz) CW radiation effects 4-67000  
 RF hazards, specific absorption rate distribution in a full-scale model of man at 350 MHz 4-115122  
 RF human whole-body absorption rates, effect of separation from ground 4-115121  
 RF power absorbed by biological samples meas., using high-power network analyser 4-85600  
 root nodulation, light-induced, in the cycadales, in vitro studies 4-62521  
 skin, wounded, of white mice, regenerative process, He-Ne laser irradiat. effects 4-72301  
 small intestine, mouse, response to X-ray and neutron irradiat. doses 4-100236  
 survival data of irradiat. animals, parametric statistical anal. (*Russian*) 4-77328  
 taste-aversion learning in rats rel. to 60 Hz elec. field exposure 4-100233  
 thyroid dysfunction following mantle radiotherapy for Hodgkin's disease 4-109911  
 time-varying mag. fields, thresholds for biological effects 4-93792  
 tissue permittivity, in vivo and in vitro expt. techniques and results 4-62640  
 track calculations, radiobiology appl., microdosimetric quantities calcs. 4-67032  
 transuranium element intake, risk estimation for radiation protection 4-111973  
 tumour induction in BALB/c mice after fractionated or protracted exposures to fission-spectrum neutrons 4-66993  
<sup>241</sup>Am, medical course after accidental exposure 4-109890  
<sup>137</sup>Cs<sup>+</sup> uptake by plants, long term fallout on grassland, soil parameters effect 4-109967  
<sup>239</sup>Pu exposed workers, human studies for health risk assessment 4-111974  
<sup>239</sup>Pu injected intramuscularly in complexon therapy conditions, behaviour and biological effect (*Russian*) 4-67015  
<sup>239</sup>Pu submicron dioxide inhalation, haemodynamics and heart mass parameters in dogs (*Russian*) 4-67014  
<sup>226</sup>Ra and bone seeking radionuclides, carcinogenicity, beagle studies 4-115221  
 Rn daughter exposure at low doses, rel. to lung cancer in rats 4-93811  
 Rn daughters rel. to lung tumours occurrence, rat. obs. 4-93810

**biological effects of ultraviolet radiation**

- see also *biomolecular effects of radiation; cellular effects of radiation*  
 corneal endothelium, rabbit, damage by UV-B 4-109878  
 diploid yeast cells, UV- and X-ray induced damage, common repair pathways 4-100256  
 DNA, transforming, UV action spectra for protection by glycerol 4-67029  
 DNA chain elongation inhibition in Chinese hamster cells on UV irradiat. 4-72312  
 DNA in proliferating and resting HeLa cells, replications and transcription, UV laser pulse effect (*Russian*) 4-66999  
 E. coli B/r Hcr<sup>+</sup> cells, error-free uvr<sup>+</sup>-dependent inducible DNA repair 4-67022  
 E. coli K-12 radC102, radiation-sensitive mutant, characterisation 4-67031  
 epidermal cells, thymocyte-activating factor/interleukin 1 prod. 4-77334  
 erythema and photoaddition due to UVB radiation 4-67023  
 eye, pterygium in Sardinia w.r.t. occupational exposure, epidemiological obs. 4-81740  
 fibroblasts, human, nondividing populations, UV exposure, transient damage repair enhancement 4-72316  
 HeLa cells on membrane filter, UV radiation apparent sensitivity increase 4-77332  
 laser radiation, max. permissible exposure estimates 4-62526  
 lymphocytes, rat blood, influence of  $\gamma$ -rays on UV fluoresc. (*Russian*) 4-77322  
 micro-irradiation of single living cells using UV and visible light 4-115326  
 non-ionising radiation dosimetry, lasers, UV, radiowaves, microwaves, ultrasound 4-105345  
 optical radiation hazards 4-100300  
 phage inactivation sensitivity to monochromatic synchrotron UV irradiat. 4-77337  
 ribulose-1,5-bisphosphate carboxylase in pea and soybean, enhanced UV-B radiation effect 4-72305  
 simian virus 40 DN, replication following UV irradiat., test of model 4-115134  
 skin tumors, work-related distrib. in Sardinia, epidemiological obs. 4-81742  
 skin tumours induced in Swiss mice by 253.7 nm UV 4-115133  
 sunburn, annotated bibliography, historical development 4-85608  
 synchrotron system for monochromatic UV irradiat. 4-67160  
 T7 bacteriophage, UV-induced small struct. changes, melting methods study 4-93808  
 yeast, radiosensitive mutants: cell inactivation by high temp., UV light and ionising radiation (*Russian*) 4-77314  
 yeast cells, dry, of different UV sensitivities, effects of vacuum-UV and far-UV synchrotron radiation 4-67034

**biological effects of X-rays**

- see also *biomolecular effects of radiation; cellular effects of radiation*  
 alveolar macrophages, rat, effects of X-irrad. on cytoskeleton in vitro 4-105290  
 ataxia-telangiectasia and normal human cells, fixation and repair of radiation damage 4-115136  
 bone marrow cells, rat, X-irrad.-induced double-strand DNA breaks (*Russian*) 4-77312  
 cell growth inhibition by irradiat. combined with hyperthermia or anticancer drugs 4-93806

**biological effects of X-rays continued**

- cells, mouse 10 T $\frac{1}{2}$ , effect on progression 4-67028  
 children, findings after in utero radiation exposure from maternal X-ray exam. 4-67050  
 Chinese hamster ovary G<sub>2</sub> cells, mitosis and survival after X-irrad. 4-77342  
 chromosome damage in Chinese hamster cells, flow cytometric determ., correl. with cell survival 4-105291  
 CNS, postnatal development after prenatal X-irrad. in mice 4-67044  
 collagen and fluid contents of mouse kidney, increases after X-irrad. 4-105298  
 conference on radiobiology, Rijswijk, Netherlands (Jan. 1984) 4-95039  
 diploid yeast cells, UV- and X-ray induced damage, common repair pathways 4-100256  
 DNA crosslinking, BCNU-induced, X-ray effects in rat brain tumour cells 4-105296  
 DNA lesion and cell inactivation caused by X-ray, hyperthermia effects at 42°C 4-77196  
 E. coli K-12 radC102, radiation-sensitive mutant, characterisation 4-67031  
 ear, mouse, long-term effect of X-rays on thermal sensitivity 4-109882  
 ectopic intestinal glands after segmental small bowel irradiation in the cat 4-93804  
 embryo cells, Golden hamster oncogenic transformation by low doses of X-rays 4-77339  
 embryos, mouse, combined effects after exposure during the preimplantation period to X-rays or  $\beta$ -rays 4-67043  
 embryos, mouse, sensitivity during pronuclear and 2-cell stages 4-67040  
 fibroblasts, normal and ataxia telangiectasia, human, thermal enhancement of radiosensitivity 4-89655  
 gene conversion in yeast as a function of LET for low LET radiation 4-89658  
 granulocyte/macrophage progenitor cell population in bone marrow and blood after total body X-irrad. 4-77340  
 hydrated lecithin membranes, X-radiation damage using wiggler-enhanced synchrotron radiation 4-93814  
 hyperthermia combined with fast neutrons or X-rays, response of mouse skin 4-100086  
 jejunum, mouse, late effects of irradiat. 4-115137  
 kidney, mouse, multifraction X-irrad. dose response 4-77344  
 lipoxygenase, wheat, radiation-induced lesion rel. to struct. organisation (*Russian*) 4-77320  
 lymphocyte radiosensitivity in vitro, age relation 4-62534  
 lymphocytes, human peripheral, X-irrad. rel. to exchanges and deletions 4-67026  
 lymphosarcoma, rapidly growing, murine, noneffectivity of roentgen irradiat. 4-93805  
 mammalian cell culture, dose-rate effect between 1 and 10 Gy/min 4-109881  
 mammalian cells, cultured, X-ray-induced DNA damage and cellular lethality 4-93817  
 microvasculature, swine skin, response to acute single exposures of X-rays 4-67033  
 multiphasic survival response of a radioresistant lepidopteran insect cell line 4-93822  
 oogonial cells in ovaries of red cotton bug, X-ray induced precocity 4-100253  
 plasma membranes, rat liver, radiation effects, IR spectroscopy obs. (*Russian*) 4-77321  
 preimplantation mouse embryos, development of cytogenetic effects and recovery after irradiat. 4-67042  
 prenatal irradiation of NMRI mice, long-term effects 4-67045  
 proliferation kinetics of cultured cells after irradiat. with X-rays and 14 MeV neutrons 4-100255  
 protein crystals, X-radiation damage reduction by polyethylene glycol 4-81822  
 radiotherapy fraction size rel. to effects on human skin 4-115178  
 skin, previously irradiated, response to combinations of X-rays, heat and cis-diamminedichloroplatinum 4-67038  
 skin, struct. and phys. props., ionising radiation effects, radiotherapy appl. 4-115141  
 small intestine, mouse, response to X-ray and neutron irradiat. doses 4-100236  
 small intestine, rat, late roentgen radiation damage, dose fractionation effects 4-81745  
 soft X-rays to investigate radiation-sensitive sites in mammalian cells 4-100254  
 T-lymphocyte colonies, PHA-induced, differential X-irrad. effects 4-93820  
 thyroid cancer, radiogenic initiation, rat expts. 4-72309  
 tumour cells, Ehrlich ascites roentgen irradiat., energy metabolism and ATP turnover time during cell cycle 4-81744  
 V79 Chinese hamster cells, sequential irradiat. with X-rays and fast neutrons 4-67018  
 vascular changes in a human malignant melanoma xenograft following single-dose irradiation 4-67035  
 vasculature, mouse intestine, effect of radiation alone or combined with hyperthermia 4-109879  
 VDU, low-background radiation meas. 4-62601  
 wheat seed radiosensitivity rel. to content of proteins and protein fractions (*Russian*) 4-67007  
 zygote, mouse, in vitro studies of radiosensitivity 4-67041

**biological fluid dynamics**

- see also *bioreology; haemodynamics*  
 alga, cell division at interface in different hydrodynamic regimes of streaming 4-66903  
 aquatic animals, actively-moving, boundary layer stability (*Russian*) 4-72280  
 aquatic animals, mechanism of flow around (*Russian*) 4-72281  
 arthropods, minute wingless, active aerial dispersal, exploitation of boundary-layer vel. gradients 4-66987  
 cerebrospinal fluid, shunt flow, quantitative evaluation using <sup>99m</sup>Tc 4-81796  
 Doppler flow meas. and processing, signal-to-noise ratio enhancement 4-100286  
 Doppler velocimeters, coded, signal-to-clutter: ratio limitation, cardiology appls. 4-100285  
 fluid velocity measurement, two-dimens., case of digital-speckle correl. techniques 4-87815

**biological fluid dynamics continued**

- hydrodynamic resistance, active control by skins of dolphins (*Russian*) 4-72278
- intracranial pressure, long-term monitoring 4-67143
- intracranial pressure, modelling by the least squares method 4-89643
- intracranial pressure during epileptic seizures 4-100190
- lung, interstitial fluid press. gradient, excised dog lung, micropuncture obs. 4-93773
- optic secretions of dolphins, nature and hydrodynamic activity (*Russian*) 4-72283
- pleural liquid pressure gradients and intrapleural distribution of injected bolus 4-93786
- protein precipitate, shear induced break-up during exposure to laminar Couette flow 4-79547
- skin, human, temp. distrib., blood flow, perspiration and metabolic heat generation effects 4-62446

**biological macromolecules** *see macromolecules; molecular biophysics***biological membranes** *see biomembranes***biological sciences** *see biology***biological specimen preparation**

- blood cells, elemental profiles, PIXE anal. 4-100387
- critical point drying technique improvement for SEM 4-93984
- cytochrome oxidase, crystalline, selective contrast in electron microscopy 4-100419
- diatom cell walls, metal coating and high resolution SEM 4-100411
- electron microscopy, frozen-hydrated specimens prep. for high resolution studies 4-115318
- ethanol coolant for rapid freezing of biological material 4-89860
- freeze-dried cryosection preparation, sublimation rates of ice in cryoultramicrotome 4-62647
- freeze-dried cryosection preparation using section press and low elemental support 4-62645
- HeLa cells, mitotic apparatus SEM studies 4-100412
- lipid extraction during freeze-substitution of bacterium cells for electron microscopy 4-89862
- microtome, instrumented for improved histological sections and fracture toughness meas. 4-62637
- monocytes, human, liq. propane jet-freezing, freeze-drying and rotary replication of cytoskeleton and membrane assoc. struct. 4-89861
- multiformat electronic cell sorting system 4-105392
- multiformat electronic cell sorting system 4-105393
- neutron activation and PIXE anal. 4-100380
- nucleic acid containing struct., selective staining using uranyl acetate-lead citrate 4-89852
- PIXE anal., preconcentration method low temp. ashing evaluation 4-100382
- PIXE determ. of Se in biological samples with preconcentration technique 4-100384
- plastic embedded hard tissues, prep. of surfaces and incident light fluoresc. microscopy 4-77429
- proteins, soluble, specimen prep. methods for electron crystallography 4-100415
- rat liver, cryoprotected, cryosectioning 4-85598
- Reichert-Jung freeze fracture apparatus, anticontamination device modification 4-89863
- SEM, high-resolution, prep. for obs. of fine struct. of biological specimens 4-100395
- slam freezer, liq. He cooled, design 4-115299
- target preparation, rel. to element distrib. deviation 4-105387
- thin cryosections, surface defects, SEM and TEM studies 4-100413
- urine, ion exchange, selective preconcentration method, PIXE anal. 4-100383
- Be coating for X-ray microanalysis 4-77431

**biological techniques and instruments**

- see also biological specimen preparation; biomedical equipment; biomedical measurement; microelectrodes; specimen preparation*
- action potential, circuit for max. rate of rise meas. 4-77432
- airflow perturbation device for measuring airways resistance of humans and animals 4-115297
- animal circadian activity plotting, microprocessor-based device, IR beam breaking 4-89865
- area detectors for protein X-ray crystallography at storage rings 4-100379
- arterial system, clinical parameters indirect determ. method using velocimetric data (*French*) 4-67154
- autoradiographic images of cerebral cortex, computerised 2D and 3D reconstructions 4-100405
- axonal transport dynamics, phys. methods for study, review 4-89851
- bacteria, aerosol, mass spectrometry anal. 4-67153
- bacteriology, use of a laser Doppler electrophoresis method 4-115288
- bacteriorhodopsin photocycle obs., using tunable pulsed dye laser cryogenic photocalorimeter 4-105005
- bag-in-box system, characterising and correcting for dynamic response 4-89858
- binaural measurement system, microcomputer-based 4-100407
- binaural fixation misalignment measured by border enhancement: a simplified technique 4-62486
- biomacromolecular crystals, HVEM for high resolution low-dose studies 4-115319
- biomembrane permeability properties, temp. depend., mass spectroscopic obs. 4-93698
- biomolecules dynamics obs., high-pressure EPR meas. of aqueous samples 4-86458
- biooptical profiling system 4-110272
- biopolymers, dielec. props. meas. 4-106332
- bioheology, new methods, conf., Nancy, France (Aug. 1983) 4-106097
- bioheology, new methods 4-106089
- biotechnology for industrial chemistry (*German*) 4-114880
- biotelemetry device linked to Apple II 4-62636
- bipolar stimulating electrode, small and atraumatic, for use on fine relatively inaccessible nerves 4-115309
- blastocysts, mouse, heavy metal incorporation and distrib., micro-PIXE anal. 4-100389
- blood, rheological properties during clotting, study methods 4-110009
- blood, smokers and non-smokers,  $\alpha$ -activity meas. by CR-39 SSNTDs 4-100371
- blood cells, mag. parameters and high gradient paramagnetic and diamagnetic phoresis 4-109848
- blood filtration measurements, recent progress in improving data processing 4-110016

**biological techniques and instruments continued**

- blood flow waveforms reproduction in vitro, digitally controlled system 4-77433
- blood rouleau formation, expt. approach, comparison of 3 methods 4-110015
- blood viscometry, co-axial, accuracy improvement 4-115279
- blue particles in cancerous organs, laser micro-Raman spectrosc. obs. 4-62455
- body fluids anal. by direct plasma emission spectrometry 4-100410
- bone mineral content measurement using dual photon absorptiometry, prototype apparatus (*French*) 4-67155
- breathing pattern and occlusion press., system for microcomputer-assisted on-line meas. 4-89857
- cadaver segments, inertial props. meas. method 4-110018
- cancer cells, laser-excited microscopic fluorescence measurement method (*Japanese*) 4-115315
- cart pushing and pulling, human motion anal., specialised laboratory 4-89645
- ceramic electrodes for ELF bioeffects studies 4-115296
- chemical concentration meas., continuous, optical fluorescence sensors 4-85584
- chemiluminescence, ultraweak, monitoring of emission from rat hearts 4-93979
- cinematography, automated, high-speed simulated vehicle-pedestrian impact motion anal. appls. 4-115098
- cochlea, guinea pig, hair cells in isolated coils, study technique 4-110017
- cochlea, rodent, computerised reconstruction of regional blood flow 4-115293
- cochlear blood flow meas. technique combining microspheres with surface prep. dissection 4-93981
- collagen fibres, histological staining as a meas. of stress 4-110020
- collagen fibres, stiffness and strength relations on maturation, clamping and stretching procedure 4-62643
- collimator for X-ray diffr. from very small samples using synchrotron radiation 4-62641
- colonial hydroid macrofouling, control by free-field US radiation 4-89866
- contrast threshold, rapid meas. system 4-105238
- coordinated locomotor behaviour in rats, automated quantitative anal. 4-100406
- cornea microscopy using soft contact lens (*Italian*) 4-81818
- cortical evoked potentials using a microcomputer for stimulation and analysis 4-115277
- Coulter volume cell sorting to improve the precision of radiation survival assays 4-67159
- cowpea mosaic virus, synchrotron radiation X-ray diffr., data collection and processing 4-81821
- crotoxin complex thin cryst., expt. strategy in 3D struct. determ. 4-100416
- crystalline lens, intact, nondestructive method for refr. index meas. 4-67161
- CW technique for elastic props. of cortical bone meas. 4-81823
- cytoskeletal components visualisation using surface refl. interference microscopy 4-62646
- dental cementum, human teeth: elemental composition, PIXE anal. 4-100390
- digital temperature controller for low-temperature light microscopy 4-115314
- dimyristoylphosphatidic acid, phase transition 4-105201
- DNA footprinting in vivo, use of light 4-85593
- DNA-containing bacteriophages, packing model using small-angle X-ray scatt. data 4-85404
- dried whole blood and blood plasma, U determ. using track detectors 4-100372
- dry aerosol production system for direct plasma emission anal. of body fluids 4-105395
- dual vial waveguide exposure facility for examining microwave effects in vitro 4-72467
- EELS for quantitative X-ray microanalysis, mass thickness determ. 4-62644
- electro-oculogram, gain calibration method using eye optical props. 4-115306
- electrodes, intraneural, coated wire, for chronic stimulation 4-100423
- electron density map, OMITMAP, for error exam. in macromolecular model 4-100064
- electron microscopic autoradiography, rapid, improved method using  $\text{En}^3\text{Hance}$  4-115301
- electron microscopy, electron beam irradiation damage rel. by cooling to 4K 4-65158
- electron microscopy, image reconstruction from projection 4-85596
- electronic rotameter for quantitative evaluation of rot. behaviour in rats 4-85590
- electrophoresis experiments on Salyut-7 orbiting space station, holographic interferometric obs. method 4-74468
- EMG, intraluminal electrodes, evaluation for oesophagus and gastrointestinal tract studies 4-115313
- EMG, respiratory muscle, fatigue anal., processing methods 4-77438
- emission tomography, utilising side information 4-72360
- ergometer, UT-7508, upgrading of automatic physical load control 4-93977
- erythrocyte aggregation, viscometric technique for meas. 4-110014
- erythrocyte deformability, assessment by constant flow filtration technique 4-115282
- erythrocyte deformability, leukocyte removal prior to study, improved method 4-115285
- erythrocyte filtration resistance at constant press., technique for continuous meas. 4-115283
- erythrocytes, human, 3D image anal. in reflection contrast 4-89525
- ESR spectroscopy, membrane and cell microrheological study appl. 4-115289
- ethanol fermentation, elec. impedance meas. as in situ sensor 4-85587
- exercising muscles, blood flow meas. by Xe clearance and microsphere trapping 4-89620
- eyes, microwave radiation hazard, metal-framed spectacles effect 4-109877
- eyetracker system for office use, performance 4-62638
- fibre Fizeau interferometer for minute biological displacements meas., tympanic membrane appl. 4-89853
- fish, spatial sonic guidance (*Russian*) 4-72464
- flash kinetic spectrophotometer employing photodiode array sensors 4-81819
- flowmeter for slow-flowing physiological liquids 4-115311

**biological techniques and instruments continued**

- fluorescent dyes, photoelectron microscopy and photoelectron quantum yields, labelled cpds. appl. 4-82869  
 fluorometer, ns, for biomembrane rheological aspects study 4-115291  
 fluorometry, multifreq. phase and modulation, in biophys., book contrib. 4-93985  
 gamma-ray scatt. techniques for NDT and imaging 4-63834  
 Gilson respirometer range increase, use of Gilmont syringe 4-81827  
 glass microelectrode coated with a ferromag. thin film, development and characts., neuroscience appl. (*Japanese*) 4-100401  
 glass microelectrodes, electroosmotic effects, rel. to electrode selection improvement 4-89854  
 glass microelectrodes, power spectrum density anal. 4-81820  
 glutamine synthetase, mois., time-resolved low dose electron microscopy 4-100420  
 grating laser microscope for microvessel blood flow vel. meas. 4-115281  
 haematocrit-erythrocyte-disaggregation apparatus 4-110013  
 hair, human, trace element incorporation, micro PIXE anal. 4-100393  
 hair, proton-induced X-ray fluorescent anal. for trace element anal. 4-89360  
 hair, trace element anal. of workers using CS<sub>2</sub> (*Chinese*) 4-72000  
 harmonic and impulse rheological tests of biomaterials 4-110012  
 hemoglobin macromolecule, STEM studies, 3-D reconstruction 4-115013  
 Hemorheometer, automated apparatus for filtration initial flow rate meas. 4-115284  
 high voltage pulsed discharge, runaway electron investigation 4-84089  
 high-power automatic network analyzer for measuring the RF power absorbed by biological samples in a TEM cell 4-115294  
 hippocampal EEG rel. to spectral anal. of hippocampal unit train 4-67152  
 human lung,  $\alpha$ -active nuclides microdistrib. using CR-39 SSNTD 4-100370  
 human skin, proton and electron microprobe analysis 4-105390  
 human tooth enamel, apatite crystals, carious dissolution, electron microscopy study 4-85599  
 hyaluronate gels, macromolecules, diffusion, methods and preliminary results 4-100366  
 image processing, shading compensation, A/D convertor appl. (*Japanese*) 4-85595  
 immunoelectron microscopy of ribosomes, book contrib. 4-93988  
 imperfect 2D crystals, 3D reconstruction 4-100417  
 implantable electric field probes, performance characts. 4-89855  
 integrating system for energy meas. from flashlamp-driven dye laser UV source 4-67158  
 interactive image analysis, neuroscience appls. 4-100409  
 intestine segment, scintigraphic assessment of intraluminal vol. and motility 4-72468  
 intracellular recording, calibration pulse appl. device 4-115310  
 ion beam and RF plasma etching effects on tissue section, ultrastructural comparison 4-77430  
 ion microscopy, lung trace elements distrib. imaging appl. 4-115316  
 Karlsruhe proton microprobe appl. to medical samples 4-105389  
 kidney, elemental conc. meas. in mouse arteries, micro-PIXE anal. 4-100385  
 knee capsule deform., microprocessor-based tissue displacement monitor 4-89864  
 laser blood Doppler velocimeter, temporal resolution estimation with optical fiber 4-66989  
 laser Doppler microscopy obs. of cytoplasmic motions in growing pollen tube tips 4-89535  
 laser method for N isotope composition determ. in biological objects 4-81825  
 laser microfluorometer, chromatin functional state study by laser fluoresc. microirrad. 4-72213  
 laser microprobe mass anal., organic mass peaks for internal standards 4-95556  
 laser microscope, design (*Japanese*) 4-82824  
 laser safety in medical appls. 4-85524  
 lenses, normal and cataractous, PIXE and microprobe anal. in rats and humans 4-100386  
 leukemia manifestation in blood cell microelement profile, nuclear microprobe determ. 4-100388  
 lifting stress calculator, microprocessor-based device 4-100408  
 linear accelerator system, microcomputer controlled, space flight induced vestibular changes appl. 4-89867  
 lipophilic cation use as membrane potential probe, critical assessment 4-77205  
 liquid crystals, electronographic images, spatial charge determ., bulk elec. props. anal. appls. 4-89850  
 liquid sample preparation, automated systems 4-63728  
 liver tissue, global element composition comparison with different cell fractions composition PIXE study 4-105391  
 living organs metabolism, in situ monitoring with laser fluorimeter system 4-85586  
 locational stereology within rat aortic wall sampling fields, microcomputer based method 4-115300  
 long bone cross-sectional moment of inertia, noninvasive meas. by photon absorptiometry 4-62642  
 low-level microwave treatment of mountain pine beetle and darkling beetle 4-115125  
 luminescence and fluoresc. methods, review 4-115324  
 lung tissue, inclusion identification by Raman microprobe 4-105380  
 macromolecular complexes, electron micrographs, 3D image reconstruction 4-85597  
 macromolecules, rheologically active, studies by: quasielastic light scatt. 4-115292  
 macromolecules, X-ray diffraction intensity meas. by photographic method (*Japanese*) 4-105384  
 maize root cells, NaCl-treated, organelles energy dispersive X-ray anal. 4-99905  
 manipulator/display system, computer-controlled, for human movement studies 4-85588  
 mass spectrometer ion flow in membrane diffusion of various molecules 4-115276  
 mechanical impulse system for myotatic reflex investigation by EMG obs. 4-115312  
 micro-irradiation of single living cells using UV and visible light 4-115326  
 microbeam design considerations for biological appl. 4-115325  
 microbiological fouling and scaling meas. with flow cell array 4-115436

**biological techniques and instruments continued**

- microdrive for extracellular recording of single neurons using fine wires 4-93980  
 microfluorometer, pulsed laser, automatic, with high spatial and temporal resolution 4-89859  
 microorganisms, enumeration by their dynamic AC conductance patterns, model and expt. method 4-62453  
 microspectrophotometer, computerised using fibre optics, for quantitative microscopy 4-62648  
 microtome, instrumented for improved histological sections and fracture toughness meas. 4-62637  
 microvessel hydraulic conductivity, meas. in microvessels, effects of compliance 4-105382  
 microwave interferometer system for biological subject displacement meas. (*Japanese*) 4-110019  
 mineral standards, Au decorated, application of XPS 4-100374  
 molecular biology, structure determination, image averaging methods comparison 4-100062  
 multi-barrel glass micropipettes prep., David-Kopf puller modification, brain recording appl. 4-115308  
 multielectrode microprobe for extracellular biopotential recording 4-115320  
 multimicroelectrode measurement system for neuron research (*Japanese*) 4-93983  
 multiplexed SQUID vectormagnetometer for biomagnetic research 4-89607  
 multiplex illumination system, controllable synchronised, for electronic speckle pattern interferometry and holography, 4-101909  
 muscle force estimation from intramuscular total press. 4-115114  
 muscular strength of upper extremity, meas. apparatus design 4-105279  
 myocardial capillaries, anisotropic, length and surface density estimation method 4-115302  
 myocardium microcirculation, indirect determ. of fluid filtration and reabsorp. 4-93771  
 nanosecond time-resolved low angle X-ray diffraction expt. facility appl. 4-115317  
 Nautilus, remote telemetry of daily vertical and horizontal movement in Palau 4-77434  
 nervous tissues, diffusely arranged, conductivities and anisotropies, determ. and importance in neurophysiological studies 4-93978  
 neuromuscular function in anaesthetised dogs in compression chambers, remote monitoring 4-100375  
 neutron scattering, quasi-elastic and inelastic, biophys. appls., book contrib. 4-93989  
 NMR, metabolic monitoring appls. 4-105321  
 NMR, solid state, of protein internal dynamics, book contrib. 4-93695  
 NMR high field spectroscopy of tissue in vivo, double reson. surface coil probe 4-81824  
 NMR image contrast, intrinsic parameters 4-89673  
 NMR imaging, basic principles and appl. (*Japanese*) 4-77368  
 nonvolatile organic molecules analysis, laser desorption technique 4-109699  
 nuclear radiations, biomedical appls. 4-77352  
 open-circuit indirect calorimetry, gaseous exchange anal. 4-85589  
 optical methods for quantitative cytochemistry 4-115322  
 optical microscopy, cell biology appl., rel. to newer methods 4-115321  
 optical sectioning microscopy, cellular architecture in three-dimens., book contrib. 4-93986  
 oyster shells, element distrib., environmental and chronological effects PIXE investigation 4-105067  
 particle and photon excited X-ray charact. spectra, appl. to trace element anal. of hair 4-99887  
 patch clamp studies of single ionic channels, book contrib. 4-93710  
 peripheral nerve impulse cond. blocking by local cooling, animal expt. method 4-115307  
 Philips EM 300 electron microscope, cold stage for biological specimens 4-95579  
 phosphate ester protons selective obs. by <sup>1</sup>H-<sup>31</sup>P spin-echo difference spectroscopy 4-95484  
 phospholipid bilayers, latent heat meas. by adiabatic compression 4-85407  
 photodiode technique for eyeball retraction latency meas. in conscious rabbits 4-81826  
 photophysical methods, continuous excitation, cellular rheology appl., interests and limits 4-115290  
 PIXE, anal. of biological and medical samples 4-105063  
 PIXE's, analytical appls., conference, Heidelberg, Germany (July 1983) 4-95034  
 PIXE anal., sample and target prep. 4-100380  
 PIXE anal., target prep. influence in rate organs 4-100381  
 PIXE and neutron activation methods in human hair material analysis 4-99895  
 PIXE semi-microprobe analysis, proton CT as means of density normalisation 4-105077  
 PIXE technique for environmental and biomedical anal. 4-99873  
 PIXE trace anal. of biological materials, using single multielement standard 4-105385  
 PIXE trace element anal., biological appls. 4-105064  
 plankton monitoring system, image analysis and silhouette photography methods 4-105779  
 plasma, human, surface rheological obs., meas. head 4-115089  
 plethysmograph for respiration rate meas. of rats with lung damage 4-105394  
 portable detectors for <sup>125</sup>I-insulin absorption measurement during subcutaneous infusion with portable pumps 4-67157  
 positron emission tomography, count normalisation methods, statistical anal. 4-72358  
 power-frequency elec. fields, system for cell suspensions exposure 4-100365  
 pressure meas. using <sup>29</sup>Si diffusion tensometers, parasitic photosensitivity 4-101829  
 probes emitting annihilation delayed fluoresc. for model and biological membrane study 4-66893  
 probing EM fields in lossy spheres and cylinders simulating biological objects 4-115295  
 protein crystallography, accuracy and resolution, probabilistic approach 4-100065  
 protein crystals, X-radiation damage reduction by polyethylene glycol 4-81822  
 protein structure fluctuations from X-ray diffr., book contrib. 4-93688

**biological techniques and instruments continued**

- proton-induced characteristic X-rays ultrasoft: X-ray source, biological appl. 4-72472
- purple membrane, surface pot. and sidedness, resonance Raman dye probe method and obs. 4-67151
- radiation protection instrumentation for medical and biochemical radionuclide laboratories 4-77403
- radiometric determination of the growth rate of *Nautilus* in nature 4-72469
- Raman microprobe, bioaccumulations in cells and tissues 4-115304
- real-time optical imaging of naturally evoked electrical activity in intact fog brain 4-72470
- red blood cells, human, Cu determ., AAS 4-100364
- red cells aggregation in space, meas., NASA Space Shuttle project 4-109970
- research reactor role in ionising radiation appls. and technology 4-74037
- respiratory calorimetry, calibration methods 4-100396
- RF power absorbed by biological samples meas., using high-power network analyser 4-85600
- rumen marker in sheep using tritiated water 4-77436
- rumen volume and volatile fatty acids prod. in sheep,  $^{14}\text{C}$ -VFA use for meas. 4-72473
- sarcomere length determ. using laser diff., effect of beam and fibre diameter 4-89849
- saturation-transfer ESR spectra, standard conditions for meas. 4-100400
- scanning CARS microscope, mol. discrimination and contrast enhancement 4-93982
- scanning microscope 'photometry' for automatic analysis of G-banded human chromosomes 4-62649
- scanning transmission soft X-ray microscopy with Fresnel zoneplate, biological specimen images 4-95585
- science with soft X-rays, conf., Upton, NY, USA (Oct. 1983) 4-90288
- sequential pulse generator for producing true biphasic stimuli for nervous tissue stimulation 4-100376
- serial section graphical reconstruction, GRIDSS programs 4-73504
- signal processing, time domain vs. spectral domain analysis, EMG 4-77437
- similar pattern two-dimensional pattern analysis, electrophoretogram data extraction appls. 4-107531
- SIMS, Ca isotopes selection 4-115303
- single photon emission computer tomography, collimation, sampling, filtering interactions 4-72359
- skeletal imaging, comparative studies on  $^{99\text{m}}$  Tc-pyrophosphate and  $^{85}\text{Sr}$ -chloride 4-93860
- skeletal maturity, syntactic recognition 4-72354
- skin conductance response analysis, microcomputer package 4-62635
- skin-surface recording electrodes, practical considerations in use 4-85557
- soft X-ray imaging, diff. pattern meas. of single micro objects 4-100369
- soft X-ray imaging of hydrated biological specimens 4-100368
- soft X-ray microscopy, TEM and SEM, imaging of blood platelets 4-100367
- solid state nuclear track detector use in radiation dosimetry, medicine and biology 4-72430
- sphere size distrib. from profile area distrib. using non-parametric method 4-86384
- spinal cord, technique for recording from single neurons in awake cats 4-115305
- strain topography of human tendon and fascia 4-110021
- surface coil spin-echo spectra without cycling the refocusing pulse through all four phases 4-100399
- sympathetic nerves, multiunit neural activity meas., assessment of 3 techniques 4-72465
- synchrotron system for monochromatic UV irradiation 4-67160
- synchrotron X-rays for digital subtraction coronary angiography 4-72367
- Technicon Ektacytometer: automated exploration of erythrocyte function 4-115286
- teeth, enamel layer, trace element distrib., PIXE and PIGE anal. 4-100391
- teeth, human, enamel pre-carious lesions, trace element surface distrib., PIXE anal. 4-100392
- thermoelectric microscope stage for meas. of supercooling points of microscopic organisms 4-100402
- thread-forming property of biological fluids, apparatus for meas. 4-115280
- time resolved modulated carrier rapid flow system for EXAFS spectroscopy 4-100377
- time-domain dielectric spectroscopy, use with lossy dielectrics, precautions in use 4-85592
- time-resolved fluoresc. anisotropy decay anal. 4-105381
- time-resolved Laue diffraction from protein crystals 4-100378
- tip growing plant cells, intracellular Ca distrib., PIXE meas. 4-100394
- tissue, broadband pulsed ultrasound appl., frequency-dependent attenuation meas. 4-100421
- tissue culture cells on deformable substrata: biomedical implications 4-100414
- tissue permittivity, in vivo and in vitro expt. techniques and results 4-62640
- tissue specimens, Pu/U quantitative assay using fission track detectors 4-100373
- tissue temp. profile reconstruction from microwave radiometry, optimisation 4-72466
- tooth enamel, human, struct., digital Fourier harmonic superposition method 4-89495
- total internal reflection fluorescence, book contrib. 4-93987
- toxic effect of Al in grape vines, PIXE, anal. 4-105388
- transducers, sensors of biological organisms, overview 4-85585
- transmembrane channels of *E. coli*, 3D reconstruction from electron micrographs 4-100418
- tumour of hamsters, time depend.  $^{10}\text{B}$  movement, in vivo meas. 4-62634
- tumour-related tissue samples, from mice, radioisotope induced X-ray fluoresc. anal. 4-105289
- TV-contrast enhancement methods for chromosome analysis 4-115223
- urea and other wastes in uremic canine dialysate canine dialysate, direct electrolytic oxidation 4-89307
- urea inclusion cmpds., Raman spectroscopic determ. 4-102684
- US pulse-echo attenuation meas. in tissue, diff. correction 4-100422
- virus microcrystalline layers, images in electron microscopy, digital storage methods 4-85594
- viscometer using mag. fluid for biological fluids meas. 4-110011
- viscometric methods for assessing red cell deformability and fragmentation 4-115287

**biological techniques and instruments continued**

- visual pigments, dense samples, method for 'peak absorbance' meas. 4-81828
- voltage clamp expts., simulation with FET analogue circuits 4-85591
- Weissenberg rheogoniometer based biorheological methods, blood appl. 4-110010
- whole-body vibr. meas. by double-pulsed holographic interferometry, human subject obs. 4-100398
- Wicksell's corpuscle problem solutions, comparison by simulation 4-115298
- X-ray beam line, double focusing for EXAFS 4-95623
- X-ray diffraction crystallography using MWPC 4-59520
- X-ray imaging system, 2-D, for very small objects, using scanning slit detection 4-111261
- X-ray microanalysis of bio-organic bulk specimens, surface roughness and use of peak to background ratio 4-100403
- X-ray microholography of biological specimens 4-72471
- X-ray scattering, small angle, from compact bone 4-97960
- X-ray tomography systems, appl. to nondestructive testing 4-71811
- $^{10}\text{B}$  loaded macromolecules in expt. physiology, tracing by neutron capture radiography 4-67156
- $\text{O}_2$  consumption rates and diffusion coeffs. in multicellular spheroids, determ. method 4-115278
- $\text{O}_2$  partial pressure meas. in vivo, fibre-optic probe method 4-62633
- Pt distrib. in black mice with adenocarcinoma, neutron activation anal. determ. 4-62639
- Ti microelectrodes, simple method for shaping 4-89856
- U conc. in urine, fluorometric meas. method 4-72438
- Y, localisation behaviour and tumours in nude mice, PIXE investigation 4-105386
- biological transport** *see* **biotransport**
- biology**
- see also biological fluid dynamics; biological techniques and instruments; biophysics; blood; cardiology; ecology; evolution (biological); medicine; physiology; zoology*
- Arctic Ocean, palaeosedimentation rate var. from amino acid epimerization 4-110130
- bacteria, near-IR spectral rel. to identification of interstellar grains 4-67780
- Belgium coastal zone, physico-chemical characts. and ecosystem dynamics 4-94137
- Bernoulli eqns., n coupled class, linearisation 4-105167
- biogeochemical processes, effect on climate 4-82227
- biosphere, global C cycle, simulation anal., effects of human interference 4-93665
- book, annual review of biophysics and bioengineering 4-90305
- conodonts, O isotopic comp., use for palaeoclimate and palaeoceanography anal. 4-110283
- coral reef biological communities influenced by sewage discharge 4-115448
- estuaries comparisons, conf. at Gleneden Beach, USA (November 1981) 4-86122
- evapotranspiration from trees, implications of gradient distributions and flux profile relations above rough forest 4-82204
- evapotranspiration from vegetation, uncoupled multi-layer model for latent heat flux density 4-105618
- forests, anthropogenic effects, implications for climate 4-94237
- heather moorland, transpiration and evaporation meas. 4-105619
- interstellar biological grains, evidence against 4-106055
- kelp culturing and utilisation for methane production 4-114887
- Ligurian Sea, colour remote sensing and surface chlorophyll 4-67266
- marine bioluminescence remote sensing, role of in-water scalar irradiation 4-85679
- marine sediment transport, effects of benthos 4-94083
- Non-equilibrium open system model, laser and biological systems (Japanese) 4-74476
- ocean, biological productivity rel. to growth and comp. of Co-rich ferromanganese crusts 4-67206
- ocean, denitrification rates and availability of organic matter in marine environments 4-67282
- ocean colour remote sensing by satellite (book) 4-78070
- ocean primary productivity fluctuations, effect on atm.  $\text{CO}_2$  conc. 4-94182
- oceanic processes, effects of Se IV and VI distrib. 4-82086
- oceans, high latit. productivity rel. to determ. of atmospheric  $\text{CO}_2$  conc. 4-62908
- OCEANS '83, utilisation of sea, conference, San Francisco, CA, USA (Aug.-Sept. 1983) 4-106113
- Pacific Ocean, atm. surface layer Hg conc., correl. with marine upwelling and biological prod. 4-105599
- Prudhoe Bay Causeway, Alaska, environmental impact assessment 4-114967
- seaweed mariculture trials, critical pathway approach 4-114966
- transuranic elements, distribution and behaviour off French Channel shore 4-105137
- tree ring C isotope record variability within and between trees 4-115607
- $\text{NO}_x$  pollutants in atm., conf. at Maastricht, Netherlands (May 1982) 4-101576
- Si geochemical processes (book) 4-78057
- U, levels in marine waters and biota, using SSNTD 4-100052
- biology computing**
- see also computerised instrumentation; computerised signal processing*
- 450-MHz RF exposure of man, specific absorption rate average and distrib. 4-115119
- autoradiographic images of cerebral cortex, computerised 2D and 3D reconstructions 4-100405
- autoradiographs of rat brain, computer-assisted video anal. 4-100404
- biotelemetry device linked to Apple II 4-62636
- breathing pattern and occlusion press., system for microcomputer-assisted on-line meas. 4-89857
- cardiac action potential sequential processing 4-81829
- cortical evoked potentials using a microcomputer for stimulation and analysis 4-115277
- didactic microcomputer simulation in cardiac dynamics 4-81737
- femur, stress distrib., three-dimensional finite element anal. (Italian) 4-81723
- ileum, rat, pendular movements of longit. musculature, computer aided Fourier spectral analysis (German) 4-62505
- locational stereology within rat aortic wall sampling fields, microcomputer based method 4-115300

**biology computing continued**

- marine ecosystems, image analysis and silhouette photography for plankton investigations. 4-105779
- molecular biology, structure determination, image averaging methods comparison 4-100062
- ophthalmotropes, computer-based 4-81666
- phrenic neurograms, computer algorithms for processing 4-100397
- polyoma virus hexamer tubes, computer image modelling of pentamer packing 4-100079
- scanning microscope photometry for automatic analysis of G-banded human chromosomes 4-62649
- serial section graphical reconstruction, GRIDSS programs 4-73504
- skin conductance response analysis, microcomputer package 4-62635
- SRT-1000, Soviet computerised tomograph, design, operation and results (Russian) 4-81811
- vestibular semicircular canal responses during righting movements of falling cat, simulation 4-81719

**biomagnetism**

- bacteria, magnetotactic,  $\text{Fe}_3\text{O}_4$  precip., mag. guidance of organisms, book contrib. 4-93769
- bacterial magnetite, struct., morphology and cryst. growth 4-100069
- behavioural studies with mice exposed to DC and 60 Hz mag. fields 4-100230
- blood cells, mag. parameters and high gradient paramagnetic and diamagnetic phoresis 4-109848
- cell biomagnetism 4-66971
- cellular magnetism, theory, expts. and appls. 4-89608
- erythrocytes, ferritin conjugate labeled, selective mag. separation 4-89523
- glass fibre sensors, appl. to mag. fields generated by human brain currents (German) 4-95409
- hyperthermia, regional, mag. induction heating, beagle dog model, thermal dosimetry anal. 4-93697
- image reconstruction from neuromagnetic fields 4-72321
- kidney, rabbit, ischemic and reperused, in vitro mag. relax. times 4-81721
- liposomes carrying paramag. species, relax. enhancement, mouse/obs. 4-105182
- lung, ferrimagnetic particles, magnetising process 4-66969
- lung, ferrimagnetic particles, relax. process 4-66970
- magnetic resonance signal intensity patterns obtained from continuous and pulsatile flow models 4-81722
- magnetometry of ingested particles in pulmonary macrophages 4-105264
- magnetosomes dynamics in magnetotactic bacteria 4-105263
- measurements, influence of thermal magnetic noise in conductors 4-80635
- medical applications of mag. phenomena, review 4-105314
- methylcholanthren carcinogenesis in mice, effect of a static uniform mag. field 4-77304
- migratory bird, transequatorial, mag. orientation and mag. sensitive material 4-72276
- multiplexed SQUID vectormagnetometer for biomagnetic research 4-89607
- plant tissue, water exchange studied by  $^1\text{H}$  NMR in presence of paramag. centres 4-66922
- plasmoid MHD wave, impossibility of excitation in physiological aq. soln. 4-66968
- random matrix theory in biological NMR spectroscopy 4-105180
- somatosensory evoked cerebral magnetic fields from SI and SII in man 4-77269
- spin-lattice relaxation of protons, freq. dependence in mag. resonance of biological materials 4-77193
- time-varying mag. fields, thresholds for biological effects 4-93792
- tissue  $^1\text{H}$  NMR relaxation times and mechanisms 4-109782
- tissues, bioelectric activity, weak mag. fields 4-109847
- urethral closure in females, magnet system 4-62631
- yellowfin tuna, Thunnus albacares, candidate mag. sense organ 4-100184
- $\text{Fe}_3\text{O}_4$ , biogenic, mag. props. (Japanese) 4-72277
- $^{15}\text{N}$  relaxation sinks in protein backbones, in vivo NMR field-cycling spectroscopy 4-72212

**biomass conversion** *see bioenergy conversion***biomechanics**

*see also biological fluid dynamics; biorheology*

- adductor pollicis, differential effects of isometric and dynamic training on mech. props. 4-93775
- aerospace biodynamic test devices and methods, AGARD report 4-78058
- aerobic energy prod. and efficiency in rats during exercise 4-93785
- anatomy constrained by elastic support, semi-empirical press. anal. 4-115106
- ankle joint biomechanics, effects of fibular shortening 4-100226
- aortas, thoracic and abdominal, human, static elastic props. 4-100206
- aortic bifurcation geometry, changes during a cardiac cycle, rabbit obs. 4-115110
- arm, phasic relations in  $90^\circ$  abduction-adduction, ARIMA representation 4-62516
- arm motion, approach to control laws 4-115099
- arterial wall distensibility rel. to flow distrib. 4-115112
- arterial wall model, 2-layer, parameter sensitivity anal. and improvement 4-105285
- arteries, 3D stress distrib. 4-77294
- arteries, elastic props. and their influence on the cardiovascular system 4-109870
- articular cartilage, fluid transport and mech. props. 4-81731
- articular cartilage, mechanical response to an oscillating load 4-115113
- articular cartilage, unconfined compression anal. 4-109868
- bacteria shape changes, surface stress theory 4-77207
- biomechanical properties meas. using random vibr. 4-66988
- biomedical and rehabilitative engng. for the phys. and/or sensory handicapped (Japanese) 4-89832
- biped landing, impact effects study 4-115101
- blood vessels, mech. strength props. functional diagnostics 4-89636
- bone, cortical, CW technique for elastic props. meas. 4-81823
- bone, human tubular, struct. features rel. to ultrasound meas. 4-89650
- bone, long, deform. rate rel. to flexural fracture behaviour 4-77276
- bone, mech. and stress adaptive props. 4-77271
- bone cement failure criteria, acetabular region appls. 4-105377
- bone cutting force, rel. to surgical instrument design 4-62503
- bone porosity and specific surface 4-58604
- brain, rotational injury study 4-109855
- cadaver segments, inertial props. meas. method 4-110018

**biomechanics continued**

- cancellous bone strength measurements with the osteopenetrometer 4-89793
- capacitive transducer for continuous measurement of vertical foot force 4-85541
- cardiac myocytes, rat, passive stiffness obs. 4-100101
- cardiopulmonary resuscitation system based on intrathoracic and abdominal press. variations 4-89826
- carotid arterial walls, aged human, dynamic radial distensibility (French) 4-66983
- cart pushing and pulling, human motion anal., specialised laboratory 4-89645
- cell interaction models based on differential adhesion 4-100103
- cell membranes, electroelastic effects 4-77206
- cellular elastic props., acoustic microscopy obs. 4-100095
- cerebral palsy, evaluation of upper extremity motion abilities (Japanese) 4-115249
- cervical spine, human, 3D model for impact simulation 4-105281
- cervical spine, normal, injured and stabilised: in vitro kinematics 4-81730
- cirral ligaments of a crinoid, nervously mediated change in mech. props. 4-66985
- cochlea isolated from guinea pig, sensory-cell hair bundles stiffness 4-109837
- cochleas used for basilar membrane mechs. studies, ultrastruct. damage 4-93758
- collagen, freeze-dried and reconstituted, mech. response under compressive loads 4-109857
- collagen fibres, histological staining as a meas. of stress 4-110020
- collagen fibres, stiffness and strength relations on maturation, clamping and stretching procedure 4-62643
- composites, biological, struct. and mech. props., book contrib. 4-66990
- conference, New Orleans, USA (April 1982) 4-73136
- coordinated locomotor behaviour in rats, automated quantitative anal. 4-100406
- cortical bone, bovine, elastic props. rel. to microstruct. 4-72290
- cortical bone, neutron irradiation effects on mech. props. (Spanish) 4-100234
- cradle and pendulum motion, study for health care appls. 4-115266
- crustaceans, bubble form. following decompression from hyperbaric gas exposures 4-93784
- didactic microcomputer simulation in cardiac dynamics 4-81737
- dura mater, glycerol-preserved, human, mech. suitability for prosthetic cardiac valves construction 4-62506
- elbow extensors, human, dynamic force during a rapid voluntary movement (Japanese) 4-93787
- electronic rotameter for quantitative evaluation of rot. behaviour in rats 4-85590
- EMG signals in gait, interpretation 4-89810
- EMG/foot force anal., real time microprocessor system 4-85549
- erythrocyte membrane, elastic area compressibility modulus determ. by cell poking 4-66907
- exercise conditioning system for paralysed leg muscle 4-100349
- exercise efficiency during arm ergometry: effects of speed and work rate 4-93781
- eye movement monitor, inexpensive, using the scleral search coil technique 4-81750
- femoral bone, human, work-of-fracture obs. 4-62515
- finger control in humans, robotic application 4-62519
- fish of scombridae family, linear parameters of body and propelling device (Russian) 4-72282
- forebrain neuron activity in cats during alternating movements 4-72235
- foundations of biomechanics, survey 4-100222
- fracture movement under supporting bandages, performance and results (German) 4-77273
- functional elec. stimulation for standing and forward progression 4-100348
- gait, linear approxs. for swing leg motion 4-109865
- gait abnormalities, human, evaluation by syntactic pattern-recognition method 4-85550
- gait analysis and alignment system for lower-limb prostheses 4-100362
- gammarid amphipods from Lake Baikal, press. effects on thermal preference behaviour 4-105193
- hammer throw, speed pattern and influence of gravity on speed fluctuations 4-115104
- hand contractions quality, meas. instrument 4-77413
- handicapped people, upper extremity motion abilities evolution 4-100189
- head and neck, human, in vitro response to impact 4-105280
- head movement, effect of external viscous load 4-66982
- hip, natural adult, contact-coupled finite element anal. 4-100207
- hip joint endoprostheses, older and modern types, remaining lifetime after loosening (German) 4-62627
- hip joint function assessment by objective gait evaluation (Japanese) 4-100208
- hopping system, one-legged, performance evaluation, simulation 4-115102
- human dynamic responses to fishing vessel motion in ocean waves (Japanese) 4-81724
- human movement biomechanics review, human locomotion study 4-62507
- hydrobionic mechanisms of optimisation of the propulsive arrangement of cetacea (Russian) 4-72279
- ileum, rat, pendular movements of longit. musculature, computer aided Fourier spectral analysis (German) 4-62505
- impulse system for myotatic reflex investigation by EMG obs. 4-115312
- insect flight muscle, cross-bridge interaction with oppositely polarized actin filaments 4-72295
- insect flight muscles, overstepping of two headed myosin bridge 4-66974
- inspiratory airflow in breathing, optimal control 4-89637
- intervertebral disks rel. to fibre stabilisation of bent cylinders 4-77298
- intervertebral joint under compression, time dependent props. 4-89613
- intestine, dog, peristalsis, intestinal movements rel. to contents (Japanese) 4-109861
- intestine segment, scintigraphic assessment of intraluminal vol. and motility 4-72468
- intramuscular fluid pressure during isometric contraction of human skeletal muscle 4-93774
- intrauterine pressure analysis in nonpregnant dysmenorrheic women, microcomputer system 4-81800
- IR diameter gauge for in vitro mech. testing of vascular grafts 4-100293
- isometric muscle force, freq. response during recruitment 4-81735
- isometric muscle force, time response during recruitment 4-81736
- joint forces in the human pelvis-leg skeleton during walking 4-100205
- joint motion in men using electrogoniometers 4-81739

**biomechanics continued**

joints, human, 1 parameter model for error in instantaneous centre of rot. meas. 4-81727  
jumping performance rel. to muscle props. in humans 4-109859  
knee capsule deform., microprocessor-based tissue displacement monitor 4-89864  
knee flexion contracture, electrostimulation, spina bifida 4-100347  
knee joint forces whilst rising from a seated position 4-62518  
knee movement determ. for external orthotic linkage design 4-100228  
laboratory, automated, appl. to rehabilitation 4-81806  
left ventricular contraction model, force length vel. relationship, time varying elastance 4-89612  
left ventricular wall motion, evaluation from cineangiograms, comparison of geometrical models 4-109904  
left ventricular wall motion analysis using operator-independent contour positioning 4-62557  
leg motion analysis during gait by multiaxial accelerometry: theoretical foundations and preliminary validations 4-77296  
lifting maximum acceptable loads, dynamic biomech. evaluation 4-72291  
lifting stress calculator, microprocessor-based device 4-100408  
ligaments, control exerted in joint integrity maintenance 4-109860  
limbs, human, literature review of vibr. anal. 4-62510  
locomotion, human, meas. using simple foot contact switch 4-72443  
long bone cross-sectional moment of inertia, noninvasive meas. by photon absorptiometry 4-62642  
lower extremity, functional evaluation using instrumented gait anal. 4-81803  
lumbar intervertebral joint, soft tissue strain and facet face interaction 4-77287  
lumbar intervertebral joint, soft tissue strain and facet face interaction 4-77286  
lung, excised, static mechs., nonlinearly elastic finite deform. anal. 4-115103  
lung tissue, mech. behaviour, constitutive eqns. 4-105283  
mammalian hearing organ sensory hairs, graded and nonlinear mech. props. 4-105255  
manipulator/display system, computer-controlled, for human movement studies 4-85588  
maximal vertical jumps by humans, control strategies 4-93789  
mechanical stresses as a factor in morphogenesis 4-81606  
mechano-mathematical model of excitation-contraction coupling in muscle tissue, cardiac appl. 4-109853  
metacarpophalangeal joint, stiffness meas., circadian variation 4-93772  
microtome, instrumented for improved histological sections and fracture toughness meas. 4-62637  
models of nonimpact type, review 4-109862  
motor control and spring-like muscles, some problems 4-93788  
motor disorder patients, computer automated evaluation 4-89812  
motor disorders, EMG anal., spectral method 4-105358  
muscle, dynamics, size principle, and stability: math. model 4-89614  
muscle, rabbit psoas, de-membranised fibre bundles, rigor tension, soln. ionic strength depend., X-ray obs. 4-89610  
muscle, rabbit psoas, rigor tension developed by demembranised fibres, depend. on soln. ionic strength 4-66976  
muscle fibres, skinned, frog, radial stiffness in relaxed and rigor conditions 4-66978  
muscle force estimation from intramuscular total press. 4-115114  
muscular strength of upper extremity, meas. apparatus design 4-105279  
myocardial material mechanics, systolic moduli variation in left ventricular dysfunction 4-115105  
neurofunction laboratory for movement disorder evaluation 4-81804  
neuromuscular disease patients, elec. muscle activity during a gradual increase in force 4-93719  
obese subjects, submax. exercise, determinants of increased energy cost 4-89619  
osteon streaming pots., anatomical model, bone electromech. effect characterisation 4-115046  
paraplegic walking via finger control of implanted multichannel-nerve-stimulation unit 4-89841  
peripheral nerve, mech. props. alteration following crush injury 4-62514  
peristalsis, strain gauge transducer for in vivo meas. (Japanese) 4-77284  
phospholipid membrane vesicles, cylindrical, thermal fluctuations 4-81643  
physiological tremor in normal man: predictions of existence, freq. and amplitude 4-77291  
posturographic measurements on children, anal. 4-85451  
posturography rel. to cerebellar diseases 4-72285  
reciprocal walking in paraplegic patients, internal functional elec. stimulation 4-100358  
respiratory mechanical impedances—methodology and interpretation 4-109852  
retropatellar surface, static press. distrib., in vitro meas. 4-77289  
right atrium contractility, nonlinear model for estimation 4-89642  
scoliosis, mech. model 4-81733  
scoliosis correction quantification, rel. to corrective force magnitude 4-89828  
scoliotic spine, finite displacement vector's method 4-100204  
semilunar valve: vibr., math. study, rel. to 2nd heart sound prod. 4-115111  
shoulder stiffness and elasticity of the muscle (Japanese) 4-100209  
simulated vehicle-pedestrian impact motion anal. using automated high-speed cinephotogrammetry 4-115098  
skeletal muscle, length change vel. rel. to tension development 4-109858  
skeletal muscle fibres, sinusoidal analysis of mechanochemical props. 4-89611  
skeletal muscle fibres, skinned, rabbit, contraction at low levels of Mg adenosine triphosphate 4-66977  
ski jumping, biomechs. of optimal flight 4-62512  
skull cavity, press. distrib. 4-66975  
skulls biomechanical analysis, stress transmission by photoelastic coatings obs. 4-66981  
soft contact lens, press. distrib. behind 4-100220  
sperm penetration, mech. hypothesis 4-66906  
spider silk as rubber 4-85453  
spinal, transcutaneous elec. neuromuscular stimulation 4-100346  
sprinting at sea level and altitude, air resistance rel. to biomechs. and energetics 4-81729  
static lifting model, relationship of leads on spine and knee 4-72292  
steady walking on level ground, human, simulation (Japanese) 4-77285  
strain topography of human tendon and fascia 4-110021  
tendon, human, mech. props. and their age dependence 4-109866

**biomechanics continued**

tendon, rat tail, tensile failure: age-dependent influence of strain rate 4-77299  
tendons and fascia from young humans, material props. 4-115107  
thoracic aortas, rat, elasticity in simple elongation 4-62504  
thoracoabdominal movements during CO<sub>2</sub> rebreathing, effect of posture 4-89623  
tibia, human, vibr. anal. using skin-mounted accelerometers 4-100211  
tibiae, human, identification of in vivo vibr. modes by modal anal. 4-77290  
tibial fracture healing assessment rel. to fracture fragments natural freq. 4-100212  
tibial lengthening device and technique based on biomechanical considerations 4-100350  
tibial surface of knee, static press. distrib., in vitro meas. 4-77288  
tissue culture cells on deformable substrata: biomedical implications 4-100414  
tissue pressure and plasma oncotic pressure during exercise 4-89624  
tympanic membrane, mech. vibrs. rel. to directional hearing in grass frogs 4-93751  
upper extremity electro-ergometer 4-89811  
upper extremity joints, functional assessment 4-81802  
vascular compliance changes during hyperthermia, dog expts. and simulation anal. 4-81636  
vascular mechanics, incremental formulations 4-109863  
velocity measurement of humans by computers 4-73196  
ventricles in diastole, incremental elastic modulus 4-115109  
visual reaction time, elec., stimulation of low threshold muscle afferents 4-72286  
walking period prediction, EMG processing method for prosthesis control (Japanese) 4-93967  
wrist, computer-simulated, range of motion 4-93790  
DNA, stress induced nonlinear struct. transition 4-100071  
**biomedical applications of computers** *see medical computing*  
**biomedical electronics**  
*see also electrocardiography; electroencephalography; microelectrodes; patient monitoring; patient treatment; prosthetics; sensory aids*  
acceptable high technology 4-67144  
anaesthesia parameters monitoring with electronic device (German) 4-72444  
auditory stimulus polarity indicator device construction 4-67136  
blind persons electronic aids, review 4-115270  
body surface potential mapping system development (Japanese) 4-72446  
circulation parameters rel. to electronic oscillography (German) 4-67133  
converter (transducer) systems for bio-data recording and bio-data processing (German) 4-77414  
cranial imaging of newborn infant, elec. resistivity tomographic technique 4-89814  
electrical nerve stimulators, meter for pulse amplitude meas. 4-93964  
electronics applications, development from idea to finished product (Danish) 4-81810  
electrostatic discharge, human body and electronic equipment effects 4-69273  
FAZYTAN automated image evaluation system, design 4-100340  
FFT signal processing IC, use for Doppler blood flow studies 4-93826  
heart, role of electronics 4-115253  
heart-rate monitors, evaluation of portable units 4-85569  
helix as RF applicator for hyperthermia, anal. 4-72215  
Japan, production growth of equipment from 1981 to 1982 (Japanese) 4-115260  
microwave radiometry, recognition of thermal structures 4-62549  
multielectrode microprobe for extracellular biopotential recording 4-115320  
neural prostheses, natural and artificial sensors development 4-115275  
NMR imaging appl., universal pulse programmer 4-105327  
optoelectronics: laser appls., fibre-optic instrumentation and IR thermography (Japanese) 4-89678  
radiometer input circuit requirements for microwave thermography, comments and reply 4-85480  
radiotherapy treatment couch rot., electronic readout 4-115193  
reading aids for the visually disabled 4-67148  
spectral analysis of short-time biomedical data using adaptive filters 4-72453  
time-scribe: universal time writer for any EEG/polygraph chart recorder 4-93942  
V-converter outlet signal, evaluation (German) 4-77420  
verification timer for AECL 780 Cobalt Unit 4-115184  
versatile simulator of evoked potentials 4-72237  
vibractile instrumentation, temporal resolution of lingual sensory modality obs. 4-89796  
video signals analogue transmission, telemedicine appl. 4-85570  
visual, evoked potentials, data archiving and analysis using electronic techniques (Italian) 4-62613  
**biomedical engineering**  
*see also biomedical electronics; biomedical equipment; orthotics; patient treatment; prosthetics; sensory aids*  
clinical laboratory, voluntary standards by consensus 4-89868  
codes and standards, role in clinical engng. 4-93946  
computers and the motor impaired physically handicapped 4-100354  
conference, Washington, USA (Apr. 1984) 4-101573  
conference on engng. and computing in health care, Columbus, USA (Sept. 1983) 4-82594  
health care, contrib. of medical phys. and engng., digital revolution 4-85572  
intensive aquaculture as candidate for bioregenerative life support systems 4-115256  
metric system, standards and practice, impact on biomedical engineers 4-86380  
perspectives in medical and biological engineering (Japanese) 4-89794  
therapeutic engineering, recent technology (Japanese) 4-89824  
United States Navy Diving Biomedical R&D Program overview 4-115255  
United States Navy diving biomedical research 4-109789  
**biomedical equipment**  
*see also biomedical electronics; biomedical measurement; orthotics; prosthetics; radiography; radioisotope scanning and imaging; sensory aids*  
accelerator design for 160 MeV proton radiotherapy 4-72408  
accelerator neutron survey, remmeter sensitivity to leakage X-rays 4-62568

## biomedical equipment continued

accelerators, high energy, neutron contamination detect. using electrochem. etching 4-72431  
 adhesionometer for instant quantitative test of blood viscosity rel. to thrombosis tendency (*German*) 4-77415  
 ambulatory monitoring system for tremor 4-67138  
 anaesthesia, mass spectrometers with spectrum overlap erasure units, possible inaccuracies 4-93851  
 anaesthetic gas monitor, chemical sensor research at the laboratory of applied physics in Linköping 4-11116  
 Anger camera, rel. to improved intrinsic resolution 4-67091  
 Anger gamma-camera for emission computerised tomography 4-63835  
 anomalouscope, portable, solid state version 4-62546  
 architectural considerations in designing a mag. resonance facility 4-105329  
 Ardian-Crooks cassette, practical experience in tube voltage determ. (*German*) 4-67082  
 arthropump with peristaltic effect and pulsatile flow 4-62616  
 audiometer screening instrument, calibration 4-85432  
 automatic artificial respirator with programmable flow curves (*Italian*) 4-105373  
 automatic light intensity regulation in photometric methods of bloodflow and oxygen saturation monitoring in peripheral blood vessels (*German*) 4-89683  
 avalanche chamber positron camera for tomographic imaging of human thyroid 4-67087  
 BGO photodiode detector, characterisation for positron emission tomography 4-59568  
 bicycle ergometer for paralysed muscle 4-85573  
 biomechanics laboratory, automated, appl. to rehabilitation 4-81806  
 blood clotting timer, automatic, optical endpoint sensing 4-115165  
 blood pressure, comparison of 2 noninvasive monitors 4-85565  
 blood pressure evaluation using screening programs 4-89795  
 blood processing machines, one-piece quick-disconnect connector 4-85536  
 body surface multielectrode for inverse problem in electrocardiography and its application (*Japanese*) 4-62621  
 capacitive transducer for continuous measurement of vertical foot force 4-85541  
 capillary tube plasma viscometer, automatic instrument for plasma viscosity meas. 4-115246  
 cardiac output, single thermistor system for continuous meas. 4-81809  
 cardiac phantom for evaluation of multigated radionuclide studies 4-72391  
 cardiopulmonary resuscitation system based on intrathoracic and abdominal press. variations 4-89826  
 catheter, US marked method for positive echographic catheter position identification 4-77354  
 collimators used for tomographic imaging of  $^{123}\text{I}$  contaminated with  $^{124}\text{I}$ , performance 4-72383  
 compensator filters made with compact Moire camera and computer 4-109916  
 conference, nuclear science and power systems, San Francisco, CA, USA (Oct. 1983) 4-58550  
 conference, optical instrumentation appl. in medicine, Atlanta, GA, USA (April 1983) 4-86103  
 controlled radiation ceiling for thermal treatment of patients 4-62545  
 critical-fusion frequency equipment using high-speed liq. cryst., prod. (*Japanese*) 4-93841  
 CT display, detectability enhancement by use of coloured illumination 4-62554  
 CT quality assurance, correlation with system performance 4-89709  
 CT scanners, evaluation of 4 machines for image quality and dose 4-85507  
 CT system quality assurance status 4-89708  
 cyclotron facilities for clinical therapy, diagnosis and analysis, general survey 4-72402  
 cyclotron for radioisotope prod. 4-77390  
 cyclotrons, medium energy research, for medical isotope production 4-77391  
 cyclotrons for radionuclide production 4-77389  
 dental plaque, instrumentation for in situ meas. 4-62617  
 diagnostic radiology image-intensifier-TV systems, performance testing 4-72414  
 differential evoked potential monitor 4-100344  
 digital fluoroscopy imaging system, performance evaluation and quality assurance 4-89706  
 digital radiography, single slit imaging, practical appls. 4-89717  
 digital radiography systems 4-89716  
 digital subtraction angiography utilising geom. and electro-optical magnification, imaging characts. 4-89705  
 digital videodensitometry system for subtraction angiography 4-89718  
 digital X-ray systems, method for MTF meas. 4-67100  
 disabled person vehicle, leg muscle propelled 4-93975  
 ECG monitors, evaluation of four machines 4-109982  
 electrocardiograph functional testing, microprocessor-controlled signal generator 4-11552  
 electromyographic equipment provision for polyclinics 4-72448  
 electronic imaging detectors performance rel. to photon transport 4-89713  
 EM field meas. probe, of submillimeter dimensions 4-106310  
 EMG, digital signal processor with adaptive decision boundaries 4-85543  
 EMG, single-fibre, meas. unit based on a personal computer 4-77412  
 EMG/foot force anal., real time microprocessor system 4-85549  
 endoscopic fibre optic surgery and therapy, appls. in USA 4-85473  
 erythrocyte deformability, device for routine meas. 4-109979  
 erythrocyte-stasis-meter, blood flow characts. universal parameter determ. 4-109976  
 Erythrometer: device for erythrocyte filterability and plasma viscosity meas. 4-109981  
 Erythrometre, evaluation, blood filtration press. and erythrocyte deformability meas. 4-115248  
 exercise conditioning system for paralysed leg muscle 4-100349  
 eye movement monitor, inexpensive, using the scleral search coil technique 4-81750  
 fast neutron therapy facilities 4-72406  
 fast scan NMR imaging, fast recovery pulse sequence method 4-77360  
 FASTBUS based data acquisition system for imaging coronary arteries 4-62570  
 fiberoptic microtip pressure transducer for medical applications 4-85531  
 fibre optic laser tunnelling device, laser catheter, for thromboembolic disease therapy 4-72343

## biomedical equipment continued

fibre-optic sensors for biomedical appls. 4-89682  
 flow transducer used in ventilatory impedance meas., transfer function modelling 4-81792  
 fluorescent lamp apparatus for photosensitivity tests 4-115172  
 fluorescent screens, energy imparted from primary and scatt. radiation, screen, thickness and comp. effects 4-67109  
 fluorometer for endoscopic diagnosis of tumors 4-109899  
 fluoroscopic image quality requirements for coronary angioplasty, high definition video system performance 4-89707  
 foil filters for equalised chest radiography 4-81779  
 foot contact switch for human locomotion meas. 4-72443  
 functional elec. stimulation system, portable 4-100357  
 functional elec. stimulator for paraplegic patient 4-100358  
 gait analysis and alignment system for lower-limb prostheses 4-100362  
 gait analysis system for functional evaluation of the lower extremity 4-81803  
 gamma camera bar phantom images, collimator design effect on moire patterns 4-67115  
 gamma-ray imaging systems, aberrations 4-67084  
 gas anal., equipment for instruments calibration (*German*) 4-77042  
 geometrically designed coded aperture mask arrays 4-67140  
 haemoglobin in blood, optothermal meas., prototype clinical instrument 4-83836  
 haemorrheology, clinical, methods and instrumentation 4-109975  
 hand contractions quality, meas. instrument 4-77413  
 health care, contrib. of medical phys. and engng., digital revolution 4-85572  
 heart rate-pressure prod. computer, microprocessor based 4-81808  
 high-field, NMR systems, installation into existing clinical facilities 4-105328  
 holographic endoscopy using gradient-index optical systems 4-83549  
 human skin, proton and electron microprobe analysis 4-105390  
 hyperthermia phantom, practical, modular 4-67066  
 image-intensifier fluorographic system, image quality 4-72399  
 impedance audiometers, laboratory and commercial, clinical comparison 4-115261  
 inductive applicator for hyperthermia using a one-turn coil with RF current 4-77424  
 infant respiration, efficacy of 5 noninvasive sensors 4-85567  
 infusion pumps, universal air-bubble detector based on modulated IR 4-109898  
 IR diameter gauge for in vitro mech. testing of vascular grafts 4-100293  
 ISM (industrial, scientific, and medical) equipment, emissions and interference caused 4-72445  
 isocentric machines, improved optical backpointer using 2 laser beams 4-109900  
 Karlsruhe proton microprobe appl. to medical samples 4-105389  
 laser dermatology, current instrumentation 4-72336  
 laser diagnostic medicine, spectroscopic techniques 4-72340  
 laser endoscopic resections in bronchology, technical problems 4-85475  
 laser medicine, injurious effects and clinical appls. 4-72341  
 laser optometer for low-luminance myopia meas. 4-100132  
 laser surgery, CO laser appls. 4-77371  
 laser surgical applications with CO<sub>2</sub> laser 4-72342  
 laser therapy in tissue contact using quartz fibres 4-85476  
 laser-Doppler blood flow monitor, diode laser source and detection in probe 4-115154  
 leg exerciser for training of paralysed muscle by closed-loop control 4-85575  
 linac electron applicator assembly, radiation leakage 4-115181  
 linear accelerator design advances, radiotherapy appl. 4-67095  
 liquid sample preparation, automated systems 4-63728  
 localised microwave hyperthermia, waveguide applicator with convergent lens 4-81753  
 low-luminance myopia meas. instrumental design and construction 4-100132  
 Magnetom, first mag. resonance tomograph 4-81754  
 mass spectrometer (*Chinese*) 4-105359  
 medical imaging with synchrotron radiation, detection of coronary artery disease 4-93956  
 metal/ceramic diagnostic X-ray tube 4-77381  
 Michelson interferometer, spectral emissivity meas. of human skin for potential early cancer detect. 4-105320  
 microcomputer-controlled microwave hyperthermia system 4-67059  
 microlens terminated optical fibres, fabrication, biomedical appls. 4-83737  
 microradiography of dental tissue, synchrotron radiation, X-ray image magnification 4-93854  
 microtrons, cyclotrons and synchrotrons appl. to radiation therapy 4-72403  
 microwave applicators, 1-10 GHz, radiometry, tissue brightness meas. (*Japanese*) 4-62553  
 microwave miniature applicators, designs for localised hyperthermia of human malignancies 4-67069  
 microwave powered electron linear accelerator, radiotherapy appls. 4-72401  
 microwave radiometric system for biomedical true temp. and emissivity meas. 4-77364  
 microwave radiometry, recognition of thermal structures 4-62549  
 microwave thermoelastic tissue imaging system design 4-115160  
 microwave thermoelastic tissue imaging system 4-85489  
 modular scintillation camera for use in nuclear medicine 4-72366  
 multichannel solid-state recorder, design and appl. to temp. meas. 4-115251  
 multidetector SPECT brain scanner, improved performance from modifications 4-100310  
 multisite elec. stimulation for paretic gait, rehabilitation program 4-100360  
 MWPC medical digital imaging system for bone densitometry 4-83273  
 myocardial blood flow and metabolism, digital film autoradiography and electronic multitracer techniques 4-77377  
 neurofunction laboratory for movement disorder evaluation 4-81804  
 neutron therapy program at cyclotron of Louvain-la-Neuve 4-72409  
 NMR imaging facility, architectural design, shielding requirements 4-89672  
 NMR imaging instrumentation, review 4-85490  
 NMR imaging system, choice of mag. field, quality and discrimination 4-89670  
 NMR system design, problems overview 4-100301  
 NMR system design, S/N ratio optimisation 4-100303

**biomedical equipment continued**

- NMR tomograph, inauguration in the Medizinische Hochschule, Hanover (German) 4-62544
- NMR whole body imaging using permanent magnets 4-89674
- ocular plethysmograph evaluation, simple time-series approach 4-81798
- OP-rheometer system for blood viscosity and viscoelasticity anal. 4-109973
- optical communication aids in rehabilitation 4-67067
- optical end-tidal air-point detector built in a nonbreathing valve 4-77367
- optical fibre thermometer for medical use 4-100292
- optical fibres, conf., Paris, France (May 1983) 4-82587
- optical fibres, enlarged taper ended, for laser radiation delivery systems, construction, surgical appls. 4-85472
- optoelectronics: laser appls., fibre-optic instrumentation and IR thermography (Japanese) 4-89678
- Osisir, computerised digital photographic apparatus, for max. information from light pictures (German) 4-77359
- perfusometer: an instrument for assessing the condition of critically ill patients 4-81799
- photo radiation therapy involving hematoporphyrin derivative, laser-fiber optic system appl. 4-85478
- photodiode array X-ray imaging system for digital angiography 4-85505
- photomultiplier tubes for nuclear radiation detectors 4-91181
- photoelectromyograph, pulsed multifreq., skin blood press. appl. 4-77366
- photothermal laser spectrometer for sensitive biomedical measurements 4-109901
- polyacrylamide as a phantom material for electromagnetic hyperthermia studies 4-67061
- polystyrene radiotherapy phantom, thermal characts. 4-67122
- polyvinylidene fluoride, transducer appls. 4-97249
- portable detectors for  $^{125}\text{I}$ -insulin absorption measurement during subcutaneous infusion with portable pumps 4-67157
- positron camera, spatial sensitivity and detection efficiency 4-62567
- positron emission ring tomograph using BGO detector, analog readout 4-62576
- positron emission tomograph, image reconstruction 4-62572
- positron emission tomograph, performance characteristics 4-62577
- positron emission tomograph design and evaluation 4-67088
- positron emission tomograph THERASCAN 3128, performance 4-62578
- positron emission tomographic unit, high resolution 4-72411
- positron emission tomography, high resolution, using analog coding 4-77375
- positron emission tomography, high resolution TOF camera 4-62573
- positron emission tomography, performance rel. to energy threshold and shielding depth 4-77376
- positron emission tomography HISPET, design features 4-62579
- positron tomographic imaging, time-of-flight method and detector technology 4-115204
- pressure sensor using buried piezoresistors, Si diaphragm 4-85530
- prosthetic heart valves, instrum. for sound anal. 4-85582
- proton microprobe, Oxford scanning medical diagnostic appl. to liver 4-105332
- pulsed-probe anemometer for meas. of vel. and flow direction in slowly moving air 4-100337
- pupil of human eye, solid-state instrument for dynamic changes meas. 4-100294
- quasi free-field audiometry, modified transducer system 4-85462
- radiation protection in modern nuclear medicine and brachytherapy departments 4-77402
- radiation protection instrumentation for medical and biochemical radionuclide laboratories 4-77403
- radiographic imaging systems, S/N ratio, dynamic range and contrast sensitivity 4-89697
- radiographic intensifying screens, preferred image characts. of various types 4-109909
- radiographic screens, photographic effect of long term persistency, ghost images 4-89701
- radioisotope diagnostic equipment, method for performance assessment 4-100317
- radioisotope imaging of the heart 4-72413
- radiologic, CT, nuclear medicine and US imaging systems, low contrast sensitivity 4-62558
- radiological video imaging, system temporal response effect 4-89700
- radionuclide cardiovascular diagnosis, micro-based system 4-109925
- radiotherapy, Hg shielded irregular field system, 4 years' experience 4-89727
- radiotherapy treatment planning, simulator-based CT system 4-89691
- radiotherapy wedge for 4 and 6 MV X-rays, dosimetry characts. 4-67119
- registration and automatic analysis apparatus for electrocardiographic QRS signals (Bulgarian) 4-93955
- respiratory gas exchange meas. systems, performance testing 4-85566
- RF coil, crossed ellipse, for head and neck NMR imaging 4-89681
- RF hyperthermia of deep-seated tumours, dipole array applicator performance study using blood flow simulator (Japanese) 4-85406
- RF shielding for NMR imagers 4-105330
- robotic arm control, speaker-dependent voice recognition unit evaluation 4-93976
- rotating X-ray collimating slit for line-scan dual-energy medical imaging 4-72362
- scintigraphy, collimated detector, effect of scatt. radiation on planar source sensitivity 4-89723
- scintillation cameras and dose calibrators, quality assurance survey 4-89733
- screen-film systems, absolute speeds and absorbed-energy constants 4-77382
- sensors and elec. props. of living bodies (Japanese) 4-89818
- sensory and motor function, computerised system for clinical assessment 4-81805
- servo ventilator, microcomputer-controlled 4-85574
- Shimadzu automated multigamma counter RAW-1600 for radioimmunoassay in clinical chem. laboratories (Japanese) 4-59578
- Shimadzu data processing system RAD-1100A for radioimmunoassay in clinical chem. laboratories (Japanese) 4-59578
- Shimadzu multichannel selective stat analyser CL-12, interference factor anal. for precision of quantitative clinical anal. (Japanese) 4-62620
- short wave diathermy equipment, stray mag. fields and power outputs using tissue equivalent phantoms 4-89755
- single photon emission computer tomography, collimation, sampling, filter-interactions 4-72359

**biomedical equipment continued**

- single-slice positron-emission tomography scanners, performance study by Monte Carlo techniques 4-62563
- skin-surface recording electrodes, practical considerations in use 4-85557
- solid state nuclear track detector use in radiation dosimetry, medicine and biology 4-72430
- spectacle indirect ophthalmoscope accessories 4-109971
- spirometer, experimental evaluation (German) 4-77278
- spirometer turbine transducer, design (Polish) 4-77279
- SRT-1000, Soviet computerised tomograph, design, operation and results (Russian) 4-81811
- student radiographers, X-ray equipment for, book 4-58599
- surgical instruments, design, bone cutting force meas. 4-62503
- syringe shields for nuclear medicine 4-93899
- TEM cell for radiofrequency radiation dosimetry studies, resonance suppression and bandwidth modification 4-77392
- TEM radiofrequency/microwave applicator for non-invasive deep body hyperthermia 4-77361
- temperature probes, inaccuracy 4-85539
- thermocouple oesophageal temperature probe, construction and position verification 4-85535
- thermoelectric cooling device for cryoprecipitation by plasma separation 4-93938
- tomoflow system for intracardiac blood flow information display, Doppler US appl. 4-85469
- tomography, time coded emission, three dimensional simulation 4-77374
- transvenous coronary angiography, synchrotron radiation imaging system 4-93957
- upper extremity electro-ergometer 4-89811
- urologic laser surgery instrumentation 4-72332
- US chirping receiver, description (Chinese) 4-62537
- US diagnostic and therapeutic equipment (Japanese) 4-89659
- US Doppler velocity meter for quantitative flow meas. and turbulence anal. 4-85464
- US imaging instrumentation, review 4-89669
- US imaging system for invasive appls. 4-89665
- US standards at NPL, power and field quantity meas. 4-93828
- V-converter outlet signal, electronic evaluation (German) 4-77420
- viscoelastometer for rheological props. of bronchial mucus study in clinical practice 4-115247
- water-immersed microwave antenna array for medical imaging and therapy, local field study 4-115159
- whole body NMR imaging system, performance specifications 4-89671
- X-ray equipment, radiation quality control 4-93849
- X-ray generators, short exposure time characts. 4-89710
- X-ray installations in Bangladesh, radiation exposure level assessment for protection 4-77400
- X-ray scanner system, dynamic spatial reconstructor, imaging characts. 4-115208
- X-ray tube filtration and kVp variation effects on mammographic examination 4-89696
- Zeiss operation microscope (German) 4-67057
- $\gamma$ -ray imaging probes for tumor detection 4-62571
- Ar laser therapy using fibre optics transmission 4-85474
- CO<sub>2</sub> electrochemical sensor for high ambient pressures, deep diving appls. 4-106311
- CO<sub>2</sub> volume per breath, evaluation (German) 4-77282
- Nd:YAG laser-fibre optic system, surgical coagulation appls. 4-85477
- Ni-Co MP35N Alloy Biowire for medical appls. 4-115263
- (Pb<sub>1-3x</sub>-Zn<sub>2x</sub>)(Ti<sub>1-y</sub>Mn<sub>y</sub>)O<sub>3</sub> ceramic ultrasonic probe 4-100341

**biomedical measurement**

- see also biological techniques and instruments; biomedical equipment; electrocardiography; electroencephalography; radiography; X-ray apparatus
- Aachen clinical haemorrhology test profile, data, documentation 4-109974
- Abris contourograph for recording of outer contour of two-dimens. human body section for radiation therapy use 4-93850
- aerosol deposition in human respiratory tract, PIXE investigation 4-105066
- ambulatory long-term blood press., recording and computerised anal. (Finnish) 4-89798
- amiodarone induced thyrotoxicosis, thyroid I content, X-ray fluoresc. 4-72389
- aperture synthesis thermography—a new approach to passive microwave temperature-measurements in the body 4-115158
- arterial O<sub>2</sub> saturation, meas. with pulse-type oximeter, multiple scatt. and peripheral circulation effects 4-115166
- artificial human respiration biosignals, microprocessor assisted automatic meas. (Polish) 4-77283
- auditory brainstem responses, averaged, quality estimation 4-115082
- auditory brainstem responses recording, artifact rejection criteria efficiency comparison 4-85546
- auditory evoked potentials, objective response detect. 4-85559
- auditory-insertion gain meas. using probe microphones in the ear canal 4-115150
- auditory level difference thresholds meas., acoustic neuroma detect. appl. 4-62536
- automatic glottal inverse filtering 4-103143
- automatic recording of biological model variables (German) 4-77419
- blood, human, from addicted and non-addicted persons, PIXE anal. 4-105365
- blood, smokers and non-smokers,  $\alpha$ -activity meas. by CR-39 SSNTDs 4-100371
- blood clotting timer, automatic, optical endpoint sensing 4-115165
- blood flow and vel. meas. in vivo by EM induction 4-77357
- blood flow meas. using digital angiography and parametric imaging 4-67098
- blood flow measurement by NMR and transcutaneous EM flowmeters 4-77362
- blood flow measurement using multichannel pulsed Doppler US, repeatability 4-72319
- blood flow monitor, diode laser source and detection in probe 4-115154
- blood pressure, indirect meas. by pulse wave vel. method (Japanese) 4-100336
- blood pressure measurement, circulation parameters made visible by electronic oscillography (German) 4-77272
- blood serum proteins, PIXE anal. using gel filtration 4-105367
- bloodstream, local velocity meas., laser method based on two or three light guides (Russian) 4-72323

**biomedical measurement continued**

- body N, H and fat, prompt and neutron activation, improved calibration 4-67104  
 bone Ca, % by mass rel. to effective at. no., dual-energy CT 4-115188  
 brain stem auditory evoked potentials, lesions location, computer analysis 4-72258  
 brainstem auditory evoked pots., human, 3-channel Lissajous' trajectory 4-67135  
 cancellous bone strength measurements with the osteopenetrometer 4-89793  
 cancer diagnosis, PIXE appl. 4-105369  
 cardiac output, thermal dilution technique for continuous meas. 4-81794  
 cardiac volumetry, computation of catheter input impedances 4-85532  
 cerebral atherosclerosis, PIXE investigation 4-105370  
 cerebral blood flow, regional, accuracy of stable Xe/CT meas. 4-67073  
 cerebrospinal fluid shunt flow, quantitative evaluation using  $^{99m}\text{Tc}$  4-81796  
 circulation parameters rel. to electronic oscillography (*German*) 4-67133  
 circulatory shunt-dilution curves, interpretation as bimodal distrib. functions 4-85452  
 computer assisted respiration tests (*German*) 4-77421  
 correlation microwave thermography principles and system tests 4-77365  
 dental calculus, human, major and trace element determ. by instrumental NAA 4-105371  
 dental plaque, instrumentation for in situ meas. 4-62617  
 diagnostic imaging in medicine, conf., Pascoli, Italy (Oct. 1981) 4-110810  
 digital radio command link for implantable biotelemetry applications 4-100299  
 diver physiological monitoring system 4-109984  
 dried whole blood and blood plasma, U determ. using track detectors 4-100372  
 dual gated nuclear cardiac images 4-72365  
 electric response audiometry, theory and appl. of weighted averaging 4-105241  
 electronics applications, development from idea to finished product (*Danish*) 4-81810  
 electrophysical meas. process for systems, and electroacupuncture 4-105354  
 EM detection and treatment of malignant disease, conf., London, England (Apr. 1984) 4-67872  
 EM field meas. probe, of submillimeter dimensions 4-106310  
 EMG, digital signal processor with adaptive decision boundaries 4-85543  
 EMG, signal charact., microcomputer anal. 4-89802  
 EMG algorithm, for sequential signal estimation and system identification 4-67141  
 EMG of patients with pathological tremors, preferential freq. detect. and determ. 4-85542  
 EMG recorded with surface electrodes, artefacts suppression 4-115245  
 EMG signal analysis rel. to upper extremity limb function discrimination 4-81661  
 EMG signal processing, algorithms comparison 4-93947  
 EMG signals in gait, interpretation 4-89810  
 EMG technique for muscle fibre cond. vel. meas. 4-105356  
 emission tomography, utilising side information 4-72360  
 end-tidal Xe conc. meas. by mass spectrometry and thermoconductivity, CT blood flow meas. appl. 4-67142  
 erythrocyte deformability, device for routine meas. 4-109979  
 erythrocyte deformability meas., improved filtration rate 4-109980  
 event-related potentials and functional assessment 4-89809  
 evoked potentials, digital signal processing 4-89808  
 eye, human, monochromatic determ. using direct photographic recording of the distorted retinal image 4-115050  
 eye movement, anal. by computer 4-85537  
 eye movement anal. system using IR fundus images (*Japanese*) 4-85486  
 eye movement meas., double mag. induction method 4-81751  
 eye optical system, binocular point spread function dynamic recording 4-100126  
 fast Walsh and Fourier transforms for bones mechanical integrity meas. 4-72458  
 feet of diabetic patients, blood flow, meas. with MWPC positron camera and  $\text{C}^{15}\text{O}_2$  4-100316  
 fiberoptic microtip pressure transducer for medical applications 4-85531  
 fibre contractility evaluation and histological analysis 4-100225  
 fluid distribution in human legs, extra- and intra-cellular fluid vol., elec. impedance meas. 4-77409  
 fluoroptic thermometry use in hyperthermia treatment of cancer 4-85470  
 formant tracking and glottal inverse filtering, two channel (speech and EGG) anal. 4-103144  
 function measurement, perspectives on approaches 4-85548  
 gait abnormalities, human, evaluation by syntactic pattern-recognition method 4-85550  
 gas anal., equipment for instruments calibration (*German*) 4-77042  
 gated cardiac scanning using limited angle image recognition technique 4-72364  
 glomerular filtration rate, meas. without blood sample, validation in renal transplant patients 4-62555  
 glucose in human serum dialysate, low-pot. voltammetry 4-89799  
 glucose measurement, implantable bidirectional telemetry system, artificial pancreas appl. 4-89834  
 haemoglobin content of blood, conductimetric procedure for assay 4-85544  
 haemoglobin in blood, optothermal meas., prototype clinical instrument 4-93836  
 haemorrhology, clinical, methods and instrumentation 4-109975  
 hair, human, elemental concs., PIXE anal. 4-105364  
 hair, human, PIXE meas. normalisation by nucl. reaction 4-105065  
 hair strands, longit. scanning PIXE anal. 4-105363  
 heart and chest wall displacement recording, laser method 4-62550  
 heavy-ion beams for biomedical studies, online characterisation with semiconductor detectors 4-85501  
 hip joint function assessment by objective gait evaluation (*Japanese*) 4-100208  
 human lung,  $\alpha$ -active nuclides microdistrib. using CR-39 SSNTD 4-100370  
 hydrogel materials, refr. indices meas. by interferometry 4-62542  
 interference EMG, characterisation 4-89803  
 intrauterine pressure analysis in nonpregnant dysmenorrheic women, microcomputer system 4-81800  
 ion induced X-ray emission spectra, medical uses (*Japanese*) 4-109924  
 knee movement determ. for external orthotic linkage design 4-100228

**biomedical measurement continued**

- laser nephelometry: development, clinical appl. and future prospects 4-81756  
 left ventricle, absolute vol. determ. by iterative build-up factor anal. of gated radionuclide images 4-81776  
 liquid cholesterol crystals for human body temperature meas. (*German*) 4-77435  
 locomotion, human, meas. using simple foot contact switch 4-72443  
 lower extremity, functional evaluation using instrumented gait anal. 4-81803  
 lung function studies, optical mapping 4-62547  
 lung residual volume, spirogramme anal. (*German*) 4-77281  
 lung water changes, radiometric technique for meas. 4-85483  
 lung water content, changes measurement by microwave, methods 4-77363  
 lung water content measurement 4-77410  
 macro EMG, use of signal representation to identify abnormal motor unit pots. 4-62615  
 microbial chromophore materials in circulating blood, identification by laser micro Raman spectroscopy 4-115156  
 microwave applicators, contact-type tissue cooling effects on brightness temp. 4-72217  
 microwave diffraction tomography for biomedical appls., analytical approach, comments 4-85481  
 microwave hyperthermia, direct temp. meas. of focused heating from phased array system 4-72349  
 microwave hyperthermia and data acquisition system 4-72348  
 microwave imagery methods for diagnostic applications 4-115170  
 microwave thermography, correlation method, thermal gradient localisation in lossy materials 4-81752  
 microwave thermography system, 3 GHz, design and clinical use 4-72346  
 microwave tomography system and use in deep hyperthermia 4-72347  
 motor disorder patients, computer automated evaluation 4-89812  
 multichannel solid-state recorder, design and appl. to temp. meas. 4-115251  
 nails, human, elemental concs., PIXE anal. 4-105364  
 neutron activation analysis, in vivo techniques, review 4-115189  
 neutron leakage measurements from a medical linear accelerator 4-109914  
 objective refraction: comparison of retinoscopy and automated techniques 4-62543  
 ophthalmic solutions lubrication props. meas., using strain gauge bridge 4-89797  
 pachometry measurements, reliability and variability 4-109792  
 peristalsis, strain gauge transducer for in vivo meas. (*Japanese*) 4-77284  
 phonocardiograms, pole-zero modelling and classification 4-85461  
 photothermal laser spectrometer for sensitive biomedical measurements 4-109901  
 PIXE, anal. of biological and medical samples 4-105063  
 PIXE, appl. in neurological diseases investigation 4-105368  
 PIXE's analytic appls., conference, Heidelberg, Germany (July 1983) 4-95034  
 PIXE anal. of biomedical samples using external piston beam 4-105362  
 PIXE trace element anal., biological appls. 4-105064  
 PIXE trace element anal., biomedical appls. 4-105361  
 positron emission tomography, count normalisation methods, statistical anal. 4-72358  
 pressure sensor using buried piezoresistors, Si diaphragm 4-85530  
 pulsed-probe anemometer for meas. of vel. and flow direction in slowly moving air 4-100337  
 pupil of human eye, solid-state instrument for dynamic changes meas. 4-100294  
 radiometer input circuit requirements for microwave thermography, comments and reply 4-85480  
 resonance thrombography, blood clotting study appl. 4-105315  
 resonance thrombography 4-109772  
 respiratory parameter anal., microprocessor assisted research tool (*German*) 4-77422  
 RF hyperthermia for tumour treatment, localised technique development 4-72345  
 scanned micro-PIXE by  $\text{H}^+$  backscatt. for local matrix thickness determ. in organic tissues 4-99889  
 sensory evoked responses, clinical appl. of dipole localisation method 4-93950  
 signal detection theory in medical imaging, limitations and applications, review 4-115203  
 single photon emission computer tomography, collimation, sampling, filtering interactions 4-72359  
 single photon emission tomography, attenuation correction, depth effect 4-72357  
 skin, human, temp. distrib., blood flow, perspiration and metabolic heat generation effects 4-62446  
 skin perfusion pressure, meas. by photoelec. technique, rel. to amputation level selection 4-72338  
 somatosensory evoked pots., recording from spinal cord and brain 4-93949  
 spectral emissivity meas. of human skin for potential early cancer detect. 4-105320  
 spirometer, experimental evaluation (*German*) 4-77278  
 splenic blood flow and platelet transit time, meas. methods using  $^{111}\text{In}$ -labelled platelets 4-81773  
 synchrotron X-rays for digital subtraction coronary angiography 4-72367  
 temperature measurements, emissivity-independent, using microwave thermographic system 4-77364  
 thermographic images, nonlinear filtering 4-85491  
 thyroid uptake meas., effect of counting system deadtime 4-85503  
 tibia, human, vibr. anal. using skin-mounted accelerometers 4-100211  
 TRU nuclides, in vivo meas. using high purity Ge detector,  $\gamma$  and X-ray meas. 4-115194  
 tympanometric middle-ear press. determ. with 2-component admittance meters 4-115254  
 upper extremity joints, functional assessment 4-81802  
 urinary bladder fullness determ. by electrical impedance meas. 4-77411  
 US tomography, practical meas. of human body temp. 4-100268  
 valvular calcification and press. drops across malfunctioning heart valves, quantitative determ. 4-81801  
 velocity measurement of humans by computers 4-73196  
 venous occlusive RN plethysmography: comparison with electrical admittance plethysmography 4-62581  
 vibrotactile instrumentation, temporal resolution of lingual sensory modality obs. 4-89796

biomedical measurement continued

vision tests, interactive 4-115244  
whole-body counter spectra from detector array, library least-squares anal. 4-109918  
whole-body determ. of <sup>57</sup>Co B<sub>12</sub> absorpt., attenuation correction 4-72379  
<sup>37</sup>Ar, release rate from human subjects following intravenous injection, meas. on volunteers 4-100313  
CO<sub>2</sub> volume per breath, evaluation (*German*) 4-77282  
Cr determ. in blood plasma, rel. to coronary heart disease, cineangiographic meas. 4-105366  
I contrast media, levels in human body, determ. via X-ray fluoresc. (*German*) 4-89724  
N and O, total body, meas. by cyclotron neutron irradiation and delayed gamma ray counting 4-67114  
N total body, meas. in critically ill, prompt gamma in vivo neutron activation analysis facility 4-67113  
O<sub>2</sub> partial pressure meas. in vivo, fibre-optic probe method 4-62633  
O<sub>2</sub> tension in muscle, meas. by microelectrode technique 4-109978  
O<sub>2</sub> transport model for transcutaneous P<sub>O2</sub> meas. (*Japanese*) 4-100108  
U conc. in urine, fluorometric meas. method 4-72438

biomedical NMR

amplitude modulated selective pulses in NMR imaging 4-89684  
architectural considerations in designing a mag. resonance facility 4-105329  
blood flow measurement by NMR and transcutaneous EM flowmeters 4-77362  
brain, rat, metabolism, <sup>13</sup>C NMR using double-tuned surface coils 4-66878  
brain, tumors and NMR, correlative study in biopsy samples 4-100295  
breast, mag. resonance imaging, work in progress 4-62552  
breast imaging in vivo using a prototype coil 4-105325  
breast tissue imaging, multiple exponential transverse relax., benign vs. malignant discrimination 4-89675  
cancer diagnosis and new medical imaging modalities (*Japanese*) 4-62580  
computer algorithm for NMR imaging simulation 4-105318  
computer analysis of NMR images, application areas 4-85488  
conference, optical instrumentation appl. in medicine, Atlanta, GA, USA (April 1983) 4-86103  
conference on clinical radiology, Las Vegas, USA (Apr. 1984) 4-101574  
conference on NMR technology, Orlando, USA (Feb. 1984) 4-95062  
contrast agents and spectroscopic probes in NMR 4-72328  
contrast material, use of MnS<sub>2</sub> colloid in rats 4-89677  
CT treatment planning for radiotherapy 4-72404  
depth pulses with polarisation transfer, sample localisation using surface coils 4-67064  
development of clinical NMR imaging, realistic expectations 4-67060  
developments in medical care and NMR as universal imaging technique (*Japanese*) 4-89679  
diagnostic imaging, state-of-the-art review 4-115171  
diagnostic imaging in medicine, conf., Pascoli, Italy (Oct. 1981) 4-110810  
diagnostic NMR 4-100296  
display of images in 3D 4-105326  
exposure limits for diagnostic use of NMR, NRPB advice 4-77397  
fast scan NMR imaging, fast recovery pulse sequence method 4-77360  
flow and motion in NMR imaging 4-100308  
flow imaging method 4-100298  
free induction decay averaging in NMR imaging, limits to S/N improvement 4-115167  
full-rotating frame NMR imaging 4-72329  
gated cardiac imaging with NMR techniques 4-105322  
glossary of NMR terms 4-105319  
head and neck imaging using crossed ellipse RF coil 4-89681  
high-field NMR systems, installation into existing clinical facilities 4-105328  
history, principles and prospects 4-85487  
image contrast, intrinsic parameters 4-89673  
image processing and display, review 4-115145  
image synthesis in real time 4-100306  
imaging, basic principles and appl. (*Japanese*) 4-77368  
imaging, pot. hazards, mag. fields rel. to cardiac function in animals obs. 4-105317  
imaging, pulse sequences optimisation by computer simulations 4-100307  
imaging facility, architectural design, shielding requirements 4-89672  
imaging system, choice of mag. field, quality and discrimination 4-89670  
imaging techniques and appls., tracers, IR imaging, NMR, X-rays, ultrasonics 4-77417  
imaging technology development: digital X-ray imaging, positron CT and NMR imaging (*Japanese*) 4-89734  
in vivo spectroscopic imaging 4-105324  
instrumentation of NMR imaging, review 4-85490  
magnetic field strength effects on imaging 4-77370  
magnetic phenomena in medical practice, review 4-105314  
magnetic resonance tomography for internal diagnostic examination 4-105312  
Magnetom, first mag. resonance tomograph 4-81754  
metabolic monitoring appls. 4-105321  
MRI, magnetic resonance imaging, for medical appls. 4-115168  
multi-exponential water proton spin-lattice relax., implications for quantitative NMR imaging 4-72210  
multinuclear NMR studies of naturally occurring nuclei 4-67062  
multiple-slice NMR imaging by 3D Fourier zeugmatography 4-100297  
orbit, mag. resonance imaging, preliminary experience 4-62551  
phase gradient modulation techniques, use for imaging true motion vel. and higher order motion quantities 4-105323  
principles of NMR 4-81755  
principles of NMR imaging 4-67063  
principles of NMR tomography, 2D and 3D Fourier imaging of protons 4-105311  
proton density meas. calibration 4-67068  
proton imaging, background and developments 4-115169  
pulse programmer, universal, for NMR imaging 4-105327  
pulse sequence considerations for computed T<sub>1</sub>, T<sub>2</sub> and spin density images 4-100305  
Radon transform and appls., book contrib. 4-106172  
reconstruction filters for 3-D NMR tomography with planar integrals 4-72325  
reconstruction principles, overview 4-100302  
resolution and contrast limits 4-72326  
respiratory gating in magnetic resonance imaging at 0.5 Tesla 4-81758

biomedical NMR continued

review of developments in in vivo diagnostic exams. using phys. methods 4-115262  
review of state of the art from the clinical engineer's viewpoint 4-115164  
RF shielding for NMR imagers 4-105330  
S/N calibration procedure for NMR imaging systems 4-67065  
selective excitation in NMR imaging, effect of AM 4-62548  
sera, human, systemic effect of cancers on relax. times 4-105316  
spatial resolution in NMR imaging 4-109895  
spin lattice relax. time in 2D NMR imaging, corrections for plane selection and pulse sequence 4-67058  
system design, problems overview 4-100301  
system design, S/N ratio optimisation 4-100303  
tissue characterisation by NMR, uncertainties in relaxation parameters meas. 4-100304  
tissues, normal and pathological proton NMR relax. times characterisation in rats 4-105181  
tomograph, inauguration in the Medizinische Hochschule, Hanover (*German*) 4-62544  
tomography, inverse problems, shift spectra, relaxation, formulation and approx. soln. (*Russian*) 4-72324  
tomography, reconstruction algorithm from truncated projections 4-77378  
whole body imaging using permanent magnets 4-89674  
whole body NMR imaging system, performance specifications 4-89671

biomedical phenomena

see also biomagnetism  
No entries

biomedical ultrasonics

3D digital display of ultrasonograms 4-100265  
A-mode speckle reduction with compound frequencies and compound bandwidths 4-105304  
abdominal, pelvic and thyroid disease prediction and imaging techniques comparison 4-115215  
abdominal US images, improvement by digital processing 4-67052  
adaptive processing for ultrasound signals 4-93834  
atherosclerosis, detection and characterisation 4-85468  
attenuation in tissue, frequency dependent, echographic A-lines, time-freq. representation 4-100241  
attenuation tomography, dual refl. technique, impediograph concept 4-100279  
Australia, ultrasonics research 4-109893  
automated diagnostic systems for outpatients clinics 4-93825  
B scans, lateral filtering before image generation 4-105303  
B-mode images, computer simulation of artifacts 4-105308  
B-mode ultrasonography, textural variations 4-105306  
B-scan images, realistic computer simulation 4-105307  
backscatter imaging, quantitative 4-89666  
bibliography 4-82621  
bibliography 4-86142  
blood flow, max. vols., noninvasive CW Doppler haemodynamic data, intracardiac jets 4-85467  
blood flow disturbance effect on ultrasonic scatt. 4-72287  
blood flow meas., freq. estimator for sampled Doppler signals 4-62538  
blood flow meas., ultrasonic Doppler effect appl. 4-105265  
blood flow measurement using multichannel pulsed Doppler US, repeatability 4-72319  
bone, human tubular, struct. features rel. to ultrasound meas. 4-89650  
cardiac tissue characterisation, stochastic approach to RF amplitude anal. 4-105302  
catheter, US marked method for positive echographic catheter position identification 4-77354  
chirping receiver, description (*Chinese*) 4-62537  
clinical hyperthermia unit utilising an array of seven focused ultrasonic transducers 4-100089  
conference on clinical radiology, Las Vegas, USA (Apr. 1984) 4-101574  
conference on radiology, Liverpool, England (Sept. 1983) 4-82584  
coronary grafts, blood flow visualisation by US method 4-100264  
crossed-transducers array for transmission ultrasonic imaging 4-100276  
diagnosis, imaging, surgery and physiotherapy appls. 4-93827  
diagnostic and therapeutic equipment (*Japanese*) 4-89659  
diagnostic imaging in medicine, conf., Pascoli, Italy (Oct. 1981) 4-110810  
diagnostic imaging physics, theory limitations and rel. to other imaging modalities 4-115152  
diagnostic imaging systems 4-109892  
diffraction corrected ultrasound tomography, freq. extrapolation algorithm 4-105310  
diffraction tomography using beam waves: Z-average reconstruction 4-100274  
Doppler flow meas. and processing, signal-to-noise ratio enhancement 4-100286  
Doppler techniques and their diagnostic appl., conf., London, England (June 1983) 4-67849  
Doppler velocimeters, coded, signal-to-clutter ratio limitation, cardiology appls. 4-100285  
Doppler velocity meter for quantitative flow meas. and turbulence anal. 4-85464  
echo cardiography, double frequency bubble-diagnostics 4-100287  
echo method for calcifications detection in breast tissues 4-100263  
echo-Doppler angle determination for noninvasive transmittal blood velocity calculations in normal and porcine bioprosthetic mitral valves 4-100192  
echo-graphics, physical principles and diagnostic applications (*Polish*) 4-100275  
echocardiograms, 2D, effective algorithm for extracting serial endocardial borders 4-85460  
echocardiograms of left ventricle, computerized 3-D finite element reconstruction 4-100272  
echocardiography, CW and pulsed Doppler, utilising a stand-alone system 4-85466  
echostructure recognition, joint transform correlation 4-93833  
endoscopic appls. of US 4-93831  
endoscopic Doppler probe for intestinal vascular studies 4-93832  
exposcoscan, parallel processing technique for high speed ultrasonic imaging 4-72454  
eye, fast B-scan diagnostics in severe trauma situations (*Italian*) 4-81749  
FFT signal processing IC, use for Doppler blood flow studies 4-93826  
fluids, US attenuation meas. 4-100266  
focused US for stimulation of nerve structures 4-72320

**biomedical ultrasonics continued**

- fetal blood flow meas. by Doppler US, methodology and basic problems 4-89662  
 foeto-placental circulation, assessment with CW Doppler 4-89663  
 glaucoma, thermal model for US treatment, rabbit obs. 4-89660  
 gray-scale ultrasonograms, relative effects of system parameters on texture 4-89661  
 heart, automatic discovery of contours in ultrasonic pictures (*German*) 4-67053  
 hyperthermia wattmeters, acoustic power o/p meas. 4-100284  
 image processing and display, review 4-115145  
 imaging instrumentation, review 4-89669  
 imaging system for invasive appls. 4-89665  
 imaging techniques and appls., tracers; IR imaging, NMR, X-rays, ultras-onics 4-77417  
 imaging techniques for diagnostics, blood flow and unborn babies appl. 4-77418  
 intraoperative US during heart surgery 4-93829  
 left ventricle, 3D reconstruction from 2D echocardiograms (*Japanese*) 4-100267  
 liver, normal and diffuse disease, ultrasound attenuation 4-105301  
 low contrast sensitivity of radiologic, CT, nuclear medicine, and ultras-ound medical imaging systems 4-62558  
 lung of fetal sheep, US attenuation and mean backscatter size meas. by digital signal processing 4-100269  
 microbubbles, nonlinear behaviour and US detection 4-62535  
 myocardial tissue characterization, US quantitative backscatter and atten-uation 4-100281  
 ophthalmology, US echographic methods (*Italian*) 4-67051  
 probes, state of the art 4-105300  
 prostate gland volume, computer assisted estimate from transrectal ultras-onic tomograms (*German*) 4-67055  
 pulse transit sonomicrometry 4-93830  
 pulsed Doppler US, freq-dependent attenuation effects 4-115149  
 pulsed fields used in diagnostic US, finite amplitude distortion 4-85465  
 PVDF polymer hydrophones in biomedical ultrasonics 4-100283  
 random backscatt. in presence of static reflection components, tissue char-acterisation 4-103059  
 real-time methods in diagnostic imaging, pulsed Doppler technique 4-115153  
 soft tissue, acoustic attenuation, modeling with minimum-phase filter 4-100270  
 speckle size and lesion signal to noise ratio 4-105305  
 spectral estimates, refl. US, diff. effects 4-115146  
 standards at NPL, power and field quantity meas. 4-93828  
 stereoscopically projected pictures, discrete data on volume (*German*) 4-67056  
 three-dimensional ultrasound images, computer system for stereopair visu-alisation 4-105309  
 thyroid gland section, automatic evaluation of ultrasonic pictures (*German*) 4-67054  
 tissue characterisation and blood flow analysis techniques, developments 4-115151  
 tissue characterisation by US scattering 4-83746  
 tissue characterization of skin utilizing high ultrasonic frequencies 4-100282  
 tissue features, computation and imaging, eye and abdominal organs anal. 4-93835  
 tissues, US scattering, analytical expressions 4-100273  
 tomoflow system for intracardiac blood flow information display, Doppler US appl. 4-85469  
 tomographic technique for the estimation of ultrasonic velocity 4-93824  
 tomography, practical meas. of human body temp. 4-100268  
 tomography, reconstruction algorithm from truncated projections 4-77378  
 tongue shape, characterisation from US image data by numerical methods 4-100271  
 transducer calibration, radiation press. meas. 4-100278  
 transducers, narrow piezoelectric parallelepiped vibr., finite element anal. 4-100280  
 variable index media, US propag. medical imaging appls. (*French*) 4-100243  
 (Pb)<sub>1-3x/2</sub>(Sm)<sub>0.5</sub>(Ti)<sub>1-y</sub>Mn<sub>y</sub>O<sub>3</sub> ceramic ultrasonic probe 4-100341

**biomembrane transport**

- see also osmosis*  
 Aplysia neurons, anomalous voltage relations of Ca 4-89511  
 ascorbic acid, struct. and biological function, rel. to Na<sup>+</sup>/K<sup>+</sup> transport 4-93682  
 axon, squid giant, current generated by backward-running electrogenic Na pump 4-77228  
 axon, squid giant, Na threshold channels 4-77227  
 bilayer lipid membranes, ionic channels formed by polymyxin B 4-66895  
 blood filtration measurements, recent progress in improving data process-ing 4-110016  
 cardiac sarcoplasmic reticulum, unidirectional Ca and nucleotide fluxes 4-89531  
 coupling between fluxes in l-particle pores with fluctuating energy profiles 4-105197  
 diffusion through membranes, effect of nonzero membrane thickness 4-72225  
 endolymph-perilymph barrier, Na<sup>+</sup> permeability 4-115039  
 erythrocyte membrane elec. breakdown through diffusion pot. difference 4-66894  
 gap junction, struct. maintenance 4-100097  
 glycerylmonoerucin membranes, elec. pot. at amphotericin channel inlet 4-66917  
 gramicidin A single-channel conductances, l-Leu<sup>+</sup>-gramicidin A analog 4-105199  
 ion currents through pores, roles of diffusion and external access steps 4-115023  
 ion transport through gramicidin A, struct. and dynamics 4-105175  
 ion-transporting channels, additively contaminated Lorentzians, anal. by integration 4-115025  
 ionising radiation effect on biomembrane structure and function 4-77335  
 lipid bilayer, cation-anion selectivity and conductivity of venom formed channels 4-66891  
 lipid bilayer, ion interaction in amphotericin channels 4-66918  
 lipid bilayers, gramicidin channels, elec. potential difference effect 4-89527  
 lipid membrane, image potential of ion-pore system, symmetrical channel 4-89528

**biomembrane transport continued**

- lipid membrane, image potential of ion-pore system, unsymmetrical chan-nels 4-89529  
 lipophilic cation use as membrane potential probe, critical assessment 4-77205  
 mass spectrometer ion flow in membrane diffusion of various molecules 4-115276  
 monoglyceride bilayer membrane conductance, thickness dependence 4-105196  
 neural membranes, ion transport, random walk model 4-62456  
 patch clamp studies of single ionic channels, book contrib. 4-93710  
 permeability properties, temp. depend., mass spectroscopic obs. 4-93698  
 precipitation membranes, review 4-114827  
 receptor membrane slope cond., transmitter-induced change 4-89543  
 retinal glial cell membrane, regional specialisation 4-72247  
 retinal rods, cation selectivity of light-sensitive conductance 4-77237  
 sarcoplasmic reticulum, permeability for monovalent cations 4-89526  
 sarcoplasmic reticulum, unidirectional Ca and nucleotide fluxes, ATPase reaction schemes 4-89530  
 sugar transport in animal cells, passive hexose transfer system 4-77217  
 transient response modelling 4-93702  
 vertebrate sensory neurons: low voltage-activated, fully inactivating Ca channel 4-100110  
 K<sup>+</sup> transport through poly(2-hydroxyethylmethacrylate) membranes, effect of whole blood interfacial interactions 4-77203

**biomembranes**

- see also biomembrane transport; lipid bilayers*  
 anisotropic two-dimensional cardiac tissue, propag. of excitation 4-89540  
 annihilation delayed fluoresc. emitting probes, for model and biological membrane study 4-66893  
 articular cartilage, mechanical response to an oscillating load 4-115113  
 basilar membrane, alteration of vibr. prod. by loud sound 4-109835  
 biological dipole oscillators, large assemblies, cell membrane modelling 4-72223  
 biomembrane systems, derivative Raman spectroscopy 4-72222  
 bladder membrane protein, 3D struct. 4-100075  
 blood, interfacial film, with vitreous body, struct., physicochemical props., in case of haemophthalmia 4-81610  
 cell membrane nonlinear response to applied elec. field 4-100093  
 cellulosic membranes, charged, membrane pots. 4-81651  
 chemiluminescence, ultraweak, monitoring of emission from rat hearts 4-93799  
 cochleas used for basilar membrane mechs. studies, ultrastruct. damage 4-93758  
 component interactions, implications for membrane function, review 4-115027  
 couple-stress fluid membrane, dynamics 4-66617  
 crambin in phospholipid vesicles: circular dichroism anal. of cryst. struct. relevance 4-77184  
 dimyristoylphosphatidic acid, phase transition 4-105201  
 DPPC lipid bilayers, <sup>1</sup>H, <sup>2</sup>H and <sup>13</sup>C spin-lattice relax. 4-62448  
 dynamic interactions between approaching surfaces of biological interest, review 4-77204  
 electric double layers interaction, metal electrolyte interface and the Don-nan membrane 4-62449  
 electroelastic effects in cell membranes 4-77206  
 electron donors and radiation protection, radiation effect modification by ascorbic acid 4-77194  
 electron microscopy, frozen-hydrated specimens prep. for high resolution studies 4-115318  
 EM radiation in dm wave range, effect on myocardium cell membranes (*Russian*) 4-77306  
 energy-transducing protein complexes, mol. aspects, review 4-66901  
 erythrocyte membrane, elastic area compressibility modulus determ. by cell poking 4-66907  
 erythrocyte membrane, shear deform. and flow, analytical solns. 4-100099  
 erythrocyte membrane, viscous dissipation inside during micropipette aspiration 4-89522  
 erythrocyte membrane viscosity, determ. from rheoscopic obs. of tank-treading motion 4-105202  
 erythrocyte plasma membrane surface, negative charge cluster detection using fluoresc. probes 4-66892  
 ESR spectroscopy, membrane and cell microrheological study appl. 4-115289  
 excitable cellular membranes, transient EM field effects, nonlinear anal. 4-100251  
 fluorometer, ns, for biomembrane rheological aspects study 4-115291  
 gramicidin A, transmembrane channel, helical librational state libration 4-69257  
 Gramicidin A transmembrane channel, conformational energy calc. 4-66861  
 hydrated lecithin membranes, X-radiation damage using wiggler-enhanced synchrotron radiation 4-93814  
 immunoglobulins G, normal and myeloma, in monomolecular layers, orientation at interfaces, comparison 4-66887  
 ionising radiation effect on biomembrane structure and function 4-77335  
 Langmuir-Blodgett films, prep. charact. and appls. 4-61245  
 lipid bilayer, cholesterol containing, reversible elec. breakdown 4-66890  
 lipid bilayers and biomembranes, nuclear spin-lattice relax. theory, dipolar relax. 4-62447  
 lipid-protein interactions in membranes, thermodynamic model 4-105171  
 lipophilic cation use as membrane potential probe, critical assessment 4-77205  
 liposomes, US absorption rel. to temp. 4-100239  
 liver mitochondrial membranes of heterothermic bat in summer and winter, thermal response 4-105190  
 lysozyme interaction with phospholipid bilayer, molecular conformation, M obs. 4-66888  
 mammalian cochlea, sensitivity modulation by LF tones, basilar membrane motion 4-109826  
 membrane fusion and interaction forces 4-93700  
 microsomal membrane structure, enzymatic crosslink influence 4-66896  
 microscope bound bromothymol blue, binding rel. to protein conformation, laser radiation effect 4-89498  
 model muscle fibre, end plate potentials, correction formulae 4-81652  
 neuronal activity, inference for diffusion models 4-89545  
 phase infection, energetics of first steps, review 4-66911  
 phosphatidylcholine multilayer liposomes,  $\gamma$ -irrad. effects: calorimetric, NMR and spectrofluorimetric obs. 4-67037

**biomembranes continued**

- phospholipid dispersions, thermotropic and high-press. phases, Raman spectroscopy, book contrib. 4-93701
- phospholipid head groups, perturbation by membrane proteins,  $^{31}\text{P}$  NMR spin lattice relax 4-89513
- phospholipid-water system, myelin figure form, pH and ion effects 4-77202
- phospholipid-water systems, calorimetric studies 4-66899
- phospholipid-water systems, calorimetric studies of water behaviour 4-66900
- plasma membranes, rat liver, radiation effects, IR spectroscopy obs. (*Russian*) 4-77321
- poly( $\alpha$ -amino acid) membranes, gas diffusivity and permeability 4-81650
- purple membrane, aq. suspensions, light activated rotation of bacteriorhodopsin 4-89500
- purple membrane, surface pot. and sidedness, resonance Raman dye probe method and obs. 4-67151
- purple membrane charged asymmetry, uranyl quenching of dansyl fluoresc. 4-89512
- retinal rod photoreceptor membranes, enzymatic processes, light scatt. probe 4-72224
- rod outer segment disc membranes, bovine; attached to lecithin bilayer, photoelec. signals generation 4-105237
- shear viscoelasticity of suspensions of biological cells with viscoelastic membrane 4-100092
- Shrapnell's membrane, comparative mechs. of hearing 4-109833
- skull cavity, press. distrib. 4-66975
- small intestine, mouse fibronectin content in basement membrane,  $^{137}\text{Cs}$   $\gamma$ -irrad. effect 4-81746
- thylakoid membranes, isolated, inactivation during freezing 4-105195
- transmembrane channels of *E. coli*, 3D reconstruction from electron micrographs 4-100418
- tympenic membrane, mech. vibrs. rel. to directional hearing in grass frogs 4-93751
- vesicles, mixed phosphatidylcholine/phosphatidylserine lipid, free energy pot. for aggregation 4-66897

**biomolecular effects of radiation**

- see also biological effects of ... (type of radiation)*
- see also photosynthesis ...*
- bacteriorhodopsin, direct meas. of ps charge separation 4-62523
- bacteriorhodopsin Biochrome film, nonlinear Weigert effect (*Russian*) 4-105184
- bilirubin, inverse Raman spectroscopy; hydrogen bonding, photoactivation 4-115016
- cell surfaces, fluoresc. reson. energy transfer, flow cytometry 4-81644
- desorption, fast heavy ion induced, mol. size effects 4-66880
- DNA, leukocyte, radiation-induced damage, fluorometric determ. (*Russian*) 4-67006
- DNA, thymus, pyrimidine cluster changes after animal  $\gamma$ -irrad. with sublethal dose (*Russian*) 4-67004
- DNA and histone within chromatin, radiation degradation (*Russian*) 4-66862
- DNA in proliferating and resting HeLa cells, replications and transcription, UV laser pulse effect (*Russian*) 4-66999
- DNA lesion and cell inactivation caused by X-ray, hyperthermia effects at 42°C 4-77196
- DNA of Chinese hamster cells, effect of 70 GeV proton secondary radiation (*Russian*) 4-67001
- electron donors and radiation protection, radiation effect modification by ascorbic acid 4-77194
- fucoxanthine layers, photocurrent action spectra 4-66863
- gum arabic, carbohydrate comp., microorganism growth and ESR spectra,  $\gamma$ -irrad. effects 4-72317
- high voltage pulsed discharge, runaway electron investigation 4-84089
- lipoygenase, wheat, radiation-induced lesion rel. to struct. organisation (*Russian*) 4-73220
- lymphoid cells, mol. mechanisms of radiation death, chromatin degradation and DNA replication (*Russian*) 4-77318
- mammalian cells, DNA repair kinetics following split dose  $\gamma$ -irrad. 4-77338
- microsome bound bromothymol blue, binding rel. to protein conformation, laser radiation effect 4-89498
- nuclear DNA segregation in *Bacillus cereus* T, radiation induced failure 4-72231
- phage  $\lambda$ , extracellular, lethal and mutagenic effects of  $^3\text{H}_2\text{O}$  and [ $^3\text{H}$ -methyl]-thymidine (*Russian*) 4-77313
- phage DNA, unpaired bases after  $\gamma$ -irrad. in-situ and in-vitro 4-77346
- poly U in aq. solns., yields of radiation-induced main chain scission 4-66872
- protein crystals, X-radiation damage reduction by polyethylene glycol 4-81822
- protein molecules, alpha-helix, Davydov solitons dissociation in EM wave field (*Ukrainian*) 4-72209
- proteins, radical formation under pulsed picosec. laser radiation action 4-109777
- quadratic field induced effects in macromol. solns. 4-85405
- radiobiology research projects, AFRR1 annual report (1982) 4-73172
- ribulose-1,5-bisphosphate carboxylase in pea and soybean, enhanced UV-B radiation effect 4-72305
- RNA, synthetic, selective nonlinear laser cutting 4-77191
- simian virus 40 DN, replication following UV irradi., test of model 4-115134
- skin optical loss influence on bilirubin, photoisomerisation during phototherapy 4-109875
- sperm whale metmyoglobin, aqs. soln., ultrasonic absorpt. 4-81614
- T7 bacteriophage, UV-induced small struct. changes, melting methods study 4-93808
- Tradescantia, somatic mutations induction using T labeled thymidine and uridine 4-72306
- tritiated water and biological systems, review 4-81619
- valyl-tRNA synthetases isolated from chick embryo and brain, difference in radiosensitivity 4-66873
- HTO ingestion, effects on mice, hexokinase isozymes in brain, liver and spleen 4-100259

**biomolecules** *see macromolecules; molecular biophysics***bionics** *see biocybernetics***biophysical effects of radiation** *see biological effects of radiation***biophysical instrumentation** *see biological techniques and instruments***biophysical techniques** *see biological techniques and instruments***biophysics**

- see also aerospace biophysics; biological fluid dynamics; biomechanics; cardiology; cellular biophysics; haemodynamics; hearing; human body physics; speech; vision*
- biophotonics, UV radiation emission from human body 4-62650
- book, annual review of biophysics and bioengineering 4-90305
- book, biophysical plant physiology and ecology 4-73191
- E-polarised RF fields, whole-body absorpt. of humans, effect of freq. and grounding 4-100229
- femur, stress distrib., three-dimensional finite element anal. (*Italian*) 4-81723
- gamma-ray tomography, medical appl. of imaging methods 4-72451
- many-body oscillators, self-synchronisation 4-93679
- muscle fibres, single glycerinated frog semitendinosus, light diff. patterns rel. to fibre rotation 4-89647
- mutually connected nervous network, recurrence eqn., bifurcation diagram 4-109772
- plant leaves, orientation depend. EPR and NMR spectra 4-72298
- review of physics in medicine and biology over 10 yrs. 4-115002
- solutes of water solns., contrib. to osmotic pot., calc. eqn. improvements, body fluids appl. 4-85399
- Stefan type free boundary problem soln. in cylindrical symm. 4-108077
- Turin Shroud image intensity correl. with the 3-D struct. of human body shape 4-89848
- vegetated randomly located vertical protrusion field, reflection 4-93795
- vegetation canopies, complete homogeneous, with various leaf-orientation distrib., directional refl. modelling 4-89649
- X-ray tomography, medical appl. of imaging methods 4-72451

**bioreology**

- Aachen clinical haemorheology test profile, data documentation 4-109974
- arterial endothelium, integrity following acute exposure to high shear stress 4-100188
- arterial system, clinical parameters indirect determ. method using velocimetric data (*French*) 4-67154
- arterial tissue, nonlinear viscoelastic props. 4-100217
- arterial wall, macromol. basis of hydraulic cond. 4-105271
- arterial wall mass transport, influencing factors 4-105272
- arteries, large, rheology rel. to press control 4-85456
- arteries, rheological approaches 4-115095
- articular cartilage, fluid transport and mech. props. 4-81731
- articular cartilage, normal, relax. and creep quasilinear viscoelastic models 4-109867
- blood, behaviour law determ., math. and numerical methods 4-115090
- blood, flows through small tubes in vitro 4-115094
- blood, reversing flow in the aorta: a theoretical model 4-109856
- blood, rheological properties during clotting, study methods 4-110009
- blood clotting, study by resonance tomography 4-105315
- blood filtration measurements, recent progress in improving data processing 4-110016
- blood filtration pressure and erythrocyte deformability meas., evaluation of the Erythrometre 4-115248
- blood flow through artery with mild stenosis, effects of couple stresses 4-100186
- blood platelets, rheological behaviour in vivo 4-115093
- blood rheological parameters, obs. using two coaxial viscometers, comparison 4-109977
- blood rouleau formation, expt. approach, comparison of 3 methods 4-110015
- blood viscometry, co-axial, accuracy improvement 4-115279
- blood viscosity in both extensional and shear flow, obs. using a falling ball viscometer 4-109851
- bone rheology, new developments 4-115096
- bronchial mucus, viscometometer for rheological props. study in clinical practice 4-115247
- bronchial secretions, human, rheological props. rel. to ciliary beat freq. 4-105276
- capillary flow resistance rel. to marginal layer width and axial core viscosity 4-115092
- capillary permeability, role of blood coagulation, fluoresc. intravital microscopy obs. 4-105208
- capillary tube plasma viscometer, automatic instrument for plasma viscosity meas. 4-115246
- cervical mucus glycoproteins macromol. architecture and hydrodynamic props. 4-105273
- conference on new methods, Nancy, France (Aug. 1983) 4-106097
- dynamic interactions between approaching surfaces of biological interest, review 4-77204
- electro-bioreology, piezoelec. in biopolymers 4-105267
- endoendothelial fibrin lining and fibrin gels rel. to transcapillary transport control 4-105270
- endothelial permeability hydrodynamic and mech. aspects 4-105209
- erythrocyte aggregation, viscometric technique for meas. 4-110014
- erythrocyte aggregation rel. to blood flow in small capillaries at low shear forces 4-109854
- erythrocyte deformability, assessment by constant flow filtration technique 4-115282
- erythrocyte deformability, device for routine meas. 4-109979
- erythrocyte deformability, leukocyte removal prior to study, improved method 4-115285
- erythrocyte deformability meas., improved filtration rate 4-109980
- erythrocyte filterability and anticoagulants 4-115097
- erythrocyte filtration resistance at constant press., technique for continuous meas. 4-115283
- erythrocyte membrane, shear deform. and flow, analytical solns. 4-100099
- erythrocyte membrane, viscous dissipation inside during micropipette aspiration 4-89522
- erythrocyte membrane viscosity, determ. from rheoscopic obs. of tank-treading motion 4-105202
- erythrocyte passage-time, dependency on pore geometry in single-pore erythrocyte rigidometer 4-109787
- erythrocyte-stasis-meter, blood flow characts. universal parameter determ. 4-109976
- erythrocytes, aggregation and agglutination 4-109786
- erythrocytes, deform. and viscoelastic props. of a concentrated suspension 4-100090
- erythrocytes, heat treatment rel. to aggregation in plasma 4-100091

**bio rheology continued**

- erythrocytes under shear, rel. to small angle light scatt. by large spheroids 4-115116
- Erythrometer: device for erythrocyte filterability and plasma viscosity meas. 4-109981
- ESR spectroscopy, membrane and cell microrheological study appl. 4-115289
- eye, vitreous humour, modelling by an oscill. viscoelastic sphere 4-105278
- fibrin gels as biological filters and interfaces 4-105269
- filtration coefficient obtained by stepwise pressure elevation in isolated dog lung 4-100194
- flowmeter for slow-flowing physiological liquids 4-115311
- fluorometer, ns, for biomembrane rheological aspects study 4-115291
- $\beta$ -galactosidase, ultrafiltration induced by pulsatile flow in variable vol. hollow-fibre enzyme reactor 4-77270
- gills, blood-circulating system rel. to effective operation (Russian) 4-72284
- grating laser microscope for microvessel blood flow vel. meas. 4-115281
- haematocrit-erythrocyte-disaggregation apparatus 4-110013
- haemoglobin 'S', abnormal, cytological and rheological characts. of drepanocytes (French) 4-115032
- haemorheology, clinical, methods and instrumentation 4-109975
- haemorheology, Copley-Scott Blair phenomenon rel. to elec. double layer 4-100185
- haemorheology, rel. to patients with chronic arterial disorders 4-109849
- haemorheology, transient, in an air-bearing viscosimeter, obs. 4-109850
- haemorheology from microcirculation to macrocirculation (Japanese) 4-72294
- harmonic and impulse rheological tests of biomaterials 4-110012
- Hemorrhometre, automated apparatus for filtration initial flow rate meas. 4-115284
- hyaluronate gels, macromolecules, diffusion, methods and preliminary results 4-100366
- invertebrate connective tissue, stress relax. behaviour rel. to ionic environment 4-62511
- macromolecules, rheologically active, studies by quasielastic light scatt. 4-115292
- methods, new, for biorheology 4-106089
- microvascular walls, permeability characts. 4-105207
- microvessel hydraulic conductivity, meas. in microvessels, effects of compliance 4-105382
- mucus glycoprotein gels, purified, cation induced changes in rheological props. 4-105275
- myocardial perfusion,  $^{82}\text{Rb}$  positron emission CT, extraction fraction and flow meas. 4-72378
- neutrophils, human, effect of colchicine on viscoelastic props. 4-115030
- O-nitrophenyl- $\beta$ -D-galactopyranoside, ultrafiltration induced by pulsatile flow 4-77270
- OP-rheometer system for blood viscosity and viscoelasticity anal. 4-109973
- photophysical methods, continuous excitation, cellular rheology appl. interests and limits 4-115290
- placental blood, capillary-tube viscometry 4-115091
- plasma, human, surface rheological obs., meas. head 4-115089
- platelets, rabbit, flowing in small arterioles, orientation and diameter distrib. 4-100187
- polysaccharide systems, rapid transport of macromols. by dissipative struts. 4-105266
- proteoglycan subunits and aggregates, viscoelastic props. in varying soln. concs. 4-81728
- pulmonary mucociliary transport, unsedated animal models 4-105277
- red cells aggregation in space, meas., NASA Space Shuttle project 4-109970
- resonance thrombography 4-109972
- shear viscoelasticity of suspensions of biological cells with viscoelastic membrane 4-100092
- skin perfusion pressure, meas. by photoelec. technique, rel. to amputation level selection 4-72338
- Technicon Ektacytometer: automated exploration of erythrocyte function 4-115286
- thoracic aortas, rat, elasticity in simple elongation 4-62504
- thread-forming property of biological fluids, apparatus for meas. 4-115280
- thrombosis tendency rel. to blood viscosity increase, adhesiometer for instant quantitative test (German) 4-77415
- tracheal gland secretions, cat, autonomic regulation of viscoelasticity 4-93779
- tracheal mucin, canine, effect of  $\text{Ca}^{2+}$  on struct. and rheology 4-105274
- tumour cells biorheology 4-105268
- viscometer using mag. fluid for biological fluids meas. 4-110011
- viscometric methods for assessing red cell deformability and fragmentation 4-115287
- wave propagation in a thin-walled liquid-filled initially stressed tube 4-77274
- Weissenberg rheogoniometer based biorheological methods, blood appl. 4-110010

**biosonic generation** see *biacoustics; mechanoeception*

**Biot-Savart law** see *electromagnetism*

**biothermics**

- 915-MHz direct contact diathermy applicator, with reduced leakage, performance 4-72327
- acclimation temperature, effects on routine metabolism muscle mitochondrial vol. density and capillary supply in elvers 4-105187
- adrenergic transmission rel. to thermal sweating in man 4-81635
- afferent temperature signals, processing in sensory ganglia and spinal cord 4-81625
- aperture synthesis thermography—a new approach to passive microwave temperature measurements in the body 4-115158
- aquatic animals, temp. control of external coverings (Russian) 4-72214
- auditory brainstem response and temperature: relationship in guinea pigs 4-77252
- auditory evoked response of cat brain stem, hypothermia effects 4-72259
- biotelemetry device linked to Apple II 4-62636
- bird and mammal coats, effects of wetting on insulation 4-105191
- brainstem, metabolic activity changes during central and peripheral thermal stimulation 4-81622
- breast, normal woman, thermal modelling 4-109783
- brown adipose tissue rel. to thermal and food efficiency regulation in rodents 4-81628

**biothermics continued**

- burn injury in blood-perfused skin, finite element model 4-77200
- cardiac output, thermal dilution technique for continuous meas. 4-81794
- cell growth inhibition by irradi. combined with hyperthermia or anticancer drugs 4-93806
- cells, normal and tumour, cooperative thermal transitions, denaturing of chromatin 4-66905
- chromaffin cells, isolated, temp. effects in stimulus-secretion process 4-66919
- clinical hyperthermia unit utilising an array of seven focused ultrasonic transducers 4-100089
- cockroach, temp. of head, thorax and abdomen during rest and flight at high ambient temps. 4-105189
- colonic temperature and operant behaviour in rhesus monkeys exposed to RF fields 4-100232
- computer modelling EM field distribution in lossy dielectrics, clinical appls. 4-109785
- conference on radiobiology, Rijswijk, Netherlands (Jan. 1984) 4-95039
- conflicts and strategy in a cold environment 4-81627
- controlled radiation ceiling for thermal treatment of patients 4-62545
- correlation microwave thermography principles and system tests 4-77365
- cutaneous vascular tone during heat load modified by exercise intensity 4-81633
- cytochrome c oxidase, electron spin-lattice relax. rate, temp. dependence 4-89499
- cytoplasm of Chinese hamster cells, thermal action of 2.45 GHz microwaves 4-100248
- dehydration, effect on circulation and temp. regulation during exercise 4-81631
- dive, response, human temp. effect rel. to cold water near-drowning 4-89510
- DNA lesion and cell inactivation caused by X-ray, hyperthermia effects at 42°C 4-77196
- DNA supercoiling, free energy rel. to enthalpy 4-77182
- ear, mouse, long-term effect of X-rays on thermal sensitivity 4-109882
- EM detection and treatment of malignant disease, conf., London, England (Apr. 1984) 4-67872
- EM heating of tissue-equivalent phantoms with thin, insulating partitions 4-100290
- EM tumour hyperthermia improvement, regional heating and systemic blood cooling 4-67070
- erythrocyte, microwave bioeffects, temp. and  $\text{pO}_2$  dependence 4-100250
- erythrocytes, heat treatment rel. to aggregation in plasma 4-100091
- erythrocytes from stored human blood, morphological changes during heating 4-105204
- exergy, engineering-thermodynamics and thermodynamics of life 4-105194
- extrahypothalamic thermal inputs to the hypothalamic thermoregulatory network 4-81640
- fibroblasts, normal and ataxia telangiectasia, human, thermal enhancement of radiosensitivity 4-89655
- fluoroptic thermometry use in hyperthermia treatment of cancer 4-85470
- forearm blood flow control during exercise in the heat, effect of mild essential hypertension 4-100196
- gammarid amphipods from Lake Baikal, press. effects on thermal preference behaviour 4-105193
- glaucoma, thermal model for US treatment, rabbit obs. 4-89660
- granulocytes, human, water permeability at subzero temps. in presence of extracellular ice 4-105212
- haemoderivative thawing, microwave heating reliability 4-72218
- haemopoietic stem cells, murine normal and leukaemic, heat sensitivities 4-72226
- heat exchange following atropine injection before and after heat acclimation 4-100088
- helix as RF applicator for hyperthermia, anal. 4-72215
- hepatoma cells, cultured, thermotolerance obs. 4-66913
- hepatoma cells, morphological response and survival during fractionated hyperthermia 4-93706
- homeothermic animal temp. regulation, five-dimensional dual butterfly catastrophe model 4-66884
- hot-humid environments, temp. regulation rel. to hydromiosis 4-81634
- human body heat balance at Polish coast of Baltic Sea 4-115019
- hydration and vascular fluid shifts during exercise in the heat 4-89509
- hydrolytic stability of biomols. at high temps., implication for life at 250°C 4-100600
- hyperthermia, mouse tumour acidity changes 4-81641
- hyperthermia, physiological mechanisms, review 4-89508
- hyperthermia, regional, mag. induction heating, beagle dog model, thermal dosimetry anal. 4-93697
- hyperthermia cancer therapy, EM local heating with HF electrical fields 4-100288
- hyperthermia combined with fast neutrons or X-rays, response of mouse skin 4-100086
- hyperthermia phantom, practical, modular 4-67066
- hyperthermic radiosensitisation of cells from a human melanoma xenograft 4-105293
- hypothalamic and thalamic neurons, responses to noxious and scrotal thermal stimulations in rats 4-81639
- hypothermia, ethanol-induced, and ethanol consumption in rats: rel. to low-level microwave irradi. 4-100247
- hypothermia, pentobarbital-induced, effects of acute low-level microwaves in rats 4-100246
- hypothermia of Chinese hamster ovary cells, survival rel. to precooling 4-77197
- hysteretic heating for the treatment of tumours 4-72322
- inductive applicator for hyperthermia using a one-turn coil with RF current 4-77424
- insect, cold-tolerant, found in a Himalayan glacier 4-93696
- interstitial hyperthermia and brachytherapy, combined technique 4-89823
- interstitial hyperthermia by RF and microwave heating 4-115162
- intestinal hyperthermia, effect in Chinese hamsters 4-89507
- IR sensors, medical appl. 4-93837
- lipid bilayers, mixed, phase transition props. rel. to those of covalent analogues 4-85408
- lipid-protein interactions in membranes, thermodynamic model 4-105171
- liposomes containing various carotenoids and chlorophyll, temp.-induced changes in spectral props. 4-115022
- liver mitochondrial membranes of heterothermic bat in summer and winter, thermal response 4-105190
- localised microwave hyperthermia, waveguide applicator with convergent lens 4-81753

# biothermics continued

- locomotor diseases, clinical appl. of advanced IR thermography 4-93839  
lung, extravascular thermal volume, effect of oedema and haemodynamic changes 4-100087  
lymphocytes, mouse, antigen-antibody complexes capping inhibition by hyperthermia 4-105210  
 $\alpha_2$ -macroglobulin, human, effect of methylamine and plasmin on conformation, differential scanning calorimetric anal. 4-66859  
magnetic induction heating of ferromag. implants for inducing localised hyperthermia in deep-seated tumours 4-62541  
magnetic induction heating of tumours with ferromag. seed implants 4-62540  
mammalian body mass and sensitivity to radiofrequency electromagnetic radiation, inverse relationship study 4-77307  
mammalian cells, occurrence of DNA strand breaks after hyperthermic treatments with or without radiation 4-66915  
marsupial, thermal balance changes during cold and warm acclimation 4-105192  
medial medullary neurons, response to preoptic and scrotal thermal stimulation 4-81624  
microcomputer-controlled microwave hyperthermia system 4-67059  
microwave applicators, 1-10 GHz, radiometry, tissue brightness meas. (Japanese) 4-62553  
microwave applicators, contact-type tissue cooling effects on brightness temp. 4-72217  
microwave heating pattern in multilayered material 4-85482  
microwave hyperthermia, direct temp. meas. of focused heating from phased array system 4-72349  
microwave hyperthermia and data acquisition system 4-72348  
microwave hyperthermia applicator, compact, design and performance 4-72351  
microwave hyperthermia applicators, field penetration limitations 4-72350  
microwave miniature applicators, designs for localised hyperthermia of human malignancies 4-67069  
microwave radiometry, recognition of thermal structures 4-62549  
microwave thermography, correlation method, thermal gradient localisation in lossy materials 4-81752  
microwave thermography system, 3 GHz, design and clinical use 4-72346  
microwave tomography system and use in deep hyperthermia 4-72347  
midbrain neurons of rats responsive to hypothalamic temperature change and their local thermosensitivity 4-81623  
mononucleosomes from replicating chromatin in heated cells, sedimentation coeff. and buoyant density 4-77198  
motility control system in algae *Euglena gracilis*, temperature masking of the circadian system 4-100104  
multichannel solid-state recorder, design and appl. to temp. meas. 4-115251  
muscle, insect, resting pot., temp. effect 4-66929  
nonshivering thermogenesis, baroreflex suppression in restrained and non-restrained rats 4-81629  
open-circuit indirect calorimetry, gaseous exchange anal. 4-85589  
paralegic men, attenuated skin blood flow response to hyperthermia 4-100202  
Passive Diver Thermal Protection System test and evaluation 4-109784  
peripheral blood leukocytes, chromatin degradation, combined effect of radiation and burn (Russian) 4-77319  
peripheral nerve impulse cond. blocking by local cooling, animal expt. method 4-115307  
pharyngo-oesophageal thermoreception rel. to water-reinforced instrumental conditioned reflex in rats 4-105185  
phased-dipole applicators for torso heating in electromagnetic hyperthermia 4-100289  
phospholipid bilayers, latent heat meas. by adiabatic compression 4-85407  
phospholipid membrane vesicles, cylindrical, thermal fluctuations 4-81643  
phospholipid-sucrose interactions, thermodynamics 4-115004  
phospholipid-water systems, calorimetric studies 4-66899  
phospholipid-water systems, calorimetric studies of water behaviour 4-66900  
photosynthesis efficiency, thermodynamic estimation 4-105205  
poly(dG)-poly(dC), DNA H bond melting, self-consistent microscopic theory 4-89276  
polyacrylamide as a phantom material for electromagnetic hyperthermia studies 4-67061  
prefrontal cortical influences on behavioural thermoregulation and thermosensitive neurons 4-81621  
preoptic thermosensitive neurons, neural inputs, histological and electrophysiological mapping in rats 4-81620  
radiation therapy dielectric-loaded rectangular waveguide applicator 4-109894  
radiometry of biological tissue, temp. profile meas. (Czech) 4-85485  
respiratory calorimetry, calibration methods 4-100396  
RF (28 MHz) CW radiation effects 4-67000  
RF hyperthermia for tumour treatment, localised technique development 4-72345  
RF hyperthermia in tumour treatment, computer simulation use 4-72344  
RF hyperthermia of deep-seated tumours, dipole array applicator performance study using blood flow simulator (Japanese) 4-85406  
sheep and man, weather influence on body heat loss 4-72220  
silkworm embryos, heat prod. and respiration 4-66883  
skeletal sarcoplasmic reticulum, thermodynamic efficiency of  $\text{Ca}^{2+}$ - $\text{Mg}^{2+}$ -ATPase 4-66912  
skin, equal thermal sensation lines determ. in evaporative regulation region (Japanese) 4-66885  
skin, human, temp. distrib., blood flow, perspiration and metabolic heat generation effects 4-62446  
skin, previously irradiated, response to combinations of X-rays, heat and cis-diamminedichloroplatinum 4-67038  
skin and coat thermalisation induced with nembutal in guinea pigs, ambient temp. effect 4-66882  
skin AVA activity and cardiac output, redistrib. in sheep during exercise and heat stress 4-81632  
skin blood flow, thermal sensation and freq. anal. of cutaneous vasomotor rhythms 4-105188  
spinal cord, thoracic and lumbosacral, effects of selective thermal stimulation on cardiovascular functions in rats 4-81626  
spinal cord thermal stimulation in rabbit, ear-skin and renal blood flow changes 4-81725  
T7 bacteriophage, UV-induced small struct. changes, melting methods study 4-93808

# biothermics continued

- TEM radiofrequency/microwave applicator for non-invasive deep body hyperthermia 4-77361  
temperature measurements, emissivity-independent, using microwave thermographic system 4-77364  
temperature probes, inaccuracy 4-85539  
temperature regulation: a theoretical consideration incorporating Sherringtonian principles of central neurology 4-81637  
thermal afferents to the hypothalamus and thermal adaptation 4-81638  
thermal strain measurement techniques, aircrew appl. 4-85526  
thermally stimulated luminescence in biochemical systems, review 4-109778  
thermoacoustic effect in dielectrics and coupling to external medium, thermodynamical formulation 4-115128  
thermocouple oesophageal temperature probe, construction and position verification 4-85535  
thermoelectric cooling device for cryoprecipitation by plasma separation 4-93938  
thermoelectric microscope stage for meas. of supercooling points of microscopic organisms 4-100402  
thermographic images, nonlinear filtering 4-85491  
thermographic tomography problem, soln. by direct substitution eqn. error technique 4-77199  
thermography, development and criteria for use 4-93838  
thermography, methodological errors rel. to diagnostic conclusions accuracy (Russian) 4-115155  
thermoradiotherapy of refractory malignant tumours 4-115163  
thermoregulation, cranial vasodilator control of lingual arteriovenous anastomoses 4-81630  
thermoregulation at high ambient temp., effect of hypercapnia in rabbits 4-105186  
thermoregulation in clothed human, transient model 4-115018  
thermoregulatory mechanisms, conf., Osaka, Japan (Aug. 1982) 4-78028  
thermotolerance, cell cycle dependence, CHO cells heated at 45.0°C 4-93707  
thermotolerance and thermosensitisation in CHO and R1H cells, comparative study 4-115020  
thermotolerant CHO cells and RIF-1 tumours, radiosensitivity and thermosensitisation 4-105297  
thylakoid membranes, isolated, inactivation during freezing 4-105195  
tissue equivalent phantom materials, thermal props. 4-89506  
tissue permittivity, in vivo and in vitro expt. techniques and results 4-62640  
tissue temp. profile reconstruction from microwave radiometry, optimisation 4-72466  
tumour microcirculation, hyperthermia-induced stoppage, time-temp. relationship 4-115021  
tumour models heated by self-regulating Ni-Cu thermoseeds, temp. distrib. 4-66886  
US hyperthermia wattmeters, acoustic power o/p meas. 4-100284  
US tomography, practical meas. of human body temp. 4-100268  
vascular compliance changes during hyperthermia, dog expts. and simulation anal. 4-81636  
vascularized tissues, 3D description of heating patterns during hyperthermic treatment 4-72219  
vasculature, mouse intestine, effect of radiation alone or combined with hyperthermia 4-109879  
villus compartment of mouse small intestine, development of thermotolerance in hyperthermal injury 4-72216  
warm-up behaviour of human extremities after cold-water immersion, model for analysis (German) 4-62445  
yeast, radiosensitive mutants: cell inactivation by high temp., UV light and ionising radiation (Russian) 4-77314
- biote** see mica
- biotransport**  
see also *biodiffusion; biological fluid dynamics; biomembrane transport; cellular transport and dynamics; neurophysiology*  
arterial wall mass transport, influencing factors 4-105272  
bronchial mucus transport, model for assessment 4-66925  
capillary permeability, role of blood coagulation, fluoresc. intravital microscopy obs. 4-105208  
glomerular filtration rate, meas. without blood sample, validation in renal transplant patients 4-62555  
inert vapours and gases, uptake, regulation and pulmonary elimination 4-115003  
intestinal uptake of bile acids, effect of external abdominal irradiation in rats 4-115139  
intestine, chicken, transport of  $^{75}\text{Se}$  selenates against conc. gradient 4-100109  
maternal-fetal exchange and transfer of radioactive compounds 4-66928  
polymer solutions, transport props., biological appl. 4-89492  
polysaccharide systems, rapid transport of macromols. by dissipative structs. 4-105266  
wall mass transport, topological anal. using a luminesc. immobilised enzymatic system 4-115037  
 $\text{O}_2$  transport model for transcutaneous  $\text{P}_{\text{O}_2}$  meas. (Japanese) 4-100108  
 $\text{O}_2$  transport system pathological functional state, minimum-power model 4-66924
- bipolar integrated circuits**  
Fahrenheit temperature sensor, monolithic IC implementation with internal offsetting function 4-95423  
I<sup>2</sup>L device circuit model with layout patterns 4-104192
- bipolar transistor circuits**  
Used for general papers and papers where use of bipolar transistors is significant  
broadband amplifier, CAD optimisation program, Gbit/s apps. 4-83723
- bipolar transistors**  
see also *bipolar integrated circuits*  
buried-collector vertical magnetotransistors, geometrical analysis of offset 4-95474  
electron microscope studies 4-103622  
homoeopitaxial structs., LPE growth, power transistor fabrication (Russian) 4-109333  
magnetotransistor effect, physical mech. 4-109052  
US thick piezoelectric transducers using bipolar transistors in avalanche mode 4-69659  
(In,Ga)As/InP n-p-n heterojunction bipolar transistors grown by LPE with high gain 4-85097  
InGaAsP/InP laser diode, monolithic integration with heterojunction bipolar transistors 4-102927

**bipolar transistors continued**

- InGaAsP/InP lateral p-n-p transistor fabrication using open diffusion technique 4-104003  
Si, shallow npn bipolar transistors fabrication by triple ion implantation 4-75460

**bipoles** *see network analysis; network synthesis*

**biquadratic filters** *see active filters*

**birefringence**

- see also flow birefringence; Kerr electro-optical effect; light polarisation; magneto-optical effects; mechanical birefringence; optical constants; optical rotation*  
trans-4-( $\beta$ -trans-4'-n-alkylcyclohexyl)-1'-ethylcyclohexane-1-carboxylates, nematic phase, physical props. 4-92359  
anisotropic artificial Kerr degenerate four-wave mixing media, 4-107757  
anisotropic media, propag. and interaction of transversely-confined beams (Russian) 4-96794  
artificial Kerr media, equilib. dielec. props. 4-97011  
benzene, Cotton-Mouton effects, temp. depend. 4-108155  
benzene, in cyclohexane, Kerr consts., mol. anisotropic polarisabilities, dielectric study 4-102721  
biaxial orthorhombic mm2 group, crystals, SHG phase matching calculation (Chinese) 4-79228  
bis-propylammonium manganese chloride, commensurate and incommensurate phase transitions, thermal expansion, birefr. meas. 4-70374  
book, optical waves in crystals, laser radiation propag. and control 4-86135  
butadiene-styrene block copolymer films, mech. and opt. props., temp. depend., superlattice fusion (Russian) 4-76547  
t-butylbenzenes, in cyclohexane, Kerr consts., mol. anisotropic polarisabilities, dielectric study 4-102721  
cholesteric, lyotropic mesophases, optical sign determinations 4-84940  
cholesteric liq. crystals, blue phases, elect. field induced birefringence 4-76426  
coiled-birefringent-fibre polarisers 4-91599  
conference on solid state optical control devices, Los Angeles, USA (Jan. 1984) 4-95024  
connector, quasi-isotropic pin-loaded, stress meas. using photoelasticity 4-69720  
copolyester of lactic and glycolic acid, strain induced crystallisation, optical and X-ray scatt. obs. 4-85186  
cyanobiphenyl liq. crystals, alignment on substrate surface by collective interactions 4-88086  
di(alkylammonium) ferrous chloride, birefringence and Brillouin scatt. at struct. phase transition 4-75661  
di(propylammonium)Mn<sub>1-x</sub>M<sub>x</sub>Cl<sub>2</sub> (M=Cd,Zn,Cu), structural phase transitions, optical studies 4-75662  
dicalcium lead propionate, ferroelec. press. induced II-III transition, polarising microscope obs., permitt. meas. 4-80879  
dicalcium strontium propionate, ferroelec. press. induced II-III transition, polarising microscope obs., permitt. meas. 4-80879  
dichroic elliptic birefringent media, Jones matrix 4-107509  
dielectric thin film birefringence measurement by prism coupler method 4-106337  
electrooptical field-measurements with linear and circular birefringent crystals 4-104572  
esters, nematic eutectic mixtures, electrooptic, dielec. and physical props. 4-108271  
extraordinary wave, self-induced transparency, relaxation effects, inverse scattering method 4-97008  
fibre lightguide, single-mode, perturbed, transfer characts. 4-83715  
fibre optic taper-polarisers, highly birefringent, finite cladding effects 4-69569  
fibre polariser, in-line birefr. 4-91606  
fibres, birefringent, with stress rods in the cladding, polarisation props. 4-74716  
fibres, polarisation-preserving high birefringence, characterisation and performance 4-91604  
filter, birefringent, development by Lockheed, solar appl. 4-97048  
3-fluoro-4-cyanophenyl 4'-n alkylbenzoates, synthesis, mesomorphic and phys. props. 4-113318  
glass fibre reinforced epoxy laminates, orthotropic, birefringent, prep. and photoelasticity 4-89022  
hexafluorobenzene, Cotton-Mouton effects, temp. depend. 4-108155  
holographic simulation of birefringent elements 4-97040  
imperfect cryst., laser irradi., thermoelastic stresses, optical polarisation study 4-61114  
inert gases, mag. birefr. meas. 4-103465  
inhomogeneous, birefringent media, polarisation transfer 4-72858  
lenses of optical instruments, permissible birefringence calc. method 4-91563  
linear birefringence induced by electric and mag. fields, mol. theory 4-102745  
linear optical birefringence of magnetic crystals, review 4-76428  
linear uniform field compensator for anisotropic body birefr. meas. 4-63774  
liquid crystals, cubic, birefringence and Frederiks effect 4-60817  
liquid crystals, IR birefringence meas. 4-80901  
liquid crystals phase transition, enthalpy and birefringence 4-98277  
Lyot birefringent filter, universal wavelength tuning formula derivation 4-97045  
magneto-optical effects, isotropic and anisotropic in crystals, review 4-61668  
methylammonium mercury trichloride, ferroelec. transition, thermal, dielec., optical meas. (French) 4-76392  
methylbenzenes, in cyclohexane, Kerr consts., mol. anisotropic polarisabilities, dielectric study 4-102721  
molecular liquid, single molecule cross-correlation functions using elec. field induced birefringence 4-93056  
monomode optical fibres, low birefr., polarisation rot. due to geometric effects 4-107859  
Mossbauer cryst. diff., at low temp. 4-88749  
nematic liquid crystal, heat convection, orientational optical nonlinearity 4-112504  
nematic liquid crystals, orientation deformations in homeotropic layers, boundary conditions 4-84154  
nematic-substrate interaction, rel. to boundary layer phase transition 4-80888  
nitrobenzene-n-hexane crit. binary mixture, shear-induced dichroism and birefringence 4-104567

**birefringence continued**

- noncentrosymmetric cubic cryst., induced birefringence anisotropy 4-88812  
nylon 66 and 6, mech. relax., elastic moduli, chain orientation, birefringence, wide angle X-ray obs. 4-93323  
optical fibre dispersion equation, direct analysis 4-107858  
optical fibres, linear polarisation preserving single-mode, birefr. meas. (French) 4-87471  
organic liquids, high field diamag. suscept., Cotton-Mouton study 4-65785  
particle characterisation by polarised light microscopy, crossed polars case 4-66532  
PET, molecular orientation, mol. wt., birefringence, density, light scatt. 4-84219  
PET films, drawn, molecular orientation, polarized IR spectra and birefringence obs. 4-84215  
polarisation, definitions and nomenclature, instrument polarisation 4-82604  
polarisation states and operators, representation by quaternions (French) 4-69306  
polydisperse particle size analysis by pulsed electric birefringence 4-84948  
polyethylene, refractive index, birefringence, orientation and morphology 4-84943  
polymer rheo-optics, conf., Seattle, WA, USA (Mar. 1983) 4-82590  
polymers, conjugated, in gels, electric field coupling to slow elastic modes 4-98198  
polypropylene, recrystallisation, morphology and birefringence studies (French) 4-103664  
polystyrene film, atactic, liq.-liq. transition, birefringence, temp. depend. 4-114241  
 $\alpha$ -quartz, synthetic, linear birefringence meas. in IR region, common beam technique appl. 4-61654  
quartz microporous glass laser active elements, optical characts. 4-79253  
semiconductors, mobile carrier optical nonlinearities 4-87391  
single mode birefringent fibres, small Stokes shift frequency conversion 4-107748  
single mode optical fibre, meas. 4-107839  
single-mode fibres, scatt. loss versus polarisation holding ability 4-69561  
single-polarisation single-mode optical fibres, absorption reducing, structure design 4-64784  
symmetric tetraavalent tensor model, transparent optically isotropic media 4-87276  
tetradecyltrimethylammonium bromide, lyotropic nematic phase, birefringence meas. 4-92088  
thiourea, memory effect, defect density waves in modulated systems 4-88163  
transient Kerr effect student apparatus 4-95103  
1,3,5-trifluorobenzene, Cotton-Mouton effects, temp. depend. 4-108155  
uniaxial crystals with isotropic period for narrow-band selective optical filters (Russian) 4-97049  
weakly ferromagnetic rhombohedral antiferromagnets, magneto-optic effects 4-114248  
BaMnF<sub>4</sub>, optical props. near incommensurate and mag. transitions 4-66004  
Ba<sub>2</sub>NaNb<sub>2</sub>O<sub>7</sub>, interaction of incommensurate modulation with mobile and fixed defects 4-75446  
Ba<sub>2-1</sub>Na<sub>0.84</sub>Nb<sub>0.99</sub>O<sub>7</sub> incommensurate system, thermal hysteresis in birefringence and permittivity 4-61656  
BaTiO<sub>3</sub>, birefr., Kerr effect 4-88805  
BiFeO<sub>3</sub> single cryst., ferroelec. domains, birefringence, and light absorption 4-71324  
Bi<sub>2</sub>SiO<sub>20</sub>, photoelectron transport props. 4-88534  
BiVO<sub>4</sub>, ferroelastic, spontaneous birefringence obs. 4-93045  
CdSiP<sub>2</sub>, chalcopyrite crystals, dispersion of temp. coeffs. of birefr. 4-61651  
Co<sub>2</sub>B<sub>2</sub>O<sub>7</sub>Br, spontaneous birefringence and Faraday effect 4-71351  
Cu<sub>2</sub>B<sub>2</sub>O<sub>7</sub>Cl, ferroelec. and paraelec. phases, optical rot., birefr., optical susceptibilities 4-109151  
Fe-Si sheets, Bitter patterns, ferrofluid birefringence studies 4-76202  
H, ground state, multipole moments, time derivative fields 4-69021  
Ho<sub>0.9</sub>Y<sub>2.2</sub>Fe<sub>2</sub>O<sub>12</sub>, spin-reorientation phase transition, Faraday effect, magnetisation study 4-88814  
K<sub>2</sub>Co<sub>2</sub>(SO<sub>4</sub>)<sub>3</sub>, langbeinite, optical props. 4-76427  
K<sub>1</sub> single cryst., birefringence induced by spatial dispersion 4-76429  
KNbO<sub>3</sub>, refractive index and polarisation 4-99081  
LiNbO<sub>3</sub> crystal, conoscopic interference pattern and refractive index (Chinese) 4-114239  
LiNbO<sub>3</sub>:Fe crystals, photoelec. and photoref. prop. control during growth by elec. current 4-80904  
MgF<sub>2</sub> single crystal refractive props. 4-93029  
NH<sub>4</sub>HCO<sub>3</sub>, relations between crystallographic characts. and cryst. struct. (Chinese) 4-75378  
Na<sub>0.5</sub>Bi<sub>0.5</sub>TiO<sub>3</sub>, crystal, birefringence and opalescence, temp. depend. 4-76425  
NaH<sub>2</sub>(SeO<sub>3</sub>)<sub>2</sub>:Cr<sup>3+</sup>, EPR spectra, temp. and external elec. field effects 4-88715  
Na<sub>5-1</sub>K<sub>1</sub>W<sub>3</sub>O<sub>9</sub>F<sub>3</sub>, Bridgman-Stockbarger growth, ferroelec. and ferroelastic props., permittivity, birefr. meas. 4-65969  
Na<sub>5-1</sub>Li<sub>1</sub>W<sub>3</sub>O<sub>9</sub>F<sub>3</sub>, Bridgman-Stockbarger growth, ferroelec. and ferroelastic props., permittivity, birefr. meas. 4-65969  
NaNH<sub>4</sub> tartrate crystals, refractive index and birefringence 4-76406  
PLZT retardation plates, nonhomogeneity of light modulation 4-61660  
PbFe<sub>0.5</sub>Ta<sub>0.5</sub>O<sub>3</sub> single cryst., ferroelec./antiferromag., spontaneous birefringence 4-71344  
Pb<sub>2</sub>GeO<sub>11</sub> crystals, spatial modulation of light 4-84941  
RbMnCl<sub>3</sub> crystals, struct. phase transition, exptl. and group theoretical study 4-75658  
SiO<sub>2</sub>-GeO<sub>2</sub> birefringent single mode fibre, optical Kerr coeff. meas. at 1.15  $\mu$ m 4-74629  
SrAl<sub>2</sub>O<sub>7</sub>(CrO<sub>4</sub>)<sub>2</sub>, flux grown, ferroelec. phase transition, domain studies, birefr., polarisation, permittivity, transition enthalpy meas. 4-65970  
Ti<sub>2</sub>SeO<sub>4</sub> ferroelec. transition, birefringence studies 4-65976  
Y<sub>3-x-y</sub>Bi<sub>x</sub>Pb<sub>y</sub>Fe<sub>3-2x-y</sub>Pt<sub>0.12</sub> garnet films, magneto-optic prop. meas. using piezobirefr. modulation 4-66013  
ZnSe cubic crystal, natural birefringence meas. 4-109153  
ZnSiAs<sub>2</sub>, ZnSiP<sub>2</sub>, chalcopyrite crystals, dispersion of temp. coeffs. of birefr. 4-61651

## bismuth

- see also nuclei with .....  
 amorphous, supercond., upper critical fields 4-76089  
 bolometers for near-MM wave IC imaging polarimeter antenna arrays 4-82827  
 colloidal, use as nucleation catalyst for mag. glass-ceramics prep. 4-71628  
 crystal growth rate of pure metals nucleated from undercooled melt 4-98042  
 decoration figures and nucleation on TGS single cryst. 4-65985  
 discontinuous thin film, electron localisation and conductivity (Russian) 4-98780  
 far-IR microbolometer, design, fabrication and characts. 4-73515  
 granules, in glass matrix, optical props. 4-88795  
 interplanetary dust collected from stratosphere, Bi content 4-115712  
 L-shell X-ray prod. cross sections,  $H^+$  induced, ratios 4-66131  
 layer struct. depth profiling, PIXE anal. 4-99874  
 liquid, propagating collective excitations, neutron scatt. study 4-65167  
 liquid, self-diffusion coeffs., temp. depend. 4-65426  
 liquid, ultrasonic vel., temp. depend., elastic moduli, vol. depend. 4-60989  
 liquid struct. determ. 4-98000  
 local-field enhancement of rough surface 4-104047  
 molecule, ground state, relativistic effective pot. CI calcs. including spin-orbit coupling 4-102601  
 muon Knight shift and relaxation 4-84888  
 muon quantum diffusion, spin relax. rate meas. 4-65900  
 PbTe:Bi, Hall study of self-compensation of donor effect 4-104242  
 Shubnikov-de Haas effect, strong anisotropic strains 4-113979  
 size-quantised film, optical absorption coeff. calc. 4-109265  
 thin film, thermopower in classical strong mag. field 4-98790  
 thin films, vacuum deposited, semiconducting props. rel. to annealing 4-65758  
 thin films strain gauge fabrication by vacuum evaporation 4-95410  
 ultrapure, muon diffusion, spin relax. rate meas. 4-80307  
 ultrathin aggregated film, cond. transition, classical percolation two-dimensional continuum model 4-104330  
 whisker crystals, nonlinear conduction props. under phonon generation 4-65687  
 whiskers, longit. magnetoresist. meas. 4-88500  
 As<sub>2</sub>Se<sub>3</sub>:Bi, extrinsic cond. and optical const. meas. 4-75971  
 Bi I,  $6p^3\ ^3S_1/3p^3\ ^2D_{3/2}$  647.5 nm forbidden transition hyperfine struct. 4-74351  
 Bi I, obs. of superfluorescence and stimulated emission after nonresonant two-photon pumping 4-107600  
 Bi II spectrum, electric quadrupole line  $\lambda=587.0$  nm, hyperfine struct. 4-102627  
 Bi:Po, impurity atom location, channelling studies with point  $\alpha$  sources 4-113470  
 Bi:Bi(0001) system, work function variation with surface coverage (French) 4-76019  
 Bi-Ne discharge, difficulties associated with stimulated emission 4-96484  
 Bi- $^{14}\text{He}^+$ , L-shell X-ray prod. cross-sections 4-107305  
 Bi<sub>2</sub>WO<sub>6</sub> bronze, microstructure and X-ray emission spectra 4-84419  
<sup>209</sup>Bi, muonic, magnetic hyperfine structure 4-91368  
 Cd-Bi, crystal growth from vapour, Bi impurities effect 4-113368  
 CdS-Bi, in photoelectrochemical cells, photovoltaic characteristics 4-93634  
 Cd<sub>2</sub>GeO<sub>4</sub>:Bi 4-84533  
 PbTe-Bi system, anomalous transport props. 4-88588  
 a-Se:Bi films, crystallisation, dark cond. and activation energy 4-88104  
 USe<sub>2</sub>Mn(Bi)(Zr),  $\alpha$ - $\beta$  phase equilibrium and elec. cond. (French) 4-103927  
 YIG:Bi epitaxial films, refr. index and optical absorption spectra at UV to near IR wavelengths 4-104553  
 YIG:Bi thin films, photoelastic birefringence, phase matching (Japanese) 4-80909

## bismuth alloys

- see also bismuth compounds  
 Al-Mg-Bi low-activation alloy development for fusion device 4-108460  
 Bi-Cd-In system, eutectic alloys, microstruct. 4-93263  
 Bi-Cd-Sn-Pb, Wood's metal, melting and solidification, US study 4-60991  
 Bi-In, liq., activities of components 4-71635  
 Bi-In, liq., activity coeff. of O 4-80242  
 Bi-In system, phase diagram and eutectic struct. 4-93264  
 Bi-Pb, strain gauge fabrication by vacuum evaporation 4-95410  
 Bi-Pb alloys, amorphous, supercond., upper critical fields 4-76089  
 Bi-Pb-Sn-Cd, Wood's metal model, inclined simulated cracks, eddy current detect. 4-66516  
 Bi-Sb, liq. alloys, activities and free energy of form., EMF obs. (Japanese) 4-61920  
 Bi-Sb, temp. effect on elastic props. 4-98171  
 Bi-Sb, US attenuation and quantum oscils. 4-92768  
 Bi-Sb single crystals, etching characts. of edge and screw dislocations on cleavage plane 4-80044  
 Bi<sub>2</sub>Ge molten alloys, ultrasonic velocity, compressibility effects 4-92303  
 n-Bi<sub>1-x</sub>Sb<sub>x</sub>, electron scatt., low temp. 4-108835  
 Bi<sub>1-x</sub>Sb<sub>x</sub>, electronic density of states and its mass 4-88439  
 Bi<sub>100-x</sub>Sb<sub>x</sub> mould grown cryst., component distrib., X-ray study 4-75694  
 Bi<sub>2</sub>Sn molten alloys, ultrasonic velocity, compressibility effects 4-92303  
 Bi<sub>0.9</sub>Tl<sub>0.1</sub>, amorphous film, quantum corrections to resistance above superconducting T<sub>c</sub> 4-84710  
 Cu-Bi, liq., Bi activity meas. by Knudsen effusion method with electrobalance 4-66312  
 Cu-Bi, segregation, grain boundary struct. and struct. transformations 4-113462  
 Fe<sub>0.1</sub>Bi<sub>0.9</sub>Si<sub>0.2</sub>C<sub>0.2</sub>, amorphous, mag. anisotropy meas. (Russian) 4-65804  
 In-Bi alloys, phase diagram and metallography 4-114483  
 In-Bi-Pb, liquid, thermodynamic props., EMF meas., 673 to 873K 4-98310  
 In-Sn and In-Bi-Sn eutectic alloy solders for Josephson packaging, mech. props. 4-71687  
 Mn-Bi hard magnets formed by rapid quenching 4-80794  
 Mn-Cu-Bi, thin film, RF sputtering prep., mag. and magneto-optical props. 4-61847  
 Mn-Ni-Bi thin film, RF sputtering prep., mag. and magneto-optical props. 4-61847  
 Pb<sub>2</sub>Bi superconducting films for Josephson junctions, microstruct. control 4-114071

## bismuth alloys continued

- Pb<sub>20</sub>Bi<sub>20</sub> superconducting filament, high transition temp., produced by glass-coated metal spinning 4-80712  
 Sb-Bi, muon spin rot. and muon Knight shift meas. 4-71235  
 Sm<sub>2</sub>Bi<sub>3</sub>, intermediate valence cpds., press.-vol. relationship 4-80554  
 Sn-Bi, binary liq., compressibility, conc. depend., expt. and theoretical invest. 4-70250  
 Sn-Bi (0.5 at.%), creep rate, grain dia. depend. 4-81259  
 Sn-Bi elastic behaviour near melting point from sound vel. and attenuation meas. 4-75597  
 Te-Bi thin films for optical data storage, optical props. and stability 4-91553  
 Tl-Bi, pre-eutectic contact fusion 4-61059

## bismuth compounds

- see also bismuth alloys  
 alkali metal fluorides, M<sub>1-1</sub>Bi<sub>1+2x</sub> (M=Na, K, Rb), elec. props. and struct. characts. 4-70452  
 BGO photodiode detector, characterisation for positron emission tomography 4-59568  
 intergrowth compounds between members of the bismuth titanate family and structures of the LiBi<sub>2</sub>O<sub>4</sub>Cl<sub>2</sub> type. An architectural approach 4-92148  
 layer-structured ferroelec. ceramics, pyroelec. props. 4-104540  
 magneto-optic prop. meas. using piezobirefr. modulation 4-66013  
 oxalate single crystals, gel growth and characterisation 4-99295  
 oxides, sillenite phase form. mag., EPR and IR studies 4-88137  
 polyacetylene:BiCl<sub>3</sub> films, morphology dopant conc. and elec. props. 4-65667  
 Ag<sub>1-x</sub>Bi<sub>x</sub>F<sub>1+2x</sub>, elec. props. and struct. characts. 4-70452  
 Ag-O-Cs (S1) and Bi-Ag-O-Cs (S-10) photocathodes, enhanced Raman scatt. 4-80920  
 Al<sub>2</sub>O<sub>3</sub>-Bi<sub>2</sub>O<sub>3</sub>-CuO system, phase relations, thick film cond. appls. 4-104770  
 BGO 4-59443  
 Ba(Bi<sub>0.5</sub>Nb<sub>0.5</sub>)O<sub>3</sub>, dielec. props. and chem. inhomogeneity, effect of sintering 4-85128  
 BaBiSe<sub>3</sub>, cryst. struct. determ. and preparation 4-80017  
 BaF<sub>2</sub> detector efficiency for monoenergetic  $\gamma$ -rays and  $\gamma$  cascades 4-68896  
 Bi-Mo-Nb oxides, complex phases, struct. determ. by high resolution electron microscopy 4-103950  
 Bi-Sb-Te, solid solutions, maximum figure of merit 4-113981  
 Bi-Se thermoelements, eutectic soldering, electron microscopy study (Russian) 4-98652  
 Bi-Se-Te system, struct. and band gap, X-ray and IR absorpt. obs. 4-104124  
 Bi-Te thermoelements, eutectic soldering, electron microscopy study (Russian) 4-98652  
 Bi-TmFeGa garnet films, anisotropy fields 4-114147  
 Bi-W bronzes, oxidation, high resolution electron microscopy study 4-89156  
 Bi-W-Mo oxides, complex phases, struct. determ. by high resolution electron microscopy 4-103950  
 Bi-W-Nb oxides, complex phases, struct. determ. by high resolution electron microscopy 4-103950  
 Bi-YIG garnet films, anisotropy fields 4-114147  
 Bi, Kr<sub>1-x</sub> mixtures, amorphous, metal-insulator transition, elec. cond., supercond. transition temp. meas., scaling theories 4-75860  
 Bi<sub>2</sub>Al<sub>2</sub>O<sub>9</sub>, luminesc. props. 4-76514  
 Bi<sub>2</sub>O<sub>6</sub>, cryst. struct., X-ray diff. study (German) 4-65233  
 Bi<sub>2</sub>CdS<sub>4</sub> film, spray pyrolysis deposited, substrate temp. effect on elec. and opt. props. 4-70962  
 Bi<sub>2</sub>CdS<sub>4</sub> films, spray pyrolysis deposition, elec. and optical props. 4-76669  
 Bi<sub>1.5</sub>Ce<sub>0.5</sub>(MoO<sub>4</sub>)<sub>3</sub>, cryst. struct., vacancies, powder neutron diff. 4-75407  
 Bi<sub>2</sub>Cr<sub>2</sub>O<sub>12</sub>, BGO scintillators for photon detection 4-107260  
 Bi<sub>2</sub>Cr<sub>2</sub>O<sub>12</sub>, BGO scintillators, timing props. 4-107259  
 Bi<sub>2</sub>Fe<sub>2-x</sub>Ga<sub>2x</sub>O<sub>12</sub> garnet layer growth by LPE, review 4-80453  
 BiFeO<sub>3</sub> single cryst., ferroelec. domains, birefringence, and light absorption 4-71324  
 Bi<sub>2</sub>Fe<sub>2</sub>O<sub>9</sub>, amorphous, mag., optical and resonant props. 4-104424  
 Bi<sub>2</sub>Fe<sub>2</sub>O<sub>9</sub> glass, IR study 4-70381  
 Bi<sub>2</sub>GeO<sub>20</sub>, circular dichroism in region of states prod. due to vacancies 4-71345  
 Bi<sub>2</sub>GeO<sub>20</sub> cryst., surface-barrier photo-EMF 4-104315  
 Bi<sub>2</sub>GeO<sub>20</sub> crystals and films, photocond. 4-65704  
 Bi<sub>2</sub>GeO<sub>20</sub>, field and charge distrib. in case of trap thermal ionisation 4-66010  
 Bi<sub>2</sub>GeO<sub>20</sub> MIS struct., elec. cond. and photoconductivity 4-98776  
 Bi<sub>2</sub>GeO<sub>20</sub>, phonon echo generation, enhancement by defects 4-70304  
 Bi<sub>2</sub>GeO<sub>20</sub> photorefractive crystals used for degenerate four-wave mixing, trapping centre conc. significance 4-87399  
 Bi<sub>2</sub>GeO<sub>20</sub> photorefractive crystals, beam coupling and decoupling in degenerate two-wave mixing in refl. geometry 4-107732  
 Bi<sub>2</sub>GeO<sub>20</sub>, piezoelectric interface, Stonely wave propagation 4-104059  
 Bi<sub>2</sub>GeO<sub>20</sub> thin films, IR spectra and lattice phonons 4-88893  
 Bi<sub>2</sub>GeO<sub>20</sub> trap parameter determ. by optical probing 4-88479  
 Bi<sub>2</sub>Ge<sub>2</sub>O<sub>9</sub>, luminesc. props. 4-76514  
 Bi<sub>2</sub>Ge<sub>2</sub>O<sub>9</sub>:Nd<sup>3+</sup>, hexagonal crystal, growth and luminesc. 4-76510  
 Bi<sub>2</sub>Ge<sub>2</sub>O<sub>12</sub>, Compton suppression spectrometer 4-91135  
 Bi<sub>2</sub>Ge<sub>2</sub>O<sub>12</sub> crystal, light scatt. from substructure 4-66050  
 Bi<sub>2</sub>Ge<sub>2</sub>O<sub>12</sub> crystal scintillators props. review 4-64292  
 Bi<sub>2</sub>Ge<sub>2</sub>O<sub>12</sub> detector efficiency for monoenergetic  $\gamma$ -rays and  $\gamma$  cascades 4-68896  
 Bi<sub>2</sub>Ge<sub>2</sub>O<sub>12</sub> optimisation for energy resolution and purity, high-energy phys. calorimeters appl. 4-59552  
 Bi<sub>2</sub>Ge<sub>2</sub>O<sub>12</sub> scintillation counters, longitudinal uniformity response 4-91153  
 Bi<sub>3</sub> crystals, screening of inverse K-like series, with two-photon carrier generation 4-114297  
 Bi<sub>2</sub>(Mo<sub>0.5</sub>Nb<sub>0.5</sub>)O<sub>6-1/2</sub>, struct. props., high resolution electron microscope studies 4-84271  
 Bi<sub>2</sub>MoO<sub>6</sub>, koechlinite, cryst. struct., neutron powder diff. profile refinement 4-88139  
 Bi<sub>2</sub>MoO<sub>6</sub>, phase transform., struct. study by X-ray diff. 4-70054  
 Bi<sub>2</sub>Mo<sub>2</sub>O<sub>9</sub>, preparation, cryst. struct., elec. and optical props. 4-84266  
 Bi<sub>3</sub>NbTiO<sub>9</sub>, stability rule and struct. 4-80245  
 Bi<sub>2</sub>O<sub>3</sub> additives in Zn plates of Ni/Zn test cells, effects 4-62325  
 Bi<sub>2</sub>O<sub>3</sub>, thin films, noise power spectra meas. 4-80638

## bismuth compounds continued

- Bi<sub>2</sub>O<sub>3</sub>-B<sub>2</sub>O<sub>3</sub> glasses, memory switching process, role of chem. reduction 4-114002  
 Bi<sub>2</sub>O<sub>3</sub>-CdO, phase relations, X-ray diffr. obs. 4-89028  
 Bi<sub>2</sub>O<sub>3</sub>-WO<sub>3</sub> layered phases, struct. props., high resolution electron microscopy studies 4-70113  
 Bi<sub>2</sub>O<sub>3</sub>-Y<sub>2</sub>O<sub>3</sub>, ionic and elec. cond. meas. 4-88547  
 Bi<sub>2</sub>O<sub>3</sub>-Y<sub>2</sub>O<sub>3</sub> system high ionic conductor, ionic cond. and electronic cond. (Chinese) 4-70879  
 Bi<sub>2</sub>O<sub>3</sub>S, synthesis and cryst. struct. 4-65227  
 Bi<sub>2</sub>Pb<sub>1-x</sub>Bi<sub>1/2</sub>Ti<sub>1/2</sub>W<sub>1/2</sub>O<sub>3</sub> perovskite ferroelec. dielec. props. 4-88783  
 (BiPbGdYb)<sub>2</sub>(FeAl)<sub>2</sub>O<sub>12</sub> garnet single cryst. films for ring laser gyroscopes (Chinese) 4-60123  
 Bi<sub>2</sub>S<sub>3</sub> films, growth by hot wall method, crystallinity, stoichiometry, temp. depend. 4-76674  
 n-Bi<sub>2</sub>S<sub>3</sub>-mPbS, long period modulated struct. with continuously variable periodicity 4-113469  
 BiSb, cryst. struct., X-ray diffr. 4-80005  
 BiSi, differential polarisability, optical reflectance ellipsometry study 4-88796  
 BiSi ferroelec. semicond., energy band struct., X-ray spectral studies 4-65609  
 Bi<sub>2</sub>(SO<sub>4</sub>)<sub>3</sub>=α,β-Bi<sub>2</sub>O(SO<sub>4</sub>)<sub>2</sub>+SO<sub>3</sub>, equil. press., α-β transform. study 4-71959  
 BiSb, acoustical nonlinearity near electronic topological transition 4-113547  
 Bi<sub>1-x</sub>Sb<sub>x</sub>, composition influence on electron scatt. intensity 4-88518  
 Bi<sub>1-x</sub>Sb<sub>x</sub> single cryst., magnetoresist. in transverse quantising mag. fields 4-98643  
 Bi<sub>0.9</sub>Sb<sub>0.1</sub>Te<sub>3</sub> films, strain-resist. effects, struct. effects 4-114052  
 Bi<sub>2</sub>Se<sub>3</sub> amorphous film, photoemission study 4-109302  
 Bi<sub>12</sub>Si<sub>2</sub>O<sub>20</sub>, circular dichroism in region of states prod. due to vacancies 4-71345  
 Bi<sub>12</sub>Si<sub>2</sub>O<sub>20</sub> cryst., dynamic image recording 4-96838  
 Bi<sub>12</sub>Si<sub>2</sub>O<sub>20</sub> cryst., surface-barrier photo-EMF 4-104315  
 Bi<sub>12</sub>Si<sub>2</sub>O<sub>20</sub> crystal volume phase holograms, light diffr. 4-83539  
 Bi<sub>12</sub>Si<sub>2</sub>O<sub>20</sub> crystals, electro-optic coeff. meas., optical activity influence 4-93055  
 Bi<sub>12</sub>Si<sub>2</sub>O<sub>20</sub>, deep impurities, photoelectric phenomena 4-113996  
 Bi<sub>12</sub>Si<sub>2</sub>O<sub>20</sub>, electron beam controlled spatial and temporal light modulator 4-60142  
 Bi<sub>12</sub>Si<sub>2</sub>O<sub>20</sub> optical amplifier, large signal effects 4-96979  
 Bi<sub>12</sub>Si<sub>2</sub>O<sub>20</sub>, optimal properties of photorefractive materials for optical data processing 4-74640  
 Bi<sub>12</sub>Si<sub>2</sub>O<sub>20</sub>, photoelectron transport props. 4-88534  
 Bi<sub>12</sub>Si<sub>2</sub>O<sub>20</sub> photorefractive crystals used for degenerate four-wave mixing, trapping centre conc. significance 4-87399  
 Bi<sub>12</sub>Si<sub>2</sub>O<sub>20</sub>, single crystal, effect of doping with Al, Ga and Cr on props. 4-76407  
 Bi<sub>12</sub>Si<sub>2</sub>O<sub>20</sub> thin films, IR spectra and lattice phonons 4-88893  
 Bi<sub>12</sub>Si<sub>2</sub>O<sub>20</sub>:Al, photocond., absorption spectra and TSC studies 4-65710  
 Bi<sub>12</sub>Si<sub>2</sub>O<sub>20</sub>:Al(Ga)(Mn)(Cr), optical absorp. spectra, photochromism (Russian) 4-114311  
 Bi<sub>12</sub>Si<sub>2</sub>O<sub>20</sub>:Nd, luminescence centres, selective excitation 4-114327  
 Bi<sub>12</sub>Si<sub>2</sub>O<sub>20</sub>:Pb PRIZ modulator, increased photosensitivity (Russian) 4-69544  
 Bi<sub>12</sub>Si(Ti)O<sub>20</sub> gyrotropic crystals, electro-optical and optical props. (Russian) 4-93058  
 Bi<sub>12</sub>Si<sub>1-x</sub>Ti<sub>x</sub>O<sub>20</sub>, optical spectra, dispersion of optical rot. 4-104627  
 Bi<sub>2</sub>(Te,Se)<sub>3</sub>, crystal growth under microgravity in SALYUT-6 space station 4-98035  
 Bi<sub>2</sub>(Te,Se)<sub>3</sub>, solidification under microgravity melt subcooling obs. 4-114382  
 Bi<sub>2</sub>Te<sub>3</sub> cryst., external shape, impurity complex effects 4-75347  
 Bi<sub>2</sub>Te<sub>3</sub>, defect-induced bonding, thermoelectric prop. anal. 4-92128  
 Bi<sub>2</sub>Te<sub>3</sub>, melting point, segregation, non-uniform comp. 4-113585  
 Bi<sub>2</sub>Te<sub>3</sub> solid, vapourisation, 719-827K, torsion and Knudsen effusion obs. 4-88273  
 n-Bi<sub>2</sub>Te<sub>3</sub>-I, free carrier mobility, Hall and Seebeck coeffs., temp. depend. 4-61369  
 Bi<sub>2</sub>Te<sub>3</sub>:Pb(Ge), doping props., elec. cond. and Seebeck measurements 4-75467  
 Bi<sub>2</sub>Te<sub>3</sub>-Sb<sub>2</sub>Te<sub>3</sub> n-type solid solution, effect of annealing in air on electro-physical props. 4-113945  
 Bi<sub>2</sub>Te<sub>3</sub>(Se<sub>3</sub>), weak-field transport, thermoelec., galvanic- and thermo-mag. coefficients 4-88613  
 Bi<sub>12</sub>Ti<sub>2</sub>O<sub>20</sub>, circular dichroism in region of states prod. due to vacancies 4-71345  
 Bi<sub>12</sub>Ti<sub>2</sub>O<sub>20</sub> single cryst., Raman spectra and phonons 4-88833  
 Bi<sub>2</sub>Ti<sub>2</sub>O<sub>7</sub> ceramics, grain orientation, ESR and thermal expansion studies 4-104482  
 Bi<sub>2</sub>Ti<sub>2</sub>O<sub>7</sub> ceramics, grain orientation by cold uniaxial method 4-104757  
 Bi<sub>12</sub>Ti<sub>2</sub>O<sub>20</sub>(SiO<sub>2</sub>)<sub>2</sub> photorefractive crystals, hologram formation, optical activity effects 4-60002  
 (BiTm)<sub>2</sub>(FeGa)<sub>2</sub>O<sub>12</sub> epitaxial film, mag. bubbles study 4-109049  
 BiVO<sub>4</sub>, ferroelastic, spontaneous birefringence obs. 4-93045  
 BiVO<sub>4</sub>, refractive index temp. depend. 4-71338  
 Bi<sub>2</sub>(W,Nb)<sub>2</sub>O<sub>6-y/2</sub>, struct. props., high resolution electron microscope studies 4-84271  
 CsBi(MoO<sub>4</sub>)<sub>2</sub> layer cryst., structural phase transitions 4-88286  
 Cs<sub>2</sub>NaBiCl<sub>6</sub> cryst. struct. and phase transitions 4-80015  
 Cs<sub>2</sub>NaBiCl<sub>6</sub>, phase transition, phonon dispersion relations 4-98269  
 (GeSe)<sub>3</sub>100-Bi<sub>2</sub>, struct. and resist. effect of dopants, high press. study 4-103660  
 (K<sub>1/2</sub>Bi<sub>3/2</sub>Bi<sub>3/2</sub>)(Bi<sub>0.2</sub><sup>3+</sup>Bi<sub>1.8</sub><sup>5+</sup>)O<sub>6-x</sub>(OH)<sub>x</sub>H<sub>2</sub>O · pyrochlore, struct. studies 4-10112  
 K<sub>2</sub>Bi<sub>0.5</sub>Er<sub>0.5</sub>(MoO<sub>4</sub>)<sub>2</sub> single crystals, Czochralski growth and optical props. (Chinese) 4-114294  
 NaBi(MoO<sub>4</sub>)<sub>2</sub>, elastic moduli, ultrasonic meas. (Russian) 4-70253  
 Na<sub>0.5</sub>Bi<sub>0.5</sub>TiO<sub>3</sub>, cryst., birefringence and opalescence, temp. depend. 4-76425  
 Na<sub>0.5</sub>Bi<sub>0.5</sub>TiO<sub>3</sub>, pure and Ba-doped, cryst. struct., ferroelec. props., neutron diffr. 4-70102  
 Na<sub>0.5</sub>Bi<sub>0.5</sub>TiO<sub>3</sub>, soft-modes and central peak, inelastic neutron scatt. studies 4-61037  
 Na<sub>0.5</sub>Bi<sub>0.5</sub>TiO<sub>3</sub> grain-oriented ferroelectric ceramics, piezoelec. props. (Japanese) 4-61625  
 Na<sub>1/2</sub>Bi<sub>1/2</sub>TiO<sub>3</sub> ceramics, pyroelectric props., perspective appl. in pyroelectric radiation detectors 4-88776  
 Na<sub>0.5x</sub>K<sub>0.5(1-x)</sub>Bi<sub>0.5</sub>TiO<sub>3</sub>, piezoelectric ceramics, microstruct., props. and phase relations 4-61629

## bismuth compounds continued

- oxides, Bi<sub>2</sub>Mo<sub>2</sub>O<sub>6</sub>, M=Ge,Ti, luminesc. props. 4-76514  
 PbO-B<sub>2</sub>O<sub>3</sub>-Bi<sub>2</sub>O<sub>3</sub>-Y<sub>2</sub>O<sub>3</sub>-Ga<sub>2</sub>O<sub>3</sub>-Fe<sub>2</sub>O<sub>3</sub>, phase diagram invest. 4-93208  
 R<sub>1-x</sub>Bi<sub>x</sub>Pb<sub>1-x</sub>Fe<sub>1-x</sub>M<sub>2</sub>O<sub>12</sub> garnet films, mag. and magneto-optical props. 4-80802  
 Sb<sub>2</sub>Te<sub>3</sub>-Bi<sub>2</sub>Te<sub>3</sub>-Sb<sub>2</sub>Se<sub>3</sub>-Se-Te, physicochemical equilibria and crystallisation 4-61053  
 Sb<sub>2</sub>Te<sub>3</sub>-Bi<sub>2</sub>Te<sub>3</sub>-Te, physicochemical equilibria and crystallisation 4-61053  
 SrBiSe<sub>3</sub>, cryst. struct. determ. and preparation 4-80017  
 SrBiTe<sub>3</sub>, cryst. struct. determ. and preparation 4-80017  
 Ti<sub>1-x</sub>Bi<sub>x</sub>Fe<sub>1-x</sub>Te<sub>2</sub>, elec. props. and struct. characts. 4-70452  
 TiBiTe<sub>3</sub>, superconducting Tc and mag. susceptibility 4-88629  
 (YBi)<sub>2</sub>(FeGa)<sub>2</sub>O<sub>12</sub> garnet, cryst. growth from flux and LPE 4-93208  
 (YBi)<sub>2</sub>(Fe)<sub>2</sub>O<sub>12</sub> film, growth induced anisotropy 4-114146  
 (YBiPb)<sub>2</sub>(FeAlP<sub>2</sub>)<sub>2</sub>O<sub>12</sub> LPE layers, lattice site determ. by channelling 4-80440  
 (YGdYbBi)<sub>2</sub>(FeAl)<sub>2</sub>O<sub>12</sub> films, magnetostrictive vibr. study 4-98927  
 ZrO<sub>2</sub>-Y<sub>2</sub>O<sub>3</sub>-Bi<sub>2</sub>O<sub>3</sub> solid electrolyte, prep. and elec. props. 4-84452

## bistable multivibrators see flip-flops

## bistable optical devices see optical bistability

## bitter patterns see magnetic domains

## bitumen see materials

## BL Lacertae-type objects

- 0215 015, absorpt. struct. at 20 km s<sup>-1</sup> resolution 4-77941  
 arcminute-scale radio emission search at 200 mm 4-63271  
 black holes, accreting, X-ray spectral signatures 4-72973  
 3C 371, N galaxy with BL Lac nucleus, multifrequency obs. 4-90222  
 classification for galaxies with active nuclei 4-73101  
 continuum spectral energy distrib., of X-ray observed sample of BL Lacertae objects 4-82546  
 double radio sources assoc. with blazars, VLA obs. 4-63329  
 H 2155-304, X-ray spectra and intensity var. 4-101483  
 JHK photometry and polarimetry 4-94961  
 BL Lacertae, flux density var. and particle injection 4-101472  
 BL Lacertae, rotation measure determ. 4-73062  
 low frequency spectral index distrib., of complete sample of extragalactic radio sources 4-73087  
 millimetre-wave emission, obs. with RT-22 at CAO and RT-14 at RHUT 4-106075  
 nuclei, γ-ray data as test for black hole accretion models 4-101484  
 nuclei X-ray emission, origin and anal. 4-77940  
 OJ 287, optical polarisation variability obs. 4-67791  
 OJ 287, variability in radio and optical emission 4-106074  
 OJ 287, visual magnitude estimates (1984 February 23 to March 9) 4-63285  
 optical monitoring of radio sources, B-band light curves 4-110763  
 optical spectra of BL Lacertae objects, possible interpretation 4-101469  
 PKS 0216-164, rapid optical variability and polarisation 4-82549  
 PKS 0548-322, X-ray spectra and intensity var. 4-101483  
 PKS 0735+17, variability in radio and optical emission 4-106074  
 PKS 2155-304, optical redshift and implications for X-ray absorpt. feature 4-86057  
 PKS 2155-304, sharp X-ray absorpt. feature obs. 4-86056  
 radio morphology and optical polarisation 4-86083  
 spectra, UV and X-ray props. anal. 4-106060  
 X-ray and gamma-ray prop. of active extragalactic objects, review (Polish) 4-63340  
 X-ray emission, Einstein Observatory obs. anal. 4-77974

## black holes

## see also gravitational collapse

- λφ<sup>4</sup> theory in curved spacetime and varying background fields, effective Lagrangian, quasiloal approx. 4-111302  
 accretion discs, contrib. to asymmetric lepton prod. 4-82500  
 accretion discs, mol. viscosity as mag. field generation mechanism 4-115742  
 accretion discs, self-gravity and global structure 4-77818  
 accretion disk, viscous transonic flow around inner edge 4-115772  
 active galactic nuclei, γ-ray data as test of black hole accretion models 4-101484  
 active galactic nuclei, emission spectra due to accretion onto massive black holes 4-106063  
 active galactic nuclei, observational props. and interpretation 4-63289  
 active galaxies nuclei, black hole accretion discs, emission contrib. to high energy background radiation 4-77985  
 V1343 Aquilae (SS 433), Einstein Observatory obs. rel. to nature of central X-ray source 4-63157  
 V1343 Aquilae (SS 433), X-ray emission anal. and W50 link 4-72958  
 asymptotically flat space-times, black holes, Hawking generalisation, strong cosmic censorship 4-63611  
 axisymmetric with parallel spins, extrinsic curvature 4-110943  
 black holes and warped spacetime, book 4-58601  
 candidates among X-ray binaries, LMC X-3 case 4-110653  
 conference on mathematical physics, Boulder, CO, USA (Aug. 1983) 4-67856  
 conference on QSOs, at Padova, Italy (March 1983) 4-101568  
 Cygnus X-1, millisecond variability rel. to black hole model 4-90181  
 Cygnus X-1, review of X-ray and gamma-ray object 4-115785  
 Cygnus X-1, SAS 3 obs. of X-ray intensity dips 4-94855  
 dynamics of N-collisions in nonsingular, asymptotically flat 3-geometry 4-68070  
 early big-bang Universe, quark-hadron and chiral transitions, review 4-73107  
 entropy in physical processes and cosmological advances 4-82622  
 evaporating black hole, calc. of Hawking radiation 4-72975  
 evolution and characts. (book) 4-78065  
 evolution and stability, review 4-72932  
 existence due to quantum effects 4-82705  
 extragalactic radio sources, theory, review 4-67908  
 formation, de Sitter space instability 4-63050  
 formation at various epochs in Universe 4-106021  
 formation rate, observational lower mass limit from X-ray binaries 4-90177  
 fourth-order gravity as general relativity plus matter, cosmology, black holes 4-110974  
 globally noncausal space-times, naked singularities and curvature conditions 4-63582  
 gravitation (book) 4-63417  
 gravitational radiation from particle plunging into Kerr black hole 4-68076

**black holes continued**

- gravitational waves from particle scatt. by Schwarzschild black hole 4-68077
- Hawking radiation and the back reaction—a first approach 4-110942
- Hawking radiation from black holes, non-thermal nature, contrib. to cosmic rays 4-106023
- Hawking thermal radiation in a stationary Riemann space-time (*Chinese*) 4-106220
- Higgs scalar field, gravitational collapse 4-115683
- Hoop conjecture on black holes 4-82502
- Kerr black hole immersed in mag. field, energy extraction, negative energy states 4-90178
- local black holes, toroidal and spherical 4-77868
- mass accretion and plasma processes,  $\gamma$ -ray emission model, 3C 273 appl. 4-101536
- massive black holes, accretion discs and radiation accel. jets 4-106020
- massive black holes accretion, cosmic rays prod., radiowave and  $\gamma$ -ray emission 4-100929
- massive black holes in clusters and galaxies nuclei, relativistic dynamics 4-77883
- massive black holes in galactic halos, contrib. to heating of stellar discs 4-67803
- massive rotating, quasimodal oscillations 4-67763
- maximal indecomposable past sets and event horizons 4-58698
- mini Schwarzschild black hole, absorption cross sections 4-90176
- neutrino energy spectra from relativistic plasma 4-110651
- new inflationary universe, Higgs scalar field fluctuation, black-hole formation 4-90452
- nonspherical accretion, finite differencing and code calibration 4-110650
- nonspherical accretion, two-dimensional numerical study 4-63195
- nucleation rate from heuristic calc. 4-115774
- origin, concept appl. to astrophysics 4-115775
- particle creation due to Casimir effect 4-73316
- Population III remnants, contrib. to D and  $^4\text{He}$  synthesis 4-67842
- pregalactic black hole remnants of Population III stars, contrib. to missing mass 4-90191
- pregalactic black holes, rel. to galaxy form. and hidden mass 4-67797
- primeval black hole formation and cosmological perturbations 4-73124
- primordial black holes, stable maximum hypothesis for form. and decay 4-63373
- primordial black holes, superheavy metastable particles 4-63376
- primordial black holes and cosmological vacuum phase transition 4-78016
- quantum black hole mining in de Sitter space, second law of thermodynamics, evaporation 4-115773
- quantum equivalence principle, black hole radiance, charge in grav. field, book contrib. 4-63616
- quantum theory of gravity, book 4-63428
- quasars, nucleus black hole, X-ray emission and stellar reverse evolution 4-77820
- quasinormal modes, black-hole oscillations, stability and late-time behaviour of radiation 4-90453
- radiating black hole, event horizon, Hawking radiation, book contrib. 4-63620
- radiating black hole in a box, thermal equilib. stability, Hawking criterion 4-101402
- relativistic MHD flows in steady gravitational field 4-103478
- Riemannian space-time, quantum field theory, value of Hawking temperature 4-95272
- rotating, pseudostationary, Kerr-Newman soln., SU(1,2) group 4-63585
- rotating distorted, axisymmetric stationary metric 4-101404
- Schwarzschild black hole, quasistationary states filling by electrons 4-77867
- Schwarzschild black hole free oscill. excitation by gravit. waves from scatt. test particle 4-94851
- Schwarzschild electrodynamics, irregular wavefunctions 4-106022
- self-gravitation in spherically symmetric accretion 4-63196
- Seyfert galaxies nuclei, cosmic ray accel. and energy spectra, photons and neutrinos as probes 4-100925
- simple gas model, superadditivity considerations, black hole thermodynamics 4-95362
- singularities and predictability in quantum gravity, book contrib. 4-63622
- small, ionisation tracks and range 4-82631
- stars tidal disruption by massive black hole, 511 keV annihilation line origin 4-101405
- theory from weak cosmic censorship 4-82501
- thermal death and entropy (*Japanese*) 4-110795
- thermal fluctuations, evaporation, mass and ang. momentum spreading, book contrib. 4-63621
- thermal radiation, max. temp. possible 4-101148
- thick discs as energy sources 4-90175
- time-asymmetric initial data for N black hole problem in general relativity 4-72974
- two Reissner-Nordstrom black holes, equilib. conditions, Einstein-Maxwell solns. 4-82503
- two Schwarzschild black holes, horizons on time symmetric spacelike hypersurface 4-101403
- unified Yang-Mills theory, topological strings, massive black holes in galactic nuclei 4-101727
- Universe and contents, evolution (book) 4-67888
- vacuum ( $\phi^2$ ) in Schwarzschild spacetime exterior to black hole 4-72868
- X-ray sources in globular clusters, Einstein obs. rel. to black hole model 4-101509
- X-ray spectral signatures of accreting black holes, bimodal spectral behaviour 4-72973
- X-ray transients, spectra and outburst models 4-110776
- blast waves** see *shock waves*
- blazars** see *BL Lacertae-type objects*
- bleaching, optical** see *optical saturable absorption*
- blending**
  - PMMA-polyethylene oxide, molten blends, thermodynamic miscibility, gas chromatography 4-80240
  - polyamide-6, blending with copolymers, effect on props. (*Polish*) 4-66433
- Block walls** see *magnetic domain walls*
- blood**
  - see also *haemodynamics*
  - Aachen clinical haemorrheology test, profile, data, documentation 4-109974
  - acute leukaemia, clinical states, mathematical model, estimation of clinical quantities (*Japanese*) 4-85411

**blood continued**

- albuminated surfaces, radiation-induced, modification toward blood compatibility 4-62630
- arterial  $\text{O}_2$  saturation, meas. with pulse-type oximeter, multiple scatt. and peripheral circulation effects 4-115166
- arterial system, clinical parameters indirect determ. method using velocimetric data (*French*) 4-67154
- arteries, large, rheology rel. to press control 4-85456
- artificial, use of perfluorochemicals as  $\text{O}_2$  carriers, interaction forces 4-59875
- atrial flutter, gated blood-pool study, Fourier anal. 4-72371
- automatic light intensity regulation in photometric methods of bloodflow and oxygen saturation monitoring in peripheral blood vessels (*German*) 4-89683
- biological fluids, US attenuation meas. 4-100266
- blood-water diffusion barrier at secondary gill lamellae in *Anabas Testudineus* 4-100106
- brain-blood barrier, microwave energy effects, review 4-115127
- capillary flow resistance rel. to marginal layer width and axial core viscosity 4-115092
- capillary permeability, role of blood coagulation, fluoresc. intravital microscopy obs. 4-105208
- capillary tube plasma viscometer, automatic instrument for plasma viscosity meas. 4-115246
- $\gamma$ -carboxyglutamic acid, role in blood clotting proteins, Mg-malonate side chain study 4-64336
- chromosome aberrations in human lymphocytes induced by fission neutrons 4-72297
- clotting, study by resonance thrombography 4-105315
- clotting timer, automatic, optical endpoint sensing 4-115165
- deoxyhaemoglobin, prosthetic group, pH-induced symmetry distortions, resonance Raman scatt. obs. 4-93683
- dried whole blood and blood plasma, U determ. using track detectors 4-100372
- elemental profiles, PIXE anal. 4-100387
- EM fields, interaction with cells, microelectrophoretic effect on ligands and surface receptors 4-100231
- endoendothelial fibrin lining and fibrin gels rel. to transcapillary transport control 4-105270
- endoscopic photocoagulation for upper gastrointestinal bleeding, Nd:YAG laser appl. 4-72334
- ERG, model and effect of vitreous haemorrhage 4-89571
- erythrocyte, microwave bioeffects, temp. and  $\text{pO}_2$  dependence 4-100250
- erythrocyte aggregation, viscometric technique for meas. 4-110014
- erythrocyte aggregation rel. to blood flow in small capillaries at low shear forces 4-109854
- erythrocyte deformability, assessment by constant flow filtration technique 4-115282
- erythrocyte deformability, device for routine meas. 4-109979
- erythrocyte deformability, leukocyte removal prior to study, improved method 4-115285
- erythrocyte deformability meas., improved filtration rate 4-109980
- erythrocyte filterability and anticoagulants 4-115097
- erythrocyte ghosts, human, microwave dielectric props. 4-85409
- erythrocyte membrane, elastic area compressibility modulus determ. by cell poking 4-66907
- erythrocyte membrane, shear deform. and flow, analytical solns. 4-100099
- erythrocyte membrane, viscous dissipation inside during micropipette aspiration 4-89522
- erythrocyte membrane elec. breakdown through diffusion pot. difference 4-66894
- erythrocyte membrane viscosity, determ. from rheoscopic obs. of tank-treading motion 4-105202
- erythrocyte passage time, dependency on pore geometry in single-pore erythrocyte rigdimeter 4-109787
- erythrocyte plasma membrane surface, negative charge cluster detection using fluoresc. probes 4-66892
- erythrocyte suspensions, LF elec. resistance rel. to Fricke's formula 4-100096
- erythrocyte-stasis-meter, blood flow characts. universal parameter determ. 4-109976
- erythrocytes, aggregation and agglutination 4-109786
- erythrocytes, anomalous diffusion in presence of polyvinylpyrrolidone 4-105203
- erythrocytes, deform. and viscoelastic props. of a concentrated suspension 4-100090
- erythrocytes, ferritin conjugate labeled, selective mag. separation 4-89523
- erythrocytes, heat treatment rel. to aggregation in plasma 4-100091
- erythrocytes, human, 3D image anal. in reflection contrast 4-89525
- erythrocytes, human,  $\text{Ca}^{2+}$ -activated  $\text{K}^+$  channels, comparison of single-channel currents with ion fluxes 4-66921
- erythrocytes, human,  $\text{O}_2$  uptake, quantitative description in 3D 4-66923
- erythrocytes and plasma, human,  $^{23}\text{Na}$  NMR, chemical shift, spin relax., intracellular Na conc. 4-66910
- erythrocytes from stored human blood, morphological changes during heating 4-105204
- erythrocytes under shear, rel. to small angle light scatt. by large spheroids 4-115116
- Erythrometer: device for erythrocyte filterability and plasma viscosity meas. 4-109981
- fibrin gels as biological filters and interfaces 4-105269
- filtration measurements, recent progress in improving data processing 4-110016
- filtration pressure and erythrocyte deformability meas., evaluation of the Erythrometer 4-115248
- filtration resistance at constant press., technique for continuous meas. 4-115283
- fish erythrocytes, reaction of intracellular matter to detergent toxicity, dielec. studies 4-72230
- flow disturbance effect on ultrasonic scatt. 4-72287
- flow through artery with mild stenosis, effects of couple stresses 4-100186
- flows through small tubes in vitro 4-115094
- fluorocarbon gas carrier (blood substitute) for biomedical appls. 4-105376
- gastrointestinal bleeding sites, detect. and localisation by  $^{99\text{m}}\text{Tc}$  labelled red blood cell scans 4-89732
- gills, blood-circulating system rel. to effective operation (*Russian*) 4-72284

## blood continued

- glomerular filtration rate, meas. without blood sample, validation in renal transplant patients 4-62555  
 granulocyte/macrophage progenitor cell population in bone marrow and blood after total body X-irrad. 4-77340  
 granulocytes, human, water permeability at subzero temps. in presence of extracellular ice 4-105212  
 grating laser microscope for microvessel blood flow vel. meas. 4-115281  
 haematocrit-erythrocyte-disaggregation apparatus 4-110013  
 haemocyanin, Limulus polyphemus, architecture soln., role of multivariate image anal. 4-100080  
 haemocyanin, Panulirus interruptus, 3.2 Å structure 4-72208  
 haemoderivative thawing, microwave heating reliability 4-72218  
 haemodialysis unit, microprocessor-controlled, for terminal renal patients 4-93963  
 haemoglobin, human, quantitative model for cooperative mechanism 4-77175  
 haemoglobin, sickle cell, polarity of 14-strand fibres, cross-correl. determ. 4-100073  
 haemoglobin 'S', abnormal, cytological and rheological characts. of drepanocytes (French) 4-115032  
 haemoglobin 'S', abnormal, mol. aspects of drepanocytosis (French) 4-115008  
 haemoglobin A, haeme pockets, exchange rates of allosterically responsive labile protons, NMR study 4-105179  
 haemoglobin content of blood, conductimetric procedure for assay 4-85544  
 haemoglobin in blood, optothermal meas., prototype clinical instrument 4-93836  
 haemoglobin in blood of normal and thalassemia patients, electronic absorpt. and reson. Raman spectra (Chinese) 4-109779  
 haemoglobin symmetry effects in a statistical equilib., model for O<sub>2</sub> binding 4-105169  
 haemopoietic stem cells, murine normal and leukaemic, heat sensitivities 4-72226  
 haemorheology, clinical, methods and instrumentation 4-109975  
 haemorheology, Copley-Scott Blair phenomenon rel. to elec. double layer 4-100185  
 haemorheology, rel. to patients with chronic arterial disorders 4-109849  
 haemorheology, transient, in an air-bearing viscosimeter, obs. 4-109850  
 haemorheology from microcirculation to macrocirculation (Japanese) 4-72294  
 heart valve bioprostheses, blood analog for in vitro testing 4-110008  
 Hemorheometre, automated apparatus for filtration initial flow rate meas. 4-115284  
 human, from addicted and non-addicted persons, PIXE anal. 4-105365  
 human mononuclear leukocytes exposure to pulse modulated microwaves 4-115126  
 hydration and vascular fluid shifts during exercise in the heat 4-89509  
 immune system, RF effects on human immunoglobulin and murine T- and B-lymphocytes 4-100252  
 interfacial film, with vitreous body, struct., physicochemical props., in case of haemophthalmia 4-81610  
 laser nephelometry: development, clinical appl. and future prospects 4-81756  
 left ventricular volume, estimates from blood-pool counts, repeatability 4-72372  
 leukemia manifestation in blood cell microelement profile, nuclear microprobe determ. 4-100388  
 leukocyte DNA, radiation-induced damage, fluorometric determ. (Russian) 4-67006  
 leukocyte uptake and release by dog lung, effect of pulmonary blood flow 4-100198  
 leukocytes, continuum mech. model during protopod form. 4-100100  
 leukocytes, peripheral blood, characts. in persons working with ionising radiation sources (Russian) 4-72302  
 lymphocyte chromosome aberrations in patients undergoing radiation therapy for mammary carcinoma 4-93844  
 lymphocyte radiosensitivity in vitro, age relation 4-62534  
 B-lymphocyte regulatory action, radiation effect rel. to nonsyngeneic stem cell inactivation (Russian) 4-66991  
 lymphocyte sister chromatid exchange, freq. to US beam exposure 4-100244  
 lymphocytes, G<sub>0</sub> human, in vitro microwave irrad., lack of clastogenic effect 4-115130  
 lymphocytes, human, chromatin functional state study by laser fluoresc. microirrad. 4-72213  
 lymphocytes, human, chromosome aberrations induced by D-T neutrons 4-93794  
 lymphocytes, human, chromosome aberrations induction by <sup>60</sup>Co γ-rays, dose response relationship 4-89656  
 lymphocytes, human, chromosome aberrations induction by β-particles from HTO 4-67025  
 lymphocytes, human, clastogenic effects of power freq. elec. fields 4-89646  
 lymphocytes, human, detrimental effects of <sup>111</sup>In labeling 4-72419  
 lymphocytes, human, lack of US effect on sister chromatid exchange in vitro 4-89651  
 lymphocytes, human, Na<sup>+</sup> self-exchange 4-115036  
 lymphocytes, human peripheral, X-irrad. rel. to exchanges and deletions 4-67026  
 lymphocytes, rat blood, influence of γ-rays on UV fluoresc. (Russian) 4-77322  
 lymphocytes, small, effects of <sup>89</sup>Sr on prod. and maturation 4-67030  
 lymphocytes of atomic bomb survivors, chromosome break nonrandom distrib. 4-77331  
 magnetic parameters of blood cells and high-gradient paramagnetic and diamagnetic phoresis 4-109848  
 microbial chromophore materials in circulating blood, identification by laser micro Raman spectroscopy 4-115156  
 microcomputer-aided patient treatment, closed-loop systems 4-89825  
 microvascular walls, permeability characts. 4-105207  
 model-base image interpretation by line structure description apps. 4-96826  
 monocytes, human, liq. propane jet-freezing, freeze-drying and rotary replication of cytoskeleton and membrane assoc. struct. 4-89861  
 myocardial perfusion, <sup>82</sup>Rb positron emission CT, extraction fraction and flow meas. 4-72378  
 neutrophils, human, effect of colchicine on viscoelastic props. 4-115030  
 OP-rheometer system for blood viscosity and viscoelasticity anal. 4-109973

## blood continued

- perfluorotributylamine, blood substitute; FC-43 emulsion, spin relax., spin probe and O effect 4-69111  
 peripheral blood leukocytes, chromatin degradation, combined effect of radiation and burn (Russian) 4-77319  
 peripheral blood mononuclear cell prematurely condensed chromosome use for biological dosimetry 4-105344  
 PIXE anal., preconcentration method low temp. ashing evaluation in humans 4-100382  
 placental blood, capillary-tube viscometry 4-115091  
 plasma, human, surface rheological obs., meas. head 4-115089  
 plasma Cr levels, rel. to coronary artery disease 4-105366  
 platelet aggregation induced in mice by whole-body hyperthermia 4-93800  
 platelets, human, fluoresc. spectroscopy obs. 4-115031  
 platelets, imaging using soft X-ray microscopy. TEM and SEM 4-100367  
 platelets, rabbit, flowing in small arterioles, orientation and diameter distrib. 4-100187  
 platelets, rheological behaviour in vivo 4-115093  
 red blood cells, human, Cu determ., AAS 4-100364  
 red blood cells, human, damage by Ar laser microbeam irrad. (Chinese) 4-109876  
 red cells aggregation in space, meas., NASA Space Shuttle project 4-109970  
 resonance thrombography 4-109972  
 reversing flow in the aorta: a theoretical model 4-109856  
 rheological parameters, obs. using two coaxial viscometers, comparison 4-109977  
 rheological properties during clotting, study methods 4-110009  
 rheology, behaviour law determ., math. and numerical methods 4-115099  
 right-ventricular function, evaluation by gated blood-pool scintigraphy 4-72377  
 rouleau formation, expt. approach, comparison of 3 methods 4-110015  
 serial tomographic images, meas. of regional tissue and blood-pool radio-racer concs. 4-72380  
 serum, analytical plasma spectrometry, dry aerosol dispersity 4-100215  
 serum lipoprotein surface charge change at atherosclerosis early development stages 4-66848  
 serum proteins, PIXE anal. using gel filtration 4-105367  
 sickle red blood cells orientation in alternating elec. field, diagnosis app. 4-93705  
 skin perfusion pressure, meas. by photoelec. technique, rel. to amputation level selection 4-72338  
 smokers and non-smokers, α-activity meas., by CR-39 SSNTDs 4-100377  
 spectral transmission studies using Ar ion laser 4-77358  
 Technicon Ektacytometer: automated exploration of erythrocyte function 4-115286  
 thermoelectric cooling device for cryoprecipitation by plasma separation 4-93938  
 thrombosis tendency rel. to blood viscosity increase, adhesiometer for instant quantitative test (German) 4-77415  
 ultrafiltration processes in blood treatment 4-81732  
 US echo cardiography, double frequency bubble diagnostics 4-100287  
 viscometric methods for assessing red cell deformability and fragmentation 4-115287  
 viscometry, co-axial, accuracy improvement 4-115279  
 viscosity in both extensional and shear flow, obs. using a falling ball viscometer 4-109851  
 Weissenberg rheogoniometer based biorheological methods, blood app. 4-110010  
 working environment aerosols in lead battery factory, toxicity monitoring by PIXE and AAS 4-105072  
 K<sup>+</sup> transport through poly(2-hydroxyethylmethacrylate) membranes, effects of whole blood interfacial interactions 4-77203  
 O<sub>2</sub> diffusion in blood, translational model of shear-induced augmentation 4-105211
- blood circulation** see haemodynamics  
**blood dynamics** see haemodynamics  
**blood flow** see haemodynamics  
**blood platelets** see blood  
**blowing problem** see boundary layers  
**blue brittleness** see brittleness  
**boilers**  
 atmospheric fluidized-bed coal combustion for electric utility applications 4-109717  
 coal-fired boiler exhaust gas heat recovery 4-64826  
 coal-liquid mixtures, possibilities and expectations as fuel for boiler installations (Dutch) 4-89374  
 coal-water slurry burner modelling and development 4-62285  
 down hole steam generator—the boiler 4-62294  
 FBR modular steam generator, dynamic loads from leaking water/steam-sodium reaction (Russian) 4-68783  
 heat pump-boiler systems for district heating, energy saving potential 4-72154  
 moving bed thermal energy storage system, appl. to fossil and solar powered boilers 4-105118  
 nuclear power station water-steam circuits gas chromatographic measurements (German) 4-85343  
 nuclear steam generator tubesheet crevices cleaning using amine borane compounds 4-111662  
 nuclear steam generator with pre-heat chambers, thermohydraulic performance and operational characts. 4-106880  
 Obrigheim nuclear power station, steam generator replacement; personnel exposure 4-86960  
 PFR steam generator experience, leaks, design basis, remedial actions 4-59357  
 PFR superheater and reheater replacement and evaporator repairs 4-68776  
 PWR and PHWR steam generator tube performance, experience during 1981 4-111651  
 PWR LOCA, decay heat removal expts. in U-tube steam generator test facility 4-83239  
 PWR LOCA decay heat removal in steam generator, condensation single inverted U-tube 4-96206  
 PWR once-through and recirculating steam generators, multidimensional model and THEDA-2 computer code 4-59309  
 PWR secondary water chemistry and damage 4-68802  
 PWR steam generator, Tricastin 1 power plant, saturation press., circulation ratio and carry-under 4-111657

- boilers continued**  
 PWR steam generator chemical cleaning database 4-83225  
 PWR steam generator corrosion denting, nonprotective magnetite formation, acid vs. neutral chloride tests 4-59333  
 PWR steam generator denting, magnetite-producing contaminant threshold tests 4-64205  
 PWR steam generator transient analysis computer code 4-59310  
 PWR steam generator units, transient modelling 4-64220  
 PWR steam generators, corrosion products under typical operating conditions 4-102371  
 PWR steam generators, denting causes, nonprotective magnetite prod. on carbon steel 4-104924  
 PWR steam generators, dilute reagent decontamination, oxide film removal 4-102385  
 PWR steam generators, simulation of FRIGG heated rod bundle expt. by ATHOS and FLOW3 4-96190  
 PWR steam generators tubes denting reduction by boric acid 4-68801  
 PWR Tricastin 1 steam generator, steady state thermal meas. on secondary side 4-111658  
 PWR U-tube steam generator transient simulation studies 4-68779  
 Sizewell B PWR steam generator design 4-86874  
 solid fuel steam generators, development trends in combustion (*German*) 4-114796  
 solid particle erosion damage, chromate conversion treatment demonstration at Long Island Lighting Company 4-89140  
 stationary combustion systems, overview of research requirements 4-72045  
 steam generator heating pipe testing and repair, tele-operated manipulator 4-86959  
 steel, austenitic stainless, WWER steam generator tubes, hardening and intergranular corrosion cracking (*Czech*) 4-85257  
 thermal power station boilers, air pollution compliance with USSR health standards 4-72199  
 water chemistry changes, PWR feedwater corrosive species conc. models 4-59378  
 water polisher systems performance at Plant Bowen, Georgia 4-59380  
 waterwall tubes root-cause failure analyses in fossil-fuel-fired power stations 4-89141
- boiling**  
*see also boiling point*  
 channel, press.-drop and density-wave instability thresholds 4-79598  
 channel, vertical, two-phase flow instabilities, effect of heater surface configs. 4-79597  
 coal-water mixtures on horizontal brass surface, film boiling of discrete droplets 4-64829  
 convection boiling, forced, flow oscillations, finite difference analysis of density-wave oscillations 4-79595  
 critical heat flux condition in high quality boiling systems 4-83803  
 cryogenic liquids flowing in tubes, heat transfer during boiling 4-69749  
 ethanol-gasoline mixtures, nucleate boiling 4-87549  
 film boiling, instability 4-112691  
 film boiling/heat transfer, radiation effect, on plane wall parallel to upward vertical flow 4-112676  
 film boiling in laminar boundary-layer flow along a horizontal plate surface 4-97473  
 flow boiling, correl. for heat transfer 4-79593  
 flow in heated channels, two-fluid model eqns. nonlinear eqns. soln. by numerical method 4-108112  
 forced convection boiling, critical heat flux in uniformly heated round tubes 4-83799  
 forced convective boiling in uniformly heated tubes, critical heat flux 4-112698  
 gas bubble generation, conductometer method monitoring 4-112985  
 heat emitting surface, influence of porous coating on heat transfer during boiling, calc. and obs. 4-108070  
 heat transmission from metal surface to boiling water under atmospheric press. 4-97295  
 helical boiler tube, full scale modelling 4-60574  
 high performance heat transfer surfaces for boiling and condensation 4-83806  
 isopropanol, boiling burnout during crossflow over horizontal cylinders, subcooling effect 4-79594  
 liquid films, flowing, critical heat flux 4-112696  
 methanol, boiling burnout during crossflow over horizontal cylinders, subcooling effect 4-79594  
 microthermosiphon, boiling heat transfer to water 4-97548  
 nucleate boiling, heat transfer, augmentation by prepared surfaces 4-83805  
 nucleate boiling heat transfer, surface configuration effect 4-112695  
 nucleate pool boiling, bubble growth rates and departure vols. 4-97649  
 nucleate pool boiling, freq. effect on bubble departure diameter 4-97644  
 pipe wall temperature effect on nucleate to film boiling transitions 4-83947  
 pool boiling heat transfer on porous surfaces, electrolytic surface prod. (*Chinese*) 4-107997  
 porous medium, film boiling, lateral mass flux effect 4-87551  
 reactive surface, oxidation in liq. flow, film boiling 4-97707  
 single tube with forced crossflow, correl. for heat transfer during subcooled boiling 4-64940  
 transient boiling heat transfer from small diameter wire and thin film flat surface 4-103321  
 two-phase flow, instabilities in horizontal boiling channel 4-97661  
 two-phase flow, instabilities in vertical boiling channel, nonlinear description 4-97660  
 vapour bubble detachment in flow boiling 4-97650  
 vapour bubbles detachment from heated walls, anal. 4-103392  
 water, nucleate to film boiling transition in pipes 4-97536  
 He, liq. pool boiling, crit. heat flux, heater thermophys. props. effects 4-69667  
 Ne, liq., limiting superheat (*Russian*) 4-98252
- boiling point**  
*see also boiling: heat of vaporisation*  
 alkanes,  $C_9$  to  $C_{11}$ , enthalpies of vaporisation, cohesive energies 4-98257  
 n-alkanois, free vol. temp. depend. and intermol. forces study using energy of vaporisation 4-84374  
 dense monatomic and molecular fluids and their mixtures, shear viscosity, thermal cond., anal. 4-113688  
 gravity perturbation effects 4-68190  
 metals, melting point, boiling point and critical point 4-92338  
 saturated vapour press. of pure substances, book 4-67890
- boiling point continued**  
 solubility props, critical temps., boiling point, predictional methods based on mol. props. 4-103939  
 CsCl, vap. press., viscosity coeff. and interdiffusion coeff. in Ar and He, Ruff-MKW-boiling point method 4-97743  
 Zn-Ag liq. alloys,  $^{109}\text{Ag}$  diffusion coeff., radiometric absorption method anal. 4-65458
- bolometers**  
 0.1-0.2K operation range bolometers cooled by adiabatic demagnetisation 4-111205  
 detector bridge ckt. appl., constant temp., frequency response optimisation 4-63735  
 European Southern Observatory IR photometer/spectrophotometer detectors 4-94624  
 far-IR microbolometer detectors 4-86481  
 ideal semiconductor bolometers, electrothermal model 4-58890  
 IR bolometers, improved fabrication techniques 4-106385  
 IR broadband detector, using pyroelectric materials 4-95514  
 submillimetre spectroscopy of stratosphere with three-channel  $^3\text{He}$ -cooled bolometer, balloon mounting 4-77663  
 Au-kapton-Au resistor bolometer for meas. UV and soft X-ray radiation 4-63783  
 Bi far-IR microbolometer, design, fabrication and characts. 4-73515  
 Bi for near-MM wave IC imaging polarimeter antenna arrays 4-82827  
 Ge bolometer, neutron-transmutation-doped, resist. meas. 4-106386  
 He-3 cooled bolometer system for 1 mm continuum obs., astron. appls. 4-105882  
 Nb superconducting films for subnanosecond bolometry 4-58891  
 YIG, doped, for thermistor-bolometers 4-68280
- Boltzmann equation**  
*see also transport processes*  
 Bloch electrons transport in const. elec. or mag. field 4-70768  
 Broadwell model, Cauchy problem for initial data 4-68179  
 charged test particle dynamics in hard rod fluid 4-111014  
 completely ionised gas, transport phenomena with large temp. gradients 4-91877  
 conference on mathematical physics, Boulder, CO, USA (Aug. 1983) 4-67856  
 constitutive equations invariance in kinetic theory of gases 4-103455  
 cosmic ray kinetics, diffusion approx. 4-94373  
 double-well pot., Fokker-Planck and BGK operators, eigenvalues 4-58790  
 Einstein's relation of transition probabilities 4-111013  
 electron-Coulomb interaction influence on electron relax. on plasma 4-108159  
 electron inelastic and elastic multiple scatt., transport eqn. description 4-66160  
 electron scattering, Boltzmann transport eqn. theory 4-66159  
 fluid dynamics relations, flows, layers and shocks 4-69730  
 gas in electric field, Boltzmann eqn. for electrons, multiterm soln. 4-69860  
 gas motion in front of a completely absorbing wall 4-60463  
 gaseous state at low temp., thermodynamics (*Russian*) 4-113096  
 hydrocarbon polymer dielectric films, hot-electron transport 4-92837  
 inert gases, electron swarm parameters calc. 4-65145  
 integral particle transport theory, tensorial diffusion approximation, Lorentz force action 4-95356  
 ion range distrib. calc. using Boltzmann transport eqn. 4-92249  
 Kac model with external force term, exact solution 4-95354  
 log gas and quantum many-body problem analogues 4-90412  
 low press., atoms and ions vel. distrib. functions, Boltzmann eqn. soln. 4-113232  
 macroscopic quantum system, nonequilibrium processes, many-body collective motion theory 4-63692  
 maser, electron cyclotron, in uniform mag. field, relativistic quantum-kinetic theory (*Korean*) 4-112370  
 metallic films with unlike surfaces, electron scatt. model 4-76051  
 metals, magnetotransport, exactly soluble model 4-75928  
 methane, electron transport calc., Boltzmann eqn. anal. 4-103461  
 Navier Stokes eqns., solution using solutions of the Boltzmann kinetic eqn. 4-97611  
 nonequilibrium gas flow, nonlinear Boltzmann eqn. soln. 4-91849  
 nonlinear, computer realisation and sputtering theory 4-73397  
 nonlinear, Kac model, odd velocity solns. (*French*) 4-95353  
 nonlinear Boltzmann eqn., exact solutions 4-86138  
 nonlinear evolution equations, H theorems, structure theorem, discrete classical system 4-95150  
 p-n junction, two-dimensional simulation of potential distrib. with graphic-computer-aid 4-76035  
 polarons, Boltzmann equation, statistical operator, eqn. of motion 4-75871  
 radial heat flow in gas, rot. effects 4-64835  
 relativistic kinetic eqns. for inelastically interacting particles in gravit. 4-73311  
 rotational averages, phased and Boltzmann-weighted 4-73338  
 semiconductors, hot carriers, Boltzmann eqn. stationary solns. 4-104214  
 semiconductors, Voigt effect and magneto-conductivity in strong elec. field 4-99099  
 small Knudsen number Boltzmann eqn., singular perturbation method anal. (*Chinese*) 4-97610  
 solid, electronic transport, appl. of resolvent method 4-84601  
 solid-state plasma, acousto-optic scatt. in nonlocal optics regime 4-71346  
 superconducting film, optical irradiation, periodic excitation, relaxation processes and response time 4-61489  
 time dependent solns. using moments method 4-101786  
 vesicles, highly charged, nonlinear Poisson-Boltzmann eqn. soln. 4-105200  
 $\text{CO}_2$ , electron transport, Monte Carlo and Boltzmann two-term calcs. 4-113109  
 $\text{CO}_2$  RF excited lasers, electron energy distrib. and transport coeffs. 4-102919  
 Cu, electronic props. of 4d transition metal and sp impurities 4-70731  
 $\text{F}_2$ , electron swarm parameters, Boltzmann eqn. calcs. 4-79713  
 K vapour, electron charact. energy and momentum transfer cross-section (*Korean*) 4-79705  
 Ne, HF plasma, electron kinetics, Fourier expansion technique 4-113242
- Boltzmann equation (gases)** *see kinetic theory of gases*  
**Boltzmann-Vlasov equation** *see Vlasov equation*
- bond angles**  
 4-amino-4'-nitrodiethylphenylsulphide, cryst. and mol. struct., X-ray diff. 4-113434

**bond angles continued**

- 4-aminophenyl N-morpholysulphone, mol. and cryst. struct., X-ray diff. 4-112293  
anomeric effect in COCOC grouping in carbohydrates, struct. criterion 4-112111  
asparagine dipeptide, quantum theory of struct. and bonding 4-87239  
aspartic acid dipeptide, unionised, quantum theory of struct. and bonding 4-87240  
bis(di-tert-butylmethyl) diselenide, dihedral angle, X-ray crystallography, UV spectra 4-65250  
2-bromo-1,3,2-dioxasolane, mol. struct. by electron diff. 4-112292  
2-bromo-1,3,2-dithiasolane, mol. struct. by electron diff. 4-112292  
2-bromo-3-chloro-1-propene, gas phase mol. struct. and conformational composition determ. by electron diff. 4-69212  
p-bromonitrobenzene, mol. struct., internal rot. barrier, gas phase electron diff. 4-112274  
2-bromopropene, mol. struct., gas-phase electron diff. and microwave spectra 4-112273  
1,3-butadiene, rot. isomerism, geometry optimisation and basis set size effect, ab initio study 4-87231  
carbohydrates, anomeric effect in COCOC grouping, struct. criterion 4-112111  
2-chloro-1,3,2-dioxasolane, mol. struct. by electron diff. 4-112292  
2-chloropropene, mol. struct., gas-phase electron diff. and microwave spectra 4-112273  
cholesterol derivatives, mesogenic, cryst. and mol. struct. 4-113437  
2,3-dibromo-1-propene, mol. struct. mechanics, electron diff. study 4-112272  
1,3-bis-(dicyanomethylene)indan-2-one, cryst. and mol. struct. 4-60906  
4,4'-difluorobiphenyl, vibrational spectra, IR and Raman studies 4-114264  
5,5-dimethyl-2-(dimethylamino)-2-oxo-1,3,2-oxazaphosphorinane config., X-ray cryst. and PMR and IR spectra in soln. 4-113432  
ethene, adsorbed on transition and noble metals, electronic struct. and conform. 4-92784  
EXAFS, bond angle determ. 4-66100  
fluorobenzene, mol. struct., ring distortion electron diff. study 4-112276  
hydrides, first- and second-row, sp hybridisation, ab initio MO study 4-102575  
isoxanine phosphate structure, CNDO MO calc. 4-107466  
isopropylisothiocyanate, conformational stability, vibr., low resol. microwave IR and Raman obs. 4-112164  
main group cpds., sp hybridisation, substitution effect on orbital utilisation 4-102576  
peptides, Karplus relationship determ. NMR study 4-102703  
polymers, semi-flexible, anisotropy induced by liq. cryst. solvent 4-84140  
N-salicylidene-p-dimethylaminoaniline, red modification, cryst. and mol. structures, X-ray diff. study 4-60911  
saturated and unsaturated mol. frameworks, vicinal  $^{13}\text{C}$ - $^{13}\text{C}$  coupling consts., dihedral angle depend. 4-64356  
silicates,  $^{29}\text{Si}$  NMR chemical shifts, bond angles and strength effects 4-114175  
tetraselenafulvalenes, substituted, cis/trans assignments, coupling consts.,  $^{77}\text{Se}$  NMR 4-102701  
tri-p-tolylphosphine, cryst. and mol. struct., X-ray study 4-60905  
trimethylplatinum iodide-carbon tetrachloride, bond lengths and angles 4-92193  
 $\text{AlPO}_4$  polymorphs, chem. shift, bond angles,  $^{27}\text{Al}$  and  $^{31}\text{P}$  NMR 4-109088  
 $\text{Br}_2\text{O}$ , thermal vibr. effect on EXAFS 4-102698  
 $\text{C}_2\text{O}_2^+$  cation radicals, matrix isolated, EPR and ab initio investig. 4-74273  
 $\text{CaZnF}_4\text{Mn}^{2+}$ , cryst. struct., axial field splitting calc., EPR, optical spectra 4-92159  
 $\text{Cs}_2\text{XO}_4$  where X=S, Cr, Mo, W, matrix isolated, IR and Raman spectra, isotope shifts, bond angles evaluation 4-96539  
 $\text{Cu}(\text{NO}_3)_2$ , gas phase, mol. struct., electron diff. 4-78965  
 $\text{C}_{60}$ (diethylenetriamine) $_2\text{Cl}_2$ ( $\text{C}_{10}\text{O}_4$ ), cryst. and mol. struct. 4-75431  
 $\text{GaSb}(110)$  surface atomic geometry and dynamics 4-70537  
a-Ge, phonon struct., inelastic electron tunnelling spectra obs. 4-61031  
a-Ge:H, bond angle disorder and optical absorption edge 4-99083  
 $^{15}\text{N}$ - $^{13}\text{C}$  spin-spin coupling consts., dihedral angle depend., INDO calcs. (German) 4-83298  
 $\text{NiO}$ , polycrystalline, density of phonon states, inelastic scatt. of cold neutrons 4-108565  
 $\text{PbCrO}_3$ , cryst. struct. determ. 4-65245  
 $\text{Pb}_2\text{H}_2$ , lone-pair interactions, rot. barriers, ab initio Gaussian basis set calcs. 4-64339  
 $\text{Si}(111)$ ,  $7\times 7$  reconstruction, strain energy, adatom model anal. 4-108685  
a-Si, phonon density of states calc., bond angle and length fluctuations 4-75631  
 $\text{SiC}_2$ , jet cooled, geom. and electronic struct., visible spectroscopy 4-69091  
 $\text{SiO}_2$  glass, struct. model, intermediate range order 4-75308  
 $\text{Sr}_2\text{Al}_2\text{SiO}_7$ , synthetic Sr-gehlenite, cryst. struct. 4-108333  
 $\text{ZnBr}_2$ , anhydrous, cryst. struct., X-ray diff. studies 4-92179

**bond energy** see ionisation potential**bond lengths**

- acetylene, adsorbed on Pt(111), struct., NMR study 4-92526  
alkali metal double molybdates and tungstates, cation-tetrahedral anion distance 4-113386  
4-amino-4'-nitrodiphenyldisulphide, cryst. and mol. struct., X-ray diff. 4-113434  
4-aminophenyl N-morpholysulphone, mol. and cryst. struct., X-ray diff. 4-112293  
annulenes, bond length alternations, MORT treatment 4-83293  
anomeric effect in COCOC grouping in carbohydrates, struct. criterion 4-112111  
benzene liq., C-C bond length, high press. compressibility study 4-65323  
benzenes, fluorinated, bond lengths, substituent effects, overtone spectra ab initio STO calcs. 4-107275  
2-bromo-1,3,2-dioxasolane, mol. struct. by electron diff. 4-112292  
2-bromo-1,3,2-dithiasolane, mol. struct. by electron diff. 4-112292  
p-bromonitrobenzene, mol. struct., internal rot. barrier, gas phase electron diff. 4-112274  
2-bromopropene, mol. struct., gas-phase electron diff. and microwave spectra 4-112273  
trans-1,3-butadiene, C-C bond lengths, K-shell EELS study 4-69229

**bond lengths continued**

- 1,3-butadiene, rot. isomerism, geometry optimisation and basis set size effect, ab initio study 4-87231  
2-butene, C-C bond lengths, K-shell EELS study 4-69229  
carbohydrates, anomeric effect in COCOC grouping, struct. criterion 4-112111  
carbonic anhydraseisozyme, human Co substituted,  $^{13}\text{C}$  NMR reson. 4-102837  
2-chloro-1,3,2-dioxasolane, mol. struct. by electron diff. 4-112292  
2-chloropropene, mol. struct., gas-phase electron diff. and microwave spectra 4-112273  
chlorotrifluoromethane, stretching and bending anharmonicity, electron diff. study 4-69042  
close-packed ordered alloys lattice consts., Pauling-Simon law 4-75365  
conjugated hydrocarbons, bond length alternations, MORT treatment 4-83293  
diatomic mols., normal vibr. calc. for inorganic cpds. 4-59696  
dibenzofuran, cryst. struct. and bond lengths, X-ray diff. studies 4-113429  
2,3-dibromo-1-propene, mol. struct. mechanics, electron diff. study 4-112272  
 $\beta$ , $\beta$ -dicyano- $\alpha$ -methylvinylferrocene, cryst. and mol. struct. 4-60909  
1,3-bis-(dicyanomethylene)indan-2-one, cryst. and mol. struct. 4-60906  
5,5-dimethyl-2-(dimethylamino)-2-oxo-1,3,2-oxazaphosphorinane config., X-ray cryst. and PMR and IR spectra in soln. 4-113432  
dioxo[15]annulenylium cation, spectra pi-electron struct. SCF MO CI calcs. 4-96458  
ethene, adsorbed on transition and noble metals, electronic struct. and conform. 4-92784  
ethylene, MO study 4-87031  
fluorobenzene, mol. struct., ring distortion electron diff. study 4-112276  
hexachloronaphthalene-1,8-disulphide, struct. refinement in space group  $P2_1/n$  4-113430  
high pressure phase transitions, X-ray absorpt. near edge struct. spectra 4-66119  
hydrides, first- and second-row, sp hybridisation, ab initio MO study 4-102575  
ionic lattices,  $\text{Mn}^{2+}\text{F}^-$  distance from isotropic superhyperfine const. for  $[\text{MnF}_6]^{4-}$  4-60883  
isoxanine phosphate structure, CNDO MO calc. 4-107466  
isoprene, struct. and conformations by vibr. spectroscopy and gas phase electron diff. 4-64606  
linear polymers, electronic props. 4-78993  
main group cpds., sp hybridisation, substitution effect on orbital utilisation 4-102576  
methoxy radical,  $^2\text{E}$  ground state, rot. mol. consts., microwave spectrum 4-107334  
methylthiocarbamate, O and S isomers, mol. and cryst. struct., IR and Raman spectra 4-80923  
molecules, total and orbital SCF energies 4-83291  
NOE spectra determ. of mol. struct. and internuclear distances 4-69123  
one electron molecules, discrete spectrum props. 4-102611  
organic mols., harmonic vibrational freq. and dipole moment derivatives, systematic GVB study 4-83300  
pentane, bond length alternations, MORT treatment 4-83293  
perfluoro-2-butene, C-C bond lengths, K-shell EELS study 4-69229  
perfluoroethylene oxide, microwave study 4-112159  
polyenes, all-trans conjugated, MO study 4-87031  
 $[\text{N}+1]\pi$ -polymethines, closed shell mol. geometry, MO LCAO calcs. 4-87048  
propynal cation geometry calc. 4-102602  
pyrochlore struct. type, ideal  $\text{A}_2\text{B}_2\text{X}_6\text{Y}$ , geometry 4-88154  
quartz,  $\alpha$  and  $\beta$  forms, struct. anal. based on Coulomb repulsion forces 4-98074  
rare earth cpds.,  $\text{R}_2\text{Zr}_{1-x}\text{O}_{2-0.5x}$  solid solns., struct. and ionic cond. 4-70445  
rare earth double molybdates and tungstates, cation-tetrahedral anion distance 4-113386  
rhodopsin chromophore, photoisomerisation, role of bond lengths change 4-99814  
scattering factors, incorrect, leading to bond length errors 4-75353  
silicates, isotropic  $^{29}\text{Si}$  chem. shift correl. with mean Si-O bond lengths 4-71199  
spinel, cations interaction on octahedral and tetrahedral sites 4-79975  
 $[\text{N}+1]\pi$ -streptopolymethines, closed and open shell ground and excited state geometries, MO-LCAO calc. 4-87047  
TCNE, monoclinic phase struct., X-ray diff. 4-65253  
thioacrolein, visible spectrum, vibronic anal. 4-74260  
toluene, aryl and alkyl C-H bonds, gas-phase overtone spectra 4-102694  
tri-p-tolylphosphine, cryst. and mol. struct., X-ray study 4-60905  
tricyclic nitroxyl biradicals,  $\text{C}_{22}\text{H}_{36}\text{N}_2\text{O}_4$ ,  $\text{C}_{22}\text{H}_{38}\text{N}_2\text{O}_4$ , cryst. and mol. structures, X-ray diff. 4-84283  
trifluoromethylisocyanide, gas phase struct., electron diff. and microwave spectra 4-69238  
trimethylplatinum iodide-carbon tetrachloride, bond lengths and angles 4-92193  
XANES for bond length determ. 4-64494  
xylenes, aryl and alkyl C-H bonds, gas-phase overtone spectra 4-102694  
 $\text{Al}_2\text{B}_2\text{F}_2\text{O}_{15}$ , Jeremejevitze, cryst. struct. refinement 4-92173  
 $\text{AlH}_3^{2+}$ , bonding, dissociation energies, CASCF calcs. 4-68948  
 $\text{B}_2\text{O}_3$  vapour, struct., photoelectron spectra, ab initio STO calcs. 4-83414  
BeF, vibr. excitation of triplet core-ionised states 4-74175  
 $\text{Bi}_2$ , ground state, relativistic effective pot. CI calcs, including spin-orbit coupling 4-102601  
CH bond length variations due to intramol. environment, isolated CH stretching freq. and ab initio calc. 4-68945  
 $\text{CO}_2$ , liq., thermodynamic state, struct., neutron diff. study 4-70017  
 $\text{CaF}_2\text{S}^{2+}(\text{Y}^{3+})$ , lattice relax. around impurities, EXAFS study 4-93140  
 $\text{CaZnF}_4$ , scheelite-type cryst. refinement and bond lengths 4-92176  
 $\text{CaZnF}_4\text{Mn}^{2+}$ , cryst. struct., axial field splitting calc., EPR, optical spectra 4-92159  
Co(III) complexes,  $\text{Co}(\text{NH}_3)_5\text{H}_2\text{P}_2\text{O}_{10}\cdot\text{H}_2\text{O}$ , hydrolysis, NMR 4-109082  
Co(II) complex,  $\mu_3$ -methoxo-(2,4-dinitrophenolato)(methanol) cobalt(II), cryst. struct., X-ray diff. 4-113420  
Co, HCP, phase transferability of Co atom pairs, EXAFS anal. 4-61771  
Co oxides, empirical bond length determ. 4-103710  
 $\text{Co}_2(\text{BO}_3)_2$ , cryst. struct. refinement, X-ray diff. (German) 4-80003  
 $\text{Co}_2\text{Nb}$ , C15 struct., phase transferability of Co atom pairs, EXAFS anal. 4-61771  
 $\text{Co}_2\text{Ta}$ , C15 struct., phase transferability of Co atom pairs, EXAFS anal. 4-61771

and lengths continued

Cr binuclear complexes, triple metal bond HF-Slater transition state method 4-59619  
Cr<sub>2</sub>, LCAO local spin density,  $\chi\alpha$  calcs. 4-87046  
Cs<sub>2</sub>Ca<sub>2</sub>(N<sub>3</sub>)<sub>2</sub>·2H<sub>2</sub>O, cryst. struct., X-ray diff. studies 4-92163  
Cs<sub>2</sub>Ca(N<sub>3</sub>)<sub>2</sub>·2H<sub>2</sub>O, cryst. struct., X-ray diff. studies 4-92164  
CsO, hyperfine interactions and bonding, semiempirical valence bond model 4-112120  
Cu oxides, empirical bond length determ. 4-103710  
Cu(NO<sub>3</sub>)<sub>2</sub>, gas phase, mol. struct., electron diff. 4-78965  
(Cu<sub>2</sub>(diethylenetriamine)<sub>2</sub>Cl<sub>2</sub>)(ClO<sub>4</sub>)<sub>2</sub>, cryst. and mol. struct. 4-75431  
Er(OH)<sub>3</sub>·0.5H<sub>2</sub>O, amorphous, short-range order struct., X-ray diff. 4-75296  
Fe complex, tris(dithiocarbamate)iron(III), vibr. motion study 4-103891  
Fe<sup>2+</sup> complex, A23187 antibiotic, cryst. and mol. struct., X-ray diff. 4-109775  
Fe(CN)<sub>6</sub><sup>4-</sup> (n=3,4), Fe-C bond lengths, EXAFS spectroelectrochemistry 4-107364  
Ga<sub>1-x</sub>In<sub>x</sub>As, bond lengths, virtual crystal approx. 4-75385  
Ge/Al interface, chemisorption and metallisation, electronic struct. 4-92527  
Ge-Si, lattice vibr. props., Raman spectra, alloying and press. depend. 4-108562  
Ge<sub>2</sub> ground state props., HF and CI calcs. 4-83289  
H<sub>2</sub>, adsorbed layers on Ni, Pd and Pt vibr. spectra 4-104073  
H<sub>2</sub>, polarisability and quadrupole moment of the mol. in a spheroidal box 4-59914  
H<sub>2</sub><sup>+</sup> ground state binding energy in intense mag. field 4-74354  
H<sub>2</sub><sup>+</sup>, pot. energy functions calc. in a strong mag. field 4-107427  
H<sub>2</sub>, photoionisation, dissoci. energy, autoionisation peaks, bond distance 4-59859  
Hg<sub>2</sub>-NbF<sub>6</sub>, cryst. struct. determ. 4-108311  
Hg<sub>2</sub>-TaF<sub>6</sub>, cryst. struct. determ. 4-108311  
HoC<sub>2</sub>, tetragonal cryst. struct., neutron diff. studies 4-108322  
KGaS<sub>3</sub>, cryst. struct., X-ray diff. 4-84253  
K<sub>2</sub>O, bond length-bond strength correlations 4-103693  
K<sub>2</sub>SiF<sub>6</sub>, cryst. struct., X-ray diff. study 4-65235  
LaHO, cryst. struct., X-ray and neutron diff. (French) 4-88149  
LaNiO<sub>3</sub>, struct. and Ni<sup>2+</sup> local environment, X-ray diff. and EXAFS studies 4-60901  
Li<sub>2</sub> A<sup>1</sup><sub>2</sub>S<sub>2</sub> state lifetime and electronic dipole moment, time-resolved spectrosc. obs. 4-83423  
Li<sub>2</sub>, semiempirical parameters, bond length depend. correls. effective valence shell Hamiltonian appl. 4-64353  
LiF·Ni<sup>2+</sup>, Ni<sup>2+</sup>-F distance for square planar and linear Ni<sup>2+</sup>-centres from isotropic superhyperfine const. 4-98581  
Li<sub>2</sub>O, bond length-bond strength correlations 4-103693  
MgAl<sub>2</sub>O<sub>4</sub> spinel, order-disorder transition at high temp. 4-92125  
Mg<sub>3</sub>(BO<sub>3</sub>)<sub>2</sub>, cryst. struct. refinement, X-ray diff. (German) 4-80003  
MgSiO<sub>3</sub>, protonstatite, cryst., struct., temp. depend. 4-92183  
Mn<sup>2+</sup> coordination polyhedra in O-containing cpds. 4-113417  
Mo binuclear complexes, triple metal bond HF-Slater transition state method 4-59619  
Mo<sub>2</sub>, LCAO local spin density,  $\chi\alpha$  calcs. 4-87046  
Mo(CO)<sub>6</sub>, cryst. struct. and bond lengths, X-ray diff. studies 4-92184  
NH<sub>3</sub> dimer, effects of basis set and electron correlation on calculated props. 4-91205  
NH<sub>3</sub>·2H<sub>2</sub>O, X-ray diff., IR spectra 4-109175  
Na<sub>2</sub>·A<sup>1</sup><sub>2</sub>S<sub>2</sub> state lifetime and electronic dipole moment, time-resolved spectrosc. obs. 4-83423  
NaF·Ni<sup>2+</sup>, Ni<sup>2+</sup>-F distance for square planar and linear Ni<sup>2+</sup>-centres from isotropic superhyperfine const. 4-98581  
Na<sub>2</sub>O, bond length-bond strength correlations 4-103693  
Na<sub>2</sub>O-SiO<sub>2</sub>-UO<sub>3</sub> glass, struct. EXAFS studies 4-65179  
Ni complexes, dibromo(N,N'-di-tert-butyl)diazabutadiene nickel, structural phase transform. 4-103717  
Ni oxides, empirical bond length determ. 4-103710  
Ni<sub>2</sub>, dimer, jet-cooled, IR gas-phase electronic spectrum 4-78839  
Ni<sub>66</sub>B<sub>33</sub>, glassy, Ni-Ni distrib., multishell modelling, EXAFS studies 4-60853  
Ni<sub>3</sub>(BO<sub>3</sub>)<sub>2</sub>, cryst. struct. refinement, X-ray diff. (German) 4-80003  
Ni(CO)<sub>4</sub>, geometry optimisation, relativistic corrections, HF approx. 4-78762  
Ni<sub>1-x</sub>Zr<sub>x</sub> amorphous alloy, local order, EXAFS studies 4-75302  
PH radicals, term energy, bond lengths, vibr. freq., visible obs. 4-87095  
 $\alpha$ -P<sub>2</sub>S<sub>3</sub>, cryst. struct. and cryst.-plastic transition, X-ray and neutron diff. studies 4-92162  
Pb<sub>2</sub>CrO<sub>5</sub>, cryst. struct. determ. 4-65245  
PbTiO<sub>3</sub>, amorphous and cryst., bond lengths, annealing effect, Raman spectra, EXAFS study 4-79935  
Pt complexes, cis-diammineplatinum  $\alpha$ -pyrrolidine green, cryst. struct., mag. susceptibility 4-98066  
Pt II complexes, bis(acetonitrile)dichloroplatinum II, mol. and cryst. struct., vibr., IR and Raman study 4-103708  
RbO, hyperfine interactions and bonding, semiempirical valence bond model 4-112120  
S<sub>n</sub> mol. and ions, n=3 to 8, geometry, MNDO calcs. 4-68961  
S<sub>4</sub>H<sub>2</sub>, lone-pair interactions, rot. barriers, ab initio Gaussian basis set calcs. 4-64339  
SbSI ferroelectric, L<sub>III</sub> edge above transition temp., EXAFS study 4-61772  
SbSI, L absorption edges, EXAFS studies 4-71475  
SbSI, paraelectric and ferroelectric phases, L-edge XANES and EXAFS obs. 4-88904  
SeF<sub>6</sub>, struct., charge redistribution model, electron diff. study 4-112275  
Si (100) 2<sup>1</sup>, pre-exposed to O in submonolayer range, chem. shifts of Si-H stretching freqs. 4-80368  
Si (100) with adsorbed O<sub>2</sub>, ab initio SCF calcs. 4-98440  
Si (111), 7 $\times$ 7 reconstruction, strain energy, adatom model anal. 4-108685  
a-Si alloys, metastable defect states,  $\chi\alpha$  scatt. wave calc. 4-113899  
a-Si, phonon density of states calc., bond angle and length fluctuations 4-75631  
a-Si:H, broken bonds and electronic density of states, H effects 4-65178  
SiC<sub>2</sub>, jet cooled, geom. and electronic struct., visible spectroscopy 4-69091  
SiO, dimerisation, ab initio quantum chemical study 4-76995  
SiO<sub>2</sub> glass, struct. model, intermediate range order 4-75308  
SiF<sub>2</sub>, struct. parameters and valence electron density distrib. 4-108331  
Sr<sub>2</sub>YRuO<sub>6</sub>, cryst. and mag. struct., time of flight neutron diff. studies 4-88141

bond lengths continued

SrZnF<sub>4</sub>, scheelite-type cryst. refinement and bond lengths 4-92176  
Ti-Nb-Ta oxides, metamict, alpha-recoil damage study by EXAFS and XANES spectroscopy 4-76559  
TiHe<sup>2+</sup>, bonding, dissoci. energies, CASSCF calcs. 4-68948  
Ti<sub>4</sub>O<sub>7</sub>, structural chem., superstructure, X-ray diff. obs. 4-88147  
U chalcogenides, electronic struct. rel. to cryst. data 4-75850  
VHe<sup>2+</sup>, bonding, dissoci. energies, CASSCF calcs. 4-68948  
V<sub>1-x</sub>Te<sub>x</sub>, cryst. struct., X-ray diff. studies 4-108324  
W binuclear complexes, triple metal bond HF-Slater transition state method 4-59619  
WOBr<sub>4</sub>, cryst. struct., X-ray diff. (German) 4-84254  
YC<sub>2</sub>, tetragonal cryst. struct., neutron diff. studies 4-108322  
Y<sub>2</sub>Ho<sub>1-x</sub>C<sub>2</sub>, tetragonal cryst. struct., neutron diff. studies 4-108322  
YbGa<sub>2</sub>Co<sub>3</sub>, cryst. struct., X-ray diff. 4-84237  
ZnBr<sub>2</sub>, anhydrous, cryst. struct., X-ray diff. studies 4-92179  
ZnS (100) surface, relations between surface states and struct. 4-80639

**bonds (adhesive)** see adhesion

**bonds (chemical)**  
see also binding energy; bond angles; bond lengths; crystal binding; hydrogen bonds; intermolecular forces; lattice energy  
3d transition metals with adsorbed CO, electronic struct. and chemical reactivity of CO 4-93552  
Al<sup>IVB</sup> cpds., cubic cryst., vibronic const. calcs. 4-61025  
acetylene, charge redistrib. in mol. vibr. M-H bond moments 4-69047  
acetylene borane, orbital interactions, charge transfer, and bond form., CNDO/2D study 4-59641  
adiabatic rate processes in condensed systems and interfaces, quantum model anal. 4-71986  
aliphatic and aromatic bisquanylhdyrazone, binding to minor groove of double stranded (dA-T), 4-62437  
aliphatic N bases, far IR continua caused by large polarisabilities of intramol. NLi<sup>+</sup>...N=...Li<sup>+</sup>N bonds 4-107346  
alkali halide dimers, electric dipole polarisabilities 4-69239  
alkali halides, elastic constants, multipole expansion 4-80139  
alkali halides, elastic const. and force const., bond deform. model 4-61034  
alkali metal, conjugated bonds, reson. energies and bond orders (Chinese) 4-84555  
alkali metal dimers, bonds, stability, nonorthogonal CI calcs. 4-64390  
alkaline earth oxides, elastic const. and force const., bond deform. model 4-61034  
n-alkanols, free vol. temp. depend. and intermol. forces study using energy of vaporisation 4-84374  
alloys, chem. bonding and heat of form., core level shift calorimetry method 4-104714  
amine-boranes, <sup>14</sup>N nuclear quadrupole double reson. and B-N bond study 4-87145  
amine-trifluoroboranes, <sup>14</sup>N nuclear quadrupole double reson. and B-N bond study 4-87145  
amino acids, <sup>13</sup>C-<sup>15</sup>N chem. bonds conc. determ. by double cross-polarisation NMR 4-96575  
amorphous solids, physics, book 4-90312  
aniline, low temp. cage effect and phosphorescence 4-96690  
antiferromagnetic Ising model, anisotropic, long-range order, quenched impurity effects 4-98848  
antiresonance phenomena in chem. bonding 4-69162  
aromatic N bases, far IR continua caused by large polarisabilities of intramol. NLi<sup>+</sup>...N=...Li<sup>+</sup>N bonds 4-107346  
aromatic radical dimer systems, charge reson. energies 4-87230  
asparagine dipeptide, quantum theory of struct. and bonding 4-87239  
aspartic acid dipeptide, ionised, quantum theory of struct. and bonding 4-87240  
astatobenzenes, substituted, C-At bond dissoci. energy calcs. 4-114779  
 $\alpha$ -B<sub>12</sub>, band struct., energy gaps, bonding, cluster approx. 4-70646  
benzenes, substituted, mol. polarisabilities calc. 4-83488  
biazoles, N,N-linked and their quaternary salts, MNDO calc. on conformation 4-107282  
binary alloy surface segregation, modelling, low index planes, steps, kinks, and chemisorption 4-92495  
binary cpds., energy gaps, polarisation and partial metallic valence 4-103697  
bis(pentadienyl)iron cpds., bonding, hyperfine interaction, Mossbauer effect 4-104512  
bisglyoximate nickel(II), solid-phase transitions and band struct. 4-88282  
borane linked polyhedral cages, B-B spin-spin coupling const., <sup>10</sup>B and <sup>11</sup>B NMR study 4-112198  
butadiene, one-end pyramidalised, sudden charact. of sudden polarisation effect 4-99751  
calcium meso-tartrate trihydrate, struct. and bonding, X-ray diff. studies 4-113428  
carbonium ions, relative stabilities and structs., computational determ. 4-112123  
carbonium ions, struct. bonding dipole moments, SINDO calcs. 4-87049  
carborane linked polyhedral cages, B-B spin-spin coupling const., <sup>10</sup>B and <sup>11</sup>B NMR study 4-112198  
charge conc. bonded and nonbonded, relation to geometry and reactivity 4-102577  
chemisorption bonds, quantum chem. studies 4-80415  
chromium methylenide cation, electronic struct. and bonding 4-112107  
complex borohydrides of Be and Mg, bonding nature, ab initio calculations 4-59911  
covalent systems, models for desorption 4-61230  
crystal stability and shape, mol. motion effect 4-113375  
cyclopentyl silanes and germanes, IR spectra, isolated SiH and GeH stretching freq., bond strength 4-112179  
cyclopropyl silanes and germanes, IR spectra, isolated SiH and GeH stretching freq., bond strength 4-112179  
diamond, vacancy formation energy, crystallisation studies 4-108354  
diarylethylenes, conformers (rotamers) proof of existence by luminesc. methods 4-104649  
2,4-diboramethylenecyclopropane, B=C double bond, ab initio SCF calcs. 4-112094  
dibromomethane, Raman spectra, reorientation and vibr. relax. 4-104605  
dichloromethylbenzene, internal rotation of dichloromethyl group, individual CH bond probe, Raman spectra studies 4-114265  
dimethyl disulphide, rot. barrier about disulphide bridge, ab initio calc. 4-74138  
N,N-dimethylaniline, low temp. cage effect and phosphorescence 4-96690

**bonds (chemical) continued**

- dimolybdenum tetracacetate, metal-metal bond, vibr. fine struct. photoelectron band 4-102739
- double bonding in main group element compounds, review 4-102815
- EELS microspectroscopy, characterisation of solids 4-66161
- enzyme-substrate bonds, transient, characterisation by reson. Raman spectroscopy, book contrib. 4-93686
- epoxide polymers, breakdown, ionisation processes role, mechanoemission mechanism 4-88952
- ester cation radicals, Freon matrix bonding, CH<sub>3</sub> group rot., EPR 4-102708
- ethane, charge redistrib. in mol. vibr. M-H bond moments 4-69047
- ethane, protonated, relative stabilities and structs., computational determ. 4-112123
- ethyl cation, relative stabilities and structs., computational determ. 4-112123
- ethylene, charge redistrib. in mol. vibr. M-H bond moments 4-69047
- ethylene, one-end pyramidalised, sudden charact. of sudden polarisation effect 4-99751
- ethynyllithium, electron density superposition errors 4-113383
- fluorinated hydrocarbon films, electron-stimulated desorption 4-98451
- fracture, environmentally assisted, atomistic models using transition rate theory 4-83855
- fused silica, high temp. intrinsic defects 4-75306
- glass forming substances, defects and glass formation 4-75299
- graphite, C bond-network defects with ring size from 3 to 9, graph theory anal. 4-92138
- graphite, conjugated bonds, reson. energies and bond orders (*Chinese*) 4-84555
- graphite, structural theory using pseudopotential local-density-functional approach 4-92135
- graphite-AsF<sub>3</sub> intercalated foils and compacted flakes, elec. resist. studies 4-92683
- group IV halides, liq. phase, vibr. hyper-Raman spectra intensities, bond hyperpolarisability theory 4-69148
- hard-disk and Lennard-Jones systems, 2-D melting, Monte Carlo studies 4-113286
- hexaaxy anions, octahedral, mol. const., force field calcs. 4-102600
- hydrocarbons, unsaturated, multiple C-C bonds, bond energies and charge distrib. 4-64557
- ice clathrate, normal and deuterated, O-H and O-D stretching and vibr., Raman studies 4-61001
- inorganic solids, stoichiometry, struct. and stability, review 4-75359
- interbond interactions, special perturbational theory for intramol. electron delocalisation 4-87027
- intermetallic compound structure, book contrib. 4-108309
- ionic crystals, diamagnetism and Van Vleck paramagnetism 4-71019
- ionic semiconductors, hydrodynamic instability at transverse optical phonon freq. (*Russian*) 4-71329
- IR active modes, electronic struct. and vibr. anal. 4-87106
- kinetic gelation model and sol-gel transition, solvent effects 4-82773
- lamellar lyotropic mesophases, mol. dynamics, <sup>2</sup>H NMR spectra 4-76271
- lamellar lyotropic mesophases, mol. dynamics, <sup>2</sup>H nuclear mag. relax. times 4-76272
- lanthanide cpds., double-double effect, rel. to bond covalency 4-112098
- lithium formate deuterate, nonlinear susceptibilities by modification of localised bond charges method 4-112507
- localized orbitals in crystals and band representations of space groups 4-88124
- margarite mica, cryst. struct. and hydroxyl group orientation 4-92175
- metal, pure, electronic and cryst. struct., bonding, book contrib. 4-108304
- metal clusters, bonding anal. 4-91378
- metalloporphyrin complexes, anomalous electronic states, crystal and mol. struct. (*Japanese*) 4-113431
- metallotetraphenylporphyrins, interaction with nitrobenzofuroxan, bonding, optical absorpt. and mag. reson. obs. 4-83381
- metals, amorphous, struct. meas. and radial distribution functions 4-92091
- metals with adsorbed CO and N<sub>2</sub>, anomalous electronic and vibr. props. 4-98441
- methane, charge redistrib. in mol. vibr. M-H bond moments 4-69047
- methane, protonated, relative stabilities and structs., computational determ. 4-112123
- methanol, gaseous, high overtone C-H and O-H transitions 4-59620
- methanol C-O stretch band, IR obs. 4-78853
- methyl mercury compounds, struct., bonding and force fields 4-59916
- methyl orange, binding by crosslinked vinylpyrrolidone-divinylbenzene copolymers, template effect 4-108289
- methyl orange, resonance Raman bands, divided disc method of meas. 4-104608
- methylsilane and isomers, stabilities, SCF calcs. 4-74146
- 1-methylsilatrane hydrochloride, Raman spectrum 4-114272
- minerals, bridging bond angle variations, qualitative MO model 4-113413
- molecular crystals, mol. packing and conformation, role of C-H...O and C-H...N interactions 4-65214
- molecules, localisable chemical bonds interaction, second-quantised theory, wave function 4-96419
- Morse oscillator systems, coupled, energy transfer between bonds, quantum dynamics 4-102774
- MOSFET, interface carrier mobility transport theory anal. 4-70944
- Mulliken's population anal., bond order and valence 4-96438
- nitroaromatic explosives, C(KVV) Auger line shapes, intra- and intermol. H bond form. 4-71928
- nucleoside derivatives, conform. equilib., difference NOE effects investig. 4-96579
- optical properties of crystals, appl. of extended model of bond charges 4-76413
- organic luminophores, chem. struct. features and directed synthesis 4-104645
- organic polyhedral mols. and ions, bonding, orbital interaction scheme 4-68953
- organosilanes covalently bonded to metal oxide surfaces, SIMS and electron stimulated desorption obs. 4-89324
- oxide glass, structure, vibr. spectroscopy 4-79945
- phosphomycin, Na salt, cryst. and mol. struct., X-ray diffr. study 4-66860
- poly(olefin sulphones), conformational origin of flexibility and stiffness, <sup>13</sup>C NMR meas. 4-61603
- cis-polyacetylene, Raman excitation profile 4-96730
- cis-polyacetylene-d<sub>8</sub>, Raman excitation profile 4-96730

**bonds (chemical) continued**

- polyethylene, fracture, simple model for chain scission 4-76849
- polyimide, cured, interfacial reaction during metallisation, XPS obs., chem. bond form. 4-88932
- polyimide surface, chem. bonding characts., annealing and desorption effects 4-88933
- polymers, computer simulation, fracture mechanism, two coupled anharmonic chains with strong interaction 4-113531
- polymers, identification by unsaturated bond form. in electron irradi. 4-79962
- polymers, ion implantation effects 4-75547
- polypyrrole, proton modification, elec. cond., optical absorpt. spectra, XPS 4-75969
- polyurethane ionomers, physical bonds (*Russian*) 4-84203
- propylene, one-end pyramidalised, sudden charact. of sudden polarisation effect 4-99751
- proteins, metal binding, <sup>25</sup>Mg and <sup>43</sup>Ca NMR study 4-77195
- rare earth sesquisulphides, energy band struct., X-ray spectral anal. 4-80492
- retinal Schiff-base, protonated, with torsion about bonds in polyene chain, optical absorption 4-77190
- semiconductors, band struct. parameters and tetrahedral const. calcs. (*Russian*) 4-88446
- semiconductors, diamagnetism and Van Vleck paramagnetism 4-71019
- semiconductors, molten, cluster-type struct. defects, review 4-60806
- semiconductors, tetrahedral, core electron binding energy, tight-binding theory anal. 4-108800
- semiconductors, tetrahedrally bonded, anisotropies of Compton profiles 4-99217
- silicates, <sup>29</sup>Si NMR chemical shifts, bond angles and strength effects 4-114175
- small clusters stability, electronic struct. 4-74371
- solid state, ionicity, XPS studies 4-66193
- solid state chemistry, correlation between struct. and phys. props. 4-70063
- solid state chemistry, struct. aspects 4-70062
- solids, dilaton mechanism for strength 4-88235
- stability and electronic struct. ab initio calc. 4-68922
- stimulated desorption spectroscopy 4-61235
- strained systems, electrostatic pots., reactive props., ab initio SCF-MO STO-5G calcs. 4-102580
- sulphenamides, N-S bonds, <sup>15</sup>N NMR investig. (*French*) 4-78865
- sulphinamides, N-S bonds, <sup>15</sup>N NMR investig. (*French*) 4-78865
- sulphonamides, N-S bonds, <sup>15</sup>N NMR investig. (*French*) 4-78865
- surface microscopic examination, Auger type emission 4-72022
- TCNQ salt, DEPA(TCNQ)<sub>4</sub>, cryst. struct., elec. cond., mag. susceptibility meas. 4-80027
- three dimensional solids, hard sphere bonding schemes 4-92136
- toluene, aryl and alkyl C-H bonds, gas-phase overtone spectra 4-102694
- transition metal carbenes, nucleophiles and electrophiles, MO and CI calcs. 4-102605
- transition metal sandwich metallocenes, correl. effects, ab initio HF calc. 4-68921
- transition metals, H absorpt. kinetics and subsurface bonding 4-75691
- transition metals, superionic metal clusters 4-74370
- tricyclo[4.2.2.2]dodeca-1,5-diene, struct. bonding, intermolecular interactions 4-96636
- triphenyl boron, sublimation and bond dissociation enthalpy 4-103919
- vacancy-interstitial pair formation in solids, phonon model 4-103895
- valency, electronic theory, 1916-1983, role of quantum mechanics (*French*) 4-63469
- vibrationally adiabatic molecules, chemical bond 4-96417
- vinyl cation, relative stabilities and structs., computational determ. 4-112123
- 4-vinylcyclohexene cation radical, retro-Diels-Alder reaction mechanism 4-81408
- vinylidene fluoride-trifluoroethylene copolymers, ferroelec. transition, statistical theory anal. 4-99053
- xylene, aryl and alkyl C-H bonds, gas-phase overtone spectra 4-102694
- 3Y<sub>2</sub>O<sub>5</sub>:Fe<sub>2</sub>O<sub>3</sub>, solid state reaction study, IR and mag. props. 4-85301
- Al (111), O chemisorption LCAO-X<sub>α</sub> method anal. 4-113799
- Al, clusters, electronic struct. and props. 4-74374
- Al-SiO<sub>2</sub>-Si struct., X-ray irradi., interface traps. 4-104281
- (AlBr<sub>3</sub>)<sub>n</sub> clusters, (n=2, 4, 6), mass spectra, stability 4-74386
- Al<sub>2</sub>CO ligand-metal bonding, charge transfer and polarisation 4-69265
- Al<sub>2</sub>NH<sub>3</sub> ligand-metal bonding, charge transfer and polarisation 4-69265
- Au/Al contacts, intermetallic bonds and contact resist. (*Russian*) 4-113819
- Bi<sub>2</sub>As<sub>2</sub>, band struct., energy gaps, bonding, cluster approx. 4-70646
- Bi<sub>2</sub>C<sub>3</sub>, <sup>13</sup>C NMR study of C distrib. 4-114182
- (BH<sub>3</sub>NO)<sub>2</sub>, orbital interactions, charge transfer, and bond form., CNDO/2D study 4-59641
- BN RF sputter deposited films, struct. and optical props. rel. to sputtering conditions 4-88415
- Bi<sub>2</sub>P<sub>3</sub>, band struct., energy gaps, bonding, cluster approx. 4-70646
- Ba<sub>0.75</sub>Al<sub>1.0</sub>O<sub>1.25</sub>, elastic const., press. and temp. derivatives, US resonance study 4-92284
- Be<sub>2</sub>, electronic struct., bonding, lifetimes, laser induced fluoresc. 4-112220
- Bi<sub>2</sub>Se<sub>3</sub> amorphous film, photoemission study 4-109302
- Bi<sub>2</sub>Te<sub>3</sub> cryst., external shape, impurity complex effects 4-75347
- Bi<sub>2</sub>Te<sub>3</sub>, defect-induced bonding, thermoelastic prop. anal. 4-92128
- C, linear polytypes, struct. aspects and conformation 4-92139
- C plasma deposited films, struct., IR spectra studies 4-98465
- C/H amorphous film, H<sub>2</sub> gas reactive RF sputtering prep. on low temp. substrates 4-76673
- C/H amorphous film prep. by H<sub>2</sub> gas reactive RF sputtering of graphite 4-76671
- C- and O-containing cpds., oxidation number, electron distrib., ab initio MO wave functions 4-107276
- CO, adsorbed on metals, bonding, EHT calcs. 4-113800
- CO, chemisorbed layer on Ni (100), vibr. spectroscopy by IR emission 4-98439
- CO, coadsorption with K on Ru (001), thermal desorption vibr. overtone spectroscopy 4-70565
- C<sup>+</sup> cation radical in Ne matrix, ESR investig. 4-78873
- CO<sub>2</sub> binding and correl. effects, gas X-ray diffr. investig. 4-102697
- CaC<sub>2</sub>O<sub>4</sub>H<sub>2</sub>O, whewellite, growth morphology 4-65213
- CaH<sub>2</sub>, bonding and electronic struct., APW calc. and photoemission studies 4-113384

onds (chemical) continued

Ca<sub>2</sub>Na<sub>1-x</sub>Al<sub>1+x</sub>Si<sub>3-x</sub>O<sub>8</sub>, intermediate plagioclase: feldspar, modulate struct. 4-84249  
CeCo<sub>2</sub>P<sub>2</sub>, cryst. struct. determ. 4-80011  
CeF<sub>3</sub> doped optical films, tensile stress: cracks and stress modification 4-76543  
Co, chemical bonding, mag. susceptibility 4-114090  
Co complexes, Co-porphyrin complex, linear free energy correl. for reversible dioxygen binding, solvent effect study 4-62178  
Co<sub>2</sub>B<sub>2</sub>O<sub>3</sub>F(OH), cryst. struct., X-ray diff. 4-65242  
CoP<sub>2</sub>, ambient press. synthesis, cryst. struct., mag. and elec. props.; bonding 4-75408  
Cr<sub>2</sub>, electron correl. effects 4-102603  
Cs selenogallates, cryst. struct. and abnormal linear oligomeric anions 4-92185  
CsEuNaNb<sub>2</sub>O<sub>15</sub>, struct. and ferroelec. props. 4-109141  
CsO, hyperfine interactions and bonding, semiempirical valence bond model 4-112120  
Cu (II) cyanates, polymeric, far IR spectra, Cu-OCN bonding, stretching and deformation bands 4-69076  
Cu (110), clean and O covered, ethylene adsorption, UPS studies 4-70548  
Cu compounds, chem. bonding and electronic struct., XPS studies 4-71524  
Cu halides, neutron irradi., defect form., EPR obs., effects of bond ionicity 4-70224  
Cu surface, lone pair ligand interaction; bonding, constrained space orbital variation method 4-114823  
Cu-L-isoleucine complex, polycryst., IR absorpt. spectra, vibr. mode assignment 4-109173  
Cu-L-tryptophan complex, polycryst., IR absorpt. spectra, vibr. mode assignment 4-109173  
Cu-Sb alloys, grain boundary segregation and cracking, Monte Carlo studies 4-114542  
CuGaSe<sub>2</sub>, thermal expansion, 301-958K 4-80266  
Cu(I)-Cu(I) intermetallic bond, in [( $\eta^5$ -C<sub>5</sub>H<sub>5</sub>)<sub>2</sub>Re(H)Cu] complex, invest. 4-96715  
Eu (III) in silica gel glass, fluoresc., cation binding and cage symm. 4-114835  
Eu-Hg, Mossbauer spectra and X-ray diff. study 4-76290  
Fe (100) with chemisorbed S, electronic struct. study 4-92779  
Fe, chemical bonding, mag. susceptibility 4-114090  
Fe oxides, six coordinated high spin Fe(IV) and Fe(V), oxidation states 4-70753  
Fe spinels, valence states, X-ray absorption and emission spectra studies 4-61341  
Fe<sup>3+</sup>-containing layer silicates, Mossbauer spectra quadrupole splitting lines, relative intensities and EFG calcs. 4-115397  
FeN<sub>2</sub>, dissoci., CAS SCF and contracted CI calc. 4-81407  
Ga-Te, molten, at. arrangement of Ga<sub>2</sub>Te<sub>3</sub> associates, metallic-like bonding, neutron scatt. obs. 4-103639  
GaAs (110), adsorption of H, EHMO method calc. (Chinese) 4-113787  
GaAs (111), adsorption of O, XPS study (Chinese) 4-85077  
GaAs, neutron irradi., defect form., EPR obs., comparison with Cu halides 4-70224  
GaAs/Al interface, electronic struct. and bonding 4-84700  
GaAs(001)-Au interface, formation by MBE and thermal stability 4-99328  
GaSb(110) surface atomic geometry and dynamics 4-70537  
Ga<sub>2</sub>Te, semicond., electronic struct. and bonding 4-84563  
Ge, clusters, electronic struct. and props. 4-74374  
Ge-As-Si glasses, chemical bonding and mag. susceptibility (Russian) 4-70041  
GeO<sub>2</sub> films, optical constns., random bonding model 4-85025  
H<sub>2</sub>, nonadiabatic quasiclassical local model, intramol. evolution 4-102588  
(H<sub>2</sub>)<sub>n</sub> (n=2, 3, 5), bound excited state form., CI calcs. 4-96740  
HCl, ground states, bond function, dissoci. energies, CI calcs. 4-74162  
HPFOH struct., bonding and internal rotation 4-68938  
H<sub>2</sub>PO, struct., bonding and internal rotation 4-68938  
H<sub>2</sub>POH, struct., bonding and internal rotation 4-68938  
H<sub>2</sub>PP, ab initio SCF and CI study of stability and electronic struct. 4-74164  
HPPH, ab initio SCF and CI study of stability and electronic struct. 4-74164  
HX-cyclopropane complex, (X=F, Cl, Br, I, CN), matrix isolation IR invest. 4-107349  
KAl(Si<sub>2</sub>)O<sub>8</sub> monoclinic feldspars, crystal growth, PBC vector analysis 4-92119  
K<sub>2</sub>O<sub>2</sub>, IR active modes, electronic struct. and vibr. anal. 4-87106  
KOD, vibr. spectrum and normal coordinate anal. 4-104607  
KOH, vibr. spectrum and normal coordinate anal. 4-104607  
K<sub>2</sub>SnTe<sub>3</sub> semicond., electronic struct. and bonding 4-84563  
LaCoP<sub>2</sub>, cryst. struct. determ. 4-80011  
La<sub>2</sub>CoO<sub>4</sub>, with K<sub>2</sub>NiF<sub>4</sub> struct., at displacements, mag. and transport props., anisotropic bonding effects 4-75358  
La<sub>2</sub>NiO<sub>4</sub>, with K<sub>2</sub>NiF<sub>4</sub> struct., at displacements, mag. and transport props., anisotropic bonding effects 4-75358  
LiNO<sub>3</sub>·3H<sub>2</sub>O, deform. electron density, X-ray and neutron diff. data 4-65232  
Mg (0001), O chemisorption, LCAO-X $\alpha$  calcs. 4-113799  
Mo compounds, La<sub>12</sub> X-ray emission lines 4-109281  
MoS<sub>2</sub>, electronic struct. and angle depend. X-ray S K-emission bands 4-98521  
MoS<sub>2</sub> type, layered compounds, valence band spectrum, crystal struct. rel. to electrophysical props. 4-75395  
N<sub>2</sub>, basis sets, diffuse s and p supplementary functions 4-68930  
N<sub>2</sub>, ground states, bond function, dissoci. energies, CI calcs. 4-74162  
N<sub>2</sub> internal subshells, rel. to bond form. and XPS struct. 4-59850  
NH<sub>2</sub>-BH<sub>3</sub>, orbital interaction, charge transfer, bond form., CNDO/2 study 4-102597  
NH<sub>4</sub><sup>+</sup>, charge redistrib. in mol. vibr. M-H bond moments 4-69047  
Na clusters under equilib. conditions with Knudsen cell, mass spectra study 4-74379  
NaFeP<sub>2</sub>O<sub>7</sub>, crystallographic, mag. and Mossbauer studies 4-108323  
Nb, chemical bonding, mag. susceptibility 4-114090  
Ni compounds, chem. bonding and electronic struct., XPS studies 4-71524  
Ni II complexes, quadridentate macrocyclic ligands, bonding cavities, X-ray struct. determ. 4-103716  
Ni-Cu alloys, grain boundary segregation and cracking, Monte Carlo studies 4-114542

bonds (chemical) continued

NiN<sub>2</sub>, dissoci., CAS SCF and contracted CI calc. 4-81407  
O<sub>2</sub>, low density discharge, bimolecular processes 4-75225  
O<sub>3</sub>, density-functional calcs. of low-lying states 4-74355  
OH groups, bridging and terminal, struct., chemical and quantum chemical calcs. 4-78768  
OH internal state distrib., prod. from O+cyclic hydrocarbons, laser induced fluoresc. study 4-77000  
OH<sup>-</sup>(CO)<sub>2</sub> clusters, (n=1, 2), ab initio invest. 4-96737  
OH<sup>-</sup>(H<sub>2</sub>O)<sub>2</sub> clusters, (n=0, 2, 3, 4), ab initio invest. 4-96736  
PCl<sub>2</sub> molecule, X-ray spectra and electronic struct. 4-112194  
PbO<sub>2</sub>,  $\alpha$  and  $\beta$  proton localisation, X-ray and neutron diff. studies. (French) 4-88142  
Pb<sub>1-x</sub>Sn<sub>x</sub>Te, defect states, impurity photoconductivity transient studies 4-80545  
PbTe cryst., external shape, impurity complex effects 4-75347  
Pd, adsorbed Xe, adsorptive bond, face specificity, s-resonance model 4-92540  
Pd-H, system, electronic struct. of small clusters, H-metal bonding 4-70624  
Pd<sub>2</sub>, electronic struct. and bonding, mass spectrosc. and ab initio HF-CI invest. 4-74167  
Pt film, sputter deposition, resistivity and struct. 4-104732  
Pt-H system, electronic struct. of small clusters, H-metal bonding 4-70624  
Rb<sub>1-x</sub>(NH<sub>4</sub>)<sub>x</sub>H<sub>2</sub>PO<sub>4</sub> single cryst. proton glasses, struct. and dielec. props. 4-76323  
RbO, hyperfine interactions and bonding, semiempirical valence bond model 4-112120  
Re (0001), adsorption of acetylene, vibrational electron energy loss spectroscopy (French) 4-75774  
Re complex, [( $\eta^5$ -C<sub>5</sub>H<sub>5</sub>)<sub>2</sub>Re(H)Cu] complex, cryst. and mol. struct., Cu(I)-Cu(I) bond 4-96715  
ReTe, semicond., electronic struct. and bonding 4-84563  
Rh, field evaporation, bonding distance and vibr. freq. determ. 4-93202  
S, allotropes, electronic states, localised orbital approach 4-92655  
SF<sub>6</sub>, force field model of stretching anharmonicities 4-68939  
SF<sub>6</sub>, laser pumped mols., electron diff. study 4-96626  
Se, allotropes, electronic states, localised orbital approach 4-92655  
Se<sub>2-x</sub>Te<sub>x</sub> alloys, amorphous, elastic constns., role of Te 4-84333  
Si (001), reconstructed, surface phonon spectrum calcs. 4-104062  
Si (100) 2 $\times$ 1, pre-exposed to O in submonolayer range, chem. shifts of Si-H stretching freqs. 4-80368  
Si (111), benzene bound state vibr. modes and chemisorption bonds 4-108714  
Si (111), surface, far UV laser induced oxidation by bond rearrangement 4-81310  
a-Si alloys, metastable defect states, X $\alpha$  scatt. wave calc. 4-113899  
Si, graphitic, structural theory using pseudopotential local-density-functional approach 4-92135  
Si, molten, electronic and bonding props. 4-98503  
Si, native oxide form. initial phase, AES study 4-104891  
Si p-n junction contrast in ultra high vacuum SEM 4-95576  
a-Si, solid phase epitaxy, bond rearrangement process, quantitative anal. 4-84534  
Si thin films on substrates, Raman study 4-99206  
a-Si:H, broken bonds and electronic density of states, H effects 4-65178  
Si:H, microcrystalline, IR absorpt. study of Si-H bond formation 4-71416  
Si:H, study of H-induced defects (Chinese) 4-103736  
a-Si:H film, hyperfine interaction, ENDOR study 4-65881  
a-Si:H films, reactive sputtering, elec. and optical props. 4-104203  
a-Si:H reactively sputtered films, H partial press. effects 4-93219  
a-Si:H Schottky diodes and nin devices, single and double carrier injection 4-114015  
a-Si:H thin films, glow discharge effects on electronic and optical props. 4-75977  
Si/Al interface, atomic redistributions, XPS studies 4-80311  
Si/Au interface, atomic redistributions, XPS studies 4-80311  
Si/SiO<sub>2</sub> interface, amorphous Si/cryst. Si facet form. during solid phase epitaxy 4-88423  
Si-Pt interface, silicide formation and chemical reactions 4-92570  
SiC<sub>2</sub>, energetically low-lying silacyclopropyne isomer, SCF and CI calc. 4-68992  
SiH<sub>4</sub>, charge redistrib. in mol. vibr. M-H bond moments 4-69047  
SiH<sub>4</sub>, unimol. decomp., Si chem. vapour deposition 4-71900  
Si<sub>2</sub>H<sub>6</sub>+m, defects, molecular cluster studies 4-84586  
Si<sub>1-x</sub>N<sub>x</sub>H<sub>2</sub> amorphous film, photoinduced ESR study 4-114161  
Si<sub>3</sub>N<sub>4</sub> films, amorphous, hydrogenated and deuterated, prepared from plasma-enhanced CVD, IR absorpt. spectra 4-81021  
Si<sub>3</sub>N<sub>4</sub> plasma deposition pres., growth mechanism, optical emission study 4-88433  
SiN<sub>1.5</sub>H<sub>0.5</sub> amorphous, localised states at conduction band edge 4-104168  
SiO<sub>2</sub>, amorphous, local electronic density of states, influence of Si-Si bonds 4-92671  
SiO<sub>2</sub> film, low temp. photochemical deposition 4-99339  
SiO<sub>2</sub>, vitreous, defects of broken-bond type 4-92097  
SiO<sub>2</sub>-Si interface, oxidation, chem. bonding in transition layer, photoemission spectra using synchrotron radiation 4-85062  
SiP<sub>2</sub>, electron density distrib. and cryst. struct. 4-79979  
Si<sub>2</sub>S<sub>3-x</sub> glass, Raman study of atomic struct. 4-92093  
SmFe<sub>2</sub>(Co<sub>2</sub>)(Ni<sub>2</sub>) cpds., bonding, X-ray emission study 4-85042  
Sn thin film, struct. and transformations during vacuum heating, RHEED and Mossbauer studies 4-75818  
SnS<sub>2</sub>, electronic struct. and angle depend. X-ray S K-emission bands 4-98521  
Te<sub>0.7</sub>Se<sub>0.3</sub>, role of temp. in struct., Raman study 4-88063  
Te<sub>1-x</sub>Se<sub>x</sub> liquid alloy, Raman study of structural transitions 4-80210  
TiB<sub>2</sub>, chemical bonding, mag. susceptibility 4-114090  
TiN, nonstoichiometric and hydrogenated, cluster calcs. of electronic states and chem. binding 4-70623  
TiN<sub>0.99</sub>, electron transfer and thermal vibr. parameters, X-ray diff. study 4-92329  
TiV, ground state in Ar matrix, bonding, hyperfine interaction, ESR 4-75871  
Ti<sub>2</sub>S-B<sub>2</sub>S<sub>3</sub> glass, NMR study and struct. 4-88726  
Ti<sub>2</sub>Ve<sub>8</sub>, NMR and topotactic redox reactions 4-84859  
UNi, ground state in Ar matrix, bonding, hyperfine interaction, ESR 4-78871  
V-Si, electron momentum distrib. and charge transfer,  $\gamma$ -ray Compton scatt. study 4-70059

**bonds (chemical) continued**

- V<sub>2</sub>, electron correl. effects 4-102603  
 V<sub>2</sub>H, normal and deuterated, shock compression to 135 GPa 4-92295  
 Vb<sub>4</sub>, ambient press. synthesis, cryst. struct., mag. and elec. props., bonding 4-75408  
 W (100), oxidised and carbided, adsorbed ethylene and acetylene 4-93553  
 W film (001), bonding of surface states, local density functional studies 4-80648  
 WO<sub>3</sub> amorphous films, electrochromic colour centres, Raman scatt. studies 4-113445  
 Y-Fe alloys, exchange interactions, coordination props. studies 4-114104  
 YPd, gaseous, disoc. energy, Knudsen-effusion mass spectrometry 4-99910  
 Yb(C<sub>2</sub>H<sub>3</sub>SO<sub>4</sub>)<sub>9</sub>H<sub>2</sub>O, cooperative absorpt. lines existence for Yb-(OH, OD) pairs, absolute oscil. strengths 4-71370  
 YbCl<sub>3</sub>·6H<sub>2</sub>O, cooperative absorpt. lines existence for Yb-(OH, OD) pairs, absolute oscil. strengths 4-71370  
 Yb(OH<sub>2</sub>), cooperative absorpt. lines existence for Yb-(OH, OD) pairs, absolute oscil. strengths 4-71370  
 Yb(OOH), cooperative absorpt. lines existence for Yb-(OH, OD) pairs, absolute oscil. strengths 4-71370  
 Zr-Ni, metallic glass, XES study of electronic states 4-80482  
 Zr-Ni-D, metallic glass, XES study of electronic states 4-80482

**bone**

- <sup>226</sup>Rn retention in mouse bone 4-77407  
 acrylic bone cement, mech. props. improvement by fibre reinforcement 4-109994  
 acrylic bone cement, tensile fatigue failure 4-105379  
 alpha-emitting radionuclides, bone incorporating, dose calcs. 4-89750  
 ankle joint biomechanics, effects of fibular shortening 4-100226  
 cancellous, broadband US attenuation obs. 4-89648  
 cancellous bone strength measurements with the osteopenetrometer 4-89793  
 carcinogenicity of <sup>22</sup>Ra and radionuclides, beagle studies 4-115221  
 cell nuclei, morphometry and location rel. to bone surfaces 4-115035  
 cement failure criteria, acetabular region appls. 4-105377  
 cervical spine, normal, injured and stabilised: in vitro kinematics 4-81730  
 composite material, elec. props. rel. to comp. 4-72232  
 conference, New Orleans, USA (April 1982) 4-73136  
 contour detection algorithm for high precision quantitative CT 4-62561  
 cortical, CW technique for elastic props. meas. 4-81823  
 cortical bone, bovine, elastic props. rel. to microstruct. 4-72290  
 cortical bone, neutron irradiation effects on mech. props. (Spanish) 4-100234  
 cutting force, rel. to surgical instrument design 4-62503  
 doses-from  $\alpha$ -emitting bone surface seeking radionuclides, calc. for radiological protection purposes 4-77395  
 electrical and dielec. props. rel. to freq. 4-66940  
 electron beam therapy, dose enhancement in bone 4-81788  
 electron density for inhomogeneity correction in radiotherapy planning using CT numbers 4-67112  
 femoral bone, human, work-of-fracture obs. 4-62515  
 femoral bone narrow, rat, loss of transportable Pu deposits from macrophages 4-77213  
 femur, stress distrib., three-dimensional finite element anal. (Italian) 4-81723  
 fibroblasts, bone, mouse, effect of <sup>241</sup>Am  $\alpha$ -particles 4-77348  
 fluid-saturated, dielec. props., immersion fluid cond. variation effect; rat expts. 4-81659  
 fracture movement under supporting bandages, performance and results (German) 4-77273  
 gamma camera energy windows for <sup>99m</sup>Tc bone scintigraphy asymmetry rel. to contrast resolution 4-81777  
 granulocyte/macrophage progenitor cell population in bone marrow and blood after total body X-irrad. 4-77340  
 hip, natural adult, contact-coupled finite element anal. 4-100207  
 human, U and <sup>226</sup>Ra contents in Russian samples 4-62607  
 human compact, water absorpt. 4-89870  
 human tubular, struct. features rel. to ultrasound meas. 4-89650  
 illium of female CBA mouse, comparison of distrib. of <sup>239</sup>Pu and calcein 4-77405  
 intervertebral joint under compression, time dependent props. 4-89613  
 limbs, human, literature review of vibr. anal. 4-62510  
 long, deform. rate rel. to flexural fracture behaviour 4-77276  
 long bone cross-sectional moment of inertia, noninvasive meas. by photon absorptiometry 4-62642  
 marrow and spleen cells, DNA struct. and catabolism, HTO and <sup>137</sup>Cs  $\gamma$ -ray effects (Russian) 4-115132  
 marrow cells, rat, X-irrad.-induced double-strand DNA breaks (Russian) 4-77312  
 marrow morphology of *Microtus oeconomicus* pall., influence of increased natural radioactivity (Russian) 4-77323  
 marrow transplant patients receiving an increased mean dose rate of total irrad., increased mortality 4-93843  
 mechanical and stress adaptive props. 4-77271  
 metastases, proton irrad. obs. (Russian) 4-93847  
 mineral content measurement using dual photon absorptiometry, prototype apparatus (French) 4-67155  
 osteon streaming pots., anatomical model, bone electromech. effect characterisation 4-115046  
 porosity and specific surface 4-58604  
 radioisotopes, <sup>239</sup>Pu and <sup>241</sup>Am, in rat bones, effect of drinking Zn-DTPA 4-77406  
 resorption by isolated rabbit osteoclasts, stereophotogrammetric obs. 4-89533  
 rheology, new developments 4-115096  
 skeletal imaging, comparative studies of <sup>99m</sup>Tc-pyrophosphate and <sup>85</sup>Sr-chloride 4-93860  
 skeletons of adult rats, long-term distrib. of <sup>239</sup>Pu, <sup>241</sup>Am and <sup>233</sup>U 4-77404  
 skull X-ray assessment of head injuries: a decision analytical approach 4-115185  
 skulls biomechanical analysis, stress transmission by photoelastic coatings obs. 4-66981  
 spinal nonunions, repair with a pulsed DC stimulator 4-93961  
 spinal section, patient-specific computer model 4-100227  
 stromal mechanocytes of human bone marrow and spleen, radiosensitivity (Russian) 4-93807  
 tibia, human, vibr. anal. using skin-mounted accelerometers 4-100211

**bone continued**

- tibia, rabbit, reference curve for axial bioelec. pots. 4-100112  
 tibiae, human, identification of in vivo vibr. modes by modal anal. 4-77290  
 tibial fracture healing assessment rel. to fracture fragments natural freq. 4-10012  
 tibial lengthening device and technique based on biomechanical considerations 4-100350  
 tumours induction, rel. to radioisotopes incorporation 4-77347  
 X-ray scattering, small angle, from compact bone 4-97960  
<sup>241</sup>Am in the beagle skeleton: microdistrib. and local dosimetry 4-77394  
<sup>241</sup>Am, microdistrib. and localised dosimetry in bones of beagle dogs 4-115242  
 Ca, % by mass rel. to effective at. no., dual-energy CT 4-115188  
<sup>241</sup>Pu, A=239, 240, body burden in Lapps, comparison with southern Finns 4-62590  
<sup>90</sup>Sr in human skeleton, uptake and turnover 4-115243

**Boolean algebra**

see also *Boolean functions*

- complete Boolean algebra of projections 4-90345  
 electron microscope image processing, Boolean algebra operations using digital frame store 4-101979

**Boolean functions**

- Boolean equations, efficient multiplication, soln. procedure (Russian) 4-63474

**Boolean lattices** see *Boolean algebra***bootstrap models** see *bootstrapping***bootstrap theory** see *bootstrapping***bootstrapping**

- density of states, statistical bootstrap model 4-86684  
 quasinuclear quark model, bootstrap procedure 4-78532  
 SU(N) principal chiral field, exact S-matrix, bootstrap method 4-90748

**bootstraps** see *bootstrapping***borate glasses**

see also *borosilicate glasses*

- alkali borate glass, thermal expansion, Gruneisen parameter 4-80272  
 alkali borate mixed glasses containing Ni, induced optical absorpt. rel. to  $\gamma$ -ray exposure 4-76502  
 binary, photoelastic consts., compositional trends 4-84945  
 multi-component oxide glasses, local environment, EXAFS studies 4-60852  
 nuclear spin stimulated echoes, pulsed NMR meas. 4-92976  
 quartz microporous glass, optical breakdown 4-107713  
 ternary photoelastic consts., compositional trends 4-84945  
 AgI-Ag<sub>2</sub>O-B<sub>2</sub>O<sub>3</sub> system, stable and metastable phases 4-113343  
 (AgI)<sub>x</sub>(Ag<sub>2</sub>O-B<sub>2</sub>O<sub>3</sub>)<sub>1-x</sub> superionic glasses, EXAFS studies 4-60855  
 (AgI)<sub>x</sub>(Ag<sub>2</sub>O·nB<sub>2</sub>O<sub>3</sub>)<sub>1-x</sub> superionic glasses, Raman scatt. study 4-61712  
 B analysis and mapping using windowless energy dispersive detector 4-66636  
 B<sub>2</sub>O<sub>3</sub>-0.5Li<sub>2</sub>O-0.7LiCl, pseudospin echoes 4-70291  
 B<sub>2</sub>O<sub>3</sub>-Li<sub>2</sub>O glass, ionic cond. meas. 4-84457  
 B<sub>2</sub>O<sub>3</sub>-Li<sub>2</sub>O(Li halides)<sub>x</sub>, fast ion cond., press. effects 4-88336  
 B<sub>2</sub>O<sub>3</sub>-Na<sub>2</sub>O-Nd<sub>2</sub>O<sub>3</sub> glasses, thermoluminescent props. 4-66086  
 B<sub>2</sub>O<sub>3</sub>-TeO<sub>2</sub> glass, Raman spectroscopic study 4-109177  
 BaO-B<sub>2</sub>O<sub>3</sub>-Fe<sub>2</sub>O<sub>3</sub> glasses, splat cooled, mag. props. 4-71107  
 BaO-B<sub>2</sub>O<sub>3</sub>-Fe<sub>2</sub>O<sub>3</sub> system, magnetic vitroceraics, prep. and props. 4-93256  
 Ba<sub>2</sub>O-Al<sub>2</sub>O<sub>3</sub>-B<sub>2</sub>O<sub>3</sub>, photochromic optical fibres 4-79329  
 Bi<sub>2</sub>O<sub>3</sub>-B<sub>2</sub>O<sub>3</sub> glasses, memory switching process, role of chem. reduction 4-114002  
 CaO-B<sub>2</sub>O<sub>3</sub>-Al<sub>2</sub>O<sub>3</sub>-Fe<sub>2</sub>O<sub>3</sub> glass system, photoacoustic spectra of Fe 4-99130  
 (CuO)<sub>x</sub>-(2B<sub>2</sub>O<sub>3</sub>-Li<sub>2</sub>O)<sub>1-x</sub> glass, EPR and mag. susceptibility meas. 4-61837  
 Fe<sub>2</sub>O<sub>3</sub>-B<sub>2</sub>O<sub>3</sub>-PbO glasses, ferric ion distrib., EPR studies 4-109064  
 (Fe<sub>2</sub>O<sub>3</sub>)<sub>x</sub>(B<sub>2</sub>O<sub>3</sub>-PbO)<sub>1-x</sub> glasses, mag. props. study 4-88654  
 GeO<sub>2</sub>-B<sub>2</sub>O<sub>3</sub> films, opt. absorpt. edge, additions influence 4-71455  
 K<sub>2</sub>O-B<sub>2</sub>O<sub>3</sub> glass, electronic spectra and coordination of Ni<sup>2+</sup>, up to 1000°C 4-61726  
 K<sub>2</sub>O-B<sub>2</sub>O<sub>3</sub>-TeO<sub>2</sub> glass, Raman spectroscopic study 4-109177  
 (Li<sub>2</sub>Na)<sub>2</sub>O-B<sub>2</sub>O<sub>3</sub> glasses, mixed alkali effect 4-84449  
 Li<sub>2</sub>O-(LiCl)-B<sub>2</sub>O<sub>3</sub>-Al<sub>2</sub>O<sub>3</sub> system, Raman spectra of glasses (Chinese) 4-93065  
 Li<sub>2</sub>O-Al<sub>2</sub>O<sub>3</sub>-B<sub>2</sub>O<sub>3</sub> glass, form. and transition temp. 4-113634  
 Li<sub>2</sub>O-B<sub>2</sub>O<sub>3</sub>-Fe<sub>2</sub>O<sub>3</sub> system, magnetic vitroceraics, prep. and props. 4-93256  
 Li<sub>2</sub>O-LiF-B<sub>2</sub>O<sub>3</sub> glasses, fast ionic cond., role of F in struct., Raman spectra 4-98025  
 Li<sub>2</sub>O-LiNbO<sub>3</sub>-B<sub>2</sub>O<sub>3</sub>, new solid electrolyte glass material, electrical conductivity 4-108649  
 Na<sup>+</sup> ion conducting glasses, activation energy and conductivity 4-113707  
 Na<sub>2</sub>O-Al<sub>2</sub>O<sub>3</sub>-B<sub>2</sub>O<sub>3</sub> glass, form. and transition temp. 4-113634  
 Na<sub>2</sub>O-B<sub>2</sub>O<sub>3</sub> glass, oxide substituted, alkali resist., porous, heat treatment, leaching, phase decomp. 4-66299  
 Na<sub>2</sub>O-B<sub>2</sub>O<sub>3</sub> glass, prep., mech., thermal and optical props. rel. to N content 4-60845  
 Na<sub>2</sub>O-B<sub>2</sub>O<sub>3</sub> glass, undoped and Co<sup>2+</sup> doped, acoustic loss and optical absorpt. spectra, matrix analysis 4-84193  
 Na<sub>2</sub>O-B<sub>2</sub>O<sub>3</sub> system, glass forming regions, roller quencher obs. 4-84191  
 Na<sub>2</sub>O-B<sub>2</sub>O<sub>3</sub>-Al<sub>2</sub>O<sub>3</sub>, aluminoborate glass, cond. max. 4-113702  
 Na<sub>2</sub>O-B<sub>2</sub>O<sub>3</sub>-Al<sub>2</sub>O<sub>3</sub>-SiO<sub>2</sub> transparent glazes, with enhanced chem. and thermal shock-resist. 4-81305  
 PbO-BaO-TiO<sub>2</sub>-B<sub>2</sub>O<sub>3</sub> glass ceramic system, crystal clamping, X-ray diffr., dilatometry 4-109386  
 Sc<sub>2</sub>O<sub>3</sub>-Na<sub>2</sub>O-B<sub>2</sub>O<sub>3</sub>, porous glass-ceramic, sintering and characterisation 4-114467  
 SiO<sub>2</sub>-B<sub>2</sub>O<sub>3</sub> glasses, sol-gel processing 4-70038  
 SiO<sub>2</sub>-B<sub>2</sub>O<sub>3</sub>-Na<sub>2</sub>O gel-derived glasses, microhomogeneity light scatt. meas. 4-114290  
 V<sub>2</sub>O<sub>5</sub>-B<sub>2</sub>O<sub>3</sub> glass, struct., IR spectra and elec. cond. 4-88107  
 V<sub>2</sub>O<sub>5</sub>-B<sub>2</sub>O<sub>3</sub> glasses, struct. study, IR spectra anal. 4-84961  
 ZnO-B<sub>2</sub>O<sub>3</sub>, cryst. and glass struct., <sup>11</sup>B NMR spectra 4-79941  
 ZnO-B<sub>2</sub>O<sub>3</sub>, X-ray diffr., density and elec. cond. obs. 4-61423  
 ZnO-B<sub>2</sub>O<sub>3</sub>-SiO<sub>2</sub> glass/Si system, surface charges, C-V characteristic meas. 4-65747

**Bordoni effect**

No entries

**boron**  
see also nuclei with .....  
amorphous, CVD diagrams, nucleus density 4-71583  
analysis and mapping using windowless energy dispersive detector 4-66636  
 $\alpha$ -B<sub>12</sub>, band struct., energy gaps, bonding, cluster approx. 4-70646  
cluster surfaces, chemisorption of H<sub>2</sub> ab initio RHF calc. 4-92555  
cosmic rays, B/C ratio, spatial and temporal variability 4-94416  
CVD, anal. 4-88985  
detection limit from capture gamma-ray meas. after preconcentration 4-105086  
diffusion coefficient determ. for drive-in in oxidising atmosphere (*Hungarian*) 4-113715  
diffusion in Si-N 4-113726  
distribution in boronised alloys VK6, T5K10 and T15K6 (*Russian*) 4-80071  
doped  $\beta$ -phase, high temp. thermoelec. materials, thermal cond. and elec. props. 4-75990  
fibre encapsulation, gas phase point by point anal. by Raman scatt. 4-71591  
fibre reinforced Al, fibre-matrix bond form: kinetics during rolling 4-71674  
fibre reinforced Al, fracture mode and shear strength rel. to interface strength 4-62022  
fibre reinforced Al, rolling in direction of reinforcement 4-66353  
fibre reinforced Al, stress-strain and failure behaviour 4-76831  
fibre reinforced Al-Mg, interaction between B and matrix 4-70577  
fibre reinforced Al-Mg alloy, fibre/matrix interface effect on fatigue, optimum processing parameters 4-114635  
fibres, chem. reaction with liq. Al 4-61891  
fibres, elastic energy absorpt. mechanism 4-66366  
geochemical cycle and basalt hydrothermal alteration 4-67191  
impact on C foil, excitation study 4-107294  
impurity diffusion in amorphous alloys, SIMS study 4-92435  
ion-induced secondary electron emission projectile incident angle depend. 4-76596  
ions, extreme UV absorption spectroscopy using two laser-produced plasmas 4-60728  
reinforcing fibres, crit. length 4-71695  
rhombohedral  $\alpha$ , electronic energy levels of icosahedron calcs. 4-113862  
segregation in Si-SiO<sub>2</sub> interface during neutral anneals 4-70387  
sputtering, ionic excitation, projectile incidence angle depend. 4-76593  
B II, Be I-like, oscillator strengths, transition wavelengths, HF relativistic calcs. 4-106127  
B ions, He- and Li-like, laser produced plasma, EUV spectra 4-83320  
B<sup>4+</sup>, H-like, elastic positron scatt., polarised orbital method 4-102798  
B<sup>+</sup>+H<sub>2</sub>, pot. energy surfaces, diatomics-in-mols. correl. diagrams 4-62166  
B<sup>3+</sup>+H, electron capture cross-sections calcs. 4-102791  
B<sup>3+</sup>+H, collisions, electron transfer, at. orbital expansion description 4-78962  
B-C/B fibre reinforced Ti-Al-V, fatigue crack growth behaviour 4-93374  
AB (A=10,11) atomic mass meas. 4-91357  
B<sup>+</sup> coatings in NPL devices, power deposition in cylindrical geometry 4-60600  
B<sup>10</sup> conc. in tumour, microanalysis 4-62634  
B<sup>10</sup> control rods, burnup characteristics 4-102361  
B<sup>10</sup> loaded macromolecules in expt. physiology, tracing by neutron capture radiography 4-67156  
B<sup>10</sup> slab and spherical sources, charged particle spectra 4-60599  
B<sup>10</sup>/B<sup>11</sup> ratio in saline lakes of Qinghai-Xizang Plateau, <sup>11</sup>B(n, $\alpha$ )<sup>7</sup>Li influence 4-10401  
Fe<sub>3</sub>Co<sub>7</sub>Si<sub>4</sub>B<sub>16</sub>, magnetic annealing kinetics 4-80795  
GaAs:B, existence of B<sub>As</sub> impurity antisite centres, IR absorption lines study 4-71413  
GaAs:B, interaction between B and defects 4-80082  
GaAs:B, interstitial centre, radiation induced, cluster-Bethe lattice treatment 4-98090  
N<sub>2</sub>+B<sup>+</sup> fast beam excitation study 4-107294  
PbTe:B, absorpt. spectra and impurity states 4-104638  
Si film, LPCVD, elec. props., effect of film thickness 4-88615  
Si:As, P, B, ion implanted, fast isothermal annealing and elec. props. 4-92224  
Si:B, (100), shallow junction implants through surface oxide, theoretical and expt. study 4-113476  
Si:B, compensated semiconductors, coalescence process, effect and rad. and heat treatment 4-65288  
Si:B, deep implanted layers, for IC appl. 4-75482  
Si:B, deep level impurities at bond centered interstitial site 4-108814  
Si:B, Fe, exciton photoluminescence study 4-109243  
Si:B, focused ion beam B<sup>+</sup> implantation 4-92222  
Si:B, heavy doping effect on band struct. and optical props. 4-92998  
Si:B, implanted, elec. activation and damage annealing by flash lamp irradi. 4-70196  
Si:B, impurity electronic struct. cluster X $\alpha$  calc. 4-65639  
Si:B, ion implant in-depth error anal., mass interference effects in' ion microprobe studies (*Chinese*) 4-111248  
p-Si:B, ion implanted, electron beam annealing 4-60960  
Si:B, ion implanted, flash-lamp annealing study 4-108395  
Si:B, ion implanted and electron beam annealed, TEM and HREM studies 4-80058  
Si:B, ion implanted shallow layers, electron beam annealing, expt. study using SIMS 4-98133  
Si:B, lattice const. meas: using X-ray double cryst. method 4-103606  
Si:B, low resistance ion implanted films 4-108398  
Si:B, magnetothermal cond. study 4-71076  
p-Si:B, p-type doping in MBE by B coevaporation 4-71561  
Si:B, phonon scatt. at acceptor ground state 4-70729  
Si:B, point defects influence on acceptor ground state splittings 4-70728  
a-Si:B, pure and doped, ion implanted, recrystallisation studies 4-88422  
Si:B, recrystallized on SiO<sub>2</sub>, laterally seeded, implantation and annealing studies 4-98121  
Si:B, retardation of B diffusion 4-88346  
Si:B, struct. of rod-like defects 4-92238  
Si:B, substrate orientation depend. of enhanced epitaxial regrowth 4-108737  
Si:B, thermal wave contrast, dopant conc. depend. 4-103978  
Si:B,C,O, impurity profiling and analysis by recoil atoms in heavy ion beams 4-108406  
Si:B,H, neutralisation of shallow acceptor levels by atomic H 4-104153  
a-Si:B film, optical props. study 4-76540

**boron continued**  
Si:B ingots, effective segregation coeff. of B, elec. studies 4-88192  
Si:B microcrystalline films, crystallinity, morphology and elec. cond. 4-108749  
Si:B neck for Josephson bridges 4-98828  
Si:B polycrystalline films, activation energy of resist., effects of grain boundary trapping state energy distrib. 4-88616  
Si:B solar cell, electron irradi., photon effects 4-93618  
Si:B solar cell material, EBIC contrast, microstruct. and composition effects 4-108878  
Si:B/Ti-W RF sputter-deposited Schottky barrier diodes 4-98691  
Si:B-SiO<sub>2</sub> MIS struct., ion bombarded, defect annealing study 4-80685  
Si:B(P)(As), dopant diffusion, numerical soln. by solving impurity, vacancy and self-interstitial continuity eqns. 4-80303  
Si:B( $\mu$ ), tetrahedral interstitial impurities, electronic struct. 4-65636  
a-Si:H, B, dark cond. and photocond., thickness depend. 4-84624  
a-Si:H, B, P, electron structure and density of states of B-P pairs, cluster calc. 4-65642  
Si:H, B(P), amorphous CVD layer, impurity doping 4-60941  
Si:H,B, amorphous, solar cells, deposition from Si<sub>2</sub>H<sub>4</sub> and B doping profiles 4-81540  
a-Si:H,B, doping effect on gap states 4-88488  
a-Si:H,B, ESR and optical props., thickness depend. 4-84853  
Si:H,B amorphous CVD films, optical props., B doping effects 4-99086  
a-Si:H,B film, optical props. study 4-76540  
a-Si:H,P,B film, drift mobility, photoconductivity meas. 4-104259  
Si/a-Si:H,B/metal junctions, current-volt. characts. 4-114033  
Si/Ti:B<sup>+</sup> ion implanted, doping effects on TiSi<sub>3</sub> formation 4-88183  
Si-SiO<sub>2</sub> interface, B drive diffusion in oxidizing ambients, segregation coeff. determ. 4-75690  
SiB, implanted, impurity depth profiles,  $\alpha$ -particle spectra, Monte Carlo calc. 4-80081  
SiC:Al, B,  $\circ$  interstitial diffusion studies 4-80302  
p-SiC:B, diffusion, track autoradiography studies 4-84466  
SiC:B, linear photogalvanic effect 4-70869  
SiC:B, shrinkage, density and phase comp. rel. to forming press. and sintering temp. 4-85130  
a-SiN<sub>x</sub>:H,B layers, prep. by glow discharge decomp. of N<sub>2</sub>/SiH<sub>4</sub> mixtures, optical and photoelectric props., effects of doping 4-114001  
SiO<sub>2</sub>:B, implanted, impurity depth profiles,  $\alpha$ -particle spectra 4-80081  
SiO<sub>2</sub>:B, low pressure CVD at quasi-high flow 4-76686  
SiO<sub>2</sub>+B<sub>2</sub>O, B-O phase stabilisation, quantum-chem. calc. 4-61325

**boron alloys**  
see also boron compounds  
rare earth alloy, RRh<sub>2</sub>B<sub>4</sub>, R=Y, Er, Ho, Tm, Dy, mag. props. and crystal field effects 4-84767  
rare earth alloys, RCo<sub>2</sub>B<sub>4</sub>, R=Gd-Tm, antiferromag. and paramag. states, NMR spectra 4-109089  
rare earth intermetallics, RPd<sub>3</sub>B<sub>x</sub>, structural and magnetic props. 4-103700  
rare earth-boron ternary and higher order systems, phase equilibria, book 4-95076  
rare earth-transition metal-boron alloys, crystallographic and mag. props. 4-75370  
transition metal-boron, amorphous and cryst., B-K $\alpha$  X-ray spectra and electronic struct. 4-71482  
transition metal-Fe-B amorphous alloys, magnetisation reversal, mech. stress effects 4-76171  
transition metal-Fe-B metallic glasses, electronic struct., XPS study 4-75837  
Udimet 700, metalloid strengthening mechanism 4-61974  
Al-Ti-B, impurity distrib. 4-114538  
Al-Ti-B alloys, Al-rich, nature and morphology of Ti- and B-rich crystals. (*French*) 4-61919  
CeB<sub>6</sub>, antiferromagnetic-quadrupole ordering 4-80763  
Co-Si-B (-Fe) metallic glasses, mag. props., annealing effects 4-109039  
Co-Si-B metallic glasses, Young's modulus, internal friction, magnetomechanical effects, permeability meas. 4-76216  
Co<sub>1-x</sub>B<sub>x</sub>, amorphous alloy, electrolytical and chemical prep., struct. 4-70603  
Co<sub>1-x</sub>B<sub>x</sub> glasses, local struct., EXAFS studies 4-60854  
Co<sub>100-x</sub>B<sub>x</sub>, amorphous alloys, mag. anisotropy, mag. annealing effects 4-76131  
Co<sub>100-x</sub>B<sub>x</sub>, metallic glass, mag. and mechanical props. 4-84841  
Co<sub>75</sub>B<sub>25</sub> amorphous alloys, mag. relax. processes 4-84825  
Co<sub>75</sub>B<sub>25</sub>, liq.-quenched amorphous, dynamic temp. crystn. 4-60835  
Co<sub>80</sub>B<sub>20</sub>, amorphous, high press. and temp. phase stability (*Chinese*) 4-103923  
CoNiFe-SiB amorphous zero magnetostrictive alloy, compositional short-range order and ordering kinetics 4-70035  
Co<sub>55</sub>Ni<sub>44</sub>Fe<sub>2</sub>B<sub>10</sub>Si<sub>6</sub> foil, thermal expansion coeff. and isothermal compressibility (*Russian*) 4-65421  
Co<sub>55</sub>Ni<sub>15</sub>Fe<sub>2</sub>B<sub>10</sub>Si<sub>6</sub>, amorphous, mag. aftereffects after field annealing 4-84823  
Co<sub>58</sub>Ni<sub>10</sub>Fe<sub>2</sub>Si<sub>1</sub>B<sub>16</sub>, amorphous, mag. hysteresis loops after heat treatment below Curie point 4-80781  
Co<sub>75</sub>Si<sub>10</sub>B<sub>15</sub>, amorphous alloys, fatigue props. 4-66424  
Co<sub>95-x</sub>Si<sub>x</sub>B<sub>5</sub>, amorphous alloys, mag. aftereffects 4-84824  
Co<sub>84</sub>Si<sub>8</sub>Fe<sub>2</sub>B<sub>25</sub>, amorphous alloy, crystn. study using DTA and elec. resist. meas. 4-65181  
Cr-B-Ni, laser deposition on steel surface for hard-facing (*Russian*) 4-85251  
Cr<sub>3</sub>C<sub>2</sub>-Ni-B electrophoretic coatings, struct. and props. 4-88430  
Er<sub>2</sub>NiB<sub>3</sub>, cryst. struct. determ. 4-75376  
ErRh<sub>2</sub>B<sub>4</sub>, ferromagnetic superconducting thin film, photoexcitation, nonequilibrium effects 4-114059  
ErRh<sub>2</sub>B<sub>4</sub>, metamagnetism, magnetisation anomaly 4-114144  
EuPd<sub>3</sub>B, valence behaviour of Eu, possible charge ordering in EuPd<sub>3</sub>B 4-80850  
EuRh<sub>2</sub>B<sub>2</sub>, X-ray absorpt. near edge struct. study 4-61769  
Fe-B, amorphous alloys, mag. anisotropy, plastic deform., annealing, Mossbauer obs. 4-65803  
Fe-B, crystalline and amorphous, cryst struct., NMR study (*Russian*) 4-79982  
Fe-B alloys,  $\alpha$ - $\gamma$  transition lines and activity coeffs., conductometric studies 4-103926  
Fe-B amorphous alloys, cryst., and press., elec. resist. study 4-60837  
Fe-B amorphous alloys, mag. anisotropy; thermal treatment effects 4-65805  
Fe-B amorphous film, ion mixing and mag. props. 4-104471

## boron alloys continued

- Fe-B metallic glass, transition-elements effect on thermal stability, crystn. activation energy 4-108283  
 Fe-Be and Fe-B-Si amorphous alloys, Mossbauer obs. of short-range order 4-92981  
 Fe-Cr-B, metallic glass, mag. props. and density 4-84773  
 Fe-Cr-B, Mossbauer study of packing fraction 4-84877  
 Fe-Cr-Co-Si-B amorphous alloys, mag. props. and hyperfine interactions (*Russian*) 4-108994  
 Fe-Ho-B, metallic glass, mag. props. and crystallisation 4-84793  
 Fe-Mo-B, amorphous, hyperfine fields mag. props. 4-92933  
 Fe-Nb-Si-B amorphous alloys, mag. props. 4-71145  
 Fe-Nd-B alloy permanent magnets, domain walls, Lorentz electron microscopy study 4-92934  
 Fe-Nd-B permanent magnet system, metallurgy 4-109381  
 Fe-Ni-P-B amorphous alloys, mag. props., proton implantation effects 4-104416  
 Fe-Ni-P-B-(Si) metallic glasses, magnetoelastic effects in ferromag. resonance 4-61581  
 Fe-Si-B metallic glass ribbons, mag. props., surface feature effects 4-76173  
 Fe-W-B, metallic glass, mag. props. and density 4-84773  
 Fe-W-B, Mossbauer study of packing fraction 4-84877  
 Fe-W-B glasses, mag. aftereffect, effect of W 4-84827  
 FeB BCC alloys, electronic struct., APW calcs. 4-108769  
 Fe<sub>1-x</sub>B<sub>x</sub> amorphous alloys, electronic struct., XPS studies 4-75838  
 Fe<sub>1-x</sub>B<sub>x</sub> amorphous films, crystallisation kinetics and mag. props. 4-75807  
 Fe<sub>1-x</sub>B<sub>x</sub> amorphous films, magnetostriction, strain-modulated FMR study 4-76217  
 Fe<sub>1-x</sub>B<sub>x</sub> glass, crystallisation, elec. cond. study 4-88109  
 Fe<sub>100-x</sub>B<sub>x</sub> amorphous alloys, mag. anisotropy, mag. annealing effects 4-76131  
 Fe<sub>100-x</sub>B<sub>x</sub> metallic glass, mag. props. meas. 4-84814  
 Fe<sub>100-x</sub>B<sub>x</sub> metallic glass, mag. and mechanical props. 4-84841  
 Fe<sub>75</sub>B<sub>25</sub>-based metallic glasses, struct., small angle X-ray scatt. studies 4-113346  
 Fe<sub>80-x</sub>B<sub>20+x</sub> metallic glasses, struct., radial distrib. function calc. from X-ray diff. 4-103657  
 Fe<sub>80</sub>B<sub>20</sub> amorphous, extended freq. anal. of permeability aftereffect 4-84822  
 Fe<sub>80</sub>B<sub>20</sub> amorphous, mag. hysteresis loops after heat treatment below Curie point 4-80781  
 Fe<sub>80</sub>B<sub>20</sub> amorphous alloy, He ion irradiat., blister and bubble form., TEM obs. 4-108434  
 Fe<sub>80</sub>B<sub>20</sub> amorphous foil, sputtered ductile, mag. and structural study 4-80782  
 Fe<sub>80</sub>B<sub>20</sub>, Fe<sub>70</sub>Cr<sub>10</sub>B<sub>20</sub> and Fe<sub>70</sub>Cr<sub>5</sub>Ni<sub>5</sub>B<sub>20</sub> amorphous alloys, elastic characts. and microplastic deform 4-93325  
 Fe<sub>80</sub>B<sub>20</sub> metallic glass, radial distrib. function asymmetry by EXAFS 4-93133  
 Fe<sub>82</sub>B<sub>18</sub>-Al<sub>2</sub>O<sub>3</sub> granular system, XPS anal., surface composition study 4-81113  
 Fe<sub>83</sub>B<sub>17</sub> ferromag., spin-polarised L<sub>23</sub>M<sub>23</sub>M<sub>23</sub> AES 4-104703  
 Fe<sub>83</sub>B<sub>17</sub> metallic glasses, struct., neutron diff. studies (*Chinese*) 4-98020  
 Fe<sub>84</sub>B<sub>16</sub> amorphous, microcrystalline domain obs. 4-113333  
 Fe<sub>86</sub>B<sub>14</sub> amorphous, thermoelectric power and elec. cond. (*Russian*) 4-65660  
 Fe<sub>86</sub>B<sub>14</sub> amorphous layer form. on surface using elec. spark 4-65180  
 Fe<sub>87</sub>B<sub>13</sub> itinerant magnetism in metallic glasses 4-104438  
 (Fe<sub>82</sub>B<sub>18</sub>)<sub>0.90</sub>La<sub>0.05</sub>Ru<sub>0.05</sub> amorphous metal alloys, ferromag. reson. and g-factor 4-71188  
 Fe<sub>87</sub>B<sub>13</sub>Si<sub>10</sub> amorphous, isothermal crystallisation and mag. props. (*Russian*) 4-65384  
 Fe<sub>82</sub>B<sub>18</sub>Si<sub>6</sub> amorphous and crystallised, UPS, XPS and EELS 4-104122  
 Fe<sub>82</sub>B<sub>18</sub>Si<sub>6</sub> ferromagnet, spin-flip Stoner excitations, EELS studies 4-104410  
 Fe<sub>80</sub>B<sub>20</sub>Si<sub>8</sub>-Al<sub>3</sub> crystallisation and mag. props. study 4-114137  
 Fe<sub>81</sub>B<sub>13</sub>Si<sub>5</sub>Si<sub>2</sub>C<sub>2</sub> glass, primary crystallisation and α-Fe dendrites, EELS studies 4-84202  
 Fe<sub>81</sub>B<sub>13</sub>Si<sub>5</sub>C<sub>2</sub>, Metglas 3605SC, mag. and hyperfine interactions 4-71223  
 Fe<sub>70</sub>Co<sub>10</sub>B<sub>20</sub> amorphous, mag. aftereffects after field annealing 4-84823  
 Fe<sub>70</sub>Co<sub>10</sub>B<sub>14</sub>Si<sub>6</sub> amorphous, extended freq. anal. of permeability aftereffect 4-84822  
 Fe<sub>70</sub>Co<sub>10</sub>Ni<sub>20</sub>-Cr<sub>2</sub>B<sub>14</sub>Si<sub>6</sub> metallic glass, mag. props. study 4-84790  
 Fe<sub>70</sub>Co<sub>10</sub>Ni<sub>10</sub>P<sub>10</sub>B<sub>10</sub> amorphous, struct. relax. processes, dilatometric anal. (*Russian*) 4-92394  
 (Fe<sub>100-x</sub>Co<sub>x</sub>)<sub>70</sub>Fe<sub>16</sub>O<sub>8</sub>, thermal effects of Co moderate substitutions 4-71124  
 (FeCo)SiB nonmagnetostriuctive amorphous ribbons for magnetic cores, DC and AC magnetic characts. 4-92939  
 Fe<sub>70</sub>Co<sub>7</sub>Si<sub>15</sub>B<sub>10</sub> amorphous, mag. noise study (*Russian*) 4-65846  
 Fe<sub>70</sub>Co<sub>7</sub>Si<sub>15</sub>B<sub>10</sub> amorphous, struct. relax. processes, dilatometric anal. (*Russian*) 4-92394  
 Fe<sub>70</sub>Co<sub>7</sub>Si<sub>15</sub>B<sub>10</sub> amorphous, mag. permeability, annealing in transverse mag. field (*Russian*) 4-104467  
 Fe<sub>70</sub>Co<sub>7</sub>Si<sub>15</sub>B<sub>10</sub>, zero magnetostrictive amorphous alloy, permeability and field-induced anisotropy 4-71056  
 Fe<sub>72</sub>Co<sub>18</sub>Si<sub>10</sub>B<sub>4</sub> metallic glass, crystn. kinetics 4-65187  
 Fe<sub>70</sub>Co<sub>10</sub>-Si<sub>15</sub>B<sub>15</sub> magnetostrictive amorphous alloys, stress-induced anisotropy and permeability 4-71055  
 (Fe<sub>80</sub>Cr<sub>10</sub>-x)<sub>70</sub> metallic glasses, onset of magnetism, Mossbauer spectra 4-71217  
 Fe<sub>80-x</sub>Hf<sub>10</sub>Si<sub>10</sub>Al<sub>3</sub> metallic glass, crystallisation and hyperfine fields 4-71030  
 Fe<sub>80</sub>M<sub>2</sub>B<sub>17</sub> (M=transition metal) metallic glass, elec. resist., transition metal effects 4-108832  
 Fe<sub>80</sub>M<sub>2</sub>B<sub>17</sub> based glassy alloys, ferromag. exchange and Curie temp. 4-76129  
 (Fe<sub>64</sub>Mn<sub>0.36</sub>)<sub>75</sub>P<sub>16</sub>B<sub>9</sub>Al<sub>3</sub> spin glass transition calcs. 4-88667  
 Fe<sub>78</sub>Mo<sub>2</sub>B<sub>20</sub> metallic glass, elec. resist., crystallisation and thermoelec. power, annealing effects 4-108831  
 (Fe<sub>80</sub>Ni<sub>20</sub>)<sub>1-x</sub>B<sub>x</sub> amorphous alloys, mag. moments, temp. variation 4-76122  
 (Fe<sub>80</sub>Ni<sub>20</sub>)<sub>1-x</sub>B<sub>x</sub> amorphous alloys, elec. cond. and struct. stability 4-92693  
 (Fe<sub>80</sub>Ni<sub>20</sub>)<sub>1-x</sub>B<sub>x</sub> metallic glass, Mossbauer and soft X-ray appearance pot. spectra studies 4-76292  
 Fe<sub>39</sub>Ni<sub>39</sub>B<sub>22</sub> metallic glass ribbon, pull-out tests in different matrices 4-71717

## boron alloys continued

- Fe<sub>80</sub>Ni<sub>20</sub>B<sub>20</sub> amorphous, mag. hysteresis loops after heat treatment below Curie point 4-80781  
 Fe<sub>80</sub>Ni<sub>20</sub>B<sub>20</sub> amorphous, structural relax., contraction and creep meas. 4-85195  
 Fe<sub>80</sub>Ni<sub>20</sub>B<sub>20</sub> amorphous alloys, neutron irradiat., mag. props. isotope effects 4-75541  
 Fe<sub>80</sub>Ni<sub>20</sub>B<sub>20</sub> amorphous alloy, ferromag. resonance and antiresonance studies 4-76256  
 Fe<sub>80</sub>Ni<sub>20</sub>B<sub>20</sub> amorphous alloys, as-quenched, mag. aftereffect 4-84826  
 Fe<sub>80</sub>Ni<sub>20</sub>B<sub>20</sub> foil, thermal expansion coeff. and isothermal compressibility (*Russian*) 4-65421  
 Fe<sub>80</sub>Ni<sub>20</sub>B<sub>20</sub> metallic glass, melt surface tension and embrittlement, effects of elemental additions and superheat 4-65184  
 Fe<sub>80</sub>Ni<sub>20</sub>B<sub>20</sub> metallic glass, amorphous-cryst. transition kinetics, elec. resist. meas. 4-70039  
 Fe<sub>80</sub>Ni<sub>20</sub>B<sub>20</sub> metallic glass, strength and plasticity, temp. depend. (*Russian*) 4-71692  
 Fe<sub>80</sub>Ni<sub>20</sub>B<sub>20</sub> metallic glass, field ion microscopic study at liq. H temp. 4-75311  
 Fe<sub>80</sub>Ni<sub>20</sub>B<sub>20</sub> sliding friction and struct. relax. 4-99606  
 Fe<sub>80-x</sub>Ni<sub>20</sub>B<sub>20</sub> amorphous sputtered films, ferromag. saturation 4-61520  
 Fe<sub>80-x</sub>Ni<sub>20</sub>B<sub>20</sub> amorphous, mag. props. study 4-84840  
 Fe<sub>80</sub>Ni<sub>20</sub>B<sub>20</sub> foil, amorphous-cryst. transition, elec. resist. variations 4-65182  
 Fe<sub>80</sub>Ni<sub>20</sub>B<sub>20</sub>Mo<sub>4</sub> Metglas 2826 MB 5 keV He implantation, bubble growth, free vol. relax. model 4-103822  
 Fe<sub>78-x</sub>Ni<sub>18</sub>Mo<sub>4</sub> metallic glasses, short range order, EXAFS studies 4-60856  
 Fe<sub>75</sub>Ni<sub>15</sub>B<sub>10</sub>Si<sub>10</sub> metallic glass, Curie point relax. study 4-84791  
 Fe<sub>80</sub>Ni<sub>20</sub>B<sub>20</sub>Si<sub>2</sub> glassy ribbon, elec. and mag. props. 4-84604  
 Fe<sub>80</sub>Ni<sub>20</sub>-xSi<sub>10</sub>Si<sub>10</sub> metallic glasses, absolute thermoelec. power meas. 4-92701  
 FeNiCrMoBSi amorphous ribbons, magnetostriction, capacitance studies 4-61580  
 Fe<sub>13</sub>Ni<sub>6</sub>Cr<sub>3</sub>P<sub>14</sub>B<sub>6</sub> amorphous alloys, flame spray quenching, coating on metal substrates 4-71797  
 Fe<sub>73</sub>Ni<sub>13</sub>Cr<sub>14</sub>P<sub>12</sub>B<sub>6</sub> metallic glass, Mossbauer study of high press. 4-84880  
 Fe<sub>80</sub>Ni<sub>18</sub>Mo<sub>4</sub>B<sub>18</sub> metallic glass, cavitation erosion resistance 4-104880  
 Fe<sub>80</sub>Ni<sub>18</sub>Mo<sub>4</sub>B<sub>18</sub> metallic glass, elec. resist., crystallisation and thermoelec. power, annealing effects 4-108831  
 Fe<sub>73</sub>Ni<sub>13</sub>Mo<sub>4</sub>Si<sub>12</sub> metallic glass, mag. props., Mossbauer studies 4-109012  
 Fe<sub>73</sub>Ni<sub>13</sub>Mo<sub>4</sub>Si<sub>12</sub> metallic glass, elec. resist., crystallisation and thermoelec. power, annealing effects 4-108831  
 Fe<sub>72</sub>Ni<sub>15</sub>P<sub>14</sub>B<sub>6</sub> metallic glass, Mossbauer study of high press. 4-84880  
 Fe<sub>80</sub>Ni<sub>20</sub>P<sub>14</sub>B<sub>6</sub> amorphous isotropic ferromag., mag. excitations 4-71043  
 Fe<sub>80</sub>Ni<sub>20</sub>P<sub>14</sub>B<sub>6</sub> amorphous alloys, flame spray quenching, coating on metal substrates 4-71797  
 Fe<sub>80</sub>Ni<sub>20</sub>P<sub>14</sub>B<sub>6</sub> amorphous ribbons, mag. props. and struct., influence of laser annealing 4-88663  
 Fe<sub>80</sub>Ni<sub>20</sub>P<sub>14</sub>B<sub>6</sub> glass transition of thin film on substrate 4-92367  
 Fe<sub>80</sub>Ni<sub>20</sub>P<sub>14</sub>B<sub>6</sub> metallic glass, dynamical power loss annealing effects 4-76175  
 Fe<sub>80</sub>Ni<sub>20</sub>P<sub>14</sub>B<sub>6</sub> metallic glass, mag. permeability with AC and DC currents 4-76176  
 Fe<sub>80</sub>Ni<sub>20</sub>P<sub>14</sub>B<sub>6</sub> metallic glass, mag. props., cold rolling effects 4-104472  
 Fe<sub>80</sub>Ni<sub>20</sub>P<sub>14</sub>B<sub>6</sub> proton irradiat., crystallisation study 4-88099  
 Fe<sub>80</sub>Ni<sub>20</sub>P<sub>14</sub>B<sub>6</sub> amorphous, explosive loading of powder, three-dimens. parts prod. 4-114443  
 Fe<sub>80</sub>Ni<sub>20</sub>-P<sub>14</sub>B<sub>6</sub> amorphous, spin glass alloys, EPR meas. and mag. props. 4-84847  
 Fe<sub>80</sub>Ni<sub>20</sub>-P<sub>14</sub>B<sub>6</sub> amorphous ferromag. and reentrant alloys, ferromag. reson. study 4-84856  
 Fe<sub>73</sub>Ni<sub>13</sub>P<sub>14</sub>B<sub>6</sub>Al<sub>3</sub> metallic glass, Mossbauer study of high press. 4-84880  
 Fe<sub>73</sub>Ni<sub>13</sub>P<sub>14</sub>B<sub>6</sub>Si<sub>2</sub> metallic glass, Mossbauer study of high press. 4-84880  
 Fe<sub>72</sub>Ni<sub>15</sub>Si<sub>10</sub>B<sub>10</sub> metallic glass, Curie temp. press. depend. 4-84792  
 (Fe<sub>80</sub>Ni<sub>20</sub>-x)Si<sub>10</sub>B<sub>14</sub> metallic glass, short range ordering study 4-88108  
 Fe<sub>80</sub>Ni<sub>20</sub>-Si<sub>10</sub>B<sub>10</sub> metallic glass, correlated hyperfine interactions 4-70761  
 Fe<sub>80</sub>Ni<sub>20</sub>-Si<sub>10</sub>B<sub>10</sub> metallic glasses, mag. props. and chemical short-range order 4-114109  
 Fe<sub>73</sub>Si<sub>13</sub>B<sub>12</sub> metallic glass, Young's modulus, internal friction, mag. hysteresis loop 4-76215  
 Fe<sub>81</sub>Si<sub>13</sub>B<sub>14</sub> metallic glass, stress pattern mag. domains 4-76161  
 Fe<sub>80-x</sub>Si<sub>10</sub>B<sub>10</sub> amorphous alloy, crystallisation behaviour 4-75309  
 Fe<sub>80</sub>Si<sub>10</sub>-P<sub>14</sub>B<sub>6</sub> metallic glasses, mag. props., chem. composition depend. 4-76135  
 (Fe<sub>1-x</sub>V<sub>x</sub>)<sub>84</sub>B<sub>16</sub> amorphous alloys, mag. and elec. props. (*Chinese*) 4-114094  
 Li-B/LiNO<sub>3</sub> anode-electrolyte system, potentiostatic studies 4-66676  
 MnB<sub>2</sub> alloy, spontaneous magnetisation changes due to amorphisation (*Russian*) 4-104407  
 Mo-Al-B-C, welded joints, long-term strength characts. effect of alloying with N 4-109513  
 Mo-Zr-B, welded joints, long-term strength characts. effect of alloying with N 4-109513  
 Nd<sub>2</sub>Fe<sub>14</sub>B, cryst. struct., mag. props. 4-65828  
 Nd<sub>2</sub>Fe<sub>14</sub>B permanent magnet, cryst. struct. 4-70069  
 Nd<sub>2</sub>Fe<sub>14</sub>B, single crystal, mag. props. study 4-114143  
 Ni-B alloys, CVD deposited, microstruct. and mech. props. 4-71581  
 Ni-Cr-B surface coatings, phase composition, X-ray diff. 4-99377  
 Ni-Cr-B-Al detonation deposited coatings, wear resist. 4-62123  
 Ni-Cr-Co-B, melt spun superalloy, annealing, castability, ductility and microstruct. rel. to B additions 4-66323  
 Ni-Mn-P-B-Al alloys, amorphous, mag. props. studies 4-71086  
 Ni-Mo-B system, phase relationships at 1223K 4-104767  
 Ni-Si-B amorphous, cryst. form. on annealing, TEM study 4-75304  
 Ni-Si-B metallic glasses, Hall effect, mag. ordering near resist. minimum 4-75933  
 Ni-W-B system, phase relationships at 1223K 4-104767  
 Ni<sub>100-x</sub>B<sub>x</sub> metallic glasses, elec. props. 4-108830  
 Ni<sub>64</sub>B<sub>36</sub> metallic glasses, struct., neutron diff. studies (*Chinese*) 4-98020  
 Ni<sub>66</sub>B<sub>33</sub> glassy, Ni-Ni distrib., multishell modelling, EXAFS studies 4-60853  
 Ni<sub>81.5</sub>B<sub>18.5</sub>-P<sub>14</sub> metallic glasses, elec. props. 4-108830  
 Ni<sub>36</sub>Fe<sub>3</sub>Cr<sub>14</sub>P<sub>16</sub>B<sub>6</sub> metallic glass, surface oxidation in crystalline and amorphous states 4-89187  
 Ni<sub>64</sub>Fe<sub>4</sub>P<sub>0.14</sub>B<sub>0.06</sub> electronic struct. extreme UV photoemission 4-85066

**boron alloys continued**

- $\text{Ni}_{40}\text{Fe}_{40}\text{P}_{14}\text{B}_6$ , glassy metal, UPS study 4-76632  
 $\text{Ni}_{78-x}\text{Fe}_{22-x}\text{Si}_{12}\text{B}_{10}$  amorphous alloys, mag. props. 4-84794  
 $\text{Ni}_{75}\text{Si}_{16}\text{B}_{10}$  amorphous alloys, fatigue props. 4-66424  
 $\text{Ni}_{72}\text{Si}_{16}\text{B}_{14}$  metallic glass, strength and plasticity, temp. depend. (Russian) 4-71692  
 Pd-Ni-Si-Be-B liquid metal ion source for maskless ion implantation 4-58913  
 $\text{Pd}_{72}\text{B}_{24}$  metallic glass, comparison with  $\text{Pd}_{72}\text{Be}_{28}$ , structural features 4-113344  
 $\text{RPd}_3\text{B}_2$  (R=rare earth,  $x < 1$ ) valence state studies 4-70748  
 a-Si-Ge-B alloys, props. and electronic device appls. (Japanese) 4-92728  
 $\text{V-B}_2\text{C}$ , neutron irradi., temp. depend. of damage microstruct. 4-108455  
 $\text{V}_2\text{CrAl}_{1-x}\text{B}_x$ , melt spinning and phase transforms 4-114450  
 $\text{Y}_2\text{Fe}_{14}\text{B}$ , single crystal, mag. props. study 4-114143

**boron compounds**

- see also boron alloys  
 alkali halide:  $\text{BH}_4^-$ , IR and Raman spectra, Fermi resonances isotope shift 4-61695  
 borane linked polyhedral cages, B-B spin-spin coupling consts.,  $^{10}\text{B}$  and  $^{11}\text{B}$  NMR study 4-112198  
 cage cpds., polyhedral struct., 2-dimens.  $^{11}\text{B}$ - $^{11}\text{B}$  NMR spectrosc. investig. 4-64503  
 carboranes, polyhedral struct., 2-dimens.  $^{11}\text{B}$ - $^{11}\text{B}$  NMR spectrosc. investig. 4-64503  
 diamond, synthesis mechanism 4-71610  
 hydrides, polyhedral struct., 2-dimens.  $^{11}\text{B}$ - $^{11}\text{B}$  NMR spectrosc. investig. 4-64503  
 III-V semiconductors, phys. data, compilation, book 4-63420  
 metallaboranes, polyhedral struct., 2-dimens.  $^{11}\text{B}$ - $^{11}\text{B}$  NMR spectrosc. investig. 4-64503  
 metallacarboranes, polyhedral struct., 2-dimens.  $^{11}\text{B}$ - $^{11}\text{B}$  NMR spectrosc. investig. 4-64503  
 small-polaron electronic transport in boron carbides 4-75988  
 $\text{Al}_2\text{O}_3$ -BN-(AlON) composite ceramics, mech. props. (French) 4-81177  
 B containing ceramic neutron absorbing materials, survey of products and appls. (German) 4-83146  
 B-C thermoelectric materials, current status 4-75989  
 $\text{B}_{12}\text{As}_2$ , band struct., energy gaps, bonding, cluster approx. 4-70646  
 $\text{B}_{1-x}\text{C}_x$ , cond. mechanism, elec. cond., Seebeck coeff., and Hall coeff. meas. 4-70811  
 $\text{B}_{12}\text{C}_3$ ,  $^{13}\text{C}$  NMR study of C distrib. 4-114182  
 $\text{B}_2\text{C}$ , absorber materials for fast breeder reactor control rod systems, physical and chemical props. 4-83147  
 $\text{B}_4\text{C}$  based materials, resist. to corrosion by  $\text{H}_2\text{SO}_4$  soln. 4-62087  
 $\text{B}_4\text{C}$  control rod performance in PFR 4-91076  
 $\text{B}_4\text{C}$ , hardness and fracture toughness rel. to stoichiometry 4-62019  
 $\text{B}_4\text{C}$ , low energy Auger transitions 4-88909  
 $\text{B}_4\text{C}$ , struct. and mech. props., hot pressing conditions effect 4-61906  
 $\text{B}_4\text{C}$ , vacuum compatible absorbing materials, submm and mm refl. spectroscopy 4-108214  
 $\text{B}_4\text{C}/\text{B}$  fibre reinforced Ti-Al-V, fatigue crack growth behaviour 4-93374  
 BCN, ground state, geometry, transition state, isomerisation reaction, ab initio calcs. 4-71908  
 $\text{BCl}_3$ , selective dissoc. due to laser irradi. at low temps. (Chinese) 4-112239  
 BF, total energies calc. using electron cloud displacement model (Chinese) 4-74136  
 $\text{BF}_3$  counters, deterioration and recovery 4-102521  
 $\text{BF}_3$ , cryst., Raman spectra, correl. method anal. 4-66022  
 $\text{BF}_3$ , electron and thermal dissoc. 4-96700  
 $\text{BF}_3$ , IR intensities, charge flux param. and transferability 4-69072  
 $\text{BF}_3\text{-CO}(\text{N}_2)$ , weakly bound complexes, Fourier transform IR spectra 4-87125  
 $(\text{BH}_2)^+$ , diatomics-in-mols. correl. diagrams 4-62166  
 BH, pot. energy curves, transition probabilities, fluoresc. obs. 4-59838  
 $\text{BH}_2$ , Renner-Teller pot. energy surfaces, analytic second derivatives 4-91250  
 $\text{B}_2\text{H}_6$ , empirical harmonic pot. function determ. 4-59871  
 $\text{BH}_2\text{NO}_2$ , electronic struct. calc. 4-87032  
 $(\text{BH}_2\text{NO})^+$ , orbital interactions, charge transfer, and bond form., CNDO/2D study 4-59641  
 BN band struct., APW calc. method appl. 4-92608  
 BN based polycrystalline materials, thermophys. props. 4-61159  
 BN coatings on silica by hexachloroborazine decomposition 4-71587  
 BN, cubic, prep. of small particles by electron irradi. of hexagonal BN in TEM 4-61895  
 BN film, CVD, on Si, as B diffusion source 4-98359  
 BN films, glow discharge prep., insulator for semicond. device passivation 4-85120  
 BN, films, interaction with Ni at high temps. 4-70583  
 BN gate insulators, CVD growth on InP, ellipsometry, XPS, AES, cond. meas. 4-80443  
 BN, low energy Auger transitions 4-88909  
 BN powders, optical props., refl. spectrum 0.2 to 25  $\mu\text{m}$  4-61730  
 BN RF sputter deposited films, struct. and optical props. rel. to sputtering conditions 4-88415  
 BN, shear strength meas., high temps. and pressures 4-81376  
 BN with adsorbed ethylene film, thermodynamic props. study 4-104068  
 BN-P film in InP, grown by CVD, elec. props. 4-99336  
 BN-InP, density of interface states 4-80443  
 $\text{B}_2\text{O}_2$ , geometrical struct., photoelectron spectra, ab initio MO calcs. 4-68932  
 $\text{B}_2\text{O}_2$  vapour, struct., photoelectron spectra, ab initio STO calcs. 4-83414  
 $\text{B}_2\text{O}_3$ , low energy Auger transitions 4-88909  
 $\text{B}_2\text{O}_3$ , molten, struct. anal. by X-ray radial distrib. method 4-113293  
 $\text{B}_2\text{O}_3$ , vapourisation, density of vapour meas., transpiration method 4-98259  
 $\text{B}_2\text{O}_3$ , vitreous, thermal expansion and specific heat 4-70417  
 $\text{B}_2\text{O}_3$ , vitreous, transition, struct., low freq. Raman spectra 4-66028  
 $\text{B}_2\text{O}_3\text{-Li}_2\text{O}$  glass, ionic cond. meas. 4-84457  
 $\text{B}_2\text{O}_3\text{-Li}_2\text{O}(\text{Li halides})_2$ , fast ion cond., press. effects 4-88336  
 $\text{B}_2\text{O}_6$ , empirical harmonic pot. function determ. 4-59871  
 BP, refractive index and elastic const. meas. 4-61647  
 $\text{B}_{12}\text{P}_2$ , band struct., energy gaps, bonding, cluster approx. 4-70646  
 $\text{BaO-B}_2\text{O}_3\text{-Fe}_2\text{O}_3$  system, magnetic vitroceraics, prep. and props. 4-93256  
 $\text{CuO-BF}_3$  van der Waals complex, microwave rot. spectrosc. obs. 4-78862  
 $(\text{CuO})_x\text{-(B}_2\text{O}_3\text{Li}_2\text{O})_{1-x}$  glass, EPR and mag. susceptibility meas. 4-61587

**boron compounds continued**

- $(\text{Fe}_2\text{O}_3)_x(\text{B}_2\text{O}_3\text{PbO})_{1-x}$  glass, mag. props. study 4-88654  
 $\text{Li}_2\text{O-B}_2\text{O}_3\text{-Fe}_2\text{O}_3$  system, magnetic vitroceraics, prep. and props. 4-93256  
 $\text{NCNN.BF}_3$  van der Waals complex, microwave rot. spectrosc. obs. 4-78862  
 $\text{NH}_3\text{-BH}_3$ , orbital interaction, charge transfer, bond form., CNDO/2 study 4-102597  
 $\text{N}_2\text{O.BF}_3$ , van der Waals complex, microwave rot. spectrosc. obs. 4-78862  
 $\text{Na}_2\text{O-B}_2\text{O}_3\text{-SiO}_2$  graded-index antirefl. coatings deposited by sol-gel process, laser damage thresholds, high power laser appls. 4-74673  
 Ni-B composites, electroless and electrodeposition 4-88990  
 $\text{PbO-B}_2\text{O}_3\text{-Bi}_2\text{O}_3\text{-Y}_2\text{O}_3\text{-Ga}_2\text{O}_3\text{-Fe}_2\text{O}_3$  phase diagram invest. 4-93208  
 $\text{Si:As}^+(\text{BF}_3)^+$ , implanted, rapid thermal annealing 4-88181  
 Si-BP-Si double heterojunction, current-voltage characteristics 4-80658  
 SiC-BN composites, thermal diffusivity anisotropy 4-84472  
 $\text{SiO}_2\text{-B}_2\text{O}_3\text{-Na}_2\text{CO}_3\text{-Fe}_2\text{O}_3$  glasses, coordination of Fe ions 4-88110  
 $\text{Ti}_2\text{S-B}_2\text{S}_3$  glass, NMR study and struct. 4-88726  
 $\text{V}_2\text{O}_5\text{-B}_2\text{O}_3$  glass, struct., IR spectra and elec. cond. 4-88107

**boronising see surface hardening**

**borosilicate glasses**

- alkali borosilicate glass rods, partially leached, abraded and unabraded strength rel. to heat treatment 4-89144  
 E-glass fabric, vol. resist. depend. on temp. and leaching parameters 4-70880  
 glass/alumina composites, density, crystallisation, elec. cond. 4-113937  
 neutron absorbing material, diffusion anal. of T thermal release 4-75536  
 nuclear waste, hot isostatic pressing 4-59330  
 radiation effects, point defects, microstructural changes, etching, leaching 4-70195  
 simulated nuclear waste glass, Na diffusion and leaching 4-11608  
 solar collector cover tubes, leached gradient index antirefl. surface use 4-114945  
 waste glasses, ion bombard., fracture toughness and leaching behaviour 4-75545  
 $\text{B}_2\text{O}_3\text{-SiO}_2\text{-TeO}_2$  glass, coordination, EXAFS and XANES studies 4-60851  
 $\text{K}_2\text{O-B}_2\text{O}_3\text{-SiO}_2$  glass, OH extinction coeff. determ., IR spectra 4-84958  
 $\text{Li}_2\text{O-B}_2\text{O}_3\text{-SiO}_2$ , phase-separated glass, dissoln. rate, influence of pH 4-84403  
 $\text{Li}_2\text{O-B}_2\text{O}_3\text{-SiO}_2$  glass, OH extinction coeff. determ., IR spectra 4-84958  
 $\text{Na}_2\text{O-B}_2\text{O}_3\text{-SiO}_2$  glass, OH extinction coeff. determ., IR spectra 4-84958  
 $\text{Na}_2\text{O-B}_2\text{O}_3\text{-SiO}_2$  glass melts, viscosity meas. 4-98329  
 $\text{Na}_2\text{O-B}_2\text{O}_3\text{-SiO}_2\text{-CaO-Al}_2\text{O}_3$  glasses UV-transmissivity of a tempered sodium-borosilicate glass (German) 4-88856  
 $\text{Na}_2\text{O-K}_2\text{O-Al}_2\text{O}_3\text{-B}_2\text{O}_3\text{-SiO}_2$  glasses, nucl. spin stimulated echoes, pulsed NMR meas. 4-92976  
 $\text{SiO}_2\text{-B}_2\text{O}_3\text{-Al}_2\text{O}_3\text{-Na}_2\text{O}$  glass, porous, precipitation of colloidal silica and pore size distrib. 4-109412  
 $\text{SiO}_2\text{-B}_2\text{O}_3\text{-Na}_2\text{CO}_3\text{-Fe}_2\text{O}_3$  glasses, coordination of Fe ions 4-88110  
 $\text{ZrO}_2\text{-La}_2\text{O}_3\text{-B}_2\text{O}_3\text{-SiO}_2$ , radioactive waste disposal, long term leaching 4-111607

**Bormann effect see X-ray crystallography; X-ray diffraction**

**Bose-Einstein statistics see quantum statistical mechanics**

**Bose gas see boson systems**

**boson fluids see boson systems**

**boson systems**

- see also liquid helium-4; quantum statistical mechanics  
 Bose fluid, excitation spectrum, struct. factor and sound vel. 4-104014  
 Bose gas phase transition, temp. depend. for ideal homogeneous gas 4-63658  
 Bose-Einstein condensation in finite noninteracting systems: a relativistic gas with pair production 4-90486  
 Bose-Einstein gases, exp. eqns. of state (German) 4-95297  
 boson hard sphere fluid, correlation functions, struct. factor 4-98380  
 bounds on exponentials of local number operators 4-78232  
 collective field treatment of confined fermions and bosons in the large- $N$  approximation 4-58736  
 free Bose fields, infrared representations 4-101745  
 gas in 1-D, correlation functions in repulsive case 4-78233  
 Gibbs phase rule, rel. to bulk and mol. props. and quantum systems 4-11086  
 ideal Bose gas, magnetised, crit. props. 4-58734  
 interacting fermion-boson systems, microscopic formulation 4-90959  
 level density fluctuations, comparison with Gaussian orthogonal ensemble 4-78236  
 many boson and many fermion systems, perturbation theory approach 4-58732  
 minimum-uncertainty coherent states, identity resolution, charged boson coherent states example 4-110932  
 nonideal Bose systems, quantum crossover behaviour 4-63652  
 number operator functions change by antinormal ordering 4-78238  
 one-dimensional, many-body props. 4-84475  
 open Bose gas, time evolution, exact kinetic equation 4-90481  
 quantum, linear response functions, density-wave-instability 4-113740  
 random field effects, critical and crossover phenomena in Hartree limit 4-111016  
 semiconductors, coherent pairing of excitons and biexciton Bose-Einstein condensation 4-88459  
 spatially periodic struct. theory, Bose excitation Green's functions 4-73340  
 spinless bosons, degeneracy splitting 4-86236  
 spinless bosons, pairwise  $\delta$ -function potentials, degeneracy splitting 4-86237  
 tachyon ideal gases, covariant statistical mechanics formalism 4-95295  
 two fluid model, symmetry breaking and Ward identities, diagrammatic anal. 4-73339  
 two level system coupled to bosons, thermodynamic props. 4-78240  
 two-dimensional system, fractional quantum Hall effect 4-92757  
 wave props. of identical particles 4-111017  
 $^4\text{He}$ , liq., momentum distrib. for Bose systems with mixture formalism, hypernetted-chain theory 4-98384

**bosons**

- see also alpha particles; boson systems; deuterons; gravitons; intermediate bosons; meson resonances; mesons; photons  
 boson mass spectrum; gauge group  $\text{SO}(d)$ , Kaluza-Klein theories on hyperspheres 4-106215

**bosons continued**

- quantum interference test of fermionic rotation props. of charged spinless boson 4-73292
- quantum mechanical Hamiltonian lower bound, relativistic kinetic energy 4-90466
- quantum-statistical distributions, R-inherent quantum mechanics, four-dimensional symmetry 4-95294
- spin-0, axion mass and couplings from macroscopic forces 4-90790
- spin-1 particle, anomalous moment Hamiltonian exact diagonalisation expression 4-73758

**boundaries** see *boundary layers; boundary value problems; grain boundaries; metal-insulator boundaries; semiconductor-insulator boundaries; semiconductor-metal boundaries*

**boundary-elements methods**

- 3D fracture mechanics, boundary integral equation-boundary element method appls. (*Chinese*) 4-97398
- acoustic scattering, boundary element methods and their asymptotic convergence 4-83751
- complex variable boundary-element method expansion into finite series of analytic functions 4-107992
- crack thermoelastic boundary integro-differential eqn. formulation 4-64882
- eddy current density, boundary-element computation in contiguous domains 4-64650
- elasticity, Signorini and friction free boundary problems using boundary elements, Trefftz approach 4-63513
- elasticity problems, appl. of weak formulation of boundary integral equations 4-78137
- function approximation, Lagrangian, spline and weighted finite difference methods 4-64848
- hybrid finite element boundary element solutions using half-space Green's functions 4-59951
- integral eqn. axisymmetric stress analysis, interior point solns. 4-63510
- plate bending, comparative analysis of boundary methods and finite element methods 4-112727
- potential theory, boundary-element method modification for singularities and Neumann eqn. 4-63509
- thermoelasticity, non-stationary, appl. of boundary element problem 4-112711
- thin plate flexure, Kirchhoff boundary-element theory 4-64847
- two-dimensional EM field problems, appl. of boundary-element method 4-83516
- two-dimensional magnetostatics, nonlinear boundary element method 4-59950
- two-dimensional plane EM wave scattering from dielec. cylinders, boundary element method 4-79019

**boundary layer flow** see *boundary layers*

**boundary layer turbulence**

- see also *atmospheric boundary layer*
- acoustic radiation anal. (*French*) 4-112632
- aerodynamic sound generation by turbulent boundary-layer flows along walls (*German*) 4-112637
- aircraft in wind tunnel, wall press. fluctuations 4-108150
- asymptotic theory of turbulent separation 4-69745
- axially rotating pipe, three dimens. turbulent boundary layer development 4-87690
- baseballs, aerodynamic drag crisis and its effect on flight 4-63440
- bodies of revolution, computation of thick axisymmetric boundary layers and wakes 4-79600
- boundary layers, three dimensional, instabilities excitation and development 4-87679
- boundary-layer interaction with shock wave at compression corner 4-87676
- buildings boundary-layer flows, near-wake parameters 4-79599
- cascade three-dimensional boundary layer approach flow, effect of degree of turbulence 4-69746
- complex three-dimensional turbulent shear flows with longitudinal vorticity 4-69747
- compliant coatings interactions with boundary-layer flows 4-60366
- cylinder, rotating, in crossflow at two turbulence level, aerodynamic forces, separation 4-103357
- cylindrical and conical flow regime, in 3D shock/boundary layer interactions 4-64978
- defining relations derivation 4-97514
- finite element formulation of thermal boundary layers 4-103305
- flat plate, boundary layer flow stability for small disturbances (*German*) 4-83883
- flat plate, turbulent boundary layer response to external flow pulsation 4-87695
- flat plate with bluff front, turbulent boundary layer response to artificial disturbances 4-112839
- flat-plate with diffusion flame, boundary layer turbulent props. 4-97507
- flow in neighbourhood of trailing edge of plate at zero angle of attack 4-112827
- fluctuating surface shear stresses on bluff bodies 4-91803
- forced convection systems, correl. of thermophoretically modified particle diffusion deposition rates 4-87703
- free stream turbulence effect 4-103311
- free-convection flow past exponentially accelerated vertical plate, theory 4-67610
- frictional drag coeffs., polymer soln. addition effects 4-112835
- fully developed turbulence inside and outside a boundary layer 4-108066
- heat transfer, temp. depend. physical props. influence 4-103312
- heat transfer and friction effect on cylinder in longitudinal turbulent air flow with variable physical props. 4-83891
- heat transfer prediction for turbulent boundary layers over rough surfaces with transpiration 4-75010
- heat transfer through turbulent and transitional boundary layers on convexly curved wall 4-60417
- hypersonic flow, three-dimens., on sharp cone at angle of attack, heat transfer interactions 4-79621
- incompressible flows over infinite swept wings, inverse mode boundary layer calcs. 4-112832
- incompressible fluid, turbulent flow, vel. and press. fluctuations 4-91804
- incompressible internal flows, inverse problem 4-87684
- interaction theory 4-97479
- intermittent separation mechanism studied by flow visualisation 4-87687
- isotropic turbulence response to spectrally local disturbance 4-112830
- jet, condensation, thermal and vel. boundary layers 4-103306

**boundary layer turbulence continued**

- laminar-turbulent boundary layer transition, thermal imaging system 4-112814
- liquid film, vaporising, laminar and turbulent boundary layers, momentum, heat and mass transfer 4-60414
- local heat transfer coeff. in turbulent boundary layer at supersonic speed 4-103308
- longitudinal flow around cylindrical body, heat exchange and friction (*Russian*) 4-74998
- mean flow field and heat transfer along cooled supersonic diffuser 4-113077
- method of calculating boundary layer in longitudinal mag. field (*Russian*) 4-112840
- MHD free-convection flow near vertical oscillating plate, theory 4-67618
- MHD free-convection oscillatory flow past porous limiting surface; effects of Joule heating and viscous dissipation 4-67616
- MHD free-convective oscillatory flow past porous limiting surface, effects of Joule heating and viscous dissipation 4-67615
- natural gaseous inhomogeneities evolution 4-79619
- near-wall similarity in a pressure-driven three-dimensional turbulent boundary layer 4-103309
- near-wall similarity models for three dimens. layers 4-87692
- ocean floor, viscous sublayer and buffer layer, turbulence spectra 4-82067
- optimisation via integral method (*French*) 4-60393
- oscillatory smooth turbulent flow against wall, model 4-108065
- periodically fluctuating flow in cascade, unsteady boundary layer 4-97510
- permeable plate with blown gas, limiting relative friction law 4-69819
- polymer fibres, cooling during melt spinning process 4-60258
- porous flat plate, isothermal turbulent flow in wake downstream of injection segment 4-75028
- pressure driven three dimens. boundary layers, direct force wall shear meas. 4-87689
- pressure driven three dimens. turbulent boundary layers, near-wall similarity 4-87693
- profile with condensation heat supply, stationary transonic flow, shock waves (*German*) 4-83922
- profiles, boundary layer calc. with laminar transition and turbulent flow zones 4-74999
- recirculating region in flow past surface-mounted obstacle 4-97516
- rotation symmetrical spaces with curved walls, frictionless stagnation flow (*German*) 4-83956
- rough surface boundary layer behaviour in turbulent wake presence 4-87724
- round jet in cross flow, initial conditions, Reynolds no. effects and near field characteristics (*German*) 4-97517
- secondary flow around unsymmetric corners 4-60391
- shear flow conf., St. Louis, Missouri, USA, June 1982 4-86119
- shear stress turbulent fluctuations at wall, hot-wire anemometry study 4-112834
- shear-driven 3D turbulent boundary layers, near-wall similarity 4-103310
- shear-driven three dimens. turbulent boundary layers, near-wall similarity 4-87694
- shock wave effects, form. of separation region, geometrical characteristics 4-112836
- skin friction meas. using hot element gauges (*French*) 4-65045
- smooth rectangular duct, experimental study 4-97513
- sound absorpt. by turbulence and other hydrodynamic flows 4-60434
- spectral analogy between temp. and vel. fluctuations 4-97511
- square building model, boundary layer flows, press. fluctuations 4-79572
- stagnation-point boundary layers, injection induced turbulence 4-64932
- steady turbulent flows in adverse pressure gradients numerical calculations 4-112837
- streamwise vel. fluctuations hot wire meas. 4-79570
- strip inserted in boundary layer, effects on plane surface heat transfer 4-87699
- supersonic boundary layers, laminar to turbulent transitions, stability 4-79554
- temperature fluctuation meas. correction, using cold wires 4-60567
- three-dimensional, near-wall similarity model 4-103301
- Tollmien-Schlichting wave, excitation in boundary layer by acoustic and vortex disturbance scatt. 4-91792
- Tollmien-Schlichting wave thermal excitation in boundary layer 4-112916
- turbomachine cascade profile, friction and heat transfer calcs. 4-112833
- turbulent flow over large-amplitude wavy surfaces, vel. meas. 4-60380
- turbulent layer near wall in presence of positive press. gradient (*Russian*) 4-87685
- unseparated shock wave/turbulent boundary-layer interaction, hot wire meas. 4-97506
- unsteady laminar and turbulent boundary layers characts. 4-60365
- unsteady layers, near wall region behavior, press. grad. 4-87691
- vibrating surface, boundary layer transition, unstable wave excitation 4-91791
- viscous laminar sublayer 4-60390
- vorticity generation and decay at rigid boundaries 4-75030
- wall heat flux, double-step change effect 4-60395
- wall jet problem, boundary layer control by means of strong injection 4-97710
- wall pressure spectra for equilib. turbulent boundary layers (*Japanese*) 4-83882
- water flow, turbulent boundary layer with gas injection, press. fluctuations 4-103316
- wave props. and shear stress 4-79611
- windfarms electric power generation capacity, effects of wind turbine generator clusters 4-114890
- He II, flowing, heat transport, transition heat flux limitations 4-80323

**boundary layer turbulent flow** see *boundary layer turbulence*

**boundary layers**

- see also *atmospheric boundary layer; boundary layer turbulence*
- air cross flow, vel. fluctuations in space between tubes in bundles 4-83892
- aquatic animals, actively-moving, boundary layer stability (*Russian*) 4-72280
- asymmetric flowfield development on slender body, laminar boundary layer separation 4-64951
- axially symmetric flow round two spherical discs by viscous noncompressible fluid flow (*Russian*) 4-67980

## boundary layers continued

- axisymmetric supersonic laval nozzles; discharge coeff., inlet conditions effect 4-103363
- Blasius boundary layer, three dims., instability calcs. 4-64917
- Boltzmann eqn. with small Knudsen number, singular perturbation method anal. (Chinese) 4-97610
- n-butanol- $N_2$ , heat and mass transfer in a laminar boundary layer under mist formation (Japanese) 4-97477
- capillary flow, hydrodynamics, no-slip boundary condition 4-60549
- cavitation phenomena within regions of flow separation 4-60468
- cholesteric liquid crystals, hydrodynamics in coarse-grained limit 4-87700
- combined flow field of moving wall with parallel wall jet 4-60472
- compressible, spatial growth of disturbances 4-87752
- compressible boundary layer on radial blade rotating at high speed 4-112929
- compressible laminar boundary layer flow, numerical soln. 4-87666
- compressible laminar boundary layers along curved walls, suction, cooling, instability 4-64912
- compressible rotating gas, viscous Ekman layer effects 4-97581
- convection, natural, from isothermal sphere submerged in infinite Bousinesq fluid 4-75022
- convective heat transfer, physical and computational aspects, book 4-86128
- convective heat transfer in laminar flow over flat plate, approx. integral methods improvement 4-75020
- cooling process of hot steel plate by laminar water bar, prediction modelling 4-93315
- Crack border-free surface intersection analysis 4-79515
- curved duct flow, secondary motion, turbulent and laminar flow, vel. meas. 4-87805
- curvilinear shallow elements of structures, optimal design problems 4-91729
- Darcian free convection boundary layer flow about semi-infinite vertical plate 4-112879
- delta wing, viscous interaction, 3D boundary layer 4-69786
- effusion-cooling, fouling rate advantages, particulate thermophoresis effect 4-65011
- Ekman layer flow during spin-up of thermally stratified fluid 4-100680
- electrostatic cooling, development of flow vel. in boundary layer (Japanese) 4-84098
- enclosed cavity, natural convection, buoyancy driven flow, boundary layers 4-87714
- entrainment rate, initial values and transverse vel. for Patankar-Spalding method 4-79553
- entry flow in weakly curved ducts 4-91841
- exterior irrotational flow, three dims., boundary layer free interaction 4-112816
- external heating of a flat plate in a convective flow 4-97555
- film boiling in laminar boundary-layer flow along a horizontal plate surface 4-97473
- finite triangular wing, hypersonic boundary layer flow 4-97606
- flat plate boundary layers, wave packet calcs. from Navier-Stokes eqns. (German) 4-83884
- flow noises, review (Chinese) 4-95123
- fluid dynamics, numerical methods, book 4-110817
- forced convection heat transfer through self-similar thermal boundary layers on plane and axisymmetric bodies 4-64914
- forced convection systems, correl. of thermophoretically modified particle diffusion deposition rates 4-87703
- free stream turbulence effect on flow round bluff bodies 4-64930
- frozen plasma boundary-layer flows over isothermal flat plates, parametric study 4-65063
- gas-liquid flows, conf., Grenoble, France (Sept. 1983) 4-58558
- glaciers obeying Glen's law, near-surface flow 4-72619
- heat flux gage calibration for skin friction meas. 4-97723
- heat transfer and friction effect on cylinder in longitudinal turbulent air flow with variable physical props. 4-83891
- horizontal cylinder floating on free surface, wave pot., expansion theory 4-108084
- hydraulic jumps, simulation in presence of rot. and mountains 4-62919
- hydromagnetic free convection with mass transfer in rotation fluid, effects of Hall current 4-101134
- hypersonic flow unsteady three. dims.: boundary layer interaction 4-112943
- hypersonic viscous gas flow, boundary layer perturbation propag., entropy layer effect 4-60457
- ice, formation on flat surfaces, convective boundary layers 4-112811
- ice formation in water flow between two horizontal parallel plates, transition phenomenon 4-64834
- incompressible flow, press. hole problem, boundary layer effects 4-79571
- incompressible flow past a semi-infinite flat plate in a stream with uniform shear 4-97478
- incompressible fluid boundary layer on moving surface of cylinder 4-112810
- incompressible two dims. pot. flow, compressor cascade, inverse boundary layer 4-97509
- inert compressible gas confined between infinite parallel planar walls, response to rapid boundary heating 4-87541
- infinite domain, steady flow round airfoil, numerical calc., grid size reduction by higher order far field asymptotics 4-87686
- interacting boundary layers and heat transfer 4-87665
- interaction theory 4-97479
- inviscid shear flow, surface wave generation 4-75052
- kinetic boundary layer, Klein-Kramers eqn. 4-111079
- laminar and incompressible boundary layer flow induced by an airfoil (German) 4-64916
- laminar boundary layer, multifold series expansion anal. appl. 4-112808
- laminar boundary-layer flow on a rotating sphere, numerical prediction 4-64913
- laminar boundary layer in rotating compressible flow over an infinite disc 4-75045
- laminar film condensation in nonuniform gravity, approximate method 4-69735
- laminar flow, Dorodnitsyn finite element formulation 4-112809
- laminar flow, separated forced convection in cavities, finite difference anal. 4-112812
- laminar free convection from vertical flat plate 4-75007
- laminar-natural convection heat transfer from slender cone to power-law fluid 4-60399
- laminar-turbulent boundary layer transition, thermal imaging system 4-112814

## boundary layers continued

- linear Gortler instability of boundary layer flow over concave wall, heating effect 4-64920
- liquid film flow over reducer surface model 4-91790
- liquid flow over chemically reactive particle, conc. and temp. fields 4-79677
- liquid flow over wavy boundary, numerical simulation 4-79608
- liquid metals, flow through channel with transverse mag. field, in elect. insulated channel 4-75093
- liquid-metal MHD open-channel flows 4-97701
- lubricated walls, boundary layer local nonsimilarity solns. 4-97471
- Marangoni boundary layers, axially symmetric 4-97524
- mass transfer effects on flow past vertical plate, variable temp. or const. heat flux 4-101130
- mass transport around a horizontal cylinder beneath waves 4-60445
- mathematic developments (German) 4-82684
- mixed convection about horizontal heated surface in fluid-saturated porous medium, non-similar boundary layer anal. 4-69752
- mixing layer, 3-dims., eqns. of motion, numerical soln. for blunt bodies (Russian) 4-64915
- NASA GA(W)-1 airfoil, separated flow study 4-97490
- natural convection in density-stratified layers in rectangular vessel, flow patterns 4-97528
- natural convection regime in rectangular cavity 4-112872
- nematic-substrate interaction, rel. to boundary layer phase transition 4-88088
- nonlinear resonant interaction of acoustic fields with Tollmien-Schlichting waves in flat channel 4-69826
- nonlinear stability, nonparallelism, three dimensionality and mode interaction effects 4-97515
- nonselfsimilar unsteady boundary-layer eqn. soln. 4-60368
- nonsimilar stratified flow over vertical flat plate unsteady incompressible laminar free convection boundary layer 4-97639
- nonspherical objects at high Rayleigh number, natural convection mass transfer 4-79577
- nonuniform approach flow, laminar boundary layer eqns., uniform suction effect 4-87664
- Oldroyd fluid, boundary layer flow along vertical wall 4-74987
- Oldroyd-B fluid, plane and axisymmetric stagnation flows 4-97476
- oscillating bluff bodies, separated flow, vortex shedding 4-91816
- oscillatory flow past infinite porous vertical plate, suction and free convection effects 4-75081
- packed spheres beds, heat transfer, local aerodynamics 4-97543
- particle deposition by diffusion and interception from boundary layer flows 4-97472
- particle deposition from laminar boundary layer, wall suction and thermophoresis effect 4-97474
- polymer fibres, cooling during melt spinning process 4-60258
- power law fluids, forced convection over a flat plate 4-108094
- power-law fluid, flow over flat plate, boundary value problems 4-87764
- profiles, boundary layer calc. with laminar transition and turbulent flow zones 4-74999
- propane gas flow around heated cylinders, heat transfer, temp. and pyrolysis effects 4-75005
- quartz glass, ablation, boundary layer, nonequilib. physicochemical processes 4-71967
- radial filling of rotating cylinder, Ekman layers 4-75036
- Rayleigh-Benard convection problem, boundary layer type solns. 4-75018
- rotating and translating cylinder, time-dependent boundary layer flow 4-75042
- rotating compressible laminar boundary layer, similar solns. and integral quantities 4-112888
- rotating disk, boundary layer transition, spiral vortices 4-83910
- second grade incompressible fluid flow past an infinite porous plate, exact soln. 4-108096
- secondary flow and vorticity, development in curved ducts, cascades and rotors 4-87739
- separating boundary layers, upstream influence, downstream influence in channel flow 4-103285
- separation criteria calc. for three dims., boundary-layer 4-97491
- shell, elastic, fluid-filled, forced vibrs., effect of viscosity 4-74946
- skin friction meas. by laser interferometer in three dims., flows 4-97505
- solid walls in 3D subsonic wind tunnels, boundary layers effect 4-79552
- spiral vortices behaviour on rot. cone in axial flow 4-112887
- steady laminar boundary layers, multifold series expansion soln. 4-60369
- Stefan type free boundary problem soln. in cylindrical symm. 4-108077
- streamlines calc. from wall press. on fusiform body 4-91793
- streamwise corner, laminar boundary layer stability 4-60374
- subsonic laminar separation from discontinuity edge of profile 4-108063
- supercritical airfoil, self-sustained oscils. of a shock wave 4-103359
- supersonic boundary layers, laminar to turbulent transitions, stability 4-79554
- supersonic flow past oscillating cone, boundary layer, blowing influence 4-69784
- supersonic impulse turbine blade cascade, flow and losses in blade passage and design criteria 4-103335
- supersonic laminar flow past flat plate, boundary layer separation 4-97603
- symmetric baroclinic instability for small Ekman numbers 4-101146
- Taylor columns over topography, temporal evolution 4-62843
- thermal, along semi-infinite plate with variable surface temp., similar solns. 4-75021
- thermopolar fluid, elec. cond., laminar free convection flow from vertical plate 4-97475
- three dimensional, instabilities excitation and development 4-87679
- time-dependent natural convection in Hele-Shaw cells, boundary layer instability (German) 4-83901
- Tollmien-Schlichting wave, excitation in boundary layer by acoustic and vortex disturbance scatt. 4-91792
- Tollmien-Schlichting waves in boundary layer nonlinear eqn. for amplitude 4-112918
- transient parallel fluid flows, finite element anal. 4-74986
- transonic potential external viscous flow over airfoils, boundary layers and wakes calcs. 4-64972
- transonic separated flows, viscous-inviscid interaction, semi-implicit and numerical methods (French) 4-64974
- turbulent boundary layer on rigid surface, dipole acoustic radiation 4-112845
- turbulent flow over vehicles at angle of attack 4-79558

**boundary layers continued**

- two dimens. hydrofoil, press. distrib. and drag reduction in dil. polymer solns. 4-87763
- two-dimensional and 3D flow, laminar instability theory 4-97480
- two-layer spin-up and frontogenesis 4-87729
- two-phase cooling film on adiabatic wall 4-83943
- two-phase critical flow, boundary layers, visualisation study, 4-60498
- unsteady free convection near a forward stagnation point at small Prandtl number 4-75012
- unsteady laminar and turbulent boundary layers charact. 4-60365
- vibrating surface, boundary layer transition, unstable wave excitation 4-91791
- viscous flow longit. to cylinder, local similarity soln. 4-97508
- viscous flow over circular cylinder, turbulence effect on heat transfer coeff. 4-97537
- viscous Stokes flows past collection of particles in circular cylinder, boundary integral eqns. 4-65026
- viscous three-dimensional flow with large secondary vel. 4-103354
- viscous-inviscid interactions on axisymmetric bodies of revolution in supersonic flow 4-60367
- volume-cycled oscillatory flow in a tapered channel 4-75088
- vortex chamber with hyperbolic end covers, hydrodynamics 4-79602
- wall jet problem, boundary layer control by means of strong injection 4-97710
- waves, weakly interacting, energy transfer eqn. 4-58655
- weakly conducting fluid, turbulent flow in pipe, boundary current fluctuations 4-108110
- CO<sub>2</sub> gasdynamic 16  $\mu$ m laser, boundary layer effects on laser gain 4-87314
- H<sub>2</sub>O-N<sub>2</sub> heat and mass transfer in a laminar boundary layer under mist formation (Japanese) 4-97477
- N<sub>2</sub> gas flow around heated cylinders, heat transfer, temp. difference effects 4-75005

**boundary-value problems**

see also initial value problems

- 3-body problem, numerical solution with Coulomb interaction 4-73261
- $\nabla \cdot (\nabla \phi) = 0$  equation boundary-value problems 4-103216
- accreting bodies subject to aging, nonlinear creep problems 4-79467
- acoustic, boundary value problems, pseudo-differential operators appl. 4-83752
- acoustics, integral equations, numerical methods 4-83748
- analytic functions, zeros determ., generalisation 4-95138
- anisotropic planar waveguides with bent optical axes, wave propag. anal. 4-83691
- aquatic velocity field interpolation from boundary and regional data 4-63518
- arch, shallow, Marguerre-type, snap-through problem 4-101625
- axial-symmetric flow through porous media with free and seepage surfaces, Volterra boundary value problems 4-113002
- beam, heavy inextensible elastic, unilateral contact problem 4-97438
- bifurcation buckling loads due to struct. geometry perturbations, first order change 4-64870
- body of revolution in liq. with jet separation, unsteady weakly perturbed motion 4-112896
- bounded region, nonlinear heat conduction eqn. with non-powered coeff. (Russian) 4-69661
- coaxial system, 1/N expansion for Dirichlet boundary problems 4-96751
- composite materials, appl. of stress and strain polarization tensors to mechanical behaviour 4-112726
- compressible fluid, with weak diffusion, Rayleigh problem (Russian) 4-112672
- conference on transport theory, Blacksburg, VA, USA (March 1983) 4-95053
- contact-line problems in fluid mechanics 4-98409
- creep damage and rupture in three dimens., strain-dependent thermodynamic foundations 4-75607
- cylinder, circular, stability when subjected to compressive end forces 4-91730
- cylinder, corrugated, transversely isotropic, of finite, dimens., stress state 4-103196
- detaching elastic body motion, boundary value problem 4-87569
- diffraction grating scattering theory, book 4-86125
- diffusion expts. using radioactive isotope method, mathematical anal. (Russian) 4-92431
- diffusion processes, nonelliptical boundary-value problems (Russian) 4-101787
- discrete ordinate method of solution of linear boundary value and eigenvalue problems 4-101634
- dynamic elastic problems, boundary integral eqn. method 4-95175
- dynamic loading of liquid impact struct., appl. to boundary integral methods (German) 4-113089
- eddy current losses, boundary value and transmission problems, Helmholtz eqn. 4-91385
- elastic bodies, optimal shape design 4-86216
- elastic wave diff. by subsurface check 4-87492
- elasticity problems, appl. of weak formulation of boundary integral equations 4-78137
- elasticity theory, boundary integral eqn. method for external boundary value problem soln. 4-106188
- elastodynamic boundary-value problems, integral eqn. method, appls. 4-60283
- electrodynamics, soln. accuracy improvement 4-78999
- electrodynamics boundary problems, combined orthogonal coordinate systems 4-112334
- electron lenses, open, computation by coupled finite element and boundary integral methods 4-91392
- EM wave propag. in stochastic medium, numerical modelling 4-112325
- filtration and heat conduction in porous bodies, related problems 4-79663
- finite elasticity, stress-boundary-value problems 4-74889
- finite element method, projection-mesh diagrams construction using soft-tened-mixed approxs. 4-63508
- function approximation, Lagrangian, spline and weighted finite difference methods 4-64848
- gases, sound propagation, boundary value problems 4-91860
- Gottlieb-Turkel time filter for Chebyshev spectral methods 4-101633
- heat conduction, inverse boundary-value problem, overdefined formulation, soln. 4-97276
- heat conduction, inverse boundary-value problem, soln. by iteration algorithm 4-97275
- high-shear grain flows, boundary conditions 4-112991
- boundary-value problems continued
- homogeneous conductors, eddy currents calc., boundary Galerkin's approach 4-59960
- homogeneous medium bounded by perfectly conducting walls, dyadic Green's function props. 4-64659
- inverse problems solution with unknown model of the process 4-79429
- inverse scatt. problems in 1-D, numerical computations 4-86235
- isotropic medium with curvilinear sections, second dynamic problem soln. in elasticity theory (Ukrainian) 4-69694
- kinked crack initiating from rigid line inclusion, stress analysis, formulation 4-108043
- Landau-Lifschitz eqn., inverse scatt. problem, boundary problem for spin waves in ferromagnet 4-92903
- linear elastic cracked body, transient elastodynamic second boundary-value problem 4-64881
- linear viscoelasticity, displacement and velocity vectors 4-91739
- local solution existence to aerodynamics equations (Chinese) 4-112933
- magnetic field problems, three-dimensional, infinite element method 4-59952
- materials parameters estimation in electrodynamic medium 4-90610
- MHD equilibria, numerical approx. of free boundary problem 4-69875
- MHD multidimensional transient flows full implicit continuous Eulerian scheme 4-87809
- microcontinuum fluid mechanics, boundary-value problems 4-110883
- mixed boundary-value problems connected with a limiting electrochemical perforation 4-89306
- moment theory of elasticity, boundary-value problems in regions with slits 4-79452
- moving contact in mechanically fastened joints, finite element anal. 4-83866
- multi-grid method numerical soln. 4-101628
- neutron transport in semiinfinite geometry, abstract boundary value problems 4-96099
- non-local dielectrics, surface exciton polaritons, dispersion relations 4-92628
- nonlinear, periodic solns. and upper and lower solns. method 4-67959
- nonlinear reflecting diffusion process, and the propagation of chaos and fluctuations associated 4-86376
- nonlinear stationary mag. fields inhomogeneous boundary conditions, Bubnov-Galerkin method appl. 4-69270
- nonlinear viscoelasticity, nonstrictly hyperbolic problem soln. existence 4-69687
- nonlocal dielectrics, generalised boundary condition, reflectivity 4-92993
- ocean, acoustic normal mode determ. method 4-103072
- one-dimensional steady shock waves in uniform and diverging ducts 4-64981
- optical fibres, multimode graded-index type, mode splitting at splices determ. 4-74740
- p-n heterojunctions, boundary conditions for excess minority carrier conc. at space charge region edges 4-88569
- p-n junction device modelling, singularly perturbed boundary value problems 4-98747
- p-n junction diodes, carrier lifetime and surface recomb. vel. determ. using transient responses 4-77093
- panel, stiffened cylindrical, nonmembrane prebuckling effects 4-91743
- penny-shaped interface crack with heat flow, imperfect contact 4-97425
- piezoelectric ceramic disc, polarised in thickness direction, free vibr. anal. (Chinese) 4-60203
- plasticity, unified framework provided by mathematical programming 4-97354
- plate, thermally stressed, vibr. anal., hybrid method calcs. 4-87617
- plates, vibrating, boundary value problem 4-91751
- power-law fluid, flow over flat plate, boundary value problems 4-87764
- quasilinear wave eqn., effect of boundary damping 4-86225
- region with curved cuts, dynamical elasticity problem 4-74879
- resonantly excited elastic tube, acoustic spectrogram and complex-freq. poles 4-87491
- Schrodinger eqn., linear bound operator, 1-D study with nonlocal potential 4-81197
- second-order fluid creeping flow 4-87767
- seepage and membrane contact problems 4-65016
- semiconductor plates, current-carrying, in magnetic field, electric field anal. 4-107482
- semiconductors, surface carrier heating, electron temp. striations and current filaments 4-84629
- shell, cylindrical, rib reinforced, static strength analysis, stress/strain state 4-64845
- shell, thin, cylindrical, laminated, in pure torsion, instability 4-103224
- shells, cylindrical, longitudinally corrugated, multilayer, thick-walled, stressed state 4-108005
- shells, cylindrical, stress-strain state investigation on basis of eqns. of elasticity theory 4-103199
- simple layer: potential method for domains having external corners 4-63511
- singular boundary value problems, numerical soln. by invariant embedding 4-101632
- small sphere motion is fluid near circular hole in plane wall 4-112904
- soap film, liquid drop suspension, simplified model 4-88376
- soap films, liquid drop suspension, general formulation 4-88375
- soil-structure interaction, far field representation, boundary element anal. 4-83817
- solids, nonlinearly locking, uniaxial strain shock waves, resultant deform. 4-113538
- sphere, inside-out elastic, equilib. stability 4-112744
- spherical bodies, elastic wave diffraction (Russian) 4-64877
- streamwise corner, laminar boundary layer stability 4-60374
- stress concentrations determ. using expt.-numerical methods 4-97445
- supersonic nonequilibrium flow channel design, plane and axisymm. 4-103420
- symmetrical modes in finite external mag. field 4-113156
- thermoelastic oscillations, initial boundary value problems (German) 4-82681
- thermoelasticity, linear, coupled dynamic theory, characterisation in terms of temp. 4-60290
- thin airfoil theory for planar inviscid shear flow 4-97594
- tubes, thin-walled, fluid-filled, wave propag. boundary value problem 4-79483
- unidirectional piston in baffle, variable impedance, directivity patterns 4-112635

# boundary-value problems continued

- upper half-plane, Dirichlet boundary-value problems, multiple scale soln. 4-97598
- viscous fluid, small-particle motion, circular disk effect 4-65013

# bending see bending

# brain

- see also *neurophysiology*
- atherosclerosis, PIXE investigation 4-105370
- auditory and visual evoked potentials in Huntington's disease 4-72244
- auditory brainstem response and temperature: relationship in guinea pigs 4-77252
- auditory brainstem responses, averaged, quality estimation 4-115082
- auditory brainstem responses, effects of stimulus rise-time and polarity 4-85440
- auditory brainstem responses and behavioural thresholds, stimulus duration effects 4-115071
- auditory brainstem responses recording, artifact rejection criteria efficiency comparison 4-85546
- auditory evoked potentials, brain stem, lesions location, computer anal. 4-72258
- auditory evoked potentials, dissociation from perception by bilateral lesions 4-77251
- auditory evoked potentials in people with perfect pitch, tone processing without P300 prod. 4-81708
- auditory evoked response of cat brain stem, hypothermia effects 4-72259
- autoradiographic images of cerebral cortex, computerised 2D and 3D reconstructions 4-100405
- autoradiographs of rat brain, computer-assisted video anal. 4-100404
- blood flow, regional, accuracy of stable Xe/CT meas. 4-67073
- blood flow meas. by intravenous  $H_2^{15}O$ , emission CT, implementation and validation 4-72374
- blood flow meas. by intravenous  $H_2^{15}O$ , emission CT, theory and error anal. 4-72373
- blood flow rel. to EEG characts. 4-89557
- blood-brain barrier, microwave energy effects, review 4-115127
- brainstem, metabolic activity changes during central and peripheral thermal stimulation 4-81622
- brainstem auditory evoked pot., amplitude, latency and waveform: effects of high-pass filter freq. 4-105242
- brainstem auditory evoked pots., human, 3-channel Lissajous' trajectory 4-67135
- brainstem auditory evoked pots., latency rel. to click phase and rate 4-100158
- brainstem auditory evoked responses, constituent components extraction 4-85433
- brainstem auditory evoked responses in chronic renal failure patients 4-100157
- brainstem modulation of hippocampal EEG activity 4-89552
- cerebellum in sheep fetus, elec. activity, acute hypoxia and sleep states effect 4-72239
- cerebrospinal fluid shunt flow, quantitative evaluation using  $^{99m}Tc$  4-81796
- cerebrovascular disease patients, haemodynamic effects of arterial by-pass, angiostographic study 4-115088
- cerebrum, mouse, dielec. props. rel. to age 4-115049
- circular ring tomograph, appl. of coded apertures to head scanning 4-72452
- CNS, postnatal development after prenatal X-irrad. in mice 4-67044
- cortical and subcortical visual areas, interactions 4-109801
- cortical evoked potentials using a microcomputer for stimulation and analysis 4-115277
- cortical indices of impaired ocular accommodation and associated convergence mechanisms 4-62475
- cortical V1 cells, monkey, spatial mapping with pure colour and luminance stimuli 4-89569
- CT images of human brain, 3D display (*Japanese*) 4-93856
- damage assessment in malnourished infants, use of visual and auditory evoked pots. 4-89821
- DNA crosslinking, BCNU-induced, X-ray effects in rat brain tumour cells 4-105296
- dynamic emission tomography of regional cerebral blood flow 4-115214
- electrical activity, mech. and interpretation 4-100116
- event-related brain pots., classification 4-85425
- event-related potential concomitants of information processing dysfunction in schizophrenic children 4-77233
- event-related potentials and functional assessment 4-89809
- extrahypothalamic thermal inputs to the hypothalamic thermoregulatory network 4-81640
- forebrain neuron activity in cats during alternating movements 4-72235
- high speed photography, videography and photonics, conf., San Diego, CA, USA (Aug. 1983) 4-106102
- hippocampal synaptic transmission, long-term potentiation rel. to behavioural learning rate 4-105228
- human brain, 3D CT image display (*Japanese*) 4-109926
- hypothalamic and thalamic neurons, responses to noxious and scrotal thermal stimulations in rats 4-81639
- illusory contours and cortical neuron responses 4-109817
- image reconstruction from neuromagnetic fields 4-72321
- inferior colliculus, cat, responses to low intensity tones 4-105248
- inferior colliculus, cat, stimulus intensity effects 4-105249
- interactive image analysis, neuroscience appls. 4-100409
- intracerebral stimulating electrodes, cylindrical coordinate Laplace's eqn., numerical soln. 4-89541
- intracranial abscesses, management by CT, radiation dose considerations 4-62586
- intracranial pressure, long-term monitoring 4-67143
- lateral geniculate neurons, cat, statistical features of impulse trains 4-105230
- medial medullary neurons, response to preoptic and scrotal thermal stimulation 4-81624
- mental retardation rel. to in utero exposure to A-bomb radiation 4-72303
- midbrain neurons of rats responsive to hypothalamic temperature change and their local thermosensitivity 4-81623
- monocularly deprived kittens, prevention of ocular dominance changes by cortical activity disruption 4-72246
- movement-related slow pots., contrast between finger and foot movements 4-100183
- multi-barrel glass micropipettes prep., David-Kopf puller modification, brain recording appl. 4-115308

# brain continued

- multidetector SPECT brain scanner, improved performance from modifications 4-100310
- neocortex, initiation of-synchronized neuronal bursting, guinea pig expts. 4-105227
- neocortical interactions, statistical mechanics, short-term memory capacity 4-85416
- neurostimulation, elec., long-term, clinical appls. 4-67147
- octopus brain, ongoing compound field pots. obs. 4-105226
- PIXE anal., target prep. influence in rate organs 4-100381
- positron emission tomography studies of cerebral blood flow-metabolism relationship, review 4-115213
- posturography rel. to cerebellar diseases 4-72285
- prefrontal cortical influences on behavioural thermoregulation and thermosensitive neurons 4-81621
- preoptic thermosensitive neurons, neural inputs, histological and electrophysiological mapping in rats 4-81620
- pressure distribution in skull cavity 4-66975
- primate superior colliculus, shift of auditory receptive fields with eye position changes 4-77261
- rat, metabolism,  $^{13}C$  NMR using double-tuned surface coils 4-66878
- real-time optical imaging of naturally evoked electrical activity in intact fog brain 4-72470
- retinotopy and orientation columns in the monkey 4-81670
- rotational injury study 4-109855
- saccade-related brain pots. in guessing tasks, late components 4-66946
- simulation using kinetic theory of neural systems 4-100119
- somatosensory evoked cerebral magnetic fields from SI and SII in man 4-77269
- somatosensory evoked potentials from the human brain-stem: origins of short latency potentials 4-77266
- somatosensory evoked pots., cortical and spinal, intraoperative monitoring 4-85576
- somatosensory evoked pots., recording from spinal cord and brain 4-93949
- somatosensory evoked pots., short latency, and central somatosensory cond. time in post-traumatic coma 4-66964
- spatial filtering of retinal images by the human visual system and its consequences for visual thresholds 4-100134
- stereotactic heavy-ion Bragg peak radiosurgery for intra-cranial vascular disorders 4-85494
- stereotactic neurosurgery, 3D image of cerebral blood vessels and tumour 4-89692
- striate cortex, cat, length summation in simple cells 4-81675
- striate cortex of macaque monkey, visual field representation 4-66948
- thermal afferents to the hypothalamus and thermal adaptation 4-81638
- thermoregulation, cranial vasodilator control of lingual arteriovenous anastomoses 4-81630
- thermoregulatory mechanisms, conf., Osaka, Japan (Aug. 1982) 4-78028
- trauma, brain management, primates, high frame rate flash X-ray cine system 4-109788
- tumors and NMR, correlative study in biopsy samples 4-100295
- tumour localisation, positron emission tomography 4-72355
- tumours, B neutron capture therapy, filtered beam 4-85515
- valyl-tRNA synthetases isolated from chick embryo and brain, difference in radiosensitivity 4-66873
- ventrolateral medullary surface blood flow,  $H_2$  clearance determ., cat obs. 4-89629
- visual cortex, mink, segregation of on- and off-centre afferents 4-77240
- visual cortical cells, cat, responses to continuously and stroboscopically illum. moving light slits 4-66949
- visual electrically evoked potential, steady-state responses 4-77234
- visual evoked potentials, steady-state, foveal Xe flash disruption 4-81669
- visual evoked potentials, variability evaluation by two statistical tests 4-100135
- visual evoked potentials in patients with well-defined occipital lesions, hemispheric asymmetry 4-93737
- visual evoked response, steady-state, factors contributing to amplitude variability 4-109797
- $^{77}Br$ , uptake by human brain, quantitation by single photon emission CT 4-93852
- HTO ingestion, effects on mice, hexokinase isozymes in brain, liver and spleen 4-100259
- $^{31}P$  NMR in vivo surface coil study of rat brain 4-72240

# brain models

- see also *neural nets*
- associative memory, hierarchical neural network model 4-93715
- associative memory model based on adaptive feature detecting cells (*Japanese*) 4-100118
- central nervous system quantisation for VLSI implementation of robotic neural systems 4-77231
- electrocortical activity controlled by lateral hypothalamus, inference of stable dispersion relation 4-93713
- electrocortical activity under lateral hypothalamic control, test for constant natural frequencies 4-93712
- global electrocortical activity, linear model, control by lateral hypothalamus 4-93711
- hippocampal neurons, segmental cable evaluation of somatic transients 4-105214
- hippocampal neurons, segmental cable model, conductance transients onto dendritic spines 4-105215
- Hodgkin-Huxley model behaviour 4-81654
- interspike interval of a cable model neuron with white noise input 4-81653
- memory model on basis of plasticity of inhibitory neurones 4-66931
- problem-solving, computer and human brain comparisons 4-62460
- spatial problem-solving, computer and human brain comparison 4-62492

# brass

- $\alpha$ - $\beta$ , superplastic alloys, two-phase, modelling of cavitation under uniaxial stress systems 4-61991
- $\alpha$ -brass, film growth in ammoniacal Cu(II) solns., early stages 4-89163
- $\alpha$ -brass 4-71793
- $\alpha$ -phase, work hardening in polycrystals 4-61956
- Admiralty, SCC, slow strain-rate, influence of deform. path 4-99654
- admiralty, slow strain rate SCC under multiaxial conditions 4-71764
- anneal-hardening of  $\alpha$ -brass, change in mechs. props. 4-99397
- beta phase, plastic deformation at He temps., capacitance meas. 4-71681
- $\alpha$ -brass, single crystal, oriented for easy glide, multiple and cross slip in stress gradient 4-80047

**brass continued**

- brittle fracture, environmentally induced, crystallographic charact. techniques 4-81383  
corrosion of Sn alloyed  $\beta$ -brass, Auger/SEM obs. 4-89172  
erosion in single particle impacts, significance of erosion parameter 4-81295  
fatigue life of M058 brass, effect of programmed load spectrum parameters (*Polish*) 4-62028  
formability, max. uniform strain, effect of matrix and second phase 4-99465  
forming limit diagrams, comparison between expt. and theoretical 4-93348  
microfractography, SEM study (*Polish*) 4-93363  
mirror, IR MTF measurements, effect of surface textures on reliability 4-97027  
neutron irradiated thin flat crystals, slip band growth and dislocation velocities 4-70164  
positron annihilation, momentum density of annihilation photons, one-dimens. Fourier transform method 4-70634  
preferential sputtering studies by AES and XPS 4-93215  
sheet, deep drawing, influence of temp. 4-66399  
sheet formability and plastic instability, effect of geometry and materials props. 4-93351  
steel-brass galvanic couple, corrosion, polarisation study 4-85245  
strain hardening exponent 4-99406  
sulphidation, atmospheric 4-79001  
surface, oxidised, Auger spectrometry and RHEED study 4-69994  
X-ray generated ultrasonic signals 4-103889  
Pb brass, precipitation and coarsening of Pb particles 4-109413

**Bravais lattice** see crystal atomic structure

**brazing bonding** see brazing

**brazing**

- see also soldering  
hardenableity of small specimens, determ. by implant method 4-76919  
Inconel 718, vacuum brazed Ni-Cr-Si joint, struct. 4-66548  
joints, welded and brazed, strain-strength charact. determ. during high-speed tearing (*Russian*) 4-78310  
leak-tight furnace brazing of intricate objects 4-78301  
steel fibre reinforced refractories, fibre-matrix bonding rel. to brazing 4-109367  
Cu, brazed, low cycle fatigue in high vacuum rel. to cold work 4-109500  
Ni-Cr-Si vacuum brazed joint of Inconel 718, struct. 4-66548  
Ti braze alloy for joining bulk graphite/solid T breeder materials to metal substrates 4-111753

**breakage** see fracture

**breakdown (electric)** see electric breakdown

**breakdown (mechanical)** see manufacturing processes

**breakdown diodes** see avalanche diodes; Zener diodes

**breeder reactors** see fission reactors

**bremsstrahlung**

- see also electron radiation; gamma-ray spectra; gamma-rays; X-ray emission spectra; X-rays  
auroral kilometric radiation, generation, theory 4-110387  
bound electrons, bremsstrahlung in field, differential cross sections calcs. 4-69221  
coherent bremsstrahlung and channelling radiation from kilovolt electrons 4-85030  
diffuse galactic  $\gamma$ -rays, bremsstrahlung component spectra and cosmic ray electrons energy spectra 4-100889  
direct-charging detector with dielectric scatterer 4-87014  
direct-photon pair production, quark bremsstrahlung contrib. to background 4-106546  
ESCA, radiation damage, bremsstrahlung contribution 4-99915  
flux dist. calcs from thin radiators 4-58657  
foil electron transport, energy loss and straggling due to at. electron collisions and bremsstrahlung 4-70249  
free-free scattering processes, inhomogeneous radiation fields effects 4-107455  
galactic cosmic ray electrons, energy spectra characts. from bremsstrahlung component of gamma ray emission anal. 4-90042  
hard scattering processes, transverse hadronic energy emission, soft gluon bremsstrahlung 4-102099  
induced bremsstrahlung radiation from plasma 4-91933  
intensities from conducting and nonconducting materials 4-59597  
inverse bremsstrahlung, Lorentz force eqn., Vlasov eqn. 4-59968  
inverse photoemission, energy depend. cross-section variations 4-109269  
Jupiter, magnetosphere trapped particles-satellite interactions,  $\gamma$ -ray emission 4-101239  
light elements, thick targets,  $H^+$  bombardment, continuous X-ray spectra 4-99214  
Maxwellian plasma, temperature-averaged Gaunt factor for bremsstrahlung energy production 4-79766  
microdosimetry of 10-15 MeV bremsstrahlung X-rays 4-85518  
Monogem Ring, extended galactic X-ray source, theory of X-ray emission 4-94992  
neutrino-pair bremsstrahlung in dense stars, BCC lattice structure 4-94849  
noble metals, unoccupied band critical point energies 4-61276  
plasma, laser produced, bremsstrahlung emission spectra meas. 4-103471  
plasma electron X-ray energy spectrum, relativistic effect 4-91977  
radiative-recombination emissivity coeff. and bremsstrahlung in non-Maxwellian plasmas 4-91883  
radiotherapy, angular distrib. and yield from bremsstrahlung targets 4-100314  
rare earth metals, 4f states in XPS and bremsstrahlung isochromat spectra 4-99277  
relativistic charged particle radiation in crystals, unified theory, quantum mech. treatment 4-96765  
surface valence states, photoemission and inverse photoemission studies, review 4-85078  
turbulent bremsstrahlung instability of whistler mode in presence of enhanced ion-acoustic fluctuations 4-103485  
X-ray galaxy clusters, isothermal bremsstrahlung model for X-ray spectrum of volume emissivity 4-86064  
X-ray microanalysis in analytical TEM, bremsstrahlung-produced fluoresc. effect 4-89365  
X-ray sources, pulsed, dose calibrations of intensifying screens and neutral density of filters 4-58927  
 $\gamma$  deep inelastic scatt., bremsstrahlung contribution 4-59067

**bremsstrahlung continued**

- $\mu p$ -X, 200 GeV, Bethe-Heitler bremsstrahlung meas. 4-73710  
Ag-Mn dilute alloys, exchange split virtual bound state 4-92680  
Al, angular distribution of particle-induced X-ray emission 4-99213  
Al, continuum X-rays produced by a few MeV proton bombardment 4-99215  
Al plasma radiative recombination, electron bremsstrahlung, VUV emission 4-83989  
Au, photon linear polarization in the elementary process of atomic-field bremsstrahlung 4-91354  
Au(100), image pot. surface states identification, inverse photoemission 4-76015  
C, continuum X-rays produced by a few MeV proton bombardment 4-99215  
C, photon linear polarization in the elementary process of electron-electron bremsstrahlung 4-91355  
Ce alloys, transition to nonmagnetic f states, bremsstrahlung isochromat spectra studies 4-113884  
Cu (001), K-resolved inverse photoelectron spectroscopy, comment 4-99219  
Cu (001), K-resolved inverse photoelectron spectroscopy, reply to comment 4-99220  
Cu (001), unoccupied surface states, inverse photoemission meas. 4-92783  
Cu (100), image-potential states observed by inverse photoemission 4-76014  
Cu, excited H reflection at grazing incidence, light emission 4-76587  
Cu, photon linear polarization in the elementary process of atomic-field bremsstrahlung 4-91354  
Cu-Mn dilute alloys, exchange split virtual bound state 4-92680  
Cu(100), image pot. surface states identification, inverse photoemission 4-76015  
 $e^+e^- \rightarrow \gamma\gamma$ , double bremsstrahlung, photon ang. distrib., radiative corrections 4-82953  
F compounds, photonuclear activation ratios as index of bremsstrahlung quality, radiology appl. 4-109913  
Fe (110), exchange split empty energy bands inverse photoemission studies 4-84551  
Fe (110), spin-dependent bremsstrahlung 4-88898  
Fe, ferromagnetic, wave-vector depend. temp. behaviour of empty bands, isochromat spectroscopy study 4-104123  
Fe fully relativistic band struct. calcs. 4-113855  
La alloys, transition to nonmagnetic f states, bremsstrahlung isochromat spectra studies 4-113884  
Ni (001) and (110), K-resolved inverse photoelectron spectroscopy, comment 4-99219  
Ni (001) and (110), K-resolved inverse photoelectron spectroscopy, reply to comment 4-99220  
Ni fully relativistic band struct. calcs. 4-113855  
Ni, polycrystalline, inverse photoemission 4-61808  
Si, gamma-irradiated, charge carrier recombination, bremsstrahlung study 4-84631  
a-Si, mobility edge, temp. depend. 4-92723  
 $^{90}\text{Tc}$  radionuclei, internal bremsstrahlung prod. probability from  $\beta$ -decay 4-83028
- brewing industry**  
raw water treatment-using stratified-bed cation-exchange filter systems 4-71915
- bridge circuits**  
see also bridge instruments  
deep-level spectroscopy by transient capacitance techniques under electrical resonance 4-58865  
frequency response optimisation of constant temp. detector system 4-63735  
half-bridge circuits, invariant, for bending moment meas. 4-97446  
Wheatstone-type bridge circuit, calorimeter dose determ. by direct voltage meas. 4-100325
- bridge instruments**  
see also bridge circuits  
direct current comparator resistance bridge automation, alloy resistivity appl. 4-90613  
electrical measuring instruments theory, moving coil, bridge and current comparison methods (*German*) 4-58863  
lattice defects in semiconductor diode structures meas. by capacitance method 4-90611
- Bridgman method** see crystal growth from melt
- brightness**  
see also sky brightness  
1983 KD, Apollo asteroid, visual magnitude estimates and light vars. 4-85887  
astigmatism errors in radiance measurements 4-86461  
atmosphere-less cosmic bodies, brightness opposition effect model 4-94565  
3C 273, quasar variability in radio and optical emission 4-106074  
3C radiogalaxies, surface photometry rel. to Abell cluster cD galaxies 4-94964  
Cassiopeia A, SNR, brightness var. and proper motions, SHF obs. 4-73010  
cathode materials for high brightness electron beams 4-71508  
Comet Austin (1984i), integrated V-magnitude (1984 July 25 and 27) 4-101266  
P/Comet Clark (1983w), total visual magnitude estimates (1984 May 6 and 7) 4-72911  
P/Comet Clark (1983w), total visual magnitude estimates (1984 May 10 to June 3) 4-85898  
P/Comet Crommelin (1983n), spectroscopic obs. and total visual magnitude estimates 4-63104  
P/Comet Crommelin (1983n), total visual magnitude estimates (1984 February 8 to 27) 4-63109  
P/Comet Encke, total visual magnitude estimates (1984 February 19 to 27) 4-63110  
P/Comet Encke, total visual magnitude estimates (1984 January 28 to February 5) 4-63106  
P/Comet Halley, brightness secular decrease and aging characts. 4-90114  
P/Comet Halley (1982i), light vars. obs. (1984 January 27 to 30) 4-77773  
P/Comet Halley (1982i), photometric obs. rel. to brightness vars. and rot. period 4-94686

## brightness continued

- P/Comet Hartley-IRAS (1983v), total visual magnitude estimate (1984 April 22) 4-67703
- P/Comet Hartley-IRAS (1983v), total visual magnitude estimates (1984 March 25 to April 9) 4-63101
- P/Comet Hartley-IRAS (1983v), total visual magnitude estimates and coma diameters (1984 February 24 to 27) 4-63108
- P/Comet Hartley-IRAS (1983v), total visual magnitude estimates (1984 April 27 to May 19) 4-77774
- Comet Meier (1984d), total visual magnitude estimate (1984 September 20) 4-115726
- P/Comet Takamizawa (1984j), total visual magnitude estimates (1984 August 8 to 21) 4-110569
- Comet Takamizawa (1984j), visual magnitude estimates (1984 August 1) 4-101265
- P/Comet Wild 3, close encounter with Jupiter rel. to magnitudes and orbital motion 4-94683
- 3CR radio galaxies, X-ray luminosities from Einstein Observatory survey 4-63269
- disk galaxies, absolute (blue) luminosity/21 cm linewidth relation 4-63276
- dwarf irregular galaxies, two-colour evolution in stochastic star form. model 4-67806
- dye penetrant inspection, brightness-colour coeff. of visibility of indications 4-109610
- efficiency function, anal. (Japanese) 4-106350
- elliptical galaxies, rotation-surface brightness relation rel. to dissipation during form. 4-67805
- equilibrium-reflectance model for clear or cloudy atmosphere 4-100729
- fireballs of 1983 April 23 and 27, Universal Times and visual magnitudes 4-72914
- flickering light sequential luminance 4-100140
- galaxy clusters brightness and spatial positions, galaxy form. implications profiles 4-67810
- global clusters, brightness distribution from narrow-slit scanning method 4-63227
- global star clusters, surface brightness profiles, electronic camera obs. 4-67777
- human eye contrast sensitivity, brightness function anal. 4-100136
- IR luminous galaxies identified with IRAS point sources, IR/optical luminosity ratios 4-77970
- luminance and saturation of equally bright colours 4-68255
- lunar radio flux data use in broadbeam antenna system meas., error anal. 4-110549
- M87 (NGC 4486), nucl. struct. 4-77914
- Mars, obs. of radiometric inhomogeneity at millimetre wavelengths 4-105898
- meteors, appl. of  $\rho I$  model to relative distrib. of radiation intensity 4-105905
- NGC 1275, flux density meas. and spectral evolution of radio nucleus (3C 84) 4-86029
- NGC 2808, NGC 6388, southern globular clusters, Reticon BVRI profiles 4-101439
- NGC 3379, elliptical galaxy, evidence for central spike of light 4-94967
- OJ 287, BL Lacertae object, variability in radio and optical emission 4-106074
- OJ 287, BL Lacertae object, visual magnitude estimates (1984 February 23 to March 9) 4-63285
- partially coherent sources, radiometric definitions 4-68258
- peripheral visual system, human light and flicker detect. at low luminance, psychophysical expts. 4-89578
- PKS 0735+17, BL Lacertae object, variability in radio and optical emission 4-106074
- polar winter stratosphere, four day oscill. in brightness temp. 4-72700
- Q 0957+561, twin QSO, CCD brightness monitoring 4-90251
- QSO 1055+018, metre-wave outburst obs. 4-94987
- QSOs,  $V/V_r$  test rel. to cosmological redshift theory 4-101494
- quasars, UV/X-ray luminosity ratio rel. to X-ray heating in broad-line region 4-90254
- quasars, X-ray variability 4-86079
- radiance standards, applic. of integrating sphere technology 4-82814
- radio sources, extragalactic, at 1 Jy at 408 MHz, estimated redshifts and radio luminosities 4-110762
- radio sources, extragalactic, struct. of hotspots from time-varying jet 4-101493
- radio sources near North Galactic Pole, flux densities from deep 4.85 GHz survey of 5C 12 area 4-110545
- radiogalaxies, multifrequency one-dimensional radio brightness distrib. in centimetre band 4-63282
- retroreflectance MAP service for coeff. of luminous intensity 4-63772
- Sagittarius A East, possible SNR, brightness, map and diameter 4-73092
- Saturn, central meridian, spectral brightness distrib. (Russian) 4-101242
- Saturn, visual photometric study of globe and rings (1943 to 1981) 4-105902
- Saturn ring system, theoretical optical thickness profile for bimodal gravitating system 4-101243
- semiconductor source, local radiance measurement, near-field method possible limits (French) 4-68262
- Seyfert galaxies, UV/X-ray luminosity ratio rel. to X-ray heating in broad-line region 4-90254
- Seyfert galaxies, variability of emission-line spectra and optical continua 4-86035
- solar radio emission calc. of brightness temp. distrib. on solar disc 4-105916
- spiral galaxies in Virgo cluster, blue-light Tully-Fisher relation rel. to dust content 4-101464
- stars, limb darkening laws, two-parametric representations, basic eqns. (Russian) 4-101315
- stars, limb darkening laws, two-parametric representations, integral quadrature coeffs. (Russian) 4-101316
- Sun, disc brightness in 160 nm continuum, features 4-90126
- Sun, prominences, brightening phenomena in H $\alpha$  line centre 4-101296
- Sun, transition region UV brightness rel. to photospheric electric current 4-105928
- video display terminal lighting 4-109790
- vision, brightness induced by opposite polarities O'Brien pattern (Japanese) 4-110506
- vision, object visibility, brightness, contrast and adaptation (Italian) 4-72248
- visual acuity in senile macular degeneration, luminance, contrast and eccentricity effect 4-72243

## brightness continued

- visual figure-ground segregation by motion contrast and by luminance contrast 4-72254
- visual response features by opposite polarization of brightness figures (Japanese) 4-100153
- D $_2$  lamps, time depend. of spectral radiance with MgF $_2$  window 4-83662
- ZnO:Nd(Yb), electrolum. brightness, voltage and freq. depend. at liq. N $_2$  temp. 4-93113
- Brillouin scattering** see Brillouin spectra
- Brillouin spectra**  
see also stimulated Brillouin scattering
- acoustic instability conditions, Brillouin scatt., width and line profile 4-61723
- p-anisaldehyde, liq., rot-trans. coupling and bulk viscosity relax., Rayleigh-Brillouin scatt. 4-71395
- carbon tetrachloride, liq., mean free path temp. depend. determ. using Brillouin scatt. expt. 4-109198
- di(alkylammonium) ferrous chloride, birefringence and Brillouin scatt. at struct. phase transition 4-75661
- dimethylammonium iron tetrachloride; phase transitions, Brillouin scatt. 4-66051
- ferroelectric, acoustic-phonon dispersion at incommensurate phase transitions, Brillouin scatt. obs. 4-61724
- fibre optic materials, scattering losses at minimum dispersion wavelength 4-79316
- ice X, high press. form occurring at 44 GPa, Brillouin scatt. 4-61057
- interfaces, Brillouin scatt., long-wavelength acoustic phonons 4-80951
- isotropic elastic plate, Brillouin scatt. 4-80956
- liquid-solid interfaces, phonons, Brillouin scatt. study 4-80955
- long scalelength laser plasma, parametric instability obs. 4-103510
- metastable liquids, transient thermodynamic props. meas. by Brillouin scatt. 4-97712
- nonequilibrium fluid undergoing planar Poiseuille-Couette flow, light scatt. 4-112520
- PET, ductile polymer, hypersonic vel. and submicrocrack formation under uniaxial tensile stress 4-114632
- phase transitions, light scatt. studies, book 4-101581
- phytol in carbon tetrachloride and toluene, liquid mixtures, Rayleigh-Brillouin spectra 4-109201
- polycarbonate, ductile polymer, hypersonic vel. and submicrocrack formation under uniaxial tensile stress 4-114632
- polycarbonate-glass interface, Brillouin spectra and photoelastic props. 4-80952
- polyvinylidene fluoride, dielectric and Brillouin spectroscopic studies 4-76483
- polyvinylidene fluoride-PMMA mixtures, dielectric and Brillouin spectroscopic studies 4-76483
- quartz, Brillouin scattering study of sound velocity at  $\alpha$ - $\beta$  transition 4-71400
- quartz, incommensurate phase, Brillouin scatt. study 4-61719
- raman and Brillouin scattering, classical reflection, and relativity in plasma 4-97799
- semiconductor materials, structural and electrical props. study using inelastic light scattering (French) 4-104621
- semiconductors, inelastic light scattering for structural/electronic props. characterisation (French) 4-84956
- semiconductors, resonant light scatt. through exciton-polaritons 4-109204
- solid-state plasma, acousto-optic scatt. in nonlocal optics regime 4-71346
- solid/liq. and solid/vacuum interfaces, surface acoustic waves 4-84501
- spatially dispersive medium, reson. Brillouin scatt. 4-80953
- squaric acid, rigid layer mode, Brillouin and Raman scatt., temp. and uniaxial stress depend. 4-98220
- stimulated Brillouin scattering in inhomogeneous flowing plasma 4-97768
- surface and interface phonon modes, light scatt. obs. 4-80361
- p-terphenyl, ferroelastic phase transition, elastic constant, Brillouin spectra 4-98180
- p-terphenyl, improper ferroelastic transition, acoustic anomalies 4-65389
- TGS, ferroelec., Brillouin spectra angular depend. studies 4-71393
- thin film waveguides, Brillouin scatt. obs. 4-79283
- thiourea, Brillouin scatt. under hydrostatic press., elastic constants. study 4-76479
- viscoelastic liquids, Rayleigh-Brillouin spectroscopy 4-114288
- BP, refractive index and elastic const. meas. 4-61647
- Ba $_2$ Na $_2$ Nb $_2$ O $_8$ , ferroelastic-incommensurate transition, Brillouin scatt. study 4-70362
- Ba $_2$ Na $_2$ Nb $_2$ O $_8$ , incommensurate, Brillouin spectra meas. 4-76482
- CdS, exciton-polaritons, resonant Brillouin scatt. studies 4-108789
- CdS, resonant Brillouin scatt. study 4-61721
- CdS, resonant Brillouin spectra calcs. 4-61722
- Co film, Brillouin scatt. from thermal magnons 4-71458
- D $_2$ O, Brillouin scattering at press. up to 34 GPa 4-80958
- Eu $_2$ Sr $_2$ S $_4$  ferromagnetic epitaxial layers, magnetooptic studies (German) 4-76441
- Fe film, epitaxially grown on GaAs; surface magnons, Brillouin scatt. study 4-88852
- Fe, thin films, Brillouin light scatt. study of magnon branch crossover 4-80959
- Ga $_2$ Al $_2$ As superlattices, acoustic modes, Brillouin and Raman scatt. study 4-80928
- InPS $_4$ , Brillouin scatt. meas. of elastic constants 4-84334
- KBr, Landau-Placzek ratio, light scatt. study 4-104623
- K $_2$ SeO $_4$ , acoustic phonon wavevector depend. near commensurate-incommensurate transition, Brillouin spectra 4-71313
- K $_2$ SeO $_4$ , Brillouin spectra, scatt. angle and press. depend. 4-76481
- (LiCl) $_x$ (H $_2$ O) $_{1-x}$  glass, hypersonic velocity and attenuation, Brillouin scatt. 4-70286
- MgSiO $_3$ , elasticity at Earth mantle pressures, Brillouin spectra study 4-100558
- Mo/Ni superlattices, magnetisation, Curie temp. and magnon spectra, Brillouin scatt. study 4-61560
- NH $_4$ Cl, hypersound attenuation and dispersion, back-and-forward Brillouin scatt. 4-76487
- NaNO $_3$ -KNO $_3$ , Brillouin scatt., sound wave attenuation and vel. meas., viscoelastic props. (French) 4-71396
- Ni $_2$ SiO $_4$ , olivine and spinel polymorphs, elasticity studies 4-98169
- SiO $_2$ , amorphous, polymorphism, optical study 4-88103
- SnTe/Sb superlattice, SAW velocity, Brillouin spectra studies 4-108694
- ZnCl $_2$ , deformation, sonic waves, hypersonic relax., Brillouin spectra 4-76485
- ZnSe, molten, potential pot. const. determ. by reson. Brillouin scatt. 4-71398

**Brillouin zones**

- see also *band structure*  
 alkali metals, BCC, thermodynamic props. at high temps. 4-92392  
 anharmonic cryst., statistical mechanics of phonons and phonon linewidths 4-70309  
 crystal Green's functions in complex energy plane, analytical tetrahedron method 4-60996  
 crystals, inhomogeneous electron damping and electron states 4-70615  
 glasses, pseudo-Brillouin zone boundaries, mol. dynamics simulations 4-80470  
 Green's function calcs., simplification through analytic continuation 4-61274  
 long-period superstructure models 4-113366  
 naphthalene, phonon harmonic dynamics, block method 4-88254  
 quasi-1D solids, band struct. shapes 4-92592  
 superlattices, Rayleigh waves, dispersion curves and displacement fields 4-92502  
 transition metal compounds, exciton satellites in photoelectron spectra 4-70665  
 Ag (110) unoccupied surface state, inverse photoemission study 4-71515  
 Ag, band structure and direct transitions, ARUPS studies 4-75842  
 Ag<sub>2</sub>Ta<sub>2</sub>S<sub>7</sub>, phonon modes, Raman spectra, valence force field model 4-104584  
 Al (111), low energy electronic excitations, EELS studies 4-99253  
 α-Al<sub>2</sub>O<sub>3</sub>, (0001) surface, hydroxylation, energy band struct. 4-108913  
 As, rhombohedral, electronic band struct., angle-resolved UPS and pseudo-pt. studies 4-113868  
 Au, band structure and direct transitions, ARUPS studies 4-75842  
 Bi<sub>12</sub>GeO<sub>20</sub> thin films, IR spectra and lattice phonons 4-88893  
 Bi<sub>12</sub>SiO<sub>20</sub> thin films, IR spectra and lattice phonons 4-88893  
 Bi<sub>12</sub>TiO<sub>20</sub> single cryst., Raman spectra and phonons 4-88833  
 Cd<sub>3</sub>As<sub>2</sub>, Raman spectrum 4-71382  
 CdSb, vibr. modes symm. and Raman scatt. (Russian) 4-99124  
 CsH<sub>2</sub>PO<sub>4</sub>, antiferroelec. fluctuations, Raman spectroscopy studies 4-71297  
 Cs<sub>2</sub>NaBiCl<sub>6</sub>, phase transition, phonon dispersion relations 4-98269  
 Cu (111), angle and energy synchronised photoemission spectrum 4-85065  
 Cu, band structure and direct transitions, ARUPS studies 4-75842  
 Cu surface, EM wave excitation spectral features 4-107811  
 Cu-Zn-Al alloys, modified phonons, calorimetry, susceptibility and inelastic neutron scatt. study 4-75636  
 Fe (100) with chemisorbed S, electronic struct. study 4-92779  
 GaAs, phonon frequencies 4-75626  
 GaAs, Raman probe of Brillouin zone for nonequil. phonons 4-66045  
 GaAs, surface electronic structure, angle resolved photoemission spectra 4-93185  
 Ge (001), metal-insulator transition, angle resolved photoemission studies 4-104126  
 Ge, elastic props., ultrasonic meas. 4-98170  
 GeS single crystal, reflectance and thermorefectance studies 4-71356  
 In<sub>2</sub>Se<sub>3</sub>, α- and γ-phases, Raman and IR spectra 4-109185  
 KHg<sub>2</sub>graphite intercalation cpd., electronic struct., Shubnikov-de Haas effect 4-92596  
 Mo (100), surface states, appl. of quick iterative scheme for transfer matrix calc. 4-76013  
 Mo (110) surface, density of states calcs. 4-70898  
 Na<sub>2</sub>Bi<sub>2</sub>TiO<sub>3</sub>, soft-modes and central peak, inelastic neutron scatt. studies 4-61037  
 NaCl, shock deform., mobility of fast dislocations 4-98109  
 NbS<sub>2</sub> (2H), phonon modes, Raman spectra, valence force field model 4-104584  
 Ni (100) surface with adsorbed O, surface phonons, EELS study 4-104086  
 Pb (111), electronic energy bands, angle resolved photoemission and self-consistent field calcs. 4-113858  
 Pb<sub>1-x</sub>Mn<sub>x</sub>Te, band struct., cyclotron reson. obs. 4-84546  
 Pb<sub>1-x</sub>Sn<sub>x</sub>Te, valence band struct. near phase transition 4-84564  
 Pd (111), chemisorption of CO, angle-resolved photoelectron spectra 4-11114  
 RbMnCl<sub>3</sub>, antiferromag. with alternating strong and weak coupling, absorpt. spectra, fluoresc. meas. 4-88659  
 Si, elastic props., ultrasonic meas. 4-98170  
 Si, far IR transmission spectrum, two-phonon difference band obs. 4-104597  
 SrAs<sub>2</sub>, monoclinic, Fermi surface determ. by Shubnikov-de Haas effect 4-108763  
 TaS<sub>2</sub> (2H), phonon modes, Raman spectra, valence force field model 4-104584  
 Te, superconducting props., energy band struct. calcs. 4-104343  
 TiO<sub>2</sub>, optically forbidden modes in Raman spectrum 4-109183  
 W (001), electronic struct., linear-augmented plane wave calc. 4-80649  
 WC (0001), bulk band struct., photoemission studies 4-80496  
 WSe<sub>2-x</sub>, zone axis patterns, changes with variations in voltage, thickness, composition and temp. 4-92157  
 ZnSiP<sub>2</sub>, valence band struct. and chem. binding 4-88445

**Brinell testing** see *hardness testing***bristles** see *fibres***brittle-ductile transitions** see *ductile-brittle transition***brittle fracture**

- see also *ductile-brittle transition; notch brittleness*  
 biaxial tension, criteria for brittle fracture 4-69704  
 α-brass, transcrystalline SCC mechanism, cleavage-like fracture surfaces 4-71793  
 cleavage fracture, Weibull probability function 4-99738  
 crack opening displacement design curves (Japanese) 4-91782  
 crack problems related to welding residual stress fields in linear elastic fracture mechanics 4-104878  
 critical brittleness of materials, use in calc. resist. to brittle fracture 4-104936  
 cyclic and dynamic loadings, fracture toughness characts. relationship 4-99536  
 elastic bodies, Novozhilov's criterion (Russian) 4-112773  
 fibre reinforced Al alloy, prep. by explosion technique, mech. props. at low temp. 4-114634  
 flaw nucleation and energetics of dynamic fragmentation 4-108509  
 fracture mechanisms, flaws, Hertzian cracks in brittle solid 4-97432  
 glass fibre reinforced PET, strength, effect of temp. and strain rate 4-93375

**brittle fracture continued**

- glass fibre reinforced polymers, electrical insulator components, damage in combined elec., mech. and chemical environments 4-66466  
 glass-glass contact, influence of brittle quartz particles 4-103271  
 glasses and ceramics, crack growth influenced by chem. environment 4-94095  
 half-space, elastic, thermal stresses 4-97408  
 inhomogeneous solids, brittle thermal fracture by high-temp. gas jet 4-97412  
 intergranular embrittlement, impurity interactions within grain boundary, MO calcs. 4-80147  
 metal, book contrib. 4-108508  
 metallic glass ribbon reinforced epoxy resin, fracture strength and ribbon shape effects 4-99479  
 metallic glass ribbon reinforced epoxy resin, strengthening by fibre pressing 4-99480  
 microstructure, influence on brittle fracture toughness 4-93388  
 Nimonic PE-16, irradi. in HFIR at 430°C, fatigue performance 4-109497  
 nuclear reactor vessels, brittle fracture resistance, calc. 4-96143  
 plastic interlayer, thin, brittle fracture in creep conditions 4-97430  
 plate, stability near sharp defect, initial biaxial stress state 4-108046  
 poly-1,4-dimethylene-trans-cyclohexyl suberate, crack propag., morphology effects 4-114661  
 polycrystals, strong and ductile, grain boundary design, overview 4-65336  
 polyethylene, linear, creep rupture and pre-rupture phenomena 4-89131  
 polyethylene, tensile stress/strain, 77-298K, crazing rel. to gas environment 4-66467  
 polyethylene fracture under long-term loading conditions, tie molecules importance in prevention 4-62041  
 polymers, fracture and rheological characteristics, interrelation 4-88232  
 polymers, fracture velocity in transient stages, US fractography study 4-99732  
 polymers, glassy, fracture speed meas. by US fractography (Japanese) 4-89235  
 pressure vessel, strength criterion in presence of prod. and service defects 4-64887  
 rock beams, combined bending and axial loading, distrib. damage approach 4-105553  
 statistical approach to brittle rupture for multiaxial states of stress 4-69708  
 steel, austenitic stainless, fracture modes under He ion and neutron irradi., temp. depend. 4-104853  
 steel, bainitic and ferritic, cleavage fracture initiation, microstruct. 4-99556  
 steel, C, cast and wrought, H induced ductility losses, annealing effects 4-85193  
 steel, C-Mn, low temp. creep crack growth, effect of cold work 4-76850  
 steel, cast, solidification, influence of AlN precip. on brittleness (Polish) 4-93270  
 steel, Cr-Mo, fracture toughness in transition region, interpretation of scatter and thickness effect 4-99603  
 steel, Cr-Mo, intergranular H stress cracking rel. to grain boundary segregation of P 4-62112  
 steel, Cr-Mo-V martensitic, liq. metal induced embrittlement, dislocation emission from crack tips 4-85210  
 steel, fracture toughness as function of temp. 4-66403  
 steel, fracture toughness tests, scatter of results, statistical model 4-81370  
 steel, heat-resistant, crack resist. characts., temp. and loading cycle asymmetry influence 4-99535  
 steel, heat-resistant, static and dynamic fracture toughness, influence of microstruct. and temp. 4-99600  
 steel, high strength, H embrittlement fracture morphology (Japanese) 4-95911  
 steel, low alloy, high-temp. brittle fracture, review 4-99562  
 steel, low C and low alloy, brittle fracture, fractographic characteristics, test temp. effects (Russian) 4-109495  
 steel, managing, influence of carbide formation on fracture struct. (Russian) 4-81273  
 steel, martensitic, press. vessel, cleavage fracture 4-71730  
 steel, martensitic stainless, cleavage fracture, micromech. mechanisms 4-104855  
 steel, Mn, 13 wt.%, prod. by powder metallurgy method 4-81169  
 steel, Ni-Mo, martensitic A533B pressure vessel, tempered, brittle fracture and fatigue crack growth, segregation effects, Auger obs. 4-66400  
 steel, reactor pressure vessel, A533B, environmentally-assisted cyclic crack growth 4-99627  
 steel, tool, brittle fracture, dopants and impurities effects, AES study 4-62063  
 steel, transformer, effect of Sb additions on texture 4-81216  
 steel, water-water power reactor vessel material, brittle fracture resist. and radiation embrittlement 4-96142  
 steel 45, plastically deformed, oriented microstresses and cold brittleness (Russian) 4-93334  
 steel with grainy cementite struct., fracture mechanism (Russian) 4-66408  
 steels, low alloy, fracture toughness studies 4-109491  
 stress intensity factors 4-97428  
 surface-coated materials, mech. props. 4-99625  
 topaz, deformation expts. indicating embrittlement by water 4-94101  
 Zircaloy-4 claddings, SCC at elevated temps., relevance to transient LWR fuel rod behaviour 4-104912  
 Al, mechanoluminescence at low loading rates 4-81019  
 Al-Cu-Li, recrystallised 2020, mech. props. rel. to soln. heat treatment 4-76781  
 Al-Mg solid solutions, ductility loss at high temps. 4-104857  
 Al-Zn-Mg single crystals, environmentally-assisted cracking 4-71762  
 C fibre reinforced plastic, damage susceptibility estimation, thermodynamic approach 4-99542  
 Ca<sub>2</sub>Ga<sub>2</sub>Ge<sub>2</sub>O<sub>12</sub>, garnet single crystals, microhardness, brittle fracture 4-65337  
 Cu, brazed, low cycle fatigue in high vacuum rel. to cold work 4-109500  
 Cu, creep and long-term strength study (Russian) 4-80146  
 Cu, dynamic tensile fracture due to impact 4-108510  
 Cu, mechanoluminescence at low loading rates 4-81019  
 Cu-Fe (2 wt.%), precipitation strengthened, high temp. creep 4-61990  
 Cu-Ga/V multifilamentary superconductors, brittle fracture, acoustic emission anal. 4-71715  
 Cu-Sb alloys, grain boundary segregation and cracking, Monte Carlo studies 4-114542

brittle fracture continued

Cu-Zn-Ni, superplastic, post-deform. tensile props., effect of cavitation 4-114621  
Cu<sub>2</sub>MnAl single crystals, Heuser alloy, compression, 77-367K, fracture slip, superlattice dislocation dissociation 4-66369  
(Fe, Co, Ni)<sub>3</sub>V, ductile ordered alloys, phys. metallurgy and mech. props. 4-114612  
(Fe,Ni)<sub>3</sub>V, ordered alloy, irradiation in HFIR, microstructure and bend ductility 4-108454  
Fe-Al-Si, Sendust, brittleness, effect of solidification and heat treatment 4-81281  
Fe-Co-Ni-Al, Alnico 5, hot workability, microstructure 4-114626  
Fe-Ni-C, fracture toughness rel. to transformation induced plasticity and grain boundary segregation 4-99585  
Fe-P alloys, intergranular fracture planes, chemical states, Auger and electron energy loss spectra 4-93385  
Fe-Si-Al, Sendust, hot workability, microstructure 4-114626  
 $\alpha$ -Fe-(C), H-induced grain boundary fracture, effect of C 4-93403  
FeCo alloy, brittleness, purity and impurity segregation effects (Russian) 4-109496  
(Fe<sub>2</sub>Co<sub>7</sub>)<sub>3</sub>V, tensile deforms, 20-1000°C, fracture mode and ductility rel. to order-disorder transform. 4-66427  
GaAs, cleaved, work function var. rel. to cooling 4-88556  
Gd<sub>3</sub>Ga<sub>5</sub>O<sub>12</sub>, garnet single crystals, microhardness, brittle fracture 4-65337  
Ge, cyclic loading near yield stress, plastic deformation (Russian) 4-113524  
LiAlSi<sub>2</sub>O<sub>6</sub>,  $\alpha$ -spodumene, microplasticity, dislocation glide and dissociation, TEM obs. 4-65331  
Mo, endurance limit in high cycle fatigue rel. to heat treatment and alloying 4-109498  
Mo, mechanoluminescence at low loading rates 4-81019  
Mo, pure and alloyed, cold deformed, softening by fast heating (Russian) 4-93316  
Nb alloy weld joints, with solid soln. and heterophase hardening, tendency toward brittle failure 4-62045  
Nb, mech. props. at low temp., Ti effect 4-93391  
Ni and alloys, fatigue lifetimes and fractography in air and liq. Hg 4-99557  
Ni and alloys, tensile fracture characters in liq. Hg 4-99558  
Ni, H embrittlement, influence of plastic deformation 4-71729  
Ni-Cu alloys, grain boundary segregation and cracking, Monte Carlo studies 4-114542  
Pb(Zr,Ti)O<sub>3</sub> ceramic, fracture mechanics evaluation of acoustic fatigue 4-95416  
W, brittle fracture, impurity effects, Auger electron and scanning electron spectroscopy (French) 4-70268  
W, powder metallurgy rods, swaging process workability rel. to texture (Japanese) 4-89068  
W-Ni-Fe, fracture behaviour, effect of substitutional impurity elements 4-89134

brittle materials see brittleness

brittleness

see also brittle fracture; embrittlement; hydrogen embrittlement; liquid metal embrittlement; notch brittleness  
basalt glass fibres, microhardness and microbrittleness 4-84342  
ceramics, N-based, innovations 1976-1981 4-71532  
composite shells, brittle, joints design in rigid systems 4-87636  
compressive surface strengthening 4-93307  
corundum single crystals, surface structure and deformation, chem. media effect 4-81314  
fatigue testing, high-temp. device 4-66527  
fibre reinforced ceramics, mech. aspects of failure (French) 4-81280  
fibre reinforced composite laminated plate, initial failure and ultimate strength theory (Japanese) 4-97417  
furfural acetate binder, highly filled composite, mech. props. 4-89080  
glass fibre reinforced plastic, roving cloth reinforced, strength in flatwise direction, temp. depend. (Japanese) 4-89087  
glass fibre reinforced polyester laminates, elastic constants rel. to fibre orientation and matrix microcracking 4-109447  
indenter loading of brittle solid, fracture mechanisms, flaws, Hertzian cracks 4-97432  
lifetime and rationalised load of brittle materials 4-69712  
microcracking brittle materials, crack-growth resist. 4-83858  
multiaxial strength tests for brittle materials 4-93491  
plane die in brittle half-plane, crack form, at edge 4-112770  
polyester unsaturated resin, surface markings in brittle plastic plate, two dimensions anal. 4-113527  
powders of brittle materials, obtained by melt spraying, temp. stresses 4-104748  
sheets, crack paths under biaxial loading 4-79497  
slag glass fibres, microhardness and microbrittleness 4-84342  
slow crack growth resistance testing with double torque method 4-81375  
spontaneous cracking of brittle matrix due to presence of thermoelastic stresses 4-108045  
statistical approach to brittle rupture for multiaxial states of stress 4-69708  
steel, alloy, reheat cracking, scanning Auger and electron microscopy study 4-71490  
steel, alloy, type 15Kh2NMFa, radiation embrittlement and temper brittleness (Russian) 4-66407  
steel, eutectoid, mech. props., effect of Si additions 4-93365  
steel, low alloy, Cr, dislocation structure and phase composition during annealing (Russian) 4-108366  
superhard materials, crack resist. determ., samples and loading 4-93494  
surface in sliding contact with spherical indenters, strength degradation 4-104881  
surface scratching in abrasive or erosive processes, effect of brittleness index and sliding speed 4-71741  
C fibre reinforced plastic, impact stability evaluation 4-89129  
Fe-Al-Si, Sendust, brittleness, effect of solidification and heat treatment 4-81281  
Fe-Cr-Mo-Ti heat-resisting alloy, Chi phase strengthened 4-71800  
 $\alpha$ -Fe-P-C solid solns., grain boundary brittleness, low-temp. reversibility (Russian) 4-104835  
FeCo alloy, brittleness, purity and impurity segregation effects (Russian) 4-109496  
MnZn ferrites, hot pressed, brittle and strength props by microindentation method 4-62044  
Ni electrodeposited from sulphate and acetate salts, hardness and structure 4-114431

brittleness continued

V-Cr-(Ti-Fe-Zr), mech. props. rel. to O contamination, fusion appls. 4-109499  
W wires, electropolished, structural changes after thermal treatment rel. to surface state (Polish) 4-85249  
WC-C, mechanical behaviour, room temp. to 1000°C 4-62002  
ZrO<sub>2</sub>, MgO partially stabilised, Weibull modulus 4-61972  
broadband amplifiers see wideband amplifiers  
broadcasting  
see also radio broadcasting; television broadcasting  
studios, sound reflections, frequency anal. 4-107953  
VLF broadcasts for clock comparison (Japanese) 4-58826  
broadside antennas see antenna arrays  
bromine  
see also nuclei with ...  
anti-Stokes Raman laser up-converter of excimer lasers using stimulated anti-Stokes Raman scattering 4-74486  
atmosphere, Br<sub>2</sub> and Br radicals in stratosphere 4-115530  
atom, ab initio calcs., spin-orbit coupling, kinetic energy operator, relativistic correction 4-102607  
atom oxidation reactions, travelling concentration waves parameters, determ. 4-62189  
atom relative photoionisation cross-section, autoionisation, Rydberg series 4-64435  
chemisorbed on Fe (110), LEED and ARUPS study 4-92518  
chemisorbed on Si (111), X-ray standing wave anal. with synchrotron radiation 4-103607  
electrodes in Zn/Br and Zn/air batteries, electrochemical calorimetry 4-104995  
gas diffusion through capillaries, laser control, energy efficiency 4-75113  
gaseous, proton and He stopping cross sections 4-92259  
laser using IBr photodissociation, solar-powered, theory and operation 4-87322  
molecule, angle- and spin-resolved photoelectron spectroscopy 4-83417  
molecule, F(O<sub>2</sub><sup>+</sup>) ion pair state, optical double resonance 4-87144  
molecule, long-range expansion coefficient, dynamical dipole polarisability 4-59625  
Br, H<sup>+</sup> impact, X-ray prod. cross sections 4-96648  
Br+Br<sub>2</sub>, collisional energy transfer, binary trajectory calcs. 4-96665  
Br+Na collisions, ion pair prod. 4-112266  
Br+Pb(U) collisions,  $\delta$ -electron spectra study 4-74321  
Br+Cl<sub>2</sub>, charge transfer and electron detachment, absolute total cross-sections meas. 4-69202  
Br<sup>+</sup>+Ne-Br<sup>+</sup>+Ne<sup>+</sup>, contribution of K-capture to Ne<sup>+</sup> production 4-83466  
Br<sub>2</sub> (B<sup>3</sup><sub>u</sub>) state, vibr. eigenenergies functional form 4-107328  
Br<sub>2</sub> absorption spectra recorded using freq. modulation spectroscopy with pulsed dye laser 4-73520  
Br<sub>2</sub> EXAFS, ab initio calcs. 4-64492  
Br<sub>2</sub> recombination gas dynamic laser, electron transitions (Russian) 4-96881  
Br<sub>2</sub><sup>-</sup>, radical in aq. soln. harmonic freq., anharmonicity constants, resonance Raman spectra 4-74247  
Br<sub>2</sub><sup>-</sup>, high resolution UV PES 4-112228  
Br<sub>2</sub><sup>-</sup> photodissociation spectra, predissociation mechanism, vibr. levels 4-87171  
Br<sub>2</sub>+Ar(Br<sub>2</sub>) collisional energy transfer, binary trajectory calcs. 4-96665  
Br<sub>2</sub>+methyl radical rate constants, product vibr. excitation and hot radical reactions 4-71893  
Br<sub>2</sub>+N<sub>2</sub>, quenching, energy exchange, rate constant, Franck-Condon factors 4-64530  
Br<sub>2</sub>(<sup>3</sup><sub>g</sub>) + Xe, laser photoassociation, XeBr(B) fluorescence 4-114772  
Br, uptake by human brain, quantitation by single photon emission CT 4-93852  
NaCl:Br, impurity-localised excitons, luminescence and absorption spectroscopy study 4-92625  
bromine compounds  
bromosodalite, visible spectra, thermal activation energy 4-109207  
ground states, MNDO calcs. 4-64378  
BrCN, photodissociation, spin-aligned CN(X<sup>2</sup> $\Sigma^+$ ) 4-114802  
BrCN+Xe, CN(B<sup>2</sup> $\Sigma^+$ ) prod., vibr. and rot. state distribution 4-89250  
BrCl laser, short wavelength 4-96883  
BrF laser, short wavelength 4-96883  
BrFO<sub>3</sub>, mol. constants, normal coordinate anal. 4-74216  
BrNCO, microwave spectrum, rot. constant, determ. from quadrupole hyperfine structure 4-91254  
Br<sub>2</sub>O, thermal vibrations, effect on EXAFS 4-102698  
CuBr, whole heated sealed-off laser, lifetime 4-107681  
Brownian motion  
see also colloids  
4-dimensional, recurrent Brownian paths with positive capacity 4-90504  
adiabatic elimination, range of validity of current procedures 4-73357  
aerosol particle, Brownian rotation, EM radiation absorption, modulation 4-85341  
aerosols, log-normally preserving size distribution for Brownian coagulation in the free-molecule regime 4-99847  
benzene, transition dipole moment, autocorrelation function, optical absorption spectra 4-114253  
bisppectrum for Brownian motion type random processes 4-73352  
charge stabilised dispersions, concentrated, self-diffusion, Brownian dynamics simulation 4-99851  
coagulation in discrete particle-size distributions, Monte Carlo simulation, Brownian motion 4-89345  
conference on transport theory, Blacksburg, VA, USA (March 1983) 4-95053  
dispersed system, kinetics of Brownian coagulation, weak hydrodynamic field 4-79638  
equilibrium and Lyapunov exponents of some Brownian flows (French) 4-110856  
extended Brownian dynamics for three dimensions, Smoluchowski diffusion 4-58739  
extremely underdamped, eigenvalues in inclined periodic potential 4-68125  
fermion diffusions 4-63664  
fluids with spin, viscoelastic models 4-112966  
interacting Brownian particles, correlation functions of infinite systems 4-111021  
interacting Brownian particles, self-diffusion coefficient, calcs. 4-85340  
kinetic boundary layer, Klein-Kramers eqn. 4-111079  
Kramers' equation, generalised function solution, convergence in type-S function spaces 4-95313  
laser-induced surface diffusion, Brownian motion model 4-70607

**Brownian motion continued**

- latex particles, scattered light intensity cross-correl. function meas. 4-79033  
 liquids, Brownian limits for tagged particle motion 4-113285  
 liquids, collective motions, interacting Brownian particle systems 4-103624  
 nematic liquid crystal, dielectric permittivity, rotational Brownian motion 4-88075  
 non-Markovian, memory effect, photon correlation method anal. (Japanese) 4-90510  
 non-Markovian stochastic differential eqns., dynamical props. 4-68134  
 nonequilibrium states, Langevin eqn. derivation, Brownian motion anal. 4-73350  
 nonlinear reaction-diffusion eqns., Brownian motion correspondence method 4-95309  
 nonstationary Brownian and molecular diffusion, described by wave eqns., variational approach 4-63662  
 phase transformation threshold analogy, effects of finite damping 4-111031  
 polydisperse scatterer number fluctuations, single-interval statistics and expt. errors 4-102888  
 polymer solutions, equilibration in momentum space in kinetic theory 4-64989  
 polystyrene suspensions, self-diffusion coeff., light scatt. meas. 4-98324  
 quantal Brownian motion in stationary and nonstationary fermionic reservoirs 4-64075  
 quantum Brownian oscillator, relaxation processes 4-78169  
 quantum Langevin eqn., noise spectrum 4-68007  
 quantum Langevin eqn. soln., return to thermal equilibrium 4-58675  
 quantum mechanics-Brownian motion analogy, relativistic expansion, Schrodinger and heat eqns. 4-95236  
 quantum system Brownian motion 4-111035  
 Riemannian geometry and Brownian motion on curved space 4-86337  
 rigid dumbbell suspensions in steady shear flow, perturbation calc. 4-74978  
 solute transport in capillary, Taylor-Aris theory 4-69829  
 spheres, rotational Brownian motion, direct obs. using NMR 4-58749  
 systems with memory effects, escape rates 4-90494  
 ultrafine chainlike or fibrous type particulate aerosols, Brownian coagulation and charge effect 4-99846  
 water, Brownian motion, translational and rot. 4-63672  
 Ar like liquid, molecular motion, fractal geometry and Brownian motion 4-70018

**Brownian movement** *see* **Brownian motion****brush discharges** *see* **discharges (electric)****bubble chambers**

- BEBC bubble chamber model, tests of two-beam holography 4-64274  
 high resolution camera for bubble chamber photography 4-68890  
 photographs evaluation using HPD automatic equipment 4-74109  
 rapid cycling bubble chamber, volume trigger 4-91183

**bubble nuclei** *see* **nuclear density****bubble point** *see* **boiling point****bubble points** *see* **bubbles****bubbles***see also* **foams**

- 10 MHz undersea sound attenuation probe for submicron bubble and particulate determ. 4-115628  
 acoustic echo effect in liquid containing gas bubbles 4-112615  
 acoustic waves nonlinear backscattering 4-103606  
 air bubbles behaviour in axial-flow pump impeller 4-103399  
 air-water bubbly flow, shear turbulence invest. for simple configs. 4-60489  
 airlift pump, bubble expansion and slip influence on performance and stability 4-60505  
 axial flow pump, entrained air effect on performance 4-97722  
 bubbly liqs., conc. waves 4-60495  
 cavitation, physical modelling using optical meas. techniques 4-60469  
 cavitation bubbles collapse between two walls in US field 4-103063  
 cavities containing Van der Waals gas, crit. radius and crit. no. of gas atoms 4-108347  
 cavity growth mechanisms, thermal and athermal processes 4-108349  
 circular cylinder, cavitating flow, erosion, trailing bubble entrainment 4-97622  
 collapse by shock wave and induced impulsive pressure 4-87757  
 column with suspended solids, gas-liq. interfacial areas 4-65003  
 critical angle laser light scatt. from bubbles in water, meas., models, appls. to bubble sizing 4-69311  
 crustaceans, bubble form. following decompression from hyperbaric gas exposures 4-93784  
 dipole oscillations of spherical particle in sound field 4-103064  
 diver decompression sickness and air embolism therapies 4-109990  
 diver decompression sickness prevention 4-109989  
 embedded-mesh pot. flow anal. 4-64971  
 equilibrium radii of small vapour bubbles and liquid droplets 4-112989  
 fluid mechanics review, book 4-90314  
 fluidised bed, particle-size effect on press. fluctuations and slugging 4-112993  
 fluidised beds, pressure and vel. meas. methods (Hungarian) 4-65043  
 fluidised beds at high temperatures, bubble size measurements and correlation 4-112983  
 fuel-air combustion in fluidised bed model 4-87787  
 furan, two-phase bubble, evaporation through immiscible liq., heat transfer 4-87781  
 gas bubble attached to solid wall, collapse by shock wave and induced impact press. 4-103400  
 gas bubble collapse near solid wall by shock wave and induced impulsive pressure 4-112954  
 gas bubble form. at submerged orifice under const. press. 4-60492  
 gas bubble generation, conductometer method monitoring 4-112985  
 gas bubble rise vel. in liq. fluidised beds, Davies-Taylor eqn. 4-87785  
 gas bubbles evolution in liquid 4-112988  
 gas bubbles formation kinetics in liquids with chemical reactions under microgravity 4-103900  
 gas content of bubbling zone in submerged-burner unit with circulation tube 4-103394  
 gas holdup in a bubble column (Chinese) 4-69816  
 gas-liquid flow in slotted disks centrifuge extractor, struct. investigation 4-103395  
 gas-liquid flows, conf., Grenoble, France (Sept. 1983) 4-58558  
 gas-liquid media, shock wave dynamics 4-60497

**bubbles continued**

- gas-solid fluidised beds, bubble- to dense-pulse mass transfer (German) 4-112994  
 gas-vapour bubbles in liquids, shape oscillations anal. 4-103387  
 glass/liquid interface, laser beam induced holographic bubble grating form. 4-83683  
 growth, in He<sup>+</sup> ion irradi. Ni, microstruct. contrib. 4-108472  
 hydro-spark forming, impulsive hydraulic press. and gas bubble motion (Japanese) 4-103594  
 infusion pumps, universal air-bubble detector based on modulated IR 4-109898  
 Langmuir circulation effect on bubble distrib. caused by breaking wind waves 4-82069  
 large particle bubbling fluidised beds, heat transfer 4-113004  
 liquid bubble motion in vertical porous tubes 4-60487  
 liquid free surface in cylinder, dynamic behavior, vertical vibr. effect 4-112913  
 liquid in bubble bed apparatus, large scale circulatory motion (Russian) 4-60442  
 liquid tensile strength, cavitation history and entrained gas effect 4-75593  
 LMFB, acoustic imaging of vapor bubbles through optically non-transparent media 4-59364  
 LMFB safety anal., core expansion studies, CARAVELLE expts. and IRIS code 4-78729  
 low press. bubble with jet attachment, transient response 4-87780  
 metallic, glasses, ion irradi., damage, He and Ar, bubble form., blistering, exfoliation 4-108481  
 metals, dislocation loop punching by He bubbles 4-103748  
 microbubbles, nonlinear behaviour and US detection 4-62535  
 microbubbles dynamic and diffusive growth, near two-dimensional hydrofoil 4-65010  
 minute gas bubbles collapse in dilute polymer solns. 4-60486  
 mixed carbide reactor fuels, irradi., defect struct., fission gas bubbles, precipitates, TEM obs. 4-83145  
 multiphase turbulent shear flows, entrapment and transport of bubbles by transient large eddies 4-60519  
 Newtonian fluid, bubble and drop motion towards deformable interface 4-60493  
 nonspherical bubble collapse, press. field generation 4-103401  
 nucleate pool boiling, bubble growth rates and departure vols. 4-97649  
 nucleate pool boiling, freq. effect on bubble departure diameter 4-97644  
 ocean surf zone, size spectra in foam patches 4-115406  
 parametric sound radiator, gas bubble effects on sound field 4-91681  
 n-pentane, two-phase bubble, evaporation through immiscible liq., 'heat transfer 4-87781  
 polyethylene films, low-density, imperfection form. during extrusion 4-113353  
 positronium bubbles in <sup>3</sup>He and <sup>4</sup>He fluids and solids 4-108672  
 pressure wave propagation in bubbly mixtures 4-83934  
 pressure wave propagation in non-Newtonian two-phase fluids (German) 4-83919  
 radially oscillating, surface dilational elasticity determ. method optimisation (German) 4-60488  
 radiative interaction of bubbles in liquids 4-79652  
 rising single bubble, gas-liquid interfacial area by chemical method (Chinese) 4-69815  
 shear viscous bubble and drop deform. 4-91835  
 shock tubes, bubbly water, pressure wave propag. (Japanese) 4-87503  
 silicate glasses, electron irradi. damage mechanism 4-70216  
 size measurement using nonlinear freqs. of two acoustic freqs. 4-74790  
 slug flow in vertical ducts, wall friction mechanism 4-60490  
 solid surfaces contacting liq.-gas soln., bubble nuclei stability 4-92477  
 sound fields, bubble phenomena 4-69615  
 spherical bubble interaction with a free surface (German) 4-83944  
 stagnant and flowing liqs., bubble rise vel. 4-60520  
 steel, austenitic stainless, irradiated, void swelling, He bubbles 4-103792  
 steel, austenitic stainless, stress rupture in-reactor creep cavity form. model 4-104854  
 swelling incubation in austenitic stainless steels, microchem., microstruct. and environmental effects 4-108413  
 thermocapillary migration normal to plane surface 4-60485  
 thermocapillary motion of two bubbles oriented arbitrarily relative to a thermal gradient 4-61188  
 three phase bubble column, axial mixing hydrodynamics, slurry props. effects 4-87782  
 transient two-component flow, modelling using four-point implicit method 4-97691  
 trapped air in polar ice, age differences 4-115475  
 turbulent flow hydrodynamics of a bubbly two-phase mixture 4-79563  
 two dims. hydrofoil, press. distrib. and drag reduction in dil. polymer solns. 4-87763  
 two-dimensional bubbles rising in a tube and jets falling from a nozzle 4-50666  
 two-phase critical flow, boundary layers, visualisation study 4-60498  
 two-phase flow, dynamics in horizontal rectangular pipe 4-97641  
 two-phase flow in large diameter pipes 4-65000  
 underwater explosion of ring charge near a free surface 4-87759  
 US echo cardiography, double frequency bubble diagnostics 4-100287  
 vapour bubble detachment in flow boiling 4-97650  
 vapour bubbles detachment from heated walls, anal. 4-103392  
 vapour bubbles in immiscible liquid, direct-contact condensation pattern 4-61062  
 vapour-gas bubble ignition in a liq. 4-71924  
 vapour-liquid medium, bubbles, wave propag. 4-91832  
 void fraction and press. waves 4-60496  
 water with bubbles, ultrasonic absorpt. and propagation (French) 4-83757  
 Al, pure, 600 MeV proton irradi., H and He bubble form. at grain boundaries 4-108479  
 Al, void and bubble form., 600 MeV proton irradi., temp. depend., 130-430°C 4-108482  
 Fe-Cr-Ni (15, 15 wt.%), He bubble form. during dual beam irradi. 4-75562  
 Fe<sub>80</sub>B<sub>20</sub> amorphous alloy, He ion irradi., blister and-bubble form., TEM obs. 4-108434  
 Fe<sub>91</sub>Ni<sub>8</sub>B<sub>1</sub>Mo<sub>1</sub> Metglas 2826 MB 5 keV He implantation, bubble growth, free vol. relax. model 4-103822  
 He bubble formation in T charged N, obs. of cylindrical cavities at dislocations 4-60913  
 He bubbles, equation of state for small cavities 4-103824  
 He bubbles at grain boundaries in austenitic alloys 4-108471

# bubbles continued

- He bubbles generated during irradiation, growth by coalescence, effect of immobilisation 4-108414
- He bubbles in Al, nucleation on dislocations during 600 MeV proton irradiation 4-113504
- He bubbles in austenitic alloy, void swelling, effect of pulsed irradiation 4-108474
- He bubbles in Fe-Cr-Ni alloy, weak beam imaging 4-103618
- He bubbles in Zr tritides, TEM study of ageing 4-75503
- He cavity growth and nucleation in Mo at 300K, expt. HDS and TEM studies 4-108348
- He I, superheated, soil interface, light induced nucleation of vapour bubbles, photoemission model 4-61163
- He in austenitic stainless steel, swelling resistance in fusion reactors 4-107012
- Nb-Ti superconductors, flux pinning by gas bubbles (Russian) 4-104381
- Ni-He, preimplanted, electron irradiation, 1 MeV, He bubble growth 4-103803
- Ni-Cr-Ti-Mo(Nb), precipitation strengthened, HFIR irradiation, ductility, microstructure 4-108457
- Ti/Ni bilayered thin films, amorphisation and ion beam mixing 4-88408
- V<sup>+</sup> charged, He bubble formation, TEM obs. 4-103825
- W, AKS-doped wire, high-temp. creep behaviour, effect of gas bubbles (German) 4-81243

bucket-brigade device arrays see charge-coupled device circuits

bucket-brigade devices see charge-coupled devices

# buckling

- beam, non-homogeneous, deep, buckling critical load 4-112739
- beam with elliptic cross section, magnetoelastic buckling 4-112737
- beams, long, thin, open section, and corrugated panels, nonlinear bending and collapse 4-103221
- bifurcation buckling loads due to struct. geometry perturbations, first order change 4-64870
- cantilever, magnetoelastic buckling, influence of finite specimen dimensions 4-74913
- caps, shallow, finite polar dimpling under sub-buckling axisymmetric pressure distribution 4-97364
- catastrophe theory, nonelementary, appl. to imperfect bifurcation problems 4-58649
- circular cylindrical shell, dynamic instability under periodic compressive force and temp. field 4-69701
- columns, unimodal, optimal, clamped-clamped, higher buckling mode determined 4-87601
- eigenvalues bound estimating 4-108027
- elastic ring, perturbation post buckling study 4-86215
- elastic structural models, potential function truncation, post-buckling response 4-64843
- elastically supported arches, lateral buckling 4-112738
- fibre reinforced composites, laminated plates, optimum design 4-97367
- films, compressed, delamination and spalling mechanics 4-79500
- girders, curved box, subjected to various loads, plastic behaviour (Japanese) 4-97337
- graphite fibre reinforced epoxy composites, buckling, hygrothermal and conditioning influence analysis 4-104810
- irreversible systems obeying max. dissipation principle, bifurcation and stability (French) 4-78139
- laminated half-plane with elastic-plastic layer deformation, surface buckling 4-97363
- large force plate characters, comprehensive force test, design problems (Japanese) 4-91746
- layered plates, delamination buckling and growth 4-79480
- linear conservative systems, loading-freq. curve, direct energetic (action) method 4-87600
- magnetoelastic buckling, interaction of two nearby ferromag. panels 4-74911
- nuclear containment-like cylindrical geometries under combined shear and bending, buckling 4-96116
- nuclear containments, buckling design research 4-96117
- nuclear reactor steel containment buckling research-program [for nuclear plants] 4-96114
- optical fibres, spring constant calculation in buckling 4-91586
- panel, stiffened cylindrical, nonmembrane prebuckling effects 4-91743
- panels, corrugated and long thin open section beams, nonlinear bending and collapse 4-103221
- panels, cylindrical, integrated-stiffened, buckling test (Chinese) 4-79475
- pipelining system buckling anal. 4-112746
- plastic buckling load approx., eigenvalue problem soln. 4-83847
- plate, circular, cylindrically orthotropic, post-buckling behaviour 4-91745
- plate, circular, isotropic, thermal post-buckling 4-91744
- plate, thick circular, post-buckling behaviour 4-97361
- plate, thin, magnetoelastic buckling, catastrophe theoretic anal. 4-112741
- plate, thin, non-homogeneous circular, variable thickness, buckling under uniform compression 4-112740
- plates, anisotropic laminated, compressive and shear loading, postbuckling anal. 4-64866
- plates, annular, stability under shear 4-112745
- plates, annular sector with variable thickness, buckling, stability anal. 4-64867
- plates, laminated, with free edge in edgewise bending and compression, buckling 4-79474
- plates, thin elastoplastic, incipient buckling study (French) 4-83846
- polyaramid fibres, compressive buckling, mech. model 4-97362
- pressure loads, displacement dependent, nonlinear finite element anal. 4-91742
- pressurised components, lower bound of creep buckling strength 4-91747
- pressurised circular tube of harmonic compressible material, finite deformation 4-79478
- prismatic beams, finite deformations, variational anal., warping stiffness effects on buckling loads 4-79479
- protective surface film, continuous, criterion for compressive failure 4-99612
- ring stiffened cylindrical shell, buckling under unsymmetrical axial loads 4-81261
- rings, circular confined, collapse under external pressure 4-112742
- rings, elastic, inextensional, postbuckling behaviour under external pressure 4-74908
- rod of elastoplastic material, dynamics of buckling 4-112743
- shell, cylindrical, with imperfections of form localised in axial direction, stability (Russian) 4-112747

# buckling continued

- shell, cylindrical, with one-sided couplings, stability under axial compression, crit. load (Russian) 4-64869
  - shell, cylindrical, with variable thickness, stability (Russian) 4-74909
  - shell, open conical sandwich, nonlinear stability under external pressure and compression 4-87598
  - shell, thin, cylindrical, laminated, in pure torsion, instability 4-103224
  - shell, zero curve, with variable thickness and elastic modulus, local buckling (Russian) 4-74910
  - shell stability 4-97365
  - shells, thin elastic, nonlinear buckling and post-buckling anal. 4-87597
  - shells, viscoplastic, cylindrical, dynamic buckling, influence of yield function nonlinearity and temp. 4-103222
  - soft ferromagnetic elastic solids, finite deformation theory 4-97312
  - sphere, inside-out elastic, equilib. stability 4-112744
  - steel, HSLA, sheet, press forming problems 4-99471
  - structure response to loading field, Newton-Raphson scheme 4-108029
  - superconducting structures, magnetoelastic buckling and Earnshaw's theorem 4-74049
  - thin elastic plate, buckling instability, mode selection, boundary conditions effects 4-79476
  - thin elastic shells, stability anal., catastrophe theory 4-87575
  - thin fluid layer undergoing end-compression, buckling 4-103452
  - thin-walled structures, crushing mechanics 4-97339
  - Timoshenko technique for estimating buckling loads, modification 4-108028
  - tubes, rectangular, plastic collapse loads 4-112722
  - vertical liquid column sinuous flow impinging on horizontal surface 4-97688
  - Si, sheet growth at high speeds, stress generation, influence of plastic deformation 4-65211
  - Si web growth, thermal stress effects, modelling 4-65210
- buffers (chemical) see pH
- building
- see also civil engineering
  - attenuation enhancement, conductive paint appl. 4-107496
  - materials, heat transfer, effect on energy conservation 4-89486
  - materials, radioactivity concs. limitation based on a practical calc. model 4-93935
  - radiation from building materials 4-93869
  - Rn, soil gas carrying, infiltration prevention in building constructions 4-93898
- bulk density see density
- bulk diffusion see diffusion in solids
- bundling see packaging
- burning see combustion
- burnout see combustion
- burst noise see random noise
- business see commerce
- BWT see backward-wave tubes
- C invariance
- Dirac equation and Hestenes' geometric algebra 4-102010
  - lepton charge conservation, massless and massive nondegenerate Majorana neutrinos 4-106490
  - Majorana particle processes, CPT, CP, and C phase effects 4-111337
- C steel see carbon steel
- cable insulation
- see also insulating oils
  - nuclear power station cables, gamma radiation and thermal ageing of polyethylene insulation 4-75526
  - polyethylene compounds, carbon black filled, IR-spectroscopic determination of stabiliser (German) 4-111222
  - polyolefins with amine additives, low temp. losses, expt. study 4-114205
  - radiation effects at CERN 4-108427
- cable jointing
- coated optical fibre for high strength splice (Japanese) 4-79302
  - dispersion-shifted single mode fibre, transmission splicing and cabling performance 4-91616
  - fibre optic connectors and joints (Italian) 4-60158
  - multi-glass rod optical fibre splicers and connectors, fabrication (Japanese) 4-79303
  - NTT's optical fibre transmission system, development (Japanese) 4-83711
  - optical fibre communication links, permanent and separable jointing (Spanish) 4-79326
  - splice enclosure for optical fibre subscriber cable (Japanese) 4-79315
  - submarine optical fibre, cable, joint box design 4-74731
  - technique for optical fibre subscriber cables (Japanese) 4-79314
- cable laying
- NTT's optical fibre transmission system, development (Japanese) 4-83711
  - optical digital transmission system for EVU news networks (German) 4-112588
  - optical subscriber loop, laying and construction technique (Japanese) 4-79300
  - power cable trenches moisture and heat transfer, physical principles and calculation methods, cable continuous loadability calc. (German) 4-69666
  - principles of cable burning 4-114799
  - SL lightweight submarine cable system sea trial, transmission tests 4-107842
- cable sheathing
- radiation effects at CERN 4-108427
- cable sheaths see cable sheathing
- cable television
- education and training appls. of information technology, Council for Educational Technology view 4-90339
  - optical fibres in broadband networks, instrumentation and urban and industrial environment appls., conf., Paris, France (May 1983) 4-78024
  - optical subscriber loop for business premises and local area appls. (Japanese) 4-79304
  - optical subscriber loop system for local area appl. (Japanese) 4-79307
- cables (electric)
- see also coaxial cables; power cables; submarine cables; superconducting cables; telecommunication cables
  - component fault testing in electro- and cable-technology, nuclear reactor appl. 4-106839
  - model for cable radiation, evaluation 4-107497

## CAD

- see also architectural CAD; circuit CAD; circuit layout CAD; computer-aided analysis; interactive systems; power system CAD
- ion optics calc. program in BASIC, for mass spectrometer design 4-78410
- MVPACK, package for computer aided design of multivariable control systems 4-68682
- nuclear power plant computer-aided design and draughting benefits 4-59311
- optical design theory and aberration, book 4-95086
- optical lens systems, intelligent program 4-102996
- optical system, complex, automated construction using a computer 4-74652
- optical system design (German) 4-74656
- phase contrast filters, construction using digital image processing system 4-79274
- reverberation characts. improvement of enclosed space, with aid of computer (Slovak) 4-60213
- ROSAT X-ray telescope thermal design features 4-85879
- shape optimal design using B-splines 4-106190
- SNOW ion beam extraction simulation program, computers for design and testing 4-73590
- soft contact lens systems, power and radius changes induced by flexure 4-77425
- solar collector, storage tank and heat exchanger design by computer, F-Chart 4-99943
- Stirling engines computer-aided design 4-66755
- two-lens cemented objective calc. using a computer 4-74653
- vision feedback and optical system design 4-97023

## CAD/CAM see CAD

## cadmium

- see also nuclei with .....
- NW Atlantic, Mn, Ni, Cu, Zn, Cd conc. in surface and deep water 4-85711
- Atlantic Ocean, As, Mn, Cd vertical profiles and correl. with phosphate 4-85712
- atom, electron impact ionisation cross-section, semi-empirical formula 4-74342
- atomic ions in laser-prod. plasma, for UV spectra 4-68997
- atomic vapour, interatomic pots., UV absorpt. spectra 4-107297
- atoms, Compton scatt., differential cross sections 4-112146
- cathode in vacuum arcs, spot region, microparticle generation 4-87977
- Congost River, Catalonia, Spain, Cd, Cu, Pb, conc. obs. 4-62430
- diffusion in Ag, isotope effect meas. 4-65476
- doppler oscills., carrier reflection influences 4-80481
- electrodeposition from acidic chloride baths, morphology and hardness rel. to addition agents 4-93238
- electroplating from acidic chloride bath, superimposed AC effect 4-93239
- film deposition through layer of liq. He 4-76677
- He-Cd laser with lateral HF discharge, different design comparative characts. (Russian) 4-69372
- impurity diffusion in solid Na 4-65475
- inversion voltammetry for metal content in river water, seawater and bottom sediments 4-100816
- laser microprobe mass analysis detection limits and lateral resolution 4-72016
- Lifshitz phase transition, muon Knight shift study 4-71230
- liquid, self-diffusion coeffs., temp. depend. 4-65426
- liquid, ultrasonic vel., temp. depend., elastic moduli, vol. depend. 4-60989
- Louisiana, USA, freshwater sediment heavy metal pollution 4-93654
- mechanisms and kinetics of dissolution in liquid Ga 4-114530
- Mediterranean, Cu, Ni, Cd concs. in surface waters 4-85717
- metastable isomer prod. for analytical work using isotopic neutron sources, Sr, Cd, In, Ba detection 4-77037
- muon Knight shift, spin rot. meas. 4-65916
- Ni-Cd batteries, construction and electric parameters of plastic bonded cells (Hungarian) 4-105102
- ocean surface waters of N Atlantic and N Pacific, Cu, Ni, Cd, Pb concs. 4-85710
- rainwater of Bermuda, trace metals content 4-67320
- seawater of Kattagat and Skagerrak, trace metal concentrations 4-85714
- seawater trace metal content meas. technique using isotope dilution mass spectrometry 4-85797
- shock-compressed, vapourisation on expansion 4-61063
- single crystal plates, low dislocation density 4-93211
- stopping power for 6.5 MeV protons and mean excitation energies 4-92271
- vacancy migration energy, exoelectron emission meas. 4-65456
- vapour, resonant freq. conversion process saturation 4-60106
- vertical distribution in Arctic Ocean rel. to Al and Fe profiles and hydrography 4-82089
- X-ray diff. data, anharmonic parameters 4-84233
- Zircaloy cladding, chemical model for cadmium liquid-metal embrittlement 4-106770
- $^{111}\text{Cd}^+$  matrix isolated, fast atom bombardment, ESR, investig. 4-74218
- Cd  $1. d_{5/2}^9 p$  electron configs., empirical Slater-Condon parameters 4-68943
- Cd $^+$ , dynamic response of inversion density to current disturbances in He-Cd discharge 4-108237
- Cd:Bi, crystal growth from vapour, Bi impurities effect 4-113368
- Cd-CdO solid solns.,  $^{113}\text{Cd}$  NMR investig. 4-98977
- Cd-He discharge, current disturbances, Cd $^+$  inversion density, dynamic response 4-108237
- Cd-Ni batteries, fast-charge, temperature-controlled characts. 4-93606
- Cd-Ni button cells, sealed, characts. for backup power source for computer memory retention 4-93600
- CdCl $_2$ , CdBr $_2$ , CdI $_2$ , melting, solid-solid transitions at high pressures 4-80195
- CdF $_2$ :Er $^{3+}$  energy transfer up-conversion 4-99162
- $^{109}\text{Cd}$  carrier free radioisotope preparation (Chinese) 4-68850
- $^{111}\text{Cd}$  self-alignment in a discharge 4-87963
- $^{113}\text{Cd}$  vapour, coherent nonlinear phenomena in random fields 4-102980
- $^{113}\text{Cd}$  vapour nonmonotonic excitation in two-photon transitions 4-91243
- $^{114}\text{Cd}/^{113}\text{Cd}$ , neutron, fluence determ. for isotopic variation meas. 4-91186
- He-Cd long lifetime laser using continuously tunable He replenisher (Chinese) 4-60089
- He-Cd-Hg system three-colour hollow cathode laser (Russian) 4-69371

## cadmium continued

- He-Cd $^+$  hollow cathode laser, population inversion mechanism 4-83570
- He-Cd $^+(Zn^{II})(Ne)$  lasers, excitation mechanisms anal. (Japanese) 4-79116
- He-Zn-Cd, hollow cathode laser, simultaneous laser oscillation by Cd II and Zn II lines (French) 4-112399
- InP-Cd crystals, bulk and surface effects of heat treatment 4-84625
- Ni-Cd accumulator batteries, technology review (French) 4-81536
- Ni-Cd batteries with polypropylene separators for space vehicles; design, development, performance and reconditioning 4-72069
- Ni-Cd cell residual charge meas. using microprocessor-based unit 4-81535
- Ni-Cd cells, analytical model for battery cycle life 4-72070
- Ni-Cd cells, degradation study using impedance measurements 4-72068

## cadmium alloys

- see also cadmium compounds
- contact materials with reduced noble metal content, corrosion behaviour (German) 4-99640
- rare earth-Cd equiatomic cpds., struct. and mag. phase transitions 4-84795
- Ag-Cd-In alloys, X-ray determ. of mean Debye-Waller factors, vibr. amp. and Debye temp. 4-84358
- Al-Cu-Cd, strengthening mechanism of Cd additions 4-61985
- Al-Cu-Li-Cd, 2020, microstruct., fracture toughness and SCC 4-76851
- Al-Cu-Li-Mn-Cd, Al 2020, fatigue crack growth behaviour 4-71728
- Au-Cd liq. and solid alloy, elec. resist. studies 4-88499
- Au-Cd, electron damage, high resolution electron microscopy study 4-92241
- Bi-Cd-In system, eutectic alloys, microstruct. 4-93263
- Bi-Cd-Sn-Pb, Wood's metal, melting and solidification, US study 4-60991
- Bi-Pb-Sn-Cd, Wood's metal model, inclined simulated cracks, eddy current detect. 4-66516
- Cd-Mg, local electron density of states, Van Hove singularities,  $\mu^+$  Knight shift 4-84887
- Cd-Ni, electrodeposition from ammoniacal baths, corrosion resist. 4-66253
- Cd-Pb, eutectic alloy thin films, growth 4-88995
- Cd-Pb, thermodynamic props. at 900°C 4-80263
- Cd-Pb composite amalgam cathode for standard cells (Japanese) 4-86439
- Cd-Pb eutectic thin films, directionally solidified, interlamellar spacing 4-93285
- Cd-Zn single crystals, critical resolved shear stress, 1.5 to 50K 4-71685
- Cd $_2$ Mg alloys; electron energy spectrum and de Haas-van Alphen effect (Russian) 4-70639
- Cd $_2$ Mg, band struct. and stability (Russian) 4-84552
- Mg-Ag-Cd, constitution diagram, eutectic transform., X-ray and thermal analysis 4-114487
- Mg-Cd, dilute alloy, solid solution hardening 4-71664
- Ni-Cd aerospace batteries, reliability determined from survival data 4-105104
- PdFeCd dilute alloys, hyperfine field at Cd, PAC spectroscopy studies 4-92681
- Sn-Cd (5 wt.%), plasticity rel. to eutectoid transform 4-114605
- Zn-Pb-Cd, cast ingots and sheets, microstructure rel. to cooling rate 4-109390

## cadmium compounds

- see also cadmium alloys
- cadmium (II) acetate dihydrate  $^{113}\text{Cd}$  and  $^{115}\text{Cd}$  chemical shift tensors, PMR 4-98958
- CdS/Cu $_2$ S heterojunction, high resolution electron microscopy characterisation 4-104294
- halides, electronic struct., UV reflectivity 4-84974
- interface states studied by electrochemical photocapacitance spectroscopy 4-98750
- oxalate trihydrate: Mn $^{2+}$ , EPR spectrum 4-104489
- sodium cadmium formate, thermal expansion, X-ray powder diff. study 4-103975
- AgCl-CdCl $_2$ , molten, electrolytic cond. 4-108638
- AgI-CdI $_2$ , pseudobinary systems, struct. and phase equil. investigs. 4-70072
- Ba(Cd $_{0.13}$ Nb $_{0.86}$ )O $_3$ , dielec. props. and chem. inhomogeneity, effect of sintering 4-85128
- Ba(PO $_3$ ) $_2$ -CdF $_2$ , high refractive index glass, optical constants, density and atomic refraction rel. to struct. 4-93043
- Bi $_2$ Cd $_3$ S $_4$  film, spray pyrolysis deposited, substrate temp. effect on elec. and opt. props. 4-70962
- (Cd,Zn)S-CuInSe $_2$  Boeing solar cells, current transport 4-81546
- (Cd,Zn)S-CuInSe $_2$  solar cells, light-induced junction modification 4-77092
- Cd complex with valine, polarographic investig. 4-72032
- Cd complexes, with dithiocarbamate and bis-(N,N-diethyl dithiocarbamate), vibr. freq., normal coordinate anal. 4-59701
- Cd-CdO solid solns.,  $^{113}\text{Cd}$  NMR investig. 4-98977
- Cd-inert gas pairs, oscillator strength, adiabatic pots., pseudopotential calcs. 4-78925
- Cd $_2$ As $_2$  crystals, growth and morphology 4-75339
- n-Cd $_2$ As $_2$ , degenerate, Debye screening length under influence of arbitrary mag. quantisation 4-70836
- Cd $_2$ As $_2$ , disordered, Mott transitions and impurity scattering (Russian) 4-88450
- n-Cd $_2$ As $_2$ , mag. quantisation effect on Einstein relation 4-92740
- Cd $_2$ As $_2$ , magnetoplasma reflectivity studies 4-92761
- Cd $_2$ As $_2$ , Raman spectrum 4-71382
- Cd $_2$ As $_2$ , role of vacancies in band struct. 4-75853
- CdBr $_2$  layered cryst., radiation defect formation 4-65299
- CdBr $_2$ :Cu, photoionis., phosphoresc., at. states 4-102632
- CdBr $_2$ :I $_2$ , absorpt. spectra and electron localisation (Russian) 4-104161
- CdBr $_2$ :Mn $^{2+}$ , phononless luminescence spectrum (Russian) 4-114328
- CdBr $_2$ -CuBr heterogeneous thin-film appls. for obtaining photographic images during phys. development (Russian) 4-82848
- CdBr $_2$ -NO $_2$ , aqueous soln., luminescence study (Russian) 4-85009
- CdCl $_2$  disubstituted thiourea complexes, appl. in fabrication of thin film solar cells 4-114909
- CdCl $_2$ :Cu, photoionis., phosphoresc., at. states 4-102632
- CdCl $_2$ -CuCl heterogeneous thin film appl. for obtaining photographic images during phys. development (Russian) 4-82848
- CdCl $_2$ -NO $_2$  aqueous soln., luminescence study (Russian) 4-85009
- CdCr $_2$ Se $_4$ , photomagnetisation study 4-99102
- CdCr $_2$ Se $_4$ , surface magnetostatic wave obs. 4-84778

**cadmium compounds continued**

CdCr<sub>2</sub>Se<sub>4</sub>In, static I-V characts. 4-70815  
Cd<sub>2</sub>Cu<sub>1-x</sub>Fe<sub>x</sub>O<sub>4</sub>, hyperfine field interactions, Mossbauer spectra 4-65885  
Cd<sub>2</sub>Cu<sub>1-x</sub>Fe<sub>x</sub>O<sub>4</sub> spinel, low temp. Mossbauer obs. of mag. interactions 4-89893  
CdD<sub>2</sub>PO<sub>4</sub>, disordered crystals undergoing structural phase transitions, at order parameter determ. by cryst. struct. anal. 4-88126  
CdF<sub>2</sub>, alkali metal doped, association and bound motion 4-80294  
CdF<sub>2</sub>, dielectric constant, temp. depend., polarisability 4-92995  
CdF<sub>2</sub>Er<sup>3+</sup>, insulator to semiconductor transition, site selective laser spectroscopy 4-99155  
CdF<sub>2</sub>Eu, deep centre characterisation by thermally controlled EPR 4-71174  
CdF<sub>2</sub>Eu, thermoluminescence processes, photo-ESR studies 4-66085  
CdF<sub>2</sub>Gd<sup>3+</sup>, EPR, anomalous high elec. field effect 4-71173  
CdFe<sub>2</sub>O<sub>4</sub>, magnetic susceptibilities meas. 4-88650  
CdFe<sub>2</sub>O<sub>4</sub>, stability in reducing atm., TGA, X-ray diffr. studies 4-76999  
CdGa<sub>1.8</sub>Fe<sub>0.2</sub>O<sub>4</sub>, magnetic susceptibilities meas. 4-88650  
CdGa<sub>2</sub>S<sub>4</sub>, effective ionic charges, optic phonon spectra 4-103894  
CdGa<sub>2</sub>S<sub>4</sub>, narrowband selective optical filter 4-107803  
CdGa<sub>2</sub>S<sub>4</sub>, optical filters using uniaxial crystals with 'isotropic' period (Russian) 4-97049  
CdGa<sub>2</sub>S<sub>4</sub>, struct. refinement and twinning 4-92167  
CdGa<sub>2</sub>S<sub>4</sub>, vibr. props., polarisation depend. IR reflectivity studies 4-75624  
CdGa<sub>2</sub>(S<sub>2</sub>Se<sub>2</sub>)<sub>2</sub>, mixed defect cryst., Raman scatt. 4-61688  
CdGa<sub>2</sub>Se<sub>4</sub>, antireflection coatings for YAG crystals (Russian) 4-97012  
CdGa<sub>2</sub>Se<sub>4</sub>, effective ionic charges, optic phonon spectra 4-103894  
CdGa<sub>2</sub>Se<sub>4</sub>, excitonic wavelength modulated reflectance 4-71336  
n-CdGeAs<sub>2</sub>, degenerate, Einstein relation, cryst. field splitting effect 4-108860  
CdGeAs<sub>2</sub>, electron scatt. by optical phonon piezoelec. pot. 4-88257  
CdGeAs<sub>2</sub> glass crystallisation, thermal anal., activation energy determ. 4-84187  
CdGeAs<sub>2</sub>, reflectivity spectra, wavelength modulation method 4-71407  
CdGeP<sub>2</sub>, photoelectrochemical cells 4-89452  
CdGe<sub>1-x</sub>Si<sub>x</sub>As<sub>2</sub> glasses, elec. props. and phase stability 4-104202  
CdHgTe, material saving method treatment for radiation sensors 4-85233  
p-Cd<sub>0.23</sub>Hg<sub>0.77</sub>Te, hopping cond. between intrinsic defects 4-104210  
Cd<sub>0.23</sub>Hg<sub>0.77</sub>Te etalon, low-power nonlinear Fabry-Perot reflection at 10 μm 4-96981  
Cd<sub>1-x</sub>Hg<sub>x</sub>Te:Mn, EPR study 4-71168  
Cd<sub>2</sub>Hg<sub>1-x</sub>Te, ellipsometric studies of interband transitions 4-92999  
Cd<sub>2</sub>Hg<sub>1-x</sub>Te, epitaxial film growth by chem. transition reactions, elec. props. 4-70965  
Cd<sub>2</sub>Hg<sub>1-x</sub>Te, galvanomagnetic effects in quantising mag. field (Russian) 4-70843  
Cd<sub>2</sub>Hg<sub>1-x</sub>Te graded energy-gap structures, interf. photoelectromag. effect 4-113992  
Cd<sub>2</sub>Hg<sub>1-x</sub>Te, ion transport and anodic oxidation (Russian) 4-70440  
Cd<sub>2</sub>Hg<sub>1-x</sub>Te, metal-organic VPE growth 4-85107  
n-Cd<sub>2</sub>Hg<sub>1-x</sub>Te, minority carrier mobility, Haynes-Shockley method 4-92714  
Cd<sub>2</sub>Hg<sub>1-x</sub>Te, narrow-gap semiconductor, internal photoeffect, quantum efficiency calc. 4-61415  
Cd<sub>2</sub>Hg<sub>1-x</sub>Te, obs. of negative luminescence 4-99190  
Cd<sub>2</sub>Hg<sub>1-x</sub>Te, phonon states, far IR absorpt. spectra study (Chinese) 4-92312  
p-Cd<sub>2</sub>Hg<sub>1-x</sub>Te, photoconductivity and photomagnetic effect 4-104268  
n-Cd<sub>2</sub>Hg<sub>1-x</sub>Te single crystals, hot electrons at strong elec. fields (Russian) 4-98628  
Cd<sub>2</sub>Hg<sub>1-x</sub>Te solid solutions, homogeneity, carrier conc., magnetic circular dichroism, temp. depend. 4-93061  
Cd<sub>2</sub>Hg<sub>1-x</sub>Te, transport and pyrolysis in MOVPE growth 4-71577  
Cd<sub>2</sub>Hg<sub>1-x</sub>Te under uniaxial deform., photoelectric props. 4-70864  
Cd<sub>2</sub>Hg<sub>1-x</sub>Te, undoped and In-doped, impurity migration 4-70468  
Cd<sub>2</sub>Hg<sub>1-x</sub>Te/In system, current noise in contact regions, defect influences 4-88595  
Cd<sub>2</sub>Hg<sub>1-x</sub>Te-CdTe heterostruct. interfaces, SIMS anal. of impurities 4-108727  
CdI<sub>2</sub>, 14 layered polytype, cryst. struct. and space group 4-92188  
CdI<sub>2</sub> layered cryst., radiation defect formation 4-65299  
CdI<sub>2</sub>, optical functions and energy band parameters (Russian) 4-88793  
CdI<sub>2</sub>, photoluminescence study of polytype layer struct. (Russian) 4-71443  
CdI<sub>2</sub>, polymorph structures, X-ray diffr. 4-84251  
CdI<sub>2</sub>, polymorph structures, optical and X-ray diffr. studies 4-84252  
CdI<sub>2</sub>, polymorph structures using mol. layer notation t-o-f 4-80000  
CdI<sub>2</sub> polymorphs, cryst. structures, X-ray diffr. determ. 4-92152  
CdI<sub>2</sub>, Raman spectra meas. 4-80944  
CdI<sub>2</sub>, soln. grown cryst., photoconductivity, nonlinear behaviour 4-61413  
CdI<sub>2</sub>(Br<sub>2</sub>), partially decomposed, electron double diff. pattern indexing 4-108252  
Cd(II) complex, xanthinium cadmium tetrachloride, thermal props. invest. 4-78846  
CdIn<sub>2</sub>(Ga<sub>2</sub>)S<sub>4</sub> visible and UV reflectivity spectra anal. 4-114295  
CdIn<sub>2</sub>S<sub>4</sub>, conduction band anisotropy, piezoresistance studies 4-98614  
CdIn<sub>2</sub>S<sub>4</sub>, luminescence kinetics study 4-104671  
CdIn<sub>2</sub>S<sub>4</sub> single cryst., photocond., photoluminescence and non-equilib. carrier recombination 4-65706  
n-CdIn<sub>2</sub>Se<sub>4</sub> single cryst. electrodes in polysulphide electrolytes, photoelectrochemical behaviour 4-77117  
CdIn<sub>2</sub>Se<sub>4</sub> single cryst., electrolyte electroreflectance in photoelectrochemical solar cell 4-89408  
Cd<sub>2</sub>Mg<sub>1-x</sub>(NO<sub>3</sub>)<sub>2</sub>·He-<sup>3</sup>He liquid boundary, thermal resistance study 4-84484  
Cd<sub>1-x</sub>Mn<sub>x</sub>S, magnetisation, s-d exchange interaction, spin-flip Raman scatt. 4-76103  
Cd<sub>1-x</sub>Mn<sub>x</sub>S, s-d exchange interaction sign, spin flip Raman scatt. studies 4-71052  
Cd<sub>1-x</sub>Mn<sub>x</sub>S semimagnetic semiconducting compounds, photoconductivity, growth techniques 4-92763  
Cd<sub>1-x</sub>Mn<sub>x</sub>S, spin-flip Raman light scatt. 4-80939  
CdMnS(Se), donor-bound mag. polarons, mag. fluctuations, spin-flip Raman scatt. 4-80759  
Cd<sub>1-x</sub>Mn<sub>x</sub>Se, far-IR obs. of electric dipole spin resonance 4-92978  
Cd<sub>1-x</sub>Mn<sub>x</sub>Se, nonlinear photoconductivity 4-70872  
Cd<sub>1-x</sub>Mn<sub>x</sub>Se, Raman scatt., magnetisation and exchange energy 4-80940  
Cd<sub>1-x</sub>Mn<sub>x</sub>Se, semimagnetic semiconductor with metallic conduction, anomalous magnetoconductivity 4-65692

**cadmium compounds continued**

Cd<sub>1-x</sub>Mn<sub>x</sub>Se, valence band, Mn 3d electron contrib. 4-75855  
Cd<sub>1-x</sub>Mn<sub>x</sub>Se(Te) semimagnetic semicond., electroreflection spectra 4-88811  
Cd<sub>2</sub>Mn<sub>0.5</sub>Te spin glass, magnon contrib. to mag. sp. ht. 4-98906  
Cd<sub>2</sub>Mn<sub>2</sub>Te, atomic layer epitaxial growth on CdTe(111)B substrates 4-76676  
Cd<sub>1-x</sub>Mn<sub>x</sub>Te, MBE growth, Auger depth profile anal. 4-71567  
Cd<sub>1-x</sub>Mn<sub>x</sub>Te mag. semicond. superlattices, MBE growth and optical props. 4-114399  
Cd<sub>1-x</sub>Mn<sub>x</sub>Te magnetic insulator, losses 4-71121  
Cd<sub>1-x</sub>Mn<sub>x</sub>Te, piezomodulation study of absorpt. edge and Mn<sup>2+</sup> transition 4-114242  
Cd<sub>1-x</sub>Mn<sub>x</sub>Te solid solns., Mn photoionisation detection 4-71349  
Cd<sub>1-x</sub>Mn<sub>x</sub>Te spin glass, dynamic behaviour, Faraday effect study 4-71354  
Cd<sub>1-x</sub>Mn<sub>x</sub>Te, struct. props., EXAFS studies 4-60902  
Cd<sub>1-x</sub>Mn<sub>x</sub>Te, ternary semiconducting random solid solutions, local structure, EXAFS 4-113414  
Cd<sub>1-x</sub>Mn<sub>x</sub>Te-CdTe multilayers grown by MBE 4-88976  
Cd<sub>2</sub>N<sub>1-x</sub>Fe<sub>x</sub>O<sub>4</sub> system, nonlinear spin struct., magnetisation and Mossbauer obs., Vafet-Kittel angles 4-71022  
Cd(NH<sub>3</sub>)<sub>6</sub>(ClO<sub>4</sub>)<sub>2</sub> and Cd(NH<sub>3</sub>)<sub>6</sub>(BF<sub>4</sub>)<sub>2</sub>, phase transitions, microscopic theory 4-61071  
Cd(NO<sub>3</sub>)<sub>2</sub> aq. solns., struct. determ. by X-ray diffr. and Raman spectrosc. 4-108265  
Cd<sub>2</sub>Nb<sub>2</sub>O<sub>7</sub>, anharmonicity of thermal vibrs., X-ray diffr. 4-65367  
Cd<sub>2</sub>Nb<sub>2</sub>O<sub>7</sub>, diffuse and sharp phase transitions, dielec., optical, and electro-optical studies 4-71309  
Cd<sub>2</sub>Nb<sub>2</sub>O<sub>7</sub>, photoconductivity and TSC meas. 4-70867  
Cd<sub>2</sub>Nb<sub>2</sub>O<sub>7</sub>, photoferroelectric phenomena 4-88785  
Cd<sub>2</sub>Nb<sub>2</sub>O<sub>7</sub>, thermo-optic and photochromic effects, phase transitions 4-99104  
Cd<sub>2</sub>Nb<sub>2</sub>O<sub>7</sub>, unusual incommensurate soft mode damping 4-113562  
Cd<sub>2</sub>Nb<sub>2</sub>O<sub>7</sub>Fe(Gd), narrow phase transitions, elec. field and impurity effects 4-71316  
Cd<sub>2</sub>Nb<sub>2</sub>O<sub>7</sub>Gd<sup>3+</sup>, ferroelec. transitions, EPR spectra 4-98945  
CdO, struct. under pressure 4-75424  
CdO-Bi<sub>2</sub>O<sub>3</sub>, phase relations, X-ray diffr. obs. 4-89028  
CdO<sub>4</sub>, rel. between electronic struct. and electron affinity, discrete variational Alpha calcs. 4-87045  
11133 CdOH matrix isolated, fast atom bombardment, ESR investig. 4-74218  
Cd(OH)<sub>2</sub>, brucite-like, struct. and IR relations 4-79996  
CdP<sub>2</sub>, absorpt. spectra and defect states (Russian) 4-71419  
CdP<sub>2</sub>, reflection and thermoreflectance spectra 4-114249  
CdP<sub>2</sub>, superionic cond. by divalent cations, electrical cond., dielec. const., studies 4-108652  
CdP<sub>2</sub> crystals, growth and morphology 4-75339  
n-Cd<sub>2</sub>P<sub>2</sub> degenerate semicond. intrinsic phonon parameters 4-92317  
CdP<sub>2</sub>, disordered, Mott transitions and impurity scattering (Russian) 4-88450  
CdRh<sub>1.8</sub>Fe<sub>0.2</sub>O<sub>4</sub>, magnetic susceptibilities meas. 4-88650  
CdS, absorptive optical bistability due to band gap shrinkage 4-69482  
CdS amorphous films, optical absorption coeff. and gap state density 4-66088  
CdS based polycrystalline thin film solar cells, future trends 4-89446  
CdS binder layers, electrophotographic props. after heat and light treatment 4-79258  
CdS, cavityless optical bistability due to light-induced absorpt. 4-102971  
CdS chemically deposited films, cubic phase, air annealing effects, XPS and XRD examination 4-99356  
CdS, colloidal crystallites, excited electronic states, size effects, optical props., Raman spectra 4-71334  
CdS coupled mode band-pass optical filters, characteristics 4-87438  
CdS, cryst. polarisabilities, quantum mech. approach 4-84596  
CdS crystal laser beam annealing 4-75508  
CdS, crystallisation kinetics, growth from CdS+CdCl<sub>2</sub> melt 4-114380  
CdS, dark current and photocurrent in strong elec. field, temp. dependence 4-113998  
CdS dispersion best fit, Sellmeier eqn., with various resonances, nonlinear regression anal. 4-93030  
CdS, edge luminesc. series emitted in elec. field 4-66068  
CdS, effect of US waves, acoustoluminescence (Russian) 4-71454  
CdS, electron beam annealing, defects diffusion 4-103801  
CdS, electron irradi., photoluminescence study 4-99189  
CdS, electroplating of Cu<sub>2</sub>S, for CdS-Cu<sub>2</sub>S photocells 4-99354  
CdS, exciton diffusion and exciton momentum scatt. 4-65616  
CdS, exciton-polaritons, resonant Brillouin scatt. studies 4-108789  
CdS, excitons in high mag. fields, gauge-invariant energy variational calc. 4-80508  
CdS film, deposited by hot wall technique, characterisation of doped and undoped films 4-114405  
CdS film, photoluminescence method of determ. minority carrier kinetics 4-61748  
CdS films grown by spray pyrolysis in an N<sub>2</sub> ambient 4-61843  
CdS, frequency tuning of far-IR radiation on hot excitons 4-69415  
CdS, ground state energies of shallow donors 4-92654  
CdS, γ-irrad., photoelectron spectra and photoconductivity (Russian) 4-71521  
CdS, HF holographic diffr. grating recording on surface 4-69339  
CdS, in Nafion film, struct., luminesc. lifetime quantum yield and quenching 4-85000  
CdS, irradiation-produced dislocation loops, HVEM study 4-75529  
CdS laser, electron-beam-pumped, excitation density distrib. 4-79162  
CdS, laser induced gratings 4-104630  
CdS, luminescence study of polaritons 4-61300  
CdS monocrytals and films, luminesc. spectra during high levels of excitation (Russian) 4-80999  
CdS, nonlinear exciton transmission, Maxwell's eqn. anal. 4-98535  
CdS, optically pumped, tunable CW mode locked laser action 4-107699  
CdS, optoelectronic switching, laser controlled, photoconductivity meas. (German) 4-84646  
CdS, particle suspensions, electronic processes, microwave probing 4-99852  
CdS, periodic precipitation in lyophilic colloid, diffusion controlled autocatalytic growth 4-71993  
CdS, piezoelec. semicond., stimulated Brillouin scatt. of electromagnetic wave, acoustic amplification 4-114291  
CdS polycrystalline films, photocorrosion in aq. solns., capacitance and action spectra meas. 4-92818

## cadmium compounds continued

- CdS, polycrystalline thin film electrodes photoelectrochemical studies 4-109747  
 CdS, radiative and nonradiative recomb., plastic deform. depend. 4-61658  
 CdS, radiative recomb. mechanisms for high density excitons 4-88458  
 CdS, resonant Brillouin scatt. study 4-61721  
 CdS, resonant Brillouin spectra calcs. 4-61722  
 CdS Schottky barrier MIS solar cells 4-62350  
 CdS, shock loaded, struct. studies 4-92293  
 CdS single, photoluminescence studies 4-109240  
 CdS single cryst., lasing action when illuminated by flashlamp 4-74520  
 CdS single cryst., photoacoustic spectra from unilluminated surface 4-109206  
 CdS interlayer layers for solar cells, prep. and annealing effects on characts. 4-62369  
 CdS, small particles, photoluminesc. 4-85004  
 CdS solar cells fabricated by reactive pulverisation 4-109738  
 CdS, spectral-time characts. of nonlinear emission (*Russian*) 4-104620  
 CdS, spin relax. of free carriers, Raman scatt. 4-104619  
 CdS, spontaneous oscils. in presence of temp.-electric instability 4-104266  
 CdS surface, clean and Au covered, surface recombination vel., photoluminescence studies 4-80600  
 CdS, thermally stimulated brightening of cryst. boundary in exciton absorption region 4-114234  
 CdS thin crystals, refr. index dispersion curve, thickness depend. (*Ukrainian*) 4-65999  
 CdS thin film, RF-sputtered, elec. props., effect of temp. and bias 4-80699  
 CdS thin films, electrodeposited in fused salt solns., struct. and morphology rel. to substrate 4-66250  
 CdS thin films prep. by spray deposition, vacuum annealing effect on elec., structural and optical props. 4-70966  
 CdS, thin plate, reflection spectrum, interference struct. anal. 4-76402  
 CdS, three-photon absorpt. with subsequent absorpt. by photogenerated carriers 4-79226  
 CdS, uniaxially deformed, current saturation and oscill. (*Russian*) 4-70818  
 CdS, wurtzite-type, hole-phonon interaction, phonon cond. calc. 4-70487  
 CdS:Cu, photoconductivity and luminescence (*Russian*) 4-84658  
 CdS:Cu<sub>2</sub>In sprayed films, topotaxial growth of Cu<sub>2</sub>S thin films, optical and structural behaviour 4-114433  
 CdS:Cu thin films, photocurrent, field quenching 4-84718  
 CdS:Cu(Cl) films, defect diffusion, luminescence study (*Russian*) 4-88875  
 CdS:In film, elec. props. meas. 4-104329  
 CdS:O<sub>2</sub>, highly photocond. films, spray pyrolysis prep. 4-88533  
 CdS:Sb films, vacuum deposited, struct., elec. and optical props., impurity conc. effect 4-98607  
 CdS/CdTe solar cell, annealing, admittance spectroscopy 4-77101  
 CdS/Cu<sub>2</sub>-S heterostruct., misfit accommodation and growth 4-108730  
 CdS/Cu<sub>2</sub>S heterojunction solar cells, electrochemical method for improving spectral response 4-109744  
 CdS/CuInSe<sub>2</sub>, solar cell interface chem. reaction, thermodynamics 4-85367  
 CdS/CuInSe<sub>2</sub> heterojunction solar cells, conduction band-lineup 4-72105  
 CdS/CuInSe<sub>2</sub> solar cells, thin film, diffusion length determ. using EBIC method 4-72110  
 n-CdS/electrolyte interface, photoelectrochem. characterisation 4-84689  
 n-CdS/n-CdSe heterojunction photoresponse, surface state effects 4-84686  
 n-CdS/S<sup>2-</sup>, S<sub>2</sub><sup>2-</sup> photoelectrochemical solar cells, quantum efficiency, theoretical model anal. 4-114913  
 CdS/Te thin film Schottky barrier diodes 4-70909  
 CdS-CdCl<sub>2</sub>, melt, crystallisation kinetics of CdS 4-114380  
 CdS-CdTe screen-printed solar cell fabrication with 12.8% efficiency and 0.78 cm<sup>2</sup> active area 4-77107  
 CdS-CdTe thin film solar cells, photocapacitance and current collection 4-81548  
 CdS-CdTe thin films, photoluminescence study 4-80987  
 CdS-Cu<sub>2</sub>S photocells formed by electroplating, prep. and props. 4-72115  
 CdS-CuInSe<sub>2</sub> thin film heterojunction solar cells, photoresponse characts. 4-77099  
 CdS-CuInSe<sub>2</sub> photovoltaic devices, short-circuit current meas. 4-88971  
 CdS-electrolyte, SAW characterisation of surface and interface states 4-98681  
 CdS-Ga<sub>2</sub>S<sub>3</sub>, phase diagram, crystallographic study, DTA, X-ray diff. 4-109387  
 CdS-InP heterojunctions, elec. and photoelec. props., solar cell appl. (*Russian*) 4-98713  
 n-CdS/n-CdSe heterojunction, photo-EMF study 4-104307  
 CdS-Se binder layer, photo and dark conductivity, modification by corona charging, expt. 4-98672  
 CdS(Bi) films, in photoelectrochemical cells, photovoltaic characteristics 4-93634  
 CdS(In) films chemical bath-deposited, electrical and optical props. 4-92832  
 Cd(SO<sub>3</sub>F)<sub>2</sub>, synthesis, Raman spectroscopic obs. 4-66020  
 CdSe, optically pumped, tunable CW mode locked laser action 4-107699  
 CdSe<sub>0.9</sub>Se<sub>0.1</sub> laser optical pumping by CdS streamer laser radiation 4-60050  
 n-CdSe<sub>0.9</sub>Se<sub>0.1</sub> electrode, liquid junction photoelectrochemical cells, props. (*Chinese*) 4-81565  
 CdS<sub>1-x</sub>Se<sub>x</sub> particles for photocatalytic production, valence bands 4-100008  
 CdS, Se<sub>1-x</sub> single cryst., elec. cond. and Hall effect studies 4-113974  
 CdSb, crystallisation front instability during laser epitaxy. (*Russian*) 4-99325  
 CdSb, cyclotron resonance of holes, effective masses 4-80477  
 CdSb, mag. band struct. in valence band 4-75849  
 CdSb, vibr. modes symm. and Raman scatt. (*Russian*) 4-99124  
 CdSb:In(Te) dopant distrib. coeffs. (*Japanese*) 4-84313  
 CdSb<sub>2</sub>, disordered, Mott transitions and impurity scattering (*Russian*) 4-88450  
 CdSe films, cell form. prior to laser induced synthesis 4-65582  
 CdSe, free exciton dynamics study 4-98788  
 CdSe, hot excitons and electron-hole pairs and Raman spectra 4-114285  
 CdSe, magnetopolaritons, dipole forbidden transmission 4-98544  
 CdSe, optically pumped, tunable CW mode locked laser action 4-107699

## cadmium compounds continued

- CdSe, particle desorpt. under laser irradi., mass and energy distrib. meas. (*Russian*) 4-113815  
 CdSe photoelectrochemical cells, surface modification using CuS 4-81566  
 CdSe photoelectrochemical solar cells, lifetime improvements 4-99969  
 CdSe, picosecond energy-relax. processes of excitons, luminesc. study 4-109244  
 CdSe, picosecond spectroscopy at high excitation densities 4-81003  
 CdSe, polycrystalline thin film electrodes photoelectrochemical studies 4-109747  
 CdSe, reaction with Pb and S containing reactive gas phase 4-105016  
 CdSe, thin films, noise power spectra meas. 4-80638  
 CdSe/ferro-ferricyanide photoelectrochemical system, I-V behaviour 4-88580  
 CdSe/poly sulphide photoelectrochemical cells, performance and stability, pronounced cation effect 4-89453  
 CdSe/sulphide-poly sulphide photoelectrochemical system, I-V behaviour 4-88580  
 CdSe-CdTe heterophase films, nonreciprocal photoelec. props. 4-108907  
 CdSe-type uniaxial cryst., excitonic absorpt. band formation (*Russian*) 4-71409  
 CdSe-VO<sub>2</sub> contact, barrier to antibarrier transition during metal-semiconductor phase transition 4-65738  
 CdSe<sub>1-x</sub>Te<sub>x</sub> thin films, vac. evaporated, for electrochemical photovoltaic cells 4-77115  
 CdSe, Te<sub>1-x</sub> hetero-photoconvertors, spectral characts. (*Russian*) 4-66692  
 CdSiAs<sub>2</sub>, impurity photoluminescence polarisation 4-88873  
 CdSiAs<sub>2</sub>, single crystal growth by chem. vapor transport, struct. and elec. props. 4-114367  
 CdSiP<sub>2</sub>, chalcopyrite crystals, dispersion of temp. coeffs. of birefr. 4-61651  
 CdSnO<sub>3</sub> and Cd<sub>2</sub>SnO<sub>4</sub>, EPR signals due to vacancies, comparison with CdO, yellow fluoresc. phenomenon 4-71179  
 Cd<sub>2</sub>SnO<sub>4</sub>, selective optical coating prod. on plastic sheet as heat reflecting films 4-112555  
 CdTe, atomic layer epitaxy on CdTe substrates, high structural perfection 4-114415  
 CdTe, cooperative processes, spontaneous and stimulated emission 4-104662  
 n-CdTe, deep levels, plastic deform. effects, DLTS studies 4-84591  
 CdTe detectors, use for qualitative anal. of diagnostic X-ray spectra 4-115192  
 CdTe, dislocations and subboundaries, etching studies 4-75451  
 CdTe doped with mag. ions, anomalous optical effects (*Russian*) 4-99103  
 n-CdTe, electron traps, DLTS study 4-80533  
 CdTe epitaxial films, MOCVD on InSb and GaAs substrates 4-81146  
 CdTe epitaxial films, OMCDV grown on sapphire, growth rates, mobilities, X-ray diff. 4-80444  
 CdTe film, composition and elec. props. 4-80696  
 CdTe films, atomic layer epitaxy and electronic struct. 4-81135  
 CdTe films, electrochem. deposited, optical props. 4-85022  
 CdTe films, MBE grown on (001) GaAs and (001) InSb, charact. 4-98471  
 CdTe films, MBE growth and elec. and optical props. 4-81136  
 CdTe films, MBE growth on InSb 4-85103  
 CdTe films, MBE growth and microstruct. characterisation 4-92578  
 CdTe films on InSb, MBE growth, charact. 4-98470  
 CdTe, growth from vapour phase, on substrate out of contact with vapour walls 4-109315  
 CdTe, heteroepitaxial, on (001) InSb, TEM studies 4-104107  
 CdTe initial growth stages on (001) GaAs, AES and RHEED obs. 4-70580  
 CdTe, ion implanted with <sup>1</sup>H, <sup>2</sup>H, <sup>4</sup>He, depth distributions, SIMS study 4-88182  
 CdTe, irradiation-produced dislocation loops, HVEM study 4-75529  
 CdTe large single crystals, grown from vapour phase, polarity 4-70048  
 CdTe, lattice dynamics, local Heine-Abarenkov model pot. 4-98222  
 CdTe, MBE films on InSb, impurity doping and photoluminesc. props. 4-88980  
 CdTe MBE growth 4-98473  
 CdTe metal-semicond.-metal struct., pot. barriers 4-84708  
 CdTe, p-type, undoped, thin dielectric films deposition as protection against decomposition during annealing 4-92755  
 CdTe photoelectrodes, photoelectrochemical props., XPS and AES studies 4-88578  
 CdTe, plastically deformed at room temp., dislocations, TEM study 4-98104  
 CdTe polycryst. film, gradient recryst. grown, photolum. 4-76522  
 CdTe, Raman characterisation 4-99106  
 CdTe, solubility in GeTe, effects of temp. 4-108622  
 CdTe, tetrahedrally bonded, anisotropy of Compton profile 4-99217  
 CdTe thin films, DC cond. rel. to H<sub>2</sub> exposure 4-76053  
 CdTe thin films, electroless deposition 4-88992  
 CdTe, thin films, noise power spectra meas. 4-80638  
 CdTe thin films for solar cell appls., deposition and elec. props. 4-76054  
 CdTe thin layers, crystal and energy structures for photoelectric transducers 4-98298  
 CdTe, two-photon absorpt. with subsequent absorpt. by photogenerated carriers 4-79226  
 p-CdTe, undoped, in situ prep. by cathodic electrochem. deposition 4-61880  
 CdTe, X-ray diffraction study, cryst. struct. (*Russian*) 4-84280  
 CdTe:Ag(Cu), deep levels, pulsed admittance spectroscopy and capture cross sections 4-92653  
 CdTe:Cl, native acceptor defects, Hall effect study 4-75899  
 CdTe:Co, optical absorpt. spectrum (*Russian*) 4-84983  
 CdTe:H-Au contacts, hydrogenation effects 4-80695  
 CdTe:In, electroconductivity at high temp. 4-61373  
 n-CdTe:In, electron traps, DLTS study 4-80533  
 CdTe:In, defect complex, IR absorption studies 4-80031  
 CdTe:Mn<sup>2+</sup>, paramag. reson., linear elec. shift 4-76243  
 CdTe/In<sub>2</sub>-xO<sub>3-y</sub> structures electrophysical characts., for photoconvertors 4-92795  
 CdTe/In<sub>2</sub>-xSn<sub>2</sub>O<sub>3-y</sub> photoconvertors, current transfer mechanism 4-93616  
 CdTe/In<sub>2</sub>O<sub>3</sub> structures electrophysical characts., for photoconvertors 4-92795  
 CdTe/InO<sub>3</sub> photoconvertors, current transfer mechanism 4-93616  
 CdTe-based thin film solar cells, elec. and spectral props. 4-93621  
 CdTe-InSb MIS struct., electronic props. 4-98778

**cadmium compounds continued**

- n-CdTe-p-Cu<sub>2</sub>Te(p-Au<sub>2</sub>Te) heterojunctions, deep levels, photocapacitance spectra 4-61410  
 CdTe-ZnTe heterojunction, interface trap depths 4-61442  
 CdTe<sub>1-x</sub>Se<sub>x</sub>, synthesis and cryst. struct. 4-84261  
 CdTiO<sub>3</sub>, electron energy struct. of cond.-band, X-ray photoemission yield spectra 4-61282  
 CdTiO<sub>3</sub>:Mn<sup>2+</sup>, ferroelec. transitions, EPR studies 4-61588  
 CdWO<sub>4</sub> crystal scintillators props. review 4-64292  
 Cd<sub>1-x</sub>Zn<sub>x</sub>Mn<sub>1-y</sub>Te, lattice parameter and energy gap 4-75847  
 CdZnS-CuInSe<sub>2</sub> polycryst. thin film solar cells 4-77088  
 Cd<sub>1-x</sub>Zn<sub>x</sub>S films, prep. at various CdZnS ion ratios, use in electrochem. photovoltaic cells 4-85099  
 Cd<sub>1-x</sub>Zn<sub>x</sub>S sprayed film, photoelectrochem. cells, Zn composition effects 4-114912  
 Cd<sub>1-x</sub>Zn<sub>x</sub>Te alloys, growth, elec. props., photoluminesc. 4-66207  
 Cd<sub>1-x</sub>Zn<sub>x</sub>Te, synthesis and cryst. struct. 4-84261  
 Cs<sub>2</sub>CdBr<sub>4</sub>, low-temp. phases and cryst. struct. 4-103712  
 Cu<sub>1-x</sub>Cd<sub>x</sub>Fe<sub>2</sub>O<sub>4</sub>, IR absorption spectra and stretching bond interatomic vibrs. 4-80933  
 Cu<sub>2</sub>S-CdS solar cells, elementary degradation mechanisms (Russian) 4-89402  
 Cu<sub>2</sub>S-CdS thin film solar cells development and transfer to industrial production 4-89429  
 (CuZn)S-CuInSe<sub>2</sub> heterojunction solar cell, interface props. 4-89401  
 (Hg,Cd)Te photovoltaic detector, near-room-temp., thermoelec. current (Chinese) 4-106382  
 (Hg,Cd)Te/Au overlayer system, deposition, interactions and diffusion, UPS study 4-80439  
 Hg-Cd-Te phase diagram, thermodynamic data, associated soln. model, book contrib. 4-89031  
 HgCdTe 0.1 eV photoconductive detector, optimum thickness 4-111204  
 HgCdTe detector technology status 4-95515  
 HgCdTe, elec. props., two stage nonmagnetic high press. equipment appl. (Chinese) 4-90607  
 HgCdTe epitaxial films, MOCVD on InSb and GaAs substrates 4-81146  
 HgCdTe, growth, props. and appls. 4-66217  
 n-HgCdTe, Haynes-Shockley expt. 4-104204  
 HgCdTe heterojunction contact photoconductor 4-88528  
 HgCdTe, IR detector arrays, state-of-the-art review 4-111202  
 HgCdTe, ion implanted with <sup>1</sup>H, <sup>2</sup>H, <sup>3</sup>He, depth distributions, SIMS study 4-88182  
 HgCdTe, optically pumped, tunable CW mode, locked laser action 4-107699  
 HgCdTe photodiode obs. by electron-beam induced voltage technique (Chinese) 4-108929  
 HgCdTe, pressure-induced epitaxial growth from soln. 4-88993  
 HgCdTe, Raman characterisation 4-99106  
 HgCdTe wide-bandwidth photodiode photomixers, 28 μm 4-68283  
 Hg<sub>0.1</sub>Cd<sub>0.9</sub>Te, LPE grown, photoluminescence study 4-80986  
 Hg<sub>0.8</sub>Cd<sub>0.2</sub>Te, (110), Raman scatt. study 4-80942  
 Hg<sub>0.8</sub>Cd<sub>0.2</sub>Te-CdTe heterojunctions, elec. characts. 4-76036  
 Hg<sub>1-x</sub>Cd<sub>x</sub>Te, annealing of radiation defects, electron irradiation 4-108442  
 Hg<sub>1-x</sub>Cd<sub>x</sub>Te, CPA calcs., Green's function calcs., simplification through analytic continuation 4-61274  
 Hg<sub>1-x</sub>Cd<sub>x</sub>Te, characterisation using transverse acoustoelectric volt. meas. 4-104275  
 Hg<sub>1-x</sub>Cd<sub>x</sub>Te, deep impurity and defect states 4-88474  
 Hg<sub>1-x</sub>Cd<sub>x</sub>Te, deep level anal. using temp. depend. of capacitance (Chinese) 4-113888  
 Hg<sub>1-x</sub>Cd<sub>x</sub>Te, dry oxidation in gas phase, predominance area phase diagrams 4-71748  
 p-Hg<sub>1-x</sub>Cd<sub>x</sub>Te, elec. resist. and Hall coeffs., low-temp. anomalies 4-108885  
 Hg<sub>1-x</sub>Cd<sub>x</sub>Te, electric subbands in the limit E<sub>G</sub>→0, for IR reson. study 4-104286  
 Hg<sub>1-x</sub>Cd<sub>x</sub>Te, electron irradiat. elec. props., heat treatment effects 4-65713  
 Hg<sub>1-x</sub>Cd<sub>x</sub>Te epitaxial layers, organometallic growth and elec. props. 4-71566  
 Hg<sub>1-x</sub>Cd<sub>x</sub>Te, Γ<sub>6</sub>Γ<sub>8</sub> band crossover under press., phase transform., thermoelec. power meas. 4-88524  
 Hg<sub>1-x</sub>Cd<sub>x</sub>Te, Hg diffusion profile meas. by heavy ion backscatt. 4-75730  
 Hg<sub>1-x</sub>Cd<sub>x</sub>Te IR detectors, 100-300 μm, mag.-field effects 4-68281  
 Hg<sub>1-x</sub>Cd<sub>x</sub>Te LPE layers, below band gap photoluminescence 4-71423  
 Hg<sub>1-x</sub>Cd<sub>x</sub>Te large area epitaxial layers, LPE growth 4-61879  
 Hg<sub>1-x</sub>Cd<sub>x</sub>Te layers, CVT growth and characterisation 4-71576  
 Hg<sub>1-x</sub>Cd<sub>x</sub>Te MBE growth 4-98473  
 Hg<sub>1-x</sub>Cd<sub>x</sub>Te, native oxides and interfaces, spectroscopic ellipsometry studies 4-80426  
 Hg<sub>1-x</sub>Cd<sub>x</sub>Te, photogenerated carrier lifetime meas. by optical modulation of IR absorpt. (Chinese) 4-84953  
 Hg<sub>1-x</sub>Cd<sub>x</sub>Te submillimeter mixing, theoretical and expt. study 4-74622  
 Hg<sub>1-x</sub>Cd<sub>x</sub>Te surface accumulation layer, cyclotron resonance studies 4-98507  
 Hg<sub>1-x</sub>Cd<sub>x</sub>Te zero-gap MIS struct., size quantisation in accumulation layers 4-65753  
 Hg<sub>1-x-y</sub>Mn<sub>y</sub>Cd<sub>x</sub>Te, spin glass phase transition, interband Faraday rot., mag. susceptibility meas. 4-61545  
 HgTe-CdTe superlattices, electronic props. 4-84680  
 HgTe-CdTe superlattice, far IR magneto-optics, band structure 4-99101  
 n-InSe/p-CdTe heterojunction, elec. props. 4-108928  
 KCdF<sub>3</sub>, phase transitions and cryst. struct. 4-84379  
 Li<sub>2-x</sub>Cd<sub>x</sub>Cl<sub>4</sub> spinel, ionic cond. and phase transition 4-75720  
 Mg<sub>1-x</sub>Cd<sub>x</sub>Fe<sub>2</sub>O<sub>4</sub> ferrite, mag. props. Mossbauer studies 4-84878  
 Mg<sub>1-x</sub>Cd<sub>x</sub>Te(Sb), synthesis and cryst. struct. 4-84261  
 (Mn<sub>1-x</sub>Cd<sub>x</sub>)<sub>2</sub>Sb<sub>2</sub>O<sub>7</sub> pyrochlores, synthesis and solid state studies 4-88140  
 (MnS)<sub>2</sub>(CdSe)<sub>2-x</sub> and (MnS)<sub>2</sub>(CdTe)<sub>1-x</sub> semimagnetic semicond., electroreflection spectra 4-88811  
 (MnSe)<sub>2</sub>(CdTe)<sub>1-x</sub> semimagnetic semicond., electroreflection spectra 4-88811  
 PbCdS tunable diode lasers, Cd diffused, multicomponent gas analysis appl. 4-112457  
 Pb<sub>1-x</sub>Cd<sub>x</sub>S tunable diode lasers for 3 to 30 μm IR operation 4-112456  
 Rb<sub>2</sub>Cd<sub>2</sub>(SO<sub>4</sub>)<sub>3</sub>, thermal expansion, 77 to 300 K 4-92396  
 Sr<sub>1-x</sub>Cd<sub>x</sub>F<sub>2</sub>Er<sup>3+</sup>, energy transfer up-conversion 4-99162  
 Zn<sub>1-x</sub>Cd<sub>x</sub>Ga<sub>2</sub>S<sub>4</sub> mixed defect cryst., Raman scatt. 4-61688  
 Zn<sub>1-x</sub>Cd<sub>x</sub>In<sub>2</sub>S<sub>4</sub> pseudoternary layered cpds., Raman spectra 4-61690  
 Zn<sub>1-x</sub>Cd<sub>x</sub>S<sub>2</sub> excitation migration between localised excitons, photoluminescence, absorpt. spectra 4-88456

**cadmium compounds continued**

- Zn<sub>1-x</sub>Cd<sub>x</sub>S solid soln., localised exciton migration, pumping intensity effects 4-92618  
 Zn<sub>1-x</sub>Cd<sub>x</sub>S, structural disorder and solid state transformations 4-103924  
 Zn<sub>1-x</sub>Cd<sub>x</sub>S/Si, p-n heterojunction photovoltaic solar cell 4-85366  
 Zn<sub>1-x</sub>Cd<sub>x</sub>S-Cu<sub>2</sub>S heterojunction, energy band diagrams 4-104296  
 Zn<sub>1-x</sub>Cd<sub>x</sub>S-Cu<sub>2</sub>S reverse-biased p-n heterojunctions, elec. props. and photodiode appls. (Russian) 4-108926  
 Zn<sub>1-x</sub>Cd<sub>x</sub>Se laser screens, crystals grown from vapour phase, receiving colour image blue component (Russian) 4-96917  
 Zn<sub>1-x</sub>Cd<sub>x</sub>Se scanning laser emitting in the blue region 4-79163  
 Zn<sub>1-x</sub>Cd<sub>x</sub>Te, solid soln., sound attenuation study 4-98208  
 Zn<sub>1-x</sub>Cd<sub>x</sub>Te, Se, Raman scatt. and phonon spectra 4-88835  
 ZnGeAs<sub>2</sub>-CdGeAs<sub>2</sub> semiconducting alloys, melt quenched, phase stability, glass form., TEM obs. 4-71641  
 ZnS-CdS system, solid solns. and phase transforms. under hydrothermal conditions 4-98264  
 ZnTe-CdTe, epitaxial film, degree of perfection and struct. 4-61250

**CAE see CAD**

**caesium**

- see also nuclei with  
 adsorbed layer on Si (111), inversion layers, positive and negative magnetoresist. 4-98645  
 adsorbed on Si (100), neutralisation of scattered He ions 4-109294  
 alkali metals, melting theory using pseudopotential calcs. 4-88268  
 are thermionic converters with multicavity anodes 4-108228  
 are thermionic converters with multicavity emitter 4-108227  
 atom, 6S→7S transition, parity-violating E1-amplitude, relativistic many-body calc. 4-91230  
 atom, electron impact excitation, light emission, Stokes parameter 4-96703  
 atom, excited 7S state, photoionisation cross section absolute meas. 4-78816  
 atom, fluorescence spectrum, inter-Doppler resonances 4-107306  
 atom, L-shell X-ray prod. cross sections for protons of energy 1-2 MeV 4-96656  
 atom, multiphoton ionisation, photoelectrons, energy resolved ang. distrib. 4-83347  
 atom, optical pumping by monochromatic light, efficiency calc. 4-107317  
 atom, polarisation spectroscopy 4-74193  
 atom hyperfine struct. intervals, relativistic many-body calcs. 4-68986  
 atomic clock characterisation in perturbed environment 4-95374  
 atomic electronic orientation after CsI photodissociation 4-93541  
 atomic frequency standard, appl. (Japanese) 4-58819  
 atomic reference frequency and clock supply, freq. keeping algorithm 4-106275  
 atoms, multiphoton process calc. (Chinese) 4-59863  
 atoms, nonreson. multiphoton ionisation in strong fields, angular distrib. and above threshold ionisation 4-74206  
 atoms, resonance lines, high press. noble gas broadening 4-74187  
 atoms, resonance lines, low press. noble gas broadening 4-74186  
 atoms, saturation spectroscopy with optical pumping for D<sub>2</sub> lines 4-111211  
 BWR spent fuel, <sup>137</sup>Cs γ-spectrometry for burn-up verification and isotopic comp., safeguards 4-106983  
 coadsorption with O on Mo (100), electronic props., EELS, UPS, work function meas. 4-61787  
 Columbia River, Oregon, USA, radioactive pollution in sediments 4-66824  
 composite surface, H<sup>+</sup> and D<sup>+</sup> ion generation rel. to surface/plasma ion source systems 4-93165  
 composite surface, partially caesiated, H<sup>+</sup> prod. in presence of H plasma 4-93166  
 determination in basaltic silicate rocks, instrumental NAA and radiochem. methods 4-66624  
 evaporated layer on Ag surface, photoelectric emission stability 4-76637  
 frequency standard, pulling by neighbouring transitions 4-101815  
 frequency standard cavity phase shift analysis 4-101814  
 Gruneisen parameters, pseudopot. calc. 4-61032  
 isoelectronic series, ions, pos., relativistic effects, core polaris. and relax. 4-68985  
 liquid, density calcs. using model-potential approach 4-92065  
 liquid, enhanced mag. susceptibility 4-92801  
 liquid, eqn. of state and pVT data up to 2000K and 600 bar 4-103898  
 liquid, struct. factor determ. using plasma reference system 4-113296  
 melting curve, high pressure calcs. 4-113583  
 molecule, first two excited <sup>2</sup>Σ<sub>g</sub><sup>+</sup> states, IR fluoresc. study 4-64525  
 molten, O<sub>2</sub> solubility study 4-113641  
 muon energy profile change upon lattice relax. 4-71232  
 optically pumped vapour, relax. depend. on detection beam radius 4-64432  
 phonon frequencies, Debye temp., Gruneisen parameter, transport props., lattice dynamical model 4-108561  
 plasma, dense, electrical conductivity 4-83985  
 plasma jet flowing into He, diagnostics 4-91993  
 radioactive caesium removal from streams with high potassium content 4-106751  
 solid and liq., Gruneisen parameter at high press., nature of isostructural electronic transition 4-61035  
 structure above s-d transition, LMTO calc. 4-75669  
 thermal expansion first-principles calcs. 4-98319  
 thermionic diodes, excited state population duration meas. 4-72140  
 vapour, plasma channels for ion beam transport initiated by XeCl laser 4-103533  
 vapour, Rydberg series in autoionising continua 4-83337  
 vapour, superfluorescence experiments, book contrib. 4-64691  
 Ag-O-Cs (SI) and Bi-Ag-O-Cs (S-I) photocathodes, enhanced Cs+(He), absolute polarisation meas., natural lifetime in Cs 7S<sub>1/2</sub> state 4-83448  
 Cs+H<sup>+</sup>(D<sup>+</sup>), spin-depend. charge transfer 4-59890  
 Cs<sup>+</sup>+Cs<sup>+</sup> inelastic collisions, Cs<sup>+</sup> prod., plasma target technique study 4-78954

## caesium continued

- <sup>133</sup>Cs vapour, spin system nonlinear interaction with radio freq. fields in presence of level crossing in a zero field 4-91238  
<sup>133</sup>Cs atom ensemble, paramag. resonance line shift in narrow band noise fields 4-91212  
<sup>133</sup>Cs, ground and excited states, Zeeman effect, optical pumping 4-91208  
<sup>137</sup>Cs, conc. in milk prod. in Channel Islands 4-105353  
<sup>137</sup>Cs, cumulative release and propagation near nuclear power plants 4-109755  
<sup>137</sup>Cs, determ. of conc. in urine samples 4-96290  
<sup>137</sup>Cs, distrib. in surface intertidal sediments of Solway Firth 4-93657  
<sup>137</sup>Cs, fallout nuclide accumulation in snails 4-62609  
<sup>137</sup>Cs, fast determination method for environment samples (Russian) 4-81604  
<sup>137</sup>Cs, in liver and lung of Lapps, comparison with southern Finns 4-62590  
<sup>137</sup>Cs movement in southern coastal plain ecosystem, Louisiana, USA 4-89788  
<sup>137</sup>Cs, nuclide conc. in animal livers consumed by man 4-62610  
<sup>137</sup>Cs, tissue accumulation and loss in mallard ducks 4-62598  
<sup>137</sup>Cs<sup>+</sup> uptake by plants, long term fallout on grassland, soil parameters effect 4-109967  
 N<sub>2</sub>+Cs plasma decay in pulse mode conditions of thermionic energy controller 4-92000

## caesium alloys

- Cs-K(Rb), volume effect, pure constituent, phonon dispersion relations, local and band modes, calcs. 4-98224  
 K<sub>2</sub>Cs, freezing temperature, crit. points 4-70349  
 Na-Cs liquid alloys, conc. fluctuations 4-92063  
 Na-Cs liquid-vapour interface struct., Monte Carlo simulation 4-88062

caesium clocks *see atomic clocks*

## caesium compounds

*see also caesium alloys*

- CsCl, Decker equations of state, polynomial representation 4-84362  
 [(CsI)<sub>2</sub>Se]<sup>+</sup> cluster ions, generation and detection ranging up to  $m/z=90000$  4-69262  
 germanates, synthesis and struct., X-ray diffr. studies 4-108320  
 selenogallates, cryst. struct. and abnormal linear oligomeric anions 4-92185  
 AgCl:CsCl, molten, electrolytic cond. 4-108638  
 α-Ag<sub>2</sub>Rb<sub>1-x</sub>Cs<sub>x</sub>I<sub>5</sub>, ionic elec. cond. and phase transitions 4-84455  
 Ba<sub>2</sub>Cs<sub>2</sub>Al<sub>2x-7</sub>Ti<sub>13-2x-y</sub>O<sub>16</sub>, hollandite phase of SYNROC, struct., X-ray analysis 4-106675  
 Ba<sub>2</sub>Cs<sub>2</sub>Ti<sub>18</sub>O<sub>40</sub>, hollandite-related superstructures 4-70085  
 Ce-Sc-Ge, phase-equilibrium diagram at 870K, X-ray data anal. 4-75644  
 CeO<sub>2</sub>, localised and extended f-symmetry states 4-92648  
 CeO<sub>2</sub>, surface exchange reactions, oxygen transport characteristics 4-98355  
 Cs<sub>2</sub>P<sub>2</sub>O<sub>14</sub>, triclinic ultraphosphate, cryst. struct. 4-70086  
<sup>222</sup>Rn<sup>+</sup> cryptates, in water, stability consts. 4-114817  
 Cs-CsI solns., electron localisation, NMR obs. 4-98965  
 Cs-Ga-Se phase diagrams, ternary cpds. obs. 4-71644  
 CsAlSi<sub>3</sub>O<sub>6</sub>, pollicite, Ar<sup>+</sup> ion irradiat., damage cross sections 4-108484  
 Cs<sub>0.5</sub>Al<sub>0.5</sub>Si<sub>2.5</sub>O<sub>6</sub>, cryst. struct., X-ray diffr. studies 4-92187  
 Cs<sub>2</sub>B<sub>6</sub>O<sub>6</sub>(OH)<sub>2</sub>·2H<sub>2</sub>O, twinned cryst. struct. X-ray diffr. determ. 4-92151  
 Cs<sub>2</sub>BiCl<sub>6</sub>, phase transitions, first phase props. 4-75657  
 CsBi(MoO<sub>4</sub>)<sub>2</sub> layer cryst., structural phase transitions 4-88286  
 CsBr, optical const. calcs. 4-99084  
 CsBr, press. induced struct. transition 4-113607  
 CsBr, scatt. primary and recoiled surface neutrals and ions, TOF spectra 4-63800  
 CsBr, total gamma-ray cross sections 4-60959  
 CsBr:TL, V<sub>K</sub> centres, thermally stimulated exoelectron emission 4-76645  
 CsBr+Ar(Kr)(Xe), collision-induced dissociation, cross sections 4-76993  
 CsCaCl<sub>2</sub>:Mn<sup>2+</sup>(Ni<sup>2+</sup>)(Co<sup>2+</sup>), fluoresc. emission, excitation, IR absorpt. spectra studies 4-99153  
 Cs<sub>2</sub>CaCl<sub>2</sub>·2H<sub>2</sub>O, struct., cryst. chemical study 4-65223  
 CsCaF<sub>3</sub>, parameter free eqn. of state calcs. 4-70336  
 CsCaF<sub>3</sub>, soft mode freq., temp. and press. depend. 4-70331  
 Cs<sub>2</sub>Ca<sub>2</sub>(N<sub>3</sub>)<sub>2</sub>·2H<sub>2</sub>O, cryst. struct., X-ray diffr. studies 4-92163  
 Cs<sub>2</sub>Ca(N<sub>3</sub>)<sub>2</sub>·2H<sub>2</sub>O, cryst. struct., X-ray diffr. studies 4-92164  
 CsCa<sub>2</sub>Nb<sub>2</sub>O<sub>10</sub>, layered ferroelastic perovskite, cryst. struct., X-ray diffr. (French) 4-75419  
 Cs<sub>2</sub>CdBr<sub>4</sub>, low-temp. phases and cryst. struct. 4-103712  
 CsCl crystals, ionic and covalent energy gaps 4-75852  
 CsCl, electron collision frequency, resonant determ. method 4-69223  
 CsCl, eqn. of state used for secondary calibration scale at low temps. 4-103897  
 CsCl, optical const. calcs. 4-99084  
 CsCl, polymorphous transitions, pseudoharmonic theory 4-61078  
 CsCl, slow electron scatt. study 4-74334  
 CsCl structure ionic crystals, plastic deformation (Japanese) 4-88228  
 CsCl structure ionic crystals, effective ionic charge, press. depend. 4-103692  
 CsCl, vap. press., viscosity coeff. and interdiffusion coeff. in Ar and He, Ruff-MKW-boiling point method 4-97743  
 CsCl-Cs liq. solns., mag. susceptibility 4-80741  
 (CsCl)<sub>2</sub>, electric dipole polarisabilities meas. 4-112294  
 CsCo(CO)<sub>4</sub>, cryst. struct. with cubic dense packing 4-92172  
 Cs<sub>2</sub>CrF<sub>3</sub>, cryst. struct. and Jahn-Teller effect 4-70095  
 Cs<sub>2</sub>CrO<sub>4</sub>, matrix isolated, IR and Raman spectra, isotope shifts, bond angles evaluation 4-96539  
 Cs<sub>2</sub>CuCl<sub>3</sub>, Jahn-Teller induced phase transition, hydrostatic press. effects 4-65392  
 CsD<sub>2</sub>PO<sub>4</sub>, quasi-one-dimensional, behaviour of thermodynamic quantities near ferroelec. phase transition 4-61634  
 CsDy(MoO<sub>4</sub>)<sub>2</sub>, layered cryst., low temp. thermal cond. (Russian) 4-70481  
 CsEuNaNb<sub>2</sub>O<sub>15</sub>, struct. and ferroelec. props. 4-109141  
 CsF-UF<sub>6</sub>, binary fused mixtures, elec. cond. 4-108847  
 CsF+Ar(Kr)(Xe), collision-induced dissociation, cross sections 4-76993  
 (CsF)<sub>2</sub>, electric dipole polarisabilities meas. 4-112294  
 Cs<sub>2</sub>FeF<sub>3</sub>, cryst. struct. and Jahn-Teller effect 4-70095  
 CsFeSe<sub>2</sub>, quasi 1-D alternating antiferromag. EPR study 4-109062  
 CsFeSe<sub>2</sub>, structure and mag. props. 4-71039  
 CsH, (A<sup>1</sup>Σ<sup>+</sup>) state, transition probabilities and radiative lifetimes ratios 4-96623  
 CsH, (A<sup>2</sup>Σ<sup>+</sup>) state, transition probabilities and radiative lifetimes calcs. 4-96624

## caesium compounds continued

- CsH<sub>2</sub>(<sub>1-2</sub>)D<sub>2</sub>PO<sub>4</sub>, ferroelectric, dielec. relaxation, activation energy, isotope effects 4-65989  
 CsH<sub>2</sub>PO<sub>4</sub> (CsD<sub>2</sub>PO<sub>4</sub>) ferroelectric phase transitions in transverse Ising model 4-93025  
 CsH<sub>2</sub>PO<sub>4</sub>, antiferroelec. fluctuations, Raman spectroscopy studies 4-71297  
 CsH<sub>2</sub>PO<sub>4</sub>, ferroelec., domain struct. relax. 4-71322  
 CsH<sub>2</sub>PO<sub>4</sub>, normal and deuterated, ferroelec. phase transition, Raman studies 4-71295  
 CsH<sub>2</sub>PO<sub>4</sub>, paraelec. phase, soft relax. mode, dielec. spectra studies 4-65986  
 CsH<sub>2</sub>PO<sub>4</sub>, pseudo-1D ferroelec., thermal cond. 4-65505  
 CsH<sub>2</sub>PO<sub>4</sub>, quasi-one-dimensional, behaviour of thermodynamic quantities near ferroelec. phase transition 4-61634  
 CsH<sub>2</sub>PO<sub>4</sub>, Raman OH stretching band shape and H-bonds, transition moment 4-66024  
 CsH<sub>2</sub>PO<sub>4</sub>, Raman scatt. study 4-71377  
 CsH<sub>2</sub>PO<sub>4</sub>, Slater-Senko model, ferroelec. transition 4-76370  
 CsH<sub>2</sub>PO<sub>4</sub>, thermal expansion, quasi-one-dimensional Ising model 4-80268  
 CsH<sub>2</sub>PO<sub>4</sub>, US absorpt. and vel., order parameter crit. fluctuations anisotropic spectrum 4-98206  
 CsHSO<sub>4</sub>, protonic superionic conductor, self-diffusion and spin-lattice relax. 4-80293  
 CsHSO<sub>4</sub>, protonic superionic conductor, self-diffusion and spin-lattice relax. 4-80293  
 CsH<sub>2</sub>(SeO<sub>2</sub>)<sub>2</sub>, antiferroelectric, elastic compliance consts., anomalies at transition point 4-108500  
 Cs<sub>2</sub>HgBr<sub>4</sub>, low-temp. phases and cryst. struct. 4-103712  
 (CsI)<sub>2</sub>, vaporisation, mass spectrometric study 4-80204  
 CsI, 60 GPa effects, UV absorpt. spectra 4-76490  
 CsI cluster ions, ultra-high mass spectrometry 4-102842  
 CsI coated photocathode in microchannel plate detector 4-73509  
 CsI fibre lightguide material, designed to operate in visible and IR spectral regions 4-74634  
 CsI, irradiated single crystals, intrinsic hole colour centres 4-114332  
 CsI, L-edge absorpt. systematics, EXAFS obs. 4-66121  
 CsI molecules, photodissociation and Cs atom electronic orientation 4-93541  
 CsI, optical absorpt. spectra, meas. at press. up to 60 GPa 4-76495  
 CsI, optical const. calcs. 4-99084  
 CsI, optical transmittancy, xenon high pressure transmitting, band closing 4-114299  
 CsI, press. induced struct. transition 4-113607  
 CsI:TL crystal scintillators props. review 4-64292  
 CsI:TL<sup>+</sup>, optical absorption and mag. circular dichroism spectra 4-99098  
 CsI-coated microchannel plate, X-ray efficiency 4-102504  
 CsI-Cs liq. solns., mag. susceptibility 4-80741  
 CsIn<sub>3</sub>, cryst. struct. study by single cryst. method (German) 4-70079  
 Cs<sub>97</sub>K<sub>13</sub>Si<sub>31</sub>Al<sub>22</sub>O<sub>192</sub> zeolites, normal and deuterated, cryst. struct. 4-92169  
 CsLiMoO<sub>4</sub>, ferroelec. phase transitions, Raman and NMR studies 4-71289  
 CsLiMoO<sub>4</sub>-type crystals, ferroelec. phase transitions 4-65979  
 CsMgCl<sub>3</sub>:Cu(II)-M(III), (M=Cr, Mo, Ru, Rh), intermetallic charge transfer spectra 4-65644  
 Cs<sub>2</sub>MgCl<sub>3</sub>, NQR spectra of Cl atoms 4-88742  
 CsMnBr<sub>3</sub> with cryst. field of low symm., spectral splittings (Chinese) 4-70754  
 CsMnBr<sub>3</sub>:Er<sup>3+</sup>, one-dimensional antiferromagnet, energy migration, luminesc. 4-99149  
 CsMnCl<sub>3</sub>, antiferromagnetic, optical absorpt. spectra, luminesc. studies 4-99133  
 CsMn<sub>1-x</sub>Co<sub>x</sub>Cl<sub>3</sub>·2H<sub>2</sub>O, random mixture with competing anisotropies, PMR meas. 4-88647  
 CsMn<sub>1/2</sub>Er<sup>3+</sup>, one-dimensional antiferromagnet, energy migration, luminesc. 4-99149  
 CsMn<sub>2</sub>Mg<sub>1-x</sub>Br<sub>3</sub>, biquadratic exchange 4-61531  
 Cs<sub>2</sub>MoO<sub>4</sub>, matrix isolated, IR and Raman spectra, isotope shifts, bond angles evaluation 4-96539  
 CsND<sub>2</sub>, molar heat capacity, X-ray and neutron diffr. study (German) 4-60997  
 CsNH<sub>2</sub>, molar heat capacity, X-ray and neutron diffr. study (German) 4-60997  
 CsNO<sub>3</sub>, ionic crystals growing from melts, morphology and kinetics 4-113370  
 CsNO<sub>3</sub>, phase II, cryst. struct. and polymorphic transitions 4-113409  
 Cs<sub>2</sub>NaBiCl<sub>6</sub>, cryst. struct. and phase transitions 4-80015  
 Cs<sub>2</sub>NaBiCl<sub>6</sub>, phase transition, phonon dispersion relations 4-98269  
 CsNa<sub>2</sub>Cl<sub>3</sub>·2H<sub>2</sub>O, struct., cryst. chemical study 4-65223  
 Cs<sub>2</sub>NaScCl<sub>6</sub>:C<sup>3+</sup> cryst., dopant fluoresc. props. 4-61745  
 Cs<sub>1-x</sub>(Na<sub>x</sub>H<sub>3</sub>O)<sub>2</sub>Cl, struct., cryst. chemical study 4-65223  
 Cs<sub>2</sub>Ni<sub>3/2</sub>Cd<sub>1/4</sub>F<sub>3</sub>, crystal struct. and linear trimers mag. interactions 4-71041  
 Cs<sub>2</sub>Ni<sub>2</sub>CdF<sub>12</sub>, hexagonal perovskites, intra- and intercluster mag. interactions 4-104405  
 Cs<sub>2</sub>Ni<sub>2</sub>CdF<sub>12</sub>, hexagonal perovskites, intra- and intercluster mag. interactions 4-104405  
 CsNiF<sub>3</sub>, failure of classical approx. for magnetisation calcs. 4-71126  
 CsNiF<sub>3</sub>, ferromagnet, optical absorption and magneto-optical properties 4-99100  
 CsNiF<sub>3</sub>, model, sp. ht. of classical easy-plane ferromag. chain 4-104452  
 CsNiF<sub>3</sub>, specific heat, sine-Gordon kinks and renormalisation 4-71100  
 CsO, hyperfine interactions and bonding, semiempirical valence bond model 4-112120  
 CsO-Al<sub>2</sub>O<sub>3</sub>-TiO<sub>2</sub> system, phase stability, TGA and DTA obs. 4-71642  
 CsO<sub>2</sub>-GeO<sub>2</sub> glass, structure, Raman spectra meas. (Japanese) 4-113347  
 CsO<sub>2</sub>-SiO<sub>2</sub> glass, vibr. spectra 4-109179  
 CsO<sub>2</sub>-Na<sub>2</sub>SiO<sub>3</sub> glass, vibr. spectra 4-109179  
 CsO<sub>2</sub>-V<sub>2</sub>O<sub>5</sub>, phase related, enthalpy of formation of vanadates 4-76758  
 CsP<sub>11</sub>, cryst. struct. and plastic phases 4-80018  
 CsPbCl<sub>3</sub> (Br<sub>3</sub>), optical props. in region of self-absorption edge (Russian) 4-93044  
 CsScN phonon dispersion relations by neutron inelastic scatt. 4-88249  
 Cs<sub>2</sub>SO<sub>4</sub>, matrix isolated, IR and Raman spectra, isotope shifts, bond angles evaluation 4-96539  
 Cs<sub>2</sub>TaOCl<sub>5</sub>, prep., fluoresc. spectra 4-108299  
 Cs<sub>2</sub>TaSCl<sub>5</sub>, prep., fluoresc. spectra 4-108299  
 Cs<sub>2</sub>Ti<sub>2</sub>Cl<sub>8</sub>, exchange interaction in orbitally degenerate binuclear units 4-71054

## cesium compounds continued

- $\text{Cs}_2\text{UO}_4$  phase, high temp., thermodynamic stability 4-113671  
 $\text{Cs}_2\text{VF}_6$ , cryst. struct. and Jahn-Teller effect 4-70095  
 $\text{Cs}_2\text{V}_2\text{X}_6$  ( $\text{X}=\text{Cl}, \text{Br}, \text{I}$ ) linear chain antiferromagnets, mag. excitations 4-65800  
 $\text{Cs}_2\text{WO}_2$ , matrix isolated, IR and Raman spectra, isotope shifts, bond angles evaluation 4-96539  
 $\text{CsI}_2\text{Xe}$ , optical absorpt. by Xe monomers and dimers. solvable one electron model 4-71404  
 $\text{Cs}_2\text{ZnI}_4$  phase transitions, Raman scatt. study 4-76470  
 $\text{Gd}_2\text{Ca}(\text{N}_3)_{15}$ , cryst. struct., single cryst. X-ray diffr. studies 4-108332  
 $(\text{Rb-Cs})\text{NO}_3$  molten binary system, internal mobilities 4-108637  
 $\text{Rb}_{1-x}\text{Cs}_x\text{D}_3\text{PO}_4$ , monoclinic, phase transitions, dielec. studies 4-109139

## cesium generators see plasma diodes

## cesium plasma diodes see plasma diodes

## calcination see heat treatment

## calcium

## see also nuclei with .....

- alkali halides:  $\text{Ca}^{2+}$ , X-irrad. effect on impurity vacancy dipoles and aggregation precipitation state, F-centre production 4-70209  
 alkali metal halides:  $\text{Mg}^{2+}(\text{Ca}^{2+})(\text{Sr}^{2+})$ , impurity complex binding energies 4-60912  
 atom, dynamic polarisabilities, semiempirical calc. methods 4-102599  
 atom, electric quadrupole transition probabilities, GTO and STO valence basis sets, CI calcs. 4-87053  
 atom, electron impact double ionisation modified binary encounter model 4-83476  
 atom, HFS, field isotope shift, multiconfigurational HF method 4-102594  
 atom, hyperfine struct. of 4s4p and 4s3d configs., pair correl. effects, ab initio calcs. 4-64368  
 atomic cascades, continuously excited, quantum beats 4-74185  
 bone Ca, % by mass rel. to effective at. no., dual-energy CT 4-115188  
 crystal structure from first principles calcs. 4-70064  
 electron scatt., collision strengths for inelastic transitions including fine struct. 4-96704  
 element analysis using charged-particle induced prompt  $\gamma$  rays 4-89362  
 FCC, phonon freqs. and binding energies, pseudopot. calc. 4-80181  
 fine particles, CESR 4-76251  
 hypersatellite X-ray spectra,  $\text{H}^+$  induced 4-107301  
 intracellular distrib. in tip growing plant cells, PIXE 4-100394  
 isotope shifts meas. using laser spectroscopy 4-78806  
 isotopes selection for SIMS of biological material 4-115303  
 isotopic analysis of refractory inclusions 4-110577  
 lattice dynamics, model-potential approach 4-61022  
 molecules, low-lying electronic states contrib. visible band spectra 4-96553  
 seawater Ca and Mg composition in seas around Italy 4-115435  
 solar corona, Ca abundance var. in X-ray flare plasma 4-105925  
 sputtering, ground and excited state, laser-fluoresc. obs. 4-93169  
 X-ray meas. of anomalous dispersion correction 4-87090  
 $\text{BaTiO}_3$ :Ca, impurity site occupancy, channelling enhanced microanal. studies 4-108394  
 Ca XVIII/Ca XIX ionisation balance in solar flares, derivation from XRP solar X-ray data 4-72916  
 Ca II, reson. electron capture to high Rydberg states 4-112268  
 Ca II emission from V711 Tau 4-94888  
 Ca II k-line, time sequence in solar flare 4-105945  
 Ca II stellar emission var. and activity 4-94824  
 Ca XIX, effective excitation and recomb. rate coeffs., appl. to Sun 4-87218  
 $\text{Ca}^+$ , 4s, 4p and 3d states, hyperfine struct., many-body perturbation theory 4-102610  
 $\text{Ca}^+$ , dielectronic recombination via 4s to 4p excitation 4-74341  
 $\text{Ca}^+$ , electron impact ionisation, excitation-autoionisation contrib., distorted-wave approx. 4-102800  
 $\text{Ca}^{17+}$ , oscillator strengths, photoionisation cross section calc. 4-83332  
 $\text{Ca}^{2+}$  domains rel. to anomalous voltage relations in Aplysia neurons 4-89511  
 $\text{Ca}^{2+}$ , effect on struct. and rheology of canine tracheal mucin 4-105274  
 $\text{Ca}^{2+}$  ion permeation mechanism through Ca channels, electrostatic repulsion 4-77215  
 $\text{Ca}^{2+}$  ions, effects on dil. aq. solns. of monosaccharides 4-112208  
 $\text{Ca}^{2+}$  second hydration shell, nonadditive effect, pot. energy surface, MO study 4-112102  
 Ca/LiCl,  $\text{LiNO}_3/\text{LiNO}_3$ ,  $\text{AgNO}_3/\text{Ni}$  thermal battery cells, discharge characts. 4-66675  
 Ca-Mg system, thermodynamic and phase diagram data 4-61079  
 $\text{Ca}^{2+}$ -activated  $\text{K}^+$  channels in human erythrocytes, comparison of single-channel currents with ion fluxes 4-66921  
 Ca +  $\text{F}_2$  reactions, crossed laser mol. beam studies and CaF prod. mol. rot. polarisation 4-91364  
 $\text{Ca}^{2+} + \text{H}_2\text{O}$ , intramol. vibr. freq., single ion effect 4-69036  
 CaI, doubly excited  $4p^2$  config. radiative lifetimes, stark shift parameters 4-91232  
 CaI, highly excited states, Stark effect, hyperfine struct., isotope shifts 4-64405  
 $^{45}\text{Ca}$  and  $^{90}\text{Sr}$  applied separately and in combination with  $^{131}\text{I}$ , tumour induction in rats (Russian) 4-67013  
 $\text{Ca}^+ + \text{HF}$  reactions, crossed laser mol. beam studies and CaF prod. mol. rot. polarisation 4-91364  
 InP:Ca crystals grown by synthesis solute diffusion, electrical and optical props. 4-85093  
 $\text{KBr}:\text{NO}_2$ ,  $\text{Ca}^{2+}$ , struct. of luminesc. and absorpt. centres (Ukrainian) 4-66059  
 KCl:Ag, Ca, X-irrad., electron centre form., luminesc., optical absorpt. studies 4-60920  
 $\text{MgO}:\text{Ca}^{2+}$ , coexistence of large- and small-radius excitons bound on defects 4-92619  
 NaCl:Ca, plastic deform. parameters, impurity conc. effect, low temp. anomaly 4-88229  
 NaCl:Ca $^{2+}$ , impurity-vacancy pairs, computer simulation of induced Snoek effect 4-75501  
 Sr + Ca collisions, multistate coupled eqn., laser-induced transition process 4-74323  
 $(\text{Y}_{1-x}\text{Gd}_x)_2\text{O}_3$ :S:Ca luminesc. study 4-81013  
 YIG:Ca epitaxial layers, elec. cond. meas. 4-80694

## calcium continued

- YIG:Ca films, charge compensation mechanism, annealing effects, behaviour on treatment with oxidising and reducing solns. 4-80799  
 YIG:Ca films, surface layer contraction, X-ray diffr. and magneto-optical studies 4-61262  
 calcium alloys  
 see also calcium compounds  
 Magnox alloys, etched, surface anal. by secondary ion mass spectrometry and ion scatt. spectroscopy 4-93456  
 Al-Ca-Zn superplastic alloy, composite, fibre reinforced, hot pressing, tensile props. 4-99369  
 Ca-Mg amorphous alloy, low-temp. elec. resist. 4-84603  
 $\text{Ca}_3\text{Cu}_2\text{Al}_7$  and  $\text{CaCr}_2\text{Al}_{10}$ , crystal structures (German) 4-75367  
 $\text{CaNi}_5$ , stability of rechargeable hydriding alloys during extended cycling 4-72190  
 $\text{CaNi}_5\text{H}_2(\text{D}_2)$ , absorption pressure-comp. isotherms, thermodynamic anal. 4-77032  
 $\text{CaSOCl}_2$  cells with anodes made from Ca/Ca-Li alloys, electrochemical studies 4-72080

## calcium compounds

## see also calcium alloys

- apatite, hexagonality to cubicity transition 4-60891  
 calcite, cleavages, Knoop and Vickers hardness numbers 4-110136  
 calcite single cryst., elasticity at calcite I-calcite II transition 4-105549  
 dicalcium barium propionate, symm. change at I-II phase transition, X-ray diffr. study 4-108607  
 dicalcium lead propionate, ferroelec. press. induced II-III transition, polarising microscope obs., permitt. meas. 4-80879  
 dicalcium lead propionate, ferroelec.-paraelec. transition, dopant conc. depend. 4-99048  
 dicalcium strontium propionate, ferroelec. press. induced II-III transition, polarising microscope obs., permitt. meas. 4-80879  
 dicalcium strontium propionate, ferroelectric phase transition, X-ray diffr. study 4-65988  
 dolomite, calsintering, effects of raw material props. and  $\text{Fe}_2\text{O}_3$  additions 4-66281  
 flashed brine geothermal system scale control 4-62298  
 2-fluorobenzoate dihydrate, intermolecular H bond, cryst. struct., X-ray diffr. 4-103733  
 formate, solid, heteronuclear zero-field NMR spectra 4-76262  
 ilvaite, cryst. and mag. struct., neutron powder diffr. study 4-113412  
 $(\text{KSCN}, \text{NaSCN}, \text{LiSCN})_2(\text{Ca}(\text{NO}_3)_2)_{0.74}\text{O}_6\text{H}_2\text{O}$  melts, mixed alkali effect 4-108642  
 oxalate, pyrolysis, rate consts., IR spectra 4-114794  
 rare earth compounds,  $\text{R}_2\text{Co}_2\text{CrO}_3$ ,  $\text{R}=\text{Ce}, \text{Pr}, \text{Nd}, \text{Sm}, \text{Eu}, \text{Gd}, \text{Tb}, \text{Dy}, \text{Ho}, \text{Er}, \text{Tm}, \text{Yb}, \text{Lu}$ , ionic cond. and thermal expansion 4-84461  
 tartrate, Raman spectrum, mode assignments, permitt. meas. 4-93011  
 tri-sarcosine calcium chloride, dielec. const. and loss meas. in paraelec. phase, behaviour near ferroelec. transition 4-71258  
 Whitestone, water-saturated, dielec. props. in MHz range, texture effects 4-82038  
 zirconolite, high resolution lattice images 4-103951  
 $\text{AgCl}:\text{CaCl}_2$ , molten, electrolytic cond. 4-108638  
 $\text{Al}_2\text{O}_3\text{MgO}:\text{CaO}$ , translucent, fracture, influence of temp. and CaO 4-92290  
 Ba-Sr-Cn carbonate suspension, rheological props. (Polish) 4-83870  
 C-CaSO $_4$  composites, for solar energy collection and storage 4-100004  
 $(\text{Ca}, \text{Na})_2\text{Al}_2\text{Si}_2\text{O}_{10} \cdot 6\text{H}_2\text{O}$ , heulandite, struct., neutron diffr. studies 4-103720  
 Ca-Si-Al-O-N system, oxynitride glasses, prep. and props. 4-76737  
 $\text{Ca}^{2+}$ -exchanged montmorillonite, intercalated mol. dynamics, quasielastic neutron scatt. 4-65154  
 $\text{CaAl}_2\text{O}_9$ ,  $\text{Ar}^+$  ion irrad., damage cross sections 4-108484  
 $\text{CaAl}_2\text{O}_9$ , solid phase synthesis 4-76668  
 $\text{CaAl}_2\text{Si}_2\text{O}_8$  glass, shock compressed, optical emission spectra 4-114305  
 $\text{CaAl}_2\text{Si}_2\text{O}_{10} \cdot 3\text{H}_2\text{O}$ , scolecite, struct. refinement, neutron diffr. studies 4-92180  
 $\text{Ca}_{0.25}\text{Ba}_{0.75}\text{Tb}_{0.05}\text{Mg}_{0.15}\text{B}_{2.05}$ , Kurchatovite struct., phosphor props. 4-66074  
 $\text{CaBeAsO}_4(\text{OH})$ , bergslagite, cryst. struct., X-ray diffr. 4-80001  
 CaBr beam, elec. quadrupole refocusing, hyperfine levels and low-J lines 4-102824  
 $\text{CaCO}_3$ , calcite, dislocation struct. and twinning 4-113467  
 $\text{CaCO}_3$ , calcite, growth rate from soln., influence of impurities 4-92116  
 $\text{CaCO}_3$ , calcite, thermal cond. and phonon scatt. by twin planes 4-65507  
 $\text{CaCO}_3$  crystallisation with chem. absorpt. 4-98038  
 $\text{CaCO}_3$ , dynamic thermogravimetric meas. using microcomputer-controlled furnace 4-111137  
 $\text{CaCO}_3$ , efficient reflection with phase conjugation in stimulated Raman scatt. 4-107754  
 $\text{CaCO}_3$ , electrolyte crystals in supersaturated aqueous soln., crystal growth kinetics 4-114373  
 $\text{CaCO}_3$ , light absorpt. coeff. anisotropy in 0.4-2.0  $\mu\text{m}$  region 4-76416  
 $\text{CaCO}_3$ , natural, luminesc. 4-80995  
 $\text{CaCO}_3$ , natural calcites, X-irradiated, thermolum., absorption and  $\text{Mn}^{2+}$  EPR spectra 4-71453  
 $\text{CaCO}_3$ , pentagonal cusp pit morphology on cleavage faces 4-75760  
 $\text{CaCO}_3$ , resonance-coupled two-wave stimulated Raman scatt. (Chinese) 4-91533  
 $\text{CaCO}_3$ , review of thermoluminesc. 4-109253  
 $\text{CaCO}_3$ , tunnel generation and locking stimulated Raman radiation components 4-112515  
 $\text{CaC}_2\text{O}_4 \cdot \text{H}_2\text{O}$ , whewellite, growth morphology 4-65213  
 $\text{CaC}_2\text{O}_4 \cdot \text{H}_2\text{O}$ , electrolyte crystals in supersaturated aqueous soln., crystal growth kinetics 4-114373  
 $\text{CaCl}_2$ , in aq. mixtures of alcohols, enthalpies of soln. at 298.15K 4-103942  
 $\text{CaCl}_2$ , solution enthalpies of divalent defects 4-98316  
 $\text{CaCl}_2\text{-LaCl}_3$  mixtures, refr. index, goniometric meas. 4-109147  
 $\text{Ca}_2\text{Cr}_2\text{Si}_2\text{O}_{12}$ , synthetic garnets, Cr coordination and vibr. props., IR study 4-65249  
 $\text{Ca}_{1-x}\text{Eu}_x\text{Ti}_{1-x}\text{Fe}_x\text{O}_3$ , perovskite solid soln. systems, prep. and charact. 4-70123  
 CaF, dissociation energy; HF STO calcs. 4-112092  
 CaF, rot. polarisation from  $\text{Ca}^+ + \text{HF}$  and  $\text{Ca} + \text{F}_2$  reactions, laser induced fluore. study 4-91364  
 CaF:He, interstitial diffusion, solubility of He, dissolution energy 4-113727  
 $\text{CaF}_2$  adsorbed on Ge, layer thickness meas. by RBS (Chinese) 4-70968  
 $\text{CaF}_2$ , antireflection coatings for YAG crystals (Russian) 4-97012

## calcium compounds continued

- CaF<sub>2</sub>, binding energy, bulk modulus and press. derivatives, interionic pot. model 4-60884  
 CaF<sub>2</sub> crystal, optical properties, 300-1600K (*Russian*) 4-61644  
 CaF<sub>2</sub>, dielectric constant, temp. depend., polarisability 4-92995  
 CaF<sub>2</sub>, electrolyte crystals in supersaturated aqueous soln., crystal growth kinetics 4-114373  
 CaF<sub>2</sub>, electron irradi., anion voidage and void superlattice 4-108350  
 CaF<sub>2</sub>, fluorite struct., inner displacement, internal strain tensor, lattice dynamic models 4-92315  
 CaF<sub>2</sub>, IR excitation of high-freq. phonons by multiphonon absorpt. 4-61027  
 CaF<sub>2</sub>, orbit-lattice coupling parameters for lanthanides 4-75903  
 CaF<sub>2</sub>, Pu and U diffusion above and below  $\lambda$  transition temp. 4-70473  
 CaF<sub>2</sub>, review of thermoluminesc. 4-109253  
 CaF<sub>2</sub>, single crystals, muonium decoupling in high transverse mag. field 4-92985  
 CaF<sub>2</sub> substrate for heteroepitaxial growth of Si 4-80448  
 CaF<sub>2</sub>, thermally induced anion disorder, neutron scatt. meas. 4-98338  
 CaF<sub>2</sub> vapour deposited thin films, TSEE, thermolum. meas. 4-81119  
 CaF<sub>2</sub> windows, bare and antirefl. coated, pulsed DF chain laser damage 4-74582  
 CaF<sub>2</sub>, Er<sup>3+</sup>, gas flow cryostat for dielectric measurements 4-63734  
 CaF<sub>2</sub>, Ce<sup>3+</sup>, O<sub>2</sub><sup>-</sup>, thermoluminescence spectra, IR effects 4-109259  
 CaF<sub>2</sub>, Dy<sup>3+</sup>, Eu<sup>2+</sup> crystals, electron-excitation relax. kinetics and nonequilibrium acoustic phonons 4-88256  
 CaF<sub>2</sub>, Er<sup>3+</sup> transferred hyperfine interaction parameters, ENDOR 4-84872  
 CaF<sub>2</sub>, Eu, phononless impurity-centre line, inhomogeneous broadening under plastic defect. conditions 4-88864  
 CaF<sub>2</sub>, Eu<sup>2+</sup>, phononless line profile under random deformations, luminesc. bands 4-70726  
 CaF<sub>2</sub>, La<sup>2+</sup>, intermediate Jahn-Teller coupling, vibronic Raman and EPR spectra 4-88491  
 CaF<sub>2</sub>, La(Er), impurity local structural environments, EXAFS determ. 4-66129  
 CaF<sub>2</sub>, Na, photochemical conversion of M<sub>A</sub>-centres, identification of M<sub>A</sub><sup>2+</sup>-centre, absorpt. and fluoresc. spectra 4-76501  
 CaF<sub>2</sub>, rare earth doped, gamma irradi., induced dielec. relax. 4-70210  
 CaF<sub>2</sub>, Sm crystal, gamma-irradiated, optical study 4-81015  
 CaF<sub>2</sub>, Sr<sup>2+</sup> (Y<sup>3+</sup>), lattice relax. around impurities, EXAFS study 4-93140  
 CaF<sub>2</sub>, Tm, NMR and dynamic nucl. pol., low-freq. modulation effects 4-65868  
 CaF<sub>2</sub>, Tm<sup>2+</sup>, Tm<sup>2+</sup> electron spin resonance line ENDOR and saturation optical detect. 4-84873  
 CaF<sub>2</sub>, U<sup>3+</sup>, diamagnetic crystal with paramag. ions, nuclear relax. rates 4-65789  
 CaF<sub>2</sub>, Y<sup>3+</sup> (Pb<sup>2+</sup>) crystals, electronic excitation decay, impurity effect 4-109209  
 CaF<sub>2</sub>/LiF isotropic interface, TE-surface polaritons 4-75869  
 CaF<sub>2</sub>/Si heterostructure interface, MBE grown, Raman spectra studies 4-98462  
 CaF<sub>2</sub>-ScF<sub>3</sub>-Nd<sup>3+</sup> system, stimulated emission channels 4-104632  
 CaF<sub>2</sub>-Si, epitaxial surface morphology, SEM study 4-113822  
 CaF<sub>2</sub>-SrF<sub>2</sub> mixed crystals, cohesion, harmonic and anharmonic elastic props. 4-92132  
 (CaF<sub>2</sub>)<sub>1-x</sub>(ErF<sub>3</sub>)<sub>x</sub>, solid soln., superstructure, ODMR and MCD study 4-75401  
 CaFe<sub>2</sub><sup>+</sup>Fe<sup>3+</sup>(Si<sub>2</sub>O<sub>7</sub>(OH)), ilvaite, electron delocalisation and Mossbauer spectra 4-98993  
 Ca<sub>3</sub>Fe<sub>2-x</sub>Mn<sub>2x</sub>O<sub>8+y</sub>, O defect perovskite struct., X-ray diff. and HREM study 4-92382  
 Ca<sub>3</sub>Ga<sub>2</sub>Ge<sub>2</sub>O<sub>12</sub>, garnet single crystals, microhardness, brittle fracture 4-65337  
 Ca<sub>3</sub>Ga<sub>2</sub>Ge<sub>2</sub>O<sub>12</sub>-Cr<sup>3+</sup> EPR spectra 4-71170  
 Ca<sub>3-x</sub>(GeO<sub>4</sub>)(O<sub>1-2x</sub>F<sub>2x</sub>), two-layer cryst. struct. 4-75393  
 CaH<sub>2</sub>, bonding and reaction studies, APW calc. and photoemission studies 4-113384  
 Ca<sub>2</sub>IrH<sub>5</sub>, H sites, geometric model 4-88155  
 Ca<sub>2</sub>KH<sub>7</sub>(PO<sub>4</sub>)<sub>2</sub>·2H<sub>2</sub>O, cryst. struct., X-ray and neutron diff. studies 4-113405  
 Ca<sub>2</sub>LaFe<sub>2</sub>O<sub>8+x</sub>, cryst. struct. determ. 4-80014  
 CaLa<sub>2</sub>S<sub>4</sub>, melt growth using Stober technique 4-108298  
 Ca<sub>1-x</sub>La<sub>1-x</sub>Fe<sub>2</sub>O<sub>8</sub>, perovskite solid soln. systems, prep. and charact. 4-70123  
 Ca<sub>3</sub>La<sub>2</sub>W<sub>2</sub>O<sub>12</sub>, rare earth, luminescence and sensitised emission 4-88871  
 CaMg(CO<sub>3</sub>)<sub>2</sub>, dolomite, interpretation of high resolution electron micrographs 4-79903  
 Ca<sub>3</sub>Mn<sub>1-x</sub>Fe<sub>1+x</sub>O<sub>8.02</sub>, struct. and frustrated antiferromag. props. 4-108998  
 Ca(NCS)<sub>2</sub>, solns. in dipolar aprotic, IR spectra and struct. 4-112175  
 Ca(NH<sub>4</sub>)<sub>2</sub>PO<sub>4</sub>·7H<sub>2</sub>O, cryst. struct., H. bonds, X-ray diff. determ. 4-92150  
 Ca(NO<sub>3</sub>)<sub>2</sub>, aqueous electrolytes, conductance, conc. depend. 4-84432  
 Ca<sub>2</sub>Na<sub>1-x</sub>Al<sub>1+x</sub>Si<sub>3-2x</sub>O<sub>8</sub>, intermediate plagioclase feldspar, modulate struct. 4-84249  
 Ca<sub>2</sub>NaMg<sub>2</sub>V<sub>2</sub>O<sub>12</sub> garnet, elec. cond. and thermopower 4-70822  
 Ca<sub>3</sub>Na<sub>2</sub>Ti<sub>3</sub>NbSi<sub>4</sub>O<sub>22</sub>F<sub>3</sub>, fersmanite, cryst. struct., X-ray diff. study 4-115396  
 Ca(NbO<sub>3</sub>)<sub>2</sub>:P<sup>3+</sup>(Er<sup>3+</sup>), stimulated emission and laser channels 4-91480  
 Ca<sub>2</sub>Nb<sub>2</sub>O<sub>7</sub>-CaTiO<sub>3</sub>, ferroelectric, crystallochemical props. 4-71288  
 CaO (100), SO<sub>2</sub> chemisorption, metal adsorbates effects, XPS study 4-113807  
 CaO, addition to Ta<sub>2</sub>O<sub>5</sub>, elec. cond., ionic transport number 4-98349  
 CaO, chemical diffusion coeff. calcs. 4-84468  
 CaO, IR-stimulated luminesc. due to O vacancies 4-81017  
 CaO, lattice defect prod. by electronic excitation 4-70213  
 CaO spin triplet, g and D values determ. in case of misalignment 4-98508  
 CaO, triplet electron spins, dipolar-induced dephasing 4-108778  
 CaO:Mn<sup>2+</sup>, zero field splitting parameter calc. method 4-65646  
 CaO-Al<sub>2</sub>O<sub>3</sub> eutectic melt, interaction with Al<sub>2</sub>O<sub>3</sub> 4-61924  
 CaO-Al<sub>2</sub>O<sub>3</sub>-P<sub>2</sub>O<sub>5</sub>-SiO<sub>2</sub>-Na<sub>2</sub>O(K<sub>2</sub>O) system glasses, opacification and crystn. 4-89021  
 CaO-Al<sub>2</sub>O<sub>3</sub>-SiO<sub>2</sub> glasses, struct. features, EXAFS and XANES studies 4-60850  
 CaO-Al<sub>2</sub>O<sub>3</sub>-SiO<sub>2</sub> glass powder, vitrification kinetics, effect of water vapour 4-92094  
 CaO-B<sub>2</sub>O<sub>3</sub> glass, photoelastic consts., compositional trends 4-84945  
 CaO-B<sub>2</sub>O<sub>3</sub>-Al<sub>2</sub>O<sub>3</sub>-Fe<sub>2</sub>O<sub>3</sub> glass system, photoacoustic spectra of Fe 4-99130

## calcium compounds continued

- CaO-Fe<sub>2</sub>O<sub>3</sub> glass, glass forming region and Fe<sup>3+</sup> coordination (*Japanese*) 4-113348  
 CaO-Fe<sub>2</sub>O<sub>3</sub>-SiO<sub>2</sub>, glass formation and props. 4-79946  
 CaO-Ga<sub>2</sub>O<sub>3</sub> glass, form. density, refr. index, crystn. temp., hardness, IR spectra 4-113635  
 CaO-NiO, chemical diffusion coeff. calcs. 4-84468  
 CaO-P<sub>2</sub>O<sub>5</sub> glass, internal friction, temp. depend. 4-61966  
 CaO-SiO<sub>2</sub>-TiO<sub>2</sub> glasses, struct. analysis, XPS 4-108286  
 Ca(OC)<sub>2</sub>, brucite-type, precursor states in phase transform. accompanying decomposition 4-113612  
 CaOH, B<sup>2+</sup>-X<sup>2+</sup> transition, dye laser spectroscopy, rot. struct. 4-59786  
 CaOH, dissoc. energy calc., HF and GTO methods 4-64347  
 Ca(OH)<sub>2</sub>, brucite-like, struct. and IR relations 4-79996  
 Ca(OH)<sub>2</sub>, proton dynamics, <sup>1</sup>H NMR relax. meas. 4-104505  
 Ca(OH)<sub>2</sub>, proton spin, nuclear dipolar mag. ordering 4-88729  
 Ca(OH)<sub>2</sub>, single cryst., preaccretion transformations, Raman studies 4-98266  
 (CaO.50P<sub>2</sub>O<sub>5</sub>)(M<sub>2</sub>O)<sub>50-55</sub>, dissolution in aq. soln. 4-84405  
 α-Ca<sub>2</sub>(PO<sub>4</sub>)<sub>2</sub>, sintering behaviour at 1200 to 1600°C 4-114458  
 β-Ca<sub>2</sub>(PO<sub>4</sub>)<sub>2</sub>:Cu<sup>2+</sup>, ESR study 4-65852  
 Ca<sub>3</sub>(PO<sub>4</sub>)<sub>2</sub>-CaNaPO<sub>4</sub> solid-solid transition equilb. 4-80221  
 Ca<sub>10</sub>(PO<sub>4</sub>)<sub>6</sub>F<sub>2</sub>, fluorapatite, radiation damage and annealing, optical studies 4-70192  
 Ca(PO<sub>3</sub>)<sub>2</sub>OH, prestressed ceramics, fatigue props. 4-62052  
 Ca<sub>10</sub>(PO<sub>4</sub>)<sub>6</sub>(OH)<sub>2</sub> coatings in Ti, comp. and struct., Auger spectroscopic analysis 4-109558  
 Ca<sub>10</sub>(PO<sub>4</sub>)<sub>6</sub>(OH)<sub>2</sub>, dissolution kinetics, effects of fluoride ions adsorption 4-98292  
 Ca<sub>2</sub>P<sub>2</sub>O<sub>7</sub>·2H<sub>2</sub>O, solid state, vibr. IR and Raman spectra 4-80922  
 Ca<sub>2</sub>RhH<sub>5</sub>, H sites, geometric model 4-88155  
 Ca<sub>2</sub>RuH<sub>5</sub>, H sites, geometric model 4-88155  
 CaS, ionic cond., Schottky defect model 4-70456  
 CaS, prep. in high purity powder form from elements 4-108298  
 CaS, single cryst. thermolum. study, 8-275K 4-104684  
 CaS:Cu, Er (Sm) electrolumins., radiation controlled enhancement of thermoluminescence 4-76529  
 CaS:Er phosphor, electrolum. spectrum and Er<sup>3+</sup> ion energy level splitting 4-71446  
 CaSO<sub>4</sub>, anhydrite, thermodynamics of solution in water 4-84400  
 CaSO<sub>4</sub> phosphors, thermoluminescence and exoelectron emission, radical effects 4-93120  
 CaSO<sub>4</sub>, review of thermoluminesc. 4-109253  
 CaSO<sub>4</sub>:Dy, photo-transfer thermoluminescence 4-104683  
 CaSO<sub>4</sub>:Dy dosimeters, TLD-900, thermolum. isothermal decay 4-68835  
 CaSO<sub>4</sub>:Dy single cryst., cryst. growth and elec. props. 4-113943  
 CaSO<sub>4</sub>:Dy Teflon discs, dosimetric parameters and comparison with MgB<sub>2</sub>O<sub>7</sub>:Dy sintered pellets 4-89757  
 CaSO<sub>4</sub>:Dy thermoluminesc. detectors response functions to γ-radiation 4-112037  
 CaSO<sub>4</sub>:Dy(Tm), Bulgarian synthesis, thermoluminescent and dosimetry props. (*Russian*) 4-78747  
 CaSO<sub>4</sub>:Dy(Tm), synthesis effect on phosphor props. (*Russian*) 4-78748  
 CaSO<sub>4</sub>:Dy(Tm) thermoluminescent detectors, sensitivity for 2-144 keV neutrons 4-96288  
 CaSO<sub>4</sub>:Eu(Sm), thermoluminesc. and radiophotoluminesc. 4-93118  
 CaSO<sub>4</sub>·4H<sub>2</sub>O, metastable crystals, growth from gels with organic additives 4-61826  
 CaSO<sub>4</sub>·2H<sub>2</sub>O, synthetic gypsum, gel growth of Herring Bone and Hour glass struct. 4-114388  
 CaSeO<sub>4</sub>·2H<sub>2</sub>O, IR spectra, vibr. anal. 4-61702  
 CaSi<sub>2</sub>, electronic density of states, XPS study 4-61272  
 CaSiO<sub>3</sub>, wollastonite, twinning, cryst. structures, polymorphism 4-89913  
 Ca<sub>2</sub>Sr<sub>1-x</sub>Al<sub>2</sub>O<sub>4</sub>(WO<sub>4</sub>)<sub>2</sub>, phase transition characs., role of cage cation substitution 4-65386  
 Ca<sub>1-x</sub>Sr<sub>x</sub>Fe<sub>2</sub>, epitaxial growth in GaAs/Ca<sub>1-x</sub>Sr<sub>x</sub>Fe<sub>2</sub>/GaAs (100) lattice-matched MBE structures 4-88562  
 Ca<sub>1-x</sub>Sr<sub>x</sub>Fe<sub>2</sub>O<sub>8</sub>, Fe<sup>4+</sup> ion electronic state, Mossbauer spectra studies 4-104171  
 CaTi<sub>3</sub>Al<sub>3</sub>O<sub>9</sub>, difficult-to-form crystal structures, preparation 4-70094  
 CaTiF<sub>6</sub>, crystal struct. and mag. props. 4-70084  
 CaTiO<sub>3</sub>, electron energy struct. of cond. band, X-ray photoemission yield spectra 4-61282  
 CaTiO<sub>3</sub>, polycryst., viscous creep deform. at elevated temps. 4-103863  
 CaTiO<sub>3</sub>-La<sub>2</sub>Ti<sub>2</sub>O<sub>7</sub>(Nd<sub>2</sub>Ti<sub>2</sub>O<sub>7</sub>), ferroelectric, crystallochemical props. 4-71288  
 CaO<sub>3</sub>Ti<sub>2</sub>P<sub>2</sub>O<sub>12</sub> ceramic, cryst. struct. determ. 4-84262  
 CaTiSiO<sub>4</sub>-La sphene-based glass-ceramics, La partitioning, Auger studies 4-88112  
 CaWO<sub>4</sub>, structural imperfection, vacancy disordering, diffusive mass transfer 4-75438  
 CaWO<sub>4</sub>, tunnel processes and assoc. of donor and acceptor centres 4-109258  
 CaWO<sub>4</sub>:Pr<sup>3+</sup>, stimulated emission and laser channels 4-91480  
 Ca<sub>3-x</sub>Y<sub>x</sub>Mn<sub>2</sub>Ge<sub>2</sub>O<sub>12</sub>, thermopower and elec. cond., 30 to 1000°C 4-70847  
 CaZnF<sub>4</sub>, scheelite-type cryst. refinement and bond lengths 4-92176  
 CaZnF<sub>4</sub>:Mn<sup>2+</sup>, 10 Dq value and isotropic superhyperfine constant 4-99080  
 CaZnF<sub>4</sub>:Mn<sup>2+</sup>, cryst. struct., axial field splitting calc., EPR, optical spectra 4-92159  
 CdTe/SnO<sub>2</sub> structures electrophysical characs., for photoconvertors 4-92795  
 CeO<sub>2</sub>-CaO solid solutions, elec. cond., temp. depend., 400-1200°C 4-61142  
 (CeO<sub>3</sub>)<sub>0.98</sub>(CaO)<sub>0.11</sub> solid solution, bulk cond. and grain boundary resist., effect of SiO<sub>2</sub> (*French*) 4-80295  
 CsCa<sub>3</sub>Mn<sub>2</sub>²⁺(Ni<sup>2+</sup>)(Co<sup>2+</sup>), fluoresc. emission, excitation, IR absorpt. spectra studies 4-99153  
 Cs<sub>2</sub>CaCl<sub>2</sub>·2H<sub>2</sub>O, struct., cryst. chemical study 4-65223  
 CsCaF<sub>3</sub>, soft mode freq., temp. and press. depend. 4-70331  
 CsCa<sub>2</sub>NbO<sub>10</sub>, layered ferroelastic perovskite, cryst. struct., X-ray diff. (*French*) 4-75419  
 CuO-CaO-P<sub>2</sub>O<sub>5</sub> glass, IR spectra 4-76446  
 (Fe,Ca,Mg)<sub>2</sub>Si<sub>2</sub>O<sub>6</sub> glass, ion bombard. effect, XPS 4-84320  
 Fe<sub>2</sub>O<sub>3</sub>-CaO-SiO<sub>2</sub> glasses, DC cond., Mossbauer and ESR. spectra 4-70807  
 K<sub>2</sub>Ca(CO<sub>3</sub>)<sub>2</sub>, butschliite, cryst. at. arrangement refinement, CO<sub>3</sub> group planarity, X-ray diff. determ. 4-92156  
 La<sub>1-x</sub>Ca<sub>x</sub>FeO<sub>3-y</sub> ferrites, mixed valence and electrochem. props. 4-70752

aluminum compounds continued

La<sub>1-x</sub>Ca<sub>x</sub>FeO<sub>3-y</sub>, high temp. order-disorder transition 4-113618  
LiF-CaF<sub>2</sub> thin film, ionic cond. meas. 4-84450  
MgO-CaTiO<sub>3</sub>-CaO.SiO<sub>2</sub> system, phase equilib. and microstruct., isothermal sections 4-114496  
Mn<sub>2</sub>Ca<sub>1-x</sub>(NO<sub>3</sub>)<sub>2</sub>.6H<sub>2</sub>O paramag. solns; conc., muon spin relax. study 4-71244  
Na<sub>1/2</sub>Ca<sub>1/2</sub>Al<sub>1/3</sub>Ti<sub>1/2</sub>O<sub>19</sub>, difficult-to-form, crystal structures, preparation 4-70094  
NaCa<sub>2</sub>Cu<sub>2</sub>V<sub>3</sub>O<sub>12</sub> garnet, mag. props. study 4-61563  
Na<sub>2</sub>CaSi<sub>3</sub>O<sub>8</sub>, cryst. struct. and isostructural cpd. relationships 4-92181  
NaCl:CaCl<sub>2</sub>, decay: props. of perturbed and unperturbed M-centres 4-92204  
NaCl:CaCl<sub>2</sub> doped cryst., dissolution at dislocation sites 4-60931  
Na<sub>2</sub>Nd<sub>2</sub>Ca<sub>2</sub>-Ga<sub>2</sub>S<sub>4</sub> luminescent props. and electron transfer 4-109233  
Na<sub>2</sub>O-B<sub>2</sub>O<sub>3</sub>-SiO<sub>2</sub>-CaO-Al<sub>2</sub>O<sub>3</sub> glasses UV-transmissivity of a tempered sodium-borosilicate glass (German) 4-88856  
Na<sub>2</sub>O-CaO glass, antireflection effects: induced by Au<sup>+</sup> implantation 4-60125  
Na<sub>2</sub>O-CaO-Al<sub>2</sub>O<sub>3</sub>-SiO<sub>2</sub> glass, leaching 4-84404  
Na<sub>2</sub>O-CaO-CO<sub>2</sub> system, calcination in air, differential thermal analysis obs. 4-99757  
Na<sub>2</sub>O-CaO-SiO<sub>2</sub>, γ radiation colouring in 600-1000 nm region 4-80948  
Na<sub>2</sub>O-CaO-SiO<sub>2</sub>, interaction with chloride melts, including MgCl<sub>2</sub> or ZnCl<sub>2</sub>, IR spectroscopic study 4-80949  
Na<sub>2</sub>O-CaO-SiO<sub>2</sub> glass, leaching kinetics, effect of divalent cations 4-109533  
Na<sub>2</sub>O-CaO-SiO<sub>2</sub> glass, stress corrosion characts., bending test 4-109535  
Na<sub>2</sub>O-CaO-SiO<sub>2</sub> glasses, ion implanted, mech. props. 4-75542  
Na<sub>2</sub>O-CaO-SiO<sub>2</sub>-Si<sub>3</sub>N<sub>4</sub> glass, prep., Fourier transform IR spectra, XPS 4-84192  
na<sub>2+x+y</sub>.Ca<sub>2(1-x-y)</sub>Ce<sub>2</sub>Tb<sub>2</sub>(PO<sub>4</sub>)<sub>3</sub> orthophosphates, luminescence and struct. relations 4-99169  
(Nd<sub>2</sub>Ca<sub>2</sub>)Ti<sub>6</sub>O<sub>20</sub>, ferroelec. cpd., perovskite-derived, crystal growth and characterisation 4-76657  
NiO-CaO eutectic, directionally solidified, crystallography 4-113658  
(Pb, Ca)TiO<sub>3</sub> piezoelectric ceramic, modified, low mech. quality factor 4-76330  
(Pb<sub>76</sub>Ca<sub>24</sub>)(Co<sub>1/2</sub>W<sub>1/2</sub>)<sub>0.04</sub>Ti<sub>0.96</sub>O<sub>3</sub> ceramics, piezoelec. props. MnO addition effects 4-104532  
(Pb<sub>76</sub>Ca<sub>24</sub>)(Mg<sub>1/3</sub>Nb<sub>2/3</sub>)<sub>0.0625</sub>Ti<sub>0.9375</sub>O<sub>3</sub>:Mn ceramics, US, elastic and dielec. props. 4-104543  
RbCaF<sub>3</sub>, soft mode freq., temp. and press. depend. 4-70331  
SiO<sub>2</sub>-CaO-Al<sub>2</sub>O<sub>3</sub>-MgO, elastic and strength props., effect of temp. 4-114597  
SiO<sub>2</sub>-CaO-Na<sub>2</sub>O glass, plastic processes 4-75602  
SiO<sub>2</sub>-CaO-Na<sub>2</sub>O-P<sub>2</sub>O<sub>5</sub> 'biological' glass, corrosion, neutral primary beam SIMS study 4-109532  
SiO<sub>2</sub>-MgO-CaO-Na<sub>2</sub>O(K<sub>2</sub>O), glass, surface alkali metals Auger anal. (French) 4-76568  
SiO<sub>2</sub>-Na<sub>2</sub>O-CaO-Fe<sub>2</sub>O<sub>3</sub> glasses, EPR study of behaviour and effect of Fe 4-88111  
SrCa<sub>1/3</sub>Nb<sub>2/3</sub>O<sub>3</sub>, defect struct., elec. and ionic cond. 4-98676  
Sr<sub>1-x</sub>Ca<sub>x</sub>TiO<sub>3</sub>, XY quantum ferroelec. with transition to randomness 4-88781  
(Sr<sub>0.50</sub>Pb<sub>0.25</sub>Ca<sub>0.25</sub>)TiO<sub>3</sub>100-x.(Bi<sub>2</sub>O<sub>3</sub>.3TiO<sub>2</sub>)<sub>x</sub>, dielectric props., HV capacitor application 4-98997  
Ta<sub>2</sub>O<sub>5</sub>-CaO sintered oxides, electronic and ionic cond. 4-92774  
(Y, Lu, Sm, Ca)<sub>3</sub>(Fe, Ge)<sub>2</sub>O<sub>12</sub> garnet system, distrib. coeffs. 4-61881  
Y<sub>3-x</sub>Ca<sub>x</sub>Fe<sub>2-x</sub>Ti<sub>x</sub>O<sub>12</sub> garnets, hyperfine fields and Mossbauer spectra 4-109098  
(Y<sub>1+2x</sub>Ca<sub>2-2x</sub>)(Fe<sub>2</sub>Zr<sub>1-2x</sub>)Fe<sub>3</sub>O<sub>12</sub> mag. atom critical conc., neutron depolarisation study 4-61514  
(YEuTmCa)<sub>3</sub>(FeGe)<sub>2</sub>O<sub>12</sub> ferrite-garnet epitaxial films, fine struct. of mag. spectra 4-76206  
(YSmCa)<sub>3</sub>(FeGe)<sub>2</sub>O<sub>12</sub> garnet films, Ne<sup>+</sup> implanted, cylindrical mag. domains obs. 4-114148  
YSmLuCaFeGe garnet film, mag. anisotropy study 4-88704  
(YSmLuCa)<sub>3</sub>(GeFe)<sub>2</sub>O<sub>12</sub> epitaxial film, cloudlike charged wall, bubble propagation 4-104473  
ZnSe-CaF<sub>2</sub> deposited by laser-assisted evaporation, as broadband gradient-index antiref. coating 4-107765  
ZrO<sub>2</sub>-Al<sub>2</sub>O<sub>3</sub>-SiO<sub>2</sub>-CaO system, compatibility relations, microscopy, energy dispersive X-ray exam. 4-61925  
ZrO<sub>2</sub>-CaO, partially stabilised, transformation-toughened, fracture toughness, crack-size depend. 4-93373  
ZrO<sub>2</sub>-CaO, partially stabilised, grain boundary chem., Auger analysis 4-109409  
ZrO<sub>2</sub>-CaO system, directionally solidified eutectic, EELS 4-72009

calculating see calculation

calculating apparatus

see also computers  
No entries

calculating machines see calculating apparatus

calculation

see also graphs; nomograms

fusion technology, measurement assurance with MIL STD 45662, quality assurance 4-111798

calculators see calculating apparatus

calculators (electronic) see electronic calculators

calculus

see also differentiation; integration; variational techniques

quantum acoustics, deformation operator, perturbation calculus 4-83759

calibration

see also measurement standards; standardisation

AC susceptibility, for cylindrical specimens 4-78347

AC voltage calibration, 0.1 to 10 Hz 4-73451

acoustic power determination using nine-point microphone array, intensity and mean square press. methods 4-103150

acoustical meas., sound spectrograph appl., control methods 4-103154

airborne IR sensing systems, modelled and empirical atmospheric propagation data comparison 4-115367

atomic absorption, calibration algorithm 4-109708

audiometer screening instrument, calibration 4-85432

Auger electron energy analyser using a cylindrical mirror with ring-to-axis focusing 4-90696

buildings, flow metering systems, on-site calibration 4-97726

calibrator for high power and high energy laser power meters and

calorimeters (Chinese) 4-112492

calibration continued

Cliff-Lorimer k factors determination by analysis of crystallised microdroplets, EDX calibration 4-62271

composites, orthotropic, elastic and photoelastic calibration, appl. of least squares method 4-69717

concrete beam, three point bending, cracking, dye penetrant obs., compliance calibration technique 4-89205

current calibrators, precision and ease of use (French) 4-58864

cylindrical mirror analyser alignment technique for Auger spectroscopy 4-95561

diagnostic radiology image-intensifier-TV systems, performance testing 4-72414

dielectric loss measurement, frequency response analyser system, minicomputer-controlled, errors and calibration technique 4-111159

diffusion battery for ultrafine aerosols, design and calibration 4-89349

diode laser spectra calibration using a confocal etalon 4-74562

direct-flow rotameters, calibration and checking by flowmeter test system 4-91853

domestic solar system instrumentation, long-term stability and performance 4-99989

dose calibrator assays discrepancies for various forms of therapeutic <sup>131</sup>I 4-89760

double ionisation chamber for fission fragment detection 4-64284

dwarf stars, gnmfm photometry system calibration 4-101332

dye laser wave-number calibration using reference lines in optogalvanic spectra of U and Th 4-83628

dye lasers, tunable, spectrosc. freq. calibration 4-78378

eddy current structurescopes testing 4-58872

EDX systems in STEM, multielement salt standards for calibration 4-72025

electric field strength meas. instruments, using parallel-plate capacitor 4-95468

electro-oculogram, gain calibration method using eye optical props. 4-115306

electron spectrometers 4-101980

electron spectroscopy, rel. to 1s ionis. energy of Ne 4-78984

electronic flow meters calibration (German) 4-60566

ESR spectroscopy, calibration methods and reference materials 4-95486

explosives, thin-pulse shock initiation threshold, meas. optimisation 4-108059

external PIXE milliprobe at Davis cyclotron, laser alignment, calibration and quality assurance 4-105076

fission and (n,α) track detectors, neutron dosimeter calibration using phantom 4-96369

fixed-point baths, commercial, exptl. determ. of precision error in temp. 4-82795

flow-microcalorimetric vessel for enthalpy of soln. meas. 4-78318

force measurement, calibration and standards 4-95417

force transducer calibrations and measurements 4-73431

force transducers, EC comparison between PTB (Braunschweig) and TNO (Delft) 4-63737

force transducers calibration, EC comparison between PTB (Braunschweig) and MD/SM (Brussels) 4-63738

force transducers calibration, EC comparison between PTB (Braunschweig) and NPL (Teddington) 4-63739

force transducers calibration, EC comparison between PTB (Braunschweig) and IMGC (Turin) 4-63740

fundamental differential pressure calibrations 4-95375

fusion reactor neutral beam heating system, water flow calorimeter, calibration system 4-11837

gamma spectrometers, radioactivity meas. of large-volume samples 4-74095

gamma-ray dosimeter calibration in equivalent dose units 4-62599

gas anal., equipment for instruments calibration (German) 4-77042

gravimetric hygrometer, calibration (Japanese) 4-101857

grazing incidence monochromator, extended relative efficiency calibration, fast-beam spectroscopy appl. 4-87439

heat flux gage calibration for skin friction meas. 4-97723

high accuracy calibration system for charge read-out electronics 4-78746

high-power automatic network analyzer for measuring the RF power absorbed by biological samples in a TEM cell 4-115294

high-resolution electron microscopes, crystalline test specimens for calibration 4-11260

hot-wire anemometer, computer-controlled 4-69842

human 4-67104

humidity measurement instruments 4-63753

image-tube spectrograms, density-to-intensity conversion using emission line intensities 4-101179

IMB proton decay detector, calibration and expt. limits 4-90874

infrared radiometers calibration using multichamber black body, geometrical characts. effect on metrological characts. 4-90657

instrument for calibration of measured velocities of angular acceleration (Russian) 4-63703

internal reference point in ICP atomic emission spectroscopy, determ. using emission spectral profiles 4-90664

intracellular recording, calibration pulse appl. device 4-115310

laser interferometer, appl. 4-95504

laser interferometer calibration at NPL 4-95508

length meas. automation, based on interference patterns analysis 4-101812

low-level photometric scale based on standardized detectors 4-90636

luminescence spectrometer, computer-controlled, for relative fluoresc. quantum yield meas. 4-106400

Makrofol Polycarbonate plastic track detector, calibration using heavy ions 4-64307

Malvern particle size calibration 4-95372

manganin gauges, piezoresistance and calibration under uniaxial stress conditions 4-90576

mass spectrometer, for partial pressures meas. 4-63805

measurement instrument yard and metrology laboratory, administrative and technical management 4-106307

measuring instruments calibration using automatic calling software system 4-106261

medical US transducer calibration, radiation press. meas. 4-100278

metal film on silica neutral density filters, re-evaluation 4-106398

microscopic particle size meas. standards, dimensional calibration 4-88813

multichannel system calibration using laser source 4-74096

NBS electron storage SURF-II, direct determ. of stored electron beam current 4-64250

NBS standard reference materials catalogue (1984-5) 4-78062

## calibration continued

- neutron multiplicity counter, absolute calibration technique for spontaneous fission sources, safeguards 4-111712  
 neutron sensitive spherical devices for radiation protection purposes, calibration technique 4-102401  
 NIMBUS 7 Stratospheric and Mesospheric Sounder 4-100802  
 NMR imaging, proton density meas. calibration 4-67068  
 NMR imaging systems, S/N calibration procedure 4-67065  
 NPL spectrofluorimeter, for fluoresc. meas. of opaque materials 4-106354  
 nuclear reactor digital control schemes, experimental evaluation 4-86932  
 nuclear safeguards, tank calibration data eval. in RITCEX, errors 4-111703  
 nucleon decay detector calibration with cosmic ray neutrinos 4-91148  
 ocean bottom seismometer, clock, correction system for clock calibration 4-82280  
 ocean wave measurement with Canadian waverider buoys 4-115633  
 optical flat, absolute calibration 4-103029  
 optical flat, absolute calibration 4-107910  
 optical imaging instruments, calibration methods in space 4-79261  
 optical system for light scattering and resonance fluorescence meas. 4-101887  
 particle elastic scattering anal. of thin samples, calibration procedure 4-99891  
 PERLA Laboratory at Ispra for nuclear safeguards performance, calibration and training 4-111697  
 photoelectric measuring microscope 4-95512  
 photoelectric photometer calibration standard 4-111174  
 photographic plate calibration, two numerical processes 4-106408  
 piezoelectric reciprocity method for absolute calibration of high frequency vibration standards 4-106269  
 piezoelectric transducer, controlled response characs., sensitivity and calibration 4-91711  
 PIXE system calibration, linearity precision and accuracy 4-95568  
 PIXE trace anal. of biological materials, using single multielement standard 4-105385  
 plasma MM and sub-MM diagnostic instruments, calibration techniques 4-75207  
 portable acoustic devices for divers, homing, surveying, navigation (French) 4-97220  
 power deposition in nuclear pumped lasers, using ozone dosimetry 4-112454  
 power reactor plumes, noble gas radionuclide concs. determ., calibration procedures 4-86974  
 precision calibrating equipment for laser power 4-96969  
 pyrometer, high-speed, freezing point determ. of Pd 4-80196  
 radio interferometer self-calibration and isoplanatism 4-115685  
 radiotherapy, calibration of high-energy photon and electron beams 4-109920  
 rare earth solutions for wavelength calibration in UV-vis. spectrophotometry 4-106399  
 reference specimens of specific elec. cond., eddy current certification 4-95471  
 refractometer, differential, calibration and checking 4-95499  
 resistivity measurements, two-probe and four-probe resistances on nonuniform structures 4-58868  
 respiratory calorimetry, calibration methods 4-100396  
 RF sputter system, substrate temp. calibration (Japanese) 4-76672  
 roundness measuring instruments filtering charact. verification using calibration standard (Chinese) 4-111115  
 S 520-3 controlled nosecone rocket-borne VUV instrumentation, characs. and obs. (Japanese) 4-94620  
 scintillation cameras and dose calibrators, quality assurance survey 4-89733  
 seawater, trace metals determ. by Zeeman graphite furnace AAS 4-114857  
 seismic channels transfer function meas. 4-67435  
 single edge notched bend specimens, deflection meas. test setup 4-76929  
 solid state track recorders, automatic scanning by computer controlled microscope, calibration 4-68882  
 space borne charged particle telescope calibration using 0.4-20 MeV protons 4-77710  
 special nuclear materials, gamma spectrometric and absorpt. meas. for safeguards 4-111717  
 SPECT: quality control procedures and artifact identification 4-67093  
 spirometer, experimental evaluation (German) 4-77278  
 steam turbine-generator, acceptance test demonstration and verification 4-87826  
 steel, hardness testing, with impact action standard-free instruments 4-99675  
 steel, stainless, standard reference material for calibrating X-ray diff. equipment 4-62153  
 steels, phase identification and anal. using SIMS (French) 4-76936  
 stellar spectrophotometry, calibration of augmented system of bright secondary standards 4-94736  
 strain transducers, calibration characteristics stability in nuclear reactor 4-102369  
 sub-beam prism for photographic photometry of faint stars (Japanese) 4-94640  
 tachometer calibration and checking equipment modernisation 4-58842  
 temperature measurement systems calibration 4-73409  
 Thematic Mapper on Landsat-4, in-flight radiometric calibration 4-82264  
 thermocouples, data processing (Japanese) 4-101837  
 thermocouples, high-temp., freezing point determ. of Pd 4-80196  
 thick target PIXE anal. review 4-99878  
 Tian-Calvet heat flow calorimeter, calibration and testing 4-95425  
 tunable diode lasers, heterodyne freq. meas. and freq. calibration standards 4-112422  
 US pulse echo thickness gauge, self calibrated 4-78308  
 UV spectrometers, wavelength calibration from H<sub>2</sub> electron impact extreme UV emissions 4-83386  
 V-converter outlet signal, electronic evaluation (German) 4-77420  
 vacuum gauges 4-58862  
 vacuum gauges 4-90606  
 vibration transducers, calibration 4-90574  
 video camera tubes, laser-formed fiducials and reticles 4-96933  
 voltage calibrators, precision and ease of use (French) 4-58864  
 vortex shedding flowmeters, for cryogenic liquids, operating principles, performance, calibration, applications 4-108151  
 VUV spectrometers, primary light standard 4-82833

## calibration continued

- X-ray fluorescence analysis, interelement effects, general eqn. for correction 4-114859  
 X-ray photoelectron spectrometers, binding energy meas. of Ni, Cu, Au and Ag (Chinese) 4-102822  
 X-ray photoelectron spectrometers, energy calibration 4-99284  
 X-ray photoelectron spectrometers, energy calibration 4-99285  
 X-ray sources, pulsed, dose calibrations of intensifying screens and neutral density of filters 4-58927  
<sup>81</sup>Br solar neutrino detector calibration, <sup>81</sup>Kr-<sup>81</sup>Br mass-difference effects 4-106565  
 C piezoresistive stress transducer, calibration by impact testing 4-106312  
 CO<sub>2</sub> coherent laser radar performance study 4-96974  
 CsCl, eqn. of state used for secondary calibration scale at low temps. 4-103897  
 Ge detector calibration from <sup>144</sup>Ce X-ray and gamma photon energies and intensities (French) 4-73850  
 Ge(Li), efficiency calibration (Chinese) 4-83268  
<sup>4</sup>He, superfluid, temperature oscils., electroacoustic meas. by reciprocity method 4-98391  
 NaCl, eqn. of state used for secondary calibration scale at low temps. 4-103897  
 phosphosilicate glass films on Si wafers, quantitative anal. for calibration of X-ray fluorescence spectrometry standards 4-105046  
 Pt resistance thermometer, long-stem and capsule-type, calibration apparatus 4-111135  
 Pu determination in MOX fuel fabrication plant wastes by passive neutron assay 4-111710  
 Rn detection in Finnish dwellings, film detectors calibration 4-93895  
<sup>222</sup>Rn and daughters, airborne, meas. with CR-39 track detectors, plated-out <sup>218</sup>Po, <sup>214</sup>Po calibration 4-66844  
 Si and blackbody-based radiometry intercomparison using a Si photodiode/filter radiometer 4-86462  
 Si p<sup>+</sup>-n-n<sup>+</sup> photodiode, oxide passivated, self-calibration 4-90652  
 Si(Li) and HpGe detectors, efficiency calibration method at low energies 4-59582  
 T extraction facility for T conc. in neutron irradiation Li metal, calibrations 4-111811  
 W, spectral emissivity, analytic expressions for 340 nm to 2.6 μm spectral region 4-60127  
 Yb piezoresistance gauges, response to shock front and calibration 4-106314
- californium**  
 see also nuclei with .....  
<sup>250</sup>Cf, L-Auger spectra meas. 4-96511  
<sup>252</sup>Cf nuclear parameters of safeguards interest, half-life, neutron multiplicity 4-106986  
<sup>252</sup>Cf(sf) use in vivo, environmental and radioecological lab. expts., prompt photon detection 4-89790
- californium compounds**  
 No entries
- calorimeters**  
 see also calorimetry  
 adiabatic, radiation fields of high-energy accelerators meas., using polyethylene detector 4-102533  
 CERN UA1 fast calorimeter trigger and minimum-bias pretrigger 4-64310  
 chromaticity coordinates, influence of Si photodiodes spectral sensitivity charact. on absolute error (Russian) 4-58884  
 cryogenic liquids, calorific props. meas. at low temps. and high press. 4-95428  
 electromagnetic and hadronic calorimeter from UA2 4-102510  
 fluid-microcalorimetric vessel for enthalpy of soln. meas. 4-78318  
 fluidic flowmeter for low flow rate electronic calorimeters for air conditioning systems 4-91854  
 fusion reactor neutral beam heating system, water flow calorimeter, calibration system 4-111837  
 heat flow calorimeters for meas. excess enthalpy 4-80237  
 heat-flow/liq. flow microcalorimeter, NaCl enthalpy of dilution appls. 4-80234  
 laser beam power measurement of high-power lasers, calorimeter development (Japanese) 4-64715  
 laser calorimeter with rapidly moving thin fluid technique, intense laser radiation meas. appls. 4-58889  
 laser calorimetric apparatus for low optical absorption meas. 4-86422  
 lead glass drift calorimeter design, Monte Carlo studies 4-64275  
 microcalorimeter for heat of solution determ., of slightly soluble gases in water 4-78319  
 Nucleon Stability Experiment (NUSEX) in Mount Blanc tunnel for proton decay expts. 4-96410  
 polystyrene-water calorimeter, absorbed dose calcs. 4-95426  
 spark calorimeter, cosmic ray muon group investigation at large zenith angles 4-110424  
 surface calorimeter for adsorbed layers heat capacities meas. 4-111136  
 Tian-Calvet heat flow calorimeter, calibration and testing 4-95425  
 Tian-Calvet type, baseline fluctuation anal. 4-95424  
 total absorption calorimeter, energy resolution for high energies 4-112058  
 tunable pulsed dye laser cryogenic photocalorimeter, for photochemical reactions obs., theory and design 4-105005  
 water calorimeter used for clinical beam dose meas., steady-state drift conditions 4-85520  
 X-ray spectroscopy, single-photon calorimeter 4-106446  
 π/e discrimination with a Pb-liquid Ar calorimeter, LEP ELECTRA appl. 4-74100  
 Ar, liq., calorimeter read-out scheme 4-68891  
 Bi<sub>2</sub>Ge<sub>2</sub>O<sub>7</sub> optimisation for energy resolution and purity, high-energy phys. calorimeters appl. 4-59552
- calorimetry**  
 see also calorimeters; specific heat; thermal analysis  
 adsorbed layers heat capacities meas., using surface calorimeter 4-111136  
 alloys, chem. bonding and heat of form., core level shift calorimetry method 4-104714  
 carbohydrates, thermal props. heat flow calorimetric obs. 4-78312  
 chromaticity coordinates, influence of Si photodiodes spectral sensitivity charact. on absolute error (Russian) 4-58884  
 dose determination by calorimeter using direct voltage meas. on a Wheatstone-type bridge circuit 4-100325  
 energy deposition meas. of intense relativistic electron beam, gas laser excitation appl. 4-69297

**calorimetry continued**

- heat transported by fluid meas. (*German*) 4-63747  
 4-heptylphenyl-4-(4-nitrobenzoxy)benzoate, smectic A<sub>1</sub>-smectic A transition, calorimetric studies 4-108619  
 hexan-1-ol-pyridine base mixtures, molar excess enthalpies 4-113647  
 n-hexane, sp. heat at const. press. in critical region determ. by flow calorimetry 4-61106  
 high temperature calorimetry of alloys with non-negligible evaporation rates 4-78320  
 high temperature procedure for alloys with non-negligible evaporation rates 4-68232  
 high-pressure AC calorimetric technique for specific heat of solids meas. 4-86423  
 isoprene-propylene copolymer, regularly alternating, thermodynamic props., stereoisomerism effects (*Russian*) 4-103970  
 liquid crystals and ordered fluids, conference, Las Vegas (USA), (March-April 1982) 4-82596  
 metallic films with adsorbed pyridine films, photocalorimetric spectroscopy and AC calorimetry 4-66629  
 open-circuit indirect calorimetry, gaseous exchange anal. 4-85589  
 phenols, enthalpies, free energies and entropies of transfer from nonpolar solvents to water 4-105009  
 p-phenylenes, homologous, liq. cryst. transitions, expts. 4-113620  
 p-phenylenes, homologous, liq. cryst. transitions, theory 4-113621  
 p-phenylenes, homologous, mixtures, liq. cryst. transitions, expts. 4-113620  
 p-phenylenes, homologous, mixtures, liq. cryst. transitions, theory 4-113621  
 polarization sensitive laser calorimetry 4-74584  
 polyethylene terephthalate, crystallisation rate, effect of silicon nucleants 4-88117  
 polymers, amorphous, thermodynamic functions, temp. depend. 4-88313  
 polymers, semicryst., thermodynamic functions, temp. depend. 4-88313  
 polystyrene film, atactic, liq.-liq. transition, birefringence, temp. depend. 4-114241  
 rare decays, low-temperature calorimetry, neutrinoless double-beta and electron decay 4-102494  
 respiratory calorimetry, calibration methods 4-100396  
 specific heat meas. method, application to organic molecular crystals 4-78321  
 stability of calorimetric circulation transducers for UHF wattmeters, stability determ. 4-58856  
 thin film absorption coefficients, calc. from laser calorimetric data 4-114333  
 thin-film laser calorimetry for optical absorpt. meas. 4-90591  
 tricosane-tetracosane, binary paraffin, X-ray diff. and calorimetric study 4-88161  
 water-methane vapour, excess enthalpies up to 698.2K and 12.6 MPa 4-113097  
 whiteness and quantum representations of calorimetry 4-73439  
 Br electrodes in Zn/Br and Zn/air batteries, electrochemical calorimetry 4-104995  
 C, graphitised, adsorpt. of sodium dodecyl sulphate (octyltetraethylene glycol), enthalpy determ. 4-70560  
 CO, catalytic oxidation on Pd, surface state effects 4-62238  
 CsLiMoO<sub>4</sub>-type crystals., ferroelec. phase transitions 4-65979  
 Cu mirrors, diamond turned and mechanically polished, intensity depend. absorpt. and laser induced catastrophic damage at 1.06  $\mu$ m 4-75519  
 KCl absorption, reversible and irreversible changes during multiple pulse 10.6  $\mu$ m irrad. 4-75518  
 NaCl absorption, reversible and irreversible changes during multiple pulse 10.6  $\mu$ m irrad. 4-75518  
 Na<sub>2</sub>O-SiO<sub>2</sub>, liquid, heat capacity, drop calorimetry meas. 4-61101  
 Nb oxides, heat of form. meas. using Tian-Calvet type calorimeter 4-81454  
 RbNO<sub>3</sub> in water, heat of soln. meas. at 298K using LKB calorimeter 4-80235  
 Zn electrodes in Zn/Br and Zn/air batteries, electrochemical calorimetry 4-104995

**calorimeters** see *calorimeters*

**CAMAC**

- COMPEX standard capabilities 4-106287  
 logarithmic charge-digital converters for operation with proportional chambers 4-68910  
 modules for controlling expt. on-line hardware with ES computer 4-58836  
 multichannel analyser, CAMAC based module for data selection 4-96412  
 multidetector alpha spectroscopy analysis system 4-59483  
 PINK PANTHER CAMAC crate controller for  $\pi^0$  spectrometers at CERN 4-78752  
 plastic scintillation counter for ray air shower array 4-91170  
 readout system for a multiwire proportional chamber (*Chinese*) 4-83274  
 Romulus compatible asynchronous time and amplitude pad acquisition system for TPC 4-96416  
 scintillation detectors data acquisition and processing, auxiliary controller ccts. design 4-90570  
 SM-3 computer interfacing to EPR spectrometer 4-90622  
 star network concept for centralised system 4-91188  
 X-ray diffractometer interfacing to SM-3 computer system 4-106289

**camera lenses** see *photographic lenses*

**camera tubes, television** see *television camera tubes*

**cameras**

see also *coronagraphs*; *television cameras*

- Anger camera, fast parallel encoding scheme 4-59556  
 Anger gamma-camera systems 4-63835  
 atmospheric Cherenkov light imaging for  $\gamma$ -ray astronomy 4-101176  
 avalanche chamber positron camera for tomographic imaging of human thyroid 4-67087  
 Cassegrain-type spectrographic cameras, near axis ray tracing, aberrations and their correction (*Japanese*) 4-94617  
 circular-scan photochron streak camera for spaceborne laser ranging applications 4-107725  
 coded aperture cameras, performance of practical designs, computer simulations 4-67638  
 compensator filters made with compact Moire camera and computer 4-109916  
 conference on astronomical instrumentation, at London, England (September 1983) 4-106099  
 demountable photocathode X-ray streak camera 4-106439

**cameras continued**

- Earth photographs, using satellite imager camera with 4 CCD sensors (*German*) 4-77643  
 electro-optical systems, moire phenomena appl. to modulation transfer function 4-79334  
 electronic still camera and recording system 4-78408  
 film camera acoustic noise characts. (*Russian*) 4-95549  
 film camera eye-piece lenses, optical characteristics (*Russian*) 4-90677  
 film camera position stability compensation (*Russian*) 4-90676  
 film shooting cameras exposure time instability (*Russian*) 4-73554  
 Fujica 645 camera review, GS645 and GSW645 Professional 4-106410  
 Fujica 645 camera review, GS645 and GSW645 Professional 4-106411  
 gamma camera bar phantom images, collimator design effect on moire patterns 4-67115  
 Gandolfi X-ray diff. camera, device for easy centring 4-58925  
 high resolution camera for bubble chamber photography 4-68890  
 high speed camera, real time error anal. by laser and position sensing system 4-111227  
 high speed photography, videography and photonics, conf., San Diego, CA, USA (Aug. 1983) 4-106102  
 modular assembly equipment for camera manufacture 4-78401  
 motion picture display, spatial correspondence 4-111233  
 NASA space telescope faint objects camera active thermal control 4-77719  
 optics for non-visible photography 4-111237  
 optics in entertainment, conf., Los Angeles, CA, USA (Jan. 1984) 4-110802  
 photochronographic camera imprecise focusing rel. to subpicosecond laser pulse shape distortions 4-64729  
 powder X-ray diff. appl. in simulating industrial furnacing 4-58923  
 professional film cameras, electric drives (*Russian*) 4-78407  
 reliability of optical instruments for cultural and general purposes, specification requirements 4-78359  
 Ricoh XR-P, general description highlighting diff. program modes available 4-78393  
 scintillation cameras and dose calibrators, quality assurance survey 4-89733  
 shadow boundary determ. photoelec. circuit 4-73547  
 soft X-ray streak cameras at Lawrence Livermore National Laboratory 4-106440  
 space telescope optical payloads accurate thermal control 4-85880  
 STEM, high resolution microdiffraction camera 4-78441  
 stereoscope three-dimensional special effects single-camera single-film system 4-111232  
 streak camera, operating at high repetition rates 4-101956  
 streak camera, optically synchronised, femtosecond optical pulses and technology 4-107696  
 streak camera, picosecond operation, design using multichannel position sensitive detector 4-101955  
 streak camera triggered by subpicosecond laser pulses, low jitter operation 4-63793  
 streak image converter camera, linear scan, direct detect. of injection laser psec pulses 4-74573  
 synchroscan streak camera sensitivity 4-106392  
 three dimensional image realisation with standard materials, appls. to medicine, industry and research 4-73542  
 three dimensional motion picture camera systems, overview 4-111230  
 time-of-flight positron emission tomography camera, BaF<sub>3</sub> scintillator appl. 4-67089  
 ultrafast voltage pulse shaping for streak and framing camera deflection 4-106415  
 uniformly redundant array coded aperture camera for ICF expts. 4-68296  
 universal holographic camera 4-64686  
 X-ray, photoregistering small-angle, for temp. depend. studies of polymers under load (*Russian*) 4-75242  
 X-ray diagnostics of laser plasma, pinhole cameras slits and apertures prep. 4-91987  
 X-ray diffraction topography camera for crystal perfection anal. 4-104727  
 X-ray goniometer of meas. in temp. range 10 to 293K 4-69988  
 X-ray lithography camera, storage ring matching optics optimisation 4-95594

**candoluminescence** see *luminescence*

**canted spin arrangements**

see also *weak ferromagnetism*

- anisotropic antiferromagnet, temp. depend. of paramag. boundary 4-84786  
 Heisenberg two-dimensional classical isotropic antiferromagnet, phase diagram in mag. field 4-109031  
 rare earth alloys, R<sub>6</sub>Fe<sub>23</sub> intermetallic cpds., magnetisation, mol. field anal. 4-71031  
 rare earth-Y alloys, mag. ordering and local mag. moments 4-61524  
 Ba<sub>2</sub>NiF<sub>6</sub>(FeF<sub>6</sub>), 2-D antiferromagnet, mag. structure 4-71028  
 Cd<sub>2</sub>Cu<sub>1-x</sub>Fe<sub>2x</sub>O<sub>4</sub> spinel, low temp. Mossbauer obs. of mag. interactions 4-98983  
 Cd<sub>2</sub>Ni<sub>1-x</sub>Fe<sub>2x</sub>O<sub>4</sub> system, nonlinear spin struct., magnetisation and Mossbauer obs., Yafet-Kittel angles 4-71022  
 CoCl<sub>2</sub>·6H<sub>2</sub>O, paramagnetic phase boundary of antiferromagnet at low temp. 4-88668  
 KMnCl<sub>3</sub>, canted antiferromagnet, mag. props. 4-88655  
 NiCl<sub>2</sub>·6H<sub>2</sub>O(4H<sub>2</sub>O), paramagnetic phase boundary of antiferromagnet at low temp. 4-88668  
 Tb<sub>2</sub>O<sub>3</sub>·SO<sub>4</sub>, magnetisation, AC susceptibility, spectroscopic Zeeman effect meas. 4-76121

**capacitance**

see also *photo capacitance*

- CoO<sub>2</sub> film, vac. deposited, dielec. parameters, temp. depend. defects role 4-99024  
 connected plates, capacitance upper bound derivation 4-74390  
 electrolyte surface struct. near critical point, free energy formalism anal. 4-92038  
 Josephson tunnel junction, overdamped, I-V characts., capacitance effects 4-108976  
 metal particles, small, Coulomb suppression of tunnelling rate 4-61441  
 metal-molten salt interface, capacitance depend. on local density profiles near electrode 4-92797  
 MOS structures, minority carrier lifetime determ. by transient capacitance measurements 4-92822  
 photoresist soln., AZ1350J, chem. and dielec. props. 4-104519

**capacitance continued**

- semiconductor isotype heterojunctions, C-V doping profiles anal. 4-75496  
 semiconductors, carrier distribution, capacitance-voltage profiling methods, review 4-75494  
 Al/Sn<sub>2</sub>O<sub>3</sub>/Al capacitor struct., dielec. props. and thermoluminescence 4-76047  
 Al-(SnO<sub>2</sub>+Sb<sub>2</sub>O<sub>3</sub>)-Al mixed thin films, dielec. studies 4-84719  
 As<sub>2</sub>S<sub>3</sub> glassy film, Schottky barrier form. at contact with metal 4-104291  
 Au-Ge-Sn structure, capacitance-voltage meas. at liq. N<sub>2</sub> temp. 4-84707  
 BaTiO<sub>3</sub> oxide perovskites, dielec. meas., surface layer effects 4-65962  
 CO<sub>2</sub> waveguide laser, RF discharge striations 4-79100  
 (Cd,Zn)-S-CuInSe<sub>2</sub> Boeing solar cells, current transport 4-81546  
 CdS/CdTe solar cell, annealing, admittance spectroscopy 4-77101  
 CuInSe In-diffused homojunctions, elec. and photovoltaic effects 4-92809  
 β-Cu<sub>2</sub>Sn, plastic deformation at He temps., capacitance meas. 4-71681  
 FeNiCrMoSi<sub>3</sub> amorphous ribbons, magnetostriiction, capacitance studies 4-61580  
 n-GaAs/Au Schottky contacts, elec. props. and interface chem., sputtering effects 4-80674  
 GaAs/native oxide interfaces, density of states, C-V meas. 4-88604  
 GaP:Zn, O LEDs, centre responsible for capacitance slow relax. 4-65735  
 Ge diodes, grain boundaries, plasma exposure effects 4-65276  
 Hg<sub>1-x</sub>Cd<sub>x</sub>Te, deep level anal. using temp. depend. of capacitance (Chinese) 4-113888  
 Hg<sub>1-x</sub>Cd<sub>x</sub>Te zero gap MIS struct., size quantisation in accumulation layers 4-65753  
 In-Hg/Si ohmic contacts, differential resistance and capacitance characts. 4-92819  
 In-Hg/insulator contacts, differential resistance and capacitance characts. 4-92819  
 P<sub>2</sub>O<sub>5</sub>-Al<sub>2</sub>O<sub>3</sub>-MgO-Nd<sub>2</sub>O<sub>3</sub> glasses, low temp. dielec. props. in mag. field 4-61638  
 Pb(Fe<sub>1/2</sub>Nb<sub>1/2</sub>)O<sub>3</sub>-Pb(Ni<sub>1/3</sub>Nb<sub>2/3</sub>)O<sub>3</sub> solid soln. system, dielec. props. 4-104517  
 Pb<sub>1-x</sub>Ge<sub>x</sub>Te, ferroelec. phase transition, high press. investigation, DC resist., capacitance meas. 4-71312  
 α-PdH<sub>x</sub>, Gorský effect and diffusion coeffs. 4-75614  
 Pt electrodes, adsorption of tripeptide, kinetics and isotherms 4-92539  
 Sb<sub>2</sub>S<sub>3</sub> glassy film, Schottky barrier form. at contact with metal 4-104291  
 Si, ion implanted, pulsed laser and thermal processing, defect anal. 4-70133  
 Si MIS struct., amorphous C covered, tunnelling to insulator gap states 4-92824  
 Si MOS inversion layers, complex capacitance in quantised resist. regime 4-98773  
 Si, plastically deformed, deep levels, capacitance, reverse current meas. 4-61319  
 Si substrates, electro-physical prop. nonuniformity (Russian) 4-65672  
 Si:Ar, carrier lifetime reduction by Ar ion implantation 4-80604  
 a-Si:H, energy distrib. of light-induced gap states, photocond. meas. 4-76004  
 a-Si:H, MIS diode, glow discharge deposited, flat-band capacitance freq. depend. 4-76042  
 a-Si:H pin solar cells, LPCVD growth, transport props. 4-114907  
 a-Si:H Schottky barriers, sputtered, freq. depend. capacitance, admittance meas. 4-98693  
 Si/ZnO-B<sub>2</sub>O<sub>3</sub>-SiO<sub>2</sub> glass system, surface charges, C-V characteristic meas. 4-65747  
 Si<sub>3</sub>N<sub>4</sub> layers, ion beam synthesised, dielec. breakdown, current density-voltage and capacitance-voltage characts. 4-80706  
 SiO<sub>2</sub>/Cr thin films, cathodoluminescence and C-V characts. (Russian) 4-99173  
 Sn<sub>2</sub>P<sub>2</sub>S<sub>6</sub> ferroelec. semicond., Curie temp. photoinduced shift 4-93017  
 SrTiO<sub>3</sub> oxide perovskites, dielec. meas., surface layer effects 4-65962  
 Ta<sub>2</sub>O<sub>5</sub>, gate insulator in MIS struct., electrophys. props. 4-61475

**capacitance measurement**

- deep-level spectroscopy by transient capacitance techniques under electrical resonance 4-58865  
 metrological research in Czechoslovakia, by TESLA, Brno 4-90614  
 SiO<sub>2</sub> film traps, microcomputer-based avalanche injection system, area density anal. 4-101870

**capacitance meters** *see* **capacitance measurement****capacitor storage**

No entries

**capacitor stores** *see* **capacitor storage****capacitors**

- see also electrolytic capacitors; thin film capacitors; varactors*  
 circular parallel plate capacitor, potential, analytical soln. 4-59954  
 electrohydrodynamic motion induced by injection from plane polymer sheets 4-97706  
 indirect plasma-enhanced CVD technique 4-104529  
 liquid dielectrics electrical conductivity, role of EHD motion, power capacitor example 4-98326  
 metal/air/semiconductor, capacitor with air as adjustable insulator 4-88596  
 metal/Si<sub>3</sub>N<sub>4</sub>/SiO<sub>2</sub>/Si capacitors, interfacial charging 4-104292  
 MIS thin gate oxide structures, direct and Fowler-Nordheim tunnelling 4-61464  
 spark-gap-driven high repetition rate laser pulser, capacitor charging power supply 4-79172  
 teaching analogy using water-filled cylinders 4-90337  
 GaAs/AlAs-GaAs superlattice/GaAs superlattice barrier capacitor: a structure for the investigation of heterojunction interfaces 4-84679  
 (Sr<sub>0.50</sub>Pb<sub>0.25</sub>Ca<sub>0.25</sub>TiO<sub>3</sub>)<sub>100-x</sub>(Bi<sub>2</sub>O<sub>3</sub>·3TiO<sub>2</sub>)<sub>x</sub> dielectric props., HV capacitor application 4-98997

**capacity, channel** *see* **channel capacity****capillarity**

- see also bubbles; contact angle; drops; foams; liquid films; surface tension*  
 aerosols, radioactivity anal. using compressible flow capillary system 4-86975  
 bi-disperse media, diffusion, effective medium approach 4-65430  
 bubble, radially oscillating, surface dilatational elasticity determ. method optimisation (German) 4-60488  
 bubbles, thermocapillary migration normal to plane surface 4-60485  
 capillary rise between closely spaced plates, effect of Van der Waals forces 4-92480  
 cavity formation by interaction between particles in a nonwetting liquid 4-61182

**capillarity continued**

- cavity formation due to a contact between particles in a nonwetting liquid 4-61181  
 contact angle, equilib. and hysteresis, smooth uniform surfaces, disjoining pressure isotherm 4-80332  
 convective thermocapillary instabilities in liq. bridges 4-75016  
 crystal growth, Czochralski configuration, buoyant, thermocapillary and forced convection expts. 4-65206  
 discharge from evaporating wall, magnetogasdynamical model 4-69973  
 discharging time measurement type capillary viscometers (Japanese) 4-75105  
 drops, slightly deformed axisymmetric, profiles 4-61186  
 evaporative process in capillary-porous structs., approx. hydrodynamic theory 4-113750  
 falling liquid films with surfactants, thermocapillary breakdown 4-60545  
 fissile and capillary materials, finite uniform strain, metaisotropic struct. 4-87588  
 flow, hydrodynamics, no-slip boundary condition 4-60549  
 immiscible fluids flow in porous media, displaced phase, capillary blocking, end effect 4-112996  
 jets, submerged of nonNewtonian fluid, laminar length meas. by flow visualisation technique 4-64997  
 liquid evaporation in small capillaries 4-61171  
 liquid-vapour interface, scaling relations 4-80337  
 metallic gauze porous materials, pore size distrib. 4-66261  
 metals, laser interaction, evaporation influence on melt behaviour 4-76566  
 myocardial capillaries, anisotropic, length and surface density estimation method 4-115302  
 myocardium microcirculation, indirect determ. of fluid filtration and reabsorption 4-93771  
 one-dimensional thermocapillary motion 4-61184  
 Poiseuille flow, shear dispersion, residence time 4-79668  
 polyethylene, high and low density blends, melt mixed, capillary flow instability 4-83871  
 polyethylene terephthalate, melt flow in capillary, vel. distrib. 4-60551  
 polymer jet, extruded from capillary die, elasticity, stretching and swelling 4-69722  
 porous bodies, transport processes, laser monitoring 4-112999  
 porous materials, geometric and mass transfer parameters determ. 4-66518  
 rarefied gas flow in long finite circular capillary 4-87761  
 resonant molecules flow through metal capillary, laser control 4-69800  
 short-wave capillary struct. parametric excitation at liq. metal surface contiguous to unstable plasma 4-84013  
 simulated floating zone configuration in reduced gravity, oscillatory thermocapillary convection 4-61834  
 solute transport in capillary, Taylor-Aris theory 4-69829  
 sphere packing, capillary hysteresis, blob movement meas. 4-61175  
 stability of the equilibrium of a capillary fluid in a horizontal slit 4-113012  
 steady axis-symmetrical thermocapillary motion of a short melting column 4-83950  
 surface and interfacial tension measurement, axisymmetric drop technique 4-98400  
 surface tension determination using double capillary method 4-67936  
 thermal photography, surface tension forces, thermally conc. capillary flows (Russian) 4-68227  
 thermocapillary convection in a two-layer system 4-69758  
 thermocapillary motion of two bubbles oriented arbitrarily relative to a thermal gradient 4-61188  
 thermogravitational and thermocapillary flows in a horizontal liquid layer under the conditions of a horizontal temperature gradient 4-103415  
 throttling in capillary tubes, laboratory equipment (Bulgarian) 4-97682  
 vapour absorption-desorption isotherms, two-dimensional network model 4-61178  
 viscosity meas. of gas-oil emulsions, semiautomatic unit based on capillary principle (German) 4-103442  
 wetting fluid, capillary spreading, asymptotic laws (French) 4-75752  
 Al<sub>2</sub>O<sub>3</sub> anodic porous films, piezo-electrocapillary effect 4-88774  
 Ar-He mixtures in microwave capillary discharges 4-87999  
 Cu-Sn-P bronze sintered permeable materials, capillary props. 4-65519  
 Ga-Al-As/GaAs, liq. epitaxy capillary effect 4-98408  
 He capillary glow discharge, collisional radiative model with atomic collisions 4-60773  
 Ne, liq., surface tension determ. (Russian) 4-98402  
 S, liquid, surface tension study 4-113749  
 W powder, activated sintering, pore size increase kinetics 4-66272

**capillary phenomena** *see* **capillarity****capillary waves**

- deep water, periodic capillary-gravity wave instability 4-75053  
 ferromagnetic liquid, capillary waves and spontaneous magnetisation (Russian) 4-113031  
 gravitational waves at homogeneous liq.-liq. interface 4-112925  
 liquid surface and interface waves 4-79613  
 liquid-vapour interface, scaling relations 4-80337  
 nonuniformly heated liquid, instability under effect of lower radiation 4-64961  
 particle trajectories in nonlinear capillary waves 4-87800  
 quasi-harmonic capillary-gravity waves, modulational instability, mag. field effect 4-91845  
 small-amplitude free-surface waves generated by moving oscillatory disturbances 4-112923  
 surface fluctuation spectroscopy, expt. technique and capillary ripple theory, comments 4-78389  
 surface fluctuation spectroscopy, liquid interface characterisation 4-78388  
 surface gravity-capillary waves, blocking effect by inhomogeneous flow 4-83917  
 surfactant solutions, interface capillary waves, neutral stability 4-108082  
 water solitary waves, capillary effects 4-103349  
 Ge, laser-induced periodic surface struct., fluence regimes, feedback and topography 4-108436

**Captains** *see* **viewdata****capture cross-sections, nuclear** *see* **nuclear reactions and scattering****Carathéodory's principle** *see* **thermodynamics****carbon**

- see also nuclei with .....*  
*see also carbon fibres; charcoal; diamond; graphite*  
 24.8 MeV electrons backscattering, energy spectra 4-88912  
 abundance in disc and halo dwarf stars 4-85915

- bon continued  
 acetylide on Li surface, electronic and geometric struct., AES and UPS study 4-92543  
 active, ACS whetlerites, porous struct. and adsorption 4-93547  
 active fluidised bed, continuous adsorpt. process 4-97651  
 adsorbed layer on Mo (001), low energy alkali ion scatt. studies 4-76582  
 adsorbed on Nb, NbC formation and synchrotron radiation study of overlayers 4-108711  
 adsorbed on Ni, Fourier transform anal. of PES, normal one beam model (Chinese) 4-75773  
 adsorbed on Ni<sup>2+</sup> (111) surface, thermal decomposition of ethylene 4-113782  
 adsorption on Ni (100), AES study 4-85331  
 adventitious, energy reference appls. 4-81106  
 amorphous, structural modelling and Raman spectra calcs. 4-108281  
 amorphous, surface diffusion of metals, in vacuo, in presence of active gases 4-98415  
 amorphous covering on Si MIS struct., tunnelling to insulator gap states 4-92824  
 amorphous film, spectral momentum density obs. using (e,2e) spectrometer 4-111257  
 amorphous film growth by CVD, methane plasma diagnostics and modelling 4-104979  
 amorphous films, ellipsometric, Raman scatt., and XPS studies 4-88418  
 amorphous hard films, growth from hydrocarbon RF plasma 4-85117  
 amorphous thin film, low energy electron attenuation length studies 4-84323  
 are evaporated amorphous film, optical const. study 4-81026  
 atom, metastable state, low energy electron inelastic scatt. 4-112279  
 atom, two photon induced VUV fluoresc. 4-83325  
 atoms, transition probability meas. for spectral lines of 3s-4p transition array 4-74194  
 Auger electron spectra 4-81050  
 BC-8 crystal phase, struct. props., phase stability and phase transistors 4-113389  
 beam-foil excitation spectra, investigation of mechanism (Chinese) 4-69192  
 biosphere, global C cycle, simulation anal., effects of human interference 4-93665  
 black dispersions, charge exchange, electrochemical/ESR studies 4-93562  
 carbonaceous selective absorber formation by catalytic deposition of pyrolytic C on Ag infrared layer 4-72174  
 ceramic materials for fusion reactor applications 4-111758  
 coating, diamond-like, development, prep. and uses 4-109525  
 coatings, diamond-like, for optical component protection 4-74677  
 continuum X-rays produced by a few MeV proton bombardment 4-99215  
 R Coronae Borealis stars, lower atm., C ionisation-chem. equilib. and condensation (Russian) 4-101358  
 cosmic rays, B/C ratio, spatial and temporal variability 4-94416  
 diffusion in metals, review 4-65474  
 doped, spark source mass spectrometric anal., ion source geometry influence 4-114863  
 elastic and inelastic electron scatt., Monte Carlo calcs. 4-97976  
 electrode use in electrochem. power sources, improved material characts. 4-62324  
 electron backscattering from thick layers 4-99249  
 filamentous growth on Fe sputtered film, surface morphology effects 4-92114  
 film, elec. cond. changes induced by pyrolysis and high energy ion irradiation 4-75966  
 film growth on Ir by vacuum sputtering, initial stages 4-61257  
 films, amorphous and graphitic, growth by ion bombardment in RF plasma 4-85116  
 films, amorphous and polycryst., plural electron scatt., Monte Carlo calc. 4-66158  
 films, as-deposited and annealed, disorder and crystallite form., Raman scatt. study 4-61254  
 films, diamondlike, ion beam deposition and props. 4-85113  
 films, diamondlike, ionized deposition from methane gas 4-65586  
 foil, excitation by fast B<sup>+</sup> beam 4-107294  
 foil, F<sup>+</sup> collisions, equilib. charge state, particle vel. depend. 4-64594  
 foil, H<sup>+</sup> and H<sub>2</sub><sup>+</sup> ion bombardment, mol. enhancement of n-state populations 4-81064  
 foil, H<sup>+</sup>, H<sub>2</sub><sup>+</sup> and H<sub>3</sub><sup>+</sup> beam-foil excitation 4-64584  
 foil, H<sup>+</sup>, H<sub>2</sub><sup>+</sup> and H<sub>3</sub><sup>+</sup> ion bombardments, continuum optical radiation emission 4-81007  
 foil, H<sup>+</sup> ion energy loss ang. depend. 4-65313  
 foil, heavy ion irradiated, charge distribution meas. 4-78945  
 foil, implanted with T, prep. and analysis w.r.t. fusion reactor safety 4-91100  
 foil, specific energy loss of <sup>16</sup>O ions, thickness depend. 4-92261  
 foils, very thin, energy loss of He<sup>+</sup> beams, nonequilibrium effects 4-103837  
 formation and oxidation on Ni exposed to ethylene 4-93440  
 gaseous, stopping power, zero-energy density effect 4-80129  
 gases/solids ignition by electrical discharges 4-69986  
 glass, stopping power, zero-energy density effect 4-80129  
 glassy, conduction band struct., core electron excitation spectra anal. 4-70647  
 glassy, electrode in LiF-KF eutectic melt, oxide ion anodic behaviour 4-66594  
 glassy, Raman spectra of oxidised and polished surfaces 4-93068  
 glassy with adsorbed H<sub>2</sub>O, adsorption depend. on substrate struct. 4-92515  
 global balance, CO<sub>2</sub> and climate interactions 4-94228  
 global cycle in atmosphere-ocean-biosphere system, models 4-72681  
 graphite particles absorption by combustion-generated C particles, sunlight absorption 4-105143  
 graphitised, adsorbed benzene, self-diffusion and nucl. spin relax. 4-61209  
 graphitised, adsorpt. of sodium dodecyl sulphate (octyltetraethylen glycol), enthalpy determ. 4-70560  
 hard coating, absorption coefficients, calc. from laser calorimetric data 4-114333  
 inhibition of deposition on stainless steel by prior selective oxidation 4-114708  
 ions, charge exchange processes 4-96694  
 ions, effective dielectric recomb. coeffs., astrophysical appl. 4-96477  
 ions in flames, origin and props. 4-71932
- carbon continued  
 isotopic anomalies in carbonate minerals due to suboxic diagenesis 4-77514  
 kaersutite, from New Zealand and USA, inert gas, H<sub>2</sub>O and C isotope geochemistry 4-105477  
 laminates, under uniaxial tension, failure behaviour, stress-strain diagram (Japanese) 4-99550  
 linear polytypes, struct. aspects and conformation 4-92139  
 midocean basaltic glass C isotope composition and origin 4-105476  
 molecule, correl. treatment with density functional theories using kinetic energy operator 4-74150  
 molecules, elementary gas phase processes, laser kinetic spectroscopy 4-69054  
 neutron irradiated, restoration of dynamic modulus of elasticity in annealing 4-65304  
 nucleosynthesis in C stars 4-85965  
 ocean C cycle, temp. and organic matter vars. effects, model 4-72614  
 overlayers on Nb, resonant photoemission and photon-induced Auger spectra 4-93182  
 overlayers on Ni (111), electronic struct. study 4-61213  
 petroleum and gas prospecting in Oklahoma, USA, by soil gas radioactivity method 4-110104  
 photon linear polarization in the elementary process of electron-electron bremsstrahlung 4-91355  
 piezoresistive stress gauge, response under shock wave conditions 4-108058  
 piezoresistive stress transducer, calibration by impact testing 4-106312  
 plasma, ionisation-chem. equilib. in R CrB stars (Russian) 4-101358  
 plasma deposited films, struct., IR spectra studies 4-98465  
 polymorphic transitions at high press. and temps. 4-113380  
 polystyrene matrix, particle elastic scattering anal. of thin samples, calibration procedure 4-99891  
 powders, Ar(N<sub>2</sub>)(CO)<sub>2</sub> adsorption, second gas-solid virial coeffs., chromatographic determ. 4-114819  
 proton stopping power, energy loss straggling, effective-charge fractions and straggling of heavy ions 4-103843  
 segregation to Ni (100) surface in presence of adsorbed S 4-61089  
 stratosphere, anomalous C, N and O cosmic ray component after 1972 4-94411  
 strip, graphitised, wetting by melts of Al and Al-Si 4-92476  
 surface, benzene adsorption equilibria 4-92512  
 target, collision of laser accelerated discs, high press. shock production 4-113257  
 targets, Cl ion-pre-equilib. charge states and charge exchange 4-75585  
 test object for electron microscopes, use of partially crystallized C 4-90692  
 thermodynamics of vapourisation and virial eqn. of state 4-103918  
 thick layers, penetration of 24.8 MeV electrons, energy spectra 4-66148  
 thin films, diamond-like, deposition on CaF<sub>2</sub> 4-74678  
 thin films, plasma induced chem. transport prep. 4-71603  
 thin foil, pre-equilibrium stopping for <sup>1</sup>H and <sup>4</sup>He ions 4-92253  
 thin targets/ stopping power for He, Li and C ions, charge state depend. 4-92252  
 trapping of sub-eV H and D atoms 4-111761  
 ultrasoft X-ray region spectroscopy 4-90700  
 Be+C(N)(O)(Ne) ions, single and double K-shell ionization cross-sections meas. 4-64583  
 C I in quasars, ground state level populations rel. to background radiation temp. at epochs (z≥2) 4-63343  
 C II, IR and UV lines, fine struct. transitions and electron collision strengths, astron. appl. 4-77701  
 C III, Be I-like, oscillator strengths, transition wavelengths, HF relativistic calcs. 4-106127  
 C III and C IV lines non-LTE anal., in hot stars 4-101320  
 C IV line broadening in dense plasmas 4-91235  
 C IV UV resonance lines in Bp-star 36 Lynx 4-67748  
 C ions, He- and Li-like, laser produced plasma, EUV spectra 4-83320  
 C material, dimensional changes, under compressive stress at high temp. 4-85182  
 C<sup>0</sup> in interstellar matter 4-110726  
 C<sup>+</sup>, branching ratios of 2s<sup>2</sup>3p <sup>2</sup>P<sup>0</sup> term, Fourier transform and VUV spectroscopy 4-87066  
 C<sup>+</sup> inelastic collisions, kinetic energy-loss spectra 4-64568  
<sup>13</sup>C diffusion investig. of intermol. struct. in solids 4-92967  
 C<sup>q+</sup> (q=6, 5, 4), incident on inert gas atoms, K-Auger electron prod. 4-78818  
 a-C:H, low emittance coatings for high temperature solar collectors 4-114950  
 C:H absorbing films, optical const. unambiguous determ. by reflectance and transmittance meas. 4-65997  
 C:H amorphous coating for IR-optical elements, optical props., thickness, density, laser damage tests 4-76422  
 C:H amorphous film, H<sub>2</sub> gas reactive RF sputtering prep. on low temp. substrates 4-76673  
 C:H amorphous film prep. by H<sub>2</sub> gas reactive RF sputtering of graphite 4-76671  
 a-C:H coating material for passive IR materials 4-74668  
 a-C:H hard thin films, RF plasma deposition 4-76681  
 a-C/Si MIS structures, DC sputter deposited, HF characts. 4-88601  
 C-Ag junctions, Schottky barrier form. 4-84694  
 C-C/TiC composite materials obtained by CVI of porous C-C substrates 4-71595  
 C-CaSO<sub>4</sub> composites, for solar energy collection and storage 4-100004  
 C-graphite materials, He ion irradiation, surface erosion 4-80120  
 C-like ions, optically allowed transitions, oscillator strengths, CI calcs. 4-74196  
 C-magnetite heterogeneous material, large-grained, step-heating technique for thermal diffusivity meas. 4-75738  
 C-Si, picosecond laser induced shock wave press. meas. 4-113259  
 C-SiC, fusion reactor first wall coatings, gas release under electron impact 4-91097  
 C-SiC alloy coated armor/limiter tiles in Doublet III 4-108178  
 C-SiC alloy coating for limiter-armor tiles on Doublet III fusion reactor, test results 4-111924  
 C+H<sub>2</sub>, CH radical prod. energetics, laser induced fluoresc. 4-114777  
 C+H<sup>+</sup>, charge transfer at large scattering angles in the strong-potential Born approximation 4-87210  
 C+NO(X<sup>2</sup>Π), collinear reaction pot. energy barrier, correl. diagram, ab initio calcs. 4-99766  
 C+SO<sub>2</sub>, chemiluminesc. reaction dynamics, vibr. energy distrib. 4-93531  
 C<sup>+</sup>+H<sub>2</sub>, reaction product rovibr. distrib., surprisal functions 4-114776

## carbon continued

- $C^+$  +  $H^+$ , ionisation cross section, PWBA 4-83461  
 $C^+$  +  $NO$ , temp. depend. of reaction from 90-450K 4-76987  
 $C^+$  +  $NO(O_2)$ , temp. depend. of reaction from 90-450K 4-76987  
 $C^{2+}$  +  $H$ , state-selective electron capture, translational energy spectroscopy 4-59891  
 $C^{2+}$  +  $Li$ , core-conserving electron capture ion excitation, metastable fraction meas. 4-83465  
 $C^{2+}$  +  $H$ , state-selective electron capture, translational energy spectroscopy 4-59891  
 $C^{4+}$  +  $H$ , electron capture, 0.25-25 keV  $amu^{-1}$  4-69205  
 $C^{4+}$  +  $H_2$ , charge transfer, polarised light emission 4-83463  
 $C^{4+}$  +  $H(Li)$ , electron transfer into  $C^{3+}(nl)$  orbitals, at. basis calcs. 4-107450  
 $C^{6+}$  +  $H$ , electron capture cross-sections calcs. 4-102791  
 $C^{6+}$  +  $H$  collisions, electron transfer, at. orbital expansion description 4-78962  
 $C^{8+}$  +  $He$ , one-electron capture at low energies, Landau-Zener model calcs. 4-96685  
 $C^{1+}$  +  $He(H)$  atoms, electron removal cross section 4-83460  
 $C_2$  in comets, excitation rates for interpreting photometric obs. 4-77766  
 $C_2$  in soot, diagnostics based on laser heating 4-93568  
 $C_2$ , radiative transition probabilities, multireference CI calcs. 4-74294  
 $C_2$  in comets, excitation rates for interpreting photometric obs. 4-77766  
 $C_2$ , vertical electron affinity and ionisation potentials 4-112295  
 $CO$ , volume per breath, evaluation (German) 4-77282  
 $^{11}C$ , prod. by photonuc. reactions for medical use 4-89746  
 $^{12}C$ , neutron scatt. cross-sections, kerma factors calc., 4-89761  
 $^{13}C$ , magnetic relax., NMR, in polystyrene solns., chain disentanglement 4-83504  
 $^{13}C$  targets prep. by cracking procedure 4-64253  
 $^{13}C$ , isotope fractionation in dense interstellar clouds, time-dependent model 4-90208  
 $^{14}C$  activity levels for low level radioactive waste 4-106731  
 $^{14}C$ , behaviour in atmosphere (Russian) 4-77162  
 $^{14}C$  dating, Chinese sucrose charcoal standard 4-68199  
 $^{14}C$  dating in tree rings, determ. of cosmic ray solar mod. cycle 4-94423  
 $^{14}C$  exchange between atmosphere and oceans 4-72682  
 $^{14}C$ , global environmental transport model review 4-83253  
 $^{14}C$  in aquatic food chain (German) 4-68911  
 $^{14}C$  in gonads of male mice, genetic effect (Russian) 4-67012  
 $^{14}C$ , low background meas., sample chamber design for liq. scintillation detector 4-87006  
 $^{14}C$ , nuclear fuel reprocessing gaseous wastes management 4-59438  
 $^{14}C$  prod. in terrestrial, atm., correl. with galactic cosmic ray var. and solar activity 4-94424  
 $^{14}C$ , volatile radionuclides from nuclear fuel reprocessing, treatment and disposal (German) 4-59318  
 $C16\alpha$  radio recomb. lines in C II regions 4-90197  
 $\alpha$ -Fe-C, martensitic, lattice deformation by C impurities (Russian) 4-103773  
 $GAs: C$ , impurity and defect anal. by IR absorpt. spectra 4-75893  
 $H_2$ /electrical power simultaneous production, using carbonaceous fuels and high-temperature nuclear process heat, thermodynamic anal. 4-89472  
 $InP:Be(C)$ , acceptor levels, photoluminesc. study 4-80543  
 $InP:C$ , acceptor impurity incorporation during organometallic VPE, photolum. obs. 4-98122  
 $MnO_2$ /active C as  $O_2$  electrode in alkaline fuel cells (Japanese) 4-89397  
 $Ni$ , thermodynamics, kinetics and props. of gases and C, data tables 4-73173  
 $Ni-C$  multilayer dispersion element performance, 80 to 500 eV 4-90698  
 $ReW-C$  multilayer dispersion element performance, 80 to 500 eV 4-90698  
 $S_{10}+C_{60}$ , disperse phase system, elec. cond., rel. to temp. and particle size 4-98680  
 $Si-^{13}C$ , muon spin rot. and TEM studies 4-71239  
 $Si:B,C,O$ , impurity profiling and analysis by recoil atoms in heavy ion beams 4-108406  
 $Si:C$ , electron irradi., optical absorpt. spectra 4-88861  
 $Si:C$ , impurity conc. determ. by IR spectroscopy 4-113484  
 $Si:C$ , self-interstitial enhanced C diffusion 4-98358  
 $Si:C,N$ , CVD thin films using di-2,2'-bipyridine silicon 4-71586  
 $Si:C$  crystals, interface shape and radial distribution of impurities 4-113371  
 $Si:C$  Czochralski, C in radiation damage centres, luminesc. study 4-93107  
 $Si:C$  layers, CVD growth, microstruct. and resist. 4-70599  
 $Si:Li$ , C, electron irradi., luminesc. decay time, absorpt., isotope splitting, and Zeeman meas. 4-71434  
 $Si:O$ , C, annealed, photoluminesc. of impurity complexes 4-88866  
 $V-C$  layered synthetic microstructure, refl. and roughness, optical consts. in X-ray region 4-93128  
 $WC/C$  system for X-ray dispersion, Auger depth profile anal. and sputter deposition 4-98466

## carbon compounds

- see also organic compounds  
 alkali halide: $CN^-$ , vibrational fluoresc., nonradiative luminesc. quenching 4-81005  
 carbides, oriented growth possibilities during reaction diffusion 4-61256  
 carborane linked polyhedral cages, B-B spin-spin coupling consts.,  $^{10}B$  and  $^{11}B$  NMR study 4-112198  
 $CO$ , pollution, climate and energy systems (book) 4-90311  
 $CO$ , adsorption on W (100), effect on EELS spectrum 4-93159  
 graphite hydrogen sulphate, stacking disorder during oxidation, X-ray diff. obs. 4-108383  
 impure carbonates, dating using decay series isotopes 4-105736  
 laser radiation detection using antenna-coupled point contact Schottky diode, responsivity study (Japanese) 4-78374  
 neutral bases,  $H^+$  and methyl- and ethyl-cation affinities, MNDO calcs. 4-64381  
 particle excitation mechanisms  $F$ ,  $Ar$ ,  $O$ ,  $N_2$ ,  $CO$  and perfluoromethyl radical in glow discharge 4-79860  
 pulsed gas lasers, high power 4-96865  
 tetracordinate C cpds., geometries calcs. 4-64346  
 CBN, abrasive grain, friction with ceramics and cemented carbide 4-109522  
 $CCl$  triplet and cold radical prod. with pulsed elec. discharge in pulsed supersonic flow 4-84090  
 $CF_4/O_2$ , emission, plasma etching systems, spatially resolved optical spectroscopy 4-79852

## carbon compounds continued

- $(C,F)_n$ , prep., struct., phys. props. and appls. in Li batteries (Japanese) 4-93246  
 $CH^+$  +  $H$ , reaction rate coeffs. 4-81427  
 $CN$  adsorbed on Ag electrode, Fourier transform IR spectra studies 4-93067  
 $CN$ , chemisorbed on Ag island film, depolarisation effects in Raman scatt., classical microscopic local field 4-88832  
 $CN$ , collisional vibr. relax. in  $A^{\Pi}$  state 4-69035  
 $CN$ , electron elastic scatt. cross section 4-83469  
 $CN$ , electronic transition moments, MCSCF-SCEP wave functions calc. 4-74166  
 $CN$  in 47 Tuc giant branch 4-85921  
 $CN$  in Comet Bowell (1982 I), spectrophotometric obs. 4-82451  
 $CN$  in comets, excitation rates for interpreting photometric obs. 4-77766  
 $CN$  plastic track detector for magnetic monopoles 4-95733  
 $CN$  radiance/column density ratio in comets, calc. from Swings effect 4-90117  
 $CN$  radical evolution in  $N_2$ -ethanol mixture pulsed discharge 4-81428  
 $CN^-$  ion, aq. soln., positronium quenching and inhibiting props. 4-103805  
 $CN^-:KBr$  solid-state vibr. laser, laser oscill. at 2054  $cm^{-1}$  4-60045  
 $CN^-e^-$ , electronic/positronic struct. examined using Hartree-Fock-Roothaan theory 4-64352  
 $CN+H_2(O_2)(CO)(CO_2)(N_2)(HCN)(methane)(cyanogen)$ , vibr. energy effect on reaction, laser meas. 4-99769  
 $C_2N^+$ , mobilities in He at 293K 4-79706  
 $C_2N_2$ , adsorption and coadsorption with  $H_2$  on Pt (111), surface chem. 4-81478  
 $C_2N_2$ ,  $H^+$  affinity, selected ion flow tube study 4-71881  
 $C_2N_2$ , thermal decomposition, shock tube study 4-76989  
 $C_2N_2^+$ , mobilities in He at 293K 4-79706  
 $CN(X^{2+})$  spin-aligned photofragment, laser induced fluoresc. 4-114802  
 $CO$ , 2.45  $\mu m$  spectral meas. using IR high-resolution cooled-optics grating spectrometer 4-95532  
 $CO$  adsorbate vibrs., Stark effect 4-98453  
 $CO$ , adsorbed Cu {100},  $2\pi^*$  associated states, angle-resolved photoemission 4-65724  
 $CO$  adsorbed layer on Ag film, adsorption process study using surface plasmons 4-80383  
 $CO$  adsorbed on 3d-transition metals, electronic struct. and chemical reactivity of  $CO$  4-93552  
 $CO$  adsorbed on  $(Ru,Si_{1-x})O_2$  surface, FT-IR study of surface acid sites 4-113783  
 $CO$ , adsorbed on Ag (110), photoemission screening effects 4-66189  
 $CO$  adsorbed on Ag film, elec. cond., effect of adsorption 4-108950  
 $CO$  adsorbed on Ir surface, oxidation,  $CO_2$  desorption ang. distrib. 4-80378  
 $CO$  adsorbed on K precovered Ru(001), EELS scatt. profiles of vibr. overtones and double losses 4-109287  
 $CO$ , adsorbed on  $LaMO_3$ , ( $M=Cr,Mn,Fe,Co$ ), IR spectra 4-104071  
 $CO$ , adsorbed on metal surfaces, XPS satellite structures 4-114361  
 $CO$ , adsorbed on metals, valence electronic excitations, EELS 4-81052  
 $CO$  adsorbed on metals, anomalous electronic and vibr. props. 4-98441  
 $CO$ , adsorbed on metals, bonding, EHT calcs. 4-113800  
 $CO$  adsorbed on Ni, anharmonicity and adsorbate vibr. lifetimes 4-104084  
 $CO$ , adsorbed on Ni (100), stretching vibr., IR emission spectroscopy study 4-92508  
 $CO$ , adsorbed on Ni (100), surface structure determ. by XANES 4-99226  
 $CO$ , adsorbed on Ni (100), Pt (111) and (110), photoelectron ang. distrib. patterns 4-109309  
 $CO$ , adsorbed on Ni (110), medium energy ion scatt. studies 4-88381  
 $CO$  adsorbed on Ni (111) surface, thermal decomposition of ethylene 4-113782  
 $CO$  adsorbed on Rh (001), photoemission, ion scatt. and secondary electron studies 4-75777  
 $CO$  adsorbed on W (110), electronic transitions, low-threshold neutral desorption,  $\alpha-\beta$  conversion, calcs. 4-113785  
 $CO$  adsorbed state over Pd/graphite catalyst, PES study of particle size effect 4-99274  
 $CO$ , adsorpt. on NiO-MgO solid soln., reactivity, spectrosc. obs. 4-113795  
 $CO$ , adsorpt. on NiO-MgO solid solns., reactivity,  $H_2$  pretreatment effects, spectrosc. obs. 4-113796  
 $CO$ , adsorpt. on Pd electrode, IR refl. spectrosc. obs. 4-107348  
 $CO$ , adsorption and desorption on Rh (111) and Rh (331), XPS and SIMS study 4-65574  
 $CO$  adsorption kinetics on perovskite-type oxide  $LaCrO_3$  4-61208  
 $CO$ , adsorption on Ag (110), AES, XPS, TDS and LEED studies 4-113810  
 $CO$  adsorption on C powders, second gas-solid virial coeffs., chromatographic determ. 4-114819  
 $CO$  adsorption on Fe (111), thermal desorpt. and LEED studies 4-65566  
 $CO$  adsorption on highly dispersed  $Rh/Al_2O_3$  catalyst, EXAFS study 4-62243  
 $CO$ , adsorption on K-doped Ni (100) 4-84509  
 $CO$  adsorption on metal surfaces, SCF calcs. 4-88398  
 $CO$ , adsorption on MgO (001), ab initio MO calcs., lattice defect methods 4-81476  
 $CO$  adsorption on Ni (111), UHV cell for Raman studies of gases adsorbed on metals 4-101947  
 $CO$ , adsorption on S-covered Ni (100), vibr. spectroscopy study 4-108720  
 $CO$  adsorption on thin Pd overlayers on Nb (110) and Ta (110) 4-92533  
 $CO$ , angle resolved thermal desorption spectra from Ni 4-70554  
 $CO$ , Auger spectra, Green's function calcs. 4-64389  
 $CO$ , bipolar gas flow in LDN 1551 IRS 5, obs. 4-115796  
 $CO$ , C 1s photoelectron spectra using soft X-ray monochromators at BESSY 4-95583  
 $CO$ , CW industrial laser, electron beam-controlled with 10 kW output power, energy characts. 4-74492  
 $CO$ , CW laser two-mode multiline stabilisation using Fabry-Perot filter under analog and digital computer control 4-60092  
 $CO$ , catalytic oxidation on Pd, surface state effects 4-62238  
 $CO$ , catalytic oxidation on Pt (100), MeV ion scatt. study 4-81069  
 $CO$  chem. laser, continuous  $CS_2-N_2O-O_2$  type with 2-m long active region output characts. 4-74496  
 $CO$ , chem. shielding and shifts,  $^{17}O$  NMR 4-102705

## Carbon compounds continued

- CO, chemisorbed, physisorbed, and free, high-resolution C 1s and O 1s core-excitation spectra 4-93125  
 CO chemisorbed layer on Ru (001), electron-induced desorption 4-104075  
 CO chemisorbed on Ni (100) and Cu (100) 4-80380  
 CO chemisorbed on Ni (100), vibr. spectroscopy by IR emission 4-98439  
 CO, chemisorbed on Pt (110), (111) and Ni (100), photoemission study 4-85055  
 CO, chemisorpt. on Ni (7 9 11) surface 4-75784  
 CO chemisorption on doped MgO {001} surfaces 4-113805  
 CO chemisorption on Ni (100), XPS study of surface electronic struct. 4-88550  
 CO, chemisorption on: Pd (111), angle-resolved photoelectron spectra 4-81114  
 CO, chemisorption on two-dimens. CO clusters 4-108725  
 CO, coadsorbed with Na on Ru (001), mol. reorientations 4-108717  
 CO, coadsorption with D<sub>2</sub> on K-predosed Ni (100) 4-92535  
 CO, coadsorption with H<sub>2</sub> on Ni, ion induced desorption study 4-92547  
 CO, coadsorption with K on Ru (001), attractive interactions 4-65548  
 CO, coadsorption with K on Ru (001), thermal desorption vibr. overtone spectroscopy 4-70565  
 CO, coadsorption with K on Rh (111), HREELS, TPD, AES and LEED study 4-84508  
 CO, coadsorption with K on Ni (100), XPS, UPS, work function, and EELS meas. 4-92552  
 CO, coadsorption with S<sub>2</sub>, H<sub>2</sub> and O<sub>2</sub> on Mo (100) and MoS<sub>2</sub> (0001) 4-80407  
 CO, collision widths of IR lines broadened by H<sub>2</sub>O vapour at elevated temps. 4-69149  
 CO conc. along urban roadsides, line-source model predictions 4-66833  
 CO condensed films, shape reson. in photoemission 4-85061  
 CO, condensed molecules, photon-stimulated ion desorption 4-61239  
 CO cryogenic electroionisation laser, energy characts. 4-69379  
 CO detection in combustion gases using two-photon absorpt. 4-62261  
 $\alpha$ -CO, dipolar reorientation and metastability in glass-like state 4-79934  
 CO, dissociative adsorption and recomb. on Ni (111) 4-93559  
 CO distribution along southern galactic plane, Galaxy spiral struct. 4-63294  
 CO distribution in southern galactic hemisphere (fourth quadrant) 4-63295  
 CO, electric dipole moments calc. using variational cellular method 4-87042  
 CO electroionisation laser, power and time characts. of light pulses, pump power depend. 4-64700  
 CO, electron (positron) impact, total cross-sections 4-107453  
 CO, electron collisions, correl. polarisation pot., parameter-free model 4-64609  
 CO, electron drift vel. at moderate E/N values 4-79712  
 CO, electron impact excitation of inner-shell excited states 4-69233  
 CO, electron scatt., R-matrix method, ab initio calcs. 4-83484  
 CO emission from M17 SW giant mol. cloud 4-73002  
 CO emission from M82, mol. halo obs. 4-86047  
 CO emission from outer Galaxy mol. clouds, distrib. 4-63309  
 CO emission from PV Cep and assoc. nebula 4-85922  
 CO, excited state lifetimes, inelastic electron-photon delayed coincidence technique 4-102644  
 CO films, structural order effects in low-energy electron transmission spectra 4-98520  
 CO, fine struct., K-shell EELS, ab initio methods 4-91346  
 CO, form. in turbulent diffusive combustion, oxidation kinetics 4-71922  
 CO, fragmentation following soft X-ray excitation 4-83440  
 CO, high coverage struct. on metal FCC (111) and HCP (0001) surfaces, LEED, HREELS and IR spectra study 4-65573  
 CO, hyperpolarisability function, derivative HF theory to all orders 4-107272  
 CO, IR absorpt. line shape and width across supersonic free jets 4-83374  
 CO, identity-forbidden two-photon transition,  $1^1\Sigma^+-X^1\Sigma^+$  states 4-91321  
 CO in atmosphere, Brazil forest fire emissions 4-67314  
 CO in Earth's atmosphere, increasing trend (1979 to 1983) 4-100045  
 CO in interstellar matter 4-107026  
 CO in southern sources 4-63261  
 CO in spiral galaxies and star formation 4-63318  
 CO, inelastic scatt. and chemisorption from Pt (111), semiclassical model 4-71495  
 CO, interstellar, absorpt. lines in spectrum of IR source (NGC 2024 IRS 2) 4-86000  
 CO, interstellar, in NGC 7538 mol. cloud, obs. of massive high-vel. outflow 4-85998  
 CO, interstellar, in peculiar galaxy M82, distrib. and kinematics 4-101471  
 CO, interstellar, obs. in mol. cloud assoc. with triple IR source (GL 437) 4-85999  
 CO, interstellar, spectral line profiles rel. to fluctuation spectrum of mol. clouds 4-115795  
 CO interstellar distrib. rel. to  $\gamma$ -ray distrib. 4-63301  
 CO interstellar distrib. and galactic spiral struct. 4-63306  
 CO isotope exchange reaction on Rh surface 4-81479  
 CO J=1-0 obs. of peculiar nebulosities and star formation regions 4-86022  
 CO J=2-1 obs. towards southern H II regions 4-63260  
 CO J=6-5 691 GHz transition, heterodyne detection 4-90218  
 CO laser, branch selected, spectral characts. at room temp., Fabry-Perot etalon meas. (Chinese) 4-112389  
 CO laser, high-power room-temp. 4-112385  
 CO laser appls. in surgery 4-77371  
 CO laser gas discharge plasma, oscillatory instability 4-64699  
 CO latitude distribution in southern galactic hemisphere 4-63308  
 $\alpha$ -CO, librational motion, anharmonic effects 4-103892  
 CO, liq., IR spectra, solvent-induced shift, Monte Carlo simulation 4-61698  
 CO lone pair ligand interaction with Cu, constrained space orbital-variation method 4-114823  
 CO mapping of giant mol. clouds 4-63264  
 CO, Massachusetts-Stony Brook survey of galactic plane 4-63307  
 CO matrix isolated Hg, electronic to vibr. energy transfer, IR emission 4-107441  
 CO near galactic centre, struct. with strong positional and kinematic gradients 4-63310  
 CO, near-threshold electron impact excitation functions 4-96702

## Carbon compounds continued

- CO, O 1s, C 1s core-level shape resonances, soft X-ray photoemission 4-96614  
 CO observations in southern galactic hemisphere H II regions 4-63263  
 CO oxidation kinetics on Ir (111), lattice gas model 4-66613  
 CO, oxidation on Ag catalyst, surface heterogeneity 4-105017  
 CO oxidation over Pd deposited on LiNbO<sub>3</sub> ferroelectrics, adsorptive and catalytic props., polarisation 4-99837  
 CO, oxidation over Pt surface, kinetic oscils., Rutherford backscattering, LEED study 4-66611  
 CO, photodissociation, interstellar mol. cloud, VUV spectra 4-83441  
 CO, photoelectron branching ratio and asymmetry parameters for two outermost MO 4-59849  
 CO, pot. functions, vibr.-rot. perturbation theory 4-102760  
 CO, prod. from formaldehyde photodissociation, collisions, IR fluoresc. study 4-78900  
 CO production from C and CO<sub>2</sub> in plasma arc reactor 4-76978  
 CO, RHF, NDDO and MOM mol. one-electron expectation values calc. using minimum basis sets 4-102598  
 CO self-exchange reaction mechanism studied using mercury photosensitisation technique 4-89270  
 CO sensing, using polymer covered interdigitated electrode structures 4-95401  
 CO, solid, adsorption of multilayers on Cu (100), epitaxial growth of new cryst. struct., LEED, IR spectra 4-113373  
 CO, solid, combined translational-rotational jumps, <sup>13</sup>C NMR obs. 4-98970  
 CO, solid, low temp. electronic sputtering by light ions and electrons 4-71502  
 CO, solid, photon-stimulated ion desorption 4-93549  
 CO, solid, range meas. of keV H ions 4-92263  
 CO supersonic expansion, coherent extreme UV and vacuum UV radiation generation using pulsed nozzles 4-107745  
 CO survey of Southern Hemisphere dark clouds, refl. nebulae and Herbig-Haro objects 4-101455  
 CO synthesis expts. from He-buffered CO<sub>2</sub> mixture by charged particle radiolysis 4-62216  
 CO, total energies calc. using electron cloud displacement model (Chinese) 4-74136  
 CO, translation rot. coupling and lattice dynamics 4-98219  
 CO triplet and cold radical prod. with pulsed elec. discharge in pulsed supersonic flow 4-84090  
 CO, VUV radiation, reson. enhanced tunable source 4-83661  
 CO, vibr. excited post discharge, electron energy distrib. function 4-92014  
 CO waveguide laser with selective resonator, emission freq. wide tuning range 4-60069  
 CO, weakly chemisorbed, correl. between anomalous electronic and vibr. props. 4-78910  
 CO<sup>+</sup>, isolated ions, IR spectra quantitative prediction 4-69075  
 CO<sup>+</sup> cation radical in Ne matrix, ESR investig. 4-78873  
 CO-Ar gas mixtures, thermal conductivity meas. 4-113102  
 CO-BF<sub>3</sub>, weakly bound complexes, Fourier transform IR spectra 4-87125  
 CO-covered Cu films, optical and elect. props. 4-80693  
 CO-H<sup>+</sup>(Li<sup>+</sup>)(Na<sup>+</sup>)(K<sup>+</sup>) struct., binding energies, ab initio HF calcs. 4-112096  
 CO-HF<sub>3</sub>-HF, photolysis, HF multiquantum vibr.-rot. relax. rates 4-102775  
 CO-He gas mixtures, thermal conductivity meas. 4-113102  
 CO-inert gas binary system, diffusion coeffs. and thermal diffusion coeffs 4-103458  
 CO-methane gas mixture, thermal conductivity meas. 4-113103  
 CO-Ne gas mixtures, thermal conductivity meas. 4-113102  
 CO-Ni interaction in presence of K, site pot. effect 4-81477  
 CO-O<sub>2</sub> mixtures, population inversion of electronic-vibr. states during adiabatic thermal explosion 4-102746  
 CO+aniline, mode-to-mode energy transfer, fluoresc. 4-83450  
 CO+Ar<sup>+</sup> collisions, integral cross section meas. 4-78929  
 CO+CN, vibr. energy effect on reaction, laser meas. 4-99769  
 CO+Cr, intramultiplet mixing collisions, fluoresc. 4-64588  
 CO+DF, vibr. relax. rate consts. determ. using flow IR chemiluminesc. technique 4-89273  
 CO+H<sub>2</sub>, CO(v=1) vibr. deactivation, influence of higher order multipole moments 4-112259  
 CO+H<sub>2</sub> collisions, rigid-rotor pot. energy surface from ab initio calcs. and rot. inelastic scatt. data 4-78940  
 CO+HF, vibr. relax. rate consts. determ. using flow IR chemiluminesc. technique 4-89273  
 CO+H(D), collisional excitation, cross sections, quasiclassical trajectory study 4-78950  
 CO+In, intramultiplet mixing collisions 4-107393  
 CO+N<sub>2</sub>, Auger and X-ray photoelectron spectra, reson. enhanced shakeup near-threshold core 4-96627  
 CO+N<sub>2</sub> vibr. relax., semiclassical dynamical model 4-107439  
 CO+N<sub>2</sub>, temp. depend. of reaction from 90-450K 4-76987  
 CO+N<sup>+</sup>, thermal and near-thermal energy charge exchange, energy disposal 4-76984  
 CO+NO reactions on Rh (111), AES, LEED, XPS, UPS and temp. programmed desorp. study 4-89326  
 CO+Rb, quenching cross sections, Rydberg electron-molecular dipole interaction 4-96604  
 CO<sup>+</sup>+CS<sub>2</sub> in flowing afterglow, charge-transfer excitation, energy reson. and Franck-Condon criteria 4-93500  
 CO<sup>+</sup>+H, reaction rate coeffs. 4-81427  
 CO<sup>+</sup>+He, electronically excited CO<sup>+</sup> collisional deactivation 4-64580  
 CO<sup>+</sup>+O<sub>2</sub>, temp. depend. of reaction from 90-450K 4-76987  
 CO<sub>2</sub> 0001 upper laser level spectroscopy based on 4.3  $\mu$ m spontaneous emission intensity modulation meas. 4-78851  
 CO<sub>2</sub> 1000-Hz mini-TEA laser, remote sensing appls. 4-107662  
 CO<sub>2</sub> absorption axial flow canister design for divers 4-109763  
 CO<sub>2</sub> absorption coefficient temp. depend. beyond edge of vibr.-rot. bands 4-83366  
 CO<sub>2</sub>, adsorbed on LaMO<sub>3</sub> (M=Cr,Mn,Fe,Co), IR spectra 4-104071  
 CO<sub>2</sub> adsorption on Ag (110), AES, XPS, TDS and LEED studies 4-113810  
 CO<sub>2</sub>, adsorption on Calgon BPL activated C, Langmuir isotherm 4-104072  
 CO<sub>2</sub> amplifier, light pulse coherent amplification 4-79101  
 CO<sub>2</sub> and global balance, climate interactions 4-94228  
 CO<sub>2</sub> and H<sub>2</sub>O laser freq.-mixing expts., beat note S/N ratio characts. 4-74608

carbon compounds continued

- CO<sub>2</sub> as an inverse greenhouse gas 4-110194
- CO<sub>2</sub> as working fluid for closed-cycle diesel engines 4-66743
- CO<sub>2</sub>, autoionisation, fluoresc. polarisation study 4-83402
- CO<sub>2</sub>, binding and correl. effects, gas X-ray diffr. investig. 4-102697
- CO<sub>2</sub> CW far IR lasers, optically pumped, using new stabilisation system 4-102954
- CO<sub>2</sub> CW high power transverse flow laser type JL6A working gas determ. and catalytic purification (*Chinese*) 4-112463
- CO<sub>2</sub> CW IR lasers, dynamics, investigation using tunable diode lasers 4-112375
- CO<sub>2</sub> CW industrial ionisation lasers, service life increase using 5-component mixtures 4-112379
- CO<sub>2</sub> CW laser, appl. of IR presensitization photography 4-111229
- CO<sub>2</sub> CW laser, gain profile, opto-voltaic representation 4-83562
- CO<sub>2</sub> CW laser, radiatively pumped 4-91494
- CO<sub>2</sub> CW RF-pumped IR laser using transverse gas flow 4-74544
- CO<sub>2</sub> CW steady-state laser model 4-112373
- CO<sub>2</sub> CW transverse flow laser, quasi two-dimens. gain distrib. (*Chinese*) 4-112376
- CO<sub>2</sub> cascade laser, 4.4 micron, resonator design 4-87313
- CO<sub>2</sub> changes in atmosphere due to marine biota at high latitude 4-115521
- CO<sub>2</sub>, chem. shielding and shifts, <sup>17</sup>O NMR 4-120705
- CO<sub>2</sub> chirp-modulated CW heterodyne laser rangefinder/velocimeter based on acousto-optic modulator 4-96963
- CO<sub>2</sub> coherent laser radar performance study 4-96974
- CO<sub>2</sub> coherent transversely excited atm. laser radar, field meas. 4-96973
- CO<sub>2</sub> commercial technological laser prod. of power 1 to 10 kW 4-107663
- CO<sub>2</sub> compact hybrid single mode TEA laser, stabilisation 4-91495
- CO<sub>2</sub> condensed films, shape reson. in photoemission 4-85061
- CO<sub>2</sub>, condensed gas solids, ion-induced chem. 4-66163
- CO<sub>2</sub> desorption, liq. film mass transfer coeffs. 4-87661
- CO<sub>2</sub>, desorption ang. distrib. from IR surface after CO oxidation 4-80378
- CO<sub>2</sub> desorption from falling aq. glycerol films, mass transfer enhancement 4-65551
- CO<sub>2</sub> diffusion in liq. heptane 4-61120
- CO<sub>2</sub> electrochemical sensor for high ambient pressures, deep diving appls. 4-106311
- CO<sub>2</sub>, electron (positron) impact, total cross-sections 4-107453
- CO<sub>2</sub>, electron collisions, correl. polarisation pot., parameter-free model 4-64609
- CO<sub>2</sub>, electron drift vel. at moderate E/N values 4-79712
- CO<sub>2</sub>, electron impact rot.-vibronic excitation by slow electrons 4-107463
- CO<sub>2</sub>, electron scatt. cross sections, CI calcs. 4-91348
- CO<sub>2</sub>, electron transport, Monte Carlo and Boltzmann two-term calcs. 4-113109
- CO<sub>2</sub>, excited vibr. states, spacing distrib., role of dynamical symmetry 4-87034
- CO<sub>2</sub>, expanding supersonic jets, condensation processes similarity 4-60474
- CO<sub>2</sub>, exposed Al, oxide formation study 4-93441
- CO<sub>2</sub>, fast axial flow laser with 1000 watt output power 4-102945
- CO<sub>2</sub>, fast flow laser plasma, electron temp. meas. 4-103466
- CO<sub>2</sub>, fluid, orthobaric props., intermol. pot. effect 4-74310
- CO<sub>2</sub>, free expansion condensation, mol. beam study 4-60561
- CO<sub>2</sub> gas, inverted, wavefront reversal, influence of excited particle diffusion 4-74623
- CO<sub>2</sub> gasdynamic 16  $\mu$ m laser, boundary layer effects on laser gain 4-87314
- CO<sub>2</sub> gasdynamic laser, Fabry-Perot resonator, mode struct. 4-60072
- CO<sub>2</sub> gasdynamic laser, regenerative elect. gas heater 4-79179
- CO<sub>2</sub> gasdynamic laser, radiation intensification in boundary layer on Laval nozzle cooled walls (*Russian*) 4-96867
- CO<sub>2</sub> gasdynamic lasers with high temp. regenerative heat-exchanger heater, generation params. 4-79178
- CO<sub>2</sub>, grating selected freq. laser, mode corrugated pipe design (*Chinese*) 4-87360
- CO<sub>2</sub>, ground state, photoionisation cross sections, linear algebraic method 4-64549
- CO<sub>2</sub>, high energy pulsed lasers, catalyst evaluation for closed cycle operation 4-96939
- CO<sub>2</sub>, high power laser optics 4-102937
- CO<sub>2</sub>, high power laser plasma investigation 4-102917
- CO<sub>2</sub>, high power laser technology overview 4-107668
- CO<sub>2</sub>, high power laser transmissive optics, failure phenomena (*Japanese*) 4-74530
- CO<sub>2</sub>, high power laser with folded resonator, computer simulation 4-102916
- CO<sub>2</sub>, high power lasers, multi-kilowatt, for use in industrial production 4-102946
- CO<sub>2</sub>, high resolution IR spectra atlas 4-91257
- CO<sub>2</sub>, high-power technological gas elec. discharge laser based on air-CO<sub>2</sub> mixture 4-107664
- CO<sub>2</sub>, hydrocarbon mixtures, Peng-Robinson eqn. of state for vapour-liquid equilib. calc. 4-70334
- CO<sub>2</sub> IR laser, freq. synthesized and continuously tunable in 9-11  $\mu$ m range 4-96947
- CO<sub>2</sub> ice, density evolution in solar system ices 4-101147
- CO<sub>2</sub>, imaging laser radar field tests 4-107870
- CO<sub>2</sub> in aqs. soln., diffusion, isotope fractionation meas. 4-87226
- CO<sub>2</sub> in atm., conc. var. due to oceanic primary productivity fluctuations 4-94182
- CO<sub>2</sub> in atm., effects on surface temperatures in long term 4-94238
- CO<sub>2</sub> in atm., effects on climate modelling 4-110243
- CO<sub>2</sub> in atm., greenhouse effect 4-82228
- CO<sub>2</sub> in atmosphere, increase, sensitivity of climate models, influence of ocean heat transport 4-67386
- CO<sub>2</sub> in atmosphere, of Pacific, concentration variations and isotopic composition 4-115520
- CO<sub>2</sub> in atmosphere, rapid vars. rel. to ocean circulation 4-62909
- CO<sub>2</sub> in atmosphere in AD 1860 to 2050 period, C cycle calcs. 4-67345
- CO<sub>2</sub> in gas mixtures, electron cloud sizes meas. 4-59519
- CO<sub>2</sub> induced climatic change and spectral vars. in outgoing IR radiation 4-115558
- CO<sub>2</sub> injection-locked TEA laser, tunable single-mode design for D<sub>2</sub>O laser pumping 4-79184
- CO<sub>2</sub>, intermolecular pots., ab initio SCF calcs. 4-96640
- CO<sub>2</sub> laser, 4.3  $\mu$ m, gain dynamics 4-79180
- CO<sub>2</sub> laser, gasdynamic, nuclear pumped heat pipe design 4-60016

carbon compounds continued

- CO<sub>2</sub> laser, gaseous medium temp., influence of high-mol. compound impurities 4-79103
- CO<sub>2</sub> laser, hybrid oscillator/electron-beam preionized amplifier config. for D<sub>2</sub>O laser pumping 4-79183
- CO<sub>2</sub> laser, hybrid TE-TEA sealed-off with corona preionisation 4-69430
- CO<sub>2</sub> laser, pulsed, miniature, with sealed-off electron source 4-102950
- CO<sub>2</sub> laser, Q-switched, electro-optic freq. shifts 4-87377
- CO<sub>2</sub> laser, quasi-CW, tunable, 1-sec pulse, optical pumping appls. 4-74536
- CO<sub>2</sub> laser, rel. to non-self-sustained discharge with a plasma cathode 4-84114
- CO<sub>2</sub> laser bands, freq. tables, rovibr. consts. 4-60015
- CO<sub>2</sub> laser development and applications at MIT Lincoln Lab. 4-90325
- CO<sub>2</sub> laser drilling of multilayer PCBs 4-87384
- CO<sub>2</sub> laser frequency stabilisation for sub-MM laser pumping by Stark modulated Lamb dip signal in methanol (*Japanese*) 4-74485
- CO<sub>2</sub> laser heterodyne bias freq. locking (*Chinese*) 4-91512
- CO<sub>2</sub> laser mixtures, electron mobility, diffusion coeffs. ratio 4-112374
- CO<sub>2</sub> laser polarimeter 4-78363
- CO<sub>2</sub> laser processing induced plasma, optical absorption prop. development 4-108189
- CO<sub>2</sub> laser produced plasma, harmonic generation study 4-102920
- CO<sub>2</sub> laser pulse shapes determ. using methyl-methacrylate plate 4-91509
- CO<sub>2</sub> laser pumped vinyl bromide, 47 CW far IR laser lines 4-96869
- CO<sub>2</sub> laser system producing single mode microsecond pulses 4-102953
- CO<sub>2</sub> laser with plasma electrodes 4-91434
- CO<sub>2</sub> laser with variable output pulse duration 4-60070
- CO<sub>2</sub> laser-target interaction expts. 4-68827
- CO<sub>2</sub> lasers, beam power measurement of high-power lasers, calorimeter development (*Japanese*) 4-64715
- CO<sub>2</sub> lasers, pulsed, damage thresholds for large irradiated spots 4-107595
- CO<sub>2</sub>, librational motion, anharmonic effects 4-103892
- CO<sub>2</sub>, light multiple scatt. contributions to depolarisation in critical region 4-112186
- CO<sub>2</sub>, liq., thermodynamic state, struct., neutron diffr. study 4-70017
- CO<sub>2</sub>, microwave spectra, intermol. interaction meas. 4-59731
- CO<sub>2</sub> mixing lasers, plasma injection controlled discharge characts. 4-83563
- CO<sub>2</sub>, O 1s, C 1s core-level shape resonances, soft X-ray photoemission 4-96614
- CO<sub>2</sub>, optical generation and detection of acoustic pulse profiles for novel ultrasonic absorpt. spectroscopy 4-103460
- CO<sub>2</sub> partial pressure in atmosphere, new model for determining role of oceans 4-62908
- CO<sub>2</sub> photoassisted reduction on aqueous suspension of TiO<sub>2</sub>, organic products formation 4-99817
- CO<sub>2</sub>, photofragment product, vibr. energy distrib., IR diode laser probes 4-107325
- CO<sub>2</sub>, pot. energy surface, rovibr. spectra inversion 4-59704
- CO<sub>2</sub> pulse periodic lasers, appl. to industrial welding 4-107660
- CO<sub>2</sub> pulse-periodic laser, wave-driven gas circulation in a gas chamber with pulse-periodic energy supply 4-60068
- CO<sub>2</sub> pulsed amplifiers, pumping process modelling in elec. discharges 4-83564
- CO<sub>2</sub> pulsed and CW laser, heterodyne freq. offset locking technique 4-96951
- CO<sub>2</sub>, pulsed discharges, energy and time characteristics 4-65149
- CO<sub>2</sub> pump laser freq. controlling method 4-96950
- CO<sub>2</sub> RF excited lasers, electron energy distrib. and transport coeffs. 4-102919
- CO<sub>2</sub>, radiation convection heat transfer problem plane channel, turbulence 4-60378
- CO<sub>2</sub> sealed TEA lasers, high peak power and sustained long life operation 4-87365
- CO<sub>2</sub> sensing, using polymer covered interdigitated electrode structures 4-95401
- CO<sub>2</sub> single-mode etalon-tuned TEA laser, optimised design for NH<sub>3</sub> laser pumping 4-79182
- CO<sub>2</sub> solid, electronic band struct., photoelectron spectra 4-85058
- CO<sub>2</sub> solid, mol. excitons, UV absorpt. and XPS spectra study 4-65613
- CO<sub>2</sub> sorption on PMMA 4-81465
- CO<sub>2</sub> spectral band contour in 4.3  $\mu$ m region (*Chinese*) 4-107337
- CO<sub>2</sub>, symmetric vibr. collision-induced IR absorpt. 4-87107
- CO<sub>2</sub> system, He-buffered, radiolytic dynamics 4-62217
- CO<sub>2</sub> TEA and continuous high power laser research and development at Battelle-Frankfurt 4-102944
- CO<sub>2</sub> TEA laser, beam expanding-grating plane cavity (*Chinese*) 4-107689
- CO<sub>2</sub> TEA laser, electron density of afterglow of pulsed discharge and UV photoionisation, meas. using microwave interferometer (*Chinese*) 4-87315
- CO<sub>2</sub> TEA laser, fine-tuned, high power, optical pumping, methanol FIR laser lines obs. 4-102918
- CO<sub>2</sub> TEA laser, injection locking studies for stable high-power operation 4-60014
- CO<sub>2</sub> TEA lasers, injection locked, transient freq. shift induced by electron density 4-102915
- CO<sub>2</sub> TEA lasers, miniature type, self modulation props. study 4-79202
- CO<sub>2</sub>, TEA lasers, multipass-prism interferometer for fine-freq.-turning, single-mode operation 4-107683
- CO<sub>2</sub> TEA repetitive tunable laser, long lifetime, without He (*Chinese*) 4-112377
- CO<sub>2</sub>, temp. and flow distrib. in self-sustained discharge, laser characts. 4-79104
- CO<sub>2</sub>, thermal averages, effective harmonic oscillator method appl. 4-112153
- CO<sub>2</sub>, thermal decomp. in Ar plasma jet 4-109631
- CO<sub>2</sub>, thermal diffusivity meas. using dynamic light scatt. (*German*) 4-65502
- CO<sub>2</sub>, thermally excited cascade laser, calc. of energy parameters, practical recommendations 4-107594
- CO<sub>2</sub> transverse flowing laser, gain coeff. meas. (*Chinese*) 4-60013
- CO<sub>2</sub> transverse-flow laser, 2.5 kW output 4-69446
- CO<sub>2</sub> transverse-flow laser vibrational and translational temp. determ. (*Chinese*) 4-112378
- CO<sub>2</sub> tunable coherent lidar for atm. aerosol backscatter and attenuation meas. 4-100763
- CO<sub>2</sub> tunable double wavelength laser study (*Chinese*) 4-91513
- CO<sub>2</sub> tunable high pressure RF excited laser 4-96938

## Carbon compounds continued

- CO<sub>2</sub> tunable high-power CW laser using compound cavity; individual transition selection 4-69366  
 CO<sub>2</sub> two-wave high-power laser 4-107684  
 CO<sub>2</sub> use in oil recovery from reservoir rocks 4-105092  
 CO<sub>2</sub> VIM theory of mol. thermodynamics, analytic eqns. of state 4-113283  
 CO<sub>2</sub> vapour press. meas. from 194 to 243K, sublimation and triple-point temp. 4-80208  
 CO<sub>2</sub> vibr. anal. photoelectron ang. distrib. 4-83416  
 CO<sub>2</sub> vibr. levels, spectrosc. consts., isotope effects 4-59711  
 CO<sub>2</sub> vibr. rot. bands in 540 to 890 cm<sup>-1</sup> region 4-64466  
 CO<sub>2</sub> vibrationally nonequilibrium 12-19 μm radiation calcs. 4-96545  
 CO<sub>2</sub> waveguide laser, continuously tunable, RF excited, high-press. 4-74542  
 CO<sub>2</sub> waveguide laser, freq. sweep stabilisation using inverted Lamb dip in NH<sub>2</sub>D 4-79098  
 CO<sub>2</sub> waveguide laser, RF discharge excited, freq. depend. 4-79099  
 CO<sub>2</sub> waveguide laser, RF discharge striations 4-79100  
 CO<sub>2</sub> waveguide laser design for max. output power at specified freq. offset 4-107679  
 CO<sub>2</sub> waveguide lasers, RF-excited sealed-off operation, Xe effects 4-96866  
 CO<sub>2</sub> working fluid in gas absorption power cycle 4-66745  
 CO<sub>2</sub><sup>+</sup> B<sup>2</sup>Σ<sub>g</sub><sup>+</sup> state, angle resolved photoelectron spectrum 4-64542  
 CO<sub>2</sub><sup>+</sup> C<sup>2</sup>Σ<sub>g</sub><sup>+</sup> state, photoion. shape reson., electron spectrosc. obs. 4-112236  
 CO<sub>2</sub><sup>+</sup> isolated ions, IR spectra quantitative prediction 4-69075  
 CO<sub>2</sub><sup>+</sup> laser induced fluorescence study 4-59832  
 CO<sub>2</sub><sup>+</sup> low-lying electronic states, linear and bent configs. 4-68980  
<sup>12</sup>C<sup>16</sup>O<sub>2</sub> Σ and II Fermi dyads in 4.5 μm region, wavenumbers, spectrosc. consts. 4-59745  
 CO<sub>2</sub>/OsO<sub>4</sub> waveguide laser with freq. stability of 10<sup>-13</sup> 4-79102  
 CO<sub>2</sub>-Ar gas proportional chamber, properties (Chinese) 4-68875  
 CO<sub>2</sub>-CO universal technological elec. ionisation laser 4-107665  
 CO<sub>2</sub>-H<sub>2</sub>O, optical generation and detection of acoustic pulse profiles for novel ultrasonic absorpt. spectroscopy 4-103460  
 CO<sub>2</sub>-He-N<sub>2</sub> electron-ion recombination 4-102794  
 CO<sub>2</sub>-hexane, excess molar enthalpies meas. 4-80236  
 CO<sub>2</sub>-SF<sub>6</sub> thermal diffusivity meas. using dynamic light scatt. (German) 4-65502  
 CO<sub>2</sub>-TEA laser, injection locking, effect of unstable resonator 4-87375  
 CO<sub>2</sub>+aniline, mode-to-mode energy transfer, fluoresc. 4-83450  
 CO<sub>2</sub>+CN, vibr. energy effect on reaction, laser meas. 4-99769  
 CO<sub>2</sub>+carbon tetrachloride, vibr. energy exchange probabilities 4-96667  
 CO<sub>2</sub>+DF, vibr. relax. rate consts. determ. using flow IR chemiluminesc. technique 4-89273  
 CO<sub>2</sub>+H<sup>-</sup> electron detachment and charge exchange to shape reson. 4-69203  
 CO<sub>2</sub>+HF(v=3, 4, 5), HF vibr. relax., fluoresc. study 4-69187  
 CO<sub>2</sub>+methane liquid mixtures, thermodynamic props. 4-70335  
 CO<sub>2</sub>+methanol gas mixture, molecular IR transitions, saturated absorpt. obs. 4-69150  
 CO<sub>2</sub>+O, translational-to-vibrational energy transfer, quantum mechanical calcs., basis set effects 4-74317  
 CO<sub>2</sub>+OH<sup>-</sup> (H<sub>2</sub>O)<sub>n</sub> reaction cross sections, translational energy depend. 4-76983  
 CO<sub>2</sub><sup>+</sup>+O<sub>2</sub> temp. depend. of reaction from 90-450K 4-76987  
 CO<sub>2</sub><sup>-</sup> radical, metastable states, unimolecular dissociation 4-76972  
 C<sub>2</sub>O<sub>2</sub><sup>+</sup> cation radicals, matrix isolated, EPR and ab initio investig. 4-74273  
 C<sub>2</sub>O J=2-1 19 GHz transition detection of interstellar molecule 4-94932  
 C<sub>2</sub>O<sub>2</sub> ligand core hole states, configuration interaction calcs. 4-83301  
 C<sub>2</sub>O<sub>2</sub> struct. and harmonic vibr. freqs., analytic derivative methods 4-96431  
 CO(J=2-1) survey of fourth galactic quadrant 4-94948  
 COS in stratosphere, meas. in El Chichon volcanic plume 4-105658  
 COS, mm-wave system for remote sensing acidic clouds and precursor gases in troposphere 4-77170  
 CO<sub>2</sub>, BF<sub>3</sub> van der Waals complex, microwave rot. spectrosc. obs. 4-78862  
 CS-Ar<sup>+</sup> emission spectra prod. from thermal energy charge transfer reactions 4-74325  
 CS<sub>2</sub> autoionisation, fluoresc. polarisation study 4-83402  
 CS<sub>2</sub> IR spectra of isotopic species 4-69065  
 CS<sub>2</sub> jet-cooled, B<sub>2</sub>(V)-Z<sub>g</sub>(X) transition, excitation and dispersed fluorescence spectra 4-64527  
 CS<sub>2</sub> liq. orientational pair correl. factors with interaction site formalism calc. 4-70009  
 CS<sub>2</sub> liq., self-focusing use for laser-induced damage prevention 4-79246  
 CS<sub>2</sub> multiphoton excitation, ionisation and photofragment fluoresc. 4-112241  
 CS<sub>2</sub> μ<sup>+</sup> state meas. by spin resonance methods 4-65932  
 CS<sub>2</sub> ν<sub>3</sub>-ν<sub>2</sub> band IR spectra, S isotope effects 4-87102  
 CS<sub>2</sub> optical nonlinear medium, spatial freq. generation 4-79232  
 CS<sub>2</sub> optical switching and n<sub>2</sub> measurements 4-87401  
 CS<sub>2</sub> optical waveguide, backward stimulated Brillouin scatt., mode and temporal characs. (Chinese) 4-112511  
 CS<sub>2</sub> polarization scrambling by the glass windows of a Raman cell up to 18 kbar 4-112187  
 CS<sub>2</sub> stimulated Raman scatt. ps pulse generation in an external cavity 4-83566  
 CS<sub>2</sub> subpicosecond Kerr effect 4-91545  
 CS<sub>2</sub> thermal averages, effective harmonic oscillator method appl. 4-112153  
 CS<sub>2</sub> tunnel generation and locking stimulated Raman radiation components 4-112515  
 CS<sub>2</sub> vibr. highly excited, UV spectra, dissociation energy 4-102695  
 CS<sub>2</sub> workers, trace element anal. of hair (Chinese) 4-72000  
 CS<sub>2</sub><sup>+</sup>, (A<sup>+</sup>-X<sup>+</sup>) emission prod. in Ar<sub>2</sub><sup>+</sup>+CS<sub>2</sub> charge transfer reactions in Ar afterglow 4-96552  
 CS<sub>2</sub><sup>+</sup> A and B states radiative lifetimes, single photon counting meas. 4-74293  
 CS<sub>2</sub><sup>+</sup> isolated ions, IR spectra quantitative prediction 4-69075  
 C<sub>3</sub>S<sub>2</sub> hydration products, obs. using cryo stage in SEM 4-71874  
 C<sub>3</sub>Si<sub>1-x</sub> amorphous film, elec. and optical props. 4-113962  
 CSiF<sub>2</sub> isomers, lowest singlet and triplet surfaces, ab initio calcs. 4-107424  
<sup>12</sup>C<sup>16</sup>O<sub>2</sub> and isotopic mols., laser transition intensity calc. 4-107593  
 CO, J=1-0 obs. of W51 molecular cloud complex 4-115806  
 CO and <sup>13</sup>CO, mapping in first galactic quadrant 4-63315

## Carbon compounds continued

- <sup>13</sup>CH<sub>3</sub>F far IR laser for microturbulence studies on TEXT Tokamak 4-75160  
<sup>13</sup>CN detection in galactic radioresources, EHF obs. 4-106072  
<sup>13</sup>CO, interstellar, J=1-0 obs. rel. to mean lifetime of mol. clouds (Chinese) 4-82543  
<sup>13</sup>CO emission from galactic disc in l=40°-60° range 4-63313  
<sup>13</sup>CO in interstellar molecular clouds, J=1-0 EHF obs. 4-67782  
<sup>13</sup>CO towards second galactic quadrant, mapping 4-63314  
<sup>13</sup>CO<sub>2</sub> laser frequency measurement chain to 30 THz using FIR Schottky diodes and submm. backward wave oscillator 4-73414  
<sup>14</sup>CO, vibr.-rot., pot. energy curves, IR spectra 4-59754  
 CS<sub>2</sub> laser-excited electronic fluorescence, quenching and self-quenching 4-69134  
 Co, condensed gas solids, electronically excited by fast light ions, nonlinear erosion yield 4-61804  
 Co, excitation in UV region, Raman scatt. cross section 4-107354  
 Co, near K-edge C is absorpt. spectra rel. to ionic fragmentation 4-96565  
 H<sub>2</sub> production, from water vapour and CO<sub>2</sub>, thermoradiation processes 4-93651  
 H<sub>2</sub>-CO mixtures for testing dissociated methanol engine 4-62290  
 H<sub>2</sub>-CO<sub>2</sub> in air, flammability and detonability in radioactive waste processing 4-106741  
<sup>3</sup>He-CO<sub>2</sub> mixture, <sup>3</sup>He numerical density on liquid-vapour boundary curve 4-70357  
<sup>3</sup>He-CO<sub>2</sub> mixture, coexisting phases near liquid-vapour transition (Russian) 4-88364  
 KBr:CN- solid-state vibr. laser, oscill. at 2054 cm<sup>-1</sup> 4-60045  
 KNCO:CN, shock-induced small mol. reactions, EPR studies 4-109655  
 Li/CF battery, electrochemical characs. 4-99955  
 N<sub>2</sub>-CO<sub>2</sub> laser mixtures, bulk discharge with ionisation multiplication of photoelectrons and light generation 4-97930  
 N<sub>2</sub>-CO<sub>2</sub> mixture, radiation amplification in continuous optical discharge plasma 4-84122  
 NCNN.BF<sub>3</sub> van der Waals complex, microwave rot. spectrosc. obs. 4-78862  
 NCO, electron impact dissociation of HNCO, UV emission spectra 4-107461  
 OCS, <sup>33</sup>S nucl. mag. shielding, chem. shift 4-102699  
 OCS, chem. shielding and shifts, <sup>17</sup>O NMR 4-102705  
 OCS, polarisability anisotropy, dipole moment, laser microwave double reson. 4-87146  
 OCS, rot. transitions and T<sub>2</sub> relax. 4-96525  
 OCS, S 2p core-level shape resonances, soft X-ray photoemission 4-96614  
 OCS, Stark effect measured by microwave Fourier transform spectroscopy 4-74278  
 OCS, vibr. rot. bands in 540 to 890 cm<sup>-1</sup> region 4-64466  
 OCS-He(Ar), rot. relax. rates for J=0-1 pure rot. transition 4-69185  
 OCS+aniline, mode-to-mode energy transfer, fluoresc. 4-83450  
 OCS+carbon tetrachloride, vibr. relax. studied by pulsed photoacoustic technique 4-87194  
 OCS+OCS(He)(Ar), IR linewidth meas., rot. levels, intermol. pot. 4-59764  
 a-Si<sub>3</sub>C<sub>4</sub>-H, low emittance coatings for high temperature solar collectors 4-114950  
 TiC as tokamak wall material, hydrogen recycling model calcs. 4-97870

## Carbon fibre reinforced composites

- eddy current equipment for aircraft maintenance 4-76943  
 epoxide matrix, hybrid composite, environmental response of flexural props. 4-76809  
 epoxy, laminates fatigue failure behaviour with edge notch 4-114669  
 epoxy matrix, acoustic emission evaluation 4-81380  
 epoxy matrix, angle-ply laminates, notch sensitivity 4-93386  
 epoxy matrix, tensile stress appl. parallel to fibres, elastic constants, failure (Japanese) 4-85199  
 epoxy matrix, tension appl. perpendicular to fibres, elastic constants, failure stresses (Japanese) 4-85200  
 epoxy matrix, unidirectional ultimate strength, influence of matrix resin 4-99455  
 epoxy matrix, unnotched laminates, fatigue and reliability evaluation 4-76846  
 epoxy matrix, vibr. damping parameters, prediction and meas. 4-80155  
 epoxy resin composites, conductivity and percolation 4-98679  
 glass-C hybrid fibre reinforced plastics, mech. props. 4-93407  
 graphic fibre reinforced epoxy, unidirectional, matrix cracking 4-74962  
 graphite fibre reinforced epoxy composites, thermomech. props., glass transition 4-92364  
 graphite fibre reinforced Al, interfacial strength meas. 4-99370  
 graphite fibre reinforced Al alloy, tensile strength rel. to gauge length 4-81239  
 graphite fibre reinforced epoxy, angle-ply laminates, long-term moisture absorpt. 4-76882  
 graphite fibre reinforced epoxy, anisotropic layered, singularities at tip of crack normal to interface 4-74952  
 graphite fibre reinforced epoxy, containing anisotropic fibres, calculated elastic consts. 4-75596  
 graphite fibre reinforced epoxy, delamination and transverse fracture 4-99577  
 graphite fibre reinforced epoxy, laminate, matrix crack growth, stochastic simulation model 4-74960  
 graphite fibre reinforced epoxy, laminated symmetric beams, damping and dynamic moduli 4-80154  
 graphite fibre reinforced epoxy, mixed mode fracture 4-99569  
 graphite fibre reinforced epoxy, orthotropic, elastic and photoelastic calibration, appl. of least squares method 4-69717  
 graphite fibre reinforced epoxy composites, buckling, hygrothermal and conditioning influence analysis 4-104810  
 graphite fibre reinforced epoxy laminate, elastoplastic response, finite element micromechanical analysis 4-87581  
 graphite fibre reinforced epoxy laminates, damage accumulation, final fracture rel. to ply thickness 4-81288  
 graphite fibre reinforced epoxy laminates, delamination, fracture mechanics 4-97431  
 graphite fibre reinforced epoxy laminates, fatigue loading damage accumulation, acoustic emission monitoring 4-81265  
 graphite fibre reinforced epoxy laminates, matrix crack growth, stochastic model 4-109506  
 graphite fibre reinforced epoxy laminates, onset of delamination, expt. and analytical study 4-76847

**carbon fibre reinforced composites continued**

- graphite fibre reinforced epoxy laminates, pin loaded holes, sizing methods, failure load 4-109507
- graphite fibre reinforced epoxy laminates, rail shear-strength, characteristic lengths 4-109478
- graphite fibre reinforced epoxy laminates, tensile failure, delamination fracture surfaces, SM obs. 4-66418
- graphite fibre reinforced epoxy laminates, thermal expansion behaviour, surface anisotropy 4-80269
- graphite fibre reinforced epoxy laminates, thermal expansion, effect of microcracks 4-80270
- graphite fibre reinforced epoxy laminates, three dimensional thermal stress distrib. 4-61943
- graphite fibre reinforced epoxy laminates, with circular holes, interlaminar stresses, effect of geometry 4-79447
- graphite fibre reinforced epoxy laminates containing pin loaded holes, failure prediction 4-109583
- graphite fibre reinforced Mg alloy, tensile strength rel. to gauge length 4-81239
- graphite fibre reinforced Ni composite electrode, concept and feasibility study 4-72065
- graphite fibre reinforced polyimide panels, high temp. fracture rel. to buffer strip use 4-62023
- graphite oxide fibres, produced by oxidation of C-graphite fibres 4-76740
- NDT, thermal method for inspecting large parts 4-71838
- plastic laminates, compression fatigue rel. to anti-buckling guides 4-89099
- plastic laminates, fault detection by X-ray NDT (*German*) 4-99693
- plastic laminates, rigidity and strength (*Japanese*) 4-99431
- plastic matrix, damage susceptibility estimation, thermodynamic approach 4-99542
- plastic matrix, generalised fatigue curve parameter estimation 4-89109
- plastic matrix, hybrid composite, unidirectional fibre, amplitude distrib. AE signatures 4-89198
- plastic matrix, impact stability evaluation 4-89129
- plastic matrix, struct. during pressure and temp. changes 4-89088
- plastic matrix, three-layer shells, stress-strain state 4-89091
- plastic matrix laminate, uniaxial tension, stress-strain diagram (*Japanese*) 4-97417
- polyester matrix, hybrid composites, flexural and fracture props. (*Japanese*) 4-99429
- polyester matrix, hybrid composites, interlaminar shear strength (*Japanese*) 4-99430
- polyimide matrix, fracture and elastic props., influence of 4-99572
- polymer based, thermal testing of struct. and mech. props. 4-85268
- stagnation-point boundary layers, injection induced turbulence 4-64932
- thermoplastic matrix, creep resistance, fatigue endurance 4-61994
- C fibre reinforced plastics, generalised fatigue curve parameter estimation 4-89109
- C matrix, pitch derived, microstruct. rel. to solvent fractionation 4-109336
- C matrix multidirectional composites, book contrib. 4-66296
- C-C fibre composites, thermal conductivity below 80K 4-97287
- C-C-TiC composite materials obtained by CVI of porous C-C substrates 4-71595

**carbon fibres**

- see also carbon fibre reinforced composites*
- activated C fibre fabrics appl. to electrodes of rechargeable battery and organic electrolyte capacitor 4-99957
- benzene derived, in-plane thermal cond., temp. variation 4-75739
- electrodeposition of metals after cation-exchange, catalysts appl. 4-76701
- field emission microscopy and mass spectrometry anal. 4-66196
- graphite fibres, intercalated, for electrical power transmission appl. 4-80562
- large area woven fibre cathodes 4-99802
- tubular growth of filaments 4-93245

**carbon microphones *see* microphones****carbon steel**

- acid corrosion inhibition by benzotriazole 4-81351
- acoustoelastic coeffs. of Rayleigh waves, US obs. 4-114733
- annealed, comparison of rotating bending and plane bending fatigue (*Japanese*) 4-89121
- bar sorting, two parametric eddy current method 4-71833
- boronising, electrolytic, boride phase form. kinetics 4-71781
- brass-steel galvanic couple, corrosion, polarisation study 4-85245
- butt-welded joint, welding stress and distortion (*Japanese*) 4-99424
- cast, fatigue, const. and variable amplitude, room temp. and -45°C 4-99551
- cast, fracture toughness, Charpy V notch test 4-99560
- cast and wrought, H induced ductility losses, annealing effects 4-85193
- cavitation erosion, decontamination of surfaces (*French*) 4-70222
- Charpy V notch impact testing with laser glazing pre-cracking 4-99681
- cold forging, materials testing 4-99714
- constructional, cyclic creep in plane stressed state, life determ. 4-99446
- constructional, strengthening using thermomech. treatment and deform. in intercrit. temp. range 4-114585
- corrosion, atm., influence of pollution, humidity, temp., solar rad. and rainfall 4-85244
- corrosion fatigue under cavitation erosion generated intermittently in salt water 4-114727
- corrosion inhibition by quaternary  $\text{NH}_4\text{Cl}$  with alkylthiomethyl radical 4-85255
- corrosion inhibition in NaCl soln. by aniline and derivatives 4-114725
- corrosion testing in PWR steam generator 4-59333
- crack growth and closure under impact fatigue 4-114630
- crevice corrosion electrochemical meas. (*Japanese*) 4-89201
- cylinder, cathodic protection in seawater, effects of flow 4-71769
- diffusion bonding below  $A_1$  transform. point, heat treatment effect on tensile strength (*Japanese*) 4-66547
- dual phase, Mn conc. profiles, EDAX obs. 4-71827
- dual phase, necking and tensile fracture, void distrib. 4-99580
- dual-phase, C-Mn, mech. props. and fracture mechanism, influence of martensite morphology 4-99530
- dual-phase, ferrite-martensitic struct., strength law 4-99399
- dual-phase, Mn-C, tensile behaviour and fracture characteristics 4-99598
- dual-phase, tempered, fracture behaviour 4-89127
- electric spark alloying, TiB, struct. influence 4-62121
- electric spark alloying with TiN-Cr, reinforced layer microhardness and comp. 4-89192

**carbon steel continued**

- electroerosion alloying with W, C influence on surface layer form. 4-114714
- emission spectrochem. anal. appl. of Grimm lamp (*Japanese*) 4-62272
- etching with  $\text{FeCl}_3$  4-76970
- etching with  $\text{Fe}(\text{ClO}_4)_3\text{-HClO}_4$  and with  $\text{Fe}(\text{H}_2\text{O})_6^{3+}$ , etching kinetics 4-76969
- eutectoid, mech. props., effect of Si additions 4-93365
- eutectoid, rail, fatigue behaviour 4-66412
- fatigue behaviour, influence of compressive mean stresses (*German*) 4-81284
- fatigue crack propagation by crack-tip plastic blunting 4-71719
- fatigue crack propagation rate, correl. with J-integral or crack opening displacement (*Japanese*) 4-114649
- fatigue damage under const. amplitude biaxial loading 4-99481
- fatigue strength, statistical analysis of S-N data (*Japanese*) 4-99500
- fatigue strength of butt welded joints with different plate thickness, stress relief effect 4-62011
- fatigue strength rel. to cold surface rolling press. (*Japanese*) 4-99514
- ferritic-pearlitic, fatigue, inelastic strain and mag. noise 4-114664
- ferrous laminated composites, steel/Fe, superplasticity 4-81235
- fracture form, shock wave exit angle effect on free surface 4-99498
- fracture toughness, stretch zone, ductility, transition region 4-99468
- high C, electric spark alloyed with refractory carbides, surface struct. 4-66503
- high C, fatigue crack growth retardation by massive eutectic carbides 4-99586
- high C, intermetallic phases formed by Sn ion implantation 4-92225
- high C, melt spun ribbon, microstructure, TEM obs. 4-81186
- high C, surface hardening by laser, technological control of surface condition parameters 4-71779
- high strength, H cracking parameters for predicting safe welding conditions 4-66404
- high tensile strength, fatigue crack growth and closure in vacuum (*Japanese*) 4-93381
- high-C tool, struct. of hardening martensite and change during low-temp. tempering 4-114583
- impact bending test, specimen shape and dimensions effect (*Japanese*) 4-99689
- laser glazed hot rolled Charpy samples, impact testing 4-81377
- laser treatment, residual stress distrib., optimum surface hardening conditions, 45 and U10 steels (*Russian*) 4-71774
- low and medium strength, crack resist. 4-62034
- low C, abnormal grain growth, decarburization treatment 4-71663
- low C, Al clad, reaction diffusion, intermetallic layer growth kinetics 4-114722
- low C, Al killed, decomp. of Mn-C dipoles during quench ageing, resist. obs. 4-71661
- low C, Al-killed, reversion and subsequent re-age-hardening 4-93308
- low C, AlN precip. identification using EELS (*French*) 4-76938
- low C, brittle fracture, fractographic characteristics, test temp. effects (*Russian*) 4-109495
- low C, carbide precip. during ageing treatments 4-114531
- low C, cold rolled, initial stage of decarburisation 4-114577
- low C, corrosion, effect of P ion implantation 4-99637
- low C, corrosion behaviour in formic and acetic acid 4-81329
- low C, deep drawing cold-rolled sheet prod. by continuous annealing, control of steel chem. 4-114565
- low C, deep-drawing, prod. by continuous annealing 4-114566
- low C, dual-phase, continuously annealed, effect of prior cold rolling 4-66350
- low C, ductile-brittle transition temp., effect of tensile prestrain (*Japanese*) 4-114650
- low C, fatigue crack initiation rel. to annealing and prestressing (*Japanese*) 4-99517
- low C, fatigue crack retardation in saltwater 4-99552
- low C, hot shortness in controlled rolling process, effect of Cu 4-89105
- low C, Mn, austenite form-mechanism during annealing 4-85151
- low C, nitrocarburising, annealing, positron annihilation, vacancy-impurity clusters in surface layer 4-66094
- low C, nitrocarburising, annealing, yield stress, brittle-ductile fracture transition 4-66384
- low C, notched, fatigue threshold prediction 4-99559
- low C, notched fatigue strength rel. to pre-straining and nitriding 4-109489
- low C, polycrystalline plasticity, self consistent relation with nonuniform matrix 4-112729
- low C, quenched, precip. kinetics 4-99394
- low C, rolling contact fatigue rel. to Tufftriding treatment 4-109517
- low C, shear band form., temp. meas. 4-99453
- low C, strain hardening behaviour, statistical anal. 4-99403
- low C, wear of Al alloy 4-114688
- low-C, structural changes during damage by surface friction 4-93424
- low-C cast, cyclic crack resist., heat treatment influence 4-62035
- magnetostriiction rel. to plane stressed state 4-71152
- mechanical properties, effect of laser quenching 4-66356
- medium C, corrosion in aq. soln. containing fluoride ions at 300°C 4-85246
- medium C, ductility anisotropy 4-60301
- medium C, H-assisted cracking after exposure to  $\text{H}_2\text{S}$ -saturated salt soln., role of MnS inclusions 4-71732
- medium C, heat treated, fatigue behaviour, overstress effects 4-62007
- medium C, laser hardening 4-114563
- medium C, short crack fatigue behaviour 4-66410
- mild, boronized pins, dry sliding wear against tool steel disc 4-114685
- mild, C-Mn, Charpy V transition temp. rel. to various material parameters 4-66431
- mild, corrosion inhibition by molybdate 4-99635
- mild, corrosion inhibition in HCl solns. by carbonyl compounds 4-104901
- mild, corrosion kinetics in  $\text{H}_2\text{SO}_4$ , thiourea inhibitor efficiency 4-89159
- mild, corrosion of plates after 20 years in New Zealand soil. 4-99655
- mild, corrosion rate in soil, IR spectra 4-109542
- mild, creep at low temp. 4-89086
- mild, cyclic creep, relationship with hysteresis loop energy 4-109456
- mild, electrodes in  $\text{H}_2\text{SO}_4$ , adsorption of thiourea 4-88390
- mild, epoxy coated, polymer-metal adhesion, appl. of X-ray photoelectron spectroscopy 4-93485
- mild, fatigue fracture, X-ray fractography (*Japanese*) 4-89123
- mild, fretting fatigue rel. to diffusion coatings from Ni-Co electrodeposits 4-114686

# carbon steel continued

- mild, H ion implanted, in H<sub>2</sub>S-free and H<sub>2</sub>S-saturated HCl, effect of acid inhibitors (*German*) 4-76897
- mild, H absorb. in H<sub>2</sub>S-saturated formic acid, effect of acid inhibitors (*German*) 4-76898
- mild, laser cavity power increases caused by reflections from workpiece surfaces 4-91519
- mild, N ion implanted, wear and friction 4-66459
- mild, panels, surface damage due to projectile impact 4-76865
- mild, plastic flow, strain hardening, changing deform. paths 4-104821
- mild, plate with small circular hole, fatigue crack propag., fracture mechanisms (*Japanese*) 4-62025
- mild, renitrogenised, cyclically deformed, prep. of thin foils for TEM 4-89233
- mild, SCC in NaH<sub>2</sub>PO<sub>4</sub> soln., effect of heat treatment and C 4-89167
- mild, sheet, axisymmetric deform., thickness effect 4-99449
- mild, Ta CVD coatings microstructure 4-71802
- mild and dual phase, post biaxially strained, residual ductility 4-104823
- mild SCC under compressive stress 4-85261
- normalised 04G2B, V additions effect on mech. props. 4-93390
- pearlitic, upper bainite varieties 4-114537
- phase identification and anal. using SIMS (*French*) 4-76936
- plastic properties, effect of nonlinear strain paths 4-99474
- plastically deformed, oriented microstresses depend. on external load direction (*Russian*) 4-93332
- plate, laser melted surface, microstruct., hardness, residual stress 4-71794
- plate, projectile impact strength critical fracture energy 4-99477
- powder metallurgical, elec. cond., thermal cond. and thermal expansion, temp. depend. 4-65658
- powders, rotating electrode process atomisation mechanisms 4-89001
- pressure vessels, steel, corrosion fatigue, development of engineering codes 4-93406
- pulsed mag. field influence on martensitic transform. (*Russian*) 4-81194
- PWR steam generators, denting causes, nonprotective magnetite prod. 4-104924
- quenching by water-air jet 4-97643
- rails, mixed fatigue-tensile surface crack growth 4-89100
- rimmed and killed, cavitation erosion resist. rel. to heat treatment and deoxidation (*Japanese*) 4-89138
- rolled, impact toughness and transition temp., effect of delamination (*Korean*) 4-76848
- SCC, simulated cracks, current and pot. meas. 4-104904
- sheet, continuous annealed cold-rolled, overaging treatment and ductility, interstitial atom supersaturation (*French*) 4-89096
- siliconised, diffusion layer formation, metallography 4-114721
- spheroidized 1090, dislocation density distrib. in tensile specimens, H effect 4-84298
- strain aging equivalent rule, hardness obs. 4-76790
- structural, fatigue fractured surfaces, residual stress, X-ray diff. (*Japanese*) 4-99513
- structural, tensile deform., ductile fracture, void nucleation 4-99426
- surface hardening by laser treatment 4-81337
- surface hardening using transversely-excited flowing CO<sub>2</sub> laser (*Chinese*) 4-62104
- surface laser hardening, struct. and property study (*Chinese*) 4-62105
- surface saturation by Cr and Ti by circulating method (*Russian*) 4-81339
- tempered, radial direction fracture surface, SEM obs. (*Japanese*) 4-89115
- torsional fatigue crack, nonpropagating phenomena (*Japanese*) 4-99549
- transformation kinetics, phenomenological approach, T-T-T and C-C-T diagrams 4-93291
- twin diffraction effects from body centred tetragonal martensite 4-65274
- US props., higher-order, influence of C content, rel. to residual stress determ. 4-99730
- wire, rolled, martensite content, microstructural stresses, EM NDT (*German*) 4-99695
- wires, stress relax., influence of work hardening (*French*) 4-81230
- yield stress rel. to C content and pearlite morphology, tensile and Charpy obs. 4-81248
- C redistribution by explosion-thermal treatment 4-71673
- C-Mn, fracture toughness studies in different regions of weld heat affected zone 4-76838
- C-Mn, grain boundary segregation of Cu, Sb and Sn at 900°C 4-93300
- C-Mn, hot-rolled, ductility and anisotropy of sulphide inclusion spacings, effect of inclusion shape 4-99437
- C-Mn, low temp. creep crack growth, effect of cold work 4-76850
- H<sub>2</sub> evolution reaction, in alkaline media 4-93533

# carbon tetrachloride, CCl<sub>4</sub> see organic compounds

# carbonitriding see surface hardening

# carburising see surface hardening

# carcinotrons

- Cherenkov relativistic electron RF sources, cyclotron reson. mode selection 4-69299

# cardiology

## see also blood; electrocardiography; haemodynamics

- action potential, circuit for max. rate of rise meas. 4-77432
- action potential generation, after the 1st ms 4-77220
- action potential sequential processing 4-81829
- action potentials, propag. along nerve axons and cardiac strands, resistive barrier effects 4-89538
- activation sequence effects simulation in heart tissue 4-81663
- anisotropic cardiac muscle, bidomain model 4-77222
- anisotropic two-dimensional cardiac tissue, propag. of excitation 4-89540
- aortic bifurcation geometry, changes during a cardiac cycle, rabbit obs. 4-115110
- arteries, elastic props. and their influence on the cardiovascular system 4-109870
- artificial and assist devices, adaptive control strategies 4-89838
- artificial heart, mag. actuated, ventricular kinetics 4-85579
- artificial heart and lung machines, review (*Japanese*) 4-110000
- artificial hearts, design problems and solutions found at Utah University 4-62632
- artificial hearts, review (*Japanese*) 4-110004
- artificial hearts and cardiac surgery 4-105374
- artificial organs and their materials, review (*Japanese*) 4-89831
- assist pump, motor-driven, with implanted compliance chamber: in vivo experience 4-89836
- assist pump applied to cardiovascular system, optimal driving conditions (*Japanese*) 4-93968

# cardiology continued

- assisted circulation and ventricular assist devices, review (*Japanese*) 4-110003
- atrial flutter, gated blood-pool study, Fourier anal. 4-72371
- automatic recording of biological model variables (*German*) 4-77419
- blood flow, max. vels., noninvasive CW Doppler haemodynamic data, intracardiac jets 4-85467
- blood vessels, mech. strength props. functional diagnostics 4-89636
- cardiac tissue characterisation, stochastic approach to RF amplitude anal. 4-105302
- cardiopulmonary resuscitation, blood flow, thoracic and abdominal press. waves effect 4-115100
- cardiopulmonary resuscitation mechanisms: a computer model 4-89641
- cardiopulmonary resuscitation system based on intrathoracic and abdominal press. variations 4-89826
- cardiovascular cine film quality 4-89699
- cardiovascular response to lower body negative press. and phys. fitness 4-89628
- cardiovascular system exercise adaptation in pilots breathing O<sub>2</sub>-poor gas mixture, haemodynamic parameters 4-66972
- cardiovascular system exercise adaptation in pilots breathing O<sub>2</sub>-poor gas mixture, polycardiographic parameters 4-66973
- catheter input impedances computation for cardiac volumetry 4-85532
- central haemodynamics, age-associated features, radiocardiographic obs. (*Russian*) 4-93770
- chemiluminescence, ultraweak, monitoring of emission from rat hearts 4-93979
- conference, New Orleans, USA (April 1982) 4-73136
- coronary angioplasty, fluoroscopic image quality requirements 4-89707
- coronary artery imaging with a computerized linear diode array radiographic system 4-85512
- coronary circulation, flow dynamics (*Japanese*) 4-62517
- coronary circulation study, differential registration of two types of radionuclides on macroautoradiograms 4-72370
- coronary grafts, blood flow visualisation by US method 4-100264
- coronary venous system, dog, dynamics 4-62513
- CT, cardiac reconstruction, conf., Santa Cruz, USA (Aug. 1983) 4-63383
- current flow patterns in 2D anisotropic bisyncytia 4-89559
- defibrillation with 10 ms trapezoidal waves of different tilts, efficacy and safety 4-81812
- didactic microcomputer simulation in cardiac dynamics 4-81737
- digital radiography developments, limitations and clinical results 4-115212
- disk-type prosthetic heart valve, turbulent flow through 4-77293
- diver decompression sickness, heart and lung injury evaluation 4-109871
- dura mater, glycerol-preserved, human, mech. suitability for prosthetic cardiac valves construction 4-62506
- echocardiograms, 2D, effective algorithm for extracting serial endocardial borders 4-85460
- echocardiograms of left ventricle, computerized 3-D finite element reconstruction 4-100272
- echocardiography, CW and pulsed Doppler, utilising a stand-alone system 4-85466
- electrical activity of the heart, implications of struct. and geometry 4-77219
- electrical propagation in cardiac muscle, discontinuous nature, quantitative model 4-73131
- electrical propagation in cardiac muscle, modelling 4-89554
- electrocardiology, oblique double layer potentials for direct and inverse problems 4-89546
- electronics appls. to heart 4-115253
- electrophysiological studies, software control of sensing and stimulation 4-85538
- EM radiation in dm wave range, effect on myocardium cell membranes (*Russian*) 4-77306
- embryonic chick heart cells, channel currents during spontaneous action pots. 4-105219
- embryonic heart cell aggregates, phase resetting of rhythmic activity 4-66908
- Fourier domain techniques for digital angiography of the heart 4-109905
- gated cardiac imaging: manual calcs. and obs. of left ventricular ejection fraction 4-67108
- gated cardiac imaging with NMR techniques 4-105322
- heart-rate monitors, evaluation of portable units 4-85569
- heart-sound processing, statistical approach 4-89664
- heart-sound processing by average and variance calc., physiological basis and clinical implications 4-115148
- intraaortic balloon pumping as cardiac assistance: simple, closed loop model 4-89827
- intraoperative US during heart surgery 4-93829
- laser blood Doppler velocimeter, temporal resolution estimation with optical fiber 4-66989
- laser method for heart and chest wall displacement recording 4-62550
- left ventricle, 3D images generated with dynamic spatial reconstructor 4-85513
- left ventricle, 3D reconstruction from 2D echocardiograms (*Japanese*) 4-100267
- left ventricle, absolute vol. determ. by iterative build-up factor anal. of gated radionuclide images 4-81776
- left ventricle, computerised model for reconstruction from cineventriculogram 4-89740
- left ventricle, parametric pictures of intravenous angiograms (*German*) 4-72400
- left ventricle, simulated emission CT using rot. slant-hole collimator and two camera positions 4-67092
- left ventricular assist device, motor-driven, digital vel. feedback control 4-89835
- left ventricular assist devices, adaptive control 4-89844
- left ventricular contraction model; force length vel. relationship, time varying elastance 4-89612
- left ventricular ejection, dynamical relations: flow rate, momentum, force and impulse 4-100219
- left ventricular regional motility anal., comparison of different methods 4-89722
- left ventricular vol. determ. count-based, utilising a left posterior oblique view 4-62582
- left ventricular volume, estimates from blood-pool counts, repeatability 4-72372
- left ventricular volume, estimation by equilb. radionuclide angiography 4-81771

## cardiology continued

left ventricular wall motion, evaluation from cineangiograms, comparison of geometrical models 4-109904  
 left ventricular wall motion analysis using operator-independent contour positioning 4-62557  
 left-ventricular ejection fractions from gate equilib. blood pool scintigrams, automated computation 4-72384  
 left-ventricular function diagnosis, computer-aided evaluation of cineangiograms 4-105331  
 LV ejection and relaxation, coupling, dog expts. 4-85455  
 magnetically actuated left ventricular assist device 4-89837  
 mammalian cardiac cells,  $K^+$  channel activation by intracellular  $Na^+$  4-77214  
 mechano-mathematical model of excitation-contraction coupling in muscle tissue, cardiac appl. 4-109853  
 medical imaging with synchrotron radiation, detection of coronary artery disease 4-93956  
 microwave effects on beating rate of isolated frog hearts 4-100249  
 models for cardiac anal. (Japanese) 4-89488  
 multichannel signal processing based on logic averaging, His-Purkinje system activity appl. 4-85534  
 muscle excitation sequence determ., evaluation of method using 2 extracellular waveforms 4-115043  
 muscle of heart, intercalated discs as a cause for discontinuous propag. 4-77221  
 myocardial  $^{201}Tl$  emission tomography, coronary artery disease localisation 4-81767  
 myocardial blood flow and metabolism, digital film autoradiography and electronic multitracer techniques 4-77377  
 myocardial emission CT using  $^{99m}Tc$ -pyrophosphate, rel. to planar imaging 4-81768  
 myocardial material mechanics, systolic moduli variation in left ventricular dysfunction 4-115105  
 myocardial perfusion,  $^{82}Rb$  positron emission CT, extraction fraction and flow meas. 4-72378  
 myocardial perfusion changes imaging, double-dose technique, evaluation in dogs 4-100312  
 myocardial scintigraphy using  $^{201}Tl$ , ECG-gated, rel. to imaging time 4-81765  
 myocardial tissue characterization, US quantitative backscatter and attenuation 4-100281  
 myocytes, rat, passive stiffness obs. 4-100101  
 NMR imaging, pot. hazards, mag. fields rel. to cardiac function in animals obs. 4-105317  
 nuclear cardiology advances 4-115200  
 open-heart surgery, practical approach to epicardial mapping 4-93959  
 output, single thermistor system for continuous meas. 4-81809  
 output of heat and skin AVA activity, redistrib. in sheep during exercise and heat stress 4-81632  
 phantom for evaluation of multigated radionuclide studies 4-72391  
 phonocardiograms, pole-zero modelling and classification 4-85461  
 pig tissue,  $^{23}Na$  NMR study 4-100081  
 pneumatic artificial ventricle, haemodynamic models 4-93971  
 pneumatic total artificial heart, new driver, in vitro testing 4-67149  
 prosthetic aortic valve, orientation rel. to arterial flow distrib. 4-109869  
 prosthetic heart valves, haemodynamic modelling 4-100356  
 prosthetic heart valves, in vitro press. drop results comparison 4-81814  
 prosthetic heart valves, instrum. for sound anal. 4-85582  
 prosthetic heart valves, pulsatile press. drop and regurgitative characts., online method for evaluation 4-81813  
 Purkinje fibre, cardiac, Ca channel blockade, photoeffect 4-81647  
 Purkinje fibre, delayed rectification, rel. to intracellular  $Ca^{2+}$  4-66933  
 Purkinje fibre, impulse functions of automaticity 4-66934  
 radiographic feature enhancement, information content and dose reduction 4-81782  
 radioisotope imaging of the heart 4-72413  
 radionuclide cardiovascular diagnosis, micro-based system 4-109925  
 radionuclide curves, 1st-transit: discrete-time, lumped-parameter math. model 4-89739  
 radionuclide determination of cardiac outputs and indices 4-67081  
 rate-pressure prod. computer, microprocessor based 4-81808  
 real-time digital angiocardiology using a temporal high-pass filter 4-81778  
 right atrium contractility, nonlinear model for estimation 4-89642  
 right-ventricular function, evaluation by gated blood-pool scintigraphy 4-72377  
 sarcoplasmic reticulum, unidirectional Ca and nucleotide fluxes 4-89531  
 second sound, spectral anal. in normal children by selective linear prediction coding 4-77353  
 semilunar valve vibr., math. study, rel. to 2nd heart sound prod. 4-115111  
 serial tomographic images, meas. of regional tissue and blood-pool radioracer concs. 4-72380  
 short-duration transients, effect on cardiac rhythm 4-77224  
 single photon emission CT, myocardial phantom, uptakes quantification, sources of overestimation 4-105333  
 spectral analysis of heart sounds, phys. characts. rel. to freq. spectra in normals and hypertensives 4-62539  
 spinal cord, thoracic and lumbosacral, effects of selective thermal stimulation on cardiovascular functions in rats 4-81626  
 thermal dilution technique for continuous meas. of cardiac output 4-81794  
 tomoflow system for intracardiac blood flow information display, Doppler US appl. 4-85469  
 total artificial heart, development, pulsatile vs. nonpulsatile flow, control algorithm 4-93972  
 transvenous coronary angiography, synchrotron radiation imaging system 4-93957  
 tricuspid regurgitation, quantitative evaluation by digital simulation of cardiac time-activity curves 4-67080  
 trileaflet heart valve prosthesis, Abiomed, in vitro fluid dynamic characts. 4-105378  
 US echo cardiography, double frequency bubble diagnostics 4-100287  
 US pictures, automatic discovery of contours (German) 4-67053  
 valve bioprostheses, blood analog for in vitro testing 4-110008  
 valve prostheses, review (Japanese) 4-110002  
 valvular calcification and press. drops across malfunctioning heart valves, quantitative determ. 4-81801  
 ventricles in diastole, incremental elastic modulus 4-115109  
 ventricular defibrillation, coeffs., of variation of 2 random variables 4-85400

## cardiology continued

ventricular performance in congenital left-to-right shunt: temporal Fourier analysis of gated blood-pool data 4-72376  
 ventricular repolarisation assessment by pot. mapping 4-89806  
 volumes and outputs, quantitative evaluation by  $^{99m}Tc$  labelled erythrocytes 4-77379  
 Walsh-Hadamard transform: an alternative of obtaining phase and amplitude maps 4-89729  
 X-ray cineangiograms, left ventricular, computer-aided anal. (Japanese) 4-67118  
 Na/K pump of cardiac cells, book contrib. 4-93725  
 $^{239}Pu$  submicron dioxide inhalation, haemodynamics and heart mass parameters in dogs (Russian) 4-67014  
**carrier avalanches** see impact ionisation  
**carrier concentration** see carrier density  
**carrier density**  
 see also current density; electron density; electron density (metals)  
 amorphous semiconductor, dispersive transport, multiple trapping model, effect of energy depend. capture cross section 4-70830  
 chalcogenide glass thin films, threshold switching effects 4-92769  
 channel-guide structures, single-stripe, anal. of closely-spaced index-guided semicond. lasers 4-69411  
 direct gap semicond., stochastic self-oscillations in two-temp. electron-hole plasma 4-98656  
 extrinsic semiconductor, drift intervalley ambipolar instability 4-104231  
 ferroelectric semicond., heavily doped, inhomogeneous state stability conditions and struct., linear approx. 4-71286  
 graphite fibres, benzene derived, transverse magnetoresistance study 4-108844  
 Hall voltages changes at high temp. meas., using AC meas. system 4-58866  
 hot electron problem, quantum field theory 4-65685  
 Hubbard, ferromagnet, narrow-band, carriers in spin wave range of temps. 4-92887  
 I $^2$ V device circuit model with layout patterns 4-104192  
 III-V semiconductor lasers, threshold current, temp. dependence 4-79132  
 III-V semiconductors, thermochemistry study of deep level defects 4-75894  
 indirect gap semiconductor, recombination in electron-hole droplets 4-70832  
 InP:Zn epitaxial layers, MOCVD grown, doping, Hall effect, SIMS, electrochemical profiling 4-80077  
 n-InSb, photoconductivity and hole trapping centre capture coeff., press. studies 4-98668  
 insulator with deep traps in carrier density dependent mobility regime, cylindrical current flow 4-98629  
 MIS structures, multicomponent, charge transport eqn. soln. using effective carrier density 4-65754  
 MOS capacitor characts., influence of Si substrate thickness and barrier height of back contact (Chinese) 4-114039  
 MOS solar cells, perform. calcs. at various temps. 4-72117  
 multistripe devices, anal. of closely-spaced index-guided semicond. lasers 4-69410  
 narrow-band mag. semicond., at operator representation 4-75961  
 one-impurity level model and carrier density temp. depend. (Russian) 4-98560  
 p-n heterojunctions, boundary conditions for excess minority carrier conc. at space charge region edges 4-88569  
 p-n junctions, space charge layer capacitance, analytical approximation 4-108935  
 PbTe:Bi, Hall study of self-compensation of donor effect 4-104242  
 polyacetylene; $_2$  ( $AsF_6$ ), millimeter-wave and far IR cond. 4-70850  
 polymer dielectrics, fast electron irradi., space-charge storage 4-71280  
 polymer films, elec. cond. changes induced by pyrolysis and high energy ion irradi. 4-75966  
 s-f model in zero bandwidth limit, complete analytical soln. 4-76101  
 semiconductor, IR flow detector, for free-carrier conc. determ., using cholesteric liq. crystals 4-89211  
 semiconductor film picosecond laser, chirp, passive pulse compression in optical fibres 4-107700  
 semiconductor isotype heterojunctions, C-V doping profiles anal. 4-75496  
 semiconductor polycrystalline thin films, with pot. barriers, Hall mobility 4-104331  
 semiconductor quantum wells, screened Coulombic impurity bound states 4-108917  
 semiconductor-ferrite interface, oblique magnetostatic surface waves 4-80752  
 semiconductor-metal contacts, Schottky barrier photosensitivity spectra in strong absorption region (Russian) 4-65741  
 semiconductors, carrier distribution, capacitance-voltage profiling methods, review 4-75494  
 semiconductors, charge carrier transfer and diffusion in strong mag. field (Russian) 4-88520  
 semiconductors, compensated, exclusive effect quenching under action of impurity illum. generating majority current carriers 4-104262  
 semiconductors, current-controlled nonequilib. processes, overview 4-92747  
 semiconductors, dopant and carrier conc. profiling, conf., London, England (May 1984) 4-73171  
 semiconductors, electrochemical carrier conc. profiling, review 4-75495  
 semiconductors, electrolytic Schottky-gated Hall effect profiling 4-75497  
 semiconductors, Hall effect in strong mag. field, percolation theory 4-88522  
 semiconductors, high resistivity, acoustoelectric interactions 4-104274  
 semiconductors, impurity profiling by SIMS, review 4-75500  
 semiconductors, locally-varying photoconductivity, visual indication 4-80622  
 semiconductors, nonuniformly doped, C-V profiling theory 4-65290  
 semiconductors, shallow donors, self-oscils. and flip-flop effect 4-108848  
 semimetallic thin wires, semimetal semicond. transition due to quantum freeze-out of carriers 4-92833  
 n-Si, radiation defect formation, annealing, defect interactions 4-113499  
 solid solutions, quaternary III-V cpd. system, optical and elec. props. 4-84929  
 spatially inhomogeneous samples, de Haas-van Alphen effect 4-113849  
 stripe geometry lasers, self-consistent model based on beam propagation method, carrier diffusion eqn. 4-112438  
 subpicosecond hot electron transport, many-body effects for high carrier density 4-108867  
 two dimensional electronic systems, cond. near mobility edge 4-80682

## carrier density continued

- AlGaAs LED, radiative, and nonradiative, recombination rates, meas. 4-112434
- AlGaAs/GaAs heterostruct., 2D magnetotransport, electron heating effects 4-98736
- n-AlGaAs/GaAs selectively doped heterojunctions, high mobility electron gas 4-80657
- Al<sub>1-x</sub>Ga<sub>x</sub>As MBE layers, free carrier conc., Raman scatt. study 4-84970
- Al<sub>1-x</sub>Ga<sub>x</sub>As, Si donor behaviour, effect of Al comp. 4-98709
- Al<sub>1-x</sub>Ga<sub>x</sub>As:Te(Sn) epitaxial films, carrier density changes due to band struct. modifications 4-61381
- Al<sub>1-x</sub>Ga<sub>x</sub>As/GaAs heterostructure, selectively doped, transient photocond. obs. 4-70862
- Al<sub>1-x</sub>Ga<sub>1-x</sub>As-GaAs double heterostructure, optically pumped laser 4-96888
- AlGaSb, LPE, substrate treatment optimisation, carrier conc., Raman spectra, photoluminesc. 4-93235
- Bi<sub>1-x</sub>Sb<sub>x</sub>, composition influence on electron scatt. intensity 4-88518
- Cd<sub>1-x</sub>Sb<sub>x</sub>, single cryst., magnetoresist. in transverse quantising mag. fields 4-98643
- C film, elec. cond. changes induced by pyrolysis and high energy ion irradi. 4-75966
- p-Cd<sub>0.7</sub>Hg<sub>0.3</sub>Te, hopping cond. between intrinsic defects 4-104210
- p-Cd<sub>1-x</sub>Hg<sub>x</sub>Te, photoconductivity and photomagnetic effect 4-104268
- Cd<sub>1-x</sub>Hg<sub>x</sub>Te solid solutions, homogeneity, carrier conc., magnetic circular dichroism, temp. depend. 4-93061
- CdS film, deposited by hot wall technique, characterisation of doped and undoped films 4-114405
- CdS film, photoluminescence method of determ. minority carrier kinetics 4-61748
- CdS:In film, elec. props. meas. 4-104329
- n-CdS<sub>0.99</sub>Se<sub>0.01</sub> electrode, liquid junction photoelectrochemical cells, props. (Chinese) 4-81565
- CdS<sub>1-x</sub>Se<sub>x</sub> single cryst., elec. cond. and Hall effect studies 4-113974
- n-CdTe, electron traps, DLTS study 4-80533
- CdTe, p-type, undoped, thin dielectric films deposition as protection against decomposition during annealing 4-92755
- CdTe thin films, DC cond. rel. to H<sub>2</sub> exposure 4-76053
- CdTe thin films for solar cell appls., deposition and elec. props. 4-76054
- n-CdTe:In, electron traps, DLTS study 4-80533
- Ce epitaxial layers, plasma enhanced CVD growth of free-standing films 4-61866
- Co<sub>0.1</sub>Li<sub>0.9</sub>, pure and doped, elec. cond., carrier mobility and conc. 4-92731
- Ga<sub>0.5</sub>Te<sub>0.5</sub>, vapour growth, thermodynamics and elec. characts. 4-71536
- CuInSe In-diffused homojunctions, elec. and photovoltaic effects 4-92809
- n-CuInSe<sub>2</sub>, optical absorption edge, influence of carrier conc. 4-80943
- CuInTe<sub>2</sub> MIS struct., field effect studies 4-80679
- CuInTe<sub>2</sub>, vapour growth, thermodynamics and elec. characts. 4-71536
- Cu<sub>2</sub>SnS<sub>4</sub>, thermal props., elec. cond. and Hall effect 4-88523
- Fe<sub>2</sub>O<sub>3</sub>, pure and doped semicond., elec. cond. and Seebeck voltage 4-92759
- Fe<sub>2</sub>O<sub>3</sub>, thin film photoanodes, carrier conc. determ. in MIS struct. 4-88505
- GaAlAs light sources, radiative coeffs., carrier dependence 4-64703
- GaAlAs/GaAs selectively doped heterojunction, electron conc., FET appl. 4-98703
- Ga<sub>1-x</sub>Al<sub>x</sub>As:Zn, (Se), doping in MOCVD growth, carrier conc. and cond. 4-88982
- GaAs, dislocations and point-defect complex formations, thermal stability 4-103758
- GaAs doping superlattices, bipolar cond., tunability 4-70914
- GaAs doping superlattices, weak localisation and magnetoresist. 4-98720
- GaAs growth using OMVPE, electronic and optical props. 4-114402
- GaAs, implanted layers, elec. props., Si<sub>3</sub>N<sub>4</sub> encapsulation effects 4-98609
- GaAs, ion implanted, transient capless annealing appl. to IC fabrication 4-103779
- GaAs, laser-induced Si diffusion from deposited Si<sub>3</sub>N<sub>4</sub> film 4-60958
- GaAs MBE films, growth and elec. props. (Chinese) 4-84523
- GaAs, MBE growth using trimethylgallium as a Ga source 4-81138
- GaAs p-n-p superlattices, LPE growth 4-80665
- GaAs, plasma-assisted epitaxial growth in H<sub>2</sub> plasma, elec. props. 4-104740
- GaAs, relaxation of hot electron energy, surface plasmons 4-98631
- GaAs:Cr, ion implanted, Cr redistrib. 4-88194
- GaAs:Cr-GaAs epitaxial junction, IR characterisation 4-109170
- GaAs:Se, deep acceptor, photoluminescence study 4-80534
- GaAs:Si, (100), vacuum annealed, free carrier reduction 4-98610
- GaAs:Si, crystal growth by horizontal gradient freeze technique, carrier and dislocation density 4-66216
- GaAs:Si, implanted, elec. props., pulse laser annealing effects 4-60953
- GaAs:Si, LEC and horizontal Bridgman growth, elec. uniformity 4-65683
- GaAs:Si, local vibr. modes and elec. activation, Raman study 4-84357
- GaAs:Si, planar channelling of Si implants 4-75483
- GaAs:Te, H ion bombarded, free carrier density, EELS studies 4-98632
- GaAs/(AlGa)As selectively doped heterostruct., transport props. 4-70913
- GaAs/AlGaAs heterostructures, carrier density, hydrostatic press. control 4-98735
- GaAs/N-AlGaAs heterostructures, selectively doped, MBE grown, tungsten-halogen lamp annealing effects 4-61444
- GaAs-Al<sub>1-x</sub>Ga<sub>x</sub>As heterostructures, electron mobility, temp. depend. from 1-10K 4-80669
- GaAs-Ga<sub>1-x</sub>Al<sub>x</sub>As multiple quantum well structs., Hall mobility, electron conc. and buffer width depend. 4-80668
- Ga<sub>0.47</sub>In<sub>0.53</sub>As, MBE planar doped barriers in InP, elec. characts. 4-98708
- Ga<sub>1-x</sub>In<sub>x</sub>AsSb<sub>1-y</sub>, epitaxial layers, reflection spectra analysis 4-114340
- GaP:Te(N)(As), impurity influence on electron-hole plasma 4-75862
- GaSb, plasma-assisted epitaxial growth in H<sub>2</sub> plasma, elec. props. 4-104740
- GaSb-InSb, behaviour of Sn in solid solns., elec. props. 4-75967
- Ge, cyclotron resonance and radiative recombination for excitons, free carriers, electron-hole droplets 4-71183
- Ge exciton condensation, microwave breakdown, one- and two-photon carrier excitation luminescence 4-70670
- Ge, exciton condensation, microwave methods using pulsed optical excitation, kinetics 4-70671
- Ge, film, RF sputtered, controlled doping 4-80059
- Ge, IR laser radiation nonlinear absorpt. and self-defocusing due to free carrier generation 4-79248

## carrier density continued

- Ge nonequilibrium current carrier microwave absorpt., carrier conc., excitons 4-70852
- Ge, phonon dispersion near melting point 4-88250
- Ge, stressed, with large electron-hole drop, magnetoacoustic props. 4-98529
- n-Ge:As, growth on Si by MBE, charact. 4-98469
- Ge:Se, impurity levels, Hall effect study 4-108804
- <sup>4</sup>He, liquid, electron mobility and surface states 4-70498
- <sup>4</sup>He, liquid, surface critical electron density 4-98385
- Hg<sub>1-x</sub>Ag<sub>x</sub>Cr<sub>2</sub>Se<sub>4</sub> mag. semicond., exchange interaction, carrier effects 4-114103
- Hg<sub>1-x</sub>Cd<sub>x</sub>Te, annealing of radiation defects, electron irradiation 4-108442
- Hg<sub>1-x</sub>Cd<sub>x</sub>Te epitaxial layers, organometallic growth and elec. props. 4-71566
- Hg<sub>1-x</sub>Cd<sub>x</sub>Te large area epitaxial layers, LPE growth 4-61879
- Hg<sub>1-x</sub>Fe<sub>x</sub>Te, negative magnetoresist. and Hall effect 4-65696
- HgS mixed films, elec. and optical props. (French) 4-84715
- InAs, electroliquid epitaxial growth, carrier density 4-93243
- InAs evaporated films, Hall mobility and carrier conc. 4-70961
- InAs-AlSb quantum wells, electron densities 4-98711
- InAs<sub>1-x</sub>Sb<sub>x</sub> epilayers, impact ionisation coeffs. 4-104333
- InGaAs epilayers, optical studies of carrier dynamics 4-98788
- InGaAs epitaxial layer, LPE growth and carrier mobility, dopant effects 4-84717
- InGaAs, high-parity, conventional LPE growth, carrier conc. and mobility 4-99353
- In<sub>0.5</sub>Ga<sub>0.47</sub>As, carrier energy relax., picosecond luminesc. studies 4-114312
- InGaAsP, 1.3  $\mu$ m bandgap, photoexcited carrier lifetime and Auger recomb. 4-108893
- InGaAsP epilayers, optical studies of carrier dynamics 4-98788
- InGaAsP laser, radiative and nonradiative, recombination rates, meas. 4-112434
- InGaAsP light sources, radiative coeffs., carrier dependence 4-64703
- InP epitaxial, deep and shallow levels due to ion irradi. 4-80531
- InP epitaxial layer, LPE growth and carrier mobility, dopant effects 4-84717
- InP epitaxial layers, MOCVD growth 4-61862
- InP, localisation of inversion electrons, Fourier transform spectra studies 4-98555
- InP single crystals and solar cells,  $\gamma$ -irrad. damage 4-62356
- InP solar cells, radiation resistant, electron irradi. damage 4-62351
- InP:Sn(Ge), (100), vacuum annealed, free carrier reduction 4-98610
- InP:Sn(Sn)(Zn)(Fe) single crystals, LEC growth, perfection, carrier conc., TEM obs. 4-71550
- InP:Se, ion implanted, annealing and transport props. 4-108397
- InP:Sn films, LPE grown, carrier saturation, Hall meas. 4-98789
- InP:Zn, electron irradi. damage, carrier conc. effects, minority carrier diffusion length 4-80107
- n-InSb, Auger recombination of holes via deep donors 4-104229
- InSb bicrystal, grain boundary barrier height and elec. cond. 4-92216
- InSb, carrier lifetime depend. on electron density 4-104228
- n-InSb, current-induced anisotropy of refractive index 4-104564
- InSb, photoconductivity under picosecond illumination (Russian) 4-88543
- InSb, Raman scatt. at high temp., diminishing energy gap near melting point 4-114274
- n-InSb, refractive index, influence of electron drift and heating 4-104561
- InSb:Ge(Si), impurity solubility, role of acceptor and donor states 4-60949
- In<sub>2-x</sub>Sn<sub>x</sub>O<sub>3-y</sub> transparent conducting films, DC reactive sputtering deposition, optical and elec. props. 4-112533
- MgO, containing dissolved traces of water, surface charges and subsurface space charge distrib. 4-80650
- MnO, stabilised and Mn<sub>1-x</sub>Zn<sub>x</sub>O solid solns., elec. props. 4-98605
- Na<sub>2</sub>Ta<sub>2</sub>W<sub>2</sub>O<sub>7</sub>, metal-nonmetal transition 4-70884
- NbN, electronic props., optical study 4-66003
- Ne solid, surface two-dimensional electron system 4-98683
- Ne, solid with adsorbed <sup>4</sup>He liquid film, electron density 4-98683
- Pb chalcogenides, carrier diffusion length and lifetime, EBIC meas. 4-92748
- Pb<sub>1-x</sub>Ge<sub>x</sub>Te, undoped and In-doped, anomalous scatt. of carriers by defects and impurities near ferroelec. phase transition 4-98622
- PbI<sub>2</sub>, photoelectric props., study using lasers 4-88532
- PbS<sub>1-x</sub>Se<sub>x</sub>, n<sup>+</sup>-p-p<sup>+</sup> injection laser, performance characts. 4-79154
- PbSe, anisotropy of Fermi surface of holes 4-104117
- PbSe film, photoelectric props. meas. 4-104267
- PbTe epitaxial films, photoluminescence characts. 4-66067
- PbTe thin films, elec. props., effect of boundary layers 4-88618
- PbTe(Si)(S), lattice thermal cond. meas. 4-98598
- Si, highly doped, modeling the intrinsic number and Fermi levels for device and process simulation 4-113966
- Sb<sub>2</sub>Te<sub>3</sub> single cryst., weak field charge transport 4-108887
- Si, excitation depend. grain boundary recombination velocity 4-104217
- Si, heavily doped, built-in elec. field for holes 4-80584
- Si, high purity, intercarrier scatt. effects, laser and electron beam excitation 4-92725
- Si, highly doped, intrinsic number and Fermi level modelling for device and process simulation 4-75983
- Si, hole space-charge layers, lifting quasipin degeneracy by surface electric field 4-98516
- Si, IR laser radiation nonlinear absorpt. and self-defocusing due to free carrier generation 4-79248
- n-Si, intervalley relax. time, elec. cond. study 4-98621
- Si inversion layers, magnetoconductance and quantised confinement 4-98764
- Si inversion layers, submicron width, quasi 1D effects 4-98765
- Si, ion implanted, CO<sub>2</sub> laser annealing, relax. characts. of metastable concentrations 4-75512
- Si MIS struct., relax. time of wave-function phase in two-dimens. electron gas 4-88605
- Si, neutron irradi., radiation defects and electrophys. parameters 4-84319
- Si, polycrystalline, elec. cond. props., I-V characts. 4-70805
- Si, polycrystalline, mobility and carrier conc. depend. on grain size and doping conc. 4-92730
- Si, profiling techniques using spreading resistance 4-75498
- Si, proton irradi. induced defects interaction with surface 4-75564
- Si, recrystallized on SiO<sub>2</sub>, laterally seeded, implantation and annealing studies 4-98121

**carrier density continued**

- Si solar cells, I-V characts. and performance between low- and high-level injection 4-81551  
 Si, surface sub-band calcs. and light scatt. meas. 4-61430  
 Si:As, high dose ion implanted, As clustering, TEM and SIMS studies 4-70384  
 Si:As, ion implanted, carrier density profiles, elec. meas., annealing behaviour 4-70179  
 Si:Au, donor level, entropy factor, resist. and DLTS meas. 4-70707  
 a-Si:H, non-substitutional dopant states and carrier density statistics 4-113902  
 Si:Mg, implanted, doping behaviour, elec. props. 4-75485  
 Si:Te, donor states, Hall effect and cond. meas. 4-104145  
 Si/a-Si:H/B/metal junctions, current-volt. characts. 4-114033  
 Si/methanol liquid junction, open circuit volt. and oxide form. 4-114030  
 Si-metal struct., scanning-tunnelling microscopy, voltage drop 4-114038  
 SiC p-n junctions, Franz-Keldysh effect on photosensitivity 4-104302  
 Sn, laser alloyed layers on GaAs substrates, elec. props., surface damage 4-99622  
 SnTe, low carrier conc., Fermi surface, Shubnikov-de Haas studies 4-98506  
 TaS<sub>2</sub> (1T), commensurate CDW state, electronic cond., Hall coeff. meas. 4-98639  
 TiO<sub>2</sub> thin film photoanodes, carrier conc. determ. in MIS struct. 4-88505  
 TiTe<sub>2</sub>, band struct., elec. and mag. props. 4-92595  
 TiBiTe<sub>2</sub>, growth, elec. and optical props. 4-65676  
 WC, semimetallic, de Haas-van Alphen effect obs. 4-104116  
 ZnO weak accumulation layers, electron transport and Hall effect 4-98686  
 ZnO:Al films, RF magnetron sputtering, elec. and optical props. 4-85100  
 Zn<sub>3</sub>P<sub>2</sub> polycryst. and single cryst., optical and photoelec. props. 4-84937  
 ZnS conductive film, MBE prep. with single effusion source, luminesc. and elec. props. 4-99323  
 n-ZnSe, OMVPE undoped films, elec. and optical props. 4-93226

**carrier diffusion length** *see carrier lifetime***carrier lifetime**

- anthracene, excitons and diffusion effects 4-92617  
 automatic measurement in 0.5 μs to 5 μs range with SEM 4-82865  
 disordered systems, field depend. charge carrier trapping process 4-104226  
 extrinsic semiconductor, drift intervalley ambipolar instability 4-104231  
 III-V semiconductor lasers, threshold current, temp. dependence 4-79132  
 MIS structures, I-V measurement and minority carrier lifetime determ. by a gated integrator 4-88597  
 MOS capacitors, charge variation rel. to voltage step, generation lifetime meas. 4-65755  
 MOS solar cells, perform. calcs. at various temps. 4-72117  
 MOS structures, minority carrier lifetime determ. by transient capacitance measurements 4-92822  
 NaCl layers, monoenergetic electron attenuation length, photoelec. studies 4-70803  
 nonequilibrium carrier effective lifetime meas. in semiconductor wafers 4-101872  
 nonohmic contacts with double injection, minority carrier lifetimes 4-88564  
 optical bistability in semicond. with density-depend. carrier lifetimes 4-87387  
 p-n junction diodes, carrier lifetime and surface recomb. vel. determ. using transient responses 4-77093  
 p-n junctions, electron beam induced short circuit currents, carrier lifetime 4-92806  
 p-n shallow junction, electron beam induced current 4-80662  
 piosecond optoelectronics, conf., San Diego, CA, USA (Aug. 1983) 4-106106  
 polyacetylene, nonequilibrium thermodynamics of photovoltaic effect, solitons 4-104265  
 recombination velocity on grain boundary, direct meas. 4-70827  
 RF sputter-deposited Schottky barrier diodes 4-98691  
 semiconductor photoanodes in aq. electrolytes, transition metal doped, photoresponse characts. 4-70875  
 semiconductor thin films, minority carrier lifetime and surface recomb. vel. meas., small-signal admittance meas. 4-68239  
 semiconductor with bipolar photoconduction, recombination parameters determ. in mag. field 4-114000  
 semiconductors, charge carrier transfer and diffusion in strong mag. field (Russian) 4-88520  
 semiconductors, large-signal photocond., Shockley-Read recomb. model 4-88537  
 semiconductors, minority carrier lifetime determ. by laser-beam induced current decay 4-80610  
 solar cells, minority carrier SEM-EBIC signal and grain boundaries 4-80609  
 solar cells, thin film, photovoltaic behaviour under space charge conditions 4-89406  
 SOS, ion implanted, elec. props., effect of heat treatment 4-98759  
 SOS films, carrier mobility, lifetime, ps photocond. meas. 4-80623  
 SOS heteroepitaxial film, surface photovoltage characterisation 4-80697  
 AlGaAs LED, radiative and nonradiative, recombination rates, meas. 4-112434  
 Al<sub>0.5</sub>Ga<sub>0.5</sub>As, cathodoluminescence study 4-71449  
 Al<sub>0.5</sub>Ga<sub>0.5</sub>As solar cell structs., photoluminescence and spectral response 4-89404  
 n-Cd<sub>3</sub>As, mag. quantisation effect on Einstein relation 4-92740  
 Cd<sub>2</sub>, soln. grown cryst., photoconductivity, nonlinear behaviour 4-61413  
 CdS film, photoluminescence method of determ. minority carrier kinetics 4-61748  
 CdS/CuInSe<sub>2</sub> solar cells, thin film, diffusion length determ. using EBIC method 4-72110  
 n-CdS/electrolyte interface, photoelectrochem. characterisation 4-84689  
 CdTe films, MBE growth and elec. and optical props. 4-81136  
 GaAlAs light sources, radiative coeffs., carrier dependence 4-64703  
 Ga<sub>1-x</sub>Al<sub>x</sub>P p-n structures, epitaxially grown, plastically and elastically deformed, quantum efficiency spectra 4-84651  
 GaAs, carrier vel. fluctuations in steady-state and transient regimes, Monte Carlo study 4-80637  
 GaAs epitaxial diode struct., nonequilibrium carrier lifetimes 4-70920  
 GaAs, free carrier lifetime from photoluminescence studies 4-80988  
 GaAs, semi-insulating, elec. and photoelectronic props., book contrib. 4-88544  
**carrier lifetime continued**  
 GaAs/AlGaAs multiple quantum well structs., photoexcited carriers intraband relax., femtosecond studies 4-88565  
 GaP, electron irradi., defect creation, luminescence and elec. studies (Chinese) 4-108441  
 p-GaP photoelectrochem. cells, absorpt. coeff. and diffusion lengths, differential photocurrent determ. 4-89455  
 GaP:N, Te VPE layers, minority carrier lifetime, photoluminesc. decay study 4-76520  
 GaP:Te(N)(As), impurity influence on electron-hole plasma 4-75862  
 GaP/GaAs<sub>1-x</sub>P<sub>x</sub> strained layer superlattices, minority carrier diffusion lengths 4-76025  
 Ge, cyclotron resonance and radiative recombination for excitons, free carriers, electron-hole droplets 4-71183  
 Ge exciton condensation, microwave breakdown, one- and two-photon carrier excitation luminescence 4-70670  
 Ge, exciton condensation, microwave methods using pulsed optical excitation, kinetics 4-70671  
 Ge nonequilibrium current carrier microwave absorpt., carrier conc., excitons 4-70852  
 Ge photo-induced complex permitt. at 9 GHz, expt. study 4-65703  
 a-Ge:H films, planar magnetron sputtering, electronic props. 4-88972  
 Ge:Hg<sub>1-x</sub>As<sub>x</sub>, hole capture cross section 4-98567  
 HgCdTe 0.1 eV photoconductive detector, optimum thickness, rel. to minority carrier diffusion length 4-111204  
 HgCdTe photodiode obs. by electron-beam induced voltage technique (Chinese) 4-108929  
 Hg<sub>1-x</sub>Cd<sub>x</sub>Te, electron irradi., elec. props., heat treatment effects 4-65713  
 Hg<sub>1-x</sub>Cd<sub>x</sub>Te, photogenerated carrier lifetime meas. by optical modulation of IR absorpt. (Chinese) 4-84953  
 InGaAs, 1.6 μm, radiative and nonradiative minority carrier lifetimes 4-70826  
 InGaAs epilayers, optical studies of carrier dynamics 4-98788  
 InGaAsP, 1.3 μm bandgap, photoexcited carrier lifetime and Auger recomb. 4-108893  
 InGaAsP epilayers, optical studies of carrier dynamics 4-98788  
 InGaAsP laser, radiative and nonradiative, recombination rates, meas. 4-112434  
 InGaAsP light sources, radiative coeffs., carrier dependence 4-64703  
 InGaAsP/GaAs, double heterojunctions, photoluminesc. studies 4-76504  
 InGaAsP/InP double heterojunctions, photoluminesc. studies 4-76504  
 InP single crystals and solar cells, γ-irrad. damage, minority carrier diffusion lengths 4-62356  
 InP solar cells, radiation resistant, electron irradi. damage 4-62351  
 InP:Fe, <sup>60</sup>He<sup>+</sup> bombarded, psec. photocond., very short free carrier lifetimes 4-108894  
 InP:Si, electron irradi.-induced deep traps, impurity conc. effects 4-88468  
 n<sup>+</sup>-InP:Si-p-InP homojunction, implanted, photoelec. props., minority carrier diffusion length 4-76034  
 InP:Zn, electron irradi. damage, carrier conc. effects, minority carrier diffusion length 4-80107  
 n-InSb, Auger recombination of holes via deep donors 4-104229  
 InSb, carrier lifetime depend. on electron density 4-104228  
 p-InSb, photomagnetolectric effect, minority carrier transport parameters 4-88530  
 Pb chalcogenides, carrier diffusion length and lifetime, EBIC meas. 4-92748  
 Pb<sub>1-x</sub>Sn<sub>x</sub>Te photoelectronic props. study using lasers 4-88532  
 PbSnTe-PbSeTe lattice-matched DH laser diodes, injected carrier lifetimes 4-112421  
 Pb<sub>1-x</sub>Sn<sub>x</sub>Te diodes, excess noise rel. to I-V characts. 4-61426  
 Si, amorphous, minority carrier diffusion length, intensity dependence 4-70829  
 Si, carrier lifetime, elec. resist. meas. by contactless method 4-61392  
 Si, carrier vel. fluctuations in steady-state and transient regimes, Monte Carlo study 4-80637  
 Si, defect and carrier lifetime, back-surface damage gettering technique 4-113972  
 Si defected substrates, minority carrier lifetime, injection level depend. 4-92753  
 Si, electron and γ irradi., influence on defect annihilation 4-98094  
 Si, electron and γ-ray irradiated, efficiency of radiation defect formation 4-92237  
 a-Si, excess carrier lifetime and mobility studies 4-104219  
 Si, excitation depend. grain boundary recombination velocity 4-104217  
 Si, gamma-irradiated, carrier recombination, dislocation effects 4-75982  
 Si, gamma-irradiated, charge carrier recombination 4-84631  
 Si, high purity, intercarrier scatt. effects, laser and electron beam excitation 4-92725  
 n-Si, irradiated by γ-rays, changes in carrier lifetime 4-104232  
 Si MIS struct., relax. time of wave-function phase in two-dimens. electron gas 4-88605  
 Si, minority carrier diffusion lengths meas. 4-70835  
 Si, minority carrier lifetime meas. using AC surface photovoltages 4-92744  
 Si photo-induced complex permitt. at 9 GHz, expt. study 4-65703  
 Si, photocurrent carrier lifetime study during ion implantation 4-75984  
 Si photovoltaic cells, photogeneration rate, minority carrier lifetime depend. 4-75997  
 Si, polycrystalline, interacting grain boundaries, surface recombination vel., EBIC study 4-70828  
 Si, polycrystalline, minority carrier diffusion length under solar illum. 4-104225  
 Si solar cells, carrier lifetime and surface recomb. vel. determ. using transient responses 4-77093  
 Si solar cells, I-V characts. and performance between low- and high-level injection 4-81551  
 Si solar cells, minority carrier lifetime meas. 4-77091  
 Si solar cells, n<sup>+</sup>-p and n<sup>+</sup>-p-p<sup>+</sup> spectral sensitivity calcs. 4-89410  
 Si solar cells, P precip. effects on open circuit voltage 4-62361  
 Si solar cells subjected to intense photoexcitation, nonequilibrium carrier lifetime determ. 4-85374  
 Si:Ar, carrier lifetime reduction by Ar ion implantation 4-80604  
 a-Si:H film, TSC and photoconductivity 4-104222  
 Si:H amorphous compensated films, xerographic discharge meas. 4-80603  
 Si:H amorphous films, glow discharge deposited, electron drift mobility, substrate temp. dependence 4-61393  
 a-Si:H films, planar magnetron sputtering, electronic props. 4-88972  
 a-Si:H p-i-n devices, EBIC decay 4-92796  
 a-Si:H surface barrier structs., photocurrent, freq. depend. 4-61418

**carrier lifetime continued**

- a-Si:H/a-Si<sub>1-x</sub>N<sub>x</sub>:H quantum well struct., luminescence and current transport 4-114024  
 Si:Li p-n junction solar cells, electron induced degradation, recovery under space conditions 4-105110  
 SiO<sub>2</sub> cryst., minority carrier lifetime, O precipitation effects, IR studies 4-113971  
 Si/methanol liquid junction, open circuit volt. and oxide form. 4-114030  
 Si-H, bonds and H-induced defects study 4-66058  
 Te photo-induced complex permit. at 9 GHz, expt. study 4-65703  
 n-TiO<sub>2</sub> anodes in photoelectrolytic cells, struct. and electronic props. 4-114031  
 n-TiO<sub>2</sub> photoelectrochemical sintered electrodes, hole diffusion length 4-70929

**carrier mean free path**

see also *electron mean free path (metals)*

- Teflon FEP, constant hole schubweg determ. 4-92742  
 GaAs, negative magnetoresist. associated with quantum localisation correction to cond. 4-61400  
 Si-Au(Ag)(Al) Schottky barrier diodes, barrier height and hot electron attenuation length meas. 4-98751

**carrier mobility**

see also *carrier mean free path; carrier relaxation time; current density; electron-hole recombination; electron mobility (metals)*

- aerosol particles, fibrous, bipolar diffusion charging, elec. mobility and charge meas. 4-89348  
 biopolymer systems, electron and hole transport mechanisms 4-108855  
 chalcogenide glasses, Hall effect studies, temperature dependence of carrier mobility 4-92756  
 cholesteryl pelargonate and chloride, charge carrier mobility meas. 4-92709  
 dielectric system, mobility and surface recombination processes of primary electrons during AES 4-93151  
 disordered lattice, cond. in strong elec. fields 4-61367  
 disordered solids, with continuous trap distrib., dispersive carrier transport 4-108874  
 disordered systems, field depend. charge carrier trapping process 4-104226  
 disordered systems, weak localisation and Coulomb interaction 4-104162  
 double-proton bombarded laser, emission properties, effect of carrier confinement 4-112437  
 electron gas, cond. near mobility edge 4-98616  
 electron-hole geminate pair in cryst. lattices, time depend. dissoc., Monte Carlo study 4-98635  
 epitaxial high-purity layers, low-pressure MOCVD growth 4-61861  
 geminate recombination on a lattice 4-111042  
 graphite fibres, benzene derived, transverse magnetoresistance study 4-108844  
 hole mobility anisotropy, temp. depend. 4-65681  
 hydrocarbon polymer dielectric films, hot-electron transport 4-92837  
 II-VI semiconductors, carrier mobility characts., displaced Maxwellian model 4-75968  
 implanted samples, applicability of van der Pauw-Hall meas. technique 4-88521  
 inversion layers, bound electron states of Coulombic impurities and effect on mobility 4-98770  
 liquid metals, ultrasound absorpt. 4-84347  
 molten salts, assoc. and mobility isotherms 4-75247  
 MOSFET, interface carrier mobility transport theory anal. 4-70944  
 organic/inorganic semicond. contact barrier diodes, I-V characts. 4-92810  
 p-n junction device modelling, singularly perturbed boundary value problems 4-98747  
 point-contact injection in an insulator 4-84672  
 polar semiconductors, electronic transport, appl. of solvent method 4-84601  
 poly-N-vinylcarbazole, charge carrier transport study 4-75999  
 polyacetylene, n-doped, DC elec. cond. 4-80576  
 polymer electrets, radiation induced charge transport 4-71264  
 semiconducting unipolar films, nonlinear elec. cond. 4-88617  
 semiconductor, elec. props., appl. of two stage nonmagnetic high press. equipment (Chinese) 4-90607  
 semiconductor heterolayers, mobility in Bloch-Grüneisen range 4-108932  
 semiconductor polycrystalline thin films, with pot. barriers, Hall mobility 4-104331  
 semiconductor superlattices, high-frequency props. theory 4-70922  
 semiconductors, charge carrier transfer and diffusion in strong mag. field (Russian) 4-88520  
 semiconductors, disordered organic and inorganic, non-equilibrium diffusive transport 4-70801  
 semiconductors, electrolytic Schottky-gated Hall effect profiling 4-75497  
 semiconductors, high resistivity, acoustoelectric interactions 4-104274  
 semiconductors, low-conductivity, carrier mobility using the travelling wave technique 4-92752  
 semiconductors, quasi-one-dimensional, low-field electron transport 4-80605  
 SIMOX films, Hall mobility and electrical conductivity, temp. dependence 4-80700  
 small polaron model with nonlinear electron-phonon interactions 4-61304  
 solid solutions, quaternary III-V cpd. system, optical and elec. props. 4-84929  
 SOS, electric props. meas. (Russian) 4-84706  
 SOS films, carrier mobility, lifetime, ps photocond. meas. 4-80623  
 TCNQ salt with N-methyl-N-ethylmorpholinium, thermoelec. power anisotropy 4-113934  
 ternary chalcopyrite semiconductors, Einstein relation, cryst. field splitting effect 4-108860  
 topologically disordered systems, localisation, self consistent theory 4-92672  
 n-(Al,Ga)As/GaAs heterojunctions, hot-electron mobility study at moderate elec. fields 4-84678  
 AlGaAs/GaAs, single quantum well heterostruct. on Al<sub>0.30</sub>Ga<sub>0.70</sub>As buffers, MBE grown, electron mobility study 4-114029  
 AlGaAs/GaAs heterostruct., 2D magnetotransport, electron heating effects 4-98736  
 n-AlGaAs/GaAs selectively doped heterojunctions, high mobility electron gas 4-80657  
 AlGaAs-GaAs modulation doped layers, 2-D electron gas, room temp. mobility, parallel conduction effects 4-70027

**carrier mobility continued**

- Al<sub>0.3</sub>Ga<sub>0.7</sub>As-GaAs heterojunction, selectively doped, persistent photocond. effect 4-98717  
 Al<sub>x</sub>Ga<sub>1-x</sub>As MBE layers, persistent photocond. centre (Chinese) 4-88529  
 Al<sub>x</sub>Ga<sub>1-x</sub>As, Si donor behaviour, effect of Al comp. 4-98709  
 Al<sub>x</sub>Ga<sub>1-x</sub>As:Si MOCVD layers, transport props. 4-92834  
 Al<sub>1-x</sub>In<sub>x</sub>As, nominally undoped, MBE growth and charact. 4-98472  
 As<sub>2</sub>Se<sub>3</sub>, amorphous, carrier diffusion, multiple-trapping limited 4-70831  
 As<sub>2</sub>Se<sub>3</sub>:Te film, transient photocurrent study 4-113991  
 Bi<sub>1-x</sub>Sb<sub>x</sub>, composition influence on electron scatt. intensity 4-88518  
 n-Bi<sub>2</sub>Te<sub>3</sub>, free carrier mobility, Hall and Seebeck coeffs., temp. depend. 4-61369  
 Ca<sub>3-x</sub>Y<sub>x</sub>Mn<sub>2</sub>Ge<sub>2</sub>O<sub>12</sub>, thermopower and elec. cond., 30 to 1000°C 4-70847  
 n-Cd<sub>3</sub>As<sub>2</sub>, mag. quantisation effect on Einstein relation 4-92740  
 n-CdGeAs<sub>2</sub>, degenerate, Einstein relation, cryst. field splitting effect 4-108860  
 Cd<sub>0.9</sub>Hg<sub>0.1</sub>Te, epitaxial film growth by chem. transport reactions, elec. props. 4-70965  
 Cd<sub>0.9</sub>Hg<sub>0.1</sub>Te, galvanomagnetic effects in quantising mag. field (Russian) 4-70843  
 n-Cd<sub>0.9</sub>Hg<sub>0.1</sub>Te, minority carrier mobility, Haynes-Shockley method 4-92714  
 n-Cd<sub>0.9</sub>Hg<sub>0.1</sub>Te single crystals, hot electrons at strong elec. fields (Russian) 4-98628  
 CdS film, deposited by hot wall technique, characterisation of doped and undoped films 4-114405  
 CdS thin film, RF-sputtered, elec. props., effect of temp. and bias 4-80699  
 CdS thin films prep. by spray deposition, vacuum annealing effect on elec., structural and optical props. 4-70966  
 CdS:In film, elec. props. meas. 4-104329  
 CdS:Se<sub>x</sub> single cryst., elec. cond. and Hall effect studies 4-113974  
 CdTe epitaxial films, MOCVD grown on sapphire, growth rates, mobilities, X-ray diff. 4-80444  
 CdTe films, MBE growth and elec. and optical props. 4-81136  
 Cd<sub>1-x</sub>Zn<sub>x</sub>Te alloys, growth, elec. props., photoluminesc. 4-66207  
 Ce epitaxial layers, plasma enhanced CVD growth of free-standing films 4-81666  
 CoO:Li, pure and doped, elec. cond., carrier mobility and conc. 4-92731  
 Cu<sub>0.9</sub>Fe<sub>0.1</sub>Cr<sub>0.5</sub>S<sub>0.5</sub> films, elec. and galvanomagnetic props. 4-70656  
 CuFe<sub>2</sub>O<sub>4</sub>, conduction mechanism, annealing effect, resist. and thermopower meas. 4-104206  
 CuGaTe<sub>2</sub>, vapour growth, thermodynamics and elec. characts. 4-71536  
 CuInTe<sub>2</sub>, MIS struct., field effect studies 4-80679  
 CuInTe<sub>2</sub>, vapour growth, thermodynamics and elec. characts. 4-71536  
 α-Fe<sub>2</sub>O<sub>3</sub>, anisotropy of elec. props., mag. order depend. 4-108853  
 Fe<sub>2</sub>O<sub>3</sub>, pure and doped semicond., elec. cond. and Seebeck voltage 4-92759  
 GaAs, plasma enhanced epitaxy, low temp. 4-99330  
 GaAs (110)-Al interface form. at low temp., electronic and struct. props. 4-84695  
 GaAs, carrier vel. fluctuations in steady-state and transient regimes, Monte Carlo study 4-80637  
 GaAs, dislocations and point-defect complex formations, thermal stability 4-103758  
 GaAs doping superlattices, bipolar cond., tunability 4-70914  
 GaAs growth using OMVPE, electronic and optical props. 4-114402  
 GaAs heterolayer, low temp. two-dimens. mobility 4-108933  
 GaAs, high field transport of holes 4-80598  
 GaAs high-field transport, model 4-88512  
 GaAs, implanted layers, elec. props., Si<sub>3</sub>N<sub>4</sub> encapsulation effects 4-98609  
 GaAs, ion implanted, transient capless annealing appl. to IC fabrication 4-103779  
 GaAs, LEC grown, improved elec. uniformity by high temp. annealing 4-65684  
 GaAs LPE layers, space-charge scatt. and mobility killers 4-84714  
 GaAs MBE films, growth and elec. props. (Chinese) 4-84523  
 GaAs p-n-p superlattices, LPE growth 4-80665  
 GaAs, plasma-assisted epitaxial growth in H<sub>2</sub> plasma, elec. props. 4-104740  
 GaAs, semi-insulating, elec. and photoelectric props., book contrib. 4-88544  
 GaAs semi-insulating substrate, inhomogeneity characterisation, expt. study 4-65759  
 GaAs, short n<sup>+</sup>nn<sup>+</sup> section, hot electron effects 4-61385  
 GaAs single domain growth on Ge (100) by MOCVD 4-99342  
 GaAs, transient hole transport, Monte Carlo study 4-80602  
 GaAs-O p-i-n structs., magnetically sensitive, elec. characts. (Russian) 4-65729  
 GaAs:Se, deep acceptor, photoluminescence study 4-80534  
 GaAs:Si, implanted, elec. props., pulse laser annealing effects 4-60953  
 GaAs:Si, implanted, radiation annealing with CW Xe arc lamp 4-75486  
 GaAs:Si, Si doping from Si<sub>3</sub>H<sub>8</sub> in MOCVD growth 4-75459  
 GaAs/(AlGa)As selectively doped heterostruct., transport props. 4-70913  
 GaAs/Al<sub>x</sub>Ga<sub>1-x</sub>As quantum well struct., low temp. electron mobility, alloy disorder scatt. contrib. 4-92808  
 GaAs/AlGaAs heterostruct., organometallic VPE growth and characterisation 4-99341  
 GaAs/AlGaAs/GaAs heterojunction barrier, MOCVD grown, electron transport 4-80661  
 GaAs/Ca<sub>1-x</sub>Sr<sub>x</sub>F<sub>2</sub>/GaAs (100) lattice-matched MBE structures 4-88562  
 GaAs/Ga<sub>1-x</sub>Al<sub>x</sub>As quantum well wires, hydrogenic impurity states 4-92815  
 GaAs/Ge single crystal layers, MBE growth and patterning on Si substrates 4-99315  
 GaAs/N-AlGaAs heterostructures, selectively doped, MBE grown, tungsten-halogen lamp annealing effects 4-61444  
 GaAs-Al<sub>x</sub>Ga<sub>1-x</sub>As heterostructures, electron mobility, temp. depend. from 1-10K 4-80669  
 GaAs-AlGaAs heterojunction, phonon emission and electron heating 4-70927  
 GaAs-Ga<sub>1-x</sub>Al<sub>x</sub>As multiple quantum well structs., Hall mobility, electron conc. and buffer width depend. 4-80668  
 GaAs-GaAlAs heterostructure, electron mobility limits 4-76030  
 GaAs-GaAlAs heterostructures, 2-D electron gas, electron mobility, temp. dependence 4-98704  
 GaAs-GaAlAs heterostructures, interband scatt. in mobility 4-98732  
 GaAs-n-AlGaAs structures, modulation doped, elec. props., effect of IR flash lamp annealing 4-98712

## carrier mobility continued

- GaAs<sub>1-x</sub>P<sub>x</sub>/GaP strained-layer superlattices, Be-implantation doping 4-80057
- GaInAsP, low field carrier mobility, book contrib. 4-61383
- GaInAsP, low field transport calcs., book contrib. 4-61384
- GaInAsP, n-type, lattice matched to InP, hot electron transport, book contrib. 4-61388
- Ga<sub>1-x</sub>In<sub>x</sub>As<sub>1-y</sub>Sb<sub>y</sub>, epitaxial layers, reflection spectra analysis 4-114340
- GaSb, plasma-assisted epitaxial growth in H<sub>2</sub> plasma, elec. props. 4-104740
- Ga<sub>2</sub>Te<sub>3</sub>, electrical and optical props. meas. 4-61380
- n-Ge, anomalous magnetoresistance study 4-108879
- Ge exciton microwave breakdown, exciton and free carrier kinetics with electron-hole drops 4-70669
- n-Ge:As, growth on Si by MBE, charact. 4-98469
- Ge:Cu, impurity states, annealing effects 4-104148
- a-Ge:H films, planar magnetron sputtering, electronic props. 4-88972
- GeS, hole drift mobility anisotropy 4-70814
- (GeS<sub>3</sub>)<sub>100-x</sub>Bi<sub>x</sub>, glass, photoconductivity meas. 4-98670
- (GeSe<sub>3</sub>)<sub>100-x</sub>Bi<sub>x</sub>, glass, photoconductivity meas. 4-98670
- He, liquid, electron mobility and surface states 4-70498
- He liquid film, electron mobility, polaronic transition 4-98399
- n-HgCdTe, Haynes-Shockley expt. 4-104204
- Hg<sub>1-x</sub>Cd<sub>x</sub>Te epitaxial layers, organometallic growth and elec. props. 4-71566
- Hg<sub>1-x</sub>Cd<sub>x</sub>Te large area epitaxial layers, LPE growth 4-61879
- HgS mixed films, elec. and optical props. (French) 4-84715
- InAs evaporated films, Hall mobility and carrier conc. 4-70961
- InAs high-field transport, model 4-88512
- InAs:Si(Te), VPE growth, morphology and elec. props. 4-109326
- InAs-AlSb quantum wells, electron densities 4-98711
- InAsP, high mobility, vapour phase heteroepitaxial growth 4-71601
- InGaAs epitaxial layer, LPE growth and carrier mobility, dopant effects 4-84717
- InGaAs, high-parity, conventional LPE growth, carrier conc. and mobility 4-99353
- In<sub>0.53</sub>Ga<sub>0.47</sub>As, 2D electron gas, alloy scatt. limited mobility 4-98620
- In<sub>0.53</sub>Ga<sub>0.47</sub>As, electron mobility, rel. to two-mode lattice vibrs. 4-80582
- In<sub>0.5</sub>Ga<sub>0.5</sub>As/InP quantum well struct., low temp. electron mobility, alloy disorder scatt. contrib. 4-92808
- InO<sub>x</sub>, amorphous, electron mobility, cond., and supercond. near metal-insulator transition 4-80710
- InP epitaxial layer, LPE growth and carrier mobility, dopant effects 4-84717
- InP epitaxial layers, MOCVD growth 4-61862
- InP, high field transport of holes 4-80598
- InP high-field transport, model 4-88512
- InP MOSFET structures, carrier channel mobility correl. with interface state meas. 4-88600
- InP:Fe, <sup>3</sup>He<sup>+</sup> bombarded, psec. photocond., very short free carrier lifetimes 4-108894
- InP:Gd(Yb) epitaxial films, doping effects on low-temp. edge photoluminescence 4-85028
- InP:Se, ion implanted, annealing and transport props. 4-108397
- InP:Si MISFETs, post-implantation capless annealing 4-113472
- n-InSb, current-induced anisotropy of refractive index 4-104564
- InSb, polycrystalline, thermomagnetic and galvanic props. (German) 4-75987
- n-InSb, strongly compensated, electron mobility meas. 4-70834
- InSe, elec. props., thickness depend. 4-88507
- n-InSe, electron scatt. mechanisms, Hall effect and magnetoresist. meas. 4-80614
- In<sub>2-x</sub>Sn<sub>x</sub>O<sub>3-y</sub>, transparent conducting films, DC reactive sputtering deposition, optical and elec. props. 4-112533
- La<sub>2</sub>Te<sub>3</sub>, electrical and optical props. meas. 4-61380
- La<sub>2</sub>CuO<sub>4</sub>, with K<sub>2</sub>NiF<sub>4</sub> struct., at displacements, mag. and transport props., anisotropic bonding effects 4-75358
- La<sub>2</sub>NiO<sub>4</sub>, with K<sub>2</sub>NiF<sub>4</sub> struct., at displacements, mag. and transport props., anisotropic bonding effects 4-75358
- La<sub>2</sub>Ti<sub>2</sub>O<sub>7</sub>:Cr<sup>3+</sup> and La<sub>2</sub>/3TiO<sub>5</sub>:Cr<sup>3+</sup>, photoelectrochem. props. 4-70874
- n-MoTe<sub>2</sub>, carrier mobility, thermoelec. power and elec. resist., one-band model anal. 4-98612
- Nd<sub>2</sub>Ti<sub>2</sub>O<sub>7</sub>:Cr<sup>3+</sup> and Nd<sub>2</sub>/3TiO<sub>5</sub>:Cr<sup>3+</sup>, photoelectrochem. props. 4-70874
- Ne solid, surface two-dimensional electron system 4-98683
- NiO:Li(Al), or undoped, elec. cond. and high temp. defect struct. 4-80617
- n-Pb<sub>1-x</sub>Ge<sub>x</sub>Te, free carrier mobility, ferroelectric phase transition 4-71317
- PbI<sub>2</sub>, photoelectronic props. study using lasers 4-88532
- n-Pb<sub>1-x</sub>Mn<sub>x</sub>Te, intraband magneto-optical transitions in epitaxial film 4-71355
- PbSnTe, negative differential mobility in high elec. fields 4-104216
- Pb<sub>1-x</sub>Sn<sub>x</sub>Te:In, elec. transport props. 4-61371
- PbTe epitaxial films, photoluminescence characs. 4-66067
- PbTe films grown by hot wall epitaxy technique, AC field effect study 4-92835
- PbTe, negative differential mobility in high elec. fields 4-104216
- Pr<sub>2</sub>Ti<sub>2</sub>O<sub>7</sub>:Cr<sup>3+</sup> and Pr<sub>2</sub>/3TiO<sub>5</sub>:Cr<sup>3+</sup>, photoelectrochem. props. 4-70874
- Sb<sub>2</sub>Te<sub>3</sub> single cryst., weak field charge transport 4-108887
- Si (100) inversion layer, electron mobility, neutral scatt. effects 4-76040
- Si, carrier vel. fluctuations in steady-state and transient regimes, Monte Carlo study 4-80637
- a-Si, cond. and thermoelectric power below mobility edge 4-108888
- a-Si, excess carrier lifetime and mobility studies 4-104219
- Si, heavily doped, built-in elec. field for holes 4-80584
- Si, high purity, intercarrier scatt. effects, laser and electron beam excitation 4-92725
- n-Si, hot electron conductivity in transverse elec. field, intervalley scatt. obs. 4-80596
- Si inversion layers, magnetoconductance and quantised confinement 4-98764
- a-Si, mobility edge, temp. depend. 4-92723
- Si, n<sup>+</sup> and p<sup>+</sup> regions, uncertainties about physical electronics, solar cell appls. 4-89428
- Si, n-type, heavily-doped, minority hole mobility, empirical expression, device modelling appl. 4-98608
- Si, polycrystalline, elec. cond. props., small signal theory 4-70804
- Si, polycrystalline, elec. cond. props., I-V characs. 4-70805
- Si, polycrystalline, mobility and carrier conc. depend. on grain size and doping conc. 4-92730

## carrier mobility continued

- Si, polycrystalline SOI structures, RF zone melting recrystn. for MOS-FET fabrication 4-88965
- n-Si, proton irradiated, electrophysical props. 4-108861
- Si, recrystallized on SiO<sub>2</sub>, laterally seeded, implantation and annealing studies 4-98121
- Si SOS structures, pulse laser irr., internal stresses, Raman scatt. studies 4-99108
- Si, solar cell, H passivation of electrically active defects (French) 4-62359
- Si solar cells, majority carrier collection in p<sup>+</sup>-p-n<sup>+</sup> and n<sup>+</sup>-p-p<sup>+</sup> structs. 4-62367
- Si solar cells, n<sup>+</sup>-p and n<sup>+</sup>-p-p<sup>+</sup> spectral sensitivity calcs. 4-89410
- Si:B, implanted, elec. activation and damage annealing by flash lamp irr. 4-70196
- Si:H, amorphous, electron mobility meas. using 4-terminal FET structures 4-75964
- a-Si:H, DC elec. cond. Meyer-Neldel rule and Staebler-Wronski effect 4-113948
- a-Si:H, extended state mobility 4-104208
- a-Si:H, geminate recombination and mobility 4-104223
- a-Si:H, glow discharge decomposition prep., electron drift mobility, photocurrent (Chinese) 4-84616
- a-Si:H, long-time drift mobility, photocurrent study 4-104221
- a-Si:H,P,B film, drift mobility, photoconductivity meas. 4-104259
- Si:H amorphous films, glow discharge deposited, electron drift mobility, substrate temp. dependence 4-61393
- a-Si:H film, drift mobility, xerographic determ. 4-104224
- a-Si:H film, hole mobility model 4-104220
- a-Si:H films, electron drift mobility, xerographic determination 4-61377
- a-Si:H films, planar magnetron sputtering, electronic props. 4-88972
- a-Si:H/a-Si<sub>1-x</sub>N<sub>x</sub> quantum well struct., luminescence and current transport 4-114024
- Si/SiO<sub>2</sub>, MOSFET, elec. props. and atomic struct. 4-80677
- Si-BP-Si double heterojunction, current-voltage characteristics 4-80658
- a-Si-based alloy p-i-n solar cells, elec. field distrib. and open circuit volt. 4-89405
- Si-SiO<sub>2</sub> phase boundary, surface hole mobility 4-104323
- SiC cubic single cryst., CVD prep. and elec. props. 4-99345
- 3C-SiC epitaxial CVD coatings, high temp. elec. props. 4-88614
- Si<sub>3</sub>Ge<sub>1-x</sub>Ga<sub>x</sub> heterojunction, interface carrier recombination velocity determ. 4-104304
- SnTe thin films, elec. cond. and Hall effect 4-84716
- Ta<sub>2</sub>S<sub>3</sub>, Peierls transition, Hall const. temp. depend. 4-75937
- TiS<sub>2</sub>, semicond.-semimetal transition at 40 kbar 4-84660
- TiS<sub>3</sub>, elec. cond. and Hall effect 4-65677
- TiS<sub>2</sub> thin films, electronic transport props., classical metallic behaviour 4-70955
- TiTe<sub>2</sub>, band struct., elec. and mag. props. 4-92595
- TlInTe<sub>2</sub>, electrophysical props., as function of temp. 4-61401
- UO<sub>2</sub>, high temp. thermoelec. power studies 4-104244
- ZnO weak accumulation layers, electron transport and Hall effect 4-98686
- ZnO:Al films, RF magnetron sputtering, elec. and optical props. 4-85100
- ZnS, nonthermalised carrier mobility rel. to bulk photovoltaic effect 4-92727
- ZnSe, crystal growth by resublimation, hole mobility meas. 4-109316
- ZnSe films, MBE growth, elec. cond., Hall effect and photoluminescence studies 4-99344
- n-ZnSe, OMVPE undoped films, elec. and optical props. 4-93226
- ZnS:In<sup>+</sup>, ion implanted, high electron mobility obs. 4-108863

## carrier relaxation time

- see also electron relaxation time (metals)
- amorphous semiconductors, picosecond electronic relaxations 4-108892
- nonequilibrium carrier effective lifetime meas. in semiconductor wafers 4-101872
- semiconducting unipolar films, nonlinear elec. cond. 4-88617
- semiconductors, shallow donors, self-oscills. and flip-flop effect 4-108848
- GaAs, negative magnetoresist. associated with quantum localisation correction to cond. 4-61400
- GaAs photoexcited carriers, femtosecond orientational relax. 4-98634
- GaAs, relaxation of hot electron energy, surface plasmons 4-98631
- Ge:Sb, wave-function phase, relax. time, temp. depend. 4-88517
- In:Fe, <sup>3</sup>He<sup>+</sup> bombarded, psec. photocond., very short free carrier lifetimes 4-108894
- NbN, electronic props., optical study 4-66003
- Pb<sub>1-x</sub>Sn<sub>x</sub>Te:In epitaxial layers, photocond. kinetics 4-88538
- Sb<sub>2</sub>Te<sub>3</sub> single cryst., weak field charge transport 4-108887
- Si MIS struct., relax. time of wave-function phase in two-dimens. electron gas 4-88605
- Si-O cryst., minority carrier lifetime, O precipitation effects, IR studies 4-113971

## carrier scattering at surfaces see surface scattering

## carrier scattering by dislocations see dislocation scattering

## carrier scattering by impurities see impurity scattering

## carrier scattering by point defects see point defect scattering

## carrier traps see electron traps; hole traps

## carry circuits see adders

## CARS see coherent antiStokes Raman scattering

## cartography

- Ada County, Idaho, USA, mapping by photogrammetric method 4-110025
- Ada County Project, Idaho, USA, photogrammetric survey 4-110026
- algorithm for error adjustment of potential field data along a survey network 4-100438
- Antarctic, German contrib: using photogrammetry and remote sensing (German) 4-72485
- aquifer layers, subterranean, data processing and representation (Italian) 4-82099
- Balt Bare Glacier, Karakoram region, surging advance, topographic mapping 4-62862
- Batura Glacier, Karakoram, surface var. mapping, stereophotogrammetric surveys 4-62867
- Batura Glacier, Karakoram Mountains, topographic map and photogrammetry 4-62860
- coastline data, point reduction in digital maps (Japanese) 4-81833
- computer applications (book) 4-90306
- dambo features in Zimbabwe, morphology, mapping, and classification 4-100576

**cartography continued**

- digitization of aerial stereo photos using interactive computer graphics system 4-62659  
 Europe, central and east regions, isoseismal maps atlas 4-62701  
 Europe, central and eastern, seismic max. observed intensity map 4-62702  
 Europe, eastern and central regions, epicentre maps and earthquake catalogue 4-62700  
 E Germany, seismic max. observed intensities and epicentres, maps 4-62703  
 height interpolation by finite elements using computer program 4-62658  
 Karokoram glaciers, fluctuations anal. techniques 4-62864  
 Lake Yli-Kitka, Finland, mapping from satellites 4-100430  
 Landsat-4, cartographic accuracy of MSS and TM instruments 4-82267  
 Landsat-4 imaging processing techniques and map making 4-82260  
 map making using photogrammetry, geodetic densification basis 4-110025  
 metallogenic maps using new realistic format 4-94247  
 model-base image interpretation by line structure description appls. 4-96826  
 ocean floor imaging and charting system 4-115638  
 orthophoto map generation from panoramic photographs 4-62660  
 photogrammetric analogue plotting, computer-assisted stereoplotting system 4-94258  
 photogrammetric analogue plotting rationalisation with DZT 90X120 digital plotting table 4-94257  
 photogrammetry, conf., conference, Washington, DC, USA (March 1984) 4-82593  
 Pine Creek Geosyncline, Australia, realistic metallogenic map 4-94247  
 placer mineral exploration and development on United States continental shelves 4-115391  
 realistic projections of sphere or rotational ellipsoid fundamental eqns. 4-85603  
 regional seismic zones, mapping and earthquake recurrence 4-62709  
 sea ice characteristics mapping with Nimbus 7 Scanning Multichannel Microwave Radiometer data 4-67480  
 seismic activity maps compilation from earthquake epicentres distrib. anal. (Russian) 4-62996  
 seismic data sets, faulted, automatic contouring 4-100735  
 seismic zoning maps compilation for France, Switzerland, West Germany and USA 4-62714  
 topography mapping from radar altimetry, appl. of surface fitting by pseudo-potential functions 4-110296  
 Wilkes Land, Antarctica, bedrock topography map and tectonic evolution 4-81962

**cascade control**

- BWR digital feedwater controller conceptual design 4-59379

**cascade showers** *see cosmic ray showers and bursts***Cassegrain antennas** *see reflector antennas***cast iron** *see iron alloys***casting**

- furnace, casting unit, heat exchange, inverse heat cond. calcs. 4-107982  
 metallurgical systems, mechanisms and kinetics of dissolution 4-114530  
 metals, stir cast microstructure 4-89049  
 metals and alloys, solidification, book contrib. 4-109393  
 Rene 95, Ni-base superalloy, fatigue, effect of processing and microstruct. 4-104843  
 steel, austenitic stainless, structure and mech. props., casting environment effects 4-109433  
 steel, boride coatings obtained in casting process, form. and wear resist. props. 4-114715  
 steel, Cu-bearing, conf., Luxembourg (May 1983) 4-86106  
 steel, low-C cast, cyclic crack resist., heat treatment influence 4-62035  
 steel, pipes, centrifugal casting, mathematical simulation 4-85148  
 steel, structural, cast, strength toughness rel. to intercritical treatment (French) 4-81222  
 ternary alloy source material for rod-fed evaporation, fabrication process 4-114581  
 Al alloy, two-component, distrib. of alloying elements between phase components 4-114482  
 Al-Cu, rheocasting, grain refinement rel. to stirrer rotation velocity (Japanese) 4-89036  
 Al-Cu (10 wt %), prod. by rheocasting, rel. between struct. and mech. props. 4-99467  
 Al-Cu (3.76 wt %), Rheocast, ageing characts. rel. to incomplete homogenisation 4-109444  
 Cu-Nb-Sn in situ superconductors, long length, Sn electroplating and processing 4-61878  
 Fe, cast, white, annealing, Fermi energy, thermoEMF obs. rel. to crystallisation in acoustic vibration field 4-76768  
 Fe, obtained at superhigh quenching rates, struct. investig., 20 to 1150°C 4-93286  
 Si ribbons, polycrystalline, prep. by fast cooling, for solar cells 4-114508  
 SiC, reaction bonded, and liq. Al, cast bonding, exchange diffusion phenomenon involving free Si 4-99741

**castings**

- IN-100, Ni-base superalloy, cast, microstruct. changes during fractional melting 4-109434  
 light alloy, radioscope for inspection 4-99671  
 solidifying, temp. meas. 4-99740  
 steel, large-scale, cylindrical, hardening after gradient heating 4-114584  
 Al alloy, two-component, distrib. of alloying elements between phase components 4-114482  
 Al-Si alloy, graphite additions influence on wear characts. 4-109520  
 Fe, grey, profilometric characterisation of microstruct. (French) 4-71820  
 Fe, hardened high-strength, with nodular graphite cryst. struct. changes during tempering 4-93260  
 Fe, high-strength, mech. props. after prior heat treatment and isothermal hardening 4-93321  
 Fe, malleable, laser treatment, residual stress distrib., optimum surface hardening conditions (Russian) 4-71774  
 Fe, obtained at superhigh quenching rates, struct. investig., 20 to 1150°C 4-93286  
 Fe, powder, laser deposition on steel surface for hard-facing (Russian) 4-85251  
 Fe, with vermicular graphite, struct. and heat treatment 4-114471  
 Mg alloy, cast ML8, surface strain hardening treatment effect on low-cycle fatigue 4-99656  
 Ti-Al-Nb-Ta-Mo, welds and castings, impact roughness, segregation and influence of B 4-114658

**cataclysmic binary stars***see also novae*

- 0623+71, nova-like variable with assoc. nebular shell, discovery on Palomar Sky Survey 4-77903  
 accretion disc eclipses, light curve model, appl. to LX Ser 4-72954  
 accretion disc model spectra, double grid 4-77848  
 accretion discs, self-gravity and global structure 4-77818  
 RX Andromedae, dwarf nova, continuum distrib., simultaneous visible and UV obs. 4-110631  
 Z Andromedae, symbiotic star, March 1984 brightening 4-67741  
 Z Andromedae, symbiotic star, visual magnitude estimates (1984 March 30 to April 9) 4-67743  
 Z Andromedae, UV spectra of cataclysmic binary after outburst 4-115763  
 EG Andromedae, UV spectral changes in symbiotic star, IUE obs. 4-115761  
 TT Arietis, nova-like variable, visual magnitude estimates during 'down' state (July to September 1984) 4-115765  
 KR Aurigae, behaviour in 1983-4 season 4-94802  
 KR Aurigae, visual magnitude estimates (1983 December 9 to 1984 January 26) 4-63173  
 bipolar outflow from disk accreting stars 4-90143  
 boundary layers, HEAO 1 X-ray constraints 4-90155  
 AT Cancri, photographic magnitude estimates (1983 December 3 to 1984 March 23) 4-82495  
 HL Canis Majoris, U Gem star, photometry and search for eclipses 4-101377  
 AM Canum Venaticorum, period changes, mass-accreting white dwarf rotation 4-63182  
 OY Carinae, eclipsing dwarf nova, light curves and accretion disc characts. 4-110632  
 OY Carinae, visible eclipses of dwarf nova central object 4-63176  
 Z Chamaeleontis, high-speed photometry of dwarf nova in quiescence 4-63175  
 CoD-48°3636, low-luminosity high-temp. variable star, photometry, spectrum and radial vel. 4-72944  
 conference on high-energy transients, at Santa Cruz, United States (July 1983) 4-106091  
 CPD-48°1577, spectroscopy and optical-IR photometry 4-82483  
 SS Cygni, dwarf nova, obs. of quasi-coherent soft X-ray oscils. 4-94785  
 SS Cygni, dwarf nova, UVB photometry and spectroscopy of anomalous outburst 4-67726  
 SS Cygni, dwarf nova, visual magnitude estimates 4-106008  
 SS Cygni, dwarf nova, visual magnitude estimates (1984 August 12 to 21) 4-110625  
 V1016 Cygni, emission lines, geometric implications for eruptive symbiotic 4-67727  
 SS Cygni, far and extreme UV flux and spectra, evidence for wind 4-85955  
 SS Cygni, far UV obs. of cataclysmic binary outbursts planned for 1984 summer 4-94805  
 SS Cygni, planned far-UV obs. during 1984 outbursts 4-77847  
 V1016 Cygni, protoplanetary nebula, electron density determ. from Si III UV emission line strengths 4-94583  
 V 1329 Cygni (HBV 475), chromospheric event and violet shifted absorpt. and emission lines detect. 4-72957  
 V1500 Cygni (Nova Cygni 1975), photometric study of short-period continuum variability 4-106003  
 dwarf novae, optical props. rel. to soft X-ray transients 4-110658  
 dwarf novae, pulsed X-ray emission 4-101375  
 dwarf novae, spectrophotometry of seven objects 4-85960  
 E 2003+225, AM Her star, obs. and model 4-85976  
 eclipsing cataclysmic variables, orbital period var. and mass transfer, photometry obs. 4-105992  
 evolution, constraints from space densities and distrib. 4-82489  
 evolution and spectral characts. rel. to planetary nebulae 4-110722  
 evolution of cataclysmic binaries and low-mass X-ray binaries, observational study 4-94737  
 U Geminorum, dwarf nova, obs. of quasi-coherent soft X-ray oscils. 4-94785  
 U Geminorum, far and extreme UV flux and spectra 4-85955  
 U Geminorum, spectrophotometry and spectra interpretation with accretion disc and accretion spot models 4-85947  
 GX 1+4, symbiotic X-ray binary star, optical emission lines obs. 4-63201  
 H 0139-68, spectral and photometric obs. of AM Herculis type system 4-67769  
 H 0139-68, X-ray emission from AM Her binary, modulation and periodic vars. 4-77873  
 H 2215-086, intermediate polar, IR and optical obs. anal. 4-110686  
 H 2215-086, intermediate polar, X-ray pulse period and white dwarf rot. period 4-110687  
 AH Herculis, dwarf nova, continuum distrib., simultaneous visible and UV obs. 4-110631  
 AM Herculis, IR and optical polarimetry 4-63204  
 AM Herculis, low state on 1984 March 9, BV obs. 4-67774  
 DQ Herculis, numerical model for absence of observable X-ray emission 4-101376  
 AM Herculis, polarization and photometric obs. 4-106040  
 YY Herculis, spectrum of symbiotic star with G8 supergiant component 4-94797  
 AM Herculis stars, collision and Thomson scattering effects 4-90182  
 AM Herculis stars, column accretion onto white dwarf, electron leak and soft X-ray excess 4-94856  
 EX Hydrae, dwarf nova, high speed photometry 4-101378  
 VW Hydril, light curve, quasi-periodic oscils. 4-63155  
 VW Hydril, SU UMa star, white dwarf characts. an accretion disc nature, obs. 4-110615  
 VW Hydril, SU UMa star, X-ray pulsations discovery during superoutburst 4-67742  
 low mass, optically identified galactic X-ray sources 4-101421  
 magnetic braking, mass transfer mechanism 4-82485  
 mass-accreting solid white dwarfs, thermonuclear ignition rel. to Type I supernovae and low-mass X-ray binaries 4-77827  
 SY Muscae, symbiotic star, periodic light vars. due to refl. effect and eclipses 4-77855  
 novae, processes in circumstellar shells during diffuse-enhanced and orion stages 4-63171  
 optical polarisation and white dwarfs mag. fields 4-110633  
 optical spectra correl. with low-mas X-ray binaries spectra 4-110658

**cataclysmic binary stars continued**

- outbursts of cataclysmic variable stars, dynamical instabilities in red dwarf component 4-82481  
 AG Pegasi, symbiotic star, new determ. of photometric period from visual and photoelectric obs. 4-67734  
 period gap of cataclysmic variables, effect of mass transfer and disrupted mag. braking 4-94811  
 PG 1550+191, spectral study of AM Her-type system 4-110683  
 progenitors as star-planet systems, evolution 4-85951  
 VV Puppis, AM Her star, X-ray emission from point of accretion onto white dwarf 4-90184  
 RX Puppis, symbiotic system with Mira component, visible and IR emission 4-72955  
 HM Sagittae, circumstellar shell struct. and wind interactions, SHF/UHF obs. 4-85910  
 HM Sagittae, emission lines, geometric implications for eruptive symbiotic 4-67727  
 HM Sagittae, X-ray emission from eruptive symbiotic system 4-67728  
 secondary stars, spectral type analysis 4-85958  
 LX Serpentis, cataclysmic variable, orbit and light curve anal; hot spot characts. 4-106010  
 UZ Serpentis, dwarf nova, continuum distrib., simultaneous visible and UV obs. 4-110631  
 supernova explosion effect on low-mass companion, momentum transfer 4-85909  
 symbiotic stars, IUE low dispersion obs. 4-67731  
 symbiotic stars, spectral characts. 4-101373  
 symbiotic stars, synthetic spectra rel. to binary models 4-94786  
 symbiotic stars, X-ray to radio obs. 4-82480  
 RR Telescopii, symbiotic star, periodic light vars. due to Mira-type pulsation 4-77855  
 TV Columbae, X-ray periodicity found in DQ Herculis star 4-110682  
 UVB colours, catalogue 4-101200  
 AN Ursae Majoris, EXOSAT obs. of AM Her binary in bright state 4-63203  
 AN Ursae Majoris, polar, polarimetric obs. 4-106038  
 SU Ursae Majoris stars, eclipse depths rel. to red component activity and superhumps 4-90163  
 PU Vulpeculae, 1979-82 optical variability, UVB photometry 4-63179  
 PU Vulpeculae, spectral vars. obs. rel. to expanding circumstellar envelope 4-101356  
 white dwarfs masses and evolutionary scheme 4-85952  
 X-ray emission from non-magnetic cataclysmic binaries 4-63206  
 WX Sagittae, recurrent nova, circumstellar shell characts. and mass ratio, spectral obs. 4-101374

**cataloguing**

- see also library mechanisation  
 optical discs systems and applications, conf., Arlington, VA, USA (June 1983) 4-90287

**catalysis**

- see also catalysts; reaction kinetics  
 160 MW OTEC plantship design for methyl alcohol production 4-114936  
 acetylene adsorbed on oxidised and carbided W (100), C-H bond activation 4-93553  
 acidic H<sub>2</sub>O<sub>2</sub> fuel cells, hydrogen-electrode processes investig. 4-105106  
 acrylamide oxidation catalysis using activated Ir electrode in H<sub>2</sub>SO<sub>4</sub> (French) 4-62247  
 anharmonic oscillators dissociation, compensation effect, a model for catalysis 4-71892  
 aromatic hydrocarbons, low-temp. oxidation on oxide catalysts, kinetics 4-109687  
 char gasification, catalytic, math. modelling 4-99831  
 combustible gas sensors, development of poison resistant type 4-95414  
 cracking process, porous catalysts, diluted, activity, dilution effect 4-66610  
 electrodes, electrochemical form. of oxide films, SEM and TEM studies 4-104908  
 fast atom bombard. mass spectroscopy for appl. surface anal. 4-82857  
 fuel cells catalysed by WC in H<sub>3</sub>PO<sub>4</sub>, corrosion resistance and catalytic activity 4-66689  
 gas sensors, MOS and catalytic, comparison 4-82787  
 graphite, catalytic oxidation: by FeSO<sub>4</sub>, electron microscopy studies 4-85328  
 hexamethyl aluminium, surface adsorbed, laser photoreactions 4-81451  
 industrial cellulose wastes conversion to diesel fuel 4-72143  
 IR spectroscopic cell for FTIR meas. at press. up to 100 MPa 4-86491  
 lanthanide films, hydridisation and catalysis 4-71984  
 microcrystalline cellulose aqueous digestion process evaluation 4-66731  
 polyacetylene, polymerisation and oxidation using Lutinger's catalyst 4-66590  
 porous catalysts, diluted, activity, dilution effect 4-66610  
 pyrolytic C catalytic deposition in formation of carbonaceous selective absorber 4-72174  
 quartz glass, ablation, boundary layer, nonequilib. physicochemical processes 4-71967  
 semiconductor particle, electron energy levels, photocatalytic activity, irrad. effect 4-77029  
 semiconductor-electrolyte interface, illuminated, catalysed reactions 4-88577  
 SIMS, static, in appl. surface anal. 4-82857  
 small clusters stability, electronic struct. 4-74371  
 solid propellant, composite, catalyst role in ignition mechanism 4-77011  
 stainless steel, Cr-Ni-Nb (20, 25, 1%), C deposits, inhibition, prior selective oxidation 4-114708  
 subtilisins, in urea presence, conformational stability, fluoresc., circular dichroism 4-59927  
 surface desorption, light induced, threshold laser intensity 4-81481  
 transition metal alloys, surface segregation predictions 4-81475  
 transition metals, surface reactions and gas adsorption on alkali-promoted surfaces 4-85329  
 1,1,2-trichloroethane, acid-catalysed and radical chain transforms. 4-109641  
 water oxidation processes at n-PtS<sub>2</sub> and n-RuS<sub>2</sub> semicond. surfaces, ns-pulse laser study 4-89308  
 Ag (110) surface catalysis of selective epoxidation of ethylene 4-93554  
 Ag, heterogeneity in CO oxidation 4-105017  
 Al-air batteries, electrochemical characteristics of air electrode with Fe phthalocyanine 4-93608

**catalysis continued**

- Bi, colloidal, use as nucleation catalyst for mag. glass-ceramics prep. 4-71628  
 CO oxidation over Pd deposited on LiNbO<sub>3</sub> ferroelectrics, adsorptive and catalytic props., polarisation 4-99837  
 CO-Ni interaction in presence of K, site pot. effect 4-81477  
 CO<sub>2</sub> high energy pulsed lasers, catalyst evaluation for closed cycle operation 4-96939  
 Cu (II) complexes, correl. of EPR parameters with thermodynamic stability 4-98937  
 Cu surface heterogeneous catalysis, adsorbed mol. surface enhanced Raman scatt. 4-105018  
 Fe catalyst for NH<sub>3</sub> synthesis, surface struct. and reactivity study 4-80355  
 H<sub>2</sub>, mobility on Pd surface during catalytic H<sub>2</sub>O-forming reactions, detection 4-71985  
 H<sub>2</sub>, ortho-para conversion on mag. surfaces, dynamical aspects 4-70555  
 H<sub>2</sub> photocatalytic prod. with CdS<sub>1-x</sub>Se<sub>x</sub> solid soln. particles 4-100008  
 H<sub>2</sub> prod. from alcohol photocatalytic reaction on Pt/TiO<sub>2</sub> 4-114820  
 H<sub>2</sub> production by photoelectrocatalysis on p-MoS<sub>2</sub> 4-114963  
 H<sub>2</sub> production from aliphatic alcohols over UV-illuminated powder Ni/TiO<sub>2</sub> catalysts, at room temperature 4-66809  
 H<sub>2</sub>/O<sub>2</sub> evolution photoelectrocatalysis 4-105112  
 H<sub>3</sub>, field promoted, surface catalyzed formation on transition metals 4-66616  
 H<sub>2</sub>O<sub>2</sub>, catalytic decomp. investig. using chemiluminesc. oxidation of luminol 4-62188  
 I<sub>2</sub>, photon-catalysed bound-continuum process, post saturation fluoresc. quenching and fragments 4-62219  
 LaMO<sub>3</sub>, (M=Cr,Mn,Fe,Co), adsorbed pyridine, CO and CO<sub>2</sub>, IR spectra 4-104071  
 Mo catalysts supported on Al<sub>2</sub>O<sub>3</sub> or SiO<sub>2</sub>, Fourier transform IR spectroscopy of sulphidation 4-105014  
 NH<sub>3</sub>, field promoted, surface catalyzed formation on transition metals 4-66616  
 NH<sub>3</sub>+Re surface, single-collision energy transfer and catalytic decomposition at high temps. 4-71971  
 NO<sub>x</sub> synthesis in low press. plasma, energy cost improvement 4-85305  
 Ni, electroless plating on metals, catalytic activity and electro-oxidation 4-66243  
 Ni, molten, diamond form. and C diffusion coeffs. 4-105013  
 Ni/S surface catalysed reactions, cyclopropane hydrogenolysis 4-85330  
 O<sub>2</sub>, reactions in aq. solns. rate and mechanism, bibliography 4-67909  
 PH<sub>3</sub>, oxidation catalysed by Cu (II) and Fe (II) halides, intermediate form., MO LCAO calcs. 4-62236  
 Pd (100), adsorpt. and catalytic reaction of H<sub>2</sub>O, O and H, EELS and LEED study 4-71969  
 Pd, catalytic oxidation of CO, surface state effects 4-62238  
 Pd-MOS struct. with adsorbed H<sub>2</sub>, use as H<sub>2</sub> sensor in catalytic reactions 4-93555  
 Pt surface, Sn underpot. deposition in H<sub>2</sub>SO<sub>4</sub> soln. 4-81480  
 Rh surface, isotope exchange reaction of CO 4-81479  
 Ru catalyst for NH<sub>3</sub> synthesis, surface struct. and reactivity study 4-80355  
 Ru electrodes, electrochemical form. of oxide films, SEM and TEM studies 4-104908  
 (Ru,Si)<sub>1-x</sub>O<sub>2</sub>, surface adsorbed CO, pyridine and acetone, FT-IR study of surface acid sites 4-113783  
 TiO<sub>2</sub>, ultra-fine, photocatalytic activity in methanol-H<sub>2</sub>O soln., particle size depend. 4-66600  
 TiO<sub>2</sub>/Cr, doping effect on elec. and catalytic props. under UV and visible illumination 4-98663  
 YIG containing magnetic glass-ceramics, prep. using colloidal Bi as nucleation catalyst, characts. 4-71628
- catalysts**  
 see also catalysis  
 cracking process, porous catalysts, diluted, activity, dilution effect 4-66610  
 dispersed particles, stacking faults and struct., electron microdiff. studies 4-88178  
 ethylene complexes with metal cations on surface of heterogeneous catalysts, IR spectra, struct. 4-64471  
 EXAFS and XANES studies 4-62241  
 flammable gas sensing elements, high methane concentrations influence obs. 4-95403  
 flammable-gas sensing elements poison resistance obs. 4-95404  
 fluidisable cracking catalyst, flow through orifices 4-64999  
 fuel cells catalysed by WC in H<sub>3</sub>PO<sub>4</sub>, corrosion resistance and catalytic activity 4-66689  
 heterogeneous catalyst, AC heating 4-89328  
 heterogeneous catalysts and catalytic surfaces characterisation 4-89335  
 metal catalysts, dispersed, ISS anal., H<sub>2</sub> effects 4-99269  
 metal catalysts, supported, particle distrib. determ. by X-ray small angle scatt. 4-97967  
 metal particles, determ. of structural parameters by EXAFS 4-93132  
 metal supported catalysts, EXAFS in situ measurements, sample cell 4-61779  
 metal-compounded semicond. photocatalysts, function of metal 4-62230  
 metal-ion exchanged layer structures, EXAFS studies 4-62196  
 nickel tetraphenylporphine compounds on  $\gamma$ -Al<sub>2</sub>O<sub>3</sub> and SiO<sub>2</sub>, reson. Raman spectra 4-105012  
 oxide, low temp. oxidation of aromatic hydrocarbons, kinetics 4-109687  
 porous catalysts, diluted, activity, dilution effect 4-66610  
 propylene complexes with metal cations on surface of heterogeneous catalysts, IR spectra, struct. 4-64471  
 sulphonated styrene-divinylbenzene resin catalysts, use in dehydration of 2-butanol 4-66580  
 1,1,2-trichloroethane, catalytic dehydrochlorination, CNDO/2, INDO and MINDO/3 calcs. 4-91202  
 Al<sub>2</sub>O<sub>3</sub> catalysts, short range order, EXAFS studies 4-62246  
 Al<sub>2</sub>O<sub>3</sub>, supported Rh catalyst, O interaction, EXAFS study 4-66097  
 C fibres, electrodeposition of metals after cation-exchange, catalysts appl. 4-76701  
 Cu/Ru(001) bimetallic catalysts, static SIMS, XPS and TPD studies 4-80411  
 Fe catalyst for NH<sub>3</sub> synthesis, surface struct. and reactivity study 4-80355  
 $\alpha$ -Fe<sub>2</sub>O<sub>3</sub> CVD coating on alumina high temp. stable catalyst for SO<sub>2</sub> conversion to SO<sub>3</sub> in hydrogen production process 4-66807  
 Fe<sub>2</sub>O<sub>3</sub>, doped, p-n assembly, water, catalytic photodissoc. 4-62207

# catalysts continued

- If electrode, activated, potentiometric behaviour in acrylamide and  $H_2SO_4$  (French) 4-62247
- Ir, for  $H_2$  production by catalytic thermal decomposition of water 4-93646
- $MgCl_2$  supported  $TiCl_3$  catalysts, fluorescence EXAFS 4-62242
- Nb films covered by Ce, catalytic oxidation, XPS 4-114830
- Ni, for pyrolytic C catalytic deposition in formation of carbonaceous selective absorber 4-72174
- Ni/ $TiO_2$  powder catalysts, UV-illuminated, for  $H_2$  production from aliphatic alcohols 4-66809
- $NiFe_2O_4$  high temp. stable catalyst for  $SO_3$  conversion to  $SO_2$  in hydrogen production process 4-66807
- $NiO-MoO_3/Al_2O_3$  catalysts, atomic distrib. studied by ion scatt. spectroscopy 4-71972
- Pd catalysts, monodisperse, adsorpt. and dissolution of  $H_2$  4-61220
- Pd, charcoal supported, used in decarbonylation of furfural to furan 4-99976
- Pd surface, catalytic  $H_2O$ -form. reaction,  $H_2$  mobility and detect. 4-71985
- Pd- $Al_2O_3$  catalyst plug of Pb/acid batteries, deterioration prevention 4-93613
- Pt, black, catalyst/pyroelectric gas sensor using heat of reaction 4-66564
- Pt catalysts, classical and inorganic cluster derived, EXAFS studies 4-62245
- Pt, epitaxial ultrathin deposits on NaCl, model catalysts appl. 4-98489
- Pt, for  $H_2$  production by catalytic thermal decomposition of water 4-93646
- Pt for p-n junction GaAs photovoltaic electrolyser for hydrogen production by water electrolysis 4-89451
- Pt layer on graphite and  $RuO_2$  substrates, ion bombard., electrocatalytic props. 4-71968
- Pt/ $\gamma-Al_2O_3$  catalyst for HI decomposition in thermochemical  $H_2$  production 4-93647
- Re, for  $NH_3$  synthesis, surface struct. sensitivity 4-109685
- Rh/ $Al_2O_3$  catalyst, highly dispersed, CO adsorption, EXAFS study 4-62243
- Ru, adsorbed  $N_2$ , temp. programmed desorption and isotopic study 4-93558
- Ru catalyst for  $NH_3$  synthesis, surface struct. and reactivity study 4-80355
- $RuO_2$  for p-n junction GaAs photovoltaic electrolyser for hydrogen production by water electrolysis 4-89451
- $Ti$ , polycryst., O<sub>2</sub> adsorption, charact. and coadsorption with Pb 4-92568
- $TiO_2$ ,  $RuO_2$  doped, for  $CO_2$  photoassisted reduction 4-99817
- $TiO_2$ , undoped n-type for  $CHCl_3/C_2HCl_3$  solar photoassisted catalytic decomposition 4-62234
- $TiO_2-V_2O_5$  catalysts, EXAFS study 4-62244
- $WO_3-Al_2O_3$ ,  $O_2$  and  $H_2O-D_2O$  exposure cycles, surface struct., O exchange, spectra studies 4-114271
- $ZnFe_2O_4$  high temp. stable catalyst for  $SO_3$  conversion to  $SO_2$  in hydrogen production process 4-66807

# cataphoresis see electrophoresis

# catastrophe theory

- asymptotically non-stationary chaos, 1-dimens. map, generalised entropy 4-90500
- beams, cantilever, elastic, with nonlinear elements, instability, butterfly catastrophe 4-87599
- conical shells, stability under large deformation (German) 4-83840
- cuspid catastrophes, Maxwell sets determ. 4-101610
- homeothermic animal temp. regulation, five-dimensional dual butterfly catastrophe model 4-66884
- hysteresis phenomena in plasmas in catastrophe theory 4-97752
- linear series and stability in astronomy 4-63091
- nonelementary, appl. to imperfect bifurcation problems 4-58649
- Pippard's rotating dipoles, contours, critical points and catastrophe 4-67942
- singular catastrophe sections, partial stability, cuspoids and conic umbilics appl. 4-90350
- thin elastic shells, stability anal., catastrophe theory 4-87575
- Thom universal catastrophe shape, intuitive geometric formation (German) 4-82653
- tilted cavities, cusp catastrophe for Benard convection numerical study 4-87715

# cathode-ray oscilloscopes

- see also oscillographs
- broadband universal sampling head construction for sampling oscilloscopes 4-64313
- colour, digital oscilloscope, Digiscope 8612, microprocessor-controlled instrument (Italian) 4-106298
- design trends, performance and user facilities (German) 4-106301
- digital storage type, Matsushita model VP-5730A (Italian) 4-106299
- operation and sampling aspects (German) 4-82788
- portable test instrumentation development, using CMOS LSI technology, flat displays and microprocessors 4-73429

# cathode-ray tube displays

- see also cathode-ray oscilloscopes
- human colour discrimination under ambient illumination 4-81686
- Japanese characters, readability on CRT and visual fatigue (Japanese) 4-93743
- large screen display by CRT projection system (Japanese) 4-107791
- VDU, low-background radiation meas. 4-62601
- Video slide printer/projector with pointer capability 4-69527
- cathode-ray tube screens see cathode-ray tubes; fluorescent screens
- cathode-ray tubes
- see also image converters; image intensifiers; image storage tubes; television camera tubes
- fine beam, specific electronic charge meas. using tangential gun 4-73197
- fine beam tubes for student expts. 4-95112
- fine-beam, electron beam physics expts. for students 4-58611

# cathode rays

- No entries

# cathodes

- see also electron emission; oxide coated cathodes; photocathodes; thermionic cathodes
- beam emittance determ. of hollow cathode ion source 4-60649
- caruba wax, thermoelectret state, charge carrier identification 4-99008
- cathode spot initiation and mass balance in near-cathode plasma 4-91876
- cathode spot retrograde motion, ampere force compensation 4-87979

# cathodes continued

- cylindrical cathode discharge in mag. field, characts. 4-113237
- externally sustained vol. discharge, cathode spot regular arrangement 4-69979
- gap closure, cathode surface impurities 4-60777
- glow discharge, sputtered atom, light emission, interferometry 4-87981
- glow-discharge-created electron beams 4-95560
- high brightness cathode materials 4-71508
- hollow cathode discharge, high purity material spectral anal. 4-81493
- hollow cathode in magnetised arc, ion source props. meas. 4-88007
- hollow cathode ion source, plasma investig. (German) 4-84102
- hollow-cathode cell for a pulsed vapor laser 4-102939
- impregnated dispenser cathodes, appearance pot. spectroscopy, XPS and AES (Chinese) 4-106437
- ion bombardment suppression effects of a field-emission cathode 4-114363
- large area woven fibre cathodes 4-99802
- material properties, simulation studies, influence on discharges 4-97918
- metal vapour arcs, cathode spot plasma, ion acceleration, Ohm's law 4-87975
- metals, boundary line, impulse discharge, cathode erosion traces 4-87985
- MHD generator, cathode wall nonuniformities on electrical characteristics, analytical models 4-77119
- moving spot in vacuum arc 4-108241
- pointed field emission cathodes, model 4-76644
- rheological properties of nitrocellulose binders as Ba-Sr-Ca carbonate suspensions (Polish) 4-83870
- sheath parameters investigation 4-84108
- steady-state externally maintained discharge cathode layer struct. form. 4-108242
- vacuum arc, cathode spot region microparticle generation 4-87977
- vacuum arcs, cathode spot lateral spread in transverse mag. field 4-87978
- vacuum discharge cathode spot, cyclicity processes 4-87980
- varigap negative electron affinity emitters, photo- and secondary emission efficiency 4-99281
- Al-air battery, rapidly refuelable, for electric vehicles, performance evaluation 4-72096
- Cu erosion coeff., cathode spots in discharge 4-87976
- Li thin film cells, solid electrolytes and cathode materials (Japanese) 4-93597
- Li/ $CrO_3$  battery, performance characts. and safety tests, for electronic applications 4-93602
- $Na_2CO_3$  electrode material, electronic processes during intercalation 4-76012
- Pb-acid battery cathodes incorporating chemically prepared  $PbO_2$  4-77073
- PdO cathodes, photoelectrolysis and electronic props. 4-85313
- W point cathodes, electron field emission instability, adsorption effects 4-61813

# cathodes, electrochemical see electrochemical electrodes

# cathodochromism

- No entries

# cathodoluminescence

- diamond, natural, type II, cathodoluminescence from dislocations 4-81012
- diamond, type IIb, individual dislocation and cathodoluminescence emission polarisation 4-99199
- garnet monocrystalline cathodoluminesc. layers 4-81010
- III-V optical sources, dislocations climbing degradation, experimental anal. 4-83654
- inert gases, solid, cathodoluminescence excitation spectra 4-85013
- phosphors, binary compounds, cathodoluminesc. efficiency calc. 4-61754
- quartz, growth sector characts. by cathodoluminesc. 4-61755
- semiconductors, cathodoluminesc. contrast formation of localized non-radiative defects 4-85016
- semiconductors, cathodoluminescence, EBIC and SIMS studies 4-76531
- voltage depend., Gaussian models 4-65303
- $Al_2Ga_{1-x}As_x$  cathodoluminescence study 4-71449
- $Al_xGa_{1-x}In_{1-x}Sb_x$  epitaxial layers, luminescence studies 4-76505
- $Al_xGa_{1-x}In_{1-x}Sb_x$ , nominally undoped, MBE growth and charact. 4-98472
- Ar, solid, cathodoluminescence excitation spectra 4-85013
- $CuInSe_2$ , radiative recombination and shallow centres 4-109250
- $Ga_{1-x}Al_xAs$  GaAs heterostructure, LPE grown, dislocation extension and density distrib. (Chinese) 4-113449
- $Ga_{1-x}Al_xP_x$  epitaxial structs., luminesc. study 4-85011
- GaAs LEC substrate, characterisation of impurities and microdefects (Japanese) 4-103778
- GaAs MBE films, growth and elec. props. (Chinese) 4-84523
- GaAs, semi-insulating LEC grown, impurity distribution, cathodoluminesc. study 4-88885
- GaAs semi-insulating substrate, inhomogeneity characterisation, expt. study 4-65759
- $Ga_{1-x}In_xP_x$  LPE growth on GaAs substrates, cathodoluminesc. and photoluminesc. spectra (Chinese) 4-113825
- $GaN:Zn$ , cathodoluminescence, anomalous kinetics 4-85015
- GaP: N epitaxial films, n-type, local cathodolum. kinetics 4-109251
- $GaP:As,Sb_{1-x}P_x$  epitaxial layers, luminescence studies 4-76505
- $HgCr_2Se_4$  ferromag. semiconductor, luminesc. study with quantum energy exceeding the forbidden band gap 4-80992
- $Hg_{1-x}In_xTe_x$ , recombination radiation 4-71447
- InP epilayers, cathodoluminescence study 4-104678
- InP, near IR cathodoluminescence in a TEM 4-81011
- KCl, impurity-localised excitons, luminesc. and absorpt. spectroscopy study 4-92625
- $LiNbO_3$  single cryst., cathodoluminescence emission, surface damage 4-93115
- $MgAl_2O_4$  spinel, cathodoluminescence induced by impurities 4-85017
- $MgO$  (100), surface dislocation, secondary electron emission study 4-80345
- $MgO$ , quenched, defect struct., plastic deform., SEM, cathodoluminescence, optical absorpt. spectra 4-71448
- $MgO$  single cryst., high anion vacancy conc., cathodoluminescence obs. 4-88886
- $NaCl:Br$ , impurity-localised excitons, luminesc. and absorpt. spectroscopy study 4-92625
- PbS film, photosensitivity and luminescence studies 4-104679
- $SiO_2$ , halogen containing layers, cathodoluminescence spectra (Russian) 4-99198

**cathodoluminescence** continued  
SiO<sub>2</sub>/Cr thin films, cathodoluminescence and C-V characts. (*Russian*) 4-99173  
(Y<sub>1-x</sub>Gd<sub>x</sub>)<sub>2</sub>O<sub>3</sub>:S:Ca luminesc. study 4-81013  
Y<sub>2</sub>(WO<sub>4</sub>)<sub>3</sub>:Eu<sup>3+</sup>, prep. and luminesc. props. 4-81009  
ZnO UV laser with longitudinal electron beam pumping 4-79164  
ZnS:Ag phosphor, phase composition effect on luminescence parameters and EPR spectrum (*Polish*) 4-85014  
ZnS:Cu film, cathodoluminescence study of annealing 4-81008

**cathodophosphorescence** *see* **cathodoluminescence**

**cathodothermoluminescence** *see* **cathodoluminescence**

**catholytes** *see* **electrolytes**

**CATV** *see* **cable television**

**Cauer filters** *see* **active filters**

**causality** *see* **physics fundamentals**

**causticity** *see* **pH**

**cavitation**  
*see also* **bubbles; vortices**  
axisymmetric cavitation problem of determ. influence of restriction of flow in vertical circular tube 4-112967  
bubble phenomena in sound fields 4-69615  
bubbles collapse between two walls in US field 4-103063  
capillary phenomena, cavity formation due to a contact between particles in a nonwetting liquid 4-61181  
capillary phenomena, interaction between particles in a nonwetting liquid 4-61182  
circular cylinder, cavitating flow, erosion, trailing bubble entrainment 4-97622  
circular cylinder, cavity/wake dynamics, noise spectra meas. 4-79631  
electrostatic technique for meas. of cavitation inception 4-103377  
ethanol in Berthelot tube at ground level, bulk nucleation obs. 4-87768  
flow separation region, cavitation phenomenon 4-60468  
gas bubble collapse near solid wall by shock wave and induced impulsive pressure 4-112954  
generation of cavitation maxima by pulsed ultrasound 4-112968  
hydrofoil, optimum shape giving max. lift in steady two dimens. fully-cavitating flow 4-103334  
laser Doppler anemometry of flow in cavitation test tank anal. (*German*) 4-103375  
liquid tensile strength, cavitation history and entrained gas effect 4-75593  
liquid through two series-connected diffusers subject to cavitation, flow states 4-103376  
liquids, cavitating, acoustic monopole and dipole radiation efficiency 4-91682  
microbubbles dynamic and diffusive growth, near two-dimensional hydrofoil 4-65010  
organic solvents, acoustic cavitation, erosion activity 4-91679  
paint, cavitation erosion, decontamination of surfaces (*French*) 4-70222  
perspex, cavitation erosion, decontamination of surfaces (*French*) 4-70222  
physical modelling of cavitation with optical measurement techniques 4-60469  
power characteristics and cavity formation in aerated agitations 4-112928  
ship propeller cavitation noise power spectra (*Chinese*) 4-107949  
steel, carbon, cavitation erosion, decontamination of surfaces (*French*) 4-70222  
steel, stainless, cavitation erosion, decontamination of surfaces (*French*) 4-70222  
two-dimens. gas-filled cavity dynamics near liq. free surface 4-112984  
underwater explosion of ring charge near a free surface 4-87759  
vapour and gas, simulation 4-97623  
variable celerity modeling by the method of characteristics 4-97624  
vortex ring collapse 4-97584  
water, acoustic cavitation threshold, dil. polymer additives effect 4-103378  
Al, cavitation erosion, decontamination of surfaces (*French*) 4-70222

**cavities (solid)** *see* **voids (solid)**

**cavity resonators**  
*see also* **acoustic resonators; laser cavity resonators**  
atomic Rydberg states interacting with MM waves in Fabry-Perot cavity 4-96474  
Cherenkov relativistic electron source for millimetre range, Bragg resonator use 4-69300  
coaxial EPR cavity for high temp. and press. studies 4-101884  
coupled resonators employing phase-conjugating and ordinary mirrors 4-107795  
dielectric measurements in 100 GHz range using resonant cavity, system config. and appl. (*Japanese*) 4-106330  
electron cyclotron resonance maser with quasioptical cavity, kinetic theory (*Chinese*) 4-83560  
ESR spectroscopy, 2 to 10 GHz, re-entrant resonator design 4-86449  
Fabry-Perot cavity, nonlinear, with nematic liquid crystal, dynamics 4-83635  
Fabry-Perot resonator, all-optical quantum system, bifurcation to chaos obs., 4-96852  
Fabry-Perot resonator, optical bistability, semiclassical approach, coupled amplitude eqns. 4-79222  
fibre-optic ring resonator for rotation sensing, passive 4-112580  
gyromonotron electron cyclotron maser with arbitrary longitudinal field distrib., kinetic theory 4-60007  
half-symmetric unstable resonator with internal axicon, reflexicon deforms effect on geom. parameters 4-69524  
irregular waveguides and open resonators theory, EM fields, variational techniques 4-102852  
low-Q cavities, cooperative behaviour of Na Rydberg atoms 4-107583  
microwave cavity design for gas breakdown characts. meas. of He-O<sub>2</sub> mixtures 4-95465  
noise Fabry-Perot cavity, absorptive optical bistability, amplitude and phase fluctuations 4-96985  
optical bistability, nondegenerate, two-photon, in Fabry-Perot cavity, large mol. dipole moments effects 4-74601  
optical resonators, narrowband absorption, demultiplexing appls. (*German*) 4-60131  
parametric amplification, intracavity and travelling-wave light fields, squeezing 4-112519  
passive and active optical systems, instabilities, Gaussian transverse intensity profile 4-112502  
quadratic Ikeda map, one-dimensional approx. 4-102976

**cavity resonators** continued  
Slater's cavity perturbation theorem, matrix formulation 4-64651  
splitring loaded resonant RF-cavity, postaccelerator sections for Van de Graaf generators 4-102415  
three-layer dielec. resonator for liquids dielec. props. meas. appl. 4-111161  
water waves propagation, analogy with EM waves 4-115413

**CCD** *see* **charge-coupled devices**

**c.c.d. circuits** *see* **charge-coupled device circuits**

**CCTV** *see* **closed circuit television**

**CDW** *see* **charge density waves**

**celestial mechanics**  
*see also* **Earth orbit; N-body problems; stellar motion**  
1983 TB, orbital evolution rel. to future observability 4-77753  
Adrastea (1979J1), orbital parameters of Jupiter satellite 4-101231  
artificial motion, synodic motion of satellites related to the Sun 4-82383  
artificial satellites, adaptive orbit estimation scheme 4-82373  
artificial satellites, atmospheric density models for orbit estimation 4-72768  
artificial satellites, autonomous orbit computation, appl. of delta-rho perturbation method 4-90058  
artificial satellites, closest approach and encounter duration for two satellites 4-82384  
artificial satellites, first order short-periodic motion due to third body perturbations, numerical evaluation 4-94561  
artificial satellites, general anomaly and time elements 4-67596  
artificial satellites, orbit prediction by vector techniques, SPIRAL program anal. 4-94642  
artificial satellites, orbit theories based on elimination of parallax 4-82371  
artificial satellites, orbit theory for LSI-11 microprocessor 4-94554  
artificial satellites, orbital mechanics, use of empirical atm. density models 4-82320  
artificial satellites, orbital perturbations due to vars. in rot. of central body 4-101212  
artificial satellites, orbits, coupled perturbations anal. appl. of Lagrange method 4-82375  
artificial satellites, synchronous orbits, appl. of extended semianalytical Kalman filter 4-90057  
artificial satellites, times of close approach between satellite pairs, prediction method 4-82382  
asteroid belt, gravit. perturbations on celestial bodies and spacecraft 4-90098  
asteroid families, ages estimation 4-90105  
asteroid families, collisional origin, effects of target's gravity 4-90104  
asteroids, dynamical evolution 4-77755  
asteroids, dynamical motions and Fundamental Reference System systematic accuracy determ. 4-82386  
asteroids, low-velocity encounters with outer planets 4-90106  
asteroids, motion and evolution, obs. database 4-101275  
asteroids, orbital elements for stability regions 4-90099  
asteroids, orbital stability 4-90100  
asteroids, resonant orbits stability 4-90101  
asteroids, stability and capture anal., use of the Lyapunov Charact. Numbers 4-82397  
autonomous satellite navigation using the stellar horizon atmospheric dispersion sensor 4-94555  
binary collisions in planar three-body problem, global regularization (*French*) 4-82387  
binary protostars, ang. momentum transfer by gravit. torques rel. to evolution 4-110598  
capture probabilities for orbit-orbit reson. problems 4-67602  
Comet Austin (1984i), discovery, orbital elements and ephemeris (1984 July 21 to 31) 4-94684  
Comet Austin (1984i), positions, magnitudes, orbital elements, ephemeris and coma diameters 4-94687  
P/Comet Boethin, capture by Jupiter 4-90119  
P/Comet Bradfield (1984a), positions, magnitude estimates and orbital elements 4-85896  
P/Comet Neujmin 3, orbit, correl. with Periodic Comet van Biesbroeck 4-67702  
comet orbit determ. by means of optimally selected observations 4-82385  
comet orbits and minimum planetary distances (*Russian*) 4-101259  
P/Comet Russel 3 (1982 IX), orbit evolution (1938 to 2028) and Jupiter encounters 4-77771  
Comet Shoemaker (1984f), astrometric obs., orbital elements and ephemeris (1984 May 30 to July 29) 4-82453  
P/Comet van Biesbroeck, orbit, correl. with Periodic Comet Neujmin 3, anal. 4-67702  
P/Comet Wild 3, orbital perturbations due to close encounter with Jupiter (May 1977) 4-94683  
comets, long period, perihelion distrib. and solar apex 4-72912  
comets, motion and evolution, obs. database 4-101275  
comets, orbits, evolution and origin 4-77780  
communications satellites, ephemeris representations 4-94560  
computational spherical astronomy (book) 4-78017  
conference at Embu, Brazil (December 1981) 4-78039  
conference on astrodynamics at Lake Placid, USA (August 1983) 4-78043  
conference on dynamical trapping and evolution in solar system, at Gerakini, Greece (August-September 1982) 4-86139  
degenerate dynamical systems and KAM-type integrals of motion disappearance 4-90077  
double resonant problem, formal soln. 4-82399  
Earth satellite in 12-hour orbit, evolution of orbit (*Russian*) 4-115678  
Enceladus orbit and interior heating, influenced by Janus and ring system 4-101246  
equality for zero vel. surfaces 4-82396  
equations of motion regularisation in central force field, appl. to artificial zonal satellites 4-90062  
equilibrium stability in problems with double reson., appl. to artificial satellites 4-82395  
extinct comets in high-inclination orbits, steady state number 4-90118  
few body problems 4-63035  
four-body problem, planar case with three fixed centres 4-63038  
four-body problem, planar symmetric case, disintegration 4-115778  
galaxies, distribution function from statistical thermodynamics of gravitationally interacting bodies 4-67801  
Galilean satellites, comparison of Sampson's theory with photographic positional observations (*Russian*) 4-101237

## celestial mechanics continued

- Galilean satellites, long-terms motion determ. via numerical integration procedure 4-82402  
 Galilean satellites, motion, analytic theory first approx. and ephemerides 4-82443  
 Galilean satellites, mutual phenomena in 1973 and 1979/80, astrometric obs. 4-63098  
 Galilean satellites, orbital evolution 4-82442  
 Galileo spacecraft for asteroid or comet rendezvous, trajectories 4-82378  
 geodynamic satellites, drag in atm., neutral and elec. components 4-82370  
 geosynchronous satellites in inclined orbits, long-term motion 4-82372  
 Giotto, pathfinder technique for targeting accuracy improvement 4-90056  
 globally optimal impulsive transfers via Green's theorem 4-115677  
 Griffiths retention theorem for N+1 body problem, correction 4-67599  
 Hamiltonian systems near equil. soln., periodic soln. stability (*French*) 4-82391  
 Hamiltonian systems near equil. soln. and periodic orbits in reson. cases, appl. to galactic dynamics (*French*) 4-82390  
 Hamiltonian transformation in quadratic Li transforms 4-67600  
 HEAO-2, definitive orbit determ. 4-82381  
 Hori auxiliary system for motion of two planets with periods commensurable (in ratio 2:1) 4-110500  
 impact ejecta from Mars, orbital evolution rel. to SNC meteorites 4-105907  
 interplanetary grains, reson. orbits trapping time with Poynting-Robertson drag 4-90112  
 interplanetary trajectory design, optimum two-impulse transfers 4-115676  
 interplanetary trajectory optimisation (*Japanese*) 4-94548  
 Janus, recent orbit evolution history 4-101246  
 Jupiter approach orbit determ. for Galileo mission 4-110494  
 Jupiter-Uranus reson. locking 4-110506  
 Kepler's equation, rapidly converging series approx. 4-94568  
 Kepler problem spinor regularisation and quantisation on the manifold  $S^2$  4-77699  
 Kirkwood gaps depletion mechanism 4-90063  
 Lagoos, orbit var. and lower mantle viscosity determ. 4-85641  
 Lagrangian singularities, appl. 4-82398  
 Landsat 4, orbit solns., ephemerides and Global Positioning System navigation results 4-94556  
 libration points of central configurations, stability 4-101123  
 Lie series, appl. as numerical integration method 4-82400  
 long-period comets, orbits, systematic and random perturbations (*Russian*) 4-94692  
 long-period comets, perihelion passages, statistical anal. 4-101263  
 lunar artificial satellites orbits anal. and Moon gravity field characts. determ. 4-101209  
 lunar secular acceleration and laser ranging data, implications for tidal deceleration of Earth rot. 4-100429  
 magnetised artificial satellite in circular polar orbit plane, eqn. of motion 4-101113  
 Mars satellites, orbital evolution and origin 4-77749  
 meteor streams evolution, effects of radiation press., Poynting-Robertson effect and comet nuclei 4-90120  
 meteoroids, orbital evolution of Perseids and Quadrantids streams 4-90121  
 Metis (1979J3), orbital parameters of Jupiter satellite 4-101231  
 Moon, recession from Earth due to ocean-induced Earth rot. decrease 4-81831  
 Moon orbit evolution, high order reson. 4-90060  
 N+ $\nu$  body problem, restricted case 4-67603  
 N-body hierarchical dynamical systems, trapping mechanism, mirror conditions asymptotic approach 4-90070  
 N-body problem, fitting to Eddington potential 4-67799  
 Neptune-Triton system, dynamical evolution 4-77763  
 orbital lifetime estimation method for near Earth satellites 4-82374  
 orbits, small perturbations determ. via estimation method 4-82403  
 ordinary differential equations numerical integration, global error estimation, stochastic approach, celestial mechanics appl. 4-82401  
 perigee elimination in satellite problem 4-67605  
 perturbed motion of spheroidal planet's satellite, approx. soln. 4-63037  
 Phoebe, ephemeris including planetary perturbations (*French*) 4-82446  
 Phoebe, orbital elements 4-82444  
 planar inverse problem for autonomous systems 4-90075  
 planet orbit perihelion shift due to electric charge of Sun 4-110507  
 planetary dynamics, appl. of VLBI obs. of extragalactic radio sources near ecliptic 4-73088  
 planetary orbits in binary star systems, periodic and quasiperiodic orbits (*German*) 4-67607  
 planetary orbits in Schwarzschild and Reissner-Nordstrom space, spherical symmetric models (*German*) 4-85865  
 planetary satellites, orbital perturbations due to vars. in rot. of central body 4-101212  
 planetary satellites orbit evolution, high order reson. 4-90060  
 planets, orbital evolution and perturbations 4-90097  
 precession, expressions using new system of astronomical const. (*Chinese*) 4-81830  
 precession dynamics in spin-orbit coupling, unified theory 4-110503  
 quasixisymmetric satellite, periodic oscil. stability in elliptical orbit plane 4-82392  
 satellite 1967-104B, orbital anal. rel. to determ. of 29th-order geopotential coeffs. 4-105398  
 satellite at libration point in restricted three-body problem, orientation 4-90061  
 Saturn, E ring dynamics 4-101247  
 Saturn, satellites in tadpole or horseshoe shaped orbits, orbital reson. effects 4-101240  
 Saturn ring system, theoretical optical thickness profile for bimodal gravitating system 4-101243  
 Saturn satellites, mutual phenomena in 1973 and 1979/80, astrometric obs. 4-63098  
 Saturn satellites, resonances evolution origin 4-90110  
 Saturn XII, XIII, XIV, orbits anal. and obs. 4-67674  
 short period comets, perihelion distances distrib. 4-90115  
 solar system, distrib. of ang. momentum vectors of comets, asteroids and meteor streams 4-101204  
 solar system, stability of three-body subsets rel. to masses and positions of possible past companions of Sun 4-101307  
 solar system dynamical evolution 4-77700  
 Space Shuttle orbital navigation expt., use of Global Positioning System geodetic receiver 4-94558

## celestial mechanics continued

- space vehicles ballistic planetary trajectories, optimisation, effect of parking orbit constraints 4-82379  
 Starlette satellite, orbital perturbations by ocean tides (*Chinese*) 4-82362  
 symmetric periodic orbits in the anisotropic Kepler problem 4-90069  
 Szebehely's equation intrinsic formulation (*French*) 4-82388  
 Szebehely's inverse problem eqn. rel. to multiple var. problem from Maupertuis' principle 4-110502  
 Szebehely's inverse problem for finite symmetrical material concentrations 4-94566  
 TDRSS satellite, navigation and orbit determ. use of dedicated VLBI system 4-82380  
 Thebe (1979J2), orbital parameters of Jupiter satellite 4-101231  
 three-body problem, collinear restricted case, capture-escape boundary 4-90073  
 three-body problem, double-averaged planar restricted case, orbit evolution 4-77697  
 three-body problem, elliptic restricted case, doubly asymptotic orbits at unstable equil. 4-90074  
 three-body problem, elliptic restricted case, equipotential curves boundaries 4-90072  
 three-body problem, elliptic restricted case, triangular points linear stability 4-90071  
 three-body problem, elliptical non-planar restricted case, periodic orbits, stability 4-90068  
 three-body problem, general case, Hill-type analytical stability surfaces shape 4-82389  
 three-body problem, isosceles soln., appl. to triple stars motion 4-82393  
 three-body problem, masses stability 4-67604  
 three-body problem, planar circular restricted case, trajectories with 2:1 reson. 4-94567  
 three-body problem, planar general case, asymmetric periodic solns. and stability 4-77698  
 three-body problem, planar general case, asymmetric periodic orbits and their stability 4-90067  
 three-body problem, planar symmetric case, disintegration 4-115778  
 three-body problem, restricted case, almost-square orbits 4-110504  
 three-body problem, restricted case, eccentricity effect on halo orbits, artificial satellite appl. 4-82404  
 three-body problem, restricted case, equil. points, perturbation effects 4-110499  
 three-body problem, restricted case, high-order reson. 4-67601  
 three-body problem, restricted case, infinite bifurcations 4-72857  
 three-body problem, restricted case, rectilinear libration point coords. 4-63036  
 three-body problem, restricted case, symm. periodic orbits, stability and bifurcations 4-90065  
 three-body problem, three-dimens. restricted case, reson. periodic solns. 4-90066  
 three-body problems, appl. to solar system 4-77700  
 three-dimensional periodic orbits, mechanism of branching from the plane 4-90064  
 Trojan asteroids, long periods in three-dimens. motion 4-90102  
 Trojan asteroids, orbital evolution 4-90103  
 two-body problem, case with variable mass, trapping theory 4-90076  
 two-body problem, case with variable masses, soln. 4-82394  
 two-body problem, perturbed planar case, generalised Sundman's transform. 4-110501  
 two-body problem with drag, semi-analytic soln., appl. to artificial satellites 4-110505  
 Uranus-Neptune system, 2:1 commensurability 4-82449  
 Venus Orbiting Imaging Radar, mission and trajectory design 4-82376  
 virial oscillations of celestial bodies, evolutionary problem in non-Newtonian time scale, soln. 4-67606
- cell model (liquids)** see *liquid theory*
- cell motility**
- algae *Euglena gracilis*, motility control system, temp. masking of the circadian system 4-100104  
 bacterial motility and flagellar motor, book contrib. 4-93708  
 bacterial rotary motor, force-generating units rel. to motB protein synthesis 4-77210  
 epidermal keratocytes, fish, and cytoplasmic fragments: motility in absence of microtubules 4-93704  
 erythrocytes, anomalous diffusion in presence of polyvinylpyrrolidone 4-105203  
 magnetic guidance of organisms, book contrib. 4-93769  
 magnetometry of ingested particles in pulmonary macrophages 4-105264  
 sperm flagella, microtubule-based motility, reversible inhibition 4-85410  
 sperm penetration, mech. hypothesis 4-66906  
 tissue culture cells on deformable substrata: biomedical implications 4-100414
- cells (electric)**
- see also *fuel cells*; *photoelectric cells*; *photoelectrochemical cells*; *primary cells*; *secondary cells*
- electrochemical batteries, basic principles and properties (*French*) 4-85362  
 electrochemical intercalation of fluorides into pyrographite, for high energy density battery cathodes 4-81444  
 electrochemical power sources, status and development 4-62322  
 load cell, method for increasing linearity (*Chinese*) 4-99953  
 non-aqueous solvents applications 4-62321  
 porous electrochemical electrode cells, potential and current density distribution study (*Hungarian*) 4-105098  
 power sources development, measures for success 4-62320  
 rechargeable electrochemical cell with polyacetylene electrodes, investig. 4-104994  
 redox-flow battery, voltage drop and elec. resist. for ion exchange membranes 4-109681  
 solid state cells, self-discharge 4-109730  
 ( $C_xF_m$ ) prep., struct., phys. props. and appls. in Li batteries, (*Japanese*) 4-93246  
 Ca/LiCl, LiNO<sub>3</sub>/LiNO<sub>3</sub>, AgNO<sub>3</sub>/Ni thermal battery cells, discharge characts. 4-66675  
 H<sub>2</sub> production by electrochemical gasification of coal 4-66814  
 Li thin film cells, solid electrolytes and cathode materials (*Japanese*) 4-93597  
 Li-B/LiNO<sub>3</sub> anode-electrolyte system, potentiostatic studies 4-66676  
 Li<sub>2</sub>O-LiNbO<sub>3</sub>-B<sub>2</sub>O<sub>3</sub>, new solid electrolyte glass material, electrical conductivity 4-108649

cells (electric) continued

Li<sub>14</sub>Zn(GeO<sub>4</sub>)<sub>4</sub> thin films, for solid state batteries, preparation and characteristics 4-93224  
Mo<sub>6</sub>S<sub>8</sub> battery examined by chronopotentiometry; X-ray diffr. and long term cycling 4-89385  
Na-S battery cells, surface degradation of β"-Na<sub>2</sub>O-Al<sub>2</sub>O<sub>3</sub> 4-65526  
Pt-ZrB<sub>2</sub>-Mo-Mo cell, thermo-EMF at 1300 to 1960K 4-61406  
ZrO<sub>2</sub>-Y<sub>2</sub>O<sub>3</sub> solid electrolyte cells, minimum working temp., thermo EMF studies 4-114898

cellular arrays

microbiological fouling and scaling meas. with flow cell array 4-115436

cellular automata *see finite automata*

cellular biophysics

*see also biomembrane transport; biomembranes; cellular effects of radiation; cellular transport and dynamics; lipid bilayers*  
acute leukaemia, clinical states, mathematical model, estimation of clinical quantities (Japanese) 4-85411  
adhesivity of cells to glass, change for unchanged density of surface charges 4-66904  
alga, cell division at interface in different hydrodynamic regimes of streaming 4-66903  
anisotropic cardiac muscle, bidomain model 4-77222  
Artemia cysts, water diffusion, quasi-elastic neutron scatt. spectra 4-81649  
ATP synthesis by proton flux in mol. machine of living cells, loose coupling mech. 4-77209  
Bacillus megaterium cultures, biologically related Raman lines absences 4-81646  
bacteria, aerosol, mass spectrometry anal. 4-67153  
bacteria shape changes, surface stress theory 4-77207  
bacterial cells, intact and living ultrastructural information from FTIR 4-100094  
bacterial magnetite, struct., morphology and cryst. growth 4-100069  
bacteriorhodopsin, Halobacterium halobium, coupling between photocycle and protonmotive force 4-89520  
bioaccumulations, Raman microprobe 4-115304  
biological dipole oscillators, large assemblies, cell membrane modelling 4-72223  
biomagnetism of cells 4-66971  
blood, erythrocytes and plasma, human, <sup>23</sup>Na NMR, chemical shift, spin relax., intracellular Na conc. 4-66910  
blood cells, elemental profiles, PIXE anal. 4-100387  
blood cells, mag. parameters and high gradient paramagnetic and diamagnetic phoresis 4-109848  
blood platelets, human, fluoresc. spectroscopy obs. 4-115031  
blood platelets, imaging using soft X-ray microscopy, TEM and SEM 4-100367  
blue particles in cancerous organs, laser micro-Raman spectrosc. obs. 4-62455  
bone cell nuclei, morphometry and location rel. to bone surfaces 4-115035  
book, biophysical plant physiology and ecology 4-73191  
brain, rat, in vivo, surface coil <sup>31</sup>P NMR study 4-72240  
breast, human, ultrastructure of mucoid carcinoma (Chinese) 4-115028  
cancer cells, laser-excited microscopic fluorescence measurement method (Japanese) 4-115315  
cancer cells, latent, phys. models of lipid membranes, ordering effects of petroleum hydrocarbons 4-85412  
cardiac myocytes, rat, passive stiffness obs. 4-100101  
cell adhesion modelling 4-89521  
cell surfaces, fluoresc. reson. energy transfer, flow cytometry 4-81644  
centrifugal cell hybridization 4-72227  
chloroplast, area of cross section fluctuations, freq. spectrum 4-66902  
chloroplast suspension, spinach, anomalous emission in photosynthetic systems 4-66916  
chromatophores and chromatophore fractions of Rhodospirillum rubrum, cell fluoresc. polarisation spectra 4-77187  
chromosome analysis, TV-contrast enhancement methods 4-115323  
chromosomes, G-banded human, automatic analysis by scanning microscope photometry 4-62649  
chromosomes, micro-Raman spectroscopy, protein and DNA contrbs. 4-115033  
cochlea, guinea pig, hair cells in isolated coils, study technique 4-110017  
cochlea isolated from guinea pig, sensory-cell hair bundles stiffness 4-109837  
cochlear hair cell density, guinea pig, rel. to freq. discrimination 4-100166  
cooperative thermal transitions in normal and tumour cells, denaturing of chromatin 4-66905  
cortical V1 cells, monkey, spatial mapping with pure colour and luminance stimuli 4-89569  
δ-crystallin accumulation in chicken embryo lens, laser light scatt. spectroscopy 4-72229  
cytogenetic data for processor digital simulation, two-stage spatial filtering for diffr. pattern anal., processor digital simulation using cytogenetic data 4-59986  
cytoskeletal components visualisation using surface refl. interference microscopy 4-62646  
diatom cell walls, metal coating and high resolution SEM 4-100411  
elastic props., acoustic microscopy obs. 4-100095  
electroelastic effects in cell membranes 4-77206  
embryonic chick heart cells, channel currents during spontaneous action pots. 4-105219  
embryonic heart cell aggregates, phase resetting of rhythmic activity 4-66908  
endothelial response to injury, simulation, phys. model 4-62454  
erythrocyte ghosts, human, microwave dielectric props. 4-85409  
erythrocyte membrane, elastic area compressibility modulus determ. by cell poking 4-66907  
erythrocyte membrane, viscous dissipation inside during micropipette aspiration 4-89522  
erythrocyte suspensions, LF elec. resistance rel. to Fricke's formula 4-100096  
erythrocytes, deform. and viscoelastic props. of a concentrated suspension 4-100090  
erythrocytes, ferritin conjugate labeled, selective mag. separation 4-89523  
erythrocytes, human, 3D image anal. in reflection contrast 4-89525  
erythrocytes from stored human blood, morphological changes during heating 4-105204  
extracellular potentials, modelled, comparative anal. 4-115048

cellular biophysics continued

fiber optics in plants 4-105206  
fish erythrocytes, reaction of intracellular matter to detergent toxicity, dielec. studies 4-72230  
GABAergic neurons in catfish proximal retina, identification and some functions 4-109805  
GABAergic neurons in the distal catfish retina, identification and some functions 4-66951  
gastrointestinal bleeding sites, detect. and localisation by <sup>99m</sup>Tc labelled red blood cell scans 4-89732  
genetic code model based on isotopic combinations of single element 4-93678  
haematocrit-erythrocyte-disaggregation apparatus 4-110013  
haemoglobin 'S', abnormal, cytological and rheological characts. of drepanocytes (French) 4-115032  
haemopoietic stem cells, murine normal and leukaemic, heat sensitivities 4-72226  
heart tissue, activation sequence effects simulation 4-81663  
heat exchanges, finned tube, microbial cell accumulation 4-60400  
HeLa cells, mitotic apparatus SEM studies 4-100412  
hepatoma cells, cultured, thermotolerance obs. 4-66913  
hepatoma cells, morphological response and survival during fractionated hyperthermia 4-93706  
horizontal cell bodies in tiger salamander retina, elec. coupling 4-89567  
hypothermia of Chinese hamster ovary cells, survival rel. to precooling 4-77197  
image enhancement in biological microscopy 4-105383  
interstellar bacteria, UV absorption and mass density constraints 4-101458  
leukemia manifestation in blood cell microelement profile, nuclear microprobe determ. 4-100388  
lipid bilayers, orientational ordering of carotenoids, resonance Raman spectroscopy 4-89514  
localational stereology within rat aortic wall sampling fields, microcomputer based method 4-115300  
macromolecular quasispices, localisation threshold calcs. from continuously distributed replication rates 4-77174  
macrophages, rat femoral bone marrow, loss of transportable Pu deposits 4-77213  
magnetism of cells, theory, expts. and appls. 4-89608  
maize root cells, NaCl-treated, organelles energy dispersive X-ray anal. 4-99905  
mammalian cells, occurrence of DNA strand breaks after hyperthermic treatments with or without radiation 4-66915  
microdrive for extracellular recording of single neurons using fine wires 4-93980  
microorganisms, enumeration by their dynamic AC conductance patterns, model and expt. method 4-62453  
mononucleosomes from replicating chromatin in heated cells, sedimentation coeff. and buoyant density 4-77198  
multiformat electronic cell sorting system 4-105392  
multiformat electronic cell sorting system 4-105393  
muscle biopsy data acquisition and display 4-85547  
NMR of intracellular metal ions in living cells, book contrib. 4-93709  
nuclei acids, multistranded structures use in information transactions 4-77172  
nucleosome, histone and DNA packing model 4-89517  
optical methods for quantitative cytochemistry 4-115322  
optical microscopy, cell biology appl. rel. to newer methods 4-115321  
optical sectioning microscopy, cellular architecture in three-dimens., book contrib. 4-93986  
organ of Corti, intercellular elec. coupling obs. 4-93752  
phage infection, energetics of first steps, review 4-66911  
phospholipid head groups, perturbation by membrane proteins, <sup>31</sup>P NMR spin lattice relax 4-89513  
phospholipid membrane vesicles, cylindrical, thermal fluctuations 4-81643  
power-law approximation and similarity properties of the regulatory characteristics of metabolism 4-89518  
reaction centres from Rhodospseudomonas sphaeroides, electron struct. of Fe<sup>2+</sup>, EPR obs. 4-89519  
rectification of distorted chromosome image: automatic determination of density profiles 4-62452  
red blood cells, human, Cu determ., AAS 4-100364  
retina, carp, L-type horiz. cell response, Ba<sup>2+</sup> ion effects (Japanese) 4-81671  
retinal ganglion cell layer and optic nerve from postmetamorphic Xenopus laevis, morphometry 4-66947  
retinal rod photoreceptor membranes, enzymatic processes, light scatt. probe 4-72224  
SEM, high-resolution, prep. for obs. of fine struct. of biological specimens 4-100395  
sickle red blood cells orientation in alternating elec. field, diagnosis appl. 4-93705  
soft X-ray imaging, diffr. pattern meas. of single micro objects 4-100369  
soft X-ray imaging of hydrated biological specimens 4-100368  
striate cortex, cat, length summation in simple cells 4-81675  
texture of cell material, anal. using UV microscopy (German) 4-72457  
thermoelectric microscope stage for meas. of supercooling points of microscopical organisms 4-100402  
thermotolerance, cell cycle dependence, CHO cells heated at 45.0°C 4-93707  
thermotolerance and thermosensitisation in CHO and RIH cells, comparative study 4-115020  
thrombi, haemodynamic forces, from incipient attachment of single cells to maturity and embolisation 4-72293  
tip growing plant cells, intracellular Ca distrib., PIXE meas. 4-100394  
tissue, in vivo, double reson. surface coil probe, <sup>13</sup>C NMR 4-81824  
tissues, intact, jump and return pulse sequence PMR study 4-72228  
total internal reflection fluorescence technique, book contrib. 4-93987  
vascular cells, living, effects of fluid flow 4-100102  
villus compartment of mouse small intestine, development of thermotolerance in hyperthermal injury 4-72216  
visual cells of Limulus, sustained discharge, current pulse effect 4-89561  
visual cortical cells, cat, responses to continuously and stroboscopically illum. moving light slits 4-66949  
X-cells in cat, receptive field organisation 4-81674  
<sup>15</sup>B loaded macromolecules in expt. physiology, tracing by neutron capture radiography 4-67156

cellular effects of radiation

see also biological effects of ... (type of radiation)  
see also photosynthesis  
adenocarcinoma in mice,  $\gamma$ -ray effects, retention of incorporated radionuclides (German) 4-81748  
age-related changes in radiosensitivity of animals and crit. cell systems (Russian) 4-77325  
alveolar macrophages, rat, effects of X-irrad. on cytoskeleton in vitro 4-105290  
ataxia-telangiectasia and normal human cells, fixation and repair of radiation damage 4-115136  
bacterial spores, anoxic, modification of radiation sensitivity by alcohols 4-72308  
barley seedlings, 1st leaf as a radiobiological test system 4-62532  
biomembrane structure and function, ionising radiation, effect 4-77335  
bone marrow and spleen cells, DNA struct. and catabolism, HTO and  $^{137}\text{Cs}$   $\gamma$ -ray effects (Russian) 4-115132  
bone marrow cells, rat, X-irrad.-induced double-strand DNA breaks (Russian) 4-77312  
bone marrow morphology of *Microtus oeconomicus* pall, influence of increased natural radioactivity (Russian) 4-77323  
cancer cell growth model, effects of radiation 4-93801  
Chinese hamster ovary  $\text{G}_2$  cells, mitosis and survival after X-irrad. 4-77342  
Chinese hamster V79 cells, RBE of neutron capture reactions, boric acid effect 4-77302  
chromatin degradation in rat thymus after irradiation with fast neutrons and  $\gamma$ -rays (Russian) 4-67005  
chromosomally aberrant cells, anal. based on  $\beta$ -binomial distrib. 4-93816  
chromosome aberrations due to radioactive air and water at Misasa Spa, Japan 4-93927  
chromosome aberrations in human lymphocytes induced by fission neutrons 4-72297  
chromosome alterations in karyotype of Ceylonese type black rat born after  $\gamma$ -irrad. 4-77336  
chromosome break nonrandom distrib. in lymphocytes of atomic bomb survivors 4-77331  
chromosome damage in Chinese hamster cells, flow cytometric determ., correl. with cell survival 4-105291  
clonogenic tumour cell release from NFS2ALM1 tumours, radiation response 4-93823  
CNS, postnatal development after prenatal X-irrad. in mice 4-67044  
concanavalin A receptors, migration in pulsed elec. fields 4-89532  
conference on cell cycle kinetics in radiobiology and radiotherapy, London, England (Nov. 1983) 4-67850  
conference on radiobiology, Rijswijk, Netherlands (Jan. 1984) 4-95039  
Coulter volume cell sorting to improve the precision of radiation survival assays 4-67159  
cytogenetic aspects of human exposure to transuranics 4-109891  
cytoplasm of Chinese hamster cells, thermal action of 2.45 GHz microwaves 4-100248  
diploid yeast cells, UV- and X-ray induced damage, common repair pathways 4-100256  
DNA, double-strand breaks, form. and repair in irrad. cells (Russian) 4-77311  
DNA, transforming, UV action spectra for protection by glycerol 4-67029  
DNA and histone within chromatin, radiation degradation (Russian) 4-66862  
DNA chain elongation inhibition in Chinese hamster cells on UV irrad. 4-72312  
DNA crosslinking, BCNU-induced, X-ray effects in rat brain tumour cells 4-105296  
DNA in proliferating and resting HeLa cells, replications and transcription, UV laser pulse effect (Russian) 4-66999  
DNA lesion and cell inactivation caused by X-ray, hyperthermia effects at  $42^\circ\text{C}$  4-77196  
DNA of Chinese hamster cells, effect of 70 GeV proton secondary radiation (Russian) 4-67001  
DNA synthesis, effect of time-varying mag. fields 4-66996  
dominant lethal induction and testicular uptake of  $^{125}\text{I}$  in mice 4-67019  
double-stranded  $\phi\text{X174}$  (RF) DNA, repair of damage due to radiation-induced water radicals 4-67021  
dual view waveguide exposure facility for examining microwave effects in vitro 4-72467  
E. coli B/r  $\text{Hcr}^+$  cells, error-free  $\text{uvr}^+$ -dependent inducible DNA repair 4-67022  
E. coli chromosomes, double-strand breaks induction by  $\gamma$ -irrad., rel. to cell lethality 4-67017  
E. coli K-12 radC102, radiation-sensitive mutant, characterisation 4-67031  
ectopic intestinal glands after segmental small bowel irradiation in the cat 4-93804  
eggs, mouse, effect of laser microbeam irrad. of nucleus on cleavage in culture 4-93799  
electron donors and radiation protection, radiation effect modification by ascorbic acid 4-77194  
EM fields, interaction with cells, microelectrophoretic effect on ligands and surface receptors 4-100231  
EM radiation in dm wave range, effect on myocardium cell membranes (Russian) 4-77306  
embryo cells, Golden hamster oncogenic transformation by low doses of X-rays 4-77339  
embryos, mouse, combined effects after exposure during the preimplantation period to X-rays or  $\beta$ -rays 4-67043  
embryos, mouse, sensitivity during pronuclear and 2-cell stages 4-67040  
epidermal cells, thymocyte-activating factor/interleukin 1 prod., UV effects 4-77334  
erythrocyte, microwave bioeffects, temp. and  $\text{pO}_2$  dependence 4-100250  
Euglena cells, X-ray induced single strand DNA breaks and their repair in chloroplasts 4-62531  
excitable cellular membranes, transient EM field effects, nonlinear anal. 4-100251  
fibroblasts, bone, mouse, effect of  $^{241}\text{Am}$   $\alpha$ -particles 4-77348  
fibroblasts, human, nondividing populations, UV exposure, transient damage repair enhancement 4-72316  
fibroblasts, normal and ataxia telangiectasia, human, thermal enhancement of radiosensitivity 4-89655  
fibrosarcoma, murine, independent effect of a mixed-beam regimen of fast neutrons and  $\gamma$ -rays 4-66995  
fibrosis in gamma irrad. rat lung, D-penicillamine modification 4-77343

cellular effects of radiation continued

fractionated radiotherapy, plateau-phase culture expts. 4-85497  
gene conversion in yeast as a function of LET for low LET radiation 4-89658  
generative cell death in mice, RBE of T low-level  $\beta$ -radiation (Russian) 4-67011  
giant algal cells exposed to X-band, absence of significant short-term EM bioeffects 4-115124  
gonads of adult *Ameba splendens*, effects of chronic  $\gamma$ -irrad. 4-100258  
gonads of male mice, genetic effect of  $^{14}\text{C}$  (Russian) 4-67012  
granulocyte/macrophage progenitor cell population in bone marrow and blood after total body X-irrad. 4-77340  
granulocytic-macrophagal cell predecessors in mouse bone marrow,  $\gamma$  post-irrad. dynamics (Russian) 4-67010  
growth inhibition by irrad. combined with hyperthermia or anticancer drugs 4-93806  
heavy ions, low-energy, photonuclear reactions used to study biological action (Russian) 4-67016  
HeLa cells, biological action of low-intensity visible light as function of coherence, dose, wavelength and irradiation regime 4-62525  
HeLa cells on membrane filter, UV radiation apparent sensitivity increase 4-77332  
hepatomas, rat, tumour-cord parameters 4-89657  
human mononuclear leukocytes exposure to pulse modulated microwaves 4-115126  
hyperthermic radiosensitisation of cells from a human melanoma xenograft 4-105293  
immune system, RF effects on human immunoglobulin and murine T- and B-lymphocytes 4-100252  
immunity in host, cell-mediated, after tumor irrad. 4-77333  
intergeneric conjugants of *Vibrio cholerae* biotype proteus X Serratia marcescens,  $\gamma$ -radiation sensitivity (Russian) 4-77324  
intestinal crypts, S-phase cell distrib., modifications after multiple daily fractionation 4-93802  
jejunum, mouse, late effects of irrad. 4-115137  
laser microbeam irrad. for cell damage (Chinese) 4-109876  
leukocyte DNA, radiation-induced damage, fluorometric determ. (Russian) 4-67006  
leukocytes, peripheral blood, characts. in persons working with ionising radiation sources (Russian) 4-72302  
linsed varieties,  $\gamma$ -ray effect on third generation 4-77349  
liver cells, intact and regenerating rat, genome mutations yield after  $\gamma$ -irrad. (Russian) 4-67002  
lymphocyte chromosome aberrations in patients undergoing radiation therapy for mammary carcinoma 4-93844  
lymphocyte radiosensitivity in vitro, age relation 4-62534  
B-lymphocyte regulatory action, radiation effect rel. to nonsyngeneic stem cell inactivation (Russian) 4-66991  
lymphocyte sister chromatid exchange, freq. to US beam exposure 4-100244  
lymphocytes,  $\text{G}_0$ , human, in vitro microwave irrad., lack of clastogenic effect 4-115130  
lymphocytes, human, chromosome aberrations induced by D-T neutrons 4-93794  
lymphocytes, human, chromosome aberrations induction by  $^{60}\text{Co}$   $\gamma$ -rays, dose response relationship 4-89656  
lymphocytes, human, chromosome aberrations induction by  $\beta$ -particles from HTO 4-67025  
lymphocytes, human, clastogenic effects of power freq. elec. fields 4-89646  
lymphocytes, human, detrimental effects of  $^{11}\text{In}$  labeling 4-72419  
lymphocytes, human, lack of US effect on sister chromatid exchange in vitro 4-89651  
lymphocytes, human peripheral, X-irrad. rel. to exchanges and deletions 4-67026  
lymphocytes, rat blood, influence of  $\gamma$ -rays on UV fluoresc. (Russian) 4-77322  
lymphocytes, small, effects of  $^{89}\text{Sr}$  on prod. and maturation 4-67030  
lymphoid cells, mol. mechanisms of radiation death, chromatin degradation and DNA replication (Russian) 4-77318  
lymphoid cells, RNA metabolism, radiation-induced disturbances during interphase death (Russian) 4-77310  
lymphosarcoma, rapidly growing, murine, noneffectivity of roentgen irrad. 4-93805  
lysis, US-induced, nontrapped bubbles in rotating culture tube, kinetics 4-100277  
malignant cells of different radiosensitivities, effectiveness of fractionated irrad. (Russian) 4-77326  
mammalian cell culture, dose-rate effect between 1 and 10 Gy/min 4-109881  
mammalian cells, cultured, X-ray-induced DNA damage and cellular lethality 4-93817  
mammalian cells, DNA repair kinetics following split dose  $\gamma$ -irrad. 4-77338  
mammalian cells, dose-response curve shape rel. to Elkind repair saturation 4-100260  
mammalian cells, occurrence of DNA strand breaks after hyperthermic treatments with or without radiation 4-66915  
mammalian cells, transient toxicity of 2-deoxy-2-[ $^{18}\text{F}$ ]fluoro-D-glucose 4-72314  
mammalian cells in vitro, stochastic model of ionising radiation effect 4-115135  
mammalian L5178Y cells, cultured, inhibition of  $\gamma$ -ray dose-rate effects 4-93819  
mean inactivation dose, rel. to human cell survival curves intercomparison 4-105294  
membrane nonlinear response to applied elec. field 4-100093  
metaphase chromosome, damage and repair of active chromatin 4-93821  
micro-irradiation of single living cells using UV and visible light 4-115326  
microvasculature, swine skin, response to acute single exposures of X-rays 4-67033  
models for cell recovery after fractionated and prolonged irradiation (Russian) 4-77327  
multicellular spheroids, appl. as model system in NSD concept based studies (Russian) 4-77315  
multiphasic survival response of a radioresistant lepidopteran insect cell line 4-93822  
mutagenicity of  $\alpha$ -particles in Ehrlich ascites tumour cells 4-105292  
neoplastic effects after prenatal irradiation 4-67046

**cellular effects of radiation continued**

- neoplastic transformation enhancement by fission-spectrum neutrons at low dose rate 4-100235  
 neuroblast destruction in mouse and man after neutron irradiation in utero 4-66997  
 neutron source reactor beam, RBE meas., comparison with cyclotron neutron and  $^{60}\text{Co}$   $\gamma$ -ray 4-77301  
 nuclear DNA segregation in *Bacillus cereus* T, radiation induced failure 4-72231  
 nuclei isolated from mixtures of heated and unheated HeLa cells, protein cross-migration 4-66914  
 oogonial cells in ovaries of red cotton bug, X-ray induced precocity 4-100253  
 peanut cells, cultured: age-dependent effects of  $\gamma$ -exposure on form, growth and peroxidase activity 4-62530  
 peripheral blood leukocytes, chromatin degradation, combined effect of radiation and burn (*Russian*) 4-77319  
 peripheral blood mononuclear cell prematurely condensed chromosomes, use for biological dosimetry 4-105344  
 peritoneal macrophages, mouse,  $\gamma$ -irrad. rel. to defect Fc-mediated phagocytosis 4-72310  
 Peyer's patch lymphocytes, rat, effect of sublethal ionising radiation 4-105295  
 pH changes in Chinese hamster cells after  $\gamma$ -irrad. 4-67020  
 phage inactivation sensitivity to monochromatic synchrotron UV irradiation 4-77337  
 photobiology of furocoumarins rel. to photochemotherapy of psoriasis, review 4-115131  
 plasma membranes, rat liver, radiation effects, IR spectroscopy obs. (*Russian*) 4-77321  
 platelet aggregation induced in mice by whole-body hyperthermia 4-93800  
 pluripotent stem cells, radiosensitivity determ. by cloning in irradiated mouse spleen (*Russian*) 4-67003  
 pneumocytes, type II, radiation induced secretion of surfactant 4-81747  
 power-frequency elec. fields, system for cell suspensions exposure 4-100365  
 preimplantation mouse embryos, development of cytogenetic effects and recovery after irradiation 4-67042  
 proliferation kinetics of cultured cells after irradiation with X-rays and 14 MeV neutrons 4-100255  
 Purkinje fibre, cardiac, Ca channel blockade, photoeffect 4-81647  
 radiobiological research projects, AFRRI annual report (1982) 4-73172  
 radiomodifying effect of hypoxia on neutron-irradiated mice (*Russian*) 4-77300  
 radiosensitivity of three goldfish cell lines, comparison using short term endpoints 4-100257  
 reproductive system of pond snail, gamma irradiation effect 4-77341  
 retinal nerve fibres in primate optic nervehead, axons degeneration obs., glaucoma causes 4-77241  
 rice, radiation-induced mutation rel. to tolerance to salinity 4-77351  
 skin, mouse, repopulation kinetics during split course MFD or daily fractionated irradiation 4-77330  
 skin, wounded, of white mice, regenerative process, He-Ne laser irradiation effects 4-72301  
 skin fibroblasts, human, of varying glutathione content, radiobiological studies 4-109880  
 small intestine, mouse, fibronectin content in basement membrane,  $^{137}\text{Cs}$   $\gamma$ -irrad. effect 4-81746  
 small intestine, rat, late roentgen radiation damage, dose fractionation effects 4-81745  
 small intestine irradiation at different times of day, S-phase cell distribution, recovery phase 4-81743  
 soft X-rays to investigate radiation-sensitive sites in mammalian cells 4-100254  
 spermatogenous epithelium of rodents and man, post-irradiation recovery regularities (*Russian*) 4-67009  
 spermatogenic stem cells, response to fission neutron irradiation 4-66992  
 spore radiobiology, conf., Amsterdam, Netherlands (July 1983) 4-63388  
 stereocilia on inner hair cells, fusion in various mammals after noise exposure 4-85437  
 stromal mechanocytes of human bone marrow and spleen, radiosensitivity (*Russian*) 4-93807  
 sublethal irradiation, recovery of cell immunity systems (*Russian*) 4-77317  
 sunburn, annotated bibliography, historical development 4-58608  
 T-lymphocyte colonies, PHA-induced, differential X-irradiation effects 4-93820  
 testicular stem cells, mouse, strain differences in response to fractionated irradiation 4-67024  
 thermotolerant CHO cells and RIF-1 tumours, radiosensitivity and thermosensitisation 4-105297  
 thyroid cancer, radiogenic initiation, rat expts. 4-72309  
 tissue properties rel. to biomedical appls. of MM waves 4-77308  
 tumour cells, Ehrlich ascites roentgen irradiation, energy metabolism and ATP turnover time during cell cycle 4-81744  
 tumour induction in rats by  $^{45}\text{Ca}$  and  $^{90}\text{Sr}$  applied separately and in combination with  $^{131}\text{I}$  (*Russian*) 4-67013  
 tumour-bearing animals, fractional irradiation rel. to survival (*Russian*) 4-62527  
 V79 Chinese hamster cells, sequential irradiation with X-rays and fast neutrons 4-67018  
 whole-body-irradiated mice, suppression of delayed-type hypersensitivity to oxazolone 4-93815  
 X-irradiation of mouse  $10^1 \text{ T}^{1/2}$  cells, effect on progression 4-67028  
 yeast, radiation sensitive mutants: cell inactivation by high temp., UV light and ionising radiation (*Russian*) 4-77314  
 yeast cells, budding haploid, exposed to ionising radiation, increased radioresistance (*Russian*) 4-77316  
 yeast cells, dry, of different UV sensitivities, effects of vacuum-UV and far-UV synchrotron radiation 4-67034  
 yeast DNA,  $\text{Si}$  nuclease-sensitive sites, assay for radiation-induced base damage 4-72311  
 zygote, mouse, in vitro studies of radiosensitivity 4-67041  
 $^3\text{H}$  toxicity, multiple parameter evaluation 4-67047

**cellular method**

- diamond, energy bands, variational cellular method 4-92598  
 Si, energy bands, variational cellular method 4-92598

**cellular transport and dynamics**

- see also cell motility  
 alveolar epithelium, effects of cell swelling on fluid flow 4-89534  
 Aplysia neurons, anomalous voltage relations of  $\text{Ca}$  4-89511  
 Artemia cysts, water diffusion, quasi-elastic neutron scattering spectra 4-81649  
 axon, squid giant, current generated by backward-running electrogenic Na pump 4-77228  
 axon, squid giant, Na threshold channels 4-77227  
 bacterial chemotaxis, phenomenological transport theory, Navier-Stokes symmetry 4-77216  
 bacteriology, use of a laser Doppler electrophoresis method 4-115288  
 blood filtration measurements, recent progress in improving data processing 4-110016  
 blood filtration pressure and erythrocyte deformability meas., evaluation of the Erythrometre 4-115248  
 blood platelets, rheological behaviour in vivo 4-115093  
 bone resorption by isolated rabbit osteoclasts, stereophotogrammetric obs. 4-89533  
 cardiac cells, Na/K pump, book contrib. 4-93725  
 cardiac Purkinje fibre, delayed rectification, rel. to intracellular  $\text{Ca}^{2+}$  4-66933  
 cardiac sarcoplasmic reticulum, unidirectional Ca and nucleotide fluxes 4-89531  
 chromaffin cells, isolated, temp. effects in stimulus-secretion process 4-66919  
 cochlea, gap junctions in the stria vascularis and effects of ethacrynic acid 4-105250  
 concanavalin A receptors, migration in pulsed elec. fields 4-89532  
 cytoplasmic motions in growing pollen tube tips, laser Doppler microscopy obs. 4-89535  
 differential adhesion based cell interaction models 4-100103  
 dynamic interactions between approaching surfaces of biological interest, review 4-77204  
 endocytosis: relation to capping and cell locomotion 4-100111  
 endothelial fibrin lining and fibrin gels rel. to transcapillary transport control 4-105270  
 endothelial permeability hydrodynamic and mech. aspects 4-105209  
 erythrocyte aggregation, viscometric technique for meas. 4-110014  
 erythrocyte aggregation rel. to blood flow in small capillaries at low shear forces 4-109854  
 erythrocyte deformability, assessment by constant flow filtration technique 4-115282  
 erythrocyte deformability, device for routine meas. 4-109979  
 erythrocyte deformability, leukocyte removal prior to study, improved method 4-115285  
 erythrocyte deformability meas., improved filtration rate 4-109980  
 erythrocyte filterability and anticoagulants 4-115097  
 erythrocyte filtration resistance at constant press., technique for continuous meas. 4-115283  
 erythrocyte membrane elec. breakdown through diffusion potential difference 4-66894  
 erythrocyte membrane viscosity, determ. from rheoscopic obs. of tank-treading motion 4-105202  
 erythrocyte passage time, dependency on pore geometry in single-pore erythrocyte rigidometer 4-109787  
 erythrocytes, aggregation and agglutination 4-109786  
 erythrocytes, heat treatment rel. to aggregation in plasma 4-100091  
 erythrocytes, human,  $\text{Ca}^{2+}$ -activated  $\text{K}^{+}$  channels, comparison of single-channel currents with ion fluxes 4-66921  
 erythrocytes, human,  $\text{O}_2$  uptake, quantitative description in 3D 4-66923  
 erythrocytes under shear, rel. to small angle light scattering by large spheroids 4-115116  
 ESR spectroscopy, membrane and cell microrheological study appl. 4-115289  
 fertilisation, time and voltage windows for reversing elec. block 4-77212  
 gap junction, struct. maintenance 4-100097  
 glycerolmonooleucin membranes, elec. potential at amphotericin channel inlet 4-66917  
 granulocytes, human, water permeability at subzero temps. in presence of extracellular ice 4-105212  
 haemorrheology from microcirculation to macrocirculation (*Japanese*) 4-72294  
 inner ear dark cells, frog, quantitative localisation of  $\text{Na-K}$  pump 4-89594  
 leukocyte uptake and release by dog lung, effect of pulmonary blood flow 4-100198  
 leukocytes, continuum mech. model during protopod form. 4-100100  
 lipid membrane, image potential of ion-pore system, symmetrical channel 4-89528  
 lipid membrane, image potential of ion-pore system, unsymmetrical channels 4-89529  
 lipophilic cation use as membrane potential probe, critical assessment 4-77205  
 lymphocytes, human,  $\text{Na}^{+}$  self-exchange 4-115036  
 lymphocytes, mouse, antigen-antibody complexes capping inhibition by hyperthermia 4-105210  
 magnetosome dynamics in magnetotactic bacteria 4-105263  
 mammalian cardiac cells,  $\text{K}^{+}$  channel activation by intracellular  $\text{Na}^{+}$  4-77214  
 membrane transient response modelling 4-93702  
 membranes of sarcoplasmic reticulum, permeability for monovalent cations 4-89526  
 microvascular walls, permeability characts. 4-105207  
 muscle, frog skeletal, model of Ca motion during sarcomere activation 4-81648  
 nematocyst discharge, ultrahigh-speed anal. of exocytosis 4-66926  
 neurophilus, human, effect of colchicine on viscoelastic props. 4-115030  
 organelle traffic, human axons, computer analysis 4-83417  
 Paramaecium caudatum, voltage dependent inward current, voltage clamp expts. (*German*) 4-66927  
 patch clamp studies of single ionic channels, book contrib. 4-93710  
 peritoneal macrophages, mouse,  $\gamma$ -irrad. rel. to defect Fc-mediated phagocytosis 4-72310  
 photophysical methods, continuous excitation, cellular rheology appl., interests and limits 4-115290  
 plant tissue, water exchange studied by  $^1\text{H}$  NMR in presence of paramagnetic centres 4-66922  
 platelets, rabbit, flowing in small arterioles, orientation and diameter distribution 4-100187  
 Purkinje fibre, cardiac, Ca channel blockade, photoeffect 4-81647

**cellular transport and dynamics continued**

- red cells aggregation in space, meas., NASA Space Shuttle project 4-109970
- retinal glial cell membrane, regional specialisation 4-72247
- retinal rods, cation selectivity of light-sensitive conductance 4-77237
- rod outer segment disks, Necturus, barrier to lateral diffusion of porphyrin 4-66920
- rouleau formation kinetics, reversible reactions 4-66909
- sarcoplasmic reticulum, unidirectional Ca and nucleotide fluxes, ATPase reaction schemes 4-89530
- Schwann cells, rabbit, neuronal-type Na<sup>+</sup> and K<sup>+</sup> channels 4-115040
- shear viscoelasticity of suspensions of biological cells with viscoelastic membrane 4-100092
- splenic blood flow and platelet transit time, meas. methods using <sup>111</sup>In-labelled platelets 4-81773
- stem of higher plant, cond. system resist. meas. during variable signal propag. 4-66932
- sugar transport in animal cells, passive hexose transfer system 4-77217
- Technicon Ektacytometer: automated exploration of erythrocyte function 4-115286
- tumour cells biorheology 4-105268
- vertebrate sensory neurons: low voltage-activated, fully inactivating Ca channel 4-100110
- yeast cells, static and dynamic dielectrophoresis 4-100105
- Ca<sup>2+</sup> ion permeation mechanism through Ca channels, electrostatic repulsion 4-77215
- O<sub>2</sub> consumption rates and diffusion coeffs. in multicellular spheroids, determ. method 4-115278

**cementation steel see alloy steel****cements (building materials)**

- used only for those materials which bind together particulate matter so as to form a coherent mass of considerable strength. For cements that cause two or more separate masses to adhere see adhesion*
- glass-ionomer dental cement, prep. and compressive strength 4-99373
- polyethylene fibrillated tape reinforced cement, mech. props. 4-109493
- natural radioactivity of cement industry materials in Hungary 4-93676
- steel fibre reinforced cement, fibre debonding and pullout, adhesional interfacial shear strength 4-66388
- steel fibre reinforced cement, free shrinkage, theoretical model 4-93255

**centrifuges**

- annular reactor with radial flow, reaction kinetics, ang. vel., gas flow rate 4-65034
- compressor operating at very low temperatures 4-95457
- gas centrifuge flow problems, finite element method 4-64952
- gas-liquid flow in slotted disks centrifuge extractor, struct. investigation 4-103395
- plasma centrifuge, vacuum-arc, element and isotope separation 4-108223
- rotating gas centrifuges, flow field, curvature effects 4-60440
- separability of highly dispersive liquids (Russian) 4-112901

**ceramics see cermets****ceramics***see also refractories*

- alkali metal phosphates, A'B<sup>+</sup>PO<sub>4</sub>, A=Na, K, B=Ca, Zn, Sr, Cd, Ba, Pb, ferroelec. phys. props. 4-65992
- aluminosilicate refractories, creep 4-81242
- aluminous electrical porcelain, doped with talc, microstruct. and mech. props. 4-114674
- apatite-based ceramics, behaviour rel. to crit. 1150-1250°C temp. range, prosthetics appl. 4-61960
- bicrystal grain boundaries, orientational relationships 4-70579
- brick, high-alumina, corrosion resist. to nitric acid, report 4-62090
- brittle, thermal stress fracture on liquid quenching rel. to thermal and mech. props. 4-109504
- ceramic-polymer composite biomaterials, fracture 4-76844
- coating for tools and sliding elements, acoustic microscopy studies 4-104957
- composite, tough, capabilities and design issues 4-66292
- composite oxides, fine particles prep. by mist decomposition method 4-109360
- crack detection by acoustic emission 4-62155
- cracking behaviour, microprocessor-controlled meas. 4-62056
- cracks in glasses and ceramics, growth influenced by chem. environment 4-94095
- design issues, material and parameter selection 4-66280
- electrolytes for electrochemical energy conversion devices 4-61141
- electron microscopy, conference, Boston, USA (Nov. 1983) 4-106124
- electron microscopy and anal., conference, Guildford, England (Aug.-Sept. 1983) 4-78034
- electrotechnical porcelain, axial compressive strength, effect of specimen dimensions 4-61944
- EM absorption and shielding props. of inhomogeneous compound layers 4-69289
- failure probability, Weibull modulus estimation 4-104928
- ferrites, polycrystalline, model of initial mag. permeability (Russian) 4-98921
- ferroelectric, diffuse phase transition, exponent  $\gamma$  determ. 4-76384
- ferroelectric, switching and hysteresis effects 4-76401
- ferroelectric ceramics, internal mechanical stresses 4-113530
- ferroelectric phase transition, thermodynamic model anal. (Russian) 4-99057
- fibre reinforced ceramics, fabrication and mech. props., book contrib. 4-66297
- fibre reinforced ceramics, mech. aspects of failure (French) 4-81280
- fine grained, containing liq. phase, superplastic flow mechanism 4-109475
- fireclay, corrosion resist. to nitric acid, report 4-62090
- flexure strength, Weibull fracture statistics 4-104954
- fracture, acoustic emission and sub-crit. events 4-62050
- fracture energy, elastic anisotropy and grain size dependence 4-60983
- friction wear, theoretical and expt. studies 4-62069
- friction with superhard abrasive grains 4-109522
- fusion reactor applications for ceramic materials 4-111758
- fusion reactor breeder blanket material developments 4-107020
- glass, brittle, disturbed surface layer parameters effect on struct. strength 4-99541
- glass ceramic, composite rod struct., glued joint, strength evaluation 4-99546
- glass ceramic Corning Macor, vacuum compatible absorbing materials, submm and mm refl. spectroscopy 4-108214
- glass ceramics, polar, for sonar transducers 4-69651
- ceramics continued
- grain and phase boundary structs. 4-108381
- high resolution electron microscopy appls. 4-108257
- high-performance, materials characterisation role 4-66279
- hot isostatic pressing, shaped part production 4-76736
- insulators, high tension, failure prediction, NDT methods comparison 4-62154
- interfacial dislocation structures, characterisation using TEM 4-108371
- IR detectors, uncooled, pyroelectric ceramic material appls. 4-90654
- isothermal hot pressing temp., effectiveness prediction 4-88999
- jet engine turbines, ceramic technology for powerplant 4-104758
- liquid phase sintering mechanisms 4-71614
- metal-piezoceramic thin composite circular plate, forced vibr. excited by voltage (Chinese) 4-60204
- mica, synthetic, sintering using hydrothermal equipment 4-89013
- microstructure, fracture toughness and thermal shock resist. relationships 4-62049
- mulite, influence of TiO<sub>2</sub> on sintering and microstruct. evolution 4-114457
- mulite-cordierite composites, sintering, hot pressing, microstruct., mech. and thermal props. 4-89017
- mulite-zirconia composites, microstruct. and mech. props 4-114672
- NASICON-type ceramics, prep. using sol-gel process and sintering 4-85124
- Nasicons, synthesis, sintering and microstruct. 4-76713
- nepheline glass-ceramic, microwave heating characts. 4-65294
- nondestructive failure prediction, fracture models 4-76964
- nuclear fuel pellets, ceramic, new hot impact densification method (German) 4-83215
- oxide, with high thermal shock resistance (German) 4-81267
- oxide glasses and ceramics, low temp. prep. from metal alkoxide sols. 4-109369
- oxides, high temperature materials for magnetohydrodynamic channels 4-109368
- oxides, tetragonal potassium-tungsten bronze struct., solid solutions 4-113599
- oxynitride glasses, prep. and props. 4-76737
- perovskite type red pigments, high temp. stability 4-104628
- piezoceramic foil attached to Al membrane adhesive delamination, photo-thermal obs. 4-114732
- piezoceramic half-space, crack-inclusion interaction 4-103259
- piezoceramic shell, reaction to concentrated effects 4-109129
- piezoceramic shell theory, symbolic integration method appl. 4-60280
- piezoceramic shells polarised along coordinate lines, boundary conditions in theory 4-60281
- piezoceramic surface with Ag film, physical mechanism of laser generated shock waves (Chinese) 4-113535
- piezoceramics, high temp. effects on props. 4-99038
- piezoelectric, elastic properties 4-60975
- piezoelectric array receivers using ceramics with high and low planar coupling, ang. response 4-97262
- piezoelectric ceramic composites, underwater transducer appls. 4-65951
- piezoelectric ceramic disc, coupled vibrations, freq. spectrum (Chinese) 4-88773
- piezoelectric ceramic disc, polarised in thickness direction, free vibr. anal. (Chinese) 4-60203
- piezoelectric ceramics, microstruct., props. and phase relations 4-61629
- piezoelectric plate, partially electrode, high resolved vibrs. 4-99036
- piezoelectric transducer, forward and backward projection of acoustic fields 4-87532
- plates and shells, piezoceramic, static stability (Ukrainian) 4-87596
- PLZT ceramics, polarisation switching characts 4-99006
- porcelain, high-alumina, for HV insulators, strength under dynamic and cyclic loads (German, English) 4-76836
- porcelain, low-voltage elec. prod. using perlite 4-81173
- porous, dielec. response, adsorbed water effects 4-65943
- preparation for elec. use based alkoxide and unidirectional solidification methods 4-104760
- prostheses, spherical surface grinding phenomena 4-115274
- PZT, electrically excitable mechanical reson. 4-114225
- PZT piezoelectric ceramic transverse acoustoelectric wave refl. 4-83796
- quartz ceramic, thermal expansion, rel. to cristobalite content 4-65422
- rare earth niobates, RnBO<sub>4</sub>, ferroelastics with the fergusonite type structure 4-76569
- red shale, corrosion resist. to nitric acid, report 4-62090
- refractory-metal carbides, high temp. oxidation at low O<sub>2</sub> press. 4-71752
- scanning piezoelectric ceramics, displacement, linearity measurement using scanning interference method (Chinese) 4-11101
- Si<sub>3</sub>N<sub>4</sub>, normally sintered, hot isostatic pressing in N<sub>2</sub> gas as pressure medium 4-114459
- $\alpha$ -silicon ceramics, hot pressing, thermal expansion, 40°-1040°C 4-88315
- silicon ceramics, liq. phase sintering, densification and transform. mechanisms 4-76724
- silicon ceramics, thermal diffusivity, effect of crystn. of grain boundary phase 4-88355
- silicon metalcutting tools, props. and appl. 4-66283
- silicon polytypoids, struct. characterisation 4-75426
- silicon X-phase, Si<sub>3</sub>Al<sub>2</sub>O<sub>5</sub>N<sub>2</sub>, cryst. struct. 4-75427
- silicons,  $\alpha$ - $\beta$  relationship 4-70123
- silicons, fabrication from Al<sub>2</sub>O<sub>3</sub>-AlN system 4-76763
- silicons, hot-pressed and reaction-bonded, phase equilib. and props. 4-76761
- $\beta$ -silicons, microstruct. evaluation by TEM, correl. to mech. props. 4-76732
- $\beta$ -silicons, oxidation behaviour in O<sub>2</sub> and CO<sub>2</sub> 4-76891
- silicate structures and atomic substitution rel. to N-based ceramics 4-70124
- slag still used in heat energetics, abrasive wear 4-81291
- slow crack growth at high temp., characterisation by double torsion method 4-62053
- slow crack growth resistance testing with double torque method 4-81375
- solidification point determ. by specular reflection and centrifugal methods (Japanese) 4-76770
- steel construction material, surface treatment and coating development (German) 4-76896
- strain around large inclusions, quantitative anal. 4-103621
- stress assisted hot form. 4-76728
- structural, characterisation requirements for math. modelling 4-66278
- structure-property relationships of the vitreous state 4-75312
- substrate and its masks, holder with thermal expansion compensator 4-88979

## ceramics continued

- surface analysis, beam techniques for poorly cond. materials 4-93575  
 surface damage, strength degradation, erosion and wear, acoustic NDT 4-76872  
 Synroc, hydrothermal attack, surface analysis 4-68760  
 thermal shock resistance and fatigue, acoustic emission study 4-62054  
 transformation-toughened, fracture toughness, crack-size depend. 4-93373  
 transition metal nitrides, ultrafine particles, growth by reactive gas evaporation technique with electron beam heating 4-61894  
 transition metal oxides, impurity diffusion and impurity-defect interactions 4-92436  
 Ts-TS-19 ceramic, gamma irradiat., influence on photovoltaic effects 4-84656  
 TsTS piezoceramic, dielec. props., influence of 90° domain struct. 4-76396  
 TsTSNV-1 ferroelec. ceramic, residual polarisation and piezo effect 4-76316  
 US shear mode piezoelectric ceramic transducer, characteristics and anal. (Japanese) 4-103169  
 willemite glass ceramic, partially crystallised, struct. and comp. 4-61910  
 zirconolite-based ceramic, self-irradiation damage 4-75546  
 AgNbO<sub>3</sub>, ferroelec. phase, dielec. props. 4-61631  
 Ag<sub>2</sub>Pb<sub>2</sub>Nb<sub>10</sub>O<sub>30</sub>, ferroelec. struct. and piezoelec. props. 4-65963  
 AlN ceramic, thermal shock resist. 4-81289  
 AlN, oxynitride bonded ceramics, sintering, microstruct., densification, flexural strength, oxide additions effect 4-76727  
 AlN powder, hot pressing kinetics, oxidation, mech. props. 4-76731  
 AlN transparent ceramics, powder and sintering characts. 4-81171  
 Al<sub>2</sub>O<sub>3</sub>, bend specimens, crack resistance curves, influence of grain size 4-62058  
 Al<sub>2</sub>O<sub>3</sub> ceramic, strength rel. to microstructure 4-62060  
 Al<sub>2</sub>O<sub>3</sub> ceramic substrate for ZnO film, SAW study 4-104053  
 Al<sub>2</sub>O<sub>3</sub> ceramics, interaction between polyvinyl butyral binder burn-out and sintering in reducing atm. 4-114460  
 Al<sub>2</sub>O<sub>3</sub> ceramics, surface topography rel. to ion beam sputtering, SEM obs. 4-76884  
 Al<sub>2</sub>O<sub>3</sub> compacts, homogeneously packed, intermediate-stage sintering 4-76702  
 Al<sub>2</sub>O<sub>3</sub>, faceted grain boundaries 4-84301  
 Al<sub>2</sub>O<sub>3</sub>, grinding ceramics for diamond wear 4-99609  
 Al<sub>2</sub>O<sub>3</sub>, internal friction and Young's modulus under thermal shock conditions 4-62009  
 Al<sub>2</sub>O<sub>3</sub>, polycrystalline, strength rel. to flow distrib. 4-109505  
 Al<sub>2</sub>O<sub>3</sub> powder, shock induced densification and sinterability 4-109350  
 Al<sub>2</sub>O<sub>3</sub>, powders, granule compaction rel. to binder glass transition temp. 4-85129  
 Al<sub>2</sub>O<sub>3</sub> powders, with bimodal particle size distrib., sintering 4-85127  
 Al<sub>2</sub>O<sub>3</sub>, sintered, fracture strength, effect of surface condition 4-62057  
 Al<sub>2</sub>O<sub>3</sub>, sintered, microstructure and optical props. 4-61649  
 β-Al<sub>2</sub>O<sub>3</sub>, sintering, microstruct. and mech. props. 4-85136  
 γ-Al<sub>2</sub>O<sub>3</sub>, spherical particles, cryst. struct. and surface morphology, electron microscopy study 4-92149  
 Al<sub>2</sub>O<sub>3</sub>, spray-dried, compaction behaviour 4-76714  
 Al<sub>2</sub>O<sub>3</sub>, strength characts. using controlled flaws, microstruct. effects 4-85205  
 Al<sub>2</sub>O<sub>3</sub> subcrit. crack propag., activation enthalpies and mechanisms (German) 4-62010  
 Al<sub>2</sub>O<sub>3</sub> tubes, multiaxial loading fracture 4-62016  
 Al<sub>2</sub>O<sub>3</sub> windows, neutron-induced RF loss meas. and thermal stress calcs. 4-113501  
 Al<sub>2</sub>O<sub>3</sub>, Young's modulus and internal friction, temp. depend. 4-61965  
 Al<sub>2</sub>O<sub>3</sub>:MgO:CaO, translucent, fracture, influence of temp. and CaO 4-92290  
 Al<sub>2</sub>O<sub>3</sub>-AlN spinel, fabrication, thermomech. props. 4-89097  
 Al<sub>2</sub>O<sub>3</sub>-AlN system, high temp. reactions and microstructs. 4-76763  
 Al<sub>2</sub>O<sub>3</sub>-AlON composite ceramic, hot pressing reaction sintering, mech. props., high temp. appls. 4-62062  
 Al<sub>2</sub>O<sub>3</sub>-BN-(AlON) composite ceramics, mech. props. (French) 4-81177  
 β/β'-Al<sub>2</sub>O<sub>3</sub>-Na<sub>2</sub>O, struct. transform. during sintering and annealing 4-93292  
 β'-Al<sub>2</sub>O<sub>3</sub>-Na<sub>2</sub>O electrolyte ceramic tubes, sintering, radial DC resist. 4-103994  
 Al<sub>2</sub>O<sub>3</sub>-PMMA (PBMA), composite biomaterials, fracture 4-76844  
 Al<sub>2</sub>O<sub>3</sub>-SiO<sub>2</sub> fibres, cristobalite form. at elevated temp. (German, English) 4-81197  
 Al<sub>2</sub>O<sub>3</sub>-ZrO<sub>2</sub> ceramics, high press. sintered, fracture toughness rel. to phase transform. 4-76839  
 Al<sub>2</sub>O<sub>3</sub>-ZrO<sub>2</sub> ceramics, strain around large inclusions, quantitative anal. 4-103621  
 Al<sub>2</sub>O<sub>3</sub>-ZrO<sub>2</sub> composite tool bit, microstruct., toughening mechanisms, performance 4-61946  
 Al<sub>2</sub>O<sub>3</sub>-ZrO<sub>2</sub> composites, grain growth hindrance by ZrO<sub>2</sub> inclusions 4-76743  
 Al<sub>2</sub>O<sub>3</sub>-ZrO<sub>2</sub> powder compacts, stresses induced by differential sintering 4-85135  
 Al<sub>2</sub>TiO<sub>3</sub> ceramics, stabilisation by cation substitution, sintering and hot pressing 4-109362  
 Al<sub>2</sub>TiO<sub>3</sub> ceramics, synthesis and sintering characts. 4-109361  
 As-Sb-Se system, glass-ceramic composites, varistor-like behaviour 4-114009  
 B containing ceramic neutron absorbing materials, survey of products and appls. (German) 4-83146  
 Ba<sub>2</sub>C, hardness and fracture toughness rel. to stoichiometry 4-62019  
 BN, cubic, prep. of small particles by electron irradi. of hexagonal BN in TEM 4-61895  
 Ba<sub>2</sub>Cs<sub>2</sub>Al<sub>24</sub>Ti<sub>18</sub>Fe<sub>18</sub>O<sub>16</sub>, hollandite phase of SYNROC, struct., X-ray analysis 4-106675  
 BaFe<sub>2</sub>O<sub>9</sub> permanent magnets, sintering temp. effect on mag. props. and density (Afrikaans) 4-76170  
 Ba(Mn<sub>1/3</sub>Ta<sub>2/3</sub>)O<sub>3</sub> ceramic, ultra-low dielec. loss at microwave freq. 4-84905  
 BaO-B<sub>2</sub>O<sub>3</sub>-Fe<sub>2</sub>O<sub>3</sub> system, magnetic vitroceraics, prep. and props. 4-93256  
 BaO-TiO<sub>2</sub>-SiO<sub>2</sub> glass-ceramics, ferroelec., depolarisation currents, dielec. and electrooptical props. 4-76317  
 BaPb<sub>0.7</sub>Bi<sub>0.25</sub>O<sub>3</sub> supercond. ceramics, heat capacity near transition temp. 4-114067  
 Ba(Pb<sub>1-x</sub>Bi<sub>x</sub>)O<sub>3</sub>, supercond: transition temp. and Mossbauer line isomeric shift 4-61486  
 BaPbO<sub>3</sub>-BaBiO<sub>3</sub> system, supercond. and ferroelec. phase transitions 4-76061

## ceramics continued

- Ba<sub>2</sub>TiGe<sub>2</sub>O<sub>8</sub>, glass ceramics, grain oriented, hydrostatic piezoelec. props. and appls. 4-84913  
 BaTiO<sub>3</sub>, centrosymmetric ceramics, elec. field induced acoustic anisotropy 4-60992  
 BaTiO<sub>3</sub> ceramics, analogy between mech. and dielec. strength distrib. 4-61942  
 BaTiO<sub>3</sub> ceramics, lanthanide doped, EPR spectra 4-109072  
 BaTiO<sub>3</sub> form. by thermal decomposition of oxalate (Japanese) 4-76718  
 BaTiO<sub>3</sub>, liquid phase sintering and composite ceramics with Pb<sub>3</sub>Ge<sub>2</sub>O<sub>11</sub> 4-104746  
 BaTiO<sub>3</sub> oxidic perovskites, dielec. meas., surface layer effects 4-65962  
 BaTiO<sub>3</sub>, PTC ceramic, strength and fracture toughness 4-62051  
 BaTiO<sub>3</sub>, piezoceramic, dielec. props., influence of 90° domain struct. 4-76396  
 BaTiO<sub>3</sub>, powder processing, grain size, ferroelec. props. 4-93253  
 BaTiO<sub>3</sub>, semicond. glass ceramics, oxidation, barrier layer form. 4-114699  
 BaTiO<sub>3</sub> synthesis, polycryst., nonstoichiometry rel. to solid-solid reaction mechanism 4-99305  
 BaTiO<sub>3</sub>:Sb(Nb), sintering, microstruct. 4-89012  
 BaTiO<sub>3</sub>-based materials, dielec. props. and chem. inhomogeneity, effect of sintering 4-85128  
 Ba<sub>2</sub>Ti<sub>2</sub>O<sub>9</sub> type ceramics, dielectric characts., microwave freqs. 4-76311  
 Ba<sub>2</sub>TiSi<sub>2</sub>O<sub>8</sub>, glass ceramics, grain-oriented, hydrostatic piezoelec. props. and appls. 4-84913  
 Ba<sub>2</sub>TiSi<sub>2</sub>O<sub>8</sub> polar glass ceramics for sonar transducers 4-69651  
 Ba(Zn,Ta)<sub>2</sub>O<sub>3</sub>-BaZrO<sub>3</sub>, complex perovskite struct., dielec. resonator with high microwave Q-value 4-84926  
 Ba(Zn<sub>1/3</sub>Nb<sub>2/3</sub>)O<sub>3</sub>-Sr(Zn<sub>1/3</sub>Nb<sub>2/3</sub>)O<sub>3</sub> solid soln., dielectric props. meas. 4-98996  
 BeO ceramics, dielec. props. in near-mm wavelength range 4-99075  
 Bi layer-structured ferroelec. ceramics, pyroelec. props. 4-104540  
 Bi<sub>2</sub>TiO<sub>12</sub> ceramics, grain orientation, ESR and thermal expansion studies 4-104482  
 Bi<sub>2</sub>TiO<sub>12</sub> ceramics, grain orientation by cold uniaxial method 4-104757  
 C, corrosion resist. to nitric acid, report 4-62090  
 C-SiC alloy coating for limiter-armor tiles on Doublet III fusion reactor, test results 4-111924  
 α-Ca<sub>3</sub>(PO<sub>4</sub>)<sub>2</sub>, sintering behaviour at 1200 to 1600°C 4-114458  
 Ca(PO<sub>4</sub>)<sub>2</sub>OH, prestressed ceramics, fatigue props. 4-62052  
 CaO<sub>2</sub>-Ti<sub>2</sub>P<sub>2</sub>O<sub>12</sub> ceramic, cryst. struct. determ. 4-84262  
 CaTiSiO<sub>5</sub>, La sphere-based glass-ceramics, La partitioning, Auger studies 4-88112  
 CdSe-Te<sub>2</sub> hetero-photoconvertors, spectral characts. (Russian) 4-66692  
 CsO-Al<sub>2</sub>O<sub>3</sub>-TiO<sub>2</sub> system, phase stability, TGA and DTA obs. 4-71642  
 FeO, high temp. corrosion scales, TEM studies 4-104927  
 FeS high temp. corrosion scales, TEM studies 4-104927  
 Hf-Al-N ternary system, phase equilib. invest. rel. to fusion reactor materials 4-76759  
 K<sub>2</sub>Li<sub>2</sub>Nb<sub>6</sub>O<sub>30</sub>, solid solns., struct. and dielec. props. 4-75381  
 K<sub>2</sub>NbO<sub>4</sub> ferroelec. semicond., positive temperature resist. coeff. 4-113958  
 K<sub>2</sub>Pb<sub>2</sub>Nb<sub>10</sub>O<sub>30</sub>, ferroelec. struct. and piezoelec. props. 4-65963  
 KTaO<sub>3</sub>, sintering with the aid of MnO 4-61901  
 La<sub>2</sub>O<sub>3</sub>-P<sub>2</sub>O<sub>5</sub> system, phase equilib. and transform. 4-61923  
 LaPd<sub>2</sub>Al<sub>2</sub>-xO<sub>3</sub>, stabilisation conditions of trivalent Pd 4-71616  
 γ-LiAlO<sub>2</sub>, breeder material, TRIO-01 expt. for in-situ T recovery 4-107023  
 γ-LiAlO<sub>2</sub>, polycrystalline, elec. cond., AC meas. 4-108645  
 Li<sub>2</sub>O breeder blanket pellet, water vapour adsorption in He sweep gas stream 4-107032  
 Li<sub>2</sub>O breeder material, neutron irradi., T release expts. 4-107030  
 Li<sub>2</sub>O breeder material, neutron irradi. behaviour and compatibility testing 4-107031  
 Li<sub>2</sub>O, Li<sub>2</sub>ZrO<sub>2</sub>, Li<sub>2</sub>SiO<sub>4</sub> and γ-LiAlO<sub>2</sub> breeder blanket material developments 4-107020  
 Li<sub>2</sub>O, LiAlO<sub>2</sub>, Li<sub>2</sub>SiO<sub>4</sub> and Li<sub>2</sub>ZrO<sub>3</sub> breeder materials, fast neutron irradi. expts. 4-107024  
 Li<sub>2</sub>O pellet, T recovery, assay techniques 4-107022  
 Li<sub>2</sub>O pellet breeder materials, in-situ T recovery expt. 4-107026  
 Li<sub>2</sub>O single cryst., breeder material, D<sub>2</sub> solubility 4-107025  
 Li<sub>2</sub>O, thermal neutron irradi. effects, lattice parameter and expansion changes, F<sup>+</sup> centres 4-107028  
 Li<sub>2</sub>O-Al<sub>2</sub>O<sub>3</sub>-SiO<sub>2</sub> glass ceramic, effective radiative thermal cond./diffusivity, role of view factor 4-84473  
 Li<sub>2</sub>O-Al<sub>2</sub>O<sub>3</sub>-SiO<sub>2</sub> glass-ceramic, superplastic ductility, rel. to hydrostatic press. and humidity 4-109474  
 Li<sub>2</sub>O-B<sub>2</sub>O<sub>3</sub>-Fe<sub>2</sub>O<sub>3</sub> system, magnetic vitroceraics, prep. and props. 4-93256  
 Li<sub>2</sub>O-SiO<sub>2</sub> glass and glass-ceramic, hydrothermal corrosion 4-85235  
 Li<sub>2</sub>O-SiO<sub>2</sub> glass ceramic systems, density, crystallisation, elec. cond. 4-113937  
 Li<sub>2</sub>O<sub>2</sub>-ZnO, ceramics system, ionic and mixed cond. rel. to comp. and humidity 4-98339  
 Li<sub>2</sub>SiO<sub>3</sub>, polycrystalline, elec. cond., AC meas. 4-108645  
 Li<sub>2</sub>SiO<sub>3</sub> glass ceramics, grain oriented, hydrostatic piezoelec. props. and appls. 4-84913  
 LiTaO<sub>3</sub>, sintering with the aid of MnO 4-61901  
 Li<sub>1-x</sub>Ti<sub>x</sub>O<sub>3</sub> ceramics, elec. and supercond. props. 4-104342  
 MgAl<sub>2</sub>O<sub>4</sub> spinel ceramics, sintering, rel. to stoichiometry 4-109363  
 MgO containing metal precipitates, optical and mech. props. 4-70161  
 MgO-CaTiO<sub>3</sub>-CaO-SiO<sub>2</sub> system, phase equilib. and microstruct., isothermal sections 4-114496  
 MgO-Cr<sub>2</sub>O<sub>3</sub> granular ceramic, sintering and phase comp. 4-81174  
 MgSiAlON ceramic powders, plasma spraying, characterisation and decomposition 4-114391  
 Mn<sub>1-x</sub>Zn<sub>x</sub>Fe<sub>2</sub>O<sub>4</sub>, hot pressed, prior heat treatment effect on props. 4-89016  
 Mn<sub>1-x</sub>Zn<sub>x</sub>Fe<sub>2</sub>O<sub>4</sub>, sintering of powders produced by different methods, mechanism and assoc. processes 4-89015  
 N-based, conf., Falmer, England (Aug. 1981) 4-67873  
 N-based, environmental degradation and gas-solid reaction kinetics 4-76888  
 N-based, innovations 1976-1981 4-71532  
 N-based, microstruct. and props. 4-76746  
 β'-Na<sub>2</sub>Al<sub>2</sub>O<sub>3</sub> ceramic, spinel block doping and ionic cond. 4-84459  
 Na<sub>2</sub>O-Bi<sub>2</sub>O<sub>3</sub>-TiO<sub>2</sub> grain-oriented ferroelectric ceramics, piezoelec. props. (Japanese) 4-61625  
 Na<sub>1/2</sub>Bi<sub>1/2</sub>TiO<sub>3</sub>, pyroelectric props., perspective appl. in pyroelectric radiation detectors 4-88776  
 Na<sub>2</sub>O, solid solubility in mullite 4-113645

## ceramics continued

- Na<sub>2</sub>O-Nb<sub>2</sub>O<sub>5</sub>-SiO<sub>2</sub> glass-ceramics, ferroelec., depolarisation currents, dielec. and electrooptical props. 4-76317
- Na<sub>2</sub>O-ZrO<sub>2</sub>-P<sub>2</sub>O<sub>5</sub>-SiO<sub>2</sub> system, ultralow expansion ceramics 4-84424
- Na<sub>1+x</sub>Zr<sub>1-x</sub>P<sub>2</sub>O<sub>7</sub>, ultralow expansion ceramics 4-84424
- Na<sub>1+x</sub>Zr<sub>1-x</sub>P<sub>2</sub>O<sub>7</sub>-SiO<sub>2</sub>, ultralow expansion ceramics 4-84424
- Na<sub>1+x</sub>Zr<sub>1-x</sub>P<sub>2</sub>O<sub>7</sub>-SiO<sub>2</sub> ceramics, prep., ionic cond., durability and strength 4-11371
- Na<sub>3</sub>Zr<sub>2</sub>Si<sub>2</sub>PO<sub>12</sub>, NASICON solid electrolyte prep. and characts. for Na-S batteries 4-62347
- NiO, high temp. corrosion scales, TEM studies 4-104927
- $\beta'$ -Nb<sub>2</sub>O<sub>5</sub>-Al<sub>2</sub>O<sub>3</sub>-ZnO ceramics, ionic cond. and activation energy 4-113708
- PLZT, ageing and space charge arising in hot poling 4-76327
- PLZT ceramic, coarse-grain light scatt. and elec. hysteresis 4-76399
- PLZT ceramic for recording of volume, amplitude-phase holograms 4-107579
- PLZT ceramics, ferroelec. and electrooptic props. 4-76353
- PLZT ceramics, hot pressed polarisation and depolarisation behaviour 4-76318
- PLZT ceramics, ion implanted, optical absorption 4-114233
- PLZT ceramics, poling strategy 4-76319
- PLZT, chemically prepared, charact. and props. 4-76712
- PLZT, ferroelec. ceramic, hot poling, polarisation, ageing rel. to space charge 4-99045
- PLZT piezoelectric ceramic, fabricated by atmospheric sintering, electrical characts. and optical transmittance (*Korean*) 4-114211
- PLZT retardation plates, nonhomogeneity of light modulation 4-61660
- PLZT, tetragonal ceramic, 90° domains under poling, XRD study 4-76398
- PZT, dielec. props. at high press., p-T phase diagrams 4-99062
- PZT, lattice site of Zn, Sc, Fe ions, X-ray anal. 4-75488
- PZT material, high density, prep. by coprecipitation technique 4-76711
- PZT, prep. using cupferron 4-61904
- PZT, sintered, densification by hot isostatic pressing 4-66286
- (Pb, Ca)TiO<sub>3</sub> piezoelectric ceramic, modified, low mech. quality factor 4-76330
- (Pb,La)(Zr,Ti)O<sub>3</sub> ceramics, stress anisotropy induced by polarisation 4-104536
- (Pb,Ba)<sub>1-x/2</sub>(1-3y/2)La<sub>y</sub>Nb<sub>2</sub>O<sub>6</sub> ceramic, dielectric, piezoelectric and optical props. 4-98999
- Pb<sub>1-x</sub>Ba<sub>x</sub>Nb<sub>2</sub>O<sub>6</sub> ceramics, hot pressed, dielec. and piezoelec. props. 4-104533
- (Pb<sub>0.76</sub>Ca<sub>0.24</sub>)<sub>2</sub>((Co<sub>1/2</sub>W<sub>1/2</sub>)<sub>0.04</sub>Ti<sub>0.96</sub>)O<sub>3</sub> ceramics, piezoelec. props. MnO addition effects 4-104532
- (Pb<sub>0.75</sub>Ca<sub>0.25</sub>)(Mg<sub>1/3</sub>Nb<sub>2/3</sub>)<sub>0.0625</sub>(Ti<sub>0.9375</sub>)O<sub>3</sub>:Mn ceramics, US, elastic and dielec. props. 4-104543
- Pb<sub>2</sub>CrO<sub>4</sub> ceramic disk, photoconductivity with surface electrodes 4-61409
- Pb(FeNb)<sub>0.5</sub>O<sub>3</sub> ceramic, prep., struct., X-ray diff., neutron powder diff., dielec. and elec. meas., SEM 4-75412
- Pb(Fe<sub>1/2</sub>Nb<sub>1/2</sub>)O<sub>3</sub>-Pb(Ni<sub>1/3</sub>Nb<sub>2/3</sub>)O<sub>3</sub> solid soln. system, dielec. props. 4-104517
- PbMg<sub>1/3</sub>Nb<sub>2/3</sub>O<sub>3</sub> ceramics, dielec. props., microstruct. rel. to sintering temp. and comp. 4-84897
- Pb(Mg<sub>1/3</sub>Nb<sub>2/3</sub>)O<sub>3</sub>-Pb(Zn<sub>1/3</sub>Nb<sub>2/3</sub>)O<sub>3</sub> solid solns., ceramic, dielec. characts. 4-76354
- PbO-BaO-TiO<sub>2</sub>-B<sub>2</sub>O<sub>3</sub> glass ceramic system, crystal clamping, X-ray diff., dilatometry 4-109386
- (Pb<sub>1-3x/4</sub>Sm<sub>x/4</sub>)(Ti<sub>1-x</sub>Mn<sub>x</sub>)O<sub>3</sub> ceramic ultrasonic probe 4-100341
- PbTiO<sub>3</sub>/synthetic rubber composites, piezoelec. and dielec. props. 4-104535
- (PbTiO<sub>3</sub>)<sub>0.9</sub>(Pb(Mg<sub>1/2</sub>W<sub>1/2</sub>)O<sub>3</sub>)<sub>0.1</sub>, photovoltaic effect and beam intensity sensor 4-98664
- Pb(Zr,Ti)O<sub>3</sub> ceramic, fracture mechanics evaluation of acoustic fatigue 4-95416
- Pb(Zr,Ti)O<sub>3</sub> ceramics, ageing and ferroelec. props., heterovalent substitution effects 4-99046
- Pb(Zr,Ti)O<sub>3</sub> ceramics, spray dried, piezoelec. props. 4-109130
- Pb(Zr,Ti)O<sub>3</sub> high-freq. transducer 4-97241
- Pb(Zr,Ti)O<sub>3</sub> piezoceramic substrate, vacuum arc-plasma deposition of Ni-Cu 4-76691
- Pb(Zr,Ti)O<sub>3</sub> porous ceramic, appl. to HF underwater transducer 4-97258
- Pb(Zr,Ti)O<sub>3</sub> ring transducer, vibr. mode anal. 4-97240
- Pb(Zr,Ti)O<sub>3</sub>/synthetic rubber composites, piezoelec. and dielec. props. 4-104535
- Pb(Zr<sub>0.5</sub>Ti<sub>0.5</sub>)O<sub>3</sub> ceramics, piezoelec. props., porous struct. effects 4-104534
- Pb(Zr<sub>1-x</sub>Ti<sub>x</sub>)O<sub>3</sub> ceramic strips, width and thickness strain meas. 4-80869
- PbZrTi<sub>1-x</sub>O<sub>3</sub> ceramics, electrostrictive coeff., time resolved X-ray diff. studies 4-71282
- Pb<sub>1-x/2</sub>(Zr<sub>1-x/2</sub>)Ti<sub>1-x/2</sub>Nb<sub>2</sub>O<sub>6</sub> ceramic transducers, pyroelec. and mechano-dielec. characts. 4-109136
- Rb<sub>2</sub>Pb<sub>2</sub>Nb<sub>10</sub>O<sub>30</sub>, ferroelec. struct. and piezoelec. props. 4-65963
- Sb<sub>2/3</sub>Zn<sub>1/3</sub>O<sub>3</sub> sintered spinel, elec. cond. and Seebeck coeff., 400-800°C 4-61368
- SeO<sub>2</sub>-Na<sub>2</sub>O-B<sub>2</sub>O<sub>3</sub>, porous glass-ceramic, sintering and characterisation 4-114467
- Si-Al-O-N 'phases', struct. studies using magic-angle-spinning NMR 4-71198
- Si<sub>3</sub>Al<sub>2</sub>O<sub>7</sub>N<sub>2</sub>, sialon X-phase, cryst. struct. 4-75427
- Si<sub>6-x</sub>Al<sub>2</sub>O<sub>7</sub>N<sub>8-x</sub>,  $\beta$ -sialon synthesis from Si<sub>3</sub>N<sub>4</sub> and Al alkoxides (*Japanese*) 4-114461
- SIC, bubble form. in oxide scales 4-62084
- SIC ceramics interfaces, contact stresses distrib. rel. to geometry 4-76873
- SIC, corrosion resist. to nitric acid, report 4-62090
- SIC, fusion reactor first wall appl., thermal and mech. props. (*German*) 4-83244
- SIC, He ion irradiation, surface erosion 4-80120
- SIC, prod. methods and parameters, report (*German*) 4-61908
- SIC, reaction bonded, and liq. Al, cast bonding, exchange diffusion phenomenon involving free Si 4-99741
- SIC, reaction bonded, high temp. creep kinetics, dislocation glide mechanism 4-109476
- $\alpha$ -SiC, sinterability, strength and oxidation 4-61899
- $\alpha$ -SiC, sintered, phenomenology of fracture 4-93372
- SIC, sintered and siliconised, microstruct. of neutron irradi. induced defects 4-108459
- SIC ultrafine powders, synthesized from colloidal silica and pitch, SEM and X-ray diff. study 4-114454
- SIC-B, shrinkage, density and phase comp. rel. to forming press. and sintering temp. 4-85130

## ceramics continued

- SiC-BN composites, thermal diffusivity anisotropy 4-84472
- SiC-based ceramics, time-temp. effects 4-76963
- Si<sub>3</sub>N<sub>4</sub>, amorphous, controlled crystn. by Ti and Cl additions 4-113334
- Si<sub>3</sub>N<sub>4</sub>,  $\alpha$ - $\beta$  relationship 4-70125
- Si<sub>3</sub>N<sub>4</sub> ceramics, liq. phase sintering, densification and transform. mechanisms 4-76724
- Si<sub>3</sub>N<sub>4</sub> ceramics interfaces, contact stresses distrib. rel. to geometry 4-76873
- Si<sub>3</sub>N<sub>4</sub>, dense compact, gas phase sintering process 4-76730
- Si<sub>3</sub>N<sub>4</sub>, determ. of  $\alpha$ -phase fraction (*Japanese*) 4-81393
- Si<sub>3</sub>N<sub>4</sub> form. from grog containing slip casts; 4-85131
- Si<sub>3</sub>N<sub>4</sub>, fracture toughness, effect of deform. 4-76868
- Si<sub>3</sub>N<sub>4</sub>, gas press. sintering, effect of oxide additions (*Japanese*) 4-81176
- Si<sub>3</sub>N<sub>4</sub>, grinding ceramics for diamond wear 4-99609
- Si<sub>3</sub>N<sub>4</sub>, hot isostatic pressing, densification, bending strength rel. to additives (*Japanese*) 4-76721
- Si<sub>3</sub>N<sub>4</sub>, hot pressed, fracture toughness, mech. props. rel. to comp. and microstruct. 4-76870
- Si<sub>3</sub>N<sub>4</sub>, hot pressing, densification and microstruct. rel. to MgO and Y<sub>2</sub>O<sub>3</sub> additions 4-76729
- Si<sub>3</sub>N<sub>4</sub>, hot-pressed, oxidation kinetics 4-76890
- Si<sub>3</sub>N<sub>4</sub>, hot-pressed, transient creep parameters, determ. by dynamic bending tests 4-81381
- Si<sub>3</sub>N<sub>4</sub>, liq. phase sintering mechanisms 4-71614
- Si<sub>3</sub>N<sub>4</sub>, microstruct. development during fabrication 4-76733
- $\beta$ -Si<sub>3</sub>N<sub>4</sub>, Mossbauer spectra, effect of heat treatment and  $\gamma$ -irrad. 4-80846
- Si<sub>3</sub>N<sub>4</sub>, multiaxial strength tests for brittle materials 4-93491
- Si<sub>3</sub>N<sub>4</sub>, nitridation of Si+Al compacts, expt. plan 4-71622
- Si<sub>3</sub>N<sub>4</sub>, polyphase, cation diffusion through intergranular phase, appl. to environmental reactions 4-76889
- Si<sub>3</sub>N<sub>4</sub> polyphase materials, high temp. deform. and fracture 4-76866
- Si<sub>3</sub>N<sub>4</sub> powder, comparison of prep. methods 4-71624
- Si<sub>3</sub>N<sub>4</sub> powder, prep. from SiO<sub>2</sub> 4-71623
- Si<sub>3</sub>N<sub>4</sub> powder, shocked, hot isostatic processing 4-71617
- Si<sub>3</sub>N<sub>4</sub> powder compacts, isostatically pressed, sintering by powder bed technique 4-76723
- Si<sub>3</sub>N<sub>4</sub>, pressureless sintered, high temp. fatigue failure 4-76867
- Si<sub>3</sub>N<sub>4</sub>, reaction bonded, creep, porosity, internal oxidation 4-76833
- Si<sub>3</sub>N<sub>4</sub>, reaction bonded, flexural strength, oxidation resist, annealing effect 4-76832
- Si<sub>3</sub>N<sub>4</sub>, reaction bonded, flexure strength, oxidation, microstruct. 4-76892
- Si<sub>3</sub>N<sub>4</sub>, reaction bonded, sintering, microstruct. and props. 4-76725
- Si<sub>3</sub>N<sub>4</sub>, reaction bonded, sintered, densification kinetics, microstruct. 4-76726
- Si<sub>3</sub>N<sub>4</sub>, reaction sintered, cyclic fatigue resist. 4-76869
- Si<sub>3</sub>N<sub>4</sub>, reaction-bonded, flow populations, effect of oxidation 4-62059
- Si<sub>3</sub>N<sub>4</sub>, reaction-bonded, infiltration by pure metals and alloys 4-76735
- Si<sub>3</sub>N<sub>4</sub>, reaction-bonded, Si nitridation reaction 4-71620
- Si<sub>3</sub>N<sub>4</sub>, reaction-bonded, sintering, review 4-71625
- Si<sub>3</sub>N<sub>4</sub>, reaction-bonded, strength-porosity relationship 4-76734
- Si<sub>3</sub>N<sub>4</sub>, reaction-bonded compacts, nitriding behaviour, influence of Si particle size 4-71621
- Si<sub>3</sub>N<sub>4</sub>, reactor ion-bonded, porous, oxidation mechanism 4-62081
- Si<sub>3</sub>N<sub>4</sub> sputter coatings, thermal oxidation resist. of reaction bonded Si<sub>3</sub>N<sub>4</sub> substrates 4-85238
- Si<sub>3</sub>N<sub>4</sub>, thermal props. and thermal shock resist. rel. to microstruct. and processing parameters 4-76871
- Si<sub>3</sub>N<sub>4</sub>, Young's modulus and internal friction, temp. depend. 4-61965
- Si<sub>3</sub>N<sub>4</sub>-based ceramics, time-temp. effects 4-76963
- Si<sub>3</sub>N<sub>4</sub>-based metalcutting tools, props. and appl. 4-66283
- Si<sub>3</sub>N<sub>4</sub>-based systems, phase equilib. calcs. 4-71645
- Si<sub>3</sub>N<sub>4</sub>-metal oxide systems, phase equilib. studies 4-71646
- Si<sub>3</sub>N<sub>4</sub>-MgO, hot pressed, fracture stress, temp. and strain rate depend. 4-85207
- Si<sub>3</sub>N<sub>4</sub>-SiC ceramic materials, high yield synthesis by pyrolysis of polyorganosilazane 4-114456
- Si<sub>3</sub>N<sub>4</sub>-SiO<sub>2</sub>-AlN-Al<sub>2</sub>O<sub>3</sub>-Y<sub>2</sub>O<sub>3</sub> system, phase relations, solid-liq. reactions 4-76762
- Si<sub>3</sub>N<sub>4</sub>-Y<sub>2</sub>O<sub>3</sub>, isostatically hot pressed, strength and microstruct. rel. to sintering additives 4-85132
- Si<sub>3</sub>N<sub>4</sub>-Y<sub>2</sub>O<sub>3</sub> based ceramics, sintering, densification, oxidation, strength and porosity 4-76835
- Si<sub>3</sub>N<sub>2</sub>O ceramic, thermal shock resist. 4-81289
- SiO<sub>2</sub>, corrosion resist. to nitric acid, report 4-62090
- SiO<sub>2</sub>, synthetic, props. under high-temp. treatment 4-81172
- SiO<sub>2</sub>-CaO-Al<sub>2</sub>O<sub>3</sub>-MgO, elastic and strength props., effect of temp. 4-114597
- SiYON ceramics, mech. props. rel. to corrosion and microstruct. 4-76834
- ((Sr<sub>0.35</sub>Pb<sub>0.25</sub>Ca<sub>0.25</sub>)TiO<sub>3</sub>)<sub>100-x</sub>(Bi<sub>2</sub>O<sub>3</sub>·3TiO<sub>2</sub>)<sub>x</sub>, dielectric props., HV capacitor application 4-98997
- SrTiO<sub>3</sub>, intrinsic ferroelectric, sp. hi. in range 0.5 to 6K 4-84420
- SrTiO<sub>3</sub>, vitroceraamics, dielectric props., low temp. meas. 4-65940
- Sr<sub>2</sub>TiSi<sub>2</sub>O<sub>7</sub> glass ceramics, grain oriented, hydrostatic piezoelec. props. and appl. 4-84913
- Ti-TiC single crystal diffusion couple, annealing, solid state reaction, C diffusion 4-85133
- TiB<sub>2</sub>, sintering and props. of samples made from powder synthesised in plasma-arc heater 4-76715
- TiC, powder prod. from Ti swarf, optimum carbidisation parameters 4-89014
- TiC, synthesis in plasma jet, effect of conditions of introduction of starting material 4-61893
- TiO<sub>2</sub>, doped, monozoned powders, synthesis and characterisation 4-114453
- TiO<sub>2</sub>, polymorphic transform. by mech. grinding 4-66328
- TiO<sub>2</sub>-based crystalline ceramic nuclear waste forms, processing and microstruct. 4-83150
- (U,Pu)O<sub>2</sub>, diffusion meas., effects of chem. surface gradient, mechanical polishing 4-98354
- UO<sub>2</sub> fuel pellets, sintering, grain growth rel. to S-content 4-85134
- WC, indented, dislocation interactions, crack nucleation, TEM obs. 4-80039
- YIG containing magnetic glass-ceramics, prep. using colloidal Bi as nucleation catalyst, characts. 4-71628
- Y<sub>2</sub>O<sub>3</sub>-Fe<sub>2</sub>O<sub>3</sub>, solid state reaction for garnet formation by sintering 4-85302
- ZnCr<sub>2</sub>O<sub>4</sub>-LiZnVO<sub>4</sub> ceramic sensors, humidity-sensitive props., microstruct. 4-82800

## ceramics continued

- ZnO varistor, high-field fine-grained, fabrication by sol-gel processing 4-66282  
 ZnO varistor, polycrystalline, elec. props. 4-104199  
 ZnO varistor ceramics, SEM EBC studies 4-75981  
 ZnO-Nb<sub>2</sub>O<sub>5</sub> ceramics, elec. props. and microstruct., wettability additives effect (*Japanese*) 4-76719  
 ZnS, polycryst., thermal cond. 4-70483  
 ZnS, polycryst. optical ceramic, thermal cond. coeff. temp. depend. 4-79254  
 ZrO<sub>2</sub> ceramics, process zone toughening by microcracking 4-62020  
 ZrO<sub>2</sub> gels, pure and MgO-doped, decomposed in vacuo, neutron and X-ray diffr. study 4-61900  
 ZrO<sub>2</sub> matrix, anion deficient stabilised, contrast from coherent precipitates 4-103945  
 ZrO<sub>2</sub>, MgO partially stabilised, Weibull modulus 4-61972  
 ZrO<sub>2</sub>, partially stabilised, Young's modulus and internal friction, temp. depend. 4-61965  
 ZrO<sub>2</sub> powder, monoclinic, prep. of ultrafine particles by hydrolysis of ZrOCl<sub>2</sub> (*Japanese*) 4-81175  
 ZrO<sub>2</sub> powders, hydrothermal prep. 4-109359  
 ZrO<sub>2</sub> system, monoclinic-tetragonal, calibration curve for quantitative anal. by X-ray diffr. 4-113657  
 ZrO<sub>2</sub>-Al<sub>2</sub>O<sub>3</sub>-SiO<sub>2</sub>-CaO system, compatibility relations, microscopy, energy dispersive X-ray exam. 4-61925  
 ZrO<sub>2</sub>-CaO, partially stabilised, grain boundary chem., Auger analysis 4-109409  
 ZrO<sub>2</sub>-P<sub>2</sub>O<sub>5</sub> system, re-examination of crystalline phases 4-84258  
 ZrO<sub>2</sub>-Y<sub>2</sub>O<sub>3</sub> single crystals, stabilised system, elastic consts., comp. and temp. depend., 20-700°C 4-85171  
 ZrO<sub>2</sub>-Y<sub>2</sub>O<sub>3</sub>-Bi<sub>2</sub>O<sub>3</sub> solid electrolyte, prep. and elec. props. 4-84452  
 ZrO<sub>2</sub>-Y<sub>2</sub>O<sub>3</sub>-HfO<sub>2</sub> ceramic powders, laser sintering 4-88998  
 ZrSiO<sub>4</sub> powder, plasma sprayed layer, heat cond. coeff. 4-114692

Cherenkov counters see Cherenkov counters

Cherenkov radiation see Cherenkov radiation

## cerium

- see also nuclei with .....  
 core EELS, surface oxidation effects 4-85048  
 dense Kondo state, spin-orbit coupling crystal field splitting 4-84613  
 electronic struct., press induced 4f occupancy enhancement 4-75844  
 europium ethylsulfate, Ce<sup>3+</sup>, Ce<sup>3+</sup> EPR spin-lattice relax. rate, press. effects 4-65855  
 impurities in fluorite deposits study by EPR and neutron activation anal. 4-80815  
 lanthanum ethylsulfate:Ce<sup>3+</sup>, energy level shift under hydrostatic press. (*Russian*) 4-84598  
 similarity hypothesis and  $\gamma \leftrightarrow \alpha$  transition (*Russian*) 4-81190  
 valence band photoemission study 4-81108  
 valence under high press., free energy depend. 4-92676  
 X-ray absorpt. near edge struct. 4-66118  
 yttrium ethylsulfate:Ce<sup>3+</sup>, Ce<sup>3+</sup> EPR spin-lattice relax. rate, press. effects 4-65855  
 Ba<sub>0.54</sub>Er<sub>0.46</sub>Nb<sub>2</sub>O<sub>6</sub>:Ce, thermally stimulated electron emission, dielec. characts., impurity effects (*Russian*) 4-114356  
 CaF<sub>2</sub>:Ce<sup>3+</sup>, O<sub>2</sub><sup>-</sup>, thermoluminescence spectra, irradi. effects 4-109259  
 $\alpha$ -Ce, local mag. susceptibility meas., TDPAD study 4-65792  
<sup>14</sup>Ce, proton impact, K-shell ionisation cross sections 4-96507  
<sup>144</sup>Ce X-ray and gamma photo energies and intensities, Ge detector calibration (*French*) 4-73850  
 Ge-Ce, spin depolarisation study 4-104722  
 Ge<sub>2</sub>Se<sub>3</sub>:Ce glass, impurity surroundings, nature of defects, positron annihilation study 4-79943  
 La<sub>2</sub>Mg<sub>3</sub>(NO<sub>3</sub>)<sub>12</sub>:Ce<sup>3+</sup>, Co<sup>2+</sup>·24H<sub>2</sub>O, paramagnetic, maser effect due to thermal excitation by pulsed mag. field 4-64692  
 MgO:Ce<sup>3+</sup>, fluoresc., thermoluminesc. and decay 4-93117  
 Nd, Cr, Ce: YAG laser props., gain coeffs. 4-79156  
 SrS:Ce:Sm, luminescence, optical and thermal stimulation 4-99174  
 YAG:Ce<sup>3+</sup>, defect emission, photoluminesc. decay time measurements 4-80971  
 YAG:Nd, Cr, Ce, laser props., gain coeffs. 4-79156

## cerium alloys

- dense Kondo state, spin-orbit coupling crystal field splitting 4-84613  
 dilute, X-ray absorpt. near edge struct. 4-66118  
 dilute magnetic alloys with Ce impurities, cryst. field interactions, low temp. thermodynamic props. 4-84801  
 misch metal alloys, Mn<sub>14</sub>Al<sub>10</sub>S<sub>5</sub>, H<sub>2</sub> desorption kinetics 4-75787  
 transition to nonmagnetic f states, bremsstrahlung isochromat spectra studies 4-113884  
 valence fluctuation dynamics, appl. of self consistent perturbation theory 4-70743  
 Ag-Ce, solid solubility, metastable extension (*Chinese*) 4-61918  
 Ag-Ce-Ce system, partial phase diagram and lattice structs. 4-71636  
 Ce-Co-Cu, magnetically hard alloys, isostructural precipitation and atomic ordering (*Russian*) 4-104784  
 Ce-Ni-Sb system, phase equilib. diagram, X-ray analysis 4-114491  
 CeAl, valence band photoemission at 3d absorption edges, reson. enhancement 4-81110  
 CeAl<sub>2</sub>, bound state between phonons and crystalline electric field states 4-104175  
 CeAl<sub>2</sub>, mixed valence system, high press. L<sub>III</sub> X-ray absorption spectra study 4-61342  
 CeAl<sub>2</sub>, phonon softening, neutron scatt. studies 4-92318  
 CeAl<sub>3</sub>, low-temp. specific heat meas. 4-75702  
 CeAl<sub>100-x</sub>, amorphous, transport and mag. props. 4-108985  
 CeB<sub>6</sub>, antiferromagnetic-quadrupole ordering 4-80763  
 CeCo<sub>2</sub>Si<sub>2</sub>, valence change, X-ray absorpt. study 4-85037  
 CeCu<sub>6</sub>, heavy-fermion system, elec. resist, susceptibility and sp. ht. meas. 4-104402  
 CeCu<sub>6</sub> Kondo lattice intermetallic compound, anisotropic negative magnetoresistance 4-76111  
 CeCu<sub>2</sub>Si<sub>2</sub>, heavy-fermion supercond., NQR spectra 4-104508  
 CeCu<sub>2</sub>Si<sub>2</sub>, heavy-fermion supercond., valence band reson. photoelectron spectra 4-104720  
 CeCu<sub>2</sub>Si<sub>2</sub>, Kondo lattice substance superconductivity 4-98797  
 CeCu<sub>2</sub>Si<sub>2</sub>, low-temp. specific heat meas. 4-75702  
 CeCu<sub>2</sub>Si<sub>2</sub>, nucl. relax., possible evidence for triplet superconductivity 4-108974  
 CeFe<sub>2</sub>Si<sub>2</sub>, valence change, X-ray absorpt. study 4-85037  
 CeGa<sub>17</sub>Ni<sub>2</sub>, cryst. struct. determ. 4-75375  
 Ce<sub>1-x</sub>Hf<sub>x</sub>Co<sub>5</sub>, anomalous mag. behaviour 4-88664

## cerium alloys continued

- CeIn<sub>3</sub>, mixed-valence system, muon Knight shift meas. 4-80852  
 Ce(In<sub>1-x</sub>Sn<sub>x</sub>)<sub>3</sub>, intermediate valence study 4-61340  
 Ce<sub>2</sub>La<sub>1-x</sub>Al<sub>2</sub>, dense Kondo state, elec. resist., mag. susceptibility meas. 4-108984  
 Ce<sub>0.8</sub>La<sub>0.2</sub>Cu<sub>2</sub>Si<sub>2</sub> disordered, low-temp. specific heat meas. 4-75702  
 Ce<sub>1-x</sub>La<sub>x</sub>Cu<sub>2</sub>Si<sub>2</sub>, mag. props. during Kondo impurity-Kondo lattice transition 4-61509  
 Ce<sub>1-x</sub>La<sub>x</sub>Ni<sub>5</sub>, mixed valence, thermopower and band struct. 4-113927  
 Ce<sub>0.9-x</sub>La<sub>0.1</sub>Th<sub>0.1</sub>,  $\gamma$ - $\alpha$  transition, x-P-T phase diagrams 4-76755  
 CeMg, antiferromagnet. cpd., magnons and phonons 4-84777  
 Ce<sub>1-x</sub>Nd<sub>x</sub>Ag mixed crystals, mag. phase diagram 4-65812  
 CeNi<sub>5</sub>, mixed valence, thermopower and band struct. 4-113927  
 CeNi<sub>5</sub>-LaNi<sub>5</sub>, phase diagram, H absorpt. characts. (*Chinese*) 4-93261  
 CeNi<sub>5-x</sub>Al<sub>x</sub> alloys, H<sub>2</sub> storage props. 4-61206  
 Ce<sub>1-x</sub>Ni<sub>2.5</sub>Cu<sub>2.5</sub> alloys, hyperstoichiometric, H<sub>2</sub> sorption 4-61207  
 CeNi<sub>2</sub>Si<sub>2</sub>, valence change, X-ray absorpt. study 4-85037  
 CeOs, Ru<sub>2-x</sub>Si<sub>2</sub>, mag. behaviour and struct. chemistry 4-103701  
 CePd<sub>3</sub>, 4f-derived photoemission study 4-81107  
 CePd<sub>3</sub>, mixed-valence system, muon Knight shift meas. 4-80852  
 CePd<sub>3</sub>B<sub>2</sub>(Si<sub>2</sub>), valence state studies 4-70748  
 CeRu<sub>2</sub>, 4f-derived photoemission study 4-81107  
 CeRu<sub>2</sub>Si<sub>2</sub>, mixed-valent system, superconductivity 4-104364  
 CeSi<sub>2</sub>, intermetallics, cryst. growth from melt 4-66219  
 CeSn<sub>3</sub>, anisotropic spin fluctuations, sp. ht., mag. susceptibility meas. 4-65819  
 CeSn<sub>3</sub>, mixed-valence system, muon Knight shift meas. 4-80852  
 Ce<sub>0.9</sub>Y<sub>0.1</sub>Cu<sub>2</sub>Si<sub>2</sub>, disordered, low-temp. specific heat meas. 4-75702  
 Ce<sub>1-x</sub>Zr<sub>x</sub>Co<sub>5</sub>, anomalous mag. behaviour 4-88664  
 Co-Ce liq. alloy, Ce valence state determ. 4-61358  
 Fe-Ce liq. alloy, Ce valence state determ. 4-61357  
 Fe-Sb-Ce alloys, Ce state at cryst. boundaries, electron diffr. studies (*Chinese*) 4-98114  
 Mg-Li-Al-Zn-Mn-Ce system, mech. props. and corrosion resist. 4-93455  
 Tb-Ce, dil., intermediate valent, temp. depend. hyperfine fields, TDPAC study 4-75907  
 Ti-Ce, rapidly solidified dispersion strengthened, struct. and props. 4-114561

## cerium compounds

see also cerium alloys

- CeO<sub>2</sub> film, vac. deposited, dielec. parameters, temp. depend., defects role 4-99024  
 dense Kondo state, spin-orbit coupling crystal field splitting 4-84613  
 hydrides, non-stoichiometric, phase transitions 4-92352  
 intermediate-valence cpds., anomalous thermo-EMF coefficient behaviour 4-61405  
 mixed valence compounds, Ce atom ground state effects of cryst. fields 4-104403  
 mononitrides, f-electron-band-electron hybridisation and anomalous cryst. field splitting 4-113913  
 valence fluctuation dynamics, appl. of self consistent perturbation theory 4-70743  
 Bi<sub>1-x</sub>Ce<sub>x</sub>(MoO<sub>4</sub>)<sub>3</sub>, cryst. struct., vacancies, powder neutron diffr. 4-75407  
 CeBi, type-I antiferromagnet., hybridisation-mediated exchange, anisotropic excitation behaviour 4-71053  
 Ce<sub>0.8</sub>Ca<sub>0.2</sub>CrO<sub>3</sub>, ionic cond. and thermal expansion 4-84461  
 Ce<sub>1-x</sub>Ca<sub>x</sub>O<sub>2-x</sub>, vacancy binding energy, polarisation contrib. 4-88165  
 CeCo<sub>2</sub>P<sub>2</sub>, cryst. struct. determ. 4-80011  
 CeCu<sub>2</sub>Si<sub>2</sub>, superconducting T<sub>c</sub> maximum 4-98800  
 CeD<sub>2+x</sub>, mag. order and cryst. field effects 4-104408  
 CeD<sub>2</sub>, order-disorder transform. and mag. struct. 4-61069  
 CeF<sub>3</sub> doped optical films, tensile stress cracks and stress modification 4-76543  
 CeF<sub>3</sub>, magnetic susceptibility and Verdet const. 4-61507  
 CeF<sub>3</sub>:Nd, NMR study, relax. time 4-71203  
 Ce<sub>1-2x</sub>Gd<sub>2x</sub>O<sub>2-x</sub>, vacancy binding energy, polarisation contrib. 4-88165  
 CeF<sub>3</sub>, X-ray absorpt. near edge struct. 4-66118  
 CeM<sub>3</sub>B<sub>2</sub> (M=Co, Ru, Rh, Ir), mixed valence, mag. and elec. props. 4-113905  
 Ce<sub>2</sub>Mg<sub>3</sub>(NO<sub>3</sub>)<sub>12</sub><sup>3</sup>He system, anomalous low temp. Kapitza resistance 4-65542  
 Ce<sub>2</sub>MoO<sub>6</sub>, valence state of Mo 4-71161  
 CeN, X-ray absorpt. near edge struct. 4-66118  
 Ce(NO<sub>3</sub>)<sub>3</sub>, aq. soln., diffusion coeffs. at 35°C 4-70422  
 CeO, electronic states, absorpt., emission and laser spectrosc. 4-59712  
 CeO<sub>2</sub> crystals, flux growth 4-71542  
 CeO<sub>2</sub>:La<sup>3+</sup>, dielectric relaxation, orientation of dipole complexes 4-114202  
 CeO<sub>2</sub>-CaO solid solutions, elec. cond., temp. depend., 400-1200°C 4-61142  
 CeO<sub>2</sub>-Ln<sub>2</sub>O<sub>3</sub> (Ln=La, Nd, Sm, Gd, Er, Y) solid solutions, elec. cond., temp. depend., 400-1200°C 4-61142  
 CeO<sub>2</sub>-Y<sub>2</sub>O<sub>3</sub>, nonstoichiometric, electronic conduction, dopant effects 4-92733  
 CeO<sub>2-x</sub>, nonstoichiometric, sp. ht. and phase diagrams 4-103957  
 (CeO<sub>0.89</sub>(CaO)<sub>0.11</sub> solid solution, bulk cond. and grain boundary resist., effect of SiO<sub>2</sub> (*French*) 4-80295  
 Ce<sub>2</sub>O<sub>3</sub> scintillating glass fiber-optic plate detectors, tracking appl. 4-59533  
 CeS, energy band struct., X-ray study 4-84565  
 Ce<sub>2</sub>(SO<sub>4</sub>)<sub>3</sub>·9H<sub>2</sub>O(D<sub>2</sub>O) single cryst. dielec. response, contact configuration effects 4-65945  
 CeSb, first order mag. phase transitions of the order-disorder type 4-65814  
 CeSb, specific heat meas., using high-pressure AC calorimetric technique 4-86423  
 CeSi<sub>8</sub>, elec. cond. and paramagnetism 4-104207  
 CeSiO<sub>3</sub>N, Ce-N- $\alpha$ -wollastonite polytypes, electron microscopy study 4-103949  
 Ce<sub>1-2x</sub>Y<sub>2x</sub>O<sub>2-x</sub>, vacancy binding energy, polarisation contrib. 4-88165  
 LiF-CeF<sub>3</sub> thin film, ionic cond. meas. 4-84450  
 na<sub>2+x+y</sub>Ca<sub>2(1-x-y)</sub>Ce<sub>2</sub>Tb<sub>2</sub>(PO<sub>4</sub>)<sub>2</sub> orthophosphates, luminescence and struct. relations 4-99169  
 NiO:CeO<sub>2</sub>, oxidation and grain boundary diffusion 4-92441  
 (U,Ce)O<sub>2</sub>, cation redistribution in thermal gradient (*French*) 4-73978  
 (U<sub>0.7</sub>Ce<sub>0.3</sub>)O<sub>2-x</sub>, thermomodification study 4-98348  
 U<sub>0.7</sub>Ce<sub>0.3</sub>O<sub>2-x</sub>, transport props. 4-104245

## cermets

- CVD-TiC coatings on hard metal, TEM study 4-71592

## cermets continued

- diffusion bonding, hot isostatic pressing 4-89239  
 friction with superhard abrasive grains 4-109522  
 hardfacing deposits, Cr<sub>3</sub>C-containing, microstruct. and abrasion resist., influence of welding process variables 4-85222  
 hardfacing deposits, Ti<sub>3</sub>C-containing, microstruct. and abrasion resist., influence of welding process variables 4-85222  
 inhomogeneous composite materials, optical props. 4-99071  
 optical props. and dielec. const., quantum size effects 4-65941  
 plasma metallising of particles, kinetics of thermophys., processes 4-61884  
 randomly distributed particles of cermet topology, optical props. 4-93039  
 solar highly absorbing coatings using graded refractive indices and textured surfaces 4-72146  
 superhard materials, crack resist. determ., samples and loading 4-93494  
 AlN/Al cermets, reactive DC planar magnetron sputtering prep., elec. transport props. 4-88607  
 Al<sub>2</sub>O<sub>3</sub>/Au cermets, optical props. and dielec. const., quantum size effects 4-65941  
 Al<sub>2</sub>O<sub>3</sub>/Au cermets, optical props. and dielec. const., quantum size effects 4-65942  
 Al<sub>2</sub>O<sub>3</sub>-Fe cermets, metal to ceramic bonding, Mossbauer studies 4-109622  
 Cr-SiO cermet films, composition and sheet resistance effect on strain sensitivity obs. 4-111117  
 Cu-Pb<sub>2</sub>, antireflecting cermets, photodecomposition, optical characts. 4-101949  
 Cu-Sn-Al<sub>2</sub>O<sub>3</sub>, abrasive composite, physicochem. props., effect of premoulding press. in elec. discharge sintering 4-89020  
 LaCrO<sub>3</sub>-Cr cermet, high-temp. creep 4-71693  
 Mo-Al<sub>2</sub>O<sub>3</sub>/Cr<sub>2</sub>O<sub>3</sub> cermet emitter electrodes, directionally solidified, development and evaluation for thermionic energy converters 4-77126  
 Mo-Al<sub>2</sub>O<sub>3</sub>/Cr<sub>2</sub>O<sub>3</sub> eutectic thermionic emitter 4-72141  
 NiB-Co, plastic deform. of compound materials based on hard phases 4-99451  
 Pt-Al<sub>2</sub>O<sub>3</sub> graded cermet selective absorber coatings, sputter-deposited 4-72171  
 Pt-Al<sub>2</sub>O<sub>3</sub> graded-cermet selective absorbers, graded infinitesimal-lamellae model 4-114948  
 SiC-Al, sintered composite interfacial reactions, joint bending strength rel. to microstruct. 4-66295  
 TaC-Co, plastic deform. of compound materials based on hard phases 4-99451  
 Ti(C,N)-Ni-Mo, hard metal, fracture toughness rel. to microstruct. 4-104873  
 TiC-Co, plastic deform. of compound materials based on hard phases 4-99451  
 TiC-Co, TiC coated, cemented carbide tools, wear studies 4-99610  
 TiC-Fe-Cr-Mo, bonded carbides, wear-resistant, produced by powder metallurgy techniques 4-66455  
 TiC-Ni tungstenless alloy powder, pressing characts., comparison with WC-Co 4-89018  
 TiN-Mo composite powders, production in low temp. plasma stream 4-89019  
 TiN-Ti coatings, reactive pulse plasma deposited, struct. and props. 4-76688  
 W hard metals, sintered, mech. props. rel. to O content (*German*) 4-61909  
 WC-(Co-Ni) hardmetals, mech. props., variation with Ni/Co ratio 4-114462  
 WC-C, mechanical behaviour, room temp. to 1000°C 4-62002  
 WC-Co, cemented carbide, hot isostatic pressing 4-66293  
 WC-Co, cemented elements of high press. apparatus, strength safety factors 4-109482  
 WC-Co, hardmetal, creation of stable cracks using bridge indentation 4-66434  
 WC-Co, hardmetals, infiltration technique 4-66294  
 WC-Co, plastic deform. of compound materials based on hard phases 4-99451  
 WC-Co cemented carbide, defect position in bending test rel. to strength variance 4-99661  
 WC-Co cemented carbide, liq. phase sintering, origins of discontinuous grain growth 4-104759  
 WC-Co hard metals, strengthening by ultrasonic vibrs. 4-62122  
 WC-Co hardmetal, grain growth rate sintering, influence of C content 4-114463  
 WC-Co powders, hypersonic flame spraying, particle vel. meas. by laser Doppler velocimetry 4-81353  
 WC-Ni, hardmetals, infiltration technique 4-66294

## CESR

- metals, acoustic excitation of spin waves due to conduction electrons (*Russian*) 4-98947  
 Al-based dilute foils, conduction electron spin resonance linewidths 4-92961  
 Ca, fine particles, CESR 4-76251  
 CuGaIn<sub>1-x</sub>Se<sub>2</sub> chalcopyritic semicond., ESR studies 4-109070  
 GaAs, doped, cond. electron spin relax. times, precession mechanism, spin splitting 4-98948  
 InSb, spin reson. of magnetoresist. and photo-EMF under stimulated Raman scatt. conditions 4-92962  
 Li-Fe film, conduction electron surface mag. relax. (*Russian*) 4-65862  
 Mg, fine particles, CESR 4-76251

## chalcogenide glasses

- amorphous solids, physics, book 4-90312  
 amorphous thin films, switching, at. and electronic processes 4-113941  
 chalcogenide glass, H<sub>2</sub>O and H<sub>2</sub> band reduction 4-107896  
 dielectric constant dispersion, freq. dependence 4-80858  
 electron microscopy of reactions with metals and electron beam induced crystn. 4-80315  
 electronic transitions in mobility gap 4-61275  
 fibre optic materials, scatt. losses, numerical estimates 4-83709  
 film vitreous chalcogenides, multilayer reflecting systems for IR lasers 4-69532  
 fluorescence and nonradiative relax. in glasses containing rare earth ions, review 4-99156  
 Hall effect studies for chalcogenide glasses, temperature dependence of carrier mobility 4-92756  
 interference narrow-band light filters 4-74689  
 metal/chalcogenide glass evaporated layers, offset printing plates, prep. processing and sensitising 4-68297

## chalcogenide glasses continued

- one-electron density of states 4-84548  
 optical fibre, preparation 4-103046  
 photodarkening and light induced anisotropy 4-112530  
 picosecond electronic relaxations 4-108892  
 quantum electronics applications, laser modulation and scanning (*Russian*) 4-79252  
 switching effects, inhomogeneous model anal. 4-88546  
 thin films, threshold switching and trap filling 4-92770  
 thin films, threshold switching effects 4-92769  
 tunnelling relax. in a.c. cond. 4-70812  
 two-step optical excitation, rel. to valence band struct. 4-85002  
 As<sub>2</sub>S<sub>3</sub> thin film, photostructural changes studied by photo-ESR 4-114162  
 Ag/As<sub>2</sub>S<sub>3</sub> evaporated layers, offset printing plates, prep. processing and sensitising 4-68297  
 Ag-As<sub>2</sub>S<sub>3</sub> multilayer struct., optical props. study 4-104563  
 Al-As<sub>2</sub>S<sub>3</sub>-Al MIM struct., bias voltage depend. of capacitance 4-104325  
 Al-chalcogenide glass structures, cathode effect in electrostimulated chem. transformations 4-88804  
 As-Ge-Sr, small conc. of Se, elec. cond. rel. to temp. 4-92729  
 As-S amorphous system, vibr. props. and network topology 4-109178  
 As-Sb-Se system, glass-ceramic composites, varistor-like behaviour 4-114009  
 As-Se, thermal cond., in solid and liq. states 4-108669  
 As-Se films, thermally-induced light scatt. (*Russian*) 4-109167  
 As<sub>2</sub>Se<sub>3</sub>, cryst. and amorphous, recomb. and excited-state absorption at photolum. centres 4-99182  
 As<sub>2</sub>S<sub>3</sub> chalcogenide glass films, photostruct. changes 4-104560  
 As<sub>2</sub>S<sub>3</sub> evap. photoresist., dissolution rate rel. to evap. conditions 4-68299  
 As<sub>2</sub>S<sub>3</sub> films, solvent-cast, morphology and thermal props. 4-84530  
 As<sub>2</sub>S<sub>3</sub> films, thermally-induced light scatt. (*Russian*) 4-109167  
 As<sub>2</sub>S<sub>3</sub> glassy film, Schottky barrier form. at contact with metal 4-104291  
 As<sub>2</sub>S<sub>3</sub>-S system, liq. and amorphous, phase diagram and short range order 4-103905  
 (As<sub>2</sub>S<sub>3</sub>)<sub>x</sub>(AsI<sub>3</sub>)<sub>1-x</sub> glasses, Raman scatt., IR and depolarisation spectra 4-109182  
 As<sub>2</sub>S<sub>3-x</sub> glass, X-ray struct. factor, temp. depend. near glass transition 4-60847  
 As<sub>2</sub>S<sub>3-x</sub>, Raman spectra and struct. 4-76455  
 As<sub>2</sub>S<sub>3-x</sub>Se<sub>2</sub> glasses, geminate recomb., picosecond electronic relaxations 4-108892  
 AsSe chalcogenide glass films, photostruct. changes 4-104560  
 AsSe vitreous chalcogenide semiconductor films, optical data storage 4-107775  
 AsSe:Sn chalcogenide glass, photostruct. transformations, Mossbauer studies 4-61075  
 As<sub>2</sub>Se<sub>3</sub> amorphous film, photo-EMF due to surface barriers 4-88541  
 As<sub>2</sub>Se<sub>3</sub>, carrier diffusion, multiple-trapping limited 4-70831  
 As<sub>2</sub>Se<sub>3</sub>, crystallisation kinetics and viscosity 4-75298  
 As<sub>2</sub>Se<sub>3</sub> glass, photoluminescence fatigue and structural disorder 4-104672  
 As<sub>2</sub>Se<sub>3</sub> glass, X-ray struct. factor, temp. depend. near glass transition 4-60847  
 As<sub>2</sub>Se<sub>3</sub>, glassy and liq., thermally generated defects 4-113335  
 As<sub>2</sub>Se<sub>3</sub>Ag, photodoping physics study 4-75464  
 As<sub>2</sub>Se<sub>3</sub>Ni(Cu)(Fe)(Bi)(Sn), extrinsic cond. and optical const. meas. 4-75971  
 As<sub>2</sub>Se<sub>3</sub>Te film, transient photocurrent study 4-113991  
 As<sub>2</sub>Se<sub>3</sub>As<sub>2</sub>S<sub>3</sub>Ag, holographic diff. grating recording (*Russian*) 4-69341  
 As<sub>2</sub>Se<sub>3</sub>Cu<sub>2</sub>Se:Mn, interaction of Mn with glass framework, mag. susceptibility, EPR spectra 4-60838  
 As<sub>2</sub>Se<sub>3-x</sub> thin films, photoinduced optical absorption, storage appls. 4-85026  
 As<sub>2</sub>Se<sub>3</sub>Ge<sub>2</sub> glassy semicond., photostructural transformations 4-61076  
 As<sub>2</sub>Se<sub>3</sub>(S<sub>2</sub>) thin films, large scale domain struct. 4-88106  
 As<sub>2</sub>Se<sub>3</sub>Te<sub>2</sub>, amorphous, radiation and thermal induced defects, electrical cond. 4-75528  
 As<sub>2</sub>Se<sub>3</sub>Tc<sub>6-x</sub> glasses, DC props., neutron and gamma-ray effects 4-103814  
 As<sub>2</sub>Te<sub>2</sub> amorphous films, electronic struct., field effect and time of flight studies 4-113852  
 Au-As<sub>2</sub>S<sub>3</sub>-Al MIM struct., bias voltage depend. of capacitance 4-104325  
 Au-Sb<sub>2</sub>S<sub>3</sub>-Al MIM struct., bias voltage depend. of capacitance 4-104325  
 Bi<sub>2</sub>Se<sub>3</sub> amorphous film, photoemission study 4-109302  
 CdGeAs<sub>2</sub> glass crystallisation, thermal anal., activation energy determ. 4-84187  
 GaSe<sub>2</sub>Ag, photodoping physics study 4-75464  
 GaSe<sub>2</sub>Ga, glassy semiconductor, doping effect, positron annihilation 4-61764  
 Ge-As-S-I glasses, chemical bonding and mag. susceptibility (*Russian*) 4-70041  
 Ge-P-S, semiconductor glass, paramagnetic centres, ESR study 4-80819  
 Ge-S glasses, narrow Lorentzian ESR signals 4-65858  
 Ge-Sb-Se glasses, dilatometric studies 4-108634  
 Ge-Se glasses, microstructure, electron microscopy obs. 4-88305  
 Ge-Se<sub>2</sub>-Se system, liq. and amorphous, phase diagram and short range order 4-103905  
 GeS<sub>2</sub> glass, struct. factor, temp. depend. 4-79944  
 GeS<sub>2</sub> glass, undoped and metal doped, impurity surroundings, nature of defects, positron annihilation study 4-79943  
 GeS<sub>2</sub>Cu(Ag), glassy, doping effect on elec. and optical props. (*Russian*) 4-98625  
 Ge<sub>2</sub>S<sub>1-x</sub> glasses, short range order model, optical gap calc., IR band intensity 4-75310  
 (GeS<sub>1.5</sub>)<sub>100-x</sub>Bi<sub>x</sub> glass, photoconductivity meas. 4-98670  
 GeS<sub>2</sub> amorphous thin film, light induced transmittance oscillation 4-76538  
 GeSe<sub>2</sub>, cryst. and glassy, photoelec. props. 4-108905  
 GeSe<sub>2</sub> glass, bulk, press. induced electronic and structural transformations 4-114004  
 Ge<sub>0.1</sub>Se<sub>0.9</sub>Ag, photodoping physics study 4-75464  
 Ge<sub>2</sub>Se<sub>7</sub>Ag layers, amorphous, photodoped, impurity lateral diffusion 4-70464  
 (GeS<sub>2</sub>S<sub>1.5</sub>)<sub>100-x</sub>Bi<sub>x</sub> glass, photoconductivity meas. 4-98670  
 (GeS<sub>2</sub>S<sub>1.5</sub>)<sub>100-x</sub>Bi<sub>x</sub> struct. and resist. effect of dopants, high press. study 4-103660  
 (GeS<sub>2</sub>S<sub>1.5</sub>)<sub>100-x</sub>Sb<sub>x</sub> struct. and resist. effect of dopants, high press. study 4-103660  
 Ge<sub>20</sub>Se<sub>80-x</sub> thin films, optical properties determ. 4-114337  
 Ge<sub>20</sub>Te<sub>80</sub> glass, bulk, elec. transport and high press. studies 4-114003  
 Ge<sub>20</sub>Te<sub>80</sub> glass, elec. cond. transition, press. and temp. depend. 4-98619  
 In<sub>30</sub>Se<sub>70</sub> films, optical absorption, heat treatment effects 4-85027

**chalcogenide glasses continued**

- P-Se<sub>1-x</sub> glasses, struct., conc. depend. of short- and intermediate-range order 4-113342  
 Sb<sub>2</sub>S<sub>3</sub> amorphous thin films, struct. and crystn. 4-60842  
 Sb<sub>2</sub>Se<sub>3</sub> glassy film, Schottky barrier form. at contact with metal 4-104291  
 Sb<sub>2</sub>Se<sub>3</sub>-Se system, liq. and amorphous, phase diagram and short range order 4-103905  
 Se-Te amorphous alloys, photogeneration and optical absorption 4-108900  
 Se-Te-As, amorphous, defect states and photoelec. behaviour 4-113903  
 Se-Te(Ge)(Sb) amorphous, DC conductivity thickness dependence 4-84620  
 Se<sub>1-x</sub>Te<sub>x</sub> glasses, electronic cond. at high press. and low temp. 4-104198  
 Se<sub>99</sub>Te<sub>1</sub>As<sub>1</sub>Li, chemical modification and elec. cond. 4-75970  
 Si<sub>2</sub>S<sub>1-x</sub> glass, Raman study of atomic struct. 4-92093  
 SiSe<sub>2</sub>, cryst. and glassy, vibr. studies 4-109191  
 SnSe-GeSe<sub>2</sub>-As<sub>2</sub>Se<sub>3</sub> glass formation, physicochemical props. 4-92365  
 Te-Ge-Pb(Sn) alloys, glass stability, cryst. struct. effect 4-60836  
 TeO<sub>2</sub>-Cu<sub>2</sub>O-(CuO), phase equilb. 4-84370  
 TiGaS<sub>2</sub>(Se<sub>2</sub>)Nd semiconducting chalcogenides, photoluminescence studies 4-99180

**change of state** *see phase transformations***channel capacity**

- corporeal information channel, ideal system 4-79068  
 nervous transmission systems 4-100122

**channel flow**

- see also pipe flow*  
 acetylene diffusion through a capillary, nonthermal effect of incoherent IR light 4-79671  
 acoustic vibrations of heat releasing medium in confined space, nonlinear stabilisation 4-69756  
 air-water drop flow in subsonic nozzles (*French*) 4-60508  
 air-water flow, annular-dispersed, in venturi, numerical model 4-60512  
 air-water two-phase upward annular flow in near horizontal tube, flow configuration (*Japanese*) 4-97655  
 annular two-phase flow, entrained liq., laser tomographic meas. 4-60527  
 asymmetric instabilities in buoyancy-driven flow in a tall vertical annulus 4-83877  
 bead spring model macromolecules in inhomogeneous flows, diffusion and migration 4-83502  
 binary gas mixture, nonisothermal motion through plane channel, kinetic phenomena 4-103368  
 boiling channel, press.-drop and density-wave instability thresholds 4-79598  
 boiling channel, vertical, two-phase flow instabilities, effect of heater surface configs. 4-79597  
 branch and bend flow, approx. treatment using elementary hydraulic theory 4-79667  
 buoyancy effects in the entrance region of horizontal rectangular channels 4-60553  
 channel wall deform. in peristaltic pumping regimes 4-113011  
 combined natural and forced convection in horizontal porous channel 4-75004  
 conduits and channels, transient free surface flow, numerical methods, TRAN6 program (*Chinese*) 4-108108  
 continuous wave motion in rough inclined channel 4-112924  
 control parameter optimisation for flows with transition through the speed of sound 4-108087  
 convection, natural, in vertical channels, finite element analysis 4-75023  
 convective heat transfer, physical and computational aspects, book 4-86128  
 convective heat transfer in vertical annular gas layers with const. heat flux on inner wall 4-60423  
 coordinate generation method based on mapping technique 4-103283  
 crevice erosion and the thermohydraulic state of slots in joints, vapour and condensate anal. 4-65027  
 critical Reynolds number in open flows 4-113010  
 curved duct flow, secondary motion, turbulent and laminar flow, vel. meas. 4-87805  
 curved duct of rectangular cross section, rot., laminar flow 4-103347  
 dispersed annular flow, press. drop, drag calc. 4-103390  
 dispersion of a soluble matter in a porous medium channel with homogeneous and heterogeneous chemical reaction 4-69823  
 downstream influence in channel flow, upstream influence in separating boundary layers 4-103285  
 duct, acoustic noise attenuator (*French*) 4-112631  
 duct, axisymmetric, flow calc. procedure (*Afrikaans*) 4-75084  
 duct, circular, abrupt expansion, self-excited flow oscillation 4-103412  
 duct, elliptical, entrance region, laminar flow 4-103422  
 duct, rectangular, acoustic attenuation of parabolic vel. profile (*French*) 4-112601  
 duct flow, near sonic, sound propagation, finite difference soln. 4-60197  
 duct flow problems, effective vorticity, numerical solution 4-87662  
 ducts, acoustic transmission, impulse method using signal synthesis and averaging 4-74786  
 ducts, regenerated noise due to closely spaced induct dampers 4-97199  
 ducts with const. wall temp., heat transfer coeff. 4-60421  
 electrically conducting incompressible liqs. in inclined open channel, nonlinear wave motion (*Russian*) 4-113055  
 electrovortex flow in a planar channel (*Russian*) 4-113049  
 elongated bluff bodies at low Reynolds number, drag and vortex shedding, transverse curvature effect 4-103345  
 entry flow in weakly curved ducts 4-91841  
 evaporative heat transfer in channel filled with porous highly conductive metal 4-83895  
 exponential law fluid, flow rate calc. in rectangular channel, form factor determ. (*German*) 4-75063  
 flames, heat transfer between hot combustion gases and cold wall in narrow channels 4-99789  
 flat rectangular duct, heat transfer response to periodic disturbances at one principal wall 4-60418  
 flow and temperature profile independence of flow measurements using long acoustic waves 4-103445  
 flow in heated channels, two-fluid model eqns. nonlinear eqns. soln. by numerical method 4-108112  
 flow of vapour in channel with porous filler, condensation process, analytic model 4-83942  
 fluctuating field in a channel, linear study (*French*) 4-69824  
 fluent/centrifugal doses, parameters of fluent streaming out (*Bulgarian*) 4-97463

**channel flow continued**

- fluid mechanics review, book 4-90314  
 free convection effects on turbulent transport of liquid in vertical channel 4-60406  
 free surface profiles for climbing, and channel flow, viscometry 4-87801  
 fully developed laminar flow and heat transfer in an arbitrarily shaped triangular duct 4-64911  
 gas, convective motion resulting from propag. of heat wave along lower boundary of closed region 4-87717  
 gas mixture flow in a cylindrical channel at intermediate Knudsen numbers 4-79670  
 gas particle flow, mathematical formulation for kinetic model 4-60534  
 gas-liquid flow, annular, pressure drop and film height meas. 4-79644  
 gas-liquid mixtures with bubbly struts, transcritical discharge 4-103393  
 gravity current upstream of buoyant influx 4-60550  
 heat transfer and friction effect on cylinder in longitudinal turbulent air flow with variable physical props. 4-83891  
 heat transfer for turbulent flow in a circular tube with uniform suction or injection 4-103319  
 heat-releasing apparatus inlet, hydromechanics 4-79669  
 horizontal cylinder in channel flow, natural convection enhancement 4-112876  
 horizontal subchannel flow, two-phase redistrib., turbulent mixing and gravity separation 4-79645  
 hydrodynamic and thermal development in square duct 4-60415  
 incompressible liquids, MHD flows, use of asymptotic methods in singular-excitation problems (*Russian*) 4-113062  
 incompressible viscous fluid stabilised laminar flow through rotating radial channel 4-112813  
 inviscid flow, exponentially derived switching schemes 4-103417  
 jets in confined spaces 4-83935  
 jumps in layered miscible fluids 4-60478  
 laminar and turbulent natural convection in an enclosed cavity 4-87660  
 laminar flow, transition control by periodic suction blowing 4-83876  
 laminar flow in channel expansion, spectral element method 4-87797  
 laminar flow stability in cylindrical channel, transversal vel. effect 4-103288  
 laminar steady flow in sinusoidal channels 4-87798  
 large-scale structural effects in developed turbulent flow through closely-spaced rod arrays 4-112861  
 liquid metals, flow through channel with transverse mag. field, in elect. insulated channel 4-75093  
 liquid-metal MHD open-channel flows 4-97701  
 macromolecular solns., time dependent. Poiseuille flow, rheological props. 4-75086  
 magnetisable fluid flow at temps. close to Curie point 4-87810  
 MHD, axisymmetric flow of cond. liquid with crossed induction and cond. currents, numerical modelling (*Russian*) 4-113044  
 MHD, conference, Riga, Latvian SSR 4-106123  
 MHD flow and heat transfer in channel with porous walls 4-87808  
 MHD flow with free surface along the substrate of liq. metal diaphragm (*Russian*) 4-113051  
 MHD instability and two-dimensional turbulence in the general hydrodynamic problem (*Russian*) 4-113032  
 mixed boundary-value problems of profiling of supersonic nozzles and channels 4-69785  
 moisture transfer in heated channels conducting flows 4-97653  
 natural convection heat transfer in complex enclosures at large Prandtl number 4-60424  
 natural convection of a viscoplastic fluid in vertical circular channels 4-112851  
 Navier-Stokes eqns., spatial stability of a class of similarity solutions 4-74983  
 Navier-Stokes eqns., steady, anal. based on Green's function approach 4-79541  
 Navier-Stokes eqns., unsteady, anal. based on Green's function approach 4-79542  
 near-one-dimensional two-phase flow 4-69814  
 non-Newtonian fluids, turbulent friction factors prediction in noncircular ducts 4-108092  
 non-Newtonian liquid, flow and heat transfer in arbitrary shape channels, conformal mapping theory (*German*) 4-97618  
 non-Newtonian viscoelastic fluid, conjugated heat transfer in flat duct 4-79627  
 noncircular duct, peripheral temp. variation in wall, heat transfer calc. 4-97552  
 nonequilibrium axial flow model for the calculation of transient behaviour in two-phase flow 4-60514  
 nonequilibrium MHD flows, radial and swirl flow configurations, wake nonuniformities 4-103475  
 nonlinear convection in high vertical channels 4-87716  
 nonlinear ducts, turbulence-driven secondary motion calcs. 4-60383  
 nonNewtonian fluid with variable physical props., channel flow, heat transfer 4-79581  
 nonrectangular inclined enclosure, convective fluid motion and heat transfer 4-64941  
 nonuniform gas flows, acoustics, variational principles 4-91673  
 n-octane, inward solid-liquid phase-change heat transfer in a rectangular cavity with conducting vertical walls 4-97554  
 open convergent channel type wavebreakers, energy transmission characteristics 4-77528  
 organised structures in transitional and developed bounded turbulent flows, mean streamwise spacing 4-112826  
 Ostwald-de-Waele liquid flow in circular tube, mass transfer 4-103372  
 parallel plates, natural convection cooled, thermally optimum spacing 4-112875  
 particle-capture coefficient at channel wall 4-113014  
 pebble bed reactors, thermohydraulic behaviour, natural convection flow expts. (*German*) 4-106875  
 physical modelling of multi-phase flow, conference, Coventry, England (April 1983) 4-58559  
 pipe, acoustic plane wave propag. with mean flow 4-112608  
 planar stationary flows in stratified liquid (*Russian*) 4-87774  
 plane channel, velocity correlations for turbulent shear flow, spectral functions 4-91802  
 plane channel with semicylindrical projections, heat transfer 4-103325  
 plate heat exchangers, U-type arrangement, flow distrib. and press. drop 4-87793  
 plate heat exchangers, Z-type arrangement, flow distrib. and press. drop 4-87794

## channel flow continued

- Poiseuille flow, laminar to shear turbulent transition, stability study 4-60546  
 polymer fluids, channel flow, unsteady, birefringence obs. 4-113018  
 polymer melts, hole pressure, flow birefringence obs. 4-113019  
 polymer soln., macromolecular in nonhomogeneous flow fields, dumbbell model 4-97619  
 polymers flexible chain in region of shear rates and stresses, rheological behaviour, elastic state 4-69721  
 polytropic gases, compressible channel flow, normal shock wave struct. 4-64982  
 ponderable liq. steady-state flow with free surface in variable-width channel 4-60547  
 pulsatile flowfield in the vicinity of an abrupt circular channel expansion 4-103421  
 radiation fluxes calc. in rectangular channels 4-113013  
 rectangular ducts, fully-developed flow, vel. distrib. and skin friction resistance 4-83948  
 rectangular flow channels, vibr. of sheet metal panels 4-83949  
 rectangular flow section downstream from mixing junction, heat transfer characteristics 4-97529  
 rigid ellipsoidal particle dil. suspension in plane channel, variable viscosity flow 4-87796  
 river system, dendritic, water depth, flow simulation, channel hydrodynamic model 4-82100  
 rod bundles, parallel flow distrib. and press. drop 4-87675  
 roll waves down an open inclined channel 4-97685  
 roll-pattern evolution in finite-amplitude Rayleigh-Benard convection in a two-dimensional fluid layer bounded by distant sidewalls 4-87730  
 rotating flow past disks and cylindrical depressions 4-75035  
 rotating wavy channels, nonlinear convective flows 4-103332  
 rotational channel flow near crit. speed, inertial flow 4-112903  
 rotationally symmetric vortex flow in a small annulus between concentric cylinders 4-60439  
 second grade non-Newtonian fluid injection/suction through long vertical channel 4-97614  
 secondary current and river-meander formation 4-105605  
 sediment transport in rivers and open channels, 2D diffusion-convection eqn. 4-60517  
 self-aeration influence on resistance in smooth and rough steep channels 4-108109  
 slot channels, two-phase flow modes 4-65007  
 smooth rectangular duct, experimental study 4-97513  
 spherical particles, lateral migration in porous flow channel, appl. to membrane filtration 4-65020  
 steady dimens. plane channel flow, governing eqns. 4-97680  
 steady secondary flow in curved open channels 4-91844  
 stratified flow channel with microcomputer monitoring and control 4-103448  
 subsonic flow, turbulent, in turbobfan lobe mixer exhaust nozzles, computational procedure 4-79559  
 subsonic flow, unsteady, through rectilinear cascades 4-112939  
 supersonic nonequilibrium flow channel design, plane and axisymm. 4-103420  
 surface gravity-capillary waves, blocking effect by inhomogeneous flow 4-83917  
 transient convective motions in a cavity with a free boundary 4-60403  
 transient two-component flow, modelling using four-point implicit method 4-97691  
 tunnel with concurrent open channel and pressurised flow, hydraulic transients anal. 4-97695  
 turbulence flow in two-dimensional channel with arbitrary inlet disturbance, numerical simulation 4-75083  
 turbulent channel flow, wall press. field calc. 4-60552  
 turbulent energy balance in linear wall region 4-65024  
 turbulent flow, fully developed, inertial layer spectral function approx. determ. 4-79562  
 turbulent flow hydrodynamics of a bubbly two-phase mixture 4-79563  
 turbulent MHD flow in planar channel between two parallel walls (*Russian*) 4-113041  
 turbulent separated flows, three-dimens., finite difference calc. procedure 4-91786  
 turbulent shear high-order vel. struct. functions 4-60382  
 turbulent Taylor-Couette flow, organised struct. 4-87735  
 two-dimensional confined channel flow, flow pattern and turbulent mixing characteristics (*Japanese*) 4-97686  
 two-phase axisymmetric flow through nozzle, anal. with correction for channel walls ablation 4-65008  
 two-phase flow, instabilities in horizontal boiling channel 4-97661  
 two-phase flow, instabilities in vertical boiling channel, nonlinear description 4-97660  
 two-phase gas-liquid flow in rectangular channels 4-87779  
 two-phase reverse flow in expanding channel, swirling effect on struct. 4-112897  
 unmixed gases in channel, supersonic combustion charact. 4-69832  
 unsteady flow eqn. as basis for extrapolation of stream flow data- 4-65028  
 unsteady flow through channel with permeable walls, solute dispersion, vel. distrib. 4-113020  
 unsteady natural concentration convection in closed region, 3D effects influence 4-112852  
 unsteady natural convection in a cavity with internal heating and cooling 4-60408  
 unsteady thermal convection in a cylindrical vessel heated from the side 4-69757  
 upward two-phase flow in vertical tubes, flow regime transition 4-87786  
 valve dynamics, computational methods for anal. 4-91843  
 viscous fluid flow hydrodynamic params. in convective problems for flow separation in channels 4-79587  
 viscous gas flowing from slit or cylindrical channels into region of lower press., interferometric study 4-113021  
 viscous gas superonic flow, cruising method calc. (*Russian*) 4-87756  
 volume-cycled oscillatory flow in a tapered channel 4-75088  
 wall confinement effects for spheres in the Reynolds number range of 30-2000 4-103348  
 wall shear stress measurements in annular two-phase flow 4-60526  
 water, evaporation under an obliquely impinging laminar ducted slot jet - a numerical model 4-108100  
 water, stably stratified turbulent flow, vertical overturns meas. 4-64928  
 water flow in rot. channel of square section, visualisation and separation meas. 4-112898

## channel flow continued

- water-solid flow in turbulent open channel, conc. distribs., stochastic models 4-60516  
 wave power absorption by oscillating water column in a channel 4-77053  
 waves, forced, in rot. fluid, open boundary conditions 4-83916  
 Br<sub>2</sub> gas diffusion through capillaries, laser control, energy efficiency 4-75113  
 CO<sub>2</sub> radiation convection heat transfer problem plane channel, turbulence 4-60378  
 He flow in horizontal channel, two-phase, hydraulic resistance calc. and obs. 4-108107  
 N<sub>2</sub> diffusion through a capillary, nonthermal effect of incoherent IR light 4-79671

## channelling radiation see channelling radiation

## channelling

- see also energy loss of particles  
 AES, crystalline effects and electron channelling 4-99243  
 alkaline earth fluorides, epitaxial growth on semiconductors, Rutherford backscatt./channelling studies 4-80438  
 automatic measurement using microprocessor (*Chinese*) 4-84325  
 axial, defect anal. appls., Lindhard model anal. 4-75587  
 axial dechannelling with dislocations, theory 4-88217  
 axial dechannelling with point defects, theory 4-88216  
 blocking effects and patterns (*Japanese*) 4-92277  
 charged particles, dynamics and their emission radiation, cryst. pot. periodicity effects 4-75577  
 crystal surfaces, electron current image diffraction at low energies 4-92034  
 crystal-assisted pair creation process, tilt-angle depend. 4-75572  
 crystal-assisted pair-creation process, const. field approx. 4-75571  
 crystalline defects in solid materials, electron channelling imaging 4-103623  
 crystallographic contrast of polycrystals using channelling micrography technique (*Chinese*) 4-60789  
 crystals, interaction pot. of light channelled particles 4-108492  
 crystals with implanted positive pions, study by lattice steering of decay muons 4-75567  
 damage profile in crystals, meas. by channelling technique 4-103840  
 dechannelling, based on stochastic theory 4-103838  
 diamond, ballistic phonon imaging 4-88387  
 diamond, etching with Ar and O ion beams 4-89149  
 EDX analysis, digital mapping appls. to channelling effect 4-81508  
 electron loss by multiply-charged ion moving at small angle to cryst. planes 4-84328  
 graphite, ion damaged, annealed, 2-D ordering, Raman study 4-70535  
 graphite, thermodynamic props., pulse-laser, melting, ion channelling 4-98315  
 ion beam-solid interactions, review of surface analytical techniques, book contrib. 4-85053  
 Kumakhov radiation in axial channelling, general case in classical theory 4-103842  
 Kumakhov radiation peculiarities in ultrarelativistic electron channelling 4-65317  
 material deformation, electron channelling obs., review 4-76807  
 molecular ion implantation in monocrystals, ion channeling prevention 4-65283  
 negatively charged GeV particles, axial channelling, kinetic approach 4-75573  
 polycrystalline foils, multiply peaked energy loss spectra of heavy ions 4-92272  
 positive pions in solid state physics studies 4-65889  
 $\alpha$ -quartz, ion bombard. damage, 50 to 295K 4-70230  
 relativistic charged particles in crystals, parametric beam instability 4-75589  
 relativistic nuclei in crystals, coherent Coulomb excitation 4-98161  
 Rutherford backscattering and channelling 4-75243  
 semiconductor interfaces, Rutherford, scatt.-channelling anal. 4-99255  
 single crystals, bent, with slowly varying curvature, GeV charged particle channelling 4-75568  
 single crystals, Kumakhov radiation in axial channelling, dipole approx. in classical theory 4-103841  
 single crystals, impurity atom localisation, Rutherford backscatt. yield in planar channelling 4-75489  
 solids, at. collisions, conf., Bad Iburg, Germany (July 1983) 4-73144  
 SOS films, material improvement process by solid phase epitaxial growth 4-81124  
 steel, stainless, N ion implanted, lattice location, nuclear reaction, channelling and RBS studies 4-75463  
 UHV system for channelling/blocking analysis of surfaces and interfaces 4-88219  
 AL-Sn(In), ion irradi., vacancy-solute atom complexes, channelling study 4-103836  
 Al, surface struct. from low energy electron channelling 4-92482  
 Al-Cu, implanted, disorder studied by ion channelling and Rutherford backscattering 4-98145  
 Al<sub>0.88</sub>Ga<sub>0.12</sub>As/GaAs:Zn diffused 'superlattice', X-ray rocking curve and backscatt. studies 4-113818  
 Al<sub>2</sub>O<sub>3</sub>, ion implantation, ion beam mixing, and annealing of metals 4-70229  
 Al<sub>2</sub>SiO<sub>5</sub>, sillimanite, absorption edge fine struct. study using electron channelling 4-80127  
 Au, ion channelling, energy stopping power depend., interatomic interaction potentials at high projectile velocities 4-80125  
 Au-Cu, real crystals with several sublattices, proton planar channelling, ang. depend. 4-70248  
 Au-In, dil., channelling effect of conversion electrons emitted from radioactive impurities 4-75569  
 BaTiO<sub>3</sub>:Ca, impurity site occupancy, channelling enhanced microanal. studies 4-108394  
 Bi-Po, impurity atom location, channelling studies with point  $\alpha$  sources 4-113470  
 Cu (001), surface semichannelling effect on energy distribs. of refl. ions 4-81056  
 Cu (001) and (011), small-angle ion refl. 4-81095  
 Cu (100), N<sub>2</sub><sup>+</sup> ions reflection, surface semichannelling obs. 4-81099  
 Cu single cryst., sputtering yields, weight loss method study 4-76620  
 Cu single-crystal films, Na<sup>+</sup>(K<sup>+</sup>)(Rb<sup>+</sup>) ion beams transmission, angular and energy distrib. 4-98159  
 Cu-In, dil., channelling effect of conversion electrons emitted from radioactive impurities 4-75569

**channelling continued**

Cu-In (0.1 at.%), vacancy trapping, PAC and ion channelling study 4-84876  
GaAs (110) and GaAs/Au(Pd) interfaces, high energy ion channelling studies 4-65318  
GaAs, crystal and amorphous, pulsed laser irradiation under O<sub>2</sub> and silane atmospheres, O incorporation and losses 4-80091  
GaAs, surface cleaning by ion bombardment Rutherford backscatt. and channelling study 4-88213  
GaAs:Si, planar channelling of Si implants 4-75483  
GaAs:Sn,Te, dual implanted damage and annealing, challenging studies 4-80116  
GaAs/Au interface struct., XPS, RHEED and ion scatt./channelling studies 4-80421  
GaAs,P<sub>1-x</sub>/GaP strained-layer superlattices, Be-implantation doping, ion channelling studies 4-80057  
Ge, ion channelling, interaction pot., stopping power, ion scatt. spectra 4-75570  
Ge,Si<sub>1-x</sub> epitaxial films on Si (100), commensurate and incommensurate struct. 4-108740  
Ge,Si<sub>1-x</sub>/Si strained layer superlattice, MBE growth 4-92576  
In<sub>0.3</sub>Ga<sub>0.7</sub>As/GaAs strained-layer superlattice, ion implanted, struct. integrity 4-113821  
InSb, ion implanted single cryst., damage study by characteristic X-ray emission 4-88214  
LiF, channelling radiation from relativistic positrons 4-65314  
Mo, BCC superlattice with and without dislocations, ion-lattice interaction potentials 4-92246  
Mo-Co dilute alloy, Co impurity location, PIXE and ion channelling studies 4-80072  
Mo-Co dilute alloy, lattice location studies by PIXE and ion channelling 4-99894  
Mo-In, dil., channelling effect of conversion electrons emitted from radioactive impurities 4-75569  
NbN<sub>1-x</sub>∞ static displacements around non-metal vacancies, channelling study 4-108355  
Nb<sub>3</sub>Sn, cryst. site determ. of dilute alloying elements, TEM studies 4-88131  
Ni (110), clean and CO covered, medium energy ion scatt. studies 4-88381  
Ni (110), surface analysis by surface channelling using ion induced Auger electron emission 4-81068  
Ni (110) and (111), adsorbed D site location, surface channelling study 4-80375  
Ni, ion implanted D trapping by vacancies, channelling studies 4-108409  
Ni-La single crystals, implanted, pulsed laser treatment studied by the <sup>4</sup>He<sup>+</sup> channelling 4-84315  
Pd-Si film, ion implanted, amorphisation, channelling anal. 4-92247  
Si (100), clean and Cs covered, neutralisation of scattered He ions 4-109294  
Si (100), energetic He ion scatt., neutralisation, channelling studies 4-76591  
Si (111)2×1 surface, MeV ion backscattering/channelling studies 4-85051  
Si, channelling electrons, energy band structure, wave functions, calcs. 4-108493  
Si channelling phenomena involved in high energy beam bending 4-98158  
Si, computer simulation, relativistic electrons, multiple scatt., axial channelling 4-108491  
Si, contamination and near-surface damage caused by reactive ion etching 4-113757  
Si curved single cryst., 1 GeV proton beam focusing in channelling regime 4-91131  
Si, elastically bent crystals, dechannelling of planar channelled protons 4-75575  
Si, epitaxial layer growth on CaF<sub>2</sub> substrates 4-80448  
Si, heavy-ion induced damage and annealing TEM and channelling studies 4-80115  
Si, ion bombarded, 14 MeV O ions, non-registered Si produced at metal-Si interface 4-114351  
Si, lateral epitaxy, electron beam annealing 4-99308  
Si, muon decay channelling positron ang. dist. studies 4-65311  
Si, muon decay channelling 4-84892  
Si reconstructed surface reordering on room temperature Ge deposition 4-98411  
Si sheets, edge-supported pulling, electron channelling and EBIC studies, rel. to solar cell appls. 4-75693  
Si single crystal, planar channelling studies (*Chinese*) 4-70245  
Si single crystal thin film, secondary recrystallisation prep. 4-88421  
Si single crystals, bent, high energy channelled proton deflection 4-75574  
Si, surface cleaning by ion bombardment, Rutherford backscatt. and channelling study 4-88213  
Si:As, implanted under channelling conditions, impurity spatial distrib., localisation, defect form. characts. 4-84321  
Si:As, ion implanted channelling Rutherford back-scatt. study (*Chinese*) 4-84324  
Si:As, low energy implanted, laser-annealed, channeling and high-resolution backscatt. studies 4-75493  
Si:B, (100), shallow junction implants through surface oxide, theoretical and expt. study 4-113476  
Si:D, anomalous muonium atom site determination 4-65277  
Si:H, lattice state and behaviour of H impurity 4-61095  
Si:Sb, ion implanted, dopant site location and profiles, channelling studies 4-108393  
Si-SiO<sub>2</sub> target, channelling effect on recoil motion 4-108488  
SiC, ion implantation, ion beam mixing, and annealing of metals 4-70229  
Si<sub>3</sub>N<sub>4</sub>, ion implantation, ion beam mixing, and annealing of metals 4-70229  
Ta, π<sup>+</sup>/μ<sup>+</sup> channelling, time depend. meas. 4-65310  
TiC<sub>1-x</sub>∞ static displacements around non-metal vacancies, channelling study 4-108355  
(U,Pu)O<sub>2</sub>, diffusion meas., effects of chem. surface gradient, mechanical polishing 4-98354  
UO<sub>2</sub> (111) and (100), surface struct. determ. 4-92483  
V:As, ion implanted, plastic deformation, channelling studies 4-70178  
(YBiPb)<sub>3</sub>(FeAlPt)<sub>2</sub>O<sub>12</sub> LPE layers, lattice site determ. by channelling 4-80440

**channelling continued**

Y<sub>3</sub>Fe<sub>5</sub>O<sub>4</sub> garnet epitaxial layers, ion implantation-induced strain and damage profiles 4-75558  
ZnSiI with adsorbed O<sub>2</sub>, surface states and LED props. 4-80643

**channelling radiation**  
asbestos, charged particle induced short-wave radiation in natural hollow crystallographic channels (*Russian*) 4-81031  
atomic collisions in solids, conf., Strasbourg, France (July 1981) 4-63398  
axial channelling radiation, mol. type, from MeV electrons 4-75582  
axially channelled electrons, photon radiation intensity calc. 4-66090  
charged particles, dynamics and their emission radiation, cryst. pot. periodicity effects 4-75577  
charged particles, relativistic plane channelled, classical emission 4-98163  
coherent bremsstrahlung and channelling radiation from kilovolt electrons 4-85030  
crystals, electron and positron channelled radiation 4-108494  
crystals, electron channelling radiation and Zeeman effect 4-65319  
crystals, interaction pot. of light channelled particles 4-108492  
crystals, relativistic particles paths simulation and radiation spectra 4-75591  
diamond, types Ia and IIa, electron and positron planar channelling radiation spectra 4-75579  
electron axial channelling, Kumakhov radiation temp. depend. 4-98162  
energy eigenvalue calc., self consistent approx. method 4-80128  
fast ions, planar channelling, characteristic X-ray radiation polarisation 4-81029  
Kumakhov radiation in axial channelling, general case in classical theory 4-103842  
Kumakhov radiation peculiarities in ultrarelativistic electron channelling 4-65317  
magnetic cryst., channelled particle radiation, appl. to laser gain 4-113513  
periodic crystal structure effects 4-113515  
periodically distorted cryst., X-ray emission by channelling electrons 4-103839  
planar channelling particle sine-squared pot. and Kumakhov radiation for charged particles (*Chinese*) 4-91390  
positron channelling radiation intensity, influence of multiple scatt. 4-75580  
QED corrections, channelling radiation, simple theory 4-68490  
relativistic charged particle radiation in crystals, unified theory, quantum mech. treatment 4-96765  
relativistic electrons and positrons, channelling phenomena (*Chinese*) 4-113514  
single crystals, Kumakhov radiation in axial channelling, dipole approx. in classical theory 4-103841  
solar system, charged particle channelling radiation 4-77762  
solids, at. collisions, conf., Bad Iburg, Germany (July 1983) 4-73144  
thin crystals, electron and positron channelling, radiation intensity 4-108489  
unguided wave Cherenkov amplifier 4-102913  
x-ray laser by channelling radiation 4-74541  
zeolite, charged particle induced short-wave radiation in natural hollow crystallographic channels (*Russian*) 4-81031

Al, Auger electron emission in LVV peak region, continuous background struct., O<sub>2</sub> partial press. effects (*French*) 4-66140  
LiF, channelling radiation from relativistic positrons 4-65314  
LiF, planar channelling radiation from relativistic positrons and electrons 4-75581  
Ni, electron axial channelling radiation spectra 4-75583  
Si, axial channelling radiation of MeV electrons 4-92276  
Si, channelled electrons, axial channelling radiation, temp. depend. 4-75576  
Si, channelling radiation emitted from 350 MeV planar channelled electrons 4-75578  
Si, channelling radiation from relativistic positrons, energy eigenvalue calc., self consistent approx. method 4-80128  
Si, mol. type axial channelling radiation from MeV electrons 4-75582  
Si, positron channelling radiation, photon intensity and polarisation, computer simulation 4-75584  
Si, relativistic positron channelling, γ ray emission 4-75588

**chaos** see random processes

**character recognition**  
see also optical character recognition  
handprinted Katakana and alphanumeric characters, human recognition performance (*Japanese*) 4-81696  
human capability of receiving character information 4-81693

**characteristic temperature** see Debye temperature

**characteristics measurement**  
see also headings for specific characteristics, e.g. gain measurement; viscosity measurement  
ferromagnetic materials, static characteristics, automatic meas. and recording, HISTEREZOGRAPH BH-1 4-106333  
field emission in microwave field visualisation 4-104724  
multimode optical fibres, baseband response characts., meas., technique and equipment (*Japanese*) 4-107913  
streamer propagation characts., meas. using photomultipliers 4-97939

**charcoal**  
see also carbon  
activated, adsorpt. from binary solns. at high press. 4-104070  
activated, adsorption isotherms and heats of adsorption of H<sub>2</sub>(Ne)(N<sub>2</sub>) 4-114821  
activated, H<sub>2</sub> adsorption at low press. and at 20K 4-99844  
activated, organic liq. adsorpt. at high press. interfacial phase props. 4-104069  
diesel engine fuel displacement by biomass producer gas 4-66652

**charge (electric)** see electric charge

**charge compensation**  
see also crystallography  
α-quartz, electrodiffusion of charge-compensating ions 4-61153  
semiconductors, momentum relax. time of Wannier-Mott excitons scatt. by charged impurities 4-61296  
silicate glasses, thermotransport, at. migration process under effect of temp. gradient 4-80283  
BaTiO<sub>3</sub>, pure and Nb-doped, elec. cond. 600-800°C, defect struct. 4-98604  
Ba<sub>0.75</sub>Al<sub>1.09</sub>O<sub>17.14</sub>, hexaaluminate phase I, cryst. struct. and nonstoichiometry 4-70087

charge compensation continued

p-Ge, nuclear doped, elec. cond., 0.06 to 300K, impurity conc. depend. 4-61382  
Ge:Zn, Sb, degree of compensation from optical absorption meas. 4-109221  
MgO, thermoluminescence charge transfer mechanism 4-71450  
NaH<sub>2</sub>(SeO<sub>3</sub>)<sub>2</sub>:Cr<sup>3+</sup>, EPR spectra, temp. and external elec. field effects 4-88715  
SrTiO<sub>3</sub>, compensated, defects and colour centres, optical study 4-92200  
YIG:Ca films, charge compensation mechanism, annealing effects, behaviour on treatment with oxidising and reducing solns. 4-80799

charge-coupled device arrays *see charge-coupled device circuits*

charge-coupled device circuits

astronomical applications, CCD/transit instrument, progress report 4-72886  
astronomical light detector characts. and future developments (*Japanese*) 4-115690  
astronomical spectrometer CCD detector, comparison of two available chips 4-110534  
astronomical telescope imaging to high resolution using cinematographic mode CCD 4-94622  
digital phase measurement interferometry using CCD image acquisition 4-106374  
electroabsorptive CCD spatial light modulator, ID, signal correlation 4-107542  
FDL 60 film scanning system, development 4-63797  
flow meas., CCD chirp-Z FFT Doppler signal processor, laser velocimetry, oceanographic appl. 4-87819  
IR astronomy, two-dimensional imaging, CCD or CID arrays 4-101159  
IR detectors, conf., San Diego, CA, USA (Aug. 1983) 4-95022  
IRCCD sensors, Schottky barrier, Earth resources features appls. 4-100759  
laser field profiles, one dimens. meas. by CCD (*Chinese*) 4-87381  
line-edge position determ. for optically effective design, CCD line appl. (*German*) 4-86385  
MEIS II multidetector electrooptical imaging scanner, airborne pushbroom imager 4-100760  
MOSAIC, Mosaicked Optical Self-Scanned Array Imaging Camera for space UV 4-110522  
optical length measurement with CCD-array (*German*) 4-90565  
scanning imagers first-order performance prediction techniques 4-97131  
sun tracking sensors for sunlight concentrators 4-66667  
TV camera for NASA Galileo mission to Jupiter 4-94615  
X-ray imaging and spectroscopy, performance 4-68340  
InSb detectors for ground-based astronomy 4-95517  
PtiSi IR CCD detector array used in digital heterodyne interferometer 4-111193  
PtiSi Schottky IR CCD evaluation for astron. appls. 4-64789  
Si strip particle detectors, junction CCD readout structure 4-68906

charge-coupled devices

*see also charge-coupled device circuits*

astronomical obs., appl. for faint planetary satellites 4-82423  
DIGITRACK, CCD based system for automatic nuclear track counting and eval. 4-96358  
IR detectors, conf., San Diego, CA, USA (Aug. 1983) 4-95022  
moire topography, sampling theory and charge-coupled devices 4-73496  
MoS<sub>2</sub> integrated sensors, electrochem. and charge-imaging effects 4-82786  
nearest neighbor hybrid deformable mirror optical computer 4-96818  
optics for non-visible photography 4-111237

charge density waves

broadband current noise and AC induced current steps by moving CDW domain 4-104279  
conduction of CDW with strong impurity pinning, permitt., threshold elec. field 4-98597  
crystals with C<sub>3v</sub><sup>5</sup> symmetry, struct. phase transitions, Landau theory (*Russian*) 4-98263  
disordered systems with periodic lattice distortion, electronic structure 4-70733  
dynamics of incommensurate structures, exact soln. 4-113842  
graphite, charge density wave and magnetoresistance anomaly 4-92639  
graphite, electronic phase transition in strong mag. field (*Japanese*) 4-92616  
impurity effects, mean field calc. 4-70687  
interacting electrons in 2k<sub>F</sub> periodic pot., one dimens. system theory 4-92703  
inversion layer width, electron-electron interactions, fractional quantum Hall effect 4-75880  
linear chain compounds, moving CDW, Josephson-type oscillations 4-92644  
metal, CDW-SDW mixing, theory 4-92640  
metals, low-dimensional, phase transitions and X-ray diffuse scatt. (*Japanese*) 4-113598  
metals, one-particle transitions and kinetic props., CDWs 4-88449  
one-dimensional electron-exciton model pairing and CDW correlations 4-104137  
one-dimensional CDW, incommensurate, in weak pinning regime, numerical study 4-75943  
one-dimensional CDW system, pinning by impurities, dynamics 4-75879  
one-dimensional electron lattice coupled system, CDW and fractional charge (*Japanese*) 4-104135  
one-dimensional system with incommensurate modulation of hopping integrals, electron localisation 4-70703  
organic conductors, correlation effects in IR props. 4-92765  
quantised Hall effect theory 4-98646  
quasi-one-dimensional metals, superconductivity and optimal phonon freq., theory 4-76066  
quasi-one-dimensional supercond. under mag. field, spin effects 4-84730  
quasi-one-dimensional systems, CDW motion, coherent pulses, microscopic model eqns. 4-80571  
secondary charge-density waves 4-108793  
superconductors, CDW, nonequilibrium states, under tunnel injection (*Russian*) 4-98818  
superconductors, nonmagnetic impurity effects 4-70683  
tetrathiosquarato nickel(II), one dimens. crystal orbital calcs., neighbour-strand interactions 4-113853  
transition metal dichalcogenides, CDW transitions and lattice vibrs. (*Japanese*) 4-92641  
TTF-TCNQ, strongly irradi., CDW fluctuations, X-ray diffuse scatt. study 4-84611

charge density waves continued

(Cr,Nb)Nb<sub>2</sub>Se<sub>10</sub>, one-dimensional systems, resistivity, structure and mag. props. 4-61364  
Cr<sub>1.45</sub>Nb<sub>2.55</sub>Se<sub>10</sub>, cryst. struct., metal-insulator transition, resist., mag. susceptibility meas. 4-88448  
CuV<sub>2</sub>S<sub>4</sub>, CDW transitions, elec. and thermal props. 4-98618  
(Fe,Nb)Nb<sub>2</sub>Se<sub>10</sub>, (Fe,V,Nb)Nb<sub>2</sub>Se<sub>10</sub> and (Fe,Ta,Nb)(Nb,Ta)Se<sub>10</sub>, one-dimensional systems, resistivity, structure and mag. props. 4-61364  
Fe<sub>1+x</sub>Nb<sub>3-x</sub>Se<sub>10</sub>, cryst. struct., metal-insulator transition, resist., mag. susceptibility meas. 4-88448  
Fe<sub>1+x</sub>Nb<sub>3-x</sub>Se<sub>10</sub>, elastic props. and Mossbauer effect 4-84881  
Fe,NbSe<sub>3</sub>, charge density waves, magnetoresistance elec. field depend. 4-70788  
GaS<sub>2</sub>, charge density wave depinning and nonlinear transport 4-70790  
K<sub>0.3</sub>MoO<sub>3</sub>, 1D, CDW modes, far IR reflectivity studies 4-108798  
K<sub>0.3</sub>MoO<sub>3</sub>, CDW deformation during sliding motion, X-ray diffr. studies 4-104188  
K<sub>0.3</sub>MoO<sub>3</sub>, quasi-one-dimensional cond., CDWs, thermodynamics 4-80257  
K<sub>0.30</sub>MoO<sub>3</sub>, electron irradi., CDW pinning in Peierls distorted state by induced defects, nonlinear cond. 4-98595  
La<sub>2</sub>CuO<sub>4</sub>, with K<sub>2</sub>NiF<sub>4</sub> struct., at displacements, mag. and transport props., anisotropic bonding effects 4-73558  
La<sub>2</sub>NiO<sub>4</sub>, with K<sub>2</sub>NiF<sub>4</sub> struct., at displacements, mag. and transport props., anisotropic bonding effects 4-73558  
Li<sub>0.9</sub>Mo<sub>0.1</sub>O<sub>7</sub>, quasi-two-dimensional electronic props. 4-104189  
Mo<sub>2</sub>Se<sub>3</sub>, elec. and mag. props. study 4-80595  
Nb<sub>2</sub>S<sub>4</sub>(Se<sub>4</sub>)(Te<sub>4</sub>), one-dimensional, thermoelectric power 4-70848  
NbSe<sub>3</sub>, AC-DC interference effects, current oscillations 4-113933  
NbSe<sub>3</sub>, anomalous elec. cond., CDW condensate dynamics 4-92705  
NbSe<sub>3</sub>, CDW conduction noise spectrum, effect of thermal gradient 4-114007  
NbSe<sub>3</sub>, CDW depinning, switching 4-75945  
NbSe<sub>3</sub>, CDW props., high-resolution synchrotron X-ray scatt. studies 4-109276  
NbSe<sub>3</sub>, chaotic response, evidence for new CDW phase 4-92706  
NbSe<sub>3</sub>, charge density waves, magnetoresistance elec. field depend. 4-70788  
NbSe<sub>3</sub>, driven CDW system, subharmonic Shapiro steps, devil's staircase 4-88501  
NbSe<sub>3</sub>, electron irradi., strandlike domains in CDW states 4-70220  
NbSe<sub>3</sub>, electronic state and Peierls transition, NMR study 4-75858  
NbSe<sub>3</sub>, negative differential resist., dynamic instability 4-88502  
NbSe<sub>3</sub>, quasi-1D metal, Hall effect and sliding Frohlich modes 4-65669  
NbSe<sub>3</sub>, sliding charge density waves and noise 4-88461  
NbSe<sub>3</sub>, stress depend. of CDW transitions 4-80498  
NbSe<sub>3</sub>, transient cond. and cond. noise 4-80574  
Nb<sub>2</sub>Te<sub>2</sub>, quasi-one-dimensional, elec. and supercond. props. 4-113930  
Ni(CN)<sub>4</sub><sup>2-</sup> system, symm. isolations in partially oxidised one dimens. transition metal polymers 4-88524  
Rb<sub>0.3</sub>MoO<sub>3</sub>, CDW transport, low frequency noise and memory effect 4-113932  
Rb<sub>0.30</sub>MoO<sub>3</sub>, electron irradi., CDW pinning in Peierls distorted state by induced defects, nonlinear cond. 4-98595  
Se crystal struct. and defects, CDW soliton model 4-70685  
Si (111) slab, interface, electron-phonon interaction and broken symm. 4-80517  
TaS<sub>2</sub>, 1T polytype single crystals, charge density wave 3D ordering, NMR studies 4-76268  
TaS<sub>2</sub> (1T), commensurate CDW state, electronic cond., Hall coeff. meas. 4-98639  
TaS<sub>2</sub>-1T, thermoelectric power in CDW phase 4-80570  
TaS<sub>3</sub>, CDW, AC cond. meas., freq. and bias depend. 4-75946  
TaS<sub>3</sub>, CDW conduction noise, quantised voltage jumps obs. 4-114006  
TaS<sub>3</sub>, CDW current induced deform. 4-84612  
TaS<sub>3</sub>, Hall effect, contrib. of moving CDW 4-113931  
TaS<sub>3</sub>, onset of current carrying CDW state, switching, hysteresis, oscill. phenomena 4-75944  
TaS<sub>3</sub>, orthorhombic, CDW state, nonlinear field-effect (*Chinese*) 4-92735  
TaS<sub>3</sub>, orthorhombic, CDW deformation relax. and thermal memory effects 4-104190  
TaS<sub>3</sub>, orthorhombic, charge density waves, current induced deformation 4-88462  
TaS<sub>3</sub>, orthorhombic, low freq. behaviour of pinned CDW condensates 4-88503  
TaS<sub>3</sub>, pure and W-doped, stable oscillations associated with CDW current 4-108841  
TaS<sub>3</sub>, quasi-1D cond. at low temp., CDW motion 4-80575  
TaS<sub>3</sub>, stress depend. of CDW transitions 4-80498  
TaS<sub>3</sub>:Ni, orthorhombic and monoclinic, CDW form., impurity effects 4-80573  
IT-TaS<sub>2</sub>(Se<sub>2</sub>), CDW states, three-dimensional orderings 4-65625  
TaS<sub>2</sub>(1T), commensurate CDW state, superlattice struct. NQR study 4-80842  
TaSe<sub>2</sub>, 1T polytype single crystals, charge density wave 3D ordering, NMR studies 4-76268  
2H-TaSe<sub>2</sub>, CDW phase transition at low temp. and high press. 4-104276  
TaSe<sub>2</sub>-2H, CDW props., high-resolution synchrotron X-ray scatt. studies 4-109276  
TaSe<sub>2</sub>-2H, charge density wave transition (*Chinese*) 4-84575  
TaSe<sub>2</sub>-2H, positron annihilation study 4-81035  
Te crystal struct. and defects, CDW soliton model 4-70685  
Ti<sub>58.7</sub>Ni<sub>37.5</sub>Al<sub>3.8</sub>, charge wave density transitions, electron microscopy study 4-98596  
TiTe<sub>2</sub>, CDW transitions and transport props. 4-80521  
VS, metal-insulator transition and elec. props. 4-84568  
VS<sub>2</sub> (1T), reflectivity, CDW band struct., Kramers-Kronig anal. 4-71401  
VS<sub>2</sub>, CDW transitions and transport props. 4-80521

charge exchange

for charge exchange in particle and nuclear physics *see elementary particle interactions and nuclear reactions and scattering*  
*see also charge transfer states; ionisation*  
3d transition metals with adsorbed CO, electronic struct. and chemical reactivity of CO 4-93552  
A=2-17, neg. ion beam form. by charge transfer in metal vapours 4-107197  
acetylene borane, orbital interactions, charge transfer, and bond form., CNDO/2D study 4-59641

## charge exchange continued

adiabatic rate processes in condensed systems and interfaces, quantum model anal. 4-71986  
 adsorbates, charge transfer instability in optical absorpt. and photoelectron spectra 4-104552  
 alkali metal vapour+H ions, spin-depend. charge transfer 4-59890  
 Anderson model, time depend., charge exchange in HF approx. 4-107448  
 aniline, low temp. cage effect and phosphorescence 4-96690  
 2-anthracene carboxylic acid alkyl ester cation radicals, charge transfer, photolysis obs. 4-102788  
 aromatic polyesters, primary thermal fragmentation, direct mass spectrosc. obs. 4-105083  
 aromatic-aliphatic polyesters, primary thermal 4-105084  
 asymmetric ion-atom collisions, charge transfer to a fast projectile in the presence of a nuclear resonance 4-96691  
 atom-ion collisions, charge exchange transitions to excited states 4-74332  
 atom-ion collisions charge transfer, laser assisted, coupled dressed quasi-molecular states approach 4-96684  
 atom-ion quasis resonant collisions, Schrodinger eqn. modelling 4-87190  
 atomic and molecular ions emerging from thin solid targets, non-equilibrated charge and excitation states 4-81065  
 atomic collisions, charge exchange processes 4-96694  
 benzoquinone-model membrane bilayer interactions, positronium chem. investig. 4-62224  
 binary alloys, charge transfer and energy of formation, CsCl intermetallic cpds. 4-77026  
 biphenyl cation-neutral acceptor, in PMMA matrix, positive charge transfer, temp. effects 4-102787  
 chemical ionisation mass spectrometry, electron impact mass spectra simulation by charge exchange 4-112241  
 cholesteryl pelargonate liq. cryst., current flow, relax. processes 4-88770  
 cyanobiphenyl liq. crystals, current flow, relax. processes 4-88770  
 cyclobutane+Ar<sup>+</sup>(Xe<sup>+</sup>), charge transfer, mass spectra 4-112267  
 density matrix formalism, quantum theory 4-99779  
 N,N-dimethylaniline, low temp. cage effect and phosphorescence 4-96690  
 electron capture decay, potential model for estimating exchange effects 4-96689  
 equilibrium charge distrib. for B, C, N ions passing through matter 4-75586  
 ethylbenzene+Ar<sup>+</sup>(Xe<sup>+</sup>), charge transfer, mass spectra 4-112267  
 fast asymmetric collisions, K and L shell charge transfer, off-shell wavefunctions effect 4-64598  
 fast ions in solids, excited state populations and charge-exchange 4-80126  
 formamide+glyoxals charge transfer, ab initio calcs., appl. electronic theory of cancer 4-87205  
 geminate recombination on a lattice 4-111042  
 graphite-AsF<sub>6</sub> intercalation cpd., X-ray absorpt. near edge struct. meas. 4-66115  
 haloanisole mol. ions, fragmentation, energy depend., charge exchange expt., breakdown graphs 4-89260  
 heavy ion charge exchange in matter, radiation calc. 4-76548  
 highly charge ion prod. and storage at room temp. appl. to electron transfer and photoionisation meas. 4-82860  
 Hubbard one-dimensional model, 2p<sub>F</sub> and 4p<sub>F</sub> instabilities 4-80467  
 inert gas atoms+H<sup>+</sup>(He<sup>+</sup>), charge transfer and direct ionisation channels, electron prod. 4-87191  
 inner-sphere reorganisation in optical electron transfer 4-83420  
 interstellar gas, ion composition and chem. reactions 4-101460  
 interstellar matter, diffuse component atomic processes 4-63258  
 ionisation equilibrium in rarefied gas, effect of charge-exchange reactions 4-94577  
 jellium, scattered and re-emitted H charged fractions, trajectory depend. 4-76597  
 MBBA liq. cryst., current flow, relax. processes 4-88770  
 methanol+Ar<sup>+</sup>(Xe<sup>+</sup>), charge transfer, mass spectra 4-112267  
 molecular complexes, complexes, electric dipole moment, IR spectra, charge distrib., polarisation effects 4-59763  
 multiply charge ion-gas target collision, charge transfer cross sections 4-102789  
 muonium form. and missing fraction in vapours 4-71956  
 muons, charge exchange in gases, density operator formalism theory 4-69201  
 muons charge exchange in gases, kinetic eqns. appl. to muon spin reson. signals 4-74330  
 outer-sphere electron transfer probability determ. using quantum-static approx. 4-66559  
 positive ion-surface scatt., negative ion form., Anderson correl. energy 4-66577  
 Princeton Large Torus, O VIII and C VI emissions due to charge-exchange processes 4-103563  
 Raman scattering, surface-enhanced charge transfer contrib. 4-88840  
 rare earth-transition metal ternary intermetallics, charge transfer, X-ray absorpt. spectra study 4-81037  
 rate constant calcs., with arbitrary dielec. loss spectrum for solvent 4-109638  
 reactive processes in condensed systems, quasia diabatic models, rel. to Franck-Condon separation (*German*) 4-81430  
 reactive sputtering plasmas, preferential ionisation, glow discharge mass spectrometry anal. 4-99313  
 red auroral arc energy transfer reactions 4-100841  
 single electron capture 4-74327  
 solid-phase charge transfer rate, intermol. vibrs. 4-81429  
 solids, heavy ion charge states and charge transfer 4-76589  
 static ionic charge in dielectric theory, scaling with ionicity parameter 4-98057  
 TCNE, on Ag film, surface-enhanced Raman scatt., charge transfer effects 4-71358  
 Tokamak limiter charge exchange flux, modelling and effects 4-60582  
 toluene and its deuterium derivatives, IR spectra, charge distrib. determ. 4-112181  
 transfer probabilities, heuristic derivation 4-64597  
 transition intermetallic alloys, heats of form. 4-99818  
 Van der Waals rare gas dimers, three-body exchange reactions, tunnelling process, WKB calcs. 4-64589  
 Al<sub>2</sub>CO ligand-metal bonding, charge transfer and polarisation 4-69265  
 Al<sub>2</sub>NH<sub>3</sub> ligand-metal bonding, charge transfer and polarisation 4-69265  
 Al<sub>2</sub>NH<sub>3</sub><sup>+</sup>, excited states in D Tokamak plasma, recombination population 4-87936

## charge exchange continued

Ar+Ar<sup>+</sup>, recoil ion charge state distrib., projectile charge state depend. 4-69204  
 Ar+H<sub>2</sub><sup>+</sup>(O<sub>2</sub><sup>+</sup>)(NO<sup>+</sup>), charge transfer reactions 4-89272  
 Ar+S<sup>13+</sup>, K vacancy transfer, interference effects 4-78961  
 Ar+Xe, correls. between charge-changing interactions and projectile K-alpha X-ray emission 4-64595  
 Ar<sup>+</sup>+CS(PN) radicals, emission spectra prod. from thermal energy charge transfer reactions 4-74325  
 Ar<sup>2+</sup>+Cu, two electron transfer collisions, Ar I VUV line intensity 4-83462  
 Ar<sup>2+</sup>+He, charge transfer processes studied by crossed-beam, expt. 4-91339  
 Ar<sup>2+</sup>(\*)+He(Ne), electron capture reactions studied by means of double translational spectroscopy 4-96686  
 Ar<sup>2+</sup>(\*)+Ar, electron capture reactions studied by means of double translational spectroscopy 4-96686  
 (BH<sub>3</sub>NO<sup>+</sup>), orbital interactions, charge transfer, and bond form., CNDO/2D study 4-59641  
 Be<sup>2+</sup>+H, charge transfer cross sections calc. using close coupling calc. 4-78959  
 Bi<sub>2</sub>SiO<sub>20</sub>:Al(Ga)(Mn)(Cr), optical absorp. spectra, photochromism (*Russian*) 4-114311  
 C black dispersions, charge exchange, electrochemical/ESR studies 4-93562  
 CO<sup>+</sup>+CS<sub>2</sub>, in flowing afterglow, charge-transfer, excitation, energy reson. and Franck-Condon criteria 4-93500  
 Cl<sub>2</sub>+Cl<sup>+</sup>(Br<sup>+</sup>)(I<sup>+</sup>) charge transfer and electron detachment, absolute total cross-sections meas. 4-69202  
 Cs<sup>+</sup>+H<sup>+</sup>(D<sup>+</sup>), spin-depend. charge transfer 4-59890  
 Cs<sup>+</sup>+Cs<sup>+</sup> inelastic collisions, Cs<sup>2+</sup> prod., plasma target technique study 4-78954  
 Cu (110), He ion reson. neutralisation into reson. states 4-76588  
 CuWO<sub>4</sub> single cryst., elec. prop., photoelectrochem. study 4-65708  
 D<sub>2</sub><sup>+</sup>+Ar(H<sub>2</sub>) collisional dissociation, correl. between channel probabilities 4-78933  
 DyFe<sub>2</sub>Al<sub>2-x</sub> Fe L<sub>III</sub> X-ray emission spectra, electron microprobe anal. 4-76563  
 F<sup>-</sup>+molecule, electron detachment and charge exchange to shape reson. 4-96687  
 F<sup>+</sup>+C(X) foils; equilb. charge state, particle vel. depend. 4-64594  
 F<sup>+</sup>+He(Ne), K Auger-electron prod. cross sections, charge-state depend. 4-96693  
 (Fe<sub>2</sub>Ni<sub>10</sub>)<sub>2</sub>, metallic glass, Mossbauer and soft X-ray appearance pot. spectra studies 4-76292  
 H<sub>2</sub> charge exchange with protons in Na, K, Rb-vapour 4-74324  
 H<sup>+</sup> charge exchange with protons in Na, K, Rb-vapour 4-74324  
 H<sup>-</sup> formation by charge transfer in alkaline earth vapours 4-73572  
 H-bonding systems, excited, electronic struct., ab initio MO-Cl calcs., charge transfer 4-96461  
 H+C<sup>+</sup>, electron transfer into C<sup>3+</sup>(nl) orbitals, at. basis calcs. 4-107450  
 H+H<sup>+</sup>, charge exchange and cross sections, symmetric orthogonalization of travelling molecular orbitals 4-64581  
 H+H<sup>+</sup> collisions, reson. electron transfer from Rydberg atom 4-74329  
 H+XZ<sub>2</sub><sup>+</sup>, charge transfer collisions, long-range secondary couplings 4-102790  
 H<sup>+</sup>+He(Ar)(H<sub>2</sub>)(N<sub>2</sub>)(O<sub>2</sub>)(CO<sub>2</sub>), electron detachment and charge exchange to shape reson. 4-69203  
 H<sup>+</sup>+C(Ne), charge transfer at large scattering angles in the strong-potential Born approximation 4-87210  
 H<sup>+</sup>+H collisions, triple-centre treatment of ionisation 4-78956  
 H<sup>+</sup>+H<sub>2</sub> collisions, two state charge transfer calc. 4-91341  
 H<sup>+</sup>+H<sup>+</sup>, mutual neutralisation, 5-2000 eV 4-64591  
 H<sup>+</sup>+He(Li<sup>+</sup>), electron capture cross sections 4-69200  
 H<sup>+</sup>+Na(K), electron transfer collisions, at. basis calcs. 4-102793  
 H<sub>2</sub> electron and positron impact, rot. excitation cross sections 4-64630  
 H<sub>2</sub>+C<sup>4+</sup>, charge transfer, polarised light emission 4-83463  
 H<sub>2</sub><sup>+</sup>+H<sub>2</sub>, symm. electron transfer reactors of state-selected ions 4-107446  
 He<sup>+</sup>+N<sub>2</sub> thermal charge transfer reaction, N<sub>2</sub><sup>+</sup> predissoc. channel 4-91317  
 He<sup>2+</sup>+H, charge transfer, laser assisted, coupled dressed quasimolecular states approach 4-96684  
 He<sup>2+</sup>+He collisions, Coriolis coupling effect in time depend. HF calcs. 4-91342  
 He<sup>2+</sup>+neutral ats., charge transfer in low-energy collisions 4-74326  
 KHg<sub>2</sub>-graphite intercalation cpd., electronic struct., Shubnikov-de Haas effect 4-92596  
 Li isoelectronic series, radiative decay following charge exchange on neutral gas targets 4-87069  
 Li-Sn liquid structure, neutron diff., cpd. form. 4-113295  
 Li+Ar<sup>+</sup>(Ne<sup>+</sup>)(Kr<sup>+</sup>)(Xe<sup>+</sup>) collisions, q=2 to 10, electron capture cross sections from slow projectiles 4-74328  
 Li+C<sup>4+</sup> electron transfer into C<sup>3+</sup>(nl) orbitals, at. basis calcs. 4-107450  
 Li<sup>+</sup>+Li, differential cross sections calc. using mol. bases, quantum effect 4-87211  
 Li<sup>+</sup>+Li<sup>+</sup> collision, charge transfer and ionis. cross-sections determ. 4-64593  
 Li<sup>3+</sup>+H, charge exchange cross-sections, low-energy calcs. 4-64592  
 Li<sup>3+</sup>+neutral ats., charge transfer in low-energy collisions 4-74326  
 MgO, F<sup>-</sup> centre, electronic point defects with self consistent lattice polarisation 4-93091  
 MnSb, electronic struct., density of states and mag. moments 4-75856  
 N<sup>2+</sup>+H, charge transfer cross sections, extreme UV radiation emission 4-64596  
 N<sub>2</sub><sup>+</sup>+Ar, state-selected charge transfer cross sections 4-87206  
 N<sub>2</sub>+N<sub>2</sub>, charge transfer reaction dynamics, crossed mol. beam study at low and intermediate energies 4-96683  
 N<sub>2</sub><sup>+</sup>+O<sub>2</sub> charge transfer study 4-87214  
 NH<sub>3</sub> on Ag electrode, surface enhanced Raman scatt., vibr. anal., charge transfer processes 4-93545  
 NH<sub>3</sub>-BH<sub>3</sub>, orbital interaction, charge transfer, bond form., CNDO/2 study 4-102597  
 NH<sub>4</sub>Cl:Co<sup>2+</sup>(Ni<sup>2+</sup>), X-irrad. effects, optical absorpt. spectra, EPR 4-70206  
 Na+Na<sup>+</sup>, differential scatt. 4-87208  
 Na<sub>2</sub>O-SiO<sub>2</sub> glass disc surfaces disturbed by ion-beam induced absorpt. currents, Na conc. changes 4-93173  
 Ne<sup>2+</sup>+Ar(Kr), low energy electron transfer collisions 4-87213

**charge exchange continued**  
Ni (100), adsorption of K, coadsorption of K and D<sub>2</sub>, work function, TDS, XPS, UPS, AES studies 4-80398  
Ni (110), He ion reson. neutralisation into reson. states 4-76588  
O+H<sup>+</sup> (H)(H<sup>+</sup>), electron capture, electron loss, excitation 4-64390  
O+O<sup>+</sup>, charge transfer calcs. 4-78958  
O<sup>+</sup>+O in atmosphere, control of auroral source of magnetospheric O<sup>+</sup> ions 4-72786  
O<sup>+</sup>+He, charge transfer at thermal energies, cross sections and rate coeff. 4-76991  
OH<sup>+</sup>, shape reson., photofragment spectroscopy 4-107417  
OH<sup>+</sup> (H<sub>2</sub>O)<sub>n</sub>+CO<sub>2</sub>(SO<sub>2</sub>), reaction cross sections; translational energy depend. 4-76983  
Ru(NH<sub>3</sub>)<sub>6</sub>Cl<sub>3</sub>, Ru L-edges, EXAFS spectra 4-66122  
SF<sub>6</sub><sup>+</sup> ion lifetime in RF quadrupole trap 4-96644  
SiF<sub>4</sub><sup>+</sup>, ion-molecule reactions, FT mass spectra 4-93518  
SiF<sub>4</sub> plasma, dissociation and charge exchange for Si ion implantation source 4-99864  
n-SrTiO<sub>3</sub>/Nb/Fe(CN)<sub>6</sub><sup>3-</sup> (IrCl<sub>6</sub><sup>2-</sup>) interfaces, electroreduction 4-65740  
TiV<sub>2</sub>S<sub>8</sub>, NMR and photoredox reactions 4-84859  
V-Si, electron momentum distrib. and charge transfer, γ-ray Compton scatt. study 4-70059  
WO<sub>3</sub> amorphous films, electrochromic colour centres, Raman scatt. studies 4-113445  
Y<sub>2</sub>FeO<sub>7</sub>, ionic structure, neutron induced transformation, calcs. 4-113415

**charge-injection device arrays** *see charge-coupled device circuits*

**charge-injection devices** *see charge-coupled devices*

**charge measurement**

*see also electrometers*  
aerosol particles, fibrous, bipolar diffusion charging, elec. mobility and charge meas. 4-89348  
airborne particle electric charge measurement, charge distribution analysis 4-95473  
centroid of charge determ., in two-side metallised electrets 4-86441  
Cherenkov counter for cosmic-ray charge and direction meas. 4-63019  
electrophotographic toner materials, one-component, specific toner charge meas. method 4-68298  
LDPE, contactless dielec. meas. of charge and current 4-106331  
MOS integrated sensors, electrochem. and charge-imaging effects 4-82786  
surface charge, using vibrating capacitor probe 4-111118  
Ni-Cd cell residual charge meas. using microprocessor-based unit 4-81535  
Si fast surface-state density determ. using CCD technique 4-76017

**charge-ordered states**

extended Hubbard model with half-filled band, ground state beyond the HF approx. 4-76147  
one-dimensional extended Hubbard model, finite-cell scaling method 4-80738  
one-dimensional extended Hubbard model, real-space renormalisation group method 4-80737  
EuPd<sub>2</sub>B<sub>4</sub>, valence behaviour of Eu, possible charge ordering in EuPd<sub>2</sub>B 4-80850  
NbSe<sub>3</sub>, AC-DC interference effects, current oscillations 4-113933  
ZnS, charge states of S vacancy, tight-binding approx. 4-61331

**charge storage diodes**

No entries

**charge transfer** *see charge exchange*

**charge-transfer device arrays** *see charge-coupled device circuits*

**charge-transfer devices** *see charge-coupled devices*

**charge transfer states**

acetylene-I(I<sub>2</sub>), Ar matrix isolated, fine struct., IR and UV spectra 4-74231  
alkali metal halides, interstitial atomic H centers in mixed config., unrelaxed excited states, MCD optical absorpt. 4-70747  
anthracene-TCND charge transfer cryst. at 1.2K, optical and ESR studies, nπ\* triplet excitation evidence 4-99146  
anthracene-TEA (DMA) complexes formed in supersonic jets, van der Waals and charge transfer states 4-112226  
anthracene-tetranitromethane complexes, charge transfer processes, photochemistry 4-66599  
aromatic silanes, 2pπ\*3dπ interactions, charge-transfer states, fluoresc. 4-64537  
atom-ion collisions, charge exchange transitions to excited states 4-74332  
N-benzylquinolinium chloride-diphenylamine hemihydrate 1:1 complex, cryst. and mol. struct. 4-60908  
9,9'-bianthryl, intramolecular electron-transfer, solvent effects; fluoresc. study 4-96598  
p-cyano-N,N-dialkylanilines in nonpolar solns., luminescence studies 4-99168  
dimethyl ether-iodide, vapour-phase charge transfer complexes 4-107356  
electric field assisted disoc. as a photocarrier prod. 4-70744  
geminate recombination on a lattice 4-111042  
molecular complex, charge transfer absorpt. bands, solvent and press. effects 4-64406  
molybdenum tetraphenylporphyrin, charge transfer absorpt., reson. Raman scatt. 4-74248  
naphthalene-tetrachlorophthalic anhydride complex, lattice vibrs., Raman obs. 4-114254  
organic solids, photogenerated charge relaxation and localisation 4-98550  
perylene-TEA (DMA) complexes formed in supersonic jets, van der Waals and charge transfer states 4-112226  
photosystem I model systems, photoprocesses 4-115014  
phthalocyanine, β-metal-free, carrier generation, photoconductivity, delayed fluoresc. study 4-70855  
poly(N-alkyl-3,3'-carbazolyl)-I<sub>2</sub> complexes, highly conducting, synthesis and I<sub>2</sub> doping 4-65664  
polymer system, doped, photogeneration anal. in terms of kinetic model for elec. field assisted disoc. of charge-transfer states 4-70745  
polyvinylcarbazole, semicond., photosensitive and charge transfer props., Mossbauer effect obs. 4-114190  
polyvinylhalocarbazole, semicond., photosensitive and charge transfer props., Mossbauer effect obs. 4-114190  
tetracene, delayed fluoresc., role of charge transfer states in triplet exciton form. 4-99191  
transition metal ions, in alkali halide matrix, lifetimes, fluoresc. spectra 4-102631

**charge transfer states continued**

transition metals, adsorption of alkali-metal atoms, electronic charge transfer 4-92554  
AG electrode, surface enhanced Raman scatt., contrib. of charge transfer complexes and photochemical effects 4-88841  
BaSO<sub>4</sub>·MnO<sub>4</sub><sup>2-</sup>, absorpt. spectra, comparison with other host lattices 4-109217  
C<sub>3</sub>O<sub>2</sub>, ligand core hole states, configuration interaction calcs. 4-83301  
CaO-B<sub>2</sub>O<sub>3</sub>-Al<sub>2</sub>O<sub>3</sub>-Fe<sub>2</sub>O<sub>3</sub> glass system, photoacoustic spectra of Fe 4-99130  
Cr(CO)<sub>6</sub>, ligand core hole states, configuration interaction calcs. 4-83301  
CsMgCl<sub>3</sub>·Cu(I)-(M(III)), (M=Cr, Mo, Ru, Rh), intermetallic charge transfer spectra 4-65644  
Eu(III) complexes, cryptates, luminesc. and UV spectra 4-80978  
FeOCl, intercalated with α-picoline, Mossbauer study 4-71226  
FeOCl, Lewis base intercalation compounds, charge transfer model, Mossbauer spectra, X-ray diffr. 4-70746  
H<sub>2</sub>O-O<sub>2</sub> triplet contact charge transfer complexes, pot. energy curves 4-91322  
NiCl<sub>2</sub>, valence-band photoemission and optical absorption 4-99279  
NiO, valence-band photoemission and optical absorption 4-99279  
(RuX<sub>3</sub>)<sub>2</sub><sup>+</sup> complexes (X=Cl, Br), spin-orbit interaction, vib. and electronic Raman effect 4-88826  
Si:H/SiN<sub>x</sub>:H amorphous semiconductor superlattices, charge transfer doping 4-92219  
TiN<sub>0.89</sub>, electron transfer and thermal vibr. parameters, X-ray diffr. study 4-92329

**charge transfer transitions** *see charge transfer states*

**charged dislocations** *see dislocation dipoles*

**charging, contact** *see static electrification*

**charm particles**

*see also D mesons; psi mesons*  
baryons mag. moments in MIT bag model, recoil corrections 4-111454  
heavy and charm particles, prod. in strong interactions, decays, review 4-90931  
book on nucleus comp., elementary particles and fields 4-82617  
conference, meson spectroscopy, Upton, NY, USA (April 1983) 4-90280  
cosmic ray EAS, role of charmed particles in creation of long flying component 4-101085  
cosmic ray prompt muons, energy spectrum and ang. distrib. from charm prod. and decay 4-115663  
decay, muon-electron universality verification 4-73745  
decays, ν and equil. μ flux 4-90864  
hadronic props. from elastic pion scatt. 4-102128  
lifetimes and production 4-68566  
oscillator-cum-generalised anharmonic potential, Klein-Gordon eqn. soln. 4-106526  
production in neutrino interactions 4-90856  
same-sign dilepton production, constraints from charm decay data 4-95787  
weak decays of charmed particles 4-95791  
B→Xμν, decay of heavy quarks, branching ratios 4-59070  
(ccc) Faddeev eqns., mass calcs. of J<sup>P</sup>=3/2 systems 4-90832  
e<sup>+</sup>e<sup>-</sup>→charm, lifetime meas. 4-90898  
η<sub>c</sub>→φφ decay obs., η<sub>c</sub> spin and parity determ. 4-78550  
F→KKπ mass and lifetime meas. 4-68567  
F meson photoproduction at SLAC 4-90890  
F<sup>±</sup> semileptonic decay widths, l=0 η and η' final states, QCD sum rules 4-95789  
F→Fγ, P-odd effects in radiative decays, P-invariance violation (Ukrainian) 4-64002  
γN→charm, inclusive cross-section, meson lifetimes 4-90891  
γp→charmed baryon+charmed meson, 5-10 GeV, cross section threshold enhancement search 4-64008  
γp→charmed baryon+charmed meson, cross section threshold enhancement 4-106534  
(KKπ) isoscalar resonances, J<sup>P</sup>C assignments 4-73727  
Λ<sub>c</sub><sup>+</sup>, Λ<sub>c</sub> inclusive nonleptonic decays, bag model, W-exchange contribs. 4-106529  
Λ<sub>c</sub><sup>+</sup> mass, decay in diffraction model 4-64149  
Λ<sub>c</sub><sup>+</sup>→K<sup>0</sup>π<sup>+</sup>π<sup>+</sup> (Λ<sup>+</sup>π<sup>+</sup>π<sup>+</sup>), branching ratios, mass 4-95830  
Λ<sub>c</sub><sup>+</sup> lifetime from γN expt. 4-73749  
νN→Λ<sub>c</sub><sup>+</sup>(Σ<sub>c</sub><sup>+</sup>Σ<sub>c</sub><sup>+</sup>), quasielastic production 4-68563  
νN→charm, inclusive production results 4-95788  
pN→charm, production cross-section from dimuon continuum 4-102138  
pN→charmed mesons, quark-fusion model 4-68586  
pN→D(Λ<sub>c</sub>)X, upper limit for charm production 4-78567  
πN→charm+X, production cross-section from dimuon continuum 4-102138  
π<sup>+</sup>p→charm, total and differential cross-section calcs. in parton model 4-90934  
π<sup>+</sup>p→γγγ, 13 GeV/c, expt. search for narrow resonances, η<sub>c</sub> prod. 4-73772  
<sup>12</sup>C(n,Λ<sub>c</sub><sup>+</sup>), 58 GeV, production cross section 4-64149

**Charpy testing** *see dynamic testing*

**charring** *see combustion*

**Chebyshev approximation**

Helmholtz eqn., Chebyshev approx. solutions 4-86226

**chelates** *see coordination complexes*

**chemical analysis**

*see also chemical analysis by nuclear reactions and scattering; chromatography; electrochemical analysis; electron probe analysis; ion microanalysis; mass spectroscopic chemical analysis; polarimetry; pollution detection and control; radioactive chemical analysis; spectrochemical analysis; thermal analysis; X-ray chemical analysis*  
acrylamide, shock loaded, chemical and ESR anal. 4-109653  
analytical and image data from SEM and STEM, integrated system for collection and processing 4-72012  
analytical electron microscopy, imaging, chem. anal. and microdiffr. 4-108255  
analytical method based on electron ionisation of thermal pulvisulisation products 4-66632  
anthracene derivatives, shock loaded, chemical and ESR anal. 4-109653  
bauxite brick, lower temp. firing, microanalyses and SEM fractographs, K<sub>2</sub>O content 4-61892  
borosilicate glasses, B analysis and mapping using windowless energy dispersive detector 4-66636  
carbon tetrachloride, solids containing acetals, gamma-irrad., .CCl<sub>3</sub> radical prod. 4-93504

**chemical analysis continued**

- condensed matter physics, research facilities in USA 4-69987  
 direct insertion type zirconia oxygen analyzer hygrometer, Fuji Electric 4-11142  
 EELS microspectroscopy, characterisation of solids 4-66161  
 electron tunnelling spectroscopy of Au films, surface state obs., chem. sensor possibility 4-88606  
 equipment for instruments calibration (*German*) 4-77042  
 exhaust emission analysis, using electrohydraulic gas sampling valve 4-78305  
 exhaust gas from petrol engine, Pb compounds distrib. 4-89478  
 film preparation and etching, vacuum or plasma technology, conf., Brighton, UK (March, 1983) 4-78031  
 fine particles in environmental samples, characterization by transmission electron microscopy (*French*) 4-81502  
 gas, CARS, principle and appls. (*Dutch*) 4-66637  
 gases in liquid streams, relative solubility determ. 4-99909  
 glasses, H depth profiling using  $^{15}\text{N}$  beam 4-64249  
 glasses, NBS standard reference materials for microanalysis 4-81498  
 Green River oil shale, organic matter chemical structure 4-81516  
 HVEM, electron scatt. and energy depend., appl. to chem. anal. 4-66162  
 II-VI semiconductor; Ag, microscopic Ag impurity quantity determ., kinetic method (*Russian*) 4-65287  
 Kevlar in conc.  $\text{H}_2\text{SO}_4$ , laser light scatt. characterisation of rod-like polymers in corrosive solvents 4-114861  
 lecture notes and study guide on process analysers and recorders, book 4-106138  
 light element anal. using energy-dispersive spectrometers 4-66635  
 lung residual volume, spirogramme anal. (*German*) 4-77281  
 magnesium nickel oxalate dihydrate powders, coprecipitation from aq. soln. 4-75683  
 Maoming oil shale kerogen, extraction by supercritical gas process, chemical structure determ. 4-78837  
 marine electrochemistry (book) 4-101599  
 marine in situ trace organic chemical-sampler 4-100058  
 material concentration in liq. media, dual freq. monitoring method (*Russian*) 4-81488  
 methylmethacrylate-vinylferrocene copolymers adsorpt. at soln./solid interface; chromatography meas. 4-85332  
 microanalysis using EELS ion electron microscope 4-68332  
 modern measurement techniques, conf., Pretoria, South Africa (May 1984) 4-101572  
 natural rubber, epoxidised, DSC, NMR, elemental and titrimetric anal. 4-114876  
 nuclear power station water-stream circuits gas chromatographic measurements (*German*) 4-85343  
 particle stimulated desorption analysis for solid surfaces (*German*) 4-92499  
 piperazine-bis-(dithiocarbamate) complexes, mag., thermogravimetric and spectral studies 4-66033  
 polyether polyol monitoring using on-line near IR process photometers 4-99930  
 polysulphide, synthesis by polycondensation of chlorinated styrene and  $\text{Na}_2\text{S}$ , struct. 4-62198  
 robots appl. prospects 4-86407  
 sediments of seafloor, heavy metal pollution meas. system 4-105165  
 semiconductor gas sensor, environmental changes effect on sensitivity 4-62431  
 single electrode atmospheric pressure microwave discharge system for elemental analysis 4-113243  
 smoke density meas., optical instrument (*Dutch*) 4-68254  
 surface analysis, conference, Teddington, UK (Nov. 1983) 4-95051  
 surface analysis techniques review and glossary 4-78063  
 trace metal anal. and speciation using plasma emission spectrosc. detectors in HPLC 4-73524  
 Ag islands, microAuger anal. interpretation by backscatt. electrons 4-71486  
 B analysis and mapping using windowless energy dispersive detector 4-66636  
 $\text{CO}_2$  conc. in air, meas. using fluidic oscillator (*Italian*) 4-114862  
 $\text{CO}_2$  volume per breath, evaluation (*German*) 4-77282  
 CdO, struct. under pressure 4-75424  
 FeOCl, Lewis base intercalation compounds, charge transfer model, Mossbauer spectra, X-ray diff. 4-70746  
 $\text{H}_2$  mobility on Pd surface during catalytic  $\text{H}_2\text{O}$ -forming reactions, detection 4-71985  
 H<sub>2</sub>S determ. in environmental samples, methods review 4-105157  
 $\gamma$ - $\text{LiAlO}_2$  breeder material, TRIO-01 expt. for in-situ T recovery 4-107023  
 $\text{Li}_2\text{O}$  pellet, T recovery, assay techniques 4-107022  
 $\text{Li}_2\text{O}$  pellet breeder materials, in-situ T recovery expt. 4-107026  
 ( $\text{Mn}_2$ ,  $\text{Cd}_2$ ),  $\text{Sb}_2\text{O}_3$ , pyrochlores, synthesis and solid state studies 4-88140  
 ( $\text{Mn}_2$ ,  $\text{Sb}_2$ ),  $\text{O}_7$ , pyrochlores, synthesis and solid state studies 4-88140  
 $\text{MoS}_3$ , prep. by solid state reaction, characts. 4-61838  
 Ni-Cr multilayer struct., depth resolution in ion sputtering 4-66168  
 Ni(II) complex, with picolines, thermogravimetric characterisation 4-81490  
 $\text{O}_2$  determination in seawater by Winkler method (iodometric volume method) 4-94268  
 $\text{O}_2$  sensors, solid-electrolyte type, review 4-101834  
 Pt, black, catalyst/pyroelectric gas sensor using heat of reaction 4-66564  
 SiC polymorphs, crust. chem. props. 4-60896  
 T gas monitoring system using digital integrating circuit (*Japanese*) 4-77043  
 T recovery expt. TRIO-01, gas anal. system design, fabrication and testing 4-111816  
 Ti:H, depth profiling and microanal. 4-81497  
 V fluorooxoperoxo complexes, elemental anal., IR and Raman spectra and X-ray powder patterns 4-79988  
 $\text{V}_3\text{Si}$  precipitates, EELS anal. using STEM and high-voltage electron microscope 4-81495  
 $\text{ZrO}_2$ -CaO system, directionally solidified eutectic, EELS 4-72009
- chemical analysis by mass spectrometry** see mass spectroscopic chemical analysis
- chemical analysis by nuclear reactions and scattering**  
 see also chemical effects of nuclear reactions and scattering; neutron activation analysis; radioactive chemical analysis  
 actinide determination by alpha spectrometry at Radiological and Environmental Sciences Lab. 4-105051  
 Allende meteorite, Mg isotope ratios,  $\text{H}^+$  microprobe anal. 4-101277

**chemical analysis by nuclear reactions and scattering continued**

- alpha spectrometric rapid radiochemical analysis method for transuranics in nuclear facilities 4-105049  
 $^{40}\text{Ar}/^{39}\text{Ar}$  dating of a basite from the Western Antarctic 4-85763  
 charged-particle induced prompt  $\gamma$ -rays in elemental analysis 4-89362  
 chemical separation techniques for alpha spectrometric meas.; review 4-105048  
 conference, alpha-particle spectrometry, low-level meas., Harwell, England, (May, 1983) 4-101565  
 deuteron activation method for element determ. 4-105089  
 fission product identification from photofission by delayed neutron and gamma emission 4-109709  
 gamma activation, X-ray line overlapping effect 4-109710  
 glass, reactivity in aqueous solns., leaching of simulated radioactive waste glass 4-93548  
 hair, human, PIXE meas. normalisation by nucl. reaction 4-105065  
 ion beam-solid interactions, review of surface analytical techniques, book contrib. 4-85053  
 LEU fuel, non-destructive assay using photoneutron interrogation, safeguards appl. 4-106990  
 materials research, nuclear physical anal. methods (*German*) 4-72030  
 metals, wear reduction and analysis, surface modification by ion beams 4-81290  
 natural radionuclides in marine environment, radiochemical anal. techniques 4-105055  
 separation procedures for alpha spectrometric meas. of environmental and biological materials 4-105050  
 standard reference materials, F content,  $^{19}\text{F}(\text{p}, \text{p}')^{19}\text{F}$  reaction anal. 4-109703  
 steel, stainless, N ion implanted, lattice location, nuclear reaction, channelling and RBS studies 4-75463  
 surface depth profiles, resonant nuclear techniques 4-113768  
 techniques and scientific impact 4-89367  
 three-dimensional nondestructive material testing using nuclear microprobe 4-99862  
 transuranic speciation in geosphere, assessment using alpha spectrometry 4-105053  
 transuranics, chemisorption from seawater, in-situ meas. technique 4-105057  
 yield tracers for alpha-emitting actinide determ. in marine environment 4-105056  
 (d,p) reactions, nuclear microprobe anal. 4-72014  
 Ag-Pt-In dilute alloys, In migration, PAC studies 4-65460  
 $^{241}\text{Am}$  concentration in  $^{239}\text{Pu}$ , alpha-spectrometry determ. 4-102438  
 Au, implanted  $^3\text{He}$  depth profiles,  $^4\text{He}$  post-bombardment effects 4-80073  
 $^{10}\text{B}$  conc. in tumour, microanalysis 4-62634  
 F determ., in near-surface region of solids using  $^{19}\text{F}(\text{p}, \text{p}')^{19}\text{F}$  reson. reaction 4-85348  
 Fe and alloys, N implanted, SIMS, Auger and nucl. reaction analysis 4-88185  
 GaAlAs, proton energy loss straggling meas. for nucl. profiling appl. 4-70246  
 GaAs, crystal and amorphous, pulsed laser irr. under  $\text{O}_2$  and silane atmospheres, O incorporation and losses 4-80091  
 H, determ. in  $\text{Si}(\text{SiO}_2)_x$  by reson. nucl. reactions 4-85347  
 InP, residual impurities determ. by charged particle activation anal. 4-85346  
 $\alpha$ - $\text{LiI}\text{O}_3$ ,  $\text{Li}^+$  migration in DC elec. field,  $^6\text{Li}(\text{n}, \alpha)^3\text{H}$  nucl. reaction anal. (*Chinese*) 4-113698  
 Nb, implanted  $^3\text{He}$  depth profiles,  $^4\text{He}$  post-bombardment effects 4-80073  
 Ni (110), chemisorption of D, saturation coverage 4-92550  
 $^{210}\text{Pb}$ , determ. in seawater and marine particulate matter 4-105059  
 $^{210}\text{Po}$ , determ. in seawater and marine particulate matter 4-105059  
 $^{238}\text{Pu}$ , A=239,240, determ. in seawater 4-105058  
 $^{238}\text{Pu}$  concentration in  $^{239}\text{Pu}$ , alpha-spectrometry determ. 4-102438  
 $^{224}\text{Ra}$ , indirect meas. by high resolution alpha spectrometry 4-105061  
 Si, impurities, activation anal. using charged particle accelerators 4-60946  
 Si, impurity characterisation using neutron activation anal. 4-60947  
 Si noncrystalline thin films, struct. props. and impurity content 4-88434  
 Si surface layers, O atom determ. by nuclear reaction (*Chinese*) 4-84491  
 a-Si:H thin films, O distrib. and modifications induced by heavy ion bombard. 4-70233  
 p-SiC:B, diffusion, track autoradiography studies 4-84466  
 SiO<sub>2</sub> amorphous films, plasma deposition from  $\text{SiH}_4$ +methane (ethylene),  $\text{H}^{15}\text{N}$ ,  $\alpha\gamma$   $^{12}\text{C}$  anal. 4-114410  
 SiO<sub>2</sub> fused, subsurface Al films, ion beam mixing,  $^{27}\text{Al}(\text{p}, \gamma)^{28}\text{Si}$  nucl. resonance broadening study 4-88189  
 Sm intestinal marker, prompt  $\gamma$  and neutron activation anal. 4-105078  
 $^{99}\text{Tc}$ , alpha spectrometric determ. in environmental samples 4-105052  
 Th, extraction from granite for alpha spectrometry 4-105060  
 $^{228}\text{Th}$ , indirect meas. by high resolution alpha spectrometry 4-105061  
 U extraction from granite for alpha spectrometry 4-105060  
 U oxidation state determ. in natural waters 4-105054  
 $\text{Y}_3\text{Fe}_2\text{O}_4$  garnet epitaxial layers, ion implantation-induced strain and damage profiles 4-75558  
 Zn compounds, activation analysis for corrosion of carburettors by alcohol 4-93442
- chemical association** see association  
**chemical batteries** see cells (electric)  
**chemical bonding** see bonds (chemical)  
**chemical bonds** see bonds (chemical)  
**chemical composition** see chemical analysis  
**chemical diffusion** see diffusion  
**chemical effects of nuclear reactions and scattering**  
 see also chemical analysis by nuclear reactions and scattering; radiation chemistry  
 No entries
- chemical effects of radiation** see radiation chemistry  
**chemical elements** see elements (chemical)  
**chemical energy conversion**  
 brown coal hydrogasification, semi-technical test plant operation 4-81572  
 coal, nuclear aided steam gasification, semi-technical pilot plant 4-81573  
 coal gasification, effect of temperature near ash melting point 4-62380  
 coal gasification, hot coal gas cleanup process 4-62376  
 coal gasification systems, developments in USA and France (*Dutch*) 4-89460

# chemical energy conversion continued

- consumption coal for fixed bed gasification (*German*) 4-85379
- cyclohexane as a liquid phase carrier in hydrogen storage and transport 4-66811
- electrochemical power sources, expected development 4-62330
- gasification of rice hulls and straw 4-66737
- Hercules coke-to-methanol plant, progress 4-62377
- high temperature methanation operation, methane from synthesis gas 4-81574
- HTR, BBC/HRB concept of nuclear process heat for coal gasification 4-81526
- HTR He/He heat exchanger, design and semitechnical testing, coal gasification 4-78711
- HTR nuclear process heat, technical assessment and future perspectives 4-81529
- HTR nuclear process heat plant, T distrib. in product gases 4-81575
- industrial cellulosic wastes conversion to diesel fuel 4-72143
- NKK coal gasification process, status report 4-62378
- oil shale gasification, optimal yield using HTR for process heat (*German*) 4-105115
- solar radiation accumulation in organic photoisomers 4-93643
- steam reformer, nuclear heated, design and semitechnical operating experiences 4-81571
- substitute natural gas production by CS/R hydrogasification process 4-62375
- thermal H<sub>2</sub> production by direct flux chemical reactor 4-66813
- thermochemical energy conversion system of inorganic aqueous salt solns., heat transfer 4-85381
- thermochemical hydrogen production, Co-Br hybrid water-splitting process (*Japanese*) 4-66806
- U-GAS gasifier dynamic response 4-62379
- underground coal, gasification, cavity growth 4-99985
- underground coal gasification, potential in USA 4-99982
- underground coal gasification, technical feasibility 4-99983
- VEW-coal conversion process: 10 ton/h-test plant (*German*) 4-85380
- water splitting, thermochemical processes using HTR, status and outlook 4-81576
- WIDCO's program for UCG commercialisation 4-99984
- H<sub>2</sub> produced from NH<sub>3</sub>, cost comparisons of various processes 4-105128
- H<sub>2</sub> production and technologies, today, tomorrow and beyond 4-93645
- H<sub>2</sub> production by HV light irradiation of H<sub>2</sub>SO<sub>4</sub> solution containing K<sub>2</sub>Cr(O<sub>2</sub>)<sub>3</sub>·3H<sub>2</sub>O and FeSO<sub>4</sub> 4-66810
- H<sub>2</sub> production from aliphatic alcohols over UV-illuminated powder Ni/TiO<sub>2</sub> catalysts, at room temperature 4-66809

## chemical engineering see chemical technology

## chemical equilibrium

- see also chemical reactions; reaction kinetics
- activity coefficient, thermodynamics at high pressures 4-81453
- affinity decay rate, temp. dependency 4-71869
- 9-alkylfluorene + (9-alkylfluorenyl)lithium, H<sup>+</sup> transfer reactions, Bronsted coeffs. 4-99754
- Belousov-Zhabotinskii reaction, random mixed modes due to fluctuations, 1-dimens. map 4-71870
- Belousov-Zhabotinsky reaction chaos, wave interactions 4-71966
- benzene, eqn. of state and optical luminosity shocked up to 210 GPa (2.1 Mbar) 4-61041
- benzene, liquid, shock compression and Hugoniot data 4-108518
- benzene-cyclodextrin inclusion complexes aq. soln., vapour press.-solubility meas. 4-99823
- benzothiazole cationic dyes, aggregation in water, equilib. consts., thermodynamics props. 4-62181
- Brusselator, chem. instability, homogeneous fluctuations 4-85288
- sec-butyl radical, chem. activated unimol. reactions, weak collisions and steady states 4-81405
- cryptands, halogen interactions, decomplexation, equilib. consts., UV and NMR study 4-104975
- diatomic cryst., equilibrium chem. reaction kinetics 4-109676
- diatomic molecular crystal dissociation, mol. dynamical studies, equilib. kinetics 4-99762
- Donnan equilibrium of 1-1 electrolyte, osmotic press., electric pot. and conc. 4-105028
- ethanal, equilb. gas-phase, role of ethanol 4-62225
- fluoroform + HOD, equilb. D distrib., temp. depend., isotope exchange 4-81419
- Ginzburg-Landau equations validity conditions in far-from equilb. kinetics 4-114768
- glass-forming melts, temp.-time dependences, chem. equilb. theory 4-92366
- halate driven chemical oscillators, skeleton mechanism 4-89241
- halide anion-organic acid (alcohol) complexes, binding energies, struct. effects, equilb. meas. 4-85293
- 2-hydroxypyridine to 2-pyridone tautomeric equilb., proton transfer mechanism 4-76977
- isobutyric acid, water solns., dissoc. at crit. soln. point 4-93523
- isothermal chemical reactions, coupling of density and internal energy - fluctuations 4-71962
- lithium benzophenone-LiBr complex form., equilb. const. 4-71906
- metallurgical thermodynamics, equilb. states and influencing factors, book contrib. 4-109375
- modified chemical vapor deposition process chemistry 4-91651
- $\alpha$ -naphthylethylene derivatives triplet state, struct. effect on triplet conformation 4-59653
- nonlinear reaction-diffusion systems, 1- and 2-component, spatial struct. form. (*German*) 4-62158
- oscillatory chemiluminescent reaction, chaos 4-109625
- polybutene, eqn. of state and optical luminosity shocked up to 210 GPa (2.1 Mbar) 4-61041
- polybutene, liquid, shock compression and Hugoniot data 4-108518
- polyelectrolyte chains, length distrib. in reversible thermodynamic equilb. 4-59924
- polyethylene, eqn. of state and optical luminosity shocked up to 210 GPa (2.1 Mbar) 4-61041
- pseudo first-order reaction diffusion systems, network thermodynamics, dissipative Lagrangian formation 4-99824
- reactive components, fluctuation thermodynamic props., species correl. function integrals 4-71965
- Schiff's base-2,2'-dipyridyl(o-phenanthroline) complexes, stability and thermodynamic props. 4-113676
- sensitivity analysis of limit cycles with application to the Brusselator 4-71960

# chemical equilibrium continued

- symmetry-breaking instabilities under nonclassical bifurcation conditions 4-66553
- 2,3,4,5-tetrachloro-6-(diethylamino)methylphenol, Mannich base, H<sup>+</sup> transfer equilb., solvent effect 4-81417
- thermal unimolecular reactions with two activation pathways 4-81400
- thermally activated crossing of a sharp potential barrier 4-114765
- thiophenol-N base H-bonds, proton polarisability and transfer 4-62226
- three-body ion-molecule association reaction rate consts., temp. variation constraints 4-85292
- Bi<sub>2</sub>(SO<sub>4</sub>)<sub>3</sub> =  $\alpha$ - $\beta$ -Bi<sub>2</sub>O(SO<sub>4</sub>)<sub>2</sub> + SO<sub>3</sub>, equilb. press.,  $\alpha$ - $\beta$  transform. study 4-71959
- Br oxidation reactions, travelling conc. waves parameters determ. 4-62189
- Fe alloy, siliconising, thermodynamic calcs. 4-89191
- HAsO<sub>3</sub>, iodate oxidation exhibiting bistability, mushrooms and isolas 4-71961
- Li breeder blanket, impure, T extraction by Y, thermochem. analysis 4-107027
- Li<sub>2</sub>O fusion reactor breeder, chem. compatibility with transition metals 4-107060
- NO<sub>2</sub><sup>-</sup>, cluster form. with HONO mols. mass spectrosc. investig. 4-69260
- N<sub>2</sub>O<sub>4</sub> = 2NO<sub>2</sub>, chem. equilb. anomalies near crit. points 4-93543
- Na<sub>2</sub>O-CaO-CO<sub>2</sub> system, calcination in air, differential thermal analysis obs. 4-99757
- Nb-N, decomposition, temp. depend. of pressure, incongruent melting 4-76981
- O<sub>4</sub><sup>+</sup> + N<sub>2</sub>, three-body reactions, O<sub>4</sub><sup>+</sup>(N<sub>2</sub>)<sub>n</sub> formation with n  $\leq$  4 4-89291
- PbO-CO<sub>2</sub>-H<sub>2</sub>O solid systems, stability and solubility rels. 4-83499
- Pu, oxidation states, coexistence in soln. 4-99931
- Si chemical behaviour in fusion reactor liq. Li systems 4-107058
- Ta film, first wall in ICF chamber, chem. reactions with pellet debris 4-107057
- Ta-N, decomposition, temp. depend. of pressure, incongruent melting 4-76981
- UF<sub>4</sub>-UF<sub>3</sub> system, vaporisation, high temp. reduction and disproportionation 4-114770
- V-N, decomposition, temp. depend. of pressure, incongruent melting 4-76981

## chemical exchanges

- see also ion exchange; isotope exchanges
- $\alpha$ -acyteric alcohols, Meyer-Schuster reaction, saddle points, transition-state struct. 4-114773
- adenosinephosphates, aq. solns., proton transfer reactions, acoustic studies 4-104985
- 9-alkylfluorene + (9-alkylfluorenyl)lithium, H<sup>+</sup> transfer reactions, Bronsted coeffs. 4-99754
- amine-HCl, H bonded complex, matrix isolation IR vibr. spectra 4-96544
- atoms, ions and mol. groups transfer in solns., activated complex theory appl. 4-66574
- 1-azacarbazole, excited-state double proton transfer, viscosity and temp. effects 4-99774
- collinear H-transfer reactions, dominant reaction probabilities evaluation 4-89245
- composite ionberg-iceberg model of aqueous nonpolar solvation and water exchange reactions 4-91326
- diaminotetrachlorotriphosphazenes + SbF<sub>3</sub>(KSO<sub>4</sub>F), fluorinating reaction, <sup>17</sup>F and <sup>1</sup>H NMR study 4-66581
- dibenzocycloheptadienyldiene radical, prod. by H abstraction 4-62212
- para-N,N-dimethylaminosalicylic acid, excited H<sup>+</sup> transfer, excitation wavelength depend. 4-62171
- N,N-dimethylaniline heat of transfer from H<sub>2</sub>O to H<sub>2</sub>O plus hexamethyl phosphorotriamide (*French*) 4-81422
- N,N-dimethylnitrosamine, gas phase <sup>1</sup>H NMR, kinetic parameters, environmental effects 4-64507
- electron transfer, rate const. calcs. with arbitrary dielec. loss spectrum for solvent 4-109638
- fluorene single crystals, doped, photochemical H-abstraction, tunnelling mechanism 4-93534
- formaldehyde + O(OH), H abstraction, pot. energy surface, ab initio HF CI calcs. 4-99770
- free radical liq. phase chem., radical structs. and reaction rates using positive muon probes 4-71885
- halogens quadrupolar nuclei, NMR spectroscopy 4-73476
- 3-hydroxylavone, intramol. excited-state H<sup>+</sup> transfer, H-bonding solvent perturbation 4-107392
- 2-hydroxypyridine to 2-pyridone tautomeric equilb., proton transfer mechanism 4-76977
- intramolecular modes, effect on rate of radiationless transitions in polar solvent 4-62184
- ion transfer between two centres of solvation, tunnelling between harmonic wells 4-66575
- methyl iodide in ocean, comparison of photolysis and substitution decomposition rates 4-100626
- nitroaniline, heat of transfer from H<sub>2</sub>O to H<sub>2</sub>O plus hexamethyl phosphorotriamide (*French*) 4-81422
- oxides, surface exchange reactions, oxygen transport characteristics 4-93855
- oxyhemoglobin, human, single cryst. NO ligand exchange, EPR study 4-105183
- polybutyleneterephthalate + polyamide interchain exchange reaction, DSC obs. of copolymers produced (*Russian*) 4-77005
- proton transfer reactions, rate consts., extinction coeffs. 4-99779
- solid-phase charge transfer reaction, intermol. vibrs. 4-81429
- 2,3,4,5-tetrachloro-6-(diethylamino)methylphenol, Mannich base, H<sup>+</sup> transfer equilb., solvent effect 4-81417
- thioacetic acid + acetic acid, H<sup>+</sup> exchange kinetics, solvent effects, PMR obs. 4-109643
- thiophenol-N base H-bonds, proton polarisability and transfer 4-62226
- three-atom reactions, Kramers' theory 4-109637
- unsaturated organic liquids, muon substituted free radicals 4-83498
- Walden inversion reactions, solvent effect 4-66558
- Ag<sub>2</sub>Mo<sub>2</sub>O<sub>7</sub>, interlayer reactions with n-alkylammonium ions 4-89284
- C + NO(X<sup>+</sup>O<sub>2</sub>), collinear reaction pot. energy barrier, correl. diagram, ab initio calcs. 4-99766
- CO self-exchange reaction mechanism studied using mercury photosensitisation technique 4-89270
- Cl + alkyl iodide, differential reaction cross-sections, collision dynamics 4-85291

## chemical exchanges continued

- Cl<sup>-</sup>H<sub>2</sub> chloride-d<sub>3</sub> (-d<sub>3</sub>), D abstraction from methyl-d<sub>3</sub> group 4-62163  
 F+DBr, collinear H-transfer reactions, dominant reaction probabilities evaluation 4-89245  
 F+H<sub>2</sub>(HD)(D<sub>2</sub>), collinear exchange reactions, probability densities, stabilisation calcs. 4-81415  
 F+I<sub>2</sub>(HI)(ICN), exchange reaction, pot. surface, I<sup>2</sup>P<sub>1/2</sub> two photon laser induced fluoresc. 4-76982  
 Fe(CO)<sub>4</sub> IR laser-induced isomerisation and Jahn-Teller effect 4-66567  
 H<sup>+</sup> transfer reactions, kinetic isotope effect, solvent depend. 4-104968  
 H<sup>+</sup> transfer reactions theory, adiabaticity effect on free energy relations 4-81406  
 H+H<sub>2</sub>(MuH), H and Mu exchange, isotope effects, semiclassical techniques 4-71884  
 H+HD-H<sub>2</sub>+D collinear reaction, competition between dissociation and exchange processes, exact quantum results 4-81409  
 H<sub>2</sub>+D<sub>2</sub>, exchange reaction on Pt (557) surface, HD ang. and vel. distrib. 4-99834  
 HCN, stripping in a packed tower, Henry's law const. meas. 4-62173  
 HO<sub>2</sub><sup>-</sup>, H-O bond energy, rel. to abstraction reactions 4-102574  
 H<sub>2</sub>O<sub>2</sub>, catalytic decomp. investig. using chemiluminesc. oxidation of luminol 4-62188  
 He+H<sub>2</sub><sup>+</sup>, exchange reaction, ab initio pot. energy surface, quasiclassical trajectory study 4-76996  
 I+H<sub>2</sub>(MuI), H and Mu exchange, isotope effects, semiclassical techniques 4-71884  
 KBr+Cl<sub>2</sub>-KCl+BrCl, nucleation and growth reaction on crystalline surface 4-71983  
 MoS<sub>3</sub>, prep. by solid state reaction, characts. 4-61838  
 NH<sub>3</sub>-HCl, H bonded complex, matrix isolated IR vibr. spectra 4-96543  
 O+H<sub>2</sub>(HD)(D<sub>2</sub>) exchange reactions, quasiclassical trajectory calcs. 4-71894  
 O<sub>2</sub>+H<sub>2</sub>(S)-OH(3π)+O(3P), reaction, primary processes, fluoresc. investig. (German) 4-99785  
 SiC, reaction bonded, and liq. Al, cast bonding, exchange diffusion phenomenon involving free Si 4-99741  
 UF<sub>6</sub>-UF<sub>4</sub> system, vaporisation, high temp. reduction and disproportionation 4-114770  
 UO<sub>2</sub><sup>2+</sup>, excited, photophysics in aq. soln., solvent exchange and H abstraction 4-112235  
 WCl<sub>3</sub>, synthesis, physicochemical props. 4-76649

## chemical industry

- advances in instrumentation, conf. Houston, Texas, USA (Oct. 1983) 4-106121  
 coal gasification, effect of temperature near ash melting point 4-62380  
 coal gasification, hot coal gas cleanup process 4-62376  
 electrical discharges and combustion, colloquium, London, England (April 1984) 4-67870  
 electrolytic H<sub>2</sub>, industrial applications, technology and economics 4-89474  
 Hercules coke-to-methanol plant, progress 4-62377  
 NKK coal gasification process, status report 4-62378  
 shell and tube slurry heat exchangers, slurry concentration and flow rates meas. 4-60554  
 substitute natural gas production by CS/R hydrogasification process 4-62375  
 U-GAS gasifier dynamic response 4-62379  
 USA hydrogen fuel industry 4-66815  
 H<sub>2</sub> thermochemical production by V/Cl<sub>2</sub> cycle, energy and exergy anal. 4-72185  
 H<sub>2</sub> thermochemical production by Y/Cl<sub>2</sub> cycle, chemical engineering aspects 4-72186

## chemical kinetics see reaction kinetics

## chemical lasers

- CW, dynamic saturation intensity, depend. on mixing rate of reagents 4-107617  
 CW flow chemical laser, generalised kinetic model 4-69392  
 I laser using photolytic O<sub>2</sub> Δ generation, kinetic model 4-112401  
 source flow chemical laser cavity performance 4-74551  
 Al photodissociation lasers using metal hydrides 4-107616  
 Br laser using IBr photodissoc., solar-powered, theory and operation 4-87322  
 BrCl laser, short wavelength 4-96883  
 BrF laser, short wavelength 4-96883  
 CO laser, type with 2-m long active region output characts. 4-74496  
 DF mid-IR waveguide lasers, RF pumped 4-74543  
 DF pulsed chain laser damage to coated window and mirror components 4-74582  
 DF RF-pumped IR laser using transverse gas flow 4-74544  
 DF-HF laser atmospheric attenuation meas. (Chinese) 4-62951  
 H<sub>2</sub>-F<sub>2</sub> pulsed laser, photolysis and electron beam method initiation efficiency 4-74499  
 HCl chemical laser system, pot. high energy, expt. demonstration 4-69394  
 HF 2-dimens. laser beam phase and intensity meas. technique 4-74564  
 HF, Blumlein discharge initiated, using SF<sub>6</sub> as F donor 4-69393  
 HF CW lasers, small signal gain meas. (Chinese) 4-112400  
 HF chemical laser, CW supersonic, shock wave effects 4-107615  
 HF chemical laser initiated by fine particle evaporation under IR radiation action 4-60028  
 HF electron beam initiated pulsed chem. laser 4-69391  
 HF laser mixtures, electron density of afterglow of pulsed discharge and UV photoionisation, meas. using microwave interferometer (Chinese) 4-87315  
 HF mid-IR waveguide lasers, RF pumped 4-74543  
 HF multiquantum vibr.-rot. relax. rates with N<sub>2</sub> and CO 4-102775  
 HF pulsed H<sub>2</sub>+F<sub>2</sub> chain reaction laser, effect of vibr. and rot. relax. mechanisms 4-91445  
 HF pulsed laser with unstable resonator (Chinese) 4-60026  
 HF pulsed nonchain laser, time-resolved spectral and energy characts. 4-74497  
 HF pulsed-discharge lasers preionised by pulse or CW X-rays 4-69387  
 HF/DF pulsed optical resonance transfer laser, theoretical simulation 4-79123  
 HgBr<sub>2</sub>/HgBr dissociation laser, discharged pumped (Japanese) 4-74490  
 I CW photolysis laser using closed-cycle gaseous C<sub>2</sub>F<sub>4</sub>/I supply system 4-69390  
 I laser, degenerate transition, self-induced transparency, coherent pulse propag. 4-96882

## chemical lasers continued

- I laser, near IR high power, pulse duration and beam flux density 4-69395  
 I laser degenerate mag. dipole transitions self-induced transparency 4-83653  
 I optically pumped laser, kinetics in optically thick medium 4-64702  
 I photodissociation laser, flashlamp-pumped, gasdynamic shock wave influence on lasing kinetics 4-60027  
 I, pulse reshaping in coherent interaction with resonant absorber homogeneous relax. time meas. 4-69511  
 I-H<sub>2</sub> laser, electron-beam-controlled 4-74498  
 I<sub>2</sub>-O<sub>2</sub> chemical laser, ICI fueled 4-91446  
 IF laser, short wavelength 4-96883  
 In photodissociation lasers using metal hydrides 4-107616  
 Kr<sub>2</sub>F photochemical laser, active medium bleaching wave optical inhomogeneities, interferometric study 4-60022  
 Xe<sub>2</sub>Cl<sup>+</sup> lasing as result of chem. radiative collisions 4-60023

## chemical potential see thermodynamic properties

## chemical reactions

- see also association; atom-atom collisions; atom-ion collisions; atom-molecule reactions; atomic inelastic collisions; catalysis; charge exchange; chemical exchanges; chemically reactive flow; chemiluminescence; chemisorption; CIDEP; CIDNP; corrosion; dissociation; electrolysis; free radical reactions; heat of reaction; ion-molecule reactions; isomerisation; molecule-molecule reactions; oxidation; photochemistry; polymerisation; pyrolysis; radiolysis; reaction kinetics; reduction (chemical); solvation  
 acrylamide, shock loaded, chemical and ESR anal. 4-109653  
 affinity decay rate, temp. dependency 4-71869  
 alkyl carboxylate-alkyltrimethylammonium mixed amphiphilic system, alkali metal and halide ion binding 4-84143  
 anthracene derivatives, shock loaded, chemical and ESR anal. 4-109653  
 atoms, ions and mol. groups transfer in solns., activated complex theory appl. 4-66574  
 Belousov-Zhabotinski reaction, relaxation oscillations in the revised Oregonator 4-89243  
 Belousov-Zhabotinskii mixed mode oscillations, variable map prediction 4-85294  
 Belousov-Zhabotinskii reaction, halate driven chemical oscillators, skeleton mechanism 4-89241  
 Belousov-Zhabotinskii reaction, random mixed modes due to fluctuations, 1-dimens. map 4-71870  
 Belousov-Zhabotinsky reaction, Oregonator model, alternative to stoichiometric factor 4-89242  
 Belousov-Zhabotinsky reaction chaos, wave interactions 4-71966  
 benzene cation radical, unimol. and bimol. reactions, kinetic energy release distrib., rate consts., PIPECO studies 4-89259  
 benzo(1,3)dioxole, electrophilic substitution, solvent depend., MNDO and MINDO calcs. (German) 4-71877  
 bistable nonequilibrium systems, plane front propag., fluctuation effect 4-63660  
 Bloch equations, generalised, for chem. reacting systems 4-91281  
 bromate-pyrogallol system+H<sub>2</sub>SO<sub>4</sub> (perchloric acids), uncatalysed oscillatory reaction, activation energy 4-66579  
 Brusselator, chem. instability, homogeneous fluctuations 4-85288  
 Brusselator chem. reaction, fluctuations stochastic simulation, ensemble statistics 4-114766  
 2-butanol, dehydration using sulphonated macroporous resin catalysts 4-66580  
 carbohydrates, thermal props. heat flow calorimetric obs. 4-78312  
 catalytic cracking process, porous catalysts, diluted, activity, dilution effect 4-66610  
 catastrophe theory, nonelementary, appl. to imperfect bifurcation problems 4-58649  
 char gasification, catalytic, math. modelling 4-99831  
 char particle and surrounding gas phase, diffusion and reaction models 4-99790  
 char particle and surrounding gas phase, diffusion and reaction, continuous model 4-99791  
 chemical quasi-equilibrium in non-isothermal plasmas 4-87953  
 chlorite+S<sub>2</sub>O<sub>8</sub><sup>2-</sup>, chemical chaos 4-66570  
 chloroethylene anions, formation and dissociation, electron attachment spectra 4-71876  
 collinear H-transfer reactions, dominant reaction probabilities evaluation 4-89245  
 complex chemical reaction, statistical models (Hungarian) 4-81401  
 comb. effects in atomic reactions in the presence of a low-frequency laser field 4-66578  
 countercurrent gas-liquid reactors near gas flooding condition, axial liq. dispersion 4-97708  
 cyclobutene/butadiene, thermally allowed electrocyclic interconversion, substituent effects, MNDO calcs. 4-85306  
 cyclopentene ozonide, synthesis, microwave spectra, elec. dipole moment and mol. struct. 4-59716  
 diamines, aromatic, hardening activity rel. to spectrosc. characts. of primary amino group 4-83372  
 diamond synthesis, ultrafast chemical reaction triggered by shock wave forming C and γ-CuBr from CBr<sub>4</sub> and Cu 4-114389  
 diatomic mols., normal vibr. calcs. for inorganic cpds. 4-59696  
 diffusion theory, nonstationary approach 4-93511  
 directed graphs of struct. stable pot. energy surfaces representing a-priori reaction pathways 4-96471  
 electrical discharges and combustion, colloquium, London, England (April 1984) 4-67870  
 endothermic gasification of a solid by thermal radiation absorbed in depth 4-103187  
 enzyme action mechanism, quantum chemical study 4-71867  
 epoxy resins, interaction with water, glass transition temp. depression 4-89157  
 exhaust gas from petrol engine, Pb compounds distrib. 4-89478  
 fluoroform+HOD, equilib. D distrib., temp. depend., isotope exchange 4-81419  
 flux-force relation for chemical processes in extended thermodynamics 4-85304  
 formaldehyde, reaction energies, pot. energy surfaces, ab initio calcs. 4-114789  
 formaldehyde-acetylcysteine-amino acid reactions studied by <sup>13</sup>C NMR 4-109635  
 fractal to classical crossover 4-85285

## chemical reactions continued

- gas bubbles formation kinetics in liquids with chemical reactions under microgravity 4-103900  
 gas hydrates, form., distrib. and appls., review 4-71912  
 glass, reactivity in aqueous solns., leaching of simulated radioactive-waste glass 4-93548  
 histidine, protonation reaction kinetics meas. using chemical relax. technique 4-89255  
 homogeneous CVD growth, review 4-88984  
 hydrocarbons plasma pyrolytical processing, kinetic optimisation, shock tube investig. 4-89288  
 impact activation of chemical reactions 4-99843  
 interstellar diffuse clouds, obs. tests for surface chemistry on gains 4-94928  
 interstellar medium, implications of 3  $\mu\text{m}$  ice band in Taurus mol. clouds 4-101457  
 intramolecular modes, effect on rate of radiationless transitions in polar solvent 4-62184  
 iodate-arsenite systems, bistability and chemical waves form. 4-85303  
 ionic reactions, reaction probability and diffusion-controlled rate consts. 4-93503  
 ions, energy selected, chem. dynamics 4-89244  
 isothermal chemical reactions, coupling of density and internal energy fluctuations 4-71962  
 kinetic boundary layer, Klein-Kramers eqn. 4-111079  
 knockout reactions, ang. and vel. distrib., hard sphere sequential impulse model 4-76985  
 metal salts, complex form. with elec. neutral ligands grafted to surface, reaction model 4-109686  
 methane- $\text{N}_2\text{O}$  mixtures, HCN form. in ion sources 4-66565  
 methyl halides, reactions of energetic  $^{11}\text{C}$ , electron density and bond polarisation effects 4-89280  
 molecular charge conc., bonded and nonbonded, relation to geometry and reactivity 4-102577  
 molecular collision, reactive, HF calcs., self-consistent time-depend. 4-77002  
 molecular struct. and conformation, book 4-67889  
 monomolecular reaction, kinetic region, rate const. depend. 4-89251  
 multidimensional systems, complex reson. energies, rational fraction analytic continuation method 4-85297  
 muon spin rot. chem. aspects 4-71947  
 muonium + OH, muonium spin rot. studies at high pH 4-81418  
 nonjective canonical transformations, use in chemical physics 4-71868  
 nonlinear reaction-diffusion systems, 1- and 2-component, spatial struct. form. (*German*) 4-62158  
 nonsymmetric linear systems, decay dynamics, quantum calcs. 4-66602  
 oil shale processing, high temp., mineral reactions 4-62195  
 opacity analysis of steric requirements in elementary chemical reactions 4-62159  
 optical surface fabrication on glass, appl. of surface anal. methods 4-91643  
 organic binary aq. mixts., solute-solute interactions, Kirkwood-Buff integrals 4-60973  
 organic luminophores, chem. struct. features and directed synthesis 4-104645  
 oscillator, chemical, 2D, computational study on limit cycle behaviour 4-104981  
 oscillatory chemiluminescent reaction, chaos 4-109625  
 outer-sphere electron transfer probability determ. using quantum-static approx. 4-66559  
 ozone synthesis, in gas discharges 4-69983  
 pentaerythritol tetranitrate, chemically reacting multiphase mixtures, detonation, statistical mechanical theory 4-104961  
 perfluoropropane- $\text{H}_2$  RF discharge, chem. mechanisms 4-108231  
 pheromones, photochem. synthesis, microcomputer interactive program appls. 4-114813  
 plasma chemical reaction rates, fluctuation anal. and correl. spectrosc. investig. 4-87943  
 poly(2,5-selenienylene), elec. cond., synthesis 4-70886  
 polyamidohydroxides, struct. transform. during thermal cyclodehydration (*Russian*) 4-62190  
 polyethylene oxide-NaSCN ionic cond., elec. props., complex reactions (*Chinese*) 4-92407  
 polyimide, cured, interfacial reaction during metallisation, XPS obs., chem. bond form. 4-88932  
 polymer analogous reactions; kinetic consts. evaluated using minicomputers (*Russian*) 4-104986  
 polypyrrole, proton modification, elec. cond.; optical absorpt. spectra, XPS 4-75969  
 polysulphonearylate block copolymers, synthesis, mech. and dielec. props. (*Russian*) 4-62191  
 porous catalysts, diluted, activity, dilution effect 4-66610  
 positive muon residual polarisation in water,  $\text{CS}_2$ , and organic liqs. under strong decoupling fields 4-71949  
 propyl acetate, protonated, fragmentation in chem. ionis. mass spectrosc., MO calcs. 4-78781  
 pseudo first-order reaction diffusion systems, network thermodynamics, dissipative Lagrangian formation 4-99824  
 quantum pendulum model mode transition, ridge effect, semiclassical array 4-110897  
 quantum-classical reaction path model for chem. reactions, theory and standardisation case 4-114764  
 quartz glass, ablation, boundary layer, nonequilib. physicochemical processes 4-71967  
 radical rearrangements in liqs., rate const. obtained by muon spin rot. 4-89282  
 radiofrequency labelling method, use in studying reaction mechanism 4-76974  
 reaction field theory, continuum models, solvent effects, desolvation contrib. 4-85286  
 reaction paths, saddle points, pot. energy surface 4-66552  
 reactive processes in condensed systems, quasiadiabatic models, rel. to Franck-Condon separation (*German*) 4-81430  
 rhodopsin, vertebrate, hydrolysis pathways 4-66950  
 $\alpha$ -selenocarbonium ions, prep., X-ray mol. struct., PMR and  $^{13}\text{C}$  NMR 4-112203  
 sensitivity analysis of limit cycles with application to the Brusselator 4-71960  
 shock tube-mass spectrometer system for chem. reaction studies 4-86499  
 simple chem. systems, complex dynamical behaviour 4-81399

## chemical reactions continued

- solid state chemistry, conf., Veldhoven, Netherlands (June 1982) 4-67863  
 solid surface, chemical and electrochemical treatment, low energy electron induced X-ray spectra 4-76572  
 solvated electrons, reaction with water in liq.  $\text{NH}_3$ , kinetics 4-104966  
 spherical shell system, facilitated transport, combined Dankohler 4-95355  
 state correlation diagrams, plotting using SCF MO LCAO method 4-107280  
 stationary wave solns. of reaction-diffusion eqn. derived from FitzHugh-Nagumo eqns. 4-71910  
 strained systems, electrostatic pots., reactive props., ab initio SCF-MO STO-5G calcs. 4-102580  
 symmetry-breaking instabilities under nonclassical bifurcation conditions 4-66553  
 thermal explosions with simultaneous parallel reactions, theory 4-62205  
 thermal ignition in porous media, convection effects 4-79657  
 thermal self-focusing of light beams, possible influence of chem. reactions 4-74633  
 thermal unimolecular reactions with two activation pathways 4-81400  
 thermally activated, internal multiplicative noise, Lindenberg-Seshadri model 4-114763  
 thiobinaphridine monomethiodides, Hofmann degradation products,  $^{13}\text{C}$  NMR 4-112205  
 three-atom reactions, Kramers' theory 4-109637  
 transformation matrices for investigating changes in electronic struct. of reacting mol. 4-85287  
 1,1,2-trichloroethane, acid-catalysed and radical chain transforms. 4-109641  
 1,1,2-trichloroethane, catalytic dehydrochlorination, CNDO/2; INDO and MINDO/3 calcs. 4-91202  
 trifluoromethyl hypochlorite, electron diffr. study 4-87215  
 triplet and cold radical prod. with pulsed elec. discharge in pulsed supersonic flow 4-84090  
 two angle dependent reactive infinite order sudden approximation 4-66551  
 unsaturated organic liquids, muon substituted free radicals 4-83498  
 vibrational intensities, G sum rule formulation 4-89277  
 vinylidene cation, generation and identification, collisionally induced mass spectrum 4-76975  
 Walden inversion reactions, solvent effect 4-66558  
 X-ray diffr. with short time resolution, appl. to chem. reactions and phase transitions 4-81489  
 zirconoanolate anion, reactivity towards ketene complex form., struct. 4-99760  
 $3\text{Y}_2\text{O}_3 \cdot 5\text{Fe}_2\text{O}_3$ , solid state reaction study, IR and mag. props. 4-85301  
 Ar afterglows, conversion reaction rate coeff. and ambipolar diffusion coeff. meas. 4-79877  
 Ar triplet and cold radical prod. with pulsed elec. discharge in pulsed supersonic flow 4-84090  
 Br oxidation reactions, travelling conc. waves parameters determ. 4-62189  
 CO production from C and  $\text{CO}_2$  in plasma arc reactor 4-76978  
 CO triplet and cold radical prod. with pulsed elec. discharge in pulsed supersonic flow 4-84090  
 $\text{CaCO}_3$  crystallisation with chem. absorpt. 4-98038  
 $\text{Cd}(\text{SO}_3\text{F})_2$ , synthesis, Raman spectroscopic obs. 4-66020  
 Co complexes, Co(II)-bisacetylal-o-phenylenediamine-pyridine-complexes,  $\text{O}_2$  interaction study on silica surface 4-62232  
 $\text{Cr} + \text{He}(\text{Ar})(\text{H}_2)(\text{D}_2)(\text{N}_2)(\text{CO})(\text{O}_2)(\text{N}_2\text{O})(\text{NH}_3)$ , intramultiplet mixing collisions, fluoresc. 4-64588  
 Cu alloy with Sn electrode, diffusion reaction, effect of additional Fe and Sn 4-71755  
 Cu-Sn-Cu-Nb composite, reaction annealing,  $\text{Nb}_3\text{Sn}$  layer growth conditions 4-61886  
 $\text{FH}_2$  reaction energies, pot. energy surfaces, ab initio calcs. 4-114789  
 Fe alloy, siliconising, thermodynamic calcs. 4-89191  
 Fe alloys, nitrogenation kinetics, mechanisms, thermodynamics 4-71988  
 GaAs/Ni reactive interface, soft X-ray photoemission spectra studies 4-113820  
 GaSe-metal interface, chem. reactivity 4-71973  
 H+formyl ion (acetyl ion), different activation energies 4-62161  
 $\text{H} + \text{O}^+ (\text{CO})^+ (\text{CH})^+$ , reaction rate coeffs. 4-81427  
 $\text{H}_2$ , ortho-para conversion on mag. surfaces, dynamical aspects 4-70555  
 $\text{HAsO}_2$ , iodate oxidation exhibiting bistability, mushrooms and isolas 4-71961  
 $\text{H}_2\text{SO}_4$  generation, standardisation and dispensing 4-89285  
 $^1\text{H}$  NMR, high resolution, appl. 4-74268  
 $\text{He} + \text{H}_3^+ (\text{D}_3^+) (\text{HD}_2^+)$ , three body dissoc. absolute cross section meas. 4-104984  
 $\text{Hg}(\text{SO}_3\text{F})_2$ , synthesis, Raman spectroscopic obs. 4-66020  
 $\text{I}_2$  photodissoc., picosecond transient spectra, chemical reactions in soln., mol. dynamics 4-85316  
 $\text{I}_2$  photodissociation in liqs., picosecond transient spectra 4-89313  
 InP-Ag interface, reactions and Schottky barrier form., XPS studies 4-92821  
 InP-metal interface, chem. reactivity 4-71973  
 Li/ $\text{SO}_2$  cells, discharge capacity at high current and temp., chem. reactions 4-66679  
 $\text{LiBH}_4$ , nonrigid rearrangement barriers, ab-initio many-body Rayleigh-Schrodinger perturbation theory calcs. 4-68925  
 $\text{Mg}(\text{H}_2\text{PO}_4)_2$  soln., complex form. and phosphate- $\text{H}_2\text{O}$  interactions 4-89256  
 $\text{Mn}_{1-x}\text{Zn}_x\text{Fe}_2\text{O}_4$ , sintering of powders produced by different methods, mechanism and assoc. processes 4-89015  
 $\text{N}_2 + \text{H}_2\text{O}$  in presence of  $\text{TiO}_2$  catalysis, effect of compounded metal on  $\text{NH}_3$  yield 4-62230  
 $\text{NH}_3\text{-N}_2\text{O-Ar}$ , shock-heated, oxidation, conc. time profiles obtained by absorpt. and emission spectra 4-89298  
 NO synthesis in DC arc plasma, modelling, temps., vels., kinetic meas. 4-71914  
 Na+inert gases, collisional relax., two-photon absorpt. spectra 4-78930  
 $(\text{NaI})_2$ , and  $(\text{NaI})$ , thermochemistry, free energy, dimerisation and trimerisation entropy 4-80205  
 $\beta\text{-Na}_2\text{O-Al}_2\text{O}_3$  solid electrolyte, surface degradation in Na-S battery cells 4-65526  
 $\text{Na}_2\text{O-CaO-CO}_2$  system, calcination in air, differential thermal analysis obs. 4-99757  
 Nb oxides, synthesis of new materials based on decomp. with  $\text{HF}_2$  4-66563

**chemical reactions continued**

- Ni(II) complex, with picolines, thermogravimetric characterisation 4-81490  
 O<sub>3</sub> generation in oxygen discharge, numerical model 4-89290  
 O<sub>3</sub> molecular formation in nonselfsustained discharge in air 4-87839  
 O<sub>3</sub>, photolysis, nuclear generation of O<sub>2</sub> 4-62222  
 O<sub>3</sub>, reactions in aq. solns. rate and mechanism, bibliography 4-67909  
 POCl<sub>3</sub>, purification by low temp. sublimation and distillation 4-66255  
 PbO-CO<sub>2</sub>-H<sub>2</sub>O solid systems, stability and solubility rels. 4-84399  
 Pt, black, catalyst/pyroelectric gas sensor using heat of reaction 4-66564  
 Sc<sub>2</sub>O<sub>3</sub>, prep. and struct. props., powder diff. studies 4-71608  
 Si chemical behaviour in fusion reactor liq. Li systems 4-107058  
 SiH<sub>4</sub>, thermal decomposition, absence of free radical processes, gas phase initiation 4-93501  
 Sm compounds, preparation and use in organic chemistry, book 4-95076  
 T recovery from tritiated water by reaction with U 4-86967  
 Ta oxides, synthesis of new materials based on decomp. with HF<sub>2</sub> 4-66563  
 Ti swarf, optimum carbidisation parameters for TiC powder power 4-89014  
 Ti-TiC single crystal diffusion couple, annealing, solid state reaction, C diffusion 4-85133  
 TiAl<sub>3</sub>, powdered, nitriding investig. 4-89189  
 Y<sub>2</sub>O<sub>3</sub>-Fe<sub>2</sub>O<sub>3</sub>, solid state reaction for garnet formation by sintering 4-85302  
 Yb compounds, preparation and use in organic chemistry, book 4-95076  
 ZnBr<sub>2</sub> in N,N-dimethylformamide soln., complex form. and solvation, electron diff. and Raman spectra 4-93502  
 Zn(SO<sub>3</sub>F)<sub>2</sub> synthesis, Raman spectroscopic obs. 4-66020

**chemical reactivity** *see* **chemical reactions****chemical relaxation**

- alkali halide molecules, collisional disoc. and chemical relax. at 2000-4200K 4-89269  
 glass-forming melts, temp.-time dependences, chem. equilib. theory 4-92366  
 glycine zwitterion protonation reactions, thermodynamic props. 4-93513  
 histidine, protonation reaction kinetics meas. using chemical relax. technique 4-9255  
 stream of recombining atoms, chemical reactions and relax. 4-108103

**chemical shift***see also* **isomer shift**

- (3,4)-dimethoxybenzaldehyde chem. shift anisotropy, switching angle sample spinning NMR 4-80826  
 alkali metals, nuclear magnetic props. and solvation, review 4-74179  
 alkaline earth metals, NMR props. 4-74180  
 alkanes, <sup>13</sup>C chem. shift, CNDO-SCF wave function calcs. 4-64375  
 alkanes, branched, isopropyl methyl C <sup>13</sup>C NMR chem. shifts, nonequivalence origin 4-78864  
 n-alkanes in urea inclusion complexes, substituent effects, NMR chem. shift study 4-112206  
 aluminosilicates, correl. between SiOSi angles and <sup>29</sup>Si NMR chemical shift 4-88730  
 N,N'-arylalkyl thioureas, conformation anal. <sup>1</sup>H NMR and IR spectra 4-112178  
 bacteriorhodopsin analogues synthesized from fluorophenyl retinals, XPS study 4-77189  
 benzoid dications, average <sup>13</sup>C chem. shifts 4-96569  
 benzoid hydrocarbons, condensed, PMR chemical shift reflection 4-98968  
 (biphenylmethyl)lithium, charge densities, struct., INDO calcs., <sup>13</sup>C NMR 4-102702  
 bisphenol-A polycarbonate, carbonate mobility, dielectric relax., NMR 4-80829  
 blood, erythrocytes and plasma, human, <sup>23</sup>Na NMR, chemical shift, spin relax., intracellular Na conc. 4-66910  
 3-(carboethoxy)carbazole, spectrochem. props. 4-112227  
 CNDO-SCF wave function calcs. 4-64375  
 copper ternary chalcopyrite semiconductors, NMR studies 4-65874  
 core electron binding energy calcs., X-ray absorpt. edge chemical shifts 4-91216  
 corticosteroids, fluorinated, chem. shifts, coupling consts., <sup>19</sup>F NMR study 4-64513  
 crambin, in organic solvents, tyrosyl ring study, PMR study 4-107476  
 cumene, long range spin-spin coupling consts., isotope shift, <sup>13</sup>C NMR 4-64497  
 3-cyanocarbazole, spectrochem. props. 4-112227  
 cyclophosphazene-diaminopropane derivatives, mass spectra, NMR 4-81423  
 dialkylphosphate ions, <sup>31</sup>P NMR chem. shift and spin-lattice relax., micellisation effects 4-112197  
 dialkylphosphate ions, conform., micellisation effects, <sup>13</sup>C NMR chem. shift and <sup>31</sup>POC<sup>13</sup>C coupling 4-107365  
 diaminotetrachlorotriphosphazenes-SbF<sub>3</sub>(KSO<sub>3</sub>F), fluorinating reaction, <sup>1</sup>F and <sup>1</sup>H NMR study 4-66581  
 diamond (111), clean and adsorbed H<sub>2</sub>, photoemission studies 4-88939  
 1,3-diketones, tautomeric equilib., H bonds, NMR spectra 4-59805  
 diphenyldiselenide, chem. shift anisotropy, <sup>77</sup>Se spin-lattice relax. 4-69112  
 1,3-dithianyllithium, 2-substituted, charge densities, struct., INDO calcs., <sup>13</sup>C NMR 4-102702  
 ethylbenzene, long range spin-spin coupling consts., isotope shift, <sup>13</sup>C NMR 4-64497  
 ethylbenzene, substituent effects, <sup>13</sup>C NMR assignment based on Karplus-Pople eqn. 4-59804  
 ethylene-1-octene (4-methyl-1-pentene), copolymers, chem. shift, <sup>13</sup>C NMR study 4-80828  
 eunicin, cembranoid diterpene, two dims. H<sup>+</sup>-C chem. shift, NMR 4-102704  
 ferrocytochrome c, <sup>1</sup>H chem. shift corrls., 2-dimens. exchange correl. spectrosc. determ. 4-91282  
 fluorenyllithium, 9-substituted, charge densities, struct., INDO calcs., <sup>13</sup>C NMR 4-102702  
 D-glucopyranosides, peracetylation effects on chem. shift, PMR study 4-64495  
 gramicidin S peptide, long range H bond, INEPT chem. shift 4-96568  
 group VI elements other than oxygen 4-73475  
 heteronuclear chemical-shift correlation utilizing homonuclear decoupling and distortionless enhancement by polarization transfer 4-69101  
 hydroxysodalite, crystallisation, high resol. NMR chem. shift 4-114174  
 isaxonine phosphate structure, CNDO MO calc. 4-107466  
**chemical shift continued**  
 lanthanide (III)-Ag (I) NMR shift reagents, secondary D isotope effects 4-102710  
 liquid crystals, mixed, opposite diamagnetic anisotropies, NMR spectra 4-109090  
 malic acid derivatives, chem. shift, <sup>13</sup>C NMR study 4-64514  
 mephobarbital, optical purity determ. and PMR spectral simplification with lanthanide shift reagent 4-87138  
 metal acetates, <sup>13</sup>C chemical shielding anisotropies 4-65871  
 metallotetraphenylporphyrins, interaction with nitrobenzofuroxan, bonding, optical absorpt. and mag. reson. obs. 4-83381  
 methoxybenzene, substituent effects, <sup>13</sup>C NMR assignment based on Karplus-Pople eqn. 4-59804  
 methyl halides, reactions of energetic <sup>11</sup>C, electron density and bond polarisation effects 4-89280  
 methyl iodide, mols. dissolved in mixture of liq. crystals, chemical shift anisotropy determ. 4-64509  
 methyl isothiocyanate, mols. dissolved in mixture of liq. crystals, chemical shift anisotropy determ. 4-64509  
 2-methylindole+mesityl oxide, reaction product, struct. two dims. NMR spectra 4-96567  
 6-methylpurine in aq. soln., relax. behaviour of self-association 4-114780  
 molecules, nuclear shielding, calc. and appl. 4-74174  
 monalkylphosphate ions, <sup>31</sup>P NMR chem. shift and spin-lattice relax., micellisation effects 4-112197  
 monoalkylphosphate ions, conform., micellisation effects, <sup>13</sup>C NMR chem. shift and <sup>31</sup>POC<sup>13</sup>C coupling 4-107365  
 monosaccharides, dil. aq. solns., Ca<sup>2+</sup> ion effects, PMR obs. 4-112208  
 α-nitride-p-tolylmethyl cations, <sup>1</sup>H, <sup>13</sup>C and <sup>15</sup>N spectroscopic data 4-112200  
 α-nitrodiarylmethyl cations, <sup>1</sup>H, <sup>13</sup>C and <sup>15</sup>N spectroscopic data 4-112200  
 NMR chemical shift meas. using heteronuclear field/freq. lock methods, vol. mag. susceptibility corrections 4-65870  
 Nuphar alkaloids, Hofmann degradation products, <sup>13</sup>C NMR 4-64506  
 1-octene copolymers, <sup>13</sup>C NMR characts. 4-65869  
 organic molecules, polarisation transfer 1D expts. for heteronuclear chemical shift correlation 4-64512  
 peptides, Karplus relationship determ. NMR study 4-102703  
 phenol, substituent effects, <sup>13</sup>C NMR assignment based on Karplus-Pople eqn. 4-59804  
 phenoxyethanol, substituent effects, <sup>13</sup>C NMR assignment based on Karplus-Pople eqn. 4-59804  
 1-phenylethanol, <sup>13</sup>C[<sup>2</sup>H] polarisation transfer, isotopic labeling NMR 4-59800  
 2-phenylethanol, substituent effects, <sup>13</sup>C NMR assignment based on Karplus-Pople eqn. 4-59804  
 2-phenylethylamine, substituent effects, <sup>13</sup>C NMR assignment based on Karplus-Pople eqn. 4-59804  
 phosphates, solids, chem. shift anisotropy, <sup>31</sup>P NMR 4-88731  
 PMMA, solns., conformations, <sup>13</sup>C NMR spectra 4-78991  
 polarisation transfer 1D expts. for heteronuclear chemical shift correlation 4-64512  
 poly(ethyl methacrylate), solns., conformations, <sup>13</sup>C NMR spectra 4-78991  
 polybenzyls, struct. characterisation by high-field <sup>13</sup>C NMR 4-105085  
 polymers, helical worm-like chains in dilute soln., NMR 4-98969  
 Propylene-isoprene alternant copolymers struct., <sup>1</sup>H and <sup>13</sup>C NMR spectra 4-112314  
 proteins, two dimensional <sup>1</sup>H-<sup>13</sup>C chemical shift correlated spectroscopy at natural abundance 4-89504  
 pyrazines and its N-oxide, <sup>15</sup>N NMR, chemical shift, shielding effects 4-96576  
 pyridine solns., ion-H<sub>2</sub>O interactions, PMR obs. 4-112207  
 rare earth-transition metal ternary intermetallics, charge transfer, X-ray absorpt. spectro study 4-81037  
 salicylaldehyde derivatives, H<sup>+</sup> spin-spin coupling and chem. shift, PMR investig. 4-64500  
 α-selenocarbenium ions, prep., X-ray mol. struct., PMR and <sup>13</sup>C NMR 4-112203  
 selenoketones, chem. shift anisotropy, <sup>77</sup>Se spin-lattice relax. 4-69112  
 silicates, <sup>29</sup>Si NMR chem. shifts correl. with MO energy differences obtained from X-ray spectra 4-65872  
 silicates, <sup>29</sup>Si NMR chemical shifts, bond angles and strength effects 4-114175  
 silicates, isotropic <sup>29</sup>Si chem. shift correl. with mean Si-O bond lengths 4-71199  
 solution-state NMR studies of group IV elements (other than carbon), review 4-74271  
 structure determination and spectral assignment by pulsed polarization transfer via long-range <sup>1</sup>H-<sup>13</sup>C coupling 4-64510  
 tetraselenafulvenes, substituted, cis/trans assignments, coupling consts., <sup>77</sup>Se NMR 4-102701  
 thermotropic mixed liq. crystals, oriented mols., NMR studies 4-84860  
 thiobinaphridine dimethiodides, stereochemistry, <sup>13</sup>C NMR 4-87135  
 thiobinaphridine monomethiodides, Hofmann degradation products, <sup>13</sup>C NMR 4-112205  
 toluene, long range spin-spin coupling consts., isotope shift, <sup>13</sup>C NMR 4-64497  
 transfer ribonucleic acid, <sup>15</sup>N labelled, PMR, dipolar coupling and chem. shift anisotropy 4-59799  
 2',3',5'-tri-O-benzoyluridine, <sup>15</sup>N labelled, PMR, dipolar coupling and chem. shift anisotropy 4-59799  
 1,2,4-triazines and its N-oxide 4-96576  
 1,3,5-tribromobenzene, mols. dissolved in mixture of liq. crystals, chemical shift anisotropy determ. 4-64509  
 trimethyl phosphate, partially oriented mols., NMR spectra, pot. energy calcs., conformation 4-69107  
 1,3,5-trinitrobenzene, mols. dissolved in mixture of liq. crystals, chemical shift anisotropy determ. 4-64509  
 van der Waals, screening contrib. to NMR chem. shift 4-59807  
 vinyl-chloride-vinyl acetate copolymers, sequential distrib., tacticity, NMR obs. (German) 4-88115  
 X-ray absorpt. edges, chemical shift calcs. 4-99228  
 Al, Ka chem. shifts, MO calcs. 4-59638  
 AlPO<sub>4</sub> polymorphs, chem. shift, bond angles, <sup>27</sup>Al and <sup>31</sup>P NMR 4-109088  
 B<sub>12</sub>C<sub>3</sub>, <sup>13</sup>C NMR study of C distrib. 4-114182  
 Bi<sub>2</sub>Se<sub>3</sub> amorphous film, photoemission study 4-109302  
 CO, chem. shielding and shifts, <sup>17</sup>O NMR 4-102705

**chemical shift continued**

- CO, chemisorbed, physisorbed, and free, high-resolution C 1s and O 1s core-excitation spectra 4-93125  
 CO, solid, combined translational-rotational jumps, <sup>13</sup>C NMR obs. 4-98970  
 CO<sub>2</sub>, chem. shielding and shifts, <sup>17</sup>O NMR 4-102705  
<sup>13</sup>C FT NMR spectra, why it cannot be phased 4-86453  
 CaTiSiO<sub>6</sub>:La sphere-based glass-ceramics, La-partitioning, Auger studies 4-88112  
<sup>113</sup>Cd NMR in bioinorganic chemistry 4-73478  
 Co (III) complex, bis(ethylenediamine) Co (III) <sup>13</sup>C NMR signals, assignment 4-91278  
 Cr complexes,  $\pi$ -electron delocalisation NMR, IR and XPS study 4-87117  
 Cu surface, organic mol. adsorption 4-80409  
 D<sub>2</sub>S, nucl. hyperfine interactions, elec. dipole moments, mol. beam elec. reson. 4-59803  
 DyFe<sub>2</sub> intermetallics, SXAPS studies 4-81039  
 ErFe<sub>2</sub> intermetallics, SXAPS studies 4-81039  
 Fe complex,  $\mu$ -oxo Fe (III) porphyrin dimers, antiferromag. coupling, <sup>13</sup>C NMR spectra 4-64508  
<sup>57</sup>Fe NMR: relax. mechanisms and chem. shifts 4-112201  
 GaAs (110), initial oxidation, core-level photoemission study 4-93195  
 GaP, spinodal decomp., <sup>31</sup>P NMR spectra, chem. shifts 4-76279  
 Ge, dislocations, deep electron levels, recursion calc. 4-70716  
 H<sub>2</sub>S (HDS), nucl. hyperfine interactions, elec. dipole moments, mol. beam elec. reson. 4-59803  
<sup>1</sup>H and <sup>13</sup>C chemical shifts, comparison between theory and expt. 4-74264  
<sup>1</sup>H-<sup>13</sup>C chemical shift correlation maps, homonuclear J couplings suppression 4-88732  
<sup>3</sup>H NMR spectroscopy 4-73472  
 In<sub>0.5</sub>Ga<sub>0.5</sub>P, spinodal decomp., phase segregation, <sup>31</sup>P NMR spectra, chem. shifts 4-76279  
 InP, spinodal decomp., <sup>31</sup>P NMR spectra, chem. shifts 4-76279  
 InP surface decomp. rel. to In M<sub>4.5</sub>N<sub>4.5</sub> Auger spectrum fine struct. 4-81046  
 KCl, gamma irradiation of single crystal, shift in K $\alpha$  line, EPR study 4-114163  
 Mg K $\alpha$  chem. shifts, MO calcs. 4-59638  
 Mo complexes, chem. shift, polar and reson. props., NMR 4-71200  
 N<sub>2</sub>O, chem. shielding and shifts, <sup>17</sup>O NMR 4-102705  
<sup>15</sup>N, (A=14, 15), NMR spectroscopy of mols. 4-74269  
 Na halide mols., vapour-phase Auger electron spectra using electron impact excitation 4-102808  
 $\beta^{\alpha}$ -Na<sub>2</sub>O-Al<sub>2</sub>O<sub>3</sub> solid electrolyte, surface degradation in Na-S battery cells 4-65526  
 (NH<sub>4</sub>)<sub>2</sub>HPO<sub>4</sub>(PO<sub>4</sub>H<sub>2</sub>)<sub>2</sub>Te(OH)<sub>6</sub>, NMR study of phase transition 4-80877  
 Ni, X-ray photoelectron and Auger electron spectra 4-109310  
 NiO, X-ray photoelectron and Auger electron spectra 4-109310  
 OCS, chem. shielding and shifts, <sup>17</sup>O NMR 4-102705  
 QF<sub>2</sub>, chem. shielding and shifts, <sup>17</sup>O NMR 4-102705  
<sup>17</sup>O NMR spectroscopy, appl. to struct. problems 4-74270  
 PbF<sub>2</sub>, cubic, electron-coupled nuclear spin-spin interactions and <sup>19</sup>F chem. shift 4-80827  
 PdH<sub>x</sub>, X-ray photoemission study of electronic struct. 4-84561  
 Pt complexes, electronic effects, PMR, IR and UV spectra 4-78866  
 Pt complexes, platinum diacetylacetonate, <sup>195</sup>Pt spin-lattice relax. and shielding anisotropy 4-96574  
 Pt surface, organic mol. adsorption 4-80409  
 Rh, oxidation adlayers, thermally and electrochemically prepared, chemical nature and thermal stability 4-93464  
 S-containing cpds., <sup>33</sup>S nucl. mag. shielding, chem. shift 4-102699  
 S<sub>2</sub>O<sub>3</sub><sup>2-</sup>, <sup>33</sup>S NMR signal assignment and T<sub>1</sub> study 4-87137  
 Sc, X-ray photoelectron and Auger electron spectra 4-109310  
 Sc<sub>2</sub>O<sub>3</sub>, X-ray photoelectron and Auger electron spectra 4-109310  
 Si (100) 2 $\times$ 1, pre-exposed to O in submonolayer range, chem. shifts of Si-H stretching freqs. 4-80368  
 Si (111)-Mo interfaces, electronic struct., XPS and X-ray excited AES study 4-85085  
 Si, dislocations, deep electron levels, recursion calc. 4-70716  
 Si<sub>3</sub>N<sub>4</sub>, low energy implant depth profiles, surface peak, Auger studies 4-80074  
 Si-Al-O-N phases, struct. studies using magic-angle-spinning NMR 4-71198  
 a-Si<sub>1-x</sub>C<sub>x</sub>-H GD thin film, plasmon behaviour studied by XPS, chem. shifts 4-65627  
 SiN<sub>x</sub>-H, amorphous, electronic struct., photoemission 4-108776  
 SiO<sub>2</sub> polymorphs, correl. between SiOSi angles and <sup>29</sup>Si NMR chemical shift 4-88730  
 Ti, X-ray photoelectron and Auger electron spectra 4-109310  
 TiO<sub>2</sub>, X-ray photoelectron and Auger electron spectra 4-109310  
 TiCl-Ti<sub>2</sub>S mixtures, <sup>205</sup>Ti NMR, shifts, linewidths and relax. 4-109080  
<sup>205</sup>Ti NMR and chem. shift in binary molten salt mixts. 4-61601  
 V, X-ray photoelectron and Auger electron spectra 4-109310  
 V<sub>2</sub>O<sub>5</sub>, X-ray photoelectron and Auger electron spectra 4-109310

**chemical structure**

- see also bonds (chemical); crystal atomic structure; crystal chemistry; molecular configurations*  
 copolyesters, aromatic, liq. cryst. props., role of sequence distrib. 4-84169  
 fast atom bombard. mass spectroscopy for appl. surface anal. 4-82857  
 ferric neurosporin, cryst., chem. and mol. struct., spectral charact. 4-102720  
 heavy oil residue utilisation, chemical aspects 4-62289  
 indandione-1,3 derivatives, substituent effects, chem. struct., IR, UV and fluoresc. study 4-78905  
 main group element cpds., double bonding, review 4-102815  
 merocyanine dyes, solar photovoltaic cells, performance correl. with mol. struct. 4-85369  
 metal-S cpds., quantitative AES, effects of chem. struct. 4-85046  
 phosphazo compounds, basicity, substituent effects 4-59662  
 polycapromide obtained in anionic polymerisation of caprolactam, chemical and physical props. 4-92056  
 polyesters, liq. cryst. props. rel. to chem. struct., DSC, miscibility, and X-ray diffr. studies 4-84170  
 polyesters, main chain, thermotropic liq. cryst. props., effect of mesogenic unit and spacer structs. 4-84168  
 pullulan, solid, thermally stimulated current 4-113969  
 SIMS, static, in appl. surface anal. 4-82857

**chemical structure continued**

- solar energy, chemical storage, demonstration using colour change 4-90334  
 transplutonium research, accomplishments and practical appl. 4-59661  
 vinyl alcohol-vinyl acetate copolymer, water-soluble, chem. and intramol. struct. (Russian) 4-102840  
 vinylpyrrolidone-divinylbenzene copolymers, template effect in binding of methyl orange 4-108289  
 $\sigma$  conjugation, chem. effects 4-74128  
 SF<sub>6</sub>, struct. exchange, intramol. vibr. redistrib., NMR investig. 4-59798  
 Se<sub>1-x</sub>Te<sub>x</sub> alloys, amorphous, elastic consts., role of Te 4-84333  
 V<sub>2</sub>O<sub>5</sub>-P<sub>2</sub>O<sub>5</sub> and V<sub>2</sub>O<sub>5</sub>-P<sub>2</sub>O<sub>5</sub>-TeO<sub>2</sub> glasses, IR absorpt. and struct. investig. 4-61670
- chemical technology**  
*see also chemical industry; chemical variables control; chemical variables measurement; oil refining*  
 biotechnology for industrial chemistry (German) 4-114880  
 bubble column with suspended solids, gas-liq. interfacial areas 4-65003  
 coal liquefaction, solvent N content effects 4-99937  
 counter-current adsorbers, continuous, axial dispersal plug flow model 4-60544  
 countercurrent gas-liquid reactors near gas flooding condition, axial liq. dispersion 4-97708  
 mobile bed contactor with low-density packing particles, hydrodynamics 4-60536  
 multitubular polymerisation reactors, uniform flow distrib. stability 4-99786  
 packed column, combined state and parameter estimation 4-65017  
 packed distillation columns, Marangoni effect 4-64935  
 PNP-500 HTR process heat installation, tritium balance and possible contamination 4-99952  
 reactor, modelling and numerical simulation 4-109335  
 sequential experimental design for model discrimination in the case of multiple responses 4-63484  
 three-phase systems, continuous contact, separation calcs. 4-99821  
 HCN, stripping in a packed tower, Henry's law const. meas. 4-62173  
 PaV extraction with 2-thenyltrifluoroacetone from strongly acidic solns. 4-72034

**chemical vapour deposited coatings** *see CVD coatings***chemical vapour deposition**

- see also vapour phase epitaxial growth*  
 cascade solar cells, future prospects using organometallic CVD growth technique 4-89414  
 cold wall reactor, temp. field determ. by holographic interferometry 4-71590  
 conference, Neuchatel, Switzerland (April 1980) 4-67868  
 convective transport in closed and open tube systems, gravity effects 4-65203  
 deposited dielectric for III-V semiconducting devices 4-84702  
 deposition diagram computation from solid solution thermodynamic functions 4-71582  
 diamond, amorphous film deposition using generation/reaction of methylene species 4-104739  
 homogeneous CVD growth, review 4-88984  
 laser CVD using CW and pulsed lasers 4-109330  
 laser induced chemical vapor deposition 4-81157  
 low pressure 4-81143  
 low pressure CVD at quasi-high flow 4-76686  
 materials for optical communications, review 4-61833  
 moderate temperature deposition using complex chloride reduction 4-71585  
 modified chemical vapor deposition process chemistry 4-91651  
 monomode diplex fibre manufacture by PCVD process 4-91657  
 monomode optical fibres and preforms, elemental distrib., electron microprobe investig. 4-79318  
 multimode diplex fibre manufacture by PCVD process 4-91657  
 multimode graded-index fibres, optical meas. during manufacture using MCVD process 4-97160  
 natural convection in sealed tube for crystal growth by gas phase transport 4-71538  
 nitride insulating films, CVD using NF<sub>3</sub> 4-85108  
 optical fibre fabrication, dehydration kinetics with soot densification in VAD process 4-97156  
 optical fibre fabrication, F doping levels in low press. PCVD process 4-91656  
 optical fibre fabrication, GeO<sub>2</sub> behaviour in dehydration and consolidation processes of VAD method 4-97155  
 optical fibre fabrication by  $\phi$  F<sub>2</sub> doping in VAD sintering process 4-91608  
 optical fibre manufacture, laser modification of thermophoretic deposition of aerosol 4-60186  
 optical fibre manufacture by MCVD and RFMCVD, developments 4-91650  
 optical fibre manufacture by PCVD, update 4-91655  
 optical fibre preform core/outside diameter ratio control using substrate glass evaporation technique 4-97157  
 optical fibre preforms fabrication by modified CVD, reactants purity problems 4-69611  
 optical fibres, radiation resistant, low-pressure PCVD fabrication process, F doping level study 4-107914  
 optical fibres, single-mode, fabrication techniques (French) 4-87469  
 optical fibres, single-mode, manufacture by VAD, latest developments 4-91646  
 optical fibres, vapour-phase axial deposition method for high numerical aperture fibres (Japanese) 4-60187  
 optical fibres manufacture by Philips Plasma-activated Chemical Vapour Deposition process (Dutch) 4-87456  
 optical VAD single-mode fibre fabrication techniques for dispersion free design 4-103040  
 optical waveguide fibre preforms, X-ray microanal. 4-79319  
 plasma fireball process for lightguide fibre production 4-74761  
 poly-p-xylylene, synthesis, epitaxial growth 4-88428  
 powder particle deposition rate rel. to flame vel. profile 4-85110  
 precautionary design of CVD systems 4-71589  
 quartz glass, synthesis from gas phase, struct. form. on surface 4-70040  
 RF plasma enhanced CVD in capacitively coupled reactor 4-81147  
 semiconductor wafer low pressure CVD processes, cylindrical sleeve technique for deposition uniformity improvement 4-71571  
 semiconductors and refractory metals, plasma enhanced CVD growth 4-88983

**chemical vapour deposition continued**

- single mode depressed cladding fibres, optical meas. during manufacture using MOCVD process 4-97160
- single mode fibre fabrication, depressed cladding, F doping in consolidation process of VAD sput preform 4-97154
- single-mode fibre fabrication techniques for large capacity transmission systems 4-64800
- stratified media technology, conf., Los Angeles, CA, USA (Jan. 1983) 4-82585
- TEXTOR liners and limiters surface conditioning by plasmachemical C deposition 4-108183
- thin gate oxides, dual two. step trichloroethylene oxidation growth 4-81151
- transition metal plasma enhanced CVD 4-88978
- transition metal silicide films plasma enhanced CVD 4-88978
- VAD graded-index optical fibre fabrication 4-103039
- VAD optical fibre preform fabrication system, improvement 4-103038
- VAD optical fibre preforms, high rate fabrication technique 4-103041
- VAD single mode fibre with depressed cladding layer, characts. 4-107832
- wafer support for low pressure CVD, stackable flat plate design 4-109328
- AlAs, MOCVD growth 4-99329
- AlN, CVD films, stability, surface morphology. CVD conditions 4-70604
- Al<sub>2</sub>O<sub>3</sub> doped VAD fibres, props. 4-103043
- Al<sub>2</sub>O<sub>3</sub> gate dielectric grown on InP using indirect plasma-enhanced CVD technique 4-104529
- Al<sub>2</sub>O<sub>3</sub> on cemented carbide, CVD coating, non-equilibrium conditions 4-71598
- B, amorphous, CVD diagrams, nucleus density 4-71583
- B, CVD, anal. 4-88985
- B fibre encapsulation, gas phase point by point anal. by Raman scatt. 4-71591
- B<sub>2</sub>C, hardness and fracture toughness rel. to stoichiometry 4-62019
- BN gate insulators, CVD growth on InP, ellipsometry, XPS, AES, cond. meas. 4-80443
- C amorphous film growth by CVD, methane plasma diagnostics and modelling 4-104979
- C-C-TiC composite materials obtained by CVI of porous C-C substrates 4-71595
- CdTe large single cryst. grown from vapour phase, polarity 4-70048
- CuAlTe<sub>2</sub> single cryst., CVD growth and elec. characterisation 4-114366
- CuGaTe<sub>2</sub>, vapour growth, thermodynamics and elec. characts. 4-71536
- CuInTe<sub>2</sub>, vapour growth, thermodynamics and elec. characts. 4-71536
- Fe films, organo-metal CVD growth from (CO)<sub>2</sub>Fe+AsH<sub>3</sub> on GaAs 4-61868
- FeAs<sub>2</sub> films, organo-metal CVD growth from (CO)<sub>2</sub>Fe+AsH<sub>3</sub> on GaAs 4-61868
- Fe<sub>2</sub>-Cr<sub>2</sub>O<sub>3</sub>, chem. transport of haematite with TeCl<sub>4</sub> as transporting agent 4-61824
- α-Fe<sub>2</sub>O<sub>3</sub> CVD coating on alumina high temp. stable catalyst for SO<sub>2</sub> conversion to SO<sub>3</sub> in hydrogen production process 4-66807
- finies in fluidized bed silane pyrolysis 4-81149
- (GaAl)As transverse-mode stabilised laser diodes, MOCVD growth 4-96912
- Ga<sub>1-x</sub>Al<sub>x</sub>As:Zn, (Se), doping in MOCVD growth, carrier conc. and cond. 4-88982
- GaAs epitaxial layers, MOCVD, surface morphology and elec. props. 4-84493
- GaAs, film growth on insulators by artificial epitaxy 4-61873
- GaAs, MOCVD growth, doping profiles, H<sub>2</sub>Se memory effects 4-81152
- GaAs, MOCVD growth 4-99329
- GaAs single domain growth on Ge (100) by MOCVD 4-99342
- GaAs:Si, Si doping from Si<sub>2</sub>H<sub>6</sub> in MOCVD growth 4-75459
- GaAs/AlGaAs, MOCVD growth and homogeneous nucleation 4-99340
- GaAs/GaAlAs DH stripe geometry lasers, Be-implanted, MOCVD growth 4-70635
- GeO<sub>2</sub>-Sb<sub>2</sub>O<sub>3</sub> optical fibres fabricated by vapour-phase axial deposition method 4-107855
- GeO<sub>2</sub>-SiO<sub>2</sub> optical fibres, CVD, gas phase equil., thermodynamics calcs. 4-109329
- HgCdTe, growth, props. and appls. 4-66217
- In<sub>2</sub>O<sub>3</sub> films, excimer laser induced CVD 4-76679
- InP films, excimer laser induced CVD 4-76679
- MgIn<sub>2</sub>Se<sub>4</sub>, layered epd., cryst. growth 4-93205
- MgO film, synthesis by CVD, textural characts. 4-71568
- Mo foil and films preparation, by decomposing MoCl<sub>5</sub> vapour 4-93231
- Nd:SiO<sub>2</sub> glasses prep. by axial injection plasma torch CVD 4-93229
- PbTiO<sub>3</sub> thin films, CVD prep. and dielec. props. 4-104736
- Pt film deposition by laser chemistry, struct., formation 4-114418
- Si alloy thin film amorphous solar cells, roll-to-roll continuous prod. 4-114903
- Si, CVD, coupled fluid mechanics and chem. kinetics, math. model 4-61867
- Si, CVD growth, solid state phase transformations 4-70598
- Si, CVD in low press. discharge, overview 4-114421
- Si, chem. vapour deposition, rel. to unimol. decomp. of SiH<sub>4</sub> 4-71900
- Si, epitaxial growth, pyrolysis of SiH<sub>4</sub>, influence of H<sub>2</sub> or Ar carrier gas 4-76682
- Si film growth from SiH<sub>4</sub> in CVD and plasma-enhanced CVD systems 4-114419
- Si, low pressure CVD growth and phys. props. 4-81150
- Si, polycrystalline, LPCVD by H reduction of dichlorosilane 4-71570
- Si, polycrystalline films formed by CVD, surface morphology 4-70588
- SiC layers, CVD growth, microstruct. and resist. 4-70599
- Si:H, amorphous, CVD growth by Si<sub>2</sub>H<sub>6</sub> pyrolysis in hot wall reactor 4-61864
- Si:H, amorphous solar cells, CVD growth 4-66694
- Si:H, B(P), amorphous CVD layer, impurity doping 4-60941
- Si:H amorphous films, laser CVD by ArF excimer laser photodissociation of Si<sub>2</sub>H<sub>6</sub> 4-61859
- a-Si:H films, CVD growth, phys. props. 4-92715
- a-Si:H/a-Ge:H/a-Si<sub>1-x</sub>C<sub>x</sub>/a-SiN<sub>x</sub>:H superlattices, CVD growth and struct. 4-114416
- Si-Mo Schottky barriers formation by Mo films CVD growth 4-89695
- SiC cubic single cryst., CVD prep. and elec. props. 4-99345
- SiC in-depth CVD within porous C-C materials 4-71594
- SiC ultrafine particle preparation by CVD method (Japanese) 4-76716
- Si<sub>3</sub>N<sub>4</sub> film deposition by plasma-enhanced CVD, appl. to GaAs LSI 4-71569
- Si<sub>3</sub>N<sub>4</sub> film deposition on Si (Rumanian) 4-81155

**chemical vapour deposition continued**

- Si<sub>3</sub>N<sub>4</sub> films, electron beam assisted CVD, conformal step coverage 4-61869
- Si<sub>3</sub>N<sub>4</sub> films, plasma enhanced CVD, transient phenomena 4-93225
- Si<sub>3</sub>N<sub>4</sub> surface oxide film growth by CVD, XPS anal. (Chinese) 4-61805
- Si<sub>3</sub>N<sub>4</sub>:F films, plasma enhanced CVD, insulating props. 4-61865
- Si<sub>3</sub>N<sub>4</sub>:H, amorphous, CVD growth 4-60941
- SiO<sub>2</sub> CVD preform for optical fibre production OH conc. profiles 4-112579
- SiO<sub>2</sub> film, low temp. CVD, etching kinetics 4-99614
- SiO<sub>2</sub> film, photo-induced CVD using direct excitation by D<sub>2</sub> lamp 4-61860
- SiO<sub>2</sub> films, chemically vapour deposited from SiH<sub>4</sub>-O<sub>2</sub>-N<sub>2</sub> mixtures 4-76885
- SiO<sub>2</sub> films, electron beam assisted CVD, conformal step coverage 4-61869
- SiO<sub>2</sub> films, plasma enhanced MOCVD, MOSFET fabrication 4-81153
- Si<sub>3</sub>O<sub>2</sub>N<sub>2</sub> thin-film waveguides, low temp. plasma CVD 4-107887
- SmS thin film phase transition material, optical switching, CVD fabrication 4-112538
- Sn film deposition by laser chemistry, struct., formation 4-114418
- TeCl<sub>4</sub>, transporting agent for CVD 4-71584
- TiC on cemented carbides, CVD layer, total C contrib. to growing layer 4-71597
- TiC-Ni<sub>3</sub>C solid solns., theoretical CVD conditions 4-61857
- TiN, deposition, factorial design method of CVD process 4-71588
- TiO<sub>2</sub> whiskers, vapour phase growth by TiF<sub>4</sub> hydrolysis 4-70609
- W, CVD, selective low press., kinetics study 4-99332
- W CVD films, selectively deposited, elec. props. 4-88609
- Zn chalcogenides, MOCVD growth 4-93227
- ZnS, CVD, vacancy-hydride complex, optical absorpt., photoluminesc. 4-60916
- ZnSe films, low press. MOCVD growth and elec. and optical props. 4-93230
- ZnSe films, MOCVD growth using diethylselenide 4-61872
- ZnSe, visual grading method, new surface and bulk absorpt. values 4-83732
- chemical variables control**  
see also pollution detection and control
- polyether polyol monitoring using on-line near IR process photometers 4-99930
- PWR power plant radioactivity, effect of coolant chemistry 4-68800
- reactively-deposited compound thin film composition control, optical emission spectroscopy monitoring 4-85101
- River Nile, decentralised control of water quality 4-105617
- O<sub>2</sub> partial pressure control by solid state electrolyte cell 4-62277
- chemical variables measurement**  
see also chemical analysis; moisture measurement; pollution detection and control
- biological systems, concentration meas., continuous, optical fluorescence sensors 4-85584
- catalytic flammable gas sensing elements, high methane concentrations influence obs. 4-95403
- catalytic flammable-gas sensing elements, poison resistance obs. 4-95404
- combustion products analysis, using dilution tunnel system 4-62266
- cyclic water splitting process, evolved H<sub>2</sub> and O<sub>2</sub> measurement by electrochemical method 4-62209
- gas selection valve for semiconductor gas sensor 4-58840
- gas sensors, MOS and catalytic, comparison 4-82787
- industrial effluent control, meas. techniques (German) 4-72203
- interdigitated electrode structures appl., polymer covered, CO, CO<sub>2</sub>, CH<sub>4</sub> and H<sub>2</sub>O sensing 4-95401
- material concentration in liq. media, dual freq. monitoring method (Russian) 4-81488
- metal refinery on-stream, X-ray fluorescence analyser appl. 4-114878
- MOS integrated sensors, electrochem. and charge-imaging effects 4-82786
- nuclear power station water-stream circuits gas chromatographic measurements (German) 4-85343
- remote fibre fluorimetry for on-stream analysis 4-72007
- seawater chem. anal., microprocessor-controlled in situ water sampler 4-72744
- seawater temperature and salinity determ. by laser Raman spectroscopy 4-77654
- sensor research at laboratory of applied physics at Linköping 4-11116
- shell and tube slurry heat exchangers, slurry concentration and flow rates meas. 4-60554
- water vapour conc. meas. by gas chromatography anal. 4-89364
- CO sensitivity and response time of SnO<sub>2</sub> gas sensors 4-86394
- CO<sub>2</sub> conc. in air, meas. using fluidic oscillator (Italian) 4-114862
- H concentration measurement, by thermocompensated ultrasonic detector 4-112660
- K, Th, U, oil reservoirs evaluation by gamma ray spectral logging and pulsed neutron application 4-62990
- KH<sub>2</sub>PO<sub>4</sub> crystal growth from aqueous solution, in-line bulk supersaturation measurement by electrical conductometry 4-114371
- NO meas. in troposphere and stratosphere, using balloon-borne chemiluminescent sonde 4-115617
- O<sub>2</sub> gas sensors using solid electrolyte, miniature rugged design 4-86401
- O<sub>2</sub> potentiometric sensor based on LaF<sub>3</sub> (Japanese) 4-86395
- T gas monitoring system using digital integrating circuit (Japanese) 4-77043
- chemically reactive flow**
- bimodal cellular flames bifurcation in vertical channels, flame propag. 4-99796
- boundary layer control by means of strong injection, wall jet problem 4-97710
- bubble columns, mass transfer meas., axial dispersion model appl. 4-75095
- centrifugal annular reactor with radial flow, reaction kinetics, ang. vel., gas flow rate 4-65034
- cocurrent and countercurrent flow wetted-wall column, chem. reaction, penetration theory soln. 4-79676
- combustible media, two dimens. nonstationary flow, visualisation study 4-69836
- combustion studying using optical techniques (Italian) 4-66591
- countercurrent gas-liquid reactors near gas flooding condition, axial liq. dispersion 4-97708
- cylindrical stretched flame, ignition-extinction behaviour 4-109650

- chemically reactive flow continued**  
 detonation waves, transmission through orifice, geometry effects 4-103366  
 diatomic gas, dissociating, coeffs. of additional terms of hydrodynamic eqns. 4-113075  
 diazo coupling reactions, mixing, models and expts. 4-65036  
 dispersion of a soluble matter in a porous medium channel with homogeneous and heterogeneous chemical reaction 4-69823  
 drops, chemically reactive, convective heat and mass transfer 4-112850  
 ethanol droplets, evap. and condensation rates deduced from struct. resonances in fluorescence spectra 4-91304  
 fast reactions in turbulent fluids, deform. of material elements 4-65035  
 flame stability inside refractory tube 4-103430  
 flames, laminar, thickness, definition 4-108141  
 free-falling multicomponent droplets, combustion and microexplosion 4-103388  
 fuel injection influence on struct. of near wake 4-97709  
 fuel-air homogeneous mixture, turbulence effects on combustion 4-97497  
 gas flows in shock tunnels, modelling 4-60560  
 gas jet, low-calorific value, combustion in cross-flow, flame stability problem 4-75096  
 gun exhaust plumes, ignition 4-81438  
 holographic interferometry method study 4-69833  
 hydrocarbon flames, ion current calc., temp. depend. 4-89296  
 iodate-arsenite systems, bistability and chemical waves form. 4-85303  
 ion current calc., temp. depend. 4-89296  
 kinetics, singularly perturbed problem 4-87814  
 laser diagnostics, techniques and appls. 4-65039  
 liquid films, falling, mass transfer kinetics, nonlinear effects influence, gas absorpt., chemical reaction 4-103433  
 liquid flow over chemically reactive particle, conc. and temp. fields 4-79677  
 mass transfer in the flow of a chemically reacting gas in a granular bed 4-79678  
 methane flames, high temp., laminar flow, stagnation point heat transfer 4-65037  
 methane-air premixed turbulent flames time resolved density meas. 4-99787  
 moving boundary diffusion problems, pseudo-steady state approx. 4-65004  
 Ostwald-de-Waele liquid flow in circular tube, mass transfer 4-103372  
 plane and curved flame stability 4-99795  
 PMMA, limiting combustion regimes in free convection absence 4-71921  
 polymerising flow, turbulent, in long pipes, laminarisation 4-87813  
 porous systems, nonstationary convective combustion eqns., qualitative anal. 4-71923  
 premixed jet flame, flow field struct. meas. 4-97628  
 propane gas flow around heated cylinders, heat transfer, temp. and pyrolysis effects 4-75005  
 radioactive flow, electric fields from ion recombination effects 4-103435  
 reacting shear layer, turbulent mixing and combustion 4-113074  
 reactive surface, oxidation in liq. flow, film boiling 4-97707  
 rocket nozzles, subsonic and transonic chemically reactive flow computation 4-87772  
 shock tube-mass spectrometer system for chem. reaction studies 4-86499  
 single particle combustion calc. 4-71925  
 solar thermal H<sub>2</sub> production by direct flux chemical reactor 4-66813  
 solid-fuel combustion in fluidised bed, two-phase model 4-71926  
 sonic detonation wave acceleration in perfect adiabatic fluids 4-112952  
 spark-ignition engine, combustion, flame photographs 4-87811  
 stationary wave solns. of reaction-diffusion eqn. derived from FitzHugh-Nagumo eqns. 4-71910  
 stream of recombining atoms, chemical reactions and relax. 4-108103  
 supersonic nonequilibrium flow channel design, plane and axisymm. 4-103420  
 thermal explosion theory for partially insulated reactants 4-87746  
 thermal ignition in porous media, convection effects 4-79657  
 turbulent combustion, in premixed flame, theory and expt. 4-103429  
 turbulent combustion, press. effect on mol. gas props. 4-71920  
 turbulent diffusive combustion, CO form. study 4-71922  
 turbulent gas flame, sound radiation mechanism 4-71919  
 turbulent nonpremixed combustion, stretched laminar flamelet model 4-103431  
 two-phase axisymmetric flow through nozzle, anal. with correction for channel walls ablation 4-65008  
 unmixed gases in channel, supersonic combustion charact. 4-69832  
 unsteady reacting muzzle exhaust flow, flow field and vel. meas. 4-60563  
 weakly conducting fluid, turbulent flow in pipe, boundary current fluctuations 4-108110  
 woodburning stoves, turbulent shear flow, two-dimens. anal. soln. 4-87688  
 H<sub>2</sub>-air mixtures, high-speed turbulent deflagration and transition to detonation 4-103432  
 K<sub>2</sub>SO<sub>4</sub>+methane, mass transfer in granular bed 4-79678  
 N+NH<sub>3</sub> (H<sub>2</sub>S) (formaldehyde), spectrophotometric studies 4-114793  
 N<sub>2</sub> dusty gas reactive flow, relax. zone behind normal shock waves 4-60460

## chemiluminescence

- alkali atom+SCl<sub>2</sub>, chemiluminesc., vibr. population inversion in B state of S<sub>2</sub> 4-89303  
 luminol, chemiluminesc. oxidation, investig. of catalytic decomp. of H<sub>2</sub>O<sub>2</sub> 4-62188  
 marine bioluminescence, remote sensing, role of in-water scalar irr. 4-85679  
 molecular luminescence and its applications, conf., Kharkov, USSR (1982) 4-106094  
 nitromethane, chemiluminesc. products form. from ArF laser-induced decomp., implications to explosive chemistry 4-89302  
 organoluminophores, solns., elec. generated chemiluminesc. 4-104687  
 oscillatory chemiluminescent reaction, chaos 4-109625  
 polycyclic aromatic hydrocarbons, nitrated, in diesel particulates, gas chromatographic obs. 4-114854  
 n-propyl nitrate, chemiluminesc. products form. from ArF laser-induced decomp., implications to explosive chemistry 4-89302  
 supersonic beam-gas conditions, chemiluminescence polarisation meas. 4-89305  
 ultraweak, monitoring of emission from rat hearts 4-93979  
 Ba+ICl(I<sub>2</sub>), chemiluminescence broad emission study 4-114801  
 Ba+N<sub>2</sub>O chemiluminescent reaction obs., quadrupole mass filter appl. (Chinese) 4-104993

## chemiluminescence continued

- BaO\* (A<sup>2</sup>Σ), vibr. relaxation and electronic quenching in Ar and N 4-107442  
 C+SO<sub>2</sub>, chemiluminesc. reaction dynamics, vibr. energy distrib. 4-93531  
 C<sub>2</sub>, elementary gas phase processes, laser kinetic spectroscopy 4-69054  
 CH+NO (O<sub>2</sub>), chemiluminesc. obs., rate const. meas. 4-93505  
 D+NO chemiluminescence reaction, DNO internal energy distrib. 4-71871  
 DF+N<sub>2</sub>(CO)(CO<sub>2</sub>)(N<sub>2</sub>O), vibr. relax. rate const. determ. using flow IR chemiluminesc. technique 4-89273  
 H+NO chemiluminescence reactions, HNO(A<sup>2</sup>A'') internal energy distrib. 4-71871  
 HF+CO, vibr. relax. rate const. determ. using flow IR chemiluminesc. technique 4-89273  
 H+HI(HBr), crossed beam reaction, chemiluminescence study 4-77012  
 NH<sub>3</sub>+O, absolute rate const. 4-66557  
 NO+O<sub>2</sub>, chemiluminescent reaction cross section, NO orientation effects 4-109666  
 NO+O<sub>2</sub>→NO<sub>2</sub>+O<sub>2</sub> reaction, O<sub>3</sub> rot. energy effect, crossed mol. beam study 4-71933  
 NO(B<sup>2</sup>Π), specific prod. from recombination of NO on Ni surface, chemiluminesc. 4-89304  
 N(S), recombination kinetics Vegard-Kaplan chemiluminescence bands 4-109629  
 Na+CCl<sub>4</sub> reaction, chemilum. spectra, quenching and vibr. relax. rates 4-66583  
 Pb+O, reaction, chemiluminesc. characterisation 4-99799  
 Xe\*+HCl, supersonic beam-gas conditions, chemiluminescence polarisation meas. 4-89305

## chemioception

- glycoprotein mucose, FIR props. 4-96727  
 olfactory bulb and cortex, spatial organisation of EEGs 4-77268  
 olfactory bulb EEG in rats, freq. anal. 4-93768  
 olfactory evoked responses, EEG obs. in malnourished rats 4-93767  
 taste-aversion learning in rats rel. to 60 Hz elec. field exposure 4-100233

## chemisorption

- acetylene, chemisorption on Pt black, vibr. modes, neutron inelastic scatt. study 4-71970  
 binary alloy surface segregation, modelling, low index planes, steps, kinks, and chemisorption 4-92495  
 bonds, quantum chem. studies 4-80415  
 complex systems, local structures, X-ray absorpt. near edge struct. spectra 4-66112  
 diatomic molecules, chemisorption processes, bond length determination using XANES 4-64494  
 dissociative chemisorption, number of involved metal atoms 4-98432  
 empty electronic states, inverse UV photoemission 4-104715  
 energy and entropy 4-80412  
 ethylene, chemisorption on Pt black, vibr. modes, neutron inelastic scatt. study 4-71970  
 graphite surface, H chemisorpt., MINDO/3 cryst. orbital LCAO SCF calc. 4-98430  
 hydrogenous species, adsorbed, vibr. spectrosc., inelastic incoherent neutron scatt. 4-70574  
 metal clusters and chemisorption on metals, LDF, X<sub>α</sub>, Hartree-Fock, CI and valence band calcs. 4-88397  
 metal surface, chemisorption, two-electron bond approach 4-113801  
 metal surfaces, electronic damping of at. and mol. vibrs. 4-70567  
 metal surfaces, electronically excited states of adsorbates, EELS 4-88917  
 metals, impurity states, positron states and chemisorption, theoretical studies 4-70706  
 metals, of nucl. spin polarised alkali atoms, NMR study 4-80374  
 metals, surface core level shifts, synchrotron radiation photoemission obs. 4-93184  
 metals with adsorbed CO and N<sub>2</sub>, anomalous electronic and vibr. props. 4-98441  
 molecular vibrations at surfaces, spectral studies, review 4-87098  
 oxides, surface props. at high temps., work function studies 4-98697  
 remote spectroscopic sensing of chem. adsorption using single multimode optical fibre 4-89355  
 semiconductor substrates, with adsorbed metallised atom submonolayers, cooperative phenomena 4-70556  
 square lattice with c(2×2) overlayer, critical temp. approx. 4-92516  
 sticking probability, coverage depend., extended Kisliuk model 4-108719  
 surface structure determ. by XANES 4-99226  
 TOF spectra, phenomenological models 4-108724  
 transition metals with chemisorbed NH<sub>3</sub>, acceptor and donor functions 4-70568  
 transuranics, chemisorption from seawater, in-situ meas. technique 4-105057  
 vibrational, electronic and struct. props., book 4-78067  
 Ag (100), chemisorbed Cl, hard square model, expt. evidence 4-88394  
 Ag, chemisorption of noble gases, excited states and decay mechanisms 4-98436  
 Ag electrode, chemisorbed cyanide molcs., surface-enhanced Raman scatt. development 4-70575  
 Ag halides, halide ion and Ag<sup>+</sup> adsorption, interaction pot. 4-75785  
 Ag surface low-index faces, normal Raman scatt. from adsorbed pyridine 4-88838  
 Al (100), of Ar, dipole moment and interaction energy 4-98452  
 Al (111), O chemisorption LCAO-X<sub>α</sub> method anal. 4-113799  
 Al, Auger electron emission in LVV peak region, continuous background struct., O<sub>2</sub> partial press. effect (French) 4-66140  
 Al, chemisorption of noble gases, excited states and decay mechanisms 4-98436  
 Al surface, of O, cluster and slab model calcs. 4-70559  
 Al thin film with chemisorbed H, chemisorption effect an elec. cond. 4-88391  
 Au, chemisorption of noble gases, excited states and decay mechanisms 4-98436  
 Au, of O<sub>2</sub>, AES, XPS, and thermal desorption study 4-92556  
 Au-TiO<sub>2</sub>-Ti structures, RF sputtered, O adsorption effects on diode I-V characts. 4-98455  
 B cluster surfaces, of H<sub>2</sub>, ab initio RHF calc. 4-92555  
 CN, chemisorbed on Ag island film, depolarisation effects in Raman scatt., classical microscopic local field 4-88832  
 CO chemisorbed layer on Ni (100), vibr. spectroscopy by IR emission 4-98439  
 CO two-dimens. clusters, of CO 4-108725

## chemisorption continued

- CO, weakly chemisorbed, correl. between anomalous electronic and vibr. props. 4-78910  
 CaO (100), SO<sub>2</sub> chemisorption, metal adsorbates effects, XPS study 4-113807  
 Cd-CdO solid solns., <sup>113</sup>C NMR investig. 4-98977  
 Cu (001) with chemisorbed K monolayers, rotational epitaxy study 4-70566  
 Cu (100) with chemisorbed CO, chemisorption bond and N<sup>+</sup>-molecule reaction 4-80380  
 Cu (110), clean and O covered, ethylene adsorption, UPS studies 4-70548  
 Cu (111), adsorption and chemisorption of water vapour, electron beam damage of adlayer 4-80397  
 Cu (111), chemisorbed acetylene, vibr. props., EELS studies 4-65567  
 Cu, chemisorption of noble gases, excited states and decay mechanisms 4-98436  
 Cu, electrode, chemisorbed cyanide mols, surface-enhanced Raman scatt. development 4-70575  
 Cu films, CO-covered, optical and elect. props. 4-80693  
 Cu surface, lone pair ligand interaction, bonding, constrained space orbital variation method 4-114823  
 Cu surface, of S and O on cylindrical crystals 4-61223  
 Fe (100) with chemisorbed S, electronic struct. study 4-92779  
 Fe (110), H chemisorbed overlayer, Monte Carlo studies 4-113816  
 Fe (110), of H, ordered struct. form. on metal surface, role of multi-atom interactions 4-80400  
 Fe (110) with chemisorbed Br, LEED and ARUPS study 4-92518  
 Fe<sub>2</sub>(10)p(2×2)-S, surface ferromagnetism, chemisorption, adsorbate-induced substrate reconstruction effect, spin-polarised LEED calcs. 4-80395  
 Fe, BCC, interaction with H, ab initio/effective core pot. cluster calc. 4-108722  
 Fe catalyst for NH<sub>3</sub> synthesis, surface struct. and reactivity study 4-80355  
 Fe surface, (111), N<sub>2</sub> chemisorbed,  $\pi$ -bonded complex, the precursor for dissociation 4-105029  
 Fe-C-Ti, liquid system, surface tension under H<sub>2</sub> atm. (Japanese) 4-65517  
 GaAs (110), H<sub>2</sub>O chemisorption and Ga and As species-specific densities of states 4-80373  
 GaAs (110), O<sub>2</sub> chemisorption, photon simulation, AES and EELS studies 4-113804  
 GaAs (110) with adsorbed H, H<sub>2</sub>, temp. programmed desorption study 4-92528  
 GaAs, MBE growth, role of As and As<sub>2</sub> in controlling quality, theoretical studies 4-98477  
 Ge (111) with chemisorbed Sm, photoemission spectra 4-80392  
 Ge/Al interface, chemisorption and metalisation, electronic struct. 4-92527  
 H<sub>2</sub>, field promoted, surface catalyzed formation on transition metals 4-66616  
 Mg (0001), O chemisorption, LCAO-X $\alpha$  calcs. 4-113799  
 MgO, doped surfaces, {001} chemisorption 4-113805  
 N<sub>2</sub>, chemisorption Al<sub>2</sub>O<sub>3</sub> supported Rh surfaces, IR spectra 4-81461  
 N<sub>2</sub> on W (110), Ru (001), Ni (100), XPS lineshapes anal. 4-104723  
 N<sub>2</sub>, weakly chemisorbed, correl. between anomalous electronic and vibr. props. 4-78910  
 NH<sub>3</sub>, field promoted, surface catalyzed formation on transition metals 4-66616  
 NH<sub>3</sub>, on Ni (111), surface Penning ionisation study 4-65575  
 Ni (001) with chemisorbed pyridine, molecular orientation effects on electronic excitations 4-93551  
 Ni (100), chemisorbed CO, angle resolved photoemission 4-85055  
 Ni (100), N<sub>2</sub> chemisorption, precursor states, XPS study 4-65569  
 Ni (100), surface electronic structure changes induced by chemisorption of CO 4-88550  
 Ni (100), with adsorbed O, CO, surface structure determ. by XANES 4-99226  
 Ni (100) with chemisorbed CO, chemisorption bond and N<sup>+</sup>-molecule reaction 4-80380  
 Ni (110), chemisorbed O<sub>2</sub>, 2×1 struct., real space obs. by scanning tunnelling microscopy 4-61212  
 Ni (110), of D, saturation coverage 4-92550  
 Ni (111), adsorption and decomposition of NO, metastable quenching electron spectroscopy 4-92567  
 Ni (111), chemisorbed acetylene, vibr. props., EELS studies 4-65567  
 Ni (111) surface, adsorbed acetylene, ab initio MO study 4-92566  
 Ni, of CO on (7 9 11) surface, SIMS and classical dynamics investig. 4-75784  
 Ni, of NH<sub>3</sub> on (110) surface, site selection by electron donor mechanism 4-70549  
 Ni surface, adsorbed O<sub>2</sub>, electron stimulated desorpt. 4-65565  
 Ni surface, of S and O on cylindrical crystals 4-61223  
 Ni surface quantum motion of chemisorbed H<sub>2</sub> 4-80385  
 Pd (110), O<sub>2</sub> chemisorbed overlayer, Monte Carlo studies 4-113816  
 Pd (111), chemisorbed acetylene, vibr. props., EELS studies 4-65567  
 Pd (111), of CO, angle-resolved photoelectron spectra 4-81114  
 Pd surface, (111), O chemisorpt., SCF MO pseudopot. studies 4-92511  
 Pd thin overlayers on Nb (110) and Ta (110), CO adsorption 4-92533  
 Pd-Si(111) interface, atomic intermixing and electronic interaction 4-70478  
 Pt (110) and (111), chemisorbed CO, angle resolved photoemission 4-85055  
 Pt (110) chemisorbed S effect on H adsorpt. (French) 4-84504  
 Pt (111), 2H<sub>2</sub>+O<sub>2</sub>→2H<sub>2</sub>O reaction, SIMS and TDS studies 4-66614  
 Pt (111), adsorbed H, He scattering studies 4-88400  
 Pt (111), CO inelastic scatt. and chemisorption, semiclassical model 4-71495  
 Pt (111), H<sub>2</sub> adsorption location from corrugation anal. and He<sup>+</sup> diffraction 4-65556  
 Pt electrodes, of aromatic mols., effect of surface pretreatment with flat oriented intermediates 4-99836  
 Pt polycrystalline surface, interaction with O<sub>2</sub>, XPS study 4-93200  
 Pt surface, Sn underpot. deposition in H<sub>2</sub>SO<sub>4</sub> soln. 4-81480  
 Pt-Si alloy, interaction with O<sub>2</sub>, XPS study 4-93200  
 Rh (0001), N<sub>2</sub> chemisorption, precursor states, XPS study 4-65569  
 Re (111), adsorption and decomposition of methanol, EELS and thermal desorption spectroscopy 4-92565  
 Ru (001), chemisorbed H<sub>2</sub>O clusters, desorption mass spectra, EELS 4-75786

## chemisorption continued

- Ru (001), incommensurate chemisorbed Na layer, orientational ordering obs. 4-88393  
 Ru (001) Na monolayer, orientational ordering 4-92525  
 Ru catalyst for NH<sub>3</sub> synthesis, surface struct. and reactivity study 4-80355  
 Si (100), of H, TDS study (Chinese) 4-92510  
 Si (100), PH<sub>3</sub> and SiH<sub>4</sub> adsorption, saturation coverage 4-88392  
 Si (100) surface, H chemisorbed, work function change, LEED expt. 4-70907  
 Si (100) surface with chemisorbed H, surface states, UVPS study 4-108709  
 Si (100) with adsorbed O<sub>2</sub>, ab initio SCF calcs. 4-98440  
 Si (100)2×1, H adsorpt., coverage and temperature-dependent vibr. spectra, EELS and LEED studies 4-80408  
 Si (111), benzene bound state vibr. modes and chemisorption bonds 4-108714  
 Si (111) surface chemisorbed Br, X-ray standing wave anal. with synchrotron radiation 4-103607  
 Si (111) with chemisorbed Sm, photoemission spectra 4-80392  
 Si, H<sub>2</sub>O dissociative chemisorption, photoemission studies 4-84514  
 Si, of water on (100), water mol. dissociation, IR spectra study 4-62233  
 Si surface, F<sub>2</sub> plasma etching, synchrotron photoemission study 4-93180  
 Si, thermal oxidation, chemisorption and linear rate const. 4-81458  
 Si with surface chemisorbed F, synchrotron photoemission study 4-108710  
 a-Si:H, of H<sub>2</sub>, work function, AES and EELS meas. 4-108715  
 SiO<sub>2</sub>, pyrogenic, of Cr<sub>2</sub>OCl<sub>2</sub>, IR spectrosc. investig. 4-109196  
 SnO<sub>2</sub>, of ketones, IR investig. 4-102681  
 Ti, polycryst., O<sub>2</sub> adsorption, charact. and coadsorption with Pb 4-92568  
 TiFe, H uptake activation, Auger electron spectroscopy 4-70558  
 W (100), N<sub>2</sub> chemisorption, precursor states, XPS study 4-65569  
 W (100), of H, two-electron bond approach 4-113801  
 W (100) with chemisorbed N<sub>2</sub>, diffusion and evaporation study 4-98434  
 W (110), clean and O covered, alkali metal chemisorption, NMR studies 4-98445  
 W (110) with surface adsorbed CO, electronic transitions, low-threshold neutral desorption,  $\alpha$ - $\beta$  conversion, calcs. 4-113785  
 W (112) with chemisorbed O<sub>2</sub>, kinetics of antiphase domain coarsening 4-98435  
 W surface, polycryst., chemisorption of NO 4-92564

## chemistry

see also atmospheric chemistry

freshmen fundamental chemical knowledge, survey 4-104960

## chemistry, physical see physical chemistry

## chemistry computing

see also computerised instrumentation; spectroscopy computing

- analytical and image data from SEM and STEM, integrated system for collection and processing 4-72012  
 Cambridge Database of molecular structures 4-64327  
 electron analytical Superprobe JCXA-733, application program 4-85344  
 electron probe microanalysis, computer program based on Gaussian curves evaluation 4-99926  
 external PIXE milliprobe at Davis cyclotron, laser alignment, calibration and quality assurance 4-105076  
 fractal to classical crossover 4-85285  
 interactive graphics application 4-95109  
 microcomputer-aided instruction and research in group theory 4-102584  
 organic photochem. synthesis, microcomputer interactive program appls. 4-114813  
 oscillator, chemical, 2D, computational study on limit cycle behaviour 4-104981  
 pesticide screening in residue analysis, BASIC program appl. 4-62273  
 polymer analogous reactions, kinetic consts. evaluated using minicomputers (Russian) 4-104986  
 reactor, modelling and numerical simulation 4-109335  
 shock wave collision with oblique ramp in shock tube, Hull computer code 4-79624  
 thermal decomposition, thermogravimetric data and effective kinetic parameters calcs. 4-81491  
 waxes gas chromatographic characts. anal. (German) 4-105087  
 X-ray microanalysis using computer controlled electron microprobe 4-72013

## Cherenkov counters

- absolute calibration for 9623B photomultipliers for atmospheric Cherenkov light intensities 4-112060  
 BUGS-4 cosmic ray detector, design, charge and energy resolution 4-101184  
 calibration using laser source 4-74096  
 cosmic ray detector, high charge and energy resolution for isotope meas. 4-102502  
 current compensation system 4-91160  
 Deep Underwater Muon and Neutrino Detection (DUMAND) expt., instrumentation 4-101181  
 directional, performance with rel. electron beams 4-59524  
 heavy antineutrino detection in cosmic ray telescope 4-112066  
 HPW water Cherenkov proton decay detector, triggers and sensitivity 4-91147  
 image intensifier system for air shower meas. 4-112059  
 IMB proton decay detector, calibration and expt. limits 4-90874  
 irradiated reactor fuel monitoring using Cherenkov methodology, safeguards surveillance 4-106977  
 Irvine-Michigan-Brookhaven proton decay detector, appl. to cosmic ray muon detect. 4-96411  
 massive water detectors for accelerator neutrino phys. 4-91182  
 NIKHEF-K, charged-pion detection systems large electron suppression 4-102451  
 ring imaging Cherenkov detectors, detection efficiency, spatial resolution 4-59523  
 silica aerogel, production studies (Japanese) 4-64309  
 silica aerogel threshold Cherenkov counters, pion detection, intermediate energies 4-102496  
 small air shower array with angular resolution system 4-112057  
 thin counter for cosmic-ray charge and direction meas. 4-63019  
 time projection ring imaging Cherenkov counter 4-87003  
 water Cherenkov based low cost 100 km<sup>2</sup> air shower detector 4-112056  
 water Cherenkov detector, HOMESTAKE mine 4-101182

Cherenkov detectors *see Cherenkov counters*

Cherenkov radiation

*see also Cherenkov counters; electron radiation*

air, microwave Cherenkov radiation 4-83511

atmospheric Cherenkov light imaging for  $\gamma$ -ray astronomy 4-101176

Cherenkov microwave generators with relativistic electron beams, plasma form. 4-91960

Compton regime Cherenkov lasers 4-96856

cosmic ray protons Cherenkov radiation and extrasolar planets IR detect. 4-77725

cosmic ray shower Cherenkov light 4-101081

electric and magnetic charges in dispersive and dissipative media, Cherenkov radiation calc. 4-69290

EM wave phenomena Fourier synthesis approach 4-95106

extensive air showers, atmospheric Cherenkov pulse-width technique 4-110428

free electron generators of coherent radiation, conf., Orcas Island, WA, USA (June 1983) 4-82588

interference between transition and Cherenkov radiation 4-59964

magnetic monopoles, Cherenkov magnon excitations 4-90768

maser experiments 4-69355

media free electron lasers for VUV and X-ray radiation production 4-96925

nonlinear optical media, electro-optic shock radiation theory 4-112498

plasma filled waveguide, Cherenkov generation at fundamental mode 4-103511

relativistic electron beam in dielectric medium 4-64663

relativistic electron RF sources, cyclotron reson. mode selection 4-69299

relativistic electron source for millimetre range, Bragg resonator use 4-69300

scintillation glass SCGIC, Cherenkov and scintillation light meas. 4-59530

spectral quantum approach to induced Cherenkov and transition radiation of electrons 4-78193

stimulated Cherenkov radiation by ultrarelativistic helical electron beams 4-63530

tandem mirror, thermal-barrier-potential measurement using the plasma Cherenkov effect 4-84043

undulator and Cherenkov free electron lasers, preliminary comparison 4-102936

unguided wave Cherenkov amplifier 4-102913

vacuum-ultraviolet Cherenkov radiation source 4-107498

chilling *see cooling*

chip carriers *see integrated circuit technology; packaging*

chiral symmetries

*see also SU<sub>N</sub> theory*

$\theta$  dependence of quark condensates, U(1) problem, chiral symm. breaking 4-111388

$\sigma$ -model, chiral invariant, soliton with valence quarks 4-63872

$\sigma$ -model, exotic structure 4-68400

abelian and nonabelian chiral anomalies, higher dimensions, and differential geometry 4-90739

asymptotically free chiral model, four dimensions, nonlinear chiral symm. 4-106470

Atiyah-Singer index, supersymmetric derivation and chiral anomaly 4-82912

bag model, c.m. motion, chiral symm. influence on hadron masses, electroweak parameters 4-106516

bag model convergence behaviour,  $\pi$ N scatt. amplitude 4-90820

bag models 4-59044

baryons, two-phase quark models, chiral Casimir effect 4-86661

boson formulation of fermion field theories 4-68414

broken SU(5)  $\otimes$  SU(5) chiral symmetry and the classification of B mesons 4-78482

chiral bag radius in strong pion fields 4-111403

collective states, structure and models 4-95877

composite models, scalar and fermion fields, large-N limit 4-106523

composite operator calculation of chiral symmetry breaking in color gauge theory 4-86642

conference on hadron substruct. in nuclear physics, Bloomington, IN, USA (Oct. 1983) 4-63381

CP<sub>N-1</sub> two-dimensional chiral models, mass gap, perturbative eval. 4-58946

d=4 and d=11 supergravity relations, supersymmetry transformation laws 4-110981

dimensional reduction of fermions, generalized grav., modification of Riemannian geometry 4-95273

Dirac fermions coupled to gauge and grav. fields, chiral anomalies, path integral derivation 4-86575

dual symmetry of chiral model and geometrical correspondence between chiral field and sine-Gordon equation (Chinese) 4-73663

dynamical symmetry breaking and particle mass generation in gauge field theories 4-82899

E<sub>8</sub>, E<sub>8</sub> gauge groups, dimensional reduction, Yang-Mills theory 4-86565

early big-bang Universe, quark-hadron and chiral transitions, review 4-73107

effective Lagrangian, symmetrical and unsymmetrical anomaly (Chinese) 4-111312

electron gas density of states in mag. field, Schwinger model chiral symmetry breaking 4-68123

exact minimal S-matrix for principal chiral model, bound state 4-73660

extended supergravity, nonlinear representations, Higgs and superHiggs effect 4-110978

extended survival hypothesis and fermion masses 4-73670

fermion determinants, chiral symmetry, and the Wess-Zumino anomaly 4-68355

fermion field theory, finite mode regularisations 4-73639

fermion gravitational interactions, chiral Lorentzian anomalies 4-90747

fermion masses in potential models of chiral symmetry breaking 4-63903

fermion models, two-dimensional curved space-time, Thirring and Schwinger models 4-90734

fermionic path-integral and chiral rotations 4-63879

finite temperature QCD, strong coupling lattice model, chiral symmetry 4-86652

G $\otimes$ G two-dimensional chiral models, mass gap, perturbative eval. 4-58946

gauge planar systems, fermion zero modes and 3-D chiral anomaly 4-78477

graded, supersymm. Kac-Moody algebra generation 4-68451

hadron vector current decay, effective Lagrangian technique 4-90757

chiral symmetries continued

high density matter, condensed  $\pi^0$  field in chiral bag model, quark spin-flavour struct. 4-83018

hybrid chiral bag models, external soliton solution 4-111413

instanton and meron fields, Dirac Hamiltonian self-adjointness 4-95673

Kac-Moody algebra struct. in Lax representation (Chinese) 4-68441

large-N chiral model reduction by dimensional reduction of gauge theories 4-95709

lattice action for Wilson fermions interacting with gauge fields 4-63862

lattice field theory, zero modes, boundary conditions and anomalies 4-86520

lattice gauge theories, confinement props. of coset pure gauge fields of nonabelian chiral group (Chinese) 4-73643

lattice gauge theories, SU(2) and SU(3), chiral symmetry breaking, deconfinement 4-82907

lattice gauge theory, Monte Carlo studies of chiral phase transition 4-68385

lattice QCD, chiral symmetry breaking at finite temp. 4-86650

lattice QCD, non-zero baryon density, chiral symm. restoration, small chemical potential 4-102062

lattice spin and gauge models, weak coupling phase for O(N), CP<sup>N-1</sup> and chiral models 4-68366

light hadron masses in chiral and cloudy bag models, N- $\Delta$  and  $\Sigma$ - $\Delta$  mass differences 4-90821

linear  $\sigma$ -model, mean field theory, chiral solitons, coupled boson-fermion fields 4-63854

massless composite fermion struct., large N limit of SU(N) gauge theory 4-90836

Minkowski space-time, d=12 compactification, left-right asymm. gauge coupling, chiral families 4-111281

MIT bag model with broken chiral symmetry, massive quarks and pions 4-59049

molecular sigma models, Einstein and chiral-field equations, exact solutions 4-95685

moving magnetic charges, electrodynamics in chiral Lagrangian theory 4-59021

muon decay, right-handed currents, exptl. search 4-68571

N=1 supergravity, flatness, superspace and linear SU(1,1) symmetry 4-58721

N=2 supergravity, dimensional reduction, compactification of D=10 to D=4 model 4-90476

N=4 extended supergravity, compactification on K<sub>3</sub>, chiral 4-68116

Nambu-Goldstone particle spectrum, supersymm. theories, chiral superfields, modified R-symm. 4-106491

natural composite models, systematic construction 4-95770

noninvertible elliptic operator, regularised determinant 4-68443

nonlinear chiral field eqns., exact solutions 4-102020

nonlinear chiral SU(2)  $\times$  SU(2) Yang-Mills Lagrangian in curved isospin space 4-102009

nonlinear fermion field, strong interaction, quark field chiral symm. breaking 4-106486

nonperturbative supersymmetry breaking in 4-dimens. model, chiral and gauge breaking 4-68455

nuclear matter, weak axial vector current, chiral filter, Gamow-Teller strengths 4-68635

nucleon as topological chiral soliton, bag models, nuclear physics 4-63855

nucleon as topological chiral soliton in bag model 4-86662

nucleon branching ratios, chiral Lagrangian calc. in supersymmetry SU(5) model 4-58995

nucleon two-body decay modes with vector mesons, chiral dynamics in SU(5) supersymmetry model 4-63995

O(2,1) chiral  $\sigma$  models, explicit solutions 4-106476

O(3) chiral  $\sigma$  models, explicit solutions 4-106476

O(n+1) hyperspherical covariant formalism, chiral anomaly in spacetime 4-58953

O(N) two-dimensional chiral models, mass gap, perturbative eval. 4-58946

perturbative pionic contrib. to nucleon observables 4-64057

pion electroproduction, current algebra-PCAC representation, chiral SU(2)  $\times$  SU(2) symm. breaking 4-111462

preon composite model with three confining hypercolor groups 4-86683

preon theories, compositeness scale lower bound, spontaneous chiral symm. breaking 4-106522

proton decay Lagrangian in SU(3)  $\times$  SU(3) theory 4-73696

pseudoscalar meson decays in theory with broken chiral symm. (Russian) 4-68569

pseudoscalar mesons, chiral Lagrangian from functional integral over quarks 4-68529

pseudoscalar mesons, nonlinear effective Lagrangian in broken SU(3)  $\times$  SU(3) 4-90750

QCD, chiral symmetry breaking model 4-63955

QCD, effective quark mass, spontaneous chiral symmetry breaking dynamics 4-82939

QCD, exotic commutators and ideal mixing 4-68500

QCD, first-order phase transition, concentration of quark matter 4-90803

QCD, quark mass gauge-parameter independence, chiral symm. breaking 4-106512

QCD chiral anomalies, effective lagrangians and differential geometry 4-86647

QCD picture of broken chiral symmetry, neutral PCAC scheme 4-73715

QCD supersymmetric, effective actions for anomalous chiral symmetries 4-59030

QED, chiral symmetry breaking in 3-D 4-73707

QED, chiral transformation, generalised, gauge conditions 4-68489

QED, gauge condition, completely covariant, consistency with field theory 4-68488

quark-hadron phase transition, QCD sum rules, chiral symm. restoration 4-111393

radiation interference theorem, photino emission, chiral superfields 4-106494

reduced finite N continuum chiral model 4-63882

Schwinger-Dyson eqns. in Landau gauge, quark confinement and chiral-symmetry breaking 4-95666

Skyrme model, strong-coupling approx., nonstrange baryons, excited states 4-106513

skyrmons and weak interactions, Weinberg-Salam Higgs field, technicolour 4-86614

SO(18) complex spinor, embedding of colour and chiral fermions, shiny quarks 4-111373

## chiral symmetries continued

- SO(3) composite fermion model with lattice gauge theory scalars, chiral symmetry breaking 4-111426  
 SO(4) invariant self-gravitating  $\sigma$ -model, flat-symmetric solns. 4-73650  
 soliton bag model with or without SU(2)×SU(2) chiral dynamics, coloured Higgs mechanism 4-59031  
 soliton bag models with nonlinear pion fields 4-78465  
 soliton fractional fermion number depletion at finite temp. and chem. pot., (1H)D chiral field theory 4-102028  
 spinor field quantisation, joint Bose-Fermi spectral problems 4-63869  
 static SU(2) gauge fields and chiral symm. breaking 4-68405  
 SU<sub>h</sub> main chiral field in two dimensions, exact solns., S-matrix 4-111325  
 SU(2)×SU(2) chiral model, proton magnetic, polarisability 4-102060  
 SU(2)×U(1) breaking constraints for vacuum misalignment, partially chiral technicolour gauge 4-111350  
 SU(2) gauge theory, scale of chiral symmetry breaking 4-58954  
 SU(2) lattice gauge theories, chiral symmetry breaking absence at high temps. 4-78494  
 SU(3) gauge theory, chiral symm. restoration transition, octet and sextet quarks 4-111300  
 SU(3) model, mass gap, Monte Carlo method 4-86603  
 SU(3) Skyrme model, static props. of baryons 4-111338  
 SU(3) symm. breaking parameter, finite-energy sum rules 4-95715  
 SU(5)×SU(3)×U(1) flavour-chiral Yang-Mills-Higgs theory, E8 dimensional reduction 4-106469  
 SU(5) model, supersymmetric, nucleon vector meson decay 4-102074  
 SU(5) SUSY GUT, chiral quarks and nucleon decay 4-102078  
 SU(N)×SU(N), chiral symmetry breaking of non-abelian gauge 4-58984  
 SU(N)×SU(N) chiral model, improved lattice action, Symanzik improvement procedure 4-95708  
 SU(N)×SU(N) chiral model, mass gap by Green's function method, 2D lattice 4-95707  
 SU(N)×SU(N) nonlinear  $\sigma$  model, exact solution 4-86561  
 SU(N) chiral model, twisted-reduced, saddle points 4-106485  
 SU(N) chiral models, mean field studies 4-106483  
 SU(N) principal chiral field, exact S-matrix, bootstrap method 4-90748  
 super self-dual Yang-Mills background, left chiral zero modes 4-86524  
 superconformal anomalies and the effective lagrangian for pure supersymmetric QCD 4-90794  
 supergravity, super b<sub>4</sub> coefficients, heat kernel superfield analogue 4-68108  
 supermetacolor, colour singlet-composite, superfields containing massless composite fermions 4-78536  
 supersymmetric field, stochastic quantisation, chiral SU(N) theory 4-90742  
 supersymmetric gauge theories, two-loop, the chiral anomaly 4-58955  
 supersymmetric gauge theory vacua and chiral fermions, SUSY breaking 4-82917  
 supersymmetric gauge-invariant interaction, nonchiral superfield, U, gauge transformation 4-90745  
 supersymmetric QCD, chiral symmetry breaking, spectral function sum rule approach 4-90800  
 SUSY QCD, massless, chiral symmetry breaking 4-90799  
 symmetric space chiral models, infinitely many symmetry generator series, Backlund transform. 4-95702  
 Thirring model, CP-asymmetric, Goldstone fields in 2-D 4-86562  
 twisted reduced chiral models at large N 4-95647  
 two-loop finite supersymmetric theories, classification 4-90771  
 U(1) chiral supergravities, unconstrained conformal superfields 4-90478  
 U(1) problem in QCD, dynamical resolution 4-86659  
 very early Universe, GUT, confinement, chiral and Weinberg phase transitions 4-63361  
 Wess-Zumino model, two-loop effective potential 4-90741  
 Yang-Mills eqn., chiral model formulation (Chinese) 4-111311  
 Yang-Mills super self-dual background, Green functions 4-78449  
 Yang-Mills supersymmetric theory, effective Lagrangian for supersymmetry breaking 4-111369  
 Yukawa two-loop beta-function in N=1 rigid supersymmetric theories 4-58988  
 $\eta$ - $3\pi$ , discrepancies due to departure from chiral symmetry, unitarity and analyticity 4-102116  
 $\eta$ - $\pi$ ,  $\pi$ - $\pi$ , current-quark mass ratios, isospin-symm. violations 4-106528  
 $\eta$  Z 4-59083  
 hh at extreme energies, light-cone QCD with axial-vector anomaly current 4-59039  
 K- $3\pi$ , matrix element quadratic terms, chiral Lagrangians, current-algebra analysis 4-106527  
 K- $\pi\pi$ ,  $\Delta I=1/2$  rule in chiral quark model, one-loop-renormalisation group eqns. 4-111444  
 K- $\pi\pi\pi$ , discrepancies due to departure from chiral symmetry, unitarity and analyticity 4-102116  
 KN low energy scatt. in cloudy bag model, SU(3) chiral generalisation 4-59106  
 $\Lambda$  nonleptonic decays, chiral bag model and weak interactions, s- and p-wave amplitudes 4-102119  
 N and  $\Delta$ , phenomenological quark model using chiral soliton model 4-63968  
 N\* and  $\Delta^*$  negative parity states, masses in chiral bag model 4-68543  
 pN, weak hadronic neutral current, right coupling consts. 4-90854  
 $\omega$ - $3\pi$ , chiral Lagrangian, nonAbelian anomaly, vector-meson decays 4-106510  
 $\omega$ - $3\pi$  contact term, QCD, low-energy theorems, broken chiral symm. 4-111446  
 $\omega$ - $3\pi$ , chiral Lagrangian, nonAbelian anomaly, vector-meson decays 4-106510  
 p mass prediction from  $\pi\pi$  scatt. data, effective chiral Lagrangians 4-102107  
 $\pi$ -N- $\pi$ N, reaction cross sections, isospin analysis, chiral-symm. breaking 4-106541  
 $\pi$ - $\pi$ , S-wave I=0 scatt. length, discrepancies due to departure from chiral symmetry, unitarity and analyticity 4-102116  
 $\pi$  scattering, low energy theorems corrections, QCD tests with current algebra 4-82940

## chlorine

see also nuclei with .....

adsorbed on Ag (001), inelastic He scatt. and surface phonons 4-99257  
 atom, reson. struct., autoionisation, photoionisation spectra 4-83339

## chlorine continued

- atoms, H-like is Lamb shift determ. by X-ray transitions meas. using beam-foil excitation 4-74195  
 atoms, photoionisation reson. struct. 4-112149  
 chemisorbed on Ag (100), hard square model, expt. evidence 4-88394  
 Cl<sub>2</sub> (D<sup>3</sup>  $\Pi_g^-$  A<sup>2</sup>  $\Pi_u$ ) transition, improved gain at 258 nm by halogen donor mixing 4-107601  
 desorption by H<sub>2</sub>, rate limiting process of GaAs VPE 4-70553  
 determination in air in presence of NH<sub>3</sub>, capillary GC method 4-114855  
 electronic Raman spectra, ion laser excitation 4-102621  
 element analysis using charged-particle induced prompt  $\gamma$  rays 4-89362  
 gas, thermal conductivity meas. by holographic interferometry 4-87546  
 gas, thermal conductivity meas. by holographic interferometry 4-87547  
 gaseous, proton and <sup>4</sup>He stopping cross sections 4-92259  
 isotopic variations in nature, determ. method 4-77651  
 liquid, struct. factor, mol. vibr., neutron diff. study 4-108263  
 molecule, E(O<sub>2</sub><sup>-</sup>) ion-pair state, stepwise two-photon excitation, rovibronically resolved E-B emission spectra 4-91319  
 molecule, electron attachment, rate const. 4-107452  
 molecule, electronic struct., EELS 4-64626  
 molecule, long-range expansion coeff., dynamical dipole polarisability 4-59625  
 molecule, photodissociation, termolecular recombination, optoacoustic detection 4-99809  
 molecule, VUV absorpt. and fluoresc. spectra 4-83389  
 X-ray meas. of anomalous dispersion correction 4-87090  
 abundance and chem. in Galaxy 4-86020  
 CdS:Cl film, defect diffusion, luminescence study (Russian) 4-88875  
 CdTe:Cl, native acceptor defects, Hall effect study 4-75899  
 Cl VII, Na-like, lifetimes, beam-foil excitation spectra 4-59677  
 Cl<sup>-</sup> in aq. soln., mol. dynamic simulation of quadrupole relax. 4-80841  
 Cl<sup>-</sup>, solvation, geometrical features, pattern recognition anal. 4-114781  
 Cl-alkyl iodide, differential reaction cross-sections, collision dynamics 4-85291  
 Cl-ethyl chloride-d<sub>3</sub> (-d<sub>4</sub>) (-d<sub>5</sub>), D abstraction from methyl-d<sub>3</sub> group 4-62163  
 Cl-ethylene, ab initio MO studies, rot. barrier, dissociation energy 4-99773  
 Cl-N<sub>2</sub>Cl reactions, rate consts. determ. at 295K 4-71863  
 Cl-NO<sub>2</sub>, kinetic growth and decay meas. using time resolved absorpt. 4-89247  
 Cl<sup>-</sup>+Cl<sub>2</sub> charge transfer and electron detachment, absolute total cross-sections meas. 4-69202  
 Cl<sup>-</sup>+H<sub>2</sub>O, intramol. vibr. freq., single ion effect 4-69036  
 Cl<sup>-</sup> inert gas atoms, positive ion prod., double electron detachment cross sections 4-87187  
 p-Cl<sub>2</sub>, <sup>35</sup>Cl NQR linewidths, dipolar second moments calc., degeneracy of  $\pm 3/2$  and  $\pm 1/2$  levels 4-71206  
 Cl<sub>2</sub><sup>-</sup> radical in aq. soln. harmonic freq., anharmonicity consts., reson. Raman spectra 4-74247  
 Cl<sub>2</sub><sup>+</sup>, high resolution UV PES 4-112228  
 Cl<sub>2</sub><sup>+</sup>, photodissoc. spectra, predissoc. mechanism, vibr. levels 4-87171  
 Cl<sub>2</sub>-N<sub>2</sub> mixtures, ion dynamics of glow discharge plasmas 4-65142  
 Cl<sub>2</sub><sup>+</sup> inert gases, spectroscopic and kinetic study with VUV synchrotron radiation excitation 4-85289  
 Cl<sub>2</sub>+Cl<sup>-</sup>(Br<sup>-</sup>)(I<sup>-</sup>) charge transfer and electron detachment, absolute total cross-sections meas. 4-69202  
 Cl<sub>2</sub>+corrugated surface scattering, mag. transition rainbows 4-66164  
 Cl<sub>2</sub>+H<sub>2</sub>, quantum classical reaction path model 4-114764  
 Cl<sub>2</sub>+H(D), oriented-averaged rot.-decoupled vibr. 4-99753  
 Cl<sub>2</sub>+methyl radical, rate consts., product vibr. excitation and hot radical reactions 4-71893  
 Cl<sub>3</sub>P<sup>+</sup>(<sup>2</sup>P<sub>1/2</sub>), collisional quenching time-resolved at. reson. VUV absorpt. 4-59665  
 KBr:Cl, and undoped crystals, anion Frenkel defect creation, luminesc. study (Russian) 4-80980  
 KBr:Cl, X-irradiated, luminesc. study (Russian) 4-80981  
 KBr+Cl<sub>2</sub>-KCl+BrCl, nucleation and growth reaction on crystalline surface 4-71983  
 Ru,Ti<sub>2</sub>-O<sub>2</sub>-Cl<sub>2</sub> coatings, solid solution formation 4-70392  
 SF<sub>6</sub>-Cl<sub>2</sub>(H<sub>2</sub>) gas mixtures, vibr. relax., US absorpt. study 4-75117  
 a-Si:Cl, H-films, photocond. spectra (Chinese) 4-113989  
 Si:P,Cl<sup>-</sup>, Cl<sup>-</sup> implantation effects on oxidation enhanced P diffusion 4-92429  
 SiO<sub>2</sub>:Cl<sub>2</sub> film on Si, impurity distrib., SIMS study 4-113485  
 V/Cl<sub>2</sub> cycle for H<sub>2</sub> production, energy and exergy anal. 4-72185  
 V/Cl<sub>2</sub> cycle for thermochemical H<sub>2</sub> production 4-72186

## chlorine compounds

- chloride pollution dynamics in Oswego River, United States 4-100014  
 chloride salt form. on Space Shuttle exhaust alumina 4-77163  
 chlorite+SO<sub>2</sub><sup>2-</sup>, chemical chaos 4-66570  
 ClCN+Xe, CN(B<sup>2</sup> $\Sigma^+$ ) prod., vibr. and rot. state distrib. 4-89250  
 ClF, Cl<sup>+</sup> and Cl<sup>+</sup>, lowest s Rydberg complex, UV spectra 4-59792  
 ClF<sub>3</sub>, mol. consts., normal coordinate anal. 4-74216  
 ClNO<sub>2</sub>, thermal energy electron capture, ECR study 4-91340  
 ClO, absolute absorpt. cross sections at high resolution in A<sup>2</sup> $\Pi$ -X<sup>2</sup> $\Pi$  band system 4-78857  
 ClO, diurnal var. in stratospheric O<sub>3</sub> layer and Cl chemistry 4-110234  
 ClO+NO<sub>2</sub>, kinetic growth and decay meas. using time resolved absorpt. 4-89247  
 ClO, absorption coefficients at <sup>12</sup>C<sup>16</sup>O<sub>2</sub> and <sup>12</sup>C<sup>18</sup>O<sub>2</sub> laser wavelengths, appl. to remote monitoring 4-114997  
 ClO<sub>2</sub>, ground excited and ionic states, force consts., vibr. anal. 4-64449  
 ClO<sub>2</sub>, trapped in  $\gamma$ -irrad. crystals, ESR temp. depend. 4-98950  
 ClONO<sub>2</sub> in N<sub>2</sub> and Ar matrices, high resolution FTIR spectra 4-74233  
 Cl<sub>2</sub>SO, <sup>35</sup>S nucl. mag. shielding, chem. shift 4-102699  
 NSCl molecule, one-electron props. from perturbative-variational wave functions in multidimensional Cl reference space 4-68968  
 NSCl, thiacyl chloride, nucl. quadrupole coupling consts. from microwave spectra and ab initio MO calc. 4-69103

## cholesteric liquid crystals

- axis instability in mag. field 4-84153  
 biphenyl, nematic liq. cryst., cholesteric mesophase induction 4-60814  
 blue mesophases, circular intensity differential scattering 4-109200  
 blue phase, morphological studies, growth of three-dimens. liq. single cryst. 4-60819  
 blue phase, optical props. 4-88791  
 blue phase, struct. anal. by optical Bragg diffraction 4-88090  
 blue phase, transmission electron microscope pictures 4-75289  
 blue phase I, cryst. habit 4-103735  
 Blue Phase I liquid crystal, order parameter optical meas. 4-103645

**cholesteric liquid crystals continued**

- blue phase liq. cryst. mixtures, lattice parameters, Bragg refl. obs. 4-88089
- blue phases, elect. field induced birefringence 4-76426
- cholesteric myristate and pelargonate, struct. studies 4-98009
- cholesterogenic mixed system, identification of monomorphic blue phase 4-113324
- cholesterol derivatives, mesogenic, cryst. and mol. struct. 4-113437
- cholesterol nonanoate-chloride mixture, blue phase struct. 4-60820
- cholesteryl  $\omega$ -arylalkanoates, liq. cryst., cholesteric-isotropic transitions, thermal props. 4-108615
- cholesteryl benzoate, liq. cryst., impurity effect, UV absorpt. spectra 4-61728
- cholesteryl chloride-cholesteryl myristate-KNO<sub>3</sub> mixtures, ferroelec. behaviour 4-109134
- cholesteryl laurate-cholesteryl capriate mixture, growth kinetics of cholesteric spherulites, applied elec. fields 4-113322
- cholesteryl laurate-cholesteryl chloride-KNO<sub>3</sub> mixtures, ferroelec. behaviour 4-109134
- cholesteryl myristate (propionate) mixed liq. crystals, compressibility, and thermal expansion anomalies 4-80227
- cholesteryl N-alkanoates, ternary system press. induced reentrant cholesteric phase 4-98002
- cholesteryl nonanoate, spherulite growth rate, effect of press. 4-92356
- cholesteryl pelargonate, current flow, relax. processes 4-88770
- cholesteryl pelargonate and chloride, charge carrier mobility meas. 4-92709
- cholesteryl pelargonate, thermally stimulated currents and phase transitions (Russian) 4-88519
- compensated liquid crystals, fluorescent guests props. 4-65168
- conference, Las Vegas (USA), (March-April 1982) 4-82596
- human body temperature meas. (German) 4-77435
- hydrodynamics, similarity to superfluids 4-88292
- hydrodynamics of cholesteric liquid crystals in the coarse-grained limit 4-87700
- inverted cholesteric phase surrounded by different types of smectic A phases, temp. conc. phase diagram 4-88073
- IR flaw detector for semiconductors free-carrier conc. determ., cholesteric liq. cryst. use 4-89211
- isotropic-cholesteric liq. cryst. phase transition, orientational ordering 4-70380
- light-induced Fredericksz transition and optical nonlinearity 4-61084
- liquid crystal-isotropic transition temperature depression by a mag. field 4-98281
- long pitch, thermal instabilities, continuum theory 4-79928
- lyotropic mesophases, optical sign determinations 4-84940
- magnetic field effects and biaxial order, theory 4-113315
- MBBA:CC mixture, pitch meas. (Chinese) 4-103642
- MBBA, with chiral component, biaxial ordering in cholesteric phase, effect of twist, <sup>2</sup>H NMR study 4-84174
- MBRA8 liquid crystal, smectic A-chiral-smectic C transition, Landau free energy 4-92358
- methoxybenzylidenebutylaniline-cholesteryl nonanoate liq. cryst. mixture, electrohydrodynamic instabilities 4-113329
- methyl 3 $\beta$ -nonanoyloxycholesterol-5-en-24-oate, cholesteric pitch, temp. depend. 4-84150
- (+)-2-methylbutyl-p((p-methoxy benzylidene)amino) cinnamate, liq. cryst., transitions and texture, enthalpy and entropy 4-113628
- micellar additions, interaction with thermotropic liq. crystals 4-113623
- monodomain, reflectance spectra 4-113299
- optical eigen mode ellipticity calcs. 4-114229
- photopolymerization in cholesteric mesophases 4-113305
- photovoltaic effects with nonmesogenic additives 4-75290
- polyester, aromatic cholesteric polymer, optical props. in elec. field 4-65176
- polymer side chain liquid crystals, struct., optical and phase transition props. 4-98013
- polymers, mesomorphic struct., miscibility studies 4-84178
- potassium 1-N-lauroyl-serinate, cholesteric lyomesophases, type II system 4-84148
- potassium 1-N-lauroyl-serinate, intrinsic cholesteric lyomesophases 4-84146
- pretransitional effects near blue phases 4-70379
- solutions circular dichroism in IR spectra 4-88806
- texture change electro-optical effect, two-freq. addressing 4-71347
- thermotropic disc-like mesogens, phase sequences 4-84181
- thermotropic liquid-crystalline polymers with mesogenic side groups, synthesis struct. and props. 4-98014
- thin large-pitch films, polar electro-optic effect 4-114246
- topological symm. breakdown in presence of defects 4-70026
- twist-induced biaxiality, Landau theory 4-84152
- AsSe<sub>3</sub>-chiral-liquid-crystal struct., phase boundary effect on electrooptical props. 4-93057

**chondrites see meteorites****choppers (circuits)**

- vehicular technology conf. Pittsburgh, PA, USA (May 1984) 4-106118
- Pb/acid batteries, influence on capacity of pulsed discharge, importance for electric vehicles 4-66683

**chopping see cutting****chromatic aberration see aberrations****chromatography**

- alkane mixtures, comparison of  $\gamma$ -radiolysis in glassy and polycryst. states 4-62215
- complex hydrocarbon mixtures separation using mixed fused silica columns, GC/FT-IR considerations 4-105037
- complex mixture charact., IR and photoionisation detector eval. 4-85349
- computerised high-speed chromatographic gas analyzer 4-105043
- dimethoxymethane, concentration meas. by chromatography for SQS- $\mu$  counter model (Chinese) 4-74116
- ethyl iodide-<sup>131</sup>I, radio-gas chromatography of labelled organic compounds (Chinese) 4-62263
- fatty acid esters, stereoisomers, laser spectrochromatographic identification 4-62269
- filterphotometric detection system for liquid chromatography 4-68259
- fuel recovery by microwave heating, heating process and chromatographic analysis 4-72041
- gas chromatographic characterization of high boiling waxes (German) 4-105087
- IMACC-8001 signal analysis system (Spanish) 4-73427
- isotope enrichment by high press. ion exchange displacement chromatography 4-59905

**chromatography continued**

- liquid, spectrophotometric detector, for HP 1090 4-68260
- liquid chromatograph injection and sampling automation 4-72005
- liquid chromatography column temperature control 4-72006
- liquid crystalline ternary mixtures, appl. in gas chromatography, eutectic composition determ. 4-113317
- liquid crystals and ordered fluids, conference, Las Vegas (USA), (March-April 1982) 4-82596
- low-dispersion liquid chromatography, HP 1090 4-72004
- methane, concentration meas. by chromatography for SQS- $\mu$  counter model (Chinese) 4-74116
- methyl 3 $\beta$ -nonanoyloxycholesterol-5-en-24-oate, cholesteric pitch, temp. depend. 4-84150
- methyl iodide-<sup>131</sup>I, radio-gas chromatography of labelled organic compounds (Chinese) 4-62263
- methylcyclopentadiene, positional isomers, laser spectrochromatographic identification 4-62269
- methylmethacrylate-vinylferrocene copolymers adsorpt. at soln./solid interface, chromatography meas. 4-85332
- microprocessor based compact economical gas chromatograph, design and performance 4-105044
- natural gas anal., high speed automated, using microcomputer controlled high resoln. gas chromatography 4-99928
- nondestructive determination of Cr by thin-layer chromatography 4-76944
- online control charts 4-105042
- organophosphorus cpd., C<sub>7</sub>H<sub>16</sub>FO<sub>2</sub>P, decomp. in silent elec. discharge 4-109630
- pentane-2-methylpentane mixtures,  $\gamma$ -irrad., energy transfer 4-76254
- perylene, Fourier transform filtering of two-dimensional fluorescence data 4-101820
- pesticide screening in residue analysis, BASIC program appl. 4-62273
- PET, crystallisation, struct. and props. 4-103666
- PMMA, viscosity average mol. wt. from gel permeation chromatography 4-59928
- PMMA-polyethylene oxide, molten blends, thermodynamic miscibility, gas chromatography 4-80240
- poly(N-alkyl-3,3'-carbazoly)-I<sub>2</sub> complexes, highly conducting, synthesis and I<sub>2</sub> doping, gel permeation chromatography study 4-65664
- polycyclic aromatic hydrocarbons, nitrated, in diesel particulates, gas chromatographic obs. 4-114854
- polydiacetylene, conducting polymer, synthesis by  $\gamma$ -ray polymerisation, gel permeation chromatography anal. 4-75958
- polymers, molecular mass determ. by thin-layer chromatography based on viscous conc. effects (Russian) 4-83507
- polystyrene, viscosity average mol. wt. from gel permeation chromatography 4-59928
- pyrene, fluoresce, and diffusion on C<sub>18</sub> reversed-phase liq. chromatographic packing 4-112219
- trace metal anal. and speciation using plasma emission spectrosc. detectors in HPLC 4-73524
- transformer insulating oil dissolved gases chromatographic anal. (Portuguese) 4-114860
- Ukraine power pools transformer equipment chromatographic testing 4-99917
- urine, ion exchange, selective preconcentration method, PIXE anal. 4-100383
- vapour-liquid equilibrium measurement, high pressure-high temp. chromatographic apparatus 4-70355
- water vapour conc. meas. by gas chromatography anal. 4-89364
- $\gamma$ -Al<sub>2</sub>O<sub>3</sub>, adsorption of alkanes and aromatic hydrocarbons, thermodynamic props., chromatography (Chinese) 4-61210
- C powders, Ar(N<sub>2</sub>)CO<sub>2</sub> adsorption, second gas-solid virial coeffs., chromatographic determ. 4-114819
- Cl<sub>2</sub>, determ. in air in presence of NH<sub>3</sub>, capillary GC method 4-114855
- I, radioelectrophoretic and chromatographic study (Chinese) 4-71934
- N<sub>2</sub>, liquid, solubility of halogen hydrocarbons at 77.4K, gas chromatography study 4-70385
- Ni electroplating bath control using saccharin additive (German) 4-66241
- SF<sub>6</sub>, decomp. by arc discharge, product meas. at sub-p.p.m. level 4-114869
- Se<sub>2</sub>O<sub>3</sub>, prep. and struct. props., powder diff. studies 4-71608
- Si noncrystalline thin films, struct. props. and impurity content 4-88434

**chromising see surface hardening****chromium****see also nuclei with .....**

- (110) with adsorbed O<sub>2</sub>, photon stimulated O<sup>+</sup> desorption 4-98438
- atom, spectral line intensities and transition probabilities (French) 4-78809
- atoms, half-filled shells, photoionisation 4-83353
- atoms, two-electron, one-photon transitions 4-74340
- Auger electron appearance potential spectroscopy 4-99230
- black, electrodeposits for heliothermic conversion (French) 4-77143
- blood plasma Cr levels, rel. to coronary artery disease 4-105366
- corrosion of pure Fe, Ni and Cr in formic acid soln., comparison with austenitic stainless steel 4-71766
- Debye-Waller factor for substitutional Mossbauer impurity 4-75633
- dimers, electron correl. effects 4-102603
- effect of mag. anisotropy on spin wave spectra (Russian) 4-80750
- electrodeposited Cu/Ni/Cr three layer coatings on steel, corrosion testing 4-66504
- electrodeposited Cu/Ni/Cr three layer protective coating on steel, corrosion testing 4-66505
- extraction of Cr and Zn from cooling tower blowdown by liq. membranes 4-81474
- film, laser induced thermochemical image recording 4-102969
- film, obliquely deposited, spectral and angular selectivity 4-112535
- film deposition, using plasma evaporator design with heated needle cathode 4-88899
- film on glass substrate, laser damage study 4-108433
- films, dissolving kinetics, plasma treatment induced changes 4-81335
- films, evaporated, internal stress, struct., substrate temp. depend., electron microscopy obs. 4-98495
- films, evaporated, mechanical stresses 4-75819
- films, laser induced metal deposition from organometallic solution 4-66239
- films electroplated on (001) Cu substrates, misfit twins and dislocations 4-108748
- glass:Cr, dominant visible absorpt. rel. to  $\gamma$ -ray irradi. 4-76503

chromium continued

impurity absorpt. spectra, crystal field, ground and excited state 4-109218  
incommensurate SDW state, mag. response function, pole at acoustic phonon energy 4-98868  
ion source, multiply charged, using heated gas discharge chamber 4-73578  
Kevlar 49:Cr<sup>3+</sup>, EPR study of stress induced free radicals 4-109076  
laser-produced plasmas, 2p<sup>3</sup>s, 3p and 3d configurations 4-102620  
magnetic moment fluctuations and magnetovol. variations 4-109026  
molecule, LCAO local spin density, X $\alpha$  calcs. 4-87046  
multilayered thin film structs., depth profiling and sputtering yields 4-81090  
Neel transition, effect and uniaxial compressive stress, US attenuation and neutron scatt. meas. 4-76208  
neutron irradi., internal friction, elastic modulus, recovery stages studied by elec. resist. meas. 4-103875  
oxidation, <sup>18</sup>O/SIMS obs. of O transport in growing  $\alpha$ -G<sub>2</sub>O<sub>3</sub> films 4-89174  
oxidation, high temp, cation diffusing scale form., SEM obs. 4-71791  
oxidation, TEM microstructural study 4-104926  
oxide film thickness and composition, AES decomposition 4-61193  
paramagnetic, angular correlation of position annihilation, radiation appl. of Lock-Crisp-West theorem 4-85031  
permeation of H and D, diffusion, permeability, and solubility (German) 4-103992  
plasma limiter, H recycling and impurity release by laser induced fluorescence 4-97867  
radiative properties at high temp. 4-84952  
reflecting layer, parasitic photosensitivity avoidance in Si diffusion tenometers 4-101829  
ruby:Cr<sup>3+</sup>, angular-modulation-induced reverse-phase first-derivative field-swept EPR spectra 4-65856  
ruby:Cr<sup>3+</sup>, cryst. fields superposition model, appl. to non-S-state impurities 4-98574  
ruby:Cr<sup>3+</sup>, phonon trapping by exchange coupled Cr<sup>3+</sup> pairs 4-65349  
sandwich with Au or Ag, superconducting and mag. props. 4-80709  
sapphire:Cr crystals, hardness 4-93393  
SDW, kink lattice struct. 4-104480  
seawater trace metal vertical profile in E tropical Pacific 4-85721  
secondary ion emission, vel. depend. 4-76626  
selective coatings thermal emittance estimation from stagnation temp. study 4-62393  
sputtering, ground and excited state, laser-fluoresc. obs. 4-93169  
surface, (001), photoemission spectra interpretation, effect of correlations 4-76635  
surface (100), mag. phase transition, angle resolved photoelectron spectra studies 4-98888  
surface (110), electronic struct., PES study 4-85064  
texture, fine structure anisotropy, X-ray method 4-93480  
thin films, hardness meas. 4-75610  
valence band and 2p core lines, XPS obs. 4-99278  
AgGaS<sub>2</sub>:Cr<sup>3+</sup>, EPR study, spin-Hamiltonian parameters 4-104488  
Al/NiSi(Pd/Si)(PtSi) Schottky barriers, Cr diffusion barrier 4-88352  
Al-Cr thin film couple, diffusion barriers, Auger study 4-88407  
AlCl<sub>3</sub>·6H<sub>2</sub>O:Cr<sup>3+</sup>, EPR study 4-84852  
Al(NO<sub>3</sub>)<sub>3</sub>:Cr<sup>3+</sup>, exchange-coupled Cr<sup>3+</sup>-Cr<sup>3+</sup> pairs, EPR obs. 4-88717  
Al<sub>2</sub>O<sub>3</sub>:Cr, grain boundary diffusion, anisotropy and doping effects 4-92443  
Al<sub>2</sub>O<sub>3</sub>:Cr, photoacoustically detected EPR (Korean) 4-114155  
Al<sub>2</sub>O<sub>3</sub>:Cr<sup>3+</sup>, Cr<sup>3+</sup> electron spin resonance line ENDOR and saturation optical detect. 4-84873  
Al<sub>2</sub>O<sub>3</sub>:Cr<sup>3+</sup>, NMR and dynamic nucl. pol., low-freq. modulation effects 4-65868  
Al<sub>2</sub>O<sub>3</sub>:Cr<sup>3+</sup> (V<sup>4+</sup>), phonons, far IR vol. generation and detection 4-61005  
Au/Cr bilayers on GaAs, interfacial chemical reactions and drive-out diffusion, AES study 4-80313  
BeAl<sub>2</sub>O<sub>4</sub>:Cr<sup>3+</sup>, alexandrite, resonant 40 cm<sup>-1</sup> phonons, lifetime and line-width 4-65356  
BeAl<sub>2</sub>O<sub>4</sub>:Cr<sup>3+</sup>, alexandrite, fluorescence of inversion site Cr<sup>3+</sup> ions 4-107647  
Bi<sub>2</sub>SiO<sub>5</sub>:Cr, optical absorpt. spectra, photochromism (Russian) 4-114311  
CaAs: Cr LEC wafer, Cr<sup>3+</sup> distribution, EPR studies 4-98124  
Ca<sub>3</sub>Ga<sub>2</sub>Ge<sub>2</sub>O<sub>14</sub>:Cr<sup>3+</sup> EPR spectra 4-71170  
Cr foil, influence of heat treatment on struct. and props. (Russian) 4-65412  
Cr II lines, Stark width and shifts 4-91222  
Cr XX, X-ray spectra in 13-15 Å region 4-69007  
Cr XXI, X-ray spectra in 13-15 Å region 4-69007  
Cr<sup>2+</sup> doped tunable vibronic lasers, overview 4-107644  
Cr<sup>2+</sup>-Be<sub>2</sub>Al<sub>2</sub>(SiO<sub>4</sub>)<sub>2</sub> laser, CW Kr laser pumped, 728.8 to 809.0 nm tuning range 4-60041  
Cr<sup>3+</sup>-BeAl<sub>2</sub>O<sub>4</sub> (alexandrite) laser rod thermal lensing anal. by moire deflectometry 4-87379  
Cr<sup>3+</sup>-BeAl<sub>2</sub>O<sub>4</sub> laser technology for chem. appls. 4-107669  
Cr<sup>3+</sup>-GdScAl-garnet, tunable room temp. CW laser action 4-74518  
Cr/Ni/Cu multilayer film system, laser mixed, AES and Rutherford backscat. studies 4-98458  
Cr/Si(100) interface, silicide growth kinetics, cross-sectional TEM 4-61146  
Cr/SiO<sub>2</sub> thin films, elec. transport props. 4-92830  
Cr-LiClO<sub>4</sub>, shock compression, physicochemical transformations 4-70273  
Cr-SiO cermet films, composition and sheet resistance effect on strain sensitivity obs. 4-11117  
Cr-SiO<sub>2</sub>-pSi capacitor, conduction and charge storage 4-61474  
Cr+He(Ar)(H<sub>2</sub>)(D<sub>2</sub>)(N<sub>2</sub>)(CO)(O<sub>2</sub>)(N<sub>2</sub>O)(NH<sub>3</sub>), intramultiplet mixing collisions, fluoresc. 4-64588  
<sup>51</sup>Cr, international fluence-rate intercomparison for 2.5 MeV and 5.0 MeV neutrons 4-102561  
CsMgCl<sub>3</sub>:Cu(I)-M(III), (M=Cr, Mo, Ru, Rh), intermetallic charge transfer spectra 4-65644  
Cs<sub>2</sub>NaScCl<sub>6</sub>:Cr<sup>3+</sup> cryst., dopant fluoresc. props. 4-61745  
Cu/a-Si:H/a-Si:H(n-type)/Cr Schottky diodes, RF magnetron sputtered 4-88557  
Cu-Ni-microporous Cr multilayer system for corrosion protection (Russian) 4-89176  
Fe/Cr redox battery; mathematical model 4-89469  
FeNi(Si,Cr,Mo), neutron irradi. effect on mag. props. 4-92907  
 $\gamma$ -Fe<sub>2</sub>O<sub>3</sub>:Cr particles for audio recording, high orientation effect 4-65832  
GaAs:Cr, Cr-related complex, photoluminesc. studies 4-88467  
GaAs:Cr, deep impurity charact., photoluminescence study 4-98557

chromium continued

GaAs:Cr, electrical properties and impurity states 4-75963  
GaAs:Cr, epitaxial layers, Cr doping and elec. parameters 4-76683  
GaAs:Cr, eval. of Cr conc. by optical absorpt. 4-104635  
GaAs:Cr, impurities, optical and transport studies 4-71444  
GaAs:Cr, impurity photocond., internal quantum efficiency 4-88540  
GaAs:Cr, ion implanted, Cr redistrib. 4-88194  
GaAs:Cr, ion irradi. effect on defect thermal annealing 4-98156  
GaAs:Cr, ionisation processes by upper conduction band electrons, mag. field effects 4-65640  
GaAs:Cr, LEC growth, mag. field effect on impurity conc. 4-114378  
GaAs:Cr, photolum. at 0.839 eV, polarisation of Zeeman spectra 4-71427  
GaAs:Cr, photoluminescence excitation spectra, Cr<sup>2+</sup> internal luminesc. 4-81004  
GaAs:Cr, semi-insulating, inhomogeneities, optical obs. 4-60944  
GaAs:Cr, semi-insulating, Four-wave mixing using photorefractive effect, optical processing appl. 4-74585  
GaAs:Cr, semi-insulating LEC grown, photoluminescence props., whole ingot annealing effects 4-84994  
GaAs:Cr, US attenuation and vel. meas. 4-98212  
GaAs:Cr, piconsecd optoelectronic switches, pulse modulation of GaAs-(GaAl)As DH diode laser 4-107701  
GaAs:Cr-GaAs epitaxial junction, IR characterisation 4-109170  
n-GaAs:Cr<sup>2+</sup>, acoustic paramagnetic resonance study 4-71171  
GaAs:Cr<sup>2+</sup>, comparison of static and dynamic Jahn-Teller models 4-61345  
GaAs:Cr<sup>2+</sup>, trigonal symmetry sites, photoluminescence spectra anal. 4-108391  
GaAs:Sn/GaAs:Cr interface, electron and hole traps, photovoltaic studies 4-104283  
 $\beta$ -Ga<sub>2</sub>O<sub>3</sub>:Cr crystals, luminesc. parameters, impurity centre electron capture effects 4-81016  
GaP:Cr, EPR study of Cr<sup>2+</sup> centre 4-104487  
InP:Cr, impurity excited states, optical absorpt. spectra, EPR 4-88863  
InP:Cr, thermal conductivity, phonon scattering (French) 4-61155  
n-InSb:Cr, Mn, impact ions in 2-mm microwave field 4-70824  
LaCrO<sub>3</sub>-Cr cermet, high-temp. creep 4-71693  
La<sub>2</sub>Ti<sub>2</sub>O<sub>7</sub>:Cr<sup>3+</sup> and La<sub>2</sub>TiO<sub>5</sub>:Cr<sup>3+</sup>, photoelectrochem. props. 4-70874  
LiNbO<sub>3</sub>:Cr<sup>3+</sup>, spin-lattice relax., EPR studies 4-114157  
LiNbO<sub>3</sub>:Cr<sup>3+</sup> (Mn<sup>2+</sup>), axial cryst. field parameters, EPR spectra 4-98579  
MgAl<sub>2</sub>O<sub>4</sub>, grain boundary diffusion, anisotropy and doping effects 4-92443  
MgO:Cr, grain boundary diffusion, anisotropy and doping effects 4-92443  
MgO:NaAl<sub>2</sub>O<sub>3</sub>:Cr(Mn), impurity ion distrib. in spinel lattice 4-84311  
NaH<sub>2</sub>(SeO<sub>3</sub>)<sub>2</sub>:Cr<sup>3+</sup>, EPR spectra, temp. and external elec. field effects 4-88715  
Na<sub>2</sub>Zn(SO<sub>4</sub>)<sub>2</sub>·4H<sub>2</sub>O:Cr<sup>3+</sup>, optical absorption spectrum of Cr<sup>3+</sup> 4-71418  
Nd<sup>3+</sup>, Cr<sup>3+</sup> (GdSc)<sub>2</sub>Ga<sub>2</sub>O<sub>12</sub> laser operating in pulse-periodic regime, output charact. 4-74521  
Nd, Cr, Ce: YAG laser props., gain coeffs. 4-79156  
Nd, Cr:Gd<sub>3</sub>Ga<sub>2</sub>O<sub>12</sub> laser props., modified Czochralski growth (Chinese) 4-112441  
Nd<sub>2</sub>Ti<sub>2</sub>O<sub>7</sub>:Cr<sup>3+</sup> and Nd<sub>2</sub>TiO<sub>5</sub>:Cr<sup>3+</sup>, photoelectrochem. props. 4-70874  
Ni-Cr multilayer struct., depth resolution in ion sputtering 4-66168  
Ni-Cr-Mo steel, high strength, stress corrosion cracking life, statistical anal. 4-60980  
Pr<sub>2</sub>Ti<sub>2</sub>O<sub>7</sub>:Cr<sup>3+</sup> and Pr<sub>2</sub>TiO<sub>5</sub>:Cr<sup>3+</sup>, photoelectrochem. props. 4-70874  
RbIn(MoO<sub>4</sub>)<sub>2</sub>:Cr, ferroelastic, structural phase transitions, EPR study 4-70372  
Si:Cr, breathing mode relax. around tetrahedral interstitial 3d impurities 4-108567  
SiO<sub>2</sub>:Cr thin films, cathodoluminescence and C-V charact. (Russian) 4-99173  
TiO<sub>2</sub>:Cr, doping effect on elec. and catalytic props. under UV and visible illumination 4-98663  
TiO<sub>2</sub>:Cr<sup>3+</sup>, dopant incorporation rel. to calcination temp., EPR obs. 4-104486  
V<sub>2</sub>O<sub>5</sub>:Cr, metallic phase-insulating phase interface, misfit dislocations 4-108373  
YAG:Nd, Cr, Ce, laser props., gain coeffs. 4-79156

chromium alloys

see also chromium compounds  
Alloy 800, fatigue, high temp., damage mechanics 4-93422  
Alloy 800H, creep of tubular components, influence of multiaxiality of stress and environmental induced degradation 4-93360  
Astroloy, Ni-base superalloy, creep fracture, effect of wavy grain boundaries (Chinese) 4-62005  
Fecralloy, Fe-Cr-Al, D permeation 4-111754  
Hastelloy X, oxidation, thermal cycling, H permeation, acoustic emission 4-76905  
Hastelloy XR for HTGR, H<sub>2</sub> permeation in simulated reactor environment 4-75732  
IN 100, Ni-base superalloy, thermal fatigue 4-93417  
IN 738, high temp. low cycle fatigue models, predictive capability 4-93411  
IN-100, Ni-base superalloy, cast, microstruct. changes during fractional melting 4-109434  
IN-617, Ni-base superalloy, fatigue, high temp. low cycle 4-66425  
IN-718, Ni-base superalloy for gas turbines, elevated temp. fatigue life estimation 4-66449  
IN-738 LC, Ni-base superalloy, creep fracture, effect of grain boundary chem. and segregation 4-81285  
IN-738LC, Ni-base superalloy, precip. of  $\beta$  phase in  $\gamma$  particles 4-114559  
Incoloy 800, compatibility with flowing Li 4-107062  
Incoloy 800, oxidation in moist air containing HCl at 800°C 4-81327  
Incoloy 802, H<sub>2</sub> permeation inhibition by corrosion oxide layers (German) 4-66506  
Inconel 600, low temp. SCC effect of thermal stabilisation 4-99633  
Inconel 617, surface crack form. and propag., effect of temp. reactor primary circuit He 4-114641  
Inconel 625, JT-60 Tokamak device, materials aspects 4-107051  
Inconel 625 as tokamak wall material, hydrogen recycling model calcs. 4-97870  
Inconel 625 for TFTR vacuum vessel bellows; eddy current testing 4-111810

## chromium alloys continued

- Inconel 718, fatigue and creep-fatigue crack propag., influence of neutron irradi. 4-99496
- Inconel 718, time-depend. fatigue crack propag., effect of small scale to large scale creep transition (*Japanese*) 4-93383
- Inconel 718, vacuum brazed Ni-Cr-Si joint, struct. 4-66548
- Inconel 718 gas turbine disc material, crack initiation from notch under creep fatigue conditions 4-99567
- Inconel MA 754, 757, environmentally induced porosity 4-85260
- Inconel X750, in BWR primary system, corrosion products release rates meas. using radiotracer technique 4-91040
- Inconel X-750, environmental, stress-state and section-size synergisms during creep 4-61995
- Inconel X-750, Ni-base superalloy, creep and fracture, prior deform. effects 4-114656
- Nimonic PE-16, irradi. in HFIR at 430°C, fatigue performance 4-109497
- Rene 95, Ni-base superalloy, fatigue, effect of processing and microstruct. 4-104843
- SDW, kink lattice struct. 4-104480
- steel, (2.25, 1 wt.%), annealed, creep-rupture props., heat-to-heat variations 4-76860
- Ti effect on rate of high-coercivity transform. 4-93296
- Udimet 700, creep-fatigue, in high temp. materials, constitutive relationships 4-93353
- Udimet 700, metalloid strengthening mechanism 4-61974
- Udimet 700, Ni-base superalloy, creep fracture, effects of wavy grain boundaries 4-93415
- Al-Cr-Ni system, phase equilib. relations, review 4-114479
- Au-Cr, cryst. struct. determ., lattice modulation 4-103703
- Ca<sub>2</sub>CoAl<sub>7</sub> and CaCr<sub>2</sub>Al<sub>10</sub>, crystal structures (*German*) 4-9367
- Co-base superalloy, MAR M509, cast, thermal fatigue 4-93416
- Co-Cr ferromagnetic thin films, high rate magnetron sputtering 4-66232
- Co-Cr films, high-rate preparation on continuous tape substrates using target facing sputtering (*Japanese*) 4-81128
- Co-Cr ion beam sputter deposition, mag. props., temp. effects 4-104469
- Co-Cr layers, mag. orientation, effect of RF sputter parameters 4-65840
- Co-Cr media, statically written magnetisation patterns, mag. field meas. 4-88696
- Co-Cr sputtered thin films, surface and vol. coercive fields 4-65841
- Co-Cr-Al(Y), Si<sup>2+</sup> implanted, 1050°C oxidation behaviour 4-62124
- Co-Cr-Mo, single-phase, low stacking fault energy, back stresses 4-76787
- Co-Cr-Mo alloy, nucleation of recryst. 4-114570
- Co-Cr-Mo for hip joint endoprostheses, fatigue strength, remaining lifetime after loosening (*German*) 4-62627
- Co(Cr,Ni)-TaC, eutectic, thermal cycling, calc. of residual stresses and strains 4-66380
- CoCrAlY alloy surface protection coating, deposited by plasma spray, for gas turbine blades (*German*) 4-99639
- CoCrAlY, low temp. hot corrosion inhibition by ZnSO<sub>4</sub>-Na<sub>2</sub>SO<sub>4</sub> deposits 4-76903
- Cr-Al BCC solid solns., valence band, XPS and X-ray emission spectra study 4-93194
- Cr-Al dilute alloys, thermal expansion, elastic consts. and mag. props. 4-80138
- Cr-B-Ni, laser deposition on steel surface for hard-facing (*Russian*) 4-85251
- Cr-Co alloys, local electron states, elec. resist. and magnetoresist. studies 4-80550
- Cr-Co(Fe)(Mo), sigma phase, pair-wise interaction model 4-84422
- Cr-Fe, antiferromagnetic spin glass, HF characs. (*Russian*) 4-71105
- Cr-Ga, dilute, mag. phase diagram, elec. cond. meas. 4-88669
- Cr-Mn austenitic stainless steels, props. for fusion reactor appls. 4-111746
- Cr-Mn-V, phase diagram, two-band models, influence of reservoir and Fermi surface 4-114107
- Cr-Ni, E1826, cyclic loading parameters influence on deform. and fracture kinetics 4-99441
- Cr-Ru(Pd)(Ir)(Pt), active dissoln. in H<sub>2</sub>SO<sub>4</sub>, effect of Pt group element additions 4-71770
- Cr-W, phase diagram, miscibility gap, BCC solid soln. decomp. 4-114477
- Cr<sub>2</sub>Ir, Debye characteristic temps. 4-70330
- CrPd, disordered alloys, spin-glass-like freezing 4-71088
- Cr<sub>2</sub>Rh, Debye characteristic temps. 4-70330
- Cr<sub>2</sub>Si single cryst., <sup>51</sup>Cr self diffusion 4-64543
- Ct<sub>1</sub>-Mn<sub>2</sub>Ge, amorphous thin films, elec. resist., Hall resist. 4-114049
- Cu-Cr, liquid alloys, enthalpies of mixing, intermetallic compound form. 4-92374
- Cu-Cr (0.8 wt.%), film, dil., thermoelec. power, thickness depend. 4-61468
- Cu-Ni-Cr (30.5 wt.%), quenching, ageing, spinodal decomp., hardness, X-ray diff. obs. 4-114526
- Cu-Ti-Cr, internal friction and precipitation morphology (*Russian*) 4-99416
- Cu-Ti-Cr (4, 0.5 wt.%), ageing, internal friction, Young's modulus, modulated structure 4-66362
- Fe, cast, white, high Cr, abrasion by quartz particles, carbide removal mechanism rel. to particle shape 4-85220
- Fe-Al-Cr, oxidation, effect of ternary alloying additions 4-85242
- Fe-base austenitic alloys, high strength evaluation for generator retaining rings 4-99448
- Fe-C-Cr, austenite, cementite dissoln., computer simulation 4-71653
- Fe-Co-Cr mag. disc., Lorentz microscopy and read/write characs. 4-80746
- Fe-Cr, accelerated oxidation in atmosphere containing water vapour 4-81356
- Fe-Cr, binding energy, CPA calcs. (*Russian*) 4-98060
- Fe-Cr, cast, surface layer alloying using laser treatment 4-109548
- Fe-Cr, corrosion and passivation, in Cl-containing H<sub>2</sub>SO<sub>4</sub> 4-85241
- Fe-Cr, mech. polishing, surface film thickness and comp., XPS obs. 4-62093
- Fe-Cr, passive film form. and props. 4-81332
- Fe-Cr, spinodal decomposition, small angle neutron scatt. studies 4-114552
- Fe-Cr, surface segregation of S, annealing and O<sub>2</sub> adsorption effect (*Japanese*) 4-61932
- Fe-Cr, thermal expansion coeff., mag. contrib. 4-84843
- Fe-Cr (26.6 at.%), sulphidation props. in H<sub>2</sub>S-H<sub>2</sub> atmospheres at temps. 973 to 1173K and S press. 10<sup>-2</sup> to 10<sup>-4</sup> Pa 4-93459
- Fe-Cr (26.6 at.%), sulphidation mechanism in H<sub>2</sub>S-H<sub>2</sub> atmospheres at temps. of 973 to 1173K and S press. 10<sup>-2</sup> to 10<sup>-4</sup> Pa 4-93460
- chromium alloys continued
- Fe-Cr (30 wt.%), high temp. corrosion mechanism, XPS and AES studies 4-62098
- Fe-Cr (8 wt.%), ferrite-austenite, isothermal transform. kinetics, grain boundary nucleation 4-109396
- Fe-Cr (9.75 wt.%), cold worked, ion beam thinned, protective oxidation in CO<sub>2</sub> 4-62095
- Fe-Cr (9.75 wt.%), protective oxidation in CO<sub>2</sub>, TEM obs. 4-62094
- Fe-Cr alloys, BCC self-diffusion of Fe 4-65449
- Fe-Cr alloys, inhomogeneous, X-ray fluoresc. intensities, Monte Carlo simulation 4-109246
- Fe-Cr alloys, pit initiation, current fluctuations obs. 4-89181
- Fe-Cr  $\alpha$  and  $\sigma$  phase alloys, sp. ht. and entropy of formation 4-103959
- Fe-Cr system, irradi., constrained equilib. thermodynamics 4-103793
- Fe-Cr-Al, oxide dispersion strengthened MA 956, fatigue crack growth 4-62031
- Fe-Cr-Al, oxide films, characterisation by soft X-ray spectroscopy and microanal. 4-76909
- Fe-Cr-Al, sulphidation in H<sub>2</sub>S, multilayered corrosion scales 4-71801
- Fe-Cr-Al alloys, sulphidation protection by Al<sub>2</sub>O<sub>3</sub> scales 4-93468
- Fe-Cr-Al-Ti alloy, Y<sub>2</sub>O<sub>3</sub> dispersed, characs. of Al<sub>2</sub>O<sub>3</sub> scales 4-89180
- Fe-Cr-Al-X, X = Cu, Ti, Ni, anodic polarization in H<sub>2</sub>SO<sub>4</sub> 4-114719
- Fe-Cr-Al-Y plasma sprayed coatings, post-treated, mech. props. 4-93471
- Fe-Cr-Al(Y), precip., small-angle neutron scatt. study 4-93304
- Fe-Cr-B, metallic glass, mag. props. and density 4-84773
- Fe-Cr-B, Mossbauer study of packing fraction 4-84877
- Fe-Cr-C, hypereutectic alloys unidirectionally solidified, hot hardness of primary carbides 4-99492
- Fe-Cr-C (10, 0.2 wt.%), austenite form., TEM and optical microscopy study 4-66331
- Fe-Cr-Co, phase separation and coarsening 4-109407
- Fe-Cr-Co (12 wt.%) permanent magnet alloys, mag. props., effect of alloying 4-84771
- Fe-Cr-Co alloys, spinodal decomposition, atom probe field ion microscopy studies 4-114553
- Fe-Cr-Co-Si-B amorphous alloys, mag. props. and hyperfine interactions (*Russian*) 4-108994
- Fe-Cr-Mo-Ti heat-resisting alloy, Chi phase strengthened 4-71800
- Fe-Cr-Ni, austenitic alloy, He bubbles at grain boundaries 4-108471
- Fe-Cr-Ni, martensitic transition and cryst. geometry (*Russian*) 4-66332
- Fe-Cr-Ni (15, 15 wt.%), He bubble form. during dual beam irradi. 4-75562
- Fe-Cr-Ni (15, 15 wt.%), weak beam imaging of He bubbles 4-103618
- Fe-Cr-Ni (20, 10 wt.%), oxidation, TEM microstructural study 4-104926
- Fe-Cr-Ni-Mo, austenitic alloy, void swelling, effect of pulsed irradi. 4-108474
- Fe-Cr-Ni-Mo, austenitic alloy, pulsed ion irradi., temp. aspects 4-108476
- Fe-Cr-Ni-W, amorphous, crystn., effect of irradi. particle mass 4-79936
- Fe-Cr-Ni(Si), acoustic emission and resist. variation during cyclic heating 4-81296
- Fe-Cr-Si(Ti), electron and ion-irradi., void and precip. struct. 4-103802
- Fe-Cr(Si), dissoln. in molten pure Al under forced flow 4-92378
- Fe-Ni-Cr, austenitic, neutron irradiated, swelling and creep 4-108452
- Fe-Ni-Cr,  $\gamma$  precip., influence on elastic limit (*French*) 4-81200
- Fe-Ni-Cr (16, 15 wt.%), void swelling, effect of C and Nb additions 4-103817
- Fe-Ni-Cr ferritic alloy, soft mag. props. and mech. strength 4-61555
- Fe-Ni-Cr-Al(Y)(Zr)(Ti), high temp. oxidation resist. influence of Y, Zr or Ti additions 4-104899
- Fe-Ni-Cr-B-C, swelling behaviour, influence of Li shell effect on microscopy determ. 4-109580
- Fe-Ni-Cr-C, butterfly martensite, TEM study 4-108363
- Fe-Ni-Cr-C, Ti-modified, void swelling, pre-irradi., ageing effects 4-104798
- Fe-Ni-Cr-C(3.6, 1.45, 0.5 wt.%) alloys, bainite formation kinetics, effect of step quenching 4-114514
- Fe-Ni-Cr-Mo-N, weld metal, annealing, precipitation, metallographic analysis 4-109417
- Fe-Ni-Cr-W amorphous alloys, corrosion resist. 4-99632
- Fe-Ni-Mn-Cr alloys with mixed exchange interactions, mag. phase transitions, sp. ht. study 4-65820
- Fe-Ni-Ti(Cr)(Al), nitrided layer, Mossbauer studies (*Russian*) 4-109555
- Fe<sub>2</sub>Co<sub>2</sub>Ni<sub>2</sub>Cr<sub>2</sub>B<sub>2</sub>Si<sub>2</sub> metallic glass, mag. props. study 4-84790
- Fe<sub>2</sub>Cr<sub>2</sub>, short range order inversion, alloy conc. depend. 4-103690
- Fe<sub>2</sub>Cr<sub>10</sub>B<sub>20</sub> and Fe<sub>2</sub>Cr<sub>3</sub>Ni<sub>3</sub>B<sub>30</sub> amorphous alloys, elastic characs. and microclastic decomp. 4-93325
- Fe<sub>2</sub>(Cr<sub>100-x</sub>)B<sub>x</sub> metallic glasses, onset of magnetism, Mossbauer spectra 4-71217
- (Fe<sub>1-x</sub>Cr<sub>x</sub>)Mn<sub>1-y</sub>, <sup>55</sup>Mn and <sup>57</sup>Fe NMR, comp. depend. 4-98960
- (Fe<sub>1-x</sub>Cr<sub>x</sub>)Mn<sub>1-y</sub>, impurity mag. state, <sup>55</sup>Mn and <sup>57</sup>Fe NMR study 4-98961
- Fe<sub>63</sub>Ni<sub>37</sub>-Cr<sub>2</sub>, magnetoresist. and ferromag-spin glass transitions 4-113924
- Fe<sub>60</sub>-Ni<sub>40</sub>Cr<sub>20</sub>, mag. phase diagram, neutron diff. study 4-71069
- FeNiCrMoBSi amorphous ribbons, magnetostriction, capacitance studies 4-61580
- Fe<sub>2</sub>Ni<sub>4</sub>Cr<sub>2</sub>P<sub>12</sub>B<sub>6</sub> amorphous alloys, flame spray quenching, coating on metal substrates 4-71797
- Fe<sub>2</sub>Ni<sub>4</sub>Cr<sub>14</sub>P<sub>12</sub>B<sub>6</sub> metallic glass, Mossbauer study of high press. 4-84880
- FePCr(Cr), structural and mag. coherence lengths 4-88100
- LaNi<sub>2</sub>Cr hydrides, H-T, H-D, D-T mixtures isotope equilibria 4-108586
- Mo-Cr, interstitial-friction, workability and ductility, effect of alloying element 4-93345
- Ni-(Al-Ti)-(Cr-Mo), pseudoternary phase diagram, phase relationship study using EPMA 4-76933
- Ni-base superalloy, DKS, directionally solidified, mech. props., influence of grain orientation 4-93420
- Ni-base superalloy, IN 100, hot corrosion inhibition by MgSO<sub>4</sub> and BaSO<sub>4</sub> 4-85254
- Ni-Co-Cr-Nb-Hf, Ni-base superalloy, MERL 76, powder metallurgy hot isostatic pressing, effect of Ar contamination 4-114447
- Ni-Co-W-Cr single crystal superalloy, crack tip plasticity, fatigue crack growth at elevated temp. 4-71727
- Ni-Co-W-Cr superalloy, single cryst., crack tip plastic strain 4-89231
- Ni-Cr, conc. FCC alloys, heterogeneous deform. mechanisms 4-81236
- Ni-Cr, environmentally induced porosity 4-85260
- Ni-Cr, internal oxidation, O transport at high temps. 4-92442
- Ni-Cr, oxidation, SIMS and XPS study of thermal oxide films 4-76908
- Ni-Cr, oxide dispersion strengthened 4-85260
- Ni-Cr (20 wt.%), reaction kinetics with SO<sub>2</sub>, 600°C-900°C 4-104905

## chromium alloys continued

- Ni-Cr base alloys, creep behaviour and microstruct. 4-71705  
 Ni-Cr detonation deposited coatings, wear resist. during sliding in dry friction 4-66457  
 Ni-Cr system, irradi., constrained equilb. thermodynamics 4-103793  
 Ni-Cr-Al,  $\gamma$  precip. growth prediction 4-71658  
 Ni-Cr-Al, recrystn. during rapid elec. heating 4-66347  
 Ni-Cr-Al (20, 4 wt.%), high temp., oxidation, tensile stress depend. 4-109572  
 Ni-Cr-Al films, highly disordered, temp. depend. resist. 4-80690  
 Ni-Cr-B surface coatings, phase composition, X-ray diffr. 4-99377  
 Ni-Cr-B-Al detonation deposited coatings, wear resist. 4-62123  
 Ni-Cr-Co, IN 939, turbine stator blades, corrosion layers, metallography 4-104948  
 Ni-Cr-Co (22, 9 wt.%) superalloy, solid solutions strengthened, development, weldability, oxidation resist. 4-61975  
 Ni-Cr-Co-Al-Ti-Nb-W-Mo-V-Hf, cryst. lattice periods mismatch determ. 4-65219  
 Ni-Cr-Co-B, melt spun superalloy, annealing, castability, ductility and microstruct. rel. to B additions 4-66323  
 Ni-Cr-Fe, alloy X-750, SCC resist. in deaerated high temp. water rel. to solution heat treatment (Japanese) 4-62110  
 Ni-Cr-Fe, Inconel X-750, HVEM irradi., void form. rel. to  $\gamma$  precipitation 4-108446  
 Ni-Cr-Mo, creep-resisting alloys, cast, grain boundary relax., effect of struct. of boundary vol. 4-71677  
 Ni-Cr-Mo superalloy, elastoplastic deform. and failure, acoustic emission obs. 4-66377  
 Ni-Cr-Mo system, isothermal sections of Ni rich portion, analytical electron microscopy 4-71638  
 Ni-Cr-Si vacuum brazed joint of Inconel 718, struct. 4-66548  
 Ni-Cr-Ti-Mo(Nb), precipitation strengthened, HFIR irradi., ductility, microstruct. 4-108457  
 Ni-Cr-W, creep-resisting alloys, cast, grain boundary relax., effect of struct. of boundary vol. 4-71677  
 Ni-Fe-Cr alloys, extraordinary Hall coeff. sign reversal and DC resist. 4-113922  
 Ni-Si-Cr, microsegregation, influence of mutual interaction of alloying elements 4-66340  
 NiAl-Cr quasibinary eutectic, rapidly solidified, microstruct. and phase solubility extension 4-66319  
 NiCr films, electrical resistance in freq. range 10-100 MHz 4-80567  
 NiCr thin films,  $\text{Cr}_2\text{O}_3$  phase appearance, electron microscopy and diffr. study 4-81344  
 $\text{Ni}_3\text{Cr}$ ,  $\text{Ni}_2\text{Cr}$ , high temp. deform., effect of ordering 4-93358  
 $\text{Ni}_3\text{Cr}$ , ordered state, annealing, elec. resist., electron diffr. obs. 4-109394  
 $\text{Ni}_3\text{Fe}_2\text{Cr}_{14}\text{Pt}_6\text{B}_6$  metallic glass, surface oxidation in crystalline and amorphous states 4-89187  
 PtCr, nonmagnetic resist. anomalies 4-113919  
 $\text{Si}_{1-x}\text{Cr}_x$  amorphous film, metal-semicond. transition, scaling behaviour and min. metallic cond. 4-70885  
 $\alpha/\beta\text{Ti-Al-Cr-Mo-V}$ , annealed, struct. and mech. props. 4-61988  
 Ti-Cr, influence of ageing on incommensurate struct. (Russian) 4-65218  
 Ti-Cr, oxidation rate and scale adherence rel. to Cr content 4-109565  
 TiC-Fe-Cr-Mo, bonded carbides, wear-resistant, produced by powder metallurgy techniques 4-66455  
 V-Cr-Fe-Zr, candidate materials for fusion appl., weldability 4-99494  
 V-Cr-Ti, candidate materials for fusion appl., weldability 4-99494  
 V-Cr-Ti, fusion materials, candidate materials for impurity control 4-91108  
 V-Cr-Ti, fusion reactor blanket use, analysis of attack by O and water vapour 4-107019  
 V-Cr-Ti, fusion reactor blanket material, neutron activation cross sections 4-107047  
 V-Cr-Ti Path C alloy for fusion reactors, V volatility, safety anal. 4-111782  
 V-Cr-Ti(Fe-Zr), mech. props. rel. to O contamination, fusion appls. 4-109499  
 V-Cr-Ti, corrosion and oxidation 4-109556  
 $\text{V}_2\text{CrAl}_{1-x}\text{B}_x$ , melt spinning and phase transforms 4-114450  
 Zr-Nb-Cr (0.5, 1%) oxidation kinetics,  $\text{H}_2$ -pickup and  $\text{O}_2$  dissolution 4-99641  
 ZrCrFe-based hyperstoichiometric alloys and hydrides, mag. props. 4-109025

## chromium compounds

see also chromium alloys

- hardfacing deposits,  $\text{Cr}_2\text{C}_3$ -containing, microstruct. and abrasion resist., influence of welding process variables 4-85222  
 $\alpha\text{-KCr}(\text{SO}_4)_2 \cdot 12\text{H}_2\text{O}$  alum, high pressure mag. resonance study of crystal fields 4-70757  
 oxides, diffusion and association of defects 4-98363  
 trisacetylacetonatochromium (III), relaxation effects on  $^{13}\text{C}$  NMR quantitative data 4-69108  
 $\text{Ag}_{50}\text{Cr}_{50}\text{PS}_{50}$ , quasi-one-dimensional antiferromagnet, electron irradi. and substitution induced disorder 4-98866  
 $\alpha\text{-Al}_2\text{O}_3\text{-Cr}_2\text{O}_3$ , ionic cond., doping effects 4-92417  
 $\text{Al}_2\text{O}_3\text{-SiO}_2\text{-TiO}_2\text{-Cr}_2\text{O}_3$ , high alumina refractory brick, creep resist. rel. to  $\text{Cr}_2\text{O}_3$  addition 4-109457  
 $\text{Ca}_2\text{Cr}_2\text{Si}_2\text{O}_{12}$ , synthetic garnets, Cr coordination and vibr. props., IR study 4-65249  
 $\text{CdCr}_2\text{Se}_4$ , photomagnetisation study 4-99102  
 $\text{CdCr}_2\text{Se}_4$ , surface magnetostatic wave obs. 4-84778  
 $\text{CdCr}_2\text{Se}_4$ :In, static I-V characts. 4-70815  
 $\text{CoO-Cr}_2\text{O}_3$ , non-stoichiometric, segregation and chem. diffusion 4-98297  
 $\text{CoO-Cr}_2\text{O}_3$ , surface segregation, ESCA studies 4-65521  
 $(\text{Cr,Nb})\text{Nb}_5\text{Se}_{10}$ , one-dimensional systems, resistivity, structure and mag. props. 4-61364  
 Cr binuclear complexes, triple metal bond HF-Slater transition state method 4-59619  
 Cr complex, HMB A Cr V radical in 1,2 propylene glycol soln., spectral and relax. time meas. at 150 GHz 4-91289  
 Cr complex, of tris(acetylacetonato), lowest doublet excited states, optical Zeeman spectra 4-66061  
 Cr complexes,  $\pi$ -electron delocalisation NMR, IR and XPS study 4-87117  
 Cr complexes, trans-diisothiocyanate(bis)ethylenediaminechromium(III) ion, absorpt. and phosphoresc. 4-107379  
 $\text{Cr}_2\text{B}_3\text{O}_{12}\text{Cl}$ , ferroelec. orthorhombic to monoclinic transition 4-71301  
 CrBr $_3$ , optical spectra near mag. transition temp. 4-61729  
 CrBr $_3$ , XPS study of core level splitting 4-109303  
 chromium compounds continued  
 $\text{Cr}_2\text{C}_3$ -Ni-B electrophoretic coatings, struct. and props. 4-88430  
 $\text{Cr}(\text{CO})_6$ , ligand core hole states, configuration interaction calcs. 4-83301  
 $\text{Cr}^{12}\text{CO}_6$ , in Ar matrix, FT-IR spectra, isotropic substitution effects 4-112183  
 $\text{Cr}^{12}\text{CO}_6$ ,  $^{13}\text{CO}$ , in Ar matrix, FT-IR spectra, isotropic substitution effects 4-112183  
 $\text{CrCl}_3$ , in organic solvents, absorpt. spectra of  $\text{Cr}^{3+}$  ion (German) 4-61731  
 $\text{CrCl}_3$ , optical spectra near mag. transition temp. 4-61729  
 $\text{CrCl}_3$ , XPS study of core level splitting 4-109303  
 $\text{CrH}_3$ , H lattice site location EXAFS 4-93137  
 $\text{Cr}_2\text{Mn}_{1-x}\text{As}$ , magnetically ordered, thermoelec. power 4-70846  
 $\text{Cr}_2\text{Mn}_{1-x}\text{As}$ , thermal and mag. props., 100 to 500K 4-92922  
 $\text{CrMo}_6\text{BrI}_3$ , preparation and cryst. struct. 4-70097  
 CrN, ultrafine particles, growth by reactive gas evaporation technique with electron beam heating 4-61894  
 $\text{CrN}_x$ , DC reactively sputtered layers with surface roughness, as selective absorbers in solar collectors 4-77147  
 $\text{Cr}_{1.4}\text{Nb}_{2.55}\text{Se}_{10}$ , cryst. struct., metal-insulator transition, resist., mag. susceptibility meas. 4-88448  
 $\text{CrO}_2$  particles for audio recording, high orientation effect 4-65832  
 $\text{CrO}_2$  particles prod. for mag. tape appls. 4-65831  
 $\text{CrO}_2$  powders, hydrothermal synthesis and charact., mag. recording appl. 4-89000  
 $\text{CrO}_2$ , reduction, struct. and textural constraints 4-71916  
 $\text{CrO}_2$ , muon capture, Cr to O ratio, amorphous or cryst. struct. effects 4-84883  
 $\text{CrO}_2$ , rel. between electronic struct. and electron affinity, discrete variational Xalpha calcs. 4-87045  
 $\text{CrO}_2^{2-}$ , totally symmetric  $\nu_1(\text{A}_1)$  mode, reson. Raman excitation profile 4-83380  
 $\text{CrO}_3$ , deviation from stoichiometry at high  $\text{O}_2$  partial press. 4-113656  
 $\text{CrO}_3$ , doped, hot pressing, annealing, elec. cond., density, grain size, XPS 4-113946  
 $\text{CrO}_3$ , exchange integrals and Hamiltonians 4-98876  
 $\text{CrO}_3$ , ferromag., Curie point transition, EPR obs. 4-109061  
 $\text{CrO}_3$ , film thickness meas. using Raman scatt. 4-104689  
 $\text{CrO}_3$  formation on Cr or Fe-Cr-Ni alloy, TEM study 4-104926  
 $\text{CrO}_3$ , muon capture, Cr to O ratio, amorphous or cryst. struct. effects 4-84883  
 $\text{CrO}_3$  plasma-sprayed deposits, IR Fourier transform specular reflection spectroscopy of surfaces 4-101942  
 $\text{CrO}_3$ , porous, thermal diffusivity, unsteady state method 4-80316  
 $\text{CrO}_3$ , thermal cond. in vicinity of Neel transition 4-113734  
 $\text{CrO}_3$  thin films, interaction with W 4-70576  
 $\text{CrO}_3\text{-Li}$ , elec. cond., O activity depend. 4-61376  
 $\text{CrO}_3\text{(TiO}_2\text{)}$ , sintering and recrystn. 4-66290  
 $\text{CrO}_x$ , mixed valence cpds., mag. and struct. studies 4-98071  
 $\text{CrOCl}_2$ , chemisorpt. on pyrogenic  $\text{SiO}_2$  surface, IR spectrosc. investig. 4-109196  
 $\text{CrO}_2\text{F}_2$ , laser induced fluoresc. spectrum in seeded mol. beam 4-91299  
 $(\text{Cr}_2\text{O}(\text{RCOO}))_n^+$  clusters, magnetic behaviour, isotropic dynamic distortion model 4-92905  
 $\text{Cr}_2\text{Ru}_{1-x}\text{O}_2$ , high press. distortion, cryst. struct. study 4-80012  
 Crsb, mag. props., mol. field theory 4-108995  
 $\text{CrSi}_2$ , AES, principal component anal. 4-77041  
 $\text{CrSi}_2$ , electronic density of states, XPS study 4-61272  
 $\text{CrSi}_2$ , form. by ion beam mixing 4-80121  
 $\text{CrSi}_2$ , optical props. and electronic struct. 4-80935  
 $\text{Cr}_2\text{TeO}_6$ , antiferromag. insulator, MM wavelength mag. reson. study 4-80812  
 $\text{Cr}_2\text{Ti}_2\text{O}_7$ , photoelectrochemical props. 4-80625  
 $\text{CrTi}_{1-x}\text{O}_2$ , high press. distortion, cryst. struct. study 4-80012  
 $\text{CrVNO}_6$ , semicond., elec. resist., mag. susceptibility meas. 4-109000  
 $\text{Cr}_2\text{WO}_6$ , antiferromag. insulator, MM wavelength mag. reson. study 4-80812  
 CrZn, rare-gas matrices, hyperfine splitting, EPR 4-102716  
 $\text{CuCr}_2\text{Se}_4$ , solid solutions, radiographic study of struct. 4-108317  
 $(\text{CuCr}_2\text{Se}_4)_x(\text{Cu}_9\text{Ga}_{10}\text{Cr}_2\text{Se}_{41})_{1-x}$ , semiconducting spin glasses, resistance, magnetoresistance, studies 4-108862  
 $(\text{CuCr}_2\text{Se}_4)_x(\text{Cu}_9\text{In}_{10}\text{Cr}_2\text{Se}_{41})_{1-x}$ , semiconducting spin glasses, resistance, magnetoresistance, studies 4-108862  
 $\text{Cu}_{1/2}\text{In}_{1/2}\text{Cr}_2\text{Se}_4$ , solid solutions, radiographic study of struct. 4-108317  
 $\text{Fe-Cr-O}$ ,  $\gamma$ -spinels, vacancy substituted, order-disorder, IR spectra (French) 4-76447  
 $\text{Fe}_2\text{-Cr}_2\text{O}_3$ , chem. transport of haematite with  $\text{TeCl}_4$  as transporting agent 4-61824  
 $\alpha\text{-G}_2\text{O}_3$ , films growing on G, O transport obs. by  $^{18}\text{O}$ /SIMS 4-89174  
 $\text{Ga}_{2/3}\text{Cr}_2\text{S}_4$ , cation deficient chalcogenide spinels, electron microscope study 4-113443  
 $\text{InCr}_{1/3}\text{S}_4$ , cation deficient chalcogenide spinels, electron microscope study 4-113443  
 $\text{KBr:Cr}(\text{CN})_6^{3-}$ , ESR, IR, Raman and emission spectra, radiative and nonradiative transition 4-65850  
 $\text{Li/CrO}_2$  battery, performance characts. and safety tests, for electronic applications 4-93602  
 $\text{LiF-CrF}_3$  thin film, ionic cond. meas. 4-84450  
 $\text{MgO-Cr}_2\text{O}_3$  granular ceramic, sintering and phase comp. 4-81174  
 $\text{MgO-Cr}_2\text{O}_3$  refractories, thermal shock damage resist., ribbon test, Young's modulus obs. 4-89195  
 $\text{MgO-Cr}_2\text{O}_3$  refractory, thermal shock resist., prod. during Frenkel effect 4-66289  
 $\text{Mo-Al}_2\text{O}_3\text{-Cr}_2\text{O}_3$  cermet emitter electrodes, directionally solidified, development and evaluation for thermionic energy converters 4-77126  
 $\text{Mo-Al}_2\text{O}_3\text{-Cr}_2\text{O}_3$  eutectic thermionic emitter 4-72141  
 $\alpha\text{-NH}_4\text{Cr}(\text{SO}_4)_2 \cdot 12\text{H}_2\text{O}$  alum, high pressure mag. resonance study of crystal fields 4-70757  
 $(\text{NH}_4)_2\text{SO}_4\text{-CrO}_3$ , phase transitions studied by EPR spectra 4-88723  
 $(\text{NH}_4)_2\text{SO}_4\text{-K}_2\text{SO}_4\text{-CrO}_3$ , phase transitions studied by EPR spectra 4-88723  
 $\text{NaCrS}_2$  cathode for secondary Li cells, props. and cyclic performance 4-93605  
 $\text{NiO}$ ,  $\text{NiO-Cr}_2\text{O}_3$ , non-stoichiometric, segregation and chem. diffusion 4-98297  
 $\text{H-Ta}_2\text{O}_5\text{-TiO}_2(\text{HfO}_2)(\text{Cr}_2\text{O}_3)$ , ionic conductivity 4-75722  
 $\text{Zn}_{1-x}\text{Ga}_{2x}\text{Cr}_2\text{Se}_4$ , magnetic semiconducting solid solutions study 4-109002  
 $\text{ZrO}_2\text{-Cr}_2\text{O}_3(\text{ZrB}_2)$ , sintering materials, rapid chem. anal. (Japanese) 4-109339

**chromosomes** *see cellular biophysics*

**chromosphere**

- active region, chromosphere and photosphere fine struct. 4-77800  
 active region, EUV struct. 4-101305  
 active regions, He I and He II line width obs. 4-77799  
 atomic spectra and oscillators, conf., Lund, Sweden, 17-19 Aug. (1983) 4-86109  
 bright points, 2-D MHD formation model 4-77793  
 charged particles acceleration region height, electrons and protons spectrum form anal. 4-100938  
 disc brightness in 160 nm continuum, features 4-90126  
 disc characteristic struct. obs. on rocket UV filtergrams 4-101186  
 electron heating, dynamical response and flares, appl. to red dwarfs 4-94838  
 emission from chromospheres, transition regions and coronae 4-67716  
 ephemeral region, HRTS II EUV obs. 4-90124  
 evaporation vels. in solar flares 4-115732  
 flare, escaping electrons from extended X-ray producing region 4-105935  
 flare emission anal., plasma characts. and sources anal. 4-94717  
 flare, numerical model based on electron beam heating of chromosphere 4-77805  
 granular structure, visible obs. 4-101293  
 limb brightening at 820 microns, radial intensity profile 4-63119  
 magneto-acoustic-gravity modes, propag. in solar atmosphere of oblique mag. field 4-115731  
 MHD waves in upper chromosphere and corona, rel. to sympathetic flare activity in distant active regions 4-105914  
 plages, Li I line strengths obs. rel. to stellar Li abundance determ. 4-63131  
 plages and magnetic field humps, correl. with radio brightness distrib. during solar min. 4-105917  
 plasma ejection, MHD motions in untwisting magnetic tubes 4-63124  
 radiative processes in cool star chromospheres 4-90152  
 radio brightness distrib. in solar disc, calc. using inhomogeneous chromospheric model 4-105916  
 resonant layer above sunspots, resonance oscillations and magnetoacoustic gravity wave transform. 4-63123  
 running penumbral waves, model based on linear transform. of magneto-acoustic-gravity waves 4-72918  
 spicules, wave propag. along mag. field in cylindrical layer 4-82460  
 sunspot oscills., propag. characts., spectral obs. 4-94701  
 sunspot transition region, oscills. distrib., spectral line and mag. field obs. 4-101289  
 sunspot umbrac, overlying chromosphere and transition region oscills. 4-105927  
 sunspot umbral oscillations and photosphere-chromosphere reson. theories 4-90134  
 sunspots, rotation determ. from radial vels. and H $\alpha$  obs. 4-105913  
 total eclipse of 1980 February 16, flash spectra obs. and instrumentation (Japanese) 4-94715  
 transient response to solar flare, gas dynamics in radial open field region 4-63114  
 transition region, Be-like ions diagnostics, effect of non-Maxwellian electron vel. distrib. 4-101288  
 transition region, heating model 4-105931  
 transition region emission lines, mass motion effects on emission measures 4-110583  
 transition region EUV line emission weakening by Lyman continuum absorpt. 4-101294  
 transition region UV brightness rel. to photospheric electric current 4-105928  
 transition zone chromosphere-photosphere spectral windows, far IR solar imaging 4-110589  
 US obs. with HRTS 4-85906  
 Wilson-Bappu effect, review (French) 4-77808  
 He I flare of 1982 September 4, nature, IR and X-ray emission 4-101299

**chronographs** *see chronometers*

**chronometers**

No entries

**CI calculations (atoms)** *see atomic electron correlations*

**CI calculations (molecules)** *see molecular electron correlations*

**CIDEP**

- benzyl radicals, stationary nutations and CIDEP during methyl benzyl ketone photolysis 4-76252  
 Heisenberg spin exchange model, CIDEP and relax. 4-88722  
 methylpyrazines radical, triplet state, photophysics and photochemistry, CIDEP 4-69115  
 polarisation, time evolution, oscillatory pattern 4-102711  
 radical pair mechanism electron spin polarisation, CIDEP 4-87142  
 radicals, spin polarised, continuous wave flash photolysis ESR spectra using time integration spectroscopy 4-74274

**CIDNP**

No entries

**cinelifilming** *see cinematography*

**cinematography**

*see also cameras*

- 3-D films development, Jaws 3D as example (German) 4-68294  
 70 millimetre motion picture films, potential of technical means for artistic creations (Russian) 4-73555  
 70 mm laser flying spot telecine projector for HDTV (Russian) 4-73557  
 70 mm sound tracks, stripping, recording and reproducing 4-73538  
 aerial, restoration of motion degraded images [in aerial cinematography] 4-58899  
 antireflection coatings, five-layer achromatic, for multicomponent movie camera lens 4-79271  
 aspect ratios consideration 4-111224  
 automated determination of correction parameters in step-by-step motion picture and photographic image printing (Russian) 4-106420  
 camera, high-speed, optical accelerator rot. mirror aerodynamic drag determ. (Russian) 4-82845  
 cardiovascular cine film quality 4-89699  
 chlorinated solvents, use in the film industry 4-95537  
 chromaticity coordinate calcs. using motion picture film characts. (Russian) 4-106419  
 cinephotogrammetry, automated, high-speed simulated vehicle-pedestrian impact motion anal. appls. 4-115098  
 Colorization, development and appl. 4-106416

**cinematography continued**

- colour release print sound track processing, use of hydroxy-ethyl-cellulose (Russian) 4-106421  
 Dallas Sound Lab, design 4-73537  
 Datadisk magnetic control surface, technological revolution in film production industry 4-101948  
 depth-compressed images production in 3D (Russian) 4-90675  
 drive systems for cine-film processors 4-95538  
 EBU/IRT and SMPTE code for film editing 4-101958  
 FDL 60 film scanning system, development 4-63797  
 feature films, stereo dubbing at Pinewood Studios 4-68292  
 film and video, use together in programme production 4-95535  
 film camera eye-piece lenses, optical characteristics (Russian) 4-90677  
 film camera position stability compensation (Russian) 4-90676  
 film production, electric energy consumption rating (Russian) 4-90680  
 film projection, release print heating evaluation (Russian) 4-73553  
 film projection equipment, advanced series (Russian) 4-78404  
 film shooting cameras exposure time instability (Russian) 4-73554  
 film studio production and technological bases development, economic considerations (Russian) 4-73549  
 film studios, measures for increased efficiency (Russian) 4-73550  
 film transport mechanisms, functional thresholds of accuracy and parametric reliability (Russian) 4-78405  
 film transport systems, static control 4-106417  
 film-scanners, dark grey shades reproduction 4-68293  
 Fujicolour motion picture negatives 4-78395  
 HDTV laser beam recording on 35 mm colour film, electro-cinematography appl. 4-106418  
 high speed video motion analysis system 4-101951  
 holography, multicolour, of animated scenes by motion synthesis using multiplexing technique 4-74454  
 image quality and artistic interpretation (Russian) 4-58909  
 Kara-Kum, filming features (Russian) 4-78406  
 Lenfilm film studio, work completed in 1983 (Russian) 4-78403  
 lenses, Cine-Xenon 1:2.0 MC (German) 4-68295  
 lighting equipment for film shooting (Russian) 4-58905  
 lighting equipment requirements 4-73543  
 motion parameters of pan-head meas. using gyroscopic sensor (Russian) 4-90678  
 motion picture equipment, technical level evaluation (Russian) 4-90681  
 motion picture film, lighting, use of discharge lamps 4-111240  
 motion picture lighting compensation filters (Russian) 4-73552  
 optical sound tracks, worn-out, spatial filtering using white light (Russian) 4-73551  
 optics in entertainment, conf., Los Angeles, CA, USA (Jan. 1984) 4-110802  
 printing system evaluation 4-101959  
 professional techniques, review of basic work done in 1983 (Russian) 4-78402  
 projector 5-element objective lens parameters, tolerances 4-90670  
 SMPTE time and edit code, appl. 4-63799  
 sound dubbing techniques for film and video: a comparison 4-78394  
 sound film, historical development (German) 4-82838  
 spatial correspondence in motion picture display 4-111233  
 standards, historical review 4-73541  
 STAR, Scene Tracking Auto Registration system for aiding cameramen 4-73540  
 stereophonic sound perception, interaural phase anomaly (Russian) 4-93761  
 Super 16 mm, UK developments 4-111225  
 telecine equipment, market trends 4-63794  
 three dimensional motion picture camera systems, overview 4-111230  
 three-dimensional cinematography 4-111231  
 Ukraina film projector looping attachment design for continuous operation (Russian) 4-73556  
 video/sound tracks, time-advanced noise reduction system (Russian) 4-90679

**circuit analysis** *see network analysis*

**circuit analysis computing**

*see also circuit CAD*

- optical fibre communications receiver, circuit noise, theoretical anal. and computer calculation (Chinese) 4-79290  
 SiO<sub>2</sub> film traps, microcomputer-based avalanche injection system, area density anal. 4-101870

**circuit breakers**

- see also circuit breaking arcs; gas blast circuit breakers*  
 microcomputer storage oscilloscope investig. of action 4-90338

**circuit-breaking arcs**

- see also circuit breakers; sparks*  
 air-blast high-current elec. arc, spectroscopic investig. 4-88017  
 dielectric recovery after interruption of a high current arc discharge 4-88018  
 SF<sub>6</sub> circuit-breaker arc channels, vel. meas. 4-88016

**circuit CAD**

*see also circuit analysis computing; circuit layout CAD*

- broadband bipolar transistor amplifier, Gbit/s appls., optimisation program development 4-83723  
 digital optical communication, numerical optimisation of equalising filters 4-83721

**circuit design** *see network synthesis*

**circuit layout CAD**

*see also circuit CAD*

- I<sup>2</sup>L device circuit model with layout patterns 4-104192

**circuit layout computer aided design** *see circuit layout CAD*

**circuit oscillations**

*see also circuit resonance*

No entries

**circuit resonance**

*see also circuit oscillations*

- nonlinear LC circuit circuit, resonant behaviour 4-95104

**circuit synthesis** *see network synthesis*

**circuit theory**

*see also filters; network analysis; network synthesis*

- electric fields and charges in elementary circuits 4-86229  
 ideal transformer, Poynting vector, consistency with elementary circuit theory 4-106148

circuits *see networks [circuits]*circular polarisation *see polarisation*

## circular waveguides

hollow waveguides with uniform curvature, wave propag. and attenuation

4-83692

pulse travelling in waveguide, absorpt. coeffs. 4-97069

## circumstellar shells

*see also stellar atmospheres; stellar winds*

0623+71, nova-like variable with assoc. nebular shell, discovery on

Palomar Sky Survey 4-77903

A 0538-66, neutron star and Be star model from light polarisation anal.

4-94858

accretion disc model spectra for cataclysmic binaries, double grid

4-77848

accretion discs, mag. field instabilities 4-63132

accretion discs, mol. viscosity as mag. field generation mechanism

4-115742

accretion discs, self-gravity and global structure 4-77818

accretion discs in close binaries, MHD anal., use of three-dimens. pseudo-

particle method 4-63209

accretion disk, viscous transonic flow around inner edge 4-115772

AGK3-0°965, central star to PN NGC 2346, IR light curves and circum-

stellar shell characts. 4-115755

anisotropically scatt. infinite uniform medium, point source 4-96799

V1343 Aquilae (SS 433), accretion ring nutation, short term periods

4-63180

V1343 Aquilae (SS 433), nutational effects of accretion disk 4-82487

Becklin-Neugebauer objects, catalogue of extremely young, massive and

compact IR sources 4-94643

bipolar outflow from disk accreting stars 4-90143

black hole, numerical study of nonspherical accretion 4-63195

black hole accretion discs, contrib. to asymmetric lepton prod. 4-82500

black hole thick discs 4-90175

OY Carinae, eclipsing dwarf nova, light curves and accretion disc char-

acts. 4-110632

 $\eta$  Carinae, spectroscopy of shell episode (1981 to 1983) 4-115760 $\gamma$  Cassiopeiae, Be star, spectrum vars., 1977 to 1979, rel. to mass ejection

into envelope 4-106004

cataclysmic binaries, HEAO 1 X-ray constraints on boundary layers

4-90155

cataclysmic binaries with accretion disc eclipses, light curve model, appl.

to LX Ser 4-72954

cataclysmic variable stars, accretion disc evolution during outbursts

4-82481

RS Cephei, eclipsing binary star, effect of circumstellar disc on UV light

curves 4-82505

RS Cephei, long-period Algol-type binary, circumstellar disc luminosity

rel. to anal. of UV light curves 4-82506

DI Cephei, T Tau star, light curve anal., effects of circumstellar extinc-

tion 4-94777

Chamaeleon I association Infrared Nebula, IR source nature and disc

characts. 4-63339

comet clouds surrounding nearby stars, constraints from isotropy of cosmic

microwave background 4-101273

composite dust shell heated by supernova, IR emission 4-105971

R Coronae Borealis stars, shell characts., IR anal. 4-72953

cyanacetylene ( $\text{HC}_3\text{N}$ ) in circumstellar shells, obs. and anal. 4-85907

CH Cygni, spectrophotometric obs. red giant with hot spot and dust shell

4-94796

V1500 Cygni (Nova Cygni 1975), photometric evidence for circumstellar

envelope 4-106003

Cygnus X-1, short period X-ray var. and accretion disc models 4-101435

Cygnus X-1, X-ray intensity dips due to absorpt. by partially ionised gas

4-94855

differentially rotating disks, turbulent magnetic field model 4-115744

dust condensation theory (*Russian*) 4-101140

early-type stars, evidence for circumstellar clouds from macrostructure of

UV continuous spectra 4-94733

early-type stars with mass loss, curve of growth method for IR and radio

spectrum 4-101312

G-type stars in Orion Ic association, IR excesses due to circumstellar dust

4-72934

U Germinorum, spectrophotometry and spectra interpretation with accretion

disc and accretion spot models 4-85947

grains formation and growth 4-77706

graphite detection method for circumstellar environment 4-101187

HD 218393, spectrophotometry of peculiar shell star revealing binary star

nature 4-82491

Herbig Ae stars CD-44°3318 and UX Ori, shell and atm. anal.

4-94792

Herbig Ae-Be stars, IR spectroscopy rel. to circumstellar H II regions

4-77830

DQ Herculis, obscuration by accretion disc as cause of absence of obser-

vable X-ray emission 4-101376

YY Herculis, spectrum of symbiotic star with G8 supergiant component

4-94797

D2 Herculis (Nova 1934), nebula characts. and star energy distrib.

4-110611

hot stars, transient components in Lyman lines rel. to ejection of shells on

very short timescales 4-115753

VW Hydri, SU UMa star, white dwarf characts. and accretion disc nature

4-110615

far-IR sources in Corona Austrina dark cloud, protostellar envelopes

model 4-86001

IRC+10216, C star,  $\text{C}_2\text{H}$  detect. in shell 4-77834IRC+10216, CN and  $\text{C}_2\text{H}$  in C star 4-94787IRC+10216 (CW Leo), C star, circumstellar  $\text{SiH}_4$  detect., IR obs.

4-82490

IRC+10420, VLA UHF obs. of OH masers assoc. with F8 supergiant

4-94759

long period variables, intrinsic polarisation var. due to flare effects on

## circumstellar shells continued

BT Monocerotis (Nova 1939), spectroscopic obs. of high and low vel. gas

streams 4-82479

MXB 1916-05, erratic X-ray var., accretion disc instability interpretation

4-110660

neutron star in X-ray binary, rot., mag. field-accretion disc plasma inter-

action effect 4-63210

neutron stars, viscous accretion discs, hydraulic jumps 4-90081

NGC 2024 No.2, IR speckle interferometry of B star with shell 4-94734

Nova Muscae 1983, shell geometry from UV obs. during early stages of

decline 4-82478

Nova Sagittarii 1982, shell geometry from UV obs. during early stages of

decline 4-82478

Nova Serpentis 1983, shell geometry from UV obs. during early stages of

decline 4-82478

novae, grain growth and destruction theory 4-101372

novae, processes in circumstellar shells during diffuse-enhanced and orion

stages 4-63171

 $\alpha$  Orionis, Be star, mass loss episode anal. 4-90156 $\alpha$  Orionis, semi-regular star, circumstellar shell photoionisation by chromo-

sphere radiation 4-85969

 $\epsilon$  Orionis (B0 la), appl. of curve of growth method to IR and radio

spectrum 4-101312

GK Persei (Nova 1901), shell radioemission detect., implications for mag.

field and plasma 4-110617

SZ Piscium, eclipsing RS CVn star, evidence for circumstellar H $\alpha$  emis-

sion 4-82504

pre-main-sequence star in dark globule B335, relation between circum-

stellar shell and  $\text{NH}_3$  emission region 4-115794

pre-main-sequence stars in Cha I assoc., IRAS obs. of two objects

4-85928

pre-main-sequence stars in young R associations NGC 1333, S68 and

NGC 7129, IR photometry 4-85993

red giant stars in globular clusters, intrinsic polarisation obs. rel. to

circumstellar shells 4-82470

red giants, circumstellar shells and mass loss 4-85936

HM Sagittae, circumstellar shell struct. and wind interactions, SHF/UHF

obs. 4-85910

SMC X-1, X-ray data anal., possible tilted precessing accretion disc

4-110666

SN 1979c and 1980k, radio and X-ray obs. as tests for circumstellar shell

models 4-72966

supergiant stars, MHD eqns. soln. rel. to form. of circumstellar envelope

4-101468

supergiant stars in Magellanic Clouds, 10-micron obs. rel. to circumstellar

dust shells 4-101334

supernova ejecta, interaction with ambient interstellar medium and

circumstellar shell 4-72963

supernovae, silicate grains in dust shells, IR emission 4-115769

supernovae, Type II, Comptonisation and UV emission lines in stellar

envelope 4-72961

 $\zeta$  Tauri, Be star, radial vel. and profile vars. of UV circumstellar lines

4-82482

 $\zeta$  Tauri, Be star, upper limit to shell size from lunar occultation obs.

4-101352

T Tauri stars, circumstellar, photometric and mass loss characts.

4-101337

T Tauri stars, circumstellar H $_2$  prod. due to ice grain-energetic particles

interactions 4-94781

T Tauri stars, intrinsic polarisation var. due to flare effects on circum-

stellar material 4-94779

T Tauri stars nebulae, frozen gases—fast particles interaction 4-94780

thick accretion disks, stability in negligible viscosity case 4-94727

thin accretion discs, nonaxisymmetric baroclinic instability 4-94732

twisted accretion disks in X-ray binaries 4-101321

W Ursae Majoris, JHK photometry and circumstellar shell evidence

4-94863

Ve2-45, WC9 star, IR dust shell model and obs. 4-85946

Vega ( $\alpha$  Lyrae), circumstellar shell of asteroids or comets 4-110602

WW Vulpeculae, rapid irregular variable star, evidence against dust

screening model 4-94789

PU Vulpeculae, spectral vars. obs. rel. to expanding circumstellar envelope

4-101356

white dwarf accretion from cool giant companion and disk properties

4-101319

white dwarfs optically thick mass losing envelopes, struct. rel. to nova

outbursts 4-72942

Wolf-Rayet ring nebulae, similarity soln. for stellar winds interaction with

surrounding interstellar medium 4-67712

X-ray binaries, periodically variable linear optical polarisation 4-94588

X-ray binary, outburst model, role of accretion disc struct., stability and

evolution 4-110661

 $\text{C}_2\text{H}$  in circumstellar envelopes of C stars, distrib. and abundance

4-72999

H-deficient binary stars, evidence for circumstellar shells, UBVRJHKI

obs. 4-90158

OH/IR stars, VLBI obs. of circumstellar shells 4-77849

OH-IR stars, circumstellar shell struct. from OH maser emission anal.

4-85970

WX Sagittae, recurrent nova, circumstellar shell characts. and mass ratio,

spectral obs. 4-101374

citation analysis *see information analysis*

## civil engineering

*see also building; dams*

Arctic offshore artificial island engineering 4-114885

glacial geology for engineers and Earth scientists, book 4-58596

rockbursts in mines and tunnels, conf., London, England (October 1983)

4-58555

United States Naval Civil Engineering Laboratory, developments

4-110175

## civil engineering computing

*see also architectural CAD; town and country planning*

linear structural systems subject to component changes, dynamic responses

anal. 4-87556

steel and concrete ocean structural design 4-114449

theodolite readings, processing using HP-41 calculator (*French*) 4-90572

## cladding techniques

steel plate, explosively bonded stainless clad pressure vessel, fatigue crack

growth (*Japanese*) 4-114643

**claddings**

- anticorrosive claddings on pressure vessel steel, fracture behaviour 4-99595  
 bond strength, multistep shear test 4-76925  
 DWR cladding (tubes, props. above annealing temp., mech. props. after thermal shock 4-106835  
 fibre optic taper-polarisers, highly birefringent, finite cladding effects 4-69569  
 fission reactor fuel and cladding relaxation during LOF accidents 4-106938  
 fission reactors, overcooling, pressure vessel cracking 4-64204  
 fuel element cans, production planning using BEKA, BIEG and NAVO programs 4-96157  
 hollow cylinder with cladding, circumferentially cracked, thermal shock resist. 4-87623  
 LMFBFR fuel element materials, swelling resist. (German) 4-83148  
 LWR large break LOCA, clad deform. and heat transfer, azimuthal effects modelling 4-102377  
 Magnox alloys, etched, surface anal. by secondary ion mass spectrometry and ion scatt. spectroscopy 4-93456  
 nuclear fuel-cladding separation by cladding-tube heating (German) 4-83218  
 PFR, B<sub>2</sub>C control rod pin performance, cladding compatibility 4-91076  
 pressure vessel cladding repairs, manual, numerical assessment of tolerance 4-66549  
 pressure vessel nozzle, crack indications in pulsed eddy current testing, spatial resolution of probe coil (German) 4-76942  
 reactor fuel pin transient deformation, cladding strains, MOX fuel appl., creep 4-102378  
 shielding, clad metals appl. 4-108836  
 space reactor fuel-cladding chemical compatibilities 4-106763  
 stainless steel clad fuel, fuel performance code 4-106772  
 stainless steel clad fuel rod anal. using NUFRAP code 4-106773  
 steel, austenitic stainless, claddings, ring test of tubes oxidised in high temp. steam 4-104816  
 steel, austenitic stainless, fast reactor fuel cladding, sigma phase form. rel. to liquid Na exposure 4-106672  
 steel, low C, Al clad, reaction diffusion, intermetallic layer growth kinetics 4-114722  
 steel, stainless, cladding, fuel rod performance, adjoint sensitivity anal. 4-111610  
 steel, stainless, claddings, fatigue crack growth rate in air and vacuum at 300°C 4-66413  
 steel, stainless, fuel cladding failures in Connecticut Yankee PWR, stress corrosion cracking 4-99659  
 steel, stainless 4-109564  
 steel plate, explosively bonded stainless clad pressure vessel, fatigue crack growth (Japanese) 4-114643  
 Superphenix FBR plant clad failure detection systems 4-111656  
 Taiwan Research Reactor, irradiated fuel rod testing 4-59326  
 Tokai Reprocessing Plant, leached fuel hull monitoring system, <sup>137</sup>Cs indicator for safeguards 4-106980  
 TRISO fuel pellet, fission product transport through cladding layers, model 4-107003  
 Zircaloy, fracture, influence of environment on form. of fluting microstruct. 4-104911  
 Zircaloy, oxide film cracking on fuel cladding tubes, strain anal. 4-91046  
 Zircaloy, textured, creep modelling under biaxial stressing 4-93354  
 Zircaloy 4, plane strain compression testing, plastic flow rel. to texture (German) 4-85270  
 Zircaloy cladding, chemical model for cadmium liquid-metal embrittlement 4-106770  
 Zircaloy cladding, fuel rod performance, adjoint sensitivity anal. 4-111610  
 Zircaloy cladding hulls, TRU contaminated; volume reduction process 4-106716  
 Zircaloy cladding tubes, ductile fracture anal. 4-106768  
 Zircaloy fuel cans, stress corrosion cracking with multiple fission product intrusion 4-96160  
 Zircaloy fuel cladding, numerical simulation of plastic deformation 4-106767  
 Zircaloy fuel rod cladding, strain rate sensitivity 4-64202  
 Zircaloy-2 cladding, localised stress-strain influence on SCC behaviour 4-106769  
 Zircaloy-2 cladding tube I-induced stress corrosion cracking time anal. 4-109549  
 Zircaloy-2 cladding tubes, stress corrosion cracking 4-106766  
 Zircaloy-4, microstruct. after air cooling from high temp.  $\beta$ -phase, effect of P impurity content 4-89071  
 Zircaloy-4, SAM determ. of O gradients, deform. modelling 4-88191  
 Zircaloy-4 claddings, SCC at elevated temps., relevance to transient LWR fuel rod behaviour 4-104912  
 Zircaloy-4/VO<sub>2</sub> chemical interaction 4-83140  
 Zircaloy-4/VO<sub>2</sub> diffusion couple, interfacial energy and work of adhesion 4-83141  
 Al-Mg (5 wt.%), direct hot extrusion of billet, pure Al cladding effect 4-109355  
 TiC-stainless steel interface, reaction zone struct. produced by vacuum annealing 4-104918  
 UO<sub>2</sub>/Zircaloy 4 reaction layer sequence, total interfacial energy 4-83142  
 Zr proton irradiation and thermal creep at elevated temps. under stress 4-75559  
 Zr, purification by electrotransport processing, resist. ratio obs. 4-85126

**classical algebra** *see algebra*

**classical field theory**

- see also classical mechanics; electromagnetic field theory; gravitation; special relativity*  
 Cauchy data space formulation 4-82689  
 classical electrodynamics, equations of motion, axiomatic deduction 4-95190  
 classical relativistic particle and field interactions 4-95682  
 correlation functions, dimensional reduction to Schwinger functions 4-101668  
 dynamical systems bound by mag. forces, math. problems, book contrib. 4-58692  
 image system of a source in no-slip sphere and cylinder 4-64908  
 instanton field, motion of particle 4-58658  
 Maxwell's eqns., hexons and octons in 6-D 4-95189

**classical field theory continued**

- Noether's theorem, equivalent conserved currents 4-86234  
 sine-Gordon systems, statistical mechanics props., boundary condition effects 4-63529

**classical mechanics**

- see also classical mechanics of continuous media; classical mechanics of discrete systems; classical theories of fluid structure*  
 book, elements of mechanics 4-63421  
 constraints, idealisation of elastic forces 4-67918  
 coupled-field dynamical system, partitioned anal., review, book contrib. 4-60359  
 cycling, frictional forces mechanical anal. 4-58636  
 Gaussian wave packet dynamics, classical interaction picture 4-106178  
 Hamilton-Jacobi eqn. derivation 4-82637  
 Hellmann-Feynman and curvature theorems 4-73257  
 interaction picture appls., canonical transform 4-106177  
 Lagrangian dynamics generalisation 4-95204  
 Lagrangian mechanics and second order eqns. 4-90372  
 multidimensional natural mechanical system 4-95152  
 power-law potential, rel. between energy and adiabatic invariants 4-82633  
 quantum mechanics classical limit coincidence with classical mechanics (French) 4-82691  
 similarity mechanics, intrinsic energy and Newton's law of gravit. as limiting cases 4-110961  
 Toda lattice type Hamiltonian systems, classical flow solutions, Lie groups 4-95315  
 transient algorithms anal. for mechanics and heat conduction, stability, book contrib. 4-60248  
 two-dimensional time-depend. classical systems, dynamical invariants 4-86195

**classical mechanics of continuous media**

- see also elasticity; fluid mechanics; mechanical contact; plasticity*  
 analytical mechanics of continua with mass, momentum and energy sources 4-73236  
 anisotropic continua, tensor representation of energy dissipation characts. (Ukrainian) 4-64839  
 arch, shallow, Marguerre-type, snap-through problem 4-101625  
 beam, infinitely long, contained in frictionless channel, flexural rigidity to axial compressive forces 4-74884  
 beam cross sections, optimal non-equal-strength shapes 4-112704  
 beam theory, higher-order, including cross-section transverse and lateral component effects (Japanese) 4-103194  
 beams, elastic, continuous, with unilateral rigid supports anal. based on classical derivatives 4-108004  
 beams with material and geometric nonlinearities, simple element for static and dynamic response 4-78141  
 bent plate containing hole with fissure from edge, stress conc. and factor (German) 4-83815  
 cables, taut, inclined, dynamics 4-101643  
 columns, unimodal, optimal, clamped-clamped, higher buckling mode determ. 4-87601  
 composite material analysis, survey 4-74862  
 composites, fibre-reinforced multilayer, delamination stress determ., iterative approach 4-112702  
 composites, fibrous, unidirectional, with initially deformed components, corrected elastic props. 4-74861  
 composites, physically nonlinear, effective dependence relationship derivation (Russian) 4-60275  
 continuum mechanics, spatial variational principles 4-87650  
 coupled shear walls, method of calc. force and displacement (Chinese) 4-79445  
 cylinder, corrugated, transversely isotropic, of finite, dimens., stress state 4-103196  
 cylindrical solids, Saint Venant theory of torsion, cross section of min. stress conc. 4-83813  
 Dirichlet problem of Laplace eqn., integral difference soln. method (Russian) 4-63517  
 distortion of a cylindrical shell in elastic casing, Flugge shell theory 4-112713  
 distributed parameter mechanical systems, minimax filtration problem soln. 4-74858  
 dynamic system stability 4-97366  
 elastic bodies of revolution with nonelliptical contact area, contact stress distrib. 4-86187  
 elastic materials, layered, strip loadings, finite layer anal. using flexibility approach 4-86211  
 Euler's foundation of continuum mechanics (German) 4-110847  
 expanded plate theories, consistency between Kirchhoff and Reissner theories (German) 4-83825  
 finite element method, projection-mesh diagrams construction using soft-tened-mixed approx. 4-63508  
 finite element strategies, classical solns., examples 4-87423  
 five-component Benard system, stochastic perturbations 4-110882  
 fluid dynamics, variational principles in Eulerian and Lagrangian descriptions 4-95180  
 focusing effect on stochastically excited beams (German) 4-82682  
 four dimens. material manifold geometric theory 4-63506  
 geodesic flow perturbations, surfaces with constant negative curvature, mixing props. 4-110898  
 granular medium static equation exact soln. 4-97303  
 gravitational interaction of bodies immersed in fluids, theory 4-101124  
 Hilbert-Schmidt's theorem, extension to unsymmetric kernel problems 4-95172  
 incompressible elastic solids, second-order problem simplification 4-67978  
 incompressible media, statically admissible stress fields 4-58644  
 integral equations, second-order reduction of continuum mech. problems (Ukrainian) 4-67976  
 internal struct. and groups 4-63507  
 irreversible systems obeying max. dissipation principle, bifurcation and stability (French) 4-78139  
 large-deformation analysis using mixed Eulerian-Lagrangian displacement model 4-79461  
 linear elastic analysis, min. norm solns. 4-86210  
 linear isotropic materials, eigenvalues and stable time steps for the uniform strain hexahedron and quadrilateral 4-95178  
 linear struct., dynamic response to a stream of random impulses 4-103195  
 low-frequency resonance curves associated with non-linear internal friction 4-110869

## classical mechanics of continuous media continued

- Mehta-Dyson one-dimensional plasma, long range interaction, thermodynamic limit 4-111087  
 membranes, elastic, circular, large axisymm. deforms. 4-112703  
 MHD, difference schemes, fully conservative, in mixed Euler-Lagrange variables (*Russian*) 4-78147  
 multicriteria structural optimisation variational formulation 4-86214  
 nonconservative general systems, nature of eigenvalues 4-95154  
 nonlinear mechanics, strange attractors and chaos 4-95164  
 nonlinearity problems, geometric and material, formulation methods 4-78142  
 overall elastic response, overall modulus operator 4-97305  
 paradoxical phenomena in vibrating fluids and solid bodies 4-101635  
 plane elastic arch, homogenisation 4-83814  
 plane problems, elasticity and plasticity law representation 4-78143  
 plate, cantilever, finite, long-time response to antisymm. dynamic surface loading 4-87563  
 plate, cantilever, finite, long-time response to dynamic surface loading 4-87564  
 plate, crack problems, weight function appl., stress intensity factors using FE calcs. (*German*) 4-83862  
 plate, isotropic circular, nonlinear transient response 4-87559  
 plate, rhombic, finite element analyses, h- and p-versions 4-112701  
 plate, round, mean flexure, appl. of method of successive approximation (*Russian*) 4-112736  
 plate and shell finite elements, Hellinger-Reissner principles 4-63514  
 plate flexure problems, relation between two-dimensional and axisymmetric loads 4-105528  
 plate or shells, unloaded hole shape optimisation, variation problem 4-86212  
 plate problems using  $C^0$  triangular plate element with one-point quadrature 4-78140  
 plates, elastic, stress intensity factors at sharp notches, path-independent integrals 4-87562  
 plates, elastic nonlinear theory, appl. to paper property characterisation 4-103201  
 plates, inelastic, fibre-reinforced, laminated, constitutive relations 4-103200  
 plates, isotropic and composite, anticlastic curvature suppression 4-83832  
 plates, laminated, anal. using mixed shear flexible finite element 4-103193  
 plates, laminated, composite, shear-flexible triangular finite element model 4-64840  
 plates, multiply connected, three-dimens. elasticity theory problems, survey 4-101652  
 plates, normally stressed, orthotropic, right angle, bending, boundary disturbance ebbing (*German*) 4-83844  
 plates, sandwich, annular, subjected to radial tensile forces, stability anal. 4-74907  
 plates, solid, elastic, optimisation problem soln. by design space restriction 4-86213  
 plates, thin, isotropic, quadrilateral, subject to bending stresses, efficient anal. 4-64837  
 plates, thin annular orthotropic, nonlinear axisymm. static anal. 4-87561  
 point wise dimension computation in multidimensional systems, isolating integrals determ. 4-95300  
 porous decomposition of deformation gradient, stretch and rot. determ. 4-90373  
 porous elastic layers, response to moving loads 4-74854  
 pressure loaded structures under large deformations 4-103202  
 regular multidimensional differential system, symmetry transformations interpretation 4-90354  
 Reissner plate function characteristics (*German*) 4-83826  
 revolution shells, fibre wound composite material, strength using finite element method (*Chinese*) 4-60271  
 Riemannian and non-Riemannian terminology, theory of yielding 4-95174  
 rigid body dynamics treatment based on continuum mechanics concept 4-95162  
 rods, plates and shells of composite materials stability, three-dimens. formulation, survey 4-79477  
 Routh equation and cyclic field variables (*Russian*) 4-67977  
 shallow arch problem for non-symmetric vertical loads 4-86204  
 shell, composite, conical, ring-reinforced, optimisation under external press. 4-103197  
 shell, shallow, simplified nonlinear eqns. of dynamics (*Ukrainian*) 4-64838  
 shell, three-layered, cylindrical, infinitely long, free wave propag. 4-74941  
 shell, wave-shaped, cylindrical, expt. investigation (*Bulgarian*) 4-79446  
 shell and plate analysis, large rotation, optimal, stable and invariant hybrid elements 4-74865  
 shell dynamics, nonlinear, intrinsic and semi-intrinsic approaches 4-74863  
 shell theory, simple edge effect description, 3D theory of elasticity 4-112719  
 shell theory, thin, nonlinear eqns. 4-106194  
 shells, circular cylindrical, linear theory, analytical methods 4-97304  
 shells, conical and cylindrical, near intersections under external pressure, limit anal. (*Chinese*) 4-60269  
 shells, cylindrical, longitudinally corrugated, multilayer, thick-walled, stressed state 4-108005  
 shells, cylindrical, stress-strain state investigation on basis of eqns. of elasticity theory 4-103199  
 shells, deformable, in presence of EM effects, nonlinear theory 4-74864  
 shells, nearly spherical, noncanonical, thin-walled, stress state 4-74856  
 shells, noncircular cylindrical, in fluid, radiation anal. 4-74787  
 shells, refined theory with allowance for curvature of the normal 4-78144  
 shells, ribbed, stability 4-108030  
 shells, shallow, theory, series-expansion method appl. as parameter for physically nonlinear problems 4-74857  
 shells, thin, arbitrary, effective nonlinear, anal. using simple finite elements 4-60273  
 shells, thin, Lagrangian description and incremental formulation in non-linear theory 4-60285  
 shells, tubular, under uniform press., stress-strain state 4-74855  
 shells from thermopiezoelectric material, generalised theory 4-103198  
 shells of rotation, axisymmetric, elastoplastic, variable loading, numerical anal. (*Russian*) 4-60274  
 soil-structure interaction, far field representation, boundary element anal. 4-83817  
 spring nonlinear theory, equivalent rod problem 4-60268

## classical mechanics of continuous media continued

- stratified media, dyadic Green's functions (*Ukrainian*) 4-87560  
 stress rate interrelationships 4-110875  
 strong coupling limit of KAM theory and the onset of turbulence 4-58634  
 structural optimisation and sensitivity anal., variational approach by means of adjoint systems, struct. shape variation 4-82678  
 structural optimisation discrete and continuum structures 4-95179  
 structures composed of composite rev. shells and axisymmetric solids, finite element anal. (*Chinese*) 4-60272  
 thermostatics, equilib. states, stability 4-95173  
 thick plates, dynamic anal., complementary energy principles appl. (*Chinese*) 4-108003  
 thin planes and shell structs., stress hybrid element anal. (*Chinese*) 4-60270  
 thin shells, nonlinear theory, incremental formulation, total lagrangian description 4-86205  
 torus, nonaxially symm. deform. anal. 4-74859  
 transient structural responses, implicit finite element methods, time integration, book contrib. 4-60276  
 trusses, minimum weight design, optimality criteria method 4-64841  
 vibrations, large amplitude 4-91750  
 vorticity, Euler equations, breakdown of smooth solutions in 3-D 4-78146

## classical mechanics of discrete systems

- see also *N-body problems*  
 affinely-connected manifolds theory and Lie theory 4-63492  
 anisotropic quantum rigid rotator, thermal evolution of specific heat 4-95151  
 autparametric system, forced nonlinear oscills., chaotic responses 4-73223  
 autparametric system, forced nonlinear oscills., periodic responses 4-73222  
 beam, vibrating, inverse problem, discrete model 4-69675  
 bifurcation phenomena near homoclinic systems, two-parameter anal. 4-111024  
 binary collisions in planar three-body problem, global regularization (*French*) 4-82387  
 bodies connected by spherical hinge, motion eqns. (*Russian*) 4-90358  
 body-fluid system, combined spatial motion problems, direct soln. method 4-74850  
 cable structures, pre-tensioned, geometrical nonlinear response 4-69676  
 cable suspended in gravitational field, vibrations, mode shapes and natural freqs. 4-74853  
 cables, taut, inclined, dynamics 4-101643  
 celtic stone, eqns. of motion, asymptotic soln. 4-60262  
 chaos and periodic doubling 4-73375  
 chaotic behaviour of deterministic systems, summer school, Les Houches, France (June-July 1981) 4-73133  
 charged systems potential and field fluctuations in 2-D 4-73213  
 circle homeomorphisms with golden ratio rotation number, functional eqns. 4-58633  
 classical mechanics in stat. background inverse temp., Lagrange multiplier, dual distrib. 4-86323  
 computational methods for transient analysis, book 4-58594  
 constrained multibody system dynamics, automated approach 4-86186  
 constrained system transform., generalised Killing's eqns. (*Chinese*) 4-90351  
 creation of non-trivial recurrence in the dynamics of diffeomorphisms 4-73230  
 critical stability anal. of dynamic systems in equilibrium (*German*) 4-83848  
 degenerate bifurcations concerning non-conservative systems 4-86198  
 diffeomorphisms on  $R^2$ , bifurcations (*French*) 4-73228  
 differentiable discrete systems, mathematical theory 4-73225  
 discrete elastic-perfectly plastic structures, dynamic shakedown by modal anal. 4-108022  
 double resonant problem, formal soln. 4-82399  
 dynamic relaxation in structural mechanics problems, review, book contrib. 4-60267  
 dynamical systems, first integrals obtention 4-73214  
 dynamical systems with time depend. constraints and Hamiltonian, approach towards quantisation 4-63544  
 dynamically tuned gyroscope interaction on an elastic platform (*Ukrainian*) 4-86189  
 elastic bodies working against rigid supports, contact effects (*German*) 4-82675  
 elastoplastic limited-ductility structs., shakedown anal. 4-108023  
 ellipsoid motion on rough surface with slippage 4-60261  
 elongated body of revolution suspended on a string, steady motion stability 4-79441  
 equation of motion, numerical methods 4-82624  
 equilibrium stability in problems with double reson., appl. to artificial satellites 4-82395  
 equivalence problem for nonconservative mechanics 4-95149  
 Fermi-Ulam problem, bounds on velocity 4-95153  
 first-order equivalent Lagrangians and conservation laws 4-101638  
 Fokker-Planck dynamics, Lagrangian representation, non-renormalised description 4-68137  
 Fokker-Planck dynamics, Lagrangian representation, renormalised description 4-68138  
 Fokker-Planck models, weak-noise limit 4-11025  
 forced oscillations, subharmonic solutions and Morse theory 4-67974  
 fountain droplets, deceleration curve 4-78125  
 frequency domain characteristics of mechanical rotors (*German*) 4-82673  
 gas flow, 1-D, infinite Lie group of symmetry, entropy distributions 4-103358  
 generalised turning points characterisation and computation 4-58638  
 generic properties of conservative systems 4-73231  
 gyro, balanced gimbal-mounted, Magnus problem, Rodrigues-Hamilton parameters (*Ukrainian*) 4-86188  
 gyroscopes, with elastic links, stabilising effect (*Russian*) 4-63497  
 gyroscopic nonperturbable system mechanics 4-79442  
 gyrostat, Euler eqns., symmetry breaking 4-82655  
 Hamilton-Jacobi equation, integrability problem 4-58635  
 Hamiltonian eqns., discrete mapping 4-90365  
 Hamiltonian mechanics, quasicoordinates, and quasimomenta 4-106161  
 hamiltonian systems, numerical studies 4-73226  
 harmonic oscillator, modulated damping or growth model in classical or quantum mechanics 4-68015

**classical mechanics of discrete systems continued**

- heavy rotating body rolling on horizontal plane, Chaplygin eqn. generalisation (*Russian*) 4-90360
- heavy solid rotation on horizontal plane with friction (*Russian*) 4-90361
- hinged rectangular rod grid, eigenfrequency computation program 4-86199
- holonomic constraint stabilisation method 4-95159
- index evaluation for dynamical systems, locating all the zeros of vector function 4-95158
- inertial rotor disc, effects of damping, stiffness anisotropy (*German*) 4-82674
- infilled frames with openings, modal analysis 4-87567
- integrability of two degree of freedom Hamiltonian system 4-101687
- kicked rotator, incommensurability in quantal and classical model 4-86197
- Klein-Gordon eqn., statistical interpretation of Weyl curvature 4-101639
- Lagrangian gyroscopes, connected by spherical hinge, motion exact solns. (*Russian*) 4-90357
- Lagrangian mechanics, conserved quantities, invariant forms, dynamical symmetries 4-86191
- Lagrangian singularities, appl. in celestial mechanics 4-82398
- lagrangians in an isotropic plane from complex coordinates 4-67944
- Lenz vector, relativistic generalisation 4-106182
- Lenz vector, relativistic generalisation 4-106183
- libration points of central configurations, stability 4-101123
- linear dynamic system: output, spectral moments calc. 4-95161
- linear structural systems subject to component changes, dynamic responses anal. 4-87556
- linear systems, extrapolated iterative methods 4-58639
- local and global behaviour near homoclinic orbits 4-111023
- local extremals of discrete functions (*Ukrainian*) 4-67971
- long rod impact onto large target, numerical study 4-91778
- low-dimensional systems, integrability and Painleve prop. 4-63494
- magnetic bearing, anal. of inertially loaded rotating systems (*German*) 4-82670
- mechanisms with nonlinear characts., dynamic models 4-73218
- modal equations, linear structural dynamics 4-86185
- momentum integrals in 2-D 4-78128
- motion stability relative to part of variables under persistent perturbations 4-58627
- multibody mechanical systems with closed loops, state-space dynamical representation 4-95142
- multibody system, reaction forces calc. (*German*) 4-82663
- multicriteria structural optimisation variational formulation 4-86214
- multiple degree of freedom systems, critical damping, computation method 4-73224
- Newtonian field, homogeneous quadratic potential, rigid rotating body integrability 4-95144
- Newtonian systems, exact polynomial invariants 4-95145
- Newtonian trajectories and quantum waves in expanding force fields 4-86246
- nonconservative dynamical systems, integrating factors and conservation laws 4-95146
- nonconservative general systems, nature of eigenvalues 4-95154
- nonconservative periodic systems close to two-dimens. Hamiltonian 4-106174
- nonequilibrium dynamics of infinite particle systems 4-73212
- nonholonomic system, conservation theorem 4-73221
- nonlinear driven oscillator, 1-D Poincare map 4-63501
- nonlinear evolution equations, H theorems, structure theorem, discrete classical system 4-95150
- nonlinear mechanical systems, random vibrations (*Russian*) 4-63499
- nonlinear mechanics, strange attractors and chaos 4-95164
- nonlinear oscillation eqns., approx. solns. on basis of Gauss principle (*Russian*) 4-110867
- nonlinear oscillators under random parametric and external excitations, cumulant-neglect closure 4-95147
- nonlinear suspensions under random excitation, identification procedure (*French*) 4-58637
- nonlinear system aperiodic vibr., incremental harmonic balance method with multiple time scales 4-95160
- nonlinear systems, random vibrations (*Russian*) 4-63500
- nonlocal maps, dynamics of interacting particles on a line 4-90364
- nonrelativistic motion, short disturbances, operator formalism 4-63491
- one-dimensional mapping, fractal basin struct. 4-68136
- one-dimensional maps, symmetries and stable periodic orbits 4-63493
- one-dimensional oscillator movement in field with periodic pot. (*Russian*) 4-90367
- one-dimensional system at equilibrium, pot. energy using Bessel polynomials 4-78129
- oscillator, discrete version of quantum mechanics, evolution operator 4-110928
- oscillator, periodically forced impact, with large dissipation 4-95157
- pendulum, double, coupled flutter and divergence bifurcation 4-60264
- periodic Ljapunov functions (*German*) 4-82668
- periodic orbits in 3-D Hamiltonians 4-90366
- plane body in central force field, steady motion stability 4-79443
- plane contact problem, formulation with wear of interacting bodies 4-74965
- plate, infinite, plate, with attached cylinder, driving-point impedance 4-87614
- plates, flexural vibrations, power series evaluation (*Russian*) 4-63498
- pointlike relativistic massive spinning particle, Hamiltonian description 4-95167
- quadratic area-preserving mappings extension to measure-preserving mappings in three dims. 4-63502
- quasixisymmetric satellite, periodic oscill. stability in elliptical orbit plane 4-82392
- random vibrations, first passage problem 4-73220
- regular multidimensional differential system, symmetry transformations interpretation 4-90354
- relativistic dynamics using wave function of classical trajectories 4-82702
- relativistic Hamilton-Jacobi theory for constrained systems 4-95166
- resonant almost-periodic systems, stability with respect to part of variables 4-58629
- resonant frequency of systems with discrete substructures (*German*) 4-82669
- rigid body dynamics treatment based on continuum mechanics concept 4-95162
- rigid body quasi-periodic motion non-degeneracy for Kovalevskaya's case (*Russian*) 4-110868

**classical mechanics of discrete systems continued**

- rigid body system, 3D, dynamic simulation using vector-network techniques 4-106180
- rigid heavy body rotating about a fixed point, eqns. of motion in Rodriguez-Hamilton parameters 4-79439
- rigid heavy body suspended on a string, eqns. of motion 4-79438
- rod, damping capacity in centrifugal force field using tuning forks 4-97302
- rod-rigid element system, longitudinal collision 4-74968
- rotational mechanics, spinor descriptions devel. from Euler's rigid body displacement theorem 4-78126
- rotors, flexible, new balancing method 4-90353
- semiclassical mechanics of regular and irregular motion 4-73227
- semidiscretisation and time integration in solid and struct. mech., book contrib. 4-60266
- separatrix loop existence in four-dimens. systems similar to the integrable Hamiltonian systems 4-106175
- Siegel centre problem, KAM estimates 4-73215
- solid body, dynamically symm., stability of steady motions at triangular point of libration 4-58630
- spherical pendulum, resonant motion 4-101640
- spring nonlinear theory, equivalent rod problem 4-60268
- stability and bifurcation theory 4-73229
- steady-state motion stabilisation of mech. systems 4-58628
- stiffness and damping matrices, frequency and time domain anal. (*German*) 4-82672
- strange repellers, escape from 4-73217
- stresses and deformations, simplified solution 4-64846
- string, nonlinear oscils. (*Russian*) 4-58641
- strip, elastic, in mechanisms with flexible couplings, mathematical models 4-74851
- strong coupling limit of KAM theory and the onset of turbulence 4-58634
- structural connections, coupling loss factors 4-87558
- structural optimisation discrete and continuum structures 4-95179
- strut, hinged, with initial curvature 4-91721
- symmetrical dynamical system asymm. periodic motion anal. 4-79444
- system with hysteresis energy dissipation, random oscils. (*Ukrainian*) 4-86190
- Szebehely's inverse problem eqn. rel. to multiple var. problem from Maupertuis' principle 4-110502
- Szebehely's inverse problem for finite symmetrical material concentrations 4-94566
- three-body problem, exact soln. 4-78080
- three-dimensional gradient conjugate systems, total periodicity 4-58640
- time-dependent evolution eqns., commuting symmetries and constants of motion 4-63495
- time-dependent harmonic oscillator, cubic and quartic invariants 4-67973
- time-dependent Lagrangian dynamics, Helmholtz conditions, geometrical version 4-67972
- torque free axisymmetric gyro, stability in short run 4-86200
- torsional vibrations in cylindrical elements, hysteresis effects (*German*) 4-82671
- transient structural responses, implicit finite element methods, time integration, book contrib. 4-60276
- transport medium, multilink, analytical description (*Russian*) 4-63496
- tricolority and quenched impurities in classical and quantum systems 4-78170
- tube, circular cylindrical, reinforced by fibres lying along helices, rotation 4-60263
- two bodies joined by a spherical linkage, eqns. of integral motion, integrability 4-79440
- two-dimensional time-dependent classical systems with confining potentials 4-67975
- two-dimensional time-dependent Hamiltonian systems with an exact invariant 4-86194
- vibration theory, field method appl. 4-95148
- vibratory conveyor, vel.-depend. function coeff. (*Japanese*) 4-103229
- wobbling Christmas tree toy 4-63441
- classical theories of fluid structure**  
see also kinetic theory; liquid theory
- collective motions, interacting Brownian particle systems 4-103624
- dimers, directional attractive forces, single mol. site, thermodynamic perturbation theory 4-95290
- dimers and s-mers, highly directional forces, statistical thermodynamics 4-95289
- free energy density functionals for non-uniform classical fluids 4-75122
- Monte Carlo method, appls. in condensed-matter physics, statistical mechanics and related fields, book 4-101584
- simple fluids, statistical mech. theory 4-75254
- thermodynamically consistent theory, pair pot. extraction 4-92043
- classification**  
see also indexing
- diogenite meteorites, multivariate statistical anal. of processes and subdivisions 4-105908
- ionic crystals, supersaturated solid solns., classification of precip. phenomena 4-75685
- plate, welded, flaw classification, US echo dynamics, multidimensional feature decision process 4-85273
- spiral galaxies, two dominant dimensions in objective classification scheme 4-86027
- steel, ferritic, impact testing, classification of absorbed energy-temperature curves 4-89230
- classification, pattern** see pattern recognition
- clathrates** see molecules; organic compounds
- clay**
- attapulgite, temp. and freq. variations of elec. props. 4-61616
- Na-beidellite, two-water-layer, struct. of hydrated clay mineral (*French*) 4-82039
- compaction into shale, and exponential porosity-depth relation 4-89914
- Cretaceous/Tertiary boundary clays, Ir-rich layer in Bidart section, France 4-105554
- Japan Trench, noncalcareous clay, Fe and Mg anal. 4-105536
- marine sediments thermal conductivity and permeability influenced by press. and temp. 4-82031
- physical struct and props., conf., London, England (Nov. 1983) 4-95048
- Late Quaternary varved clay, remanent magnetism, stress induced var. 4-110133
- sea floor embedded object breakout resistance prediction 4-115390

- clay continued  
 surficial deposits in Athabasca Tar Sands area, Canada, mineralogy and O isotopes 4-62726  
 water permeability of fault gouge, effect of confining press. 4-85724  
 cleaning see surface treatment  
 cleanliness see hygiene  
 cleavage fracture see brittle fracture  
 Clebsch-Gordan coefficients  
   see also elementary particle theory  
   compact Lie groups, representation spaces, Wigner-Racah calculus 4-95710  
   Gelfand basis Clebsch-Gordan coeffs., isoscalar factors for group chain 4-95940  
   magnetic point group symmetry, spectroscopic coeffs. tables 4-58674  
   nuclear collective basis functions, recurrent reconstruction 4-115154  
   one-body coeff. of fractional parentage for group chains  $U(mn) \supset U(m) \times U(n)$  and  $U(mp+nq/mq+np) \supset U(m/n) \times U(p/q)$  4-68020  
   SU(1,1) Clebsch-Gordan coeffs., Racah coefficients, Poschl-Teller wavefunctions 4-95208  
   SU(2) Clebsch-Gordan coeffs., Racah coefficients, Poschl-Teller wavefunctions 4-95208  
   time Dirac pulse excited system, Schrodinger eqn. soln., Wigner function 4-95107  
   Wigner-Racah algebra of arbitrary group 4-68055  
 climatology  
   see also atmospheric humidity; atmospheric precipitation; sunlight; wind  
   aerosol influence on general circulation model of climate (Russian) 4-100723  
   afforestation and deforestation effects on climate 4-94237  
   air-sea interactions, monitoring for climatic anal., strategy 4-82226  
   air-sea interactions in global climate and prediction 4-82224  
   Allan Hills, meteorites distrib., implications for climatology 4-82230  
   anomalies in climate and zonal circulation (Spanish) 4-115563  
   Antarctic, weather and climate (book) 4-67905  
   Arctic Ocean, climatic response to Soviet river diversions 4-94234  
   arid lands and droughts 4-82222  
   Athens, Greece, monthly rainfall statistics 4-77571  
   Atlantic ocean, glacial to interglacial changes in carbonate and clay sedimentation from  $^{230}\text{Th}$  meas. 4-110129  
   NE Australia, coastal rainfall record in coral fluorescent bands 4-105673  
   Australia, monthly estimates of wind speed and wind run 4-110191  
   Baffin Bay and Labrador Sea, palaeoclimate from sediment foraminifera 4-72690  
   Bay of Bengal coast, cyclonic storms incidence (1877-1980) 4-110216  
   biogeochemical processes, effect on climate 4-82227  
   book 4-82618  
   central Canada, temperature records from 1768 to 1910 AD 4-62944  
   Carpathian Mountains, Poland, orographic patterns refl. in meso- and microclimatic conditions 4-94236  
   Chimborazo, Ecuador, climate record in glacier ice core 4-115560  
   China, long-range weather forecasts, geophysical factors, appl. 4-72671  
   climate and weather in tropics, book 4-106135  
   climatology and water supply, book 4-90326  
   cloud-radiation interactions 4-82220  
   conference on atm. radiation at Toronto, Canada (June 1981) 4-90300  
   conference on climate and offshore energy resources at London, England (October 1980) 4-78044  
   continent distribution influence of global temperature 4-105701  
   continental thermal energy storage in a zonally averaged global thermodynamic model 4-110242  
   continuum sea ice model for a global climate model 4-89936  
   Cretaceous climate model sensitivity, geographic variables effect 4-72692  
   Cretaceous-Tertiary boundary, isotope variations rel. to climate changes 4-89892  
   cryosphere, effect on climate 4-82223  
   Czechoslovakia, precipitation statistics from 1881 to 1980 (German) 4-77573  
   data for offshore industry 4-77625  
   dendroclimatology, average value of correlated time series 4-100665  
   dynamical heat fluxes and climate model sensitivity 4-115561  
   energy balance climate model with cloud feedback 4-89988  
   energy consumption, pollution and climate (book) 4-90310  
   energy systems and climate (book) 4-90311  
   central England, homogeneity of annual temp. (1659 to 1973) 4-110187  
   equatorial forcing of climate telecommunications, dynamical anal. 4-72652  
   Etesians, 1892-1981 records, possible solar signature 4-77624  
   NW Europe, evidence for pre-Weichselian glaciation, stratigraphy 4-110176  
   extratropical cyclone activity in Northern Hemisphere, anal. for four mid-season months 4-110190  
   few-parameter climate model including thermal fluctuation influences 4-105703  
   Florida, USA land use rel. to surface temp. fluctuations 4-115499  
   France, Holocene climates of Alps and Massif Central, pollen study (French) 4-85752  
   general circulation climate models including hydrologic cycles 4-77626  
   general circulation models in climatology 4-82219  
   tropical glacier ice cores for palaeoclimatic studies 4-115560  
   glaciology and climatology, conf., Evanston, Illinois, USA (June-July 1983) 4-110803  
   global climate, space research projects involving RAL 4-100724  
   global climate (book) 4-78051  
   global climate research 4-82217  
   global response to orbital forcing and atm. CO<sub>2</sub> var. 4-110243  
   global temperature field, long-term time evolution (Chinese) 4-67363  
   global warming influence on northern hemisphere meteorological variables 4-105704  
   Goddard general circulation model climatology, effects of sea ice var. 4-89990  
   greenhouse effect 4-82228  
   Greenland and Canadian Arctic Holocene precipitation rate from ice core obs. 4-110306  
   Hadley circulation subject to climate perturbations, GCM model 4-94203  
   heat storage and poleward transport in ocean-atmos. system, interannual variability 4-110197  
   Huacaran, Peru, climate record in glacier ice core 4-115560  
   Hunza Valley, ancient trees dendroclimatic pot. 4-62949  
 climatology continued  
   ice age, rapid atmospheric CO<sub>2</sub> vars. and ocean circulation 4-62909  
   ice age climate, European/Atlantic correlations during last interglacial 4-85754  
   ice ages, role of oceans in determining atmospheric CO<sub>2</sub> partial press. 4-62908  
   ice edge latitude, sensitivity to var. in solar const. 4-72691  
   Iceland, climate and sea-ice record (AD 870 to 1780) 4-94235  
   India, climatic features from anal. of trees annual growth rings 4-67387  
   India, droughts and famine (1769 to 1974) 4-110241  
   India, rainfall quantities rel. to sunspot cycle (1871 to 1978) 4-77621  
   S Indian Ocean, plankton and water circulation since 127000 yr BP 4-77550  
   Intertropical Convergence Zone dynamics, GLAS climate model symm. version anal. 4-72643  
   Japan, summer temperature low rel. to 100 mb height var. 4-110239  
   Krakatau, 1883 eruption and effects (book) 4-101587  
   Lamb's Dust Veil Index, formulation 4-105699  
   land surface processes and climate, conf., Greenbelt, Maryland, USA (Jan. 1981) 4-73159  
   land surface remote sensing for climate model application 4-77677  
   land surface shortwave albedo and surface emissivity data for climate models 4-77620  
   Lower Beskid Range, Poland, mesoclimatic and thermal relations 4-94253  
   Lower Palaeozoic palaeoclimatology, book contrib. 4-63415  
   Lower Palaeozoic palaeoclimatology 4-67390  
   Lower Rhine Basin, Germany, Plio-Pleistocene climatic conditions 4-110036  
   Madhya Maharashtra, India, rainfall heterogeneity, orographic effects 4-110218  
   Marion Island, Quaternary glaciation of island near Antarctic convergence 4-82142  
   Mesozoic climate, significance of fossil flora on Alexander Island 4-82229  
   Milankovitch theory tested using 3-D seasonal energy balance climate model 4-62947  
   model, sensitivity to atm. CO<sub>2</sub> increase, effect of oceanic heat transport 4-67386  
   Mount St. Helens, 1980 eruptions effect on climate 4-105706  
   Late Neogene climate of Arctic, from sediment record 4-94155  
   Nevada, glacial chronology of Ruby Mountains-East Humboldt Range 4-94176  
   W North America, 18.6-yr lunar nodal drought in past millennium 4-72665  
   North America, evidence for enhanced atmospheric circulation during Early Holocene 4-100712  
   nuclear war, climatic consequences, computational expt. (Russian) 4-67389  
   nuclear war, climatic effects, global nuclear winter 4-105702  
   nuclear winter, prolongation by snow and ice feedbacks 4-105674  
   numerically simulated climates, sensitivity to land surface boundary conditions 4-82221  
   ocean circulation, role in climate 4-82225  
   ocean-atmosphere dynamical models for climate studies 4-115559  
   oceans role in climate 4-81831  
   oscillatory behaviour and predictability in climate model with external forcing 4-89987  
   N Pacific Ocean cyclones, central press. rel. to sea surface temp. and land coverage 4-110240  
   Padova, Italy, AD 1725 to 1981 rainfall records analysis 4-62945  
   palaeoclimate (book) 4-95070  
   palaeoclimate analysis, use of conodonts O isotopic comp. 4-110283  
   palaeoclimatic change chronology at end of last glaciation 4-115562  
   palaeoclimatic indicators for weathered cratons, use of tropical stone lines and podzolised sand plains 4-110275  
   palaeoclimatology, Quercy Lias Formation relationships (French) 4-72583  
   late Pleistocene and early Holocene climate of Washington, USA 4-115557  
   Late Pleistocene climate at Marsworth, UK, evidence of two temperate episodes 4-89989  
   Pleistocene climate of Arctic and N Canada, from sediment record 4-115335  
   polar ice-trapped air age difference at Siple Station 4-115475  
   quasi-periodic oscillations in a symmetric general circulation model 4-72644  
   Quebec, relation between dunes, fire and climate recorded in Holocene deposits 4-85753  
   Quelccaya Ice Cap, Peru, climate record in glacier ice core 4-115560  
   radiative flux balance, effect of antiscreening of outgoing thermal radiation by clouds (Russian) 4-67392  
   rainfall to World Ocean, estimation of annual mean rainfall 4-115500  
   river flows reconstruction from precipitation data in UK 4-77560  
   N Scotland, blocked summer weather in AD 1967 to 1982 period 4-82208  
   sea ice cover, freq. locking in periodically forced thermal two-phase oscillator 4-62841  
   sea ice seasonal cycle influences on CO<sub>2</sub> increase models 4-62943  
   sea surface temperature long term trends 4-100580  
   sensitivity, energy balance models and oscillatory climate models 4-72693  
   short-term fluctuations, effects, of sea surface temperature anomalies 4-72601  
   soil types on regional and global scale for climate modeling purposes 4-77627  
   solar radiation long-term variability and climate, review 4-115739  
   solar variability, weather and climate, review 4-101601  
   solar-terrestrial influence 4-77809  
   Southern Hemisphere sea level pressure data set for use in climatic studies 4-77622  
   Southern Oscillation, signal and noise 4-100722  
   Sudan, rainfall 2000 years ago 4-72694  
   surface temperatures, effects of CO<sub>2</sub>, volcanic aerosols and solar radiation var. 4-94238  
   temperature variations, correl. with monsoon rainfall and sea surface temp. 4-82218  
   three-component zonal model of Earth climate 4-62948  
   time dependent models, variational formulation for diffusion 4-77623  
   transitions in climate states, asynchronicity due to sea ice-ocean interaction 4-110238  
   tropical air-sea heat flux, usefulness of shipboard meas. for detect. of secular changes 4-100582

**climatology continued**

- tropical cloud clusters mesoscale circulation, implications for large-scale dynamics and climate 4-72651
- tropical regions (book) 4-90318
- United Kingdom network design 4-67331
- United States, climatological contingency anal. and seasonal forecasting skill 4-77586
- United States, pressure spectral anal. as indicator of synoptic-scale activity climatic var. 4-100756
- United States, role of January in character. of recent winters (1975 to 1982) 4-100663
- eastern USA, rainfall patterns 4-62946
- USA, severe winters rel. to global radiation and heating degree days 4-115498
- Valle Ricca Pits, Italy, Plio-Pleistocene deposits and climatic conditions 4-110036
- variations due to solar const. var. 4-101304
- volcanic eruption S and Cl releases and climatic impact of basalt eruptions 4-115366
- volcanic eruptions effect on climate 4-105514
- volcanic particles in atmosphere, climatic effects 4-105705
- Washington, tephrochronology of Late Wisconsin deglaciation and Holocene glacier fluctuations near Glacier Peak 4-94177
- Washington State, USA, late Pleistocene and early Holocene climate 4-115557
- Western Mediterranean Sea, ozone climatology, 1968-1976 4-105668
- World Climate Research Programme 4-82216
- worldwide marine temperature fluctuations, 1856 to 1981, anal. 4-105569
- zonal circulation annual variation by small component spectral model (Russian) 4-100682
- C isotope record in pinyon pine tree rings, variability within and between trees 4-115607
- CO<sub>2</sub> in Earth's atmosphere, indirect effects of increasing trend on climate 4-100045
- CO<sub>2</sub> and global C balance, climate interactions 4-94228
- CO<sub>2</sub> as an inverse greenhouse gas 4-110194
- CO<sub>2</sub> global concentration influence on air temp. and precipitation 4-67388
- CO<sub>2</sub> in atm., conc. var. due to oceanic primary productivity fluctuations 4-94182
- CO<sub>2</sub> induced climatic change and spectral vars. in outgoing IR radiation 4-115558
- CO<sub>2</sub> variation induced climate change, marine biota and Earth orbit 4-115521
- O isotopes in glacier ice cores, atmospheric model for isotopes in falling snow 4-115522

**climb, dislocation** *see* **dislocation climb**

**clinical equipment** *see* **biomedical equipment**

**clinical measurement** *see* **biomedical measurement**

**clock paradox** *see* **special relativity**

**clocks**

- see also* **atomic clocks; chronometers; time measurement**
- Geostationary Operational Environmental Satellite, time transfer appl. 4-73426
- GPS time data recording system using a multi-task minicomputer (Japanese) 4-90566
- ocean bottom seismometer, clock, correction system for clock calibration 4-82280
- satellite-aided time comparison methods (Japanese) 4-58827
- time-scribe: universal time writer for any EEG/polygraph chart recorder 4-93942
- VLF broadcasts for clock comparison (Japanese) 4-58826

**closed circuit television**

- classroom optics demonstration 4-110837
- ultrashort pulse TPF pattern meas. and anal. using closed circuit TV with memory system (Chinese) 4-60057

**closed loop control systems** *see* **closed loop systems**

**closed loop systems**

- see also* **feedback**
- CCD sun tracking sensors for sunlight concentrators 4-66667
- constrained multibody system dynamics, automated approach 4-86186
- intensive aquaculture as candidate for bioregenerative life support systems 4-115256
- leg exerciser for training of paralysed muscle by closed-loop control 4-85575
- synergistic control system for paralyzed extremity joint 4-100359
- thermal simulation method for use in RF hyperthermia treatment of tumours 4-72344

**cloud chambers**

No entries

**cloud physics** *see* **clouds****clouds**

- see also* **atmospheric precipitation; sky**
- amounts of cloud, NIMBUS 7 THIR/CLE and AF 3-D nephanalysis 4-100695
- anticyclonic stratocumulus, sympathetic fluctuations of cloud water content and cloud top height 4-62926
- Bay of Bengal, monsoon depression core struct. 4-72637
- Bay of Bengal cyclone, cloud anal. from satellite imagery 4-67340
- Bay of Bengal monsoon depression cloud distributions 4-72638
- Belgium, AD 1983 weather conditions 4-115553
- Bermuda area of North Atlantic, AD 1981 meteorological obs. 4-105682
- blue-green propagation through clouds (French, English) 4-67399
- Boundary Layer Experiment-1983, characts. 4-110255
- broken cloudiness, model, Poisson indicator field, optical radiation transfer 4-85756
- characteristics assoc. with hazardous weather phenomena for aviation 4-110222
- cirrus cloud, depolarisation, backscatt. and attenuation of IR laser radiation 4-110248
- cloud clusters in NW Australia, comparative study rel. to tropical cyclogenesis 4-62917
- cloudiness effects on photolysis and O<sub>3</sub> formation in unpolluted troposphere 4-72669
- clusters in tropical easterly wave, precipitation struct. 4-100657
- computer study of clouds and aerosol vertical distribution 4-110330
- condensation nuclei measurements within clouds 4-82152

**clouds continued**

- convective cloud echo bands, merging rel. to heavy rain prod. (Chinese) 4-67369
- cumulonimbus, surface outflow numerical model 4-77579
- cumulus, downdrafts from tropical oceanic clouds 4-77575
- cumulus clouds, numerical simulation of cloud seeding with salt particles (Chinese) 4-67365
- cumulus clouds in atmospheric fronts, convective and boundary layer parametrizations 4-82198
- cumulus convection, anelastic and Boussinesq approx. comparison 4-82188
- cumulus momentum transport effects in tropical cyclones 4-94208
- darkness at midday in southern England, 6 August 1981 event 4-67334
- deep convection, three-dimens. nonhydrostatic cloud model 4-94224
- diffuse solar radiation from cloudy skies, anisotropy of sky radiance 4-62925
- condensational drop growth, efficient numerical calc. 4-94219
- electrically charged water droplet production expts. 4-85734
- Elton, Louisiana, 1976 March 24 tornado, storm characts. 4-105665
- energy conditions for cloud development, stability criterion for moist compressible atmosphere (Russian) 4-67310
- equilibrium-reflectance model for clear or cloudy atmosphere 4-100729
- ER-2 airborne LIDAR, NASA/CNES potential project 4-110326
- Florida, USA, cumulus convection, radar echo study 4-72632
- general circulation models with cloud parametrizations, sensitivity study 4-105633
- global cloud water maps from Nimbus 7 obs. 4-67411
- hail growth in storm cloud over Westplains, Colorado, USA 4-82154
- height determination techniques for optically thin ice clouds 4-105734
- hoar frost on cylinder, specific mass var. rel. to ang. position 4-94222
- hydrometeor characteristics, radar backscattering anisotropy coeff. anal. (Russian) 4-115601
- ice clouds, effects of horizontal orientation of crystals on radiative props. (Chinese) 4-67397
- ice nucleation in supercooled water sample, laboratory expts. 4-115545
- ice nucleation on surfaces, predictions 4-94221
- ice-forming nuclei in continental-maritime air 4-89971
- identification by NIMBUS 7 ERB, effect on albedo 4-100694
- Indian Ocean, cloudiness var. rel. to SW Monsoon rainfall in India 4-110223
- Indian Ocean, SW monsoon season cloud distrib. 4-100708
- IR, cloud, radiance model, high-altitude sensor systems, appl. 4-115566
- IR imaging of sea surface temp., atm. effects 4-67405
- IR radiances from broken fields of cumulus, angular distrib. 4-72662
- Ivory Coast, convective cloud model for precipitation occurrence 4-115543
- laboratory clouds, control of liq. water content and drop size distrib. 4-62927
- laser beam propagation, form. of elevated transmission zone in weakly-absorbing water aerosol 4-77633
- LIDAR, spaceborne, meteorology and environmental studies appl. 4-110321
- liquid water content meas., appl. of passive optical device 4-62978
- merging, historical perspective 4-67297
- mesoscale convective bands behind cold fronts, cloud and microphysical struct. 4-82199
- mesoscale convective cloud bands behind cold fronts, mesoscale organisation 4-62918
- mesoscale stability of entrainment into cloud-topped mixed layers 4-72649
- monsoon depressions, equivalent pot. temp., convection, cloud heights and humidity zones 4-110224
- natural cumulus clouds, importance of cloud top lifetime in description of cloud characts. 4-100670
- noctilucent cloud phenomena, solar illumination screening by troposphere 4-82236
- noctilucent clouds observed from Scotland, July 1979 obs. 4-82236
- nocturnal stratocumulus cloud, simultaneous meas. of turbulent and microphysical struct. 4-62914
- optical properties of broken cloud cover, calc. of mean photon path lengths (Russian) 4-100731
- photochemistry of marine stratiform cloud 4-115524
- Poisson indicator field model, stochastic props. 4-85755
- radar differential reflectivity and raindrops and graupel, rel. to hydrometeor size 4-85783
- radar scattering properties of hydrometeors, meas. by dual-polarisation radar 4-85782
- radiation-cloud interactions, implications for climate 4-82220
- radiative budget of atmosphere, influence of clouds 4-94242
- radiative fluxes in atmosphere and monthly mean cloudiness 4-115523
- radiative properties, accuracy of approx. computation method of radiative fluxes with broken cloud (Russian) 4-67393
- radiative transfer, effect of antiscreening of outgoing thermal radiation (Russian) 4-67392
- radiative transport, Palm point fluxes anal. (Russian) 4-82171
- raindrop shape affected by elec. charge and elec. field 4-85743
- reflected solar radiance from broken cloud scenes 4-72663
- remote sensing of low stratus by satellite IR radiometry method (German) 4-82276
- satellite remote sensing of cloud shapes, computer shape recognition 4-72707
- seasonal var. of cloudiness rel. to Southern Oscillation persistence 4-94226
- Sicily, high-cloud occurrence and design of solar energy concentrators 4-110226
- solar radiation in Arctic stratus, obs. and theory 4-82231
- solar radiation model using total cloud cover and percentage sunshine meas. 4-62942
- spectral absorpt. by clouds, improved shortwave parameterization scheme 4-94243
- spectrometry from Meteor-Priroda satellite 4-77587
- stereo-pair photographic technique and observations of monsoon clouds 4-90000
- stratiform clouds of S Carolina, USA, acidity and chem. composition 4-67322
- stratocumulus-topped marine boundary layer, mixed layer modeling 4-115516
- stratus clouds, lidar determ. of extinction 4-94239
- subtropical cloud cluster, development into Typhoon 8010 (LEK) (Chinese) 4-67370

clouds continued

temperature and motion meas. technique, by mm wave remote sensing 4-100797  
thermal radiation upward flux, effects of three-layer cloudiness model (Russian) 4-82169  
thunderstorm cloud height-rainfall rate relations, for use with satellite rainfall estimation techniques 4-100671  
tropical cloud cluster, influence of radiative forcing 4-72639  
tropical cloud clusters mesoscale circulation, implications for large-scale dynamics and climate 4-72651  
turbulent mixing, effects on cloud dynamics and microphys. 4-72661  
vaulted storms in NE Colorado, radar and other obs. 4-72658  
wet equivalent potential temp. and enthalpy as cloud model prognostic variables 4-94213  
winter-maritime cumulonimbus cloud anvil observational study 4-62916  
AgI cloud seeding, laboratory expts. 4-115503  
O<sub>2</sub> in boundary layer of Philadelphia, USA, transport by turbulence and clouds 4-115525

Clusius-Dickel columns see isotope separation

cluster analysis see pattern recognition

cluster approximation

adsorbates, surface electronic excitations and dynamic spectral properties 4-108708  
alkali halides, polarisation energy by point defects, INDO cluster calc. 4-80861  
alloys, binary, equilib. short-range order, effect of lattice geometry (Russian) 4-92142  
alloys, nonrandom, substitutionally disordered, densities of states calcs. 4-113843  
 $\alpha$ -B<sub>2</sub> band struct., energy gaps, bonding, cluster approx. 4-70646  
binary alloys, kinetics of first order phase transition 4-75642  
Blume-Capel model, two spin cluster approx., expansion of free energy, tricritical point 4-95343  
carbonium ions, relative stabilities and struct., computational determ. 4-112123  
density of states, effective medium approx., percolation networks spectral dims. 4-95333  
disordered alloy, magnetisation, susceptibility in cluster-variational method 4-92900  
electronic density of states, Bethe-lattice approach, cluster size depend. 4-70621  
finite chain with arbitrary conc. of pure absorbers, random walk problem, exact soln. 4-73365  
grain boundary model, impurity effects, cluster variation method calcs. 4-113465  
II-IV semiconductor compounds and alloys, cluster-Bethe-lattice approach to electronic struct. 4-70625  
Ising square, two-dimens., cluster variation method calcs. of crit. temp. (Turkish) 4-114126  
low-level atom, time-depend. cluster variation method calcs. (Turkish) 4-112082  
magnetic transition temperature determ. by cluster variation method (Turkish) 4-114114  
nonrandom substitutionally disordered alloys, cluster density of states 4-70737  
one-dimensional disordered binary alloys, cluster mean-field theory 4-92599  
percolation and self-avoiding walks, Gaussian-cluster models 4-68160  
percolation cluster hulls, fractal dims. 4-68155  
random substitutional alloys with environmental disorder, muffin-tin potentials, self-consistent approx. 4-61269  
self-avoiding walks on percolation clusters 4-68156  
semiconductor, electronic struct. and hyperfine interaction of muonium 4-65633  
solutions, strictly regular, conc. profile of boundary, cluster approach 4-80333  
transition metal alloys, binary alloys, multiatom interactions, relevance for determ. of stability of ordered structures and short range order 4-88444  
transition metal alloys, electronic struct. and multiatom interaction calcs. 4-113863  
transition metals and their cpds., electronic struct. and muon hyperfine field calcs. 4-65643  
Al (111), O chemisorption LCAO-X $\alpha$  method anal. 4-113799  
Al, positive muon pot., self-consistent cluster calc. 4-71236  
 $\alpha$ -Al<sub>2</sub>O<sub>3</sub>, electronic energy levels from Al L-edge photoabsorption, small-cluster CNDO calcs. 4-81038  
B<sub>12</sub>As<sub>2</sub> band struct., energy gaps, bonding, cluster approx. 4-70646  
B<sub>12</sub>P<sub>2</sub> band struct., energy gaps, bonding, cluster approx. 4-70646  
Be, 1s binding energy, core levels, state-specific many-electron theory 4-75887  
CaF<sub>2</sub>, thermally induced anion disorder, neutron scatt. meas. 4-98338  
Cu, positive muon pot., self-consistent cluster calc. 4-71236  
Cu-Au alloys, (100) surface, order-disorder transitions and segregation 4-98268  
Cu-Ni-Zn, L<sub>10</sub> and L<sub>12</sub> alloys, order-disorder transitions, microstructure obs. 4-114511  
CuCl, electronic struct., cryst. cluster model 4-61280  
Fe, BCC, interaction with H, ab initio/effective core pot. cluster calc. 4-108722  
FeO, wustite, struct. props., cluster component method anal. 4-70109  
Ga<sub>4</sub>In<sub>4</sub>(SbAsP)<sub>4</sub> short-range clustering, thermodynamic anal. 4-61093  
GaP:Ni, Jahn-Teller coupling forces, self consistent LCAO calc. 4-98577  
GaP:O, electronic struct. of single neutral ideal P vacancy 4-92657  
Ge:H-based impurity complexes, charge state determ. 4-92663  
K complex, K<sub>2</sub>Pt(CN)<sub>4</sub>Br<sub>3</sub>·3H<sub>2</sub>O, electronic struct., multiple scatt. generalised partitioning mol. cluster model 4-70629  
K complex, K<sub>2</sub>Pt(CN)<sub>4</sub>·3H<sub>2</sub>O, electronic struct., multiple scatt. generalised partitioning mol. cluster model 4-70629  
KH<sub>2</sub>PO<sub>4</sub> type crystals, ferroelec. phase transition, stress effects 4-76365  
Li, muon interactions with lattice defects, mol. cluster calcs. 4-65255  
LiCl, substitutional defects, molecular cluster-INDO calcs. 4-108806  
LiF, substitutional defects, molecular cluster-INDO calcs. 4-108806  
Mg (0001), O chemisorption, LCAO-X $\alpha$  calcs. 4-113799  
NaCl, substitutional defects, molecular cluster-INDO calcs. 4-108806  
NaCl with U-centre, deep impurity states, cryst. cluster method 4-61324  
NaF, substitutional defects, molecular cluster-INDO calcs. 4-108806  
Ne, solid 4-61042  
PbF<sub>2</sub>, thermally induced anion disorder, neutron scatt. meas. 4-98338

cluster approximation continued

Pd-H, electronic structure; cluster anal. using SW-X $\alpha$  method, relativistic effects 4-65605  
Pd-H, system, electronic struct. of small clusters; H-metal bonding 4-70624  
PdH<sub>2</sub>, non-stoichiometric, heat of form., cluster-Bethe lattice approx. 4-75355  
Pt-H, electronic structure, cluster anal. using SW-X $\alpha$  method, relativistic effects 4-65605  
Pt-H system, electronic struct. of small clusters; H-metal bonding 4-70624  
Se clusters, electronic and vibr. struct., Raman spectra, cluster method 4-74387  
a-Se, electronic and vibr. struct., Raman spectra, cluster method 4-74387  
Si (100) with adsorbed O<sub>2</sub>, ab initio SCF calcs. 4-98440  
a-Si alloys, metastable defect states, X $\alpha$  scatt. wave calc. 4-113899  
Si, deep impurity levels, cluster method of pseudoatomic orbitals (Chinese) 4-84583  
a-Si, electronic struct. of defects, cluster Bethe lattice method 4-70739  
Si:B, impurity electronic struct. cluster X $\alpha$  calc. 4-65639  
Si:F, amorphous, electronic struct. theory 4-92600  
a-Si:H, B, P, electron structure and density of states of B-P pairs, cluster calc. 4-65642  
Si:H (100)(2 $\times$ 1), surface IR studies 4-99116  
Si:Mg(Al)(S), third-period interstitials, electronic struct. calcs. 4-108808  
SiO<sub>2</sub>, amorphous; local electronic density of states, influence of Si-Si bonds 4-92671  
SiO<sub>2</sub>+B<sub>2</sub>O, B-O phase stabilisation, quantum-chem. calc. 4-61325  
SrCl<sub>2</sub>, thermally induced anion disorder, neutron scatt. meas. 4-98338  
SrTiO<sub>3</sub>:Fe<sup>2+</sup>-V<sub>O</sub> pairs, electronic struct. calcs. 4-113890  
TiC, C KVV and Ti L<sub>2,3</sub>M<sub>2,3</sub>V Auger spectra, discrete variational X $\alpha$  anal. 4-66136  
TiC<sub>2</sub>, Ti L<sub>2,3</sub>M<sub>2,3</sub>V Auger spectra 4-88910  
TiN, nonstoichiometric and hydrogenated, cluster calcs. of electronic states and chem. binding 4-70623  
TiO<sub>x</sub>, K-edge photoabsorp. cross section, effect of vacancies 4-93139  
VO<sub>x</sub>, K-edge photoabsorp. cross section, effect of vacancies 4-93139  
ZnS:Cu<sup>2+</sup> Jahn-Teller coupling forces, self consistent LCAO calc. 4-98577

cluster model (nuclear) see nuclear cluster model

clustering, impurity see segregation

clustering, solute see segregation

clusters, atomic see atomic clusters

clusters, globular (stellar) see globular star clusters

clusters, metal see metal clusters

clusters, molecular see molecular clusters

clusters, stellar see stellar clusters and associations

clusters of galaxies

see also galaxies; intergalactic matter  
0016+16, microwave background influenced by galaxy cluster 4-73104  
Abell 1142, poor cluster, redshift survey 4-73085  
Abell 1367, galaxy UGC 6697 intergalactic medium interaction 4-115818  
Abell 1367, radial gradients in props. of spiral galaxies 4-82553  
Abell 1367, ram pressure stripping and gas content 4-77944  
Abell 2141, evidence of hard X-ray emission 4-86065  
Abell 2151, Hercules Cluster, IRAS obs. 4-86068  
Abell 2197+Abell 2199 supercluster, red shift anal. 4-77954  
Abell 2218, microwave background influenced by galaxy cluster 4-73104  
Abell 2634, dynamics of 3C 465 wide-angle-tail radio source 4-77918  
Abell 2634, interaction of ambient cluster gas with radio galaxy 3C 465 (NGC 7720) 4-86072  
Abell 576, X-ray line emission, temp. and elemental abundances 4-86067  
Abell 665, microwave background influenced by galaxy cluster 4-73104  
Abell cluster cD galaxies, surface photometry rel. to 3C radiogalaxies 4-94964  
Abell clusters, catalogue of membership in superclusters, red shift anal. 4-77732  
Abell clusters, X-ray spectrum of volume emissivity 4-86064  
alignments as probe for superclusters and their evolution 4-86094  
binding, effects of Newtonian gravit. modification 4-105869  
blue galaxies in distant clusters, nature from spectral obs. 4-77933  
Bootes void survey, 231 galaxies red shift obs. 4-77936  
bound hypothetical particles, decay, X-ray and UV emission, contrib. to background radiation 4-101154  
brightness profiles and spatial positions, galaxy form. implications 4-67810  
3C 129, evidence of hard X-ray emission 4-86065  
CEDAG, data centre aims and methods 4-94974  
Cl 1447+2619, blue galaxies spectral characts. and star form. anal. 4-94976  
collisions between clusters, numerical simulation 4-77945  
Coma, radial gradients in props. of spiral galaxies 4-82553  
Coma cluster, centimetre-wavelength obs. of extended radio source near Coma A 4-73091  
Coma cluster, evidence of hard X-ray emission 4-86065  
Coma cluster, velocity dispersion anisotropy, constraints from stripping characts. 4-90246  
Coma-type radio halos form., role of galactic cosmic ray electrons 4-90248  
compact groups dominated by dark matter, N-body simulation 4-86070  
cooling flows leading to star form. and central galaxy growth 4-110759  
cosmological pair correlation, exact closed eqn. 4-63324  
dark matter, evidence for non-baryonic nature 4-67795  
dark matter, galaxies, superclusters and voids, review 4-63379  
dense clusters, galaxy props. rel. to galaxies in voids 4-77937  
distant clusters, photometry and morphology 4-77946  
distant clusters detect. on photographic plates 4-94638  
distribution and Universe large-scale struct. 4-78008  
dynamical development from primordial density fluctuations, correl. with present-day cosmic background radiation 4-78003  
early-type galaxies in clusters, bright end of colour-magnitude relation from UBVR photometry 4-86026  
envelopes, unseen matter existence as substellar bodies 4-77942  
faint galaxies distrib., Monte Carlo simulation 4-78010  
filaments in galaxy counts, reality anal. 4-78005  
formation, role of pregalactic activity and hidden mass 4-67797  
formation (book contribution) 4-63352  
formation and structure growth in Universe 4-73127

**clusters of galaxies continued**

- galaxy correlation hierarchy in perturbation theory 4-86033  
 general characteristics 4-101489  
 gravitational lensing, screen model for spatial fluctuations of cosmic microwave background 4-63344  
 Hercules Cluster, IRAS obs. 4-86068  
 hierarchical structure of Metagalaxy, review of problems 4-63327  
 interacting galaxies groups, morphological features investigation 4-94939  
 intergalactic gas of rich galaxy clusters, He separation from D (*Russian*) 4-94971  
 intervening cluster towards QSO 0957+561 A,B 4-110772  
 intervening cluster towards quasar pairs, absorpt. lines anal. and nature of intervening objects 4-77966  
 intervening clusters towards quasars, absorpt. lines origin 4-106081  
 intracluster gas-active galaxies interactions, radio-trail galaxies form. 4-94968  
 large-scale distrib. of rich clusters and superclusters 4-73086  
 Local Group infall towards Virgo cluster, evidence from Sc I galaxies obs. 4-90220  
 Local Group motion rel. to background of galaxies 4-77938  
 Local Group motion towards Virgo cluster, evidence in microwave background anisotropy 4-77983  
 Local Supercluster, dynamics and overdensity from red shift survey anal. 4-77935  
 Local Supercluster, galaxy form characts. and ang. momentum effects 4-110756  
 Local Supercluster, identification of absorption lines with small redshifts in spectra of quasars 4-94984  
 Local Supercluster, mass, cosmological implications 4-73081  
 M81 group, discovery of low surface brightness galaxies in region (1046+65) 4-94952  
 M81/M82 group, luminosity profiles of dwarf galaxies 4-94953  
 masses, cosmological implications 4-73081  
 massive black holes in clusters and galaxies nuclei, relativistic dynamics 4-77883  
 microwave background, cooling of brightness of temp. in direction of clusters of galaxies 4-73104  
 missing mass problem 4-90268  
 monopole dominated universe, galaxy formation, clusters, perturbation growth 4-115844  
 morphology-density relation for galaxies 4-110732  
 multiple imaging of quasars by galaxies and rich clusters 4-94988  
 N-point correlation function 4-94973  
 N-point correlation functions, theoretical amplitudes for arbitrary N 4-63326  
 neighbouring superclusters, struct. determ. methods 4-77950  
 NGC 6166 and 7720, brightest cluster galaxies and their multiple nuclei, orbit anal. 4-86066  
 nonlinear gravitational clustering 4-94975  
 numerical experiments for different Universe expansion histories 4-78011  
 optical contour maps correl. with X-ray struct. 4-77947  
 pancake theory and massive neutrinos 4-110791  
 Perseus supercluster, filamentary structures, red shift survey 4-77951  
 Perseus supercluster, north extension evidence 4-101488  
 protogalactic eddies, structure 4-63290  
 in quasar fields, catalogue of objects discovered in imaging survey 4-94644  
 quasars clustering, anal. for quasars with known redshifts 4-101495  
 quasars host galaxies, direct imaging obs. and assoc. with galaxy clusters 4-86078  
 radial velocities, determ., using submm spectrophotometry (*Russian*) 4-86071  
 ram pressure stripping and gas content 4-77944  
 remote superclusters, dynamics and red shift survey, cosmological implications 4-77953  
 rotation of galaxies and clusters, prod. by tidal torques 4-67804  
 self-similar gravitational clustering 4-78009  
 self-similar spherical voids in an expanding Universe 4-110789  
 size in neutrino-dominated Universe 4-95005  
 small groups, N-body simulations 4-63325  
 southern clusters of galaxies, survey 4-77731  
 supercluster catalog 4-63086  
 supercluster-void struct. topology in the Universe, cluster chains 4-94977  
 superclusters, gravit. imaging theory 4-86069  
 superclusters and voids, struct. 4-77943  
 superclusters as nondissipative pancakes, N-body simulations 4-77948  
 superstructures, props. of nearby objects 4-73086  
 Ursa Major supercluster, red shift survey and radio obs. 4-77952  
 violent relaxation, galaxies interactions and form. 4-90247  
 Virgo; distance from disk galaxies, absolute (blue) luminosity/21 cm line-width relation 4-63276  
 Virgo cluster, evidence for low dust content in spiral galaxies 4-101464  
 Virgo cluster, galaxies infall, cosmological eqns. soln. 4-77949  
 Virgo Cluster, galaxies infall and cosmological constraints 4-110755  
 Virgo cluster, meas. of four photoelectric UBVRI sequences near cluster galaxies 4-94741  
 Virgo cluster and field galaxies, H I and optical diameters 4-77939  
 Virgo cluster dwarfs, classification system and illustrated atlas 4-115827  
 Virgo cluster supernovae and origin of first metals in Galaxy 4-90137  
 Virgo supercluster and cosmic ray sources 4-100925  
 voids evolution from primordial density var., correl. with present-day cosmic background radiation 4-78003  
 voids origin as consequence of adiabatic perturbations 4-78002  
 X-ray emission, appl. as probe of intergalactic medium 4-63266  
 X-ray emission, Einstein Observatory obs. anal. 4-77974  
 Zwicky's near clusters, red shifts list 4-101197  
 Zwicky clusters, WSRT 1415 MHz obs. 4-67808  
 $\gamma$ -ray emission, contrib. to background 4-82554

**clutter**

see also radar clutter

- atmospheric clutter modelling for down-looking satellite platform 4-115565

c.m.o.s. integrated circuits see field effect integrated circuits

c.m.o.s.l.c. see field effect integrated circuits

**CNDO calculations**

- acetylide borane, orbital interactions, charge transfer, and bond form., CNDO/2D study 4-59641  
 L-alanine, vibr. circular dichroism, MO calc. 4-69125  
 alkanes,  $^{13}\text{C}$  chem. shift, CNDO-SCF wave function calcs. 4-64375

**CNDO calculations continued**

- alkylamines and cation radicals, electronic and spatial struct., CNDO/2 calcs. 4-59647  
 aniline, low temp. cage effect and phosphorescence 4-96690  
 annulene, anions and derivatives, elec. polarisability, CHF-CNDO calcs. 4-64373  
 bacteriorhodopsin analogues synthesized from fluorophenyl retinals, XPS study and CNDO/S calcs. 4-77189  
 benzene, substituted, two-photon props., CNDO/s CI calcs. 4-78779  
 carboanions and dianions, elec. susceptibilities, extended basis CNDO calc. using coupled HF perturbation energy 4-64380  
 chemical shift, CNDO-SCF wave function calcs. 4-64375  
 conjugated-bond molecules, UV spectra, CNDO/S and PPP calcs. 4-59705  
 cycloocta-1,5-diene, anions and derivatives, elec. polarisability, CHF-CNDO calcs. 4-64373  
 diamond:Fe, electronic struct. calcs. 4-113894  
 10,10-dichloro-10-germa-9-oxa-9,10-dihydroanthracene, conjugation effects calcs. 4-59648  
 6,7-dihydroxycoumarin, molecular electronic props. calcs. 4-78778  
 10,10-dimethyl-10-germa-9-thia-9,10-dihydroanthracene, conjugation effects calcs. 4-59648  
 N,N-dimethylaniline, low temp. cage effect and phosphorescence 4-96690  
 dimethylbenzaldehydes- $d_6(d_4)$  in durene cryst., vibronic intensities, phosphorescence spectra 4-96596  
 enamine aldehydes (ketones) (amides), UV spectra, CNDO/S CI calcs. 4-78789  
 geometry optimisation, symmetry coordinates 4-68979  
 inorganic ion-exchange materials, selective action, simulation of solvation interactions 4-62185  
 ion+ molecule interactions, low-frequency vibrations, geometries and energetics calcs. 4-107432  
 isoxanine phosphate structure, CNDO MO calc. 4-107466  
 isocyanic acid, electron impact dissoci., fragment emission spectra 4-107461  
 methyl dichlorophosphite, PES and electronic struct., orbital model of conformational isomerism 4-112118  
 methyl dichlorothiosphite, PES and electronic struct., orbital model of conformational isomerism 4-112118  
 methylamine, intensity and electro-optical parameters, CNDO calc. 4-83397  
 molecular models, electrostatic pot., evaluation by conventional, vector and array processors 4-69172  
 1-nitronaphthalene, second hyperpolarisability, electronic contrib., CHF-PT-EB-CNDO calcs. 4-68959  
 nitroso cpds., closed and open forms, relative ionicity, XPS, NDO calcs. 4-107402  
 organic molecules, dipole moments and polarisabilities of lowest singlet and triplet states, CNDO CI calcs. (*Russian*) 4-112119  
 organophosphorus compounds, PES and electronic struct., orbital model of conformational isomerism 4-112118  
 PCIO framework, modified using CNDO/Boyd-Whitehead parametrisation 4-78759  
 poly(trimethylene sulphide), conformational stability, CNDO/2 tight binding calcs. 4-78992  
 polyatomic molcs., IR vibr. freqs. and intensities, semiempirical NDO calcs. 4-64387  
 polyglycine and its model systems, hydrogen bonds theoretical study 4-59931  
 porphyrin dianions +  $\text{H}^+$  donors (alkyl halides), reaction products electron density distrib. 4-107284  
 pyrene, two-photon spectrum, vibronic activity, CNDO/S CI calc. 4-74156  
 p-quinonemethide, electronic struct., CNDO calc. 4-112117  
 thioamides, CN stretching freq. in rel. to reson., CNDO/2 calc. (*German*) 4-83297  
 transition metal compounds, Jahn-Teller distortions, NDDO calcs. 4-87050  
 1,3,5,2 $\lambda^2$ -triazaphosphorines, substituted,  $^{35}\text{Cl}$  NQR and CNDO/2 investigation 4-59808  
 s-triazine,  $e^-$  modes, vibronic activity CNDO/S and MINDO/3 calcs. 4-59640  
 tribromoaetonitrile and  $^{15}\text{N}$  isotopic derivative, IR and Raman vibr. spectra 4-69081  
 1,1,2-trichloroethane, catalytic dehydrochlorination, CNDO/2, INDO and MINDO/3 calcs. 4-91202  
 uracil- $d_6(d_2)$ , vibr. force consts. CNDO/2 calcs., IR spectra 4-59699  
 Al, adsorpt. of H atoms, on (100) surface, CNDO/BW calcs. 4-61222  
 $\alpha\text{-Al}_2\text{O}_3$ , electronic energy levels from Al L-edge photoabsorption, small-cluster CNDO calcs. 4-81038  
 (BH $_3$ NO) $_2$ , orbital interactions, charge transfer, and bond form., CNDO/2D study 4-59641  
 (H $_2$ O) $_2$ , electronic struct., semiempirical linear combination of MO's method calc. 4-112116  
 H $_2$ O-O $_2$  triplet contact charge transfer complexes, pot. energy curves 4-91322  
 NH $_3$ -BH $_3$ , orbital interaction, charge transfer, bond form., CNDO/2 study 4-102597  
 PtCl $_2$ CO, electronic struct., semiempirical linear combination of MO's method calc. 4-112116  
 SiF $_4$ , dipole moment derivatives, polar tensors and effective charges 4-107283  
 TiC refractories, electronic struct., CNDO/2 calc. 4-75848  
 WC refractories, electronic struct., CNDO/2 calc. 4-75848  
 WC refractories, wetting by transition metal ions, CNDO/2 study 4-75756

**coagulation**

- aerosols, log-normally preserving size distribution for Brownian coagulation in the free-molecule regime 4-99847  
 blood clotting timer, automatic, optical endpoint sensing 4-115165  
 branched polymers, Smolouchowski's eqn. and  $\theta$ -exponent 4-90523  
 colloidal suspensions, stability and coagulation in shear fields 4-91836  
 dilute polydisperse system of sedimenting spheres; coagulation rate 4-112990  
 discrete particle distrib., coagulation, Monte Carlo simulation, Brownian motion 4-89345  
 dispersed system, kinetics of Brownian coagulation, weak hydrodynamic field 4-79638

**coagulation continued**

- grains, nucleation, growth, coagulation and condensation, astrophysical appl. 4-77706
- graphite suspensions, aggregation processes, conductometric study 4-109691
- interparticle forces and quasi-stationary equilibrium hypothesis 4-89346
- ultrafine chainlike or fibrous type particulate aerosols, Brownian coagulation and charge effect 4-99846
- Au colloids, aqueous, fractal structures formed by kinetic aggregation 4-62258

**coal**

- see also mining*
- brown coal hydrogasification, semi-technical test plant operation 4-81572
- brown coal-oil suspensions, rheology, moisture effect 4-60352
- charcoal as an alternative energy carrier: net energy and cost analyses 4-114882
- clastic sedimentary sequences, quantification in time series anal. 4-94042
- coal, drying, Stefan model comparison with two-phase model 4-103186
- coal-fired boiler exhaust gas heat recovery 4-64826
- coal-natural gas fuel mixture, combustion characts. and viability 4-77052
- coal-oil suspensions, rheological study 4-97458
- coal-water mixtures on horizontal brass surface, film boiling of discrete droplets 4-64829
- coal-water slurry burner modelling and development 4-62285
- combustion products, collision integrals for ions and electrons with neutral particles 4-114797
- comparison with coal-liquid mixtures, possibilities and expectations as fuel for boiler installations (*Dutch*) 4-89374
- consumption coal for fixed bed gasification (*German*) 4-85379
- conversion wastewater treatment by wet oxidation 4-62415
- electromagnetic techniques for remote detection, monitoring and mapping coal derived energy resources 4-72042
- elemental concentration determ. in coal using synchrotron radiation 4-100785
- fluidised bed combustion of solid fuels 4-99935
- fly ash, elemental particle size distrib. in thick samples, PIXE anal. 4-105069
- French Coal Board, efforts in developing market for coal (*French*) 4-77049
- gasification, effect of temperature near ash melting point 4-62380
- gasification combined cycle power plant 4-109716
- gasification systems, developments in USA and France (*Dutch*) 4-89460
- Hercules coke-to-methanol plant, progress 4-62377
- hot coal gas cleanup process in coal gasification 4-62376
- HTR, BBC/HRB concept of nuclear process heat for coal gasification 4-81526
- HTR He/He heat exchanger, design and semitechnical testing, coal gasification 4-78711
- IR microspectroscopy, specimen prep. technique, computer-controlled microspectrophotometer 4-93572
- lignite, with fractal props., small-angle X-ray scatt. study 4-103602
- liquefaction, solvent N content effects 4-99937
- low-grade fuels—Swedish energy option 4-89376
- MHD coal combustor development for low preheat operation 4-72130
- microwave energy interaction for upgrading fuel precursors, chemical product analysis 4-72040
- mining, Netherlands, present state (*Dutch*) 4-114883
- NKK coal gasification process, status report 4-62378
- nuclear aided steam gasification, semi-technical pilot plant 4-81573
- Pennsylvania, USA, elec. props. and radar attenuation of coal measure rocks 4-72582
- recreational fishing reef construction from coal waste blocks 4-114974
- shell and tube slurry heat exchangers, slurry concentration and flow rates meas. 4-60554
- solid fuel steam generators, development trends in combustion (*German*) 4-114796
- solid-fuel combustion in fluidised bed, two-phase model 4-71926
- steam power stations, fuel consumption, environmental problems (*Hungarian*) 4-109761
- steam power stations, high sulphur coal burning, strategies for compliance with SO<sub>2</sub> emission standards, economics 4-89480
- steam reformer, nuclear heated, design and semitechnical operating experiences 4-81571
- Stirling engines, coal-burning, large-scale, possible applications 4-72148
- substitute natural gas production by CS/R hydrogasification process 4-62375
- thermal and thermoelastic props., photoacoustic microscopy studies 4-105552
- U-GAS gasifier dynamic response 4-62379
- underground gasification, cavity growth 4-99985
- underground gasification, potential in USA 4-99982
- underground gasification, technical feasibility 4-99983
- VEW-coal conversion process: 10 ton/h-test plant (*German*) 4-85380
- Weller Coal Measures, Victoria Land, Antarctica, geological study 4-81942
- WIDCO's program for UCG commercialisation 4-99984
- wind erosion from coal surfaces, computer simulation program 4-82211
- X-ray emission spectroscopy for trace element anal. 4-89361
- H<sub>2</sub> production by electrochemical gasification 4-66814

**coating processes** *see coating techniques***coating techniques**

- see also anodisation; cladding techniques; coatings; electrodeposition; electrophoretic coating techniques; encapsulation; epitaxial growth; metallisation; spray coating techniques; vapour deposition*
- acoustic levitation based coating technology 4-99306
- glasses and ceramics, preparation for elec. use based alkoxide and unidirectional solidification methods 4-104760
- ICF target fabrication using polystyrene mandrels, plastic coated metal shells prep. 4-91962
- IR window manufacturing technology 4-106381
- Langmuir-Blodgett alternating multilayer film, prep. method 4-81164
- metallic surfaces, coatings by powder deposition of explosive condensed substances 4-61839
- microwave plasma generator for polymerisation and surface treatment, experimental evaluation 4-75171
- Newtonian fluids, dip coating finite element simulation 4-113088
- non-Newtonian fluids, dip coating, finite element simulation 4-112963
- optical fibre, high-speed drawing and coating techniques 4-103042
- optical fibre coating materials and high speed coating techniques 4-91661

**coating techniques continued**

- optical fibres high-speed coated, strength tests 4-91662
  - optical films and antirefl. coatings deposited from solns. mech. strength 4-74670
  - oxide coating deposition using sol-gel technology 4-76697
  - x-phthalocyanine, organic photocond., inhomogeneous deposition Pt particles 4-81449
  - plasma sputtering to produce metal coatings 4-66231
  - PVDF piezoelectric layers, deposition from soln., US transducer fabrication 4-60242
  - radioautographic coating apparatus for monolayer emulsion coating 4-58920
  - silicate filler for polymers, tridecylamine coating treatment, ang. depend. XPS obs. 4-109526
  - solar cells, electrodeless Ni metallisation, process reliability, experimental analysis 4-62363
  - solar highly absorbing coatings using graded refractive indices and textured surfaces 4-71746
  - steel, C, electric spark alloying, TiB<sub>2</sub> struct. influence 4-62121
  - Al, chemical colouring by conversion coating process 4-81349
  - Be coating for biological X-ray microanalysis 4-77431
  - CdCl<sub>2</sub> disubstituted thiourea complexes, appl. in fabrication of thin film solar cells 4-114909
  - CdTe thin films, electrodeless deposition 4-88992
  - Co<sub>3</sub>O<sub>4</sub>-based selective surfaces prep. by dip-coating process for solar absorber-convertors 4-72172
  - Cr films, laser induced metal deposition from organometallic solution 4-66239
  - GaAs, thick-film silk-screen deposition technique 4-109320
  - HfO<sub>2</sub> optical films and antirefl. coatings deposited from solns. mech. strength 4-74670
  - Mo films, laser induced metal deposition from organometallic solution 4-66239
  - Ni detonated coatings, metastable phase form. in Ni-C system 4-71554
  - Ni-B composites, electrodeless and electrodeposition 4-88990
  - Si solar cells, thick film metallisation technique, structure and electrical properties analysis 4-62365
  - a-Si:H films, thickness effects on electrical and photoelectrical properties 4-98484
  - SiO<sub>2</sub> optical films and antirefl. coatings deposited from solns. mech. strength 4-74670
  - SnO<sub>2</sub>:Sb film deposition by sol-gel technique, optical and elec. characts. 4-71604
  - TiO<sub>2</sub> optical films and antirefl. coatings deposited from solns. mech. strength 4-74670
- coatings**
- see also anodised layers; antireflection coatings; claddings; decorative coatings; electrodeposits; electrophoretic coatings; epitaxial layers; insulating coatings; protective coatings; spray coatings; sputtered coatings; vapour deposited coatings; varnish*
  - deposited dielectric for III-V semiconducting devices 4-84702
  - epoxide resin coatings, internal stress, network struct., glass transition temp., rel. to curing process (*Japanese*) 4-88966
  - fretting wear and fretting fatigue, relationship 4-65339
  - hard coating flaking under shear stress, fracture mech. anal. 4-69713
  - hard coatings on steel substrate, fatigue testing using (*German, English*) 4-71822
  - Infrablack improved optical black for stray light rejection from 0.3 to 500 µm reflectance meas. 4-74667
  - inorganic thin coatings on metals, Fourier transform IR spectra 4-104688
  - laser induced damage in optical materials, conf., Boulder, CO, USA (Nov. 1981) 4-73169
  - layer with winker-type coating, contact problems in the theory of elasticity 4-79523
  - mirror coating reflectivity meas. using mirror reflectometer 4-78364
  - multilayer 3.8 µm coatings, pulsed damage and optical characts., influence of cleaning solvents, sunlight, humidity and HF gas 4-75523
  - multilayer filter coating light scatt. 4-74413
  - nondestructive materials monitoring instruments (*Russian*) 4-81384
  - optical coating standards 4-83673
  - optical coatings, laser induced damage, physical aspects 4-74566
  - optical fibres in adverse environments, conf., Paris, France (May 1983) 4-78025
  - optical specifications, components and systems, conf., Arlington, VA, USA (Apr. 1983) 4-82586
  - optical-black coating specular reflectance in the far-IR 4-97030
  - organic coatings on optical fibres, contributions and effects 4-81299
  - poly(styrene-co-divinylbenzene) beads coating with styrene-divinylbenzene copolymers 4-114691
  - stainless steel, permeation of T, suppression by Au(Ni) plating 4-61261
  - steel, Cr-Mn, diffusion reaction with Al coating, Si content effect 4-114723
  - stratified media technology, conf., Los Angeles, CA, USA (Jan. 1983) 4-82585
  - surface layers of bases for standard measures of coating depth 4-81315
  - thickness measurements, X-ray studies 4-63717
  - thin film technologies, conf., Geneva, Switzerland (Apr. 1983) 4-73137
  - Ag<sub>2</sub>S films on Ag, spectrally selective props. for solar absorber convertors 4-99211
  - Al<sub>2</sub>O<sub>3</sub> thin films, interaction with W 4-70576
  - Be coating for biological X-ray microanalysis 4-77431
  - C-SiC alloy coating for limiter-armor tiles on Doublet III fusion reactor, test results 4-111924
  - C-SiC coating on graphite tiles for Doublet III armour/limiters, process evaluation and characterisation 4-111755
  - Ca<sub>10</sub>(PO<sub>4</sub>)<sub>6</sub>(OH)<sub>2</sub> coatings in Ti, comp. and struct., Auger spectroscopic analysis 4-109558
  - Cr<sub>2</sub>O<sub>3</sub> thin films, interaction with W 4-70576
  - GaAs, laser alloyed Sn layers, elec. props., surface damage 4-99622
  - Ni detonated coatings, metastable phase form. in Ni-C system 4-71554
  - Ni-coated Nb, hardening and fracture initiation, resulting from H<sub>2</sub> adsorpt.-desorpt. cycling 4-81282
  - Pd-coated Nb, hardening and fracture initiation, resulting from H<sub>2</sub> adsorpt.-desorpt. cycling 4-81282
  - SiC coatings of nuclear fuel particles, characterisation (*German*) 4-78702
  - ZrO<sub>2</sub> amorphous coatings, prep. from metal-organic solns. 4-76696

coatings, protective *see protective coatings*

# coaxial cables

- diode-switchable coaxial cable delay system for a synthesis radio telescope 4-101164
- infinitely long radiators carrying electric and mag. currents, comparative anal., geophys. prospecting appls. (*Russian*) 4-102875
- lightwave undersea transmission systems, development (*French*) 4-103018
- pairs, study of interference arising from radio wave induction (*Chinese*) 4-107484
- permittivity meas. of liquid materials, broad-band meas. equipment for 1 MHz to 1 GHz range 4-111153

coaxial lines *see coaxial cables*

# cobalt

- see also nuclei with*.....
- atom, quartet states, electron impact excitation cross sections 4-78970
- atom, two-electron one-photon excitation, X-ray absorpt. spectra 4-83324
- atoms, two-electron, one-photon transitions 4-74340
- band structure, interpolation scheme (*Rumanian*) 4-98513
- chemical bonding, mag. susceptibility 4-114090
- clusters, two-dimens., chemisorption of CO 4-108725
- Columbia River, Oregon, USA, radioactive pollution in sediments 4-66824
- diffusion in  $\alpha$ -Fe, effect of mag. transition 4-65481
- distribution in boronised alloys VK6, TSK10 and T15K6 (*Russian*) 4-80071
- electrochemical oxidation in NaOH soln., ion passivation mechanisms 4-109540
- electrolytic films, mag. props. and struct. (*Russian*) 4-80797
- electrolytic method for making thick foils 4-104742
- electronic struct., magnetism and Curie temps. 4-75843
- FCC cryst., phonon dispersion, magnetic interactions 4-61018
- film, Brillouin scatt. from thermal magnons 4-71458
- films, elec. cond. temp. depend. (*Russian*) 4-88613
- HCP, effects of systematic reflections on diff. contrast 4-92035
- HCP, phase transferability of Co atom pairs, EXAFS anal. 4-61771
- K-absorption edge, X-ray absorpt. near edge struct. obs. 4-66123
- Kramers-Kronig relation of measured atomic scatt. factors 4-98063
- LWR primary circuits, Co release from component wear, radiation field buildups 4-102383
- many-domain magnetically ordered media, nucl. distrib. functions and enhancement factors (*Russian*) 4-114183
- mechanisms and kinetics of dissolution in liquid Cu 4-114530
- Pacific seafloor Mn crust containing Co, in USA economic zones 4-110107
- polycrystalline, approach to saturation at intermediate fields, role of internal demagnetising fields 4-76183
- polycrystalline, ferromagnetic, density of unoccupied states, SXAPS study 4-85039
- polyfluorocarbon films containing Co(Al) clusters, plasma polymerisation 4-81433
- radiative properties at high temp. 4-84952
- single crystals, spin polarised Auger electrons 4-85044
- stainless steel, <sup>60</sup>Co content control in fission reactors 4-64198
- surface, bonding of Al flame-sprayed coating, emission Mossbauer spectroscopy study 4-92979
- thin-film magnetic domain obs. with differential phase contrast Lorentz scanning transmission microscope using double gap objective lens 4-86506
- transition metal oxides: Co, electronic struct. and cryst. field transitions 4-113891
- Al<sub>2</sub>O<sub>3</sub>:Co, thermoluminescence and trap parameters 4-76532
- BaTiO<sub>3</sub>:Co, impurity valence states, EPR 4-75901
- $\beta$ -Co, creep mechanism maps, expt. 4-93359
- CdTe:Co, optical absorpt. spectrum (*Russian*) 4-84983
- Co I lines, Stark width and shifts 4-91223
- Co I oscillator strengths from Fraunhofer line equivalent widths 4-63125
- Co III, transition probabilities for forbidden lines in 3d<sup>7</sup> ground configuration 4-63041
- Co:MgF<sub>2</sub> CW tunable mode-locked lasers, 1.65-2.01  $\mu$ m range 4-60043
- Co:MgF<sub>2</sub> tunable lasers, recent advances 4-69447
- Co-Al<sub>2</sub>O<sub>3</sub> coevaporated thin films, solar selectivity 4-72169
- Co-Al<sub>2</sub>O<sub>3</sub> with adsorbed N<sub>2</sub>, FT-IR studies 4-113786
- Co-Mo oxide film, immersion coated, for selective absorber 4-72173
- Co-Nb amorphous films, electron beam deposited, ion mixed, FMR, magnetisation meas. 4-71138
- Co-Nb multilayered compositionally modulated films, e-beam deposited, FMR, magnetisation, B-H loop meas. 4-71139
- Co-Sb multilayered films, cpd. form., interface magnetism, <sup>59</sup>Co NMR obs. 4-109095
- <sup>57</sup>Co, no-carrier-added, indirect prod. using <sup>59</sup>Co(p,n)<sup>57</sup>Ni 4-89744
- <sup>57</sup>Co ultra-thin  $\alpha$ -source, preparation by adsorption 4-68853
- <sup>60</sup>Co, fallout nuclide accumulation in snails 4-62609
- <sup>60</sup>Co  $\gamma$ -rays, fatal accidental exposure, dose estimation from watch jewels thermolum. 4-89754
- <sup>60</sup>Co, low-cost hot facility for high-Cl gamma-source processing 4-74084
- <sup>60</sup>Co, tissue accumulation and loss in mallard ducks 4-62598
- <sup>60</sup>Co tracer diffusion in austenitic stainless steel 4-75731
- CsCaCl<sub>2</sub>:Mn<sup>2+</sup>(Ni<sup>2+</sup>)(Co<sup>2+</sup>), fluoresc. emission, excitation, IR absorpt. spectra studies 4-99153
- Cu-Co composites, magnetoelectric, mech. props. 4-98934
- $\gamma$ -Fe<sub>2</sub>O<sub>3</sub>:Co, textural and surface props. rel. to mag. recording appls. 4-65833
- $\gamma$ -Fe<sub>2</sub>O<sub>3</sub>:Co magnetic powder, perpendicular orientation, Mossbauer study 4-65838
- $\gamma$ -Fe<sub>2</sub>O<sub>3</sub>-Fe<sub>2</sub>O<sub>4</sub>:Co thin films, coercivity study 4-114145
- GaSe:Co, injection and thermopolarisation currents 4-70833
- InP:Co, impurities, optical and transport studies 4-71444
- La<sub>2</sub>Mg<sub>3</sub>(NO<sub>3</sub>)<sub>12</sub>Ce<sup>3+</sup>Co<sup>2+</sup>24H<sub>2</sub>O, paramagnetic, maser effect due to thermal excitation by pulsed mag. field 4-64692
- LiNbO<sub>3</sub>:<sup>57</sup>Co, Fe<sup>3+</sup>, electron capture, non-equilibrium population, Mossbauer spectra studies 4-108807
- LiTaO<sub>3</sub>:<sup>57</sup>Co, Fe<sup>3+</sup>, electron capture, non-equilibrium population, Mossbauer spectra studies 4-108807
- MgF<sub>2</sub>:Co tunable lasers, recent advances 4-69447
- MgO:Co, electronic Raman spectrum and perturbation calcs. 4-114281
- MgO:Co<sup>2+</sup>, g value, Jahn-Teller effect 4-88492
- Mn/Co compositionally modulated layered structures, enhanced unidirectional spin-glass behavior, mech. 4-71087
- NH<sub>4</sub>Cl:Co<sup>2+</sup>(Ni<sup>2+</sup>), X-irrad. effects, optical absorpt. spectra, EPR 4-70206

# cobalt continued

- Na<sub>2</sub>O-B<sub>2</sub>O<sub>3</sub> glass, undoped and Co<sup>2+</sup> doped, acoustic loss and optical absorpt. spectra, matrix analysis 4-84193
  - Si:Co, breathing mode relax around tetrahedral interstitial 3d impurities 4-108567
  - WC-Co composites, carbide-carbide grain boundaries, microanal. 4-80052
- # cobalt alloys
- see also cobalt compounds*
  - Alnico magnets, microstruct., comp., atom probe field ion microscopy 4-71828
  - amorphous ribbon, as-cast, crystn. and heat treatment effect (*Chinese*) 4-84190
  - amorphous sputtered films, mag. props. 4-84836
  - amorphous thin films for longitudinal recording, preparation and props. 4-80798
  - Co-W-Mn alloy electrodeposited coatings struct., effect of electrolytes containing Na<sub>2</sub>WO<sub>4</sub>, NaWO<sub>3</sub> (*Russian*) 4-65593
  - IN 100, Ni-base superalloy, thermal fatigue 4-93417
  - IN 738, high temp. low cycle fatigue models, predictive capability 4-93411
  - IN-100, Ni-base superalloy, cast, microstruct. changes during fractional melting 4-109434
  - IN-617, Ni-base superalloy, fatigue, high temp. low cycle 4-66425
  - IN-738 LC, Ni-base superalloy, creep fracture, effect of grain boundary chem. and segregation 4-81285
  - IN-738LC, Ni-base superalloy, precip. of  $\beta$  phase in  $\gamma'$  particles 4-114559
  - Inconel 617, surface crack form. and propag., effect of temp. reactor primary circuit He 4-114641
  - metallic glass ribbons, relax. damping, mag. charact. 4-76186
  - metallic glasses, low magnetostriction, crystallisation composition depend. 4-84196
  - oceanic ferromanganese crust database 4-115402
  - rare earth alloys, R-Co, hexagonal phases, abnormal mag. props. and mixed valence states 4-113907
  - rare earth alloys, RCo<sub>2</sub>, R=rare earth metals, paramagnetic props. calcs. 4-61508
  - rare earth alloys, RCo<sub>2</sub>Si<sub>2</sub>, R-Ce, Eu, valence change, X-ray absorpt. study 4-85037
  - rare earth alloys, RCo<sub>2</sub>B<sub>4</sub>, R=Gd-Tm, antiferromag. and paramag. states, NMR spectra 4-109089
  - rare earth alloys, RCo<sub>2</sub>Sn<sub>2</sub>, R=Y, Tb, Dy, Ho, Er, Tm, Lu, cryst. struct. and mag. props. (*Russian*) 4-88135
  - rare earth alloys RCoGe, R=Y, Yb, Tb, Dy, Ho, Er, Tm, Lu, cryst. struct., mag. and elec. props. (*Russian*) 4-88134
  - rare earth-Co intermetallics, RCo<sub>2</sub> type, domain struct. 4-114133
  - Rene 95, Ni-base superalloy, fatigue, effect of processing and microstruct. 4-104843
  - Stellite, Co-based wear-resistant alloy, liq. phase sintered, carbide comp. 4-99365
  - Ti effect on rate of high-coercivity transform. 4-93296
  - Udimet 700, metalloid strengthening mechanism 4-61974
  - Udimet 700, Ni-base superalloy, creep fracture, effects of wavy grain boundaries 4-93415
  - wear resistant, optical constns. of carbides and borides, interference microscopy 4-104949
  - Al-Co, sputtering, surface comp., quantitative AES anal. 4-104045
  - Al-Co-Fe, Alcor 122, magnetostrictive, piezomagnetic coeffs., annealing, mag. field depend. 4-76214
  - Al-Fe-Ni-Co, prep. from atomised powder, prod. struct. and props. 4-114446
  - AuCo, impurity lineshapes in dilute alloys, UPS study 4-113893
  - Co-Cu, magnetically hard alloys, isostructural precipitation and atomic ordering (*Russian*) 4-104784
  - Ce<sub>1-x</sub>Hf<sub>x</sub>Co<sub>2</sub>, anomalous mag. behaviour 4-88664
  - Ce<sub>1-x</sub>Zr<sub>x</sub>Co<sub>2</sub>, anomalous mag. behaviour 4-88664
  - Co (Fe, Mn)-Nb system, amorphous sputtered films, magnetostriction and HF permeability 4-71147
  - Co-Ag-Pd, transient films, g-factor, gyromagnetic ratios 4-113914
  - Co-Al, directionally solidified eutectic, compressive yield stress rel. to lamellar termination density 4-81263
  - Co-Al, long range 21R struct. during martensitic transform. (*Chinese*) 4-103699
  - Co-base alloy coating, contact fatigue resist. 4-93426
  - Co-base alloys, gaseous corrosion in H<sub>2</sub>O-HCl environment 4-89164
  - Co-base superalloy, MAR M509, cast, thermal fatigue 4-93416
  - Co-based heat resisting alloys, radiative and optical props. 4-74847
  - Co-C, hyper-eutectic alloy, diamond form. at high press. 4-109374
  - Co-Ce liq. alloy, Ce valence state determ. 4-61358
  - Co-Co<sub>17</sub>Gd<sub>2</sub>, off-eutectic, growth by floating zone techniques 4-99304
  - Co-Cr ferromagnetic thin films, high rate magnetron sputtering 4-66232
  - Co-Cr films, high-rate preparation on continuous tape substrates using target facing sputtering (*Japanese*) 4-81128
  - Co-Cr ion beam sputter deposition, mag. props., temp. effects 4-104469
  - Co-Cr layers, mag. orientation, effect of RF sputter parameters 4-65840
  - Co-Cr media, statically written magnetisation patterns, mag. field meas. 4-88696
  - Co-Cr sputtered thin films, surface and vol. coercive fields 4-65841
  - Co-Cr-Al(Y), Si<sup>3+</sup> implanted, 1050°C oxidation behaviour 4-62124
  - Co-Cr-Mo, single-phase, low stacking fault energy, back stresses 4-76787
  - Co-Cr-Mo alloy, nucleation of recrystn. 4-114570
  - Co-Cr-Mo for hip joint endoprostheses, fatigue strength, remaining lifetime after loosening (*German*) 4-62627
  - Co-Cu, small diffusion coeff. meas. using SIMS 4-65459
  - Co-Fe-Mo-B-Si, metallic glass, fatigue crack propag. and overload effect 4-109511
  - Co-Fe-Mo-Ni, phase equilib., Gibbs energy and activity coeff., SOLGAS-MIX program 4-84369
  - Co-Fe-V, Wiegand wire sensor characts. (*German*) 4-101830
  - Co-Gd amorphous films, tunnelling, zero bias anomalies 4-76049
  - Co-Ge eutectics, X-ray spectral investigation (*Russian*) 4-76564
  - Co-Ir sputtered films, mag. props. 4-71141
  - Co-Mn, binary liquid alloys, thermodynamic props., formalism appls. 4-114478
  - Co-Nb amorphous film, ion mixing and mag. props. 4-104471
  - Co-Nb-Ti system, amorphous sputtered films, magnetostriction and HF permeability 4-71147
  - Co-NbC eutectic alloy, comp., microstruct. and tensile strength 4-66320
  - Co-Ni, equilib., activities at 1273K 4-80265

## cobalt alloys continued

- Co-Ni-P, amorphous thin films, small planar domains, nucleation and equilib. conditions 4-71123
- Co-P, amorphous, microstruct., TEM and small angle X-ray scatt. study 4-113332
- Co-P, amorphous electroplated alloy, mag. domain struct. obs. (*Spanish*) 4-88694
- Co-P amorphous alloys, NMR enhancement factor and multiple echoes 4-76270
- Co-P amorphous electrodeposited layers, Barkhausen effect, torsion effects 4-76198
- Co-P amorphous electrodeposits, elastic props. and struct. relax. 4-92282
- Co-P amorphous layers, mag. and struct. props. 4-76199
- Co-P electrodeposited amorphous alloys, reorientation kinetics of induced mag. anisotropy 4-84783
- Co-Si-B (-Fe) metallic glasses, mag. props., annealing effects 4-109039
- Co-Si-B metallic glasses, Young's modulus, internal friction, magnetomechanical effects, permeability meas. 4-76216
- Co-Ta, welded joints, electrolytic polishing investig. (*Russian*) 4-71777
- Co-Ti-C system, phase relations, diffusion paths, 1273K 4-109382
- Co-V(Cr)(Mo), sigma phase, pair-wise interaction model 4-84422
- Co-W-Mn thin mag. film deposition, electrocrystallisation (*Russian*) 4-65592
- Co-Zn system,  $\alpha$ -solid soln., interdiffusion study 4-98368
- Co<sub>1-x</sub>B<sub>x</sub> amorphous alloy, electrolytical and chemical prep., struct. 4-70603
- Co<sub>1-x</sub>B<sub>x</sub> glasses, local struct., EXAFS studies 4-60854
- Co<sub>100-x</sub>B<sub>x</sub> amorphous alloys, mag. anisotropy, mag. annealing effects 4-76131
- Co<sub>100-x</sub>B<sub>x</sub> metallic glass, mag. and mechanical props. 4-84841
- Co<sub>75</sub>B<sub>25</sub> amorphous alloys, mag. relax. processes 4-84825
- Co<sub>75</sub>B<sub>25</sub> liq.-quenched amorphous, dynamic temp. crystn. 4-60835
- Co<sub>80</sub>B<sub>20</sub> amorphous, high press. and temp. phase stability (*Chinese*) 4-103923
- Co(Cr,Ni)-TaC, eutectic, thermal cycling, calc. of residual stresses and strains 4-66380
- CoCrAlY alloy surface protection coating, deposited by plasma spray, for gas turbine blades (*German*) 4-99639
- CoCrAlY, low temp. hot corrosion inhibition by ZnSO<sub>4</sub>-Na<sub>2</sub>SO<sub>4</sub> deposits 4-76903
- Co<sub>66</sub>Fe<sub>4</sub>(MO, Si, B)<sub>30</sub> alloys, amorphous, mag. props., influence of induced anisotropy 4-84782
- Co<sub>2</sub>MnAl(Si), spin echo study of hyperfine interactions 4-71209
- Co<sub>1-x</sub>Nb<sub>x</sub> amorphous alloys, magnetic moments, Friedel's model 4-76123
- Co<sub>2</sub>Nb, C15 struct., phase transferability of Co atom pairs, EXAFS anal. 4-61771
- CoNiFe-SiB amorphous zero magnetostrictive alloy, compositional short-range order and ordering kinetics 4-70035
- Co<sub>55</sub>Ni<sub>14</sub>Fe<sub>3</sub>B<sub>10</sub>Si<sub>16</sub> foil, thermal expansion coeff. and isothermal compressibility (*Russian*) 4-65421
- Co<sub>55</sub>Ni<sub>15</sub>Fe<sub>3</sub>B<sub>10</sub>Si<sub>16</sub> amorphous, mag. aftereffects after field annealing 4-84823
- Co<sub>55</sub>Ni<sub>10</sub>Fe<sub>5</sub>Si<sub>16</sub>B<sub>16</sub> amorphous, mag. hysteresis loops after heat treatment below Curie point 4-80781
- Co<sub>5</sub>Ni<sub>1-x</sub>MnGe, magnetic transforms., effect of external press. 4-104418
- CoP, amorphous alloy characterisation using SEM 4-76937
- CoSi<sub>3</sub> film, elec. transport props., metallic cond. 4-70950
- CoSi<sub>3</sub>, formation and Schottky barrier heights 4-108922
- CoSi<sub>3</sub> single cryst. films, <sup>4</sup>He irradi., elec. cond. studies 4-98782
- Co<sub>75</sub>Si<sub>10</sub>B<sub>15</sub> amorphous alloys, fatigue props. 4-66424
- Co<sub>95-x</sub>Si<sub>5-x</sub>B<sub>x</sub> amorphous alloys, mag. aftereffects 4-84824
- Co<sub>85</sub>Si<sub>15</sub>Fe<sub>2</sub>B<sub>25</sub> amorphous alloy, crystn. study using DTA and elec. resist. meas. 4-65181
- Co<sub>2</sub>Ta, C15 struct., phase transferability of Co atom pairs, EXAFS anal. 4-61771
- CoTi, amorphous thin films, small planar domains, nucleation and equilib. conditions 4-71123
- Co<sub>100-x</sub>Ti<sub>x</sub> thin films, field induced anisotropy 4-71133
- CoTi<sub>1-x</sub>Al<sub>x</sub>, transition from nonmag.-ferromag. state, magnetisation and NMR meas. 4-76133
- CoTiSi<sub>3</sub> mag. props., magnetometry, neutron diffr. studies 4-71025
- Co<sub>84</sub>Zr<sub>15</sub>Nb<sub>10</sub>SiO<sub>2</sub> multilayered struct. amorphous films, mag. props. 4-104462
- Cr-Co alloys, local electron states, elec. resist. and magnetoresist. studies 4-80550
- Cu-Al-Co, with noncoherent particles, crit. shearing stresses, temp. depend. rel. to slip and twinning (*Russian*) 4-93333
- Cu-Al-Co (15.2 at.%), with non-coherent particles, superelasticity effects due to twinning 4-76795
- Cu-Be-Co (2, 0.2 wt.%), precip. hardening investigation by microhardness and elec. resist. meas. 4-61947
- Cu-Co (2 at.%) single crystals, age hardened, fatigue limit 4-104860
- Cu-Co alloys, Co precipitate coarsening, electron microscope studies 4-114544
- Cu-Co system, coarsening of semi-coherent precipitates 4-114525
- Cu-Co-Si alloys, dil., diffusion of <sup>59</sup>Co 4-65447
- Dy<sub>1-x</sub>Y<sub>x</sub>Co<sub>2</sub>, magnetically ordered, satellite struct. in <sup>59</sup>Co spin-echo NMR spectrum 4-88743
- (Fe, Co, Ni)<sub>2</sub>V, ductile ordered alloys, phys. metallurgy and mech. props. 4-114612
- (Fe, Co)<sub>2</sub>V single crystals, flow stress, temp. and orientation depend. 4-71699
- Fe-Co, mech. polishing, surface film thickness and comp., XPS obs. 4-62093
- Fe-Co alloys, magnetostriction, recrystn., heat treatment, and strain texture effects (*Russian*) 4-104476
- Fe-Co based metallic glasses, nearly magnetostrictive, disaccommodation 4-84828
- Fe-Co disordered alloys, magnetisation, tight-binding calc. 4-98924
- Fe-Co electrodeposited films, field induced mag. anisotropy 4-92943
- Fe-Co-C, ternary systems, phase equilib. 4-76750
- Fe-Co-Cr mag. disc., Lorentz microscopy and read/write characts. 4-80746
- Fe-Co-Ni-Al, Alnico 5, hot workability, microstruct. 4-114626
- Fe-Cr-Co, phase separation and coarsening 4-109407
- Fe-Cr-Co (12 wt.%) permanent magnet alloys, mag. props., effect of alloying 4-84771
- Fe-Cr-Co alloys, spinodal decomposition, atom probe field ion microscopy studies 4-114553

## cobalt alloys continued

- Fe-Cr-Co-Si-B amorphous alloys, mag. props. and hyperfine interaction (*Russian*) 4-108994
- Fe-Ni-Co film, mag. domain walls, dynamic props. 4-88705
- FeAl-CoAl, length changes rel. to heat treatment, phase transform. vacancy annihilation 4-109442
- FeCo alloy, brittleness, purity and impurity segregation effects (*Russian*) 4-109496
- FeCo based alloys, strength and mag. props. rel. to cold rolling and heat treatment 4-98918
- FeCo, coupling between chemical and mag. interactions, NMR study 4-114173
- FeCo, self-diffusion, influence of order-disorder transition 4-113695
- Fe<sub>2</sub>Co<sub>75</sub>B<sub>20</sub> amorphous, mag. aftereffects after field annealing 4-84823
- Fe<sub>60</sub>Co<sub>10</sub>B<sub>14</sub>Si<sub>16</sub> amorphous, extended freq. anal. of permeability aftereffect 4-84822
- Fe<sub>2</sub>Co<sub>51</sub>Ni<sub>20</sub>-Cr<sub>2</sub>B<sub>4</sub>Si<sub>3</sub> metallic glass, mag. props. study 4-84790
- (FeCoNi)SiB nonmagnetostrictive amorphous ribbons for magnetic cores, DC and AC magnetic characts. 4-92939
- Fe<sub>2</sub>Co<sub>58</sub>Ni<sub>10</sub>Si<sub>11</sub>B<sub>16</sub> amorphous, struct. relax. processes, dilatometric anal. (*Russian*) 4-92394
- (Fe<sub>100-x</sub>Co<sub>x</sub>)<sub>76</sub>Pr<sub>16</sub>O<sub>8</sub>, thermal effects of Co moderate substitutions 4-71124
- (FeCo)SiB nonmagnetostrictive amorphous ribbons for magnetic cores, DC and AC magnetic characts. 4-92939
- Fe<sub>2</sub>Co<sub>75</sub>Si<sub>15</sub>B<sub>10</sub> amorphous, mag. noise study (*Russian*) 4-65846
- Fe<sub>2</sub>Co<sub>75</sub>Si<sub>15</sub>B<sub>10</sub> amorphous, struct. relax. processes, dilatometric anal. (*Russian*) 4-92394
- Fe<sub>2</sub>Co<sub>70</sub>Si<sub>15</sub>B<sub>10</sub> amorphous, mag. permeability, annealing in transverse mag. field (*Russian*) 4-104467
- Fe<sub>2</sub>Co<sub>75</sub>Si<sub>15</sub>B<sub>10</sub> magnetic annealing kinetics 4-80795
- Fe<sub>2</sub>Co<sub>75</sub>Si<sub>15</sub>B<sub>10</sub> zero magnetostrictive amorphous alloy, permeability and field-induced anisotropy 4-71056
- Fe<sub>60</sub>Co<sub>15</sub>Si<sub>15</sub>B<sub>10</sub> metallic glass, crystn. kinetics 4-65187
- FeCo<sub>80-x</sub>Si<sub>15-x</sub>B<sub>5</sub> magnetostrictive amorphous alloys, stress-induced anisotropy and permeability 4-71055
- (Fe<sub>1-x</sub>Co<sub>x</sub>)<sub>90</sub>Zr<sub>10</sub> amorphous alloy, elec. resist. minima and mag. props. 4-75922
- (Fe<sub>22</sub>Co<sub>78</sub>)<sub>3</sub>V, tensile deforms, 20-1000°C, fracture mode and ductility rel. to order-disorder transform. 4-66427
- FeNiCo thin film, multiple spin echo study 4-84870
- Gd-Co amorphous films, spontaneous Hall effect in vicinity of the compensation composition 4-75929
- Gd-Fe-Co amorphous film, struct. and mag. props. 4-80434
- Gd-Ni-Co amorphous film, struct. and mag. props. 4-80434
- GdCo amorphous cosputtered film, surface versus bulk magnetisation curves 4-71131
- Gd<sub>2</sub>Co<sub>3</sub> crystn., cryst. struct. and mag. props. in microgravity 4-98915
- GdCo<sub>2-x</sub>Al<sub>x</sub> magnetoelastic interactions (*Russian*) 4-65845
- Gd(Co,Ni)<sub>1-x</sub> paramagnetic reson. lineshape anal. 4-88714
- GdCo<sub>2</sub>Si<sub>2</sub> charge transfer, X-ray absorpt. spectra study 4-81037
- (Gd<sub>0.5</sub>Tb<sub>0.5</sub>)<sub>3</sub>Co, crystn., cryst. struct. and mag. props. in microgravity 4-98915
- Gd<sub>2</sub>Y<sub>1-x</sub>Co<sub>2</sub> cluster glasses, mag. props. and magnetovolume effects 4-76207
- Ho-Co amorphous films, with perpendicular anisotropy, planar Hall effect 4-75932
- Ho-Co sputtered amorphous films with perpendicular mag. anisotropy 4-80796
- HoCo thin amorphous films, perpendicular anisotropy near compensation temp. 4-84835
- Ho<sub>2</sub>Co<sub>7</sub> intermetallics, cryst. growth from melt 4-66219
- LaCo<sub>2</sub>-H system, two-phase coexistence region, H chemical pot., interface rel. effect 4-104769
- LuCo<sub>2</sub>, quenching of spin fluctuations, heat capacity and magnetisation meas. 4-80744
- Mo-Co dilute alloy, Co impurity location, PIXE and ion channelling studies 4-80072
- Mo-Co dilute alloy, lattice location studies by PIXE and ion channelling 4-99894
- NbC-Co, plastic deform. of compound materials based on hard phases 4-99451
- NdCo, elastic and magnetoelastic props. (*Russian*) 4-80806
- Ni-base superalloy, DKS, directionally solidified, mech. props., influence of grain orientation 4-93420
- Ni-base superalloy, IN 100, hot corrosion inhibition by MgSO<sub>4</sub> and BaSO<sub>4</sub> 4-85254
- Ni-Co, FCC, elastical eigenstrains, X-ray study 4-71716
- Ni-Co, oxidation, parabolic growth of oxide solid solutions 4-109563
- Ni-Co electroplating, US agitation effect on mech. props. and comp. 4-114430
- Ni-Co MP35N Alloy Biowire for medical appls. 4-115263
- Ni-Co matrix, ThO<sub>2</sub> particles, oxide growth inhibition 4-104796
- Ni-Co-Cr-Nb-Hf, Ni-base superalloy, MERL 76, powder metallurgy hot isostatic pressing, effect of Ar contamination 4-114447
- Ni-Co-Nb, damping capacity, mag. and mech. props. 4-61564
- Ni-Co-W-Cr single crystal superalloy, crack tip plasticity, fatigue crack growth at elevated temp. 4-71727
- Ni-Co-W-Cr superalloy, single cryst., crack tip plastic strain 4-89231
- Ni-Cr-Co, IN 939, turbine starter blades, corrosion layers, metallography 4-104948
- Ni-Cr-Co (22, 9 wt.%) superalloy, solid solutions strengthened, development, weldability, oxidation resist. 4-61975
- Ni-Cr-Co-Al-Ti-Nb-W-Mo-V-Hf, cryst. lattice periods mismatch determ. 4-65219
- Ni-Cr-Co-B, melt spun superalloy, annealing, castability, ductility and microstruct. rel. to B additions 4-66323
- Ni-Fe-Co-Ti, Incalloy, domain struct. study by differential phase contrast Lorentz microscopy, max. specimen thickness 4-65825
- Ni-Fe-Co-Ti, STEM study of mag. domain walls 4-80779
- Ni<sub>100-x</sub>Co<sub>x</sub>-Ni<sub>81</sub>Fe<sub>19</sub> mag. films, exchange-coupled, mag. reversal characts. 4-76200
- PdCo dil. solns of H<sub>2</sub>(D<sub>2</sub>), thermodynamics 4-70411
- Pd<sub>0.83-x</sub>Co<sub>0.17</sub> metallic glasses, form., crystallisation and elec. props. 4-92685
- PdCuSiCo alloys, spin glasses, exptl. evidence for mag. two level systems 4-71082
- Pd(Fe, Co) dilute, Mossbauer study of relax., spin glass props. 4-104514
- Pr-Fe-Co alloy sheets, rapid quenching, magnetic properties (*Japanese*) 4-114141

## cobalt alloys continued

- Pt-Mn-Co system, Mn solubility, isothermal section, X-ray crystallography 4-11449
- Pt-Co dilute alloys, resistance thermometers with low magnetoresistive effects 4-11132
- Pt<sub>3</sub>Co, mag. transition temp., influence of plastic deform. 4-84785
- ScCo<sub>2</sub>, exchange enhanced Pauli paramagnet, mag. susceptibility, Knight shift meas. 4-10893
- ScCo<sub>2</sub>, quenching of spin fluctuations, heat capacity and magnetisation meas. 4-80744
- Sm-Co, powder particles and agglomerates, individual mag. props. and particle size effect 4-88702
- Sm-Co amorphous films, mag. props. 4-65842
- Sm-Co ferromagnetic thin films, high rate magnetron sputtering 4-66232
- Sm-Fe-Co alloy sheets, rapid quenching, mag. props. (*Japanese*) 4-114141
- Sm(Co,Fe,Cu,Zr)<sub>7.5</sub> magnets, high resolution electron microscopy study 4-61098
- SmCo<sub>5</sub> magnets, thermal remagnetisation, domain rearrangement 4-71074
- SmCo<sub>5</sub> permanent alloys, metallographic study, improved phase and grain boundary etching 4-114754
- SmCo<sub>5</sub> permanent magnets, magnetic field fluctuations, spin wave theory 4-61565
- Sm<sub>2</sub>Co<sub>17</sub>, high-temp. modification study (*Russian*) 4-80213
- Sm<sub>2</sub>Co<sub>17</sub> permanent magnets, rotational hysteresis 4-92940
- Sm(Co<sub>1-x</sub>Cu<sub>x</sub>)<sub>5</sub> cellular permanent magnets, coercivity 4-76191
- Sm<sub>2</sub>Fe<sub>7-9</sub>Co<sub>x</sub>, magnetic cooling near Curie temperatures above 300K 4-88677
- SmFe<sub>2</sub>(Co<sub>2</sub>)(Ni<sub>2</sub>) cpds., bonding, X-ray emission study 4-85042
- Ta-C-Co, plastic deform. of compound materials based on hard phases 4-99451
- TbCo amorphous films, perpendicular mag. anisotropy 4-61569
- TbCo<sub>2</sub>, mag. moments, susceptibility meas. 4-61525
- TbCo<sub>2</sub>, valence band photoemission at 3d absorption edges, reson. enhancement 4-81110
- TbCo<sub>2</sub>, intersublattice exchange parameters (*Russian*) 4-80743
- Tb<sub>2</sub>Y<sub>1-x</sub>Co<sub>2</sub>, magnetic phase transition studies 4-109020
- Th-Co, hexagonal phases, abnormal mag. props. and mixed valence states 4-113907
- Ti-C-Co, plastic deform. of compound materials based on hard phases 4-99451
- Ti-C-Co, TiC coated, cemented carbide tools, wear studies 4-99610
- TiNi<sub>3</sub>M<sub>1-x</sub> (M=Co, Fe, Cu), multiphase diffusion 4-61136
- UGaCo, mag. props., temp. depend. 4-71033
- WC-(Co-Ni) hardmetals, mech. props., variation with Ni/Co ratio 4-114462
- WC-C, mechanical behaviour, room temp. to 1000°C 4-62002
- WC-Co, cemented carbide, hot isostatic pressing 4-66293
- WC-Co, cemented elements of high press. apparatus, strength safety factors 4-109482
- WC-Co, hardmetal, creation of stable cracks using bridge indentation 4-66434
- WC-Co, hardmetals, infiltration technique 4-66294
- WC-Co, plastic deform. of compound materials based on hard phases 4-99451
- WC-Co cemented carbide, defect position in bending test rel. to strength variance 4-99661
- WC-Co cemented carbide, liq. phase sintering, origins of discontinuous grain growth 4-104759
- WC-Co hard metals, strengthening by ultrasonic vibrs. 4-62122
- WC-Co hardmetal, grain growth rate-sintering, influence of C content 4-114463
- WC-Co powders, hypersonic flame spraying, particle vel. meas. by laser Doppler velocimetry 4-81353
- WC-Co-P, wear resist., P addition influence 4-66458
- Y<sub>2</sub>(Co, Fe, Cu)<sub>17</sub>, single cryst. cpds., growth conditions and characterisation 4-66220
- Y<sub>2</sub>(Co, Mn)<sub>17</sub>, M=Al, Fe, single cryst. cpds., growth conditions and characterisation 4-66220
- YCo<sub>5</sub>, electronic struct. and mag. props. 4-92602
- YCo<sub>5</sub>, itinerant metamagnetism 4-84788
- YCo<sub>5</sub>, quenching of spin fluctuations, heat capacity and magnetisation meas. 4-80744
- Y<sub>2</sub>Co<sub>3</sub>, very weak itinerant ferromag., spin fluctuations, susceptibility and resistivity 4-76117
- Y<sub>9</sub>Co<sub>7</sub> ferromag. inhomogeneous supercond., sample size and meas. power effects 4-76065
- Y<sub>9</sub>Co<sub>7</sub>, paramag. close to ordering, supercond. transition temp. 4-92852
- YCo<sub>2</sub>Fe, H absorption in 0-40°C temp. range (*Russian*) 4-75775
- YCo<sub>2</sub>Ni, H absorption in 0-40°C temp. range (*Russian*) 4-75775
- Y<sub>0.5</sub>Dy<sub>0.5</sub>Co<sub>5</sub>, H absorption in 0-40°C temp. range (*Russian*) 4-75775
- Y<sub>2</sub>Fe<sub>17-x</sub>Co<sub>x</sub>, magnetic cooling near Curie temperatures above 300K 4-88677
- Y(Mn<sub>1-x</sub>Co<sub>x</sub>)<sub>12</sub>, mag. struct., neutron diff. study (*Chinese*) 4-92892
- YbGa<sub>2</sub>Co<sub>2</sub>, cryst. struct., X-ray diff. 4-84237
- Zr-Co, fast diffusion of Co atoms, quasielastic neutron scatt. meas. 4-113725
- Zr-Co amorphous alloys, crystallisation, DSC and elec. resist. studies (*Chinese*) 4-103658
- Zr-Co base eutectic, mech. props. rel. to microstruct. 4-89135

## cobalt compounds

- see also cobalt alloys
- acetate dihydrate, protiated and deuterated, IR spectra, H-bonds 4-61703
- formate dihydrates, Evans holes, IR spectra 4-66019
- intercalation cpd. with graphite, graphite-CoCl<sub>3</sub>, mag. order, neutron diff. studies 4-61511
- oxides, empirical bond length determ. 4-103710
- rhodamine-6G, aq. soln., triplet state quenching by inorganic ions, appl. to lasers 4-79159
- Ba<sub>2</sub>MgCrF<sub>6</sub> and Ba<sub>2</sub>MgFeF<sub>6</sub> (M=Ni, Co, Fe), crystal structure and mag. props. 4-71040
- BaRu<sub>1-x</sub>Co<sub>x</sub>O<sub>3-y</sub>, cryst. struct. and elec. cond. (*German*) 4-84265
- Co III complexes, 2-(5-cyanotetraazolato) pentaamminecobalt (III) perchlorate, solid high explosives, detonation front meas. 4-66592
- CeCo<sub>2</sub>P<sub>2</sub>, cryst. struct. determ. 4-80011
- (Co,Fe)<sub>1-x</sub>O, defects, thermodynamic calcs. 4-98087
- Co (III) complex, bis(ethylenediamine) Co (III) <sup>13</sup>C NMR signals, assignment 4-91278

## cobalt compounds continued

- Co (III) complexes, Co(NH<sub>3</sub>)<sub>5</sub>H<sub>2</sub>P<sub>2</sub>O<sub>10</sub>·H<sub>2</sub>O, hydrolysis, NMR 4-109082
- Co (II) complex,  $\mu_3$ -methoxo-(2,2,4-dinitrophenolato)(methanol) cobalt (II), cryst. struct., X-ray diff. 4-113420
- Co complex, Co(ethylenediamine)<sub>3</sub><sup>3+</sup>, rot. motion and ion interactions, NMR obs. 4-59802
- Co complexes, Co-porphyrin complex, linear free energy correl. for reversible dioxygen binding, solvent effect study 4-62178
- Co complexes, Co(II)-bis(acyl-o-phenylenediamine-pyridine) complexes, O<sub>2</sub> interaction study on silica surface 4-62232
- Co complexes, mag. susceptibilities determ. in temp. region below 77K. 4-71029
- Co complexes, oxygenated X-ray photoelectron spectra 4-107404
- Co complexes containing 2,2,3,4,4-pentamethylphosphetanic acid, IR, Raman, UV and NMR spectra 4-79989
- Co II complex, ethyl  $\alpha$ -ketocyclopentylcarboxylate, V-UV spectrosc. investigation 4-112191
- Co II complexes, IR spectra, mag. susceptibility meas., antiferromag. interactions 4-80918
- Co-Ni-Zn ferrites, microstruct., mag. props., BaO additions effect 4-88302
- Co-O perpendicular magnetic film by evaporation 4-92941
- Co<sub>2</sub>AlO<sub>4</sub> spinel, cryst. struct. and IR absorption bands 4-88145
- CoAs<sub>3</sub> skutterudites, far IR refl. spectra, temp. depend. 4-104595
- Co<sub>2</sub>(BO<sub>3</sub>)<sub>2</sub>, cryst. struct. refinement, X-ray diff. (*German*) 4-80003
- Co<sub>2</sub>B<sub>2</sub>O<sub>7</sub>Br, spontaneous birefringence and Faraday effect 4-71351
- Co<sub>2</sub>B<sub>2</sub>O<sub>7</sub>F(OH), cryst. struct., X-ray diff. 4-65242
- CoBr<sub>2</sub>, high freq. dielec. const. 4-61646
- CoBr<sub>2</sub>, XPS study of core level splitting 4-109303
- CoCo<sub>3</sub>, K-absorption edge, X-ray absorpt. near edge struct. obs. 4-66123
- Co<sub>2</sub>(CO)<sub>8</sub> adsorbed on AlO, glove box deposition system and study 4-101860
- CoCl solns., US relax. mechanisms 4-92308
- CoCl<sub>2</sub>, high freq. dielec. const. 4-61646
- CoCl<sub>2</sub> intercalation cpds. with graphite, sp. ht. and thermal expansion 4-80260
- CoCl<sub>2</sub>, XPS study of core level splitting 4-109303
- CoCl<sub>2</sub>-FeCl<sub>3</sub>-graphite intercalation cpds. mag. phase transitions, susceptibility meas. 4-98881
- CoCl<sub>2</sub>-LiCl aq. solns. X-ray diff. study 4-60805
- CoCl<sub>2</sub>·6H<sub>2</sub>O, paramagnetic phase boundary of antiferromagnet at low temp. 4-88668
- CoCl<sub>2</sub>·6H<sub>2</sub>O, anisotropic antiferromagnet, temp. depend. of paramag. boundary 4-84786
- CoF<sub>2</sub>, antiferromagnets, hyperfine fields, muon spin relax. 4-71253
- CoF<sub>2</sub>, mag. props., localisation of implanted positive muons,  $\mu$ SR obs. 4-98994
- CoF<sub>2</sub>, sublattice magnetisation and phase transitions, muon probe studies 4-98864
- CoFe<sub>2</sub>-Ni<sub>2</sub>O<sub>4</sub> spinel system, cryst. struct., elec. cond. and mag. susceptibility 4-70121
- CoFe<sub>2</sub>O<sub>4</sub>, small particle ferrites, mag. hyperfine fields 4-61568
- CoFe<sub>2</sub>O<sub>4</sub> thin films, interference enhanced magneto-optic Kerr rotation, storage appls. 4-93059
- CoFe<sub>2</sub>O<sub>4</sub> ultra-fine spinel ferrites, prep. and characterisation 4-71130
- Co<sub>10</sub>Fe<sub>23</sub>O<sub>4</sub> ferrite, mag. anisotropy, torque meas. 4-114105
- Co<sub>2</sub>Fe<sub>3</sub>-O<sub>4</sub>, ceramic ferrite, mag. props. (*Spanish*) 4-88649
- CoH<sub>2</sub>, low and high spin pot. energy surface, CI calcs. 4-96459
- CoI<sub>2</sub>, d-excitations, vibr. struct., IR and Raman spectra studies 4-113873
- CoI<sub>2</sub>, single cryst., permittivity, electronic states, UV reflectivity 4-84975
- Co(II) complex with 1-phenyl-3,5-dimethylpyrazole, cond., electronic and IR spectra, mag. susceptibility meas. 4-76104
- CoMn<sub>2</sub>-Ni<sub>2</sub>O<sub>4</sub> spinel system, cryst. struct., elec. cond. and mag. susceptibility 4-70121
- Co<sub>2</sub>Mo<sub>2</sub>O<sub>9</sub>, crystal growth, mag. and elec. props. 4-71537
- CoMo<sub>2</sub>S<sub>2</sub>Br<sub>2</sub>(I), preparation and cryst. struct. 4-70097
- Co(NH<sub>3</sub>)<sub>4</sub>(BeF<sub>4</sub>)<sub>2</sub>·6H<sub>2</sub>O, optical absorption spectrum 4-104588
- Co(NH<sub>3</sub>)<sub>4</sub>(SO<sub>4</sub>)<sub>2</sub>·6H<sub>2</sub>O·VO<sup>2+</sup>, paramag. Tutton salts, EPR studies 4-71167
- CoNbOF<sub>6</sub>·6H<sub>2</sub>O, optical spectra, obs. 4-71402
- CoNbOF<sub>6</sub>·6H<sub>2</sub>O:Mn(II), host spin-lattice relax. narrowing in EPR, phase transition 4-71162
- CoNi(Cu) EDTA complexes, one-dimensional ordered bimetallic chains, mag. props. 4-71036
- Co<sub>2</sub>(NiZn)<sub>1-x</sub>Fe<sub>2</sub>O<sub>4</sub> ferrites, magnetostrictive props. 4-84839
- CoO, 3d impurity excitation spectra, separation of one- and many-electron effects 4-75900
- CoO, band or Mott insulators and magnetism 4-70699
- CoO, eqn. of state and Gruneisen parameters 4-92331
- CoO film, on metallic substrate, solar thermal absorbing props. 4-89465
- CoO solar selective thermal absorbers, optical props. and selective absorption mechanism 4-99212
- CoO, surface morphology changes during vacancy relax. processes 4-75445
- CoO:Li, pure and doped, elec. cond., carrier mobility and conc. 4-92731
- CoO-Al<sub>2</sub>O<sub>3</sub>-SiO<sub>2</sub> insulating spin glass, light-induced mag. effects 4-71085
- CoO-Cr<sub>2</sub>O<sub>3</sub>, non-stoichiometric, segregation and chem. diffusion 4-98297
- CoO-Cr<sub>2</sub>O<sub>3</sub>, surface segregation, ESCA studies 4-65521
- CoO-NiO solid solns., equilib., activities at 1273K 4-80265
- Co<sub>1-x</sub>O, high-temp. deformation, point defects role 4-92287
- Co<sub>1-x</sub>O, chem. diffusion, creep meas. 4-92418
- Co<sub>1-x</sub>O:Ni single cryst., Ni impurity diffusion and interaction with vacancies 4-92437
- Co<sub>3</sub>O<sub>4</sub>, point defects and transport props. 4-98366
- Co<sub>3</sub>O<sub>4</sub>-based selective surfaces prep. by dip-coating process for solar absorber-convertors 4-72172
- Co(OH)<sub>2</sub>, brucite-like, struct. and IR relations 4-79996
- CoF<sub>2</sub>, ambient press. synthesis, cryst. struct., mag. and elec. props., bonding 4-75408
- Co<sub>90</sub>P<sub>10</sub>, galvanomagnetic characs. temp. depend. 4-84635
- CoRh<sub>2</sub>Ga<sub>2</sub>-O<sub>4</sub>, oxide spinel solid soln., cation distrib. study 4-80016
- CoS<sub>2</sub>, band struct. calcs., Mossbauer spectra 4-92611
- CoS<sub>2</sub>, electronic struct., reflectivity spectra, optical consts., meas. between 0.2-4.4 eV 4-80963
- Co(Si<sub>1-x</sub>Se<sub>x</sub>)<sub>2</sub>, mag. prps. modelling (*Russian*) 4-80762
- CoSb<sub>3</sub> skutterudites, far IR refl. spectra, temp. depend. 4-104595
- CoSi<sub>2</sub>, electronic density of states, XPS study 4-61272
- CoSi<sub>2</sub>, epitaxial growth on Si (111) surface 4-61844
- CoSi<sub>2</sub> films, solid-phase epitaxial growth, patterning effects 4-84537
- CoSi<sub>2</sub> formation from evaporated Si, kinetics 4-104099

## cobalt compounds continued

- CoTiO<sub>3</sub>, ilmenite-type cryst., electron density distrib. 4-65224  
 Co<sub>2</sub>V<sub>2</sub>O<sub>8</sub> single crystals, flux growth, X-ray charact. 4-76651  
 Co<sub>1-x</sub>Zn<sub>x</sub> complex, (C<sub>2</sub>H<sub>5</sub>NO)<sub>2</sub>(NO)<sub>2</sub> Co<sub>1-x</sub>Zn<sub>x</sub> ant. ferromag., AC susceptibility 4-61517  
 Co<sub>2</sub>Zn<sub>1-x</sub>Al<sub>2</sub>O<sub>4</sub>, oxidic spinel solid soln., cation distrib. study 4-80016  
 CuO-CoO-P<sub>2</sub>O<sub>5</sub>, ESR in phosphate glasses containing mixed transition metal ions 4-65851  
 Fe-Co complexes, high spin to low spin transition, thermally induced, metal dilution effect 4-65815  
 Fe-Co-O, γ-spins, vacancy substituted, order-disorder, IR spectra (French) 4-76447  
 Fe<sub>1-x</sub>Co<sub>x</sub>Br<sub>2</sub> antiferromag., random mixture with competing spin anisotropies, uniform and localised mag. modes 4-109066  
 Fe<sub>1-x</sub>Co<sub>x</sub>Br<sub>2</sub>, randomly mixed antiferromag. with competing Ising and XY spin anisotropies, mag. transitions 4-104446  
 Fe<sub>0.72</sub>Co<sub>0.28</sub>Cl<sub>2</sub>, disordered spin-flop phase obs. 4-104420  
 Fe<sub>1-x</sub>Co<sub>x</sub>Cl<sub>2</sub>, competing anisotropy system, Fe<sup>2+</sup> spin orientation, Mossbauer spectra 4-92906  
 Fe<sub>1-x</sub>Co<sub>x</sub>Cl<sub>2</sub>, nondiluted random-field Ising system, neutron diff. study 4-108992  
 Fe<sub>1-x</sub>Co<sub>x</sub>Cl<sub>2</sub>, random mixture with competing spin anisotropies, AFMR, FMR obs. 4-76259  
 Fe<sub>2</sub>Co<sub>1-x</sub>Cr<sub>2</sub>S<sub>8</sub>, magnetisation and Curie point meas. 4-104461  
 Fe<sub>1-x</sub>Co<sub>x</sub>S, single cryst. solid solutions, homogeneity studies 4-75693  
 α-Fe<sub>1-x</sub>Co<sub>x</sub>Si<sub>10</sub>O<sub>19</sub>, hematite, resonant and static mag. props., Co<sup>2+</sup> doping effects 4-92938  
 Fe<sub>2</sub>Co<sub>1-x</sub> complex, hexa(pyridine-N-oxide) (ClO<sub>4</sub>)<sub>2</sub>, decoupled mag. sub-systems 4-98895  
 Fe<sub>4.48</sub>Ni<sub>4.57</sub>Co<sub>0.03</sub>S<sub>8</sub>, cryst. struct. determ. 4-103714  
 Fe<sub>0.003</sub>Co<sub>0.998</sub>Cl<sub>2</sub> magnetoelastic coupling at Fe<sup>2+</sup> ions Mossbauer spectrum 4-92948  
 In<sub>2</sub>O<sub>3</sub>-Fe<sub>2</sub>O<sub>3</sub>-CoO, phase relations and cryst. structures 4-98242  
 In<sub>2</sub>O<sub>3</sub>-Ga<sub>2</sub>O<sub>3</sub>-CoO, phase relations and cryst. structures 4-98242  
 K<sub>2</sub>Co<sub>0.27</sub>Fe<sub>0.73</sub>F<sub>4</sub>, magnetic ordering, elastic neutron study 4-104404  
 K<sub>2</sub>Co<sub>2</sub>(SO<sub>4</sub>)<sub>3</sub>, langbeinite, optical props. 4-76427  
 KZn<sub>1-x</sub>Co<sub>x</sub>F<sub>3</sub>, Fourier transform IR spectroscopy of Co<sup>2+</sup> excitations 4-104596  
 LaCo<sub>2</sub>F<sub>7</sub>, cryst. struct. determ. 4-80011  
 LaCu<sub>2</sub>Al<sub>11</sub>O<sub>18+x</sub>, struct., substitution effects, X-ray diff. studies 4-103722  
 Na<sub>2</sub>Co<sub>2-x</sub>, intercalation cpd., transport props. 4-92734  
 Nd-Co-B system, cryst. struct. of ternary compounds, isothermal cross sections of phase diagram 4-65244  
 Ni<sub>0.988</sub>Co<sub>0.012</sub>Mn<sub>0.02</sub>Fe<sub>2</sub>O<sub>4</sub>, magnetostriuctive, magnetomechanical props., hysteresis loop, elastic moduli, internal friction, influence of mag. history 4-76212  
 Ni<sub>0.98-x</sub>Mn<sub>0.02</sub>Co<sub>0.02</sub>Cu<sub>0.98</sub>Fe<sub>2</sub>O<sub>4</sub>, stress sensitivity coeff. 4-76213  
 Ni<sub>0.953</sub>Mn<sub>0.047</sub>Co<sub>0.027</sub>Fe<sub>2</sub>O<sub>4</sub> ferrites, ΔE effect 4-76229  
 Rb<sub>2</sub>Co<sub>0.85</sub>Mg<sub>0.15</sub>F<sub>4</sub>, crossover scaling and specific heat 4-68175  
 Rb<sub>2</sub>Co<sub>1-x</sub>Mg<sub>x</sub>F<sub>4</sub>, 2D mag. alloys, neutron scatt., computer simulation 4-84768  
 Rb<sub>2</sub>Co<sub>0.5</sub>Mn<sub>0.5</sub>F<sub>4</sub>, 2D mag. alloys, neutron scatt., computer simulation 4-84768  
 Rb<sub>2</sub>Co<sub>0.5</sub>Ni<sub>0.5</sub>F<sub>4</sub>, 2D mag. alloys, neutron scatt., computer simulation 4-84768  
 Si/CoSi<sub>2</sub>/Si epitaxial monolithic structures, transistor effect 4-114036  
 SrZn<sub>2-x</sub>Co<sub>x</sub>Fe<sub>10</sub>O<sub>27</sub> hexaferrite, mag. and crystallographic studies 4-88697  
 WO<sub>3</sub>-Al<sub>2</sub>O<sub>3</sub>-SiO<sub>2</sub> glasses, insulating spin glass, field cooled magnetisation, cooling rate effect 4-71084  
 γ-(Zn<sub>0.5</sub>Co<sub>0.5</sub>)(PO<sub>4</sub>)<sub>2</sub>, farringtonite-type phases, crystallographic studies 4-84242  
 γ-Zn<sub>0.5</sub>Co<sub>0.5</sub>(PO<sub>4</sub>)<sub>2</sub>, farringtonite-type phases, crystallographic studies 4-84242  
 Zn<sub>1-x</sub>Co<sub>x</sub>S, single cryst. solid solutions, homogeneity studies 4-75693

## cochlea see ear

- codes  
 see also cryptography; encoding; error correction codes; error detection codes  
 Doppler velocimeters, coded, signal-to-clutter ratio limitation, cardiology appls. 4-100285  
 EBU/IRT and SMPTE code for film editing 4-101958  
 MST radar sounding, quasi-complementary codes technique 4-85789  
 SMPTE time and edit code motion-picture production appl. 4-63799

## coding see encoding

## coefficient of thermal expansion see thermal expansion

## coercive force

## see also magnetic hysteresis

- acicular particles, anisotropy field and coercivity 4-65837  
 dust samples, remanent magnetism and coercive force meas. using micro-computer controlled magnetometer 4-86447  
 ferromagnetic components quality control by coercive field strength meas. 4-93475  
 ferromagnets, amorphous and polycrystalline, microeddy currents with point defects (Russian) 4-109037  
 field strength, coercivity and loss meas., effective mag. path length 4-73463  
 garnet epitaxial layers, coercivity phenomena 4-76204  
 hydrothermal particles for mag. recording, mag. props. 4-65834  
 magnetic recording particles, acicular, temp. depend. of reduced anisotropy 4-61566  
 metallic glasses, mag. props. 4-114139  
 natural remanent magnetisation, stress sensitivity 4-62804  
 oxide dispersions, rheological, mech., and mag. props. 4-65830  
 Permalloy, mag. domain struct., complex permeability meas. 4-76164  
 Permalloy evaporated films, coercive force and mag. domains (Japanese) 4-104474  
 Permalloy thin films, micron size, magnetisation dynamics 4-61573  
 Perminvar, mag. domain struct., complex permeability meas. 4-76164  
 rare earth alloys, R-Fe-based metallic glasses, anomalous mag. hysteresis and coercive force 4-114140  
 rare earth intermetallics, RFe<sub>2</sub>H<sub>x</sub> (R=Gd, Ho, Er, Tm, Lu), mag. props. and cryst. struct., absorbed H<sub>2</sub> effects (Russian) 4-104458  
 rare earth-transition metal-boron alloys, crystallographic and mag. props. 4-75370  
 soft magnetic materials, coercivity, composite numerical model 4-61559  
 soft magnetic materials, coercivity, composite numerical model 4-84818  
 steel, ferrite-martensite, dual phase, Bauschinger effect, coercivity meas. (Chinese) 4-93330

## coercive force continued

- steel, NDT, residual magnetic field above surface, tangential component distrib. 4-71843  
 steel, stainless, ferritic-austenitic, embrittlement, mag. inspection 4-99704  
 thermomagnetic recording material perpendicular domain stability 4-92914  
 thin films, domain-wall pinning mechanisms (Russian) 4-109047  
 thin films, perpendicular hysteresis models 4-71132  
 viscosity coefficient, irreversible susceptibility and Barbier plots 4-92937  
 Ba-ferrite films deposited using Targets-Facing sputtering method, ion substitution effects (Japanese) 4-61851  
 BaFe<sub>2</sub>O<sub>9</sub> permanent magnets, sintering temp. effect on mag. props. and density (Afrikaans) 4-76170  
 Ce-Co-Cu, magnetically hard alloys, isostructural precipitation and atomic ordering (Russian) 4-104784  
 Co electrolytic films, mag. props. and struct. (Russian) 4-80797  
 Co-Cr ferromagnetic thin films, high rate magnetron sputtering 4-66232  
 Co-Cr ion beam sputter deposition, mag. props., temp. effects 4-104469  
 Co-Cr sputtered thin films, surface and vol. coercive fields 4-65841  
 Co-Ir sputtered films, mag. props. 4-71141  
 Co-Nb multilayered compositionally modulated films, e-beam deposited, FMR, magnetisation, B-H loop meas. 4-71139  
 Co-Si-B (-Fe) metallic glasses, mag. props., annealing effects 4-109039  
 CoSm amorphous thin films for longitudinal recording 4-80798  
 CrO<sub>2</sub> particles for audio recording, high orientation effect 4-65832  
 CrO<sub>2</sub> particles prod. for mag. tape appls. 4-65831  
 Eu<sub>2</sub>Sr<sub>1-x</sub>S ferromagnetic epitaxial layers, magnetooptic studies (German) 4-76441  
 Fe alloys, Fe-M, M=Al, Si, Nb, Ti, Zr, coercive field rel. to solid solubilities and nucleation behaviour 4-76185  
 Fe ferromagnetic thin films, high rate magnetron sputtering 4-66232  
 Fe fine particles, prep. from goethite microcrysts., morphology and mag. props. 4-65835  
 Fe sintered materials, coercive force, influence of microstruct. 4-66461  
 Fe Z 4-65836  
 Fe-Cr-Co alloy, Ti effect on rate of high-coercivity transform. 4-93296  
 Fe-P (0.8 wt.%), sintered, mag. props., influence of processing parameters 4-66266  
 Fe-Si (6.5 wt.%) rapidly quenched ribbons, mag. props. and preparation 4-84819  
 Fe-Si multilayered films, mag. props. and domain struct. 4-61574  
 Fe<sub>72</sub>B<sub>12</sub>Si<sub>10</sub>, amorphous, isothermal crystallisation and mag. props. (Russian) 4-65384  
 FeCo based alloys, strength and mag. props. rel. to cold rolling and heat treatment 4-98918  
 Fe<sub>2</sub>Co<sub>51</sub>Ni<sub>20-x</sub>Cr<sub>2</sub>B<sub>28</sub>Si<sub>8</sub> metallic glass, mag. props. study 4-84790  
 (Fe<sub>100-x</sub>Co<sub>x</sub>)<sub>76</sub>Pr<sub>16</sub>O<sub>8</sub>, thermal effects of Co moderate substitutions 4-71124  
 Fe<sub>2</sub>Co<sub>6</sub>Sn<sub>4</sub>N<sub>0.7</sub>C<sub>0.3</sub> ferromag. material for magnetic recording 4-104644  
 Fe<sub>2</sub>Ni pigments, mag. props. rel. to specific surface area 4-65836  
 Fe<sub>20</sub>Ni<sub>80</sub>B<sub>13</sub>Si<sub>7</sub> glassy ribbon, elec. and mag. props. 4-84604  
 γ-Fe<sub>2</sub>O<sub>3</sub>-Co, textural and surface props. rel. to mag. recording appls. 4-65833  
 γ-Fe<sub>2</sub>O<sub>3</sub>-Cr particles for audio recording, high orientation effect 4-65832  
 γ-Fe<sub>2</sub>O<sub>3</sub>-Fe<sub>2</sub>O<sub>4</sub>-Co thin films, coercivity study 4-114145  
 Fe<sub>2</sub>S<sub>8</sub> (pyrrhotite), mag. hysteresis of sized dispersed monoclinic grains 4-100541  
 GdFe/TbFe amorphous double-layer films, magneto-optical characts. 4-61665  
 GdTbFe amorphous sputtered films, mag. props. 4-65843  
 Mn-Al(Bi) hard magnets formed by rapid quenching 4-80794  
 Mn-Cu-Bi, thin film, RF sputtering prep., mag. and magneto-optical props. 4-61847  
 Mn-Ni-Bi thin film, RF sputtering prep., mag. and magneto-optical props. 4-61847  
 Ni-Co-Nb, damping capacity, mag. and mech. props. 4-61564  
 Ni<sub>2</sub>B<sub>2</sub>O<sub>7</sub>Br, magnetoelec. effect, mag. and elec. meas. 4-71144  
 NiZn ferrites, prod. by shock hot working, props. 4-61905  
 Pr-Fe-Co alloy sheets, rapid quenching, magnetic properties (Japanese) 4-114141  
 Sm-Co amorphous films, mag. props. 4-65842  
 Sm-Co ferromagnetic thin films, high rate magnetron sputtering 4-66232  
 Sm-Fe-Co alloy sheets, rapid quenching, mag. props. (Japanese) 4-114141  
 Sm(Co<sub>1-x</sub>Cu<sub>x</sub>)<sub>2</sub> cellular permanent magnets, coercivity 4-76191  
 TbFe thin films, amorphous, ageing phenomena, hysteresis cycles 4-71134  
 TbFe<sub>2</sub>, mag. and magnetomech. hysteresis 4-76219  
 Tb<sub>0.5</sub>Y<sub>0.5</sub>Ni, metamagnetism and coercivity 4-71070

## coercivity see coercive force

## coexistent superconductors see magnetic superconductors

## coherence

## see also light coherence

- electron Mollenstedt biprism interferometer interference pattern, effects of chromatic aberration and partial coherence 4-87265  
 quantum acoustics, deformation operator, perturbation calculus 4-83759  
 quantum coherence in electron beams 4-112338

## coherence distance see coherence length

## coherence length

- filamentary metals, theory of mixed state (Russian) 4-84753  
 normal-superconducting multifilm struct., tunnelling and T<sub>c</sub> (Chinese) 4-104368  
 superconductor/semicond./supercond. structs., carrier coherence length 4-65774  
 In whiskers, charge imbalance relax. in phase slip centre, effect of super-current 4-92863  
 Nb-Cu composite superlattice superconductor, dimensional crossover 4-71005  
 NbZr multilayers, struct. and superconductivity 4-70594  
 Pb-Ag<sub>1-x-y</sub>Mn<sub>x</sub>Al<sub>y</sub>-Pb, S-N-S junction, pair-breaking mechanism 4-98824  
 UPt<sub>3</sub>, heavy-fermion supercond., upper crit. mag. field meas. 4-104380  
 coherent accelerators see collective accelerators  
 coherent anti-Stokes Raman scattering  
 accurate convolutions of coherent anti-Stokes Raman spectra 4-79236  
 combustion studying using optical techniques (Italian) 4-66591  
 excimer laser up-conversion via stimulated anti-Stokes Raman scatt. 4-74486

**coherent anti-Stokes Raman scattering** continued

- flame, N<sub>2</sub> temp. determ., broadband rot. and vibr. CARS comparison 4-102983  
 gas, CARS, principle and appls. (*Dutch*) 4-66637  
 harmonic emission,  $\omega_0/2$  and  $3\omega_0/2$ , from 526 nm laser produced plasmas 4-79840  
 jet engine augmented exhausts, CARS temp. and species meas. 4-73436  
 laser diagnostics; techniques and appls. 4-65039  
 laser field statistics effects on coherent anti-Stokes Raman spectroscopy intensities 4-78392  
 methane free jet expansion, picosec. coherent anti-Stokes Raman spectroscopy 4-74251  
 methyl iodide in CS<sub>2</sub>, time-resolved picosecond CARS spectra 4-66025  
 molecular gases, coherent Raman scatt., saturation spectroscopy 4-83641  
 RDX decomposition, CARS probe study 4-99788  
 rhodamine 6G dye solns., inverse pre-resonance Raman spectrum 4-78894  
 rhodamines, reson. CARS spectra of lowest excited singlet states 4-91269  
 scanning CARS microscope, mol. discrimination and contrast enhancement 4-93982  
 shock compressed material, diagnostics by Raman scatt. 4-109713  
 state-of-the-art review w.r.t. multiple-wavelength generation and spectroscopic diagnosis 4-68286  
 surface polaritons, transient CARS 4-92630  
 turbulence and combustion studies, laser scatt. for conc. and temp. determ. 4-68289  
 D<sub>2</sub> in small volumes, coherent anti-Stokes Raman scatt. 4-78856  
 H<sub>2</sub>, time-domain CARS in Dicke narrowing region 4-69090  
 H<sub>2</sub>O vapour, high temp. and press., CARS spectra rot. diffusion model appl. 4-69085  
 N<sub>2</sub> CARS based temp. meas. inside firing internal combustion engine, optical multichannel anal. with rapid mass spectral storage 4-73437  
 N<sub>2</sub> CARS spectra, two-color dye laser appl., fast temp. meas. 4-91264  
 N<sub>2</sub> CARS thermometry in ethylene-air diffusion flames 4-77008  
 N<sub>2</sub> flow, spatially and spectrally resolved multipoint CARS 4-112516  
 N<sub>2</sub> in methane/O<sub>2</sub>/N<sub>2</sub> flame, coherent anti-Stokes Raman spectra, accurate convolutions 4-79236  
 NH<sub>3</sub>(X<sup>+</sup>B<sup>-</sup>) free radical detect. by CARS spectroscopy 4-62262  
 O<sub>2</sub> flow, spatially and spectrally resolved multipoint CARS 4-112516  
 PbSe epitaxial narrow-gap semicond. films, optical four-wave mixing 4-83640  
 PbTe epitaxial narrow-gap semicond. films, optical four-wave mixing 4-83640  
 SF<sub>6</sub> CARS thermometry 4-78854  
 Si intensified photodiode array detector linearity, appl. to coherent anti-Stokes Raman spectroscopy 4-95513

**coherent optical transients** *see optical coherent transients*

**coherent potential approximation** *see CPA calculations*

**cohesive energy** *see binding energy*

**coils**

*see also inductors; solenoids*

- ENDOR coil, for RF generation 4-63763  
 Faraday rotators and modulators design 4-79282  
 Fourier-analyzing coil arrays for pulsed relativistic electron beam experiments, plasma diagnostics appl. 4-113222  
 inductive applicator for hyperthermia using a one-turn coil with RF current 4-77424  
 RF coil, crossed ellipse, for head and neck NMR imaging 4-89681  
 superconducting structures, magnetoelastic buckling and Earnshaw's theorem 4-74049  
 tandem mirror reactor, drift-pump coil design 4-111827  
 tokamak reactor plasmas, bean-shaped magnet systems 4-111825  
 toroidal-field coil in SNUT-79 Tokamak, homopolar generator as power supply (*Korean*) 4-113228

**coincidence circuits**

*see also counters*

- frequency comparison by pulse coincident method, errors analysis 4-58815  
 multilayer spherical ring positron emission tomography, mega-channel coincidence circuit 4-74122

**cold-cathode tubes**

*see also counting tubes; photomultipliers; phototubes*

No entries

**cold rolling**

- metals, polycrystalline cubic, cold rolled, recrystallised, state of anisotropy, X-ray obs. 4-76784  
 metals and alloys, plastic deformation, mech. props. and struct. (*Russian*) 4-109468  
 steel, dual-phase, cold-rolled sheet, recrystn. kinetics 4-93310  
 steel, fatigue strength rel. to cold surface rolling press. (*Japanese*) 4-99514  
 steel, having preferred orientation, residual stress evaluation with X-rays 4-114749  
 steel, HSLA, tensile strength and ductility, dependence on microstruct. 4-114603  
 steel, low C, cold rolled, initial stage of decarburisation 4-114577  
 steel, low C, deep drawing cold-rolled sheet prod. by continuous annealing, control of steel chem. 4-114565  
 steel, low C, deep-drawing, prod. by continuous annealing 4-114566  
 steel, low C, dual-phase, continuously annealed, effect of prior cold rolling 4-66350  
 steel, maraging, tensile strength and ductility, dependence on microstruct. 4-114603  
 steel, stainless, texture development during annealing and rolling 4-76786  
 steel sheet, cold-rolled, spatial orientation distrib. of crystallites during cold-rolling (*Chinese*) 4-61952  
 steel sheet, continuous annealed cold-rolled, overaging treatment and ductility, interstitial atom supersaturation (*French*) 4-89096  
 Al-Fe-Si (0.31, 0.11 wt.%), recovery and recrystn., DSC study 4-85167  
 Al-Mg, cold rolled strip, texture, X-ray diff. obs., defocusing corrections 4-92029  
 Al-Mg alloys, heat treated and cold rolled, oxidation, AES study 4-66474  
 Al-Zn-Mg alloys, struct. and mech. props., effect of low-temp. thermomech. treatment 4-66352  
 Cu, cold rolled, 50%, orientation depend. of stored energy of cold work 4-99404  
 Cu-Be, work hardened thin sheets, determ. of plastic characts. 4-104938

**cold rolling** continued

- Fe, cold-rolled and recrystallised, metallographic methods for studying crystallographic orientation 4-114576  
 Fe, pure, orthogonally planed surface layer, X-ray lattice strains rel. to texture (*Japanese*) 4-114567  
 Fe-Ag composite sheets, anisotropy of phys. and mech. props. 4-99368  
 Fe-Co alloys, magnetostriction, recrystn., heat treatment, and strain texture effects (*Russian*) 4-104476  
 Fe-Si (3.4 wt.%), cold workability, effect of struct. and texture (*Chinese*) 4-61950  
 Fe-Si (3 wt.%), texture development and final mag. props., effect of secondary cold-reduction ratios (*Korean*) 4-81215  
 FeCo based alloys, strength and mag. props. rel. to cold rolling and heat treatment 4-98918  
 Fe<sub>40</sub>Ni<sub>40</sub>P<sub>14</sub>B<sub>6</sub> metallic glass, mag. props., cold rolling effects 4-104472  
 Fe<sub>40</sub>Ni<sub>40</sub>P<sub>14</sub>B<sub>6</sub>, Metglas 2826, struct. factor, influence of cold rolling 4-61954  
 Nb<sub>50</sub>Zr<sub>15</sub>Si<sub>15</sub>, Nb<sub>70</sub>, Zr<sub>15</sub>Si<sub>15</sub>, amorphous alloys, supercond. and electronic props., cold rolling effect 4-61480  
 Ni, H embrittlement, influence of plastic deform. 4-71729  
 Ni-Fe-V, thin sheets, effective mag. permeability and its stress sensitivity, effect of heat treatment and comp. 4-104883  
 Ni<sub>3</sub>Al, cold-rolled, recrystn. annealing 4-81213  
 Ti alloy OT4, cold rolling, texture and elastic modulus anisotropy change 4-93314  
 Ti-Al-V (6, 4 wt.%), evolution of  $\alpha+\beta$  struct. rel. to thermomech. treatment 4-109431

**cold shortness** *see brittleness*

**cold working**

- see also bending; cold rolling; plastic deformation; slip; work hardening*  
 Al-Fe, cold worked, damping capacity, mech. props. rel. to heat treatment and comp. (*Japanese*) 4-61968  
 brass, erosion in single particle impacts, significance of erosion parameter 4-81295  
 FCC crystal, cold worked, recrystn., effect of stacking fault energy 4-81221  
 materials testing for cold forging 4-99714  
 metals, cubic, fibre, texture, quantitative representation (*Korean*) 4-104946  
 polypropylene, isotactic, cold drawn, annealing, superstructure, SAXS obs. 4-61955  
 pure, cold worked, annealing characts rel. to trace element additions 4-109438  
 specimens with flat ends, region of appl. of method of upsetting 4-109597  
 steel, austenitic stainless, cold worked and irradiated, correl. of fracture toughness with tensile props. 4-93376  
 steel, austenitic stainless, dual-ion and/or electron irradi. in HVEM, in-situ obs. of cavity growth process 4-98134  
 steel, austenitic stainless, dual-ion irradi., microstruct. evolution under various He injection schedules 4-98150  
 steel, austenitic stainless, irradiation, fracture toughness, SEM obs. 4-104836  
 steel, austenitic stainless, metallographic revelation of  $\sigma$ -phase and  $\delta$ -ferrite, etching and mag. techniques (*German, English*) 4-66540  
 steel, austenitic stainless, PCA, unirr., tensile props. from room temp. to 700°C 4-104812  
 steel, austenitic stainless, swelling and cavity microstruct. development, irradi. in EBR-II and HFIR 4-98131  
 steel, austenitic stainless, thermal creep and stress-affected precip. 4-99428  
 steel, austenitic stainless, TiC precipitation, influence on creep rupture strength, ductility and He embrittlement 4-99388  
 steel, austenitic stainless, void swelling, effects of C and N 4-98149  
 steel, austenitic stainless, Path A-type alloys, neutron irradi., mech. props. 4-98139  
 steel, C-Mn, low temp. creep crack growth, effect of cold work 4-76850  
 steel, Cr, ledeburitic cold work, microstruct. and abrasive wear 4-114679  
 steel, ferritic stainless, recrystn. and deform. inhomogeneities, effect of twinning (*Polish*) 4-93309  
 steel, low C, notched fatigue strength rel. to pre-straining and nitriding 4-109489  
 steel, martensitic stainless, Mo, H embrittlement, effect of surface condition 4-85202  
 steel, mild, creep at low temp. 4-89086  
 steel, structural, fine-grained, low cycle fatigue, influence of cold forming 4-104841  
 steels, tool, hot isostatic pressing powder metallurgy fabrication method 4-89004  
 trioxane-dioxolane copolymer, conform., press. and mech. treatment effect, IR spectra 4-70043  
 zircaloy-4, cold worked, creep, eqn. of state appl. 4-109462  
 Al, shock loaded, microstructure and hardness 4-109515  
 Al-Cu-Mg, low cycle fatigue, influence of cold forming 4-104841  
 Al-Cu-Mg, thermomech. treatment, age hardening rel. to Mg/Cu ratio (*Japanese*) 4-89064  
 Al-Si, cold worked, damping capacity, mech. props. rel. to heat treatment 4-61967  
 Al-Zn-Mg (4.25, 2.75 wt.%), SCC by slow strain-rate method 4-66495  
 Al-Zn-Mg-Cu, cold working, recovery and recrystn. (*German*) 4-71670  
 Cu, brazed, low cycle fatigue in high vacuum rel. to cold work 4-109500  
 Cu, recrystallisation, effect of prior cold work on the influence of elec. current pulses 4-61957  
 Cu-Mn-Sn, microstructure study after cold working 4-108385  
 Cu-Ni bands, nonisothermal recrystn., activation energy (*Polish*) 4-85163  
 Cu-(Al), cold-worked, recrystn., effect of stacking fault energy 4-81221  
 Fe-Cr (9.75 wt.%), cold worked, ion beam thinned, protective oxidation in CO<sub>2</sub> 4-62095  
 Nb, superconducting, flux pinning mechanism of grain boundaries (*Japanese*) 4-76094  
 Nb-Ti multifilamentary supercond. composites, cold drawn, heat treatment, precip. morphology, TEM obs. 4-71657  
 Ni<sub>3</sub> dislocation/obstacle interaction during low dose D irradi. creep 4-104813  
 Ni-Cu alloy, domain wall-dislocation interaction behaviour, role of Cu atoms 4-104457  
 Ni-Mn, stabilisation of flow stress during cold working, struct. reasons (*Polish*) 4-93328  
 Pt-Pt/10%Rh and Pt-Pt/13%Rh thermocouples, thermoelectric effects of cold work obs. 4-101839

**cold working continued**

- Ti, texture evolution during deform., influence on formability (*French*) 4-71669  
 W-Ni alloys, diffusion induced recrystn. 4-61958  
 Zr, texture evolution during deform., influence on formability (*French*) 4-71669  
 Zr-Nb (2.5 wt.%), CANDU pressure tubes, high temp. creep model for loss of coolant accident 4-109473

**collagen** *see proteins***collections of physical data**

- A=110 nuclear data sheets, levels,  $J^\pi$ , transitions 4-73177  
 A=129, nuclear data sheets, levels,  $J^\pi$  and transitions 4-101590  
 A=157, nuclear data sheets, levels,  $J^\pi$ , transitions 4-58582  
 A=198, data sheet, levels, spin, parity, configuration assignments 4-106128  
 A=230, data sheet, levels, spin, parity, configuration assignment 4-106129  
 A=231, 235, 239, nuclear data sheets levels,  $J^\pi$  and transitions 4-101593  
 A=45, nuclear data sheets, levels,  $J^\pi$  and transitions 4-101594  
 A=59, nuclear data sheets, levels,  $J^\pi$  and transitions 4-101591  
 A=61 nuclear data sheets, levels,  $J^\pi$ , transitions 4-73176  
 A=66, nuclear data sheets, levels,  $J^\pi$ , transitions 4-58581  
 A=67, nuclear data sheets, levels,  $J^\pi$  and transitions 4-101592  
 A=98, nuclear data sheets, levels,  $J^\pi$  and transitions 4-101589  
 actinide fuel materials, fissile and fertile, nuclear data, resonances and cross sections 4-73955  
 alkali metal oxides, binary, high temp. vaporisation behaviour 4-98260  
 astronomical methods, constants and solar system, Landolt-Bornstein series 4-82603  
 atoms, highly ionised, spectral classification for 1980-3 period 4-67875  
 certified radioactive sources, international directory 4-58580  
 charged particle in various substances, ionisation energy loss, density effect 4-95073  
 earthquakes, centroid-moment tensor solutions (for October to December 1983) 4-105459  
 elastic, piezoelectric and related constants of crystals, book 4-58593  
 electron states and Fermi surfaces of homogeneously strained metallic elements, data compilation 4-73178  
 elemental semiconductors, physical data, compilation, book 4-63420  
 even open-shell nuclei, ground state band energies, generalised variable moment of inertia models 4-67882  
 gases and carbon in metals, thermodynamics, kinetics and props., Ag and Au 4-73174  
 geomagnetic activity and variations during 1980 AD 4-62671  
 geomagnetic activity obs. made during 1981 in Czechoslovakia 4-62672  
 Georgia (USA) estuaries circulation survey (1980) 4-115432  
 III-V semiconductors, physical data, compilation, book 4-63420  
 intermediate Voigt broadening, tables for direct determ. of spectral line parameters 4-112141  
 magnetic and other props. of oxides and related cpds., data collection 4-67886  
 magnetic transitions, critical exponents and amplitude ratios, numerical data compilation 4-67884  
 marine pollution data archiving, user preferences 4-115455  
 mass spectral database (EPA/NIH), supplement 4-67896  
 mineralogy encyclopaedia 4-95087  
 nontetrahedrally bonded binary and ternary cpds., collection of physical data 4-58587  
 nontetrahedrally bonded elements and binary cpds., physical data collection 4-58586  
 nuclear data sheets, 1983 references, levels,  $J^\pi$  and transitions 4-101588  
 nuclear data sheets, recent references, May-August 1983 4-73175  
 nuclear decay data sources and inconsistencies 4-73859  
 nuclear reactor control materials and light coolants, cross section data 4-73956  
 nuclear reactor dosimetry, gas prod. and activation cross-section data 4-73958  
 nuclear reactor heavy coolants, structural and shielding materials, cross section data 4-73957  
 Ocean Pollution Data and Information Network (OPDIN) 4-109758  
 Ocean Wave Statistics, update plans 4-77555  
 oceanic ferromanganese crust database 4-115402  
 particle properties review, masses, decays and lifetimes 4-67885  
 phonon states of metallic compounds, disordered alloys, data compilation 4-73178  
 saturated vapour press. of pure substances, book 4-67890  
 standard neutron cross section data for nuclear reactor materials 4-73954  
 stellar photometry, data compilation at Lausanne Institute of Astronomy 4-94636  
 thermal expansion data for binary oxides with fluorite, rutile and antiferroelectric str. 4-84428  
 thermodynamics, kinetics and props. of gases and C in Ni 4-73173  
 transition metal borides, thermochemical and phase diagram data, coupled pair pot. 4-85324  
 transition metal complexes, mag. susceptibility data collection 4-63419  
 U, neutral, oscillator strengths 4-74192  
 UK Meteorological Office archive for marine enquiries 4-115556  
 USA Northeast Area Remote Sensing System, NEARSS 4-110174  
 valence shell molecular photoelectron branching ratios, energy depend. 4-78048  
 water, fluid, viscosity, rel. to thermodynamic props., eqns. 4-98328  
 water, fluid phase thermophys. props. 4-98314  
 Westinghouse PWR plant radiation field data 4-59455  
 X-ray powder diffraction patterns for 71 substances 4-67893  
 Be-like ion, isoelectronic series, oscillator strengths, wavelengths, energy levels 4-67881  
 Be-like ions, fine struct. transitions between  $2L_s2L_p$  and  $2L_s3L_p$  configurations, collision and line strengths 4-95072  
 Be-like isoelectronic series, oscillator strengths, transition wavelengths, HF relativistic calcs. 4-106127  
 CO<sub>2</sub> high resolution IR spectra atlas 4-91257  
 H<sup>+</sup> atom collisions, L-shell X-ray prod. and ionisation cross sections 4-67883  
 H<sub>2</sub>, band transition moments between excited singlet states, spontaneous emission 4-95074  
 H<sub>2</sub>, transition probabilities for D and B vibr. levels to X vibr. levels and continuum 4-95075  
 NaCl, aq. soln., thermodynamic props. 4-98313  
 O<sub>2</sub>, Schumann-Runge absorpt. bands, 175-205 nm, atlas 4-96562

**collections of physical data continued**

- P-like ions, energy levels, transition probabilities, multiconfiguration Dirac study 4-106126  
 Th, spectral atlas (312.4 nm to 904.8 nm) 4-101195  
 U III, wavelength and energy level meas. using Fourier-transform spectrometer 4-102623  
 V II spectrum  $3d^3(^4F)4f$  config. 4-96479  
**collective accelerators**  
 charged beam propagating through relativistic annular electron beam 4-64664  
 collective free electron lasers 4-112449  
 collective ion acceleration using slow space charge waves 4-60754  
 compressed ring accelerators, azimuthal stability 4-60758  
 diagnostic system using scintillator-streak camera system 4-111982  
 electron beam wave accelerators 4-111979  
 high power particle beam conf., San Francisco, CA, USA, (Sept. 1983) 4-110808  
 high-current plasma accelerators, expt. examination of crisis 4-87948  
 imploding linear driven ring accelerators, stability 4-111980  
 ion acceleration theory in Luce diode 4-111983  
 ion beam diode, anode heating with CO<sub>2</sub> laser 4-111976  
 ion sources, collective acceleration, Thomson spectrometer anal. 4-107180  
 multicharge and negative ion generation and accel. by collective effects 4-111985  
 multimode accelerator, X-ray prod. anal. 4-60757  
 near-wall conduction in closed drift systems 4-83986  
 plasma, inhomogeneous, electron acceleration by laser driven plasma waves 4-96299  
 plasma cluster acceleration in additional mag. field 4-92002  
 plasma clusters, mag. induction, appls. 4-60740  
 reflexing electron beam type, model and scaling 4-96300  
 relativistic electron beam propag. through a plasma region into vacuum 4-97808  
 relativistic partly neutralised electron hollow beam, accelerating process 4-86983  
 Ba ions, accel. to GeV energies 4-111984  
**collective states, nuclear** *see nuclear collective states and giant resonances*  
**collimators (optical)** *see optical collimators*  
**collision processes**  
*see also atom-surface impact; atomic inelastic collisions; charge exchange; chemical reactions; elastic scattering of atoms and molecules; elastic scattering of electrons by atoms and molecules; electron attachment; electron impact; elementary particle interactions; intermolecular mechanics; ion-surface impact; molecular inelastic collisions; molecule-surface impact; negative ions; Penning ionisation; plasma collision processes; potential energy surfaces for collision processes; quantum field theory; quasimolecules; radiation quenching*  
 atomic and molecular database system, AMDS program 4-102813  
 chaotic bands, Feigenbaum cascades collisions 4-90502  
 charged particle small-angle refl. from plane scatterer of finite thickness 4-81102  
 corrugated hard wall, scatt. GR method 4-99268  
 decay of a state, effect of frequent collisions 4-101740  
 galaxies, elliptical, collision model for form. of optical shells 4-86041  
 galaxies and galaxy clusters, tidal torques rel. to rot. 4-67804  
 inner shell ionisation, wave function effects 4-99235  
 mass ratio dependence of the mixed species collision integral 4-79701  
 Saturn ring system, theoretical optical thickness profile for bimodal gravitating system 4-101243  
 steel balls, overhead projector expts. 4-73202  
 Kr, dynamic struct. factor determ. 4-83968  
**collision sequences, focused** *see sputtering*  
**colloid chemistry** *see colloids*  
**colloids**  
*see also Brownian motion; coagulation; electrophoresis; electroviscous effect; emulsions; gels; magnetic fluids; thixotropy*  
 acridine, micelle stabilised room temp. phosphoresc., heavy atom and complexation effects 4-96609  
 alkali metal halides, radiolysis process 4-70194  
 alkyltrimethylammonium bromide colloids, viscosity, light scatt. studies 4-89344  
 anthracene, micelle stabilised room temp. phosphoresc., heavy atom and complexation effects 4-96609  
 aqueous soln., aromatic hydrocarbon fluoresc. quenching by counterions, ion exchange relationship 4-62248  
 charged colloidal dispersions, liq.-gas transitions, perturbation theory anal. 4-62256  
 colloidal suspensions, stability and coagulation in shear fields 4-91836  
 concentrated colloidal dispersions, one-component macrofluid theory 4-113288  
 crystals, osmotic press. bulk modulus, charge renormalisation 4-85339  
 decyltrimethylammonium bromides, aq. soln., critical micelle conc., elec. cond. 4-98325  
 dialkylphosphate ions, <sup>31</sup>P NMR chem. shift and spin-lattice relax., micellisation effects 4-112197  
 diamond formation, martensitic mechanism, in colloidal systems 4-80212  
 dispersion in nonpolar solvents, light scatt. 4-114837  
 n-dodecylcetoxyethylene glycol monoether isotropic amphiphilic solns., micelle struct. 4-114834  
 double layer contrib. to diffusion effects 4-103979  
 electrical double-layer interactions in concentrated colloidal systems 4-114838  
 ferromagnetic colloids, anisotropic theory 4-93563  
 ferromagnetic fine particle colloid dispersions, mag. props., Monte Carlo calc. 4-109044  
 glycine-Al<sub>2</sub>O<sub>3</sub>-H<sub>2</sub>O mixtures, points of zero charge (*German*) 4-85314  
 hexyltrimethylammonium bromide, aq. soln., critical micelle conc., elec. cond. 4-98325  
 hydration forces near charged surfaces 4-99841  
 interacting Brownian particles, self-diffusion coeff. calcs. 4-85340  
 interacting particles, dynamic struct. correl. study 4-89340  
 ionic micelle soln., counterion fluoresc. quenching 4-81485  
 mechanical stability of tenuous objects 4-93564  
 metal colloid, surface enhanced Raman scatt. 4-88842  
 micellar systems photoionisation yields, interfacial elect. charge effect 4-62249  
 micelle-stabilized room-temperature phosphorescence with synchronous scanning 4-78885  
 micelles and vesicles, partition and binding constants, from fluoresc. quenching data 4-99845

## colloids continued

- monalkylphosphate ions,  $^{31}\text{P}$  NMR chem. shift and spin-lattice relax., micellisation effects 4-112197  
 naphthoquinone, in micelle, photochem. reaction, internal mag. field effect of lanthanoid ions 4-11942  
 nonionic micellar solns., phase diagrams, statistical model, osmotic compressibility, virial coeff. 4-89337  
 phenazine, micelle stabilised room temp. phosphoresc., heavy atom and complexation effects 4-96609  
 phenothiazine in aq. and reversed micelles, femtosecond and ps. time resolved electron solvation 4-99804  
 phospholipid bilayer solns. at ordered-fluid phase transition, microwave dielectric spectrum 4-91255  
 PMMA colloids, sterically stabilised, shear viscosity, temp. depend. 4-112789  
 polyethylene oxide soln., long-range attractive forces between mica surfaces 4-70563  
 polymer adsorption on colloidal particles 4-62250  
 polymer colloids, fluorescence techniques 4-85342  
 polymer solutions and blends, long range correlation's, low angle X-ray and neutron scatt. 4-75262  
 polyoxyethylene, micelle soln., cloud point transition, light scatt. 4-81486  
 polystyrene (polyballs) colloidal crysts. and glasses, solidification 4-89353  
 polystyrene colloids, charged, viscosity and self-diffusion const. meas. 4-89354  
 polystyrene latex, liq. like ordered suspension, struct. factor temp. depend. 4-114845  
 polystyrene monodisperse colloids, light diff. and cryst. struct. 4-103661  
 pyrene in tetradecyltrimethylammonium bromide and sodium dodecyl sulphate, triplet-state lifetimes 4-96469  
 pyrene-sodium lauryl sulphate micellar system, caffeine effect on photo-induced reactions 4-104998  
 rodlike micelles, sheared soln., vel. gradient influence on small angle neutron scatt. 4-71992  
 semiconductor colloidal electrode particles, photogenerated carrier transport and kinetics 4-65671  
 shear-induced partial translational ordering of colloidal solid 4-108582  
 surfactant micelles in aq. soln., adiabatic compressibility 4-113516  
 suspensions, colloidal, electric-field jump studies, negative second Wien effect theory 4-99850  
 Triton X-100 micelles effect on  $\text{Fe}^{2+}$ /thionine photogalvanic cell 4-105113  
 Ag, adsorpt. of rhodamine 6G, surface fluoresc. and surface Raman scatt. 4-108704  
 Ag microcrystallites, optial props., size depend. and matrix effects 4-109168  
 Ag small particles, colloidal, surface enhanced Raman scatt. of adsorbed guanine 4-87129  
 Ag sols, adsorbed cyanine dye, surface enhanced Raman scatt. 4-75779  
 Au colloids, aqueous, fractal structures formed by kinetic aggregation 4-62258  
 $\text{BaSO}_4$  dispersion, effect on colloid stability of adsorpt. of amphoteric polymer 4-66619  
 Bi, use as nucleation catalyst for mag. glass-ceramics, prep. 4-71628  
 CdS, colloidal crystallites, excited electronic states, size effects, optical props., Raman spectra 4-71334  
 CdS, periodic precipitation in lyophilic colloid, diffusion controlled autocatalytic growth 4-71993  
 $\alpha\text{-Fe}_2\text{O}_3$  colloidal particles, Mossbauer parameters, size effects 4-65886  
 KCl-iodine interface, Raman scatt., Rayleigh line broadening 4-80925  
 $\text{KCl}(\text{Br})\text{I}$ :Ag, surface-enhanced Raman scatt. from Ag colloids, optical absorpt. spectra 4-99117  
 MnS colloid, use as an NMR contrast material in rats 4-89677  
 NaCl, electron irradi., appl. to radioactive waste repositories 4-75532  
 NaCl:Ag, surface-enhanced Raman scatt. from Ag colloids, optical absorpt. spectra 4-99117  
 $\text{SiO}_2$  colloidal dispersion in nonpolar solvents, light scatt. 4-114837  
 $\text{SiO}_2$  small particles, colloidal aggregates, fractal geometry 4-89352  
 $\text{SiO}_2$ , sterically stabilised colloidal dispersions in toluene, phase separation 4-93561  
 $\text{TiO}_2$  colloidal, trapped positive holes and electrons, absorpt. spectra, flash photolysis obs. 4-89341

## colorimeters

- see also colorimetry  
 analyzer of transmitted, reflected and diffused light, using optical fibres (French) 4-82813  
 continuous flow anal. system, microcomputer-controlled, matching colorimeter output to A/D converter 4-97717  
 laboratory instruments for colour characts. meas. 4-63770  
 photoelectric colorimeters, performance factors and current status (Japanese) 4-86466  
 tristimulus colorimeter accuracy improvement method 4-111169

## colorimetry

- see also colorimeters; spectrochemical analysis; spectrophotometry  
 Ceramic Colour Standards, thermochromic props. 4-68256  
 chromaticness estimation of const. luminance central field colours on  $D_{65}$  surround 4-72250  
 combustion detection with a semiconductor color sensor 4-82812  
 cone excitations, system of photometry and colorimetry 4-111176  
 dichromatic colour discrimination, filter-aided, expt. test 4-77246  
 dichromats, filter-aided, quantitative tool development 4-77245  
 document examination, colour matching by microspectrophotometry 4-90640  
 electro-optical instrumentation for industrial applics., conf., Arlington, USA (Apr. 1983) 4-90286  
 Fourier holograms, computer generated, colour study 4-96846  
 frequency-limited function chromaticity coordinates 4-100142  
 geometric considerations w.r.t. illumination 4-90639  
 geometric tolerances influence on  $45^\circ/0^\circ$  and  $0^\circ/45^\circ$  meas. 4-111179  
 heads for colour difference meters, consequences of adjustments errors on quality 4-111178  
 historical survey of colour metrics 4-110846  
 Hunterlab SC 520 spectrophotometer in colorimetry appls. (Hungarian) 4-78361  
 industrial whiteness measurement (Hungarian) 4-58883  
 light source colour characteristics, international standards and determ. using spectrometer/computer program (Bulgarian) 4-87406  
 luminance and saturation of equally bright colours 4-68255  
 orthogonal polarization and colour states for information processing 4-102892

## colorimetry continued

- reflecting specimens colours with  $45^\circ/0^\circ$  illumination and observation conditions 4-90644  
 spectral reflectance factor, absolute meas. in  $45^\circ/0^\circ$  illumination and viewing conditions (Hungarian) 4-78360  
 spectrophotometry, light and colour meas. principles and systems 4-101899  
 tristimulus colorimetry of white papers, Monte-Carlo study of errors 4-111170  
 TV picture colour rendition, meas. and evaluation method 4-106349  
 TV sets, colorimetric errors correction (Polish) 4-101894  
 Cu, temperature dependent absorpt., calorimetric meas. 4-76420  
 Fe complex, tris-1,10-phenanthroline Fe (II), colorimetric detect., laser thermal lensing method 4-66623  
 $\text{SO}_2$  colorimetric detect., laser thermal lensing method 4-66623  
 $\text{ZrO}_2\text{-Cr}_2\text{O}_3(\text{ZrB}_2)$  sintering materials, rapid chem. anal. (Japanese) 4-109339

## colour

- see also colour vision  
 aberration theory, chromatic coordinates 4-59992  
 Ceramic Colour Standards, thermochromic props. 4-68256  
 dye penetrant inspection, brightness-colour coeff. of visibility of indications 4-109610  
 luminance and saturation of equally bright colours 4-68255  
 nematichiral thermochromic mixtures for thermography appls. 4-75276  
 physiological human response to colour, critical review 4-72249  
 polychromatic signal detection by complex spatial filtering 4-74435  
 polydiacetylene in dil. toluene soln., rod-to-coil transition theory, optical absorpt. spectra 4-75261  
 reflecting specimens colours with  $45^\circ/0^\circ$  illumination and observation conditions 4-90644  
 thermoplastic films, interf. colour creation using diff. gratings for embossing 4-69558  
 Al, chemical colouring by conversion coating process 4-81349  
 Cu, surface characterisation by polysulphide reagent, corrosion pot. rel. to colour change 4-81352  
 $\text{Cu}_6\text{-PS}_3\text{I}$ , photointercalation and optical information storage 4-79058

## colour blindness see colour vision; vision defects

## colour cameras, television see colour television cameras

## colour centre lasers see solid lasers

## colour centres

- see also F-centres;  $\text{OH}^-$ -centres; paramagnetic resonance of colour centres; U-centres; V-centres  
 alkali halide crystals, colour centre IR luminesc. and stimulated emission 4-80997  
 alkali halide crysts., colour centre form. dynamics under ionising radiation 4-80085  
 alkali halide mixed crystals, growth and characterisation, microhardness, colour centres, radiation hardening 4-70152  
 alkali halides, point defects, elastic dipole tensor 4-60924  
 alkali halides, polarisation energy by point defects, INDO cluster calc. 4-80861  
 alkali halides, stability and optical props. of self-trapped exciton 4-104129  
 alkali metal halide microcrystalline powders, reduced stability of coloration, dislocation model 4-60926  
 glass:Cr, dominant visible absorpt. rel. to  $\gamma$ -ray irradi. 4-76503  
 glass:Yb $^{3+}$ , statistical modelling, luminescence and absorpt. spectra 4-109247  
 quartz, E-centre prod. by ionising radiation, ESR and optical studies 4-70145  
 quartz, synthetic, irradi. induced coloration (Turkish) 4-114307  
 quartz crystals, radiation induced transient anisotropy loss 4-70279  
 sapphire, neutron irradi. and thermochem. treated, colour centres, visible luminescence study 4-81000  
 triplet electron spins, dipolar-induced dephasing 4-108778  
 Ag halide microcrystals, spectroscopic identification of localised electrons and holes 4-114308  
 $\text{Al}_2\text{O}_3\text{:Co}$ , thermoluminescence and trap parameters 4-76532  
 $\text{CaF}_2$ , electron irradi., anion voidage and void superlattice 4-108350  
 $\text{CaF}_2\text{:Ce}^{3+}$ ,  $\text{O}^{2-}$ , thermoluminescence spectra, irradi. effects 4-109259  
 $\text{CaO}$ , triplet electron spins, dipolar-induced dephasing 4-108778  
 CsI, irradiated single crystals, intrinsic hole colour centres 4-114332  
 $\text{Cu}_6\text{-PS}_3\text{I}$ , photointercalation and optical information storage 4-79058  
 GaAs, irradi., E3 centre accumulation, effect of defect charge state 4-60966  
 K halides, Ba-doped, impurity colour centres, absorpt. spectra 4-88865  
 KBr:Cl, X-irradiated, luminesc. study (Russian) 4-80981  
 KCl:Ag, Ca, X-irradi., electron centre form., luminesc., optical absorpt. studies 4-60920  
 KCl:Ag, X-irradi., electron centre form., luminesc., optical absorpt. studies 4-60920  
 $\text{KClO}_4$ , fluoresc. time depend. study 4-109239  
 KCl:Sr, X-irradiated, struct. of  $(\text{Cl}_3)^-_{\text{Z}}$ -centres. optical study (Russian) 4-80968  
 KCl:Ti, lattice defects creation and corrosion during annihilation of electronic excitations (Russian) 4-80035  
 $\text{LaMgAl}_2\text{O}_9$ , thermally stimulated phenomena 4-113967  
 $\text{LiNbO}_3$  cryst. growth, melt composition effect on props. 4-84227  
 $\text{Li}_2\text{SiO}_3$ , coloration of irradiated samples, during isothermal annealing (Russian) 4-98100  
 $\text{MgO}$ , point defects, elastic dipole tensor 4-60924  
 Na/Na cells, elec. and chem. degradation of  $\beta$ - and  $\beta''$ -alumina, ESR studies 4-109735  
 Na/S cells, elec. and chem. degradation of  $\beta$ - and  $\beta''$ -alumina, ESR studies 4-109735  
 NaA and NaX zeolites, luminescent, migration of electronic excitations (Russian) 4-80983  
 $\text{Na}_2\text{O-CaO-SiO}_2$ ,  $\gamma$  radiation colouring in 600-1000 nm region 4-80948  
 $\text{NaPO}_3$  glass, alpha-particle induced damage, vibr. Raman spectra 4-70237  
 $\text{NaYF}_6$ , polycryst. powder, X-irradi., thermolum. and colour centre obs. 4-61757  
 Rb halides, Ba-doped, impurity colour centres, absorpt. spectra 4-88865  
 $\text{Rb}_2\text{ZnCl}_4$ , colour centre production by additive colouring and X-ray irradi. 4-70144  
 n-Si, gamma and neutron irradi., radiation defect interactions 4-92227  
 n-Si, irradiated, Si-Si centre, optical excitation and relaxation, EPR study 4-109075  
 Si, substitutional and interstitial donors, many electron effect 4-113895

# lour centres continued

- n-Si:H, neutron irradiated, deep levels study (*Chinese*) 4-92649
- Si/SiO<sub>2</sub>/Al capacitors, radiation-induced oxide defects, ESR study, bias effects 4-70205
- Si-SiO<sub>2</sub> MIS structures, hole traps, trivalent Si centres, EPR meas. 4-80817
- Si-SiO<sub>2</sub> MOS struct., microstructural variations in oxides, electron spin reson. obs. 4-61590
- Si<sub>1-x</sub>N<sub>x</sub>H amorphous film, photoinduced ESR study 4-114161
- SiO<sub>2</sub>, amorphous, X- and gamma-irrad., E'-centre variants, EPR obs. 4-70207
- SiO<sub>2</sub> glass, alpha-particle induced damage, vibr. Raman spectra 4-70237
- SiO<sub>2</sub>, ion implanted, damage recovery, EPR studies 4-92245
- SiO<sub>2</sub>, ion implanted, E' defects, isothermal annealing studies 4-70146
- SiTiO<sub>3</sub>, compensated, defects and colour centres, optical study 4-92200
- SiTiO<sub>3</sub>, variable colour centre density, Raman spectra studies (*Chinese*) 4-109169
- TiO<sub>2</sub>, colour centre accumulation under electron exposure 4-60927
- WO<sub>3</sub> amorphous films, colour centres, EPR study 4-84291
- WO<sub>3</sub> amorphous films, electrochromic colour centres, Raman scatt. studies 4-113445
- Y<sub>3</sub>Al<sub>5</sub>O<sub>12</sub>:Nd<sup>3+</sup> garnets,  $\gamma$ -ray irrad., colour centres and optical props. 4-114310
- Y(PO<sub>3</sub>)<sub>3</sub> glass, alpha-particle induced damage, vibr. Raman spectra 4-70237

## lour filters *see optical filters*

# lour model

- 1<sup>++</sup> QQ $\bar{q}\bar{q}$  states, bag model, QQ state mixing, hadronic transitions (*Chinese*) 4-102089
- $\theta$  dependence of quark condensates, U(1) problem, chiral symm. breaking 4-111388
- Altarelli-Parisi eqns., jet-calculus propagators, transverse-momentum calcs. 4-106518
- anisotropic chromodynamics, extension of QCD 4-68525
- anomalous inequivalence of phenomenological theories, QCD with SU(3) matrix 4-111370
- anomalous Ward identities solns. in QCD framework 4-59033
- axion and mag. monopole theories 4-59010
- bag model, nucleon and pion form factors 4-78530
- Baker-Ball-Zachariasen gluon propagator eqn. linearisation, QCD dielectric constant 4-86640
- baryon spectrum in quenched QCD on 16<sup>4</sup> lattice 4-68555
- baryonic quark-gluon bag system, deconfinement phase transition model 4-59035
- beauty and charm particles, prod. in strong interactions, decays, review 4-90931
- BEBC structure function, QCD fit in Baulieu-Kounnas approach 4-73757
- book, hadron interactions, current theories, expt. results 4-110822
- book on nucleus comp., elementary particles and fields 4-82617
- bound heavy-quark systems, relativistic quasipotential approach, mass spectra 4-95764
- BRS algebra representations for gauge theory canonical formulation, colour confinement 4-82874
- CERN-collider Z<sup>0</sup> anomalous decays, conjectured second strong force on heavy quarks 4-106508
- Chern-Simons topological Lagrangians, odd dimensions, Kaluza-Klein reduction 4-95262
- chromomagnetic vacuum fields, influence on high energy hadron-hadron reactions 4-111484
- classical Yang-Mills, theories with external sources, colour screening 4-68420
- collective states, structure and models 4-95877
- colour breaking non-Abelian monopoles, SU(5) GUT, field theory and quantum mech. 4-86630
- colour-breaking non-Abelian monopoles in unified theories, classical mechanics 4-86629
- composite operator calculation of chiral symmetry breaking in color gauge theory 4-86642
- composite quarks and leptons, lower and upper bounds on radius 4-63984
- conference, Corfu, Greece (Sept. 1982) 4-95015
- conference, few body problems, Karlsruhe, Germany (Aug. 1983) 4-58553
- conference, meson spectroscopy, Upton, NY, USA (April 1983) 4-90280
- conference on hadron substruct. in nuclear physics, Bloomington, IN, USA (Oct. 1983) 4-63381
- conference on higher energy physics, Austin, TX, USA (Nov. 1982) 4-67857
- conference on mathematical physics, Boulder, CO, USA (Aug. 1983) 4-67856
- conference on particles and fields, Banff, Canada (Aug. 1981) 4-63404
- conference on quark matter in rel. nucleus-nucleus collisions, Long Island, NY, USA (Sept. 1983) 4-67855
- conference on semiclassical methods in nuclear physics, Grenoble, France, (Mar. 1984) 4-101567
- confinement, Yang-Mills theories, gauge-invariant quantisation procedure 4-86651
- constant gauge field configurations and Galilean gauge theories 4-58950
- contact interaction limit for massive Yang-Mills fields 4-68423
- Coulomb-gauge Gribov horizon, non-Abelian gauge model, colour charge terms 4-95674
- decay constants, pseudoscalar mesons and scalar diquarks 4-90819
- decay constants and SU(2) mass splittings of pseudoscalar mesons 4-68533
- deconfinement in the baryon rich region 4-68641
- deconfining transition, flux tube model 4-78522
- deep inelastic Compton scatt., QCD corrections, single photon spectrum, photon-hadron correlations 4-111461
- deep inelastic lepton-interactions QCD anal. 4-90887
- deep inelastic scatt., Q<sup>2</sup>-dependent parametrizations of parton distribution functions 4-90824
- deep inelastic singlet struct. functions and scaling violation (*Chinese*) 4-68573
- deep-inelastic lepton scattering, clustering and quark distributions in nuclei 4-64077
- deuteron, six-quark compound state in QCD 4-83000
- direct photon production at CERN ISR, CERN collider, and Fermilab Tevatron energies 4-86669
- direct-photon pair production, higher-order QCD corrections 4-106546

# colour model continued

- Drell-Yan process, lepton pair P<sub>T</sub> distrib. is asymptotically free scalar field theory 4-59043
- dynamical symmetry breaking and particle mass generation in gauge field theories 4-82899
- e<sup>+</sup>e<sup>-</sup> annihilation, energy-energy correlations in perturbative QCD 4-59112
- early Universe, GUT quark-hadron phase transition, fluctuations 4-67832
- effective field theory and weak non-leptonic interactions 4-90804
- electric versus scalar confinement for  $\bar{c}c$  and  $\bar{b}b$  systems 4-111406
- EM mass splittings in QCD 4-68572
- EMC effect, dynamical rescaling, hadron structure function universality 4-68520
- EMC effect, quark confinement scale gluon distribution functions, electroproduction results 4-68521
- energy dependent potentials, quark confinement 4-68515
- energy scales in GUTs, QCD, technicolor and SU(2)×U(1) breaking 4-68477
- energy-energy correlation function, test of perturbative QCD, pp collider 4-86667
- Euclidean gauge theories, behaviour in strong fields, functional determinants 4-68413
- excited quarks, production cross-sections and decay signatures 4-78524
- external source problem, massless quarks, stability and fluctuations 4-90797
- fermionic quark boundaries, surface description of QCD 4-82937
- field theory in elementary particles, conf., Coral Gables, FL, USA (Jan. 1982) 4-67869
- finite energy dispersion sum rules, QCD 4-95756
- first-order phase transition, concentration of quark matter 4-90803
- flavour changing neutral currents and mass generation in Technicolour theories 4-95741
- flavour changing suppression in technicolour, pseudo-Goldstone bosons, Cabibbo mixing 4-102075
- four-fermion operators, matrix elements, nonleptonic decays 4-86665
- four-quark states in the bag model 4-82938
- fragmentation functions of discrete particles on Artru-Mennessier string 4-59050
- fragmentation model comparison, hadronic distributions, 3-jet parton events 4-111420
- fundamental interactions in nuclei using hybrid quark-gauge field model 4-64053
- $\bar{g}$  and  $\bar{t}$  states, decay and spectroscopy, possible detection of supersymmetric particles 4-58987
- gauge hierarchy problem, technicolor supersymmetry and SUSY breaking, review 4-68478
- generation structure for quarks and leptons, rishon model, CP violation 4-63922
- global colour in GUTs, demise in presence of mag. monopoles 4-63924
- glueball discovery in  $\pi^+p \rightarrow \phi\phi\pi$  4-63973
- glueball EM decay in MIT bag model 4-90884
- glueball mass in mixed action SU(2) lattice gauge theory 4-111407
- glueball masses in SU(2) lattice gauge theory, Monte Carlo study 4-111409
- glueball model, heavy quarkonium <sup>3</sup>S, state pion cascades, OZI violation 4-95771
- glueball props., level ordering, mass, production, decay 4-90807
- glueballs, candidate states, mixing with quarkonia, elementary considerations 4-68523
- gluino production signature, pp collider, lower limit on gluino mass 4-86740
- gluon and quark jets, particle multiplicity ratios,  $\sqrt{\alpha(Q^2)}$  corrections in QCD 4-86660
- gluon fragmentation contrbs. to small P<sub>T</sub> hadron-hadron inclusive single particle distrib. 4-82944
- gluon thermodynamics near the continuum limit 4-78470
- gluon wave functions, internal structure in composite model 4-90830
- gluonic excitations in hadron spectroscopy 4-59026
- hadron energy eigenvalues and coupling strengths determ. with duality, Shifman-Vainshtein-Zakharov method 4-59059
- hadron mass inequalities, extended form based on lattice QCD 4-95765
- hadron masses in lattice QCD 4-59061
- hadron struct. functions universality and dynamical rescaling 4-68575
- hadron structure functions, dynamical rescaling 4-90882
- hadron-hadron scattering, high energy, unitarity, U-matrix approach 4-95815
- hadronic compound-systems in cumulative production processes, clusters, colour confinement 4-102130
- hadronic jet fragmentation including soft gluon interference, QCD parton model 4-82945
- hadronic mass spectrum, computer calcs. in lattice QCD 4-59060
- hadronic mass spectrum, Monte Carlo computations 4-68557
- hadronic matter, two-phase description using relativistic mean field theory and perturbative QCD 4-59034
- hadronic wave functions in QCD 4-63974
- hard scattering processes, transverse hadronic energy emission, non-leading QCD corrections 4-102099
- heavy hadron production, diffraction dissociation 4-90842
- heavy ion collisions, nuclear-matter transition to quark-gluon plasma, hydrodynamical model 4-111552
- heavy ion relativistic collisions, quark-matter form., spectator temp. signature 4-90966
- heavy ion ultra-relativistic collisions, quark-gluon plasma form. in central rapidity region, finite size effects 4-95767
- heavy mesons, semileptonic decay and minimum invariant mass 4-78529
- heavy quark threshold effects, two-loop beta function, Landau gauge 4-102090
- heavy quark vacuum expectation values, Q condensate, light quark QCD sum rules 4-68532
- heavy quarkonium, relativistic effects, fine struct. splittings 4-90811
- heavy quarks, properties, exchange (*German*) 4-95753
- heavy-quark jets and their semi-leptonic fragmentation 4-73721
- high density matter, condensed  $\pi^0$  field in chiral bag model, quark spin-flavour struct. 4-83018
- high energy nucleus-nucleus collisions, dual parton model, quark-gluon plasma 4-86843
- hot twisted Eguchi-Kawai model, deconfinement transition at large N, SU(54) 4-86558
- hybrid mesons in colour SU(3) 4-90806
- hybrid mesons with excited glue from SU(3) lattice gauge theory 4-102033

## colour model continued

hydrodynamic theory,  $t$ -mass and quark number restrictions,  $e^+e^-$  and  $pp$  comparison 4-86664  
 hydrodynamics of hadronic matter in heavy ion collisions 4-68640  
 hypercharged quark states in SU(3) theory (*Chinese*) 4-111368  
 hypercolor unification without cosmological domains, GUTs, [SU(9)]<sup>3</sup> semisimple theory 4-86631  
 ICL DAP parallel processor, Monte Carlo simulations in solid-state and elementary particle physics 4-59029  
 infinite nuclear matter, quantum hydrodynamics, rel. quantum field-theory 4-64080  
 infinite temperature limit, renormalisable 4-dimensional Euclidean QFT 4-90706  
 initial state interactions, factorization, and the Drell-Yan process 4-63967  
 instanton and meron fields, Dirac Hamiltonian self-adjointness 4-95673  
 integer charge quark model, heavy meson radiative decay, muon anomalous mag. moment 4-68537  
 jet calculus beyond leading order for gluon sector 4-59040  
 jets, hadronic average multiplicities, QCD predictions 4-111386  
 Kaluza-Klein theory, G and H. invariant metrics, colour and Higgs charges 4-110960  
 Kobayashi-Masakawa matrix, CP violation 4-111377  
 KRVS supersymmetric theories with false vacua, extension to three space dims. 4-58986  
 large  $p_T$  hadronic reactions, jets, lowest order QCD quark/gluon scatt. 4-90812  
 large-N QCD, confined phase temp. independ. 4-68510  
 large-N QCD, single point model, hot twists, twisted Eguchi-Kawai model 4-63956  
 lattice fermions, axial anomaly, Wilson and Kogut-Susskind actions, lattice QCD<sub>4</sub> 4-111267  
 lattice field theories, review 4-102043  
 lattice gauge QCD theories 4-95694  
 lattice gauge theory Monte Carlo evaluation of hadron masses and decay consts. 4-68439  
 lattice QCD, chiral symmetry breaking at finite temp. 4-86650  
 lattice QCD, current normalisation 4-63856  
 lattice QCD, hadron spectra, random walk approx. 4-63857  
 lattice QCD, Monte Carlo calc. of hadron masses, light dynamical quarks 4-111392  
 lattice QCD, Monte Carlo calc. with unquenched Wilson fermions 4-68507  
 lattice QCD, quarks and hadron mass formulae 4-73716  
 lattice QCD, renormalisation group behaviour, perturbative corrections, two-loop contrib. 4-86559  
 lattice QCD at finite temp., dynamical light quark incorporation 4-86646  
 leading-logarithm model, QCD, mesons containing one heavy and one light quark 4-106519  
 lepton signatures for top quark, QCD radiation effects,  $pp$  events 4-95827  
 light meson mass formulae from QCD 4-59062  
 mass singularities, minimal subtraction, gluonic operator coeff. in light quark currents 4-95754  
 massless two-dimens. gauge theories, nonlinear sigma model, QCD<sub>2</sub> zero mass bound states 4-95671  
 meson and isobar degrees of freedom in nuclear forces, review 4-64054  
 meson configurations in bag model, transitions and mixing 4-78528  
 meson exchange, equivalent interactions between quarks, transition potential (*Chinese*) 4-111510  
 meson exchange currents, energy transfer effects for electroweak nuclear processes, review 4-64055  
 meson wave function in QCD, and the constituent quark model 4-78527  
 meson-meson scattering in nuclei, quark scatt., confining forces and quantum mech. effects 4-64056  
 meson-nucleon high  $p_T$  exclusive scatt., perturbative QCD appl. 4-90815  
 MIT bag model, confinement of non-Abelian monopoles, colour singlet bag size 4-86680  
 MIT bag model, improved study of lowest lying hadrons 4-59052  
 MIT bag model, zeroth order, smaller  $\alpha_s$ , Coulomb spike effect 4-59053  
 monopole induced baryon number violating transitions, complete QFT treatment 4-86616  
 Monte Carlo simulations in SU(3) 4-86590  
 multi-hadron systems, many-body confinement pot. model, nuclear forces 4-64050  
 multicolour QCD in terms of random surfaces 4-63959  
 multiplicity-generating function, hadron-nucleus collisions, QCD and dual topological unitarization 4-111383  
 muon  $g-2$  anomalous magnetic moment, hadronic part, QCD eval. 4-73759  
 naive quark model for an arbitrary number of colors 4-90802  
 natural composite models, systematic construction 4-95770  
 negative absolute press., axiomatic thermodynamics 4-73659  
 neutron electric dipole moment induced by strong CP violation 4-111453  
 NN low energy states, quark and potential models 4-90810  
 non-Abelian gauge theory, long range scatt. of quantum particle 4-68430  
 non-Abelian Klein-Kaluza theories, spinor fields 4-58702  
 non-relativistic quark cluster model of the isospin-violating two-nucleon interaction 4-86641  
 non-singlet electromagnetic structure functions, QCD analysis 4-111456  
 nonlocal light-cone expansion in deep inelastic scatt. processes 4-73719  
 nonperturbative QCD, Monte Carlo anal. 4-59025  
 nonsinglet quark longitudinal structure function, fourth-order QCD contribution 4-106507  
 nontopological chiral soliton bag for hedgehog model 4-63954  
 nontopological solitons, Green's functions and bound states, self-interacting scalar field 4-90831  
 nucleon, vector meson dominance, EM structure 4-90843  
 nucleon as topological chiral soliton, bag models, nuclear physics 4-63855  
 nucleon model with relativistic oscillator interaction between quarks 4-68516  
 nucleon-meson vertex function, nonrel. quark model, meson probability distrib. from qg interaction (*Chinese*) 4-82942  
 one-dimensional nonlinear lattice, critical props. and hadron phys. 4-59032  
 order  $g^4$  QCD corrections to longitudinal structure function 4-63961  
 parity conservation in QCD 4-102057  
 particles and interactions, supersymmetric theories, quarks, leptons, W, Z, Winos, Zinos and Higgs 4-73674  
 parton jets, colour correlations in decay 4-90833

## colour model continued

partons, multiplicities and correls. in jets taking into account coherence effects, QCD calcs. 4-82951  
 Peccei-Quinn symmetry in QCD 4-95758  
 perturbative graph summation by Legendre transform 4-68518  
 perturbative pionic contrib. to nucleon observables 4-64057  
 perturbative QCD, ambiguity resolution, Stevenson's principle of minimal sensitivity 4-90798  
 perturbative QCD, factorisation, soft and collinear divergences,  $e^+e^-$  appl. 4-63966  
 perturbative QCD, jet Monte Carlo simulation and soft gluon radiation 4-102086  
 perturbative QCD, leading log approximations 4-82936  
 perturbative QCD, small  $x$  behaviour of deep inelastic structure functions 4-95757  
 perturbative QCD, three quark interaction in inhomogeneous evolution equations 4-111398  
 perturbative QCD 4-95759  
 perturbative QCD ambiguity, integration path depend. 4-78521  
 perturbative quantum chromodynamics at short distances, review 4-78525  
 PETRA  $e^+e^-$  storage ring, review of experimental investigations 1978-83 4-90851  
 phenomenological model description of expt. data 4-59012  
 pion electroproduction, Goldberger-Treiman discrepancy, Dashen-Weinstein sum rules, PCAC representation 4-111462  
 potential quark model with cloud, QCD, N and  $\Delta$  isobar appl. 4-73723  
 power-suppressed contributions to deep-inelastic processes 4-86668  
 $pp$ -jets, missing  $p_T$  events, possible  $\bar{q}-q\gamma$  decay 4-102135  
 preon composites and their interactions in SU(7)@SU(7) unified preon model, postons 4-78535  
 primordial SU(5) SUSY GUT plasma, strongly coupled nature, inflationary scenarios 4-73112  
 proton decay, next to leading corrections in SU(5) model 4-59072  
 proton valence quarks, SU(6) symmetry and quark forces in perturbative QCD 4-86663  
 protons, QCD perturbation theory of confined sea quarks and gluons 4-106506  
 pseudo-Goldstone boson masses in technicolor model with massive techniquarks 4-73691  
 pseudoscalar  $J^{PC}=0^{-+}$  spectrum,  $\eta$ ,  $\eta'$ ,  $\eta(1275)$ ,  $\eta(1440)$  4-90805  
 pseudoscalar mesons, chiral Lagrangian from functional integral over quarks 4-68529  
 pseudoscalar mesons, nonlinear effective Lagrangian in broken SU(3)×SU(3) 4-90750  
 QCD, (3+1)-dimens., variational methods in master field formulation 4-86656  
 QCD, chiral symmetry breaking model 4-63955  
 QCD, collective, stochastic and nonequilibrium behavior of highly excited hadronic matter 4-68504  
 QCD, cosmological constraints on GUTs 4-59009  
 QCD, description of hadron world 4-59038  
 QCD, dimens. quantities from Monte Carlo calcs. 4-68503  
 QCD, effective quark mass, spontaneous chiral symmetry breaking dynamics 4-82939  
 QCD, exotic commutators and ideal mixing 4-68500  
 QCD, extracting hidden fermions from bosonic effective theories 4-111378  
 QCD, finite temp., effective spin model, deconfining phase transition 4-63958  
 QCD, glueballs, hybrids and baryonia,  $\chi(1440)$ ,  $\theta(1700)$  and  $\xi(2220)$  exotic states 4-102084  
 QCD, hadron wavefunctions, large momentum transfer interactions, deep inelastic lepton scatt. 4-63975  
 QCD, large  $P_T$  hadron prod., effective interaction scale, qq partonic sub-processes 4-95762  
 QCD, lattice gauge theory, strong coupling expansion of SU(3) and U(3) 4-73664  
 QCD, light quark masses, model independ. determ. 4-111375  
 QCD, noncompact with stochastic gauge fixing, Monte Carlo simulation 4-78451  
 QCD, nonperturbative confinement, improved gluon propagator 4-102082  
 QCD, perturbative, predictions from spacelike to timelike regime 4-95752  
 QCD, phenomenology of coloured scalars,  $1^{--}$  state 4-73720  
 QCD, prospects and problems 4-68522  
 QCD, quarks and gluons, book 4-63425  
 QCD, reduction of nonabelian gauge theory through bare coupling 4-68514  
 QCD, static SU(2) gauge fields and chiral symm. breaking 4-68405  
 QCD, strong and weak coupling expansions for low-energy 4-68506  
 QCD, sum rules and exclusive form factors, review 4-82941  
 QCD, supersymmetric, nonperturbative nonrenormalisation theorem 4-86643  
 QCD, supersymmetric with massless quarks 4-68509  
 QCD, variational study of vacuum wave functional 4-59036  
 QCD branching processes and hadronisation, differential-difference eqn. 4-111374  
 QCD chiral anomalies, effective lagrangians and differential geometry 4-86647  
 QCD cluster model of hadronization for  $e^+e^-$  annihilation 4-90792  
 QCD deconfining phase transition, supersaturated pion vapour, ultrarelativistic heavy ion collisions 4-102095  
 QCD duality, moments, and Regge trajectories in nonrelativistic quantum mechanics 4-68553  
 QCD effects in few nucleon systems, high energy electron expts. 4-59027  
 QCD hard-scattering-jet effect on the gamma-ray families observed at mountain altitudes 4-110457  
 QCD high  $p_T$  physics, Lund Monte Carlo method 4-78566  
 QCD in few nucleon systems 4-59024  
 QCD in Veneziano limit, elfin theory, string model, baryon dynamics 4-59037  
 QCD interacting partons 4-95760  
 QCD jet simulation in  $10^{13}$ - $10^{17}$  eV hadron collisions, Monte Carlo approach 4-110458  
 QCD jets, matching to fragmentation models 4-102083  
 QCD jets, Monte Carlo simulation with soft gluon interference 4-68502  
 QCD jets, soft gluon emission 4-68501  
 QCD Lagrangian, background gauge formalism, quarks in background mean-field 4-111380  
 QCD lattice field theory, string tension 4-68408

## colour model continued

- QCD lattice gauge theory, statistical mechanical view 4-86540  
 QCD long distance behaviour, field theoretical gauge model description, UV divergences 4-86655  
 QCD mass spectrum, numerical. computations in lattice gauge theory 4-68349  
 QCD modelling with soliton bag model, nuclear matter and forces calcs. 4-63953  
 QCD on a random lattice 4-68527  
 QCD parameters on lattice and in continuum 4-86645  
 QCD perturbation series convergence, PMS and FAC procedures 4-86654  
 QCD picture of broken chiral symmetry, neutral PCAC scheme 4-73715  
 QCD potential due to small size vacuum fluctuations 4-78523  
 QCD SU(3) deconfining transition, with closed quark loops 4-86644  
 QCD sum rules, factorisation and related topics 4-63957  
 QCD sum rules, introduction and appls. 4-82935  
 QCD sum rules implications for nucleon and  $\Delta$  size 4-95773  
 QCD supersymmetric, effective actions for anomalous chiral symmetries 4-59030  
 QCD vacuum and bound state problem, colour confinement 4-68511  
 quantum chromodynamics, chiral symmetry and bag models 4-102085  
 quark and gluon propagators, IR divergence 4-73714  
 quark degrees of freedom in nuclear phenomena 4-64065  
 quark fragmentation with different recombination functions, QCD jets 4-68528  
 quark mass gauge-parameter independence, chiral symmetry breakdown 4-106512  
 quark masses, effect on perturbative thrust in QCD 4-86653  
 quark problems in nuclear physics 4-102189  
 quark-antiquark charge distributions and confinement, hadronic structure, 2 dimens. QCD 4-102094  
 quark-antiquark spectra, relativistic treatment 4-68512  
 quark-based phenomenology of strong and electromagnetic particle mixing 4-68535  
 quark-cluster potential model with relativistic kinematics 4-63952  
 quark-gluon plasma, colour-singlet partition function, finite baryon density 4-111381  
 quark-gluon higher twist contributions, parton diagrams 4-90823  
 quark-gluon matter in heavy ion collisions, thermodynamics, finite temp. field theory 4-68637  
 quark-gluon model with conformal symmetry 4-82947  
 quark-gluon plasma, boost-invariant motion of relativistic perfect fluid 4-102087  
 quark-gluon plasma, characteristics of hadronic phase transition 4-68505  
 quark-gluon plasma, confinement effect on sound vel. 4-68508  
 quark-gluon plasma, meson radiation using chromoelectric flux tube model 4-64082  
 quark-gluon plasma, strangeness prod., perturbative QCD anal. 4-68531  
 quark-gluon plasma, Vlasov eqn., Wigner transform. to nonAbelian Yang-Mills symmetries 4-102285  
 quark-gluon plasma formation, energies and mass numbers for heavy ion collisions 4-95766  
 quark-gluon plasma in ultra-relativistic nucleus-nucleus collisions, hydrodynamics, review 4-68638  
 quark-hadron phase transition, QCD sum rules, quark dynamical mass 4-111393  
 quark-hadron phase transition in Bianchi type-I cosmologies 4-63353  
 quark-quark interaction in nonrelativistic QCD 4-63964  
 quark-quark scatt., duality, flavour SU(3)  $\otimes$  colour SU(3) algebra, polarised electrod. appl. 4-73722  
 quarkless QCD, Monte Carlo mass calculations, lattice gauge dynamics 4-68524  
 quenched, reduced,  $N=\infty$ , lattice QCD Wilson loops 4-78520  
 quenched QCD on  $16^4$  lattice, meson spectrum 4-63970  
 relativistic charmonium model, gluonic corrections to mass spectrum 4-90814  
 relativistic fermion systems, superfluidity and superconductivity, colour superconducting quark matter 4-90489  
 relativistic heavy ion collisions, entropy production 4-68716  
 relativistic heavy ion collisions, quark-gluon plasma temp. meas. using detector meson resonances 4-64157  
 renormalisation-scheme dependence problem, effective charges method for QCD and QED 4-78526  
 review, Z 4-67907  
 scalar glueball, existence below 1 GeV in QCD 4-111397  
 scattering, large angle, Regge theory and QCD 4-59058  
 screened charge and phase transition in QCD quark matter 4-63965  
 semiclassical QCD-Lagrangian for nuclear physics 4-102187  
 single tag two-photon expts. at PETRA, quark charges, integer and fractional charge models 4-95866  
 Skyrme model, strong-coupling approx., nonstrange baryons, excited states 4-106513  
 skyrmion breathing mode, phase shifts, QCD large-N limit,  $N(1440)$  and  $\Delta(1600)$  resonances 4-111283  
 skyrmions and weak interactions, Weinberg-Salam Higgs field, technicolour 4-86614  
 SO(18) complex spinor, embedding of colour and chiral fermions, shiny quarks 4-111373  
 soft gluons in semi-inclusive deep inelastic experiments 4-90793  
 soft quantum-chromodynamics radiation and the weak-boson transverse momentum 4-73717  
 soliton bag model with or without SU(2)  $\times$  SU(2) chiral dynamics, coloured Higgs mechanism 4-59031  
 spinorial model with composite bosons, mag. monopole soln. 4-68530  
 stability of charmonium spectrum calculations from QCD sum rules 4-63963  
 strange particles, nonleptonic decays in supersymmetric theories 4-111330  
 straton, heavy, interaction potentials, QCD calc.,  $\psi$  and T spectrum (Chinese) 4-111382  
 strong coupling lattice model, chiral symmetry 4-86652  
 strong CP violation and axion mechanism 4-95714  
 structure functions,  $Q^2$  dependence due to  $q\bar{q}$  annihilation and gluon absorption 4-82961  
 structure functions of mesons for  $x \rightarrow 1$ , in QCD leading log approx. 4-68539  
 SU(3) mass differences and axial vector coupling const., QCD sum rules 4-73679  
 SU(2)  $\times$  U(1) breaking constraints for vacuum misalignment, partially chiral technicolour group 4-111350

## colour model continued

- SU(2) gauge theory, constant fields and invariants 4-90754  
 SU(2) lattice gauge theories, variant action independence of phys. quantities 4-58968  
 SU(2) Yang-Mills theory, colour screening 4-78498  
 SU(3) flux-tube quark model of hadrons 4-63951  
 SU(3) gauge theory with next-to-nearest neighbour interactions on  $12^4$  lattice, Monte Carlo study 4-111288  
 SU(3) lattice gauge theory, phase transition of pure glue, Monte Carlo calcs. 4-68384  
 SU(3) lattice gauge theory, QCD simulation using 1080 element subgroup 4-106456  
 SU(3) meson decouplets, mass formulae,  $S^*$  (975) structure, gluonium 4-111431  
 SU(5) SUSY GUT, chiral quarks and nucleon decay 4-102078  
 SU(8) grand unification with technicolour, evolution of coupling consts. 4-68465  
 SU(N) lattice gauge theory, quark-gluon partition function 4-95712  
 SU(N)  $\times$  SU(N), chiral symmetry breaking of non-abelian gauge 4-58984  
 SU(N) colour gauge theory, P and CP violation with massive fermions 4-78496  
 SU(N) gauge theory, colour screening at finite temp. 4-68382  
 SU(N) lattice QCD, non-zero baryon density, chiral symm. restoration 4-102062  
 SU(n) multiplet, weight diagram by means of Young tableaux 4-78519  
 Summer School, Chilton, Didcot, England (Sept. 1983) 4-58542  
 superconformal anomalies and the effective lagrangian for pure supersymmetric QCD 4-90794  
 supercooled quark-gluon plasma, hadron bubble growth mechanism 4-63980  
 supermetacolour, colour singlet composite, superfields containing massless composite fermions 4-78536  
 supersymmetric QCD, chiral symmetry breaking, spectral function sum rule approach 4-90800  
 supersymmetric QCD, instanton-induced vacuum structure 4-86649  
 supersymmetric QCD, non-renormalisation theorem, non-perturbative breakdown 4-63960  
 supersymmetric QCD model spectrum, false vacua, extended field configurations 4-95700  
 supersymmetry and fundamental interactions in the region of the Fermi scale 4-63919  
 supersymmetry breaking, superpotential production by instantons 4-90796  
 Susskind fermions, mass term symmetry properties 4-90816  
 SUSY QCD, coloured scalar quarks and hadrons, cosmological implications 4-111371  
 SUSY QCD, massless, chiral symmetry breaking 4-90799  
 technicolour, supersymmetry and physics 4-95718  
 technicolour model, fermion degeneracy, flavour 4-111346  
 technijets structure, QCD anal., expt. signals 4-111387  
 three point QCD sum rules, single borelisation procedure 4-68519  
 three-colour quarks and paraquarks, parastatistics and internal symmetries 4-95755  
 twisted Eguchi-Kawai model, numerical study of Langevin eqn. 4-106451  
 two-gluino bound states 4-86670  
 two-nucleon systems, resonating group quark cluster model, nuclear chromodynamics 4-64066  
 U(1) problem in QCD, dynamical resolution 4-86659  
 U(1) symmetry breaking, soln. to domain wall problem 4-58930  
 ultra-relativistic heavy ion collisions, hydrodynamical space-time evol. of central rapidity region 4-64156  
 ultrarelativistic heavy ion central collisions, energy densities, quark-gluon plasma 4-96045  
 ultrarelativistic heavy ion collisions, colour plasma and QCD descriptions 4-68719  
 ultrarelativistic nuclear collisions, new phenomena signatures, quark-gluon plasma 4-68713  
 vacuum fluctuations and impulse approximation in QCD 4-86648  
 very high energy heavy ion collisions, quark matter form., review 4-68636  
 weak decays, one-gluon corrections in QCD 4-86639  
 weak quark decays, diagrammatic approach 4-73718  
 weak quark decays, gluonic corrections, leading log summation 4-73724  
 Wentzel pair theory, massless scalar field, renormalised self-energy, radiative corrections 4-95775  
 Wilson string dist. in hot gluodynamics, Monte Carlo calcs. 4-90840  
 Yang-Mills classical equations with external charges, perturbative soln., colour charges 4-95635  
 Yang-Mills supersymmetric theory, effective Lagrangian for supersymmetry breaking 4-111369  
 Yang-Mills theory, colour screening, solutions with external charge and current densities 4-78454  
 Yang-Mills theory, free-energy density at finite temp. 4-73640  
 Yang-Mills theory, Wilson loop operators, path integral formalism 4-90801  
 $\alpha\alpha$  collisions, multiplicity dist. and coloured strings 4-59122  
 B decays, KM matrix cabibbo mixing 4-90863  
 B meson mixing props. and CP-violating effects, charge current couplings, QCD 4-111320  
 $b\bar{b}$ , fine-hyperfine structure of spectra 4-86675  
 $c\bar{c}$ , fine-hyperfine structure of spectra 4-86675  
 $D^+$  semileptonic decay widths,  $1=0$   $\eta$  and  $\eta'$  final states, QCD sum rules 4-95789  
 $\delta(980)$ ,  $0^{++}$  scalar meson, gluonia candidate 4-68538  
 $\Delta N$ , radiative decay, effect of quark-quark tensor and spin-spin force 4-64003  
 $\Delta N$ ,  $\Delta T=3/2$  amplitudes, effective weak Hamiltonian, QCD short distance corrections 4-111449  
 E(1420) completion of the 1p meson nonet 4-90808  
 $e^+e^-$  annihilation, energy-energy correl. function, higher order QCD corrections 4-59092  
 $e^+e^-$  annihilation, quark flavour separation, appl. to electroweak asymmetries, quark lifetimes 4-95768  
 $e^+e^-$  annihilation, quark mass effects for energy-energy correlations 4-90904  
 $e^+e^-$  annihilation jets at PETRA, 9.4-31.6 GeV CM, transverse particle momenta meas. 4-59091  
 $e^+e^- \rightarrow b\bar{b}$ , lifetime meas. 4-90898  
 $e^+e^- \rightarrow c\bar{c}$ , charm, lifetime meas. 4-90898

colour model continued

- $e^+e^- \rightarrow e^+e^-X$ , photon structure function,  $x$  depend, QCD scale parameter 4-95796  
 $e^+e^- \rightarrow e^+e^- + \text{hadrons}$ , photon structure function, comparison with QCD models 4-111455  
 $e^+e^- \rightarrow \text{hadrons}$ , narrowness of hadronic multiplicity distrib., cell theory, KNO scaling 4-59088  
 $e^+e^- \rightarrow \text{hadrons}$ , supersymmetry QCD theory 4-59087  
 $e^+e^-$  in Upsilon region,  $\Xi$  and  $\Lambda$  prod. from T decay, gluon and quark fragmentation 4-90900  
 $e^+e^- \rightarrow \text{jets}$ , flavour independence of quark-gluon coupling const. 4-59090  
 $e^+e^- \rightarrow \text{jets}$ , lepton and quark asymmetries, weak neutral currents 4-90897  
 $e^+e^- \rightarrow \text{jets}$ , QCD Monte Carlo code PARJET 4-78560  
 $e^+e^- \rightarrow q\bar{q}g$ , MARK-J at PETRA, expt. results, evidence for gluons 4-111434  
 $e^+e^- \rightarrow q\bar{q}g$ , model depend. of coupling const. in 2nd order QCD 4-59089  
 $e^+e^- \rightarrow q\bar{q}g$ , coloured quark electric charge assignments, expt. implications 4-73765  
 $\eta$  and  $\eta'$  radiative decays, light quark mass ratios, vacuum flavour symmetry breaking 4-73761  
 $\eta \rightarrow \pi^+ \pi^- \pi^0$ , current-quark mass ratios, mass matrix element,  $\rho$ -dominance assumption 4-106528  
 $\eta$  Z 4-59083  
 $F^+$  semileptonic decay widths,  $I=0$ ,  $\eta$  and  $\eta'$  final states, QCD sum rules 4-95789  
 $G(1590)$  scalar meson, glueball features, decay mechanisms and branching ratios 4-111419  
 $g_8(1240)$  glueball state, coupling to Goldstone mesons in QCD 4-111390  
 $gg \rightarrow gg$ , single-jet events at pp collider, gluino production, QCD calcs. 4-111402  
 $\gamma^* \gamma^* \rightarrow \pi^0$  in  $e^+e^-$ , form factor, QCD sum rule method and perturbative QCD comparison 4-82946  
 $\gamma\gamma \rightarrow \text{baryon} + \text{antibaryon}$ , high  $p_T$  exclusive scatt., perturbative QCD appl. 4-90815  
 $\gamma\gamma$  collisions, QCD test through parton-parton scatt., jet prod. 4-111376  
 $\gamma\gamma \rightarrow \eta \pi^0$ , gluonic contribs. to two photon exclusive processes, gg Fock states 4-59123  
 $\gamma\gamma \rightarrow \pi^+ \pi^-$ , partial width,  $Q^2$  dependence, comparison with QCD 4-111489  
 $\eta \rightarrow V X$  polarization in large- $p_T$  photoproduction of vector mesons 4-90892  
 $h$  at extreme energies, light-cone QCD with axial-vector anomaly current 4-59039  
 $h$ -jets, experimental props., comparison with QCD 4-73774  
 $h$ -jets, QCD Monte Carlo simulation, COJETs program 4-95763  
 $h$ - $W^{\pm}(Z^0)$  in Weinberg model with QCD bremsstrahlung, Monte Carlo program WIZJET 4-95825  
 $h$ - $X$ , exclusive multistring fragmentation model 4-73734  
 $h_1(1440) \rightarrow Xh_2$  process, two-gluon exchange model 4-59113  
 $h(1440)$ , glueball candidate, status report 4-68540  
 $h(1440)$ , with glueball, identification in simple quarkonium-glueball mass matrices 4-68534  
 $h$  meson, production and decay rates, gluonium component 4-111458  
 $J/\psi \rightarrow \gamma + \text{pseudogluon}$ , pseudomeson glueball component, process width (Chinese) 4-102098  
 $k(1500)$ ,  $0^{++}$  scalar meson, glukonia candidate 4-68538  
 $K \rightarrow 3\pi$ , matrix element quadratic terms, chiral Lagrangians, current-algebra analysis 4-106527  
 $K^0 \bar{K}^0$  mixing, CP violation, dispersive contributions 4-68536  
 $(K\bar{K}\pi)$  isoscalar resonances,  $J^P$  assignments 4-73727  
 $K^- \rightarrow K^*(K^*) (890) X$ ,  $E=175$  GeV, integrated cross-sections, quark counting rules 4-102142  
 $ld$  deep inelastic scatt., QCD parametrizations, nucleon structure functions 4-95801  
 $IN$  deep inelastic scatt., in Fe, C, QCD parametrizations, nucleon structure function 4-95801  
 $IN$  deep inelastic scatt., struct. function, nuclear effects 4-111460  
 $IN$ -IX, electroweak structure functions, deep inelastic scatt., quark-parton model 4-102103  
 $IN$ -IX, electroweak structure functions, deep inelastic scatt., quark-parton model 4-102103  
 $lp$  deep inelastic scatt., QCD parametrizations, nucleon structure functions 4-95801  
 $\Delta(1405)$  reson., QCD sum rules appl. 4-59041  
 $\Lambda_c$ ,  $\Lambda_b$  inclusive nonleptonic decays, bag model, W-exchange contribs. 4-106529  
 $N$  and  $\Delta$ , phenomenological quark model using chiral soliton model 4-63968  
 $N$ - $e^+b(\text{nonstrange})$ , nonstandard fermion mass matrices, branching ratios 4-90776  
 $N$ -III + mesons within SU(4) of colour unifying quarks with leptons 4-59073  
 $NN$ , multiparticle production, quark-gluon plasma 4-68593  
 $NN$ , short-range part of interaction, quark-gluon vs. meson exchange 4-64058  
 $NN$  forces using relativistic quark model for low-lying hadrons, review 4-64052  
 $NN$  interactions, colour, Van de Waals force, coupling eqns. soln. (Chinese) 4-82943  
 $NN$  scatt., description in OBE- $\pi NN$  dynamics 4-86723  
 $NN$  scattering, compound bag model, P-matrix analysis, Wigner-Breit condition 4-106517  
 $\nu(p,N)$ , nucleon longitudinal structure function in charged particle interactions 4-86709  
 $\nu N$ -X, hadron up-down asymmetry 4-111439  
 $\omega \rightarrow 3\pi$ , chiral Lagrangian, nonAbelian anomaly, vector-meson decays 4-106510  
 $\omega \rightarrow 3\pi$  contact term, QCD, low-energy theorems, broken chiral symm. 4-111446  
 $\omega \rightarrow \pi^0 \gamma$ , chiral Lagrangian, nonAbelian anomaly, vector-meson decays 4-106510  
 $pN$ -mesons at large momentum transfer in QCD 4-90933  
 $pN$ -pN, parity nonconservation in total cross-section, comparison with QCD 4-111468  
 $pp$ , 1-jet inclusive cross section in QCD, supersymmetric enhancement factor 4-73786  
 $pp$ , 540 GeV, very high energy density events at CERN SPS, quark-gluon plasma relevance 4-68592  
 $pp$ ,  $\sqrt{s}=540$  GeV, electron and hard jet prod., large missing  $p_T$ ,  $W^{\pm}$  prod., QCD processes 4-68595

colour model continued

- $pp$ , neutrino species counting,  $Z$  and  $W$  production ratios 4-73726  
 $pp$ , t-quark prod. simulation by hard 3-parton final states 4-68594  
 $pp \rightarrow 2$  jets in multi-TeV range, cross sections, parton model with QCD corrections 4-73780  
 $pp \rightarrow (gg)X$ , gluino production rates 4-102137  
 $pp$  background to t-quark signals from higher-order QCD contributions 4-73725  
 $pp$  collider at CERN, supersymmetric partners of gluons, quarks, W-bosons 4-90749  
 $pp \rightarrow F^+ X$ ,  $E=27.4$  GeV and 43.4 GeV, QCD calc. of interaction cross section 4-106509  
 $pp \rightarrow \gamma(\gamma\gamma)$  large  $p_T$  production, QCD predictions 4-78568  
 $pp \rightarrow \text{heavy flavours and multihadronic final states}$  4-90919  
 $pp \rightarrow l^+ l^- X$ , lepton pair production with  $M(l^+ l^-) < M_X$  4-86739  
 $pp \rightarrow lX$ , Drell-Yan parton-quark model relation, two gluon radiation modification 4-111476  
 $pp \rightarrow pK^+ K^- \pi^0$  ( $p\pi^+ \pi^-$ ) resonances in glueball-glueball collisions 4-95818  
 $pp(pp) \rightarrow \gamma X$ , prompt photon hadroprod. at large  $p_T$  in QCD,  $O(\alpha_s^2)$  calc. 4-73779  
 $pp \rightarrow pp\pi^+ \pi^-$  ( $ppK^+ K^-$ ), exclusive central collisions,  $f(1270)$  prod., resonance gluonium content 4-59109  
 $pp \rightarrow pp\pi\pi$ , glueball search in final state interactions below 1 GeV 4-59110  
 $pp \rightarrow \psi X$  inclusive  $\psi$  cross section, bb prod., gluon distrib. 4-106547  
 $pp \rightarrow \theta$ , glueball production cross-sections 4-86736  
 $pp \rightarrow W^{\pm}(Z^0)$  X review of COLLIDER project 4-102134  
 $pp \rightarrow WX \rightarrow tbX$ , top particle weak production, mass  $\approx 35$  GeV 4-111482  
 $pp \rightarrow Z^0 X$ , scaling violations in intermediate boson prod., QCD deviations 4-95828  
 $\pi$  evolution kernel beyond leading order, QCD correction, exclusive process anal. 4-111385  
 $\pi \rightarrow e^+ e^- \gamma(e^+ e^-)$ , form factor slope and decay amplitude calc. using quark triangle mechanism 4-59069  
 $\pi N$  interaction, Born-Oppenheimer cluster calc., one gluon exchange, cloudy bag model 4-111430  
 $\pi^- N \rightarrow K^*(K^*) (890) X$ ,  $E=175$  GeV, integrated cross-sections, quark counting rules 4-102142  
 $\pi^- N \rightarrow \psi DD X$ , cross section calc. in  $O(\alpha_s^4)$  QCD 4-95831  
 $\pi^- N \rightarrow \psi X$ , production in quark-parton model 4-90918  
 $\pi^- p \rightarrow \text{charm}$ , total and differential cross-section calcs. in parton model 4-90934  
 $\pi^- p \rightarrow \eta \eta$ , 38 GeV/c, glueball search, G(1590) decays 4-78565  
 $\pi^- p \rightarrow \gamma(\gamma\gamma)$  large  $p_T$  production, QCD predictions 4-78568  
 $\pi^- p \rightarrow \phi \phi$ , glueball resonance production, couplings to  $\phi\phi$  4-90913  
 $\pi^- p \rightarrow \phi \phi$ , glueballs, partial wave anal. 4-90912  
 $\pi^- p \rightarrow \phi \phi$ , Okubo-Zweig-Iizuka rule, glueball evidence 4-111480  
 $\pi^-$  scattering, low energy theorems corrections, QCD tests with current algebra 4-82940  
 $\pi^+ \pi^- \rightarrow \pi^+ \pi^-$ , leading order QCD calc. 4-102129  
 $\Psi$  production, signal for quark-gluon plasma formation 4-59042  
 $q\bar{q} \rightarrow q\bar{q}$ , possible decay for pp missing  $p_T$  events 4-102135  
 $q\bar{q} \rightarrow 0^{++}$  mesons in unitarised quark model 4-90809  
 $q$  bound states, Salpeter eqn. in position space, arbitrary confining potentials 4-106474  
 $QQ \rightarrow gg$ , gluino production, decay rates 4-86752  
 $qq \rightarrow gg$ , single-jet events at pp collider, gluino production, QCD calcs. 4-111402  
 $Q\bar{Q}$  mesons, mass spectra from Bethe-Salpeter confinement dynamics 4-68432  
 $Q^2 Q^2$  state production, colour-spin structure, potential and bag models 4-106511  
 $QQ$  hybrid meson spectroscopy, potential model, excited states 4-102100  
 $S^*(980)$ ,  $0^{++}$  scalar meson, glukonia candidate 4-68538  
 $\Sigma \rightarrow N\pi$ ,  $\Delta T=3/2$  amplitudes, effective weak Hamiltonian, QCD short distance corrections 4-111449  
 $\theta(1640)$ , glueball candidate, status report 4-68540  
 $\theta(1640)$ , with glueball, identification in simple quarkonium-glueball mass matrices 4-68534  
 $T \rightarrow ll$ , leptonic branching ratios 4-90863  
 $T$  system, new coloured particles, contributions to width and hyperfine splitting 4-90817  
 $T(T)$  decays, direct photons obs. and QCD scale parameter determ. 4-64004  
 $W$  decay in QCD and Weinberg model, constraint on  $N_c$  species 4-68467  
 $\xi(2220)$ , bound state of massive coloured scalars 4-63971  
 $\xi(222)$ , from  $\psi$  radiative decay, properties consistent with  $L=3$  ss meson. 4-86666  
 $\Xi \rightarrow \Lambda \pi$ ,  $\Delta T=3/2$  amplitudes, effective weak Hamiltonian, QCD short distance corrections 4-111449  
 $Z$  decay in QCD and Weinberg model, constraint on  $N_c$  species 4-68467  
 $Z \rightarrow ll \gamma\gamma$ , Z mixing with degenerate bound colour quarkonium 4-111486  
 $Z^0 \rightarrow e^+ e^- \gamma$ , composite boson coloured constituents, hypercolour binding 4-111425  
 $Z^0 \rightarrow \gamma + \text{quarkonium}$ , production of  $^1S_0$  squarkonium states, gluon jets 4-111487  
 $^1H(\alpha\alpha')$ , 63 GeV, central rapidity region, quark-gluon plasma search, ISR results 4-68700  
 $^2H(e,e)$ , form factors, signatures for QCD in nuclear physics 4-90949  
 $^4He(\alpha\alpha')$ , 63 GeV, central rapidity region, quark-gluon plasma search, ISR results 4-68700  
 $J$  muonproduction, spin-spin asymmetries, gluon helicity distribution function 4-95803  
 $NN$  scattering, quark-struct. effects, relevance to bag models and nuclear data 4-64051

colour perception see colour vision

colour photography

- Eastman Color LC Print Film 5380/7380 4-63798  
 electronic analyser for film enlargement checking (German) 4-63796  
 electrophotographic photoreceptor surface pot. decay meas. using X-Y recorder (Japanese) 4-95546  
 electrophotography, color imaging process using filter beads (Japanese) 4-95543  
 electrostatic latent image characts., tone improving process, colour reproduction in copier (Japanese) 4-95542  
 fading of images irradi. by white fluorescent lamp (Japanese) 4-111236  
 Fujicolor HR 1600 colour negative film, high speed 4-106409

**colour photography continued**

- HID lamps design and evaluation for colour photographic purposes 4-90673
- Illuminating Engineering Society Annual Conf., Los Angeles, USA (Aug. 1983) 4-90291
- image separation into respective colour forming layers (*Japanese*) 4-73545
- image storage and display, stability analysis (*Japanese*) 4-111235
- Konica Color SR 100 colour negative film, review 4-86493
- material structure and photographic characts., charact. curve, colour granularity (*Russian*) 4-68312
- paper, exposure measuring, and control equipment (*German*) 4-86495
- photomicrography procedures using colour reversal film emulsions 4-63795
- two-color electrophotography with multilayer photoreceptor (*Japanese*) 4-95544

**colour receivers, television** *see colour television receivers***colour television**

- signal transmission, chrominance pattern movement masking appl. 4-105239
- TV picture colour rendition, meas. and evaluation method 4-106349

**colour television cameras**

- Fujinon lenses, technological advances 4-107788
- Schneider-Kreuznach lenses, review 4-107789

**colour television receivers**

- colorimetric errors convection (*Polish*) 4-101894
- optical meas., TV pictures evaluation (*Japanese*) 4-106345

**colour tv** *see colour television***colour tv receivers** *see colour television receivers***colour vision***see also eye*

- Abney effect: chromaticity coordinates of unique and other constant hues 4-66953
- accommodation and convergence under high pressure sodium illumination 4-93739
- anomaloscope, portable, solid state version 4-62546
- chromatic adaptation for light grey background, nonlinear model 4-115053
- chromaticity, Broca-Sulzer effect, temporal transient response of colour mechanism (*Japanese*) 4-93742
- chromaticness estimation of const. luminance central field colours on D<sub>65</sub> surround 4-72250
- colour-matching functions for  $\lambda \geq 540$  nm: incompatibility with blue fundamental 4-89575
- computerised visual function data manipulation system, VF-DMS 4-89820
- cone excitations, system of photometry and colorimetry 4-111176
- cone oil droplets of Emydoidea blandingii: pigment types, densities and cones. 4-81685
- cone retina, vertebrate, electronic simulation of cones, horizontal cells and bipolar cells 4-105231
- cones, rel. to rod saturation with flashed backgrounds 4-66955
- cones of different spectral types in turtle retina, direct excitatory interactions 4-105236
- contrast sensitivity, effect of yellow bitter 4-100148
- cortical V1 cells, monkey, spatial mapping with pure colour and luminance stimuli 4-89569
- CRT display, human colour discrimination under ambient illumination 4-81686
- dichoptic masking, selective colour effects 4-89584
- dichromatic colour discrimination, filter-aided, expt. test 4-77246
- dichromats, filter-aided, quantitative tool development 4-77245
- flicker-photometric spectral sensitivity in the presence of chromatic surrounds 4-100143
- frequency-limited function chromaticity coordinates 4-100142
- ganglion cells of generalised vertebrate cone retina, electronic simulation 4-105232
- green rod pigment of the bullfrog, Rana catesbeiana 4-62484
- historical survey of colour metrics 4-110846
- horizontal cells in goldfish retina, depolarising, responses under intense chromatic background 4-109804
- lateral chromatic aberration of the eye 4-100130
- luminance and saturation of equally bright colours 4-68255
- motion photometry 4-111177
- moving pattern perception of chromaticness channel, psychophysical expt. (*Japanese*) 4-100152
- multiple sclerosis patients, colour discrimination and visual acuity 4-62482
- perceived velocity of moving chromatic gratings 4-100151
- perception under chromatic adaptation, supersensitivity with dim backgrounds 4-66954
- photoreceptors, hyperpolarising, of giant clam Tridacna, UV sensitivity 4-77238
- physiological human response to colour, critical review 4-72249
- pigments, dense samples, method for peak absorbance meas. 4-81828
- short-wave cone pathways, sensitivity to different spatial freqs., adaptive processes 4-109811
- spectral colour hue change by dilution with white light, Abney effect 4-62483
- spectral sensitivity and wavelength discrimination of the human peripheral visual field 4-72251
- spectral sensitivity of single cones in the retina of Macaca fascicularis 4-77247
- stereoscopic acuity rel. to chromatic light illum. 4-100145
- temporal integration of the  $\pi_1/\pi_3$  pathway in normal and dichromatic vision 4-89568
- temporal sensitivities rel. to colour theory 4-72252
- threshold temporal integration of chromatic stimuli 4-89574
- TV signal transmission, chrominance pattern movement masking appl. 4-105239
- whiteness and quantum representations of colorimetry 4-73439

**columbium** *see niobium***coma** *see aberrations***combination scattering spectra** *see Raman spectra***combinational mathematics** *see combinatorial mathematics***combinatorial mathematics***see also graph theory; trees (mathematics)*

- Coniglio's lemma 4-68163

**combustion***see also explosions; flames; heat of combustion; reaction kinetics*

- 8th Australasian Fluid Mechanics Conference, Newcastle, NSW, Australia (Nov.-Dec. 1983) 4-67858
- acetaldehyde-air mixture, two-stage ignition during rapid compression 4-71930
- alkali metal combustion gas plasmas, atomic density meas. by near-resonant Rayleigh scatt. 4-113218
- Allison 501-KB gas turbine engine, Brayton cycle, Cheng dual-fluid cycle effects on power and thermal efficiency 4-66744
- American Power Conference, Chicago, USA (April 1983) 4-86112
- analysis of combustion products, using dilution tunnel system 4-62266
- arc generated plasma 4-69984
- automotive Stirling engine development program—overview and status report 4-66777
- ball powders, convective combustion in strong confinement numerical simulation 4-114795
- cable burning 4-114799
- char particle and surrounding gas phase, diffusion and reaction models 4-99790
- char particle and surrounding gas phase, diffusion and reaction, continuous model 4-99791
- coal combustion products, collision integrals for ions and electrons with neutral particles 4-114797
- coal-natural gas fuel mixture, combustion characts. and viability 4-77052
- coal-water slurry burner modelling and development 4-62285
- colour sensor, semiconductor chip for detect. appls. 4-82812
- coronas in combustion due to application of electrical fields 4-69985
- diesel-cycle engine, H<sub>2</sub>-fueled, two-stroke, performance improvements 4-62404
- distillate liquid fuels, chemical and physical properties during combustion in gas turbine 4-114884
- distributed combustion effects on particle damping 4-79616
- double cyclone furnace 4-86424
- electrohydraulic gas sampling valve 4-78305
- enclosed deflagrations, one dimens. homogeneous and heterogeneous, numerical modelling 4-89300
- ethylene-air flame fuel-rich combustion zone N<sub>2</sub> CARS thermometry 4-77008
- exhaust gas from petrol engine, Pb compounds distrib. 4-89478
- flame, OH meas. using photoacoustic deflection spectroscopy 4-62204
- flame temperature in intermittent-combustion chamber 4-85312
- flames, heat transfer between hot combustion gases and cold wall in narrow channels 4-99789
- flames, turbulent, stability, coalescence/dispersion model 4-81437
- fluidised bed combustion of solid fuels 4-99935
- fluidised bed gas burner for dust laden air in lime kiln 4-97666
- fluidised bed single particle combustion calc. 4-71925
- forced oscillation experiments in supercritical diffuser flows 4-97626
- framing high-speed shearing interferography with pulsed He-Ne lasers, flow, shock, combustion and explosion problem appls. 4-68275
- free-falling multicomponent droplets, combustion and microexplosion 4-103388
- fuel injection influence on struct. of near wake 4-97709
- fuel-air combustion in fluidised bed model 4-87787
- fuel-air homogeneous mixture, turbulence effects on combustion 4-97497
- gas turbine combustion chambers, flame radiation 4-114798
- gaseous detonation, dynamic parameters 4-91822
- gases/solids ignition by electrical discharges 4-69986
- gasification of rice hulls and straw 4-66737
- heat transfer in flames 4-83808
- heterogeneous explosives, shock-induced initiation, burning topology 4-109660
- HMX explosive, thermal initiation and burning prior to detonation 4-109656
- HMX explosive grain burning behaviour, velocity interferometer obs. 4-101908
- industrial explosions, detonation wave intensity, influence of humidity and air excess, using gaseous phase spherical detonation mathematical model 4-109652
- intracavity laser spectroscopy, combustion diagnostics appls. 4-73519
- ionizing additive, physico-chemical transformation simulation (*French*) 4-81567
- ions in flames, origin and props. 4-71932
- jet engine augmented exhausts, CARS temp. and species meas. 4-73436
- jet wall cooling, protective layer, temp. distrib., boundary conditions effect 4-60405
- laser diagnostics, techniques and appls. 4-65039
- LWR containment, H<sub>2</sub> behaviour during accidents, production, mixing, combustion 4-64221
- methane flames, high temp., laminar flow, stagnation point heat transfer 4-65037
- methane-air flame CO detect. using two-photon absorpt. 4-62261
- MHD coal combustor development for low preheat operation 4-72130
- MHD heterogeneous combustion plasma equilibrium composition 4-108166
- microwave plasma incinerator for burning hazardous organic liquids 4-71931
- nonuniqueness of stationary propagation modes of combustion waves 4-99793
- nuclear reactor containment building, H<sub>2</sub> combustion and control 4-111666
- oil shale combustion retorting 4-62287
- open and closed vessels, turbulent combustion, flame propag. 4-89301
- optical techniques for studying combustion (*Italian*) 4-66591
- petrol engine, homogeneous combustion parameters and emissions control, computer simulation 4-77171
- PMMA, limiting combustion regimes in free convection absence 4-71921
- polydisperse liq. fuel diffusional combustion, self-similar conditions kinetics 4-81439
- porous powdered fuel, nonstationary convective combustion regimes 4-81442
- porous systems, nonstationary convective combustion eqns., qualitative anal. 4-71923
- premixed fuel-oxidiser flames, microwave effects 4-109649
- pulsed combustion, phase relationships 4-104992
- radiation fluxes calc. in rectangular channels 4-113013
- radioactive low level combustible waste incineration facility 4-106748
- ramjet combustion efficiencies comparison (*German*) 4-99797
- reacting shear layer, turbulent mixing and combustion 4-113074
- slag explosive condensation kinetics in MHD generator channel 4-113025

## combustion continued

- solid fuel steam generators, development trends in combustion (*German*) 4-114796  
 solid propellant, high freq. press. oscills., combustion instabilities (*French*) 4-66593  
 solid-fuel combustion in fluidised bed, two-phase model 4-71926  
 soot particles formation, growth and oxidation, sonic sampling technique and flat flames 4-104990  
 soot particles formation, growth and oxidation 4-104989  
 spark-ignition engine, combustion, flame photographs 4-87811  
 spatial dynamic structure of combustion zone, frequency charact. matrix determ. 4-85311  
 spherical mass of gas, compression optimisation 4-87837  
 stationary combustion systems, overview of research requirements 4-72045  
 swirl combustor flow meas. with and without combustion 4-103436  
 swirl-combustion chamber with shaped end walls 4-64967  
 swirling flow in closed vessels, flame development 4-75029  
 thermal sciences conference, Miami, USA (Apr. 1982) 4-73165  
 thermal self-ignition of system of hot foci, 4-97301  
 thermally protective materials, thermophys. characts., inverse heat cond. problem calcs 4-97269  
 thermionic converters, combustion-heated, development for fopping and cogeneration application 4-77124  
 turbulence and combustion studies, laser scatt. for conc. and temp. determ. 4-68289  
 turbulent, Bray-Moss-Libby model 4-87747  
 turbulent combustion, in premixed flame, theory and expt. 4-103429  
 turbulent combustion, press. effect on mol. gas props. 4-71920  
 turbulent diffusive combustion, CO form. study 4-71922  
 turbulent gas flame, sound radiation mechanism 4-71919  
 turbulent nonpremixed combustion, stretched laminar flamelet model 4-103431  
 two dimens. nonstationary flow, visualisation study 4-69836  
 United Stirling 4-95/4-275 heat engines for underwater use, characts. 4-66775  
 unmixed gases in channel, supersonic combustion charact. 4-69832  
 woodburning stoves, turbulent shear flow, two-dimens. anal. soln. 4-87688  
 Al flaming particles produced by rocket propellant in accel. field, high speed photography 4-111226  
 H combustion test program in nuclear pressure vessel 4-106927  
 H<sub>2</sub> flame propagation model in 1-D, pressure transients in reactor vessel 4-106926  
 H<sub>2</sub>/electrical power simultaneous production, using carbonaceous fuels and high-temperature nuclear process heat, thermodynamic anal. 4-89472  
 H<sub>2</sub>-air mixtures, high-speed turbulent deflagration and transition to detonation 4-103432  
 H<sub>2</sub>-CO<sub>2</sub> in air, flammability and detonability in radioactive waste processing 4-106741  
 N<sub>2</sub> CARS based temp. meas. inside firing internal combustion engine, optical multichannel anal. with rapid mass spectral storage 4-73437  
 OH concentration measurement in combustion environment using laser-induced fluoresc., collisional effects,  $\nu=1$  excitation effects 4-77007  
 OH spatially resolved meas. in flame using cross-beam saturated absorpt. spectroscopy 4-77006  
 Ti, laser ignition and combustion, optical props. and scale growth kinetics 4-77009

## comets

- angular momenta in solar system, statistical distrib. for comets, asteroids and meteor streams 4-101204  
 P/Arend-Rigaux (1984k), precise position (August 1984) 4-110567  
 P/Arend-Rigaux (1984k), recovery and accurate position (1984 August 9) 4-110571  
 P/Arend-Rigaux (1984k), recovery positions and ephemeris 4-101269  
 Austin (1982 VI), H I Balmer  $\alpha$  production rate in corona 4-94681  
 Austin (1982 VI), spectrophotometry during post-perihelion period 4-77770  
 P/Austin (1982 VI), spectropolarimetric observations 4-115714  
 Austin (1982 VI) plasma tail orientation, solar wind effect 4-82452  
 Austin (1984i), discovery, orbital elements and ephemeris (1984 July 21 to 31) 4-94684  
 Austin (1984i), discovery and semi-accurate positions (1984 July 8) 4-94685  
 Austin (1984i), IR magnitudes and ephemeris (1984 August 28 to October 15) 4-101272  
 Austin (1984i), July 1984 comet observations and ephemeris 4-101264  
 Austin (1984i), OH molecule radioemissions and visual magnitude 4-101268  
 Austin (1984i), parabolic orbital elements and ephemeris (1984 August 28 to October 2) 4-101262  
 Austin (1984i), photometric and spectroscopic obs. (1984 July 25 and 27) 4-101266  
 Austin (1984i), positions, magnitudes, orbital elements, ephemeris and coma diameters 4-94687  
 Austin (1984i), positions, orbital elements, ephemeris magnitudes and tail obs. 4-115725  
 Austin (1984i), total visual magnitude and tail length (1984 Aug.) 4-101270  
 Austin (1984i), total visual magnitude estimates (1984 August 25 to 28) 4-110570  
 Austin (1984i), visual magnitudes and tail lengths (1984 Aug.-Sept.) 4-110573  
 P/Boethin, capture by Jupiter 4-90119  
 Bowell (1980b), coma properties from stellar occultation obs. 4-115716  
 Bowell (1982 I) optical filter photometry and optical and UV spectrophotometry 4-82451  
 Bradfield (1984a), elliptical orbital elements and ephemeris (1984 March 21 to August 28) 4-63111  
 Bradfield (1984a), ephemeris (1984 March 1 to June 29) 4-67684  
 P/Bradfield (1984a), positions, magnitude estimates and orbital elements 4-85896  
 Bradfield (1984a), precise positions, orbital elements and ephemeris 4-67687  
 capture from molecular clouds, dynamical constraints on star and planet formation 4-77779  
 Cernis (1983i), coma icy grains detect. in IR 4-101258  
 P/Churyumov-Gerasimenko (1982 VIII), spectropolarimetric observations 4-115714  
 comets continued  
 P/Clark (1983w), ephemeris for 1984 April 30 to August 28 in 10 day intervals 4-77777  
 P/Clark (1983w), total visual magnitude estimates (1984 May 10 to June 3) 4-85898  
 P/Clark (1983w), total visual magnitude estimates (1984 May 6 and 7) 4-72911  
 column densities from brightnesses through CN, C<sub>3</sub> and C<sub>2</sub> filters 4-77766  
 P/Comet Halley (1982i), VEGA mission, profile and instrumentation 4-101117  
 composition determ., implications for solar nebula characts. 4-101207  
 P/Crommelin (1983n), ephemeris continuation (1984 April 10-June 9) 4-63112  
 P/ Crommelin (1983n), IUE spectrum features and total visible magnitude estimates 4-63102  
 P/ Crommelin (1983n), spectra and visual magnitude estimates 4-67692  
 P/Crommelin (1983n), spectroscopic obs. and total visual magnitude estimates 4-63104  
 P/Crommelin (1983n), total visual magnitude estimates (1984 February 8 to 27) 4-63109  
 P/ Crommelin (1983n), total visual magnitude estimates and occultation prediction 4-67697  
 P/Crommelin (1983n), trial run for Periodic Comet Halley (1982i) in International Halley Watch 4-82455  
 P/Crommelin (1983n), UV and visible spectra, mag. estimates (1984 Feb.-March) 4-67686  
 dust ejecta and its evolution (*Japanese*) 4-110563  
 ejected grains, destruction near Sun 4-77765  
 emission features of 17 comets 4-63099  
 P/Encke, 1984 March visual magnitudes and 1984 April 10 to June 29 ephemeris 4-67699  
 P/ Encke, total visual magnitude estimates 4-67695  
 P/Encke, total visual magnitude estimates (1984 April) 4-82454  
 P/Encke, total visual magnitude estimates (1984 February 19 to 27) 4-63110  
 P/Encke, total visual magnitude estimates and ephemeris 4-63106  
 extinct comets in high-inclination orbits, steady state number 4-90118  
 P/Faye (1984h), precise and prerecovery positions 4-115718  
 P/Faye (1984h), recovery, approximate positions, and ephemeris 4-85897  
 P/Faye (1984h), total visual magnitude obs. 4-115720  
 Galileo spacecraft for asteroid or comet rendezvous, trajectories 4-82378  
 P/Gehrels 3 (1984i), recovery, precise position, and orbital elements 4-110568  
 P/ Giacobini-Zinner (1984e), position from CCD images (1984 July 21) 4-110572  
 P/Giacobini-Zinner (1984e), recovery and precise positions (January to April 1984) 4-63100  
 P/Halley, brightness secular decrease and aging characts. 4-90114  
 P/Halley, dust drag and perturbations on Giotto 4-77689  
 P/Halley, Giotto spacecraft mission, navigation problems 4-90048  
 P/Halley, Giotto spacecraft terminal navigation problem 4-90091  
 P/Halley, orbit determ. by means of optimally selected observations 4-82385  
 P/Halley (1910 II), coma morphology and dust-emission pattern 4-82450  
 P/halley (1910 II), photographs (1910 May 5 to June 6) 4-77768  
 P/Halley (1982i), astrometry (1984 March 4) and flux 4-67700  
 P/Halley (1982i), autonomous tracking of nucleus during spacecraft flyby 4-105865  
 P/ Halley (1982i), electronographic bi-dimensional photometry 4-67694  
 P/Halley (1982i), Giotto mission and comet characts. 4-101274  
 P/Halley (1982i), International Halley Watch trial run involving Periodic Comet Crommelin (1983n) 4-82455  
 P/Halley (1982i), light vars. obs. (1984 January 27 to 30) 4-77773  
 P/Halley (1982i), occultations of stars (for period 1985 to 1986) 4-90116  
 P/Halley (1982i), photometric obs. rel. to brightness vars. and rot. period 4-94686  
 P/Halley (1982i), precise positions (1983 December 31 to 1984 January 30) 4-63105  
 P/Hartley-IRAS (1983v), emission spectra and brightness 4-67690  
 P/ Hartley-IRAS (1983v), total visual magnitude estimate 4-67698  
 P/Hartley-IRAS (1983v), ephemeris (1984 April 20 to June 19) 4-72910  
 P/Hartley-IRAS (1983v), ephemeris and total visual magnitude estimate 4-67703  
 P/Hartley-IRAS (1983v), magnitude estimate 4-85895  
 P/Hartley-IRAS (1983v), total visual magnitude estimates (1984 March 25 to April 9) 4-63101  
 p/Hartley-IRAS (1983v), total visual magnitude estimates (1984 April 27 to May 19) 4-77774  
 P/Hartley-IRAS (1983v), total visual magnitude estimates and coma diameters (1984 February 24 to 27) 4-63108  
 P/Hartley-IRAS (1983v), total visual magnitude obs. 4-67685  
 impacts as causes of mass extinctions, periodicity rel. to Sun's motion perpendicular to galactic plane 4-72591  
 impacts of large asteroids and comets on Earth, geological implications, conference, Snowbird, Utah (1981 October 19 to 22) 4-100577  
 IRAS (1983k), positions, parabolic orbit elements, and ephemeris (1984 Feb.-Aug.) 4-67688  
 IRAS (1983o), ephemeris for 1984 April 10 to August 28 in 10 day intervals 4-63103  
 IRAS (1983o), visual magnitude estimate (11 March 1984) 4-67701  
 IRAS fast mover program 4-101227  
 IRAS fast-moving object search 4-77691  
 IRAS-Araki-Alcock (1983d), atomic oxygen spectral obs. 4-115715  
 IRAS-Araki-Alcock (1983d), close Earth encounter, review (*French*) 4-115713  
 IRAS-Araki-Alcock (1983d), IRAS 12-100  $\mu$ m obs. 4-85893  
 IRAS-Araki-Alcock (1983d), new molecules in visible spectrum 4-94691  
 IRAS-Araki-Alcock (1983d), spectroscopic obs. and molecular identifications 4-67683  
 P/Kopff, rendezvous mission 4-115670  
 P/Kowal-Mrkos (1984n), discovery observations, orbit and ephemeris 4-115724  
 long period comets, perihelion distrib. and solar apex 4-72912  
 long-period comets, orbits, systematic and random perturbations (*Russian*) 4-94692  
 long-period comets, perihelion passages, statistical anal. 4-101263

## comets continued

- magnetospheres of different astronomical objects, comparative study 4-72897  
 magnitudes, coma and tail details for sixteen objects, visual obs. 4-101260  
 Meier (1984c), precise positions, parabolic orbital elements, ephemeris, and visual magnitude estimate 4-115726  
 motion and evolution, obs. database 4-101275  
 P/Neujmin 1 (1984c), June to Dec. 1984 ephemeris 4-77776  
 P/Neujmin 1 (1984c), recovery and precise positions (1984 February 26) 4-63107  
 P/Neujmin 1 (1984c), visual magnitude and coma size 4-115723  
 P/Neujmin 3, orbit, correl. with Periodic Comet van Biesbroeck 4-67702  
 nuclei, formaldehyde form. due to cosmic ray interactions 4-94682  
 nuclei particles, effect on meteor streams evolution 4-90120  
 nucleus, friable sponge model 4-90113  
 nucleus sample return mission 4-115674  
 observations (1946 August 6 to 1984 January 30) 4-77769  
 Oort cloud, perturbations by distant solar companion rel. to periodic mass extinctions on Earth 4-72593  
 Oort cloud rel. to solar system gravitational boundary 4-115696  
 orbits, evolution and origin 4-77780  
 origins, constraints from isotropy of microwave background and other meas. 4-101273  
 periodic comet showers rel. to terrestrial mass extinctions, role of solar companion star 4-72594  
 Periodic Comets lost for more than one apparition 4-94690  
 planetary distances and Jupiter family velocities (*Russian*) 4-101259  
 precise posns. on Minor Planet Circulars 8579-8690 for 21 objects 4-63095  
 precise posns. on Minor Planet Circulars 8827-8946 for 16 objects 4-101228  
 precise posns. on Minor Planet Circulars 8947-9036 for 16 objects 4-105900  
 precise posns. on Minor Planet Circulars for 19 objects 4-77754  
 P/Russell 3 (1982 IX), orbit evolution (1938 to 2028) and Jupiter encounters 4-77771  
 P/Russell 4 (1984d), precise positions, orbit, and ephemeris 4-67696  
 P/Russell 4 (1984d), precise positions (1984 March 12) 4-67691  
 P/Russell (1984d), discovery, precise positions, orbit and ephemeris 4-67689  
 P/Schaumasse (1976XV, 1984m), orbital elements and ephemeris 4-115722  
 P/Schaumasse (1976XV, 1984m), recovery obs. in 1976 and 1984 and orbit 4-115721  
 Shoemaker (1984f), astrometric obs., orbital elements and ephemeris (1984 May 30 to July 29) 4-82453  
 Shoemaker (1984f), ephemeris continuation (1984 July-October) 4-94688  
 Shoemaker (1984f), May 1984 discovery of new comet 4-77775  
 Shoemaker (1984f), precise position (1984 May 31) 4-77778  
 short period comets, perihelion distances distrib. 4-90115  
 solar wind and radiation interaction 4-77686  
 structure and chem. processes 4-101274  
 Sugano-Saigusa-Fujikawa (1983e), close Earth encounter, review (*French*) 4-115713  
 sungrazing comets, orbits and origin (*Polish*) 4-63113  
 Takamizawa (1984j), discovery, approximate positions, and visual magnitude estimates 4-101265  
 P/Takamizawa (1984j), elliptical orbital elements and ephemeris (1984 August 18 to September 27) 4-101261  
 P/Takamizawa (1984j), orbital elements and ephemeris 4-110566  
 P/Takamizawa (1984j), positions, elements and ephemeris (1984 June-Aug.) 4-110574  
 Takamizawa (1984j), possible short period comet, astrometry, orbit and ephemeris 4-101267  
 P/Takamizawa (1984j), precise positions (1984 July-August) 4-101271  
 P/Takamizawa (1984j), total visual magnitude estimates (1984 August 8 to 21) 4-110569  
 P/Takamizawa (1984j), visual magnitude estimates 4-105903  
 P/Takamizawa (1984j), visual magnitude estimates 4-115719  
 p/Tempel 2, tail obs. during IRAS fast mover program 4-101227  
 thermal stresses and cracking of cometary nuclei 4-110565  
 P/van Biesbroeck, orbit, correl. with Periodic Comet Neujmin 3, anal. 4-67702  
 West (1976 VI), dust in secondary tail 4-72913  
 P/Wild 2 (1983s), dust coma and tail structure 4-67693  
 P/Wild 2 (1983s), total visual magnitude, estimates (1984 April) 4-94689  
 P/Wild 3, orbital perturbations due to close encounter with Jupiter (May 1977) 4-94683  
 P/Wolf-Harrington, rediscovery in June 1984 and obs. of tail 4-85894  
 P/Wolf-Harrington (1984g), visual magnitude and ephemeris 4-115717  
 CN radiance/column density ratio calc. from Swings effects 4-90117  
 O 1, 557.7 nm forbidden line detect. 4-77772

## command and control systems

- weather support role 4-72675

## commensurate-incommensurate transformations

- asymmetric clock model on Cayley tree 4-68158  
 bis-propylammonium manganese chloride, commensurate and incommensurate phase transitions, thermal expansion, birefr. meas. 4-70374  
 bis-tetramethylammonium tetrachlorozincate:  $Mn^{2+}$ , soliton density in incommensurate phase, EPR, temp. depend. 4-109065  
 cholesteryl 2,2,3,3-tetrafluoropropionate, dielec. props. under hydrostatic press., commensurate-incommensurate transition obs. 4-80853  
 cholesteryl 2,2,3,3-tetrafluoropropionate, successive phase transitions and cryst. struct., X-ray diff. study 4-61068  
 di-(tetramethylammonium- $d_4$ ) cobalt tetrachloride, commensurate-incommensurate transition 4-80023  
 dielectric substances, incommensurate transition sequence 4-84366  
 discrete Frenkel-Kontorova chain, non-Kolmogorov-Arnold-Moser incommensurate states 4-80191  
 displacive incommensurate phase, field theory anal. (*Chinese*) 4-98239  
 dynamics of incommensurate structures, exact soln. 4-113842  
 ferroelectric, acoustic-phonon dispersion at incommensurate phase transitions, Brillouin scatt. obs. 4-61724  
 fluctuation effects as a cause for the incommensurate phase formation 4-76371  
 graphite, adsorbed methane submonolayer, commensurate-incommensurate transition, neutron diff. study 4-65559

## commensurate-incommensurate transformations continued

- graphite intercalation compounds, modification of material props. 4-60890  
 graphite with adsorbed methane, commensurate-incommensurate transition model 4-70572  
 insulators, approx. method in theory of incommensurate phases 4-70344  
 Ising model, next-nearest neighbour, soliton pinning and annealing 4-82764  
 Ising nearest neighbour model, with uniaxial incommensurate phase and Lifshitz point 4-71115  
 light scattering near phase transitions, book 4-101581  
 lock-in transitions, successive, in incommensurate systems 4-76379  
 magnetic films, uniaxial, with Lifshitz crit. point, phase transitions from homogeneous to inhomogeneous states in external mag. field 4-71140  
 methane adsorbed on graphite, model of commensurate-incommensurate transitions 4-80394  
 modulated phases, Ginzburg-Levanyuk criterion for phase transition 4-98274  
 organic halides,  $[(CH_3)_4N]_2MX_4$ , ferroelectricity and antiferroelectricity 4-65957  
 orientational instability of higher-order commensurate lattices 4-103947  
 original-incommensurate-commensurate phase transition sequence 4-88285  
 Percival variational principle for invariant meas. 4-101795  
 phase diagrams for incommensurate systems 4-113571  
 Potts model, asymmetric three-state, phase struct. 4-111075  
 quartz, incommensurate phase, Brillouin scatt. study 4-61719  
 quartz, incommensurate phase formation, fluctuation effect mechanism 4-76371  
 quartz, incommensurate transition, thermal expansion, permitt. meas. 4-108604  
 quartz, intermediate phase, refined obs. of satellite reflections 4-98265  
 quartz, thermodynamical behaviour around transition between  $\alpha$ , incommensurate and  $\beta$  phases 4-113619  
 random walkers, phase transition in 1-D 4-86335  
 rippled commensurate state, new type of incommensurate state 4-65372  
 soliton structures, phase diagram in 2-D 4-86357  
 superspace symmetry in incommensurate structures, Landau theory 4-103689  
 susceptibility anomalies in the vicinity of a nonpolar commensurate phase 4-114219  
 tetramethylammonium tetrachlorozincate, deuterated, ferroelec., temp.-press. phase diagram 4-76377  
 thermal hysteresis near commensurate-incommensurate phase transition, interpretation 4-76382  
 thiourea, Brillouin scatt. under hydrostatic press., elastic constants, study 4-76479  
 thiourea, deuterated, neutron diff. study under high elec. field 4-109142  
 thiourea, incommensurate phase transitions, phase mode dynamics, neutron and Raman scatt. studies 4-65966  
 (TMTSF) $_2PF_6$ , one-dimensional conductivity, temp. dependence anal. 4-75939  
 transition metal dichalcogenides, CDW transitions and lattice vibr. (*Japanese*) 4-92641  
 TTF-TCNQ, one-dimensional conductivity, temp. dependence anal. 4-75939  
 two-dimensional ANNNI type models, Monte Carlo studies 4-113608  
 $Ag_3AsS_3$ , proustite, incommensurate phase in region of second-order phase transition, NQR, sp. ht. meas. 4-71314  
 $AlPO_4$ , berlinite, incommensurate phase, colorimetric and neutron scatt. studies 4-84277  
 $BaMnF_4$ , incommensurate phase, neutron scatt. study, press. effect 4-75654  
 $BaMnF_4$ , optical props. near incommensurate and mag. transitions 4-66004  
 $Ba_2NaNb_2O_{10}$ , ferroelastic-incommensurate transition, Brillouin scatt. study 4-93062  
 $Ba_2NaNb_2O_{10}$ , incommensurate, Brillouin spectra meas. 4-76482  
 $Ba_2NaNb_2O_{10}$ , tetragonal bronze-like struct., modulated phases and domain struct. 4-113616  
 $Cd_3Nb_2O_7$ , unusual incommensurate soft mode damping 4-113562  
 $Cs_2ZnI_4$ , phase transitions, Raman scatt. study 4-76470  
 Ge, Si, epitaxial films on Si (100), commensurate and incommensurate struct. 4-108740  
 $K_2SeO_4$ , acoustic phonon wavevector depend. near commensurate-incommensurate transition, Brillouin spectra 4-71313  
 $K_2SeO_4$ , Brillouin spectra, scatt. angle and press. depend. 4-76481  
 $K_2SeO_4$ , incommensurate phase, SHF Obs. 4-61635  
 $K_2SeO_4$ , incommensurate phase transitions, phase mode dynamics, neutron and Raman scatt. studies, review 4-65966  
 $K_2SeO_4$ , incommensurate-ferroelec. transition, struct. study 4-76381  
 $K_2SeO_4$ , incommensurate transition, order parameter, EPR lineshape anal. 4-99056  
 $K_2SeO_4$ , incommensurate-ferroelectric transition, structural study 4-109138  
 $K_2SeO_4$ , phonon-soliton interaction, discommensurations at lock-in transition 4-70299  
 $K_2ZnCl_4$ , metastable chaotic state close to incommensurate-commensurate transition,  $^{51}Cr$  NQR obs. 4-76285  
 Kr layer on graphite in one-to-two layer regime, phase diagram, freezing transitions 4-103910  
 Kr monolayer, on graphite, commensurate-incommensurate transition, X-ray scatt. study 4-61215  
 $LiKSO_4$ , incommensurate phase (*Chinese*) 4-70359  
 $LiKSO_4$ , incommensurate-commensurate phase transitions, superstructure, X-ray diff., neutron diff., thermal anal. 4-103929  
 $(NH_4)_2BeF_6$ , incommensurate phase, SHF Obs. 4-61635  
 $(NH_4)_2BeF_6$ , incommensurate phase, in applied elec. field 4-76376  
 $(NH_4)_2BeF_6$ , sp. ht. in region of incommensurate phase transition 4-61104  
 $(NH_4)_2ZnBr_4$ , ferroelec., Raman scatt. study of phase transitions 4-104589  
 $(NH_4)_2ZnCl_4$ , incommensurate phase transition, dielec. props., X-ray diff. study 4-93021  
 Nb (110)-Pd interface, electronic struct. 4-84674  
 NbSe $_3$ , CDW props., high-resolution synchrotron X-ray scatt. studies 4-109276  
 $NiBr_2$ , helimag, and antiferromag., mag. excitations, neutron scatt. studies 4-104409  
 $Pb_2NaNb_2O_{10}$ , tetragonal bronze-like struct., modulated phases and domain struct. 4-113616

**incommensurate-incommensurate transformations continued**

- RbD<sub>2</sub>(SeO<sub>3</sub>), ferroelectric phase transition, dielec. anomaly 4-65987  
 Rb<sub>2</sub>ZnCl<sub>4</sub>, ferroelec., phase transitions, dielec. and DTA studies, rel. to cryst. growth conditions 4-76374  
 Rb<sub>2</sub>ZnCl<sub>4</sub>, incommensurate, modulation wave floating, NMR meas. 4-65991  
 Rb<sub>2</sub>ZnCl<sub>4</sub>, incommensurate-ferroelec. phase transition, X-ray study 4-76373  
 Rb<sub>2</sub>ZnCl<sub>4</sub>, incommensurate phase, dynamic dielec. props., pinning effects 4-109140  
 Rb<sub>2</sub>ZnCl<sub>4</sub>, modulated ferroelec., thermal hysteresis and pinning 4-76380  
 Rb<sub>2</sub>ZnCl<sub>4</sub>, nucleation processes at commensurate-incommensurate transition 4-80874  
 Rb<sub>2</sub>ZnCl<sub>4</sub> type crystals, phase transitions, Landau pot. 4-75653  
 Sr<sub>2</sub>KNb<sub>2</sub>O<sub>7</sub>, tetragonal bronze-like struct., modulated phases and domain struct. 4-113616  
 Sr<sub>2</sub>NaNb<sub>2</sub>O<sub>7</sub>, tetragonal bronze-like struct., modulated phases and domain struct. 4-113616  
 Sr<sub>2</sub>Nb<sub>2</sub>O<sub>7</sub>, ferroelec., incommensurate-polar transition 4-76375  
 TaS<sub>2</sub>-IT, phase transition at 282K, DSC, elec. cond. and Hall effect meas. 4-92349  
 IT-TaS<sub>2</sub>(Se<sub>2</sub>), CDW states, three-dimensional orderings 4-65625  
 2H-TaSe<sub>2</sub>, CDW phase transition at low temp. and high press. 4-104276  
 TaSe<sub>2</sub>-2H, CDW props., high-resolution synchrotron X-ray scatt. studies 4-109276  
 TaSe<sub>2</sub>-2H, charge density wave transition (*Chinese*) 4-84575  
 ThBr<sub>4</sub>, incommensurate phase, Gd<sup>3+</sup> EPR study 4-76246  
 ThBr<sub>4</sub>Gd<sup>3+</sup>, incommensurate, phase fluctuations near transition temp., phase pinning, EPR meas. 4-92956  
 Ti<sub>8/7</sub>Ni<sub>37/5</sub>Al<sub>1/8</sub>, charge wave density transitions, electron microscopy study 4-98596  
 TiInS<sub>2</sub> crystal, incommensurate phase transition 4-113601  
 W (001), adsorbed H-induced surface reconstruction, LEED and EELS study 4-92492  
 α-ZnP<sub>2</sub>, commensurate-incommensurate-commensurate phase transition 4-113600

**inference**

- see also* marketing  
 40 MWe OTEC pilot plant programme status report 4-114932  
 diving operations, regulation and safety organisation 4-106169  
 lobster culture development and commercial viability 4-115446

**communication channels**

- see also* channel capacity  
 corpuscular information channel, ideal system 4-79068  
 dispersive optical fibre, digital pulse position transmission anal. 4-60177  
 Fabry-Perot etalon, use as RF freq. channeliser 4-95507  
 monofrequency optical carrier, modulated by frequency multiplexed voice channels, spectral anal. 4-102889  
 underwater acoustic channels characterisation 4-60201

**communication networks**

- see also* computer networks; television networks  
 advances in instrumentation, conf. Houston, Texas, USA (Oct. 1983) 4-106121  
 Ocean Pollution Data and Information Network (OPDIN) 4-109758  
 optical fibres in broadband networks, instrumentation and urban and industrial environment apps., conf., Paris, France (May 1983) 4-78024  
 optical fibres in the industrial and commercial environment, review 4-79292  
 transmitters and receivers for fibres optics transmission (*Italian*) 4-69562  
 USA Northeast Area Remote Sensing System, NEARSS 4-110174

**communication overhead lines**

- see also* telecommunication cables  
 optical fibre cable, transmission characts. (*Japanese*) 4-79312

**communication overhead transmission lines** *see* communication overhead lines**communication theory** *see* information theory**communications applications of computers** *see* communications computing**communications applications of control**

- see also* communications computer control; telephony  
 laser radar beam control with holographic diffraction gratings 4-107720

**communications computer control**

- see also* communications computing  
 laser diode rangefinder, target acquisition and tracking system, functional model/demonstration model 4-107727

**communications computing**

- see also* communications computer control  
 radar, coverage and anomalous propag. through inhomogeneous atmospheres (*French, English*) 4-67384  
 vehicular technology conf. Pittsburgh, PA, USA (May 1984) 4-106118

**community planning** *see* town and country planning**compacting** *see* densification**comparators (circuits)**

- automatic polarity switching of DC voltmeter using op-amp comparator (*Spanish*) 4-73430

**compasses**

- see also* navigation  
 ships, magnetic compass card movement, referring to bowl motion (*Japanese*) 4-78345

**compensation**

- see also* error compensation  
 biological image processing, shading compensation, A/D convertor appl. (*Japanese*) 4-85595  
 cryogenic sensor-amplifier interfaces, hybrid circuit freq. compensation modules 4-90573  
 film camera position stability compensation (*Russian*) 4-90676  
 gas laser, steady state synchronisation of lateral modes (*Russian*) 4-60079  
 measurement results processing (*German*) 4-101822  
 optical fibres, single mode, step index and W-profile, refractive index optimisation for dispersion compensation (*German*) 4-83713  
 optical phase conjugate techniques, distortion compensation and props./appl. review 4-74624  
 single-mode fibre-optic holography 4-60004  
 temperature compensated coupled cavity diode lasers 4-107691  
 Si sensors with on-chip signal processing for long-term stability 4-68225  
 n-Si:Au, elec. cond. and photoconductivity 4-104213

**compensation, charge** *see* charge compensation**complementarity**

- time-dependent neutron interferometry, Aharonov-Bohm and Wheeler-type delayed choice expts. 4-68012

**complementary metal-oxide-semiconductor integrated circuits** *see* field effect integrated circuits**complete computer programs***see also* subroutines

- biotelemetry device linked to Apple II, program in BASIC, 6502 assembly language 4-62636  
 Commodore Pet, appl. school physics lab., program in machine code 4-78074  
 decibel calculation program for TI 59 calculator 4-83768  
 glomerular filtration rate, determ. using <sup>99m</sup>Tc-DTPA, in-house computer program 4-89730  
 graph plotting, best straight line, BASIC programs for BBC Microcomputer 4-82647  
 ion optics calc. program in BASIC, for mass spectrometer design 4-78410  
 loudness, British Standard 4198-Method A, BASIC computer program for calculations 4-69636  
 loudness measurements, BASIC program for execution of International Standard ISO 532 B 4-79403  
 macromolecules, linear, heat capacity, theta temps. and group vibrs. obs. 4-80254  
 multicomponent systems, mixing effects, subregular eqn. in FORTRAN 4-84401  
 music on the BBC Micro, programs in BASIC 4-69635  
 pesticide screening in residue analysis, program in BASIC 4-62273  
 planetary remote sensing, computer program package 4-101114  
 water-air mixture flow in vertical pipe, hydrodynamic calc. 4-60515

**complex angular momentum plane**

- see also* angular momentum theory; Pomeranchuk poles and trajectories; Regge poles and trajectories  
 No entries

**compliance constants** *see* elastic constants**composite insulating materials**

- glass fibre reinforced polymers, electrical insulator components, damage in combined elec., mech. and chemical environments 4-66466  
 organic, electron and neutron irradi. effects on mech. props. 4-75533  
 power capacitors, electrohydrodynamic motion induced by injection from plane polymer sheets 4-97706

**composite materials**

- see also* cermets; composite insulating materials; composite superconductors; concrete; eutectic alloys; fibre reinforced composites; fibres; filled polymers; laminates  
 aerospace structures, conf., Boston, MA, USA (Nov. 1983) 4-73167  
 annular plates, vibr. anal. by integral eqn. technique 4-112756  
 anodised layer, spectrally selective, solar collector appl., ESCA studies 4-66789  
 beams, reinforced, failure in combined loading 4-87629  
 biaxially stressed, inconsistency in max. strain theory of failure 4-112769  
 bielastic strip, edge crack anal. 4-87628  
 biological composites, struct. and mech. props., book contrib. 4-66990  
 body with hard sharp-angled inclusion and interface crack, longit displacement 4-97414  
 bone composite material, elec. props. rel. to comp. 4-72232  
 capillary and fissile materials, finite uniform strain, metamorphic struct. 4-87588  
 ceramic, high-performance, materials characterisation role 4-66279  
 ceramic-polymer composite biomaterials, fracture 4-76844  
 ceramic/ceramic, tough, capabilities and design issues 4-66292  
 composites, cement-based, modified instrumented Charpy test 4-89204  
 conducting/insulating particulate mixture, elec. cond. model 4-84662  
 conducting/insulating sphere mixture, AC cond., percolation approach 4-108911  
 damaged, affine equivalence of local stress and displacement distrib. 4-79448  
 design, reliability-based, fatigue-proof 4-99392  
 dielectric constant, complex, of two-phase composite 4-114197  
 diffusion bonding, hot isostatic pressing 4-89239  
 elastic body with long thin cylindrical inclusions, stress conc. 4-97416  
 elastic moduli determ. using flexural tests 4-112784  
 elastoplastic media with microstruct., singular approx. 4-108018  
 EM and elastic props., correlation, microgeometries corresponding with effective medium approx. 4-70251  
 fatigue failure, probabilistic modelling employing Markov process 4-74961  
 fatigue-proof design, reliability-based 4-99604  
 fibre/matrix, acoustic emission waveforms in isotropic and orthotropic plates 4-97188  
 fibrous cross-reinforced materials, heat conduction anal. using double periodic harmonic functions (*Ukrainian*) 4-87537  
 glass bead reinforced epoxy, acoustic emission evaluation 4-81380  
 glass-ionomer dental cement, prep. and compressive strength 4-99373  
 glass-metal particulate composites, preparation and props. 4-104761  
 granular composites, fluid saturated, US propagation 4-79357  
 graphite composites in reactors, influence of neutron and α-particle bombardment 4-96141  
 inelastic, delayed failure 4-97434  
 insertion electrodes using solid electrolytes, theory 4-89386  
 Iosipescu shear test 4-71807  
 Jones-Nelson-Morgan, nonlinear composite materials model, incremental stress-strain rels. (*Chinese*) 4-108021  
 layer compression development on compression 4-79514  
 layered composites, elastic and viscoelastic, transient wave propag. 4-79492  
 layered composites with transversely isotropic constituents, annular crack problem 4-103263  
 layered structures, adhesion bond strength, US study (*French*) 4-62136  
 lignin/paper composites, temp. depend. of tensile props. 4-109451  
 matrix/inclusion composite, overall elastic response, quasicrystalline approx. appl. 4-103207  
 metal particles, small, in composite material, far-IR absorption 4-61708  
 metal-dielectric composites, effective dielec. const. 4-99002  
 metallic, generalised classif., book contrib. 4-109357  
 metallic composites, endurance of matrix during thermal fatigue loading 4-71722  
 micromechanical test machine for high temperatures 4-89218  
 model, thermal-moisture stresses 4-69677

## composite materials continued

- mullite-zirconia composites, microstruct. and mech. props 4-114672  
 multicriterial optimisation models of structuring 4-87566  
 multilayer, plasticity and fracture 4-70267  
 nonsymmetric anisotropic hardening for composite materials 4-87592  
 oriented reinforcement composites, thermal diffusivity anal. 4-104010  
 oriented reinforcement composites, thermal props., flash method meas. 4-104009  
 orthotropic, resistance-foil strain gauge technology 4-68223  
 orthotropic flat sandwich plates, thick faces theory 4-69692  
 overall elastic response, overall modulus operator 4-97305  
 panels, cylindrical, integrated-stiffened, buckling test (*Chinese*) 4-79475  
 periodic, effective elasticity tensor 4-91728  
 photographic follow-up system for measuring thermal deform. 4-112787  
 physically nonlinear composite composites, effective dependence relationship derivation (*Russian*) 4-60275  
 piezoelectric ceramic composites, underwater transducer appls. 4-65951  
 piezoelectric composites, periodic, dynamic behaviour, generalised Floquet theory 4-99037  
 plasticity of composition material with spherical inclusions 4-112733  
 plate, thick, transversely isotropic, ductile penny-shaped crack 4-83856  
 plates, cantilevered, with bending-torsion coupling, freq. determ. techniques 4-79481  
 plates, isotropic and composite, anticlastic curvature suppression 4-83832  
 plates, laminated, composite, shear-flexible triangular finite element model 4-64840  
 polycrystalline aggregates, grain growth, computer simulation studies 4-113665  
 polymer composites, thermal cond. meas. to high temp. using line-source technique 4-108668  
 polymer/Li salt hybrids as superionic conductors 4-75723  
 polymeric, thick-wall cylinders, allowance for rheology 4-87590  
 polymers, molded, percolation conductivity for orientation detection 4-92777  
 porous composite materials for vacuum appl. 4-95446  
 refractory oxides, oriented eutectics, microstruct. and related props. 4-71627  
 revolution shells, fibre wound composite material, strength using finite element method (*Chinese*) 4-60271  
 rods, plates and shells, stability, three-dimens. formulation, survey 4-79477  
 sandwich structure, penny shaped cracks, stress analysis 4-60339  
 secant stiffness meas., peak-valley detector appl. 4-66514  
 shells, brittle, joints design in rigid systems 4-87636  
 silicone composite material, glassy film conversion, humidity-sensing props. rel. to elec. resistance 4-63752  
 skeletal structure, thermal expansion 4-61116  
 steel, stainless, composite detonation deposited coatings, wear resist. 4-62123  
 structures composed of composite rev. shells and axisymmetric solids, finite element anal. (*Chinese*) 4-60272  
 superhard materials, crack resist. determ., samples and loading 4-93494  
 survey from applied mech. and engineering science point of view 4-74862  
 symmetric rail shear test, mode II fracture toughness, finite element analysis 4-109582  
 thermal conductivity, nonlinear inverse problem, accuracy of soln. anal. 4-97277  
 three-layer sample, thermal diffusivity meas. by modulated heating method 4-97289  
 triglycine sulphate/polymer composites, dielec. const. and pyroelec. props. 4-109132  
 viscoelastic, thick-wall cylindrical shell, optimal nonsteady cooling process 4-87589  
 void content, optical assessment techniques 4-89199  
 Ag-KCl random composite materials, EM propag. 4-71331  
 Al welds, miniature, in composite structures, nondestructive inspection 4-66529  
 Al-glass composite, produced by powder metallurgy route, mech. props. 4-66275  
 Al-Mg-Al<sub>2</sub>O<sub>3</sub>, incorporation of Al<sub>2</sub>O<sub>3</sub> particles by stirring in melt 4-93522  
 Al<sub>3</sub>Ni whisker reinforced Al, effects of morphology of Al<sub>3</sub>Ni whiskers on tensile strength 4-88133  
 Al<sub>2</sub>O<sub>3</sub>-AlON composite ceramic, hot pressing reaction sintering, mech. props., high temp. appls. 4-62062  
 Al<sub>2</sub>O<sub>3</sub>-BN(-AlON) composite ceramics, mech. props. (*French*) 4-81177  
 Al<sub>2</sub>O<sub>3</sub>-glass composite, hot isostatically pressed, macropore struct. 4-71629  
 Al<sub>2</sub>O<sub>3</sub>-PMMA (PBMA), composite biomaterials, fracture 4-76844  
 Al<sub>2</sub>O<sub>3</sub>-ZrO<sub>2</sub>, transformation-toughened, fracture toughness, crack-size depend. 4-93373  
 Al<sub>2</sub>O<sub>3</sub>-ZrO<sub>2</sub> composites, grain growth hindrance by ZrO<sub>2</sub> inclusions 4-76743  
 Al<sub>2</sub>O<sub>3</sub>-ZrO<sub>2</sub> powders, prep. by evaporative decomp. of solns. 4-85137  
 As-Sb-Se system, glass-ceramic composites, varistor-like behaviour 4-114009  
 Au-SiO<sub>2</sub> composite granular films, conductivity and crossover effects 4-114047  
 BaTiO<sub>3</sub>, liquid phase sintering and composite ceramics with Pb<sub>3</sub>Ge<sub>2</sub>O<sub>11</sub> 4-104746  
 Bi granules, in glass matrix, optical props. 4-88795  
 C-C porous materials, in-depth CVD of SiC 4-71594  
 C-CaSO<sub>4</sub> composites, for solar energy collection and storage 4-100004  
 Co-Al<sub>2</sub>O<sub>3</sub> coevaporated composite films, solar selectivity 4-72169  
 Cu/CuO(N<sub>2</sub>) composites, reactive ion beam sputter deposited, optical recording appl. 4-79249  
 Cu-Su filled crystalline glass composite, frictional and strength props. 4-66456  
 CuCl(Al<sub>2</sub>O<sub>3</sub>) composites, elec. cond., particle size effects 4-88548  
 Fe<sub>3</sub>B<sub>12</sub>-Al<sub>2</sub>O<sub>3</sub> granular system, XPS anal., surface composition study 4-81113  
 In(In<sub>2</sub>O<sub>3</sub>(N<sub>2</sub>)) composites, reactive ion beam sputter deposited, optical recording appl. 4-79249  
 MgO, pitch-bonded refractories, oxidation and Mg diffusion 4-114698  
 MgO, resin-bonded, C-bearing magnesia, mech. props. 4-114673  
 MgO-graphite, C-bearing magnesia, mech. props. 4-114673  
 Nb-Ti multifilamentary supercond. composites, cold drawn, heat treatment, precip. morphology, TEM obs. 4-71657  
 Ni-B composites, electroless and electrodeposition 4-88990  
 Ni-Mo-Al eutectic alloy, unidirectionally solidified composite,  $\gamma/\gamma'$  phases, microstruct. changes 4-114493

## composite materials continued

- PZT/semi-crystalline polymer composite piezoelectrics 4-71283  
 PZT-polymer composites, piezoelec., with two dimensional periodicity, reson. modes of vibr. 4-76331  
 PbTiO<sub>3</sub>/synthetic rubber composites, piezoelec. and dielec. props. 4-104535  
 Pb(Zr,Ti)O<sub>3</sub>/synthetic rubber composites, piezoelec. and dielec. props. 4-104535  
 Pd small particle composites, far IR absorption studies 4-99073  
 SiC particle reinforced Al alloy, composite strengthening, influence of microstruct. 4-99398  
 SiC-BN, thermal diffusivity anisotropy 4-84472  
 SiO<sub>2</sub>-AgCl, diphasic photosensitive xerogel prep. method 4-71990  
 V-MoSe<sub>2</sub>, and V-NbSe<sub>2</sub>, volume changes in sintering 4-66271  
 W-Cu composites, sintering 4-66270  
 Zr-Al composite-cathode sputter-ion pump 4-78332  
 ZrO<sub>2</sub>-Y<sub>2</sub>O<sub>3</sub>-Al<sub>2</sub>TiO<sub>3</sub> refractory composites, props. 4-71626

## composite models of elementary particles

- see also composite models of hadrons  
 boson wave functions, internal structure in composite model 4-90830  
 boson-fermion duality, neutrino and photon construction from new massless boson 4-95777  
 chiral symmetry, composite models, scalar and fermion fields, large-N limit 4-106523  
 composite leptons, mag. moment CM corrections 4-102091  
 conference on higher energy physics, Austin, TX, USA (Nov. 1982) 4-67857  
 conference on particles and fields, Banff, Canada (Aug. 1981) 4-63404  
 dynamical models in QFT, negative metric ghost fields 4-95776  
 dynamical symmetry breaking through preons 4-111417  
 extended structure of quarks and leptons 4-68547  
 fermion and weak boson masses 4-90826  
 fermions, masses and anomalous mag. moments, non-renormalizable supersym. interactions 4-111421  
 flavon-chromon preon model, mechanisms 4-111423  
 flavour mixing and masses of leptons and quarks 4-63981  
 fourth-generation quarks and leptons, production, decay and detection 4-111411  
 fractionally charged particles, proton-nucleus, neutrino-nucleus collisions 4-111427  
 generation structure for quarks and leptons, rishon model, CP violation 4-63922  
 grand unification model of quarks and leptons from one of preons 4-90783  
 hard scattering processes, transverse hadronic energy emission, non-leading QCD corrections 4-102099  
 Higgs models, custodial SU(2) theory, SU(2)×U(1) and U(1) gauge interactions 4-111424  
 hypercolour instantons, fermion mass generation and supercomplementarity in preon model 4-90834  
 Kobayashi-Masakawa matrix, CP violation 4-111377  
 large magnetic moment effects at high energies and composite particle models 4-68576  
 left-right symmetric composite model, fermion mass relation and t-quark mass 4-73730  
 leptons and quarks,  $\tau$  anomalous magnetic moment limits 4-68548  
 light composite fermions, review 4-68549  
 massless composite fermion struct., large N limit of SU(N) gauge theory 4-90836  
 N=1 supersymmetric theories, Goldstone fields, global internal symmetry breakdown 4-82910  
 N-quantum approx., massless bound states normalisation problems 4-68550  
 natural composite models, systematic construction 4-95770  
 noncompact sigma model, dynamical mass generation, composite gauge bosons, supergravity theories 4-111299  
 preon composite model with three confining hypercolor groups 4-86683  
 preon composites and their interactions in SU(7)@SU(7) unified preon model, postons 4-78535  
 preon model,  $m \gg 1$  relation from SU(2) gauge theory monopole result 4-78533  
 preon theories, weak residual low-energy interactions, compositeness scale lower bound 4-106522  
 quark and lepton composite models, motivation, hopes and difficulties, review 4-68546  
 quark fragmentation, neutrino and antineutrino charged current interactions, Lund model 4-102102  
 quarks and leptons, SU(3)×SU(2)×U(1) to rishon model 4-63985  
 radius of composite quarks and leptons, lower and upper bounds 4-63984  
 SLAC PEP, Bhabha scatt., muon pair prod., supersym. scalar electrons 4-106502  
 SO(3) composite fermion model with lattice gauge theory scalars, chiral symmetry breaking 4-111426  
 SU(2)@U(1) rishon model with quadruplets 4-78534  
 SU(5)×SU(3) GUT, composite quark and lepton model 4-90835  
 sub-quark models, CERN tests (*French*) 4-90837  
 substructure effects, composite leptons, quarks and W bosons, W couplings 4-111422  
 substructure of leptons, quarks, W<sup>±</sup>, Z bosons, e<sup>±</sup>e<sup>-</sup> collider tests 4-111428  
 supermetacolour, colour singlet composite, superfields containing massless composite fermions 4-78536  
 supersymmetric composite models, 't Hooft anomaly constraints-Nambu-Goldstone mech. interplay 4-63982  
 three-fermion model for quarks and leptons with three families 4-63983  
 triplet code model of leptons and quarks, electroweak gauge theory 4-95778  
 twistor theory, dual relations 4-78538  
 (bbb) Faddeev eqns., mass calcs. of J<sup>P</sup>=3/2 systems 4-90832  
 (ccc) Faddeev eqns., mass calcs. of J<sup>P</sup>=3/2 systems 4-90832  
 d Faddeev eqns., mass calcs. of J<sup>P</sup>=3/2 systems 4-90832  
 gg→Z<sup>0</sup> $\gamma$ , composite Z-scheme cross section 4-86682  
 IN→IX, electroweak structure functions, deep inelastic scatt., quark-parton model 4-102103  
 IN→ $\nu$ X, electroweak structure functions, deep inelastic scatt., quark-parton model 4-102103  
 $\mu$  rare and normal decays, standard model, left-right symmetric theories 4-102120  
 $\Omega$  Faddeev eqns., mass calcs. of J<sup>P</sup>=3/2 systems 4-90832

# composite models of elementary particles continued

- pp-K<sup>+</sup>X, parton fragmentation model: with diffractive resonance prod. 4-111483  
pp- $\pi^+$ X, parton fragmentation model: with diffractive resonance prod. 4-111483  
pp-Z<sup>0</sup>X, test of Z<sup>0</sup> composite nature 4-86682  
W bosons,  $\rho$ -parameter in weak interactions 4-73731  
tt mass prediction in rishon model, mass formula 4-95779

# composite models of hadrons

- see also parton model; quark models  
chemical-like structures of hadrons and nuclei 4-68499

# composite particles

- see also alpha-particles; deuterons; nuclei with mass number 1 to 5; tritons  
classical many particle system, composite particle scattering 4-90758

# composite superconductors

- filamentary metals, theory of mixed state (Russian) 4-84753  
multifilamentary in situ superconductor, longitudinal field loss, twist effects 4-61496  
multifilamentary superconducting cables, coupling losses calc. 4-70983  
multifilamentary superconducting wire, energy losses by current and mag. field sweeps 4-76068  
multifilamentary superconductors, coupling current losses calc. 4-71006  
small particle composites, magnetoresist., strong mag. field behaviour 4-76071  
surface resistance influence on current-carrying characts. 4-114079  
Ag-M-Ag sandwiches, M-Pd, Cr, V, superconducting and mag. props. 4-80709  
Au-M-Au sandwiches, M-Pd, Cr, V, superconducting and mag. props. 4-80709  
Cu-Ga/V multifilamentary superconductors, brittle fracture, acoustic emission anal. 4-71715  
Cu-Nb<sub>3</sub>Sn in situ superconductors, long length, Sn electroplating and processing 4-61878  
Cu-Nb-Sn multifilamentary superconductors for superconducting magnets, powder metallurgy processing 4-80731  
Cu-Sn-Cu-Nb composite, reaction annealing, Nb<sub>3</sub>Sn layer growth conditions 4-61886  
KCl/Sn granular supercond., far IR absorption spectrum 4-76076  
Nb-Al multifilamentary superconductors for superconducting magnets, powder metallurgy processing 4-80731  
Nb-Cu composite superlattice superconductor, dimensional crossover 4-71005  
Nb-Sn supercond wires, processed, electromag. props., stress effects (Japanese) 4-84759  
Nb-Ta/Sn liquid-infiltration multifilamentary superconductors 4-98832  
Nb-Ti supercond. wires, electromag. props., stress effects (Japanese) 4-84759  
Nb-Ti superconductor, acoustic emission (Chinese) 4-92855  
Nb<sub>3</sub>Sn composite superconds., prep. and high field supercond. props. 4-92881  
Nb<sub>3</sub>Sn, growth kinetics by bronze process 4-114451  
Nb<sub>3</sub>Sn in situ composite superconducting wire of internal diffusion type, fabrication 4-61890  
Nb<sub>3</sub>Sn, multifilamentary bronze composites, diffusion reaction growth kinetics, supercond. critical temp. 4-76064  
Nb<sub>3</sub>Sn phase formation, influence of thermal regime of multifilamentary wire prep. 4-76063  
Nb<sub>3</sub>Sn-Cu, superconducting wire, welded annular region of Nb<sub>3</sub>Sn filaments 4-99363  
Nb<sub>3</sub>-Ta<sub>2</sub>Sn multifilamentary superconductor, crit. current and upper crit. field 4-98834  
NbTi composite supercond., pulsed mag. field influence on stability (Chinese) 4-76075  
NbZr multilayers, struct. and superconductivity 4-70594  
V<sub>2</sub>Ga composite superconductors, in situ, prep. by external diffusion, microstruct. and supercond. props. 4-92844  
V<sub>2</sub>Ga composite superconds., prep. and high field supercond. props. 4-92881
- composite systems** see large-scale systems
- composition measurement** see chemical analysis
- compressibility**  
see also compressibility of gases; compressibility of liquids; compressive strength  
alkali halide crystals, compression; theory 4-75604  
balanced vane pump pressure pulsation, fluidborne noise generation characts. 4-112843  
brittle solids with interacting cracks, estimate of stress intensity factors 4-74963  
calcite single cryst., elasticity at calcite I-calcite II transition 4-105549  
crack propagation under variable amplitude loading, influence of compressive loads 4-69707  
dimers, directional attractive forces, single mol. site, thermodynamic perturbation theory 4-95290  
dynamic material response to shock wave propagation 4-108531  
electron liquids, electron-hole pseudopotentials, polarisation pot. theory 4-75884  
graphite intercalation compound, KHgC<sub>8</sub>, compressibility and phonon spectra 4-80183  
halide glasses, thermal and elastic props., molecular dynamics calc. 4-109455  
hard disks, finiteness effects, Monte Carlo method assessment 4-106250  
hyperelastic bodies in large deformations, equilib. problems (French) 4-74875  
ice sheet, stress-strain state estimation by acoustic probe pulse 4-115428  
III-V covalent semicond. crystals, equation of state, bulk modulus press. derivative 4-98236  
incompressible Newtonian fluids, numerical simulation 4-91801  
isothermal third-order elastic consts., linear and vol. compressibilities 4-108499  
magnetic tape coatings, Hg porosimetry anal. 4-65839  
Mg-Mn ferrite, elastic behaviour at room temp. 4-65327  
pentaerythritol tetranitrate explosive, shock initiation sensitivity, cryst. orientation effect 4-70272  
plate, biaxially compressed rectangular flat, vibrs., geometric imperfection effects 4-97391  
poly(vinylidene fluoride), mech. and phys. props. at high press. and temp. 4-98167  
polymers, constitutive eqns. and failure conditions 4-98034

# compressibility continued

- polymers, piezoelectric, pyroelec. and ferroelec. props., conf., Honolulu, USA (July 1983) 4-95030  
pressure-generating system, MASS OB-8 mechanism 4-78341  
pTS, lattice props. as function of polymer content 4-75321  
PVC-chlororubber-20 blends, dielec., ultrasonic and X-ray diff. 4-113352  
rock bulk modulus, pore-space model 4-82106  
rubber elasticity entanglement models, uniaxial extension-compression 4-61971  
shell, cylindrical, radial compression plastic flow energy loss 4-64855  
shell, fluid-filled spherical, compression by rigid indenters 4-97441  
shock wave generation in solid laser targets 4-84345  
solids, dynamic compression, thermodynamic props. 4-70409  
steel, austenitic stainless, strain rate effect on plastic props. (Russian) 4-89094  
steel, Fe-Si (3 wt.%), grain oriented, compression effects on domain struct. 4-80774  
steel, ferrite-martensite, dual phase, Bauschinger effect, coercivity meas. (Chinese) 4-93330  
substrates, finite compressibility effects on monatomic film adsorption 4-61218  
vortex tube, temp. separation characts., estimation method 4-97573  
Al, damage simulation in high velocity impact 4-108529  
Al, dynamic heterogeneous response to stress waves 4-108540  
Al, lattice dynamics, second-order perturbation theory 4-92320  
Al, shock compressibility in range 0.4 to 4 Gbar, reflection method 4-92294  
CaAl<sub>2</sub>Si<sub>2</sub>O<sub>8</sub> glass, shock compressed, optical emission spectra 4-114305  
Co<sub>2</sub>Ni<sub>4</sub>Fe<sub>2</sub>B<sub>10</sub>Si<sub>16</sub> foil, thermal expansion coeff. and isothermal compressibility (Russian) 4-65421  
Cu, dynamic heterogeneous response to stress waves 4-108540  
Fe-based amorphous alloys, magnetoelastic props., X-ray diff. studies 4-76209  
Fe<sub>20</sub>Ni<sub>40</sub>B<sub>20</sub> foil, thermal expansion coeff. and isothermal compressibility (Russian) 4-65421  
KBr, fused, partial struts. and compressibilities of ions 4-92061  
MgO, shock compressed, optical emission spectra 4-114305  
MgO, static P-T-V meas. and shock wave data 4-108574  
NH<sub>4</sub>Br(Cl)(I), cohesion and thermodynamic props. calcs. 4-92126  
NH<sub>4</sub>Cl, critical exponents, Pippard relations, Raman spectra 4-61694  
Na<sub>2</sub>WO<sub>3</sub>, compressibilities and high-press. phase transitions 4-88276  
Na<sub>2</sub>WO<sub>3</sub>F<sub>3</sub>, ferroelastic transition and detwinning 4-80226  
 $\alpha$ -O<sub>2</sub>, solid, high press. props. 4-61066  
Sc, elastic props. under static compression up to 6 GPa (Russian) 4-108515  
Si, partial dislocations, glide forces, climb forces, geometrical study 4-113446  
UC, fast reactor fuel, critical constants, sensitivity anal. 4-68757  
UO<sub>2</sub>, fast reactor fuel, critical constants, sensitivity anal. 4-68757  
V<sub>2</sub>H, normal and deuterated, shock compression to 135 GPa 4-92295  
YFe, interionic distance effect on local fields, NMR study 4-84869
- compressibility of gases**  
see also high pressure phenomena and effects  
gas vibrations, nonlinear, in closed pipe, rel. to thermoacoustic effects 4-69853  
inert compressible gas confined between infinite parallel planar walls, response to rapid boundary heating 4-87541  
spherical mass of gas, compression optimisation 4-87837  
Na compression by laser beam, semipermeable optical piston demonstration 4-87092  
SF<sub>6</sub> compressed, breakdown voltage and timelags under corona stabilisation 4-79727
- compressibility of liquids**  
alcohol-alkane (1,2-dichloroethane) mixtures, adiabatic compressibilities and viscosities, US meas. 4-92298  
alkali metals, liquid, influence of many-body interactions 4-98204  
aqueous binary non-electrolyte mixtures, compressive and dielec. props. (Japanese) 4-99001  
benzene liq., C-C bond length, high press. compressibility study 4-65323  
benzene-d<sub>6</sub>(d<sub>6</sub>), solns. and mixtures, isotope effects, isothermal compressibility 4-84330  
binary liquid mixture, osmotic press. and models 4-114829  
butyloxy phenylphenyl oxybenzoate, ferroelastic smectic A-smectic C transition 4-80229  
butyloxyphenyl noniloxymyristate, smectic A liq. cryst., elastic, nonlinear and plastic behaviour 4-92070  
cholesteryl myristate (propionate) mixed liq. crystals, compressibility and thermal expansion anomalies 4-80227  
classical liquid struct., thermodynamically consistent theory, pair pot. extraction 4-92043  
coal liquids, vap. press. incorporating renormalisation group formulations with corresponding state principle 4-88271  
cyclohexane-d<sub>6</sub>(d<sub>6</sub>), solns. and mixtures, isotope effects, isothermal compressibility 4-84330  
cyclohexylamine-water mixture, positron annihilation, compressibility, US meas. 4-103635  
3,6-dioxaoctane-n-heptane mixtures, excess volumes and US speeds 4-98202  
dynamic loading of liquid impact struct., appl. to boundary integral methods (German) 4-113089  
glycine, aq. soln., adiabatic compressibility and US vel., temp. depend. 4-108495  
methyl ethyl ketone-n-nonane-1-alkanols, mixtures, compressibilities, US meas. 4-92297  
methylcyclohexane-toluene (cyclohexane) mixtures, thermodynamics, isothermal compressibility meas. 4-98301  
molten alloys, ultrasonic velocity, compressibility effects 4-92303  
nonionic micellar solns., phase diagrams, statistical model, osmotic compressibility, virial coeff. 4-89337  
octyloxycyanobiphenyl, smectic A liq. cryst., elastic, nonlinear and plastic behaviour 4-92070  
organic binary aq. mixts., solute-solute interactions, Kirkwood-Buff integrals 4-60973  
PEBAB, phase transition studies 4-98280  
PMBAB, phase transition studies 4-98280  
polyethylene glycol solutions, US absorpt. 4-103881  
polystyrene solutions, US studies and Rao formalism 4-103883  
polyvinyl acetate, solutions, US absorpt. 4-103881

**compressibility of liquids continued**

- propyl alcohol, thermodynamic props. at atm. press. 4-80251  
 PVC, vol. viscosity, compressibility, elastic modulus 4-70426  
 surfactant micelles in aq. soln., adiabatic compressibility 4-113516  
 1,1,2,2-tetrachloroethane-ketone mixtures, US vel. investig. 4-108549  
 thermodynamic props. calc. of fluids in mol. dynamics expts. 4-113666  
 virial eqn. conformity condition and compressibility (*Russian*) 4-70332  
 Ar. liquid, thermodynamic Gruneisen parameter, mol. compressibility and sound speed 4-60974  
 n-D<sub>2</sub> liquid and liquid mixtures, intermolecular free length, acoustic study 4-88059  
 n-H<sub>2</sub> liquid and liquid mixtures, intermolecular free length, acoustic study 4-88059  
 KOH, conc. aq. solns., heat capacities, vols., expansibilities and compressibilities 4-103954  
 Kr, compressional viscosity, US absorpt., modified hole theory 4-103884  
 Kr, dense gas, struct. factor, bridge contribs. and many-body effects 4-75263  
 LiOH, conc. aq. solns., heat capacities, vols., expansibilities and compressibilities 4-103954  
 N<sub>2</sub> fluid, equation of state near critical points, scaling props. 4-98238  
 NaBr water soln., compressibility meas. 4-84329  
 NaCl water soln., compressibility meas. 4-84329  
 NaI water soln., compressibility meas. 4-84329  
 NaOH, conc. aq. solns., heat capacities, vols., expansibilities and compressibilities 4-103954  
 Ne fluid, equation of state near critical points, scaling props. 4-98238  
 Ne, liquid and liquid mixtures, intermolecular free length, acoustic study 4-88059  
 Sn-Bi, binary liq., compressibility, conc. depend., expt. and theoretical invest. 4-70250  
 Sn-Pb, binary liq., compressibility, conc. depend., expt. and theoretical invest. 4-70250

**compressible flow**

- see also compressibility*  
 1-D transonic flow, multiple steady states 4-64973  
 adjustable fixed-flow restrictor with wide turndown ratio 4-87825  
 aerosols, radioactivity anal. using compressible flow capillary system 4-86975  
 airlift pump, bubble expansion and slip influence on performance and stability 4-60505  
 Bloch's expansion for a two-fluid medium (*French*) 4-112935  
 boundary layer on radial blade rotating at high speed 4-112929  
 boundary layers, compressible, spatial growth of disturbances 4-87752  
 columnar vortices instability 4-112908  
 computer extended series, appl. to fluid flow 4-91858  
 concentrated gas suspensions, weakly nonlinear disturbances 4-91818  
 flow around blunt bodies, press. fluctuations 4-60451  
 frozen plasma boundary-layer flows over isothermal flat plates, parametric study 4-65063  
 heat exchangers, flow reversible, temp.-entropy bond graph modelling 4-112938  
 homogeneous, isotropic turbulent flow field, mass conservation principle 4-91798  
 homogeneous isotropic two dimes. turbulence, numerical simulation (*French*) 4-64931  
 hypersonic aerodynamics at low Mach numbers 4-60450  
 infinite domain, steady flow round airfoil, numerical calc., grid size reduction by higher order far field asymptotics 4-87686  
 internal, book 4-108086  
 inviscid perfect fluids, conservation laws, higher dimensions and axisymmetric case (*French*) 4-112934  
 laminar and turbulent flow time-split finite element method 4-112932  
 laminar boundary layer flow, numerical soln. 4-87666  
 laminar boundary layers along curved walls, suction, cooling, instability 4-64912  
 low-dimensional isotropic fluid eqns., higher-order symmetries 4-63519  
 Navier-Stokes eqns., generalised forms, numerical soln. 4-108061  
 nonuniform compressible fluid, shear flow, wave theory 4-60449  
 nozzles, choking phenomena in multi-flow nozzle with or without viscosity effects (*French*) 4-97635  
 polytropic gases, compressible channel flow, normal shock wave struct. 4-64982  
 potential flow over circular cylinder in a wind tunnel 4-91787  
 rotating compressible laminar boundary layer, similar solns. and integral quantities 4-112888  
 rotating gas, viscous Ekman layer effects 4-97581  
 Stirling engine analysis using mathematical model 4-66754  
 symmetric impact of compressible fluid streams, jet form. and penetration in steady flow 4-91821  
 transient analysis of compressible and incompressible flow, implicit finite difference method 4-97690  
 transient flow, acoustic noise emission 4-97193  
 transient pressure waves in liq. transmission line, radial and axial variations 4-97693  
 transonic potential external viscous flow over airfoils, boundary layers and wakes calcs. 4-64972  
 turbulent boundary layers, defining relations derivation 4-97514  
 two-dimensional unsteady compressible flows, computational technique 4-112931  
 two-phase flow, appl. to flow metering 4-97656  
 unsteady compressible flow, shock waves and wakes, numerical prediction 4-97483  
 viscous three-dimensional flow with large secondary vel. 4-103354  
 N<sub>2</sub> superheated liqs., explosive flashing in discharge through short nozzles 4-112936  
 O<sub>2</sub> superheated liqs., explosive flashing in discharge through short nozzles 4-112936

**compression, bandwidth *see* bandwidth compression****compressive strength**

- see also compressibility*  
 acrylic plastic, strength under complex stress state 4-99543  
 Arctic offshore structures, lightweight concrete props. 4-114464  
 brick, high-alumina, corrosion resist. to nitric acid, report 4-62090  
 brittle materials, compressive surface strengthening 4-93307  
 cancellous bone strength measurements with the osteopenetrometer 4-89793  
 composite materials, biaxially stressed, inconsistency in max. strain theory of failure 4-112769  
 contact friction forces, effect in compressive tests of specimens 4-109596

**compressive strength continued**

- crack propagation under variable amplitude loading, influence of compressive loads 4-69707  
 fibre reinforced composites, mech. props. at elevated temps., model for prediction 4-81240  
 fibre reinforced materials, failure criterion, macroscopic 4-81266  
 fireclay ceramic, corrosion resist. to nitric acid, report 4-62090  
 glass, toughened, thin thermally polished, strength asymmetry 4-89103  
 glass-ionomer dental cement, prep. and compressive strength 4-99373  
 graphite, neutron irradi., relationship between strength characts. 4-66443  
 graphite, nuclear-grade, mech. and phys. props., influence of prehydrostatic loading 4-102353  
 graphite, thin layer, compression testing method 4-104939  
 graphite short bars with hemispherical seals failure mechanism 4-78694  
 HTR graphitic component corrosion in operating and accident conditions 4-96163  
 impact-tension compression test using split-Hopkinson bar 4-87639  
 large force plate characts., comprehensive force test, design problems (*Japanese*) 4-91746  
 porcelain, electrotechnical, axial compressive strength, effect of specimen dimensions 4-61944  
 protective surface film, continuous, criterion for compressive failure 4-99612  
 red shale, ceramic, corrosion resist. to nitric acid, report 4-62090  
 SPAULRAD-S laminate for fusion reactor appls., irradiation and mech. props. 4-111768  
 steel, austenitic stainless, claddings, ring test of tubes oxidised in high temp. steam 4-104816  
 strain determ. in dynamic compression test 4-112780  
 thermoplastics testing using computerised machine 4-104934  
 Al, dynamic heterogeneous response to stress waves 4-108540  
 Al-Cu (10 wt.%), prod. by rheocasting, rel. between struct. and mech. props. 4-99467  
 Al-glass composite, produced by powder metallurgy route, mech. props. 4-66275  
 B<sub>2</sub>C, struct. and mech. props., hot pressing conditions effect 4-61906  
 Be, neutron irradi. at various temps., compression props. and swelling 4-108458  
 C ceramic, corrosion resist. to nitric acid, report 4-62090  
 C fibre reinforced plastics, unidirectional ultimate strength, influence of matrix resin 4-99455  
 C material, dimensional changes, under compressive stress at high temp. 4-85182  
 Cu, dynamic heterogeneous response to stress waves 4-108540  
 Ni superalloy Mar-M 200 powder, shock induced compaction, mech. props. 4-109430  
 SiC ceramic, corrosion resist. to nitric acid, report 4-62090  
 $\beta$ -SiC powders, sintering, hot pressing, densification and mech. props. rel. to prep. 4-109366  
 SiO<sub>2</sub> ceramic, corrosion resist. to nitric acid, report 4-62090  
 SiO<sub>2</sub>, hydrothermal hot pressing, aggregate form., shrinkage 4-109370  
 WC-Co, cemented elements of high press. apparatus, strength safety factors 4-109482
- compressors**  
 metal hydride/hydrogen compressor, four-stage, design, fabrication and testing 4-66818  
 photovoltaic solar panel optimal coupling to compression cold room with ZnSO<sub>4</sub> energy storage 4-63749  
 refrigeration compressor development for domestic heat pump appl. 4-89461
- Compton effect**  
 V1343 Aquilae (SS 433), inverse Compton scatt. rel. to extended X-ray emission 4-72948  
 classical theory and quantum rules, interaction of EM waves with charged particles 4-67941  
 deep inelastic Compton scatt., QCD corrections, single photon spectrum, photon-hadron correlations 4-111461  
 excited state hadron Compton scatt. amplitudes 4-86715  
 free electron laser amplifier performance in Compton regime 4-87338  
 gamma ray ang. flux, appl. of P<sub>0</sub>-method 4-86373  
 graphite, electron momentum distrib., Compton profile 4-109268  
 graphite intercalated with Li, electron momentum distrib., Compton profile 4-109268  
 graphite-Li intercalation cpd. LiC<sub>6</sub>, Compton profile, X-ray scatt. meas. 4-61765  
 Heisenberg's microscope and Compton scatt. 4-67919  
 inhomogeneous media, scatt. of collimated  $\gamma$  radiation 4-99708  
 inverse Compton interaction, cosmic-ray electrons with interstellar photons 4-101088  
 inverse Compton scattering in high freq. region, coherent effects 4-96764  
 isotropic electrons, Compton scatt. 4-78556  
 laser, non-collinear Compton, effects of saturation and inhomogeneous broadening 4-60052  
 methane, electron and X-ray scatt., incoherent scatt. factors, Waller-Hartree calcs. 4-112271  
 NGC 4151, Seyfert galaxy, synchrotron self-Compton model for HEAO 1 obs. 4-86038  
 nonrelativistic Compton scatt. in Furry's picture, sudden impulse approx. 4-83426  
 optically thick plasma X-ray emission, Comptonisation contrib. 4-101153  
 photon cross-section processor for relativistic electrons using MAXWEL program 4-102123  
 Radon transform and appls., book contrib. 4-106172  
 semiconductors, tetrahedrally-bonded, anisotropies of Compton profiles 4-99217  
 single-photon emission CT, subtraction of Compton-scatt. photons 4-72387  
 solid state Compton profiles by inelastic ion-electron scattering 4-81071  
 solids, electron Compton scatt. 4-71463  
 supernovae, Type II, Comptonisation and UV emission lines in stellar envelope 4-72961  
 transition metals, Compton scatt., exchange-correlation energy functional, gradient expansion 4-98552  
 ( $\gamma,\gamma$ ), intermediate energy, Compton scatt.,  $\Delta$ -hole approach, dynamical model 4-86668  
 $\gamma e^- \rightarrow \gamma e^-$ , cross-sections from QED on lattice 4-90849  
 $\pi^+ N \rightarrow \pi^+ \gamma N$ , Primakoff formalism veracity evidence 4-86727  
 Ar, self interaction corrected Compton profiles 4-96495  
 As, amorphous and polycryst., Compton profile studies 4-99218  
 Cd, Compton scatt. differential cross sections 4-112146

**Compton effect continued**

- Cu Compton scatt. differential cross sections 4-112146
- Cu, total Compton profile, nonlocal exchange-correlation effects 4-81032
- Fe, mag. Compton profile meas. using circularly polarised  $\gamma$ -rays from oriented  $^{191}\text{Ir}$  nuclei 4-71462
- $\text{H}_2$ , spherically averaged molecular-electron momentum density, Compton profile 4-83489
- $\text{H}_2^+$  momentum distrib., nodal struct. 4-78766
- $\text{H}_2\text{O}$ , electron and X-ray scatt., incoherent scatt. factors, Waller-Hartree calcs. 4-112271
- $\text{Li}_3\text{N}$ , electronic struct., Hartree-Fock studies 4-98522
- $\text{Li}_2$ , spherically averaged molecular-electron momentum density, Compton profile 4-83489
- $\text{NH}_3$ , electron and X-ray scatt., incoherent scatt. factors, Waller-Hartree calcs. 4-112271
- Ne, self interaction corrected Compton profiles 4-96495
- Ni, spin-polarised Compton profile, relativistic corrections to classical Hamiltonian 4-71464
- Pb, Compton scatt. differential cross sections 4-112146
- Pt, Compton scatt. differential cross sections 4-112146
- Sn, Compton scatt. differential cross sections 4-112146
- U, Compton scatt. differential cross sections 4-112146
- V-Si, electron momentum distrib. and charge transfer,  $\gamma$ -ray Compton scatt. study 4-70059
- W, Compton scatt. differential cross sections 4-112146
- Zn, Compton scatt. differential cross sections 4-112146

**Compton profile** *see* **Compton effect****Compton scattering** *see* **Compton effect****computation** *see* **calculation****computational complexity**

- boundary function approximation, Lagrangian, spline and weighted finite difference methods 4-64848
- boundary integral eqn. axisymmetric stress analysis, interior point solns. 4-63510

**computational linguistics**

- gap parsing in speech 4-69634
- phonological processor for Italian 4-69633

**computer-aided analysis**

- see also analogue simulation; CAD; circuit analysis computing; digital simulation; hybrid simulation*
- 2-D magnetostatic program TRIM converted into RIPS, accuracy of computation (*Japanese*) 4-64648
- 3D fracture mechanics, boundary integral equation-boundary element method appls. (*Chinese*) 4-97398
- absorption heat pumps, STASAN program for computerised simulation (*German*) 4-114920
- acoustic arrays, computer analysis using STARPAC package 4-107965
- ambulatory long-term blood press., recording and computerised anal. (*Finnish*) 4-89798
- antireflection coatings, two-film, stable optical props., CAD method (*Russian*) 4-109261
- automatic light intensity regulation in photometric methods of bloodflow and oxygen saturation monitoring in peripheral blood vessels (*German*) 4-89683
- cell material texture anal. using UV microscopy (*German*) 4-72457
- electron diffraction pattern, automatic computer anal. 4-60792
- external PIXE milliprobe at Davis cyclotron, laser alignment, calibration and quality assurance 4-105076
- Fresnel lenses, design for low concentration photovoltaic conversion (*French*) 4-105107
- infrared spectra of organic compounds, automated structure analysis 4-91258
- laboratory, EMI investigation 4-106165
- pictures taken by electron microscopes (*German*) 4-63823
- plastically deformed cryst. at low temp., thermal effects, response to strain rate changes, computer calcs. 4-98179
- prostate gland volume, computer assisted estimate from transrectal ultrasonic tomograms (*German*) 4-67055
- radiobiology publications growth, computer analysis (*Russian*) 4-109884
- Ringom-Stirling engine, free displacer dynamics determ. 4-66771
- single-mode lightguides fabrication systematic approach 4-107895
- sound emission analysis using MPS 4944 microprocessor system (*German*) 4-79377
- sound reinforcement system, computer model and ray-tracing, speech transmission index prediction 4-79409
- Stirling analysis code validation using free-piston engine base line data 4-77141
- thyroid gland section, automatic evaluation of ultrasonic pictures (*German*) 4-67054
- visual recognition performance, computer simulation 4-81684
- X-ray cineangiograms, left ventricular, computer-aided anal. (*Japanese*) 4-67118
- Si induced-inversion layer MOS solar cells 4-77102

**computer-aided circuit analysis** *see* **circuit analysis computing****computer-aided circuit design** *see* **circuit CAD****computer-aided design** *see* **CAD****computer-aided instruction***see also* **education**

- Apple II microcomputer, laboratory instrument for physics teaching 4-95113
- BBC microcomputer, analogue port, laboratory measuring and monitoring appls. 4-63460
- circuit breakers, microcomputer storage oscilloscope investig. of action 4-90338
- $F=M/A$ , Newton's law, computer simulation expt. 4-73199
- geometry and S-bends, teaching using computers 4-101607
- learning key concepts in physics and mathematics through computer graphic simulation, preliminary results 4-73203
- physics education, interactive graphics package, appl. to collision phenomena 4-86149
- physics problem assignments using BASIC and word processor computer programs 4-63438
- radiation, education programmes, computer controlled slide and activities-oriented presentation 4-78086
- reactor operator diagnostic ability, training using knowledge based CAI 4-106883
- student attitudes and scientific curiosity improvement by computer studies 4-110824
- velocity measurement of humans by computers 4-73196

**computer architecture**

- control systems, memory intensive functional architecture 4-59600
- molecular physics, computers and computation 4-59612
- weather forecasting, numerical prediction model implementation on Cray-1 supercomputer, computational aspects 4-62912

**computer-generated holography**

- aspheric surface testing with interference type, computer-generated holograms (*Chinese*) 4-87427
- binary Fourier transform holograms, quantisation and phase encoding errors reduction 4-107557
- binary holograms, generated using halftone screen method 4-96842
- coherent Doppler tomography expts. simulation 4-107573
- continuous tone holograms by halftoning 4-107562
- digital hologram recording, using an electron beam exposure system 4-107561
- Fourier hologram efficiency and versatility 4-107556
- Fourier holograms, colour study 4-96846
- geometric transformations appl. 4-107567
- hybrid time and space integration method 4-107565
- image encoding by a computer generated holographic filter 4-107569
- image formation using high efficiency multifacet holographic optical elements 4-107570
- image processing through computer made hologram, appls. 4-107536
- interpolation approach 4-107558
- laser scanner for 2D graphics 4-69332
- Lissajous coding for computer generated and longwave holography 4-107559
- microwave kinoform for magnetic fusion 4-107571
- multiplex holograms made of computer processed images, medical appls. 4-74452
- nonlinear photolayer props. effect in holography, Spektr set of programs for computer calc. 4-69340
- one-dimensional computer generated hologram using a line printer 4-102906
- optical correlator using computer generated holograms, micromech. quality control appls. 4-107572
- optical data processor using computer generated holograms, high energy physics expt. appls. 4-107535
- optical logic system space-variant interconnection appls. 4-107568
- optical pattern recognition, use of E-beam written computer generated holography 4-107533
- performance and appls., conf., San Diego, CA, USA (Aug. 1983) 4-106105
- polarisation holography 4-107564
- polygonal scanner using flat-field linearised scans with reflection dichromated gelatin holographic grating 4-91418
- rainbow hologram synthetic generation 4-96839
- real time holography, cellular array processor approach 4-107560
- review, digressions, applications, limitations 4-107555
- synthetic digital-phase gratings—design, features, applications 4-107563
- tandem component with optimum light efficiency, combination of lens and phase filters 4-79077
- Wigner distribution function and optical geometrical transformation 4-79028

**computer graphic equipment***see also* **interactive terminals; plotters; remote consoles**

- 3-D graphic display devices for X-ray crystal structural analysis reproduction 4-97943
- colour data projector, using single lens 4-102997
- colour display and analysis system for hydrographic surveying 4-67452
- mEDS online graphics system 4-67500
- slide production from computer graphics (*German*) 4-101954

**computer graphics***see also* **curve fitting; interactive systems**

- 3-D graphic display devices for X-ray crystal structural analysis reproduction 4-97943
- aquifer layers, subterranean, data processing and representation (*Italian*) 4-82099
- Broken Hill Field geology, mining and metallurgy, conference, Broken Hill, NSW, Australia (July, 1983) 4-58562
- chemistry, interactive graphics 4-95109
- crystals, electron density, electrostatic field characts., machine graphics methods 4-84123
- learning key concepts in physics and mathematics through computer graphic simulation, preliminary results 4-73203
- longhole open stopes stability assessment using computer models 4-62806
- magnetic field analysis, computer graphics using finite element method 4-59956
- mine geology, design and survey applications 4-62815
- modular laser graphics projection system, animated laser show appls. 4-111165
- molecules, electron density, electrostatic field characts., machine graphics methods 4-84123
- near IR scan data, regression anal., best-pair wavelengths selection, colour graphics 4-95534
- nuclear power plant computer-aided design and draughting benefits 4-59311
- optics in entertainment, conf., Los Angeles, CA, USA (Jan. 1984) 4-110802
- photogrammetry, digitization of aerial stereo photos using interactive computer graphics system 4-62659
- seismic data sets, faulted, automatic contouring 4-100735
- serial section graphical reconstruction, GRIDSS programs 4-73504
- terrain perspectives, exaggerated vertical scale 4-81703
- three-dimensional flow visualisation, computer graphics techniques 4-103450

**computer interfaces***see also* **CAMAC**

- A/D converter—D3-28 microcomputer interface 4-106288
- A/D converter and data input ccts. for 15VSM5 minicomputer and Elektronika D3-28 4-90569
- adapter for attaching laser meas. system to computer 4-58835
- Apple II microcomputer interface for Mossbauer spectroscopy 4-63726
- BBC microcomputer, analogue port, laboratory measuring and monitoring appls. 4-63460
- controller for automatic data acquisition on magnetic tape using an ES-9002 recorder 4-86391
- D/A converter interface to Apple II computer, 16-bit, low-noise design 4-78300

**computer interfaces continued**

- EPR spectrometer automation, interfaces for JRA-5 and SM-3 computers 4-90622
- FASTBUS, ADC for pulse height data from EM calorimeter 4-59604
- FASTBUS, data acquisition system for 256 wire MWPC 4-59603
- FASTBUS and data acquisition for MARK II detector 4-59605
- FASTBUS based data acquisition system for imaging coronary arteries 4-62570
- general purpose photon-counting minicomputer interface 4-101897
- IEEE-488 bus for data acquisition in undergraduate expts. 4-58609
- multichannel A/D interface for ion beam phase volume meas., using Elektronika-1001 computer 4-91130
- oceanographic data rationalising system using IEEE 488 standard interface 4-115580
- Paks Nuclear Power Plant, air activity measurement computerised system, using basic (Hungarian) 4-96289
- pulse counting interface for scanning Auger microscopy 4-78432
- X-ray diffractometer interfacing to SM-3 computer system 4-106289
- Z80-based microcomputer, interface for adding signal averaging facility 4-58837

**computer internal arrangement** *see computer architecture***computer languages** *see programming languages***computer networks**

- see also distributed processing*
- Canadian Marine Environmental Data Service, achievements of first decade 4-115578
- magnetic fusion energy research, centralized supercomputer support, computer codes 4-59415
- optical fibres in the industrial and commercial environment, review 4-79292
- GaAIs BH 100 Mbit/s laser diode terminal with optical gain for fibre-optic LANs 4-112586

**computer operator training** *see training***computer printers** *see printers***computer programming** *see programming***computer programs, complete** *see complete computer programs***computer programs (listings)** *see complete computer programs***computer science education**

- BASIC programming, learning, course evaluation 4-101603
- FORTTRAN programming and computer simulation teaching by diffusion in percolative lattice 4-78076

**computer software**

- not used for applications software for which see specific applications*
- see also programming; software engineering*
- No entries

**computer subroutines** *see subroutines***computerised communications control** *see communications computer control***computerised control**

- see also command and control systems; communications computer control; computerised materials handling; electrical engineering computing; mechanical engineering computing; nuclear engineering computing; power system computer control*
- AC high-stability microprocessor-based temperature controller for use at high temperatures 4-11119
- advances in instrumentation, conf. Houston, Texas, USA (Oct. 1983) 4-106121
- channelling expts., automatic measurement using microprocessor (Chinese) 4-84325
- clinical hyperthermia unit utilising an array of seven focused ultrasonic transducers 4-100089
- conference on fusion engineering, Philadelphia, PA, USA (Dec. 1983) 4-110807
- conference on nuclear track registration, Richland, WA, USA (Jul. 1982) 4-67851
- digital heterodyne interferometer for analysis and control of adaptive optics 4-111194
- EBT-P control/interlock/display system using commercially available equipment 4-111848
- electron microprobe control program, software system design 4-68327
- exercise conditioning system for paralysed leg muscle 4-100349
- functional elec. stimulation system, portable 4-100357
- functional elec. stimulator for paraplegic patient 4-100358
- JT-60, communications in control systems, D-port 4-111846
- KEK NODAL users guide for TRISTAN accelerator (Japanese) 4-102565
- leg exerciser for training of paralysed muscle by closed-loop control 4-85575
- linear accelerator system, microcomputer controlled, space flight induced vestibular changes appl. 4-89867
- liquid sample preparation, automated systems 4-63728
- manipulator/display system, computer-controlled, for human movement studies 4-85588
- metals, strain controlled creep-fatigue tests 4-89209
- microcomputer-controlled furnace for obtaining dynamic thermogravimetric measurements 4-111137
- microcomputer-controlled scanning of a laser beam at constant speed 4-64717
- microprobes, automation, software system designed, control program 4-68326
- microprocessor laboratory in a physics department 4-78075
- microprocessor-aided remoulding of field emitters 4-111250
- optical discs systems and applications, conf., Arlington, VA, USA (June 1983) 4-90287
- optoelectronic correlator based on modified Michelson interferometer with computer control (Russian) 4-107527
- paralysed limbs, elec. stimulation under feedback computer control 4-93958
- prosthetic arm control by EMG pattern recognition 4-77427
- scan radiometer operation controlled by single board microcomputer (Chinese) 4-106384
- Small Angle Scattering Spectrometer, SAMPLE control program suite 4-64271
- solid state track recorders, automatic scanning by computer controlled microscope 4-68881
- solid state track recorders, automatic scanning by computer controlled microscope, calibration 4-68882
- solid state track recorders, track counting, automated scanning electron microscopy 4-68883

**computerised control continued**

- surface testing with shearing interferometer using computer controlled interference phase measuring technique 4-112592
- TMX-Upgrade, computer control of Ti getter system 4-111845
- TMX-Upgrade, systems control, small computer appl. 4-111840
- Tritium Systems Test Assembly, control logic specification, structured flowcharts 4-111851
- vacuum measurement, and control, Joint European Torus project 4-86970
- vehicular technology conf., Pittsburgh, PA, USA (May 1984) 4-106118
- H maser frequency standards, NR series microprocessor monitor and control system 4-68202

**computerised instrumentation**

- see also astronomy computing; astrophysics computing; automatic test equipment; biology computing; chemistry computing; computerised monitoring; computerised spectroscopy; computerised tomography; electronics engineering computing; electronic engineering computing; geophysics computing; nuclear engineering computing; physics computing*
- aberration polynomials for computer anal. of interferograms 4-97148
- absolute spectroradiometer, fully automatic 4-95528
- adapter for attaching laser meas. system to computer 4-58835
- analog video signal processor for an automatic nuclear photoemulsion scanning system 4-107261
- analytical electron microscope for elemental imaging 4-101987
- angular windowing system for rotating equipment tests 4-86392
- animal circadian activity plotting, microprocessor-based device, IR beam breaking 4-89865
- anomaly search using plastic track detectors and automatic measuring technique 4-96051
- area meas. using microcomputer based system 4-82781
- arrhythms monitoring on electrocardiogram, digital cardiomonitor appl. 4-72447
- aspherical surface testing with shearing interferometer using fringe scanning detection method 4-107909
- automated data handling and instrument control using low-cost desktop computers and an IEEE 488 compatible version of the ODETA V 4-97149
- automated scanning systems for SSNTD and emulsions, current states 4-96347
- automatic balance beam rest position determining microcomputer system (Slovak) 4-86383
- automatic developing machine for large photographic plates (Japanese) 4-90682
- automatic light intensity regulation in photometric methods of bloodflow and oxygen saturation monitoring in peripheral blood vessels (German) 4-89683
- automatic track analysis for large area plastic nuclear track detectors 4-96362
- automatic track counting for LR-115 detectors 4-96350
- binaural measurement system, microcomputer-based 4-100407
- biomechanics laboratory, automated, appl. to rehabilitation 4-81806
- breathing pattern and occlusion press., system for microcomputer-assisted on-line meas. 4-89857
- BWR, traversing incore probe automatic scanning operation system 4-59376
- CA8015 plastic detectors, pseudocolour techniques for nuclear track differentiation 4-96360
- calibration of a three-element hot-wire anemometer, digital system 4-69842
- cardiac electrophysiological studies, software control of sensing and stimulation 4-85538
- chromatographic analyser, highspeed 4-105043
- chromatography, online control charts 4-105042
- colour characteristics meas. laboratory instruments 4-63770
- colour digital oscilloscope, Digiscope 8612, microprocessor-controlled instrument (Italian) 4-106298
- colour graphic US imaging device, DRUID 4-69637
- combined X-ray/beta sensor, nuclear gauging technology appl. 4-82790
- Commodore Pet, appl. school physics lab. 4-78074
- complex FFT processor for image synthesis in radio astronomy (Japanese) 4-94639
- conference on solid state nuclear track detectors, Acapulco, Mexico (Sept. 1983) 4-95027
- continuous flow anal. system, microcomputer-controlled, matching colorimeter output to A/D converter 4-97717
- cosmic ray automatic data collection system 4-72891
- CR-39 detector, heavy nuclei tracks, automatic meas. system 4-96363
- CR-39 proton and alpha etch pits, automated assessment techniques 4-96354
- CR-39 SSNTD, scanning by a sampling method, automated country 4-96357
- CR-39 track detector, automatic PEPR device for counting  $\alpha$ -tracks 4-96349
- CRO, digital storage type, Matsushita model VP-5730A (Italian) 4-106299
- dead-time correction method, short-lived radioisotopes, gamma-ray spectrometry 4-102543
- deep-sea sediment shear strength meas. vane system 4-115635
- dielectric loss measurement, frequency response analyser system, minicomputer-controlled, errors and calibration technique 4-111559
- dielectric response meas., computer controlled method for low-freq. meas. 4-95467
- digital heterodyne interferometer for analysis and control of adaptive optics 4-111194
- digital image processing for diameter distribution evaluation of nuclear tracks 4-96356
- digital low-noise DC power supply for tunnelling spectrometers 4-95469
- digital phase measurement interferometry using CCD image acquisition 4-106374
- digital Talbot interferometer for lateral aberration meas. 4-87409
- DIGITRACK, CCD based system for automatic nuclear track counting and eval. 4-96358
- direct current comparator resistance bridge automation, alloy resistivity appl. 4-90613
- Doppler current profiler, theory and performance 4-72758
- DZT 90X120 digital plotting table 4-94257
- electro-optical instrument, sensitivity improvement techniques for electric field strength measurement (Japanese) 4-78298
- electrocardiograph functional testing, microprocessor-controlled signal generator 4-115252

**computerised instrumentation continued**

- electron analytical Superprobe JXA-733, application program 4-85344
- electron guns and detectors, for analytical instruments 4-111999
- electron microprobe control program, software system design 4-68327
- electron microscope, computer interfaced, control, image processing and struct. anal. 4-106430
- electronic thermometer with single-chip microprocessor (*German*) 4-90586
- EMG, single-fibre, meas. unit based on a personal computer 4-77412
- EMG/foot force anal., real time microprocessor system 4-85549
- eyes, microwave radiation hazard, metal-framed spectacles effect 4-109877
- FASTBUS and data acquisition for MARK II detector 4-59605
- ferroelectric switching current meas., microprocessor controlled data acquisition system 4-76369
- ferroelectrics, hysteresis curve tracer using a single-board microcomputer 4-95461
- FIDES automated U-enrichment meter for nuclear safeguards inspection 4-106992
- fluid mechanics research, data acquisition system, minicomputer-based 4-69845
- fluorometer, fibre optic, absorption corrected, microcomputer controlled, appls. 4-78376
- haemodialysis unit, microprocessor-controlled, for terminal renal patients 4-93963
- Hall effect meas. in specimens of any shape 4-101873
- heart rate-pressure prod. computer, microprocessor based 4-81808
- high polymer materials, VLF dielectric meas. using microcomputer-controlled system 4-111158
- holographic interferometry system, microprocessor control/data acquisition, real-time signal processing, NDT appl. 4-73501
- hybrid experiments with short-lived particles, emulsion techniques, automation 4-96341
- IMACC-8001 signal analysis system (*Spanish*) 4-73427
- interfacing 15VSM5 minicomputer and Elektronika D3-28 to expt. equipment, using TTL ICs 4-90569
- laser beam polarisation meas. apparatus using TP801 microcomputer (*Chinese*) 4-91514
- leg exerciser for training of paralysed muscle by closed-loop control 4-85575
- lifting stress calculator, microprocessor-based device 4-100408
- linear accelerator system, microcomputer controlled, space flight induced vestibular changes appl. 4-89867
- liquid sample preparation, automated systems 4-63728
- logarithmic charge-digital converters for operation with proportional chambers 4-68910
- low-dispersion liquid chromatography, HP 1090 4-72004
- magnetic props. meas. of Permalloy ring cores, using microcomputer 4-58879
- magnetometer, microcomputer-controlled rotating-sample, appl. to meas. of remanent magnetism and coercive force of dust samples 4-86447
- magnetometer for palaeomagnetic and rock magnetism studies, superconducting instrument 4-90006
- magnetostriction measurement of crystalline specimens, using 13 T superconducting solenoid, microcomputer-controlled system 4-58876
- manipulator/display system, computer-controlled, for human movement studies 4-85588
- MFTF-B plasma diagnostics, data acquisition and control system 4-111838
- microcomputer controlled decoupler for NMR spectroscopy 4-90620
- microcomputer photoacoustic data-acquisition system for multiphoton absorption 4-111112
- microcomputer-controlled microwave hyperthermia system 4-67059
- microphotometer, automated, for photoplate reading for spark-source mass spectrosc. 4-63771
- microprobes, automation, software system designed, control program 4-68326
- microprocessor-based thin film thickness meas. system 4-95388
- microprocessor based compact economical gas chromatograph, design and performance 4-105044
- microprocessor based nuclear track measuring system 4-96361
- microprocessor-based multipoint data recorders (*French*) 4-63736
- minority carrier lifetime automatic measurement in 0.5  $\mu$ s to 5  $\mu$ s range with SEM 4-82865
- modular system use for microtopographical surface meas. 4-111104
- modules for controlling expt. on-line hardware with ES computer 4-58836
- MOS capacitors, charge variation rel. to voltage step, generation lifetime meas. 4-65755
- multichannel A/D interface for ion beam phase volume meas., using Elektronika-1001 computer 4-91130
- multichannel automated system for mag. field nonuniformity index meas. of synchrotron 4-59460
- multichannel solid-state recorder, design and appl. to temp. meas. 4-115251
- narrowband dye laser with a large scan range 4-91489
- natural gas anal., high speed automated, using microcomputer controlled high resoln. gas chromatography 4-99928
- NODAPEC, online system for low temp. nuclear orientation expts. 4-102563
- nuclear commercial, appl. of advanced instrumentation and control technology 4-102373
- nuclear power station control and instrumentation, future trends review 4-111654
- nuclear reaction commercial instrumentation, research and development projects at EPRI 4-102374
- nuclear reactor active zone temp. field meas. (*Slovak*) 4-83221
- nuclear track profile determination by direct digital processing of SEM images 4-96359
- nuclear track pseudocoloring by illumination wavefront angle variation on CR-39 detectors 4-96353
- ophthalmologic department instrumentation of municipal polyclinic, automated control system prerequisites 4-93953
- optical fluid distribution measurement system, application in nuclear reactor loss-of-coolant experiment 4-106315
- opto-electronic system for automatic track counting for plastic SSNTD 4-96351
- Paks Nuclear Power Plant, air activity measurement computerised system, using basic (*Hungarian*) 4-96289
- particulate material, automated electron microprobe anal. 4-81500

**computerised instrumentation continued**

- personal computer based signal compression method for sound field meas. in pipes (*Japanese*) 4-97209
- photoelectric photometers, computer controlled, three statistical tests 4-94630
- photoluminescence intensities, computer-controlled mapping 4-104650
- programmable data-acquisition and stepping motor control system 4-97968
- prosthetic heart valves, instrum. for sound anal. 4-85582
- pulse counting interface for scanning Auger microscopy 4-78432
- pulse-counting system, microcomputer-based, construction 4-112076
- pyrometer, alternating light for temps. below 600K, microcomputer appls. (*German*) 4-95427
- quartz crystals vibration amplitudes meas., using speckle effect 4-70542
- quartz doubly rotated crystals, angle of cut meas. using automated X-ray orientation system 4-58814
- radiometer development fully automated 4-111182
- real-time six-port reflectometer 4-78343
- recorders, modular instruments, design developments and microprocessor control (*German*) 4-106303
- relativistic heavy ion streamer chamber expts., data acquisition of high multiplicity events 4-74101
- respiratory parameter anal., microprocessor assisted research tool (*German*) 4-77422
- reverberation characts. improvement of enclosed space, with aid of computer (*Slovak*) 4-60213
- rheogoniometer, Weissenberg model R17, modification and computerisation 4-114745
- sampling of events in research experiments on mu-atomic and mesomolecular processes 4-74123
- satellite borne charge-composition instrumentation, data processing unit 4-112077
- scan radiometer operation controlled by single board microcomputer (*Chinese*) 4-106384
- scintillation detectors data acquisition and processing, auxiliary controller ccts. design 4-90570
- seawater, quantitative anal. of low organic pollutant levels by automated Raman scatt. 4-105166
- selective image analyser for use in particle metrology employing TV monitor and computer equipment (*German*) 4-101985
- SEM-microcomputer system for quantitative morphological analysis, single object case 4-111251
- SEM-microcomputer system for quantitative morphological analysis, complex images case 4-111252
- sensory and motor function, computerised system for clinical assessment 4-81805
- servo ventilator, microcomputer-controlled 4-85574
- Shimadzu automated multigamma counter RAW-1600 for radioimmunoassay in clinical chem. laboratories (*Japanese*) 4-59578
- Shimadzu data processing system RAD-1100A for radioimmunoassay in clinical chem. laboratories (*Japanese*) 4-59578
- Shimadzu multichannel selective stat analyser CL-12, interference factor anal. for precision of quantitative clinical anal. (*Japanese*) 4-62620
- shuttle infrared telescope facility, secondary mirror, microprocessor based position control system 4-85873
- skin conductance response analysis, microcomputer package 4-62635
- Small Angle Scattering Spectrometer, SAMPLE control program suite 4-64271
- sonar side-scan device for mapping sea-floor topography 4-72737
- sound emission analysis using MPS 4944 microprocessor system (*German*) 4-79377
- spherical EM ocean current meter 4-115625
- SSNTD semiautomatic track counting, use of commercial bacterial colony counter 4-96352
- standards maintenance, personal computer appl. (*Japanese*) 4-106260
- STEM, computer-controlled analytical microscopy 4-82868
- surface cleaning and sample addition for surface balances automation 4-63853
- TECRON TEF System 10 acoustic analyser, appl. 4-97221
- temperature biotelemetry, Apple II programs 4-62636
- temperature measurement, microcomputer-based system using SAB 80215 device and Si sensor (*Italian*) 4-86418
- thermophysics, exptl. data processing, hardware and software struct. 4-95420
- thermopower and electrical conductivity of liquid semiconductors meas. 4-68241
- three dimensional spatial coordinate measurement from survey data 4-78292
- time domain transmission test apparatus, computer-controlled, for SAW filters testing 4-103175
- time-domain EM induction system 4-86442
- TMX-Upgrade, X-ray detection system development, hardware and software 4-111839
- tomoflow system for intracardiac blood flow information display, Doppler US appl. 4-85469
- transmission electron microscopy, time shared television digital image processing system 4-106431
- underwater modular acoustic measurement electronics system 4-112625
- universal programmable deep ocean transceiver 4-115623
- US diagnostic systems, automated, for outpatients clinics 4-93825
- US-1000 computer controlled US test system, reactor component appl. 4-109621
- VATPOL, microcomputer-controlled photoelectric polarimeter 4-105884
- volume transformer for flowmeters with frequency-analogue output signal (*German*) 4-69840
- weather station using BBC microcomputer for online data acquisition 4-110256
- X-ray diffractometer interfacing to SM-3 computer system 4-106289
- X-ray microanalysis using computer controlled electron microprobe 4-72013
- CO CW laser two-mode multiline stabilisation using Fabry-Perot filter under analog and digital computer control 4-60092
- Ni-Cd cell residual charge meas. using microprocessor-based unit 4-81535

**computerised materials handling**

- liquid chromatograph injection and sampling automation 4-72005

**computerised monitoring**

- arrhythms monitoring on electrocardiogram, digital cardiometer appl. 4-72447

**computerised monitoring continued**

- CCTV solid state storage system for nuclear material safeguards 4-106976
- channelling expts., automatic measurement using microprocessor (*Chinese*) 4-84325
- computerised radiation data acquisition and management system at Seabrook nuclear power station, USA 4-78739
- computers for heart, electronics in intensive care 4-109986
- distributed system for the monitoring of critically ill patients 4-67146
- knee capsule deform., microprocessor-based tissue displacement monitor 4-89864
- minewide 2000-channel data acquisition system 4-62956
- multichannel spectrometer for process monitoring and control (*German*) 4-82836
- nuclear safeguards, automatic identification in containment and surveillance 4-106972
- polyether polyol monitoring using on-line near IR process photometers 4-99930
- respiration, noninvasive monitoring by microcomputer 4-89801
- sequential probability ratio controllers for nuclear safeguards radiation monitors 4-111694
- stratified flow channel with microcomputer monitoring and control 4-103448
- transcutaneous monitoring, computerised, incorporating laser Doppler velocimetry 4-81797

**computerised navigation**

- Kingfisher charts of sea-bed, around British Isles, electronic chart display 4-72736

**computerised numerical control**

- diamond machining developments for small optical workshops 4-83727
- diamond tool flycutter, computer controlled 4-107900
- large optics diamond turning machine, motion control system 4-107905
- optical machine tool precision air temp. control techniques 4-107906
- optical machine tool precision computerised numerical control evolution 4-107907
- optical manufacturing and testing, conf., San Diego, CA, USA (Aug. 1983) 4-106104

**computerised pattern recognition**

- 3-D digital images, noise reduction techniques 4-107544
- analog video signal processor for an automatic nuclear photoemulsion scanning system 4-107261
- automated scanning systems for SSNTD and emulsions, current states 4-96347
- automatic track analysis for large area plastic nuclear track detectors 4-96362
- automatic track counting for LR-115 detectors 4-96350
- CA8015 plastic detectors, pseudocolour techniques for nuclear track differentiation 4-96360
- cell material texture anal. using UV microscopy (*German*) 4-72457
- cellulose nitrate track detectors,  $\alpha$ -track anal. using Interactive Image Analysis System 4-96348
- CR-39 detector, heavy nuclei tracks, automatic meas. system 4-96363
- CR-39 proton and alpha etch pits, automated assessment techniques 4-96354
- CR-39 SSNTD, scanning by a sampling method, automated country 4-96357
- CR-39 track detector, automatic PEPR device for counting  $\alpha$ -tracks 4-96349
- digital image processing for diameter distribution evaluation of nuclear tracks 4-96356
- DIGITRACK, CCD based system for automatic nuclear track counting and eval. 4-96358
- discrete binary image thinning algorithm 4-112345
- ECG processing, symptom pattern recognition 4-105372
- EEG epileptic spikes, computerised classification method 4-93952
- EEG spike and shape wave detection 4-109987
- heart, automatic discovery of contours in ultrasonic pictures (*German*) 4-67053
- hybrid optical-digital pattern recognition 4-74426
- image enhancement algorithms, incorporating human visual response 4-107545
- machine vision 4-89580
- medical diagnosis, image enhancement 4-105360
- microprocessor based nuclear track measuring system 4-96361
- multiple circular harmonic component based pattern discrimination 4-64677
- nuclear track profile determination by direct digital processing of SEM images 4-96359
- nuclear track pseudocoloring by illumination wavefront angle variation on CR-39 detectors 4-96353
- optical image analysis algorithms with stress analysis and medical applications (*German*) 4-69318
- opto-electronic system for automatic track counting for plastic SSNTD 4-96351
- pictures taken by electron microscopes, computer anal. (*German*) 4-63823
- prostate gland volume, computer assisted estimate from transrectal ultrasonic tomograms (*German*) 4-67055
- prosthetic arm control by EMG pattern recognition 4-77427
- random textures visual ranking computer algorithm 4-107547
- rotation-invariant pattern recognition using a vector reference 4-64676
- shape perception rel. to oriented reference frame 4-66956
- spectral domain, optical numerical computation 4-96817
- SSNTD semiautomatic track counting, use of commercial bacterial colony counter 4-96352
- stereoscopically projected pictures, discrete data on volume (*German*) 4-67056
- surface feature classification using ZS region growing method (*Chinese*) 4-100757
- thyroid gland section, automatic evaluation of ultrasonic pictures (*German*) 4-67054
- two-stage spatial filtering for diff. pattern anal., processor digital simulation using cytogenetic data 4-59986
- University of Maryland computer vision research, 20-year retrospective study 4-107543
- Pb/acid battery lifetime prediction, computerised pattern recognition application to life-cycling test data 4-81530

**computerised picture processing**

- see also *computer-generated holography*
- 3-D digital images, noise reduction techniques 4-107544

**computerised picture processing continued**

- 3D moulded surface views, reconstructed from sequential CT scans 4-85509
- abdominal US images, improvement by digital processing 4-67052
- achromatic images, high contrast, perceptual models, filtering 4-109814
- angiography, digital subtraction, imaging characs. using geom. and electro-optical magnification techniques 4-72396
- astronomical image processing 4-82422
- automatic track analysis for large area plastic nuclear track detectors 4-96362
- autoradiographic images of cerebral cortex, computerised 2D and 3D reconstructions 4-100405
- autoradiographs of rat brain, computer-assisted visual anal. 4-100404
- biological microscopy, image enhancement 4-105383
- CA8015 plastic detectors, pseudocolour techniques for nuclear track differentiation 4-96360
- cell material texture anal. using UV microscopy (*German*) 4-72457
- CLEAN, deconvolution algorithm enhancement 4-115694
- cloud shape recognition in satellite remote sensing, computer programming 4-72707
- Colorization, development and appl. 4-106416
- colour graphic US imaging device, DRUID 4-69637
- computer analysis of pictures taken by electron microscopes (*German*) 4-63823
- conference on nuclear track registration, Richland, WA, USA (Jul. 1982) 4-67851
- conference on solid state nuclear track detectors, Acapulco, Mexico (Sept. 1983) 4-95027
- contrast enhancement, preprocessing TV-scanned images electron beam microscopy 4-106291
- cosinusoidal transforms in white light 4-59987
- CR-39 detector, heavy nuclei tracks, automatic meas. system 4-96363
- cranial imaging of newborn infant, elec. resistivity tomographic technique 4-89814
- CT image of human brain, 3D display (*Japanese*) 4-93856
- current trends in optical and hybrid processing methods 4-74434
- digital fluoroscopy imaging system, performance evaluation and quality assurance 4-89706
- digital fluoroscopy with a conventional fluoroscopic room and a nuclear medicine computer system 4-96869
- digital grey-scale fluorography: a new approach to digital radiographic imaging 4-85496
- digital image enhancement/restoration efficiency meas. by human performance 4-81704
- digital image processing for diameter distribution evaluation of nuclear tracks 4-96356
- digital imaging technique in conventional radiography: present and future possibilities 4-81761
- digital medical image processing, automated pattern recognition (*French*) 4-115143
- digital processing of dynamic imagery for photogrammetric applications 4-58902
- digital radiographic data acquisition for radiation therapy treatment planning 4-89704
- digital radiography, basic imaging props., MTF 4-85502
- digital radiography, optimal dose utilisation with variable X-ray intensity 4-89702
- digital radiography, single slit imaging, practical appls. 4-89717
- digital radiography of flow patterns in phantoms and canine arteries 4-89711
- digital subtraction angiography: principles, techniques and applications 4-72394
- digital subtraction angiography, motion correction 4-81783
- digital subtraction angiography, noise reduction methods for hybrid subtraction 4-85500
- digital subtraction angiography, spatial freq. filtering by real-time digital video convolution 4-89703
- digital subtraction angiography utilising geom. and electro-optical magnification, imaging characs. 4-89705
- digital video framestore system, slow scan imaging applications 4-78429
- digital videodensitometry system for subtraction angiography 4-89718
- directional terrain textures invariant under translation rotation and change of scale, optical-digital processing 4-67412
- disc, deform. analysis, grid and grating methods, digital image processing (*German*) 4-64896
- dynamic spatial reconstructor, 3D images of left ventricle 4-85513
- echocardiograms, 2D, effective algorithm for extracting serial endocardial borders 4-85460
- electron microscope, computer interfaced, control, image processing and struct. anal. 4-106430
- electron microscope image processing, Boolean algebra operations using digital frame store 4-101979
- environmental problem solving using satellite imagery 4-93675
- fibre fusion splice loss estimation using image processing technique for graded-index fibres 4-87479
- Fourier processed images of dynamic lung function from list mode data 4-89741
- fringe pattern analysis by image processing using personal computer (*Japanese*) 4-111197
- heart, automatic discovery of contours in ultrasonic pictures (*German*) 4-67053
- heart, left ventricle, parametric pictures of intravenous angiograms (*German*) 4-72400
- hip, three-dimensional reconstruction, CT scans 4-85508
- HIPAS, interactive image processing in geophysical analysis 4-77674
- holographic interferograms, sandwich, ultrahigh resolution of surface deform. 4-79074
- holography interferometry by spatial carrier-fringe-pattern anal. 4-101917
- hybrid optical-digital image processing method (*French*) 4-68270
- hybrid optical-digital pattern recognition 4-74426
- image analyser, Olympus-Cambridge Quantimet 10 4-106293
- image enhancement algorithms, incorporating human visual response 4-107545
- image reconstruction algorithm for time varying X-ray projection image sequences 4-105335
- image restoration and processing methods 4-67637
- image restoration by an iterative regularised pseudoinverse method 4-64679
- INSAT meteorological imagery, data processing 4-100764
- interactive image analysis, neuroscience appls. 4-100409

**computerised picture processing continued**

International Ultraviolet Explorer, SWP camera spectra, order overlap problem, correction algorithm 4-77723  
 IR data analysis, cost-effective approach using Apple II computer 4-106284  
 iterative digital, statistically weighted non-local method 4-100309  
 laser fusion experiments, holographic interferograms, fringe patterns tracing 4-96821  
 left ventricle, 3D reconstruction from 2D echocardiograms (*Japanese*) 4-100267  
 left ventricle, computerised model for reconstruction from cineventriculogram 4-89740  
 mammographic imaging, dual energy techniques 4-89715  
 marine ecosystems, image analysis and silhouette photography for plankton investigations 4-105779  
 medical diagnosis, image enhancement 4-105360  
 medical imaging, image processing and display, review 4-115145  
 medical imaging, meas. depend. filtering, improved S/N ratio 4-62559  
 medical imaging, multiprocessor system for digital data analysis 4-100339  
 medical imaging technology development: digital X-ray imaging, positron CT and NMR imaging (*Japanese*) 4-89734  
 microaneurysms in retinopathy fluoro-angiogram, automatic detection 4-100338  
 microfractography of fibrous fracture, automatic image analyses appl. 4-89212  
 microscope image processing in general purpose microcomputer 4-111253  
 microscopy, quality assurance appl. 4-95563  
 mineralogical measuring procedures automation 4-114879  
 modular laser graphics projection system, animated laser show appls. 4-111165  
 moire contouring, 3D surface automatic reconstruction 4-78290  
 moire method for penetration depth profiles obs., on corroded metal surface (*Japanese*) 4-104942  
 molecular biology, structure determination, image averaging methods comparison 4-100062  
 moulded 3D representations from sequential CT sections 4-81781  
 multidimensional scaling for metric information obtaining from nonmetric data, EEG as example (*German*) 4-72241  
 multidimensional signal processing, projection theorem appls. 4-79037  
 muscle biopsy data acquisition and display 4-85547  
 nearest neighbor hybrid deformable mirror optical computer 4-96818  
 NMR image contrast, intrinsic parameters 4-89673  
 nuclear medicine images, fast count-dependent digital filtering 4-72381  
 nuclear track profile determination by direct digital processing of SEM images 4-96359  
 nuclear track pseudocoloring by illumination wavefront angle variation on CR-39 detectors 4-96353  
 ocean wave image spectra extraction from SAR data, digital processing efficiency improvement 4-67434  
 optical discs systems and applications, conf., Arlington, VA, USA (June 1983) 4-90287  
 optical image analysis algorithms with stress analysis and medical applications (*German*) 4-69318  
 optics in entertainment, conf., Los Angeles, CA, USA (Jan. 1984) 4-110802  
 orbital mosaic IR image simulation and processing 4-97129  
 organelle traffic, human axons, computer analysis 4-85417  
 Osiris, computerised digital photographic apparatus, for max. information from light pictures (*German*) 4-77359  
 phase contrast filters, construction using digital image processing system 4-79274  
 phase-only matched filtering 4-59990  
 photodiode array X-ray imaging system for digital angiography 4-85505  
 photoelastic data, automatic acquisition and calculation (*Chinese*) 4-83869  
 photograph enhancement and deblurring, image processing system 4-91413  
 piecewise constant images, interactive reconstruction from few projections 4-107537  
 planetary remote sensing, digital anal. of spacecraft imaging data 4-101114  
 porous media, impregnated, serial sectioning and digitisation for two- and three-dimens. analysis 4-114744  
 problem-oriented digital image processing system 4-83547  
 projected interference fringes applied to nonoptical surface microscopic topography, computer image processing techniques 4-111099  
 prostate gland volume, computer assisted estimate from transrectal ultrasonic tomograms (*German*) 4-67055  
 radiation damage microstructure, microcomputer system for quantitative image analysis 4-103617  
 radiocolloid liver images, digitised, automatic analysis of diagnostic features 4-115216  
 radiographs, digital tomographic filtering 4-67078  
 radiography, digital mammographic imaging 4-89714  
 radiography, digital tomographic filters, design and implementation 4-67079  
 radiography, digital tomosynthesis system 4-89712  
 radiography, selective exposure, using digitally formed X-ray beam attenuators 4-89719  
 random textures visual ranking computer algorithm 4-107547  
 real-time digital angiocardiology using a temporal high-pass filter 4-81778  
 real-time digitally subtracted fluoroscopy for cervical myelography 4-77384  
 relative elevation determination from Landsat imagery 4-100833  
 remote sensing, digital image processing techniques, book 4-86132  
 scanning Auger microscope digital images, noisy and sparse, comparison of smoothing techniques 4-78434  
 sea-ice analysis of NOAA satellite image using ice breaker Shirase's meteorological data processing system 4-85762  
 segmentation, use of speckle statistics in real hlogram reconstructions (*German*) 4-69342  
 SEM image information extraction by digital processing 4-75245  
 SEM studies of surface processes, digital data acquisition and anal. system 4-78433  
 serial section graphical reconstruction, GRIDSS programs 4-73504  
 small low resolution optical images, model-based restoration procedure 4-91412  
 solid liquid interface, freezing solutions, motion of interface 4-108592

**computerised picture processing continued**

solid state track recorders, automatic scanning by computer controlled microscope 4-68881  
 solid state track recorders, automatic scanning by computer controlled microscope, calibration 4-68882  
 solid state track recorders, track counting, automated scanning electron microscopy 4-68883  
 spatial domain filtering algorithm, clinical appls. 4-72390  
 statistical image recognition using new optical transforms 4-79038  
 steel inclusion classification by automatic picture analysis system according to standard specifications (*German*) 4-81363  
 STEM image processing system 4-78430  
 stereoscopically projected pictures, discrete data on volume (*German*) 4-67056  
 stomach region extraction in double contrast radiography (*Japanese*) 4-109927  
 surface feature classification using ZS region growing method (*Chinese*) 4-100757  
 television speckle interferometer with real-time digital image processing 4-63072  
 temporomandibular joint in vitro and in vivo, three-dimensional imaging 4-85510  
 three-dimensional flow field anal. using image processing techniques 4-97719  
 thyroid gland section, automatic evaluation of ultrasonic pictures (*German*) 4-67054  
 tomographic filters, 2-D digital filtering 4-62622  
 tomography images segmentation, 3D anal. 4-105337  
 tomosynthesis in dental appls. 4-85511  
 transmission electron microscopy, time shared television digital image processing system 4-106431  
 University of Maryland computer vision research, 20-year retrospective study 4-107543  
 US, tissue features, computation and imaging, eye and abdominal organs anal. 4-93835  
 US imaging of defects, high resolution portable system using synthetic aperture focusing 4-93474  
 volcano calderas, LANDSAT imaging 4-94060  
 Walsh-Hadamard transform: an alternative of obtaining phase and amplitude maps 4-89729  
 weak-contrast electron microscopic image restoration (*Russian*) 4-58918  
**computerised power station control** see power station computer control  
**computerised power system control** see power system computer control  
**computerised process control** see process computer control  
**computerised signal processing**  
 see also biology computing; computerised pattern recognition; computerised picture processing; medical diagnostic computing  
 acoustic, alternate low-level primitive structures (ALPS), architectural approach 4-69629  
 acoustic arrays, digital signal processor module architecture, implementation using VLSIs 4-103122  
 acoustic signals, personal computer based signal compression method for sound field meas. in pipes (*Japanese*) 4-97209  
 ADMF (average magnitude difference function) concept, pitch detection algorithm implementation 4-103137  
 algorithm design for real-time audio signal processing 4-103111  
 analogue data recording and processing, for high-resolution frequency analysis 4-63725  
 bearings-only tracking, recursive vs. batch processing algorithms 4-107942  
 cardiac action potential sequential processing 4-81829  
 cardiogram signal compression with AZTEC algorithm (*Chinese*) 4-105355  
 complex FFT processor for image synthesis in radio astronomy (*Japanese*) 4-94639  
 differential evoked potential monitor 4-100344  
 digital signal processing for precision wide-swath bathymetry 4-67432  
 ECG, high resolution, signal averaging system 4-85563  
 editing digital audio 4-103112  
 EEG 16 channel telephone transmission system with cassette recording and CRT display (*Spanish*) 4-62619  
 electrophysiological meas., signal processing unit 4-100343  
 EMG, decomposition, automatic signal processing method 4-93948  
 EMG, digital signal processor, theoretical results 4-81790  
 EMG, on-line signal processing system 4-62614  
 EMG, signal charact., microcomputer anal. 4-89802  
 EMG interference pattern, automatic anal. 4-67134  
 EMG of patients with pathological tremors, preferential freq. detect. and determ. 4-85542  
 EMG processing method for prosthesis control, walking period prediction (*Japanese*) 4-93967  
 EMG signal decomposition system 4-93943  
 EMG signal processing, algorithms comparison 4-93947  
 evoked potential processing, system identification techniques for noise reduction 4-105357  
 evoked potentials, digital signal processing 4-89808  
 FFT signal processing IC, use for Doppler blood flow studies 4-93826  
 FFT-based signal processor for 6502 microcomputers 4-106146  
 folded spectrum analysis 4-79047  
 glottal volume-velocity waveform, automatic determ. method 4-89668  
 hippocampal EEG rel. to spectral anal. of hippocampal unit train 4-67152  
 holographic interferometry system, microprocessor control/data acquisition, real-time signal processing, NDT appl. 4-73501  
 IMACC-8001 signal analysis system (*Spanish*) 4-73427  
 interface for Z80-based computer, for adding signal averaging facility 4-58837  
 IR coatings and multilayer thin-film filter vac. deposition optical reflectance excursion interpretation using Kalman filter algorithm 4-74752  
 multiprocessor EEG analyser, distrib. system 4-85560  
 multiwavelength LIDAR system, computer system for data acquisition and processing 4-74583  
 phrenic neurograms, computer algorithms for processing 4-100397  
 QRS detection in ambulatory monitoring, review 4-85540  
 sea-echo data, surface current mapping radar system 4-67433  
 seismic data, digital processing of analogue high-freq. data 4-77673  
 seismic data, pulse estimation and deconvolution, adaptive least-squares for parametric spectral estimation 4-105766  
 sound emission analysis using MPS 4944 microprocessor system (*German*) 4-79377

**computerised signal processing continued**

- spectral analysis of short-time biomedical data using adaptive filters 4-72453
- speech, new time-domain real-time pitch detector implemented in hardware and software 4-74818
- wideband ocean noise and propagation loss, real-time digital signal processing algorithms 4-107938
- Wordfit, digital audio signal processing system, for automatic time alignment of post-synchronised dialogue 4-69628

**computerised spectroscopy**

- see also spectroscopy computing*
- array-processor-based Fourier-transform ion cyclotron resonance mass spectrometer 4-101965
- ASPECT, area spectroscopy technique in astronomy 4-105889
- coal, IR microspectroscopy, specimen prep. technique, computer-controlled microspectrophotometer 4-93572
- computer-controlled 'Stearat' X-ray spectrometer 4-106444
- computerized laser Raman spectrometer 4-58895
- dielectric relaxation spectroscopy, nitrocellulose/nitroglycerine propellants meas. appl. 4-111152
- DLTS, using low-cost personal computer 4-70721
- EPR spectrometer automation, interfaces for JRA-5 and SM-3 computers 4-90622
- ESR Bruker spectrometer, using digital phase-sensitive detection and Aspect 2000 minicomputer 4-68253
- Fourier transform spectroscopy, microcomputer expl. control and data analysis 4-106406
- FT-IR absorbance subtraction from mixtures, automated procedure 4-105036
- ICP emission spectroscopy 4-105041
- IKS-29 based computers-controlled grid spectrometer, 400-4200  $\text{cm}^{-1}$  range (Russian) 4-68291
- infrared spectra of organic compounds, automated structure analysis 4-91258
- ion-translational-energy spectrometer control cts. 4-106423
- laser photoacoustic microspectrometer 4-101929
- lateral trace element distrib. determ. with Bochum proton microprobe 4-105075
- luminescence spectrometer, computer-controlled, for relative fluoresc. quantum yield meas. 4-106400
- mass spectrometer ion current meas. automation 4-68316
- microcomputer data acquisition system for mass spectrometry 4-106422
- microcomputers in Fourier transform spectroscopy 4-101928
- microfluorometer, pulsed laser, automatic, with high spatial and temporal resolution 4-89859
- microspectrophotometer, computerised using fibre optics, for quantitative microscopy 4-62648
- multichannel spectrometer for process monitoring and control (German) 4-82836
- multidetector alpha spectroscopy analysis system 4-59483
- multiprocessor leased data acquisition and processing system for photon counting expts. 4-59606
- near IR scan data, regression anal., best-pair wavelengths selection, colour graphics 4-95534
- near-IR reflectance analysis for individual component spectra from complex mixtures 4-101818
- NMR imaging systems and spectrometers, use of IBM S9000 computer 4-106335
- photoacoustic correlation spectroscopy, tunable laser induced, online system (Japanese) 4-106389
- photoacoustic resonance expts., computer-controlled performance 4-101946
- photoelectron spectrometer, short-lived gas phase intermediates detection 4-106427
- photon counting system, low-intensity spectral line registration using programmable timer 4-111175
- polymer deformation studies by FT-IR spectroscopy, mechanical stretcher interface 4-103850
- polymer deformation studies by time-resolved FT-IR spectroscopy 4-103851
- programmed quantity markers (Italian) 4-63801
- real-time-resolved scanning spectrophotometer with spectrum averaging capabilities 4-86487
- scanning microscope photometer for automatic analysis of G-banded human chromosomes 4-62649
- smoothing methods comparison for Raman spectral data 4-106286
- spectrophotometer, double-beam, with computer response correction, optical transmission meas. appl. 4-68264
- spectrophotometer, microprocessor-controlled, for film thickness and color analyzer 4-63767
- spectrophotometer computer controlled, software package 4-101924
- spectroradiometer, fully automated continuous operation in broad wavelength band (Chinese) 4-95523
- thin film design and production software packages for use with computerised Perkin-Elmer 983 IR spectrophotometer 4-74663
- triple quadrupole mass spectrometer, artificial intelligence appl. 4-58912

**computerised test equipment *see automatic test equipment*****computerised tomography**

- 2-D digital filters 4-62622
- 3D moulded surface views, reconstructed from sequential CT scans 4-85509
- abdominal, pelvic and thyroid disease prediction and imaging techniques comparison 4-115215
- adaptive grey level assignment in CT scan display 4-67076
- algorithm for evaluation of regions of interest and statistical uncertainty 4-72397
- analog and tomographic 3-D simulations using NORA 4-89685
- Anger gamma-camera for emission computerised tomography 4-63835
- angled-collimator SPECT for cranial appl. 4-105334
- BGO photodiode detector, characterisation for positron emission tomography 4-59568
- blood flow determination, validation of a CT method 4-81775
- bolus geometry after intravenous contrast medium injection, dynamic and quantitative meas. 4-67075
- bone Ca, % by mass rel. to effective at. no., dual-energy CT 4-115188
- brain, human, 3D display, of CT images (Japanese) 4-93856
- brain, human,  $^{45}\text{Ca}$  uptake quantitation by single photon emission CT 4-93852
- cancer diagnosis and new medical imaging modalities (Japanese) 4-62580
- cardiac reconstruction, conf., Santa Cruz, USA (Aug. 1983) 4-63383

**computerised tomography continued**

- cerebral blood flow, regional, accuracy of stable Xe/CT meas. 4-67073
- cerebral blood flow, regional, dynamic emission tomography 4-115214
- circular ring tomography, appl. of coded apertures to head scanning 4-72452
- circularly coded X-ray tomography 4-77372
- coded aperture 3-D imaging in 3-D 4-72356
- coherent Doppler tomography expts. simulation using computer-generated holograms 4-107573
- collimator malpositioning effects in 7 pinhole tomography 4-89731
- collimators used for tomographic imaging of  $^{123}\text{I}$  contaminated with  $^{124}\text{I}$ , performance 4-72383
- conference, nuclear science and power systems, San Francisco, CA, USA (Oct. 1983) 4-58550
- conference, optical instrumentation appl. in medicine, Atlanta, GA, USA (April 1983) 4-86103
- conference on clinical radiology, Las Vegas, USA (Apr. 1984) 4-101574
- contrast-detail diagram meas., empirical investigation of variability 4-89698
- contrast-detail studies of CT scanners, use of multivariate regression anal. 4-109912
- diagnostic imaging systems 4-109892
- diffraction tomography, distortion caused by multiple scatt. 4-62564
- digital image processing, statistically weighted non-local method 4-100309
- display, detectability enhancement by use of coloured illumination 4-62554
- dosimetry system using ionisation chambers 4-89764
- dual energy attenuation correction for single photon emission computed tomography (SPECT) 4-72368
- dual gated nuclear cardiac images 4-72365
- dual-energy CT scanning, discrimination between thorotrast and I contrast medium 4-115187
- dynamic spatial reconstructor, 3D images of left ventricle 4-85513
- electrical impedance imaging of the body with nonlinear reconstruction 4-89813
- EM reconstruction algorithms for emission and transmission tomography 4-67077
- emission and transmission tomography, image quality improvement by scatt. photon reduction 4-67086
- emission and transmission tomography, overview 4-67085
- emission tomography, utilising side information 4-72360
- emission tomography by linear-aperture nuclear-image data inversion 4-85514
- end-tidal Xe conc. meas. by mass spectrometry and thermoconductivity, CT blood flow meas. appl. 4-67142
- energy imparted rel. to radiation risk 4-115225
- film analysis systems and medical imaging applications, review 4-115211
- first-order diffraction, limitations of imaging 4-115257
- fluid mechanics, modern optical techniques, review 4-91856
- full-rotating frame NMR imaging 4-72329
- gamma-ray tomography, medical appl. of imaging methods 4-72451
- gated cardiac scanning using limited angle image recognition technique 4-72364
- high precision quantitative CT, fast contour detect. algorithm 4-62561
- high resolution PET detection system, small detectors geometrical study 4-72363
- hip, three-dimensional reconstruction, CT scans 4-85508
- human brain, 3D CT image display (Japanese) 4-109926
- image processing and display, review 4-115145
- image quality and dose, evaluation of 4 scanners 4-85507
- image quality of an analog radiation therapy simulator-based tomographic scanner 4-109915
- image reconstruction algorithm for time varying X-ray projection image sequences 4-105335
- image reconstruction from projections of small number of views, props. (Japanese) 4-67117
- image reconstruction methods in X-ray computed tomography 4-115177
- image reconstruction technique from limited sampled data, use of a priori knowledge 4-59994
- image resemblance to original object rel. to filter function, noise interf. case 4-72395
- images segmentation, 3D anal. 4-105337
- imaging system, 2-D X-ray, for very small objects, using scanning slit detection 4-111261
- imaging system, effect of  $\gamma$ -ray camera nonlinearity 4-72450
- imaging techniques and appls., tracers, IR imaging, NMR, X-rays, ultrasounds 4-77417
- imaging technology development: digital X-ray imaging, positron CT and NMR imaging (Japanese) 4-89734
- intracranial abscesses, management by CT, radiation dose considerations 4-62586
- iterative convolution based tomography, empirical study and appl. to interferometry 4-95503
- iterative correction algorithm of incomplete projections 4-93857
- left ventricle, simulated emission CT using rot. slant-hole collimator and two camera positions 4-67092
- limited-angle tomographic imaging, non-iterative, using eigenfunctions adapted to space-limited objects 4-69326
- liver, segmental assessment on ordinary scintigrams and SPECT images 4-81763
- liver and spleen volume meas. by single photon emission CT 4-93859
- low contrast sensitivity of radiologic, CT, nuclear medicine, and ultrasound medical imaging systems 4-62558
- magnetic phenomena in medical practice, review 4-105314
- magnetic resonance tomography for internal diagnostic examination 4-105312
- maximum likelihood PET with real data 4-89815
- medical imaging advances, state of art 4-81784
- microwave diffraction tomography, reconstruction method 4-100291
- moulded 3D representations from sequential CT sections 4-81781
- multidetector SPECT brain scanner, improved performance from modifications 4-100310
- multilayer spherical ring positron emission tomography, mega-channel coincidence circuit 4-74122
- myocardial  $^{201}\text{Tl}$  emission tomography, coronary artery disease localisation 4-81767
- myocardial emission CT using  $^{99m}\text{Tc}$ -pyrophosphate, rel. to planar imaging 4-81768
- myocardial perfusion,  $^{82}\text{Rb}$  positron emission CT, extraction fraction and flow meas. 4-72378

**computerised tomography** continued  
 neovascy, 3D CT of nevi and melanomas by transillumination 4-109896  
 NMR imaging, development (*Japanese*) 4-82810  
 NMR tomography, inverse problems, shift spectra, relaxation, formulation and approx. soln. (*Russian*) 4-72324  
 noise and contrast detect. in CT images 4-67110  
 nonlinear, for three-dimens. image reconstruction of dense plasma 4-84069  
 object reconstruction from its coded image and object constraints 4-67071  
 optical tomography, expt. verification of noise theory 4-91414  
 optimum wavelength selection for an X-ray tomography system 4-67072  
 parameter estimation for dynamic systems in emission-tomography systems having list-mode data 4-89816  
 photoacoustic correlation spectroscopy, tunable laser induced, online system (*Japanese*), 4-106389  
 piecewise constant images, interactive reconstruction from few projections 4-107537  
 positron computed tomography, developments in detectors 4-67090  
 positron emission ring tomograph using BGO detector, analog readout 4-62576  
 positron emission tomograph, image reconstruction 4-62572  
 positron emission tomograph, performance characteristics 4-62577  
 positron emission tomograph design and evaluation 4-67088  
 positron emission tomograph THERASCAN 3128, performance 4-62578  
 positron emission tomographic unit, high resolution 4-72411  
 positron emission tomography, count normalisation methods, statistical anal. 4-72358  
 positron emission tomography, high resolution, using analog coding 4-77375  
 positron emission tomography, high resolution TOF camera 4-62573  
 positron emission tomography, image reconstruction procedure 4-62574  
 positron emission tomography, modelling of coincidences 4-62575  
 positron emission tomography, performance rel. to energy threshold and shielding depth 4-77376  
 positron emission tomography, time-of-flight, effect of accidental coincidences 4-109906  
 positron emission tomography HISPET, design features 4-62579  
 positron emission tomography of regional tissue using short lived cyclotron produced isotopes 4-72410  
 positron emission tomography tumour localisation 4-72355  
 positron tomography, in-vivo vol. meas. 4-67087  
 positron transmission tomograph, design considerations for non-medical appl. 4-71815  
 postreconstruction beam hardening correction, comparative study of two methods 4-62560  
 proton CT as means of density normalisation in PIXE semi-microprobe anal. 4-105077  
 pulmonary nodules, CT images, problems of attenuation and area meas. 4-67074  
 pulsed meson beam, 2D profile meas. by computerised tomography method 4-74073  
 quality assurance, correlation with system performance 4-89709  
 quality assurance status for CT systems 4-89708  
 radiation therapy, user requirements on CT based computed dose planning systems 4-81760  
 radiation treatment planning 4-72404  
 radioisotope CT, iterative method for verifying systematic nonuniformities in refillable flood sources 4-72393  
 radiotherapy planning using computers 4-62565  
 radiotherapy planning using CT numbers, electron density of bone for inhomogeneity correction 4-67112  
 radiotherapy treatment planning, simulator-based CT system 4-89691  
 Radon transform and appls., book contrib. 4-106172  
 reconstruction algorithm from truncated projections 4-77378  
 reconstruction filters for 3-D NMR tomography, with planar integrals 4-72325  
 reconstruction of image from incomplete view data by convex protections and direct Fourier inversion 4-109908  
 regional blood flow, first-pass positron emission tomography with external detectors, modelling 4-72388  
 restoration of images by the method of generalised projections 4-112348  
 restoring spline interpolation of CT images 4-62562  
 retroperitoneal lymph nodes evaluation by CT (*Russian*) 4-89687  
 review of 10 years of CT 4-81762  
 review of developments in in vivo diagnostic exams. using phys. methods 4-115262  
 review-of in vivo imaging systems based on tissue resistivity distrib. 4-115259  
 review of medical imaging techniques 4-72412  
 scanned projection radiography developments 4-115205  
 serial tomographic images, meas. of regional tissue and blood-pool radiotracer concs. 4-72380  
 signal detection theory in medical imaging, limitations and applications; review 4-115203  
 single photon emission computer tomography, collimation, sampling, filtering interactions 4-72359  
 single photon emission CT, 2 algorithms for use with an orthogonal-view coded-aperture system 4-100311  
 single photon emission CT, myocardial phantom, uptakes quantification, sources of overestimation 4-105333  
 single photon emission CT, performance test conditions 4-93858  
 single photon emission CT, review 4-89742  
 single photon emission CT, rotating gamma camera capability, image reconstruction software 4-89738  
 single photon emission CT for estimates of liver and spleen vol. 4-81772  
 single photon emission tomography, attenuation correction, depth effect 4-72357  
 single photon tomography, attenuated Radon transform inversion formula 4-72361  
 single-photon emission CT, subtraction of Compton-scatt. photons 4-72387  
 single-slice positron-emission tomography scanners, performance study by Monte Carlo techniques 4-62563  
 SPECT: a practical guide for users 4-67094  
 SPECT: quality control procedures and artifact identification 4-67093  
 SPECT resolution and uniformity improvements by noncircular orbit 4-72375  
 SRT-1000, Soviet computerised tomograph, design, operation and results (*Russian*) 4-81811

**computerised tomography** continued

stereotactic neurosurgery, 3D image of cerebral blood vessels and tumour 4-89692  
 synchrotron radiation, use in X-ray computed tomography 4-93855  
 temporomandibular joint in vitro and in vivo, three-dimensional imaging 4-85510  
 THERAPLAN-L radiation therapy treatment planning system 4-115174  
 thorax computerised electrical impedance imaging 4-77416  
 three dimensional X-ray pictures (*Swedish*) 4-77373  
 three-dimensional image reconstruction from planar projections with application to optical data processing 4-79052  
 time coded emission, three dimensional simulation 4-77374  
 timer smear corrected multiplex holographic display of computerized tomography data 4-74460  
 tomographic technique for the estimation of ultrasonic velocity 4-93824  
 tomosynthesis in dental appls. 4-85511  
 transmission tomography, CT and digital vol. scanning 4-115207  
 twin BGO detectors for high resolution positron emission tomography 4-74105  
 ultrasonics research in Australia 4-109893  
 US tomography, practical meas. of human body temp. 4-100268  
 wave-front tomography by Zernike polynomial decomp. 4-91640  
 X- and  $\gamma$ -ray computed tomography for nondestructive evaluation 4-71810  
 X- and  $\gamma$ -ray tomography for nondestructive evaluation 4-71809  
 X-ray and  $\gamma$ -ray imaging techniques, Int. Workshop, Southampton, England (July 1983) 4-63386  
 X-ray CT image reconstruction method from projection data with quantum noise (*Japanese*) 4-67116  
 X-ray tomography, live tree annual ring meas. 4-71812  
 X-ray tomography, medical appl. of imaging methods 4-72451  
 X-ray tomography systems, appl. to nondestructive testing 4-71811  
 BaF<sub>2</sub> scintillator characts. for time-of-flight positron emission tomography 4-67089  
 I<sub>2</sub> vapour density mapping using optical fan beam tomography 4-108157  
**computerised traffic control** *see* traffic computer control  
**computers**  
*see also* computer architecture; computer software; data handling; digital computers; file organisation; special purpose computers  
 electrical and electronic phenomena and devices, book 4-67952  
 technological revolution and impact on society 4-58615  
**computing applications to aerospace engineering** *see* aerospace computing  
**computing applications to architectural design** *see* architectural CAD  
**computing applications to astronomy** *see* astronomy computing  
**computing applications to astrophysics** *see* astrophysics computing  
**computing applications to biology** *see* biology computing  
**computing applications to biomedical engineering** *see* medical computing  
**computing applications to business** *see* administrative data processing  
**computing applications to chemistry** *see* chemistry computing  
**computing applications to circuit analysis** *see* circuit analysis computing  
**computing applications to circuit design** *see* circuit CAD  
**computing applications to circuit layout design** *see* circuit layout CAD  
**computing applications to civil engineering** *see* civil engineering computing  
**computing applications to command and control systems** *see* command and control systems  
**computing applications to communications engineering** *see* communications computing  
**computing applications to education** *see* educational computing  
**computing applications to electrical engineering** *see* electrical engineering computing  
**computing applications to electronic engineering** *see* electronic engineering computing  
**computing applications to engineering** *see* engineering computing  
**computing applications to geophysics** *see* geophysics computing  
**computing applications to government** *see* government data processing  
**computing applications to history** *see* history  
**computing applications to legal research** *see* government data processing; social and behavioural sciences computing  
**computing applications to linguistics** *see* linguistics  
**computing applications to mathematics** *see* numerical analysis  
**computing applications to mechanical engineering** *see* mechanical engineering computing  
**computing applications to medical administration** *see* medical administrative data processing  
**computing applications to medical diagnostics** *see* medical diagnostic computing  
**computing applications to medicine** *see* medical computing  
**computing applications to music** *see* music  
**computing applications to natural sciences** *see* natural sciences computing  
**computing applications to nuclear engineering** *see* nuclear engineering computing  
**computing applications to physics** *see* physics computing  
**computing applications to police** *see* police data processing  
**computing applications to power system design** *see* power system CAD  
**computing applications to psychology** *see* psychology  
**computing applications to social and behavioural sciences** *see* social and behavioural sciences computing  
**computing applications to town and country planning** *see* town and country planning  
**computing military applications** *see* military computing  
**concentration measurement** *see* chemical analysis; chemical variables measurement  
**concepts (index language)** *see* vocabulary  
**concrete**  
 Arctic offshore structures, lightweight concrete props. 4-114464  
 beam, rectangular reinforced, behaviour and ultimate strength under combined torsion, bending and shear 4-62046  
 beam, three point bending, cracking, dye penetrant obs., compliance calibration technique 4-89205  
 cement-based composites, modified instrumented Charpy test 4-89204  
 conference on structural and mechanical engineering for nuclear power plants, Chicago, IL, USA (Aug. 1983) 4-95044  
 crack growth detection, vertical-displacement gage fixture for J<sub>IC</sub> testing 4-104933

## concrete continued

- ferro-concrete structures for nuclear facilities, computer simulation for impact loadings 4-107006  
 fibre reinforced cements, mech. props. and fabrication, book contrib. 4-66298  
 hypothetical core-melt through in concrete foundations, core-concrete interactions 4-91088  
 impact testing, meas. device effect on curve shape (*German*) 4-66535  
 liner construction for pre-stressed concrete reactor pressure vessels, anchors 4-106840  
 LMFBR safety anal., Na-concrete reaction data appl. 4-83231  
 LWR core-melt interaction with concrete foundations, crust form., long-time behaviour 4-96236  
 nuclear reactor core melt-concrete foundations interaction, gas outflow 4-96237  
 nuclear reactor cracked reinforced concrete containments under seismic loads, displacements and stresses 4-96112  
 nuclear reactor reinforced concrete containment design, allowable stresses to limit shearing deformation 4-96111  
 nuclear reactor reinforced concrete containments, tangential shear design, research results and appls. 4-96110  
 nuclear reactors, reinforced concrete double cantilevers testing and finite element verification anal. 4-96113  
 ocean structural design 4-114449  
 photon backscattering, energy albedo meas. 4-61782  
 plain, in direct tension, method for determining cracking stress, cracking strain and Young's modulus 4-81369  
 porous materials, improvement of sound-absorpt. props. 4-87513  
 prestressed lightweight concrete barrier for cryogenic containment vessel 4-114675  
 radioactivity induction in constituents by high energy particle irradi. 4-115230  
 natural radioactivity of cement industry materials in Hungary 4-93676  
 seawater pressure resistant concrete structure test data and trends 4-114760  
 specimen in multiaxial compression finite element failure analysis (*Japanese*) 4-99686  
 thermophysical and transport props. 4-111613  
 utilisation in energy-efficient buildings (*German*) 4-66739  
 Rn exhalation rel. to flyash additives and porosity 4-93902

concurrency (computers) *see multiprocessing systems*

## condensation

- see also clouds; drops; fog*  
 adsorbed atoms, two-dimensional condensation, crit. temp. calc., lattice incompatibility effects 4-65561  
 aerosols, random fluctuations, effects on behaviour 4-82189  
 air-water vapour mixture in greenhouse environment, thermal behaviour 4-87545  
 Arctic OTEC plant scheme 4-114931  
 binary liquid condensation, steady state nucleation kinetics 4-70339  
 canonical partition function, virial expansion 4-97991  
 DC electric field heat transfer during condensation of nonconducting fluids 4-97561  
 desuperheaters, injection-type operation 4-97549  
 direct contact condensation of vapor to falling cooled droplets 4-112697  
 drag of evaporating or condensing droplets in low Reynolds number flow 4-83933  
 dropwise condensation on upper surface of horizontal tube, heat transfer 4-97292  
 ethanol droplets, evap. and condensation rates deduced from struct. resonances in fluorescence spectra 4-91304  
 falling film evaporator, heat transmission meas. for condensation and evaporation (*German*) 4-111126  
 film condensation, heat and mass transfer, mathematical modelling 4-107996  
 film condensation in vertical tube with closed top 4-75009  
 film condensation with lateral mass flux about a body of arbitrary shape in a porous medium 4-108598  
 fission reactor, multicomponent phase transition modeling 4-106943  
 flow of vapour in channel with porous filler, condensation process, analytic model 4-83942  
 gas cooling and condensation in vortex flow 4-69764  
 gas-liquid phase transition and singularities, space of undercritical states 4-65381  
 geothermal power station turbine hydrocarbon vapour expansions condensation behaviour 4-60250  
 grains, nucleation, growth, coagulation and condensation, astrophysical appl. 4-77706  
 heat transfer intensification (*German*) 4-112689  
 high performance heat transfer surfaces for boiling and condensation 4-83806  
 high-performance surfaces for non-boiling heat transfer, review 4-83800  
 homogeneous condensation, droplet growth study 4-60506  
 ice, formation on flat surfaces, convective boundary layers 4-112811  
 interphase layer, mass, momentum and energy conservation law, surface parameters 4-112692  
 jet, turbulent, condensation, thermal and vel. boundary layers 4-103306  
 laminar film condensation in nonuniform gravity, approximate method 4-69735  
 Laval nozzle for absolute humidity of air determ. 4-65046  
 metal vapour condensation studies 4-84377  
 phase separation late stage, dynamics in two dims. 4-98254  
 PWR LOCA decay heat removal in steam generator, condensation in single inverted U-tube 4-96206  
 reflux condensation in a two-phase closed thermosyphon 4-112688  
 review 4-84376  
 single-pass aircooled or gascooled condensers, temp. distrib. and vapour flow distrib. calc. 4-103192  
 slag explosive condensation kinetics in MHD generator channel 4-113025  
 spontaneous droplet nucleation in clean saturated moist air at atmospheric press. 4-80200  
 steam, Wilson line at low press. condensation onset 4-97658  
 steam-air mixture, air absorption during condensation in nuclear reactor 4-106874  
 supersonic jet expansion, gas condensation, mol. beam study 4-60561  
 supersonic nozzles, condensation processes from air-water vapour mixture (*German*) 4-83938  
 surface, evaporation and condensation, mass and heat transfer, kinetic anal. 4-88270  
 theory of evaporation and condensation 4-64833

## condensation continued

- thermosyphon, two-phase flow, noncondensate gas effect 4-97647  
 transient film condensation on a vertical surface in a porous medium, heat transfer 4-87713  
 turbulent film condensation on horizontal circular cylinder 4-69744  
 turbulent filmwise condensation on vertical plate, heat transfer 4-97534  
 vapour absorption-desorption isotherms, two-dimensional network model 4-61178  
 vapour bubbles in immiscible liquid, direct contact condensation pattern 4-61062  
 vapour condensation, waves in interphase surface, calc. 4-108597  
 vapour interaction with densely packed spherical particles, modelling, relative permeability 4-61179  
 water, phase transitions parameterisation, deep concern eqns. 4-79578  
 Ag electroplated surfaces, dropwise condensation of steam 4-112694  
 Ar, homogeneous condensation in He studied using nozzle flow of cryogenic Ludwig tube 4-98251  
 CO<sub>2</sub>, expanding supersonic jets, condensation processes similarity 4-60474  
 CdTe thin layers, crystal and energy structures for photoelectric transducers 4-98298  
 H<sub>2</sub>SO<sub>4</sub>, vapour condensation in cooled tube, mathematical model 4-80199  
 a-Se, condensates, kinetics of crystallisation 4-109327  
 Si-H-Cl system, Si condensation, equilibrium calcs., 300 to 3000K 4-61107  
 SiO<sub>2</sub>, reactive film deposition, surface processes, planar magnetron sputtering 4-113798  
 ZnO (0001), interaction with methanol at low temp., XPS and UPS study 4-92542
- condensers (electric) *see capacitors*
- condensers (steam plant)  
 biomass/MSW augmented OTEC systems 4-62373  
 OTEC closed system optimisation with dual-zoned condenser and reverse osmosis desalination unit 4-66740  
 water polisher systems performance at Plant Bowen, Georgia 4-59380
- condensing *see condensation*
- conductance, electric *see electric admittance*
- conductance, electric, measurement *see electric admittance measurement*
- conductance measurement, electric *see electrical conductivity measurement*
- conducting materials  
*see also bimetallic; electrolytes; metals; semiconductor materials; superconducting materials*  
 No entries
- conduction, heat *see heat conduction*
- conduction bands  
*see also Fermi level; semiconductor materials*  
 biglyximate nickel(II), solid phase transitions and band struct. 4-88282  
 chalcogenide glasses, one-electron density of states 4-84548  
 diamond, conduction band struct., core electron excitation spectra anal. 4-70647  
 ferroelectric materials space-charge limited currents, fundamental assumptions and results of theory (*Polish*) 4-65690  
 graphite, conduction band struct., core electron excitation spectra anal. 4-70647  
 inert gas, solids, conduction band states, excitons, photoemission 4-85057  
 d-metal carbides, Auger C lines 4-93149  
 metallic rare earth valence fluctuating systems model 4-80468  
 MIS structure, interface electron state calc. 4-108912  
 narrow band gap semiconductor, two-photon interband electron transitions via deep impurity levels 4-88477  
 PbTe:Bi, Hall study of self-compensation of donor effect 4-104242  
 trans-polyacetylene, electronic struct. studied by transfer matrix technique, localised state 4-87243  
 semiconductor crystallites, electron-electron and electron-hole interactions, size depend. of excited electronic state 4-70660  
 semiconductors, excited quasistationary states relax. as source of exoelectron emission 4-99290  
 semiconductors, multivalley polar with impurities, optical absorption by electron plasmas 4-114230  
 semiconductors, Raman characterisation 4-99106  
 space charge limited currents, fundamental assumptions and results of theory (*Polish*) 4-65964  
 TCNQ salt, TTF-TCNQ, <sup>13</sup>C NMR studies and spin susceptibility 4-92975  
 tetraza porphyrin polygermyloxane:halogen, band struct. studied by crystal orbital formalism and CNDO approx. 4-65606  
 tetraza porphyrin polysiloxane:halogen, band struct. studied by crystal orbital formalism and CNDO approx. 4-65606  
 titanates, electron energy struct. of cond. bands, X-ray photoemission yield spectra 4-61282  
 transition metals, liquid, Muffin-tin model, local density of states, calcs. 4-108755  
 Al<sub>3</sub>Ga<sub>1-x</sub>As<sub>2</sub>Te(Sn) epitaxial films, carrier density changes due to band struct. modifications 4-61381  
 Am, localisation of 5f electrons, XPS study 4-70892  
 Ar, solid, cond. band struct., floating 1-s gaussian basis functions calcs. 4-92609  
 Au-Si-SiO<sub>2</sub> interface, Au surface-state energy level determ. 4-80640  
 C, glassy, conduction band struct., core electron excitation spectra anal. 4-70647  
 CO, solid, electronic band struct., photoelectron spectra 4-85058  
 CdIn<sub>2</sub>Se<sub>4</sub>, conduction band anisotropy, piezoresistance studies 4-98614  
 Cd<sub>1-x</sub>Mn<sub>x</sub>Se, far-IR obs. of electric dipole spin resonance 4-92978  
 Cd<sub>1-x</sub>Mn<sub>x</sub>Se, Raman scatt., magnetisation and exchange energy 4-80940  
 CdS, spontaneous oscils. in presence of temp.-electric instability 4-104266  
 CuInSe<sub>2</sub>/CdS heterojunction solar cells, conduction band-lineup 4-72105  
 GaAs, conduction band splitting for k along [110] 4-108777  
 GaAs, conduction bands, strain-induced splitting 4-75854  
 GaAs, deep level wavefunctions, behaviour in shallow energy region (*Chinese*) 4-92650  
 GaAs, deep levels associated with vacancy-impurity pairs 4-92662  
 GaAs, doped, cond. electron spin relax. times, precession mechanism, spin splitting 4-98948  
 n-type GaAs free-carrier absorption, quantum mechanical perturbation theory 4-80893  
 GaAs, k,p interaction and effective mass, band gap depend. 4-113850

## conduction bands continued

- GaAs, optical spin orientation of  $[^{115}\text{In}]$  conduction band electrons, photoemission study 4-66188  
 GaAs, photoexcited conduction electron spin polarisation precession in band-bending region 4-88945  
 GaAs pnp quantum well strucs., reson. tunnelling 4-104299  
 n-GaAs, power broadening and nonlinear far IR magnetophotocond. 4-108897  
 GaAs:Cr, ionisation processes by upper conduction band electrons, mag. field effects 4-65640  
 n-GaAs:Se, free electron optical absorpt. theory 4-104637  
 GaAs- $\text{P}_2\text{N}_2$ , excitons and excitonic mols. bound to impurity, calcs. 4-108785  
 $\text{Ga}_{0.47}\text{In}_{0.53}\text{As}/\text{Al}_{0.48}\text{In}_{0.52}\text{As}$  heterojunction, conduction band discontinuity, photoluminescence study 4-76028  
 GaP, donor wave functions and band struct. 4-98519  
 GaS, EXAFS spectra and near edge struct. 4-66128  
 GaSb, conduction bands, strain-induced splitting 4-75854  
 Hg $_{1-x}\text{Te}$ , EXAFS spectra and near edge struct. 4-66128  
 GeSb(As), impurity state breakdown under uniaxial compression 4-70715  
 Ge $_{1-x}\text{Se}_x$  glass, photoluminescence characts. 4-76513  
 Hg $_{1-x}\text{Te}$ , Fe, Te cryst., negative magnetoresist. and Hall effect 4-65696  
 Hg $_{1-x}\text{In}_x\text{Sb}$ , thermoelec. power and Fermi level 4-104243  
 Hg $_{1-x}\text{Mn}_x\text{Te}$ , Cd, Te, spin glass phase transition, interband Faraday rot., mag. susceptibility meas. 4-61545  
 Hg $_{1-x}\text{Mn}_x\text{Te}$ , spin glass phase transition, interband Faraday rot., mag. susceptibility meas. 4-61545  
 HgTe, zero-gap, intrinsic cond. theory 4-70813  
 In $_{1-x}\text{Ga}_x\text{As}$ , indirect conduction band minima determ. 4-98517  
 In $_{1-x}\text{Ga}_x\text{As}$ , P $_{1-y}\text{As}_y$ , indirect conduction band minima determ. 4-98517  
 In $_{1-x}\text{Ga}_x\text{Sb}$ , indirect conduction band minima determ. 4-98517  
 InP, k,p interaction and effective mass, band gap depend. 4-113850  
 n-InSb, Auger recombination of holes via deep donors 4-104229  
 InSb, two photon interband magnetoabsorption, level transitions, photoconductivity meas. 4-71350  
 InSe, EXAFS spectra and near edge struct. 4-66128  
 NbC, C vacancy electronic struct., tight binding calculations 4-92661  
 NbN, electronic props., optical study 4-66003  
 Ne, solid, cond. band struct., floating 1-s gaussian basis functions calcs. 4-92609  
 Ni (111) with adsorbed graphite and C overlayers, electronic struct. study 4-61213  
 P, black, electronic struct., polarised X-ray emission and absorption studies 4-108771  
 PbSnTe, negative differential mobility in high elec. fields 4-104216  
 Pb $_{1-x}\text{Sn}_x\text{Te}$ , longitudinal magnetoresist., magnetophonon oscils. 4-65694  
 Pb $_{1-x}\text{Sn}_x\text{Te}$ :In, Gunn effect, threshold field rel. to cond. band struct. 4-88513  
 PbTe, negative differential mobility in high elec. fields 4-104216  
 PbTe Schottky barriers, resonant magneto-optical transitions from a deep level 4-76440  
 PbTe:B, absorpt. spectra and impurity states 4-104638  
 Se $_{50}\text{Te}_{50}\text{As}_{50}\text{Li}_{50}$ , chemical modification and elec. cond. 4-75970  
 Si (100) surface electronic excitations, EELS study 4-108914  
 Si, deep level wavefunctions, behaviour in shallow energy region (Chinese) 4-92650  
 a-Si, film, gap density of states determ. 4-80551  
 Si, plastically deformed, deep levels, capacitance, reverse current meas. 4-61319  
 Si surface two-photon photoemission 4-85076  
 Si:Au, transient capacitance of Au acceptor energy level under uniaxial stress (Chinese) 4-75888  
 Si:Cu/Au Schottky diode, stress effects, photoelec. meas. 4-88591  
 a-Si:H, radiative combination at dangling bonds, quantitative model, expt. study 4-114326  
 Si:Mn, Cu, impurity energy levels, DLTS and capacitance studies 4-88471  
 SiN $_x$ :H, amorphous, electronic struct., photoemission 4-108776  
 Si $_3\text{N}_4$  amorphous, electronic struct., X-ray emission and XPS studies 4-75839  
 SiNi $_x$ :H, amorphous, localised states at conduction band edge 4-104168  
 SiO $_2$ , strong elec. field heating of cond. band electrons 4-61386  
 n-SrTiO $_3$ :Nb, electronic struct., PES and IPES studies 4-108775  
 Ti cpds., electronic relax. effects, X-ray absorpt. 4-66114  
 TiN $_{1-x}$ , electronic struct., PES study, stoichiometry effect 4-84560  
 TiO $_2$  (110), surface defects, XPS, X-ray induced AES, EELS study 4-80351  
 TiO $_2$ , electronic struct. of O $_2$  vacancy 4-88475  
 Ti $_{0.9}\text{Ru}_{0.05}\text{O}_2$  biphasic cryst. in aq. soln., photoelec. props. 4-84648  
 TiTe $_2$ , band struct., elec. and mag. props. 4-92595  
 Y $_3$ , Gd, Fe $_2\text{O}_3$ , noncrystalline garnet films, electron transport and thermopower 4-108958  
 Yb $_2\text{O}_3$ , 4f $^{13}$  config., strong intrasite interaction, pseudopot. model anal. 4-80495  
 ZnS:Fe $^{2+}$ , impurity states, EPR meas. 4-84588  
 ZrN $_{1-x}$ , electronic struct., PES study, stoichiometry effect 4-84560

## conduction electron spin resonance see CESR

## conduction in solids, ionic see ionic conduction in solids

## conductivity, electrical see electrical conductivity

## conductivity, thermal see thermal conductivity

## conductors (electric)

see also bimetal; overhead line conductors; wires (electric)

Ampere tension in electric conductors 4-79001

cylinders with rectangular cross-section, EM wave scattering, expt. study (Japanese) 4-83525

EM scattering by conducting circular cylinders 4-102858

homogeneous, eddy currents calc., boundary Galerkin's approach 4-59960  
 nondestructive testing of moving sheet conductors, speed effects on solid coil impedance 4-71806

## configuration interactions (atoms) see atomic electron correlations

## configuration interactions (molecules) see molecular electron correlations

## confinement, plasma see plasma confinement

## connecting see joining processes

## conservation laws

see also C invariance; CP invariance; CPT invariance; elementary particle symmetry; P invariance; T invariance

$^{76}\text{Ge}$  double beta decay, Battelle-Carolina expt. status 4-90976

## conservation laws continued

- Backlund transformations, infinitesimal, gauge symmetries and conserved currents 4-82890  
 baryon number violating nuclear decay 4-68476  
 baryon number violation, Higgs mediated in GUT's 4-90780  
 baryon number violation in SU(2) gauge theory, mag. monopole interactions 4-68457  
 baryon number violation in SU(5) theory, monopole catalysts of proton decay 4-78514  
 composite particle scattering, classical many-particle system, space-time conservation laws 4-90758  
 conference on low energy tests of conservation laws, Blacksburg, VA, USA (Sep. 1983) 4-90281  
 field theories, identities and conservation laws 4-78431  
 first-order equivalent Lagrangians and conservation laws 4-101638  
 four-dimensional statistical mechanics, Poincare invariant Hamiltonian dynamics. 4-95169  
 free electromagnetic field, conservation laws 4-110891  
 instanton induced compactification, 8-dimens. Einstein-SU(2) Yang-Mills,  $\text{P}_4\text{SO}(5)$  4-95644  
 interphase layer, mass, momentum and energy conservation law, surface parameters 4-112692  
 KAMIOKANE nucleon decay expt., status and performance 4-90875  
 kaon decay review of recent results, electroweak theory, lepton number violation 4-73685  
 Lagrangian symmetry, eqns. of motion, Noether's theorem 4-111324  
 lattice field theory, zero modes, boundary conditions and anomalies 4-86520  
 lepton conservation in weak interaction processes 4-90756  
 lepton generation puzzle, lepton universality and conservation, double  $\beta$ -decay 4-63944  
 linear field equation, relation to algebra of space-time symmetry group 4-95703  
 linear thermoelasticity appl. (French) 4-112700  
 Lorentz invariance, breakdown in preferred time-like vector-field 4-95701  
 monopole induced baryon number violating transitions, complete QFT treatment 4-86616  
 muon decay, review of recent results, electroweak theory, lepton number violation 4-73685  
 N=2 supergravity, superspace formulation, superfield Lagrangian 4-101737  
 Noether's theorem, equivalent conserved currents in classical field theories 4-86234  
 nonlinear  $O(n)$ - $\sigma$  model, symmetry relations, dual transformation and Noether symmetry 4-95660  
 nonlinear sigma models, Einstein and chiral-field equations, exact solutions 4-95685  
 Peccei-Quinn symmetry, horizontal symmetry, domain wall problem 4-86560  
 pion decay review of recent results, electroweak theory, lepton number violation 4-73685  
 proton decay and  $\Delta B=2$  processes, expt. limits at IMB detector 4-90874  
 proton-positron oscils. 4-68472  
 quantum gravity, S-matrix theory, symmetry principles and conservation laws 4-58708  
 SL(2,C) gauge theory of gravit., conservation laws, Noether's theorem 4-110968  
 softly broken supersymmetry, lepton number violation 4-63936  
 solitons, adiabatic stability, matching of conservation laws 4-101661  
 strong equivalence principle and its violation 4-78019  
 SU(3) $\times$ SU(2) $\times$ U(1) gauge group, baryon number non-conservation, low mass scale 4-111363  
 time-dependent mechanical symmetries and extended Hamiltonian systems 4-58989  
 two-dimensional quantum field theory, infinite conformal symmetry 4-90710  
 world-line condition, spinning particle in superspace, Grassmann variables description 4-110870  
 $e^+e^-$  annihilation, 14-36.7 Gev, local compensation of baryon number,  $p$ - $p$  pair prod. 4-68578  
 $\eta$ - $\mu$   $\mu$   $\gamma$ , rare decays, conservation law tests, neutral currents 4-102113  
 $\mu$ -e conversion search, time projection chamber at TRIUMF 4-102467  
 $\mu^+$ - $e^+$   $\nu$ , positron polarisation vectors, preliminary results 4-102122  
 $\mu$   $p$ - $n$ , PCAC and muon-electron universality 4-102264  
 n- $\bar{n}$  oscillation expts. using ultra-cold neutrons 4-90762  
 n- $\bar{n}$  oscillations, Grenoble high flux reactor expt. 4-90761  
 n- $\bar{n}$  oscillations, unified models, baryon number nonconservation 4-90760  
 n- $\bar{n}$  transition searches, field compensation as alternative to mag. shielding 4-59004  
 $\pi^0$  and  $\eta$  rare decays, conservation law tests, neutral currents 4-102113  
 $\pi^0$ - $e^+e^-$  ( $e^+e^-e^+e^-$ ) ( $e^+e^- \gamma$ ), rare decays, conservation law tests, neutral currents 4-102113  
 $^{76}\text{Ge}$ , double  $\beta$ -decay calcs. in GUT, B-L violation 4-102069  
 $^{76}\text{Ge}$ , neutrinoless double  $\beta$ -decay, Mont Blanc expt.,  $\nu$  mass effects 4-90974  
 $^{76}\text{Ge}$ , neutrinoless double  $\beta$ -decay, CIT results, lepton number conservation,  $\nu$  mass 4-90975  
 $^1\text{H}(\mu^- \nu)$ , PCAC and muon-electron universality 4-102264  
 $\pi^+$ - $\mu^+$   $\nu$ , at rest, neutrino mass and  $\pi^+$  rest mass 4-102111  
 $^{82}\text{Se}$ , double  $\beta$ -decay calcs. in GUT, B-L violation 4-102069  
 $^{127}\text{Te}$  A=128, 130 double  $\beta$ -decay calcs. in GUT, B-L violation 4-102069

## consoles, remote see remote consoles

## constant current modulation see amplitude modulation

## constant voltage diodes see avalanche diodes; Zener diodes

## constants

- see also elastic constants; gravitational constant; lattice constants; optical constants  
 astronomical constants, Landolt-Bornstein series 4-82603  
 Avogadro constant determ. by unit cell measurements on Si single crystal (German) 4-79980  
 fundamental constants and SI units, quantum phenomena anal. 4-106259  
 magnetic flux quantum, absolute determination using superconducting magnetic levitation system 4-73410  
 Planck const. to neutron mass ratio determ. 4-63704

- constituent interchange model *see* quark models
- constitution diagrams *see* phase diagrams
- construction *see* building
- construction industry  
*see also* civil engineering  
 earth dams, provision of reliability in design and construction 4-77457
- constructional engineering *see* civil engineering
- contact (mechanical) *see* mechanical contact
- contact angle  
*see also* capillarity; surface tension; wetting  
 albuminated surfaces, radiation-induced, modification toward blood compatibility 4-62630  
 contact angle, equilib. and hysteresis, smooth uniform surfaces, disjoining pressure isotherm 4-80332  
 droplet spreading, liquid-air interface (French) 4-75753  
 drops, slightly deformed axisymmetric, profiles 4-61186  
 liquid drops on smooth and rough circular cylinders, equilib. 4-61187  
 liquid partial wetting of solid surface contact angle hysteresis model 4-98404  
 liquids, on polymers, effect of surface roughening 4-98401  
 polyethylene, determ. of free surface energy 4-104039  
 polyethylene terephthalate films, photooxidation and ageing, ESCA and contact angle obs. 4-61806  
 porosimetry, Hg, hysteresis theory 4-73418  
 powders, dynamic critical surface tension of wetting 4-108677  
 solid surfaces contacting liq.-gas soln., bubble nuclei stability 4-92477  
 surface free energy, contact angle meas., spreading press. effects 4-61173  
 Ag films and particles on MgO, surface diffusion under intense electron irradiation 4-98412  
 C strip, graphitised, wetting by melts of Al and Al-Si 4-92476  
 Cu-Sn-P bronze sintered permeable materials, capillary props. 4-65519
- contact e.m.f. *see* contact potential
- contact lenses  
 cornea microscopy using soft contact lens (Italian) 4-81818  
 hydrogel contact lens wearers, qualitative vision rel. to qualitative overkeratometry 4-109793  
 hydrogel materials, refr. indices meas. by interferometry 4-62542  
 ophthalmic solutions lubrication props. meas., using strain gauge bridge 4-89797  
 pachometry measurements, reliability and variability 4-109792  
 soft contact lens, press. distrib. behind 4-100220  
 soft contact lens systems, power and radius changes induced by flexure 4-77425  
 soft contact lenses, toric, double-thin zone, flexure effects 4-109992  
 types, advantages and disadvantages 4-62644
- contact potential  
*see also* contact resistance  
 Josephson point contacts, freq. locking 4-80727  
 Schottky contact formed on back contact-semiconductor interface of degraded solar cells, barrier height 4-109745  
 water drop collisions, charge separation, contact-balloelectric mechanism 4-72676  
 GaAs (110)-Al interface form. at low temp., electronic and struct. props. 4-84695  
 Ni surface, sputter-cleaned, work function meas. 4-114017  
 Si-metal struct., scanning-tunnelling microscopy, voltage drop 4-114038
- contact resistance  
*see also* contact potential  
 closed contact temp. rise with regard to skin effect, calc. (Russian) 4-84671  
 III-V semiconductors, contact resistance profiling 4-75499  
 measurement for two different metals, allowing for thermal EMF 4-92794  
 solar cell contact resist., review 4-81544  
 solar cells, contact resist. meas. and importance rel. to power loss 4-81545  
 Al, fretting in elec. contacts 4-92798  
 Al-Si/ $n^+$ -Si system, metallisation by fast heat pulse alloying, hillock elimination 4-114034  
 Au electrodeposits on contacts, performance eval. 4-76020  
 Au/Al contacts, intermetallic bonds and contact resist. (Russian) 4-113819  
 Au-Ge-Ni ohmic contacts on GaAs, CO<sub>2</sub> laser alloying 4-76038  
 a-Ni<sub>2</sub>W<sub>64</sub> contacts on Si, elec. charact. 4-104311  
 Pd-Ni electrodeposits on contacts, performance eval. 4-76020  
 Si-Mo-Ni contacts, elec. charact. study 4-80653  
 W-Ti/Si direct contact system, contact resist., heat treatment effects 4-114032
- contacts, electrical *see* electrical contacts
- context-free grammars  
 skeletal maturity, syntactic recognition 4-72354
- continuous creation hypothesis *see* cosmology
- continuum hypothesis *see* set theory
- continuum mechanics *see* classical mechanics of continuous media
- contours, surface *see* surface contours
- contrast transfer function *see* optical transfer function
- control system synthesis  
*see also* correlation methods; frequency-domain synthesis; frequency response; linearisation techniques; perturbation techniques; poles and zeros; root loci; sensitivity analysis; stability; state-space methods; step response; transfer functions  
 nuclear reactor, suboptimal stochastic control 4-102346  
 nuclear reactor optimal feedback control by frequency-domain methods 4-64197
- control systems  
*see also* adaptive systems; closed loop systems; distributed parameter systems; multidimensional systems; multivariable control systems; optimal control; physical instrumentation control; sampled data systems; time-varying systems  
 advances in instrumentation, conf. Houston, Texas, USA (Oct. 1983) 4-106121  
 automotive Stirling engine development program—overview and status report 4-66777  
 gas driven heat pumps in public buildings (German) 4-81580  
 MOD I automotive Stirling engine development 4-66776  
 optical layer fabrication process automated control 4-74751  
 underground mining vehicle hydrogen engine fuel control 4-62406
- controllers  
*see also* cryostats; instruments; servomechanisms; thermostats  
 AC high-stability microprocessor-based temperature controller for use at high temperatures 4-111119  
 advances in instrumentation, conf. Houston, Texas, USA (Oct. 1983) 4-106121  
 annealing furnaces AC power supply, temp. controller 4-106297  
 automatic liquid N<sub>2</sub> filler controller 4-86402  
 baseline sail system controller 4-72751  
 domestic solar system instrumentation, long-term stability and performance 4-99989  
 environmental and thermal control for space vehicles, conf. Toulouse, France (Oct. 1983) 4-73162  
 functional neuromuscular stimulation, pulse-train controllers 4-89845  
 high technology electronics exhibition and conference, Detroit, MI, USA (June, 1983) 4-95014  
 neuroprostheses, controllers for electrically activated muscle 4-89843  
 nuclear reactor digital control schemes, experimental evaluation 4-86932  
 optical discs systems and applications, conf., Arlington, VA, USA (June, 1983) 4-90287  
 PID controllers for solar total energy experimental facility, operating characteristics 4-72183  
 precision programmable temperature regulator 4-101826  
 temperature controller design, for surface phenomena exam. by electron spectroscopy 4-78304  
 two-shutter controller for investigation of the kinetics of the recording of dynamic holograms 4-87303  
 vehicular technology conf. Pittsburgh, PA, USA (May 1984) 4-106118
- convection  
*see also* convection in liquids  
 advection-diffusion equations, space-time least-square finite element scheme 4-64903  
 air, free convection along nonuniformly heated vertical plate, transpiration effects 4-97279  
 air pollutant distrib., 2-dimens., convection and diffusion 4-62417  
 air refrigeration, transient natural convection heat and mass transfer 4-75006  
 alloys, solidifying, convection, anal. in two-phase zone 4-98276  
 arterial wall mass transport to viscous fluid flow 4-89609  
 atmosphere, convective and boundary layer parametrizations in diagnostic model of fronts 4-82198  
 atmosphere, stability criterion for moist compressible atmosphere and energy conditions for cloud development (Russian) 4-67310  
 axisymmetric and 3-dimens. convection anal. using penalty finite elements, computer code (Japanese) 4-64193  
 ball powders, convective combustion in strong confinement numerical simulation 4-114795  
 Benard convection and the Cattaneo law of heat conduction 4-69665  
 Benard convection with time-periodic heating 4-64946  
 Benard-Marangoni problem, nonlinear stability analysis 4-112863  
 binary fluid mixtures, Benjamin-Feir instability convection onset 4-6494  
 boiling, forced, flow oscillations, finite difference analysis of density-wave oscillations 4-75955  
 boundary layer natural convection regime in rectangular cavity 4-11287  
 cellular, in fluid layer between horizontal porous plates with nonuniform heat source 4-75082  
 channel, vertical, natural convection, finite element analysis 4-75023  
 chemical reactions, dynamics of parabolic eqns. describing diffusion and convection 4-89240  
 closed areas with high side ratios, hydrodynamic and heat flow characteristics (Russian) 4-64938  
 collocation method for convection dominated flows 4-79576  
 combined heat and mass transfer in natural convection on a horizontal surface 4-87718  
 combined Marangoni- and natural convection in a variable micro-gravity field 4-112675  
 combined natural and forced convection in horizontal porous channels 4-75004  
 conducting liq. (Russian) 4-113061  
 convection loop, chaotic flow regimes 4-87680  
 convection-diffusion problem porous medium, strong solns. in 3D case (French) 4-87698  
 convective heat transfer in complex turbulent flows, time to abandon wall functions 4-112856  
 coupled heat-mass transfer in natural convection under flux conditions along vertical cone 4-69754  
 crystal growth, conference, Stuttgart, Germany (Sept. 1983) 4-58552  
 crystal growth, interfacial transport, parametric comparison of convective effects 4-60872  
 crystal growth from vapours, diffusive-convective vapour transport 4-114368  
 cylinder, horizontal, transient behaviour of natural behaviour 4-75024  
 cylinder system, convective heat transfer between vertical concentric cylinders, rot. effects 4-75026  
 cylinder system, natural convection between two vertical concentric cylinders 4-75025  
 Czochralski crystal growth method, crystn. rate during fluctuations of melt temp. 4-71545  
 Darcian free convection boundary layer flow about semi-infinite vertical plate 4-112879  
 dielectric fluid vertical layer in horiz. AC elec. field, stability of natural convection 4-79583  
 dielectric liq., plane layer, electrothermal convection, cond. mod. 4-112877  
 dielectric liq. layers subjected to electric field, oscillatory convective instability, dielectric constant 4-103427  
 drops, chemically reactive, convective heat and mass transfer 4-112850  
 Earth mantle, admittance for convection in layered spherical shell 4-67204  
 Earth mantle, convection with press. and temp. dependent non-Newtonian rheology 4-67203  
 EHD flows, properties and convective mechanism of current transfer (Russian) 4-113073  
 electrostatic cooling, development of flow vel. in boundary layer (Japanese) 4-84098  
 enclosed cavity, natural convection, buoyancy driven flow, boundary layer 4-87714  
 enclosed concentric vertical cylinders natural convection, laminar flow pattern visualisation 4-97531  
 external heating of a flat plate in a convective flow 4-97555

## convection continued

fast jet furnace with top-mounted burners, heat exchange 4-97629  
 film condensation with lateral mass flux about a body of arbitrary shape in a porous medium 4-108598  
 fin geometry optimisation, simultaneous, convective and radiative heat transfer 4-97280  
 finite-difference solutions of convection-diffusion problems in irregular domains, using a nonorthogonal coordinate transformation 4-107991  
 finned tube, cross flow, convection heat transfer and press. drop 4-103329  
 finned tube staggered-array banks, in transverse arrays, heat transfer and hydraulic resistance 4-112679  
 flow through porous medium, effects of Hall current on heat and mass transfer 4-101125  
 fluid convective sheath, oscillations and bifurcations in 2-D 4-91794  
 fluid in nearly spherical cavity, convective motions 4-91808  
 fluid interfaces with elec. double layers, coupled longitudinal and transverse wave motion 4-64944  
 fluid layer overlying layer of porous medium, vel. and temp. distrib. 4-103410  
 fluid motion in a cavity, Benard problem, finite element study 4-65025  
 fluid particle pair, relative diffusion in turbulence 4-91807  
 fluidised bed tubular flow, twisted tape heat transfer augmentation 4-97530  
 forced convection heat and momentum transfer to dendritic struts. 4-97557  
 forced convection of non-Newtonian flow past a nonisothermal needle 4-60426  
 forced convection systems, correl. of thermophoretically modified particle diffusion deposition rates 4-87703  
 forced convective boiling in uniformly heated tubes, critical heat flux 4-112698  
 free convection and mass transfer through porous medium, rot. and Hall currents effect 4-108074  
 free convection between concentric spheres, Navier Stokes and energy eqns. 4-79588  
 free convection effects on turbulent transport of liquid in vertical channel 4-60406  
 free convection of non-Newtonian fluids over non-isothermal two-dimensional bodies 4-87712  
 free liquid surface response induced by fluctuations of thermal Marangoni convection 4-79606  
 free-convection flow past exponentially accelerated vertical plate, theory 4-67610  
 furnace, thermal processes, numerical study 4-107985  
 gas, convective motion resulting from propag. of heat wave along lower boundary of closed region 4-87717  
 gas layer, planar, convective instability in absence of external forces 4-74840  
 geophysical convection processes 4-105677  
 glacial ice in saline water, mixed convection melting, heat and mass transfer 4-87701  
 glycerin, laminar free convection in a vertical tube with temperature-dependent viscosity 4-112860  
 heat accumulators with solid filler, heat transfer by air stream 4-93640  
 heat exchangers, open-topped, closed-sided, with vertical fins, heat transfer rates enhancement, for use in electronic equipment cooling 4-79420  
 heat transfer coeff. in highly circulating reheating furnace, aerodynamic props. 4-103318  
 heated chimney under conditions of natural convection, dynamic stability (German) 4-83902  
 high-performance surfaces for non-boiling heat transfer, review 4-83800  
 honeycomb structure transparent insulation rel. to solar energy use, heat loss mechanisms 4-114946  
 horizontal Bridgman cryst. growth, thermal convection and longit. macrosegregation, order of magnitude analysis 4-98040  
 horizontal Bridgman cryst. growth, thermal convection and longit. macrosegregation, practical laws 4-98041  
 horizontal cylinder in channel flow, natural convection enhancement 4-112876  
 horizontal finned tubes in cylindrical container, free convection heat transfer 4-103330  
 horizontal line heat source, laminar natural convection flow, stability characts. 4-75013  
 horizontal square cylinder, natural convection, temp. inversions 4-87702  
 human lung airways, convective gas mixing, laminar rel. to turbulent dispersion 4-89615  
 hydromagnetic free convection past on impulsively started vertical plate in rot. fluid 4-108114  
 hypersonic boundary layer, turbulent, three-dimens., on sharp cone at angle of attack, heat transfer interactions 4-79621  
 ice, formation on flat surfaces, convective boundary layers 4-112811  
 incompressible Newtonian fluids, numerical simulation 4-91801  
 initial heating period for a massive body in a high-temperature oven 4-74838  
 intensification of heat transfer (German) 4-112689  
 isothermal cylinder in conditions of natural convection, heat transfer 4-79579  
 jet wall cooling, protective layer, temp. distrib., boundary conditions effect 4-60405  
 laminar and turbulent natural convection in an enclosed cavity 4-87660  
 laminar Benard convection by energy integral method 4-97533  
 laminar duct flow development with external radiation and convection 4-97468  
 laminar flow, heat transfer from rot. cylinder with external longitudinal fins 4-60413  
 laminar flow, internal heat generation in vertical triangular channel, combined free and forced convection 4-103327  
 laminar flow, separated forced convection in cavities, finite difference anal. 4-112812  
 laminar flow with convective heat transfer, over flat plate, approx. integral methods improvement 4-75020  
 laminar fluid convection between concentric and eccentric heated rot. cylinders 4-79550  
 laminar free convection from vertical flat plate 4-75007  
 laminar free convection in a vertical tube with temperature-dependent viscosity 4-112860  
 laminar natural convection heat transfer from slender cone to power-law fluid 4-60399  
 laminar three-dimensional flow, temp. profiles and heat transfer rates, matched asymptotic solns. 4-75001

## convection continued

liquid metals, MHD convection in two-layer systems heated from below 4-108135  
 local heat transfer coeffs. distrib. of cylinder covered with close-fitting fabrics 4-112674  
 locally analytic differencing scheme to test convection-diffusion problems 4-107990  
 long horizontal pipes with different end temperatures, anal. (Chinese) 4-78276  
 low Prandtl number convection, transition to turbulence, numerical anal. 4-69765  
 macromolecules, membrane rejection coeffs., conc. and charge effects 4-89333  
 Magneto-Boussinesq approximation by scale anal. 4-101144  
 magnetoconvection in a rotating fluid between walls of very low thermal conductivity 4-97577  
 mantle with heterogeneous distrib. of heat prod. elements 4-72549  
 Marangoni boundary layers, axially symmetric 4-97524  
 Marangoni effect in the Couette flow 4-64945  
 Marangoni thermal convection, numerical anal. of microgravity expts. 4-97526  
 Marangoni-Stokes flows in Plateau configurations, gravity level effects 4-97525  
 marginal stability curve and linear growth rate for rotating Couette-Taylor flow and Rayleigh-Benard convection 4-64921  
 mass transfer effects on flow past vertical plate, variable temp. or const. heat flux 4-101130  
 methane flames, high temp., laminar flow, stagnation point heat transfer 4-65037  
 MHD convection, mag. field and temp. modulation effects 4-103428  
 MHD free convection with mass transfer in rot. fluid, effects of Hall current 4-101134  
 MHD free-convection flow near vertical oscillating plate, theory 4-67618  
 MHD free-convection oscillatory flow past porous limiting surface; effects of Joule heating and viscous dissipation 4-67616  
 MHD free-convection oscillatory flow past porous limiting surface, effects of Joule heating and viscous dissipation 4-67615  
 mixed convection about horizontal heated surface in fluid-saturated porous medium, non-similar boundary layer anal. 4-69752  
 mixed convection modes in a vertical layer with unsteadily deformable boundaries 4-108068  
 multiphase two-dimensional flow, finite element study, five-spot problem 4-103389  
 natural convection, 3D, in inclined cylindrical annulus, flow visualisation 4-87710  
 natural convection along isothermal vertical surface 4-112859  
 natural convection effects in the continuous casting of a horizontal cylinder 4-87707  
 natural convection from a cooling vertical sheet 4-69762  
 natural convection from an isothermal downward facing horizontal plate 4-69755  
 natural convection heat transfer from vertical plate, approx. soln. 4-69753  
 natural convection heat transfer in complex enclosures at large Prandtl number 4-60424  
 natural convection in a rectangular cavity, analytical soln. 4-108078  
 natural convection in density-stratified layers in rectangular vessel, flow patterns 4-97528  
 natural convection in inclined air layer 4-103317  
 natural convection in inclined water layer, thermal instability and heat transfer, interferometric study 4-112855  
 natural convection in porous media in rectangular cavity, transient characts. 4-60397  
 natural convection in rectangular cavity, wall conductance effect 4-103323  
 natural convection in saturated porous layers with internal heat sources 4-87705  
 natural convection in sealed tube for crystal growth by gas phase transport 4-71538  
 natural convection of a viscoplastic fluid in vertical circular channels 4-112851  
 neutrally buoyant anisotropic particles for flow visualization 4-65015  
 nonDarcy regime for vertical boundary layer natural convection in a porous medium 4-87709  
 nonlinear convection in high vertical channels 4-87716  
 nonlinear steady-state thermal anal., reduction methods 4-91714  
 nonlinear thermal anal., hybrid perturbation/Bubnov-Galerkin technique 4-64818  
 nonlinear thermal convection in spherical shell 4-108076  
 nonNewtonian fluid, free convection motion studied by interferograms 4-103326  
 nonrectangular inclined enclosure, convective fluid motion and heat transfer 4-64941  
 nonsimilar stratified flow over vertical flat plate unsteady incompressible laminar free convection boundary layer 4-97639  
 nonspherical objects at high Rayleigh number, natural convection mass transfer 4-79577  
 nucleate pool boiling, bubble growth rates and departure vols. 4-97649  
 ocean, turbulence meas. in convective mixed layer 4-100615  
 optical method for local heat transfer coeffs. estimation 4-97286  
 oscillatory flow past infinite porous vertical plate, suction and free convection effects 4-75081  
 packed distillation columns, Marangoni effect 4-64935  
 parallel plates, natural convection-cooled, thermally optimum spacing 4-112875  
 particle-fluid mixture with temp. gradient, oscills., thermal convection instability 4-87697  
 periodic heat flow, in infinite cylinder 4-112673  
 phase-change problems, implicit/explicit numerical soln., convective heating 4-80197  
 physical and computational aspects of convective heat transfer, book 4-86128  
 planar or radial freezing with solid-solid transitions and convective heating at the solid-liquid interface 4-80198  
 plasma, collisionless, energy vars. and elec. fields rel. to convection 4-100868  
 plasma convection, effect on charged particle transport in random mag. fields 4-94569  
 polymer melts, laminar, three-dimensional flow, temp. profiles and heat transfer rates, matched asymptotic solns. 4-75001

## convection continued

- porous powdered fuel, nonstationary convective combustion regimes 4-81442
- porous slab, single-period oscillatory convection (*French*) 4-112998
- porous systems, nonstationary convective combustion eqns., qualitative anal. 4-71923
- power law fluids, forced convection over a flat plate 4-108094
- power-law fluid, axisymmetric stagnation point flow, mass transfer 4-87765
- rarefied gas, Hall current effects on convective flow in slip flow regime 4-101128
- Rayleigh-Benard convection, externally modulated, Lorenz eqns. 4-91809
- Rayleigh-Benard convection, symmetries and pattern selection 4-87672
- Rayleigh-Benard convection in vertical rotation and mag. field, stability 4-79591
- Rayleigh-Benard convection onset, nonlinear pattern formation 4-91810
- Rayleigh-Benard convection problem, boundary layer type solns. 4-75018
- Rayleigh-Bernard convector between insulating boundaries, free boundary conditions 4-79590
- recirculation of fluid in porous layer heated from below 4-97673
- roll-pattern evolution in finite-amplitude Rayleigh-Benard convection in a two-dimensional fluid layer bounded by distant sidewalls 4-87730
- rotating fluid, natural convective flow, Hall current and wall temp. oscils. effects 4-97575
- rotating porous layer, thermal convection 4-60429
- rotating wavy channels, nonlinear convective flows 4-103332
- salt gradient solar pond, stability, effective insulation, heat loss 4-105120
- salt-finger convection in shear flow 4-64947
- saturated porous medium, thermal convective instabilities, temp. distrib. 4-112878
- segregated media, combined convection-radiation anal. 4-64934
- semi-infinite plate with uniform surface heat flux, MHD free convection flow 4-60558
- shear flow turbulence modelling, buoyancy effects 4-79575
- sheetlike plumes near a heated bottom plate at large Rayleigh number 4-64943
- similarity solution for combined forced and free convection 4-112847
- single-brain solar still coupled to flat-plate collector, water flow over glass cover, transient anal. 4-99994
- softwood, high temp. convective drying, transfer phenomena 4-87540
- solar collection, flat plate, natural convection visualisation 4-100002
- solar dryer, radiatively convective type, design, construction and testing to avoid 'burn-up' 4-62390
- solar energy utilisation in heating installations with air convection (*German*) 4-62300
- solar pond, saturated, laboratory-scale, self-generation 4-62396
- solar ponds, intrinsic movement under convection (*Spanish*) 4-75002
- solar ponds, operating at different latitudes, performance characts. 4-105119
- solid phase change material, melting in rectangular enclosures, convection 4-112866
- solid-liquid interface, convective coupling in internally heated vertical cylinder 4-97562
- sound absorpt. by turbulence and other hydrodynamic flows 4-60434
- sound scattering by convection, perturbation theory 4-74794
- sphere, isothermal, submerged in infinite Boussinesq fluid, natural convection heat transfer 4-75022
- square cylinder, natural convection heat transfer in 'laminar' and turbulent regions 4-87696
- stationary constant coefficient diffusion-convection reaction eqn., difference scheme errors 4-69766
- steady natural convection in cavities, oscillatory approach 4-112873
- steam, high press. high temp., convection-radiation interaction 4-74018
- surface-layer similarity in turbulent circular Couette flow 4-103307
- thermal convection, stabilising solute gradient effect 4-75017
- thermal convection in a porous medium with horizontal cracks 4-97551
- thermal ignition in porous media, convection effects 4-79657
- thermally and hydrodynamically developing flow in horizontal curved pipes, convection 4-112871
- thermals with large density difference, turbulent thermal theory 4-112848
- thermocapillary convection in a two-layer system 4-69758
- thermocapillary instabilities in liq. bridges 4-75016
- thermogravitational convection, struct. in flat variously oriented layers of liq. and on vertical wall 4-112815
- thermohaline columns, layered, wave motion at boundaries 4-87742
- thermohaline convection with rot. and mag. field, semicircle theorems 4-97700
- thermopolar fluid, elec. cond., laminar free convection flow from vertical plate 4-97475
- thermosiphon solar domestic hot water system performance 4-62394
- tilted cavities, cusp catastrophe for Benard convection numerical study 4-87715
- time-dependent natural convection in Hele-Shaw cells, boundary layer instability (*German*) 4-83901
- transient boiling heat transfer from small diameter wire and thin film flat surface 4-103321
- transient convective motions in a cavity with a free boundary 4-60403
- transient laminar convective heat transfer inside circular duct 4-60427
- transient natural convection in a cavity 4-103324
- transition from conduction to convection around a horizontal cylinder experiencing a ramp excursion in internal heat generation 4-97268
- tubes, elliptical, heat transfer with natural convection 4-103331
- turbulence, spectral analogy between temp. and vel. fluctuations 4-97511
- turbulent channel flow, wall press. field calc. 4-60552
- turbulent film condensation on horizontal circular cylinder 4-69744
- two dims. turbulence, enstrophy convection region (*German*) 4-64924
- two-phase droplet flow, convective and radiative heat transfer 4-75073
- unsteady free convection flow of a visco-elastic fluid past a vertical porous flat plate 4-69763
- unsteady free convection near a forward stagnation point at small Prandtl number 4-75012
- unsteady laminar natural convection, MAC scheme in boundary-fitted curvilinear coordinates 4-60409
- unsteady natural concentration convection in closed region, 3D effects influence 4-112852
- unsteady natural convection in a cavity with internal heating and cooling 4-60408
- unsteady thermal convection in a cylindrical vessel heated from the side 4-69757

## convection continued

- vacuum-shield heat insulation, multilayer, radiative-molecular-conductive heat transfer 4-112684
- vapour growth systems, convective transport, gravity effects 4-65203
- vertical annular gas layers with const. heat flux on inner wall, heat transfer 4-60423
- vertical layer with uniform volumetric heat source, thermal stability of natural convection 4-75019
- vertical transient natural convection flows in cold water 4-112858
- vertical vorticity, influence on thermal convection 4-60396
- viscous fluid flow hydrodynamic params. In convective problems for flow separation in channels 4-79587
- viscous fluid local swirling, convective heat transfer intensification by axial flow bladed swirling unit 4-79585
- visualisation of convective heat transfer 4-60425
- water, combined forced and free convective flow at 4°C past semiinfinite vertical plate 4-64942
- water, phase transitions parameterisation, deep concern eqns. 4-79578
- weakly absorbing dielectrics and semiconductors, convective instability and self-focusing 4-97009
- CO<sub>2</sub>, radiation convection heat transfer problem plane channel, turbulence 4-60378
- He II, thermohydrodynamics eqns. and reduced density matrices 4-84480
- In-Ga-Sn, natural convection, mag. field orientation influence (*Russian*) 4-113061
- Na surface fires in reactor containment, convection current computation, KONVEC 4-91083
- convection in liquids**
- Benard convection in very dilute polyacrylamide solns., holographic study (*German*) 4-83900
- book 4-82606
- cholesteric liquid crystals, hydrodynamics in coarse-grained limit 4-87700
- cholesteric liquid crystals, long pitch, thermal instabilities, continuum theory 4-79928
- crystal growth, Czochralski configuration, buoyant, thermocapillary and forced convection expts. 4-65206
- crystal growth, finite-element simulation of Czochralski bulk flow 4-65207
- crystal growth from solution, growth kinetics, comp. inhomogeneity, morphological stability, convection effects 4-65205
- crystal growth from solution, top seeded method, hydrodynamics in high temp. solns., simulation 4-65208
- crystal-melt interfaces, coupled convective instabilities 4-88120
- cylindrical floating zone, steady flow under low gravity, computer simulation 4-61837
- Czochralski cryst. growth, melt. convection suppression using heater-mag. solenoid coils 4-71546
- dielectric liquids, central-symmetry convection in microgravity, simulation 4-97523
- edge defined film fed crystal growth, lateral solute segregation 4-88119
- film boiling heat transfer, radiation effect, on plane wall parallel to upward vertical flow 4-112676
- fluid fueled marine nuclear reactor, convection and heat dissipation, numerical anal. 4-86938
- fluid velocity measurement in convection flows, thermistor anemometer appl. 4-97729
- forced convection boiling, critical heat flux in uniformly heated round tubes 4-83799
- forced Lorenz system, limit cycles 4-103292
- heat transfer consideration in energy resources 4-85387
- heated fluid, oscils. and chaos at free surface 4-83886
- n-heptane, supercrit. coolant, forced convection heat transfer 4-83898
- ice layer, melted, vertical, with variable viscosity, onset of convection 4-79592
- Maxwell-Cattaneo fluid, Benard-Marangoni instability 4-112864
- melt growth systems, convective transport, review 4-65204
- melting heat transfer with regard to different geometric arrangements 4-108072
- melting process, coupling of natural convection and phase change (*French*) 4-112854
- nematic liquid crystal, heat convection, orientational optical nonlinearity 4-112504
- nonchaotic Rayleigh-Benard convection with four and five incommensurate frequencies in water 4-97560
- n-octadecane, melting from cavity wall, heat transfer meas. 4-112865
- one-dimensional thermocapillary motion 4-61184
- pattern selection in single-component systems coupling Benard convection and solidification 4-103322
- semi-insulating liquids, electrokinetic streaming current, induction sensing 4-65033
- simulated floating zone configuration in reduced gravity, oscillatory thermocapillary convection 4-61834
- solidification, transport processes and growth morphology under microgravity 4-89051
- solidifying binary melt, thermoconcentrational gravitational convective motion and solute distrib 4-61049
- stagnation zone effects (*Spanish*) 4-69751
- subcooled small metallic drops, rapid solidification, internal nucleation 4-71648
- thermoconvection loop, L.L.O.-7, for studying corrosion behaviour of stainless steel in liq. Li 4-107059
- transparent liquids, separation due to interface convection (*German*) 4-112880
- viscous liquid, flow through porous bed, analogy with unsteady MHD convective diffusion 4-75080
- water, natural convection in inclined rectangular cavity at density extremum 4-112874
- water, superheat, natural convection effect on freezing around isothermal horizontal cylinder 4-108588
- water in inclined square cavity density inversion, natural convection 4-79584
- weakly-conducting fluid, isothermal flow in nonuniform elec. field (*Russian*) 4-83958
- Al-Cu, directional solidification, off-eutectic composite growth, segregation, convection effects 4-71647
- Ga<sub>0.4</sub>Al<sub>0.6</sub>As-GaAs heterostructures, LPE growth, layer height profiles related to convection and cooling rates 4-66248
- GaAs crystal, numerical simulation of horizontal Bridgman growth 4-66212
- He II, flowing, heat transport, transition heat flux limitations 4-80323

**convection in liquids continued**

- He, liquid, supercritical, mixed convection heat transfer to upflow in vertical tube 4-69750  
<sup>3</sup>He-<sup>4</sup>He mixtures, convection onset near  $\lambda$  line, effect of parametric modulation 4-104031  
<sup>4</sup>He, liq., convection in rot. cell, stability and heat transfer study 4-113736  
 Hg, chaotic phases, mag. order and Rayleigh-Benard convection 4-69761  
 SrF<sub>2</sub>, electrolyte crystals in supersaturated aqueous soln., crystal growth kinetics 4-114373

**convergence**

- see also *convergence of numerical methods*  
 bearings-only tracking, recursive vs. batch processing algorithms 4-107942  
 four-point vertex, convergence of crossing-symmetric perturbation series 4-63866  
 Fredholm eqns. solns. through nonlinear iterative processes 4-67960  
 probability density function estimates, derivatives and mode, convergence rate 4-63488  
 Thomas-Fermi eqns. soln. using imaginary time step method 4-68627

**convergence of numerical methods**

- acoustic scattering, boundary element methods and their asymptotic convergence 4-83751  
 computer-extended series, bad behaviour and counter measures 4-67981  
 diatomic mol., pot. function, inverse problem convergence 4-59874  
 EELS, plural scattering removal techniques 4-73601  
 electrostatic rotationally symmetric lens systems, potential and field strength calc. by convergent Fourier-Bessel series 4-96772  
 few group two-dimens. HEXAB-II-30K, outer iteration convergence acceleration (*Russian*) 4-78660  
 inviscid and viscous flow computations, multiple-grid convergence acceleration 4-60455  
 Navier-Stokes eqns., explicit system convergence (*Russian*) 4-87656  
 plates, thin, viscoelastic, finite element anal. 4-112721  
 power-law fluid, flow over flat plate, boundary value problems 4-87764  
 ring laser, bidirectional homogeneously broadened, stability analysis 4-107690  
 tectonics, Signorini problem without friction in linear thermoelasticity 4-67199  
 two dimensional transonic flow, solution of Euler equations by multigrid method 4-60453

**conversion electron spectra**

- conversion electron Mossbauer spectrometer for depth selective spectroscopy 4-74089  
 steel, corrosion products in H<sub>2</sub>S-N<sub>2</sub>(-O<sub>2</sub>), chem. anal. by conversion electron Mossbauer spectroscopy 4-66473  
 steel, corrosion products in SO<sub>2</sub>, chem. anal. by conversion electron Mossbauer spectroscopy 4-66472  
<sup>241</sup>Am nucl. structure study with ( $\gamma$ , $\gamma$ ) reaction 4-68651  
<sup>106</sup>Cd, A=106, 108, levels study from  $\beta^+$ /EC decay of <sup>106</sup>In<sup>m+8</sup> and <sup>108</sup>In<sup>m+8</sup> 4-68645  
<sup>108</sup>Cd( $\alpha$ ,n)<sup>111</sup>Sn, excited states, in-beam spectroscopic methods, shell model predictions 4-102221  
<sup>134</sup>Ce level structure study using  $\gamma$  and e<sup>-</sup> spectroscopic methods 4-59127  
<sup>201</sup>Hg(d,pn $\gamma$ ), A=202, 204, 25 MeV, gamma ray and conversion electron spectra, yrast state population 4-102162  
<sup>201</sup>Pb(d,pn $\gamma$ ), A=196,198, 25 MeV, gamma ray and conversion electron spectra, yrast state population 4-102162  
<sup>228</sup>Th, A=228,230, rotational levels from ( $\alpha$ , $\alpha'$ ,n) reactions 4-68609  
<sup>232</sup>Th(d,pn $\gamma$ ), 25 MeV, gamma ray and conversion electron spectra, yrast state population 4-102162  
<sup>128</sup>Xe, low-lying states, internal conversion study from <sup>128</sup>Cs decay 4-95962  
<sup>174</sup>Yb(d,pn $\gamma$ ), 25 MeV, gamma ray and conversion electron spectra, yrast state population 4-102162

**convertors**

- see also *analogue-digital conversion; digital-analogue conversion; direct energy conversion; frequency convertors; image convertors; magnetohydrodynamic convertors; solar absorber-convertors*  
 dual differential discriminator with accurate time linkage to a time-to-height converter 4-107265  
 laser anemometer gas streak vel. meas. electro-optical convertor and photoelectric controller appl. (*Russian*) 4-60564  
 transducer systems for bio-data recording and bio-data processing (*German*) 4-77414  
 UV convertor transients induced by electrons 4-110520  
 V-convertor outlet signal, electronic evaluation (*German*) 4-77420

**cooling**

- see also *Joule-Thomson effect; low-temperature production; magnetic cooling; quenching (thermal); refrigeration; supercooling*  
 air saturated porous media in short cylinder, transient heat transfer 4-108073  
 Aquaplast aq. soln., cooling capacity investig. 4-83899  
 boundary layer natural convection regime in rectangular cavity 4-112872  
 building cooling using air tubes 4-62319  
 composite materials, viscoelastic, thick-wall cylindrical shell, optimal non-steady cooling process 4-87589  
 composites, polymeric, thick-wall cylinders, allowance for rheology 4-87590  
 convective heat transfer, physical and computational aspects, book 4-86128  
 cyclopropane, jet-cooled, IR laser spectrosc. 4-83373  
 cylinder, long two layer, temp. field, Newton's law appl. 4-107988  
 deep-sea water pumping for onshore facility cooling 4-115445  
 desiccant dehumidifier cooling system, sorption props. effect on performance 4-88404  
 effusion-cooling, fouling rate advantages, particulate thermophoresis effect 4-65011  
 electronic controls for solar heating and heat/cool storage systems 4-93642  
 electrostatic cooling, development of flow vel. in boundary layer (*Japanese*) 4-84098  
 film cooling effectiveness and turbulence distribution of discrete holes on a convex surface 4-112829  
 film cooling of walls, effect of cooling-gas injection arrangement 4-65137  
 finite solid radiant cooling 4-107978  
 fluid fueled marine nuclear reactor, convection and heat dissipation, numerical anal. 4-86938

**cooling continued**

- forced convection systems, correl. of thermophoretically modified particle diffusion deposition rates 4-87703  
 frost layers on cold surfaces, growth rate and props. 4-60259  
 fuel-element assemblies, cooled with N<sub>2</sub>O<sub>4</sub> disoc., thermophysical transients cal. 4-83887  
 gas cooling and condensation in vortex flow 4-69764  
 gas driven heat pumps in public buildings (*German*) 4-81580  
 gases, relaxation times calc. using kinetic cooling data 4-64577  
 He-Cd laser with lateral HF discharge, different design comparative charts. (*Russian*) 4-69372  
 heat and mass transfer on filament-type packing in contact-type exchangers 4-83894  
 heat conduction of coolant in flow direction (*Chinese*) 4-83885  
 heat exchangers, open-topped, closed-sided, with vertical fins, heat transfer rates enhancement, for use in electronic equipment cooling 4-79420  
 heat pump future development prospects 4-77135  
 hybrid desiccant air conditioning systems for commercial buildings, performance influencing factors 4-72166  
 hybrid desiccant vapor compression cooling system 4-86416  
 hydromagnetic free convection past on impulsively started vertical plate in rot. fluid 4-108114  
 ice formation in water flow between two horizontal parallel plates, transition phenomenon 4-64834  
 industrial thermoelectric water cooling 4-77130  
 Infrared Space Observatory dual liquid H<sub>2</sub>/2 superfluid He coding system thermal design 4-73441  
 Infrared Telescope in Space, mirror testing apparatus and cooling effects (*Japanese*) 4-91565  
 integrated passive systems of heating and cooling buildings by natural energies 4-81522  
 inverse problems solution with unknown model of the process 4-79429  
 isopropanol, boiling burnout during crossflow over horizontal cylinders, subcooling effect 4-79594  
 jet wall cooling, protective layer, temp. distrib., boundary conditions effect 4-60405  
 Joule Thomson coolers at very low powers 4-101855  
 Large Coil Test Facility, pulse coil coolant system design 4-111884  
 laser mirrors, cooled, thermoelastic stability 4-102940  
 laser mirrors, high intensity, heat carrier use in powder and felt porous structs. 4-74659  
 linear Gortler instability of boundary layer flow over concave wall, heating effect 4-64920  
 liquid desiccant heating and cooling system, operational experience in residential use 4-72167  
 liquid metal cooling system, mass transfer in presence of strong mag. field (*Russian*) 4-113035  
 local pore cooling, steady-state problem 4-79664  
 magnetic disk files cooling-air diffuser for noise abatement 4-83763  
 materials for radiative cooling to low temperatures 4-112683  
 mean flow field and heat transfer along cooled supersonic diffuser 4-113077  
 methanol, boiling burnout during crossflow over horizontal cylinders, subcooling effect 4-79594  
 microcomputer simulation of thermal performance of a solar cooling system 4-93596  
 natural convection from a cooling vertical sheet 4-69762  
 nuclear power plants, emergency reactor core cooling system 4-97704  
 passively cooled shelters for unattended telecommunication sites 4-73435  
 peripheral nerve impulse cond. blocking by local cooling, animal expt. method 4-115307  
 phase separator for zero-g environment, design and test 4-73442  
 polymer fibres, cooling during melt spinning process 4-60258  
 polypropylenes, isotactic quenched melts, cooling rate effect on morphology 4-108291  
 Pratt's transient cooling soln. 4-97298  
 radiative cooling with selectively IR emitting gases 4-87834  
 radioisotope thermoelectric generator, fins and shell temp-time distribution and thermal stresses during water cooling 4-72139  
 relativistic electron beam, propag. in gases, return. current 2-dimens. mapping 4-69301  
 residential earth coupled heat pump in New York, field test 4-72152  
 residential heating and cooling, combinations of passive solar and energy conservation measures 4-66660  
 rewetting of a hot surface by a falling liquid film—effects of liquid subcooling 4-98403  
 roof-mounted solar distillation and water heating/cooling system performance 4-62301  
 semiconductor detectors, charged particles in outer space detection 4-91179  
 semiinfinite body with nonlinear heat liberation from surface, cooling 4-103190  
 slab with thermal contraction and progressive loss of contact with cold surface, cooling 4-60260  
 solar air conditioning system, with liquid desiccant, performance computer simulation 4-114944  
 solar desiccant residential cooling system high performance dehumidifier 4-72165  
 solar heat pumps for room and water heating (*Japanese*) 4-85385  
 solar heating and cooling systems, Japan's research and development status 4-77065  
 solid-state thermoelectric and thermomagnetic cooling below 200K 4-77131  
 spacecraft thermal control using Giotto shutter 4-83810  
 stable compositional gradient, heating and cooling from one side 4-97733  
 steel, CrMn, acoustic emission in H origin defects flux. 4-99534  
 synchrotron radiation, X-ray beam lines, high flux, grain boundary diffusion of coolants 4-95626  
 TEM, TV image recording system, SIT camera tube, cooling device 4-86505  
 thermoelectric cooler as power generator, configuration, capability and performance 4-77132  
 thermoelectric cooling device for cryoprecipitation by plasma separation 4-93938  
 thermoelectric residential heat pump, solar driven, feasibility 4-72151  
 tokamak reactor, swimming-pool type, radiation shielding for repair and maintenance 4-96250  
 trapped ion, laser cooled, steady state in Lamb-Dicke limit 4-69020  
 trapped two-level particle system, laser cooling, master eqn. 4-107315  
 turbomolecular pump, water cooling, lubrication, use with corrosive gases (*Japanese*) 4-73447

**cooling continued**

- two-phase cooling film on adiabatic wall 4-83943
- unsteady natural convection in a cavity with internal heating and cooling 4-60408
- water-air mixture jet, quenching 4-97643
- Zimmerman-Stirling cryogenic cooler, construction and operation 4-72146
- $\text{Fe}_{40}\text{Ni}_{40}\text{P}_{14}\text{B}_6$ , glass transition of thin film on substrate 4-92367
- GaAs/GaAlAs monolithically Peltier-cooled laser diodes 4-74540
- H, liq., target cooled by flowing He 4-59473
- $\text{H}_2\text{PO}_4$  pressurised fuel cell stacks, gas-cooled, performance evaluation 4-72103
- He II, flowing, heat transport, transition heat flux limitations 4-80323
- He cooling heat exchangers, comparison of Cu, Ag and Pd 4-95433
- LiBr-water double effect absorption cooling cycle modelling 4-72159
- Si surface, paramag. centre form. during strong cooling 4-65861

**cooling, splat** *see splat cooling***cooling towers**

- see also water supply*
- drift-measuring devices compared 4-62432
- extraction of Cr and Zn from cooling tower blowdown by liq. membranes 4-81474
- mechanical draft cooling towers, thermal performance capability calcs. 4-112849
- plume dispersion, advanced integral model 4-100016
- visible plume rise anal., use of time integrated photographs 4-100017

**Cooper Hewitt lamps** *see mercury vapour lamps***Cooper pairing** *see Cooper pairs***Cooper pairs**

- see also BCS theory; Josephson effect*
- BCS theory, Cooper pairing, crit. temps. calc. 4-104359
- dirty nearly ferromagnetic metallic films, triplet supercond., weak localisation effect 4-98798
- phonon anomalies in supercond. and ferroelectrics 4-65351
- quasi-one-dimensional supercond. under mag. field, spin effects 4-84730
- superconductors, Cooper pairing in the presence of antiferromagnetism 4-88631
- $\text{EuMo}_6\text{S}_8$ , bulk superconductivity obs. under pressure, multiple pair-breaking theory 4-71004
- Nb, phonon singularities on I-V curves, point contact spectroscopy 4-71000
- Nb-Ta, global pinning force density saturation 4-80730

**coordination complexes**

- inorganic complexes are indexed under the appropriate metal compound headings*
- organic molecules-electrically neutral metal complexes, outer-sphere coordination 4-62228

**copolymerisation** *see polymerisation***copolymers** *see polymers***copper**

- see also nuclei with .....*
- (001) with chemisorbed K monolayers, rotational epitaxy study 4-70566
- 24.8 MeV electrons backscattering, energy spectra 4-88912
- (100), surface dynamic processes, excitation of electron-hole pairs 4-70902
- (100), surface electronic struct. and 3d-band hole screening 4-70895
- (110) surface diffraction of Ne atoms, surface states 4-104706
- (111) substrate for Ag epitaxial film, interfacial effects in electron transmission 4-114050
- absorptivity of 10.6  $\mu\text{m}$ , temp. depend., computed from Drude theory 4-76405
- adhesion to sputtered  $\text{Al}_2\text{O}_3$  coating 4-76967
- adsorbed on Ag, electronic props., surface refl. spectroscopy study 4-85023
- adsorbed pyridine, evidence of surface enhanced Raman scatt. active sites 4-88839
- adsorbed pyridine, surface enhanced Raman scatt., effect of surface roughness, SEM obs. 4-76473
- adsorption and chemisorption of water vapour on (110), electron beam damage of adlayer 4-80397
- adsorption of CO multilayers on (100) surface, epitaxial growth of new cryst. struct., LEED, IR spectra 4-113373
- adsorption of  $\text{O}_2$  on (110) surface, influence of  $\text{Ne}^+$  ion bombard. 4-108723
- adsorption of water vapour on (110), electron beam damage to adlayer 4-80396
- adsorption on Au(111), underpotential region, LEED and RHEED investigation. 4-108702
- adsorption on W, work function changes 4-61202
- alkali chloride:  $\text{Cu}^+$ , two-photon spectra, impurity states 4-109215
- annealing texture development 4-109425
- anode foils disruption by high-current relativistic electron beams irradi. 4-108195
- arc, in air, absolute spectral intensity meas. (Japanese) 4-97924
- NW Atlantic, Mn, Ni, Cu, Zn, Cd conc. in surface and deep water 4-85711
- atom, angle dependent energy loss of 7-MeV protons, stopping powers meas., geometrical effect 4-96658
- atom, optically excited, in inert gas matrices, radiative lifetimes 4-102642
- atom, two-electron, one-photon transitions 4-74340
- atomic oscillator-amplifier systems, negative image characts. formed using Cu green and yellow lines 4-79335
- atoms, Compton scatt. differential cross sections 4-112146
- atoms, in slotted hollow cathode discharge Cu II laser, diffusion meas. 4-83569
- Auger electron spectra 4-81050
- band struct. calc. using linearised APW method using quadratic energy expansions 4-98504
- band structure, interpolation scheme (Rumanian) 4-98513
- band structure and direct transitions, ARUPS studies 4-75842
- band structure SCF calc. by LMTO method 4-61277
- Bauschinger effect, influence of surface removal 4-114616
- brazed, low cycle fatigue in high vacuum rel. to cold work 4-109500
- brittle fracture, environmentally induced, crystallographic charact. techniques 4-81383
- cathode in vacuum arcs, spot region, microparticle generation 4-87977
- chemisorbed CO, chemisorption bond and  $\text{N}^+$ -molecule reaction 4-80380

**copper continued**

- chemisorption of noble gases, excited states and decay mechanisms 4-98436
- clusters, equilib. geom., binding energy and ionisation pots. 4-74373
- clusters on graphite, valence bands and core levels, XPS, Auger and EELS studies 4-113860
- coating on ultrahigh strength maraging steels, H embrittlement (Japanese) 4-89114
- cold rolled, 50%, orientation depend. of stored energy of cold work 4-99404
- cold worked FCC crystals, recrystn., effect of stacking fault energy 4-31221
- concentrations in sub-Arctic waters of NW Pacific, fluxes and origin 4-82088
- Congost River, Catalonia, Spain, Cd, Cu, Pb, conc. obs. 4-62430
- contamination by oxidation and sulphuration, kinetics, ESCA obs. 4-81462
- cooling  $^3\text{He}$  heat exchangers, comparison 4-95433
- creep and long-term strength study (Russian) 4-80146
- creep at cryogenic temps. 4-99423
- creep cavitation, grain boundary void growth, small angle neutron scatt. obs. 4-85197
- creep fatigue, failure life and microdamage mode rel. to wave shape 4-109508
- creep mechanism maps, expt. 4-93359
- cyclic creep, relationship with hysteresis loop energy 4-109456
- cyclic deformation of single crystals, oriented for double slip 4-98174
- cyclically deformed [001], dislocation struct. 4-108362
- damage structures, evolution under 14 MeV neutron, 4 MeV ion and 1.25 MeV electron irradi. 4-108418
- deposition from cyanide bath, selective case hardening 4-104744
- determination in human red blood cells by AAS 4-100364
- diffusivity of In along stationary and migrating grain boundaries 4-65484
- dislocation drag, mag. field effect 4-103763
- doped, trapping of muons and protons, effect of substitutional impurities 4-65631
- dynamic heterogeneous response to stress waves 4-108540
- dynamic plastic response and press.-shear impact 4-109485
- dynamic tensile fracture due to impact 4-108510
- dynamically deformed, annealing-induced struct. variations 4-71667
- electrode, chemisorbed cyanide mols. surface-enhanced Raman scatt. development 4-70575
- electrodeposited Cu/Ni/Cr three layer coatings on steel, corrosion testing 4-66504
- electrodeposited Cu/Ni/Cr three layer protective coating on steel, corrosion testing 4-66505
- electrodeposition on Pt (111), LEED and AES studies 4-66244
- electrodeposits of dendritic type on point cathode, fractal behaviour 4-75825
- electrolytic, single cryst. elastic consts., cubic polycryst. orientation distrib. function 4-61197
- electron and positron slowing down 4-108486
- electron backscatt., Monte Carlo calcs. 4-66157
- electron backscattering from thick layers 4-99249
- electron scatt., X-ray intensity calc. by Monte Carlo simulation (Chinese) 4-71480
- electronic properties of 4d transition metal and sp impurities 4-70731
- electronic stopping power, excitation energy alpha-particle time of flight expt. 4-67916
- electroplated coating on maraging steel, H embrittlement (Japanese) 4-89113
- electroplating, mag. field influence on elec. transfer of metal in galvanic baths (Russian) 4-85252
- electroplating on Fe powder, coating props. 4-89188
- epitaxial growth on Ni (100), morphology in initial stages, XPS study 4-88416
- epitaxial layers, quantum size effects, surface and interface roughness influence, LEED study 4-84526
- erosion morphology, solid particle impact and particle shape effect 4-114682
- excited H reflection at grazing incidence, light emission 4-76587
- fatigue crack propagation by crack-tip plastic blunting 4-71719
- fatigue crack propagation rate, correl. with J-integral or crack opening displacement (Japanese) 4-114649
- fatigue of single crystals in air and vacuum, fatigue crack propag. 4-99522
- fatigue of single crystals in air and vacuum, persistent slip bands and dislocation microstruct. 4-99521
- FCC metal lattice dynamics, nine-parameter model, specific heats 4-75625
- Fermi surface maps, phonon anomalies 4-70312
- fibre texture, quantitative representation (Korean) 4-104946
- film, aggregated, on Al substrate, solar selective behaviour 4-61760
- film, epitaxial growth, effects of low energy ion bombardment 4-98478
- film, optical consts. meas. in visible using dispersive Fourier transform spectroscopy 4-101934
- film, proton and deuteron stopping cross section 4-92260
- film deposition, using plasma evaporator design with heated needle cathode 4-88989
- film in liq. He, heat flux density emission 4-70491
- film on glass substrate, laser damage study 4-108433
- films, CO-covered, optical and elect. props. 4-80693
- films, oxidation, optical transmittance studies 4-71796
- films, structure and resistivity, transverse elec. field effect (German) 4-76052
- fine powders, electrodeposition, organic additions influence 4-61888
- foil, stopping power of 7 MeV protons, geometrical effects 4-92264
- foil melting by laser-guided discharges 4-75219
- formability, max. uniform strain, effect of matrix and second phase 4-99465
- fracture form, shock wave exit angle effect on free surface 4-99498
- fracture strain and flow stress, invest. by tension and torsion methods (Polish) 4-93362
- fracture stresses time depend. during spall 4-99499
- fusion reactor material applics., DOE-OFE workshop report 4-107014
- hexaimidozolecadmium (II) nitrate: Cu (II), Jahn-Teller distortion, EPR 4-71165
- high temp. oxidation, scale morphology, SEM obs. 4-62113
- impact of He atoms, interaction potentials 4-99256
- impurity diffusion, isotope effect meas. 4-65476
- inert gas atoms, metastable states, quenching by Cu atoms 4-96485

- copper continued
- inversion voltammetry for metal content in river water, seawater and bottom sediments 4-100816
- ion bombard., temp. effects in fast recoil ejection 4-65309
- ion implantation of Au and Ta at non-normal incidence, sputtering yields 4-76619
- ion-induced, inner-shell ionisation, nonperturbative effects 4-99260
- irradiated, stored energy, calorimetric determ. 4-103829
- K and L X-rays prod. by Ar ion impact 4-99216
- K-absorption edge, X-ray absorpt. near edge struct. obs. 4-66123
- Kevlar 49; Cu<sup>2+</sup>, EPR study of stress induced free radicals 4-109076
- Kramers-Kronig relation of measured atomic scatt. factors 4-98063
- laser chamber wall temp. meas. in Cu-vapour laser, using optical pyrometer 4-102951
- lightning conductor plates, corrosion in soil, over 50 years 4-109543
- liquid, mechanisms and kinetics of dissolution of Fe, Co or Ni 4-114530
- liquid, structural props., elec. resist., X-ray diff. 4-79925
- liquid, thermal expansion 4-84425
- local-field enhancement of rough surface 4-104047
- low energy N atom implantation, profiles, ranges and straggling 4-80062
- luminescence during static loading 4-99204
- M2, tensile stresses behind spalling plane, meas. 4-89222
- many-electron systems, ground state energy and X-ray scatt. cross sections 4-114344
- matrix, W fibre reinforced, fracture, acoustic emission obs. (Japanese) 4-62024
- mechanoluminescence at low loading rates 4-81019
- Mediterranean, Cu, Ni, Cd concs. in surface waters 4-85717
- melting influence on shocked free surface behaviour 4-108541
- metallisation of polyimide, adhesion, nuclear scattering eval. 4-71749
- microfractography, SEM study (Polish) 4-93363
- mirrors, bare and carbyne coated, pulsed DF chain laser damage 4-74582
- mirrors, diamond machined, laser damage at nonnormal incidence 4-75520
- mirrors, diamond turned and mechanically polished intensity depend., absorpt. and laser induced catastrophic damage at 1.06  $\mu\text{m}$  4-75519
- muon energy profile change upon lattice relax. 4-71232
- muon mobility below 2K 4-65896
- muon motion appl. of quantum theory of diffusion 4-65892
- muon spin rotation, zero-field, and low temp.  $\mu^+$  diffusivity 4-65894
- muon-spin relax. due to transitions between metastable and stable  $\mu^+$  sites 4-65890
- neutral Cu<sub>2</sub> dimer sputtering by Ar<sup>+</sup> ion bombardment 4-104711
- neutron cross sections for defect prod. by high energy displacement cascades 4-108462
- neutron irradi., microhardness, resistivity, electron microscopy 4-103811
- neutron-irradiated thin flat crystals, slip band growth and dislocation velocities 4-70164
- Ni diffusion along grain boundaries in Cu 4-70428
- ocean surface waters of N Atlantic and N Pacific, Cu, Ni, Cd, Pb concs. 4-85710
- OHFC, fusion materials, candidate materials for impurity control 4-91108
- one-electron states, dispersion and lifetime calcs. 4-70701
- oxidation, collision model for fume formation 4-62114
- oxidation, high temp, cation diffusing scale form., SEM obs. 4-71791
- oxidation, high-temp., in situ obs. of whiskers, pyramids and pits 4-93463
- oxidation, initial; stage, Cu<sub>2</sub>O metastable oxide struct., electron microscopic study 4-65228
- oxidation early stages by CW CO<sub>2</sub> laser irradi. 4-99653
- oxidation rel. to imidazole treatment, surface oxide layers effect 4-99646
- oxide-metal-oxide low-emittance films on glass, industrial realisation 4-112531
- oxidised surface solar absorber, thermal stability, AES and refl. meas. 4-114951
- Pacific seafloor Mn crust containing Co, in USA economic zones 4-110107
- particle characteristics, effect on bulk powder props. 4-66259
- photoacoustic spectra, reflectance effects 4-80961
- photointercalation and photodeposition in p-type lamellar InSe 4-93539
- photon linear polarization in the elementary process of atomic-field bremsstrahlung 4-91354
- pipes, corrosion of soldered and brazed joints in hot tap water 4-109538
- plastic deformation caused by cone indentation of {100} face 4-88176
- plastic flow and dynamic recrystallisation in single crystals 4-66394
- plastically deformed, dislocation struct., ultrasonic study 4-66520
- plates, Bridgman growth, temp. distrib., computer calc. 4-66224
- polycrystalline, cyclic creep accel. and retardation, threshold stress temp. depend. 4-66372
- polycrystalline, He porosity, profilometric investigations 4-103834
- polycrystalline, XPS spectra, background intensities 4-114362
- positive muon diffusion studied by zero field  $\mu\text{SR}$  4-65895
- positive muon pot., self-consistent cluster calc. 4-71236
- positron experiments, computational anal. 4-76554
- positron lifetime after annealing and cooling (Russian) 4-109270
- potential at at. boundaries in Thomas-Fermi model and eqns. of states (Chinese) 4-70333
- powder, compaction by rolling 4-66268
- powder, Kapitza resist. to <sup>3</sup>He-4He dilute mixtures, size effect 4-65514
- powder compacts, rel. between compacting press., green density and green strength 4-114444
- powders, rotating electrode process atomisation mechanisms 4-89001
- powders, sintering behaviour 4-76703
- probe for thermal conductivity meas. of pyrotechnic compositions 4-111128
- pure, cold worked, annealing characts. rel. to trace element additions 4-109438
- quartz:Ag(Cu), X-ray irradi. induced optical absorpt., impurity electrolysis effect 4-70208
- rainwater of Bermuda, trace metals content 4-67320
- recrystallisation, effect of prior cold work on the influence of elec. current pulses 4-61957
- relativistic electron beam propag., energy absorpt. 4-70221
- resonant emission processes, theory 4-85068
- resonant photoemission at 3-p thresholds 4-85070
- Sea of Japan, Fe, Mn, Zn, Cu in seawater of USSR coast 4-94171
- seawater of Kattegat and Skagerrak, trace metal concentrations 4-85714
- seawater trace metal content meas. technique using isotope dilution mass spectrometry 4-85797
- copper continued
- secondary ion emission, vel. depend. 4-76626
- selective optical coating prod. on plastic sheet as heat reflecting films 4-112555
- selective plating Mo structs. on multilayer ceramic substrates 4-66242
- self-diffusion, equilb. defect parameters and characts. 4-65445
- self-ion sputtering yields 4-76628
- separation from Ni in estuaries, role of sediments and seawater 4-82093
- shock-compressed, vapourisation on expansion 4-61063
- single cryst., oxidation, electron microscopy and RHEED studies 4-85259
- single cryst., sputtering yields, weight loss method study 4-76620
- single crystal, elastic consts., US transducer appl. 4-114729
- single crystal, strain bursts in cyclic creep at ambient temp. 4-66371
- single crystal plates, as-grown, micromosaics, neutron rocking curves 4-65413
- single crystals, close packed, dislocation drag 4-103762
- single crystals, cyclically strained, dislocation microstruct. rel. to plastic strain amplitude 4-66373
- single Frenkel-pair production by neutrino recoil 4-98089
- single-crystal films, Na<sup>+</sup>(K<sup>+</sup>)(Rb<sup>+</sup>) ion beams transmission, angular and energy distrib. 4-98159
- sintering, characterisation of particle stacking 4-76709
- small-angle X-ray scatt. by small clusters of intrinsic point defects, intensity calc. 4-98129
- soft surface vibr. of fine particles 4-61201
- spall fracture, models applicability 4-98192
- specimens with flat ends, region of appl. of method of upsetting 4-109597
- sputtered material composition transients, oxide and segregation effects 4-76606
- sputtering, atomic excitations and level populations 4-76590
- stabiliser materials, magnetoresistivity, fusion neutron effects 4-113502
- strain hardening exponent 4-99406
- strain hardening in microdeform., dislocation density, internal friction obs. 4-66397
- stress measurement methods, for cyclic internal and effective stresses 4-71817
- surface, {100}, adsorbed CO, 2 $\pi^*$  associated states, angle-resolved photoemission 4-65724
- surface, (001), Ar<sup>+</sup> beam bombardment induced cascade mixing and importance of post-cascade relaxation 4-65403
- surface, (001), Ar<sup>+</sup> sputtering fine struct. ang. depend. 4-88928
- surface, (001), azimuthal X-ray photoelectron diff. from Cu<sub>2</sub>P<sub>3/2</sub> core level 4-76639
- surface, (001), semichannelling effect on energy distrib., of refl. ions 4-81056
- surface, (001), unoccupied surface states, inverse photoemission meas. 4-92783
- surface, (001) and (011), small-angle ion refl. 4-81095
- surface, (100), 2p core-level binding energy shifts, XPS 4-76016
- surface, (100), image pot. surface states identification, inverse photoemission 4-76015
- surface, (100), long-range electron-phonon coupling at metal surfaces, EELS meas. 4-80647
- surface, (100), N<sub>2</sub><sup>+</sup> ions reflection, surface semichannelling obs. 4-81099
- surface, (100), time of flight mass spectra study on IR laser photodesorption of NH<sub>3</sub> 4-80384
- surface, (100) image-potential states observed by inverse photoemission 4-76014
- surface, (110), adsorbed O<sub>2</sub>, reconstruction, angle-resolved UPS study 4-85083
- surface, (110), He atom scatt., validity of Esbjerg-Norskov approach to pots. 4-93176
- surface, (110), reconstruction determ. with impact-collision alkali ion scatt. 4-81100
- surface, (111), chemisorbed acetylene, vibr. props., EELS studies 4-65567
- surface, adsorbed Ar, He scatt. time depend. wavepacket calcs. 4-88918
- surface, adsorbed CO, bonding, EHT calcs. 4-113800
- surface, adsorbed S, surface struct. determ. by photoelectron diff. 4-85082
- surface, adsorp. of S and O on cylindrical crystals. 4-61223
- surface, diffraction of He atoms, anticorruating effect 4-104709
- surface, EM wave excitation spectral features 4-107811
- surface, He scatt., time-depend. wavepacket scatt. calcs., isolated impurities effect 4-61794
- surface, heterogeneous catalysis, adsorbed mol. surface enhanced Raman scatt. 4-105018
- surface, lattice relax., effect of strong elec. field 4-75766
- surface, lone pair ligand interaction, bonding, constrained space orbital variation method 4-114823
- surface, organic mol. adsorption 4-80409
- surface, target adatom form. during quenching of energetic Ar ion induced cascade 4-88209
- surface (001), K-resolved inverse photoelectron spectroscopy, comment 4-99219
- surface (001), K-resolved inverse photoelectron spectroscopy, reply to comment 4-99220
- surface (001), Sn ordered overlayers, homogeneous intermediate valence, LEED and XPS study 4-61807
- surface (100), angle-resolved photoemission extended fine structure from S 4-93186
- surface (100), band struct., synchrotron radiation study 4-85074
- surface (100), ion scattering spectrometry, shadowing effects 4-81088
- surface (100), keV-Ne<sup>+</sup> and H<sub>2</sub>O<sup>+</sup> ion scatt., neutralisation study 4-81082
- surface (110), adsorbed (2 $\times$ 1) $\times$ 1, azimuthal and polar angle depend. surface EXAFS 4-61770
- surface (110), clean and O covered, ethylene adsorption, UPS studies 4-70548
- surface (110), He ion reson. neutralisation into reson. states 4-76588
- surface (110), low-energy ion scatt., 100 to 600K, temp. effects 4-81089
- surface (111) CO overlayers, band dispersion, multielectron effects 4-85056
- surface atom core level shifts, photoemission obs. 4-93183
- surface berylling, Cu-Be diffusion coating formation 4-62127
- surface characterisation by polysulphide reagent, corrosion pot. rel. to colour change 4-81352
- surface energy, SCLO calc. 4-88388
- surface light absorpt., effects of roughness 4-88797

## copper continued

- surface periodic gratings, light scattering, field enhancement and SERS 4-114292
- surface struct. generation by laser pulses 4-80358
- surface with adsorbed O, SEXAFS spectra using soft X-ray monochromators at BESSY 4-95583
- surface with S monolayer, attenuation of substrate Auger signal and recovery rates determ. (French) 4-66143
- target, impact craters due to glass pellets 4-108689
- targets, fast ionised recoils, directional effects 4-109297
- temperature dependent absorpt., calorimetric meas. 4-78420
- thermal neutron irr., defect production efficiencies 4-108463
- thermo spray technology of undercoat (Chinese) 4-99629
- thin layers, penetration of 24.8 MeV electrons, energy spectra 4-66148
- thin film, optical props. of grain boundaries (German) 4-71461
- thin film bounded by InSb, nonlinear surface plasmon propag., dispersion relations 4-79219
- thin films, 2000 Å thick, electron localisation and interaction, electronic cond., dimensionality crossover 4-80689
- tilt boundary energy and segregation, computer simulation studies 4-114540
- torsion test, interpretation based on Krupkowski's eqn. (Polish) 4-85164
- total Compton profile, nonlocal exchange-correlation effects 4-81032
- tough-pitch, drawn and extruded, stress/strain props. 4-104824
- tubes, corrosion in hot water, prediction of pit initiation from water comp. 4-81328
- tubes, creep deform. under combined tension-torsion at 300°C 4-76806
- tubes, OFHC, Bauschinger effect model for large computer codes 4-108504
- twist boundaries (100), calc. energy and struct., effect of interatomic pot. 4-65272
- two-hole core-level satellite obs. 4-70896
- ultrafast chemical reaction triggered by shock wave forming C and  $\gamma$ -CuBr from CBr<sub>4</sub> and Cu, for diamond synthesis 4-114389
- ultrasonic particles, correlation between position age and momentum of annihilating pairs 4-76555
- ultrahigh-pressure laser-driven shock-wave experiments at 0.26  $\mu$ m wavelength 4-75180
- ultrapure, muon diffusion, spin relax. rate meas. 4-80307
- vacancies and interstitials, energy and vol. characts. (Russian) 4-92199
- vacancy migration energy, electrochemical meas. 4-65456
- vapour diffusion in N<sub>2</sub> arc chamber 4-88019
- vapour laser, picosecond pulses amplification 4-96952
- vapour laser, pulsed, use in high-speed video 4-112494
- vapour laser, self-heating, numerical anal. of parameters 4-112393
- vapour laser with 230 kHz pulse repetition rate 4-69378
- vapour lasers with unstable cavities and short inversion times, kinetics 4-96877
- whiskers, sound emission 4-113839
- wire, exploding current pause 4-87905
- wire explosive emission, MHD processes in the initial stage 4-75226
- wire with current, MHD instability and evaporation 4-79817
- work hardening in polycrystals 4-61956
- X-ray absorption and dispersion at K-edge, interferometric meas. 4-61775
- X-ray anomalous scattering factors from X-ray absorption data by Kramers-Kronig analysis 4-61768
- X-ray generated ultrasonic signals 4-103889
- X-ray L<sub>III</sub> absorption edge, one-electron approx. 4-71478
- Ag/Cu biccystal, two-phase, oriented, prod. by diffusion bonding technique 4-61244
- Ag+Cu smoke particles, coalescence growth, DSC study 4-114836
- Al, liquid, pair pots., Monte Carlo simulation 4-92047
- Al-Au(Cu) thin film bilayers, ion beam bombarded, interfacial phase formation 4-70241
- Al-Cu couple, galvanic corrosion in uninhibited aq. glycol soln. 4-66480
- Al-I-Cu tunnel junction, fast light emission, plasmon polaritons (French) 4-80998
- Al+Cu smoke particles, coalescence, electron microscopy study 4-81483
- As<sub>2</sub>Se<sub>3</sub>-Cu, extrinsic cond. and optical const. meas. 4-75971
- Au/Cu bilayers, ion-induced solid solutions and ordered cpd. form. 4-108470
- $\beta$ -Ca<sub>3</sub>(PO<sub>4</sub>)<sub>2</sub>-Cu<sup>2+</sup>, ESR study 4-65852
- CaS-Cu, Er (Sm) electrolumins., radiation controlled enhancement of electroluminescence 4-76529
- CdBr<sub>2</sub>-Cu, photoionis., phosphoresc., at. states 4-102632
- CdCl<sub>2</sub>-Cu, photoionis., phosphoresc., at. states 4-102632
- CdS-Cu, photoconductivity and luminescence (Russian) 4-84658
- CdS-Cu,In sprayed films, topotaxial growth of Cu<sub>2</sub>S thin films, optical and structural behaviour 4-114433
- CdS-Cu film, defect diffusion, luminescence study (Russian) 4-88875
- CdS-Cu thin films, photocurrent, field quenching 4-84718
- CdTe:Ag(Cu), deep levels, pulsed admittance spectroscopy and capture cross sections 4-92653
- Cr/Ni/Cu multilayer film system, laser mixed, AES and Rutherford backscatt. studies 4-98458
- Cr-coated, hardness meas. of coating 4-75610
- CsMgCl<sub>3</sub>:Cu(I)-M(II), (M=Cr, Mo, Ru, Rh), intermetallic charge transfer spectra 4-65644
- Cu (111), angle and energy synchronised photoemission spectrum 4-85065
- Cu foils, neutron irr., damage prod. rate meas. at liq. He temp. 4-65307
- Cu, H<sup>+</sup> impact, X-ray prod. cross sections 4-96648
- Cu I, lifetimes of some excited levels, beam foil spectra 4-87082
- Cu I lines, rel. oscill. strengths, hook and emission meas. 4-69000
- Cu II, lifetimes of some excited levels, beam foil spectra 4-87082
- Cu/a-Si:H/a-Si:H(n-type)/Cr Schottky diodes, RF magnetron sputtered 4-88557
- Cu/Al thin film interface reactions, X-ray diffr. and Rutherford backscatt. studies 4-88409
- Cu/Cu<sub>2</sub>O photovoltaic cells, backwall type, preparation and props. 4-99970
- Cu/CuO<sub>x</sub>(N<sub>2</sub>) composites, reactive ion beam sputter deposited, optical recording appl. 4-79249
- Cu/Fe systems, wear study 4-76875
- Cu/ $\gamma$ -Fe/Cu epitaxial sandwich layers, struct. and Mossbauer studies 4-84531
- Cu/Ni diffusion couple, bulge and dent zones formation 4-61150
- Cu/Ru(001) bimetallic catalysts, static SIMS, XPS and TPD studies 4-80411

## copper continued

- Cu-Cu composites, magnetoelastic, mech. props. 4-98934
- Cu-Cu<sub>2</sub>O-CuO catalyst evaluation for closed cycle operation of high energy pulsed CO<sub>2</sub> laser 4-96939
- Cu-Ne hollow cathode glow discharge at intermediate currents 4-75224
- Cu-Ni interface, electronic struct. and mag. props. 4-80645
- Cu-Ni-microporous Cr multilayer system for corrosion protection (Russian) 4-89176
- Cu-p-CuInSe<sub>2</sub> contacts, elec. props., solar cell appls. 4-70935
- Cu-Pb thin proximity layers, electron localisation and superconductivity 4-76083
- Cu-PbI<sub>2</sub>, antireflecting cermets, photodecomposition, optical characts. 4-101949
- Cu-SiO<sub>2</sub>/GeO<sub>2</sub>-Cu sandwich structures, elec. props. time, temp. press. depend. 4-108949
- Cu-Sn-Cu-Nb composite, reaction annealing, Nb<sub>3</sub>Sn layer growth conditions 4-61886
- Cu-Ti interface, electron probe anal. of diffusion zones 4-62151
- Cu<sup>2+</sup>-semiquinones interaction in aq. solns. relax. and complex formation 4-99777
- Cu+Ar<sup>2+</sup>, two electron transfer collisions, Ar I VUV line intensity 4-83462
- Cu+H<sup>+</sup> collisions, K-shell ionisation, angular depend. 4-74322
- Cu+O collisions, K-shell ionisation, angular depend. 4-74322
- Cu<sub>2</sub><sup>+</sup> and Cu<sub>3</sub><sup>+</sup> form. from monoatomic secondary ions emitted after primary impact 4-66608
- Cu<sub>2</sub><sup>+</sup> clusters, equilib. geom., binding energy and ionisation pots. 4-74373
- CuH<sub>2</sub>, cryogenic material, heat losses due to H ortho-para conversion (German) 4-106326
- Cu(I)-Cu(I) intermetallic bond, in [( $\eta^5$ -C<sub>5</sub>H<sub>5</sub>)<sub>2</sub>Re(H)Cu]I<sub>2</sub> complex, investigation 4-96715
- Cu(II) dimers, singlet-triplet accidental degeneracy vs. two local doublets problem, EPR study 4-92953
- <sup>64</sup>Cu radioisotope, production and preparation (Chinese) 4-68849
- D<sup>+</sup> irradiated, two-level fracture in blistering 4-75560
- Fe meteorites, group IIIE resolution from IIIAB, Cu as taxonomic parameter and elemental comp. 4-77787
- GaAs<sub>1-x</sub>P<sub>x</sub>-Cu, LEDs, Cu impurities, thermal redistribution 4-80080
- Ge-Cu, impurity contamination reduction by heat treatments above 700°C 4-71535
- Ge-Cu, impurity states, annealing effects 4-104148
- Ge-Cu, nonradiative multiphonon capture of carriers by deep traps 4-75889
- Ge-Cu, quenched-in deep acceptors 4-70713
- Ge<sub>2</sub>S<sub>3</sub>-Cu, glassy, doping effect on elec. and optical props. (Russian) 4-98625
- InP (110)-Cu(Ag)(Au) interface, soft X-ray photoemission study 4-85080
- LiF:Mg,Cu,P, high sensitivity thermoluminesc. dosimeter, environmental monitoring appl. 4-109934
- LiNbO<sub>3</sub>-Cu holographic refl. gratings, angular and spectral selectivities 4-74692
- LiNbO<sub>3</sub>:Cu<sup>2+</sup>, EPR and optical absorption spectra, Jahn-Teller effect 4-71166
- LiNbO<sub>3</sub>:Cu<sup>2+</sup>, single crystal, Jahn-Teller effect 4-108825
- LiNbO<sub>3</sub>:Cu<sup>2+</sup>, spin-lattice relax., EPR studies 4-114157
- LiTaO<sub>3</sub>, degenerate four-wave parametric light scatt. (Russian) 4-88851
- MnI<sub>2</sub>-Cu, pseudo-Zeeman splitting of excited states 4-104579
- NH<sub>4</sub>LiCu<sup>+</sup>, anomalous positive g-shift 4-92952
- NaF:Cu<sup>2+</sup>, excited state dynamics 4-108803
- Na<sub>2</sub>Zn(SO<sub>4</sub>)<sub>2</sub>·4H<sub>2</sub>O:Cu<sup>2+</sup> single cryst., electronic absorption spectrum 4-80967
- Nb-Cu composite superlattice superconductor, dimensional crossover 4-71005
- Ni powder, nonequilibrium vacancy formation during plastic flow (Russian) 4-80030
- Ni/Cu (001) interface, electronic struct., magnetism, muon spin relax. 4-70888
- Ni/Cu metal/metal interfaces, electronic struct. and interface energy 4-114019
- Pr-Cu point contacts low temp., high purity, I-V characteristics 4-114018
- Si-Cu, impurity effect on dislocation motion 4-70187
- Si/Cu/Au Schottky diode, stress effects, photoelec. meas. 4-88591
- Si:Mn, Cu, impurity energy levels, DLTS and capacitance studies 4-88471
- SiO<sub>2</sub>-Cu films, elec. breakdown strength, Cu precipitates effect 4-99022
- ZnS-Cu, Er phosphor, electroluminescence and photoluminescence emission spectra 4-76512
- ZnS-Cu,Sm electroluminescent phosphors, Alfrey-Taylor relation 4-114331
- ZnS-Cu conductive film, MBE prep. with single effusion source, luminesc. and elec. props. 4-99323
- ZnS-Cu film, cathodoluminescence study of annealing 4-81008
- ZnS-Cu<sup>2+</sup>, Jahn-Teller coupling forces, self-consistent LCAO calc. 4-98577
- ZnS,Se<sub>1-x</sub>Te<sub>x</sub>-Cu, photoluminescence study 4-93095
- ZnSiF<sub>6</sub>·6H<sub>2</sub>O:Cu<sup>2+</sup>, EPR, dynamical peculiarities of Jahn-Teller effect (Russian) 4-98938

## copper alloys

see also brass; copper compounds

- binary alloys, effective vacancy formation energy and solute-vacancy binding energy 4-65260
- bronzes, atmospheric sulphidation 4-76901
- contact materials with reduced noble metal content, corrosion behaviour (German) 4-99640
- Coronze 638, strain-enhanced grain growth during superplastic flow 4-71686
- electroplated with Sn, diffusion reaction, effect of additional Fe and Sn 4-71755
- fusion reactor material applcs., DOE-OFE workshop report 4-107014
- laser melted, microstruct. and props. 4-109553
- laser treatment, strengthening and microstruct. (Russian) 4-71665
- rare earth alloys, R<sub>2</sub>Cu<sub>2</sub>, high pressure crystn. 4-75369
- RIGGATRON tokamak, material and design aspects 4-107052
- seawater intake canal antifouling material test results 4-114705
- shape-memory alloy, mech. and elec. props., sonic studies 4-76773
- solid solutions and intermetallic phases, mech. of deforming 4-93449
- thermal diffusivity and sp. ht., 400-850K 4-75926
- thermo spray technology of undercoat (Chinese) 4-99629

copper alloys continued

- Ag-Cu, internal oxidation mechanism 4-93305  
 Ag-Cu (7.5 to 16.5 wt.%), reaction mechanism with  $H_2S$ , 0-220°C 4-66475  
 Ag-Cu dilute alloys, defect production and annealing 4-75442  
 Ag-Cu dilute alloys, electron irradi., defect prod. and annealing 4-75441  
 Ag-Cu-Zn, ternary  $\beta$ -phase alloys, ordering and phase separation, EM obs. 4-66310  
 AgCu, conc. layered, amorphous thin films, diffusional mixing, elec. resist. meas. 4-92687  
 Al bronze on steel, sliding friction break-in curves, effect of flat-on-ring sample alignment 4-81294  
 Al/Al<sub>2</sub>Cu biccystal, two-phase, oriented, prod. by diffusion bonding technique 4-61244  
 Al-Al<sub>2</sub>Cu, eutectic alloy thin films, growth 4-88995  
 Al-Al<sub>2</sub>Cu eutectic thin films, directionally solidified, interlamellar spacing 4-93285  
 Al-Cu, and thermal cond., 400 to 850K 4-75927  
 Al-Cu, columnar crystals, unidirectionally solidified in flowing melt 4-81181  
 Al-Cu, dendritic solidification and segregation in accordance with Krupkowski's formula (*Polish*) 4-85146  
 Al-Cu, dil., quenched, positive muon spin depolarisation 4-65910  
 Al-Cu, directional solidification, off-eutectic composite growth, segregation, convection effects 4-71647  
 Al-Cu, droplet solidification on chill block, predendrite form. rel. to supercooling 4-89037  
 Al-Cu, dynamic recovery and recrystn. (*Korean*) 4-76785  
 Al-Cu, fatigue crack growth anal., cycle counting 4-104839  
 Al-Cu, implanted, disorder studied by ion channelling and Rutherford backscattering 4-98145  
 Al-Cu, liq., structural props., elec. resist., X-ray diffr. 4-79925  
 Al-Cu, phase transform., thermoelec. power study 4-114473  
 Al-Cu, rapidly solidified, decomp. struct. 4-104775  
 Al-Cu, rheocasting, grain refinement rel. to stirrer rotation velocity (*Japanese*) 4-89036  
 Al-Cu,  $\theta'$  phase form., departures from Matthiessen's rule, elec. resist. obs. 4-71660  
 Al-Cu (10 wt.%), prod. by rheocasting, rel. between struct. and mech. props. 4-99467  
 Al-Cu (2 to 5 wt.%), precip. effects on thermopower 4-99384  
 Al-Cu (3.6 wt.%), aged, coarsening kinetics of rod shaped  $\theta$  particles, LSW theory 4-71652  
 Al-Cu (3.76 wt.%), Rheocast, ageing characts. rel. to incomplete homogenisation 4-109444  
 Al-Cu (4 wt.%), dissoln. kinetics of  $\theta$  phase using thermoelec. power meas. 4-114533  
 Al-Cu (4 wt.%), plastically deformed, stability of GP zones 4-61992  
 Al-Cu (4.3 wt.%), randomly nucleated two-dimens. grain struct., effect of grain growth anisotropy 4-104774  
 Al-Cu (5 wt.%), with and without Ti, stress corrosion cracking, electrochemical aspects 4-104920  
 Al-Cu alloy, BEELS for GP zones and precipitates 4-61786  
 Al-Cu alloys, Guinier-Preston zones and solute clusters, high resolution lattice images 4-114543  
 Al-Cu casting alloys, cold cracking mech., plasticity-elasticity transition (*Chinese*) 4-62026  
 Al-Cu eutectic, rapid solidification, with nonhomogeneous thermal contact 4-93276  
 Al-Cu films, microstructure and electromigration studies 4-88413  
 Al-Cu films deposited by sputtering techniques, microstruct. 4-108733  
 Al-Cu system, metastable states controlled by diffusion 4-65463  
 Al-Cu-Cd, strengthening mechanism of Cd additions 4-61985  
 Al-Cu-Fe(Mg), strain meas. near growing fatigue crack tip 4-114651  
 Al-Cu-Li, recrystallised 2020, mech. props. rel. to soln. heat treatment 4-76781  
 Al-Cu-Li alloys, mech. props., effect of minor alloying additions of Zr, Cd or Fe 4-99526  
 Al-Cu-Li-Cd, 2020, microstruct., fracture toughness and SCC 4-76851  
 Al-Cu-Li-Mg-Zr, splat-quenched, microstruct. and tensile props. 4-114620  
 Al-Cu-Li-Mn-Cd, Al 2020, fatigue crack growth behaviour 4-71728  
 Al-Cu-Mg, 2017, surface characterisation as vacuum vessel for nuclear fusion devices 4-96266  
 Al-Cu-Mg, 2024, plates, flow stress under quasi-static compression by steel punches 4-76827  
 Al-Cu-Mg, 2024 sheets, plastic energy dissipation and toughness, size effect 4-89102  
 Al-Cu-Mg, fatigue crack propag., overload-induced 4-99482  
 Al-Cu-Mg, fatigue crack propag., statistical characts. (*Japanese*) 4-99501  
 Al-Cu-Mg, low cycle fatigue, influence of cold forming 4-104841  
 Al-Cu-Mg, near threshold fatigue crack growth, stress intensity factors, crack closure 4-99583  
 Al-Cu-Mg, notch fatigue, limits to applicability of LEFM 4-71721  
 Al-Cu-Mg, RR-58, anelastic creep at 180°C 4-99472  
 Al-Cu-Mg, shot peening effect on fatigue crack initiation by fretting 4-66448  
 Al-Cu-Mg, thermomech. treatment, age hardening rel. to Mg/Cu ratio (*Japanese*) 4-89064  
 Al-Cu-Mg alloy D16 plates, struct. strength, chem. comp. and heat treatment effects 4-61986  
 Al-Cu-Mg wrought alloy 1163, props. 4-62038  
 Al-Cu-Mg-Ag, precipitate struct. and orientation relationship, effect of Ag additions 4-93303  
 Al-Cu-Si, Al 2014, punch-stretching behaviour, 250 to 500°C 4-76817  
 Al-Cu-Si, Al 2014, tensile props., 250 to 500°C 4-76816  
 Al-Cu-Si, low temp. deposition and SiO<sub>2</sub> film growth 4-71783  
 Al-Cu-Si sputtered thin film conductors electromigration resistance 4-88611  
 Al-CuAl<sub>2</sub> eutectic alloys, melting mechanism 4-114507  
 Al-CuAl<sub>2</sub>, lamellar eutectic composites, high temp. yield strength rel. to microstruct. 4-81247  
 Al-CuAl<sub>2</sub> system, directionally solidified, faceting behaviour 4-76766  
 Al-Cu(4 wt.%), polycryst. containing  $\theta'$  precipitates, cyclic deform., grain size depend. and correl. with single crystals 4-66379  
 Al-Fe-Mg-Cu, periodic load serrations in tensile curve, occurrence conditions 4-85194  
 Al-Li-Cu-Mg-Zr, powder metallurgy produced, superplastic behaviour 4-76820  
 Al-Mg-Cu, tubes, biaxial yield and flow, evaluation of anisotropic effective stress-strain criteria 4-104826

copper alloys continued

- Al-Si-Cu, reactive ion etching, rel. to film deposition characteristics 4-81357  
 Al-Si-Cu-Mg, strengthening with continuous CO<sub>2</sub> laser 4-62117  
 Al-Zn-Cu, tribological props. (*Polish*) 4-85216  
 Al-Zn-Mg-Cn, phase identification, X-ray analysis, sequential etching 4-104950  
 Al-Zn-Mg-Cu, cold working, recovery and recrystn. (*German*) 4-71670  
 Al-Zn-Mg-Cu, corrosion, effect of water-displacing corrosion preventives 4-114720  
 Al-Zn-Mg-Cu, ERGAL 7075, plastic deformation at high strain rates 4-84337  
 Al-Zn-Mg-Cu, precip. and quench sensitivity, effect of Cu additions 4-85155  
 Al-Zn-Mg-Cu, SCC, nature of occluded cell 4-85248  
 Al-Zn-Mg-Cu, V95, microstruct. at early stages of spalling 4-114665  
 Al-Zn-Mg-Cu (7.8, 2.6, 1.5 wt.%), 7049 notch sensitivity (*French*) 4-81251  
 Al-Zr-Mg-Cu-Mn, supersaturation of Mn solid soln. 4-61935  
 AlCuZr, AlCu eutectic, fine grained superplastic alloys, anelastic strains, grain boundary cavity distrib., sintering 4-66359  
 Au-Cu, real crystals with several sublattices; proton planar channelling, ang. depend. 4-70248  
 Au-Cu minerals, study using electron probe anal. 4-76934  
 Au-Cu-M metallic glasses, (M=Mg, Si, Sn, Sb), liq.-quenched, form. and low temp. electronic props. 4-75919  
 Ca<sub>2</sub>Cu<sub>3</sub>Al<sub>7</sub> and CaCr<sub>2</sub>Al<sub>10</sub>, crystal structures (*German*) 4-75367  
 Ce-Co-Cu, magnetically hard alloys, isostructural precipitation and atomic ordering (*Russian*) 4-104784  
 CeCu<sub>8</sub>, heavy-fermion system, elec. resist. susceptibility and sp. ht. meas. 4-104402  
 CeCu<sub>8</sub>, Kondo lattice intermetallic compound, anisotropic negative magnetoresistance 4-76111  
 CeCu<sub>5</sub>Si<sub>3</sub>, heavy-fermion supercond., NQR spectra 4-104508  
 CeCu<sub>5</sub>Si<sub>3</sub>, heavy-fermion supercond., valence band reson. photoelectron spectra 4-104720  
 CeCu<sub>5</sub>Si<sub>3</sub>, Kondo lattice substance superconductivity 4-98797  
 CeCu<sub>5</sub>Si<sub>3</sub>, low temp. specific heat meas. 4-75702  
 CeCu<sub>5</sub>Si<sub>3</sub>, nucl. relax., possible evidence for triplet superconductivity 4-108974  
 Ce<sub>0.8</sub>La<sub>0.2</sub>Cu<sub>2</sub>Si<sub>2</sub>, disordered, low-temp. specific heat meas. 4-75702  
 Ce<sub>0.8</sub>La<sub>0.2</sub>Cu<sub>2</sub>Si<sub>2</sub>, mag. props. during Kondo impurity-Kondo lattice transition 4-61509  
 Ce<sub>1-x</sub>Ni<sub>2-x</sub>Cu<sub>2.5</sub> alloys, hyperstoichiometric, H<sub>2</sub> sorption 4-61207  
 Ce<sub>0.9</sub>Co<sub>0.1</sub>Cu<sub>2</sub>Si<sub>2</sub>, disordered, low-temp. specific heat meas. 4-75702  
 Co-Cu, small diffusion coeff. meas. using SIMS 4-65459  
 Cu/Sn-Cu diffusion couple, electron microprobe anal. (*Chinese*) 4-104008  
 Cu-Ag (3.93 wt.%), electron-positron annihilation study (*Russian*) 4-99223  
 Cu-Ag alloy plate, thermal fatigue behaviour 4-111931  
 Cu-Ag isovalent solid soln., elastic core effects, EXAFS studies 4-60886  
 Cu-Al, Ar<sup>+</sup> ions impact in ultrahigh vacuum, secondary ion and Auger electron emission (*French*) 4-66170  
 Cu-Al, cold worked, recrystn., effect of stacking fault energy 4-81221  
 Cu-Al, neutron irradi., microhardness, resistivity, electron microscopy 4-103811  
 Cu-Al, sliding wear induced residual stresses, X-ray diffr. analysis methods 4-76927  
 Cu-Al, strain hardening in microdeform., dislocation density, internal friction obs. 4-66397  
 Cu-Al, vacancies obs. by positive muons trapping (*Japanese*) 4-104515  
 Cu-Al (14 at.%), plastic flow instability boundaries at low temps. 4-99421  
 Cu-Al (3 wt.%), surface chemistry of wear scars 4-99830  
 Cu-Al system, dual-phase, deform. behaviour 4-61993  
 Cu-Al<sub>2</sub>O<sub>3</sub>, dispersion hardened, tensile failure, temp. depend., grain boundary fracture 4-66405  
 Cu-Al-Co, with noncoherent particles, crit. shearing stresses, temp. depend. rel. to slip and twinning (*Russian*) 4-93333  
 Cu-Al-Co (15.2 at.%), with non-coherent particles, superelasticity effects due to twinning 4-76795  
 Cu-Al-Fe (10, 1 wt.%), corrosion and mech. props., effect of solidification struct. 4-85243  
 Cu-Al-Fe alloys, laser surface melted, microstruct., X-ray diffr. study 4-108628  
 Cu-Al-Ni shape memory alloy, martensitic transform., effects of parent phase aging 4-66334  
 Cu-Al-Ni single crystals, regions of thermoelastic phase stability, comp. depend. 4-66311  
 Cu-Al-Ti, internal oxidation, dispersion hardening (*Japanese*) 4-89065  
 Cu-Al-Zn,  $\beta$ -phase, damping capacity rel. to mech. props. and martensite morphology 4-99414  
 $\beta$ -Cu-Al-Zn (8.7, 12.0 wt.%), with reversible martensite in struct., effect of ageing on damping capacity 4-109452  
 Cu-Al-Zn system, high damping  $\beta$  alloys, effect of aging in martensite condition on mech. props. 4-114588  
 Cu-Au, liquid, elec. resist., conc. depend., role of pseudopot. refinements 4-84605  
 Cu-Au alloys, (100) surface, order-disorder transitions and segregation 4-98268  
 Cu-base alloys, Suzuki segregation, TEM study 4-89054  
 Cu-Be, fusion materials, candidate materials for impurity control 4-91108  
 Cu-Be, struct. transform. mechanisms during ageing, internal friction and resist. obs. 4-114536  
 Cu-Be, work hardened thin sheets, determ. of plastic characts. 4-104938  
 Cu-Be (1.0 wt.%), aged, twinned microstruct. 4-89070  
 Cu-Be (1.1, 1.5 wt.%),  $\gamma$ -phase boundary 4-76754  
 Cu-Be (1.35 at.%), undersaturated, irradiated, formation of precipitates 4-104791  
 Cu-Be alloys, Guinier-Preston zones and solute clusters, high resolution lattice images 4-114543  
 Cu-Be alloys, precipitation, elec. resist. and thermopower 4-114549  
 Cu-Be diffusion coating on Cu formed by surface berylliding 4-62127  
 Cu-Be/Fe systems, wear study 4-76875  
 Cu-Be-Co (2, 0.2 wt.%), precip. hardening investigation by microhardness and elec. resist. meas. 4-61947  
 Cu-Be(Ni)(Mn), dil., chem. redistrib. under simulation irradi. 4-108478  
 Cu-Bi, segregation, grain boundary struct. and struct. transformations 4-113462

## copper alloys continued

- Cu-Bi(Sb), liq., Bi and Sb activity meas. by Knudsen effusion method with electrobalance 4-66312
- Cu-Co (2 at.%) single crystals, age hardened, fatigue limit 4-104860
- Cu-Co alloys, Co precipitate coarsening, electron microscope studies 4-114544
- Cu-Co system, coarsening of semi-coherent precipitates 4-114525
- Cu-Co-Si alloys, dil., diffusion of  $^{59}\text{Co}$  4-65447
- Cu-Cr (0.8 wt.%), film, dil., thermoelec. power, thickness depend. 4-61468
- Cu-Fe, elastic distortion of  $\alpha$ -Fe particles by Orowan loops, moiré fringes, TEM obs. 4-66358
- Cu-Fe (1.59 wt.%),  $\alpha$ - $\gamma$  martensitic transform. of Fe particles, magnetisation obs. 4-66355
- Cu-Fe (2 wt.%), precipitation strengthened, high temp. creep 4-61990
- Cu-Fe dilute alloy, exchange-circulation electron current between Fe atoms (*Chinese*) 4-114102
- Cu-Ga/V multifilamentary superconductors, brittle fracture, acoustic emission anal. 4-71715
- Cu-Ge, shock loaded, dislocations and plastic response 4-108370
- Cu-H, electron irradi., elec. resist. meas., annealing behaviour 4-92240
- Cu-In, dil., channelling effect of conversion electrons emitted from radioactive impurities 4-75569
- Cu-In, free enthalpy of impurity-vacancy binding, solvent diffusion meas. 4-84465
- Cu-In, interdiffusion, thermodynamic factor and vacancy flow term 4-70479
- Cu-In, precip. of  $\delta$ -phase on ageing 4-81201
- Cu-In (0.1 at.%), vacancy trapping, PAC and ion channelling study 4-84876
- Cu-In system, volume In diffusion, SIMS studies 4-65457
- Cu-La, liquid alloys, enthalpies of mixing, intermetallic compound form. 4-92374
- Cu-Li alloy, surface material for fusion devices 4-97888
- Cu-Lu, liquid alloys, enthalpies of mixing, intermetallic compound form. 4-92374
- Cu-Mg amorphous alloys, mag. susceptibility rel. to comp., quenching rate and tempering 4-92890
- Cu-Mn, binary liquid alloys, thermodynamic props., formalism appls. 4-114478
- Cu-Mn, elec. resist. max. and thermo-EMF, short-range antiferromagnetism (*Russian*) 4-84608
- Cu-Mn, neutron irradi., microhardness, resistivity, electron microscopy 4-103811
- Cu-Mn (0.25 at.%), spin-glass transition revisited from partial derivative of sp. ht. 4-84807
- Cu-Mn dilute alloys, exchange split virtual bound state 4-92680
- Cu-Mn spin glasses, irreversibility onset, torque meas. 4-84805
- Cu-Mn spin glasses, zero-field muon spin relax. rel. to neutron and susceptibility meas. 4-104435
- Cu-Mn-Zn, microstructure study after cold working 4-108385
- Cu-Nb<sub>3</sub>Sn in situ superconductors, long length, Sn electroplating and processing 4-61878
- Cu-Nb-Sn multifilamentary superconductors for superconducting magnets, powder metallurgy processing 4-80731
- Cu-Ni, disordered, positron spatial distrib. effects 4-104170
- Cu-Ni, forming limit diagrams, comparison between expt. and theoretical 4-93348
- Cu-Ni, neutron irradi., microhardness, resistivity, electron microscopy 4-103811
- Cu-Ni, paramagnetic, thermoelec. power, elastic strain effects (*Russian*) 4-108838
- Cu-Ni, recrystn. at fast continuous heating, thermokinetics (*Russian*) 4-85161
- Cu-Ni, small diffusion coeff. meas. using SIMS 4-65459
- Cu-Ni, twin boundary dislocations, determ. of Burgers vector by weak beam method 4-80051
- Cu-Ni (Al)(Zn), dendritic solidification and segregation in accordance with Krupkowski's formula (*Polish*) 4-85146
- Cu-Ni (25 wt.%), sintered and pressed coinage alloy, tensile props., SEM and X-ray obs. 4-71697
- Cu-Ni (30 wt.%), corrosion in 3% NaCl soln., energy dispersive X-ray analysis (*French*) 4-76895
- Cu-Ni alloys, sputtering by Cu and Ni ions, binary collision cascade calc. 4-76604
- Cu-Ni bands, nonisothermal recrystn., activation energy (*Polish*) 4-85163
- Cu-Ni surface segregation, modelling, low index planes, steps, kinks, and chemisorption 4-92495
- Cu-Ni vapour deposited composition modulated film, long-range interaction effect on diffusion 4-70476
- Cu-Ni-Cr (30.5 wt.%), quenching, ageing, spinodal decomp., hardness, X-ray diffr. obs. 4-114526
- Cu-Ni-Fe, coarsening of extremely small particles 4-113588
- Cu-Ni-Fe, internal friction and precipitation morphology (*Russian*) 4-99416
- Cu-Ni-Fe (9.4, 1.7 wt.%), corrosion behaviour in air-saturated aqueous NaCl soln. 4-93447
- Cu-Ni-Fe (9.4, 1.7 wt.%), corrosion in aqueous NaCl soln., effect of sulphide 4-93448
- Cu-Ni-Fe alloys, decomposition neutron scatt. studies 4-114539
- Cu-Ni-Fe alloys, electron irradi., clustering and decomposition, neutron scatt. studies 4-114555
- Cu-Ni-Fe alloys, short-range clustering and decomposition, dynamic scaling props. 4-114554
- Cu-Ni-Mn alloy, intergranular precipitation and ageing phenomena 4-114550
- Cu-Ni-P equilib. diagram, Cu corner 4-114486
- Cu-Ni-S melts, thermodynamics analysis by associated solution model 4-109380
- Cu-Ni-Si, cellular precip., effect of B and P additions 4-66342
- Cu-Ni-Sn (9, 6 wt.%), ageing, internal friction, Young's modulus, modulated structure 4-66362
- Cu-Ni-Sn alloys, atmospheric sulphidation 4-76902
- Cu-Ni-Sn alloys, spinodal decomposition, applied stress effects 4-114551
- Cu-Ni-Sn spinodal alloys, deformation behaviour, ageing treatment effects 4-114628
- Cu-Ni-Sn system, supersaturated solid soln. decomposition 4-81210
- Cu-Ni-Zn, L<sub>10</sub> and L<sub>12</sub> alloys, order-disorder transitions, microstructure obs. 4-114511
- Cu-Ni-Zn system, diffusion at 775°C, zero-flux planes and flux reversals 4-65496

## copper alloys continued

- Cu-Ni(Al)(Zn) alloys, microsegregation, solidification effects 4-61940
- Cu-O-Pb system, thermodynamics of O<sub>2</sub> miscibility gap, 1200°C 4-108631
- Cu-P, annealing texture development 4-109425
- Cu-P alloys, extruded, microstruct. and mech. props. 4-114574
- Cu-Pb, irregular monotectic struct., effects of temp. gradient and growth vel. 4-66321
- Cu-Pb engine bearings, multilayer diffusion barriers 4-98331
- Cu-Pd binary alloys, quantitative AES anal., backscatt. factors and matrix corrections 4-99241
- Cu-Pd random substitutional alloy, [111] neck radius on the Fermi surface 4-80476
- Cu-Pt, electronic structure and surface comp., ion etching, X-ray photoelectron spectra 4-66187
- Cu-Sb, free enthalpy of impurity-vacancy binding, solvent diffusion meas. 4-84465
- Cu-Sb (1 wt.%), creep rupture life, effects of pre-existing grain boundary cavities 4-62042
- Cu-Sb alloys, grain boundary segregation and cracking, Monte Carlo studies 4-114542
- Cu-Sc, liquid alloys, enthalpies of mixing, intermetallic compound form. 4-92374
- Cu-Si, dil. alloy, internal oxidation, grain boundary cavitation under creep or fatigue loading 4-71726
- Cu-Si (6 at.%), tilt boundaries, (110), asymm.,  $\Sigma 9$ ,  $\Sigma 27a$  and  $\Sigma 81d$ , disloc. 4-65273
- Cu-Sn, free enthalpy of impurity-vacancy binding, solvent diffusion meas. 4-84465
- Cu-Sn, interdiffusion, thermodynamic factor and vacancy flow term 4-70479
- Cu-Sn, phosphor bronze, surface durability upper limit studies 4-104879
- Cu-Sn (14.8%), austenitic and martensitic phase, thermally activated processes, kinetics 4-61963
- Cu-Sn dil. alloys, vacancy jump freq. ratios 4-65448
- Cu-Sn-Al<sub>2</sub>O<sub>3</sub>, abrasive composite, physicochem. props., effect of premoulding press. in elec. discharge sintering 4-89020
- Cu-Sn-P bronze sintered permeable materials, capillary props. 4-65519
- Cu-Su filled crystalline glass composite, frictional and strength props. 4-66456
- Cu-Ti, internal friction and precipitation morphology (*Russian*) 4-99416
- Cu-Ti (3.5 wt.%), age hardening 4-76782
- Cu-Ti alloys, tensile deform., acoustic emission 4-66390
- Cu-Ti glasses, surface composition, composition profiles, Auger electron spectroscopy 4-113758
- Cu-Ti system, cellular decomp. and Ti solid solubility 4-71633
- Cu-Ti/diamond interface, struct. microanal. (*Chinese*) 4-61242
- Cu-Ti/graphite interface, struct. microanal. (*Chinese*) 4-61242
- Cu-Ti-Cr, internal friction and precipitation morphology (*Russian*) 4-99416
- Cu-Ti-Cr (4, 0.5 wt.%), ageing, internal friction, Young's modulus, modulated structure 4-66362
- Cu-Ti(P)(Si), Portevin-Le Chatelier effects 4-66374
- W-electrodes, arcing phenomena, current density 4-87984
- Cu-Y, liquid alloys, enthalpies of mixing, intermetallic compound form. 4-92374
- Cu-Zn, high energy electron irradi., radiation enhanced diffusion, interstitialcy mechanism, elec. resist. meas. 4-92239
- Cu-Zn, interdiffusion, thermodynamic factor and vacancy flow term 4-70479
- Cu-Zn, interdiffusion coeffs., high press. effect 4-88353
- $\beta$ -Cu-Zn, single cryst., deformed in compression, dislocation struct. 4-70162
- $\beta$ -Cu-Zn-Al,  $\gamma$ -brass-type precipitates, origin of incommensurate electron diffr. pattern 4-76775
- Cu-Zn-Al, obs. using scanning electron acoustic microscopy imaging, depend. on chopping and detect. freq. 4-69639
- Cu-Zn-Al, shape memory alloys, ageing and stabilisation of martensite 4-109441
- Cu-Zn-Al, sliding contact with steel, micro-indentation hardness gradients of worn surface 4-76842
- Cu-Zn-Al (25, 6 wt.%), isothermal decomp. of  $\beta'$  phase 4-99387
- Cu-Zn-Al (26.3, 4 wt.%), shape memory alloy for wires and springs 4-114517
- Cu-Zn-Al alloy, shape-memory effect, practical appls. 4-104782
- Cu-Zn-Al alloys, martensitic transformations, positron annihilation studies 4-89053
- Cu-Zn-Al alloys, softened phonons, calorimetry, susceptibility and inelastic neutron scatt. study 4-75636
- Cu-Zn-Al single crystals, second martensitic transform., stress-induced 4-81195
- Cu-Zn-Al single crystals, tensile test, stress-strain curve anal. 4-81260
- Cu-Zn-Au, ordered, two-dimensional antiphase struct., electron diffr. study 4-113397
- Cu-Zn-Ni, superplastic, post-deform. tensile props., effect of cavitation 4-114621
- Cu-Zn-Ni, superplastic alloys, two-phase, modelling of cavitation under uniaxial stress systems 4-61991
- $\alpha/\beta$ -Cu-Zn-Ni-Mn alloy, superplastic, cavity size distrib., effect of strain and temp. 4-61978
- Cu-Zr, amorphous, local struct., EXAFS study 4-88101
- Cu-Zr amorphous alloys, mag. susceptibility rel. to comp., quenching rate and tempering 4-92890
- CuAg alloys, cone form. during Ar<sup>+</sup> ion sputtering 4-75552
- CuAl, dil. disordered, diffuse size effect scatt. in high voltage electron diffr. 4-113395
- CuAl<sub>2</sub>, second-phase particles, dissoln. rates in various microstruct. 4-89059
- CuAl<sub>2</sub>, amorphous, elec. resist. and temp. coeff., pseudopot. theory 4-92692
- CuAu, microstructure, field ion microscopy study 4-88177
- Cu<sub>3</sub>Au (100), keV Ne scatt., atom layer effects 4-76580
- Cu<sub>3</sub>Au alloy, first-order phase transitions, nucleation-growth processes, scaling laws (*Japanese*) 4-113568
- Cu<sub>3</sub>Au, displacement cascade collapse at low temps. 4-103835
- Cu<sub>3</sub>Au, substitutionally disordered, electronic struct. calcs. 4-70644
- Cu<sub>3</sub>Au, Zener relax. anisotropy 4-103874
- CuBe<sub>2</sub>, age hardened, discontinuous flow studies, low temp. 4-113520
- CuMn (1.1 at.%), spin glass, static and dynamic effects, muon spin relax. 4-71250

## copper alloys continued

- CuMn, dilute alloy spin glass, susceptibility, neutron scatt. and muon spin rot. 4-71249  
 CuMn, spin glass dynamics, muon spin relax., neutron spin echo meas. 4-71080  
 Cu<sub>2</sub>MnAl, Heusler alloy, decomposition during isochronal annealing 4-61916  
 Cu<sub>2</sub>MnAl single crystals, Heusler alloy, compression, 77-367K, fracture slip, superlattice dislocation dissociation 4-66369  
 CuNi compositionally modulated foils, electron and X-ray diffraction studies 4-80455  
 CuNi impurity lineshapes in dilute alloys, UPS study 4-113893  
 CuNi, ion bombard., secondary ion and proton yields 4-81097  
 Cu<sub>2</sub>NiZn, superlattice dislocations, TEM microstruct. study 4-75450  
 CuPt, sputtered material composition transients, oxide and segregation effects 4-76606  
 CuPt, sputtering angular distrib. and surface segregation 4-76611  
 (Cu<sub>2</sub>Pt)<sub>1-x</sub>Mn, spin glasses, high temp. susceptibility behaviour 4-71097  
 CuRh, valence band photoelectron spectra 4-88941  
 Cu<sub>49</sub>Ti<sub>40</sub>, amorphous, crystallisation, quenching method effects 4-84185  
 CuZn, antiphase boundary energy, superlattice dislocations, slip systems, weak-beam electron microscopy obs. 4-104792  
 β-CuZn, disordered, vibr. spectra study (Russian) 4-65366  
 CuZn, electronic struct. 4-61278  
 β-CuZn, martensite start temp., effect of Ti additions 4-61928  
 β-CuZn, self-diffusion, influence of order-disorder transition 4-113695  
 β-CuZn, single crystal, yield point phenomenon, high temp. 4-113521  
 CuZn, yield stress, slip, orientation and temp. dependences 4-71709  
 Cu<sub>2</sub>Zr phase in Cu-Zr alloys, identification 4-114534  
 Cu<sub>57</sub>Zr<sub>43</sub> amorphous alloy, deformed, dilatational defects 4-84201  
 Cu<sub>60</sub>Zr<sub>40</sub> alloy system, amorphous, crystallisation kinetics 4-108279  
 Cu<sub>60</sub>Zr<sub>40</sub> metallic glass, elastic props. and thermal expansion 4-84335  
 Cu<sub>9</sub>Zr<sub>91</sub>, 3D long-period superstructure, electron diff., electron microscopy obs. 4-70068  
 Cu<sub>2</sub>Zr<sub>1-x</sub> metallic glass, electronic struct. calcs. 4-104120  
 DyCu amorphous alloy film, mag. transition, small angle mag. scatt. 4-71064  
 DyCu<sub>2</sub>Ge<sub>2</sub>, mag. and cryst. struct., neutron diff. studies 4-65794  
 EuCu<sub>2</sub>Si<sub>2</sub>, mixed valent, isomer shift, mag. susceptibility 4-98573  
 Fe-Cr-Al-Cu, anodic polarisation in H<sub>2</sub>SO<sub>4</sub> 4-114719  
 Fe-Cu, Cu role in radiation damage 4-108423  
 Fe-Cu, H permeation in H<sub>2</sub>SO<sub>4</sub> with and without H<sub>2</sub>S, electrochem. and surface anal. studies 4-104898  
 Fe-Cu, liq. phase sintering, Ostwald ripening, effect of vol. fraction on coarsening kinetics 4-99362  
 Fe-Cu, strengthening effect of Cu 4-89062  
 Fe-Cu (10 wt.%), powder compacts, liq. phase sintering, dimens. changes 4-66267  
 Fe-Cu (2 wt.%), needle-precip. growth directions, invariant line strain 4-66336  
 Fe-Cu powders, liquid phase sintering, pore-filling process 4-99361  
 Fe-Cu-C, ternary systems, phase equilib. 4-76750  
 Fe-Cu-Ni, sintered, fracture mechanics behaviour, influence of specimen size 4-81372  
 Fe-P-Cu, mech. props. and microstructure rel. to sintering atmosphere 4-109354  
 Fe-P-Cu, powder compacts, anisotropic shrinkage during liq. phase sintering 4-104752  
 GdCu<sub>2</sub>Ge<sub>2</sub>, charge transfer, X-ray absorpt. spectra study 4-81037  
 GdCu<sub>2</sub>Si<sub>2</sub>, charge transfer, X-ray absorpt. spectra study 4-81037  
 GdCu<sub>2-x</sub>Zn<sub>x</sub>Si<sub>2</sub>, cryst. struct., mag. and elec. props. 4-92145  
 LaNi<sub>3</sub>Cu<sub>2</sub> hydrides, H-T, H-D, D-T mixtures isotope equilibria 4-108586  
 LaNi<sub>3</sub>Cu<sub>2</sub> hydrides, H-T, H-D, D-T mixtures isotope equilibria 4-108586  
 Mg-Cu-Si system, ordered struct., X-ray diff. study 4-113400  
 MgCu<sub>2</sub> family, sharp homeotypism 4-98118  
 Mn-Cu, high-damping-capacity alloy, martensitic and mag. transitions after powder metallurgical prep. (Russian) 4-109403  
 Mn-Cu-Bi, thin film, RF sputtering prep., mag. and magneto-optical props. 4-61847  
 Mn-Zr-Cu amorphous alloys, local Mn moment, supercond. props. 4-114091  
 Nb<sub>3</sub>Sn-Cu, superconducting wire, welded annular region of Nb<sub>3</sub>Sn filaments 4-99363  
 Ni-Cu, anomalous resistivity, 4.2 to 1100K 4-92708  
 Ni-Cu, bonding and enthalpy studies 4-79978  
 Ni-Cu, Cu diffusion after dynamic and static deformation (Russian) 4-108658  
 Ni-Cu, electronic structure and surface comp., ion etching, X-ray photoelectron spectra 4-66187  
 Ni-Cu, repassivation in alkaline soln., oxidation rates 4-104909  
 Ni-Cu, repassivation in H<sub>2</sub>SO<sub>4</sub> 4-71760  
 Ni-Cu, thermoelectric power and sp. ht. near Curie temp., AC method meas. 4-75934  
 Ni-Cu, vacuum arc-plasma deposition, on Pb(Zr,Ti)O<sub>3</sub> piezoceramic substrate 4-76691  
 Ni-Cu (22 at.%), annealed and quenched, creep behaviour and miscibility gap 4-66387  
 Ni-Cu alloy, domain wall-dislocation interaction behaviour, role of Cu atoms 4-104457  
 Ni-Cu alloys, grain boundary segregation and cracking, Monte Carlo studies 4-114542  
 Ni-Cu fine particle mixture, sintering vel., collective effects during diffusion interactions 4-61887  
 Ni-Cu-Zn alloys, electrodeposition from sulphate bath, effect of additions 4-81163  
 Ni-Mn-Cu, intermetallic form., alloying elements influence (Russian) 4-76757  
 NiCuM (M=Zn, Al, Si) alloys, spontaneous magnetisation, thermal variation 4-65796  
 Ni<sub>49</sub>Zn<sub>50</sub>Cu<sub>10</sub>, martensite, tempering, morphology and recovery 4-109404  
 Pb-Cu films, localisation and superconducting fluctuations 4-80719  
 Pd-Cu, bonding and enthalpy studies 4-79978  
 Pd-Cu (60 wt.%), field ion imaging of surface atoms 4-88384  
 Pd-Cu-Ni alloys, elec. resist., atomic ordering effects (Russian) 4-108833  
 Pd-Y-Cu system, phase equilib., corrosion resist. to nitric acid soln. 4-114490  
 PdCuAg, phase transition, field ion microscopy study (Russian) 4-81189  
 Pd<sub>3</sub>Cu<sub>2</sub>P, cryst. struct. and phase equilib. 4-70070  
 Pd<sub>75</sub>Cu<sub>25</sub>Si<sub>16.5</sub> metallic glass, elastic props. and thermal expansion 4-84335

## copper alloys continued

- PdCuSiMn alloys, (M=Fe, Co, Mn), spin glasses, exptl. evidence for mag. two level systems 4-71082  
 Pd<sub>67.5</sub>Cu<sub>32.5</sub>Si<sub>16.5</sub>Mn<sub>10</sub>, (M=Fe or Mn), glasses, ferro- and antiferromagnetism study 4-71063  
 Pd<sub>0.775</sub>Si<sub>0.165</sub>Cu<sub>0.06</sub> metallic glass, low-freq. elastic loss at low temp. 4-70289  
 Pd<sub>0.775</sub>Si<sub>0.165</sub>Cu<sub>0.060</sub>, amorphous and cryst. states, two-level tunnelling system, US study 4-98024  
 Pt-Cu, bonding and enthalpy studies 4-79978  
 Sb-Cu, Sb, eutectic alloys, melting mechanism 4-114507  
 Si-Fe-Cu high permeability grain oriented steel, recrystallisation and grain sizes 4-61953  
 SiC fibre reinforced Al alloy, squeeze cast, thermal expansion, elastic to plastic deformation, transition 4-108635  
 Sm(Co,Fe,Cu,Zr)<sub>7.5</sub> magnets, high resolution electron microscopy study 4-61098  
 Sm(Co<sub>1-x</sub>Cu<sub>x</sub>)<sub>2</sub>, cellular permanent magnets, coercivity 4-76191  
 Sn<sub>1-x</sub>Cu<sub>x</sub> amorphous films, quench-condensed, low temp. sp. ht. 4-70403  
 (Sn<sub>1-x</sub>Cu<sub>x</sub>)<sub>1-x</sub>H<sub>x</sub>, superconductivity and cond. studies 4-92840  
 Te<sub>64</sub>Ni<sub>20</sub>Cu<sub>10</sub>Si<sub>6</sub> amorphous alloy, TTT-curve construction 4-93287  
 Ti-Ni-Cu system, dissipative props. and struct., martensitic transform. 4-66361  
 TiBe<sub>2</sub>-Cu<sub>2</sub>, onset of ferromagnetism, neutron small angle scatt. study 4-84797  
 Ti<sub>2</sub>Cu<sub>1-x</sub> alloys, electrochemical and thermal oxidation and electrochemical O<sub>2</sub> evolution 4-93452  
 Ti<sub>61</sub>Cu<sub>16</sub>Ni<sub>23</sub>, amorphous, X-ray diff. pattern prepeak, temp. depend. 4-79942  
 Ti<sub>62.5</sub>Cu<sub>17.5</sub>Ni<sub>12.5</sub>Si<sub>7.5</sub>, amorphous, X-ray diff. pattern prepeak, temp. depend. 4-79942  
 TiNi<sub>1-x</sub>M<sub>1-x</sub> (M=Cu, Fe, Co), multiphase diffusion 4-61136  
 UBe<sub>12.94</sub>Cu<sub>0.06</sub>, heavy fermion supercond., sp. ht. meas. 4-104363  
 W-Cu composites, sintering 4-66270  
 W-Cu pseudoballoys, thermophys. props. calc. 4-61115  
 W-Ni-Cu, liq. phase sintered, interphase boundary precip. 4-99364  
 Y-Cu-Fe metallic glasses, XPS study of electronic struct. 4-104121  
 Y<sub>2</sub>(Co, Fe, Cu)<sub>17</sub>, single cryst. cpds., growth conditions and characterisation 4-66220  
 Zn-Al-Cu alloys, vol. change on ageing 4-114592  
 Zn-Cu-Ti alloys, bendability, struct. aspects (French) 4-81252  
 Zr-Cu, amorphous, sputtered, low-energy excitations, thermal cond., sp. ht. meas. 4-70987  
 Zr-Cu-Ni and Zr-Cu-Sn, amorphous, anodic electrochem. treatment 4-114716  
 Zr<sub>70</sub>Cu<sub>30</sub>, amorphous, thermal cond., phonon-electron contrib., heat treatment effects 4-70988  
 Zr<sub>76</sub>Cu<sub>24</sub>, amorphous, sputtered, structural relax. induced by annealing X-ray diff. 4-84189  
 Zr<sub>76</sub>Cu<sub>24</sub>, amorphous sputtered alloys supercond. critical field and normal state resist. 4-114077  
 Zr<sub>1-x</sub>Cu<sub>x</sub> metallic glass, sp. ht., thermal cond. props. after structural relax. 4-70406
- copper compounds**  
 see also copper alloys  
 acetylacetonate, vapour, laser action and fluorescence (Japanese) 4-60019  
 chalcogenides, electronic struct., X-ray spectra and X-ray photoemission studies 4-61283  
 chem. bonding and electronic struct., XPS studies 4-71524  
 copper (I) complexes with some disubstituted acetylenes and dimethylsulphoxide, <sup>1</sup>H NMR, UV and IR spectra 4-76467  
 γ-CuBr, diamond synthesis, ultrafast chemical reaction triggered by shock wave forming C and γ-CuBr from CBr<sub>4</sub> and Cu 4-114389  
 dodecanoate, disclotic mesophase, X-ray diff. study 4-92076  
 formate tetrahydrate, first order paraelectric-antiferroelectric transition, X-ray topography 4-65990  
 halides, anharmonic props., interionic pot. model 4-98056  
 halides, deformation pots., relativistic LMO calc. 4-80473  
 halides, electron-phonon interaction and optical props., Raman spectra studies 4-66008  
 halides, ionic compounds photo-induced covalency 4-88931  
 halides, neutron irradiat., defect form., EPR obs., effects of bond ionicity 4-70224  
 halides, superionic, phase transition and soft mode behaviour 4-92330  
 oxides, empirical bond length determ. 4-103710  
 oxides, K absorption edge, extended fine struct. 4-71477  
 oxides, mixed, ionicity, XPS studies 4-66193  
 oxides, resonant photoemission at 3-p thresholds 4-85070  
 phthalocyanine, chlorinated, mol. energetics of epitaxial growth on KCl 4-98480  
 phthalocyanine, vapour press. determ. (German) 4-80209  
 phthalocyanine thin films, surface enhanced Raman scatt. 4-66036  
 8-quinolinedithiocarbonylate salt, liquid membranes, extraction and electrode props. 4-81446  
 ternary chalcopryrite semiconductors, NMR studies 4-65874  
 ternary sulphides and selenides, symmetry and dislocations, electron microscopy studies 4-95580  
 Ag<sub>2</sub>Te-Cu<sub>2</sub>Te, thin film, high and low temp. modifications 4-75800  
 Al<sub>2</sub>O<sub>3</sub>-Bi<sub>2</sub>O<sub>3</sub>-Cu<sub>2</sub>O system, phase relations, thick film cond. appls. 4-104770  
 As<sub>2</sub>Se<sub>3</sub>-Cu<sub>2</sub>Se:Mn, interaction of Mn with glass framework, mag. susceptibility, EPR spectra 4-60838  
 CdBr<sub>2</sub>-CuBr heterogeneous thin-film appls. for obtaining photographic images during phys. development (Russian) 4-82848  
 CdCl<sub>2</sub>-CuCl heterogeneous thin film appl. for obtaining photographic images during phys. development (Russian) 4-82848  
 Cd<sub>2</sub>Cu<sub>1-x</sub>Fe<sub>x</sub>O<sub>4</sub>, hyperfine field interactions, Mossbauer spectra 4-65885  
 Cd<sub>2</sub>Cu<sub>1-x</sub>Fe<sub>x</sub>O<sub>4</sub> spinel, low temp. Mossbauer obs. of mag. interactions 4-98983  
 CdS/Cu<sub>2</sub>S heterojunction solar cells, electrochemical method for improving spectral response 4-109744  
 CdS/CuInSe<sub>2</sub>, solar cell interface chem. reaction, thermodynamics 4-85367  
 CdS-CuInSe, photovoltaic devices, short-circuit current meas. 4-88971  
 CeCu<sub>2</sub>Si<sub>2</sub>, superconducting T<sub>c</sub> maximum 4-98800  
 Cu<sub>2</sub>Rb<sub>2</sub>Cu<sub>16</sub>Cl<sub>13</sub>/Rb<sub>2</sub>Cu<sub>16</sub>Cl<sub>13</sub>/Cu<sub>2</sub>Se solid electrolyte cells, single- and multilayer, performances (Russian) 4-99956  
 Cu (II) complex, CuMn (thioxalato)<sub>2</sub>·7.5H<sub>2</sub>O, quasi-one-dimens. ferrimagnetic, magnetisation and susceptibility study 4-80748

## copper compounds continued

- Cu (II) complexes, correl. of EPR parameters with thermodynamic stability 4-98937  
 Cu (II) complexes, five-coord., distortion, optical absorpt. and ESR obs. 4-78872  
 Cu (II) cyanates, polymeric, far IR spectra, Cu-OCN bonding, stretching and deformation bands 4-69076  
 Cu (I) complexes, bis(N-methyl)-dithioformamidinium, IR spectra 4-66032  
 Cu ( $\pi$ ) complexes, crystal struct., EPR and optical study, stereochemistry (French) 4-70075  
 Cu complex, 2DMSO.CuCl<sub>2</sub>, 1D Heisenberg antiferromag., mag. susceptibility 4-61516  
 Cu complex, bis-(propylammonium) copper(II) tetrachloride, cryst. growth from soln., Oswald ripening along faceted bridge 4-75336  
 Cu complex, bis(2,9-diphenyl-1,10-phenanthroline) copper(II), solid, luminesc. 4-99148  
 Cu complex, bis(di-ethanol-dithiocarbamate) Cu(II), intermol. interactions, EPR obs. 4-64516  
 Cu complex, Cu<sub>2</sub>OCl<sub>2</sub>(triphenylphosphine oxide)<sub>2</sub>, excited S=2 manifold cubic field splitting 4-76240  
 Cu complexes, bis-piperidinium tetrachlorocuprate, ESR linewidth ang. depend. 4-71160  
 Cu complexes, Cu-phthalocyanine single cryst., visible absorpt. band, temp. depend. 4-76489  
 Cu complexes, diacetyl-bis(thiosemicarbazone)Cu(II), electronic struct. and intermol. interactions 4-61586  
 Cu complexes, methylglyoxal-bis(thiosemicarbazone)Cu(II), electronic struct. and intermol. interactions 4-61586  
 Cu complexes, polyamine Cu (II) in soln., ESR hyperfine linewidth anal. 4-83394  
 Cu complexes, with dithiocarbamate and bis-(N,N-diethyl dithiocarbamate), vibr. freq., normal coordinate anal. 4-59701  
 Cu halide clusters, ionisation, fragmentation, mass spectra 4-69264  
 Cu halide vapour long-lived sealed-off lasers, operating characts. and projected lifetimes 4-69386  
 Cu II complexes, IR spectra, mag. susceptibility meas., antiferromag. interactions 4-80918  
 Cu II complexes, in Ni II host lattice and toluene-d<sub>8</sub> solns., <sup>1</sup>H and <sup>31</sup>P ENDOR spectra 4-91292  
 Cu II complexes of N<sup>4</sup>, N<sup>4</sup>-disubstituted thio- and selenosemicarbazones of 2-acetylpyridine, EPR spectra 4-89841  
 Cu tetraclusters, adiabatic pot., mag. props., Jahn-Teller effect 4-108823  
 Cu/CuO(N<sub>2</sub>) composites, reactive ion beam sputter deposited, optical recording appl. 4-79249  
 Cu-Cu<sub>2</sub>O-CuO catalyst evaluation for closed cycle operation of high energy pulsed CO<sub>2</sub> laser 4-96939  
 Cu-III-VI<sub>2</sub> chalcopyrites, valence bands study, photoemission and X-ray emission spectra, electronic structure calcs. 4-65608  
 Cu-In-S layers, electrodeposition, photoelectrochemical characterisation 4-99355  
 Cu-L-glutamine complex, IR spectra, band assignments 4-107339  
 Cu-L-histidine complex, IR spectra, band assignments 4-107339  
 Cu-L-isoleucine complex, polycryst., IR absorpt. spectra, vibr. mode assignment 4-109173  
 Cu-L-lysine complex, IR spectra, band assignments 4-107339  
 Cu-L-tryptophan complex, polycryst., IR absorpt. spectra, vibr. mode assignment 4-109173  
 CuAg<sub>4</sub> matrix isolated, ESR spectra 4-107371  
 CuAg<sub>3</sub> matrix isolated, ESR spectra 4-107371  
 (Cu<sub>1-x</sub>Ag<sub>x</sub>)(Ga<sub>1-x</sub>In<sub>x</sub>)(Se<sub>1-x</sub>Te<sub>x</sub>)<sub>2</sub>, lattice parameter and energy gap 4-75847  
 CuAlO<sub>2</sub> 2H stacking variant, synthesis and cryst. struct. 4-92177  
 CuAlTe<sub>2</sub> single crystal, CVD growth and elec. characterisation 4-114366  
 Cu<sub>3</sub>B<sub>2</sub>O<sub>7</sub>Cl ferroelec. and paraelec. phases, optical rot., birefr., optical susceptibilities 4-109151  
 CuBr, bixciton two-photon absorpt., Raman scatt., perturbation theory calc. 4-75864  
 CuBr, interdependence of buffer gas pressure and optimum interpulse delay in a burst-mode copper halide laser 4-112396  
 $\beta$ -CuBr, microwave AC cond. of superionic conductors 4-88527  
 CuBr, whole heated sealed-off laser, lifetime 4-107681  
 7CuBr.C<sub>6</sub>H<sub>4</sub>(N<sub>2</sub>CH<sub>3</sub>Br) solid superionic conductors, transport props. 4-113983  
 CuBr<sub>2</sub>.1, spin-order splitting energy, exciton spectra, disorder effects 4-88457  
 CuCNS photocathodes, dye sensitisation in aq. KCNS 4-104257  
 Cu<sub>1-x</sub>Cd<sub>x</sub>Fe<sub>2</sub>O<sub>4</sub>, IR absorption spectra and stretching bond interatomic vibrs. 4-80933  
 Cu<sub>2</sub>Cd<sub>1-x</sub> superionic conductor, Raman and far IR studies 4-109195  
 CuCl (110), angle resolved photoemission 4-85071  
 CuCl complex with acrylamide, cryst. struct., X-ray diff. 4-113419  
 CuCl complex with fumarodinitrile, cryst. struct., X-ray diff. 4-113419  
 CuCl, dense exciton-bicxicon system, optical bistability 4-64732  
 CuCl, dielec. function, exciton-bicxicon transitions and population effects 4-80525  
 CuCl, electronic struct., cryst. cluster model 4-61280  
 CuCl exciton-excitonic mol. system, optical bistable behaviour 4-96993  
 CuCl, excitonic absorpt. edge, IR laser radiation induced electroabsorpt. 4-61287  
 CuCl excitonic optical bistability, effects of mirror reflectivity 4-83632  
 CuCl, excitonic polaritons, picosecond spectroscopy (Japanese) 4-76403  
 CuCl in H<sub>2</sub>-O<sub>2</sub> flames, emission intensity mag. quenching 4-78891  
 CuCl, interdependence of buffer gas pressure and optimum interpulse delay in a burst-mode copper halide laser 4-112396  
 CuCl, multiphoton optical bistability and phase conjugacy, oscillator models 4-69509  
 CuCl, nonlinear optical props. of bixictons, degenerate four-wave mixing 4-69488  
 CuCl, optical nonlinearity due to Z<sub>1</sub> and Z<sub>1,2</sub> excitons, study by reflected four-wave mixed light generation 4-79217  
 CuCl, resonant Raman scatt. in region of edge excitons 4-76472  
 CuCl/CuBr piezoelectric composition-modulated structures 4-99040  
 CuCl<sub>2</sub> intercalation cpds. with graphite, Sp. ht. and thermal expansion 4-80260  
 CuCl<sub>2</sub>(Al<sub>2</sub>O<sub>3</sub>) composites, elec. cond., particle size effects 4-88548  
 CuCl<sub>2</sub>.2H<sub>2</sub>O, antiferromagnetic, magnon amplitude oscillations under parallel microwave pumping 4-65798  
 CuCrS<sub>2</sub>, reversible phase transitions, X-ray diffraction studies 4-65397  
 Cu<sub>2</sub>Cr<sub>2</sub>Se<sub>4</sub>, nuclear quadrupole interaction, NMR spin echo, study 4-61352

## copper compounds continued

- CuCr<sub>2</sub>Se<sub>4</sub> solid solutions, radiographic study of struct. 4-108317  
 (Cu<sub>1-x</sub>Cr<sub>x</sub>)<sub>2</sub>(Cu<sub>0.5</sub>Ga<sub>0.5</sub>Cr<sub>2</sub>Se<sub>4</sub>)<sub>1-x</sub>, semiconducting spin glasses, resistance magnetoresistance, studies 4-108862  
 (Cu<sub>1-x</sub>Cr<sub>x</sub>)<sub>2</sub>(Cu<sub>0.5</sub>In<sub>0.5</sub>Cr<sub>2</sub>Se<sub>4</sub>)<sub>1-x</sub>, semiconducting spin glasses, resistance magnetoresistance, studies 4-108862  
 CuFe<sub>2</sub>Al<sub>2</sub>O<sub>4</sub>, orthorhombic distortions due to doping 4-70103  
 Cu<sub>2</sub>Fe<sub>1-x</sub>Cr<sub>x</sub>S<sub>4</sub> films, elec. and galvanomagnetic props. 4-76056  
 CuFe<sub>2</sub>O<sub>4</sub>, conduction mechanism, annealing effect, resist. and thermoelectric power meas. 4-104206  
 CuFe<sub>2</sub>O<sub>4</sub> single crystals, flux growth, X-ray charact. 4-76651  
 Cu<sub>2</sub>Fe<sub>1-x</sub>O<sub>4</sub>, oxidation states, <sup>57</sup>Fe Mossbauer study 4-71225  
 Cu<sub>2</sub>Fe<sub>1-x</sub>O<sub>4</sub>, X-ray spectra, K-absorpt. edge 4-66130  
 CuFeS<sub>2</sub>/Ag<sub>2</sub>S system, electron probe anal., detection limit, vol. and surface impurity diffusion effects 4-99918  
 CuGa<sub>1-x</sub>In<sub>x</sub>S<sub>2</sub>, LPE growth on ZnSe substrate 4-80436  
 CuGa<sub>1-x</sub>In<sub>x</sub>Se<sub>2</sub> chalcopyritic semicond., ESR studies 4-109070  
 CuGaS<sub>2</sub>-CuInS<sub>2</sub> solute for LPE growth of CuGa<sub>1-x</sub>In<sub>x</sub>Se<sub>2</sub> on ZnSe substrate 4-80436  
 CuGaSe<sub>2</sub>, thermal expansion, 301-958K 4-80266  
 CuGaTe<sub>2</sub>, vapour growth, thermodynamics and elec. characts. 4-71536  
 Cu<sub>1-x</sub>Ge<sub>0.5</sub>Fe<sub>0.5</sub>O<sub>4</sub>, orthorhombic distortions due to doping 4-70103  
 p-Cu<sub>2</sub>Fe<sub>2</sub>P<sub>3</sub>, optical lattice modes and IR reflectivity 4-88834  
 CuH in H<sub>2</sub>-O<sub>2</sub> flames, emission intensity mag. quenching 4-78891  
 CuH<sub>2</sub>, low and high spin pot. energy surface, CI calcs. 4-96459  
 CuH<sub>2</sub>, Renner-Teller pot. energy surfaces, analytic second derivative 4-91250  
 Cu<sub>2</sub>HgI<sub>4</sub>, Raman and IR spectra, ionic cond. studies 4-99119  
 Cu(I) complex with 1-phenyl-3,5-dimethylpyrazole, cond., electronic and IR spectra, mag. susceptibility meas. 4-76104  
 CuI, interdependence of buffer gas pressure and optimum interpulse delay in a burst-mode copper halide laser 4-112396  
 CuI laser with supraoptical wall temp. metastable Cu atom conc. relaxation in afterglow 4-60021  
 CuI single crystal, band-edge emission 4-80994  
 CuI single crystals and thin films, excitons, uniaxial stress effects 4-98539  
 CuI solid superionic conductors, transport props. 4-113983  
 CuI-Cu<sub>2</sub>O-P<sub>2</sub>O<sub>5</sub> glass, fast ion cond. study 4-88339  
 Cu(II) complex with 1-phenyl-3,5-dimethylpyrazole, cond., electronic and IR spectra, mag. susceptibility meas. 4-76104  
 Cu(II) square planar complexes, K-absorption edge study 4-104698  
 Cu<sub>1-x</sub>In<sub>1-x</sub>Cr<sub>2</sub>Se<sub>4</sub> solid solutions, radiographic study of struct. 4-108317  
 CuInS<sub>2</sub>, defect chemistry, elec. and Mossbauer studies 4-70730  
 CuInS<sub>2</sub>, Raman study of optical phonons 4-80917  
 CuInS<sub>2</sub>, single crystal growth by travelling heater method 4-71539  
 p-Cu<sub>2</sub>In<sub>2</sub>S<sub>3</sub>/p-GaSe heterojunctions, elec. and photoelec. props. 4-88573  
 CuIn(S<sub>2</sub>Se<sub>2</sub>Te<sub>2</sub>), solid solubility, optical energy gap values 4-70074  
 CuInSe<sub>2</sub> in-diffused homojunctions, elec. and photovoltaic effects 4-9280  
 n-CuInSe<sub>2</sub>, elec. and thermal conductivity 4-75974  
 CuInSe<sub>2</sub> film form. by chemical spray pyrolysis, kinetic effects 4-81165  
 CuInSe<sub>2</sub> films, rheotaxial growth on liquid In film 4-61877  
 n-CuInSe<sub>2</sub>, optical absorption edge, influence of carrier conc. 4-80943  
 CuInSe<sub>2</sub>, radiative recombination and shallow centres 4-109250  
 CuInSe<sub>2</sub>, reactive sputtering for photovoltaic applications 4-88971  
 CuInSe<sub>2</sub> semicond., Se self-diffusion studies 4-88335  
 CuInSe<sub>2</sub> single crystal, electrode, solar cell performance, surface chemistry 4-66696  
 CuInSe<sub>2</sub>, sintered, grain size, SEM obs., resist., Hall obs. 4-66284  
 CuInSe<sub>2</sub>, sphalerite-chalcopyrite order-disorder transitions, group theory anal. 4-84383  
 CuInSe<sub>2</sub> sputtered surface characterisation using AES, O<sub>2</sub> adsorption 4-93147  
 CuInSe<sub>2</sub>, surface photocond. and positive cryst. splitting 4-65649  
 CuInSe<sub>2</sub> thin films, flash evaporated, photocond. 4-104264  
 CuInSe<sub>2</sub>/CdS heterojunction solar cells, conduction band-lineup 4-72105  
 CuInSe<sub>2</sub>/CdS solar cells, thin film, diffusion length, determ., using EBIC method 4-72110  
 p-CuInSe<sub>2</sub>/n-ZnIn<sub>2</sub>S<sub>4</sub> heterojunction solar cell, ZnIn<sub>2</sub>S<sub>4</sub> use as a window layer 4-114911  
 n-CuInSe<sub>2</sub>/p-CuInSe<sub>2</sub> solar cells, 12% conversion efficiency by interphase restructuring 4-93614  
 CuInSe<sub>2</sub>(Cd,Zn)S solar cells, light-induced junction modification 4-77092  
 CuInSe<sub>2</sub>(Cd,Zn)S Boeing solar cells, current transport 4-81546  
 CuInSe<sub>2</sub>(Cd,Zn)S thin film heterojunction solar cells, photoreponse charact. 4-77099  
 CuInSe<sub>2</sub>-CdZnS polycryst. thin film solar cells 4-77088  
 p-CuInSe<sub>2</sub>-metal contacts, elec. props., solar cell appls. 4-70935  
 CuInTe<sub>2</sub> MIS struct., field effect studies 4-80679  
 CuInTe<sub>2</sub>, thermal expansion coeffs. 30 to 300K 4-103974  
 CuInTe<sub>2</sub>, vapour growth, thermodynamics and elec. characts. 4-71536  
 Cu<sub>2</sub>Mg<sub>1-x</sub>Al<sub>x</sub>O<sub>4</sub>, oxide spinel solid soln., cation distrib. study 4-80016  
 Cu<sub>2</sub>Mg<sub>1-x</sub>Al<sub>x</sub>O<sub>4</sub>, phase transitions, ionic cond. study 4-88287  
 CuMn(Co) EDTA complexes, one-dimensional ordered bimetallic chain mag. props. 4-71036  
 CuMo<sub>2</sub>S<sub>4</sub>Br(I), preparation and cryst. struct. 4-70097  
 Cu<sub>2</sub>Mo<sub>2</sub>Se<sub>4</sub> single crystals, growth, comp. inhomogeneity and superconductivity 4-80708  
 Cu(NO<sub>3</sub>)<sub>2</sub>, aq. solns., Cu(II) coordination, X-ray diff. study 4-75260  
 Cu(NO<sub>3</sub>)<sub>2</sub>, gas phase, mol. struct., electron diff. 4-78965  
 Cu<sub>2</sub>(NO<sub>3</sub>)(OH), monoclinic cryst. struct. and H-bonds 4-92166  
 CuNa<sub>3</sub>P<sub>3</sub>O<sub>10</sub>.12H<sub>2</sub>O, cryst. struct. determ. (French) 4-75392  
 CuNbO<sub>3</sub> cryst., struct. with stepped NbO<sub>3</sub> layers, X-ray obs. 4-108310  
 Cu<sub>2</sub>Nb<sub>2</sub>O<sub>7</sub> single crystals, flux growth, X-ray charact. 4-76651  
 Cu<sub>1-x</sub>Ni<sub>x</sub>Mo<sub>2</sub>Se<sub>4</sub> superconducting Tc changes 4-61481  
 CaO electronic valence states, energy level diagram 4-64394  
 CuO electronic valence states, radiative lifetimes of A<sub>1</sub>, A<sub>2</sub>, C, and D states 4-64545  
 CuO, K-absorption edge, X-ray absorpt. near edge struct. obs. 4-66123  
 CuO, porous, thermal diffusivity, unsteady state method 4-80316  
 CuO/Li/ZnO junctions I-V characteristics, humidity effects, humidity sensor appl. 4-63750  
 CuO/C physical mixture thermal behaviour anal. using thermogravimetry and X-ray diffraction 4-99784  
 CuO/stainless steel tandem solar absorber converters, optical properties and spectral selectivity 4-99999  
 CuO-CaO-P<sub>2</sub>O<sub>5</sub> glass, IR spectra 4-76446  
 CuO-CoO-P<sub>2</sub>O<sub>5</sub>, ESR in phosphate glasses containing mixed transition metal ions 4-65851

## copper compounds continued

- CuO-NiO-P<sub>2</sub>O<sub>5</sub>, ESR in phosphate-glasses containing mixed transition metal ions 4-65851  
 CuO-SnO<sub>2</sub>-SiO<sub>2</sub>, ruby, colouring process study by optical and EPR spectroscopy 4-65859  
 CuO-Ta<sub>2</sub>O<sub>5</sub>, struct. of Ta<sub>2</sub>O<sub>5</sub>-rich phases, electron-optical and X-ray powder diffr. studies 4-108329  
 CuO<sub>2</sub>, photochem. and struct. in inert gas matrices 4-109672  
 (Cu<sub>0.9</sub>-(2Bz<sub>0.3</sub>O<sub>1.2</sub>Li<sub>2</sub>O))<sub>1-x</sub> glass, EPR and mag. susceptibility meas. 4-61587  
 Cu<sub>2</sub>O, ESCA and Auger spectroscopy determ. of binding energy. (French) 4-66638  
 Cu<sub>2</sub>O, excited spectra in mag. fields upto 9.77 T. (Japanese) 4-107307  
 Cu<sub>2</sub>O, K-absorption edge, X-ray absorpt. near edge struct. obs. 4-66123  
 Cu<sub>2</sub>O, ortho-exciton states, time-resolved hot luminesc., reson. Raman scatt. 4-71438  
 Cu<sub>2</sub>O, para-exciton luminesc. polarisation in mag. field 4-92624  
 Cu<sub>2</sub>O thin films on Cu, defect luminesc. 4-66062  
 Cu<sub>2</sub>O, triplet states, photoluminescence ODMR obs. 4-61608  
 Cu<sub>2</sub>O/Cu photovoltaic cells, backwall type, preparation and props. 4-99970  
 Cu<sub>2</sub>O/CuO selective surface optical props. and surface composition 4-72170  
 Cu<sub>2</sub>O/stainless steel tandem solar absorber-convertors, optical properties and spectral selectivity 4-99999  
 Cu<sub>2</sub>-O, elec. cond. meas. 4-98624  
 Cu<sub>2</sub>O metastable oxide formed in initial Cu oxidation, struct., electron microscopic study 4-65228  
 Cu<sub>4</sub>(OH)<sub>6</sub>(SO<sub>4</sub>)<sub>2</sub>H<sub>2</sub>O, langite, cryst. struct. determ. 4-108313  
 Cu<sub>2</sub>P<sub>7</sub>, preparation and cryst. struct. 4-80008  
 Cu<sub>6</sub>-P<sub>2</sub>S<sub>8</sub>, photointercalation and optical information storage 4-79058  
 Cu<sub>2</sub>PS<sub>2</sub>Br<sub>7</sub>, solid superionic conductors, transport props. 4-113983  
 CuRb<sub>2</sub>Br<sub>2</sub>H<sub>2</sub>O, mag. props. meas. 4-98925  
 Cu<sub>16</sub>Rb<sub>4</sub>I<sub>2</sub>Cl<sub>13</sub> solid electrolyte, thermoelec. power 4-80298  
 CuS, surface modification of CdSe photoelectrochemical cells 4-81566  
 CuS-GaS system, phase diagram and CuGaS, phase field range 4-71640  
 CuS<sub>2</sub>, band struct. calcs., Mossbauer spectra 4-92611  
 Cu<sub>2</sub>S, adsorption of ethyl xanthate XPS study 4-85090  
 Cu<sub>2</sub>S solar cells fabricated by reactive pulverisation 4-109738  
 Cu<sub>2</sub>S/CdS heterojunctions, characterisation by high resolution electron microscopy 4-104294  
 Cu<sub>2</sub>S-CdS solar cells, elementary degradation mechanisms. (Russian) 4-89402  
 Cu<sub>2</sub>S-CdS thin film solar cells development and transfer to industrial production 4-89429  
 Cu<sub>2</sub>S-Cu<sub>2</sub>Te, molten, thermal cond. meas. 4-104193  
 Cu<sub>2</sub>S-Zn<sub>2</sub>Cd<sub>1-x</sub>S heterojunction, energy band diagrams 4-104296  
 Cu<sub>2</sub>-S ionic conductor, Cu electromigration 4-88354  
 Cu<sub>2</sub>-S, long period modulated struct. with continuously variable periodicity 4-113469  
 Cu<sub>2</sub>-S/CdS heterostruct., misfit accommodation and growth 4-108730  
 Cu<sub>2</sub>S cathodes in organic electrolyte Li batteries, electrochem. behaviour 4-104996  
 Cu<sub>2</sub>S electroplating on CdS for CdS-Cu<sub>2</sub>S heterojunction photocells 4-99354  
 Cu<sub>2</sub>S films, photocond. and solar cell props. 4-113988  
 Cu<sub>2</sub>S thin films, topotaxially grown on CdS:Cu<sub>2</sub>In sprayed films, optical and structural behaviour 4-114433  
 Cu<sub>2</sub>S-CdS photocells formed by electroplating, prep. and props. 4-72115  
 CuSO<sub>4</sub> aq. solns., elec. resist. fluctuations 4-75713  
 CuSO<sub>4</sub>, gel medium electrolyte-diffusion and self-diffusion, transition state theory 4-89339  
 CuSO<sub>4</sub> soln. electron spin echoes, phase shifted excitation 4-98936  
 CuSO<sub>4</sub>/C physical mixture thermal behaviour anal. using thermogravimetry and X-ray diffraction 4-99784  
 CuSO<sub>4</sub>.5H<sub>2</sub>O, dehydration reactions, kinetic studies using quartz cryst. microbalance 4-99778  
 Cu<sub>2</sub>S(Se), ionic thermoelectromotive force, rel. to temp. and mobile ion conc. 4-75719  
 Cu<sub>2</sub>S-Zn<sub>2</sub>Cd<sub>1-x</sub>S reverse-biased p-n heterojunctions, elec. props. and photodiode appls. (Russian) 4-108926  
 Cu<sub>2</sub>-S-ZnS p-n heterojunctions, elec. and photoelec. props., UV detector appls. (Russian) 4-108927  
 Cu<sub>2</sub>-Se, mixed conductor, DC ionic cond. meas. 4-88340  
 Cu<sub>2</sub>-Se, superionic transition, DSC study 4-88338  
 Cu<sub>2</sub>-Se, thermal expansion, dilatometer study 4-88319  
 Cu<sub>2</sub>Se<sub>2</sub> (010) crystal, high resolution transmission electron microscopic images 4-88044  
 Cu<sub>2</sub>SnS<sub>4</sub>, thermal props., elec. cond. and Hall effect 4-88523  
 Cu<sub>2</sub>Ta<sub>2</sub>(Se<sub>4</sub>)<sub>2</sub>, isomer shifts of 6.2 keV nucl. transition, Mossbauer spectra 4-109104  
 Cu<sub>2</sub>-Te<sub>2</sub>, long period modulated struct. with continuously variable periodicity 4-113469  
 p-Cu<sub>2</sub>Te-n-CdTe heterojunction, deep levels, photocapacitance spectra 4-61410  
 CuTeBr, phase transitions, ionic cond. study 4-88287  
 β-Cu<sub>2</sub>V<sub>2</sub>O<sub>7</sub>, bipolaron ordering, X-ray scatt. study 4-80519  
 CuV<sub>2</sub>S<sub>4</sub>, CDW transitions, elec. and thermal props. 4-98618  
 CuV<sub>2</sub>S<sub>4</sub>, valence band holes 4-70653  
 Cu<sub>0.75</sub>VS<sub>2</sub>, long period modulated struct. with continuously variable periodicity 4-113469  
 Cu<sub>0.75</sub>VS<sub>2</sub>, phase transitions and cryst. struct. 4-80224  
 CuWO<sub>4</sub> single cryst., elec. props., photoelectrochem. study 4-65708  
 (CuZn)S-CuInSe<sub>2</sub> heterojunction solar cell, interface props. 4-89401  
 Fe<sub>1-x</sub>Cu<sub>x</sub>C<sub>4</sub>S<sub>4</sub>, ferrimagnetic to ferromagnetic order transition, ion valence states, NMR 4-88670  
 In<sub>2</sub>O<sub>3</sub>-Fe<sub>2</sub>O<sub>3</sub>-Cu<sub>2</sub>O, phase relations and cryst. structures 4-98242  
 In<sub>2</sub>O<sub>3</sub>-Ga<sub>2</sub>O<sub>3</sub>-Cu<sub>2</sub>O, phase relations and cryst. structures 4-98242  
 KCuNb<sub>2</sub>(Ta<sub>2</sub>)O<sub>6</sub>, pentagonal tunnel structs., X-ray diffr. and electron microscopy studies 4-98069  
 LaCu<sub>2</sub>Al<sub>10</sub>O<sub>18+x</sub>, struct., substitution effects, X-ray diffr. studies 4-103722  
 Li/Cu<sub>2</sub>V<sub>2</sub>O<sub>7</sub> battery with 1-M LiClO<sub>4</sub>-propylene carbonate/1,2-dimethoxyethane electrolyte 4-93607  
 Li/CuMoO<sub>4</sub> voltage compatible battery, performance 4-77074  
 NaCa<sub>2</sub>Cu<sub>2</sub>V<sub>2</sub>O<sub>7</sub>O<sub>19</sub> garnet, mag. props. study 4-61563  
 Na<sub>2</sub>O-Cu<sub>2</sub>O-GeO<sub>2</sub> glass, elec. cond., chem. content depend. 4-98673  
 Nd<sub>2-x</sub>Ba<sub>1+x</sub>Cu<sub>2</sub>Y<sub>2</sub>O<sub>5-x</sub>, cryst. struct., mag. susceptibility, elec. cond. (French) 4-75418  
 NdCu<sub>3-x</sub>Mn<sub>1+x</sub>, synthesis, composition and mag. props. 4-108997  
 Ni<sub>0.98-x</sub>Mn<sub>0.02</sub>Co<sub>0.02</sub>Cu<sub>0.98</sub>Fe<sub>2</sub>O<sub>4</sub>, stress sensitivity coeff. 4-76213

## copper compounds continued

- TeO<sub>2</sub>-Cu<sub>2</sub>O-(CuO), phase equilib. 4-84370  
 TiCu<sub>2-x</sub>M<sub>x</sub>Se<sub>2</sub> (M=Fe, Mn), valence band holes 4-70653  
 TiCu<sub>2</sub>Se<sub>2</sub>, p-type metal with layer struct. 4-70652  
 copper zinc alloys *see brass*  
 copying *see reproduction (copying)*  
 Corbino effect  
*see also Hall effect*  
 TiSi<sub>2</sub> thin films, electronic transport props., classical metallic behaviour 4-70955  
 core levels *see localised electron states*  
 Coriolis force  
*see also rotation*  
 benzene, intramolecular vibr. relax., high resol. spectra 4-78825  
 benzene, rot. linewidths, Doppler free two-photon spectra 4-74302  
 benzene-d<sub>6</sub>(-d<sub>6</sub>), vibr. anal., force const. 4-91246  
 cubane, force consts., vibr., IR and Raman spectra, HF level calcs. 4-59694  
 dichloromethane-d<sub>2</sub>(d<sub>2</sub>), force consts. thermodynamic props., vibr. anal. 4-64448  
 difluorocarbene, ν<sub>3</sub> band, IR diode laser spectroscopy 4-59740  
 formaldehyde, S<sub>1</sub>, rovibr. levels, Coriolis perturbations, fluoresc. excitation spectrosc. obs. 4-102731  
 formaldehyde-d<sub>2</sub>, collision induced vibr. energy transfer, IR-UV double reson. 4-78875  
 Goryachev-Chaplygin gyrostat in quantum mech. 4-68006  
 hexaquo anions, octahedral, mol. consts., force field calcs. 4-102600  
 methoxy radical, <sup>2</sup>E ground state, rot. mol. consts., microwave spectrum 4-107334  
 nonsteady state axisymmetrical surface gravitational waves propag. (Russian) 4-86276  
 rot. Zeeman effect and Coriolis coupling, spin-rot. const. 4-59823  
 rotating liq. drop, Coriolis force, oscils. 4-79648  
 symmetric and spherical top molecules, rot. energy levels, Jahn-Teller and L-uncoupling effects 4-59690  
 BrFO<sub>3</sub>, mol. consts., normal coordinate anal. 4-74216  
 ClFO<sub>3</sub>, mol. consts., normal coordinate anal. 4-74216  
 ClO<sub>2</sub>, ground excited and ionic states, force consts., vibr. anal. 4-64449  
 GeH<sub>3</sub>F, excited vibr. states Coriolis reson., MM wave spectra 4-59719  
 He<sup>2+</sup>+He collisions, Coriolis coupling effect in time depend. HF calcs. 4-91342  
 ND<sub>4</sub>, rot. energy levels, Jahn-Teller and L-uncoupling effects 4-59690  
 NF<sub>3</sub>(X<sup>2</sup>B<sub>1</sub>), ν<sub>3</sub> band, IR laser spectroscopy 4-69082  
<sup>18</sup>N<sup>16</sup>O<sub>2</sub>, ν<sub>1</sub> band, line positions and intensities, Fourier transform IR spectra 4-59755  
 NeHCl, rot. Zeeman effect and Coriolis coupling, spin-rot. const. 4-59823  
 OPCl<sub>3</sub>, millimeter wave spectrum 4-64457  
 PCl<sub>3</sub>F<sub>2</sub>, valence force field pot. consts., vibr. anal. 4-102661  
 ReBrO<sub>3</sub>, mol. consts., normal coordinate anal. 4-74216  
 SbF<sub>3</sub>Cl<sub>2</sub>, valence force field pot. consts., vibr. anal. 4-102661  
 corona *see eye*  
 corona  
*see also electric breakdown; flashover; solar corona*  
 air, positive corona breakdown, residual streamer channel 4-108233  
 air, positive DC corona, breakdown parameters and current-voltage characts. 4-79887  
 air, RF corona discharge, pulsed, spatiotemporal spectrosc. obs. 4-79846  
 air pulsed RF corona, ns. image intensifier investigation 4-84105  
 circular pipe placed in air jet and corona wind, heat transfer coeff. 4-97527  
 convective stimulated Raman scattering instability in UV laser plasmas 4-113127  
 CW arc pluming at high-power aerials, pulsed RF plasmas obs. 4-69970  
 detection by electrostatic probe 4-84061  
 discharge, EGD flow and its influence on motion of dispersed particles 4-103425  
 discharge effects on gasdynamical flow rate 4-69975  
 distributed source corona photoionization calculations applicable to finite element computer models 4-96506  
 electrical fields application to combustion systems 4-69985  
 electrical wind velocity field meas. using multicomponent laser Doppler velocimeter (Russian) 4-69837  
 electrodes subjected corona discharges, corrosion products anal. by Raman microprobe spectroscopy 4-76910  
 electron avalanche-corona transition temporal characts., electrode radius of curvature effects 4-84104  
 electrostatic, precipitator rods, DC corona discharge and ion flow distribution characts. 4-97933  
 electrostatic cooling, development of flow vel. in boundary layer (Japanese) 4-84098  
 negative corona current and trichel pulses, time depend. 4-84107  
 negative corona discharges, negative ion extraction 4-84106  
 negative ions mass spectrometry in negative corona discharge in air-O<sub>3</sub> mixtures 4-87227  
 organic insulation, tracking discharges, light emission, corona, scintillation and arc discharges 4-84097  
 overhead line conductors, surface treated conductors for reduced corona losses (Japanese) 4-60776  
 polystyrene films charged by friction and corona discharge, surface charge densities 4-92800  
 polyvinylidene fluoride, conductivity, constant current corona charging studies 4-108857  
 positive glow corona in atmospheric air, simple theoretical model 4-97935  
 positive wire to plane coronas, atmospheric humidity effect on inception voltage 4-97937  
 PVDF, corona poling, piezoelec. activities 4-109117  
 self corona discharge of sharp edged ellipsoidal particles in electric field 4-97934  
 spontaneous megaGauss magnetic field detect. in laser plasma created by 0.53 μ radiation 4-79843  
 N<sub>2</sub> pulsed RF corona, ns. image intensifier investigation 4-84105  
 N<sub>2</sub>, RF corona discharge, pulsed, spatiotemporal spectrosc. obs. 4-79846  
 O<sub>3</sub> production during corona discharges in air and other gases, experimental study 4-97938  
 SF<sub>6</sub>, compressed, breakdown voltage and timelags under corona stabilisation 4-79727

**corona continued**

- SF<sub>6</sub>, corona discharge under switching impulse, insulator in gap effects 4-79888  
 SF<sub>6</sub>, positive DC corona, breakdown parameters and current-voltage characteristics 4-79887

**coronagraphs**

- see also solar corona  
 No entries

**corpuscular streams** see cosmic rays; solar wind**correlation methods**

## see also correlators

- BASIC program for bootstrap analysis of correlation coeff., laboratory microcomputers appl. 4-106290  
 curve fitting, least squares and utmost correl. methods comparison 4-67967  
 differential-modulation correlator for extracting 4-74441  
 diffraction grating autocorrelator for meas. single ultrashort light pulses 4-107807  
 electroabsorptive CCD spatial light modulator, 1D, signal correlation 4-107542  
 galaxy correlation hierarchy in perturbation theory 4-86033  
 hybrid optical-digital pattern recognition 4-74426  
 LPC voiced-speech synthesis, improved algorithm using iterative method 4-74817  
 near IR scan data, regression anal., best-pair wavelengths selection, colour graphics 4-95534  
 photoacoustic spectroscopy and thermal wave imaging, tutorial review 4-106391  
 polychromatic signal detection by complex spatial filtering 4-74435  
 radio interferometry, high-sensitivity correl. receiver, cosmic radio source meas. 4-72887  
 scene matching using photon-limited images 4-69319  
 speech, discrimination between /mo/ and /no/, canonical correl. anal. 4-79380  
 speech, discrimination of nasal consonants and voiced stop consonants by using transitions 4-79387  
 tactical targeting by structural and correlation analysis 4-96829

**correlation theory**

## see also correlators; information theory

- autocorrelation and lattice deform. simulation, appl. in rock struct. 4-105544  
 average value of correlated time series, appls. in dendroclimatology and hydrometeorology 4-100665  
 functional standpoint of simultaneous order in nervous nets 4-81656  
 geometrical structures determined by the functional order in nervous nets 4-81657  
 neural spike trains, estimation of correlation function 4-93716  
 optical image reconstruction from autocorrel. 4-96836  
 speckle pattern correlations with double-beam and polychromatic illumination 4-74424

**correlators**

## see also correlation methods; correlation theory; information theory

- 64-channel, laser Doppler anemometry signal processing appl. 4-78299  
 cross correlator loss of optimality 4-59995  
 digital sign correlator for a very long baseline radiointerferometer 4-94609  
 image recognition, optical-electronic system with operational input and preliminary processing of images for recognition (Russian) 4-107526  
 joint transform real time optical correlator using As<sub>2</sub>S<sub>3</sub> noncrystalline film 4-74461  
 laminar flow velocity determ. using photon correlator, systematic errors (Russian) 4-108142  
 matched holographic filtering in FTIROS 4-79080  
 optical correlator using computer generated holograms, micromech. quality control appls. 4-107572  
 optical correlator using holographic lens 4-107576  
 optical data processor using computer generated holograms, high energy physics expt. appls. 4-107535  
 optoelectronic correlator based on modified Michelson interferometer with computer control (Russian) 4-107527  
 picosecond rotating-mirror autocorrelator, optimisation study 4-107793  
 SAW finite amplitude waves, resonators, convolvers and correlators, appl. 4-74792  
 signal processing using laser light and SAW interaction 4-74565  
 squared signal correlation and possible acoustooptic implementation 4-59988  
 Van der Lugt correlator with spherical wave illum. 4-74439

**correspondence principle**

- conformal mappings using Schwartz-Christoffel integral 4-91382  
 viscoelastic crack analysis by boundary integral eqn. 4-112766

**corrosion**

## see also corrosion protection; corrosion testing; electrochemistry; stress

- corrosion cracking; surface chemistry  
 activation product transport in fusion reactors, radiation fields calc. around plant components 4-107153  
 advanced HTR systems, alloys eval., creep, fatigue, corrosion, neutron effects 4-78699  
 Alloy 800H, creep of tubular components, influence of multiaxiality of stress and environmental induced degradation 4-93360  
 anodised layer, spectrally selective, solar collector appl., ESCA studies 4-66789  
 applied surface anal., conf., Dayton, USA (June 1983) 4-95016  
 borosilicate glasses containing ZrO<sub>2</sub>, radioactive waste disposal, long term leaching 4-111607  
 brass, atmospheric sulphidation 4-76901  
 $\beta$ -brass, Sn alloyed, Auger/SEM obs. of corrosion 4-89172  
 brass-steel galvanic couple, corrosion, polarisation study 4-85245  
 brick, high alumina, corrosion resist. to nitric acid, report 4-62090  
 bronzes, atmospheric sulphidation 4-76901  
 ceramic oxides, high temperature materials for magnetohydrodynamic channels 4-109368  
 contact materials with reduced noble metal content, corrosion behaviour (German) 4-99640  
 corrosion products solubility in O<sub>2</sub> containing aq. solns. under extreme conditions 4-113642  
 crevice erosion and the thermohydraulic state of slots in joints, vapour and condensate anal. 4-65027  
 dielectric film degradation by XeF excimer laser intermediates 4-74534  
 electrical insulation degradation for chem. sprays in loss of coolant accidents 4-68799

**corrosion continued**

- electrodes subjected corona discharges, corrosion products anal. by Raman microprobe spectroscopy 4-76910  
 ferrous alloys, dissoln. in molten pure Al under forced flow 4-92378  
 fibre reinforced metal matrix composites, directionally solidified, book contrib. 4-66277  
 fireclay ceramic, corrosion resist. to nitric acid, report 4-62090  
 fission reactors, surface states of constructional materials in RBMK-1000 4-102356  
 fluorides, organic and inorganic chemistry and energy storage 4-72184  
 fuel cells catalysed by WC in H<sub>3</sub>PO<sub>4</sub>, corrosion resistance and catalytic activity 4-66689  
 fusion reactor blankets, liquid metal corrosion product transfer, MHD effects, safety 4-111786  
 fusion reactor materials, conf., Albuquerque, NM, USA (Sept. 1983) 4-90290  
 fusion reactors, liquid breeders, compatibility of structural materials 4-111750  
 galvanised reinforcements, immersed in soln. with pH range 12.6 to 13.6  
 SEM study of corrosion product 4-66481  
 glass, in weak-acid and weak-alkali solns., effects of electrolyte additions 4-81316  
 glass fibres, leaching and local comp., SEM study 4-81303  
 glass radwaste forms, leaching backfill materials effects; glass powder backfill 4-59328  
 glass-bentonite nuclear waste interfaces after one year burial in STRIPAL 4-111605  
 glass-glass nuclear waste interfaces after one year burial in STRIPAL 4-111604  
 graded-index fibre light pipes, lifetime estimation model 4-69581  
 heat resistant alloy sheets, corrosion props. in He environment (Japanese) 4-96136  
 HVDC transmission systems caused corrosion, prediction possibilities 4-81334  
 Incoloy 800, compatibility with flowing Li<sup>+</sup> 4-107062  
 Incoloy 802, H<sub>2</sub> permeation inhibition by corrosion oxide layers (German) 4-66506  
 Inconel 617, surface crack form. and propag., effect of temp. reactor primary circuit He 4-114641  
 Inconel 750, nuclear reactor construction material 4-66476  
 Inconel X750, in BWR primary system, corrosion products release rates, meas. using radiotracer technique 4-91040  
 intergranular corrosion of steels and alloys, book 4-95084  
 LWR low-pressure steam turbines, corrosive salt solubility in dry steam 4-111692  
 Magnox alloys, etched, surface anal. by secondary ion mass spectrometry and ion scatt. spectroscopy 4-93456  
 MARS, liquid Li<sub>2</sub>Pb<sub>3</sub> cooled fusion reactor blanket, corrosion product cleanup system 4-111785  
 metal, dry corrosion, linear kinetics 4-99660  
 metals, atmospheric corrosion monitoring using electrochemical sensors 4-109544  
 metals, corrosion, high temp., role of diffusion of sulphides 4-66509  
 metals, passive, pit initiation, halide nuclei theory 4-66491  
 metals, passive, pit repassivation during pitting corrosion 4-89182  
 mild steel plates, corrosion after 20 years in New Zealand soil. 4-99655  
 nuclear power stations, single-loop, low-pressure heater system  
 08Cr18Ni10Ti steel replacement by carbon steel feasibility 4-93469  
 nuclear steam generator tubesheet crevices cleaning using amine borane compounds 4-111662  
 pressure vessels, steel, corrosion fatigue, development of engineering code 4-93406  
 PWR and PHWR steam generator tube performance, experience during 1981 4-111651  
 PWR coolant, chemical additive role in corrosive impurity transport in steam 4-96189  
 PWR steam generator chemical cleaning database 4-83225  
 PWR steam generators, corrosion products under typical operating conditions 4-102371  
 radioactive waste disposal container materials, corrosion in synthetic groundwater (French) 4-59338  
 radioactive waste materials, ion implantation effects on dissolution props. simulation of internal irradi. due to  $\alpha$ -decay 4-75544  
 rate calc. by computer program 4-109545  
 red shale ceramic, corrosion resist. to nitric acid, report 4-62090  
 Ringbom-Stirling air engine, design and operational experience with water as lubricant 4-66770  
 semiconductor device manufacture, Raman microprobe applic. 4-93573  
 semiconductor electrodes, oxidation, corrosion, elec. double layer mode 4-62235  
 semiconductors, photoelectrochemistry, book contrib. 4-88585  
 simulated nuclear waste glass, Cm doped, radiation damage, annealing short term leach test 4-83149  
 solidified TRU-contaminated incinerator ash, leach rates and Pu release 4-106714  
 steam power plant chemical water treatment equipment, wastewater and fresh water corrosion comparison 4-71795  
 steel, acid corrosion inhibition by benzotriazole 4-81351  
 steel, alloy, chemical reactor cooling coils, corrosion, X-ray radiographic test (Chinese) 4-62141  
 steel, austenitic, AM-2, various properties and products of nonmagnetic steels 4-114590  
 steel, austenitic and ferritic, corrosion behaviour in eutectic Pb-Li environment 4-107056  
 steel, austenitic and ferritic, for use in fusion reactor liq. metal blankets compatibility, review 4-107054  
 steel, austenitic stainless, Alloy 800 H, surface crack form. and propag. effect of temp. reactor primary circuit He 4-114641  
 steel, austenitic stainless, corrosion rate in liquid Na environment (Japanese) 4-96138  
 steel, austenitic stainless, creep of tubular components, influence of multiaxiality of stress and environmental induced degradation 4-93360  
 steel, austenitic stainless, crevice corrosion and SCC, metallography 4-109566  
 steel, austenitic stainless, crevice corrosion behaviour in seawater and related environments 4-99638  
 steel, austenitic stainless, in formic acid soln., comparison with pure Fe, Ni and Cr 4-71763  
 steel, austenitic stainless, Incoloy 800, H<sub>2</sub> permeation inhibition by corrosion oxide layers (German) 4-66506

## corrosion continued

- steel, austenitic stainless, meas. of low corrosion rates, comparison of AC impedance and thin layer activation methods 4-62139
- steel, austenitic stainless, nuclear reactor construction materials, Co release rates in oxidising and reducing water environments 4-66476
- steel, austenitic stainless, oxide layer structure, formed in simulated LWR conditions 4-76893
- steel, austenitic stainless, pitting corrosion detection using double layer activation technique 4-81368
- steel, austenitic stainless, pitting corrosion in water-organic solvent mixtures 4-81348
- steel, austenitic stainless, sintered, anodic behaviour in  $\text{H}_2\text{SO}_4$  soln. rel. to carburisation 4-62096
- steel, austenitic stainless, structure and mech. props., casting environment effects 4-109433
- steel, austenitic stainless, thermal and radiation-stimulated ageing, kinetics 4-66354
- steel, austenitic stainless in BWR primary system, corrosion products release rates meas. using radiotracer technique 4-91040
- steel, austenitic stainless superalloy, as-cast, corrosion in molten sulphates, influence of Si and W additions 4-71759
- steel, austeno-ferritic stainless, sulphidation kinetics, triplex scale form. 4-109560
- steel, C, atm. corrosion, influence of pollution, humidity, temp., solar rad. and rainfall 4-85244
- steel, carbon, in PWR steam generators, denting causes, nonprotective magnetite prod. 4-104924
- steel, cathodic polarisation curves, S content influence (French) 4-71792
- steel, corrosion products in  $\text{H}_2\text{S}$ - $\text{N}_2$ -( $\text{O}_2$ ), chem. anal. by conversion electron Mossbauer spectroscopy 4-66473
- steel, corrosion products in  $\text{SO}_2$ , chem. anal. by conversion electron Mossbauer spectroscopy 4-66472
- steel, Cr-Mn austenitic, phase stability and corrosion on exposure to pure Li 4-107061
- steel, Cr-Mo, reduction of rust in high temp. liq. Na 4-104914
- steel, ferritic and type 316, exposed to static Pb-Li, corrosion reactions, surface analysis 4-107064
- steel, ferritic stainless, corrosion and passivation, in Cl-containing  $\text{H}_2\text{SO}_4$  4-85241
- steel, ferritic stainless, intergranular corrosion susceptibility, etching method 4-85265
- steel, ferritic stainless, resistance welded, corrosion resist. under detergent exposure 4-104895
- steel, ferritic stainless, stabilisation breakdown 4-114718
- steel, H corrosion, theory of void growth limited by C diffusion 4-81338
- steel, low C, corrosion behaviour in formic and acetic acid 4-81329
- steel, medium C, corrosion in aq. soln. containing fluoride ions at 300°C 4-85246
- steel, mild, corrosion rate in soil, IR spectra 4-109542
- steel, mild, electrodes in  $\text{H}_2\text{SO}_4$ , adsorption of thiourea 4-88390
- steel, simulated atmospheric corrosion, Mossbauer spectroscopic study of rust 4-104896
- steel, stainless, austenitic, modified PCA, mass transfer behaviour in Li 4-107063
- steel, stainless, austenitic, type 316, flowing Li environment effect on fatigue and tensile props. 4-107055
- steel, stainless, corrosion by liq. Li using LILO-7 thermoconvection loop 4-107059
- steel, stainless, crevice corrosion in 3% NaCl soln, accelerated tests (Japanese) 4-99652
- steel, stainless, localised corrosion propag., Cr and Mo effects 4-104903
- steel, stainless, Ni-free, alloyed with rare-earth metals and Ca, struct. and props. 4-62116
- steel, stainless, type 316, chem. compatibility with  $\text{Li}_2\text{O}$  fusion reactor breeder 4-107060
- steel, Ti ion implanted, corrosion resist. of amorphous Fe-Ti-C surface 4-76917
- steel, use of surface behavior diagrams to study hydration/corrosion of aluminum and steel surfaces 4-89171
- steel, weathering, preetched, electrochemical and corrosion props. 4-62092
- steel, weathering performance, effect of Cu 4-89175
- steel, welded patinable, atm. corrosion, passivating capabilities of rust film (French) 4-62126
- steel bar reinforcements in concrete, corrosion rate, AC impedance meas. by spectrum analyser 4-109546
- steel fibre reinforced monolithic refractories, selection and service life 4-109458
- steel pressure vessels, corrosion fatigue crack growth 4-93405
- steels, heat-resisting, surface layer fatigue failure, protective effect of alloy coatings 4-93470
- transition metal, chem. compatibility with  $\text{Li}_2\text{O}$  fusion reactor breeder 4-107060
- US reflection from natural defects propagating from surface, echo signal amplitude 4-109615
- water chemistry changes, PWR feedwater corrosive species conc. models 4-59378
- Zircaloy-4, anodic behaviour in conc.  $\text{H}_2\text{SO}_4$ , form. of two surface films 4-76899
- 4-104916
- Ag-Cu (7.5 to 16.5 wt.%), reaction mechanism with  $\text{H}_2\text{S}$ , 0-220°C 4-66475
- Al alloy, surface preparation, adhesive bonding and corrosion developments 4-89173
- Al alloys, corrosion behaviour in HCl, inhibitive effect of heterocyclic compounds 4-104919
- Al, corrosion resistance of oxide layers rel. to impurity content 4-62102
- Al, galvanic corrosion kinetics in  $\text{H}_2\text{SO}_4$ , gas evolution role 4-114726
- Al, hydration/corrosion, surface behaviour diagrams, dissolution of adsorbed inhibitor 4-89171
- Al, with small Sn additions, microstruct. and corrosion behaviour 4-99630
- Al-Cu couple, galvanic corrosion in uninhibited aq. glycol soln. 4-66480
- Al-Mg, 5083 alloy plates, mech. props. and stress corrosion cracking, anisotropy effects (Japanese) 4-66496
- Al-Mo alloys, ion implanted, corrosion resist., AES studies 4-99626
- Al-Sn (0.1 wt.%), corrosion resist., electrochemical props. rel. to alloying additions 4-81342
- Al-Zn-Mg single crystals, environmentally-assisted cracking 4-71762
- $\text{Al}_2\text{O}_3$ - $\text{ZrO}_2$ - $\text{SiO}_2$  glass refractory, fusion-cast high  $\text{ZrO}_2$ , corrosion resistance in soda lime glass 4-62080

## corrosion continued

- $\text{Al}_2\text{O}_3$ - $\text{ZrO}_2$ - $\text{SiO}_2$  refractory, corrosion by Pb glass 4-71753
- Au electrodeposits on contacts, performance eval. 4-76020
- B<sub>2</sub>C based materials, resist. to corrosion by  $\text{H}_2\text{SO}_4$  soln. 4-62087
- C ceramic, corrosion resist. to nitric acid, report 4-62090
- C-SiC alloy coating for limiter-armor tiles on Doublet III fusion reactor, test results 4-111924
- CaSOCl<sub>2</sub> cells with anodes made from Ca/Ca-Li alloys, electrochemical studies 4-72080
- Cd-Ni, electrodeposition from ammoniacal baths, corrosion resist. 4-66253
- CDS polycrystalline films, photocorrosion in aq. soln., capacitance and action spectra meas. 4-92818
- Co-base alloys, gaseous corrosion in  $\text{H}_2\text{O}$ -HCl environment 4-89164
- Cr-Ru(Pd)(Ir)(Pt), active dissoln. in  $\text{H}_2\text{SO}_4$ , effect of Pt group element additions 4-71770
- CrN<sub>x</sub> DC reactively sputtered layers with surface roughness, as selective absorbers in solar collectors 4-77147
- Cu base solid solutions and intermetallic phases, mech. of dealloying 4-93449
- Cu, lightning conductor plates, corrosion in soil, over 50 years 4-109543
- Cu pipes, corrosion of soldered and brazed joints in hot tap water 4-109538
- Cu, surface characterisation by polysulphide reagent, corrosion pot. rel. to colour change 4-81352
- Cu tubes, corrosion in hot water, prediction of pit initiation from water comp. 4-81328
- Cu-Al-Fe (10, 1 wt.%), corrosion and mech. props., effect of solidification struct. 4-85243
- Cu-Ni (30 wt.%), corrosion in 3% NaCl soln., energy dispersive X-ray analysis (French) 4-76895
- Cu-Ni-Fe (9.4, 1.7 wt.%), corrosion behaviour in air-saturated aqueous NaCl soln. 4-93447
- Cu-Ni-Fe (9.4, 1.7 wt.%), corrosion in aqueous NaCl soln., effect of sulphide 4-93448
- Cu-Ni-Sn alloys, atmospheric sulphidation 4-76902
- (Fe, Co, Ni)<sub>3</sub>V, ductile ordered alloys, phys. metallurgy and mech. props. 4-114612
- Fe alloy surfaces in acid media,  $\text{H}_2$  evolution kinetics, metallurgical and electrochem. factors 4-85335
- Fe, corrosion in molten carbonate, electrochem. studies 4-104917
- Fe, corrosion in molten chloride, electrochem. studies 4-104915
- Fe, corrosion in molten sulphate, electrochem. studies 4-104916
- Fe corrosion products solubility in  $\text{O}_2$  containing aq. solns. under extreme conditions 4-113642
- Fe, electrochem. behaviour, effect of  $\text{Br}^-$  4-89165
- Fe, H electrochemical penetration, effect of As additions to electrolyte 4-66497
- Fe, high temp. corrosion scales, TEM studies 4-104927
- Fe, passive films, in borate solns., electrochemical and ellipsometric studies, film growth 4-89178
- Fe powders, chem. instability and corrosion, mag. tape appls. (Chinese) 4-98982
- Fe, pure, corrosion pit growth, early stages, meas. of shape change 4-104897
- Fe, pure and siliconised, corrosion and oxidation kinetics in  $\text{SO}_2$  atm. 4-109554
- Fe, sulphidation, microstruct. and growth rates of FES 4-88304
- Fe-Al, anodic polarisation characteristics in 1N  $\text{H}_2\text{SO}_4$  4-85247
- Fe-Al-Si, anodic polarisation characteristics in 1N  $\text{H}_2\text{SO}_4$  4-85247
- Fe-base alloy, gaseous corrosion in  $\text{H}_2\text{O}$ -HCl environment 4-89164
- Fe-C, dissoln. in molten pure Al under forced flow 4-92378
- Fe-Cr, accelerated oxidation in atmosphere containing water vapour 4-81356
- Fe-Cr, corrosion and passivation, in Cl-containing  $\text{H}_2\text{SO}_4$  4-85241
- Fe-Cr (26.6 at.%), sulphidation props. in  $\text{H}_2\text{S}$ - $\text{H}_2$  atmospheres at temps. 973 to 1173K and S press.  $10^{-10}$  to  $10^{-6}$  Pa 4-93459
- Fe-Cr (26.6 at.%), sulphidation mechanism in  $\text{H}_2\text{S}$ - $\text{H}_2$  atmospheres at temps. of 973 to 1173K and S press.  $10^{-4}$  to  $10^{-6}$  Pa 4-93460
- Fe-Cr (30 wt.%), high temp. corrosion mechanism, XPS and AES studies 4-62098
- Fe-Cr alloys, pit initiation, current fluctuations obs. 4-89181
- Fe-Cr-Al, sulphidation in  $\text{H}_2\text{S}$ , multilayered corrosion scales 4-71801
- Fe-Cr-Al-X, X=Cu, Ti, Ni, anodic polarisation in  $\text{H}_2\text{SO}_4$  4-114719
- Fe-Cr(Si), dissoln. in molten pure Al under forced flow 4-92378
- Fe-Cu, H permeation in  $\text{H}_2\text{SO}_4$  with and without  $\text{H}_2\text{S}$ , electrochem. and surface anal. studies 4-104898
- Fe-Ni-Cr ferritic alloy, soft mag. props. and mech. strength 4-61555
- Fe-Sb-Ce alloys, Ce state at cryst. boundaries, electron diff. studies (Chinese) 4-98114
- Fe-Si, anodic polarisation characteristics in 1N  $\text{H}_2\text{SO}_4$  4-85247
- Fe-Zr amorphous films, corrosion props. in 1N  $\text{H}_2\text{SO}_4$  4-76904
- HfF<sub>4</sub>-BaF<sub>2</sub>-LaF<sub>3</sub>-AlF<sub>3</sub> glass, IR transparent, stability in humid air, AES study 4-109534
- LaF<sub>3</sub>-BaF<sub>2</sub>-ZrF<sub>4</sub>, fluoride glass, surface crystals formed by reaction with water 4-81298
- $\text{Li}_2\text{O}$ - $\text{B}_2\text{O}_3$ - $\text{SiO}_2$ , phase-separated glass, dissoln. rate, influence of pH 4-84403
- $\text{Li}_2\text{O}$ - $\text{SiO}_2$  glass and glass-ceramic, hydrothermal corrosion 4-85235
- Mg-Li-Al-Mn and Mg-Li-Al-Zn-Mn-Ce system alloys, mech. props. and corrosion resist. 4-93455
- MoSi<sub>3</sub> based materials, resist. to corrosion by  $\text{H}_2\text{SO}_4$  soln. 4-62087
- $\text{Na}_2\text{CO}_3$ - $\text{SiO}_2$  melts, dissolution of  $\text{SiO}_2$  4-84402
- $\text{Na}_2\text{O}$ - $\text{Al}_2\text{O}_3$ - $\text{SiO}_2$ , alkali resistance, effects of alkali metal and zinc oxide additions 4-81317
- $\text{Na}_2\text{O}$ - $\text{MO}$ - $\text{Al}_2\text{O}_3$ - $\text{SiO}_2$  glass, M=Ca, Mg, Zn, leaching 4-84404
- $\text{Na}_2\text{O}$ - $\text{MO}$ - $\text{SiO}_2$  glass, (M=Ca, Mg, Zn), leaching kinetics, effect of divalent cations 4-109533
- $\text{Na}_{1-x}\text{Zr}_x\text{P}_{3-x}\text{Si}_4\text{O}_{12}$  ceramics, prep., ionic cond., durability and strength 4-113711
- Nb, surface oxide films, influence of  $\text{Cl}^-$  ion conc. 4-71767
- Ni alloy surfaces in acid media,  $\text{H}_2$  evolution kinetics, metallurgical and electrochem. factors 4-85335
- Ni, corrosion in molten carbonate, electrochem. studies 4-104917
- Ni, corrosion in molten chloride, electrochem. studies 4-104915
- Ni, high temp. corrosion scales, TEM studies 4-104927
- Ni, light purity, reaction mechanism with  $\text{O}_2$ + $\text{SO}_2$ , grain boundary diffusion in scale 4-109561
- Ni, pitting and crevice corrosion in NaCl soln., effect of temp. 4-81355
- Ni, pitting susceptibility, influence of incorporated  $\text{Cl}^-$  in NiO 4-89179
- Ni, sintered porous, usage, manufacture and props. 4-104751

**corrosion continued**

- Ni-base alloys, gaseous corrosion in H<sub>2</sub>O-HCl environment 4-89164  
 Ni-base superalloys, corrosion in molten chloride, electrochem. studies 4-104915  
 Ni-base superalloys, corrosion in molten sulphate, electrochem. studies 4-104916  
 Ni-base superalloys, corrosion in molten carbonate, electrochem. studies 4-104917  
 Ni-Cr (20 wt.%), reaction kinetics with SO<sub>2</sub>, 600°C-900°C 4-104905  
 Ni-Cr-Co, IN 939, turbine stator blades, corrosion layers, metallography 4-104948  
 Ni-Mo (13 wt.%), pitting corrosion, surface segregation of Mo 4-71765  
 O<sub>2</sub> electrochemical meter for liquid Na 4-89370  
 Pb, corrosion in tap water and aq. solns. 4-109573  
 Pb/acid cells, rotating ring-disc electrode study of impurity effects on lead corrosion in sulphuric acid 4-81533  
 Pb/acid stationary battery, reliability 4-93609  
 Pb-acid batteries, with fibre reinforced Pb composites, corrosion behaviour analysis, obs. 4-72099  
 Pd-Ni electrodeposits on contacts, performance eval. 4-76020  
 Pd-Y-Cu system, phase equilib., corrosion resist. to nitric acid soln. 4-114490  
 SiC ceramic, corrosion resist. to nitric acid, report 4-62090  
 Si<sub>3</sub>N<sub>4</sub> based materials, resist. to corrosion by H<sub>2</sub>SO<sub>4</sub> soln. 4-62087  
 Si<sub>3</sub>N<sub>4</sub>, polyphase, cation diffusion through intergranular phase, appl. to environmental reactions 4-76889  
 SiO<sub>2</sub> ceramic, corrosion resist. to nitric acid, report 4-62090  
 SiO<sub>2</sub> fibres, degradation modes and protection 4-79294  
 SiO<sub>2</sub>-B<sub>2</sub>O<sub>3</sub>-Al<sub>2</sub>O<sub>3</sub>-Na<sub>2</sub>O glass, porous, precipitation of colloidal silica and pore size distrib. 4-109412  
 SiO<sub>2</sub>-CaO-Na<sub>2</sub>O-P<sub>2</sub>O<sub>5</sub> 'biological' glass, corrosion, neutral primary beam SIMS study 4-109532  
 SiYON ceramics, mech. props. rel. to corrosion and microstruct. 4-76834  
 steel, Cr-Mo and 316 types, compatibility with flowing Li 4-107062  
 Ti alloy, surface preparation, adhesive bonding and corrosion developments 4-89173  
 Ti anodic oxide film, corrosion reaction in HCl soln. 4-89169  
 Ti, corrosion in H<sub>2</sub>-H<sub>2</sub>S atmospheres, TGA, X-ray diff. 4-109559  
 Ti, corrosion reaction at anodic oxide film in HCl soln. 4-89169  
 Ti overpacks, corrosion assessment for radioactive waste containers 4-64244  
 Ti, oxidation in O<sub>2</sub>, multilayered corrosion scales 4-71801  
 Ti, oxide scale morphology 4-93458  
 Ti, weight loss measurement, interpretation for alloys showing time-delay activation 4-99662  
 Ti-Al alloy VTI-0, anodic soln. under potentiostatic conditions (*Russian*) 4-71778  
 Ti-base alloys, gaseous corrosion in H<sub>2</sub>O-HCl environment 4-89164  
 Ti-Mo-Ni corrosion props. for nuclear waste containers 4-109569  
 Ti-Ni-Mo, weight loss measurement, interpretation for alloys showing time-delay activation 4-99662  
 U-Nb (6 wt.%), microstruct., mech. props. and corrosion, effect of quench rate 4-114558  
 V-base alloys, corrosion and oxidation 4-109556  
 Zr-Ni alloys in halide media, electrochemical behaviour, influence on corrosion resistance 4-104921  
 Zn compounds, activation analysis for corrosion of carburettors by alcohol 4-93442  
 Zn, electrodisso. in acidic chloride solns. 4-89166  
 Zn, high purity, passivity breakdown in buffered NaCl soln., localised acidification mechanism 4-89161  
 Zn, pitting in borate buffered dil. NaCl solns., transport processes in passivity breakdown 4-89160  
 Zn-Al (21 wt.%), lamellar, superplastic and cast dendritic, water vapour corrosion 4-62097  
 Zn-based alloys, review of commercial alloys 4-88954  
 Zr 702, gaseous corrosion in H<sub>2</sub>O-HCl environment 4-89164  
 ZrF<sub>4</sub>-BaF<sub>2</sub>-LaF<sub>3</sub>-AlF<sub>3</sub> glass, IR transparent, stability in humid air, AES study 4-109534

**corrosion control** *see corrosion protection*

**corrosion fatigue** *see stress corrosion cracking*

**corrosion fatigue testing** *see corrosion testing*

**corrosion prevention** *see corrosion protection*

**corrosion protection**

- see also anodisation; corrosion; corrosion protective coatings; packaging; pH control*  
 cathodic protection theory, appl. to practical corrosion systems 4-66479  
 intergranular corrosion of steels and alloys, book 4-95084  
 metals, hard facing methods and appl. (*German*) 4-62066  
 rusty-bolt intermodulation interference, chemical suppression 4-109574  
 steel, austenitic stainless, surface alloying with Ta using powerful monochromatic radiation 4-71782  
 steel, C, corrosion inhibition by quaternary NH<sub>4</sub>Cl with alkylthiomethyl radical 4-85255  
 steel, C, corrosion inhibition in NaCl soln. by aniline and derivatives 4-114725  
 steel, Cr-Mo, cast, corrosion fatigue strength in fresh water, freq. and inhibitor effect (*Japanese*) 4-99650  
 steel, improved corrosion resist. in water after abrasive blasting with Al<sub>2</sub>O<sub>3</sub> 4-62099  
 steel, low C, corrosion, effect of P ion implantation 4-99637  
 steel, mild, corrosion inhibition by molybdate 4-99635  
 steel, mild, corrosion inhibition in HCl solns. by carbonyl compounds 4-104901  
 steel, mild, corrosion kinetics in H<sub>2</sub>SO<sub>4</sub>, thiourea inhibitor efficiency 4-89159  
 steel, mild, H absorpt. in H<sub>2</sub>S-free and H<sub>2</sub>S-saturated HCl, effect of acid inhibitors (*German*) 4-76897  
 steel, mild, H absorpt. in H<sub>2</sub>S-saturated formic acid, effect of acid inhibitors (*German*) 4-76898  
 steel, stainless, corrosion resistance and mech. props. rel. to Mo additions 4-109541  
 steel cylinder, cathodic protection in seawater, effects of flow 4-71769  
 surface saturation by Cr and Ti by circulating method (*Russian*) 4-81339  
 Al 1100 alloys, in HCl, thiourea and derivative corrosion inhibitors 4-99643  
 Al alloys, corrosion, effect of water-displacing corrosion preventives 4-114720

**corrosion protection continued**

- Al-Mg (4 wt.%), corrosion in chloride containing electrolytes, inhibitor efficiency 4-109537  
 Al-Zn-Mg-Cu, corrosion, effect of water-displacing corrosion preventives 4-114720  
 Cu-Ni-Sn alloys, atmospheric sulphidation 4-76902  
 Fe-Ni-Cr-W amorphous alloys, corrosion resist. 4-99632  
 Ni-base superalloy, IN 100, hot corrosion inhibition by MgSO<sub>4</sub> and BaSO<sub>4</sub> 4-85254  
 Ti, corrosion by cathodic currents in NaCl solns. 4-99631  
 Zr alloy, amorphous, anodic electrochem. treatment 4-114716  
 Zr, electrochem. corrosion protection 4-99634
- corrosion protective coatings**  
 alloy coatings on heat-resisting steels, surface layer fatigue failure 4-93470  
 aluminide coating on Ni-base superalloy, low cycle fatigue in air and corrosive environment 4-99657  
 black layers on steel, anal. using conversion electron Mossbauer spectroscopy 4-104943  
 claddings on pressure vessel steel, fracture behaviour 4-99595  
 electrospray alloying of tool steel, erosion of interstitial carbide phase 4-71780  
 enamel, corrosion of glass in weak-acid and weak-alkali solns., effects of electrolyte additions 4-81316  
 galvanised steel,  $\delta_1$  phase form. and growth 4-80314  
 glass enamel used in heat energetics, abrasive wear 4-81291  
 metal sprayed coatings in cold regions, corrosion resistance 4-104906  
 metals, wear reduction and analysis, surface modification by ion beams 4-81290  
 slag silt used in heat energetics, abrasive wear 4-81291  
 solder coating for steel plate 4-99644  
 steel, electrodeposited protective Cu/Ni/Cr coatings; corrosion testing 4-66505  
 steel, electrodeposited protective three layer Cu/Ni/Cr coatings, corrosion testing 4-66504  
 steel, mild, Ta CVD coatings microstructure 4-71802  
 steel, Ni-Co-Mo maraging, H embrittlement rel. to coating and heat treatment (*Japanese*) 4-89113  
 steel, stainless, claddings, fatigue crack growth rate in air and vacuum at 300°C 4-66413  
 steel, stainless high-alloy, black coatings produced by chem. methods 4-69606  
 steel, sulfidizing corrosion protection by Al<sub>2</sub>O<sub>3</sub>, diffusion model 4-93467  
 steel structures, corrosion protection using inorganic Zn-rich paint, testing methods 4-62109  
 steel superheater tubes, chromate conversion treatment, exfoliation control and scale growth limitation 4-89140  
 steels, heat-resisting, surface layer fatigue failure, protective effect of alloy coatings 4-93470  
 strip electrode deposited metal, controlling ease of slag removal 4-81325  
 Al, anodised and its alloys, permanent black coatings, corrosion resistant 4-104922  
 Al film, using inexpensive rotating barrel 4-66494  
 Al flame sprayed coating on CO<sub>2</sub> bonding, emission Mossbauer spectroscopy study 4-92979  
 Al, ion plated on maraging steel, H embrittlement 4-114671  
 Al sprayed coatings in cold regions, corrosion resistance 4-104906  
 Al-Al<sub>2</sub>O<sub>3</sub> film ion plating, using inexpensive rotating barrel 4-66494  
 Al-Zn alloy coated sheet steel, composition of chromate passivation films, XPS anal. 4-93453  
 Al-Zn film, using inexpensive rotating barrel 4-66494  
 Cr<sub>3</sub>C<sub>2</sub>-Ni-B electrophoretic coatings, struct. and props. 4-88430  
 Cu-Ni-microporous Cr multilayer system for corrosion protection (*Russian*) 4-89176  
 Fe based Y<sub>2</sub>O<sub>3</sub> dispersed alloys, characts. of Al<sub>2</sub>O<sub>3</sub> scales 4-89180  
 Fe-Cr (9.75 wt.%), protective oxidation in CO<sub>2</sub>, TEM obs. 4-62094  
 Fe-Cr-Al alloys, sulphidation protection by Al<sub>2</sub>O<sub>3</sub> scales 4-93468  
 Fe-Si (10 at.%) solid soln., corrosion and oxidation kinetics in SO<sub>2</sub> atm. 4-109554  
 Ni base superalloys, diffusion coated, crack initiation, acoustic emission obs. (*German*) 4-62140  
 Si<sub>3</sub>N<sub>4</sub> sputter coatings, thermal oxidation resist. of reaction bonded Si<sub>3</sub>N<sub>4</sub> substrates 4-85238  
 TiN-TiC multilayer coatings on Nb tubes, nucl. reactor fuel pin accidental behaviour 4-68771  
 Zn sprayed coatings in cold regions, corrosion resistance 4-104906  
 Zn-based coatings for corrosion protection of steel sheet and strip 4-89185  
 ZnSO<sub>4</sub>-Na<sub>2</sub>SO<sub>4</sub> deposits on CoCrAlY, low temp. hot corrosion inhibition 4-76903
- corrosion testing**  
 apparatus for nonisothermal systems with programmable principle of temp. change along metal surface (*Russian*) 4-85266  
 atmospheric corrosion monitoring using electrochem. methods in lab. environment 4-76923  
 fluid flow, rotating cylinder electrode for velocity sensitivity testing 4-89197  
 high level radwaste form, chemical durability, testing methods (*Czech*) 4-59332  
 intergranular corrosion of steels and alloys, book 4-95084  
 metal surface, penetration depth profiles obs. using moire method (*Japanese*) 4-104942  
 metals, fatigue test method for cyclic and pulsating torsional load 4-66525  
 OTEC heat exchanger biofouling, corrosion and heat resistive expts. 4-114935  
 PWR steam generator corrosion denting, nonprotective magnetite formation, acid vs. neutral chloride tests 4-59333  
 PWR steam generator denting, magnetite-producing contaminant threshold tests 4-64205  
 refractory, vertical honeycomb corrosion resist. in glass furnaces, stat. testing method 4-89207  
 refractory lining in glass-melting furnaces, corrosion monitoring method 4-89208  
 steel, austenitic stainless, meas. of low corrosion rates, comparison of AC impedance and thin layer activation methods 4-62139  
 steel, crevice corrosion electrochemical meas. (*Japanese*) 4-89201  
 steel, electrodeposited protective Cu/Ni/Cr coatings, corrosion testing 4-66505

**corrosion testing continued**

- steel, electrodeposited protective three layer Cu/Ni/Cr coatings, corrosion testing 4-66504
- steel, ferritic stainless, intergranular corrosion susceptibility, etching method 4-82565
- steel, stainless, crevice corrosion in 3% NaCl soln, accelerated tests (*Japanese*) 4-99652
- steel structures, corrosion protection using inorganic Zn-rich paint, testing methods 4-62109
- weight loss measurement, interpretation for alloys showing time-delay activation 4-99662

**corundum**

- see also ruby; sapphire*
- (0001) surface, hydroxylation, energy band struct. 4-108913
- aluminous electrical porcelain, doped with talc, microstruct. and med. props. 4-114674
- crystal morphology, effect of trivalent rare-earth ions 4-75349
- diffusion coeff. of S, slow discharge spectrometry (*French*) 4-80300
- emerald:Cr<sup>3+</sup> impurity absorpt. spectra, crystal field, ground and excited state 4-109218
- monocrystalline, dislocations, chem. etching studies 4-60933
- monocrystals, polished surfaces structure and thermal treatment 4-113763
- mullite-corundum refractories, thermomech. props. 4-66437
- single crystals, cracking resist. rel. to dislocation density 4-93370
- sintered, behaviour in vac. at high temps. 4-76717
- surface structure and deform., chem. media effect 4-81314
- $\alpha$ -Al<sub>2</sub>O<sub>3</sub>:Er(Gd)(Tb) crystals., radiative and thermochem. effects 4-76491
- Cu-Sn-Al<sub>2</sub>O<sub>3</sub>, abrasive composite, physicochem. props., effect of premoulding press. in elec. discharge sintering 4-89020

**cosmic background radiation**

- see also radiofrequency cosmic radiation*
- 3K background in far-IR (900-2000 microns) 4-77981
- 3K background radiation in 400-1100 microns range, large scale anisotropy 4-77982
- angular distribution in homogeneous cosmological models 4-90093
- anisotropy in open model Universe 4-101540
- dark matter consisting of collisionless particles and pancake mass 4-101553
- diffuse  $\gamma$ -ray background, contrib. of Seyfert galaxies nuclei 4-82562
- diffuse  $\gamma$ -ray background origin 4-100891
- diffuse galactic  $\gamma$ -ray background, origin 4-77975
- diffuse galactic  $\gamma$ -rays, bremsstrahlung component spectra and cosmic ray electrons energy spectra 4-100889
- diffuse galactic and extragalactic radiation in far-IR, balloon meas. 4-86091
- diffuse galactic gamma-ray emission and cosmic ray-interstellar matter interactions 4-100890
- diffuse low-energy gamma-ray background, contrib. of normal galaxies 4-82561
- diffuse soft X-ray background, possible origin from galactic corona 4-73103
- diffuse X-ray background, anisotropy 4-101542
- fluctuations rel. to primordial density fluctuations, voids and galaxy clusters form. 4-78003
- galactic far-IR emission, large-scale struct. of southern galactic disc. 4-115833
- galactic soft X-ray and EUV background spectra, appl. to superbubble model of local interstellar medium 4-94926
- gamma-ray background, meas. at balloon altitudes above Beijing area (*Chinese*) 4-82355
- gamma-ray diffuse component meas. by high-altitude balloon 4-100888
- gravitational radiation due to cosmic string 4-115840
- high-energy background, contrib. of black hole accretion discs in active galaxies nuclei 4-77985
- interstellar radiation field, rel. to OH photodissociation in interstellar clouds 4-90207
- IR diffuse background, IRAS obs. 4-86092
- isotropic X-ray and  $\gamma$ -ray backgrounds, contrib. of zero-point field accel. 4-100887
- near IR background and early Universe obs. (*Japanese*) 4-115837
- soft X-ray background 4-101541
- soft X-ray diffusion background (100 to 1000 eV), contrib. of supernova remnants 4-73105
- spectrum distortions 4-67814
- UV background, contrib. of decaying hypothetical particles emission 4-101154
- UV background due to decay of galactic halo massive neutrinos 4-77912
- UV photons, emission by massive neutrinos and photinos 4-63375
- X-ray background, contrib. of decaying hypothetical particles emission 4-101154
- X-ray background, contrib. of hot intergalactic medium 4-63266
- X-ray background, contributing sources, possible electron-positron annihilation line emission 4-77976
- X-ray background, implications of obscuration of cosmologically distant objects by dust 4-86025
- X-ray background, X-ray spectrum of volume emissivity arising from Abell clusters 4-86064
- X-ray background and Universe large scale struct. 4-78007
- X-ray background radiation from intergalactic matter, zero-point field effect in quantum theory 4-63044
- $\gamma$ -ray, contrib. of galaxy clusters 4-82554
- $\gamma$ -ray diffuse spectra and positronium annihilation 4-63045
- $\gamma$ -ray spectrum, balloon-borne spectrometer meas. 4-59482
- $\gamma$ -ray background as obs. test for baryon symm. cosmology 4-78012

**cosmic dust**

- see also meteoroids*
- 2021+614, narrow-line radiogalaxy, dust content, core luminosity and visible spectra 4-86045
- AGK3-0°965, central star to PN NGC 2346, IR light curves and circumstellar shell characts. 4-115755
- BD+30°3639, planetary nebula, far IR spatial anal. and optical obs. 4-90203
- bipolar reflection nebulae, Monte Carlo simulations of radiative transfer 4-85995
- 3C 109, broad-line radiogalaxy, dust characts. from visible and IR obs. 4-90223
- $\eta$  Carinae, circumstellar dust form. during shell episode (1981 to 1983) 4-115760
- cosmic dust continued
- circumstellar composite dust shell heated by supernova, IR emission 4-105971
- column density fluctuations scale, anal. of interstellar reddening in direction of globular cluster (M71) 4-101441
- Comet Bowell (1980b), coma properties from stellar occultation obs. 4-115716
- Comet Bowell (1982 I), grain props. from optical and UV obs. 4-82451
- Comet Cernis (1983I), coma icy grains detect. in IR 4-101258
- P/Comet Halley, dust drag and perturbations on Giotto 4-77689
- P/Comet Halley (1910 II), coma morphology and dust-emission pattern 4-82450
- Comet West (1976 VI), dust in secondary tail 4-72913
- condensation theory (*Russian*) 4-101140
- Cygnus A, nucleus struct. and dust distrib. 4-82551
- deep-sea sediment spherules with Pt group nuggets 4-85900
- electrostatic charge on dust particles in plasma, theoretical limitation and appl. to Saturn ring particles 4-101141
- ESO 210-6A, dark globule in Gum Nebula, star form. anal. 4-63262
- fluff on cosmic grains, effects on field emission, charge and particle levitation 4-94578
- G-type stars in Orion Ic association, IR excesses due to circumstellar dust 4-72934
- grain formation in stellar winds, rapid computation method rel. to graphite condensation 4-72927
- grain temperature in IR sources, determ. from 1-millimetre continuum obs. 4-115834
- grains, nucleation, growth, coagulation and condensation 4-77706
- grains alignment towards NGC 6334/6357 region, results from polarimetric obs. 4-115792
- graphite, interstellar and circumstellar, spectroscopic method for detect. 4-101187
- Herbig Ae-Be stars, IR spectroscopy rel. to thermal emission from dust 4-77830
- ice, detect. in IR spectrum of OH-IR star (OH 32.8-0.3) 4-110764
- in interacting galaxies, JHKL photometry rel. to warm dust and recent star form. 4-94959
- interplanetary dust collected from stratosphere, Bi content 4-115712
- interplanetary dust distrib. in Solar System 4-90115
- interplanetary dust grains, origin, size distrib. and evolution (*Japanese*) 4-110563
- interplanetary dust particle size and solar coronal IR polarization 4-63121
- interplanetary grains, reson. orbits trapping time with Poynting-Robertson drag 4-90112
- interplanetary grains from comets, heterogeneous destruction near Sun 4-77765
- interplanetary LOW CA hydrated particle, transmission electron microscopy 4-110564
- interstellar biological grains, evidence against 4-106055
- interstellar dust, effect on meas. of 3K background radiation in 400-1100 microns range 4-77982
- interstellar dust, meas. of diffuse galactic radiation in far-IR 4-86091
- interstellar grains, evidence for surface reactions from 3  $\mu$ m ice band in Taurus mol. clouds 4-101457
- interstellar grains, identification of 'unidentified' IR emission features 4-115790
- interstellar grains, obs. tests for contrib. of surface reactions to diffuse cloud chemistry 4-94928
- interstellar grains, scatt. props. rel. to OH photodissociation in interstellar clouds 4-90207
- interstellar grains, spectroscopic identification 4-67780
- interstellar grains as bacteria, discussion meeting, London, England (November 1983) 4-95046
- interstellar grains-shock wave interactions, effects on gaseous C<sup>18</sup>O:CO ratio 4-110726
- interstellar needle-shaped grains and thermalisation of microwave background 4-78001
- far-IR sources in Corona Austrina dark cloud; protostellar envelopes model 4-86001
- long period variables, intrinsic polarisation var. due to flare effects on circumstellar material 4-94779
- lunar soil electrostatic erosion 4-94656
- $\alpha$  Lyrae, IRAS obs. of circumstellar dust, possible pre-planetary system 4-86088
- M2-9, bipolar nebula, polarisation, nebula struct. and grains characts. 4-94918
- M51, spiral galaxy SHF radio maps 4-94979
- Mars, albedo changes due to dust fallout, laboratory expts. 4-115702
- Mars, dust storms (1973), polarimetric anal. 4-94664
- metallic dust grains, far-IR props. 4-67779
- meteoroid capture cell technique for satellite deployment 4-77722
- micro-meteoroids, capture-cell expt. on Long Duration Exposure Facility (LDEF) mission 4-105876
- NGC 1068, Seyfert 2 galaxy, IR spectropolarimetry rel. to grain polarisation model 4-106068
- NGC 7027, planetary nebula, dust grains populations from 10-micron obs. 4-86002
- NGC 7538 molecular cloud, dust absorpt. in ultracompact H II region 4-85998
- in novae, grain growth and destruction theory 4-101372
- obscuration of cosmologically distant objects by dust, test using quasars 4-86025
- in planetary nebulae, near-IR scans rel. to dust thermal emission 4-73001
- Pleiades cluster, polarisation and reddening of brighter stars 4-115787
- Population III radiation-dust interaction and microwave background distortion 4-77880
- RX Puppis, symbiotic system with Mira component, visible and IR emission 4-72955
- Saturn B-ring, particles surface microstructure, polarimetric model appl. 4-94680
- Seyfert galaxies, nuclei extinction, colours and axial ratios anal. 4-106061
- small dark clouds, evidence from magnitude discrepancies in Almagest star catalogue 4-110691
- solar nebula, planetesimals formation from dust 4-77737
- solar nebula, thickness and evolution of dust layer during origin of solar system (*Chinese*) 4-82426
- spectral features near 10  $\mu$ m in galactic IR sources, extinction estimation 4-86018

**cosmic dust continued**

- structure and evolution 4-94935
- supergiant stars in Magellanic Clouds, 10-micron obs. rel. to circumstellar dust shells 4-101334
- supernovae, silicate grains in dust shells, IR emission 4-115769
- T Tauri stars, circumstellar H<sub>2</sub> prod. due to ice grain-energetic particles interactions 4-94781
- T Tauri stars, intrinsic polarisation var. due to flare effects on circumstellar material 4-94779
- T Tauri stars nebulae, frozen gases—fast particles interaction 4-94780
- TMC-1, dark dust cloud, methyldiacetylene detect., SHF obs. 4-94915
- in Virgo cluster spiral galaxies, evidence for low dust content 4-101464
- WW Vulpeculae, rapid irregular variable star, evidence against dust screening model 4-94789

**cosmic radiation see cosmic background radiation****cosmic radiations, radiofrequency see radiofrequency cosmic radiation****cosmic radio waves see radiofrequency cosmic radiation****cosmic ray absorption see cosmic ray propagation****cosmic ray alpha-particles and helium nuclei**

- anomalous components in low energy spectra 4-94461
- distant terrestrial magnetosphere, protons, He and heavy ion obs. with ISEE-3 4-94323
- galactic, spectra 1965-79 as modulation theory tests 4-94407
- isotopic composition at high rigidity 4-94484
- low energy ions, mean free path in front of interplanetary shock waves 4-100933
- low energy propagation of flare accelerated protons and alpha particles 4-100950
- modulation asymmetries over two solar cycles, 1965-81 4-94409
- pregalactic <sup>4</sup>He nuclei, contrib. to synthesis of D and <sup>3</sup>Li 4-67841
- solar flare <sup>3</sup>He particles, heating in atm. and characts. 4-101302
- solar proton and alpha differential energy spectra 4-105820
- He cosmic ray anomalous component, short- and long-term variations, Voyager data 4-94417
- He<sup>+</sup> and He<sup>2+</sup> in Earth's outer radiation belts, temporal and spatial variations 4-94324
- He<sup>3</sup>/He<sup>4</sup> abundance ratios in solar energetic events 4-105959
- <sup>3</sup>He isotope search in solar flares 4-105822
- <sup>3</sup>He rich solar energetic events, He ionisation states 4-105958
- <sup>3</sup>He rich solar events, 27 day recurrence 4-105955
- <sup>3</sup>He rich solar flares, role of spallation reactions 4-105956
- <sup>3</sup>He/<sup>4</sup>He ratio in solar events, dependence on energy 4-105957
- <sup>4</sup>He, A=3, 4, energy spectra deformation in traverse through solar plasma 4-67580
- <sup>4</sup>He anomalous component in heliosphere in 1972-7 and 1965 solar modulation minima 4-94410
- <sup>4</sup>He, A=3, 4, relative intensities in 1973-9, propagation, energy spectra 4-94481

**cosmic ray apparatus****see also particle detectors**

- 24 NM 64 neutron supermonitor on Musala 4-112063
- absolute calibration for 9623B photomultipliers for atmospheric Cherenkov light intensities 4-112060
- ADC CR-39 detector module for Space Shuttle/Spacelab 3 cosmic ray expt. 4-101180
- Anger camera, coded aperture gamma ray optics studies 4-112065
- antiproton experiment, data eval. 4-94491
- atmospheric Cherenkov pulse-width technique, extensive air showers 4-110428
- automatic data collection system 4-72891
- automatic track analysis for large area plastic nuclear track detectors 4-112053
- balloon borne  $\gamma$ -ray telescope, background induced by neutron-payload interactions 4-101171
- balloon borne detector, background  $\gamma$ -ray spectra origin 4-100720
- Bristol University detector for anomalous component comp. meas. 4-101185
- BUGS-4 detector, design, charge and energy resolution 4-101184
- cellulose acetate butyrate as a detector for cosmic ray heavy nuclei 4-112049
- charged particles telescope to observe proton albedos 4-101039
- Cherenkov  $\Delta E/\Delta X$  expt. for isotope meas. 4-94629
- Cherenkov counter for cosmic-ray charge and direction meas. 4-63019
- Cherenkov light image intensifier system for air shower meas. 4-112059
- conference on nuclear track registration, Richland, WA, USA (Jul. 1982) 4-67851
- conference on solid state nuclear track detectors, Acapulco, Mexico (Sept. 1983) 4-95027
- CR-39, high resolution study in transmediterranean balloon flight 4-112048
- CR-39, response variation due to registration temp. 4-112052
- CR-39 detector module for Indian cosmic ray experiment aboard Space Shuttle Spacelab-3 4-112050
- CR-39 with dinonyl phthalate as dopant for cosmic ray studies 4-96390
- Deep Underwater Muon and Neutrino Detection (DUMAND) expt., instrumentation 4-101181
- detectors of ultraheavy cosmic rays 4-101183
- digital recording system for the pulse waveforms of fast scintillation counter in EAS 4-112072
- drift chamber telescope for heavy ion track detection in cosmic ray isotope expt. 4-68898
- EAS muon energy spectra meas. in ANI magnetic spectrometer 4-112035
- Elbrus spectrograph detectors, coupling function, meteorological coeffs. 4-101055
- EM cascade obs. using Thermoluminescent Calorimeters 4-105838
- emulsion chamber design for cosmic ray expts. at balloon altitudes 4-72890
- emulsion chamber experiment at Mt. Kanbala 4-110435
- flight-time system for recording cosmic radiation 4-77721
- galactic ultra-heavy nuclei, particle identification using SSNTD 4-101070
- gamma ray detector using position-sensitive Ge detector 4-63078
- heavy antinuclei detection in cosmic ray telescope 4-112066
- high energy particle detection using transition radiation intensity growth in plate stacks 4-112075
- hodoscope, design, performance for isotopic meas. 4-102502
- hodoscope, fine grained scintillator, EM-shower position and size 4-59531
- hodoscope, time of flight plastic scintillators, resolution 4-59550

**cosmic ray apparatus continued**

- integral and differential response functions 4-101056
- Irvine-Michigan-Brookhaven proton decay detector, appl. to cosmic ray muon detect. 4-96411
- large temporal scintillation counter for cosmic ray ionizing radiation meas. 4-112062
- latitude observations with lead free neutron monitor 4-101046
- Lexan polycarbonate, response variation due to registration temp. 4-112052
- liquid scintillation counter, 1000 tons, for solar neutrino detection 4-91149
- liquid scintillator detector in Mount Blanc tunnel for cosmic neutrinos detect. 4-96410
- microprocessor control of a cosmic-ray hadron spectrometer 4-112073
- multi-channel pulse height recorder for EAS arrays 4-112079
- multiplicity distribution parameters in neutron monitor, energy spectrum relevance 4-112064
- multiplicity response function of the double neutron monitor at Turku 4-101058
- muon chamber detection system with surface air shower array 4-110540
- muon spectrometer, spark chamber-scintillation counter system 4-107258
- neutron intensity observations by Pb-less counters 4-101047
- neutron monitors on board r/v Academician Aleksander Nesmeyanov 4-101049
- nucleon energy distribution, Ottawa large zenith angle muon telescope array 4-101057
- Pair Meter proportional counter stack, muon energy spectrum meas. 4-110416
- plastic scintillators, cosmic ray air shower array 4-91170
- proportional counter in radiochemical detector of solar neutrino, automated system for rare pulse recording 4-63020
- proton decay detector, appl. to detect. of supernova neutrinos 4-101095
- pulse timing system, high-precision, for meas. of arrival time of ultrahigh-energy photons 4-105885
- recording system for scintillation counter pulses over a wide dynamic range 4-112078
- relativistic electron observation expt. in upper atmosphere 4-101044
- satellite borne charge-composition instrumentation, data processing unit 4-112077
- small air shower array with angular resolution system 4-112057
- solid state nuclear track detectors, aerospace appls., microcircuit dosimetry 4-68880
- spark calorimeter, muon group investigation at large zenith angles 4-110424
- SSNTD array for ultra-heavy cosmic ray nuclei aboard NASA LDEF 4-96389
- super neutron monitors for cosmic ray intensity distribns. meas. 4-101007
- telescope neutrino events, correlation with acceleration pulses 4-101097
- thermoluminescent sheet to detect the high energy electromagnetic cascades 4-112067
- thin plastic scintillation counter design and performance 4-112061
- total absorption calorimeter, energy resolution for high energies 4-112058
- ultra heavy cosmic ray experiment on the NASA Long Duration Exposure Facility (LDEF) 4-112051
- underground cosmic ray detectors, characts. 4-101182
- water Cherenkov based low cost 100 km<sup>2</sup> air shower detector 4-112056
- Yakutsk EAS complex array modernisation 4-115693
- Z=10-92 relativistic nuclei, identification using various nuclear track detectors 4-96388
- Z $\geq$ 6 nuclei meas. using CR=39 4-94466
- BaSO<sub>4</sub>/Eu thermoluminescent detectors, screening in cosmic ray expts. 4-102523
- U ion registration temp. effect in doped CR-39, Lexan and Tuffak SSNTDs 4-96387

**cosmic ray composition**

- see also cosmic ray alpha-particles and helium nuclei; cosmic ray deuterons; cosmic ray electrons; cosmic ray mesons; cosmic ray muons; cosmic ray neutrinos; cosmic ray nuclei; cosmic ray photons*
- (4/3)e charged lepton search in cosmic rays 4-101071
- abundance calculations, implications of total inelastic cross sections of interactions 4-101093
- acceleration in magnetotail 4-94325
- altitude and latitude variations obs. by airborne detectors 4-101024
- anomalies in chemical composition and low energy spectrum 4-94522
- anomalous component meas., possible mol. ion component 4-101185
- antiparticles of extragalactic origin 4-72841
- atmospheric hadron cascades, spectra calcs. 4-67581
- BUGS-4 detector, design, charge and energy resolution 4-101184
- Cherenkov density spectra interpretation, primary mass composition energy depend. 4-82359
- coincidence accompanied hadrons in sea-level detectors 4-67582
- cross section uncertainties effect on source composition derivations 4-94344
- EAS, K<sub>e</sub>/K distribution in nucleon interactions 4-101087
- EAS high energy hadrons, energy spectrum, possible heavy particle 4-82360
- emulsion chamber design for cosmic ray expts. at balloon altitudes 4-72890
- Fermi shock acceleration, Coulomb losses, Monte Carlo calcs. 4-105819
- flare events, elemental composition 4-105825
- fluctuations exceeding 2 hours, spectral anal., relation to solar activity 4-94428
- galactic anomalous low-energy component, origin 4-94361
- galactic cosmic rays, diffusion and relative abundances 4-94362
- galactic cosmic rays, origin and acceleration characts. 4-94363
- galactic cosmic rays 4-94354
- galactic nuclei, age and source characts., isotopic comp. anal. 4-94357
- galactic nuclei, comp. and nucleosynthesis 4-94356
- galactic nuclei, energy spectra and comp. 4-94355
- galactic ultra-high energy cosmic rays 4-94360
- gravitinos, decay and lifetimes, X-ray emission, appl. to galaxy clusters and background radiation 4-101154
- hadron component of cosmic rays at mountain altitude 4-105826
- hadron flux intensity, 200 GeV-2 TeV, at mountain altitude 4-105827
- heavy ions comp. in solar energetic particle events 4-100939
- high energy, >10 TeV, composition and energy spectrum 4-94500
- intensities of accompanied particles in sea-level detectors 4-105832
- ionization effects shaping the elemental cosmic-ray source composition 4-100914
- leptons, search for 4/3.e charge 4-101078

**cosmic ray composition continued**

low-energy cosmic rays from stellar X-ray sources 4-101512  
 massive particle search in extensive air showers 4-101083  
 multiple phenomena, Monte Carlo study 4-110423  
 muons, comp. and energy spectra, determ. of primary cosmic ray characts. 4-94524  
 particle acceleration by flare-induced interplanetary shocks 4-94377  
 particle charge evolution during acceleration and implications on mass and charge spectra 4-101074  
 photinos, decay and lifetimes, X-ray emission, appl. to galaxy clusters and background radiation 4-101154  
 primaries of cosmic ray showers, mass distrib. study 4-101081  
 primary cosmic rays, comp. and energy spectra from muons anal. 4-94524  
 primary cosmic rays, neutral particle detection 4-100923  
 primary mass composition in  $E=10^{15}$ - $10^{16}$  eV range from EAS data 4-94506  
 primary mass composition in energy interval  $10^{15}$ - $10^{18}$  eV, EAS meas. anal. 4-94508  
 primary mass composition in energy range  $10^{16}$  to  $10^{17}$  eV from EAS data 4-94507  
 primary ray composition at  $10^{14}$ - $10^{16}$  eV from EAS data 4-94503  
 primary ray composition at  $E \sim 10^{15}$  eV from delayed hadrons in air showers 4-94505  
 primary rays, at  $E \sim 10^{15}$ - $10^{17}$  GeV 4-94502  
 primary rays at  $E \sim 10^{15}$ - $10^{17}$  GeV 4-94501  
 QCD, neutron star quark-matter cosmic ray component 4-90803  
 scaling violation in fragmentation region of pp collisions 4-105834  
 shock wave acceleration from hot interstellar medium, charge state effect on composition 4-94353  
 slepton production cross-section limits in hadron-nucleus collisions 4-101079  
 solar cosmic ray enrichment mechanism by heavy ions 4-105950  
 solar cosmic ray particles, elemental and isotopic composition 4-105951  
 solar flare event, elemental composition, acceleration mechanisms 4-105821  
 solar flare nucleon abundances, implications for acceleration and coronal propagation 4-105949  
 solar flare particles anal. 4-94395  
 solar flare particles of coronal origin, comp. and energy spectra 4-90043  
 solar flares, isotopic composition in solar flares 4-105953  
 source abundance determ., effects of nucl. cross-section uncertainties 4-100928  
 source abundances above 10 GeV per nucleon, air-shower meas. implications 4-67583  
 source spectra from supernova blast waves 4-94352  
 spallation cross-sections and fragment yields, appl. to cosmic ray abundances and confinement calcs. 4-96039  
 stratosphere, anomalous C, N and O cosmic ray component after 1972 4-94411  
 ultraheavy cosmic rays, abundances and propag. model, role of nucleosynthesis 4-85846  
 ultraheavy cosmic rays, tracks in minerals and comp. determ. 4-101098  
 unaccompanied hadrons, 1-20 TeV neutral to charged particle ratio 4-105828  
 very high energy, mass composition, energy dependence, energy spectrum 4-90045  
 Fe(p,X) 0.5-5.0 TeV, cosmic ray hadron component composition at mountain altitudes 4-102325  
 Fe( $\pi$ ,X), 0.5-5.0 TeV, cosmic ray hadron component composition at mountain altitudes 4-102325  
 He<sup>3</sup>-rich solar particle events, ionic charge state meas. 4-110587  
<sup>3</sup>He and <sup>4</sup>He, relative abundance in cosmic radiation 4-101072  
<sup>3</sup>He rich solar energetic events, He ionisation states 4-105958  
<sup>3</sup>He rich solar flares, role of spallation reactions 4-105956  
<sup>3</sup>He-rich solar particle events, ionic charge distrib., ISEE 3 meas. 4-110586  
<sup>22</sup>Ne/<sup>20</sup>Ne ratio, isotopic studies in solar flare 4-105952  
<sup>22</sup>Ne/<sup>20+21</sup>Ne isotopic abundance in solar flares 4-105954

**cosmic ray deuterons**

No entries

**cosmic ray effects and interactions**

see also high-energy cosmic ray interactions  
 balloon borne detector, background  $\gamma$ -ray spectra origin, role of crystal-cosmic ray interactions 4-100720  
 biological tissue, cosmic ray exposure in space, doses and LET distrib. rel. to shielding 4-77393  
 Biostack Experiments, HZE particles effects on biological systems 4-100334  
 black holes, small, ionisation tracks and range 4-82631  
 comet nuclei, formaldehyde form. due to cosmic ray interactions 4-94682  
 cross-sections, implications for propag. calcs. 4-101093  
 fossil record by <sup>10</sup>Be accelerator mass spectrometry 4-90047  
 galactic cosmic ray interactions and gamma ray emission 4-101525  
 galactic cosmic rays-interstellar matter interactions, diffuse  $\gamma$ -ray background origin 4-77975  
 galactic source abundance determ., effects of nucl. cross-section uncertainties 4-100928  
 galactic X-ray emissivity due to cosmic ray-interstellar matter interactions 4-100886  
 hadron-nucleus collision process, expt. data 4-102277  
 interstellar interactions 4-94362  
 inverse Compton interaction, cosmic-ray electrons with interstellar photons 4-101088  
 molecular clouds, gamma-ray line emission and cosmic ray interactions 4-101463  
 muon interactions with rock, flux of background neutrons 4-110469  
 muon multiple events, simulation calcs. 4-110465  
 muons, electron pair production cross-section in iron 4-110466  
 neutrino interactions, proton decay and neutrino oscillation limits 4-110474  
 neutrons-balloon borne  $\gamma$ -ray telescope interactions, induced  $\gamma$ -ray background 4-101171  
 nucleon emission from high energy cosmic hadron-nucleus interactions 4-102278  
 pion formation in atmosphere, rel. to form. of high-energy electron aureole 4-110399  
 radiation history of meteoritic and lunar material by track data 4-115665

**cosmic ray effects and interactions continued**

solar protons, nuclear interactions in atmosphere rel. to determ. of absolute fluxes above  $E=100$  MeV 4-110397  
 spallation cross-sections and fragment yields, appl. to cosmic ray abundances and confinement calcs. 4-96039  
 $\mu$ N-cascades, cross-sections, shadowing coeff. 4-110471  
 $\mu$ N-cascades, hadron flux characteristics 4-110468  
 $\mu$ N cosmic ray interactions, photonic energy loss term calcs. 4-110472  
 $\mu$ N-hX, hadroproduction by cosmic rays, cross-sections 4-110473  
 $\mu$ N-showers, interaction process and energy spectrum 4-110470  
 $\bar{\nu}$ - $\nu$ sX, neutrino yield calcs. 4-110475  
 Be concentration and deposition in lower atmosphere over Kaohsiung City, Taiwan 4-62418  
 (<sup>2</sup>C,  $\alpha$ X) anomalous interaction mean free path of relativistic alpha-particles 4-96077  
 $\mu$ N- $\mu$ N inelastic scatt., cross-sections 4-110467

**cosmic ray electrons**

acceleration conditions in solar flares 4-100953  
 acceleration in interplanetary space 4-94376  
 acceleration in supernova remnants, evolution as radio sources 4-63246  
 acceleration of electrons in supernova remnants 4-100909  
 Akeno extensive air shower expt., primary spectrum, cosmic ray electrons and muons 4-110410  
 automatic data collection system, response to muons and electrons 4-72891  
 density spectrum at sea level 4-72891  
 diffusion from local galactic sources 4-94342  
 diffusive shock acceleration of energetic electrons subject to synchrotron losses 4-115661  
 distribution in face-on spiral galaxies 4-110749  
 Earth electron aureole with energies of hundred of MeV, mechanism of form. 4-110399  
 EAS arrival direction and muon to electron ratio 4-94528  
 energy spectrum from radio loop III 4-94516  
 energy spectrum of galactic electrons, new meas. rel. to cosmic ray confinement 4-94460  
 extragalactic cosmic rays origin, role of radioastronomy 4-105816  
 flux,  $E > 30$  MeV in equatorial region 4-101041  
 flux bidirectional opposite streamings in noon low latitude magnetosheath 4-67570  
 flux intensity variations, solar effects 4-94429  
 flux variations in geosynchronous orbit 4-100974  
 fluxes at 500 km in equatorial region 4-67569  
 galactic, spectra 1965-79 as modulation theory tests 4-94407  
 galactic cosmic rays, distrib. and diffusion,  $\gamma$ -ray anal. 4-101487  
 galactic electron-photon interactions EM cascade showers initiation 4-101537  
 galactic electron-positron component and lepton prod. in black hole accretion discs 4-82500  
 galactic electrons, density near galactic centre from gamma ray emission 4-63300  
 galactic electrons, energy spectra characts. from bremsstrahlung component of gamma ray emission anal. 4-90042  
 galactic electrons distrib., H I maps and  $\gamma$ -ray distrib. 4-90237  
 galactic electrons prod. at massive black holes, radioemission characts. 4-100929  
 galactic electrons producing diffuse galactic  $\gamma$ -ray bremsstrahlung component, energy spectra 4-100889  
 galactic positrons and electrons, propag. and energy spectra anal. 4-94358  
 galaxy clusters, Coma-type radio halos form., role of galactic cosmic ray electrons 4-90248  
 high energy electrons and photons, intensity-depth relation 4-105854  
 high energy obs. beyond 1 TeV 4-94489  
 high energy spectrum 4-94488  
 inverse Compton interaction, cosmic-ray electrons with interstellar photons 4-101088  
 Jovian electron events, interplanetary transport, modulation in Earth's orbit 4-94434  
 magnetosphere boundary penetration 4-67575  
 motion in neutral sheet 4-100937  
 positron fluxes from densely shrouded sources, consequences in leaky box model 4-94328  
 positron sources, accretion powered, constraints 4-94329  
 primary energy spectrum, arrival direction in EAS 4-94510  
 prolonged injection effect on solar flare generated particle propagation 4-100931  
 propagation on leaky box model with truncated pathlength distrib. 4-94490  
 radiosources, electron energy spectra produced by turbulent reson. accel. 4-94978  
 radiosources, visible-IR spectra cutoff due to cosmic ray electrons energy spectra evolution 4-106073  
 relativistic solar electron and proton, arrival time differences at Earth 4-100956  
 solar flare electrons, energy spectrum 4-105962  
 solar flare particles acceleration region height, electrons and protons spectrum form anal. 4-100938  
 solar modulation 1978-83 of 1 GeV electrons 4-94408  
 solar modulation of cosmic ray electrons (1978 to 1983) 4-85851  
 spectral index variations in the galactic radio continuum emission 4-94335  
 statistical acceleration of electrons in the galactic halo 4-100911  
 Sun, flare, 1978 November 8, X-ray producing electrons and escaping electrons, energy spectra 4-105935  
 supernova remnants, radio emission and electrons accel. at various evolutionary stages 4-73025  
 supernova remnants, radioemission evolution, role of relativistic electrons accel. by MHD turbulence 4-73026  
 young supernovae remnants as acceleration sites of cosmic ray electrons 4-100906

**cosmic ray energy spectra**

acceleration by diffusive shocks and cut-off energy 4-94525  
 active galaxies nuclei,  $\gamma$ -ray and relativistic particles prod. and spectra anal. 4-100891  
 active galaxies nuclei, gamma-ray emission characts. due to cosmic ray interactions 4-101537  
 air showers,  $E > 10^{19}$  eV, sub-luminal pulses, energy deposition 4-101080

## cosmic ray energy spectra continued

- Akeno extensive air shower expt., primary spectrum, cosmic ray electrons and muons 4-110410  
 anisotropy of cosmic rays of superhigh energies 4-94515  
 anomalies in chemical composition and low energy spectrum 4-94522  
 anomalous components in low energy spectra 4-94461  
 antiproton/proton ratio, energy depend. in 4.4-13.4 GeV range 4-94494  
 arrival direction and origin of multi-joule cosmic rays 4-94333  
 atmospheric hadron cascades, spectra calcs. 4-67581  
 black holes, mass accretion and plasma processes,  $\gamma$ -ray emission model, 3C 273 appl. 4-101536  
 black holes, neutrino energy spectra from relativistic plasma 4-110651  
 bump in energy spectra due to extragalactic antiparticles 4-72841  
 CG 195+04,  $\gamma$ -ray line emission search 4-101521  
 2CG 195+4, gamma ray flux periodicity and energy spectra, EAS obs. 4-101527  
 Crab Nebula, search for  $\gamma$ -ray lines 4-101462  
 diffuse galactic  $\gamma$ -rays, bremsstrahlung component spectra and cosmic ray electrons energy spectra 4-100889  
 diffusion coefficient derived from individual spectra 4-94366  
 distant terrestrial magnetosphere, protons, He and heavy ion obs. with ISEE-3 4-94323  
 distribution in galactic diffusion model 4-94517  
 EAS, long flying component investigation 4-101084  
 EAS, role of charmed particles in creation of long flying component 4-101085  
 EAS arrival direction and muon to electron ratio 4-94528  
 EAS Cherenkov radiation density spectrum, primary energy spectrum 4-94509  
 EAS high energy hadrons, energy spectrum, possible heavy particle 4-82360  
 EAS muon energy spectra meas. in ANI magnetic spectrometer 4-112035  
 electron energy spectrum from radio loop III 4-94516  
 electron high energy spectrum 4-94488  
 electron propagation in leaky box model with truncated pathlength distrib. 4-94490  
 electrons, acceleration in interplanetary space 4-94376  
 electrons, energy spectrum meas. rel. to cosmic ray confinement 4-94460  
 electrons, high energy obs. beyond 1 TeV 4-94489  
 electrons, spectral index variations in the galactic radio continuum emission 4-94335  
 energy spectrum, charge ratio in horizontal showers 4-110419  
 equator-pole anisotropy, semi-analytical analysis 4-94443  
 fluctuations in diffusion approx., low freq. limit 4-67578  
 Forbush decrease, global spectrography method 4-94442  
 Forbush decrease, muon-anomalous anisotropy 4-94446  
 Forbush decrease, pitch angle anisotropy, spectrographic global survey 4-94458  
 Forbush decreases, energy dependence 4-94455  
 Forbush decreases, energy dist. 4-94444  
 Forbush decreases, time profile differences by neutron monitors and ion chambers 4-94452  
 galactic centre, 2-20 MeV gamma-ray map and energy distrib. 4-101523  
 galactic cosmic rays, diffusion and obs. anal. 4-94362  
 galactic cosmic rays, modulation by solar wind in spherically symmetric nonstationary diffusive model 4-94402  
 galactic cosmic rays, power spectra variations, correlation with Sun's activity 4-94436  
 galactic cosmic rays 4-94354  
 galactic e,p and He spectra 1965-79 as modulation theory tests 4-94407  
 galactic electrons, energy spectra characts. from bremsstrahlung component of gamma ray emission anal. 4-90042  
 galactic electrons producing diffuse galactic  $\gamma$ -ray bremsstrahlung component 4-100889  
 galactic energy spectra from HEAO-3 meas. 4-94469  
 galactic nuclei propagation and accel., energy spectra anal. 4-94355  
 galactic positrons and electrons, propag. and energy spectra anal. 4-94358  
 galactic ultra-heavy nuclei, particle identification using SSNTD 4-101070  
 galactic ultra-high energy cosmic rays 4-94360  
 gamma ray burst sources observed by Hinotori satellite, energy spectra, time history and origin 4-101513  
 gamma ray energy spectra at highest energies, galactic plane events contrib. 4-85845  
 gamma ray line obs., statistical reliability 4-101190  
 gamma-ray burst of 1978 March 25, absorpt. feature characts. 4-101522  
 gamma-ray bursts, high time resolution  $\gamma$ -ray spectral obs. with Solar Maximum Mission 4-101514  
 gamma-ray intensity rel. to interstellar column density of H and  $^{12}\text{C}$ O 4-110409  
 gamma-ray sources, absorpt. features, effects of emitted photons-interstellar photon interactions 4-101535  
 gamma-ray spectra recorded by balloon borne detector, background origin 4-100720  
 gamma-rays from interstellar  $\text{H}_2$  and  $\text{H I}$  4-101486  
 giant air shower primaries, energy estimation methods 4-94512  
 hadron energy determination in X-ray emulsion chamber with C block 4-105847  
 hadron energy spectra, atmospheric depth depend. 4-105836  
 hadron energy spectra in atmosphere 4-105833  
 high energy, >10 TeV, composition and energy spectrum 4-94500  
 high energy cosmic ray hadrons, systematic errors in energy determ. 4-112081  
 high energy spectra, Mt. Fuji data 4-105829  
 high energy spectra Mt. Kanbala obs. 4-105830  
 horizontal muon spectrum, charge ratio, atmos. propagation 4-110402  
 intensities, energy spectra and interactions of 10-30 GeV/n nuclei 4-94470  
 intensity anisotropy for  $E > 10^{17}$  eV rays 4-94398  
 intergalactic protons, zero-point field accel. and energy spectra 4-100887  
 interplanetary space, nonstationary modulation for constant radial gradient 4-94405  
 leptons, search for 4/3c charge 4-101078  
 massive black holes, 511 keV annihilation line, origin due to tidally disrupting stars 4-101405  
 median primary energies for hadrons in the atmosphere 4-101059  
 medium energy cosmic nuclei,  $10 \leq Z \leq 26$ , elemental composition 4-94464  
 medium mass nuclei, flux in near-Earth space 4-94462

## cosmic ray energy spectra continued

- modulation coefficient during 1954, 1965 and 1976 minima in solar activity 4-94427  
 molecular clouds, gamma-ray line emission and cosmic ray interactions 4-101463  
 multiplicity distribution parameters in neutron monitor, energy spectrum relevance 4-112064  
 multiplicity response function of the double neutron monitor at. Turku 4-110158  
 muon angular distribution meas. underground 4-110417  
 muon differential spectrum correspondence to pion-kaon spectra 4-110415  
 muon energy spectrum, meas. by Pair Meter proportional stack 4-110416  
 muon energy spectrum at sea level, flux limits 4-110418  
 muon group investigation at large zenith angles 4-110424  
 muon group spatial separation dist. and energy spectrum 4-110420  
 muon multiple events in Kolar gold mines 4-110421  
 muon multiple events underground, Monte Carlo simulations 4-110422  
 muon north-south anisotropy, high rigidities, 27-day recurrence 4-94459  
 muon spectra, derivation at large zenith angles from primary flux 4-110389  
 muon spectral indices in  $E > 1$  TeV region 4-94499  
 muon spectrum, high multiplicity model 4-110411  
 muon spectrum meas., analysis of techniques 4-110412  
 muon underwater intensities depth range, momentum spectrum 4-110406  
 muons, absolute vertical density and momentum spectrum at sea level, Beijing district, China 4-67586  
 muons, charge ratio of low energy particles 4-110414  
 muons, comp. and energy spectra, determ. of primary cosmic ray characts. 4-94524  
 muons, depth-intensity relation, Monte Carlo simulation 4-110404  
 neutron anisotropies, 3-D anal. method during solar rotation period 4-94440  
 neutron harmonic components, best fit rigidity spectra during solar rotation 4-94523  
 neutron-proton flux ratio in atmosphere, depth depend. 4-105835  
 nucleon energy distribution, Ottawa large zenith angle muon telescope array 4-101057  
 Pamir expt.,  $\gamma$ -ray energy spectra and ang. distrib. 4-110438  
 photon spectral indices in  $E > 1$  TeV region 4-94499  
 pitch angle distributions and energy spectral for solar particle effects 4-100951  
 power spectra of cosmic ray variations in the region of  $3 \times 10^{-8}$ - $10^{-4}$  Hz 4-67579  
 primary arrival direction meas. for  $10^{13}$ - $10^{17}$  eV rays 4-94514  
 primary cosmic rays, comp. and energy spectra from muons anal. 4-94524  
 primary cosmic rays, energy spectrum study in 600 TeV-50 PeV range (Chinese) 4-115662  
 primary cosmic rays, neutral particle detection 4-100923  
 primary energy spectrum, arrival direction in EAS 4-94510  
 primary nucleons, spectrum determ. from muons sea level intensity at Mt. Blanc underground expt. 4-82356  
 primary ray induced cascades in emulsion chamber, energy spectra 4-94527  
 primary spectrum above 1 TeV from Cherenkov light images 4-94526  
 prompt lepton production, atmos. muon and neutrino spectra 4-110403  
 prompt muon cosmic ray, total flux anal. 4-110413  
 prompt muons, energy spectrum and ang. distrib. from charm prod. and decay 4-115663  
 proton energetic spectra, associated planetary shock waves 4-94389  
 proton spectra, propagation and acceleration 4-94391  
 PSR 0531+21, 1-20, MeV pulsed  $\gamma$ -ray emission anal. 4-101391  
 PSR 0531+21,  $\gamma$ -ray flux and energy spectra, Cherenkov radiation obs. 4-101393  
 PSR 0833-45 and 0950+08,  $\gamma$ -ray emission, Cherenkov radiation anal. 4-101396  
 quasars,  $\gamma$ -ray and relativistic particles prod. and spectra anal. 4-100891  
 quasars, gamma-ray emission characts. due to cosmic ray interactions 4-101537  
 radioisotopes, electron energy spectra produced by turbulent reson. accel. 4-94978  
 radioisotopes, visible-IR spectra cutoff due to cosmic ray electrons energy spectra evolution 4-106073  
 scaling violation in fragmentation region of pp collisions 4-105834  
 sea level muon spectrum, derivation from all-particle primary spectrum 4-101094  
 semidirectional variation, energy spectrum 4-100995  
 Seyfert galaxies nuclei, cosmic ray accel. and energy spectra, photons and neutrinos as probes 4-100925  
 shower energy spectrum above  $10^{17}$  eV 4-94511  
 shower excess from Crab nebula 4-94513  
 slepton production cross-section limits in hadron-nucleus collisions 4-101079  
 small air showers, arrival direction meas. 4-94529  
 soft muon intensity variations, geophysical effects 4-110405  
 solar cosmic ray neutron event, flux and intensity 4-105964  
 solar flare electrons, energy spectrum 4-105962  
 solar flare particle events, correlation with radio bursts 4-105946  
 solar flare particle fluences during solar cycles 19, 20 and 21 4-105961  
 solar flare particles acceleration region height, electrons and protons spectrum form anal. 4-100938  
 solar flare particles anal. 4-94395  
 solar flare particles of coronal origin, comp. and energy spectra 4-90043  
 solar flare protons, spectral and temporal characts. rel. to coronal mag. field struct. 4-110396  
 solar flares, gamma-ray obs., energy spectra 4-105968  
 solar neutron event, emission spectrum, ion acceleration 4-105963  
 solar proton and alpha differential energy spectra 4-105820  
 solar proton events of 1977 November 22 and 1978 May 7, comparison 4-72839  
 solar proton spectrum dynamics, time evolution 4-105944  
 solar protons, absolute fluxes and energy spectra above  $E=100$  MeV 4-110397  
 solar protons,  $E > 100$  MeV, stratospheric meas. 4-100961  
 solar protons, energy spectra from balloon and neutron monitor data 4-101077  
 solar protons associated with solar wind shock waves, accel. and energy spectra 4-72837  
 source abundances above 10 GeV per nucleon, air-shower meas. implications 4-67583

**cosmic ray energy spectra continued**

- source energy spectra from HEAO-3 meas. 4-94519  
 source spectra and mean path-length of primary high energy cosmic rays 4-101076  
 spectrography method, variation parameter determ. 4-94441  
 Sun, flare of 1978 November 8, X-ray producing electrons and escaping electrons 4-105935  
 ultra-high energy,  $\gamma$ -ray component for detection-anal. technique 4-90044  
 ultraheavy nuclei, energy spectra, HEAO-3 meas. 4-94479  
 upstream protons, energy spectra 4-94393  
 very high energy, mass composition, energy dependence, energy spectrum 4-90045  
 very high energy cosmic ray events, primary spectral changes, anomalous interactions 4-72842  
 Z=10-26 multiply charged cosmic ray nuclei, 160-759 MeV/n, solar modulation in interplanetary region 4-94412  
 NN cosmic ray interactions, ang. dist., fractional energy spectra 4-101092  
 A=1-4, relative intensities in 1973-9, propagation, energy spectra 4-94481  
 Fe rich solar energetic events, ionic charge dist. 4-105960  
 $\text{He}^{2+}$  and  $\text{He}^{3+}$  in Earth's outer radiation belts, temporal and spatial variations 4-94324  
 $\text{He}^{2+}/\text{He}^{3+}$  abundance ratios in solar energetic events 4-105959  
 $^3\text{He}/^4\text{He}$  ratio in solar events, dependence on energy 4-105957  
 $^4\text{He}$ , A=3, 4, energy spectra deformation in traverse through solar plasma 4-67580

**cosmic ray geophysical effects** *see geophysical aspects of cosmic rays***cosmic ray jets** *see cosmic ray showers and bursts***cosmic ray mesons**

No entries

**cosmic ray muons**

- absolute vertical density and momentum spectrum at sea level, Beijing district, China 4-67586  
 air showers,  $E > 10^{19}$  eV, sub-luminal pulses, energy deposition 4-101080  
 Akeno extensive air shower expt., primary spectrum, cosmic ray electrons and muons 4-110410  
 angular distribution meas. underground 4-110417  
 automatic data collection system, response to muons and electrons 4-72891  
 chamber detection system with surface air shower array 4-110540  
 charge ratio of low energy particles 4-110414  
 composition and energy spectra, determ. of primary cosmic ray characts. 4-94524  
 Deep Underwater Muon and Neutrino Detection (DUMAND) expt., instrumentation 4-101181  
 depth-intensity relation, Monte Carlo simulation 4-110404  
 differential spectrum correspondence to pion-kaon spectra 4-10415  
 EAS arrival direction and muon to electron ratio 4-94528  
 EAS muon energy spectra meas. in ANI magnetic spectrometer 4-112035  
 electron pair production cross-section in iron 4-110466  
 energy loss by ionisation, track lengths 4-110425  
 energy spectrum, charge ratio in horizontal showers 4-110419  
 energy spectrum, meas. by Pair Meter proportional stack 4-110416  
 energy spectrum at sea level, flux limits 4-110418  
 flux at different zenith angles and from east and west 4-72891  
 Forbush decrease, muon anomalous anisotropy 4-94446  
 group investigation at large zenith angles using spark calorimeter 4-110424  
 high energy muon anal. in air showers 4-94502  
 horizontal muon spectrum, charge ratio, atmos. propagation 4-110402  
 interactions with rock, flux of background neutrons 4-110469  
 Irvine-Michigan-Brookhaven proton decay detector, appl. to cosmic ray muon detect. 4-96411  
 low energy muon anal. in air showers 4-94501  
 multiple events, simulation calcs. 4-110465  
 multiple events in Kolar gold mines 4-110421  
 multiple events underground, Monte Carlo simulations 4-110422  
 multiple phenomena, Monte Carlo study 4-110423  
 north-south anisotropy, high rigidities, 27-day recurrence 4-94459  
 primary energy spectrum, arrival direction in EAS 4-94510  
 prompt lepton production, atmos. muon and neutrino spectra 4-110403  
 prompt muon cosmic ray to total flux anal. 4-110413  
 prompt muons, energy spectrum and ang. distrib. from charm prod. and decay 4-115663  
 sea level intensity at Mt. Blanc underground expt., primary nucleon spectrum determ. 4-82356  
 sea level muon spectrum, derivation from all-particle primary spectrum 4-101094  
 soft muon intensity variations, geophysical effects 4-110405  
 spatial separation dist. and energy spectrum in muon groups 4-110420  
 spectra, derivation at large zenith angles from primary flux 4-110389  
 spectral indices in  $E > 1$  TeV region 4-94499  
 spectrometer, spark chamber-scintillation counter system 4-107258  
 spectrum, high multiplicity model 4-110411  
 spectrum meas., analysis of techniques 4-110412  
 underground cosmic ray detectors, characts. 4-101182  
 underwater, depth-intensity curve, sea-level momentum 4-78751  
 underwater intensities depth range, momentum spectrum 4-110406  
 vertical muon spectrum, charge ratio from primary spectrum 4-110388  
 zenith angle distribution of the cosmic ray muon component 4-67585  
 $\mu\text{N}$ -cascades, cross-sections, shadowing coeff. 4-110471  
 $\mu\text{N}$ -cascades, hadron flux characteristics 4-110468  
 $\mu\text{N}$  cosmic ray interactions, photonuclear energy loss term, calcs. 4-110472  
 $\mu\text{N}$ -hX, hadroproduction by cosmic rays, cross-sections 4-110473  
 $\mu\text{N}$ -showers, interaction process and energy spectrum 4-110470  
 $\text{Fe}(\mu, \mu')$ , cosmic ray muon scatt., virtual photon shadowing 4-85852  
 $\mu\text{N}$ - $\mu\text{N}$  inelastic scatt., cross-sections 4-110467
- cosmic ray neutrinos**  
 antineutrino fluxes from collapsing stars 4-110426  
 atmospheric fluxes, effects of oscillations 4-110408  
 atmospheric neutrino fluxes, effects of oscillations 4-90775  
 atmospheric neutrinos, ang. distrib. and flux, nucleon decay expt. appl. 4-63023  
 atmospheric neutrinos and astrophysical neutrinos in proton decay experiments 4-63024  
 black holes, neutrino energy spectra from relativistic plasma 4-110651  
 Davis' experiment, galactic cosmic rays, solar neutrino flux 4-101096

**cosmic ray neutrinos continued**

- decay and lifetimes, UV emission, appl. to galaxy clusters and background radiation 4-101154  
 Deep Underwater Muon and Neutrino Detection (DUMAND) expt., instrumentation 4-101181  
 $E > 10^{19}$  eV neutrinos, flux limit from upward EAS data anal. 4-110476  
 extraterrestrial neutrinos, upper limit on muon flux from neutrinos 4-110390  
 flux calcs. in atmos. 4-110407  
 interactions, proton decay and neutrino oscillation limits 4-110474  
 liquid scintillation counter, 1000 tons, for solar neutrino detection 4-91149  
 liquid scintillator detector in Mount Blanc tunnel for cosmic neutrinos detect. 4-96410  
 mass from spectroscopic meas. and oscillations,  $\beta$ -decay, solar neutrinos 4-59016  
 nucleon decay detector calibration with cosmic ray neutrinos 4-91148  
 oscillation parameters, experimental sensitivity 4-110427  
 prompt lepton production, atmos. muon and neutrino spectra 4-110403  
 Seyfert galaxies nuclei, cosmic ray accel. and energy spectra, photons and neutrinos as probes 4-100925  
 solar flare neutrinos, flux estimations 4-110591  
 solar neutrino flux, periodic change 4-100963  
 solar neutrino flux, quasiannual variation 4-110394  
 supernova neutrinos, detectability with existing proton decay detector 4-101095  
 telescope neutrino events, correlation with acceleration pulses 4-101097  
 underground cosmic ray detectors, characts. 4-101182  
 $\text{py} \rightarrow \nu \text{SX}$ , neutrino yield calcs. 4-110475  
 $^3\text{Cl}$  neutrino counting rate, P-P chain reactions, quasi-non-degenerate distrib. 4-101090

**cosmic ray neutrons**

- albedo at  $E < 1$  MeV 4-115664  
 anisotropies, 3-D anal. method during solar rotation period 4-94440  
 balloon borne  $\gamma$ -ray telescope, background induced by neutron-payload interactions 4-101171  
 capture line limb darkening at 2.22 MeV in solar flares 4-100940  
 coupling coefficients, expt. determ. 4-101054  
 equator-pole anisotropy, semi-annual variation 4-94443  
 fluctuations exceeding 2 hours, spectral anal. 4-94428  
 Forbush decrease, anisotropic intensity waves 4-94445  
 Forbush decrease, diurnal and semi-diurnal anisotropies 4-94438  
 Forbush decrease, jet plane obs. 4-94453  
 Forbush decrease, neutron monitoring, correlation with solar activity 4-94457  
 Forbush decrease, rigidity dependence 4-94454  
 Forbush decreases, energy dependence 4-94455  
 Forbush decreases, time profile differences by neutron monitors and ion chambers 4-94452  
 harmonic components, best fit rigidity spectra during solar rotation 4-94523  
 intensity increases during geomagnetic storms 4-94448  
 intensity observations by Pb-less counters 4-101047  
 Jupiter, cosmic ray contribution 4-94394  
 latitude distributions during solar minima 1954, 1965, 1976 4-94371  
 latitude observations with lead free neutron monitor 4-101046  
 lunar-diurnal variation of high-energy cosmic rays 4-101000  
 modulation, shock related diffusion-acceleration models 4-94392  
 modulation coefficient during 1954, 1965 and 1976 minima in solar activity 4-94427  
 multiplicity response function of the double neutron monitor at Tüürku 4-101058  
 neutron-proton flux ratio in atmosphere, depth depend. 4-105835  
 NN fragmentation collisions, EM contrib. 4-86748  
 nucleon-nucleon interactions at high-energies, short- and long-range corrls. 4-78576  
 semiannual variations of nucleonic components 4-100994  
 solar cosmic ray neutron event, flux and intensity 4-105964  
 solar flare flux from interplanetary charged particle meas. 4-100942  
 solar neutron event, emission spectrum, ion acceleration 4-105963  
 solarflare neutrons and gamma ray lines 4-100943  
 underground occurrence of thermal neutrons 4-110142

**cosmic ray nuclei**

- see also cosmic ray alpha-particles and helium nuclei; cosmic ray neutrons; cosmic ray protons*  
 abundances in  $26 \leq Z \leq 42$  range, HEAO-3 meas. results 4-94473  
 abundances of  $75 \leq Z \leq 79$  and  $81 \leq Z \leq 83$ , HEAO-3 meas. 4-94478  
 abundances of Sn, Te, Xe, Ba, Ce, HEAO-3 meas. 4-94477  
 abundances of unstable cosmic-ray isotopes 4-94485  
 anomalous components in low energy spectra 4-94461  
 anti-proton obs. in emulsion stack exposed to primary rays 4-94492  
 BUGS-4 detector, design, charge and energy resolution 4-101184  
 detectors of ultraheavy cosmic rays 4-101183  
 diffusion coefficient derived from individual spectra 4-94366  
 distant terrestrial magnetosphere, protons, He and heavy ion obs. with ISEE-3 4-94323  
 elemental composition from Be to Ni 4-94468  
 flux of  $Z > 50$ , Ariel VI meas. 4-94476  
 flux on  $32 < Z < 50$  range, Ariel VI meas. 4-94475  
 Forbush decreases, time profile differences by neutron monitors and ion chambers 4-94452  
 galactic, mean masses of C, N, Ne, Mg, Si, S, Fe, HEAO-3 meas. 4-94482  
 galactic cosmic rays, intensity depression, effect of solar wind disturbances 4-94451  
 galactic cosmic rays, origin and acceleration characts. 4-94363  
 galactic cosmic rays, reson. diffusion 4-94362  
 galactic flux variation deduced from  $^{22}\text{Na}$ - $^{26}\text{Al}$  data of lunar samples 4-67577  
 galactic nuclei, age and source characts., isotopic comp. anal. 4-94357  
 galactic nuclei, comp. and nucleosynthesis 4-94356  
 galactic nuclei distrib., H I maps and  $\gamma$ -ray distrib. 4-90237  
 galactic nuclei propagation and accel., energy spectra anal. 4-94355  
 galactic rays, acceleration and propagation, HEAO-3 meas. implications 4-94347  
 galactic source abundance determ., effects of nucl. cross-section uncertainties 4-100928  
 galactic ultra-heavy nuclei, particle identification using SSNTD 4-101070  
 heavy nuclei flux in low energy rays 4-94496

**cosmic ray nuclei continued**

- heavy nuclei meas. above 20 GeV/nuc. 4-94471  
 high energy Fe spectrum 4-94472  
 intensities, energy spectra and interactions of 10-30 GeV/n nuclei 4-94470  
 ionic charge composition influence on heavy ion abundance variations 4-100949  
 isotopic anomalies due to solar system being anomalous 4-100968  
 medium energy cosmic nuclei,  $10 \leq Z \leq 26$ , elemental composition 4-94464  
 medium mass nuclei, flux in near-Earth space 4-94462  
 particle charge evolution during acceleration and implications on mass and charge spectra 4-101074  
 primary heavy nuclei, obs. above 5 GeV/n 4-94467  
 primary nuclei  $8 \leq Z \leq 26$ , charge composition 4-94463  
 primary ray induced cascades in emulsion chamber, energy spectra 4-94527  
 primary spectrum determ. from muons sea level intensity at Mt. Blanc underground expt. 4-82356  
 rare earth/lead-platinum ratio, nucleosynthesis at cosmic ray source 4-94521  
 secondary element abundances from HEAO-3 meas. 4-94520  
 size dependence determ. in marine sediments 4-101101  
 solar flare nucleon abundances, implications for acceleration and coronal propagation 4-105949  
 source spectra and mean path-length of primary high energy cosmic rays 4-101076  
 SSNTD array for ultra-heavy cosmic ray nuclei aboard NASA LDEF 4-96389  
 stratosphere, anomalous C, N and O cosmic ray component after 1972 4-94411  
 superheavy nuclei abundances in meteoritic crystal tracks 4-94480  
 time- and space-averaged cosmic ray flux experienced by meteorites 4-101102  
 two-stage acceleration and propagation at low energy 4-100912  
 ultra high energy nuclear interaction producing multiple large  $P_T$  components (Chinese) 4-77685  
 ultraheavy cosmic ray origin and propagation 4-94348  
 ultraheavy nuclei, energy spectra, HEAO-3 meas. 4-94479  
 ultraheavy source abundances, first ionisation pot. correlations 4-101073  
 very high energy cosmic ray events, primary spectral changes, anomalous interactions 4-72842  
 Z=10-26 multiply charged cosmic ray nuclei, 160-759 MeV/n, solar modulation in interplanetary region 4-94412  
 Z=10-92 relativistic nuclei, identification using various nuclear track detectors 4-96388  
 Z>26 abundances, HEAO-3 expt. results 4-94474  
 Z≥6 nuclei meas. using CR=39 4-94466  
 NN cosmic ray interactions, ang. dist., fractional energy spectra 4-101092  
 B, mass and isotopic abundances, HEAO-3 meas. 4-94483  
 B/C nuclei ratio, spatial and temporal variability 4-94416  
 Be, mass and isotopic abundances, HEAO-3 meas. 4-94483  
<sup>10</sup>Be abundance in ice cores, cosmic ray intensity variation obs. 4-101099  
<sup>10</sup>Be, conc. in deep sea sediments, intensity variation meas. 4-101100  
 Fe flux in 10<sup>18</sup> eV cosmic rays 4-94504  
 Fe group nuclei track density and lengths in meteorites 4-101106  
 Fe high energy nuclei obs. 4-94465  
 Fe rich solar energetic events, ionic charge dist. 4-105960  
<sup>60</sup>Fe, cosmic ray clock 4-101075  
<sup>4</sup>H, A=1, 2, relative intensities in 1973-9, propagation, energy spectra 4-94481  
<sup>4</sup>H, A=2, 3 isotope search in solar flares 4-105822  
 Mn isotopes, cosmic ray age determ. method 4-94487  
 N abundance in cosmic ray source 4-94486  
 Ne-Fe isotope meas. using Cherenkov ΔE/ΔX expt. 4-94629  
 O cosmic ray anomalous component, short-and long-term variations, Voyager data 4-94417  
<sup>50</sup>V, cumulative production by cosmic ray spallation 4-94337

**cosmic ray-nucleus reactions**

- for inelastic cosmic ray-nucleus scattering, see "cosmic ray-nucleus scattering"  
 anomalous nuclei events observed in the JACEE emulsion chambers 4-102312  
 anomalous relativistic ion interactions, cosmic rays in photoemulsions, nucl. pionisation model 4-110429  
 cross-section uncertainties, effects on galactic source abundance determ. 4-100928  
 cross-sections, implications for cosmic ray propag. and abundance calcs. 4-101093  
 diffractive dissociation in multi TeV hadron-hadron and hadron-nucleus collisions 4-102145  
 hadron-nucleus collision process, expt. data 4-102277  
 heavy ion relativistic central collisions on heavy targets 4-102315  
 high energy nuclei interactions in emulsion 4-102309  
 high energy nucleon-nucleus collisions, scaling violation 4-105857  
 multiparticle clustering in hadron-nucleus collisions at cosmic ray energies 4-102279  
 multiplicity correlation coefficients, energy depend. in high energy hadron-nucleus collisions 4-102281  
 nucleon emission from high energy cosmic hadron-nucleus interactions 4-102278  
 nucleon-nucleus collisions, multihadron production, collective mechanism 4-102313  
 nucleon-nucleus collisions, multihadron production, collective mechanism 4-102313  
 nucleon-nucleus collisions, phase transition simulation 4-102314  
 nucleus-nucleus interactions above 1 TeV/n in the JACEE emulsion chamber 4-102311  
 nucleus-nucleus reactions, 20 GeV/nuc., balloon expt. 4-102310  
 pregalactic <sup>4</sup>He nuclei, contrib. to synthesis of D and <sup>3</sup>Li 4-67841  
 proton relativistic central collisions on heavy targets 4-102315  
 pseudorapidity correlation in hadron-nucleus interaction at cosmic ray energies 4-102280  
 self induced nuclear transparency in mult TeV hadronic interactions 4-102319  
 spallation cross-sections and fragment yields, appl. to cosmic ray abundances and confinement calcs. 4-96039  
 ultra-relativistic heavy ion collisions, high multiplicity events 4-102316  
 (p,X), total and partial inelastic cross sections 4-94534

**cosmic ray-nucleus reactions continued**

- Fe(p,X) 0.5-5.0 TeV, cosmic ray hadron component composition at mountain altitudes 4-102325  
 Fe(π,X), 0.5-5.0 TeV, cosmic ray hadron component composition at mountain altitudes 4-102325  
**cosmic ray-nucleus scattering**  
 No entries  
**cosmic ray origin**  
 see also cosmology; element origin  
 accelerated particles and hard radiation generation during solar flare 4-100944  
 acceleration to ultra high energies in magnetospheres of young pulsars 4-100900  
 adiabatic expansion, consequences for secondary cosmic rays 4-94332  
 antiproton, annihilation and non-annihilation cross sections energy depend. origin models implications 4-94331  
 antiproton interstellar flux, nonuniform galactic disk model 4-94497  
 antiprotons, low energy, origin 4-94495  
 antiprotons of extragalactic origin 4-72841  
 arrival direction and origin of multi-joule cosmic rays 4-94333  
 baryon symmetric cosmology testing on a supergalactic scale 4-100920  
 charged particle transport in random mag. fields, effect of convection 4-94569  
 cross section uncertainties, effect on source composition derivations 4-94344  
 delayed energetic particle event of June 6, 1979 interplanetary shock effect 4-100952  
 energetic rays, 10<sup>14</sup>-10<sup>19</sup> eV, propagation and origin 4-100902  
 excess charge hypothesis, high energy particle source of contracting cosmic cloud 4-100918  
 extraterrestrial neutrinos, upper limit on muon flux from neutrinos 4-110390  
 galactic anomalous low-energy component 4-94361  
 galactic cosmic ray electrons, distrib. and diffusion, γ-ray anal. 4-101487  
 galactic cosmic rays, origin and acceleration characts. 4-94363  
 galactic cosmic rays 4-94354  
 galactic nuclei, age and source characts., isotopic comp. anal. 4-94357  
 galactic nuclei, comp. and nucleosynthesis 4-94356  
 galactic possibilities of rays of energy up to 10<sup>19</sup> eV 4-94336  
 galactic ultra-high energy cosmic rays 4-94360  
 gamma-ray bursters, assoc. X-ray emission, neutron star model 4-101517  
 Hawking radiation from black holes, non-thermal nature, contrib. to cosmic rays 4-106023  
 ionization effects shaping the elemental cosmic-ray source composition 4-100914  
 LMC, cosmic rays origin, models and expected radio and γ-ray emission 4-101485  
 low-energy cosmic rays from stellar X-ray sources, comp. 4-101512  
 multiple supernova I galactic source of ultra high energy particles 4-94350  
 OB association, upper mass limit, cosmic ray implication and cosmic abundances 4-101208  
 particle acceleration in interplanetary space, contribs. of shock accel. and turbulent accel. 4-110392  
 photon damping in cosmic ray acceleration in active galactic nuclei 4-94349  
 positron fluxes from densely shrouded sources, consequences in leaky box model 4-94328  
 positron sources, accretion powered, constraints 4-94329  
 rapid X-ray burster as a source of cosmic rays 4-100915  
 relativistic electron beam propag. through a plasma region into vacuum 4-97808  
 secondary galactic antiprotons, flux from propag. models and origin anal. 4-94359  
 shock acceleration, theory of cosmic-ray-mediated shocks with variable compression ratio 4-63021  
 shock wave acceleration from hot interstellar medium, charge state effect on composition 4-94353  
 solar flare increases in current cycle 4-100959  
 source abundances, direct determ. method 4-94345  
 source of ultra-high energy cosmic rays in galactic centre (Russian) 4-85847  
 source spectra and mean path-length of primary high energy cosmic rays 4-101076  
 source spectra from supernova blast waves 4-94352  
 sources and propagation 4-100905  
 star types for dominant cosmic ray injectors 4-100913  
 ultra high energy ray source 4-100919  
 ultraheavy cosmic ray origin and propagation 4-94348  
 X-ray binary stars, clues from photonuclear time scale on nature of particle accelerators 4-101503  
 young supernovae remnants as acceleration sites of cosmic ray electrons 4-100906  
**cosmic ray photons**  
 see also cosmic ray X-rays; solar cosmic ray photons  
 active galaxies nuclei, γ-ray and relativistic particles prod. and spectra anal. 4-100891  
 altitude variation of the derived electron photon intensity 4-105852  
 background γ-ray spectrum balloon-borne spectrometer meas. 4-59482  
 black holes, mass accretion and plasma processes, γ-ray emission model, 3C 273 appl. 4-101536  
 CG 195+04, γ-ray line emission search 4-101521  
 2CG 195+4, gamma ray flux periodicity and energy spectra, EAS obs. 4-101527  
 CG 195+4, gamma-ray var., obs. of Cherenkov radiation due to air showers 4-101528  
 Crab Nebula, search for γ-ray lines 4-101462  
 Cygnus X-3, γ-ray emission, period from EAS data anal. 4-101531  
 Cygnus X-3, γ-ray emission var., small air showers arrival directions obs. 4-101529  
 Cygnus X-3, gamma ray var., Cherenkov radiation due to air showers 4-101528  
 diffuse γ-ray background origin 4-100891  
 diffuse galactic gamma-ray emission and cosmic ray-interstellar matter interactions 4-100890  
 galactic γ-rays prod. in quasars and active galactic nuclei 4-100929  
 galactic anticentre direction γ-ray sources, obs. 4-101524  
 galactic centre, 2-20 MeV gamma-ray map and energy distrib. 4-101523  
 galactic gamma-ray-photon interactions, EM cascade showers initiation 4-101537

## cosmic ray photons continued

- gamma ray background of balloon borne  $\gamma$ -ray telescope, origin 4-101171
- gamma ray burst sources, distance model 4-101518
- gamma ray burst sources observed by Hinotori satellite, energy spectra, time history and origin 4-101513
- gamma ray imaging via detect. of atm. Cherenkov radiation due to air showers 4-101176
- gamma ray line obs., statistical reliability 4-101190
- gamma ray production in EAS 4-67584
- gamma ray sources, excess fluxes search, EAS data anal. 4-101533
- gamma rays, 1000 GeV, from M31 (Andromeda galaxy), Dugway array obs. 4-101470
- gamma rays in atmosphere, due to cosmic ray interactions 4-110400
- gamma rays of very high energy, galactic plane events 4-85845
- gamma-ray astronomy, review 4-106084
- gamma-ray background, meas. at balloon altitudes above Beijing area (Chinese) 4-82355
- gamma-ray burst of 1978 March 25, absorpt. feature characts. 4-101522
- gamma-ray bursts, high time resolution  $\gamma$ -ray spectral obs. with Solar Maximum Mission 4-101514
- gamma-ray diffuse component meas. by high-altitude balloon 4-100888
- gamma-ray discrete sources ( $E > 10^{15}$  eV), search in EAS data 4-101530
- gamma-ray emission from interstellar clouds 4-100892
- gamma-ray intensity rel. to interstellar column density of H and  $^{12}\text{CO}$  4-110409
- gamma-ray spectra recorded by balloon borne detector, background origin 4-100720
- gamma-rays from celestial sources, Cherenkov radiation obs. 4-101532
- gamma-rays from interstellar  $\text{H}_2$  and H I, energy spectra anal. 4-101486
- high energy electrons and photons, intensity-depth relation 4-105854
- inverse Compton interaction, cosmic-ray electrons with interstellar photons 4-101088
- massive black holes, 511 keV annihilation line, origin due to tidally disrupting stars 4-101405
- molecular clouds, gamma-ray line emission and cosmic ray interactions 4-101463
- Pamir expt.,  $\gamma$ -ray energy spectra and ang. distrib. 4-110438
- photon damping in cosmic ray acceleration in active galactic nuclei 4-94349
- PSR 0531+21, 1-20, MeV pulsed  $\gamma$ -ray emission anal. 4-101391
- PSR 0531-21,  $\gamma$ -ray flux and energy spectra, Cherenkov radiation obs. 4-101395
- PSR 0531+21, gamma ray emission, possible sporadicity, Cherenkov radiation anal. 4-101392
- PSR 0531+31 and 1937+214 (millisecond pulsar),  $\gamma$ -ray emission, Cherenkov radiation obs. 4-101394
- PSR 0532+31,  $\gamma$ -ray periodicity, EAS data anal. 4-101534
- PSR 0833-45, 1-20 MeV pulsed gamma-rays obs. 4-101390
- PSR 0833-45, possible transient  $\gamma$ -ray emission obs. 4-101395
- PSR 0833-45 and 0950+08,  $\gamma$ -ray emission, Cherenkov radiation anal. 4-101396
- pulsars,  $\gamma$ -ray luminosity anal. and distrib. in Galaxy 4-101526
- quasars,  $\gamma$ -ray and relativistic particles prod. and spectra anal. 4-100891
- Seyfert galaxies nuclei, cosmic ray accel. and energy spectra, photons and neutrinos as probes 4-100925
- solar flare gamma-ray events, associated proton fluxes 4-105967
- solar flares, gamma-ray line 2.22 MeV 4-105965
- solar flares, gamma-ray meas. above 10 MeV 4-105966
- solar flares, gamma-ray obs., energy spectra 4-105968
- solar flares, mechanisms for proton acceleration 4-105824
- spectral indices in  $E > 1$  TeV region 4-94499
- ultra-high energy,  $\gamma$ -ray component for detection-anal. technique 4-90044
- ultrahigh-energy photons, high-precision system for meas. of arrival time 4-105885
- UV photons, emission by massive neutrinos and photinos 4-63375

## cosmic ray propagation

- accelerated particles and hard radiation generation during solar flare 4-100944
- accelerated particles spectrum, influence on shock front structure 4-100896
- acceleration, turbulent dynamo  $\alpha$ -effect 4-94379
- acceleration and drift in latitude at the solar-wind termination shock 4-94383
- acceleration and transport in stellar winds with terminal shocks 4-100897
- acceleration between approaching shock fronts 4-94380
- acceleration by collapsing molecular clouds 4-100904
- acceleration by diffusive shocks and cut-off energy 4-94525
- acceleration by interplanetary shock waves 4-67572
- acceleration by pulsars 4-100903
- acceleration by supernova remnant shock 4-73049
- acceleration efficiency by supernovae remnants 4-100907
- acceleration in interplanetary medium, associated solar wind disturbances 4-94378
- acceleration in magnetotail 4-94325
- acceleration mechanisms 4-94327
- acceleration of electrons in supernova remnants 4-100909
- acceleration to ultra high energies in magnetospheres of young pulsars 4-100900
- anisotropic stage of cosmic ray propagation 4-94372
- anisotropy distributions associated with interplanetary shocks 4-94387
- anomalous cosmic ray component, acceleration, numerical model 4-94375
- antiproton equilibrium spectra in cosmic ray propagation models 4-94330
- antiproton interstellar flux, nonuniform galactic disk model 4-94497
- atmospheric propagation, geomagnetic field effect 4-101050
- azimuthal heliosphere, two-dimens. steady state cosmic ray transport eqn. 4-94368
- blast waves with cosmic ray pressure, steep energy spectrum case 4-100910
- Burgers' equation and cosmic ray shocks 4-105815
- charged particle transport, solar wind convection effects 4-100930
- charged particle transport in random mag. fields, effect of convection 4-94569
- coherent regime near Sun, cosmic ray modulation 4-94399
- coronal and interplanetary transport 4-100947
- coronal and interplanetary transport model 4-100948
- coronal propagation model, radiation characteristics, mag. field depend. 4-67571
- coupled hydromagnetic wave excitation and cosmic ray acceleration at interstellar shocks 4-94351
- cross section uncertainties effect on source composition derivations 4-94344
- delayed energetic particle event of June 6, 1979 interplanetary shock effect 4-100952
- diffusion coefficient derived from individual spectra 4-94366
- diffusion from local galactic sources 4-94342
- diffusive shock acceleration of energetic electrons subject to synchrotron losses 4-115661
- diurnal variation, 27-day recurrences 4-94435
- electron acceleration in supernova remnants, evolution as radio sources 4-63246
- electron motion in neutron sheet 4-100937
- electron propagation in leaky box model with truncated pathlength distrib. 4-94490
- electrons, acceleration in interplanetary space 4-94376
- electrons in radiosources, propag. effects and visible-IR spectra cutoff 4-106073
- energetic rays,  $10^{14}$ - $10^{19}$  eV, propagation and origin 4-100902
- energetic storm particle events, shock wave anisotropies 4-94390
- energy changes in solar wind, diffusion-convection modulation eqn. 4-94401
- excess charge hypothesis, high energy particle source of contracting cosmic cloud 4-100918
- extragalactic cosmic rays, sources characts. and intergalactic propag. 4-100926
- Fermi acceleration at interplanetary shocks 4-94381
- Fermi shock acceleration, Coulomb losses, Monte Carlo calcs. 4-105819
- Forbush decreases, energy dist. 4-94444
- Forbush decreases, solar flare induced, depend. on shock wave geometry 4-85850
- frictional acceleration of high-energy particles in pulsar vicinity 4-100901
- galactic confinement, interpretation of electron energy spectra meas. 4-94460
- galactic cosmic ray anisotropies during solar cycle 20 4-94437
- galactic cosmic ray modulation by solar wind, subsonic streaming transition in nonlinear model 4-94404
- galactic cosmic rays, origin and acceleration characts. 4-94363
- galactic cosmic rays, power spectra variations, correlation with Sun's activity 4-94436
- galactic cosmic rays, propagation analysis and solar modulation, use of matrix methods 4-100927
- galactic cosmic rays, reson. diffusion 4-94362
- galactic cosmic rays, source abundance determ., propag. model 4-100928
- galactic cosmic rays 4-94354
- galactic electrons, distrib. and diffusion,  $\gamma$ -ray anal. 4-101487
- galactic nuclei, age and source characts., isotopic comp. anal. 4-94357
- galactic nuclei propagation and accel., energy spectra anal. 4-94355
- galactic positrons and electrons, propag. and energy spectra anal. 4-94358
- galactic rays, acceleration and propagation, HEAO-3 meas. implications 4-94347
- galactic secondary/primary ratio and energy-dependent truncation of the pathlength distribution 4-94346
- galactic ultra-high energy cosmic rays 4-94360
- global radio continuum of nearby galaxies 4-94334
- heliocentric radial gradient of cosmic ray intensity 4-94364
- heliosphere, galactic cosmic ray propag., electric field effects, modulation 4-94400
- high energy solar particle events, isotropic and anisotropic diffusion models 4-100960
- horizontal muon spectrum, charge ratio, atmos. propagation 4-110402
- intensity transient decreases, solar wind stream interfaces 4-94449
- intensity variations in magnetosphere 4-94326
- interactions cross-sections, implications for propag. calcs. 4-101093
- intergalactic protons, zero-point field accel. and energy spectra 4-100887
- interplanetary mean free path, rigidity dependence 4-100934
- interplanetary medium, estimate of cosmic ray latit. gradient (1981-1982) 4-85849
- interplanetary medium, shock waves accel. of cosmic ray particles 4-110392
- interplanetary pitch angle scattering, absolute value, functional depend. 4-100936
- interplanetary propagation, effect of anisotropy of random component of mag. field 4-110393
- interplanetary propagation during steady and transient solar wind conditions 4-94365
- interplanetary propagation of galactic cosmic rays 4-67566
- interplanetary propagation of galactic cosmic rays 4-72838
- interplanetary solar proton propagation 4-100935
- interplanetary space, nonstationary modulation for constant radial gradient 4-94405
- interstellar cloud accretion and evaporation, implication for cosmic rays and  $\gamma$ -ray emission 4-100892
- ion acceleration at interplanetary shocks, hydromagnetic wave excitations 4-94384
- ion acceleration in solar flares, magnetosonic plasma waves 4-63042
- ion anisotropies associated with interplanetary shocks 4-94385
- ionic charge composition influence on heavy ion abundance variations 4-100949
- isotope search in solar flares 4-105822
- Jovian electron events, interplanetary transport, modulation in Earth's orbit 4-94434
- Jupiter, cosmic ray contribution 4-94394
- kinetics, diffusion approx. 4-94373
- kinetics in anisotropic mag. field 4-94374
- local superbubble model of cosmic ray propagation 4-94339
- localized nature of the galactic cosmic rays 4-94340
- low energy ions, mean free path in front of interplanetary shock waves 4-100933
- low energy propagation of flare accelerated protons and alpha particles 4-100950
- magnetospheric propagation 4-101029
- mean lifetime in dynamical halo model 4-94341
- medium energy cosmic nuclei,  $10 \leq Z \leq 26$ , elemental composition 4-94464
- models for  $10^8$ - $E < 10^{14}$  eV particles 4-94338
- modulation, solar activity effects in 19-21 cycles 4-94433
- muon spectra, derivation at large zenith angles from primary flux 4-110389
- nested leaky box model 4-94343

## cosmic ray propagation continued

- neutrons, solar flare flux from interplanetary charged particle, meas. 4-100942
- OB association, upper mass limit, cosmic ray implication and cosmic abundances 4-101208
- OB associations, mechanical energy output, cosmic ray accel. at wind shocks 4-101447
- oblique MHD shock waves modified by cosmic-rays 4-100894
- onion-shell model of cosmic ray acceleration in supernova remnants 4-100908
- particle acceleration by flare-induced interplanetary shocks 4-94377
- particle acceleration in local magnetic structures on the Sun 4-105943
- pathlength distribution, energy depend. evidence in short pathlengths 4-94518
- pitch angle distributions and energy spectral for solar particle effects 4-100951
- prolonged injection effect on solar flare generated particle propagation 4-100931
- proton acceleration mechanisms, associated interplanetary shocks 4-94386
- proton energetic spectra, associated planetary shock waves 4-94389
- proton spectra, propagation and acceleration 4-94391
- protons, intensity increases, associated planetary shocks 4-94388
- quantum theory of EM interactions in intergalactic space, effect of zero-point field 4-63044
- rare earth/lead-platinum ratio, nucleosynthesis at cosmic ray source 4-94521
- relativistic electron beam propag. through a plasma region into vacuum 4-97808
- relativistic solar electron and proton, arrival time differences, at Earth 4-100956
- secondary galactic antiprotons, flux from propag. models and origin anal. 4-94359
- Seyfert galaxies nuclei, cosmic ray accel. and energy spectra, photons and neutrinos as probes 4-100925
- shock acceleration, theory of cosmic-ray-mediated shocks with variable compression ratio 4-63021
- shock acceleration, time depend. approx. and exact soln. 4-100898
- shock acceleration events, association with interplanetary proton events 4-105864
- shock profiles with variable compression ratio 4-100893
- shock wave acceleration from hot interstellar medium, charge state effect on composition 4-94353
- shock wave ensemble formation of cosmic ray spectrum 4-100895
- solar cosmic ray diffusion in solar wind 4-72840
- solar cosmic ray flare event, features 4-105948
- solar flare event, elemental composition, acceleration mechanisms 4-105821
- solar flare gamma-ray events, associated proton fluxes 4-105967
- solar flare neutrinos, flux estimations 4-110591
- solar flare nucleon abundances, implications for acceleration and coronal propagation 4-105949
- solar flare particle fluences during solar cycles 19, 20 and 21 4-105961
- solar neutrino flux, quasi-biennial variation 4-110394
- solar proton and alpha differential energy spectra 4-105820
- solar protons, interplanetary mean free paths and diffusion coeffs. 4-105823
- solar protons associated with solar wind shock waves, accel. and energy spectra 4-72837
- solar wind energetic particle acceleration mechanisms 4-72847
- source abundances, direct determ. method 4-94345
- sources and propagation 4-100905
- spallation cross-sections and fragment yields, appl. to cosmic ray abundances and confinement calcs. 4-96039
- spatial distribution of the solar particles during the 7 May 1978 flare 4-100958
- spurious sidereal daily variation due to stationary anisotropy of solar origin 4-63022
- statistical acceleration of electrons in the galactic halo 4-100911
- steady state shock structure, mediation and particle escape 4-100899
- storm particle events, effects of adiabatic deceleration and shock lifetime 4-94382
- supernova remnants, radio emission and electrons accel. at various evolutionary stages 4-73025
- supernova remnants, radioemission evolution, role of relativistic electrons accel. by MHD turbulence 4-73026
- supernova remnants, radio sources, mag. field amplification and particle accel. (Russian) 4-67786
- three dimensional transport. eqn. for energetic particles in EM fields 4-94367
- three-dimensional diffusion of high-energy solar cosmic rays 4-100932
- two-stage acceleration and propagation at low energy 4-100912
- ultraheavy cosmic ray origin and propagation 4-94348
- ultraheavy cosmic rays, abundances and propag. model, role of nucleosynthesis 4-85846
- young supernovae remnants as acceleration sites of cosmic ray-electrons 4-100906
- A=1-4, relative intensities in 1973-9, propagation, energy spectra 4-94481
- C(<sup>20</sup>Ne,X), 500 MeV/nuc fragmentation, charge and isotropic cross sections, cosmic ray propagation appl. 4-91022
- C(<sup>16</sup>O,X), 500 MeV/nuc fragmentation, charge and isotropic cross sections, cosmic ray propagation appl. 4-91022
- (Fe,X), 710 and 1050 MeV/nuc, fragmentation, cosmic ray propagation appl. 4-91021
- He<sup>3</sup> and He<sup>4</sup> in Earth's outer radiation belts, temporal and spatial variations 4-94324
- <sup>3</sup>He rich solar energetic events, He ionisation states 4-105958
- <sup>3</sup>He rich solar events, 27 day recurrence 4-105955
- <sup>3</sup>He/<sup>4</sup>He ratio in solar events, dependence on energy 4-105957
- <sup>4</sup>He, A=3, 4, energy spectra deformation in traverse through solar plasma 4-67580

## cosmic ray protons

- acceleration between approaching shock fronts 4-94380
- acceleration during solar flares, plausible mechanisms 4-105824
- acceleration mechanisms, associated interplanetary shocks 4-94386
- anomalous cosmic ray component, acceleration, numerical model 4-94375
- antiparticles of extragalactic origin 4-72841
- antiproton, annihilation and non-annihilation cross sections energy depend., origin models implications 4-94331

## cosmic ray protons continued

- antiproton equilibrium spectra in cosmic ray propagation models 4-94330
- antiproton experiment, data eval. 4-94491
- antiproton flux and positron fluxes from densely shrouded sources, consequences in leaky box model 4-94328
- antiproton flux in low energy rays 4-94496
- antiproton interstellar flux, nonuniform galactic disk model 4-94497
- antiproton/proton ratio, energy depend. in 4.4-13.4 GeV range 4-94494
- antiprotons, 50-200 MeV abundance 4-94493
- antiprotons, low energy, origin 4-94495
- antiprotons, low-energy, large abundances 4-94498
- antiprotons in primary cosmic rays, characts. (French) 4-105817
- charged particles telescope to observe proton albedos 4-101039
- distant terrestrial magnetosphere, protons, He and heavy ion obs. with ISEE-3 4-94323
- energetic spectra, associated planetary shock waves 4-94389
- flux bidirectional opposite streamings in noon low latitude magnetosheath 4-67570
- flux dependence on solar activity cycle 4-100954
- flux intensity variations, solar effects 4-94429
- Forbush decreases, solar flare induced, depend. on shock wave geometry 4-85850
- galactic, Cherenkov radiation and extrasolar planets IR detect. 4-77725
- galactic, spectra 1965-79 as modulation theory tests 4-94407
- galactic cosmic rays, estimate of helioliat. gradient (1981-1982) 4-85849
- geomagnetic storm effect on trapped protons at 500 km 4-67568
- heliosphere, long term cosmic ray modulation, 1-25 AU, Pioneer, Voyager, ISEE-3 and Helios data 4-94421
- intensity increases, associated planetary shocks 4-94388
- intergalactic protons, zero-point field accel. and energy spectra 4-100887
- interplanetary shock event Nov. 11-12, 1978, test of acceleration theory 4-94543
- interplanetary solar proton propagation 4-100935
- ion anisotropies associated with interplanetary shocks 4-94385
- low energy ions, mean free path in front of interplanetary shock waves 4-100933
- low energy propagation of flare accelerated protons and alpha particles 4-100950
- magnetosphere boundary penetration 4-67575
- modulation asymmetries over two solar cycles, 1965-81 4-94409
- modulation coefficient during 1954, 1965 and 1976 minima in solar activity 4-94427
- modulation diffusion, stochastic instability in inner radiation belt 4-101038
- neutron-proton flux ratio in atmosphere, depth depend. 4-105835
- NN fragmentation collisions, EM contrib. 4-86748
- nucleon-nucleon interactions at high-energies, short- and long-range correls. 4-78576
- penetration of solar particles into magnetosphere 4-100975
- photon-dominated Universe, cosmic-ray antiprotons 4-105818
- pitch angle distributions and energy spectral for solar particle effects 4-100951
- primary proton flux coordination with flux of hadrons without shower accompany 4-105831
- primary spectrum model 4-94499
- in QS 0630+180, proton quasar model rel. to identification of 206.5 nm emission line 4-90252
- relativistic solar electron and proton, arrival time differences at Earth 4-100956
- secondary galactic antiprotons, flux from propag. models and origin anal. 4-94359
- semidural variations of nucleonic components 4-100994
- Seyfert galaxies nuclei, cosmic ray proton characts. 4-100925
- shock acceleration events, association with interplanetary proton events 4-105864
- sign alternating solar proton anisotropy 4-101067
- solar cosmic ray flare event, features 4-105948
- solar cosmic ray proton fluxes in last 10<sup>5</sup> years 4-100970
- solar cosmic rays, magnetosphere penetration, use in ring current characts. determ. 4-94303
- solar flare gamma-ray events, associated proton fluxes 4-105967
- solar flare particles acceleration region height, electrons and protons spectrum form anal. 4-100938
- solar flare proton events, correlation with coronal mass ejections 4-105942
- solar flare proton fluxes, deduced from <sup>26</sup>Al depth profile in lunar rocks 4-100971
- solar flare proton fluxes, secular variations 4-100972
- solar flare protons, spectral and temporal characts. rel. to coronal mag. field struct. 4-10396
- solar particles associated with solar wind shock waves, energy spectra and accel. 4-72837
- solar proton, quasistationary injection obs. during small Forbush decreases 4-101068
- solar proton and alpha differential energy spectra 4-105820
- solar proton events of 1977 November 22 and 1978 May 7, comparison 4-72839
- solar proton spectrum dynamics, time evolution 4-105944
- solar protons, absolute fluxes above E=100 MeV from meas. in stratosphere and with neutron monitors 4-110397
- solar protons, E>100 MeV, stratospheric meas. 4-100961
- solar protons, energy spectra from balloon and neutron monitor data 4-101077
- solar protons, flux at polar caps 4-67576
- solar protons, high-latitude profiles in Earth magnetosphere 4-100965
- solar protons, interplanetary mean free paths and diffusion coeffs. 4-105823
- spectra, propagation and acceleration 4-94391
- spectra of solar proton ground level events recorded at Sanae 4-100957
- stratosphere, anomalous C, N and O cosmic ray component after 1972 4-94411
- upstream protons, energy spectra 4-94393
- NN cosmic ray interactions, ang. dist., fractional, energy spectra 4-101092
- (p,X), total and partial inelastic cross sections 4-94534
- py-ν<sub>s</sub>X, neutrino yield calcs. 4-110475
- pp cross section at 30 TeV from EAS 4-64021
- <sup>37</sup>Cl neutrino counting rate, P-P chain reactions, quasi-non-degenerate distribution 4-101090

## cosmic ray showers and bursts

see also cosmic ray electrons; cosmic ray X-rays  
 Akeno extensive air shower expt., primary spectrum, cosmic ray electrons and muons 4-110410  
 altitude variation of the derived electron photon intensity 4-105852  
 anisotropy of cosmic rays of superhigh energies 4-94515  
 arrival directions of large EAS in the Southern Hemisphere 4-94532  
 atmosphere Cherenkov light emission imaging, appl. to  $\gamma$ -ray astronomy 4-101176  
 atmospheric Cerenkov 'pulse-width technique', extensive air showers 4-110428  
 atmospheric propagation and energy deposition detectors 4-105856  
 cascade curve and energy flow properties in two layer absorber 4-105846  
 cascades and atmospheric propagation 4-105855  
 celestial arrival directions of primary cosmic rays of median energy  $2.10^{15}$  eV 4-94530  
 Cerenkov density spectra interpretation, primary mass composition energy depend. 4-82359  
 CG 195+4, gamma-ray var., obs. of Cherenkov radiation due to air showers 4-101528  
 Cygnus X-3,  $\gamma$ -ray emission, period from EAS data anal. 4-101531  
 Cygnus X-3,  $\gamma$ -ray emission and air showers, arrival directions anal. 4-101529  
 Cygnus X-3, gamma ray var., Cherenkov radiation due to air showers 4-101528  
 $E > 10^{19}$  eV, sub-luminal pulses, energy deposition 4-101080  
 EAS,  $K_{\gamma}/K$  distribution in nucleon interactions 4-101087  
 EAS, long flying component investigation 4-101084  
 EAS, Poisson branching point processes 4-90046  
 EAS, role of charmed particles in creation of long flying component 4-101085  
 EAS, search for discrete  $\gamma$ -ray sources ( $E > 10^{15}$  eV) in Kiel data 4-94991  
 EAS, tachyon production in primary interaction 4-101086  
 EAS arrival direction and muon to electron ratio 4-94528  
 EAS at Akeno, lateral distrib. of electrons 4-82358  
 EAS Cherenkov radiation density spectrum, primary energy spectrum 4-94509  
 EAS hadron, role in muon pair production 4-101091  
 EAS high energy hadrons, energy spectrum, possible heavy particle 4-82360  
 EAS muon energy spectra meas. in ANI magnetic spectrometer 4-112035  
 EAS upward obs. use for  $E > 10^{19}$  eV neutrino flux determ. 4-110476  
 electron lateral distribution problem, cascade theory approx. A soln. 4-105850  
 electron time struct. in extensive air showers due to long-lived massive particle production 4-94533  
 electron-photon cascades, calc. by Monte Carlo method 4-105849  
 EM 10 TeV cascades, lead X-ray emulsion chamber meas. 4-105839  
 EM cascade development in matter 4-105840  
 EM cascade obs. using Thermoluminescent Calorimeters 4-105838  
 EM cascades, particle number distrib. function variation 4-105845  
 EM showers at superhigh energies, mean characteristics and fluctuations 4-105842  
 EM superhigh energy cascades, particle angular distrib. 4-105844  
 energy spectrum, charge ratio in horizontal showers 4-110419  
 gamma ray production in EAS 4-67584  
 gamma ray sources, excess fluxes search, EAS data anal. 4-101533  
 gamma rays in atmosphere, due to cosmic ray interactions 4-110400  
 gamma-ray discrete sources ( $E > 10^{15}$  eV), search in EAS data 4-101530  
 gamma-ray sources at  $E = 10^{15}$  eV, search, EAS data anal. 4-101534  
 gamma-ray sources emission, Cherenkov radiation obs. 4-101532  
 giant air shower primaries, energy estimation methods 4-94512  
 hadron cascades in the atmosphere 4-105851  
 hadron energy determination in X-ray emulsion chamber with C block 4-105847  
 high energy electrons and photons, intensity-depth relation 4-105854  
 high energy muon anal. in air showers 4-94502  
 inelasticity effects in EAS nucleon number, an analytic solution 4-105853  
 intensity anisotropy for  $E > 10^{17}$  eV rays 4-94398  
 Landau-Pomeranchuk-Migdal effect, X-ray emulsion chamber expt. 4-105841  
 Landau-Pomeranchuk-Migdal effect for EM cascade showers in Pb 4-105843  
 long-lived particles produced in extensive air showers 4-94533  
 longitudinal cascade of high-energy showers, from Cherenkov light observations 4-101081  
 low energy muon anal. in air showers 4-94501  
 massive particle search in extensive air showers 4-101083  
 meson-nucleon cascades in atmos. including geomag. field effect 4-101050  
 Monte Carlo simulation, energy determ. 4-105837  
 muons charact. anal. and primary cosmic rays charact. determ. 4-94524  
 primary arrival direction meas. for  $10^{12}$ - $10^{17}$  eV rays 4-94514  
 primary energy spectrum, arrival direction in EAS 4-94510  
 primary mass composition in  $E = 10^{15}$ - $10^{16}$  eV range from EAS data 4-94506  
 primary mass composition in energy interval  $10^{13}$ - $10^{18}$  eV, EAS meas. anal. 4-94508  
 primary mass composition in energy range  $10^{16}$  to  $10^{17}$  eV from EAS data 4-94507  
 primary ray composition at  $10^{14}$ - $10^{16}$  eV from EAS data 4-94503  
 primary ray composition at  $E \sim 10^{15}$  eV from delayed hadrons in air showers 4-94505  
 primary ray induced cascades in emulsion chamber, energy spectra 4-94527  
 primary spectrum above 1 TeV from Cherenkov light images 4-94526  
 proton generated cascade, possibilities of distinguishing from electron generated cascade 4-105848  
 PSR 0531+21,  $\gamma$ -ray flux and energy spectra, Cherenkov radiation obs. 4-101393  
 PSR 0531+21, gamma ray emission, possible sporadicity, Cherenkov radiation anal. 4-101392  
 PSR 0531+31 and 1937+214 (millisecond pulsar),  $\gamma$ -ray emission, Cherenkov radiation obs. 4-101394  
 PSR 0532=31,  $\gamma$ -ray periodicity, EAS data anal. 4-101534

## cosmic ray showers and bursts continued

PSR 0833-45 and 0950+08,  $\gamma$ -ray emission, Cherenkov radiation anal. 4-101396  
 quark flux estimation at sea level 4-101082  
 scaling violation in fragmentation region of pp collisions 4-105834  
 shower excess from Crab nebula 4-94513  
 small air showers, arrival direction meas. 4-94529  
 small scale anisotropies in cosmic rays near  $10^{16}$  eV 4-94531  
 source abundances above 10 GeV-per-nucleon, air-shower meas. implications 4-67583  
 pN-cosmic ray cascades, nuclear target effects 4-95859  
 pp cross section at 30 TeV from EAS 4-64021

cosmic ray solar modulation  
 anisotropy, component discrimination using crossed telescopes 4-101006  
 anisotropy variation on solar activity cycle 4-101005  
 azimuthal heliosphere, two-dimens. steady state cosmic ray transport eqn. 4-94368  
 coherent regime near Sun, cosmic ray modulation 4-94399  
 daily variation harmonics of galactic cosmic rays 4-100991  
 daily variations, average behaviour, recent trends 4-100987  
 daily variations, first three harmonics, day-to-day correlated changes, statistical study 4-100988  
 density gradients, long term variations, solar mag. field induced 4-94425  
 diurnal and semi-diurnal anisotropy variation 4-100997  
 diurnal and semi-diurnal variations, upper cutoff rigidity determ. 4-100999  
 diurnal anisotropy, 11 and 22 year periodic variation 4-100990  
 diurnal anisotropy, 22 year recurrence tendency during maximum solar activity periods 4-100993  
 diurnal anisotropy, solar polar mag. field polarity effect 4-101004  
 diurnal anisotropy inferred from Elbrus spectrograph data 4-100986  
 diurnal effect on galactic ray intensity from stratospheric meas. 4-100985  
 diurnal variation, 27-day recurrences 4-94435  
 diurnal variation, long term changes 4-100983  
 diurnal variation, relation to interplanetary mag. field 4-100982  
 diurnal variation Feb-Mar. 1977, anomalous change 4-100989  
 diurnal variations, harmonics from interplanetary transport processes 4-100981  
 electron flux variations in geosynchronous orbit 4-100974  
 electrons, 1 GeV, solar modulation 1978-83 4-94408  
 electrons, solar modulation meas. (1978 to 1983) 4-85851  
 energetic hysteresis of galactic cosmic ray intensity during solar mag. field inversion 4-94406  
 energy changes in solar wind, diffusion-convection modulation eqn. 4-94401  
 equatorial anisotropy inside fast solar wind streams 4-101001  
 flare effects on 1975-9 decreases 4-100978  
 flux intensity variations, solar effects 4-94429  
 Forbush decrease, diurnal and semi-diurnal anisotropies 4-94438  
 Forbush decrease, global spectrography method 4-94442  
 Forbush decrease, rigidity dependence 4-94454  
 Forbush decrease July 13/14 1983, intensity periodicities 4-100973  
 Forbush decrease of galactic cosmic ray intensity 4-67566  
 Forbush decreases in heliosphere, full trajectory integration, comparison with obs. 4-94431  
 galactic, intensity modulation from: anal. of tree rings  $^{14}\text{C}$  dating 4-94423  
 galactic cosmic ray anisotropies during solar cycle 20 4-94437  
 galactic cosmic ray behaviour in solar wind 4-72838  
 galactic cosmic ray gradient and modulation effects obs. by Voyager and Pioneer spacecraft 4-94415  
 galactic cosmic ray modulation by solar activity processes, shock wave steady-state model 4-94413  
 galactic cosmic ray modulation by solar wind, subsonic streaming transition in nonlinear model 4-94404  
 galactic cosmic ray radial gradients, Pioneer 10 meas. at 1 to 29 AU through solar maximum 4-94418  
 galactic cosmic rays, Forbush decreases, technique to study anisotropy 4-94439  
 galactic cosmic rays, intensity var. and terrestrial atm.  $^{14}\text{C}$  prod. var. 4-94424  
 galactic cosmic rays, modulation by solar wind in spherically symmetric nonstationary diffusive model 4-94402  
 galactic cosmic rays, power spectra variations, correlation with Sun's activity 4-94436  
 galactic cosmic rays 4-94354  
 galactic c.p. and He spectra 1965-79 as modulation theory tests 4-94407  
 galactic intensity variations, relation to solar mag. field 4-94370  
 galactic rays, heliolongitudinal asymmetry of solar activity and cosmic ray distribution 4-101003  
 galactic rays, sidereal daily variation, seasonal variation due to heliomagnetosphere 4-101008  
 galactic rays anisotropy in high velocity solar wind fluxes 4-100976  
 global modulation in interplanetary space 4-94430  
 heliosphere, galactic cosmic ray propag., electric field effects, modulation 4-94400  
 heliosphere, long term cosmic ray modulation, 1-25 AU; Pioneer, Voyager, ISEE-3 and Helios data 4-94421  
 high energy cosmic rays, solar and meteorological effects 4-101033  
 inner heliosphere, galactic cosmic ray modulation by solar flare disturbances 4-94419  
 integral radial cosmic ray gradients (1972 to 1982) 4-85848  
 intensity time depend. from tree-ring data 4-100967  
 intensity variations, solar wind velocity correlations 4-100977  
 interplanetary magnetic field sector structure and second harmonic of cosmic ray intensity 4-100998  
 interplanetary modulation effect of anisotropy of random component of mag. field 4-110393  
 interplanetary propagation, review of theory 4-78072  
 interplanetary space, nonstationary modulation for constant radial gradient 4-94405  
 irradiation parameters of accelerated particles during solar system evolution 4-100969  
 latitude distributions during solar minima 1954, 1965, 1976 4-94371  
 long term intensity variations, relation to different indices of solar activity 4-110398  
 low frequency fluctuations of the cosmic ray intensity 4-100979  
 lunar-diurnal variation of high-energy cosmic rays 4-101000

**cosmic ray solar modulation continued**  
 measurement stations for cosmic ray variation studies, necessary geographic distrib. 4-110539  
 model constraints from anomalous cosmic ray component meas. 4-101185  
 models, use of matrix methods 4-100927  
 modulation coefficient during 1954, 1965 and 1976 minima in solar activity 4-94427  
 modulation during 1970-4, anomalous phenomena due to coronal holes 4-94422  
 neutrino flux, periodic change 4-100963  
 north-south anisotropy, Earth latitudinal ang. distance from heliospheric current sheet effect 4-101002  
 nucleon energy distribution, Ottawa large zenith angle muon telescope array 4-101057  
 outer heliosphere, cosmic ray gradients from Pioneer data 4-94414  
 pathlength distribution, energy depend. evidence in short pathlengths 4-94518  
 power spectral variations, ambient power 4-100992  
 preferred solar longitude zones in affecting solar activity and geophysical parameters 4-101053  
 primary cosmic rays, zonal modulation rel. to solar mag. field 4-94396  
 proton flux dependence on solar activity cycle 4-100954  
 proton modulation asymmetries over two solar cycles, 1965-81 4-94409  
 protons, penetration of solar particles into magnetosphere 4-100975  
 relativistic interplanetary particle anisotropy, 50 day periodicity, Pioneer data 4-94420  
 relativistic solar cosmic ray flux, anisotropic distrib. 4-101065  
 sector-dependent sidereal diurnal variation produced from solar anisotropy of cosmic rays 4-101014  
 semi-diurnal anisotropy, rigidity spectrum 4-100984  
 semi-diurnal variation, energy spectrum 4-100995  
 semi-diurnal variation during days of low and high diurnal amplitude wave trains 4-100996  
 semi-diurnal variations of nucleonic components 4-100994  
 sidereal diurnal variation, galactic origin 4-100921  
 sidereal diurnal variation measured underground in London 4-101009  
 sidereal time and solar variation meas. 4-101010  
 sidereal time daily variation meas. 4-101016  
 sidereal variations, interplanetary mag. field direction effects 4-101015  
 sign alternating solar proton anisotropy 4-101067  
 solar activity effects in 19-21 cycles 4-94433  
 solar cosmic ray proton fluxes in last 10<sup>8</sup> years 4-100970  
 solar diurnal anisotropy, 22 year variation in diffusion-convection model 4-94403  
 solar flare proton fluxes, deduced from <sup>26</sup>Al depth profile in lunar rocks 4-100971  
 solar flare proton fluxes, secular variations 4-100972  
 solar mag. field effects 4-94432  
 solar proton, quasistationary injection obs. during small Forbush decreases 4-101068  
 spectral time analysis, cosmic ray intensity and solar activity correlation 4-101064  
 spurious sidereal daily variation due to stationary anisotropy of solar origin 4-63022  
 sunspot number, solar activity relations 4-94426  
 variations in heliosphere from radioactivity meas. of meteorites 4-94369  
 Z=10-26 multiply charged cosmic ray nuclei, 160-759 MeV/n, solar modulation in interplanetary region 4-94412  
 B/C nuclei ratio, spatial and temporal variability 4-94416  
<sup>10</sup>Be abundance in ice cores, cosmic ray intensity variation obs. 4-101099  
 He nuclei, modulation asymmetries over two solar cycles, 1965-81 4-94409  
 He<sup>+</sup> and He<sup>2+</sup> in Earth's outer radiation belts, temporal and spatial variations 4-94324  
<sup>4</sup>He anomalous component in heliosphere in 1972-7 and 1965 solar modulation minima 4-94410  
 O cosmic ray anomalous component, short- and long-term variations, Voyager data 4-94417

# cosmic ray variations

*see also geomagnetism*  
 acceleration by interplanetary shock waves 4-67572  
 anisotropic stage of cosmic ray propagation 4-94372  
 anisotropy, component discrimination using crossed telescopes 4-101006  
 anisotropy distributions associated with interplanetary shocks 4-94387  
 anisotropy of cosmic rays of superhigh energies 4-94515  
 anisotropy variation on solar activity cycle 4-101005  
 annual cosmic ray variations at various atmospheric levels 4-101061  
 anomalies due to solar system being anomalous 4-100968  
 arrival direction and origin of multi-joule cosmic rays 4-94333  
 arrival directions of large EAS in the Southern Hemisphere 4-94532  
 azimuthal heliosphere, two-dimens. steady state cosmic ray transport eqn. 4-94368  
 bidirectional anisotropy, galactic origin 4-100922  
 2CG 195+4, gamma ray flux periodicity and energy spectra, EAS obs. 4-101527  
 CG 195+4, gamma-ray var., obs. of Cherenkov radiation due to air showers 4-101528  
 Chacaltaya, Bolivia, variation meas. 4-94397  
 coherent regime near Sun, cosmic ray modulation 4-94399  
 Cygnus X-3,  $\gamma$ -ray emission, period from EAS data anal. 4-101531  
 Cygnus X-3,  $\gamma$ -ray emission var., small air showers arrival directions obs. 4-101529  
 Cygnus X-3, gamma ray var., Cherenkov radiation due to air showers 4-101528  
 daily variation, harmonics of galactic cosmic rays 4-100991  
 daily variations, average behaviour, recent trends 4-100987  
 daily variations, first three harmonics, day-to-day correlated changes, statistical study 4-100988  
 density gradients, long term variations, solar mag. field induced 4-94425  
 diffusion from local galactic sources 4-94342  
 diurnal and semi-diurnal anisotropy variation 4-100997  
 diurnal and semi-diurnal variations, upper cutoff rigidity determ. 4-100999  
 diurnal anisotropy, 11 and 22 year periodic variation 4-100990  
 diurnal anisotropy, 22 year recurrence tendency during maximum solar activity periods 4-100993  
 diurnal anisotropy, solar polar mag. field polarity effect 4-101004  
 diurnal anisotropy inferred from Elbrus spectrograph data 4-100986

# cosmic ray variations continued

diurnal effect on galactic ray intensity from stratospheric meas. 4-100985  
 diurnal variation, 27-day recurrences 4-94435  
 diurnal variation, long term changes 4-100983  
 diurnal variation, relation to interplanetary mag. field 4-100982  
 diurnal variation Feb.-Mar. 1977, anomalous change 4-100989  
 diurnal variations, harmonics from interplanetary transport processes 4-100981  
 electron energy spectrum from radio loop III 4-94516  
 electron flux variations in geosynchronous orbit 4-100974  
 electrons, 1 GeV, solar modulation 1978-83 4-94408  
 energetic hysteresis of galactic cosmic ray intensity during solar mag. field inversion 4-94406  
 energy changes in solar, wind, diffusion-convection, modulation, eqn. 4-94401  
 equator-pole anisotropy, semi-annual variation 4-94443  
 equatorial anisotropy inside fast solar wind streams 4-101001  
 fluctuations exceeding 2 hours, spectral anal., relation to solar activity 4-94428  
 fluctuations in diffusion approx., low freq. limit 4-67578  
 flux decreases, heliosphere cold plasma effects 4-101069  
 flux intensity variations, solar effects 4-94429  
 Forbush decrease, anisotropic intensity waves 4-94445  
 Forbush decrease, diurnal and semi-diurnal anisotropies 4-94438  
 Forbush decrease, global spectrography method 4-94442  
 Forbush decrease, jet plane obs. 4-94453  
 Forbush decrease, muon anomalous anisotropy 4-94446  
 Forbush decrease, neutron monitoring, correlation with solar activity 4-94457  
 Forbush decrease, pitch angle anisotropy, spectrographic global survey 4-94458  
 Forbush decrease, rigidity dependence 4-94454  
 Forbush decrease July 13/14 1983, intensity periodicities 4-100973  
 Forbush decrease of galactic cosmic ray intensity 4-67566  
 Forbush decreases, effect on atmospheric elec. field and air-Earth current 4-89970  
 Forbush decreases, energy dependence 4-94455  
 Forbush decreases, energy dist. 4-94444  
 Forbush decreases, solar flare induced, depend. on shock wave geometry 4-85850  
 Forbush decreases, time profile differences by neutron monitors and ion chambers 4-94452  
 Forbush decreases in heliosphere, full trajectory integration, comparison with obs. 4-94431  
 galactic, intensity solar modulation from anal. of tree rings <sup>14</sup>C dating 4-94423  
 galactic anomalous low-energy component, origin 4-94361  
 galactic cosmic ray anisotropies during solar cycle 20 4-94437  
 galactic cosmic ray density distribution in heliosphere, quasistationary asymmetry 4-67573  
 galactic cosmic ray gradient and modulation effects obs. by Voyager and Pioneer spacecraft 4-94415  
 galactic cosmic ray intensity variation, effect of equatorial coronal holes 4-94450  
 galactic cosmic ray modulation by solar activity processes, shock wave steady-state model 4-94413  
 galactic cosmic ray modulation by solar wind, subsonic streaming transition in nonlinear model 4-94404  
 galactic cosmic ray radial gradients, Pioneer 10 meas. at 1 to 29 AU through solar maximum 4-94418  
 galactic cosmic ray variations in heliosphere from radioactivity meas. of meteorites 4-94369  
 galactic cosmic rays; Forbush decreases, technique to study anisotropy 4-94439  
 galactic cosmic rays, Forbush decreases, variations in IMF and solar wind velocity 4-94456  
 galactic cosmic rays, intensity depression, effect of solar wind disturbances 4-94451  
 galactic cosmic rays, long-term intensity vars. rel. to different indices of solar activity 4-101398  
 galactic cosmic rays, modulation by solar wind in spherically symmetric nonstationary diffusive model 4-94402  
 galactic cosmic rays, power spectra variations, correlation with Sun's activity 4-94436  
 galactic cosmic rays, weak modulation a few million years ago 4-100916  
 galactic cosmic rays solar modulation var. and terrestrial atm. <sup>14</sup>C prod. 4-94424  
 galactic e.p. and He spectra 1965-79 as modulation theory tests 4-94407  
 galactic intensity variations, relation to solar mag. field 4-94370  
 galactic rays, heliogeomagnetic asymmetry of solar activity and cosmic ray distribution 4-101003  
 galactic rays, sidereal daily variation, seasonal variation due to heliomagnetosphere 4-101008  
 galactic rays anisotropy in high velocity solar wind fluxes 4-100976  
 gamma ray burst sources observed by Hinotori satellite, energy spectra, time history and origin 4-101513  
 gamma ray sources, excess fluxes search, EAS data anal. 4-101533  
 gamma-ray bursts, high time resolution  $\gamma$ -ray spectral obs. with Solar Maximum Mission 4-101514  
 gamma-ray intensity rel. to interstellar column density of H and <sup>12</sup>CO 4-110409  
 gamma-ray sources at E=10<sup>15</sup> eV, search, EAS data anal. 4-101534  
 global modulation in interplanetary space 4-94430  
 heliosphere; galactic cosmic ray prop., electric field effects, modulation 4-94400  
 heliosphere, long term cosmic ray modulation, 1-25 AU, Pioneer, Voyager, ISEE-3 and Helios data 4-94421  
 inner heliosphere, galactic cosmic ray modulation by solar flare disturbances 4-94419  
 intensity anisotropy for E>10<sup>17</sup> eV rays 4-94398  
 intensity increases during geomagnetic storms 4-94448  
 intensity time depend. from tree-ring data 4-100967  
 intensity transient decreases, solar wind stream interfaces 4-94449  
 intensity variations in magnetosphere 4-94326  
 interplanetary magnetic field effects 4-100980  
 interplanetary magnetic field sector structure and second harmonic of cosmic ray intensity 4-100998  
 interplanetary propagation, review of theory 4-78072  
 interplanetary space, nonstationary modulation for constant radial gradient 4-94405

## cosmic ray variations continued

- ionospheric F-region, corpuscular ionisation, latitudinal depend. during Forbush decrease 4-101051  
irradiation parameters of accelerated particles during solar system evolution 4-100969  
isotope production in meteorites and cosmic ray variation 4-101104  
Jovian electron events, interplanetary transport, modulation in Earth's orbit 4-94434  
kinetics in anisotropic mag. field 4-94374  
long term variations, Earth's mag. field effects 4-101030  
low frequency fluctuations of the cosmic ray intensity 4-100979  
lower atmosphere asymmetry, time variations 4-101032  
lunar-diurnal variation of high-energy cosmic rays 4-101000  
measurement stations for cosmic ray variation studies, necessary geographic distrib. 4-110539  
meteorites, induced thermoluminescence 4-101103  
methodical principles in studying cosmic ray variations 4-101060  
modulation, solar mag. field effects 4-94432  
modulation coefficient during 1954, 1965 and 1976 minima in solar activity 4-94427  
modulation during 1970-4, anomalous phenomena due to coronal holes 4-94422  
multiplicity response function of the double neutron monitor at Turku 4-101058  
muon north-south anisotropy, high rigidities, 27-day recurrence 4-94459  
neutron anisotropies, 3-D anal. method during solar rotation period 4-94440  
neutron intensity observations by Pb-less counters 4-101047  
neutron modulation, shock related diffusion-acceleration models 4-94392  
neutron monitor data, Seoul and Tokyo, critical comparisons 4-101048  
neutron monitors on board r/v Akademian Aleksander Nesmeyanov 4-101049  
north-south anisotropy, Earth latitudinal ang. distance from heliospheric current sheet effect 4-101002  
nucleon energy distribution, Ottawa large zenith angle muon telescope array 4-101057  
outer heliosphere, cosmic ray gradients from Pioneer data 4-94414  
pitch angle distributions and energy spectral for solar particle effects 4-100951  
power spectra of cosmic ray variations in the region of  $3 \times 10^{-8} - 10^{-4}$  Hz 4-67579  
power spectral variations, ambient power 4-100992  
preferred solar longitude zones in affecting solar activity and geophysical parameters 4-101053  
primary cosmic rays, zonal modulation rel. to solar mag. field 4-94396  
proton modulation asymmetries over two solar cycles, 1965-81 4-94409  
protons, acceleration mechanisms, associated interplanetary shocks 4-94386  
protons, penetration of solar particles into magnetosphere 4-100975  
PSR 0531+21, gamma ray emission, possible sporadicity, Cherenkov radiation anal. 4-101392  
PSR 0531+31 and 1937+214 (millisecond pulsar),  $\gamma$ -ray emission, Cherenkov radiation obs. 4-101394  
PSR 0532=31,  $\gamma$ -ray periodicity, EAS data anal. 4-101534  
PSR 0833-45, possible transient  $\gamma$ -ray emission obs. 4-101395  
PSR 0833-45 and 0950+08,  $\gamma$ -ray emission, Cherenkov radiation anal. 4-101396  
radionuclide size dependence determ. in marine sediments 4-101101  
relativistic interplanetary particle anisotropy, 50 day periodicity, Pioneer data 4-94420  
relativistic solar cosmic ray flux, anisotropic distrib. 4-101065  
rigidity spectrum, spatial anisotropy May 7, 1978 ground level event meas. 4-101066  
sector-dependent sidereal diurnal variation produced from solar anisotropy of cosmic rays 4-101014  
secular variations, implications of  $^{10}\text{Be}$  measurements in deep-sea sediments 4-110128  
semi-diurnal anisotropy, rigidity spectrum 4-100984  
semi-diurnal variation, energy spectrum 4-100995  
semi-diurnal variation during days of low and high diurnal amplitude wave trains 4-100996  
semi-diurnal variations of nucleonic components 4-100994  
shock acceleration events, association with interplanetary proton events 4-105864  
sidereal daily variation, statistical scatt. effect 4-101013  
sidereal diurnal variation, galactic origin 4-100921  
sidereal diurnal variation measured underground in London 4-101009  
sidereal time and solar variation meas. 4-101010  
sidereal time daily variation meas. 4-101016  
sidereal variation, Tasmanian meas. 4-101012  
sidereal variations, interplanetary mag. field direction effects 4-101015  
sidereal variations, interplanetary mag. field effect 4-101011  
sign alternating solar proton anisotropy 4-101067  
small scale anisotropies in cosmic rays near  $10^{16}$  eV 4-94531  
soft muon intensity variations, geophysical effects 4-110405  
solar activity effects in 19-21 cycles 4-94433  
solar activity relations 4-94426  
solar cosmic ray flare event, features 4-105948  
solar diurnal anisotropy, 22 year variation in diffusion-convection model 4-94403  
solar flare effects on 1975-9 decreases 4-100978  
solar flare proton events, correlation with coronal mass ejections 4-105942  
solar flare protons, spectral and temporal characs. rel. to coronal mag. field struct. 4-110396  
solar modulation of cosmic ray electrons (1978 to 1983) 4-85851  
solar neutrino flux, quasi-biennial variation 4-110394  
solar proton, quasistationary injection obs. during small Forbush decreases 4-101068  
solar proton events of 1977 November 22 and 1978 May 7, comparison 4-72839  
solar ray variations by Meteor satellite obs. 4-67574  
solar system integral radial cosmic ray gradients (1972 to 1982) 4-85848  
solar wind velocity correlations 4-100977  
spectrography method, variation parameter determ. 4-94441  
spurious sidereal daily variation due to stationary anisotropy of solar origin 4-63022  
stratospheric soundings, 240 day variation dynamics 4-101062  
sudden storm commencement and Forbush decreases, correlation to solar wind and IMF 4-94447  
super neutron monitors for cosmic ray intensity distrib. meas. 4-101007

## cosmic ray variations continued

- time- and space-averaged cosmic ray flux experienced by meteorites 4-101102  
Z=10-26 multiply charged cosmic ray nuclei, 160-759 MeV/n, solar modulation in interplanetary region 4-94412  
zenith angle distribution of the cosmic ray muon component 4-67585  
zonal modulation, north-south asymmetry, energy selectivity 4-101052  
B/C nuclei ratio, spatial and temporal variability 4-94416  
 $^{10}\text{Be}$  abundance in ice cores, cosmic ray intensity variation obs. 4-101099  
 $^{10}\text{Be}$ , conc. in deep sea sediments, intensity variation meas. 4-101100  
Fe group nuclei track density and lengths in meteorites 4-101106  
He cosmic ray anomalous component, short- and long-term variations, Voyager data 4-94417  
He nuclei, modulation asymmetries over two solar cycles, 1965-81 4-94409  
 $\text{He}^+$  and  $\text{He}^{2+}$  in Earth's outer radiation belts, temporal and spatial variations 4-94324  
 $^4\text{He}$  anomalous component in heliosphere in 1972-7 and 1965 solar modulation minima 4-94410  
 $^{81}\text{Kr}$  production rate in the atmosphere 4-101105  
O cosmic ray anomalous component, short- and long-term variations, Voyager data 4-94417  
**cosmic ray X-rays**  
background radiation from intergalactic matter, zero-point field effect in quantum theory 4-63044  
gamma-ray bursts, assoc. X-ray emission, neutron star model 4-101517  
production from electron acceleration conditions in solar flares 4-100953  
soft X-ray precursors of solar flares 4-100945  
X-ray background, contrib. of hot intergalactic medium 4-63266  
**cosmic rays**  
*see also cosmic ray apparatus; cosmic ray composition; cosmic ray effects and interactions; cosmic ray energy spectra; cosmic ray origin; cosmic ray propagation; cosmic ray showers and bursts; cosmic ray solar modulation; cosmic ray variations; galactic cosmic rays; geophysical aspects of cosmic rays; high-energy cosmic ray interactions; primary cosmic rays; solar cosmic ray particles*  
18th International Cosmic Ray Conference at Bangalore, India (August-September 1983) 4-95059  
baryon decay, magnetic monopole catalysed, Rubakov interaction 4-95734  
Cherenkov radiation from cosmic ray showers 4-101081  
conference at Eric, Sicily (June 1982) 4-90298  
indoor exposure rate, NaI(Tl) scintillation counter, building material perturbation 4-109936  
indoor exposure rates to gamma and cosmic rays, Ge spectrometer and ionisation chamber obs. 4-93893  
magnetic monopole cosmic ray detection, hybrid detector 4-95730  
magnetic monopole detection using proportional counters 4-95732  
magnetic monopole flux determ. from baryon decay expt. 4-95735  
magnetic monopoles, detection with plastic scintillators 4-95729  
magnetic monopoles, flux limitation in cosmic rays at large zenith angles 4-95731  
magnetic monopoles, plastic track detector 4-95733  
magnetic monopoles, slowly moving, velocities, ionisation threshold for detection 4-95728  
quantum theory of EM interactions in intergalactic space, effect of zero-point field 4-63044  
radiation doses and biological effects of cosmic rays 4-100261  
spaceflights, dosimetric radiation meas., absorbed dose, dose rates 4-68834  
superheavy mag. monopoles, search at underground telescope 4-95727  
 $\text{D}^0$  semileptonic decays, lifetimes 4-95790  
**cosmic X-rays** *see cosmic ray X-rays*  
**cosmogony** *see cosmology*  
**cosmology**  
*see also black holes; element origin; general relativity; red shift*  
(2+1) space-time vacuum field solutions in general relativity 4-67825  
 $\lambda\phi^4$  theory in curved spacetime and varying background fields, effective Lagrangian, quasiloocal approx. 4-111302  
 $\lambda\phi^4$  theory in Robertson-Walker space-times, symmetry behaviour at finite temp. 4-63372  
Abell 2197+Abell 2199 supercluster, red shift anal. 4-77954  
Abell cluster cD galaxies and 3C radiogalaxies, brightness implications for cosmology 4-94964  
active galactic nuclei, evolution 4-106062  
antibang, accel. and dissolution of stars 4-78014  
asymptotically flat space-times, black holes, Hawking generalisation, strong cosmic censorship 4-63611  
axion and mag. monopole theories 4-59010  
axion cosmology 4-90274  
baryon generation at low temps.,  $\text{SU}(3) \times \text{SU}(2) \times \text{U}(1)$  calcs., 1 TeV physics 4-90264  
baryon number origin and related problems 4-72875  
baryon symmetric cosmology, nature depend. on CP violation type, obs. tests 4-78012  
baryon symmetric cosmology testing on a supergalactic scale 4-100920  
Bianchi class A models, quantisation formalism 4-67826  
Bianchi type II, VIII and IX models, exact Brans-Dicke stiff matter solns. 4-67614  
Bianchi type II, VIII and IX space-times, viscous and nonviscous fluids 4-67824  
Bianchi type IX EM cosmology, diagonal, Hamiltonian formalism 4-90278  
Bianchi type V cosmological model with tilt, He form., D abundances 4-90265  
Bianchi type-I models, solution to Einstein's eqns. 4-90447  
Bianchi type-I universe, Coleman-Weinberg symmetry breaking in an anisotropic spacetime 4-90270  
Bianchi type- $\text{VI}_h$  cosmologies, isotropic singularities and isotropization 4-101732  
Bianchi-Brans-Dicke-Maxwell field eqns., mag. radiation solns. 4-72862  
big bang, element yields, nucl. uncertainties 4-94999  
Big Bang, hot or cold, evidence from microwave background 4-78001  
Big Bang nucleosynthesis, implications of chemical evolution of light elements 4-67843  
big bang supersymmetric relics, neutral gauge/Higgs fermion mass 4-77988  
black hole theory from weak cosmic censorship 4-82501  
black holes, formation at various epochs in Universe 4-106021  
black holes, small, ionisation tracks and range 4-82631

## cosmology continued

- black holes 4-115775
- black holes and warped spacetime, book 4-58601
- blue galaxies, large scale distrib., red shift anal. (*Russian*) 4-67830
- book on nucleus comp., elementary particles and fields 4-82617
- Bootes void survey, 231 galaxies red shift obs. 4-77936
- Bose-Einstein condensate due to light bosons and heavy photons 4-86099
- Brans-Dicke Bianchi type-I vacuum exact solns. with cosmological const. 4-82568
- Brans-Dicke cosmologies exact solns. with cosmological const. 4-82566
- Brans-Dicke solutions with cosmological constant in 'Bianchi type-I space-time 4-77996
- Brans-Dicke-Bianchi type II models, exact solns. 4-78217
- Brans-Dicke-Bianchi type-I soln. 4-82565
- bubble boundaries, eqn. of motion from embedding four geometries 4-73115
- bubble nucleation and the Coleman-Weinberg model 4-67818
- Cauchy horizons, compact 4-77992
- chaotic inflation scenario in  $N=1$  supergravity 4-68111
- classical tests and galaxy evolution 4-73121
- closed Universe, physical space topology, breakdown of connectedness 4-73322
- Coleman-Weinberg GUT model, phase transitions and fluctuation in inflationary universe 4-115838
- conference, gravity, gauge theories, supergravity, Caracas, Venezuela (Dec. 1982) 4-86117
- conference, particles and fields, Blacksburg, VA, USA (Sept. 1983) 4-73135
- conference on grand unification, Philadelphia, PA, USA, (April 1983) 4-58573
- conference on higher energy physics, Austin, TX, USA (Nov. 1982) 4-67857
- conference on particles and fields, Banff, Canada (Aug. 1981) 4-63404
- conference on quark matter in rel. nucleus-nucleus collisions, Long Island, NY, USA (Sept. 1983) 4-67855
- conference on the very early Universe, Cambridge, England, (June-July 1982) 4-58571
- conference on Universe early evolution and present struct., at Kolymbari, Crete (August-September 1982) 4-73160
- conference on Universe struct. and galaxies form. and evolution at La Plagne, France (March 1983) 4-63401
- cosmic baldness, relaxation to de Sitter space, early Universe appl. 4-63365
- cosmic censorship, future asymptotic predictability, absence of naked singularities 4-67823
- cosmic horizons, book 4-63432
- cosmic string network from GUT phase transition for expanding universe, stretching 4-73113
- cosmic strings, phase transition in early Universe 4-63360
- cosmological constant as a canonical variable in grav. field coupled to gauge field 4-110973
- coupled scalar field on Robertson-Walker background, Riemannian approach and cosmological singularity 4-68097
- dark matter, evidence for non-baryonic nature 4-67795
- dark matter, galaxies, superclusters and voids, review 4-63379
- dark matter consisting of collisionless particles and pancake mass 4-101553
- dark matter in Universe, role in galaxy form. 4-67838
- de Sitter space instability, quantum gravity, Euclidean formulation 4-63050
- deceleration of nearby galaxies 4-73080
- deceleration parameter, determ. via correl. procedure for identification of cosmological mol. clouds 4-67790
- density perturbations, evolution through cosmological phase transitions, gauge invariant formalism 4-95010
- determination of cosmological parameters 4-73120
- dileptonic system, mass bounds from cosmology, cosmic mass density 4-67625
- Dirac cosmology, gravitational theory in atomic scale units 4-73106
- Dirac cosmology, var. of fund. interactions coupling const. 4-82567
- Dirac equation of free particles in Friedmann space-time, spinor null tetrad formalism (*Chinese*) 4-86095
- disc galaxies formation, neutrino accretion effects 4-67840
- dust-radiation Universe, Friedmann eqns. with  $\Lambda$ -term, exact solns. 4-63350
- early big-bang Universe, quark-hadron and chiral transitions, review 4-73107
- early cosmos, bifurcation in autonomous nonlinear differential eqns. 4-95003
- early Universe, diffuse material and background radiation 4-73128
- early Universe, effective pot. in de Sitter space 4-63370
- early Universe, generation of primordial perturbations 4-63369
- early Universe, GUT quark-hadron phase transition, fluctuations 4-67832
- early Universe, importance of quantum gravity 4-63356
- early Universe, inhomogeneities evolution and superheavy particles in cosmology 4-63376
- early Universe, locally supersymmetric model, primordial inflation and supercosmology 4-67831
- early Universe, mag. monopoles and bubbles, phase transitions, review 4-67846
- early Universe, particle production evidence 4-73125
- early Universe, SU(5) GUT model, CP domain wall problem, matter-antimatter domains soln. 4-115842
- early Universe rel. to near IR background obs. (*Japanese*) 4-115837
- Einstein's equations with cosmological constant, higher dimensional vacuum solns. 4-90451
- Einstein's field equations, static, spherically symmetric solutions, massless scalar field 4-95275
- Einstein eqns., inhomogeneous solutions, de Sitter 'space-time generalisation 4-90450
- Einstein eqns. solns. taking into account vacuum effects of quantised field 4-73312
- Einstein universe, closed cosmology with massive mag. field 4-77997
- Einstein-Maxwell eqns., EM fields invariant to duality rot. under isometry group 4-86286
- Einstein-Maxwell eqns., exact solns. 4-67815
- Einstein-Weyl field equations in a Bianchi type-IX space-time 4-90454
- electrified viscous fluid, class one cosmological model 4-115841
- element origin, D and  $^3\text{Li}$  from Population III remnants 4-67842
- element origin, possible synthesis of D and  $^3\text{Li}$  by pregalactic massive stars 4-67841

## cosmology continued

- elliptical galaxies, form. and evolution (*Japanese*) 4-63275
- entropy in physical processes and cosmological advances 4-82622
- eternal Universe from generalised soln. of Maxwell-Einstein eqns. 4-101549
- event horizons, nonequilibrium thermodynamics 4-90273
- evolution of the Universe 4-67820
- ex nihilo creation 4-73109
- exact Brans-Dicke-Bianchi type-V solutions 4-86098
- expanding or collapsing Universe, early stages 4-110793
- expanding Universe, order and entropy increases 4-77991
- faint galaxies, colour distrib. and evolution 4-77932
- faint galaxies distrib., Monte Carlo simulation 4-78010
- field equations of massless particles with arbitrary spin in spinor null tetrad formalism (*Chinese*) 4-82569
- filaments in galaxy counts, reality anal. 4-78005
- finite rotating universe, null geodesics, caustics and galaxies' apparent motion 4-67822
- fourth-order gravity as general relativity plus matter, cosmology, black holes 4-110974
- Friedmann cosmology and hadron properties, unified approach 4-82575
- Friedmann space-time, scalar conformally noninvariant particles, quantum effects 4-82582
- Friedmann universe, closed, with scalar field as source 4-101543
- Friedmann universes and cosmological const. 4-67833
- Friedmann-Robertson-Walker space-times in Brans-Dicke theory, exact perfect fluid solns. 4-67611
- G-variable cosmologies, galaxy form. in Hoyle-Narlikar and 'Brans-Dicke theories 4-101547
- galaxies, field, ( $B \leq 22.5$ ), red shift survey and evolution 4-77934
- galaxies, large-scale distrib. of rich clusters and superclusters 4-73086
- galaxies, secular dynamical evolution over Hubble time 4-67800
- galaxies and clusters form., origin of present-day unseen matter as sub-stellar bodies 4-77942
- galaxies and globular clusters formation 4-67839
- galaxies dissipationless collapse and initial conditions 4-110731
- galaxies form. and interactions during cluster violent relax. 4-90247
- galaxies formation, role of missing matter (*Japanese*) 4-110790
- galaxies luminosity function and cosmological tests  $N(z)$  and  $N(m)$  4-82564
- galaxies N-point correlation function 4-94973
- galaxy clustering, numerical expts. for different Universe expansion histories 4-78011
- galaxy clusters, compact groups dominated by dark matter, N-body simulation 4-86070
- galaxy clusters evolution, evidence from subclustering anal. 4-77947
- galaxy correlation hierarchy in perturbation theory 4-86033
- galaxy form. via adiabatic fluctuations and pancake collapse, microwave background problem 4-78004
- galaxy formation, role of dark matter 4-90262
- galaxy formation, role of muon neutrino mass 4-115826
- galaxy formation, role of pregalactic activity and hidden mass 4-67797
- galaxy formation, topologically stable strings, grand unification phase transition 4-95264
- galaxy formation and low-mass collisionless particles in expanding Universe 4-67622
- galaxy formation and strings evolution within GUT 4-78017
- galaxy formation in matter and radiation dominated universes 4-73082
- galaxy formation in neutrino dominated universes, adiabatic theory 4-78006
- galaxy formation seeded by cosmic string 4-115840
- galaxy mass distrib. from gravitational light deflection and open Universe 4-115820
- galaxy pair correlation, exact closed eqn. 4-63324
- galaxy superclusters, total linear density rel. to gravit. imaging effects 4-86069
- general relativity, spherically symmetric perfect fluid distrib. 4-73308
- generalized Klein-Gordon equation and the Mach principle 4-82731
- global time in the general theory of relativity 4-95257
- globular star clusters form., role of dark matter 4-90262
- Godel cosmological model, nonstationary generalisation, Einstein eqn. soln. 4-82572
- Gowdy  $T^3$  cosmology, stress-energy tensor, combined system symm. bounce 4-101546
- grand unified symmetry breakdown and creation of Universe 4-73129
- gravitation (book) 4-63417
- gravitational constant, energy depend. at high energy and unified field theory 4-82406
- gravitational instability in the presence of a magnetic field in the expanding universe 4-90275
- gravitino and photino masses in supersymmetric cosmology, galaxy form. 4-67845
- gravitino regeneration and decay, supersymm. standard model, cosmological nucleosynthesis 4-110975
- GUT, cosmological constraints 4-59009
- GUT scale influence on early Universe thermal history 4-59008
- GUTs in curved space-time, renormalisation group anal., coupling constants 4-68091
- heterogeneous model, macroscopic gravitational eqn. soln. (*Russian*) 4-101558
- hierarchical structure of Metagalaxy, review of problems 4-63327
- Higgs field at finite temp., time development 4-78513
- Higgs scalar field, gravitational collapse 4-115683
- higher dimensional cosmologies search in 6D Einstein-Maxwell theory and 11D supergravity 4-115847
- homogeneous models, background radiation ang. distrib. 4-90093
- hot Universe, monopole-proton bound state formation, effects on monopole detection 4-115843
- Hubble const. value from obs. of Sc I galaxies 4-90220
- Hubble parameter, implications of low dust content of Virgo cluster spiral galaxies 4-101464
- Hubble parameter upper limit from QSO 0957+561 gravitational lens obs. 4-77960
- inflation model based on quantum gravity 4-110792
- inflation scenario circa 1983 4-63378
- inflationary cosmology, cosmological constant smallness, principle of naturalness 4-73108
- inflationary cosmology, mass hierarchy in locally supersymmetric theories 4-106086
- inflationary model with correct density fluctuations and CP problem soln., SU(5) field 4-73110

## cosmology continued

- inflationary universe, bubbles in de Sitter space 4-63347
- inflationary Universe, conditions for effective scalar potential 4-82579
- inflationary universe, density fluctuations from quantum effects 4-73689
- inflationary Universe, Euclidean approach, quantum state 4-63367
- inflationary Universe, GUTs, supersymmetry and galactic astronomy 4-90268
- inflationary universe, Higgs field evolution, SU(5) Coleman-Weinberg model 4-115845
- inflationary Universe, Minkowski space candidate for primeval config. 4-82571
- inflationary Universe, origin of density fluctuation 4-63368
- inflationary Universe, primordial sound waves and galaxy formation 4-78015
- inflationary Universe, quantum creation in elementary particle theories 4-77990
- inflationary Universe 4-86100
- inflationary Universe model, quantum fluctuations and phase transitions 4-63371
- inflationary universe models, cosmological perturbations 4-82580
- inflationary universe scenario, SU(5) GUT, Higgs field dynamical evol. 4-101554
- inflationary Universe scenario 4-106088
- inflationary universe scenario from class of GUTs, broken symmetry minima 4-90271
- inflationary Universe scenario in supersymmetric models without unnatural fine-tuning 4-63363
- inhomogeneous cosmological model in gen. rel., perfect solution 4-115839
- inner space-outer space connection, review 4-77986
- interacting quantum field theory in curved space-time, renorm., symmetry breaking, book contrib. 4-63619
- intergalactic clouds evolution with red shift, QSO absorpt. lines anal. 4-77964
- intergalactic medium density, implications of sharp X-ray absorpt. in BL Lacertae object (PKS 2155-304) 4-86056
- intergalactic medium density, probing via X-ray emission from clusters of galaxies 4-63266
- intermediate vector bosons and neutrino cosmology 4-68485
- invisible axions, domain walls, energy crisis and galaxy form. 4-59018
- isotropic homogeneous universe, scale factor 4-95000
- isotropy of Universe, spatially homogeneous anisotropic minisuperspace model 4-102039
- Jordan-Thiry theory, nonsymmetric, nonabelian, gravitation and Yang-Mills unification 4-68094
- Kaluza-Klein cosmologies, entropy from extra compact dimensions 4-90269
- Kaluza-Klein cosmologies and inflation 4-115846
- Kaluza-Klein cosmologies at late times, equilibrium solution 4-101730
- Kaluza-Klein cosmology, dimensional reduction 4-58705
- Kaluza-Klein theories, quantum effective action, cosmological evolution, curved spacetime 4-90465
- Kerr metric in de Sitter space-time 4-68072
- left hand of creation, book 4-77998
- Local Supercluster, galaxy form characts. and ang. momentum effects 4-110756
- LM, globular cluster, age from deep CCD photometry of main sequence stars 4-63215
- Mach-Einstein-universes, equilibr. statistical mech. 4-67816
- magnetic monopoles, evolution in expanding universe 4-101559
- mass density of Universe rel. to binary pairs of dwarf irregular galaxies 4-90243
- mass scales and cosmological coincidences 4-101545
- masses of galaxies and clusters of galaxies 4-73081
- massive neutrinos and photinos in cosmology and galactic astronomy 4-63375
- massive neutrinos and Universe mass density 4-67836
- massless scalar particles, gravitational creation by vacuum bubble 4-73111
- matter filled de Sitter Universe, small metric perturbations 4-63364
- matter-antimatter asymmetry in Universe 4-105873
- microphysical cosmology, foundations and working pictures, galaxies and microwave background 4-73117
- microphysical cosmology, foundations and working pictures 4-63354
- microwave background, cooling of brightness of temp. in direction of clusters of galaxies 4-73104
- microwave background, sky-temp. fluctuations from VLA survey of  $\alpha=08^{\circ} 52^m 15^s$ ,  $\delta=+17^{\circ} 16'$  field 4-101192
- microwave background at 3K, anisotropy and perturbations of Friedmann cosmology 4-94997
- microwave background spatial fluctuations, galaxy cluster gravit. screen model 4-63344
- microwave background temperature at epochs  $z \geq 2$ , determ. from quasars C1 spectra 4-63343
- mirror particles effect 4-63046
- models rel. to obs. 4-73119
- Moller's tetrad theory of gravity and Universe open or closed state-4-86097
- monopole dominated universe, galaxy formation, clusters, perturbation growth 4-115844
- monopole-antimonopole bound state, lifetime in early universe 4-95726
- multiply connected Universe, evidence from periodicity in quasars redshift distrib. (Chinese) 4-82558
- N=1 supergravity models, cosmological baryon prod., matter stability, gravitino decay 4-111002
- N-body simulations 4-73123
- neighbouring superclusters, struct. determ. methods 4-77950
- neutrino degeneracy and nucleosynthesis 4-72873
- neutrino flavors, cosmological constraints, relation to  $Z^0$  width 4-95009
- neutrino halos formation, role of cosmological const. 4-67817
- neutrino mass upper limit astrophysical consequences 4-72874
- neutrino role in cosmology 4-77999
- neutrino-dominated Universe, cluster size 4-95005
- neutrino-dominated Universe, consistency with standard big-bang cosmology 4-106085
- neutrinos, massive, cosmological bounds 4-95008
- new inflationary Universe scenario, bubbles, phase transitions and GUTs 4-63362
- non-Abelian gauge theories in curved space-time, renormalisation 4-58932
- nonequilibrium universe of stars and radiation, Robertson-Walker metric appl. 4-101551

## cosmology continued

- noninflationary cosmological models, mag. monopole suppression 4-63374
- nonlinear gravitational clustering 4-94975
- nonlinear photons, anisotropic case 4-86279
- nucleosynthesis in primordial Universe 4-63293
- O(5) gravitational gauge fields, cosmological constant, quantum theory 4-68098
- open model Universe, background radiation anisotropy and large scale perturbations 4-101540
- oscillating universe, dust-like model, one-loop approximation 4-94998
- pancake model with massive neutrinos, microwave background distortions 4-67835
- pancake theory of galaxy form., role of massive neutrinos 4-110791
- particle in early Universe 4-72877
- particle physics in cosmology, inflationary Universe and baryon asymmetry 4-77705
- perpetually bouncing universes, fractal set 4-90266
- Perseus supercluster, filamentary structures, red shift survey 4-77951
- perturbations and primeval black hole formation 4-73124
- perturbed expanding Universes, relativistic dynamics 4-77883
- phase transitions, from spontaneously broken global symmetries and cosmology 4-73116
- photon-dominated Universe, cosmic-ray antiprotons 4-105818
- physical cosmology, Les Houches Session XXXII, France (July 1979) 4-67874
- planar numerical cosmology, difference eqns. and numerical tests 4-95001
- Planckian seconds of the universe (German) 4-86093
- plane-symmetric Einstein-Dirac cosmology containing classical spinor field, exact nonghost soln. 4-90267
- Population II stars, form. via thermal instability 4-67717
- Population III, dust and distortions in microwave background 4-77880
- Population III massive stars, evolution and nucleosynthesis 4-63090
- Population III stars, cosmological consequences 4-90191
- power asymptote singularities, orthogonal spatially homogeneous cosmologies, Einstein field eqns. 4-101711
- pregalactic chemical abundances, determ. from element abundances in interstellar medium 4-101459
- primeval plasma recombination, supersymm. light-inos, universe expansion rate 4-110794
- primordial black holes and cosmological vacuum phase transition 4-78016
- primordial Coleman-Weinberg inflation, energy density fluctuations 4-90459
- primordial cosmological inflation versus local supersymmetry breaking in SUSY GUTs coupled to N=1 supergravity 4-73324
- primordial density variations rel. to voids and galaxy clusters form. 4-78003
- primordial helium abundance and grand unification schemes 4-110796
- primordial inflation, fluctuations in cosmological models 4-90460
- primordial inflation, rapid phase transitions with flat supergravity potentials 4-101731
- primordial nucleosynthesis 4-63255
- primordial perturbations of Universe, spectral anal. of RATAN-600 obs. 4-63346
- primordial SU(5) SUSY GUT plasma, strongly coupled nature, inflationary scenarios 4-73112
- primordial Universe density fluctuations and microwave background distortion 4-77880
- protogalactic eddies, structure 4-63290
- protogalaxies ang. momentum and elliptical galaxies rot. origin 4-101481
- QCD, first-order phase transition, concentration of quark matter 4-90803
- QSOs, cosmological evolution of sharp metal-rich absorpt. lines 4-73096
- QSOs, luminosities at 1 mm and in X-rays, depend. on red shift 4-77962
- quantum black hole mining in de Sitter space, second law of thermodynamics, evaporation 4-115773
- quantum conformal cosmology, vanishing likelihood of a space-time singularity 4-82570
- quantum creation of universes, cosmological wave function, minisuperspace model 4-101555
- quantum fluctuations in the early Universe 4-90277
- quantum mechanics pilot wave interpretation rel. to cosmology 4-95006
- quantum theory of gravity, book 4-63428
- composite quark and lepton, cosmological constraint on radius upper bound 4-63984
- quark-hadron phase transition in Bianchi type-I cosmologies 4-63353
- quasar population evolution, research at Royal Observatory, Edinburgh 4-106079
- quasar red shifts, interpretation 4-106081
- quasar redshifts, implications of  $V/V_m$  test for bright QSOs 4-101494
- quasar redshifts, neutrino objects-lack of effect, cosmological significance 4-73097
- quasars, evolution and colour distrib. 4-77932
- quasars, evolution and red shift cut-off 4-78000
- quasars, Hubble diagrams for flat and steep spectrum radio sources from optical monitoring 4-110763
- quasars, red shift survey and evolution 4-77934
- quasars, surveys and evolution 4-77961
- quasars clustering, anal. for quasars with known redshifts 4-101495
- quasars distribution inhomogeneity 4-101497
- quasars luminosity evolution 4-101498
- quasars properties, effects of obscuration of cosmologically distant objects by dust 4-86025
- quasars radio luminosity function, depend. on cosmological evolution 4-106078
- radiation era, spatial density fluctuations 4-82563
- radiative breaking of cosmologically acceptable GUT through supergravity terms 4-111354
- radio source population, luminosity and space density evolution anal. from 1-Jy sample 4-110762
- radiogalaxy population, evolution from deep radio-optical surveys 4-77929
- distant radiosource alignment, survey of 300 sources 4-73079
- radiosources, extragalactic, evolution and red shift cut-off 4-78000
- radiosources, red shift survey and evolution 4-77934
- radiosources evolution model 4-77959
- red shifts not assoc. with Universe expansion, evidence 4-77928
- Reissner-Nordstrom metric modification in Einstein-De Sitter cosmology (Spanish) 4-73118
- relativistic cosmology, Dirac quantisation 4-67821
- relativistic cosmology, metrics for spherically symmetric solns. 4-101550

## cosmology continued

- relativistic cosmology (book) 4-82609
- relaxation of the cosmological constant 4-63348
- remote superclusters, dynamics and red shift survey, cosmological implications 4-77953
- Riemann tensor, peeling-off property of gravity 4-95007
- Robertson-Walker geometry, quantum mechanics 4-77993
- Robertson-Walker geometry coupled to fermionic matter, quantisation 4-86302
- Robertson-Walker universe, causal cosmological perturbations, Sachs-Wolfe effect in microwave background 4-73114
- Robertson-Walker universe, three equiv. definitions for spin-1 massive particles 4-82576
- rotating homogeneous universe with an electromagnetic field 4-82573
- scalar-tensor theory 4-77989
- Schwarzschild mass, imbedding into cosmological perfect fluid, geodesic fluid appl. 4-90272
- Segal's mechanism for the red shift and its physical bases 4-90086
- self-cancellation of cosmological terms 4-63377
- self-similar gravitational clustering 4-78009
- self-similar gravitational collapse in an expanding Universe 4-110788
- self-similar spherical voids in an expanding Universe 4-110789
- self-similarity principle, definition and evidence 4-82574
- shocked pancakes and dark matter 4-67834
- singularity avoided oscillating bouncing cosmological model 4-63351
- size of Universe, theory 4-101544
- SL(N,C) gauge interactions, linear descrpt., cosmological implications, hadrons made from vector bosons 4-111284
- SO<sub>3</sub> exact magnetic monopole solns. in expanding Universe 4-67827
- Space science and cosmology 4-77693
- spacetime thermodynamics and inflationary Universe, theory 4-90263
- spatial curvature of background Friedmann Universe, effect on background radiation anisotropy 4-77984
- static spherical symmetric space-times, geodesic deviation eqn. soln. 4-67608
- string in Universe, gravitational interactions, gravitational radiation and Yang-Mills symmetry breaking 4-115840
- strings and microwave background anisotropy 4-101552
- strong equivalence principle and its violation 4-78019
- structure growth in Universe 4-73127
- SU(5) GUT, inflation with gravity coupling 4-78212
- SU(5) GUT in curved space-time, effective couplings 4-58703
- SU(5) supersymmetric cosmology, masses and coupling consts. 4-78502
- Sunyaev-Zeldovich effect, obs. of microwave background 4-73104
- supercluster-void struct. topology in the Universe, cluster chains 4-94977
- superclusters and voids, struct. 4-77943
- superclusters as nondissipative pancakes, N-body simulations 4-77948
- superclusters form- and evolution from anal. of clusters alignment 4-86094
- supercooled quark-gluon plasma, hadron bubble growth mechanism, implications to early cosmology 4-63980
- supergravity, cosmological pot. 4-58724
- superheavy mag. monopole production in inflationary Universe 4-78512
- supernovae for cosmological distance determ. 4-72967
- supersymmetric inflationary cosmology, GUT and SUSY breaking, N=1 supergravity framework 4-63349
- SUSY QCD, coloured scalar quarks and hadrons, cosmological implications 4-111371
- symmetric matter-antimatter model of Universe 4-73126
- Taub model, exact soln. 4-90276
- ten dimensional cosmologies, supergravity Maxwell-Einstein theory 4-67829
- thermal equilibrium of different vol. of primordial gas, microwave background anal. 4-77977
- thermodynamical history of the Universe 4-86096
- three-dimensional cosmological gravity: dynamics of constant curvature 4-63345
- topological mapping properties of collisionless potential and vortex motion 4-69773
- topological struct., mathematics of three-dimensional manifolds 4-101557
- topological supergravity, fermio mass term, three layered model, book contrib. 4-63645
- tunnelling Universe, particle creation from quantised fields 4-95002
- two neutral fermion system, constraints from cosmology, SUSY GUT relevance 4-63925
- unclustered matter on supercluster scale and open nature of Universe 4-82577
- uncoupled fluids, gauge invariant cosmological fluctuations, early Universe axions 4-67819
- unified field theories in models of early Universe 4-101556
- unified Yang-Mills theory, topological strings, massive black holes in galactic nuclei 4-101727
- unit gravitational charge existence consequences in big bang theory 4-67828
- universal age determ. methods 4-73122
- Universe, contents (book) 4-67892
- Universe, flatness, reconciling theoretical prejudices with obs. data 4-82578
- Universe, large scale structure, mass distribution 4-77987
- Universe, locally supersymmetric theory, SUSY breaking sector, energy density, entropy crisis 4-77995
- Universe, matter-antimatter partition 4-78018
- Universe, quantum metrics and matter field configurations 4-78202
- Universe, thermal death and entropy (Japanese) 4-110795
- Universe adiabatic fluctuations, late evol., pancake scenario, Big Bang collisionless relics 4-63380
- Universe age and galaxies infall to Virgo Cluster, constraints 4-110755
- Universe and contents, evolution (book) 4-67888
- Universe closure, effects of Newtonian gravit. modification 4-105869
- Universe expansion and red shift (Norwegian) 4-73071
- Universe expansion nature, role of gravit. and elementary particles (Russian) 4-82581
- Universe expansion rate 4-95004
- Universe in pregalactic era, large-scale struct. form. 4-67837
- Universe initial singularity and particle phase transitions 4-78013
- Universe large scale struct. from X-ray background anal. 4-78007
- Universe large-scale struct. and galaxies distrib. 4-78008
- Universe origin and evolution (book) 4-63352
- Universe size and age, Tully Fisher relation use, errors 4-106087
- Universe with non-trivial topology and the possibility of its quantum creation (Russian) 4-95011

## cosmology continued

- unstable photino mass bound from cosmology 4-78505
  - Ursa Major supercluster, red shift survey and radio obs. 4-77952
  - vacuum Bianchi models, types  $\text{I}_{III}$ ,  $\text{IV}$  and  $\text{VI}_h$ , inhomogeneous generalisations, exact solns. 4-68059
  - vacuum bubble collisions in false 'background vacuum', general relativity 4-63366
  - vacuum energy in a squashed Einstein universe, book contrib. 4-63618
  - variable G, scale covariant gravitation and cosmology 4-72876
  - very early Universe, astrophysical scale, isotropy and baryonic and non-baryonic content 4-63355
  - very early Universe, cosmological aspects of quantum gravity, book contrib. 4-63617
  - very early Universe, GUT, confinement, chiral and Weinberg phase transitions 4-63361
  - very early Universe, GUTs and SUSY-GUTs, baryosynthesis, inflation 4-63357
  - very early Universe, Kaluza-Klein and self-consistent models, dimensions reduction dynamics 4-77994
  - very early Universe, mag. monopole flux, role and props. in cosmology, GUTs 4-63358
  - very early Universe, specific features 4-63373
  - very early Universe, strings, GUTs and galaxy form. 4-63359
  - Virgo cluster, galaxies infall, cosmological eqns. soln. 4-77949
  - voids evolution from primordial density var., correl. with present-day cosmic background radiation 4-78003
  - voids origin as consequence of adiabatic perturbations 4-78002
  - X-ray background, X-ray spectrum of volume emissivity arising from Abell clusters 4-86064
  - X-ray quasars and Seyferts evol. 4-67812
  - He abundance in globular cluster M15, determ. from photographic photometry of RR Lyrae variables 4-101368
  - He and D synthesis in early Universe 4-101548
  - He primordial abundance, determ. from mass meas. of components of  $\mu$  Cassiopeiae 4-72977
  - $^{18}\text{Re}$ - $^{187}\text{Os}$  cosmochronology, validity of local approximation for s-process in Os region 4-115680
  - $^{238}\text{U}$ ( $^{238}\text{U}$ , X), ultra-relativistic collisions, possible vacuum catastrophic phase transition 4-68714
- cosmotrons**  
No entries
- Costa Ribeiro effect** see *dielectric phenomena; phase transformations*
- Cotton-Mouton effect** see *birefringence; magneto-optical effects*
- Cottrell atmospheres**  
impurities, Cottrell atmospheres, dislocation interactions, internal friction and US meas. 4-65486  
steel, low C, ductile-brittle transition temp., effect of tensile prestrain (Japanese) 4-114650  
Al-Mg, creep, stress range of Class I behaviour 4-81249
- Cottrell locking** see *Cottrell atmospheres*
- Couette flow**  
see also *jets*  
axisymmetric Couette flow at large Taylor numbers 4-103296  
batch crystallisation process, optimisation via Legendre polynomials 4-88122  
boundary conditions for high-shear grain flows 4-112991  
convergent flows, rot. process (Russian) 4-112910  
cylinder, Couette spiral forming disturbances and Poiseuille flow, instabilities (German) 4-83954  
granular material rapid flow, kinetic model 4-60484  
granular materials, Couette flow, inelastic and slightly inelastic particles, collisional distrib. function 4-60362  
hydrodynamic stability 4-97488  
in space partly filled with porous medium 4-87790  
incompressible flow, reference press. location, finite element anal. 4-64909  
marangoni effect in the Couette flow 4-64945  
marginal stability curve and linear growth rate for rotating Couette-Taylor flow and Rayleigh-Benard convection 4-64921  
non-Newtonian fluid flow, heat and mass transfer, power function vel. profiles 4-60464  
nonequilibrium fluid undergoing planar Poiseuille-Couette flow, light scatt. 4-112520  
nonNewtonian fluid, relax. props. and stability 4-97469  
onset of turbulence, quasilinear approx. 4-108113  
Orr-Sommerfeld equation asymptotic solns., error estimates 4-103419  
planar Couette flow, nonlinear-response theory 4-112807  
protein precipitate, shear induced break-up during exposure to laminar Couette flow 4-79547  
pseudoplastic crude oil, thixotropy, grid-shell theory 4-69723  
shearing fluids, instability mechanism at interface 4-103291  
stratified plane Couette flow, stability 4-97638  
surface-layer similarity in turbulent circular Couette flow 4-103307  
Taylor-vortex flow, wave speeds 4-75039  
transient parallel fluid flows, finite element anal. 4-74986  
turbulent Taylor-Couette flow, organised struct. 4-87735  
viscoplastic fluid, modes of generalised MHD Couette flow 4-108125  
viscous liquid between rotating coaxial cylinders, pointwise nonlinear stability 4-79603
- counter accessories**  
see also *counting circuits*  
No entries
- counters**  
see also *Cherenkov counters; counting tubes; fission counters; Geiger counters; proportional counters; scintillation counters; semiconductor counters; spark counters*  
differential counting, practical estimation methods 4-91187  
electronic counting scales employing count-by-weight method 4-63722  
pulse-counting system, microcomputer-based, construction 4-112076
- counters (circuits)** see *counting circuits*
- counting circuits**  
see also *coincidence circuits; pulse height analysers; scaling circuits*  
activity determination, modulo-2 counting technique, alternative to coincidence method 4-102542  
frequency meters and timer-counters (German) 4-106328  
radiation monitoring system for separation of transplutonium elements 4-102537

- counting tubes**  
 see also *dekagrams*  
 No entries
- country planning** see *town and country planning*
- county planning** see *town and country planning*
- coupled superconductor devices** see *superconducting junction devices*
- coupling (process)** see *joining processes*
- CP invariance**  
 baryogenesis,  $SU(3)_C \times SU(2)_L \times U(1)$  model, CP breaking, GUT scale 4-111336  
 conference on particles and fields, Banff, Canada (Aug. 1981) 4-63404  
 $CP^{N-1}$  lattice model, topology in strong coupling 4-102031  
 CP violation and CPT violation limits, status and prospects 4-82908  
 early Universe,  $SU(5)$  GUT model, CP domain wall problem, matter-antimatter domains soln. 4-115842  
 electroweak theory, intermediate bosons, currents, CP violation 4-95736  
 fundamental interactions, unity, summer school, Erice, Italy, (July-Aug. 1981) 4-86102  
 gauge models of CP nonconservation, GUT constraints, strong CP, Kobayashi-Maskawa model, review 4-63921  
 generation structure for quarks and leptons, rishon model, CP violation 4-63922  
 hypercolor unification without cosmological domains, GUTs,  $[SU(9)]^3$  semisimple theory 4-86631  
 inflationary model with correct density fluctuations and CP problem soln.,  $SU(5)$  field 4-73110  
 instanton and meron fields, Dirac Hamiltonian self-adjointness 4-95673  
 invisible axion detection, properties, P- and CP-conservation 4-90767  
 invisible axions, domain walls, energy crisis and galaxy form. 4-59018  
 $K_L$ - $K_S$  mass difference and CP-violation in supersymmetric models 4-111331  
 leptonic CP violation and left-right symmetry 4-63940  
 Majorana particle processes, CPT, CP, and C phase effects 4-111337  
 $N=1$  supergravity and strong CP violation, axion soln. 4-95279  
 natural composite models, systematic construction 4-95770  
 neutrino mass eigenstates, CP properties 4-86605  
 neutron electric dipole moment, triangle graph contribution 4-86711  
 neutron electric dipole moment induced by strong CP violation 4-111453  
 non-Abelian Klein-Kaluza theories, spinor fields 4-58702  
 Peccei-Quinn symmetry as flavour symmetry and grand unification 4-59001  
 Peccei-Quinn symmetry in QCD 4-95758  
 quark mass scale,  $\theta$  calculation, CP violation, Kobayashi-Maskawa mechanism 4-106504  
 quark mixing and CP violation in heavy quark system 4-90759  
 $S_4$  permutation symmetry, CP nonconservation, rare decays and quark/lepton electric moments 4-86600  
 six-quark model based on  $SO(10) \times U(1)_{PQ}$ , mixing angles, B-meson life-time 4-63937  
 $SO(10) \times U(1)_{PQ}$  model, mixing angles and CP violation 4-59002  
 $SO(10)$  theory, CP-violation parameters in a left-right-symmetric model 4-111361  
 soft-pion skyrmion lagrangian and strong CP violation 4-68407  
 status, historical and current 4-86612  
 strong CP problem in grand unified models without Peccei-Quinn symmetry 4-95705  
 strong CP soln. in UT, small  $\theta$  and invisible axion 4-63946  
 strong CP violation and axion mechanism 4-95714  
 $SU(1,1)$  supergravity models, Yukawa coupling, matrix, CP violation 4-90473  
 $SU(2)_C \times U(1)$  gauge theory, permutation group, CP violation, quark mass matrices 4-111342  
 $SU(N)$  colour gauge theory, P and CP violation with massive fermions 4-78496  
 super Kobayashi-Maskawa C P-violation 4-86621  
 supersymmetric models, CP problem and generation of mass term 4-63939  
 violation in baryon symm. cosmology 4-78012  
 $b$ - $c$   $\bar{u}$ , Fritsch-type quark mass matrices, CP violation strength parameter 4-111394  
 $B$  decay, CP violation, mixing angles, t-quark mass, in six-quark model 4-82959  
 $B$  meson mixing props. and CP-violating effects, charge current couplings, QCD 4-111320  
 $b$ - $u$   $\bar{u}$ , Fritsch-type quark mass matrices, CP violation strength parameter 4-111394  
 $\eta$  Z 4-59083  
 $h$ - $\phi$  decay mode, parity and signature determ. 4-90870  
 $K$  decays, symmetry violation studies at Brookhaven 4-102051  
 $K^0$ - $\bar{K}^0$  mixing, CP violation, dispersive contributions 4-68536  
 $K_L^0$ - $\mu^+$  $\mu^-$ , six-quark scheme tests, CP violation, quark mixing matrix 4-111389  
 $Z^0$ - $\tau^+\tau^-$  limits on composite structure, CP violation 4-90937  
 $T$   $\beta$ -decay and neutrinoless double  $\beta$ -decay, CP violation 4-111528
- CPA calculations**  
 alloy, Auger spectra, core-valence-valence, CPA theory, disorder-induced vertex corrections role 4-71491  
 alloys, Auger spectra, partial long range order effects 4-99238  
 alloys, nonrandom, substitutionally disordered, densities of states calcs. 4-113843  
 anthracene, isotopically mixed, disordered crystals, exciton transport in rel. correl. functions 4-113872  
 disordered Hubbard alloys, spin glass behaviour 4-92928  
 disordered systems, field depend. charge carrier trapping process 4-104226  
 metallic glasses, elec. resist. and sp. ht. due to interaction of cond. electrons with two-level systems 4-92689  
 naphthalene, isotopically mixed, disordered crystals, exciton transport in rel. correl. functions 4-113872  
 randomly distributed particles of cermet topology, optical props. 4-93039  
 semiconductors, hopping conduction, multiple scatt. theory, continuous time random walks and CPA approx. 4-61366  
 solid solutions, quaternary III-V cpd. system, optical and elec. props. 4-84929  
 transition metal, local spin fluctuations-CPA model of mag. 4-71016  
 transition metal alloy, disordered, Eliashberg eqns., CPA calc., supercond. crit. temp. depend. factors 4-70976  
 transition metal alloy, second-order perturbation treatment of correls. and disorder 4-70645  
 transition metal alloys, binding energy, CPA calcs. (Russian) 4-98060
- CPA calculations continued**  
 transition metals, magnetism and electronic struct., validity of simple alloy model 4-98865  
 $Ag, Pd_{1-x}$ , elec. cond. and thermopower calcs. 4-70776  
 $Ag, Pd_{1-x}$ , Hall coeff. and band struct. calcs. 4-70780  
 $Au, Pt_{1-x}(Ni_{1-x})$ , substitutionally disordered, electronic struct. calcs. 4-70644  
 Cu-Ni, disordered, positron spatial distrib. effects 4-104170  
 Cu-Au, substitutionally disordered, electronic struct. calcs. 4-70644  
 Fe-Cr(Mn), binding energy, CPA calcs. (Russian) 4-98060  
 $GaAs-Ga_{1-x}Al_x$ , lateral superlattice struct. 4-92816  
 $Hg_{1-x}Cd_xTe$ , CPA calcs., Green's function calcs., simplification through analytic continuation 4-61274  
 Ni-Cr alloys, mag. struct. amplitudes, polarised neutron studies 4-108989  
 $Ni, Pt_{1-x}$ , substitutionally disordered, electronic struct. calcs. 4-70644  
 Tm intermediate valence cpds., mag. susceptibility and sp. ht. 4-108999
- CPT invariance**  
 CP violation and CPT violation limits, status and prospects 4-82908  
 Majorana particle processes, CPT, CP, and C phase effects 4-111337  
 Majorana particles from CPT invariance, constraints on interactions 4-59006  
 nonlinear fermion field, strong interaction, wave duality causing discrete symm. conservation 4-106486  
 nontrivial weakly local massive Wightman field class with interpolating props. 4-95637  
 $K^0 \rightarrow 3\pi^0$ , CPT symmetry, Bell-Steinberger unitarity relation 4-73748
- crack detection**  
 see also *cracks*  
 AC field technique, skin depth effect 4-114728  
 acoustic emission, for crack resistance evaluation in steady loading 4-99699  
 acoustic holography appl. to defect evaluation (French) 4-76922  
 adhesive bonded joint, strength tests using acoustic emission method 4-109614  
 automatic flow detection, X-ray TV system, interface unit and software 4-76950  
 cable inspection using electro-optical technique and microprocessing technology 4-106347  
 capillary and bubble methods for detection of through-defects 4-76956  
 capillary flaw inspection, appl. of aq. soln. of detergents 4-76955  
 castings, light alloy, radioscope for inspection 4-99671  
 ceramic materials, crack detection by acoustic emission 4-62155  
 ceramics, nondestructive failure prediction, fracture models 4-76964  
 ceramics, surface damage, strength degradation, erosion and wear, acoustic NDT 4-76872  
 coating for tools and sliding elements, acoustic microscopy studies 4-104957  
 colour graphic US imaging device, DRUID 4-69637  
 colour penetrant system, new method (German) 4-89228  
 concrete, vertical-displacement gauge fixture for  $J_{Ic}$  testing 4-104933  
 concrete beam, three point bending, cracking, dye penetrant obs., compliance calibration technique 4-89205  
 defect location and sizing by US diffr. based time-of-flight meas. 4-71803  
 dye penetrant inspection, brightness-colour coeff. of visibility of indications 4-109610  
 eddy current equipment for aircraft maintenance 4-76943  
 eddy current impedance plane testing appls. 4-109588  
 eddy current testing of hot pipe welds 4-76960  
 elastic discontinuities, acoustic microscopy 4-60237  
 electron-optical converters in flaw detection with ionizing radiation 4-71854  
 EM field of defect in form of cylindrical cavity 4-76952  
 energy flux density during transverse-shear crack propag. 4-109617  
 fatigue damage inspection in stainless steel VNS-25, by positron annihilation method 4-81390  
 ferrosonde flaw detector, appl. to welded joints 4-71835  
 fibre reinforced plastic, NDT with acoustic flaw detector (German) 4-76941  
 flaw detection in conducting half space, eddy current coil impedance 4-62133  
 flaw in elastic medium, US scatt., time domain Born approx. 4-62134  
 flaw parameters in real time in case of random perturbations 4-71836  
 flaw sizing and characterisation, US holography and synthetic aperture focusing techniques 4-85274  
 fusion reactor first wall, crit. flaw size prediction methodology 4-96268  
 glass fibre reinforced plastics, fatigue crack growth, environmental effect, compliance and moire techniques 4-89200  
 glass fibre reinforced polyamide, fracture mechanism, acoustic emission and microscopy obs. 4-66417  
 grazing longitudinal US wave pulse scattering by crack 4-99723  
 inspection of transmission pipelines, electromag. field distrib. in flaw detector 4-81389  
 magnetic inspection method, mag. leakage flux as function of orientation between direction of defect and mag. field direction 4-81392  
 metal, surface, AC field perturbation by plane cracks, skin effect 4-62131  
 metal, surface crack depth, AC field meas., probe characs. 4-62130  
 metals, surface current distrib. around surface flaws 4-60984  
 metals, US checking instruments 4-109601  
 microwave detection from extended objects using shape of spacial frequency spectrum 4-71837  
 NDT techniques, vibrational 4-81367  
 noncontact crack detection method (French) 4-93478  
 nondestructive materials monitoring instruments (Russian) 4-81384  
 optical method for flaw detect., reflected images determ. on curved surfaces 4-107538  
 optical tomogram synthesis 4-71840  
 piping welds, flaw cracks, using US satellite pulses 4-85272  
 plate, surface cracks originating at open hole, shape and growth rate meas. 4-87625  
 plate, welded, flaw classification, US echo dynamics, multidimensional feature decision process 4-85273  
 polymers, NDT, remote testing by photothermal anal. of thermal waves 4-81374  
 positional small angle X-ray scattering from flaws 4-85278  
 pulsed eddy current testing, crack indications, spatial resolution of probe coil (German) 4-76942  
 pulsed self-excited oscillator for electromagnetic flaw inspection devices 4-109604

**crack detection continued**

- radiometer flaw detector for welded joints monitoring 4-62149
- reactor pressure vessel, quality assurance, NDT, human reliability models 4-68781
- reactor pressure vessels, thick walled components, US inspection, time of flight data evaluation, ALOK system 4-71804
- scintillation monitoring with pulsed sources, effects of nonideal adder on data accumulation 4-78444
- semiconductor, IR flaw detector, for free-carrier conc. determ., using cholesteric liq. crystals 4-89211
- shear waves, linearly polarised, reflection and transform. by plane and flaws 4-74827
- spark erosion, reference defects for nondestructive inspection (*German*) 4-114746
- steam pipe bends flaws, ultrasonic inspection 4-66545
- steam turbine rotor steel crack growth detection and monitoring by acoustic emissions meas. 4-76961
- steel, austenitic stainless, creep crack propag., DC pot. meas. of crack length (*Japanese*) 4-99688
- steel, austenitic stainless, crit. flaw size prediction methodology 4-96268
- steel, austenitic stainless, pitting corrosion detection using double layer activation technique 4-81368
- steel, austenitic stainless, radiographic crack detection in thick sections using linear accelerator source 4-89224
- steel, austenitic stainless weldments, US inspection, compression crack closure effect; 4-85277
- steel, crack length monitoring using AC potential drop system 4-114741
- steel, reflection and transformation of linearly polarized shear waves at defects 4-81386
- steel, stainless, fatigue test, IR monitoring 4-109585
- steel, stainless, US inspection, flaw visibility, split spectrum processing, grain size effect 4-89226
- steel, tool alloy, magnetographic inspection, flaw image rel. to heat treatment 4-71834
- steel, US testing, smallest detectable defect, sensitivity of technique 4-85267
- steel block, US flaw detection, photoelastic visualisation, railway appls. 4-62138
- steel plate, crack type defects, US inspection with inclined transducers 4-71850
- steel plates, fatigue crack sizing by double inclination US probe 4-109589
- subsurface flaw in joined fluid-solid half spaces, US wave scatt. 4-97178
- subsurface hole location and size, Rayleigh surface wave scatt. 4-62135
- superfine defect detection, feasibility of US method 4-76949
- surface breaking cracks, location and sizing by synthetic aperture acoustic imaging system 4-85276
- surface crack depth meas., alternating potential method and measuring instrument appl. (*Chinese*) 4-81366
- surface crack growth monitoring, DC potential technique (*Japanese*) 4-93489
- surface defect, acoustic wave scatt., fibre optic detection 4-85275
- surfaces, quality control, automated interference meas. 4-81391
- time-of-flight diffraction technique and portable US digital recording system 4-114736
- two-frequency eddy current method, interfering factor effects suppression (*Russian*) 4-104947
- ultrasonic nondestructive evaluation methods 4-99716
- US, characterisation using phase information in . US spectroscopy 4-99720
- US, probabilistic approach to inverse problems 4-99724
- US, steel, stainless heat-treated samples, evaluation by split-spectrum processing 4-99721
- US characterization of edge cracks using near-field acoustic displacement amplitude and fibre optics 4-99725
- US flaw detection scheme for long rod using remote inspection 4-99719
- US flaw detector with acoustic bond monitor attachment 4-109598
- US flaw detectors, performance indices, metrological support 4-99710
- US imaging, high resolution portable system using synthetic aperture focusing 4-93474
- US mode-conversion phenomena at surface-breaking cracks for defect characterization 4-99727
- US Rayleigh critical angle method to meas. metal surface props. 4-97235
- US reflection from natural defects propagating from surface, echo signal amplitude 4-109615
- US scattering and P/SV-conversion of elastic waves by a plane crack of finite width 4-99722
- weld heat affected zone, acoustic emission testing of cold crack initiation and growth (*German*) 4-99718
- welded joints, magnetic particle testing 4-76959
- welded joints, X-ray flaw detection, photographic paper appl. 4-99670
- welded joints in ship hulls, radiographic inspection by  $\gamma$ -flaw detector 4-109603
- welds, flaw characterisation, nondestructive inspection, international codes and standards 4-89225
- X-ray images, statistical method of estimating detectability of small and low-contrast details 4-71839
- Zipscon system for defect detection and sizing 4-109577
- Al alloy, high strength, notch fatigue, limits to applicability of LEFM 4-71721
- Al alloy sheet, flaw inspection, fatigue crack parameter selection in setting specimens 4-109605
- Al radiators, quality assurance by IR thermography 4-66531
- Bi-Pb-Sn-Cd, Wood's metal model, inclined simulated cracks, eddy current detect. 4-66516
- C fibre reinforced plastic, thermal NDT method for inspecting large parts 4-71838
- C fibre reinforced plastic laminates, fault detection by X-ray NDT (*German*) 4-99693
- Fe, nodular, cast, fatigue crack growth obs., using bonded-resistance gauges 4-93477
- Ni base superalloys, diffusion coated, crack initiation, acoustic emission obs. (*German*) 4-62140

**crack-edge stress field analysis**

- see also penny-shaped cracks
- 3D fracture mechanics, boundary integral equation-boundary element method appls. (*Chinese*) 4-97398
- acrylic polymers, fracture in water 4-76881
- adhesive joints, mode I and II fracture 4-93387

**crack-edge stress field analysis continued**

- annular crack, flat, axisymm. response to normal impact waves 4-69695
- antiplane shear in adhesively bonded semi-finite media with transverse cracks 4-60337
- axial beltline flaws, pseudo-elastic anal. 4-97406
- axial cracks in thin walled hollow cylinder, stress intensity factors 4-60334
- bars, round, loaded in mode III, fracture and procedure for fracture toughness determ. 4-69709
- beam, edge-cracked, ductile fracture under EM bending force 4-91763
- elastisitic strip, edge crack anal. 4-87628
- body with hard sharp-angled inclusion and interface crack, longit displacement 4-97414
- boundary of elastic materials, subsonic propag. of shear displacement edge with friction 4-108049
- brittle fracture, criteria in biaxial tension 4-69704
- brittle fracture toughness, influence of microstruct. 4-93388
- brittle material sheets, crack paths under biaxial loading 4-79497
- brittle materials, compressive surface strengthening 4-93307
- brittle materials, microcracking, crack-growth resist. 4-83858
- central crack element in fracture mechanics 4-60338
- centre cracked tensile panel in net section yield, crack tip opening displacement calc. 4-60335
- ceramics, cracking behaviour, microprocessor-controlled meas. 4-62056
- ceramics, fracture energy, elastic anisotropy and grain size dependence 4-60983
- ceramics, slow crack growth at high temp., characterisation by double torsion method 4-62053
- circular crack opening, effect of initial stresses 4-60327
- collocation procedure for determining fracture mechanics parameters at a corner 4-60340
- compact specimen, Dugdale plastic zone size, crack tip opening displacement eqns. 4-60333
- compact specimen, fatigue crack closure, finite element analysis 4-97433
- composite laminates, matrix crack growth, stochastic simulation model 4-74960
- composite materials, delamination, fracture mechanics 4-97431
- composites, fatigue failure, probabilistic modelling employing Markov process 4-74961
- composites, unidirectional, matrix cracking 4-74962
- concordant displacement at crack tip, finite element method employing singular element 4-69711
- Crack border-free surface intersection analysis 4-79515
- crack growth under creep, stress field nonstationarity influence 4-97407
- crack opening displacement design curves (*Japanese*) 4-91782
- creep, crack growth, comparison of finite element predictions with expt. data 4-97410
- creep crack growth at high temp., void coalescence and growth 4-79505
- creep crack growth in damaged material, biaxial test facility 4-93490
- cyclical loads, crack growth theory 4-112771
- cylinder, cracked, under internal pressure, finite element calc. evaluation by speckle photography 4-97450
- cylinders, autofretted, fatigue crack initiation from holes, R-ratio effect 4-87626
- cylinders, thin-walled, butt-welded, stress intensity factor for internal circumferential crack 4-97418
- cylinders with axial cracks, vibrating 4-97396
- development of crack stopped by small elastic inclusions (*Russian*) 4-112772
- dislocations of opposite sign at crack tip, dislocation-free zone image force theory (*Chinese*) 4-91762
- double slip plane model crack, explicit calc. of crack tip stress intensity factor 4-60329
- ductile materials, crack blunting and initiation, microvoid nucleation 4-60981
- ductile penny-shaped crack in a thick transversely isotropic plate 4-83856
- edge-crack under action of cyclic temperature 4-97413
- edge-crack, oblique, dynamic behaviour under impact loading 4-91770
- elastic body containing a flaw, dimensional analysis 4-103255
- elastic body with long thin cylindrical inclusions, stress conc. 4-97416
- elastic-plastic analysis of rel. between  $K_I$  and CTOD 4-103267
- elastic-plastic finite element analysis of voids and inclusions 4-92195
- elastic-plastic fracture, energy flux into process region 4-69705
- elastic-plastic material, power-law, near tip dynamic fields for 4-60328
- embrittlement and pitting, environmentally-induced, possible role of surface stress 4-62086
- energy flux density during transverse-shear crack propag. 4-109617
- epoxide composite, alumina particle filled, fractography (*Japanese*) 4-99512
- external circular crack form. by normal impact or sudden twisting, dynamic stress intensity factors 4-87622
- fatigue crack growth, near threshold, at elevated temps., oxide wedging effect 4-91775
- fatigue crack growth and crack closure in structural materials (*Japanese*) 4-112767
- fatigue crack growth at high strain amplitudes 4-103265
- fatigue crack propagation, residual stress distrib., X-ray meas. (*Japanese*) 4-99685
- fatigue crack propagation by crack-tip plastic blunting 4-71719
- fatigue cracks, general crack opening stress equation 4-60342
- fatigue cracks, growth rate and closure in incipient short and elastic-plastic long cracks (*Japanese*) 4-92291
- fatigue striation numerical analysis, crack tip plasticity 4-64883
- fibre reinforced composite, anisotropic layered, singularities at tip of crack normal to interface 4-74952
- fibre reinforced composites, unidirectional, fracture toughness in mode II 4-93366
- fibre reinforced plastics, stable crack growth, influence of fibre orientation 4-99570
- finite difference technique for solving crack problems 4-69710
- flexible samples, cracks, determ. of zones of distrib. 4-60344
- fracture, unified theory, book 4-63426
- fracture in biaxial fields, higher order approx. for T-criterion 4-79495
- fracture mechanics, new approaches 4-103266
- geometry of deformed crack tip rel. to crack parameters 4-79504
- glass, elliptical crack, transient growth, mathematical model 4-104845
- glass, fatigue, crack growth and crack tip sharpening models 4-89101
- glass fibre reinforced epoxy resin laminates, transverse cracking rel. to mech. props. of matrix 4-99489
- glass fibre reinforced polyester, laminated hybrid, crack growth resist., flexural strength 4-62012

# crack-edge stress field analysis continued

graphite fibre reinforced epoxy, mixed mode fracture 4-99569  
Griffith crack in orthotropic plate, bending stress intensity factors (Chinese) 4-97397  
half plane with partially contracting crack, thermoelasticity problem 4-97415  
half-space, surface deflection due to crack presence 4-69703  
hard coating flaking under shear stress, fracture mech. anal. 4-69713  
hollow cylinder with cladding, circumferentially cracked, thermal shock resist. 4-87623  
HSLA, fatigue threshold, thermally activated behaviour of effective stress intensity 4-76853  
inclusion, elastic, model problem of stopped cracks (Russian) 4-74959  
Inconel 718, time-depend. fatigue crack propag., effect of small scale to large scale creep transition (Japanese) 4-93383  
inhomogeneously ageing bodies, asymptotics near crack tip 4-60325  
interacting cracks, estimate of stress intensity factors 4-74963  
interface of dissimilar media, biaxial-load effects on isopachics for crack 4-112764  
interfacial crack between two dissimilar elastic orthotropic solids, transient stress intensity factors 4-97422  
interferometry for elastic and plastic anal. of cracked specimens (Chinese) 4-83854  
J-integral for arbitrary geometry and loading, laser moire determ. 4-60348  
J-integral meas. in plane stress state by strain gauge system 4-79531  
J-integral path depend. for blunt crack 4-79499  
J-R curve, direct determ. from load-displacement record 4-104959  
kinetic equation of crack growth, theoretical method of estimating parameters 4-108055  
kinked crack initiating from rigid line inclusion, stress analysis, formulation 4-108043  
kinked crack initiating from rigid line inclusion, stress analysis, propag. direction 4-108044  
layered composite, penny-shaped interface crack, torsional impact response 4-79498  
linear elastic cracked body, transient elastodynamic second boundary-value problem 4-64881  
material aspects of crack tip yielding and subcrit. crack growth in eng. alloys 4-93408  
metals, fatigue crack propag. rate, correl. with J-integral or crack opening displacement (Japanese) 4-114649  
micropolar elastic solids, crack propag. 4-91768  
mixed mode crack propag. studies, double nodding technique 4-79502  
mixed mode fracture studies, evaluation of compact shear specimen 4-103277  
mixed-mode elastic crack analysis, extended weight function method 4-97427  
nonhomogeneous plane, crack problem 4-74957  
nonlinear viscoelastic media, deform., fracture analysis, generalised J integral, correspondence principles 4-103253  
notch fatigue, limits to applicability of LEFM 4-71721  
orthotropic medium, cracked, impact response 4-74967  
orthotropic structures, adhesive bonded, with part through crack, stress intensity factors analysis 4-79494  
panel, centre cracked, plane stress tensile deform., J-integral estimation 4-103262  
path-independent integral and moving isoparametric elements for dynamic crack propagation 4-79493  
penny-shaped crack, symmetric indentation by embedded rigid circular disc inclusion 4-79506  
penny-shaped interface crack with heat flow, imperfect contact 4-97425  
pipe, longit. crack, finite element analysis of leak areas using ADINA program 4-103254  
planar crack of arbitrary shape at interface of two anisotropic elastic half spaces 4-79508  
plane cut in elastic medium with slip and adhesion of surfaces, 3D mixed problems 4-60326  
plane die in brittle half-plane, crack form. at edge 4-112770  
plane elastic media, curvilinear cracks tip stress intensity factors 4-64886  
plane elasticity crack problems, isochromatic fringe determ. method 4-60347  
plastic zone and tip opening displacement in notches, effect of geometry and finite root radius 4-69706  
plate, homogeneous isotropic elastic, stress conc. at circular porous inclusion 4-79519  
plate, infinite with broken or branching crack, stress determ. 4-64884  
plate, orthotropic, bending stress intensity factors for Griffith crack (Chinese) 4-97397  
plate, orthotropic, thermoelastic problem of uniform heat flow disturbed by central crack 4-79511  
plate, semi-infinite, edge cracks, plastic zone size estimation 4-60341  
plate, stability near sharp defect, initial biaxial stress state 4-108046  
plate containing circular hole, Fredholm integral eqn. 4-103251  
plate of finite width under bending, internal and edge cracks 4-74958  
plate structures with through-wall cracks, J-integral anal. using thick shell elements 4-79496  
plate with a moving slit and heat source, thermoelastic state 4-108016  
plates, cracked polygonal, stress intensity factors determ. by use of Westergaard's functions 4-91765  
plates, finite, approx. weight functions for centre and edge cracks 4-91764  
Plexiglas with deposited Al, macrocrack opening, residual compressive stress study 4-64885  
PMMA, dynamic fracture toughness, determ. by impact bending test (Japanese) 4-93488  
PMMA, fatigue crack closure, dependence on fracture features 4-80149  
power-law hardening material, optical shadow spot method for tensile crack 4-97449  
pressure vessel, strength criterion in presence of prod. and service defects 4-64887  
pressure vessel, stress intensity factor solns. for internal longitudinal semi-circular surface flaws 4-76859  
reliability analysis and design, crack growth model (Japanese) 4-99687  
rolling contact fatigue, pitting model 4-64888  
sandwich structure, penny shaped cracks, stress analysis 4-60339  
SCC growth rate correlation with crack tip opening angle 4-62108  
screw dislocations, inclined pileup at crack tip without a dislocation-free zone 4-80148  
semi-infinite composite with long reinforced phase, edge crack analysis 4-97400

# crack-edge stress field analysis continued

semi-infinite plane crack with wavy front, stress-intensity factors 4-83860  
semielliptic surface flaws, fatigue life prediction 4-103261  
semiminfinite plane crack, pair of point forces appl. to crack faces 4-83859  
shaft, elastic cylindrical, containing circular cracks, nonsteady stress state under torque 4-108047  
shell structures with through-wall cracks, J-integral anal. using thick shell elements 4-79496  
short cracks effect on fatigue limit, analytical soln. 4-66440  
short fatigue crack behaviour and the concept of absolute and relative fatigue thresholds 4-84344  
single edge notch specimens, compliant drawbar loading, Mode I stress intensity factors 4-89203  
single edge notch tensile specimens loaded through frictionless pins, ductile fracture 4-60336  
singularity powers, finite element anal. for cracks terminating at finite width interfaces 4-87621  
solid, infinite, three dims. crack, stress conditions 4-87627  
spontaneous cracking of brittle matrix due to presence of thermoelastic stresses 4-108045  
steel, austenitic stainless, crack initiation and growth anal. by direct optical obs. during slow strain rate tests in high temp. water 4-71768  
steel, austenitic stainless, ductile fracture resistance, assessment based on engineering approach 4-104876  
steel, austenitic stainless, fatigue crack propag. threshold 4-99590  
steel, austenitic stainless, fatigue crack propagation in specimens subjected to thermal shock 4-93413  
steel, austenitic stainless, SCC propag. rate, fracture mechanics parameters (Japanese) 4-99649  
steel, C, fracture toughness, stretch zone, ductility, transition region 4-99468  
steel, C-Mn, fracture toughness studies in different regions of weld heat affected zone 4-76838  
steel, Cr-Mo-V martensitic, lig. metal induced embrittlement, dislocation emission from crack tips 4-85210  
steel, eutectoid, rail, fatigue behaviour 4-66412  
steel, high C, fatigue crack growth retardation by massive eutectic carbides 4-99586  
steel, high strength, H embrittlement fracture morphology (Japanese) 4-99511  
steel, high strength, SCC, growth mechanisms 4-81333  
steel, HSLA, fatigue threshold, effect of strength and surface asperities on closure 4-76852  
steel, low alloy, crack branching 4-109490  
steel, low alloy, small scale yielding, crack tip opening displacement determ. 4-81270  
steel, low alloy mild, ductile fracture, rel. between J-integral and COD 4-104842  
steel, low C, notched, fatigue threshold prediction 4-99559  
steel, martensitic stainless, crack opening displacement, stretched zone size and  $J_{IC}$  4-104875  
steel, medium C, heat treated, fatigue behaviour, overstress effects 4-62007  
steel, medium C, short crack fatigue behaviour 4-66410  
steel, mild SCC under compressive stress 4-85261  
steel, Ni-Cr-Mo, crack paths and H assisted crack growth in  $H_2$  and  $H_2S$ , temp. and press. depend. 4-66429  
steel, stainless type 304, circumferentially cracked pipe, tearing instability simplified analysis 4-99566  
steel, strain rate effects on ductile fracture 4-103250  
steel rails, mixed fatigue-tensile surface crack growth 4-89100  
strain fields around propagating cracks, determ. by hybrid methods 4-91766  
strain hardening materials, toughness meas., J-estimation formulae 4-81378  
stress field around penny shaped crack, couple stresses effect 4-97402  
stress intensity factors, interrelation between static and dynamic, evaluation by caustics 4-97411  
stress intensity factors 4-97428  
stress intensity factors for cracks at loaded holes, effect of load distrib. 4-97409  
stress intensity factors for curved crack fronts in compact tension specimens 4-99680  
stress intensity factors for slender surface cracks 4-60332  
stress intensity factors of crack between two nonhomogeneous materials with antiplane shear loading 4-79516  
stress intensity rel. to fracture toughness 4-79507  
stress intensity variation and compression load, influence on crack propag. 4-69707  
subcritical crack growth in viscoelastic medium with nonlinear stress distrib. in crack end zone 4-103260  
subsurface horizontal crack subjected to time harmonic excitation stress intensity factors, resonance effects 4-97421  
surface cracks, three-dims. structures, stress intensity factor analyses 4-71738  
surface intersection of cracks, linear elastic fracture mechanics 4-79503  
thermoelastic body, crack growth, contour invariants in fracture theory 4-108042  
thermoelastic boundary integro-differential eqn. formulation 4-64882  
three dimensional crack problem, crack front elastic stress state 4-97403  
three-point bend specimen, effect of inclusion or hole on approaching crack 4-91767  
threshold stress intensity factor, crit. assessment 4-103264  
tip singularity modeling by quarter point quadrilateral element 4-103252  
transparent materials, dynamic optical and mech. props., evaluation by interferometry 4-79529  
two dimensional elastic crack, fracture mechanics analysis using localised finite element method 4-87624  
Udimet 700, Ni-base superalloy, creep fracture, effects of wavy grain boundaries 4-93415  
uniaxially reinforced composite, stress distrib. near cracks, shear lag theory 4-79518  
virtual crack extension technique for stress intensity factors and energy release rate calculations for mixed fracture mode 4-97404  
viscoelastic crack analysis by boundary integral eqn. 4-112766  
wedge, elastic, subjected to rapid tearing, transient shear waves 4-91769  
wedge opening loaded specimens, applied crack tip stress intensity effect of loadline shift 4-79530  
weight functions and stress intensity magnification factors for elliptical and semi-elliptical cracks under variable normal stress 4-60331

- crack-edge stress field analysis continued**
- welding residual stress fields, crack problems, linear elastic fracture mechanics 4-104878
  - work hardening materials, crack tip opening displacement 4-97405
  - Al alloys, fatigue crack growth, thermoactivation anal. 4-99597
  - Al-Cu-Mg, near threshold fatigue crack growth, stress intensity factors, crack closure 4-99583
  - Al-Zn-Mg, fatigue crack advance model, crack tip parameters 4-66401
  - Al<sub>2</sub>O<sub>3</sub>, bend specimens, crack resistance curves, influence of grain size 4-62058
  - Fe, crack tip under mixed mode loading, atomic model 4-62013
  - Fe, sintered, crack propag. and processes near crack tip 4-66435
  - Fe-Ni-C, fracture toughness rel. to transform. induced plasticity and grain boundary segregation 4-99585
  - Fe-(Si), fatigue threshold, effect of strength and surface asperities on closure 4-76852
  - Fe-(Si), fatigue threshold, thermally activated behaviour of effective stress intensity 4-76853
  - LiF single crystal, crack tip deform. 4-84343
  - Ni, crack propag., plastic zone, dislocation struct. 4-99488
  - Ni-base superalloy, single cryst., crack tip plastic strain 4-89231
  - Ni-Co-W-Cr single crystal superalloy, crack tip plasticity, fatigue crack growth at elevated temp. 4-71727
  - $\alpha$ -SiC, sintered, phenomenology of fracture 4-93372
  - ZrO<sub>2</sub> ceramics, process zone toughening by microcracking 4-62020
- crack inspection** *see crack detection*
- crack-tip stress field analysis** *see crack-edge stress field analysis*
- cracking** *see cracks; fracture*
- cracking, stress corrosion** *see stress corrosion cracking*
- cracking, thermal stress** *see thermal stress cracking*
- cracks**
- see also crack detection; crack-edge stress field analysis; crazing; fatigue cracks; penny-shaped cracks; stress corrosion cracking; thermal stress cracking*
  - $\nabla \cdot (\nabla \phi) / \nabla \phi = 0$  equation boundary-value problems 4-103216
  - alkali halide, crack edge contact restoration phenomena 4-98191
  - alkali halides, fracture-induced luminesc. and crack vel. 4-104685
  - alloys, amorphous, plastic deform. and failure, in situ electron microscopy 4-93481
  - brittle solid, fracture mechanisms, flaws, Hertzian cracks 4-97432
  - brittle surface in sliding contact with spherical indenters, strength degradation 4-104881
  - cast Fe, SG, fracture mechanics, cracks, elasticity anal., microtension tests (Chinese) 4-62027
  - ceramics, N-based 4-76746
  - ceramics, transformation-toughened, fracture toughness, crack-size depend. 4-93373
  - ceramics clay-based, fracture props., practical technique using diamond indentation 4-62144
  - circle bounded plane region, arbitrary system of cracks 4-97317
  - circular discs, with central hole, impact loading, crack initiation and propag. 4-97439
  - coating for tools and sliding elements, acoustic microscopy studies 4-104957
  - composite layer compression development on compression 4-79514
  - concrete, plain, in direct tension, method for determining cracking stress, cracking strain and Young's modulus 4-81369
  - continuum damage role in creep crack growth 4-71736
  - creep crack C\* integrals, evaluation 4-91783
  - dilatation model of thermal fluctuation crack nucleation 4-88236
  - elastic beam, dynamic flexural fracture, crack propag. path 4-97401
  - elastic discontinuities, acoustic microscopy 4-60237
  - elastic plane, cut opening under moving load 4-97313
  - elastic solids, cracks, acoustic wave diffraction anal. 4-74779
  - elastic wave diff. by subsurface crack 4-87492
  - elastic wave scattering by surface-breaking or subsurface planar crack 4-97378
  - elastic waves, multiple scatt. formalism, scatt. by spheres 4-87611
  - environmental crack growth, temp.-depend., specimen and expt. design 4-109575
  - extended elastic material, deformations and stress intensities due to a craze 4-97424
  - ferrites for magnetic recording heads, toughness evaluation 4-104951
  - ferroelectric ceramics, internal mechanical stresses 4-113530
  - fibre reinforced composite laminates, onset of delamination, expt. and analytical study 4-76847
  - fibre reinforced composite laminates, thermal expansion, effect of microcracks 4-80270
  - fibre reinforced composites model, acoustic emission evaluation 4-81380
  - fracture, environmentally assisted, atomistic models using transition rate theory 4-83855
  - fracture mechanics, microscopic, appl. of J-integral concept 4-97435
  - fully plastic crack problems, consistency check appl. 4-97420
  - fully plastic crack problems, penalty method solns. 4-97419
  - fusion reactor first wall, crit. flaw size prediction methodology 4-96268
  - glass, acoustic emission signal characteristics of Hertzian and unloading cracks 4-75617
  - glass, soda-lime silicate, Vickers indented, delayed fracture in deionised water 4-81268
  - glass fibre reinforced epoxy, thin-walled tubes, deform. and failure after transverse indentation 4-99573
  - glass fibre reinforced PET, strength, effect of temp. and strain rate 4-93375
  - glass fibre reinforced plastics, filament wound pipes, acoustic emission under long-term loading 4-99457
  - glass fibre reinforced polyester, laminated hybrid, crack growth resist., flexural strength 4-62012
  - glass fibre reinforced polyester, panels, surface damage due to projectile impact 4-76865
  - glass fibre reinforced polyester laminates, elastic consts. rel. to fibre orientation and matrix microcracking 4-109447
  - glass grinding damage, single- and multi-point comparison 4-85206
  - glasses and ceramics, crack growth influenced by chem. environment 4-94095
  - grain boundary cavitation in creeping body containing macroscopic crack 4-92289
  - granite from Japan, microcrack growth in aqueous environments 4-94100
  - graphite fibre reinforced epoxy laminates, matrix crack growth, stochastic model 4-109506
  - growth under rolling contact, defect installing technique 4-85284
- cracks continued**
- hard coating flaking under shear stress, fracture mech. anal. 4-69713
  - hardmetal, creation of stable cracks using bridge indentation 4-66434
  - Inconel 617, surface crack form. and propag., effect of temp. reactor primary circuit He 4-114641
  - insulators, high tension, failure prediction, NDT methods comparison 4-62154
  - interface cracks, atomistic versus continuum models 4-113532
  - internal stress energy and fracture characteristics of inhomogeneous solids (German) 4-83861
  - isotropic elastic layer, thermal crack problem, dual integral eqns. 4-112765
  - J-integral estimation procedures for inelastic crack growth 4-76858
  - layered composites with transversely isotropic constituents, annular crack problem 4-103263
  - line contact between a rigid indenter and a damaged elastic body 4-103272
  - materials strain, plastic cracking (Polish) 4-84341
  - metal, book contrib. 4-108508
  - metal hydride solubility, elastic and plastic accommodation effects 4-108620
  - metals, crack-containing, failure mechanism under the effect of electro-mag. field 4-81274
  - metals, fracture mechanism, energetic anal. (Spanish) 4-70269
  - microcrack density function, deformations and thermodynamics, statistical mechanics 4-60330
  - micromechanics, thermodynamic approach 4-88234
  - mixed mode crack propag. studies, double nodding technique 4-79502
  - mixed-mode break mechanics, crack ductility level and deflection angle (German) 4-83864
  - multiple crack problem solns. using Fredholm integral eqns. 4-79509
  - notched bar, creep rupture, continuum damage 4-71735
  - nozzle corner crack, three-dimens. J-integral evaluation under thermal transient loading (Japanese) 4-91772
  - PET, ductile polymer, hypersonic vel. and submicrocrack formation under uniaxial tensile stress 4-114632
  - piezoceramic half-space, crack-inclusion interaction 4-103259
  - pipelines, catastrophic fracture 4-95122
  - plane strain dynamic crack bifurcation 4-83857
  - plate, freely supported, bending in presence of cracks 4-108026
  - plate, multiconnected, anisotropic, with holes and internal cracks, elasticity theory problem 4-74954
  - plate, tensile, small scale, with centre crack tensile test, elastic-plastic FEM computation 4-114737
  - plate, weight function appl., stress intensity factors using FE calcs. (German) 4-83862
  - Plenelj formulas appl. 4-87630
  - PMMA, secondary cracks, form. mechanism, X-ray microanal. and acoustic emission 4-66421
  - PMMA, uniaxial tensile stress, time dependent small angle X-ray scatt. 4-76805
  - poly(1,4-dimethylene-trans-cyclohexyl suberate), crack propag. and morphology 4-114662
  - poly-1,4-dimethylene-trans-cyclohexyl suberate, crack propag., morphology effects 4-114661
  - polycaprolactam, oriented crystalline film, accumulation and enlargement of submicrocracks 4-114667
  - polycarbonate, ductile polymer, hypersonic vel. and submicrocrack formation under uniaxial tensile stress 4-114632
  - polycarbonate, hot water ageing, form. of internal cracks and microvoids 4-81225
  - polyester unsaturated resin, surface markings in brittle plastic plate, two dimens. anal. 4-113527
  - polyethylene films and thick sections, micromechanisms of crack initiation 4-99491
  - polyethylene fracture under long-term loading conditions, tie molecules importance in prevention 4-62041
  - polyimide films, fracture-crack resist. by high mol. weight incorporation 4-89108
  - polymers, brittle, fragmentation due to shock waves 4-108528
  - polymers, fracture and emission of electrons, ions and photons 4-98189
  - polymers, fracture velocity in transient stages, US fractography study 4-99732
  - polymethylmethacrylate, evolution of fractures, prolonged action of electric field 4-108507
  - polystyrene, evolution of fractures, prolonged action of electric field 4-108507
  - polystyrene films, crosslinked, crazing and shear deform. 4-66468
  - porous solids, strength, rel. to pore vol. and max. pore length 4-71714
  - powder compacts, bimodal, sintering behaviour 4-99359
  - prefracture zone, influence of local hardening on plastic deform. 4-70262
  - propagation, double cantilever beam technique 4-103256
  - PWR pipework, unstable crack propagation and stoppage behaviour 4-96225
  - pyrophyllite, shear cracks and seismic conditions in specimens containing long-strength inclusions 4-100554
  - quartz, crack propagation affected by chem. environment 4-94097
  - quartz, diffusional crack healing in aqueous environment 4-94098
  - rock-like material, using rigid body spring model (Japanese) 4-105545
  - rocks, crack growth during unroofing of crustal rocks 4-94102
  - rocks, elec. resist. during crack form. rel. to pore water surface cond. 4-62801
  - rocks, fracture mechanics and acoustic emission of anti-plane shear cracks 4-77507
  - rocks, subcritical crack growth and influence of aqueous environment 4-94099
  - rocks, ultrasonic propagation in cracked rocks (French) 4-62796
  - SH wave diff. by cuts in non-homogeneous solids 4-103257
  - solid/solid interfaces, computer simulations, conf., Philadelphia, USA (Oct. 1983) 4-110806
  - solidification cracking, remedies causes and transverse restraint test 4-85215
  - solids, dilatation mechanism for strength 4-88235
  - sound radiation by growing cracks 4-103258
  - steel, alloy, arc shaped specimens of pipe, errors in J-integral determ. 4-62142
  - steel, alloy, environmental crack growth, temp.-depend., specimen and expt. design 4-109575
  - steel, alloy, reheat cracking, scanning Auger and electron microscopy study 4-71490
  - steel, austenitic, explosion hardened high Mn, residual stress distribution (Japanese) 4-114645

cracks continued  
 steel, austenitic and ferritic stainless, fusion reactor material, crack growth modelling 4-104851  
 steel, austenitic stainless, Alloy 800 H, surface crack form. and propag., effect of temp. reactor primary circuit He 4-114641  
 steel, austenitic stainless, creep crack growth 4-104837  
 steel, austenitic stainless, creep crack initiation and growth 4-99584  
 steel, austenitic stainless, crit. flaw size prediction methodology 4-96268  
 steel, austenitic stainless, fracture modes under He ion and neutron irradi., temp. depend. 4-104853  
 steel, C-Mn, low temp. creep crack growth, effect of cold work 4-76850  
 steel, Cr-Mo, nitrided cases, fracture process, acoustic emission obs. 4-99587  
 steel, Cu-bearing, hot shortness in controlled rolling process 4-89105  
 steel, Cu-Ni-Cr, compact and surface-flawed specimens, fracture toughness meas. comp. 4-104858  
 steel, dynamic toughness, drop weight nil ductility transition test 4-99679  
 steel, elastic wave refl. by infinitely long ribbon crack 4-98197  
 steel, fracture toughness meas. using specimen strength ratio 4-81371  
 steel, high strength, H cracking parameters for predicting safe welding conditions 4-66404  
 steel, high strength structural, stress relief cracking susceptibility 4-109509  
 steel, HSLA, Cu-bearing, hot shortness 4-89104  
 steel, HSLA, shear failure, development of fractographic features 4-76837  
 steel, HT80 weldments, fracture toughness evaluation of heterogeneous bond region 4-99713  
 steel, low alloy, high-temp. brittle fracture, review 4-99562  
 steel, low C and low alloy, brittle fracture, fractographic characteristics, test temp. effects (Russian) 4-109495  
 steel, maraging, ultrahigh strength, delayed failure 4-93402  
 steel, martensitic stainless, Mo, H embrittlement, effect of surface condition 4-85202  
 steel, medium C, ductility anisotropy 4-60301  
 steel, medium C, H-assisted cracking after exposure to H<sub>2</sub>S-saturated salt soln., role of MnS inclusions 4-71732  
 steel, Mn-Si-Cu low-alloy, low-cycle surface cracks exam. under tensile loadings 4-89214  
 steel, oxide-scale cracking and spallation, initiation conditions 4-62100  
 steel, pressure vessel, A 508 2 and A 533 B, comparison of stress relief cracking 4-109510  
 steel, reactor pressure vessel, A533B, environmentally-assisted cyclic crack growth 4-99627  
 steel, rimmed and killed, cavitation erosion resist. rel. to heat treatment and deoxidation (Japanese) 4-89138  
 steel, rotor forgings, unstable fracture, effect of small clustered flaws (Japanese) 4-93378  
 steel, sintered, fracture mechanics behaviour, influence of specimen size 4-81372  
 steel, stainless, type 304, crack opening, stable growth, instability, elastoplastic anal. 4-76822  
 steel, textured, residual stress meas. using US vel. combinations technique 4-89237  
 steel fibre reinforced mortar, polystyrene impregnated, interfacial failure 4-99571  
 steel panels, surface damage due to projectile impact 4-76865  
 stress intensity factor determ. by surface reflected Caustics 4-74970  
 sub-surface crack, elastic wave diff. 4-74926  
 subcritical crack growth in viscoelastic medium with nonlinear stress distributions in crack end zone 4-103260  
 subsurface horizontal crack subjected to time harmonic excitation stress intensity factors, resonance effects 4-97421  
 sucrose, fracture, electron and positive ion emission, triboluminescence 4-104686  
 sucrose, fracture and emission of electrons, ions and photons 4-98189  
 superalloy, IN 100, crack growth under sustained load, statistics 4-99555  
 thermal convection in a porous medium with horizontal cracks 4-97551  
 thermoelastic crack fracture problem (German) 4-83824  
 thick walled tube, branching-out pressures, additional axial forces effect on fissures (German) 4-83863  
 TMI-1, OTSG unplugged tubes, mechanical integrity analysis using linear elastic fracture mechanics 4-86877  
 wear, surface dislocation model 4-60985  
 Wint-o-green Lifesavers, fracture, electron and positive ion emission, triboluminescence 4-104686  
 Al alloy panels, surface damage due to projectile impact 4-76865  
 Al alloys, anisotropic material response on continuum damage, expt. evaluation 4-99565  
 Al-Cu casting alloys, cold cracking mech., plasticity-elasticity transition (Chinese) 4-62026  
 Al-Mg alloy welded joint, crack resistance limit determ. by the moment of crack displacement (Russian) 4-81275  
 Al<sub>2</sub>O<sub>3</sub> ceramics, subcrit. crack propag., activation enthalpies and mechanisms (German) 4-62010  
 Al<sub>2</sub>O<sub>3</sub>, crack kinetics of bend specimens 4-62061  
 Al<sub>2</sub>O<sub>3</sub>, polycrystalline, strength rel. to flow distrib. 4-109505  
 Al<sub>2</sub>O<sub>3</sub>-ZrO<sub>2</sub> ceramics, high press. sintered, fracture toughness rel. to phase transform. 4-76839  
 Al<sub>2</sub>TiO<sub>3</sub> ceramics, synthesis and sintering characts. 4-109361  
 Au/Al contacts, intermetallic bonds and contact resist. (Russian) 4-113819  
 C fibre reinforced epoxy, angle-ply laminates, notch sensitivity 4-93386  
 C fibre reinforced plastic, impact stability evaluation 4-89129  
 CeF<sub>3</sub> doped optical films, tensile stress cracks and stress modification 4-76543  
 Cu-Ga/V multifilamentary superconductors, brittle fracture, acoustic emission anal. 4-71715  
 Cu-Sb alloys, grain boundary segregation and cracking, Monte Carlo studies 4-114542  
 Cu<sub>2-x</sub>S/CdS heterostruct., misfit accommodation and growth 4-108730  
 Fe-Ni austenitic alloys, crack growth and plasticity, influence of mag. ordering (Russian) 4-93368  
 Fe-Ni(-C), martensitic transform., amplitude distrib. of acoustic emission 4-71651  
 Fe-P, segregated grain boundaries crack propag. mol. dynamics calcs. 4-114663  
 Fe-Si (3.25 at.%) alloy, mechanisms of crack origin and twins role in dynamic loading, 77-573K 4-99539  
 Fe-Zn system, formation and growth of  $\delta$  phase, cracks 4-89026

## cracks continued

GaAs, ductile brittle transition in (001) surface layers in single crystals, effect of medium 4-70266  
 GaP, thermal oxidation, surface topography and oxide interface struct. 4-80342  
 H induced delayed cracking in weldments (Chinese) 4-99478  
 KH<sub>2</sub>PO<sub>4</sub> crystals, laser induced damage, X-ray topography 4-65296  
 KNbO<sub>3</sub>, ferroelec. domain struct., IR spectra anal. 4-71323  
 LiF bicrystals, fracture at plastic deform. 4-75609  
 LiF cryst., dislocation band interactions with a healed crack 4-113492  
 LiFe<sub>2</sub>O<sub>3</sub>, mag. domain walls interaction with microstruct. features 4-71122  
 LiNbO<sub>3</sub> cryst. growth, melt composition effect on props. 4-84227  
 MgO crystals, microhardness indentation cracks, energy dissipation, X-ray topography 4-75608  
 (Mn,Zn)Fe<sub>2</sub>O<sub>4</sub>, mag. domain walls interaction with microstruct. features 4-71122  
 Na<sub>2</sub>O-CaO-SiO<sub>2</sub> glasses, ion implanted, mech. props. 4-75542  
 Ni, crack propag., plastic zone, dislocation struct. 4-99488  
 Ni, electrodeposition, hardness, microstruct. 4-66252  
 Ni superalloy Mar-M 200 powder, shock induced compaction, mech. props. 4-109430  
 Ni-Co-Cr-Nb-Hf, Ni-base superalloy, MERL 76, powder metallurgy hot isostatic pressing, effect of Ar contamination 4-114447  
 Ni-Cu alloys, grain boundary segregation and cracking, Monte Carlo studies 4-114542  
 PbO<sub>2</sub> vacuum evaporated films, electron emission and I-V characts. (Japanese) 4-76643  
 Si, dislocation sources, oxidation induced stacking faults (Russian) 4-113457  
 Si<sub>3</sub>N<sub>4</sub>, reaction-bonded, flaw populations, effect of oxidation 4-62059  
 Si<sub>3</sub>N<sub>4</sub>, sintered, static and cyclic fatigue strength (Japanese) 4-99502  
 SiO<sub>2</sub>, fracture and emission of electrons, ions and photons 4-98189  
 SiO<sub>2</sub> glass, crack growth under dynamic loading, temp. and humidity effects 4-62018  
 SiO<sub>2</sub> glass film, crack tip geometry, water ageing, high resolution electron microscopy 4-71724  
 Sn, laser alloyed layers on GaAs substrates, elec. props., surface damage 4-99622  
 Ti<sub>2</sub>VS<sub>4</sub>, reduction of cracking by directional solidification 4-103869  
 W bicrystals, dynamic fracture resist., effect of crack vel. 4-99528  
 W polycrystals, dynamic fracture resist., effect of crack vel. 4-99528  
 W single crystals, dynamic fracture resist., effect of crack vel. 4-99527  
 WC, indented, dislocation interactions, crack nucleation, TEM obs. 4-80039  
 WC-Co, hardmetal, creation of stable cracks using bridge indentation 4-66434

## cranes

TMI-2 reactor building polar crane repair procedures 4-59395

cranking model see nuclear cranking model

## crazing

see also stress corrosion cracking  
 ABS polymers, craze formation and texture 4-104889  
 acrylic polymers, fracture in water 4-76881  
 extended elastic material, deformations and stress intensities due to a craze 4-97424  
 glass fibre reinforced PET, strength, effect of temp. and strain rate 4-93375  
 glassy polymers, ductile, max., strain for craze initiation 4-85227  
 hybrid composite, unidirectional fibre, amplitude distrib. AE signatures 4-89198  
 PMMA, fatigue loaded, crack propag., craze zone, optical interference obs. 4-66422  
 polycarbonate blends with ABS and SAN, tensile and impact tests, energy absorpt. 4-66389  
 polyethylene, tensile stress/strain, 77-298K, crazing rel. to gas environment 4-66467  
 polyethylene terephthalate in liq. media, strain kinetics in creep conditions (Russian) 4-62089  
 polymers, fracture micromechanisms, direct obs. in SEM 4-99578  
 polymers, notched, deform. and fracture, effect of temp. 4-81276  
 polystyrene, glass bead filled, craze form., microscopic in situ obs., interfacial adhesion 4-62073  
 polystyrene, isotactic, craze behaviour, craze-spherulite interaction 4-80150  
 polystyrene films, crosslinked, crazing and shear deform. 4-66468  
 positional small angle X-ray scattering from flaws 4-85278  
 PVC, craze development and breakdown during cyclic loading 4-66465  
 PVC, fatigue loaded, crack propag., craze zone, optical interference obs. 4-66422  
 LiNbO<sub>3</sub>, magnetron sputtered film, prep., crazing rel. to tensile stress 4-81130

creation hypothesis, continuous see cosmology

creation of electron pairs see electron pair production

## creep

see also creep fracture; creep testing; diffusion creep; elastic aftereffect; irradiation induced creep; recovery-creep; stress relaxation  
 accreting bodies subject to aging, nonlinear creep problems 4-79467  
 acrylonitrile-butadiene copolymers,  $\alpha$  relax. kinetics near glass transition temp. 4-81231  
 acrylonitrile-butadiene rubber C reinforcement, static fatigue, statistical analysis 4-99683  
 advanced HTR systems, alloys eval., creep, fatigue, corrosion, neutron effects 4-78699  
 alloy, multiphase, mech. props., book contrib. 4-109424  
 Alloy 800H, creep of tubular components, influence of multiaxiality of stress and environmental induced degradation 4-93360  
 alloys, plastic eqn. of state rel. to scaling behaviour 4-109462  
 aluminosilicate refractories, creep 4-81242  
 anisotropic creep damage in the framework of continuum damage mechanics, reactor appls. 4-102338  
 anisotropic creep damage theory, appl. of continuum damage mechanics 4-65335  
 anisotropic materials, secondary and tertiary creep behaviour, constitutive eqns. 4-91740  
 articular cartilage, normal, relax. and creep quasilinear viscoelastic models 4-109867  
 articular cartilage, unconfin ed compression anal. 4-109868  
 beams, viscoplasticity theory based on overstress 4-60308  
 brittle fracture of thin plastic interlayer in creep conditions 4-97430

## creep continued

butadiene elastomers, relax. process assoc. with supermol. struct., creep meas. (*Russian*) 4-85175  
 butadiene-(methyl)(styrene) elastomers, relax. process assoc. with supermol. struct., creep meas. (*Russian*) 4-85175  
 C\* integrals for creep cracks, evaluation 4-91783  
 Carrara Marble, high temp. flow, grain boundary sliding model 4-110132  
 cavitation damage, influence on high temp. creep, model description 4-103865  
 cavitation damage, influence on high temp. creep at const. load and const. true stress 4-103866  
 ceramics, N-based 4-76746  
 ceramics, stress assisted hot form. 4-76728  
 columns, clamped-clamped, bimodal optimal design under creep conditions 4-83833  
 crack growth under creep, stress field nonstationarity influence 4-97407  
 deformation with multicyclic loading 4-74899  
 deformation-rate law, classical rate-theory-based 4-99417  
 diffusion bonding, development of theoretical model 4-114762  
 ductile materials containing small volume of voids or inclusions, estimates for constitutive moduli 4-98172  
 elastomers, temp. induced creep, hysteresis in thermoelasticity 4-113525  
 ethylene-propylene copolymer, deformation, structural heterogeneity effect (*Russian*) 4-109461  
 ethylene-propylene elastomers, relax. process assoc. with supermol. struct., creep meas. (*Russian*) 4-85175  
 fatigue behaviour, effect of creep prestress 4-104856  
 fusion reactor materials for INTOR and DEMO, first wall lifetime, effect of material props. and operating conditions variations 4-96265  
 glass fibre reinforced plastics, filament wound pipes, acoustic emission under long-term loading 4-99457  
 glass fibre reinforced polyester, creep behaviour of reinforced and non-reinforced resins 4-99456  
 glass fibre reinforced polyester, laminates, creep characts. (*Japanese*) 4-114615  
 grain boundary cavitation in creeping body containing macroscopic crack 4-92289  
 grain boundary migration during high temp. deform. 4-98115  
 Harper-Dorn creep in Earth's mantle, artifact of low-amplitude temp. cycling 4-94089  
 high temperature creep and diffusion, nonstoichiometry depend. 4-92440  
 hot pressing kinetics, semilogarithmic law 4-85123  
 IN 100, Ni-base superalloy, thermal fatigue 4-93417  
 IN-738LC, Ni-base superalloy, precip. of  $\beta$  phase in  $\gamma$  particles 4-114559  
 Inconel 617, surface crack form. and propag., effect of temp. reactor primary circuit He 4-114641  
 Inconel 718, fatigue and creep-fatigue crack propag., influence of neutron irradi. 4-99496  
 Inconel 718, time-depend. fatigue crack propag., effect of small scale to large scale creep transition (*Japanese*) 4-93383  
 Inconel X-750, environmental, stress-state and section-size synergisms during creep 4-61995  
 Inconel X-750, Ni-base superalloy, creep and fracture, prior deform. effects 4-114656  
 inelastic design anal., constitutive eqns. 4-91737  
 inelastic solids and structures, plasticity and creep methods, reactor appls. 4-102339  
 inhomogeneously ageing bodies, asymptotics near crack tip 4-60325  
 macrocrack motion, influence of creep void growth 4-98194  
 mantle, viscosity-depth profiles and creep 4-72550  
 material squeezed between parallel plates, power law creep, perturbation scheme 4-87586  
 materials behaviour at high temperatures 4-99473  
 mechanical behaviour of materials, conf., Stockholm, Sweden (Aug. 1983) 4-90297  
 metal, book contrib. 4-109484  
 metallic material, nonsteady creep, system of kinetic eqns. 4-65334  
 metallic materials, creep, determ. for 'long-service' lives by multistage process 4-114624  
 metals, creep mechanism maps, expt. 4-93359  
 metals, cyclic creep, relationship with hysteresis loop energy 4-109456  
 metals, hardening and degradation rules under monotonic and cyclic loading 4-65333  
 metals, high-temp. creep, reln. between Orowan and Bailey-Orowan eqns. 4-92209  
 metals, plastic deform. constitutive eqn., recovery, dislocation creep, stress relax. 4-66370  
 metals, strain controlled creep-fatigue tests 4-89209  
 metals, with memory of maximal prestress, creep-hardening rule 4-76806  
 metals and alloys, dislocations and strength at very low temps., book contrib. 4-99452  
 metals and alloys, stress-rupture strength in complex stressed state, criteria development 4-99540  
 metamorphic rocks, pressure solution creep 4-94113  
 nonlinear materials, dilutely voided, constitutive potentials 4-87583  
 periclase refractories, creep 4-66396  
 petroleum pitches, fractionated and blended, creep and glass transition, influence of mol. wt. distrib. 4-103864  
 plastic deformation, low-temperature anomalies in crystalline materials 4-70256  
 plates, circular, simply supported, creep anal., variational principles (*Chinese*) 4-60305  
 PMMA, rubber particle toughened, kinetics and mechanism of deform. 4-76813  
 polyethylene, high density, mechanical loss factor, transient behaviour during creep and relax. 4-71710  
 polyethylene, thermally stimulated creep 4-84339  
 polyethylene mixtures, ultrahigh mol. wt. and medium density, rheological and mech. props. 4-84414  
 polyethylene terephthalate in liq. media, strain kinetics in creep conditions (*Russian*) 4-62089  
 polyethylene-propylene copolymers and blends, thermally stimulated creep 4-84339  
 polymer, thermally stable, viscoelastic behaviour under isothermal creep, governing laws 4-66367  
 polymer blends, conf., Ottawa, Ontario, Canada (April 1983) 4-82591  
 polymer solutions, nonlinear creep and recovery, strain criterion 4-85183  
 polymers, fracture and rheological characteristics, interrelation 4-88232

## creep continued

polymers, viscoelastic, transient creep, nonlinear constitutive eqns. 4-88230  
 polyoxadiazole, viscoelastic behaviour under isothermal creep, governing laws 4-66367  
 polypropylene, isotactic,  $\alpha$  and  $\beta$  relax. kinetics 4-81255  
 polypropylene, long term creep tests at 120°C 4-109466  
 polypropylene, physical ageing by freezing-in of nonequib. values of limiting compliances 4-81254  
 polypropylene, thermally stimulated creep 4-84339  
 polystyrene latex dispersions, conc., sterically stabilised, free polymer addition, rheological investigation 4-112788  
 polystyrenes of narrow mol. wt. distrib., blending, creep flow and recovery in elongation 4-97454  
 polyurethane foam, compressive creep rel. to particulate reinforcement 4-89084  
 powder compacts, bimodal, sintering behaviour 4-99359  
 pressurised components, lower bound of creep buckling strength 4-91747  
 quartz, creep, dislocation mobility stress depend. 4-70265  
 quartz, hydrolytically weakened, plasticity and rheology 4-92286  
 Heavirtre quartzite, creep behaviour, water content effects 4-94112  
 reactor fuel pin transient deformation, cladding strains, MOX fuel appl., creep 4-102378  
 reactor structure optimisation problems under creep conditions, math. models, plates appl. 4-102354  
 reinforced thermoplastic composites, creep resistance, fatigue endurance 4-61994  
 relaxation creep, computer model for high temp. 4-84340  
 rods, nonuniformly-heated, under creep conditions, combined extension and flexion (*Russian*) 4-79465  
 shell, reinforced, cylindrical, stability in creep 4-74896  
 shells of revolution, thick, under asymm. loading creep anal. 4-74891  
 sialon, fracture toughness, effect of deform. 4-76868  
 sialons, hot-pressed and reaction-bonded, phase equilib. and props. 4-76761  
 $\beta$ -sialons, microstruct. evaluation by TEM, correl. to mech. props. 4-76732  
 solid solutions and intermetallics, mech. props. book contrib. 4-109423  
 steel, alloy, reheat cracking, scanning Auger and electron microscopy study 4-71490  
 steel, austenitic, Cr-Ni type, reactor irradi. effect on refractory characts. 4-66398  
 steel, austenitic stainless, Alloy 800 H, surface crack form. and propag., effect of temp. reactor primary circuit He 4-114641  
 steel, austenitic stainless, creep, applicability of creep J-integral to microscale propag. (*Japanese*) 4-93384  
 steel, austenitic stainless, creep, Portevin-Le Chatelier effect and dynamic strain ageing 4-114617  
 steel, austenitic stainless, creep and plasticity, constitutive eqns. 4-93347  
 steel, austenitic stainless, creep exposure, influence of regenerative heat treatment on remaining life 4-114602  
 steel, austenitic stainless, creep of tubular components, influence of multiaxiality of stress and environmental induced degradation 4-93360  
 steel, austenitic stainless, creep-fatigue, in high temp. materials, constitutive relationships 4-93353  
 steel, austenitic stainless, creep-fatigue studies under biaxial stress state at elevated temps. 4-66409  
 steel, austenitic stainless, cumulative fatigue damage at high temps., effect of cyclic strain 4-93414  
 steel, austenitic stainless, cyclic creep and life 4-99445  
 steel, austenitic stainless, fatigue crack propagation in specimens subjected to thermal shock 4-93413  
 steel, austenitic stainless, high temp. creep, biaxial expts., constitutive laws 4-93352  
 steel, austenitic stainless, high temp. creep rel. to carbide precipitates 4-76802  
 steel, austenitic stainless, low cycle fatigue, elevated temps., crack propag. and fracture modes (*Japanese*) 4-89125  
 steel, austenitic stainless, low cycle fatigue, notch effect in creep-fatigue interaction at elevated temp. 4-66444  
 steel, austenitic stainless, Nb-bearing, creep props., effect of Fe<sub>2</sub>Nb precip. 4-114619  
 steel, austenitic stainless, plasticity at elevated temps., effect of prior creep 4-104828  
 steel, austenitic stainless, thermal creep and stress-affected precip. 4-99428  
 steel, austenitic stainless, TiC precipitation, influence on creep rupture strength, ductility and He embrittlement 4-99388  
 steel, C-Mn, low temp. creep crack growth, effect of cold work 4-76850  
 steel, constructional, cyclic creep in plane stressed state, life determ. 4-99446  
 steel, Cr-Mo, creep and precip. (*German*) 4-66375  
 steel, Cr-Mo, creep failure, influence of state of stress 4-93419  
 steel, Cr-Mo-V, crack growth, influence of cyclic loading 4-93421  
 steel, Cr-Mo-V, creep recovery by reheat treatment, carbide distrib., X-ray analysis 4-66392  
 steel, Cr-Ni-Mo-V, cyclic creep in complex stress state 4-99447  
 steel, creep and plasticity, constitutive eqns. 4-93347  
 steel, creep damage and embrittlement at high temp., US meas. (*French*) 4-61973  
 steel, ferritic, welded joints, creep behaviour 4-93357  
 steel, H attack, invest. of models 4-104847  
 steel, low alloy, cast, thermal-mech. fatigue crack propag., effect of strain wave shape 4-66445  
 steel, low alloy, creep fatigue and environmental interactions 4-99593  
 steel, low alloy, fracture under corrosive environment, high temp. creep, fatigue, creep-fatigue 4-99592  
 steel, low alloy ferritic, low cycle fatigue, elevated temps., crack propag. and fracture modes (*Japanese*) 4-89125  
 steel, martensitic stainless, HT-9, thermal creep deform., constitutive design eqns. 4-93338  
 steel, martensitic stainless, welded joints, creep behaviour 4-93357  
 steel, microduplex stainless, rapidly solidified, superplastic response rel. to ferrite-austenite content 4-99433  
 steel, mild, creep at low temp. 4-89086  
 steel, pressure vessel, A 508 2 and A 533 B, comparison of stress relief cracking 4-109510  
 steel, structural, nonlinear elasto-plastic creep, stress and temp. depend. 4-109465  
 steel, viscoplasticity at room temp., crit. uniaxial expt. 4-93336

creep continued

strain-dependent creep damage and rupture in three dims., thermodynamic foundations 4-75607

structural materials, mech. props. at low temps. rel. to stressed state and mode of loading 4-93350

super alloys, super alloys, oxide dispersion strengthened, developments in prod. 4-114452

thermally unstable alloy, thermal fatigue 4-93417

thin layers, steady-state nonlinear creep, contact problems 4-64856

Udimet 700, creep-fatigue, in high temp. materials, constitutive relationships 4-93353

Udimet 700, metalloid strengthening mechanism 4-61974

viscoelastic bodies, subcritical growth of microscopic fatigue cracks 4-108048

viscoelasticity, regularisation and inverse problems 4-103220

viscoplasticity at room temp., crit. uniaxial expt. 4-93336

voids, creep, mechanism of sintering out during subsequent annealing 4-92213

welded joints, creep behaviour 4-93356

Zircaloy, textured, creep modelling under biaxial stressing 4-93354

Zircaloy-2, creep activation energy rel. to dynamic strain ageing 4-81250

Zircaloy-4, cold worked, creep, eqn. of state appl. 4-109462

Zircaloy-4, creep at 673K, texture evolution 4-114613

Ag-Al (10 at %), transient creep, effect of  $\mu$  phase precip. 4-114618

Al alloy, type 2618, 48 hour multiaxial creep and creep recovery at 200°C 4-104830

Al alloy, type 2618-T61 multiaxial creep under proportional loading steps 4-104831

Al biaxial creep behaviour, thermodynamic aspects (*French*) 4-85187

Al, creep substructure effect on stress exponent following stress reductions 4-104820

Al creep velocity, high-energy ion irradiation effects 4-70243

Al single crystal, dislocation multiplication during creep 4-98106

Al-Al<sub>2</sub>O<sub>3</sub>-(Si), creep deform., stress and temp. depend. 4-81246

Al-glass composite, produced by powder metallurgy route, mech. props. 4-66275

Al-Mg, creep, stress range of Class I behaviour 4-81249

Al-Mg (1.74 at %), creep, strain transients in stress drop tests 4-85196

Al-Mg alloys, steady-state creep, stress components 4-85181

Al-Mg class I high temp. creep alloys, internal and friction stresses 4-85185

Al-Mg solid solution alloys, high stress levels, breakdown in creep 4-113526

Al-Mg-Si, creep life prediction, long-time, role of microstruct. instability 4-114622

Al-Zn solid solns., creep and Zn self-diffusion 4-65461

Al<sub>2</sub>O<sub>3</sub>-SiO<sub>2</sub>-TiO<sub>2</sub>-Cr<sub>2</sub>O<sub>3</sub>, high alumina refractory brick, creep resist. rel. to Cr<sub>2</sub>O<sub>3</sub> addition 4-109457

CaTiO<sub>3</sub>, polycryst., viscous creep deform. at elevated temps. 4-103863

Cd-Zn single crystals, critical resolved shear stress, 1.5 to 50K 4-71685

Co-Co, creep mechanism maps, expt. 4-93359

Co<sub>3</sub>O<sub>4</sub>, chem. diffusion, creep meas. 4-92418

Cr-Ni alloy, El826, cyclic loading parameters influence on deform. and fracture kinetics 4-99441

Cu, creep and long-term strength study (*Russian*) 4-80146

Cu, creep at cryogenic temps. 4-99423

Cu, creep cavitation, grain boundary void growth, small angle neutron scatt. obs. 4-85197

Cu, creep mechanism maps, expt. 4-93359

Cu, polycrystalline, cyclic creep accel. and retardation, threshold stress temp. depend. 4-66372

Cu, single crystal, strain bursts in cyclic creep at ambient temp. 4-66371

Cu-Fe (2 wt %), precipitation strengthened, high temp. creep 4-61990

Cu-Sb (1 wt %), creep rupture life, effects of pre-existing grain boundary cavities 4-62042

Cu-Si, dil. alloy, internal oxidation, grain boundary cavitation under creep or fatigue loading 4-71726

$\beta$ -CuZn, plastic deformation at He temps., capacitance meas. 4-71681

(Fe, Co, Ni)<sub>3</sub>V, ductile ordered alloys, phys. metallurgy and mech. props. 4-114612

$\alpha$ -Fe, creep-induced dislocation subgrain arrangement in ferrite, effect of stress changes 4-76799

Fe-base superalloys, creep-rupture of candidate Stirling engine alloys 4-99553

Fe-Cr-Al-Y plasma sprayed coatings, post-treated, mech. props. 4-93471

Fe-Mo (6.3 at %), high temp. creep, stress exponent and substruct. 4-76821

Fe<sub>40</sub>Ni<sub>60</sub>B<sub>20</sub>, amorphous, structural relax., contraction and creep meas. 4-85195

LiF, single crystal, IR transmission spectra at 300K, effect of stepped creep on exhaustion of dislocations 4-65271

Mg, creep mechanism maps, expt. 4-93359

MgO powder, hot pressing, densification, dislocation creep mechanism 4-114455

MgO spinel refractories, creep 4-66396

Mo, high temp. creep, surface relief form. and growth in single crystals. 4-71689

Nb alloy, plastic deform. with subsequent nitriding effect on mech. props. 4-114713

Ni, creep mechanism maps, expt. 4-93359

Ni superalloy, creep and recovery kinetics, report 4-62000

Ni-Al<sub>2</sub>O<sub>3</sub>, electron beam evaporated condensates, creep props. 4-93361

Ni-base alloys with high vol. fraction of  $\gamma'$ , flow stress and creep props. 4-114611

Ni-base superalloy, single cryst., creep-fatigue behaviour, effect of orientation 4-109512

Ni-Co-Cr-Nb-Hf, Ni-base superalloy, MERL 76, powder metallurgy hot isostatic pressing, effect of Ar contamination 4-114447

Ni-Cr base alloys, effect of microstruct. and microstruct. 4-71705

Ni-Cr-Al (20, 4 wt %), high temp., oxidation, tensile stress depend. 4-109572

Ni-Cu (22 at %), annealed and quenched, creep behaviour and miscibility gap 4-66387

Ni<sub>3</sub>Al, ordered alloy, flow stress and creep props. 4-114611

Re, creep tested, dislocation struct., X-ray divergent beam obs., TEM studies 4-99420

SIC fibres, mech. props. and struct. (*French*) 4-62003

SIC, fusion reactor first wall appl., thermal and mech. props. (*German*) 4-83244

SIC, reaction bonded, high temp. creep kinetics, dislocation glide mechanism 4-109476

## creep continued

Si<sub>3</sub>N<sub>4</sub>, fracture toughness, effect of deform. 4-76868

Si<sub>3</sub>N<sub>4</sub>, hot-pressed, transient creep parameters, determ. by dynamic bending tests 4-81381

Si<sub>3</sub>N<sub>4</sub>, pressureless sintered, high temp. fatigue failure 4-76867

Si<sub>3</sub>N<sub>4</sub>, reaction bonded, creep, porosity, internal oxidation 4-76833

SiYON ceramics, mech. props. rel. to corrosion and microstruct. 4-76834

Sn, white, single crystals, dislocation motion in pre-multiplication region, creep, etching 4-108375

Sn-Bi (0.5 at %), creep rate, grain dia. depend. 4-81259

Sn-Cd (5 wt %), plasticity rel. to eutectoid transform 4-114605

Sn-Pb (38.1 wt %), eutectic, fine-grained, accelerated coarsening of microstruct. during superplastic deform. 4-61997

$\alpha$ -Ti, creep mechanism maps, expt. 4-93359

Ti-Al-V (6.4 wt %), superplastic, solid state bonding 4-61989

Ti-Er, rapidly solidified dispersion strengthened, tensile and creep props. 4-114562

Ti-Nd, rapidly solidified dispersion strengthened, tensile and creep props. 4-114562

Ti-V solid solutions, creep, microstruct. 4-109464

UO<sub>2</sub>, creep deform. behaviour, 2100 to 2600°C 4-76814

UO<sub>2</sub>, indentation creep before and after irradiation, sintered pellets 4-61977

V-Cr-Ti(Fe-Zr), mech. props. rel. to O contamination, fusion appls. 4-109499

W, AKS-doped wire, high-temp. creep behaviour, effect of gas bubbles (*German*) 4-81243

W, creep in single crystals at moderate temps., struct changes 4-65269

Zr proton irradiation and thermal creep at elevated temps. under stress 4-75559

Zr-Nb (2.5 wt %), CANDU pressure tubes, high temp. creep model for loss of coolant accident 4-109473

## creep fracture

anisotropic creep damage theory, appl. of continuum damage mechanics 4-65335

Astrolay, Ni-base superalloy, creep fracture, effect of wavy grain boundaries (*Chinese*) 4-62005

biaxial test facility for creep crack growth in damaged material 4-93490

brittle fracture of thin plastic interlayer in creep conditions 4-97430

C\* integrals for creep cracks, evaluation 4-91783

cavitation damage, influence on high temp. creep, model description 4-103865

cavitation damage, influence on high temp. creep at const. load and const. true stress 4-103866

continuum damage role in creep crack growth 4-71736

crack growth, comparison of finite element predictions with expt. data 4-97410

crack growth at high temp., void coalescence and growth 4-79505

defect sizes in plant at elevated temp. 4-91773

epoxide composite, alumina particle filled, fractography (*Japanese*) 4-99512

ferromagnetic amorphous ribbon, simultaneous magnetic meas. and torsional creep 4-111163

fusion reactor first walls, lifetime calc., creep-fatigue design criteria 4-96254

grain boundary cavitation in creeping body containing macroscopic crack 4-92289

IN-738 LC, Ni-base superalloy, creep fracture, effect of grain boundary chem. and segregation 4-81285

Inconel 718, time-depend. fatigue crack propag., effect of small scale to large scale creep transition (*Japanese*) 4-93383

Inconel 718 gas turbine disc material, crack initiation from notch under creep fatigue conditions 4-99567

Inconel X-750, environmental, stress-state and section-size synergisms during creep 4-61995

Inconel X-750, Ni-base superalloy, creep and fracture, prior deform. effects 4-114656

Kevlar 29 braid, bending fatigue life rel. to resin impregnation 4-93394

macrocrack motion, influence of creep void growth 4-98194

materials behaviour at high temperatures 4-99473

metal, book contrib. 4-109484

metals, dissipative criterion for creep rupture 4-88231

notched bar, creep rupture, continuum damage 4-71735

plant life prediction at elevated temp., creep-fatigue and thermal shock failure 4-91774

polyamide 66 fibre, loading criteria for fatigue failure, acceleration of creep failure 4-62008

polycrystals, strong and ductile, grain boundary design, overview 4-65336

polyethylene, linear, creep rupture and pre-rupture phenomena 4-89131

polymeric materials, creep damage eqn., stress effect 4-92288

steel, (2.25, 1 wt %), annealed, creep-rupture props., heat-to-heat variations 4-76860

steel, alloy, reheat cracking, scanning Auger and electron microscopy study 4-71490

steel, austenitic stainless, crack growth under creep-fatigue interaction (*Japanese*) 4-99507

steel, austenitic stainless, creep, applicability of creep J-integral to microscale propag. (*Japanese*) 4-93384

steel, austenitic stainless, creep crack growth 4-104837

steel, austenitic stainless, creep crack initiation and growth 4-99584

steel, austenitic stainless, creep crack propag., DC pot. meas. of crack length (*Japanese*) 4-99688

steel, austenitic stainless, creep crack propag. after boiler service (*Japanese*) 4-99510

steel, austenitic stainless, irradiation creep, light ion simulation 4-104815

steel, austenitic stainless, Nb-bearing, creep props., effect of Fe<sub>2</sub>Nb precip. 4-114619

steel, austenitic stainless, stress rupture in-reactor creep cavity form. model 4-104854

steel, austenitic stainless, stress rupture strength, statistical prediction 4-99701

steel, austenitic stainless, TiC precipitation, influence on creep rupture strength, ductility and He embrittlement 4-99388

steel, C-Mn, low temp. creep crack growth, effect of cold work 4-76850

steel, Cr-Mo, creep failure, influence of state of stress 4-93419

steel, Cr-Mo-V, crack growth, influence of cyclic loading 4-93421

steel, Cr-Mo-V, creep recovery by reheat treatment, carbide distrib., X-ray analysis 4-66392

steel, ferritic, welded joints, creep behaviour 4-93357

steel, low alloy, creep fatigue and environmental interactions 4-99593

**creep fracture continued**

- steel, low alloy, fracture under corrosive environment, high temp. creep, fatigue, creep-fatigue 4-99592  
 steel, martensitic stainless, HT-9, thermal creep deform., constitutive design eqns. 4-93338  
 steel, martensitic stainless, welded joints, creep behaviour 4-93357  
 steel, Mn-Mo-Ni, creep fracture and rupture life (*Japanese*) 4-114647  
 steel, Ni-Cr-Mo-V, creep rupture and service properties improvement (*German*) 4-76862  
 steel, stainless, austenitic, kinetic damage and failure at sharp notch tip in creep conditions 4-66441  
 steel, steam turbine casing and rotor, mech. props. rel. to service life (*Japanese*) 4-89119  
 steel, steam turbine rotor type, creep-fatigue damage, report 4-62047  
 strain-dependent creep damage and rupture in three dims., thermodynamic foundations 4-75607  
 stress rupture strength prediction, damage accumulation theory 4-98193  
 structural materials, mech. props. at low temps. rel. to stressed state and mode of loading 4-93350  
 Udimet 700, Ni-base superalloy, creep fracture, effects of wavy grain boundaries 4-93415  
 welded joints, creep behaviour 4-93356  
 welded joints, high temp. deform. and failure 4-93409  
 Cr-Ni alloy, E1826, cyclic loading parameters influence on deform. and fracture kinetics 4-99441  
 Cu, creep fatigue, failure life and microdamage mode rel. to wave shape 4-109508  
 Cu-Fe (2 wt.%), precipitation strengthened, high temp. creep 4-61990  
 Cu-Sb (1 wt.%), creep rupture life, effects of pre-existing grain boundary cavities 4-62042  
 Fe-base superalloys, creep-rupture of candidate Stirling engine alloys 4-99553  
 Fe-Cr-Al, oxide dispersion strengthened MA 956, fatigue crack growth 4-62031  
 Ni-Nb-NbC, eutectic alloys, powder metallurgy, physical props., high temp. use 4-85125

**creep-recovery see recovery-creep****creep testing**

- biaxial test facility for creep crack growth in damaged material 4-93490  
 braided orthodontic tensioning device, creep and stress relax. props. 4-115269  
 cryogenic creep testing, equipment 4-104930  
 organic plastic, unidirectionally reinforced, creep strain prediction 4-89234  
 plastic, creep testing and eval. method in static bending fatigue tests (*German*) 4-71821  
 polymers, strength and deform. under artificial weathering (*German*) 4-89229  
 polypropylene, long term creep tests at 120°C 4-109466  
 recovery rate meas., strain transient dip test, computer simulation 4-114734  
 shortened test method for creep eval. during static bending fatigue tests (*German*) 4-71821  
 steel, austenitic stainless, creep of cylindrical specimens, dia. deviations (*German*) 4-99697  
 tensile testing of materials at elevated temps., threshold stress, struct., recovery models 4-66528  
 urethane TPE monofilament, orthodontic tensioning device, creep and stress relax. props. 4-115269  
 wood, creep testing and eval. method in static bending fatigue tests (*German*) 4-71821  
 Al-Mg solid solution alloys, high stress levels, breakdown in creep 4-113526  
 Re, creep tested, dislocation struct., X-ray divergent beam obs., TEM studies 4-99420  
 Si<sub>3</sub>N<sub>4</sub>, hot-pressed, transient creep parameters, determ. by dynamic bending tests 4-81381

**crestatrons see travelling-wave-tubes****crimping**

No entries

**critical constants, thermal see critical points****critical current density (superconductivity)**

- composite superconduc., prep. and high field supercond. props. 4-92881  
 composite superconductor, surface resistance influence on current-carrying characts. 4-114079  
 hexagonal to quadratic vortex lattice transition, pinning on surfaces and large grain boundaries 4-80729  
 multifilamentary in situ superconductor, longitudinal field loss, twist effects 4-61496  
 Mo<sub>1-x</sub>Si<sub>x</sub> getter, sputtered films, superconducting props. (*Chinese*) 4-114054  
 NbN-Nb Josephson junction with plasma oxidised barrier, growth and props. 4-84747  
 Nb<sub>3</sub>Sn, bronze processed pure and alloyed, supercond. crit. current density at very high mag. fields 4-71008  
 Nb<sub>3</sub>Zr<sub>35</sub>Si<sub>15</sub>, Nb<sub>3</sub>O, Zr<sub>15</sub>Si<sub>15</sub>, amorphous alloys, supercond. and electronic props., cold rolling effect 4-61480  
 Pb-Ag<sub>1-x</sub>Mn<sub>x</sub>Al<sub>1-x</sub>Pb, S-N-S junction, pair-breaking mechanism 4-98824  
 Ti-Nb-Ni-(Ge), struct. and supercond. props. (*Russian*) 4-92143  
 V<sub>3</sub>Ga composite superconduc., prep. and high field supercond. props. 4-92881  
 V<sub>3</sub>Ga wire, supercond. props. and modified jelly roll prep. 4-104749  
 V<sub>3</sub>Si layers, superconducting props. study 4-88623

**critical currents**

- see also critical current density (superconductivity); flux creep; flux flow; flux pinning*  
 losses in multifilament superconducting wire at increasing transport current and magnetic field 4-92879  
 magnetic superconductors, phase transitions, critical characteristics (*Bulgarian*) 4-80732  
 quantum Hall regime, critical currents 4-98644  
 superconducting broad films, resistive state, vortex changes 4-65780  
 type II supercond. plate, longitudinal critical current and critical thickness (*Chinese*) 4-98833  
 Cu-Nb-Sn multifilamentary superconductors for superconducting magnets, powder metallurgy processing 4-80731  
<sup>3</sup>He, B-phase, flowing superfluid, dissipation mechanism crossover near tricritical press. 4-113746

**critical currents continued**

- In supercond. film, resistive transition in mag. field, symmetry breakdown 4-65779  
 Nb film, supercond. crit. current in weak mag. field (*Russian*) 4-92880  
 Nb, film Dayem microbridges, critical current, metallurgical transformation effects (*French*) 4-84760  
 Nb-Al multifilamentary superconductors for superconducting magnets, powder metallurgy processing 4-80731  
 Nb-Sn supercond wires, processed, electromag. props., stress effects (*Japanese*) 4-84759  
 Nb-Ta/Sn liquid-infiltration multifilamentary superconductors 4-98832  
 Nb-Ti supercond. wires, electromag. props., stress effects (*Japanese*) 4-84759  
 Nb-Ti superconductors, flux pinning by gas bubbles (*Russian*) 4-104381  
 NbN film, supercond. crit. current in weak mag. field (*Russian*) 4-92880  
 Nb<sub>3-x</sub>Ta<sub>x</sub>Sn multifilamentary superconductor, crit. current and upper crit. field 4-98834  
 Y<sub>6</sub>Co<sub>7</sub> ferromag. inhomogeneous supercond., sample size and meas. power effects 4-76065  
 Zr-Si, amorphous, upper critical field meas. 4-84754

**critical field, superconducting see superconducting critical field****critical fluctuations**

- see also fluctuations in superconductors*  
 antiferromagnet, weakly anisotropic, phase diagram and critical lines (*Russian*) 4-71062  
 binary fluid, nonlinear effects in supercritical quenches 4-61043  
 Dicke-like models, fluctuations and phase transitions 4-92923  
 ferroelectric semiconductors, photoferroelectric phenomena caused by fluctuations and phasons 4-70856  
 glass, anomalous thermal, acoustic and dielec. props. at low temp. 4-60994  
 Heisenberg, magnetic materials, intermediate ordered phases, calcs. 4-114132  
 low-dimensional phase transition, droplet theory 4-78283  
 massless quantum field theory, conformal symmetry of critical fluctuations in 2-D 4-86539  
 metallic rare earth valence fluctuating systems model 4-80468  
 modulated phases, Ginzburg-Levanyuk criterion for phase transitions 4-98274  
 noncollinear antiferromagnet, spin-flip transitions 4-104425  
 one-dimensional systems, Ising model, fluctuation study 4-98849  
 order-disorder phase transitions, crit. anomalies of vibr. lineshape 4-103893  
 transition metals, paramagnetic, temp. fluctuations of electron spin density (*Russian*) 4-65791  
 uniaxial crystals, with defects, crit. fluctuations and phase transitions 4-71308  
 uniaxial ferroelectrics, US absorpt. and vel., order parameter crit. fluctuations anisotropy spectrum, appl. to CsH<sub>2</sub>PO<sub>4</sub> 4-98206  
 Fe, Gilbert damping, critical fluctuation effects, ferromag. resonance study 4-61539  
<sup>3</sup>He, liq., critical fluctuations near gas-liq. critical point, decay rates 4-92468  
<sup>3</sup>He-<sup>4</sup>He liq. mixtures, critical fluctuations near gas-liq. critical point, decay rates 4-92468  
<sup>4</sup>He, superfluid, turbulent, fluctuations of a negative ion current 4-113737  
 K<sub>2</sub>CoF<sub>4</sub> 2D Ising model, critical fluctuations, neutron scatt. meas. 4-92927  
 Ni, stress effects on mag. phase transitions 4-114106  
 Pb<sub>3</sub>Ge<sub>2</sub>O<sub>11</sub>, soft modes rel. to crit. fluctuations, neutron and Raman scatt. meas. 4-65370  
 Rb<sub>2</sub>ZnCl<sub>4</sub>, soft modes rel. to crit. fluctuations, X-ray scatt. meas. 4-65370  
 SrTiO<sub>3</sub>, soft modes rel. to crit. fluctuations, neutron scatt. meas. 4-65370  
**critical mixtures**  
 agarose, gel saturated with binary liq. mixtures, critical behaviour 4-93365  
 binary fluid, nonlinear effects in supercritical quenches 4-61043  
 binary fluid mixture, anisotropic spinodal decomposition under shear flow 4-69738  
 carbon tetrachloride/coconut oil, complex binary mixtures, crit. point, US study 4-80161  
 methanol-cyclohexane mixtures, turbidity near critical point 4-66052  
 methanol-n-heptane, critical dielectric const. meas. as function of temp. 4-92989  
 microemulsion, three-component, struct. in critical region, small-angle neutron scatt. obs. 4-66620  
 nitrobenzene-n-hexane crit. binary mixture, shear-induced dichroism and birefringence 4-104567  
 polyacrylamide gel saturated with binary liq. mixtures, critical behaviour 4-93565  
 polyoxyethylene, micelle soln., cloud point transition, light scatt. 4-81486  
 silica gel saturated with binary liq. mixtures, critical behaviour 4-93565  
 turbulent critical binary mixtures 4-60386

**critical opalescence**

- BMOA-isooctane mixture, extinction, optical props. of highly opalescent systems 4-84936  
 multiple light-scattering near the critical point, critical opalescence 4-84938  
 oil-water microemulsion model 4-99849  
 polyvinyl methyl ether-deuterated polystyrene mixture, critical opalescence (*German*) 4-104565  
 N<sub>2</sub>O<sub>4</sub>-2NO<sub>2</sub>, chem. equilib. anomalies near crit. points 4-93543

**critical phenomena**

- see also critical fluctuations; critical mixtures; magnetic transitions; phase equilibrium; phase transformations; renormalisation*  
 (1+1)-dimensional Ashkin-Teller model, phase diagram and critical props. 4-68162  
 1d quantum ground state, Monte Carlo renormalisation group simulation 4-58762  
 aliphatic carboxylic acid monolayers, critical phenomena, mol. theory 4-75755  
 Ashkin-Teller model, time-continuous Hamiltonian, finite size studies 4-111046  
 asymmetric clock model on Cayley tree 4-68158  
 Baxter model, impure, universal behaviour, Monte Carlo studies 4-104388  
 bond percolation critical probability determ. based on star-triangle transformation 4-68161

## critical phenomena continued

Bose system, random field effects, critical and crossover phenomena in Hartree limit 4-111016  
 chaos, statistical mech. formalism, window phenomenon, critical phenomena 4-90501  
 cluster aggregation, diffusion-limited, dynamic scaling relation 4-68173  
 complex models, linked-cluster series expansion and phase transitions 4-58800  
 condensed matter physics, Iberian Symposium, Lisbon, Portugal (Sept. 1983) 4-78036  
 conductivity, critical exponents rel. to static exponents 4-95323  
 conference on mathematical physics, Boulder, CO, USA (Aug. 1983) 4-67856  
 Coulomb gas, spin models in 2-D, charge asymmetry, critical behaviour 4-86356  
 d-dimensional lattice, critical exponents for long-range interactions 4-68169  
 defect space,  $\epsilon$  expansion, critical phenomena and renormalisability 4-82761  
 dilute antiferromag. chain, critical dynamic response 4-71119  
 dilute magnets, phase transitions, critical behaviour, percolation, random fields 4-88690  
 diluted ANNNI models, modulated phases, conc. depend., spin configs., percolation 4-80770  
 diluted quantum transverse Ising model in two dimensions 4-63681  
 dimensional crossover in directed percolation position space renormalisation group 4-111047  
 dipolar fluids, coexistence curve, orientation correl., effective pair pot. 4-88055  
 eight-vertex SOS model and generalized Rogers-Ramanujan-type identities 4-101766  
 EPPCB, smectic B-nematic phase transition, X-ray scatt. studies 4-75675  
 equilibrium statistical mechanics, theories, and appls., book 4-58589  
 ferromagnet, cubic, critical behaviour, Potts model anal. 4-61546  
 field theory, critical phenomena, constructive approach 4-68393  
 finite-size scaling, conformal invariance and universality 4-68157  
 first-order phase transitions, nucleation-growth processes, scaling laws (Japanese) 4-113568  
 flat square lattice, multiphase behaviour of large interacting molecules, Percus-Yevick approx. 4-73396  
 fluid viscosity meas. in critical region, rotating disc viscometer appl. 4-60568  
 fractal lattices, dilute Ising models, phase diagram and critical exponents 4-90516  
 fractal lattices, infinitely ramified, phase transitions 4-58771  
 hard hexagon model, generalised, deviations from critical density 4-90518  
 Heisenberg model, mean field renormalisation, critical temp. 4-98850  
 hierarchical lattice spin systems, phase transition phenomena 4-95364  
 hypercubic lattices, bond percolation, extended mean cluster size series anal. 4-111071  
 ideal Bose gas, magnetised, crit. props. 4-58734  
 interface stability critical phenomena and scalar order parameters 4-58802  
 irreversible kinetic gelation, crossover between random and kinetic growth, computer simulation 4-62251  
 Ising ferromagnet, 2-D, universality, Monte Carlo renormalisation group studies 4-114085  
 Ising lattices, cluster expansions in (2+1)D, high-temp. series 4-78254  
 Ising model, critical exponent universality, renormalisation group theory 4-95326  
 Ising model, Green function ansatz for K-space pair correl. function 4-58763  
 Ising model, random field, domain growth and self-similar scaling breakdown 4-82763  
 Ising model, random field on Bethe lattice, critical behaviour 4-98844  
 Ising model, simple cubic, critical behaviour, Monte Carlo renormalisation group calcs. 4-71114  
 Ising random model, magnetisation, critical temp. and percolation thresholds 4-58759  
 Ising two-dimensional model, detailed balance and the dynamical crit. exponent 4-73382  
 isotropic random elastic medium, critical properties from fractal model of percolating backbone 4-103209  
 isotropic-nematic liq. cryst. phase transition, tricritical phenomena (Russian) 4-113632  
 kinetic gelation model and sol-gel transition, solvent effects 4-82773  
 lattice gas model, critical behaviour 4-78266  
 lattice gas model, order-disorder transitions, layering, and multicritical phenomena 4-101779  
 lattice kinetic spin models, dynamical renormalisation through classical equations of motion 4-58765  
 liquid films, critical thickness, rupture and black spot 4-61191  
 metal-insulator transition, kinetic coefficients, DC cond. and diffusion 4-80501  
 metricization of thermodynamic-state space and the renormalization group 4-82772  
 Monte Carlo method, appls. in condensed-matter physics; statistical mechanics and related fields, book 4-101584  
 multi-state models, interfacial adsorption, Monte Carlo studies 4-113812  
 N-mode truncated Navier-Stokes eqns., fixed point limit behaviour for increasing N 4-103280  
 nitrobenzene solns., critical props. study by elec. cond. method 4-113954  
 nitrobenzene solns., elec. resist. anomaly near critical point 4-113955  
 one dimensional bond percolation with further neighbour bonds, transfer matrix approach 4-58772  
 one-dimensional nonlinear lattice, critical props. and hadron phys. 4-59032  
 organic compounds, critical temperature estimates 4-70340  
 percolation, critical probabilities, branching processes 4-95332  
 percolation clusters, segment distribution in self-similar patterns 4-86350  
 percolation lattices, acoustic wave absorpt. enhancement near a percolation threshold 4-69614  
 phase transitions with order parameter having six or eight components, phenomenological and crit. behaviour 4-68185  
 polyisobutylene, semidilute benzene soln., osmotic press. near  $\theta$  point 4-99835  
 polymer solns. dilute to semidilute behaviour transition, critical conc. study 4-103921  
 polystyrene, semidilute cyclohexane soln., osmotic press. near  $\theta$  point 4-99818

## critical phenomena continued

Potts lattice-gas, multicritical behaviour in q-state 4-78257  
 Potts model, p-component, with correlated impurities, crit. behaviour 4-101780  
 Potts model, q-state, free energy critical amplitude 4-73394  
 Potts model of magnetism, critical dimensionalities and props. 4-61499  
 Potts model with quadratic symmetry breaking, crossover exponents 4-111070  
 proximity effect sandwiches, local spin fluctuations, renormalisation group anal. 4-114073  
 pseudospin model Hamiltonians, critical props. 4-98838  
 quantised Hall effect, critical fluctuations in disordered electronic system, field theory 4-104235  
 quantum crit. behaviour, quenched impurity influence 4-63656  
 quantum spin systems, low temp. critical behaviour (Russian) 4-71013  
 quantum systems with long-range correlated impurities, dynamical critical exponent 4-68168  
 random systems, electron localisation and diffusion 4-98572  
 renormalisation group studies review 4-101999  
 renormalisation groups, Monte Carlo simulation, critical phenomena 4-86362  
 self-avoiding random surfaces, scaling behaviour, renormalisation group calcs. 4-90531  
 self-avoiding walk, critical exponents in two- and three-dimensional lattices 4-86343  
 self-avoiding walk, homotopy parameter expansion appl., critical phenomena 4-106247  
 self-avoiding walk, universality on square lattice 4-95329  
 self-avoiding walks on percolation clusters at criticality and lattice animals 4-101760  
 singlet-triplet paramagnet, Curie point vicinity, mode-mode coupling effects 4-98854  
 six-state Potts model, 2D, phase transitions and critical props. 4-58760  
 solid-gas interface, adsorbed liq. phase wetting, critical exponents 4-98407  
 space correlated quenched defects critical behaviour 4-111048  
 spherical model in  $d=r+1$  dimensions, Hamiltonian formulation 4-73404  
 spin  $1/2$  anisotropic Heisenberg model in infinite lattice dimens., time depend. behaviour 4-68172  
 spin systems, correlated random fields, crossover to random critical behaviour 4-114120  
 spin systems with impurities, static and dynamic crit. props., two-loop approx. 4-61541  
 strip-these for random systems 4-58751  
 super-normal conductors, conduction in random networks, nonlinearity 4-98584  
 supercritical fluids; solubility parameters 4-88297  
 surface-induced order and disorder, critical phenomena and phase transitions 4-58803  
 TGS, ferroelec. transition, critical behaviour, defect influence 4-65983  
 TGS group ferroelectrics, mean field to critical behaviour crossover (Japanese) 4-93012  
 TGSe, ferroelec. transition, critical behaviour, defect influence 4-65983  
 thermodynamic system, Monte Carlo renormalization book contrib. 4-63679  
 thermotropic mixed liq. crystals, oriented mols., NMR studies 4-84860  
 three-dimensional lattice model with directional bonding, renormalization group study 4-111052  
 tricriticality and quenched impurities in classical and quantum systems 4-78170  
 two electron binding at fixed centre with one- and two-body pots., criterion 4-75896  
 universal combinations between thermodynamic crit. amplitudes for Ising-like systems 4-102023  
 X-Y one-dimensional S=1 model with single-ion anisotropy, crit. behaviour 4-104454  
 Z<sub>3</sub> Potts model, critical behaviour and associated conformal algebra 4-86358  
 Ar, Rayleigh wing spectrum, crit. effect 4-84971  
<sup>3</sup>He, superfluid A and B phases, persistent current expts. 4-92465  
 K<sub>2</sub>FeO<sub>4</sub>, mag. ordering and critical slowing down, Mossbauer studies 4-76148  
 NH<sub>4</sub>AlF<sub>6</sub>, clusters and critical slowing down near T<sub>c</sub>, EPR study 4-65982  
 Ni, ferromagnet, critical phenomena, muon spin relax. study 4-71252  
 SF<sub>6</sub>, PVT props. in gas-liquid critical region 4-111089  
 TiCdF<sub>3</sub>Gd<sup>3+</sup>O<sub>2</sub><sup>-</sup>, critical phenomena above and below T<sub>c</sub>, EPR studies 4-65854

critical phenomena, magnetic see magnetic transitions

## critical points

see also boiling point; melting point

A-15 compounds, structural phase transitions, renormalisation group anal. 4-70360  
 adsorbed solid film, multilayer, layering critical points, renormalisation group anal. 4-104082  
 binary liq. mixtures, H bonded, lower critical soln. points 4-75641  
 Blume-Capel model, linked-cluster series anal. 4-78272  
 classical fluids, triplet correl. function at crit. point 4-75251  
 classical liquid struct., thermodynamically consistent theory, pair pot. extraction 4-92043  
 coal liquids, vap. press. incorporating renormalisation group formulations with corresponding state principle 4-88271  
 conformal invariance, unitarity, and critical exponents in two dimensions 4-68189  
 critical behaviour for phase transitions with four-components order parameters 4-78285  
 dimyristoyl phosphatidylcholine-water system, phase transitions, high press. study 4-113624  
 elastic stresses due to point defects, anomalous properties of crystals near phase transition points 4-113609  
 electrolyte surface struct. near critical point, free energy formalism anal. 4-92038  
 ferromagnet, cubic, with fourth- and sixth-order anisotropy, crit. behaviour, Potts models 4-98897  
 ferromagnetic q-state Potts model on BCC and FCC lattice, critical points 4-80734  
 finite-size scaling, universal critical amplitudes and free energy 4-95365  
 fluids, vibr. bands, critical contrib., Raman spectral linewidth 4-88823

## critical points continued

- Fokker-Planck eqn., asymptotic properties near crit. points, Hopf bifurcation 4-101785  
 Fokker-Planck eqn., asymptotic properties near Hopf bifurcation 4-101784  
 frustrated spin-glass model with random couplings, renormalisation group 4-71078  
 gas-liquid phase transition and singularities, space of undercritical states 4-65381  
 graphite, ethylene adsorption, layering, prewetting and wetting 4-98450  
 n-hexane, sp. heat at const. press. in critical region determ. by flow calorimetry 4-61106  
 Hubbard model, magnetic and Mott transitions 4-88673  
 Ising model, three dimensional, cell distribution functions, Monte Carlo study 4-76155  
 Ising model, two-dimensional, tricritical behaviour, finite size scaling anal. 4-61547  
 Ising model decorated hypercubic lattice with multiple transitions, transition point location 4-109034  
 Ising pair correlation functions at critical temp. 4-111061  
 isobutyric acid, water solns., dissoc. at crit. soln. point 4-93523  
 Jahn-Teller crystals, antiferrodistortive ordering in external mag. field 4-108608  
 lattice gas, tricritical point from low temp. series expansions 4-95322  
 liquid, caloric eqn. of state near crit. point (*Russian*) 4-84360  
 liquid crystals, nematic-smectic A-smectic C multicritical points 4-88292  
 low-dimensional phase transition, droplet theory 4-78283  
 2,6-lutidine, binary aq. mixture, lower critical point, dielectric study 4-80855  
 magnetic films, uniaxial, with Lifshitz crit. point, phase transitions from homogeneous to inhomogeneous states in external mag. field 4-71140  
 magnetic lattice gas of molecules with internal structure, phase diagrams 4-111060  
 metals, melting point, boiling point and critical point 4-92338  
 methane, adsorbed on graphite, two-dimens. liq.-vapour crit. point exponent, sp. ht. study 4-92341  
 methanol-n-heptane, critical dielectric const. meas. as function of temp. 4-92989  
 modulated phases, Ginzburg-Levanyuk criterion for phase transitions 4-98274  
 molecular liquid, nonpolar, nonlinear dielect. effect 4-71257  
 Monte Carlo renormalised group methods for critical points and flow diagrams determ. 4-68406  
 multiple light-scattering near the critical point, critical opalescence 4-84938  
 nematic liquid crystals, pressure effects, reentrant phenomena, tricritical point 4-70033  
 oil-water microemulsion model 4-99849  
 organic compounds, critical temperature estimates 4-70340  
 organic liquid droplet, evap., low and high mass flux data, wet bulb temp. 4-80341  
 paradichlorobenzene-paradibromobenzene, polymorphic behaviour, mixing phenomena 4-108302  
 phase rule for critical coexistence manifolds 4-78286  
 polar molecular fluids, interaction sites, critical points 4-70011  
 polymer blends, lower crit. soln. temp. determ. using Raman spectrometer 4-103899  
 polymer soln., coexistence curve universality 4-97997  
 Potts model, three-component ferromagnetic, Yang-Lee zeros 4-101769  
 Potts models, pseudodimensional var. and tricriticality by hierarchical breaking of translational invariance 4-101804  
 pressure, extrapolation and estimation using principle of corresponding states and ref. fluids 4-80190  
 pyridine, binary aq. mixture, lower critical point, dielectric study 4-80855  
 quasibinary fluid mixtures, tricritical points 4-103901  
 random field Ising model in dimens. 2, possible line of crit. points 4-88691  
 seawater, critical point and two-phase boundary, 200 to 500°C 4-67219  
 semiconductors, thermal breakdown critical temp. determ. method 4-98599  
 singular manifolds of the star potential in the six-dim space 4-78284  
 smectic A-smectic C transition, heat capacity behaviour, effect of tricrit. region 4-84394  
 superparamagnetic localised moments, magnetisation, temp. and field depend. 4-76193  
 surface tension of non-critical interfaces near crit. end points 4-88371  
 tetramethylammonium chlorides, normal and deuterated, III-II phase transition, Raman spectra studies 4-113604  
 Tolman's length for surface tension, critical exponent at liquid-gas critical point 4-61172  
 triangular magnetic configs. at OK in various mag. fields 4-92895  
 universal vector scaling in one-dimensional maps 4-106243  
 unsteady stagnation-point heat transfer for a variable freestream temperature 4-60404  
 water droplet, evap., low and high mass flux data, wet bulb temp. 4-80341  
 wetting, crit., in systems with long-range forces 4-88374  
 X-Y model, eqn. of state and quantal crossover in longit. mag. field 4-63682  
 Ar, liquid and gas, viscosity determ. 4-61125  
 Ar triple point, appl. to resistance thermometer calibration 4-111135  
 CO<sub>2</sub>, vapour press. meas. from 194 to 243K, sublimation and triple-point temp. 4-80208  
 Ca<sub>3</sub>Sr<sub>2</sub>-Al<sub>2</sub>O<sub>3</sub>(WO<sub>4</sub>)<sub>2</sub>, phase transition characters., role of cage cation substitution 4-65386  
 Ce<sub>99</sub>-La<sub>1</sub>Th<sub>0.1</sub>  $\gamma$ - $\alpha$  transition, x-P-T phase diagrams 4-76755  
 Co<sub>2</sub>Ni<sub>1-x</sub>Mn<sub>x</sub>, magnetic transforms., effect of external press. 4-104418  
 CuVSe<sub>4</sub>, CDW transitions, elec. and thermal props. 4-98618  
 ErRh<sub>2</sub>B<sub>4</sub>, ferromagnetic superconducting thin film, photoexcitation, nonequilibrium effects 4-114059  
 Fe, work hardening characts., plastic behaviour depend. on temp., strain rate, cryst. orientation 4-99418  
 H bonded cryst., isotope effect on critical temp. 4-70341  
 H<sub>2</sub>, liquid and gas, viscosity determ. 4-61125  
<sup>3</sup>He, liq., critical fluctuations near gas-liq. critical point, decay rates 4-92468  
<sup>3</sup>He-<sup>4</sup>He liq. mixtures, critical fluctuations near gas-liq. critical point, decay rates 4-92468  
 In triple point, appl. to resistance thermometer calibration 4-111135  
 KCl, vapour and liq., critical point and vapour press. 4-60972

## critical points continued

- KMnF<sub>3</sub>, multicritical points 4-65385  
 Kr monolayer, on graphite, commensurate-incommensurate transition, X-ray scatt. study 4-61215  
 LaAlO<sub>3</sub>, multicritical points 4-65385  
 LiKSO<sub>4</sub>, press. effect on phase transitions 4-104546  
 N<sub>2</sub>, fluid, equation of state near critical points, scaling props. 4-98238  
 N<sub>2</sub>, liquid and gas, viscosity determ. 4-61125  
 NH<sub>4</sub>Cl<sub>1-x</sub>Br<sub>x</sub> solid solns., heat capacity near  $\gamma$ - $\beta$  transition 4-103958  
 N<sub>2</sub>O<sub>4</sub>-2NO<sub>2</sub>, chem. equilb. anomalies near crit. points 4-93543  
 NaCl, vapour and liq., critical point and vapour press. 4-60972  
 Ne adsorbed layer on exfoliated graphite, 2-D press.-temp. phase diagram 4-92523  
 Ne fluid, equation of state near critical points, scaling props. 4-98238  
 O chemisorbed on W, lattice gas-model, finite size scaling study 4-84513  
 PZT, dielec. props. at high press., p-T phase diagrams 4-99062  
 Rb, liq., struct. factors calc. using optimised random-phase approx. 4-84142  
 Rb, triple point standard, temp. reference standard near 39.30°C 4-78288  
 RbCaF<sub>3</sub>, multicritical points 4-65385  
 S liquid solutions, symm. and nonsymm. tricrit. points 4-92342  
 Sb, phase transitions at hydrostatic press. up to 9 GPa 4-75666  
 SrTiO<sub>3</sub>, multicritical points 4-65385  
 SrTiO<sub>3</sub>, US attenuation and vel. near ferroelec. transition 4-65345  
 TlFe<sub>2</sub>-Al<sub>2</sub>O<sub>3</sub>, magnetic props., influence of mag. vacancies 4-104414  
 UC, fast reactor fuel, critical constants, sensitivity anal. 4-68757  
 UO<sub>2</sub>, fast reactor fuel, critical constants, sensitivity anal. 4-68757  
 V-Te, thermodynamic props. isopiestic method determ. 4-103966  
 Xe, liq., nonlinear dielect. effect 4-71257  
 critical temperature, superconducting *see superconducting transition temperature*  
 CRO *see cathode-ray oscilloscopes*  
 crocidolite *see asbestos*  
 crops *see farming*  
 cross-sections (nuclear) *see nuclear reactions and scattering*  
 crossed-field tubes *see microwave tubes*  
 crosstalk  
 optical fibre, low crosstalk polarisation-maintaining optical fibre with an 11 km length 4-112574  
 optical single-mode fibres for WDM communication systems, crosstalk due to stimulated Raman scatt. 4-107857  
 LiNbO<sub>3</sub>:Ti directional coupler based low-crosstalk waveguide polarisation multiplexer/demultiplexer for 1.32  $\mu$ m 4-60183  
 crowsdons  
 binary cryst., displacement domains caused by defects (*Chinese*) 4-70254  
 CaF<sub>2</sub>, electron irradi., anion voidage and void superlattice 4-108350  
 TiO<sub>2</sub>, rutile, threshold radiation damage, computer simulation 4-108420  
 CRT *see cathode-ray tubes*  
 crushing  
 MnB<sub>2</sub> alloy, spontaneous magnetisation changes due to amorphisation (*Russian*) 4-104407  
 crushing strength *see compressive strength*  
 cryobiology *see biothermics*  
 cryogenic cables *see superconducting cables*  
 cryogenic pumps *see cryopumping*  
 cryogenics  
*see also cryopumping; cryoscopy; cryostats; cryotrons; Joule-Thomson effect; low-temperature production; low-temperature techniques; magnetic cooling; refrigeration*  
 20 MW superconducting cryoturbogenerator/cryogenic support system, cooling techniques and reliability 4-111141  
 Dow Corning Silicon Oil No. 704, low temp. sp. ht., 2 to 18K 4-74848  
 energy-dispersive X-ray diffraction with synchrotron radiation at cryogenic temperatures 4-103608  
 environmental and thermal control for space vehicles, conf. Toulouse, France (Oct. 1983) 4-73162  
 Infrared Space Observatory dual liquid H<sub>2</sub>/2 superfluid He coding system thermal design 4-73441  
 liquid N<sub>2</sub> transferring, passive level indicator and valve 4-95434  
 liquids flowing in tubes, heat transfer during boiling 4-69749  
 microminiature refrigeration, fabrication, design and appl. 4-78324  
 microscopy specimens, simple and inexpensive 4-95572  
 mirror mount design for cryogenic environments 4-87413  
 phase separator for zero-g environment, design and test 4-73442  
 prestressed lightweight concrete barrier for cryogenic containment vessel 4-114675  
 sensor-amplifier interfaces, hybrid circuit freq. compensation modules 4-90573  
 specific heat of solids measurement, Robotron K 1510 microcomputer applications (*German*) 4-91720  
 subroutine for cryogenic temperature natural logarithm computation on K 1510 microcomputer (*German*) 4-90595  
 superfluid He dewar use in Infrared Astronomical Satellite cryogenic system 4-77718  
 telescope on IRAS 4-110525  
 temperature control of a cryogenic torsion pendulum 4-95431  
 uracil, monomeric, trapped in Ar and N<sub>2</sub> cryogenic matrices, IR spectra 4-64472  
 vacuum and cryogenic techniques, review 4-95448  
 vacuum and cryogenic technologies, conference, Grenoble, France (April 1984) 4-95055  
 voltage standard utilisation, based on Josephson effect (*Czech*) 4-82805  
 Zimmerman-Stirling cryogenic cooler, construction and operation 4-72146  
 Ar, homogeneous condensation in He studied using nozzle flow of cryogenic Ludwig tube 4-98251  
 CuH<sub>2</sub>, cryogenic material, heat losses due to H ortho-para conversion (*German*) 4-106326  
 H, liq., target cooled by flowing He 4-59473  
 He, liq. pool boiling, crit. heat flux, heater thermophys. props. effects 4-69667  
 Si:P IR detector field enhanced photoresponse up to 43  $\mu$ m, at cryogenic temp. 4-90656  
 SrTiO<sub>3</sub> detector of liquid <sup>4</sup>He level 4-101833  
 cryopumping  
 centrifugal compressor operating at very low temperatures 4-95457  
 colliding beam accelerator, first string full cell vacuum system 4-91125

## cryopumping continued

- Doublet III neutral beam injector cryopumping system 4-90603  
fusion research appl. 4-95453  
JET, large cryopump systems construction 4-95456  
MFTF-B axicell, vacuum vessel and cryopumping, design features 4-111859  
neutral beam injection lines, multimegawatt, vacuum pumping 4-90602  
neutral beam test-bed cryopump appl. 4-95455  
optical coating deposition, coater modernisation using cryopump 4-71562  
principle, types and aerospace appl. 4-101861  
refrigerator-cooled cryopumps and their applications in industry 4-95458  
reliability, of cryopumps, principles of operation and advantages (Japanese) 4-73448  
review 4-95452  
review of physical basis 4-95451  
sputtering plants, refrigerator-cooled cryopumps appl. 4-78331  
vacuum coater technology, fast-cycle pump design 4-71563  
vibration measurements on cryopumps for cryogenerators 4-95441  
He cryopumping in fusion power systems, charcoal sorbents development 4-111861  
He, liquid pool cryopump 4-68236

cryoscopes *see cryoscopy*

## cryoscopy

No entries

cryosorption *see sorption*

## cryostats

- continuous flow cryostat for Mossbauer meas., 77-300K 4-101854  
gas flow cryostat for dielectric measurements 4-63734  
high-field magnetic for low-temperature low-field cryostats 4-95430  
insert for use with He transport vessel, 1.5 to 300K 4-101853  
insulation, cooled shield props. effect 4-101850  
metal bath type liq. He cryostat 4-90593  
Milan Superconducting Cyclotron, cryostat pressure behaviour following coil quench 4-64251  
miniature optical cryostat for a semiconductor laser with temperature stabilization 4-91486  
polarised Raman spectroscopy of crystals, using cryostat 4-78323  
refrigerators and their applications 4-95436  
superconducting linear accelerator cryostat 4-111977  
superconducting transition temp. measurement system based on Meissner effect 4-90594  
thermal conductivity, thermoelectric power, and thermal diffusivity from the same apparatus 4-82646  
He cryostat (Chinese) 4-101849  
He gas flow-type cryostat, adsorbed layers of gases obs., under ultrahigh vacuum 4-68224  
He, liquid, cryostat, interfacing to closed-cycle refrigerators 4-58858  
He, mass spectrometer attachment to field ionisation source 4-101963  
He transfer gas-liquid separator for cryostat appl. 4-73440  
He-He dilution refrigerator with <sup>3</sup>He cryogenic circulation cycle 4-58859

## cryotrons

No entries

## cryptography

- safeguard seals for surveillance and containment of nuclear materials 4-106975

## crystal atomic structure

- see also crystal atomic structure of alloys; crystal atomic structure of elements; crystal atomic structure of inorganic compounds; crystal atomic structure of organic compounds; electron diffraction crystallography; lattice constants; neutron diffraction crystallography; space groups; superlattices; X-ray crystallography*  
analytical electron microscopy, imaging, chem. anal. and microdiff. 4-108255  
anharmonic temperature factors of atoms with 4 mm and 42 m site symmetries 4-113377  
Atomic Resolution Microscope, design and performance 4-108254  
binary compounds, cryst. struct. maps, chem. scale 4-84228  
bond length errors resulting from incorrect struct. factors 4-75353  
composite symmetry, formed by two identical point groups with common origin 4-75342  
convergent beam electron diff. determ. of point and space groups (Japanese) 4-92033  
convergent beam electron diffraction, cryst. struct. and defect appls. 4-79906  
cubic point configs., geometrical classification 4-79968  
disordered crystals undergoing structural phase transitions, at. order parameter determ. by cryst. struct. anal. 4-88126  
extinction effects 4-97944  
ferroic crystals, non-magnetic, tensorial classification 4-75344  
heteropolyanion and isopolyanion, struct. stability index 4-79967  
hypercubic cryst. systems, point symm. of holohedries in four-dimensional space 4-98049  
incommensurate phases, structural anal. group theory 4-98051  
ionic substitution, MEB and X-ray microanal. investig. 4-79889  
lattice distortion and crystallite size calcs. 4-84226  
light diffraction, materials science appls., microdiff. techniques and cryst. struct. determ. 4-88043  
LUCH-77 program system, random direct methods, use of tangent formula 4-113261  
modulated atomic displacement description and easy structural factor computing 4-113365  
molecular cryst. struct., translation problem solving by fragmentary-implicational method, appl. to chromene 4-113263  
nanocrystalline structure, proposed new material struct. (German) 4-70045  
point groups of four-dimensional Euclidean space, geometric symbols (French) 4-103688  
point-symmetry operations in four-, five- and six-dimensional spaces 4-98048  
polydomain crystals, TWIN program for refining at. structures 4-113262  
representations method of struct. invariants, triplet relationships strengthening 4-75330  
SEM stage for crystal orientation and struct. determ. 4-108253  
solid state chemistry, conf., Veldhoven, Netherlands (June 1982) 4-67863  
space group symm., international tables for crystallography, book 4-58583  
stability, valence and cryst. chem. systematics 4-92137  
thin films, anal. techniques, review 4-113832

## crystal atomic structure continued

- two-coloured point and rod groups containing 8- or 12-fold symm. axes 4-75343  
X-ray diff., secondary extinction, absolute struct. factors, determ. by polarisation var. 4-75241  
X-ray powder diffraction patterns for 71 substances 4-67893
- crystal atomic structure of alloys**  
alkali-group IV alloys, liq. and solid, electronic struct. and cluster form. 4-92601  
binary substitutional alloys, FCC struct., interstitial impurity effect on atomic ordering 4-60919  
catalyst dispersed particles, stacking faults and struct., electron microdiff. studies 4-88178  
close-packed ordered alloys lattice const., Pauling-Simon law 4-75365  
intermetallic compound structure, book contrib. 4-108309  
intermetallic compounds, AB<sub>2</sub> binary, three-dimens. struct. diagram 4-70080  
MoBe<sub>2</sub>, cryst. struct., X-ray diff. 4-84236  
omega phase, struct. and X-ray diffuse scatt. (Japanese) 4-113390  
plane two-networks hexagonal structures, homologous series, cryst., chem. anal. 4-84278  
rare earth alloys, R<sub>4</sub>Cu<sub>23</sub>, high pressure crystn. 4-75369  
rare earth alloys, R-Mn-based, cryst. struct., X-ray diff. studies 4-113394  
rare earth alloys, RCo<sub>2</sub>Sn<sub>6</sub>, R=Y, Tb, Dy, Ho, Er, Tm, Lu, cryst. struct. and mag. props. (Russian) 4-88135  
rare earth alloys, RNiGe, R=Y, Yb, Tb, Dy, Ho, Er, Tm, Lu, cryst. struct., mag. and elec. props. (Russian) 4-88134  
rare earth alloys RCoGe, R=Y, Yb, Tb, Dy, Ho, Er, Tm, Lu, cryst. struct., mag. and elec. props. (Russian) 4-88134  
rare earth intermetallic binary phases of 5:3 composition, crystal structures 4-103705  
rare earth intermetallics, RFe<sub>2</sub>H<sub>x</sub> (R=Gd, Ho, Er, Tm, Lu), mag. props. and cryst. struct., absorbed H<sub>2</sub> effects (Russian) 4-104458  
rare earth intermetallics, RPd<sub>2</sub>B<sub>x</sub>, structural and magnetic props. 4-103700  
rare earth rhodium stannides, mag. superconductors, cryst. chemistry 4-70071  
rare earth-transition metal-boron alloys, crystallographic and mag. props. 4-75370  
short-range order fluctuations and Fermi surface effects. (Japanese) 4-113391  
solid soln., partial impurity volume and lattice deform. 4-108390  
solid solution structure, book contrib. 4-108308  
standardization of inorganic crystal-structure data 4-75386  
steel, stainless powder particles, droplet processed, rapid solidification struct., STEM obs. 4-71649  
steel, type Kh17N8, phase transitions during deform. press. effect (Russian) 4-81188  
superalloys single crystal thin films, X-ray microanal. (French) 4-81496  
transition metal alloys, sigma phase, pair-wise interaction model 4-84422  
transition metal binary alloys, stoichiometric, struct. maps 4-108307  
Ag<sub>2</sub>Ce-Ce system, partial phase diagram and lattice structs. 4-71636  
Al sheet, prod. by elec. bursting method, struct. 4-93250  
Al-Cu-Mg-Ag, precipitate struct. and orientation relationship, effect of Ag additions 4-93303  
Al-Mg-Sc, electron irradi., precipitation and struct. (Russian) 4-66339  
Al-Sc (0.3 at.%) alloy, ageing, precipitation obs. (Russian) 4-104786  
Al-Ti long-period one-dimensional antiphase structures, electron diff. and microscopy, X-ray diff. 4-113398  
Au-Mn long-period ordered structures, electron microscopy study 4-113396  
Au-Mn partially disordered, high resolution electron microscopy images 4-92146  
Au<sub>4</sub>Cr, cryst. struct. determ., lattice modulation 4-103703  
Bi<sub>100-x</sub>Sb<sub>x</sub>, mould grown cryst., component distrib., X-ray study 4-75694  
Ca<sub>2</sub>Cu<sub>2</sub>Al<sub>3</sub> and CaCr<sub>2</sub>Al<sub>10</sub>, crystal structures (German) 4-75367  
Ce-Co-Cu, magnetically hard alloys, isostructural precipitation and atomic ordering (Russian) 4-104784  
Ce-Ni-Sb system, phase equilib. diagram, X-ray analysis 4-114491  
Ce<sub>2</sub>Ga<sub>17</sub>Ni<sub>2</sub>, cryst. struct. determ. 4-75375  
CeOs<sub>2</sub>Ru<sub>2</sub>-Si<sub>2</sub>, mag. behaviour and struct. chemistry 4-103701  
Co-Al, long range 21R struct. during martensitic transform. (Chinese) 4-103699  
Cu-Ag isovalent solid soln., elastic core effects, EXAFS studies 4-60886  
Cu-Bi, segregation, grain boundary struct. and struct. transformations 4-113462  
β-Cu-Zn-Al, γ-brass-type precipitates, origin of incommensurate electron diff. pattern 4-76775  
CuAl, dil. disordered, diffuse size effect scatt. in high voltage electron diff. 4-113395  
CuAu, microstructure, field ion microscopy study 4-88177  
CuNi compositionally modulated foils, electron and X-ray diffraction studies 4-80455  
Cu<sub>2</sub>Zr<sub>2</sub>, 3D long-period superstructure, electron diff., electron microscopy obs. 4-70068  
DyCu<sub>2</sub>Ge<sub>2</sub>, mag. and cryst. struct., neutron diff. studies 4-65794  
Dy<sub>2</sub>(Fe<sub>1-x</sub>Al<sub>x</sub>)<sub>17</sub>, pseudobinary intermetallic cpd., mag. props. 4-71032  
Er<sub>2</sub>NiB<sub>12</sub>, cryst. struct. determ. 4-75376  
Eu-He, Mossbauer spectra and X-ray diff. study 4-76290  
EuPd<sub>2</sub>Sb<sub>2</sub>, cryst. struct. determ. 4-79985  
Fe-Al-Mo, Mossbauer study of atomic struct. and mag. polarisation 4-80848  
Fe-B, crystalline and amorphous, cryst. struct., NMR study (Russian) 4-79982  
Fe-Be system, B32 metastable precip., identification by APFIM and TEM 4-61922  
Fe-Co electrodeposited films, field induced mag. anisotropy 4-92943  
Fe<sub>0.56</sub>Cr<sub>0.23</sub>Ni<sub>0.23</sub>, stainless steel, local order, neutron diffuse scatt. meas. 4-75364  
Gd-Pd, effect of H<sub>2</sub> absorpt. on mag. and cryst. props. 4-104412  
Gd<sub>2</sub>Co, crystn., cryst. struct. and mag. props. in microgravity 4-98915  
GdCu<sub>1-x</sub>Zn<sub>x</sub>Si<sub>2</sub>, cryst. struct., mag. and elec. props. 4-92145  
(Gd<sub>0.7</sub>Tb<sub>0.3</sub>)<sub>2</sub>Co, crystn., cryst. struct. and mag. props. in microgravity 4-98915  
HoAlGa, mag. transitions, mag. and cryst. structures, X-ray diff., thermal expansion meas. 4-114113  
In-Sb system, high press. intermediate phases, form., struct., stability, supercond. props. 4-89029  
La-Rh-Si system, superconducting study 4-80713

**crystal atomic structure of alloys continued**

- Fe<sub>2</sub>(Al<sub>1-x</sub>)<sub>13</sub>, metamagnetic transitions and struct. aspects 4-92910  
 LaNi<sub>5</sub>-NdNi<sub>5</sub>(CeNi<sub>5</sub>), phase diagrams, grain size anisotropy, H absorpt. characts. (Chinese) 4-93261  
 LaNi<sub>5</sub>Sb<sub>2</sub>, cryst. struct. determ. 4-79985  
 Li-Tl(In)(Ga), cryst. struct. determ. 4-79986  
 LiMg, pair ordering pots., Clapp and Moss approx. inadequacy 4-92129  
 LuNiSn<sub>2</sub>, cryst. struct. determ. 4-75374  
 Mg-Cu-Si system, ordered struct., X-ray diffr. study 4-113400  
 Mg-Zn isovalent solid soln., elastic core effects, EXAFS studies 4-60886  
 Mn<sub>11</sub>Ge<sub>8</sub>, cryst. struct. and lattice const. temp. depend. 4-103702  
 Mn<sub>2</sub>Ge<sub>2</sub>, cryst. struct., X-ray diffr. 4-65216  
 Mo-Ga phase diagram, binary Mo<sub>3</sub>Ga<sub>41</sub> cpd. 4-76753  
 Nb-Sn A15 alloys, struct. and supercond. props. 4-104344  
 Nb<sub>3</sub>Al, low temp. diffusion, supercond. and struct. props. 4-65498  
 Nb<sub>3</sub>Ge<sub>2</sub> hexagonal phase, X-ray diffr. study 4-76751  
 NbH<sub>2</sub>, symm. anal. of H ordering process (Russian) 4-65217  
 Nb<sub>3</sub>Sn, cryst. site determ. of dilute alloying elements, TEM studies 4-88131  
 NbZr multilayers, EXAFS struct. studies 4-70595  
 NbZr multilayers, struct. and superconductivity 4-70594  
 Nd<sub>2</sub>Fe<sub>14</sub>B, cryst. struct., mag. props. 4-65828  
 Nd<sub>2</sub>Fe<sub>14</sub>B, permanent magnet, cryst. struct. 4-70069  
 Nd<sub>2</sub>Ga<sub>17</sub>Ni<sub>3</sub>, cryst. struct. determ. 4-75375  
 Ni-Al-Hf system, β-(Ni<sub>2</sub>Al)<sub>2</sub>Hf<sub>2</sub> eutectic struct., cryst. morphology, struct., stacking faults, TEM, X-ray diffr. obs. 4-81182  
 Ni-base superalloys, struct. and space groups by convergent beam electron diffr. 4-88132  
 Ni-Cr-Co-Al-Ti-Nb-W-Mo-V-Hf, cryst. lattice periods mismatch determ. 4-65219  
 Ni-Fe, low temp. lattice parameters 4-108306  
 Ni-P amorphous, hexagonal metastable phase formed during crystallisation (Chinese) 4-103698  
 Ni-P electrodeposited alloy struct., X-ray diffr. (Chinese) 4-75363  
 Ni-Rh alloys, magnetism and atomic short range order 4-98899  
 NiGa<sub>4</sub> vacancy controlled γ-brass phase, struct. determ. 4-60885  
 Ni<sub>3</sub>(Ti<sub>1-x</sub>)<sub>2</sub> alloys, long period structs., electron diffr. studies (Chinese) 4-95064  
 Ni<sub>3</sub>Ti<sub>2</sub>V<sub>1-x</sub> polymorphs, ordered struct., stacking sequence, high resolution electron microscopy study 4-79984  
 Os-Sn, intermediate phases, effects of high pressure on crystn. 4-75366  
 Pd-Ag-H, struct. and elec. props. (Russian) 4-79981  
 Pd-Cu-Ni alloys, elec. resist., atomic ordering effects (Russian) 4-108833  
 Pd<sub>2</sub>Cu<sub>2</sub>S<sub>2</sub>P, cryst. struct. and phase equilib. 4-70070  
 Pr-Mn-Co system, Mn solubility, isothermal section, X-ray crystallography 4-114489  
 RGa<sub>2</sub>Ni<sub>2-x</sub> (1 ≤ x ≤ 2, R = La-Lu), phase form. struct., comp., X-ray analysis 4-114488  
 Re-Al alloys, phase relations and cryst. struct., X-ray diffr. studies 4-70066  
 ReO<sub>2</sub>Be<sub>16</sub>, cryst. struct., X-ray diffr. 4-84235  
 Sr<sub>6</sub>Al<sub>2</sub>Sb<sub>6</sub>, Zintl phases with complex anions (German) 4-70067  
 Sr<sub>2</sub>Pb<sub>3</sub>, cryst. struct., X-ray diffr. 4-75373  
 Sr<sub>3</sub>Pb<sub>5</sub>, cryst. struct., X-ray diffr. 4-75373  
 TaH<sub>2</sub>, symm. anal. of H ordering process (Russian) 4-65217  
 Ti-Cr(V)(Mn)(Fe)(Mo), influence of ageing on incommensurate struct. (Russian) 4-65218  
 Ti-Nb-Ni-(Ge), struct. and supercond. props. (Russian) 4-92143  
 TiAl, cryst. struct. determ. 4-113401  
 Ti(Fe<sub>1-x</sub>)<sub>2</sub>, paramagnetic props. study (Russian) 4-71020  
 Ti<sub>1-x</sub>Mn<sub>x</sub>D<sub>2</sub>, structure and mag. props., neutron diffr. study 4-75368  
 V<sub>2</sub>Si, perfect, A15 supercond., structure imaging by high resolution electron microscopy 4-70065  
 W-Re, electronic and fine cryst. struct. (Russian) 4-75377  
 Y<sub>13</sub>Pd<sub>40</sub>Sn<sub>31</sub>, cryst. struct., X-ray diffr. determ. 4-92141  
 YbGa<sub>2</sub>Co<sub>2</sub>, cryst. struct., X-ray diffr. 4-84237  
 Zn-Nb, electronic and fine cryst. struct. (Russian) 4-75377  
 Zr-based Frauf-Laves phases, lattice const. and H absorption capacities 4-84234  
 Zr-Fe, hydride formation, X-ray diffr., Mossbauer spectra, gas anal. 4-113392  
 Zr<sub>2</sub>Nb<sub>3</sub>Ge<sub>4</sub>, crystal struct., X-ray diffr. studies 4-113393

**crystal atomic structure of elements**

- elements, FCC or HCP to BCC transitions, at high press. interatomic distance contraction 4-80215  
 graphite, C bond-network defects with ring size from 3 to 9, graph theory anal. 4-92138  
 graphite, structural theory using pseudopotential local-density-functional approach 4-92135  
 metal, pure, electronic and cryst. struct., bonding, book contrib. 4-108304  
 Al, charge densities, interionic pot., phonon freq., calcs. 4-113856  
 Al, structure factors obtained from X-ray diffr. methods, Debye-Waller factors 4-92158  
 Au small particles, crystalline struct., STEM microdiffraction studies 4-108305  
 Ba, cryst. struct. from first principles calcs. 4-70064  
 Be, cryst. struct. from first principles calcs. 4-70064  
 Be, electron density distrib., diffr. study 4-84232  
 C, BC-8 crystal phase, struct. props., phase stability and phase transistors 4-113389  
 C, linear polytypes, struct. aspects and conformation 4-92139  
 C material, dimensional changes, under compressive stress at high temp. 4-85182  
 Ca, cryst. struct. from first principles calcs. 4-70064  
 Cd, X-ray diffr. data, anharmonic parameters 4-84233  
 Co Kramers-Kronig relation of measured atomic scatt. factors 4-98063  
 Cu Kramers-Kronig relation of measured atomic scatt. factors 4-98063  
 Eu, cryst. struct. from first principles calcs. 4-70064  
 Fe, cast, obtained a superhigh quenching rates, struct. investig., 20 to 1150°C 4-93286  
 α-Fe-C, martensitic, lattice deformation by C impurities (Russian) 4-103773  
 Ge, high-press. structural phase transitions and cryst. struct. 4-92350  
 Li, crystal struct. at 4.2K 4-92140  
 Mg, cryst. struct. from first principles calcs. 4-70064  
 NbH<sub>2</sub>, H permeability and struct. (Russian) 4-65406  
 Ni electrodeposits, struct., X-ray diffr. and Mossbauer studies 4-104102  
 Ni electrodeposits, struct., positron lifetime meas. 4-104103  
 Ni Kramers-Kronig relation of measured atomic scatt. factors 4-98063

**crystal atomic structure of elements continued**

- Ra, cryst. struct. from first principles calcs. 4-70064  
 Se, orthorhombic mol. crystal, IR and Raman studies 4-98062  
 Si, BC-8 crystal phase, struct. props., phase stability and phase transistors 4-113389  
 Si, graphitic, structural theory using pseudopotential local-density-functional approach 4-92135  
 Si, high-press. structural phase transitions and cryst. struct. 4-92350  
 Si, microscopic defects using DTS-1 X-ray topographic spectrometer 4-75362  
 Si single crystal, planar channelling studies (Chinese) 4-70245  
 Si single crystal, unit cell parameters determ. (German) 4-79980  
 Si substrates, electro-physical prop. nonuniformity (Russian) 4-65672  
 Si, unit cell parameters determ. by precision meas. of Bragg plane spacings 4-113388  
 Si:As, X-ray standing wave anal. with synchrotron radiation 4-103607  
 Si:H, grown by zone melting, A-centre distrib. study 4-76666  
 Sn thin film, struct. and transformations during vacuum heating, RHEED and Mossbauer studies 4-75818  
 Sr, cryst. struct. from first principles calcs. 4-70064  
 Ti, quenched, beta to alpha transition, electron microscopy study (Russian) 4-104776  
 Ti thin foil, cryst. symmetry, convergent beam electron diffr. studies 4-80456  
 U, hkl indices determ. in polychromatic beam by wavelength markers method, neutron diffr. study 4-97972  
 α-U, modulated phase, easy struct. factor computing and atomic displacement description 4-113365  
 Yb, cryst. struct. from first principles calcs. 4-70064  
 Zn, X-ray diffr. data, anharmonic parameters 4-84233
- crystal atomic structure of inorganic compounds**  
 alkali metal halogenoformates, MFeS<sub>2</sub> (M=K, Rb, Cs) and Na<sub>3</sub>FeS<sub>3</sub>, structure and mag. props. 4-71039  
 alkali metal fluorides, M<sub>1-x</sub>BiF<sub>1+2x</sub> (M=Na, K, Rb), elec. props. and struct. characts. 4-70452  
 alkali metal pyrophosphates, M<sup>I</sup>M<sup>III</sup>P<sub>2</sub>O<sub>7</sub>, vibr. spectra and crystal struct. 4-65247  
 alkali metal-rare earth phyllosilicates, MR<sub>2</sub>Cl<sub>2</sub>, crystallographic characterisation and phase transitions 4-70077  
 alkaline earth niobates, electronic cond. rel. to complex perovskite structs. 4-70821  
 alkaline earth pnictides, cryst. struct. and plastic phases 4-80018  
 alkaline hexahydroaluminate, struct. chemistry 4-70119  
 alumina, metastable phases, TEM, X-ray diffr. obs. 4-113661  
 Na-beidellite, two-water-layer, struct. of hydrated clay mineral (French) 4-82039  
 ceramics, N-based, conf., Falmer, England (Aug. 1981) 4-67873  
 cryst. struct. and mag. props. 4-70082  
 CsCl, Decker equations of state, polynomial representation 4-84362  
 delafossite type compounds, deform. of octahedral layers (Japanese) 4-75606  
 dicalcium strontium propionate, ferroelectric phase transition, X-ray diffr. study 4-65988  
 epsilosite struct. single crystals, ferroelastic phase transitions 4-65387  
 ferric neoprosin, cryst., chem. and mol. struct., spectral charact. 4-102720  
 framework silicate zeolites, cryst. struct., 4-1 chain and 2D nets 4-92121  
 graphite intercalation compounds, modification of material props. 4-60890  
 graphite-K(NH<sub>3</sub>), intercalation cpd., K(NH<sub>3</sub>)<sub>2</sub>C<sub>24</sub>, tuneable sandwich thickness, cryst. struct. 4-70101  
 heulandite, natural and partially dehydrated, struct., neutron diffr. studies 4-103720  
 ice, Monte Carlo calcs. for ice-rule model 4-103973  
 ilvaite, cryst. and mag. struct., neutron powder diffr. study 4-113412  
 inorganic salts, charge and magnetisation densities study by X-N diff. method and by polarised neutrons 4-71027  
 intergrowth compounds between members of the bismuth titanate family and structures of the LiBi<sub>2</sub>O<sub>4</sub>Cl<sub>2</sub> type. An architectural approach 4-92148  
 lanthanide oxyhalides, Matlockite-type struct., lattice dynamics calcs. 4-108560  
 layered metal oxides, cryst. chemistry and mag. props. 4-98070  
 margarite mica, cryst. struct. and hydroxyl group orientation 4-92175  
 NASICON-type ceramics, prep. using sol-gel process and sintering 4-85124  
 nonstoichiometric compounds, transport processes, conf., Cracow, Poland (Aug. 1980) 4-95060  
 oxides, deviation from stoichiometry, control and meas. 4-98078  
 oxides, ferroelec., antiferroelectric, Seignettomagnetic, phys. props., phase transitions 4-65974  
 oxides, tetragonal potassium-tungsten bronze struct., solid solutions 4-113599  
 phase transitions in MM'Bx<sub>4</sub> type crystals, structural aspects 4-65241  
 plane two-networks hexagonal structures, homologous series, cryst., chem. anal. 4-84278  
 pyrochlore struct. type, ideal A<sub>2</sub>B<sub>2</sub>X<sub>2</sub>Y, geometry 4-88154  
 quartz, α and β forms, struct. anal. based on Coulomb repulsion forces 4-98074  
 rare earth aluminates, solid state reaction prep. and struct. 4-92186  
 rare earth antimonates, R<sub>3</sub>SbO<sub>7</sub>, structural studies by vibrational spectroscopy 4-65248  
 rare earth borates, RAl<sub>3</sub>(BO<sub>3</sub>)<sub>4</sub>, R=Y, Nd, Gd, structures, polymorphic relationships 4-84279  
 rare earth cpds., R<sub>2</sub>Zr<sub>1-x</sub>O<sub>2-0.5x</sub> solid solns., struct. and ionic cond. 4-70445  
 rare earth ionic conductors, K<sub>8-x</sub>R<sub>3</sub>(SiO<sub>4</sub>)<sub>2</sub>(OH)<sub>1-x</sub>, R=Gd, Ho, Yb, cryst. struct. and chem., X-ray diffr., study 4-60895  
 rare earth iron borides, RFe<sub>2</sub>B, with struct. of CeCo<sub>2</sub>B type, unit cell parameters determ. 4-65243  
 rare earth sulphofluorides, RSF, R=La-Lu, Y, precision lattice const., X-ray powder diffr. 4-108327  
 rare earth-transition metal ternary borides, silicides and homologues, cryst. struct. and crystal chemistry, book 4-95076  
 refractory compounds, phys. props. depend. on electronic struct. (Russian) 4-75423  
 sialon polytypoids, struct. characterisation 4-75426  
 sialon X-phase, Si<sub>3</sub>Al<sub>2</sub>O<sub>7</sub>N<sub>2</sub>, cryst. struct. 4-75427  
 sialons, α-β relationship 4-70125

## crystal atomic structure of inorganic compounds continued

- silicate minerals, structure prediction using energy-minimisation techniques 4-84244
- silicate structures and atomic substitution rel. to N-based ceramics 4-70124
- silicates,  $^{29}\text{Si}$  NMR chemical shifts, bond angles and strength effects 4-114175
- sodalite frameworks, cubic, tetragonal tetrahedra distortions 4-84241
- solid electrolytes, diffusion tunnels and cryst. field pot., diffraction expts. 4-70442
- standardization of inorganic crystal-structure data 4-75386
- stoichiometry, struct. and stability, review 4-75359
- ternary semiconductors, relationship between physicochemical and electro-physical props. 4-108856
- three dimensional skeleton phosphates, ionic cond., phase transitions and struct. 4-70448
- $\text{TiO}_2$ , rutile, crystallographic shear phase, high-resolution electron microscopy study of disorder 4-84303
- tooth enamel, human, struct., digital Fourier harmonic superposition method 4-89495
- transition metal chalcogenides, exhibiting quasi-one-dimensional behaviour 4-88136
- transition metal fluorides, ionic and mag. ordering 4-70096
- transition metal monoarsenides, struct. trends, tight binding model anal. 4-92160
- transition metal oxides, struct. prediction using energy-minimisation techniques 4-84243
- transition metals, supersonic metal clusters 4-74370
- VA transition metal oxides of V, Nb, and Ta, oxidation mechanism, phase form., cryst. struct., electron microscopy, electron and X-ray diff. studies 4-62119
- VA transition metal oxides of V, Nb, and Ta, oxidation mechanism in nonequilibrium conditions, structural correlations 4-62120
- $\beta$ -Mg-Si-Al-O-N system, X-ray and electron diff., rhombohedral struct. 4-65246
- $\text{Ag}_3\text{AsS}_3$ , cryst. struct. determ. (Russian) 4-70104
- $\text{Ag}_{1-x}\text{Bi}_x\text{F}_{1+2x}$ , elec. props. and struct. charact. 4-70452
- $\text{Ag}_2\text{CdI}_4$  in  $\text{AgI}-\text{CdI}_2$  pseudobinary system, struct. and phase equilib. invests. 4-70072
- $\text{Ag}_2\text{HgI}_4$  in  $\text{AgI}-\text{HgI}_2$  pseudobinary system, struct. and phase equilib. invests. 4-70072
- $\alpha$ - $\text{AgI}$ , dynamic struct., ionic motion 4-88341
- $\text{AgI}$ , superionic conductor, struct., EXAFS 4-66125
- $\text{AgPO}_4$ , low temp. ionic cond., rel. to struct. 4-113712
- $\text{Ag}_2\text{PbNb}_2\text{O}_{10}$ , ferroelec. struct. and piezoelec. props. 4-65963
- $\text{Ag}_3\text{Sc}(\text{PO}_4)_2$ , rhombic double phosphate, cryst. struct. 4-75399
- $\text{AgSm}(\text{PO}_3)_4$ , cryst. struct. and IR spectra 4-98249
- $\text{Ag}_2\text{Ta}_2\text{S}_7$ , Ag intercalation, electron diffraction studies 4-80068
- $\text{Ag}_2\text{TeCu}_2\text{Te}_2$ , thin film, high and low temp. modifications 4-75800
- $\text{AgTlX}$  ( $X=\text{S}, \text{Se}, \text{Te}$ ), elec. and crystallographic props. 4-70111
- $\text{Ag}_2\text{ZnI}_4$  in  $\text{AgI}-\text{ZnI}_2$  pseudobinary system, struct., and phase equil. invests. 4-70072
- $\text{Al}_6\text{B}_3\text{F}_3\text{O}_{15}$ , Jeremejevitze, cryst. struct. refinement 4-92173
- $\text{Al}_2\text{O}_3$  powder, shock loaded densification, X-ray study 4-114439
- $\gamma$ - $\text{Al}_2\text{O}_3$  spherical particles, cryst. struct. and surface morphology, electron microscopy study 4-92149
- $\text{Al}_2\text{O}_3\text{:SiO}_2$ , struct. and surface comp. X-ray diff. and SIMS investigation 4-113764
- $\beta$ - $\text{Al}_2\text{O}_3$ - $\text{BaO}$ , short-range ordering in  $\text{Ba}^{2+}$  ion distrib at 295K 4-84245
- $\beta$ - $\text{Al}_2\text{O}_3$ - $\text{La}_2\text{O}_3$ : $\text{Eu}^{3+}$  structure, laser excited fluorescence study 4-66071
- $\text{Al}_2\text{O}_3$ - $\text{Na}_2\text{O}$ ,  $\beta$  and  $\beta'$  phases, ion-rich, high temp. struct. and elec. cond. props. 4-70454
- $\beta$ - $\text{Al}_2\text{O}_3$ - $\text{Na}_2\text{O}$ , struct. transform. during sintering and annealing 4-93292
- $\text{AlPO}_4$ , berlinite, incommensurate phase, colorimetric and neutron scatt. studies 4-84277
- $\text{AlPO}_4$ , cation ordering and struct. anal. based on Coulomb repulsion forces 4-98074
- $\text{Al}_2\text{SiC}_4$  mixed carbide, prep. and struct. studies 4-88144
- Ar and Kr, clathrate hydrate formation in struct. II modification 4-112251
- Ar, clusters, electron diff. patterns 4-74367
- (Au,Ag) $\text{Te}_2$ , krennerite, modulated struct., electron microscopic studies 4-108319
- $\text{B}_{12}\text{C}_3$ ,  $^{13}\text{C}$  NMR study of C distrib. 4-114182
- $\text{BaABNb}_2\text{O}_3$  ( $A=\text{Ca}$  or  $\text{Sr}$ ;  $B=\text{K}$  or  $\text{Ti}$ ) ferroelectric materials, synthesis and characteristics 4-104547
- $\text{Ba}_{0.75}\text{Al}_{1.0}\text{O}_{7.5}$ , cryst. struct., X-ray diff. determ. 4-92155
- $\text{Ba}_{0.75}\text{Al}_{1.0}\text{O}_{7.14}$ , hexaaluminate phase I, cryst. struct. and nonstoichiometry 4-70087
- $\alpha$ - $\text{BaB}_2\text{O}_4$ , low temp. phase, space group and refractive index 4-92165
- $\text{BaBiSe}_4$ , cryst. struct. determ. and preparation 4-80017
- $\text{Ba}_2\text{C}_{2-x}\text{Al}_{2x+y}\text{Ti}_{8-2x-y}\text{O}_{16}$ , hollandite phase of SYNROC, struct., X-ray analysis 4-106675
- $\alpha$ - $\text{Ba}_2\text{Ti}_8\text{O}_{40}$ , hollandite-related superstructures 4-70085
- $\text{BaFBr}$ , Matlockite-type struct., lattice dynamics calcs. 4-108560
- $\text{BaFCl}$ , Matlockite-type struct., lattice dynamics calcs. 4-108560
- $\text{BaFe}_{1-x}\text{Mn}_x\text{O}_{10}$ , bipyrarnidal site occupancy, Mossbauer spectra 4-75420
- $\text{BaFe}_{12}\text{O}_{19}$ , ferrite, M phase, superstruct. obs. 4-84275
- $\text{Ba}_3\text{Ga}_2\text{S}_6$ , prep., cryst. struct., X-ray diff. (German) 4-75415
- $\text{Ba}_3\text{Ga}_2\text{S}_7$ , prep., cryst. struct., X-ray diff. (German) 4-75415
- $\text{Ba}_2\text{MgCrF}_9$  and  $\text{Ba}_2\text{MgFeF}_9$  ( $M=\text{Ni}, \text{Co}, \text{Fe}$ ), crystal structure and mag. props. 4-71040
- $\text{BaMnF}_5\text{H}_2\text{O}$  and  $\text{Ba}_4\text{Fe}_3\text{F}_{17}\cdot 3\text{H}_2\text{O}$ , hydrated fluorometallates (III), one-dimens. antiferromagnet 4-71035
- $\text{Ba}(\text{NO}_2)_2\cdot x\text{H}_2\text{O}$ , anisotropy of imaginary parts of N at. scatt. factors (German) 4-80004
- $\text{Ba}_2\text{Ni}(\text{N}_3)_6\cdot 3\text{H}_2\text{O}$ , cryst. struct., X-ray diff. studies 4-92182
- $\text{BaO-Li}_2\text{O-Nb}_2\text{O}_5$ , phase equilibria in crystn. region, tetragonal phase 4-114495
- $\text{BaP}_2\text{O}_8(\text{WO}_3)_{2m}$ , X-ray diff. and high-temperature electron microscopy study of struct. 4-84250
- $\text{Ba}_2(\text{ReO}_3)_3\text{X}$  ( $X=\text{I}, \text{Br}, \text{Cl}, \text{F}, \text{NO}_3, \text{CO}_3, \text{O}_2$ ), apatite like phases, structure and physical props. 4-70115
- $\text{BaRu}_{1-x}\text{M}_x\text{O}_{3-y}$ ,  $M=\text{Rh}, \text{Ir}, \text{Mn}, \text{Fe}, \text{Co}, \text{Ni}$ , cryst. struct. and elec. cond. (German) 4-84265
- $\text{BaSb}_2\text{S}_4$ , struct., SbS $_2$  strings 4-103724
- $\text{BaSnF}_6$ , fluoride ionic cond. with  $\alpha$ - $\text{PbSnF}_6$  struct., ionic cond. and Mossbauer study 4-92411

## crystal atomic structure of inorganic compounds continued

- $\text{BaSnFe}_2\text{O}_{13}$ , cryst. struct., neutron diff., Mossbauer spectra, magnetisation meas. 4-75406
- $\text{BaSn}_{1-x}\text{Hf}_x\text{O}_3$ , solid solns., cryst. struct. determ. 4-70122
- $\text{BaSn}_{1-x}\text{Ti}_x\text{O}_3$ , solid solns., cryst. struct. determ. 4-70122
- $\text{BaSn}_{1-x}\text{Zr}_x\text{O}_3$ , solid solns., cryst. struct. determ. 4-70122
- $\text{Ba}_2\text{SrRu}_2\text{O}_8$ , cryst. struct., Rietveld refinement of neutron powder diff. data 4-84256
- $\text{BaTiF}_3$ , crystal struct. and mag. props. 4-70084
- $\text{BaTi}_2\text{Fe}_2\text{O}_{11}$ , cryst. struct., neutron diff., Mossbauer spectra, magnetisation meas. 4-75406
- $\text{BaTiO}_3$  thin films, crystallisation from amorphous phase, electron microscopy study 4-113830
- $\text{BaTiO}_3$  single cryst., struct. refinement, X-ray diff. studies 4-113408
- $\text{Ba}_6\text{Ti}_2\text{O}_{19}$  single cryst., struct. refinement, X-ray diff. studies 4-113408
- $\text{Ba}_{15}\text{WO}_3$ , pentagonal tunnel struct. bronze, cryst. data X-ray diff., electron microscopy studies 4-75404
- Bi oxides, sillenite phase form. mag., EPR and IR studies 4-88137
- Bi-Se-Te system, struct. and band gap, X-ray and IR absorpt. obs. 4-104124
- $\text{Bi}_2\text{O}_6$ , cryst. struct., X-ray diff. study (German) 4-65233
- $\text{Bi}_{1-x}\text{Ce}_x(\text{MoO}_4)_3$ , cryst. struct., vacancies, powder neutron diff. 4-75407
- $\text{Bi}_2(\text{Mo},\text{Nb}_2)\text{O}_{6-y/2}$ , struct. props., high resolution electron microscope studies 4-84271
- $\text{Bi}_2\text{MoO}_6$ , koechlinite, cryst. struct., neutron powder diff. profile refinement 4-88139
- $\text{Bi}_2\text{MoO}_6$ , phase transform., struct. study by X-ray diff. 4-70054
- $\text{Bi}_2\text{Mo}_2\text{O}_8$ , preparation, cryst. struct., elec. and optical props. 4-84266
- $\text{Bi}_2\text{NbTiO}_8$ , stability rule and struct. 4-80245
- $\text{Bi}_2\text{O}_3$ - $\text{WO}_3$  layered phases, struct. props., high resolution electron microscopy studies 4-70113
- $\text{Bi}_2\text{O}_3\text{S}$ , synthesis and cryst. struct. 4-65227
- $\text{BiSb}$ , cryst. struct., X-ray diff. 4-80005
- $\text{Bi}_2\text{Sb}_2\text{Te}_3$  films, strain-resist. effects, struct. effects 4-114052
- $\text{Bi}_2(\text{W},\text{Nb}_2)\text{O}_{6-y/2}$ , struct. props., high resolution electron microscope studies 4-84271
- (C,F) $\text{M}_n$  prep., struct., phys. props. and appls. in Li batteries (Japanese) 4-93246
- $\text{CaAl}_2\text{Si}_2\text{O}_8\cdot 3\text{H}_2\text{O}$ , scolecite, struct. refinement, neutron diff. studies 4-92180
- $\text{CaBeAsO}_4(\text{OH})$ , bergslagite, cryst. struct., X-ray diff. 4-80001
- $\text{Ca}_2\text{Cr}_2\text{Si}_2\text{O}_{12}$ , synthetic garnets, Cr coordination and vibr. props., IR study 4-65249
- $\text{Ca}_{1-x}\text{Eu}_x\text{Ti}_{1-x}\text{Fe}_2\text{O}_9$ , perovskite solid soln. systems, prep. and charact. 4-70123
- $\text{CaF}_2\text{:La}(\text{Er})$ , impurity local structural environments, EXAFS determ. 4-66129
- ( $\text{CaF}_2$ ) $_x$ ( $\text{ErF}_3$ ) $_x$ , solid soln., superstructure, ODMR and MCD study 4-75401
- $\text{Ca}_{1-x}(\text{GeO}_4)(\text{O}_{1-2x}\text{F}_{2x})$ , two-layer cryst. struct. 4-75393
- $\text{Ca}_2\text{IrH}_6$ , H sites, geometric model 4-88155
- $\text{Ca}_2\text{KH}_7(\text{PO}_4)_4\cdot 2\text{H}_2\text{O}$ , cryst. struct., X-ray and neutron diff. studies 4-113405
- $\text{Ca}_2\text{LaFe}_2\text{O}_8$ , cryst. struct. determ. 4-80014
- $\text{Ca}_{1-x}\text{La}_x\text{Ti}_{1-x}\text{Fe}_2\text{O}_9$ , perovskite solid soln. systems, prep. and charact. 4-70123
- $\text{CaMg}(\text{CO}_3)_2$ , dolomite, interpretation of high resolution electron micrographs 4-79903
- $\text{Ca}_3\text{Mn}_{13}\text{Fe}_{1.65}\text{O}_{82}$ , struct. and frustrated antiferromag. props. 4-108998
- $\text{Ca}(\text{NH}_4)\text{PO}_4\cdot 2\text{H}_2\text{O}$ , cryst. struct., H bonds, X-ray diff. determ. 4-92150
- $\text{Ca}_2\text{Na}_3\text{Al}_4\text{Si}_3\text{O}_{20}$ , intermediate plagioclase feldspar, modulate struct. 4-84249
- $\text{Ca}_2\text{Na}_3\text{Ti}_3\text{NbS}_4\text{O}_{22}\text{F}_3$ , fersmanite, cryst. struct., X-ray diff. study 4-115396
- $\text{Ca}_2\text{Nb}_2\text{O}_7$ - $\text{CaTiO}_3$ , ferroelectric, crystallochemical props. 4-71288
- $\text{Ca}_2\text{RhH}_6$ , H sites, geometric model 4-88155
- $\text{Ca}_2\text{RuH}_6$ , H sites, geometric model 4-88155
- $\text{CaSiO}_3$ , wollastonite, twinning, cryst. structures, polymorphism 4-89913
- $\text{Ca}_2\text{Sr}_4\text{Al}_2\text{O}_{24}(\text{WO}_4)_2$ , phase transition charact., role of cage cation substitution 4-65386
- $\text{CaTi}_2\text{Al}_2\text{O}_8$ , difficult-to-form crystal structures, preparation 4-70094
- $\text{CaTiF}_3$ , crystal struct. and mag. props. 4-70084
- $\text{Ca}_2\text{Ti}_2\text{P}_2\text{O}_{12}$  ceramic, cryst. struct. determ. 4-84262
- $\text{CaZnF}_6$ , scheelite-type cryst. refinement and bond lengths 4-92176
- $\text{CaZn}_2\text{Mn}^{2+}$  cryst. struct., axial field splitting calc., EPR, optical spectra 4-92159
- $\text{CdD}_2\text{PO}_4$  disordered crystals undergoing structural phase transitions, at. order parameter determ. by cryst. struct. anal. 4-88126
- $\text{CdGa}_2\text{S}_4$ , struct. refinement and twinning 4-92167
- $\text{CdI}_2$ , 14 layered polytype, cryst. struct. and space group 4-92188
- $\text{CdI}_2$ , photoluminescence study of polytype layer struct. (Russian) 4-71443
- $\text{CdI}_2$ , polymorph structures, X-ray diff. 4-84251
- $\text{CdI}_2$ , polymorph structures, optical and X-ray diff. studies 4-84252
- $\text{CdI}_2$  polymorphs, cryst. structures, X-ray diff. determ. 4-92152
- $\text{CdI}_2$ - $\text{MnTe}$ , struct. props., EXAFS studies 4-60902
- $\text{CdI}_2$ - $\text{MnTe}$ , ternary semiconducting random solid-solutions, local structure, EXAFS 4-113414
- $\text{CdO}$ , struct. under pressure 4-75424
- $\text{CdS}$ , in Nafion film, struct., luminesc. lifetime quantum yield and quenching 4-85000
- $\text{CdS}$ , shock loaded, struct. studies 4-92293
- $\text{CdSiAs}_2$ , single crystal growth by chem. vapor transport, struct. and elec. props. 4-114367
- $\text{CdTe}$ , X-ray diffraction study, cryst. struct. (Russian) 4-84280
- $\text{CdTe}_{1-x}\text{Se}_x$ , synthesis and cryst. struct. 4-84261
- $\text{Cd}, \text{Zn}, \text{Mn}_{1-x-y}\text{Te}$ , lattice parameter and energy gap 4-75847
- $\text{Cd}_{1-x}\text{Zn}_x\text{Te}$ , synthesis and cryst. struct. 4-84261
- $\text{CeCo}_2\text{P}_2$ , cryst. struct. determ. 4-80011
- $\text{CeD}_3$ , order-disorder transform. and mag. struct. 4-61069
- $\text{Ce}_2\text{MoO}_6$ , valence state of Mo 4-71161
- $\text{Ce}_2\text{O}_4$ , triclinic ultraphosphate, cryst. struct. 4-70086
- $\text{Co}(\text{III})$  complexes,  $\text{Co}(\text{NH}_3)_5(\text{H}_2\text{P}_2\text{O}_7)$ , hydrolysis, NMR 4-109082
- $\text{Co}(\text{II})$  complex,  $\mu_2$ -methoxo (2,4-dinitrophenolato)(methanol)cobalt (II), cryst. struct., X-ray diff. 4-113420
- $\text{Co}_2\text{AlO}_4$  spinel, cryst. struct. and IR absorption bands 4-88145
- $\text{Co}_3(\text{BO}_3)_2$ , cryst. struct. refinement, X-ray diff. (German) 4-80003
- $\text{Co}_3\text{O}_3\text{F}(\text{OH})$ , cryst. struct., X-ray diff. 4-65242

## crystal atomic structure of inorganic compounds continued

- CoFe<sub>2</sub>-Ni<sub>2</sub>O<sub>4</sub> spinel system, cryst. struct., elec. cond. and mag. susceptibility 4-70121  
 CoMn<sub>2</sub>-Ni<sub>2</sub>O<sub>4</sub> spinel system, cryst. struct., elec. cond. and mag. susceptibility 4-70121  
 CoMo<sub>2</sub>Br(I), preparation and cryst. struct. 4-70097  
 CoP<sub>2</sub>, ambient press. synthesis, cryst. struct., mag. and elec. props., bonding 4-75408  
 CoRh<sub>2</sub>Ga<sub>2</sub>-O<sub>4</sub>, oxide spinel solid soln., cation distrib. study 4-80016  
 CoTiO<sub>3</sub>, ilmenite-type cryst., electron density distrib. 4-65224  
 Co<sub>2</sub>Zn<sub>1-x</sub>Al<sub>2</sub>O<sub>4</sub>, oxide spinel solid soln., cation distrib. study 4-80016  
 (Cr,Nb)Nb<sub>2</sub>Se<sub>10</sub>, one-dimensional systems, resistivity, structure and mag. props. 4-61364  
 CrH<sub>2</sub>, H lattice site location EXAFS 4-93137  
 CrMo<sub>2</sub>Br(I), preparation and cryst. struct. 4-70097  
 Cr<sub>1.45</sub>Nb<sub>0.55</sub>Se<sub>10</sub>, cryst. struct., metal-insulator transition, resist., mag. susceptibility meas. 4-88448  
 Cr<sub>2</sub>O<sub>3</sub>, mixed valence cpds., mag. and struct. studies 4-98071  
 Cr<sub>2</sub>Ru<sub>2</sub>-O<sub>3</sub>, high press. distortion, cryst. struct. study 4-80012  
 Cr<sub>2</sub>Ti<sub>1-x</sub>O<sub>3</sub>, high press. distortion, cryst. struct. study 4-80012  
 Cs germanates, synthesis and struct., X-ray diff. studies 4-108320  
 Cs selenogallates, cryst. struct. and abnormal linear oligomeric anions 4-92185  
 Cs-Ga-Se phase diagrams, ternary cpds. obs. 4-71644  
 Cs<sub>0.35</sub>Al<sub>0.65</sub>Si<sub>2</sub>S<sub>6</sub>O<sub>8</sub>, cryst. struct., X-ray diff. studies 4-92187  
 Cs<sub>2</sub>B<sub>2</sub>O<sub>7</sub>(OH)<sub>2</sub>·2H<sub>2</sub>O, twinned cryst. struct. X-ray diff. determ. 4-92151  
 Cs<sub>2</sub>CaCl<sub>4</sub>·2H<sub>2</sub>O, struct., cryst. chemical study 4-65223  
 Cs<sub>2</sub>Ca<sub>2</sub>(N<sub>3</sub>)<sub>2</sub>·2H<sub>2</sub>O, cryst. struct., X-ray diff. studies 4-92163  
 Cs<sub>2</sub>Ca<sub>2</sub>(N<sub>3</sub>)<sub>2</sub>·2H<sub>2</sub>O, cryst. struct., X-ray diff. studies 4-92164  
 Cs<sub>2</sub>Ca<sub>2</sub>Nb<sub>2</sub>O<sub>10</sub>, layered ferroelectric perovskite, cryst. struct., X-ray diff. (French) 4-75419  
 Cs<sub>2</sub>CdBr<sub>4</sub>, low-temp. phases and cryst. struct. 4-103712  
 CsCo(CO)<sub>4</sub>, cryst. struct. with cubic dense packing 4-92172  
 Cs<sub>2</sub>CrF<sub>3</sub>, cryst. struct. and Jahn-Teller effect 4-70095  
 CsEuNaNb<sub>2</sub>O<sub>15</sub>, struct. and ferroelec. props. 4-109141  
 Cs<sub>2</sub>FeF<sub>3</sub>, cryst. struct. and Jahn-Teller effect 4-70095  
 Cs<sub>2</sub>HgBr<sub>4</sub>, low-temp. phases and cryst. struct. 4-103712  
 CsIn<sub>3</sub>, cryst. struct. study by single cryst. method (German) 4-70079  
 Cs<sub>97</sub>K<sub>130</sub>Si<sub>12</sub>Al<sub>22</sub>O<sub>192</sub> zeolites, normal and deuterated, cryst. struct. 4-92169  
 CsNO<sub>3</sub>, phase II, cryst. struct. and polymorphic transitions 4-113409  
 Cs<sub>2</sub>NbCl<sub>6</sub>, cryst. struct. and phase transitions 4-80015  
 CsNa<sub>2</sub>Cl<sub>3</sub>·2H<sub>2</sub>O, struct., cryst. chemical study 4-65223  
 Cs<sub>1-x</sub>(Na<sub>1-x</sub>H<sub>2</sub>O)Cl, struct., cryst. chemical study 4-65223  
 Cs<sub>2</sub>Ni<sub>3</sub>/Cd<sub>1/4</sub>F<sub>3</sub>, crystal structure and linear trimers mag. interactions 4-71041  
 Cs<sub>2</sub>VF<sub>3</sub>, cryst. struct. and Jahn-Teller effect 4-70095  
 Cu tetraclusters, adiabatic pot., mag. props., Jahn-Teller effect 4-108823  
 (Cu<sub>1-x</sub>Ag<sub>x</sub>)(Ga<sub>1-y</sub>In<sub>y</sub>)(Se<sub>1-z</sub>Te<sub>z</sub>)<sub>2</sub>, lattice parameter and energy gap 4-75847  
 CuAlO<sub>2</sub>, 2H stacking variant, synthesis and cryst. struct. 4-92177  
 CuCl complex with acrylamide, cryst. struct., X-ray diff. 4-113419  
 CuCl complex with fumardinitrile, cryst. struct., X-ray diff. 4-113419  
 CuCr<sub>2</sub>Se<sub>4</sub>, solid solutions, radiographic study of struct. 4-108317  
 CuFe<sub>2</sub>Al<sub>2</sub>O<sub>4</sub>, orthorhombic distortions due to doping 4-70103  
 CuGaSe<sub>2</sub>, thermal expansion, 301-958K 4-80266  
 Cu<sub>12</sub>Ge<sub>0.2</sub>Fe<sub>1.8</sub>O<sub>4</sub>, orthorhombic distortions due to doping 4-70103  
 Cu<sub>12</sub>In<sub>1.2</sub>Cr<sub>0.8</sub>Se<sub>4</sub>, solid solutions, radiographic study of struct. 4-108317  
 CuIn(S<sub>2</sub>Se<sub>2</sub>Te<sub>2</sub>)-x-y<sub>2</sub>, solid solubility, optical energy gap values 4-70074  
 Cu<sub>2</sub>Mg<sub>1-x</sub>Al<sub>2</sub>O<sub>4</sub>, oxide spinel solid soln., cation distrib. study 4-80016  
 CoMo<sub>2</sub>Br(I), preparation and cryst. struct. 4-70097  
 Cu<sub>2</sub>(NO<sub>3</sub>)(OH)<sub>2</sub>, monoclinic cryst. struct. and H-bonds 4-92166  
 CuNa<sub>3</sub>P<sub>3</sub>O<sub>10</sub>·12H<sub>2</sub>O, cryst. struct. determ. (French) 4-75392  
 Cu<sub>2</sub>NbO<sub>3</sub>, cryst. struct., with stepped NbO<sub>5</sub> layers, X-ray obs. 4-108310  
 CuO-CaO-P<sub>2</sub>O<sub>5</sub> glass, IR spectra 4-76446  
 CuO-Ta<sub>2</sub>O<sub>5</sub>, struct. of Ta<sub>2</sub>O<sub>5</sub>-rich phases, electron-optical and X-ray powder diff. studies 4-108329  
 Cu<sub>2</sub>O metastable oxide formed in initial Cu oxidation, struct., electron microscopic study 4-65228  
 Cu<sub>4</sub>(OH)<sub>4</sub>(SO<sub>4</sub>)<sub>2</sub>·2H<sub>2</sub>O, langite, cryst. struct. determ. 4-108313  
 Cu<sub>2</sub>P<sub>7</sub>, preparation and cryst. struct. 4-80008  
 Cu<sub>2</sub>S<sub>3</sub>VS<sub>3</sub>, phase transitions and cryst. struct. 4-80224  
 Er<sub>2</sub>Si<sub>5</sub>, mag. phase transition, elec. cond. and cryst. struct. 4-88675  
 Er<sub>2</sub>V<sub>10</sub>O<sub>28</sub>·25H<sub>2</sub>O, cryst. struct. 4-75387  
 EuAlO<sub>3</sub>, perovskite struct., vibr. study, force field calc. 4-113416  
 EuBr<sub>2</sub>-EuI<sub>2</sub>, preparatory and crystallographic studies using X-ray diff. 4-88143  
 EuCl<sub>2</sub>-EuI<sub>2</sub>, preparatory and crystallographic studies using X-ray diff. 4-88143  
 EuEr<sub>2</sub>S<sub>4</sub>, band gap width, rel. to short-range environment of S atom 4-80493  
 EuGd<sub>2</sub>S<sub>4</sub>, band gap width, rel. to short-range environment of S atom 4-80493  
 Eu<sub>2</sub>Ge<sub>2</sub>O<sub>7</sub>, hydrothermal synthesis and cryst. struct. 4-60900  
 EuHo<sub>2</sub>S<sub>4</sub>, band gap width, rel. to short-range environment of S atom 4-80493  
 Eu<sub>2</sub>Ir<sub>2</sub>S<sub>4</sub>, H sites, geometric model 4-88155  
 EuLa<sub>2</sub>S<sub>4</sub>, band gap width, rel. to short-range environment of S atom 4-80493  
 EuPr<sub>2</sub>S<sub>4</sub>, band gap width, rel. to short-range environment of S atom 4-80493  
 (Fe,Nb)Nb<sub>2</sub>Se<sub>10</sub>, (Fe,V,Nb)Nb<sub>2</sub>Se<sub>10</sub> and (Fe,Ta,Nb)(Nb,Ta)Se<sub>10</sub>, one-dimensional systems, resistivity, structure and mag. props. 4-61364  
 Fe<sup>2+</sup> complex, A23187 antibiotic, cryst. and mol. struct., X-ray diff. 4-109775  
 Fe<sup>3+</sup>Fe<sub>2</sub>(H<sub>2</sub>O)<sub>2</sub>, cryst. struct. and idle spin behaviour 4-108321  
 Fe<sub>2</sub>Ge<sub>2</sub>O<sub>7</sub>, mixed valent, prep. struct., mag. props. (French) 4-88148  
 Fe<sub>2.96</sub>Mg<sub>0.04</sub>O<sub>4</sub>, magnetite, annealing and cryst. struct., X-ray diff. studies 4-113402  
 Fe<sub>2</sub>Mn<sub>1-x</sub>S<sub>2</sub>, metal-insulator transition study 4-98527  
 FeNH<sub>4</sub>HP<sub>2</sub>O<sub>10</sub>, unit cell parameters, anion packing 4-113410  
 Fe<sub>1+x</sub>Nb<sub>1-x</sub>Se<sub>10</sub>, cryst. struct., metal-insulator transition, resist., mag. susceptibility meas. 4-88448  
 Fe<sub>4.40</sub>Ni<sub>4.57</sub>Co<sub>0.03</sub>S<sub>8</sub>, cryst. struct. determ. 4-103714  
 Fe<sub>50</sub>0N<sub>40</sub>0S<sub>10</sub>, cryst. struct. determ. 4-103714  
 FeO, wustite, struct. props., cluster component method anal. 4-70109  
 γ-Fe<sub>2</sub>O<sub>3</sub>, particle product from iron (III) benzoate thermal decomposition, Mossbauer study 4-114868  
 Fe<sub>2</sub>O<sub>3</sub>, thermal decomposition from β-FeOOH, struct. props. 4-109636  
 Fe<sub>2</sub>O<sub>3</sub>-MgFe<sub>2</sub>O<sub>4</sub> system, cation distrib., thermoelec. coeff., 600-1300°C 4-61402

## crystal atomic structure of inorganic compounds continued

- Fe<sub>3.005</sub>O<sub>4</sub>, magnetite, annealing and cryst. struct., X-ray diff. studies 4-113402  
 Fe<sub>9</sub>(PO<sub>4</sub>)<sub>6</sub>, mixed valent, prep., cryst. struct., mag. props., Mossbauer spectra (French) 4-88146  
 Fe<sub>2</sub>S<sub>4</sub>-γ-Fe<sub>2</sub>S<sub>3</sub> mixture, cryst. struct. and defect struct. 4-75422  
 Fe<sub>2</sub>TiO<sub>4</sub> and Fe<sub>2</sub>Ti<sub>0.9</sub>O<sub>4</sub>, neutron diffraction study of cryst. struct. and mag. props. 4-100540  
 Fe<sub>2</sub>TiO<sub>3</sub>, cryst. struct., TEM, electron diff., X-ray powder diff. studies 4-103726  
 Fe<sub>2</sub>TiSe<sub>2</sub>, intercalation cpd., cryst. struct., mag. ordering, susceptibility meas., X-ray diff. 4-76119  
 Ga<sub>1-x</sub>Al<sub>x</sub>As, crystalline struct., two-phonon Raman spectra study 4-71385  
 Ga<sub>1-x</sub>Al<sub>x</sub>As-GaAs/GaAs (001) superlattices, structural parameters, X-ray diff. 4-84257  
 GaAs, crystal struct. determ. using convergent beam electron diff. 4-103612  
 GaAs:B, interstitial centre, radiation induced, cluster-Bethe lattice treatment 4-98090  
 (GaAs)<sub>2</sub>-Ge<sub>2</sub>, bond and struct. models 4-108772  
 Ga<sub>1-x</sub>In<sub>x</sub>As, bond lengths, virtual crystal approx. 4-75385  
 Ga<sub>0.5</sub>Mo<sub>0.5</sub>S<sub>4</sub> spinel, cryst. struct., mag. props., temp. depend. 4.2-300K 4-114110  
 GaP<sub>2</sub>-As<sub>2</sub>, crystalline struct., two-phonon Raman spectra study 4-71385  
 GaP<sub>2</sub>-CdS<sub>2</sub>, phase diagram, crystallographic study, DTA, X-ray diff. 4-109387  
 Gd-Ni-Si, X-ray phase anal. of compounds formed 4-114494  
 Gd<sub>2</sub>Ga<sub>2</sub>O<sub>7</sub>-Pr(Bi) garnet epitaxial layers, site selectivity, dichroism studies 4-84533  
 Gd<sub>2</sub>Ga<sub>2</sub>SiO<sub>7</sub>, pyrochlore prep., cryst. struct., X-ray diff. 4-75400  
 GdMnSi, M=first row transition metal, cryst. struct., mag. and elec. props. 4-70083  
 Gd<sub>2</sub>(MoO<sub>4</sub>)<sub>3</sub>, lattice parameters, thermal expansion, DSC and X-ray investig. 4-108315  
 Ge<sub>2</sub>Fe<sub>3</sub>-O<sub>4</sub>, mixed valent, prep., struct., mag. props. (French) 4-88148  
 Ge<sub>20</sub>Te<sub>80</sub> glass, elec. cond. transition, press. and temp. depend. 4-98619  
 Ge<sub>2</sub>Ca<sub>2</sub>(N<sub>3</sub>)<sub>2</sub>, cryst. struct., single cryst. X-ray diff. studies 4-108332  
 HCl oxides, thermally grown on Si, XPS study of Cl incorporation 4-76640  
 H<sub>2</sub>FeRu<sub>3</sub>(CO)<sub>13</sub>, cryst. struct. study 4-75390  
 H(NH<sub>4</sub>)<sub>2</sub>SbO<sub>3</sub>, proton cond. and cryst. struct. (French) 4-84451  
 H<sub>3</sub>O<sup>+</sup>·NO<sub>2</sub><sup>-</sup>·(ClO<sub>4</sub>)<sub>2</sub>, cryst. struct. determ. (French) 4-92147  
 H<sub>2.5</sub>V<sub>2</sub>O<sub>5</sub>, cryst. struct., inelastic neutron scatt. study 4-108326  
 H<sub>3.3</sub>V<sub>2</sub>O<sub>5</sub>, cryst. struct., inelastic neutron scatt. study 4-108326  
 HgCl<sub>2</sub>·K<sub>2</sub>Cr<sub>2</sub>O<sub>7</sub>, cryst. struct. determ. 4-75391  
 HgCl<sub>2</sub>(NH<sub>4</sub>)<sub>2</sub>Cr<sub>2</sub>O<sub>7</sub>, cryst. struct. determ. 4-75391  
 HgGa<sub>2</sub>Se<sub>4</sub>, crystal growth and refinement (French) 4-75380  
 Hg<sub>3</sub>-NbF<sub>6</sub>, cryst. struct. determ. 4-108311  
 Hg<sub>3</sub>-TaF<sub>6</sub>, cryst. struct. determ. 4-108311  
 Hg<sub>1-x</sub>Zn<sub>x</sub>Te, synthesis and cryst. struct. 4-84261  
 HoC<sub>2</sub>, tetragonal cryst. struct., neutron diff. studies 4-108322  
 HoP<sub>2</sub>O<sub>4</sub>, crystal, spectra and struct. (Chinese) 4-60887  
 In-Sb system, high press. intermediate phases, form., struct., stability supercond. props. 4-89029  
 In<sub>2</sub>MoS<sub>2</sub> (0≤x≤1) intercalation compound, synthesis and characts 4-104200  
 In<sub>2</sub>O<sub>3</sub>-Fe<sub>2</sub>O<sub>3</sub>-CuO(CoO), phase relations and cryst. structures 4-98242  
 In<sub>2</sub>O<sub>3</sub>-Ga<sub>2</sub>O<sub>3</sub>-CuO(CoO), phase relations and cryst. structures 4-98242  
 InSb, X-ray diffraction study, cryst. struct. (Russian) 4-84280  
 InSe films, flash and thermal evaporation growth, struct. and elec. characterisation 4-114409  
 In<sub>2</sub>S<sub>3</sub>S<sub>7</sub>, cryst. struct., X-ray diff. (French) 4-84255  
 InY<sub>2</sub>Cl<sub>7</sub>, crystallographic characterisation and phase transitions 4-70077  
 KAlF<sub>6</sub>, structural phase transition and cryst. struct. 4-80225  
 KAl<sub>2</sub>(Si<sub>2</sub>)<sub>8</sub> monoclinic feldspars, crystal growth, PBC vector analysis 4-92119  
 K<sub>1.5</sub>Al<sub>1.5</sub>Ti<sub>0.5</sub>O<sub>16</sub>, hollandite, one-dimens. ionic cond., three-dimens. long range order, diffuse X-ray scatt. 4-98067  
 (K<sub>1.22</sub>Bi<sub>0.78</sub>)(Bi<sub>0.22</sub><sup>3+</sup>Bi<sub>1.5</sub><sup>3+</sup>)O<sub>6-x</sub>(OH)<sub>2</sub>·xH<sub>2</sub>O, pyrochlore, struct. studies 4-70112  
 K<sub>2</sub>Bi<sub>2</sub>Er<sub>0.1</sub>(MoO<sub>4</sub>)<sub>3</sub>, single crystals, Czochralski growth and optical props (Chinese) 4-114294  
 KCN, diffuse neutron scatt., cryst. struct. 4-70297  
 K<sub>2</sub>Ca(CO<sub>3</sub>)<sub>2</sub>, butschliite, cryst. at. arrangement refinement, CO<sub>3</sub> group planarity, X-ray diff. determ. 4-92156  
 KCdCl<sub>3</sub>, crystal oriented intergrowth, struct. interpretation (French) 4-65201  
 KCdCl<sub>3</sub>·H<sub>2</sub>O, crystal oriented intergrowth, struct. interpretation (French) 4-65201  
 KCdCl<sub>3</sub>·H<sub>2</sub>O, normal and anhydrous, cryst. struct., X-ray diff. studies 4-92170  
 KCdF<sub>3</sub>, phase transitions and cryst. struct. 4-84379  
 KCl<sub>1-x</sub>Br<sub>x</sub>, lattice relax. and local environment near Br<sup>-</sup> ions, EXAFS studies 4-60903  
 K<sub>2</sub>CrF<sub>3</sub>, cryst. struct. and Jahn-Teller effect 4-70095  
 K<sub>2</sub>CuNb<sub>3</sub>(Ta<sub>3</sub>)O<sub>19</sub>, pentagonal tunnel structs., X-ray diff. and electron microscopy studies 4-98069  
 K<sub>2</sub>FeF<sub>3</sub>, cryst. struct. and Jahn-Teller effect 4-70095  
 KGaS<sub>2</sub>, cryst. struct., X-ray diff. 4-84253  
 KGd(WO<sub>4</sub>)<sub>2</sub>·Nd<sup>3+</sup>, struct., morphological and optical characts. 4-69518  
 K<sub>2</sub>GeTe<sub>4</sub>, telluridgermanate with chain struct. (German) 4-70091  
 KIO<sub>4</sub>, Raman spectra and cryst. struct. (Russian) 4-84968  
 KIO<sub>3</sub>, HIO<sub>3</sub> polymorphs, NQR, IR absorpt. spectra and thermograms rel. to cryst. struct. 4-60897  
 K<sub>2</sub>LiNb<sub>3</sub>O<sub>10</sub>, solid solns., struct. and dielec. props. 4-75381  
 KLiSO<sub>4</sub>, cryst. struct. at room temp., neutron diff. study (Chinese) 4-75379  
 K<sub>2</sub>Li<sub>2</sub>(OH)<sub>2</sub>[Si<sub>8</sub>O<sub>20</sub>], cryst. struct. determ. 4-75421  
 K<sub>1.33</sub>Mg<sub>0.33</sub>Sb<sub>4.33</sub>O<sub>16</sub>, supercell ordering study 4-80006  
 KMg<sub>2</sub>Si<sub>3</sub>Al<sub>2</sub>O<sub>10</sub>F<sub>2</sub>-Ba<sub>0.2</sub>Mg<sub>0.8</sub>Si<sub>3</sub>Al<sub>2</sub>O<sub>10</sub>F<sub>2</sub> system, solid solns., lattice const., melting temp. 4-109384  
 KMnF<sub>3</sub>, cryst. struct., X-ray diff. 4-75413  
 KNaCO<sub>3</sub>·6H<sub>2</sub>O, crystal structure 4-103729  
 K<sub>2</sub>Na<sub>1-x</sub>MnF<sub>3</sub>, cryst. struct., X-ray diff. 4-75413  
 K<sub>0.9</sub>NbF<sub>3</sub>, chem. prep., cryst. struct., X-ray diff. study 4-88156  
 K<sub>2</sub>Pb<sub>2</sub>Nb<sub>10</sub>O<sub>30</sub>, ferroelec. struct. and piezoelec. props. 4-65963  
 K<sub>2</sub>SeO<sub>4</sub>, incommensurate-ferroelec. transition, struct. study 4-76381  
 K<sub>2</sub>SeO<sub>4</sub>, incommensurate-modulated struct., X-ray diff. obs. 4-108318  
 K<sub>2</sub>SeO<sub>4</sub>, incommensurate-ferroelectric transition, structural study 4-109138

## crystal atomic structure of inorganic compounds continued

- K<sub>2</sub>SiF<sub>6</sub>, cryst. struct., X-ray diffr. study 4-65235  
 K<sub>2</sub>TeBr<sub>6</sub>, high temp. phases, polymorphism and phase transitions, X-ray diffr. study 4-70052  
 K<sub>2</sub>ThNb<sub>2</sub>O<sub>15</sub>, tetragonal tungsten bronze phase, cryst. struct., elec. and optical props. 4-70116  
 K<sub>2</sub>VF<sub>3</sub>, cryst. struct. and Jahn-Teller effect 4-70095  
 K<sub>2</sub>V<sub>2</sub>S<sub>8</sub>, prep., cryst. struct., and props. 4-84269  
 K<sub>2</sub>YF<sub>5</sub>, cryst. struct., X-ray anal. 4-60898  
 La<sub>0.827</sub>Al<sub>1.19</sub>O<sub>19.09</sub>, cryst. struct., single cryst. X-ray diffr. studies 4-103723  
 La<sub>2</sub>Ba<sub>2</sub>Cu<sub>6</sub>O<sub>14+y</sub>, struct., electron transport and mag. props. 4-70110  
 La(ClO<sub>4</sub>)<sub>3</sub>·3H<sub>2</sub>O, cryst. struct., X-ray diffr. determ. 4-92153  
 LaCo<sub>2</sub>P<sub>2</sub>, cryst. struct. determ. 4-80011  
 LaCo<sub>2</sub>P<sub>2</sub>, flux growth and cryst. struct. 4-108335  
 La<sub>2</sub>CuO<sub>4</sub>, with K<sub>2</sub>NiF<sub>4</sub> struct., at displacements, mag. and transport props., anisotropic bonding effects 4-75358  
 La<sub>1-x</sub>Eu<sub>x</sub>FeO<sub>3</sub>, perovskite solid soln. systems, prep. and charact. 4-70123  
 LaGaOSe<sub>2</sub>, cryst. struct., X-ray diffr. study (French) 4-65234  
 LaHO, cryst. struct., X-ray and neutron diffr. (French) 4-88149  
 LaM<sub>2</sub>Al<sub>11</sub>O<sub>18+y</sub> (M = Mn, Co, Cu), struct., substitution effects, X-ray diffr. studies 4-103722  
 LaNiO<sub>3</sub>, struct. and Ni<sup>2+</sup> local environment, X-ray diffr. and EXAFS studies 4-60901  
 La<sub>2</sub>NiO<sub>4</sub>, with K<sub>2</sub>NiF<sub>4</sub> struct., at displacements, mag. and transport props., anisotropic bonding effects 4-75358  
 LaTi<sub>2</sub>Al<sub>2</sub>O<sub>19</sub>, difficult-to-form crystal structures, preparation 4-70094  
 La<sub>2</sub>Ti<sub>2</sub>O<sub>7</sub>-CaTiO<sub>3</sub>, ferroelectric, crystallochemical props. 4-71288  
 Li ferromagnetic ordered struct., uniqueness 4-79994  
 Li<sub>2</sub>B<sub>2</sub>O<sub>7</sub>, growth and props. for SAW devices 4-98419  
 LiBiO<sub>3</sub>, ionic cond., cryst. struct., and sp. ht. studies 4-70455  
 Li<sub>2</sub>Cr<sub>2</sub>O<sub>7</sub>·2H<sub>2</sub>O, struct., neutron diffr. investigations 4-60899  
 LiFe phengite, mica, cryst. struct. of di-trioctahedral 1M polymorphic modification, electron diffr. study 4-60894  
 Li<sub>2</sub>Fe<sub>2</sub>O<sub>3</sub>, struct. charact. 4-70120  
 Li<sub>2</sub>Fe<sub>2</sub>O<sub>3</sub>, struct. charact. 4-70120  
 LiFePO<sub>4</sub>·(OH, F), tavorite, hydrothermally grown, cryst. struct., X-ray diffr. study 4-113418  
 Li<sub>2</sub>FeSb<sub>2</sub>O<sub>8</sub>, cryst. struct., X-ray powder diffr. 4-108325  
 Li<sub>2</sub>H<sub>2</sub>BO<sub>3</sub>, struct. changes, X-ray diffr. studies 4-84272  
 LiKSO<sub>4</sub>, cryst. and domain struct., neutron diffr. studies 4-88159  
 LiKSO<sub>4</sub>, single cryst., unit cell correl. effects, polarised Raman spectra 4-71374  
 LiMnMF<sub>2</sub> (M = Fe, V, Ti, Cr, Ga), cationic distribution and mag. behaviour 4-71026  
 Li<sub>2</sub>Mn<sub>2</sub>O<sub>7</sub>, struct. charact. 4-70120  
 LiMo<sub>2</sub>S<sub>2</sub>Br(l), preparation and cryst. struct. 4-70097  
 Li<sub>2</sub>N, electronic struct., Hartree-Fock studies 4-98522  
 LiNO<sub>3</sub>·3H<sub>2</sub>O, deform. electron density, X-ray and neutron diffr. data 4-65232  
 LiNaSO<sub>4</sub>, single cryst., unit cell correl. effects, polarised Raman spectra 4-71374  
 Li<sub>2</sub>NiP<sub>2</sub>S<sub>6</sub>, prep. and structural studies, powder X-ray diffr. studies 4-113421  
 Li<sub>2</sub>O<sub>3</sub>-ZnO, ceramics system, ionic and mixed cond. rel. to comp. and humidity 4-98339  
 LiPN<sub>2</sub>, crystal structure 4-70114  
 LiSM(PO<sub>3</sub>)<sub>4</sub>, cryst. struct. and IR spectra 4-98249  
 Li<sub>2</sub>SO<sub>4</sub>, superionic cond. phase, neutron struct. factor, simulations 4-98068  
 Li<sub>2</sub>SeO<sub>4</sub>, cryst. struct., X-ray diffr. 4-88153  
 LiTi<sub>2</sub>O<sub>4</sub>, cryst. struct., neutron diffr. powder profile anal. 4-88151  
 Li<sub>2</sub>Ti<sub>2</sub>O<sub>4</sub>, cryst. struct., neutron diffr. powder profile anal. 4-88151  
 MgAl<sub>2</sub>Fe<sub>2-x</sub>O<sub>4</sub>, Mossbauer study of spin struct. 4-84875  
 MgAl<sub>2</sub>O<sub>4</sub> spinel, anharmonic thermal vibrs. of atoms up to 1933K, struct. refinement 4-65225  
 Mg<sub>2</sub>Al<sub>2</sub>Si<sub>2</sub>O<sub>18</sub>, cordierite, Al-Si ordering, Raman studies 4-98073  
 Mg<sub>3</sub>(BO<sub>3</sub>)<sub>2</sub>, cryst. struct. refinement, X-ray diffr. (German) 4-80003  
 Mg<sub>1-x</sub>Cd<sub>x</sub>Te(Se), synthesis and cryst. struct. 4-84261  
 MgCl<sub>2</sub>, microcrystalline, structural disorder, X-ray diffr. 4-79992  
 Mg<sub>2</sub>PN<sub>3</sub>, crystal structure 4-70114  
 MgSO<sub>4</sub>·6H<sub>2</sub>O, cryst. struct., neutron diffr. refinement 4-65239  
 MgSO<sub>4</sub>·7H<sub>2</sub>O, synthetic epsomite, complementary [111] forms, absolute config. and surface features 4-84247  
 (Mg<sub>(x-12)/3</sub>Sc<sub>4</sub>)(Li<sub>1/3</sub>Si<sub>(x-4)/3</sub>)O<sub>8</sub>, enstatite-IV series, superstruct., cryst. struct. study and twinning 4-65229  
 (Mg<sub>-(x-7.5)/3</sub>Sc<sub>3</sub>)(Mg<sub>2/3</sub>Si<sub>(x-4)/3</sub>)O<sub>8</sub>, enstatite-IV Sc series, superstruct., cryst. struct. determ. 4-65230  
 MgSeO<sub>3</sub>·6H<sub>2</sub>O, cryst. struct., X-ray diffr. 4-65240  
 MgSiO<sub>3</sub>, enstatite, twinning, cryst. structures, polymorphism 4-89913  
 MgSiO<sub>3</sub>, protoenstatite, cryst. struct., temp. depend. 4-92183  
 Mg<sub>2</sub>SiO<sub>4</sub>, olivine and spinel polymorphs, structural and phys. props., computer simulations 4-89912  
 Mg<sub>2</sub>SiO<sub>4</sub>, olivine and spinel forms, struct. and elastic const., computer modelling 4-113411  
 Mg<sub>2</sub>TeO<sub>3</sub>·6H<sub>2</sub>O, cryst. struct., X-ray diffr. 4-65240  
 Mn<sup>2+</sup> coordination polyhedra in O-containing cpts. 4-113417  
 MnFeF<sub>8</sub>(H<sub>2</sub>O)<sub>2</sub>, cryst. struct. and idle spin behaviour 4-108321  
 MnO-ZnO solid solutions, diffuse reflectance spectra, struct. 4-76488  
 MnPS<sub>2</sub>, layered cpd., disorder effects by cation intercalation, EXAFS studies 4-61773  
 Mn<sub>2</sub>Sb<sub>2</sub>O<sub>7</sub>, pyrochlores, synthesis and solid state studies 4-88140  
 MnTiO<sub>3</sub>, electron density distrib., cryst. struct. determ. 4-103709  
 Mo complex, MoCl<sub>3</sub>(OC(NH<sub>2</sub>)<sub>2</sub>)<sub>3</sub>, crystal and molecular structure 4-70089  
 Mo complex, triammonium hexathiocyanate molybdate (III), cryst. struct. 4-70090  
 Mo VI complexes, crystal struct. 4-79990  
 Mo(CO)<sub>6</sub>, cryst. struct. and bond lengths, X-ray diffr. studies 4-92184  
 MoO<sub>3</sub>·2D<sub>2</sub>O, D-atom positions, powder neutron diffr. determ. 4-92154  
 MoS<sub>2</sub>, type layered compounds, valence band spectrum, crystal struct. rel. to electrophysical props. 4-75395  
 Mo<sub>2</sub>Se<sub>2</sub>S<sub>3</sub>, cryst. struct. determ. 4-80007  
 N<sub>2</sub> clusters, electron diffr. patterns 4-74367  
 NH<sub>4</sub>AlF<sub>6</sub>, structural phase transition and cryst. struct. 4-80225  
 NH<sub>4</sub>HCO<sub>3</sub>, relations between crystallographic charact. and cryst. struct. (Chinese) 4-75378  
 NH<sub>4</sub>H<sub>2</sub>PO<sub>4</sub>, monoclinic, cryst. struct. 4-75389  
 NH<sub>4</sub>HSeO<sub>4</sub>, ferroelec. transitions, Raman spect. and vibr. props. 4-93066  
 NH<sub>4</sub>IO<sub>4</sub>, Raman spectra and cryst. struct. (Russian) 4-84968

## crystal atomic structure of inorganic compounds continued

- NH<sub>4</sub>MnFeF<sub>6</sub>, crystal structure and mag. props. 4-71038  
 NH<sub>4</sub>NO<sub>3</sub>, single-cryst. disorder diffuse X-ray scatt. 4-103711  
 (NH<sub>4</sub>)<sub>2</sub>NaFeF<sub>6</sub>, phase transition, X-ray diffr. and <sup>57</sup>Fe Mossbauer study 4-65398  
 NH<sub>3</sub>·2H<sub>2</sub>O, X-ray diffr., IR spectra 4-109175  
 Na<sub>2</sub>Bi<sub>2</sub>TiO<sub>3</sub>, pure and Ba-doped, cryst. struct., ferroelec. props., neutron diffr. 4-70102  
 NaCN, diffuse neutron scatt., cryst. struct. 4-70297  
 Na<sub>1/2</sub>Ca<sub>1/2</sub>Al<sub>1/2</sub>Ti<sub>1/2</sub>O<sub>19</sub>, difficult-to-form crystal structures, preparation 4-70094  
 Na<sub>2</sub>CaSi<sub>2</sub>O<sub>9</sub>, cryst. struct. and isostructural cpd. relationships 4-92181  
 NaCl, Decker equations of state, polynomial representation 4-84362  
 Na(ClO<sub>3</sub>)<sub>0.7</sub>(BrO<sub>3</sub>)<sub>0.3</sub> solid soln., cryst. struct., size effect, X-ray diffr. study 4-80002  
 Na<sub>2</sub>D<sub>2</sub>SiO<sub>8</sub>·8D<sub>2</sub>O, D atom location and anisotropic refinement, H bonding, neutron diffr. study 4-75394  
 NaFeP<sub>2</sub>O<sub>7</sub>, crystallographic, mag. and Mossbauer studies 4-108323  
 Na<sub>2</sub>(H<sub>2</sub>O)<sub>13</sub>Ta<sub>2</sub> Hendricks-Teller disordered layer lattice, X-ray diffr. studies 4-98075  
 NaH<sub>2</sub>(SeO<sub>3</sub>)<sub>4</sub>, cryst. data, X-ray powder diffr. 4-79993  
 NaIO<sub>4</sub>, Raman spectra and cryst. struct. (Russian) 4-84968  
 NaMg(PO<sub>3</sub>)<sub>3</sub>, cryst. struct. determ. 4-98077  
 NaMoO<sub>3</sub>F, single cryst., new oxyfluoromolybdate, synthesis and growth 4-76663  
 NaN<sub>3</sub>, low-temp. phase, cryst. struct., ferroelastic transition 4-84246  
 NaNO<sub>2</sub>, struct. of incommensurate modulated phase 4-103707  
 NaNO<sub>3</sub>, cryst. struct., near order-disorder transition 4-103719  
 NaNbO<sub>3</sub>, ilmenite-type allotropic 4-70092  
 NaNb<sub>2</sub>O<sub>8</sub>, cryst. struct. deduced from HREM images and X-ray powder diffr. data 4-65222  
 Na<sub>2</sub>Nb<sub>2</sub>W<sub>13</sub>O<sub>40</sub>, cryst. struct. determ. 4-108312  
 NaOH-ZrO<sub>2</sub>-SiO<sub>2</sub>-H<sub>2</sub>O system, struct. of mineral analogues and synthetic phases 4-79997  
 Na<sub>2</sub>P<sub>2</sub>O<sub>7</sub>(WO<sub>3</sub>)<sub>m</sub>, m = 4, 6, cryst. struct., X-ray diffr. 4-65236  
 Na<sub>2</sub>Se<sub>2</sub>(PO<sub>4</sub>)<sub>2</sub> solid electrolyte, struct. and cond. 4-61130  
 Na<sub>2</sub>Si<sub>2</sub>O<sub>7</sub>·0.5H<sub>2</sub>O, magadiite, synthesis by crystallisation 4-76653  
 NaSm(PO<sub>3</sub>)<sub>3</sub>, cryst. struct. and IR spectra 4-98249  
 NaVO<sub>3</sub>, β-phase, prep. by dehydration of NaVO<sub>3</sub>·2H<sub>2</sub>O, cryst. struct. study 4-65226  
 Na<sub>2</sub>V<sub>2</sub>Ti<sub>2</sub>Si<sub>2</sub>O<sub>12</sub>, structural, elec., mag., NMR studies (French) 4-75414  
 Na<sub>2</sub>Zr<sub>2</sub>Ge<sub>2</sub>O<sub>16</sub>·H<sub>2</sub>O, cryst. struct. determ. 4-79998  
 Na<sub>1+x</sub>Zr<sub>2</sub>Si<sub>2</sub>P<sub>3-x</sub>O<sub>12</sub> system, crystallographic charact. 4-103706  
 Na<sub>2+x</sub>Ca<sub>2</sub>(1-x)Ge<sub>2</sub>Tb<sub>2</sub>(PO<sub>4</sub>)<sub>2</sub> orthophosphates, luminescence and struct. relations 4-99165  
 Nb polychalcogenides, struct. and XPS studies 4-71525  
 Nb-Ni-P, isothermal section, at 1070K, struct. of compounds formed 4-114509  
 NbC-base complex carbides, struct. and thermal expansion 4-88318  
 NbC<sub>v</sub>, NMR spectra of <sup>93</sup>Nb and cryst. struct. determ. 4-84871  
 Nb<sub>2</sub>Ge, CVD grown via heteroepitaxial process, growth morphology, cryst. struct., supercond. transition temp. 4-88624  
 Nb<sub>2</sub>O<sub>7</sub>, structure anal. using high resolution electron microscopy 4-70105  
 NbP(As), stacking disorder, X-ray diffr. study 4-75398  
 β-NbPO<sub>3</sub>, IR and Raman spectra, cryst. struct. 4-61669  
 Nb<sub>2</sub>Pd<sub>2</sub>Se<sub>8</sub>, structure and elec. props. 4-70088  
 Nb<sub>2</sub>S<sub>3</sub>, structural anisotropy, sp. ht. meas. 4-80258  
 (NbSe<sub>2</sub>)<sub>n</sub>I, struct. electron microscopy study, rel. to elec. props. 4-79995  
 NbTe<sub>4</sub>, evidence for deform. modulated struct. 4-113424  
 NbWO<sub>6</sub>, structure anal. using high resolution electron microscopy 4-70105  
 Nd-Co-B system, cryst. struct. of ternary compounds, isothermal cross sections of phase diagram 4-65244  
 NdAl<sub>3</sub>(BO<sub>3</sub>)<sub>4</sub>, struct. and growth morphology 4-108297  
 Nd<sub>2-x</sub>Ba<sub>1+x</sub>Cu<sub>(1-x)/2</sub>O<sub>8-2x</sub>, cryst. struct., mag. susceptibility, elec. cond. (French) 4-75418  
 NdCu<sub>2-x</sub>Mn<sub>x</sub>, synthesis, composition and mag. props. 4-108997  
 Nd<sub>2</sub>O<sub>3</sub>-Al<sub>2</sub>O<sub>3</sub> hexaaluminate cryst. struct., X-ray diffr. studies 4-103725  
 Nd<sub>2</sub>Ti<sub>2</sub>O<sub>7</sub>-CaTiO<sub>3</sub>, ferroelectric, crystallochemical props. 4-71288  
 Nd<sub>2</sub>Zr<sub>2</sub>O<sub>7</sub>, anionic disorder, neutron diffr. and ionic cond. study 4-70108  
 Ni complex, TTF(Ni(dmit)<sub>2</sub>), mol. metallic cond., cryst. struct. 4-70786  
 Ni complexes, dibromo(N,N'-di-tert-butylidiazabutadiene) nickel, structural phase transform. 4-103717  
 Ni II complexes, quadridentate macrocyclic ligands, bonding cavities, X-ray struct. determ. 4-103716  
 Ni<sub>3</sub>(BO<sub>3</sub>)<sub>2</sub>, cryst. struct. refinement, X-ray diffr. (German) 4-80003  
 Ni<sub>2</sub>Fe<sub>2-x</sub>O<sub>4</sub>, cation-site occupancy, effect of Ni content 4-98079  
 NiH<sub>2</sub>, H lattice site location EXAFS 4-93137  
 Ni<sub>2</sub>(Mn<sub>2</sub>As<sub>2</sub>), G-type phase, crystallographic structure determ. (French) 4-75411  
 Ni<sub>3</sub>(PO<sub>4</sub>)<sub>2</sub>-based solid solns., crystallographic studies, X-ray and neutron diffr. studies 4-92178  
 Ni<sub>1-x</sub>S, cryst. struct., electron and optical diffr. studies 4-88152  
 NiTeMoO<sub>6</sub>, mag. props. and electronic reflectance spectra 4-76106  
 NpO<sub>2</sub><sup>+</sup> complex with mellic acid, crystal struct. 4-75397  
 P<sub>2</sub>O<sub>8</sub>(WO<sub>3</sub>)<sub>2m</sub> bronzes, struct. props., electron microscopy studies 4-103721  
 α-P<sub>2</sub>S<sub>3</sub>, cryst. struct. and cryst.-plastic transition, X-ray and neutron diffr. studies 4-92162  
 Pb<sub>2</sub>CrO<sub>5</sub>, cryst. struct. determ. 4-65245  
 Pb<sub>2</sub>RF<sub>3</sub>, R = La, Nd, Gd, Ho, Yb and Y, synthesis, cryst. struct., electron diffr. obs. (French) 4-75405  
 Pb(FeNb)<sub>0.5</sub>O<sub>3</sub>, ceramics and single crystals, prep., struct., X-ray diffr., neutron powder diffr., dielec. and elec. meas., SEM 4-75412  
 Pb<sub>2</sub>Ge<sub>2</sub>O<sub>11</sub>, hydrothermally grown crystals, dielec., pyroelectric props., X-ray diffr. 4-84915  
 Pb<sub>2</sub>Ge<sub>2</sub>O<sub>11</sub>, metastable form, hydrolysis, X-ray diffr. studies 4-65220  
 Pb<sub>1-x</sub>Ge<sub>x</sub>Te, synthesis and cryst. struct. 4-84261  
 Pb<sub>2</sub>InNbO<sub>6</sub>, single crystal, perovskite and pyrochlore modifications, prep. and props. 4-76662  
 PbMg<sub>1/3</sub>Nb<sub>2/3</sub>O<sub>3</sub>, mean square displacements, thermal expansion coeff. in diffuse ferroelec. transition region, X-ray diffr. meas. 4-65971  
 Pb<sub>1/67</sub>Nb<sub>1/3</sub>Zn<sub>0.23</sub>O<sub>6.66</sub>, crystal structure 4-103727  
 PbO-Bi<sub>2</sub>O<sub>3</sub> system, crystallographic parameters, Mossbauer studies 4-61614  
 PbO-PbXO<sub>4</sub> (X = S, Cr, Mo) cryst. struct., neutron powder diffr. studies 4-84268  
 PbO<sub>2</sub>, α and β, proton localisation, X-ray and neutron diffr. studies. (French) 4-88142  
 β-PbO<sub>2</sub>, struct. parameters and Pb-acid battery failure 4-103718

## crystal atomic structure of inorganic compounds continued

- Pb<sub>2</sub>P<sub>2</sub>S<sub>6</sub>, far IR, IR and Raman spectra, crystal struct. and vibr. spectra (*German*) 4-70073  
 PbS, at. vibr. amplitudes, Debye-Waller factor 4-98232  
 PbSO<sub>4</sub>-PbO, high temp.  $\beta$  phase, struct. study (*French*) 4-98065  
 Pb<sub>1-x</sub>Sn<sub>x</sub>Te(Se), synthesis and cryst. struct. 4-84261  
 PbTe:Ti, pure and doped, defect struct., X-ray double cryst. studies 4-75383  
 PbTe<sub>1-x</sub>Se<sub>x</sub>, synthesis and cryst. struct. 4-84261  
 Pb<sub>2-x</sub>Th<sub>x</sub>KTa<sub>0.5</sub>, crystallographic and dielec. props. (*French*) 4-79987  
 Pb<sub>2-x</sub>Th<sub>x</sub>Ta<sub>0.5</sub>, crystallographic and dielec. props. (*French*) 4-79987  
 PbTiO<sub>3</sub> thin films, CVD prep. and dielec. props. 4-104736  
 PbTiAs<sub>2</sub>S<sub>6</sub>, cryst. struct. and coordination polyhedra 4-92174  
 Pb<sub>2</sub>Ti<sub>2</sub>O<sub>7</sub> electrodeposit, cryst. structure (*Japanese*) 4-88138  
 Pb<sub>2</sub>V<sub>2</sub>O<sub>7</sub>, cryst. struct. of ferroelectric  $\alpha$  phase (*French*) 4-84259  
 Pb<sub>6</sub>V<sub>2</sub>O<sub>13</sub> and Pb<sub>6</sub>V<sub>2(1-x)</sub>P<sub>2x</sub>O<sub>13</sub>, ferroelectric props. and crystal struct. 4-70264  
 Pb(Zr,Ti)O<sub>3</sub> ceramics: ageing and ferroelec. props., heterovalent substitution effects 4-99046  
 Pd<sub>2</sub>P<sub>80</sub>H<sub>17</sub>, H crystallographic positions, neutron powder diff. obs. 4-75409  
 Pd<sub>4</sub>HP<sub>30</sub>, H crystallographic positions, neutron powder diff. obs. 4-75409  
 PrAlO<sub>3</sub>Gd<sup>3+</sup>, order parameter behaviour, EPR study 4-70076  
 PrF<sub>3</sub>Pr<sup>3+</sup>, tysonite struct. and cryst.-field anal. 4-113909  
 Pt complexes, [Pt<sub>2</sub>S<sub>2</sub>(PMe<sub>2</sub>)<sub>2</sub>Ph<sub>2</sub>][BEt<sub>4</sub>]<sub>2</sub>, cryst. and mol. struct. and <sup>31</sup>P and <sup>195</sup>Pt NMR 4-108338  
 Pt complexes, cis-diamminoplatinum  $\alpha$ -pyrrolidine green, cryst. struct., mag. susceptibility 4-98066  
 Pt II complexes, bis(acetonitrile)dichloroplatinum II, mol. and cryst. struct., vibr., IR and Raman study 4-103708  
 PtMnGa, cryst. struct. and mag. props. 4-70082  
 $\beta$ -P<sub>2</sub>O<sub>5</sub>, new high-pressure form 4-70081  
 Rb germanates, synthesis and struct., X-ray diff. studies 4-108320  
 RbAlF<sub>4</sub>, structural phase transition and cryst. struct. 4-80225  
 Rb<sub>2</sub>CrF<sub>6</sub>, cryst. struct. and Jahn-Teller effect 4-70095  
 Rb<sub>2</sub>PO<sub>4</sub>, intermediate paraelec. phase, crystal struct. 4-75388  
 Rb<sub>2</sub>FeF<sub>6</sub>, cryst. struct. and Jahn-Teller effect 4-70095  
 RbIO<sub>3</sub>, Raman spectra and cryst. struct. (*Russian*) 4-84968  
 RbLiMoO<sub>4</sub>, cryst. struct. determ. and phase transition 4-79999  
 RbMgF<sub>3</sub>Ni<sup>2+</sup>(6H), cryst. struct., EPR spectra 4-109063  
 RbMnCl<sub>3</sub>, crystal and mag. structure heterogeneities 4-84276  
 RbMnFeF<sub>6</sub>, cryst. struct. and mag. props. 4-71038  
 RbMo<sub>2</sub>P<sub>3</sub>S<sub>15</sub>O<sub>25</sub>, intersecting tunnel struct., with ion-exchange props., struct. determ. 4-84240  
 RbNO<sub>3</sub>, phase IV, cryst. struct. and polymorphic transitions 4-113409  
 Rb<sub>2</sub>Pb<sub>2</sub>Nb<sub>10</sub>O<sub>30</sub>, ferroelec. struct. and piezoelec. props. 4-65963  
 Rb<sub>2</sub>TeBr<sub>6</sub>, cryst. struct., phase transition, rotary phonon softening 4-75403  
 Rb<sub>2</sub>VF<sub>6</sub>, cryst. struct. and Jahn-Teller effect 4-70095  
 Rb<sub>2</sub>ZnBr<sub>4</sub> type cpds., comparison of superstruct. phases 4-113423  
 Re-As-P system, phase equilibria, cryst. growth, struct. refinements, props. 4-88150  
 Re-P system, phase equilibria, cryst. growth, struct. refinements props. 4-88150  
 ReO<sub>3</sub>, struct. above 'compressibility collapse' transition 4-70099  
 Re<sub>2</sub>P, cryst. struct. determ. 4-80009  
 Rh<sub>2</sub>Ru<sub>1-x</sub>O<sub>2</sub>, high press. distortion, cryst. struct. study 4-80012  
 Ru<sub>2</sub>Ti<sub>1-x</sub>O<sub>2</sub>Cl coatings, solid solution formation 4-70392  
 SbCl<sub>3</sub>-graphite intercalation cpd., lattice expansion, phase transition effects, X-ray diff. studies 4-98076  
 Sb<sub>0.57</sub>Mo<sub>2</sub>O<sub>4</sub>, preparation, cryst. struct., elec. and optical props. 4-84266  
 Sb<sub>2</sub>Mo<sub>6</sub>, cryst. struct., X-ray and powder neutron diff. studies 4-108334  
 Sb<sub>2</sub>O<sub>3</sub>Cl<sub>2</sub>, onoratoite, pure and hydrated, cryst. struct. and twin planes 4-113407  
 SbSI ferroelectric, L<sub>III</sub> edge above transition temp., EXAFS study 4-61772  
 SbTel, cryst. struct., full matrix least squares refinement 4-92168  
 Se<sub>2</sub>OC, prep. and struct. props., powder diff. studies 4-71608  
 Se<sub>2</sub>S<sub>3</sub>, cryst. struct., electron irradi. induced disorder 4-103713  
 Si, low pressure CVD growth and phys. props. 4-81150  
 Si:As, ion implanted and laser annealed, struct. changes, X-ray diff. study 4-75461  
 Si:As implanted layers, struct., total external reflection spectra studies 4-108330  
 Si-Al-O-N phases, struct. studies using magic-angle-spinning NMR 4-71198  
 Si<sub>192-x</sub>Al<sub>x</sub>O<sub>384</sub> Linde Y-zeolites, struct., neutron diff. studies 4-113403  
 Si<sub>3</sub>Al<sub>2</sub>O<sub>7</sub>N<sub>2</sub> sialon X-phase, cryst. struct. 4-75427  
 SiC, lattice imaging of 201R polypolyte 4-75384  
 SiC polymorphs, crust. chem. props. 4-60896  
 SiC, polytype and its intergrowth structures, high resolution electron microscopic studies 4-65231  
 SiC powders, prep. from glass and C black, lattice constants 4-109365  
 SiC synthetically coalesced polytype structs., growth mechanisms 4-75382  
 Si<sub>3</sub>N<sub>4</sub>,  $\alpha$ - $\beta$  relationship 4-70125  
 SiO<sub>2</sub> film, low temp. photochemical deposition 4-99339  
 SiP<sub>2</sub>, electron density distrib. and cryst. struct. 4-79979  
 SiP<sub>2</sub>, struct. parameters and valence electron density distrib. 4-108331  
 SmAlO<sub>3</sub>, perovskite struct., vibr. study, force field calc. 4-113416  
 Sn complexes, solid state configurations, cond. behaviour in nonaqueous solvents 4-76466  
 SnO<sub>2</sub>, high temp. struct. of rutile-type oxides 4-113422  
 Sn<sub>3</sub>(PO<sub>4</sub>)<sub>2</sub>, monoclinic, <sup>119</sup>Sn Mossbauer spectrum 4-61610  
 Sn<sub>3</sub>Sb<sub>2</sub>S<sub>6</sub>, cryst. struct., TEM, X-ray diff. 4-65238  
 Sn<sub>3</sub>Sb<sub>2</sub>S<sub>6</sub>, cryst. struct. determ. 4-84263  
 Sr<sub>2</sub>(ReO<sub>4</sub>)<sub>2</sub>F, apatite like phases: structure and physical props. 4-70115  
 Sr-Al<sub>2</sub>SiO<sub>6</sub>, synthetic Sr-gehlenite, cryst. struct. 4-108333  
 SrBiSe<sub>3</sub>, cryst. struct. determ. and preparation 4-80017  
 SrBiTe<sub>3</sub>, cryst. struct. determ. and preparation 4-80017  
 SrCeO<sub>3</sub>-SrZrO<sub>3</sub> solid solutions, X-ray characterisation and elec. cond. 4-84239  
 SrCl<sub>2</sub>-SrI<sub>2</sub>, preparatory and crystallographic studies using X-ray diff. 4-88143  
 SrCl<sub>2</sub>·6H<sub>2</sub>O, cryst. struct., X-ray diff. 4-65237  
 Sr<sub>2</sub>IrD<sub>3</sub>, H sites, geometric model 4-88155  
 Sr<sub>2</sub>IrH<sub>3</sub>, H sites, geometric model 4-88155  
 Sr<sub>2</sub>KNb<sub>2</sub>O<sub>15</sub>(TiNb<sub>2</sub>O<sub>15</sub>), ferroelectric materials, synthesis and characteristics 4-104547

## crystal atomic structure of inorganic compounds continued

- SrMnF<sub>3</sub>·H<sub>2</sub>O, hydrated fluorometallates (III), one-dimens. antiferromagnet 4-71035  
 Sr<sub>2</sub>MnGe<sub>2</sub>O<sub>7</sub>, synthesis and cryst. struct. 4-109358  
 Sr<sub>2</sub>Nd<sub>1-x</sub>FeO<sub>3-y</sub>, cryst. struct. determ. 4-80013  
 Sr<sub>2</sub>RhH<sub>3</sub>, H sites, geometric model 4-88155  
 Sr<sub>2</sub>RuD<sub>3</sub>, H sites, geometric model 4-88155  
 Sr<sub>2</sub>RuH<sub>3</sub>, H sites, geometric model 4-88155  
 Sr<sub>2</sub>YRuO<sub>6</sub>, cryst. and mag. struct., time of flight neutron diff. studies 4-88141  
 SrZnF<sub>4</sub>, scheelite-type cryst. refinement and bond lengths 4-92176  
 Ta-N-O films, DC reactive sputtered, elec. resist., microstruct., oxidation 4-80704  
 TaP(As), stacking disorder, X-ray diff. study 4-75398  
 $\beta$ -TaPO<sub>3</sub>, IR and Raman spectra, cryst. struct. 4-61669  
 TaS<sub>2</sub>(Se<sub>2</sub>), struct. and XPS studies 4-71525  
 TaS<sub>2</sub>(IT), commensurate CDW state, superlattice struct. NQR study 4-80842  
 TaSe<sub>2</sub>, 1T- and 2H-, angle-resolved XPS, azimuthal orientations 4-104718  
 (TaSe<sub>4</sub>)<sub>n</sub>, struct., electron microscopy study, rel. to elec. props. 4-79995  
 TaTe<sub>4</sub>, evidence for deform. modulated struct. 4-113424  
 Tc phosphides, crystal struct. determ. 4-80010  
 Te-Se, solid solutions, ordering near melting temp. 4-60878  
 Te(OH)<sub>6</sub>·2KH<sub>2</sub>PO<sub>4</sub>·K<sub>2</sub>HPO<sub>4</sub>, cryst. struct., X-ray diff. study 4-60888  
 Te(OH)<sub>6</sub>·2NH<sub>4</sub>H<sub>2</sub>AsO<sub>4</sub>·(NH<sub>4</sub>)<sub>2</sub>HAsO<sub>4</sub>, cryst. struct., X-ray diff. study 4-60888  
 Te(OH)<sub>6</sub>·2NH<sub>4</sub>H<sub>2</sub>PO<sub>4</sub>·(NH<sub>4</sub>)<sub>2</sub>HPO<sub>4</sub>, cryst. struct., X-ray diff. study 4-60888  
 ThNH<sub>3</sub>, chemical struct. and composition 4-70078  
 ThS<sub>2</sub>, cryst. struct., single cryst. diffractometric obs. 4-108316  
 ThS<sub>2</sub>Gd<sup>3+</sup>, cryst. struct., single cryst. diffractometric obs. 4-108316  
 Ti complexes, solid state configurations, cond. behaviour in nonaqueous solvents 4-76466  
 TiC, electron density, density of states and chem. binding, APW calc. 4-75356  
 TiC<sub>0.9</sub>H<sub>0.1</sub>, prod. of electric bursting, phase comp. and lattice spacing 4-93259  
 Ti<sub>1-x</sub>Li<sub>x</sub>M<sub>2</sub>O<sub>2</sub> (M=Nb, Ta, Sb) rutile solid solns., X-ray characterisation 4-84274  
 TiNb<sub>2</sub>O<sub>7</sub>, struct. refinement, cation distrib., X-ray diff. study (*French*) 4-88157  
 TiO<sub>2</sub>, high temp. struct. of rutile-type oxides 4-113422  
 TiO<sub>2</sub> powder, shock loaded densification, X-ray study 4-114439  
 TiO<sub>2</sub>V<sub>2</sub>O<sub>7</sub>, crystallographic shear phase, high-resolution electron microscopy study of disorder 4-84303  
 TiO<sub>2</sub>-based solid solns., struct., X-ray diff. and thermogravimetric studies 4-70107  
 TiO<sub>2</sub>-FeNb<sub>2</sub>O<sub>7</sub>-NbO<sub>2</sub> system, rutiles, struct., mag. and electron transport props. 4-84238  
 Ti<sub>4</sub>O<sub>7</sub>, structural chem., superstructure, X-ray diff. obs. 4-88147  
 Ti<sub>2</sub>Ru<sub>1-x</sub>O<sub>2</sub>, high press. distortion, cryst. struct. study 4-80012  
 TiS<sub>2</sub>, formation by deintercalation of Na<sub>2</sub>TiS<sub>2</sub>, cryst. struct. and mag. susceptibility 4-75425  
 TiS<sub>2</sub>, nonstoichiometric, Raman spectra, struct. and composition depend. 4-109186  
 TiS<sub>2</sub> films, sputter deposition at high substrate temps., elec. and struct. props. 4-114393  
 Ti ternary chalcogenides, cryst. struct., X-ray, IR and photoacoustic studies 4-84273  
 Ti-based quaternary chalcogenide 4-84270  
 TiAlF<sub>4</sub>, structural phase transition and cryst. struct. 4-80225  
 Ti<sub>1-x</sub>Bi<sub>x</sub>F<sub>1+2x</sub>, elec. props. and struct. characts. 4-70452  
 TiCo(CO)<sub>4</sub>, cryst. struct. with cubic dense packing 4-92172  
 TiCu<sub>2</sub>Se<sub>2</sub>, p-type metal with layer struct. 4-70652  
 Ti<sub>2</sub>Fe<sub>2</sub>S<sub>2</sub>, phase relationships 4-104772  
 TiH<sub>2</sub>(SeO<sub>3</sub>)<sub>2</sub>, cryst. struct., phys. props., phase transitions 4-84921  
 TiH<sub>2</sub>(SeO<sub>3</sub>)<sub>2</sub>, dielec. props., phase transitions, cryst. struct. 4-65965  
 TiMO<sub>2</sub>P<sub>3</sub>Si<sub>2</sub>O<sub>25</sub>, intersecting tunnel struct., with ion-exchange props., struct. determ. 4-84240  
 Ti<sub>2</sub>O<sub>3</sub>·3V<sub>2</sub>O<sub>5</sub>, cryst. struct., X-ray diff. study 4-60892  
 Ti<sub>2</sub>(Sb<sub>2</sub>As<sub>2</sub>)<sub>2</sub>O<sub>10</sub>, perovskite, cryst. struct., least squares determ. 4-92171  
 Ti<sub>2</sub>Se-TiX (X=Cl, Br, I), phase diagram and Ti<sub>2</sub>Se<sub>2</sub>I cryst. struct. 4-71643  
 Ti<sub>2</sub>SnS<sub>4</sub>, cryst. struct., X-ray diff. (*French*) 4-75416  
 Ti<sub>2</sub>SnS<sub>4</sub>, cryst. struct., X-ray diff. (*French*) 4-75417  
 TiP(As)Se<sub>2</sub>, cryst. struct., neutron time of flight diff. studies 4-113406  
 (U, Pu)C, mixed carbide fuel, irradi., X-ray diff. study 4-83138  
 (U, Pu)O<sub>2</sub>, mixed oxide fuel, irradi., X-ray diff. study 4-83138  
 US<sub>2</sub>, cryst. struct., X-ray diff. data 4-75402  
 US<sub>2</sub>, cryst. struct., X-ray diff. data 4-75402  
 V<sub>4</sub>N, crystal struct. from 1 MV electron microscopy 4-92161  
 VNH<sub>4</sub>HP<sub>3</sub>O<sub>10</sub>, unit cell parameters 4-113410  
 V<sub>2</sub>Nb<sub>2</sub>O<sub>9</sub> 4-70105  
 V<sub>2</sub>O<sub>5</sub>Sb<sub>2</sub>O<sub>3</sub>, nonstoichiometric rutile-type phase, ESR and X-ray diff. studies 4-71163  
 V<sub>2</sub>O<sub>5</sub>, mixed valence oxide, metal-insulator transition (*French*) 4-70655  
 V<sub>2</sub>O<sub>5</sub>(V<sub>2</sub>O<sub>5</sub>) insertion cpds. with H<sub>2</sub> 4-70093  
 V<sub>4</sub>, ambient press. synthesis, cryst. struct., mag. and elec. props., bonding 4-75408  
 VS, metal-insulator transition and elec. props. 4-84568  
 VS<sub>2</sub>, struct. and XPS studies 4-71525  
 V<sub>2</sub>S<sub>3</sub>, cryst. struct. determ. 4-84260  
 V<sub>1-x</sub>Te<sub>x</sub>, cryst. struct., X-ray diff. studies 4-108324  
 W bronze, struct. props., review 4-70106  
 W bronze tetragonal struct. non-stoichiometric phases, dielec., ferroelastic and nonlinear optical props. 4-65972  
 W<sub>2</sub>C, crystal structure and dislocation climb obs. by TEM 4-98072  
 WCl<sub>3</sub>, synthesis, physicochemical props. 4-76649  
 WOBr<sub>4</sub>, cryst. struct., X-ray diff. (*German*) 4-84254  
 WSe<sub>2</sub>-x, zone axis patterns, changes with variations in voltage, thickness, composition and temp. 4-92157  
 YC<sub>2</sub>, tetragonal cryst. struct., neutron diff. studies 4-108322  
 Y<sub>2</sub>Fe<sub>2</sub>O<sub>7</sub>, ionic structure, neutron induced transformation, calcs. 4-113415  
 Y<sub>2</sub>Ho<sub>1-x</sub>C<sub>2</sub>, tetragonal cryst. struct., neutron diff. studies 4-108322  
 Y<sub>2</sub>O<sub>3</sub>, undoped single cryst., struct., crystal-chemical anal. 4-65221  
 Y<sub>2</sub>Rh<sub>2</sub>Si<sub>2</sub>, cryst. struct. determ. 4-108314  
 YbGa<sub>2</sub>S<sub>4</sub>, cryst. struct., polymorphic modifications, X-ray diff. study 4-60893  
 YbMoS<sub>6</sub>, crystal growth and crystal structure refinement 4-75396

**crystal atomic structure of inorganic compounds continued**

- ZnBr<sub>2</sub>, anhydrous, cryst. struct., X-ray diffr. studies 4-92179  
 Zn<sub>1-x</sub>Cd<sub>x</sub>(S)(Mn<sub>1-x</sub>S), structural disorder and solid state transformations 4-103924  
 γ-(Zn<sub>0.5</sub>Co<sub>0.5</sub>)<sub>2</sub>(PO<sub>4</sub>)<sub>2</sub>, farringtonite-type phases, crystallographic studies 4-84242  
 γ-Zn<sub>2</sub>Co(PO<sub>4</sub>)<sub>2</sub>, farringtonite-type phases, crystallographic studies 4-84242  
 (Zn<sub>0.70</sub>Fe<sub>0.30</sub>)<sub>2</sub>(PO<sub>4</sub>)<sub>2</sub>, farringtonite struct., cation distrib., neutron powder diffr., Rietveld technique 4-60889  
 Zn<sub>0.36</sub>Mn<sub>0.57</sub>Fe<sub>2.07</sub>O<sub>4</sub>, non-stoichiometric ferrite spinel, mag. props. 4-108996  
 ZnMoS<sub>4</sub>Br(I), preparation and cryst. struct. 4-70097  
 ZnO RF sputtered film on Au/quartz, crystalline props., X-ray diffr. studies 4-104101  
 ZnO-B<sub>2</sub>O<sub>3</sub>, cryst. and glass struct., <sup>11</sup>B NMR spectra 4-79941  
 β-Zn<sub>2</sub>P<sub>2</sub>, X-ray study of phase transitions 4-84385  
 ZnS:Mn electroluminesc. thin layers, doping and cryst. struct. 4-75810  
 ZnS-type crystal struct. determ. using convergent beam electron diffr. 4-103612  
 ZnTe, growth forms, chem. transport reactions 4-109314  
 ZnTe-CdTe, epitaxial film, degree of perfection and struct. 4-61250  
 Zn<sub>3</sub>[Fe<sup>II</sup>(CN)<sub>6</sub>]<sub>2</sub>, cryst. structure and phase transformations 4-103728  
 Zr<sub>2</sub>Be<sub>17</sub>, cryst. struct., X-ray diffr. studies 4-113404  
 Zr<sub>2</sub>F<sub>2.67</sub>O<sub>6.67</sub>, cryst. struct. determ. (*French*) 4-84264  
 Zr<sub>2</sub>FeO<sub>6</sub>, hydride formation, X-ray diffr., Mossbauer spectra, gas anal. 4-113392  
 ZrGeO<sub>4</sub>, cryst. struct., neutron powder diffr. 4-108328  
 Zr<sub>2</sub>GeO<sub>8</sub>, cryst. struct., neutron powder diffr. 4-108328  
 Zr(MoO<sub>4</sub>)<sub>2</sub>, polymorphism, X-ray diffr. and vibr. spectroscopy study 4-70053  
 ZrO<sub>2</sub>-based systems, ordered defect-fluorite cpds., TEM studies 4-108336  
 ZrO<sub>2</sub>-P<sub>2</sub>O<sub>5</sub> system, re-examination of crystalline phases 4-84258  
 ZrO<sub>2</sub>-ZrF<sub>4</sub> system, nonstoichiometric Zr(O,F)<sub>3+y</sub> phase, structure 4-70117  
 Zr(YO<sub>1.862</sub>), cryst. struct. determ. 4-103715

**crystal atomic structure of organic compounds**

- all-trans-n-alkanes, cryst. struct. and C-H stretching modes 4-70126  
 4-amino-4'-nitrodiphenyldisulphide, cryst. and mol. struct., X-ray diffr. 4-113434  
 4-aminophenyl N-morphylsulphone, mol. and cryst. struct., X-ray diffr. 4-112293  
 azahydrocarbons, nonbonded potentials and Coulombic interaction 4-103731  
 benzene, cryst. struct. at -3°C, calc. by mol. interaction anal. (*French*) 4-80026  
 benzene chromium tricarbonyl, substituted derivatives, mol. stackings, struct. relationships (*French*) 4-75428  
 benzene-cyclophosphazene inclusion compound, struct. and mobility, D NMR line shape study 4-113433  
 2-benzyl-1,7,10,13,19-pentaaza-4,16-diazacycloicosane-3,17,21-trione hydrate, cryst. and mol. struct., X-ray diffr. 4-113436  
 N-benzylquinolinium chloride-diphenylamine hemihydrate 1:1 complex, cryst. and mol. struct. 4-60908  
 biethylenedithiylene-TTF compounds, cryst. struct. and elec. props. 4-75430  
 biological specimens in frozen aq. solns., mol. struct. determ. 4-100072  
 bis(di-tert-butylmethyl) diselenide, dihedral angle, X-ray crystallography, UV spectra 4-65250  
 bis(ethylene dithiol)tetrahydrofulvalene triiodide, cryst. struct. determ. 4-92191  
 bismuth oxalate single crystals, gel growth and characterisation 4-99295  
 bromoacetamide, cryst. struct. and radical anion stability 4-70130  
 bromotrifluoromethane, IR and Raman spectra, cryst. struct. 4-104690  
 calcium 2-fluorobenzoate dihydrate, intermolecular H bond, cryst. struct., X-ray diffr. 4-103733  
 calcium meso-tartrate trihydrate, struct. and bonding, X-ray diffr. studies 4-113428  
 catenadiquabis-μ-(isonicotinato N-oxide), crystal and mol. struct. 4-80019  
 chloroacetamide, cryst. struct. and radical anion stability 4-70130  
 chlorocoumarins, solid-state photodimerisation rel. to cryst. engineering 4-109669  
 cholesteric myristate and pclarogonate, struct. studies 4-98009  
 cholesterol derivatives, mesogenic, cryst. and mol. struct. 4-113437  
 cholesteryl 2,2,3,3-tetrafluoropropionate, successive phase transitions and cryst. struct., X-ray diffr. study 4-61068  
 chromene, molecular cryst. struct., translation problem solving by fragmentary-implicational method 4-11263  
 conference, Charlotte, NC, USA (Nov. 1983) 4-73146  
 copper dodecanoate, discotic mesophase, X-ray diffr. study 4-92076  
 β-copper phthalocyanine, vapour phase cryst. growth, struct. and morphology 4-76647  
 copper phthalocyanines, localised mol. arrangements, electron microscopy study 4-80028  
 (Crypt 2,2,2-K<sup>+</sup>)<sub>2</sub>As<sub>2</sub>Te<sub>6</sub><sup>-</sup> complex, cryst. struct. (*French*) 4-98082  
 cyanofamide, mol. and cryst. struct., least squares anal. 4-108346  
 cyclohexanol, plastic and glassy crystalline phases, structure, X-ray diffr. study 4-60866  
 cyclophosphazenes-polyamine binding, antineoplastic activity 4-81609  
 di-(tetramethylammonium-d<sub>12</sub>) cobalt tetrachloride, commensurate-incommensurate transition 4-80023  
 sym-dibenzo-14-crown-4-oxycetate-Li<sup>+</sup> complex, cryst. and mol. struct., X-ray diffr. 4-103732  
 dibenzofuran, cryst. struct. and bond lengths, X-ray diffr. studies 4-113429  
 p-dibromobenzene, cryst. struct., powder data 4-80024  
 p-dichlorobenzene, cryst. struct., powder data 4-80024  
 p-dichlorobenzene-p-dibromobenzene mixed crystals, cryst. struct., powder data 4-80024  
 dichlorophenols, H-bonded cryst. substituent effects, cryst. struct. 4-113425  
 β,δ-dicyano-α-methylvinylferrocene, cryst. and mol. struct. 4-60909  
 1,3-bis-(dicyanomethyl)endian-2-one, cryst. and mol. struct. 4-60906  
 5,5-dimethyl-2-(dimethylamino)-2-oxo-1,3,2-oxazaphosphorinane config., X-ray struct. and PMR and IR spectra in soln. 4-113432  
 dipeptides, glycine-containing, influence of N-methylation 4-109776  
 ethyl thiocyanate, gas and solid, conform. investig. and vibr. anal. 4-69044

**crystal atomic structure of organic compounds continued**

- 3-ethyl-5-(2-(3-ethyl-2-benzothiazolylidene)ethyl-(idene))rhodamine, crystal and mol. struct. 4-59910  
 ethynyllithium, electron density superposition errors 4-113383  
 ferrirocen, Fe (III) binding peptide from *Aspergillus versicolor*, cryst. struct., X-ray diffr. study 4-85401  
 fluoroacetamide, cryst. struct. and radical anion stability 4-70130  
 fluorform, Raman and IR spectra, crystal field splitting, struct. 4-61671  
 α-Dglucopyranose, H bonds, stretching vibr., IR spectra 4-88824  
 H-bond distances and angles in organic cryst. structures 4-84231  
 hexachloronaphthalene-1,8-disulphide, struct. refinement in space group P2<sub>1</sub>/n 4-113430  
 hexahydro-1,3,5-trinitro-s-triazine, mol. struct. in vapour. soln. and solid phases, IR obs. 4-69064  
 hexaquinazolin(II)isonicotinate N-oxide, crystal and mol. struct. 4-80019  
 n-hexatriacontane, melt crystn. in temp. gradient 4-65376  
 hexavinylsiloxane, cryst. struct. 4-60907  
 hydrogen bis (phthalocyaninato) neodymium (III), iodination effect on elec. cond. 4-70808  
 indolizine and azaindolizines struct. relationship and their ability to undergo rearrangement 4-59907  
 N-iodomidosulphinyl difluoride, cryst. and mol. struct., X-ray diffr. study 4-65251  
 lithium hydrogen malate, cryst. struct. and hydrogen bonds 4-92192  
 α,ω-lors(methyldodeca-1,12-diylammonio)hexane. dibromide, conformation, X-ray struct. 4-98083  
 magnesium bis(hydrogen maleate)hexahydrate, cryst. struct., X-ray diffr. studies 4-113427  
 magnesium nickel oxalate dihydrate powders, coprecipitation from aq. soln. 4-75683  
 metalloporphyrin complexes, anomalous electronic states, crystal and mol. struct. (*Japanese*) 4-113431  
 methane, clusters, electron diffr. patterns 4-74367  
 7-methoxycoumarin, topochem. dimerisation in solid state 4-109628  
 9-methoxyanthracene in 9-cyanoanthracene host, mixed cryst. packing calc. 4-113382  
 methylcoumarins, solid-state photodimerisation rel. to cryst. engineering 4-109669  
 methylthiocarbamate, O and S isomers, mol. and cryst. struct., IR and Raman spectra 4-80923  
 neodymium acetate tricarbamide hydrate, cryst. struct., X-ray diffr. study 4-60910  
 6-(4-nitrobenzyl)thioinosine, anomalous dispersion factor for S, X-ray diffr. meas. 4-98081  
 organolithium compounds, crystal struct. 4-80020  
 oxazine derivatives, crystallographic investig. rel. to pharmacological activity 4-60904  
 n-pentylphenyl cyano-thiolbenzoates, cryst. struct. and nematic phases 4-84281  
 pepsin, cryst. struct. determ. 4-98085  
 syn-9-phenyl-2,11-dithia[3,3]metacyclopentane, cryst. and mol. struct. 4-108337  
 1-phenyl-3,5-dimethylpyrazole-oxalic acid adducts, H-bonding in cryst. struct. 4-108339  
 1-phenyl-3,5-dimethylpyrazole-perchloric acid adducts, H-bonding in cryst. struct. 4-108339  
 phosphomycin, Na salt, cryst. and mol. struct., X-ray diffr. study 4-66860  
 picolyltricyanoquinodimethan, cryst. and mol. struct. 4-70132  
 poly(γ-methyl L-glutamate)-dimethyl, phthalate, cryst. complex. struct. 4-88429  
 poly(cyclopentane-β-carboxyamine), crystalline struct., electron diffr. study 4-84214  
 polyamidohydroxides, struct. transform. during thermal cyclodehydration (*Russian*) 4-62190  
 polydiacetylene cryst., radiation damage and high resolution electron microscopy 4-80111  
 polyethylene, crystal block size change during single axial extension 4-76800  
 polyethylene, FT-IR study of soln. grown crystals. 4-108343  
 polyethylene, neutron scatt. studies on soln. grown crystals. 4-108342  
 polypivalolactone morphology 4-108344  
 polypropylene, crystal block size change during single axial extension 4-76800  
 polypropylenes, isotactic quenched melts, cooling rate effect on morphology 4-108291  
 proceaine, cryst. struct., X-ray diffr. obs. 4-92190  
 protein structure fluctuations from X-ray diffr., book contrib. 4-93688  
 proteins, cryst. struct. determ., optimum X-ray wavelength 4-62438  
 pyridine dichromates (IV), synthesis and characterisation 4-104615  
 roseotoxin B, secondary struct., X-ray and NMR study 4-115015  
 roseotoxin B, struct. and conformation 4-115009  
 N-salicylidene-p-dimethylaminoaniline, red modification, cryst. and mol. structures, X-ray diffr. study 4-60911  
 semicarbazones, oxidation prods., struct. studied using X-ray crystallography 4-92189  
 sodium hydrogen maleate trihydrate, cryst. struct., neutron diffr. study 4-113426  
 sodium hydrogen oxalate monohydrate, cryst., electron density, intermolecular interactions, ab initio LCAO-MO-SCF calcs. 4-88160  
 struct. and EXAFS studies 4-70129  
 TCNE, monoclinic phase cryst. struct., X-ray diffr. 4-65253  
 TCNQ salt, DEPA(TCNQ)<sub>4</sub>, cryst. struct., elec. cond., mag. susceptibility meas. 4-80027  
 TCNQ salt, DIT-TCNQ, optical props., cond. and cryst. struct. 4-113435  
 TCNQ salts, (1,1'-bis(p-fluorophenyl)-4,4'-bipyridinium)<sup>2+</sup>(TCNQ)<sub>2</sub><sup>2-</sup>, elec. cond. and cryst. struct. 4-65254  
 TCNQ salts, Cs<sub>2</sub> (TCNQ)<sub>2</sub>(II), synthesis, anal., novel isomeric struct. 4-114376  
 TCNQ salts, elec. mag. and struct. characterisation 4-88162  
 TCNQ salts, heterofulvalene-TCNQ, cryst. struct., Madelung energy calcs. 4-70131  
 tetramethylammonium manganese (iron) cyanide octahydrate, chain struct. and magnetism 4-71073  
 tetraphenylarsonium aquatetrachlorooxoborate(V), cryst. struct. refinement (*German*) 4-65252  
 tetraselenonaphthalene, cryst. and mol. struct. 4-70127  
 tetrahydrofulvalene-pyromellitic dianhydride complex, cryst. struct. study 4-108345  
 TGS crystals, repeated switching-induced fatigue, struct. props. 4-71300

**crystal atomic structure of organic compounds continued**

- thioacetamide,  $^{13}\text{C}$  and  $^{15}\text{N}$  substituted species, Raman spectrum, struct. 4-66030
- thioacetamide, cryst. struct., rotamers, neutron diff. study, ab-initio MO Mf calcs. 4-103734
- thiosemicarbazide hydrobromide, cryst. struct., X-ray diff. studies 4-113438
- thiosemicarbazones, oxidation prods., struct. studied using X-ray crystallography 4-92189
- thiourea, deuterated, neutron diff. study under high elec. field 4-109142
- thorium (1-phenyl-4,4,4-trifluoro-1,3-butanedione):U (IV), polarised high resolution spectra, struct. 4-108341
- thorium phthalocyanine, high resoln. electron microscopy of struct. defects 4-75429
- thorium tetrakis- $\beta$  diacetate:U (IV), polarised high resolution spectra, struct. 4-108341
- (TMTSF) $_2\text{ClO}_4$ , cavity size versus anion size, anion ordering 4-75432
- (TMTSF) $_2\text{X}$  salts, anion size, structural props., intracolumnar effects, assoc. 4-98084
- tri-p-tolylphosphine, cryst. and mol. struct., X-ray study 4-60905
- 1,3,5-tribromobenzene, cryst. struct., powder data 4-80025
- tribromomethane, polycryst., IR spectrum 4-114255
- 1,3,5-trichlorobenzene, cryst. struct., powder data 4-80025
- tricosane-tetracosane, binary paraffin, X-ray diff. and calorimetric study 4-88161
- tricyclic nitroxyl biradicals,  $\text{C}_{22}\text{H}_{36}\text{N}_2\text{O}_4$ ,  $\text{C}_{22}\text{H}_{38}\text{N}_2\text{O}_4$ , cryst. and mol. structures, X-ray diff. 4-84283
- tricyclo[4.2.2.2<sup>2,2</sup>]dodeca-1,5-diene, struct. bonding, intermolecular interactions 4-96636
- trimethylammonium manganese copper trichloride, polarised cryst. spectra and cryst. struct. 4-88825
- trimethylplatinum iodide-carbon tetrachloride, bond lengths and angles 4-92193
- triphenylmethylsulphane, single cryst., struct., photolysis, ESR of radical pairs 4-88724
- (TSeF) $_3(\text{ClO}_4)_2$ , cryst. struct., X-ray diff. 4-84282
- TTF-FeOCl intercalation cpd., struct. and EXAFS studies 4-70129
- TTF-FeOCl intercalation cpd., struct. and EXAFS studies 4-70129
- urea, charge density determ. by neutron diff. 4-103730
- zinc hexacyanoferrite (III), cryst. struct. determ. 4-108340
- Ar and Kr, clathrate hydrate formation in struct. II modification 4-112251
- $\text{Au}_3\text{Ru}_4(\mu\text{-H})(\text{CO})_{12}(\text{PPh})_3$ , synthesis, mol. and cryst. struct. 4-104969
- Cu ( $\pi$ ) complexes, crystal struct., EPR and optical study, stereochemistry (French) 4-70075
- $\text{Cu}_2(\text{diethylenetriamine})_2\text{Cl}_2(\text{ClO}_4)_2$ , cryst. and mol. struct. 4-75431
- $2\text{NaPF}_6$ , dibenzo-36-crown-12-complex, isolation, X-ray cryst. struct. determ. 4-98080
- Ni complex, TTF(Ni(dmit)) $_2$ , mol. metallic cond., cryst. struct. 4-70786
- Re complex,  $[\eta^2\text{-C}_3\text{H}_5\text{H}_2\text{Re}(\text{H})\text{CuI}]_2$ , cryst. and mol. struct., Cu(I)-Cu(I) bond 4-96715
- Re complex, hydrogen cis-diacetyl(tetracarbonyl)rhene, single cryst. TOF neutron diff. obs. 4-80222
- (TMTTF) $_2\text{M}_6$  (M=P, As, Sb), structural and electrical props. 4-70783
- U complex, dicyclohexyl-(18-crown-6) $\text{UO}_2(\text{ClO}_4)_2$  and hydrolysis product, cryst. struct. 4-80021

**crystal binding**

- see also binding energy; lattice energy
- alkali halide crystals, compression, theory 4-75604
- alkali metal double molybdates and tungstates, cation-tetrahedral anion distance 4-113386
- benzil in bibenzyl, cryst. forces, conformation, ENDOR study 4-88745
- binary alloys, charge transfer and energy of formation, CsCl intermetallic cpds. 4-77026
- chalcopyrite type E1, phases, lattice consts. and Pearson plots 4-75352
- cubic single crystals, microhardness and interatomic binding 4-113528
- density functional method (German) 4-103694
- dilute oxide solid solns., acid site form. and stoichiometry 4-88129
- fluorite-type lattice, cubo-octahedral cluster, simulation study 4-88128
- heteropolyanion and isopolyanion, struct. stability index 4-79967
- II-VI tetrahedral semicond. cpds., lattice dynamics, local Heine-Abarenkov model pot. 4-98222
- III-V tetrahedral semicond. cpds., lattice dynamics, local Heine-Abarenkov model pot. 4-98222
- inorganic solids, stoichiometry, struct. and stability, review 4-75359
- ionic crystals, Van der Waals potentials, review 4-75360
- ionic crystals, effective ionic charge, press. depend. 4-103692
- ionic-covalent cryst. pot. function struct., force const. method 4-92130
- metal, pure, electronic and cryst. struct., bonding, book contrib. 4-108304
- 9-methoxyanthracene in 9-cyanoanthracene host, mixed cryst. packing calc. 4-113382
- nonmetallic solids, amorphisability under heavy ion bombard., covalent-ionic transition 4-80122
- pyrochlore families, force fields, vibr. spectra and cryst. defects 4-98055
- rare earth double molybdates and tungstates, cation-tetrahedral anion distance 4-113386
- static ionic charge in dielectric theory, scaling with ionicity parameter 4-98057
- three dimensional solids, hard sphere bonding schemes 4-92136
- transition metals, bonding energy, pair pots. 4-103691
- transition metals, HCP, FCC and BCC structs., relative stability and entropy 4-113677
- transition metals and group B elements, valency relations 4-98054
- $\text{AgCl}(\text{Br})(\text{I})$ , anharmonic props., interionic pot. model 4-98056
- BP, refractive index and elastic const. meas. 4-61647
- $\text{CdGa}_2\text{S}_4$ , effective ionic charges, optic phonon spectra 4-103894
- $\text{CdGa}_2\text{Se}_4$ , effective ionic charges, optic phonon spectra 4-103894
- $\text{CuCl}(\text{Br})(\text{I})$ , anharmonic props., interionic pot. model 4-98056
- $\text{CuO-CaO-P}_2\text{O}_5$  glass, IR spectra 4-76446
- HBr mol. crystal, lattice dynamical model in phase III, H bond strengths 4-88246
- HCl molecular crystal, lattice dynamical model in phase III, H bond strengths 4-88246
- HF mol. crystal, lattice dynamical model in phase III, H bond strengths 4-88246
- $\text{Hg}_{3-2}\text{NbF}_6$ , cryst. struct. determ. 4-108311
- $\text{Hg}_{3-2}\text{TaF}_6$ , cryst. struct. determ. 4-108311
- $\text{KM}_3\text{F}_{10}$  (M=Y, Bi), cubo-octahedral cluster and extended defects 4-88128

**crystal binding continued**

- LiMg, pair ordering pots., Clapp and Moss approx. inadequacy 4-92129
- $\text{NH}_3$  halides, struct. stability and static props. 4-98059
- $\text{NH}_4$  halides, ionic compressibilities and static polarizabilities 4-88130
- Ni II complexes, quadridentate macrocyclic ligands, bonding cavities, X-ray struct. determ. 4-103716
- Ni-Cu(Ga)(Ag)(Au), bonding and enthalpy studies 4-79978
- NiAs phase, systematics and bonding 4-79974
- Pd-Cu(Ga)(Ag)(Au), bonding and enthalpy studies 4-79978
- PdH $_2$ , non-stoichiometric, heat of form., cluster-Bethe lattice approx. 4-75355
- Pt-Cu(Ga)(Ag), bonding and enthalpy studies 4-79978
- SiP $_2$ , struct. parameters and valence electron density distrib. 4-108331
- $\text{SrTiO}_3$ ,  $\text{V}^{5+}$  partial substitution for  $\text{Ti}^{4+}$ , ion-deficient perovskites, elec. and optical props. 4-80589
- $\text{ThCl}(\text{Br})(\text{I})$ , anharmonic props., interionic pot. model 4-98056
- TiC, electron density, density of states and chem. binding, APW calc. 4-75356
- Ti( $\text{Fe,Al}_{1-x}$ ) $_2$ , paramagnetic props. study (Russian) 4-71020
- $\text{Ti}_4\text{O}_7$ , structural chem., superstructure, X-ray diff. obs. 4-88147
- $\text{VO}_x$ , cation valence 4-88127
- Zn chalcogenides, CVD using elemental source materials, struct. props. 4-98481
- $\text{ZnSiP}_2$ , valence band struct. and chem. binding 4-88445
- crystal chemistry**
- see also crystallography
- alkali metal phosphates,  $\text{A}^1\text{B}^1\text{PO}_4$ , A=Na, K, B=Ca, Zn, Sr, Cd, Ba, Pb, ferroelec. phys. props. 4-65992
- alkaline hexahydroaluminate, struct. chemistry 4-70119
- benzene chromium tricarboxyl, substituted derivatives, mol. stackings, struct. relationships (French) 4-75428
- delafossite type compounds, deform. of octahedral layers (Japanese) 4-75606
- layered metal oxides, cryst. chemistry and mag. props. 4-98070
- linear electro-optic effect, crystallographic aspects 4-80905
- plane two-networks hexagonal structures, homologous series, cryst., chem. anal. 4-84278
- rare earth rhodium stannides, mag. superconductors, cryst. chemistry 4-70071
- rare earth-transition metal ternary borides, silicides and homologues, cryst. struct. and crystal chemistry, book 4-95076
- solid state chemistry, conf., Veldhoven, Netherlands (June 1982) 4-67863
- stability, valence and cryst. chem. systematics 4-92137
- VA transition metal oxides of V, Nb, and Ta, oxidation mechanism, phase form., cryst. struct., electron microscopy, electron and X-ray diff. studies 4-62119
- $\text{BaTiO}_3$  synthesis, polycryst., nonstoichiometry rel. to solid-solid reaction mechanism 4-99305
- $\text{Ca}_2\text{Nb}_2\text{O}_7\text{-CaTiO}_3$ , ferroelectric, crystallochemical props. 4-71288
- $\text{CeO}_3\text{Ru}_2\text{-Si}_3$ , mag. behaviour and struct. chemistry 4-103701
- $\text{Cs}_2\text{CaCl}_4\cdot 2\text{H}_2\text{O}$ , struct., cryst. chemical study 4-65223
- $\text{CsNa}_3\text{Cl}_3\cdot 2\text{H}_2\text{O}$ , struct., cryst. chemical study 4-65223
- $\text{Cs}_{1-x}(\text{Na}_2\text{H}_2\text{O})_x\text{Cl}$ , struct., cryst. chemical study 4-65223
- Fe spinels, Fe-M-O (M=Al, Cr, Zn, Co, Mn), vacancy substituted, order-disorder, IR absorpt. spectra (French) 4-76447
- $\text{In}_2\text{O}_3\text{-Fe}_2\text{O}_3\text{-CuO}(\text{CoO})$ , phase relations and cryst. structures 4-98242
- $\text{In}_2\text{O}_3\text{-Ga}_2\text{O}_3\text{-CuO}(\text{CoO})$ , phase relations and cryst. structures 4-98242
- $\text{LaB}_6$ , X-ray reflections intensity, nonstoichiometry effect 4-61099
- $\text{La}_2\text{Ti}_2\text{O}_7\text{-CaTiO}_3$ , ferroelectric, crystallochemical props. 4-71288
- $\text{Li}_2\text{O-M}_2\text{O}_3\text{-M}'_2\text{O}_4$ , M=Nb, Ta, M'=Ti, Zr, non-stoichiometric phases, cryst. chem. and ferroelec. props. 4-65968
- $\text{Nd}_2\text{Ti}_2\text{O}_7\text{-CaTiO}_3$ , ferroelectric, crystallochemical props. 4-71288
- SiC polymorphs, crust. chem. props. 4-60896
- $\text{Y}_2\text{O}_3$ , undoped single cryst., struct., crystal-chemical anal. 4-65221
- crystal classes** see crystal symmetry
- crystal cleavage** see brittle fracture
- crystal defects**
- see also Cottrell atmospheres; crowdions; crystal inclusions; crystal microstructure; defect electron energy states; disclinations; dislocations; grain boundaries; impurity-defect interactions; phonon-defect interactions; point defects; stacking faults; twinning
- alkali halides, defect creation mechanisms 4-60915
- alkali metal fluorides and chlorides, solution enthalpies of divalent defects 4-98316
- bent crystal, high resolution electron microscope structure images around pole pattern 4-113277
- binary solid solutions, high conc., lattice dilatation 4-75410
- catalyst dispersed particles, stacking faults and struct., electron microdiff. studies 4-88178
- chain systems, H-bonded, proton cond. mechanism 4-80285
- chemical diffusion in binary FCC solid solutions 4-65434
- close-packed crystals, types of one-dimensional disorder, diffractive indications 4-113440
- condensed matter physics, Iberian Symposium, Lisbon, Portugal (Sept. 1983) 4-78036
- corundum monocrystals, polished surfaces structure and thermal treatment 4-113763
- damage profile in crystals, meas. by channelling technique 4-103840
- defect-induced anomalies near phase transitions 4-80189
- diamond, natural, platelet defects, electron microscopy study 4-103740
- diffusion under high pressures, rel. to defect mech. 4-65435
- electromagnetic elastic continua, multipolar lattice defects 4-75449
- FCC metals, defect melting in 3-dimens. crystals, Monte Carlo method 4-61055
- ferroelectric, polarised defects, effects near Curie point 4-70134
- ferroelectric symmetrical phase, forbidden Raman lines 4-66026
- fluorides, perovskite-type, wide band gap expts., excitation of thermally stimulated luminesc. and conductivity 4-85018
- glass forming substances, defects and glass formation 4-75299
- graphite, C bond-network defects with ring size from 3 to 9, graph theory anal. 4-92138
- graphite-AsF $_3$  intercalated foils and compacted flakes, elec. resist. studies 4-92683
- hierarchical lattice spin systems, phase transition phenomena 4-95364
- high-temperature analysis techniques, surface characteristics 4-99927
- ice, Monte Carlo calcs. for ice-rule model 4-103973
- ice, thermal patterns obs. under dynamic loading 4-106320
- insulators, radiation effects, conf., Albuquerque, NM, USA (May-June 1983) 4-73143

crystal defects continued

- insulators, track damage and erosion by ion-induced electronic interactions 4-75551
- ion beam-solid interactions, review of surface analytical techniques, book contrib. 4-85053
- magnetic resonance studies, book contrib. 4-84845
- magnetic thin films, law of approach to saturation, Green's function calc. 4-71136
- measurement of lattice defects in semiconductor diode structures, by capacitance method 4-90611
- metallic thin films, crystal growth, initial steps, microscopic studies 4-98486
- metals, defects, hyperfine interaction studies, review, book contrib. 4-70135
- metals, defects, positron annihilation studies, book contrib. 4-85034
- metals, relation between self-diffusion, equilb. defect parameters and characts. 4-65445
- metals, stress-strain curves, anal. by macroscopic nonlinear defect model 4-103857
- metals, surfaces, impurities and defects, embedded atom method 4-92590
- metals and alloys grain boundaries and cryst. defects, interatomic pots. 4-113464
- mica, oriented U ion nuclear tracks, small angle X-ray and neutron scatt. studies 4-75554
- microstructure, book contrib. 4-109377
- naphthalene cryst., excitons, defects and intramolecular phonon interactions (Russian) 4-98532
- neutron scattering studies, book contrib. 4-84129
- nonmetallic solids, amorphisability under heavy ion bombard., covalent-ionic transition 4-80122
- nuclear methods in solid state physics, book 4-82605
- optical defects in glass, removal by reaction with H<sub>2</sub> 4-83659
- organic molecular crystals, excitonic processes (Russian) 4-98531
- oxides, ionic, particle bombard., defects and defect processes 4-70190
- oxides, non-stoichiometry at high temp., thermal emission of electrons 4-92973
- p-n junction isolation, breakdown characts., mask misalignment and crystal defects 4-92813
- n-paraffins, electron beam damage quasi-thermal mechanism, electron diff. studies 4-98135
- pentaerythritol tetrakisulfate crystals, soln. growth and defects 4-113452
- polydiacetylene cryst., radiation damage and high resolution electron microscopy 4-80111
- pyrochlore families, force fields, vibr. spectra and cryst. defects 4-98055
- quartz, natural, struct. defects and impurities diffusion 4-80055
- quartz, natural, wide band gap expts., excitation of thermally stimulated luminesc. and conductivity 4-85018
- quartz, phonon echo generation, enhancement by defects 4-70304
- rare earth fluoride cryst., ionic thermocurrents and ionic cond. 4-70443
- rare earth mixed valence cpds., struct. props. 4-70751
- Rene 95, Ni-based superalloy, fatigue, effect of processing and microstruct. 4-104843
- ripple structures, laser-induced, associated with ordered surface defects 4-80090
- sapphire, synthetic, wide band gap expts., excitation of thermally stimulated luminesc. and conductivity 4-85018
- semiconductor characterisation, EPR and spontaneous Raman scatt. 4-104485
- semiconductor defects, use of linear predictive modelling for anal. of transients from expts. 4-80528
- semiconductor wafer surface defects, automated detection by laser scanning 4-113773
- semiconductor/metal Schottky barrier struct., defects and elec. props. 4-108924
- semiconductors, appl. of electron microscope techniques 4-103622
- semiconductors, defect form., electron gas heating effects 4-84284
- semiconductors, defect formation as a result of isovalent doping 4-70181
- semiconductors, localised defects, electronic struct. and stability 4-80538
- semiconductors, thermal wave imaging anal. of defects 4-86414
- shock wave effects, conf., Santa Fe, USA (July 1983) 4-106116
- solid solution structure, book contrib. 4-108308
- solid solutions, supersaturated, radiation swelling 4-108421
- solid state chemistry, conf., Veldhoven, Netherlands (June 1982) 4-67863
- SOS films, material improvement process by solid phase epitaxial growth 4-81124
- spinel films, epitaxial growth by solid state reactions 4-61252
- TEM, book contrib. 4-109620
- tetracene, delayed fluoresc., role of charge transfer states in triplet exciton form. 4-99191
- TGS, cryst., phys. props., influence of defects 4-76329
- TGS, ferroelec. transition, critical behaviour, defect influence 4-65983
- TGSe, cryst., phys. props., influence of defects 4-76329
- TGSe, ferroelec. transition, critical behaviour, defect influence 4-65983
- thiourea, memory effect, defect density waves in modulated systems 4-88163
- transition metal alloys, sigma phase, pair-wise interaction model 4-84422
- transition metal carbides, nitrides and oxides, structural defects, influence on character of mutual solubility 4-113643
- triglycine fluoroberyllate, cryst., phys. props., influence of defects 4-76329
- TTF-TCNQ, strongly irradi., CDW fluctuations, X-ray diffuse scatt. study 4-84611
- two-phase system, ionic cond. enhancement and space charge region defects 4-80286
- type II supercond., elemental-flux pinning pot. 4-76093
- type II superconductors, vortex motion and effect of controllable defects 4-84757
- uniaxial ferroelectrics, spin-lattice relax. at phase transitions, effect of relaxing defects, appl. to TGS 4-99059
- x-ray and neutron scattering, book contrib. 4-108250
- Al-based thin films, ultramicrohardness and internal stresses 4-92582
- (Al,Ga)As heterojunctions, laser-induced defects, photochem. etching 4-113439
- (Al,Ga)As, interrupted MBE growth, epitaxial, InAs protection layer 4-114400
- Al<sub>1-x</sub>Ga<sub>x</sub>As<sub>1-y</sub>Sb<sub>y</sub> heterostruct., conditions for LPE growth 4-114429
- Al<sub>2</sub>O<sub>3</sub>/Ti, sintering and densification, defect models 4-109364
- Al<sub>2</sub>O<sub>3</sub>/Zr, sintering and densification, defect models 4-109364
- Au-based thin films, ultramicrohardness and internal stresses 4-92582

crystal defects continued

- Au-Cd liq. and solid alloy, elec. resist. studies 4-88499
- Ba<sub>2</sub>Na<sub>0.84</sub>Nb<sub>0.99</sub>O<sub>15</sub>, incommensurate system, thermal hysteresis in birefringence and permittivity 4-61656
- BaTiO<sub>3</sub> doped single cryst., ferroelec. transition, substitutional defect influence 4-65984
- BaTiO<sub>3</sub> synthesis, polycryst., nonstoichiometry rel. to solid-solid reaction mechanism 4-99305
- Bi whiskers, longit. magneto-resist. meas. 4-88500
- Bi<sub>2</sub>GeO<sub>20</sub>, phonon echo generation, enhancement by defects 4-70304
- CaF<sub>2</sub>, Pu and U diffusion above and below  $\lambda$  transition temp. 4-70473
- Ca<sub>10</sub>(PO<sub>4</sub>)<sub>6</sub>F<sub>2</sub>, fluorapatite, radiation, damage and annealing, optical studies 4-70192
- CaSO<sub>4</sub>/Dy single cryst., cryst. growth and elec. props. 4-113943
- CdBr<sub>2</sub> layered cryst., radiation defect formation 4-65299
- Cd,Hg<sub>1-x</sub>Te/In system, current noise in contact regions; defect influences 4-88595
- CdI<sub>2</sub> layered cryst., radiation defect formation 4-65299
- Cd<sub>3</sub>Nb<sub>2</sub>O<sub>7</sub>, unusual incommensurate soft mode damping 4-113562
- CdS, electron beam annealing, defects diffusion 4-103801
- (Co,Fe)<sub>1-x</sub>O<sub>x</sub>, defects, thermodynamic calcs. 4-98087
- CoSi<sub>2</sub> single cryst. films, <sup>4</sup>He irradi., elec. cond. studies 4-98782
- CrO<sub>2</sub>, reduction, struct. and textural constraints 4-71916
- CsDy(MoO<sub>4</sub>)<sub>2</sub> layered cryst., low temp. thermal cond. (Russian) 4-70481
- Cu halides, neutron irradi., defect form., EPR obs., effects of bond ionicity 4-70224
- Cu, thermal neutron irradi., defect production efficiencies 4-108463
- CuAg alloys, cone form. during Ar<sup>+</sup> ion sputtering 4-75552
- CuInS<sub>2</sub>, defect chemistry, elec. and Mossbauer studies 4-70730
- CuInSe<sub>2</sub> semicond., Se self-diffusion studies 4-88335
- Cu<sub>2</sub>S-CdS solar cells, elementary degradation mechanisms (Russian) 4-89402
- Cu<sub>2-x</sub>S, long period modulated struct. with continuously variable periodicity 4-113469
- Cu<sub>2-x</sub>Te<sub>2</sub>, long period modulated struct. with continuously variable periodicity 4-113469
- Cu<sub>2-x</sub>VS<sub>2</sub>, long period modulated struct. with continuously variable periodicity 4-113469
- Fe-base superalloy,  $\alpha$ -phase, planar faults, domain structures, high resolution electron microscopy obs. 4-104793
- Fe<sub>1-x</sub>O<sub>x</sub>, chem. and self diffusion coeff. calc. 4-98356
- Fe<sub>1-x</sub>O<sub>x</sub>, self-diffusion and defects 4-98343
- Fe<sub>2</sub>O<sub>3</sub>, pure and doped semicond., elec. cond. and Seebeck voltage 4-92759
- Fe<sub>3-x</sub>O<sub>4</sub>, self-diffusion and defects 4-98343
- Fe<sub>1-x</sub>VS<sub>2</sub>, chem. and self diffusion coeff. calc. 4-98356
- Fe<sub>3-4x</sub>γ-Fe<sub>2</sub>S<sub>3</sub> mixture, cryst. struct. and defect struct. 4-75422
- GaAs (100) etch pits and cryst. defects, ellipsometry and reflectivity studies 4-84492
- GaAs, crystal and amorphous, pulsed laser irradi. under O<sub>2</sub> and silane atmospheres, O incorporation and losses 4-80091
- GaAs, defect visualisation by oxidation in water 4-92194
- GaAs, electron irradi., electronic struct. of E3-defects 4-70720
- GaAs, interrupted MBE growth, epitaxial InAs protection layer 4-114400
- GaAs LEC substrate, characterisation of impurities and microdefects (Japanese) 4-103778
- GaAs MBE layers, elec. props. of oval defects, FET appl. 4-92574
- GaAs, MBE layers, spatially-resolved luminescence at oval defects 4-75803
- GaAs, magnetic circular dichroism-ODMR study, of EL<sub>2</sub> defect 4-104151
- GaAs, photoluminescence characterisation of impurities and defects 4-88876
- GaAs Schottky diodes, transport mechanism, deep centre effects 4-88558
- n-GaAs:Si,  $\alpha$ -irradi., positron annihilation study 4-104696
- GaAs:Si, implanted, elec. props., pulse laser annealing effects 4-60953
- Ga<sub>2-3</sub>Cr<sub>3</sub>S<sub>4</sub>, cation deficient chalcogenide spinels, electron microscope study 4-113443
- Ga<sub>0.47</sub>In<sub>0.53</sub>As, ion implanted, annealing, TEM obs. 4-70228
- GaInAsP, defect motion and growth of extended non-radiative defect structs., book contrib. 4-60914
- GaP crystal quality in soln. growth P press. effects 4-103685
- Ge, radiation-induced rod-like defects 4-92238
- Ge single cryst.,  $\alpha$ -particle irradi., defects and photoelectromag. effects 4-84654
- In supercond. film, resistive transition in mag. field, symmetry breakdown 4-65779
- InCr<sub>3</sub>S<sub>4</sub>, cation deficient chalcogenide spinels, electron microscope study 4-113443
- In<sub>0.4</sub>Ga<sub>0.6</sub>As/GaAs strained layer superlattice, MBE growth, strain and layer thickness effects 4-93919
- InGaAsP-InGaP rapidly degraded DH laser grown by LPE, dark-line defects 4-69406
- InP p<sup>+</sup>-n junctions,  $\gamma$ -ray irradi., electron trap annealing 4-98748
- InSb, ion implanted single cryst., damage study, by characteristic X-ray emission 4-88214
- KH<sub>2</sub>(SeO<sub>3</sub>)<sub>2</sub>, ferroelastic domain struct. dynamics, internal friction meas. 4-80156
- KM<sub>3</sub>F<sub>10</sub> (M=Y, Bi), cubo-octahedral cluster and extended defects 4-88128
- K<sub>0.3</sub>MoO<sub>3</sub>, electron irradi., CDW pinning in Peierls distorted state by induced defects, nonlinear cond. 4-98595
- LaCrO<sub>3</sub>/Mg, defect struct., model and thermogravimetric meas. 4-75434
- LaF<sub>3</sub>Er<sup>3+</sup>, high freq. phonon dynamics, optical detection methods 4-65357
- LaMo<sub>6</sub>S<sub>8</sub> films, supercond. props. and normal state resist. 4-92876
- LiNbO<sub>3</sub>:Ti(Mg), single cryst., chemical and microscopical studies 4-103777
- MgO (001), adsorption of CO and simple organic mols., ab initio MO calcs., lattice defect methods 4-81476
- MgO:Ca<sup>2+</sup>, coexistence of large- and small-radius excitons bound on defects 4-92619
- Mo, isochronal annealing study of neutron induced defects; positron annihilation obs. 4-65305
- Mo, thermal neutron irradi., defect production efficiencies 4-108463
- MoO<sub>3</sub>, impurities, defect form. and charge compensation; EPR studies 4-80054
- (NH<sub>4</sub>)<sub>2</sub>BeF<sub>4</sub>, dielectric hysteresis and anomalous temperature 4-93026
- NH<sub>4</sub>Cl:Co<sup>2+</sup>(Ni<sup>2+</sup>), X-irrad. effects, optical absorpt. spectra, EPR 4-70206

## crystal defects continued

- Na<sub>2</sub>Mo<sub>2</sub>O<sub>7</sub>, impurities, defect form. and charge compensation, EPR studies 4-80054  
 Nb, electron-irradiated, muon diffusion and trapping by defects 4-65905  
 NbO<sub>2+x</sub>, phase equilibria and defect struct. 4-98246  
 Ni electrodeposits, struct., positron lifetime meas. 4-104103  
 NiO, cationic self-diffusion and oxidation 4-92419  
 Ni<sub>1-x</sub>O ceramic, grain boundaries, TEM studies 4-108382  
 NiSi<sub>2</sub> single cryst. films, <sup>4</sup>He irradiat., elec. cond. studies 4-98782  
 Ni<sub>3+2x</sub>Te<sub>2</sub>, long period modulated struct. with continuously variable periodicity 4-113469  
 PbF<sub>2</sub>-R, R=rare earth, dielec. spectrum study, 5.5 to 380K 4-71272  
 Pb<sub>1-x</sub>Ge<sub>x</sub>Te, undoped and In-doped, anomalous scatt. of carriers by defects and impurities near ferroelec. phase transition 4-98622  
 mPbS-nBi<sub>2</sub>Si<sub>3</sub>, long period modulated struct. with continuously variable periodicity 4-113469  
 Pb<sub>0.2</sub>Sn<sub>0.8</sub>S multilayer single cryst. semiconductor, X-ray effects, Mossbauer investig. 4-109106  
 PrCrO<sub>3</sub>, defect struct. 4-75436  
 RbM<sub>3</sub>F<sub>10</sub> (M=Y, Bi), cubo-octahedral cluster and extended defects 4-88128  
 Rb<sub>0.10</sub>MoO<sub>3</sub>, electron irradiat., CDW pinning in Peierls distorted state by induced defects, nonlinear cond. 4-98595  
 Se crystal struct. and defects, CDW soliton model 4-70685  
 Si, defect and carrier lifetime, back-surface damage gettering technique 4-113972  
 Si, defect delineation by chem. etching 4-88171  
 Si, electron and γ-ray irradiated, efficiency of radiation defect formation 4-92237  
 Si, fast neutron irradiation effects on resistivity in single crystals 4-98138  
 Si, float-zone dislocation-free single crystal, microdefects effect on positron lifetimes (Chinese) 4-104694  
 Si, floating-zone crystals, microdefects, metallographic and electron microscopical anal. 4-103737  
 p-Si high-purity quenched samples, defect photoluminesc. 4-80979  
 Si, ion implanted, pulsed laser and thermal processing, defect anal. 4-70133  
 Si, lattice defects, μSR study 4-84885  
 Si MOS struct., implantation-induced defects, RF annealing using H plasma 4-84308  
 Si, monocrystalline films grown on SiO<sub>2</sub>, defect characterisation 4-61251  
 Si, neutron irradiat., radiation defects and electrophys. parameters 4-84319  
 Si, photoluminescence characterisation of impurities and defects 4-88876  
 Si, polycrystalline, defect etching 4-81308  
 Si, radiation-induced rod-like defects 4-92238  
 Si surface, paramag. centre form. during strong cooling 4-65861  
 Si, swirl defect formation during zone growth 4-71552  
 Si VLSI circuit processing, material phenomena 4-103738  
 Si, with structure defects, X-ray scatt. in Laue geometry, dynamical effects 4-75435  
 Si:As, implanted under channelling conditions, impurity spatial distrib., localisation, defect form. charact. 4-84321  
 Si:As, ion implanted, IR radiation annealing of extended defects 4-92228  
 Si:As, ion implanted through screen oxide, residual disorder after high temp. anneal 4-113511  
 Si:As<sup>+</sup>(Sb<sup>+</sup>), ion implanted and laser annealed, defects, photoluminescence studies 4-75433  
 Si:H, study of H-induced defects (Chinese) 4-103736  
 a-Si:H p-n devices, EBIC decay 4-92796  
 Si:H single cryst., defect distrib. and density, X-ray projection topography studies (Chinese) 4-98086  
 Si:muonium, interstitial atom mobility, radiation defect effects 4-65256  
 SiC, structural defects and grain boundaries, electron microscope study 4-92217  
 Si<sub>3</sub>N<sub>4</sub> CVD films, fault struct., TEM studies 4-108389  
 Si<sub>3</sub>N<sub>4</sub>, structural defects and grain boundaries, electron microscope study 4-92217  
 SiO, amorphous, optical study of defects 4-88862  
 SiO<sub>2</sub>, layers, defect density, influence of halogens in thermal oxidation of Si (Russian) 4-99624  
 Sm<sub>2</sub>B<sub>6</sub>, defect single crystals, galvanomagnetic props., press. effect 4-70840  
 Sn, single crystal, lattice defect kinetics (Russian) 4-80029  
 SrTiO<sub>3</sub> polycrystalline anodes, photoelectrochemical props., influence of mech. polishing 4-75998  
 SrTiO<sub>3</sub>:La, oxidation-reduction behaviour 4-103739  
 steel, Mn-Mo-Ni, for reactor pressure vessels, neutron irradiation effects on mech. props. 4-108467  
 Ta, electron-irradiated, muon diffusion and trapping by defects 4-65905  
 Ta<sub>2</sub>O<sub>5</sub>, stabilised with TiO<sub>2</sub>, HfO<sub>2</sub> and Cr<sub>2</sub>O<sub>3</sub>, ionic cond. studies 4-70435  
 Te crystal struct. and defects, CDW soliton model 4-70685  
 TiO<sub>2</sub>, reduced rutile crystal energy calcs. for planar faults 4-98088  
 ZnO, non-stoichiometric, diffusion processes 4-98352

crystal dislocations *see dislocations*crystal electron states *see electron energy states (condensed matter)*crystal energy *see lattice energy*crystal etching *see etching*

## crystal faces

- alloys, BCC binary, bulk decomposition, surface monolayer ordering 4-65383  
 bismuth oxalate single crystals, gel growth and characterisation, vicinal faces 4-99295  
 corundum, crystal morphology, effect of trivalent rare-earth ions 4-75349  
 ice crystals, vapour grown, morphological instability, SEM obs. 4-88125  
 ice single crystal, vapour growth mechanisms, morphological stability 4-60868  
 kinetic equations of normal growth near equil. 4-60870  
 Ag<sub>2</sub>S, high temp. phase, equil. roughening transition 4-60877  
 Bi<sub>2</sub>Te<sub>3</sub> cryst., external shape, impurity complex effects 4-75347  
 Cu complex, bis-(propylammonium) copper(II) tetrachloride, cryst. growth from soln., Oswald ripening along faceted bridge 4-75336  
 GaSb cryst., facet regions and Czochralski growth 4-75348  
 NaCl (100) cleavage faces, time evolution of non-circular islands, simulation 4-60871  
 PbTe cryst., external shape, impurity complex effects 4-75347  
 Si/SiO<sub>2</sub> interface, amorphous Si/cryst. Si facet form. during solid phase epitaxy 4-88423  
 YIG single crystal spheres, dissoln. forms in H<sub>3</sub>PO<sub>4</sub> and HBr 4-75687

## crystal field interactions

*see also crystal hyperfine field interactions*

- alkali halide phosphors, S<sup>2+</sup> ion impurity centres with O<sub>h</sub>, D<sub>4h</sub>, C<sub>4v</sub> and C<sub>2v</sub> symm., cryst. field theory 4-61346  
 alkaline halogenides with admixture halogenide anions, electron transitions in C<sub>4v</sub> symm. centres, formed from S<sup>2+</sup> ions 4-76404  
 Anderson Hamiltonian with cryst. field splitting and spin-orbit interactions, ground state props. 4-108821  
 cadmium oxalate trihydrate: Mn<sup>2+</sup>, EPR spectrum 4-104489  
 centrosymmetric complexes, radiative transitions, symmetry adapted crystal field approach 4-61751  
 Coqblin-Schrieffer model in cryst. field, ground state props. 4-98837  
 covalent semiconductors, spectroscopy of 3d impurities 4-70712  
 cyclopropane-1,1-d<sub>2</sub> and cyclopropane-1,1,2,2-d<sub>4</sub> IR and Raman spectra, splitting patterns, vibr. modes 4-66029  
 erbium hexa antipyrine tri-iodide:Gd<sup>3+</sup>, soft mode dynamics, phase transition, EPR 4-109068  
 ferric complexes, quantum mixed-spin, EPR param. 4-92951  
 fluoroform, Raman and IR spectra, crystal field splitting, struct. 4-61671  
 hexaimidazolecadmium(II) nitrate: Mn(II), EPR study in a cubic ligand field 4-76241  
 ionic crystals and complexes, decreased repulsion of localised electrons, nephelauxetic effect 4-70759  
 α-KCr(SO<sub>4</sub>)<sub>2</sub>·12H<sub>2</sub>O alum, high pressure mag. resonance study of crystal fields 4-70757  
 lanthanum ethylsulphate:Ce<sup>3+</sup>, energy level shift under hydrostatic press. (Russian) 4-84598  
 linear Ising model, crystal field effect, ferromag. and antiferromag. susceptibilities 4-98845  
 magnetic alloys, dil. low temp. thermodynamic props., anomalous contrib., in presence of cryst. field 4-84801  
 metalloporphyrin complexes, anomalous electronic states, crystal and mol. struct. (Japanese) 4-113431  
 molecular crystals, mixing Frenkel excitons with charge-transfer excitons 4-108784  
 muon spin rot., possibility for cryst. field levels study 4-71229  
 noncubic symmetries, cryst. field splitting calc. 4-75905  
 point charge model, modified, cryst. field parameters 4-104176  
 rare earth alloy, R<sub>2</sub>Rh<sub>2</sub>B<sub>2</sub>, R=Y, Er, Ho, Tm, Dy, mag. props. and crystal field effects 4-84767  
 rare earth alloys, R<sub>3</sub>Rh<sub>2</sub>, R-Gd, Tb, Dy, Ho, Er, mag. props. meas. 4-61521  
 rare earth compounds, crystal-field parameters, extended charge contrib. 4-113912  
 rare earth metals, alloys and compounds, giant magnetostriction, influence of magnetoelastic interaction, review 4-71151  
 rare earth oxyhalides, doped, crystal field, quadrupole moments, ab initio calc. 4-65650  
 ruby:Cr<sup>3+</sup>, cryst. fields superposition model, appl. to non-S-state impurity ions 4-98574  
 semiconductors, deep levels, expt. and theoretical studies, review 4-84593  
 solid electrolytes, diffusion tunnels and cryst. field pot., diffraction expts. 4-70442  
 squarilum dye, polymorphs, cryst. field influence on UV spectra 4-104626  
 ternary chalcopyrite semiconductors, Einstein relation, cryst. field splitting effect 4-108860  
 tetraphenylsilane, vibr., Raman spectra, IR dichroism 4-84963  
 thioacetamide, <sup>13</sup>C and <sup>15</sup>N substituted species, Raman spectrum, struct. 4-66030  
 transition metal based alloys, dipole force tensor, cryst. field effect 4-84597  
 transition metal compounds, band struct. calcs., Mossbauer spectra 4-92611  
 transition metal oxides: Co, electronic struct. and cryst. field transitions 4-113891  
 2,4,5-trimethylbenzaldehyde in dureac single crystals, doublet phosphoresc., Stark splitting 4-64526  
 trivalent ion, position-depend. antishielding factors 4-70762  
 unitary group approach, use of projection operator techniques 4-80556  
 UV-visible and IR spectra, radiative transition probabilities for fluoresc. level 4-114309  
 ytterbium hexa antipyrine tri-iodide:Gd<sup>3+</sup>, soft mode dynamics, phase transition, EPR 4-109068  
 zircon-structure crystals, internal strain, orbit-lattice coupling and phase transitions 4-80220  
 Ag-Gd(Er), dil., impurity-induced muon depolarisation, mag. field depend. 4-71228  
 Au-Gd, dil., impurity-induced muon depolarisation, mag. field depend. 4-71228  
 AuNi(Co), impurity lineshapes in dilute alloys, UPS study 4-113893  
 BaSO<sub>4</sub>:MnO<sub>2</sub><sup>2+</sup>, absorpt. spectra, comparison with other host lattices 4-109217  
 BaTiO<sub>3</sub>, lattice deformation induced cryst. field variations, Mossbauer and EPR studies 4-71159  
 BiFeO<sub>3</sub> single crystal, ferroelec. domains, birefringence, and light absorption 4-71324  
 CaO:Mn<sup>2+</sup>, zero field splitting parameter calc. method 4-65646  
 CaS:Er phosphor, electrolum. spectrum and Er<sup>3+</sup> ion energy level splitting 4-71446  
 CaZn<sub>2</sub>F<sub>6</sub>:Mn<sup>2+</sup> cryst. struct., axial field splitting calc., EPR, optical spectra 4-92159  
 n-CdGeAs<sub>2</sub>, degenerate, Einstein relation, cryst. field splitting effect 4-108860  
 Cd(NH<sub>3</sub>)<sub>2</sub>(ClO<sub>4</sub>)<sub>2</sub> and Cd(NH<sub>3</sub>)<sub>6</sub>(BF<sub>4</sub>)<sub>2</sub>, phase transitions, microscopic theory 4-61071  
 CdS, cryst. polarisabilities, quantum mech. approach 4-84596  
 Ce intermediate-valence cpds., anomalous thermo-EMF coefficient behaviour 4-61405  
 Ce ion in cubic environment, ground state, effects of cryst. fields 4-104403  
 Ce metal, alloys and compounds, dense Kondo state, spin-orbit coupling crystal field splitting 4-84613  
 Ce mononitrides, f-electron-band-electron hybridisation and anomalous cryst. field splitting 4-113913  
 CeAl<sub>3</sub>, bound state between phonons and crystalline electric field states 4-104175  
 CeAl<sub>3</sub>, phonon softening, neutron scatt. studies 4-92318  
 CeAl<sub>100-x</sub>, amorphous, transport and mag. props. 4-108985  
 CeD<sub>2+x</sub>, mag. order and cryst. field effects 4-104408  
 CeF<sub>3</sub>, magnetic susceptibility and Verdet const. 4-61507

## crystal field interactions continued

- CeMg, antiferromag. cpd., magnons and phonons 4-84777  
 CeSi<sub>0.86</sub>, elec. cond. and paramagnetism 4-104207  
 Co-P amorphous alloys, NMR enhancement factor and multiple echoes 4-76270  
 Co(NH<sub>4</sub>)<sub>2</sub>(BeF<sub>4</sub>)<sub>2</sub>·6H<sub>2</sub>O, optical absorption spectrum 4-104588  
 CoO solar selective thermal absorbers, optical props. and selective absorption mechanism 4-99212  
 Cr<sup>3+</sup> impurity absorpt. spectra, crystal field, ground and excited state 4-109218  
 CsMnBr<sub>3</sub> with cryst. field of low symm., spectral splittings (*Chinese*) 4-70754  
 CuInSe<sub>2</sub>, surface photocond. and positive cryst. splitting 4-65649  
 CuNi impurity lineshapes in dilute alloys, UPS study 4-113893  
 DyAl<sub>2</sub>, ferromag., magnetisation, NMR studies 4-80787  
 Er<sup>3+</sup> in ionic crystals, nephelauxetic effect and radial expectation values, dielec. screening model 4-61344  
 ErNi<sub>5</sub>, crystal electric field splitting, inelastic neutron scatt. study 4-65648  
 ErTiO<sub>3</sub>, single cryst., magnetisation and mag. susceptibility 4-88652  
 Eu complex, tris(ethylsulphate) ennehydrate, elec. dipole intensity parameters 4-70756  
 Fe complex, halobis(diethylselenocarbamate)iron(III), mag. props. 4-76124  
 Fe-C, induced mag. moment by tetragonally elongated lattice expansion, magnetisation, Mossbauer spectra meas. 4-98930  
 Fe-N, induced mag. moment by tetragonally elongated lattice expansion, magnetisation, Mossbauer spectra meas. 4-98930  
 Fe-Ni-C, induced mag. moment by tetragonally elongated lattice expansion, magnetisation, Mossbauer spectra meas. 4-98930  
 Fe<sub>3</sub>Co<sub>3</sub> complex, hexa(pyridine-N-oxide) (ClO<sub>4</sub>)<sub>2</sub>, decoupled mag. sub-systems 4-98895  
 Fe(NH<sub>4</sub>)<sub>6</sub>(ClO<sub>4</sub>)<sub>2</sub> and Fe(NH<sub>3</sub>)<sub>6</sub>(BF<sub>4</sub>)<sub>2</sub>, phase transitions, microscopic theory 4-61071  
 α-Fe<sub>2</sub>O<sub>3</sub>, anisotropy of elec. props., mag. order depend. 4-108853  
 Fe<sub>2</sub>TiO<sub>3</sub>, spin glass, irreversible phenomena, effect of cryst. field anisotropy 4-104432  
 GaAs:Cr, Cr-related complex, photoluminesc. studies 4-88467  
 GaP: transition metal, impurity electron states calcs. 4-70711  
 GdAl<sub>3</sub>, ferromag., magnetisation, NMR studies 4-80787  
 HoAlGa, mag. transitions, mag. and cryst. structures, X-ray diffr., thermal expansion meas. 4-114113  
 HoTiO<sub>3</sub>, single cryst., magnetisation and mag. susceptibility 4-88652  
 InP, excitons bound to neutral acceptors, stress effects, photoluminesc. study 4-61294  
 In III complexes, <sup>1</sup>H and <sup>13</sup>C NMR, cond. and mag. susceptibility meas. 4-71192  
 α-KAl(SO<sub>4</sub>)<sub>2</sub>·12H<sub>2</sub>O alum, high pressure mag. resonance study of crystal fields 4-70757  
 KCrO<sub>2</sub>, EPR linewidths and exchange integrals 4-76244  
 K<sub>2</sub>FeO<sub>4</sub>, mag. ordering and critical slowing down, Mossbauer studies 4-76148  
 K<sub>3</sub>Pr<sub>2</sub>(NO<sub>3</sub>)<sub>9</sub>, single cryst., absorpt. and circular dichroism spectra 4-114240  
 LaCoO<sub>3</sub>, spin-state transitions at low temp., near-neighbour impurity effect 4-88643  
 LaF<sub>3</sub>:Pr<sup>3+</sup>, two-photon transition from <sup>3</sup>H<sub>4</sub> to <sup>5</sup>S<sub>0</sub> 4-104636  
 LiCrO<sub>2</sub>, EPR linewidths and exchange integrals 4-76244  
 LiNH<sub>2</sub>SO<sub>4</sub>:Mn<sup>2+</sup>, impurity electronic absorpt. spectrum 4-66055  
 LiNbO<sub>3</sub>:Cr<sup>3+</sup> (Mn<sup>2+</sup>), axial cryst. field parameters, EPR spectra 4-98579  
 LiNbO<sub>3</sub>:Cu<sup>2+</sup>, EPR and optical absorption spectra, Jahn-Teller effects 4-71166  
 LiNbO<sub>3</sub>:Cu<sup>2+</sup>, single crystal, Jahn-Teller effect 4-108825  
 LiNbO<sub>3</sub>:Ni<sup>2+</sup>, cryst. field splitting of impurity levels 4-65647  
 LiYF<sub>4</sub>:Br<sup>3+</sup>, crystal-field energy levels, splitting chain calc. (*Chinese*) 4-113908  
 MgCO<sub>3</sub>:<sup>57</sup>Fe (II), orbit-lattice interaction effect on Mossbauer studies 4-71222  
 Mg(NH<sub>3</sub>)<sub>6</sub>(ClO<sub>4</sub>)<sub>2</sub> and Mg(NH<sub>3</sub>)<sub>6</sub>(BF<sub>4</sub>)<sub>2</sub>, phase transitions, microscopic theory 4-61071  
 MgO:Er<sup>3+</sup>, strain results, superposition model of orbit-lattice interaction 4-80557  
 Mn<sup>2+</sup> ion in crystalline environment with C<sub>3</sub> symm., relativistic crystal field model 4-113911  
 MnO, antiferromag., muon spin precession obs., local fields and phase transition 4-65921  
 α-NH<sub>4</sub>Al(SO<sub>4</sub>)<sub>2</sub>·12H<sub>2</sub>O alum, high pressure mag. resonance study of crystal fields 4-70757  
 NH<sub>4</sub>Cl:Co<sup>2+</sup>(Ni<sup>2+</sup>), X-irrad. effects, optical absorpt. spectra, EPR 4-70206  
 α-NH<sub>4</sub>Cr(SO<sub>4</sub>)<sub>2</sub>·12H<sub>2</sub>O alum, high pressure mag. resonance study of crystal fields 4-70757  
 NaAl(SO<sub>4</sub>)<sub>2</sub>·12H<sub>2</sub>O:Fe<sup>3+</sup>, single crystal EPR, resonance linewidths, crystal field splittings 4-84851  
 NaCrO<sub>2</sub>, EPR linewidths and exchange integrals 4-76244  
 Na<sub>2</sub>Eu(MO<sub>4</sub>)<sub>4</sub>, M=Mo, W, cryst. field effect, mag. susceptibility, fluorescence study 4-88667  
 Na<sub>2</sub>Zn(SO<sub>4</sub>)<sub>4</sub>·4H<sub>2</sub>O:Cr<sup>3+</sup>, optical absorption spectrum of Cr<sup>3+</sup> 4-71418  
 Nb/Au/Nb Josephson tunnel junction, ESR study 4-92871  
 NdAl<sub>2</sub>, cryst. elec. fields, conduction electron screening effects 4-75906  
 Nd(BrO<sub>3</sub>)<sub>3</sub>·9H<sub>2</sub>O, single cryst., mag. susceptibility, cryst. field effect and calcs. 4-71018  
 NdCl<sub>3</sub>(F<sub>3</sub>)(OCl), paramagnetic anisotropy, optical spectra study 4-65790  
 NdF<sub>3</sub>, magnetic susceptibility and Verdet const. 4-61507  
 NdP(S), paramagnet, mag. susceptibility and cryst. field effects 4-80742  
 NdSm<sub>1-x</sub>Fe<sub>2</sub>, Laue phase, spin-reorientation temp., mag. anisotropy, Mossbauer spectra (*Japanese*) 4-61533  
 NiCl<sub>2</sub>, valence-band photoemission and optical absorption 4-99279  
 Ni<sub>2</sub>Fe<sub>2-x</sub>O<sub>4</sub>, cation-site occupation, effect of Ni content 4-98079  
 Ni(NH<sub>3</sub>)<sub>6</sub>(ClO<sub>4</sub>)<sub>2</sub> and Ni(NH<sub>3</sub>)<sub>6</sub>(BF<sub>4</sub>)<sub>2</sub>, phase transitions, microscopic theory 4-61071  
 Ni<sub>2</sub>NbBO<sub>6</sub>, polarised absorpt. spectra of Ni<sup>2+</sup> ion 4-93085  
 NiO solar selective thermal absorbers, optical props. and selective absorption mechanism 4-99212  
 NiO, valence-band photoemission and optical absorption 4-99279  
 Ni<sub>3</sub>(PO<sub>4</sub>)<sub>2</sub>-based solid solns., crystallographic studies, X-ray and neutron diffr. studies 4-92178  
 Pd II complexes, <sup>1</sup>H and <sup>13</sup>C NMR, cond. and mag. susceptibility meas. 4-71192  
 PrD<sub>1.95</sub>, mag. order and cryst. field effects 4-104408

## crystal field interactions continued

- PrF<sub>3</sub>, magnetic susceptibility and Verdet const. 4-61507  
 PrF<sub>3</sub>:Pr<sup>3+</sup>, tysonite struct. and cryst.-field anal. 4-113909  
 PrP(S), paramagnet, mag. susceptibility and cryst. field effects 4-80742  
 Pr<sub>2</sub>Sm<sub>1-x</sub>Fe<sub>2</sub>, Laue phase, spin-reorientation temp., mag. anisotropy, Mossbauer spectra (*Japanese*) 4-61533  
 Pt II complexes, <sup>1</sup>H and <sup>13</sup>C NMR, cond. and mag. susceptibility meas. 4-71192  
 RbCdF<sub>3</sub>, competition between ferroelectricity and ferroelasticity 4-76355  
 RbMgF<sub>3</sub>:Ni<sup>2+</sup> (6H), cryst. struct., EPR spectra 4-109063  
 Rb<sub>2</sub>ZnCl<sub>4</sub>:Mn<sup>2+</sup>, incommensurate phase, quadrupolar cryst. field modulation, EPR study 4-76239  
 Rh III complexes, <sup>1</sup>H and <sup>13</sup>C NMR, cond. and mag. susceptibility meas. 4-71192  
 Se-<sup>57</sup>Fe, Mossbauer study of electric field gradient 4-88754  
 Si, substitutional and interstitial donors, many electron effect 4-113895  
 TbNi<sub>5</sub>, crystal electric field splitting, inelastic neutron scatt. study 4-65648  
 Tb<sub>2</sub>O<sub>3</sub>SO<sub>4</sub>, magnetisation, AC susceptibility, spectroscopic Zeeman effect meas. 4-76121  
 ThBr<sub>4</sub>, incommensurate phase, Gd<sup>3+</sup> EPR study 4-76246  
 ThBr<sub>4</sub>:Pa<sup>4+</sup>, incommensurate phase, single cryst., Pa<sup>4+</sup> optical spectroscopy 4-71422  
 ThS<sub>2</sub>:Gd<sup>3+</sup>, cryst. struct., single cryst. diffractometric obs. 4-108316  
 TmAsO<sub>4</sub>, crystal-field parameters, Mossbauer meas. 4-61350  
 TmAsO<sub>4</sub>, optical and mag. studies of lowest levels 4-88831  
 TmMO<sub>2</sub> (M=Al, Fe, Cr, V), mag. and cryst. field props., Mossbauer studies 4-98988  
 U dipnictides, mag. props., cryst. field interpretation 4-76146  
 U monopnictides, antiferromagnetic transition theory 4-88672  
 U<sub>1-x</sub>Pr<sub>x</sub>(Nd<sub>2</sub>P) solid soln., paramagnet, mag. susceptibility and cryst. field effects 4-80742  
 V<sub>2</sub>O<sub>5</sub>, antiferromag., muon spin precession obs., local fields and phase transition 4-65921  
 YIG single cryst. and epitaxial film, sublattice anisotropy and mag. linear dichroism 4-61667  
 YbF<sub>3</sub><sup>2-</sup> (n=6,8), mol. hyperfine interactions, Dirac scatt. wave calcs. 4-68982  
 ZnNi, impurity lineshapes in dilute alloys, UPS study 4-113893  
 ZnO: transition metal, impurity electron states calcs. 4-70711  
 ZnS: transition metal, impurity electron states calcs. 4-70711  
 ZnS:Ni<sup>2+</sup>, photolum. band arising from <sup>3</sup>T<sub>1</sub>(P)→<sup>3</sup>T<sub>1</sub>(F) transition 4-104664  
 ZnSiF<sub>6</sub>·6H<sub>2</sub>O:Cu<sup>2+</sup>, EPR, dynamical peculiarities of Jahn-Teller effect (*Russian*) 4-98938  
 ZrSiO<sub>4</sub>:Pr<sup>4+</sup>, ESR, hyperfine interactions and g-values 4-71175
- crystal field splitting** *see* crystal field interactions  
**crystal field theory** *see* crystal field interactions  
**crystal fields** *see* crystal field interactions  
**crystal filters**  
 SAW diffraction compensation on YZ-LiNbO<sub>3</sub> 4-97183  
 LiNbO<sub>3</sub>, (YX)128°, SAW filters, residual bulk mode levels 4-104049
- crystal growth**  
*see also* crystal growth from melt; crystal growth from solution; crystal growth from vapour; crystal purification; crystallisation; dendrites; epitaxial growth; nucleation  
 alkali halide crystals, dislocation etching, etch pits, crystal growth, review 4-70159  
 alkali halide mixed crystals, growth and characterisation, microhardness, colour centres, radiation hardening 4-70152  
 biethylenedithiolyene-TTF, electrochemical cryst. synthesis 4-76646  
 binary alloy, dil. plane crystallisation front stability 4-98044  
 chemical driving force, role in discontinuous coarsening 4-113651  
 chemisorbed and physisorbed systems, island growth kinetics, computer simulation studies 4-113813  
 circular crystal growth in circular region 4-113372  
 diamond, formation at high press. in Co-C hypereutectic alloy 4-109374  
 diamond synthesis, ultrafast chemical reaction triggered by shock wave forming C and γ-CuBr from CBr<sub>4</sub> and Cu 4-114389  
 electrochemical nucleation and cryst. growth parameters, integral eqn. anal. 4-66595  
 explosive, self-sustained and laser driven, front propag. 4-103686  
 FCC crystals, mechanisms and shapes of cryst. growth 4-75340  
 ferrite powder, form. mechanism in fused salts, SEM studies 4-70399  
 forced convection heat and momentum transfer to dendritic structs. 4-97557  
 Green function techniques appl. 4-60871  
 growth mechanisms, morphology and nucleation (*Japanese*) 4-92118  
 II-VI semiconductors, crystal growth, optical and surface, props. (*Japanese*) 4-88957  
 III-V ternary antimonides, material prep., cryst. and epitaxial growth, review 4-98045  
 interfacial transport, parametric comparison of convective effects 4-60872  
 kinetic equations of normal growth near equilb. 4-60870  
 kinetics of crystal growth, review 4-88956  
 liquid-solid transition, absolute kinetic coeffs., mol. theory 4-65374  
 metallic thin films, crystal growth, initial steps, microscopic studies 4-98486  
 molecular mechanisms, review 4-60869  
 morphology rel. to growth mechanisms (*Japanese*) 4-103687  
 n-octacosane crystals, spiral step patterns, stress field effect 4-103680  
 oxide, two-phase, growth on pure metals 4-98047  
 oxide film, low temp. oxidation of metal, diffusion mechanism 4-98350  
 oxide films grown on Si surface, TEM and EELS study (*French*) 4-75809  
 poly-ε-caprolactone-polyvinylmethylether-polystyrene, phase diagram and crystal growth behaviour obs. (*Japanese*) 4-103665  
 sealed silica pressure ampoules for crystal growth 4-88955  
 SEM studies of surface processes, digital data acquisition and anal. system 4-78433  
 stearic acid, intermolecular potential and surface energies of crystalline polymorph 4-113379  
 stochastic model 4-79965  
 synchrotron topography of growth defects 4-65212  
 synthetic metals, crystal growth 4-61816  
 VLSI technology, textbook 4-82610  
 YAG crystal, specially doped growth and multi-function props. (*Chinese*) 4-114364  
 Al, internal friction originated by grain boundaries 4-103872

## crystal growth continued

- $\text{Ba}_3\text{Ga}_2\text{S}_6$ , prep., cryst. struct., X-ray diffr. (*German*) 4-75415  
 $\text{Ba}_2\text{Ga}_2\text{S}_7$ , prep., cryst. struct., X-ray diffr. (*German*) 4-75415  
 $\text{BaO-Li}_2\text{O-Nb}_2\text{O}_5$ , phase equilibria in crystn. region, tetragonal phase 4-114495  
 $\text{BaTiO}_3$  synthesis, polycryst., nonstoichiometry rel. to solid-solid reaction mechanism 4-99305  
 $\text{Bi}_2\text{O}_3\text{-CdO}$ , phase relations, X-ray diffr. obs. 4-89028  
 $\text{CaAl}_2\text{O}_9$ , solid phase synthesis 4-76668  
 $\text{CaS}$ , prep. in high purity powder form from elements 4-108298  
 $\text{CaTi}_3\text{Al}_5\text{O}_{19}$ , difficult-to-form crystal structures, preparation 4-70094  
 $\text{CoP}_2$ , ambient press. synthesis, cryst. struct., mag. and elec. props., bonding 4-75408  
 $\text{Cs}_2\text{O-V}_2\text{O}_5$ , phase ratios, enthalpy of formation of vanadates 4-76758  
 $\text{Cs}_2\text{TaOCl}_5$ , prep., fluoresc. spectra 4-108299  
 $\text{Cs}_2\text{TaSCl}_5$ , prep., fluoresc. spectra 4-108299  
 $\text{Cu}$ , dendritic electrodeposits, fractal behaviour 4-75825  
 $\text{Cu}_2\text{-S/CdS}$  heterostruct., misfit accommodation and growth 4-108730  
 $\text{Er}_2\text{S}_3$ , prep. in high purity powder form from elements 4-108298  
 $\text{Fe}_2\text{Ge}_2\text{O}_8$ , mixed valent, prep., struct., mag. props. (*French*) 4-88148  
 $\alpha\text{-Fe}_2\text{O}_3$ , topotactic conversion of  $\gamma\text{-FeOOH}$  and comparative transform. methods of iron oxide in mag. spinels 4-109632  
 $\text{Fe}_3(\text{PO}_4)_2$ , mixed valent, prep., cryst. struct., mag. props., Mossbauer spectra (*French*) 4-88146  
 $\text{Gd}_2\text{GaSbO}_7$ , pyrochlore prep., cryst. struct., X-ray diffr. 4-75400  
 $\text{Fe}_2\text{Fe}_{1-x}\text{O}_4$ , mixed valent, prep., struct., mag. props. (*French*) 4-88148  
 $\text{HgGa}_2\text{Se}_4$ , crystal growth and refinement (*French*) 4-75380  
 $\text{InBO}_3$ , cryst. growth 4-61817  
 $\text{KAl}_4(\text{Si}_4)_3\text{O}_{20}$  monoclinic feldspars, crystal growth, PBC vector analysis 4-92119  
 $\text{KdCl}_3$ , crystal oriented intergrowth, struct. interpretation (*French*) 4-65201  
 $\text{KdCl}_3\text{-H}_2\text{O}$ , crystal oriented intergrowth, struct. interpretation (*French*) 4-65201  
 $\text{K}_{0.30}\text{NbF}_3$ , chem. prep., cryst. struct., X-ray diffr. study 4-88156  
 $\text{LaM}_2\text{Al}_2\text{O}_{10+x}$  ( $\text{M}=\text{Mn, Co, Cu}$ ), struct., substitution effects, X-ray diffr. studies 4-103722  
 $\text{La}_2\text{S}_3$ , prep. in high purity powder form from elements 4-108298  
 $\text{LaTi}_3\text{Al}_5\text{O}_{19}$ , difficult-to-form crystal structures, preparation 4-70094  
 $\text{MnTe-Te}$  system, crystallographic phase diagram and single cryst. growth 4-61045  
 $\text{MoS}_3$ , prep. by solid state reaction, characts. 4-61838  
 $\text{Na}$  metal single crystals, formation during decomposition of  $\text{NaAlH}_4$  4-108296  
 $\text{Na}_{1/2}\text{-Ca}_{1/2}\text{Al}_{1/2}\text{Ti}_{1/2}\text{O}_{19}$ , difficult-to-form crystal structures, preparation 4-70094  
 $\text{NdAl}_2(\text{BO}_3)_4$ , struct. and growth morphology 4-108297  
 $\text{PbF}_2\text{-RF}_3$ ,  $\text{R}=\text{La, Nd, Gd, Ho, Yb}$  and  $\text{Y}$ , synthesis, cryst. struct., electron diffr. obs. (*French*) 4-75405  
 $\text{Rb}_2\text{ZnCl}_4$ , ferroelec., phase transitions, dielec. and DTA studies, rel. to cryst. growth conditions 4-76374  
 $\text{SbCl}_3$ -graphite intercalation cpd., de Haas-van Alphen effect meas. 4-88440  
 $\text{Si}$ , crystalline, production for solar cells (*German*) 4-81121  
 $\text{Si}$ , dislocation behaviour, X-ray topography study 4-88175  
 $\text{Si}$  single crystal thin film, secondary recrystallisation prep. 4-88421  
 $\text{SiC}$  syntactically coalesced polytype structs., growth mechanisms 4-75382  
 $\text{U}_3\text{O}_8$ , production of high density powder for MTR fuel by special crystal growth 4-96171  
 $\text{VF}_4$ , ambient press. synthesis, cryst. struct., mag. and elec. props., bonding 4-75408  
 $\text{Y}_3\text{Al}_5\text{O}_{12}\text{:Nd}^{3+}$  garnets,  $\gamma$ -ray irradiat., colour centres and optical props. 4-114310  
 $\text{Y}_3\text{Fe}_5\text{O}_{12}$  garnet, cryst. growth 4-61818  
 $\text{ZnO}$  crystallite growth during annealing, morphological anal. 4-61902

## crystal growth from gel

- bismuth oxalate single crystals, gel growth and characterisation 4-99295  
 $\text{CaSO}_4\cdot 4\text{H}_2\text{O}$ , metastable crystals, growth from gels with organic additives 4-61826  
 $\text{CaSO}_4\cdot 2\text{H}_2\text{O}$ , synthetic gypsum, gel growth of Herring Bone and Hour glass struct. 4-114388  
 $\text{SiO}_2\text{-AgCl}$ , diphasic photosensitive xerogel prep. method 4-71990  
 $\text{Sn}$ , single crystal growth in silica gel in elec. field 4-93209  
 $\text{Sn}_2$ , single crystal growth in silica gel in elec. field, elec. cond., mag. props. 4-93209  
 $\text{SnI}_4$ , single crystal growth in silica gel in elec. field, elec. cond., mag. props. 4-93209

## crystal growth from melt

- see also liquid phase epitaxial growth; zone melting  
 alloy, binary, freezing, periodic growth rate effect on morphological stability 4-98039  
 anthracene crystals, reduction of grown-in dislocation density due to heat treatment and growth conditions 4-113450  
 automatic Czochralski growth, parameter meas. and process control 4-66218  
 Bridgman-type crystal growth, vertical, one-dimens. thermal modelling 4-75341  
 carbothermic silica reduction process, computer simulation 4-66200  
 conference, Stuttgart, Germany (Sept. 1983) 4-58552  
 convective transport, review 4-65204  
 crucibleless crystal growth techniques, review 4-66214  
 crystal rods with high melting points, prep. by RF floating zone technique, temp. distrib. 4-75338  
 crystal-melt interfaces, coupled convective instabilities 4-88120  
 Czochralski cable puller, crystal orbiting elimination with coax. magnet and mag. weight 4-85096  
 Czochralski configuration, buoyant, thermocapillary and forced convection expts. 4-65206  
 Czochralski cryst. growth, melt. convection suppression using heater-mag. solenoid coils 4-71546  
 Czochralski growth, crystal pulling apparatus 4-104727  
 Czochralski growth, historical review of technique, impurity conc. and distrib. 4-66213  
 Czochralski growth by the double container technique 4-66215  
 Czochralski method, crystn. rate during fluctuations of melt temp. 4-71545  
 Czochralski process, contamination reduction method 4-66210  
 Czochralski technique, growth programming optimal control 4-99298  
 edge defined film fed crystal growth, lateral solute segregation 4-88119

## crystal growth from melt continued

- finite-element simulation of Czochralski bulk flow 4-65207  
 graphite substrate, resistance to molten Si in RAD process (*French*) 4-61835  
 heat transfer analysis of Bridgman-Stockbarger config., radial temp. variations 4-114381  
 horizontal Bridgman cryst. growth, thermal convection and longit. macrosegregation, order of magnitude analysis 4-98040  
 horizontal Bridgman cryst. growth, thermal convection and longit. macrosegregation, practical laws 4-98041  
 horizontal directional crystallization, height of cryst. growth from melt 4-71544  
 II-VI chalcogenides, iodide prep. method in flow reactor 4-76660  
 impurity distribution and inclusions (*Russian*) 4-113483  
 ionic crystals, morphology and kinetics 4-113370  
 IV-VI chalcogenides, iodide prep. method in flow reactor 4-76660  
 kinetics of crystal growth, review 4-88956  
 lanthanide hexaaluminates,  $\text{RMgAl}_{11}\text{O}_{19}$ , crystal growth by Verneuil and floating zone methods and spectroscopic props. 4-66054  
 large-area sheet technology for photovoltaic cells and arrays 4-62352  
 leucosapphire, growth by horizontal solidification, temp. fields 4-90587  
 metals, non-cubic, single crystal plates, low dislocation density 4-93211  
 metals, pure, nucleated from undercooled melt, cryst. growth rate 4-98042  
 metals and alloys, solidification, book contrib. 4-109393  
 non-orbiting Czochralski crystal puller 4-61832  
 polyethylene terephthalate, crystallisation rate, effect of silicon nucleants 4-88117  
 profiled components, appl. in solar water heating 4-99944  
 rapid solidification, computer simulation 4-114383  
 rare earth compound single crystal growth in high press. furnace (*Japanese*) 4-109319  
 rare earth intermetallics, cryst. growth from melt 4-66219  
 rare earth vanadates, single cryst. synthesis using IR-radiation converging furnace 4-61828  
 ribbon-shaped crystals, melt-grown, shape of phase boundary 4-103681  
 semiconductor photovoltaic material bulk single cryst. and epitaxial multilayer growth 4-71548  
 Si solar cells manufacture, technological and economic aspects 4-89403  
 single crystals, shaped, melt growth by Stepanov method, dislocation struct. form. 4-98108  
 solid-liquid interface, convective coupling in internally heated vertical cylinder 4-97562  
 substrates, LEC growth, optical communication requirements, review 4-61833  
 succinonitrile, solid-liquid interface, convective coupling in internally heated vertical cylinder 4-97562  
 thermal stresses in crystals grown by Stockbarger method, generated by different thermal expansion coeffs. 4-70046  
 thermoelastic stresses in crystals grown by Stockbarger method 4-66208  
 variable crystallisation rate, impurity distrib. 4-75492  
 $\text{BeAl}_2\text{O}_4$ , chrysoberyl, Czochralski grown, dislocation form. and distrib. laws, X-ray diffr. topography method 4-113453  
 $\text{Bi}_2\text{Ge}_2\text{O}_5\text{:Nd}^{3+}$ , hexagonal crystal, growth and luminesc. 4-76510  
 $\text{Bi}_2\text{Mo}_2\text{O}_8$ , preparation, cryst. struct., elec. and optical props. 4-84266  
 $\text{Bi}_3\text{Si}_2\text{O}_{10}$ , single crystal, effect of doping with Al, Ga and Cr on props. 4-76407  
 $\text{Bi}_2(\text{Te,Se})_3$ , crystal growth under microgravity in SALYUT-6 space station 4-98035  
 $\text{Bi}_2(\text{Te, Se})_3$ , solidification under microgravity melt subcooling obs. 4-114382  
 $\text{Ca}_3\text{Ga}_2\text{Ge}_2\text{O}_{14}\text{:Cr}^{3+}$  EPR spectra 4-71170  
 $\text{CaLa}_2\text{S}_4$ , melt growth using Stober technique 4-108298  
 $\text{CdS}$ , crystallisation kinetics, growth from  $\text{CdS}+\text{CdCl}_2$  melt, 4-114380  
 $\text{CeSi}_2$ , intermetallics, cryst. growth from melt 4-66219  
 $\text{CsI}$ , irradiated single crystals, intrinsic hole colour centres 4-114332  
 $\text{CsMnCl}_3$ , antiferromagnetic, optical absorpt. spectra, luminesc. studies 4-99133  
 $\text{Cu}$  plates, Bridgman growth, temp. distrib., computer calc. 4-66224  
 $\text{Cu}$  single crystal plates, as-grown, micromosaics, neutron rocking curves 4-65413  
 $\text{Cu}_2\text{Mo}_6\text{Se}_8$  single crystals, growth, comp. inhomogeneity and supercond. props. 4-80708  
 $\text{GaAs}$ , Bridgman ingots, photocond., 80-300K, CR and O impurity effects 4-65705  
 $\text{GaAs}$ , contour maps of EL2 deep level, dislocations 4-80530  
 $\text{GaAs}$  crystal, numerical simulation of horizontal Bridgman growth 4-66212  
 $\text{GaAs}$ , crystallisation from melt, rate, elec. current effects 4-71551  
 $\text{GaAs}$ , dislocations and point-defect complex formations, thermal stability 4-103758  
 $\text{GaAs}$ , electrical properties and impurity states 4-75963  
 $\text{GaAs}$ , growth from melt and elec. props. 4-99300  
 $\text{GaAs}$ , LEC crystal growth in mag. field (*Japanese*) 4-88960  
 $\text{GaAs}$ , LEC grown, EPR identification of  $\text{As}_{\text{Ga}}$  antisite defects 4-71178  
 $\text{GaAs}$ , LEC grown, improved elec. uniformity by high temp. annealing 4-65684  
 $\text{GaAs}$ , LEC growth in vertical mag. field, homogeneity anal. 4-76661  
 $\text{GaAs}$  LEC wafers, undoped, defect characterisation by electron-beam-induced charge collection microscopy 4-60932  
 $\text{GaAs}$ , liquid encapsulated Czochralski growth, deep level study 4-98569  
 $\text{GaAs}$ , semi-insulating, undoped and low Cr doped, LEC grown, photoluminescence props., whole ingot annealing effects 4-84994  
 $\text{GaAs}$ , semi-insulating LEC grown, impurity distribution, cathodoluminesc. study 4-88885  
 $\text{GaAs}$  semi-insulating single crystal growth by LEC method, IC appls. (*Japanese*) 4-104728  
 $\text{GaAs}$ , single cryst. growth of large size, vertical mag. field appl. LEC apparatus 4-85094  
 $\text{GaAs}$ , single cryst. growth by liquid encapsulated Czochralski method 4-114377  
 $\text{GaAs}$  substrates for GaAs ICs, growth processes 4-99299  
 $\text{GaAs}$  wafer production, crystal fabrication device using supercond. mag. field 4-114379  
 $\text{GaAs:Cr}$ , LEC growth, mag. field effect on impurity conc. 4-114378  
 $\text{GaAs:Cr(O)}$ , electrical properties and impurity states 4-75963  
 $\text{GaAs:Ge(Si)}$ , LEC grown, dislocation structure etching rel. to dopant conc. 4-114351  
 $\text{GaAs:Si}$ , crystal growth by horizontal gradient freeze technique, carrier and dislocation density 4-66216

## ystal growth from melt continued

- GaAs:Si, LEC and horizontal Bridgman growth, elec. uniformity 4-65683
- GaP, crystal growth under microgravity in SALYUT-6 space station 4-98035
- GaP, large single crystals, LEC growth, LEDs 4-99301
- GaSb cryst., facet regions and Czochralski growth 4-75348
- Gd<sub>2</sub>Ga<sub>2</sub>O<sub>7</sub>:Nd,Cr, laser props., modified Czochralski growth (Chinese) 4-112441
- Gd<sub>2</sub>Sc<sub>2</sub>Al<sub>2</sub>O<sub>7</sub>:Cr<sup>3+</sup>, tunable room temp. CW laser action 4-74518
- Ge, high-purity, purification, cryst. growth and annealing props. 4-61831
- Ge:Ga, crystal growth characts. in vertical Bridgman system 4-70049
- He, crystal growth and surface tension 4-61169
- HgCdTe, growth, props. and appls. 4-66217
- Ho<sub>2</sub>Co<sub>17</sub>, intermetallics, cryst. growth from melt 4-66219
- InAs<sub>1-x</sub>P<sub>x</sub>, LEC growth and characterisation 4-99302
- InP, residual impurities determ. by charged particle activation anal. 4-85346
- InP:Zn(Si) single crystal growth, LEC technique, perfection, preferential etching, SEM and X-ray analysis 4-71549
- InP-Au Schottky barriers, semicond. LEC growth, deep level defects (Chinese) 4-61320
- InSb, Czochralski growth, Peltier coeff. at crystal/melt interfaces 4-70845
- InSb, Czochralski: pulling, numerical modelling of elec. current induced growth layers 4-88121
- InSe Bridgman grown crystals, growth parameters, improvement rel. to defects 4-98043
- InSe:Sn(Zn)(Ga)(S), dopant segregation and distrib. study 4-103940
- K<sub>2</sub>Bi<sub>9</sub>ErO<sub>11</sub>(MoO<sub>4</sub>)<sub>4</sub> single crystals, Czochralski growth and optical props. (Chinese) 4-114294
- KCl:Li single crystal growth, colour centre laser appls. (Chinese) 4-61829
- KI very thin cryst., melt grown, optical absorpt. and refl. spectra 4-93035
- (K<sub>1-x</sub>Na<sub>x</sub>)<sub>0.4</sub>(Sr<sub>1-x</sub>Ba<sub>x</sub>)<sub>0.8</sub>Nb<sub>2</sub>O<sub>6</sub>, single cryst. growth and phys. props. 4-76352
- LaMgAl<sub>11</sub>O<sub>19</sub>, thermally stimulated phenomena 4-113967
- La<sub>2</sub>Nd<sub>2</sub>O<sub>7</sub>:MgAl<sub>11</sub>O<sub>19</sub> grown by Czochralski method, continuous laser effect obs. (French) 4-79155
- Li<sub>2</sub>B<sub>2</sub>O<sub>3</sub>, growth and props. for SAW devices 4-98419
- LiNbO<sub>3</sub>, congruently grown, temp.-depend. dispersion eqn., three beam parametric mixing appls. 4-88801
- LiNbO<sub>3</sub> cryst. growth, melt composition effect on props. 4-84227
- LiNbO<sub>3</sub>:Fe crystals, photorefr. and photorefr. prop. control during growth by elec. current 4-80904
- Mg alloys, structure and physicochemical props. different methods of Stepanov crystallisation effect 4-99297
- Na<sub>2</sub>-K<sub>2</sub>W<sub>2</sub>O<sub>6</sub>F<sub>2</sub>, Bridgman-Stockbarger growth, ferroelec. and ferroelastic props., permittivity, birefr. meas. 4-65969
- Na<sub>2</sub>-Li<sub>2</sub>W<sub>2</sub>O<sub>6</sub>F<sub>2</sub>, Bridgman-Stockbarger growth, ferroelec. and ferroelastic props., permittivity, birefr. meas. 4-65969
- NaMoO<sub>3</sub>F, single cryst., new oxyfluoromolybdate, synthesis and growth 4-76663
- NaNbO<sub>3</sub>, bladed crystallisation in Na<sub>2</sub>O-Nb<sub>2</sub>O<sub>5</sub>-B<sub>2</sub>O<sub>3</sub> system 4-61061
- Nd:YAG crystals, Czochralski, vertical distrib. conc. determ. of Nd ion (Chinese) 4-84310
- Nd<sub>2</sub>Ga<sub>2</sub>O<sub>7</sub>, crystal growth by floating zone method 4-76665
- (Pb, Sn)Te, crystal growth by Bridgman method and by travelling heater method 4-103678
- Pb<sub>2</sub>InNbO<sub>6</sub>, single crystal, perovskite and pyrochlore modifications, prep. and props. 4-76662
- PbMoO<sub>4</sub>, stoichiometry deviation, electron transfer, elec. cond. meas. 4-80591
- PbSnTe, crystal growth under microgravity, segregation obs. 4-98036
- Pb<sub>2</sub>-Sn<sub>2</sub>Te large homogeneous single crystals, growth by vapour-melt-solid mechanism 4-71547
- PbTe, crystal growth by Bridgman method and by travelling heater method 4-103678
- PbTe, iodide prep. method in flow reactor 4-76660
- PbTe:Ga, elec. and optical meas. (Russian) 4-84636
- R<sub>2</sub>CoO<sub>4</sub>, R<sub>2</sub>CoO<sub>3</sub>, synthesis and high-temperature study (French) 4-85095
- RbMnCl<sub>3</sub>, antiferromagnetic, optical absorpt. spectra, luminesc. studies 4-99133
- Sb<sub>0.57</sub>Mo<sub>2</sub>O<sub>4</sub>, preparation, cryst. cryst., elec. and optical props. 4-84266
- Si and sapphire ribbons, produced by EFG, comparison of growth characts. 4-66222
- Si, clusters of electrically active centres and impurity states 4-70183
- Si, conference, San Jose, CA, USA (Jan. 1982) 4-10812
- Si, crystal growth and processing technology 4-114365
- Si, crystal growth and wafer prep., book contrib. 4-85098
- Si crystals, Czochralski pulled, O precipitation, diffusion mechanism, etching optical and neutron scatt. obs. 4-65209
- Si crystals, interface shape and radial distribution of impurities 4-113371
- Si, Czochralski crystal growth, computer controlled 4-66211
- Si, Czochralski grown compensated thermodons, EPR and Hall studies 4-75898
- Si, Czochralski growth, impurity clouds, microdefects, scatt. light intensity and etch pit density after annealing 4-84312
- Si, Czochralski growth, O segregation control by combining mag. field and cryst. rot. 4-104729
- Si, Czochralski single crystal growth in mag. field (Japanese) 4-88959
- Si, growth of ultra-large-area crystals using EFG technique, low cost photovoltaics appl. 4-88961
- Si, impurity incorporation during Czochralski growth 4-114385
- Si ingots and ribbons, cryst. growth techniques, review 4-93210
- Si, large-diameter Czochralski growth 4-114384
- Si layer growth from melt on graphitised fabric substrates 4-66240
- Si polycrystalline sheet growth by melt spinning, solar cell appl. (Japanese) 4-62368
- Si ribbon growth processes for solar cell/module technology 4-66724
- Si sheet, EFG in production 4-66221
- Si, sheet growth at high speeds; stress generation, influence of plastic deform. 4-65211
- Si sheets, large-grain, growth by improved spinning method 4-66223
- Si tubes, drawn from melt using wettable shaper 4-61830
- Si web growth, thermal stress effects, modelling 4-65210
- Si:N(O), microdefect formation during single crystal growth, influence of impurities on nucleation 4-114386
- Si:O Czochralski crystals, O precipitation and microdefects 4-84411
- Si:Re, Czochralski grown cryst., thermal stability study 4-109318

## crystal growth from melt continued

- SnO<sub>2</sub> whiskers, growth by VLS mechanism 4-70610
- U intermetallics, cryst. growth from melt 4-66219
- UGe<sub>2</sub>, intermetallics, cryst. growth from melt 4-66219
- UNi<sub>2</sub>, intermetallics, cryst. growth from melt 4-66219
- UPt<sub>3</sub>, intermetallics, cryst. growth from melt 4-66219
- UPt<sub>3</sub>, spin fluctuations, superconductivity and elec. cond. 4-114057
- UPt<sub>3</sub> whiskers, unusual form. and morphology, screw dislocation growth mechanism 4-98496
- W, plasma growth of single crystals, removal of interstitial impurities 4-66209
- YAG cryst., impurity distrib. and Bridgman-Stockbarger growth 4-60950
- YAG refractories, heat transfer during growth 4-76664
- Y<sub>2</sub>(Co, M)<sub>17</sub>, M=Al, Fe; single cryst. cpds., growth conditions and characterisation 4-66220
- YIG, crystal growth by floating zone method 4-76665
- YbMo<sub>6</sub>S<sub>8</sub>, crystal growth and crystal structure refinement 4-75396
- crystal growth from solution**
- see also crystal growth from gel; liquid phase epitaxial growth
- batch crystallisation process, optimisation via Legendre polynomials 4-88122
- calcium oxalate monohydrate, crystallisation kinetics 4-103684
- camphor, cryst. growth from soln. in elec. fields 4-113367
- conference, Stuttgart, Germany (Sept. 1983) 4-58552
- corundum, crystal morphology, effect of trivalent rare-earth ions 4-75349
- dislocation-controlled facet growth, microscopic studies 4-76659
- electrolyte crystals in supersaturated aqueous soln., crystal growth kinetics 4-114373
- flux growth, review of present status 4-76654
- growth kinetics, comp. inhomogeneity, morphological stability, convection effects 4-65205
- guanidinium aluminium sulfate hexahydrate, ferroelectric, cleavage surfaces, spiral patterns 4-103677
- hydrothermal particles for mag. recording, mag. props. 4-65834
- magneto-optical materials, flux cryst. growth 4-61820
- optical microscope stage, low-temp., for solidification studies in aqueous soln. 4-111199
- oxide solid solutions, cryst. growth and appl. 4-76655
- polyacrythritol tetranitrate crystals, soln. growth and defects 4-113452
- poly(vinylene fluoride), solution growth, ionic impurity effects 4-98037
- polyethylene, cryst. growth kinetics and lateral growth habits 4-88123
- polyethylene, FT-IR study of soln. grown crystals 4-108343
- polyethylene, neutron scatt. studies on soln. grown crystals 4-108342
- potash alum small crystals, decreasing number suspended in agitated supersaturated soln. 4-92117
- quartz, cultured, random elec. twinning, non-destructive obs., resonator appl. 4-70170
- quartz, hydrothermally weakened, plasticity and rheology 4-92286
- quartz, hydrothermal growth, p-V-T behaviour of H<sub>2</sub>O-NaOH-SiO<sub>2</sub> system 4-60875
- quartz, hydrothermally grown, Q determ., IR meas. and etch channel meas. 4-61627
- quartz, seed treatment effect on dislocations 4-61827
- quartz crystals, temp.-induced growth striations, X-ray topography study 4-75333
- rare earth perovskites, flux grown single crystals, microhardness, indentation tests 4-99493
- TCNQ salts, Cs<sub>2</sub> (TCNQ)<sub>2</sub>(II), synthesis, anal., novel isomeric struct. 4-114376
- TGS, doped cryst., dielec. permittivity nonlinearity, rel. to growth conditions 4-76297
- TGS, L-α alanine doped, polarisation, influence of growth conditions 4-76314
- top seeded technique, hydrodynamics in high temp. solns., simulation 4-65208
- AlCl<sub>3</sub>·6H<sub>2</sub>O:Cr<sup>3+</sup>, EPR study 4-84852
- BaFCl:Na crystals, flux grown thermoluminesc. glow curves, emission spectra 4-99200
- BaMoO<sub>4</sub> single cryst., flux evaporation growth and morphology 4-114369
- BaPb<sub>1-x</sub>Bi<sub>x</sub>O<sub>3</sub>, superconducting cryst., crystal growth from solution 4-61825
- BaTiO<sub>3</sub> type oxide fluoride growth at low temp. using LiF-BaF-LiBO<sub>2</sub> mixture flux 4-99296
- CaCO<sub>3</sub>, calcite, growth rate from soln., influence of impurities 4-92116
- CaCO<sub>3</sub> crystallisation with chem. absorpt. 4-98038
- CaC<sub>2</sub>O<sub>4</sub>·H<sub>2</sub>O, whewellite, growth morphology 4-65213
- CaSO<sub>4</sub>·Dy single cryst., cryst. growth and elec. props. 4-113943
- CdI<sub>2</sub>, polymorph structures, X-ray diff. 4-84251
- CdI<sub>2</sub> polymorphs, cryst. structures, X-ray diff. determ. 4-92152
- Cd<sub>2</sub>Nb<sub>2</sub>O<sub>7</sub>, photoconductivity and TSC meas. 4-70867
- Cd<sub>2</sub>-Zn<sub>2</sub>Te alloys, growth, elec. props., photoluminesc. 4-66207
- Co<sub>2</sub> crystals, flux growth 4-71542
- CoV<sub>2</sub>O<sub>8</sub> single crystals, flux growth, X-ray charact. 4-76651
- Cu complex, bis(propylammonium) copper(II) tetrachloride, cryst. growth from soln., Oswald ripening along faceted bridge 4-75336
- CuFe<sub>2</sub>O<sub>4</sub> single crystals, flux growth, X-ray charact. 4-76651
- CuInS<sub>2</sub> single crystal growth by travelling heater method 4-71539
- Cu<sub>2</sub>Nb<sub>2</sub>O<sub>7</sub> single crystals, flux growth, X-ray charact. 4-76651
- Ga-N crystal growth, vapor-liquid-solid mechanism, NH<sub>3</sub> reaction with Ga 4-61823
- GaN, crystals, high pressure soln. growth, equilib. N<sub>2</sub> press. over Ga-GaN mixtures 4-61822
- GaP crystal quality in soln. growth P press. effects 4-103685
- HgCdTe, growth, props. and appls. 4-66217
- HgS, hydrothermal crystal growth 4-104726
- InP:Mg(Ca,Zn) crystals grown by synthesis solute diffusion, electrical and optical props. 4-85093
- K<sub>2</sub>Cr<sub>2</sub>O<sub>7</sub>, crystal growth from aq. soln., macrospiral layers and macrosteps on surface 4-75335
- KH<sub>2</sub>PO<sub>4</sub>, in-line bulk supersaturation measurement by electrical conductometry 4-114371
- KH<sub>2</sub>PO<sub>4</sub> single cryst. growth from supersaturated boiling solns. 4-66205
- LaCo<sub>5</sub>P<sub>3</sub>, flux growth and cryst. struct. 4-108335
- Li-Mn-O compounds, crystal growth, hydrothermal and flux synthesis 4-71541
- LiFePO<sub>4</sub>(OH, F), tavorite, hydrothermally grown, cryst. struct., X-ray diff. study 4-113418
- LiH<sub>2</sub>(SeO<sub>3</sub>)<sub>2</sub>, ferroelec., single cryst. growth from soln. (Korean) 4-114375
- LiIO<sub>3</sub>, single crystal growth, properties, appls. (Russian) 4-75394

**crystal growth from solution continued**

- Li<sub>2</sub>Ta<sub>2</sub>S<sub>7</sub> intercalation cpds., (1T<sub>4</sub>Hb), elec. resist. meas., metallic and supercond. states 4-84726  
 Mg<sub>2</sub>FPO<sub>4</sub>:Ni single crystals, flux growth, X-ray charact. 4-76651  
 Mg<sub>2</sub>P<sub>2</sub>O<sub>7</sub>:Ni single crystals, flux growth, X-ray charact. 4-76651  
 Mg<sub>2</sub>V<sub>2</sub>O<sub>7</sub>:Ni single crystals, flux growth, X-ray charact. 4-76651  
 (NH<sub>4</sub>)<sub>2</sub>Cr<sub>2</sub>O<sub>7</sub> crystals grown from aqueous soln., morphology and charact. 4-103679  
 NH<sub>4</sub>H<sub>2</sub>PO<sub>4</sub> crystallisation, supersaturation, soln. velocity, crystal habit and growth rate 4-114372  
 NH<sub>4</sub>H<sub>2</sub>PO<sub>4</sub> microcrystal growth in aq. soln. under nonstationary conditions 4-71540  
 NH<sub>4</sub>H<sub>2</sub>PO<sub>4</sub> oriented crystallisation, electron-microscope study 4-65202  
 NH<sub>4</sub>HSeO<sub>4</sub>, ferroelec., with varying D content, phase transitions, dielec. anomalies 4-99061  
 Na<sub>2</sub>O-Al<sub>2</sub>O<sub>3</sub>, effect of F<sup>-</sup>, Co<sup>2+</sup> and Ti<sup>4+</sup> on synthesis and props. 4-114370  
 Na<sub>2</sub>Si<sub>4</sub>O<sub>9</sub>·10H<sub>2</sub>O, magadiite, synthesis by crystallisation 4-76653  
 Nb<sub>2</sub>Sn, cryst. growth by top-seeded solution method 4-76658  
 (Nd<sub>1-x</sub>La<sub>x</sub>)P<sub>2</sub>O<sub>7</sub>, large good-quality laser crystals, growth methods 4-71543  
 (Nd<sub>0.9</sub>Ca<sub>0.1</sub>)Ti<sub>2</sub>O<sub>7</sub>, ferroelec. cpd., perovskite-derived, crystal growth and characterisation 4-76657  
 Nd<sub>2</sub>Ga<sub>2</sub>O<sub>7</sub>, single cryst. growth 4-66206  
 Os<sub>2</sub>(Se<sub>2</sub>)(Te<sub>2</sub>), single cryst. synthesis by solvent method 4-99294  
 Pb(FeNb)<sub>2</sub>O<sub>7</sub> ceramics and single crystals, prep., struct., X-ray diffr., neutron powder diffr., dielec. and elec. meas., SEM 4-75412  
 Pb<sub>2</sub>Ge<sub>2</sub>O<sub>7</sub>, hydrothermally grown crystals, dielec., pyroelectric props., X-ray diffr. 4-84915  
 PbMg<sub>1/3</sub>Nb<sub>2/3</sub>O<sub>3</sub>, single cryst., growth by mass crystallisation method, elec. relax. study 4-76315  
 Pb<sub>2</sub>SnO<sub>4</sub> single crystals, flux growth, X-ray charact. 4-76651  
 Pb<sub>2</sub>V<sub>2</sub>O<sub>7</sub>, crystn. in Pt crucible, DTA study 4-109317  
 Pt crucible surface, nucleation sites in flux growth 4-109317  
 Re-P system, phase equilibria, cryst. growth, struct. refinements props. 4-88150  
 RuS<sub>2</sub>(Se<sub>2</sub>)(Te<sub>2</sub>), single cryst. synthesis by solvent method 4-99294  
 SnO<sub>2</sub> film, impurity phases, hydrolysis of SnCl<sub>4</sub> 4-113829  
 Sr<sub>2</sub>Al<sub>2</sub>O<sub>4</sub>(CrO<sub>4</sub>)<sub>2</sub>, flux grown, ferroelec. phase transition, domain studies, birefr., polarisation, permittivity, transition enthalpy meas. 4-65970  
 SrSO<sub>4</sub>, precipitation from aq. solns. and cryst. growth 4-75684  
 Te(OH)<sub>6</sub>·2NH<sub>4</sub>H<sub>2</sub>PO<sub>4</sub>·(NH<sub>4</sub>)<sub>2</sub>HPO<sub>4</sub>, single cryst. growth and morphology 4-61821  
 ThO<sub>2</sub> crystals, flux growth 4-71542  
 TiH<sub>3</sub>(SeO<sub>3</sub>)<sub>2</sub>, cryst. struct., phys. props., phase transitions 4-84921  
 U-Al-O, synthesis by precipitation of hydroxides 4-76652  
 (YBi)<sub>2</sub>(FeGa)<sub>2</sub>O<sub>12</sub> garnet, cryst. growth from flux and LPE 4-93208  
 Y<sub>2</sub>Fe<sub>2</sub>O<sub>12</sub> single crystal, top seeded soln. growth method and mag. props. 4-93207  
 YIG, seed and unseeded, growth from high temp. solns., studied by growth striations 4-76656  
 ZnO, cryst. growth by hydrothermal decomp. of Zn-EDTA 4-114374  
 ZnO, hydrothermal crystal growth 4-104726  
 α-Zn<sub>3</sub>(PO<sub>4</sub>)<sub>2</sub>·4H<sub>2</sub>O, hopeite, crystn. kinetics 4-75337  
 ZnS, hydrothermal crystal growth 4-104726  
 ZnS(Se), solution growth and photoluminesc. props. 4-88958

**crystal growth from vapour**

see also vapour phase epitaxial growth

- bulk single crystals, vapour growth for high perfection struct. 4-76648  
 closed ampoule vapor crystal growth, mass transfer, one dimensional diffusion model 4-60873  
 conference, Stuttgart, Germany (Sept. 1983) 4-58552  
 convective transport in closed and open tube systems, gravity effects 4-65203  
 β-copper phthalocyanine, vapour phase cryst. growth, struct. and morphology 4-76647  
 diffusive-convective vapour transport 4-114368  
 high-field crystal growth on held emitting electrode in plasma atmosphere (Japanese) 4-76650  
 ice crystal, vapour growth kinetics, morphology, review 4-60867  
 ice crystals, vapour grown, morphological instability, SEM obs. 4-88125  
 ice single crystal, vapour growth mechanisms, morphological stability 4-60868  
 kinetics of crystal growth, review 4-88956  
 methylammonium mercury trichloride, ferroelec. transition, thermal, dielec., optical meas. (French) 4-76392  
 β-phthalocyanines, cryst. growth from vapour in closed ampoules 4-76647  
 semiconductors, organometallic crystal growth, review 4-98046  
 sputtered film, filamentous C. growth, surface morphology effects 4-92114  
 transition metal molybdates, M<sub>2</sub>Mo<sub>2</sub>O<sub>8</sub> (M=Mn, Fe, Co, Ni), crystal growth, mag. and elec. props. 4-71537  
 transparent furnace for vapour transport expts. 4-93206  
 Ag<sub>2</sub>S, high temp. phase, equil. roughening transition 4-60877  
 β-Ag<sub>2</sub>S whiskers, growth mechanism and growth form 4-70608  
 Cd:Bi, crystal growth from vapour, Bi impurities effect 4-113368  
 Cd<sub>3</sub>As<sub>2</sub> crystals, growth and morphology 4-75339  
 Cd<sub>3</sub>P<sub>2</sub> crystals, growth and morphology 4-75339  
 CdSiAs<sub>2</sub>, single crystal growth by chem. vapour transport, struct. and elec. props. 4-114367  
 CdTe, growth from vapour phase, on substrate out of contact with vapour walls 4-109315  
 CdTe large single crystals, grown from vapour phase, polarity 4-70048  
 CuGaTe<sub>2</sub>, vapour growth, thermodynamics and elec. characts. 4-71536  
 CuInTe<sub>2</sub>, vapour growth, thermodynamics and elec. characts. 4-71536  
 EuSe, chem. transport growth in I<sub>2</sub> atm. 4-109313  
 EuTe, chem. transport growth in I<sub>2</sub> atm. 4-109313  
 Fe<sub>2</sub>·Cr<sub>2</sub>O<sub>3</sub>, chem. transport of haematite with TeCl<sub>4</sub> as transporting agent 4-61824  
 GeSe, crystal growth from GeSe-I vapour, complex equilibria anal. 4-81122  
 α-HgI<sub>2</sub>, cryst. growth, space-charge relax. in appl. elec. field 4-66204  
 HgI<sub>2</sub>, crystal growth and appl. 4-66203  
 MgIn<sub>2</sub>Se<sub>4</sub>, layered cpd., cryst. growth 4-93205  
 Mo<sub>4</sub>O<sub>11</sub>, cryst. growth from vapour, transparent furnace 4-93206  
 Nb<sub>2</sub>S<sub>4</sub> single crystals, quasi-one-dimensional, growth by chem. vapour transport 4-99293  
 Pb<sub>1-x</sub>Sn<sub>x</sub>Te large homogeneous single crystals, growth by vapour-melt-solid mechanism 4-71547

**crystal growth from vapour continued**

- Si, carbothermic silica reduction process, computer simulation 4-66200  
 Si films, cryst. oriented by metal patterns on planar amorphous substrates 4-66202  
 Si, solar-grade, growth by Zn reduction of SiCl<sub>4</sub>, morphology 4-66199  
 SnO<sub>2</sub> whiskers, growth by VLS mechanism 4-70610  
 TiO<sub>2</sub> whiskers, vapour phase growth by TiF<sub>4</sub> hydrolysis 4-70609  
 TiS<sub>2</sub>, intercalation cpd. with Mn, chemical vapor growth and EPR studies 4-66201  
 WCl<sub>6</sub>, synthesis, physicochemical props. 4-76649  
 Zn<sub>0.9</sub>Cd<sub>0.1</sub>Se laser screens, crystals grown from vapour phase, receiving colour image blue component (Russian) 4-96917  
 Zn<sub>1-x</sub>Mn<sub>x</sub>S single crystals, vapour phase grown, stacking faults, structural transform. 4-88278  
 β-Zn<sub>2</sub>P<sub>2</sub>, X-ray study of phase transitions 4-84385  
 Zn<sub>3</sub>P<sub>2</sub> crystals, growth and morphology 4-75339  
 ZnSe, crystal growth by resublimation, hole mobility meas. 4-109316  
 ZnSe, IR transparent polycrystal, deposited by low purity reagent, props. (Chinese) 4-107767  
 ZnTe, growth forms, chem. transport reactions 4-109314

**crystal habit see crystal morphology****crystal hyperfine field interactions**

- anthracene, cryst., carrier pairs prod. and recombination by VUV radiation 4-84571  
 l-asparagine-H<sub>2</sub>O, single cryst., X-irrad., free radical ESR-ENDOR study 4-76253  
 copper ternary chalcopyrite semiconductors, NMR studies 4-65874  
 cubic crystal: rare earth ion crystals, forbidden two-photon transitions 4-84972  
 diamond, transition from isotropic muonium state to axially symm. anomalous muonium state 4-71237  
 difluoranthrylphosphorhexafluoride, Overhauser shift, hyperfine interaction 4-76235  
 dimethylbenzylaldehydes-d<sub>6</sub>(d<sub>1</sub>) in durenene cryst., vibronic intensities, phosphoresc. spectra 4-96596  
 dislocations in solids, NMR studies, book contrib. 4-98111  
 dodecamethylferrocene, paramag., electronic and mag. props., Mossbauer meas. and MO calcs. 4-80845  
 electric field gradient, charge shift model calc., validity regions 4-113915  
 ENDOR and EPR, g-tensors and A-tensors, anisotropic and non-coincident, least squares fitting 4-61607  
 fluorite: Pb<sup>2+</sup> crystals, hyperfine interactions 4-88494  
 Heusler alloys, band struct., mag. moments, hyperfine fields, local spin density method 4-108767  
 hexaimidazolecadmium (II) nitrate: Cu (II), Jahn-Teller distortion, EPR 4-71165  
 ice: muonium single cryst. hyperfine interaction and spin relax. 4-65924  
 ionic lattices, Mn<sup>2+</sup>-F<sup>-</sup> distance from isotropic superhyperfine const. for [MnF<sub>6</sub>]<sup>4-</sup> 4-60883  
 isomeric nuclei and μ emitters as probes in condensed matter, review, book contrib. 4-71197  
 martensite, elec. cond., thermoelectric power and electronic struct. (Russian) 4-65657  
 metals, defects, hyperfine interaction studies, review, book contrib. 4-70135  
 metals, ferromagnetic, muon hyperfine fields, influence of lattice relax. and zero-point motion 4-65919  
 metals, muon states, recent progress 4-65902  
 metals, noncubic, elec. quadrupole interaction studies, review, book contrib. 4-70764  
 muonium, anomalous, nuclear hyperfine struct. 4-65653  
 muonium hyperfine interaction meas. using μSR 4-65931  
 oxides, mag., muon hyperfine interactions, spin rot. studies 4-65917  
 quartz, neutron irrad., EPR study of electron centres 4-88721  
 quartz, rose-coloured, Al<sup>3+</sup>-O<sup>2-</sup>-P radiation defect, EPR study 4-71180  
 radioactive nuclei, hyperfine interactions, condensed matter studies, book 4-67877  
 radioactive nuclei for hyperfine interactions study, book contrib. 4-70763  
 rare earth alloys, RCo<sub>2</sub>B<sub>2</sub>, R=Gd-Tm, antiferromag. and paramag. states, NMR spectra 4-109089  
 rare earth oxyhalides, doped, crystal field, quadrupole moments, ab initio calc. 4-65650  
 rare earth trifluoride single crystal, electric field gradient at Gd nucleus, integral perturbed angular correlation studies 4-98991  
 ruby, inhomogeneous reson. lines, effectiveness of spectral diffusion 4-98940  
 semiconductor, electronic struct. and hyperfine interaction of muonium 4-65633  
 sodium methylpentanoates, thermotropic liq. cryst., struct., NMR study 4-84862  
 TCNQ salt with quinolinium, mag. props. and electron-nuclear interaction 4-76126  
 TCNQ salt with triphenyl methyl arsenic cation triplet excitation radical, exchange anomaly resolution 4-70760  
 Tempone nitroxide radical, in MBBA liq. cryst., mag. field induced distrib., ESR 4-80820  
 transition metal, cubic, relativistic APW calcs. of nucl. spin-lattice relax. rates 4-71204  
 transition metals and their cpds., electronic struct. and muon hyperfine field calcs. 4-65643  
 Tutton salts: VO<sub>4</sub><sup>3-</sup>, zero mag. field EPR 4-109060  
 urea-ammonium ion complexes: Mn<sup>2+</sup>, zero-field splittings and site distortions, EPR studies 4-98580  
 Ag-Fe (001), interface magnetism, self-consistent spin-polarised localised spin-density calcs. using APW method 4-98863  
 Ag-Gd(Er), dil., impurity-induced muon depolarisation, mag. field depend. 4-71228  
 Ag-Tm, crystal field parameters, Mossbauer spectroscopy 4-114189  
 Al crystal with vacancies, elec. field gradient, adjustable parameter free calc. 4-61347  
 Al-Mg(Ga)(In)(Si)(Ge)(Sn), distribution of electric field gradients around impurities, conduction electron screening lattice strain 4-113910  
 Al<sub>2</sub>O<sub>3</sub>, single crystals, muonium decoupling in high transverse mag. field 4-92985  
 Al<sub>2</sub>O<sub>3</sub>:V<sup>3+</sup>, zero-field hyperfine splitting by Josephson phonon spectroscopy 4-61353  
 AlPO<sub>4</sub> polymorphs, chem. shift, bond angles, <sup>27</sup>Al and <sup>31</sup>P NMR 4-109088  
 Au-Gd, dil., impurity-induced muon depolarisation, mag. field depend. 4-71228

## crystal hyperfine field interactions continued

- AuFe alloys, spin glass freezing, PAC study 4-71216  
 BaF<sub>2</sub>Mn<sup>2+</sup>, annealed, EPR spectra 4-71169  
 BaSnFe<sub>2</sub>O<sub>13</sub>, cryst. struct., neutron diffr., Mossbauer spectra, magnetisation meas. 4-75406  
 BaTi<sub>2</sub>Fe<sub>2</sub>O<sub>11</sub>, cryst. struct., neutron diffr., Mossbauer spectra, magnetisation meas. 4-75406  
 BaTiO<sub>3</sub>, lattice deformation induced cryst. field variations, Mossbauer and EPR studies 4-71159  
 Be-HfO<sub>2</sub>, Hf<sup>3+</sup> implanted, O gettering, Rutherford backscatt. studies 4-92218  
 CaF<sub>2</sub>, single crystals, muonium decoupling in high transverse mag. field 4-92985  
 CaF<sub>2</sub>Er<sup>3+</sup>, transferred hyperfine interaction parameters, ENDOR 4-84872  
 CaFe<sub>2</sub><sup>2+</sup>Fe<sup>3+</sup>(Si<sub>2</sub>O<sub>7</sub>(OH)O), ilvaite, electron delocalisation and Mossbauer spectra 4-98993  
 Cd<sub>2</sub>Cu<sub>1-x</sub>Fe<sub>x</sub>O<sub>4</sub>, hyperfine field interactions, Mossbauer spectra 4-65885  
 Cd<sub>2</sub>Cu<sub>1-x</sub>Fe<sub>x</sub>O<sub>4</sub> spinel, low temp. Mossbauer obs. of mag. interactions 4-98983  
 Co-Ag-Pd, transient fields, g-factor, gyromagnetic ratios 4-113914  
 CoF<sub>2</sub>, antiferromagnets, hyperfine fields, muon spin relax. 4-71253  
 CoFe<sub>2</sub>O<sub>4</sub>, small particle ferrites, mag. hyperfine fields 4-61568  
 Co<sub>2</sub>MnAl(Si), spin echo study of hyperfine interactions 4-71209  
 CsMn<sub>1-x</sub>Co<sub>x</sub>Cl<sub>3</sub>·2H<sub>2</sub>O, random mixture with competing anisotropies, PMR meas. 4-88647  
 Cs<sub>2</sub>Ni<sub>3</sub>CdF<sub>12</sub>, hexagonal perovskites, intra- and intercluster mag. interactions 4-104405  
 Cs<sub>2</sub>Ni<sub>4</sub>CdF<sub>15</sub>, hexagonal perovskites, intra- and intercluster mag. interactions 4-104405  
 Cu complex, Cu<sub>2</sub>OC(Ph)<sub>3</sub>(triphenylphosphine oxide)<sub>4</sub>, excited S=2 manifold cubic field splitting 4-76240  
 Cu II complexes of N<sup>4</sup>, N<sup>4</sup>-disubstituted thio- and selenosemicarbazones of 2-acetylpyridine, EPR spectra 4-98941  
 CuCr<sub>2</sub>Se<sub>4</sub>, nuclear quadrupole interaction, NMR spin echo study 4-61352  
 (CuO)<sub>2</sub>(2B<sub>2</sub>O<sub>3</sub>Li<sub>2</sub>O)<sub>1-x</sub> glass, EPR and mag. susceptibility meas. 4-61587  
 Dy<sub>1-x</sub>Y<sub>x</sub>Co<sub>2</sub>, magnetically ordered, satellite struct. in <sup>59</sup>Co spin-echo NMR spectrum 4-88743  
 EuCoO<sub>3</sub>, quadrupole interactions, <sup>151</sup>Eu Mossbauer spectroscopy 4-76295  
 EuCrO<sub>3</sub>, quadrupole interactions, <sup>151</sup>Eu Mossbauer spectroscopy 4-76295  
 EuFeO<sub>3</sub>, quadrupole interactions, <sup>151</sup>Eu Mossbauer spectroscopy 4-76295  
 EuMnO<sub>3</sub>, quadrupole interactions, <sup>151</sup>Eu Mossbauer spectroscopy 4-76295  
 Eu<sub>2</sub>Sc<sub>2</sub>Fe<sub>2</sub>O<sub>12</sub>, EFG sign at <sup>57</sup>Fe nuclei, Mossbauer spectra 4-84599  
 EuScO<sub>3</sub>, quadrupole interactions, <sup>151</sup>Eu Mossbauer spectroscopy 4-76295  
 EuVO<sub>4</sub>, stoichiometric, nucl. quadrupole optical hole-burning 4-80969  
 Fe complex, halobis(diethylselenocarbamate)iron(III), mag. props. 4-76124  
 Fe, hyperfine interactions of interstitial <sup>125</sup>B, asymmetric  $\beta$  decay studies 4-65651  
 Fe, impurity hyperfine fields and adiabatic pot., self-consistent calc. 4-65632  
 Fe surface layer at nonmag. material interfaces, magnetisation, temp. depend. 4-61575  
 Fe-<sup>175</sup>Ta(177Ta), mag. hyperfine splitting frequencies, mag. moments, NMR-ON obs. 4-109083  
 Fe-Ag-Pd, transient fields, g-factor, gyromagnetic ratios 4-113914  
 Fe-based 3d-metal alloys, impurity charge screening 4-98562  
 Fe-Be and Fe-B-Si amorphous alloys, Mossbauer obs. of short-range order 4-92981  
 Fe-Mg multilayered films with superlattice, mag. props. study 4-80791  
 Fe-Ni Invar alloys, Mossbauer spectra 4-88748  
 Fe<sup>3+</sup>-containing layer silicates, Mossbauer spectra quadrupole splitting lines, relative intensities and EFG calcs. 4-115397  
 Fe<sub>1-x</sub>Co<sub>x</sub>Cl<sub>2</sub>, competing anisotropy system, Fe<sup>2+</sup> spin orientation, Mossbauer spectra 4-92906  
 Fe(Cr<sub>1-x</sub>Al<sub>x</sub>)<sub>2</sub>O<sub>4</sub> spinels, next-nearest-neighbour effects, Mossbauer studies 4-98987  
 (Fe<sub>1-x</sub>Cr<sub>x</sub>)<sub>2</sub>Mn<sub>1-x</sub>, <sup>55</sup>Mn and <sup>57</sup>Fe NMR, comp. depend. 4-98960  
 FeF<sub>3</sub>·0.33 H<sub>2</sub>O, normal and anhydrous, mag. ordering, Mossbauer studies 4-109103  
 Fe<sup>17</sup>Fe<sub>1-x</sub>Fe<sub>x</sub>(H<sub>2</sub>O)<sub>2</sub>, cryst. struct. and idle spin behaviour 4-108321  
 Fe<sub>3-x</sub>Ga<sub>x</sub>BO<sub>6</sub> boroferrite, hyperfine interactions, Mossbauer studies 4-109099  
 Fe<sub>3</sub>Ni<sub>9</sub>Mo<sub>5</sub>Si<sub>6</sub>B<sub>12</sub> metallic glass, mag. props., Mossbauer studies 4-109012  
 (Fe<sub>1-x</sub>Ni<sub>x</sub>)<sub>2</sub>Sb, antiferromag., mag. props. 4-104422  
 Fe<sub>2</sub>O<sub>3</sub>, hematite, quadrupole shifts, temp. depend.,  $\gamma$ -ray spectra anal. 4-65888  
 FeOCl, Lewis base intercalation compounds, charge transfer model, Mossbauer spectra, X-ray diffr. 4-70746  
 FeSiF<sub>6</sub>·6H<sub>2</sub>O, phase transition and cryst. field effects, Mossbauer study 4-75668  
 FeV<sub>2</sub>Se<sub>4</sub>, Mossbauer spectra, 4.8 to 700K 4-80849  
 Fe<sub>0.92</sub>Co<sub>0.08</sub>Cl<sub>2</sub> magnetoelectric coupling at Fe<sup>2+</sup> ions Mossbauer spectrum 4-92948  
 GaP single crystals, muonium decoupling in high transverse mag. field 4-92985  
 Gd, electric field gradient at Gd nucleus, integral perturbed angular correlation studies 4-98991  
 Gd with s-p impurities, hyperfine field systematics 4-70758  
 GdCl<sub>3</sub>Pr<sup>3+</sup>, crystal field levels, coord. geometry depend. 4-70755  
 GdCrO<sub>3</sub>, NQR and spin-flip transition 4-104509  
 Ge, anomalous muonium hyperfine interaction, temp. depend., 5 to 100K 4-71240  
 Ge, isotopically enriched, low-field anomalous muonium depolarisation 4-71241  
 GeNi<sub>2</sub>O<sub>4</sub>, mag. hyperfine interaction, <sup>61</sup>Ni Mossbauer spectra 4-98986  
 HoVO<sub>4</sub>, hyperfine-enhanced nuclear spin ordering, neutron diffr. studies (Japanese) 4-92988  
 InP, electron irradi., antisite defects, EPR study 4-80816  
 InSe, electric field gradients, nuclear quadrupole freqs., anomalous temp. behaviour 4-71221  
 KAl(SO<sub>4</sub>)<sub>2</sub>·12H<sub>2</sub>O, <sup>27</sup>Al NMR press. depend. 4-98955  
 KCl, single crystals, muonium decoupling in high transverse mag. field 4-92985  
 KIO<sub>3</sub>, low temp. ferroelec. transition under press. NQR studies 4-93019  
 KTaO<sub>3</sub>Fe<sup>3+</sup>, EPR spectra, superhyperfine struct., spin Hamiltonian parameters 4-98942

## crystal hyperfine field interactions continued

- KTaO<sub>3</sub>Li, impurity ion quasi-reorientational dynamics, NMR spectrum 4-98973  
 LaCl<sub>3</sub>Pr<sup>3+</sup>, crystal field levels, coord. geometry depend. 4-70755  
 LaF<sub>3</sub>Eu<sup>2+</sup>, fine struct. parameters, hyperfine splittings, X-band EPR meas. 4-71176  
 LiF-Ni<sup>2+</sup>, Ni<sup>2+</sup>-F<sup>-</sup> distance for square planar and linear Ni<sup>2+</sup>-centres from isotropic superhyperfine const. 4-98581  
 MgAl<sub>2</sub>Fe<sub>2-x</sub>O<sub>4</sub>, Mossbauer study of spin struct. 4-84875  
 Mg<sub>1-x</sub>Cd<sub>x</sub>Fe<sub>2</sub>O<sub>4</sub> ferrite, mag. props. Mossbauer studies 4-84878  
 Mn II complex, di(aminophenazone)MnCl<sub>4</sub>, cryst., photoexcitation and photoluminescence spectra 4-80976  
 Mn II complex, di(phenazone)MnCl<sub>4</sub>, cryst., photoexcitation and photoluminescence spectra 4-80976  
 MnF<sub>2</sub> antiferromagnets, hyperfine fields, muon spin relax. 4-71253  
 Mn<sub>1-x</sub>Fe<sub>x</sub>CO<sub>3</sub>, mixed antiferromag. system, competing anisotropy and random field effects 4-109019  
 MnFe<sub>2</sub>F<sub>8</sub>(H<sub>2</sub>O)<sub>2</sub>, cryst. struct. and idle spin behaviour 4-108321  
 MnFe<sub>2</sub>O<sub>4</sub>, small particle ferrites, mag. hyperfine fields 4-61568  
 Mn<sub>0.90</sub>Fe<sub>0.10</sub>P, mag. phases, Mossbauer spectroscopy study 4-88753  
 Mn<sub>1-x</sub>Fe<sub>x</sub>Si<sub>2</sub>, Mossbauer effect, magnetisation meas., in external mag. fields 4-98879  
 Mn<sub>2</sub>Sb, NMR of <sup>55</sup>Mn <sup>121</sup>Sb and <sup>123</sup>Sb, hyperfine fields 4-114167  
 NH<sub>4</sub>LiMn<sup>2+</sup>, Q-band EPR study 4-114154  
 NaF-Ni<sup>2+</sup>, Ni<sup>2+</sup>-F<sup>-</sup> distance for square planar and linear Ni<sup>2+</sup>-centres from isotropic superhyperfine const. 4-98581  
 NaOH, orthorhombic phase, quadrupole interactions, NMR 4-76266  
 Nb/Au/Nb Josephson tunnel junction, ESR study 4-92871  
 Ni (III) complex, dichloro bis-o-phenylene bis-dimethyl arsino nickelate (III) chloride, exchange interaction, EPR 4-71164  
 Ni,  $\mu$  spin precession and giant hyperfine anomaly 4-71254  
 NiCr<sub>2</sub>O<sub>4</sub>, mag. hyperfine interaction, <sup>61</sup>Ni Mossbauer spectra 4-98986  
 NiFe<sub>2</sub>Cr<sub>1-x</sub>O<sub>4</sub>, mag. hyperfine interaction, <sup>61</sup>Ni Mossbauer spectra 4-98986  
 NiFe<sub>2</sub>O<sub>4</sub>, mag. hyperfine interaction, <sup>61</sup>Ni Mossbauer spectra 4-98986  
 NiRh<sub>2</sub>O<sub>4</sub>, mag. hyperfine interaction, <sup>61</sup>Ni Mossbauer spectra 4-98986  
 Ni<sub>1-x</sub>Zn<sub>x</sub>Fe<sub>2</sub>O<sub>4</sub>, hyperfine fields NMR spin echo studies 4-61351  
 Pb, muon Knight shift, 20 to 785K 4-71233  
 Pb<sub>2</sub>Ge<sub>2</sub>O<sub>11</sub>Gd<sup>3+</sup>, superhyperfine interaction, ESR and ENDOR studies 4-114159  
 (Pd<sub>1-x</sub>Au<sub>x</sub>)<sub>2</sub>Fe, hyperfine mag. field study 4-88493  
 Pd(Fe, Co) dilute, Mossbauer study of relax., spin glass props. 4-104514  
 PdFeCd dilute alloys, hyperfine field at Cd, PAC spectroscopy studies 4-92681  
 Pd<sub>2</sub>FeH<sub>4</sub>, Mossbauer study of hyperfine interactions 4-88756  
 Rb<sub>2</sub>CrCl<sub>4</sub>, ferromagnet, CI NMR study (Japanese) 4-98967  
 Rb<sub>2</sub>ZnBr<sub>4</sub>, isomorphs, EFG tensor modulation, model calc. 4-75904  
 Rh complexes, tetrakis(trisopropylphosphite)rhodium, zero valent, EPR at X- and Q-band ranges 4-98944  
 ScCo<sub>2</sub>, exchange enhanced Pauli paramagnet, mag. susceptibility, Knight shift meas. 4-108983  
 Si<sup>13</sup>C, muon spin rot. and TEM studies 4-71239  
 SiB<sub>2</sub>( $\mu^+$ ), tetrahedral interstitial impurities, electronic struct. 4-65636  
 SiF<sub>4</sub>, amorphous and cryst., ion implanted, elec. quadrupole hyperfine interaction at impurity sites 4-92675  
 Si muon, spin polarised electron struct. of positive muon, LCAO-Green's function anal. 4-65634  
 Si<sub>1-x</sub>Ge<sub>x</sub>P, EPR study and spin-lattice relax. (Russian) 4-71177  
 Sr(NO<sub>3</sub>)<sub>2</sub>, X-irradiated, colour centres, ESR study 4-61589  
 Ta, hyperfine interactions of interstitial <sup>125</sup>B, asymmetric  $\beta$  decay studies 4-65651  
 Tb-Ce, dil., intermediate valent, time depend. hyperfine fields, TDPAC study 4-75907  
 TiS<sub>2</sub>, intercalation cpd. with Mn, chemical vapor growth and EPR studies 4-66201  
 TlBr, valence band, 5d ligand field splittings, UPS 4-66186  
 TlCl, valence band, 5d ligand field splittings, UPS 4-66186  
 TlI, valence band, 5d ligand field splittings, UPS 4-66186  
 TmNi<sub>2</sub>(Rh<sub>2</sub>)I<sub>2</sub>, <sup>169</sup>Tm Mossbauer spectra, quadrupole splitting, static or dynamic distortion 4-114188  
 V, hyperfine interactions of interstitial <sup>125</sup>B, asymmetric  $\beta$  decay studies 4-65651  
 VBr<sub>2</sub>, 2-D triangular Heisenberg antiferromag., heat capacities 4-76156  
 VCl<sub>2</sub>, 2-D triangular Heisenberg antiferromag., heat capacities 4-76156  
 VCl<sub>3</sub>(Br<sub>2</sub>)<sub>2</sub>, triangular Heisenberg antiferromagnet in paramag. state, hyperfine field, <sup>51</sup>V nucl. relax., NMR 4-92973  
 VLi<sub>2</sub>, 2-D triangular Heisenberg antiferromag., heat capacities 4-76156  
 VO<sup>2+</sup> ion impurities in crystalline solids, EPR spectra and spin Hamiltonian parameters 4-104490  
 V<sub>2</sub>O<sub>5</sub>-Sb<sub>2</sub>O<sub>3</sub>, nonstoichiometric rutile-type phase, ESR and X-ray diffr. studies 4-71163  
 W (110), clean and O covered, alkali metal chemisorption, NMR studies 4-98445  
 Y<sub>3-x</sub>Ca<sub>x</sub>Fe<sub>5-x</sub>Ti<sub>x</sub>O<sub>12</sub> garnets, hyperfine fields and Mossbauer spectra 4-109098  
 YFe, interionic distance effect on local fields, NMR study 4-84869  
 YIG, amorphous, appl. of hyperfine and exchange field distrib. in amorphous speromagnets 4-104413  
 YbF<sub>3</sub><sup>3-</sup> (n=6,8), mol. hyperfine interactions, Dirac scatt. wave calcs. 4-68982  
 Zn, single crystal, level crossing reson. on <sup>69</sup>Gd 4  $\mu$ s (9/2)<sup>+</sup> isomer, in-beam study 4-76289  
 Zn-In, diffusion and hyperfine interactions 4-61134  
 ZnFe<sub>2</sub>O<sub>4</sub> ferrite, mag. struct. and Neel temp. 4-108986  
 Zn<sub>0.25</sub>Ni<sub>0.75-x</sub>Ti<sub>x</sub>Fe<sub>2-2x</sub>O<sub>4</sub>, hyperfine field, meas., Mossbauer effect study 4-71224  
 ZnSeI, vacancy-I complex hyperfine interactions, ESR study 4-70150  
 ZrSiO<sub>4</sub>Pr<sup>3+</sup>, ESR, hyperfine interactions and g-values 4-71175

## crystal imperfections see crystal defects

## crystal inclusions

- binary cryst., displacement domains caused by defects (Chinese) 4-70254  
 brittle fracture toughness, influence of microstruct. 4-93388  
 brittle matrix, spontaneous cracking due to presence of thermoelastic stresses 4-108045  
 ceramics, strain around large inclusions, quantitative anal. 4-103621  
 cerams, optical props. and dielec. const., quantum size effects 4-65941  
 crystal growth from melt, impurity distribution and inclusions (Russian) 4-113483  
 ductile materials containing small volume of voids or inclusions, estimates for constitutive moduli 4-98172

**crystal inclusions continued**

- edge dislocation inside elliptical inclusion 4-60928  
 elastic-plastic finite element analysis of voids and inclusions 4-92195  
 ferromagnetic components quality control by coercive field strength meas. 4-93475  
 fracture mechanics, microscopic, appl. of J-integral concept 4-97435  
 garnet epitaxial layers, coercivity phenomena 4-76204  
 grain boundary shape, pinned by spherical particle 4-84302  
 infinite solid with thin foreign inclusion, integral eqns. for stress determ. (Ukrainian) 4-69680  
 interaction of rigid indenter and near-surface void or inclusion 4-74966  
 minerals containing water, IR spectral studies 4-93071  
 pentaerythritol tetrakisphosphate crystals, soln. growth and defects 4-113452  
 plastically deforming matrix, stress and strain fields around inclusions 4-97360  
 quartz, diffusional crack healing in aqueous environment 4-94098  
 quartz containing water, IR spectral studies 4-93071  
 solid solution, supersaturated, radiative swelling problem, inclusion growth and impurity pump mechanisms 4-70197  
 steel, alloy, fracture strain and characteristic fracture distance, microstruct. interpretation 4-85211  
 steel, alloy type, Ca treated resulphurised, mech. props. and machinability, S and sulphide shape effect, report 4-62048  
 steel, C, cast and wrought, H induced ductility losses, annealing effects 4-85193  
 steel, C-Mn, hot-rolled, ductility and anisotropy of sulphide inclusion spacings, effect of inclusion shape 4-99437  
 steel, HSLA, shear failure, development of fractographic features 4-76837  
 steel, inclusion assessment technique using image analyser (Korean) 4-104945  
 steel, low alloy, cavity initiation criteria at inclusions 4-104874  
 steel, medium C, H-assisted cracking after exposure to H<sub>2</sub>S-saturated salt soln., role of MnS inclusions 4-71732  
 steel, microalloyed, fracture micromechanics 4-99602  
 steel, Ni-Cr-Mo maraging, nitrogen effect on struct. and mech. props. 4-114532  
 steel, Ni-Cr-Mo-V, fracture toughness, overheating, effect of S content (Japanese) 4-93377  
 steel, roll type 9Kh, small N and B additions effect on struct. and mech. props. 4-93342  
 steel, rolled, impact toughness and transition temp., effect of delamination (Korean) 4-76848  
 steel, rotor forgings, unstable fracture, effect of small clustered flaws (Japanese) 4-93378  
 steel, seamless tubes, anal. of oxide inclusion responsible for internal defects (French) 4-76935  
 steel, submerged arc welds, inclusion anal. using EPMA and TEM 4-76744  
 steel, tool, brittle fracture, dopants and impurities effects, AES study 4-62063  
 steel, weld metal deposits, austenite decomposition products, influence of O-rich inclusions 4-114513  
 steel inclusion classification by automatic picture analysis system according to standard specifications (German) 4-81363  
 subsurface flaw in joined fluid-solid half spaces, US wave scatt. 4-97178  
 subsurface layers, thermal evolution of trapped gas, during linear tempering schedule 4-89073  
 superconducting small particle composites, magnetoresist., strong mag. field behaviour 4-76071  
 Ag<sub>3</sub>MnAl, Al<sub>3</sub>Manal, magnetic phase growth (Russian) 4-109014  
 Al superconducting thin film, N ion implanted, critical temp. 4-61485  
 Al, with small Sn additions, microstruct. and corrosion behaviour 4-99630  
 Al-Zn-Mg, 7075, heat-treated, acoustic emission during deform. 4-93343  
 Fe, cast, spheroidal graphite, cavity initiation criteria at inclusions 4-104874  
 Fe, cast, with vermicular graphite, struct. and heat treatment 4-114471  
 Fe-Si-C, cast, fracture micromechanism 4-62036  
 Gd-Ni-Si, X-ray phase anal. of compounds formed 4-114494  
 Ge:Ga, migration of molten inclusion 4-108659  
 InP(ZnS) single crystal growth, LEC technique, perfection, preferential etching, SEM and X-ray analysis 4-71549  
 KCl, grain boundary influence on motion of cryst. inclusions 4-75455  
 KH<sub>2</sub>PO<sub>4</sub> crystals, laser induced damage, X-ray topography 4-65296  
 NH<sub>4</sub>H<sub>2</sub>PO<sub>4</sub>, cryst. perfection, flow visualisation expts. 4-65042  
 Nb-Ti superconductors, flux pinning by gas bubbles (Russian) 4-104381  
 Ti<sub>3</sub>VS<sub>4</sub>, reduction of cracking by directional solidification 4-103869  
 W-Re, prep., sintering, phase comp., microhardness, SEM obs. 4-89010  
 WC, sintered, Co inclusions, magnetisation curves 4-109040

**crystal internal fields** see crystal field interactions

**crystal interstitials** see interstitials

**crystal lattice structures** see crystal atomic structure

**crystal microphones** see microphones

**crystal microstructure**

- for microstructural changes; see also phase transformations, hardening, heat treatment, metalworking  
 see also crystal defects; crystal inclusions; crystallites; dendritic structure; domain boundaries; domains; electron microscope examination of materials; eutectic structure; grain boundaries; grain size; Guinier-Preston zones; mosaic structure (microstructure); noncrystalline state structure; precipitation; segregation; subboundary structure; superlattices; texture; X-ray diffraction examination of microstructure  
 alloys, monotectic, solidification, microstruct. and phase spacings 4-93284  
 alloys, oxidation rel. to inert dispersoids and rare earth additions 4-114710  
 alloys, precipitation rel. to elec. resist. 4-114546  
 alloys, rapid solidification, research and appls., review 4-66322  
 alloys, rapidly quenched, struct. and thermal props., review 4-109443  
 Alnico magnets, microstruct., comp., atom probe field ion microscopy 4-71828  
 $\beta$ -alumina compacts, second phase particle struct., high resolution TEM studies 4-108627  
 aluminous electrical porcelain, doped with talc, microstruct. and med. props. 4-114674  
 antigorite, microstruct., high resolution electron microscopy study 4-103952  
 bauxite brick, lower temp. firing, microanalyses and SEM fractographs, K<sub>2</sub>O content 4-61892  
 book contribution 4-109377

**crystal microstructure continued**

- boronised alloys, types VK6, TSK10, T15K6, distrib. of B, W, Ti and Co (Russian) 4-80071  
 ceramics, high resolution electron microscopy appls. 4-108257  
 ceramics, microstructure, fracture toughness and thermal shock resist. relationships 4-62049  
 ceramics, N-based, conf., Falmer, England (Aug. 1981) 4-67873  
 ceramics, N-based, innovations 1976-1981 4-71532  
 ceramics, slow crack growth at high temp., characterisation by double torsion method 4-62053  
 creep damage theory, anisotropic, appl. of continuum damage mechanics 4-65335  
 dendritic and cooperative growth, conf., Atlanta, GA, USA (Mar. 1983) 4-90292  
 diamond formation in presence of Ni, high press. and temp., rel. to starting C crystallinity 4-66256  
 FCC [111] traces, Euler angles, grain orientation (Korean) 4-79969  
 filtered multipolar model of microstructural medium with coupled fields 4-84418  
 flow localisation and plastic instability, microstruct. aspects 4-85192  
 fracture surfaces fractal charact. 4-71734  
 fusion reactor materials, conf., Albuquerque, NM, USA (Sept. 1983) 4-90290  
 fusion reactor materials, radiation damage, pulse ion irradi. microstruct. 4-103821  
 grain growth, grain size distrib., topology and local dynamics, computer simulation 4-66306  
 grain growth kinetics, computer simulation 4-66305  
 graphite intercalation compounds, ultrastructure. 4-84417  
 hardfacing deposits, Cr<sub>7</sub>C<sub>3</sub>-containing, microstruct. and abrasion resist., influence of welding process variables 4-85222  
 hardfacing deposits, Ti<sub>3</sub>C<sub>2</sub>-containing, microstruct. and abrasion resist., influence of welding process variables 4-85222  
 magnetism conference, Eger, Hungary (Sept. 1983) 4-78029  
 metal, arc fusion welding, solidification microstruct. 4-89050  
 metal powder under shock compression, microstructural modifications 4-109342  
 metals, FCC, inhomogeneous deform., mech. and struct. effects (Polish) 4-84336  
 metals, shock wave treatment, texture anal. (Russian) 4-103878  
 metals, surface phenomena induced by intense laser irradi. 4-81044  
 multite-cordierite composites, sintering, hot pressing, microstruct., mech. and thermal props. 4-89017  
 nanocrystalline structure, proposed new material struct. (German) 4-70045  
 pearlite interlamellar spacing, review of data 4-93293  
 peritectic alloys, solidification mechanism, microstruct. aspects 4-93273  
 phase transformations in solids, Crete, Greece (June-July 1983) 4-110811  
 piezoelectric ceramics, microstruct., props. and phase relations 4-61629  
 pore channel stability, dihedral angle effects 4-114434  
 precipitate dissolution, anal. of microstruct. dynamic 4-109408  
 precipitation, discontinuous, interlamellar spacing 4-93302  
 qualitative and quantitative surface microscopy, book contrib. 4-109619  
 radiation damage microstructure, microcomputer system for quantitative image analysis 4-103617  
 rapid solidification microstructures 4-89046  
 recovery and recrystallization, book contrib. 4-109429  
 Rene 95, Ni-base superalloy, fatigue, effect of processing and microstruct. 4-104843  
 sialon polytypoids, struct. characterisation 4-75426  
 sialons,  $\alpha$ - $\beta$  relationship 4-70125  
 $\beta$ '-sialons, microstruct. evaluation by TEM, correl. to mech. props. 4-76732  
 solidification, modelling of heat flow 4-88266  
 steel, alloy, fracture strain and characteristic fracture distance, microstruct. interpretation 4-85211  
 steel, austenitic stainless, fatigue crack propag. threshold 4-99590  
 steel, austenitic stainless, H induced slow crack growth rel. to  $\alpha'$  martensite form. 4-66428  
 steel, austenitic stainless, heat resistant, precip. and carbide transform. (German) 4-81196  
 steel, austenitic stainless, metallographic revelation of  $\alpha$ -phase and  $\delta$ -ferrite, etching and mag. techniques (German, English) 4-66540  
 steel, austenitic stainless, nitrided, microstructure, optical microscopy, TEM obs. 4-81359  
 steel, austenitic stainless, stress relax. in bending at 773K 4-81229  
 steel, austenitic stainless, structure and mech. props., casting environment effects 4-109433  
 steel, austenitic stainless, swelling and cavity microstruct. development, irradi. in EBR-II and HFIR 4-98131  
 steel, bainitic and ferritic, cleavage fracture initiation, microstruct. 4-99556  
 steel, C, tempered, radial direction fracture surface, SEM obs. (Japanese) 4-89115  
 steel, C, yield stress rel. to C content and pearlite morphology, tensile and Charpy obs. 4-81248  
 steel, C-Mn, fracture toughness studies in different regions of weld heat affected zone 4-76838  
 steel, Cr-Mn austenitic, thermally aged, phase instability, precip. reactions 4-109410  
 steel, Cr-Mn-Ti, carburised, struct. and hardness rel. to cyclic heat treatment 4-66406  
 steel, dual-phase, C-Mn, mech. props. and fracture mechanism, influence of martensite morphology 4-99530  
 steel, dual-phase, deform., heterogeneity in ferrite phase 4-71712  
 steel, dual-phase, fatigue crack propag., effect of microstruct. on crack path morphology 4-99525  
 steel, dual-phase, martensite-ferrite, tensile strength, shear-lag anal. 4-71704  
 steel, electric spark alloying with TiN-Cr, reinforced layer microhardness and comp. 4-89192  
 steel, electrotechnical, grain oriented, microstructure and mag. props. 4-80247  
 steel, ferritic, Cr-Mo-V-Nb, microstruct. after irradi. to 36 dpa at elevated temps. in HFIR 4-98153  
 steel, ferritic stainless, resistance welded, corrosion resist. under detergent exposure 4-104895  
 steel, heat-resistant, static and dynamic fracture toughness, influence of microstruct. and temp. 4-99600

## crystal microstructure continued

- steel, high strength, heat-treatable, fatigue at +20°C and -70°C 4-93364
- steel, high-C tool, struct. of hardening martensite and change during low-temp. tempering 4-114583
- steel, hypereutectoid, Mode III fracture initiation toughness, depend. on strength and microstruct. 4-71720
- steel, ion-nitrided structure, electron microscopic studies (*Bulgarian*) 4-81354
- steel, low alloy, HY-80, microstruct. after small plastic strains, TEM characterisation 4-93340
- steel, low alloy, reversible temper embrittlement, role of microstructure, scanning Auger microcopy study 4-81286
- steel, low C, Al killed, decomp. of Mn-C dipoles during quench ageing, resist. obs. 4-71661
- steel, low C, cold rolled, initial stage of decarburisation 4-114577
- steel, managing, influence of carbide formation on fracture struct. (*Russian*) 4-81273
- steel, maraging, Ni, fracture toughness, effect of treatment condition 4-76856
- steel, martensitic transformations in 18KhNVA steel, residual austenite (*Russian*) 4-104779
- steel, mech. props., effect of laser quenching 4-66356
- steel, microalloyed, cast, microstruct. and mech. props., influence of phase changes (*French*) 4-81278
- steel, microalloyed, charact. of low temp. transform. products 4-103948
- steel, microalloyed, rel. between microstruct. and H embrittlement 4-99605
- steel, Mn, 13 to 19 wt.%, sinter-forged, mech. props. 4-81283
- steel, Mn, 13 wt.%, prod. by powder metallurgy method 4-81169
- steel, Mn, controlled hot rolling and intercrit. annealing, time-temp.-reaction diagrams 4-66351
- steel, Mn-V-Cu austenitic, microstructure rel. to heat treatment and alloying additions 4-89066
- steel, Nb-microalloyed and medium C, laser hardening 4-114563
- steel, Nb-V, low C, controlled-rolled, transform. textures 4-99405
- steel, Ni-Co-Mo-Ti, controlled hot rolling and intercrit. annealing, time-temp.-reaction diagrams 4-66351
- steel, Ni-Cr-Mo-V, creep rupture and service properties improvement (*German*) 4-76862
- steel, Ni-Mo, martensitic A533B pressure vessel, tempered, brittle fracture and fatigue: crack growth, segregation effects, Auger obs. 4-66400
- steel, nonoriented electric, composition effect on loss, elec. cond. and texture 4-81219
- steel, nuclear structural, A-203D, low temp. deform., effect of microstruct. 4-66386
- steel, pearlite growth, by combined vol. and phase boundary diffusion 4-114470
- steel, pearlitic, upper bainite varieties 4-114537
- steel, stainless, Cr-Mn, ferritic-austenitic, superplasticity 4-61984
- steel, stainless, hardenable, microstruct.-strength relationship 4-114560
- steel, stainless, microanalysis by EELS, comparison with EDX 4-80248
- steel, stainless, Ni-free, alloyed with rare-earth metals and Ca, struct. and props. 4-62116
- steel, stainless, shock loaded, residual struct. and props. 4-109516
- steel, stainless, transition and martensitic-class, superplasticity 4-61983
- steel, stainless and bearing, surface analysis, ion implantation and tribological processes 4-99607
- steel, stainless powder particles, droplet processed, rapid solidification struct., STEM obs. 4-71649
- steel, structural, cast, strength toughness rel. to intercritical treatment (*French*) 4-81222
- steel, structural, weldability, effect of residual elements 4-85214
- steel, submerged arc welds, inclusion anal. using EPMA and TEM 4-76744
- steel, Ti-modified, prep. by rapid solidification processing, microstruct. response to neutron irradi. 4-98143
- steel, transformer, effect of Sb additions on texture 4-81216
- steel, twin diffraction effects from body centred tetragonal martensite 4-65274
- steel wire, rolled, martensite content, microstructural stresses, EM NDT (*German*) 4-99695
- steels, austenitic stainless, 316 and 253MA, high temp. low cycle fatigue, comparison between mech. props. and microstruct. 4-93410
- steels, low alloy, fracture toughness studies 4-109491
- strain softening, materials model with appl. in modelling strain localisation 4-99407
- superalloys, powder metallurgy, book 4-86129
- textured materials, kinetic props., grain interaction effects 4-60938
- thin films, anal. techniques, review 4-113832
- thin foils, electron beam spreading in STEM-EDS X-ray micro anal. 4-85279
- transformations due to shock loading, temp. and deform. 4-113611
- transport model systems, microstruct. form. investigation (*German*) 4-81183
- welds, ferritic stainless steel,  $\gamma$ - $\alpha$  transform temp., direct determ. method 4-114752
- willemitte glass ceramic, partially crystallised, struct. and comp. 4-61910
- Zircaloy, fracture, influence of environment on form. of fluting microstruct. 4-104911
- zirconolite, high resolution lattice images 4-103951
- Ag-Cu-Zn, ternary  $\beta$ -phase alloys, ordering and phase separation, EM obs. 4-66310
- Ag-Pd-Ag multilayered films, microstructure changes rel. to layer spacing, TEM obs. 4-80432
- Ag<sub>3</sub>Ce-Ce system, partial phase diagram and lattice struts. 4-71636
- Al alloy, laser treatment, strengthening and microstruct. (*Russian*) 4-71665
- Al alloys, homogenising ingots, struct. changes 4-61961
- Al, impact by steel spheres, velocity propagation 4-108532
- Al, shock loaded, microstructure and hardness 4-109515
- Al-Ag, age hardened, persistent slip bands, energy dispersive spectra 4-104794
- Al-Cu, phase transform., thermoelec. power study 4-114473
- Al-Cu (10 wt.%), prod. by rheocasting, rel. between struct. and mech. props. 4-99467
- Al-Cu (3.6 wt.%), aged, coarsening kinetics of rod shaped  $\theta$  particles, LSW theory 4-71652
- Al-Cu (3.76 wt.%), Rheocast, ageing characts. rel. to incomplete homogenisation 4-109444
- Al-Cu films deposited by sputtering techniques, microstruct. 4-108733

## crystal microstructure continued

- Al-Cu-Cd, strengthening mechanism of Cd additions 4-61985
- Al-Cu-Li, recrystallised 2020, mech. props. rel. to soln. heat treatment 4-76781
- Al-Cu-Li-Cd, 2020, microstruct., fracture toughness and SCC 4-76851
- Al-Fe-Ni-Co, prep. from atomised powder, prod. struct. and props. 4-114446
- Al-Li, microcrystal evolution, DSC obs. 4-71659
- Al-Li-Si system, liquidus surface, thermal and microstructural analysis 4-61921
- Al-Mg-Si, creep life prediction, long-time, role of microstruct. instability 4-114622
- Al-Mg-Si-Sn, ageing, clustering process rel. to Sn addition, elec. resist., TEM obs. 4-114529
- Al-Sc alloys, age hardening kinetics 4-61949
- Al-Si-Cu-Mg, strengthening with continuous CO<sub>2</sub> laser 4-62117
- Al-Si-Mg-Sr, struct. and props., comp. and Sr addition effects 4-61987
- Al-Si-Sb, eutectic, struct. rel. to Sb addition, electron beam microanalysis (*German, English*) 4-66314
- Al-Zn-Mg-Cu, phase identification, X-ray analysis, sequential etching 4-104950
- Al-Zn(Mg), neutron irradi., radiation damage 4-80112
- AlN, oxynitride bonded ceramics, sintering, microstruct., densification, flexural strength, oxide additions effect 4-76727
- AlN powder, shock compression study 4-109349
- AlN powder, shock effects, TEM study 4-109345
- Al<sub>2</sub>O<sub>3</sub> membranes, prep. and microstruct. 4-66285
- Al<sub>2</sub>O<sub>3</sub> powder, shock induced densification and sinterability 4-109350
- Al<sub>2</sub>O<sub>3</sub> thin microporous layers, prep. and characterisation 4-70601
- Al<sub>2</sub>O<sub>3</sub>-AlN system, high temp. reactions and microstructs. 4-76763
- $\beta/\beta'$ -Al<sub>2</sub>O<sub>3</sub>-Na<sub>2</sub>O, struct. transform. during sintering and annealing 4-93292
- Al<sub>2</sub>O<sub>3</sub>-SiO<sub>2</sub> fibres, cristobalite form. at elevated temp. (*German, English*) 4-81197
- Al<sub>2</sub>O<sub>3</sub>-ZrO<sub>2</sub> ceramics, high press. sintered, fracture toughness rel. to phase transform. 4-76839
- Al<sub>2</sub>O<sub>3</sub>-ZrO<sub>2</sub> composite tool bit, microstruct., toughening mechanisms, performance 4-61946
- Al<sub>2</sub>TiO<sub>3</sub> ceramics, stabilisation by cation substitution, sintering and hot pressing 4-109362
- Au-Ag-Au multilayered films, microstructure changes rel. to layer spacing, TEM obs. 4-80432
- B<sub>4</sub>C, hardness and fracture toughness rel. to stoichiometry 4-62019
- Bi-Mo-Nb oxides, complex phases, struct. determ. by high resolution electron microscopy 4-103950
- Bi-W-Mo oxides, complex phases, struct. determ. by high resolution electron microscopy 4-103950
- Bi-W-Nb oxides, complex phases, struct. determ. by high resolution electron microscopy 4-103950
- Bi<sub>2</sub>Ti<sub>2</sub>O<sub>12</sub> ceramics, grain orientation, ESR and thermal expansion studies 4-104482
- Bi<sub>2</sub>Ti<sub>2</sub>O<sub>12</sub> ceramics, grain orientation by cold uniaxial method 4-104757
- Bi<sub>2</sub>WO<sub>3</sub> bronze, microstructure and X-ray emission spectra 4-84419
- Ca<sub>2</sub>Fe<sub>3-x</sub>Mn<sub>2x-1</sub>O<sub>8+y</sub>, O defect perovskite struct., X-ray diffr. and HREM study 4-92382
- Ca<sub>2</sub>LaFe<sub>3</sub>O<sub>8+y</sub>, cryst. struct. determ. 4-80014
- CdTe films, MBE growth and microstruct. characterisation 4-92578
- CdTe thin layers, crystal and energy structures for photoelectric transducers 4-98298
- CeSiO<sub>3</sub>N, Ce-N- $\alpha$ -wollastonite polytypes, electron microscopy study 4-103949
- Co, polycrystalline, approach to saturation at intermediate fields; role of internal demagnetising fields 4-76183
- Co<sub>2-x</sub>O, chem. diffusion, creep meas. 4-92418
- Cr films, evaporated, mechanical stresses 4-75819
- Cr foil, influence of heat treatment on struct. and props. (*Russian*) 4-65412
- Cr, oxidation, TEM microstructural study 4-104926
- Cu alloy, laser treatment, strengthening and microstruct. (*Russian*) 4-71665
- Cu, polycrystalline, cyclic creep accel. and retardation, threshold stress temp. depend. 4-66372
- Cu-Al-Fe alloys, laser surface melted, microstruct., X-ray diffr. study 4-108628
- Cu-Al-Ti, internal oxidation, dispersion hardening (*Japanese*) 4-89065
- Cu-Be (1.0 wt.%), aged, twinned microstruct. 4-89070
- Cu-Co system, coarsening of semi-coherent precipitates 4-114525
- Cu-Mn-Zn, microstructure study after cold working 4-108385
- Cu-Ni-Sn (9, 6 wt.%), ageing, internal friction, Young's modulus, modulated structure 4-66362
- Cu-Ni-Zn, L1<sub>0</sub> and L1<sub>2</sub> alloys, order-disorder transitions, microstructure obs. 4-114511
- Cu-Ti-Cr (4, 0.5 wt.%), ageing, internal friction, Young's modulus, modulated structure 4-66362
- CuAl<sub>3</sub>, second-phase particles, dissoln. rates in various microstruct. 4-89059
- CuAu, microstructure, field ion microscopy study 4-88177
- (Fe,Ni)V, ordered alloy, irradi. in HFIR, microstruct. and bend ductility 4-108454
- Fe alloy, diffusion carburizing, growth of carbide fibres 4-93454
- Fe, cast, graphite morphology, appl. of secondary ion mass spectrometry 4-66343
- Fe, cast, grey, profilometric characteris. of microstruct. (*French*) 4-71820
- Fe, cast, metallographic differences between compacted and vermicular graphite 4-114753
- Fe, cast, Mg treated, graphite nodularisation and graphitisation during solidification under 145 atm. Ar pressure 4-66325
- Fe, cast, microstruct. and phase comp. after irradi. by pulsed or continuous rad. of optical quantum generator 4-66485
- Fe, cast, with vermicular graphite, struct. and heat treatment 4-114471
- Fe powder, Ni-coated, compacted, phase identification by colour etching 4-114755
- Fe, sulphidation, microstruct. and growth rates of FES 4-88304
- Fe-base superalloy,  $\alpha$ -phase, planar faults, domain structures, high resolution electron microscopy obs. 4-104793
- Fe-C martensite, incommensurate direction of modulated struct., strain energy, lattice distortion 4-109454
- Fe-Cr-C, hypereutectic alloys unidirectionally solidified, hot hardness of primary carbides 4-99492
- Fe-Cr-Co (12 wt.%) permanent magnet alloys, mag. props., effect of alloying 4-84771

## crystal microstructure continued

- Fe-Cr-Ni, martensitic transition and cryst. geometry (*Russian*) 4-66332  
 Fe-Cr-Ni (20, 10 wt.%), oxidation, TEM microstructural study 4-104926  
 Fe-Mo, lattice imaging of solute atom clusters, electron microscopy obs. 4-81362  
 Fe-Nb, lattice imaging of solute atom clusters, electron microscopy obs. 4-81362  
 Fe-Nb, nitrided, void form., mech. props., optical microscopy, SEM, TEM obs. 4-81361  
 Fe-Ni Invar alloys, phase transforms. 4-70373  
 Fe-Ni-C, shock induced martensitic transform. 4-109406  
 Fe-Ni-Mn (21, 4 wt.%), isothermal lath martensite growth at  $-80^{\circ}\text{C}$ , cinemicrophotography 4-81193  
 Fe-Ni-Mn (21.1, 4.0 wt.%), athermal martensitic transform. with isothermal component 4-89052  
 Fe-P-Cu, mech. props. and microstructure rel. to sintering atmosphere 4-109354  
 Fe-Sb-Ce alloys, Ce state at cryst. boundaries, electron diff. studies (*Chinese*) 4-98114  
 Fe-Si (3 wt.%), reversible magnetisation curve at any angle to rolling direction 4-61558  
 Fe-Ti alloys, ion implanted,  $\text{C}^{+}$  implantation effects on surface mech. props. 4-114707  
 Fe-Zn system, formation and growth of  $\delta$  phase, cracks 4-89026 ( $\text{Fe}_{23}\text{Co}_{78}$ ), V, tensile deformis,  $20-1000^{\circ}\text{C}$ , fracture mode and ductility rel. to order-disorder transform. 4-66427  
 FeO, high temp. corrosion scales, TEM studies 4-104927  
 $\text{Fe}_2\text{O}_3$ , oxidation and reduction influences on grain morphology 4-93436  
 $\gamma$ - $\text{FeOOH}$  powder, grinding, lepidocrocite to hematite transform., morphology and mag. props., Mossbauer obs. 4-66329  
 FeS high temp. corrosion scales, TEM studies 4-104927  
 $\text{Fe}_2\text{TiO}_4$  and  $\text{Fe}_2\text{Ti}_2\text{O}_4$ , neutron diffraction study of cryst. struct. and mag. props. 4-100540  
 GaAs(001)-Au interface, formation by MBE and thermal stability 4-99328  
 InP:Sn(Zn)(Fe) single crystals, LEC growth, perfection, carrier conc., TEM obs. 4-71550  
 InSb films, MBE growth and microstruct. characterisation 4-92578  
 $\text{La}_{1-x}\text{Ca}_x\text{FeO}_{3-y}$ , high temp. order-disorder transition 4-113618  
 $\text{LiKSO}_4$ , cryst. and domain struct., neutron diff. studies 4-88159  
 $\text{Li}_2\text{TiSi}_2$ , intercalation study by TEM 4-103953  
 $\text{Li}_2\text{V}_2\text{O}_7$ , intercalation study by TEM 4-103953  
 $\text{MgAl}_2\text{O}_4$  spinel ceramics, sintering, rel. to stoichiometry 4-109363  
 $\text{MgO-CaTiO}_3\text{-CaO-SiO}_2$  system, phase equilb. and microstruct., isothermal sections 4-114496  
 $\text{MnO}_{1-x}$ , oxidation and reduction influences on grain morphology 4-93436  
 $\text{Mn}_{1-x}\text{Zn}_x\text{Fe}_2\text{O}_4$  ferrite, microstruct. and permeability during sintering 4-109432  
 Mo alloys, structure formation during internal oxidation (*Russian*) 4-81336  
 Mo, pulse ion irradi., void nucleation 4-103826  
 Na(Tl) deformed cryst., relationships among stresses, microstruct. and photolum. 4-71441  
 Nb-Ti multifilamentary supercond. composites, cold drawn, heat treatment, precip. morphology, TEM obs. 4-71657  
 Ni alloys, high-alloy, microstruct. and comp. charact. of eutectic  $\gamma'$  phase (*Russian*) 4-92380  
 Ni foils, He injected, self-ion irradi., annealing, voids, TEM obs. 4-103827  
 Ni, pure, heavy ion irradi. damage, in situ electron microscopy 4-103828  
 Ni superalloy Mar-M 200 powder, shock induced compaction, mech. props. 4-109430  
 Ni/SiC mixed layers, ion and laser irradi., microstruct. anal. 4-84415  
 Ni-Al thin foils, pre-martensitic phase, electron diff. study 4-114518  
 Ni-B alloys, CVD deposited, microstruct. and mech. props. 4-71581  
 Ni-base superalloy, DKS, directionally solidified, mech. props., influence of grain orientation 4-93420  
 Ni-base superalloy, microstruct. effects of fatigue crack propag., TEM study 4-104871  
 Ni-based amorphous alloys, crystallisation processes, microstruct. anal. 4-84183  
 Ni-Cr-Co-B, melt spun superalloy, annealing, castability, ductility and microstruct. rel. to B additions 4-66323  
 Ni-Mo ordered alloys, phys. metallurgy, microstruct. and props., review 4-114556  
 Ni-Mo-Al eutectic alloy, unidirectionally solidified composite,  $\gamma/\gamma'$  phases, microstruct. changes 4-114493  
 Ni-Mo-Al unidirectionally solidified eutectic, microstruct. instability 4-61926  
 Ni-Nb-Al  $\gamma-\gamma'$  eutectic composite, prep. and morphology 4-114500  
 Ni-Ni<sub>3</sub>Al-Mo eutectic composite, crystallographic orientation of phases 4-114501  
 NiO, high temp. corrosion scales, TEM studies 4-104927  
 NiO-CaO eutectic, directionally solidified, crystallography 4-113658  
 NiO-Y<sub>2</sub>O<sub>3</sub> system, composite microstruct. and interface struct. 4-70578  
 PZT material, high density, prep. by coprecipitation technique 4-76711  
 Pb-acid battery active mass, microstruct. model anal. 4-105103  
 Pb-Sn (7.6 wt.%) role of excess vacancies in discontinuous precipitation (*Russian*) 4-81199  
 Pb( $\text{Sc}_{0.5}\text{Ta}_{0.5}$ )O<sub>3</sub> single cryst., ordered domains, TEM obs. 4-65411  
 Pt ultrathin drawn wires, struct. and elec. props. 4-92696  
 Si sheets, edge-supported pulling, electron channelling and EBIC studies, rel. to solar cell appls. 4-75695  
 Si, swirl defect formation during zone growth 4-71552  
 Si-B microcrystalline films, crystallinity, morphology and elec. cond. 4-108749  
 Si-B solar cell material, EBIC contrast, microstruct. and composition effects 4-108878  
 Si-C layers, CVD growth, microstruct. and resist. 4-70599  
 $\text{Si}_2\text{-Al}_2\text{O}_3\text{-N}_2$   $\beta$ -sialon synthesis from  $\text{Si}_3\text{N}_4$  and Al alkoxides (*Japanese*) 4-114461  
 SiC fibres, mech. props. and struct. (*French*) 4-62003  
 SiC:B, shrinkage, density and phase comp. rel. to forming press. and sintering temp. 4-85130  
 SiC-Al, sintered composite interfacial reactions, joint bending strength rel. to microstruct. 4-66295  
 SiFe, polycrystalline, approach to saturation at intermediate fields, role of internal demagnetising fields 4-76183  
 $\text{Si}_3\text{N}_4$ ,  $\alpha$ - $\beta$  relationship 4-70125  
 $\text{Si}_3\text{N}_4$ , determ. of  $\alpha$ -phase fraction (*Japanese*) 4-81393

## crystal microstructure continued

- $\text{Si}_3\text{N}_4$ , hot pressed, fracture toughness, mech. props. rel. to comp. and microstruct. 4-76870  
 $\text{Si}_3\text{N}_4$ , hot pressing, densification and microstruct. rel. to MgO and Y<sub>2</sub>O<sub>3</sub> additions 4-76729  
 $\text{Si}_3\text{N}_4$ , microstruct. development during fabrication 4-76733  
 $\text{Si}_3\text{N}_4$  polypase materials, high temp. deform. and fracture 4-76866  
 $\text{Si}_3\text{N}_4$ , reaction bonded, flexure strength, oxidation, microstruct. 4-76892  
 $\text{Si}_3\text{N}_4$ , reaction bonded, sintering, microstruct. and props. 4-76725  
 $\text{Si}_3\text{N}_4$ , reaction bonded, sintered, densification kinetics, microstruct. 4-76726  
 $\text{Si}_3\text{N}_4$ , thermal props. and thermal shock resist. rel. to microstruct. and processing parameters 4-76871  
 $\text{Si}_3\text{N}_4\text{-Y}_2\text{O}_3$  based ceramics, sintering, densification, oxidation, strength and porosity 4-76835  
 $\text{SiO}_2$  film RF magnetron sputtering, film growth and struct. 4-88967  
 $\text{SiO}_2$ , synthesis using ion implantation into Si 4-70175  
 SiYON ceramics, mech. props. rel. to corrosion and microstruct. 4-76834  
 Sm( $\text{Co,Fe,Cu,Zr}$ )<sub>7.5</sub> magnets, high resolution electron microscopy study 4-61098  
 SmCo<sub>5</sub> permanent alloys, metallographic study, improved phase and grain boundary etching 4-114754  
 Ta-N-O films, DC reactive sputtered, elec. resist., microstruct., oxidation 4-80704  
 Ti alloys, plasticity of coarse grained type VT30 alloy in  $\beta$ -region (*Russian*) 4-81241  
 Ti alloys, polygonisation and recrystallisation obs. (*Russian*) 4-80246  
 Ti alloys, rapid solidification by melt spinning technique, alloy additives selection 4-89034  
 Ti, pure, electron beam welding, mech. props., fusion reactor appls. 4-109471  
 Ti thin films, struct. and elec. props. 4-80441  
 Ti-Al-V (6, 4 wt.%), electron beam welding, mech. props., fusion reactor appls. 4-109471  
 Ti-Al-V (6, 4 wt.%), evolution of  $\alpha+\beta$  struct. rel. to thermomech. treatment 4-109431  
 Ti-Al-V (6, 4 wt.%), tensile props. and fracture mode, temp. depend. 4-109488  
 Ti-Al-V (6.4 wt.%), erosion by spherical particles at  $90^{\circ}$  impact angles, effect of microstruct. 4-76876  
 $\alpha+\beta$  Ti-Al-V and Ti-Al-Cr-Mo-V, annealed, struct. and mech. props. 4-61988  
 Ti-Cr(V)(Mn)(Fe)(Mo), influence of ageing on incommensurate struct. (*Russian*) 4-65218  
 Ti-Ni-Cu system, dissipative props. and struct., martensitic transform. 4-66361  
 Ti-V solid solutions, creep, microstruct. 4-109464  
 TiAl intermetallic, ductility, strength and microstruct., Ag addition effect (*Japanese*) 4-66391  
 TiB<sub>2</sub>, implanted with 1-MeV Ni<sup>+</sup> ions, microstruct. and surface mech. props. 4-70232  
 Ti(C,N)-Ni-Mo, hard metal, fracture toughness rel. to microstruct. 4-104873  
 TiC, low Z films, correl. of residual stress with microstruct. 4-114695  
 TiC powder, shock induced densification study 4-109351  
 TiN, low Z films, correl. of residual stress with microstruct. 4-114695  
 TiN-TiC solid soln. powder, shock compaction study 4-109341  
 TiNi, martensitic transform., mech. props., struct. rel. to thermomech. treatment 4-66376  
 TiO<sub>2</sub> thin films, plasma-enhanced CVD, photoelectrochemical props. 4-80627  
 TiO<sub>2</sub>-based crystalline ceramic nuclear waste forms, processing and microstruct. 4-83150  
 TiO<sub>2</sub> thin films, struct. and elec. props. 4-80441  
 U-Nb (6 wt.%), microstruct., mech. props. and corrosion, effect of quench rate 4-114558  
 V, neutron irradi., temp. depend. of damage microstruct. 4-108455  
 V-B<sub>4</sub>C, neutron irradi., temp. depend. of damage microstruct. 4-108455  
 W, powder metallurgy rods, swaging process workability rel. to texture (*Japanese*) 4-89068  
 W-Ni alloys, diffusion induced recrystn. 4-61958  
 W-Ni-Fe, dynamic strength calcs. based on grain deform. 4-108511  
 W-Re, prep., sintering, phase comp., microhardness, SEM obs. 4-89010  
 W-C, crystal structure and dislocation climb obs. by TEM 4-98072  
 WO<sub>3</sub>-Nb<sub>2</sub>O<sub>5</sub>(Ta<sub>2</sub>O<sub>5</sub>)(Nb<sub>2</sub>O<sub>5</sub>-Ta<sub>2</sub>O<sub>5</sub>), TEM study of microstructs. 4-113655  
 Y<sub>2</sub>(Co, M)<sub>17</sub>, M=Al, Fe, single cryst. cpds., growth conditions and characterisation 4-62220  
 Zn-Al-Cu alloys, vol. change on ageing 4-114592  
 Zn-Al-SO alloys, quench-aged, phase transforms., rel. to hardness 4-114515  
 ZnO-Nb<sub>2</sub>O<sub>5</sub> ceramics, elec. props. and microstruct., wettability additives effect (*Japanese*) 4-76719  
 Zr-Nb, nuclear reactor pressure tubes, fracture micromechanisms, use of J<sub>R</sub> curves 4-99582  
 Zr-Nb (20 wt.%),  $\beta$ -phase decomp. rel. to thermal treatment 4-109411  
 ZrO<sub>2</sub> glaze coatings, microstruct. effect on whiteness 4-81304  
 ZrO<sub>2</sub> powder, shock modified, microstructure study 4-109343  
 ZrO<sub>2</sub>, shock modified, energy release and phase transform. 4-108612

## crystal morphology

- alkali halide crystals, dislocation etching, etch pits, crystal growth, review 4-70159  
 alkali halide crystals, etch pit studies of dislocations, dissolution kinetics and impurity effects 4-70158  
 alloy, binary, freezing, periodic growth rate effect on morphological stability 4-98039  
 $\beta$ -copper phthalocyanine, vapour phase cryst. growth, struct. and morphology 4-76647  
 corundum, crystal morphology, effect of trivalent rare-earth ions 4-75349  
 crystal growth, molecular mechanisms, review 4-60869  
 crystal stability and shape, mol. motion effect 4-113375  
 cyclotrimethylene-trinitramine single cryst., density and thermal expansion 4-88222  
 epitaxial growth, atomic pair correlation function during early stages 4-92577  
 ferrite powder, form. mechanism in fused salts, SEM studies 4-70399  
 flux growth, review of present status 4-76654  
 growth mechanisms, morphology and nucleation (*Japanese*) 4-92118  
 growth mechanisms rel. to morphology (*Japanese*) 4-103687  
 ice crystal, vapour growth kinetics, morphology, review 4-60867

**crystal morphology continued**

- ice crystals, vapour grown, morphological instability, SEM obs. 4-88125  
ice single crystal, vapour growth mechanisms, morphological stability 4-60868  
ionic crystals growing from melts, morphology and kinetics 4-113370  
phase form, thermodynamics in crystals in external stress field 4-84386  
polymers, natural, liq., liq.-crystalline and crystalline phase equilibria, phase diagrams, morphology (*Russian*) 4-103913  
polyvaliolactone morphology 4-108344  
polypropylenes, isotactic quenched melts, cooling rate effect on morphology 4-108291  
quartz, twinned crystals, morphology, re-entrant corner effect 4-60935  
sapphire, dislocation dissociation, TEM studies 4-108374  
semiconductors, organometallic crystal growth, review 4-98046  
small particles, equilibrium shapes calc. 4-113378  
solution growth kinetics, comp. inhomogeneity, morphological stability, convection effects 4-65205  
zinc phthalocyanine film, charge transfer complex with piperidine, unit cell const., crystal habit 4-88425  
Ag<sub>2</sub>S, high temp. phase, equil. roughening transition 4-60877  
Al-Zn alloys, plastic deformation, precipitation and precipitate morphology 4-114548  
Al-Zr alloys, precipitation reactions 4-114545  
BaMoO<sub>4</sub> single cryst., flux evaporation growth and morphology 4-114369  
BaTiO<sub>3</sub> type oxide fluoride growth at low temp. using LiF-BaF-LiBO<sub>2</sub> mixture flux 4-99296  
Bi<sub>2</sub>Te<sub>3</sub> cryst., external shape, impurity complex effects 4-75347  
CaCO<sub>3</sub>, pentagonal etched pit morphology on cleavage faces 4-75760  
CaC<sub>2</sub>O<sub>4</sub>·H<sub>2</sub>O, whewellite, growth morphology 4-65213  
Cd:Bi, crystal growth from vapour, Bi impurities effect 4-113368  
Cd<sub>2</sub>As<sub>2</sub> crystals, growth and morphology 4-75339  
Cd<sub>2</sub>P<sub>2</sub> crystals, growth and morphology 4-75339  
Co-Co<sub>2</sub>-Gd<sub>2</sub>, off-eutectic, growth by floating zone techniques 4-99304  
Cu, epitaxial growth on Ni (100), morphology in initial stages, XPS study 4-88416  
Fe sputtered film, filamentous C growth, surface morphology effects 4-92114  
GaAs, reactive ion etching in CCl<sub>4</sub>/H<sub>2</sub> and CCl<sub>4</sub>/O<sub>2</sub>, AES, Raman spectra 4-81306  
Ge single cryst. film growth on SiO<sub>2</sub> by laterally seeded heteroepitaxy 4-93234  
KAl<sub>3</sub>(Si<sub>4</sub>)O<sub>8</sub> monoclinic feldspars, crystal growth, PBC vector analysis 4-92119  
KGd(WO<sub>4</sub>)<sub>2</sub>·Nd<sup>3+</sup>, struct., morphological and optical charact. 4-69518  
(NH<sub>4</sub>)<sub>2</sub>Cr<sub>2</sub>O<sub>7</sub> crystals grown from aqueous soln., morphology and charact. 4-103679  
NH<sub>4</sub>H<sub>2</sub>PO<sub>4</sub> crystallisation, supersaturation, soln. velocity, crystal habit and growth rate 4-114372  
NaCl, anisotropic interface diffusion and precipitation morphology 4-61088  
(NaK)Cl, melt-grown mixed single cryst., precipitation, etching study 4-61090  
Nb<sub>3</sub>Ge, CVD grown via heteroepitaxial process, growth morphology, cryst. struct., supercond. transition temp. 4-88624  
NdAl<sub>3</sub>(BO<sub>3</sub>)<sub>4</sub>, struct. and growth morphology 4-108297  
Ni-Al-Hf system, β+(Ni,Al)<sub>2</sub>Hf<sub>2</sub> eutectic struct., cryst. morphology, struct., stacking faults, TEM, X-ray diff. obs. 4-81182  
NiAl on Ni, coatings struct. and morphology 4-70605  
PbTe cryst., external shape, impurity complex effects 4-75347  
Rb<sub>2</sub>ZnBr<sub>4</sub>, modulated-cell parameters, morphological determ. 4-92122  
Si, solar-grade, growth by Zn reduction of SiCl<sub>4</sub>, morphology 4-66199  
Si:B microcrystalline films, crystallinity, morphology and elec. cond. 4-108749  
Si:C layers, CVD growth, microstruct. and resist. 4-70599  
Te(OH)<sub>2</sub>·2NH<sub>4</sub>H<sub>2</sub>PO<sub>4</sub>·(NH<sub>4</sub>)<sub>2</sub>HPO<sub>4</sub>, single cryst. growth and morphology 4-61821  
UPt<sub>3</sub> whiskers, unusual form. and morphology, screw dislocation growth mechanism 4-98496  
YIG, seed and unseeded, growth from high temp. solns., studied by growth striations 4-76656  
Zn-Ge eutectic alloy, (100) textured Ge crystallites, morphology 4-76783  
Zn<sub>3</sub>P<sub>2</sub> crystals, growth and morphology 4-75339  
Zn<sub>3</sub>P<sub>2</sub> single crystals grown by recrystallisation, morphological and structural properties 4-113369

**crystal orientation**

- alkali halide crystals, etch pit studies of dislocations, dissolution kinetics and impurity effects 4-70158  
anthracene cryst., fluoresce. excitation and absorpt. spectra relationship for photon energies up to 10 eV 4-84988  
α-brass, single crystal, oriented for easy glide, multiple and cross slip in stress gradient 4-80047  
eggshell calcite crystals, domestic fowl, preferred orientation development 4-105173  
electrodeposits, struct., X-ray diff. and Mossbauer studies 4-104102  
electrooptic spatial light modulators, theoretical resolution limitations, effects of crystallographic orientation 4-87441  
FCC [111] traces, Euler angles, grain orientation (*Korean*) 4-79969  
FCC crystal containing mech. twin lamellae, shear band formation 4-70263  
FCC crystals, annealing texture development by multiple twinning 4-98113  
ice I, III, IV, V and VI, orientational correlation tensor 4-98053  
ice surfaces, epitaxial freezing of supercooled droplets 4-98052  
pentaerythritol tetratrate explosive, shock initiation sensitivity, cryst. orientation effect 4-70272  
quartz, hydrothermally weakened, plasticity and rheology 4-92286  
quartz doubly rotated crystals, angle of cut meas. using automated X-ray orientation system 4-58814  
SEM stage for crystal orientation and struct. determ. 4-108253  
steel, Ni-Mo-Si, 300M, occurrence of blocky martensite 4-114582  
succinic acid, β-α polymorphic transform, polarisation thermomicroscopy, X-ray anal. 4-84387  
texture anal. 4-92381  
unit cell parameter refinement from two-circle diffractometer meas. 4-108251  
Al single crystal, cutting mechanism rel. to orientation, slip theory 4-80144  
α-Al<sub>2</sub>O<sub>3</sub> growth from transition Al<sub>2</sub>O<sub>3</sub> matrix 4-84380  
Ca<sub>3</sub>Ga<sub>2</sub>Ge<sub>2</sub>O<sub>12</sub>, garnet single crystals, microhardness, brittle fracture 4-65337

**crystal orientation continued**

- CdTe epitaxial films, OMCD grown on sapphire, growth rates, mobilities, X-ray diff. 4-80444  
Co-Cr ion beam sputter deposition, mag. props., temp. effects 4-104469  
Co-Cr-Mo alloy, nucleation of recrystn. 4-114570  
Cu, cold rolled, 50%, orientation depend. of stored energy of cold work 4-99404  
Cu, cyclic deformation of single crystals, oriented for double slip 4-98174  
Cu, plastic flow and dynamic recrystallisation in single crystals 4-66394  
Cu-Zn-Al single crystals, second martensitic transform., stress-induced 4-81195  
Cu<sub>2</sub>MnAl single crystals, Heusler alloy, compression, 77-367K, fracture slip, superlattice dislocation dissociation 4-66369  
(Fe, Co, V) single crystals, flow stress, temp. and orientation depend. 4-71699  
Fe, cold-rolled and recrystallised, metallographic methods for studying crystallographic orientation 4-114576  
Fe, work hardening charact., plastic behaviour depend. on temp., strain rate, cryst. orientation 4-99418  
Fe-Mn-Si (19, 1.2 wt.%), stretched, anomaly of α/γ orientation ratio (*Russian*) 4-93289  
Fe-Ni-Cr-C, butterfly martensite, TEM study 4-108363  
Fe-P (0.1 wt.%), single crystals, deform. behaviour, effect of orientation and temp. 4-71702  
Fe-P-Ti (0.1, 0.16 wt.%) 4-71702  
Fe-Si (3.5 wt.%), single crystals, high strain rate deform. and positron annihilation 4-99434  
Gd<sub>3</sub>Ga<sub>2</sub>O<sub>7</sub>, garnet single crystals, microhardness, brittle fracture 4-65337  
LiNbO<sub>3</sub>:Ti, impurity diffusion as a function of stoichiometry 4-80304  
Mo sheet, MgO- and CaO-doped, secondary recrystn. kinetics 4-71668  
Nb surface, UV laser-activated oxidation 4-99810  
Ni, electron axial channelling radiation spectra 4-75583  
Ni, grain boundaries, Σ distrib. in polycryst. prep. by strain annealing 4-108377  
Ni-base superalloy, single cryst., creep-fatigue behaviour, effect of orientation 4-109512  
NiO-CaO eutectic, directionally solidified, crystallography 4-113658  
PbO layers, microscopic appearance, preferred orientation, and platelet thickness, X-ray diff. and SEM obs. (*Chinese*) 4-88411  
Pt-Al single crystal, plastic flow, temp. range from liq. He to 1080K 4-76798  
Si single cryst., dislocation etching, orientation depend. 4-113454  
Si-C layers, CVD growth, microstruct. and resist. 4-70599  
Si:P<sup>+</sup>, implanted, dislocation struct. development, effect of cryst. orientation, TEM obs. 4-80040  
Sn single cryst., penetration depth anisotropy, temp. variation 4-76072  
TiNi single crystals, shape memory alloys, deform. behavior 4-76819  
W, dislocation struct. after rolling, TEM obs. 4-99440
- crystal oscillators** *see* **crystal resonators**
- crystal properties**  
*see also* **crystal chemistry**  
No entries
- crystal purification**  
*see also* **zone refining**  
quartz, seed treatment effect on dislocations 4-61827  
semiconductors, heterogeneous anisotropic, electrodiffusion purification 4-71533  
Ge:Cu, impurity contamination reduction by heat treatments above 700°C 4-71535  
Zr, purification by electrotransport processing, resist. ratio obs. 4-85126  
ZrO<sub>2</sub>, electrotransport purification, contamination and cold ends effects 4-61819
- crystal resonant gamma-ray interactions** *see* **Mossbauer effect**
- crystal resonators**  
*see also* **piezoelectric oscillations**  
double mode resonators, acoustic coupling in thickness twist mode 4-97222  
Lamb wave transducer using piezoelec. resonator 4-97260  
mass meas. appl., temp. and stresses changes effects 4-111106  
quartz, cultured, random elec. twinning, non-destructive obs., resonator appl. 4-70170  
quartz crystal microbalance for thin film thickness monitoring 4-95378  
quartz crystals, radiation induced transient acoustic loss 4-70279  
quartz crystals as mechanical sensors for force meas. 4-95407  
quartz fifth-overtone resonators, 5 MHz, Q capability 4-61626  
quartz plates, lateral field excitation 4-99035  
quartz trapped energy resonators, AT- and SC-cut, transient thermally induced freq. excursions 4-61628  
SAW filters, general diff. anal. 4-97184  
SAW finite amplitude waves, resonators, convolvers and correlators, appl. 4-74792  
very low temperature design (*Japanese*) 4-58860  
vibration amplitudes meas., using speckle effect 4-70542  
H<sub>2</sub> maser frequency standards, limitations due to receiver noise 4-96854  
Li<sub>2</sub>B<sub>4</sub>O<sub>7</sub>, bulk acoustic wave props., SAW appls. 4-70280
- crystal structure**  
*see also* **crystal atomic structure**; **crystal microstructure**; **crystal morphology**; **crystal orientation**; **crystal symmetry**; **crystallography**; **granular structure**; **polymorphism**  
modulated structures in a homogeneous field, phenomenological theory 4-88118  
periodic ground states, one dimension, Lennard-Jones-type potentials 4-95336  
phosphate group interactions, cryst. refined H-bond pots. 4-60879  
solid state chemistry, correlation between struct. and phys. props. 4-70063  
solid state chemistry, struct. aspects 4-70062
- crystal surface and interface vibrations**  
acetylene, chemisorption on Pt black, vibr. modes, neutron inelastic scatt. study 4-71970  
acoustic high-energy phonon lifetime calcs. 4-104051  
adsorbed layers on metal surfaces, survey of vibr. spectroscopic methods 4-104065  
adsorbed molecules, vibrational properties 4-80413  
adsorption on solid surfaces, vibrational, electronic and struct. props., book 4-78067  
atom dynamics of cryst. surfaces, cluster-Bethe lattice method investig. 4-84502

## crystal surface and interface vibrations continued

- atomic row with correlated thermal vibr., surface backscattering yield 4-81075  
benzoic acid monolayers adsorbed on Al oxide inelastic electron tunnelling spectra studies 4-75782  
bilayer systems, p-polarised guided wave phonon-polaritons and guided wave surface phonon-polaritons 4-92629  
4,4'-bipyridine, on Ag electrodes, redox behaviour, Raman and cyclic voltammetry study 4-75778  
Brillouin scatt. at interfaces, long-wavelength acoustic phonons 4-80951  
chemisorbed molecules, vibr. spectroscopy by IR emission 4-98439  
diamond, ballistic phonon imaging 4-88387  
dielectric crystals, anisotropic effects in spectra of surface polaritons and phonons 4-108699  
diffuse surface scatt. of thermal phonons 4-65540  
ethane monolayers adsorbed on graphite (0001) surfaces, collective excitations 4-104061  
ethylene, chemisorption on Pt black, vibr. modes, neutron inelastic scatt. study 4-71970  
FCC solid surfaces, memory function parameterisation in generalized Langevin eqn.-ghost atom function 4-92493  
ferroelectric materials, surface modes 4-61632  
ferroelectrics, surface modes, dispersion curves and soft mode temp., Ising model anal. 4-65538  
formic acid monolayers adsorbed on Al oxide inelastic electron tunnelling spectra studies 4-75782  
graphite with surface adsorbed ethylene, surface diffusional and vibr. motion study 4-104078  
ideal interfaces, phonon transitions, reciprocity theorem with acoustic mismatch model 4-65539  
inelastic scatt. of heteropolar rotor, effect of initial rot. distrib. and surface softness 4-109298  
interface dynamics, conf., Lille, France (Sept. 1983) 4-78030  
ionic crystals, surface dynamics, surface Green function matching method 4-108700  
IR laser photoacoustic spectroscopy for surface studies 4-86490  
isotropic interface, TE-surface polaritons 4-75869  
metal surface, laser induced electron-phonon processes 4-75873  
metals, FCC, surface vibr. modes at high Miller index surfaces 4-92507  
metals, thermal desorption, phonon and electron-hole pair excitations 4-88401  
metals, vibrations of adsorbed atoms and molecules 4-113778  
mismatched overlayers, collective modes and dislocation ordering, mol. dynamics study 4-108555  
mixed valence compounds, vibrations of adsorbed atoms and molecules 4-113778  
molecular vibrations at surfaces, spectral studies, review 4-87098  
phonon focusing maximum, asymptotic depend. 4-104063  
phonon modes, light scatt. obs. 4-80361  
phonon spectroscopy, recent developments 4-61200  
phonons at crystal interfaces, elasticity theory (French) 4-80362  
piezoelectric transducer, vibration and acoustic radiation, finite element method-equivalent circuit anal. 4-60241  
plasmons, props. and appls. (French) 4-80360  
polar crystals, semi-infinite, polarons and their dead layers 4-70681  
polar double heterostructures, interface optic phonons and magnetophonon effects 4-98739  
polaritons, props. and appls. (French) 4-80360  
polaritons, transient CARS 4-92630  
rhodamine-590 physisorbed thin films, surface photoacoustic wave spectra 4-104693  
sapphire, phonon reflection imaging study 4-80367  
solid surface/<sup>4</sup>He system, Kapitza resistance, spectral depend. between 0.5 and 2.3K 4-65512  
solid/solid interfaces, thermal phonons, critical cone channelling 4-65541  
spatially dispersive medium, reson. Brillouin scatt. 4-80953  
superlattices, surface vibrations and dispersion theory 4-80365  
surface desorption, light induced, threshold laser intensity 4-81481  
thin films, light scatt. by acoustic surface phonons, asymmetric lineshape 4-80954  
Ag (001), inelastic He scatt. and surface phonons 4-99257  
Ag (001) with adsorbed Cl, inelastic He scatt. and surface phonons 4-99257  
Ag (110), adsorbed layers, vibr. props., He atom scatt. 4-65570  
Ag (111), phonon inelastic scatt. from He atom impact 4-98426  
Ag (111) and (100), surface at. vibrs., phonon dispersion, interatomic forces 4-92506  
Ag, soft surface vibr. of fine particles 4-61201  
Al-Al<sub>2</sub>O<sub>3</sub>-metal junctions, thermally shorted, point contact spectroscopy 4-80687  
 $\alpha$ -Al<sub>2</sub>O<sub>3</sub> (0001), high resolution EELS meas., surface phonons 4-99247  
Au (111) and (100), surface at. vibrs., phonon dispersion, interatomic forces 4-92506  
Au, soft surface vibr. of fine particles 4-61201  
Au/Ni, superlattices, dynamical props., computer simulations 4-113777  
CO adsorbate vibrs., Stark effect 4-98453  
CO adsorbed on K recovered Ru (001), EELS scatt. profiles of vibr. overtones and double losses 4-109287  
CO chemisorbed layer on Ni (100), vibr. spectroscopy by IR emission 4-98439  
Cd<sub>3</sub>Mg<sub>1-x</sub>(NO<sub>3</sub>)<sub>2</sub>·<sup>3</sup>He-<sup>4</sup>He liquid boundary, thermal resistance study 4-84484  
Cu (100), long-range electron-phonon coupling at metal surfaces, EELS meas. 4-80647  
Cu (111), chemisorbed acetylene, vibr. props., EELS studies 4-65567  
Cu, soft surface vibr. of fine particles 4-61201  
Ga<sub>1-x</sub>Al<sub>x</sub>As superlattices, acoustic modes, Brillouin and Raman scatt. study 4-80928  
GaAs, Raman scatt. study of phonon-surface polaritons 4-80931  
GaAs-Ag, high resolution EELS study 4-99248  
GaAs-Al<sub>x</sub>Ga<sub>1-x</sub>As superlattices, Raman probing of phonons and interfaces 4-80927  
GaAs-AlGaAs superlattice and interface, acoustic props. 4-80366  
GaInAs/InP(AlInAs) heterojunctions and superlattices, 2-D magnetophonon resonance 4-98740  
GaP powders, surface phonons, Raman scatt. 4-109193  
GaP, Raman scatt. by surface EM waves 4-80930  
GaP, Raman scatt. study of phonon-surface polaritons 4-80931  
GaSb(110) surface atomic geometry and dynamics 4-70537  
GaSe, phonon inelastic scatt. from He atom impact 4-98426  
GaSe, Raman scatt. study of phonon-surface polaritons 4-80931

## crystal surface and interface vibrations continued

- He phonon induced desorption, thermodynamic and perturbation theory anal. 4-65577  
<sup>4</sup>He, solid-liq. interface, phonon, transmission and Kapitza resist. 4-70501  
<sup>4</sup>He, solid-liquid interface, sound transmission 4-70502  
In<sub>0.5</sub>Ga<sub>0.5</sub>As-GaAs strained-layer superlattices, phonon frequencies, Raman scatt. meas. 4-99121  
InP (100), optical surface phonons obs. using high res. electron energy loss spectroscopy 4-70546  
n-InSb film, amplification of total reflection mode surface phonons 4-70547  
KI-K collod interface, Raman scatt., Rayleigh line broadening 4-80925  
LiF (001), inelastic He scatt., eikonal approx., surface dynamics 4-108700  
LiNbO<sub>3</sub>-ZnO piezoelectric interface, Stoneley wave propagation 4-104059  
LiTaO<sub>3</sub>-ZnO piezoelectric interface, Stoneley wave propagation 4-104059  
MgO (001), IR optical const., EELS meas. 4-71337  
MgO (100), surface dislocation, secondary electron emission study 4-80345  
NO adsorbed on Pt (111) vibr. excitation and deexcitation rates 4-98443  
NaClO<sub>3</sub>, radiative surface phonon-polariton dispersion, ATR studies 4-80514  
NaF (001), inelastic He scatt., eikonal approx., surface dynamics 4-109300  
NaF, phonon inelastic scatt. from He atom impact 4-98426  
Na<sub>2</sub>WO<sub>4</sub>, surface phonon features in high-resolution EELS 4-93158  
Nb, phonon singularities in I-V curves, point contact spectroscopy 4-71000  
Ni (100), adsorbed CO, stretching vibr., IR emission spectroscopy study 4-92508  
Ni (100), clean and O-covered, surface vibr. dispersion, EELS study 4-109288  
Ni (100), clean and with adsorbed O, surface vibr. dispersion curves, EELS study 4-80363  
Ni (100), long-range electron-phonon coupling at metal surfaces, EELS meas. 4-80647  
Ni (100), N<sub>2</sub> adsorption, thermodynamic meas. 4-92563  
Ni (100), p(2×2) adsorbed O<sub>2</sub>, vibrational props., cluster anal. 4-113809  
Ni (100), S-covered, adsorption of CO, vibr. spectroscopy study 4-10872  
Ni (100) surface with adsorbed O, surface phonons, EELS study 4-104086  
Ni (110), H<sub>2</sub>(D<sub>2</sub>) adsorption, EELS study 4-65564  
Ni (111), chemisorbed acetylene, vibr. props., EELS studies 4-65567  
Ni (111) and (100), surface at. vibrs., phonon dispersion, interatomic forces 4-92506  
Ni surface quantum motion of chemisorbed H<sub>2</sub> 4-80385  
Ni, surface vibr. modes at high Miller index surfaces 4-92507  
Pb, soft surface vibr. of fine particles 4-61201  
Pd (111), chemisorbed acetylene, vibr. props., EELS studies 4-65567  
Pt (111), H<sub>2</sub> adsorption, vibr. props., EELS and inelastic neutron scatt. studies 4-113806  
Rh, field evaporation, bonding distance and vibr. freq. determ. 4-93202  
Si (001), reconstructed, surface phonon spectrum calcs. 4-104062  
Si (100) 2×1, pre-exposed to O in submonolayer range, chem. shifts of Si-H stretching freqs. 4-80368  
Si (100)2×1, H adsorp., coverage and temperature-dependent vibr. spectra, EELS and LEED studies 4-80408  
Si (100)(2×1), chemisorbed H<sub>2</sub>O and D<sub>2</sub>O, multiple vibr. excitations, high resolution EELS study 4-109289  
Si (111), (2×1) to (7×7) to (1×1) phase transitions, rel. to defect-phonon interactions 4-108686  
Si (111), benzene bound state vibr. modes and chemisorption bonds 4-108714  
Si (111), surface phonons and surface reconstruction 4-80364  
Si (111), surface phonons and reconstruction 4-92509  
Si (111) (7×7), NO adsorption and reactions, EELS, LEED and AES studies 4-65562  
Si, laser-annealed surface, Kapitza resist. at liq. <sup>4</sup>He interface 4-70500  
Si on sapphire, phonon boundary scatt. at interface 4-104050  
Si surface, excess carriers, light-induced recombination 4-76005  
Si:H (100)(2×1), surface IR studies 4-99116  
TiC, ion surface scatt. near 180° scatt. angle, thermal vibrs. effect, two-atom scatt. model 4-81072  
TiN (001), anomalies in surface-phonon dispersion 4-75771  
W (100), adsorption of H, surface reconstruction, symm. effects, refl. EELS study 4-80382  
W (110), adsorbed O<sub>2</sub>, vibrational modes, EELS study 4-80402  
WO<sub>3</sub>, surface phonon features in high-resolution EELS 4-93158  
ZnTe, surface phonon polaritons, Raman intense increase on rough surfaces 4-98427

## crystal symmetry

- see also crystallography; group theory  
alkali cyanides, symmetry reduction in phase transitions 4-92344  
alkali metal phosphates, A'B'PO<sub>4</sub>, A=Na, K, B=Ca, Zn, Sr, Cd, Ba, Pb, ferroelec., phys. props. 4-65992  
anharmonic temperature factors of atoms with 4 mm and  $\bar{4}2m$  site symmetries 4-113377  
apatite, hexagonality to cubicity transition 4-60891  
apatially loaded crystals in n-fold symmetry, first and second order anal. 4-88233  
benzene chromium tricarbonyl, substituted derivatives, mol. stackings, struct. relationships (French) 4-75428  
beryl, hexagonality to cubicity transition 4-60891  
bicrystal symm. var. due to relative displacements of components, analytical method 4-75794  
bicrystals, symmetry determ. using convergent beam electron diff. 4-80431  
composite symmetry formed by two identical point groups with common origin 4-75342  
convergent beam diff., lattice parameter and cryst. symmetry appls. (French) 4-88041  
cubic point configs., geometrical classification 4-79968  
equilibrium crystal shape, interfacial phase diagrams, transitions, review 4-60876  
ferroelectric perovskites, phase transition influence on oscillation spectrum 4-76362  
ferroelectricity and crystal symmetry 4-65955

## crystal symmetry continued

- four-dimensional crystal classes, Hermann-Mauguin type notation 4-98050
- framework silicate zeolites, cryst. struct., 4-1 chain and 2D nets 4-92121
- freezing, density wave theory with crystal symmetry 4-70350
- graphite, hexagonality to cubicity transition 4-60891
- hypercubic cryst. systems, point symm. of holohedries in four-dimensional space 4-98049
- improper magnetostructural phase transitions, symmetry breaking 4-65810
- incommensurate crystal phases, superspace groups and representations 4-113376
- incommensurate crystals, symmetry, 4-dimensional superspace approach 4-75346
- incommensurate phases, structural anal. group theory 4-98051
- incommensurate structure, irreducible representations of space groups and superspace symmetry 4-75345
- incommensurate structures superspace symmetry and Landau theory 4-103689
- linear electro-optic effect, crystallographic aspects 4-80905
- magnesium bis(hydrogen maleate)hexahydrate, cryst. struct., X-ray diffr. studies 4-113427
- one-phase seminvariants of first rank, algebraic conditions 4-92120
- perovskite ferroelectrics, existence of ferroelectric phases of different symmetries 4-114221
- physical properties, symmetry description 4-63451
- point groups of four-dimensional Euclidean space, geometric symbols (French) 4-103688
- point-symmetry operations in four-, five- and six-dimensional spaces 4-98048
- quartz,  $\alpha$  and  $\beta$  forms, struct. anal. based on Coulomb repulsion forces 4-98074
- space group symbols, symmetry operation derivation, SYMOP computer program 4-108301
- space group symm., international tables for crystallography, book 4-58583
- two-coloured point and rod groups containing 8- or 12-fold symm. axes 4-75343
- Au (111), electronic band struct., photoemission spectra determ., cryst. symm. effect 4-84549
- $\text{Ca}_2\text{Sr}_8\text{Al}_2\text{O}_{24}(\text{WO}_4)_2$ , phase transition characts., role of cage cation substitution 4-65386
- $\text{CsH}_2\text{PO}_4$ , normal and deuterated, ferroelec. phase transition, Raman studies 4-71295
- $\text{CsNO}_3$ , phase II, cryst. struct. and polymorphic transitions 4-113409
- Cu ternary sulphides and selenides, symmetry and dislocations, electron microscopy studies 4-95580
- $\text{CuInSe}_2$ , sphalerite-chalcopyrite order-disorder transitions, group theory anal. 4-84383
- Life phengite, mica, cryst. struct. of di-trioctahedral 1M polymorphic modification, electron diffr. study 4-60894
- $\text{Mo}(\text{CO})_6$ , cryst. struct. and bond lengths, X-ray diffr. studies 4-92184
- $\text{Na}_{1-x}\text{Hf}_x\text{Si}_2\text{P}_3\text{O}_{13}$ ,  $\text{Na}^+$  ion cond. and crystallographic cell characterisation 4-113706
- $(\text{Nd}_2\text{Ca}_2)\text{Ti}_6\text{O}_{20}$ , ferroelec. cpd., perovskite-derived, crystal growth and characterisation 4-76657
- $\text{RbNO}_3$ , phase IV, cryst. struct. and polymorphic transitions 4-113409
- Ti thin foil, cryst. symmetry, convergent beam electron diffr. studies 4-80456

crystal vacancies *see vacancies (crystal)*crystal whiskers *see whiskers (crystal)*crystalline-amorphous transformations *see amorphisation*

## crystallisation

- see also crystal growth; dendrites; heat of crystallisation; nucleation*
- amorphous alloys, crystallisation, activation energies from elec. resist. meas., review 4-108285
- amorphous alloys, crystn., effect of irrad. particle mass 4-79936
- amorphous film, rapid crystallisations, dynamics, nonlinear heat conduction model 4-103686
- atomic system, quenched condensation, computer simulation 4-75295
- batch crystallisation process, optimisation via Legendre polynomials 4-88122
- binary alloy, dil., plane crystallisation front stability 4-98044
- bisphenol-A polycarbonate 4-108292
- calcium oxalate monohydrate, crystallisation kinetics 4-103684
- carbohydrates, thermal props. heat flow calorimetric obs. 4-78312
- chalcogenide glasses, electron microscopy of reactions with metals and electron beam induced crystn. 4-80315
- cholesterol crystallisation in bile, dislocation growth mechanism 4-89491
- copolyester of lactic and glycolic acid, strain induced crystallisation, optical and X-ray scatt. obs. 4-85186
- crystal grown from melt with variable crystallisation rate, impurity distrib. 4-75492
- crystal growth from melt, rapid solidification, computer simulation 4-114383
- Czochralski technique, growth programming optimal control 4-99298
- diamond, natural, metastable autotaxial crystallisation 4-70592
- diamond, vacancy formation energy, crystallisation studies 4-108354
- ethylene propylene diene terpolymers, elastomeric networks, crystallisation, stress optical coeffs., DSC, X-ray obs. 4-92105
- glass, laser induced crystallisation kinetics, Raman scatt. studies 4-108288
- glass, thermodynamics of grain boundary crystallisation 4-75314
- glass forming substances, defects and glass formation 4-75299
- glass-forming metallic melts, undercooled, free energy approx. 4-70414
- glass/alumina composites, density, crystallisation, elec. cond. 4-113937
- glasses, crystn. and props., prep. from Illinois coal fly ash 4-79940
- glycerol, normal and metastable supercooling liq., fluctuating voltage spectrum, crystn. process 4-92991
- growth from melt, impurity distribution and inclusions (Russian) 4-113483
- n-hexatriacontane, melt crystn. in temp. gradient 4-65376
- hydroxysodalite, crystallisation, high resol. NMR chem. shift 4-114174
- ice, amorphous, nonexistent glass transition 4-88098
- isobutylamine monohydrate, vibr. spectroscopy 4-104611
- Lennard-Jones, supercooled liquid homogeneous nucleation, periodic boundary conditions, computer simulation 4-98247
- liquid crystal, cholesteryl nonanoate, spherulite growth rate, effect of press. 4-92356
- liquid crystals, cholesteric, blue phase, morphological studies, growth of three-dimens. liq. single cryst. 4-60819

## crystallisation continued

- melt, one-component, self-modelling crystallisation front instability 4-103683
- metallic glasses, optimised domain pattern by heat treatment and surface crystallisation 4-76160
- N-methylcarbazole/naphthalene transparent glass, microcryst. formation and triplet-triplet energy transfer (German) 4-75297
- model polyisobutylene networks, strain induced crystallisation 4-75324
- PET, crystallisation, struct. and props. 4-103666
- PET films, uniaxially drawn, crystallisation kinetics, DSC obs. 4-92103
- PET yarn, oriented, deform., melting-recrystallisation mechanism, SAXS using synchrotron radiation 4-71691
- phthalein films, amorphous vacuum deposited, crystn. and optical props. 4-71565
- poly(vinylidene fluoride), crystallisation and melting, head-to-head defect effects 4-98027
- poly- $\epsilon$ -caprolactone-polyvinylmethylether-polystyrene, phase diagram and crystal growth behaviour obs. (Japanese) 4-103665
- poly-p-xylylene, synthesis, epitaxial growth 4-88428
- polyester yarn, spin-oriented, differential scanning calorimetry, obs. 4-79952
- polyester yarn, spun and drawn, differential scanning calorimetric obs. 4-79953
- polyethylene, branched, isothermal crystallisation kinetics 4-60862
- polyethylene, cryst., growth kinetics and lateral. growth habits 4-88123
- polyethylene, crystallisation at high supercooling, fold length, habit 4-84212
- polyethylene, crystallisation theory, twin morphology importance 4-113350
- polyethylene, electron irrad., melting and crystallisation, calorimetric study (Russian) 4-84223
- polyethylene, high press. extended chain crystallisation kinetics, NMR obs. 4-65191
- polyethylene, non-isothermal crystallisation kinetics 4-60863
- polyethylene films, melt-drawn, microstruct., TEM and X-ray diffr. study 4-92102
- polyethylene fractions, crystallization and melting behavior 4-84139
- polyethylene oxide-PMMA blends, crystallisation, microstruct., phase separation, IR spectra, calorimetry 4-92107
- polyethylene terephthalate, chemical nucleation applied to crystallisation 4-108292
- cis-polyisoprene, equilb. melting temp. 4-61058
- polymer conformation and morphology, small angle neutron scatt., review 4-92110
- polymer melts, crystallisation layer growth on cold surface 4-79950
- polymer rheo-optics, conf., Seattle, WA, USA (Mar. 1983) 4-82590
- polymers, piezoelectric, pyroelec. and ferroelec. props., conf., Honolulu, USA (July 1983) 4-95030
- polyolefins, semicrystalline,  $^1\text{H}$  NMR spectra, spin-lattice relax. rel. to morphology 4-65877
- polypropylene, crystallization, effect of talc on nucleation 4-79966
- polypropylene, isotactic, isothermal crystallisation from melt 4-113580
- polypropylene, isotactic  $\alpha$  form, crystalline order, melting behaviour 4-84211
- polypropylene, non-isothermal crystallisation kinetics 4-60863
- polypropylene, reversible secondary crystallisation during cooling, UV microscopy obs. 4-113374
- polypropylene-polyethylene blends, polypropylene spherulite morphology and growth rate changes 4-65193
- polyurethane elastomer, MDI/diol-based, hard-segment polymorphism 4-65195
- polyvinylidene fluoride, reversible pyroelectricity in melting and crystn. regions 4-88775
- polyvinylidene fluoride film, piezoelectric and ferroelectric props. under shock wave action 4-109131
- polyvinylidene fluoride-PMMA blends, melting pt., crystalline morphology, light scatt. obs. 4-84217
- quasibinary semiconductor solns. component distrib. calcs. 4-108585
- rare earth alloys,  $\text{R}_2\text{Cu}_{23}$ , high pressure crystn. 4-75369
- semiconductors, molten, cluster-type struct. defects, review 4-60806
- silica ceramics, thermal diffusivity, effect of crystn. of grain boundary phase 4-88355
- trans 1,4-polyisoprene, crystallisation from solution, melting endotherm, heat of fusion, density 4-75315
- Wigner cryst., two-dimensional, on He film, static and dynamical props. 4-98549
- $\text{Al}_2\text{O}_3$  fibres, polycryst., prod. 4-71618
- $\text{Al}_2\text{O}_3$  films on Au, Al, and Si, vibr. props., IR refl. absorpt. spectroscopy study 4-71459
- $\text{Al}_2\text{O}_3\text{-Fe}_2\text{O}_3\text{-MnO-SiO}_2$  glass, crystallisation and mag. props. 4-65188
- $\text{Al}_2\text{O}_3\text{-SiO}_2$  fibres, cristobalite form. at elevated temp. (German, English) 4-81197
- $\text{As}_2\text{Se}_3$ , crystallisation kinetics and viscosity 4-75298
- $\text{BaF}_2\text{-LaF}_3\text{-ZrF}_4\text{-AlF}_3$  glass, crystallisation, devitrification on reheating 4-84194
- $\text{BaO-Li}_2\text{O-Nb}_2\text{O}_5$ , phase equilibria in crystn. region, tetragonal phase 4-114495
- $\text{BaO-SiO}_2$  glasses, cryst. nucleation kinetics, effect of amorphous phase separation 4-65185
- $\text{BaO-VO}_2\text{-PO}_2\text{s}$ , semiconductor glass, crystallisation rel. to composition, temp. and duration of heat treatment 4-92096
- $\text{BaTiO}_3$  thin films, crystallisation from amorphous phase, electron microscope study 4-113830
- $\text{CaCO}_3$  crystallisation with chem. absorpt. 4-98038
- $\text{CaO-Al}_2\text{O}_3\text{-P}_2\text{O}_5\text{-SiO}_2\text{-Na}_2\text{O-K}_2\text{O}$  system glasses, opacification and crystn. 4-89021
- $\text{CdGeAs}_2$  glass crystallisation, thermal anal., activation energy determ. 4-84187
- $\text{CdGe}_{1-x}\text{Si}_x\text{As}_2$  glasses, elec. props. and phase stability 4-104202
- Co based amorphous ribbon, as-cast, crystn. and heat treatment effect (Chinese) 4-84190
- Co-based metallic glasses, low magnetostriction, crystallisation composition depend. 4-84196
- Co-P amorphous layers, mag. and struct. props. 4-76199
- Co-Si-B (-Fe) metallic glasses, mag. props., annealing effects 4-109039
- Co-W-Mn thin mag. film: deposition, electrocrystallisation (Russian) 4-65592
- $\text{Co}_2\text{B}_{21}$ , liq.-quenched amorphous, dynamic temp. crystn. 4-60835
- $\text{Co}_{40}\text{Si}_{18}\text{Fe}_2\text{B}_{25}$ , amorphous alloy, crystn. study using DTA and elec. resist. meas. 4-65181
- $\text{Cu}_{60}\text{Ti}_{40}$ , amorphous, crystallisation, quenching method effects 4-84185

## crystallisation continued

- $\text{Cu}_{40}\text{Zr}_{60}$  alloy system, amorphous, crystallisation kinetics 4-108279  
 $\text{Eu}_2\text{O}_3$ , hydrothermal synthesis and cryst. struct. 4-60900  
 Fe base amorphous ribbon, as-cast, crystn. and heat treatment effect (Chinese) 4-84190  
 Fe, cast, obtained a superhigh quenching rates, struct. investig., 20 to  $1150^\circ\text{C}$  4-93286  
 Fe, electronic struct., XPS studies 4-75838  
 Fe-B amorphous alloys, cryst., and press., elec. resist. study 4-60837  
 Fe-B metallic glass, transition elements effect on thermal stability, crystn. activation energy 4-108283  
 Fe-base metallic glasses, thermal embrittlement model 4-89098  
 Fe-Cr-Co-Si-B amorphous alloys, mag. props. and hyperfine interactions (Russian) 4-108994  
 Fe-Hf based amorphous alloys, crystallisation and hyperfine fields 4-71030  
 Fe-Ho-B, metallic glass, mag. props. and crystallisation 4-84793  
 Fe-Nb-Si-B amorphous alloys, mag. props. 4-71145  
 Fe-Ni-Cr-W amorphous alloys, corrosion resist. 4-99632  
 $\text{Fe}_{1-x}\text{B}_x$  amorphous alloys, electronic struct., XPS studies 4-75838  
 $\text{Fe}_{1-x}\text{B}_x$  amorphous films, crystallisation kinetics and mag. props. 4-75807  
 $\text{Fe}_{1-x}\text{B}_x$  glass, crystallisation, elec. cond. study 4-88109  
 $\text{Fe}_2\text{B}_{12}\text{Si}_{10}$ , amorphous, isothermal crystallisation and mag. props. (Russian) 4-65384  
 $\text{Fe}_2\text{B}_{12}\text{Si}_8$ ,  $\text{Al}_2$ , crystallisation and mag. props. study 4-114137  
 $\text{Fe}_8\text{B}_{13}\text{Si}_5\text{C}_2$  glass, primary crystallisation and  $\alpha$ -Fe dendrites, EELS studies 4-84202  
 $\text{Fe}_7\text{Co}_{18}\text{Si}_{14}$ , metallic glass, crystn. kinetics 4-65187  
 $\text{Fe}_{78}\text{Mo}_{20}$ , metallic glass, elec. resist., crystallisation and thermoelec. power, annealing effects 4-108831  
 $\text{Fe}_{40}\text{Ni}_{40}\text{B}_{20}$  metallic glass, amorphous-cryst. transition kinetics, elec. resist. meas. 4-70039  
 $\text{Fe}_{40}\text{Ni}_{40}\text{B}_6$  foil, amorphous-cryst. transition, elec. resist. variations 4-65182  
 $\text{Fe}_{40}\text{Ni}_{38}\text{Mo}_2\text{B}_{18}$ , metallic glass, elec. resist., crystallisation and thermoelec. power, annealing effects 4-108831  
 $\text{Fe}_{39}\text{Ni}_{39}\text{Mo}_2\text{Si}_6\text{B}_{12}$  metallic glass, mag. props., Mossbauer studies 4-109012  
 $\text{Fe}_{39}\text{Ni}_{39}\text{Mo}_2\text{Si}_6\text{B}_{12}$ , metallic glass, elec. resist., crystallisation and thermoelec. power, annealing effects 4-108831  
 $\text{Fe}_{40}\text{Ni}_{40}\text{P}_{14}\text{B}_6$  amorphous ribbons, mag. props. and struct., influence of laser annealing 4-88663  
 $\text{Fe}_{40}\text{Ni}_{40}\text{P}_{14}\text{B}_6$  glass transition of thin film on substrate 4-92367  
 $\text{Fe}_{40}\text{Ni}_{40}\text{P}_{14}\text{B}_6$ , proton irradi., crystallisation study 4-88099  
 $\text{Fe}_{1-x}\text{O}_x$  oxidation and reduction influences on grain morphology 4-93436  
 $\text{Fe}_{88-x}\text{Si}_x\text{B}_{12}$  amorphous alloy, crystallisation behaviour 4-75309  
 $(\text{Fe}_{1-x}\text{V}_x)_{84}\text{B}_{16}$  amorphous alloys, mag. and elec. props. (Chinese) 4-114094  
 $\text{Fe}_{90}\text{Zr}_{10}$  amorphous alloy, struct. and mech. props. rel. to heat treatment 4-75305  
 GaAs crystallisation by nonequilibrium electroliq. epitaxy, molten soln. parameter determ. 4-75817  
 $\text{Ga}_2\text{O}_3$ -CaO glass, form. density, refr. index, crystn. temp., hardness, IR spectra 4-113635  
 $(\text{GaSb})_{1-x}(\text{Ge}_2)_{2x}$  semicond. alloys, phase transforms. 4-92347  
 Gd-Fe amorphous alloy films, crystallisation and ferromag. reson. behaviour 4-71189  
 Gd-Fe evaporated films, crystn. behaviour 4-80445  
 $\text{Gd}_2\text{Co}$ , crystn., cryst. struct. and mag. props. in microgravity 4-98915  
 $(\text{Gd}_{0.2}\text{Tb}_{0.8})_3\text{Co}$ , crystn., cryst. struct. and mag. props. in microgravity 4-98915  
 Ge amorphous film, laser enhanced crystallisation, nucleation, growth velocity, recombination enhanced diffusion 4-65295  
 Ge single cryst. film growth on  $\text{SiO}_2$  by laterally seeded heteroepitaxy 4-93234  
 \*He, equilibrium crystallisation, interface problem 4-108670  
 \*He liquid-solid interface, evidence for new quantum state, crystallisation waves 4-70520  
 In photoionic laser epitaxy, purity and nucleation conditions of cryst. films 4-76694  
 $\text{In}_{1-x}\text{Ga}_x\text{P}_{1-x}\text{As}_x$ , solid solution, LPE, crystn. and optical props. 4-108736  
 $\text{KMg}_2\text{Si}_2\text{AlO}_6\text{F}_2\text{BaO}_3\text{Mg}_2\text{Si}_3\text{AlO}_{10}\text{F}_2$  system, solid solns., lattice const., melting temp. 4-109384  
 $\text{KMnO}_4$  thermostability var. during crystn. in elec. field 4-70047  
 $\text{K}_2\text{YF}_6$ , cryst. struct., X-ray anal. 4-60898  
 $\text{Li}_2\text{O-Nb}_2\text{O}_5$  amorphous dielectrics, crystallisation, elastic and dielec. props. 4-104518  
 $\text{Li}_2\text{O-SiO}_2$  glass and glass-ceramic, hydrothermal corrosion 4-85235  
 $\text{Li}_2\text{O-SiO}_2$  glass ceramic systems, density, crystallisation, elec. cond. 4-113937  
 Mg alloys, structure and physicochemical props. different methods of Stepanov crystallisation effect 4-99297  
 Mg-Si-O-N glass, crystallisation and microstruct. 4-75313  
 $\text{Mg}(\text{OH})_2$ , periodic crystallisation in agar-agar gel., temp. depend. 4-66621  
 $\text{Mg}_{0.7}\text{Zn}_{0.3-x}\text{Ga}_x$  simple metallic glasses, electronic props. 4-75920  
 $\text{MnO}_{1+x}$  oxidation and reduction influences on grain morphology 4-93436  
 $\text{Mo}_2\text{Ge}_{1-x}(\text{Si}_{1-x})_x$  amorphous sputtered films, supercond. transition temp. (Chinese) 4-98794  
 $\text{NH}_4\text{Cl-NaCl-NH}_4\text{HCO}_3\text{-NaHCO}_3\text{-H}_2\text{O}$  ( $-(\text{NH}_4)_2\text{CO}_3\text{-Na}_2\text{CO}_3\text{-H}_2\text{O}$ ) systems, phase diagrams 4-104773  
 $\text{NH}_4\text{H}_2\text{PO}_4$  crystallisation, supersaturation, soln. velocity, crystal habit and growth rate 4-114372  
 $\text{NH}_4\text{H}_2\text{PO}_4$ , oriented crystallisation, electron-microscope study 4-65202  
 Na, martensitic nucleation and growth, mol. dynamics simulation studies 4-114520  
 $\text{NaNbO}_3$ , bladed crystallisation in  $\text{Na}_2\text{O-Nb}_2\text{O}_5\text{-B}_2\text{O}_3$  system 4-61061  
 $\text{Na}_2\text{O-B}_2\text{O}_3\text{-Al}_2\text{O}_3$ , aluminoborate glass, cond. max. 4-113702  
 $\text{Na}_2\text{O-B}_2\text{O}_3\text{-Al}_2\text{O}_3\text{-SiO}_2$  transparent glazes, with enhanced chem. and thermal shock-resist. 4-81305  
 $\text{Na}_2\text{O-BaO-SiO}_2$  glass system, glass transition temp. and devitrification behaviour 4-98285  
 $\text{NaOH-ZrO}_2\text{-SiO}_2\text{-H}_2\text{O}$  system, struct. of mineral analogues and synthetic phases 4-79997  
 $\text{Na}_2\text{WO}_3$  bronzes, rapidly quenched, DTA and X-ray diff. study 4-93277  
 Ni alloys, directional crystn. and grain boundary diffusion (Russian) 4-108643

## crystallisation continued

- Ni-based amorphous alloys, crystallisation processes, microstruct. anal. 4-84183  
 Ni-P amorphous, hexagonal metastable phase formed during crystallisation (Chinese) 4-103698  
 Ni-P amorphous alloys, crystn. phases, electron diff. study (Chinese) 4-113331  
 Ni-Si-B, amorphous, cryst. form. on annealing, TEM study 4-75304  
 NiTi memory alloy, aging-induced precipitations, neutron diff. study 4-89055  
 $\text{NiZr}_2$  glasses, quenched, phase separation and supercond. props. 4-60839  
 $\text{Ni}_3\text{Zr}_{16}$ , proton irradi., crystallisation study 4-88099  
 4-octyloxy-4'-cyanobiphenyl, liq. crysts., crystallisation kinetics, Raman spectrosc. obs. 4-88846  
 Os-Sn, intermediate phases, effects of high pressure on crystn. 4-75366  
 $\text{PbF}_2\text{-ZnF}_2$  system, amorphous phase form. by roller splat cooling 4-85122  
 $\text{PbO-BaO-TiO}_2\text{-B}_2\text{O}_3$  glass ceramic system, crystal clamping, X-ray diff., dilatometry 4-109386  
 $\text{Pd}_{36}\text{Au}_{54}\text{Si}_{18}$  amorphous alloy, crystn., SAXS study 4-65186  
 $\text{Pd}_{0.83-x}\text{Co}_{0.17}$  metallic glasses, form., crystallisation and elec. props. 4-92685  
 $\text{Pd}_{0.83-x}\text{Fe}_{0.17}$  metallic glasses, form., crystallisation and elec. props. 4-92685  
 $(\text{Pd}_{100-x}\text{Ni}_x)_{83}\text{Si}_{17}$  amorphous material, isothermal crystallisation study 4-113336  
 $\text{Pd}_{0.83-x}\text{Ni}_{0.17}$  metallic glasses, form., crystallisation and elec. props. 4-92685  
 Rh-Si amorphous alloy film, form. and crystallisation 4-108750  
 Sb, amorphous film, vacuum-deposited, isochronous annealing, crystallisation 4-61854  
 Sb amorphous films, obliquely vacuum deposited, growth and crystn. 4-98491  
 $\text{Sb}_2\text{S}_3$  amorphous thin films, struct. and crystn. 4-60842  
 $\text{Sb}_2\text{Te}_3\text{-Bi}_2\text{Te}_3\text{-Bi}_2\text{Se}_3\text{-Se-Te}$ , physicochemical equilibria and crystallisation 4-61053  
 $\text{Sb}_2\text{Te}_3\text{-Bi}_2\text{Te}_3\text{-Te}$ , physicochemical equilibria and crystallisation 4-61053  
 a-Se, condensates, kinetics of crystallisation 4-109327  
 Se, epitaxial crystallisation on linear polyphenyls 4-65590  
 a-Se:Bi films, crystallisation, dark cond. and activation energy 4-88104  
 Si, amorphous, ion implanted, crystn. growth velocities, charged dangling bonds 4-88093  
 Si amorphous film, laser enhanced crystallisation, nucleation, growth velocity, recombination enhanced diffusion 4-65295  
 Si, CVD growth, solid state phase transformations 4-70598  
 a-Si film, epitaxial crystallisation on GaP substrate 4-80452  
 Si films, UHV deposited, crystn. temp. 4-88410  
 Si growth of insulating  $\text{SiO}_2$  films by oxidation 4-98485  
 Si, ion implanted, explosive liq. phase crystallisation by double pulse laser irradi. 4-84188  
 Si, ion implanted, pyrometric temp. meas. during laser annealing 4-70203  
 Si monocrystalline island growth on insulating substrates 4-76670  
 Si, noncrystalline, explosive crystallisation 4-98019  
 a-Si, pulsed laser irradiation, melting temp. and explosive crystallisation 4-88201  
 a-Si, solid phase epitaxy, bond rearrangement process, quantitative anal. 4-84534  
 a-Si, vacuum deposited, solid-phase epitaxial growth anisotropy 4-75811  
 Si(BiAs), low resistance ion implanted films 4-108398  
 Si:H, Al-covered, solid-state reaction between film and substrate 4-92498  
 Si/ $\text{SiO}_2$  interface, amorphous Si/cryst. Si facet form. during solid phase epitaxy 4-88423  
 $\text{Si}_3\text{N}_4$  amorphous, controlled crystn. by Ti and Cl additions 4-113334  
 $\text{Si}_{1-x}\text{Sn}_x$  amorphous, vapour deposited, struct., resist. characts., density, electron diff. meas. 4-61424  
 Sn-Ge-Pb, nonequilibrium crystn., rel. to cooling rate 4-61054  
 Te-Ge-Pb(Sn) alloys, glass stability, cryst. struct. effect 4-60836  
 $\text{Te}_{64}\text{Ni}_{36}\text{Cu}_{64}\text{Si}_{36}$  amorphous alloy, TTT-curve construction 4-93287  
 Ti alloys, rapid solidification by melt spinning technique, alloy additives selection 4-89034  
 Ti-Fe-Ni, sintering processes, Ni effect 4-61889  
 Ti-Ni amorphous alloys, thermal stability, short-range order effects 4-88096  
 $\text{Ti}_{62}\text{Cu}_{12}\text{Ni}_{23}\text{Si}_3$ , amorphous, X-ray diff. pattern prepeak, temp. depend. 4-79942  
 $\text{Ti}_{62}\text{Cu}_{12}\text{Ni}_{23}\text{Si}_3$ , amorphous, X-ray diff. pattern prepeak, temp. depend. 4-79942  
 $\text{Ti}_{80}\text{Si}_{20}$  amorphous, crystallisation study (Chinese) 4-103922  
 $\text{U-Al-O}_2$  synthesis by precipitation of hydroxides 4-76652  
 $\text{V}_2\text{O}_5\text{-B}_2\text{O}_3$  glasses, struct. study, IR spectra anal. 4-84961  
 $\text{V}_2\text{O}_5\text{-P}_2\text{O}_5$  glass, synthesis and course of crystn. 4-81178  
 $\text{V}_2\text{O}_5\text{-P}_2\text{O}_5$  glasses, crystallisation study 4-65183  
 $\text{V}_2\text{O}_5\text{-As}_2\text{O}_5$  glasses, IR study 4-104614  
 $\text{WO}_3$  anodic films, electrochromic, TEM, RHEED and Raman studies 4-99114  
 $\text{WO}_3\cdot x(\text{H}_2\text{O})$  films, influence of crystallisation as hydration 4-88424  
 YAG refractories, heat transfer during growth 4-76664  
 YIG containing magnetic glass-ceramics, prep. using colloidal Bi as nucleation catalyst, characts. 4-71628  
 Zr-Ba-La-Al-F glass, crystn. kinetics 4-70037  
 Zr-Ni cryst. and amorphous alloys, enthalpies of form. and crystallisation 4-88097  
 Zr-Ni(Co) amorphous alloys, crystallisation, DSC and elec. resist. studies (Chinese) 4-103658  
 $\text{ZrF}_4\text{-BaF}_2$ -based fluorozirconate glasses, crystallisation, X-ray diff., and DSC studies 4-84197  
 $\text{ZrO}_2$  powders, hydrothermal prep. 4-109359  
 $\text{ZrO}_2$ , short-range struct., radial distrib. curve of atomic density 4-75801  
 $\text{ZrO}_2\text{-Al}_2\text{O}_3\text{-SiO}_2\text{-CaO}$  system, compatibility relations, microscopy, energy dispersive X-ray exam. 4-61925

## crystallite texture see texture

## crystallites

## see also crystal microstructure

- t-butyl bromide, dielec. permitt. meas., crit. comparison with incoherent quasielastic neutron scatt. results 4-88761  
 t-butyl chloride, dielec. permitt. meas., crit. comparison with incoherent quasielastic neutron scatt. results 4-88761  
 t-butyl cyanide, dielec. permitt. meas., crit. comparison with incoherent quasielastic neutron scatt. results 4-88761

## crystallites continued

- dye oriented film, laser marking process based on microcrystallite photo-thermal transform., 4-107773  
 expansion during appearance of stresses in thin films 4-98479  
 ferromagnet, cubic single-domain crystallites, skew-symmetric stresses 4-76228  
 glass, laser induced crystallisation kinetics, Raman scatt. studies 4-108288  
 glycine, radiothermoluminesc., ESR investig. 4-61758  
 lattice distortion and crystallite size calcs. 4-84226  
 nanocrystalline structure, proposed new material struct. (German) 4-70045  
 plastic deformation, in situ TEM obs. method 4-62148  
 PMMA:Si ion implanted film, struct. anal. using differential etching 4-79951  
 poly(vinylidene fluoride) films,  $\alpha$ - $\beta$  phase transition, crystallite orientation effects 4-98262  
 polycapromide, oriented, amorphous-crystalline, loaded, mol. dynamics investig. (Russian) 4-103676  
 polycrystalline specimens, multiple-beam diffr. of fast electrons, calc. of reflected intensities 4-113273  
 polyethylene, oriented, amorphous-crystalline, loaded, mol. dynamics investig. (Russian) 4-103676  
 polyethylene, oriented, linear, crystallite distrib. function, X-ray diffr. investig. (Russian) 4-60864  
 semiconductor crystallites, electron-electron and electron-hole interactions, size depend. of excited electronic state 4-70660  
 semiconductor polycrystalline thin films, with pot. barriers, Hall mobility 4-104331  
 surface phenomena, rel. to props. of materials 4-98416  
 AgBr, evap. layers, Rh ions influence on photographic parameters (German) 4-71954  
 Al<sub>2</sub>O<sub>3</sub>, shock-modified powders, X-ray line-broadening 4-113539  
 Au films, growth on Ni as function of substrate temp., AES study (French) 4-65581  
 BaF<sub>2</sub>-LaF<sub>3</sub>-ZrF<sub>4</sub>-AlF<sub>3</sub> glass, crystallisation, devitrification on reheating 4-84194  
 BaTiO<sub>3</sub>, semicond. glass ceramics, oxidation, barrier layer form. 4-114699  
 C films, as-deposited and annealed, disorder and crystallite form., Raman scatt. study 4-61254  
 C films, diamondlike, ionized deposition from methane gas 4-65586  
 CdS, colloidal crystallites, excited electronic states, size effects, optical props., Raman spectra 4-71334  
 Fe fine particles, prep. from goethite microcrysts., morphology and mag. props. 4-65835  
 Fe<sub>3</sub>Fe<sub>0.6</sub>Sn<sub>0.4</sub>N<sub>0.7</sub>C<sub>0.3</sub> ferromag. material for 'magnetic' recording 4-104464  
 $\beta$ -FeOOH, thermal decomposition into hematite, struct. props. 4-109636  
 KCl crystallites, graphoeptaxial alignment in presence of water vapour 4-92571  
 KCl powders, coloration stability, particle size depend. 4-60921  
 LiF, cold-worked, microstrains, X-ray diffr. lines anal. (French) 4-79892  
 Nb<sub>3</sub>Ge superconducting films, bias sputtered, film growth process 4-98804  
 Ni crystallites, distributed, vacuum deposition on SnO<sub>2</sub> island nucleation sites 4-88432  
 Ni-based amorphous alloys, crystallisation processes, microstruct. anal. 4-84183  
 Pb-acid battery active mass, microstruct. model anal. 4-105103  
 $\beta$ -PbO<sub>2</sub>, struct. parameters and Pb-acid battery failure 4-103718  
 Sb amorphous films, obliquely vacuum deposited, growth and crystn. 4-98491  
 Si:B microcrystalline films, crystallinity, morphology and elec. cond. 4-108749  
 Si:C layers, CVD growth, microstruct. and resist. 4-70599  
 TiO<sub>2</sub>, shock-modified powders, X-ray line-broadening 4-113539  
 W-Fe, dil. segregation of Fe to grain boundaries, elec. resist., thermo-power, AES meas. 4-103943  
 Zn-Ge eutectic alloy, (100) textured Ge crystallites, morphology 4-76783  
 ZnO crystallite growth during annealing, morphological anal. 4-61902  
 ZnTe polycryst. films, resonant light scatt. spectra 4-99207  
 ZrF<sub>4</sub>-BaF<sub>2</sub>-based fluorozirconate glasses, crystallisation, X-ray diffr. and DSC studies 4-84197  
 ZrN powder, prep. from ZrCl<sub>4</sub>-N<sub>2</sub> system using reducing agents (Japanese) 4-76720  
 ZrO<sub>2</sub> gels, pure and MgO-doped, decomposed in vacuo, neutron and X-ray diffr. study 4-61900

## crystallographic shear

- FCC crystal containing mech. twin lamellae, shear band formation-4-70263  
 pyrochlore families, force fields., vibr. spectra and cryst. defects 4-98055  
 steel, bainitic, shape memory and structural inheritance effects. (Russian) 4-109400  
 Al single crystal, cutting mechanism rel. to orientation, slip theory 4-80144  
 Bi<sub>2</sub>(Mo<sub>2</sub>Nb<sub>2</sub>)O<sub>6-y/2</sub>, struct. props., high resolution electron microscope studies 4-84271  
 Bi<sub>2</sub>(W<sub>2</sub>Nb<sub>2</sub>)O<sub>6-y/2</sub>, struct. props., high resolution electron microscope studies 4-84271  
 Fe-Ni alloys, Ni redistribution by diffusion precipitation. (Russian) 4-104785  
 MgCu<sub>2</sub> family, shear homeotypism 4-98118  
 SnO<sub>2</sub>, mechanical activation, defect formation 4-75456  
 Ta<sub>2</sub>O<sub>5</sub>-WO<sub>3</sub>(Nb<sub>2</sub>O<sub>5</sub>-WO<sub>3</sub>), TEM study of microstruts. 4-113655  
 TiO<sub>2</sub>, mechanical activation, defect formation 4-75456  
 TiO<sub>2</sub>, rutile, crystallographic shear phase, high-resolution electron microscopy study of disorder 4-84303  
 TiO<sub>2</sub>:V<sub>2</sub>O<sub>3</sub>, crystallographic shear phase, high-resolution electron microscopy study of disorder 4-84303  
 TiO<sub>2</sub>:V<sup>4+</sup>, extended defects, EPR and TEM study 4-75457  
 TiO<sub>2-x</sub>, interaction of small and extended defects 4-75443  
 WO<sub>3</sub>, mechanical activation, defect formation 4-75456  
 WO<sub>3</sub>, nonstoichiometric, point defect to shear plane evolution 4-92202  
 WO<sub>3-x</sub>, interaction of small and extended defects 4-75443

## crystallography

- see also crystal atomic structure; electron diffraction crystallography; gamma-ray diffraction; isomorphism; lattice constants; neutron diffraction crystallography; space groups; X-ray crystallography  
 apo-D-glyceraldehyde 3-phosphate dehydrogenase, struct. refinement, appl. of mol. symm. constraints to CORELS 4-100063  
 Debye diffr. scatt. by crystals with thin twins 4-113466  
 direct methods of cryst. struct., solution, conf. Trapani, Italy (April 1984) 4-101571  
 electron density, electrostatic field characts., machine graphics methods 4-84123  
 finite cryst. diffr., general Laue-Bragg case, comparison with approximate extinction theories 4-75230  
 geometrical method for charact. nature of puckering in pyrrolidine and furanose rings 4-65151  
 history of crystallography in North America 4-67951  
 hypercubic cryst. systems, point symm. of holohedries in four-dimensional space 4-98049  
 LUCH-77 program system, random direct methods, least-squares refinement of starting sets of phases 4-113260  
 LUCH-77 program system, random direct methods, use of tangent formula 4-113261  
 macromolecular struct. determ., ROCKS crystallographic program system, VAX adaptation 4-81613  
 molecular cryst. struct., translation problem solving by fragmentary-implicational method, appl. to chromene 4-113263  
 particle characterisation by polarised light microscopy, crossed polars case 4-66532  
 Patterson synthesis, probabilistic coeffs., anomalous scatterers, determ. of positions 4-75231  
 phase transformations in solids, Crete, Greece (June-July 1983) 4-110811  
 photomicrography procedures using colour reversal film emulsions 4-63795  
 point-symmetry operations in four-, five- and six-dimensional spaces 4-98048  
 ROCKS system of computer programs for macromolecular crystallography 4-81612  
 single crystals, degree of perfection, gamma-ray and neutron diffr. methods 4-65155  
 solvent contrast var. expts., scaling and phase-difference determ. 4-60779  
 texture, computer simulation of pole figures 4-66512  
 three dimensional disordered systems, theory of power spectrum and scatt. props. 4-75244  
 Si-SiO<sub>2</sub> interface structure, oxidation of singular and vicinal surfaces of Si 4-104317
- crystals**  
 see also bicrystals; crystal structure; crystallography; dendrites; epitaxial layers; liquid crystals; plastic crystals; whiskers (crystal)  
 No entries
- Curie point** see Curie temperature; ferroelectric Curie temperature
- Curie point writing** see thermomagnetic recording
- Curie temperature**  
 see also ferroelectric Curie temperature  
<sup>1</sup>H NMR and mag. susceptibility 4-71202  
 amorphicity, heterogeneity, and the Arrott plots 4-71065  
 amorphous ribbon, simultaneous magnetic meas. and torsional creep 4-111163  
 Bethe lattice, statistical mech. 4-76151  
 FCC lattice, Curie temp., specific heat, single band Hubbard model high temp. series 4-84764  
 ferromagnetic materials, phase transitions, 2nd order near Curie point 4-98890  
 Heisenberg ferromagnet, amorphous, short-range order and mag. props. 4-76157  
 Heisenberg planar ferromag., biquadratic interactions 4-88641  
 Hubbard model, magnetic and Mott transitions 4-88673  
 intermediate valence systems, ferromagnetism stability 4-71061  
 magnetisable fluid flow at temps. close to Curie point 4-87810  
 methylammonium aluminum alum, dielectric props. meas. 4-76312  
 NpAsTe, mag. props. (French) 4-84766  
 rare earth alloys, R<sub>3</sub>Rh<sub>2</sub>, R-Gd, Tb, Dy, Ho, Er, mag. props. meas. 4-61521  
 rare earth alloys, RCo<sub>2</sub>, R= rare earth metals, paramagnetic props. calcs. 4-61508  
 rare earth compounds, pressure effect on Curie temp. 4-114108  
 rare earth intermetallics, RFe<sub>2</sub>H<sub>2</sub> (R=Gd, Ho, Er, Tm, Lu), mag. props. and cryst. struct., absorbed H<sub>2</sub> effects (Russian) 4-104458  
 rare earth-transition metal alloys, magnetic cooling near Curie temperatures above 300K 4-88677  
 singlet-triplet paramagnet, Curie point vicinity, mode-mode coupling effects 4-98854  
 spinel ferrites Curie point, O param. effect 4-84798  
 transition metal compounds, pressure effect on Curie temp. 4-114108  
 transition metals, magnetism and electronic struct., validity of simple alloy model 4-98865  
 BaFe<sub>2</sub>O<sub>7</sub> glassy ferrites, effects of mag. quenching 4-61898  
 BaTiO<sub>3</sub>, PILC ceramic, strength and fracture toughness 4-62051  
 Bi oxides, silicene phase form. mag., EPR and IR studies 4-88137  
 Bi<sub>2</sub>Fe<sub>2</sub>O<sub>7</sub>, amorphous, mag., optical and resonant props. 4-104424  
 CdCr<sub>2</sub>Se<sub>4</sub>In, static I-V characts. 4-70815  
 CeF<sub>3</sub>, magnetic susceptibility and Verdet const. 4-61507  
 Ce<sub>1-x</sub>Hf<sub>x</sub>Co<sub>2</sub>, anomalous mag. behaviour 4-88664  
 Ce<sub>2</sub>La<sub>1-x</sub>Al<sub>2</sub>, dense Kondo state, elec. resist., mag. susceptibility meas. 4-108984  
 CeM<sub>2</sub>B<sub>2</sub> (M=Co, Ru, Rh, Ir), mixed valence, mag. and elec. props. 4-113905  
 Co<sub>1-x</sub>Zr<sub>x</sub>Co<sub>2</sub>, anomalous mag. behaviour 4-88664  
 Co<sub>2</sub>, electronic struct., magnetism and Curie temps. 4-75843  
 Co-Si-B (-Fe) metallic glasses, mag. props., annealing effects 4-109039  
 Co<sub>2</sub>Ni<sub>1-x</sub>Mn<sub>x</sub>Co<sub>2</sub>, magnetic transforms., effect of external press. 4-104418  
 Co<sub>8</sub>Si<sub>8</sub>Fe<sub>2</sub>B<sub>2</sub>, amorphous alloy, crystn. study using DTA and elec. resist. meas. 4-65181  
 CrBr<sub>3</sub>, optical spectra near mag. transition temp. 4-61729  
 Cr<sub>2</sub>Mn<sub>1-x</sub>As, thermal and mag. props. 100 to 500K 4-92922  
 Cr<sub>2</sub>O<sub>3</sub>, ferromag., Curie point transition, EPR obs. 4-109061  
 Cu<sub>2</sub>(O<sub>2</sub>)-(2B<sub>2</sub>O<sub>3</sub>.Li<sub>2</sub>O)<sub>1-x</sub> glass, EPR and mag. susceptibility meas. 4-61587  
 DyCu<sub>2</sub>Ge<sub>2</sub>, mag. and cryst. struct., neutron diffr. studies 4-65794  
 Dy<sub>2</sub>(Fe<sub>1-x</sub>Al<sub>x</sub>)<sub>17</sub>, pseudobinary intermetallic cpd., mag. props. 4-71032

## Curie temperature continued

- Eu,  $\text{Sr}_{1-x}\text{S}$  ferromagnetic epitaxial layers, magnetooptic studies (*German*) 4-76441
- Fe, electronic struct., exchange splitting, spin- and angle-resolved photoemission spectra 4-38944
- Fe, electronic struct., magnetism and Curie temps. 4-75843
- Fe-Al (48 at%), mag. props. rel. to heat treatment 4-109003
- Fe-Cr-B, metallic glass, mag. props. and density 4-84773
- Fe-Cr-Co-Si-B amorphous alloys, mag. props. and hyperfine-interactions (*Russian*) 4-108994
- Fe-graphite system, carbide form. high press. and temp., mag. props. 4-99371
- Fe-Ho-B, metallic glass, mag. props. and crystallisation 4-84793
- Fe-Nb-Si-B amorphous alloys, mag. props. 4-71145
- Fe-Ni Elinvar alloys, dispersion-hardened, mag. and physical props. (*Russian*) 4-104800
- Fe-Ni-P-B amorphous alloys, mag. props., proton implantation effects 4-104416
- Fe-W-B, metallic glass, mag. props. and density 4-84773
- Fe-Zr amorphous films, elec. and mag. props. 4-75923
- $\text{Fe}_3\text{B}_{13}\text{Si}_3\text{C}_2$ , Metglas 3605SC, mag. and hyperfine interactions 4-71223
- $\text{FeCo}_{1-x}\text{Cr}_x\text{S}_2$ , magnetisation and Curie point meas. 4-104461
- $\text{FeCo}(\text{Mn})(\text{V})$ , coupling between chemical and mag. interactions, NMR study 4-114173
- $\text{Fe}_2\text{Co}_5\text{Ni}_{20-x}\text{Cr}_x\text{B}_4\text{Si}_3$  metallic glass, mag. props. study 4-84790
- $(\text{Fe}_{100-x}\text{Co}_x)_{76}\text{Pr}_{16}\text{O}_8$ , thermal effects of Co moderate substitutions 4-71124
- $(\text{Fe}_{1-x}\text{Co}_x)_{90}\text{Zr}_{10}$  amorphous alloy, elec. resist. minima and mag. props. 4-75922
- $(\text{Fe}_2\text{Cr}_{100-x})\text{B}_y$  metallic glasses, onset of magnetism, Mossbauer spectra 4-71217
- $\text{Fe}_2\text{Ge}_2\text{O}_5$ , mixed valent, prep., struct., mag. props. (*French*) 4-88148
- $\text{Fe}_{80}\text{Mn}_{17}\text{B}_3$  based glassy alloys, ferromag. exchange and Curie temp. 4-76129
- $\text{Fe}_2\text{Mg}_{1-x}\text{Cl}_2$  phase diagram, mag. susceptibility meas. 4-61535
- $\epsilon\text{-Fe}_2\text{N}$ , ( $x=2-3$ ), mag. props., Mossbauer obs. 4-61611
- FeNi, neutron irradiation effect on mag. props. 4-92907
- FeNi: (Si, Cr, Mo), neutron irradiation effect on mag. props. 4-92907
- $\text{Fe}_{66}\text{Ni}_{34}$ , Curie point at ultrahigh press. 4-88676
- $(\text{Fe}_{80}\text{Ni}_{20})_{1-x}\text{B}_x$  amorphous alloys, mag. moments, temp. variation 4-76122
- $\text{Fe}_2\text{Ni}_5\text{B}_{10}\text{Si}_{10}$  metallic glass, Curie point relax. study 4-84791
- $\text{Fe}_2\text{Ni}_{80-x}\text{B}_{10}\text{Si}_{10}$  metallic glasses, absolute thermolec. power meas. 4-92701
- FeNiCrMoBSi amorphous ribbons, magnetostriction, capacitance studies 4-61580
- $(\text{Fe}_{1-x}\text{Ni}_x)_2\text{Ge}$ , magnetisation, Curie temp., mag. moments, X-ray diffraction studies 4-98862
- $(\text{Fe}_{1-x}\text{Ni}_x)_2\text{Ge}$ , magnetisation, Curie temp., mag. moments, X-ray diffraction studies 4-98862
- $(\text{Fe}_2\text{Ni}_{1-x})\text{M}$ ,  $\text{M}=\text{P}, \text{B}, \text{Si}$  or  $\text{Al}$ , metallic glass, Mossbauer study of high press. 4-84880
- $\text{Fe}_{39}\text{Ni}_{59}\text{Mo}_2\text{Si}_8\text{B}_{12}$  metallic glass, mag. props., Mossbauer studies 4-109012
- $\text{Fe}_{23}\text{Ni}_5\text{Si}_{10}\text{B}_{10}$  metallic glass, Curie temp. press. depend. 4-84792
- $(\text{Fe}_{1-x}\text{Ni}_x)_{90}\text{Zr}_{10}$  amorphous alloy, elec. resist. minima and mag. props. 4-75922
- $\gamma\text{-Fe}_2\text{O}_3$  (maghemite), stability to change to  $\alpha$ -phase for heating up to  $600^\circ\text{C}$  4-100539
- $(\text{Fe}_2\text{O}_3)_x(\text{B}_2\text{O}_3\text{PbO})_{1-x}$  glass, mag. props. study 4-88654
- $\text{FePCr}(\text{Cr})$ , structural and mag. coherence lengths 4-88100
- $\text{Fe}_2\text{P}_{1-x}\text{Si}_x$ , hexagonal-orthorhombic transition, Mossbauer studies 4-109102
- $\text{Fe}_2\text{Si}_{90-x}\text{B}_{10}$  metallic glasses, mag. props., chem. composition depend. 4-76135
- $(\text{Fe}_{1-x}\text{V}_x)_{84}\text{B}_{16}$  amorphous alloys, mag. and elec. props. (*Chinese*) 4-114094
- $\text{Ga}_2\text{O}_3\text{Mo}_2\text{Si}_2$  spinel, cryst. struct., mag. props., temp. depend. 4-2-300K 4-114110
- $\text{GaMo}_4\text{X}_2$  chalcogenides, electron-phonon contrib. to Stoner enhancement 4-84803
- Gd, positron lifetime near ferromag. transition temp. 4-93127
- Gd-Pd, effect of  $\text{H}_2$  absorpt. on mag. and cryst. props. 4-104412
- $\text{Gd}_{1-x}\text{La}_x\text{Al}_2$ , loss of ferromagnetism 4-98885
- $\text{Gd}_{1-x}\text{Th}_x\text{Al}_2$ , loss of ferromagnetism 4-98885
- $\text{Gd}_{1-x}\text{U}_x\text{Al}_2$ , loss of ferromagnetism 4-98885
- $\text{Ge}_2\text{Fe}_{3-x}\text{O}_4$ , mixed valent, prep., struct., mag. props. (*French*) 4-88148
- $\text{Hg}_{1-x}\text{Ag}_x\text{Cr}_2\text{Se}_4$  mag. semicond., exchange interaction, carrier effects 4-114103
- $\text{HgCr}_2\text{Se}_4$ , ferromagnetic semicond., elec. cond., photocond. meas., temp. depend. 4-61375
- $\text{KD}_2\text{PO}_4$ , photon emission during uniaxial deform., Curie temp. 4-81028
- $\text{KH}_2\text{PO}_4$ , photon emission during uniaxial deform., Curie temp. 4-81028
- $\text{Li}_{0.5-2/3}\text{Zn}_{2/3}\text{Fe}_{2.5-2/3}\text{O}_4$  ferrites, Curie temp. and mag. moments 4-109013
- $\text{Mn}_{12}\text{Al}_8\text{-xFe}_x$ , thermal expansion, atomic order effects (*Russian*) 4-103971
- $\text{Mn}_{90}\text{Fe}_{10}\text{P}$ , mag. phases, Mossbauer spectroscopy study 4-88753
- $\text{Mn}_2\text{Ge}_3$ , thermal expansion meas., 4.2-800K, Curie point, press. shifts 4-98320
- $\text{Mn}_2\text{Mo}_2\text{O}_8$ , crystal growth, mag. and elec. props. 4-71537
- $\text{MnRhAs}$ , antiferromagnetic-ferromagnetic transition, mag. props., elec. resist. meas. 4-104417
- MnSb, solid solns., evidence of critical Mn-Mn distance for onset of ferromagnetism 4-84780
- MnSb-based solid solns., recording media in optical memory appls. 4-61572
- Mo/Ni superlattices, magnetisation, Curie temp. and magnon spectra, Brillouin scatt. study 4-61560
- $\text{Nd}(\text{BrO}_3)_3\cdot 9\text{H}_2\text{O}$ , single cryst., mag. susceptibility, cryst. field effect and calcs. 4-71018
- $\text{NdFe}_3$ , magnetic susceptibility and Verdet const. 4-61507
- Ni, Curie point at ultrahigh press. 4-88676
- Ni, electronic struct., magnetism and Curie temps. 4-75843
- Ni, thermoelectric power and sp. ht. near Curie temp., AC method meas. 4-75934
- Ni-Cu, anomalous resistivity, 4.2 to 1100K 4-92708
- Ni-Cu, thermoelectric power and sp. ht. near Curie temp., AC method meas. 4-75934
- Ni-Ti, forced vol. magnetostriction, press. coeffs. 4-88711

## Curie temperature continued

- Ni-V, forced vol. magnetostriction, press. coeffs. 4-88711
- Ni-Al, weak itinerant ferromagnet, de Haas-van Alphen effect, Curie temp. 4-113848
- $\text{Ni}_3\text{MnGa}$ , ferromagnetic order and martensitic transformations 4-61512
- $\text{Ni}_3\text{MnIn}$  Heusler alloy, elec. resist. and magnetisation 4-92695
- $\text{Ni}_3\text{-xMnSb}$ , chemical order and mag. props. 4-88666
- $\text{Ni}_2\text{Zn}_{1-x}\text{SiF}_6\cdot 6\text{H}_2\text{O}$ , mag. interactions, paramagnetic Curie temp. studies 4-88645
- Pd-Fe, ion implanted, ferromagnetism study 4-71137
- PrAg, elec. mag. and struct. props. meas. 4-80566
- Pr $_3$ , magnetic susceptibility and Verdet const. 4-61507
- Pt-Co dilute alloys, resistance thermometers with low magnetoresistive effects 4-111132
- $\text{Pt}_3\text{FeMn}_{1-x}$ , elec. cond. and mag. props. 4-104180
- $\text{PtMnAl}$ , cryst. struct. and mag. props. 4-70082
- $\text{PtMnGa}$ , cryst. struct. and mag. props. 4-70082
- $\text{Rb}_2\text{Mn}_{1-x}\text{Cr}_x\text{Cl}_4$  mixed insulating ferromag. and antiferromag., ferromag. resonance studies 4-65863
- $\text{Se}_3\text{In}$  weak itinerant electron ferromag., negative magnetoresistance 4-75931
- Si:P, EPR study of low-temp. mag. props. 4-84854
- $\text{SrZn}_{2-x}\text{Co}_x\text{Fe}_{10}\text{O}_{27}$  hexaferrite, mag. and crystallographic studies 4-88697
- IT-Ta $\text{S}_2(\text{S}_{1/2}\text{Se}_{3/2})$ , paramagnetic susceptibility in Anderson localised states 4-65786
- $\text{Tb}_{75}\text{Gd}_{25}$ , Hall effect and elec. resist. near Curie point 4-61361
- $\text{Tb}_2\text{Si}_2$ , polycrystalline, antiferromag., Neel temp., paramag. Curie temp., mag. struct. 4-109017
- $\text{Tb}_2\text{Ir}_2\text{Si}_8$ , antiferromag., Neel temp., paramag. Curie temp. 4-109017
- $\text{Te}(\text{OH})_2\cdot 2\text{NH}_4\text{H}_2\text{PO}_4\cdot (\text{NH}_4)_2\text{HPO}_4$ , dielec., thermal and optical props. 4-61636
- $\text{TiBe}_{2-x}\text{Cu}_x$ , onset of ferromagnetism, neutron small angle scatt. study 4-84797
- $\text{TiO}_2\text{-FeNbO}_6\text{-NbO}_2$  system, rutiles, struct., mag. and electron transport props. 4-84238
- UGaCo, mag. props., temp. depend. 4-71033
- $\text{UM}_2\text{B}_2$  ( $\text{M}=\text{Co}, \text{Ru}, \text{Ir}$ ), mixed valence, mag. and elec. props. 4-113905
- $\text{UNiAlH}_3$ ,  $^1\text{H}$  NMR and mag. susceptibility 4-71202
- $\text{U}_2\text{Th}_{1-x}\text{Se}$  solid solns., mag. props. 4-104419
- Y-Fe alloys, exchange interactions, coordination props. studies 4-114104
- $\text{Y}_2\text{FeO}_{12}$  ionic structure, neutron induced transformation, calcs. 4-113415
- YIG, influence of pre-sintering on mag. props. 4-84789
- Curie-Weiss law** see magnetic susceptibility; paramagnetic properties of substances; paramagnetism
- curium**  
see also nuclei with .....  
alpha-spectrum anal., peak ratio's 4-68865  
fission reactor fuel, burnup and isotopic composition determ. in VVER-440 4-102355  
measurement in marine samples 4-105158  
simulated nuclear waste glass, Cm doped, radiation damage, annealing, short term leach test 4-83149  
 $^{248}\text{Cm}$  carcinogenic effect in rat expts. (*Russian*) 4-67008  
 $^{248}\text{Cm}$  ultra-thin  $\alpha$ -source, preparation by adsorption 4-68853
- curium compounds**  
No entries
- current (electric)** see electric current
- current algebra**  
see also elementary particle theory; hadron current; light cones; quantum field theory  
Bjorken  $x$  and  $y$  distributions in neutral and charged current  $\nu_\mu$  interactions 4-73739  
electroweak theory, introduction 4-59011  
electroweak theory, intermediate bosons, currents, CP violation 4-95736  
fermion masses in potential models of chiral symmetry breaking 4-63903  
functional integral and anomalies in theories with S, P, V and A currents 4-111343  
ground state mesons, radiative decays, covariant quark model, hadron currents 4-90883  
hadron final states in neutrino weak charged current interaction 4-90857  
hadron mass inequalities, extended form based on lattice QCD 4-95765  
lattice gauge theories, confinement props. of coset pure gauge fields of nonabelian chiral group (*Chinese*) 4-73643  
lattice QCD, chiral symmetry breaking at finite temp. 4-86650  
lattice QCD, current normalisation 4-63856  
Lie algebra over physical space 4-58990  
massless pion in modified bag model 4-59048  
MIT bag model, axial form factors, pion field 4-111408  
MIT bag model with broken chiral symmetry, massive quarks and pions 4-59049  
muon decay, right-handed currents, exptl. search 4-68571  
neutrino charged current inclusive interactions 4-90858  
open b-flavour states, hadronic couplings 4-68542  
PCAC picture of MIT bag model, symmetry breaking phenomena 4-90829  
pion decay, rel. to massive neutrinos 4-111442  
pion electroproduction, current algebra-PCAC representation, chiral  $\text{SU}(2)\times\text{SU}(2)$  symm. breaking 4-11462  
pseudoscalar mesons, nonlinear effective Lagrangian in broken  $\text{SU}(3)\times\text{SU}(3)$  4-90750  
QCD modelling with soliton bag model, nuclear matter and forces calcs. 4-63953  
QCD picture of broken chiral symmetry, neutral PCAC scheme 4-73715  
 $\text{SU}_4$  main chiral field in two dimensions, exact solns., S-matrix 4-11325  
supersymmetric  $\text{CP}_{N-1}$  model, gauge-invariant currents 4-111279  
symmetric space chiral models, infinitely many symmetry generator series, Backlund transform. 4-95702  
U(1) problem, pseudoscalar mass spectrum 4-86591  
vector indexed supercurrents in extended supersymmetry 4-86593  
B meson mixing props. and CP-violating effects, charge current couplings, QCD 4-111320  
 $F\text{-}\phi\pi$ , current algebra upper bound on decay rate 4-102117  
 $K\text{-}3\pi$ , matrix element quadratic terms, chiral Lagrangians, current-algebra analysis 4-106527  
 $\mu^+\mu^-\nu$ , PCAC and muon-electron universality 4-102264  
 $\nu_N(\bar{\nu}_N)$  charged current total cross section 4-90853  
 $\omega\text{-}3\pi$ , chiral Lagrangian, nonAbelian anomaly, vector-meson decays 4-106510

**current algebra continued**

- $\omega \rightarrow \pi^0 \gamma$ , chiral Lagrangian, nonAbelian anomaly, vector-meson decays 4-106510  
 $p \rightarrow e^+ \pi^0$ , baryon wave functions, currents uncertainties, GUTs, lifetime 4-82922  
 $\pi^+ \rightarrow \pi^0 e^+ \nu$ , conserved vector current hypothesis test for electroweak theories 4-102114  
 $\pi\pi$  scattering, low energy theorems corrections, QCD tests with current algebra 4-82940  
 $^1H(\mu, \nu)$ , PCAC and muon-electron universality 4-102264

**current control, electric** *see electric current control***current density**

- see also critical current density (superconductivity); electron density*  
 Bitter plate tokamaks, coupled EM and thermal problems, transient non-linear solns. 4-59412  
 eddy current computation with EDDYNET 4-59958  
 eddy current density, boundary-element computation in contiguous domains 4-64650  
 electric cells with porous electrochemical electrodes, potential and current density distribution study (Hungarian) 4-105098  
 electrical stimulation of living body, spatial distrib. of current density in vol. conductor model (Japanese) 4-77230  
 electrodes, intracerebral stimulating, cylindrical coordinate Laplace's eqn., numerical soln. 4-89541  
 electron tunnelling, from potential well, in electric field 4-86247  
 fine-focused electron beam profile meas. using semiconductor detector 4-87263  
 Josephson tunnel junctions, current density distrib. (German) 4-84750  
 MHD generators, diagonal, electrodynamic parameters determ. (Chinese) 4-89457  
 shell, cylindrical, eddy current problem, integral eqn. approach 4-102850  
 Sun, photosphere electric current density profile and transition region UV brightness 4-105928  
 vacuum-arc cathode spot, current density estimation 4-97902  
 Bi whiskers, longit. magnetoresist. meas. 4-88500  
 Fe, apparent H diffusivity, effect of cathodic charging current density 4-104005  
 Pb-acid batteries, with fibre reinforced Pb composites, corrosion behaviour analysis, obs. 4-72099  
 PbSnTe-PbSeTe lattice-matched DH laser diodes, threshold current density 4-112421  
 Sn single cryst., penetration depth anisotropy, temp. variation 4-76072

**current distribution**

- see also current density*  
 bipolar disc electrode with many holes, network model components 4-109668

**current fluctuations**

- see also noise*  
 Knudsen diode, surface ionisation, nonlinear self-consistent oscills. and ion vel. distrib. function 4-108225  
 Ge, compensated, thermoelec. current instability 4-61404

**current measurement, electric** *see electric current measurement***current transformers**

- see also electric current control; electric current measurement*  
 small rated secondary currents, errors determ., meas. techniques (German) 4-86444

**current transients** *see transients***currents algebra** *see current algebra***curvature measurement**

- drop, curvature parameter, theory of nucleation on charged nuclei 4-80331  
 engraved straight-edge rectilinearity checking instrument 4-63719  
 epoxy beam, residual stresses and warp generated by one-sided quench 4-71672  
 grid-reflection technique for surface curvature anal. 4-68209  
 mirrors of X-ray satellite ROSAT, manufacture and testing, roundness 4-115686  
 multiperture speckle shearing arrangements for stress analysis 4-58888  
 speckle shearing interferometer, three-aperture, slope and curvature simultaneous meas. 4-73411

**curvature of field** *see aberrations***curve fitting**

- chi-square and likelihood functions in fitting curves to histograms 4-67966  
 cubic spline techniques for curve fitting X-ray photoelectron cross sections 4-59682  
 data smoothing, matrix formulation, least-squares principle 4-102557  
 fatigue life, data fitting to Bernstein and inverse normal distributions 4-99672  
 least squares and utmost correl. methods comparison 4-67967  
 positron annihilation lifetime spectrum anal. using multiple-exponential function model (Chinese) 4-71466  
 spectroscopic curve smoothing and differentiation using spline functions 4-101819  
 strain determ. in dynamic compression test 4-112780  
 tongue shape, characterisation from US image data by numerical methods 4-100271  
 US measurement of grain size, estimation of scatterer spacing using non-linear least-squares technique 4-99726  
 wavelength dispersive spectrometer, deconvolution method for overlapping spectral peaks 4-82872  
 Al<sub>2</sub>O<sub>3</sub> anodised films, breakdown statistics 4-109128

**cutting**

- see also machine tools; machining*  
 bone cutting force, rel. to surgical instrument design 4-62503  
 BTA deep hole machining, analytical time domain evaluation of cutting forces using thin shear plane model 4-99742  
 carbide cutting tools, in-situ CVD method appl. 4-71599  
 industrial applications of high power lasers, conf., Linz, Austria (Sept. 1983) 4-101561  
 laser gas cutting, physical models and technological aspects 4-107718  
 piacryl cutting by laser beam (German) 4-112596  
 sialon metalcutting tools, props. and appl. 4-66283  
 steel, tool, high-speed 4-93437  
 Al single crystal, cutting mechanism rel. to orientation, slip theory 4-80144  
 Si<sub>3</sub>N<sub>4</sub>-based metalcutting tools, props. and appl. 4-66283

**cutting continued**

- TiC CVD coatings on cemented carbides, differences in appearance 4-71596  
 TiC coatings of cemented carbide tools by halide-activated pack cementation process, props. 4-71600

**CVD** *see chemical vapour deposition***CVD coatings**

- carbide cutting tools, in-situ CVD method appl. 4-71599  
 cavitation erosion of coated steels 4-99611  
 conference, Neuchatel, Switzerland (April 1980) 4-67868  
 fusion reactor first wall coatings, gas release under electron impact 4-91097  
 moderate temperature deposition using complex chloride reduction 4-71585  
 phosphosilicate glass film, void formation and IR absorpt. after heat treatment in H<sub>2</sub> atmosphere 4-60840  
 SOS films, material improvement process by solid phase epitaxial growth 4-81124  
 steels, tool, CVD temp. influence on transformation behaviour in martensite and bainite 4-71593  
 transition metal plasma enhanced CVD 4-88978  
 transition metal silicide films plasma enhanced CVD 4-88978  
 Al films, prep. by low press. MOCVD 4-81156  
 AlGaAs/GaAs quantum wells, photoluminescence studies 4-93105  
 Al<sub>0.5</sub>Ga<sub>0.5</sub>As, correlation of photoluminescence and deep trapping 4-80537  
 Al<sub>0.5</sub>Ga<sub>0.5</sub>As:Si MOCVD layers, transport props. 4-92834  
 Al<sub>0.5</sub>Ga<sub>0.5</sub>As:Zn, CVD deposited, luminescence study 4-80985  
 AlN, CVD films, stability, surface morphology. CVD conditions 4-70604  
 Al<sub>2</sub>O<sub>3</sub> thin film deposition by UV laser photolysis 4-99337  
 BN coatings on silica by hexachloroborazine decomposition 4-71587  
 BN film, CVD, on Si, as B diffusion source 4-98359  
 BN gate insulators, CVD growth on InP, ellipsometry, XPS, AES, cond. meas. 4-80443  
 BN:P film in InP, grown by CVD, elec. props. 4-99336  
 a-C:H, low emittance coatings for high temperature solar collectors 4-114950  
 CdS-InP heterojunctions, elec. and photoelec. props., solar cell appl. (Russian) 4-98713  
 Ga<sub>1-x</sub>Al<sub>x</sub>As-GaAs, Raman scatt. theory 4-76460  
 GaAs, lateral growth over W gratings by CVD, application to FET transistors 4-81148  
 GaAs, MOCVD grown, deep electron traps, DLTS obs. 4-84585  
 GaAs single quantum wells, low temp: exciton trapping on interface defects, photolum. 4-93111  
 GaAs:Si MOCVD films, free carrier profile synthesis by atomic plane doping 4-92221  
 GaAs/AlGaAs/GaAs heterojunction barrier, MOCVD grown, electron transport 4-80661  
 GaAs-AlAs semiconductor superlattices, MOCVD prep., interface struct. study 4-108726  
 GaAs-In<sub>0.5</sub>Al<sub>0.5</sub>As MOCVD strained-layer superlattices, lattice distortion, TEM study 4-88406  
 GaAsP strained-layer superlattice structures and their buffer layers, comparison of trapping levels 4-113885  
 Ga<sub>0.47</sub>In<sub>0.53</sub>As-InP, Raman scatt. theory 4-76460  
 InP epilayers, cathodoluminescence study 4-104678  
 InP layers, prep. by chloride-hydride reaction 4-93232  
 InP-Al<sub>2</sub>O<sub>3</sub>, MIS struct. CVD growth and elec. props. 4-80680  
 MgO film, synthesis by CVD, textural characters 4-71568  
 Mo-MoO<sub>3</sub> black CVD film, roughness effect on absorbing surface selectivity 4-76537  
 Ni-B alloys, CVD deposited, microstruct. and mech. props. 4-71581  
 NiAl on Ni, coatings struct. and morphology 4-70605  
 Re, chem. deposition from gas phase 4-114417  
 Si, amorphous CVD films, H<sub>2</sub> plasma annealing localized state density 4-61337  
 a-Si film, CVD CO<sub>2</sub> laser deposition process 4-114412  
 Si film, LPCVD, elec. props., effect of film thickness 4-88615  
 Si film plasma enhanced chemical vapour deposition 4-114423  
 a-Si films, polarisability, refr. index meas. 4-93001  
 Si, polycrystalline films, X-ray and electron diff., anal. 4-61258  
 Si, reduced pressure chemical vapour deposition 4-114422  
 a-Si:B film, optical props. study 4-76540  
 Si:B(As), low resistance ion implanted films 4-108398  
 Si:C,N, CVD thin films using di-2,2'-bipyridine silicon 4-71586  
 p-Si:H, amorphous, prepared by photo-CVD, electronic and optical props. 4-70959  
 Si:H,B amorphous CVD films, optical props., B doping effects 4-99086  
 a-Si:H,B film, optical props. study 4-76540  
 a-Si:H pin solar cells, LPCVD growth, transport props. 4-114907  
 a-Si:O,H CVD films, struct. model 4-88427  
 poly-Si:P film, CVD deposition, trench coverage characters 4-114413  
 Si:P film, deposition by thermal decomposition of silane 4-114414  
 n-Si:P polycrystalline CVD films, elec. props., grain size and impurity conc. effects 4-70963  
 SiC, epitaxial and chemical vapour growth for optoelectronic devices 4-109331  
 SiC, fusion reactor first wall material, permeation of H 4-92403  
 p-SiC:H, amorphous, prepared by photo-CVD, electronic and optical props. 4-70959  
 a-Si<sub>0.8</sub>C<sub>0.2</sub>H, amorphous, CVD prep., XPS and optical studies 4-70600  
 a-Si<sub>0.8</sub>C<sub>0.2</sub>H, low emittance coatings for high temperature solar collectors 4-114950  
 Si<sub>3</sub>N<sub>4</sub> CVD films, fault struct., TEM studies 4-108389  
 Si<sub>3</sub>N<sub>4</sub> films, amorphous, hydrogenated and deuterated, prepared from plasma-enhanced CVD, IR absorpt. spectra 4-81021  
 Si<sub>3</sub>N<sub>4</sub> MNOS structures using atmospheric press. and plasma enhanced CVD coatings 4-98760  
 Si<sub>3</sub>N<sub>4</sub> plasma-enhanced CVD films, anomalously high etch rate, optical props. 4-104108  
 Si<sub>3</sub>N<sub>4</sub>, sputtering with H<sup>+</sup> and H<sub>2</sub><sup>+</sup> ions, reactive ion beam etching 4-71497  
 Si<sub>3</sub>N<sub>4</sub> thin film deposition by UV laser photolysis 4-99337  
 Si<sub>3</sub>N<sub>4</sub> films, photo-CVD, props. study 4-99338  
 SiO<sub>2</sub> film, low temp. photochemical deposition 4-99339  
 SiO<sub>2</sub> films, chemically vapour deposited from Si<sub>3</sub>N<sub>4</sub>-O<sub>2</sub>-N<sub>2</sub> mixtures 4-76885  
 SiO<sub>2</sub> films, IR transmission spectra, nitridation effects 4-81022  
 SiO<sub>2</sub> films, photo-CVD, props. study 4-99338

## CVD coatings continued

- SiO<sub>2</sub>, low temp. CVD, etching kinetics 4-99614  
 SiO<sub>2</sub> thin film deposition by UV laser photolysis 4-99337  
 SiO<sub>2</sub>:B, low pressure CVD at quasi-high flow 4-76686  
 SiO<sub>2</sub>:Cr thin films, cathodoluminescence and C-V characts. (Russian) 4-99173  
 SiO<sub>2</sub>:P, low pressure CVD at quasi-high flow 4-76686  
 SnS thin film phase transition material, optical switching, CVD fabrication 4-112538  
 SnO<sub>2</sub>:F conducting glass film for SIS solar cells, optical props. 4-88894  
 Ta-steel, coatings microstructure 4-71802  
 TiC CVD coatings on cemented carbides, differences in appearance 4-71596  
 TiC coatings of cemented carbide tools by halide-activated pack cementation process, props. 4-71600  
 TiC, low Z films, correl. of residual stress with microstruct. 4-114695  
 TiC, low Z films, residual stress measurement by X-ray diffractometry 4-114694  
 TiC on cemented carbides, CVD layer, total C contrib. to growing layer 4-71597  
 TiC on hard metal, CVD coatings, TEM study 4-71592  
 TiC, on type 316 stainless steel, void form. near interface by diffusion annealing 4-109557  
 TiC<sub>x</sub>N<sub>1-x</sub> solid solns., theoretical CVD conditions 4-61857  
 TiN, low Z films, correl. of residual stress with microstruct. 4-114695  
 TiN, low Z films, residual stress measurement by X-ray diffractometry 4-114694  
 TiN-TiC multilayer coatings on Nb tubes, nucl. reactor fuel pin accidental behaviour 4-68771  
 TiO<sub>2</sub> thin films, plasma-enhanced CVD, photoelectrochemical props. 4-80627  
 WSi<sub>3</sub>-poly-Si-SiO<sub>2</sub>-Si MOS struct., interface reaction and resistivity 4-114040

CVD epitaxial growth *see vapour phase epitaxial growth*CVD thin films *see CVD coatings*cyanogen, C<sub>2</sub>N<sub>2</sub> *see carbon compounds*cyclopentadienylides *see organometallic compounds*

## cyclotron resonance

- for ion cyclotron resonance spectroscopy see mass spectroscopy; for ion cyclotron resonance heating see plasma heating*  
*see also diamagnetism; dopplers*  
 Cherenkov relativistic electron RF sources, cyclotron reson. mode selection 4-69299  
 electron gas, 2D, lifted spectral degeneracy 4-92638  
 layer crystal, cyclotron resonance theory 4-71184  
 line shape theories 4-61593  
 magnetized high-intensity electron beam, cyclotron resonance of pumping wave, induced rad. 4-69293  
 maser with opposing waves, nonsteady processes 4-79085  
 metal, compensated, plate, bound EM and sonic waves (Russian) 4-98951  
 metal plate, electromag. generation of sound in perpendicular mag. field 4-80632  
 MOS device, IR FT spectroscopy of two dimens. space charge layers 4-99109  
 noble metal, electron-phonon and electron-electron scatt. investigations on Fermi surface 4-70798  
 semiconductor superlattices, quantum wells, and heterostructs., elec. and optical props. 4-80666  
 semiconductor superlattices, Stark cyclotron-phonon oscillations of sound absorption 4-70276  
 semiconductors, cyclotron, intervalley cyclotron-impurity and spin resons. at submm. wavelengths 4-114165  
 transition metal, electron-phonon and electron-electron scatt. investigations on Fermi surface 4-70798  
 two-dimensional systems, electronic props., conf., Oxford, England (Sept. 1983) 4-95050  
 Ag, doppleron oscils., carrier reflection influences 4-80481  
 Al<sub>x</sub>Ga<sub>1-x</sub>As/GaAs heterojunction FET, 2D electrons, cyclotron resonance studies 4-98743  
 Cd, doppleron oscils., carrier reflection influences 4-80481  
 CdSb, cyclotron resonance of holes, effective masses 4-80477  
 GaAs, neutral impurity scatt., far-IR cyclotron resonance study 4-71185  
 GaAs neutral impurity scatt., far-IR cyclotron reson. study 4-92964  
 GaAs/(GaAl)As two-dimens. electron gas, cyclotron reson. study 4-104297  
 GaAs/Al<sub>x</sub>Ga<sub>1-x</sub>As heterostruct., photcond. studies 4-98744  
 GaAs/AlGaAs heterojunction, 2D electron gas, cyclotron resonance studies 4-76032  
 GaAs/AlGaAs heterostruct., screening and polaron effects, cyclotron resonance studies 4-98741  
 GaAs-GaAlAs interface, 2D electron gas, cyclotron reson. 4-109077  
 GaInAs/AlInAs heterojunctions, cyclotron resonance and polaron effects 4-98742  
 GaInAs/InP heterojunctions and superlattices, cyclotron resonance and polaron effects 4-98742  
 Ge, cyclotron resonance and radiative recombination for excitons, free carriers, electron-hole droplets 4-71183  
 Ge exciton condensation, microwave studies, biexcitons and electron-hole droplets 4-70668  
 Ge, hot hole submillimetre emission in transverse mag. field 4-71412  
 Hg<sub>1-x</sub>Cd<sub>x</sub>Te, electric subbands in the limit E<sub>G</sub>→0, for IR reson. study 4-104286  
 Hg<sub>1-x</sub>Cd<sub>x</sub>Te surface accumulation layer, cyclotron resonance studies 4-98507  
 n-InP, cyclotron resonance, impurity conc. and compensation effects (Russian) 4-98952  
 Ni<sub>3</sub>Al, weak itinerant ferromagnet, de Haas-van Alphen effect, Curie temp. 4-113848  
 Pb<sub>1-x</sub>Mn<sub>x</sub>Te, band struct., cyclotron reson. obs. 4-84546  
 n-Pb<sub>1-x</sub>Mn<sub>x</sub>Te, intraband magnetooptical transitions in epitaxial film 4-71355  
 PbTe/Pb<sub>1-x</sub>Sn<sub>x</sub>Te superlattices, struct. and electronic props. 4-98463  
 PbTe/Pb<sub>1-x</sub>Sn<sub>x</sub>Te superlattices, optical and elec. props. 4-99209  
 Si, quantum cyclotron reson. 4-108762  
 Si-SiO<sub>2</sub> interface cyclotron resonance lineshape distortion (Chinese) 4-84701  
 ZnSe, millimeter and submillimeter cyclotron resonance study 4-92963

## cyclotrons

*see also microtrons; synchrocyclotrons*

- <sup>23</sup>Na beam prod., cold cathode PIG source for use with cyclotron 4-74072  
 design for 160 MeV proton radiotherapy 4-72408  
 giant particle accelerators, circular and straight, beam focusing and accelerating, parameters 4-68841  
 half-quadrupoles for SIN cyclotron beam lines 4-83263  
 medical facilities for clinical therapy, diagnosis and analysis, general survey 4-72402  
 medical isotope production, medium energy research cyclotron use 4-77391  
 Milan Superconducting Cyclotron, cryostat pressure behaviour following coil quench 4-64251  
 Milan superconducting cyclotron, mag. field design, beam dynamics 4-96306  
 neutron therapy program at cyclotron of Louvain-la-Neuve 4-72409  
 pilot CW superconducting electron accelerator design, fabrication and test 4-102409  
 radioactivation of heavy ion cyclotron central region 4-91116  
 radiofrequency amplifier, requirements 4-111987  
 radioisotope production for medical appls., cyclotron use in Rio de Janeiro 4-77390  
 radionuclide production cyclotrons for medical appls. 4-77389  
 Tokyo University cyclotron, neutron, skyshine spectra and dose distrib. 4-96293  
 variable energy cyclotron at Calcutta, high power wideband RF system 4-59465  
 VEC, variable energy cyclotron, central region parameters study 4-59464
- cytology** *see cellular biophysics*
- Czochralski method** *see crystal growth from melt*
- D-layer** *see D-region*
- D mesons**  
 beauty and charm particles, prod. in strong interactions, decays, review 4-90931  
 conference, meson spectroscopy, Upton, NY, USA (April 1983) 4-90280  
 resonance in K $\bar{K}\pi$  system 4-90905  
 D(1285)→K<sup>+</sup>K<sup>-</sup> $\pi^0$ ,  $\delta$ -dominance model, K<sup>+</sup>K<sup>-</sup> effective mass spectrum 4-111445  
 D(1285)→K<sup>+</sup>K<sup>-</sup> $\pi^0$ , invariant mass distrib. and differential spectrum 4-90867  
 D<sup>0</sup> lifetime and mass from  $\gamma$ N expt. 4-73750  
 D<sup>0</sup> lifetime following e<sup>+</sup>e<sup>-</sup> 29 GeV annihilation 4-78549  
 D<sup>+</sup> semileptonic decay widths, 1=0  $\eta$  and  $\eta'$  final states, QCD sum rules 4-95789  
 D<sup>±</sup> lifetime from  $\gamma$ N expt. 4-73749  
 D<sup>+</sup>→D<sup>0</sup> $\pi^+$ , P-odd effects in radiative decays, P-invariance violation (Ukrainian) 4-64002  
 D<sup>±</sup> semileptonic decays, lifetimes 4-95790  
 D<sup>0</sup>→D<sup>0</sup> $\pi^0$ (D<sup>0</sup> $\gamma$ ), decay widths and excited meson props. 4-111443  
 D<sup>0</sup>→D<sup>0</sup> $\pi^0$ (D<sup>0</sup> $\pi^0$ ), decay widths and excited meson props. 4-111443  
 D<sup>±</sup>(D<sup>0</sup>) mesons masses and decay widths 4-111443  
 e<sup>+</sup>e<sup>-</sup>→DX, lifetime meas. 4-90898  
 e<sup>+</sup>e<sup>-</sup>→heavy quarks, D meson tagging 4-90896  
 $\gamma\gamma$ →DX, lifetimes, cross-sections 4-90890  
 $\gamma$ N→charm, inclusive cross-section, meson lifetimes 4-90891  
 $\gamma$ N→D<sup>±</sup> $\pi^0$ , cross section threshold enhancement 4-106534  
 pN→D(Δ)X, upper limit for charm production 4-78567  
 pp→DD $\pi$ , model for central charm prod. 4-59121  
 $\pi^-$ N, 278 GeV, on Fe, forward prod. of charm states and prompt single muons 4-64023  
 $\pi^-$ N→ $\gamma$ DDX, cross section calc. in O( $\alpha_s^4$ ) QCD 4-95831
- D-region**  
 A1 absorption data reduction, validity of George's method 4-90019  
 auroral absorption, day/night absorpt. ratio in auroral and subauroral zone riometer meas. 4-90018  
 auroral region, heated patch, effect on VLF propag. 4-85820  
 coupling to lower atmosphere planetary waves, radioabsorpt. study (Chinese) 4-63006  
 electron density inhomogeneities, turbulent spreading 4-115657  
 electron density profile, test of International Reference Ionosphere using single-freq. Al absorpt. data 4-90020  
 electron density profile estimation with VLF refl. coeffs., improved technique (Japanese) 4-85827  
 ELF waves generated during radiowave heating of auroral electrojet 4-67538  
 ion chemistry of E- and D-regions, photochemical aspects 4-72774  
 ion line spectra, EISCAT meas. during CAMP 4-100840  
 negative ion zone at 88 km altitude 4-115647  
 radar probing technique at HF freqs. using pulse compression techniques 4-94278  
 NO chemistry and ionization influenced by planetary waves 4-82318
- D/A conversion** *see digital-analogue conversion*
- damage, radiation** *see radiation effects*
- damping** *see dams*
- damping**  
*see also dislocation damping; internal friction*  
 alloys, noise and vibration control appl., service condition parameters (German) 4-66365  
 composite materials for damping, development 4-76797  
 damped simple pendulum of const. amplitude, nonlinear differential eqn. 4-86184  
 discrete linear mechanical systems, weak damping (German) 4-82661  
 eddy current damping due to linear period array of mag. poles 4-69277  
 fibre reinforced composites, laminated symmetric beams, damping and dynamic moduli 4-80154  
 frequency domain characteristics of mechanical rotors (German) 4-82673  
 gas flow pulsation, freq. limits 4-103447  
 inertial rotor disc. effects of damping, stiffness anisotropy (German) 4-82674  
 joints, nonlinear oscillation damping (German) 4-82660  
 laminated plates and beams, fibre vol. fraction, dynamic mech. props. 4-89078  
 magnetic bearing, anal. of inertially loaded rotating systems (German) 4-82670  
 magnetic suspension systems, radial viscous damper 4-78348  
 multiple degree of freedom systems, critical damping, computation method 4-73224

# damping continued

- oscillations, damped, holographic subtraction (*Chinese*) 4-112362
- passive mechanical oscillating systems (*German*) 4-82664
- plasma Langmuir wave damping, collisional, quasilinear relax. of electron beam 4-69921
- plates, C and glass fibre reinforced laminates, vibr. damping parameters, prediction and meas. 4-80155
- plates, rectangular with hysteresis damping large-amplitude vibrs., effects of geometric imperfections 4-97389
- PVDF polarised films, high-freq. piezoelec. strain response 4-99025
- quasilinear wave eqn., effect of boundary damping 4-86225
- rod, damping capacity in centrifugal force field using tuning forks 4-97302
- rod elements, damping capacity determ. in biharmonic oscillations 4-97447
- shell structure, immersed, scaling relations for structural frequency response 4-91759
- steel 40 Kh, damping capacity and residual life, preliminary cyclic loading influence 4-99544
- stiffness and damping matrices, frequency and time domain anal. (*German*) 4-82672
- strangled harmonic oscillator, decaying Hamiltonian for damping 4-82706
- Timoshenko beam, coupled thermoelastic vibr. and damping (*Japanese*) 4-74944
- viscosity meas., damping and period eval. method 4-87822
- weakly-coupled nonlinear oscillators, transitions 4-78157
- Al-Si, cold worked, damping capacity, mech. props. rel. to heat treatment 4-61967
- $\beta$ -Cu-Al-Zn (8.7, 12.0 wt.%), with reversible martensite in struct., effect of ageing on damping capacity 4-109452
- Cu-Al-Zn alloy,  $\beta$ -phase, damping capacity rel. to mech. props. and martensite morphology 4-99414
- Cu-Al-Zn system, high damping  $\beta$  alloys, effect of aging in martensite condition on mech. props. 4-114588
- Ni-Co-Nb, damping capacity, mag. and mech. props. 4-61564
- Ti alloy, damping capacity, energy scatt. mechanism,  $\beta \leftrightarrow \alpha'$  transform. by twinning 4-93326

# dams

- see also civil engineering; hydroelectric power stations
- earth dams, provision of reliability in design and construction 4-77457
- Idukki reservoir catchment, Kerala, India, valley slumping, sedimentation and reservoir capacity 4-100628
- El Limoner dam site, Malaga, Spain, seismic risk and expected strong motion (*Spanish*) 4-115342
- Vilyui River, flow rates, linear model for data transformation 4-72620

# dark space see discharges (electric)

# DASD see magnetic disc and drum storage

# data acquisition

- see also CAMAC; data handling; indicators; recorders
- A/D converter-D3-28 microcomputer interface 4-106288
- air-launched expendable seawater conductivity and temp. profiler 4-115629
- analytical and image data from SEM and STEM, integrated system for collection and processing 4-72012
- angular windowing system for rotating equipment tests 4-86392
- Argos meteorological and oceanographic data collection buoy system 4-105725
- atmospheric particle size meas. probe (*French*) 4-85761
- instrumented data handling and instrument control using low-cost desktop computers and an IEEE 488 compatible version of the ODETA V 4-97149
- autonomous computer controlled ice drill performance tests 4-115640
- baseline sail system controller 4-72751
- BBC microcomputer, analogue port, laboratory measuring and monitoring appls. 4-63460
- Broken Hill Field geology, mining and metallurgy, conference, Broken Hill, NSW, Australia (July, 1983) 4-58562
- calorimeter array, data acquisition system 4-59602
- CAMAC star network concept for centralised system 4-91188
- cardiac tissue characterisation, stochastic approach to RF amplitude anal. 4-105302
- coherent digital data acquisition system (CODDAS), a general purpose oceanographic instrument 4-67493
- COMPEX standard capabilities 4-106287
- computerized radiation data acquisition and management system at Seabrook nuclear power station, USA 4-78739
- conference, nuclear science and power systems, San Francisco, CA, USA (Oct. 1983) 4-58550
- control systems, memory intensive functional architecture 4-59600
- controller for automatic data acquisition on magnetic tape using an ES-9002 recorder 4-86391
- core logging safety and productivity improvement by microelectronics 4-62957
- data quality assessment using empirical orthogonal functions 4-67507
- deep ocean ambient noise spectra recording instrument 4-67494
- deep-sea sediment shear strength meas. vane system 4-115635
- digital heterodyne interferometer for analysis and control of adaptive optics, automatic data acquisition 4-111194
- digital recording system for the pulse waveforms of fast scintillation counter in EAS 4-112072
- domestic solar system instrumentation, long-term stability and performance 4-99989
- Doppler acoustic profiling current meter 4-72761
- Doublet III Big-Dee upgrade, diagnostic data acquisition computer system 4-111842
- electro-oculography data acquisition system, microcomputer-based neurological diagnosis 4-89819
- electron microscopy and anal., conference, Guildford, England (Aug.-Sept. 1983) 4-78034
- EMG, reference signal acquisition system 4-93944
- ES-1030 system at Obninsk Central-Seismological Observatory, USSR 4-100752
- ESR Bruker spectrometer, using digital phase-sensitive detection and Aspect 2000 minicomputer 4-68253
- FASTBUS, ADC for pulse height data from EM calorimeter 4-59604
- FASTBUS, data acquisition system for 256 wire MWPC 4-59603
- FASTBUS and data acquisition for MARK II detector 4-59605
- FASTBUS based data acquisition system for imaging coronary arteries 4-62570

# data acquisition continued

- ferroelectric switching current meas., microprocessor controlled data acquisition system 4-76369
- filterphotometric detection system for liquid chromatography 4-68259
- fluid mechanics research, data acquisition system, minicomputer-based 4-69845
- formal metrology and data-acquisition facilities 4-90556
- gamma-ray spectral anal., computerised acquisition system 4-59484
- geology, computer techniques use (book) 4-85793
- geomagnetic micropulsations, data acquisition procedures used at L'Aquila, Italy 4-110301
- global positioning system and marine geophysical research 4-67499
- HB 1040A, high-speed spectrophotometric LC detector 4-68260
- heterodyne interferometry, generalised data reduction 4-106371
- holographic interferometry system, microprocessor control/data acquisition, real-time signal processing, NDT appl. 4-73501
- IEEE-488 bus for data acquisition in undergraduate expts. 4-58609
- intelligent data selection system 4-72754
- KEK proton synchrotron data acquisition online program (*Japanese*) 4-102564
- left-ventricular ejection fractions from gate equilib. blood pool scintigrams, automated computation 4-72384
- Marc I data acquisition system for oceanographic applications 4-72760
- metals, strain controlled creep-fatigue tests 4-89209
- microcomputer data acquisition system for mass spectrometry 4-106422
- microcomputer photoacoustic data-acquisition system for multiphoton absorption 4-111112
- micropores, automation, software system designed, control program 4-68326
- microprocessor for a high-speed X-ray digital data collection system 4-107268
- microprocessor-controlled remote data acquisition unit for hyperbaric environment 4-109985
- micropulsation data acquisition and primary processing at Adolf Schmidt Observatory (*German*) 4-72704
- microwave thermoelastic tissue imaging-system design 4-115160
- minewide 2000-channel data acquisition system 4-62956
- modules for controlling expt. on-line hardware with ES computer 4-58836
- monitoring oceanographic data in real time 4-67503
- Mossbauer data collection using an Apple II microcomputer 4-63726
- multichannel analyser, CAMAC based module for data selection 4-96412
- multichannel analyser with touch sensitive video display 4-59591
- multilayer semiconductor spectrometer, automated electronic system 4-87009
- multiprocessor leased data acquisition and processing system for photon counting expts. 4-59606
- multiwavelength LIDAR system, computer system for data acquisition and processing 4-74583
- NODAPEC, online system for low temp. nuclear orientation expts. 4-102563
- nutrient determination in seawater, data acquisition system 4-72755
- ocean floor imaging and charting system 4-115638
- ocean waved, direction measurement, design of solid state meter 4-67495
- oceanographic data rationalising system using IEEE 488 standard interface 4-115580
- oceanographic equipment for real time data telemetry 4-62955
- oceanographic remote acquisition system lifetime extension by in-situ data selection and compression 4-115579
- OCEANS '83, utilisation of sea, conference, San Francisco, CA, USA (Aug.-Sept. 1983) 4-106113
- particle detector system, neutron time of flight meas. 4-59601
- personal noise exposure, database construction (*Japanese*) 4-93668
- photoelastic data, automatic acquisition and calculation (*Chinese*) 4-83869
- photon counting system, low-intensity spectral line registration using programmable timer 4-111175
- PINK PANTHER CAMAC crate controller for  $\pi^0$  spectrometers at CERN 4-78752
- portable data logger for severe environments 4-100738
- profiling system for oceanographic research 4-72759
- programmable data-acquisition and stepping motor control system 4-97968
- radionuclide laboratory, data acquisition system 4-74124
- RATAN-600 radio, surveys, data collecting and processing system 4-63077
- reactor pressure vessels, thick walled components, US inspection, time of flight data evaluation, ALOK system 4-71804
- read-out system on 6-bit fast ADC for MWPC and drift chambers 4-91165
- real time data acquisition systems for very short range weather forecasting 4-105662
- real-time digital data acquisition system for free-piston Stirling engine/linear compressor system parametric testing and evaluation 4-66779
- real-time telemetry system for hydrographic and meteorological data collection in the South Atlantic Bight 4-72752
- relativistic heavy ion streamer chamber expts., data acquisition of high multiplicity events 4-74101
- rheogoniometer, Weissenberg model R17, modification and computerisation 4-114745
- ROCKS system of computer programs for macromolecular crystallography 4-81612
- Romulus compatible asynchronous time and amplitude pad acquisition system for TPC 4-96416
- SAIL protocol for shipboard data acquisition 4-72753
- SAIL systems in IOS ships 4-72756
- sampling of events in research experiments on mu-atomic and mesomolecular processes 4-74123
- scintillation detectors data processing, auxiliary controller ccts. design 4-90570
- scintillator hodoscopic systems, optimal data encoding 4-59573
- SEASAT-data acquisition and processing by the Royal Aircraft Establishment 4-82241
- seismic recording stations, technical improvement of data assembly and transmission (*Russian*) 4-100737
- SEM image information extraction by digital processing 4-75245
- SEM studies of surface processes, digital data acquisition and anal. system 4-78433
- shipboard data management, SAIL 4-67506

**data acquisition continued**

- solid state current meter for wave direction sensing 4-67495
- solid surface, Auger spectra data acquisition improvement (*French*) 4-71488
- sound emission analysis using MPS 4944 microprocessor system (*German*) 4-79377
- spectrophotometer, five-channel, expansion of dynamic range of data-gathering and measuring system 4-105880
- steel, duplex austenitic-ferritic stainless, weld solidification routes, thermal analysis, high speed data acquisition 4-85150
- thermal decomposition, thermogravimetric data and effective kinetic parameters calcs. 4-81491
- tomographic acoustic microscopy, data acquisition 4-103162
- TOPEX satellite project, end-to-end ground data system 4-77657
- towed oceanographic sampler 4-67496
- towed thermistor system for marine research 4-67497
- triple quadrupole mass spectrometer, artificial intelligence appl. 4-58912
- TRS-80 colour computer as 4-channel data logger 4-82644
- universal programmable deep ocean transceiver 4-115623
- vector averaging electromagnetic current meter for near surface measurement 4-72757
- visual evoked potentials data collection and storage, database 4-81679
- weak radiation spectrometry, using data acquisition and processing system (*Japanese*) 4-11216
- weather station using BBC microcomputer for online data acquisition 4-110256
- X-ray diffractometer interfacing to SM-3 computer system 4-106289
- Al-Si-Mg casting alloys, quality evaluation, thermal analysis, data acquisition system (*French*) 4-81365

**data communication systems**

- see also cryptography*
- EEG 16 channel telephone transmission system with cassette recording and CRT display (*Spanish*) 4-62619
- expanded beam directional couplers for LAN 4-107844
- fibre optic communication line with multimode waveguides for data transfer up to 8 km distance 4-107866
- optical data transmission, industrial appl. 4-97118
- optical fibres in broadband networks, instrumentation and urban and industrial environment apps., conf., Paris, France (May 1983) 4-78024
- optical fibres in the industrial and commercial environment, review 4-79292
- optical subscriber loop for business premises and local area apps. (*Japanese*) 4-79304
- optical subscriber system for business premises appl. (*Japanese*) 4-79306
- receiver concepts for data transmission at 10 microns 4-107884
- semiconductor laser for space optical data links 4-107882
- semiconductor lasers for data links between satellites 4-107881
- TV picture quality and data processing, subjective assessment (*Japanese*) 4-109815
- CO<sub>2</sub> laser intersatellite data link system, low IF translation loop concept 4-107552
- CO<sub>2</sub> laser transceiver with Gbit/s capability, space-to-space communication appl. 4-107883

**data compression**

- see also information theory*
- coastline data, point reduction in digital maps (*Japanese*) 4-81833
- ECG data compression, Fourier descriptors 4-89800
- oceanographic remote acquisition system lifetime extension by in-situ data selection and compression 4-115579
- underwater images compression for transmission on low bit rate acoustic channel 4-103079

**data dictionaries *see database management systems*****data handling**

- see also cryptography; data reduction and analysis*
- automated data handling and instrument control using low-cost desktop computers and an IEEE 488 compatible version of the ODETA V 4-97149
- calorimeter array, data acquisition system 4-59602
- Doublet III, neutral beam data archiving for offline analysis and access 4-111841
- FASTBUS, ADC for pulse height data from EM calorimeter 4-59604
- FASTBUS, data acquisition system for 256 wire MWPC 4-59603
- gamma-ray spectral anal., computerised acquisition system 4-59484
- image data processed by descriptive multidimensional anal. 4-68328
- JT-60, diagnostics data management facility 4-111850
- microprocessor laboratory in a physics department 4-78075
- multichannel analyser with touch sensitive video display 4-59591
- optical discs systems and applications, conf., Arlington, VA, USA (June 1983) 4-90287
- particle detector system, neutron time of flight meas. 4-59601
- Shimadzu data processing system RAD-1100A for radioimmunoassay in clinical chem. laboratories (*Japanese*) 4-59578

**data loggers**

- ocean, current meter, bottom mounted Doppler acoustic equipment 4-115620
- portable data logger for severe environments 4-100738
- seismometer for ocean deployment, event recording data logger design 4-67491
- TRS-80 colour computer as 4-channel data logger 4-82644

**data processing (administrative) *see administrative data processing*****data reduction and analysis**

- see also data acquisition*
- AMD-1 automatic densitometer spectra, scanning and processing software 4-94635
- analytical and image data from SEM and STEM, integrated system for collection and processing 4-72012
- BASIC program for bootstrap analysis of correlation coeff., laboratory microcomputers appl. 4-106290
- Bayesian method for data anal. and application to oceanographic data 4-94266
- beta-ray spectra, data anal. using response function 4-59481
- CLEAN, deconvolution algorithm enhancement 4-115694
- compensation of measurements series (*German*) 4-101822
- EEG and EMG signals, data reduction technique 4-85561
- electrostatic precipitator for the study of airborne radioactivity 4-89786
- Fourier transform filtering of two-dimensional fluorescence data 4-101820
- Fourier transform spectroscopy, microcomputer expt. control and data analysis 4-106406
- geology, computer techniques use (book) 4-85793

**data reduction and analysis continued**

- heterodyne interferometry, generalised data reduction 4-106371
  - high-resolution frequency analysis of analogue signals 4-63725
  - image processing, data anal. 4-115611
  - interferogram analysis, lateral shearing, for testing aspheric elements 4-113594
  - IR data analysis, cost-effective approach using Apple II computer 4-106284
  - maximal entropy method 4-63487
  - measurement data processing, error analysis (*German*) 4-101806
  - meteorology, GARP level III data processing 4-72728
  - metrological reliability, use of hyperelliptical coordinates in specific DP algorithms 4-95370
  - microprobs., automation, software system designed, control program 4-68326
  - Mossbauer spectra anal., expression for fitting and stripping 4-71220
  - multiwavelength LIDAR system, computer system for data acquisition and processing 4-74583
  - NMR relaxation data, reduction program, in FORTRAN 4-78124
  - nuclear safeguards, software, data structs. and data eval. for verification system 4-111700
  - oceanographic data acquisition, analysis and presentation standards 4-77676
  - palaeomagnetic transitional data display and analysis method 4-115603
  - pattern recognition techniques, remote sensing data anal. 4-115612
  - PINK PANTHER CAMAC crate controller for  $\pi^0$  spectrometers at CERN 4-78752
  - pole figures evaluation, data processing 4-106292
  - potential field data, 3-D automatic interpretation using Hilbert transforms 4-110289
  - potential field data analysis, continuation between arbitrary surfaces 4-110039
  - Raman spectroscopy, white noise and single outlier contamination, robust smoothing 4-101817
  - reactor pressure vessels, thick walled components, US inspection, time of flight data evaluation, ALOK system 4-71804
  - remote sensing pattern recognition and image processing anal. 4-115610
  - ROCKS system of computer programs for macromolecular crystallography 4-81612
  - SEASAT-data acquisition and processing by the Royal Aircraft Establishment 4-82241
  - seismic data interpretation, interactive system use 4-100774
  - SEM image information extraction by digital processing 4-75245
  - SEM studies of surface processes, digital data acquisition and anal. system 4-78433
  - smoothing methods as preprocessing for iterative deconvolution (*Japanese*) 4-95396
  - spectral functions estimation for normal random noises 4-68197
  - spikes in data sets, elimination by median filtering method 4-94261
  - rational splines for vertical interpolation of data 4-94267
  - surface photometry of galaxies, digital processing techniques (*Russian*) 4-115695
  - thermocouples calibration, data processing (*Japanese*) 4-101837
  - time series data editing method using Kalman filter 4-100736
  - VISAR, data reduction method 4-111191
  - X-ray photoelectron spectra processing (*Chinese*) 4-101821
  - Al-Si-Mg casting alloys, quality evaluation, thermal analysis, data acquisition system (*French*) 4-81365
- data structures**
- human brain, 3D CT image display (*Japanese*) 4-109926
  - nuclear safeguards, software, data structs. and data eval. for verification system 4-111700
- data tables *see collections of physical data***
- data transmission systems *see data communication systems***
- database management systems**
- AMDS program, atomic and molecular database system 4-102813
  - Landsat data and database approach, apps. 4-77658
  - low-level waste management information, system, system description 4-111645
  - mass spectrometry-mass spectrometry, instrument database system 4-114853
  - optical discs systems and applications, conf., Arlington, VA, USA (June 1983) 4-90287
  - SIMBAD data base at CDS, 1984 software capabilities for stellar astronomy 4-94900
- dating, Earth *see geochronology***
- dating, radioactive *see radioactive dating***
- Davydov splitting**
- t-butanol, cryst., torsion band, IR obs. 4-61691
  - cyclohexanol, cryst., torsion band, IR obs. 4-61691
  - cyclopentanol, cryst., torsion band, IR obs. 4-61691
  - methanol, cryst., torsion band, IR obs. 4-61691
  - naphthalene, phonon harmonic dynamics, block method 4-88254
  - naphthalene-indole soln., IR spectra (*Russian*) 4-84969
  - n-terphenyl, pure and impure crystals, exciton, visible absorpt. and fluores. spectra 4-99141
  - GeSe, layer crystals, Jahn-Teller effect 4-108824
- Davydov states *see Davydov splitting***
- dawn *see twilight***
- dawn chorus *see atmospheric***
- dayglow *see airglow***
- DBR lasers *see distributed Bragg reflector lasers***
- d.c. amplifiers**
- matching calorimeter output to A/D convertor, continuous flow anal. system, microcomputer-controlled 4-97717
- d.c. generators**
- see also homopolar generators*
  - kinematic dynamic in a sphere with separate toroidal and poloidal motions (*Russian*) 4-113065
  - transformation coeff. of poloidal field into toroidal one due to differential rot. of conducting media (*Russian*) 4-113068
  - ZT-40M RFP dynamo, plasma resistivity calcs. 4-69963
- d.c. motors**
- gamma-ray telescopes, choice of astatic system for controlling DC motor speed for altazimuth mountings 4-105886
- d.c. sputtering**
- DC reactive magnetron sputtering technique for thin film production (*Polish*) 4-93217

- d.c. sputtering continued**  
planar magnetron sputtering system, poles exposing type, DC discharge characts. *[Japanese]* 4-61852  
PLZT, ferroelec. films, reactive sputtering prep. and dielec. props. 4-104731  
polyimide, metallisation by Ni and Cu, adhesion, nuclear scattering eval. 4-71749  
Al-Si interconnects, DC magnetron-sputtered, influence of residual gas composition on lifetime 4-71560  
AlN/Al cermets, reactive DC planar magnetron sputtering prep., elec. transport props. 4-88607  
Au, adsorption of  $O_2$ ,  $Au_2O_3$  prod. by DC reactive sputtering, EELS, AES, and XPS study 4-93161  
a-C/Si MIS structures, DC sputter deposited, HF characts. 4-88601  
CrN<sub>x</sub> DC reactively sputtered layers with surface roughness, as selective absorbers in solar collectors 4-77147  
In<sub>2</sub>-Sn<sub>2</sub>O<sub>3</sub>- transparent conducting films, DC reactive sputtering deposition, optical and elec. props. 4-112533  
Mo films, DC magnetron sputtering with RF substrate bias 4-81126  
Nb-Si Al<sub>5</sub> films, compositionally graded, synthesis by co-sputtering 4-93214  
Pb(Zr,Ti)O<sub>3</sub> ferroelec. films, reactive sputtering prep. and dielec. props. 4-104731  
a-Si:H films, DC planar magnetron reactive sputtering and characterisation 4-93218  
Ta-N-O films, DC reactive sputtered, elec. resist., microstruct., oxidation 4-80704  
W films, DC magnetron sputtering with RF substrate bias 4-81126
- de Broglie waves** *see wave mechanics*
- de Haas-van Alphen effect**  
*see also diamagnetic properties of substances; diamagnetism*  
modulation-doped heterostructures, two-dimensional phenomena 4-98721  
plasma, semi-infinite, degenerate, linear response function in external mag. field 4-92643  
spatially inhomogeneous samples, de Haas-van Alphen effect 4-113849  
two-dimensional electron systems, sound propag. in strong mag. fields 4-65718  
two-dimensional interacting fermions in uniform mag. field 4-70686  
Al, surface acoustic waves and de Haas-van Alphen meas. 4-70540  
AlGaAs-GaAs superlattices, magnetisation meas., de Haas-van Alphen oscils. 4-98734  
Cd,Mg alloys, electron energy spectrum and de Haas-van Alphen effect *(Russian)* 4-70639  
Cu, electronic props. of 4d transition metal and sp impurities 4-70731  
Ga, surface acoustic waves and de Haas-van Alphen meas. 4-70540  
Hg<sub>1-x</sub>AsF<sub>6</sub>, incommensurate, mag. breakdown 4-84543  
Ni<sub>3</sub>Al, weak itinerant ferromagnet, de Haas-van Alphen effect, Curie temp. 4-113848  
SbCl<sub>2</sub>-graphite intercalation cpd., de Haas-van Alphen effect meas. 4-88440  
Si inversion layers, de Haas-van Alphen effect obs. 4-98771  
WC, semimetallic, de Haas-van Alphen effect obs. 4-104116
- Debye-Huckel theory**  
colloidal crystals, osmotic press. bulk modulus, charge renormalisation 4-85339  
polystyrene charged spheres in dilute soln., fluorescence labeled, electrolyte friction meas. 4-98323  
He<sup>+</sup>, electron impact excitation in dense plasma 4-112281
- Debye-Scherrer cameras** *see cameras; X-ray crystallography apparatus*
- Debye temperature**  
*see also specific heat*  
1,1'-diacetylferrocene in cold smectic C liq. crystal, Mossbauer temp. study 4-109105  
ionic cryst., lattice and thermodynamic props., overlap repulsion pot. 4-92327  
metallic solid solutions, thermodynamics, vibr. and configurational contribs. 4-103962  
metals and alloys, liquid, entropy, expansion coeff., sp. ht. and Debye temp. 4-103963  
Mg-Mn ferrite, elastic behaviour at room temp. 4-65327  
solids, nucl. stopping power, binding force effect 4-65316  
Ag-Cd-In alloys, X-ray determ. of mean Debye-Waller factors, vibr. amp. and Debye temp. 4-84358  
BaPb<sub>1-x</sub>Bi<sub>x</sub>O<sub>3</sub>, sp. ht. and supercond. 4-108972  
Cr<sub>3</sub>Ir, Debye characteristic temps. 4-70330  
Cr<sub>3</sub>Rh, Debye characteristic temps. 4-70330  
Cs, phonon frequencies, Debye temp., Gruneisen parameter, transport props., lattice dynamical model 4-108561  
Cu (001), azimuthal X-ray photoelectron diffr. from Cu<sub>2</sub>p<sub>3/2</sub> core level 4-76639  
Fe, electron irradi., internal friction *(Polish)* 4-92234  
Gd<sub>2</sub>Ga<sub>2</sub>O<sub>7</sub>, hypersonic wave attenuation 4-75620  
Ge, elastic props., ultrasonic meas. 4-98170  
HfC, X-ray Debye temps. and mean square atomic displacements 4-88260  
KTaO<sub>3</sub>, anharmonic interactions, X-ray diffr. study 4-61036  
NH<sub>4</sub>Br(Cl)(I), cohesion and thermodynamic props. calcs. 4-92126  
Nb, plastic deform. effect on superconducting T<sub>c</sub> 4-108960  
Sc, elastic props. under static compression up to 6 GPa *(Russian)* 4-108515  
Si, elastic props., ultrasonic meas. 4-98170  
Si-metal interface, dislocation mediated melting 4-103912  
Sn<sub>1-x</sub>Cu<sub>x</sub>, amorphous films, quench-condensed, low temp. sp. ht. 4-70403  
Ta, plastic deform. effect on superconducting T<sub>c</sub> 4-108960  
Ti<sub>3</sub>Al and TiAl, Young's modulus and Debye temp., 300 to 1300K *(Russian)* 4-92281  
TiN<sub>0.99</sub>, electron transfer and thermal vibr. parameters, X-ray diffr. study 4-92329  
V, plastic deform. effect on superconducting T<sub>c</sub> 4-108960  
α-W<sub>2</sub>C, X-ray Debye temps. and mean square atomic displacements 4-88260  
YAG, hypersonic wave attenuation 4-75620  
ZnIn<sub>2</sub>S<sub>4</sub> layered cpd., energy gap, temp. depend., optical meas. 4-88803
- Debye-Waller factors**  
*see also lattice dynamics*  
alkali halide crystals, colour centre IR luminesc. and stimulated emission 4-80997  
disordered binary alloys, diffuse X-ray scatt., separation of thermal component 4-103704  
EXAFS, Debye-Waller factors in R-space analysis 4-65368

- Debye-Waller factors continued**  
metallic solids, Debye-Waller factor for substitutional Mossbauer impurity 4-75633  
metallic solids with small conc. of impurities, Mossbauer oscillator strengths, Debye-Waller factor 4-75634  
metals, thermalised He atom-surface scatt., electronic Debye-Waller effect 4-93172  
solids, γ-ray scatt. and diffr. due to thermal vibrs. of atoms *(Japanese)* 4-113275  
three-atom system, thermal vibr. effect on EXAFS 4-64491  
triatomic system, thermal vibrs. effect on EXAFS 4-102698  
Ag-Cd-In alloys, X-ray determ. of mean Debye-Waller factors, vibr. amp. and Debye temp. 4-84358  
Al, structure factors obtained from X-ray diffr. meas., Debye-Waller factors 4-92158  
Br<sub>2</sub>O, thermal vibrs. effect on EXAFS 4-102698  
Cr<sub>3</sub>Ir, Debye characteristic temps. 4-70330  
Cr<sub>3</sub>Rh, Debye characteristic temps. 4-70330  
Cu (001), azimuthal X-ray photoelectron diffr. from Cu<sub>2</sub>p<sub>3/2</sub> core level 4-76639  
He liq. surface, two-dimens. electron cryst., liq.-solid transition, coupled electron-ripple vibrs., RF absorpt. spectra 4-88358  
La<sub>100-x</sub>Al<sub>x</sub>, amorphous, supercond., thermodynamic and transport props. 4-70986  
MnPS<sub>3</sub> layered cpd., disorder effects by cation intercalation, EXAFS studies 4-61773  
PbS, at. vibr. amplitudes, Debye-Waller factor 4-98232  
Si, with structure defects, X-ray scatt. in Laue geometry, dynamical effects 4-75435
- decay periods (radioactive)** *see radioactive decay periods*
- decay schemes (radioactive)** *see radioactive decay schemes*
- decay theory (nuclear)** *see nuclear decay theory*
- decision theory** *see decision theory and analysis*
- decision theory and analysis**  
*see also Bayes methods; dynamic programming*  
building retrofit, optimal strategies identification 4-72048  
countable state Markov decision chains with total strategy *(Russian)* 4-73348  
optical communications, conditional probability and conditional expectation in quantum mech., expressions 4-74445  
skull X-ray assessment of head injuries: a decision analytic approach 4-115185
- decoding**  
*see also demodulation*  
zone plate coded imaging, theory and appls., book contrib. 4-107501
- decomposition**  
*microstructure features and processes only; for other aspects see dissociation and pyrolysis*  
*see also spinodal decomposition*  
alloys, BCC binary, bulk decomposition, surface monolayer ordering 4-65383  
alloys, magnetisation and phase decomposition, structural diagrams 4-76138  
ionic crystals, supersaturated solid solns., classification of precip. phenomena 4-75685  
pearlite interlamellar spacing, review of data 4-93293  
solid solution, supersaturated, radiative swelling problem, intensified recomb. of unlike defects 4-70188  
solid solution, supersaturated, radiative swelling problem, inclusion growth and impurity pump mechanisms 4-70197  
steel, austenitic stainless, weld metal, ferrite decomp., effect of Mo additions 4-99374  
steel, high C and stainless, intermetallic phases formed by Sn ion implantation 4-92225  
steel, high-C tool, struct. of hardening martensite and change during low-temp. tempering 4-114583  
steel, low C, Al killed, decomp. of Mn-C dipoles during quench ageing, resist. obs. 4-71661  
steel, microalloyed, hot-rolled, isothermal decomp. of austenite 4-99409  
steel, weld metal deposits, austenite decomposition products, influence of O-rich inclusions 4-114513  
Ag-based thin films, ultramicrohardness and internal stresses 4-92582  
AgI, polymorphic transform. and decomposition *(Russian)* 4-70376  
Al-Cu, rapidly solidified, decomp. struct. 4-104775  
Al-Zn, cellular decomp., TEM, DSC obs. 4-114528  
Al-Zn dilute alloys, α<sub>2</sub>-Zn rich precipitate shape, small angle neutron scatt. studies 4-114547  
Al-Zr (9.4 wt.%), melt-quenched, decomp. study using TEM 4-93262  
Al-Zr-Mg-Cu-Mn, supersaturation of Mn solid soln. 4-61935  
β<sup>+</sup>-Al<sub>2</sub>O<sub>3</sub>-Na<sub>2</sub>O:Fe, decomposition processes, microscopic mechanisms 4-109415  
Al<sub>2</sub>O<sub>3</sub>-SiO<sub>2</sub> fibres, cristobalite form. at elevated temp. *(German, English)* 4-81197  
Al<sub>2</sub>O<sub>3</sub>-ZrO<sub>2</sub>-SiO<sub>2</sub> refractory, corrosion by Pb glass 4-71753  
Au-based thin films, ultramicrohardness and internal stresses 4-92582  
BaTiO<sub>3</sub> form. by thermal decomposition of oxalate *(Japanese)* 4-76718  
Bi<sub>2</sub>O<sub>3</sub>-CdO, phase relations, X-ray diffr. obs. 4-89028  
Cr-W, phase diagram, miscibility gap, BCC solid soln. decomp. 4-114477  
Cu-Be alloy, struct. transform. mechanisms during ageing, internal friction and resist. obs. 4-114536  
Cu-Ni-Fe alloys, decomposition neutron scatt. studies 4-114539  
Cu-Ti system, cellular decomp. and Ti solid solubility 4-71633  
Cu-Zn-Al (23, 6 wt.%), isothermal decomp. of β' phase 4-99387  
Cu<sub>2</sub>MnAl, Heusler alloy, decomposition during isochronal annealing 4-61916  
Fe, cast, hardened high-strength, with nodular graphite cryst. struct. changes during tempering 4-93260  
Fe, cast, obtained a superhigh quenching rates, struct. investig., 20 to 1150°C 4-93286  
Fe, cast, with vermicular graphite, struct. and heat treatment 4-114471  
Fe, intermetallic phases formed by Sn ion implantation 4-92225  
Fe-Al-Si (6, 9 at.%), ordering with phase separation, annealing, TEM, X-ray diffr. study 4-114472  
Fe-C, high purity, forced veld. pearlite, expt. 4-93294  
Fe-C, high purity, forced velocity pearlite, theoretical 4-93295  
Fe-Co-Ni-Al, Alnico 5, hot workability, microstruct. 4-114626  
FeSi-Fe<sub>2</sub>Si<sub>3</sub> eutectic alloy, sintered, annealing, FeSi<sub>2</sub> form., elec. props. 4-109414

## decomposition continued

- Gd-Sn phase diagram, intermetallic cpds. and peritectic and eutectic reactions (*Chinese*) 4-114476  
 InP surface decomp. rel. to In  $M_{4.5}N_{4.5}N_{4.5}$  Auger spectrum fine struct. 4-81046  
 MgSiAlON ceramic powders, plasma spraying, characterisation and decomposition 4-114391  
 $NH_3$ , on Ru (001) and Ru (1,1,10) surfaces 4-65572  
 NO, on Ru (001) and Ru (1,1,10) surfaces 4-65572  
 Ni-La-Ni<sub>3</sub>-Zr<sub>3</sub>Ni<sub>7</sub>, peritectic equilibrium studies 4-76749  
 Ru-Rh system, constitution, solid solubility and lattice const. 4-70390  
 V-MoSe<sub>2</sub>, and V-NbSe<sub>2</sub>, volume changes in sintering 4-66271  
 ZrO<sub>2</sub>-Y<sub>2</sub>O<sub>3</sub>-Al<sub>2</sub>TiO<sub>3</sub> refractory composites, props. 4-71626

## decomposition, spinodal see spinodal decomposition

## decomposition, thermal see pyrolysis

## decorative coatings

- Al, chemical colouring by conversion coating process 4-81349  
 Bi decoration figures and nucleation on TGS single cryst. 4-65985  
 Sn, electrodeposition on Al alloys (*Russian*) 4-88991

## deep level transient spectra see deep level transient spectroscopy

## deep level transient spectroscopy

## see also deep levels

- computerised, using low-cost personal computer 4-70721  
 MIS, tunnel capacitor, leakage current effects on DLTS 4-70938  
 MIS structures, current DLTS spectra due to dielec. polarisation of the insulator 4-76043  
 resonance method using variable-frequency impedance bridges 4-58865  
 RF sputter-deposited Schottky barrier diodes 4-98691  
 semiconductor defects, use of linear predictive modelling for anal. of transients from expts. 4-80528  
 semiconductors, DLTS and deep level optical spectroscopy 4-108815  
 Al-SiO<sub>2</sub>-Si structures, dipolar relax. effects, transient capacitance spectroscopy study 4-80683  
 n-AlGaAs, MBE grown, deep electron traps 4-98570  
 AlGaAs:Si MBE layers, donor levels anal. 4-61316  
 AlGaAs-GaAs heterojunction interfaces, deep levels, forward I-V and DLTS meas. 4-70915  
 Al<sub>0.3</sub>Ga<sub>0.8</sub>As:Si MBE layers, electron trap conc., DLTS study 4-61317  
 n-Al<sub>0.3</sub>Ga<sub>0.8</sub>As, MBE grown, deep electron traps, growth conditions and alloy composition influence 4-98558  
 Al<sub>0.3</sub>Ga<sub>0.8</sub>As p-n junctions, organometallic VPE, anomalous light sensitivity 4-92817  
 Au-Si nucl. detectors, gamma-ray effects on rise time 4-59566  
 CdS-CdTe thin film solar cells, photocapacitance and current collection 4-81548  
 n-CdTe, deep levels, plastic deform. effects, DLTS studies 4-84591  
 n-CdTe, electron traps, DLTS study 4-80533  
 n-CdTe:In, electron traps, DLTS study 4-80533  
 CdTe-ZnTe heterojunction, interface trap depths 4-61442  
 GaAs, LPE growth, deep intrinsic centers, anisotropic capture 4-113897  
 GaAs, liquid encapsulated Czochralski growth, deep level study 4-98569  
 GaAs, MOCVD grown, deep electron traps, DLTS obs. 4-84585  
 GaAs MOS structures with anodic oxides, defect states, DLTS study 4-114043  
 GaAs, scanning DLTS investig. 4-75892  
 GaAs, sputter etch induced electrically active defects, H passivation 4-108918  
 GaAs, trap parameters meas. by photo-excited DLTS (*Japanese*) 4-80544  
 GaAs:Fe, Cu, epilayers, deep states, DLTS study 4-108802  
 GaAs-Al(Au) Schottky barrier contacts, LEC grown, electron traps, DLTS signals, effect of metal 4-84691  
 GaAsP strained-layer superlattice structures and their buffer layers, comparison of trapping levels 4-113885  
 GaP, scanning DLTS investig. 4-75892  
 Ge, neutron transmutation doped, annealing, DLTS study 4-60942  
 Ge, sputter etch induced electrically active defects, H passivation 4-108918  
 Ge:Ar(Sb), neutron-transmutation-doped, defects 4-60967  
 InP, electron irradiation induced defects, energy and orientation depend. 4-108810  
 InP:Si, electron irradi.-induced deep traps, impurity conc. effects 4-88468  
 InP:Zn, grown-in defects, annealing effects, DLTS studies 4-84287  
 InP-Au Schottky barriers, semicond. LEC growth, deep level defects (*Chinese*) 4-61320  
 Si, a-centre and thermal donor levels, Hall effect, DLTS meas., press. depend. 4-80529  
 Si,  $\gamma$ -ray irradi., trapping centres, DLTS studies 4-104147  
 Si, ion implanted, laser or electron beam annealing, electronically active defects, DLTS 4-80527  
 Si, ion implanted, pulsed laser and thermal processing, defect anal. 4-70133  
 Si MIS struct., X-ray irradi., interface traps, DLTS studies 4-104282  
 Si, point defects due to laser annealing, DLTS study (*Chinese*) 4-84584  
 Si, sputter etch induced electrically active defects, H passivation 4-108918  
 Si:Au, donor and acceptor levels, DLTS meas. 4-88473  
 n-Si:Au, doping by laser (*Chinese*) 4-113473  
 Si:Au, photocurrent deep level transient spectra 4-80535  
 Si:Au, transient capacitance of Au acceptor energy level under uniaxial stress (*Chinese*) 4-75888  
 p-Si:B, ion implanted, electron beam annealing, DLTS study 4-60960  
 Si:B solar cell, electron irradi., photon effects 4-93618  
 n-Si:H, neutron irradiated, deep levels study (*Chinese*) 4-92649  
 a-Si:H, resolution of DLTS energy scale controversy 4-104166  
 a-Si:H:B, doping effect on gap states 4-88488  
 Si:Li solar cells, counterdoped, increased radiation resistance to electron irradi. 4-81539  
 Si:Mn, Cu, impurity energy levels, DLTS and capacitance studies 4-88471  
 SiO<sub>2</sub>, O thermal donor, symmetry and electronic props., DLTS studies 4-113886  
 Si:P,O, trap spectrum of O donor, DLTS study 4-92651  
 Si:Pd, deep levels, DLTS study (*Chinese*) 4-113887  
 Si-Mo contacts, ion beam sputter deposition, defects, DLTS and EBIC studies 4-61848  
 Si-SiO<sub>2</sub> interface states, degeneracy and capture cross sections, DLTS studies 4-76039  
 Si-SiO<sub>2</sub>-Mo MOS diodes, carrier trapping centres and interface states induced by RF sputtering of Mo 4-88603

## deep level transient spectroscopy continued

- Si-SiO<sub>2</sub>-Na, Na<sup>+</sup>-induced surface states, DLTS study 4-61463  
 ZnSe:N, acceptor levels, optically excited DLTS study 4-61322

## deep levels

## see also deep level transient spectroscopy

- amorphous semiconductors, picosecond electronic relaxations 4-108892  
 chalcogenide glass thin films, threshold switching and trap filling 4-92770  
 depletion regions, carrier capture from free-carrier tails 4-92746  
 III-V semiconductors, antisite defect energy levels 4-80548  
 III-V semiconductors, thermochemistry study of deep level defects 4-75894  
 III-V semiconductors, wide band-gap, deep levels, review, book contrib. 4-88484  
 insulator with deep traps in carrier density dependent mobility regime, cylindrical current flow 4-98629  
 MIS structures, hole traps, trivalent Si centres, EPR meas. 4-80817  
 narrow band gap semicond., two-photon interband electron transitions via deep impurity levels 4-88477  
 ODMR and photoluminescence detection (*Japanese*) 4-80844  
 p-n junctions, tunnel capture influence on impurity-level recombination of charge carriers (*Russian*) 4-70923  
 pulsed admittance spectroscopy and capture cross sections 4-92653  
 semiconductor, deep centre problem, analytic soln. by method of continued fractions 4-61333  
 semiconductor, deep centres, carrier capture cross section meas. method (*Chinese*) 4-92741  
 semiconductors, compensated, exclusive effect quenching under action of impurity illum. generating majority current carriers 4-104262  
 semiconductors, compensated, spatial distrib. of impurities 4-103784  
 semiconductors, deep impurities, final state effects 4-84982  
 semiconductors, deep levels, expt. and theoretical studies, review 4-84593  
 semiconductors, deep levels and interface states, electrochem. photocapacitance spectroscopy method 4-65635  
 semiconductors, DLTS and deep level optical spectroscopy 4-108815  
 semiconductors, dynamic defect reactions induced by multiphonon nonradiative recomb. of injected carriers at deep levels 4-70316  
 semiconductors, nonradiative multiphonon capture of carriers by deep traps 4-75889  
 semiconductors, p-type, impact recombination by deep and shallow acceptors 4-84632  
 semiconductors, recombination through deep centers in electron-hole scattering 4-113970  
 SOS, ion implanted, elec. props., effect of heat treatment 4-98759  
 SOS heteroepitaxial film, surface photovoltaic characterisation 4-80697  
 tunneling negative-U centers and photo-induced reactions in solids 4-108816  
 (Al,Ga)As heterojunctions, laser-induced defects, photochem. etching 4-113439  
 AlGaAs-GaAs heterojunction interfaces, deep levels, forward I-V and DLTS meas. 4-70915  
 n-Al<sub>0.3</sub>Ga<sub>0.8</sub>As, MBE grown, deep electron traps, growth conditions and alloy composition influence 4-98558  
 Al<sub>0.3</sub>Ga<sub>0.8</sub>As solar cell structs., photoluminescence and spectral response 4-89404  
 Al<sub>0.3</sub>Ga<sub>0.8</sub>As/GaAs heterostructure, selectively doped, transient photocond. obs. 4-70862  
 CdIn<sub>2</sub>S<sub>4</sub> single cryst., photocond., photoluminescence and non-equilib. carrier recombination 4-65706  
 CdSe, interface states studied by electrochemical photocapacitance spectroscopy 4-98750  
 n-CdTe, deep levels, plastic deform. effects, DLTS studies 4-84591  
 n-CdTe, electron traps, DLTS study 4-80533  
 CdTe:Ag(Cu), deep levels, pulsed admittance spectroscopy and capture cross sections 4-92653  
 n-CdTe-p-Cu<sub>2</sub>Te(p-Au<sub>2</sub>Te) heterojunctions, deep levels, photocapacitance spectra 4-61410  
 GaAs, plasma enhanced epitaxy, low temp. 4-99330  
 GaAs, compensation resulting from N ion implantation 4-104150  
 GaAs, contour maps of EL2 deep level, dislocations 4-80530  
 GaAs, deep centre point defect introduction 4-108819  
 GaAs, deep centres, electron probe method anal. 4-104158  
 GaAs, deep impurity levels, ENDOR and ESR spectra 4-84594  
 GaAs, deep level wavefunctions, behaviour in shallow energy region (*Chinese*) 4-92650  
 GaAs, deep-level wavefunctions with energies near band edges 4-92656  
 GaAs, electroluminescence and photoluminescence in aq. redox electrolyte 4-88584  
 GaAs epitaxial structs., photomemory effect, influence of deep levels 4-104261  
 GaAs heterojunctions and homojunctions, deep levels, tunnel spectra meas. 4-84685  
 GaAs, impurity photocurrent and deep level spectroscopy 4-70865  
 GaAs, irradi., E3 centre accumulation, effect of defect charge state 4-60966  
 GaAs, LEC grown, EPR identification of As<sub>2</sub>C antisite defects 4-71178  
 GaAs LEC substrate, characterisation of impurities and microdefects (*Japanese*) 4-103778  
 GaAs, LPE growth and nonequilib. deep centre trapping 4-108744  
 GaAs, liquid encapsulated Czochralski growth, deep level study 4-98569  
 GaAs Schottky diodes, deep levels, photocapacitance spectra 4-61410  
 GaAs Schottky diodes, transport mechanism, deep centre effects 4-88558  
 GaAs, semi-insulating, 0.635 eV photoluminescence band, EL2 level 4-114315  
 GaAs, undoped, deep donor EL2, beam coupling at 1.06  $\mu$ m using photorefractive effect 4-96987  
 GaAs: Mn, spin-dependent recombination, optical pumping studies 4-99183  
 GaAs:Cr, eval. of Cr conc. by optical absorpt. 4-104635  
 GaAs:Cr, impurity photocond., internal quantum efficiency 4-88540  
 GaAs:O p-n structs., magnetically sensitive, elec. characs. (*Russian*) 4-65729  
 GaAs:Si, ion implanted, and semi-insulating GaAs, deep levels, photoconductivity study 4-88469  
 GaAs:Sn/GaAs:Cr interface, electron and hole traps, photovoltaic studies 4-104283  
 GaAs/(Al,Ga)As selectively doped heterostruct., transport props. 4-70913  
 GaAs/AlGaAs heterostructures, carrier density, hydrostatic press. control 4-98735  
 GaP, deep impurity levels, ENDOR and ESR spectra 4-84594

## deep levels continued

- GaP:Ni<sup>2+</sup> Jahn-Teller coupling forces, self consistent LCAO calc. 4-98577  
GaP:Zn, O LEDs, centre responsible for capacitance slow relax. 4-65735  
Ge, deep impurity conc., elec. resist. and Hall coeff. meas. 4-65638  
Ge, deep level impurities, low temp. passivation techniques 4-59561  
Ge, dislocations, deep electron levels, recursion calc. 4-70716  
Ge:Cu(Au), nonradiative multiphonon capture of carriers by deep traps 4-75889  
Ge:D, plasma treated, D diffusion and interaction with point defects, deep level recombination centres 4-60951  
Ge:Zn, nonohmic hopping cond. in strong elec. fields 4-88515  
Hg<sub>1-x</sub>Cd<sub>x</sub>Te, deep level anal. using temp. depend. of capacitance (*Chinese*) 4-113888  
InP, electron irradi. induced deep traps, deep level optical spectroscopy 4-104156  
InP photoelectrodes, surface states, photocapacitance spectra studies 4-114010  
InP, transition metal diffusion, photoluminesc. study, deep acceptor levels obs. 4-70461  
InP:Si, electron irradi.-induced deep traps, impurity conc. effects 4-88468  
InP-Au Schottky barriers, semicond. LEC growth, deep level defects (*Chinese*) 4-61320  
La, photoionisation, local density-based random phase approx. calc. 4-102656  
NaCl with U-centre, deep impurity states, cryst. cluster method 4-61324  
PbTe Schottky barriers, resonant magneto-optical transitions from a deep level 4-76440  
Se, amorphous, defect states and photoelec. behaviour 4-113903  
Se:Te, As glassy films, pure and doped, deep level defects, xerographic spectra studies 4-61339  
Si, deep impurity levels, cluster method of pseudoatomic orbitals (*Chinese*) 4-84583  
Si, deep impurity levels, ENDOR and ESR spectra 4-84594  
Si, deep level impurities, low temp. passivation techniques 4-59561  
Si, deep level wavefunctions, behaviour in shallow energy region (*Chinese*) 4-92650  
Si deep-level wavefunctions with energies near band edges 4-92656  
Si, defect states, T<sub>2</sub> symmetric deep level wave functions 4-108801  
Si, dislocations, deep electron levels, recursion calc. 4-70716  
Si, ESR meas. of chalcogen pairs, theory 4-104493  
n-Si, ion implanted with He<sup>+</sup>, deep donor levels 4-61323  
Si, ion implanted with noble gases, optical defects, photoluminesc. study 4-71429  
Si, irradiated, excitation spectroscopy on 0.79 eV (C) line defect 4-93112  
Si, plastically deformed, deep levels, capacitance, reverse current meas. 4-61319  
a-Si, space charge limited current rel. to density of states 4-98637  
Si surface, excess carriers, light-induced recombination 4-76005  
Si:B, deep level impurities at bond centered interstitial site 4-108814  
Si:B( $\mu^+$ ), tetrahedral interstitial impurities, electronic struct. 4-65636  
n-Si:H, neutron irradiated, deep levels study (*Chinese*) 4-92649  
a-Si:H Schottky barriers, sputtered, freq. depend. capacitance, admittance meas. 4-98693  
a-Si:H Schottky solar cells, gap state density 4-88438  
Si:H wide optical gap binary alloy films, elec. props. 4-113956  
Si muon, spin polarised electron struct. of positive muon, LCAO-Green's function anal. 4-65634  
Si:S, deep levels, DLTS meas. 4-84592  
Si:Te, donor states, Hall effect and cond. meas. 4-104145  
a-Si-based field effect transistors, flat-band volt. and surface states 4-92825  
Si<sub>3</sub>Ge<sub>1-x</sub> alloys, substitutionally sp<sup>3</sup>-bonded defects, deep energy levels 4-108813  
Si<sub>3</sub>Ge<sub>1-x</sub>:P(As)(Sb), paired donor impurities energy levels 4-61315  
Si<sub>3</sub>N<sub>4</sub>:F films, plasma enhanced CVD, insulating props. 4-61865  
Th, photoionisation, local density-based random phase approx. calc. 4-102656  
U, photoionisation, local density-based random phase approx. calc. 4-102656  
ZnO, nonlinear light absorpt., two-photon absorpt. spectra 4-96992  
ZnS conductive film, MBE prep. with single effusion source, luminesc. and elec. props. 4-99323  
ZnS:Cu<sup>2+</sup> Jahn-Teller coupling forces, self consistent LCAO calc. 4-98577  
ZnS,Se<sub>1-x</sub>, deep impurity, trap embedding, luminesc. spectra 4-61321  
ZnSe, VPE growth, photoluminesc. props. 4-61858

## defect electron energy states

- see also colour centres; deep levels  
alkali halides, stability and optical props. of self-trapped exciton 4-104129  
alkali halides, with F-centres, hopping-type electronic processes in pre-breakdown elec. fields 4-108868  
alkali metal halides, F-centre states, hybrid method with floating 1-s Gaussian basis 4-70709  
diamond:Fe, electronic struct. calcs. 4-113894  
diamond, type IIb, individual dislocation and cathodoluminescence emission polarisation 4-99199  
III-V semiconductors, antisite defect energy levels 4-80548  
III-V semiconductors, thermochemistry study of deep level defects 4-75894  
infinite cryst. with charged point defects, total energy, Green's function calc. 4-108812  
insulators, defect states, hybrid method with floating 1-s Gaussian basis 4-70709  
metal, positron annihilation characteristics for positron in divacancies and vacancy clusters 4-70742  
metal semiconductor interface, electronic props., contrib. of defects 4-84697  
multiwell one-dimensional struct., tunnelling theory 4-70912  
naphthalene cryst., excitons, defects and intramolecular phonon interactions (*Russian*) 4-98532  
nonmetallic crystals, optically stimulated electron jumps, between local electron centres 4-65641  
organic-molecular crystals, excitonic processes (*Russian*) 4-98531  
oxides, ionic, particle bombard., defects and defect processes 4-70190  
quartz, rose-coloured, Al<sub>2</sub>O<sub>3</sub>-P radiation defect, EPR study 4-71180  
quartz, vacuum swept, Al and OH<sup>-</sup> defect centres 4-61335  
quenching centre form., host interstitial injection by oxidising surface 4-65258

## defect electron energy states continued

- semiconductors, charged dislocations, electronic props. 4-98565  
semiconductors, dislocation electronic props., review 4-92205  
semiconductors, DLTS and deep level optics, spectroscopy 4-108815  
semiconductors, excited quasistationary states relax. as source of exoelectron emission 4-99290  
semiconductors, localised defects, electronic struct. and stability 4-80538  
semiconductors, negative-U tunnelling centres and photostimulated reactions 4-113892  
n-Si, radiation defect formation, annealing, defect interactions 4-113499  
space groups, band representations, appl. in theory of electronic states of crystalline solids 4-75833  
titanates, Fe doped, point defects and semicond. behaviour 4-70137  
two electron binding at fixed centre with one- and two-body pots., criterion 4-75896  
two electron binding criteria for two-dimens., many-body bound state 4-75897  
two-level systems, interconversion valence-alternation pair originated, anomalous interaction with phonons 4-92309  
(Al,Ga)As heterojunctions, laser-induced defects, photochem. etching 4-113439  
Al<sub>1-x</sub>Ga<sub>x</sub>As p-n junctions, organometallic VPE, anomalous light sensitivity 4-92817  
Al<sub>1-x</sub>Ga<sub>x</sub>As:Si, grown by MBE, photoluminesc. composition depend. 4-84996  
Al<sub>1-x</sub>Ga<sub>x</sub>As:Si, grown by MBE, photoluminesc. spectra, defect-related emissions 4-84997  
As<sub>2</sub>Se<sub>3</sub>Te<sub>6-x</sub> glasses, DC props., neutron, and gamma-ray effects 4-103814  
BaTiO<sub>3</sub>, pure and Nb-doped, elec. cond. 600-800°C, defect struct. 4-98604  
Bi oxides, Bi<sub>2</sub>MO<sub>20</sub>, M=Ge,Ti, luminesc. props. 4-76514  
Bi<sub>2</sub>Al<sub>4</sub>O<sub>9</sub>, luminesc. props. 4-76514  
Bi<sub>2</sub>Ge<sub>2</sub>O<sub>9</sub>, luminesc. props. 4-76514  
CaF<sub>2</sub>:Na, photochemical conversion of M<sub>A</sub>-centres, identification of M<sub>A</sub><sup>+</sup>-centre, absorpt. and fluoresc. spectra 4-76501  
Cd<sub>3</sub>As<sub>2</sub>, role of vacancies in band struct. 4-75853  
CdP<sub>2</sub>, absorpt. spectra and defect states (*Russian*) 4-71419  
CdS amorphous films, optical absorption coeff. and gap state density 4-66088  
n-CdTe, deep levels, plastic deform. effects, DLTS studies 4-84591  
CuInS<sub>2</sub>, defect chemistry, elec. and Mossbauer studies 4-70730  
CuInSe<sub>2</sub>, radiative recombination and shallow centres 4-109250  
Fe, grain boundary with impurity segregation, atomic and electronic structs., 4-113463  
GaAs, acceptor level, 78 meV, luminescence and Raman scatt. studies 4-70704  
GaAs, contour maps of EL2 deep level, dislocations 4-80530  
GaAs, deep acceptor, Hall effect obs. and photoluminescence 4-80532  
GaAs, deep centre point defect introduction 4-108819  
GaAs, deep level wavefunctions, behaviour in shallow energy region (*Chinese*) 4-92650  
GaAs, deep levels associated with vacancy-impurity pairs 4-92662  
GaAs, deep-level wavefunctions with energies near band edges 4-92656  
GaAs, defect anisotropy following electron irradiation 4-75534  
GaAs, EL2 defect: technological and physical aspects 4-75891  
GaAs, electron irradi., electronic struct. of E3-defects 4-70720  
GaAs, electron traps, props. and nature 4-75890  
GaAs, magnetic circular dichroism-ODMR study of EL2 defect 4-104151  
GaAs, midgap level surface density, heat treatment and capping effects 4-114011  
GaAs, muonium states, positive muon depolarisation 4-71243  
GaAs, photoluminescence characterisation of impurities and defects 4-88876  
GaAs Schottky diodes, transport mechanism, deep centre effects 4-88558  
GaAs, sputter etch induced electrically active defects, H passivation 4-108918  
GaAs, vacancy energy levels, impurity state pinning, tight-binding calcs., local density theory 4-88470  
GaAs:B, interaction between B and defects 4-80082  
GaAs:C(Si), impurity and defect anal. by IR absorpt. spectra 4-75893  
GaAs<sub>1-x</sub>P<sub>x</sub>, EL2 metastable state, photocapacitance quenching study 4-70717  
GaP, defect electronic struct. calcs. 4-61326  
GaP, localised vacancies, electronic struct. and stability 4-80539  
GaP, symm. deep level wavefunction for defect pairs (*Chinese*) 4-104144  
GaP:O, electronic struct. of single neutral ideal P vacancy 4-92657  
Ge (111)-(2×1), dangling bond states, HREELS and photoelectron spectra study 4-65725  
Ge, dislocations, deep electron levels, recursion calc. 4-70716  
Ge, gamma-irradiated, hole traps 4-103799  
Ge, p<sup>+</sup>-n junction irradi. with γ-rays, capacitance spectroscopy 4-104287  
Ge single cryst., α-particle irradi., defects and photoelectromag. effects 4-84654  
Ge, sputter etch induced electrically active defects, H passivation 4-108918  
Ge:Si, ultrapure and doped, muonium state, positive muon spin precession signals 4-71242  
Hg<sub>1-x</sub>Cd<sub>x</sub>Te, deep impurity and defect states 4-88474  
InP, electron irradiation induced defects, energy and orientation depend. 4-108810  
InP epitaxial, deep and shallow levels due to ion irradi. 4-80531  
n-InP, self-trapping and metastable M-centre 4-108809  
InP:Mg(Fe,Mg), implanted, effect on photoluminescence props. 4-85007  
InP:Si, electron irradi.-induced deep traps, impurity conc. effects 4-88468  
InP-Au Schottky barriers, semicond. LEC growth, deep level defects (*Chinese*) 4-61320  
InSb/Al<sub>2</sub>O<sub>3</sub>-SiO<sub>2</sub> system, slow states, field effect studies 4-65752  
KBr, excited F-centre emission, effect of CO<sub>2</sub> laser light 4-61742  
KCN, electric dipole ordering 4-61633  
KCl:Li, optically excited colour centres, relaxation dynamics 4-113896  
KI, F-centre luminesc., mag. circular polarisation, anomalous effect 4-93062  
LiCl, substitutional defects, molecular cluster-INDO calcs. 4-108806  
LiF, substitutional defects, molecular cluster-INDO calcs. 4-108806  
LiNbO<sub>3</sub>, electrooptic cells, γ-irrad. effect on optical inhomogeneity 4-76438  
NaCN, electric dipole ordering 4-61633  
NaCl, cryst., X-irrad., F-centre decay during photoannealing 4-80036  
NaCl, substitutional defects, molecular cluster-INDO calcs. 4-108806

**defect electron energy states continued**

- NaF polycrystalline thin films, neutron and X-irrad., photochemical hole burning 4-76518  
 NaF, substitutional defects, molecular cluster-INDO calcs. 4-108806  
 NaI(Tl) deformed cryst., relationships among stresses, microstruct. and photolum. 4-71441  
 NbC, C vacancy electronic struct., tight binding calculations 4-92661  
 Ne, solid, self-trapped excitons, electronic struct., hybrid method with floating 1-s Gaussian basis 4-70709  
 Pb oxides, PbM<sub>2</sub>O<sub>4</sub>, M-Al, Ga, luminesc. props. 4-76514  
 PbGeO<sub>7</sub>, luminesc. props. 4-76514  
 Pb-, Sn-Te, defect states, impurity photoconductivity transient studies 4-80545  
 PbTe Schottky barriers, resonant magneto-optical transitions from a deep level 4-76440  
 PbTe:B, absorpt. spectra and impurity states 4-104638  
 PbTe:Ga, elec. and optical meas. (Russian) 4-84636  
 S, allotropes, electronic states, localised orbital approach 4-92655  
 Se, allotropes, electronic states, localised orbital approach 4-92655  
 Se, amorphous, defect states and photoelec. behaviour 4-113903  
 Se:Te, As glassy films, pure and doped, deep level defects, xerographic spectra studies 4-61339  
 Se-Te-As, amorphous, defect states and photoelec. behaviour 4-113903  
 Si (100) 2X1, dissociative adsorption of water, IR spectra obs. 4-93557  
 a-Si alloys, metastable defect states, X $\alpha$  scatt. wave calc. 4-113899  
 Si, amorphous, ion implanted, crystn. growth velocities, charged dangling bonds 4-88093  
 Si, clusters of electrically active centres and impurity states 4-70183  
 Si, deep level wavefunctions, behaviour in shallow energy region (Chinese) 4-92650  
 Si deep-level wavefunctions with energies near band edges 4-92656  
 Si, defect states, T<sub>1</sub> symmetric deep level wave functions 4-108801  
 Si, dislocations, deep electron levels, recursion calc. 4-70716  
 a-Si, electronic struct. of defects, cluster Bethe lattice method 4-70739  
 Si, grain boundaries, spin-depend. trapping, effects of light and modulation freq. 4-104155  
 Si,  $\gamma$ -ray irrad., trapping centres, DLTS studies 4-104147  
 Si, ideal vacancy, electronic struct. calcs. 4-70722  
 Si, ion implanted, laser or electron beam annealing, electronically active defects, DLTS 4-80527  
 n-Si, ion implanted with He<sup>+</sup>, deep donor levels 4-61323  
 Si, ion implanted with noble gases, optical defects, photoluminesc. study 4-71429  
 Si, localised vacancies, electronic struct. and stability 4-80539  
 Si, partial 90° dislocation, structural and elec. props. 4-108368  
 Si, photoluminescence characterisation of impurities and defects 4-88876  
 Si, proton irrad., acceptor level positions of divacancy 4-70725  
 n-Si, proton irradiated, electrophysical props. 4-108861  
 Si, self interstitials, electronic struct. and total energy migration barriers 4-108811  
 Si, solar cell, H passivation of electrically active defects (French) 4-62359  
 Si, sputter etch induced electrically active defects, H passivation 4-108918  
 Si, submicron epitaxial films quality, for device fabrication 4-88567  
 Si surface, excess carriers, light-induced recombination 4-76005  
 Si, vacancy energy levels, impurity state pinning, tight-binding calcs., local density theory 4-88470  
 Si, vacancy energy spectrum calc. by semiempirical technique using MO approach 4-88478  
 Si:Al, electronically simulated defect migration 4-113730  
 Si:B, impurity electronic struct. cluster X $\alpha$  calc. 4-65639  
 a-Si:H, correlated defects and steady-state photoconductivity 4-61417  
 a-Si:H, deep recombination centres, luminescence and EPR studies 4-104164  
 Si:H, RF sputtered amorphous film, dark cond. and photocond., annealing effects 4-70960  
 a-Si:H,O(N) alloys, electron trapping states, tight binding formalism calcs. 4-113901  
 a-Si:H,P, defect states and carrier capture processes 4-104165  
 Si:In(Tl), isoelectronic bound excitons, transient photoluminesc. study 4-80507  
 Si:Li and Si:Li, C, electron irrad., luminesc. decay time, absorpt., isotope splitting, and Zeeman meas. 4-71434  
 Si:Mg(Al)(S), third-period interstitials, electronic struct. calcs. 4-108808  
 Si-SiO<sub>2</sub>, MOS struct., H passivation of implantation defects using a-Si:H film 4-71744  
 Si<sub>3</sub>H<sub>2n+2</sub>, defects, molecular cluster studies 4-84586  
 SiN<sub>x</sub>H<sub>y</sub>, amorphous, electronic struct., photoemission 4-108776  
 SiO<sub>2</sub>, amorphous, local electronic density of states, influence of Si-Si bonds 4-92671  
 SiO<sub>2</sub>, amorphous, X- and gamma-irrad., E'-centre variants, EPR obs. 4-70207  
 SrTiO<sub>3</sub>:Fe<sup>2+</sup>-V<sub>O</sub> pairs, electronic struct. calcs. 4-113890  
 Te, neutron irrad. induced defects, optical props. near fundamental energy gap 4-84318  
 Ti-V, positron annihilation with stacking faults (Russian) 4-71473  
 TiO<sub>2</sub>, electronic struct. of O<sub>2</sub> vacancy 4-88475  
 TiO<sub>2</sub>, K-edge photoabsorpt. cross section, effect of vacancies 4-93139  
 VO<sub>2</sub>, K-edge photoabsorpt. cross section, effect of vacancies 4-93139  
 ZnS, charge states of S vacancy, tight-binding approx. 4-61331  
 ZnSe, localised vacancies, electronic struct. and stability 4-80539  
 ZnR<sub>n</sub>, non-stoichiometric, electronic struct., XPS study 4-76638

**defectoscopy see crack detection****defects, crystal see crystal defects****defibrillators**

see also patient treatment

reduced mortality after automatic defibrillator implantation 4-81817

**deformation**

see also bending; cold working; creep; drawing (mechanical); elastic deformation; elongation; ferroelasticity; plastic deformation; shape memory effects; thermomechanical treatment

anisotropic elastoplastic materials, finite deform., effects of plastic rotation 4-60302

anisotropic materials, generalisation of Mindlin's kinematic plate theory 4-91741

arch, shallow, Marguerre-type, snap-through problem 4-101625

axisymmetric combined backward-forward, upper-bound solutions (Chinese) 4-81212

beam bending theory, shear deformation, strain and stresses 4-112723

**deformation continued**

- beams, curved, large-rot. nonlinear problems, mixed models and reduction techniques 4-101637  
 capillary and fissile materials, finite uniform strain, metaisotropic struct. 4-87558  
 classical rate-theory-based deformation-rate law 4-99417  
 coupled shear walls, method of calc. force and displacement (Chinese) 4-79445  
 deformation kinetics of ageing materials 4-60278  
 defofofossite type compounds, deform. of octahedral layers (Japanese) 4-75606  
 diamond, synthetic, single-cryst. deform. evaluation using Kossel pseudopatterns (Ukrainian) 4-88226  
 DWR cladding tubes, props. above annealing temp., mech. props. after thermal shock 4-106835  
 Earth crust, method for quantifying deform. of given faulted volume (French) 4-105556  
 Earth crust deformation assoc. with earthquake cycle, models of viscoelastic flow in asthenosphere 4-110068  
 elastic body, simply connected, action of rigid smooth stamps 4-79525  
 elastomer, stretched, recovery of surface layers during ageing in ozone (German) 4-65554  
 elastomer, surfactant-modified, slow phys. relax. processes effect on props. in wide temp. range (Russian) 4-75327  
 epoxy mirrors for astronomical telescopes, mechanical stability and usefulness (Russian) 4-101169  
 Ericksen's problem of elasticity, iterative soln. method 4-110874  
 FCC crystal containing mech. twin lamellae, shear band formation 4-70263  
 fibre reinforced composites, microstress redistrib. due to time-depend. processes 4-97329  
 fibre reinforced laminated plates, design for max. stiffness 4-75599  
 fibre reinforced plastics, tensile tests, at cryogenic temps., acoustic emission 4-76804  
 finite elasticity, equilb. solns. 4-97328  
 finite plasticity, constitutive results 4-69690  
 fluid particles, deformation in contact zone under linear tension 4-109690  
 free elastic body systems with isoperimetric constraints, vibr. anal. 4-103244  
 fusion reactor components, dynamic deform. due to EM forces, finite element anal. 4-74050  
 glass fibre reinforced phenolformaldehyde, laminate plates, shrinkage strains 4-61915  
 glass-plastic plates, deform. during static loading and interaction with a shock 4-79533  
 grain deformation 4-76745  
 graphite, deform. under hydrostatic states 4-103859  
 graphite epoxy alignment tube, thermal structural deform., optimisation 4-87415  
 helical coil springs, stress and vibr. anal., shearing deform. and rot. inertia effects (Japanese) 4-103228  
 homogeneous systems under shock compression, heterogeneous deform. (Japanese) 4-103880  
 incompressible space with vertical circular cylindrical cavity containing a fluid, stability in case of large uniform subcritical deformations. 4-74905  
 interface surfaces, characteristics modelling using finite element method 4-79521  
 internal strain of cryst. lattice; contrib. to elastic const. and piezoelec. coeffs. 4-80135  
 Jones-Nelson-Morgan nonlinear composite materials model, incremental stress-strain rels. (Chinese) 4-108021  
 knee capsule deform., microprocessor-based tissue displacement monitor 4-89864  
 laminated plates, natural freq. prediction by higher order shear deform. theory 4-79491  
 liquid crystalline polymers, deform. studies 4-113303  
 mechanical systems with distributed parameters, minimax filtration problem soln. 4-74858  
 membrane, circular, impact response to blunt projectile 4-87634  
 metal reinforced plastics, struct. during pressure and temp. changes 4-89088  
 metals, FCC, inhomogeneous deform., mech. and struct. effects (Polish) 4-84336  
 metals, mechanical instability of cellular dislocation structure 4-65268  
 microcrack density function, deformations and thermodynamics, statistical mechanics 4-60330  
 minerals barycentre alignment in deformed rocks 4-105544  
 moire fringe techniques in engineering metrology 4-78366  
 nematic liquid crystal, deformation in elec. and mag. fields as seen by proton NMR 4-113321  
 oceanic lithosphere, numerical simulation of interaction between trench and seamount 4-105526  
 optical fibres, single-mode, microdeform. losses 4-69556  
 plate, cantilever, finite, long-time response to antisymm. dynamic surface loading 4-87563  
 plate, cantilever, finite, long-time response to dynamic surface loading 4-87564  
 plate, room temp., thermal deformation by misfocus speckle method (Chinese) 4-60350  
 plate, spalling fracture under shock loading 4-89112  
 plates, elastoplastic, large deflection, incremental model (French) 4-74890  
 plates, flat, strains determ. by moire displacement patterns 4-87642  
 plates, laminated composite, mixed finite element anal. 4-74904  
 plates and shells, piezoceramic, static stability (Ukrainian) 4-87596  
 poly  $\alpha$ -olefins, spherulitic, dynamic tensile deform., X-ray diff. obs. 4-85173  
 polycrystals, microdeform. anal. 4-65328  
 polymer, mech. strained, temp. depend. studies using photoregistering small-angle X-ray camera (Russian) 4-75242  
 polymer deformation studies by FT-IR spectroscopy, mechanical stretcher interface 4-103850  
 polymer deformation studies by time-resolved FT-IR spectroscopy 4-103851  
 polymer fibres, mech. props. rel. to conform. compositions (Russian) 4-103862  
 polymer-metal bilayer deform. recording process, optical storage appls. 4-79251  
 polymeric films, biaxial stretching instability, appl. of Swift criterion (French) 4-92581

- deformation continued**  
 polymeric network, uniformly strained, mol. orientation (*Russian*) 4-75326  
 polypropylene-ultrahigh molecular weight polyethylene, deformation orientation 4-98176  
 porous elastic material, finitely strained periodic, macroscopic props. 4-74887  
 porous materials, thermoelastoplastic deform. 4-60306  
 powder compaction, deform. meas. by scanning-moire method 4-87643  
 prismatical beams, finite deforms., variational anal., warping stiffness effects on buckling loads 4-79479  
 PVC composites, filled, deform. thermodynamics 4-89089  
 quartz powders, shock-loaded, deform., X-ray line broadening obs. 4-65324  
 reactor fuel pin transient deformation, cladding strains, MOX fuel appl., creep 4-102378  
 rocks, fracture mechanics and acoustic emission of anti-plane shear cracks 4-77507  
 shell, cylindrical, hanging on ropes, deformation and stress anal. 4-112705  
 shell, open-conical sandwich, nonlinear stability under external press. and compression 4-87598  
 shell and plate analysis, large rotation, optimal, stable and invariant hybrid elements 4-74865  
 shells of revolution, anisotropic, with transverse shear, stressed state 4-74860  
 shrinkage and molecular extension 4-75600  
 stainless steel, deformation and failure from neutron irradiation 4-102357  
 steel plates deform. during static loading and interaction with a shock 4-79533  
 strain softening, materials model with appl. in modelling strain localisation 4-99407  
 stress-boundary value problems in finite elasticity 4-74889  
 stretching of plane fluid film 4-97453  
 strip, semi-infinite, decaying states of plane strain and boundary conditions for plate theory 4-83822  
 symmetric stresses and strains, graphical representations (*Japanese*) 4-101651  
 thin films, strain relaxation mechanisms 4-80463  
 topaz, deformation expts, indicating embrittlement by water 4-94101  
 C fibre reinforced plastics, struct. during pressure and temp. changes 4-89088  
 In, deformed, low-temp., recovery activation enthalpy, positron annihilation meas. 4-76556  
 Pb and Pb-alloy thin films on Si, strain relaxation mechanisms 4-80463  
 Pb alloys, lattice correspondence of  $\delta$ - $\alpha$  displacive transform. 4-75351  
 Si, crystal whiskers, cyclically deformed, relaxation spectrum 4-61264  
 Si:Au, transient capacitance of Au acceptor energy level under uniaxial stress (*Chinese*) 4-75888  
 W-Ni-Fe (5.5 wt.%) heavy alloy, precipitation hardening 4-114564
- deformation lines** *see Luder's bands*
- degenerate semiconductor materials** *see degenerate semiconductors*
- degenerate semiconductors**  
*see also heavily doped semiconductors; superconducting semiconductors*  
 ferromagnetic semiconductors, degenerate, spin waves at low temps. 4-114096  
 piezoelectrics, even elec. cond. with streaming, separation of shift and ballistic contributions 4-113951  
 n-Cd<sub>3</sub>As<sub>2</sub>, degenerate, Debye screening length under influence of arbitrary mag. quantisation 4-70836  
 (CuCr<sub>7</sub>Se<sub>4</sub>)<sub>2</sub>(Cu<sub>0.5</sub>Ga<sub>0.5</sub>Cr<sub>2</sub>Se<sub>4</sub>)<sub>1-2x</sub>, semiconducting spin glasses, resistance, magnetoresistance, studies 4-108862  
 (CuCr<sub>7</sub>Se<sub>4</sub>)<sub>2</sub>(Cu<sub>0.5</sub>In<sub>0.5</sub>Cr<sub>2</sub>Se<sub>4</sub>)<sub>1-2x</sub>, semiconducting spin glasses, resistance, magnetoresistance, studies 4-108862  
 n-CuInSe<sub>2</sub>, optical absorption edge, influence of carrier conc. 4-80943
- dektrons**  
 No entries
- delay lines**  
*see also acoustic delay lines*  
 diode-switchable coaxial cable delay system for a synthesis radio telescope 4-101164  
 optical fibre delay line signal processing, overview 4-97093  
 optical fibre macrobend tapped delay lines for high-speed signal processing 4-97094  
 self-aligning scanning optical delay line for picosec. spectroscopy 4-86485  
 single mode fibre optic recirculating delay line with bandwidth >1 GHz 4-97114  
 Nd:YAG laser pulses, freq. doubled, 80X single-stage compression using single-mode fibre and grating-pair delay line 4-64726
- delayed neutrons**  
 asymptotically stable solutions of 1-D space-time kinetics in the presence of delayed neutrons 4-64192  
 emission probability determ. using  $\beta$ - $\gamma$  spectroscopic method 4-5595  
 fission product identification from photofission by delayed neutron and gamma emission 4-109709  
 MWPC, cylindrical, <sup>3</sup>He filled, for delayed neutron registration (*Russian*) 4-83270  
 proton pairing in fission yields, delayed neutron yields versus proton, neutron and mass numbers 4-96084  
<sup>86</sup>As,  $\beta$ -decay, 2n emission probability, from half-life 4-95967  
<sup>92</sup>Ba, mass-separated short-lived fission products, half-life meas. 4-59204  
<sup>92</sup>Br,  $\beta$ -decay, 2n emission probability, from half-life 4-95967  
<sup>13</sup>K, A=50-52,  $\beta$ -decay, 2n emission probability, from half-life 4-95967  
<sup>13</sup>N,  $\beta$ -decay, 2n emission probability, from half-life 4-95967  
<sup>14</sup>Rb, A=98-100,  $\beta$ -decay, 2n emission probability, from half-life 4-95967  
<sup>156</sup>Sb,  $\beta$ -decay, 2n emission probability, from half-life 4-95967  
<sup>91</sup>Se,  $\beta$ -decay, 2n emission probability, from half-life 4-95967  
<sup>85</sup>Sr, A=93, 94, mass-separated short-lived fission products, half-life meas. 4-59204
- delayed protons**  
<sup>33</sup>Ar  $\beta$ -delayed proton spectra, cross sections, half-life, from <sup>24</sup>Mg(<sup>12</sup>C,3n) (*Chinese*) 4-73858  
<sup>123</sup>C, mass and beta-delayed proton emission 4-64103  
<sup>14</sup>Dy, A=141, 143, mass and beta-delayed proton emission 4-64103  
<sup>147</sup>Er beta delayed proton activity, half-life from <sup>142</sup>Nd(<sup>12</sup>C,7n) 4-106594  
<sup>147</sup>Er beta delayed proton activity, half-life from <sup>144</sup>Sm(<sup>12</sup>C,7n) 4-106594  
<sup>49</sup>Fe  $\beta$ -delayed proton spectra, cross sections from <sup>40</sup>Ca(<sup>12</sup>C,3n) (*Chinese*) 4-73858

- delayed protons continued**  
<sup>141</sup>Gd, mass and beta-delayed proton emission 4-64103  
<sup>141</sup>La, A=120, 122, mass and beta-delayed proton emission 4-64103
- delays**  
*see also distributed parameter systems*  
 radiowave propagation delays study due to tropospheric water vapour 4-89966
- demagnetisation**  
*see also magnetisation*  
 magnetic thin films minimum energy states, Permalloy films and bubble films 4-109050  
 recording media, stress-induced demagnetisation, magnetostriction 4-104477  
 Co, polycrystalline, approach to saturation at intermediate fields, role of internal demagnetising fields 4-76183  
 Fe, Gilbert damping, critical fluctuation effects, ferromag. resonance study 4-61539  
 Fe, sintered, mag. suscep. and porosity, semi-empirical rel. 4-84774  
 ribbon, 6.5%, rapidly quenched, mag. props. stability (*Japanese*) 4-76196  
 SiFe, polycrystalline, approach to saturation at intermediate fields, role of internal demagnetising fields 4-76183  
 WC, sintered, Co inclusions, magnetisation curves 4-109040
- demagnetisation, adiabatic** *see magnetic cooling*
- Dember effect**  
 anisotropic semiconductors, Dember and photon-drag effects (*German*) 4-92766
- demodulation**  
*see also demodulators; modulation*  
 fibre-coupled heterodyne detect. at 10  $\mu$ m preliminary expts. 4-64787  
 heterodyne detection phase and amplitude uncertainties 4-96851  
 heterodyne detection SNR in turbulent atm., matrix formalism calcs. 4-72201  
 heterodyne interferometry, generalised data reduction 4-106371  
 heterodyne receiver with open struct. mixer at 324 GHz and 693 GHz 4-86482  
 heterodyne speckle interferometry 4-106370  
 homodyne and heterodyne detection, noise 4-79069  
 multimode Y-coupler for heterodyne detection 4-112566  
 optical heterodyne profilometer 4-106346  
 photoelectron statistics for two independ. nonuniform random-phase sinusoids plus additive Gaussian noise, appl. to optical heterodyne detect. 4-87289  
 quadrature demodulation in laser Doppler velocimetry 4-83960  
 SIR heterodyning using Ag halide fibres 4-107854  
 GaAs, photoacoustic signal meas. by laser heterodyne at high temps. 4-106388  
 GaAs Schottky diode heterodyne receiver for plasma diagnosis 4-103541  
 HF 2-dimens. laser beam phase and intensity meas. technique using acousto-optic modulator, heterodyne detector and raster-scanning mirrors 4-74564
- demodulators**  
*see also demodulation; discriminators*  
 fibre-optic interferometric detection of slow temperature change using unlimited phase compensation 4-107862  
 synchronous demodulator circuitry and autoranging circuit for photothermal spectrometer 4-106401
- demonstrations**  
*includes student experiments*  
*see also student laboratory apparatus*  
 air, sound vel. variation with temp., US meas. 4-86163  
 alpha-particle, time of flight expt. for determ. excitation energy for stopping power of Al, Cu, Ag and Au 4-67916  
 alpha-particle-induced, inner-shell ionization measurements for the undergraduate laboratory 4-82625  
 angular displacement meas. using holographic interferometry 4-90336  
 atomic spectroscopy and holography, laboratory expt. 4-67927  
 atomic structure theory, teaching approach using game board and rubber rings 4-90331  
 cathode-ray tube, fine-beam, student expt. 4-95112  
 circuit breakers, microcomputer storage oscilloscope investig. of action 4-90338  
 closed circuit television for optics demonstration 4-110837  
 coefficients and spontaneous polarisation meas. 4-82634  
 coupled pendulums, overhead projector expts. 4-73202  
 CRT, fine-beam, electron beam physics expts. for students 4-58611  
 cryostat, modified, for meas. thermal cond., thermoelectric power and thermal diffusivity 4-82646  
 diffusion in liqs., holographic interferometry student expts. 4-106151  
 digital pendulum, attached to rotary potentiometer, student demonstrations 4-86153  
 Dunnington's  $e/m_0$  meas. method, undergraduate expt. 4-106144  
 F=M/A, Newton's law, computer simulation expt. 4-73199  
 fine-beam cathode ray tube for meas. Earth's mag. field 4-63463  
 fishing trawl design and demonstration tanks 4-113086  
 fraunhofer diffraction patterns of microparticles 4-82628  
 Fresnel diff. fields, television technique study 4-86157  
 galvanometer, forced simple harmonic motion 4-90335  
 gauge-length meas. interferometer for classroom demonstrations 4-82642  
 holographic setup using planoconvex lens having short focal length 4-82645  
 human velocity, power and accel. meas. using computers 4-73196  
 integrals for determination of integrals and areas 4-67933  
 Langmuir probe characteristics in various mag. field configs. 4-106156  
 light wave propag., group and phase vel., interference effects 4-106157  
 microwave-plasma interaction expt. for laboratory courses 4-106145  
 missing fundamental in harmonically rel. sounds 4-67934  
 nonlinear optical effects in absorbing fluids, undergraduate expts. 4-110825  
 physiological optics, expts. for Weber's law verification 4-110826  
 polarised light demonstration 4-95115  
 prisms, right-angle, use in total internal reflection and interference meas. 4-63458  
 reaction times, meas. by balancing or dropping sticks 4-73198  
 resonances in string instruments 4-67935  
 Schlieren optical system using single spherical mirror and two Ronchi rulings 4-67932  
 second law of thermodynamics expt. 4-106147  
 soil, albedo effect on surface temps., outdoor expt. 4-106153  
 solar cells, open-circuit voltage, temp. depend. 4-67924

**demonstrations continued**

- solar energy, chemical storage, demonstration using colour change 4-90334
- solar radiometer for meas. horizontal global solar irradiance 4-82636
- specific electronic charge meas. using tangential gun in cathode-ray tube 4-73197
- steel balls, overhead projector expts. 4-73202
- surface tension determination using double capillary method 4-67936
- thermal radiation from land surface, to clear night sky, teaching expt. 4-73200
- thermodynamics, second law, expt. using thermoelectric device 4-86151
- United States Naval Academy alternative energy conversion demonstration laboratory 4-63464
- He-Ne laser, mode struct. optical spectrum analyser study, undergraduate expt. 4-106152

**dendrites**

- see also crystal growth*
- cholesterol crystallisation in bile, dislocation growth mechanism 4-89491
- metal dendrites, electrocrystallisation rate under galvanostatic conditions 4-61265
- metals, FCC, void nucleation kinetics, mol. dynamics simulation 4-92197
- solid liquid interface, freezing solutions, motion of interface 4-108592
- $\beta$ -Ag<sub>2</sub>S whiskers, growth mechanism and growth form 4-70608
- Cu, dendritic electrodeposits, fractal behaviour 4-75825
- Fe<sub>81</sub>B<sub>13</sub>Si<sub>3</sub>C<sub>2</sub> glass, primary crystallisation and  $\alpha$ -Fe dendrites, EELS studies 4-84202
- Mo, FCC needle crystals, Auger and electron diff. studies 4-92584
- Ru dendrites, form. by electrolysis of chloride melt, morphology 4-80465
- Zn-Ge eutectic alloy, (100) textured Ge crystallites, morphology 4-76783

**dendritic crystals *see dendrites*****dendritic structure**

- alloys, microsegregation model, dendritic struct., undercooling, temp. depend. diffusion 4-89056
- alloys, monotectic, solidification, microstruct. and phase spacings 4-93284
- alloys, solidification and cooling, dendritic segregation development (Polish) 4-85144
- castings, columnar to equiaxed transition, determ. from cooling curves 4-93271
- conference, Atlanta, GA, USA (Mar. 1983) 4-90292
- constrained dendritic growth and spacing 4-89043
- dynamics of dendritic pattern formation 4-89040
- free dendritic growth 4-89041
- IN-100, Ni-base superalloy, cast, microstruct. changes during fractional melting 4-109434
- IN-738LC, Ni-base superalloy, precip. of  $\beta$  phase in  $\gamma'$  particles 4-114559
- metallurgical systems, mechanisms and kinetics of dissolution 4-114530
- metals, solidification, undercooling, dendritic struct. 4-89047
- metals, stir cast microstructure 4-89049
- microstructure formation, investigation using transparent model systems (German) 4-81183
- Ostwald ripening and relaxation in dendritic struct. 4-93283
- solidification, directional, interdendritic spacing, comparison of theory and expt. 4-93281
- solidification, directional, interdendritic spacing, expt. 4-93280
- solidification, pattern selection 4-93279
- solidification, steady-state cellular and dendritic growth, numerical finite difference model 4-93282
- steady-state columnar and equiaxed growth 4-89044
- steady-state dendritic growth at non-zero capillarity 4-85149
- steel, austenitic stainless, melt layer form. under repetitive electron beam heating, simulation of plasma disruption 4-75535
- steel, cast, solidification, influence of AlN precip. on brittleness (Polish) 4-93270
- steel, high speed, powders, morphology and struct. of splat caps (German, English) 4-71615
- steel, martensitic stainless, HT-9, weldments, microstruct., hardness and fracture toughness, effect of preheat 4-99495
- Stellite, Co-based wear-resistant alloy, liq. phase sintered, carbide comp. 4-99365
- succinonitrile-acetone system, solidification, directional, interdendritic spacing, expt. 4-93280
- undercooled alloy melts, dendritic growth 4-89042
- Al-Cu, columnar crystals, unidirectionally solidified in flowing melt 4-81181
- Al-Cu, droplet solidification on chill block, predendrite form. rel. to supercooling 4-89037
- Al-Cu, rheocasting, grain refinement rel. to stirrer rotation velocity (Japanese) 4-89036
- Al-Cu (4.3 wt.%), randomly nucleated two-dimens. grain struct., effect of grain growth anisotropy 4-104774
- Al-Zn (Cu)(Mg), dendritic solidification and segregation in accordance with Krupkowski's formula (Polish) 4-85146
- Al-Zn (40 wt.%), dendritic segregation and solidification (Polish) 4-85147
- Al-Zn alloys, microsegregation, solidification effects 4-61940
- Cu-Al-Fe (10, 1 wt.%), corrosion and mech. props. effect of solidification struct. 4-85243
- Cu-Ni (Al)(Zn), dendritic solidification and segregation in accordance with Krupkowski's formula (Polish) 4-85146
- Cu-Ni(Al)/(Zn) alloys, microsegregation, solidification effects 4-61940
- Fe alloy, diffusion carburizing, growth of carbide fibres 4-93454
- Fe, gray and nodular cast, laser surface hardening, erosion resist., near surface microstructure 4-64533
- Fe-Mn-Al-C (15, 8, 2 wt.%), rapidly solidified, phase struct. and morphology 4-114504
- Ni base superalloys, directional solidification morphology 4-89048
- Ni-Cr-Si vacuum brazed joint of Inconel 718, struct. 4-66548
- Ni-Nb-Al  $\gamma$ - $\gamma'$  eutectic composite, prep. and morphology 4-114500
- Ni<sub>3</sub>Al powders, rapidly solidified and annealed 4-93278
- Pb-Sb ingot casting, equiaxed zone form.; dendritic solidification front 4-99379
- Si-on-insulator, subgrain boundary free, strip heater recrystn. 4-75796
- Sn-Pb droplets, highly undercooled, solidification 4-114502
- Zn-Al, diecasting alloy, fracture 4-89128
- Zn-Al (21 wt.%), lamellar, superplastic and cast dendritic, water vapour corrosion 4-62097
- Zn-Pb-Cd, cast ingots and sheets; microstructure rel. to cooling rate 4-109390
- dense fluids, theory *see liquid theory*
- densification**
- see also density; powders; sintering*
- alloys, amorphous, compaction process, stability, DSC obs. 4-114448
- ceramics, stress assisted hot form. 4-76728
- compacts, homogeneously packed, intermediate-stage sintering 4-76702
- dolomite, calcinering, effects of raw material props. and Fe<sub>2</sub>O<sub>3</sub> additions 4-66281
- energetic materials, porous, compaction at deflagration-detonation transition 4-108546
- fibre reinforced Al-Mg alloy, fibre/matrix interface effect on fatigue, optimum processing parameters 4-114635
- hot pressing kinetics, semilogarithmic law 4-85123
- liquid phase sintering mechanisms 4-71614
- LWR fuels, low temp. swelling and densification 4-102352
- materials structure role (Russian) 4-76707
- melting consolidation thermodynamics, interparticle binding 4-76706
- metal powder, compaction by rolling 4-66268
- metal powder under shock compression, microstructural modifications 4-109342
- metal powders, densification kinetics in hot pressing in porous shells 4-61885
- metal powders, densification kinetics in hot pressing in porous shells 4-66260
- metal powders, sintering behaviour 4-76703
- metal unsintered powders, Hugoniot meas. using C gauges 4-108578
- mica, synthetic, sintering using hydrothermal equipment 4-89013
- multilite-cordierite composites, sintering, hot pressing, microstruct., mech. and thermal props. 4-89017
- Nasicons, synthesis, sintering and microstruct. 4-76713
- nuclear fuel pellets, ceramic, new hot impact densification method (German) 4-83215
- olivine-basalt partially molten aggregates, diffusion creep during hot pressing 4-110137
- optical fibre fabrication, dehydration kinetics with soot densification in VAD process 4-97156
- polyacetylene:1, IR refl. spectra, effect of sample densification 4-99120
- polymer glasses, press. effects, densification and dielectric losses 4-65190
- polymeric powders, cold compaction in tapered dies 4-76738
- porous gas diffusion electrodes prep. and characts. for alkaline low-temp. H<sub>2</sub>-O<sub>2</sub> fuel cells 4-62349
- powder, shell stripping from compacts by pulse mag. field forces, model 4-89002
- powder compaction, deform. meas. by scanning-moire method 4-87643
- powder compacts, bimodal, sintering behaviour 4-99359
- powder compacts, rearrangement phenomenon, theoretical model expressing assoc. shrinkage 4-104747
- powders, gravitational compaction, discharges appearance 4-93247
- quasistatic and explosion compacting, density calc. method 4-81167
- refractory metals and alloys, powder metallurgy production 4-66264
- shock wave consolidation of powders, theory 4-109337
- Si<sub>3</sub>N<sub>4</sub>, normally sintered, hot isostatic pressing in N<sub>2</sub> gas as pressure medium 4-114459
- sialon ceramics, liq. phase sintering, densification and transform. mechanisms 4-76724
- sialons, hot-pressed and reaction-bonded, phase equilib. and props. 4-76761
- $\beta$ -sialons, microstruct. evaluation by TEM, correl. to mech. props. 4-76732
- sintering, liq. phase, densification and microstructural development 4-99360
- sintering, temp. depend. 4-66262
- sintering of refractory metals and alloys, conf., Atlanta, GA, USA (Mar. 1983) 4-95042
- sintering processes, book contrib. 4-109340
- steel, Mn, 13 to 19 wt.%, sinter-forged, mech. props. 4-81283
- steel, Mn, 13 wt.%, prod. by powder metallurgy method 4-81169
- steel, powder, shock induced densification, mechanical props. 4-109347
- steel, powder, shock induced densification 4-109346
- steel powder, rapidly solidified, shock consolidation 4-109353
- superalloys, powder metallurgy, book 4-86129
- superalloys, superalloys, oxide dispersion strengthened, developments in prod. 4-114452
- Teflon 7C porous bed compaction, strain rate sensitivity 4-109487
- Al-Fe-Ni-Co, prep. from atomised powder, prod. struct. and props. 4-114446
- AlN, oxyinitride bonded ceramics, sintering, microstruct., densification, flexural strength, oxide additions effect 4-76727
- AlN powder, hot pressing kinetics, oxidation, mech. props. 4-76731
- AlN powder, shock compression study 4-109349
- AlN powder, shock effects, TEM study 4-109345
- AlN, powder, surface area after shock treatment 4-109344
- Al<sub>2</sub>O<sub>3</sub> compacts, homogeneously packed, intermediate-stage sintering 4-76702
- Al<sub>2</sub>O<sub>3</sub> powder, shock induced densification and sinterability 4-109350
- Al<sub>2</sub>O<sub>3</sub> powder, shock loaded densification, X-ray study 4-114439
- Al<sub>2</sub>O<sub>3</sub>, powder, surface area after shock treatment 4-109344
- Al<sub>2</sub>O<sub>3</sub>, powders, granule compaction rel. to binder glass transition temp. 4-85129
- Al<sub>2</sub>O<sub>3</sub> powders, with bimodal particle size distrib., sintering 4-85127
- Al<sub>2</sub>O<sub>3</sub>, spray-dried, compaction behaviour 4-76714
- Al<sub>2</sub>O<sub>3</sub>:Ti, sintering and densification, defect models 4-109364
- Al<sub>2</sub>O<sub>3</sub>:Zr, sintering and densification, defect models 4-109364
- Al<sub>2</sub>O<sub>3</sub>:ZrO<sub>2</sub> powder compacts, stresses induced by differential sintering 4-85135
- Al<sub>3</sub>SiC mixed carbide, prep. and struct. studies 4-88144
- Al<sub>3</sub>TiO<sub>2</sub> ceramics, synthesis and sintering characts. 4-109361
- BaFe<sub>2</sub>O<sub>19</sub> permanent magnets; sintering temp. effect on mag. props. and density (Afrikaans) 4-76170
- C fibre reinforced C multidirectional composites, book contrib. 4-66296
- $\alpha$ -Ca<sub>3</sub>(PO<sub>4</sub>)<sub>2</sub>, sintering behaviour at 1200 to 1600°C 4-114458
- Ca<sub>3</sub>(PO<sub>4</sub>)<sub>2</sub> powder compacts, rel. between compacting press., green density and green strength 4-114444
- Cu-Sn-Al<sub>2</sub>O<sub>3</sub> abrasive composite, physicomech. props., effect of premoulding press. in elec. discharge sintering 4-89020
- Fe-Cu (10 wt.%), powder compacts, liq. phase sintering, dimens. changes 4-66267
- Fe-Si-C powder compacts; sintered and carburised; graphite growth 4-93306

## densification continued

- Fe<sub>30</sub>Ni<sub>40</sub>P<sub>10</sub>B<sub>6</sub>, amorphous, explosive loading of powder, three-dimens. parts prod. 4-114443  
 LaCrO<sub>3</sub>-Cr cermet, high-temp. creep 4-71693  
 MgO powder, hot pressing, densification, dislocation creep mechanism 4-114455  
 Mn<sub>1-x</sub>Zn<sub>x</sub>Fe<sub>2</sub>O<sub>4</sub> ferrite, microstruct. and permeability during sintering 4-109432  
 Mn<sub>1-x</sub>Zn<sub>x</sub>Fe<sub>2</sub>O<sub>4</sub>, hot pressed, prior heat treatment effect on props. 4-89016  
 Mn<sub>1-x</sub>Zn<sub>x</sub>Fe<sub>2</sub>O<sub>4</sub>, sintering of powders produced by different methods, mechanism and assoc. processes 4-89015  
 Mo, activated sintering, retarded grain boundary mobility 4-99366  
 Mo powder, shock induced densification study 4-109348  
 Na<sub>2</sub>Zr<sub>2</sub>Si<sub>2</sub>PO<sub>6</sub>, NASICON solid electrolyte prep. and characs. for Na-S batteries 4-62347  
 Ni, sintering kinetics after explosive compacting 4-93249  
 Ni-Co matrix, ThO<sub>2</sub> particles, oxide growth inhibition 4-104796  
 PZT, sintering, densification by hot isostatic pressing 4-66286  
 Si<sub>6-x</sub>Al<sub>2</sub>O<sub>8-x</sub>N<sub>8-x</sub>, β-sialon, hot pressed, flexural strength, phase struct., comp. depend. (Japanese) 4-76828  
 Si<sub>6-x</sub>Al<sub>2</sub>O<sub>8-x</sub>N<sub>8-x</sub>, β-sialon synthesis from Si<sub>3</sub>N<sub>4</sub> and Al alkoxides (Japanese) 4-114461  
 β-SiC powders, sintering, hot pressing, densification and mech. props. rel. to prep. 4-109366  
 SiC, prod. methods and parameters, report (German) 4-61908  
 SiC:B, shrinkage, density and phase comp. rel. to forming press. and sintering temp. 4-85130  
 Si<sub>3</sub>N<sub>4</sub> ceramics, liq. phase sintering, densification and transform. mechanisms 4-76724  
 Si<sub>3</sub>N<sub>4</sub>, dense compact, gas phase sintering process 4-76730  
 Si<sub>3</sub>N<sub>4</sub>, hot isostatic pressing, densification, bending strength rel. to additives (Japanese) 4-76721  
 Si<sub>3</sub>N<sub>4</sub>, hot pressing, densification and microstruct. rel. to MgO and Y<sub>2</sub>O<sub>3</sub> additions 4-76729  
 Si<sub>3</sub>N<sub>4</sub>, liq. phase sintering mechanisms 4-71614  
 Si<sub>3</sub>N<sub>4</sub> polyphase materials, high temp. deform. and fracture 4-76866  
 Si<sub>3</sub>N<sub>4</sub> powder, shock induced densification study 4-109352  
 Si<sub>3</sub>N<sub>4</sub> powder, shocked, hot isostatic processing 4-71617  
 Si<sub>3</sub>N<sub>4</sub> powder compacts, isostatically pressed, sintering by powder bed technique 4-76723  
 Si<sub>3</sub>N<sub>4</sub> powders, sintering, densification rel. to processing parameters 4-76722  
 Si<sub>3</sub>N<sub>4</sub>, reaction bonded, sintered, densification kinetics, microstruct. 4-76726  
 Si<sub>3</sub>N<sub>4</sub>-Y<sub>2</sub>O<sub>3</sub> based ceramics, sintering, densification, oxidation, strength and porosity 4-76835  
 SiO<sub>2</sub> film, low temp. photochemical deposition 4-99339  
 Ti powders, coarse, compacting phenomenology 4-66274  
 Ti-Al-V (6, 4 wt%), powder metallurgical prod. 4-104750  
 TiB<sub>2</sub>, powder, surface area after shock treatment 4-109344  
 TiB<sub>2</sub>, sintering and props. of samples made from powder synthesised in plasma-arc heater 4-76715  
 TiC powder, shock induced densification study 4-109351  
 TiC, powder, surface area after shock treatment 4-109344  
 TiC-Ni tungstenless alloy powder, pressing characs., comparison with WC-Co 4-89018  
 TiC-Ti, reactive liq. phase sintering 4-61896  
 TiC-Ti, reactive solid-state hot pressing 4-61897  
 TiN-TiC solid soln. powder, shock compaction study 4-109341  
 TiO<sub>2</sub> powder, shock loaded densification, X-ray study 4-114439  
 (U,Pu)C fuel, swelling, densification and creep under irradiation 4-83144  
 UO<sub>2</sub>, irradiat., densification algorithm 4-59329  
 W-Re, prep., sintering, phase comp., microhardness, SEM obs. 4-89010  
 ZnO varistor, high-field fine-grained, fabrication by sol-gel processing 4-66282  
 ZrO<sub>2</sub> powder, shock modified, microstructure study 4-109343  
 ZrO<sub>2</sub> powder under shock compression, phase transformation 4-108611  
 ZrO<sub>2</sub>-Y<sub>2</sub>O<sub>3</sub>-HfO<sub>2</sub> ceramic powders, laser sintering 4-88998

densimeters see densitometry

densitometers see densitometry

## densitometry

- see also photometry  
 AMD-1 automatic densitometer spectra, scanning and processing software 4-94635  
 BWR LOCA, instantaneous pipe rupture, void fraction meas. with X-ray densitometer 4-74036  
 digital subtraction angiography, spatial freq. filtering by real-time digital video convolution 4-89703  
 digital videodensitometry system for subtraction angiography 4-89718  
 K-edge-densitometer for nuclear safeguards 4-111709  
 multichannel, gas phase electron diffraction pattern intensities investig. 4-79901  
 soil wet density meas. using ND-A densimeter (Chinese) 4-72715  
 Yale PDS 2020G microdensitometer, use of high speed photometer 4-110538  
 Pu solution characterisation by γ-spectrometry, densitometry and isotopic anal., safeguards 4-111707

## density

- see also atmospheric pressure and density; density measurement; density of gases; density of liquids; density of solids  
 charged particle in various substances, ionisation energy loss, density effect 4-95073  
 simple layer potential method for domains having external corners 4-63511

density, atmospheric see atmospheric pressure and density

density, vapour see density of gases

## density measurement

- see also hydrometers  
 air, temperature and density fluctuation meas. feasibility using laser-induced O<sub>2</sub> fluorescence 4-78311  
 apparatus for liq. density and dielec. const. meas. to 35 MPa 4-63761  
 axisymmetric optical material density determ. from X-ray photographs (Russian) 4-106435  
 compressed fluids by combining hydrostatic weighing and mag. levitation 4-95390  
 damaged nuclear fuel rods from CABRI distortion expts., quantitative radiography 4-106836  
 fluids, vibrating tube flow densimeter for up to 700K and 40 MPa 4-68215

## density measurement continued

- gaseous species density gradient meas. technique, STROPE 4-79698  
 holographic moiré deflectometry for stiff density fields anal. 4-64684  
 lecture notes and study guide on process analysers and recorders, book 4-106138  
 methane-air premixed turbulent flames time resolved density meas. 4-99787  
 molten liquids, density measurement, high temp. techniques 4-95389  
 porous particles in powders, apparent density meas. using simple, inexpensive microvolumeter 4-63723  
 quasistatic and explosion compacting, density calc. method 4-81167  
 reference standard, solid 4-106274  
 vibration transducer transfer constant determ. on shaker with plane circular motion of table 4-90579  
 H<sub>2</sub>, liq. density meas. using microwave open ended cavity tuned oscillator (Chinese) 4-73425  
 I<sub>2</sub> vapour density mapping using optical fan beam tomography 4-108157

## density of gases

- atomic vapour density meas. by least-squares fit to spectra 4-102825  
 dense gases, viscosity and thermal cond., density depend. 4-87832  
 dense monatomic and molecular fluids and their mixtures, shear viscosity, thermal cond., anal. 4-113688  
 hexane, liquid-gaseous coexistence, specific refraction (Russian) 4-99087  
 species density gradient meas. technique, STROPE 4-79698  
 sphere-plane gaps in dry air, impulse breakdown, 0.25 to 2 atm. 4-79718  
 target for radionuclide prod. in nucl. medicine, charged particle penetration, density reduction 4-89745  
 Ar, high press. PVT meas. 4-97737  
 C, gaseous, stopping power, zero-energy density effect 4-80129  
 H<sub>2</sub>, solid, adiabatic eqn. of state at 150 kbar 4-113567  
 I<sub>2</sub> vapour density mapping by optical tomography, noise theory expt. verification 4-91414  
 I<sub>2</sub> vapour density mapping using optical fan beam tomography 4-108157  
 KCl, vapour and liq., critical point and vapour press. 4-60972  
 Kr, dense gas, density fluctuation calcs. 4-83967  
 NH<sub>3</sub>, expanding jet, rotational temp. and mol. density determ. by IR absorpt. 4-83490  
 NO density quantitative meas. by reson. three-photon ionisation 4-75108  
 NaCl, vapour and liq., critical point and vapour press. 4-60972  
 Rb saturated-vapour density meas. at 302-351K 4-107298

## density of liquids

see also hydrometers

- acetone, soln., partial molar and molar vols., D isotope effect 4-65322  
 acetonitrile, soln., partial molar and molar vols., D isotope effect 4-65322  
 N-acetyl amino acids, aq. solns., apparent molar volumes 4-62433  
 alcohol-alkane (1,2-dichloroethane) mixtures, adiabatic compressibilities and viscosities, US meas. 4-92298  
 alcohol-water mixtures, density and viscosity, press. depend. (Japanese) 4-98327  
 n-alkanol-N-formylmorpholine mixtures, excess volumes 4-103847  
 n-alkanone-n-alkane mixtures excess molar vols. and heat capacity study 4-103955  
 amino acids, aq. solns., apparent molar volumes 4-62433  
 benzene, liq., residual Helmholtz energies between 390 and 465K and up to 60 MPa 4-88309  
 benzene, US vels., density, high press. (Japanese) 4-98203  
 benzene+2-ethoxyethanol, excess volumes at 303.15, 313.15 and 323.15K 4-98294  
 benzene+n-hexane, excess molar volume at 298.15 and 323.15K 4-98295  
 benzene-cyclohexane, density meas., excess thermodynamic quantities calc., equation of state 4-80261  
 benzene-d<sub>6</sub>(d<sub>12</sub>), solns. and mixtures, isotope effects, isothermal compressibility 4-84330  
 benzene-hexa-n-alkanoate discotic nematogen, phase diagrams, regular soln. theory 4-84393  
 bromobenzene+chloroethane mixtures, excess vols. meas. 4-113639  
 t-butyl chloride+tetrachloromethane, excess volumes, at 298.15K 4-98296  
 butyl-p-(p-ethoxyphenoxycarbonyl) phenyl carbonate, local electric field anisotropy in nematic phase 4-113313  
 chlorobenzene+chloroethane mixtures, excess vols. meas. 4-113639  
 chlorolanes, liq., viscous flow, acoustic wave studies (Russian) 4-92402  
 cholesteryl myristate (propionate) mixed liq. crystals, compressibility and thermal expansion anomalies 4-80227  
 cyclohexane, soln., partial molar and molar vols., D isotope effect 4-65322  
 cyclohexane+1,3-diphenylbutane, excess volumes, at 301.47K 4-98296  
 cyclohexane+triethylamine mixtures, keto-enol tautomerism 4-113589  
 cyclohexane-d<sub>6</sub>(d<sub>12</sub>), solns. and mixtures, isotope effects, isothermal compressibility 4-84330  
 dense monatomic and molecular fluids and their mixtures, shear viscosity, thermal cond., anal. 4-113688  
 1,2-dichloroethane-based mixtures, excess molar vol., temp. coeffs. 4-103846  
 3,6-dioxaoctane-n-heptane mixtures, excess volumes and US speeds 4-98202  
 fluids, orthobaric props. of spherical and linear mols., intermol. pot. effect 4-74310  
 graphite intercalation compound with K, liq.-solid transitions, in-plane liq. K density 4-70348  
 hard-sphere fluid, two particle distrib. approx. near hard wall at low densities 4-97989  
 hexamethylphosphotriamide-water mixtures, heat of dilution, sp. heat and ultrasonic vel. calc. (French) 4-80250  
 hexane, liquid-gaseous coexistence, specific refraction (Russian) 4-99087  
 HOAB, density meas. across liq. cryst. phase transformations 4-108496  
 isopropanol, in aqueous soln., in tetrachloroethylene soln., Raman line-width, conc. depend. 4-114268  
 (KSCN,NaSCN)<sub>1-x</sub>(Cs)<sub>x</sub>(Ca(NO<sub>3</sub>)<sub>2</sub>)<sub>0.7</sub>4.06H<sub>2</sub>O melts, mixed alkali effect 4-108642  
 liquid-solid interface, press., density functional, integral eqns. 4-108258  
 methane, liquid, self-diffusion and shear viscosity theory 4-88327  
 nematic liquid crystals, local electric field anisotropy 4-113313  
 organic binary aq. mixts., solute-solute interactions, Kirkwood-Buff integrals 4-60973  
 PEBAB, phase transition studies 4-98280  
 peptides, aq. solns., apparent molar volumes 4-62433  
 perfluorobenzene, liq., acoustic relax. mechanism 4-92301  
 PMBAB, phase transition studies 4-98280

**density of liquids continued**

- poly(dimethyl siloxanes), cyclic and linear, static dielect. meas. and dipole moments 4-61620  
 polystyrene solutions, US studies and Rao formalism 4-103883  
 polystyrene solutions, US vel. and absorpt. 4-80162  
 4-n-propoxybiphenyl-4-ethyl carboxylate, smectic A-smectic B transition, optical effects 4-61086  
 propyl alcohol, thermodynamic props. at atm. press. 4-80251  
 rare earth metals, liquid, density, surface tension, periodic depend. 4-113517  
 small pores, superfluid density and transition temp. 4-92463  
 tetraalkylammonium bromide, water-KCl solns., partial molar vols. meas. (French) 4-80130  
 thermodynamic props. calc. of fluids in mol. dynamics expts. 4-113666  
 toluene, US vels., density, high press. (Japanese) 4-98203  
 tributylphosphite-alkane mixtures, excess vol. meas. 4-103848  
 vibrating tube flow densimeter, for up to 700K and 40 MPa 4-68215  
 $\text{AlCl}_3\text{-SOCl}_2$  based electrolytes, transport props. 4-88323  
 $\text{B}_2\text{O}_3$  molten, struct. anal. by X-ray radial distrib. method 4-113293  
 Cs, eqn. of state and pVT data up to 2000K and 600 bar 4-103898  
 Cs, liquid, density calcs. using model-potential approach 4-92065  
 HCl-N<sub>2</sub>O liquid mixtures, thermodynamics and densities 4-98311  
 He, liquid, charged surface stability in a condenser (Russian) 4-70489  
 \*He, superfluid, dilute interacting, critical behaviour theory 4-104020  
 \*He, superfluid density, velocity depend., roton liq. theory 4-80322  
 K, liquid, density calcs. using model-potential approach 4-92065  
 KCl, vapour and liq., critical point and vapour press. 4-60972  
 KOH, conc. aq. solns., heat capacities, vols., expansibilities and compressibilities 4-103954  
 LiOH, conc. aq. solns., heat capacities, vols., expansibilities and compressibilities 4-103954  
 Na<sub>2</sub> fluid, equation of state near critical points, scaling props. 4-98238  
 Na, liquid, density calcs. using model-potential approach 4-92065  
 NaCl, vapour and liq., critical point and vapour press. 4-60972  
 NaCl-LaCl<sub>3</sub> binary melt, density (Korean) 4-80131  
 NaOH, conc. aq. solns., heat capacities, vols., expansibilities and compressibilities 4-103954  
 Ne fluid, equation of state near critical points, scaling props. 4-98238  
 Rb, liquid, density calcs. using model-potential approach 4-92065  
 Sc, liquid, density, surface tension studies 4-113517  
 SnBr<sub>4</sub> binary mixtures, molar excess enthalpies and volumes 4-108630  
 Xe+methyl chloride liquid mixture, thermodynamic props. meas. 4-70408  
 Y, liquid, density, surface tension studies 4-113517

**density of solids**

- absorber materials for fast breeder reactor control rod systems, physical and chemical props. 4-83147  
 amorphous polymer density fluctuation theory in a glass transition region and photon correlation spectroscopy 4-98026  
 Arctic offshore structures, lightweight concrete props. 4-114464  
 bisphenol A polycarbonate samples, specific vol. depend. on mol. characts. 4-103663  
 ceramics, brittle, thermal stress fracture on liquid quenching rel. to thermal and mech. props. 4-109504  
 chamotte refractories, high-strength lightweight, prod. 4-71619  
 cyclotrimethylene-trinitramine single cryst., density and thermal expansion 4-88222  
 glass fibre-reinforced composites, thermal testing of struct. and mech. props. 4-85268  
 glass/alumina composites, density, crystallisation, elec. cond. 4-113937  
 glasses, alkali silicate and aluminosilicate, Young's modulus, effect of vol. and struct. 4-85170  
 graphite fibres, intercalated, for electrical power transmission appl. 4-80562  
 melt-spun ribbons, form. control, thermal transport, momentum transport 4-114441  
 organic crystal density, empirical calc. (Chinese) 4-108497  
 particulate materials dielectric props., density dependence 4-71256  
 PET, molecular orientation, mol. wt., birefringence, density, light scatt. 4-84219  
 phosphate glasses, containing fluorides of Group I-IV elements, optical and spectral props. rel. to struct. 4-92098  
 poly aryl-ether-ether-ketone, crystalline struct., powder X-ray diffr. 4-92099  
 poly p-phenylene terephthalamide films, extruded and drawn, tensile strength, void struct. rel. to heat treatment 4-81257  
 polyamide-6, blending with copolymers, effect on props. (Polish) 4-66433  
 polyethylene, thermal characts., electron and gamma-neutron irradi. effects (Russian) 4-103977  
 polymer-based composites, thermal testing of struct. and mech. props. 4-85268  
 polymers, amorphous, vol. structural relax. theory 4-84396  
 pulse spectrum technique, simultaneous determ. of bulk and shear modulus, and density for nondestructive evaluation 4-66515  
 quartz, reflected shocks and density transitions 4-108520  
 quartz powders, shock-loaded, deform., X-ray line broadening obs. 4-65324  
 radioactive waste glass, simulated, density changes under ion, electron, and gamma irradi. 4-73974  
 refractory materials, fibrous, specific thermal cond. rel. to temp. and apparent density 4-98379  
 silicate glasses containing TiO<sub>2</sub>, refractive index, density, thermal expansion and IR spectra 4-84199  
 sintered, behaviour in vac. at high temps. 4-76717  
 tellurite-halide ternary systems, glass-forming region, density and thermal expansion 4-80273  
 trans 1,4-polyisoprene, crystallisation from solution, melting endotherm, heat of fusion, density 4-75315  
 Al-Si (3 wt.%) ingots, quality and feedability during solidification 4-109389  
 Al<sub>2</sub>O<sub>3</sub> ceramics, interaction between polyvinyl butyral binder burn-out and sintering in reducing atm. 4-114460  
 Al<sub>2</sub>TiO<sub>3</sub> ceramics, synthesis and sintering characts. 4-109361  
 Ar, solid, volume and isothermal bulk modulus, press. depend. 4-92278  
 Ba(PO<sub>3</sub>)<sub>2</sub>-CdF<sub>2</sub>, high refractive index glass, optical constants, density and atomic refraction rel. to struct. 4-93043  
 C fibre reinforced polymer composites, thermal testing of struct. and mech. props. 4-85268  
 C, stopping power, zero-energy density effect 4-80129  
 CaSiO<sub>3</sub>, wollastonite, twinning, cryst. structures, polymorphism 4-89913

**density of solids continued**

- Cr<sub>2</sub>O<sub>3</sub>, doped, hot pressing, annealing, elec. cond., density, grain size, XPS 4-113946  
 Cu fine powders, electrodeposition, organic additions influence 4-61888  
 Cu-Ni (25 wt.%), sintered and pressed coinage alloy, tensile props., SEM and X-ray obs. 4-71697  
 Cu<sub>2</sub>Zr<sub>3</sub> amorphous alloy, deformed, dilatational defects 4-84201  
 Fe-Cr-B, metallic glass, mag. props. and density 4-84773  
 Fe-W-B, metallic glass, mag. props. and density 4-84773  
 Fe<sub>2</sub>O<sub>3</sub>, wustite, Fe-rich phase boundary, press. and temp. var. effects 4-66318  
 Ga<sub>2</sub>O<sub>3</sub>-CaO glass, form. density, refr. index, crystn. temp., hardness, IR spectra 4-113635  
 Ge, elastic props., ultrasonic meas. 4-98170  
 Li<sub>2</sub>O-SiO<sub>2</sub> glass ceramic systems, density, crystallisation, elec. cond. 4-113937  
 Mg alloys, structure and physicochemical props. different methods of Stepanov crystallisation effect 4-99297  
 MgO powder, hot pressing, densification, dislocation creep mechanism 4-114455  
 MgO-Cr<sub>2</sub>O<sub>3</sub> refractory, thermal shock resist., prod. during Frenkel effect 4-66289  
 MgSiO<sub>3</sub>, enstatite, twinning, cryst. structures, polymorphism 4-89913  
 MnZn ferrites, hot-pressed, powder particle size distrib. and heterogeneity 4-61907  
 Mo powder, shock induced densification study 4-109348  
 N<sub>2</sub>-Kr solid mixtures, phase diagrams, X-ray study (Russian) 4-84372  
 NH<sub>4</sub>HCO<sub>3</sub>, relations between crystallographic characts. and cryst. struct. (Chinese) 4-75378  
 Na<sub>2</sub>O-B<sub>2</sub>O<sub>3</sub> glass, prep., mech., thermal and optical props. rel. to N content 4-60845  
 Na<sub>2</sub>O-B<sub>2</sub>O<sub>3</sub>-Al<sub>2</sub>O<sub>3</sub>-SiO<sub>2</sub> transparent glazes, with enhanced chem. and thermal shock-resist. 4-81305  
 Na<sub>2</sub>O-SiO<sub>2</sub> glass, nature of dissolved water, effect on phys. props. 4-109180  
 Ni-Nb-NbC, eutectic alloys, powder metallurgy, physical props., high temp. use 4-85125  
 Ni<sub>80</sub>P<sub>20</sub>, amorphous powder, warm pressing consolidation kinetics 4-81168  
 NiZn ferrites, prod. by shock hot working, props. 4-61905  
 Si, elastic props., ultrasonic meas. 4-98170  
 a-Si, ion implantation form. and optical state characterisation 4-88186  
 SiC polymorphs, crust. chem. props. 4-60896  
 β-SiC powders, sintering, hot pressing, densification and mech. props. rel. to prep. 4-109366  
 SiC-B<sub>4</sub>, shrinkage, density and phase comp. rel. to forming press. and sintering temp. 4-85130  
 Si<sub>3</sub>N<sub>4</sub>, hot isostatic pressing, densification, bending strength rel. to additives (Japanese) 4-76721  
 Si<sub>3</sub>N<sub>4</sub> powder, shocked, hot isostatic processing 4-71617  
 Si<sub>3</sub>N<sub>4</sub> powder compacts, isostatically pressed, sintering by powder bed technique 4-76723  
 Si<sub>3</sub>N<sub>4</sub> powders, sintering, densification rel. to processing parameters 4-76722  
 SiO<sub>2</sub> polymorphs, relationship between refr. index and density 4-66001  
 SiO<sub>2</sub>, properties of high-press. fluorite struct. phase 4-110135  
 SiO<sub>2</sub>, synthetic, props. under high-temp. treatment 4-81172  
 Si<sub>1-x</sub>Sn<sub>x</sub>, amorphous, vapour deposited, struct., resist. characts., density, electron diff. meas. 4-61424  
 Ti plate, shock wave-induced temp. rise, thermoviscoplastic model anal. 4-108527  
 Ti<sub>1-x</sub>Li<sub>x</sub>M<sub>3</sub>O<sub>2</sub> (M=Nb, Ta, Sb) rutile solid solns., X-ray characterisation 4-84274  
 TiN-TiC solid soln. powder, shock compaction study 4-109341  
 TiO<sub>2</sub>-SiO<sub>2</sub>, RF sputtered amorphous films, density, refractive index, thermal expansion, X-ray spectra 4-61263  
 V<sub>2</sub>O<sub>5</sub>-B<sub>2</sub>O<sub>3</sub> glass, struct., IR spectra and elec. cond. 4-88107  
 WC-Co-P, wear resist., P addition influence 4-66458  
 WO<sub>3</sub> thick films, elec. cond. and electrochromism 4-65674  
 ZnO-B<sub>2</sub>O<sub>3</sub> glass, X-ray diffr., density and elec. cond. obs. 4-61423  
 Zr(MoO<sub>4</sub>)<sub>2</sub>, polymorphism, X-ray diffr. and vibr. spectroscopy study 4-70053  
 ZrO<sub>2</sub> powder under shock compression, phase transformation 4-108611  
 ZrSiO<sub>4</sub>, swelling induced by alpha and gamma irradi. 4-75543
- density of states, electron** see *electronic density of states*  
**deoxyribonucleic acids** see *DNA*  
**deperming** see *demagnetisation*  
**desalination**  
 photovoltaic array supplied desalination plant, with management strategies, simulation 4-77062  
 solar lake-condensation tower system (SL/CT system), application to land irrigation water production 4-72182  
**desalting** see *desalination*  
**descriptors** see *vocabulary*  
**design aids**  
 see also *design engineering; nomograms*  
 fishing trawl design and demonstration tanks 4-113086  
 holographic NDT as mech. design aid 4-114739  
**design engineering**  
 composite materials, fatigue-proof design, reliability-based 4-99604  
 composite materials, reliability-based, fatigue-proof 4-99392  
 holographic NDT as mech. design aid 4-114739  
 Jamaican 1 MWe OTEC pilot plant 4-114929  
**desk calculators** see *calculating apparatus; electronic calculators*  
**desk-top computers** see *minicomputers*  
**desorption**  
 acetylene, condensed molecules, photon-stimulated ion desorption 4-61239  
 acetylene adsorbed on oxidised and carbided W (100), C-H bond activation 4-93553  
 alkali halide surfaces, electronic desorption of excited alkali atoms 4-61236  
 alkanes, branched, solid, electron stimulated desorption 4-61240  
 biological mols., mol. size effects in fast heavy ion induced desorption 4-66880  
 colloidal suspensions, electric-field jump studies, negative second Wien effect theory 4-99850  
 composite surface, H<sup>+</sup> and D<sup>-</sup> ion generation rel. to surface/plasma ion source systems 4-93165

- desorption continued
- composite surface, partially caesiated,  $H^-$  prod. in presence of  $H$  plasma 4-93166
- condensed gas solids, electronically excited by fast light ions, nonlinear erosion yield 4-61804
- condensed gases, desorption by electronic processes 4-61238
- covalent systems, models for desorption 4-61230
- cyclohexane film, photon and electron-stimulated desorption, mech. of ion formation and desorption 4-61241
- degassing rate of materials, compensated meas. method. (Polish) 4-111145
- electrode/electrolyte interface, desorption rates and electrochem. meas. 4-104066
- electron stimulated, mechanisms 4-61227
- electronic, mechanisms, overview 4-61229
- electronic desorption, anal. 4-61225
- electronic transition-induced desorption, laser induced fluorescence studies 4-75780
- electronically induced, of ions and neutrals, mechanisms 4-61228
- field adsorption kinetics of gas atoms of mols. 4-92541
- fluorinated hydrocarbon films, electron-stimulated desorption 4-98451
- fundamental excitations in solids pertinent to desorption induced by electronic transitions 4-61224
- fusion reactor first wall coatings, gas release under electron impact 4-91097
- gas diffusion in imperfect crystals, effective coeff. determ. in time depend. expts. 4-65433
- glass/liquid interface, laser beam induced holographic bubble grating form. 4-83683
- glycerol films, falling,  $CO_2$  desorption, mass transfer enhancement 4-65551
- grain boundary model, impurity effects, cluster variation method calcs. 4-113465
- graphite, adsorbed methane, intermol. pot. and lattice sums 4-80393
- graphite, enhanced sputtering yield at elevated temps., time of flight mass spectra studies 4-76610
- 2-hydroxyethylmethacrylate-methylmethacrylate copolymers, water sorption and desorption 4-88348
- induced by electronic transitions, role of excited state and time evolution 4-61231
- induced by electronic transitions, workshop, Williamsburg, VA, USA (May 1982) 4-58556
- insulating thin films, Auger electron spectra, electron and ion beam effects 4-109283
- insulin, bovine, fast heavy ion-induced desorption, damage cross sections 4-77188
- interacting dimers, first-order thermal desorption 4-92522
- ion desorption, photon stimulated mechanism, review 4-88389
- ion desorption processes, effect of image interaction 4-92557
- ion formation from organic solids, conf., Munster, Germany (Sept. 1982) 4-86114
- ion impact desorption mechanisms, substrate role, fusion device relevance 4-93164
- ion impact stimulated desorption 4-61237
- local density formalism 4-92548
- metal surfaces, nature of electron stimulated desorption active species 4-61232
- metal-metalloid system, thermodynamics, kinetics and props. of gases and  $C$  in  $Ag$  and  $Au$ , data collection 4-73174
- metallic thin films, crystal growth, initial steps, microscopic studies 4-98486
- metals, thermal desorption, phonon and electron-hole pair excitations 4-88401
- methanol, condensed molecules, photon-stimulated ion desorption 4-61239
- methanol film, photon and electron-stimulated desorption, mech. of ion formation and desorption 4-61241
- mica, muscovite, nuclear track detector, ion stimulated desorption 4-68900
- molecular Coulomb explosion and mol. decomposition study methods, appl. to desorption studies 4-62223
- molecular desorption by reson. laser-mol. vibr. coupling, time-of-flight spectra calcs. 4-93556
- molecular structure at surfaces, determ. using angle resolved electron- and photon-stimulated desorption, review 4-61234
- molecule-surface interactions and dynamics 4-99828
- one-dimensional quantum model 4-98431
- optical surfaces, laser desorption analysis of  $H_2O$  and other contaminants 4-74777
- organic molecules, desorption by electronic processes 4-61238
- organosilanes covalently bonded to metal oxide surfaces, SIMS and electron stimulated desorption obs. 4-89324
- phonon-induced  $He$  desorption, thermodynamic and perturbation theory anal. 4-65577
- photodesorption and negative ion ESD 4-61233
- photodesorption of weakly bound molecules 4-92553
- photon stimulated desorption, surface characterization, instrumentation 4-90703
- polydimethylsiloxane, of  $SO_2$  sorption-desorption isotherms (Russian) 4-104091
- polyethylene, vacuum outgassing study 4-86426
- polyimide surface, chem. bonding characts., annealing and desorption effects 4-88933
- polymers, fracture and emission of electrons, ions and photons 4-98189
- polyvinyl trimethylsilane, of  $SO_2$  sorption-desorption isotherms (Russian) 4-104091
- PVC, chlorinated, vacuum outgassing study 4-86426
- quartz, surface and vol. centres, optical and paramag. props. 4-66057
- sapphire (1-102), surface treatment for Si MBE growth 4-71743
- sapphire with surface adsorbed  $Na$ , laser irradi., photostimulated desorption 4-113793
- secondary electron multipliers, T adsorption and desorption, fusion reactor appl. 4-59413
- semiconductors, electron stimulated desorption 4-66150
- small molecules, laser pulse-induced field desorption 4-80418
- stimulated, direct and indirect mechanisms 4-61226
- stimulated desorption spectroscopy 4-61235
- sucrose, fracture and emission of electrons, ions and photons 4-98189
- surface desorption, light induced, threshold laser intensity 4-81481
- surface structure, particle stimulated desorption analysis for solid surfaces (German) 4-92499
- desorption continued
- surface study by resonant microwave cavity detuning, hysteresis effect obs. 4-70552
- TEXTOR first wall characts. w.r.t.  $H$  recycling 4-91968
- thermal desorption from heterogeneous surfaces; normalized curve treatment 4-65563
- thin film deposition, ion-surface interactions 4-80437
- trimethylsilyl aerosol, thermodesorption of water (methanol), mass spectrometric investig. 4-62259
- valine, amino acid, fast heavy ion-induced desorption, damage cross sections 4-77188
- vapour absorption-desorption isotherms, two-dimensional network model 4-61178
- vapour interaction with densely packed spherical particles, modelling, relative permeability 4-61179
- water film, photon and electron-stimulated desorption, mech. of ion formation and desorption 4-61241
- $Ag$  (110) surface catalysis of selective epoxidation of ethylene 4-93554
- $Ag$  (111) with adsorbed  $NO$ , adsorption and decomposition study 4-98433
- $AgBr(Cl)$ , photon-stimulated desorption of neutral species 4-61216
- $Al$ , adsorbed water, electron stimulated desorption,  $H^+$  ion energy distrib. 4-92536
- $Al$ , clean and  $H_2$  exposed,  $H_2$  adsorption, electron stimulated desorption study 4-75792
- $Al$ , diffusion of  $H$ , desorption study 4-65489
- $Al-Cu-Mg$ , 2017, surface characterisation as vacuum vessel for nuclear fusion devices 4-96266
- $AlGa_{1-x}As$  MBE growth, Ga desorpt., AES and photoluminesc. studies 4-93220
- $Ar$ , solid, cathodoluminescence excitation spectra, desorption, exciton creation 4-85013
- $Ar$  solid, electron stimulated desorpt., luminesc. and exciton creation 4-80381
- $Au$  adsorption and thermal decomposition of tricesylphosphate, XPS studies 4-98428
- $Au$ , adsorption of  $O_2$ , AES, XPS, and thermal desorption study 4-92556
- $C$  fluidised bed, continuous adsorpt. process 4-97651
- $C$ , trapping of sub-eV  $H$  and  $D$  atoms 4-111761
- $CO$  chemisorbed layer on  $Ru$  (001), electron-induced desorption 4-104075
- $CO$  clusters, two-dimens., chemisorption of  $CO$  4-108725
- $CO$ , condensed molecules, photon-stimulated ion desorption 4-61239
- $CO$ , solid, photon-stimulated ion desorption 4-93549
- $CO_2$  desorption, liq. film mass transfer coeffs. 4-87661
- $CaTiSiO_5$ :La sphere-based glass-ceramics, La partitioning, Auger studies 4-88112
- $CdSe$ , particle desorpt. under laser irradi., mass and energy distrib. meas. (Russian) 4-113815
- $Ce_{1-x}Ni_xCu_{2.5}$  alloys, hyperstoichiometric,  $H_2$  sorption 4-61207
- $Cr$  (110) with adsorbed  $O_2$ , photon stimulated  $O^+$  desorption 4-98438
- $Cr$  (100), time of flight mass spectra study on IR laser photodesorption of  $NH_3$  4-80384
- $Cu$  (110), adsorption of water vapour, electron beam damage to adlayer 4-80396
- $Cu$  (110), clean and  $O$  covered, ethylene adsorption, UPS studies 4-70548
- $Cu/Ru(001)$  bimetallic catalysts, static SIMS, XPS and TPD studies 4-80411
- $D_2O$ , condensed molecules, photon-stimulated ion desorption 4-61239
- $Fe$  (111),  $CO$  interaction, thermal desorpt. and LEED studies 4-65566
- $Fe$ , adsorption and thermal decomposition of tricesylphosphate, XPS studies 4-98428
- $Fe$  films,  $H_2$  adsorption, surface pot. and thermal desorpt. spectra study 4-65555
- $Fe-Si$  (3 wt.%) (100) surfaces, interaction with  $O_2$  and electron stimulated desorption 4-92560
- $GaAs$  (110),  $H_2O$  adsorption, TDS and LEED studies 4-65568
- $GaAs$  (110) with adsorbed  $H$ ,  $H_2$ , temp. programmed desorption study 4-92528
- $GaAs$ , VPE,  $Cl$  desorption by  $H_2$ , quantum chemistry 4-70553
- $Ge$  (111)- $Pb$  interface form, dynamics and oxidation 4-84518
- $Ge$  substrate, carbon tetrachloride, IR laser stimulated desorption, time of flight distrib. 4-61203
- $H_2$ , electron-stimulated field desorption 4-92532
- $H_2$ , electron-stimulated field desorption 4-92532
- $HD$ , prod. from  $H_2+D_2$  reactions on  $Pt$  (557), ang. and vel. distrib. 4-99834
- $^4He$  thin film on sapphire, desorption studies 4-98398
- $Ir$  (111),  $CO$  oxidation kinetics, lattice gas model of thermal desorpt. spectra 4-66613
- $Ir$  surface,  $CO$ , desorption ang. distrib. from  $CO$  oxidation 4-80378
- $KI$ , photon-stimulated desorption of neutral species 4-61216
- $LaNi_2-NdNi_2(CeNi_2)$ , phase diagrams, grain size anisotropy,  $H$  absorpt. characts. (Chinese) 4-93261
- $LaNi_2(Ni_{1-x}Al_x)_2$  and misch metal analogues,  $H_2$  desorption kinetics 4-75787
- $LiF$ , photon-stimulated desorption study 4-70571
- $LiF$  surfaces,  $F^+$  ejection by ion bombardment 4-61800
- $Mo$  (100) and  $MoS_2$  (0001),  $CO$  coadsorption with  $S_2$ ,  $H_2$ , and  $O_2$ , LEED, AES and TDS studies 4-80407
- $Mo$ , low energy heavy ion bombardment, self-interstitial generation 4-80117
- $MoO_3$  with adsorbed methanol, desorption, oxidation to formaldehyde 4-92520
- $N_2$ , condensed molecules, photon-stimulated ion desorption 4-61239
- $N_2$ , solid, photon-stimulated ion desorption 4-93549
- $NH_3$ , condensed molecules, photon-stimulated ion desorption 4-61239
- $N_2O$  chemisorbed layer on  $Ru$  (001), electron-induced desorption 4-104075
- $N_2O$ , condensed molecules, photon-stimulated ion desorption 4-61239
- $Na_3(AlO_2)_4(SiO_2)_{40}24H_2O:Eu^{2+}$ , adsorption of  $O_2$ , fluorescence study 4-84511
- $NaCl$  with adsorbed methyl fluoride, IR laser induced desorption, momentum distrib. study 4-80419
- $NaF$ , photon-stimulated desorption study 4-70571
- $Na_2O-SiO_2$  glass surface, electron stimulated desorption mechanisms 4-92514
- $Na_2WO_3$ , photon stimulated  $O^+$  ion desorption 4-84503
- $Nb$ ,  $Pd$ - and  $Ni$ -coated, hardening and fracture initiation, resulting from  $H_2$  adsorpt.-desorpt. cycling 4-81282

## desorption continued

- Ne, 585.2 nm line intensity variation due to return to gas phase from glass bulb 4-69006  
 Ni (100), adsorption of K, coadsorption of K and D<sub>2</sub>, work function, TDS, XPS, UPS, AES studies 4-80398  
 Ni (100), K-doped, CO and D<sub>2</sub> adsorpt., XPS, UPS, TDS, EELS and work function studies 4-84509  
 Ni (100), K-predosed, coadsorption of CD and D<sub>2</sub> 4-92535  
 Ni (100), S-covered, adsorption of CO, vibr. spectroscopy study 4-108720  
 Ni (100) with adsorbed N<sub>2</sub>, core level binding energy shift anal. 4-92517  
 Ni (110), desorption of H<sub>2</sub>, influence of magnetisation 4-104081  
 Ni (110), oxidised, electron stimulated desorption of O<sup>+</sup> ions, role of inner shell excitations 4-108718  
 Ni (110), oxygen dosed, H<sub>2</sub>O adsorption, OH(ad) formation and orientation 4-66615  
 Ni (110), phase transitions obs. 4-88395  
 Ni (110) surface, adsorbed H, dual path surface reconstruction study 4-108716  
 Ni (111), adsorption and decomposition of NO, metastable quenching electron spectroscopy 4-92567  
 Ni (111), dissociative adsorption and recomb. of CO, N<sub>2</sub>, SO, and O<sub>2</sub> 4-93559  
 Ni, angle resolved thermal desorption spectra for CO and H<sub>2</sub> 4-70554  
 Ni, coadsorption of H<sub>2</sub> and CO, ion induced desorption study 4-92547  
 Ni, ion bombardment-induced O<sup>-</sup> desorption, energy distrib. 4-75781  
 Ni, ion desorption spectrometry for surface anal. 4-66609  
 Ni, low energy heavy ion bombardment, self-interstitial generation 4-80117  
 Ni, polycrystalline, O<sub>2</sub> adsorption, temperature programmed desorpt. study 4-84515  
 Ni surface, adsorbed O<sub>2</sub>, electron stimulated desorpt. 4-65565  
 Ni, thermodynamics, kinetics and props. of gases and C, data tables 4-73173  
 O<sub>2</sub>, adsorption and desorption, generation and feeding (German) 4-114822  
 PBS film, photosensitivity and luminescence studies 4-104679  
 Pd (110) with adsorbed H<sub>2</sub>O, photon stimulated desorption of H<sup>+</sup> 4-98437  
 Pd (111), O<sub>2</sub> adsorption, AES, EELS, TDS, ESD and work function studies 4-80410  
 Pd, adsorbed Xe, adsorptive bond, face specificity, s-resonance model 4-92540  
 Pd-MOS struct. with adsorbed H<sub>2</sub>, use as H<sub>2</sub> sensor in catalytic reactions 4-93555  
 PdH<sub>x</sub> powder, thermal desorption spectra 4-84510  
 Pt (100), electrodeposition of Ag, thermal desorption, Auger effect, LEED 4-80449  
 Pt (100) and (111), O<sub>2</sub> adsorption, XPS and TDS studies 4-80406  
 Pt (100) with adsorbed O<sub>2</sub>, interactions, XPS and work function 4-92521  
 Pt (110) with adsorbed H<sub>2</sub>O, photon stimulated desorption of H<sup>+</sup> 4-98437  
 Pt (111), 2H<sub>2</sub>+O<sub>2</sub>→2H<sub>2</sub>O reaction, SIMS and TDS studies 4-66614  
 Pt (111), adsorbed NO, vibr. excitation and deexcitation rates 4-98443  
 Pt (111), adsorption and decomp. of methyl isocyanide, EELS and thermal desorption study 4-108721  
 Pt (111), adsorption of C<sub>2</sub>N<sub>2</sub>, coadsorption with H<sub>2</sub>, surface chem. 4-81478  
 Pt (111), cyclopentene adsorpt., cyclopentadienyl obs. by EELS and TDS 4-65558  
 Pt (111), of O and O<sub>2</sub>, local density formalism 4-92548  
 Pt electrodes, adsorption of tripeptide, kinetics and isotherms 4-92539  
 Pt/TiO<sub>2</sub>, H<sub>2</sub> and D<sub>2</sub> isotope scrambling, thermal desorption 4-80377  
 Ra, trace adsorpt. and desorpt. on freshwater sediments and their mineral components 4-80376  
 RbBr(I), photon-stimulated desorption of neutral species 4-61216  
 Re (0001), O<sub>2</sub> predosed, H<sub>2</sub>O adsorption, TDS study 4-113803  
 Re (0001) and stepped surfaces, adsorption and dissoc. of water, TDS, LEED, AES, ESD/AD studies 4-80401  
 Rh (111), adsorption and decomposition of methanol, EELS and thermal desorption spectroscopy 4-92565  
 Rh (111), CO and K coadsorption, HREELS, TPD, AES and LEED study 4-84508  
 Rh (111), NO+CO reactions, AES, LEED, XPS, UPS and temp. programmed desorpt. study 4-89326  
 Rh (111) and (331), CO adsorption and desorption, XPS and SIMS study 4-65574  
 Rh (111) with surface adsorbed HNCO, effects of preadsorbed O 4-113781  
 Rh surface, isotope exchange reaction of CO 4-81479  
 Ru (001), chemisorbed H<sub>2</sub>O clusters, desorption mass spectra, EELS 4-75786  
 Ru (001), coadsorption of CO and Na, mol. reorientations 4-108717  
 Ru (001) surface, coadsorption of K and CO, thermal desorption vibr. overtone spectroscopy 4-70565  
 Ru (001) surface, K covered, thermal desorption of CO 4-65548  
 Si (100), chemisorption of H, TDS study (Chinese) 4-92510  
 Si (100), PH<sub>3</sub> and SiH<sub>4</sub> adsorption, saturation coverage 4-88392  
 Si (100), surface treatment for Si MBE growth 4-71743  
 Si (111) and (100), Cs, K, Na, Li desorption kinetics and surface phase changes, surface ionisation studies 4-65571  
 Si, doping kinetics from atomic beam in vacuum, desorption 4-113479  
 Si, MBE growth, use of In for surface cleaning 4-99616  
 Si MBE layer, Sb adsorption, LEED, AES and TDS study 4-65560  
 Si/SiO<sub>2</sub>/Si<sub>3</sub>N<sub>4</sub>/electrolyte system, static and dynamic volt-ampere charact. (Russian) 4-65739  
 SiO<sub>2</sub>, fracture and emission of electrons, ions and photons 4-98189  
 SiO<sub>x</sub>, reactive film deposition, surface processes, planar magnetron sputtering 4-113798  
 SrF<sub>2</sub> cryst., He diffusion and solubility, trivalent impurity effect 4-108663  
 Ti (0001), clean and oxidised, electron emission and ion desorption spectroscopy 4-92561  
 Ti film, characterisation in TMX-U 4-93579  
 Ti, thermal cycling in D<sub>2</sub> atmosphere 4-99497  
 TiMn<sub>1.5</sub>, desorption of H<sub>2</sub> and D<sub>2</sub> at low press. (Japanese) 4-65552  
 TiO<sub>2</sub>, electron stimulated desorption of neutral OH radicals 4-108713  
 W (100), H<sub>2</sub> and O<sub>2</sub> coadsorpt., temperature-programmed desorpt. study 4-84507  
 W (100) stepped surfaces, adsorbed K, desorption kinetics and directional depend. of surface diffusion 4-92545

## desorption continued

- W (110) with surface adsorbed CO, electronic transitions, low-threshold neutral desorption, α-β conversion, calcs. 4-113785  
 W, adsorbed water, electron stimulated desorption, H<sup>+</sup> ion energy distrib. 4-92536  
 W, low energy heavy ion bombardment, self-interstitial generation 4-80117  
 W point cathodes, electron field emission instability, adsorption effects 4-61813  
 W surface polycryst., chemisorption of NO desorption, FEM and work function meas. 4-92564  
 WC, electron stimulated desorption of O<sup>+</sup>, AES study 4-92569  
 ZnO (0001), interaction with methanol at low temp., XPS and UPS study 4-92542  
 Zr with surface adsorbed H, sticking coefficients, binding states, desorption studies 4-113784
- detection (demodulation) see demodulation**
- detectors**  
 see also electric sensing devices; hydrophones; infrared detectors; microwave detectors; nonelectric sensing devices; particle detectors; photodetectors; ultraviolet detectors  
 fibre-optic magnetic-field sensor detect. scheme free from ambiguity due to material mag. hysteresis 4-78303  
 IR and MM waves, conf., Miami Beach, FL, USA (Dec. 1983) 4-73154
- determinants**  
 see also matrix algebra  
 noninvertible elliptic operator, regularised determinant 4-68443
- detonation**  
 see also explosions; shock waves  
 atmospheric buoyant materials, temp.-field struct. 4-75056  
 Composition B-3 and PBXW-109(I), unreacted Hugoniot and shock ignition 4-109654  
 cyclohexane, shock wave diagnostics by Raman and IR meas. 4-109712  
 deflagrations and detonations for small heat release 4-79618  
 EM stress gauge, effect of stress discontinuities 4-106313  
 energetic materials, porous, compaction at deflagration-detonation transition 4-108546  
 explosives, decomposition rates, multiple wave effects 4-109663  
 explosives, detonation initiation by imploding shock waves, high speed photographic obs. 4-112951  
 Freon 22, superheated, explosive phase transitions 4-108600  
 gaseous detonation, dynamic parameters 4-91822  
 gases, light-induced detonation, thermodynamic props. 4-97796  
 granular porous explosives, shock sensitivity, grain size effects 4-108548  
 heterogeneous explosives, shock-induced initiation, burning topology 4-109660  
 hexanitrostilbene, impact initiation, photographic investig. 4-109648  
 HMX explosive, thermal initiation and burning prior to detonation 4-109656  
 HNS porous explosive, shock initiation, mixture theory appls. 4-109658  
 industrial explosions, detonation wave intensity, influence of humidity and air excess, using gaseous phase spherical detonation mathematical model 4-109652  
 light induced detonation of gas, lateral expansion, optical discharge 4-113252  
 LX-10, LX-1, and RX-26-AF, spherically diverging detonation wave vel. 4-108544  
 oblique shock wave incidence on a semi-infinite detonating medium (Russian) 4-112957  
 overdriven expts., product EOS above Chapman Jouguet press. 4-109664  
 PBX and PBXW, elec. resist. and dielec. breakdown meas. 4-108865  
 pentaerythritol tetranitrate, chemically reacting multiphase mixtures, detonation, statistical mechanical theory 4-104961  
 pentaerythritol tetranitrate, shock wave diagnostics by Raman and IR meas. 4-109712  
 porous systems, nonstationary convective combustion eqns., qualitative anal. 4-71923  
 reactive explosive mixtures, initiation and growth-to-detonation 4-109657  
 RX-26-AF, shock initiation, detonation wave propag. and metal acceleration 4-109662  
 RX-26-AF, shock initiation, reactive flow lagrange anal. 4-109661  
 shaped explosive charges, detonation wave shaping, computer simulation anal. 4-108545  
 shock compressed material, diagnostics by Raman scatt. 4-109713  
 shock-detonation transitions, Lagrangian method anal. using thermodynamic quantities 4-108547  
 solid high explosives, detonation front meas. 4-66592  
 sonic detonation wave acceleration in perfect adiabatic fluids 4-112952  
 spin detonation, theoretical study (Ukrainian) 4-87812  
 TEN, explosive density effect on air shock wave parameters 4-99792  
 thin-pulse shock initiation threshold, meas. optimisation 4-108059  
 triaminotrinitrobenzene explosive, short-duration shock initiation 4-108543  
 triaminotrinitrobenzene-based explosives, shock initiation, particle size and temp. depend. 4-109659  
 water cannon, internal ballistics 4-69792  
 waves, transmission through orifice, geometry effects 4-103366  
 Ar, weak imploding shock waves, streak camera obs. 4-112950  
 H<sub>2</sub>-air mixtures, high-speed turbulent deflagration and transition to detonation 4-103432  
 H<sub>2</sub>-CO<sub>2</sub> in air, flammability and detonability in radioactive waste processing 4-106741  
 N<sub>2</sub>, vibrationally excited, nonstationary shock waves propag. 4-108090
- detonation spraying see powder spraying**
- deuterium**  
 adsorbed layer on W (111), diffusion, fluctuation method anal. 4-104088  
 adsorbed on Ni (110) and (111), site location, surface channelling study 4-80375  
 adsorption on K-dosed Ni (100) 4-84509  
 adsorption on Ni (110), EELS study 4-65564  
 Bianchi type V cosmological model with tilt, He form., D abundances 4-90265  
 Big Bang nucleosynthesis, implications of model of chemical evolution of cosmic abundance 4-67843  
 chemisorption on Ni (110), saturation coverage 4-92550  
 coadsorption of D<sub>2</sub> and K on Ni (100), work function, TDS, XPS, UPS, AES studies 4-80398  
 coadsorption with CO on K-predosed Ni (100) 4-92535  
 diffusion, in β-Pd, Fick's coefficient 4-98334  
 dilute solutions in Pd alloys, thermodynamics 4-70411

## uterium continued

- frozen polarised target 4-64262  
 gas, DC breakdown strength, isotope depend. 4-79723  
 glow discharge, high voltage, planar 1D model 4-60767  
 intergalactic gas of rich galaxy clusters, He separation from D (Russian) 4-94971  
 lamps, time depend. of spectral radiance with  $MgF_2$  window 4-83662  
 liquid metallic, two-component quantum fluid, equil. props. 4-104036  
 mass spectroscopic determination in heavy wakes 4-109706  
 metals, D implanted, reemission and permeation 4-113721  
 migration process of H isotopes in BCC metals, realistic calc. 4-65465  
 molecular fluid equil. props. in semiclassical limit 4-103632  
 molecule, electron-polarised-photon coincidence excitation of  $C^{19}H$ , state 4-83483  
 molecule, high-resolution spectroscopy at 83 nm 4-64490  
 molecules adsorbed in NaCaA zeolites, induced IR overtone and fundamental bands 4-102678  
 muonic molecule, resonant formation, hyperfine effects 4-59917  
 optical fibres, single-mode,  $H_2$  and  $D_2$  gas-in-glass effects 4-97121  
 plasma time evolution of transport processes, computer codes 4-87848  
 primordial nucleosynthesis, D and  $^7Li$  from Population III remnants 4-67842  
 primordial nucleosynthesis and interstellar D 4-63255  
 primordial nucleosynthesis by pregalactic massive stars 4-67841  
 solid, proton irradi., electron trapping, IR absorption studies 4-75751  
 solid, rot. excitation under high press., anharmonic theory 4-108674  
 solid, rotation-libration transition, modified Ree-Bender pot. effects 4-92475  
 solubility in single cryst.  $Li_2O$  breeder material 4-107025  
 sorption in  $TiMn_{1.5}$  at low press. (Japanese) 4-65552  
 steel, austenitic stainless, D permeation, plasma-driven, effect of surface comp. 4-113718  
 steel, H and D diffusion under fission reactor radiation 4-113503  
 thermal desorption from  $Pt/TiO_2$ , isotope scrambling 4-80377  
 trapping of sub-eV H and D atoms in C 4-111761  
 tunnelling in Nb, sp. ht. meas. 4-61103  
 Be-D, retention and thermal release of implanted D 4-113477  
 $CaNi_5H_x(D_x)$ , absorption pressure-comp. isotherms, thermodynamic anal. 4-77032  
 D-, generation on composite surfaces rel. to surface/plasma ion source systems 4-93165  
 D-, ion source development, sheet plasma 4-78415  
 D- Lamb-shift polarised ion sources 4-107239  
 D-, very-low-energy electron detachment 4-91336  
 D+ polarised ion source, ECR technique 4-107242  
 D/H ratio in solar neighbourhood, implications for solar nebula characts. 4-77733  
 D/H ratio in upper atmosphere, meas. from optical detect. by Spacelab. I mission 4-90016  
 D- $^3He$  fuel ignition in high-field OMITRON type Tokamaks 4-59405  
 D- $^3He$  fusion plasmas, nuclear elastic scatt. effects 4-103543  
 D-D catalysed fuel ignition in high-field OMITRON type Tokamaks 4-59405  
 D-D fusion plasmas, nuclear elastic scatt. effects 4-103543  
 D-H isotope separation between hydrogen and liq. methanols 4-59904  
 D-T plasma depolarisation by recycling in material walls 4-91096  
 D-T spin-polarised fuel, fusion gains using homogeneous ignition and central ignition model 4-59409  
 D+CO, collisional excitation, cross sections, quasiclassical trajectory study 4-78950  
 D+Cl $_2$ , oriented-averaged rot.-decoupled vibr. 4-99753  
 D+FD reactive reson., partial widths and isotope effects calc. by reaction path Hamiltonian model 4-71890  
 D+H $_2$ , BKLT eqn. for reactive scatt. of collinear nonsymm. systems 4-114787  
 D+H $_2$ , initial and state to state cross sections, quantum chemical study, rate consts. 4-62160  
 D+H $_2$ , reactive differential cross sections in rot. linear model, ang. distrib. 4-99775  
 D+He, H(D) 2s and 2p excitation, integral cross sections 4-102786  
 D+NO chemiluminescence reaction, DNO internal energy distrib. 4-71871  
 D+Cs, spin-depend. charge transfer 4-59890  
 D $_2$  gas permeability in polymer microballoons, interferometric meas. 4-70469  
 D $_2$  gas-in-SiO $_2$  fibre Raman laser, synchronously pumped, operating at 1.56  $\mu m$  4-79181  
 D $_2$ , H $_2$  solid soln., H and D behaviour at liq. He temp. 4-70517  
 D $_2$  in mixtures of nematic liq. crystals, D NMR spectra, quadrupole moment, orientational ordering 4-91276  
 D $_2$  in small volumes, coherent anti-Stokes Raman scatt. 4-78856  
 n-D $_2$ , liquid and liquid mixtures, intermolecular free length, acoustic study 4-88059  
 D $_2^+$  ion beams, high conc., prod. using short multicusp ion source, use in heating 4-60673  
 D $_2^+$ , UV laser photodissoc. 4-69157  
 D $_2^+$ +Ar, rotationally inelastic cross sections, anisotropic interaction pot. determ. 4-83452  
 D $_2$ +F, collinear exchange reactions, probability densities, stabilisation calcs. 4-81415  
 D $_2$ +F, reactive infinite order sudden approx. calc., cross-sections and vibr. branching ratios 4-66571  
 D $_2$ +H, nascent HD prod. quantum state distrib., pulsed laser photolysis, Raman spectra 4-104977  
 D $_2$ +H, opacity analysis of steric requirements in elementary chemical reactions 4-62159  
 D $_2$ +H, vibr. and rot. energy disposal reaction at 1.3 eV, surprisal anal. 4-76973  
 D $_2$ +H $_2$ , exchange reaction on Pt (557) surface, HD ang. and vel. distrib. 4-99834  
 D $_2$ +HD, vibr. relax., mechanisms and rate consts. 4-96669  
 D $_2$ +HF( $v=3, 4, 5$ ), HF vibr. relax., fluoresc. study 4-69187  
 D $_2$ +H $_2$ -HD+D reaction, coupled state quantum calc. at  $E_{rel}(\nu=0, j=0)=0.55$  eV 4-99750  
 D $_2$ +H $_2$ -HD+D reaction, distorted wave calcs. at  $E_{trans}(\nu=0, j=0)=0.55$  and 1.3 eV 4-99749  
 D $_2$ +I $_2$ , state-to-state rot. transfer rates; induced fluoresc. 4-91333  
 D $_2$ +Mg reactions, MgD nascent internal energy distrib. 4-71872  
 D $_2$ +O reaction dynamics, reduced dimensionality quantum and quasiclassical rate consts. 4-114784  
 D $_2$ +O $_2$ , in Ar shock tube, O $_2$  vibr. relax. study 4-96668

## deuterium continued

- D $_2$ +O $_2$ D $_2^+$ , forward and reverse rate coeff., enthalpy and entropy changes 4-62165  
 D $_2$ +OH, electronic quenching, rot. level depend., fluoresc. 4-74281  
 D $_2$ +O( $^3P$ ), exchange reactions, quasiclassical trajectory calcs. 4-71894  
 D $_2$ +T $_2$ -2DT, reaction rate meas. 4-109624  
 D $_3$ , dissociative recombination coeffs. 4-112285  
 D $_3$ +Ar(H $_2$ ) 4-78933  
 D $_3$ +He, three body dissoc. absolute cross section meas. 4-104984  
 DT, muonic, reaction kinetics, hyperfine effects 4-59918  
 D\*, electron impact dissoc. of D $_2$ O, emission cross section 4-107462  
 Ge:D, plasma treated, D diffusion and interaction with point defects 4-60951  
 H+D $_2$  reaction dynamics, product state distrib. determ. at collision energy of 1.3 eV 4-71896  
 HD, high-resolution spectroscopy at 83 nm 4-64490  
 Ni, D segregation, surface and grain boundary SIMS study 4-76774  
 Si:D, anomalous muonium atom site determination 4-65277  
 a-Si:D thin films, coupled local mode vibr., IR absorpt. study 4-88259  
 SiO $_2$ -GeO $_2$ -P $_2$ O $_5$  optical fibres, H and D absorption losses, expt. study 4-91589  
 T-D pumping at TSTA using U beds 4-86968  
 Zr:D, ion implantation, lattice defect trapping, binding enthalpy, migration 4-108400  
 Zr-V-Fe alloys, bulk getters, H and D diffusion 4-113719  
 Zr-Ni-D, metallic glass, XES study of electronic states 4-80482

## deuterium compounds

- see also heavy water  
 far IR laser, pulsed, optically pumped effects of pumping pulse width (Chinese) 4-112391  
 propyne-DF, microwave spectrum and props. 4-74229  
 triethylamine-DCN system, CN $^+$  rot., IR study 4-64463  
 D $_2$  spin system, strongly coupled, partially ordered, quadrupolar and Zeeman order relax. 4-91279  
 DBR+F, collinear H-transfer reactions, dominant reaction probabilities evaluation 4-89245  
 DCN CW waveguide laser operating at 195, 190  $\mu m$ , quartz tube cavity (Chinese) 4-107604  
 DCN laser interferometer for plasma electron density meas. 4-113220  
 DCI+H $_2$ , vibr. energy transfer probabilities, temp. depend. 4-91332  
 DF mid-IR waveguide lasers, RF pumped 4-74543  
 DF pulsed chain laser damage to coated window and mirror components 4-74582  
 DF RF-pumped IR chemical laser using transverse gas flow 4-74544  
 DF-B series complexes, B=proton acceptor mol., rot., hyperfine and quadrupole coupling consts. 4-112195  
 DF-HF chemical laser atmospheric attenuation meas. (Chinese) 4-62951  
 DF+I\*, quenching, time resolved IR fluoresc. used to determ. rate const. 4-102730  
 DF+N $_2$ (CO)(CO $_2$ )(N $_2$ O), vibr. relax. rate consts. determ. using flow IR chemiluminesc. technique 4-89273  
 DNO, internal energy distrib. formed in D+NO reaction 4-71871  
 DNO, predissoc. and bond dissoc. energy for DNO-D+NO 4-96628  
 D $_2$ N $_2$ O $_2$ , D hyperfine struct. microwave Fourier transform spectroscopy study 4-96719  
 D $_2$ O, condensed gas solids, ion-induced chem. 4-66163  
 D $_2$ O laser, TEA CO $_2$  laser pumped, development, plasma in temp. meas. appl. 4-79184  
 D $_2$ O optically pumped laser with unstable resonator, high-energy design for plasma diagnostics 4-79183  
 D $_2$ O submm laser for single shot ion temp. meas. by Thomson scatt. 4-103569  
 D $_2$ O $^+$ , UV laser photodissoc. 4-69157  
 D $_2$ O+OH, electronic quenching, rot. level depend., fluoresc. 4-74281  
 (D $_2$ S) $_2$ , 4-69154  
 D $_2$ S, nucl. hyperfine interactions, elec. dipole moments, mol. beam elec. reson. 4-59803  
 HCl-DCI, dipolar correlation times, NQR study 4-80171  
 HF/DF pulsed optical resonance transfer laser, theoretical simulation 4-79123  
 H $_2$ O gas, transport props. prediction at high temps. 4-60576  
 N $_2$ -DF, rot., hyperfine and quadrupole coupling consts. 4-112195  
 N(D $_2$ H $_{1-2}$ )+(D $_2$ H $_{1-2}$ ) $_2$ PO $_4$ , dielectric and electro-optical props. meas. 4-76313  
 OD $^+$ , vibr. fine struct. in collisionally induced charge reversal and fragmentation 4-71875  
 SiO $_2$ GeO $_2$ -OD 4-64779

## deuteron effects

- CR-39 plastic track detectors, light charged particle registration characts. 4-64306  
 Ag film, proton and deuteron stopping cross section 4-92260  
 Au film, proton and deuteron stopping cross section 4-92260  
 Cu, D $^+$  irradi., two-level fracture in blistering 4-75560  
 Cu film, proton and deuteron stopping cross section 4-92260  
 Cu, irradi., stored energy, calorimetric determ. 4-103829  
 Ni, dislocation/obstacle interaction during low dose D irradi. creep 4-104813

deuteron interactions see deuteron-nucleus reactions; hadron-deuteron interactions; lepton-deuteron interactions; meson-deuteron interactions; photon-deuteron interactions; proton-deuteron interactions

## deuteron-nucleus reactions

- for inelastic deuteron-nucleus scattering, see 'deuteron-nucleus scattering'  
 see also nuclear fusion  
 charged particle fusion cross sections, data status for reactor design 4-111772  
 Coulomb dissociation at nonrelativistic and relativistic energies 4-95980  
 (d, $\alpha$ ) reactions, D-state and nuclear struct. effects, DWBA calcs. 4-96041  
 (d, $n$ ), on A=255-258, fission fragments and mechanisms 4-106637  
 (d $^+$ ,He), 52 MeV, Zr region, deeply bound hole states, p-h strength 4-73794  
 (d $^+$ ,Li), A=90 region,  $\alpha$ -pick up at 45 MeV, clustering, high resolution data 4-86815  
 (d,p), differential cross-sections, vector analysing powers 4-73904  
 (d,pf), on A=255-258, fission fragments and mechanisms 4-106637  
 (d,X), quasideuteric 3-body dynamics of stripping and breakup reactions 4-59248  
 (d,X) on C, Cu, Pb, neutron energy spectra, anal. 4-73908

**deuteron-nucleus reactions continued**

- (d,x) on C, Fe, Cu, Pb, neutron and photon prod., expt., Monte Carlo calcs. 4-73907  
 $(\mu^+d)^+$  system, muon<sup>+</sup> decay, muon catalysed fusion appl. 4-59079  
 PP (d,p), reaction, deuteron distorting potentials 4-102283  
<sup>197</sup>Au(d,pn), E=12 MeV, breakup in Coulomb field of heavy nuclei, DWBA comparison 4-111536  
<sup>10</sup>B(d,<sup>6</sup>Li), 13.6 MeV, differential cross, sections, ang. depend. 4-96040  
<sup>10</sup>B(d,<sup>7</sup>Be), 13.6 MeV, differential cross, sections, ang. depend. 4-96040  
<sup>209</sup>Bi(d,<sup>3</sup>He), <sup>208</sup>Pb isoscalar character of 5845 MeV 1<sup>+</sup> state, 4-68683  
<sup>12</sup>C(d,pn), 56 MeV, p-n coincidence cross section and p spectrum, CC approach to breakup 4-83072  
<sup>12</sup>C(d,p), 17.7 MeV, <sup>14</sup>C isoscalar transition rates, stripping probabilities, and spectroscopic factors, DWBA anal. 4-111519  
<sup>48</sup>Ca(d,<sup>3</sup>He), 80 MeV, <sup>48</sup>K 7/2<sup>+</sup> state, spectroscopic factor, <sup>48</sup>Ca proton ground state correl. 4-64035  
<sup>4</sup>(d,<sup>4</sup>Li) microscopic cluster form factor in DWBA calcs. 4-64161  
<sup>4</sup>(d,p) stripping reaction, antisymmetry in 3-body model 4-102241  
<sup>2</sup>(d,d,n)<sup>3</sup>He muon catalysed, yield ratios 4-86634  
<sup>2</sup>(d,p)<sup>3</sup>T muon catalysed, yield ratios 4-86834  
<sup>4</sup>(d,n)<sup>3</sup>He, cross-section calcs., resonating group method 4-78638  
<sup>3</sup>Fe(d,p) depolarisation param., two-component cross-section model 4-64139  
<sup>1</sup>H(d,<sup>3</sup>He), <sup>3</sup>HeD state study 4-83078  
<sup>1</sup>H(d,<sup>3</sup>He), tensor analysing power, D-state effects 4-73915  
<sup>1</sup>H(d,p)n, reaction cross section, charge dependence 4-91009  
<sup>2</sup>H(d,2p), 80 MeV, four-body breakup process, two spectator quasifree scatt. 4-64153  
<sup>2</sup>H(d,n) neutron polarisation meas. using fast neutron polarimeter (Chinese) 4-83266  
<sup>2</sup>(d,n)<sup>3</sup>He, charge symmetry violation study 4-83077  
<sup>2</sup>H(d,p)<sup>3</sup>He, charge symmetry violation study 4-83077  
<sup>3</sup>H(d,X), muon catalysed fusion, high density mixtures, temp. depend. 4-106641  
<sup>3</sup>H(d,X), muon catalysed fusion,  $\alpha$ -sticking fraction 4-106642  
<sup>3</sup>H(d,X), muon catalysed fusion,  $\alpha$ -sticking probability 4-106644  
<sup>3</sup>H(d, $\gamma$ ), 45, 146 keV ground state  $\gamma$ -ray branching ratio at low energies 4-102282  
<sup>3</sup>H(d,n)<sup>3</sup>He, cross-section meas. 12.5-117 keV 4-83074  
<sup>3</sup>H(d,n)<sup>3</sup>He, muon catalysed in DT system at high density 4-59294  
<sup>3</sup>H(d,n)<sup>3</sup>He, muon catalysed high temp. fusion cross section 4-59296  
<sup>3</sup>H(d,n)<sup>3</sup>He, muon catalysed, point kinetics anal. 4-59297  
<sup>3</sup>H(d,n)<sup>3</sup>He, muon catalysed fusion 4-59918  
<sup>3</sup>H(d,x), muon catalysed fusion, low density expts. 4-106640  
<sup>3</sup>He(d,p)<sup>3</sup>He, proton energy spectrum in Tokamak by ICRF 4-86833  
<sup>4</sup>H(d,pn $\gamma$ ), A=202, 204, 25 MeV, gamma ray and conversion electron spectra, yrast state population 4-102162  
<sup>82</sup>Kr(d,<sup>3</sup>He), <sup>81</sup>Kr, <sup>81</sup>Br ground state mass difference, <sup>81</sup>Br solar neutrino detector calibration 4-106565  
<sup>82</sup>Kr(d,t), <sup>81</sup>Kr, <sup>81</sup>Br ground state mass difference, <sup>81</sup>Br solar neutrino detector calibration 4-106565  
<sup>6</sup>Li(d, $\alpha$ ), low-energy cross sections, optical model 4-106600  
<sup>6</sup>Li(d,n)<sup>3</sup>He $\alpha$ , low-energy cross sections, optical model 4-106600  
<sup>6</sup>Li(d,n)<sup>3</sup>Be(GS)+<sup>3</sup>Be\*, low-energy cross sections, optical model 4-106600  
<sup>6</sup>Li(d,p)<sup>7</sup>Li+<sup>7</sup>Li\*, low-energy cross sections, optical model 4-106600  
<sup>6</sup>Li(d,pt) $\alpha$ , low-energy cross sections, optical model 4-106600  
<sup>7</sup>Li(d,n)<sup>8</sup>Be neutron polarisation source at low energy, DWBA calcs. 4-83075  
<sup>25</sup>Mg(d,p)<sup>26</sup>Mg ang. dist., spectroscopic factors, DWBA calcs. 4-83073  
<sup>144</sup>Nd(d,p $\gamma$ ), <sup>145</sup>Nd low-lying vibrational states study 4-59133  
<sup>144</sup>Nd(d,t), A=148, 150, <sup>147</sup>,<sup>149</sup>Nd low-lying vibrational states study 4-59133  
<sup>20</sup>Ne(d, $\alpha$ )<sup>18</sup>F, density reduction in gas targets for medical radionuclide prod. 4-89745  
<sup>58</sup>Ni(d, $\alpha$ ), 6.75-9.5 MeV, tensor anal. powers, <sup>56</sup>Co levels and J<sup>π</sup> 4-111503  
<sup>58</sup>Ni(d, $\alpha$ )<sup>56</sup>Co, 16 MeV, cross section ang. distrib., vector and tensor analysing powers meas. 4-68698  
<sup>4</sup>Pt(d,pn $\gamma$ ), A=196,198, 25 MeV, gamma ray and conversion electron spectra, yrast state population 4-102162  
<sup>193</sup>Pt(d,p), multi-j supersymmetry scheme breaking, forbidden transitions 4-106621  
<sup>4</sup>Ru(d,<sup>6</sup>Li), 45 MeV, <sup>96,98,100</sup>Mo levels, J<sup>π</sup>, transitions, DWBA and IBA anal. 4-86760  
<sup>118</sup>Sn(d,pn), 56 MeV, p-n coincidence cross section and p spectrum, CC approach to breakup 4-83072  
<sup>126</sup>Te(d,t)<sup>125</sup>Te pick-up reactions, nucl. level struct. investig. 4-78637  
<sup>4</sup>Th(d,<sup>6</sup>Li), A=230, 232,  $\alpha$ -pick up at 45 MeV, clustering, high resolution data 4-86815  
<sup>230</sup>Th (d,pf), obs. of new states in the third well 4-106636  
<sup>232</sup>Th(d, fission) fission fragment ang. distribution, momentum transfer 4-86869  
<sup>232</sup>Th(d,pn $\gamma$ ), 25 MeV, gamma ray and conversion electron spectra, yrast state population 4-102162  
<sup>4</sup>Th(d,<sup>6</sup>Li), 45 MeV, <sup>226,228</sup>Ra levels, transitions and  $\alpha$ -clustering search, DWBA anal. 4-86759  
<sup>49</sup>Ti(d,p), 6 MeV, <sup>50</sup>Ti excited levels, J<sup>π</sup>, decay scheme and lifetimes 4-78606  
<sup>50</sup>Ti(d, $\alpha$ )<sup>48</sup>Sc, 16 MeV, cross section ang. distrib., vector and tensor analysing powers meas. 4-68698  
<sup>238</sup>U(d,pn), <sup>238</sup>U<sup>m</sup> shape isomer,  $\gamma$ -decay branch 4-73851  
<sup>51</sup>V (d,pn), 56 MeV, p-n coincidence cross section and p spectrum, CC approach to breakup 4-83072  
<sup>174</sup>Yb(d,pn $\gamma$ ), 25 MeV, gamma ray and conversion electron spectra, yrast state population 4-102162

**deuteron-nucleus scattering**

- <sup>4</sup>H(d,d)H off-shell effects in polarisation observables 4-83079  
<sup>6</sup>Li(d,d') differential cross-sections calcs. in diffraction model 4-91007

**deuteron photodisintegration**

- $\gamma$ d-pn, 0.4-0.8 GeV, cross-section asymmetry, dibaryon resonances 4-111464  
 $\gamma$ d-pn, polarisation expts. in nuclear resonance region 4-102257  
<sup>2</sup>H( $\gamma$ , pn), meson exchange currents, energy transfer effects for electroweak nuclear processes, review 4-64055  
<sup>2</sup>H( $\gamma$ , pn), polarisation expts. in nuclear resonance region 4-102257  
<sup>2</sup>H( $\gamma$ ,n)H, asymmetry function at low energy 4-68671  
<sup>2</sup>H( $\gamma$ ,np) two-body effects from meson exchanges 4-59221

**deuteron photodisintegration continued**

- <sup>2</sup>H( $\gamma$ ,pn), photodisintegration in  $\Delta$  resonance region, total cross section, polarisation 4-68670  
<sup>3</sup>H( $\gamma$ ,pn), forward disintegration, matrix anal., meson exchange currents, rel. corrections 4-106609

**deuteron polarisation**

No entries

**deuteron scattering** *see deuteron-nucleus scattering; hadron-deuteron scattering; lepton-deuteron scattering; meson-deuteron scattering; photon-deuteron scattering; proton-deuteron scattering*

**deuterons**

*see also cosmic ray deuterons*

- Bethe-Salpeter amplitude, symmetry 4-106568  
 low energy parameters 4-59082  
 quark struct. and relativistic quark dynamics 4-95800  
 quasi-deuterons, potential barrier tunnel superpenetrability 4-95911  
 relativistic effects, manifestation in ed-enp 4-59086  
 six quark compound bag component, nuclear chromodynamics 4-86779  
 six-quark component from structure function comparison 4-59047  
 six-quark compound state in QCD 4-83000  
 two-nucleon systems, resonating group quark cluster model, nuclear chromodynamics 4-64066  
 NN-d $\sigma$ , >800 MeV, amplitude energy depend. for <sup>3</sup>P<sub>2</sub>, <sup>1</sup>D<sub>2</sub>, <sup>3</sup>S<sub>0</sub>, <sup>3</sup>F<sub>2</sub> and <sup>3</sup>F<sub>3</sub> 4-78561  
 $\pi$ NN coupling constant, deuteron D/S ratio, nucleon-nucleon interactions 4-106535  
 $\pi$ NN coupling constant, deuteron props., one-pion exchange 4-106536  
<sup>2</sup>H, EM form factors and tensor force, non-relativistic calc. 4-90951  
<sup>2</sup>H wavefunction asymptotic S-state amplitude, one-pion exchange 4-95891

**developers (photographic)** *see photographic materials*

**development, photographic** *see photographic process*

**development management** *see research and development management*

**DFB lasers** *see distributed feedback lasers*

**diagnosis, patient** *see patient diagnosis*

**diagnostics, particle beam** *see particle beam diagnostics*

**diagnostics, plasma** *see plasma diagnostics*

**diagrams**

*see also Feynman diagrams; flowcharting; nomograms; phase diagrams*

No entries

**dialogue systems** *see interactive systems*

**diamagnetic properties of substances**

*see also de Haas-van Alphen effect; diamagnetism*

- biyotropic nematic mesophases, diamag. anisotropy, effect of aromatic surfactants 4-84171  
 graphite, intercalated, stage depend. of mag. susceptibility 4-104400  
 inert gases, mag. props., local exchange correl. pot. calcs. (German) 4-108156  
 liquid crystals, mixed, opposite diamagnetic anisotropies, NMR spectra 4-109090  
 metalloporphyrin complexes, anomalous electronic states, crystal and mol. struct. (Japanese) 4-113431  
 organic liquids, high field diamag. suscept., Cotton-Mouton study 4-65785  
 polyacetylene, cis and trans, electronic states, muon spin resonance studies 4-65922  
 rare earth garnets, R<sub>3</sub>Fe<sub>2</sub>O<sub>12</sub>, Faraday effect in strong mag. fields 4-80908  
 rare earth garnets, R<sub>x</sub>Y<sub>3-x</sub>Fe<sub>2</sub>O<sub>12</sub>, Faraday effect in strong mag. fields 4-80908  
 tetradecyltrimethylammonium bromide, lyotropic nematic phase, birefringence meas. 4-92088  
 (TMTSF)<sub>2</sub>FSO<sub>3</sub>, diamagnetism and superconductivity 4-98855  
 zinc-blende semiconductors, localised lattice instability, microscopic model for large lattice relax. and high temp. anomalous diamagnetism 4-70718  
 As<sub>2</sub>Se<sub>3</sub>-Cu<sub>2</sub>Se:Mn, interaction of Mn with glass framework, mag. susceptibility, EPR spectra 4-60838  
 CdS, cryst. polarisabilities, quantum mech. approach 4-84596  
 CoP<sub>2</sub>, ambient press. synthesis, cryst. struct., mag. and elec. props., bonding 4-75408  
 Cr, magnetic moment fluctuations and magnetovol. variations 4-109026  
 Cu<sub>2</sub>P<sub>3</sub>, preparation and cryst. struct. 4-80008  
 Ga<sub>2</sub>In<sub>2</sub>Se<sub>8</sub> system, magneto-optical props. near fundamental band gap 4-109166  
 In<sub>2</sub>MoS<sub>7</sub> (0 $\leq$ x $\leq$ 1) intercalation compound, synthesis and characts. 4-104200  
 KBr, F-centres, mag. permeab. change, ang. freq. and temp. depend. 4-60922  
 NaCl cryst. ionic crystals, diamag. susceptibility and electron polarisability, X-ray diff. studies 4-114089  
 Ni<sub>2</sub>Zn<sub>1-x</sub>SiF<sub>6</sub>H<sub>2</sub>O, mag. interactions, paramagnetic Curie temp. studies 4-88645  
 Pd<sub>2</sub>-Si, liq. alloy, mag. susceptibility, diamagnetism and paramagnetism 4-76107  
 Re-P system, phase equilibria, cryst. growth, struct. refinements props. 4-88150  
 Re<sub>2</sub>P, cryst. struct. determ. 4-80009  
 Sn<sub>2</sub>, single crystal growth in silica gel in elec. field, elec. cond., mag. props. 4-93209  
 Sn<sub>4</sub>, single crystal growth in silica gel in elec. field, elec. cond., mag. props. 4-93209  
 TmAsO<sub>4</sub>, optical and mag. studies of lowest levels 4-88831

**diamagnetic resonance** *see cyclotron resonance*

**diamagnetism**

*see also cyclotron resonance; de Haas-van Alphen effect; diamagnetic properties of substances*

- crystal with paramag. ions, nuclear relax. rates 4-65789  
 fractional quantized Hall effect, alternating diamagnetism and paramagnetism, magnetoresistance and Hall resistance studies 4-113977  
 ionic crystals, diamagnetism and Van Vleck paramagnetism 4-71019  
 magnetic field in cavity of perfect diamagnetic material, integral eqn. method 4-105811  
 metal acetates, <sup>13</sup>C chemical shielding anisotropies 4-65871  
 picolityricanoquindimethan, cryst. and mol. struct. 4-70132  
 semiconductors, diamagnetism and Van Vleck paramagnetism 4-71019  
 superconductors, type I, infinite conductivity and perfect diamagnetism 4-88633

**superdiamagnetism continued**  
 superdiamagnetism in non-supercond. substances, possibility of existence 4-76102  
 superlattice, layered, mag. susceptibility 4-104399  
 surface sheath of superconductivity, diamagnetism calcs. 4-84736  
 thermotropic mixed liq. crystals, oriented mols., NMR studies 4-84860

**diameter measurement**  
 electron beam profile meas., in SEM 4-58919  
 fine-focused electron beam profile meas. using semiconductor detector 4-87263  
 IR diameter gauge for in vitro mech. testing of vascular grafts 4-100293  
 metal rods, EM-acoustic excitation for radial resonances 4-68213  
 optical fibre, single mode, automated mode radius meas. using variable aperture method in far field 4-97107  
 optical fibre diameter measurement using diffraction method (Russian) 4-107851

**diamond**  
 abrasive grain, friction with ceramics and cemented carbide 4-109522  
 amorphous film deposition using generation/reaction of methylene species 4-104739  
 aspheric surface generation, diamond machining applications and capabilities 4-107899  
 Auger line shape 4-66138  
 ballistic phonon imaging 4-88387  
 boron diamond, synthesis mechanism 4-71610  
 cohesive and struct. props., ab initio LCAO calc. 4-60881  
 conduction band struct., core electron excitation spectra anal. 4-70647  
 diamond:Fe, electronic struct. calcs. 4-113894  
 diamond:H, interstitial muons anal. impurity states 4-80541  
 energy bands, variational cellular method 4-92598  
 etching with Ar and O ion beams 4-89149  
 formation, martensitic mechanism, in colloidal systems 4-80212  
 formation at high press. in Co-C hyperitectic alloy 4-109374  
 formation in graphite/metal mixtures under shock compression and flash heating 4-108516  
 formation in molten Ni, C diffusion coefficients 4-105013  
 formation in presence of Ni, high press. and temp., ref. to starting C crystallinity 4-66256  
 geological origin of diamonds, from old enriched mantle 4-94050  
 graphite-diamond polymorphic transitions at high press. and temps. 4-113380  
 IIa, space-charge-induced optoelectronic switching 4-98660  
 ion stopping cross-section in solids, effects of electronic struct. 4-92273  
 ionising radiation detector, TSC current and polarisation 4-104230  
 Mbuji Mayi kimberlite district, Zaire, diamond C and N isotopes 4-89893  
 muonium, transition from isotropic state to axially symm. anomalous state 4-71237  
 muonium formation, asymmetry and relax. temp. depend. 4-65925  
 natural, metastable autotaxial crystallisation 4-70592  
 natural, platelet defects, electron microscopy study 4-103740  
 natural, type II, cathodoluminescence from dislocations 4-81012  
 nuclear spin-lattice relax.,  $^{13}\text{C}$  NMR 4-80838  
 Ohmic conductivity of electrons calc. 4-108864  
 one-electron excitations, exchange-correlation pot. 4-84579  
 organic, synthetic, adsorp. of organic compounds, IR spectroscopy, (Russian) 4-75791  
 secondary electron emission props., synthetic and natural material (Chinese) 4-109285  
 semiconducting and insulating natural, picosec. photoconductive switching 4-108895  
 sintered compacts, grain size, internal strain, photoluminesc. spectra 4-99160  
 surface, (111), clean and adsorbed  $\text{H}_2$ , photoemission studies 4-88939  
 surface, (111), total energy minimisation, support for undimerised  $\pi$ -bonded chain reconstruction 4-92489  
 surface, (111)  $2\times 1$ , structure determ. by energy minimisation 4-88382  
 synthesis, ultrafast chemical reaction triggered by shock wave forming C and  $\gamma$ -CuBr from  $\text{CBr}_4$  and Cu 4-114389  
 synthetic, single-cryst. deform. evaluation, using Kossel pseudopatterns (Ukrainian) 4-88226  
 synthetic, surface study using reflection electron microscopy, slip and growth steps, microcrystals 4-65523  
 type Ia, defect-induced one-phonon absorption 4-84981  
 type IIb, individual dislocation and cathodoluminescence emission polarisation 4-99199  
 types Ia and IIa, electron and positron planar channelling radiation spectra 4-75579  
 vacancy formation energy, crystallisation studies 4-108354  
 wear of single point diamond for grinding ceramics 4-99609  
 $\text{Al}_2\text{O}_3$ , diamond dispersed composite, very high press. sintered, fracture toughness, phase transform. 4-99372  
 Cu-Ti/diamond interface, struct. microanal. (Chinese) 4-61242  
 Si X-ray optical elements, prod. using diamond turning 4-58924

**diaphragms**  
 see also valves  
 electroacoustic transducers, vibration distrib. at diaphragms, quantitative determ. by holographic interferometry methods (German) 4-74829  
 nonuniform influence on rotating single-sector scanning field (Russian) 4-63768  
 vibratory displacement meas. apparatus with projection reading diaphragm and remote scale 4-63742  
 X-ray diagnostics of laser plasma, pinhole cameras slits and apertures prep. 4-91987

**dibaryons** see baryon resonances

**dichroism**  
 see also magnetic circular dichroism; pleochroism  
 L-alanine, vibr. circular dichroism, MO calc. 4-69125  
 anthraquinone dichroic dyes, liq. cryst. characterisation and synthesis 4-84156  
 azo dye Langmuir multimolecular layers, optical anisotropy, visible absorpt. spectra 4-109208  
 chitosan-azo dye complexes, induced optical activity 4-103736  
 cholesteric solutions circular dichroism in IR spectra 4-88806  
 $\alpha$ -chymotrypsin-dyes assoc., fluoresc. circular polarisation, Cotton effect 4-102838  
 crambin in phospholipid vesicles: circular dichroism anal. of cryst. struct. relevance 4-77184  
 4-cyano-4'-pentylbiphenyl, nematic liq. cryst., orientation distrib., two-photon dichroism 4-113326

**dichroism continued**  
 cytosine, in-plane vibr., transition moments, fixed partial charge model calcs. 4-107326  
 dichroic elliptic birefringent media, Jones matrix 4-107509  
 epoxypropane, mid-IR vibr. circular dichroism, bond moment model predictions 4-102722  
 ferric neurosporin, cryst., chem. and mol. struct., spectral charact. 4-102720  
 ferrite garnet epitaxial films, dichroic axis, and magnetisation rotation 4-93047  
 halomethanes, in MBBA matrix, local field anisotropy meas. 4-83375  
 (2-hydroxy-born-2-yl)phenylacetic acids, diastereoisomerism, circular dichroism curves, configurations 4-64524  
 impurity mol. embedded in crystal lattice, electronic circular dichroism lineshapes theory 4-76424  
 d-limonene, excited states, circular dichroism, VUV absorpt. and photoelectron spectra 4-107400  
 linear dichroism using polarisation modulation FT-IR technique 4-104566  
 liquid crystals, heteroaromatic azo dyes exhibiting negative dichroism 4-93046  
 magneto-optical effects, isotropic and anisotropic in crystals, review 4-61668  
 (R)-2-methylcyclobutanone, circular dichroism, solvent electrostatic interaction, RPA approx. 4-69124  
 methylsilanes, in MBBA matrix, local field anisotropy meas. 4-83375  
 molecular systems, cooperative two-photon absorpt. 4-74304  
 (R)(+)-neopentyl-1-d bromide, vibr. circular dichroism 4-69126  
 (R)(-)-neopentyl-1-d chloride, vibr. circular dichroism 4-69126  
 nitrobenzene-n-hexane crit. binary mixture, shear-induced dichroism and birefringence 4-104567  
 (IS,4R)-norecamphor, circular dichroism, solvent electrostatic interaction, RPA approx. 4-69124  
 peptides, conformation, circular dichroism, PMR, fluoresc. meas. 4-102736  
 perylene dichroic dyes, liq. cryst. characterisation and synthesis 4-84156  
 polarisation, definitions and nomenclature, instrument polarisation 4-82604  
 poly( $\alpha$ -L-glutamic acid), for UV linear dichroism in helical and coiled conforms. 4-112313  
 poly-L-lysine-DNA complexes, conformation, circular dichroism spectra 4-89497  
 polymers, bulk, mol. viscoelasticity determ. by neutron scatt., IR dichroism and fluoresc. polarisation 4-114596  
 polypeptides,  $\alpha$ -helical,  $n\pi^*$  circular dichroism, solvent effects, linear response theory 4-64642  
 polypeptides,  $\alpha$ -helical  $\pi\pi^*$  circular dichroism, solvent effects, linear response theory 4-64641  
 polypropylene films, uniaxially and biaxially oriented, IR internal reflection spectroscopy 4-93073  
 poly(tetrafluoroethylene) films, chain orientation param. from IR-dichroism and X-ray data (Russian) 4-84536  
 polyurethane-urea elastomers, segmented, struct. and props. 4-113356  
 subtilisins, in urea, presence, conformational stability, fluoresc., circular dichroism 4-59927  
 T7 bacteriophage, UV-induced small struct. changes, melting methods study 4-93808  
 tetraphenylsilane, IR dichroism and Raman meas., vibr. anal. 4-61653  
 tetraphenylsilane, vibr., Raman spectra, IR dichroism 4-84963  
 thioketones, chiroptical props., circular dichroism spectra and ab-initio RPA calcs. 4-78916  
 thymine, in-plane vibr., transition moments, fixed partial charge model calcs. 4-107326  
 uracil, in-plane vibr., transition moments, fixed partial charge model calcs. 4-107326  
 vibrational circular dichroism meas. of single enantiomer on FT-IR spectrometers 4-102816  
 vibrational circular dichroism measurements by optical subtraction FT-IR spectrometry 4-101938  
 vinylidene cyanide-vinyl acetate copolymer, piezoelectricity and remanent polarisation 4-99028  
 $\text{Bi}_2\text{GeO}_{20}$ , circular dichroism in region of states prod. due to vacancies 4-71345  
 $\text{Bi}_2\text{SiO}_{20}$ , circular dichroism in region of states prod. due to vacancies 4-71345  
 $\text{Bi}_2\text{TiO}_{20}$ , circular dichroism in region of states prod. due to vacancies 4-71345  
 $\text{CaF}_2\text{:Na}$ , photochemical conversion of  $\text{M}_A$ -centres, identification of  $\text{M}_A^+$ -centre, absorpt. and fluoresc. spectra 4-76501  
 $\text{Er}^{3+}$  complexes, diglycollate, circular dichroism, optical density 4-80902  
 $\text{Er}^{3+}$  complexes, pyrogermanate, circular dichroism, optical density 4-80902  
 $\text{Gd}_3\text{Ga}_5\text{O}_{12}\text{:Pr(Bi)}$  garnet epitaxial layers, site selectivity, dichroism studies 4-84533  
 $\text{H}_2\text{O}$  in liq. crystal, polarised FT-IR spectra 4-64473  
 $\text{K}_2\text{Co}_2(\text{SO}_4)_3$ , langbeinite, optical props. 4-76427  
 $\text{K}_2\text{Pr}_2(\text{NO}_3)_4$ , single cryst., absorpt. and circular dichroism spectra 4-114240  
 $\text{LiIO}_3\text{:H}_2\text{O}$  system, influence of growth conditions on optical props. 4-76430  
 $\text{SrF}_2$ , photo-induced transform. of close Frenkel pairs, absorption and luminesc. props. 4-76500

**dictionaries** see glossaries

**die steel** see tool steel

**dielectric breakdown** see electric breakdown

**dielectric constant** see permittivity

**dielectric depolarisation**  
 see also dielectric polarisation  
 alanine-TGS ferroelectric crystals, pyroelec. props. (Chinese) 4-114213  
 ferroelectric hysteresis, loop tracer for instantaneous meas. 4-95460  
 order-disorder transitions of dipolar relaxations, entropy change 4-93002  
 poly(vinylidene fluoride), solution growth, ionic impurity effects 4-98037  
 rare earth fluorite cryst., ionic thermocurrents and ionic cond. 4-70443  
 TGS, and deuterated, ferroelec. crystals, pyroelec. props. (Chinese) 4-114213  
 TGS, ferroelec., Brillouin spectra angular depend. studies 4-71393  
 TGS, pyroelectric response relax., role of viscous phenomena 4-71284  
 $\text{Ce}_2(\text{SO}_4)_3\cdot 9\text{H}_2\text{O(D}_2\text{O)}$  single cryst. dielec. response, contact configuration effects 4-65945

**dielectric depolarisation continued**

- PLZT ceramics, hot pressed polarisation and depolarisation behaviour 4-76318  
 (Pb,Lu)(Zr,Ti)O<sub>3</sub> ceramics, stress anisotropy induced by polarisation 4-104536

**dielectric devices**

- see also capacitors; ferroelectric devices; insulators; piezoelectric devices; pyroelectric devices; space-charge limited devices  
 EHF aplanatic zoned dielectric lens antenna, anal. 4-102998  
 optical polarisers, 3-refl., use of dielectric-coated metallic mirrors 4-97035  
 resonator, stabilisation of microwave oscillator, B<sub>2</sub>Ti<sub>2</sub>O<sub>20</sub> type ceramics 4-76311

**dielectric-filled waveguides** see dielectric-loaded waveguides**dielectric function**

- atomic inelastic electron scatt. cross sections, electron microscopy aspects 4-64623  
 bilayer systems, surface plasma polaritons 4-108795  
 complex cryst. lattice with Frenkel excitons, 0-99 energy bands (Japanese) 4-75865  
 dielectric function and spin susceptibility, exchange effects 4-70692  
 electron gas, metallic densities, exchange and correlation 4-88464  
 electron liquids, correlation energy plasmon dispersion, static and dynamic form factors 4-75885  
 electron liquids, electron-hole pseudopotentials, polarisation pot. theory 4-75884  
 fusion plasmas, inertially confined, ion density correlations, thermonuclear reaction rate 4-91974  
 glasses, semiconductor doped, optical nonlinearities, phenomenological theory 4-102984  
 inert gas solids, optical const., self-consistent anal. 4-71332  
 macroscopic dielectric tensor at crystal surfaces 4-70894  
 metal, LMTO approach to optical props. calc. 4-71341  
 metal surface electrodynamics, dielec. responses 4-88552  
 metal targets, proton irradi., electronic energy loss, impact parameter depend. 4-108485  
 metal-dielectric composites, effective dielec. const. 4-99002  
 polyacetylene:1, IR refl. spectra, effect of sample densification 4-99120  
 polyacetylene:1<sub>2</sub> (AsF<sub>6</sub>), millimeter-wave and far IR cond. 4-70850  
 quartz, lattice vibr., dielec. function, ellipsometry 4-75627  
 quartz, vitreous and cryst., LO-TO phonon mode splitting, many-particle effects 4-98223  
 randomly distributed particles of cermet topology, optical props. 4-93039  
 semiconductor quantum wells, screened Coulombic impurity bound states 4-108917  
 semiconductor thin films, dielec., function calc., screening effect 4-70693  
 semiconductors, core exciton resons. at inner-shell thresholds, dynamical scanning effects 4-80506  
 semiconductors, undoped, Thomas-Fermi-Dirac statistics of dielectric screening 4-61314  
 semiinfinite cryst., exciton-polariton theory 4-70667  
 small dielectric clusters, resonance optical response 4-74388  
 surface polariton amplification and instability due to DC current 4-61433  
 three-level systems, dispersion and absorption anomalies 4-99072  
 three-level systems under high excitation, dielectric funct. determ. 4-65629  
 Ag film, dielectric function by ATR technique 4-88463  
 Al, (200)-zone boundary collective mode, perturbation theory anal. 4-104139  
 Al,Ga<sub>1-x</sub>As, Fourier anal. of optical spectra 4-99131  
 AuSn diffusion produced alloys, optical props. 4-80897  
 C, stopping power, zero-energy density effect 4-80129  
 n-Cd,P, degenerate semicond. intrinsic phonon parameters 4-92317  
 CoCl<sub>2</sub>(Br<sub>2</sub>), high freq. dielec. const. 4-61646  
 Cu (100), surface dynamic processes, excitation of electron-hole pairs 4-70902  
 CuCl, dielec. function, exciton-biexciton transitions and population effects 4-80525  
 CuCl, nonlinear optical props. of biexcitons, degenerate four-wave mixing 4-69488  
 FeAl and FeRh, ordered, LMTO approach to optical props. 4-71342  
 FeCl<sub>2</sub>(Br<sub>2</sub>), high freq. dielec. const. 4-61646  
 Ga<sub>1-x</sub>Al<sub>x</sub>As, spatial dielec. functions, site and comp. depend. 4-104136  
 GaAs<sub>1-x</sub>P<sub>x</sub>, Fourier anal. of optical spectra 4-99131  
 Ge, dielectric function, temp. depend. 4-109111  
 In films on mica substrates, surface plasmon modes and energy loss function 4-85024  
 InP, far IR optical props. at 6 and 300 K 4-109174  
 In<sub>2-x</sub>Sn<sub>x</sub>O<sub>3-y</sub> transparent and heat-reflecting films, optical props. 4-114334  
 KCl/Sn granular supercond., far IR absorption spectrum: 4-76076  
 MgO (001), IR optical const., EELS meas. 4-71337  
 MoSi<sub>2</sub>, dielec. function, spectroscopic ellipsometry 4-93041  
 NaClO<sub>3</sub>, radiative surface phonon-polariton dispersion, ATR studies 4-80514  
 Na<sub>2</sub>WO<sub>3</sub>, surface phonon features in high-resolution EELS 4-93158  
 NbN, electronic props., optical study 4-66003  
 Ni (100), surface dynamic processes, excitation of electron-hole pairs 4-70902  
 NiBr<sub>2</sub>, high freq. dielec. const. 4-61646  
 NiCl<sub>2</sub>(Br<sub>2</sub>)(I<sub>2</sub>), UV reflectance and electronic states 4-71406  
 P, black, band struct. and optical props. 4-70650  
 Pb chalcogenides, electron scatt. interaction and elementary excitations 4-70694  
 Pd small particle composites, far IR absorption studies 4-99073  
 WO<sub>3</sub>, surface phonon features in high-resolution EELS 4-93158  
 α-Zr, band structure, APW calcs., optical props., superconducting props. 4-113857
- dielectric hysteresis**  
 alkali metal phosphates, A'B'PO<sub>4</sub>, A=Na, K, B=Ca, Zn, Sr, Cd, Ba, Pb, ferroelec. phys. props. 4-65992  
 ammonium Rochelle salt, deuterated, dielec. and pyroelec. props. 4-114220  
 betaine arsenate and phosphate, deuterated, ferroelectric props. 4-80876  
 betaine calcium chloride dihydrate, phase transitions, crit. dielec. phenomena and hysteresis effects 4-76304  
 ceramics, ferroelectric, switching and hysteresis effects 4-76401  
 diglycine nitrate, low-temp. dielec. props., freq. depend. 4-76299  
 ferroelectric hysteresis, loop tracer for instantaneous meas. 4-95460

**dielectric hysteresis continued**

- ferroelectric polymers, props. and applications 4-65954  
 ferroelectrics, hysteresis curve tracer using a single-board microcomputer 4-95461  
 methylammonium mercury trichloride, ferroelec. transition, thermal, dielec., optical meas. (French) 4-76392  
 MIS structures hysteresis effects reduction method in meas. 4-88602  
 polyvinylidene fluoride, ferroelec. and 33 ferroelastic hysteresis 4-99066  
 polyvinylidene fluoride film, piezoelectric and ferroelectric props. under shock wave action 4-109131  
 rare earth niobates, RNbO<sub>4</sub>, ferroelastics with the fergusonite type structure 4-75659  
 ruby, electric domains due to laser irradi., hysteresis 4-114224  
 squaric acid, thermal expansion, high resolution meas. along b-axis 4-92393  
 tetramethylammonium tetrachlorozincate, deuterated, ferroelec., temp.-press. phase diagram 4-76377  
 TGS, L-α alanine doped, polarisation, influence of growth conditions 4-76314  
 TGSe, phase transition rel. to deuterisation 4-76387  
 trissarcosine calcium chloride, iodinated, dielec. props., temp. and press. depend. 4-76310  
 TST piezoceramic, dielec. props., influence of 90° domain struct. 4-76396  
 vinylidene fluoride-trifluoroethylene copolymer, ferroelec. hysteresis 4-99065  
 Al-SiO<sub>2</sub>-Si MIS structures, with plasma deposited SiO<sub>2</sub>, alkali ion motion, C-V characts. (Russian) 4-114042  
 BaTiO<sub>3</sub>, piezoceramic, dielec. props., influence of 90° domain struct. 4-76396  
 LiH<sub>3</sub>(SeO<sub>3</sub>), ferroelec., single cryst. growth from soln., hysteresis loops (Korean) 4-114375  
 LiNH<sub>4</sub>SO<sub>4</sub>, normal and deuterated, II-III phase transition, elec. field effects 4-65396  
 (NH<sub>4</sub>)<sub>2</sub>BeF<sub>4</sub>, dielectric hysteresis and anomalous temperature 4-93026  
 PLZT ceramic, coarse-grain light scatt. and elec. hysteresis 4-76399  
 PLZT ceramics, poling strategy 4-76319  
 (Pb,Ba<sub>1-x</sub>)<sub>1-3y</sub>La<sub>2</sub>Nb<sub>2</sub>O<sub>6</sub> ceramic, dielectric, piezoelectric and optical props. 4-98999  
 PbTiO<sub>3</sub> thin films, CVD prep. and dielec. props. 4-104736  
 PbZrO<sub>3</sub>, with O vacancies, phase transitions, dielec. props. 4-76391  
 PbZrO<sub>3</sub>, with vacancies, para, ferro and antiferroelectric phase transitions, influence of hydrostatic press. 4-76390  
 Pb<sub>(1-y/2)</sub>Zr<sub>(1-y/2)</sub>Ti<sub>y</sub>Nb<sub>2</sub>O<sub>3</sub> ceramic transducers, pyroelec. and mechano-dielec. characts. 4-109136  
 Rb<sub>2</sub>ZnCl<sub>4</sub>, modulated ferroelec., thermal hysteresis and pinning 4-76380  
 Te(OH)<sub>4</sub>·2NH<sub>4</sub>H<sub>2</sub>PO<sub>4</sub>·(NH<sub>4</sub>)<sub>2</sub>HPO<sub>4</sub>, dielec., thermal and optical props. 4-61636
- dielectric-loaded waveguides**  
 cellulose acetate, water sorption and pore vol. 4-97067  
 dielectric-loaded rectangular waveguide applicator for radiation therapy 4-109894  
 unilateral fin lines with dielectric layers, dispersion anal. 4-79006
- dielectric loss angle** see dielectric losses
- dielectric loss-angle measurement** see dielectric loss measurement
- dielectric loss measurement**  
 see also dielectric losses  
 computer controlled method for low-freq. meas. 4-95467  
 frequency response analyser system, minicomputer-controlled, errors and calibration technique 4-111159  
 insulators, apparatus for measuring tan δ and ε 4-101874  
 MM-wave meas. of complex refractive index, complex dielectric permittivity and loss tangent 4-82820  
 open resonators for measuring permittivity and moderate dielectric loss 4-111160  
 TE<sub>01n</sub> helical cavity, loss tangent calc. for dielec. meas. 4-84910
- dielectric losses**  
 see also loss angle  
 alkali halide mixed crystals, growth and characterisation, microhardness, colour centres, radiation hardening 4-70152  
 attapulgite, temp. and freq. variations of elec. props. 4-61616  
 benzenes, substituents, in glassy forming solvents, β process study 4-92990  
 carbazole:trinitrobenzene, piezoelec. charge transfer complex, phase transition obs. 4-70364  
 cellulose fibres, pineapple, mech. and dielec. props. 4-104807  
 CeO<sub>2</sub> film, vac. deposited, dielec. parameters, temp. depend, defects role 4-99024  
 chalcogenide glasses, dispersion of dielectric constant, freq. dependence 4-80858  
 chlorophyll-a, surface cond. in various ambient gases 4-108921  
 conducting/insulating sphere mixture, AC cond., percolation approach 4-108911  
 cyclohexane, liq., dielec. loss in millimetre and submillimetre wavelength region 4-99015  
 cyclohexanol, rotor and glassy cryst. phase, mol. motion, PMR linewidth study 4-84863  
 diglycine nitrate, low-temp. dielec. props., freq. depend. 4-76299  
 electron transfer, rate const. calcs. with arbitrary dielec. loss spectrum for solvent 4-109638  
 erythrocyte ghosts, human, microwave dielectric props. 4-85409  
 ethylene-vinyl alcohol copolymer, struct., mech. and dielec. props., temp. depend. (German) 4-71261  
 glycerol-water system, microwave field meas. in ESR and saturation-transfer ESR spectroscopy 4-96572  
 n-heptane, liq., dielec. loss in millimetre and submillimetre wavelength region 4-99015  
 n-hexane, liq., dielec. loss in millimetre and submillimetre wavelength region 4-99015  
 insulator wetted by liq. dielec., surface cond. and losses 4-108920  
 Levy distrib. and Williams-Watts model of dielec. relax. 4-61623  
 liquids, dielectric props., resonator method meas. in microwave range 4-61617  
 lossy dielectric slab, EM plane wave diffraction by slit 4-79005  
 low-frequency dispersion dielectric effects of moisture in layered and porous materials 4-109118  
 3-methyl-1,5-diphenyl-1,4-pentadien-3-ol, soln. and solid, dielectric props., IR study 4-99017  
 monodisperse semicond. system, amplitude size effect 4-88526  
 natural rubber vulcanisation, effects on dielectric props. 4-114468  
 nepheline glass-ceramic, microwave heating characts. 4-65294

**electric losses continued**

- Nylon 5.7 films, dielec. and pyroelec. props., mol. orientation depend. 4-99043  
 n-octane, liq., dielec. loss in millimetre and submillimetre wavelength region 4-99015  
 organic charge transfer complexes, dielectric const. and loss meas. 4-76308  
 outer-sphere electron transfer probability determ. using quantum-static approx. 4-66559  
 oxides, ferroelec., antiferroelectric, Seignettomagnetic, phys. props., phase transitions 4-65974  
 PMMA, dielec. relax., crosslinking and branching effects 4-104528  
 poly(vinylidene fluoride), stress and dielec. relax. studies 4-99014  
 poly 4,4'-oxydiphenylene pyromellitimide, low temp. dielec. relax., anhydride end-group effect 4-104527  
 poly-N-vinylcarbazole, nonpolar crosslinking agent effect on relax. processes, hopping mechanism of transport (*Polish*) 4-65948  
 polyacrylamide, dielec. relax., crosslinking and branching effects 4-104528  
 polyethylene terephthalate, dielec. loss, expt. study 4-111158  
 polymer blends, struct. and dielec. props. (*German*) 4-71269  
 polymer glasses, press. effects, densification and dielectric losses 4-65190  
 polyolefins with amine additives, low temp. losses, expt. study 4-114205  
 polypropylene and polycarbonate, study of dielectric relaxation in polymer blends—transient current approach 4-99021  
 polystyrene, dielec. relax., crosslinking and branching effects 4-104528  
 PVC-poly- $\alpha$ -methyl- $\alpha$ -n-propyl- $\beta$ -propiolactone blends, dielec. props. 4-84909  
 quartz, elec. cond., relax. dielec. losses, temp. depend. due to electrolysis 4-113959  
 quartz, electrical and optical props., neutron,  $\gamma$ , and electron irradi. effects 4-60968  
 quartz crystals, electrical conductivity and dielectric loss, effect of alkali ions 4-71271  
 TE<sub>01n</sub> helical cavity, loss tangent calc. for dielec. meas. 4-84910  
 tris-sarcosine calcium chloride, dielec. const. and loss meas. in paraelec. phase, behaviour near ferroelec. transition 4-71258  
 trissarcosine calcium chloride, iodinated, dielec. props., temp. and press. depend. 4-76310  
 universal response of EM, acoustic, and mech. influences 4-90540  
 water-oil microemulsions, DSC, permitt., dielec. loss tangent meas. 4-89343  
 wheat seeds, deuterium effect in dielectric losses 4-89544  
 Ag halide emulsion-microcrystals, dielec. loss obs. of ionic cond. (*Japanese*) 4-113699  
 AgNbO<sub>3</sub>, ceramic, ferroelec. phase, dielec. props. 4-61631  
 Al/Sm<sub>2</sub>O<sub>3</sub>/Al capacitor struct.; dielec. props. and thermoluminescence 4-76047  
 Al-(SnO<sub>2</sub>+Sb<sub>2</sub>O<sub>3</sub>)-Al mixed thin films, dielec. studies 4-84719  
 Al<sub>2</sub>O<sub>3</sub> windows, neutron-induced RF loss meas. and thermal stress calcs. 4-113501  
 Al(PO<sub>3</sub>)<sub>3</sub>-Li<sub>2</sub>O-K<sub>2</sub>O glasses, mixed-alkali effect 4-80296  
 Ba(Mn<sub>1/3</sub>Ta<sub>2/3</sub>)O<sub>3</sub> ceramic, ultra-low dielec. loss at microwave freq. 4-84905  
 BaO-Al<sub>2</sub>O<sub>3</sub>-SiO<sub>2</sub> thick film crossover dielec.-compositions, dielec. props. rel. to multiple refring. 4-109113  
 BaO-PbO-Nd<sub>2</sub>O<sub>3</sub>-TiO<sub>2</sub>, dielec. resonators, microwave characts 4-84908  
 Ba<sub>2</sub>Sr<sub>1-x</sub>Nb<sub>2</sub>O<sub>6</sub>, pyroelectric effect, ferroelectric transition 4-114214  
 BaTiO<sub>3</sub>, liquid phase sintering and composite ceramics with Pb<sub>2</sub>Ge<sub>2</sub>O<sub>11</sub> 4-104746  
 BaTiO<sub>3</sub>:Yb, dielec. and X-ray diff. study 4-84896  
 Bi<sub>2</sub>Pb<sub>1/3</sub>Bi<sub>2/3</sub>Ti<sub>4/3</sub>W<sub>2/3</sub>O<sub>3</sub> perovskite ferroelec., dielec. props. 4-88783  
 CDS, particle suspensions, electronic processes, microwave probing 4-99852  
 EuF<sub>2</sub>, permitt., dielec. loss tangent, cond. meas. 4-104523  
 EuS, FIR dielec. energy loss function 4-84895  
 KCl:Sn, single cryst., dielectric props. meas. 4-93006  
 KH<sub>2</sub>PO<sub>4</sub>, ferroelec., domain struct., dielec. and loss consts. 4-65994  
 KTaO<sub>3</sub>:Li single cryst., dielec. dispersion, dielec. spectra studies 4-76322  
 LiKSO<sub>4</sub>, phase transitions at low temp., domain textures, dielec. meas. 4-75655  
 MgO, dipolar defect ordering due to dissolved CO<sub>2</sub> 4-71287  
 (Pb<sub>0.75</sub>Ca<sub>0.25</sub>)(Mg<sub>1/3</sub>Nb<sub>2/3</sub>O<sub>0.6625</sub>Ti<sub>0.3375</sub>)O<sub>3</sub> Mn ceramics, US, elastic and dielec. props. 4-104543  
 Pb(FeNb<sub>0.5</sub>)O<sub>3</sub> ceramics and single crystals, prep., struct., X-ray diff., neutron powder diff., dielec. and elec. meas., SEM 4-75412  
 Pb(Fe<sub>1/2</sub>Nb<sub>1/2</sub>)O<sub>3</sub>-Pb(Ni<sub>1/3</sub>Nb<sub>2/3</sub>)O<sub>3</sub> solid soln. system, dielec. props. 4-104517  
 Pb<sub>2</sub>Ge<sub>2</sub>O<sub>11</sub>, hydrothermally grown crystals, dielec., pyroelectric props., X-ray diff. 4-84915  
 Pb<sub>2</sub>(MF<sub>6</sub>)<sub>2</sub> (M=Ti, V, Cr, Fe, Ga), ferroelectric phase transitions 4-71311  
 RbCl, single cryst., dielec. props. 4-104522  
 Rb<sub>1-x</sub>(NH<sub>4</sub>)<sub>x</sub>H<sub>2</sub>PO<sub>4</sub> single cryst. proton glasses, struct. and dielec. props. 4-76323  
 Rb<sub>1-x</sub>(NH<sub>4</sub>)<sub>x</sub>H<sub>2</sub>PO<sub>4</sub> glass, H-bonded, NMR relax. study 4-98974  
 Se, particle suspensions, electronic processes, microwave probing 4-99852  
 SrTiO<sub>3</sub> vitroceraamics, dielectric props., low temp. meas. 4-65940  
 TGSe, audiofrequency dielec. dispersion, universal behaviour and temp. depend. 4-76303  
 TiO<sub>2</sub> particle suspensions, electronic processes, microwave probing 4-99852  
 (Zr, Sn)TiO<sub>4</sub>, dielec. resonators, microwave characts 4-84908

**dielectric materials**

- see also *antiferroelectric materials; dielectric thin films; electrets; ferroelectric materials; glass; insulating materials; insulation; piezoelectric materials*  
 complex permittivity measurement, time-domain reflectivity techniques 4-111156  
 complex permittivity of dielectric mixture, Fricke's formula based on logarithmic law of mixing 4-61618  
 conduction and breakdown, conf., Toulouse, France (July 1983) 4-106109  
 erosion by high-energy ions 4-61802  
 IR and MM waves, conf., Miami Beach, FL, USA (Dec. 1983) 4-73154  
 polyolefins with amine additives, low temp. losses, expt. study 4-114205  
 Sylgard 184 containing hollow microspherical fillers, high temp. elec. cond. and thermal decomp. 4-92710  
 Al-based sputtered solar selective absorbing surfaces, props., effects of various antireflection coatings 4-114954

**dielectric materials continued**

- BaO-PbO-Nd<sub>2</sub>O<sub>3</sub>-TiO<sub>2</sub>, dielec. resonators, microwave characts 4-84908  
 (Zr, Sn)TiO<sub>4</sub>, dielec. resonators, microwave characts 4-84908  
**dielectric measurement**  
 see also *dielectric loss measurement; permittivity measurement*  
 anisotropic materials, dielec. response function determ., direct method using time-domain spectroscopy 4-111157  
 biopolymers, dielec. props. meas. 4-106332  
 dielectric materials, measurements anal appls., conf., Lancaster, England (Sept. 1984) 4-106120  
 ferroelectric hysteresis, loop tracer for instantaneous meas. 4-95460  
 ferroelectrics, hysteresis curve tracer using a single-board microcomputer 4-95461  
 films, radiation charged, methods for charge- or field-distrib. studies 4-71826  
 high polymer materials, VLF dielectric meas. using microcomputer-controlled system 4-111158  
 high-resistance, probing methods of strong current fields 4-71825  
 impedance meter use for dielectric meas. 4-58841  
 LDPE, contactless dielec. meas. of charge and current 4-106331  
 liquids, microwave range meas. technique using three-layer dielec. resonator 4-111161  
 microcomputer-based dielectric relaxation spectroscopy, nitrocellulose/nitroglycerine propellants meas. appl. 4-111152  
 microwave measurement in 100 GHz range using resonant cavity, system conf. and appl. (*Japanese*) 4-106330  
 piezoelectric coeff. meas. using electrostriction cell 4-78342  
 time-domain dielectric spectroscopy, use with lossy dielectrics, precautions in use 4-85592  
**dielectric phenomena**  
 see also *dielectric hysteresis; dielectric losses; dielectric properties of substances; dielectric relaxation; dielectric resonance; electric strength; ferroelectricity; photodielectric effect; piezoelectricity; solvated electrons*  
 NH<sub>4</sub>HSeO<sub>4</sub>, high temp. phase transition, ionic motion 4-108651  
 RbHSeO<sub>4</sub>, high temp. phase transition, ionic motion 4-108651  
**dielectric polarisation**  
 see also *Barkhausen effect; dielectric depolarisation*  
 acetic acid, dipole assoc. in nonpolar solvents (*German*) 4-109116  
 alanine-TGS ferroelectric crystals, pyroelec. props. (*Chinese*) 4-114213  
 alkali glass and halide crystal, cond. polarization characts. and comparison 4-99003  
 alkali halides, polarisation energy by point defects, INDO cluster calc. 4-80861  
 alkali halides, space charge elec. field form. during cleaving 4-76021  
 benzene, in cyclohexane, Kerr consts., mol. anisotropic polarisabilities, dielectric study 4-102721  
 betaine arsenate, dielec. props. near ferroelec. transition 4-71307  
 betaine arsenate and phosphate, deuterated, ferroelectric props. 4-80876  
 t-butylbenzenes, in cyclohexane, Kerr consts., mol. anisotropic polarisabilities, dielectric study 4-102721  
 chalcogenide glasses, dispersion of dielectric constant, freq. dependence 4-80858  
 cholesteric liq. cryst.-KNO<sub>3</sub> mixtures, ferroelec. behaviour 4-109134  
 dicalcium lead propionate, ferroelec.-paraelec. transition, dopant conc. depend. 4-99048  
 dicalcium strontium propionate, ferroelectric phase transition, X-ray diff. study 4-65988  
 DOBA-1-MBC, ferroelec. liq. cryst. with large spontaneous polarisation 4-60813  
 elastic dielectrics with polarisation gradient, dynamical problems 4-80152  
 electrolytic aqueous solutions, dielec. effects, kinetic depolarisation, saturation and solvent relax. 4-80859  
 ferroelectric crystals, optical rot., microscopic model 4-65959  
 ferroelectric materials, electric aging, low freq. polarisation relaxation (*Russian*) 4-99010  
 ferroelectric polymers, props. and applications 4-65954  
 ferroelectric semicond., heavily doped, inhomogeneous state stability conditions and struct., linear approx. 4-71286  
 ferroelectric smectic liquid crystals, struct. and design 4-113307  
 ferroelectrics, dipole-dipole mechanism of energy transfer 4-88482  
 ferroelectrics, monoaixial, with second order phase transition, nonlinear pyroelectric response 4-88777  
 ferroelectrics, polarisation fluctuations correlation function 4-88766  
 ferroelectrics, weakly ferromag., static and dynamic props. of mag. domain walls (*Russian*) 4-92936  
 ferroelectrics and ferroelastics, viscous phenomena 4-76367  
 fluorite structure crystals, dielectric constant, temp. depend., polarisability 4-92995  
 labyrinthine instability in dielectric fluids 4-99011  
 liquid crystals, relaxation current increase study 4-75291  
 methylammonium aluminum alum., dielectric props. meas. 4-76312  
 methylammonium mercury trichloride, ferroelec. transition, thermal, dielec., optical meas. (*French*) 4-76392  
 methylbenzenes, in cyclohexane, Kerr consts., mol. anisotropic polarisabilities, dielectric study 4-102721  
 MIS structures, current DLTS spectra due to dielec. polarisation of the insulator 4-76043  
 narrow-band cryst., polarisation features in external mag. field 4-114200  
 natural rubber vulcanisation, effects on dielectric props. 4-114468  
 optical, microwave, rf and dielectric spectra (*Russian*) 4-114303  
 order-disorder transitions of dipolar relaxations, entropy change 4-93002  
 pentachlorophenol in soln., IR dispersion of H-bonded systems, dielec. function for weak complexes 4-102676  
 photoresist soln., AZ1350J, chem. and dielec. props. 4-104519  
 PLZT ceramics, polarisation switching characts 4-99006  
 polar liquids, molecular dynamics study of dielectric props. 4-88057  
 poly(dimethyl siloxanes), cyclic and linear, static dielec. meas. and dipole moments 4-61620  
 poly(vinylidene fluoride),  $\beta$ -phase, polar axis rotation under high elec. field 4-99007  
 poly(vinylidene fluoride) film, dipolar orientation study 4-65946  
 poly(vinylidene fluoride) film, struct. under high elec. fields 4-98029  
 poly(vinylidene fluoride) films, piezoelectric studies 4-65952  
 poly(vinylidene fluoride) piezoelec. and pyroelec. props. under high press. 4-99027  
 polymeric dielectrics, giant polarisation 4-104526  
 polypropylene and polycarbonate, study of dielectric relaxation in polymer blends—transient current approach 4-99021  
 polystyrene films, underwater, interfacial polaris. in bilamellar struct., dielec. anal. 4-84901

## dielectric polarisation continued

- polyvinylidene fluoride,  $\alpha$ -form unstretched films, anomalous discharging current 4-99004
- polyvinylidene fluoride film, piezoelectric and ferroelectric props. under shock wave action 4-109131
- PVDF, complex polarisation distributions 4-76320
- PVDF, corona poling, piezoelec. activities 4-109117
- random media, response kernels, dielectric polarisation, Onsager-Kirkwood function 4-99009
- remnant memory systems, relax. and polarisation 4-99020
- solutions, optical electron transfer, dispersion spectroscopy 4-80854
- surface layers, electrostatics, with spontaneous polarisation 4-80654
- surface polarization induced by an adatom in a dielectric 4-70551
- susceptibility anomalies in the vicinity of a nonpolar commensurate phase 4-114219
- TGS, and deuterated, ferroelec. crystals, pyroelec. props. (Chinese) 4-114213
- TGS, doped single crystals, pyroelec. and dielec. props. meas. 4-76346
- TGS, ferroelec., Brillouin spectra angular depend. studies 4-71393
- TGS, ferroelec. switching current, effect of time between polarisation reversals 4-76368
- TGS, L- $\alpha$  alanine doped, polarisation, influence of growth conditions 4-76314
- TGS, single crystal, metal ion doped, pyroelec. response relax. 4-76344
- TGS, universal behaviour of dynamic relax. 4-80863
- TGS crystal, polarisation current, domain width distrib. 4-71262
- TGS crystals, repeated switching-induced fatigue, struct. props. 4-71300
- THSe, dielec. props., elec. cond., thermodynamical 4-88779
- triglycine sulphate: L- $\alpha$  alanine ferroelec. cryst., piezooptical props. 4-76431
- triglycine sulphate/polymer composites, dielec. const. and pyroelec. props. 4-109132
- 2,4,6-trimethylphenol in soln., IR dispersion of H-bonded systems, dielec. function for weak complexes 4-102676
- trissarcosine calcium chloride, iodinated, dielec. props., temp. and press. depend. 4-76310
- trissarcosine calcium chloride (bromide), polarisation reversal 4-88780
- TsTS piezoceramic, dielec. props., influence of 90° domain struct. 4-76396
- TsTSNV-1 ferroelec. ceramic, residual polarisation and piezo effect 4-76316
- vinylidene cyanide-vinyl acetate copolymer, piezoelectricity and remanent polarisation 4-99028
- vinylidene fluoride-trifluoroethylene copolymer, ferroelec. hysteresis 4-99065
- vinylidene fluoride-trifluoroethylene copolymer, ferroelec. switching 4-109137
- vinylidene fluoride-trifluoroethylene copolymer rolled films, piezoelec. props. 4-99029
- vinylidene fluoride-trifluoroethylene copolymers, ferroelec. transition, statistical theory anal. 4-99053
- vinylidene fluoride/trifluoroethylene copolymer, ferroelec. transitions 4-99050
- AgNbO<sub>3</sub>, ceramic, ferroelec. phase, dielec. props. 4-61631
- Al-(SnO<sub>2</sub>+Sb<sub>2</sub>O<sub>3</sub>)-Al mixed thin films, dielec. studies 4-84719
- BaPbO<sub>3</sub>-BaBiO<sub>3</sub> system, supercond. and ferroelec. phase transitions 4-76061
- BaTiO<sub>3</sub> crystals,  $\gamma$ -irradiated, with equilb. domain struct., polarisation state 4-76395
- BaTiO<sub>3</sub>, piezoceramic, dielec. props., influence of 90° domain struct. 4-76396
- BaTiO<sub>3</sub> poly. and single cryst. dielec. after-effects and domain walls 4-71267
- Cd<sub>2</sub>Nb<sub>2</sub>O<sub>7</sub>:Gd<sup>3+</sup>, ferroelec. transitions, EPR spectra 4-98945
- Ce<sub>2</sub>(SO<sub>4</sub>)<sub>3</sub>.9H<sub>2</sub>O(D<sub>2</sub>O) single cryst. dielec. response, contact configuration effects 4-65945
- CsEuNaNb<sub>2</sub>O<sub>15</sub>, struct. and ferroelec. props. 4-109141
- CsH<sub>2</sub>PO<sub>4</sub>, Raman scatt. study 4-71377
- CsH<sub>2</sub>PO<sub>4</sub>, Slater-Senko model, ferroelec. transition 4-76370
- FeF<sub>3</sub> granular thin films, localised electronic state spatial distrib., polarisation study 4-104334
- Gd<sub>2</sub>(MoO<sub>4</sub>)<sub>3</sub>, ferroelectric-ferroelastic, acoustic emission and domain wall dynamics 4-84925
- Gd<sub>2</sub>(MoO<sub>4</sub>)<sub>3</sub>, polydomain ferroelec., quadrupole fields 4-80882
- (KBr)<sub>0.5</sub>(KCN)<sub>0.5</sub>, dielectric response, distribution of relaxation times 4-114203
- KCl:Sn, single crystal, dielectric props. meas. 4-93006
- KH<sub>2</sub>PO<sub>4</sub>, acoustic soft mode, piezoacoustic obs. 4-71266
- KNbO<sub>3</sub>, electrostatics, polarisable point-ion model 4-80860
- KNbO<sub>3</sub>, refractive index and polarisation 4-99081
- K<sub>2</sub>SeO<sub>4</sub>, incommensurate-ferroelectric transition, structural study 4-109138
- KTaO<sub>3</sub>:Li, single crystal, dielec. dispersion, dielec. spectra studies 4-76322
- LiNH<sub>2</sub>SO<sub>4</sub>, normal and deuterated, II-III phase transition, elec. field effects 4-65396
- LiNbO<sub>3</sub>, laser irradi., photovoltaic effects 4-70868
- LiNbO<sub>3</sub>, spontaneous polarisation screening on free surface 4-88767
- LiTaO<sub>3</sub> crystals, poling using interdigital electrodes, appl. to bulk wave transducers 4-99068
- (ND<sub>3</sub>)<sub>2</sub>D(SO<sub>4</sub>)<sub>2</sub>, successive phase transitions studied by VO<sup>2+</sup> ion and SeO<sub>3</sub> radical EPR 4-76388
- (NH<sub>4</sub>)<sub>2</sub>H(SO<sub>4</sub>)<sub>2</sub>, successive phase transitions studied by VO<sup>2+</sup> ion and SeO<sub>3</sub> radical EPR 4-76388
- NH<sub>4</sub>HSeO<sub>4</sub>, dielec. nonlinearity, ferroelec. transition 4-76366
- NaH<sub>2</sub>(SeO<sub>3</sub>)<sub>2</sub>:Cr<sup>3+</sup>, EPR spectra, temp. and external elec. field effects 4-88715
- Na<sub>2</sub>O-Al<sub>2</sub>O<sub>3</sub>-SiO<sub>2</sub>-S cluster cryst., Raman, ESR spectra and dielec. permittivity 4-61714
- Ni<sub>2</sub>B<sub>2</sub>O<sub>7</sub>:Br, magnetoelec. effect, mag. and elec. meas. 4-71144
- PLTZ ceramics, hot pressed polarisation and depolarisation behaviour 4-76318
- PLTZ ceramics, poling strategy 4-76319
- PLTZ, chemically prepared, charact. and props. 4-76712
- PLTZ, ferroelec. ceramic, hot poling, polarisation, ageing rel. to space charge 4-99045
- PLTZ piezoelectric ceramic, fabricated by atmospheric sintering, electrical characts. and optical transmittance (Korean) 4-114211
- PLTZ, tetragonal ceramic, 90° domains under poling, XRD study 4-76398
- PZT, dielec. props. at high press., p-T phase diagrams 4-99062
- PZT, doped, diffuse phase transition, ultrasound meas. 4-76385

## dielectric polarisation continued

- PZT material, high density, prep. by coprecipitation technique 4-76711
- Pb, Ca/TiO<sub>3</sub> piezoelectric ceramic, modified, low mech. quality factor 4-76330
- (Pb,Li,Ti)O<sub>3</sub> ceramics, stress anisotropy induced by polarisation 4-104536
- (Pb,Ba<sub>1-x</sub>)<sub>1-3/2</sub>La<sub>3/2</sub>Nb<sub>2</sub>O<sub>6</sub> ceramic, dielectric, piezoelectric and optical props. 4-98999
- (Pb<sub>0.76</sub>Ca<sub>0.24</sub>)(Co<sub>1/2</sub>W<sub>1/2</sub>)<sub>0.04</sub>Tu<sub>0.96</sub>O<sub>3</sub> ceramics, piezoelec. props. MnO addition effects 4-104532
- Pb<sub>2</sub>Ge<sub>2</sub>O<sub>11</sub>, ferroelec., surface states role in polarisation reversal 4-71325
- PbMg<sub>1/3</sub>Nb<sub>2/3</sub>O<sub>3</sub>, single crystal, growth by mass crystallisation method, elec. relax. study 4-76315
- PbZrO<sub>3</sub>, with O vacancies, phase transitions, dielec. props. 4-76391
- PbZrO<sub>3</sub>, with vacancies, para, ferro and antiferroelectric phase transitions, influence of hydrostatic press. 4-76390
- Pb(Zr<sub>1-x</sub>Ti<sub>x</sub>)O<sub>3</sub> ceramic strips, width and thickness strain meas. 4-80869
- Pb<sub>(1-y/2)</sub>[Zr<sub>1-(x+y/2)</sub>Ti<sub>x</sub>Nb<sub>y</sub>]O<sub>3</sub> ceramic transducers, pyroelec. and mechano-dielec. characts. 4-109136
- Rb<sub>1-x</sub>(NH<sub>4</sub>)<sub>x</sub>H<sub>2</sub>PO<sub>4</sub> single cryst. proton glasses, struct. and dielec. props. 4-76323
- Rb<sub>2</sub>ZnCl<sub>4</sub>, incommensurate and ferroelec. phases, electro-optical props. 4-104574
- Si/SiO<sub>2</sub>/Si<sub>3</sub>N<sub>4</sub>/electrolyte system, static and dynamic volt-ampere characts. (Russian) 4-65739
- Sr<sub>2</sub>Al<sub>2</sub>O<sub>7</sub>(CrO<sub>4</sub>)<sub>2</sub>, flux grown, ferroelec. phase transition, domain studies, birefr., polarisation, permittivity, transition enthalpy meas. 4-65970
- Sr<sub>1-x</sub>Ca<sub>x</sub>TiO<sub>3</sub>, XY quantum ferroelec. with transition to randomness 4-88781
- Tb<sub>2</sub>(MoO<sub>4</sub>)<sub>3</sub>, ferroelectric-ferroelastic, acoustic emission and domain wall dynamics 4-84925
- Te(OH)<sub>2</sub>.2NH<sub>4</sub>H<sub>2</sub>PO<sub>4</sub>.(NH<sub>4</sub>)<sub>2</sub>HPO<sub>4</sub>, dielec., thermal and optical props. 4-61636
- Xe soft X-ray absorpt., dielec. screening and core hole relax. 4-64414
- dielectric properties of gases**
- net ionisation rates, meas. by transient techniques 4-79728
- SF<sub>6</sub> in rod-rod gap, impulse breakdown, insulated barrier shielding 4-79715
- dielectric properties of liquids and solutions**
- acetic acid, dipole assoc. in nonpolar solvents (German) 4-109116
- aqueous binary non-electrolyte mixtures, compressive and dielec. props. (Japanese) 4-99001
- aromatic compounds, dipolar association as a function of molecular structure studied by nonlinear dielectric effect 4-89253
- aromatic cpds., dil. solns., dielectric behaviour on freezing 4-88759
- artificial Kerr media, equilb. dielec. props. 4-97011
- benzene, in cyclohexane, Kerr const., mol. anisotropic polarisabilities, dielectric study 4-102721
- benzenes, substitutes, in glassy forming solvents,  $\beta$  process study 4-92990
- benzylperoxyl radical, dipole meas. by microwave dielect. absorpt. 4-59915
- binary mixtures, conductive components, static permittivity 4-109109
- bis(4-nitrophenyl) ether in glassy o-terphenyl, anomalous dielectric relaxations, Eyring activation barriers 4-87060
- n-butanol, binary polar mixtures, dielec. props. and excess thermodynamic functions 4-114195
- t-butylbenzenes, in cyclohexane, Kerr const., mol. anisotropic polarisabilities, dielectric study 4-102721
- butyrophenones and related cpds., assoc. with I<sub>2</sub>, dielectric study 4-104971
- complex permittivity of liquids, determ. using inverse numerical treatment of microwave refl. meas. 4-114198
- 4-cyano-3-fluorophenyl-4-heptylbenzoate, nematic liq. cryst., dielectric const. 4-99000
- cyanobiphenyl liq. cryst. mixtures, alignment near smectic A-nematic transition 4-88087
- cyclohexane, liq., dielec. loss in millimetre and submillimetre wavelength region 4-99015
- cyclohexane + triethylamine mixtures, keto-enol tautomerism and permittivity 4-113589
- decyltrimethylammonium bromides, aq. soln., critical micelle conc., elec. cond. 4-98325
- diaryl ethers in polystyrene matrix, anomalous dielectric relaxations, Eyring activation barriers 4-87060
- dielectric liq. layers subjected to electric field, oscillatory convective instability, dielectric constant 4-103427
- dipolar two centre Lennard-Jones mol. liqs., dielec. behaviour and multi-body orientational correl. 4-97988
- DNA solution, dielec. behaviour at radio and microwave freqs. at 20°C 4-105213
- electrical conductivity of liquid dielectrics role of EHD motion, power capacitor example 4-98326
- electrohydrodynamic behaviour of viscous dielectric fluid and current response to voltage changes 4-97702
- electrolyte solution, charged aggregates interaction, Monte Carlo simulation 4-97986
- electrolytic aqueous solutions, dielec. effects, kinetic depolarisation, saturation and solvent relax. 4-80859
- electrostriction press. dynamics near spherical electrode 4-93010
- ferroelectric liquid crystals, permittivity 4-76307
- 3-fluoro-4-cyanophenyl 4'-n alkylbenzoates, synthesis, mesomorphic and phys. props. 4-113318
- glycerol-water system, microwave field meas. in ESR and saturation-transfer ESR spectroscopy 4-96572
- n-heptane, liq., dielec. loss in millimetre and submillimetre wavelength region 4-99015
- n-hexane, liq., dielec. loss in millimetre and submillimetre wavelength region 4-99015
- hexyltrimethylammonium bromide, aq. soln., critical micelle conc.; elec. cond. 4-98325
- insulin in sol., relative permittivity at 6 temps. in 0.2-50 MHz freq. range 4-72211
- ions moving through compressible polar solvents, electrostriction and dielectric friction 4-61124
- linear dipole molecules in inert solvents, dielec. susceptibility dispersion, model 4-83316
- liquid crystal displays, dual-frequency addressable 4-88763
- liquid crystals, dielectric relax. and permittivity, book contrib. 4-93000
- liquid crystals, polymorphism, NMR, dielec. props. and presence in living tissue, book 4-90313

# dielectric properties of liquids and solutions continued

- liquids, dielectric props., resonator method meas. in microwave range 4-6167
- liquids, high-permittivity, dual-channel time domain spectroscopy, dielectric characterisation 4-88760
- 2,6-lutidine, binary aq. mixture, lower critical point, dielectric study 4-80855
- 3,4-lutidine, polar mols. at microwave freq., relax. time, viscosity effect 4-91325
- methanol-acetonitrile mixtures, dielec. relax. 4-99013
- methanol-n-heptane, critical dielectric const. meas. as function of temp. 4-92989
- methyl nitrite conformational kinetics, phase depend. NMR 4-69104
- 3-methyl-1,5-diphenyl-1,4-pentadien-3-ol, soln. and solid, dielectric props., IR study 4-99017
- methylbenzenes, in cyclohexane, Kerr const., mol. anisotropic polarisabilities, dielectric study 4-102721
- microwave range meas. technique using three-layer dielec. resonator 4-111161
- molecular liquid, nonpolar, nonlinear dielect. effect 4-71257
- nematogens, monoester and diester, dielec. obs. 4-88764
- n-octane, liq., dielec. loss in millimetre and submillimetre wavelength region 4-99015
- optical, microwave, rf and dielectric spectra (*Russian*) 4-114303
- optical electron transfer, dispersion spectroscopy 4-80854
- organic charge transfer complexes, dielectric const. and loss meas. 4-76308
- organic polar cpds., dielectric relax., nucl. spin-lattice relax., NMR 4-88768
- outer-sphere electron transfer probability determ. using quantum-static approx. 4-66559
- pentachlorophenol in soln., IR dispersion of H-bonded systems, dielec. function for weak complexes 4-102676
- permittivity meas. apparatus 4-63761
- phenylpyridines, dielec. relax. mechanism and internal rot. 4-99012
- phospholipid bilayer solns. at ordered-fluid phase transition, microwave dielectric spectrum 4-91255
- photoresist soln., AZ1350J, chem. and dielec. props. 4-104519
- phthalates in benzene solns., dielec. absorpt. in viscous liqs. at 9.2 GHz, viscoelastic behaviour 4-84906
- polar fluids, dielectric props., static and freq. depend., computer simulation 4-71259
- polar liquid, dielectric const. determ. by simulation of microscopic drops 4-76302
- polar liquid dielectrics, temp. depend. of elec. conductance 4-98995
- polar liquids, molecular dynamics study of dielectric props. 4-88057
- poly(dimethyl siloxanes), cyclic and linear, static dielect. meas. and dipole moments 4-61620
- poly N-vinylcarbazole soln., dipole moment, Kerr const., stereoregularity 4-93053
- polymers, helical worm-like chains in dilute soln., dielec. relax. 4-99016
- polyvinylidene fluoride, DC cond. and dielec. absorption 4-80588
- 1-propanol, aq. solns., dielec. relax., time-domain meas. 4-65947
- pyridine, binary aq. mixture, lower critical point, dielectric study 4-80855
- quadrupolar fluids, polarisable, single particle props. and static dielectric const. 4-61619
- salicylates in benzene solns., dielec. absorpt. in viscous liqs. at 9.2 GHz, viscoelastic behaviour 4-84906
- smectogenic cpds., dielectric and X-ray studies 4-92077
- spheres with thin double layers, dilute suspension in asymmetric electrolyte, dielec. response 4-105031
- Stockmayer 3D fluid, permittivity, thermodynamic props., mol. dynamics simulation 4-70002
- 1,1,2,2-tetrachloroethane binary systems, dielec. props. at 308.15K 4-104521
- tetramethylammonium chloride, in 1-butanol, viscosity determ. 4-103987
- thiocyanates, sodium, potassium and ammonium in 1-butanol, viscosity determ. 4-103987
- 2,4,6-trimethylphenol in soln., IR dispersion of H-bonded systems, dielec. function for weak complexes 4-102676
- n-valeric acid, association study from dielec. props. 4-76998
- water, charge injection and transport anal. 4-99023
- CdS, particle suspensions, electronic processes, microwave probing 4-99852
- p-H<sub>2</sub>, dielectric const., density depend. (*Chinese*) 4-76300
- KCl-glycerol supercooled liq. solns., ionic mobility and dielec. relax. 4-88326
- LiAsF<sub>6</sub> in 2-methyltetrahydrofuran, mol. relax., US absorpt. investig. 4-109108
- LiBF<sub>4</sub> in 2-methyltetrahydrofuran, mol. relax., US absorpt. investig. 4-109108
- LiClO<sub>4</sub> in 2-methyltetrahydrofuran, mol. relax., US absorpt. investig. 4-109108
- Se, particle suspensions, electronic processes, microwave probing 4-99852
- TiO<sub>2</sub>, particle suspensions, electronic processes, microwave probing 4-99852
- tri-n-alkylammonium nitrates, benzene solns., dielec. obs. at 298.15K 4-114196
- Xe, liq., nonlinear dielect. effect 4-71257

# dielectric properties of solids

- antiferromagnetic dielect., hybrid excitations, anal. of mag. and optical props. 4-76233
- aromatic cpds., dil. solns., dielectric behaviour on freezing 4-88759
- attapulgite, temp. and freq. variations of elec. props. 4-61616
- betaine arsenate, dielec. props. near ferroelec. transition 4-71307
- bone, fluid-saturated, dielec. props., immersion fluid cond. variation effect, rat. expts. 4-81659
- bone composite material, elec. props. rel. to comp. 4-72232
- t-butyl bromide, dielec. permitt. meas., crit. comparison with incoherent quasielastic neutron scatt. results 4-88761
- t-butyl chloride, dielec. permitt. meas., crit. comparison with incoherent quasielastic neutron scatt. results 4-88761
- t-butyl cyanide, dielec. permitt. meas., crit. comparison with incoherent quasielastic neutron scatt. results 4-88761
- cellulose fibres, pineapple, mech. and dielec. props. 4-104807
- Co<sub>2</sub>O<sub>3</sub> film, vac. deposited, dielec. parameters, temp. depend. defects role 4-99024
- copoly(butyl-L-aspartate-benzyl-L-aspartate), dielec. props. 4-114201
- 1-cyanoadamantane, plastic phases, low freq. dielectric props. 4-71260

# dielectric properties of solids continued

- cycloaliphatic epoxy resin,  $\gamma$ -irrad. under vacuum, phys. props., ageing 4-103800
- cyclohexanol, rotor and glassy cryst. phase, mol. motion, PMR linewidth study 4-84863
- dipolar dielectrics, TCS driven by temp. gradients 4-109115
- elastic dielectrics, variational principle 4-78145
- ethylene-vinyl alcohol copolymer, struct., mech. and dielec. props., temp. depend. (*German*) 4-71261
- glass, anomalous thermal, acoustic and dielec. props. at low temp. 4-60994
- ice, hexagonal, translational lattice vibrs. and permittivity, temp. and press. 4-76309
- insulating solids, conduction and breakdown phenomena, role of electrodes 4-108869
- IV-VI compounds, electronic and dynamical props., book contrib. 4-61003
- multilayer-cordierite composites, sintering, hot pressing, microstruct., mech. and thermal props. 4-89017
- natural rubber vulcanisation, effects on dielectric props. 4-114468
- nonlocal dielectrics, generalised boundary condition, reflectivity 4-92993
- particulate materials dielectric props., density dependence 4-71256
- photogalvanomagnetic phenomena 4-65702
- PMMA, dielec. relax., crosslinking and branching effects 4-104528
- poly 4,4'-oxydiphenylene pyromellitimide, low temp. dielec. relax., anhydride end group effect 4-104527
- poly-N-vinylcarbazole, nonpolar crosslinking agent effect on relax. processes, hopping mechanism of transport (*Polish*) 4-65948
- poly-p-phenylene oxides, chlorinated, solid, dielec., mech. and thermal props. 4-88769
- polyacrylamide, dielec. relax., crosslinking and branching effects 4-104528
- polymeric dielectrics, giant polarisation 4-104526
- polymers dielectrics, elec. breakdown rel. to high-mobility states 4-109119
- polypyromellitimide films, struct.-property rels. 4-103667
- polystyrene, dielec. relax., crosslinking and branching effects 4-104528
- polysulphonearylate block copolymers, synthesis, mech. and dielec. props. (*Russian*) 4-62191
- pullulan, solid, thermally stimulated current 4-113969
- PVC-chlororubber-20 blends, dielec., ultrasonic and X-ray diff. 4-113352
- quartz crystals, electrical conductivity and dielectric loss, effect of alkali ions 4-71271
- rock, complex resistivity and dielectric behaviour 4-100538
- static ionic charge in dielectric theory, scaling with ionicity parameter 4-98057
- structural aspects of phase transitions in MM'B<sub>x</sub>A type crystals 4-65241
- synthetic foams, three phase, mech. props., dielec. const. 4-89077
- thermoelastic dielectrics, generalised, acceleration waves propag. 4-80151
- transition metal halide, single cryst., permittivity, electronic states, UV reflectivity 4-84975
- tris-sarcosine calcium chloride, dielec. const. and loss meas. in paraelec. phase, behaviour near ferroelec. transition 4-71258
- Whitstone, water-saturated, dielec. props. in MHz range, texture effects 4-82038
- (As<sub>2</sub>S<sub>3</sub>)<sub>x</sub>(As<sub>2</sub>S<sub>3</sub>)<sub>1-x</sub> glasses, Raman scatt., IR and depolarisation spectra 4-109182
- Au thin films, dynamic scaling near percolation threshold, AC cond. and dielectric const. 4-98525
- BaO-PbO-Nd<sub>2</sub>O<sub>3</sub>-TiO<sub>2</sub> dielec. resonators, microwave characts 4-84908
- Ba(Zn,Ta)O<sub>3</sub>-BaZrO<sub>3</sub> complex perovskite struct., dielec. resonator with high microwave Q-value 4-84926
- BeO dielectric props. in NMMW range, refract. index and absorpt. coeff. 4-73491
- Cd halides, electronic struct., UV reflectivity 4-84974
- D<sub>2</sub>O ice, hexagonal, translational lattice vibrs. and permittivity, temp. and press. 4-76309
- KCl:Sn, single cryst., dielectric props. meas. 4-93006
- Mn,Zn,Fe<sub>2</sub>O<sub>4</sub> ferrites, mag. and dielec. relax. 4-84904
- Ni<sub>2</sub>B<sub>2</sub>O<sub>7</sub>Br, magnetoelec. effect, mag. and elec. meas. 4-71144
- PLZT, ferroelec. ceramic, hot poling, polarisation, ageing rel. to space charge 4-99045
- PbFe<sub>2</sub>R, R=rare earth, dielec. spectrum study, 5.5 to 380K 4-71272
- Pb(Fe<sub>1/2</sub>Nb<sub>1/2</sub>O<sub>3</sub>)<sub>2</sub>Pb(Nb<sub>1/3</sub>Nb<sub>2/3</sub>O<sub>3</sub>) solid soln. system, dielec. props. 4-104517
- n-Pb<sub>1-x</sub>Ge<sub>x</sub>Te, free carrier mobility, ferroelectric phase transition 4-71317
- PbMg<sub>1/3</sub>Nb<sub>2/3</sub>O<sub>3</sub> ceramics, dielec. props., microstruct. rel. to sintering temp. and comp. 4-84897
- RbCl, single cryst., dielec. props. 4-104522
- SrTiO<sub>3</sub>:La, oxidation-reduction behaviour 4-103739
- ZnS:Er(Mn,Er) phosphors, electro- and photo-luminescence props. 4-104652
- (Zr, Sn)TiO<sub>4</sub> dielec. resonators, microwave characts 4-84908

# dielectric properties of substances

- see also antiferroelectricity; dielectric depolarisation; dielectric function; dielectric materials; dielectric measurement; dielectric phenomena; dielectric polarisation; dielectric properties of gases; dielectric properties of liquids and solutions; dielectric properties of solids; electric strength; optical susceptibility; permittivity; piezoelectricity; pyroelectricity
- bone, elec. and dielec. props. rel. to freq. 4-66940
- ceramics, porous, dielec. response, adsorbed water effects 4-65943
- computer simulations, reaction field calcs. 4-80856
- fish erythrocytes, reaction of intracellular matter to detergent toxicity, dielec. studies 4-72230
- polymer blends, conf., Ottawa, Ontario, Canada (April 1983) 4-82591
- PVC-poly- $\alpha$ -methyl- $\alpha$ -n-propyl- $\beta$ -propiolactone blends, dielec. props. 4-84909
- BaTiO<sub>3</sub> ceramics, analogy between mech. and dielec. strength distrib. 4-61942

# dielectric relaxation

- see also dielectric resonance
- adenosine diarsenate, deuterated, dielectric relax. meas. 4-93004
- adipic acid-hexanedioic copolymers, dielec. relax. 4-80866
- anisotropic materials, dielec. response function determ., direct method using time-domain spectroscopy 4-111157
- benzene halogenic derivatives, molecular reorientation studies 4-91275
- bis(4-nitrophenyl) ether in glassy o-terphenyl, anomalous dielectric relaxations, Eyring activation barriers 4-87060

**dielectric relaxation continued**

- bisphenol-A polycarbonate, carbonate mobility, dielectric relax., NMR 4-80829  
breakdown, Weibull statistics, theoretical basis and appls. 4-109121  
cholesteryl 2,2,3,3-tetrafluoropropionate, dielec. props. under hydrostatic press. 4-80853  
cholesteryl paragonate liq. cryst., current flow, relax. processes 4-88770  
copoly(butyl-L-aspartate-benzyl-L-aspartate), dielec. props. 4-114201  
cyanobiphenyl liq. crystals, current flow, relax. processes 4-88770  
cyclohexanol, rotor and glassy cryst. phase, mol. motion, PMR linewidth study 4-84863  
decyltrimethylammonium bromides, aq. soln., critical micelle conc., elec. cond. 4-98325  
diaryl ethers in polystyrene matrix, anomalous dielectric relaxations, Eyring activation barriers 4-87060  
dibenzoyl in p-xylene, dielectric relax. process mechanism 4-71268  
dielectrics, electron irradiated, vol. electrification meas. 4-71270  
distributed layers, dielec. relax. 4-84907  
DOBA-1-MBC, ferroelec. liq. cryst. with large spontaneous polarisation 4-60813  
electrolytic aqueous solutions, dielec. effects, kinetic depolarisation, saturation and solvent relax. 4-80859  
ferroelectric materials, electric aging, low freq. polarisation relaxation (*Russian*) 4-99010  
flexible molecule with intramol. interaction, dielect. relax. 4-93005  
hexyltrimethylammonium bromide, aq. soln., critical micelle conc., elec. cond. 4-98325  
Kapton-H polymer thin film, space charge and dipolar relax. 4-76328  
Levy distrib. and Williams-Watts model of dielec. relax. 4-61623  
liquid crystals, dielectric relax. and permittivity, book contrib. 4-93000  
liquid crystals, relaxation current increase study 4-75291  
2,6-lutidine, binary aq. mixture, lower critical point, dielectric study 4-80855  
3,4-lutidine, polar mols. at microwave freq., relax. time, viscosity effect 4-91325  
MBBA, metastable solid, dielectric props. under press. 4-80865  
MBBA liq. cryst., current flow, relax. processes 4-88770  
methanol-acetonitrile mixtures, dielec. relax. 4-99013  
3-methyl-1,5-diphenyl-1,4-pentadien-3-ol, soln. and solid, dielectric props., IR study 4-99017  
microcomputer-based dielectric relaxation spectroscopy, nitrocellulose/nitroglycerine propellants meas. appl. 4-11152  
nematogens, monoester and diester, dielec. obs. 4-88764  
nitrocellulose-nitroglycerine mixture, dielec. studies 4-109110  
Nylon 5,7 films, dielec. and pyroelec. props., mol. orientation depend. 4-99043  
nylons, dielectric and ultrasonic absorpt. meas. 4-92987  
octylcyanobiphenyl, dielectric props., time domain spectroscopy study 4-104520  
one-dimensional rotator-type polar molecules, dielec. relaxation model 4-112253  
organic polar cpds., dielectric relax., nucl. spin-lattice relax., NMR 4-88768  
p-pentobenzylidene alkylaniline, dielectric relaxation and nematic order in liquid crystals 4-76326  
phenylpyridines, dielec. relax. mechanism and internal rot. 4-99012  
phospholipid bilayer solns. at ordered-fluid phase transition, microwave dielectric spectrum 4-91255  
photoresist soln., AZ1350J, chem. and dielec. props. 4-104519  
phthalates in benzene solns., dielec. absorpt. in viscous liqs. at 9.2 GHz, viscoelastic behaviour 4-84906  
PMMA, dielec. relax., crosslinking and branching effects 4-104528  
polar liquids, molecular dynamics study of dielectric props. 4-88057  
poly(vinylidene fluoride), stress and dielec. relax. studies 4-99014  
poly 4,4'-oxydiphenylene pyromellitimide, low temp. dielec. relax., anhydride end group effect 4-104527  
poly-N-vinylcarbazole, nonpolar crosslinking agent effect on relax. processes, hopping mechanism of transport (*Polish*) 4-65948  
poly-p-phenylene oxides, chlorinated, solid, dielec., mech. and thermal props. 4-88769  
polyacrylamide, dielec. relax., crosslinking and branching effects 4-104528  
polyesters, aliphatic, dielec. relax. is oriented specimens 4-80158  
polymer blends, struct. and dielec. props. (*German*) 4-71269  
polymers, helical worm-like chains in dilute soln., dielec. relax. 4-99016  
polypropylene and polycarbonate, study of dielectric relaxation in polymer blends - transient current approach 4-99021  
polypyromellitimide films, struct.-property rels. 4-103667  
polystyrene, dielec. relax., crosslinking and branching effects 4-104528  
1-propanol, aq. solns., dielec. relax., time-domain meas. 4-65947  
PVC-poly- $\alpha$ -methyl- $\alpha$ -propyl- $\beta$ -propiolactone blends, dielec. props. 4-84909  
pyridine, binary aq. mixture, lower critical point, dielectric study 4-80855  
quartz crystals, electrical conductivity and dielectric loss, effect of alkali ions 4-71271  
quasi-DC ionic conduction in dielec. materials 4-108656  
remnant memory systems, relax. and polarisation 4-99020  
salicylates in benzene solns., dielec. absorpt. in viscous liqs. at 9.2 GHz, viscoelastic behaviour 4-84906  
smectic A phase, induced, dielec. relax. studies 4-92078  
smectogenic cpds., dielectric and X-ray studies 4-92077  
TGS, pyroelectric response relax., role of viscous phenomena 4-71284  
TGS, universal behaviour of dynamic relax. 4-80863  
trifluoromethane, dielectric and thermodynamic props. near critical temp. 4-88758  
vinylidene fluoride-trifluoroethylene copolymers, ferroelec. transition and dielec. props. 4-99052  
Williams-Watts function of dielectric relaxation 4-76325  
Al-SiO<sub>2</sub>-Si structures, dipolar relax. effects, transient capacitance spectroscopy study 4-80683  
BaO-Al<sub>2</sub>O<sub>3</sub>-SiO<sub>2</sub> thick film crossover dielec.-compositions, dielec. props. rel. to multiple refiring 4-109113  
BaTiO<sub>3</sub> poly and single cryst. dielec. after-effects and domain walls 4-71267  
BaTiO<sub>3</sub>:Fe(Nb), dielectric relax. meas. 4-80864  
CaF<sub>2</sub>:rare earth doped, gamma irradi. induced dielec. relax. 4-70210  
CdF<sub>2</sub>, alkali metal doped, association and bound motion 4-80294  
CeO<sub>2</sub>:La<sup>3+</sup>, Nb<sup>5+</sup>, dielectric relaxation, orientation of dipole complexes 4-114202

**dielectric relaxation continued**

- CsH<sub>2(1-x)</sub>D<sub>2</sub>PO<sub>4</sub>, ferroelectric, dielec. relaxation, activation energy, isotope effects 4-65989  
CsH<sub>2</sub>PO<sub>4</sub> ferroelec., domain struct. relax. 4-71322  
CsH<sub>2</sub>PO<sub>4</sub>, paraelec. phase, soft relax. mode, dielec. spectra studies 4-65986  
KBr:S<sup>2-</sup>, impurity-vacancy dipoles, dielec. relaxation 4-99019  
(KBr)<sub>0.5</sub>(KCN)<sub>0.5</sub>, dielectric response, distribution of relaxation times 4-114203  
KCl:Sn, single cryst., dielectric props. meas. 4-93006  
KCl:glycerol supercooled liq. solns., ionic mobility and dielec. relax. 4-88326  
KH<sub>2</sub>PO<sub>4</sub> ferroelec., domain struct. relax. 4-71322  
La<sub>1-x</sub>Ba<sub>x</sub>F<sub>3-x</sub> solid solns., elec. props., small-signal AC response and TSDC meas. 4-70449  
La<sub>1-x</sub>Ba<sub>x</sub>F<sub>3-x</sub> solid solutions, small signal AC response 4-92424  
LiNbO<sub>3</sub> amorphous films, dielec. and elec. props. 4-104531  
Mn<sub>2</sub>Zn<sub>2</sub>Fe<sub>2</sub>O<sub>4</sub> ferrites, mag. and dielec. relax. 4-84904  
(NH<sub>4</sub>)<sub>2</sub>BeF<sub>4</sub>, incommensurate phase, dielec. dispersion in microwave range 4-104524  
Na<sub>2</sub>O-MgO-SiO<sub>2</sub> glass, dielec. relax. and dispersion 4-114204  
Ni<sub>2</sub>B<sub>2</sub>O<sub>7</sub>, piezoelec. and dielec. relax. at low temp. 4-76324  
PbF<sub>2</sub>:Na(K)(Rb), ionic cond., dielec. relax. and activation vol. 4-113701  
PbF<sub>2</sub>:R, R=rare earth, dielec. spectrum study, 5.5 to 380K 4-71272  
PbTiO<sub>3</sub> amorphous films, dielec. and elec. props. 4-104531  
Rb<sub>1-x</sub>(NH<sub>4</sub>)<sub>x</sub>H<sub>2</sub>PO<sub>4</sub> single cryst. proton glasses, struct. and dielec. props. 4-76323  
(Rb)(NH<sub>4</sub>)<sub>1-x</sub>SO<sub>4</sub>, dielectric relax. meas. 4-80862  
Rb<sub>2</sub>ZnCl<sub>4</sub>, incommensurate phase, dynamic dielec. props., pinning effects 4-109140  
SiO<sub>2</sub>, thermally grown layers, halogen-containing, relaxation processes (*Russian*) 4-99018
- dielectric resonance**  
see also *dielectric relaxation; paraelectric resonance*  
liquids, dielectric props., resonator method meas. in microwave range 4-61617  
materials with uniaxial anisotropy, dielec. resonator meas. 4-65944  
PZT, electrically excitable mechanical reson. 4-114225
- dielectric strength** see *electric strength*
- dielectric susceptibility** see *optical susceptibility*
- dielectric thin films**  
see also *ferroelectric thin films; insulating thin films; optical films; piezoelectric thin films*  
alumina humidity sensor, moisture effect on dielectric props. analysis 4-95442  
birefringence measurement by prism coupler method 4-106337  
charge centroids determ. in two-side metallised electrets 4-86441  
columnar structure films, refr. index vars. 4-109148  
decomposition preventing films on p-CdTe, annealing 4-92755  
distributed layers, dielec. relax. 4-84907  
division-of-wavefront polarising beam splitter and half-shade device using dielectric thin film on dielectric substrate 4-74679  
hydrocarbon polymer dielectric films, hot-electron transport 4-92837  
ice films, enhanced erosion by high energy <sup>19</sup>F ion sputtering 4-80123  
ionic transport, transient current calc. 4-70433  
IR ray path visualisation 4-87269  
Kapton-H polymer thin film, space charge and dipolar relax. 4-76328  
multilayer dielectric coatings of unequal thickness 4-87432  
organic translucent thin films, optical microscopy, visibility enhancement using fibre-optic cables 4-106378  
poly(vinylidene fluoride) film, dipolar orientation study 4-65946  
polyolefins with amine additives, low temp. losses, expt. study 4-114205  
radiation charged, methods for charge- or field-distrib. studies 4-71826  
surface layers, electrostatics, with spontaneous polarisation 4-80654  
transparent single layers on glass substrates, light scatt. 4-99205  
Al<sub>2</sub>O<sub>3</sub> anodised films, breakdown statistics 4-109128  
Al<sub>2</sub>O<sub>3</sub> gate dielectric grown on InP using indirect plasma-enhanced CVD technique 4-104529  
Al<sub>2</sub>O<sub>3</sub> thin film deposition by UV laser photolysis 4-99337  
Au-polymers, prep. by plasma polymerisation 4-81162  
Ba<sub>2</sub>Si<sub>1-x</sub>F<sub>2-x</sub> lattice-matched single cryst. film growth on InP (001) by MBE 4-70582  
Ba<sub>2</sub>Si<sub>1-x</sub>F<sub>2-x</sub> single cryst. dielec. films, MBE growth on InP (001) 4-81137  
a-C/Si MIS structures, DC sputter deposited, HF characts. 4-88601  
CeO<sub>2</sub>, vac. deposited, dielec. parameters, temp. depend, defects role 4-99024  
KNbO<sub>3</sub> ferroelec. films, liquid phase epitaxy growth 4-76695  
Si<sub>3</sub>N<sub>4</sub> dielectric film: electron conduction; expt. study 4-114053  
Si<sub>3</sub>N<sub>4</sub> thin film deposition by UV laser photolysis 4-99337  
SiO<sub>2</sub> gate dielect., charge build-up and breakdown 4-109124  
SiO<sub>2</sub> gate oxide breakdown, expt. study 4-114207  
SiO<sub>2</sub>, thermally grown layers, halogen-containing, relaxation processes (*Russian*) 4-99018  
SiO<sub>2</sub> thin film deposition by UV laser photolysis 4-99337  
Ta<sub>2</sub>O<sub>5</sub> film form., thermally stable on Si substrates 4-85256  
Ta<sub>2</sub>O<sub>5</sub> films on Si, electrical props. 4-84720  
Ta<sub>2</sub>O<sub>5</sub>/Si, film struct., reflection and electroreflection spectra 4-109266  
Y<sub>2</sub>O<sub>3</sub> films, struct. and phys. props. 4-65585
- dielectric triodes** see *space-charge limited devices*
- dielectric waveguides**  
see also *optical waveguides*  
cellulose acetate, water sorption and pore vol. 4-97067  
circular hollow waveguides with uniform curvature, wave prop. and attenuation 4-83692  
circular metallic dielectric-coated waveguides for IR transmission, design theory 4-74704  
degenerate four-wave mixing with surface guided waves 4-96982  
open dielectric strip waveguides, leakage and resonance effects, expt. study (*Japanese*) 4-60168  
HCN waveguide laser and HCN laser-excited oversized hollow dielec. waveguide submm radiation pattern study 4-107709
- dielectrics** see *dielectric materials*
- diesel engines** see *internal combustion engines*
- difference equations**  
advection-diffusion equation, finite difference schemes, stability anal. 4-68183  
boundary problems in generalised analytical functions, variational-difference method (*Russian*) 4-63490

# ference equations continued

boundary value problems, multi-grid method numerical soln. 4-101628  
 computational methods for transient analysis, book 4-58594  
 convection boiling, forced, flow oscillations, finite difference analysis of density-wave oscillations 4-79595  
 counterflow heat exchanger dynamics calc. using difference equations; errors 4-91719  
 crack problems, solution using finite difference technique 4-69710  
 Dirichlet problem of Laplace eqn., integral difference soln. method (*Russian*) 4-63517  
 dispersion of semidiscretized and fully discretized systems, book contrib. 4-58626  
 fluids, US field propag. calc. using finite difference techniques 4-98205  
 gasdynamics with gravity allowance, operator-difference scheme-stability 4-87753  
 high resolution total variation stable finite difference schemes 4-58620  
 Ising pair correlation functions at critical temp. 4-111061  
 light absorption by outer segment of retinal rods 4-81680  
 MHD multidimensional transient flows full implicit continuous Eulerian scheme 4-87809  
 multi-dimensional nonlinear Schrodinger eqns., numerical calc. 4-63571  
 nonlinear filtration, difference schemes 4-87789  
 nuclear reactor design, computational techniques 4-111598  
 overlapping Gaussian peaks, generalised difference eqn. method 4-59479  
 parabolic eqns. with singular coeffs., projected difference schemes with split operator (*Russian*) 4-63480  
 parametric correction method for finite difference schemes (*Russian*) 4-63481  
 partial difference eqns. with constant coeffs. and appl., system decoupling 4-86182  
 periodic particle transport eqn., solution smoothness, space functions with differential-difference characts. (*Russian*) 4-111077  
 planar numerical cosmology, difference eqns. and numerical tests 4-95001  
 plates, thin, viscoelastic, finite element anal. 4-112721  
 radiative transfer, difference eqns. and linearisation methods 4-94598  
 Raman-Nath eqns., operational identities and soln. 4-110852  
 recirculating flow, two and three dims. numerical methods 4-103453  
 Riemann solvers, the entropy condition, and difference approximations 4-68192  
 semiconductor lasers, stationary characts., numerical anal. (*Chinese*) 4-112419  
 spherical Raman-Nath eqn. soln. 4-67998  
 stationary constant coefficient diffusion-convection reaction eqn., difference scheme errors 4-69766  
 Stokes and Navier-Stokes equations, finite-difference methods 4-64900  
 strange attractors, perturbation calcs. of the fractal dimension 4-86341  
 stress, shock and acceleration waves in various materials, explicit Lagrangian finite diff. method 4-60324  
 two-dimensional eddy current problems, direct soln. 4-69276  
 viscous gas, heat conducting, difference schemes, stability and convergence (*Russian*) 4-69660

**difference frequency generation (optical)** *see optical frequency conversion*

**differential calculus** *see differentiation*

## differential equations

*see also boundary-value problems; difference equations; Green's function methods; integro-differential equations; linear differential equations; Navier-Stokes equations; nonlinear differential equations; partial differential equations*  
 adiabatic approx. validity in nucl. problems 4-59168  
 barotropic perturbations, general solns. (*Turkish*) 4-115504  
 chaotic trajectories, bifurcations near homoclinic orbits with 'symm. 4-90495  
 chemical reactions, dynamics of parabolic eqns. describing diffusion and convection 4-89240  
 cold plasmas, nonlinear EM wave processes, transform. to space independent frame 4-91899  
 compressed stratified liquid, plane wave propag. and diffraction at half-plane (*Russian*) 4-69776  
 cone-shaped bodies, plastic axisymm. flow 4-60300  
 coupled-channel Schrodinger eqn. soln. using const. linear and quadratic reference pot. with corrected magnus propagators 4-73270  
 creation of non-trivial recurrence in the dynamics of diffeomorphisms 4-73230  
 delay-differential equations, singularly perturbed 4-78118  
 diffusive Volterra delay differential eqn., travelling waves, pulses and relax. oscils. 4-95357  
 dihydroindolizines photochromic systems, photokinetic examinations 4-99093  
 discrete linear mechanical systems, weak damping (*German*) 4-82661  
 discrete ordinate method of solution of linear boundary value and eigenvalue problems 4-101634  
 elastic system small vibrs., Hilbert-Schmidt theorem extension to problems with unsymmetric kernels 4-110865  
 fermion diffusions 4-63664  
 gauge theories, first order differential equations, integration conditions 4-102016  
 generalised 12-matrix propagation program, coupled 2nd order differential eqns., computer code 4-78107  
 graded mixed crystals, quasi-Bloch functions as basis functions 4-92585  
 Hamiltonian eqns., discrete mapping 4-90365  
 harmonic Raman-Nath eqn., non-trivial perturbative soln. 4-60051  
 heat exchangers, parallel flow, multichannel, coeff. matrix of differential eqns. 4-75011  
 Helmholtz eqn., Chebyshev approx. solutions 4-86226  
 Hirota-Satsuma system, prolongation algebra 4-63478  
 injection laser, multimode homogeneously broadened, analytic description 4-112439  
 integrable many-body system in external field, functional differential equation 4-82656  
 integral representation for the product of two Jacobi functions with different order and arguments 4-86264  
 intermittency, control-parameter modulation 4-63675  
 inverse scattering problem, integration of differential eqn. linear hyperbolic system (*Ukrainian*) 4-63574  
 inviscid magnetofluid, stationary finite-beta equilb. 4-91891  
 Ito's theorem and stochastic simulation 4-58741  
 Lagrangian dynamics generalisation 4-95204  
 Lie-Backlund symmetry of linear ordinary differential equations 4-86596

## differential equations continued

magnetised plasma, mode conversions 4th order differential solutions 4-83994  
 mechanics, affinely-connected manifolds theory and Lie theory 4-63492  
 membranes; elastic, circular, large axisymm. deforms. 4-112703  
 n-vector model, pair correlation function eqn. 4-90527  
 nonseparable Sturm-Liouville operator, deficiency indices and spectrum (*Russian*) 4-95136  
 ordinary differential equations numerical integration, global error estimation, stochastic approach, celestial mechanics appl. 4-82401  
 parabolic eqns. with singular coeffs., projected difference schemes with split operator (*Russian*) 4-63480  
 parabolic equation with Bessel operator, existence of periodic soln. 4-112673  
 period doublings and possible chaos in neutral models 4-68141  
 periodic particle transport eqn., solution smoothness, space functions with differential-difference characts. (*Russian*) 4-111077  
 power cable trenches moisture and heat transfer, physical principles and calculation methods, cable continuous loadability calc. (*German*) 4-69666  
 resonances in oscillation describing differential equations (*German*) 4-82659  
 rigid body mechanics, numerical simulation of time-dependent contact and friction problems 4-82654  
 Schrodinger equation power law potentials from classical treatment of 2nd order linear diff. eqn. 4-58668  
 Schrodinger group invariant linear and nonlinear differential eqn. systems 4-73298  
 shell, circular cylindrical, elastically restrained, by axially spaced springs, free vibr. 4-74947  
 shell theory, simple edge effect description, 3D theory of elasticity 4-112719  
 shells, thin elastic spherical, free vibrations, rederivation of differential eqns. in invariant form 4-112753  
 shells of revolution, axisymm. vibrs. in fluid under conc. stimuli 4-112761  
 solvent diffusion in shrinking or swelling bodies, differential eqn. 4-75716  
 source function identification by B-spline regularisations 4-106171  
 spatial dynamic structure of combustion zone, frequency charact. matrix determ. 4-85311  
 spherical Raman-Nath eqn. soln. 4-67998  
 stiffness and the automatic selection of ODE codes 4-67968  
 stochastic, nonlinear systems, dual frequency vibrations with random actions (*Russian*) 4-63665  
 stochastic systems, adiabatic elimination of variables 4-73366  
 stochastic systems, adiabatic elimination of variables 4-73367  
 stochastic systems, adiabatic elimination of variables 4-73368  
 thermoelasticity two-point problem decoupling of coupled systems of abstract differential eqns. (*Ukrainian*) 4-86209  
 three-dimensional imaging, differential operator 4-87286  
 toroidal plasma, continuous double adiabatic spectrum 4-91885  
 turbomachine cascade profile, friction and heat transfer calcs. 4-112833  
 two-dimensional time-depend. classical systems, dynamical invariants 4-86195  
 two-dimensional time-dependent Hamiltonian systems with an exact invariant 4-86194  
 WKB method for Airy differential eqn. soln. 4-78116  
 Ca<sup>+</sup>, 4s, 4p and 3d states, hyperfine struct., many-body perturbation theory 4-102610

**differential scanning calorimetry** *see thermal analysis*  
**differential thermal analysis** *see thermal analysis*  
**differentiation**  
*see also differential equations*  
 quantum mechanics, weak semi-differentiability 4-73269

**diffraction**  
*see also acoustic wave diffraction; diffraction gratings; diffractometers; electromagnetic wave diffraction; electron diffraction; neutron diffraction*  
 compressed stratified liquid, plane wave propag. and diffraction at half-plane (*Russian*) 4-69776  
 plane wave diff. by prolate solid of revolution 4-95187  
 seismic waves, three-dimensional diff. of plane P, SV and SH waves by hemispherical alluvial valley 4-110075

**diffraction gratings**  
*see also holographic gratings*  
 acoustic reflection phase grating diffuser, design theory and appl. 4-64810  
 autocorrelator for meas. single ultrashort light pulses 4-107807  
 binary optical elements, developments in fabrication 4-107808  
 blazed concave gratings, relative efficiency distrib. over grating surface 4-105881  
 book, scattering theory for diff. gratings 4-86125  
 Bragg-grating optical-waveguide lenses, out-of-phase props. 4-87444  
 centro-symmetry and partial coherence 4-102881  
 chirped grating lens on BeO glass waveguide using ion beam etching 4-62071  
 circularly ruled for general surface metrology 4-112559  
 coated crossed gratings, transformation formalism, interf. type polar-selective absorber appls. 4-60141  
 coherence peaks in picosecond sampling experiments 4-79227  
 corrugated metal surface, IR surface EM wave reflection 4-83519  
 coupler diffracted field anal. using coarse grating made from cylindrical elements 4-79280  
 DFB laser, quarter-wave shifted grating type, wavelength selectivity analysis 4-64716  
 dichromated gelatin holographic mirrors, diff. efficiency 4-107578  
 dielectric surface-relief gratings with high diffraction efficiency 4-97055  
 disc, deform. analysis, grid and grating methods, digital image processing (*German*) 4-64896  
 duplexer/isolator, near-mm wave polarising 4-103000  
 Duruy diffraction micrometer for double star work (*French*) 4-101157  
 dye laser, pulsed single-mode, cavity of prism-grating-mirror combination, spectral linewidth 4-112477  
 dye lasers, prismatic, pulsed, multi-pass dispersion theory 4-69398  
 efficiencies, differential methods for mag. field parallel to grooves 4-69541  
 efficiencies in soft X-ray region, comparison of different theories 4-69542  
 EM wave phenomena Fourier synthesis approach 4-95106  
 fluoromethane grazing-incidence far-IR laser 4-96949  
 Fresnel diffraction and white-light processing based system for real-time depth meas. and display 4-73412

## diffraction gratings continued

- Fresnel diffraction by two-dimensional periodic structures 4-107514  
Fresnel images of periodic objects, lateral shift under coherent plane wave illum. 4-96831  
garnet film with submicron domains, appl. as laser light deflector 4-103002  
grazing incidence far IR gas laser, config. and characts. 4-79187  
grazing incidence spectroscopy focusing, by elastic deformation of the grating 4-82834  
grazing-incidence dye lasers with and without intracavity lenses, comparative study 4-91447  
grazing-incidence grating cavities with Brewster-prism beam preexpander for pulsed dye lasers (Chinese) 4-112481  
heterodyning method using diff. grating optical mixer, dynamic operating mode 4-69543  
holographic common-path interferometer using movable grating and two spatial filters 4-79073  
image instability analysis using low cost moire pattern sheet 4-111195  
incoherent light optical processing techniques using diff. gratings 4-74437  
integrated optical device patterns, quadrupole electron-beam exposure technology 4-107889  
interferometric processor, grating based for real-time optical Fourier transformation 4-95500  
International Ultraviolet Explorer echelle grating, blaze function ripple correction 4-110542  
IR high-resolution cooled-optics grating spectrometer 4-95532  
laser Doppler vibrometer, two dimens., with a grating modulator (Chinese) 4-86460  
linearly chirped grating lenses, of medium Q in dielec. waveguides, perturbation and iterative perturbation anal. 4-79262  
liquid crystal device, variable grating mode, for optical processing and computing functions, physical characterisation 4-74690  
magnetic diffraction coating parameter meas. by double-beam photometer 4-63769  
MBBA, liq. cryst., laser induced thermal grating (Chinese) 4-91523  
metal gratings, CO<sub>2</sub> laser radiation absorption 4-114232  
metallic, surface polariton attenuation and dispersion 4-92632  
MM-wave grating spectrometer, plasma electron cyclotron emission diagnostic systems 4-75203  
moire gratings fabrication and testing, high-reflectance 4-103036  
moire interferometry with  $\pm 45$  deg. gratings 4-69540  
movable diffraction grating, rot. effect in linear-displacement convertor operation 4-64763  
moving chromatic grating perceived vel. 4-100151  
multiple interaction bandstop filters based on the Talbot effect 4-74687  
multiple-beam grating interferometer for coating thickness meas. 4-111188  
narrowband dye laser with a large scan range 4-91489  
nonclassical concave gratings in fixed-slit monochromators, parameter calc. 4-74691  
nonlinear optics, energy balance criterion for diff. 4-79221  
nonlinear resonant media, spatially inhomogeneous radiation propag., diff. by self-induced gratings 4-74605  
nonsinusoidal absorption gratings in photographic materials 4-91572  
optical logical processing in parallel with theta modulation, encoding of pixel information by grating structures 4-112349  
periodic structures on solid surfaces, laser irradi., temporal and spatial evolution 4-104702  
periodically corrugated surface, EM wave propagation, plasmons 4-79279  
phase behaviour in Wood anomalies 4-60140  
phase grating use in moire interferometry 4-73492  
phase gratings hidden by diffusers detect. using intensity interferometry 4-59980  
phase object measurement using Talbot effect and moire techniques 4-95501  
phase transmission grating, diff. radiation reflection (Russian) 4-69307  
photon-correlation techniques to detect gratings hidden by diffusers 4-112560  
photorefractive ferroelectrics, nonlinear optical expts., optical device applications, review 4-64744  
photorefractive laser beamsteering using thick diff. gratings, configurations 4-96968  
photorefractive materials, optimal props. for optical data processing 4-74640  
planar periodic structures, higher-order mode interaction 4-79278  
plane diffraction gratings and optical aberrations 4-69302  
polarisation, definitions and nomenclature, instrument polarisation 4-82604  
polychromatic signal detection by complex spatial filtering 4-74435  
polymer gratings preparation, by vacuum-UV photoetching 4-91570  
progress in optics, book, vol.XXI 4-106130  
pulses as short as 16 fs, compression with short optical fibre and grating pair 4-69460  
radiation pattern of an element in diffraction grating theory and Rayleigh's hypothesis 4-74418  
range measurement using Talbot diffraction imaging of gratings 4-63707  
rippled interface, intense light wave diff. 4-74422  
S 520-3 controlled nosecone rocket-borne VUV instrumentation, grating characts. (Japanese) 4-94620  
slanted anisotropic gratings, scatt. and waveguiding props. analysis 4-69539  
Smith-Purcell radiation enhancement from a grating with surface-plasmon excitation 4-87260  
spatial frequency pseudocolour encoding using coarse gratings 4-74431  
stationary Fresnel diff. field of ultrasonic progressive wave 4-103003  
stationary reference grating based optical detection method for SAW detect. 4-60180  
strip gratings, simple formulae for transmittance 4-107809  
strip gratings, Talbot effect 4-107810  
submillimetre laser couple, strip grating type, design, photolithographic fabrication and transmission meas. 4-74693  
surface grating formation under action of laser radiation on metal, semi-cond. and insulator surfaces 4-107813  
tandem scanning methods for gratings of unequal ang. dispersion 4-97054  
thermoplastic films, interf. colour creation using diff. gratings for embossing 4-69538  
toroidal grating monochromators at BESSY 4-83677  
transient orientational grating technique for fast mol., relax. process investigation 4-83625

## diffraction gratings continued

- transversely stratified sinusoidal dielectric grating, diffraction anal. using modal expansion theory (Japanese) 4-83684  
vector theories, book contrib. 4-107519  
volume phase gratings, optical anisotropy, phase shift between S, P polarisation components 4-91571  
VUV radiation physics, conf., Jerusalem, Israel, 8-12 Aug. (1983) 4-82583  
waveguide grating lenses for optical couplers 4-87443  
wide-band laser spectrum depend. on selective loss profile 4-74483  
X-ray grating spectrometer with point source and crossed-grating configuration, efficiency 4-63819  
X-ray transmission gratings and zone plates, free-standing fabrication using UV holography and X-ray lithography 4-97147  
XUV grating contamination due to overlapping orders: a study through the electromagnetic theory 4-83682  
Al rough surface, s-polarised surface polariton propagation 4-80510  
CO<sub>2</sub> waveguide laser with selective resonator, emission freq. wide tuning range 4-60069  
CO<sub>2</sub> grating selected freq. laser, mode corrugated pipe design (Chinese) 4-87360  
CO<sub>2</sub> TEA laser, beam expanding grating plane cavity (Chinese) 4-107689  
CdS, laser induced gratings 4-104630  
Cu surface, EM wave excitation spectral features 4-107811  
GaP, Raman scatt. by surface EM waves 4-80930  
Ge, surface periodic structures on intense laser bombardment 4-70201  
H, atomic spectroscopy and holography, laboratory expt. 4-67927  
InGaAsP/InP heterostructure waveguides integrated with optical devices 4-97146  
InSb, surface periodic structures on intense laser bombardment 4-70202  
 $\alpha$ -LiIO<sub>3</sub>, phase-type gratings induced by electro-optical effect, space charge fluctuation 4-66012  
LiKSO<sub>4</sub> single cryst., light diff. from vol. phase gratings (Chinese) 4-96784  
LiNbO<sub>3</sub> grating, annealing effect on surface relief 4-107812  
LiNbO<sub>3</sub> optical waveguide surface, rippled grating coupling efficiency 4-107824  
LiNbO<sub>3</sub> planar waveguide prep. with dip coating method and embossing technique, grating coupler fabrication 4-69602  
LiNbO<sub>3</sub>/Fe, polarisation-anisotropic light-induced light scatt. 4-87395  
NaCl rough surface, s-polarised surface polariton propagation 4-80510  
Nd:YAG laser pulses, freq. doubled, 80X single-stage compression using single-mode fibre and grating-pair delay line 4-64726  
Nd<sub>2</sub>La<sub>1-x</sub>P<sub>2</sub>O<sub>14</sub>, four wave mixing and exciton dynamics 4-83638  
SiO<sub>2</sub>-TiO<sub>2</sub> integrated optical planar waveguide based switches and gas sensors using grating couplers and Bragg reflector grating 4-60182  
SiO<sub>2</sub>-TiO<sub>2</sub> planar waveguide prep. with dip coating method and embossing technique, grating coupler fabrication 4-69602

## diffraction instruments see diffractometers

## diffraction model

- CERN ISR, charged multiplicity distribution, split-field-magnet detector 4-106545  
coherent particle production in nuclei, Drell-Hildre-Deck model 4-78615  
diffractive dissociation in multi TeV hadron-hadron and hadron-nucleus collisions 4-102145  
heavy hadron production, diffraction dissociation 4-90842  
KNO scaling, QCD branching processes and hadronisation, differential-difference eqn. 4-111374  
relativistic contraction effects in multiple diffraction scatt. model 4-78616  
small angle, high energy hadron scatt., spin effects, total cross section strength 4-78544  
strongly interacting particles, elastic scatt. at GeV energies, diffraction peak width bound 4-73736  
 $K^+p$ , 32 GeV/c,  $K_s^0$ ,  $\Lambda$  and  $\bar{\Lambda}$  prod., total and semi-inclusive cross sections 4-95829  
 $K^+p \rightarrow K^+p\pi^+\pi^-$ , 32 GeV/c, diffraction peaks cross sections, diffraction excitation 4-86732  
 $\bar{p}N$  in Ne, semi-inclusive coherent diffractive charged current interactions 4-73741  
 $pp$  (pp) elastic scatt.,  $E=10$ -1000 GeV, nucleon valence core model 4-95814  
 $pp$  and  $p\bar{p}$  diffractive peak comparison at ISR energies 4-102136  
 $pp \rightarrow \Delta^+ \pi^- p$ , diffractive dissociation in Deck model, slope-mass-cos  $\theta_{GJ}$  correlation 4-86725  
 $pp \rightarrow K^+X$ , parton fragmentation model with diffractive resonance prod. 4-111483  
 $pp \rightarrow \pi^+X$ , parton fragmentation model with diffractive resonance prod. 4-111483  
 $\pi^-N \rightarrow K_s^0 K_s^0 \pi^+ \pi^-$ , 200 GeV, diffractive production 4-73773

## diffractometers

## see also X-ray diffractometers

- moderator choice for pulsed neutron source 4-92031

## diffusion

- see also bioidiffusion; diffusion in gases; diffusion in liquids; diffusion in solids; electromigration; membranes; osmosis; permeability; self-diffusion; surface diffusion; thermal diffusion; turbulent diffusion  
 $\nabla \cdot (\nabla \phi) \nabla \phi = 0$  equation boundary-value problems 4-103216  
advection, simple positive definite, algorithm with small implicit diffusion 4-73400  
advection-diffusion equation, finite difference schemes, stability anal. 4-68183  
advection-diffusion equations, space-time least-square finite element scheme 4-64903  
aerosol particles, fibrous, bipolar diffusion charging, elec. mobility and charge meas. 4-89348  
aerosol particles, fibrous, bipolar diffusion charging, theory 4-89347  
aerosols, bipolar diffusion charging of monodisperse particles 4-62254  
aerosols, ultrafine, diffusion battery design and calibration 4-89349  
aggregates, fractal dimension of random walk, possible breakdown of Alexander-Orbach rule 4-86368  
aggregation, diffusion limited, position space renormalisation group 4-78278  
aggregation, diffusion-controlled, continuum approx. calcs. 4-65408  
aggregation, diffusion-limited, stirred percolation, contact prop. regime, prop. rel. scaling 4-111036  
anomalous diffusion in intermittent chaotic systems 4-73364  
bead spring model macromolecules in inhomogeneous flows, diffusion and migration 4-83502

## diffusion continued

- biased correlated walks, long-time asymptotic probability distrib. 4-68142  
 Brusselator with diffusion term, approx. analytical soln. 4-58794  
 capillary Poiseuille flow, shear dispersion, residence time 4-79668  
 catastrophe theory, nonelementary, appl. to imperfect bifurcation problems 4-58649  
 cellular confluence, Landau-Ginsburg model 4-90538  
 chaotic systems, diffusion and intermittency 4-82748  
 chaotic systems, statistical props. of intermittent diffusion 4-90490  
 char particle and surrounding gas phase, diffusion and reaction models 4-99790  
 char particle and surrounding gas phase, diffusion and reaction, continuous model 4-99791  
 charged particles in turbulent electric fields, relative diffusion, scaling prop. 4-79020  
 chemical reactions, diffusion theory, nonstationary approach 4-93511  
 chemical reactions, dynamics of parabolic eqns. describing diffusion and convection 4-89240  
 classical diffusion in random environments, numerical method 4-111076  
 classical diffusion on random chains, exact soln. 4-58797  
 cluster growing, active zone, diffusion-limited aggregation, Eden model 4-95310  
 cluster growth on the Cayley tree, diffusion controlled processes 4-95347  
 coefficients determ. from interference fringes 4-81459  
 compressible fluid, with weak diffusion, Rayleigh problem (*Russian*) 4-112672  
 coupled reaction-diffusion system, stability of steady-state solns. 4-68178  
 current relaxation theory, validity near percolation threshold 4-86374  
 deterministic random walk, chaotic behaviour 4-101748  
 diffusion-controlled reactions, perturbation anal. of Wilemski-Fixman approx. 4-62157  
 diffusiophoresis in nonuniform medium, motion of near-spherical body 4-109667  
 diffusive Volterra delay differential eqn., travelling waves, pulses and relax. oscils. 4-95357  
 directed diffusion-controlled aggregation versus directed animals 4-95346  
 discrete ordinates problems, diffusion synthetic acceleration methods, review 4-95361  
 disordered diffusive systems, fixed points and universality 4-78282  
 disordered lattice, 1-dimens., diffusion, renormalisation-group calcs. 4-63683  
 disordered materials, continuous time random walk aspects in reaction and transport 4-58738  
 elastomer-phenolformaldehyde oligomers, adhesion strength, diffusion and phase equilb. (*Russian*) 4-103906  
 elastomers, penetration swelling interaction in diffusion of liquids 4-98030  
 electrically modulated membrane permeability 4-99839  
 excited particles, combination rules in light-induced drift theory 4-107410  
 extended Brownian dynamics for three dimens. Smoluchowski diffusion 4-58739  
 fermion diffusions 4-63664  
 ferroparticles, mag. microconvection on diffusion front 4-108129  
 finite-difference solutions of convection-diffusion problems in irregular domains, using a nonorthogonal coordinate transformation 4-107991  
 flat-plate with diffusion flame, boundary layer turbulent props. 4-97507  
 forced convection systems, correl. of thermophoretically modified particle diffusion deposition rates 4-87703  
 FORTRAN programming and computer simulation teaching by diffusion in percolative lattice 4-78076  
 fractal and directed percolation clusters, spreading dimens., lattice animals analogy 4-58767  
 fractals, percolation and anomalous diffusion 4-86361  
 free-falling multicomponent droplets, combustion and microexplosion 4-103388  
 gravitational field effects on diffusion eqn. solns. 4-95352  
 hard-sphere suspensions, diffusion investigation 4-114839  
 heterodiffusion and polyrelaxation 4-101789  
 high-inlet-blockage diffusers, performance 4-113007  
 homogeneous diffusive systems, discrete eqns. of motion, fixed points 4-78281  
 hydrology, nonlinear diffusion with linearly varying diffusivity 4-100640  
 inertial corrections using Fokker-Planck eqn. 4-78280  
 interacting Brownian particles, correl. functions of infinite systems 4-111021  
 ionic micelle soln., counterion fluoresc. quenching 4-81485  
 ionic reactions, reaction probability and diffusion-controlled rate consts. 4-93503  
 kinetic boundary layer, Klein-Kramers eqn. 4-111079  
 Kramers' problem of diffusion over pot. barriers, transition rate, uniform expansion 4-101791  
 localized partial traps in diffusion processes and random walks 4-58793  
 locally analytic differencing scheme to test convection-diffusion problems 4-107990  
 mean flow field and heat transfer along cooled supersonic diffuser, 4-113077  
 micromixing theory, bounding theorem 4-66550  
 Monte Carlo method, appls. in condensed-matter physics, statistical mechanics and related fields, book 4-101584  
 moving boundary diffusion problems, pseudo-steady state approx. 4-65004  
 N-body decay, diffusion-controlled multiparticle reactions, scaling approach 4-114767  
 Nolan-Pollak condensation nucleus counter, particle loss by diffusion 4-86519  
 nonelliptical boundary-value problems (*Russian*) 4-101787  
 nonlinear reaction-diffusion eqns., Brownian motion correspondence method 4-95309  
 nonlinear reaction-diffusion systems, 1- and 2-component, spatial struct. form. (*German*) 4-62158  
 nonlinear reflecting diffusion process, and the propagation of chaos and fluctuations associated 4-86376  
 nonlinear stability of a diffusion equation 4-110884  
 one-dimensional bond-percolation model, hopping, cond. in const. field 4-68182  
 one-dimensional random walk, dispersive transport and conc. depend. diffusivity from mutual blocking of diffusants 4-58799  
 particle deposition by diffusion and interception from boundary layer flows 4-97472  
 particle traps, kinetics of diffusion controlled reaction 4-78228

## diffusion continued

- percolation clusters in two dimensions, random walks, exact-enumeration approach 4-101758  
 percolation lattices, mobility and linear response theory, particle motion 4-58777  
 periodically kicked rotator, quantum dynamics 4-63560  
 plasma cross-field diffusion problems, shape functions for separable solutions 4-97761  
 poly( $\alpha$ -amino acid) membranes, gas diffusivity and permeability 4-81650  
 polymer chain, dynamic exponent in good solvents 4-86375  
 polymer films, diffusion coeff. determ. using interionic apparatus (*Russian*) 4-103674  
 pore interactions and distrbs., effects on diffusion and permeation in membranes 4-98332  
 porous media, diffusion-limited aggregation and two-fluid displacements 4-69820  
 positronium quenching reaction mechanism, quantum effects 4-114815  
 power-law fluid, axisymmetric stagnation point flow, mass transfer 4-87765  
 processes, quantum dynamical semigroups, and classical KMS condition 4-68180  
 pseudo first-order reaction diffusion systems, network thermodynamics, dissipative Lagrangian formation 4-99824  
 purely diffusive systems, mode-coupling theory, 1D lattice gas appl. 4-101790  
 pyrene, fluoresc. and diffusion on  $C_{18}$  reversed-phase liq. chromatographic packing 4-112219  
 quantum mechanical diffusion coeff., fundamental constraint 4-101698  
 radiation diffusion, flux limited, one-D calcs. 4-73398  
 radioactive waste, radionuclide time-dependent mass transfer into ground-water 4-106720  
 radionuclide migration, mathematical modelling 4-64199  
 random chain with correlated hopping rates, diffusion const. 4-101793  
 random media, dielectric polarisation methods for coeffs. of same generic type 4-99009  
 random percolating systems, classical diffusion, drift and trapping 4-101778  
 random vel. field, perturbation expansion 4-95358  
 random walks, diffusion at percolation threshold 4-73353  
 reaction-diffusion eqns., spherically symmetric solns. 4-86371  
 recombining particles of two types, asymptotic behaviour of late stages of decay 4-89286  
 separation nozzles, flow and diffusion processes, appls. 4-75068  
 shear flow, tagged particle diffusion tensor in fluids 4-112838  
 soils, moist, unsaturated, heat and mass transfer coeff., diffusion coeff. 4-97556  
 soot particles formation, growth and oxidation, sonic sampling technique and flat flames 4-104990  
 soot particles formation, growth and oxidation 4-104989  
 spherical shell system, facilitated transport, combined Damkohler 4-95355  
 stationary constant coefficient diffusion-convection reaction eqn., difference scheme errors 4-69766  
 stationary diffusion over multidimensional pot. barrier, Kramers' formula generalisation 4-58792  
 stationary random media, diffusion, long time tails appl. using mode-coupling theory 4-101754  
 stationary random media, long time tails 4-73355  
 stationary wave solns. of reaction-diffusion eqn. derived from FitzHugh-Nagumo eqns. 4-71910  
 stellar interiors, neutrinos diffusion coeffs. during core collapse 4-101313  
 stochastic systems, adiabatic elimination of variables 4-73367  
 suspension, concentrated, diffusion of spheres 4-111081  
 terephthalic acid aromatic polyesters solns., conformational props. 4-103636  
 toluene, spin-rot. relax. study of mol. reorientation in presence of rot. diffusion 4-87134  
 transient three dimens. turbulent flowfields press.-vel. finite difference code 4-87682  
 transonic turbulent diffusion transport 4-103457  
 triangular percolation lattice, diffusion, renormalisation study 4-101771  
 turbulent shear flows, passive scalar diffusion, statistical theory 4-74997  
 two dimensional random lattice hopping model, diffusion and conduction 4-90492  
 two-dimensional percolation clusters, diffusion-limited aggregation 4-70394  
 unbounded systems, intermittent diffusion, chaotic scenario 4-63676  
 underdamped metastable wells, thermally activated escape, comments and reply 4-58796  
 unimolecular dissociation as diffusion with a radiation boundary condition 4-76994  
 unsteady flow through channel with permeable walls, solute dispersion, vel. distrib. 4-113020  
 vortex chamber, turbulent rot. air flow, particle diffusion 4-97572  
 white dwarf stars, effects of diffusion on surface comp. 4-94754  
 CdS, periodic precipitation in lyophilic colloid, diffusion controlled autocatalytic growth 4-71993  
 CuSO<sub>4</sub> gel medium electrolyte-diffusion and self-diffusion, transition-state theory 4-89339  
 MnCl<sub>2</sub> and MnSO<sub>4</sub> gel medium electrolyte-diffusion and self-diffusion, transition state theory 4-89339  
 SiO<sub>2</sub> colloidal dispersion in nonpolar solvents, light scatt. 4-114837

diffusion coefficient *see* diffusion

## diffusion creep

- creep mechanism maps, expt. 4-93359  
 olive-basalt partially molten aggregates, diffusion creep during hot pressing 4-110137  
 polycrystalline materials, creep at low stresses and intermediate temp., diffusion flow mechanism 4-71701  
 CaTiO<sub>3</sub>, polycryst., viscous creep deform. at elevated temps. 4-103863  
 LaCrO<sub>3</sub>-Cr cermet, high-temp. creep 4-71693

## diffusion in gases

- see also self-diffusion in gases; thermal diffusion in gases*  
 acetylene diffusion through a capillary, nonthermal effect of incoherent IR light 4-79671  
 air pollutant distrib., 2-dimens., convection and diffusion 4-62417  
 air-water gas transfer models 4-75754  
 alkali closed shell ions, repulsive interactions with Ar, Kr and Xe, beam and transport meas. comparison 4-96653

**diffusion in gases continued**

- binary fluid, mutual diffusion coeff. in presence of macroparticles 4-97740  
 closed ampoule vapor crystal growth, mass transfer, one dimensional diffusion model 4-60873  
 excited donor molecule, direct energy transfer 4-96662  
 gas mixtures, barodiffusion 4-69856  
 halogen closed shell ions, repulsive interactions with Ar, Kr and Xe, beam and transport meas. comparison 4-96653  
 n-heptane, electron mobility, diffusion coeff. 4-79711  
 n-hexane, electron mobility, diffusion coeff. 4-79711  
 inert gas mixtures, equilibrium and transport props. at low density 4-97744  
 inert gases, equilibrium and transport props. at low density 4-97744  
 negative differential cond., generalised Einstein relation 4-79710  
 nonstationary Brownian and molecular diffusion, described by wave eqns., variational approach 4-63662  
 n-octane, electron mobility, diffusion coeff. 4-79711  
 n-pentane, electron mobility, diffusion coeff. 4-79711  
 thermosyphon, two-phase flow, noncondensate gas effect 4-97647  
 turbulent combustion, press. effect on mol. gas props. 4-71920  
 Ar<sup>+</sup> and Ar<sup>2+</sup> in Ar, transverse diffusion coeff. 4-83969  
 Br<sub>2</sub> gas diffusion through capillaries, laser control, energy efficiency 4-75113  
 CO-inert gas binary system, diffusion coeffs. and thermal diffusion coeffs 4-103458  
 CO<sub>2</sub> laser mixtures, electron mobility, diffusion coeffs. ratio 4-112374  
 CO<sub>2</sub>, RF excited lasers, electron energy distrib. and transport coeffs. 4-102919  
 CS optically pumped vapour, relax. depend. on detection beam radius 4-64432  
 CsCl, vap. press., viscosity coeff. and interdiffusion coeff. in Ar and He, Ruff-MKW-boiling point method 4-97743  
 Cu atoms, in slotted hollow cathode discharge Cu II laser, diffusion meas. 4-83569  
 H diffusion coeff. in He, interaction pot. 4-103456  
 H, diffusion cross sections in He gas, interatomic pot. 4-103454  
 K vapour, electron charact. energy and momentum transfer cross-section (Korean) 4-79705  
 N<sub>2</sub> diffusion through a capillary, nonthermal effect of incoherent IR light 4-79671  
 N<sub>2</sub>, electron transmission, drift vel. depend. 4-79714  
 N<sub>2</sub>-Ar gas mixture, investigation of viscomagnetic diffusion flux 4-112960  
 N<sub>2</sub>-Ar mixtures, viscous diffusion in mag. field 4-112959  
 N<sub>2</sub>-He gas mixture, investigation of viscomagnetic diffusion flux 4-112960  
 N<sub>2</sub>-He mixtures, viscous diffusion in mag. field 4-112959  
 Na atoms and ions, diffusion coeff. in inert gases 4-75111  
 Ne-Ar, interatomic pot., dilute gas bulk and microscopic props. 4-96638  
 O+H mixture, mutual diffusion coeff. 4-110517  
 O<sub>2</sub>-inert gas binary system, diffusion coeffs. and thermal diffusion coeffs 4-103458

**diffusion in liquids**

- see also *electromigration; self-diffusion in liquids; thermal diffusion in liquids*  
 acetone, aromatic cpds., diffusion, mol. shape mass and dipole moment effect 4-84431  
 air-water gas transfer models 4-75754  
 alkyltrimethylammonium bromide colloids, viscosity, light scatt. studies 4-89344  
 5 $\alpha$ -androstane steroids, mol. tumbling internal rot., diffusion const., NMR 4-61602  
 benzene, in water, limiting interdiffusion coeffs. in water, 298-368K 4-84434  
 benzocyclobutyl, mol. diffusion in alcohol solns., solvation effects 4-83396  
 benzofuran, methyl-substituted, rot. diffusion tensors determ. 4-107332  
 binary fluid, mutual diffusion coeff. in presence of macroparticles 4-97740  
 binary fluid mixture, diffusion coeff. meas. using an optical method 4-75712  
 binary isothermal electrolyte solns., linear vector transport processes (German) 4-108640  
 carbon tetrabromide in di-isobutyl phthalate, temp. depend. of viscosity and interdiffusion coeffs. 4-103980  
 $\kappa$ -carrageenan, aq. soln., light scatt. invest. 4-104622  
 colloids, double layer contrib. to diffusion effects 4-103979  
 compensation effect in diffusion, chem. pot. and entropy 4-65439  
 concentration profiles near a wall at Pr>1 4-97734  
 dissolved-gas diffusion in normal alkanes, corresponding states correl. 4-113683  
 electrolytes, aqueous, diffusion const., intermolecular dipolar spin relax., microdynamical models 4-88321  
 ethanol, aromatic cpds., diffusion, mol. shape mass and dipole moment effect 4-84431  
 ethylbenzene, in water, limiting interdiffusion coeffs. in water, 298-368K 4-84434  
 ferrous alloys, dissoln. in molten pure Al under forced flow 4-92378  
 hard sphere liq. mixtures, diffusion coeff., mol. dynamics simulation 4-92399  
 heptane, liq., diffusion of dissolved CO<sub>2</sub> 4-61120  
 hexafluorobenzene, in water, limiting interdiffusion coeffs. in water, 298-368K 4-84434  
 holographic interferometry student expts. 4-106151  
 ion hydration and mobility in soln. 4-62176  
 liquid suspensions, small electrophoretic mobilities by light scatt. and phase struct. function anal. 4-114844  
 liquid-solid composition, diffusion effects (Russian) 4-113685  
 MBBA, liq. cryst., laser induced thermal grating (Chinese) 4-91523  
 MBBA liquid crystal, diffusion constants meas. by forced Rayleigh scatt., homodyne detection 4-61718  
 metals, laser glazing, mass transfer, role of diffusion in liq. state 4-71790  
 moving drop with variable surface tension, diffusion 4-80339  
 naphthalene, in di-isobutyl phthalate, temp. depend. of viscosity and interdiffusion coeffs. 4-103980  
 nonideal systems, diffusive permeation rates and selectivity, computer simulation 4-89331  
 nonstationary Brownian and molecular diffusion, described by wave eqns., variational approach 4-63662

**diffusion in liquids continued**

- poly(vinylpyrrolidone)-dextran-H<sub>2</sub>O, structured flow, diffusion coeff. 4-97615  
 poly- $\gamma$ -benzyl-L-glutamate, semidilute solns., diffusion coeffs., dynamic light scatt. study 4-76486  
 poly-m-oxyphenyl benzoxazoterephthalamide moles. in H<sub>2</sub>SO<sub>4</sub>, hydrodynamic props. and conformation (Russian) 4-84438  
 polybutadiene N-mer stars diffusing in highly entangled melt of linear polyethylene 4-112310  
 polydimethylsiloxanes, cyclic and linear, diffusion coeffs. from network sorption meas. 4-113684  
 polyethers, viscosity and diffusion, <sup>1</sup>H<sup>+</sup> nucl. mag. relax. invest. (Russian) 4-104507  
 polyethylene oxide, diffusion in water, mol. wt. depend., light scatt. obs. 4-84430  
 polymer chain translational diffusion, universality failure 4-88322  
 polymer membrane, formation mechanisms, diffusion during precipitation process 4-61912  
 polymer solns., semi-dilute, diffusion, conc. depend. 4-88849  
 polyoxyphenylbenzoxazol terephthalamide in soln., macromolecular hydrodynamics and conformation (Russian) 4-79919  
 polystyrene charged spheres in dilute soln., fluorescence labeled, electrolyte friction meas. 4-98323  
 polystyrene in dibutylphthalate, cooperative diffusion of semi-dilute solns., conc. solns. and swollen networks 4-61122  
 polystyrene in toluene and methyl ethyl ketone soln., conc. fluctuation dynamics 4-103637  
 polystyrene latex, aq. solns., diffusion temp. depend., light scatt. 4-80275  
 polyvinylidene fluoride-PTEF copolymer, randomly branched, vol. effects on hydrodynamic dims. (Russian) 4-102839  
 positronium, reactions and tunnelling in liquids 4-66606  
 serum albumin soln., bovine, osmotic susceptibility, mutual diffusion coeff. 4-72205  
 solid-liquid metal interaction, phase layer formation, effect of gravity 4-70386  
 solutions, concentration fluctuations, acoustic wave propag. and light scatt. 4-92302  
 synchrotron radiation, X-ray beam lines, high flux, grain boundary diffusion of coolants 4-95626  
 Tempone in glycerol, mol. motion, two dims. electron spin echo spectra 4-109055  
 terephthalic acid aromatic polyesters solns., conformational props. 4-103636  
 terephthaloyl chloride-1,10-decanediol spin-labelled copolymer in soln., mol. mobility, ESR study 4-112308  
 n-tetradecane, aromatic cpds., diffusion, mol. shape mass and dipole moment effect 4-84431  
 tetramethyl ammonium ion-paramagnetic anion pair, motion in aq. solns., NMR study 4-88735  
 toluene, in water, limiting interdiffusion coeffs. in water, 298-368K 4-84434  
 tracer diffusion coeffs., solute solvent interaction effects 4-103981  
 volatile solutes, diffusion coefficients, resistometric methods 4-65427  
 water, diffusive motions, incoherent quasielastic neutron scatt. 4-108639  
 CO<sub>2</sub> in aq. soln., diffusion, isotope fractionation meas. 4-87226  
 Ce(NO<sub>3</sub>)<sub>3</sub> aq. soln., diffusion coeffs. at 35°C 4-70422  
 Fe-C, dissoln. in molten pure Al under forced flow 4-92378  
 Fe-Cr(Si), dissoln. in molten pure Al under forced flow 4-92378  
 Ga-P solution-melt system, diffusion coeff. determ. by X-ray microanalysis 4-83820  
 HCl aq. solns., fast H<sup>+</sup>-ion motion, neutron scatt. study 4-80278  
 He, liq., surface, diffusion of H atoms 4-88357  
 In, liquid, solubility and diffusivity of oxygen 4-92373  
 LiF-AlF<sub>3</sub> cryolite melts, interdiffusion 4-88324  
 LiF-KF eutectic melt, oxide ion anodic behaviour at glassy C electrode 4-66594  
 Mg(OH)<sub>2</sub>, periodic crystallisation in agar-agar gel, temp. depend. 4-66621  
 Ni, molten, diamond form. and C diffusion coeffs. 4-105013  
 O<sub>2</sub>, diffusion in water and hydrocarbons, ESR spin-label obs. 4-65423  
 Si:As(Sb)(In), ion implanted, pulsed electron beam annealing, impurity diffusion 4-103984  
 Sn, liquid, solubility and diffusivity of oxygen 4-92373  
 SrF<sub>2</sub>, electrolyte crystals in supersaturated aqueous soln., crystal growth kinetics 4-114373  
 W-Ni alloys, liq. phase sintering, chem. induced migration of molten Ni films between W grains 4-114435  
 ZnCl<sub>2</sub> aq. soln., diffusive motions, incoherent quasielastic neutron scatt. 4-108639

**diffusion in plasma** see *plasma transport processes***diffusion in solids**

- see also *electromigration; ionic conduction in solids; self-diffusion in solids; surface diffusion*  
 actinide carbides, point defects and transport props. 4-98097  
 aggregates, diffusion limited, dynamical scaling and growth 4-113644  
 alkali alkaline earth phosphate glasses, He migration, thermal expansion, glass transition temp. 4-108661  
 alkali metal halides, diffusion along grain boundaries and dislocations 4-92439  
 alkali silicate glasses, ion bombard., alkali depletion, ion beam mixing 4-70239  
 alkali silicate glasses, ion irradi., glass comp. modification by alkali ion migration 4-70238  
 alloys, dilute, free enthalpy of impurity-vacancy binding, solvent diffusion meas. 4-84465  
 amorphous semiconductor, physico-chemical props., review 4-93038  
 anisotropic diffusion of point defects to edge dislocations 4-104007  
 anodic oxide films, diffusion and transport numbers 4-104001  
 anthracene, single cryst., singlet exciton transport transient grating meas. 4-65611  
 atomic mixing, collective atom current concept 4-80284  
 atomic mixing induced by ion beams, atomic collisions 4-80118  
 austenite, cementite dissoln., computer simulation 4-71653  
 austenitic alloys, He bubbles at grain boundaries 4-108471  
 benzene, adsorption in Na mordenite, quasielastic neutron scatt. study 4-92537  
 bi-disperse media, diffusion, effective medium approach 4-65430  
 bicrystals, two-phase, oriented, prod. by diffusion bonding technique 4-61244

# diffusion in solids continued

- binary interdiffusion, frame of reference and intrinsic diffusion coeffs. 4-65436
- ceramics, stress assisted hot form. 4-76728
- chalcogenide glasses, electron microscopy of reactions with metals and electron beam induced crystn. 4-80315
- chemical diffusion coeff. calcs. 4-84468
- chemical driving force, role in discontinuous coarsening 4-113651
- coarsening models, incorporating both diffusion geometry and volume fraction of particles 4-61936
- compensation effect in diffusion, chem. pot. and entropy 4-65439
- conference, Alanya, France (June-July 1982) 4-95052
- conference, Bombay, India (Jan. 1984) 4-67864
- Cottrell atmospheres of impurities, dislocation interactions, internal friction and US meas. 4-65486
- cyclohexane, diffusion and sorption in SBS and SBR copolymers 4-113724
- cyclohexane, NMR echoes of slow motion region 4-104511
- defect mechanism, diffusion under high pressures 4-65435
- dislocation effects on diffusion in crystals 4-65438
- dislocation-particle elastic interactions, diffusionaly-modified 4-98125
- disordered media, atomic particle delocalisation effect 4-92405
- disordered systems, elec. cond. and diffusion processes, freq. depend. 4-61356
- disperse systems, concentration distrib. during diffusion 4-70428
- dye adsorption on SiO<sub>2</sub>, aq. soln.-solid diffusion model 4-65546
- electron probe analysis, detection limit, vol. and surface impurity diffusion effects 4-99918
- epoxy resins, interaction with water, glass transition temp. depression 4-89157
- epoxy resins, water sorption and diffusion 4-81470
- FCC metals, diffusion activation energies using Morse pot. function 4-84445
- FeCrAlloy, Fe-Cr-Al, D permeation 4-111754
- Fick's laws, conc. depend. 4-63457
- fusion reactor materials, nucleation of voids and precipitates under cascade damage 4-103794
- gas diffusion in imperfect crysts., effective coeff. determ. in time depend. expts. 4-65433
- gas transport through polyethylene membranes 4-112992
- glass, borosilicate, neutron absorbing material, diffusion anal. of T thermal release 4-75536
- glass, reactivity in aqueous solns., leaching of simulated radioactive waste glass 4-93548
- glassy materials, temp. coeffs. of transport props. 4-92409
- Gorsky relaxation of light interstitials, linear response anal. 4-75613
- grain boundary diffusion, struct. props. and point defect mobility, mol. dynamics simulations 4-80305
- graphite fibre reinforced epoxy, angle-ply laminates, long-term moisture absorpt. 4-76882
- graphite-alkali metal intercalation cpds. stage-one, Thomas-Fermi density functional theory 4-92131
- Hastelloy X, oxidation, thermal cycling, H permeation, acoustic emission 4-76905
- Hastelloy XR for HTGR, H<sub>2</sub> permeation in simulated reactor environment 4-75732
- n-hexane sorpt. in polystyrene, time-temp. superposition 4-81469
- high temperature creep and diffusion, nonstoichiometry depend. 4-92440
- hot isostatic pressing all diffusion bonding 4-89239
- 2-hydroxyethylmethacrylate-methylmethacrylate copolymers; water sorption and desorption 4-88348
- ice:muonium single crystal. hyperfine interaction and spin relax. 4-65924
- implantation as tool to introduce tracer 4-65432
- impurity particle kinetics in low-temp. matrices 4-92434
- Incoloy 800 H, oxidation, thermal cycling, H permeation, acoustic emission 4-76905
- Incoloy 802, H<sub>2</sub> permeation inhibition by corrosion oxide layers (German) 4-66506
- Inconel sheathed Nicrosil, thermocouples, failure mode, SIMS anal. 4-111125
- InP:Zn epitaxial layers, MOCVD grown, doping, Hall effect, SIMS, electrochemical profiling 4-80077
- integrated optics, diffused thin films, realisation and meas. 4-103025
- interstitial atom soliton state (Ukrainian) 4-88351
- interstitial impurity diffusion in crystals under action of shock waves 4-65342
- ion propagation in crystals, diffusion coefficient, Monte Carlo simulation 4-88332
- ionic conductors, nonequilibrium steady states of stochastic lattice gas 4-73385
- ionic crystals, simple diffusion model for charge transport by moving dislocations 4-75448
- LiNbO<sub>3</sub> optical waveguides, out-diffused, fabrication at low temps. in molten salts 4-112569
- mass transfer, kinetics, across interface, effect of surface processes 4-98464
- mass transfer coeff. of gases and vapours in polymers, extremal and anomalous temp. depend. (Russian) 4-84442
- metal matrix composites, fabrication, book contrib. 4-66276
- metal overlayer/metal structures, sputtering, AES and EELS studies 4-76617
- metal-insulator transition, kinetic coefficients, DC cond. and diffusion 4-80501
- metal/insulator/metal structure formation, upper electrode effects 4-61466
- metallic bilayers, ion mixing, chemically enhanced diffusion 4-92445
- metals,  $\pi^+$  diffusion 4-84891
- metals, anomalous fast diffusion 4-65440
- metals, BCC and FCC, H and He impurities, self-trapping phenomena 4-80056
- metals, BCC migration process of H isotopes calc. 4-65465
- metals, corrosion, high temp., role of diffusion of sulphides 4-66509
- metals, D implanted, reemission and permeation 4-113721
- metals, diffusion and conc. of H, electrochem. permeation method (Japanese) 4-65467
- metals, diffusion coeff. and conc. of dissolved H, electrochem. permeation method (Japanese) 4-65466
- metals, diffusion coeff. and conc. of dissolved H, electrochemical permeation method (Japanese) 4-65468
- metals, diffusion of C, N and O, review 4-65474
- metals, diffusion of H, trapping model analysis 4-70470

# diffusion in solids continued

- metals, diffusion of positive muons and light particles 4-65893
- metals, diffusion of very light particles, NMR studies 4-65472
- metals, grain boundaries, diffusion mechanisms, review 4-65492
- metals, light atom diffusion and tunnelling 4-65473
- metals, mass transfer during pulse loading 4-70429
- metals, muon motion, appl. of quantum theory of diffusion 4-65892
- metals, muon motion, limitations of diffusion approx. 4-65897
- metals, positive muon diffusion theory, at low temps. 4-65898
- metals, pure, impurity diffusion, models, review 4-65471
- metals, pure, two-phase oxide growth 4-98047
- metals and alloys, book contrib. 4-113689
- metals and alloys, diffusion, conf., Tihany, Hungary (Aug.-Sept. 1982) 4-63405
- metals and semiconductors, low temperature oxidation, Cabrera-Mott theory anal. 4-104910
- models, enhancements and retardations, book contrib. 4-84467
- muon localisation and trapping, kinetics and dynamics 4-65891
- Nicrosil, stainless steel sheathed, failure mode, SIMS anal. 4-111125
- Nilil, Inconel sheathed, thermocouples, failure mode, SIMS anal. 4-111125
- Nilil, stainless steel sheathed, thermocouples, failure mode, SIMS anal. 4-111125
- nonequilibrium sorption dynamics with allowance for longitudinal diffusion 4-88403
- nonstoichiometric compounds, transport processes, conf., Cracow, Poland (Aug. 1980) 4-95060
- nuclear fuel, fission product behaviour under normal and accident conditions, improved model 4-74032
- nylon-6 membranes, grafted, permeability of KCl, selectivity 4-114832
- nylon-6 membranes, grafted, permeability of urea and KCl, selectivity 4-114831
- optical fibres, H<sub>2</sub> diffusion constant temp. and press. depend. 4-107861
- optical fibres, single mode, H<sub>2</sub> exposure, long-term loss stability, expt. study 4-83704
- oxide, exchange of O between gas and solid, electrochemical study 4-98357
- oxides, binary and ternary, point defects and transport props. 4-98366
- oxides, chemical diffusion coeff. calcs. 4-98370
- oxides, defect energetics and nonstoichiometry 4-92201
- oxides, diffusion and association of defects 4-98363
- oxides, non-stoichiometric, segregation and chem. diffusion 4-98297
- oxides and carbides, diffusion along grain boundaries and dislocations 4-92439
- phase coarsening, statistical mechanics study 4-113573
- PMMA films, ion beam induced decomp. and diffusion 4-70234
- poly(vinyl alcohol) networks, swollen, diffusion of bovine serum albumin, diffusive props. 4-81472
- poly-para-phenylene, 'conducting' oriented fibres, synthesis, struct. and AsF<sub>5</sub> doping 4-65666
- polyacetylene, electrochemical doping, transient effects, EPR obs. 4-84846
- cis-polyacetylene, Li doping, diffusion EPR and Raman study 4-88345
- polyacetylene films, doped, morphology-props. correlations 4-80306
- polycrystalline film, impurity diffusion, Monte Carlo calcs. 4-108660
- polycrystalline solids, grain-boundary diffusion study (Russian) 4-80309
- polyethylene films, treed and crosslinked, anal. of water 4-71281
- polymer composites, fluid absorpt., NMR imaging 4-109584
- polymer films, solvent diffusion, oscillatory diffusion expt. 4-81468
- polymer microballoons, interferometric meas. of D<sub>2</sub>, T<sub>2</sub>, Ar gas permeability 4-70469
- polymer systems, multiphase 4-84441
- polymer-metal adhesion compounds, spontaneous increase in strength 4-81396
- polymer-polymer diffusion couples, intrinsic and interdiffusion coeff. 4-80312
- polymers, glassy, diffusivities. dual model sorption model 4-81463
- polymers, glassy, model for diffusion 4-84463
- polymers, non-Fickian transport, statistical anal. 4-70561
- polypropylene, highly oriented, sorption and diffusion of toluene 4-65553
- porous materials, Ra diffusion coeff. determ. 4-75504
- profile determ. by sputtering techniques 4-65432
- quartz, hydrothermally weakened, plasticity and rheology 4-92286
- quartz, natural, struct. defects and impurities diffusion 4-80055
- radioactive isotope method, mathematical anal. (Russian) 4-92431
- radioisotope diffusion in metal grain textures, finite element formulation 4-73399
- radiotracer techniques in solid-state physics, book contrib. 4-84443
- refractory metal silicides, AES, principal component anal. 4-77041
- Schottky-barrier diode, EBIC contrast from individual surface-parallel dislocations, temp. depend. 4-103749
- semiconductor, diffusion coefficient, rel. to conc. (Rumanian) 4-70467
- semiconductor, near surface layer, role in diffusion studies 4-98333
- semiconductor impurity diffusion simulation, adaptation of stiff methods 4-75734
- semiconductor-metal boundary, radiation and voltage effects on interlayer props. (Russian) 4-104316
- semiconductors, electronic and atomic diffusion, D grad  $\nu$  and grad(D $\nu$ ) descriptions 4-104195
- semiconductors, heterogeneous anisotropic, electrodiffusion purification 4-71533
- semiconductors, impurity atom diffusion, two-dimensional numerical anal. 4-92432
- semiconductors, microkinetics of two-component diffusion 4-88350
- semiconductors, surface diffusion impurity profiles, consecutive diffusion 4-70184
- n-Si, radiation defect formation, annealing, defect interactions 4-113499
- silica glasses, diffusion of water at low temp. 4-84464
- silicate glasses, thermotransport, at migration process under effect of temp. gradient 4-80283
- silicide formation, radioactive marker, mathematical model 4-92404
- silicides and germanides with FeB and ZrSi<sub>2</sub> structures, texture in diffusion-grown layers 4-61147
- sintering, diffusional activated, quantitative theory 4-76704
- soda-lime silicate glass, stress relax. and ion exchange 4-108284
- solid solutions, phase stability under irradiation, ballistic effects 4-103796
- solid state chemistry, conf., Veldhoven, Netherlands (June 1982) 4-67863
- solid-liquid metal interaction, phase layer formation, effect of gravity 4-70386

## diffusion in solids continued

- solid/solid interfaces, computer simulations, conf., Philadelphia, USA (Oct. 1983) 4-110806
- solvent diffusion in shrinking or swelling bodies, differential eqn. 4-75716
- stainless steel, permeation of T, suppression by Au(Ni) plating 4-61261
- steel, austenitic stainless,  $^{60}\text{Co}$  tracer diffusion 4-75731
- steel, austenitic stainless, D permeation, plasma-driven, effect of surface comp. 4-113718
- steel, austenitic stainless, Incoloy 800,  $\text{H}_2$  permeation inhibition by corrosion oxide layers (German) 4-66506
- steel, austenitic stainless, repassivation kinetics, effect of Mo alloying 4-81331
- steel, austenitic stainless, swelling incubation, effect of microchem., microstruct. and environmental mechanisms 4-108413
- steel, austeno-ferritic stainless, sulphidation kinetics, triplex scale form. 4-109560
- steel, C, boronising, electrolytic, boride phase form. kinetics 4-71781
- steel, Cr-Mn, diffusion reaction with Al coating, Si content effect 4-114723
- steel, H and D diffusion under fission reactor radiation 4-113503
- steel, H corrosion, theory of void growth limited by C diffusion 4-81338
- steel, low C, Al clad, reaction diffusion, intermetallic layer growth kinetics 4-114722
- steel, martensitic transformation in alloy 40N25, diffuse-mobile H effects (Russian) 4-104780
- steel, mild, fretting fatigue rel. to diffusion coatings from Ni-Co electrodeposits 4-114686
- steel, of W, during electrolytic plasma coating process (Russian) 4-71775
- steel, pearlite growth, by combined vol. and phase boundary diffusion 4-114470
- steel, sintered, Mn diffusion coatings 4-89186
- steel, stainless, H transport 4-113722
- steel, stainless,  $\text{TiO}_2$  sputter coated, H embrittlement prevention 4-62033
- steel, stainless, type 316, with  $\text{TiC}$  coating, void form. near interface by diffusion annealing 4-109557
- steel, structural 45, boronisation, B diffusion processes (Russian) 4-93311
- steel, sulfidizing corrosion protection by  $\text{Al}_2\text{O}_3$ , diffusion model 4-93467
- steel, tribologically induced effect of H effusion and penetration 4-109521
- stilbene, mol. cryst., triplet exciton  $\alpha$  particle excitation, diffusion coeff. 4-104130
- structural alloys, austenitic, T permeation barrier development 4-113717
- structural alloys, H isotope permeation 4-113720
- supersaturated alloys, spherical precipitates, growth kinetics anal. 4-61939
- surface exposed to fusion reactor plasmas, steady state H transport 4-74041
- ternary solid solutions, solutions with diffusion coeff. linearly dependent on conc. 4-113690
- ternary systems, interdiffusion coeff. calc. using computer program (Korean) 4-75735
- TEXTOR first wall charact. w.r.t. H recycling 4-91968
- textured materials, kinetic props., grain interaction effects 4-60938
- theoretical model of diffusion bonding 4-114762
- thin film analysis by low energy proton induced X-ray emission 4-109705
- tracer diffusion, continued fraction expansion, exact soln. 4-88331
- transition metal carbides, point defects and transport props. 4-98097
- transition metal oxides, impurity diffusion and impurity-defect interactions 4-92436
- transition metal oxides, nonstoichiometric, point defects and diffusion 4-98096
- transition metal oxides and sulphides, chemical diffusion studies 4-98347
- transition metal silicides on Si, thermal oxidation and diffusion, review 4-66464
- VA transition metal oxides of V, Nb, and Ta, oxidation mechanism, phase form., cryst. struct., electron microscopy, electron and X-ray diff. studies 4-62119
- vacancy mechanism for self-diffusion and tracer diffusion, phenomenological anal. 4-113692
- VLSI technology, textbook 4-82610
- zeolites, synthetic, surface diffusion of metals, in vacuo, in presence of active gases 4-98415
- Zircaloy membrane, D transport kinetics, surface oxides influence 4-89325
- Zircaloy-4, SAM determ. of O gradients, deform. modelling 4-88191
- Zircaloy-4/ $\text{UO}_2$  chemical interaction 4-83140
- Zircaloy-4/ $\text{UO}_2$  diffusion couple, interfacial energy and work of adhesion 4-83141
- Ag, impurity diffusion, isotope effect meas. 4-65476
- Ag-Mg(Cu), internal oxidation mechanism 4-93305
- AgCu, conc. layered amorphous thin films, diffusional mixing, elec. resist. meas. 4-92687
- ( $\text{AgI}_x$ )( $\text{Ag}_2\text{O} \cdot \text{B}_2\text{O}_3$ ) $_{1-x}$  superionic glasses, EXAFS studies 4-60855
- Al bicrystals, grain boundaries diffusivity 4-65485
- Al, diffusion of  $^{65}\text{Zn}$ , effects of hydrostatic press. 4-65483
- Al, diffusion of H, desorption study 4-65489
- Al, diffusion of Mo and W 4-65477
- Al, electron irradi., incoherent tunnelling of positive muons and trapping by vacancies, muon spin relax. meas. 4-65909
- Al, muon trapping by dislocations, spin depolarisation rate meas. 4-65911
- Al/Ag system, react diffusion, effect of high press. 4-108666
- Al/Mo thin films, reactions 4-61148
- Al/NiSi(PdSi)(PtSi) Schottky barriers, Cr diffusion barrier 4-88352
- Al-Ag, solubility of Ag in Al, effect of high press. 4-81179
- Al-Au(Cu) thin film bilayers, ion beam bombarded, interfacial phase formation 4-70241
- Al-Cr thin film couple, diffusion barriers, Auger study 4-88407
- Al-In; dil., He localised diffusion around In impurities, PAC obs. 4-65470
- Al-Mg, dil., muon spin relax. 4-65907
- Al-Mg (0.047 at. %), dil., positive muon spin relax. meas., diffusion, trapping and detrapping 4-65908
- Al-Mn dilute alloys,  $^{65}\text{Zn}$  diffusion 4-65482
- Al-Si interdiffusion ohmic contact achieved by capacitance discharge (Chinese) 4-98752
- Al-SiO $_2$ -Si MIS structures, with plasma deposited SiO $_2$ , alkali ion motion, C-V charact. (Russian) 4-114042
- Al-steel interface, Al diffusion, mech. activation effects 4-61151

## diffusion in solids continued

- Al-Zn (Cu)(Mg), dendritic solidification and segregation in accordance with Krupkowski's formula (Polish) 4-85146
- $\text{Al}_{0.8}\text{Ga}_{0.2}\text{As}/\text{GaAs}/\text{Zn}$  diffused superlattice, X-ray rocking curve and backscatt. studies 4-113818
- $\alpha\text{-Al}_2\text{O}_3$ , diffusion coeff. of S, glow discharge spectrometry (French) 4-80300
- $\text{Al}_2\text{O}_3\text{-Cr}$ , grain boundary diffusion, anisotropy and doping effects 4-92443
- $\alpha\text{-Al}_2\text{O}_3\text{-Cr}_2\text{O}_3(\text{Y}_2\text{O}_3)$ , ionic cond., doping effects 4-92417
- $\text{Al}_2\text{O}_3\text{-ZrO}_2\text{-SiO}_2$  refractory, corrosion by Pb glass 4-71753
- Ar crystals, low temp. internal friction 4-60987
- $\text{As}_2\text{S}_3/\text{Ag}$ , photostimulated diffusion kinetics (Russian) 4-70471
- Au, diffusion of He 4-65488
- Au films deposited by electron beam evaporation or sputtering; Si outdiffusion, annealing ambients effects 4-70459
- Au, impurity diffusion, isotope effect meas. 4-65476
- Au on GaAs, alloying behaviour 4-80454
- Au thin films, diffusion of Fe, Ni and Co, XPS study 4-81115
- Au/Cr bilayers on GaAs, interfacial chemical reactions and drive-out diffusion, AES study 4-80313
- Au/Fe interface boundary, interdiffusion 4-65497
- Au/Ga thin film couples, room temp. interdiffusion 4-61149
- Au-Ag thin film, grain boundary diffusion coeff. from Ag surface coverage, AES 4-92430
- Au-Fe alloys; chemical interdiffusion at interface with Au 4-65497
- Au-Ge/Au ohmic contact struct., grain boundary diffusion of Ge through Au, Auger anal. 4-88344
- Au-Ge(-Ni) on GaAs, alloying behaviour 4-80454
- AuSn diffusion produced alloys, optical props. 4-80897
- AuY(Zr)(Nb)(Rh)(Pt)(Pd), dil. alloys, thermoelectric power, resistivity, low temp. studies 4-113925
- BN film, CVD, on Si, as B diffusion source 4-98359
- BaF $_2$ -He, interstitial diffusion, solubility of He, dissolution energy 4-113727
- BaF $_2$ -LaF $_3$ -ZrF $_4$ -AlF $_3$  glass, crystallisation, devitrification on reheating 4-84194
- BaTiO $_3$ -SrTiO $_3$ , high-temp. reactions, EPMA and SEM investig. 4-80292
- BaZrO $_3$ -BaTiO $_3$ , high-temp. reactions, EPMA and SEM investig. 4-80292
- Bi, muon quantum diffusion, spin relax. rate meas. 4-65900
- Bi, ultrapure, muon diffusion, spin relax. rate meas. 4-80307
- C, amorphous, of metals, in vacuo, in presence of active gases 4-98415
- C foil, implanted with T, prep. and analysis w.r.t. fusion reactor safety 4-91100
- $\text{Ca}^{2+}$ -exchanged montmorillonite, intercalated mol. dynamics, quasielastic neutron scatt. 4-65154
- CaF $_2$ -He, interstitial diffusion, solubility of He, dissolution energy 4-113727
- CaF $_2$ , Pu and U diffusion above and below  $\lambda$  transition temp. 4-70473
- CaO, chemical diffusion coeff. calcs. 4-84468
- $\text{Ca}_{10}(\text{PO}_4)_6\text{F}_2$  fluorapatite, radiation damage and annealing, optical studies 4-70192
- $\text{CaWO}_4$ , structural imperfection, vacancy disordering, diffusive mass transfer 4-75438
- Cd,Hg $_2$ -Te, undoped and In-doped, impurity migration 4-70468
- CdS, electron beam annealing, defects diffusion 4-103801
- CdS:Cu(Cl) films, defect diffusion, luminescence study (Russian) 4-88875
- CdTe, p-type, undoped, thin dielectric films deposition as protection against decomposition during annealing 4-92755
- Co-Sb multilayered films, cpd. form., interface magnetism,  $^{59}\text{Co}$  NMR obs. 4-109095
- Co-Zn system,  $\alpha$ -solid soln., interdiffusion study 4-98368
- CoO, surface morphology changes during vacancy relax. processes 4-75445
- CoO-Cr $_2\text{O}_3$ , non-stoichiometric, segregation and chem. diffusion 4-98297
- $\text{Co}_{1-x}\text{O}$ :Ni single cryst., Ni impurity diffusion and interaction with vacancies 4-92437
- $\text{Co}_3\text{O}_4$ , point defects and transport props. 4-98366
- Cr, permeation of H and D, diffusion, permeability, and solubility (German) 4-103992
- Cr/Si (100) interface, silicide growth kinetics, cross-sectional TEM 4-61146
- Cr $_2\text{O}_3$ , deviation from stoichiometry at high  $\text{O}_2$  partial press. 4-113656
- CrSi $_2$ , form. by ion beam mixing 4-80121
- Cu alloy with Sn electrodeplate, diffusion reaction, effect of additional Fe and Sn 4-71755
- Cu, diffusivity of In along stationary and migrating grain boundaries 4-65484
- Cu, impurity diffusion, isotope effect meas. 4-65476
- Cu, muon mobility below 2K 4-65896
- Cu, muon spin rotation, zero-field, and low temp.  $\mu^+$  diffusivity 4-65894
- Cu, positive muon diffusion studied by zero field  $\mu\text{SR}$  4-65895
- Cu, surface berylliding, Cu-Be diffusion coating formation 4-62127
- Cu, ultrapure, muon diffusion, spin relax. rate meas. 4-80307
- Cu/Al thin film interface reactions, X-ray diff. and Rutherford backscatt. studies 4-88409
- Cu/Ni diffusion couple, bulge and dent zones formation 4-61150
- Cu/Sn-Cu diffusion couple, electron microprobe anal. (Chinese) 4-104008
- Cu-Ni (Al)(Zn), dendritic solidification and segregation in accordance with Krupkowski's formula (Polish) 4-85146
- Cu-Ni-Fe, coarsening of extremely small particles 4-113588
- Cu-Ni-Zn system, diffusion at 775°C, zero-flux planes and flux reversals 4-65496
- Cu-Pb engine bearings, multilayer diffusion barriers 4-98331
- Cu-Sn dil. alloys, vacancy jump freq. ratios 4-65448
- Cu-Ti interface, electron probe anal. of diffusion zones 4-62151
- Cu-Zn, interdiffusion coeffs., high press. effect 4-88353
- CuInSe In-diffused homojunctions, elec. and photovoltaic effects 4-92809
- Fe alloy, diffusion carburizing, growth of carbide fibres 4-93454
- Fe, apparent H diffusivity, effect of cathodic charging current density 4-104005
- Fe base alloys, inoculation particles dissolution, carbide precipitation 4-89057
- $\alpha$ -Fe, Co diffusion, effect of mag. transition 4-65481
- Fe, H electrochemical penetration, effect of As additions to electrolyte 4-66497
- $\gamma$ -Fe, high purity, thermotransport, isotope effect 4-108664

## diffusion in solids continued

- $\alpha$ -Fe, nitriding, heterogeneous, dislocation production and oriented precip. 4-66498  
 Fe, permeation of T, reduction by Al implantation 4-88184  
 $\alpha$ -Fe, positive muon quantum diffusion 4-104516  
 Fe, sintered, apparent diffusion coeff. of C during gas carburising process 4-103989  
 Fe/Ni system, interdiffusion, activation energy and freq. factor 4-65495  
 Fe/Zn system,  $\delta$  phase form. and growth 4-80314  
 Fe-Al alloys, segregation to static and migrating diffuse antiphase boundaries 4-114541  
 Fe-C, high purity, forced velocity pearlite, theoretical 4-93295  
 Fe-C(Cr), austenite, cementite dissol., computer simulation 4-71653  
 Fe-Cr (26.6 at.%), sulphidation mechanism in  $H_2S$ -H<sub>2</sub> atmospheres at temps. of 973 to 1173K and S press.  $10^{-4}$  to  $10^{-6}$  Pa 4-93460  
 Fe-Cu, H permeation in  $H_2SO_4$  with and without  $H_2S$ , electrochem. and surface anal. studies 4-104898  
 Fe-Cu (10 wt.%), powder compacts, liq. phase sintering, dimens. changes 4-66267  
 Fe-graphite, sintering, C absorpt. by Fe 4-114437  
 Fe-graphite, sintering, mechanism of C absorpt. by Fe 4-114438  
 Fe-Ni, H<sub>2</sub> charged, internal friction 4-104802  
 Fe-Ni-C, martensitic transform., B effusion in subzero temp. 4-85153  
 Fe-Ni-Cr-Al-(Y)(Zr)(Ti), high temp. oxidation resist. influence of Y, Zr or Ti additions 4-104899  
 Fe-Ni-P alloys, growth of intragranular ferrite 4-76777  
 Fe-P-C amorphous alloys, B impurity diffusion, SIMS studies 4-92435  
 Fe-Si-C powder compacts, sintered and carburised, graphite growth 4-93306  
 Fe-W dilute alloy wires, diffusion coefficients, resistometric methods 4-65427  
 Fe<sub>3</sub>C, diffusion coeff. meas. 4-98345  
 Fe<sub>3</sub>O<sub>4</sub>, magnetite, diffusion of cations and point defects 4-99378  
 Fe<sub>2</sub>O<sub>3</sub>, point defects and transport props. 4-98366  
 Fe<sub>2</sub>Si/Zn diffusion couples, periodic structs. and two phase band form. 4-65499  
 G, with growing  $\alpha$ -G<sub>2</sub>O<sub>3</sub> films, <sup>18</sup>O/SIMS obs. of O transport 4-89174  
 GaAs/Ni reactive interface, soft X-ray photoemission spectra studies 4-113820  
 GaAlAs buried multiquantum well lasers fabricated by diffusion-induced disordering 4-91452  
 GaAs, crystal and amorphous, pulsed laser irradi. under O<sub>2</sub> and silane atmospheres, O incorporation and losses 4-80091  
 GaAs, ion implanted, ion implanted, diffusion of Be and Mn during damage recovery 4-104002  
 GaAs, laser-induced Si diffusion from deposited Si<sub>3</sub>N<sub>4</sub> film 4-60958  
 GaAs:Mn, Mn redistribution, interstitial-substitutional model anal. 4-92433  
 GaAs:Si, Si diffusion using rapid thermal processing, encapsulant effects 4-65464  
 GaAs:Sn with SiO<sub>2</sub> cap, thermal diffusion, doping mechanism 4-104006  
 GaAs:V, semi-insulating, V redistribution during heat treatment 4-80070  
 GaAs:Zn, reproducible leaky tube Zn diffusion with submicron junction depths 4-98361  
 GaAs:Zn, thermal pulse diffusion of Zn from elemental source 4-98360  
 GaAs/AuGe ohmic contact, Ge and Au profiles, SIMS studies 4-103782  
 GaAs/Ni-Ta interfacial reactions, metallisation appl. 4-98367  
 GaAs-AlAs:Zn superlattice, Zn impurity diffusion, X-ray study 4-75729  
 GaAs<sub>1-x</sub>P<sub>x</sub>, internal elec. field-enhanced impurity diffusion and p-n junction form. 4-84469  
 GaAs(001)-Au interface, formation by MBE and thermal stability 4-99328  
 GaInAsP, defect motion and growth of extended non-radiative defect structs., book contrib. 4-60914  
 Ge, positron diffusion const., temp. depend. 4-99222  
 Ge single cryst. film growth on SiO<sub>2</sub> by laterally seeded heteroepitaxy 4-93234  
 Ge:Cu, impurity states, annealing effects 4-104148  
 Ge:D, plasma treated, D diffusion and interaction with point defects 4-60951  
 Ge:Ga, migration of molten inclusion 4-108659  
 Ge:Si, ultrapure and doped, muonium state, positive muon spin precession signals 4-71242  
 Ge<sub>2</sub>Se<sub>7</sub>:Ag layers, amorphous, photodoped impurity lateral diffusion 4-70464  
 H diffusivity in metals meas. by resistance technique 4-68343  
 H<sub>2</sub> in D<sub>2</sub> solid soln., H and D behaviour at liq. He temp. 4-70517  
 H<sub>2</sub>, mobility on Pd surface during catalytic H<sub>2</sub>O-forming reactions, detection 4-71985  
 He isotropic mixture, configurational relax. and quantum diffusion (*Russian*) 4-70516  
 Hf-Ni films, amorphisation by thin film solid state reaction 4-80428  
 (Hg,Cd)Te/Au overlayer system, deposition, interactions and diffusion, UPS study 4-80439  
 Hg<sub>1-x</sub>Cd<sub>x</sub>Te, Hg diffusion profile meas. by heavy ion backscatt. 4-75730  
 In<sub>0.5</sub>Ga<sub>0.5</sub>As planar diodes, fabrication using open tube method for Zn diffusion 4-95519  
 InP (110)-Cu(Ag)(Au) interface, soft X-ray photoemission study 4-85080  
 InP, open diffusion technique using Zn<sub>3</sub>P<sub>2</sub>, appl. to lateral p-n-p transistor 4-104003  
 InP planar diodes, fabrication using open tube method for Zn diffusion 4-95519  
 InP, semi-insulating, simulation of anomalous Be diffusion 4-88193  
 InP, transition metal diffusion, photoluminesc. study 4-70461  
 InP:Cd crystals, bulk and surface effects of heat treatment 4-84625  
 InP:Fe, thermally annealed, Fe redistribution and diffusion coeff. 4-70460  
 InP:Zn, temp-dependent Zn diffusion mechanism using semiclosed diffusion method 4-80301  
 InP:Zn crystals, bulk and surface effects of heat treatment 4-84625  
 InP/metal interfaces, chem. reactions, photoemission study 4-80310  
 KI, UV irradi., V<sub>K</sub> motion and luminesc. quenching 4-66063  
 LaCrO<sub>3</sub>-Cr cermet, high-temp. creep 4-71693  
 LaNi<sub>5</sub>H<sub>2</sub>, muon diffusion, spin rot. meas. 4-65914  
 LaO<sub>1-x</sub>F<sub>1+x/2</sub>, <sup>19</sup>F NMR study of anion mobility 4-114168  
 Li, muon interactions with lattice defects, mol. cluster calcs. 4-65255  
 Li-Al, T release on heating or NaOH dissolving liq. to Li conc. 4-75733  
 Li-Al electrode secondary cell at room temp., Li-Al alloy electrochemical formation kinetics 4-72059

## diffusion in solids continued

- LiF:U, pure and doped, preferential sputtering and ion induced comp. changes 4-71501  
 LiNbO<sub>3</sub> and LiTaO<sub>3</sub>, waveguide fabrication by proton diffusion from benzoic acid soln. 4-69553  
 LiNbO<sub>3</sub>:Ti, impurity diffusion as a function of stoichiometry 4-80304  
 LiNbO<sub>3</sub>:Ti, indiffused, planar waveguide modes, water vapour effects 4-103008  
 LiNbO<sub>3</sub>:Ti, indiffused, optical waveguides, in-plane scattering 4-112565  
 Li<sub>2</sub>O breeder material, neutron irradi., T release expts. 4-107030  
 Li<sub>2</sub>O single cryst., breeder material, D<sub>2</sub> solubility 4-107025  
 LiTaO<sub>3</sub>:Ti, changes in refractive index due to diffusion 4-99085  
 MgAl<sub>2</sub>O<sub>4</sub>, grain boundary diffusion, anisotropy and doping effects 4-92443  
 Mg<sub>2</sub>Ni-H<sub>2</sub>, H<sub>2</sub> diffusion and localisation, PMR study (*French*) 4-70462  
 MgO, vacancies and multiphonon IR-absorpt. spectra (*Russian*) 4-71420  
 MgO:Cr, grain boundary diffusion, anisotropy and doping effects 4-92443  
 Mg<sub>2</sub>Si form., thin film reaction kinetics, AES and SIMS 4-81131  
 MnO, point defects and transport props. 4-98366  
 Mo, diffusion of N at low temps., internal friction meas. 4-65487  
 Mo diffusion through graphite in HTGR 4-111631  
 Mo-Si interface, silicide form. kinetics induced by ion bombard. 4-61243  
 Mo-Si system, thin-film reactions and phase diagrams 4-88263  
 NH<sub>4</sub>HSeO<sub>4</sub>, high temp. phase transition, ionic motion 4-108651  
 Na, impurity diffusion 4-65475  
 NaCl, anisotropic interface diffusion and precipitation morphology 4-61088  
 NaCl, cryst., X-irrad., F-centre decay during photoannealing 4-80036  
 NaCl, F-centre form., excitonic pot. surface, absorpt. spectra 4-71415  
 Na<sub>2</sub>O-NaF-SiO<sub>2</sub> glass, mol. dynamics simulation 4-98023  
 Na<sub>2</sub>O-SiO<sub>2</sub> glass, electron irradiated, evidence of enhanced diffusion process 4-80108  
 Na<sub>2</sub>O-SiO<sub>2</sub>-H<sub>2</sub>O glass, hygroscopicity study 4-76997  
 Nb, electromigration of Nb, Fe, Co, Ta and Cr 4-65500  
 Nb, electron-irradiated, muon diffusion and trapping by defects 4-65905  
 Nb, H permeation, surface effects 4-113723  
 Nb-Si interface, silicide form. kinetics induced by ion bombard. 4-61243  
 Nb<sub>2</sub>Al, low temp. diffusion, supercond. and struct. props. 4-65498  
 NbH<sub>x</sub>, dynamic muon-H correlations, positive muon as a tracer 4-65431  
 NbH<sub>x</sub>, H permeability and struct. (*Russian*) 4-65406  
 2H-NbSe<sub>2</sub>:In, in thermal diffusion 4-88347  
 Nb<sub>2</sub>Sn, growth kinetics by bronze process 4-114451  
 Nb<sub>2</sub>Sn, multifilamentary bronze composites, diffusion reaction growth kinetics, supercond. critical temp. 4-76064  
 Nb<sub>2</sub>Sn phase formation, influence of thermal regime of multifilamentary wire prep. 4-76063  
 Ni, D implanted, reemission and permeation 4-113721  
 Ni, H permeation and diffusion, effect of press. modulation on flow of gas through solid membrane 4-65469  
 Ni, light purity, reaction mechanism with O<sub>2</sub>+SO<sub>2</sub>, grain boundary diffusion in scale 4-109561  
 Ni, monocrystals, volume diffusion of simple and transition metal impurities 4-65478  
 Ni powder, low-temp. diffusion, positron annihilation study 4-98365  
 Ni, thermodynamics, kinetics and props. of gases and C, data tables 4-73173  
 Ni/Si interfaces, silicide form., atom-probe study 4-70475  
 Ni-Al, internal oxidation, O transport at high temps. 4-92442  
 Ni-Au films, ion-induced comp. change, role of grain boundary diffusion at elevated temps. 4-108475  
 Ni-Co, oxidation, parabolic growth of oxide solid solutions 4-109563  
 Ni-Cr, internal oxidation, O transport at high temps. 4-92442  
 Ni-Cr, Cu diffusion after dynamic and static deformation (*Russian*) 4-108658  
 Ni-Cu fine particle mixture, sintering vel., collective effects during diffusion interactions 4-61887  
 Ni-P, amorphous alloys, B impurity diffusion, SIMS studies 4-92435  
 Ni-Si (111) interface, Ni<sub>2</sub>Si islands growth, ion scatt. study 4-92444  
 Ni-Ti foils, electron irradi., precipitation characts. 4-108625  
 Ni-Yb films, ion beam mixing, radiation enhanced diffusion by Kr<sup>+</sup> and O<sub>2</sub><sup>+</sup> bombard. 4-103832  
 Ni-(Cr), oxidation, SIMS and XPS study of thermal oxide films 4-76908  
 Ni<sub>3</sub>Fe<sub>1-x</sub>O<sub>4</sub>, cation-site occupancy, effect of Ni content 4-98079  
 NiO, chemical diffusion coeff. calcs. 4-84468  
 NiO, interaction with O<sub>2</sub>, H<sub>2</sub>S and SO<sub>2</sub>, surface and vol. processes 4-98372  
 NiO, NiO-Cr<sub>2</sub>O<sub>3</sub>, non-stoichiometric, segregation and chem. diffusion 4-98297  
 NiO:CeO<sub>2</sub>, oxidation and grain boundary diffusion 4-92441  
 NiO-O<sub>2</sub>, interaction, elec. cond., thermal flux 4-98627  
 NiSi, Ni<sub>2</sub>Si, thin films, metal silicide form., AES and SIMS study 4-75795  
 NiSi thin film form. in Ni<sub>2</sub>Si/Si system, diffusion mechanisms 4-92446  
 Pb<sub>1-x</sub>Eu<sub>x</sub>Te, MBE growth and elec. and optical props. 4-81142  
 Pb<sub>1-x</sub>Ag<sub>x</sub>, exciton spectrum, photodoping effects (*Russian*) 4-92626  
 PbS<sub>1-x</sub>Se<sub>x</sub>, DH diode lasers fabricated by compositional interdiffusion 4-102952  
 PbTiO<sub>3</sub>-PbZrO<sub>3</sub>, high-temp. reactions, EPMA and SEM investig. 4-80292  
 Pd-H, H diffusion, induced Hall voltage 4-70463  
 Pd-Al alloys, T mobility and permeability, influence of struct. of segregation overlayers 4-70472  
 Pd-Si(111) interface, atomic intermixing and electronic interaction 4-70478  
 Pd<sub>3</sub>Au<sub>3</sub>Si<sub>3</sub>, amorphous alloy, crystn., SAXS study 4-65186  
 $\alpha$ -PdH<sub>2</sub>, Gorsky effect and diffusion coeffs. 4-75614  
 PdH<sub>2</sub>, muon diffusion, spin rot. meas. 4-65914  
 Pt layer on graphite and RuO<sub>2</sub> substrates, ion bombard., electrocatalytic props. 4-71968  
 PtSi, Pt<sub>2</sub>Si, thin films, metal silicide form., AES and SIMS study 4-75795  
 PuO<sub>2-x</sub>, O<sub>2</sub> diffusion meas. 4-98369  
 RbHSeO<sub>4</sub>, high temp. phase transition, ionic motion 4-108651  
 Rn, exhalation and diffusion from building materials 4-93908  
<sup>\*</sup>Rn, A=220, 222, diffusion and exhalation from building materials 4-93901  
<sup>\*</sup>Rn, A=220, 222, emanating power and specific surface area of building materials 4-93907

## diffusion in solids continued

- <sup>222</sup>Rn exhalation from porous materials, diffusion transport theory 4-93911
- Si, atomic diffusion mechanisms theory 4-70430
- a-Si, atomic partial delocalisation effect in disordered media 4-92405
- Si CMOS active lateral diffusion and linewidth test struct. 4-108665
- Si crystals, Czochralski pulled, O precipitation, diffusion mechanism, etching optical and neutron scatt. obs. 4-65209
- Si, defect and carrier lifetime, back-surface damage gettering technique 4-113972
- Si, disorder profiles at high sputtering dose by oxide growth rate profiling 4-66470
- Si, excess interstitial distribution during thermal oxidation, two-dimensional model 4-84286
- Si film, polycryst., ion implanted, dopant diffusion (*Russian*) 4-108657
- Si, impurity diffusion, fraction of interstitial mechanism 4-80308
- Si, impurity diffusion, impurity conc. doping effects 4-113728
- Si, impurity migration, effect of elastic stresses 4-88349
- Si, intrinsic point defects and diffusion processes 4-108358
- Si, MBE growth, use of In for surface cleaning 4-99616
- p-Si, O low-temp. diffusion coeff. 4-70458
- Si with adsorbed Ag, growth and diffusion, SEM, study 4-80417
- Si:Al, electronically simulated defect migration 4-113730
- Si:As, P, B, ion implanted, fast isothermal annealing and elec. props. 4-92224
- Si:As, P, ion implanted, diffusion modelling 4-113729
- Si:As, shallow implants, depth profiling using SIMS 4-108408
- Si:As thin films, As fast diffusion during rapid thermal annealing 4-113714
- Si:As/Al interface, sintering and diffusion, As dopant effect 4-80427
- Si:As/Ti interface, As implantation, As out-diffusion during TiSi<sub>2</sub> formation 4-65493
- Si:As<sup>+</sup>(BF<sub>3</sub>), implanted, rapid thermal annealing 4-88181
- Si:Au, effect of mobile dislocations on surface saturation (*Russian*) 4-98107
- Si:B, P, compensated semiconductors, coalescence process, effect and rad. and heat treatment 4-65288
- Si:B, retardation of B diffusion 4-88346
- Si:B(P)(As), dopant diffusion, numerical soln. by solving impurity, vacancy and self-interstitial continuity eqns. 4-80303
- Si:C, self-interstitial enhanced C diffusion 4-98358
- Si:Ge, bulk impurity diffusion, SIMS study 4-70465
- Si:Ge, Ge diffusion, isotope effects, SIMS studies 4-65491
- Si:Ge, Ge diffusion and conc. profiles, SIMS studies 4-65490
- Si:H, Al-covered, solid-state reaction between film and substrate 4-92498
- Si:H, dislocated, impurity exodiffusion 4-103788
- Si:H, lattice state and behaviour of H impurity 4-61095
- Si:muonium, interstitial atom mobility, radiation defect effects 4-65256
- Si:N, B diffusion profile 4-113726
- Si:N, low energy implant depth profiles, surface peak, Auger studies 4-80074
- Si:N(O), microdefect formation during single crystal growth, influence of impurities on nucleation 4-114386
- Si:P, diffusion study, influence of internal electric field 4-108662
- Si:P, ion implanted, diffusion during rapid thermal annealing 4-113713
- Si:P, P diffusion from solid source for solar cell fabrication 4-77085
- Si:P, Sb, P diffusion, self-interstitial supersaturation and vacancy under-saturation 4-70457
- Si:P, Cl<sup>+</sup>, Cl<sup>+</sup> implantation effects on oxidation enhanced P diffusion 4-92429
- Si:S, deep levels, DLTS meas. 4-84592
- Si:Sb, electrolytical Sb diffusion in MQS structures 4-80299
- Si:Xe, implanted Xe reemission by He<sup>+</sup> ion bombardment 4-75462
- Si/Ag system, atomic mixing using 45 keV Ar<sup>+</sup> ion beam 4-80119
- Si/Al interface, atomic redistributions, XPS studies 4-80311
- Si/Au interface, atomic redistributions, XPS studies 4-80311
- Si/methanol liquid junction, open circuit volt. and oxide form. 4-114030
- Si/Pd-Si system, contact growth and elec. charact., dry etching effects 4-104313
- Si-Er interface, ErSi<sub>3</sub> formation using electron beam heating 4-65494
- Si-metal struct., scanning-tunnelling microscopy, voltage drop 4-114038
- Si-SiO<sub>2</sub> interface, B drive diffusion in oxidizing ambients, segregation coeff. determ. 4-75690
- Si-Ti interface, TiSi<sub>2</sub> formation by fast radiative processing 4-113731
- SiC, CVD coating, fusion reactor first wall material, permeation of H 4-92403
- SiC, reaction bonded, and liq. Al, cast bonding, exchange diffusion phenomenon involving free Si 4-99741
- SiC:Al, B(Be), interstitial diffusion studies 4-80302
- p-SiC:B, diffusion, track autoradiography studies 4-84466
- Si<sub>3</sub>N<sub>4</sub>, polyphase, cation diffusion through intergranular phase, appl. to environmental reactions 4-76889
- Si<sub>3</sub>N<sub>4</sub> sputter coatings, thermal oxidation resist. of reaction bonded Si<sub>3</sub>N<sub>4</sub> substrates 4-85238
- SiO, surface diffusion of metals, in vacuo, in presence of active gases 4-98415
- SiO-V<sub>2</sub>O<sub>5</sub> thin films, memory elements, metallic conducting filaments in low resist. state 4-75804
- SiO<sub>2</sub> glass, anomalous diffusion behaviour of Na 4-98362
- SiO<sub>2</sub> glass, water diffusion, effect of stress 4-61145
- SiO<sub>2</sub>:As, shallow implants, depth profiling using SIMS 4-108408
- SrF<sub>2</sub>:He, interstitial diffusion, solubility of He, dissolution energy 4-113727
- SrF<sub>2</sub> cryst., He diffusion and solubility, trivalent impurity effect 4-108663
- Ta, electron-irradiated, muon diffusion and trapping by defects 4-65905
- Ta-Si system, thin-film reactions and phase diagrams 4-88263
- Ta<sub>2</sub>O<sub>5</sub>, ionic transport number, effect of CaO addition 4-98349
- Te/metal binary thin film systems, Te cpd. formation 4-98371
- Ti diffusion process in LiNbO<sub>3</sub> 4-64804
- Ti-Nb (5 to 20 wt.%), oxidation resist., 500-850°C, influence of Nb (*French*) 4-71788
- Ti-Si system, thin-film reactions and phase diagrams 4-88263
- Ti-TiC single crystal diffusion couple, annealing, solid state reaction, C diffusion 4-85133
- Ti-V binary alloy, oxidation resistance, diffusion anal. (*French*) 4-71786
- TiC-stainless steel interface, reaction zone struct. produced by vacuum annealing 4-104918
- TiC<sub>0.97</sub>O, O diffusion coeff. and conc. profile, SIMS studies 4-92438
- TiO<sub>2</sub>, vacancies and multiphonon IR-absorpt. spectra (*Russian*) 4-71420
- TiSi<sub>2</sub> formation, effect of O<sub>2</sub> distrib. 4-80447

## diffusion in solids continued

- (u,Pu)<sub>2</sub>O<sub>3</sub>, nuclear fuel oxide, diffusion processes, surface effects 4-98353
- U, oxidation reactions, activation energy and reaction rates 4-71785
- UO<sub>2</sub>, CeO<sub>2</sub>, transport props. 4-104245
- UO<sub>2</sub>(U,Pu)O<sub>2</sub>, chem. interdiffusion coeff., O pot. depend. 4-92447
- UO<sub>2</sub>/Zircaloy 4 reaction layer sequence, total interfacial energy 4-83142
- UO<sub>2</sub>/Zircaloy 4, diffusion couple, interfacial energy and work of adhesion 4-83141
- UO<sub>2</sub>/Zircaloy-4 chemical interaction 4-83140
- UO<sub>2+x</sub>, nuclear fuel oxide, diffusion processes, surface effects 4-98353
- UO<sub>2+x</sub>, O<sub>2</sub> diffusion meas. 4-98369
- V and V-Cr-Ti alloy, fusion reactor blanket use, analysis of attack by O and water vapour 4-107019
- V/Al thin film couples, phase form. and diffusion in couples prep. under varying deposition conditions 4-75736
- V<sub>2</sub>O<sub>5</sub>-GeO<sub>2</sub>, sp. heat, thermal cond. and diffusivity coeff. 4-92384
- VSi<sub>3</sub> form., thin film reaction kinetics, AES and SIMS 4-81131
- W (110) field emitter, diffusion of H at low temp. 4-92549
- W, diffusion of W, Ta, Re, Os, and Ir in single crystals 4-65479
- W, range distrib. of Xe ions, expt. and computer simulation studies 4-92256
- W-<sup>182</sup>He, ion implanted, diffusivity study 4-104004
- W-K, dispersion hardened materials, diffusional stress relax. around second phase K particles, expt. study 4-61948
- W-Ni alloys, diffusion induced recryst. 4-61958
- W-Ni alloys, liq. phase sintering, chem. induced migration of molten Ni films between W grains 4-114435
- W-Si system, thin-film reactions and phase diagrams 4-88263
- WO<sub>3</sub> thin films, diffusion of H 4-70474
- Y, H diffusivity, 960 to 1160K 4-113716
- Y-Nb, H diffusivity, 960 to 1160K 4-113716
- Y-Th, H diffusivity, 960 to 1160K 4-113716
- YAG cryst., impurity distrib. and Bridgman-Stockbarger growth 4-60950
- YIG:H, H diffusion, optical absorption and mag. circular dichroism studies 4-61144
- Y<sub>2</sub>O<sub>3</sub>-Fe<sub>2</sub>O<sub>3</sub>, solid state reaction for garnet formation by sintering 4-85302
- Yb-Al interdiffusion cpds, dil., surface segregation and mixed valency, photoemission study 4-108688
- Zn-In, diffusion and hyperfine interactions 4-61134
- ZnS (Se)(Te), chemoeptaxy, reactive diffusion, struct. and growth kinetics 4-80442
- ZnS:Mn thin films, electrolum., diffusion and trapping 4-104677
- ZnS, diffusion coeff. determ. in Zn-Sn alloy from conc. distrib. near diffusion interface, conc. effect 4-88330
- Zr membrane, D transport kinetics, surface oxides influence 4-89325
- Zr, oxidation in O<sub>2</sub> atmosphere, temp. and press. depend. 4-114709
- Zr, pure, fast solute diffusion 4-65480
- Zr with surface adsorbed H, sticking coefficients, binding states, desorption studies 4-113784
- Zr:D, ion implantation, lattice defect trapping, binding enthalpy, migration 4-108400
- Zr:O, electrotransport purification, contamination and cold ends effects 4-61819
- Zr-Co, fast diffusion of Co atoms, quasielastic neutron scatt. meas. 4-113725
- Zr-Ti alloy, fast solute diffusion 4-65480
- Zr-V-Fe alloys, bulk getters, H and D diffusion 4-113719
- diffusion pumps**
- MBE growth in diffusion pumped systems, GaAs appl. 4-85105
- oil, comparison with other vacuum pumps (*Japanese*) 4-73445
- oil diffusion pumped large UHV system 4-63756
- oil gas beaming effect, pumping speed meas., effective conductance 4-86430
- diffusivity** see *diffusion*
- diffusivity, thermal** see *thermal diffusivity*
- digital-analogue conversion**
- see also *analogue-digital conversion*
- dispersive models for A-to-D and D-to-A conversion systems 4-79378
- interface for Apple II computer, 16-bit, low-noise design 4-78300
- Wordfit, digital audio signal processing system, for automatic time alignment of post-synchronised dialogue 4-69628
- digital arithmetic**
- optical architecture for performing matrix algebra 4-96815
- parallel digital optical adder construction method 4-60001
- quadratic-like complex residue number system arithmetic appls. to ultrasounds 4-103116
- digital circuits**
- see also *adders; digital integrated circuits; pulse circuits; switching circuits*
- integrating circuit design for T gas monitoring appl. (*Japanese*) 4-77043
- pulse-shape discriminating unit for neutron-gamma discrimination with NE213 liq. scintillator 4-64312
- digital communication systems**
- 1.3 μm optical transmission system, modal noise influence 4-64775
- A-to-D and D-to-A conversion systems, dispersive models 4-79378
- DIKOS digital communication system for office use 4-97116
- Earth-space links, digital, effect of ice-induced cross polarisation 4-62904
- editing digital audio 4-103112
- fibre optic junction, digital data harmonic distortion 4-107865
- integrated optical broadband, experimental results and review 4-60170
- long-wavelength optical communication systems, avalanche photodiode and PIN-FET receivers 4-97133
- optical communication, numerical optimisation of equalising filters 4-83721
- optical digital transmission system for EVU news networks (*German*) 4-112588
- optical fibre communication, APD digital receiver, non-Gaussian design methods (*Chinese*) 4-97132
- optical fibre digital telecommunication link, reliability and economics 4-69588
- optical fibres in broadband networks, instrumentation and urban and industrial environment appls., conf., Paris, France (May 1983) 4-78024
- wide-band communication network with optical fibre conductors, strategy for introduction (*Danish*) 4-79344
- digital computers**
- for computer applications see *under relevant applications e.g. administrative data processing; computerised control; natural sciences computing*

# digital computers continued

see also *digital systems; electronic calculators; microcomputers; mini-computers; special purpose computers*

CRAY-1 supercomputer, weather forecasting appl. 4-77592

# digital control

BWR digital feedwater controller conceptual design 4-59379

fusion reactor digital control and power supply system (*Japanese*) 4-111765

gamma-ray telescopes, choice of astatic system for controlling DC motor speed for altazimuth mountings 4-105886

MTR-II 5-MWt nuclear reactor digital control schemes, experimental evaluation 4-86932

SiO<sub>2</sub> film traps, microcomputer-based avalanche injection system, area density anal. 4-101870

# digital discs see video and audio discs

# digital filters

see also *signal processing*

A-to-D and D-to-A conversion systems, dispersive models 4-79378

achromatic images, high contrast, perceptual models, filtering 4-109814

acoustic noise cancellation, adaptive, digital filter implementation using modified Widrow-Hoff algorithm 4-103114

audio filter design, appl. of simple hearing model 4-105260

audio signal enhancement, digital techniques appl. 4-103109

audio signal processing, digital, CMOS-VLSI rate conversion digital filter appl. 4-103121

biological microscopy, image enhancement 4-105383

discrete stationary stochastic process, modelling using digital lattice filter (*Japanese*) 4-73374

modelling thickness-mode piezoelectric transducers using *z* transforms 4-97256

noise reduction by nonlinear digital filtering, estimation method 4-91694

real-time signal processing with digital bandpass filters 4-97206

recursive digital filters, IIR design for velocity selection/rejection in seismic signals 4-115592

sea-level survey data, digital filtering (*Chinese*) 4-85680

soft tissue, acoustic attenuation, modeling with minimum-phase filter 4-100270

spatial domain filtering algorithm, clinical appls. 4-72390

speech signal, frequency domain adaptive noise cancellation 4-69632

wideband ocean noise and propagation loss, real-time digital signal processing algorithms 4-107938

# digital instrumentation

see also *digital readout; digital voltmeters*

atmospheric transparency meas. using automated digital instrument 4-78358

blood flow waveforms reproduction in vitro, digitally controlled system 4-77433

calibration of a three-element hot-wire anemometer, computer-controlled system 4-69842

depth meter, differential, portable, using pressure sensors 4-72724

digital pendulum, attached to rotary potentiometer, student demonstrations 4-86153

digital recording system for wind vel. meas. 4-86165

dissector-based tracking device, appl. to meas. of star jitter 4-94254

health care, contrib. of medical phys. and engng., digital revolution 4-85572

infrasound digital vibration meter, seismic instruments inspection appl. 4-62973

laminar flow velocity determ. using photon correlator, systematic errors (*Russian*) 4-108142

magnetic props. meas. of Permalloy ring cores, using microcomputer 4-58879

medical X-ray systems, method for MTF meas. 4-67100

photogrammetric analogue plotting, computer-assisted stereoplotting system 4-94258

photogrammetric analogue plotting rationalisation with DZT 90X120 digital plotting table 4-94257

portable test instrumentation development, using CMOS LSI technology, flat displays and microprocessors 4-73429

programmed quantity markers (*Italian*) 4-63801

real-time digital data acquisition system for free-piston Stirling engine/linear compressor system parametric testing and evaluation 4-66779

registration and automatic analysis apparatus for electrocardiographic QRS signals (*Bulgarian*) 4-93955

RF pulse method apparatus for US meas. in liqs. (*Japanese*) 4-95119

sonic pile-testing system, digital, hand held, NDT appls. 4-89220

television speckle interferometer with real-time digital image processing 4-63072

# digital instruments see digital instrumentation

# digital integrated circuits

see also *integrated logic circuits; microprocessor chips*

integrated optoelectronic devices for high-speed IC interconnects 4-97139

pulse-position modulator for a microwave spectrometer 4-101881

# digital modulation see pulse modulation

# digital readout

see also *digital instrumentation*

humidity metering circuit with digital displays of the relative humidity and limiting value transducers (*German*) 4-101856

magnification-indicating unit for the REM-200 scanning electron microscope 4-101982

maximum/minimum thermometer, using analogue/digital readout 4-58848

min-max indicator 4-106304

spectral ratio peak intensity meter, appl. of A/D linear colour-temp./freq. convertor (*Russian*) 4-101847

# digital signal processing see computerised signal processing; signal processing

# digital signals

computerised digital signal processing for precision wide-swath bathymetry 4-67432

dynamic imagery processing for photogrammetric appl. 4-58902

# digital simulation

1d quantum ground state, Monte Carlo renormalisation group simulation 4-58762

450-MHz RF exposure of man, specific absorption rate average and distrib. 4-115119

acetone, carbon disulphide soln., Monte Carlo simulation using quantum mech. intermol. pot. 4-65160

# digital simulation continued

acoustical shallow water propag., computer simulation 4-87502

adsorption kinetics, stochastic numerical simulation 4-75776

aggregates, diffusion limited, dynamical scaling and growth 4-113644

air to water heat pumps for domestic space heating, use of floor panel energy storage 4-89462

alloys, FCC random, atom transport, phenomenological coeffs. computer simulation 4-84444

American Power Conference, Chicago, USA (April 1983) 4-86112

amorphous and liq. struct., computer simulation by Markov chain method 4-75301

amorphous solar cells, efficiency, computer simulation 4-99962

amorphous target, ion beam bombardment, SASAMAL computer code using liquid model (*Japanese*) 4-109295

anisotropic two-dimensional cardiac tissue, propag. of excitation 4-89540

aquifer seasonal energy storage—results and simulation of moderate temperature field experiments 4-66795

atomic clusters, melting behaviour Metropolis Monte Carlo simulations 4-113579

axons, myelinated and demyelinated, computer simulation of cond., review 4-89550

B-mode images, computer simulation of artifacts 4-105308

B-scan images, realistic computer simulation 4-105307

ball powders, convective combustion in strong confinement numerical simulation 4-114795

bicrystal, grain boundary phase equilib., computer mol. dynamics simulation 4-113461

binary alloys, kinetics of first order phase transition 4-75642

biped landing, impact effects study 4-115101

Boltzmann nonlinear eqn., computer realisation and sputtering theory 4-73397

S-bromochlorofluoromethane, liq., translational motion, external elec. field effect 4-103625

2-bromonaphthalene glassy films, spectral diffusion and triplet exciton localisation 4-98538

sec-butyl chloride, supercooled, rise transient dynamics, computer simulation 4-65161

BWR cores adaptive simulation using 3-D coarse-mesh neutron diffusion theory 4-86933

cardiac 1st-transit radionuclide curves discrete-time, lumped-parameter math. model 4-89739

Cartesian two dimensional phase change, fixed mesh finite element solution 4-112669

cementite dissolution in austenite, computer simulation 4-71653

charge excess in 1/r 2-dimens. plasma, grand canonical Monte Carlo calcs. 4-65053

chemisorbed and physisorbed systems, island growth kinetics, computer simulation studies 4-113813

coal-fired boiler exhaust gas heat recovery 4-64826

coded aperture cameras, performance of practical designs, computer simulations 4-67638

coded aperture imaging, advanced deconvolution techniques 4-67636

complex ocean environment, acoustic propagation loss calc. for simulator based training 4-60200

computer generated imagery, terrain perspectives, exaggerated vertical scale 4-81703

computerised tomography, iterative correction algorithm of incomplete projections 4-93857

conformal mappings using Schwartz-Christoffel integral 4-91382

continuous systems, discrete simulation, implementation of noise 4-58758

creep recovery rate meas., strain transient dip test, computer simulation 4-114734

crystals, accumulation kinetics of Frenkel defects 4-70141

CT image resemblance to original object rel. to filter function, noise interf. case 4-72395

cylindrical floating zone, steady flow under low gravity, computer simulation 4-61837

damped elastic string, nonlinear free vibr. 4-87507

dense gases, mol. dynamics simulations, continuous pots. effects 4-63648

dense polymer systems, liq. glass-type transition, dynamic Monte Carlo simulation 4-98286

desalination plant supplied by photovoltaic array with management strategies 4-77062

didactic microcomputer simulation in cardiac dynamics 4-81737

dipolar two centre Lennard-Jones mol. liqs., dielec. behaviour and multi-body orientational correl. 4-97988

distorted cryst., three wave X-ray images, numerical simulation 4-60780

dye laser, intensity corrls. for laser with fluctuating pump 4-69400

ECG, autoregressive model with abnormal values, order estimation (*Japanese*) 4-67145

elastic-plastic materials, isotropic, Bauschinger effect model for large computer codes 4-108504

electrically driven heat pump 4-66742

electron ring trapping in mirror fields, simulation 4-60715

electron-hole geminate pair in cryst. lattices, time depend. dissoc., Monte Carlo study 4-98635

EM mass-accelerator development, impact fusion 4-107135

endothelial response to injury, simulation, phys. model 4-62454

equatorial spherical band with pulsating surface, radiation field 4-107927

F=M/A, Newton's law, computer simulation expt. 4-73199

fluid dynamical equations solving, computer model 4-91785

fluid thin films, disjoining press. oscils. 4-75759

fluorochloroacetone, racemic mixture, rot. translation coupling obs. 4-92049

fluorochloroacetone, supercooled liq. fall transients field-induced acceleration 4-92048

flywheel energy storage system, peak reducing potential 4-66791

FORTTRAN programming and computer simulation teaching by diffusion in percolative lattice 4-78076

fractal to classical crossover 4-85285

free electron laser pulse propagation, model for noise introduction into computer simulations 4-87346

free electron lasers, computer simulation of lasers with variable Wigglers 4-102935

GABA:Zn<sup>2+</sup> complex, hydration, Monte Carlo simulation 4-99759

GABA, hydration, Monte Carlo simulation 4-99759

grain growth, grain size distrib., topology and local dynamics, computer simulation 4-66306

grain growth kinetics, computer simulation 4-66305

graphite with surface adsorbed ethylene, molecular dynamics calcs. 4-104079

## digital simulation continued

- hard disk systems, two-dimens., long-range correl., nonequilib. mol. dynamics calcs. 4-103633  
 hard sphere liq. mixtures, diffusion coeff., mol. dynamics simulation 4-92399  
 heart tissue, activation sequence effects simulation 4-81663  
 heat exchanger performance simulation using programmable calculator 4-111127  
 heavy ion beam fusion, target study 4-102388  
 high energy density ion cascades, surface damage, computer simulation studies 4-75553  
 n-hydrocarbon chains in bilayer system; struct. and conformation 4-85402  
 Illuminating Engineering Society Annual Conf., Los Angeles, USA (Aug. 1983) 4-90291  
 image enhancement/restoration efficiency meas. by human performance 4-81704  
 infinitely thin hard platelets, isotropic-nematic transition, Monte Carlo study 4-108616  
 inorganic ion-exchange materials, selective action, simulation of solvation interactions 4-62185  
 irreversible kinetic gelation, crossover between random and kinetic growth, computer simulation 4-62251  
 Ising antiferromagnet, FCC, hysteresis and free energy, computer simulation 4-114127  
 laser ranging meas., system anal. and computer simulation 4-107723  
 learning key concepts in physics and mathematics through computer graphic simulation, preliminary results 4-73203  
 Lennard-Jones, supercooled liquid homogeneous nucleation, periodic boundary conditions, computer simulation 4-98247  
 light-ion and heavy-ion sputtering, threshold energies, incidence angle depend. 4-76612  
 linear algebraic equations, direct and indirect optical solutions, error source modelling 4-96816  
 liquid alkali metals near freezing point, liquid structure factor calcs. 4-113296  
 longhole open slope stability assessment using computer models 4-62806  
 luminescence decay data deconvolution 4-59824  
 MAXI-LILLIPUT: a simplified model of a French pressurized water reactor power plant 4-83222  
 MCP photomultiplier tubes, timing props., computer anal. 4-64298  
 membrane column, continuous, computer simulation 4-81473  
 metal/Si<sub>3</sub>N<sub>4</sub>/SiO<sub>2</sub>/Si capacitors, interfacial charging 4-104292  
 metallic semicontinuous thin films, resist. based on computer model of thin film formation 4-80692  
 metals, amorphous, atomic struct. model, computer simulation 4-103653  
 metals, BCC, vacancy loop unfauling in radiation damage 4-108353  
 metals, cryst. and amorphous, indirect exchange interaction, computer simulation 4-84779  
 metals, vacancy-two boundary interactions, computer simulation studies 4-113491  
 microcomputer simulation of thermal performance of a solar cooling system 4-93596  
 MIS, tunnel capacitor, leakage current effects on DLTS 4-70938  
 multicomponent targets, sputtering, implanted ion range and profiles, TRI-DYN TRIM 4-80076  
 multiparticle diffusive fractal aggregation, computer simulation studies 4-95345  
 multiple pulse and 2 dimens. Fourier transform NMR computer simulation 4-78352  
 muonium in water, computer simulation 4-83510  
 neuron model, analogue threshold, pattern separability (*Japanese*) 4-100117  
 nitroxide radicals in soln., superhyperfine struct., ESR spectra, computer simulation 4-96578  
 NMR imaging, pulse sequences optimisation by computer simulations 4-100307  
 NMR imaging simulation, computer algorithm 4-105318  
 noise reduction by nonlinear digital filtering, estimation method 4-91694  
 non-Newtonian flow, numerical simulation, book 4-108097  
 nonideal systems, diffusive permeation rates and selectivity, computer simulation 4-89331  
 nuclear reactor digital control schemes, experimental evaluation 4-86932  
 nucleic acid-base interactions, solvent effects, Monte Carlo simulation 4-64559  
 ocean cable systems simulations 4-114677  
 one dimensional transonic flow, numerical simulation employing micro-computer 4-91825  
 one-dimensional disordered system, dynamic cond. freq. depend. 4-84610  
 optical etch-rate monitoring, computer simulation of reflectance 4-81952  
 optokinetic reflex, cat. modelling and computer simulation 4-93736  
 p-n junction, reverse-biased, switching to high cond. state, computer simulation 4-61452  
 p-n junction, two-dimensional simulation of potential distrib. with graphic-computer-aid 4-76035  
 PEP and PETRA, single beam stability, computer simulation 4-68843  
 petrol engine, homogeneous combustion parameters and emissions control, computer simulation 4-77171  
 phase coarsening, statistical mechanics study 4-113573  
 plasma, conditional-probability function for elec. fields 4-91980  
 plasma deposited films, step coverage calc. by computer simulation 4-104096  
 plasmas, computer simulation techniques 4-91979  
 polar fluids, dielectric props., static and freq. depend., computer simulation 4-71259  
 polarisable polar systems, dielectric const., computer simulation 4-76301  
 polycrystalline aggregates, grain growth, computer simulation studies 4-113665  
 polymer solutions, polydisperse systems, computer simulation (*Russian*) 4-79920  
 polymers, computer simulation, fracture mechanism, two coupled anharmonic chains with strong interaction 4-113531  
 polymers, transient radiation-induced cond., computer simulation and analytic solns. 4-104263  
 polyvinylidene fluoride and copolymers, ferroelec. switching, computer simulation 4-99049  
 prediction of turbulent fluid flows using computers 4-91788  
 pulsed microwave annealing, power distribution effects (*French*) 4-61781  
 PVC, thermodegraded, UV-visible electronic absorpt. spectrum (*Russian*) 4-84978

## digital simulation continued

- PWR spatial power oscillations, Xe-induced, time optimal control 4-111652  
 pyrazine, fluoresc. yield, rot. level depend. 4-69131  
 quantised noisy systems and room acoustics, general state estimation algorithm 4-103092  
 radioisotope thermoelectric generator, computer predictions of ground storage effects 4-77133  
 RE 1-11 rotary expander engine testing and analysis 4-66746  
 reactor, modelling and numerical simulation 4-109335  
 relaxation creep, computer model for high temp. 4-84340  
 reverberant room, sound absorbing coeffs. evaluation 4-107951  
 RF hyperthermia in tumour treatment, computer simulation use 4-72344  
 road traffic noise in Hiroshima 4-103095  
 room acoustics, image source computer model 4-79370  
 semiconductor films, impurity distrib. studied by computer simulation 4-75806  
 semiconductor impurity diffusion simulation, adaptation of stiff methods 4-75734  
 semiconductor laser regular pulsations in time-averaged spectra, intrinsic manifestation 4-83578  
 shaped explosive charges, detonation wave shaping, computer simulation anal. 4-108545  
 sheared suspensions, dynamic simulation 4-74975  
 shock recovery fixture, two-dimensional simulation 4-108536  
 shock wave recovery, three-dimensional computer modelling 4-108535  
 short term memory as metastable state 4-100124  
 Shuttle IR Telescope Facility, thermal modelling 4-110488  
 signal processing for precision wide-swath bathymetry 4-67432  
 silica glass, radiation-induced defects, mol. dynamics study (*French*) 4-88113  
 silicide formation, radioactive marker, mathematical model 4-92404  
 solid/solid interfaces, computer simulations, conf., Philadelphia, USA (Oct. 1983) 4-110806  
 solids, laser induced shock struct. simulation 4-113540  
 solvation, geometrical features, pattern recognition anal. 4-114781  
 spacecraft guidance and control techniques, conf., Florence, Italy (Sept. 1983) 4-73164  
 spark sources, high voltage, current waveforms simulation, rel. to gap dynamic impedance 4-79854  
 spatial problem-solving, computer and human brain comparison 4-62492  
 spectral estimation for short data sequence, fast algorithm of maximum entropy method 4-63678  
 speech analysis, phonemic errors simulation 4-89603  
 speech signal, frequency domain adaptive noise cancellation 4-69632  
 spin glass, 3-D planar, computer studies of two-level systems 4-84802  
 spin glasses, short range three-dimensional nearest-neighbour Ising model, Monte Carlo simulations 4-92926  
 Stirling cycle machine anal. methods review 4-66751  
 superconducting transient system with topological surface irregularities 4-80714  
 target adatom form. during quenching of energetic Ar ion induced cascade 4-88209  
 texture, computer simulation of pole figures 4-66512  
 thickness mode piezoelectric ultrasonic transducer, systems model 4-112662  
 tomography, first-order diffraction, limitations of imaging 4-115257  
 tomography, nonlinear, for three-dimens. image reconstruction of dense plasma 4-84069  
 tomography, time coded emission, three dimensional simulation 4-77374  
 travelling salesman problem, optimization by simulated annealing 4-79433  
 tricuspid regurgitation, quantitative evaluation by digital simulation of cardiac time-activity curves 4-67080  
 two-dimensional percolation clusters, diffusion-limited aggregation 4-70394  
 ultrasound speckle size and lesion signal to noise ratio 4-105305  
 vestibular semicircular canal responses during righting movements of falling cat 4-81719  
 water, liq., H bonded networks, percolation model, computer simulation 4-88056  
 weakly compensated classical impurity band, neutral donor energies 4-92658  
 weather radar simulator, for pilot training 4-85794  
 wind erosion from coal surfaces, computer simulation program 4-82211  
 wrist, computer-simulated, range of motion 4-93790  
 zirconolite, high resolution lattice images 4-103951  
 Ag<sub>2</sub>Te, electronic-ionic cond. calcs. 4-98675  
 Al, damage simulation in high velocity impact 4-108529  
 Al, FCC tilt boundary, vacancy migration, computer simulation studies 4-113694  
 Al, grain boundary struct., computer simulation studies 4-113459  
 Al, liquid, pair pots., Monte Carlo simulation 4-92047  
 Al target, laser-driven shock wave evolution 4-113258  
 Al-plexiglass target, high speed water jet penetration simulation 4-108533  
 Ar, liquid, pair pots., Monte Carlo simulation 4-92047  
 Au, tilt boundary energy and segregation, computer simulation studies 4-114540  
 Au/Ni, superlattices, dynamical props., computer simulations 4-113777  
 BaTiO<sub>3</sub>, surface domains, double Laue pattern topography 4-104548  
 Be foil, stopping power of 7 MeV protons, geometrical effects 4-92264  
 C target, collision of laser accelerated discs, high press. shock production 4-113257  
 CO, liq., IR spectra, solvent-induced shift, Monte Carlo simulation 4-61698  
 Cr film, laser induced thermochemical image recording 4-102969  
 Cu (100), ion scattering spectrometry, shadowing effects 4-81088  
 Cu foil, stopping power of 7 MeV protons, geometrical effects 4-92264  
 Cu, liquid, pair pots., Monte Carlo simulation 4-92047  
 Cu, tilt boundary energy and segregation, computer simulation studies 4-114540  
 Cu<sub>2</sub>Au (100), keV Ne scatt., atom layer effects 4-76580  
 Fe-Cr alloys, inhomogeneous, X-ray fluoresc. intensities, Monte Carlo simulation 4-109246  
 Fe-Ni, single particle martensitic growth, computer simulation studies 4-114521  
 H nonequilibrium positive columns, state transitions, two-temp. model 4-92007  
 H solvation by H<sub>2</sub>O mols. 4-62175

**digital simulation continued**

- InGaAsP/InP buried crescent laser, dynamic characis., computer simulation method (*Chinese*) 4-96887  
 KCl:Li, optically excited colour centres, relaxation dynamics 4-113896  
 KMnF<sub>3</sub> (M=Y, Bi), cubo-octahedral cluster and: extended defects 4-88128  
 K<sub>1.33</sub>Mg<sub>3.11</sub>Sb<sub>4.89</sub>O<sub>16</sub>, supercell ordering study 4-80006  
 Kr, adsorbed on graphite domain growth, Monte Carlo simulations 4-98444  
 Kr dense gas, dynamic struct. 4-91859  
 LiNbO<sub>3</sub> planar ion implanted optical waveguides, computer simulation 4-69547  
 Mo (001), clean and adsorbate covered, low energy alkali ion scatt. 4-76582  
 Mo, atom sputtering at grazing incidence, spherical angular distrib. 4-76613  
 Mo, low energy heavy ion bombardment, self-interstitial generation 4-80117  
 Mo, tilt grain boundary struct., computer simulation studies 4-113459  
 Mo-Co dilute alloy, Co impurity location, PIXE and ion channelling studies 4-80072  
 Mo-N ion implanted single cryst., computer simulation anal. 4-108402  
 NH<sub>4</sub>Cl, librational motion of NH<sub>4</sub><sup>+</sup> 4-60865  
 Na atoms trapped in Ar and Xe solids, site form., computer simulation 4-96472  
 NaCl-type mixed cryst., vacancy-pair diffusion, Monte Carlo simulations 4-84454  
 Na<sup>+</sup>-HPO<sub>4</sub><sup>-</sup>, tightly bound system, cation hydration, polarisation effects 4-69167  
 Nb Josephson junction, thin film point-contact, Stewart-McCumber model 4-114072  
 Ni, atom sputtering at grazing incidence, spherical angular distrib. 4-76613  
 Ni hexamine complex, EPR powder spectra, computer simulation 4-76242  
 Ni, ion bombardment-induced O<sup>-</sup> desorption, energy distrib. 4-75781  
 Ni, low energy heavy ion bombardment, self-interstitial generation 4-80117  
 Ni, tilt boundary energy and segregation, computer simulation studies 4-114540  
 NiO-Y<sub>2</sub>O<sub>3</sub> system, composite microstruct. and interface struct. 4-70578  
 Pb-acid batteries for photovoltaic systems, math. model and computer simulation 4-72092  
 β-PbF<sub>2</sub>, point defect stability, computer simulation 4-103744  
 RbMgF<sub>10</sub> (M=Y, Bi), cubo-octahedral cluster and extended defects 4-88128  
 S<sub>n</sub> polymers, flexible networks, rubberlike elasticity 4-74872  
 Se<sub>n</sub> polymers, flexible networks, rubberlike elasticity 4-74872  
 a-Si, amorphous layer effect on lattice images of dislocations 4-79939  
 Si, carbothermic silica reduction process, computer simulation 4-66200  
 Si, computer simulation, relativistic electrons, multiple scatt., axial channelling 4-108491  
 Si, ion bombardment, sputtered particles and cascade recoils 4-76621  
 Si multiply implanted targets, range distrib., Rutherford scatt. studies 4-92268  
 Si, plasma etching using CF<sub>4</sub>, computer simulation and chem. reactions 4-109683  
 Si, positron channelling radiation, photon intensity and polarisation, computer simulation 4-75584  
 Si, self-interstitial scatt. and imaging 4-80033  
 a-Si:H, F-p-n junctions, generation, recombination currents, computer simulation 4-84683  
 SiO<sub>2</sub> glass, struct. model, intermediate range order 4-75308  
 TiO<sub>2</sub> powder, fixtures for controlled explosive loading 4-108538  
 TiO<sub>2</sub> rutile, threshold radiation damage, computer simulation 4-108420  
 W, low energy heavy ion bombardment, self-interstitial generation 4-80117  
 W, molecular ion collision cascades, spatial configurations, computer simulation studies 4-75557  
 W, noble gas atom implanted, cascade annealing, computer simulation studies 4-75556  
 W, range distrib. of Xe ions, expt. and computer simulation studies 4-92256  
 W surface, interstitial atom interactions, field-ion microscopy studies 4-61798  
 W(110)+K<sup>+</sup> ion impact, angle and energy resolved, rainbows 4-81092  
 YIG, spin wave excitation by EM field pulses (*Russian*) 4-65797  
 Zr-Al alloys, inhomogeneous, X-ray fluoresc. intensities, Monte Carlo simulation 4-109246

**digital systems**

- see also computer networks; digital computers; multiprocessing systems; real-time systems; sampled data systems  
 astatic system, for control of DC motors for altazimuth mountings of gamma-ray telescopes 4-105886

**digital voltmeters**

- 3<sup>1</sup>/<sub>2</sub> digit voltmeter, kit design using CMOS A/D convertor (*French*) 4-95408  
 double-integrating DVM, A/D convertor interf. suppression and error considerations (*Bulgarian*) 4-86398

**digitisers** see analogue-digital conversion**digraphs** see directed graphs**dilatometers** see extensometers**dilute alloys**

- see also impurity electron states; Kondo effect; magnetic properties of dilute systems  
 diffusion in dilute alloys, review 4-65441  
 free enthalpy of impurity-vacancy binding, solvent diffusion meas. 4-84465  
 impurity diffusion in pure metals, review of models 4-65471  
 magnetic alloys, dil., low temp. thermodynamic props., anomalous contrib., in presence of cryst. field 4-84801  
 magnets, phase transitions, critical behaviour, percolation, random fields 4-88690  
 orbitally anisotropic exchange interaction, magnetic ions, creation-annihilation operators 4-109008  
 plane crystallisation front stability 4-98044  
 Ag based dilute alloys, interaction of trivalent solutes with vacancies 4-65259  
 Ag-Cu dilute alloys, defect production and annealing 4-75442  
 Ag-Cu dilute alloys, electron irradi., defect prod. and annealing 4-75441

**dilute alloys continued**

- Ag-Gd(Er), dil., impurity-induced muon depolarisation, mag. field depend. 4-71228  
 Ag-Mn dilute alloys, exchange split virtual bound state 4-92680  
 Ag-Pr-In dilute alloys, In migration, PAC studies 4-65460  
 Ag-Sn(In) dilute alloys, correlated impurity diffusion jump processes, isotope effect 4-84446  
 Al-Ag, dil., single cryst., doped, muon localisation, transverse μSR linewidth study 4-65906  
 Al-based dilute foils, conduction electron spin resonance linewidths 4-92961  
 Al-Cu, dil., quenched, positive muon spin depolarisation 4-65910  
 Al-In, dil., He localised diffusion around In impurities, PAC obs. 4-65470  
 Al-Mg, dil., muon spin relax. 4-65907  
 Al-Mg, dil., quenched, positive muon spin depolarisation 4-65910  
 Al-Mg, neutron irradi., internal friction, elastic modulus, recovery stages studied by elec. resist. meas. 4-103876  
 Al-Mg dilute alloys, oxidation behaviour, ESCA studies 4-76907  
 Al-Mn dilute alloys, <sup>65</sup>Zn diffusion 4-65482  
 Al-Mo alloys, ion implanted, corrosion resist., AES studies 4-99626  
 Al-Si, dil., quenched, positive muon spin depolarisation 4-65910  
 Al-Sn, small Sn additions effect on microstruct. and corrosion behaviour 4-99630  
 Al-Zn dilute alloys, α<sub>2</sub>-Zn rich precipitate shape, small angle neutron scatt. studies 4-114547  
 Au based dil. alloys, interaction of trivalent solutes with vacancies 4-65259  
 Au-Fe dilute alloy, exchange-circulation electron current between Fe atoms (*Chinese*) 4-114102  
 Au-Gd, dil., impurity-induced muon depolarisation, mag. field depend. 4-71228  
 Au-In, channelling effect of conversion electrons emitted from radioactive impurities 4-75569  
 AuNi(Co), impurity lineshapes in dilute alloys, UPS study 4-113893  
 AuY(Zr)(Nb)(Rh)(Pd), dil. alloys, thermoelectric power, resistivity, low temp. study, phase-shift anal. 4-113926  
 AuY(Zr)(Nb)(Rh)(Pt)(Pd), dil. alloys, thermoelectric power, resistivity, low temp. studies 4-113925  
 Ce alloys, dil., X-ray absorpt. near edge struct. 4-66118  
 Cr-Al dilute alloys, thermal expansion, elastic const. and mag. props. 4-80138  
 Cr-Ga, dilute, mag. phase diagram, elec. cond. meas. 4-88669  
 Cu-Cr (0.8 wt.%), film, thermoelec. power, thickness depend. 4-61468  
 Cu-Fe dilute alloy, exchange-circulation electron current between Fe atoms (*Chinese*) 4-114102  
 Cu-In, dil., channelling effect of conversion electrons emitted from radioactive impurities 4-75569  
 Cu-In (0.1 at.%), vacancy trapping, PAC and ion channelling study 4-84876  
 Cu-Mn dilute alloys, exchange split virtual bound state 4-92680  
 Cu-Pd random substitutional alloy, [111] neck radius on the Fermi surface 4-80476  
 Cu-Si, dil. alloy, internal oxidation, grain boundary cavitation under creep or fatigue loading 4-71726  
 Cu-Sn dil. alloys, vacancy jump freq. ratios 4-65448  
 CuAl, disordered, diffuse size effect scatt. in high voltage electron diffr. 4-113395  
 CuNi impurity lineshapes in dilute alloys, UPS study 4-113893  
 Fe alloys, dil., electron irradi., muon spin rot. obs. 4-65913  
 Fe dilute alloys, vacancy-impurity interaction, μSR study 4-84886  
 Fe-<sup>173</sup>Ta(<sup>177</sup>Ta), mag. hyperfine splitting frequencies, mag. moments, NMR-ON obs. 4-109083  
 Fe-Ni dilute alloys, electron and neutron irradiated, low-temp., mag. relax. spectra 4-84831  
 Fe-Sn dil. alloys, tracer diffusion coeffs. meas. 4-65450  
 Fe-W dilute alloy wires, diffusion coefficients, resistometric methods 4-65427  
 FeCo(Mn)(V), coupling between chemical and mag. interactions, NMR study 4-114173  
 Mg based dil. alloys, interaction of trivalent solutes with vacancies 4-65259  
 Mg-Cd, dilute alloy, solid solution hardening 4-71664  
 Mo-Co, lattice location studies by PIXE and ion channelling 4-99894  
 Mo-Co dilute alloy, Co impurity location, PIXE and ion channelling studies 4-80072  
 Mo-In, channelling effect of conversion electrons emitted from radioactive impurities 4-75569  
 Mo-Nb dilute alloys, thermoelec. props. at low temps. 4-92700  
 Mo-Se, dilute alloy, arc melted, workability and ductility 4-76808  
 Nb<sub>2</sub>Sn, cryst. site determ. of dilute alloying elements, TEM studies 4-88131  
 Ni-Ge dilute alloys, defect reactions, diffuse X-ray scatt. studies 4-75440  
 Ni-Si dilute alloys, defect reactions, diffuse X-ray scatt. studies 4-75439  
 Pb-Au dil. solutions, bulk equilib. lattice parameters, neutron diffr. meas. 4-75372  
 Pb-Au dilute solutions, single cryst., struct. in quenched state, X-ray and neutron diffr. studies 4-75371  
 Pd(Fe, Co) dilute, Mossbauer study of relax., spin glass props. 4-104514  
 PdFeCd dilute alloys, hyperfine field at Cd, PAC spectroscopy studies 4-92681  
 PdMn dilute alloy, spin glass peak heights, field depend. 4-76144  
 Pt-Co dilute alloys, resistance thermometers with low magnetoresistive effects 4-111132  
 PtCr, nonmagnetic resist. anomalies 4-113919  
 Sn-Ge dilute alloys, semiconductor-metal transition, press. effects 4-92613  
 Sn-Ge dilute alloys, semiconductor-metal transition under press. 4-113871  
 Sn-Pb sputtering alloy, effect of ion mass and energy on the surface composition 4-98493  
 Tb-Ce, dil., intermediate valent, time depend. hyperfine fields, TDPAC study 4-75907  
 W-Fe, segregation of Fe to grain boundaries, elec. resist., thermopower, AES meas. 4-103943  
 W-Ta dilute alloys, thermoelec. props. at low temps. 4-92700  
 Yb-Al interdiffusion cpds., dil., surface segregation and mixed valency, photoemission study 4-108688  
 Yb-Es dilute alloys, thermodynamics, Henry's Law vaporisation studies 4-92390  
 ZnNi, impurity lineshapes in dilute alloys, UPS study 4-113893

**dimensions**

- tutorial paper on dimensions and units 4-68198
- Al-Si Schottky barrier diodes, barrier height and hot electron attenuation length meas. 4-98751

**dimer lasers** *see excimer lasers***dimerisation** *see association***dimers** *see molecules***dineutrons** *see neutrons***Dingle temperature**

- Bi whiskers, longit. magnetoresist. meas. 4-88500
- Cd/Mg alloys, electron energy spectrum and de Haas-van Alphen effect (Russian) 4-70639
- Cu, electronic props. of 4d transition metal and sp impurities 4-70731
- Pb-, Sn-, Te, Shubnikov-de Haas effect, temp. depend. scatt. parameter 4-113978

**diode lasers** *see semiconductor junction lasers***diode sputtering**

- ZnO transparent conductive films, prep. by RF diode sputtering (Japanese) 4-113831
- Zr-Pd(Ni), amorphous, electronic density of states and superconducting props. 4-70738

**diode tubes** *see diodes***diodes**

- see also plasma diodes; rectifier tubes; semiconductor diodes*
- intensifier tube designed for scintillation detection 4-64301
- magnetic insulation time for coaxial diodes 4-73580

**dipole antennas**

- field intensity meas., geometric asymmetry effects determ. 4-58834
- human head, absorbed power distrib. inside simulating sphere in near field of  $\lambda/2$  dipole antenna 4-89653

**dipole moment, electric** *see electric moments***dipole moments, magnetic** *see magnetic moments***Dirac electron theory** *see Dirac equation; electron theory***Dirac equation**

- see also electron theory*
- (1+1) dimensional Dirac equation, fractional charges in confinement 4-111286
- $\sigma$ - $\omega$  model, electromagnetic interactions in nucl. dynamics, Dirac-based theories 4-111365
- atoms, neutral, ns'-nsp radiative transition rates, correl. and relax. effects 4-96492
- bag models, Dirac eqn. and solutions for confined quarks in SO(3,2) 4-111414
- bag-like solutions to Dirac equation with fractional nonlinearity 4-86679
- canonical transforms., relativistic particles 4-95670
- charged spin 3/2 particle coupled to homogeneous mag. fields, eigenvalues 4-86637
- classical model of the Dirac electron 4-78188
- conformal spinors and semispinors, book contrib. 4-58976
- conservation laws, relation to algebra of space-time symmetry group 4-95703
- conserved quantity partition for Dirac's equation 4-111313
- crystal-assisted pair creation process, tilt-angle depend. 4-75572
- crystal-assisted pair-creation process, const. field approx. 4-75571
- De Donder-Weyl Hamilton-Jacobi theory appl. to relativistic field theories 4-68374
- Dirac monopole, Abelian Higgs model 4-68496
- Dirac particle in central field, inclusion of anomalous mag. moment term. 4-95672
- Dirac-Coulomb problem, exact path-integral soln. 4-90426
- electron in nonuniform mag. field, supersymmetry 4-111326
- electron-positron field, interaction with const. mag. field (Spanish) 4-73620
- elementary derivation, electrodynamic hydrogen field transversality 4-95188
- Feynman checkerboard model, hypergeometric series and Jacobi polynomial soln. 4-90707
- free atoms, Auger transitions, kinetic energies calc. using multiconfig. Dirac-Fock method 4-107323
- free particles in Friedmann space-time, spinor null tetrad formalism (Chinese) 4-86095
- free spin 1/2 particle, trembling motion 4-68033
- grassmannian  $\alpha$  models, classical solns. props. 4-63860
- Hestenes' geometric algebra 4-102010
- hydrogenic fine struct. spectrum in space of const. negative curvature 4-102591
- instanton and meron fields, Dirac Hamiltonian self-adjointness 4-95673
- interface states, relativistic, in one-dimens. solid 4-65730
- inverse scattering problem, integration of differential eqn. linear hyperbolic system (Ukrainian) 4-63574
- Klein-Gordon equation, bound-state solns. for strong pots. 4-106461
- leading-logarithm model, QCD, mesons containing one heavy and one light quark 4-106519
- linear potential, asymptotic behaviour in nonrelativistic regime 4-102017
- localization props. of relativistic wave functions, Dirac particles 4-111278
- Lorentz-Dirac eqn. 4-67923
- massless monopole in central electric field, Dirac relation, spin 1/2 monopole nonlinear eqn. (French) 4-68486
- momentum space, relativistic wave eqn. 4-101700
- monopole charge quantisation, Aharonov-Bohm effect 4-101998
- neutrino and Dirac eqns., separation of variables and symmetry operators 4-68064
- nonlinear Dirac equations, integrability from soliton theory 4-95656
- nonlinear Dirac field models of extended particles, book contrib. 4-58977
- operators with decaying potential and dense point spectrum (Russian) 4-101900
- particle propagation, path integral approach 4-101685
- particle with 'anomalous moment, Hamiltonian exact diagonalisation 4-102079
- path integral formulation of the propagator for a two-dimensional Dirac particle 4-73630
- plane-symmetric Einstein-Dirac cosmology containing classical spinor field, exact nonghost soln. 4-90267
- quantum mechanics-Brownian motion analogy, relativistic expansion, Schrodinger and heat eqns. 4-95236
- quantum physical origin of the gauge idea (German) 4-82932
- radial eqns. for confirming interaction 4-73642
- recurrent formulae and some exact relations for radial integrals with Dirac and Schrodinger waves functions (Russian) 4-90442

**Dirac equation continued**

- reduced Dirac Green function for Coulomb pot. 4-68009
  - relativistic cosmology, Dirac quantisation 4-67821
  - relativistic density-functional theory, quantum fluid dynamic, many-electron systems 4-110881
  - Riemann space-time, Dirac equation deduction 4-82893
  - Schouten space-time, Dirac eqn. formulation 4-68397
  - single-particle mag. moments in relativistic shell model 4-64071
  - solution by expansion methods 4-68983
  - solution in field of general spherically symmetric monopole 4-111307
  - solutions of Dirac eqn. and Green's electron function in external EM field 4-73648
  - space-curvature effects in atomic fine- and hyperfine-structure calculations 4-74352
  - spectral asymmetry on open space for family of Dirac operators 4-111304
  - spin 1/2 fields with gauge freedom, indefinite metric field quantisation 4-73628
  - spin-1/2 fields, causal stochastic theory, hydrodynamical analysis 4-95229
  - spinor analysis of Yang-Mills theory in the Minkowski space 4-73654
  - spinor chain path integral, Dirac eqn., Feynman's checkerboard rule 4-111271
  - spinor superfield equations of motion 4-95711
  - spinorial relativistic rotor, transformation from quasi-Newtonian to Minkowski coordinates 4-90735
  - stability properties for static potentials 4-68487
  - stationary solutions for electron in EM field (Spanish) 4-73619
  - strong coupling theory for external time-depend. pot., pair creation 4-111273
  - SU(1,1) symmetry as subgroup of SL(2,C) 4-68424
  - SU(5) GUT, colourless and finite mass dyon soln., fermion Dirac eqn. 4-63923
  - superposed scalar pot. 4-102004
  - supersymmetric Grassmannian sigma models, 2-dimens., classical solns. for SUSY Dirac eqn. 4-78461
  - symmetry operators for neutrino and Dirac fields on curved spacetime 4-90733
  - total vacuum charge eigenvalue, Dirac fermion in bounded background soliton field 4-106471
  - transformation matrix for Dirac spinors and spinorial amplitudes calc. 4-63868
  - two-dimensional one-component plasma, free energy and correlation functions 4-90485
  - unified gauge theories approach using generalised Dirac eqn., symmetry breaking to general relativity 4-111357
  - variational safety, kinetic balance partial soln. 4-112088
  - qq spectroscopy with power law pot. in Dirac eqn., rel. quark model 4-90845
  - H-like heavy ions, energies calc. of 1s, 2s and 2p states 4-83307
  - H<sub>2</sub><sup>+</sup>, Dirac eqn., two dimens. numerical soln. 4-112093
  - HeH<sup>2+</sup>, Dirac eqn., two dimens. numerical soln. 4-112093
- direct access storage devices** *see magnetic disc and drum storage*
- direct coupled amplifiers** *see d.c. amplifiers*
- direct current amplifiers** *see d.c. amplifiers*
- direct current generators** *see d.c. generators*
- direct current motors** *see d.c. motors*
- direct energy conversion**
- see also bioenergy conversion; cells (electric); chemical energy conversion; magnetohydrodynamic conversion; photothermal conversion; plasma diodes; solar energy conversion; thermionic conversion; thermoelectric conversion*
  - photoelectrochemical energy conversion, review 4-72125
  - power for the future, overview 4-62281
  - solid state chemistry, conf., Veldhoven, Netherlands (June 1982) 4-67863
  - thermodynamic generators, numerical anal. 4-100006
- direct nuclear reactions and scattering**
- see also pick-up reactions; stripping reactions*
  - conference on highly excited states and nuclear struct., Orsay, France (Sept. 1983) 4-73145
  - conference on quark matter in rel. nucleus-nucleus collisions, Long Island, NY, USA (Sept. 1983) 4-67855
  - energy averaged cross sections and durations, imprints of compound nucleus and direct interaction processes 4-111533
  - fission after p, d, t, <sup>3</sup>He and  $\alpha$  induced reactions, fragments, mechanisms for A=255-258 4-106637
  - hadron-nucleus high energy data review, fragmentation, extrapolation to ultrarelativistic heavy ion collisions 4-68685
  - heavy ion quasi-elastic reactions, DWBA diffractive model, direct cross sections,  $\alpha$ -transfer 4-86851
  - heavy ion relativistic collisions, limiting fragmentation and transparency, hydrodynamical anal. 4-59274
  - heavy-ion collisions, wave packet scatt. model with quantum friction 4-59260
  - incomplete fusion, heavy-ion induced, break-up and sum-rules models anal. 4-59277
  - multiparameter-evaporation model for intermediate energy nuclear collisions 4-96068
  - multiple scattering direct reactions, 3-body approach, continuum spectrum statistical theory 4-106606
  - neutron energy spectra in (p,X), (d,X), (<sup>3</sup>He,X), ( $\alpha$ ,X), phenomenological anal. 4-73908
  - nucleus-nucleus collisions, medium mass fragment apparent temp., hot spots 4-106608
  - quasi-elastic heavy ion reactions, SU<sub>A</sub>-invariant model 4-102303
  - quasi-free direct knock-out mechanism for photoreactions 4-102243
  - quasielastic knock-on model, appl. to cumulative fragment spectra, clusters 4-95991
  - single-particle states, continuum strength, optical-model potential 4-90939
  - ( $\alpha$ , $\alpha'$ X), nucleon emission deexcitation of highly excited states and giant resonances 4-73668
  - (e,e'N), knock-out reactions, coincidence form factors interpretation 4-68677
  - ( $\gamma$ ,N) pre-equilib. emission and quantum 4-83043
  - (p,pn), 150 MeV, A=2-90, neutron deep hole states, separation energy and cross-sections 4-73795
  - (p,X), high energy, nuclear recoil velocity and neutron-deficient-fragments 4-102266
  - Ag(n,n'), statistical multistep direct emission theory 4-86828

**direct nuclear reactions and scattering continued**

- <sup>27</sup>Al(<sup>14</sup>N, HI+light particles), 30 MeV/N, projectile fragmentation processes, multifragmentation 4-59264
- <sup>27</sup>Al(<sup>19</sup>F, pny)<sup>44</sup>Se excited state lifetime meas. 4-68654
- Au(<sup>12</sup>C, X), 25 GeV, <sup>37</sup>Ar and <sup>127</sup>Xe fragment ang. distrib. and fragmentation mechs. 4-96066
- B( $\alpha$ , X), A=10, 11, X=p, d, t, 31.2 MeV ang. distrib. and reaction mech. (Chinese) 4-73884
- B(p,  $\gamma$ ),  $\gamma$ -spectra, direct-semidirect anal., ang. distrib., anal. powers 4-106615
- <sup>12</sup>C( $\gamma$ , n), direct knockout, orthogonality, antisymmetry, c.m. effects 4-83044
- <sup>12</sup>C(p,  $\gamma$ ),  $\leq 1$  MeV, direct-semidirect capture anal., <sup>13</sup>N resonances and ground state spectroscopic factor 4-96012
- <sup>12</sup>C(p,  $\gamma$ ),  $\gamma$ -spectra, direct-semidirect anal., ang. distrib., anal. powers 4-106615
- <sup>4</sup>Ca(p, pn) A=40, 48 4-96025
- <sup>48</sup>Ca(p, n), 160 MeV, forward angle energy spectra, microscopic 1p1h doorway anal., giant resonance quenching 4-73899
- Gd, N=88 isotones, proton occupation amplitudes and proton stripping spectroscopic factors determ. 4-59147
- <sup>2</sup>H(p, pn) <sup>1</sup>H, knockout reactions, neutron-hole states 4-96025
- (<sup>3</sup>He, t), broad structure in t spectra, breakup-pickup reaction mechanism 4-59253
- <sup>4</sup>He(p, 2p), 350, 500 MeV, ang. distrib., mech. from nonrel. diagram summing 4-96016
- (<sup>8</sup>Kr, X), 1.52 GeV/N, Z $\geq 15$  projectile fragments, anomalous behaviour 4-86856
- Kr(p, X), high energy, fragmentation as critical phenomenon, fragment kinetic energy spectra 4-68664
- <sup>6</sup>Li(<sup>3</sup>Li,  $\alpha$ ), 2.4, 4.2 MeV, direct mechanism, quasifree effects 4-106607
- <sup>25</sup>Mg(d, p)<sup>26</sup>Mg ang. dist., spectroscopic factors, DWBA calcs. 4-83073
- <sup>23</sup>Na( $\pi$ , xN $\gamma$ ), nucleon removal, gamma spectra analysis, direct and cascade/evaporation processes 4-106631
- <sup>93</sup>Nb(n, n), statistical multistep direct emission theory 4-86828
- <sup>93</sup>Nb(n, p), 14 MeV, proton preequil. emission, ang. distrib., stat. model anal. 4-96019
- Nd, N=88 isotones, proton occupation amplitudes and proton stripping spectroscopic factors determ. 4-59147
- <sup>58</sup>Ni(<sup>32</sup>S, X), 355 MeV, light particle emission and fragmentation process, kinematic anal. 4-111550
- <sup>58</sup>Ni(<sup>32</sup>Ni, X) subbarrier fusion in direct reaction technique 4-73930
- <sup>58</sup>Ni(<sup>64</sup>Ni, X), subbarrier fusion in direct reaction technique 4-73930
- <sup>58</sup>Ni( $\alpha$ , d), breakup-fusion description, continuum spectra fit, ( $\alpha$ , p) comparison 4-102242
- <sup>58</sup>Ni( $\alpha$ , p), breakup-fusion description, continuum spectra fit, ( $\alpha$ , d), ( $\alpha$ , t) comparison 4-102242
- <sup>58</sup>Ni( $\alpha$ , t), breakup-fusion description, continuum spectra fit, ( $\alpha$ , p) comparison 4-102242
- <sup>58</sup>Ni(p, 2p)<sup>57</sup>Co, 198 MeV, multiple scatt. direction reactions, three-body approach 4-68695
- <sup>16</sup>O( $\alpha$ ,  $\gamma$ )<sup>20</sup>Ne direct capture reaction at low energies 4-102284
- (p, x) exchange effects in DWBA models of direct nuclear reactions 4-78636
- <sup>31</sup>P( $\pi$ , xN $\gamma$ ), nucleon removal, gamma spectra analysis, direct and cascade/evaporation processes 4-106631
- <sup>209</sup>Pb high excitation energy struts., direct excitation process from HI scatt. 4-102239
- <sup>209</sup>Pb(<sup>7</sup>Li, <sup>7</sup>Li), (<sup>7</sup>Li, <sup>7</sup>Li), 68 MeV, <sup>7</sup>Li excitation, Coulomb and nucl. contrib. 4-68725
- <sup>32</sup>S(<sup>3</sup>He, n)<sup>34</sup>Ar, interference between direct and compound reactions, excitation curves 4-59251
- <sup>32</sup>S( $\pi$ , xN $\gamma$ ), nucleon removal, gamma spectra analysis, direct and cascade/evaporation processes 4-106631
- <sup>28</sup>Si(p, p), polarisation and cross-section statistical correlation 4-78622
- Sm, N=88 isotones, proton occupation amplitudes and proton stripping spectroscopic factors determ. 4-59147
- <sup>23</sup>Th(<sup>40</sup>Ar, X), quasi-elastic multistep heavy ion processes, random matrix model 4-91013
- <sup>238</sup>U( $\alpha$ ,  $\alpha$ , X), X=p or fission fragment, 172 MeV, direct N knockout, precompound emission 4-83084
- Xe(p, X), high energy, fragmentation as critical phenomenon, fragment kinetic energy spectra 4-68664
- <sup>90</sup>Zr( $\alpha$ ,  $\alpha$ ),  $\alpha$ -clustering probe in statistical multistep direct theory 4-83082
- <sup>90</sup>Zr(p, n), 200 MeV, forward angle energy spectra, microscopic 1p1h doorway anal., giant resonance quenching 4-73899

**direct graphs**

- potential energy surfaces representing a-priori reaction pathways, directed graphs 4-96471

**direction finders, radio see radio direction-finding**

**directional antennas see directive antennas**

**directional couplers**

- acoustooptical couplers for an optical time-domain reflectometer 4-74703
- expanded beam directional couplers for LAN 4-107844
- fibre-optic polarising directional coupler 4-74726
- general planar guiding struct. at 10.6  $\mu$ m 4-91639
- graded-index (GRIN) rod-lens, design 4-74742
- power divider by two-step K<sup>+</sup>-ion exchange 4-107822
- InGaAsP/InP gigahertz-bandwidth optical modulators/switches with DH waveguides 4-112585
- LiNbO<sub>3</sub> high-speed modulators, design 4-64764
- LiNbO<sub>3</sub> high-speed modulator with low insertion loss for 1.3  $\mu$ m 4-64765
- LiNbO<sub>3</sub>:Ti channel waveguides and directional couplers, 3-D anal. 4-79286
- LiNbO<sub>3</sub>:Ti coupler based low-crosstalk waveguide polarisation multiplexer/demultiplexer for 1.32  $\mu$ m 4-60183
- LiNbO<sub>3</sub>:Ti directional coupler travelling wave optical modulator, high-speed pulse generation 4-69596

**directional patterns see antenna radiation patterns**

**directive antennas**

- see also lens antennas; loop antennas
- lunar radio flux data use in broadband antenna system meas., error anal. 4-110549
- microwave propagation and antenna characts. for solar power satellite (Japanese) 4-62932

**dirty superconductors**

- disordered narrow band, spin and density fluctuations 4-104355

**dirty superconductors continued**

- gapless superconductivity, vortex-antivortex pair dissociation in 2-D 4-92875
- metallic nearly ferromagnetic films, triplet supercond., weak localisation effect 4-98798
- pairing condensates, exciton mediated, phonon effect on T<sub>c</sub> 4-70974
- transition temp., upper crit. field, theory in weakly localised regime 4-108964
- triplet pairing supercond., possible diminution of impurity pair breaking in weakly localised 2D nearly mag. systems 4-104357
- two-dimensional, vortex pair unbinding and surface effects 4-108979
- Bi, amorphous, supercond., upper critical fields 4-76089
- Bi-Pb alloys, amorphous, supercond., upper critical fields 4-76089
- Nb, phonon singularities on I-V curves, point contact spectroscopy 4-71000
- Zr-Si, amorphous, upper critical field meas. 4-84754

**discharge lamps**

- see also arc lamps; flash lamps; fluorescent lamps; metal vapour lamps
- coaxial high-freq. electrodeless lamp, Kr filled, spectral distrib. of radiation 4-78385
- HID lamps design and evaluation for colour photographic purposes 4-90673
- Illuminating Engineering Society Annual Conf., Los Angeles, USA (Aug. 1983) 4-90291
- metal halide projection lamp 4-91555
- motion picture film, lighting, use of discharge lamps 4-111240
- rare earth halide, high press. lamp plasma, radiation mechanism 4-97940

**discharge lasers see gas lasers**

**discharge tubes see gas discharge tubes**

**discharges (electric)**

- see also arcs (electric); electric breakdown; exploding wires and foils; flashover; glow discharges; high-frequency discharges; lightning; positive column; sparks; surface discharges; Townsend discharge
- AC plasma display, transient phenomena 4-91999
- air, discharge plasma, electron gas, transport coeff., binary collision rates 4-97759
- air discharge, low pressure, VUV obs. (Chinese) 4-87954
- air gap discharges, phys. props. of leaders 4-79885
- air streamer inception field strength, area and time effect 4-79879
- anode sheath ionisation average freq. in crossed field discharge 4-92012
- atmospheric pressure discharge plasma, semi-self-sustained, electron energy distrib. function 4-79875
- battery state-of-charge determ. (Polish) 4-99959
- beam plasma discharge in crossed elec. and mag. fields, spatial characts. 4-113235
- bounded plasma, pot. form., dynamical behaviour 4-91875
- bulk discharge with ionisation multiplication of photoelectrons and light generation 4-97930
- capillary discharge from evaporating wall, magnetogasdynamic model 4-69973
- cataphoresis, steady-state density profile collapse with large cylindrical end volumes 4-60774
- cathode processes in exploding electron emission, cyclic nature 4-79872
- cathode spot initiation and mass balance in near-cathode plasma 4-91876
- cathode spot struct., Cu cathode erosion coeff. 4-87976
- charged particle density determ. in induced discharges 4-108247
- chromatic dispersion in the negative glow-cathode fall space transition zone 4-79864
- conductivity change at hollow cathode illuminated by ns. laser pulses 4-75227
- conference, energy removal and particle control in fusion devices, Princeton, NJ, USA (July 1983) 4-95041
- current oscillations in plane gas-filled diode with pulsing discharge 4-87856
- cylindrical cathode discharge in mag. field, characts. 4-113237
- cylindrical cathode discharge in mag. field, plasma parameters study 4-113238
- DC discharge, isotope separation in longit. mag. field 4-88011
- detector for gas and volatile liqs. leakage from pipes and containers under press. 4-78306
- dielectric materials, measurements anal. appls., conf., Lancaster, England (Sept. 1984) 4-106120
- dielectric surface charge field after discharge in adjoining gas gap 4-87988
- discharge threshold and space charge distrib., with electron beam emission 4-84109
- diverted ASDEX discharges, particle balance 4-97855
- divertor discharges, electron density and temperature meas. 4-97841
- divertor discharges, heat load reduction 4-97851
- divertor discharges, neutral beam heated in tokamak, high confinement 4-97850
- divertor discharges, neutral beam heated in tokamak, power balance 4-97853
- divertor discharges, particle recycling in beam heated expanded boundary 4-97856
- divertor discharges in D-III Langmuir probe meas. 4-97839
- divertor discharges in PDX tokamak, energy balance 4-97852
- drift-tearing modes control in Tokamak discharges 4-87867
- EGD flow of gas in corona discharge and its influence on motion of dispersed particles 4-103425
- electrical discharges and combustion, colloquium, London, England (April 1984) 4-67870
- electrochemical intercalation of fluorides into pyrographite, for high energy density battery cathodes 4-81444
- electrode discharges, simulation studies basic eqns. and soln. 4-75218
- electrode erosion phenomena in a high-energy pulsed discharge 4-60772
- electrode evaporated in vacuum 4-87972
- electrodeless discharge, stability in EM wave 4-103600
- electrodeless discharges, wall charge variations in 60 Hz fields 4-69981
- electron beam ionised, with added attaching gases, characts. 4-84118
- electron cyclotron emission from high density discharges in ASDEX Tokamak 4-75196
- electron density fluctuation spectrum, CO<sub>2</sub> laser light scatt. 4-65133
- electron energisation in crit. vel. discharge expt. 4-91863
- electron energy distribution in gases 4-79702
- electrostatic, electronic equipment immunity 4-69272
- electrostatic, geosynchronous spacecraft protection 4-69271
- electrostatic, human body and electronic equipment effects 4-69273
- electrostatic, precipitator rods, DC corona discharge and ion flow distribution characts. 4-97933

## discharges (electric) continued

- electrostatic discharges, charged insulator minimum potential for incendiary discharges 4-97936  
 electrostatic simulation, test facility development 4-69274  
 energy confinement with neutral beam heating, impurity effects 4-97843  
 externally sustained vol. discharge, cathode spot regular arrangement 4-69979  
 gap closure, cathode surface impurities 4-60777  
 gas discharge in electric field, kinetic theory 4-79876  
 gas discharges, charged particles, spacetime distrib. calc. (Russian) 4-84103  
 gas discharges containing excited atoms at low press., theoretical description 4-75223  
 gas expansion effect on contraction of a  $N_2$  discharge 4-113247  
 gas flow cond. development during  $N_2$  injection from capillary plasmatoms 4-87969  
 gas fueling in PDX tokamak 4-97854  
 gas temperature profile in discharge, laser beam deflection meas. 4-84086  
 gases/solids ignition by electrical discharges 4-69986  
 heterogeneous alloys, selective erosion, rel. to emission spectral anal. 4-81292  
 high voltage pulsed discharge, runaway electron investigation 4-84089  
 hollow anode ion-electron source 4-103528  
 hollow cathode discharge, high purity material spectral anal. 4-81493  
 hollow-cathode cell for a pulsed vapor laser 4-102939  
 HV electrode systems, post streamer stage of discharge in a nonuniform field (Russian) 4-69968  
 ignition conditions in transverse axisymmetric slightly uniform mag. field 4-69980  
 inert gases, electrical discharge, externally maintained, preionised, IR radiation generation, laser efficiency 4-64695  
 inert gases, nonequilibrium pulsed discharge plasma, ionisation relax. 4-60765  
 intense radiation transmission along, track of interrupted laser breakdown in gas 4-75167  
 ion beam current amplification, numerical soln. (Russian) 4-83538  
 laser plasmatron, steady-state optical discharge plasma, diagnostics 4-103577  
 laser-triggered elec. breakdown of gases, fundamental processes 4-75221  
 laser-triggered switching, recent advances 4-69471  
 light induced detonation of gas, lateral expansion, optical discharge 4-113252  
 low press., atoms and ions vel. distrib. functions, Boltzmann eqn. soln. 4-113232  
 low-pressure gas discharge, current break in transverse axially symm. mag. field 4-88003  
 metal vapour, nonequilibrium pulsed discharge plasma, ionisation relax. 4-60765  
 metals, energy deposition by laser-guided discharges 4-75219  
 microcomputer DC discharge intensity stabilization 4-108248  
 molecular gases in self-sustained pulse discharge, holographic interferometric investigation 4-79845  
 multiplier discharge with high plasma density 4-97926  
 multipolar discharge, primary electron trajectories 4-87957  
 nanosecond volume discharge form. with UV radiation preionisation 4-79732  
 negative ion formation and extraction in Cs-H discharge 4-58915  
 net ionisation rates, meas. by transient techniques 4-79728  
 non-self-sustained discharge with a plasma cathode 4-84114  
 nonpreionised gas in cylindrical discharge tube, wave breakdown, electron prod. kinetics 4-60766  
 onset levels in strongly electroneg. gases and gas mixtures, Paschen's law calcs. 4-79880  
 optical emissions from laboratory beam plasma discharge 4-67526  
 optically controlled discharges, recent advances 4-113256  
 organic cpds., plasma-beam discharges, electron beam longitudinal excitation 4-78977  
 organophosphorus cpd.,  $C_7H_{16}FO_2P$ , decomp. in silent elec. discharge 4-109630  
 ozone synthesis, in gas discharges 4-69983  
 phenomena in ionised gases, conference, Dusseldorf, Germany (Sept. 1984) 4-82598  
 planar magnetron sputtering system, poles exposing type, DC discharge characts. (Japanese) 4-61852  
 plasma density uniformity in multipolar discharges 4-75124  
 plasma diagnostics, in ion-assisted physical vapour deposition systems 4-79853  
 plasma discharge behaviour in TEXTOR, carburization 4-97885  
 plasma focus discharge, sheath build-up, temp. and density spectral meas. 4-87951  
 plasma focus discharge, sheath polarisation fields 4-87950  
 plasma focus discharges, initiation, energy compression and neutron prod. 4-87949  
 plasma in inert gas ion thruster (Japanese) 4-103589  
 plasma neutral beam-heated limiter discharges in D-III tokamak, power flow 4-97877  
 plasma parameters of cylindrical cathode discharge, mag. field effects 4-88012  
 plasma poloidal divertor plates, thermomechanical evaluation for long pulses 4-97891  
 plasma pump limiters, particle removal in ISX-B tokamak 4-97872  
 plasmatron, high freq. induction, heating of porous wall, math. modelling 4-60742  
 PLT Tokamak, thermal and slideway discharges, resistivity 4-60778  
 polyethylene, low-density, anomalous discharge current 4-114206  
 polythene films, space-charge limited charge distrib., discharge currents 4-88621  
 positive wire to plane coronas, atmospheric humidity effect on inception voltage 4-97937  
 pulsed discharge, diagnostics, using multicolour laser interferometer 4-60727  
 pulsed discharge sound source for acoustic measurements, stability (Japanese) 4-112663  
 pulsed discharges, energy and time characteristics 4-65149  
 pulsed hollow cathode discharge in cylindrical geometry 4-113253  
 quasisteady flow behind intense shock waves, air ionisation meas. using electrostatic probes 4-60640  
 rare-gas-halide lasers, X-ray preionisation 4-74488  
 resonance cones, kinetic effects, diagnostic appls. 4-91992

## discharges (electric) continued

- resonant atomic state excitation rate const., depend. on plasma ionisation degree 4-69977  
 self corona discharge of sharp edged ellipsoidal particles in electric field 4-97934  
 self-focusing electron beams, plasma-beam discharge 4-84022  
 self-sustaining discharge condition at the transition from high-energy to low-energy electron beam 4-92017  
 semi-self-sustained discharge form., X-ray effects 4-84110  
 semiconductor etching in gas discharge 4-76878  
 similarity laws in cylindrical cathode discharges 4-87989  
 single electrode atmospheric pressure microwave discharge system for elemental analysis 4-113243  
 space-charge-limited electron current flow in curved geometries with ion. prod. 4-92006  
 spherical magnetic-discharge cell for low-density gas flow meas. 4-86433  
 static filf TEA lasers, high repetition rate, gas density perturbations 4-91443  
 stationary potential jump on weak double layer in discharge plasmas 4-108186  
 steady-state externally maintained discharge cathode layer struct. form. 4-108242  
 streamer development at large E/P in drift approx. 4-69978  
 streamer propagation characts., meas. using photomultipliers 4-97939  
 subsonic optical discharge, two gasdynamic propag. regimes 4-60775  
 supersonic propagation of an ionization wave along a laser beam 4-97931  
 Thomson scatt. diagnostics of atm. press. discharges 4-79836  
 tokamak, FT-2, with slowly increasing vortical field in prebreakdown phase, discharge development 4-75192  
 triplet and cold radical prod. with pulsed elec. discharge in pulsed supersonic flow 4-84090  
 tube, diffusion, steady state cataphoretic profile 4-79878  
 uniform high-current creeping discharge 4-113246  
 vacuum breakdown under impulse voltages 4-69982  
 vacuum capacitor, metal particles collisions, self-oscillatory motion 4-97932  
 vacuum channels, form. of plasma near wall 4-97816  
 water, HV discharge in limited volume, quasistatic press. calc. (Russian) 4-84095  
 water, pulse discharge, decontaminating factors influence (Russian) 4-84094  
 weakly ionised gas, discharge threshold and space charge distrib., with electron beam emission 4-84109  
 Z-pinch high-current discharge current struct. diagnostics 4-91976  
 Ar, electrical discharge, externally maintained, preionised, IR radiation generation, laser efficiency 4-64695  
 Ar, flow of a nonequilibrium recombining plasma in a magnetogasdynamic duct 4-60602  
 Ar high-voltage discharge in crossed inhomogeneous mag. field 4-88004  
 Ar 1, 2p level lifetime determ. 4-107310  
 Ar ICP, vacuum UV emission spectra, 85 to 200 nm 4-90665  
 Ar low-current discharge with two parallel plane cathodes, electron motion simulation 4-91981  
 Ar plasma, Cs seeded, MHD channels, discharge struct., load change characts. 4-97912  
 Ar triplet and cold radical prod. with pulsed elec. discharge in pulsed supersonic flow 4-84090  
 Ar-plasma, discharge column, low-press., nonlinear behaviour, density changes 4-60771  
 Bi-Ne discharge, difficulties associated with stimulated emission 4-96484  
 CN radical evolution in  $N_2$ -ethanol mixture pulsed discharge 4-81428  
 CO CW industrial laser, electron beam-controlled with 10 kW output power, energy characts. 4-74492  
 CO triplet and cold radical prod. with pulsed elec. discharge in pulsed supersonic flow 4-84090  
 CO, vibr. excited, post discharge, electron energy distrib. function 4-92014  
 CO<sub>2</sub> CW high power transverse flow laser type JL6A working gas determ. and catalytic purification (Chinese) 4-112463  
 CO<sub>2</sub> CW transverse flow laser, quasi two-dimens. gain distrib. (Chinese) 4-112376  
 CO<sub>2</sub> laser, quasi-CW, tunable, 1-sec pulse, optical pumping appls. 4-74536  
 CO<sub>2</sub> mixing lasers, plasma injection controlled discharge characts. 4-83563  
 CO<sub>2</sub> pulse-periodic laser, wave-driven gas circulation in a gas chamber with pulse-periodic energy supply 4-60068  
 CO<sub>2</sub> pulsed amplifiers, pumping process modelling in elec. discharges 4-83564  
 CO<sub>2</sub> pulsed discharges, energy and time characteristics 4-65149  
 CO<sub>2</sub> RF excited lasers, electron energy distrib. and transport coeffs. 4-102919  
 CO<sub>2</sub>, temp. and flow distrib. in self-sustained discharge, laser characts. 4-79104  
 CO<sub>2</sub> waveguide laser, RF discharge excited, freq. depend. 4-79099  
 Cd-He discharge, current disturbances, Cd<sup>+</sup> inversion density, dynamic response 4-108237  
<sup>111</sup>Cd self-alignment in a discharge 4-87963  
 Cs plasma triodes, electron beam heating, switching transient theory 4-108226  
 F<sup>+</sup> laser, discharge-pumped, intense laser generation 4-60062  
 H<sup>+</sup>, honeycomb surface-plasma source 4-101975  
 H<sub>2</sub> discharge, spatial and temporal current growth: 4-79883  
 H<sub>2</sub> vibrationally excited generation by H<sub>2</sub><sup>+</sup> wall collisions 4-76574  
 HF pulsed-discharge lasers preionised by pulse or CW X-rays 4-69387  
 He DC discharge anode plasma, propag. phenomena 4-92020  
 He filled spark chamber, ionisation meas. and time depend. discharge characts. study 4-59570  
 He high-voltage discharge in hollow cathode 4-103591  
 He, liq., dielectric breakdown delay time, superconductivity effect 4-109125  
 He, spark discharge formation time, discharge gap ionisation, depend. 4-69974  
 He-F<sub>2</sub>-Kr atmospheric discharge, electron density, streak interferometric method 4-84092  
 He-Ne gas discharge cell, He-Ne probe laser intensity perturbation transverse distribution investigation 4-79207  
 He-Ne lasers, small, striation-onset condition investigation 4-64694  
 He-Ne small bore discharge, radial optical gain distrib. 4-102921  
 He-plasmas, discharge column, nonlinear behaviour, density changes 4-60771

# discharges (electric) continued

- He-Xe mixture, pulse discharge, nonequilib. plasma, electron energy distrib. 4-79874
- Hg, effective lifetimes of  $6^3\text{P}_1$  level in low press. discharges 4-91233
- Hg low press. discharge,  $6^3\text{P}_1$  state direct electron impact excitation cross section 4-102801
- Hg-He high-press. discharge, electron loss rate meas. 4-65143
- Hg-Tl discharge temp. determ. by reabsorpt. method 4-84100
- HgBr<sub>2</sub>/HgBr dissociation laser, discharged pumped (*Japanese*) 4-74490
- KrF<sup>+</sup> electrodischarge, excimer laser plasmas, runaway electron current and form. of spatial struct. 4-97929
- Li anode cells, primary and secondary, review 4-72054
- Li/Cu<sub>2</sub>V<sub>2</sub>O<sub>7</sub> battery with 1-M LiClO<sub>4</sub>-propylene carbonate/1,2-dimethoxyethane electrolyte 4-93607
- Li-Al electrode secondary cell, cycling behaviour in LiClO<sub>4</sub>-propylene carbonate solutions 4-72058
- MnO<sub>2</sub>-Zn rechargeable alkaline cells, test cell construction and development, cycling tests 4-81531
- N<sub>2</sub>, active, expt. evidence for  $\text{N}_2(\text{X}^1\Sigma_g^+)$ , by multichannel pulsed-laser Raman spectroscopy 4-96551
- N<sub>2</sub>, C<sup>+</sup> and B<sup>+</sup> levels, in pulsed self-sustained discharge, low ionisation pot. additives effects 4-83294
- N<sub>2</sub>, compact capacitively coupled laser with new electrode design 4-60067
- N<sub>2</sub> discharge, volume-dominated, UV preionisation effect 4-84112
- N<sub>2</sub> discharge laser, model calc. and expts. 4-83568
- N<sub>2</sub>, E state deactivation 4-92010
- N<sub>2</sub>, pulse laser gas discharge, plasma decay 4-113236
- N<sub>2</sub>, pulsed discharges, energy and time characteristics 4-65149
- N<sub>2</sub> pulsed-discharge lasers preionised by pulse or CW X-rays 4-69387
- N<sub>2</sub>, pure, discharge form. and development 4-79886
- N<sub>2</sub>-CO<sub>2</sub> mixture, radiation amplification in continuous optical discharge plasma 4-84122
- Na, vapour, laser initiated discharge channels 4-113255
- Nd:glass laser discharge supersonic propag. away from region of microsec. breakdown in air in beam direction 4-79823
- Ne, contracted, compression ionisation waves 4-91914
- Ne diffusion coeff. meas. at 530K in low press. Na-Ne discharge 4-79760
- Ne discharge, constricted, ionisation waves 4-92018
- Ne gas discharge cell, He-Ne probe laser intensity perturbation transverse distribution investigation 4-79207
- Ne hollow cathode discharge, optogalvanic effect, Langmuir probe meas. 4-84063
- Ne RF discharge, plasm polarisation spectroscopy 4-87933
- Ne streamer breakdown, electron avalanche critical radius 4-103595
- Ne-H<sub>2</sub> pulsed transverse elec. discharge, Ne<sup>+</sup> recomb. pumping (*Russian*) 4-112133
- Ni-Cd accumulator batteries, technology review (*French*) 4-81536
- O<sub>2</sub> generation in oxygen discharge, numerical model 4-89290
- O<sub>2</sub> molecular formation in nonsustained discharge in air 4-87839
- O<sub>2</sub> production during corona discharges in air and other gases, experimental study 4-97938
- Pb/acid batteries, influence on capacity of pulsed discharge, importance for electric vehicles 4-66683
- Pb/acid battery lifetime prediction, computerised pattern recognition application to life-cycling test data 4-81530
- Pb/acid sealed recombination cells for standby power 4-93610
- SF<sub>6</sub>, compressed, leader development in short point-plane gaps 4-69972
- SF<sub>6</sub>, low press., long path breakdown and discharge development 4-79730
- Si:H amorphous compensated films, xerographic discharge meas. 4-80603
- SiH<sub>4</sub> multiple discharges, positive and negative extraction, mass spectra study 4-79857
- SiH<sub>4</sub> multiple discharges, positive and negative extraction, mass spectra study 4-79857
- Ti/Fe redox flow battery discharge performance 4-81534
- TlHg laser, discharge excited 4-69389
- U, Penning ionisation in hollow cathode discharge 4-88006
- Xe, energy distribution function of electron swarm in binary encounter region 4-79757
- XeCl<sup>+</sup> laser, discharge stability 4-91441

# disclinations

- curved space formalism for dislocation density 4-80037
- ferroelectric smectic C\* liq. crystals, helicoidal struct., field induced processes 4-65171
- magnetic thin films, amorphisation of regular domain structures at second-order phase transitions, dislocation-disclination mechanism 4-98928
- MBBA, disclinations during shear flow, optical microscopy studies 4-75279
- metals, wedge disclination systems, elastic interaction with grain boundaries 4-65292
- methoxybenzylidenbutylaniline-cholesteryl nonanoate liq. cryst. mixture, electrohydrodynamic instabilities 4-113329
- noncrystalline sphere packings, defect struct. model 4-108280
- plasticity and fracture, deform. modes 4-98177
- potassium 1-N-lauroyl-serinate, cholesteric lyomesophases, type II system 4-84148
- potassium 1-N-lauroyl-serinate, intrinsic cholesteric lyomesophases 4-84146
- rectangular disclination loops, elastic props. 4-70155
- smectic B and E phases, disclinations and ovals near clearing temp. 4-75268
- smectic C\* liq. cryst., twist disclinations 4-70027
- smectic C\* phase, dispirations, disclinations and dislocations 4-79926
- smectic-C, monopole struct. and droplet shapes 4-103650
- thermo-piezoelectric continua, moving dislocations and disclinations, mechanical electrical and thermal fields 4-98102

# discontinuous control systems see sampled data systems

# discontinuous metallic thin films

- columnar and polycrystalline, resist., TCR and Hall coeff. 4-70952
- electrical conductivity, unlike surfaces effect, Cottey model 4-70951
- electrical conductivity of discontinuous thin metal films and conducting filaments 4-98785
- ion beam mixing of metal films on SiO<sub>2</sub> 4-108732
- laser-induced surface diffusion Brownian motion model 4-70607
- mass fluctuations meas. 4-82759
- optical storage material, laser induced coalescence writing mechanism 4-97010

# discontinuous metallic thin films continued

- photosensitive glass, discontinuous/continuous metal films growth by ion exchange 4-87404
- semi-continuous metallic films, vapour deposition simulation, submicron hemisphere sintering model 4-66237
- semicontinuous thin films, resist. based on computer model of thin film formation 4-80692
- trilayer with island metal film recording layer as optical data disc 4-91548
- Ag aggregated film on Al substrate, solar selective behaviour 4-61760
- Ag discontinuous film, freq. shift of electric dipole resonances 4-104326
- Ag epitaxial films on Ge (001), superconductivity and electron localisation 4-114062
- Ag film, adsorbed on Cu, electronic props., surface refl. spectroscopy study 4-85023
- Ag island film, adsorbed rhodamine 6G dye molecule, picosecond fluorescence decay 4-87156
- Ag island film, chemisorbed CN, depolarisation effects in Raman scatt., classical microscopic local field 4-88832
- Ag island films, deposited copper phthalocyanine thin films, surface enhanced Raman scatt. 4-66036
- Ag islands, microAuger anal. interpretation by backscatt. electrons 4-71486
- Au discontinuous films, epitaxial deposition on mica substrates 4-70597
- Au fine grained target, sputtering by heavy multicharged ions 4-109296
- Au, granular films, relax. phenomena 4-108747
- Au island film, charge transport and conductance oscill. 4-84712
- Au semicontinuous thin films, 2D percolation system, conduction and Hall coeffs. 4-70957
- Au submonolayer film, optical absorption,  $\epsilon_{\text{bound}}$  size depend. in small island particles 4-66089
- Au thin films, agglomerated, phys. and optical props. 4-76545
- Bi discontinuous thin film, electron localisation and conductivity (*Russian*) 4-98780
- CO clusters, two-dimens., chemisorption of CO 4-108725
- Cu aggregated film on Al substrate, solar selective behaviour 4-61760
- Cu film, adsorbed on Ag, electronic props., surface refl. spectroscopy study 4-85023
- H<sub>2</sub> production by photoelectrocatalysis on p-MoS<sub>2</sub> 4-114963
- MnO films, C supported, XPS and Ar ion etching study 4-93192
- Pb granular films, SAW attenuation in normal and supercond. states 4-98422

# discrete symmetries

- see also *C invariance*; *CP invariance*; *CPT invariance*; *P invariance*; *parity*; *T invariance*
- boson-fermion duality, neutrino and photon construction from new massless boson 4-95777
- complex Grassmannian and CP<sup>N-1</sup> nonlinear sigma models, classical and exact solution 4-102047
- Dirac and Majorana fermions, pseudo-Dirac neutrinos, discrete symmetries 4-106531
- dynamical charge conjugation, Weinberg-Salam SU(2)×U(1) gauge symm. 4-106449
- normal units of large symmetry group 4-106488
- reflectivity positivity and modified Migdal-Kadanoff procedure, lattice gauge theories 4-95675
- Susskind fermions, mass term symmetry properties 4-90816
- unified theories, mirror fermions, SU(3)×SU(2)×U(1) gauge symmetry 4-86604

# discrete systems

- see also *sampled data systems*
- astatic system, for control of DC motors for altazimuth mountings of gamma-ray telescopes 4-105886
- dynamical systems with stochastic parameters, Lyapunov's direct method appl. 4-73211
- oil stratum dynamic model, parameter correction 4-110145

# discriminators

- see also *demodulators*
- digital pulse-shape discriminating unit for neutron-gamma discrimination with NE213 liq. scintillator 4-64312
- dual differential discriminator with accurate time linkage to a time-to-height converter 4-107265
- speech signal, discriminator of informative features 4-112646
- X-ray position sensitive detectors, discriminator performance characts. 4-86518

# disinclinations see disclinations

# disintegration (radioactive) see radioactivity

# disintegration energies see radioactivity

# dislocation anchoring see dislocation pinning

# dislocation arrays

- austenitic alloys, He bubbles at grain boundaries 4-108471
- FCC/BCC interfaces, semicoherent and incoherent, electron diff. obs. of dislocation arrays 4-70160
- fracture, unified theory, book 4-63426
- Al-Al<sub>3</sub>Ni eutectics, directionally solidified, interfacial microstructures, TEM obs. 4-81187
- Li<sub>2</sub>CO<sub>3</sub>, single cryst., sub-boundaries on (002) cleavages 4-103751
- Ni/Cu/(001)Ni triple layer films, tensile props. 4-99324
- Ni<sub>3</sub>Cr, Ni<sub>2</sub>Cr, high temp. deform., effect of ordering 4-93358
- Si polycrystalline islands on fused SiO<sub>2</sub>, crack elimination by recrystn. 4-80461

# dislocation breakaway, pinned see dislocation damping

# dislocation climb

- Carrara Marble, high temp. flow, grain boundary sliding model 4-110132
- Harper-Dorn creep, artifact of low-amplitude temp. cycling 4-94089
- III-V optical sources, defects degradation, experimental anal. 4-83654
- metals, high-temp. creep, reln. between Orowan and Bailey-Orowan eqns. 4-92209
- metals and alloys, book contrib. 4-108361
- relaxation creep, computer model for high temp. 4-84340
- sapphire, dislocation dissociation, TEM studies 4-108374
- steel, A liq. cryst., screw dislocation lines, helical instability 4-60822
- steel, austenitic stainless, proton irradiation creep of thin foil specimens, thickness effects on mech. props. 4-103820
- steels, austenitic stainless, 316 and 253MA, high temp. low cycle fatigue, comparison between mech. props. and microstruct. 4-93410
- Al, internal friction originated by grain boundaries 4-103872

**dislocation climb continued**

- Al-Mg solid solution alloys, high stress levels, breakdown in creep 4-113526
- Cu, creep and long-term strength study (*Russian*) 4-80146
- GaAs, contour maps of EL2 deep level, dislocations 4-80530
- Ni superalloy, creep and recovery kinetics, report 4-62000
- NiAl, vacancy dislocation loops, annealing effect, TEM obs. 4-103756
- PbTe,  $\text{Se}_{1-x}\text{Te}_x$ /PbTe heterojunctions, epitaxially grown, misfit dislocations 4-88431
- Si, partial dislocations, glide forces, climb forces, geometrical study 4-113446
- SiC, reaction bonded, high temp. creep kinetics, dislocation glide mechanism 4-109476
- W<sub>2</sub>C, crystal structure and dislocation climb obs. by TEM 4-98072

**dislocation damping**

see also Bordoni effect

- Al-Fe, cold worked, damping capacity, mech. props. rel. to heat treatment and comp. (*Japanese*) 4-61968
- alloys, superdislocation traps in inhomogeneous glide plane (*Russian*) 4-92210
- LiF crystal,  $\gamma$ -ray irradiation effects on dislocation damping coeff. 4-65267
- NaCl,  $\gamma$  and laser irradiation, internal friction and dislocation damping 4-80153
- Si-Cu, impurity effect on dislocation motion 4-70187

**dislocation density**

- anthracene crystals, reduction of grown-in dislocation density due to heat treatment and growth conditions 4-113450
- axial dechanneling with dislocations, theory 4-88217
- corundum single crystals, cracking resist. rel. to dislocation density 4-93370
- crack near a free surface, resonance effects 4-97421
- crack tip stress intensity factor for double slip plane model crack, explicit calc. 4-60329
- crystalline solid dynamic plasticity 4-98183
- crystals, mechanoluminescence, microhardness and disloc. density depend. 4-85020
- garnet epitaxial layers, coercivity phenomena 4-76204
- HSLA, fatigue threshold; thermally activated behaviour of effective stress intensity 4-76853
- inclined pileup at crack tip without a dislocation-free zone 4-80148
- Luders band propagation, constitutive eqns. for inhomogeneous plastic flow 4-65329
- magnetic transition temperature of Li<sub>2</sub>-type materials, influence of plastic deform. 4-84785
- metals, fatigued, elastic strain distrib. and X-ray reflex profiles 4-76796
- metals, high-temp. creep, reln. between Orowan and Bailey-Orowan eqns. 4-92209
- metals, non-cubic, single crystal plates, low dislocation density 4-93211
- NMR studies of dislocations in solids, book contrib. 4-98111
- pentaerythritol tetratrate crystals, soln. growth and defects 4-113452
- quartz, seed treatment effect on dislocations 4-61827
- relaxation creep, computer model for high temp. 4-84340
- solids, stress relax., dislocation dynamics 4-64854
- steel, austenitic stainless, low cycle fatigue damage at high temp., X-ray obs. (*Japanese*) 4-114642
- steel, austenitic stainless, stress relax. in bending at 773K 4-81229
- steel, austenitic stainless, swelling resistance under HFIR irradiation, improvement through microstruct. control 4-103791
- steel, austenitic stainless, work hardening rel. to grain size 4-81220
- steel, bainitic and ferritic, cleavage fracture initiation, microstruct. 4-99556
- steel, C redistribution by explosion-thermal treatment 4-71673
- steel, cast Mn, shock wave loaded, struct. and residual props. 4-93369
- steel, dual-phase, dislocation substruct. as function of strain 4-99435
- steel, HSLA, Mn, bearing, strengthening mechanisms rel. to treatment and microstruct. 4-81209
- steel, low C, cold rolled, initial stage of decarburisation 4-114577
- steel, low C, ductile-brittle transition temp., effect of tensile prestrain (*Japanese*) 4-114650
- steel, martensitic, precip. and mech. props., influence of high temp. thermomechanical treatment 4-114522
- steel, microalloyed, structural, yield props., influence of dislocation density and precip. 4-114601
- steel, Nb, strengthening mechanisms, influence of rolling variables 4-71666
- steel, spheroidized 1090, dislocation density distrib. in tensile specimens, H effect 4-84298
- substrates and epilayers, growth, optical communication requirements, review 4-61833
- tensile testing of materials at elevated temps., threshold stress, struct., recovery models 4-66528
- weld metal, globular silicates effect on ductility and microstruct. 4-114607
- X-ray diffraction patterns, Kossel line broadening anal. 4-70157
- Ag-Sn alloys, rapidly quenched, TEM study of struct. defects, depend. on internal residual stresses 4-88172
- Al, plastic deformation at high strain rates 4-84337
- Al, shock loaded, microstructure and hardness 4-109515
- Al wires, low cycle fatigue, lattice defects, resist., temp. depend. (*Japanese*) 4-99508
- Al-Fe-Mg-Cu, periodic load serrations in tensile curve, occurrence conditions 4-85194
- Al-Zn-Mg, fatigue crack advance model, crack tip parameters 4-66401
- Al-Zn-Mg-Cu, ERGAL 7075, plastic deformation at high strain rates 4-84337
- Cd, Hg<sub>1-x</sub>Te under uniaxial deform., photoelectric props. 4-70864
- n-CdTe, deep levels, plastic deform. effects, DLTS studies 4-84591
- CdTe, dislocations and subboundaries, etching studies 4-75451
- CdTe, plastically deformed at room temp., dislocations, TEM study 4-98104
- CdTe, X-ray diffraction study, cryst. struct. (*Russian*) 4-84280
- Cu and Cu-Al alloys, strain hardening in microdeform., dislocation density, internal friction obs. 4-66397
- Cu, dynamically deformed, annealing-induced struct. variations 4-71667
- Cu, single crystal, strain bursts in cyclic creep at ambient temp. 4-66371
- Cu-Ge, shock loaded, dislocations and plastic response 4-108370
- Cu-Mn-Zn, microstructure study after cold working 4-108385
- $\beta$ -CuZn, single crystal, yield point phenomenon, high temp. 4-113521
- Fe, dislocation loop form. by self-ion irradiation at 40K, electron microscopy obs. 4-70242
- dislocation density continued
- $\alpha$ -Fe, nitriding, heterogeneous, dislocation production and oriented precip. 4-66498
- Fe-Nb-C-(B), isothermally transformed, microstruct. 4-114510
- Fe-(Si), fatigue threshold, thermally activated behaviour of effective stress intensity 4-76853
- (Ga,Al)As/GaAs double heterostructures, LPE, struct. and lasing characteristics, rel. to As vapour press. 4-66249
- Ga<sub>1-x</sub>Al<sub>x</sub>As-GaAs heterostructure, LPE grown, dislocation extension and density distrib. (*Chinese*) 4-113449
- GaAs epitaxial selective regions in Si substrate windows, struct. perfection 4-75812
- GaAs, growth from melt and elec. props. 4-99300
- GaAs, semi-insulating, deep donor conc., dislocations and elec. resist. 4-103781
- GaAs semi-insulating substrate, inhomogeneity characterisation, expt. study 4-65759
- GaAs, single cryst. growth by liquid encapsulated Czochralski method 4-114377
- GaAs substrates for GaAs ICs, growth processes 4-99299
- GaAs:Cr, semi-insulating, inhomogeneities, optical obs. 4-60944
- GaAs:Si, crystal growth by horizontal gradient freeze technique, carrier and dislocation density 4-66216
- GaAs/Ge single crystal layers, MBE growth and patterning on Si substrates 4-99315
- GaP, large single crystals, LEC growth, LEDs 4-99301
- $\alpha$ -HgI<sub>2</sub> crystal, growth, space-charge relax. in appl. elec. field 4-66204
- InAs, P<sub>1-x</sub>As<sub>x</sub>, LEC growth and characterisation 4-99302
- InP/Ga<sub>1-x</sub>Sb crystals, dislocation density reduction by isoelectronic double doping 4-60940
- InSb, X-ray diffraction study, cryst. struct. (*Russian*) 4-84280
- KCl powders, coloration stability, particle size depend. 4-60921
- LiF single crystals, grinding, surface layer, strain hardening, dislocation density, microhardness 4-93312
- MgO single crystals, dislocation motion under plate impact 4-65265
- Mo, shock loaded, dislocations and plastic response 4-108370
- Mo-Re, shock loaded, dislocations and plastic response 4-108370
- NaCl-type crystals, flexibility of dislocation forest to deformation resistance 4-84293
- Ni alloys, high-alloy, microstruct. and comp. characts. of eutectic  $\gamma'$  phase (*Russian*) 4-92380
- Ni, H embrittlement, influence of plastic deform. 4-71729
- Ni, laser irradiation, defect struct. and surface alloys 4-75509
- PbTe epitaxial films, photoluminescence characts. 4-66067
- PbTe,  $\text{Se}_{1-x}\text{Te}_x$ /PbTe heterojunctions, epitaxially grown, misfit dislocations 4-88431
- Si, amplitude depend. of ultrasonic absorpt. 4-70278
- n-Si, defect characterisation, SEM-CCM studies 4-113278
- p-Si high-purity quenched samples, defect photoluminesc. 4-80979
- n-Si, irradiated by  $\gamma$ -rays, changes in carrier lifetime 4-104232
- Si on sapphire, phonon boundary scatt. at interface 4-104050
- Si:P<sup>+</sup>, implanted, dislocation struct. development, effect of cryst. orientation, TEM obs. 4-80040
- SiC fibre/platelet reinforced Al-Mg-Si, magnitude and mechanism of strengthening 4-76710
- SiC reinforced Al alloy, fibres and particles, composite strengthening, influence of microstruct. 4-99398
- TiB<sub>2</sub>, implanted with 1 MeV Ni<sup>2+</sup> ions, microstruct. and surface mech. props. 4-70232
- W, creep in single crystals at moderate temps., struct. changes 4-65269
- WC, indented, dislocation interactions, crack nucleation, TEM obs. 4-80039
- Y<sub>2</sub>O<sub>3</sub>, undoped single crystal, struct., crystal-chemical anal. 4-65221
- dislocation dipoles
- cell wall form. mechanism 4-80038
- prefecture zone, influence of local hardening on plastic deform. 4-70262
- steel, Mn pearlitic ferrite, fatigue dislocation structure (*Chinese*) 4-85201
- CdTe, plastically deformed at room temp., dislocations, TEM study 4-98104
- Cu<sub>2</sub>NiZn, superlattice dislocations, TEM microstruct. study 4-75450
- GaAs:Te, deformed, precip., defect struct., electron microscopy obs. 4-103752
- InGaAsP-InGaP rapidly degraded DH laser grown by LPE, dark-line defects 4-69406
- KBr(Cl), electric field influence on dynamic yield point 4-75605
- LiF, electric field influence on dynamic yield point 4-75605
- NaCl, electric field influence on dynamic yield point 4-75605
- Ni<sub>3</sub>Cr, Ni<sub>2</sub>Cr, high temp. deform., effect of ordering 4-93358
- dislocation drag
- anisotropic BCC metal, mobile interstitial internal friction and viscosity 4-70271
- dynamic dragging of dislocations, effect of impurities 4-98127
- metals, close packed, dislocation displacements under stress pulses 4-103762
- metals and alloys, book contrib. 4-108361
- phonon drag of dislocations near phase transition points 4-60929
- superconductors, US attenuation, electron drag on dislocations, energy gap meas. 4-92862
- US attenuation meas. of dislocation drag ultrasonic absorption metals 4-103764
- Al single crystal, dislocation displacements under stress pulses 4-103762
- Al-Mg (1.74 at.%), creep, strain transients in stress drop tests 4-85196
- Cu, dislocation drag, mag. field effect 4-103763
- Cu single crystal, dislocation displacements under stress pulses 4-103762
- MgO, dislocation motion and plasticity 4-80043
- MgO single crystals, dislocation motion under plate impact 4-65265
- NaCl, shock deform., mobility of fast dislocations 4-98109
- Ni, yield point, temp. depend., mag. field effects 4-80807
- Si sheets, coated, dislocation movement 4-70166
- Zn, dislocation drag, mag. field effect 4-103763
- Zn, dislocation drag mech. 4-103761
- Zn, electron dislocation drag during low temp. plastic deform. 4-98128
- Zn single crystal, dislocation displacements under stress pulses 4-103762
- dislocation energy
- two-dimensional systems, melting, Monte Carlo simulation studies 4-113586
- dislocation etching
- alkali halide, crack edge contact restoration phenomena 4-98191
- alkali halide crystals, dislocation etching, etch pits, crystal growth, review 4-70159

**dislocation etching continued**

- alkali halide crystals, etch pit studies of dislocations, dissolution kinetics and impurity effects 4-70158
- anthracene crystals, reduction of grown-in dislocation density due to heat treatment and growth conditions 4-113450
- gallium aluminium sulfate hexahydrate, ferroelectric, cleavage surfaces, spiral patterns 4-108367
- organic explosive, dislocation etching, microhardness, primary slip systems 4-65266
- quartz, hydrolytically weakened, plasticity and rheology 4-92286
- $\alpha\text{-Al}_2\text{O}_3$ , monocrystalline, dislocations, chem. etching studies 4-60933
- Bi-Sb single crystals, etching characts. of edge and screw dislocations on cleavage plane 4-80044
- $\text{CaCO}_3$ , calcite, dislocation struct. and twinning 4-113467
- CdTe, dislocations and subboundaries, etching studies 4-75451
- Cu, cyclic deformation of single crystals, oriented for double slip 4-98174
- $\text{Ga}_{1-x}\text{Al}_x\text{As}$ -GaAs heterostructure, LPE grown, dislocation extension and density distrib. (Chinese) 4-113449
- GaAs, dislocations and point-defect complex formations, thermal stability 4-103758
- GaAs, MBE grown, surface defects obs. 4-61246
- GaAs, semi-insulating, deep donor conc., dislocations and elec. resist. 4-103781
- GaAs:Ge(Si), LEC grown, dislocation structure etching rel. to dopant conc. 4-113451
- InP:Zn(S) single crystal growth, LEC technique, perfection, preferential etching, SEM and X-ray analysis 4-71549
- InSe Bridgman grown crystals, growth parameters, improvement rel. to defects 4-98043
- $\text{Li}_2\text{CO}_3$ , single crystal, sub-boundaries on (002) cleavages 4-103751
- LiF, dislocation mobility at low temps., etch pit obs., Peierls mechanism 4-98105
- MgO, dislocation motion and plasticity 4-80043
- MgO single crystals, dislocation motion under plate impact 4-65265
- NaCl single crystals, etching, solvent impurity effects 4-65264
- NaCl:CaCl<sub>2</sub> doped cryst., dissolution at dislocation sites 4-60931
- (NaK)Cl, melt-grown mixed single cryst., precipitation, etching study 4-61090
- Si crystals, Czochralski pulled, O precipitation, diffusion mechanism, etching optical and neutron scatt. obs. 4-65209
- Si, defect delineation by chem. etching 4-88171
- n-Si, irradiated by  $\gamma$ -rays, changes in carrier lifetime 4-104232
- Si single cryst., dislocation etching, orientation depend. 4-113454
- Si:P, dislocation motion, onset delay times, etching study 4-70163
- Sn, white, single crystals, dislocation motion in pre-multiplication region, creep, etching 4-108375

**dislocation glide** *see slip*

**dislocation interactions**

*see also impurity-dislocation interactions; vacancy-dislocation interactions*

- activation-free dislocation motion, deviation from Friedel law (Russian) 4-65270
- alkali metal halide microcrystalline powders, reduced stability of coloration, dislocation model 4-60926
- anisotropic diffusion of point defects to edge dislocations 4-104007
- diffusionally-modified dislocation particle elastic interactions 4-98125
- dislocation-point defect interaction, lattice dynamics model 4-103786
- ionic crystals, simple diffusion model for charge transport by moving dislocations 4-75448
- metals, dislocation interactions and deform. theory 4-113489
- metals, HCP, dislocations, forest intersection, flow stress calc. 4-70153
- metals, internal friction peaking effect due to electron or  $\gamma$ -ray irradi. 4-103873
- metals, radiation-induced swelling, point defect-dislocation interactions, preference parameters (Russian) 4-108411
- metals and alloys, book contrib. 4-108361
- phonon drag of dislocations near phase transition points 4-60929
- phonon scattering by dislocations, book contrib. 4-98227
- phonon-dislocation interaction, frictional force, fluttering mechanism 4-103750
- phonon-dislocation scatt. and thermal cond. review 4-70189
- plastic deformation, quantum effects at low temp., dislocation transition rates over obstacles 4-70255
- positron studies of dislocations, book contrib. 4-99224
- single crystals, plasticity, effects of dislocation collective behaviour 4-98101
- steel, austenitic stainless,  $\gamma'$  precip., influence on elastic limit (French) 4-81200
- steel, austenitic stainless, Alloy 800, low cycle fatigue at 600°C, influence of dislocation-precip. interaction 4-99529
- steel, austenitic stainless, creep, Portevin-Le Chatelier effect and dynamic strain ageing 4-114617
- superconductors, dislocation phonon interactions, viscosity effects in plastic flow and internal friction 4-103861
- thermally activated motion of dislocations through random array of point obstacles, review 4-65261
- Al, muon trapping by dislocations, spin depolarisation rate: meas. 4-65911
- Al, plastic deformation at high strain rates 4-84337
- Al-Zn-Mg-Cu, ERGAL 7075, plastic deformation at high strain rates 4-84337
- Be, acoustic emission due to deform. (Russian) 4-92304
- Cu, cyclic deformation of single crystals, oriented for double slip 4-98174
- Cu, tough-pitch, drawn and extruded, stress/strain props. 4-104824
- $\text{CuBe}_2$ , age hardened, discontinuous flow studies, low temp. 4-113520
- Fe, ferromagnetic, high purity, magnetomechanical damping, influence of struct. defects 4-76226
- In, electron-dislocation interaction during plastic deform. at supercond. transitions 4-98178
- KCl-KBr model crystals, solid soln. softening and hardening 4-80140
- LiF bicrystals, fracture at plastic deform. 4-75609
- LiF cryst., dislocation band interactions with a healed crack 4-113492
- LiF, dislocation strain-field scatt. of fast-transverse acoustic phonons 4-84355
- MgO, dislocation motion and plasticity 4-80043
- NaCl crystals, doped, solution hardening due to fixed and rotating impurity-vacancy dipoles 4-75502
- Nb, electron-dislocation interaction during plastic deform. at supercond. transitions 4-98178

**dislocation interactions continued**

- Ni, dislocation/obstacle interaction during low dose D irradi. creep 4-104813
- Ni, mag. small-angle neutron scatt. by dislocations 4-84299
- Ni-Cu alloy, domain wall-dislocation interaction behaviour, role of Cu atoms 4-104457
- Pb, electron-dislocation interaction during plastic deform. at supercond. transitions 4-98178
- Pb-In, electron-dislocation interaction during plastic deform. at supercond. transitions 4-98178
- Si, plastically deformed, thermostimulated depolarization spectra 4-114199
- Si:B(In), point defects influence on acceptor ground state splittings 4-70728
- W, AKS-doped wire, high-temp. creep behaviour, effect of gas bubbles (German) 4-81243
- W, dislocation struct. after rolling, TEM obs. 4-99440
- W, interstitial atom interaction with grain boundaries (Russian) 4-65293
- WC, indented, dislocation interactions, crack nucleation, TEM obs. 4-80039
- Zn, electron dislocation drag during low temp. plastic deform. 4-98128

**dislocation jog motion** *see dislocation jogs*

**dislocation jogs**

- metals and alloys, book contrib. 4-108361
- Al, muon trapping by dislocations, spin depolarisation rate: meas. 4-65911
- InGaAsP-InGaP rapidly degraded DH laser grown by LPE, dark-line defects 4-69406
- LiF single crystal, crack tip deform. 4-84343
- MgO, dislocation motion and plasticity 4-80043
- Mo, deformation mechanism and dislocation struct., HVEM study 4-71682
- Ni superalloy, creep and recovery kinetics, report 4-62000
- Si:Cu, impurity effect on dislocation motion 4-70187

**dislocation locking**

*see also Cottrell atmospheres*

- Ni-Cr-Mo superalloy, elastoplastic deform. and failure, acoustic emission obs. 4-66377

**dislocation loops**

*see also vacancy condensation loops*

- anisotropic media, elastic fields of rational dislocation elements 4-84294
- cascade region structs., role of replacement sequences 4-108419
- defect cluster nucleation kinetics in materials under continuous and cyclic irradi. conditions 4-92229
- glissile dislocation loops ensemble, thermodynamics 4-60930
- II-VI compounds, irradiation-produced dislocation loops, HVEM study 4-75529
- instability model for plastic deform. at constant cross-head velocity 4-80143
- metals, BCC, vacancy loop unfaulting in radiation damage 4-108353
- metals, dislocation loop punching by He bubbles 4-103748
- metals, non-cubic, single crystal plates, low dislocation density 4-93211
- mixed carbide reactor fuels, irradi., defect struct., fission gas bubbles, precipitates, TEM obs. 4-83145
- sphere-plane contact, nonstationary formation stages, dislocation mechanism, thermal fluctuation relax. 4-92212
- steel, austenitic stainless, cavity formation during electron irradi., effect of pre-implanted He 4-108444
- steel, austenitic stainless, dislocation struct. during radiation creep (Russian) 4-80041
- steel, austenitic stainless, Ti- and Si-modified, microstruct. evolution, effects of pulsed and/or dual ion irradi. 4-98154
- steel, Mn pearlitic ferrite, fatigue dislocation structure (Chinese) 4-85201
- thorium phthalocyanine, high resolu. electron microscopy of struct. defects 4-75429
- Al-Mn alloy, commercial, quenched-in vacancy defects 4-108365
- Al-Mn-Zr, rapidly quenched from melt transform. behaviour 4-81185
- Al-Zn(Mg), neutron irradi., radiation damage 4-80112
- $\text{Au}_3\text{Cd}$ , electron damage, high resolution electron microscopy study 4-92241
- $\text{Au}_3\text{Mn}$ , electron damage, high resolution electron microscopy study 4-92241
- Cu-Fe, elastic distortion of  $\alpha$ -Fe particles by Orowan loops, moire fringes, TEM obs. 4-66358
- $\text{Cu}_3\text{Au}$ , displacement cascade collapse at low temps. 4-103835
- Fe, dislocation loop form. by self-ion irradi. at 40K, electron microscopy obs. 4-70242
- Fe-Cr-Ni (15.15 wt.%), weak beam imaging of He bubbles 4-103618
- Fe-Cr-Si(Ti), electron and ion-irrad., void and precip. struct. 4-103802
- Fe-Cu (2 wt.%), needle-precip. growth directions, invariant line strain 4-66336
- Fe-Ta(Mn), neutron irradi. at 325K, defect annealing stages (Russian) 4-92242
- $(\text{Fe}_{0.49}\text{Ni}_{0.51})_3\text{V}$ , ordered alloys, microstruct. and creep rel. to implanted He 4-108399
- Ge:H(He), ion irradi., structural defect study 4-88164
- $^3\text{He}$ , HCP, dislocation pinning by large US stresses 4-70523
- InGaAsP and InGaP LPE layers, dislocation loops, TEM studies 4-92206
- InGaAsP/GaAs, LPE grown, defects, TEM and STEM studies 4-108387
- InGaAsP-InGaP rapidly degraded DH laser grown by LPE, dark-line defects 4-69406
- InGaP/GaAs, LPE grown, defects, TEM and STEM studies 4-108387
- InP:Zn(S) single crystal growth, LEC technique, perfection, preferential etching, SEM and X-ray analysis 4-71549
- $\text{Li}_2\text{TiS}_2$ , intercalation study by TEM 4-103953
- MgO containing metal precipitates, optical and mech. props. 4-70161
- MgO, electron irradi., point defect kinetics, HVEM study 4-70214
- Mo, neutron irradiated, positron annihilation temp. dependence 4-61763
- NaCl,  $\gamma$ -irrad., interstitial dislocation loops (Russian) 4-113455
- Nb single crystal, neutron and electron irradi., dislocation sweeping of defects 4-103810
- Ni, dislocation/obstacle interaction during low dose D irradi. creep 4-104813
- Ni, pure, heavy ion irradi. damage, in situ electron microscopy 4-103828
- Ni:He, preimplanted, electron irradi., 1 MeV, He bubble growth 4-103803
- Ni-based alloys, HVEM irradi., void form. rel. to  $\gamma'$  precipitation 4-108446

**dislocation loops continued**

- Ni-Cr-Ti-Mo(Nb), precipitation strengthened, HFIR irradi., ductility, microstruct. 4-108457  
 Ni-Si (12.7 at.%), solute redistrib. under irradi., TEM invest. 4-108416  
 NiAl, Ni-rich, extruded, deform. struct., TEM study 4-93341  
 Si, dislocation sources, oxidation induced stacking faults (*Russian*) 4-113457  
 Si, dislocations, isolated, mobility meas., half-loops obs. 4-70156  
 Si:As, high dose ion implanted, As clustering, TEM and SIMS studies 4-70384  
 Si:Cu, impurity effect on dislocation motion 4-70187  
 Si:O, Czochralski grown, annealed, impurity precipitates, induced defects, TEM obs. (*Chinese*) 4-92368  
 Si:O Czochralski crystals, O precipitation and microdefects 4-84411  
 Si:P(Sb), ion implanted, flash lamp annealing 4-108735  
 SiC, sintered and siliconised, microstruct. of neutron irradi. induced defects 4-108459  
 Si<sub>3</sub>N<sub>4</sub>, precipitated film, dislocation propagation 4-60934  
 V, neutron irradi., hardness, tensile props. 4-103809  
 V, neutron irradi., temp. depend. of damage microstruct. 4-108455  
 V, T charged, <sup>3</sup>He bubble formation, TEM obs. 4-103825  
 V, T-charged, obs. of cylindrical cavities at dislocations 4-60913  
 V-B<sub>2</sub>C, neutron irradi., temp. depend. of damage microstruct. 4-108455  
 Zr, electron irradi., disloc. loops, electron microscopy studies 4-84296

**dislocation motion**

- for dislocation relaxation see dislocation damping  
 see also dislocation climb; slip  
 activation-free dislocation motion, deviation from Friedel law (*Russian*) 4-65270  
 alkali halides, space charge elec. field form. during cleaving 4-76021  
 alkali metal halide microcrystalline powders, reduced stability of coloration, dislocation model 4-60926  
 alloys, oxidation rel. to inert dispersoids and rare earth additions 4-114710  
 anthracene crystals, reduction of grown-in dislocation density due to heat treatment and growth conditions 4-113450  
 crystallite, thin, plastic deform., in situ TEM obs. method 4-62148  
 dislocation-point defect interaction, lattice dynamics model 4-103786  
 dynamically loaded media, vel. distrib. of dislocations, quasiequilibrium function 4-65263  
 instability model for plastic deform. at constant cross-head velocity 4-80143  
 ionic crystals, simple diffusion model for charge transport by moving dislocations 4-75448  
 Luders band propagation, constitutive eqns. for inhomogeneous plastic flow 4-65329  
 metals, BCC, impurity-dislocation interactions, influence of elastic anisotropy 4-98126  
 metals, plastic deform. constitutive eqn., recovery, dislocation creep, stress relax. 4-66370  
 metals and alloys, dislocations and strength at very low temps., book contrib. 4-99452  
 modulated system, dynamic behaviour of bound dislocation pairs 4-88167  
 NMR studies of dislocations in solids, book contrib. 4-98111  
 piezoelectric solids, sonoluminescence mechanisms 4-88890  
 plastic shock waves, finite amplitude, treated with summed infinitesimal amplitude elastic-plastic waves through dislocation dynamics 4-60988  
 Portevin-Le Chatelier effect, kinetic theory 4-108502  
 screw dislocation motion, transient, in anisotropic medium 4-84292  
 single crystals, plasticity, effects of dislocation collective behaviour 4-98101  
 slip-line formation and collective dislocation motion, book contrib. 4-98110  
 sphere-plane contact, nonstationary formation stages, dislocation mechanism, thermal fluctuation relax. 4-92212  
 steel, austenitic stainless, annealed, load relax. near 563K, thermally activated dislocation motion 4-99413  
 thermally activated motion of dislocations through random array of point obstacles, review 4-65261  
 thermo-piezoelectric continua, moving dislocations and disclinations, mechanical electrical and thermal fields 4-98102  
 Al single crystal, dislocation multiplication during creep 4-98106  
 Al-Cu-Mg, RR-58, anelastic creep at 180°C 4-99472  
 Al-Li (22 wt.%), dislocation dynamics, mean jump distance and activation length of moving dislocations 4-108364  
 AlN powder, shock effects, TEM study 4-109345  
 Fe, work hardening charact., plastic behaviour depend. on temp., strain rate, cryst. orientation 4-99418  
 Fe-Ni, H<sub>2</sub> charged, internal friction 4-104802  
 Fe, solid, plastic flow, dislocation motion mechanism (*Japanese*) 4-70519  
 KCl, screw dislocation segment displacement distrib. (*Russian*) 4-84297  
 KCl-KBr model crystals, solid soln. softening and hardening 4-80140  
 LiF crystals, annealed and aged, dislocation behaviour 4-103759  
 LiF, dislocation mobility at low temps., etch pit obs., Peierls mechanism 4-98105  
 LiF:OH<sup>-</sup>, mechanical props., dislocation motion anal. 4-70257  
 MgO containing metal precipitates, optical and mech. props. 4-70161  
 MgO, dislocation motion and plasticity 4-80043  
 MgO powder, hot pressing, densification, dislocation creep mechanism 4-114455  
 NaCl, shock deform., mobility of fast dislocations 4-98109  
 NaCl:OH<sup>-</sup>, mechanical props., dislocation motion anal. 4-70257  
 NaCl-type crystals, flexibility of dislocation forest to deformation resistance 4-84293  
 Nb, plastic deform. effect on superconducting T<sub>c</sub> 4-108960  
 Nb, twinning at low temp., elec. effects obs. 4-70168  
 Si, dislocation behaviour, review 4-88169  
 Si, dislocation behaviour, X-ray topography study 4-88175  
 Si, dislocation slip planes, EBIC contrast in SEM 4-103754  
 Si, heat treatment influence on dislocation motion kinetics (*Russian*) 4-88173  
 Si, oxidation induced stacking faults, dislocations, effects of Cl<sup>+</sup> and F<sup>+</sup> implantation, X-ray topography 4-80053  
 Si:Au, effect of mobile dislocations on surface saturation (*Russian*) 4-98107  
 Si:P, dislocation motion, onset delay times, etching study 4-70163  
 SiC, partial dislocation motion under electron irradi. in TEM 4-75453  
 Sn, white, single crystals, dislocation motion in pre-multiplication region, creep, etching 4-108375  
 Ta, plastic deform. effect on superconducting T<sub>c</sub> 4-108960

**dislocation motion continued**

- V, plastic deform. effect on superconducting T<sub>c</sub> 4-108960  
 W, dislocation struct. after rolling, TEM obs. 4-99440  
 Zn, dislocation drag mech. 4-103761  
 Zn, electron dislocation drag during low temp. plastic deform. 4-98128  
 Zn, plastic deformation, point defect diffusion 4-61137  
**dislocation motion, nonconservative** see dislocation climb  
**dislocation motion hindrance** see dislocation drag  
**dislocation multiplication**  
 BCC metals, yielding and plastic flow, model, rel. to thermal activation 4-103860  
 Al single crystal, dislocation multiplication during creep 4-98106  
 Be, acoustic emission due to deform. (*Russian*) 4-92304  
 Cu, touch-pitch, drawn and extruded, stress/strain props. 4-104824  
 Fe, yielding and plastic flow, model, rel. to thermal activation 4-103860  
 LiF crystals, annealed and aged, dislocation behaviour 4-103759  
 LiF, single cryst., IR transmission spectra at 300K, effect of stepped creep on exhaustion of dislocations 4-65271  
**dislocation nucleation**  
 defect cluster nucleation kinetics in materials under continuous and cyclic irradi. conditions 4-92229  
 Cu, neutron irradiated thin flat crystals, slip band growth and dislocation velocities 4-70164  
 Cu-Zn, neutron irradiated thin flat crystals, slip band growth and dislocation velocities 4-70164  
 Fe-Ni, single particle martensitic growth, computer simulation studies 4-114521  
 (NaK)Cl, melt-grown mixed single cryst., precipitation, etching study 4-61090  
 Si:Cu, impurity effect on dislocation motion 4-70187  
 SiC, 3C-6H solid-state transform., nonrandom microtwinning, X-ray diffr., calcs. 4-113606  
**dislocation pile-ups**  
 alkali halides, space charge elec. field form. during cleaving 4-76021  
 metal, neutron irradi., localised plastic flow characterisation with indentation hardness 4-109581  
 metals and alloys, book contrib. 4-108361  
 sphere-plane contact, nonstationary formation stages, dislocation mechanism, thermal fluctuation relax. 4-92212  
 steel, C-Mn, low temp. creep crack growth, effect of cold work 4-76850  
 Co-Cr-Mo, single-phase, low stacking fault energy, back stresses 4-76787  
 Cu-Si, dil. alloy, internal oxidation, grain boundary cavitation under creep or fatigue loading 4-71726  
 Fe-Si (3 wt.%), electrical engineering steel, anisotropic, mag. losses, annealing and elongation effects (*Russian*) 4-104459  
 LiF single crystal, crack tip deform. 4-84343  
 MgO crystals, microhardness indentation cracks, energy dissipation, X-ray topography 4-75608  
 Nb, twinning at low temp., elec. effects obs. 4-70168  
 Ni, crack propag., plastic zone, dislocation struct. 4-99488  
 Ni-Cr, conc. FCC alloys, heterogeneous deform. mechanisms 4-81236  
 W, dislocation struct. after rolling, TEM obs. 4-99440  
**dislocation pinning**  
 see also dislocation damping  
 metals, internal friction peaking effect due to electron or γ-ray irradi. 4-103873  
 mismatched overlayers, collective modes and dislocation ordering, mol. dynamics study 4-108555  
 modulated system, dynamic behaviour of bound dislocation pairs 4-88167  
 steel, carbon, strain ageing, influence of high press. (*Russian*) 4-85168  
 SiC, tool, wear resistance, effect electron irradi. 4-71740  
 Udmet 700, metalloid strengthening mechanism 4-61974  
 Al-Mg, dil., neutron irradi., internal friction, elastic modulus, recovery stages studied by elec. resist. meas. 4-103876  
 Cr, neutron irradi., internal friction, elastic modulus, recovery stages studied by elec. resist. meas. 4-103875  
 Cu, tough-pitch, drawn and extruded, stress/strain props. 4-104824  
<sup>3</sup>He, HCP, dislocation pinning by large US stresses 4-70523  
 InP/InGaAsP DHE, LPE grown, misfit dislocations, TEM study 4-113826  
 MgO containing metal precipitates, optical and mech. props. 4-70161  
 NaCl, γ and laser irradi., internal friction and dislocation damping 4-80153  
 Ni-Cr, conc. FCC alloys, heterogeneous deform. mechanisms 4-81236  
 Si:Cu, impurity effect on dislocation motion 4-70187  
 W, field ion study of mixed dislocations 4-108369  
**dislocation relaxation** see dislocation damping  
**dislocation scattering**  
 used for carrier scattering by dislocations  
 carrier recombination velocity on grain boundary, direct meas. 4-70827  
**dislocation sources**  
 see also Frank-Read sources  
 metals, mechanical instability of cellular dislocation structure 4-65268  
 metals and alloys, book contrib. 4-108361  
 slip-line formation and collective dislocation motion, book contrib. 4-98110  
 Al-Mn alloy, commercial, quenched-in vacancy defects 4-108365  
 Cu, Baushinger effect, influence of surface removal 4-114616  
 MgO containing metal precipitates, optical and mech. props. 4-70161  
**dislocation structure**  
 alloys, microstructure, classification, overview 4-66309  
 diamond, natural, type II, cathodoluminescence from dislocations 4-81012  
 FCC alloys, Suzuki segregation, TEM study 4-89054  
 FCC crystals, stability of dislocation cell boundaries 4-108376  
 friction and wear, appl. of dislocation concepts to alloy systems, book contrib. 4-98103  
 IN-617, Ni-base superalloy, fatigue, high temp. low cycle 4-66425  
 low C, Al-killed, reversion and subsequent re-age-hardening 4-93308  
 metals, BCC, screw dislocation core struct. and plastic deformation 4-70154  
 metals, cubic, subgrain-forming, evolution of plastic resist in large strain plastic flow 4-98175  
 metals, mechanical instability of cellular dislocation structure 4-65268  
 mixed carbide reactor fuels, irradi., defect struct., fission gas bubbles, precipitates, TEM obs. 4-83145  
 pentaerythritol tetranitrate crystals, soln. growth and defects 4-113452  
 semiconductors, dislocation electronic props., review 4-92205  
 single crystals, dislocation struct. formed under indentation (*Russian*) 4-88168

## dislocation structure continued

- single crystals, shaped, melt growth by Stepanov method, dislocation struct. form. 4-98108  
 solids, stress relax., dislocation dynamics 4-64854  
 steel, austenitic stainless, C or N ion irradi., double peak of voidage depth profile 4-98147  
 steel, austenitic stainless, cavity formation during electron irradi., effect of pre-implanted He 4-108444  
 steel, austenitic stainless, creep, Portevin-Le Chatelier effect and dynamic strain ageing 4-114617  
 steel, austenitic stainless, dislocation struct. during radiation creep (*Russian*) 4-80041  
 steel, austenitic stainless, irradiated, void swelling, He bubbles 4-103792  
 steel, austenitic stainless, TiC precipitation, influence on creep rupture strength, ductility and He embrittlement 4-99388  
 steel, carbon, strain ageing, influence of high press. (*Russian*) 4-85168  
 steel, constructional, near-threshold fatigue, struct. influence 4-93397  
 steel, dual-phase, dislocation substruct. as function of strain 4-99435  
 steel, ferritic stainless, recrystn. and deform. inhomogeneities, effect of twinning (*Polish*) 4-93309  
 steel, H embrittlement by cathodic charging 4-66420  
 steel, high strength, heat-treatable, fatigue at +20°C and -70°C 4-93364  
 steel, low alloy, Cr, dislocation structure and phase composition during annealing (*Russian*) 4-108366  
 steel, low alloy, HY-80, microstruct. after small plastic strains, TEM characterisation 4-93340  
 steel, plastic properties, effect of nonlinear strain paths 4-99474  
 steel, stainless, austenitic, previous deform. effect on yield point in low-temp. loading 4-99444  
 steel, surface plastic deformation, structural change in case-hardened layers 4-66484  
 steels, austenitic stainless, 316 and 253MA, high temp. low cycle fatigue, comparison between mech. props. and microstruct. 4-93410  
 twin boundary dislocations, determ. of Burgers vector by weak beam method 4-80051  
 wear, surface dislocation model 4-60985  
 Al, dislocation internal friction hysteresis 4-70165  
 Al single crystal, dislocation multiplication during creep 4-98106  
 Al-Mg-Mn, hot deform. and dynamic recrystn. 4-109479  
 Al-Si-Fe, Luders band deform., stress relax., load suppression effect 4-76801  
 Al-Zr (9.4 wt.%), melt-quenched, decomp. study using TEM 4-93262  
 Al-(Mg), shear bands, localised flow 4-99460  
 $\alpha$ -Al<sub>2</sub>O<sub>3</sub>, monocrystalline, dislocations, chem. etching studies 4-60933  
 Au thin films 4-75814  
 BaTiO<sub>3</sub>, surface domains, double Laue pattern topography 4-104548  
 CaCO<sub>3</sub>, calcite, dislocation struct. and twinning 4-113467  
 CdO, struct. under pressure 4-75424  
 CdTe large single crystals, grown from vapour phase, polarity 4-70048  
 Cr films electroplated on (001) Cu substrates, misfit twins and dislocations 4-108748  
 Cu, cyclic deformation of single crystals, oriented for double slip 4-98174  
 Cu, cyclically deformed [001], dislocation struct. 4-108362  
 Cu, fatigue of single crystals in air and vacuum, persistent slip bands and dislocation microstruct. 4-99521  
 Cu, plastic flow and dynamic recrystallisation in single crystals 4-66394  
 Cu, plastically deformed, dislocation struct., ultrasonic study 4-66520  
 Cu, polycrystalline, cyclic creep accel. and retardation, threshold stress temp. depend. 4-66372  
 Cu, single crystal, strain bursts in cyclic creep at ambient temp. 4-66371  
 Cu single crystals, cyclically strained, dislocation microstruct. rel. to plastic strain amplitude 4-66373  
 Cu-Al-Co (15.2 at.%), with non-coherent particles, superelasticity effects due to twinning 4-76795  
 Cu-Ni, twin boundary dislocations, determ. of Burgers vector by weak beam method 4-80051  
 Cu-Ni-Zn, Li<sub>0</sub> and Li<sub>2</sub> alloys, order-disorder transitions, microstructure obs. 4-114511  
 Cu-Ti (3.5 wt.%), age hardening 4-76782  
 $\beta$ -Cu-Zn, single cryst., deformed in compression, dislocation struct. 4-70162  
 Cu<sub>2</sub>MnAl single crystals, Heusler alloy, compression, 77-367K, fracture slip, superlattice dislocation dissoc. 4-66369  
 Cu<sub>2</sub>NiZn, superlattice dislocations, TEM microstruct. study 4-75450  
 $\alpha$ -Fe, creep-induced dislocation subgrain arrangement in ferrite, effect of stress changes 4-76799  
 Fe-Al-Si (20.5 at.%), DO<sub>3</sub>-ordered alloys, tensile behaviour 4-93337  
 Fe-Cr-Si(Ti), electron and ion-irradi., void and precip. struct. 4-103802  
 Fe-Mn alloys,  $\gamma$ - $\epsilon$  martensitic transformations, recrystn. (*Russian*) 4-109398  
 Fe<sub>2</sub>Si, DO<sub>3</sub>-ordered alloys, tensile behaviour 4-93337  
 GaAs, ductile brittle transition in (001) surface layers in single crystals, effect of medium 4-70266  
 GaAs semi-insulating substrate, inhomogeneity characterisation, expt. study 4-65759  
 GaAs:Ge(Si), LEC grown, dislocation structure etching rel. to dopant conc. 4-113451  
 InP:S(Sn)(Zn)(Fe) single crystals, LEC growth, perfection, carrier conc., TEM obs. 4-71550  
 KH<sub>2</sub>PO<sub>4</sub> crystals, laser induced damage, X-ray topography 4-65296  
 LiF bicrystals, fracture at plastic deform. 4-75609  
 LiF, dislocation struct. evolution at premelting temp. (*Russian*) 4-88174  
 LiF, single cryst., IR transmission spectra at 300K, effect of stepped creep on exhaustion of dislocations 4-65271  
 LiF single crystals, grinding, surface layer, strain hardening, dislocation density, microhardness 4-93312  
 Mg alloy, strain induced grain boundary migration 4-85198  
 MgO crystals, microhardness indentation cracks, energy dissipation, X-ray topography 4-75608  
 MgO, quenched, defect struct., plastic deform., SEM, cathodoluminescence, optical absorpt. spectra 4-71448  
 MgO-ZrO<sub>2</sub>, directionally solidified eutectic microstruct., misfit dislocations, TEM obs. (*Japanese*) 4-66324  
 Mo, deformation mechanism and dislocation struct., HVEM study 4-71682  
 Mo, high temp. neutron irradi., annealing, void form., mech. props. 4-108456  
 NaCl-type crystals, flexibility of dislocation forest to deformation resistance 4-84293

## dislocation structure continued

- Ni alloys, high-alloy, microstruct. and comp. characts. of eutectic  $\gamma'$  phase (*Russian*) 4-92380  
 Ni, crack propag., plastic zone, dislocation struct. 4-99488  
 Ni, deformed, dislocation struct. and fracture behaviour, effect of H<sub>2</sub> and He 4-62043  
 Ni eutectic alloys,  $\gamma$ - $\gamma'$ ,  $\gamma$ - $\gamma'$  and  $\gamma$ - $\alpha'$ , yield stress and deform. struct., temp. depend. 4-93346  
 Ni, He<sup>+</sup> ion irradiated, bubble growth, microstruct. contrib. 4-108472  
 Ni, laser irradiation, defect struct. and surface alloys 4-75509  
 Ni-Cr base alloys, creep behaviour and microstruct. 4-71705  
 Ni-TiO<sub>2</sub>, dispersion hardened, work hardening 4-66349  
 Ni<sub>3</sub>Al, cold-rolled, recrystn. annealing 4-81213  
 NiO, dislocation core region in grain boundaries, mean inner pot. charge, electron microscope obs. 4-103755  
 PbSnTe-PbTeSe lasers with high efficiencies, lattice-matching to reduce misfit dislocations 4-112420  
 PbTiO<sub>3</sub>, single crystal, dislocation and domain struct. 4-75452  
 Re, creep tested, dislocation struct., X-ray divergent beam obs., TEM studies 4-99420  
 Si, dislocation behaviour, review 4-88169  
 Si, dislocation behaviour, X-ray topography study 4-88175  
 Si solar cells, electrical microcharacterisation using SEM 4-81560  
 SiP<sup>+</sup>, implanted, dislocation struct. development, effect of cryst. orientation, TEM obs. 4-80040  
 SiC, sintered and siliconised, microstruct. of neutron irradi. induced defects 4-108459  
 SiC whiskers, planar faults, cavities, TEM obs. 4-108754  
 Sn, laser alloyed layers on GaAs substrates, elec. props., surface damage 4-99622  
 Sn-Bi (0.5 at.%), creep rate, grain dia. depend. 4-81259  
 SnO<sub>2</sub>, mechanical activation, defect formation 4-75456  
 Ti-Al-Sn (5, 2.5 wt.%), stressed at room temp., hydride precip., dislocation substruct. 4-71655  
 Ti-Mo (V)(Al), stacking fault energies and dislocation structure (*Russian*) 4-108384  
 TiO<sub>2</sub>, mechanical activation, defect formation 4-75456  
 W, dislocation struct. after rolling, TEM obs. 4-99440  
 W, field ion study of mixed dislocations 4-108369  
 W<sub>2</sub>C, high temp. plastic deform., expt. determ. of constitutive law 4-62001  
 WO<sub>3</sub>, mechanical activation, defect formation 4-75456

dislocation translation *see slip*

## dislocations

- For pipe diffusion, see diffusion in solids. See also dislocation ..... see also Bordoni effect; Cottrell atmospheres; disclinations; edge dislocations; grain boundaries; prismatic dislocations; screw dislocations*  
 alkali halide crystals, etch pit studies of dislocations, dissolution kinetics and impurity effects 4-70158  
 alkali halide crystals, localised phonon mode associated with dislocations 4-70321  
 alkali halide mixed crystals, growth and characterisation, microhardness, colour centres, radiation hardening 4-70152  
 alkali metal halides, diffusion along grain boundaries and dislocations 4-92439  
 anisotropic media, elastic fields of rational dislocation elements 4-84294  
 application to metallurgy and materials science problems, recent advances, book 4-95067  
 axial channelling, defect anal. appls., Lindhard model anal. 4-75587  
 bicrystal, grain boundary slip at high temp., dislocation model (*Russian*) 4-92211  
 cell wall form. mechanism 4-80038  
 cholesterol crystallisation in bile, dislocation growth mechanism 4-89491  
 convergent beam electron diffraction, cryst. struct. and defect appls. 4-79906  
 crack tip with dislocations of opposite sign, dislocation-free zone image force theory (*Chinese*) 4-91762  
 crystalline solid dynamic plasticity 4-98183  
 diamond, type IIb, individual dislocation and cathodoluminescence emission polarisation 4-99199  
 diffusion in crystals with dislocations 4-65438  
 diffusion in metals and alloys, conf., Tihany, Hungary (Aug.-Sept. 1982) 4-63405  
 dislocation kinetics and viscosity of liquids, laminar flow, nonequilibrium dynamics 4-84437  
 double sure-Gordon dislocation, Peierls energy 4-75447  
 electromagnetic elastic continua, multipolar lattice defects 4-75449  
 electron channelling imaging of crystalline defects in solid materials 4-103623  
 epitaxial layers, dislocation-free, growth, book contrib. 4-98492  
 fatigue, appl. of dislocation concepts, book contrib. 4-99564  
 freezing, density wave theory with crystal symmetry 4-70350  
 grain boundary diffusion, struct. props. and point defect mobility, mol. dynamics simulations 4-83035  
 ice, melting of crystalline solids, US study 4-70351  
 inhomogeneous, cryst., local phase transition points, fluctuation enhancement 4-65373  
 interfacial dislocation structures, characterisation using TEM 4-108371  
 interfacial dislocations and coherency, interpretation of discrete atomic positions 4-113447  
 interphase boundary migration, dislocations and steps 4-108372  
 lamellar systems, B-phases, restacking phase transitions, dislocation model 4-98283  
 magnetic thin films, amorphisation of regular domain structures at second-order phase transitions, dislocation-disclination mechanism 4-98928  
 metals, FCC, interfacial free energy between dislocation core and bulk material 4-65262  
 metals, grain boundaries, diffusion mechanisms, review 4-65492  
 metals, spalling microdamage initiation, critical loading conditions 4-89111  
 metals and alloys, book contrib. 4-108361  
 NMR studies of dislocations in solids, book contrib. 4-98111  
 oxides and carbides, diffusion along grain boundaries and dislocations 4-92439  
 plasticity and fracture, deform. modes 4-98177  
 positron studies of dislocations, book contrib. 4-99224  
 quantum crystals, pure, plasticity mechanism (*Russian*) 4-92473  
 quartz, creep, dislocation mobility stress depend. 4-70265

## dislocations continued

- radiation damage microstructure, microcomputer system for quantitative image analysis 4-103617  
 random distrib., X-ray Debye profiles 4-88170  
 Schottky-barrier diode, EBIC contrast from individual surface-parallel dislocations, temp. depend. 4-103749  
 semi-infinite composite with long reinforced phase, edge crack analysis 4-97400  
 semiconductor technology, book 4-86123  
 semiconductors, cathodoluminesc. contrast formation of localized non-radiative defects 4-85016  
 semiconductors, charged dislocations, electronic props. 4-98565  
 semiconductors, dislocation electronic props., review 4-92205  
 semiconductors, electroacoustic effects due to charged dislocations 4-65717  
 shock loaded solids, thermodynamic props., influence of defects 4-113680  
 single metals elec. resistivity and scatt. theory 4-92694  
 solid/solid interfaces, computer simulations, conf., Philadelphia, USA (Oct. 1983) 4-110806  
 steel, Cr-Mo-V martensitic, liq. metal induced embrittlement, dislocation emission from crack tips 4-85210  
 steel, siliconised, diffusion layer formation, metallography 4-114721  
 steel, stainless, dislocation microstruct. and power-law breakdown 4-113456  
 steel, stainless, duplex austenite-ferrite, fatigue crack propag. 4-81287  
 steel, weld metal deposits, austenite decomposition products, influence of O-rich inclusions 4-114513  
 switching and oscillations, threshold behaviour 4-113448  
 two-dimensional systems, melting, Monte Carlo simulation studies 4-113586  
 X-ray diffr. contrast and ray-paths for dislocation in particular position 4-103753  
 X-ray imaging, plane wave imaging of dislocations parallel to diff. vector 4-84295  
 Ag halide grains twinned, tabular, disorder, photolytic Ag patterns 4-80050  
 Al, He bubble nucleation on dislocations during 600-MeV proton irradi. 4-113504  
 Al, high purity, polygonised, TEM, internal friction peak 4-113534  
 Al, void and bubble form., 600 MeV proton irradi., temp. depend., 130-430°C 4-108482  
 Al-Cu, implanted, disorder studied by ion channelling and Rutherford backscattering 4-98145  
 Al-Mg solid solution alloys, high stress levels, breakdown in creep 4-113526  
 Al<sub>2</sub>O<sub>3</sub> powders, sintering behaviour, positron annihilation studies 4-114436  
 Al<sub>2</sub>O<sub>3</sub>-Cr, grain boundary diffusion, anisotropy and doping effects 4-92443  
 Au (111), direct atomic imaging after in situ C etching 4-113770  
 BeAl<sub>2</sub>O<sub>4</sub>, chrysoberyl, Czochralski grown, dislocation form. and distrib. laws, X-ray diffr. topography method 4-113453  
 BeO powders, sintering, positron annihilation study 4-71469  
 CaF<sub>2</sub>-Eu, phononless impurity-centre line, inhomogeneous broadening under plastic deform. conditions 4-88864  
 Ca<sub>10</sub>(PO<sub>4</sub>)<sub>6</sub>F<sub>2</sub>, fluorapatite, radiation damage and annealing, optical studies 4-70192  
 CdTe films, MBE growth and microstruct. characterisation 4-92578  
 Cu, positron lifetime after annealing and cooling (Russian) 4-109270  
 Cu-Al-Co, with noncoherent particles, crit. shearing stresses, temp. depend. rel. to slip and twinning (Russian) 4-93333  
 Cu-Ni-Sn spinodal alloys, deformation behaviour, ageing treatment effects 4-114628  
 Cu-Zn-Al alloys, martensitic transformations, positron annihilation studies 4-89053  
 CuZn, antiphase boundary energy, superlattice dislocations, slip systems, weak-beam electron microscopy obs. 4-104792  
 β-CuZn, plastic deformation at He temps., capacitance meas. 4-71681  
 Fe, BCC, grain boundary diffusion, mol. dynamics simulation studies 4-80287  
 Fe, cold rolled, defect annealing, alloying element effects, positron studies 4-76550  
 Fe, thick foil, mag. domain wall obs. 4-80780  
 Fe-Cr-Ni (15.15 wt.%), weak beam imaging of He bubbles 4-103618  
 Fe-Ni, positron lifetime after annealing and cooling (Russian) 4-109270  
 Fe-P, segregated grain boundaries crack propag., mol. dynamics calcs. 4-114663  
 FeCo alloy, brittleness, purity and impurity segregation effects (Russian) 4-109496  
 GaAs (100), reconstructed, electron microscopy and diffr. studies 4-108690  
 GaAs (110), cleaved, surface steps and dislocations, reflection electron microscopy study 4-65529  
 GaAs, electron traps, props. and nature 4-75890  
 GaAs LEC wafers, undoped, defect characterisation by electron-beam-induced charge collection microscopy 4-60932  
 GaAs, stoichiometry, X-ray intensity meas. of quasi-forbidden reflections 4-84416  
 GaAs:In, isoelectric doping, X-ray and electron microprobe anal. 4-75491  
 GaAs:Te, deformed, precip., defect struct., electron microscopy obs. 4-103752  
 GaAs-In<sub>0.3</sub>Ga<sub>0.7</sub>As MOCVD-strained-layer superlattices, lattice distortion, TEM study 4-88406  
 GaAs,P<sub>1-x</sub>/GaP superlattices, strain depth profiles, misfit dislocations obs 4-104095  
 Ge, dislocations, deep electron levels, recursion calc. 4-70716  
 Ge, electronically neutral impurities on muonium, low temp. meas. 4-65279  
 Ge<sub>2</sub>Si<sub>3</sub>, epitaxial films on Si (100), commensurate and incommensurate struct. 4-108740  
 \*He, liquid, dislocation mediated melting of 2-d electron lattice 4-98386  
 InP-In<sub>0.3</sub>Ga<sub>0.7</sub>As-InP DH wafers, LPE grown, misfit dislocations, X-ray and photoluminescence topography 4-80042  
 InSb films, MBE growth and microstruct. characterisation 4-92578  
 KCl, grain boundary influence on motion of cryst. inclusions 4-75455  
 K<sub>2</sub>MoO<sub>4</sub>, 1D, CDW modes, far IR reflectivity studies 4-108798  
 LiAlSi<sub>2</sub>O<sub>6</sub>, α-spodumene, microplasticity, dislocation glide and dissoci., TEM obs. 4-65331  
 MgAl<sub>2</sub>O<sub>4</sub>, grain boundary diffusion, anisotropy and doping effects 4-92443

## dislocations continued

- MgO (100), surface dislocation, secondary electron emission study 4-80345  
 MgO-Cr, grain boundary diffusion, anisotropy and doping effects 4-92443  
 Mo single cryst., dislocation-induced vel. dispersion of US waves 4-113546  
 NaCl:Ba, thermoluminescence, pre- and post-irrad. deformation effects 4-66083  
 Pb single cryst., boundary and dislocation phonon scatt. 4-65365  
 PbTe:Ti, pure and doped, defect struct., X-ray double cryst. studies 4-75383  
 Si (111), reconstructed, electron microscopy and diffr. studies 4-108690  
 a-Si, amorphous layer effect on lattice images of dislocations 4-79939  
 Si, deformed, EBIC/TEM study of defects 4-80045  
 Si dislocation stress distrib., effects on pendulum fringes 4-60783  
 Si, dislocations, deep electron levels, recursion calc. 4-70716  
 Si, gamma-irradiated, carrier recombination, dislocation effects 4-75982  
 Si, oxidation model, stacking faults and dislocations 4-104888  
 Si, partial 90° dislocation, structural and elec. props. 4-108368  
 Si photovoltaic cells, photogeneration rate, minority carrier lifetime depend. 4-75997  
 Si, plastically deformed, deep levels, capacitance, reverse current meas. 4-61319  
 Si wafer props., influence of laser marking 4-113498  
 Si:Al, solid solution, nuclear-spin lattice relaxation 4-76282  
 Si-metal interface, dislocation mediated melting 4-103912  
 SiO<sub>2</sub>-Cu films, elec. breakdown strength, Cu precipitates effect 4-99022  
 Te(OH)<sub>6</sub>·2NH<sub>4</sub>H<sub>2</sub>PO<sub>4</sub>·(NH<sub>4</sub>)<sub>2</sub>HPO<sub>4</sub>, single cryst. growth and morphology 4-61821  
 ThBr<sub>3</sub>:Gd<sup>3+</sup>, incommensurate, phase fluctuations near transition temp., phase pinning, EPR meas. 4-92956  
 Ti, proton irradi., positron annihilation study (Russian) 4-85033  
 Ti-Sn, proton irradi., positron annihilation study (Russian) 4-85033  
 Ti-V solid solutions, creep, microstruct. 4-109464  
 TiC<sub>0.97</sub>O, O diffusion coeff. and conc. profile, SIMS studies 4-92438  
 TiO<sub>2</sub>, interaction of small and extended defects 4-75443  
 V<sub>2</sub>O<sub>5</sub>-Cr, metallic phase-insulating phase interface, misfit dislocations 4-108373  
 WO<sub>3</sub>, interaction of small and extended defects 4-75443  
 Zn, single crystal, deformation stress and electrical resistance change due to dislocation 4-60978  
 α-Zr, hydride form., an α-phase, pendulum technique investig. 4-70398
- disordered systems, vibrational states** see vibrational states in disordered systems
- disperse systems**  
 see also aerosols; Brownian motion; colloids; dust; emulsions; foams; fog; gels; powders; smoke; soots; suspensions  
 acrylic and copolymer and allyl pentacrythrite ether dispersion in water, rheological behaviour (Russian) 4-64985  
 air, compressed, with metal vapour and particles at high temp., elec. breakdown (Japanese) 4-103463  
 atmospheric vapour dispersion, affect of molecular props. 4-114991  
 bi-disperse media, diffusion, effective medium approach 4-65430  
 Brownian coagulation kinetics, weak hydrodynamic field 4-79638  
 cellulose dispersions, rheological behaviour, temp. relationships 4-108105  
 charge stabilised dispersions, concentrated, self-diffusion, Brownian dynamics simulation 4-99851  
 combustion products analysis, using dilution tunnel system 4-62266  
 dilute polydisperse system of sedimenting spheres, coagulation rate 4-112990  
 dry cohesionless granular materials in annular shear cell, stress development 4-79629  
 dusty gases, fully dispersed shock waves 4-112953  
 fluid particles, deformation in contact zone under linear tension 4-109690  
 fly ash, radiative transfer scatt. data 4-79428  
 foam flooding process for heavy oil recovery, interfacial phenomena 4-61097  
 gas-liquid dispersions, mass transfer determ. methods (German) 4-78277  
 gas-solid fluidised beds, mixing, lateral dispersion coeffs. 4-87783  
 heated particle cloud, precipitation on horizontal plane 4-71995  
 hydrocarbon-electrolyte systems in pulsed electric field, hydrodynamic behaviour 4-79675  
 liquid jet mixing with drifting gas flow 4-60475  
 metal catalysts, supported, particle distrib. determ. by X-ray small angle scatt. 4-97967  
 metal chlorides, aq. solns., refractive index, transmission spectra 4-80899  
 metallic particles, IR absorption coeff., nonlocal theory anal. 4-93042  
 monodisperse semicond. system, amplitude size effect 4-88526  
 nonequilibrium gas-surface solid relax. gasdynamics 4-60562  
 oscillatory pipe flows, dispersion coeff. meas. 4-75090  
 oxide dispersions, rheological, mech., and mag. props. 4-65830  
 particle charging by ultraviolet ray exposure 4-99854  
 phase separation, droplet growth rates, crossover, locking-in and intermittency 4-108099  
 polydisperse fluids, thermodynamic props., statistical mechs. 4-70410  
 polydisperse liq. fuel diffusional combustion, self-similar conditions kinetics 4-81439  
 polydisperse mixtures, electromagnetic separation, conc. effects 4-103424  
 polydisperse systems, random systems of particles concept 4-114843  
 polyfractional, irregularly shaped particles, rheological props. 4-79639  
 polymer film, two-phase, structural charges during heat treatment 4-80435  
 polynuclear aromatic hydrocarbons, in cyclodextrins, room-temp. phosphoresc. 4-78884  
 polystyrene latex conc. dispersion, weakly flocculated, sedimentation, viscous flow 4-114841  
 polystyrene latex dispersions, conc., sterically stabilised, free polymer addition, rheological investigation 4-112788  
 polyvinylacetate dispersions, flow behaviour and anomalies, meas. methods and role in polymer manufacturing (German) 4-75062  
 pulsation velocities correl. of disperse phase in jet flows 4-69808  
 small metal particles, energy calcs. 4-77035  
 spherocylindrical aggregates in single- and multi-component amphiphilic systems 4-109689  
 spin diffusion (Russian) 4-80765  
 three phase bubble column, axial mixing hydrodynamics, slurry props. effects 4-87782

**perse systems continued**

- unsteady flow through channel with permeable walls, solute dispersion, vel. distrib. 4-113020
- BA<sub>2</sub>O<sub>3</sub> dispersion, effect on colloid stability of adsorpt. of amphoteric polymer 4-66619
- C black dispersions, charge exchange, electrochemical/ESR studies 4-93562
- KCl<sub>19</sub> + Ag<sub>19</sub>, elec. cond., rel. to temp. and particle size 4-98680
- Pd catalysts, monodisperse, adsorpt. and dissolution of H<sub>2</sub> 4-61220
- S<sub>10</sub> + C<sub>60</sub>, elec. cond., rel. to temp. and particle size 4-98680
- SF<sub>6</sub> with metal vapour and particles at high temp., elec. breakdown (Japanese) 4-103463

**perspersion (wave)**

- see also acoustic dispersion; optical dispersion
- auroal kilometric radiation, relativistic dispersion of extraordinary mode waves 4-94312
- directional wave spectra from heave/pitch/roll data buoys 4-105585
- EM pulse envelope change with pulse packet in dispersive medium 4-69914
- EM wave dispersion props. in unsteady-state inhomogeneous media 4-91387
- gravity waves, algorithm for nonlinear dispersion relation 4-72772
- particle dispersion due to water wave motion, Monte Carlo model 4-110885
- plasma sphere, diffraction of plane TM wave, spatial dispersion 4-79799
- TE/TM waves obliquely incident on plasma cylinder, spatial dispersion effects 4-84005
- unilateral fin lines with dielectric layers, anal. 4-79006
- wave fronts in dispersive dissipative media, theory (Russian) 4-67221

**dispersion hardening**

- see also precipitation hardening
- alloy, multiphase, mech. props., book contrib. 4-109424
- ceramics, transformation-toughened, fracture toughness, crack-size depend. 4-93373
- deformation-rate law, classical rate-theory-based 4-99417
- diamond dispersed alumina composite, very high press. sintered, fracture toughness, phase transform. 4-99372
- elastic/plastic body, longitudinal shear loading, singular stress field at ribbon like inclusion 4-60304
- metallic composite materials, generalised classif., book contrib. 4-109357
- steel, Mn-V-Cu austenitic, microstructure rel. to heat treatment and alloying additions 4-89066
- steel, nitriding, diffusion layer props. form. peculiarities 4-114712
- superalloys, powder metallurgy, book 4-86129
- superalloys, superalloys, oxide dispersion strengthened, developments in prod. 4-114452
- tensile testing of materials at elevated temps., threshold stress, struct., recovery models 4-66528
- weld metal, globular silicates effect on ductility and microstruct. 4-114607
- Ag-MgO, dispersion hardened, qualitative analysis of fracture 4-114633
- Al-Al<sub>2</sub>O<sub>3</sub>-(Si), creep deform., stress and temp. depend. 4-81246
- Al<sub>2</sub>O<sub>3</sub>-AlON composite ceramic, hot pressing reaction sintering, mech. props., high temp. appls. 4-62062
- Al<sub>2</sub>O<sub>3</sub>-ZrO<sub>2</sub> ceramics, high press. sintered, fracture toughness rel. to phase transform. 4-76839
- Al<sub>2</sub>O<sub>3</sub>-ZrO<sub>2</sub> ceramics, strain around large inclusions, quantitative anal. 4-103621
- Al<sub>2</sub>O<sub>3</sub>-ZrO<sub>2</sub> composite tool bit, microstruct., toughening mechanisms, performance 4-61946
- Al<sub>2</sub>O<sub>3</sub>-ZrO<sub>2</sub> powders, prep. by evaporative decomp. of sols. 4-85137
- Cu-Al<sub>2</sub>O<sub>3</sub> dispersion hardened, tensile failure, temp. depend., grain boundary fracture 4-66405
- Cu-Al-Ti, internal oxidation, dispersion hardening (Japanese) 4-89065
- Cu-Fe, elastic distortion of  $\alpha$ -Fe particles by Orowan loops, moire fringes, TEM obs. 4-66358
- Fe-Cr-Al, oxide dispersion strengthened MA 956, fatigue crack growth 4-62031
- Fe-Ni Elinvar alloys, dispersion-hardened, mag. and physical props. (Russian) 4-104800
- Mo alloys, dispersion hardened, strength and elasticity, effect of heating 4-114600
- Ni-Cr, oxide dispersion strengthened 4-85260
- Ni-TiO<sub>2</sub> dispersion hardened, work hardening 4-66349
- Ti-Er, rapidly solidified dispersion strengthened, tensile and creep props. 4-114562
- Ti-Nd, rapidly solidified dispersion strengthened, tensile and creep props. 4-114562
- Ti-R, R=Ce, Dy, Er, Gd, La, Nd or Y, rapidly solidified dispersion strengthened, struct. and props. 4-114561
- W-HfC, dispersion and solid solution hardening of vacuum-melted W 4-66346
- W-K, diffusional stress relax. around second phase K particles, expt. study 4-61948
- W-ZrC, dispersion and solid solution hardening of vacuum-melted W 4-66346
- W-ZrC(HfC), produced by powder metallurgy, mech. props. 4-71694

**dispersion power, rotatory see optical rotation****dispersion relations**

- see also dispersion (wave); Kramers-Kronig relations; Mandelstam representation; N/D method; phonon dispersion relations; phonons; plasma instability; plasma waves; S-matrix theory
- annular pipes, sound propagation, rotational flow effects (French) 4-97520
- antiferromagnetic spin waves in system with helical ordering (Russian) 4-71049
- classical Toda lattice, finite-temp. excitation spectrum, soliton-phonon phenomenology 4-111067
- complex discrete eigenvalues, neutron transport eqn. with anisotropic scatt. 4-96092
- crystal/overlay system, elastic surface waves, Green's function anal. 4-108695
- crystals, use of Raman scatt. in condition of total reflection 4-80932
- electron liquids, correlation energy plasmon dispersion, static and dynamic form factors 4-75885
- ferroelectric domain layer surface wave, dispersion eqns. 4-88787
- gravity waves, algorithm for nonlinear dispersion relation 4-72772
- inter-surfaceband plasmon, dispersion relations, SCF calc. 4-65630
- ionosphere travelling disturbances, dispersion relations rel. to determ. of thermospheric wind vectors 4-90015

**dispersion relations continued**

- layered dielectric struct., surface and guided polaritons 4-80512
- layered electron-hole liq., ground state correlations 4-92620
- longitudinally magnetized antiferromagnet, exchange-free spin waves 4-71047
- metallic gratings, surface polariton attenuation and dispersion 4-92632
- non-local dielectrics, surface exciton polaritons, dispersion relations 4-92628
- nonpropagating hydrodynamic soliton theory 4-86231
- one-dimensional disordered binary alloys, cluster mean-field theory 4-92599
- p-n junctions, surface acoustic plasmons, dispersion 4-92642
- periodically corrugated surface, EM wave propagation, plasmons 4-79279
- piezoelectric semicond. magnetised plasma, high-power helicon wave parametric decay 4-98657
- Raman free electron laser, three-dimens. theory 4-96924
- relativistic electron beam in dielectric medium 4-64663
- scalar  $\phi^4$  model, imaginary coupling, high-order behaviour of critical exponents 4-86533
- semiconducting piezoelectric plasma, parametric EM wave conversion into acoustic wave 4-65716
- semiconductor interfaces, dispersion and instability of localised polaritons 4-80511
- semiconductor superlattices, collective excitations theory 4-61451
- shell, three-layered, cylindrical, infinitely long, free wave propag. 4-74941
- short-range NN repulsion, omega and eta meson exchange, Regge behaviour 4-106576
- scolecite natural zeolite, IR vibr. spectra studies 4-76445
- soliton surfaces, topological charge 4-86541
- stratifying sols., acoustic wave dispersion and absorption by conc., fluctuations 4-80164
- superlattices, Rayleigh waves, dispersion curves and displacement fields 4-92502
- superlattices, surface vibrations and dispersion theory 4-80365
- surface plasmon-polariton dispersion, influence of collisional damping 4-80522
- thin rough film, local resonances and optical props. 4-81024
- tubes, thin walled, liquid-filled, approx. dispersion eqns. 4-60299
- waveguide properties of an atmosphere with a monotonically varying temperature 4-63047
- Ag film, electroreflectance meas. of bulk plasmon dispersion 4-113883
- Al film on LiNbO<sub>3</sub> substrate, elastic const. study 4-104052
- Al-Al<sub>2</sub>O<sub>3</sub>-Ag tunnel junctions, surface plasmons and light emission 4-98553
- AlGaAs injection laser, dispersion of linewidth enhancement factor 4-112425
- Ar, liquid, sound nonanalytic dispersion relations 4-103887
- Bi size-quantised film, optical absorption coeff. calc. 4-109265
- Co film, Brillouin scatt. from thermal magnons 4-71458
- CsVX<sub>3</sub> (X=Cl, Br, I) linear chain antiferromagnets, mag. excitations 4-65800
- GaAs-Si interface, nonlinear surface EM waves 4-80892
- GaP, volume plasmon dispersion, transmission electron energy loss studies 4-88465
- <sup>4</sup>He, superfluid, nonanalytic hydrodynamic dispersion relations, mode-coupling theory 4-75746
- InGaAsP, quadratic electro-optic Kerr effects, dispersion 4-109159
- InP, volume plasmon dispersion, transmission electron energy loss studies 4-88465
- InSb, magnetised plasma, parametric excitation of electron-acoustic waves 4-88545
- LiF, X-ray refractive index meas. 4-104557
- Mo film on LiNbO<sub>3</sub> substrate, elastic const. study 4-104052
- NiBr<sub>2</sub>, helimag, and antiferromag., mag. excitations, neutron scatt. studies 4-104409
- PbSe, anisotropy of Fermi surface of holes 4-104117
- Si (100) surface electronic excitations, EELS study 4-108914
- Si-Ag interface, nonlinear surface EM waves 4-80892
- SiF, X-ray refractive index meas. 4-104557
- SrTeO<sub>3</sub>, dielectric const. dispersion study (Russian) 4-88762
- Zn piezoelectric membranes, SAW characts. and transducers 4-104058

**dispersions see disperse systems****dispersoids see disperse systems****displacement measurement**

- accelerometer signals, displacement measurement by double integration 4-73416
- acoustic transducers, surface displacement, fibre optic meas. 4-97261
- angle-to-code measurement transducers, high-precision, testing 4-90577
- angular displacement meas. using holographic interferometry 4-90336
- angular displacement optical measurement method for case when axis of rot. inclines 4-78356
- diffraction grating movement, rot. effect in linear-displacement convertor operation 4-64763
- disc, deform. analysis, grid and grating methods, digital image processing (German) 4-64896
- displacement sensors: which technologies? (French) 4-63710
- fibre optic Doppler velocimeter, mixed-fibre interferometric sensor with microretroreflectors 4-91618
- fibre optic optimised microband displacement sensor 4-91617
- fluidic micrometer for vacuum chamber, pressure-related transfer characteristics 4-111144
- fringe carrier method for displacement derivative determ. in hologram interferometry 4-79078
- fringe pattern analysis by image processing using personal computer (Japanese) 4-111197
- heart and chest wall displacement recording, laser method 4-62550
- instantaneous phase measuring interferometer, displacement meas. appls. 4-106373
- instantaneous phase measuring interferometry 4-106362
- interior warping measurement by holographic interferometry 4-95383
- laser interferometer, appl. 4-95504
- lateral extensometer long-term accuracy assessment using optical technique 4-78296
- linear displacement measurement transducers 4-101835
- metal bar, impacted, meas. transient vibration by high speed laser interferometry 4-111189
- micropiezometer for use with liquids 4-90561
- microwave interferometer system for biological subject displacement meas. (Japanese) 4-110019

**displacement measurement continued**

- moire fringe techniques in engineering metrology 4-78366
- multiaperture speckle shearing arrangements for stress analysis 4-58888
- multifunctional laser displacement-measuring instruments 4-63721
- non-contact displacement measurement system having one microinch resolution 4-95377
- object repositioning using hybrid moire system 4-86476
- optical fibre, displacement monitor for use in characterization of single mode fibres 4-107830
- optical method of angular displacement meas. 4-68207
- pulsed laser velocimetry, 2-D particle displacement meas. using orthogonal compression and 1-D anal. techniques 4-83962
- scanning piezoelectric ceramics, displacement, linearity measurement using scanning interference method (Chinese) 4-11101
- speckle shear interferometry, multiplexing 4-101915
- surface displacement measurement by white speckle photography (Polish) 4-58903
- surface distortion with extreme dynamic loads, laser-optical meas. (German) 4-73415
- vibratory displacement meas. apparatus with projection reading diaphragm and remote scale 4-63742
- Al rods impaction on PMMA target, radial displacement meas. method 4-106280
- W, field ion study of mixed dislocations 4-108369

**displace transformations**

- see also martensitic transformations; polymorphic transformations; reverse martensitic transformations; soft modes
- anthracene-TCNB, charge transfer complexes, order-disorder and displacive transitions 4-70367
- dislocations, phonon drag near phase transition points 4-60929
- incommensurate displacive phase, field theory anal. (Chinese) 4-98239
- metallic system, book contrib. 4-109405
- rock, calcite, stress-wave induced phase transformations, nonhydrostatic effects 4-110138
- tris-sarcosine calcium chloride (bromide), ferroelec. phase transition, IR and Raman studies 4-93023
- Ba<sub>2</sub>NaNbO<sub>15</sub>, ferroelec. transition, critical narrowing of central peak, Raman studies 4-71291
- BaTiO<sub>3</sub>, displacive type ferroelastic, lattice model 4-76394
- BaTiO<sub>3</sub>, displacive/order-disorder crossover, soft mode temp. depend., contrib. to low freq. permittivity 4-65369
- CoP<sub>2</sub>, ambient press. synthesis, cryst. struct., mag. and elec. props., bonding 4-75408
- CsCaF<sub>3</sub>, soft mode freq., temp. and press. depend. 4-70331
- K<sub>2</sub>Fe(CN)<sub>6</sub>, cryst., Raman scatt. and phase transition 4-71375
- KNbO<sub>3</sub>, displacive/order-disorder crossover, soft mode temp. depend., contrib. to low freq. permittivity 4-65369
- K<sub>2</sub>ZnCl<sub>4</sub>, incommensurate ferroelec., phase transitions, lattice dynamics, Raman effect 4-84922
- KZnF<sub>3</sub>, soft mode freq., temp. and press. depend. 4-70331
- RbCaF<sub>3</sub>, soft mode freq., temp. and press. depend. 4-70331
- VP<sub>4</sub>, ambient press. synthesis, cryst. struct., mag. and elec. props., bonding 4-75408

**display devices**

- see also gas-discharge displays; liquid crystal displays
- auto-stereoscopic holographic display devices 4-74459
- miniature readout devices for metal-cutting lathes 4-58844
- optical schemes for display and demonstration 4-112557
- optics in entertainment, conf., Los Angeles, CA, USA (Jan. 1984) 4-110802
- timer smear corrected multiplex holographic display of computerized tomography data 4-74460
- Er complex, Er-diphthalocyanine films, electrochromism for all solid display cells 4-74635
- Fe garnet magneto-optic spatial light modulator in optical image processor or display system 4-74696
- SnO<sub>2</sub>:Sb electrocond. film deposited by sol-gel technique, transparent electrodes for display appls. 4-71604

**display equipment see display instrumentation****display instrumentation**

- see also cathode-ray tube displays; display devices; screens (display)
- array-mapped display system for Fourier transform IR spectroscopy 4-101945
- biocular magnifiers for electro-optic displays, visual comfort assessment 4-97024
- colour display and analysis system for hydrographic surveying 4-67452
- colour imaging thermal video system 4-58839
- CT display, detectability enhancement by use of coloured illumination 4-62554
- EPM-1 Milliwatt Power Meter for 10 Hz to 300 MHz 4-95472
- high technology electronics exhibition and conference, Detroit, MI, USA, (June, 1983) 4-95014
- hologram as an electronic display 4-107566
- holographic stereograms for three-dimens. imaging 4-74453
- manipulator/display system, computer-controlled, for human movement studies 4-85588
- object visibility in presence of strobe illum. 4-81695
- optics in entertainment, conf., Los Angeles, CA, USA (Jan. 1984) 4-110802
- three dimensional display fundamentals 4-74448
- three-dimensional imaging, conf., Geneva, Switzerland (April 1983) 4-73140
- visual tasks requiring three dimensional stereoscopic displays 4-115054

**display instruments see display instrumentation****display systems see display instrumentation****disruptive voltage see electric breakdown****dissipation (heat) see cooling****dissociation**

- see also electrolytic dissociation; heat of dissociation; ionisation; molecular dissociation; molecular dissociation energies; photodissociation
- alkali halides solid in microwave-induced plasma afterglow, lattice atomisation, temp. depend. 4-79862
- alkane eliminations from radical cations through ion-radical complexes 4-114778
- carbohydrates, thermal props. heat flow calorimetric obs. 4-78312
- graphite-FeCl<sub>3</sub> interstitial cpds., isobaric thermal anal. 4-81425
- ionic cryst., lattice and thermodynamic props., overlap repulsion pot. 4-92327

**dissociation continued**

- metal surfaces, decomposition of main group organometallic compounds 4-89323
  - metal-metalloid system, thermodynamics, kinetics and props. of gases and C in Ag and Au, data collection 4-73174
  - nucleation kinetic theory, pot. energy barrier 4-85326
  - PMMA films, ion beam induced decomp. and diffusion 4-70234
  - polyhexamethylene sebacamide, struct. changes during ageing (Russian) 4-62239
  - polypropylene, mech. future, ionic product form. 4-114660
  - RDX decomposition, CARS probe study 4-99788
  - reactive components, fluctuation thermodynamic props., species correl. function integrals 4-71965
  - solids, acceleratory degradation, non-steady state kinetics 4-104980
  - VUV radiation physics, conf., Jerusalem, Israel, 8-12 Aug. (1983) 4-82583
  - CoCl solns., US relax. mechanisms 4-92308
  - DyMnO<sub>3</sub>, decomposition, O partial press. and elec. cond. 4-85290
  - Fe surface, (111), N<sub>2</sub> chemisorbed,  $\pi$ -bonded complex, the precursor for dissoci. 4-105029
  - Fe(NH<sub>4</sub>)<sub>2</sub>(SO<sub>4</sub>)<sub>2</sub>·6H<sub>2</sub>O-Ni(NH<sub>4</sub>)<sub>2</sub>(SO<sub>4</sub>)<sub>2</sub>, co-precipitated, thermal decomp. Mossbauer investig. 4-65883
  - LiClO<sub>4</sub>-Mg(Al)(Fe)(Cr)(Ni), shock compression, physicochemical transformations 4-70273
  - NaAlH<sub>4</sub>, decomposition, Na single cryst. form., electron microscopic study 4-108296
  - Na<sub>2</sub>O-CaO-CO<sub>2</sub> system, calcination in air, differential thermal analysis obs. 4-99757
  - Ni (111), dissociative adsorption and recomb. of CO, N<sub>2</sub>, SO, and O<sub>2</sub> 4-93559
  - Ni, thermodynamics, kinetics and props. of gases and C; data tables 4-73173
  - Pt-electrolyte interface, laser induced processes 4-81452
  - SnO<sub>2</sub>, mechanical activation, defect formation 4-75456
  - TiO<sub>2</sub>, mechanical activation, defect formation 4-75456
  - WO<sub>3</sub>, mechanical activation, defect formation 4-75456
- dissolution see dissolving**
- dissolving**
- see also solubility; solutions; solvation
  - alkali halide crystals, etch pit studies of dislocations, dissolution kinetics and impurity effects 4-70158
  - alloys, carbide precipitates, computer simulated dissoln. 4-109416
  - alloys, preferred sputtering, segregation effects 4-81203
  - borosilicate waste glasses, ion bombard., fracture toughness and leaching behaviour 4-75545
  - $\alpha$ -brass, film growth in ammoniacal Cu(II) solns., early stages 4-89163
  - cementite dissolution in austenite, computer simulation 4-71653
  - ferrous alloys, dissoln. in molten pure Al under forced flow 4-92378
  - fusion reactor breeder materials, solid, irradiated, retained He and T meas. technique 4-107021
  - glass, reactivity in aqueous solns., leaching of simulated radioactive waste glass 4-93548
  - glass fibres, leaching and local comp., SEM study 4-81303
  - Incoloy 800, compatibility with flowing Li 4-107062
  - iron phthalocyanine film electrodes, anodic dissolution in H<sub>2</sub>SO<sub>4</sub> 4-61453
  - landfill leachate,  $\gamma$ -irrad. conditions required in combined radiation-microbial process 4-93677
  - metallurgical systems, mechanisms and kinetics of dissolution 4-114530
  - metals, diffusion coeff. and conc. of dissolved H, electrochem. permeation method (Japanese) 4-65466
  - metals, diffusion coeff. and conc. of dissolved H, electrochemical permeation method (Japanese) 4-65468
  - nuclear fuel-cladding separation by cladding-tube heating (German) 4-83218
  - nuclear waste storage materials, radiation effects 4-73973
  - optical fibres, single-mode, H<sub>2</sub> and D<sub>2</sub> gas-in-glass effects 4-97121
  - precipitate dissolution, anal. of microstruct. dynamic 4-109408
  - radioactive waste, radionuclide transport, time-temperature dissolution 4-106719
  - radioactive waste materials, ion implantation effects on dissolution props., simulation of internal irradiation due to  $\alpha$ -decay 4-75544
  - simulated nuclear waste glass, Cm doped, radiation damage, annealing, short term leach test 4-83149
  - sintering, liq. phase, densification and microstructural development 4-99360
  - steel, Cr-Mo-V-W, HT-9, austenitising and microstruct. 4-93320
  - steel, alloy, high C, optimisation of heat treatment (French) 4-81224
  - steel, austenitic stainless, repassivating in acid solutions, film growth and dissoln. kinetics 4-81330
  - steel, austenitic stainless, repassivation kinetics, effect of Mo alloying 4-81331
  - steel, Cr-Mo and 316 types, compatibility with flowing Li 4-107062
  - steel, high speed, W-Mo-V, transform. in matrix during austenitising and quenching, influence of Mo 4-114516
  - steel, HSLA, small fatigue crack initiation and growth, in various environments (Japanese) 4-89124
  - steel, low alloy, fatigue crack propag. in viscous environment 4-99579
  - steel, low alloy, sulphide stress cracking, role of H 4-89168
  - steel, low C, Mn, austenite form-mechanism during annealing 4-85151
  - steel, mild, SCC in NaH<sub>2</sub>PO<sub>4</sub> soln., effect of heat treatment and C 4-89167
  - steel, stainless, austenite-ferrite duplex, preferential phase dissolution in H<sub>2</sub>SO<sub>4</sub>-NaCl soln. rel. to heat treatment and comp. 4-81341
  - steel, stainless, austenitic, modified PCA, mass transfer behaviour in Li 4-107063
  - steel, stainless high-alloy, black coatings produced by chem. methods 4-69606
  - steel, Ti-modified, prep. by rapid solidification processing, microstruct. response to neutron irradiation 4-98143
  - steel, use of surface behavior diagrams to study hydration/corrosion of aluminum and steel surfaces 4-89171
  - Synroc, hydrothermal attack, surface analysis 4-68760
  - Zircaloy-4, SCC in neutral aq. chloride soln. 4-66478
  - Ag-Pb, liq., thermodynamic study of dissolved O 4-92379
  - Al, hydration/corrosion, surface behaviour diagrams, dissolution of adsorbed inhibitor 4-89171
  - Al-Cu (4 wt.%), dissoln. kinetics of  $\theta$  phase using thermoelec. power meas. 4-114533
  - Al-Fe alloys, Fe precipitation and dissolution, thermoelec. study 4-61938
  - Al-Li, microcrystal evolution, DSC obs. 4-71659

# dissolving continued

- Al<sub>2</sub>O<sub>3</sub>, thermal-dissolution of layers on W and Mb substrates in elec. field 4-80405  
As<sub>2</sub>S<sub>3</sub> evap. photoresist., dissolution rate rel. to evap. conditions 4-68299  
(CaO,50P<sub>2</sub>O<sub>5</sub>),(M<sub>2</sub>O)<sub>50-x</sub>, dissolution in aq. soln. 4-84405  
Ca<sub>10</sub>(PO<sub>4</sub>)<sub>6</sub>(OH)<sub>2</sub>, dissolution kinetics, effects of fluoride ions adsorption 4-98292  
Cr films, dissolving kinetics, plasma treatment induced changes 4-81335  
Cr-Ru(Pd)(Ir)(Pt), active dissoln. in H<sub>2</sub>SO<sub>4</sub>, effect of Pt group element additions 4-71770  
Cu complex, bis-(propylammonium) copper(II) tetrachloride, cryst. growth from soln., Oswald ripening along faceted bridge 4-75336  
CuAl<sub>2</sub>, second-phase particles, dissoln. rates in various microstruct. 4-89059  
Fe base alloys, inoculation particles dissolution, carbide precipitation 4-89057  
Fe, electrochem. behaviour, effect of Br<sup>-</sup> 4-89165  
Fe-C, dissoln. in molten pure Al under forced flow 4-92378  
Fe-C(Cr), austenite, cementite dissoln., computer simulation 4-71653  
Fe-Cr-C (10, 0.2 wt.%) austenite form., TEM and optical microscopy study 4-66331  
Fe-Cr(Si), dissoln. in molten pure Al under forced flow 4-92378  
Fe-Cu, H permeation in H<sub>2</sub>SO<sub>4</sub> with and without H<sub>2</sub>S, electrochem. and surface anal. studies 4-104898  
Fe-Ni, H<sub>2</sub> charged, internal friction 4-104802  
Fe-Ni-Cr-W amorphous alloys, corrosion resist. 4-99632  
Fe-C, SCC in NaH<sub>2</sub>PO<sub>4</sub> soln., effect of heat treatment and C 4-89167  
Gd-Ni-Si, X-ray phase anal. of compounds formed 4-114494  
In-Bi alloys, phase diagram and metallography 4-114483  
Li<sub>2</sub>O, activity coeff. of dissolved LiOH, water press.-temp. regime, breeder material 4-107029  
Li<sub>2</sub>O pellet, T recovery, assay techniques 4-107022  
Li<sub>2</sub>O-B<sub>2</sub>O<sub>3</sub>-SiO<sub>2</sub>, phase-separated glass, dissoln. rate, influence of pH 4-84403  
Na-W bronze, anodic behaviour in neutral soln. 4-81346  
Na<sub>2</sub>CO<sub>3</sub>-SiO<sub>2</sub>, melts, dissolution of SiO<sub>2</sub> 4-84402  
NaCl:CaCl<sub>2</sub> doped cryst., dissolution at dislocation sites 4-60931  
Na<sub>2</sub>O-MO-Al<sub>2</sub>O<sub>3</sub>-SiO<sub>2</sub> glass, M=Ca, Mg, Zn, leaching 4-84404  
Ni-Fe, dissoln. and passivation, influence of S adsorpt. 4-71756  
Ni-Fe, dissoln. and passivation, influence of S adsorpt. 4-71757  
Ni<sub>53</sub>Fe<sub>47</sub>O<sub>4</sub>, ferrite, dissoln. in EDTA soln. 4-88295  
Ni<sub>40</sub>P<sub>60</sub>, dissolution of H, vol. changes 4-70396  
Ni<sub>47</sub>Al<sub>53</sub>P<sub>18</sub>, dissolution of H, vol. changes 4-70396  
Pd catalysts, monodisperse, adsorpt. and dissolution of H<sub>2</sub> 4-61220  
Pd<sub>3</sub>Si<sub>20</sub>, dissolution of H, vol. changes 4-70396  
Si, dissoln. kinetics in Cr<sub>2</sub>O<sub>3</sub>-HF-H<sub>2</sub>O soln. 4-62082  
SiO<sub>2</sub> glass film, crack tip geometry, water ageing, high resolution electron microscopy 4-71724  
(Th, U)O<sub>2</sub>, mixed oxide fuel, dissoln. in conc. HNO<sub>3</sub> 4-83217  
Ti anodic oxide film, corrosion reaction in HCl soln. 4-89169  
Ti-Al alloy VT1-0, anodic soln. under potentiostatic conditions, {Russian} 4-71778  
YIG, seed and unseeded, growth from high temp. solns., studied by growth striations 4-76656  
YIG single crystal spheres, dissoln. forms in H<sub>3</sub>PO<sub>4</sub> and HBr 4-75687  
Zn anodic dissolution in alkaline electrolytes, three step model 4-103941  
Zn, electrodisoln. in acidic chloride solns. 4-89166

# distance measurement

- absolute distance interferometer using dye laser heterodyne interferometer and spatial separation of beams 4-106366  
deep sound channel time-delay ranging, multilayer sound speed profile model 4-107940  
dispersion method using Nd<sup>3+</sup>:YAG laser 4-106272  
EM, atmospheric refraction effects determ. 4-110313  
FEN 2000 family of instruments using pulse-timing meas. {German} 4-62967  
geodetic distance meas. with Mekometer laser instrument, atmos. corrections and data reduction 4-89998  
Hyades star cluster, distance, moduli of oft-occulted binary stars 4-101407  
IC production, photomasks, absolute measurements of structure widths in micrometer range with the optical microscope 4-95386  
laser ranging meas., system anal. and computer simulation 4-107723  
laser ranging plotter for close-range applications 4-91520  
M3 (NGC 5272), globular cluster, distance determ. using variable stars {Russian} 4-101445  
phase phototachymeters having different types of photodetectors, distance meas. error 4-60135  
polyvinylidene fluoride transducers for acoustic ranging and imaging in air 4-97251  
portable acoustic devices for divers, homing, surveying, navigation {French} 4-97220  
radiation device for distance and velocity measurements 4-73413  
self-detecting light-emitting diode optical sensor for object proximity meas. 4-95411  
sensor for distance and velocity meas., laser speckle pattern motion appl. {Japanese} 4-58845  
sensor with optical-fibre-array spatial filter {Japanese} 4-78309  
space laser systems for geodetic appls. accuracy requirements 4-110322  
stars, distances determ. using rigorous formulae for proper motion calc. {German} 4-67715  
stellar parallaxes and proper motions from McCormick Observatory, 45th list 4-82464  
stellar trigonometric parallaxes, determ. from obs. in hour angles {Russian} 4-101118  
ultrasonic waves appl. to distance meas. method 4-103153  
US distance measurement using compensated digital US sensor in air 4-97225  
US piezoelectric air transducers for distance measurement 4-91706  
US transducers for HF acoustic wave meas. in air 4-97252  
visual binary stars, dynamical parallax and orbital inclination determ. from obs. of short arc {Russian} 4-101414

# distillation

- see also isotope separation  
binary azeotropic distillation design 4-65379  
entropy production minimisation 4-87555  
packed distillation columns, Marangoni effect 4-64935  
roof-mounted solar distillation and water heating/cooling system performance 4-62301

# distillation continued

- POCl<sub>3</sub>, purification by low temp. sublimation and distillation 4-66255  
T enrichment in metallic Li, distillation column design, fusion fuel: appl. {German} 4-64237  
distortive transformations see solid-state phase transformations  
distributed Bragg reflector lasers  
GaInAsP/InP phase adjusted active distributed reflector laser, 1.5 μm, for dynamic single mode operation 4-69437  
GaInAsP-InP BH but-jointed built-in integrated, lasers, 1.5-1.6 μm operation, static characts. 4-60065  
GaInAsP-InP DH lasers, review, book contrib. 4-60037  
InGaAsP/InP DFB laser diodes, cleaved facet, grating phase effects 4-60063  
PbSnTe-PbSeTe DBR diode lasers grown by LPE 4-112460  
distributed control  
memory intensive functional architecture 4-59600  
River Nile, decentralised control of water quality 4-105617  
distributed feedback lasers  
chirp effect on optical systems, wavelength shift 4-91521  
dye laser, distributed feedback, picosecond pulses generation using grating hologram 4-112405  
dye laser, ultrashort-pulse, travelling-wave-pumped 4-83571  
dye laser N<sub>2</sub> laser oscillator-amplifier system 4-69439  
dye laser pulses, directional and wavelength sweep 4-69466  
fluoromethane grazing-incidence far-IR laser 4-96949  
fluoromethane laser, optically pumped 496 μm, linear DFB, helical DFB and grazing-incidence types {Chinese} 4-107677  
helical DFB far IR gas laser, theory, realisation and mode characts. 4-79186  
IR laser particle accelerators, linear and helical DFB structs., theory and feasibility 4-74062  
optical schemes of pumping beams {Russian} 4-96936  
quarter-wave shifted grating type, wavelength selectivity analysis 4-64716  
resonance frequencies and threshold gains calc. with strong modulations 4-107589  
rhodamine B DFB dye laser, amplified spontaneous emission 4-83572  
semiconductor DFB lasers, overgrowth of gratings, adducts in MOVPE 4-71575  
single pulse selection in amplifiers 4-69470  
single-frequency cleaved-coupled cavity and DFB laser, direct modulation transient chirping study 4-83627  
threshold gains and resonance freqs. calc. for strong modulation 4-79095  
{AlGa}As heterolasers with distrib. feedback, polarisation effects 4-64708  
AlGaAs heterostructure laser with distributed feedback 4-74538  
Al<sub>0.3</sub>Ga<sub>0.7</sub>As-GaAs distributed feedback surface-emitting laser diode 4-112424  
GaInAsP heterostructure laser with distributed feedback 4-74538  
GaInAsP/InP 1.3 μm distributed feedback lasers, LPE growth 4-96913  
GaInAsP/InP DFB lasers, 1.3 μm, monolithic integrated struct., WDM optical communication appl. 4-83618  
GaInAsP/InP laser, 1.5 μm range, longitudinal mode behaviour 4-74512  
InGaAsP 1.53 μm DFB lasers made by mass transport 4-102947  
{InGa}AsP heterolasers with distrib. feedback, polarisation effects 4-64708  
InGaAsP heterostructure laser with distributed feedback 4-74538  
InGaAsP tunable DFB laser pumped by heterostructure injection laser 4-96907  
InGaAsP/InP DFB ridge-waveguide laser, 1.2 Gbit/s optical fibre transmission over 113.7 km 4-107847  
InGaAsP/InP laser diode lasing characts. at 1.5 μm, effect of mirror facets 4-74513  
InGaAsP-InP single-longitudinal-mode 1.3 μm DFB-DC-PBH diodes 4-91467  
InP/InGaAsP DFB double-channel PBH laser diode, 1.55 μm, single longit. mode operation 4-87358  
LiF F<sub>2</sub> centre tunable laser with distributed feedback 4-107651  
distributed parameter systems  
curvilinear shallow elements of structures, optimal design problems 4-91729  
hydraulic systems, errors in simulation of pressure transients 4-83952  
inverse problems for hyperbolic systems, spline-based approximation method appl. 4-85637  
reactor, modelling and numerical simulation 4-109335  
distributed processing  
see also computer networks; multiprocessing systems  
COMPEX standard capabilities 4-106287  
control systems, memory intensive functional architecture 4-59600  
multiprocessor EEG analyser 4-85560  
patients monitoring system 4-67146  
radionuclide laboratory, data acquisition system 4-74124  
wave dynamics and surface weather data transmission between radio-linked microprocessors 4-115622  
distributions, statistical see statistical analysis; statistics  
district heating  
community solar heating system performance in southern Finland 4-62302  
heat pump-boiler systems for district heating, energy saving potential 4-72154  
heat pumps, MW range, present possibilities and limitations {German} 4-81577  
Organic Rankine Cycle for district heating reactor 4-91038  
peat fuel for district heating in Finland 4-93584  
pipeline configurations, design improvements 4-103180  
power stations with heat pumps using refrigerant, market opportunities {German} 4-85382  
diversity reception  
see also fading  
atmospheric effects meas. on satellite links at very low elevation angle {French, English} 4-67380  
site diversity model, for satellite communications systems, evaluation 4-100687  
DLTS see deep level transient spectroscopy  
DNA  
B and Z, interaction energies between purine and pyrimidine bases, ab initio SCF LCAO calcs. 4-66851  
bacteriophages, DNA containing, packing model using small-angle X-ray scatt. data 4-85404  
band structure 4-77178

## DNA continued

- base components, electrostatic interactions, pot. derived point-charge model study 4-107271  
base pairs, H bonding, effect of carcinogenic epoxides 4-76980  
bending, sequence-directed and protein-induced, locus 4-62439  
bone marrow and spleen cells, DNA struct. and catabolism, HTO and  $^{137}\text{Cs}$   $\gamma$ -ray effects (*Russian*) 4-115132  
bone marrow cells, rat, X-irrad.-induced double-strand DNA breaks (*Russian*) 4-77312  
cell damage, Ar laser microbeam irrad. (*Chinese*) 4-109876  
chain elongation inhibition in Chinese hamster cells on UV irrad. 4-72312  
chromosomes, micro-Raman spectroscopy, protein and DNA contribs. 4-115033  
crosslinking, BCNU-induced, X-ray effects in rat brain tumour cells 4-105296  
dielectric behaviour of DNA soln. at radio and microwave freqs. at 20°C 4-105213  
diploid yeast cells, UV- and X-ray induced damage, common repair pathways 4-100256  
DNA-ethidium, binding constns., elec. pots. 4-109774  
B-DNA-polyglycine, interaction energies, complex struct. and stability 4-77181  
double helices, solitary excitation 4-91377  
double-strand breaks, form. and repair in irrad. cells (*Russian*) 4-77311  
double-stranded  $\phi\text{X174}$  (RF) DNA, repair of damage due to radiation-induced water radicals 4-67021  
E. coli B/r Hcr<sup>+</sup> cells, error-free uvr<sup>+</sup>-dependent inducible DNA repair 4-67022  
E. coli K-12 radC102, radiation-sensitive mutant, characterisation 4-67031  
elastic and inelastic electron scatt., Monte Carlo calcs. 4-97976  
electron crystallographic studies 4-100074  
equilibrium sedimentation distrib. scaling in dense solns. 4-66850  
Euglena cells, X-ray induced single strand DNA breaks and their repair in chloroplasts 4-62531  
evolution and tertiary protein structures, book contrib. 4-93690  
footprinting in vivo, use of light 4-85593  
hyperthermia at 42°C, effects on DNA lesion and cell inactivation caused by X-ray 4-77196  
interaction with molcs., steric surface, electrostatic contours 4-72206  
leukocyte DNA, radiation-induced damage, fluorometric determ. (*Russian*) 4-67006  
lymphoid cells, mol. mechanisms of radiation death, chromatin degradation and DNA replication (*Russian*) 4-77318  
mammalian, of Chinese hamster cells, effect of 70 GeV proton secondary radiation (*Russian*) 4-67001  
mammalian cells, cultured, X-ray-induced DNA damage and cellular lethality 4-93817  
mammalian cells, DNA repair kinetics following split dose  $\gamma$ -irrad. 4-77338  
mammalian cells, occurrence of DNA strand breaks after hyperthermic treatments with or without radiation 4-66915  
mononucleosomes from replicating chromatin in heated cells, sedimentation coeff. and buoyant density 4-77198  
multistranded structures use in information transactions 4-77172  
nuclear DNA segregation in *Bacillus cereus* T, radiation induced failure 4-72231  
nucleic acid containing struct., selective staining using uranyl acetate-lead citrate 4-89832  
nucleosome, histone and DNA packing model 4-89517  
oligo-DNA, conformation, two dimens. double quantum spectra, PMR 4-81617  
phase DNA, unpaired bases after  $\gamma$ -irrad. in-situ and in-vitro 4-77346  
poly-L-lysine-DNA complexes, conformation, circular dichroism spectra 4-89497  
radiation degradation of DNA and histone within the chromatin (*Russian*) 4-66862  
replication and transcription of DNA in proliferating and resting HeLa cells, UV laser pulse effect (*Russian*) 4-66999  
sequence-determined separations, electrophoretic mobility in gels obs., book contrib. 4-93689  
simian virus 40 DN, replication following UV irrad., test of model 4-115134  
stress induced nonlinear struct. transition 4-100071  
structures, information decoding (*French*) 4-77185  
supercoiling, free energy rel. to enthalpy 4-77182  
synthesis, effect of time-varying mag. fields 4-66996  
synthesis in HeLa cell culture under biological action of low-intensity visible light 4-62525  
thymus DNA, pyrimidine cluster changes after animal  $\gamma$ -irrad. with sublethal dose (*Russian*) 4-67004  
transforming, UV action spectra for protection by glycerol 4-67029  
yeast DNA, S1 nuclease-sensitive sites, assay for radiation-induced base damage 4-72311

document retrieval *see information retrieval*

documentation, program and system *see program and system documentation*

## domain boundaries

- for boundaries between magnetic domains and electric domains *see magnetic domain walls and electric domain walls respectively*  
*see also antiphase boundaries*  
crystals, phase transitions, X-ray topography, review 4-65990  
graphite intercalation cpd., domain walls, elastic plates model anal. 4-113660  
9-hydroxyphenalene, phase transitions and ferroelasticity 4-113614  
interface stability critical phenomena and scalar order parameters 4-58802  
MBBA, nematic liq. cryst. structural phase transitions, energy-dispersive X-ray diff. 4-75673  
random-field Ising model, domain wall width, lower bounds 4-78269  
 $\text{Gd}_2(\text{MoO}_4)_3$ , acoustic wave reflection from ferroelastic domain walls 4-98209  
 $\text{KFe}(\text{MoO}_4)_2$ , ferroelastic domain switching 4-92343  
 $\text{KH}_2(\text{SeO}_3)_2$ , ferroelastic, light deflection by domain walls 4-104550  
 $\text{KIn}(\text{MoO}_4)_2$ , ferroelastic domain switching 4-92343  
 $\text{KSc}(\text{MoO}_4)_2$ , ferroelastic domain switching 4-92343  
 $\text{NaO}_2$ , phase transitions, phenomenological theory 4-92348  
 $\text{NdP}_2\text{O}_{14}$ , acoustic wave reflection from ferroelastic domain walls 4-98209

## domain boundaries continued

- $\text{Pb}(\text{Se}_{0.5}\text{Ta}_{0.5})\text{O}_3$  single cryst., ordered domains, TEM obs. 4-65411  
 $\text{ZrO}_2\cdot\text{Y}_2\text{O}_3$ , domain boundaries generated by cubic-tetragonal transition, TEM study 4-70378  
*domains*  
*see also antiphase domains; crystal microstructure; domain boundaries; electric domains; magnetic domains*  
alloys (*Japanese*) 4-113391  
p-azoxyanisole nematic liq. cryst., domains, threshold characters 4-113330  
Na-beidellite, two-water-layer, struct. of hydrated clay mineral (*French*) 4-82039  
binary cryst., displacement domains caused by defects (*Chinese*) 4-70254  
bis-tetramethylammonium tetrachlorozincate: $\text{Mn}^{2+}$ , soliton density in incommensurate phase, EPR, temp. depend. 4-109065  
crystals, first order transition, domain walls' structure, formation and activation energies 4-65394  
double sine-Gordon chain, damped, uniformly moving domain walls 4-90391  
p-ethoxy phenyl azophenyl butyrate, nematic liq. cryst., mol. alignment in elec. and mag. fields 4-108277  
ferroelastic domain regular struct., bulk acoustic wave interaction 4-108551  
first-order phase transitions, nucleation-growth processes, scaling laws (*Japanese*) 4-113568  
graphite intercalation compounds, ultramicrostruct. 4-84417  
growth, temp. depend., Ising model Monte Carlo simulation 4-58761  
growth kinetics, universality of kinetic exponents, Potts model 4-58779  
p-n-heptyloxybenzoic acid smectic C liq. cryst., electrohydrodynamic transient instability 4-75270  
Ising model, random field, domain growth and self-similar scaling breakdown 4-82763  
kink, uniformly driven, in damped  $\phi^4$ -chain 4-68148  
liquid crystalline polymers, deform. studies 4-113303  
polyarylenesulphonoxide-polybutadiene block copolymer films, morphology (*Russian*) 4-61100  
quartz powders, shock-loaded, deform., X-ray line broadening obs. 4-65324  
simple layer potential method for domains having external corners 4-63511  
thermotropic liquid crystalline polymers, domains and walls 4-79933  
 $\text{As}_2\text{Se}_3(\text{S}_x)$  thin films, large scale domain struct. 4-88106  
 $\text{AuGa}_2(001)$ , surface net characterisation and electronic struct. 4-80642  
 $\text{Ba}_2\text{NaNb}_2\text{O}_{15}$ , tetragonal bronze-like struct., modulated phases and domain struct. 4-113616  
 $\text{CaF}_2$  vapour deposited thin films, TSEE, thermolum. meas. 4-81119  
 $\text{Cu}_2\text{Zr}_2$ , 3D long-period superstructure, electron diff., electron microscopy obs. 4-70068  
DNA, stress induced nonlinear struct. transition 4-100071  
Fe-Al (40 at %), ion implantation, phase changes, TEM studies 4-108403  
Fe-Al-Si (6, 9 at %), ordering with phase separation, annealing, TEM, X-ray diff. study 4-114472  
Fe-base superalloy,  $\sigma$ -phase, planar faults, domain structures, high resolution electron microscopy obs. 4-104793  
FeCo alloy, brittleness, purity and impurity segregation effects (*Russian*) 4-109496  
Ge-Se glasses, microstructure, electron microscopy obs. 4-88305  
 $^3\text{He-A}$ , superfluid, solitons as bound states on domain walls 4-70505  
 $\text{KFe}(\text{MoO}_4)_2$ , ferroelastic domain switching 4-92343  
 $\text{KH}_2(\text{SeO}_3)_2$ , ferroelastic domain struct. dynamics, internal friction meas. 4-80156  
 $\text{KIn}(\text{MoO}_4)_2$ , ferroelastic domain switching 4-92343  
 $\text{KSc}(\text{MoO}_4)_2$ , ferroelastic domain switching 4-92343  
Kr, adsorbed on graphite domain growth, Monte Carlo simulations 4-98444  
Kr monolayer, on graphite, commensurate-incommensurate transition, X-ray scatt. study 4-61215  
 $\text{La}_{1-x}\text{Ca}_x\text{FeO}_{3-y}$ , high temp. order-disorder transition 4-113618  
 $\text{LiF}$  vapour deposited thin films, TSEE, thermolum. meas. 4-81119  
 $\text{LiKSO}_4$  cryst. and domain struct., neutron diff. studies 4-88159  
 $\text{LiKSO}_4$ , phase transitions at low temp., domain textures, dielec. meas. 4-75655  
 $\text{Mg}_2\text{Al}_4\text{Si}_2\text{O}_{18}$ , cordierite, Al-Si ordering, Raman studies 4-98073  
 $(\text{ND}_4)_2(\text{SO}_4)_2$ , successive phase transitions studied by  $\text{VO}^{2+}$  ion and  $\text{SeO}_3$  radical EPR 4-76388  
 $\text{NH}_4\text{BeF}_3$ , ferroelastic, domain struct., polarising microscope obs. 4-108629  
 $(\text{NH}_4)_2\text{H}(\text{SO}_4)_2$ , successive phase transitions studied by  $\text{VO}^{2+}$  ion and  $\text{SeO}_3$  radical EPR 4-76388  
 $\text{NaH}_2(\text{SeO}_3)_2$  biaxial ferroelec., ferroelastic and ferroelec. domains 4-93027  
 $\text{NbSe}_3$ , electron irrad., strandlike domains in CDW states 4-70220  
 $\text{NbSe}_3$ , negative differential resist., dynamic instability 4-88502  
Ni (110), chemisorbed  $\text{O}_2$ , 2X1 struct., real space obs. by scanning tunnelling microscopy 4-61212  
 $\text{Pb}_2\text{NaNb}_2\text{O}_{15}$ , tetragonal bronze-like struct., modulated phases and domain struct. 4-113616  
 $\text{Pb}(\text{Se}_{0.5}\text{Ta}_{0.5})\text{O}_3$  single cryst., ordered domains, TEM obs. 4-65411  
 $\text{Pb}_2\text{V}_{2-3}\text{O}_{13}$  and  $\text{Pb}_2\text{V}_{2(1-x)}\text{P}_{2-x}\text{O}_{13}$ , ferroelastic props. and crystal struct. 4-70264  
 $\text{Pr}_2\text{O}_{12}$  to  $\text{Pr}_2\text{O}_{16}$  phase transition, hysteresis and kinetics 4-108606  
 $\text{RbAg}_2\text{I}_5$ , domain struct. below phase transition point 4-70402  
 $\text{RbMnCl}_3$ , crystal and mag. structure heterogeneities 4-84276  
 $\text{Sr}_2\text{KNb}_2\text{O}_{15}$ , tetragonal bronze-like struct., modulated phases and domain struct. 4-113616  
 $\text{Sr}_2\text{NaNb}_2\text{O}_{15}$ , tetragonal bronze-like struct., modulated phases and domain struct. 4-113616  
*domestic appliances*  
*see also ovens; refrigerators*  
Swedish residential energy use and conservation (1963-80) 4-66644  
*donor levels* *see impurity electron states*  
*doping, semiconductors* *see semiconductor doping*  
*doping profiles*  
III-V semiconductors, contact resistance profiling 4-75499  
 $\text{InP}$ :Zn epitaxial layers, MOCVD grown, doping, Hall effect, SIMS, electrochemical profiling 4-80077  
 $n^+n^-p^+$  structure, I-V characters, dopant profile effects 4-88572  
optical fibres and preforms, Raman microanalysis 4-79320  
polyacetylene, electrochemical  $(\text{IrCl}_6)^{2-}$  doping, elec. cond. meas. 4-65661  
polyacetylene morphology upon  $\text{I}_2$  doping, SEM 4-60861

## doping profiles continued

- semiconductor, sputtered ions during ion implantation, SIMS system anal. 4-111244
- semiconductor doping processes, two-dimensional numerical anal., appl. to MOS processing 4-75470
- semiconductor isotype heterojunctions, C-V doping profiles anal. 4-75496
- semiconductors, carrier distribution, capacitance-voltage profiling methods, review 4-75494
- semiconductors, dopant and carrier conc. profiling, conf., London, England (May 1984) 4-73171
- semiconductors, electrochemical carrier conc. profiling, review 4-75495
- semiconductors, electrolytic Schottky-gated Hall effect profiling 4-75497
- semiconductors, impurity distribution anal. by IR spectroscopy 4-76478
- semiconductors, impurity profiling by SIMS, review 4-75500
- semiconductors, nonuniformly doped, C-V profiling theory 4-65290
- semiconductors, surface diffusion impurity profiles, consecutive diffusion 4-70184
- semiconductors, surface diffusion impurity profiles, mutual diffusion 4-70185
- $\text{Al}_{0.99}\text{Ga}_{0.01}\text{As/GaAs:Zn}$  diffused superlattice, X-ray rocking curve and backscatt. studies 4-113818
- $\text{Al}_2\text{O}_3$  synthesis by  $\text{O}_2^-$  ion implantation into Al 4-70174
- B, diffusion coefficient determ. for drive-in in oxidising atmosphere (*Hungarian*) 4-113715
- GaAs:Cr LEC wafer,  $\text{Cr}^{2+}$  distribution, EPR studies 4-98124
- GaAlAs-GaAs heterostructure, nuclear profiling of Al 4-98123
- GaAs, gas phase epitaxy, doping and impurity trapping 4-108745
- GaAs, ion implanted, transient capless annealing appl. to IC fabrication 4-103779
- GaAs, MOCVD growth, doping profiles,  $\text{H}_2\text{Se}$  memory effects 4-81152
- GaAs:Be, ion implanted, reduced damage generation 4-113474
- GaAs:Be, ion implanted, annealing behaviour, spectroscopic ellipsometry and Raman scatt. 4-113482
- GaAs:Cr, epitaxial layers, Cr doping and elec. parameters 4-76683
- GaAs:Cr, ion implanted, Cr redistrib. 4-88194
- GaAs:Cr, LEC growth, mag. field effect on impurity conc. 4-114378
- GaAs:Cr, semi-insulating, inhomogeneities, optical obs. 4-60944
- GaAs:In, isoelectric doping, X-ray and electron microprobe anal. 4-75491
- GaAs:Si, (100), vacuum annealed, free carrier reduction 4-98610
- GaAs:Si, planar channelling of Si implants 4-75483
- GaAs:V, semi-insulating, V redistribution during heat treatment 4-80070
- GaAs/Al $_x$ Ga $_{1-x}$ As quantum wells, Be doped, photoluminescence studies 4-104653
- Hg $_{1-x}$ Cd $_x$ Te, Hg diffusion profile meas. by heavy ion backscatt. 4-75730
- InP, implant depth profiles 4-65289
- InP, semi-insulating, simulation of anomalous Be diffusion 4-88193
- InP:GaSb crystals, dislocation density reduction by isoelectronic double doping 4-60940
- InP:S(Sn)(Ge), (100), vacuum annealed, free carrier reduction 4-98610
- InP:Si MISFETs, post-implantation capless annealing 4-113472
- LiNbO $_3$ :Ti(Mg), single cryst., chemical and microscopical studies 4-103777
- $\text{Na}_2\text{O-CaO}$  glass, antireflection effects induced by  $\text{Ar}^+$  implantation 4-60125
- PZT, lattice site of Zn, Sc, Fe ions, X-ray anal. 4-75488
- Si crystals, interface phase and radial distribution of impurities 4-113371
- Si, dopant distributions, direct imaging by STEM 4-113481
- Si epitaxial layers, formation of transitional conc. regions 4-76678
- Si, implant depth profiles 4-65289
- Si, polycrystalline, implantation under thermal and laser annealing, sheet resist. and doping profiles 4-75487
- Si, profiling techniques using spreading resistance 4-75498
- Si solar cell, ion implanted, laser annealed 4-72121
- Si solar cell junction profiles in ion-implanted texture-etched surfaces 4-93620
- Si, submicron epitaxial films quality, for device fabrication 4-88567
- Si:As, high dose ion implanted, As clustering, TEM and SIMS studies 4-70384
- Si:As, ion implanted regions, 2-D shape, etching and EBIC studies 4-88187
- Si:As, low energy implanted, laser-annealed, channeling and high-resolution backscatt. studies 4-75493
- Si:As, P, B, ion implanted, fast isothermal annealing and elec. props. 4-92224
- Si:As/Al interface, sintering and diffusion, As dopant effect 4-80427
- Si:As $^+$ (BF $_3$ ), implanted, rapid thermal annealing 4-88181
- Si:As $^+$ , shallow dopant profile production by low-angle ion implantation 4-108396
- Si:B, (100), shallow junction implants through surface oxide, theoretical and expt. study 4-113476
- Si:B, deep implanted layers, for IC appl. 4-75482
- Si:B, ion implanted, flash-lamp annealing study 4-108395
- Si:B, retardation of B diffusion 4-88346
- Si:B,C,O, impurity profiling and analysis by recoil atoms in heavy ion beams 4-108406
- Si:B ingots, effective segregation coeff. of B, elec. studies 4-88192
- Si:Ge(Sb)(W), electron beam doping, SIMS and RBS studies (*Japanese*) 4-108401
- Si:H,B, amorphous, solar cells, deposition from Si $_2$ H $_6$  and B doping profiles 4-81540
- a-Si:H,F films, F incorporation during glow discharge deposition 4-114426
- Si:Mg, implanted, doping behaviour, elec. props. 4-75485
- Si:P, ion implanted, diffusion during rapid thermal annealing 4-113713
- Si:P(B), substrate orientation depend. of enhanced epitaxial regrowth 4-108737
- Si:Sb, electrolytic Sb diffusion in MOS structures 4-80299
- Si:Sb, ion implanted, dopant site location and profiles, channelling studies 4-108393
- a-Si-based alloy p-i-n solar cells, performance enhancement rel. to B profiling 4-77087
- Si-SiO $_2$  interface, B drive diffusion in oxidizing ambients, segregation coeff. determ. 4-75690
- Si-SiO $_2$ :P interface, Auger study of P pile-up 4-103780
- SIB, implanted, impurity depth profiles,  $\alpha$ -particle spectra, Monte Carlo calc 4-80081
- SiC p-n junctions, Franz-Keldysh effect on photosensitivity 4-104302
- a-Si $_3$ N $_4$ :H layers, prep. by glow discharge decomp. of N $_2$ /SiH $_4$  mixtures, optical and photoelectronic props., effects of doping 4-114001

## doping profiles continued

- Si $_3$ N $_4$  films, amorphous, hydrogenated and deuterated, prepared from plasma-enhanced CVD, IR absorpt. spectra 4-81021
- SiO $_2$ :B, implanted, impurity depth profiles,  $\alpha$ -particle spectra 4-80081
- TiB $_2$ , implanted with 1 MeV Ni $^{2+}$  ions, microstruct. and surface mech. props. 4-70232
- TiO $_2$ :Cr $^{3+}$  dopant incorporation rel. to calcination temp., EPR obs. 4-104486
- ZnS:Mn electroluminesc. thin layers, doping and cryst. struct. 4-75810

## Doppler broadening see Doppler effect

## Doppler effect

- see also atomic spectra; red shift; spectral line breadth
- acoustic Doppler current profiling systems, sea-truth expts. 4-110166
- acoustic holographic imaging, Doppler effect influence (*Chinese*) 4-83779
- atom driven by standing-wave laser field, reson. fluoresc. 4-102633
- atomic collisions, line broadening, final state distrib. 4-102768
- atoms, forces in standing-wave laser field calcs. 4-96497
- bacteriology, use of a laser Doppler electrophoresis method 4-115288
- blood flow, max. vels., noninvasive CW Doppler haemodynamic data, intracardiac jets 4-85467
- blood flow meas., ultrasonic Doppler effect appl. 4-105265
- blood flow measurement using multichannel pulsed Doppler US, repeatability 4-72319
- blood velocity measurement in normal and porcine bioprosthetic mitral valves 4-100192
- cathode glow, sputtered atom light emission, interferometry 4-87981
- coherent Doppler tomography expts. simulation using computer-generated holograms 4-105773
- combustion studying using optical techniques (*Italian*) 4-66591
- coronary grafts, blood flow visualisation by US method 4-100264
- differential laser Doppler anemometer with semiconductor laser (*Russian*) 4-69476
- echocardiography, CW and pulsed Doppler, utilising a stand-alone system 4-85466
- endoscopic Doppler probe for intestinal vascular studies 4-93832
- ethylene, neutron inelastic scatt. 4-70314
- Fabry-Perot velocimetry techniques, Doppler shift rel. to surface normal direction 4-101904
- fast ion beam velocity meas., Doppler-shift technique 4-86988
- FFT signal processing IC, use for Doppler blood flow studies 4-93826
- fibre optic Doppler velocimeter, mixed-fibre interferometric sensor with microretroreflectors 4-91618
- fibre optic laser Doppler anemometry device for gas/liquid flow and solid surface velocity meas. 4-108152
- fibre optic laser Doppler velocimeter using external-cavity semiconductor laser 4-97096
- flexible discs, rotating, characterization using a laser Doppler vibrometer 4-108054
- flow meas. and processing, signal-to-noise ratio enhancement 4-100286
- foetal blood flow meas. by Doppler US, methodology and basic problems 4-89662
- foeto-placental circulation, assessment with CW Doppler 4-89663
- intensity-fluctuation spectroscopy of optical fields with non-Gaussian statistics 4-95530
- intruder detection using pulsed-Doppler ultrasonic motion detector for limited area surveillance in an unconfined region 4-64817
- Klein-Gordon radio, Doppler effect, bound on photon mass 4-95748
- laser diagnostics, techniques and apps. 4-65039
- laser Doppler anemometry, burst mode, flow related data processing (*German*) 4-103375
- laser Doppler anemometry, Mie scattering functions for milk fat globules 4-79682
- laser Doppler anemometry, signal processing requirements (*German*) 4-78294
- laser Doppler anemometry signal processing, using processor operated correlator 4-78299
- laser Doppler microscopy obs. of cytoplasmic motions in growing pollen tube tips 4-89535
- laser Doppler tissue flowmeters, signal processor 4-85484
- laser Doppler velocity meter signal processing using automatically controlled filter (*Russian*) 4-106277
- laser Doppler vibration amplitude meas. with optical fibre probe (*Japanese*) 4-112781
- laser theory and Doppler effects 4-91432
- laser velocimeter, multicomponent, for vel. meas. of gas and liq. currents in strong elec. fields (*Russian*) 4-69837
- laser velocimetry, (book contrib.) 4-79687
- laser-Doppler blood flow monitor, diode laser source and detection in probe 4-115154
- light clocks, relativistic Doppler effect, possible result of prior acceleration 4-106185
- medical US, Doppler techniques and their diagnostic appl., conf., London, England (June 1983) 4-67849
- metal plate, electromag. generation of sound in perpendicular mag. field 4-80632
- metals, defects, positron annihilation studies, book contrib. 4-85034
- Mitsubishi fiber-optic laser Doppler velocimeter 4-106279
- Mossbauer spectra, Doppler velocities anal. 4-88747
- nonpremixed turbulent flame, vel. and scalars, laser Doppler velocimetry and Raman scatt. 4-75101
- ocean, current meter, bottom mounted Doppler acoustic equipment 4-115620
- ocean current profiling with 115 kHz shipboard Doppler acoustic back-scatter system 4-110314
- oceanography, pulsed-Doppler current profiling systems, spatial properties 4-105771
- particle transverse vel. meas. using laser Doppler-anemometers 4-97724
- phenyl ether, angular correl. and Doppler broadening, positronium bubble state, temp. depend. 4-76551
- plasma, Doppler-broadened spectral lines for temperature determination 4-60726
- plasma impurities meas. in neutral beam by laser-induced fluoresc. 4-91985
- positron annihilation, Doppler-broadening data, stabilisation 4-88899
- pulse Doppler flow imaging using a SAW CZT processor 4-97728
- pulsed Doppler US, freq.-dependent attenuation effects 4-115149
- relativistic Doppler effect of subluminal and superluminal sources in 8-D 4-90371
- special relativity 4-63455

**Doppler effect** continued

- sporadic-E layers, vertical and horiz. struct. using HF Doppler technique 4-100867
- three-dimensional current and scattering strength distribution mapping system 4-105774
- transcutaneous monitoring, computerised, incorporating laser Doppler velocimetry 4-81797
- transverse Doppler acoustic current profiler design and operation 4-115626
- US blood flow meas., freq. estimator for sampled Doppler signals 4-62538
- US Doppler velocity meter for quantitative flow meas. and turbulence anal. 4-85464
- US inspection, Doppler shift of echo signal freq. 4-71847
- velocimeter, backscatter-modulated Doppler, S/N ratio 4-91850
- velocimeters, coded, signal-to-clutter ratio limitation, cardiology appls. 4-100285
- <sup>9</sup>Be<sup>+</sup> ions laser cooled, appl. in freq. standard 4-68204
- Ca target, ground and excited state sputtering obs. using laser-fluoresc. 4-93169
- Cr target, ground and excited state sputtering obs. using laser-fluoresc. 4-93169
- Cs, fluorescence spectrum, inter-Doppler resonances 4-107306
- Fe, sputtered atom vel. and electronic state distrib. by laser-induced fluorescence spectroscopy 4-93168
- Fe sputtered neutrals, ionisation length near wall in ISX-B using laser-induced fluoresc. 4-91971
- H plasma, ion temp., spectral line broadening (*Chinese*) 4-87840
- HCF, A<sup>1</sup>A<sup>0</sup> state, mag. props., Zeeman splittings, laser induced fluoresc. 4-69129
- <sup>199</sup>Hg trapped ion freq. standards, exptl. and theoretical results 4-68203
- La, depend. of <sup>140</sup>Ce recoil motion on phonon spectrum, nucl. reson. fluorescence study 4-98216
- LaF<sub>3</sub>, depend. of <sup>140</sup>Ce recoil motion on phonon spectrum, nucl. reson. fluorescence study 4-98216
- Mo, alpha-irrad., defect annealing, positron annihilation, Doppler broadening 4-70227
- NH<sub>3</sub>, electron impact dissoc., H\* energy distrib., Balmer emission 4-69226
- Na collision induced coherence, high resol. four-wave light mixing 4-102767
- Na, virtually excited state, inelastic collisions 4-74316
- OH, fragment from HONO photodissociation, Doppler and polarisation laser spectra 4-77017
- SH<sup>+</sup>, hyperfine struct., laser predissociation spectrum 4-107416
- <sup>29</sup>SiH<sub>4</sub>, silane, mol. transitions, stimulated Raman scatt. studies (*French*) 4-59785
- Tl, coinduced press. broadening and shift of 535 nm line 4-78801

**Doppler shift** see Doppler effect**dopplers**

- metal, compensated, plate, bound EM and sonic waves. (*Russian*) 4-98951

**dosimeters** see dosimeters**dosimetry**

- see also dosimetry; thermoluminescent dosimeters
- ascorbic acid, aq. solns., chemical dosimetry appls. by UV spectrophotometry 4-74118
- beta spectrometer-dosimeter, description 4-59442
- combination track etch neutron dosimeter/spectrometer, spectra evaluation improvement 4-96372
- conference on solid state nuclear track detectors, Acapulco, Mexico (Sept. 1983) 4-95027
- CR-39, electrochemically etched, manufacturing parameter effects on neutron dosimetry 4-96364
- CR-39 as a gamma ray dosimeter, bulk etch rates 4-102475
- CR-39 damage track detectors for personnel neutron dosimetry, etching processes 4-96377
- CR-39 detector, proton track characts., implications for neutron dosimeter 4-96371
- CR-39 fast neutron flat dose-equivalent-response dosimeter, expt. approach 4-96375
- CR-39 fast neutron flat dose-equivalent-response dosimeter, math. model 4-96376
- CR-39 foils, improved production parameters and dosimetry appl. 4-102482
- CR-39 neutron spectrometer, sensitivity 1 mrem at 100 keV-20 MeV, personal dosimetry appl. 4-96378
- CR-39 recoil track etch detectors as supplement of universal albedo neutron dosimeter 4-96374
- dose equivalent determination for 4 to 10 MeV photons 4-62589
- dose-equivalent meters based on microdosimetric principles, development 4-89766
- fibre optic solid state dosimeters 4-78738
- fission and (n,α) track detectors, neutron dosimeter calibration using phantom 4-96369
- Fuji Electric's pocket dosimeter with alarm REM MASTER-S 4-111971
- gamma-ray dosimeter calibration in equivalent dose units 4-62599
- high dose MOS dosimeter for space use, design criteria 4-63026
- Indian glass dosimeter for thermal neutron fluence meas. 4-59451
- ion exchange resins, high-dose radiation dosimeter appls. 4-74119
- ionisation chamber, collection efficiency in a pulsed and mag. swept electron beam 4-109938
- LR115 coloured cellulose nitrate detectors, etching parameter optimisation for processing 4-96332
- LR(115) track detector with (n,α) converters, neutron sensitivity meas. 4-96404
- LR-115 as hadron detector, 2 years practical experience at CERN 4-96373
- Makrofol-E recoil track etch detectors as supplement of universal albedo neutron dosimeter 4-96374
- neutron dosimeter, electret ionisation chamber, sensitivity 4-91118
- neutron monitor, performance 4-59439
- perfluoromethylcyclohexane, chemical dosimeter, magaGray range 4-102403
- polycarbonate neutron personnel dosimeters, track electrochem. etching, etchant optimisation 4-102472
- portable microdosimetric radiation. protection monitor, development 4-59449
- radiochromic dye film, appl. as radiation dose meter 4-74120
- solid-state, ionising energy storage, rel. to trapping levels 4-68838
- dosimeters continued
- SSNTD, CR-39, CN-85, CA 80-15, LR 115 and Melinex O, high energy charged particle response 4-102484
- SSNTD, use of different Mexican commercial polymers, etching, dosimeters 4-102476
- terephthalate dosimeter for X, γ and β-radiation 4-74117
- UV film badge dosimeter, diazochrome KBL film, sensitivity and processing 4-89763
- water calorimeter used for clinical beam dose meas., steady-state drift conditions 4-85520
- n-γ dose rate, NDK 601 instrument dosimetric characts. 4-59454
- FeSO<sub>4</sub>·7H<sub>2</sub>O dosimeter, ε(Fe<sup>3+</sup>) determ. (*Chinese*) 4-68833
- dosimetry
- see also dosimeters; radiation detection and measurement; radiation monitoring
- A150 plastic proportional counters, performance of A150 plastic-equivalent gases, neutron dosimetry appl. 4-109937
- airborne radionuclides, recovery and storage, dose commitments versus costs 4-106808
- ALARA application to normal radioactive emissions from nuclear facilities 4-96222
- alpha-emitting radionuclides, bone incorporating, dose calcs. 4-89750
- Argentine nuclear programme radwaste management, radiological impact (*Spanish*) 4-86921
- atmospheric radionuclide releases, CRRIS computerised system 4-64242
- atomic bomb survivor data anal., effects of random dose meas. errors 4-93888
- backscatter factors for X-rays generated at voltages between 10 and 100 kV 4-72429
- bibliography: radionuclide diagnosis, radiation therapy, dosimetry and radiation protection (*Russian*) 4-86141
- bibliography: radionuclide diagnosis, radiation therapy and dosimetry (*Russian*) 4-86140
- bladder dose during direct radionuclide cystography 4-105342
- bleomycin, <sup>57</sup>Co and <sup>55</sup>Co, absorbed doses 4-72425
- bone doses from α-emitting bone surface seeking radionuclides, calc. for radiological protection purposes 4-77395
- brachytherapy, remote after loading technique, safety aspects and dosimetry 4-72405
- brain tumours, B neutron capture therapy, filtered beam 4-85515
- building materials, radiation from, methods of evaluation 4-93869
- calorimeter dose determ. by direct voltage meas. on a Wheatstone-type bridge circuit 4-100325
- Canadian radiation protection conf., Banff, Alberta, Canada (May, 1984) 4-86115
- cardiac catheterisation laboratory, radioprotection using TLD system 4-100327
- cervical carcinoma, meas. of dose distrib. around Fletcher-Suit-Delcos colposts 4-85521
- charge storage effect on dose in insulating phantoms irradiated with electrons 4-115226
- conference, nuclear science and power systems, San Francisco, CA, USA (Oct. 1983) 4-58550
- conference, radiation protection in medicine, Jodhpur, Rajasthan, India (Feb. 1984) 4-73156
- conference on nuclear track registration, Richland, WA, USA (Jul. 1982) 4-67851
- contact radiation therapy, distrib. of doses near radiation sources (*Russian*) 4-115219
- cosmic ray exposure in space, doses and LET distrib. rel. to shielding 4-77393
- cosmic rays, indoor exposure rate, NaI:Tl scintillation counter, building material perturbation 4-109936
- CT, image quality and dose, evaluation of 4 scanners 4-85507
- CT dosimetry system using ionisation chambers 4-89764
- CT examinations, energy imparted rel. to radiation risk 4-115225
- cylindrical tissues, γ-ray absorpt. with off-axis linear source 4-62592
- de minimis concept appl. in risk management 4-107161
- de minimis dose limits acceptance, implications on nuclear radiation practice 4-107162
- de minimis level criteria for radiation protection and risk assessment 4-107160
- dental inspection priority program for radiation exposure 4-100330
- diagnostic radiology, dose, Monte Carlo simulation studies 4-109939
- diethylenetriaminopentaacetic acid, <sup>99m</sup>Tc labelled, radiation absorbed dose 4-72426
- digital radiographic data acquisition for radiation therapy treatment planning 4-89704
- digital radiography, optimal dose utilisation with variable X-ray intensity 4-89702
- dose buildup factors of collimated gamma radiation behind steel and aluminum plates 4-107154
- dose calibrator assays discrepancies for various forms of therapeutic <sup>131</sup>I 4-89760
- dose component separation in mixed field using spherical proportional counters 4-109944
- dose equivalent determination for 4 to 10 MeV photons 4-62589
- dose reduction in diagnostic radiology 4-109948
- effective dose equivalent, evaluation using Ci.Mc 4-89768
- effective-dose dosimeter based on thermoluminescent aluminophosphate glasses 4-107267
- electron beam radiotherapy, intercomparison of absorbed dose by Fricke dosimetry 4-85523
- electron beam therapy, dose enhancement in bone 4-81788
- electron contamination due to Lucite in a 45-MV photon beam 4-109919
- electron dosimetry associated with the beam scanning technique in linacs, approach to overcome inconveniences 4-100323
- electron dosimetry with thermally stimulated exoelectron emission 4-115224
- electron irradiated plastic phantoms, dose errors due to charge storage 4-67120
- electron therapy, central axis per cent depth dose for 4-29 MeV electrons, beam angulation effect 4-115223
- electron therapy, dosimetric effects on field shaping and shield positioning 4-72434
- electrons, central axis depth-dose 4-67124
- electrons, low energy, elastically scatt. from water vapour, angular distrib. 4-64608
- EM dosimetry and energy deposition, RF and microwave exposure (*Japanese*) 4-62524

## dosimetry continued

- EM field dosimetry in biomedical investigs. 4-115227  
 endometrial cancer, combined, radiation therapy using Agat-B unit, dose distrib. (*Russian*) 4-93862  
 energy-absorption coefficients for  $\gamma$ -rays in compounds or mixtures 4-100324  
 exposure rate and distrib. in rooms, determ. 4-93871  
 exposures from radiotherapy procedures 4-109953  
 external dose equivalent from radioactive finite clouds 4-89775  
 external radiation exposure from aquatic pathways, simple models for prediction 4-105338  
 fast neutron beam propag. in water phantom using SSNTDs 4-96380  
 fast neutron dosimetry using solid state track detectors (*Czech*) 4-59453  
 film badge accuracy determ. 4-62591  
 fluoroscopy, finger doses in special procedures 4-89751  
 fusion material irradiation facilities, neutron dosimetry and radiation damage calc. developments 4-107043  
 gamma background, natural, in Poland, exposure of urban populations 4-100320  
 gamma beam therapy, shield block use for field form. (*Russian*) 4-72352  
 gamma radiation, levels in dwellings in the Republic of Ireland 4-93880  
 gamma ray exposure in wooden houses, indoor rel. to outdoor 4-93874  
 gamma-ray dose equivalent rate estimates due to natural radioactivity sources in Saudi Arabia 4-72433  
 gastro-intestinal tract, radiation exposure to patients during radiological exam. 4-62585  
 general cavity theory, Burlin-Horowitz modification 4-67125  
 general cavity theory, modified Burlin-Horowitz, refinements in appl. to  $^{60}\text{Co}$  thermolum. dosimetry 4-67127  
 global environmental transport model review for  $^3\text{H}$ ,  $^{14}\text{C}$ ,  $^{85}\text{Kr}$  and  $^{129}\text{I}$  4-83253  
 Gundremmingen BWR power-station, shut-down, decommissioning and scrap decontamination 4-86980  
 gynaecological intracavitary therapy, current practice for low, medium and high dose rate dosimetry 4-72435  
 hand radiation dose monitoring at a nuclear power plant 4-89753  
 high energy electron beams, radiobiological and microdosimetric characs., radiotherapy appls. 4-72417  
 Hiroshima and Nagasaki bombings survivors, dosimetric studies, book 4-110813  
 hyperthermia, regional, mag. induction heating, beagle dog model, thermal dosimetry anal. 4-93697  
 ICRU sphere, dose equivalent quantities 4-67128  
 ICRU sphere, dose equivalent quantities 4-67129  
 ICRU sphere, mean values of dose equivalent for limiting effective dose equivalent 4-100321  
 indoor dose in Milan 4-93878  
 indoor environments, radiation aspects, related radioecological problems, Netherlands situation 4-93884  
 indoor exposure in a region of central Italy 4-93875  
 indoor exposure rates to gamma and cosmic rays, Ge spectrometer and ionisation chamber obs. 4-93893  
 indoor exposure to natural radiation, conf., Anacapri, Italy (Oct. 1983) 4-90285  
 indoor gamma exposure measurements in Italy 4-93881  
 indoors radiation surveys in the UK, rel. to  $^{222}\text{Rn}$  decay prods. and terrestrial  $\gamma$ -rays 4-93883  
 inhomogeneous media, scatt. of collimated  $\gamma$  radiation 4-99708  
 internal dosimetry of tritiated hydrogen gas 4-89769  
 internal exposure of patients and staff in diagnostic nuclear medicine procedures 4-81786  
 intracavitary  $\gamma$ -therapy, methods of dose distrib. form. (*Russian*) 4-89749  
 intracranial abscesses, management by CT, radiation dose considerations 4-62586  
 ionising radiation appls., conf., Riyadh, Saudi Arabia (March 1982) 4-67859  
 kerma factors calc.,  $^{12}\text{C}$ , neutron scatt. cross-sections 4-89761  
 laryngeal tumours, gamma ray treatment, phantom dosimetry obs. 4-72407  
 LD<sub>50</sub> for uniform low LET irradiation of man 4-72420  
 leakage and scattered dose equivalent during 25-MV radiation treatments 4-89756  
 linear accelerator therapy system, microwave interference effects 4-89737  
 low level exposure to radioactive pollutants, health risk assessment 4-109965  
 low level radiation, atmospheric ions and probable indirect biological effect 4-72315  
 low level radwaste sea disposal, NEA research and environmental surveillance programme 4-83210  
 LR-115 SSNTD with (n, $\alpha$ ) converter as passive environmental neutron spectrometer 4-96322  
 lung cancer induction by Rn daughters inhalation, dose required 4-93809  
 lung dose, improved calc. using tissue-max. ratios in Batho correction 4-85519  
 lymphocytes, human, chromosome aberrations induction by  $^{60}\text{Co}$   $\gamma$ -rays, dose response relationship 4-89656  
 mammalian cell culture, dose-rate effect between 1 and 10 Gy/min 4-109881  
 mammalian cells, dose-response curve shape rel. to Elkind repair saturation 4-100260  
 mammographic examination, effects of kVp variation and X-ray tube filtration 4-89696  
 mammographic quality assurance in a National Breast Screening Study in Canada 4-89694  
 mammographic screening, low dose, benefit/risk ratios 4-89693  
 mean inactivation dose, rel. to human cell survival curves intercomparison 4-105294  
 medical accelerator neutron survey, remmeter sensitivity to leakage X-rays 4-62568  
 microdistribution of  $\alpha$ -active nuclides in the human lung by autoradiography 4-105349  
 microdosimetric distributions for nm-size targets in water 4-67130  
 microdosimetry of 10-15 MeV bremsstrahlung X-rays 4-85518  
 monoenergetic neutrons, Q-factors for interactions in tissue 4-105343  
 natural indoor gamma background in an urban environment of Southern Poland 4-93873  
 natural irradiation in dwelling places in France:  $\gamma$ -rays, Rn and Rn daughters obs. 4-93882  
 natural radiation in Belgian houses 4-93876  
 neutron contamination detect. from high energy medical accelerators using electrochem. etching 4-72431

## dosimetry continued

- neutron kerma values above 15 MeV, calc. with nuclear model for light nuclei 4-67126  
 NMR proton imaging, background and developments 4-115169  
 non-ionising radiation dosimetry, lasers, UV, radiowaves, microwaves, ultrasound 4-105345  
 nuclear facility design, impact of potential for criticality, safety, doses 4-106923  
 nuclear medical procedures, dose and risk to patients in the GDR 4-89752  
 nuclear medicine, exposure sources 4-100332  
 Nuclear Medicine Department, radiation safety program 4-115234  
 nuclear power industry radionuclide emissions, environmental aspects 4-83252  
 nuclear reactor dosimetry, gas prod. and activation cross-section data 4-73958  
 nuclear waste disposal in hard crystalline bedrock, radiological impact 4-106830  
 Obrigheim nuclear power station, steam generator replacement, personnel exposure 4-86960  
 off-axis planes, dose calc. using off-axis ratios 4-67121  
 off-site dose rates estimation using BWR containment high range monitor after accident 4-106890  
 Ontario Hydro's survey meters and dosimetry/dose control devices, response characteristics 4-86977  
 optimisation for radiodiagnostic and radiotherapeutic rooms, doses (*Czech*) 4-59452  
 oral agents used in upper gastrointestinal disease, radiation dose estimates 4-72423  
 organ doses rel. to X-ray exam. schedule (*Russian*) 4-89688  
 organ transformation calc. after radioactive aerosol inhalation 4-62593  
 paediatric radiography, relative dose efficiencies of antiscatter grids and air gaps 4-109941  
 paediatric radiopharmaceutical dose calc. and display 4-89765  
 passive track detectors for Rn dosimetry, plate-out effects 4-96402  
 peripheral blood mononuclear cell prematurely condensed chromosomes, use for biological dosimetry 4-105344  
 personnel portal monitoring, proposed standard for Ontario Hydro's power stations 4-89770  
 phantom geometry, effect on conversion factor from exposure to absorbed dose 4-105341  
 phantom irradiations, neutron kerma and spectra meas. (*Hungarian*) 4-86976  
 photon and electron dosimetry at Physikalisches Technische Bundesanstalt 4-96295  
 photon dose distrib. in an inhomogeneous medium, shortening of calc. time 4-109943  
 photon dosimetry in radioprotection and radiotherapy, accuracy requirements 4-72436  
 Point Lepreau generating station Dose Records System 4-89781  
 polystyrene radiotherapy phantom, thermal characs. 4-67122  
 population exposure due to natural radiation in an urban district of West Germany 4-93877  
 population exposure to Pacific nuclear tests fallout, on Rongelap and Utrik, environmental and personnel monitoring 4-62611  
 portable RF data terminal operators exposure eval. methods and instrumentation 4-109949  
 public radiation exposure impact of TRU nuclides from Sellafield liquid wastes 4-83211  
 PVDF polymer hydrophones in biomedical ultrasonics 4-100283  
 PWR, heavy load drop consequences, critical and radiological anal., safety 4-106915  
 RAD-80 automatic digital dose metering system for use at Gundremmingen nuclear power plant (*German*) 4-68830  
 radiation exposure and radioactive emissions from United States DoE operations 4-83202  
 radiation exposures, Sieverts and safety 4-115228  
 radiation medical exposure and occupational exposure in AEE of Egypt, intercomparison 4-77401  
 radiation therapy, user requirements on CT based computed dose planning systems 4-81760  
 radio oncology irradiation parameters, monitoring and documenting using Dynabaver systems 4-115142  
 radioactive emissions and radiation exposures from nuclear power prod., collective dose 4-83250  
 radioactive emissions from nuclear plants, permitted levels, ICRP-26 effects 4-91120  
 radioactive waste disposal, long-term radiation protection objectives 4-106815  
 radioactive waste management, radiation protection optimisation 4-106817  
 radioactive wastes from nuclear reprocessing plants, management in UK 4-106797  
 radiobiology research projects, AFRR1 annual report (1982) 4-73172  
 radioecological calcs., reliability, parameter variability 4-115233  
 radiographic feature enhancement, information content and dose reduction 4-81782  
 radiography, digital mammographic imaging 4-89714  
 radioisotope atmospheric transport from notional nuclear plants, European doses, MESOS code 4-77612  
 radionuclide kinetics in MIRD dose calculations 4-72427  
 radionuclide releases, environmental impact, release limits, assessment principles 4-83201  
 radionuclide transport, human exposure, health risk calc. 4-109952  
 radionuclides in dust cloud from Mount St. Helens eruptions, doses to individuals 4-105697  
 radiotherapy, buildup region outside primary beam, dose obs. 4-85522  
 radiotherapy, dosimetric apparatus, energy dependence for long-wave X-rays (*Russian*) 4-115220  
 radiotherapy, electron beam isodose distribns., analytic calc. 4-85517  
 radiotherapy, fractionated, total doses, implications of new radiobiological data, review 4-115222  
 radiotherapy, integral dose and evaluation of irradiation tissue vol. (*Russian*) 4-115218  
 radiotherapy, low energy electron beams, depth doses improvement 4-89759  
 radiotherapy linear accelerator, 20 MeV, modified neutron shield, neutron leakage meas. 4-62569  
 radiotherapy personnel, ALARA- and personnel dosimetry 4-109947  
 radiotherapy planning using computers 4-62565

**dosimetry continued**

- radiotherapy treatment rooms, leakage through shielding window gaps 4-89772
- radiotherapy wedge for 4 and 6 MV X-rays, dosimetry characts. 4-67119
- reference phantoms for in-vivo monitoring calibrations 4-89782
- roentgenotherapy, close-focus, with moving sources, skin tumour irradi. (Russian) 4-72353
- rotational photon fields with gravity-oriented eye blocks, dose distrib. and tissue-air ratios 4-81787
- rotational total skin electron irradi., surface dose calc. 4-109942
- salt dome radwaste repository, radiation exposure due to radioactive releases 4-83205
- shielding device for radiation reduction to the hands 4-109957
- shielding geometry, dose factors of  $\gamma$ -ray build up 4-102406
- short wave diathermy equipment, stray mag. fields and power outputs using tissue equivalent phantoms 4-89755
- skin dose assessment, TLD response to beta radiation 4-89762
- skin dose from diagnostic X-ray procedures, calc. 4-109932
- skin dosimetry research with TLD chips 4-72437
- small intestine, mouse, response to X-ray and neutron irradi. doses 4-100236
- solid state nuclear track detector use in radiation dosimetry, medicine and biology 4-72430
- spaceflights, dosimetric, radiation meas., absorbed dose, dose rates 4-68834
- spent fuel shipping casks, shielding characts., CRIEPI cask appl. 4-96294
- standard mortality ratios for CRNL long-term employees in relation to lifetime occupational dose 4-89780
- steel pipe barrier, radiographic inspection, dose build up factors of isotropic point source 4-99707
- stopping power for protons and alpha particles rel. to dosimetry of fast neutrons and actinides 4-68840
- stratified shields, transmitted and interface dose buildup factors 4-68831
- styrylcyanine dye solns., radiation dosimetry appls. 4-68836
- TEM cell for radiofrequency radiation dosimetry studies, resonance suppression and bandwidth modification 4-77392
- TEM cells bandwidth limitations due to resonances 4-72300
- therapeutic  $\gamma$ -ray units, radiation field sizes determ. (Russian) 4-93848
- THERAPLAN-L radiation therapy treatment planning system 4-115174
- tissue-equivalence of various materials for negative pions 4-67123
- TLD, fast neutron sensitivities (Hungarian) 4-83249
- TLD, uncommon materials, review 4-109933
- Tokyo University cyclotron, neutron skyshine spectra and dose distrib. 4-96293
- track calculations, radiobiology appl., microdosimetric quantities calcs. 4-67032
- UV film badge dosimeter, diazochrome KBL film, sensitivity and processing 4-89763
- UV radiation online monitoring system for photosensitivity test dose control 4-67131
- vehicular technology conf. Pittsburgh, PA, USA (May 1984) 4-106118
- walls of buildings, math. models of emitted  $\gamma$ -rays, congruence of meas. 4-93868
- walls of room, radioactivity inhomogeneities rel. to external  $\gamma$ -doses 4-93870
- workers in medical institutions, radiation dose profiles 4-109946
- Wurgassen BWR power station, steam and feedwater pipelines replacement 4-86955
- X-ray installations, breast exposure rates, image quality survey 4-100329
- X-ray installations in Bangladesh, radiation exposure level assessment for protection 4-77400
- X-ray penumbra, high-energy, associated phys. parameters anal. 4-109940
- xeromammography, absorbed dose and image quality 4-89695
- $n$ - $\gamma$  dose rate, NDK 601 instrument dosimetric characts. 4-59454
- <sup>241</sup>Am in the beagle skeleton: microdistrib. and local dosimetry 4-77394
- <sup>241</sup>Am, microdistrib. and localised dosimetry in bones of beagle dogs 4-115242
- <sup>77</sup>Br-p-bromospiperone 4-100319
- <sup>60</sup>Co  $\gamma$ -rays, fatal accidental exposure, dose estimation from watch jewels thermolum. 4-89754
- <sup>60</sup>Co, tissue accumulation and loss in mallard ducks 4-62598
- <sup>137</sup>Cs, determ. of conc. in urine samples 4-96290
- <sup>137</sup>Cs, tissue accumulation and loss in mallard ducks 4-62598
- FeSO<sub>4</sub> G-values for photons and electrons, ionisation dosimetry 4-89773
- <sup>125</sup>I dosimetry using LiF 4-72432
- <sup>129</sup>I, in human thyroid tissues of Utah populations, 1947-54 4-109888
- <sup>129</sup>I in waterfowl muscle, collection from radioactive leaching pond, SE Idaho 4-115231
- <sup>131</sup>I, radioiodine exposure to families of hyperthyroid therapy patients 4-109954
- <sup>192</sup>Ir wire, standard planar implants, dosimetry tables 4-85516
- <sup>192</sup>Ir wire used in interstitial radiation therapy, activity meas. intercomparison 4-81759
- LiF, phototransferred thermoluminesc. for high LET radiation dosimetry 4-105339
- MgB<sub>2</sub>O<sub>7</sub>:Dy, some advantages and disadvantages for practical dosimetry 4-105340
- <sup>20</sup>Ne ion beam, depth dose relations in water 4-109935
- O<sub>2</sub>, for calibration of power deposition in nuclear pumped lasers 4-112454
- <sup>232</sup>Pb colloids, intraperitoneal administration, whole-body distrib. of radioactivity 4-72421
- Pu isotope concentration in human tissues of Northern Utah 4-109889
- PuO<sub>4</sub> particles in lungs of hamsters, rats, and dogs, microscopic dose distrib. 4-89767
- <sup>241</sup>Pu, A=239, 240, body burden in Lapps, comparison with southern Finns 4-62590
- <sup>239</sup>PuO<sub>2</sub> particle in lung,  $\alpha$ -particle microdosimetry 4-62595
- <sup>226</sup>Ra and bone seeking radionuclides, carcinogenicity, beagle studies 4-115221
- <sup>226</sup>Ra content in drinking water, Denmark 4-94173
- Rn and Tn, dosimetry and monitoring, public exposure to natural radiation, OECD/NEA programme 4-93865
- Rn, daughter activities, meas. instrumentation 4-93867
- Rn daughter collection and passive monitors calibration 4-93673
- Rn daughter dose: environmental vs. underground exposure 4-93887
- Rn daughter product, passive detection rel. to plateau 4-93863
- Rn daughters, indoor exposure, design and interpretation of large surveys 4-93879

**dosimetry continued**

- Rn daughters, indoor exposure, dosimetric approaches to risk assessment 4-93886
- Rn daughters, population exposure, annual dose assessment problems 4-93885
- Rn, environmental impact on buildings, mining dumps sources 4-93906
- Rn, indoor exposure meas. system using ionisation chamber 4-93894
- Rn, indoor exposure rel. to way of living: methodological study 4-93872
- <sup>222</sup>Rn and decay products, active and passive dosimetry, international intercomparison 4-93864
- <sup>222</sup>Rn content in drinking water, Denmark 4-94173
- Si planar diffused diodes for dosimetry of irradiation of pourable bulk materials (German) 4-68832
- <sup>90</sup>Sr, determ. of conc. in urine samples 4-96290
- T concentrations in urine and hair use for dose estimation from chronic T exposure 4-62588
- T distrib. and excretion after intratracheal installation of glass microballoon fragments in rats 4-62594
- T, internal contamination of radiological workers at two Netherlands universities, urinalysis dosimetry 4-62597
- <sup>99</sup>Tc, relative radiation and chemical hazards when used as NaTcO<sub>4</sub> 4-62533
- <sup>99m</sup>Tc flood phantom, personnel exposure during quality assurance procedures 4-72428
- <sup>99m</sup>Tc S colloid radioaerosol inhalation, dose to lung calcs. 4-72422
- Ti in-breath monitoring, multicompartment lung model anal. 4-89774
- <sup>201</sup>Tl, local absorbed dose due to low energy electrons from Auger and Coster-Kronig transitions 4-72424
- U mill tailings, long-term management and dose limitations 4-106821
- <sup>131</sup>Xe, personnel exposure in nuclear medicine laboratories, instrument evaluation 4-62596
- <sup>13</sup>Xe, released effluent, sector averaged plume, gamma dose rate from side sectors 4-115240
- double heterostructure lasers** *see semiconductor junction lasers*
- double layers (electric)** *see electrochemistry; liquid theory*
- double nuclear magnetic resonance**  
*see also INDORE*
- A, X, spin systems, density matrix description of heteronuclear decoupling 4-98980
- acetylene, adsorbed on Pt (111), struct., NMR study 4-92526
- amine-boranes, <sup>13</sup>N nuclear quadrupole double reson. and B-N bond study 4-87145
- amine-trifluoroboranes, <sup>14</sup>N nuclear quadrupole double reson. and B-N bond study 4-87145
- meso-1,1'-bi(2-methylpiperidine)s, barriers to rotation and inversion <sup>13</sup>C DNMR obs. 4-78877
- 2-butanol, spin decoupling, modified sequence 4-78880
- catechol, struct., double transition, NQR spectra 4-69109
- DOUBTFUL double quantum coherence expt., multiple selection selectivity 4-90630
- hydroquinone, struct., double transition, NQR spectra 4-69109
- J coupling in <sup>13</sup>C NMR, instrumental imperfection anal. 4-78355
- J scaling in <sup>13</sup>C NMR, multiplicity determ. 4-78354
- organic cpds., long-range couplings in heteronuclear two dimens. J spectra 4-78879
- resorcinol, struct., double transition, NQR spectra 4-69109
- spin decoupling, modified sequence 4-78880
- squaric acid, order-disorder transition, <sup>17</sup>O nucl. quadrupole double reson. obs. 4-92977
- tissue, in vivo, double reson. surface coil probe, <sup>13</sup>C NMR 4-81824
- CD<sub>2</sub> systems, coupled <sup>2</sup>D-<sup>13</sup>C DEPT spectra 4-78878
- NaCl, doped, point defect, pulsed DNMR obs. 4-71211
- double refraction** *see birefringence*
- double refraction, electric** *see electro-optical effects*
- double refraction, magnetic** *see magneto-optical effects*
- double resonance, electron nuclear** *see ENDOR*
- doublet antennas** *see dipole antennas*
- DPPH, diphenylpicrylhydrazyl** *see organic compounds*
- drag reduction**
- baseballs, aerodynamic drag crisis and its effect on flight 4-63440
- capsule transport wake and drag interaction in pipe flow 4-112882
- compliant surfaces and surface-active substances 4-91796
- flow past blunt obstacles of circular section placed on a plane boundary (Japanese) 4-112823
- spirally fluted tube flow computation 4-103413
- Toms effect research into friction loss of turbulent liquids flow (Rumanian) 4-69740
- turbulent boundary layer, frictional drag coeffs., polymer soln. addition effects 4-112835
- turbulent flows over flat plate, drag reducing compliant walls 4-79560
- two dimens. hydrofoil, press. distrib. and drag reduction in dil. polymer solns. 4-87763
- drawability** *see ductility*
- drawing (mechanical)**
- chalcogenide optical fibre, preparation 4-103046
- deep-drawing forming limits, three-dimens. ductile damage model 4-99596
- forming limit diagrams, comparison between expt. and theoretical 4-93348
- metal matrix composites, fabrication, book contrib. 4-66276
- metals, plastic strain ratio relation with limiting draw ratio 4-104808
- metals, sheet, deep drawing, influence of temp. 4-66399
- metals and alloys, plastic deformation, mech. props. and struct. (Russian) 4-109468
- monomode fibres, fabrication conditions, performance sensitivity 4-107834
- multi-glass rod optical fibre splicers and connectors, fabrication (Japanese) 4-79303
- optical fibre, high-speed drawing and coating techniques 4-103042
- optical fibres, tensile strength anal. 4-74736
- PET film, amorphous, extrusion drawn, irreversible spontaneous elongation 4-109440
- PET films, drawn, molecular orientation, polarized IR spectra and birefringence obs. 4-84215
- PET films, extrusion drawn amorphous and semi-crystalline, linear thermal expansion analysis 4-109439
- plastic optical fibres, preparation 4-103047
- PMMA, stress relaxation under uniaxial tension 4-114599

**drawing (mechanical)** continued  
 poly(ethylene terephthalate), viscoelastic props. on homogeneous and plastic deformations 4-114593  
 poly p-phenylene terephthalamide films, extruded and drawn, tensile strength, void struct. rel. to heat treatment 4-81257  
 poly p-xylylene, high temp. phase transform. and struct., EM obs. 4-66330  
 polycarbonate blends with ABS and SAN, tensile and impact tests, energy absorpt. 4-66389  
 polyethylene, linear oriented, stiffness, relax., US meas. 4-81232  
 polyethylene copolymers; tensile drawing behaviour rel. to branch conc. 4-61980  
 polyethylene resin, low density blown film grade; rheological props. 4-79535  
 polymer fibres, orientational drawing termination rel. to supermolecular struct., X-ray obs. 4-75316  
 polyoxymethylene; cryst. modulus estimation using ultradrawn tapes 4-76793  
 polypropylene, isotactic, cold drawn, annealing, superstructure, SAXS obs. 4-61955  
 polystyrene, stress relaxation under uniaxial tension 4-114599  
 PVC composites, filled, deform. thermodynamics 4-89089  
 shrinkage and molecular extension 4-75600  
 silica core optical fibres,  $\gamma$ -ray induced absorpt. band at 770 nm 4-79296  
 silica optical fibers, high-strength long-length, drawing study 4-74762  
 steel, low C, deep drawing cold-rolled sheet prod. by continuous annealing, control of steel chem. 4-114565  
 steel, low C, deep-drawing, prod. by continuous annealing 4-114566  
 thermal expansion 4-80271  
 viscoplastic materials, rate effects in steady forming processes 4-83831  
 Al sheets, square cup drawing characs. 4-61941  
 BaF<sub>2</sub>-GdF<sub>3</sub>-ZrF<sub>4</sub> optical fibre, preparation 4-103045  
 Cu, tough-pitch, drawn and extruded, stress/strain props. 4-104824  
 Nb, thin wires, heat treatment 4-66355  
 Nb-Ti, thin wires, heat treatment 4-66355  
 Nb-Ti multifilamentary supercond. composites, cold drawn, heat treatment, precip. morphology, TEM obs. 4-71657  
 PdH<sub>x</sub>, reverse mech. aftereffects during hydrogenation; synergism obs. (Russian) 4-109469  
 Pt ultrathin drawn wires, struct. and elec. props. 4-92696  
 SiO<sub>2</sub> fibres, induced absorpt. due to drawing and irradi., Raman study 4-80919  
 V-Ti, thin wires, heat treatment 4-66355

**drift chambers** see position sensitive particle detectors; proportional counters

**drives**  
 see also electric drives; propulsion  
 magnetic, for mechanical booster pump, for radioactive and other dangerous gases 4-86432  
 turbine drive sample spinner for X-ray diffraction 4-78442

**drop model (nuclear)** see nuclear liquid drop model

**droplets** see drops

**drops**  
 air-water drop flow in subsonic nozzles (French) 4-60508  
 air-water two-phase downward annular flow config. (Japanese) 4-97654  
 axisymmetric drop technique, surface and interfacial tension meas. 4-98400  
 chemically reactive, convective heat and mass transfer 4-112850  
 cloud droplet spectra, effects of turbulent mixing 4-72661  
 clouds droplet content, ground-based meas. via passive optical device 4-62978  
 coal-water mixtures on horizontal brass surface, film boiling of discrete droplets 4-64829  
 collisions between rapidly-moving droplets in gas flows 4-65022  
 compressed gases in centrifugal precipitator, droplet removal 4-60482  
 condensation on upper surface of horizontal tube, heat transfer 4-97292  
 continuum theory of the free and forced oscillations of a magnetic drop 4-108128  
 cumulus clouds, importance of cloud top lifetime in description of cloud characs. 4-100670  
 curvature parameter, theory of nucleation on charged nuclei 4-80331  
 cylindrical drop, differentially rotated at moderate Reynolds number 4-103397  
 deformation, external and internal streamlines in linear 2-D. flows 4-60438  
 direct contact condensation of vapor to falling cooled droplets 4-112697  
 dispersed liquid jet mixing with drifting gas flow 4-60475  
 drag of evaporating or condensing droplets in low Reynolds number flow 4-83933  
 droplet spreading, liquid-air interface (French) 4-75753  
 electrically charged water droplets produced by electrical dispersion 4-85734  
 electrospray, remelting, metal droplets, form. and transport 4-64832  
 equilibrium radii of small vapour bubbles and liquid droplets 4-112989  
 fluid mechanics review, book 4-90314  
 fluid particles, deformation in contact zone under linear tension 4-109690  
 fog droplets, spatial distrib. investigation by holographic method 4-62979  
 free liquids, fluid dynamical studies using acoustic levitation 4-97621  
 free vibrations of a drop in partial contact with a solid support 4-75757  
 free-falling multicomponent droplets, combustion; and microexplosion 4-103388  
 fuel, droplet, evaporation dynamics, press. effect 4-103914  
 furan, two-phase bubble, evaporation through immiscible liq., heat transfer 4-87781  
 gas-liquid media, shock wave dynamics 4-60497  
 Hele-Shaw cell, interfaces and falling drops 4-95101  
 homogeneous condensation, droplet growth study 4-60506  
 hot gas stream, spray vaporisation, laser diff. techniques 4-87776  
 hot spray, evaporation rate const. laser diff. technique meas. 4-87777  
 ideal liq., colliding drop stability 4-91828  
 kinetics of droplet growth in systems with arbitrary degeneracy 4-65380  
 laboratory clouds, control of liq. water content and drop size distrib. 4-62927  
 Laval nozzles, gas flow effect on rels. governing breakup of droplets 4-65009  
 liquid drop suspension, simplified model for soap film 4-88376  
 liquid droplets undercooling, nucleation and solidification 4-88267  
 liquid drops, Lennard-Jones pot. surface tension, mol. dynamics study 4-97987  
 liquid drops on smooth and rough circular cylinders, equilib. 4-61187

## drops continued

liquid films, asymmetrical thinning beneath liq. drop 4-79694  
 liquid free surface in cylinder, dynamic behavior, vertical vibr. effect 4-112913  
 liquid-liquid jet breakup, drops size, mass transfer and solute adsorpt. effects 4-64993  
 magnetic liquid drop, singly connected axisymmetrical forms, numerical simulation 4-108131  
 magnetic liquid drop, trapped, MHD instability in free surface, numerical simulation 4-108127  
 microemulsions, droplet sizes 4-77034  
 microscopic, spreading laws (French) 4-80328  
 microstructure of flow inside minute drops evaporating on a surface 4-60467  
 moisture transfer in heated channels conducting flows 4-97653  
 moving drop with variable surface tension, diffusion 4-80339  
 nematic/isotropic interfacial energy, determ. from Frenkel relation for droplet coalescence 4-75758  
 Newtonian fluid, bubble and drop motion towards deformable interface 4-60493  
 nocturnal stratocumulus cloud, turbulent struct. rel to droplet concs. and size distrib. 4-62914  
 nonaxisymmetric equilibrium shapes of a drop on a plane 4-70529  
 nonvolatile liquids, spreading over flat solid surface 4-108678  
 nucleation on charged nuclei in strong field 4-108595  
 organic liquid droplet, evap., low and high mass flux data, wet bulb temp. 4-80341  
 n-pentane, two-phase bubble, evaporation through immiscible liq., heat transfer 4-87781  
 phase separating systems, droplet growth processes, self-similarity and intermittency 4-83932  
 phase separation, droplet growth rates, crossover, locking-in and intermittency 4-108099  
 phase separation late stage, dynamics in two dims. 4-98254  
 polymer liq. drops, wetting laws, interpretation of foot 4-88369  
 raindrop axial and backscatter ratios, collisional probability model 4-94187  
 rotating liq. drop, Coriolis force, oscils. 4-79648  
 shear viscous bubble and drop deform. 4-91835  
 slender drops, tip streaming in nonlinear extensional flow 4-103278  
 slightly deformed axisymmetric, profiles 4-61186  
 slowly evaporating droplet near hot plate 4-97620  
 spherical drop motion in viscous liq. at small Reynolds and Hartman nos., MHD eqns. (Russian) 4-113072  
 spherical fluid-vapour interfaces, surface tension, curvature corrections 4-88372  
 spontaneous droplet nucleation in clean saturated moist air at atmospheric press. 4-80200  
 steam, Wilson line at low press. condensation onset 4-97658  
 steel, stainless powder particles, droplet processed, rapid solidification struct., STEM obs. 4-71649  
 subcooled small metallic drops, rapid solidification, internal nucleation 4-71648  
 surface tension curvature corrections 4-84489  
 suspension by soap films, general formulation 4-88375  
 transparent liquids, separation due to interface convection (German) 4-112880  
 turbulent and inertial deposition in ducts, coalescence influence 4-60507  
 two-phase droplet flow, convective and radiative heat transfer 4-75073  
 unsteady-state extraction from a falling droplet with nonlinear dependence of distribution coefficient on concentration 4-103374  
 water, droplet on heated surfaces, behaviour heat transfer characteristics 4-87711  
 water drop collisions, charge separation, contact-balloelectric mechanism 4-72676  
 water droplet, evap., low and high mass flux data, wet bulb temp. 4-80341  
 water droplet trajectory around air intake, calcs. (German) 4-113006  
 water droplets supercooling 4-97294  
 wet steam, transient thermal processes, interphase transfer influence 4-60509  
 Al-Cu, droplet solidification on chill block, predendrite form. rel. to supercooling 4-89037  
 H<sub>2</sub>SO<sub>4</sub>, vapour condensation in cooled tube, mathematical model 4-80199  
 InSb-InTe, spreading of droplets of eutectic melt 4-113752

**drying**  
 biological critical point drying technique improvement for SEM 4-93984  
 coal, drying, Stefan model comparison with two-phase model 4-103186  
 coated films, IR drying, internal heating effect 4-97293  
 fruit solar drying, optical characs. of fruit 4-93595  
 grains, pneumatic drying, const. rate, mathematical anal. 4-76965  
 grains, pneumatic drying, falling rate, mathematical anal. 4-76966  
 heat pump future development prospects 4-77135  
 nonsteady heat and mass transfer in drying by reduced pressure 4-74849  
 single moving fibre, drying kinetics in longitudinal or transverse hot air flow 4-83896  
 softwood, high temp. convective drying, transfer phenomena 4-87540  
 solar crop drying systems, field performance studies 4-77063  
 solar dryer, radiative convective type, design, construction and testing to avoid 'burn-up' 4-62390  
 solar-dehumidification drying anal. 4-87552  
 C<sub>2</sub>S, hydration products, obs. using cryo stage in SEM 4-71874

**DSC** see thermal analysis

**DTA** see thermal analysis

**dual resonance model** see duality and dual models

**duality (mathematics)**  
 IRF models, duality transformations 4-78231

**duality and dual models**  
 see also Veneziano model  
 baryon exchange processes, pole exchange, duality and broken SU(3), review 4-63987  
 baryonium physics 4-95761  
 bose string actions construction 4-59051  
 boson-fermion duality, neutrino and photon construction from new massless boson 4-95777  
 charge-monopole duality, Coulomb phase of gauge theories 4-111298  
 Coulomb interaction, string potential, static quarks on random lattice, strong coupling limit 4-111292

## duality and dual models continued

dual symmetry of chiral model and geometrical correspondence between chiral field and sine-Gordon equation (*Chinese*) 4-73663  
 extended supergravity, light-cone superfields in 10-D, type II superstrings 4-110980  
 extended supergravity in 10-D, spontaneous compactification 4-68088  
 fermionic degrees of freedom on a lattice; particles and strings for Ising model 4-58948  
 fermionic quark boundaries, surface description of QCD 4-82937  
 fragmentation functions of discrete particles on Artru-Mennessier string 4-59050  
 gauge theories, charges in spacelike cones 4-102000  
 generalised Bose string models, semiclassical approx. 4-68552  
 GUT, vector products, duality and octonionic identities in 8-D 4-82924  
 hadron energy eigenvalues and coupling strengths determ. with duality, Shifman-Vainshtein-Zakharov method 4-59059  
 hadron-hadron scattering, high energy, unitarity, U-matrix approach 4-95815  
 Harari-Freund duality, validity 4-86685  
 high energy nucleus-nucleus collisions, dual parton model, quark-gluon plasma 4-86843  
 highly excited mesons, partial decay widths, duality scheme with quark model spectrum 4-90868  
 Kac-Moody algebras and exact solvability in hadronic physics, review 4-111339  
 Liouville string field theory, scatt. amplitudes, Green's functions 4-73617  
 Liouville string field theory, triangle relation, absence of tachyons 4-68356  
 meson spectrum and automodelity in a dual approach (*Russian*) 4-82952  
 multicolour QCD in terms of random surfaces 4-63959  
 multiplicity-generating function, hadron-nucleus collisions, QCD and dual topological unitarization 4-111383  
 N=8 supergravity, supersymmetric Kaluza-Klein, coset structure and duality invariance 4-111004  
 non-Abelian gauge field, string-like config. with quarks at ends 4-82901  
 non-Abelian gauge theories, electric-magnetic duality 4-58933  
 nonlinear string eqns. in d-dimensional space-time, gauge description 4-63898  
 point charges as electric monopoles in dual Maxwell field 4-95693  
 Polyakov model for closed string 4-68551  
 preon composites and their interactions in SU(7)@SU(7) unified preon model, postons 4-78535  
 QCD, finite energy dispersion sum rules 4-95756  
 QCD, light quark masses, model independ. determ. 4-111375  
 QCD, reduction of nonabelian gauge theory through bare coupling 4-68514  
 QCD duality, moments, and Regge trajectories in nonrelativistic quantum mechanics 4-68553  
 QCD in Veneziano limit, elfin theory, string model, baryon dynamics 4-59037  
 QCD jets, matching to fragmentation models 4-102083  
 QCD lattice field theory, string tension 4-68408  
 quark-quark scatt., duality, flavour SU(3)@ colour SU(3) algebra, polarised electrod. appl. 4-73722  
 relativistic string, Backlund transformation for Liouville eqn. and gauge conditions 4-63894  
 relativistic string, inverse scatt. method 4-106525  
 relativistic string, restricted class of motions 4-63895  
 scalar and antisymmetric tensor field theories, quantum equivalence 4-68412  
 self-dual gauge field eqns. on N dimens. manifolds, book contrib. 4-58974  
 self-dual monopoles in SU(5) 4-95680  
 self-dual Yang-Mills and general relativity Einstein eqns., R gauge parametrisation 4-110948  
 'string' formation in gas of Feynman diagrams 4-68545  
 string motion, nonlinear Klein-Gordon eqns. 4-78539  
 strings, classical Liouville theory, soln. sectors and minimal energies 4-86686  
 SU(2) lattice gauge theory, strings in 3-D 4-102038  
 SU(2) lattice gauge theory in three dimens., obs. of string 4-58980  
 SU(2) string tension from large Wilson loops 4-63881  
 SU(3) gauge theory with next-to-nearest neighbour interactions on 12<sup>4</sup> lattice, Monte Carlo study 4-111288  
 SU(3) lattice gauge theory, renormalisation group improved action, string tension, Wilson loops 4-111287  
 SU(3) lattice gauge theory, string tension coeff., Monte Carlo calcs. 4-68503  
 SU(N) Eguchi-Kawai model, string tension Monte Carlo calcs. in 4-D 4-68459  
 super self-dual Yang-Mills background, left chiral zero modes 4-86524  
 superstring theories, props. of covariant formulation 4-106454  
 superstrings, covariant, light-cone anal. 4-59056  
 supersymmetric Liouville string theory, monodromy matrix, poisson brackets 4-90729  
 supersymmetric string theories, spontaneous supersymmetry breaking 4-63861  
 symmetric space chiral models, infinitely many symmetry generator series, Backlund transform. 4-95702  
 topological strings, massive black holes in galactic nuclei, unified Yang-Mills theory 4-101727  
 topologically massive gauge theories, self-duality 4-78515  
 topologically stable strings, grand unification phase transition, galaxy formation 4-95264  
 twistor theory, dual relations 4-78538  
 U(1) lattice, monopole-antimonopole potential, Monte Carlo simulation 4-111301  
 Wilson string dist. in hot gluodynamics, Monte Carlo calcs. 4-90840  
 $\alpha\alpha$  collisions, multiplicity dist. and coloured strings 4-59122  
 hh $\rightarrow$ X, exclusive multistring fragmentation model 4-73734  
 K $\bar{p}\rightarrow\pi^+$ s, string fragmentation model predictions at 110 GeV 4-59111  
 pp multiplicity distrib., high order moments in dual parton model, KNO scaling 4-73787  
 $\pi^+\pi^-\rightarrow\pi^+\pi^-$ X, inclusive cross sections in dual parton model 4-111474  
 $\pi\pi$ , Born approximation of dual model with quantized slope Regge trajectories 4-78540  
 $\pi^+\pi^-\rightarrow\pi^+\pi^-$ X, inclusive cross sections in dual parton model 4-111474  
 qq bound states, Salpeter eqn. in position space, arbitrary confining potentials 4-106474  
 $e^+e^-\rightarrow qqX$ , sum over resonances, Thomas-Fermi model, local duality 4-90899

## ductile-brittle transition

see also embrittlement  
 brittle fracture resistance, calc. using crit. brittleness 4-104936  
 brittle fracture toughness, influence of microstruct. 4-93388  
 critical brittleness temperatures determined on specimens with different stress raisers 4-104937  
 critical transition temperature, determ. using criterion of meeting plane strain conditions 4-104935  
 epoxy polymers, elastic constants under impact loading, plasticiser content effect 4-66364  
 fracture toughness,  $J_{IC}$  test procedures in transition temp. region (*Japanese*) 4-93486  
 glass fibre reinforced PET, strength, effect of temp. and strain rate 4-93375  
 polycrystals, strong and ductile, grain boundary design, overview 4-65336  
 steel, as-rolled, tensile tests in mixed fracture range (*German*) 4-66511  
 steel, austenitic stainless, creep crack growth 4-104837  
 steel, austenitic stainless, fracture modes under He ion and neutron irradi., temp. depend. 4-104853  
 steel, austenitic stainless, H induced slow crack growth rel. to  $\alpha'$  martensite form. 4-66428  
 steel, austenitic stainless, irradiation, fracture toughness, SEM obs. 4-104836  
 steel, C, yield stress rel. to C content and pearlite morphology, tensile and Charpy obs. 4-81248  
 steel, Cr-Mo, fracture toughness in transition region, interpretation of scatter and thickness effect 4-99603  
 steel, Cr-Mo-V-W, ferritic, impact props., effect of specimen size and Ni content 4-104848  
 steel, Cr-Mo-V-W, ferritic-martensitic, reduction of ductile-brittle transition temp. 4-104849  
 steel, Cr-Ni ferritic, rapidly solidified, struct. and mech. props. 4-109388  
 steel, dynamic toughness, drop weight nil ductility transition test 4-99679  
 steel, ferritic stainless, irradi. embrittlement 4-93392  
 steel, fracture toughness,  $J_{IC}$  test procedures in transition temp. region (*Japanese*) 4-93486  
 steel, low C, ductile-brittle transition temp., effect of tensile prestrain (*Japanese*) 4-114650  
 steel, low C, nitrocarburising, annealing, yield stress, brittle-ductile fracture transition 4-66384  
 steel, martensitic, low C, controlled rolled and quenched, strengthening effects 4-99393  
 steel, martensitic, press. vessel, cleavage fracture 4-71730  
 steel, martensitic stainless, HT-9, weldments, microstruct., hardness and fracture toughness, effect of preheat 4-99495  
 steel, mild, C-Mn, Charpy V transition temp. rel. to various material parameters 4-66431  
 steel, Nb, strengthening mechanisms, influence of rolling variables 4-71666  
 steel, nuclear structural, A-203D, low temp. deform., effect of microstruct. 4-66386  
 steel, powder metallurgy, prod. by dynamic hot pressing, design strength 4-89011  
 steel, rolled, impact toughness and transition temp., effect of delamination (*Korean*) 4-76848  
 Fe-Al-Si (20.5 at.%), DO<sub>3</sub>-ordered alloys, tensile behaviour 4-93337  
 (Fe<sub>2</sub>Co<sub>7</sub>)<sub>3</sub>V, tensile deformations, 20-1000°C, fracture mode and ductility rel. to order-disorder transform. 4-66427  
 Fe<sub>2</sub>Si, DO<sub>3</sub>-ordered alloys, tensile behaviour 4-93337  
 GaAs, ductile brittle transition in (001) surface layers in single crystals., effect of medium 4-70266  
 Mo, deformed, mechanical props. anisotropy under cross rolling, texture 4-66378  
 Mo, neutron irradiation embrittlement, influence of irradi. temp. and heat treatment 4-108453  
 Mo, purification by arc melting, mech. props. (*Japanese*) 4-89116  
 Mo-Se, dilute alloy, arc melted, workability and ductility 4-76808  
 Mo-Ti-Zr, TZM, neutron irradiation embrittlement, influence of irradi. temp. and heat treatment 4-108453  
 Mo-V(Zr)(Ti)(Nb)(Ru)(Cr), interstitial-free, workability and ductility, effect of alloying element 4-93345  
 Ni and alloys, tensile fracture characs. in liq. Hg 4-99558  
 Ni base superalloys, diffusion coated, crack initiation, acoustic emission obs. (*German*) 4-62140  
 Si thin single-crystals, anomalous plasticity in the visco-brittle transition temp. range, 500-700°C (*Ukrainian*) 4-88227  
 V-base alloys, candidate materials for fusion appl., weldability 4-99494  
 W, bicrystal, intrinsic grain boundary brittleness (*French*) 4-99476  
 W bicrystals, oriented, brittle-ductile transition temp. rel. to O and C content, AFS 4-104859  
 W, brittle fracture, impurity effects, Auger electron and scanning electron spectroscopy (*French*) 4-70268  
 Zn, tensile deformation testing with a high press. apparatus (*Japanese*) 4-62147  
 Zn-Cu-Ti alloys, bendability, struct. aspects (*French*) 4-81252

## ductile fracture

see also ductile-brittle transition; notch ductility  
 beam, edge-cracked, ductile fracture under EM bending force 4-91763  
 deep-drawing forming limits, three-dimens. ductile damage model 4-99596  
 defect sizes in plant at elevated temp. 4-91773  
 deformation and fracture at isolated holes in plane-strain tension 4-61976  
 fusion reactor materials for INTOR and DEMO, first wall lifetime, effect of material props. and operating conditions variations 4-96265  
 local stress and strain fields near a spherical elastic inclusion in a plastically deforming matrix 4-60303  
 mechanical behaviour of materials, conf., Stockholm, Sweden (Aug. 1983) 4-90297  
 metal, book contrib. 4-108508  
 metal, ductile, tearing, essential work of fracture 4-62014  
 polymers, fracture and rheological characteristics, interrelation 4-88232  
 rings, rapidly expanding, ductile fracture 4-74956  
 single edge notch tensile specimens loaded through frictionless pins, ductile fracture 4-60336  
 steel, alloy, fracture strain and characteristic fracture distance, microstruct. interpretation 4-85211  
 steel, austenitic stainless, ductile fracture resistance, assessment based on engineering approach 4-104876

## ductile fracture continued

- steel, austenitic stainless, edge-cracked beam, ductile fracture under EM bending force 4-91763  
 steel, austenitic stainless, fatigue crack propag. threshold 4-99590  
 steel, ductile, static resistance to cracking calc. under ductile fracture conditions (*Russian*) 4-66415  
 steel, ductile fracture and fracture toughness, effect of stress triaxiality and temp. (*Japanese*) 4-93379  
 steel, failure predictions, tearing instability and limit load 4-99589  
 steel, low alloy, cavity initiation criteria at inclusions 4-104874  
 steel, low alloy mild, ductile fracture, rel. between J-integral and COD 4-104842  
 steel, medium C, ductility anisotropy 4-60301  
 steel, microalloyed, fracture micromechanics 4-99602  
 steel, Mn, 13 wt.%, prod. by powder metallurgy method 4-81169  
 steel, pressure vessel, unstable ductile fracture under combined load of thermal shock and tension (*Japanese*) 4-93380  
 steel, quasiamellar and quasimonolithic, character of fracture 4-114659  
 steel, strain rate effects on ductile fracture 4-103250  
 steel structural, tensile deform., ductile fracture, void nucleation 4-99426  
 steels, low alloy, fracture toughness studies 4-109491  
 tensile deformation, acoustic emission response and interpret. 4-114608  
 weld metal, globular silicates effect on ductility and microstruct. 4-114607  
 Zircaloy cladding tubes, ductile fracture anal. 4-106768  
 Zircaloy-4, SCC in neutral aq. chloride soln. 4-66478  
 Ag-MgO, dispersion hardened, qualitative analysis of fracture 4-114633  
 Cu, brazed, low cycle fatigue in high vacuum rel. to cold work 4-109500  
 Cu-Zn-Ni, superplastic, post-deform. tensile props., effect of cavitation 4-114621  
 Fe, cast, spheroidal graphite, cavity initiation criteria at inclusions 4-104874  
 Fe-Cr-Al, oxide dispersion strengthened MA 956, fatigue crack growth 4-62031  
 Fe-P alloys, intergranular fracture planes, chemical states, Auger and electron energy loss spectra 4-93385  
 Fe<sub>22</sub>Co<sub>78</sub>V, tensile deform., 20-1000°C, fracture mode and ductility rel. to order-disorder transform. 4-66427  
 In-Sn and In-Bi-Sn eutectic alloy solders for Josephson packaging, mech. props. 4-71687

## ductility

see also ductile fracture; notch ductility

- brass, Admiralty, SCC, slow strain-rate, influence of deform. path 4-99634  
 brass, admiralty, slow strain rate SCC under multiaxial conditions 4-71764  
 $\alpha$ -brass, anneal-hardening, change in mechs. props. 4-99397  
 coated and uncoated, low cycle fatigue in air and corrosive environment 4-99657  
 discrete elastoplastic limited-ductility structs., shakedown anal. 4-108023  
 ductile-brittle transition temperature, determ. using criterion of meeting plane strain conditions 4-104935  
 dynamically loaded media, vel. distrib. of dislocations, quasiequilibrium function 4-65263  
 failure of ductile materials, effect of yield surface vertex 4-69689  
 fibre reinforced composite laminated plate, initial failure and ultimate strength theory (*Japanese*) 4-97417  
 glass fibre reinforced plastic, roving cloth reinforced, strength in flatwise direction, temp. depend. (*Japanese*) 4-89087  
 glassy polymers, ductile, max., strain for craze initiation 4-85227  
 graphite fibre reinforced epoxy, delamination and transverse fracture 4-99577  
 ice, columnar grained, ductile deform., yield function coeffs. 4-89954  
 IN 100, Ni-base superalloy, thermal fatigue 4-93417  
 Inconel X-750, Ni-base superalloy, creep and fracture, prior deform. effects 4-114656  
 metal sheets, rate-sensitive, formability limits 4-93349  
 perforated casing, finite element anal. of collapse 4-91736  
 PET, ductile polymer, hypersonic vel. and submicrocrack formation under uniaxial tensile stress 4-114632  
 PMMA, rubber particle toughened, kinetics and mechanism of deform. 4-76813  
 polycarbonate, ductile polymer, hypersonic vel. and submicrocrack formation under uniaxial tensile stress 4-114632  
 polycarbonate blends with ABS and SAN, tensile and impact tests, energy absorpt. 4-66389  
 polyethylene, high-density, moulded sheets tear strength 4-104846  
 power-law hardening material, optical shadow spot method for tensile crack 4-97449  
 Rene 93, Ni-base superalloy, fatigue, effect of processing and microstruct. 4-104843  
 sheet-metal forming, plastic instability 4-99462  
 steel, alloy type, Ca treated resulphurised, mech. props. and machinability, S and sulphide shape effect, report 4-62048  
 steel, austenitic, neutron irradi., high temp. deform. behaviour (*German*) 4-81262  
 steel, austenitic stainless, claddings, ring test of tubes oxidised in high temp. steam 4-104816  
 steel, austenitic stainless, Nb-bearing, creep props., effect of Fe<sub>2</sub>Nb precip. 4-114619  
 steel, austenitic stainless, PCA, unirrad., tensile props. from room temp. to 700°C 4-104812  
 steel, austenitic stainless, TiC precipitation, influence on creep rupture strength, ductility and He embrittlement 4-99388  
 steel, austenitic stainless, tubular specimens, endurance and long-term ductility, effect of prior irradi. 4-92243  
 steel, austenitic stainless, Path A-type alloys, neutron irradi., mech. props. 4-98139  
 steel, C, cast and wrought, H induced ductility losses, annealing effects 4-85193  
 steel, C, fracture toughness, stretch zone, ductility, transition region 4-99468  
 steel, C-Mn, grain boundary segregation of Cu, Sb and Sn at 900°C 4-93300  
 steel, C-Mn, hot-rolled, ductility and anisotropy of sulphide inclusion spacings, effect of inclusion shape 4-99437  
 steel, constructional, strengthening using thermomech. treatment and deform. in intercrit. temp. range 4-114585  
 steel, Cu-bearing, conf., Luxembourg (May 1983) 4-86106  
 steel, Cu-bearing, hot shortness in controlled rolling process 4-89105

## ductility continued

- steel, ductile fracture and fracture toughness, effect of stress triaxiality and temp. (*Japanese*) 4-93379  
 steel, effect on wear resist. in abrasive friction 4-93425  
 steel, HSLA, Cu-bearing, hot shortness 4-89104  
 steel, HSLA, tensile strength and ductility, dependence on microstruct. 4-114603  
 steel, maraging, tensile strength and ductility, dependence on microstruct. 4-114603  
 steel, martensitic, low C, controlled rolled and quenched, strengthening effects 4-99393  
 steel, martensitic hypereutectoid, rapid heat hardening using incomplete homogenisation effect 4-71671  
 steel, martensitic stainless, Mo, H embrittlement, effect of surface condition 4-85202  
 steel, medium and low strength, ductile behaviour, computer simulation 4-104832  
 steel, medium C, ductility anisotropy 4-60301  
 steel, mild and dual phase, post biaxially strained, residual ductility 4-104823  
 steel, Ni-Cr-Mo maraging, nitrogen effect on struct. and mech. props. 4-114532  
 steel, Ni-Cr-Mo-V, creep rupture and service properties improvement (*German*) 4-76862  
 steel, Ni-Cr-Mo-V, fracture behaviour effect of S content 4-99601  
 steel, normalised 04G2B, Y additions effects on mech. props. 4-93390  
 steel, plastic properties, effect of nonlinear strain paths 4-99474  
 steel, roll type 9Kh, small N and B additions effect on struct. and mech. props. 4-93342  
 steel, stainless, austenitic, type 316, flowing Li environment effect on fatigue and tensile props. 4-107055  
 steel, stainless, metastable austenitic, preliminary plastic deform. effect on mech. props. at low temp. 4-99443  
 steel, stainless, Ni-free, alloyed with rare-earth metals and Ca, struct. and props. 4-62116  
 steel, stainless, transition and martensitic-class, superplasticity 4-61983  
 steel sheet, continuous annealed cold-rolled, overaging treatment and ductility, interstitial atom supersaturation (*French*) 4-89096  
 steel weld metal, globular silicates effect on ductility and microstruct. 4-114607  
 steels, austenitic stainless and high Mn austenitic, neutron irradiated, comparison of tensile props. 4-103807  
 wear equation, mechanical, formulation 4-64891  
 Zircaloy-4 claddings, SCC at elevated temps., relevance to transient LWR fuel rod behaviour 4-104912  
 Al-Cu (10 wt.%), prod. by rheocasting, rel. between struct. and mech. props. 4-99467  
 Al-Cu-Li, recrystallised 2020, mech. props. rel. to soln. heat treatment 4-76781  
 Al-Cu-Mg alloy D16 plates, struct. strength, chem. comp. and heat treatment effects 4-61986  
 Al-Cu-Si, Al 2014, tensile props., 250 to 500°C 4-76816  
 Al-Mg solid solutions, ductility loss at high temps. 4-104857  
 Al-Mg-Bi, Al-Mg-Li and Al-Li-Mg low-activation alloy development for fusion device 4-108460  
 Al-Si-Mg-Sr, struct. and props., comp. and Sr addition effects 4-61987  
 Al-Zn-Mg-Cu (7.3, 2.6, 1.5 wt.%), 7049 notch sensitivity (*French*) 4-81251  
 Be, neutron irradi. at various temps., compression props. and swelling 4-108458  
 Cu-Al system, dual-phase, deform. behaviour 4-61993  
 Cu-Al<sub>2</sub>O<sub>3</sub>, dispersion hardened, tensile failure, temp. depend., grain boundary fracture 4-66405  
 Cu-Zn-Ni, superplastic, post-deform. tensile props., effect of cavitation 4-114621  
 Cu<sub>2</sub>MnAl single crystals, Heusler alloy, compression, 77-367K, fracture slip, superlattice dislocation dissociation 4-66369  
 (Fe,Ni)V, ordered alloy, irradi. in HFIR, microstruct. and bend ductility 4-108454  
 (Fe,Ni)<sub>3</sub>V alloy, long-range ordered, strain rate and ageing effect on mech. props. 4-109501  
 Fe, sintered, crack propag. and processes near crack tip 4-66435  
 Fe-base austenitic alloys, high strength evaluation for generator retaining rings 4-99448  
 Fe-Nb, nitrided, void form., mech. props., optical microscopy, SEM, TEM obs. 4-81361  
 Fe-Si (3.4 wt.%), cold workability, effect of struct. and texture (*Chinese*) 4-61950  
 Fe-Si (6.5 wt.%) rapidly quenched ribbons, mag. props. and preparation 4-84819  
 (Fe<sub>22</sub>Co<sub>78</sub>)<sub>3</sub>V, tensile deforms, 20-1000°C, fracture mode and ductility rel. to order-disorder transform. 4-66427  
 Hg, solid, mechanical props. at cryogenic temp. 4-80142  
 In-Sn and In-Bi-Sn eutectic alloy solders for Josephson packaging, mech. props. 4-71687  
 Li<sub>2</sub>O-Al<sub>2</sub>O<sub>3</sub>-SiO<sub>2</sub> glass-ceramic, superplastic ductility, rel. to hydrostatic press. and humidity 4-109474  
 Mg-Li-Al-Mn and Mg-Li-Al-Zn-Mn-Ce system alloys, mech. props. and corrosion resist. 4-93455  
 MgO containing metal precipitates, optical and mech. props. 4-70161  
 Mo, ductility transition temp. rel. to alloying elements (*Japanese*) 4-61979  
 Mo-Hf-C, electron beam welded joint, tensile strength, ductility, comp. depend. 4-109470  
 Mo-Nb-C, electron beam welded joint, tensile strength, ductility, comp. depend. 4-109470  
 Mo-Re-C, Z 4-109470  
 Mo-Sc, dilute alloy, are melted, workability and ductility 4-76808  
 Mo-V(Zr)(Ti)(Nb)(Ru)(Cr), interstitial-free, workability and ductility, effect of alloying element 4-93345  
 Nb alloy, plastic deform. with subsequent nitriding effect on mech. props. 4-114713  
 Nb, mech. props. at low temp., Ti effect 4-93391  
 Nb, thin wires, heat treatment 4-66355  
 Nb-Ti, thin wires, heat treatment 4-66355  
 Ni-Co electroplating, US agitation effect on mech. props. and comp. 4-114430  
 Ni-Cr-Co-B, melt spun superalloy, annealing, castability, ductility and microstruct. rel. to B additions 4-66323  
 Ni-Cr-Ti-Mo(Nb), precipitation strengthened, HFIR irradi., ductility, microstruct. 4-108457

**ductility continued**

- Ni-Fe electroplating, US agitation effect on mech. props. and comp. 4-114430  
 Ni<sub>3</sub>Cr, Ni<sub>3</sub>Cr, high temp. deform., effect of ordering 4-93358  
 SiC fibre/platelet reinforced Al-Mg-Si, magnitude and mechanism of strengthening 4-76710  
 Sn-Cd (5 wt.%), plasticity rel. to eutectoid transform 4-114605  
 Ti, plastic flow and fracture at low temps. 4-76803  
 Ti, texture evolution during deform., influence on formability (*French*) 4-71669  
 Ti-Al-Nb-Ta-Mo, Widmanstätten struct., effect on 'deform.' modes and mech. props. 4-99436  
 TiAl intermetallic, ductility, strength and microstruct., Ag addition effect (*Japanese*) 4-66391  
 U-Nb (6 wt.%), microstruct., mech. props. and corrosion, effect of quench rate 4-114558  
 V-Cr-Ti(Fe-Zr), mech. props. rel. to O contamination, fusion appls. 4-109499  
 V-Ti, thin wires, heat treatment 4-66355  
 W alloys, dispersion and solid solution hardening of vacuum-melted W 4-66346  
 W hard metals, sintered, mech. props. rel. to O content (*German*) 4-61909  
 W, powder metallurgy rods, swaging process workability rel. to texture (*Japanese*) 4-83968  
 W-Mo(Re), produced by vacuum melting, mech. props. 4-71694  
 W-Ni-Fe, sintered mixed powders, ductility and pore struct. rel. to sintering atm. 4-66393  
 W-ZrC(HfC), produced by powder metallurgy, mech. props. 4-71694  
 Zn-Cu-Ti alloys, bendability, struct. aspects (*French*) 4-81252  
 Zr, texture evolution during deform., influence on formability (*French*) 4-71669

**duplicating** *see reproduction (copying)***Duralumin** *see aluminium alloys***dusk** *see twilight***dust***see also cosmic dust*

- air dust, chemical species identification by X-ray powder diffractometry 4-105164  
 Arctic Haze during 1948-61 'Ptarmin' weather reconnaissance flights, origin 4-77631  
 Asian dust storm detection in Japan in April 1980, PIXE anal. 4-105661  
 atmosphere, dust storms over SE Australia and associated cold fronts 4-72685  
 atmosphere, haematite dust at 60 km altitude, spectra and particle size 4-94227  
 atmosphere, Mount St. Helens, volcanic plume disposal over USA and Atlantic 4-115482  
 atmosphere, El Chichon volcanic debris in Arctic atmosphere 4-105649  
 atmosphere of Arabian Sea, heating due to radiation absorpt. by aerosol 4-94241  
 atmosphere of Grand Canyon, Arizona, USA, pollution, particulates, and visibility 4-115564  
 atmosphere sediment transport, conf. at Istanbul, Turkey (July 1982) 4-78047  
 atmospheric dust of Central Mediterranean, wind blown dust 4-72672  
 Boulder, Colorado, atm. dust from Mount St. Helens 1980 May 18 eruption, optical effects 4-105719  
 deposition in power plants catchment area 4-114984  
 El Chichon volcanic dust cloud, twilight optical studies at Ahmedabad, India 4-89969  
 El Chichon dust cloud, effect on received solar IR/radio radiation at Fairbanks, Alaska 4-67296  
 electrostatic prism for microparticle beam steering, on 2 MV Van der Graaf dust accelerator 4-64263  
 gases, dusty, fully dispersed shock waves 4-112953  
 Hanford, Washington, dust from Mount St. Helens 1980 May 18 eruption, conc. 4-105698  
 Lamb's Dust Veil Index, formulation 4-105699  
 laser systems, high power, electrostatic technology for dust and hydrocarbon vapour control 4-74533  
 Manatee Glacier, BC, Canada, cryoconite hole thermodynamics 4-72615  
 Mars, dust storms, historical record and atmospheric modelling 4-82432  
 Mediterranean atmosphere, soil-sized particulates, ferrimagnetic minerals distrib. 4-100715  
 millimetre-wave propagation, effects of low-altitude nuclear burst (*French, English*) 4-67379  
 Mount St. Helens, 1980 April dust incursion to SW USA, movement pattern and visibility 4-105720  
 Mount St. Helens, 1980 May 18 eruption plume dispersion 4-105691  
 Mount St. Helens, 1980 May eruptions, atm. ash loading and insolation at Hanford, Washington 4-105718  
 Mount St. Helens, dust cloud from 1980 May 18 eruption, downwind deposition and radiation doses 4-105697  
 Mount St. Helens, eruption loud (April 1980), chem. comp. and ash characts. 4-105515  
 Mount St. Helens, stratospheric clouds, physical and chem. processes modelling (May-June 1980) 4-105692  
 Mount St. Helens, stratospheric particles due to 1980 eruptions, climatic implications 4-105706  
 Mount St. Helens 1980 eruptions, stratospheric aerosols time var. 4-105685  
 Mount St. Helens 1980 May 18 eruption, fine particles generation and electrification 4-105693  
 Mount St. Helens 1980 May eruptions, dust distrib. in atm. 4-105690  
 Mount St. Helens 1980 May eruptions, stratospheric tephra and aerosols, comp. and plume characts. 4-105687  
 Mount St. Helens dust cloud (1980) over Wyoming, particles size and conc. evolution 4-105686  
 Northern Ireland, Saharan dust washout in rain, Sept. 1983 obs. 4-82209  
 nuclear war, climatic consequences, computational expt. (*Russian*) 4-67389  
 nuclear war, climatic effects, global nuclear winter 4-105702  
 Saharan dust in atmosphere, mobilisation, transport, and deposition, conference, Gothenburg, Sweden (1977 April 25 to 28) 4-90302  
 Saharan dust incursion over the Tyrrhenian Sea 4-94180  
 solid phase sampling and deposition measurements (*German*) 4-72202
- dust continued**  
 stratospheric dust from El Chichon, optical sky polarimetry and photometry at Mauna Loa 4-62950  
 volcanic particles effect on sunlight extinction, climatic implications 4-105705
- dust storms** *see storms*
- DVM** *see digital voltmeters*
- dwarf stars**  
*see also white dwarfs*  
 active chromosphere dwarf stars, quiescent coronae and mag. fields 4-94818  
 active dwarf stars, mag. fields and atm. characts. 4-94817  
 active dwarf stars, photospheric parameters, evolutionary status, rot. and oscils. 4-94816  
 active red dwarfs, atm. emission, rot. and duplicity, X-ray and UV data anal. 4-94819  
 RX Andromedae, dwarf nova, continuum distrib., simultaneous visible and UV obs. 4-110631  
 BD+25°2511, spectroscopic binary star, discovery of light variability 4-82515  
 black dwarf inside red giant envelope, inward spiral anal. 4-110685  
 black dwarfs, initial mass function 4-110724  
 black dwarfs, struct. evolution, masses and luminosities 4-77823  
 ξ Bootis A, Li star, comp. determ. from spectrophotometric study 4-105985  
 AT Cancari, brightness variability like dwarf nova 4-105996  
 HL Canis Majoris, U Gem star, photometry and search for eclipses 4-101377  
 Capella HL, red dwarfs, X-ray and UV emission anal. 4-85932  
 OY Carinae, eclipsing dwarf nova, light curves and accretion disc characts. 4-110632  
 OY Carinae, visible eclipses of dwarf nova central object 4-63176  
 μ Cassiopeiae, astrometric binary, speckle interferometry and mass meas. 4-72977  
 μ Cassiopeiae, binary star orbit, parallax and proper motion 4-110688  
 cataclysmic binary stars, struct. and evolution 4-94737  
 cataclysmic variable stars, dynamical instabilities rel. to outbursts 4-82481  
 cataclysmic variable stars, mass transfer and disrupted mag. braking rel. to period gap 4-94811  
 UV Ceti stars, activity, correl. with Sun 4-94834  
 UV Ceti stars, flare models, magnetic fields and plasma characts. 4-94835  
 UV Ceti stars, flare spectra and photometry 4-94829  
 UV Ceti stars, negative preflares, theory and obs. 4-94837  
 UV Ceti stars, UV colours at flare max. 4-106006  
 Z Chamaeleontis, high-speed photometry of dwarf nova in quiescence 4-63175  
 common-proper-motion pairs, nearby, UBVR photometric study 4-94876  
 conference on red dwarf stars and related objects activity, of Catania, Italy (August 1982) 4-90295  
 contact and near-contact binary stars, Reticon spectroscopy rel. to orbital parameters and min. masses 4-110684  
 contact binary stars, X-ray survey 4-63197  
 cool dwarfs, mag. field strengths in spots 4-90145  
 dMe stars, flare triggering mechanism 4-94836  
 dMe stars, flares UV and visible obs. 4-94831  
 dMe stars, quiescent and flaring radio emission 4-94833  
 dwarf novae, optical props. rel. to soft X-ray transients 4-110658  
 dwarf novae, pulsed X-ray emission 4-101375  
 dwarf novae, spectrophotometry of seven objects 4-85960  
 FG-type dwarf stars, Li isotope ratio determ. 4-101327  
 flare star characts., relevance of Solar Maximum Mission results 4-94716  
 flare stars, atm. characts. from visible and UV spectra anal. 4-94828  
 flare stars, flares low-temperature emission and energy balance 4-94713  
 flare stars, H lines and continuum time variations during flares 4-94830  
 flare stars, nature, emission mechanism and evolutionary status 4-106012  
 flare stars, optical photometry and polarisation characts. 4-94822  
 flare stars, visible and UV spectroscopy of flares rel. to solar flare data 4-94827  
 flare stars, X-ray coronal emission anal. and obs. 4-94820  
 flare stars, X-ray emission, models and mag. fields anal. 4-94832  
 flare stars, X-ray emission comparison with solar flares X-ray emission 4-94718  
 flare stars discovery in Orion Trapezium region 4-106000  
 flare stars in Pleiades, probable numbers 4-63083  
 flare stars is soft X-ray sources 4-101507  
 G-type stars in Orion IC association, incidence of IR excesses 4-72934  
 U Geminorum, far and extreme UV flux and spectra 4-85955  
 U Geminorum, spectrophotometry and spectra interpretation with accretion disc and accretion spot models 4-85947  
 Gliese 890, rapidly rot. field M-type dwarf, spot activity 4-101379  
 gnmfu photometry system calibration 4-101332  
 halo subdwarfs, evidence for form. of Population II stars via thermal instability 4-67717  
 HD 282773, flare observed in G5 star 4-105997  
 HD 29697 (K3 V), possible BY Draconis star, light vars. obs. 4-105986  
 HD 5210, comparison star for RS CVn system HD 5303, photometric evidence for light variability 4-94764  
 HD 86590 short-period RS CVn star, recognition as triple system 4-101406  
 AH Herculis, dwarf nova, continuum distrib., simultaneous visible and UV obs. 4-110631  
 high-proper-motion stars, spectral classification 4-101308  
 high-tangential-velocity stars, catalogue 4-101193  
 Hyades dwarf stars, X-ray flare activity, influence of duplicity 4-94906  
 EX Hydrae, dwarf nova, high speed photometry 4-101378  
 VW Hydril, light curve, quasi-periodic oscils. of dwarf nova 4-63155  
 VW Hydril, SU UMa star, white dwarf characts. an accretion disc nature, obs. 4-110615  
 VW Hydril, SU UMa star, X-ray pulsations discovery during superoutburst 4-67742  
 Kpr 75, rapid visual binary, orbit and magnitude 4-110689  
 EV Lacertae, flare star, X-ray emission anal. 4-85961  
 EV Lacertae, flare star as possible eclipsing binary (*Russian*) 4-85956  
 EV Lacertae, October 1979 flare characts. 4-94826  
 late type disc and halo dwarf stars, C and N abundances 4-85915  
 late-type dwarf stars, spots, spot cycles and mag. fields 4-94821  
 late-type dwarf stars, Zeeman broadening of spectra 4-85923

## dwarf stars continued

- late-type dwarfs, mean colours and effective temps. 4-94772  
 AD Leonis, flare star, photometric anal. of flare activity 4-77836  
 AD Leonis, UV Cet star, flare activity anal. (1971 to 1982) 4-85962  
 M4, globular clusters, deep CCD photometry of main sequence stars 4-63215  
 M dwarfs, X-ray coronal activity 4-63146  
 metal-deficient F-M stars, new catalogues 4-94650  
 nearby stars, photometric systems used, catalogue 4-94766  
 NGC 2808, southern globular cluster, main-sequence photometry 4-72991  
 open clusters red giants and dwarfs, radial vel. anal. 4-63222  
 $\chi^1$  Orionis (GO V), IUE obs. rel. to rot. modulation of chromospheric activity 4-63142  
 parallaxes and proper motions from McCormick Observatory, 45th list 4-82464  
 AE Phoenicis, contact binary star, anal. from deconvoluted spectra 4-82513  
 UV Piscium, RS CVn-type eclipsing binary star, UVB photometry 4-82519  
 Pleiades variable K-type stars, VBLUV photometry anal. 4-94775  
 red dwarf star flares, chromosphere dynamic response to heating by electrons 4-94838  
 red dwarfs, search for photometric variations 4-94823  
 red dwarfs, spectral types, absolute magnitudes and colour indices in Cousins photometric system 4-63149  
 red dwarfs, trigonometric parallaxes determ. from obs. in hour angles (Russian) 4-101118  
 red dwarfs, turbulent sound generation from outer convection zones 4-94782  
 red dwarfs activity, models 4-94839  
 red dwarfs activity and magnetic fields 4-94771  
 RT Sculptoris, eclipsing binary, UVB photometry rel. to configuration, mass ratio, and evolutionary state 4-101409  
 UZ Serpentis, dwarf nova, continuum distrib., simultaneous visible and UV obs. 4-110631  
 solar companion star, orbital elements rel. to periodic mass extinctions on Earth 4-72593  
 solar companion star, rel. to periodic comet showers and terrestrial mass extinctions 4-72594  
 solar neighbourhood, dwarf evolution 4-94770  
 solar-type dwarf stars, activity, rot. and Ca II emission 4-94824  
 solar-type stars of known age, sample 4-82471  
 SU Ursae Majoris stars, eclipse depths rel. to red component activity and superhumps 4-90163  
 EQ Virginis, flare star, X-ray emission anal. 4-85961  
 EV Lacertae, flare star, activity rel. to possible planet-like companion 4-94825  
 Li abundance determin., effects of chromospheric activity 4-63131  
 $^6\text{Li}/^7\text{Li}$  in metal-deficient stars 4-63147  
 N abundances in disk and halo dwarfs 4-94755  
 WX Sagittae, recurrent nova, circumstellar shell characts. and mass ratio, spectral obs. 4-101374

## dye lasers

- amplified spontaneous emission, effect of  $\text{O}_2$  (Japanese) 4-112404  
 benzoxazinone derivatives, new laser dyes 4-107622  
 cascade pumped picosecond dye laser system 4-91448  
 cavity configuration for dispersion on two output beams 4-74554  
 cavity length detuning properties in synchronous mode locking 4-96964  
 coumarin 1-acriflavine-uranine-rhodamine 6G dye mixture systems, continuously tunable energy transfer laser generation 4-107619  
 coumarin derivatives for blue-green spectral band lasers 4-69397  
 coumarin laser dyes, photodegradation products 4-91449  
 CW, with standing wave and travelling wave cavities, single freq. output (Chinese) 4-107621  
 CW laser for intracavity state selection of atomic and molecular gases 4-60095  
 CW laser with self pumped phase-conjugating resonator cavity, self scanning 4-107692  
 CW mode-locked, small Stokes shift freq. conversion in birefr. fibres 4-107748  
 DFB dye laser, ultrashort-pulse, travelling-wave-pumped 4-83571  
 DFB laser pulses, directional and wavelength sweep 4-69466  
 distributed feedback, picosecond pulses generation using grating hologram 4-112405  
 double-wavelength pulsed tunable dye laser (Chinese) 4-112465  
 dye CW mode-locked lasers, role of cavity dispersion 4-79124  
 excimer pumped, picosec. pulse amplification (Japanese) 4-83574  
 femtosecond cavity, quarter-wave dielec. mirror dispersion analysis 4-102957  
 femtosecond duration pulse generation with a passively mode locked dye laser 4-79130  
 femtosecond pulse generation by mode locking (Japanese) 4-74560  
 flash lamp, high power vortex gas flow, for dye laser pumping 4-64718  
 flashlamp-driven dye laser UV source, integrating system for energy meas. 4-67158  
 flashlamp-pumped laser for laser damage meas. at 492 nm 4-74549  
 fluid jet stream of high optical quality, wire guided 4-112969  
 grazing-incidence lasers with and without intracavity lenses, comparative study 4-91447  
 high power blue-green LD-490 laser, pumped by hypocycloidal pinch plasma 4-79125  
 intensity correls. for laser with fluctuating pump 4-69400  
 IR dye laser,  $\text{N}_2$  laser pumped, efficiency improvement by energy transfer excitation 4-107620  
 IR picosecond pulses, narrow-band, tunable between 1.2-1.4  $\mu\text{m}$ , generated by travelling-wave dye laser 4-74569  
 linear anisotropy induced by polarised pumping radiation 4-79126  
 linewidths meas. using optical spectrum analyser 4-60093  
 longitudinally pumped laser with grazing-incidence holographic grating, stimulated emission characts. 4-74504  
 merocyanine cyclised new laser dye family from an old family of fluors 4-91450  
 9-methylanthracene-erylene laser dye mixture soln., energy transfer mechanism (Japanese) 4-74502  
 4-methylumbelliferone dye solns., two-component, lasing spectrum, UV radiation effects 4-60029  
 narrow band spectrum locked to compound atomic absorption lines (Russian) 4-69396  
 narrowband dye laser with a large scan range 4-91489
- dye lasers continued  
 Nile Blue-cyranine energy transfer laser,  $\text{N}_2$  laser pumped, efficiency improvement by energy transfer excitation 4-107620  
 Nile Blue-HITC energy transfer laser,  $\text{N}_2$  laser pumped, efficiency improvement by energy transfer excitation 4-107620  
 nonlinear laser model with multiplicative coloured noise, distrib. function 4-87312  
 Oxazine 750, Ar ( $^3P_2$ ) atoms orientation by optical pumping 4-112148  
 passively mode locked, calc. of light pulses with chirp inc. absorber and amplifier phase memory 4-107695  
 perylene-3,4,9,10-tetracarboxylic acid-bis-N,N'(2',6'-xylyldi)diimide laser dye, high stability and broad band lasing action pot. 4-107623  
 2-phenylbenzoxazole, spectral-luminesc. and lasing props. rel. to struct. 4-87155  
 picosecond mode-locked dye laser oscillator-amplifier synchronisation with a streak camera system 4-112475  
 planar self-waveguiding flashlamp-pumped dye laser (Chinese) 4-107675  
 polymer matrices with dye based active media, passive and generation characts. 4-107618  
 POPOP vapour phase laser performance, effect of triplet quenchers 4-74500  
 prismatic pulsed lasers, multi-pass dispersion theory 4-69398  
 pulsed dye lasers, grazing-incidence grating cavities with Brewster-prism beam preexpander (Chinese) 4-112481  
 pulsed longitudinal pumping theory 4-79128  
 pulsed single-mode, cavity of prism-grating-mirror combination, spectral linewidth 4-112477  
 pump system using  $\text{N}_2$  laser oscillator-amplifier system 4-69439  
 pumping, radiation 605 to 725 nm region pumped by 544 nm fluorescein dye laser 4-112402  
 radiation concentration in spectrum of dye laser with intracavity absorpt. cell 4-74505  
 radiation polarisation, steady-state approx. theory 4-79131  
 raman amplification spectroscopy using pulsed dye lasers 4-61696  
 rhodamine 560, 6G tunable picosec. laser oscillator-amplifier system, spatial and temporal props. 4-91488  
 rhodamine 590 laser oscillators, narrow linewidth, high PRF Cu laser pumped 4-74535  
 Rhodamine 6G,  $^{12}\text{I}_2$ -stabilized design, 576 nm, characts. 4-87324  
 rhodamine 6G, longit. pumped laser with grazing-incidence holographic grating, stimulated emission characts. 4-74504  
 rhodamine 6G colliding pulse mode locking ring laser anal. 4-96884  
 rhodamine 6G continuous high-power dye laser exptl. design. (Russian) 4-69432  
 rhodamine 6G CW ring laser with a Mach-Zehnder interferometer, efficient single mode operation 4-91496  
 rhodamine 6G CW single-mode laser radiation freq. doubling with an external auxiliary active cavity (Chinese) 4-60107  
 rhodamine 6G CW tunable ring laser, passively mode-locked, picosec. pulse SHG correl. meas. (Chinese) 4-87354  
 rhodamine 6G double wavelength laser,  $\text{N}_2$  laser pumped (Chinese) 4-91492  
 rhodamine 6G dye laser, CW, single longitudinal mode oscill. (Korean) 4-112483  
 rhodamine 6G femtosecond laser, expt. and theoretical study 4-107627  
 rhodamine 6G homogeneously broadened laser, higher order dynamical states 4-69399  
 rhodamine 6G laser superradiance and lasing spectra under longit. excitation, reabsort. effect. 4-107624  
 rhodamine 6G multimode pulsed laser, single-shot spectral meas. and mode correls. 4-69467  
 rhodamine 6G ring laser saturable amplification, picosec. pulse intracavity degenerate four-wave mixing 4-91524  
 rhodamine 6G subpicosecond dye laser pumped by Xe ion laser 4-96937  
 rhodamine 6G thin layer two-frequency tunable laser 4-107626  
 rhodamine 6G tunable dye jet laser pumped synchronously by second harmonic of Nd:YAG laser 4-60031  
 rhodamine 6G tunable single-mode picosec. laser with ultra-short cavity (Chinese) 4-112468  
 rhodamine 6G-saffrin T-cresyl violet-Nile blue dye mixture systems, continuously tunable energy transfer laser generation 4-107619  
 rhodamine 700 laser, flashlamp-pumped, passive mode locking in near IR 4-60030  
 rhodamine dyes, solns., lasing efficiency solvent effects 4-79129  
 rhodamine-6G, aq. solns., triplet state quenching by inorganic ions, appl. to lasers 4-78793  
 rhodamine-6G dye laser, use of Mather type plasma focus for optical pumping 4-64720  
 ring dye laser, rapid-tuning, freq.-doubled, for high resolution absorpt. spectroscopy in shock-heated gases 4-83607  
 ring dye laser/amplifier, two-stage injection-locked; for coherent image amplification 4-69452  
 ring dye lasers, CW, injection locking 4-74501  
 ring laser, pulsed, intensity stabilisation by controlled self-injection 4-60076  
 ring lasers, femtosecond, multilayer dielec. mirror generated chirp 4-83573  
 short-cavity dye laser design, piezoelec. tuned 4-69434  
 single pulse selection in amplifiers 4-69470  
 solvent deuteration effects, fluoresc., laser efficiency 4-79127  
 styryl 9, subpicosecond generation via hybrid mode locking in near IR 4-60083  
 styryl 9 laser, flashlamp-pumped 4-87323  
 synchronously pumped, rate eqn. simulation 4-74503  
 synchronously pumped dye laser, picosecond pulse amplification: 4-60032  
 tunable, spectrosc. freq. calibration 4-78378  
 tunable dye laser resolution for laser spectroscopy of H 4-64412  
 tunable laser stabilisation techniques for ultrahigh-resolution spectroscopy 4-63789  
 tunable pulsed dye laser cryogenic photocalorimeter, for photochemical reactions obs., theory and design 4-105005  
 two freq. tunable laser with high efficiency intrasensor radiation divider 4-79192  
 two-wavelength narrow-band dye laser, independently tunable (Chinese) 4-112464  
 VUV radiation, reson. enhanced tunable source 4-83661  
 wave-number calibration using reference lines in optogalvanic spectra of U and Th 4-83628  
 white light operation (Chinese) 4-112403  
 xanthene dyes, solvent deuteration effects, fluoresc., laser efficiency 4-79127

**dye lasers continued**

- Cu vapour laser pumped dye laser for spectroscopic appl., conversion efficiency 4-107666
- Nd<sup>3+</sup>:YAG pumped, cavity configuration for dispersion on two output beams 4-74554
- rhodamine B DFB laser, amplified spontaneous emission 4-83572
- Xe ion-pumped open dye stream laser time resolved spectrum 4-107625

**dye penetrant tests** *see nondestructive testing***dynamic nuclear polarisation**

- see also CINDP; Overhauser effect; solid effect*
- Al<sub>2</sub>O<sub>3</sub>:Cr<sup>3+</sup>, NMR and dynamic nucl. pol., low-freq. modulation effects 4-65868
- CaF<sub>2</sub>:Tm, NMR and dynamic nucl. pol., low-freq. modulation effects 4-65868
- <sup>3</sup>He, adsorbed on fluorocarbon microspheres, dynamic polarisation effects, EPR study 4-80324
- <sup>3</sup>He gas, nuclear polarisation by optical pumping 4-108675
- Si:Au, solid solution, optical nuclear polarisation 4-76282

**dynamic programming**

- coastline data, point reduction in digital maps (*Japanese*) 4-81833
- continuous speech recognition using dynamic programming, parameters comparison 4-79393
- continuous speech recognition using dynamic programming, postprocessing 4-79392
- countable state Markov decision chains with total strategy (*Russian*) 4-73348

**dynamic response**

- linear structural systems subject to component changes, dynamic responses anal. 4-87556
- ocean cable systems simulations 4-114677
- shell, thin stiffened, resonance response, nonlinear interactions 4-87607

**dynamic stability** *see stability***dynamic testing**

- see also fatigue testing*
- Borssele reactor vessel, neutron embrittlement Charpy tests 4-96132
- capacitive deformation gauge, for 10<sup>4</sup> sec<sup>2</sup> deform. rates 4-89219
- fishing trawl net design, hydrodynamic testing facility development 4-115639
- piezoresistive stress transducer, calibration by impact testing 4-106312
- steel, hardness testing, with impact action standard-fee instruments 4-99675
- strain determ. in dynamic compression test 4-112780
- strain measurement, equipment on German market (*German*) 4-76939
- Si<sub>3</sub>N<sub>4</sub>, hot-pressed, transient creep parameters, determ. by dynamic bending tests 4-81381

**dynamical symmetry**

- action equivalent Hamiltonians, dynamical symmetries 4-110918
- composite model, dynamical symmetry breaking through preons 4-111417
- conference on collective states in nuclei, Suzhou, China (Sept. 1983) 4-95043
- dynamical symmetry breaking and particle mass generation in gauge field theories 4-82899
- equivalent Hamiltonians, accidental degeneracies and dynamical symmetries 4-95199
- general relativity, space-time theories and symmetry groups 4-63578
- IBFM, symm. connected with U(5) limit, nuclear collective states 4-95918
- interacting Bose-Fermi model, dynamical supersymmetry, collective nuclear structure 4-95930
- interacting boson model, dynamical supersymmetry, collective nuclear structure 4-95930
- microscopic collective states, dynamical group, coherent state representations 4-102192
- space time, null geodesic motion, conformal dynamical symmetry 4-63589
- symmetry operators for neutrino and Dirac fields on curved spacetime 4-90733
- time-dependent mechanical symmetries and extended Hamiltonian systems 4-58989
- two-dimensional N=1 supergravity theories, dynamical supersymmetry breaking 4-68115

**dynamics**

- see also ballistics; fluid dynamics; force; friction; haemodynamics; impact (mechanical); kinematics; resonance; rotating bodies; rotation; vibrating bodies; vibrations*
- Arp 91, interacting galaxy pair, dynamical model rel. to optical morphology and kinematics 4-90230
- beam structure, multilayer, dynamics under moving conc. load 4-108002
- disc galaxies, transient spiral wave heating rel. to discs thickness 4-67802
- discrete dynamic systems with stochastic parameters, Liapunov's direct method 4-73211
- dynamical systems, first integrals obtention 4-73214
- elliptical galaxies, rotation-surface-brightness relation rel. to dissipation during form. 4-67805
- elliptical galaxies, stellar dynamical models 4-115813
- Fermi-Ulam problem, bounds on velocity 4-95153
- five body problem, model for singularity without collisions 4-86192
- galaxies, secular dynamical evolution over Hubble time 4-67800
- galaxies, stellar discs heating by massive objects 4-67803
- galaxies, stellar dynamical model of ring struct. and stability 4-94944
- generalized modal shock spectra with indeterminate interface 4-110859
- index evaluation for dynamical systems, locating all the zeros of vector function 4-95158
- laser systems, chaos in nonlinear dynamics 4-79097
- linear dynamic system output, spectral moments calc. 4-95161
- long term dynamic irregularity, statistical anal. 4-78198
- mechanisms with nonlinear characts., dynamic models 4-73218
- multibody dynamics 4-95165
- nonconservative dynamical systems, integrating factors and conservation laws 4-95146
- nonconservative system, mass distrib. effect on stability (*Russian*) 4-64836
- nonlinear dynamic systems, time-domain quasilinear identification 4-110858
- nonlinear oscillators, dynamically determined force functions 4-106179
- numerical time integration in dynamics 4-87557
- one-dimensional oscillator movement in field with periodic poi. (*Russian*) 4-90367

**dynamics continued**

- planar 3-body problem, parabolic orbits 4-86193
- planar collisions, particle and rigid body, friction, restitution and energy loss 4-101646
- planetary nebulae, expansion vels. rel. to evolution and formation rate 4-115793
- protogalaxies, dynamical constraints during violent relaxation and effects on final state 4-94956
- random vibration survey of recent developments 4-95163
- rigid heavy body suspended on a string, eqns. of motion 4-79438
- Ringbom-Stirling engine, free displacer dynamics determ. 4-66771
- rod of elastoplastic material, dynamics of buckling 4-112743
- rods, elastic, soln. of nonlinear cases of motion (*Russian*) 4-79437
- separatrix loop existence in four-dimens. systems similar to the integrable Hamiltonian systems 4-106175
- Seyfert galaxies, dynamics of narrow line regions 4-86034
- solar filaments dynamics, anal. of steady flows in H $\alpha$  and C IV lines 4-101281
- solar nebula, thickness and evolution of dust layer during origin of solar system (*Chinese*) 4-82426
- solid with ellipsoidal cavity filled with mag. fluid, dynamics, astrophysical appls. 4-106176
- spatial screw motion (*German*) 4-82662
- spherical stellar system, numerical study of gravit. collapse 4-101438
- stellar systems, cooling and heating by binary stars rel. to dissipative evolution 4-63211
- stellar systems, influence of binary stars on evolution of globular clusters and galactic nuclei 4-63212
- stellar systems, numerical study of, relaxation of one-dimensional gravit. systems 4-106044
- stellar systems, relaxation time 4-72989
- stochastic vibrations of dynamical systems, Green's multi-dimens. function appl. 4-90352
- systems with elastic elements of large stiffness, dynamics 4-78130
- technical stability of motion with the aid of Newton potentials 4-106181
- triaxial galaxies, fitting of N-body potentials to Eddington pot. 4-67799
- triaxial galaxies, struct. and evolution 4-67798

**dynamometers**

- see also force measurement*
- feedback dynamometers with differential scale conversion 4-90581
- interpolation criteria comparison, hysteresis influence 4-111124

**dynamos** *see d.c. generators***dyprosium**

- see also nuclei with .....*
- atoms, isotope shift, parametric description appl. 4-74191
- films, hydridisation and catalysis 4-71984
- thin films, struct., effect of ion irradi. 4-70240
- total and photoelectric cross sections 4-91244
- BaSO<sub>4</sub>:Dy, thermoluminesc. detectors response functions to  $\gamma$ -radiation 4-112037
- CaF<sub>2</sub>:Dy<sup>3+</sup>, Eu<sup>2+</sup> crystals, electron-excitation relax. kinetics and nonequilibrium acoustic phonons. 4-88256
- CaSO<sub>4</sub>:Dy, photo-transfer thermoluminescence 4-104683
- CaSO<sub>4</sub>:Dy dosimeters, TLD-900, thermolum. isothermal decay 4-68835
- CaSO<sub>4</sub>:Dy single cryst., cryst. growth and elec. props. 4-113943
- CaSO<sub>4</sub>:Dy Teflon discs, dosimetric parameters and comparison with MgB<sub>2</sub>O<sub>7</sub>:Dy sintered pellets 4-89757
- CaSO<sub>4</sub>:Dy thermoluminesc. detectors response functions to  $\gamma$ -radiation 4-112037
- CaSO<sub>4</sub>:Dy(Tm), Bulgarian synthesis, thermoluminescent and dosimetry props. (*Russian*) 4-78747
- CaSO<sub>4</sub>:Dy(Tm), synthesis effect on phosphor props. (*Russian*) 4-78748
- CaSO<sub>4</sub>:Dy(Tm) thermoluminescent detectors, sensitivity for 2-144 keV neutrons 4-96288
- MgB<sub>2</sub>O<sub>7</sub>:Dy, some advantages and disadvantages for practical dosimetry 4-105340
- MgB<sub>2</sub>O<sub>7</sub>:Dy sintered pellets, dosimetric parameters and comparison with CaSO<sub>4</sub>:Dy Teflon discs 4-89757
- Zn-like ions from Ru<sup>14+</sup> to Dy<sup>3+</sup>, 4s<sup>2</sup> 1S-4s4p<sup>1</sup>P<sub>1</sub> transitions 4-102626

**dyprosium alloys**

- Dy-Tb-Fe, elastic props. nonlinearity and magnetostriction (*Russian*) 4-80133
- DyAl<sub>2</sub>, ferromag., magnetisation, NMR studies 4-80787
- DyCoSn<sub>6</sub>, cryst. struct. and mag. props. (*Russian*) 4-88135
- DyCu amorphous alloy film, mag. transition, small angle mag. scatt. 4-71064
- DyCu<sub>2</sub>Ge<sub>2</sub>, mag. and cryst. struct., neutron diffr. studies 4-65794
- Dy, Er, ..., Ni<sub>5</sub>, mag. struct. characts. (*Russian*) 4-92894
- DyFe<sub>2</sub> intermetallics, SXAPS studies 4-81039
- DyFe<sub>2</sub>Al<sub>1-x</sub>, Fe L<sub>III</sub> X-ray emission spectra, electron microprobe anal. 4-76563
- Dy<sub>2</sub>(Fe<sub>1-x</sub>Al<sub>x</sub>)<sub>17</sub>, pseudobinary intermetallic cpd., mag. props. 4-71032
- Dy<sub>2</sub>Rh<sub>2</sub>, mag. props. meas. 4-61521
- DyRh<sub>2</sub>B<sub>4</sub>, mag. props. and crystal field effects 4-84767
- Dy<sub>2</sub>Si<sub>3</sub>, low-temp. phase transitions and mag. ordering 4-71071
- (Dy<sub>0.7</sub>Tb<sub>0.3</sub>)<sub>2</sub>Fe<sub>2</sub>, mechanostriuctive strain as a function of magnetic field and mechanical elastic stresses 4-113523
- DyXGe, X=Ni, Co, cryst. struct., mag. and elec. props. (*Russian*) 4-88134
- Dy<sub>1-x</sub>Y<sub>x</sub>Co<sub>2</sub>, magnetically ordered, satellite struct. in <sup>59</sup>Co spin-echo NMR spectrum 4-88743
- Gd<sub>1-x</sub>Dy<sub>x</sub>Al<sub>2</sub>, NMR spectra, dipole field rot. 4-109084
- Sc-Dy, spin glasses with uniaxial anisotropy 4-71099
- Ti-Dy, rapidly solidified dispersion strengthened, struct. and props. 4-114561
- Y-Dy, spin glasses with uniaxial anisotropy 4-71099
- Y<sub>0.5</sub>Dy<sub>0.5</sub>Co<sub>2</sub>, H absorption in 0-40°C temp. range (*Russian*) 4-75775

**dyprosium compounds**

- see also dyprosium alloys*
- CaDy(MoO<sub>4</sub>)<sub>2</sub>, layered cryst., low temp. thermal cond. (*Russian*) 4-70481
- Dy<sup>3+</sup> cpds. nonq. solns., absorpt. spectral intensity anal. 4-78858
- DyAg, EPR at far IR wavelengths 4-76249
- Dy<sub>2</sub>Al<sub>2</sub>O<sub>12</sub>, far IR EPR study 4-71214
- Dy<sub>2</sub>B<sub>6</sub> antiferromagnet, elec. resist. and thermoelec. power studies 4-113982
- DyB<sub>6</sub>, low temp. resistivity and mag. props. 4-108859
- Dy<sub>0.8</sub>Ca<sub>0.2</sub>CrO<sub>3</sub>, ionic cond. and thermal expansion 4-84461
- Dy<sub>2</sub>Co<sub>4</sub>, Dy<sub>2</sub>Co<sub>3</sub>, synthesis and high-temperature study (*French*) 4-85095

**prosium compounds continued**

- DyF<sub>3</sub>, optically excited, fluorescent excitation and absorpt. spectra 4-99154  
 DyFeO<sub>3</sub>, muon site determ. 4-71227  
 DyMnO<sub>3</sub>, decomposition, O partial press. and elec. cond. 4-85290  
 DyMoS<sub>8</sub>, two-stage flux penetration 4-108971  
 Dy<sub>2</sub>O<sub>3</sub> thin films, high resolution CTEM images, effect of slight disorientation on image aspect 4-70602  
 Dy<sub>2</sub>O<sub>3</sub>, total gamma-ray cross sections 4-60959  
 Dy<sub>2</sub>Se<sub>2</sub>Fe<sub>2</sub>O<sub>3</sub> orthoferrites, mag. props., Se substitution effects 4-104463  
 DyVO<sub>4</sub>, zircon-structure crystals, internal strain, orbit-lattice coupling and phase transitions 4-80220

**E-region** *see E-region*

**E-region**

*see also sporadic-E layer*

- A1 absorption data reduction, validity of George's method 4-90019  
 afternoon auroral oval, field-aligned currents, electron beams and density enhancements 4-82338  
 auroral electrojet, elec. field and plasma density meas. 4-72783  
 auroral electrojet irregularities studied using STARE radar 4-67523  
 auroral electron density vars., power spectra rel. to electron drift vel. in eastward electrojet 4-72777  
 auroral region, electrostatic plasma wave energy propag. 4-85818  
 E<sub>z</sub> formation, effects of longitudinal currents 4-94289  
 electron density, EISCAT data rel. to GEOS 2 electron flux vars. 4-100857  
 electron density profile, test of International Reference Ionosphere using single-freq. A1 absorpt. data 4-90020  
 electron density profiles, effects of longitudinal currents 4-94289  
 electron gas heating due to magnetosphere convection, effect on cond. 4-100847  
 electron temperature profile at high latitude 4-105800  
 electrons, low energy, in E and F-regions, nonthermal components obs. 4-63008  
 ELF waves generated during radiowave heating of auroral electrojet 4-67538  
 HF ray tracing at high-latitudes using observed meridional electron density distrib. 4-85823  
 ion chemistry of E- and D-regions, photochemical aspects 4-72774  
 ionization and elec. cond. at high latitudes rel. to solar flux and zenith angle 4-94301  
 L equivalent current systems, seasonal vars. 4-72785  
 morning sector convection reversal, SABRE obs. during mag. storm 4-110364  
 radiowave heating expt. using 430 MHz radar, obs. of enhanced plasma lines 4-85825  
 rocket radiowave propag. expt. for nighttime electron density profiles 4-94280  
 spread-F irregularities generated in E-region in post-sunset period 4-82326  
 VHF intensity scintillation of transionospheric signals, due to F- and E-regions 4-115648  
 N<sub>2</sub> + O<sub>2</sub> charge transfer study 4-87214  
 O<sub>2</sub> conc. at lower ionosphere altitudes in auroral zone 4-100835

**ear**

*see also hearing*

- acoustic props., short-time power spectra parametric representation 4-103141  
 acoustic reflex, math. model 4-109823  
 adaptation, long-term, in hearing impaired ears, cat obs. 4-93755  
 antibodies, Met-enkephalin and Leu-enkephalin, immunofluoresc. in guinea pig cochlea 4-105246  
 basilar membrane, alteration of vibr. prod. by loud sound 4-109835  
 cats, dorsal and posteroventral cochlear nuclei, postnatal development 4-77255  
 cochlea, anatomical correlates of impulse noise-induced mech. damage 4-89592  
 cochlea, Bronx waltzer mutant mouse, age-related struct., electron microscopy obs. 4-105245  
 cochlea, gap junctions in the stria vascularis and effects of ethacrynic acid 4-105250  
 cochlea, guinea pig, hair cells in isolated coils, study technique 4-110017  
 cochlea, guinea pig, water permeability of endolymph-perilymph barrier 4-109840  
 cochlea, hypothyroid developing rat, microtubules obs. 4-89589  
 cochlea, rodent, computerised reconstruction of regional blood flow 4-115293  
 cochlea, single fibre responses in guinea pigs with long-term endolymphatic hydrops 4-93759  
 cochlea generated distortion, ear canal acoustic and round window elec. correlates 4-109828  
 cochlea isolated from guinea pig, sensory-cell hair bundles stiffness 4-109837  
 cochlea of Mongolian gerbil, auditory function development 4-89596  
 cochlear blood flow meas. technique combining microspheres with surface prep. dissection 4-93981  
 cochlear function in guinea pigs with long-term endolymphatic hydrops, electrophysiological meas. 4-93760  
 cochlear hair cell density, guinea pig, rel. to freq. discrimination 4-100166  
 cochlear innervation in the cat, fine struct. 4-93745  
 cochlear microphonic responses prod. by noise exposure in guinea pigs, nonlinearity modifications 4-93756  
 cochlear nerve and nucleus, single units, noise masking of tone responses and crit. ratios 4-93757  
 cochlear nonlinearities, inference from 2-tone distortion prods. in alligator lizard ear canal 4-105247  
 cochlear nucleus, unit responses to elec. stimulation through a cochlear prosthesis 4-93753  
 cochlear nucleus neurons, tone-evoked activity reduction by baclofen 4-105244  
 cochlear nucleus of deaf quivering mouse, single unit responses 4-109830  
 cochlear potentials, gross, rel. to hair cell pathology in waltzing guinea pig 4-115060  
 cochlear shunts in birds, comparative mechs. of hearing 4-109832  
 cochlear stereocilia, dimensions in man and guinea pig 4-109834  
 cochleas used for basilar membrane mechs. studies, ultrastruct. damage 4-93758  
 eardrum surfaces, stereo reconstruction from photomicrographs 4-85492

**ear continued**

- endolymph-perilymph barrier, Na<sup>+</sup> permeability 4-115039  
 frequency dependence of directional amplification at the cat's pinna 4-93754  
 human, quantum limits to oscillator stability, acoustic emission 4-115079  
 inner ear dark cells, frog, quantitative localisation of Na-K pump 4-89594  
 insertion gain meas. using probe microphones in the ear canal 4-115150  
 mammalian cochlea, sensitivity modulation by LF tones, basilar membrane motion 4-109826  
 mammalian cochlea, sensitivity modulation by LF tones, inner hair cell receptor pots. 4-109825  
 mammalian cochlea, sensitivity modulation by LF tones, primary afferent activity 4-109824  
 mammalian hearing organ sensory hairs, graded and nonlinear mech. props. 4-105255  
 multichannel cochlear prosthesis for profound-to-total hearing loss 4-109993  
 organ of Corti, elec. circuit props., anal. including reactive elements 4-100163  
 organ of Corti, guinea pig, cross-links between stereocilia, rel. to sensory transduction 4-115058  
 organ of Corti, intercellular elec. coupling obs. 4-93752  
 organ of Corti of guinea pig, hair cell counts 4-115068  
 oto-acoustic emissions anal. 4-62501  
 primary fibres, discharge pattern with elec. stimulation of cochlea in cats 4-109829  
 shock-proof ear, comparative mechs. of hearing 4-109831  
 Shrapnell's membrane, comparative mechs. of hearing 4-109833  
 sound localisation, influence of pinnae-based spectral cues 4-72265  
 spinal cord thermal stimulation in rabbit, ear-skin and renal blood flow changes 4-81725  
 spontaneous oto-acoustic emission, use of aspirin 4-115069  
 spontaneous otoacoustic emissions in a dog 4-89598  
 stapedius reflex and brainstem auditory evoked responses in multiple sclerosis patients 4-85439  
 stereocilia on inner hair cells, fusion in various mammals after noise exposure 4-85437  
 stimulated acoustic emissions in gerbil and man, suppressibility 4-109827  
 thermal sensitivity of mouse ear, long-term effect of X-rays 4-109882  
 tympanic membrane, fibre Fizeau interferometer for minute biological displacements meas. 4-89853  
 tympanic membrane, mech. vibrs. rel. to directional hearing in grass frogs 4-93751  
 tympanometric middle-ear press. determ. with 2-component admittance meters 4-115254  
 tympanometry, ear drum mobility and middle ear vol. meas. 4-115080  
 vestibular semicircular canal responses during righting movements of falling cat 4-81719  
 wave propagation and dispersion in the cochlea 4-105243

**ear microphones** *see microphones*

**earphones**

*see also hearing aids*

No entries

**Earth**

*see also Earth composition; Earth orbit; Earth rotation; Earth structure; earthquakes; geochemistry; geochronology; geodesy; geomagnetic variations; geomagnetism; terrestrial atmosphere; terrestrial electricity; terrestrial heat*

- accretion characts. 4-110099  
 accretionary event at Cretaceous-Tertiary boundary, siderophile-rich mag. spheroids chem. anal. 4-100509  
 antineutrino production by Earth interior and possibility of observing them 4-94136  
 atmosphere, land and ocean interaction 4-77662  
 early hydrosphere of Earth, origin and physical state, review 4-110254  
 elastic constant from satellite orbital inclination analyses 4-77474  
 free oscillations, inverse problems for torsional modes 4-110070  
 free oscillations, upper limit of undertone periods 4-67174  
 geoid shape in Sudan 4-89872  
 Moon origin by fission from fast rotating proto-Earth 4-101211  
 neutrino geophysics, Earth's projected mass density meas. 4-77642  
 neutrino tomography of Earth interior, feasibility of method 4-72721  
 origin of Earth-Moon system 4-77742  
 Pamirs-Hindu Kush region, tectonic features from seismic obs. 4-62771  
 position, effect on solar flare isolated shock wave arrival time 4-94536  
 reference ellipsoid, formulae for great elliptic line 4-72479  
 satellite exploration, ground stations features (German) 4-110284  
 solar system, book 4-58598  
 tidal evolution of Earth's gravit. field and figure, theory 4-105399

**earth (electric)** *see earthing*

**earth (soil)** *see soil*

**Earth age** *see geochronology*

**Earth atmosphere** *see terrestrial atmosphere*

**Earth composition**

*see also Earth structure*

- abundances in core and upper mantle, equilibration 4-110106  
 NE Africa, Proterozoic crustal evolution from model Nd ages 4-89900  
 Archean mantle fractionation, evidence from Nd-isotopic ratios in igneous rocks 4-100499  
 basalts of continental arches in eastern USSR distinctive petrochemical features 4-100563  
 Bowers Supergroup volcanics, geochemistry rel. to Early Palaeozoic tectonic evolution of N Victoria Land, Antarctica 4-67215  
 Cantal, France, coexisting alkaline magma series, isotope geochemistry and magma chamber characts. 4-110098  
 cretaceous dyke rocks, Pyrenees, geochemical characts. and relation to Sillon Houlier (French) 4-82043  
 crystalline basement rocks of Norilsk area, NW Siberian platform, comp. and age 4-100514  
 Late Devonian mass extinction horizon, no geochemical evidence for asteroid impact 4-62811  
 felsic magmas, extreme fractionation through liq.-state diffusion or fractional crystallisation 4-67217  
 geochemistry (book) 4-73192  
 gneiss complexes, Lower Precambrian, of Yenisei Ridge region, USSR, geochemistry 4-100561  
 gneisses of Georgia Inner Piedmont, scale of Sr isotopic diffusion during post-metamorphic cooling 4-67216

**Earth composition continued**

- granite from Gabal Mueilha, Egypt, post-magmatic alteration, trace element distrib. 4-85674  
 Hawaiian tholeiite, element abundances rel. to metasomatic model for origin 4-85650  
 igneous rocks, phase equilib. controls on tholeiitic and calc-alkaline differentiation trends 4-85651  
 Ivrea Zone, NW Italy, amphibolites, chem. comp., petrogenesis and tectonic anal. 4-110146  
 kimberlites of Daldyn field, comp. rel. to principal stages of form. 4-100565  
 mantle composition, large-scale Sr and Pb isotope anomaly in Southern Hemisphere 4-89899  
 mantle heterogeneity, implications of inverse relationship between Sr isotope diversity and rate of oceanic volcanism 4-77490  
 mantle siderophile elements depletion, evidence from W and Mo abundances 4-110099  
 measurements in deep-sea sediments 4-110128  
 Mount Isa Inlier, Australia, batholiths geochemistry and age, implications for magmatism 4-94032  
 Mount St. Helens, 1980 May eruptions, ash and magma, comp.-chem. 4-105513  
 Mount St. Helens, eruption loud (April 1980), chem. comp. and ash characts. 4-105515  
 ocean chemistry, water column anomalies assoc. with hydrothermal activity in Guaymas Basin, Gulf of California 4-67218  
 oceanic ferromanganese crusts, influence of carbonate dissolution rate on metal comp. 4-67206  
 Oklo reactor characts. (book) 4-78049  
 Phanerozoic basite volcanism of Transbaikai, USSR, comp. evolution 4-100515  
 Queriguit, France, granite-granodiorite complex genesis, recycling processes, Nd-Sr isotopic systematics 4-110096  
 radioactive elements distrib. and ores prospecting (*Russian*) 4-100819  
 Seychelles, granites and xenoliths, Nd and Pb isotopic comp. 4-110102  
 Zacatecas, Mexico, mid-tertiary felsic volcanic rocks, Sr and Nd isotopic comp. 4-110113  
 Ar loss predictors in basic rocks, test of two alteration indices 4-110140  
 Hf/rare earth elements fractionation in sediments, evidence for crustal recycling into mantle 4-110100  
 Hg annual flux from Kilauea main vent, estimate from Hg/SO<sub>2</sub> ratio 4-72559  
 Ir anomaly at nonmarine Cretaceous-Tertiary boundary sites, Raton Basin 4-72588  
 K-rich volcanic rocks, <sup>18</sup>O/<sup>16</sup>O and chem. relationships, mantle implications 4-110094  
 Ne isotopic variation in Mid-Atlantic Ridge basalt, mantle component 4-110095  
 Ra fluxes from salt marsh, meas. in Bly Creek, South Carolina 4-77557  
 Ra, occurrence and behaviour in saline formation water of US Gulf Coast region 4-110179  
<sup>230</sup>Th in Atlantic ocean sediments, glacial to interglacial changes in carbonate and clay sedimentation 4-110129  
<sup>232</sup>Th behaviour during magma formation and volcanism 4-67190  
<sup>238</sup>U decay chain nuclides, behaviour during magma formation and volcanism 4-67190  
 V concentrations in N Pacific Ocean, profiles of particulate and dissolved V 4-77556

**Earth core**

- boundary diffusion skin layer and short-period geomagnetic secular variations 4-94000  
 chemical equilibration 4-110106  
 coupling with mantle and geomag. impulse anal. 4-105413  
 dynamics, dynamo theory, review 4-100512  
 dynamo action in a stably stratified core 4-105410  
 fluid upwelling at core-mantle boundary resolvability for geomag. secular var. obs. 4-105486  
 formation mechanisms, constraints from mantle Mo and W abundance anal. 4-110099  
 geomagnetic dynamo during early Archaean, implications for core size, comp. and convective flow 4-94004  
 geomagnetism and lower mantle convection, implications of mag. reversal time scales 4-85620  
 slow hydromagnetic oscillations in outer core 4-77449  
 hydromagnetic planetary-gravity waves in zonal wind-magnetic shears, instability 4-62940  
 liquid core dynamics, upper limit of undertone periods 4-67174  
 Love numbers partial derivatives for inner core 4-72535  
 pendulum mode oscillation of inner core, seismic data spectra anal. 4-81865  
 perfectly conducting core and secular geomag. var. 4-77446  
 pyrrhotite (Fe<sub>9</sub>S), eqn. of state at Earth core conditions 4-115395  
 South Magnetic Pole, secular motion and core struct. 4-81856  
 structure, dynamics and thermal state, seismic data anal. 4-105483  
 SiO<sub>2</sub>, existence and properties in Earth core 4-110135

**Earth crust**

see also *geology; oceanic crust*

- Aberdeen Newer Gabbros, Scotland, slow post-organic cooling, palaeomagnetic signature 4-77489  
 Adamaoua Plateau, Cameroon, crustal struct. (*French*) 4-94029  
 Adamello complex, N Italy, country rock assimilation into magma body 4-62734  
 Adriatic microplate, margin crustal struct. (*German*) 4-81984  
 Adriatic microplate, struct. and evolution (*Italian*) 4-81983  
 Adriatic region, Mesozoic-Tertiary deform. history 4-100522  
 Adriatic Sea and crustal struct., conf. at Trieste, Italy (September 1983) 4-78027  
 Aeolian Islands, Italy, seismic activity and stress characts. 4-100451  
 Afar nascent passive margin, palaeomag. and geochronological evidence for episodic spreading and rift propag. 4-85655  
 southern Africa, crustal evolution (book) 4-78052  
 northeast Africa, Pan-African crustal accretion 4-77481  
 NE Africa, Proterozoic crustal evolution from model Nd ages 4-89900  
 NW Africa continental margin, geology (book) 4-78059  
 African geology, conf., Nairobi, Kenya (Dec: 1982) 4-73141  
 NW African platform, Aptian-Albian mesohaline facies, an aborted evaporitic basin (*French*) 4-115355  
 African-Adriatic promontory, geological and tectonic anal. (*Italian*) 4-81985

**Earth crust continued**

- Aigurande Plateau, French Massif Central, Pb isotopes indicating Upper Brioverian age (*French*) 4-81877  
 Alabama Appalachians, polyphase Late Palaeozoic deform. 4-105516  
 Alabama Piedmont, USA, amphibolite petrography, geochem. and tectonic significance 4-94024  
 SW Alaska, relations between plate motions and Late Cretaceous to Palaeogene magmatism 4-94131  
 Algerie granite quarry, Massachusetts, USA, in situ rock strain obs. 4-62802  
 S Alpine tectonic deformation (*Italian*) 4-81982  
 Alpine-Himalayan belt, tectonics and seismology 4-62789  
 Alps, crust deep struct. from teleseismic obs. 4-62695  
 E Alps, evolution, plate tectonics modelling 4-100493  
 W Alps, profiles and tectonic struct. 4-85665  
 Amchitka Island, Aleutians, teleseismic obs. and crustal structure 4-94012  
 North America, combined correlation anal. of geophys. fields 4-72541  
 Amur territory, USSR, ring structures of magmatogenic origin spatial distribution 4-115363  
 W Anabar area, USSR, paragenesis of rocks and facies and palaeogeographic features 4-105497  
 Andean conductivity anomaly, effect of depth of non-conducting layer on induced mag. field 4-62668  
 Central Andes, plate tectonics, volcanism and continental crust 4-105530  
 Andes volcanic rock petrogenesis, geochemical considerations 4-62741  
 Antarctic Earth science, conf., Adelaide, Australia (Aug. 1982) 4-78045  
 East Antarctic metamorphic shield, Precambrian geological evolution, review 4-81920  
 N Antarctic Peninsula, evolution of Late Mesozoic sedimentary basins 4-81946  
 Antarctic Peninsula, tectonic evolution of magmatic arc 4-82019  
 Antarctic Peninsula region, age of post-Gondwana calc-alkaline volcanism 4-81947  
 Antarctic sedimentary basins, struct. and morphology 4-81961  
 Antarctica, crust struct. and tectonics from geophys. evidence 4-81957  
 Antarctica, crustal struct. 4-81956  
 West Antarctica, geomag. anomalies and subglacial geology 4-81853  
 Antarctica, gravity and geomagnetic studies between 45 and 65 degrees East 4-81959  
 Antarctica, major structural provinces and metallogenic provinces 4-81951  
 Antarctica, metallogenic provinces 4-81950  
 Antarctica, petroleum prospects and geology and geophysics studies 4-81952  
 Antarctica, position in Gondwana, Palaeozoic orogenic development anal. 4-82022  
 Antarctica between Ellsworth Mts. and Antarctic Peninsula, subglacial morphology 4-81945  
 Antarctica Peninsula, active plate margin geological history 4-82021  
 E Antarctica-W Antarctica boundary region, geology and tectonics 4-81930  
 Appalachian orogen, Alabama, geodynamic transect geology 4-85677  
 Appalachian orogen, N Newfoundland, geotransverse tectonic characts. 4-85668  
 S Appalachian Piedmont, geophysical anomalies along strike rel. to crustal struct. and tectonics 4-93990  
 Southern Appalachian Piedmont, USA, gabbro-metagabbro assoc. geology 4-94025  
 Appalachian Plateau, New York State, USA, foreland deformation 4-67201  
 N Appalachian traverses, Canada, geology and tectonic evolution 4-85675  
 Appalachian-Caledonian orogen, palaeomagnetic evidence against large-scale Carboniferous strike-slip faulting 4-110123  
 Appalachians, orocline hypothesis v. thin skin rotation 4-94070  
 S Appalachians, USA, mafic rock geology, review 4-90319  
 Southern Appalachians, USA, mafic-ultramafic complex geology 4-94027  
 Appin earthquake, 1981 November 15, seismicity and mechanism anal. 4-89880  
 Apuseni Mountains, Cretaceous tectono-magnetic evolution, K-Ar dating 4-77492  
 Arab region, seismology and seismotectonics, summary and future plans 4-110060  
 Arabian platform, regional joint sets as indicators of intraplate processes 4-94132  
 Archaean crustal thicknesses and metamorphic mineral assemblages anal. 4-81896  
 Archaean-Proterozoic boundary, geological characts. 4-82048  
 Pre-Archaeon times, existence of surface water, palaeoclimate and plate tectonics 4-105564  
 NW Argentina, 1200 km magnetotelluric profile 4-85614  
 Armorica, Devonian palaeomagnetic pole, red beds anal. in Spain 4-77503  
 artificial mines, induced stress fields rel. to nature of mining tremors 4-77458  
 Arunta Inlier, Australia, Proterozoic crustal events, Rb-Sr geochronology 4-94034  
 Asal-Ghoubbet rift, Djibouti, Africa, strain accumulation study 4-115380  
 Ashe Metamorphic Suite, N Carolina, USA, metamorphism and tectonic history 4-94022  
 Central Asia, surface relief and orogenesis rel. to lateral inhomogeneities of upper mantle 4-100505  
 Asia-N Pacific transition zone, heat flow and geodynamics 4-81916  
 assimilation of country rock into intruded magma body 4-62734  
 asthenosphere lateral density heterogeneity estimation from geophys. data 4-105500  
 NE Atlantic, seafloor topography of Orphan Knoll 4-62793  
 Atlas Mountains, Morocco, Tertiary and Quaternary volcanism and tectonic events dating 4-100517  
 SE Australia, crustal deformation from geodetic evidence? 4-89871  
 central Australia, crustal struct. and teleseismic travel time anomalies 4-72547  
 Australia, lithosphere, seismic refl. anal. 4-82278  
 Australia-SW Pacific crust-mantle boundary, teleseismic obs. 4-89888  
 Australian Continent, northern margin, rifting and ages of events 4-110125  
 Avalonian terrain of Rhode Island region, USA, geology and tectonic characts. 4-85676  
 W Baikal area, USSR, interruptions in Riphean (Precambrian) sedimentation 4-105494

Earth crust continued

- Baikal megashear, USSR, overthrust struct. form. mechanism 4-100567  
 Baja California, Mexico, geotect. obs. of fault motions 4-72483  
 basement fault reactivation in young fold mountain belts 4-62790  
 eastern Basin Range, USA, intraplate extensional tectonics 4-110109  
 bauxite deposits in S America, Africa, India, formed in Early Tertiary 4-77483  
 Bay of Islands ophiolite complex, Newfoundland, Canada, geology 4-115358  
 Benue Trough, SE Nigeria, tectonics and sedimentation history 4-77479  
 Benue-Chad Basin, Cretaceous rift valley system 4-115371  
 Betic Cordilleras, S Spain, wrenching tectonics of external zone 4-105533  
 block rotation by strike-slip faulting, geophys. evidence 4-115382  
 Blue Ridge Province, N Carolina, USA, compositional layering of Precambrian rocks 4-67188  
 Brese graben, Vignoble, France, overlapping by Jura formations 4-89909  
 Briançonnais Carboniferous, subsidence of NS groove (French) 4-77473  
 Bristol Channel area, SW Britain, seismic study of deep geological struct. 4-110141  
 Britain, provenance and crustal residence ages of sediments in rel. to palaeogeographic reconstructions 4-89895  
 British Tertiary Volcanic Province, crustal contamination and granite problem 4-62745  
 Buchan area, Scotland, Caledonides, major shear zones and autochthonous Dalradian 4-110143  
 Builth Volcanic Series, Wales, Permo-Carboniferous and Ordovician palaeomagnetic remanence and pole position var. 4-110038  
 Bulgaria, fault systems and earthquake foci migration (Russian) 4-62708  
 Burma and surrounding regions, active faulting and tectonics 4-81989  
 Caledonian intrusion of Scotland and N England, geochem. and magma sources 4-62743  
 central California, correl. between geological record and computed plate motions 4-94127  
 S California, fault friction, regional stress, coupling to mantle 4-81991  
 S California, USA, Pn velocities and crust and mantle struct. 4-81861  
 S California, USA, regional deformation near Palmdale 4-72562  
 Campanian Apennines, Italy, neotectonics and crust struct. (French) 4-81878  
 Canada, geothermal meas. in N British Columbia and S Yukon Territory 4-105474  
 Canada, Lithoprobe seismic and drilling project to study crust 4-115576  
 Canning Basin, Western Australia, faults, temp. and subsidence, seismic geohistory anal. 4-100772  
 Cantal, France, coexisting alkaline magma series, mantle material characts. and crustal contamination 4-110098  
 Cape Fold Belt, South Africa, geodynamics, review 4-85660  
 Carpathian arc region, seismic wave velocity struct. 4-105467  
 Carrara Range region, N.T., Australia, preserved Proterozoic landforms 4-94038  
 Caucasus Alpine cycle, geology, crustal movements and magmatism evolution 4-85666  
 Chars sheet nappe zone, Irtys-Zaisan fold region, tectonic struct. 4-77494  
 Charlevoix zone, St. Lawrence Valley Canada. Seismicity and faulting 4-105436  
 Chattolance Baltimore Gneiss Dome, Maryland, USA, gravity survey 4-81834  
 chemical composition of continental crust, empirical estimate of elemental composition 4-105491  
 NW China, magnetotelluric studies of He-Xi Corridor (Chinese) 4-85611  
 China, tectonics of shear fracture zones 4-110108  
 N China Plain, seismic velocity struct. of lower lithosphere (Chinese) 4-62673  
 Chuckanut Formation, NW Washington, USA, stratigraphy, age and palaeogeography 4-62727  
 Church Bay Anticline, Co. Cork, Ireland, tectonics and cleavage geometry 4-67185  
 coal measure rocks of Pennsylvania, USA, rock elec. props. and radar attenuation props. 4-72582  
 Coalinga, California, surface folding and seismic potential 4-110089  
 Colombia-Ecuador coast, 1942, 1958, 1979 earthquakes, seismicity and rupture models 4-105435  
 Columbia Plateau, Washington, palaeomag. study of post 12 Myr clockwise rot. 4-94130  
 computational seismology, workshop, Glenenden Beach, OR, USA, (March 1981) 4-67854  
 conference on arc volcanism at Tokyo and Hakone, Japan (August-September 1981) 4-95032  
 conference on earthquakes at Varenna, Italy (June-July 1982) 4-67871  
 conference on geodesy, at Hamburg, West Germany (August 1983) 4-86111  
 conglomerate pebble previous strain history from pebble microstructure 4-62813  
 continental arches in eastern USSR, petrochemical features of basaltoid lavas 4-100563  
 continental crust, Phanerozoic addition rates rel. to crustal growth 4-94044  
 continental lithosphere, flexural models based on long-term erosional decay of topography 4-67189  
 continental lithosphere, flexure beneath Apennine and Carpathian foredeep basin 4-72563  
 continental margins and extent and number of continents 4-110111  
 continental tectonic geology, use of earthquake studies 4-72552  
 continental tectonics correl. with plate motions, Laramide orogeny to Basin and Range province 4-94062  
 continents evolution 4-81897  
 cratonization of continental crust throughout geologic time 4-105493  
 Cretaceous dyke rocks, Pyrenees, geochemical characts. and relation to Siliceous Houiller (French) 4-82043  
 Middle Cretaceous formation, polyphased synsedimentary tectonic evidence (French) 4-77501  
 Crimean continental slope, geology of lower Cretaceous dredged rocks 4-94052  
 Daldyn kimberlite field, USSR, struct., comp. and principal stages of form. 4-100565  
 Damara orogen, model 4-85661  
 Deccan volcanism, evolution and surface heat flow 4-81967  
 deep crustal fault zones, seismic reflectivity 4-85634  
 deep fault zones, fluid regimes 4-94072

Earth crust continued

- deep-seated diapirism theory as alternative to tectonics (Russian) 4-81894  
 Deer Lake basin, Newfoundland, Canada, gravity and magnetic interpretation 4-62653  
 Deer Lake Group, Newfoundland, Early Carboniferous palaeomagnetism, tectonic implications 4-110037  
 deformation and Earth natural oscills., meas. with laser deformographs 4-62969  
 deformation assoc. with earthquake cycle, models of viscoelastic flow in asthenosphere 4-110068  
 deformation of foreland fold and thrust belts, pore water circulation effects 4-94071  
 deformation of rock masses of near-surface crust, tensors 4-77497  
 Demon Fault, NSW, Australia, transcurrent fault dextral motion 4-62730  
 density model, effects of thermodynamic conditions and density depend. on seismic vel. 4-77496  
 Dinantian anhydritic form., Hercynian domain, tectonics, paleogeography (French) 4-82044  
 displacement and strain calc. from survey meas. 4-62752  
 Donnybrook Anticline, Australia, seismic-gravity interpretation and tectonic settings 4-94121  
 Doppler satellite system for Earth surface position meas. 4-63001  
 earthquake prediction model and crustal mechanisms 4-72528  
 earthquake rupture model (Chinese) 4-110046  
 earthquake source theory, review 4-72519  
 earthquakes, seismic moments, rupture lengths, stress drops and magnitudes, intercomparisons (Chinese) 4-110048  
 southwest Egypt, geology of migmatite and metamorphic units 4-77480  
 Egypt, hydrocarbon generation and prospects in Western Desert 4-77482  
 Egypt and Sudan, bedrock below sand layer in desert, satellite radar obs. 4-100793  
 El Asnam, earthquake, Algeria, 1980 October 10, rupture process anal. 4-77467  
 Ellsworth Mts., W Antarctica, structural and metamorphic history 4-81944  
 EM induction sounding, Frechet derivatives 4-85622  
 Enderby Land, Antarctica, geological history of Napier Complex 4-81921  
 Enderby land, Antarctica, metamorphism of Napier Province 4-81924  
 Eurasian continent, earthquake depth distrib., crust struct., tectonics 4-72503  
 Central Europe, Cretaceous apparent polar wander path rel. to palaeomag. study of Hoheifel Tertiary volcanics 4-105419  
 Europe, central and eastern regions, earthquake sources, distrib. and characts. 4-62707  
 evolution of structures formed by vertical movements, mathematical model 4-100504  
 Eye-Dasha pluton, Ontario, Canada, geology of radioactive waste disposal site 4-81919  
 Eyre Peninsula, South Australia, magnetotelluric obs. indicating deep shear zone 4-94006  
 Farallon plate subduction beneath North America, determ. from relative plate motions 4-94061  
 Fari'a Anticline, structural evolution in Central Israel 4-94068  
 fault asperities inferred from seismic body waves 4-72522  
 fault coherent and incoherent rupture, seismic directivity 4-81872  
 fault model of earthquake occurrence, influence of asperities and barriers 4-110083  
 fault zone, cutoff depth for microseismic activity 4-110121  
 fault zone modifications due to fracturing, water circulation and chem. alteration 4-110082  
 Fennoscandian uplift and glacial isostasy, gravity and seismicity anal. 4-81994  
 Forsyth area, Queensland, Australia, heavy metal mineralisation survey by helicopter 4-94037  
 Freemans Cove volcanic suite, Bathurst Island, petrochemistry and tectonic setting rel. to rifting 4-94124  
 French Alps (Briançonnais zone), high press.-low temp. metamorphic evolution 4-81888  
 Fyfe Hills-Khmara Bay region of Enderby Land, Antarctica, geology 4-81922  
 Gangdese plutonism, Lhasa-Xigaze region, Tibet, U-Pb geochronology and assoc. tectonics 4-110097  
 Gavarnie nappe, France, struct. and thrust sheets emplacement ages 4-105470  
 Gebel El Mueilha, Egyptian Central Eastern Desert, crust radioactivity and lineaments 4-77486  
 geodynamical processes in earthquake focal regions, symposium, Potsdam, Germany (1981 November 2 to 7) 4-73142  
 geophysical predictions (book) 4-90308  
 George V continental margin, Antarctica, marine geology and glaciology 4-82035  
 global seismicity and plate motion 4-72533  
 Gondwana reconstruction between Antarctica and South Africa 4-82023  
 Gorda plate subduction beneath Cape Mendocino, California, seismic evidence 4-105519  
 Gran Paradiso, Italian Alps, tectonometric shear folds (French) 4-82045  
 granitoid magma origin and influence of mantle 4-105498  
 gravity and geomagnetic anomalies due to subsurface struct., computation method 4-85604  
 gravity field representation by finite grid of mascons, approx. 4-93995  
 Great Basin province, USA, regional tectonics during Quaternary 4-110120  
 Greece, Atalanti region, microgravity network, crustal movements and precursors to earthquakes 4-77440  
 SW Greenland, Archaean crust evolution, review based on Buksefjorden region 4-81899  
 Guadeloupe Archipelago, Neogene tectonic evolution of limestone islands (French) 4-115374  
 Gulf of Aden, lithosphere flexure and isostatic compensation, bathymetry and gravity profiles anal. 4-105484  
 Gulf of Aqaba earthquake swarm, 1983 January to April, tectonic implications 4-110066  
 Gulf of Corinth, 1981 February-March earthquake sequence, tectonic features and stress var. 4-105429  
 Gulf of Taranto, seismic profiling of crust and sediments 4-81858  
 Gundahil Complex, New England Fold Belt, Australia, tectonic melange form. 4-105471  
 helvetic thrust belt of Switzerland, crustal strain partitioning 4-67184

## Earth crust continued

- Hercynian Europe, Late Palaeozoic plate and intraplate processes 4-105532
- High Himalaya-Yarlung Zangbo Jiangbo suture unit, upper lithosphere seismic struct. 4-100489
- Highland Border Fracture Zone, Scotland, ophiolite rock tectonic history 4-89904
- Himachal Himalayas, India, foreshock activity migration rel. to presence of micro tear faults 4-94019
- Himalaya, earthquake activity, mechanisms and plate tectonics 4-62715
- Himalaya, Moho tracing from P-wave propag. 4-100490
- Himalaya, tectonic evolution 4-81993
- NW Himalaya (N Pakistan),  $^{39}\text{Ar}/^{40}\text{Ar}$  ages of Alpine tectonometamorphic events 4-94043
- Himalaya zone of crustal interaction, explosion seismology obs. 4-100491
- Himalayan arc, continental subduction of central and NW portions 4-62774
- Himalayan collision zone, seismotectonics 4-85643
- N Himalayan foredeep, sequential structural disruption in late Cainozoic 4-115383
- Himalayan front, continental subduction 4-81995
- Himalayas, Pamirs, Karakorum and Tien Shan, lithospheric struct. and orogenesis 4-62718
- Himalayas (Toksotgul-Srinagar profile) crust struct. from seismic sounding obs. 4-62678
- Himalayas of USSR, crust struct. from explosion seismology obs. 4-62682
- Hungary, scalar audio-magnetotelluric observations of crust 4-100440
- Ibaraki Prefecture, Japan, offshore region, seismicity and seismic wave characts. 4-81870
- Ibaraki Prefecture, Japan, Philippine and Eurasian plates seismic coupling and earthquake parameters 4-81868
- Iberian plate position in Lower Cretaceous, plate tectonic reconstruction (French) 4-81978
- Ibero-Armorian Variscan arc, W Europe, geotraverses characts. 4-85664
- Iceland, anomalous focal mechanisms and tensile crack form. on accreting plate boundary 4-94015
- Imperial Valley, California, seismic refr. and gravity survey 4-85644
- India, lithosphere, elec. cond. struct. and magnetomet. anal. 4-81850
- India, Phanerozoic palaeomagnetism, implications for India-Asia collision 4-81997
- Indian lithosphere, gravity anomalies and compensation 4-81901
- Indian Shield, thermal evolution and mantle thermal props. 4-81906
- Indian shield and Himalaya, lithosphere mag. anomalies 4-81849
- S Indian Shield thermo-mechanical struct. rel. to Precambrian basin form. 4-81898
- Indian teleseismic observations and crust and mantle struct. 4-62697
- Indian/Pacific plate boundary, microseismicity and tectonics in New Zealand 4-67180
- Indo-Asian plate convergence and triangulation surveys anal., errors determ. 4-62788
- E Indonesia, Cenozoic tectonic devel. 4-82011
- Indonesia, earthquake stress directions 4-82013
- E Indonesia collision zone, tectonic, bathymetric, seismic, volcanic and palaeomagnetic features 4-82012
- Indore-Khandwa profile, Narmada basin, crust seismic struct. and microearthquake locations 4-67198
- International Karakoram Project, crust deform. and surveying 4-62662
- NE Iowa, USA, geology and erosion of Palaeozoic Plateau area 4-77491
- Iowa, USA, geology of Driftless Area, conf., Decorah, IA, USA (April 1983) 4-73149
- SE Iran, Golbaf-Sirch 1981 earthquakes, faulting and earthquake characts. 4-77465
- W Irian Jaya, oblique plate convergence and resulting crust struct. 4-89908
- Irtysk lineament, USSR, structural metamorphic zoning 4-115362
- N Israel, block rotation by strike-slip faulting, geophys. evidence 4-115382
- Italian region, seismicity and tectonics 4-72553
- Italy continental shelf next to Tyrrhenian Sea, tectonic struct. from seismic obs. 4-115351
- Ivrea body and Insubric Line, Alps, tectonic anal. 4-100494
- Ivrea Zone, NW Italy, amphibolites, chem. comp., petrogenesis and tectonic anal. 4-110146
- Japan, cross sections of earthquakes, focal mechanism and tectonic features 4-81917
- SW Japan, crust struct. and Mesozoic orogeny (French) 4-115373
- Japan, oblique subduction and strike-slip tectonics 4-82008
- Japan, seismic hazard anal., use of quaternary faulting meas. 4-105440
- NE Japan, vertical crustal movements since Middle Miocene 4-82009
- Jemez volcanic zone, New Mexico, detailed magnetotelluric and audio-magnetotelluric study 4-85619
- Jordan-Dead Sea Rift, horizontal crustal movements detection using MA 100 Tellurometer 4-94252
- Jurassic volcanism, Aspro Vrissi unit, Greek Macedonia (French) 4-77499
- S Kanto District, Honshu, Japan strain buildup after 1923 Kanto earthquake 4-85630
- Kanto District, Japan, earthquake generating stresses 4-72496
- Kanto Mountains, SW Japan, pre-Cretaceous tangential structs. (French) 4-81979
- Kanto-Tokai area, Japan, hydraulic fracturing stress meas. and seismic activity 4-81908
- Kanto-Tokai area, Japan, stress anal. and plate tectonics 4-81909
- Karakoram region, microearthquake survey and crustal activity 4-62716
- Karakoram region, plate motion and stress field, seismic anal. 4-62791
- South Karakoram synclinalium, geology and tectonic development 4-62723
- W Karakorum, Pakistan, geological struct. and tectonics 4-62722
- Karakorum and Kashmir Himalayas, geology and tectonics 4-62720
- Karakorum Range, crust struct. from seismic sounding obs. 4-62679
- Central Karelia, USSR, magnetotelluric sounding of Baltic Shield area 4-85612
- Kashmir Himalayas, crust struct. from deep seismic sounding obs. 4-62680
- western Kenya, kimberlite pipes in greenstone belt 4-77444
- Kofu Basin, Honshu, earthquakes seismic intensity, implications for plate interactions 4-105534
- Kohistan island arc, N Pakistan, geological evolution 4-62721
- Kohistan region, Pakistan, earthquakes, sources anal. and tectonics 4-62717

## Earth crust continued

- komatiite magmas, petrogenesis and evolution 4-100564
- S Kootenay Arc, SE British Columbia, geochronology and tectonic implications of magmatism and metamorphism 4-105473
- Kuril-Kamchatka deep-sea trench, tectonics, magnetic anomalies, bathymetry and seismic struct. 4-82006
- Kuznets Basin, USSR, linear and intersecting folding 4-77495
- Labrador, Canada, Grenville lithotectonic regions and with Sweden 4-115349
- Lachlan Fold Belt, SE Australia, source rocks of granites 4-62742
- Lake Malawi, Africa, structural evolution 4-62732
- Lakejford Nappe, Finnmark, finite strain patterns generation and modification by progressive thrust faulting 4-110031
- palaeo-latitude determination technique using vertical drill core samples 4-100821
- Lebanon-Syria area, geologic interpretation of SIR-A radar obs. from space (French) 4-62965
- lithosphere, tectonic stress origin 4-81895
- lithosphere extension over continental margins, initial stretching phase, thermal consequences 4-105485
- lithosphere stress caused by topography and its isostatic compensation, appl. to Apennines 4-72554
- lithospheric flexure due to thrust loading, sedimentologic effects 4-100532
- lithospheric plate motion, load induced cyclic volume changes 4-62782
- Los Angeles region, California, Earth model regional deform., seismic, tectonic and geodetic meas. 4-110032
- Louisiana continental shelf, USA, gas deposits extent 4-110103
- Louisiana-Mississippi, USA, modern uparching of coastal plain 4-115381
- Lutzw-Holm Bay, Antarctica, gravity, geomag. intensity anomalies and crust tilt 4-81841
- Lutzw-Holm Bay region, E Antarctica, tectonic and metamorphic history 4-81926
- Lutzw-Holm Bay region, E Antarctica, tectonic history and relevance to Gondwanaland 4-82015
- magma chamber evolution fluid dynamics, review 4-58606
- magma chamber location techniques, review 4-58605
- magma genesis, geochemical indications 4-62736
- magma source identification isotope geochemistry, review 4-58607
- Mahabaleshwar area, Deccan Traps, India, flood basalt, magma origin 4-62738
- Maine Appalachians, USA, Acadian synorogenic mafic intrusions 4-94026
- Malaita, Solomon Islands, isotope geochemistry of volcanics and xenoliths and mantle stratigraphy 4-72543
- Marie Byrd Land, Antarctica, Cretaceous volcanic rocks, palaeomagnetism and palaeopole position anal. 4-81963
- Marie Byrd Land, Antarctica, glacial and tectonic events, chronology recorded by rocks 4-82024
- S McArthur Basin, Australia, crustal struct. from deep seismic sounding 4-94030
- McMurdo Sound area of Antarctica, crust and upper mantle struct. 4-81941
- Mediterranean, continental margin of Israel, bathymetry, crust struct., seafloor topography 4-72567
- Western Melville Peninsula, NW Territories, Canada, Precambrian geology 4-78068
- Mesozoic geology of the world, book 4-73187
- Messinian compression, tectonics, Rif, Morocco (French) 4-77500
- meta-ophiolitic zone of Hokkaido, struct., right lateral strike slip movement (French) 4-81976
- Michipicoten plutonic-volcanic terrain, Ontario, volcanism, tectonics evolution 4-94059
- microstructures and fabrics due to rock deformation, conf., Zurich, Switzerland (August-September 1982) 4-63382
- microwave dielectric constants meas. method for substances of Earth's surface (Chinese) 4-77638
- Minnelusa sands hydrocarbon deposits, Wyoming, USA, seismic exploration 4-109715
- Miramichi earthquake, New Brunswick, Canada, 1982 January 9, after-shocks characts. and tectonics 4-105438
- Miura and Boso peninsulas, Kanto, Japan, geodetic survey obs. (Japanese) 4-72481
- Mizuho Plateau, E Antarctica, seismic sounding of crust struct. 4-81874
- Moine thrust zone, NW Scotland, Assynt region tectonics 4-67186
- Montana-Idaho region, crustal struct., from reversed seismic refr. line meas. 4-100500
- Montenegro region (Yugoslavia), effects of freq., depth and time windowing on seismic Q of lithosphere 4-105461
- Morrow formation, New Mexico, USA, seismic profiling of natural gas deposits 4-100457
- Mount Isa, Queensland, geology of Proterozoic rift zone and implications for mineralisation 4-94117
- mountain isostatic equilibrium calc. method 4-105529
- Mozambique Belt, N Tanzania, petrochemistry of geotectonic evolution 4-77475
- Mugodzhir region of Urals, parallel dike intrusion, rock magnetism study 4-100503
- Murray Fault Zone tectonics, implication of Southern Province cross sections, Lake Huron 4-94039
- Nanga Parbat area of Himalayas, crust struct. from DSS obs. 4-62687
- Napier and Rayner complexes, Enderby Land, Antarctica, metamorphism and tectonism 4-81923
- west-central Nevada, palaeomag. assessment of oroflexural deform. 4-94128
- New Madrid seismic zone, crustal vel. structure 4-94049
- New Zealand, horizontal kinematics and seismic activity 4-82014
- S New Zealand, overriding of Indian-Antarctica ridge rel. to migration of Late Cainozoic volcanism 4-94082
- New Zealand, subduction regression and volcanism oceanward migration 4-85657
- central Nigeria, geological interpretation of Landsat images 4-77478
- SE Nigeria, hydrology and chemistry of water resources of Agwata area 4-115466
- SW Nigeria, metavolcano-sedimentary sequence east of Ife and Ilesha and metal deposits 4-115353
- southeast Nigeria, Rb-Sr dating and age of Pan-African orogenesis 4-77485
- eastern Nigeria, upper mantle character inferred from ultramafic xenoliths 4-77484
- Niigata earthquake, Japan, 1964 June 16, fault model 4-72512

## Earth crust continued

- Ninmaroo Formation, Australia, late diagenetic history and related tectonics 4-94120
- Norilsk area, NW Siberian platform, comp. and age of crystalline basement and overlying sedimentary rocks 4-100514
- SW North America, rel. to mid-Tertiary extensional orogeny 4-94129
- North Himalayan Belt, Tibet, metamorphism and deformation 4-110101
- North Sea, geoid, gravity measurement anomalies and SEASAT sea surface heights 4-81840
- North Sea gravity field observations 4-81839
- North Sea near Denmark and Norway, crust salt tectonic structures 4-105505
- Northwest Territories, Canada, palaeomag. positions of continental plates during Early Proterozoic 4-105407
- Norwegian Caledonides, geodynamic implications of coesite in clinopyroxene 4-105560
- Norwegian-Danish Basin of North Sea, salt dome and other tectonic struts. 4-105505
- NTS explosions, tectonic release, effect on short-period P-waves amplitude patterns 4-110050
- number and extent of continents 4-110111
- northeast Nyanza rift valley, Kenya, genesis and tectonics 4-77502
- Oklo reactor charact. (book) 4-78049
- Olgyidakh River-Mirny-Lenski profile, USSR, deep seismic sounding studies 4-100513
- Ometepe, Guerrero, Mexico, 1982 June 7 earthquake doublet anal. and tectonic setting 4-72517
- Omsukchan basin, NE, USSR, struct. and geological nature 4-115361
- NW Ontario, Canada, gravity profile across English River Subprovince 4-72482
- Ontong Java Plateau, isotope geochem. and stratigraphy of mantle 4-72543
- ophiolite rock origin, importance of magma in forearcs 4-105503
- Ordes Block, N China, crust stress field and intraplate tectonics (*Chinese*) 4-85638
- Oregon Cascades, USA, P-wave velocity model 4-85632
- W Oregon-Washington, volcano-tectonic evolution rel. to Cainozoic plate motions 4-94065
- orogenic belt profiles (book) 4-82602
- orogenic granulites, French Hercynian, typology (*French*) 4-77472
- orogeny, theories and petrology (book) 4-63430
- Orville Coast and E Ellsworth Land, Antarctica, geology and plate tectonics 4-82017
- P-wave scattering beneath SCARLET, S California 4-105451
- SW Pacific porphyry Cu deposits, geochem. of submarine formation and uplift 4-81887
- W Pacific region, tectonic charact. from seismicity and focal mechanism anal. 4-82000
- Pakistan, lithosphere evolution 4-81903
- Pakistan to Soviet Union triangulation connection, error anal. and plate motion 4-62661
- Pamir and Tien-Shan, Quaternary tectonics and deep struct. 4-62784
- Pamir-Himalaya struct. from Karakul Lake explosion seismic obs. 4-62681
- Pamirs, crust struct. from seismic sounding obs. 4-62678
- Pamirs and S Tien Shan, crust struct. and tectonics 4-62719
- Pamirs region, crust struct. from seismic obs. 4-62683
- Pamirs Syntaxis poorly correlated with surface geology and orogenic belts 4-62776
- Pamirs-Himalayas syntaxis, geological lineaments seen by LANDSAT 4-62724
- Pamirs-Hindu Kush region, crust struct. from obs. of earthquakes 4-62685
- Pamirs-Hindu Kush region, tectonic features from seismic obs. 4-62771
- Pangano Nunatak and Hart Hills area, Antarctica geology 4-81943
- Pannonian Basin, Hungary, modelling of elec. cond. anomalies 4-85613
- Pannonian Basin and surrounding mountain belts, neotectonics 4-100492
- Papuan Fold Belt, seismic zone charact. and tectonic activity 4-94008
- Patia Valley, SW Colombia, geochronology of basic rocks and emplacement 4-105506
- S Peru, Benioff zone struct., earthquakes epicentres positions anal. 4-105518
- S Peru, Pb isotope study of magma-crust interaction in Andes 4-105475
- Phyllites nappes, S Peloponnese, Greece, Alpine metamorphism and deform. geodynamic implications 4-62731
- Pilbara craton, Australia, lithosphere seismic vel.-depth models 4-94031
- plate flexure problems, relation between two-dimensional and axisymmetric loads 4-105528
- plate tectonics and continents (book) 4-73182
- Port Hacking estuary, Sydney, Australia, bedrock depth and sediment geology 4-77498
- Portuguese margin, diapiric intrusion of Caldas da Rainha and Jurassic halokinetic movement (*French*) 4-105559
- postglacial rebound, gravity anomalies Lagoes obs., lower mantle effective viscosity determ. 4-85641
- postseismic deformation due to subcrustal viscoelastic relaxation following dip-slip earthquakes 4-94080
- Precambrian granulite rocks, origin of magma 4-62737
- Prince Olav Coast, Earth Antarctica, geology and petrology 4-81925
- Princess Elizabeth Land, Antarctica, Archaean and Late Proterozoic rocks extent and crust struct. 4-89889
- N Pyrenean mag. anomaly and crustal current channel nature 4-100433
- Pyrenees, crust deep struct. from teleseismic obs. 4-62695
- Quebec Appalachians, reflected turbidity currents seen in Ordovician rocks 4-115359
- Quebec Appalachians, seismic profile, gravity and crust struct. 4-72502
- Queen Maud Batholith, central Transantarctic Mts., geology and Ross Orogeny 4-81936
- Queen Maud Land, Antarctica, Sr isotope studies of Ahlmann Ridge and Amundagstoppane 4-81927
- Querigut, France, granite-granodiorite complex genesis, recycling processes, Nd-Sr isotopic systematics 4-110096
- Rainy Lake region, Ontario, Canada, geochem. of mantle-derived Archaean rocks 4-94051
- Rajasthan, India, Proterozoic Delhi and pre-Delhi rock groups. struct. history 4-82050
- Ramshorn Peak area, Idaho-Wyoming thrust belt, United States, fault related folding 4-105517
- recycling of crustal material, sedimentary Hf/rare earth elements fractionation anal. 4-110100

## Earth crust continued

- recycling through mantle, mean life of continents is not constrained by Nd and Hf isotopes 4-94047
- regional metamorphism and deformation, fluid pressures 4-94048
- rheology, isostasy and eustasy conf., Stockholm (July-August 1977) 4-101580
- Riddleville Basin, tectonic struct., seismic data anal. 4-100531
- ring structures of magmatogenic origin spatial distribution, analysis methods 4-115363
- ring-like structures on planetary surfaces, inherited from previous tectonic processes 4-110550
- rock porosity meas. technique for in-situ rocks, EM tomography method 4-110292
- rock props. influenced by water, conf., Carmel, California, USA (June 1982) 4-90289
- E Rouergue, French Massif Central, thrust tectonics and metamorphics (*French*) 4-81876
- rupture complexity, effect on source size estimates 4-85625
- Russian platform, seismic boundary velocities of basement 4-100466
- San Andreas fault near Monarch Peak, California, creep rate geodetic meas. 4-110116
- San Andreas fault zone, California, USA, crust struct. model 4-110122
- San Andreas fault zone materials, California, USA, geological model 4-110110
- Sardinia, Mesozoic-Cenozoic struct. evolution and geodynamic implications (*French*) 4-105524
- NW Sardinia, Pyrenean thrust faulting (*French*) 4-115372
- Saskatchewan, crustal elec. cond. meas. rel. to Proterozoic plate margin 4-105406
- Saudi Arabia, seismic velocity struct. of lower lithosphere (*Chinese*) 4-62673
- Scandinavian Caledonides, geotraverse charact. 4-85663
- Scotia arc tectonic evolution, review 4-82018
- Sea of Okhotsk, plate tectonics and geology 4-82004
- Seal Nunataks, W Antarctica, active volcanism and heat flow 4-81971
- seismic rupture zones, stress redistrib. rel. to earthquake triggering during preparation for great earthquakes 4-100464
- seismic slow source processes, fault charact. 4-72526
- seismic sounding of crust, discrepancies between surface and borehole methods 4-100467
- seismic structure over ocean-continent margins, US modeling 4-77468
- Setouchi volcanic belt, Japan, high magnesian andesites prod. rel. to Shikoku Basin evolution 4-81970
- Seve-Koli Nappe Complex of Norway and Sweden, strain discontinuities 4-67187
- Seychelles, granites and xenoliths, dating and parental magma mantle origin with crustal interactions 4-110102
- Shackleton Range, Antarctica, tectonics and Precambrian struct. stages 4-81938
- Shackleton Range, Coats Land, Antarctica, Precambrian and Early Proterozoic history 4-81939
- shale diapirism in accretionary terrains, role in melange prod. 4-72586
- Shelleng-Numan area, Nigeria, geology remote sensing by radar 4-100483
- Shikine Island, Japan, Late Holocene uplift and seismic activity 4-81910
- Shizuoka-Seibu, Japan, stress conditions and source charact. assoc. with 1981 January 16 earthquake 4-105437
- shorelines and isostasy (book) 4-67903
- short period seismology, Earth structure modeling 4-72505
- SE Siberia, Early Precambrian crustal development, role of endogenous processes 4-85667
- W Siberia, EM core sounding rel. to hydrocarbon deposits 4-100448
- Siberia, lead ore deposits, Pb isotope study 4-105499
- Western Siberian Platform, formation of crustal arches and megaswells 4-105501
- W Siberian Platform, USSR, salt deposit distrib. 4-105496
- Singhbum area, India, gravity field, geology, tectonic history 4-89907
- small local earthquake in randomly inhomogeneous lithosphere, seismograms, attenuation and envelope form 4-85627
- Snake River Plain, Idaho, USA, origin of flood basalts 4-62739
- Snake River Plain-Yellowstone volcanic system, crust and upper mantle seismic struct. 4-81904
- Soufriere, Guadeloupe, faulting and stress (*French*) 4-105525
- South China Sea, crustal struct. from seismic refl. study (*Chinese*) 4-85639
- Southern Province, Lake Huron, regional cross section, implications for Murray Fault Zone tectonics 4-94039
- space/airborne laser ranging system for geodesy and crust deform. anal. 4-110324
- statistical tests of additional plate boundaries from plate motion inversions 4-110117
- stochastic slip-predictable model for earthquake occurrences 4-105442
- stress concentrations and fracture processes, theory of earthquake premonitory phenomena 4-77459
- stress drops and seismic radiated energy 4-105427
- stress field changes due to hydraulic pressure applied to a borehole (*Chinese*) 4-85678
- stress measurement, appl. of fracture mechanics to hydraulic fracturing stress meas. 4-77509
- structure inferred from surface seismic waves 4-72525
- subcrustal layer density nonuniformities from seismic data, for USSR 4-100502
- subducting lithospheric slab, interaction with chemical or phase boundary 4-94073
- subducting slabs, stress and earthquakes distrib. with depth 4-105522
- subducting slabs stress, earthquakes 4-77466
- northwest Sudan, geology of migmatitic and metamorphic units 4-77480
- Sudbury Basin, meteorite impact site in Ontario, Canada 4-115405
- surface deformation approximation from long buried kinked crack or intrusive body, simple method 4-94283
- surface deformation from buried strike-slip fault or shear crack 4-110092
- surface displacement patterns associated with asthenospheric stress relaxation following major underthrust earthquakes 4-81907
- survey techniques for moving terrain, appl. to glaciology and tectonics 4-63000
- Svalbard Archipelago, palaeomagnetism of late Mesozoic dolerite sills rel. to microplate model 4-110040
- Taiwan, tectonic evolution 4-82010
- Tanna fault, Izu, Japan, trenching study of previous fault activity 4-105445
- Tarr Complex, Sinai Peninsula, folding, thrusts and melanges 4-77487

## Earth crust continued

- Tasman orogen, Australia, fault struct. 4-85659  
 tectonic deformation quantification, method for given faulted volume (French) 4-105556  
 tectonic displacement, topographic amplification, implications for geodetic meas. of strain changes 4-85642  
 tectonic stress, correl. with groundwater discharge and precipitation 4-81998  
 tectonic stresses rel. to remagnetisation in diabase dykes, evidence from mag. susceptibility anisotropy data 4-94088  
 tectonics, mechanical modelling, similarity criteria use 4-100533  
 Tethys, European margin, distensional movements during Jurassic. (French) 4-115354  
 Thorsmork ignimbrite of S Iceland, geology of volcanic deposits 4-62763  
 thrust belt transport calculation 4-62786  
 thrust tectonics, mechanistic view from West and Central Alps 4-94057  
 Tibet, crust struct. from PL seismic propagation 4-85633  
 Tibetan plateau, model of neotectonics 4-94066  
 Tien Shan, USSR, palutimite rebedd formations of intermontaine basins 4-115364  
 tilt determ. from US levelling data base, characts. 4-110033  
 Togo, magnetite and haematite mineralisation of atacorian series rocks (French) 4-77477  
 Tokai region, Japan, predicted earthquake, corresponding mantle, tectonic, thermal and seismic features 4-81873  
 Tokai region, Japan, vertical crustal movements and tectonic stress, levelling data anal. 4-81999  
 Transantarctic Mountains, uplift due to E Antarctica overriding W Antarctica anomalously hot asthenosphere 4-85656  
 Earth Transbaikial, USSR, injection relief structures 4-115360  
 transition zones to oceanic crust, struct. and evolution 4-81992  
 Trinity peridotite, California, USA, Nd-Sr isotope study and mantle evolution 4-89890  
 Umbrian Maiolica Formation, Italy, palaeomagnetic and biostratigraphical study 4-105408  
 Umnak Island, Aleutians, Alaska, geology and geochronology 4-72537  
 W United States, Mesozoic struts. in western Cordillera rel. to kinematics of plate convergence 4-94064  
 NW United States, seismicity assoc. with Juan de Fuca subduction zone 4-110055  
 W United States, tectonic reconstructions from palaeomag. results from Sierra Nevada 4-93998  
 SW United States, thermal regime of lithosphere 4-94058  
 Uppington Geotraverse, South Africa, tectonic features 4-85662  
 Urukawa-Oki earthquake, Hokkaido, 1982 March 21, aftershock distrib. determ. from ocean bottom seismograph and land obs. 4-105452  
 western USA, origin of Mesozoic and Tertiary granitic rocks 4-62744  
 USSR Far East, mountain areas isostatic equilibrium 4-105529  
 Vendee eclogites, France, tectonic dispersion during continent-continent collisions (French) 4-67214  
 N Venezuela, Bocono-Moron-El Pilar fault and basin formation 4-110119  
 Venezuela, Margarita Island, kinematic emplacement of Cerro Matasiete unit (French) 4-115375  
 N Vermont, USA, metamorphic schists of Ordovician and Devonian age 4-94023  
 Vermont and Massachusetts, USA, tectonic emplacement of pre-Silurian eugeoclinal belt 4-94028  
 Vestfold Block, E Antarctica, Sr-Nd isotopes, lithology and crust evolution 4-81929  
 N Victoria Land, Antarctica, age of Bowers Supergroup 4-81933  
 N Victoria Land, Antarctica, airborne gamma-ray survey 4-81953  
 N Victoria Land, Antarctica, geochemistry of Cambrian volcanics to Early Palaeozoic tectonic evolution 4-67215  
 N Victoria Land, Antarctica, geology of pre-Beacon bedrocks 4-81931  
 S Victoria Land, Antarctica, granite geology and orogenies 4-81935  
 N Victoria Land, Antarctica, tectonics of Robertson Bay Group deformations 4-81932  
 N Victoria Land, post-Ross orogeny cratonisation 4-81934  
 Villefranche-de-Rouergue fault, France, Tertiary sedimentary deposits evidence for fault motion (French) 4-100482  
 Wadi Kid metamorphic complex, SE Sinai, stratigraphy and tectonic history 4-72540  
 Wadi Natash Volcanic series, Eastern Desert, Egypt, geology and geochemistry 4-115352  
 Wasatch Front, Utah, horizontal strain, geodetic obs., 4-85608  
 S Weddell Sea Basin, crust struct. and geologic history 4-81940  
 Weller Coal Measures, Victoria Land, Antarctica, geological study 4-81942  
 Wilkes Land, Antarctica, bedrock topography map and tectonic evolution 4-81962  
 Williston Basin, USA, mechanical and thermal model for tectonic evolution 4-94067  
 Wind River Mts., Wyoming, USA, deformed foreland tectonics 4-67200  
 S Wyoming, Early Proterozoic volcanic arc succession, tectonic setting and origin, geochemical modelling 4-94123  
 Yamasaki microearthquakes, Japan, fracture units characts. 4-105535  
 Yellowstone region, United States, hypocentres and lateral vel. var. simultaneous inversion 4-85645  
 Yenisei Ridge region, USSR, geochemistry of Lower Precambrian gneiss complexes 4-100561  
 Yugoslavia coastal region, Moho discontinuity mapping, seismic and tectonic anal. 4-81879  
 Zacatecas, Mexico, mid-Tertiary felsic volcanism, mantle origin and crustal interactions 4-110113  
 Pb ore deposits in Siberia, isotope geochemistry study 4-105499

## Earth electricity see terrestrial electricity

## Earth electrodes

- Cu, lightning conductor plates, corrosion in soil, over 50 years 4-109543

## Earth heat see terrestrial heat

## Earth interior

- see also Earth core; Earth crust; Earth mantle; tectonics; volcanology  
 deformations of an elastic Earth, book 4-86133  
 diopside, mineral elastic const. at pressures up to 2 GPa 4-72577  
 fluid dynamics of rotating atmosphere and planetary interiors 4-110208  
 free modes and relax. of self-gravitating planet 4-77464  
 free oscillations anal. from crust deform. meas. by laser deformographs 4-62969  
 geodynamical effects on Earth rotation, implications of tidal deceleration of Moon 4-100429

## Earth interior continued

- geodynamical processes in earthquake focal regions, symposium, Potsdam, Germany (1981 November 2 to 7) 4-73142  
 geoid anomalies in a dynamic Earth 4-110024  
 geomagnetic field generation via battery effects 4-101138  
 Harper-Dorn creep in mantle, artifact of low-amplitude temp. cycling 4-94089  
 inner core pendulum mode oscillation, spectral anal. of seismic data 4-81865  
 Jeffreys-Lomnitz transient creep law and application to seismology and mantle flow 4-81859  
 Love numbers of inner core 4-72535  
 upper mantle, heterogeneity and azimuthal anisotropy mapping rel. to convective flow 4-100529  
 mantle convection in layered spherical shell, admittance of gravity over topography 4-67204  
 mantle convection with press. and temp. dependent non-Newtonian rheology 4-67203  
 mantle convective mixing of passive heterogeneities 4-81890  
 neutrino mapping of Earth interior, feasibility method 4-72721  
 nonlinear thermal convection in spherical shell 4-108076  
 normal-mode theory for seismic sources parameters determ. 4-72762  
 phonon thermal conductivity in upper mantle, behaviour at seismic discontinuities 4-100555  
 point mass model constructed to represent gravity field (Russian) 4-115332  
 radially stratified Earth, surface waves and global oscillation 4-110076  
 rocks at Earth interior conditions, physical properties press. depend. (Russian) 4-72578  
 seismic discontinuities, inverse problems for torsional modes 4-110070  
 seismic travel times, new average global P and PcP travel times 4-105460  
 structure and models (book) 4-63427  
 structure dynamics 4-105483  
 thermal evolution of Earth interior, regionalized model 4-89896  
 viscoelastic flow in asthenosphere, models rel. to crustal deformation assoc. with earthquake cycle 4-110068  
 viscosity of upper mantle, press. and temp. dependence rel. to stability of oceanic lithosphere 4-105492
- Earth lower mantle** see Earth mantle
- Earth magnetic field** see geomagnetism
- Earth magnetic field variations** see geomagnetic variations
- Earth mantle**
- Alpine front, upper mantle shear-wave rel. lateral var. 4-77488  
 anisotropy and shear-velocity heterogeneities in upper mantle, long-period surface wave studies 4-94046  
 Archean mantle fractionation, evidence from Nd isotopic ratios in igneous rocks 4-100499  
 NW Argentina, 1200 km magnetotelluric profile 4-85614  
 Central Asia, lateral inhomogeneities of upper mantle and possible relation to orogenesis 4-100505  
 Asia-N Pacific transition zone, heat flow and geodynamics 4-81916  
 asthenosphere, viscoelastic flow models rel. to crustal deformation assoc. with earthquake cycle 4-110068  
 asthenosphere lateral density heterogeneity estimation from geophys. data 4-105500  
 asthenosphere stress relax. following major underthrust earthquakes, assoc. surface displacement patterns 4-81907  
 Mid-Atlantic Ridge basalt, Ne isotopic var. and mantle component 4-110095  
 Australia, lithosphere, seismic refl. anal. 4-82278  
 Australia-SW Pacific crust-mantle boundary, teleseismic obs. 4-89888  
 Backus' mantle filter theory and the 1969 geomagnetic impulse 4-105413  
 Bay of Islands ophiolite complex, Newfoundland, Canada, geology 4-115358  
 S California, fault friction, regional stress, coupling to mantle 4-81991  
 S California, USA, Pn velocities and crust and mantle struct. 4-81861  
 Canadian Shield area, upper mantle seismic velocity struct. 4-105454  
 Cantal, France, coexisting alkaline magma series, mantle material characts. and crustal contamination 4-110098  
 Carpathian arc region, seismic wave velocity struct. 4-105467  
 Caucasus Alpine cycle, crust vertical movements and mantle thermal activation 4-85666  
 chemical equilibration of upper mantle 4-110106  
 chemical heterogeneity, implications of inverse relationship between Sr isotope diversity and rate of oceanic volcanism 4-77490  
 NW China, magnetotelluric studies of He-Xi Corridor (Chinese) 4-85611  
 N China Plain, seismic velocity struct. of lower lithosphere (Chinese) 4-62673  
 composition, large-scale SR and Pb isotope anomaly in Southern Hemisphere 4-89899  
 composition of upper mantle, petrological models 4-100498  
 convection, constraints placed by isotope and geophysical data 4-115376  
 convection cells, numerical and dynamical stability 4-100523  
 convection cells of small-scale laboratory experiments in centrifuge 4-100524  
 convection in layered spherical shell, admittance of gravity over topography 4-67204  
 convection in lower mantle, implications of mag. reversal time scales 4-85620  
 convection in lowermost mantle, numerical model 4-100525  
 convection in mantle, conf., Strasbourg, France (March 1983) 4-95029  
 convection in mantle with heterogeneous distrib. of heat prod. elements 4-72549  
 convection in regionalized thermal evolution model of Earth interior 4-89896  
 convection in upper mantle, mapping via long-period seismic surface waves 4-100529  
 convection indicated by gravity anomalies across subduction zones 4-100526  
 convection lag, and related geoid anomalies and mantle structure 4-105520  
 convection plumes, theory for free convective boundary layers 4-62781  
 convection processes 4-105677  
 convection with press. and temp. dependent non-Newtonian rheology 4-67203  
 convective mixing of passive heterogeneities 4-81890  
 crustal recycling through mantle, mean life of continents is not constrained by Nd and Hf isotopes 4-94047

# Earth mantle continued

D<sup>2</sup>-layer and deep plumes in non-Newtonian mantle, dynamic struct. 4-72548  
 deep-seated diapirism theory as alternative to tectonics (*Russian*) 4-81894  
 density model, effects of thermodynamic conditions and density depend. on seismic vel. 4-77496  
 diapirism under continental arches in eastern USSR, relation to petrochemical features of basaltoid lavas 4-100563  
 double layer convection by numerical model 4-62780  
 elastic properties of lower mantle, rigid ion lattice models anal. 4-72551  
 electrical cond. of upper mantle, from satellite mag. data 4-81845  
 electrical conductivity profile of upper mantle, from magnetotelluric data 4-105417  
 electrical properties of partial melt zone 4-105551  
 Fennoscandian shield, mantle rheological props. 4-81994  
 fluid upwelling at core-mantle boundary resolvability for geomag. secular var. obs. 4-105486  
 Fram and Makarov basins, Arctic Ocean, crust struct. from seismic obs. 4-81860  
 geoid anomalies due to subduction zones, constraints on mantle rheology 4-115330  
 geoid anomalies in a dynamic Earth 4-110024  
 geoid heights and lithospheric stresses for a dynamic Earth 4-100495  
 grain-size distribution and rheology of upper mantle 4-62747  
 granitoid magma origin and influence of mantle 4-105498  
 Gulf of Aden, crust and mantle thermal struct. 4-105484  
 Harper-Dorn creep in mantle, artifact of low-amplitude temp. cycling 4-94089  
 Hawke's Bay area, New Zealand tectonics of Pacific plate subduction 4-105466  
 High Himalaya-Yarlung Zangbo Jiangbo suture unit, upper lithosphere seismic struct. 4-100489  
 Himalayas, Pamirs, Karakorum and Tien Shan, lithospheric struct. and orogenesis 4-62718  
 Hindu Kush region, upper mantle seismic velocity struct. 4-62686  
 India, lithosphere, elec. cond. struct. and magnetometer anal. 4-81850  
 Indian Shield, thermal evolution and mantle thermal props. 4-81906  
 Indian teleseismic observations and crust and mantle struct. 4-62697  
 inhomogeneity parameter and implications for thermally driven processes 4-72542  
 Jeffreys-Lomnitz transient creep law and application to seismology and mantle flow 4-81859  
 Central Karelia, USSR, magnetotelluric sounding of Baltic Shield area 4-85612  
 Kashmir Himalayas, crust struct. from deep seismic sounding obs. 4-62680  
 komatiite magmas, petrogenesis and evolution 4-100564  
 Kuril-Japan region, asthenosphere seismic struct. 4-82005  
 lateral heterogeneity of upper mantle, results from waveform inversion of mantle Love waves 4-110064  
 Laurentide (N America) glacial rebound and mantle rheology 4-105527  
 Lomonosov Ridge, Arctic Ocean, crust struct. from seismic obs. 4-81860  
 lower mantle lateral density inhomogeneities from teleseismic data 4-110105  
 magma genesis, geochemical indications 4-62736  
 magma sources of crust rocks, constraints imposed by experimental petrology 4-62733  
 mantle 400 km discontinuity and Mg orthosilicate elastic props. 4-100558  
 transient mantle convection model of plate tectonics 4-100527  
 McMurdo Sound area of Antarctica, crust and upper mantle struct. 4-81941  
 midocean ridge uppermost mantle, mineralogic variability 4-105478  
 Mizuho Plateau, E Antarctica, seismic sounding of crust struct. 4-81874  
 New Zealand, seismic velocity model of upper mantle 4-62785  
 New Zealand area, teleseismic obs. of upper mantle 4-62698  
 eastern Nigeria, upper mantle character inferred from ultramafic xenoliths 4-77484  
 oceanic mantle, initial-value approach to convective stability with variable viscosity 4-105492  
 oceanic mantle, metasomatic model for origin of Hawaiian tholeiite 4-85650  
 Olgyidakh River-Mirnyi-Lensk profile, USSR, deep seismic sounding studies 4-100513  
 Ontong Java Plateau, isotope geochem. and stratigraphy of mantle 4-72543  
 orogeny, theories and petrology (book) 4-63430  
 Orozco transform zones of E Pacific Rise, crust struct. from seismic profiles 4-81893  
 oxidation state from anal. of basaltic magma O fugacity meas. 4-100519  
 P-wave scattering beneath SCARLET, S California 4-105451  
 P-wave struct. of lower mantle 4-105481  
 P-wave vel. of upper mantle rel. to Adamaoua Plateau, Cameroon, crustal struct. (*French*) 4-94029  
 NW Pacific, subducting slab penetration into lower mantle, teleseismic study 4-85652  
 W Pacific margin, extensional basins form., mantle flow and gravimetric data anal. 4-82002  
 Pamirs-Hindu Kush region, seismic obs. of upper mantle struct. 4-62684  
 Pamirs-Hindu Kush region, tectonic features from seismic obs. 4-62771  
 S Peru, Benioff zone struct., earthquakes epicentres positions anal. 4-105518  
 phonon thermal conductivity in upper mantle, behaviour at seismic discontinuities 4-100555  
 Querigut, France, granite-granodiorite complex genesis, recycling processes, Nd-Sr isotopic systematics 4-110096  
 recycling of crustal material, sedimentary Hf/rare earth elements fractionation anal. 4-110100  
 rheological structure from glacial rebound data from N America 4-105527  
 Saudi Arabia, seismic velocity struct. of lower lithosphere (*Chinese*) 4-62673  
 Sayan-Altay zone, upper mantle seismic vel. struct. 4-62729  
 seismic anisotropy in Japan islands area, teleseismic obs. 4-85636  
 seismic discontinuities in upper mantle, inverse problems for torsional modes 4-110070  
 seismic shear wave triplication in lower mantle 4-110074  
 seismic velocities in lower mantle, extremal bounds 4-77461  
 seismic velocity 3-D struct. of upper mantle 4-110088  
 seismic velocity lateral heterogeneity of lower mantle 4-110087

# Earth mantle continued

seismic wave velocities anal. and correl. with heat flow and non-hydrostatic geoid 4-105488  
 seismic waves, short period S to p-wave conversion at depth near 700 km 4-67181  
 Seychelles, granites and xenoliths, dating and parental magma mantle origin with crustal interactions 4-110102  
 siderophile elements depletion, evidence from W and Mo abundances 4-110099  
 Snake River Plain-Yellowstone volcanic system, crust and upper mantle seismic struct. 4-81904  
 structure, seismic vel. anal. 4-105483  
 structure from stress and seismicity in subducting slabs 4-105522  
 structure inferred from surface seismic waves 4-72525  
 subcrustal layer density nonuniformities from seismic data, for USSR 4-100502  
 subducting lithospheric slab, interaction with chemical or phase boundary 4-94073  
 subducting slab penetration into lower mantle, teleseismic study 4-85652  
 subducting slab stress state deduced from deep earthquake data 4-105521  
 subduction zone thermomechanical convection cell model 4-100528  
 tau estimates for mantle P- and S-waves from global travel-time observations 4-77460  
 tectonic transition zones, volatile mantle products at surface 4-81992  
 thermal boundary layer for lower mantle, seismic Q-profile anal. 4-100507  
 thermal profile of mid-mantle 4-105482  
 Transantarctic Mountains, uplift due to E Antarctica overriding W Antarctica anomalously hot asthenosphere 4-85656  
 transition zone, obs. of converted seismic phases at European stations 4-105456  
 Trinity peridotite, California, USA, Nd-Sr isotope study and mantle evolution 4-89890  
 SW United States, chronology of asthenospheric intrusion rel. to thermal regime of lithosphere 4-94058  
 upper mantle, clues from xenoliths in kimberlites 4-110112  
 central Vanuatu Islands, Pacific Ocean, upper mantle P-wave vel. and crust thickness 4-110093  
 viscosity determ. from Lagoes obs. of gravity anomalies due to postglacial rebound 4-85641  
 viscosity-depth profiles and creep 4-72550  
 Zacatecas, Mexico, mid-Tertiary felsic volcanism, mantle origin and crustal interactions 4-110113  
 K-rich volcanic rocks, <sup>18</sup>O/<sup>16</sup>O and chem. relationships, mantle implications 4-110094  
<sup>238</sup>U behaviour during magma formation and volcanism 4-67190  
<sup>238</sup>U decay chain nuclides, behaviour during magma formation and volcanism 4-67190

## Earth orbit

Hippolyte Fizeau and the movement of the Earth: a tentative misunderstanding (*French*) 4-110844  
 Milankovitch theory tested using 3-D seasonal energy balance climate model 4-62947  
 variations, effect on climatic var. 4-110243

## Earth rotation

*see also time and latitude*  
 angular velocity, rel. to upper limit of undertone periods for liq. core dynamics 4-67174  
 astrometric and geodetic reference systems, linking from space 4-72856  
 atmosphere angular momentum and ocean currents responsible for rot. changes 4-110030  
 atmosphere torques, friction torque and mountain torque estimates from global atmospheric data 4-72654  
 Cagliari Danjon astrolabe, pre-MERIT time and latitude obs. 4-110498  
 core-mantle coupling and geomag. impulse anal. 4-105413  
 detection using superfluid interferometer 4-58728  
 earthquake occurrence correl. with Earth rot. changes (*Chinese*) 4-62675  
 general relativistic gravitomagnetic field, Foucault pendulum expt., at South Pole 4-110110  
 gyroscope precession on Earth surface, existence of mag. type gravit. 4-94587  
 interannual length-of-day variation; relation to Southern Oscillation/El Nino 4-105396  
 nutation of precession, book 4-86133  
 parameter comparison from different observational techniques 4-85610  
 polar motion and 30 year latitude var. (*Russian*) 4-100424  
 precession, alternative derivation of influence on stellar equatorial coordinates (*German*) 4-67597  
 precession, expressions using new system of astronomical consts. (*Chinese*) 4-81830  
 principal axes of inertia, motion within elastic triaxial Earth 4-77439  
 satellite orbital perturbations due to vars. in Earth rotation, theory 4-101212  
 spin slow-down, effect of oceans 4-81831  
 symmetry of the spinning Earth 4-78084  
 tidal deceleration, anal. of lunar secular accel. and laser ranging data 4-100429  
 tidal deceleration, appl. to evolution of Earth's gravit. field and figure 4-105399  
 time and latitude, simultaneous determ. from visual obs. with zenith telescope (*German*) 4-67598  
 Tokyo Astronomical Obs., Time and Latitude Bulletins (October-December 1983) 4-101122  
 variations and their prediction (*Japanese*) 4-93994

## Earth satellites

*see artificial satellites; Moon*

## Earth structure

*see also Earth composition; Earth interior*  
 crust-mantle structure inferred from surface seismic waves 4-72525  
 crustal structures, mathematical model of form. by vertical movements 4-100504  
 density inhomogeneities on large-scale, gravity field effect on geoid 4-62657  
 lateral heterogeneity of upper mantle, results from waveform inversion of mantle Love waves 4-110064  
 lateral variations, use of wave-form inversion method 4-72764  
 mantle, short period S to p-wave conversion at depth near 700 km 4-67181  
 lower mantle thermal boundary layer, seismic Q-profile anal. 4-100507

**Earth structure continued**

mantle transition zone, obs. of converted seismic phases at European stations 4-105456

seismic discontinuities, inverse problems for torsional modes 4-110070

short period seismology, Earth structure modeling 4-72505

synthetic seismograms, theory and appl. to Earth struct. determ. 4-72520

**earth surface processes** *see geomorphology*

**Earth third layer** *see Earth mantle*

**Earth upper layer** *see Earth mantle*

**earthring**

*see also earth electrodes*

steel plate, corrosion-protective solder coating 4-99644

**earthquake recorders** *see seismometers*

**earthquakes**

*see also seismology*

adjacent slip zones on fault, interaction causing amplification of seismic energy release 4-110080

Aegean Sea area, seismic faults 4-89906

Aeolian Islands, Italy, seismic activity and stress characts. 4-100451

aftershocks immediately following underground nuclear explosion, teleseismic obs. 4-67177

Alaska, source parameters and coda waves 4-105431

Aleutian Islands, long-term probabilities for future great earthquakes 4-100465

Alpine-Himalayan belt, tectonics and seismology 4-62789

North America, ground motion prediction form earthquakes Lg phase displacement spectral density corner periods 4-105443

Appin, 1981 November 15, seismicity and mechanism anal. 4-89880

N Arabian Sea and Pakistan, plate motions constrained by earthquake mechanisms 4-72561

Central Asia, seismicity distrib. rel. to lateral inhomogeneities of upper mantle 4-100505

Asia (Central and Eastern), earthquake faulting and tectonics 4-115340

asperities and barriers in fault slip model of earthquake occurrence 4-110083

asperity model 4-72522

asthenosphere stress relax. following major underthrust earthquakes, assoc. surface displacement patterns 4-81907

Mid Atlantic Ridge event on 4 July 1966, fault length and rupture velocity (*Spanish*) 4-94274

rock avalanches due to earthquakes 4-82059

Azores-Gibraltar region of N Atlantic, earthquakes and seismotectonics (*Spanish*) 4-94018

Baikal-Amur trunk railway line, seismotectonics of Khani and Katugin areas 4-100479

Belchatow, Poland, seismic risk in surface coal mine area 4-77451

Benioff zone geometry, by hypocentral trend surface analysis 4-115337

Bulgaria, fault systems and earthquake foci migration (*Russian*) 4-62708

N California, focal mechanisms, evidence for plate subduction 4-105519

central California, seismic moments, local magnitudes and coda-duration magnitudes 4-105428

California earthquakes, seismic moment-magnitude relations 4-115341

Canada and Greenland, AD 1981 earthquakes and seismicity 4-81867

Canada and surrounding region, catalogue of 1979 earthquakes and characts. 4-105463

NE Caribbean, aseismic ridge subduction, max. possible shock 4-94078

catalogue generation by ES-1030 system at Obninsk Central Seismological Observatory, USSR 4-100752

centroid-moment tensor solns. and deep seismicity anal. 4-77466

centroid-moment tensor solns. for 1983 July-September 4-72514

centroid-moment tensor solutions (October to December 1983) 4-105459

Charlevoix zone, St. Lawrence Valley Canada. Seismicity and faulting 4-105436

China, magnitude estimates and short period wave attenuation 4-110057

Coalinga, California, 2 May 1983, surface folding and seismic potential 4-110089

Colombia-Ecuador coast, 1942, 1958, 1979 earthquakes, seismicity and rupture models 4-105435

computational seismology, workshop, Glenenden Beach, OR, USA, (March 1981) 4-67854

conference on earthquakes at Varenna, Italy (June-July 1982) 4-67871

continental tectonic geology, use of earthquake studies 4-72552

Coyote Lake earthquake, California, USA, seismic velocity monitoring before earthquake 4-110298

depth distribution of quakes, tectonics and crust struct. of Eurasian continent 4-72503

distribution and seismic risk 4-72532

distribution with depth in subducting slabs and stress 4-105522

Earth rotation correl. with occurrence of island arc and trench zone earthquakes (*Chinese*) 4-62675

East Pacific Rise event on 18 Nov. 1970, fault length and rupture velocity (*Spanish*) 4-94274

El Asnam, Algeria, 1980 October 10, rupture process anal. 4-77467

electrotelluric precursors, characts. depend. on earthquake energy 4-62692

Europe, central and east regions, isoseismal maps atlas 4-62701

Europe, central and eastern, seismic activity spatial characts. and physical characts. 4-62706

Europe, central and eastern, seismic max. observed intensity map 4-62702

Europe, central and eastern regions, earthquake sources, distrib. and characts. 4-62707

Europe, central and eastern regions, isoseismal surface rel. to epicentral intensity 4-62710

Europe, eastern and central regions, epicentre maps and earthquake catalogue 4-62700

event detection computer algorithms (*Spanish*) 4-115618

far-field acceleration radiated from circular cracks, implications for stress drop assoc. with high-freq. radiation 4-100474

fault behaviour and earthquakes, conf.; Snowbird, USA (Oct. 1982) 4-106110

fault coherent and incoherent rupture, seismic directivity 4-81872

fault displacement detection using aerial-triangulation methods 4-110282

fault length and rupture vel. determ. by Love and Rayleigh wave method (*Spanish*) 4-94274

fault rupture, shear cracks and seismic conditions in specimens containing low-strength inclusions 4-100554

fault rupture spreading model (*Chinese*) 4-110046

fault zone modifications due to fracturing, water circulation and chem. alteration 4-110082

**earthquakes continued**

faulting process, calc. of stress and displacement of elliptical plane shear crack 4-89883

faulting process, frictional instabilities seen in laboratory expts. 4-110079

Fiordland, New Zealand, Benioff seismic zone and tectonics 4-62785

Flores, 23 December 1978, focal mechanism and plate tectonics 4-115379

focus parameters: determ. from composite waves amplitude spectra 4-100480

geodynamical processes in earthquake focal regions, symposium, Potsdam, Germany (1981 November 2 to 7) 4-73142

East Germany, mining induced earthquakes 4-110071

E Germany, seismic max. observed intensities and epicentres, maps 4-62703

E Germany, seismicity and max. intensity earthquakes 4-62705

The Geysers geothermal area, California, seismicity induced by geothermal activity 4-85626

global seismicity and plate motion 4-72533

gravity anomalies associated with faulting processes 4-81866

Greece, magnitude scales 4-110058

ground motion, three-dimensional diff. of plane P, SV and SH waves by hemispherical alluvial valley 4-110075

Gulf of Aqaba earthquake swarm, 1983 January to April, focal mechanism 4-110066

Gulf of Corinth, 1981 February-March earthquake sequence, source processes and distrib. 4-105429

Hawke's Bay, New Zealand, Sept. 1982 event and related tectonics 4-105466

HF radiation from dislocation model of rupture propag. at earthquake source 4-105434

Himachal Himalayas, India, seismic wave amplitude changes and seismic activity prior to earthquakes 4-94019

Himalaya, earthquake activity, mechanisms and plate tectonics 4-62715

Himalayan collision zone, seismotectonics 4-85643

Hindu Kush region, earthquake mechanisms and tectonics 4-62696

Honshu arc, Japan, earthquakes mechanisms and tectonic settings 4-72511

hydrodynamic precursors, groundwater level meas. in Leninabad Region, Tadzhikistan 4-100471

hypocentre and seismic velocity struct. simultaneous inversion, theory and method (*Chinese*) 4-85623

S Ibaraki earthquake, Japan, damage and intensity distrib. of Feb. 1983 event 4-105446

Ibaraki Prefecture, Japan, offshore region, seismicity and seismic wave characts. 4-81870

Ibaraki Prefecture, Japan, Philippine and Eurasian plates seismic coupling and earthquake parameters 4-81868

Ibaraki region, Japan, paired earthquakes, tectonic mechanism 4-81871

Iceland, anomalous focal mechanisms and tensile crack form. on accreting plate boundary 4-94015

Imperial fault, California, USA, large earthquake occurrence probability 4-110086

Imperial Valley, 1979 October 15, faulting model 4-94014

Imperial Valley, California, 1940 earthquake rel. to vertical movements 4-94079

S Indian Ocean, off-ridge normal faulting earthquakes 4-72509

Indonesia, earthquake stress directions 4-82013

Indore-Khandwa profile, Narmada basin, crust seismic struct. and microearthquake locations 4-67198

intensity, use of food store as indicator 4-110276

ionospheric disturbances due to great earthquakes in Japan area 4-105801

Iran, focal mechanism soln. 4-72515

SE Iran, Golbaf-Sirch 1981 earthquakes, faulting and earthquake characts. 4-77465

Italy, seismic activity during the 1900s 4-72530

Izu Peninsula, Japan, geodetic strain obs. and tectonics (*Japanese*) 4-72480

Jalisco, Mexico, 1932 June, Rivera plate seismicity and tectonics 4-94013

Japan, cross sections of earthquakes, focal mechanic and tectonic features 4-81917

Japan, seismic hazard anal., use of quaternary faulting meas. 4-105440

S Kanto District, Honshu, Japan strain buildup after 1923 Kanto earthquake 4-85630

Kanto District, Japan, earthquake generating stresses 4-72496

Karakoram region, earthquakes distrib. and parameter rel. to tectonics 4-62791

Karakoram region, microearthquake survey and crustal activity 4-62716

Kashmir and Himachal Pradesh, seismicity and recent earthquakes 4-100476

Kii Peninsula area, Japan, offshore earthquake swarm 4-105455

Kofu Basin, Honshu, earthquakes seismic intensity, implications for plate interactions 4-105534

Kohistan region, Pakistan, earthquakes, sources anal. and tectonics 4-62717

Koyna, India, reservoir-induced earthquakes, foreshocks anal. 4-110052

Kuril-Japan region, geodynamics and earthquake hypocentres distrib. 4-82005

large shallow earthquakes during 1980, source mechanisms 4-110049

Leipzig, E Germany, 20 Feb. 1982, earthquake source parameters 4-110072

location of local earthquakes, least squares procedure 4-105728

magnitude determ. for shallow events, JMA EM seismograph model 76, Tsuboi constant (*Japanese*) 4-72712

magnitude scales, station corrections for longit., transverse and surface waves 4-100470

mapping of regional seismic zones and earthquake recurrence 4-62709

E Mediterranean, seismic risk and forecasting 4-105450

Messina, Italy, 1908, seismicity and source characts. 4-72531

microtremors of 1-5 second period, correl. with sea waves 4-81869

mining induced earthquakes 4-110071

mining tremors, stress distrib., source parameters, and synthetic seismograms 4-77458

Miramichi, New Brunswick, Canada, 1982 January 9, aftershocks characts. and tectonics 4-105438

Montenegro (Yugoslavia), 1979 April 15, seismic Q-factor determ. for lithosphere 4-105461

Monticello, S Carolina, 1979, focal mechanisms and radiated energy partitioning 4-105425

Mount Erebus, Ross Island, seismic activity (1980 to 1981) 4-81975

# earthquakes continued

- Nankai Trough, SW Japan, earthquake deformation cycle 4-85629  
 New Madrid seismic zone, fault tectonics from microearthquake survey 4-94049  
 New Zealand, horizontal kinematics and seismic activity 4-82014  
 Nihon-kai Chubu earthquake, Japan, May 1983 event, damage study 4-105447  
 Nihonkai-Chubu, Japan Sea, May 1983 event and tsunami generation (Japanese) 4-72500  
 Nihonkai-Chubu earthquake, Japan, damage caused by May 1983 event (Japanese) 4-72501  
 Niigata, Japan, 1964 June 16, fault model 4-72512  
 Niigata, Sea of Japan, 1964, June 16 earthquake, aftershocks distrib. 4-105468  
 North Sea, high-gain seismometer on sea bed, preliminary results 4-77471  
 nuclear power plant pipework system behaviour during earthquakes, comparison with calcs. 4-96231  
 nuclear power plants, seismic risk models, sensitivity studies 4-96220  
 nuclear reactor core with spherical fuel elements, earthquake behaviour using SAMSON vibr. test bed 4-96246  
 Oaxaca, Mexico, source mechanisms of 1965, 1968 and 1978 earthquakes 4-81862  
 occurrence, correl. with groundwater discharge and precipitation 4-81998  
 Ometepe, Guerrero, Mexico, 1982 June 7 earthquake doublet anal. and tectonic setting 4-72517  
 Orozco transform fault, lateral vel. var. effect on source parameters 4-77462  
 circum Pacific region, precursory seismic activity prior to great earthquakes 4-110056  
 W Pacific region, tectonic characts. from seismicity and focal mechanism anal. 4-82000  
 central Pakistan, earthquake mechanisms and depths rel. to tectonics 4-72510  
 S Pakistan and Arabian Sea, plate motions constrained by earthquake mechanisms 4-72561  
 Parkfield, California, USA, earthquake recurrence models 4-85628  
 S Peru, Benioff zone struct., earthquakes epicentres positions anal. 4-105518  
 S Peru, tectonic implications of seismicity and fault plane solns. 4-115378  
 phenomena preceding the seismic events. II. Instrumentation and measuring techniques (Italian) 4-67170  
 plate boundary earthquakes, Shumagin seismic gap, tilt and subduction 4-94077  
 postseismic deformation due to subcrustal viscoelastic relaxation following dip-slip earthquakes 4-94080  
 precursory phenomena, EM emission from rocks undergoing fracture (Russian) 4-72579  
 prediction, appl. of portable continuously working Rn meas. system 4-93671  
 prediction, estimation of parameters in statistical prediction theory 4-100475  
 prediction, fracture mechanics and acoustic emission of anti-plane shear cracks in rocks 4-77507  
 prediction model and crustal mechanisms 4-72528  
 premonitory phenomena, theory of stress distrib. and fracture process 4-77459  
 PWR containment vessel mechanical behaviour during core-melt accidents and earthquakes ROTMEM code 4-96240  
 recording bridge, design of buildings to withstand earthquakes (French) 4-105726  
 recurrence relations for great earthquakes 4-110077  
 recurrence relationships, use of maximum entropy principle 4-105729  
 RF emissions from rocks, hypervel. impact simulation 4-72581  
 rupture complexity, effect on source size estimates 4-85625  
 Ryukyu Island Arc region, microearthquake obs. 4-105469  
 San Andreas fault, California, USA, large earthquake occurrence probability 4-110086  
 San Andreas fault, seismic hazard var. 4-105441  
 San Andreas fault zone, USA, fault behaviour, seismicity and characteristic earthquakes 4-110078  
 San Jacinto fault, California, USA, Anza seismic gap study 4-110084  
 San Jacinto fault, California, USA, large earthquake occurrence probability 4-110086  
 Santa Barbara Island, California, 1981 September 4, strong motion and source parameters 4-110059  
 seismic activity and change of baric field 4-115343  
 seismic activity maps compilation from earthquake epicentres distrib. anal. (Russian) 4-62996  
 seismic hazard calcs. 4-62711  
 seismic linear moment inversion method for obtaining double couple focal mechanisms 4-81864  
 seismic moments, rupture lengths, stress drops and magnitudes, intercomparisons (Chinese) 4-110048  
 seismic shock effects on nuclear installations, mech. system dynamic behaviour in plastic regime 4-96232  
 seismic sources parameters determ., use of normal-mode theory 4-72762  
 seismic waves from circular fault, calc. of high. freq. seismic radiation 4-89882  
 shallow large earthquakes, magnitudes anal. (1904 to 1980) 4-72516  
 Shizuoka-Seibu, Japan, 1981 January 19, foreshocks and aftershocks anal. 4-105437  
 short period seismology, Earth structure modeling 4-72505  
 signals frequency compression 4-100749  
 slow source processes, models 4-72526  
 small local earthquake in randomly inhomogeneous lithosphere, seismograms, attenuation and envelope form 4-85627  
 Songpan, China, 1976 August 16, precursory activity and prediction (Chinese) 4-110045  
 source mechanisms, deviation from double-couple model in high seismicity subduction zones 4-72527  
 source mechanisms and depth retrieval from low-freq. Rayleigh waves 4-105727  
 source parameters, use of seismic waveforms joint inversion 4-72764  
 source parameters of small earthquakes, determ. method (Chinese) 4-110273  
 source properties determ. from surface waves inversion 4-72524  
 source theory, review 4-72519  
 space laser applications in geophysics 4-110319  
 Stiegler's Gorge area, Tanzania, seismicity and fault process 4-81863

# earthquakes continued

- stochastic slip-predictable model for earthquake occurrences 4-105442  
 strong earthquakes, near-zone investigation, instrument deployment and techniques 4-100748  
 strong ground motion from stochastic source model 4-72523  
 strong shallow earthquakes, heterogeneities of instrumental seismicity catalogue (1904-80) 4-105439  
 strong-motion seismology 4-72521  
 subducting plate double-planned seismic zone, thermal stress model 4-105453  
 subducting 'slab' stress' state deduced from deep earthquake data 4-105521  
 synthetic seismograms, theory and appl. to Earth struct. determ. 4-72520  
 Szechwan province, China, earthquake source mechanisms and faulting 4-100477  
 Tangshan, China, July 28, 1976, magnitude determination 4-72513  
 Tanna fault, Izu, Japan, trenching study of previous fault activity 4-105445  
 tectonic analysis of fault slip data sets 4-110081  
 Tokai region, Japan, predicted earthquake, corresponding mantle, tectonic, thermal and seismic features 4-81873  
 Tokyo University historical seismogram archive, microfilming programme 4-105724  
 triggering of precursory events during preparation for great earthquakes 4-100464  
 NW United States, seismicity assoc. with Juan de Fuca subduction zone 4-110055  
 Urakawa-Oki, Hokkaido, 1982 March 21, aftershock distrib. determ. from ocean bottom seismograph and land obs. 4-105452  
 volcanic earthquakes, seismogram interpretations, appl. to Mount St. Helens 4-72529  
 Vrancea, Romania, intermediate earthquakes, intensity attenuation 4-62712  
 Vrancea type, dislocation, slip fault type at ground level 4-67183  
 Wasatch fault zone, Utah, USA, fault behaviour, seismicity and characteristic earthquakes 4-110078  
 SE Wellington province, New Zealand, microseismicity and tectonics at Indian/Pacific plate boundary 4-67180  
 Working Group 4.3.5 KAPG Meeting at Bratislava, Czechoslovakia (October 1979) 4-58572  
 Yamasaki microearthquakes, Japan, fracture units characts. 4-105535  
 Yellowstone region, United States, hypocentres and lateral vel. var. simultaneous inversion 4-85645
- EAS** see cosmic ray showers and bursts  
**Eberhard effect** see photographic materials  
**ebullition** see boiling  
**e.c.g.** see electrocardiography  
**echelles** see diffraction gratings  
**echelons** see diffraction gratings  
**echo**  
 see also anechoic chambers; architectural acoustics; clutter; reverberation; sonar  
 auditoria in Ljubljana, acoustic props., echographic study (German) 4-79369  
 correlation detection, optimally phase-fluctuation tolerant waveforms (Japanese) 4-103106  
 cylinder, immersed,insonification at large Ka (French) 4-107917  
 cylinder, US detection, influence of reflectivity of sea bottom (French) 4-107937  
 dolphin echolocation critical interval 4-103074  
 echocardiograms of left ventricle, computerized 3-D finite element reconstruction 4-100272  
 echosonde pattern synthesis study 4-112661  
 liquid containing gas bubbles, echo effect 4-112615  
 radar echo from anisotropically turbulent air, theory 4-85750  
 radar echo power from rain, estimates rel. to quantitative rainfall-rate meas. (Chinese) 4-67450  
 reverberant room, sound absorbing coeffs. evaluation 4-107951  
 reverberation times of closed sound paths with low damping 4-91664  
 sonar echo fading in shallow water, rel. perform. of incoherent and coherent processing 4-69619  
 subsonic passage above reflecting ground surface, expanding sound due to time-varying source 4-74795  
 underwater spherical targets, echo classification (Chinese) 4-107932  
 US echo method for calcifications detection in breast tissues 4-100263  
 US pulse echo systems, range resolution improvement by deconvolution 4-60199  
 B<sub>2</sub>O<sub>3</sub>-0.5Li<sub>2</sub>O-0.7LiCl glass, pseudospin echoes 4-70291
- echolocation (physiological)** see bioacoustics; mechanoreception  
**eclipses**  
 see also solar eclipses  
 HL Canis Majoris, U Gem star, photometry and search for eclipses 4-101377  
 eclipsing binary stars, times of minima (1980 to 1983) 4-94865  
 Galilean satellite eclipse timings (1975-82), ALPO report 4-110558  
 Galilean satellite eclipses (1652-1982), manuscripts anal. 4-90109  
 Galilean satellites, 1975-1982 eclipse timings 4-63096  
 Galilean satellites, mutual phenomena in 1973 and 1979/80, astrometric obs. 4-63098  
 AM Herculis (3U 1809+50), IUE obs. of eclipses of UV continuum 4-101433  
 Io, eclipse observations collected by Delambre (1775 to 1802) 4-101229  
 lunar, predictions, 1984-2000 (book) 4-101596  
 Pluto-Charon system, eclipses 4-110560  
 Pluto-Charon system speckle obs. of positions, orbit and eclipse prediction 4-115710  
 Saturn satellites, mutual phenomena in 1973 and 1979/80, astrometric obs. 4-63098  
 SU Ursae Majoris stars, eclipse depths rel. to red component activity and superhumps 4-90163
- eclipsing binary stars**  
 AGK3-0°965, central star to PN NGC 2346, IR light curves and circumstellar shell characts. 4-115755  
 AM Herculis, visual magnitude estimates of eclipsing X-ray binary 4-101415  
 RX Andromedae, dwarf nova, continuum distrib., simultaneous visible and UV obs. 4-110631  
 EG Andromedae, UV spectral changes in symbiotic star, IUE obs. 4-115761

## eclipsing binary stars continued

- AB Andromedae, W UMa star, light curve anal., starspot effects 4-72983
- AO Camelopardalis, light curve of eclipsing contact binary star 4-67766
- Ap stars in eclipsing binary systems, review of props. 4-90162
- V1343 Aquilae, (SS 433), periodic and secular changes, review 4-72960
- V822 Aquilae, spectroscopic obs. 4-106039
- V1343 Aquilae (SS 433), 11.1-cm and 3.7-cm flux density vars. 4-82475
- V1343 Aquilae (SS 433), accretion ring nutation, short term periods 4-63180
- V1343 Aquilae (SS 433), correl. with SNR W50 extended radio emission 4-73057
- V1343 Aquilae (SS 433), Einstein Observatory obs. rel. to nature of central X-ray source 4-63157
- V1343 Aquilae (SS 433), jet instabilities rel. to nonthermal emission 4-72948
- V1343 Aquilae (SS 433), radio flux density and structure variations 4-101371
- V1343 Aquilae (SS 433), relativistic radial velocities, precessional period, modulation 4-72959
- V1343 Aquilae (SS 433), X-ray emission anal. and W50 link 4-72958
- SS Arietis, W UMa star, period var., V-photometry 4-106035
- E Aurigae, eclipsing binary B V R I J H K photometric obs. 4-94866
- ε Aurigae, high dispersion spectra (1982 September-1983 March) 4-94870
- ε Aurigae, IR obs. during eclipse 4-72980
- ε Aurigae, light curve anomaly in eclipsing binary star 4-106034
- ε Aurigae, optical photometry between second and third contacts 4-63202
- ε Aurigae, spectroscopic study during 1982/3 ingress/totally 4-82520
- ε Aurigae, winds P Cyg theoretical profiles atlas 4-67644
- 44-i Bootis, contact binary, period change, IR photometric anal. 4-115781
- R Canis Majoris, orbital elements and absolute dimensions from photometric and spectroscopic study 4-82518
- RS Canum Venaticorum, Catania Observatory photometric obs., starspots, rot. and orbital motion 4-94884
- AM Canum Venaticorum, interacting binary white dwarfs, light curve and rot./orbital period 4-90159
- RS Canum Venaticorum eclipsing stars, migrating waves, rot. and mag. activity 4-94885
- OY Carinae, eclipsing dwarf nova, light curves and accretion disc characts. 4-110632
- GW Carinae, photometric obs. and light curve soln. 4-82516
- OY Carinae, visible eclipses of dwarf nova central object 4-63176
- YZ Cassiopeiae, detached eclipsing binary, model of age and composition 4-94861
- RZ Cassiopeiae, October 1977 energy distrib. (Russian) 4-94880
- SX Cassiopeiae, origin and status of semi-detached binary 4-82524
- TX Cassiopeiae, photoelectric photometry and epochs of primary minimum (1982 to 1983) 4-106031
- V368 Cassiopeiae, photometric elements and orbit anal. 4-90189
- cataclysmic binaries, evolutionary constraints from space densities and distrib. 4-82489
- cataclysmic binaries with accretion disc eclipses, light curve model, appl. to LX Ser 4-72954
- cataclysmic variables, orbital period var. and mass transfer, photometry obs. 4-105992
- BH Centauri, masses and dimensions, photometric anal. 4-110654
- V701 Centauri, UVB photometry 4-110679
- CQ Cephei, eclipsing WR star, models, spectra, photometry and secondary nature 4-77832
- RS Cephei, long-period Algol-type binary, UVB light curves 4-82505
- RS Cephei, long-period Algol-type binary, UVB light curves anal. 4-82506
- GK Cephei, obs. of secondary eclipse using photoelectric photometer 4-105883
- VW Cephei, photoelectric minima times of eclipsing binary 4-82527
- VW Cephei, W UMa star, bright spot and flare obs. 4-94897
- VW Cephei, W UMa star, HK photometry anal. 4-94863
- VW Cephei, W UMa star, orbital var. and light curve var. 4-94898
- VV Cephei stars, winds P Cyg theoretical profiles atlas 4-67644
- Z Chamelaentis, high-speed photometry of dwarf nova in quiescence 4-63175
- classical Algol-type mass ratio-log period distrib. 4-82523
- contact and near-contact binary stars, Reticon spectroscopy rel. to orbital parameters and min. masses 4-110684
- contact binary stars, review (Turkish) 4-115782
- contact binary stars, X-ray survey 4-63197
- SX Corvi, W UMa star, period and UVB obs. 4-90185
- W Crucis, W Ser star, radial vel., mass and spectra anal. 4-85977
- SS Cygni, dwarf nova, obs. of quasi-coherent soft X-ray oscils. 4-94785
- SS Cygni, dwarf nova, UVB photometry and spectroscopy of anomalous outburst 4-67726
- SS Cygni, dwarf nova, visual magnitude estimates 4-106008
- CG Cygni, eclipsing RS CVn star, new light curve from B-band photometry (August 1982) 4-94869
- SS Cygni, far and extreme UV flux and spectra, evidence for wind 4-85955
- Cygnus X-1 (V1357 Cygni), shallow partial eclipse light curve soln. 4-63207
- RW Doradus, UVB photometry 4-110679
- UX Draconis, light and radial vel. var. in C star 4-77843
- U Geminorum, dwarf nova, obs. of quasi-coherent soft X-ray oscils. 4-94785
- U Geminorum, far and extreme UV flux and spectra 4-85955
- U Geminorum, spectrophotometry and spectra interpretation with accretion disc and accretion spot models 4-85947
- HD 184035, eclipsing binary, preliminary orbital elements 4-106029
- HD 191765, eclipsing WR star, low mass companion characts. (Russian) 4-94813
- HD 199497, W Ursae Majoris star, photoelectric light curves and orbital period 4-106030
- Hercules X-1, cyclotron line energy var. correl. with continuum luminosity 4-106025
- Hercules X-1, energy spectrum hard X-ray feature 4-85974
- Hercules X-1, March 1984 X-ray observations 4-67770
- Hercules X-1, X-ray pulsation obs. (1984 March 1) 4-67768
- Hercules X-1 (HZ Herculis), high-resolution soft X-ray spectra with objective grating spectrometer aboard Einstein Observatory 4-101170
- AM Herculis, IR and optical polarimetry 4-63204
- HZ Herculis, IUE obs. and spectra 4-101426

## eclipsing binary stars continued

- AM Herculis, low state on 1984 March 9, BV obs. 4-67774
- u Herculis, narrow band light curves 4-110681
- DQ Herculis, numerical model for absence of observable X-ray emission 4-101376
- V624 Herculis, spectra of double-lined eclipsing Am system 4-115759
- AM Herculis, visual magnitude obs. of eclipsing X-ray binary 4-67767
- AM Herculis (3U 1809+50), high resolution soft X-ray spectra with objective grating spectrometer aboard Einstein Observatory 4-101170
- AM Herculis (3U 1809+50), obs. of UV continuum by IUE satellite 4-101433
- HZ Herculis (Her X-1), active/inactive states (1928-79) 4-77871
- HZ Herculis (Her X-1), cyclotron feature model 4-101437
- HZ Herculis (Her X-1), short period X-ray var. and models 4-101435
- HZ Herculis (Hercules X-1), Ariel V obs. of eclipsing X-ray binary 4-101425
- D2 Herculis (Nova 1984), nebula characts. and star energy distrib. 4-110611
- HR 3337, UVB photometry 4-106026
- HR 7464, detached eclipsing binary with very unequal members, mass ratio anal. 4-90188
- EX Hydrae, dwarf nova, high speed photometry 4-101378
- EZ Hydrae, UVB photometry 4-110679
- AR Lacertae, eclipsing RS CVn star, Ha obs. 4-82504
- EV Lacertae, flare star as possible eclipsing binary (Russian) 4-85956
- AR Lacertae, RS CVn star, corona modelling 4-94893
- RT Lacertae, RS CVn star, Ha profiles and gas streaming evidence 4-85988
- AR Lacertae, RS CVn star, VLA obs. 4-72976
- SW Lacertae, W-type W UMa contact binary, IUE spectra 4-77872
- light curves rel. to binary asteroids, comparison 4-82435
- FT Lupi, short period eclipsing binary, system parameters, radial vel. and secondary nature 4-72984
- TU Monocerotis, origin and status of semi-detached binary 4-82524
- BT Monocerotis (Nova 1939), spectroscopic obs. 4-82479
- SY Muscae, symbiotic star, periodic light vars. due to refl. effect and eclipses 4-77855
- MXB 1659-29, discovery of eclipses and normal star mass anal. 4-110663
- VV Orionis, detached early-type binary star, geometric and photometric elements 4-82514
- FZ Orionis, period and light-curve of close eclipsing binary 4-106036
- EE Pegasi, component masses and radii and triple nature 4-110652
- V436=1 Persei, 1983-4 V photometry 4-94868
- DM Persei, eclipsing binary, photometric obs. and parameters 4-77877
- 1 Persei, light curves of variable star, eclipsing binary 4-77728
- DM Persei, origin and status of semi-detached binary 4-82524
- β Persei (Algol), photoelectric UVB photometry (September to December 1983) 4-82528
- β Persei AB, orbit plane orientation 4-101412
- AE Phoenicis, contact binary star, anal. from deconvoluted spectra 4-82513
- photometric observations by automatic photoelectric telescope (October to December 1983) 4-77816
- SZ Piscium, eclipsing RS CVn star, Ha obs. 4-82504
- UV Piscium, RS CVn-type eclipsing binary star, UVB photometry 4-82519
- SZ Piscium RS CVn star, IR light curve, JHK photometry 4-90186
- VV Puppis, AM Her star, X-ray emission from point of accretion onto white dwarf 4-90184
- VV Pyxidis, double-lined eclipsing binary, radii, masses and orbit 4-77869
- rotational velocity changes, implications for mass transfer 4-106042
- V861 Scorpii, β Lyr star, JHKL photometry 4-77878
- RT Sculptoris, UVB photometry rel. to configuration, mass ratio, and evolutionary state 4-101409
- RY Scuti, IUE low dispersion obs. 4-67731
- RS Scuti, photometric obs. and light curve soln. 4-82516
- LX Serpentis, cataclysmic variable, orbit and light curve anal; hot spot characts. 4-106010
- SMC X-1, X-ray data anal., possible tilted precessing accretion disc 4-110666
- spectral types, determ. for 37 eclipsing binaries 4-106027
- spectral types, of eclipsing binaries in optical coincidence with clusters and associations 4-106028
- GR Tauri, BV photometry and spectroscopy of noncontact close binary 4-115783
- times of minima of eclipsing variables, photometric obs. (1980 to 1983) 4-94865
- unevolved close binary systems, period distrib. 4-77870
- AW Ursae Majoris, A-type W UMa contact binary, IUE spectra 4-77872
- AN Ursae Majoris, EXOSAT obs. of AM Her binary in bright state 4-63203
- W Ursae Majoris, IRVBU obs. 4-94871
- W Ursae Majoris, JHK photometry and circumstellar shell evidence 4-94863
- AN Ursae Majoris, polar, polarimetric obs. 4-106038
- XY Ursae Majoris, short period eclipsing RS CVn-like star, flare-like event characts. 4-94889
- W Ursae Majoris stars, amplitude-wavelength dependence 4-106033
- W Ursae Majoris stars, atm. activity and fluxes 4-94895
- W Ursae Majoris stars, atm. struct., UV and X-ray emission 4-94894
- SU Ursae Majoris stars, eclipse depths rel. to red component activity and superhumps 4-90163
- W Ursae Majoris stars, radio obs. 4-94854
- W Ursae Majoris stars; rot.-atm. activity relations 4-94896
- W Ursae Majoris stars in open cluster NGC 188, spectra anal. 4-85984
- Vela X-1, supergiant-neutron star eclipsing system, X-ray pulse and orbit characts. 4-90187
- FO Virginis, eclipsing binary star, light curve observations 4-106037
- DM Virginis, evolutionary status, comp., radii, masses, orbit and atm. parameters, photometric anal. 4-115780
- FO Virginis, orbit characts. and masses, spectral and photometric obs. 4-94867
- AX Virginis (BD+4°2748), possible eclipsing Ap star, position, magnitudes and spectral type 4-106032
- ε Aurigae, eclipsing supergiant, UVB photometry from ingress to, third contact phase 4-63200

## eclipsing binary stars continued

- EV Lacertae, flare star, activity rel. to possible planet-like companion 4-94825  
 WX Sagittae, recurrent nova, circumstellar shell characts. and mass ratio, spectral obs. 4-101374

## ecology

- artificial reef module for marine environmental quality enhancements 4-114972  
 book, biophysical plant physiology and ecology 4-73191  
 coral reef biological communities influenced by sewage discharge 4-115448  
 Gulf of Mexico organic geochem. and ecological processes, tracing by stable isotopes 4-110173  
 indoor environments, radiation aspects, related radioecological problems, Netherlands situation 4-93884  
 intensive aquaculture as candidate for bioregenerative life support systems 4-115256  
 marine biology, pollutant bioaccumulation in marine organisms 4-115451  
 marine ecosystem resistance to pollutants 4-115452  
 plankton monitoring system, image analysis and silhouette photography methods 4-105779  
 Prudhoe Bay Causeway, Alaska, environmental impact assessment 4-114967  
 seaweed mariculture trials, critical pathway approach 4-114966  
<sup>14</sup>C in aquatic food chain (*German*) 4-68911  
<sup>137</sup>Cs movement in southern coastal plain ecosystem, Louisiana, USA 4-89788  
 NO<sub>x</sub> pollutants in atm., conf. at Maastricht, Netherlands (May 1982) 4-101576

## economic and sociologic effects

- see also personnel  
 air pollution in the Netherlands, SO<sub>2</sub> and NO<sub>x</sub> emission standards 4-72193  
 Andrei Sakharov, American physical society meeting in Baltimore, 18-21 April 1983 4-67956  
 electrical and electronic phenomena and devices, book 4-67952  
 Friedel-Anderson model, dynamics and development 4-95128  
 marine recreational facilities, activities, activities and technological advances 4-115001  
 Mexico's economic crisis, scientific community problems 4-110850  
 microelectronics technological revolution and impact on society 4-58615  
 Newport Yachting Center, RI, USA, waterfront development 4-114971  
 scientific activity in underdeveloped countries (*Portuguese*) 4-67949

## economics

- 1970's energy data and anal. 4-72046  
 alkaline storage battery aspects of air electrode research, appl. 4-66687  
 American Power Conference, Chicago, USA (April 1983) 4-86112  
 Baden-Wuerttemberg power stations SO<sub>2</sub> emission reduction, cost/benefit anal. (*German*) 4-114988  
 biogas installations using farm animal waste, design and costs (*Italian*) 4-77048  
 biogas plant economics in developing countries 4-66651  
 building retrofit, optimal strategies identification 4-72048  
 charcoal as an alternative energy carrier: net energy and cost analyses 4-114882  
 coal conversion wastewater treatment by wet oxidation 4-62415  
 cogeneration with steam turbines in citrus engineering plants 4-89487  
 commercialisation chances after Department of Environment 4-62296  
 direct-use geothermal systems, life cycle cost anal. 4-99940  
 district heating power stations with heat pump using refrigerant, market opportunities (*German*) 4-85382  
 Dixie Valley geothermal energy project, development 4-62297  
 domestic heating in Austria, economic aspects and use of heat pumps (*German*) 4-81578  
 electrolytic H<sub>2</sub>, economics and potential applications in the future 4-114961  
 energy generation economics, comparison of various sources (*German*) 4-66643  
 European Communities' medium-term energy modelling, Netherlands results of Reference Case II 4-77046  
 European Communities' medium-term energy modelling, Irish results of Reference Case II 4-72035  
 evaporation source distrib. and material usage efficiency rel. to costs 4-76675  
 film studio production and technological bases development, economic considerations (*Russian*) 4-73549  
 floating-log method of harnessing coastal wave energy 4-66655  
 forestal biomass, importance as energy resource/raw material, utilisation possibilities (*Hungarian*) 4-99995  
 Fort Calhoun: PWR, extended burn-up fuel design, economic goals 4-106681  
 fossil fuel industries and energy policy, 1973-83 4-77050  
 fuels from biomass 4-81518  
 fusion breeders, economics 4-59353  
 gamma-source processing, high Ci, using low-cost hot facility 4-74084  
 greenhouse heating with low temperature geothermal water 4-99941  
 ground water source heat pumps for space heating, economic and comparative analysis 4-62384  
 Gulf Coast geopressure geothermal wells operational testing 4-62299  
 heat pump installations with gas motors in residential buildings, cost effectiveness (*German*) 4-81579  
 heat pumps, space heating, developments and economic aspects, general overview 4-62382  
 heat pumps, temperature and heat flow effects on performance and running costs (*Swedish*) 4-77136  
 heat supply from nuclear power stations, economics and sensitivity anal. 4-89383  
 heavy metals recovery from waste water 4-99802  
 high temperature fluids, transport system, new pipeline design 4-66803  
 industrial cellulosic wastes conversion to diesel fuel 4-72143  
 Japanese industries, energy anal., time series methods 4-72191  
 LMFBR design, cost reduction potential 4-68750  
 LWR low-leakage fuel management, Westinghouse experience, loading pattern designs 4-106695  
 macroeconomic energy model EURECA and modifications 4-66646  
 marine mineral exploration and mining, progress and problems 4-115403  
 Maritsa East 2 thermal power station SO<sub>2</sub> emissions reduction (*Bulgarian*) 4-100042  
 measuring instruments, purchase and rental considerations (*German*) 4-106316

## economics continued

- metal hydride hydrogen storage in automobiles, technio-economic aspects 4-105130  
 microcrystalline cellulose aqueous digestion process evaluation 4-66731  
 mosaic glass reflector solar furnace 4-109727  
 natural energy resources, economic method for studying future conditions and present extraction 4-66645  
 Nepalese biogas developments and prospects 4-66650  
 nuclear fuel cycle cost, current data and developments (*French*) 4-91064  
 nuclear power, electricity generation costs compared to coal 4-99951  
 on-site spent fuel storage options, cost comparisons 4-102364  
 optical communication, anal. (*Polish*) 4-83716  
 optical fibre digital telecommunication link, reliability and economics 4-69588  
 p-n junction GaAs photovoltaic electrolyser for hydrogen production by water electrolysis 4-89451  
 palm oil processing for fuel augmentation and substitution 4-66649  
 photovoltaic concentration, efficiency and costs 4-66663  
 photovoltaic systems design, impact of solar cell efficiency, fabrication costs 4-72118  
 photovoltaics, economic and technology trends 4-89433  
 photovoltaics, installation cost reduction, small scale reflector augmented systems 4-99965  
 physics teaching in developing countries, problems and needs 4-90327  
 power plant flue gas desulphurisation system evaluations and cost calculations 4-66839  
 power plants, nondestructive testing of metal equipment, practical and economic optimisation analysis 4-71855  
 PWR low-leakage fuel management, Florida Power and Light Company experience 4-106692  
 Rankine-cycle heat engine, low-temp., technical and economic study 4-66747  
 shielding hospital rooms for brachytherapy patients, design, regulatory and cost/benefit factors 4-62604  
 Si solar cells manufacture, technological and economic aspects 4-89403  
 single-family residences energy conservation and renewable options anal. 4-72051  
 small fusion reactor concepts, economy of scale 4-111829  
 solar, thermal energy storage systems, value and cost analyses 4-66800  
 solar energy systems, economic analysis 4-77061  
 solar power plant heliostat facets installation and adjustment costs anal. 4-93593  
 solar/gas industrial process heat and cogeneration systems comparison 4-72052  
 space heating, economic comparison of heat pumps and gas/oil boiler systems (*German*) 4-72145  
 space heating, energy and cost savings with air/air heat pumps 4-62387  
 spent fuel reprocessing methods and economics (*Hungarian*) 4-78707  
 steam power stations, fuel consumption, environmental problems (*Hungarian*) 4-109761  
 steam power stations, high sulphur coal burning, strategies for compliance with SO<sub>2</sub> emission standards, economics 4-89480  
 thermal energy storage in aquifers, short-term, system description 4-66804  
 Turkish active solar house heating systems, economic analysis 4-66661  
 Cu<sub>2</sub>S-CdS thin film solar cells development and transfer to industrial production 4-89429  
 H storage economy, technoeconomic comparisons 4-66817  
 H<sub>2</sub> fuel comparison with synthetic fossil fuels, economic and environmental aspects 4-66648  
 H<sub>2</sub> produced from NH<sub>3</sub>, cost comparisons of various processes 4-105128  
 H<sub>2</sub> production and use for rural Alaskan community, programme design and planning 4-89473  
 H<sub>2</sub> production by catalytic thermal decomposition of water 4-93646  
 NO<sub>x</sub> synthesis in low press. plasma, energy cost improvement 4-85305  
 Rn progeny conc. indoors, cost evaluation of control measures 4-115229  
 SO<sub>2</sub> emission by power stations in Baden-Wuerttemberg, reduction measures, costs and efficiency 4-89481  
 Si solar cells as energy source, economic and technical considerations (*Italian*) 4-62305
- eddy current braking**  
 damping due to linear period array of mag. poles 4-69277
- eddy current losses**  
 boundary value and transmission problems, Helmholtz eqn. 4-91385  
 magnetisation and eddy current losses, general statistical approach 4-76179  
 magnetisation and eddy current losses, space-time correlation props. for fine wall spacing 4-88698  
 magnetisation and eddy current losses, space-time correlation props. for large wall spacing 4-88699  
 metallic glasses, optimised domain pattern by heat treatment and surface crystallisation 4-76160  
 watt-hour efficiency of system loop inductor-ferromagnetic plate 4-102851  
 Fe<sub>2</sub>Co<sub>10</sub>-Si<sub>3</sub>B<sub>15</sub>, magnetostrictive amorphous alloys, stress-induced anisotropy and permeability 4-71055  
 Fe<sub>2</sub>Si strips, mag. props. and domain struct., laser scribing effects 4-61550
- eddy current testing** see eddy currents; nondestructive testing
- eddy currents**  
 see also induction heating  
 aircraft maintenance, eddy current equipment 4-76943  
 alloys, soft magnetic, domain wall motion modelling 4-76162  
 crack detection, two-frequency eddy current method, interfering factor effects suppression (*Russian*) 4-104947  
 crack indications in pulsed eddy current testing, spatial resolution of probe coil (*German*) 4-76942  
 damping due to linear period array of mag. poles 4-69277  
 density, boundary-element computation in contiguous domains 4-64650  
 double layered plate, eddy current calculations 4-88692  
 EDDYNET computation developments 4-59958  
 ferromagnets, amorphous and polycrystalline, microeddy currents with point defects (*Russian*) 4-109037  
 flaw detection in conducting half space, eddy current coil impedance 4-62133  
 fusion reactor components, dynamic deform. due to EM forces, finite element anal. 4-74050  
 fusion reactors EM anal., status and need 4-111818  
 heavily doped semicond. diffusion layers, surface resist. eddy current meter for non-contact meas. (*Russian*) 4-111555

**eddy currents continued**

- homogeneous conductors, eddy currents calc., boundary Galerkin's approach 4-59960
- hybrid finite element boundary element solutions using half-space Green's functions 4-59951
- impedance plane testing appls. 4-109588
- inspection of transmission pipelines, electromag. field distribns. in flow detector 4-81389
- interfaces, acoustic and EM wave scattering anal. 4-83754
- interstellar dust, eddy current contrib. to far-IR absorpt. by metallic grains 4-67779
- JT-60 tokamak, eddy current anal. using EDDYMULT program 4-68818
- magnetic field problems, nonlinear transient, comparison of lumped and distributed solns. 4-59959
- metal, surface, AC field perturbation by plane cracks, skin effect 4-62131
- monitoring of laser-heated metals, pot. process control use 4-71808
- moving conductor system, eddy-currents, variational formulation 4-74391
- naval structures, underwater NDT methods 4-114759
- NDT, eddy current probe signal superposition, automatic processing 4-89227
- NDT mag. field intensity vector direction 4-71844
- nondestructive testing of moving sheet conductors, speed effects on solenoid coil impedance 4-71806
- nonsymmetric coil above conducting half-space, eddy currents 4-91383
- reference specimens of specific elec. cond., eddy current certification 4-95471
- shell, cylindrical, eddy current problem, integral eqn. approach 4-102850
- steel, grading by combined eddy current and thermoelec. methods 4-99705
- steel bar sorting, two parametric eddy current method 4-71833
- symmetrical half-closed EM shield, mag. field and eddy current anal. 4-91381
- test lines, integration of microcomputers, review 4-62137
- testing equipment for eddy current structurescopes 4-58872
- three-dimensional problems, soln. methods 4-112321
- two-dimensional eddy current problems, direct soln. 4-69276
- welding, eddy current testing of hot pipe joints 4-76960
- Al welds, miniature, in composite structures, nondestructive inspection 4-66529
- AlGaAs-GaAs superlattices, magnetisation meas., de Haas-van Alphen oscills. 4-98734
- Bi-Pb-Sn-Cd, Wood's metal model, inclined simulated cracks, eddy current detect. 4-66516
- Si,  $\gamma$ -ray irradi., conductivity, eddy current meas. 4-104201
- YIG films, electrical props. 4-80698

**edge-defined film fed growth** *see crystal growth from melt***edge dislocations**

- alkali halide, crack edge contact restoration phenomena 4-98191
- anisotropic diffusion of point defects to edge dislocations 4-104007
- binary cryst., displacement domains caused by defects (*Chinese*) 4-70254
- Carrara Marble, high temp. flow, grain boundary sliding model 4-110132
- ceramics, grain and phase boundary struct. 4-108381
- compact tension specimen, 2-dimens. stress distrib., elastic soln. 4-112709
- elliptical inclusion containing edge dislocation 4-60928
- facet growth, dislocation-controlled, microscopic studies 4-76659
- FCC crystals, stability of dislocation cell boundaries 4-108376
- metals, anelastic interaction between moving kink and point defect pairs (*Chinese*) 4-103785
- metals, high-temp. creep, reln. between Orowan and Bailey-Orowan eqns. 4-92209
- relaxation creep, computer model for high temp. 4-84340
- single crystals, plasticity, effects of dislocation collective behaviour 4-98101
- smectic A liq. cryst., screw dislocation lines, helical instability 4-60822
- smectic C\* phase, dispirations, disclinations and dislocations 4-79926
- surface slip lines and dislocation glide planes in deformed crystals, theory (*Russian*) 4-108360
- tilt boundary struct., struct. unit/grain boundary dislocation model anal. 4-113460
- Al, FCC tilt boundary, vacancy migration, computer simulation studies 4-113694
- Au, tilt boundary energy and segregation, computer simulation studies 4-114540
- Bi-Sb single crystals, etching characts. of edge and screw dislocations on cleavage plane 4-80044
- Cu, tilt boundary energy and segregation, computer simulation studies 4-114540
- Cu-Bi, segregation, grain boundary struct. and struct. transformations 4-113462
- Cu-Sb alloys, grain boundary segregation and cracking, Monte Carlo studies 4-114542
- Fe, BCC crystal, irradiation creep, stress induced edge dislocation-interstitial atom interaction 4-104814
- LiF bicrystals, fracture at plastic deform. 4-75609
- LiF, dislocation mobility at low temps., etch pit obs., Peierls mechanism 4-98105
- LiF, dislocation strain-field scatt. of fast-transverse acoustic phonons 4-84355
- Mo, BCC superlattice with and without dislocations, ion-lattice interaction potentials 4-92246
- Mo, He trapping at low-angle tilt boundary 4-113505
- Mo, tilt grain boundary struct., computer simulation studies 4-113459
- Ni, tilt boundary energy and segregation, computer simulation studies 4-114540
- Ni-Cu alloys, grain boundary segregation and cracking, Monte Carlo studies 4-114542
- Si<sub>3</sub>N<sub>4</sub> precipitated film, dislocation propagation 4-60934
- Zn, dislocation drag mech. 4-103761

**education**

- see also computer science education; educational aids; educational courses; teaching; training*
- acoustics conference, Paris, France (July 1983) 4-78035
- computer-to-computer communication using light pulses, cheap demonstration for schools 4-63461
- freshmen fundamental chemical knowledge, survey 4-104960
- information technology in education and training, Council for Educational Technology view 4-90339

**education continued**

- intuitive science, investigation, review 4-67910
- NDT, university development, teaching and research, in UK 4-90330
- physics education in China 4-90328
- Saudi Arabian engineering education, role of physics 4-90329
- science, differential uptake in schools in England, Wales and N Ireland 4-67911
- science and engineering graduate utilisation in energy-related employment 4-66647
- simulation games in science education 4-67937
- educational aids**
  - see also student laboratory apparatus*
  - cathode-ray tube, fine-beam, student expt. 4-95112
  - digital displays for the overhead projector 4-63459
  - IEEE-488 bus for data acquisition in undergraduate expts. 4-58609
  - lung model, medical education appls. 4-110827
  - radiation, education programme, computer controlled slide and activities-oriented presentation 4-78086
  - spectrograph for educational purposes utilising a holographic transmission grating 4-67948
  - TRS-80 colour computer as 4-channel data logger 4-82644
  - versatile laboratory aid apparatus evaluation 4-95118
- educational computing**
  - see also computer-aided instruction*
  - chemistry, interactive graphics 4-95109
  - Commodore Pet, appl. school physics lab. 4-78074
  - graph plotting, best straight line, BASIC programs for BBC Microcomputer 4-82647
  - IEEE-488 bus for data acquisition in undergraduate expts. 4-58609
  - microprocessor laboratory in a physics department 4-78075
  - missing fundamental in harmonically rel. sounds 4-67934
- educational courses**
  - alternative energy sources and environmental effects, course development 4-63465
  - BASIC programming, learning, course evaluation 4-101603
  - Delhi schools, class X students, evaluation of achievement in algebra 4-101604
  - mathematics, precollege, modular, multimedia course 4-101605
  - microprocessors use in electronics, undergraduate laboratory course 4-95100
  - physical sciences and mathematics, primary university courses 4-106141
- e.g.* *see electroencephalography*
- EELS* *see electron energy loss spectra*
- effective mass (band structure)**
  - abrupt heterojunction, Hermitian effective mass Hamiltonian 4-104118
  - antiferromagnet, conduction electrons, ground state, strong mag. field effect 4-108981
  - antiferromagnetic semiconductors, mag. polaron study (*Russian*) 4-70682
  - binary alloys, electronegativity in local density functional formalism 4-70061
  - graded mixed semicond., extended Wannier-Slater theorem 4-75836
  - layer crystal, cyclotron resonance theory 4-71184
  - many-valley semicond., shallow donor polarisabilities 4-92666
  - metallic rare earth valence fluctuating systems model 4-80468
  - MOS solar cells, perform. calcs. at various temps. 4-72117
  - narrow band gap semicond., effective electron mass in inversion layers, surface elec. field effect, appl. to InSb 4-104280
  - quantum-well struct., resonant impurity states 4-61327
  - semiconductor superlattices, narrow, breakdown of three dimens. effective mass approx. 4-84681
  - semiconductors, position-dependent effective masses in semicond. theory 4-75835
  - semiconductors, Raman characterisation 4-99106
  - two-photon resonant Raman scattering of light involving free electron-hole pairs 4-66039
  - Ag film, dielectric function by ATR technique 4-88463
  - Bi<sub>2</sub>Sb<sub>3</sub>, electronic density of states and its mass 4-88439
  - Cd<sub>3</sub>Mg alloys, electron energy spectrum and de Haas-van Alphen effect (*Russian*) 4-70639
  - CdSb, cyclotron resonance of holes, effective masses 4-80477
  - CdSb, mag. band struct. in valence band 4-75849
  - p-CuGeP<sub>3</sub>, optical lattice modes and IR reflectivity 4-88834
  - GaAs, deep level wavefunctions, behaviour in shallow energy region (*Chinese*) 4-92650
  - GaAs, k,p interaction and effective mass, band gap depend. 4-113850
  - GaAs, shallow acceptors, ground state calc., allowing for valence band corrugations 4-108817
  - GaAs/AlGaAs heterostruct., screening and polaron effects, cyclotron resonance studies 4-98741
  - GaAs-Al<sub>x</sub>Ga<sub>1-x</sub>As quantum well struct., exciton binding energy 4-75868
  - GaAs-Al<sub>x</sub>Ga<sub>1-x</sub>As quantum wells, energy-gap discontinuities and effective masses 4-92623
  - GaAs-Ga<sub>1-x</sub>Al<sub>x</sub>As heterojunction, electron energy level calcs. 4-108915
  - GaInAs/AlInAs heterojunctions, cyclotron resonance and polaron effects 4-98742
  - GaInAs/InP heterojunctions and superlattices, cyclotron resonance and polaron effects 4-98742
  - Ga<sub>x</sub>In<sub>1-x</sub>Se system, magneto-optical props. near fundamental band gap 4-109166
  - GaP, donor wave functions and band struct. 4-98519
  - GaP:O(Zn), size effects and impurity electronic struct. 4-70723
  - Ge, shallow acceptors, ground state calc., allowing for valence band corrugations 4-108817
  - HgS mixed films, elec. and optical props. (*French*) 4-84715
  - n-HgTe zero gap semicond., effective electron mass, mag. quantisation effects 4-88442
  - In, electron-phonon mass-enhancement parameter anisotropy and cyclotron mass 4-84344
  - InP, k,p interaction and effective mass, band gap depend. 4-113850
  - InP:Ge(Sn), donor identification, photolum. and far IR photocond. in high mag. fields 4-70705
  - KH<sub>2</sub> graphite intercalation cpd., electronic struct., Shubnikov-de Haas effect 4-92596
  - Pb<sub>1-x</sub>Mn<sub>x</sub>Te, band struct., cyclotron reson. obs. 4-84546
  - Pb<sub>1-x</sub>Sn<sub>x</sub>Te, band struct. changes during struct. and band inversion transitions 4-65607
  - Pb<sub>1-x</sub>Sn<sub>x</sub>Te, Shubnikov-de Haas effect, temp. depend. scatt. parameter 4-113978
  - Si, deep level wavefunctions, behaviour in shallow energy region (*Chinese*) 4-92650

## effective mass (band structure) continued

- Si:P(As)(Sb), many-valley semiconductor, shallow donor polarisabilities 4-92666  
 Si/SiO<sub>2</sub>/metal struct., electron inversion layers, tunnelling spectra of Landau levels 4-98772  
 n-Si-tunnel oxide-metal struct. with MOSFET for meas. elec. cond. of SiO<sub>2</sub> films 4-61476  
 SrAs<sub>2</sub>, monoclinic, Fermi surface determ. by Shubnikov-de Haas effect 4-108763  
 TiBiTe<sub>2</sub>, growth, elec. and optical props. 4-65676  
 UPTs, spin fluctuations, superconductivity and elec. cond. 4-114057  
 ZnSe, millimeter and submillimeter cyclotron resonance study 4-92963

## effusion

- flow conductance of shielded circular channel 4-83927  
 flow parameters calc., scatt. chambers with rectangular apertures 4-87653

## EFG see crystal growth from melt

## EHD see electrohydrodynamics

## EHT calculations

- ferriocytochrome, hyperfine struct., self-consistent charge EHT calcs. 4-64384  
 iron-tyrosinate proteins, X-ray absorpt. spectra, EHT MO calcs. 4-102835  
 metmyoglobin, N hyperfine interaction ENDOR, EHT calcs. 4-59644  
 molecules, ionisation pots., dipole moments geometries and binding energies calc. extended Huckel theories (*German*) 4-83299  
 polyazine, pi system, band props., EHT calcs. 4-108765  
 polyazobenzene, pi system, band props., EHT calcs. 4-108765  
 B cluster surfaces, chemisorption of H<sub>2</sub> ab initio RHF calc. 4-92555  
 BeH, pot. curves, spin-extend HF study 4-64383  
 CO, adsorbed on metals, bonding, EHT calcs. 4-113800  
 GaAs (110), adsorption of H, EHTMO method calc. (*Chinese*) 4-113787  
 Ir<sub>8</sub> clusters, electronic struct., Xa-SW and EHT calcs. 4-92603  
 Li<sub>2</sub>, pot. curves, spin-extend HF study 4-64383  
 LiH, pot. curves, spin-extend HF study 4-64383  
 Pt<sub>6</sub> clusters, electronic struct., Xa-SW and EHT calcs. 4-92603  
 Si (100) surface with chemisorbed H, surface states, UVPS study 4-108709  
 UFe<sub>6</sub>, electronic struct., ESCA shake-up, X $\alpha$  and EHT calcs. 4-107401

## eigenfunctions see eigenvalues and eigenfunctions

## eigenvalues and eigenfunctions

- action equivalent Hamiltonians, dynamical symmetries 4-110918  
 Aharonov-Bohm effect, charged-boson, magnetic-flux-tube composite, angular momentum 4-110926  
 anharmonic oscillator, bound state energies, perturbation theory 4-63570  
 anharmonic oscillator, ground state eigenvalue, summation of divergent power series 4-95216  
 anharmonic oscillator, quartic and sextic, operator method and eigenvalues 4-78162  
 anharmonic oscillator eigenvalues and Green's functions, 1/N series 4-63533  
 anharmonic oscillator eigenvalues from variational functional method 4-63545  
 arrow matrices, eigenvalue problem 4-63537  
 atomic spectra multiple terms, eigenfunction struct. 4-83318  
 axially symmetric incompressible viscous flow, with perturbations, numerical stability anal. 4-83874  
 bars, tapered, with end mass, vibr. freqs. 4-103247  
 beam, cantilever, constrained, vibr. freqs. and mode shapes 4-103248  
 bearing estimation in shallow water using eigenvector decomposition method 4-103080  
 bound state energies, relativistic corrections for spin 1/2 particles 4-91358  
 boundary problems in generalised analytical functions, variational-difference method (*Russian*) 4-63490  
 Brownian motion, extremely underdamped, eigenvalues in inclined periodic pot. 4-68125  
 buckling and vibration, eigenvalues bound estimating 4-108027  
 sec-butyl radical, chem. activated unimol. reactions, weak collisions and steady states 4-81405  
 composite media heat transfer, solns. of transcendental eqn. 4-63691  
 coupled resonators employing phase-conjugating and ordinary mirrors, calc. of eigenfrequencies 4-107795  
 crystals, inhomogeneous electron damping and electron states 4-70615  
 cylinder, two-layered hollow, thermoelasticity, dynamical problem 4-103206  
 d-dimensional heavy positive ions, energy relations in density functional theory 4-90545  
 deformed nuclei, two-rotor model reformulation 4-64074  
 degree of randomness of the sequence of eigenvalues 4-110930  
 density matrices, geometry, eigenstates 4-95238  
 diatomic mol., composite struct. excitation model 4-106154  
 Dirac eqn. superposed scalar pot. 4-102004  
 Dirac equation, soln. by expansion methods 4-68983  
 discrete ordinate method of solution of linear boundary value and eigenvalue problems 4-101634  
 discrete Schrödinger eqn., Cauchy soln. and positivity of Lyapunov exponent 4-63539  
 discrete spectra in 2-Coulomb centre problem, asymptotic expansion of eigenfunctions (*Russian*) 4-110933  
 disordered diffusive systems, fixed points and universality 4-78282  
 double-well pot., Fokker-Planck and BGK operators, eigenvalues 4-58790  
 electron, wavefunctions and eigenvalues in three-body problem 4-101132  
 electron gas, thermodynamic and mag. props. in inhomogeneous mag. field H<sup>-1</sup> 4-90788  
 electrostatic capacity and eigenvalues of the Laplacian 4-87246  
 electrostatic stability of nonrelativistic non-neutral electron flow in cylindrical diode 4-91902  
 Feynman propagator for time-dependent Lagrangian with invariant quadratic in momentum 4-110910  
 finite element analysis, computational aspects, book 4-110821  
 fluid agitation in rotating cavities, approx. soln. method 4-75044  
 fluid oscillations, analytic soln. for continuous spectrum in differentially rotating perfect fluids 4-94581  
 flux gate sensors, capacitively loaded, steady state characs. 4-101876  
 Fokker-Planck equation, with bistable pot., discrete ordinate method of soln. 4-106234  
 four-centre tetrahedral cluster, Hubbard model, eigenvalue calc. 4-113841  
 generalised anharmonic oscillator, energy eigenvalues 4-58663

## eigenvalues and eigenfunctions continued

- geomagnetic pulsations, eigenperiods rel. to diurnal period var. of mid-latitude ULF pulsations 4-105812  
 graded mixed crystals, quasi-Bloch functions as basis functions 4-92585  
 hadron energy eigenvalues and coupling strengths determ. with duality, Shifman-Vainshtein-Zakharov method 4-59059  
 harmonic oscillator, quasiprobability operator defined quantisation procedure, properties 4-90435  
 Hellmann-Feynman and curvature theorems 4-73257  
 Hilbert-Schmidt's theorem, extension to unsymmetric kernel problems 4-95172  
 hinged rectangular rod grid, eigenfrequency computation program 4-86199  
 homogeneous diffusive systems, discrete eqns. of motion, fixed points 4-78281  
 homogeneous one-speed transport eqn., closed-form formulae for discrete eigenvalues 4-101792  
 homogeneous sphere, 1-speed neutron transport eqn., complex time eigenvalues, criticality 4-83125  
 hydrogen centres in metals 4-92652  
 hypersurfaces, minima location, Levenberg-Marquardt method 4-78120  
 incommensurate potential, quantum motion, solvable model 4-90437  
 infinite cryst. with charged point defects, total energy, Green's function calc. 4-108812  
 infinite strip confocal resonator filled with a saturable-absorpt. gas, lowest-order eigenvalue evaluation 4-87400  
 interface states, relativistic, in one-dimens. solid 4-65730  
 isotropic bending vibrs.; description of radial portion, Gaussian pot. function anal. 4-102666  
 JWKB approximations, quartic oscillator, effective potential method 4-110913  
 Kohn-Sham theory, adiabatic connection approach 4-63654  
 laser resonator oscillation characs. (*Chinese*) 4-87372  
 lattice gas interface, field dependence of eigenvalues of correlation function matrices 4-78253  
 light atoms, density functional exchange correlation pots. and orbital eigenvalues 4-74169  
 linear isotropic materials, eigenvalues and stable time steps for the uniform strain hexahedron and quadrilateral 4-95178  
 linear transport in nonhomogeneous media, discrete eigenfunctions 4-82768  
 magnetic energy, explosive growth in turbulent medium, theory 4-108118  
 Maxwell eqns., source free, on compact space S<sup>3</sup>×S<sup>1</sup>, eigenfunctions and eigenvalues 4-96744  
 metastability and analyticity in drop-like model 4-58805  
 mixed valence compounds, magnetic impurity spin interaction with conduction electrons 4-104173  
 modified kV solitons with non-zero vacuum parameter from ZS-AKNS inverse scatt. method 4-68002  
 molecular bound and continuum systems; statisticality 4-71866  
 molecules, vibr. eigenvalues, G-matrix redundant conditions 4-59700  
 momentum space, relativistic wave eqn. 4-101700  
 multidimensional systems; complex reson. energies, rational fraction analytic continuation method 4-85297  
 nonconservative general systems, nature of eigenvalues 4-95154  
 nonrelativistic Coulomb problem, Sturmian propagator 4-63561  
 nonrelativistic quantum mechanics, inverse methods and solitons 4-90398  
 one electron molecules, discrete spectrum props. 4-102611  
 one-body coeff. of fractional parentage for group chains U(mn)⊃U(m)×U(n) and U(mp+nq/mq+np)⊃U(m/n)×U(p/q) 4-68020  
 optical resonators with nonuniform magnification 4-87373  
 n-paraffins, approx. method for zero-point energy appl. 4-112108  
 partitioning solutions, eigenvalue problem 4-78172  
 perfectly conducting cylinder of infinite length, eigenfunction expansion of electric and magnetic dyadic Green's functions 4-102847  
 periodic functions, interpolation, differentiation and soln. of eigenvalue problems 4-73207  
 photon statistical distribution evolution in laser radiation field 4-107592  
 photonic atom, relativistically corrected Schrödinger eqn. with Coulomb interaction 4-69250  
 plasma, semi-infinite, degenerate, linear response function in external mag. field 4-92643  
 Poiseuille flow, stationary perturbation, eigenvalues, initial value method calcs. 4-97683  
 polyatomic molcs., rot. energy surfaces and high-J eigenvalue structs. 4-69168  
 polyenes, infinite, monoexcited CI spectrum, Hubbard approx. 4-68965  
 positive symmetry matrices, renormalisation group transformation 4-106235  
 quantum mechanical resonances, perturbation 4-110908  
 quantum mechanics, inversion symmetry and time reversal, secular eqn. solution 4-73262  
 quantum mechanics, matrix eigenvector methods 4-58694  
 quantum spectra and transition from regular to chaotic classical motion 4-95307  
 quantum systems, bound, energy eigenvalues 4-67926  
 quantum theory, energy levels and eigenvalues, simple approx. 4-58670  
 quantum theory, two-centre problem, noncompact groups and Sturm solutions 4-90439  
 quantum-mechanical models, eigenvalues obtained using algebraic technique 4-63444  
 radiative transfer models, eigenvalue calcs. including polarisation 4-90541  
 random media, eigenvalues of the Laplacian 4-101751  
 Rayleigh piston, discrete point spectrum of linear gas model 4-90480  
 recursion method with plane wave basis, band struct. calc. appls. 4-80471  
 reduced Dirac Green function for Coulomb pot. 4-68009  
 regularity of low-lying quantum eigenstates in a classically mixing system 4-67990  
 relativistic equations for spin-1/2 particles 4-90722  
 resonance width 4-73300  
 resonator, eigenstate flipping effects (*French*) 4-74553  
 rotation matrix and eigenvalue problem 4-63452  
 Schell-model sources, coherent-mode eigenfunctions, completeness 4-107517  
 Schrödinger eqn., eigenfunctions and wavefunctions with rational potentials 4-63557  
 Schrödinger eqn., eigenvalues, complementary tight upper and lower bounds 4-58660

**eigenvalues and eigenfunctions continued**

- Schrodinger equation, eigenvalue calcs. by numerical integration using DIFEQ program 4-95196  
 Schrodinger equation, hyperviral-Pade scheme, energy eigenvalues of general potential 4-95197  
 Schrodinger equation, nonlinear, bound state solns. 4-68018  
 Schrodinger equation, periodic, with nonperiodic boundary conditions, eigenvalues, semiclassical anal. 4-73259  
 Schrodinger operator spectrum and eigenfunctions with zero range potential 4-106212  
 separating boundary layers, upstream influence, downstream influence in channel flow 4-103285  
 shell, thin, self-oscills. problem numerical soln. (Ukrainian) 4-69693  
 short range pots., eigenvalues, perturbation and numerical methods 4-82693  
 Shrodinger eqn., one-dimensional, embedded eigenvalues 4-101694  
 sine-Gordon eigenvalue problem, squared eigenstates 4-101660  
 spherical optical resonator, incident wave coupling coeffs. and modes, in case of mismatching and misalignment 4-74550  
 spherically symmetric pots., energy eigenstates using shifted 1/N expansion 4-68044  
 square step pots., eigenvalues upper and lower bounds 4-106210  
 Stirling engine, free-piston, design and optimisation using non-linear state space stability anal. 4-66759  
 stratified viscous fluid, oscills., spectral problem (Russian) 4-87775  
 strongly anharmonic oscillator and oscillator with double-well pot., analytical formulae for eigenenergies 4-68004  
 sufficiency of the anticorrelation identities 4-63565  
 supersymmetry and the bistable Fokker-Planck equation 4-73402  
 swirling flow above infinite rot. disc., similarity soln. stability 4-103340  
 symmetry-breaking instabilities under nonclassical bifurcation conditions 4-66553  
 thermally activated crossing of a sharp potential barrier 4-114765  
 three-wave resonant interaction, eigenvalue problem via prolongation Lie algebra 4-90383  
 Timoshenko shaft, stepped thickness, natural freqs. 4-74935  
 tomographic imaging, non-iterative, limited-angle, using eigenfunctions adapted to space-limited objects 4-69326  
 transient heat cond. problems, eigenvalue method 4-60245  
 two-level atom, transition probabilities, eigenvalue problem 4-64330  
 two-photon ionisation: interference and population trapping 4-74203  
 unitary equivalence and scattering theory for Stark-like Hamiltonians 4-63547  
 Waller-Hartree-Fock spatial wave function derivation 4-64331  
 waveguide properties of an atmosphere with a monotonically varying temperature 4-63047  
 Wigner's semicircle law for eigenvalues of non-random Hamiltonians 4-73833  
 $\text{Br}_2^+$  ( $\text{Br}^+\text{Br}^+$ ) state, vibr. eigenenergies functional form 4-107328  
 $\text{H}_2\text{O}(\text{HDO})(\text{D}_2\text{O})$ , local mode pot. function 4-74223  
 He fluids, dimers and trimers, unified framework anal. 4-104013  
 He isoelectronic series, autoionis. states and widths 4-69024  
 $^4\text{He}$  with Paris pot., variational calc. 4-64064  
 $\text{O} + \text{H}_2(\text{D}_2)$  reaction dynamics, reduced dimensionality quantum and quasi-classical rate consts. 4-114784

**eigenvectors** *see eigenvalues and eigenfunctions***eightfold way** *see  $\text{SU}_3$  theory***Einstein-de Haas effect***see also gyromagnetic ratio*

No entries

**einsteinium***see also nuclei with .....*

No entries

**einsteinium compounds**

No entries

**elastic aftereffect**

No entries

**elastic constants***see also elastic moduli*

- alkali halides, elastic constants, multipole expansion 4-80139  
 alkali halides, elastic consts. and force const., bond deform. model 4-61034  
 alkali halides, lattice energies calc. from elastic constants 4-79971  
 alkaline earth oxides, elastic consts. and force const., bond deform. model 4-61034  
 anisotropic materials, generalisation of Mindlin's kinematic plate theory 4-91741  
 beam, cantilever, constrained, vibr. freqs. and mode shapes 4-103248  
 betaine borate, ferroelastic phase transition 4-61072  
 bilayer smectic-A liq. crystals, crit. behaviour of smectic elastic const. 4-75288  
 bis(methylammonium) transition metal chlorides, layered perovskite-type crystals, elastic constants, temp. dependence near struct. transitions 4-65391  
 calcite single cryst., elasticity at calcite I-calcite II transition 4-105549  
 cerium ethyl sulphate, US vel. and attenuation near cooperative Jahn-Teller dilation 4-70292  
 cohesive energy, elastic const. and Gruneisen coeff. calcs. 4-84230  
 composite materials, secant stiffness meas., using peak valley detector 4-66514  
 composites, fibrous, unidirectional, with initially deformed components, corrected elastic props. 4-74861  
 composites, orthotropic, elastic and photoelastic calibration, appl. of least squares method 4-69717  
 composites, unidirectional, matrix cracking 4-74962  
 crystals, data tables, book 4-58593  
 cubic crystals, fourth-order elastic consts. and uniaxial stresses 4-80137  
 cyano derivative/azoxy cpd. liq. cryst. mixtures, elastic consts. 4-60830  
 cyclohexane, liq. and cryst., ultrasonic sound vel. and elastic consts. 4-98200  
 dimethylammonium iron tetrachloride, phase transitions, Brillouin scatt. 4-66051  
 diopside, mineral elastic consts. at pressures up to 2 GPa 4-72577  
 dynamic analysis of elastic-plastic structures by mode-superposition and equivalent plastic load 4-97350  
 epoxy polymers, elastic constants under impact loading, plasticiser content effect 4-66364  
 fibre reinforced composite laminates, material design with required flexural stiffness 4-99391

**elastic constants continued**

- fibre reinforced composites, containing anisotropic fibres, calculated elastic consts. 4-75596  
 fibre reinforced composites, nondestructive evaluation, design philosophy 4-99734  
 fibre reinforced composites, short fibres, mech. behaviour 4-98173  
 fibre reinforced composites, stiffness reduction due to fibre breakage 4-80136  
 fibre reinforced laminated plates, design for max. stiffness 4-75599  
 fibre reinforced plastic, plates, stresses around partial contact pin-loaded holes 4-79520  
 fibre reinforced Ti matrix composites, fabrication and mech. props., review 4-81170  
 fluoride structure crystals, anharmonic elastic props. 4-80132  
 glass fibre reinforced epoxy laminate, elastic consts., stress-strain relations, failure stresses (Japanese) 4-99415  
 glass fibre reinforced polyester, creep behaviour of reinforced and non-reinforced resins 4-99456  
 glass fibre reinforced polyester, laminates, creep charactrs. (Japanese) 4-114615  
 glass fibre reinforced polyester laminates, elastic consts. rel. to fibre orientation and matrix microcracking 4-109447  
 graphite intercalation cpds.,  $\text{K}_1$ -,  $\text{Rb}$ -,  $\text{C}_8$ , phonon softening, inelastic neutron scatt. 4-92319  
 halide glasses, thermal and elastic props., molecular dynamics calc. 4-109455  
 hexa-n-octyloxytriphenylene, discotic liq. cryst., column buckling instability 4-113325  
 hexaony anions, octahedral, mol. consts., force field calcs. 4-102600  
 interface cracks, atomistic versus continuum models 4-113532  
 internal strain of cryst. lattice; contrib. to elastic consts. and piezoelec. coeffs. 4-80135  
 ionic cryst., lattice and thermodynamic props., overlap repulsion pot. 4-92327  
 isothermal third-order elastic consts., linear and vol. compressibilities 4-108499  
 laminated plates and beams, fibre vol. fraction, dynamic mech. props. 4-89078  
 Lennard-Jones solid, second-order elastic const. calcs. 4-70252  
 liquid crystal, columnar-crystalline phase transition, elastic degrees of freedom 4-80230  
 liquid crystal bistable cell, Clausius eqn. and thermodynamics 4-88065  
 liquid crystals, Frank elastic consts., mol. struct. 4-103641  
 liquids, elastic constants calc. from structure functions 4-103844  
 MBBA, nematic liq. cryst., flexoelectric coeffs., bend curvature elastic const. meas. 4-65169  
 metal plates, residual deform. stress, US meas. using SAW 4-99731  
 metals, polycrystalline, elastic deform., X-ray strain analysis (Japanese) 4-114598  
 metals, stresses and elastic consts. with classical ion motion 4-98181  
 metals, surfaces, impurities and defects, embedded atom method 4-92590  
 metals and alloys grain boundaries and cryst. defects, interatomic pots. 4-113464  
 methane- $\text{d}_4$ , liq. and cryst., ultrasonic sound vel. and elastic consts. 4-98200  
 monolayer smectic-A liq. crystals, crit. behaviour of smectic elastic const. 4-75288  
 nematic hybrid aligned cell, influence of surface-like volume elasticity on critical thickness 4-108270  
 nematic liq. crystals, electric field induced flow, surface forces 4-70528  
 nematic liquid crystals, anisotropy induced director refraction inside inversion walls 4-103644  
 p-n-octyloxy-p-cyanobiphenyl, nematic liq. cryst., flexoelectric coeffs., bend curvature elastic const. meas. 4-65169  
 optical fibres, spring constant calculation in buckling 4-91586  
 piezoelectric ceramics, elastic properties 4-60975  
 polyethylene, linear oriented, stiffness, relax., US meas. 4-81232  
 polymer liquid cryst., splay and bend elastic consts., mol. wt. depend. 4-84332  
 polystyrene (polyballs) colloidal crystals and glasses, solidification 4-89353  
 quartz, AT- and SC-cuts, transient thermally induced freq. excursions 4-61628  
 quartz, Brillouin scattering study of sound velocity at  $\alpha$ - $\beta$  transition 4-71400  
 quartz, elastic stiffness temp. derivatives, freq.-temp. behaviour anal. 4-108498  
 quartz, nonlinear acoustic props. and third-order elastic consts. 4-74793  
 residual stress evaluation with X-rays in steels having preferred orientation 4-114749  
 ribbons, amorphous, under torsion, elastic and magnetoelastic effects 4-103854  
 rigid ion lattice models anal. and lower mantle elastic props. 4-72551  
 rock core samples, acoustoelastic consts., interferometric meas. using pulsed phase-locked US instrument 4-97237  
 rubber, frequency-depend. elastic props. 4-103853  
 sphere, spherically isotropic thermoelastic properties, transient thermal stresses 4-112716  
 p-terphenyl, ferroelastic phase transition, elastic constant., Brillouin spectra 4-98180  
 p-terphenyl, improper ferroelastic transition, acoustic anomalies 4-65389  
 thallium acid phthalate, elastic const. meas. 4-92279  
 thiourea, Brillouin scatt. under hydrostatic press., elastic constants, study 4-76479  
 US meas. methods appl. in science and industry 4-104932  
 vinylidene fluoride/trifluoroethylene copolymers, piezoelec. and pyroelec. props. 4-99031  
 Ag-Zn HCP e-phase, elastic constants and phase stability using US method 4-75598  
 AgBr, anharmonic behaviour study 4-92280  
 AgCl, anharmonic behaviour study 4-92280  
 AgCl(Br), interaction pots. and van der Waals forces 4-98058  
 AgCl(Br)(I), anharmonic props., interionic pot. model 4-98056  
 AgI, anharmonic behaviour study 4-92280  
 Al, charge densities, interionic pot., phonon freq., calcs. 4-113856  
 Al film on  $\text{LiNbO}_3$  substrate, elastic const. study 4-104052  
 Al, lattice dynamics, second-order perturbation theory 4-92320  
 Al, polycrystalline aggregates with transverse isotropy, US acoustoelastic response 4-62129  
 $\text{AlH}_3$ , electronic contrib. to elastic consts. 4-65326  
 BP, refractive index and elastic const. meas. 4-61647

elastic constants continued

Ba<sub>0.75</sub>Al<sub>1.1</sub>O<sub>3.25</sub>, elastic consts., press. and temp. derivatives, US resonance study 4-92284  
 BaF<sub>2</sub>, ultrasonic transverse meas. 4-88241  
 Ba(NO<sub>3</sub>)<sub>2</sub>, cohesive energy, elastic const. and Gruneisen coeff. calcs. 4-84230  
 Ba<sub>2</sub>NaNb<sub>2</sub>O<sub>10</sub>, ferroelastic-incommensurate transition, Brillouin scatt. study 4-70362  
 Ba<sub>2</sub>NaNb<sub>2</sub>O<sub>10</sub>, incommensurate, Brillouin spectra meas. 4-76482  
 Ba<sub>0.95</sub>Sr<sub>0.05</sub>Nb<sub>2</sub>O<sub>6</sub>, elastic compliances, temp. depend., 4-76336  
 Be, temp. and press. induced phase transitions 4-70369  
 BrF<sub>3</sub>, mol. const., normal coordinate anal. 4-74216  
 C fibre reinforced epoxy composite, tensile stress appl. parallel to fibres, elastic constants, failure (*Japanese*) 4-85199  
 C fibre reinforced epoxy composite, tension appl. perpendicular to fibres, elastic constants, failure stresses (*Japanese*) 4-85200  
 CaF<sub>2</sub>-SrF<sub>2</sub>, mixed crystals., cohesion, harmonic and anharmonic elastic props. 4-92132  
 CeMg, antiferromag. cpd., magnons and phonons 4-84777  
 ClF<sub>3</sub>, mol. const., normal coordinate anal. 4-74216  
 Co-P amorphous electrodeposits, elastic props. and struct. relax. 4-92282  
 Cr-Al dilute alloys, thermal expansion, elastic const. and mag. props. 4-80138  
 CsCl, eqn. of state used for secondary calibration scale at low temps. 4-103897  
 CsH<sub>2</sub>(SeO<sub>3</sub>)<sub>2</sub>, antiferroelectric, elastic compliance const., anomalies at transition point 4-108500  
 Cu, electrolytic, single cryst. elastic const., cubic polycryst. orientation distrib. function 4-61197  
 Cu single crystal, elastic const., US transducer appl. 4-114729  
 CuCl(Br)(I), anharmonic props., interionic pot. model 4-98056  
 Fe-P amorphous electrodeposits, elastic props. and struct. relax. 4-92282  
 Gd<sub>2</sub>Ga<sub>2</sub>O<sub>12</sub>, hypersonic wave attenuation 4-75620  
 Ge<sub>2</sub>Si<sub>1-x</sub> solid solutions, local and band mode freqs. 4-70307  
 In-Tl, premartensitic phenomena, role of Fermi surface 4-84384  
 InP<sub>3</sub>, Brillouin scatt. meas. of elastic constants 4-84334  
 KBr<sub>1-x</sub>(CN)<sub>x</sub>, dipole glass phase, dielec., thermal, elastic, and struct. props. (*Japanese*) 4-104525  
 KH<sub>2</sub>PO<sub>4</sub>, C<sub>33</sub> anomaly near ferroelec. transition, US attenuation studies 4-65325  
 KH<sub>2</sub>PO<sub>4</sub>, US study near press. induced tricritical point 4-76386  
 K<sub>1-x</sub>Li<sub>x</sub>TAO<sub>3</sub>, dipole glass phase, dielec., thermal, elastic, and struct. props. (*Japanese*) 4-104525  
 (K<sub>1-x</sub>Na<sub>x</sub>)<sub>0.4</sub>(Sr<sub>1-y</sub>Ba<sub>y</sub>)<sub>0.8</sub>Nb<sub>2</sub>O<sub>6</sub>, single cryst. growth and phys. props. 4-76352  
 K<sub>2</sub>SeO<sub>4</sub>, phonon-soliton interaction, discommensurations at lock-in transition 4-70299  
 KTAO<sub>3</sub>Li, incipient ferroelec., off-centre impurity induced phase transition 4-76383  
 LiNbO<sub>3</sub>, ballistic heat pulse propag., effect of piezoelec. 4-76335  
 LiNbO<sub>3</sub>, nonlinear acoustic props. and third-order elastic const., 4-74793  
 Mg<sub>2</sub>SiO<sub>4</sub>, olivine and spinel polymorphs, structural and phys. props., computer simulations 4-89912  
 Mg<sub>2</sub>SiO<sub>4</sub>, olivine and spinel forms, struct. and elastic const., computer modelling 4-113411  
 Mo film on LiNbO<sub>3</sub> substrate, elastic const. study 4-104052  
 NH<sub>4</sub>Br, third order elastic const. near λ-point 4-88223  
 NaCl, eqn. of state used for secondary calibration scale at low temps. 4-103897  
 NaH<sub>2</sub>(SeO<sub>3</sub>)<sub>2</sub> crystals, ferroelec., existence of interphase between α- and β-phases 4-104544  
 Rb<sub>1-x</sub>(NH<sub>4</sub>)<sub>x</sub>H<sub>2</sub>PO<sub>4</sub>, dipole glass phase, dielec., thermal, elastic, and struct. props. (*Japanese*) 4-104525  
 Rb<sub>2</sub>NaHfF<sub>6</sub>(TmF<sub>6</sub>), struct. phase transition 4-75651  
 ReBrO<sub>3</sub>, mol. const., normal-coordinate anal. 4-74216  
 Se<sub>1-x</sub>Te<sub>x</sub> alloys, amorphous, elastic const., role of Te 4-84333  
 Sr(NO<sub>3</sub>)<sub>2</sub>, cohesive energy, elastic const. and Gruneisen coeff. calcs. 4-84230  
 ThCl(Br)(I), anharmonic props., interionic pot. model 4-98056  
 TiH<sub>3</sub>(SeO<sub>3</sub>)<sub>2</sub>, cryst. struct., phys. props., phase transitions 4-84921  
 TiNO<sub>2</sub>, dipole glass phase, dielec., thermal, elastic, and struct. props. (*Japanese*) 4-104525  
 YAG, hypersonic wave attenuation 4-75620  
 ZrO<sub>2</sub>-Y<sub>2</sub>O<sub>3</sub> single crystals, stabilised system, elastic const., comp. and temp. depend., 20-700°C 4-85171

elastic deformation

see also bending; elasticity; electrostriction; stress/strain relations; torsion  
 aortic pulse wave velocity analysis 4-66979  
 body with hard sharp-angled inclusion and interface crack, longit displacement 4-97414  
 calcite single cryst., elasticity at calcite I-calcite II transition 4-105549  
 ceramics, friction wear, theoretical and expt. studies 4-62069  
 compressible hyperelastic bodies in large deformations, equilib. problems (*French*) 4-74875  
 compressible isotropic elastic material, incremental shear modulus, shear waves 4-60295  
 cylinder, microinhomogeneous, axisymmetrical deform. problem (*Russian*) 4-91733  
 cylindrical rod of semi-infinite solid and hollow cylinders, torsion problem 4-114606  
 diamond formation, martensitic mechanism, in colloidal systems 4-80212  
 diffusion bonding, development of theoretical model 4-114762  
 ductile materials, failure, effect of yield surface vertex 4-69689  
 dynamic stress intensity factor of elastic plane. with cut, Mazja-Plamenevski's calc. method (*Russian*) 4-74885  
 Earth crust, relation between two-dimensional and axisymmetric loads in plate flexure problems 4-105528  
 elastic strain rate at finite elastic-finite plastic deform. 4-64862  
 elastic-plastic analysis, small deform. effects 4-97353  
 elastic-plastic behaviour with work-hardening appropriate model for structural software 4-74894  
 elastic-viscoplastic materials, idealised, constitutive restrictions 4-97338  
 epoxide polymers, breakdown, ionisation processes role, mechanoemission mechanism 4-88952  
 external load differentiated determ. for elastically deformed struct. from strain-gauge meas. 4-108056  
 fibre reinforced beams, dynamic loading 4-99454  
 fibre reinforced composites, discontinuous, strength, probabilistic theory 4-81244

elastic deformation continued

fibre reinforced metal composites, thermoplasticity 4-97348  
 frames with Timoshenko members, second order analysis 4-112712  
 glass cloth reinforced polyester panels, elastic props. under low velocity impact 4-89079  
 glass fibre reinforced epoxy, thin-walled tubes, deform. and failure after transverse indentation 4-99573  
 glass fibre reinforced plastics, wound, transverse thermoelastic characts. 4-89082  
 hollow sphere of linear elastic-perfectly plastic material, large deformations (*German*) 4-83843  
 incremental thermoelasticity with small deformations, existence and uniqueness 4-79454  
 inelastic design anal., constitutive eqns. 4-91737  
 laminated half-plane with elastic-plastic layer deform., surface buckling 4-97363  
 membranes, elastic, circular, large axisymm. deforms. 4-112703  
 metal rod thermodynamic model for plastic properties (*German*) 4-84338  
 metallic sample, fatigued mesoscopic vol. elements, plastic deform. spectrum, X-ray method 4-71708  
 metals, acoustoelastic response, plastic deform. effect 4-74903  
 metals, BCC, impurity-dislocation interactions, influence of elastic anisotropy 4-98126  
 metals, dislocation interactions and deform. theory 4-113489  
 metals, fatigued, elastic strain distrib., and X-ray reflex profiles 4-76796  
 metals, polycrystalline, elastic deform., X-ray strain analysis (*Japanese*) 4-114598  
 metals, polycrystalline, finite elastic-plastic deformation 4-89093  
 metals, stresses and elastic const., with classical in motion 4-98181  
 metals, wedge disclination systems, elastic interaction with grain boundaries 4-65292  
 micro-inhomogeneous half-space elastic anisotropic, deform. problem 4-108007  
 nonlinear loading calcs., horizontal structure under bending (*German*) 4-83836  
 plane finite elastic deformations, analogy with certain MHD flows 4-60297  
 plane problems, elasticity and plasticity law representation 4-78143  
 plate, deformation in generalised linear thermoelasticity theory 4-69684  
 plate, thick circular in contact with isotropic elastic half-space, exam. using variational method 4-112775  
 polydimethylsiloxane copolymers, elastic, strain-strength and thermoelastic props. (*Russian*) 4-103673  
 polyethylene fibres, X-ray irradi., hyperfine interactions, EPR studies 4-114164  
 polymers, entangled, elastic response 4-98168  
 pressurized circular tube of harmonic compressible material, finite deformation 4-79478  
 rings, circular confined, collapse under external pressure 4-112742  
 rods, plane assembly, heat transfer, elastic deform., coupled thermoelastic kinematic problem (*French*) 4-74878  
 sandwiched solid-metal flat gasket between two discs, contact stresses 4-112774  
 SBR vulcanisates, mech. props. under finite deformation 4-60282  
 semi infinite solid with heat supply, three-dimens. thermoelastic analysis 4-112715  
 shell, cylindrical, rib reinforced, static strength analysis, stress/strain state 4-64845  
 shells, circular cylindrical, analysis of free vibrations, shear deformation 4-112752  
 shells, cylindrical, effect of shear deformation on thermal stresses 4-60294  
 shells, thin, Lagrangian description and incremental formulation in non-linear theory 4-60285  
 shells, thin-walled, with stress concentrators, elastic-plastic state in cases of small and large strains 4-74898  
 soft ferromagnetic elastic solids, finite deform. theory 4-97312  
 sphere, hollow, elastic and plastic deformation 4-83827  
 steel, ferritic-pearlitic, fatigue, inelastic strain and mag. noise 4-114664  
 stress-induced first-order phase transforms., thermodynamics 4-92351  
 stresses and deformations, simplified solution 4-64846  
 strut, hinged, with initial curvature 4-91721  
 surface thermoelastic deformations caused by a laser 4-103798  
 V-die bending, large elastic deflection of thin strips and onset of plasticity 4-79464  
 Al alloys, D-16 sample, particle vel. distrib. in elastic precursor of compression wave 4-92296  
 Cu, cold rolled, 50%, orientation depend. of stored energy of cold work 4-99404  
 Cu-Fe, elastic distortion of α-Fe particles by Orowan loops, moire fringes, TEM obs. 4-66358  
 (Dy<sub>0.7</sub>Tb<sub>0.3</sub>)<sub>2</sub>Fe<sub>2</sub>, mechanostriuctive strain as a function of magnetic field and mechanical elastic stresses 4-113523  
 Fe-C martensite, incommensurate direction of modulated struct., strain energy, lattice distortion 4-109454  
 Ga<sub>1-x</sub>Al<sub>x</sub>P p-n structures, epitaxially grown, plastically and elastically deformed, quantum efficiency spectra 4-84651  
 Ni-Cr-Mo superalloy, elastoplastic deform. and failure, acoustic emission obs. 4-66377  
 RbAg<sub>2</sub>I<sub>3</sub>, domain struct. below phase transition point 4-70402  
 Si single cryst., elastically deformed, Pendellosung fringes 4-88035  
 SiC fibre reinforced Al alloy, squeeze cast, thermal expansion, elastic to plastic deform. transition 4-108635  
 SmFe<sub>2</sub>, mechanostriuctive strain as a function of magnetic field and mechanical elastic stresses 4-113523  
 Tb<sub>2</sub>Fe<sub>2</sub>, mechanostriuctive strain as a function of magnetic field and mechanical elastic stresses 4-113523  
 Zn, single crystal, deformation stress and electrical resistance change due to dislocation 4-60978

elastic hysteresis

fatigue crack growth at high strain amplitudes 4-103265  
 impact-tension compression test using split-Hopkinson bar 4-87639  
 metals, cyclic creep, relationship with hysteresis loop energy 4-109456  
 polyvinylidene fluoride, ferroelec. and 33 ferroelastic hysteresis 4-99066  
 rod of elastoplastic material, dynamics of buckling, friction properties and hysteresis 4-112743  
 steel, austenitic stainless, strain hardening, hysteresis, constitutive eqns. 4-104805  
 steel, strain meas. near growing fatigue crack tip 4-114651  
 Al alloys, strain meas. near growing fatigue crack tip 4-114651

**elastic hysteresis continued**

- Al, dislocation internal friction hysteresis 4-70165  
 Cu-Al-Co (15.2 at.%), with non-coherent particles, superelasticity effects due to twinning 4-76795  
 In-Pb single crystal, superelastic, irreversible twinning transition 4-85174  
 KFe(MoO<sub>4</sub>)<sub>2</sub>, ferroelastic domain switching 4-92343  
 KH<sub>2</sub>(SeO<sub>4</sub>)<sub>2</sub>, ferroelastic domain struct. dynamics, internal friction meas. 4-80156  
 KIn(MoO<sub>4</sub>)<sub>2</sub>, ferroelastic domain switching 4-92343  
 KSc(MoO<sub>4</sub>)<sub>2</sub>, ferroelastic domain switching 4-92343  
 SiC fibre reinforced Al alloy, squeeze cast, thermal expansion, elastic to plastic deform. transition 4-108635

**elastic limit**

- plastics, limit hardening modulus determ. (Bulgarian) 4-66368  
 rings, circular confined, collapse under external pressure 4-112742  
 steel, austenitic stainless,  $\gamma$ , precip., influence on elastic limit (French) 4-81200  
 steel, dual-phase, deform., heterogeneity in ferrite phase 4-71712  
 steel, dual-phase, work hardening at small plastic strains 4-114568  
 steels, plastically deformed, orientation microstresses depend. on external load direction (Russian) 4-93332  
 Fe<sub>30</sub>B<sub>70</sub>, Fe<sub>70</sub>Cr<sub>10</sub>B<sub>20</sub> and Fe<sub>70</sub>Cr<sub>5</sub>Ni<sub>5</sub>B<sub>20</sub> amorphous alloys, elastic characts. and microplastic deform 4-93325

**elastic moduli**

- see also Poisson ratio; shear modulus; Young's modulus  
 alkali metal alloys, MAu (M=Li, Na, K, Rb, Cs), electronic props., self-consistent relativistic band struct. calcs. 4-92604  
 alkali metal halides, short-range repulsive pot. anal. 4-75361  
 alkali metals, BCC, thermodynamic props. at high temps. 4-92392  
 alkali metals, lattice props., Heisenberg Hamiltonian studies 4-108501  
 Arctic offshore structures, lightweight concrete props. 4-114464  
 bars, nonlinear longitudinal waves 4-87608  
 borate glasses, photoelastic consts., compositional trends 4-84945  
 brittle materials, microcracking, crack-growth resist. 4-83858  
 cardiac ventricles in diastole, incremental elastic modulus 4-115109  
 ceramic-polymer composite biomaterials, fracture 4-76844  
 ceramics, cracking behaviour, microprocessor-controlled meas. 4-62056  
 composite laminates, fatigue damage parameter using stiffness change 4-76864  
 composite material, singular approx. in theory of elastoplastic media with microstruct. 4-108018  
 composite materials for damping, development 4-76797  
 composite materials meas., using flexural tests 4-112784  
 composites, EM and elastic props., correlation, microgeometries corresponding with effective medium approx. 4-70251  
 compressive tests of specimens, effect of contact friction forces 4-109596  
 cooperative model of relaxation behaviour, appl. to elastic and viscoelastic materials 4-65340  
 ductile, cohesive and struct. props., ab initio LCAO calc. 4-60881  
 ductile materials containing small volume of voids or inclusions, estimates for constitutive moduli 4-98172  
 ethylene-vinyl alcohol copolymer, struct., mech. and dielec. props., temp. depend. (German) 4-71261  
 2-ethylhexadecyl-1,3, viscoelastic relaxation, US studies 4-98213  
 fibre reinforced composites, elastic props., rule of mixtures 4-109448  
 fibre reinforced composites, inelasticity, effect on strength in static loading 4-71678  
 fibre reinforced composites, laminated, quasi-isotropic, thermal expansion behaviour, surface anisotropy 4-80269  
 fibrous materials, high-modulus, shear anomalies 4-108014  
 fufurrol acetate binder, highly filled composite, mech. props. 4-89080  
 glass fibre reinforced plastic, sheet moulding cpd., impact damage 4-76829  
 glass fibre reinforced plastics, reinforced in three directions with variable placement angle with depth, mech. props. 4-89081  
 glass fibre reinforced polyester laminates, elastic consts. rel. to fibre orientation and matrix microcracking 4-109447  
 glass fibre reinforced polyurethane foam, flexural strength and modulus, thermal and photodegradation (Japanese) 4-99623  
 glass fibre reinforced thermoplastic alloy, mech. props. at elevated temps. 4-76855  
 graphite, structural theory using pseudopotential local-density-functional approach 4-92135  
 graphite, thermomechanical treatment, neutron irradiation-induced changes in props. 4-108451  
 graphite fibre reinforced polyimide, fracture and elastic props., influence of 4-99572  
 graphite fibres, intercalated, for electrical power transmission appl. 4-80562  
 graphite oxide fibres, produced by oxidation of C-graphite fibres 4-76740  
 graphite-alkali metal intercalation cpds. stage-one, Thomas-Fermi density functional theory 4-92131  
 high temperature deform., Zener-Holloman hyperbolic eqn., consts. determ. 4-109463  
 hybrid fibre reinforced epoxide composite, environmental-response of flexural props. 4-76809  
 III-V covalent semicond. crystals, equation of state, bulk modulus press. derivative 4-98236  
 isotropic random elastic medium, critical properties from fractal model of percolating backbone 4-103209  
 J-R curve, direct determ. from load-displacement record 4-104959  
 joint, bolted, contact stress distrib. anal. in beam model (Japanese) 4-103268  
 joint, bolted, contact stress distrib. in bolted column (Japanese) 4-103269  
 metals, polycrystalline, finite elastic-plastic deformation 4-89093  
 metals, solid and liq., ultrasonic vel., temp. depend., elastic moduli, vol. depend. 4-60989  
 metals, thermodynamic props. when Fermi surface is close to Brillouin zone surfaces 4-70404  
 Mg-Mn ferrite, elastic behaviour at room temp. 4-65327  
 model polyisobutylene networks, strain induced crystallisation 4-75324  
 mullite-cordierite composites, sintering, hot pressing, microstruct., mech. and thermal props. 4-89017  
 noble metals, lattice props., Heisenberg Hamiltonian studies 4-108501  
 nuclear reactor pressure tubes, fracture micromechanisms, use of J<sub>R</sub> curves 4-99582  
 nuclear waste glasses, fracture toughness, hardness, elastic recovery, indentation testing 4-104844  
 nylon 66 and 6, mech. relax., elastic moduli, chain orientation, birefringence, wide angle X-ray obs. 4-93323

**elastic moduli continued**

- n-octacosane crystals, spiral step patterns, stress field effect, shear modulus estimated 4-103680  
 orthoferrosilite (FeSiO<sub>3</sub>), elastic moduli of single crystal 4-94115  
 oxide dispersions, rheological, mech., and mag. props. 4-65830  
 periodically modulated nonlinear medium opacity to acoustic waves 4-91680  
 PET, crystallisation, struct. and props. 4-103666  
 plate, homogeneous, cylindrical bending, asymptotic method 4-79458  
 polybutadiene, reinforcement with inorganic fillers, mech. characts. 4-61914  
 polycarbonate blends with ABS and SAN, tensile and impact tests, energy absorpt. 4-66389  
 polydimethylsiloxane, trifunctional model networks, elongation moduli 4-93324  
 polyethylene, high-density, moulded sheets tear strength 4-104846  
 polymer, press. effect on mech. props., glassy parameters substitution for occupied vol. parameters 4-61964  
 polymers, entangled, elastic response 4-98168  
 polypropylene, mica-filled, mech. props. influence of particle size 4-81279  
 polystyrene latex dispersions, conc., sterically stabilised, free polymer addition, rheological investigation 4-12788  
 polyvinylidene fluoride films, unoriented, piezoelec. props., plasticizer effects 4-99026  
 porous material, elastic, periodic, finitely strained, macroscopic props. 4-74887  
 porous materials, elastoplasticity theory 4-87585  
 pulse spectrum technique, simultaneous determ. of bulk and shear modulus, and density for nondestructive evaluation 4-66515  
 PVC, vol. viscosity, compressibility, elastic modulus 4-70426  
 PVC-ethylacrylate 4-vinylpyridine copolymers blends, miscibility, interactions, mech. props. 4-103670  
 quartz plates, elastic stiffness temp. derivatives from frequency-temp. behaviour 4-60977  
 random percolating systems, elastic props. 4-74876  
 ring polymer liqs. elastic coupling, modified Rouse eqn. of motion 4-98164  
 rock, heavily jointed, mechanical props. 4-77508  
 rubber, noncrystalline networks, EPDM, linear thermoviscoelasticity rel. to degree of crosslinking 4-61969  
 shell, zero curve, with variable thickness and elastic modulus, local buckling (Russian) 4-74910  
 solid suspension of spheres, effective moduli in lowest multipole approx. 4-110876  
 steel, austenitic stainless, ductile fracture resistance, assessment based on engineering approach 4-104876  
 steel, powder, shock induced densification, mechanical props. 4-109347  
 steel, structural, deform. mechanisms using high temp. tests 4-109481  
 steel wire reinforced Al alloy, KAS-1A composite, resources eval. 4-66442  
 strain fields around propagating cracks, determ. by hybrid methods 4-91766  
 strain wave propagation in non-Hookian media with yield delay 4-60976  
 syntactic foams, three phase, mech. props., dielec. const. 4-89077  
 transition metals, multi-ion interaction using empirical N-body pot. 4-103695  
 transparent materials, dynamic optical and mech. props., evaluation by interferometry 4-79529  
 two-dimensional electron solids, static and dynamic props., effects of anharmonicities and broken time-reversed invariance 4-70689  
 type II superconductors, two-vortex interactions and elastic consts. 4-92877  
 vinylidene fluoride-trifluoroethylene copolymer, ferroelec. transition, bulk modulus anomaly, thermal expansion, press. depend. 4-84917  
 vinylidene fluoride-trifluoroethylene copolymer rolled films, piezoelec. props. 4-99029  
 vinylidene fluoride-trifluoroethylene copolymers, ferroelec. transition and dielec. props. 4-99052  
 AgCl(Br), interaction pots. and van der Waals forces 4-89058  
 Al, crystallographic transitions and equilib. props., Gaussian-orbital calcs. 4-92353  
 Al-Al<sub>3</sub>Ni eutectic composites, work hardening in stage II, 293-673K (Japanese) 4-89067  
 Al-Mg dil., neutron irradiation, internal friction, elastic modulus, recovery stages studied by elec. resist. meas. 4-103876  
 Al-Mg(Ga)(In)(Si)(Ge)(Se), distribution of electric field gradients around impurities, conduction electron screening lattice strain 4-113910  
 Al<sub>2</sub>O<sub>3</sub> fibre reinforced Mg, tensile and fatigue behaviour, fibre fraction and orientation 4-114652  
 Al<sub>2</sub>O<sub>3</sub>-PMMA (PBMA), composite biomaterials, fracture 4-76844  
 Ar, solid, volume and isothermal bulk modulus, press. depend. 4-92278  
 B fibres, elastic energy absorpt. mechanism 4-66366  
 BaF<sub>2</sub>, binding energy, bulk modulus and press. derivatives, interionic pot. model 4-60884  
 BeO, structural and electronic props., phase transform., pseudopotential calcs. 4-70100  
 Bi-Sb, temp. effect on elastic props. 4-98171  
 C fibre reinforced epoxy, angle-ply laminates, notch sensitivity 4-93386  
 C materials, neutron irradiated, restoration of dynamic modulus of elasticity in annealing 4-65304  
 CaF<sub>2</sub>, binding energy, bulk modulus and press. derivatives, interionic pot. model 4-60884  
 Cr, neutron irradiation, internal friction, elastic modulus, recovery stages studied by elec. resist. meas. 4-103875  
 Cr-Al dilute alloys, thermal expansion, elastic consts. and mag. props. 4-80138  
 Cu halides, deformation pots., relativistic LMT0 calc. 4-80473  
 D, liquid metallic, two-component quantum fluid, equilib. props. 4-104036  
 Fe<sub>2</sub>O<sub>3</sub>, wustite, Fe-rich phase boundary, press. and temp. var. effects 4-66318  
 Ge, elastic props., ultrasonic meas. 4-98170  
 Ge, electronic and structural props., non-local density functional theory 4-108760  
 LiH, ground-state props., LCAO HF study using polarisable basis set 4-60882  
 Mg alloys, structure and physicochemical props. different methods of Stepanov crystallisation effect 4-99297  
 Mg<sub>2</sub>SiO<sub>4</sub>, elastic props. of modified spinel phase at Earth mantle pressures 4-100558

**elastic moduli continued**

- $Mn_{1-x}Mg_xFe_2O_4$ , elastic behaviour, comp. and mag. field depend.,  $\Delta E$  effect 4-98929  
 NaBi(MoO<sub>4</sub>)<sub>2</sub>, elastic moduli, ultrasonic meas. (*Russian*) 4-70253  
 NdCo<sub>2</sub>, elastic and magnetoelastic props. (*Russian*) 4-80806  
 $Ni_{0.968}Co_{0.012}Mn_{0.02}Fe_2O_4$ , magnetostrictive, magnetomechanical props., hysteretic loop, elastic moduli, internal friction, influence of mag. history 4-76212  
 $Ni_{0.953}Mn_{0.02}Co_{0.027}Fe_2O_4$  ferrites,  $\Delta E$  effect 4-76229  
 Ni<sub>2</sub>SiO<sub>4</sub>, olivine and spinel polymorphs, elasticity studies 4-98169  
 Sc, elastic props. under static compression up to 6 GPa (*Russian*) 4-108515  
 Si, elastic props., ultrasonic meas. 4-98170  
 Si, electronic and structural props., non-local density functional theory 4-108760  
 Si, graphitic, structural theory using pseudopotential, local-density-functional approach 4-92135  
 SiO<sub>2</sub>-CaO-Al<sub>2</sub>O<sub>3</sub>-MgO, elastic and strength props., effect of temp. 4-114597  
 SrF<sub>2</sub>, binding energy, bulk modulus and press. derivatives, interionic pot. model 4-60884  
 TaSi<sub>x</sub>,  $x=1.4, 2.4$ , thin film, in situ stress meas. during sintering 4-70416  
 THs, high press. transitions and bulk modulus, X-ray diff. study 4-70371  
 TiC refractories, electronic struct., CNDO/2 calc. 4-75848  
 TiSi<sub>2</sub>, thin film, in situ stress meas. during sintering 4-70416  
 US, high press. bulk modulus and phase transitions, X-ray diff. studies 4-70370  
 W fibre reinforced Cu composite, fracture, acoustic emission obs. (*Japanese*) 4-62024  
 W, total energy full potential linearised APW method 4-104143  
 WC refractories, electronic struct., CNDO/2 calc. 4-75848  
 WSi<sub>2.4</sub>, thin film, in situ stress meas. during sintering 4-70416  
 Yb, pressure-volume relations up to 9 GPa, FCC-BCC transition obs. 4-103925  
 ZrC-Co-base eutectic, mech. props. rel. to microstruct. 4-89135  
 ZrO<sub>2</sub>, MgO partially stabilised, Weibull modulus 4-61972  
 ZrV<sub>2</sub>, structural instability, elastic moduli meas. 4-88224

**elastic moduli measurement**

- composite materials, secant stiffness meas. using peak valley detector 4-66514  
 concrete, plain, in direct tension, method for determining cracking stress, cracking strain and Young's modulus 4-81369  
 sea floor sediment shear modulus meas. using boundary waves 4-115636  
 single edge notched bend specimens, deflection meas. test setup 4-76929  
 wood, elastic constants meas. by US method (*French*) 4-60229  
 Cu, plastically deformed, dislocation struct., ultrasonic study 4-66520  
 Cu single crystal, elastic consts., US transducer appl. 4-114729  
 MgO-Cr<sub>2</sub>O<sub>3</sub> refractories, thermal shock damage resist., ribbon test, Young's modulus obs. 4-89195

**elastic scattering of atoms and molecules**

- atomic processes, rel. to fusion plasma diagnostics and modelling, conf., Nagoya, Japan (August 1982) 4-67866  
 complex high-order semiclassical phase integrals 4-112244  
 cross sections ratio to capture cross sections 4-64597  
 molecular elastic circular intensity differential scattering, quantum mechanical treatment 4-112254  
 H<sup>+</sup>, three particle system with Coulomb interaction, elastic scatt. 4-102763  
 H+H<sup>+</sup>, elastic scatt., intermediate energies, model calcs. 4-107430  
 He+H<sup>+</sup>, elastic scatt., Glauber approx. 4-83447  
 Xe+iodomethane scattering, elastic and inelastic differential cross sections at superthermal collision energies 4-87186  
 Yb+Ne (Xe), collisional study, stimulated photon echo 4-78928

**elastic scattering of electrons by atoms and molecules**

- see also gas phase electron diffraction  
 atomic electron scatt. in strong laser field 4-69209  
 atoms, local exchange pot. for low-energy electron scatt. 4-64601  
 correlation-polarisation pot., parameter-free model 4-64609  
 coupled-channel scattering eqns., L<sup>2</sup> soln. 4-69208  
 cross sections, classical and quantum mechanical calcs. 4-64612  
 ethylene, elastic electron scatt. cross section, ab initio SCF HF calcs. 4-112270  
 free-free scattering processes, inhomogeneous radiation fields effects 4-107455  
 gas discharge resonant atomic state excitation rate const., depend. on plasma ionisation degree 4-69977  
 inert gases, electron scatt., optical model pot., investig. of the shape of the imaginary part 4-78966  
 linear molecules, electron scatt. cross sections, CI calcs. 4-91348  
 methane, elastic electron scatt. 20-500 eV, cross sections, pots., quantum mechanical calcs. 4-96698  
 methane, electron and X-ray scatt., incoherent scatt. factors, Waller-Hartree calcs. 4-112271  
 methane, electron elastic scatt., differential 4-83468  
 methane elastic electron scatt. cross sections, GO and HF wave function calcs. 4-64334  
 polar. mols., electron scatt., eigenphase sum 4-102811  
 positron scattering in gases 4-64565  
 scattering amplitude properties, N-body Schrodinger eqn. 4-91349  
 tetrafluoromethane, elastic electron scatt. cross sections, GO and HF wave function calcs. 4-64334  
 Ar, low energy positron scatt., critical points 4-74313  
 Ar, photoionisation, electron source, collision processes 4-83338  
 Be<sup>3+</sup>, H-like, elastic positron scatt., polarised orbital method 4-102798  
 Be<sup>3+</sup>, H-like, elastic positron scatt., polarised orbital method 4-102798  
 CN, electron elastic scatt. cross section 4-83469  
 CO, electron (positron) impact, total cross-sections 4-107453  
 CO<sub>2</sub>, electron (positron) impact, total cross-sections 4-107453  
 CsCl, slow electron scatt. study 4-74334  
 Cu, oxidation, collision model for fume formation 4-62114  
 F<sub>2</sub>, electrons elastic scatt., cross sections, polarisation effects 4-78963  
 H, elastic electron and positron scatt. in intermediate energy range 4-78968  
 H, elastic electron scatt. in intense laser field, cross sections 4-83474  
 H, elastic scatt., two-electron wave functions, combined hyperspherical and close-coupling description 4-64566  
 H, electron scattering, pseudostate expansions convergence 4-102805

**elastic scattering of electrons by atoms and molecules continued**

- H, muonic, e<sup>-</sup> scattering amplitude estimated below  $\mu^-$  excitation threshold 4-64611  
 H, positron elastic scatt. mechanism, field-theoretic optical pit. calcs. 4-69211  
 H, positron elastic scatt. and positronium form. cross sections 4-83471  
 H<sup>+</sup> positron, elastic scatt. and positronium form. cross sections 4-78964  
 H<sub>2</sub>, electron elastic scatt. and rot. excitation at 10 to 100 eV, optical pot. model 4-96697  
 H<sub>2</sub>, electron scatt., Eikonal amplitude with effective complex pot. 4-96643  
 H<sub>2</sub> gas, subexcitation electron thermalisation, Monte Carlo simulation 4-83470  
 H<sub>2</sub>, positron scatt., coupled-state method calcs. 4-64616  
 H<sub>2</sub>O, angular distrib. of elastically scatt. low energy electrons, Monte Carlo transport codes 4-64608  
 H<sub>2</sub>O, electron and X-ray scatt., incoherent scatt. factors, Waller-Hartree calcs. 4-112271  
 He, elastic electron and positron scatt., model pot. method study 4-78967  
 He, electron scattering, 11-state r-matrix calcs. 4-69210  
 He<sup>+</sup>, H-like, elastic positron scatt., polarised orbital method 4-102798  
 Hg, approx. phase shift formula calc. 4-102797  
 Kr, electron elastic scattering calcs. 4-107456  
 Kr, low energy elastic electron scatt. cross section calcs. 4-83472  
 Kr, low energy positron scatt., critical points 4-74313  
 Li<sup>2+</sup>, H-like, elastic positron scatt., polarised orbital method 4-102798  
 LiH, electron elastic scatt. cross section 4-83469  
 Me, low energy positron scatt., critical points 4-74313  
 N<sub>2</sub>, elastic electron scatt., HF and multiconfiguration SCF CI calcs. 4-102796  
 N<sub>2</sub>, electron (positron) impact, total cross-sections 4-107453  
 N<sub>2</sub>, electron scatt., complex reson. poles calc. using separable T-matrix expansions 4-87223  
 N<sub>2</sub>, electron scatt. low energy, correl. effects studied using linear-algebraic-optical pot. method 4-96699  
 N<sub>2</sub>, epithelial electron thermalisation, Monte Carlo simulation 4-96708  
 NH<sub>3</sub>, electron and X-ray scatt., incoherent scatt. factors, Waller-Hartree calcs. 4-112271  
 N<sub>2</sub>O, electron scatt. cross sections in low energy region 4-91347  
 Ne, elastic electron scatt., cross sections in 5 to 100 eV range 4-64610  
 O<sub>3</sub>, electron elastic scatt. cross section 4-83469  
 OCS, electron scatt. cross sections in low energy region 4-91347  
 Rb, elastic and inelastic electron scatt. cross section meas. 4-83473  
 Xe, low energy elastic electron scatt. cross section calcs. 4-83472

**elastic waves**

- see also acoustic waves; Love waves; magnetoelastic waves; Rayleigh waves; seismic waves; vibrations  
 anharmonic solids, compressive and shock-waves, nonlinear eqn. anal. 4-108519  
 anisotropic materials, stress wave propag. in plates, study by dynamic photoelasticity 4-108037  
 bar, finite length, variable cross-section, elastic wave propag., impact loading effects 4-112750  
 bars, nonlinear longitudinal waves 4-87608  
 beams, Timoshenko type, with cross-section discontinuities, transient response 4-83850  
 Bleustein-Gulyaev waves propag. in nonhomogeneous piezoelectric half-space 4-98196  
 composite materials, appl. of stress and strain polarization tensors to mechanical behaviour, wave attenuation 4-112726  
 compressible fluid, transient elastostatic problem 4-91686  
 compressible isotropic elastic material, incremental shear modulus, shear waves 4-60295  
 crack, annular flat, axisymm. response to normal impact waves 4-69695  
 curve-linear section, high-freq. elastic wave diff. (*Russian*) 4-112763  
 cylinder, multilayer, wave propag. rel. to anisotropy and viscosity 4-108040  
 cylindrical bodies with spherical cavity, elastic/viscoplastic, stress wave propag. 4-97368  
 disc, extremely flexible, spinning with a transverse load, steady-state soln. 4-74852  
 discontinuity wave propagation in elastic solid 4-91761  
 dynamic behaviour of oblique edge-crack under impact loading 4-91770  
 dynamic elasticity, finite element simulation 4-106192  
 dynamically loaded media, vel. distrib. of dislocations, quasiequilibrium function 4-65263  
 elastic dielectrics with polarisation gradient, dynamical problems 4-80152  
 elastodynamic theory and anal., review 4-97394  
 EM-acoustic excitation for radial resonances in metal rods 4-68213  
 equipartition of energy for anisotropic elastic waves 4-64872  
 fibres, elastic, sub-surface, elastic wave scatt. 4-97385  
 free wave propagation in a three-layered cylindrical shell containing a fluid 4-74941  
 half-space, with horizontal elastic cylindrical inclusion, elastic wave excitation 4-64876  
 harmonic waves in homogeneous isotropic medium, exterior problem 4-82679  
 homogeneous solid, lattice dynamics and elastic wave propagation 4-80175  
 hyperelastic materials, exceptional waves 4-91760  
 impact-tension compression test using split-Hopkinson bar 4-87639  
 incompressible flow in elastic tubes, wave phenomena 4-60541  
 incompressible isotropic material, regularity of one-dimens. elastic waves 4-60312  
 induced discontinuities behind shock waves, isotropic linear viscoelastic materials 4-95184  
 isotropic medium with curvilinear sections, second dynamic problem soln. in elasticity theory (*Ukrainian*) 4-69694  
 laminate, viscoelastic, attenuation of stresses in uniform harmonic loading 4-64879  
 layered composites, elastic and viscoelastic, transient wave propag. 4-79492  
 metals, acoustoelastic response, plastic deform. effect 4-74903  
 mode conversion and resonance scatt. from fluid-filled cavity 4-91748  
 multiple scatt. formalism, scatt. by spheres 4-87611  
 multiple scatt. theory application to subsurface defects 4-87612  
 nonaxisymmetrical wave propag. in orthotropic hollow cylinder 4-74940  
 nonhomogeneous elastic wall, mech. wave propag., reflexion and transmission coeffs. (*Rumanian*) 4-74915

**elastic waves continued**

- nonlinear waves in rate-depend. viscoelastic media, asymptotic anal. 4-69699
- periodically ribbed elastic structures under fluid loading, energy transmission 4-97380
- plane polarised wave diff. on a noncircular cavity 4-74937
- plate, elastic, under torsional moment and horizontal force, waves generation 4-60315
- plates, finite, elastic wave, diffuse field assumption 4-91752
- plates, longitudinal, shear and flexural waves attenuation by-periodic inhomogeneities 4-103242
- plates, stability of nonlinear wave propag. 4-87609
- prestressed elastic half-space, P and SV wave reflection at free surface 4-112755
- pulse spectrum technique, simultaneous determ. of bulk and shear modulus, and density for nondestructive evaluation 4-66515
- radiation wavelength influence on laser excited elastic pulses 4-108437
- rare earth compounds, HF elastic waves, props. 4-76222
- reflection and transformation of linearly polarized shear waves at defects 4-81386
- rocks, fluid saturated, elastic wave dissipation 4-72572
- rod, semiinfinite, cylindrical, connected to infinite elastic stratum longit. wave reflection 4-87610
- rods and pipes, separation of dynamically-induced low freq. stresses 4-69696
- rotor vibration: excitation by seismic waves 4-87606
- S-waves scattering on low-contrast spherical inclusion, theory for plane polarised waves 4-100469
- scattering by a sub-surface elastic fibre 4-97385
- scattering by surface-breaking or subsurface planar crack 4-97378
- seismic plane wave interaction with elastic medium section 4-62689
- seismic wave calculations by Fourier method 4-110053
- seismic waves, anisotropy and dispersion in periodically layered media 4-100452
- seismic waves propag. over ocean-continent margins, US modeling 4-77468
- SH wave diff. by cuts in non-homogeneous solids 4-103257
- shear wave and longitudinal wave disappearance in solid body subject to high stresses and large strains 4-74934
- shell, circular cylindrical, fluid filled beam-type, fluid filled, bending vs. membrane theory 4-87580
- shell, three-layer, cylindrical, effect of press. wave velocity 4-103204
- shells, noncircular cylindrical, in fluid, radiation anal. 4-74787
- shells, stability of nonlinear wave propag. 4-87609
- soft gels, shear wave propagation 4-97379
- soil-structure wave propag., silent boundary methods for transient anal., book contrib. 4-60323
- solid-liquid interface under residual stresses, plane waves reflection and refraction 4-87618
- spherical bodies, elastic wave diffraction (*Russian*) 4-64877
- stamp, vibrating, wave excitation in medium with inhomogeneous initial stresses 4-108032
- steel, elastic wave refl. by infinitely long ribbon crack 4-98197
- stress, shock and acceleration waves in various materials, explicit Lagrangian finite diff. method 4-60324
- sub-surface crack, elastic wave diff. 4-74926
- thermoelastic dielectrics, generalised, acceleration waves propag. 4-80151
- thermoelastic wave generation, effects of backing material elastic props. 4-103870
- thermoelasticity problems, dynamic coupled, with relax. times, finite element analysis 4-97322
- three dims. scatterer, exterior Radon transform 4-73307
- transversely isotropic materials, acoustoelasticity 4-88240
- ultrasonic nondestructive evaluation methods 4-99716
- US wave speed in elastic bodies 4-87619
- velocities in heavily jointed rock, meas. 4-77508
- wave vectors, formal power series and iterative methods 4-67179
- weak discontinuity waves in electro-magnetoelastic materials 4-76221
- wedge, elastic, subjected to rapid tearing, transient shear waves 4-91769
- Al cylinder, acoustic wave excitation by low energy electrons 4-80168
- BaTiO<sub>3</sub>, reversed c-domain patterns and elastic wave velocity surfaces 4-84924
- LiNbO<sub>3</sub>, complex elastoelectric effect 4-80629
- LiTaO<sub>3</sub>, complex elastoelectric effect 4-80629
- NH<sub>4</sub>HSeO<sub>4</sub>, dielectric, piezoelectric and elastic props. 4-80878
- a-Si film, elastic and inelastic props. 4-88225
- Ta, shocked, rarefaction velocities and high press. melting point 4-108524
- ZnO triode sputtered films, stress relax. study 4-104109

**elasticity**

- for crack problems in elasticity see crack-edge stress field analysis
- see also elastic constants; elastic moduli; elasticity of liquids; elastoplasticity; photoelasticity; rheology; thermoelasticity
- anisotropic materials, stress wave propag. in plates, study by dynamic photoelasticity 4-108037
- anisotropic solids, statistical ensembles and mol. dynamics studies, sp. ht., thermodynamic tension 4-70368
- aortas, thoracic and abdominal, human, static elastic props. 4-100206
- aramide fibres, struct. and mechanical props. (*Dutch*) 4-92283
- asymmetric rotation of a penny-shaped rigid inclusion embedded at a bi-material elastic interface 4-79456
- asymmetric theory, axial-symmetric contact problem 4-91776
- axially loaded stiffened cylindrical panels with elastic restraints, vibration anal. 4-74916
- bar, elastic in uniaxial tension, bifurcation absence study 4-87570
- bar, linear, elastic, isotropic, nonlinear bending, two fundamental cases 4-74895
- beam, heavy inextensible elastic, unilateral contact problem 4-97438
- beam, infinitely long, contained in frictionless channel, flexural rigidity to axial compressive forces 4-74884
- beam with unilateral supports, optimal design 4-106189
- beams, cantilever, elastic, with nonlinear elements, instability, butterfly catastrophe 4-87599
- beams, elastic, continuous, with unilateral rigid supports anal. based on classical derivatives 4-108004
- beams, elastic, reciprocal Backlund transformations 4-91757
- bodies of revolution, involute, axisymm. stress fields 4-74888
- bone, cortical, CW technique for elastic props. meas. 4-81823
- boundary integral eqn. axisymmetric stress analysis, interior point solns. 4-63510

**elasticity continued**

- boundary integral eqn. method for external boundary value problem soln. 4-106188
- boundary integral equations appl. 4-78137
- boundary layer effect on infinitely long plates hydroelastic instability 4-74873
- boundary of elastic materials, subsonic propag. of shear displacement edge with friction 4-108049
- brittle fracture of elastic bodies, Novozhilov's criterion (*Russian*) 4-112773
- bundles of elastic rods, random coupled vibr., stress-displacement anal. 4-69700
- calcite single cryst., elasticity at calcite I-calcite II transition 4-105549
- cardiac myocytes, rat, passive stiffness obs. 4-100101
- cast FE, SG, fracture mechanics, cracks, elasticity anal., microtension tests (*Chinese*) 4-62027
- cavities, rotationally symmetric, elastostatics as limit of elastodynamic matrix formulation 4-86206
- cellular elastic props., acoustic microscopy obs. 4-100095
- cholesteryl myristate shear elasticity in region of solid-liq. cryst. transition 4-61060
- circle bounded plane region, arbitrary system of cracks 4-97317
- circular beam on Wiegardt-type elastic foundation, dynamic response, vibrs. 4-103249
- circular crack opening, effect of initial stresses 4-60327
- circular cylindrical shell, dynamic instability under periodic compressive force and temp. field 4-69701
- circular hole in an infinite plane elastic sheet, optimum reinforcement under an arbitrary stress system at infinity 4-74874
- coaxial elastic materials, inequalities sufficient to ensure strong ellipticity 4-74871
- cochlea isolated from guinea pig, sensory-cell hair bundles stiffness 4-109837
- collagen fibres, stiffness and strength relations on maturation, clamping and stretching procedure 4-62643
- columnar discotic liq. crystals, Saint-Venant principle 4-60823
- compact tension specimen, 2-dimens. stress distrib., elastic soln. 4-112709
- composite, periodic, effective elasticity tensor 4-91728
- composite laminate elasticity problems with singularities, hybrid finite element approach 4-97324
- composite layer compression development on compression 4-79514
- composite material analysis, survey 4-74862
- composite materials, overall elastic response, overall modulus operator 4-97305
- compressible hyperelastic bodies in large deformations, equilib. problems (*French*) 4-74875
- compressible isotropic elastic material, incremental shear modulus, shear waves 4-60295
- conference on mathematical physics, Boulder, CO, USA (Aug. 1983) 4-67856
- consolidation around a lined circular tunnel 4-83865
- contact problem between elastic bodies 4-108050
- contact problem of elastic layer on rigid base with cylindrical protrusion or pit 4-87631
- contact stresses between two thick plates with a circular hole and a sandwiched solid-metal flat gasket 4-74870
- container, spherical, surrounded by infinite elastic medium, blast loading 4-97390
- cortical bone, bovine, elastic props. rel. to microstruct. 4-72290
- crack development stopped by small elastic inclusions (*Russian*) 4-112772
- crack stopped by elastic inclusion, model problem (*Russian*) 4-74959
- curvilinear, shallow elements of structures, optimal design problems 4-91729
- cyclic loading, inelastic analysis of structures 4-91731
- cylinder, circular, stability when subjected to compressive end forces 4-91730
- cylinder, corrugated, transversely isotropic, of finite, dimens., stress state 4-103196
- cylinder, elastic circular finite, torsion by annular rigid stamp, stress anal. 4-97310
- cylinder, elastic solid, with one or two semicircular grooves, torsion anal. 4-110860
- cylinders, elastic, with grooves, stress state anal. 4-79453
- cylinders, hollow curvilinearly orthotropic, stress-strain state 4-97316
- cylinders, multilaminate finite, nonaxisymmetric loading, stress state algorithm 4-108011
- cylindrical bodies with wear, contact problem in the theory of elasticity 4-103273
- detaching elastic body motion, boundary value problem 4-87569
- dielectrics, variational principle 4-78145
- diisocyanates, polycyclotrimerisation, gel form. and rheology (*Russian*) 4-62203
- dipolar elastic solid, equilib. soln. uniqueness, compatibility theorem 4-69683
- disc, extremely flexible, spinning with a transverse load, steady-state soln. 4-74852
- disc, nonlinear vibrations of elastic disc rotating in viscous fluid 4-112754
- disc inclusion, rigid, elliptical, embedded, in transversely isotropic elastic solid, asymm. rot. 4-110866
- disclination loops, rectangular, elastic props. 4-70155
- distortion of a cylindrical shell in elastic casing, Flugge shell theory 4-112713
- dynamic elastic problems, boundary integral eqn. method 4-95175
- dynamic elasticity, boundary-element methods for transient response analysis, book contrib. 4-60298
- dynamic elasticity, finite element simulation 4-106192
- dynamic impact of an elastically supported beam-large area contact 4-79527
- dynamic stress intensity factor of elastic plane with cut, Mazja-Plamenevski's calc. method (*Russian*) 4-74885
- dynamic system stability 4-97366
- dynamically tuned gyroscope interaction on an elastic platform (*Ukrainian*) 4-86189
- edge dislocation inside elliptical inclusion 4-60928
- elastic bodies, optimal shape design 4-86216
- elastic plane, cut opening under moving load 4-97313
- elastic ring, perturbation post buckling study 4-86215
- elastic waves in solids, elastodynamics, review 4-97394

## elasticity continued

- elastic-plastic materials, isotropic, Bauschinger effect model for large computer codes 4-108504  
 elastodynamic boundary-value problems, integral eqn. method appls. 4-60283  
 elliptical disc inclusion embedded in transversely isotropic bi-material interface, stiffness bounds 4-60296  
 empty skeleton in granular collector, elastic props. 4-87573  
 energy expressions for singular elastic states 4-87578  
 engineering problems, numerical soln. based on finite elements 4-110857  
 Ericksen's problem soln., iterative soln. method 4-110874  
 expanded plate theories, consistency between Kirchhoff and Reissner theories (German) 4-83825  
 extended elastic material, deformations and stress intensities due to a craze 4-97424  
 exterior domains, traction problem for linear elastostatics 4-69682  
 FCC crystal, low-angle [001] twist boundary, Volterra-type dislocation model 4-75454  
 fibre stability in an elastic matrix with nonuniform subcritical state 4-108031  
 fibres, elastic, sub-surface, elastic wave scatt. 4-97385  
 finite elasticity, equilib. solns. 4-97328  
 finite element method in elasticity, appl. of displacement function (Chinese) 4-79449  
 free boundary problems using boundary elements, Trefftz approach 4-63513  
 free elastic body systems with isoperimetric constraints, vibr. anal. 4-103244  
 half space, elastic, nonhomogeneous, indentation of a system of stamps, press. anal. 4-108051  
 half space having spheroidal inhomogeneity under all-around tension, stress field 4-97321  
 half-space, nonuniform, with an elastic cylinder, torsion 4-101644  
 hydroelastic systems, stability (Russian) 4-63515  
 hyperelastic solid with circular hole, displacement and stress fields 4-69685  
 hypoelastic isotropic relativistic medium, prop. of infinitesimal discontinuity waves 4-82680  
 hypoelasticity, with isotropic or kinematic hardening, constitutive relations at finite strain 4-79459  
 impact problems, lumped parameter method 4-97393  
 incompressible elastic solids, second-order problem simplification 4-67978  
 inextensible fibre reinforced material, stability, finite plane, strain 4-87579  
 infinite solid with thin foreign inclusion, integral eqns. for stress determ. (Ukrainian) 4-69680  
 inhomogeneously ageing bodies, asymptotics near crack tip 4-60325  
 interfacial crack between two dissimilar elastic orthotropic solids, transient stress intensity factors 4-74222  
 isotropic cube, finite element analysis of elasticity 4-86217  
 isotropic elastic layer, thermal crack problem, dual integral eqns. 4-112765  
 isotropic medium with curvilinear sections, second dynamic problem soln. in elasticity theory (Ukrainian) 4-69694  
 isotropic random elastic medium, critical properties from fractal model of percolating backbone 4-103209  
 J-integral estimation procedures for inelastic crack growth 4-76858  
 kinematic hardening and induced anisotropy in large elastoplastic strain (French) 4-79463  
 laminated composites, strength and elastic props., macroscopic description 4-97399  
 laminates, specially orthotropic, stacking combination stiffness matrices 4-60288  
 lattice and spin dynamical theories 4-76357  
 layer with winker-type coating, contact problems in the theory of elasticity 4-79523  
 layered composites with transversely isotropic constituents, annular crack problem 4-103263  
 layered elastic materials, strip loadings, finite layer anal. using flexibility approach 4-86211  
 line contact between a rigid indenter and a damaged elastic body 4-103272  
 linear elastic analysis, min. norm solns. 4-86210  
 linear elastic cracked body, transient elastodynamic second boundary-value problem 4-64881  
 linear homogeneous isotropic elastostatics, conservation laws 4-86208  
 liquid films, Gibbs elasticity of multicomponent solutions 4-108681  
 local elastic property determ. in solids, laser based method 4-60233  
 low-frequency theory of elastic wave scatt. 4-110877  
 lung compliance changes on HF ventilation in normal dogs 4-93783  
 magnesium orthosilicate, elastic props. of modified spinel phase at Earth mantle pressures 4-100558  
 magnetised medium/magnetically inactive medium interface, US transmission 4-92307  
 matrix/inclusion composite, overall elastic response, quasicrystalline approx. appl. 4-103207  
 mechanics, boundary layers and function spaces 4-63512  
 membranes, elastic, circular, large axisymm. deforms. 4-112703  
 membranes, linear elastic circular, small deflections under lateral pressure 4-97319  
 membranes, plane, under lateral press., variation principles and bounds for approx. analysis 4-97320  
 metacarpophalangeal joint, stiffness meas., circadian variation 4-93772  
 metal hydride solubility, elastic and plastic accommodation effects 4-108620  
 metal-polymer two-layer plate, circular 4-108010  
 metallic glasses, atomic size effect on formability 4-75300  
 metals, inelastic deformations, elastic-plastic effects during manufacture (German) 4-83838  
 n-methyl methacrylate copolymers slightly struct. by dimethacrylic esters of glycol, synthesis and props. (Russian) 4-85176  
 microvessel hydraulic conductivity, meas. in microvessels, effects of compliance 4-105382  
 mixed-mode elastic crack analysis, extended weight function method 4-97427  
 moment theory of elasticity, boundary-value problems in regions with slits 4-79452  
 multiple crack problem solns. using Fredholm integral eqns. 4-79509  
 muscle fibres, skinned; frog, radial stiffness in relaxed and rigor conditions 4-66978  
 nearly spherical cavities in an elastic medium, stress conc. 4-103211

## elasticity continued

- network model of elastic body with boundary load sources 4-95177  
 nodal forces in elements under surface and body loads in axisymmetric and planar elasticity theory problems 4-95176  
 nonhomogeneous elastic wall, mech. wave propag., reflexion and transmission coeffs. (Rumanian) 4-74915  
 nonlinear analysis, stiffness matrix extrapolation strategy 4-79451  
 nonlinear bending of corrugated annular plates 4-110878  
 nonlinear three-dimensional elasticity, unilateral problems (French) 4-97308  
 nonlinearity problems, geometric and material, formulation methods 4-78142  
 optical fibres, spring constant calculation in buckling 4-91586  
 piecewise-homogeneous space, spherically symm. wave propag. 4-78153  
 piezoceramic shell, reaction to concentrated effects 4-109129  
 piezoceramic shell theory, symbolic integration method appl. 4-60280  
 piezoceramic shells polarised along coordinate lines, boundary conditions in theory 4-60281  
 piezoelectric transducer, vibration and acoustic radiation, finite element method-equivalent circuit anal. 4-60241  
 pipe, thick-walled, in-plane vibr. problems 4-97392  
 pipes, cylindrical, resist. stress distrib. (French) 4-74877  
 plane contact problem formulation with wear of interacting bodies 4-74965  
 plane cut in elastic medium with slip and adhesion of surfaces, 3D mixed problems 4-60326  
 plane elastic arch, homogenisation 4-83814  
 plane elastic media, curvilinear cracks tip stress intensity factors 4-64886  
 plane finite elastic deformations, analogy with certain MHD flows 4-60297  
 plane polarised wave diff. on a noncircular cavity 4-74937  
 plane stamp indentation into elastic halfspace, self-similar problem 4-79524  
 plane wave interaction with a cut in an elastic medium under transseismic conditions 4-78152  
 plasticity hypoelastic formulation using past max. of stress 4-97344  
 plastics, prestressed, tensile strength investig. 4-89083  
 plate, cantilever, finite, long-time response to antisymm. dynamic surface loading 4-87563  
 plate, cantilever, finite, long-time response to dynamic surface loading 4-87564  
 plate, elastic thick circular, torsion by annular rigid stamp, stress anal. 4-97310  
 plate, homogeneous isotropic elastic, stress conc. at circular porous inclusion 4-79519  
 plate, infinite with broken or branching crack, stress determ. 4-64884  
 plate, multiconnected, anisotropic, with holes and internal cracks, elasticity theory problem 4-74954  
 plate, orthotropic circular thin, nonlinear axisymmetric transient anal. 4-103208  
 plate, orthotropic thin circular, with elastically restrained edge under central load, nonlinear static and transient analysis 4-60286  
 plate, rot. circular elastic, transient displacement and stresses 4-64844  
 plate, stability near sharp defect, initial biaxial stress state 4-108046  
 plate, stress conc. region near notches, photoelasticity, least squares analysis 4-103276  
 plate, thick circular, three dims. elastic stress anal. 4-97309  
 plate, thick circular in contact with isotropic elastic half-space, exam. using variational method 4-112775  
 plate reinforced by symm. system of radial ribs, nonsymm. bending 4-108008  
 plate theory, boundary conditions 4-83822  
 plate von Karman eqns. for Poisson ratio one-third, closed-form axisymm. soln. 4-97327  
 plate with thin-walled inclusion, stress state along arc of circle 4-60279  
 plate with two circular holes connected by narrow slit, stress conc. 4-108012  
 plates, annular, stability under shear 4-112745  
 plates, elastic, in-plane thermal stresses 4-97314  
 plates, elastic, laminated, isotropic and anisotropic, mixed variational theorem and appls. 4-90374  
 plates, elastic, stress intensity factors at sharp notches, path-independent integrals 4-87562  
 plates, infinite orthotropic, optimum quasi-rectangular holes under inplane loading 4-97325  
 plates, multiply connected, three-dims. elasticity theory problems, survey 4-101652  
 plates, solid, elastic, optimisation problem soln. by design space restriction 4-86213  
 plates, thin, elastic, nonlinear free flexural vibrations 4-87616  
 plates, viscoelastic, multilaminated, piezoelectric, geometrically nonlinear theory 4-79470  
 Plemelj formulas appl. 4-87630  
 poked cylinder, nonlinear bending and collapse anal. 4-74881  
 poly(dimethylsiloxane), bimodal networks, elasticity, stress-strain curve, Monte Carlo calcs. 4-71680  
 polycarbonate films, physical modification by compatible and incompatible cpds. (Russian) 4-103852  
 polymer liquid crystals, macroscopic phenomena, Fredericks transition 4-75284  
 polypropylene-polyethylene blends, rheological characts. 4-114595  
 porous elastic material, finitely strained periodic, macroscopic props. 4-74887  
 potential theory, boundary-element method modification for singularities and Neumann eqn. 4-63509  
 PU rigid foam, elastic props. at low temp. (Chinese) 4-105030  
 rate type polymers, stress relaxation, elastic energy 4-74892  
 region with curved cuts, dynamical elasticity problem 4-74879  
 Reissner plate function characteristics (German) 4-83826  
 resolvent finite element eqns., divergence-curl scheme 4-106193  
 rigid ring bonded to hollow cylinder, 3-dims. contact problem 4-112708  
 ring of arbitrary shape, in-plane vibr. problems 4-97392  
 rings, circular confined, collapse under external pressure 4-112742  
 rod, semiinfinite, cylindrical, connected to infinite elastic stratum longit. wave reflection 4-87610  
 rods, elastic, soln. of nonlinear cases of motion (Russian) 4-79437  
 rough body two-dims. contact problem soln. 4-108052  
 rubber elasticity entanglement models, uniaxial extension-compression 4-61971

**elasticity continued**

- sandwiched solid-metal flat gasket between two discs, contact stresses 4-112774  
 second order fluid, unsteady laminar flow due to flat plate movement 4-97484  
 semidiscretisation and time integration in solid and struct. mech., book contrib. 4-60266  
 shaft, elastic cylindrical, containing circular cracks, nonsteady stress state under torque 4-108047  
 shaft with annular groove, under tension, stress conc. problem 4-60284  
 shape optimal design using B-splines 4-106190  
 shell, cylindrical, elastically restrained, by axially spaced springs, free vibr. 4-74947  
 shell, cylindrical, contact problem, primary and dual formulation 4-64889  
 shell, cylindrical, made of rings, equilib. problem (*Russian*) 4-91732  
 shell, elastic spherical, interaction with plane acoustic wave 4-97382  
 shell, reinforced, cylindrical, stability in creep 4-74896  
 shell panel, thin, elastic, sloping with rigid inclusion, vibr. anal. 4-74943  
 shell stability 4-97365  
 shell theory, simple edge effect description, 3D theory of elasticity 4-112719  
 shells, multi-layered cylindrical, with adhesively bonded longit. stiffeners 4-79455  
 shells, shallow, theory, series-expansion method appl. as parameter for physically nonlinear problems 4-74857  
 shells, spherical, elastic stability anal. 4-87595  
 shells, thin, Lagrangian description and incremental formulation in non-linear theory 4-60285  
 shells, thin, linear elastodynamics, coupled primal-dual variational principles (*French*) 4-79450  
 shells, triple-layer, with delaminations, stability problems, filler three-dimens., model appl. 4-87603  
 shells, viscoelastic, multilaminate, piezoelectric, geometrically nonlinear theory 4-79470  
 shells of revolution, crit. load calc., variational difference method 4-60311  
 shoulder stiffness and elasticity of the muscle (*Japanese*) 4-100209  
 simple layer potential method for domains having external corners 4-63511  
 single degree of freedom elastic system with rate and state depend. friction, slip motion and stability 4-64890  
 solid suspension of spheres, effective moduli in lowest multipole approx. 4-110876  
 space with cut along spherical band surface, elasticity theory, axisymm. problem (*Ukrainian*) 4-87571  
 spatial elastic problems, soln. in deterministic and stochastic form (*Russian*) 4-73239  
 sphere, inside-out elastic, equilib. stability 4-112744  
 stamps, rigid smooth, action on simply connected elastic body 4-79525  
 stepped finite element analysis for elastic thin plate equations (*Chinese*) 4-106191  
 stochastic structural dynamics methods, critical review of reactor appls. 4-102336  
 stress concentration determ. using expt.-numerical methods 4-97445  
 stress measurement, acoustoelastic method using US waves (*Japanese*) 4-87648  
 stress tensor function for dynamic equilibrium (*German*) 4-67979  
 stress-boundary value problems in finite elasticity 4-74889  
 stresses and deformations, simplified solution 4-64846  
 stresses around a hole in a linear elastic material with voids 4-103203  
 strip, semi-infinite, decaying states of plane strain and boundary conditions for plate theory 4-83822  
 strip with row of circular holes subjected to tension, stress conc. 4-112707  
 structural models, potential function truncation, post-buckling response 4-64843  
 structural optimisation and sensitivity anal., variational approach by means of adjoint systems, struct. shape variation 4-82678  
 superlattices, surface vibrations and dispersion theory 4-80365  
 symmetry groups and conservation laws 4-86207  
 system small vibrations, Hilbert-Schmidt theorem extension to problems with unsymmetric kernels 4-110865  
 systems with elastic elements of large stiffness, dynamics 4-78130  
 tangentially loaded structures, critical forces, multi-modal anal. 4-87574  
 thermal elastohydrodynamic problems, lubrication theory 4-91779  
 thick composite shells, elastomechanics 4-87576  
 thin elastic shells, stability anal., catastrophe theory 4-87575  
 thin-walled cylinders, min. wt., of given torsional and flexural rigidity 4-97326  
 torus, nonaxially symm. deform. anal. 4-74859  
 transversely isotropic materials, acoustoelasticity 4-88240  
 transversely isotropic medium, stress conc. near a hyperboloid, notch in pure shear and bending 4-103210  
 trusses, elastic, bicriterion optimum design method 4-83820  
 tube deformation in noncontact zones during broaching 4-79471  
 two-dimensional elastic half-space, dynamic response, freq. domain anal. (*Japanese*) 4-103205  
 uniform asymptotic solns. of 2D problems of elasticity for domain exterior to thin region 4-69686  
 universal relations, local and global 4-83823  
 US wave speed in elastic bodies 4-87619  
 vascular compliance changes during hyperthermia, dog expts. and simulation anal. 4-81636  
 vibration problems for elastic body immersed in slightly compressible fluid 4-97381  
 weighted residuals based general soln. method 4-73235  
 Al-Cu casting alloys, cold cracking mech., plasticity-elasticity transition (*Chinese*) 4-62026  
 $\text{Pd}_{0.775}\text{Si}_{0.165}\text{Cu}_{0.06}$  metallic glass, low-freq. elastic loss at low temp. 4-70289  
 $\text{S}_x$  polymers, flexible networks, rubberlike elasticity 4-74872  
 $\text{S}_x$  polymers, flexible networks, rubberlike elasticity 4-74872  
 $\text{SiO}_2$  vitreous, low-freq. elastic loss at low temp. 4-70289  
 Sn-Bi elastic behaviour near melting point from sound vel. and attenuation meas. 4-75597  
 ZnS, multispectral, chemically vapour-deposited, initial characterisation 4-76418

**elasticity of liquids**

- see also compressibility of liquids  
 butyloxyphenyl noniloxypbenzoate, smectic A liq. cryst., elastic, nonlinear and plastic behaviour 4-92070  
 elastic constants calc. from structure functions 4-103844  
 hexa-n-octyloxytriphenylene, discotic liq. cryst., column buckling instability 4-113325  
 hydroelastic fluctuations in two-phase flow in tube bundles 4-103336  
 liquid crystals, Frank elastic const., mol. struct. 4-103641  
 MBBA, nematic liq. cryst., flexoelectric coeffs., bend curvature elastic const. meas. 4-65169  
 nematic liq. crystals, electric field induced flow, surface forces 4-70528  
 p-n-octyloxy-p-cyanobiphenyl, nematic liq. cryst., flexoelectric coeffs., bend curvature elastic const. meas. 4-65169  
 octyloxycyanobiphenyl, smectic A liq. cryst., elastic, nonlinear and plastic behaviour 4-92070  
 Oldroyd-B fluid, extruded and axisymmetric stagnation flows 4-97476  
 polymer jet, extruded from capillary die, elasticity, stretching and swelling 4-69722  
 polymers, conjugated, in gels, electric field coupling to slow elastic modes 4-98198  
 polymers flexible chain in region of shear rates and stresses, rheological behaviour, elastic state 4-69721  
 polyvinylidene fluoride-PMMA blends, homogeneous and inhomogeneous, rheological props. (*Russian*) 4-84331  
 PVC, vol. viscosity, compressibility, elastic modulus 4-70426  
 shear modulus meas. in freq. range 80-2500 Hz using torsion pendula 4-69726  
 surface waves and struct. of liq. surfaces 4-64963

**elasto-optical effects** see photoelasticity; piezo-optical effects**elastomers**

- see also rubber  
 butadiene elastomers, relax. process assoc. with supermol. struct., creep meas. (*Russian*) 4-85175  
 butadiene-(methyl)(styrene) elastomers, relax. process assoc. with supermol. struct., creep meas. (*Russian*) 4-85175  
 creep, temp. induced, hysteresis in thermoelasticity 4-113525  
 end-linked, bulk cured tetrafunctional networks 4-66585  
 ethylene propylene diene terpolymers, elastomeric networks, crystallisation, stress optical coeffs., DSC, X-ray obs. 4-92105  
 ethylene-propylene elastomers, long-time dynamic compatibility with liq.  $\text{N}_2\text{H}$  4-114609  
 ethylene-propylene elastomers, relax. process assoc. with supermol. struct., creep meas. (*Russian*) 4-85175  
 glass bead filled, failure processes near rigid spherical inclusion 4-76841  
 membranes, pervaporation separation of benzene-n-heptane mixtures 4-71978  
 model polyisobutylene networks, strain induced crystallisation 4-75324  
 peeling, spontaneous, fracture mechanics concepts (*French*) 4-114761  
 penetration swelling interaction in diffusion of liquids 4-98030  
 perforated viscoelastic elastomers, press. effects on dynamic props. 4-103879  
 poly(dimethylsiloxane), bimodal networks, elasticity, stress-strain curve, Monte Carlo calcs. 4-71680  
 polyacetylene/elastomer blends, electrically conductive 4-75940  
 polybutadiene, fracto-emission, effect of cross-linking 4-66419  
 polydiethyleneglycol terephthalate, elastomeric network, random coil config., stress birefr. obs. 4-84209  
 polydimethylsiloxane, trifunctional cross linkers, computer simulation 4-66584  
 polydimethylsiloxane, trifunctional model networks, elongation moduli 4-93324  
 polypropylene, impact modified elastomer blends and block copolymers, phase separation optical microscopy 4-66308  
 polyurethane, MDI/diol-based, hard-segment polymorphism 4-65195  
 polyurethane elastomers, chain segment orientation rel. to tensile strain, constitutive eqns. 4-76815  
 polyurethane-urea elastomers, segmented, struct. and props. 4-113356  
 radiation aging, time-temp. superposition 4-108431  
 stretched, recovery of surface layers during ageing in ozone (*German*) 4-65554  
 styrene-butadiene copolymer, fracto-emission, effect of cross-linking 4-66419  
 surfactant-modified, slow phys. relax. processes effect on props. in wide temp. range (*Russian*) 4-75327  
 Viton E60C, stress relax. response, shear modulus, dynamic meas. 4-71676

**elastoplasticity**

- acoustic emission, for crack resistance evaluation in steady loading 4-99699  
 adhesive bonded joints, elastoplastic stress anal., microcomputer program (*Japanese*) 4-103218  
 alloys, fatigue failure curves, centre portion anal. 4-92292  
 anisotropic elastoplastic materials, finite deform., effects of plastic rotation 4-6302  
 beam, elasto-viscoplastic response accounting for shear effect, numerical formulation 4-64849  
 beam, thin, transient finite elastic-viscoplastic deform, numerical simulation 4-97341  
 beam with unilateral supports, optimal design 4-106189  
 ceramics, friction wear, theoretical and expt. studies 4-62069  
 classical solutions guiding finite element strategies, examples 4-87423  
 composite material, singular approx. in theory of elastoplastic media with microstruct. 4-108018  
 constitutive relations finite strains, elastoplasticity with kinematic or isotropic hardening 4-79459  
 constitutive restrictions for idealized elastic-viscoplastic materials 4-97338  
 crack opening displacement design curves (*Japanese*) 4-91782  
 crystalline solids and geomaterials, finite plastic flow 4-98184  
 cylinder, two-layer, long, with nonsteady cooling, residual stresses problem soln. 4-64864  
 cylindrical bodies with spherical cavity, elastic/viscoplastic, stress-wave propag. 4-97368  
 deforming elastic-plastic materials, proof of normality condition 4-91735  
 disc, rotating, elastic-plastic stress, Tresca's yield condition 4-74902  
 discrete elastic-perfectly plastic structures, dynamic shakedown by modal anal. 4-108022  
 discrete limited-ductility structs., shakedown anal. 4-108023

**elastoplasticity continued**

- dislocation dynamics, finite amplitude plastic shock wave treated with summed infinitesimal amplitude elastic-plastic waves 4-60988  
displacement, equilibrium and hybrid finite element models, unified approach 4-103215  
ductile materials, failure, effect of yield surface vertex 4-69689  
dynamic analysis of elastic-plastic structures by mode-superposition and equivalent plastic load 4-97350  
dynamically loaded media, vel. distrib. of dislocations, quasiequilibrium function 4-65263  
elastic strain rate at small elastic-finite plastic deform. 4-64862  
elastic-plastic transition in shells under internal pressure and steady state temperature 4-64860  
fatigue crack propagation by crack-tip plastic blunting 4-71719  
fatigue cracks, growth rate and closure in incipient short and elastic-plastic long cracks (*Japanese*) 4-92291  
fibre reinforced composite, elastoplastic response, finite element micromechanical analysis 4-87581  
fibre reinforced composite pressure vessel, elastic-plastic solns. (*Chinese*) 4-112725  
finite deformation effects in elastic-plastic analysis 4-97353  
finite plasticity, constitutive results 4-69690  
finite strain theory 4-83828  
fracture, elastic-plastic, energy flux into process region 4-69705  
fracture in biaxial fields, higher order approx. for T-criterion 4-79495  
fracture toughness, elastic-plastic analysis of rel. between  $K_{Ic}$ ,  $J$  and CTOD 4-103267  
frames, dynamically side-loaded, rigid-plastic and simplified elastic-plastic solns. 4-97358  
frames, plane elastic-plastic, influence of discretisation density 4-79460  
hardening material under longitudinal shear, ribbon like inclusion, singular stress field 4-60304  
heterogeneity macroscopic effects at finite strain 4-64859  
hollow sphere of linear elastic-perfectly plastic material, large deformations (*German*) 4-83843  
incremental elastoplastic stiffness matrix for materials obeying the principal stress yield criterion 4-112731  
indentation fracture, indenter geometry effects 4-60346  
inelastic solids and structures, plasticity and creep methods, reactor appls. 4-102339  
J-integral estimation procedures for inelastic crack growth 4-76858  
J-integral path depend. for blunt crack 4-79499  
kinematic hardening and induced anisotropy in large elastoplastic strain (*French*) 4-79463  
laminated half-plane with elastic-plastic layer deform., surface buckling 4-97363  
local stress and strain fields near a spherical elastic inclusion in a plasticity-deforming matrix 4-60303  
mass with a vertical incline, elastic-plastic problem 4-79468  
material inhomogeneity and surface roughening during plastic deform. 4-99458  
mechanical behaviour of materials, conf., Stockholm, Sweden (Aug. 1983) 4-90297  
mechanics of material behaviour 4-95069  
metals, acoustoelastic response, plastic deform. effect 4-74903  
metals and alloys, strain hardening, plastic deform., elastic-plastic problem soln. 4-114623  
nonassociated elastoplasticity, finite elements, axisymm. necking in void-containing materials 4-79462  
nonlinear structural stability, finite element method appls. (*Polish*) 4-60310  
nonlinearity problems, geometric and material, formulation methods 4-78142  
oscillatory shearing of a class of elastic-plastic materials 4-79473  
perfectly plastic anti-plane straining, theory 4-87584  
plane problems, elasticity and plasticity law representation 4-78143  
plastic struct., one dimens., dynamic problem soln. 4-64857  
plate, notched, cyclic elastoplastic strain fields, endochronic analysis 4-97342  
plate, tensile, small scale, with centre crack tensile test, elastic-plastic FEM computation 4-114737  
plates, elastic-plastic anal., triangular assumed-stress finite element (*Chinese*) 4-79457  
plates, large deflection, incremental model (*French*) 4-74890  
plates, thin elastoplastic, incipient buckling study (*French*) 4-83846  
plates, transversal-isotropic circular, elastic-plastic bending (*Russian*) 4-112735  
porous materials, elastoplasticity theory 4-87585  
porous materials, thermoelastoplastic deform. 4-60306  
power-law elastic-plastic material, near tip dynamic fields for 4-60328  
power-law hardening material, optical shadow spot method for tensile crack 4-97449  
quasi-statically moving surfaces, restrictions of strong discontinuity in elastic-plastic solids 4-97347  
rings, circular confined, collapse under external pressure 4-112742  
rod, elastoplastic state rel. to loading path 4-108024  
rod, solid, failure, effect of yield surface vertex 4-69689  
rod of elastoplastic material, dynamics of buckling 4-112743  
rods, nonlinear, elastic-plastic, under cyclic loading, stress accumulation (*German*) 4-83845  
rotating annulus, elastic-plastic stress distrib. under external press. 4-87577  
shell, cylindrical, coiled, loaded by internal press., elastoplastic deform. analysis 4-97335  
shell, double-walled elastoplastic, with complex nonisothermal loading, stress/strain state 4-64865  
shells, shallow, theory, series-expansion method appl. as parameter for physically nonlinear problems 4-74857  
shells, thin-walled, with stress concentrators, elastic-plastic state in cases of small and large strains 4-74898  
shells, unevenly heated, elastic-plastic design, applicability of Kirchhoff-Love hypothesis 4-60309  
shells of rotation, axisymmetric, elastoplastic, variable loading, numerical anal. (*Russian*) 4-60274  
solid body, elastic-perfectly plastic, dynamic shakedown for set of alternative loading histories 4-97332  
stability of geometrically non-linear elastic-plastic shells 4-87593  
start-thrust module with axial expansion, plastic-hypelastic model anal., stresses (*German*) 4-83842  
steel, austenitic stainless, ductile fracture resistance, assessment based on engineering approach 4-104876

**elastoplasticity continued**

- steel, austenitic stainless, strain hardening, hysteresis, constitutive eqns. 4-104805  
steel, C, fracture toughness, stretch zone, ductility, transition region 4-99468  
steel, Cu-Ni-Cr, compact and surface-flawed specimens, fracture toughness meas. comp. 4-104858  
steel, fracture toughness meas. using specimen strength ratio 4-81371  
steel, stainless, type 304, crack opening, stable growth, instability, elastoplastic anal. 4-76822  
steel, structural, nonlinear elasto-plastic creep, stress and temp. depend. 4-109465  
strain hardening materials, determ. of post yield stresses from strains 4-64897  
strain-hardening topography of elastic-plastic materials 4-97343  
stress, shock and acceleration waves in various materials, explicit Lagrangian finite diff. method 4-60324  
stress analysis of structures subject to elastic and plastic deform., appropriate model for structural software 4-74894  
stress and strain fields around inclusions in plastically deforming matrix 4-97360  
stress calculation in finite element anal. 4-91734  
stress frame specimens, thermo-elastic-plastic anal. of dynamic stress (*Chinese*) 4-60349  
structure response to loading field, Newton-Raphson scheme 4-108029  
thermomechanical deformation, stress/strain relations over period with isothermal uniaxial loads 4-64863  
thick walled tube, branching-out pressures, additional axial forces effect on fissures (*German*) 4-83863  
thin-walled cross sections under pure torsion, elastoplastic stress conc. at reentrant corners 4-97345  
Tresca and Mohr-Coulomb yield functions, removal of singularities 4-97359  
tubes, eccentric, elastic-plastic strain stress state 4-97334  
tubular specimen, failure, effect of yield surface vertex 4-69689  
viscoelastic-plastic material behaviour, intermediate configs., strains, reactor appls. 4-102337  
viscoplastic materials, advanced deformations and fracture initiation, constitutive modelling 4-103856  
viscoplastic materials, isoclinic parameters under cyclic stress, expt. invest. 4-87641  
voids and inclusions, elastic-plastic finite element anal. 4-92195  
Al alloys, fatigue crack growth, thermoactivation anal. 4-99597  
Al, dynamic yield strength meas. 4-89110  
Ti-Al-V (6.4 wt.%), dynamic yield strength meas. 4-89110

**elastoresistance**

No entries

**ELDOR**

- naphthalene in decalin soln., sensitized photolysis ELDOR electron spin echo study 4-112212  
nitroxyl type radicals, glassy solns., ELDOR electron spin echo study 4-112212  
2,2,6,6-tetramethyl-4-piperidone-N-oxyl, liq. solns., spin relax., EPR and ELDOR obs. 4-107373

**electrets**

- see also dielectric devices; electrostatics; photoelectrets; thermoelectrets*  
centroid of charge determ., in two-side metallised electrets 4-86441  
ethylene propylene fluorinated copolymer, positive charge stabilisation 4-65688  
polyethylene terephthalate electrets, AC elec. field form. and TSC studies 4-84902  
polymer, radiation induced charge transport 4-71264  
PVDF, complex polarisation distributions 4-76320  
transducers, electromechanics anal. 4-73432  
Si, plastically deformed, thermostimulated depolarization spectra 4-114199  
SiO<sub>2</sub> backplate electret transducer 4-69655  
TaO<sub>2</sub>, amorphous film, electret state relax. 4-88765

**electric admittance**

- microorganisms, enumeration by their dynamic AC conductance patterns, model and expt. method 4-62453  
resistive susceptibility of 3-D random diode-insulator network 4-78261  
semiconductors, grain-boundary admittance theory 4-108849  
Fe<sub>2</sub>O<sub>3</sub>, electrochemical kinetic studies 4-99803  
PZT-polymer composites, piezoelec., with two dimensional periodicity, reson. modes of vibr. 4-76331  
Pt electrodes, adsorption of tripeptide, AC admittance meas. 4-92538  
a-Si:H Schottky barriers, sputtered, freq. depend. capacitance, admittance meas. 4-98693

**electric admittance measurement**

- lattice defects in semiconductor diode structures meas. by capacitance method 4-90611  
semiconductor thin films, minority carrier lifetime and surface recomb. vel. meas., small-signal admittance meas. 4-68239

**electric amplifiers** *see amplifiers***electric arc welding** *see arc welding***electric arcs** *see arcs (electric)***electric breakdown**

- see also electric breakdown of gases; electric-breakdown of liquids; electric breakdown of solids*  
dielectric materials, measurements anal. appls., conf., Lancaster, England (Sept. 1984) 4-106120  
MHD generator interelectrode breakdown obs. 4-66728  
optical aerosol breakdown producing extended plasma region, collective mode 4-113187  
vacuum, impulsive breakdown, electrode vapor resonance radiation emission 4-65146  
vacuum breakdown initiation, by fast microscopic particles impact 4-108245  
vacuum gap triggered by exploding wire, delay time 4-87960  
Weibull statistics, theoretical basis and appls. 4-109121  
Al, anodic films, pore filling, elec. breakdown characts. 4-81350

**electric breakdown of gases**

- see also electron avalanches*  
air, compressed, with metal vapour and particles at high temp., elec. breakdown (*Japanese*) 4-103463  
air, laser induced breakdown thresholds by admixing electronegative gas 4-79708

**electric breakdown of gases continued**

- air, laser-produced breakdown interferograms, high-speed recording 4-75120  
 air, positive corona breakdown, residual streamer channel 4-108233  
 air, positive DC corona, breakdown parameters and current-voltage char-acts. 4-79887  
 atomic gases, laser breakdown near metal surfaces 4-113111  
 breakdown plasma in air, induced by pulsed TEA-CO<sub>2</sub> laser radiation, evolution 4-79824  
 breakdown waves, spatiotemporal luminous investigations 4-79729  
 bulk discharge with ionisation multiplication of photoelectrons and light generation 4-79730  
 corona discharges in air and other gases, experimental O<sub>3</sub> production study 4-79738  
 CW arc pluming at high-power aerials, pulsed RF plasmas obs. 4-69970  
 CW arc pluming at high-power aerials, scale-model studies 4-69971  
 dry air, formative time lags calc. for crossed electric and magnetic fields 4-84096  
 electrodeless breakdown with pre-breakdown current-flow 4-79731  
 electron gas, electric breakdown waves 4-87836  
 fast waves, breakdown in long tubes, 4-60769  
 high-voltage breakdown investigation 4-79724  
 laser produced converging shocks and consequent plasma effects in gases 4-84121  
 laser-triggered elec. breakdown of gases, fundamental processes 4-75221  
 light induced detonation of gas, lateral expansion, optical discharge 4-113252  
 long spark formation in optical discharge plasma channel 4-108238  
 methane gas, DC breakdown strength, isotope depend. 4-79723  
 methane-d<sub>4</sub> gas, DC breakdown strength, isotope depend. 4-79723  
 microwave breakdown threshold lowering in periodic-pulse operation 4-87967  
 nonpreionised gas in cylindrical discharge tube, wave breakdown, electron prod. kinetics 4-60766  
 in one-turn solenoid, initial stage investigation 4-79725  
 positive wire to plane coronas, atmospheric humidity effect on inception voltage 4-79737  
 RF ion sources, breakdown behaviour 4-78417  
 rod-rod gap, sparkover, impulse voltage induced stress and humidity effects 4-79716  
 space-charge-limited electron current flow in curved geometries with ion. prod. 4-92006  
 sphere-plane gaps in dry air, impulse breakdown, 0.25 to 2 atm. 4-79718  
 stellator, nonplanar, gas breakdown and plasma form. 4-79726  
 Townsend ionization coeff. determ., initial photoelec. current rel. to gas press. 4-60770  
 Ar gas, breakdown threshold near metal target by laser heating 4-69933  
 Ar, picosecond laser-induced breakdown study 4-103462  
 D<sub>2</sub> gas, DC breakdown strength, isotope depend. 4-79723  
 H<sub>2</sub> gas, DC breakdown strength, isotope depend. 4-79723  
 He, low pressure breakdown, stepwise voltage drop 4-69976  
 He, threshold near metal target by laser heating 4-69933  
 He-F<sub>2</sub>(SF<sub>6</sub>) mixtures, elec. breakdown 4-79720  
 He-Ne low breakdown voltage lasers, capillary gas breakdown modelling (Chinese) 4-112380  
 He-O<sub>2</sub> mixtures, breakdown characts. meas. using improved microwave cavity design 4-95465  
 N<sub>2</sub> breakdown in strongly nonuniform elec. field at nanosec. voltage pulsing 4-79719  
 N<sub>2</sub> gas, elec. breakdown at high uniform field strength 4-79717  
 N<sub>2</sub> prebreakdown ionis., quenching mechanisms investigation 4-79722  
 N<sub>2</sub>-O<sub>2</sub>(SF<sub>6</sub>) breakdown in strongly nonuniform elec. field at nanosec. voltage pulsing 4-79719  
 ND<sub>3</sub> gas, DC breakdown strength, isotope depend. 4-79723  
 NH<sub>3</sub> gas, DC breakdown strength, isotope depend. 4-79723  
 Na, vapour, laser initiated discharge channels 4-113255  
 Ne streamer breakdown, electron avalanche critical radius 4-103595  
 SF<sub>6</sub>, breakdown voltage and time to breakdown under impulse voltage, insulator support effect 4-65150  
 SF<sub>6</sub> compressed, breakdown voltage and timelags under corona stabilisation 4-79727  
 SF<sub>6</sub> in rod-rod gap, impulse breakdown, insulated barrier shielding 4-79715  
 SF<sub>6</sub> insulations, AC breakdown voltage calcs. area effect 4-79721  
 SF<sub>6</sub>, low press., long path breakdown and discharge development 4-79730  
 SF<sub>6</sub> negative ions, electron detachment and its importance in elec. breakdown 4-91337  
 SF<sub>6</sub> positive DC corona, breakdown parameters and current-voltage char-acts. 4-79887  
 SF<sub>6</sub>, positive leader propagation 4-79881  
 SF<sub>6</sub> prebreakdown avalanche pulses under uniform field 4-113244  
 VOCl<sub>3</sub>, pulsed CO<sub>2</sub> laser induced chemistry 4-114808  
 Xe, picosecond laser-induced breakdown study 4-103462

**electric breakdown of liquids**

- aerosol medium optical breakdown, low-threshold; comprehensive diagnos-tics 4-65109  
 alkanes, anomalous positive point prebreakdown behaviour 4-84911  
 aqueous aerosols, weakly absorbing, disruption and optical breakdown in intense light field 4-65108  
 high pressure, electroexplosive action influence (Russian) 4-71273  
 laser-induced breakdown, shock wave production 4-61624  
 liquid metal films, electromag. induced breakdown during free flow on surface (Russian) 4-114210  
 oil, aged transformer, DC cond. under nonuniform high fields 4-88771  
 organic fluid, surface discharge use for resistor fragment creation (Rus-sian) 4-71274  
 viscous dielectric fluid electrohydrodynamic behaviour and current response to voltage changes 4-97702  
 He dielectric breakdown delay time, superconductivity effect 4-109125

**electric breakdown of solids**

- see also impact ionisation; Zener effect  
 dielectrics, conduction and breakdown, conf., Toulouse, France (July 1983) 4-106109  
 electrofracture mechanics and aging 4-93007  
 explosives, PBX and PBXW, elec. resist. and dielec. breakdown meas. 4-108865  
 glass, electron irradiated, discharge form. 4-71275  
 glass, electron-irradiated, discharge phenomena 4-71277

**electric breakdown of solids continued**

- glass fibre reinforced polymers, electrical insulator components, damage in combined elec., mech. and chemical environments 4-66466  
 insulating solids, conduction and breakdown phenomena, role of electrodes 4-108869  
 insulating thin films, breakdown, rel. to recording mech. in thin-film breakdown counters 4-102525  
 LV thermoplastic/thermosetting insulating materials for industrial use, laboratory tests (Italian) 4-99410  
 n<sup>+</sup>-p<sup>+</sup> structure, I-V characts., dopant profile effects 4-88572  
 p-n junction isolation, breakdown characts., mask misalignment and crys-tal defects 4-92813  
 PMMA Plexiglas insulator, breakdown phenomena in vacuum and N<sub>2</sub> gas gap 4-65950  
 polyethylene, dielec. breakdown at elevated temps. 4-109123  
 polyethylene, tree initiation rel. to DC prestressing effects, needle-shaped voids 4-84912  
 polyethylene, water tree propag., effect of physicochem. factors 4-109120  
 polyethylene films, treed and crosslinked, anal. of water 4-71281  
 polymers, electric breakdown, review 4-114208  
 polymers, electrical cond. and carrier traps, review 4-108854  
 polymers dielectrics, elec. breakdown rel. to high-mobility states 4-109119  
 polystyrene thin layers, dielec. breakdown, definition and characts. 4-109122  
 polythene, impulse elec. strength, comments 4-109126  
 prebreakdown electron emission currents, switching and other nonlinear phenomena 4-76641  
 PVC:Al(OH)<sub>3</sub>(Al<sub>2</sub>O<sub>3</sub>), resist. to tracking study 4-69969  
 soil, arc initiation characteristics, effect of ambient gas 4-62799  
 soil, elec. breakdown, high resolution studies 4-62797  
 soil, elec. breakdown initiation by water vapourisation 4-62798  
 weakly absorbing dielectrics and semiconductors, convective instability and self-focusing in laser-induced breakdown 4-97009  
 Ag thin films, electroformed, humidity sensitive switching 4-108908  
 Al-(SnO<sub>2</sub>+Sb<sub>2</sub>O<sub>3</sub>)-Al mixed thin films, dielec. studies 4-84719  
 Al<sub>2</sub>O<sub>3</sub> anodised films, breakdown statistics 4-109128  
 Al<sub>2</sub>O<sub>3</sub> thin film deposition by UV laser photolysis 4-99337  
 Al<sub>2</sub>O<sub>3</sub> thin layers, dielec. breakdown, definition and characts. 4-109122  
 BaF<sub>2</sub> epitaxial films, vacuum deposition on PbSe 4-99316  
 Fe powder, porous, type P2h-2-MZ high-voltage breakdown 4-80867  
 GaAs, p-n junctions, spectral distrib. of avalanche breakdown radiation (Russian) 4-98715  
 GaTe, amorphous films, elec. breakdown in pulsed fields 4-114209  
 Ge:Sb(As), impurity state breakdown under uniaxial compression 4-70715  
 InTe, amorphous films, elec. breakdown in pulsed fields 4-114209  
 Mo electrodes, selective SiO<sub>2</sub> form. for MOS struct. 4-98467  
 Si oxide films, elec. props. and oxidation characts. 4-65762  
 Si, plasma anodic nitridation in N<sub>2</sub>-H<sub>2</sub> system, struct. and optical props. 4-81307  
 Si<sub>3</sub>N<sub>4</sub> layers, ion beam synthesised, dielec. breakdown, current density-voltage and capacitance-voltage characts. 4-80706  
 Si<sub>3</sub>N<sub>4</sub>:F films, plasma enhanced CVD, insulating props. 4-61865  
 Si<sub>3</sub>N<sub>4</sub> thin film deposition by UV laser photolysis 4-99337  
 Si<sub>3</sub>N<sub>4</sub> films, photo-CVD, props. study 4-99338  
 SiO<sub>2</sub>/SnO<sub>2</sub> coeap. films in sandwich struct., high-field cond. and opt. absorpt. 4-108948  
 SiO<sub>2</sub> films, photo-CVD, props. study 4-99338  
 SiO<sub>2</sub> films, plasma enhanced MOCVD, MOSFET fabrication 4-81153  
 SiO<sub>2</sub> gate dielects., charge build-up and breakdown 4-109124  
 SiO<sub>2</sub> gate oxide breakdown, expt. study 4-114207  
 SiO<sub>2</sub> thin film deposition by UV laser photolysis 4-99337  
 SiO<sub>2</sub> thin layers, dielec. breakdown, definition and characts. 4-109122  
 SiO<sub>2</sub>, vitreous, flashover model (French) 4-65949  
 SiO<sub>2</sub>/Cu films, elec. breakdown strength, Cu precipitates effect 4-99022  
 Ta, anodic oxidation, electron injection and avalanche breakdown 4-89183  
 Zr electrolytic porous powder, high-voltage breakdown 4-80867
- electric cables** see cables (electric)  
**electric capacity** see capacitance  
**electric cells** see cells (electric)  
**electric charge**  
 see also space charge  
 airborne particle electric charge measurement, charge distribution analysis 4-95473  
 circumstellar dust grains in nova ejecta, effect of elec. charge on growth and destruction 4-101372  
 Dunnington's e/m<sub>0</sub> meas. method, undergraduate expt. 4-106144  
 dust particles in plasma, limitation of electrostatic charging 4-101141  
 electric neutrality of matter, results summary, quark searches, e-p charge difference 4-59080  
 electrostatic precipitators, aerosol particle charging by free electrons, charge potential limit model 4-99853  
 electrostatics, four dimensional, multipole expansions for charge distrib. 4-59953  
 Fredholm's method for determ. of electrostatic fields and equipotentials 4-87245  
 Saturn ring particles, limitation of electrostatic charge and elec. current transport 4-101141  
 self corona discharge of sharp edged ellipsoidal particles in electric field 4-97934  
 He<sup>+</sup> rich solar particle events, ionic charge state meas. 4-110587  
 He-rich solar particle events, ionic charge distrib., ISEE 3 meas. 4-110586  
 Ni-Cd cell residual charge meas. using microprocessor-based unit 4-81535
- electric coils** see coils  
**electric condensers** see capacitors  
**electric conductance** see electric admittance  
**electric conductance measurement** see electric admittance measurement  
**electric conduction processes** see electrical conductivity  
**electric conductors** see conductors (electric)  
**electric current**  
 see also arcs (electric); corona; critical currents; current density; current distribution; current fluctuations; eddy currents; electrojets; leakage currents; short-circuit currents; sparks  
 current heating coefficient M and its application (Polish) 4-112670

**electric current continued**

- diagonal MHD channel, problems associated with consolidation of electrode currents 4-85378  
 flame, time-dependent elec. current 4-71929  
 Hall current, effects on free convection with mass transfer in rot. fluid 4-101134  
 Hall current, effects on heat and mass transfer in flow through porous medium 4-101125  
 Hall current, effects on natural convective flow in slip flow regime 4-101128  
 Saturn ring particles, limitation of electrostatic charge and elec. current transport 4-101141  
 solar corona, electric currents generation by convective motions in photosphere 4-63116  
 solar corona, heating by reconnection in DC current systems 4-115730  
 transformer loaded with single phase half-wave rectifier, theoretical anal. (Chinese) 4-107481

**electric current control**

- AlGaAs semiconductor laser, frequency stabilization by thermal and current feedback control 4-60071

**electric current measurement**

- see also ammeters; galvanometers  
 air-hare current meas., design for eliminating displacement currents 4-90007  
 automatic DC measurement instrument 4-77641  
 cable radiation, evaluation model 4-107497  
 calibrators, precision and ease of use (French) 4-58864  
 charge flux intensity in vacuum, meas. by counting method (Polish) 4-111149  
 DC ammeter using Hall effect transducers 4-111120  
 isolated current monitor for low-frequency asymmetrical current waveforms 4-58869  
 large current measurement using digital multimeter, shunt technique (Spanish) 4-101875  
 LDPE, contactless dielec. meas of charge and current 4-106331  
 monomode optical fibres, low birefr., polarisation rot. due to geometric effects, use in current sensor 4-107859  
 NBS (Gaithersburg) developments 4-63702  
 NPL moving-coil ampere determination (Japanese) 4-101824  
 Permalloy thin film sensor, design, construction and appl. 4-111123  
 rail gun arc armature, spatial distributions meas. 4-78346  
 techniques and instruments, review (German) 4-82807  
 transformers, small rated secondary currents, errors determ., meas. techniques (German) 4-86444

**electric discharges** see discharges (electric)**electric domain walls**

- ferroelectric crystals, soliton propag. and electroacoustic interactions (French) 4-99047  
 ferroelectrics, domain struct. influence on elec. cond. 4-99067  
 polydomain ferroelectrics, uniaxial, soft local vibrs. 4-93028  
 semiconductor, multivalley, anomalous Hall effect and multivalued Sasaki effect 4-80615  
 thermal hysteresis near commensurate-incommensurate phase transition, interpretation 4-76382  
 BaTiO<sub>3</sub> poly and single cryst. dielec. after-effects and domain walls 4-71267  
 Gd<sub>2</sub>(MoO<sub>4</sub>)<sub>3</sub>, ferroelectric-ferroelastic, acoustic emission and domain wall dynamics 4-84925  
 LiNH<sub>4</sub>SO<sub>4</sub>, ferroelec. domain struct., SEM studies 4-71321  
 PbTiO<sub>3</sub>, single crystal, dislocation and domain struct. 4-75452  
 Tb<sub>2</sub>(MoO<sub>4</sub>)<sub>3</sub>, ferroelectric-ferroelastic, acoustic emission and domain wall dynamics 4-84925

**electric domains**

- see also electric domain walls; ferroelectric materials  
 alanine-TGS ferroelectric crystals, pyroelec. props. (Chinese) 4-114213  
 antiferromagnetic ferroelectric, equilibrium state of mag. subsystem 4-71150  
 ceramics, ferroelectric, switching and hysteresis effects 4-76401  
 cyanoadamantane, glassy cryst. phase and plastic phase, local mol. order, diffuse X-ray scatt. anal. 4-98022  
 ferroelectric crystals, soliton propag. and electroacoustic interactions (French) 4-99047  
 ferroelectric domain layer surface wave, dispersion eqns. 4-88787  
 ferroelectric smectic C\* liq. crystals, helicoidal struct., field induced processes 4-65171  
 GASH single cryst., ferroelec. domain struct., SEM studies 4-71320  
 nematic liq. cryst., longitudinal domain struct., laser diff. studies 4-60829  
 octylcyanobiphenyl, dielectric props., time domain spectroscopy study 4-104520  
 poly(vinylidene fluoride), solution growth, ionic impurity effects 4-98037  
 polyvinylidene fluoride and copolymers, ferroelec. switching, computer simulation 4-99049  
 ruby, electric domains due to laser irradiation, hysteresis 4-114224  
 ruby, electric domains due to laser irradiation 4-114223  
 surface distortions near phase transition points, quadrupole moment anomalies 4-88385  
 TGS, and deuterated, ferroelec. crystals, pyroelec. props. (Chinese) 4-114213  
 TGS, doped cryst., dielec. permittivity nonlinearity, rel. to growth conditions 4-76297  
 TGS, ferroelec. switching current, effect of time between polarisation reversals 4-76368  
 TGS, lateral struct. of domains, obs. using laser probe technique with high pyroelectric signal 4-88786  
 TGS, pyroelectric response relax., role of viscous phenomena 4-71284  
 TGS crystal, polarisation current, domain width distrib. 4-71262  
 TSTs piezoceramic, dielec. props., influence of 90° domain struct. 4-76396  
 vinylidene fluoride/trifluoroethylene copolymer, ferroelec. transitions 4-99050  
 (Ba,Sr)TiO<sub>3</sub> heteroepitaxial ferroelec. films, domain struct. 4-65993  
 BaTiO<sub>3</sub> cryst., ferroelec. domain struct., SEM and optical microscopy studies 4-71319  
 BaTiO<sub>3</sub> crystals, γ-irradiated, with equilb. domain struct., polarisation state 4-76395  
 BaTiO<sub>3</sub>, piezoceramic, dielec. props., influence of 90° domain struct. 4-76396  
 BaTiO<sub>3</sub>, reverse switching effect 4-76393

**electric domains continued**

- BaTiO<sub>3</sub>, reversed c-domain patterns and elastic wave velocity surfaces 4-84924  
 BaTiO<sub>3</sub>, surface domains, double Laue pattern topography 4-104548  
 BaTiO<sub>3</sub> thick film, grain boundaries, TEM obs. 4-84300  
 BiFeO<sub>3</sub> single cryst., ferroelec. domains, birefringence, and light absorption 4-71324  
 Cd<sub>2</sub>Nb<sub>2</sub>O<sub>7</sub>, diffuse and sharp phase transitions, dielec., optical, and electro-optical studies 4-71309  
 Cd<sub>2</sub>Nb<sub>2</sub>O<sub>7</sub>:Gd<sup>3+</sup>, ferroelec. transitions, EPR spectra 4-98945  
 Cr<sub>2</sub>B<sub>2</sub>O<sub>3</sub>Cl, ferroelec. orthorhombic to monoclinic transition 4-71301  
 CsH<sub>2</sub>PO<sub>4</sub> ferroelec., domain struct. relax. 4-71322  
 Gd<sub>2</sub>(MoO<sub>4</sub>)<sub>3</sub>, domain walls, SAM and SPAM study 4-99064  
 Gd<sub>2</sub>(MoO<sub>4</sub>)<sub>3</sub> polydomain ferroelec., quadrupole fields 4-80882  
 H<sub>2</sub>(UO<sub>2</sub>)(AsO<sub>4</sub>)<sub>4</sub>H<sub>2</sub>O, phase transition temps. and ferroelec. domain struct. 4-76400  
 KH<sub>2</sub>PO<sub>4</sub>, ferroelec., domain struct., dielec. and loss consts. 4-65994  
 KH<sub>2</sub>PO<sub>4</sub>, ferroelec., domain struct. relax. 4-71322  
 KNbO<sub>3</sub>, ferroelec. domain struct., IR spectra anal. 4-71323  
 K<sub>2</sub>SeO<sub>4</sub>, incommensurate phase, SHF Obs. 4-61635  
 LiNH<sub>4</sub>SO<sub>4</sub>, ferroelec. domain struct., SEM studies 4-71321  
 LiNbO<sub>3</sub> cryst. growth, melt composition effect on props. 4-84227  
 LiNbO<sub>3</sub>, single cryst., phys. props. 20-200°C 4-76397  
 LiNbO<sub>3</sub>, spontaneous polarisation screening on free surface 4-88767  
 LiNbO<sub>3</sub>:Fe, photocurrent jumps due to domain struct. (Russian) 4-75996  
 LiTaO<sub>3</sub> crystals, poling using interdigital electrodes, appl. to bulk wave transducers 4-99068  
 MgO, dipolar defect ordering due to dissolved CO<sub>2</sub> 4-71287  
 (NH<sub>4</sub>)<sub>2</sub>BeF<sub>4</sub>, incommensurate phase, SHF Obs. 4-61635  
 NaH<sub>2</sub>(SeO<sub>3</sub>)<sub>2</sub> biaxial ferroelec., ferroelastic and ferroelec. domains 4-93027  
 NaH<sub>2</sub>(SeO<sub>3</sub>)<sub>2</sub>:Cr<sup>3+</sup>, EPR spectra, temp. and external elec. field effects 4-88715  
 NdP<sub>2</sub>O<sub>4</sub>, domain walls, SAM and SPAM study 4-99064  
 PLZT ceramics, poling strategy 4-76319  
 PLZT, tetragonal ceramic, 90° domains under poling, XRD study 4-76398  
 PZT, dielec. props. at high press., p-T phase diagrams 4-99062  
 (Pb,Li)(Zr,Ti)O<sub>3</sub> ceramics, stress anisotropy induced by polarisation 4-104536  
 (Pb<sub>0.75</sub>Ca<sub>0.25</sub>)(Co<sub>0.1</sub>W<sub>0.2</sub>Mo<sub>0.4</sub>Ta<sub>0.3</sub>)O<sub>3</sub> ceramics, piezoelec. props. MnO addition effects 4-104532  
 Pb<sub>2</sub>GeO<sub>11</sub>, ferroelec., surface states role in polarisation reversal 4-71325  
 Pb<sub>2</sub>Ge<sub>2</sub>Te, rhombohedral phase, energy surfaces and domain struct. 4-76010  
 PbTiO<sub>3</sub>, delayed phenomena in transient pyroelectric response derived from cylindrical shaped domains 4-61630  
 PbTiO<sub>3</sub> heteroepitaxial ferroelec. films, domain struct. 4-65993  
 RbHSeO<sub>4</sub>, ferroelec. ferroelastic, light deflection 4-80883  
 Sn<sub>2</sub>P<sub>2</sub>S<sub>6</sub> ferroelec. semicond., Curie temp. photoinduced shift 4-93017  
 Sr<sub>8</sub>Al<sub>12</sub>O<sub>24</sub>(CrO<sub>4</sub>)<sub>2</sub>, flux growth, ferroelec. phase transition, domain studies, birefr., polarisation, permittivity, transition enthalpy meas. 4-65970  
 Sr<sub>1-x</sub>Ca<sub>x</sub>TiO<sub>3</sub>, XY quantum ferroelec. with transition to randomness 4-88871  
 TGS, ferroelec. transition and domains, positron annihilation, TEM and decoration studies 4-65985  
 TGSe, audiofrequency dielec. dispersion, universal behaviour and temp. depend. 4-76303  
 Te(OH)<sub>6</sub>·2NH<sub>4</sub>H<sub>2</sub>PO<sub>4</sub>·(NH<sub>4</sub>)<sub>2</sub>HPO<sub>4</sub>, single cryst. growth and morphology 4-61821  
 TiH<sub>2</sub>PO<sub>4</sub>, ferroelastic phase transition, permittivity meas. 4-65393  
 Ti<sub>2</sub>SeO<sub>4</sub>, ferroelec. transition, birefringence studies 4-65976

**electric double layers** see electrochemistry; liquid theory**electric double refraction** see electro-optical effects**electric drives**

- see also electric propulsion  
 electrodynamic drive for a Mossbauer spectrometer 4-101996  
 stepping motor control ckt. for monochromator scanning system 4-101828

**electric field effects**

- see also acoustoelectric effects; discharges (electric); electrical conductivity; electro-optical effects; electrochemistry; electrodynamics; electrokinetic effects; electroluminescence; electromechanical effects; electromigration; electron field emission; electrophoresis; field emission in micro-spaces; field evaporation; field ion emission; field ionisation; high field effects; magnetoelectric effects; particle optics  
 artificial satellites, elec. drag 4-82370  
 atoms, dynamic response in elec. field, Born-Oppenheimer and Feynman-Hellmann approx. 4-102589  
 S-bromochlorofluoromethane, liq., translational motion, external elec. field effect 4-103625  
 cell surface, concanavalin A receptors, migration in pulsed elec. fields 4-89532  
 ceramic electrodes for ELF bioeffects studies 4-115296  
 chiral liquid-crystal mixture, electric-field-induced helix uncoiling 4-75292  
 cholesteryl laurate-cholesteryl capitate mixture, growth kinetics of cholesteric spherulites, applied elec. fields 4-113322  
 dipole tom, electric field commutation rel. 4-64445  
 electrically modulated membrane permeability 4-99839  
 electron tunnelling, from potential well, in electric field 4-86247  
 electroseparator, slotted, field strength distrib. calc. (Russian) 4-82806  
 ferromagnetic semicond., nonequilibrium system of electrons and magnons, fluctuations in strong elec. fields 4-98870  
 human body, overhead power line 50-Hz elec. field, physiological effects 4-62520  
 LF stray fields, EM smog (German) 4-59971  
 lymphocytes, human, clastogenic effects of power freq. elec. fields 4-89646  
 metal surface, lattice relax., effect of strong elec. field 4-75766  
 plasma weakly ionised, electron energies under alternating elec. fields 4-60583  
 polarisation nuclear magnetic shielding in elec. field 4-107368  
 polymer macromol. degradation in elec. fields and under mech. loading (Russian) 4-104869  
 polymers, conjugated, in gels, electric field coupling to slow elastic modes 4-98198  
 polymethylmethacrylate, evolution of fractures, prolonged action of electric field 4-108507

**electric field effects continued**

- polypropylene and polycarbonate, study of dielectric relaxation in polymer blends—transient current approach 4-99021
- polystyrene, evolution of fractures, prolonged action of electric field 4-108507
- power-frequency elec. fields, system for cell suspensions exposure 4-100365
- quadratic field induced effects in macromol. solns. 4-85405
- Rydberg atoms with large orbital ang. momentum, prod. 4-59655
- semiconductors, heterogeneous anisotropic, electrodiffusion purification 4-71533
- surface tension, two-phase liquids, influence of arbitrarily oriented elec. field 4-80330
- taste-aversion learning in rats rel. to 60 Hz elec. field exposure 4-100233
- thiourea, deuterated, neutron diff. study under high elec. field 4-109142
- turbulent heating by low pulsed elec. field in Tokamak plasma, trapped electron effect 4-79813
- Ag films, structure and resistivity, transverse elec. field effect (*German*) 4-76052
- Al-chalcogenide glass structures, cathode effect in electrostimulated chem. transformations 4-88804
- CaS:Cu, Er (Sm) electroluminsors, radiation controlled enhancement of electroluminescence 4-76529
- Cu films, structure and resistivity, transverse elec. field effect (*German*) 4-76052
- H atoms, second-order perturbation theory in crossed elec. and mag. fields 4-83329
- H, dynamic response in elec. field, Born-Oppenheimer and Feynman-Hellmann approx. 4-102589
- H photoionisation in elec. field, reson. and interference effects 4-69028
- H photoionisation in elec. field, overlapping resons. and interference effects 4-69029
- He, dense gas, electron delocalisation by external elec. field 4-75119
- <sup>4</sup>He, superfluid, charged vortex ring nucleation by exotic negative ions in strong electric fields 4-75742
- KMnO<sub>4</sub>, thermostability var. during crystn. in elec. field 4-70047
- ZrO<sub>2</sub>, electrotransport purification, contamination and cold ends effects 4-61819
- electric field gradient (condensed matter)** *see crystal hyperfine field interactions; hyperfine field interactions (condensed matter)*
- electric field measurement**  
*see also field plotting*  
atmospheric boundary layer potential, Hy-wire measurement system 4-67437
- broadband high-power MM to CM-wave spectrometer 4-68284
- calibration equipment with parallel-plate capacitor 4-95468
- dielectric films, radiation charged, methods for charge-or field-distrib. studies 4-71826
- dielectrics, high-resistance, probing methods of strong current fields 4-71825
- dipole antennas appl., geometric asymmetry effects determ. 4-58834
- electro-optical instrument, sensitivity improvement techniques (*Japanese*) 4-78298
- EM field strength probe, noise anal. 4-106309
- EM near-field sensor for simultaneous electric and magnetic field meas. 4-112317
- field emission in microwave field visualisation 4-104724
- half-wave dipole standard system meas. of elec. field in continuous range 100-300 MHz 4-58871
- implantable electric field probes, performance characts. 4-89855
- magnetosphere electric field measurement with spherical double probes on satellites 4-82367
- microwave spectrometer, broadband, mm-to-cm range 4-78373
- oceanographic meter, using AgCl miniature electrodes 4-62974
- probe for EM field meas., of submillimeter dimensions 4-106310
- probes, miniature type, size limitations, sensitivity 4-95462
- radio stations, EM radiation meas. 4-106281
- spherical dipole probe system, 30 Hz 1 MHz EM fields meas. 4-106282
- vacuum space potential meas. using emissive probe 4-69956
- He-O<sub>2</sub> mixtures, breakdown characts. meas. using improved microwave cavity design 4-95465
- electric field strength measurement** *see electric field measurement*
- electric fields**  
*see also electric field effects; electric field measurement; electromagnetic fields; electromagnetic waves; field plotting*  
charge simulation method for exterior problems of narrow regions (*Japanese*) 4-112318
- conducting surface, small or comparable to wavelength, E-field solution 4-87250
- coplanar electrode systems, electric-field distribution 4-96748
- cosmic grains fluff, effects on field emission, charge and particle levitation 4-94578
- dielectric polarisation, labyrinthine instability in dielectric fluids 4-99011
- Earth radio noise spectral characts., few hertz to 50 kHz., expt. data-review 4-89879
- EHD induction pumps, stability study 4-97703
- electric fields and charges in elementary circuits 4-82629
- electrofluidised beds, small wave propagation and, reflection analysis 4-97677
- electrostatic discharges, charged insulator minimum potential for incendiary discharges 4-97936
- electrostatic fluidised bed behaviour under radioactive gas flow conditions 4-97678
- EM wave focusing through dielectric interface, distribution of electric fields 4-112323
- equilibrium step junction, surface and field variables, general soln. 4-92805
- external equipotential lines, shape determ. of electrode system producing the field (*Russian*) 4-102846
- ferromagnetic cylindrical conductor with weak nonlinearity in harmonic quasistationary regime, weak skin effect (*French*) 4-65698
- field eqns. comparison with mechanical material eqns. (*German*) 4-83512
- heat transfer during condensation of nonconducting fluids in DC electric field 4-97561
- ice polymorphs, electrostatic field and mol. dipole moments 4-70051
- industrial electric/magnetic fields, effects on health (*French, German*) 4-72299
- ionosphere, double layer-like and soliton-like structures; rocket obs. 4-105791
- ionosphere, double layer-like structures at rocket altitudes 4-105792

**electric fields continued**

- isolated collector sphere for charged aerosol collection, electrostatic field direction effect 4-95464
- photovoltaic modules, method for calculating multidimensional elec. fields 4-77104
- Quincke rotation of spheres in liquid dielectrics with electrostatic field applied 4-96749
- radioactive flow, electric fields from ion recombination effects 4-103435
- rotating charge distrib., mag. and elec. fields 4-106160
- self corona discharge of sharp edged ellipsoidal particles in electric field 4-97934
- solar wind, elec. field penetration rel. to field-aligned current in magnetosphere polar cap 4-110372
- solar wind field, penetration to magnetosphere and ionosphere 4-94305
- stars, photospheric sources of magnetic field aligned currents 4-94748
- static fields measurements, extrapolation using finite element method 4-83514
- three-dimensional electric field calculation by means of surface charges and surface currents 4-102849
- transition scattering of velocity waves from stationary sources of the electric and magnetic fields 4-112326
- Venus ionosheath, PVO plasma and electric field meas. 4-94659
- water, dielec. props., charge injection and transport anal. 4-99023
- electric filters** *see filters*
- electric furnaces**  
*see also resistance furnaces*  
AC high-stability microprocessor-based temperature controller for use at high temperatures 4-111119
- microcomputer-controlled furnace for obtaining dynamic thermogravimetric measurements 4-111137
- resistance furnace for vacuum metallurgy facility (*Chinese*) 4-106327
- electric generators**  
*see also d.c. generators; magnetohydrodynamic converters; turbogenerators; Van de Graaff generators*  
American Power Conference, Chicago, USA (April 1983) 4-86112
- Stirling engine-generator sets development for the US Army 4-66780
- electric glow** *see corona*
- electric heaters** *see electric heating*
- electric heating**  
*see also domestic appliances; drying; electric furnaces; induction heating; ovens; radiofrequency heating; space heating*  
oil recovery, electrothermic system for heavy viscosity oil 4-72044
- residential solar/electric water heater simulation model development and evaluation 4-72050
- C, vitreous, strip heater annealing of ion implanted Si:Sb 4-92375
- electric ignition**  
No entries
- electric impedance**  
*see also electric reactance; electric resistance*  
catheter input impedances computation for cardiac volumetry 4-85532
- coaxial system, 1/N expansion for Dirichlet boundary problems 4-96751
- humidity sensitivity of sintered porous alumina and alumina-boria (*Japanese*) 4-66642
- metal surface impedance calc. in IR domain 4-104251
- perineurium of frog sciatic nerve, AC impedance 4-105217
- polystyrene films, underwater, interfacial polaris. in bilamellar struct., dielec. anal. 4-84901
- posts in waveguide, impedance calc. by current simulation method (*Japanese*) 4-83526
- skeletal muscle, impedance from 1 Hz to 1 MHz 4-85414
- source impedances and errors in voltage measurements, theoretical and expt. study (*Spanish*) 4-106329
- spark sources, high voltage, current waveforms simulation, rel. to gap dynamic impedance 4-79854
- US transducer with Gaussian field profile and improved electrode impedance characts. 4-97250
- vascular thoracic impedance, meas. after complete obstruction of pulmonary artery (*French*) 4-66984
- BaTiO<sub>3</sub> oxide perovskites, dielec. meas., surface layer effects 4-65962
- Ge, compensated, photoresponse to local optical excitation 4-108904
- Nd<sub>2</sub>Zr<sub>2</sub>O<sub>7</sub>-Nd<sub>2</sub>Ce<sub>2</sub>O<sub>7</sub> system, anion cond., order/disorder effects 4-70447
- Pb<sub>1-x</sub>Ge<sub>x</sub>R, R=rare earth, dielec. spectrum study, 5.5 to 380K 4-71272
- Pb<sub>1-x</sub>Ge<sub>x</sub>Te, rhombohedral phase, energy surfaces and domain struct. 4-76010
- SrTiO<sub>3</sub> oxide perovskites, dielec. meas., surface layer effects 4-65962
- electric impedance measurement**  
*see also electric reactance measurement; electric resistance measurement*  
biological tissue, applied potential tomography review 4-115259
- computerised impedance tomography imaging of the body with nonlinear reconstruction 4-89813
- ethanol fermentation, elec. impedance meas. as in situ sensor 4-85587
- fluid distribution in human legs, extra- and intra-cellular fluid vol., elec. impedance meas. 4-77409
- high-power automatic network analyzer for measuring the RF power absorbed by biological samples in a TEM cell 4-115294
- meter use for dielectric meas. 4-58841
- metrological research in Czechoslovakia, by TESLA, Brno 4-90614
- quaternary lasers, high-speed transient effects 4-79200
- steel bar reinforcements in concrete, corrosion rate, AC impedance meas. by spectrum analyser 4-109546
- thorax computerised electrical impedance imaging 4-77416
- urinary bladder fullness determ. by electrical impedance meas. 4-77411
- Li/CF battery, electrochemical characts. 4-99955
- Ni-Cd cells, degradation study using impedance measurements 4-72068
- electric load** *see load (electric)*
- electric moments**  
*see also atomic electric moment; molecular moments; nuclear electric moment*  
antiferromagnetic dielec., hybrid excitations, anal. of mag. and optical props. 4-76233
- methane, IR transition moments, isotopic depend. 4-69146
- neutron charge, search method 4-64000
- neutron elec. dipole moment, strong CP violating soft-pion nucleon coupling constant contrib. 4-68407
- neutron electric dipole moment, expt. search 4-63998
- neutron electric dipole moment, triangle graph contribution 4-86711
- neutron electric dipole moment meas. method 4-64321
- neutron electric dipole moment search 4-63999
- non-Abelian Klein-Kaluza theories, spinor fields 4-58702

**electric moments continued**

- nonlinear optical susceptibility, calculus, of 7 and 9-order, without fine struct. consideration (*Rumanian*) 4-69494
- poly N-vinylcarbazole soln., dipole moment, Kerr consts., stereoregularity 4-93053
- Quincke rotation of spheres in liquid dielectrics with electrostatic field applied 4-96749
- $S_4$  permutation symmetry, CP nonconservation, rare decays and quark/lepton electric moments 4-86600
- strong CP violation, neutron electric dipole moment 4-111453
- $\eta$  Z 4-59083
- Eu complex, tri(ethylsulphate) enneahydrate, elec. dipole intensity parameters 4-70756

**electric motors**

- see also d.c. motors; stepping motors
- photoelectric tachometer test set, review (*Japanese*) 4-106296
- vehicular technology conf. Pittsburgh, PA, USA (May 1984) 4-106118

**electric networks** see networks (circuits)**electric noise measurement**

- avalanche photodiodes with separate absorption, grading and multiplications, excess noise statistics meas. 4-112587
- conductivity fluctuations, probe size effects 4-80636
- NMR pickup coil design, noise current meas. and S/N improvement, low-temp. expts. 4-68252
- optical fibre communications receiver, circuit noise, theoretical anal. and computer calculation (*Chinese*) 4-79290
- UHF radio environment, man-made noise level meas. 4-107972
- H<sub>2</sub> maser frequency standards, limitations due to receiver noise 4-96854

**electric potential**

- see also contact potential; overvoltage; surface potential; voltage control; voltage measurement
- AC potential drop system for steel crack length monitoring 4-114741
- cellulose acetate membrane, membrane charge and Donnan distrib. of ions by EMF 4-105027
- circular parallel plate capacitor, potential, analytical soln. 4-59954
- electric cells with porous electrochemical electrodes, potential and current density distribution study (*Hungarian*) 4-105098
- electrostatic discharges, charged insulator minimum potential for incendiary discharges 4-97936
- electrostatic precipitators, aerosol particle charging by free electrons, charge potential limit model 4-99853
- electrostatics, four dimensional, multiple expansions for charge distrib. 4-59953
- EMF and potential difference: an illustrative example 4-78078
- external equipotential lines, shape determ. of electrode system producing the field (*Russian*) 4-102846
- Fredholm's method for determ. of electrostatic fields and equipotentials 4-87245
- glycerol, normal and metastable supercooling liq., fluctuating voltage spectrum, crystn. process 4-92991
- Hall plates and anisotropic layers with arbitrary geometries, pot. distrib. 4-64649
- nonuniformly magnetised long rod moving through scanning coils, EMF 4-76953
- polyethylene-Al contact, elec. pot. distrib., SEM study 4-104314
- semiconductor complex structs., EMF due to dynamic deformation 4-65953
- solid electrolyte mixed potential phenomena 4-71939
- Na-S batteries, molten polysulphide electrodes, pot. distrib. and electrochem. reaction rate 4-66678
- W wires, electropolished, struct. changes after thermal treatment rel. to surface state (*Polish*) 4-85249

**electric power generation**

- see also direct energy conversion; ocean thermal energy conversion; power stations; wave power generation
- biogas in agriculture and production of power and heat (*German*) 4-99980
- forecasting system, intermediate future, conf. Washington DC, USA (Aug. 1982) 4-78038
- generic solar thermal conversion configurations for large power appls., comparative analysis 4-114923
- heat transfer problems in advanced systems 4-85388
- moving bed thermal energy storage system, appl. to fossil and solar powered boilers 4-105118
- nuclear fuel cycle cost, current data and developments (*French*) 4-91064
- photovoltaic electricity generation, work by AEG-Telefunken, overview (*German*) 4-85365
- pressure retarded osmosis for electrical power generation from salinity gradients 4-62399
- renewable energy sources for power generation, Italian experience 4-81514
- Stirling engines, coal-burning, large-scale, possible applications 4-72148
- thermionic cogeneration burner design 4-77123
- waste resource recovery and energy generation 4-93585
- H<sub>2</sub> production and use for rural Alaskan community, programme design and planning 4-89473
- H<sub>2</sub>/electrical power simultaneous production, using carbonaceous fuels and high-temperature nuclear process heat, thermodynamic anal. 4-89472

**electric propulsion**

- see also electric drives; electric vehicles; traction
- nuclear electric propulsion missions 4-115675
- secondary cells for electric vehicle propulsion and load levelling applications, progress 4-62338
- LiAl/FeS cells with molten salt electrolyte for elec. vehicle propulsion (*German*) 4-77076
- Pb/acid cells for electric vehicles, comparison with alternate cells 4-62335

**electric reactance**

- see also capacitance; inductance
- No entries

**electric reactance measurement**

- see also capacitance measurement; inductance measurement
- No entries

**electric resistance**

- erythrocyte suspensions, LF elec. resistance rel. to Fricke's formula 4-100096
- silicone composite material, glassy film conversion, humidity-sensing props. rel. to elec. resistance 4-63752
- solar cells, series resistance determinations, review 4-85373

**electric resistance continued**

- BaTiO<sub>3</sub>, combined doping, electron-conduction compensation 4-113475
- GaAs concentrator solar cells, resistance effects and cell performance 4-77086
- In-Hg/Si ohmic contacts, differential resistance and capacitance characts. 4-92819
- In-Hg/insulator contacts, differential resistance and capacitance characts. 4-92819

**electric resistance furnaces** see resistance furnaces**electric resistance measurement**

- see also ohmmeters
- contact resistance measurement for two different metals, allowing for thermal EMF 4-92794
- diffusivity of H in metals meas. 4-68343
- direct current comparator resistance bridge automation, alloy resistivity appl. 4-90613
- heavily doped semicond. diffusion layers, surface resist. eddy current meter for non-contact meas. (*Russian*) 4-111155
- metrological research in Czechoslovakia, by TESLA, Brno 4-90614
- ohmic contacts, specific contact resistivity from contact end resist. meas. 4-84673
- semiconductor diffused layers, surface resist. meter for non-contact meas. (*Russian*) 4-111154
- solar cell, series resist. meas. methods 4-81555
- solar cells, contact resist. meas. and importance rel. to power loss 4-81545
- solar cells sheet resist., nondestructive meas. using laser scanner 4-73450
- square-wave method for measuring very low resistances at low temperatures (*Chinese*) 4-90567
- thermometer testing standardisation in USSR, using GOST 8.461-8.2 standard 4-58851
- thin metal films, using transient hot-strip method 4-68242
- two-probe and four-probe resistances on nonuniform structures 4-58868

**electric resistors** see resistors**electric sensing devices**

- see also instruments; measurement
- absolute layer thickness gauges, comparative study 4-95381
- biomedical pressure sensor using buried piezoresistors, Si diaphragm 4-85530
- buried-collector vertical magnetotransistors, geometrical analysis of offset 4-95474
- chemical sensor research at the laboratory of applied physics in Linköping 4-111116
- combustible gas sensors, development of poison resistant type 4-95414
- combustion detection with a semiconductor color sensor 4-82812
- computerised time-domain EM induction system 4-86442
- cryogenic sensor-amplifier interfaces, hybrid circuit freq. compensation modules 4-90573
- displacement sensors: which technologies? (*French*) 4-63710
- dual in-line package spectrophotometric sensor 4-68261
- EM field meas. probe, of submillimeter dimensions 4-106310
- EM field strength probe, noise anal. 4-106309
- EM induction coil detector, time domain response analysis and obs. 4-100790
- EM near-field sensor for simultaneous electric and magnetic field meas. 4-112317
- EM stress gauge, effect of stress discontinuities 4-106313
- ethanol fermentation, elec. impedance meas. as in situ sensor 4-85587
- Fahrenheit temperature sensor, monolithic IC implementation with internal offsetting function 4-95423
- FET humidity sensor incorporates temperature sensor 4-73443
- fiber optic sensors in industrial applications. An update 4-107878
- force, small values, precise meas., dist. meas., direct conversion and zero defl. sensor types 4-82785
- frequency response optimisation of constant temp. detector system 4-63735
- gas sensors, MOS and catalytic, comparison 4-82787
- high technology electronics exhibition and conference, Detroit, MI, USA, (June, 1983) 4-95014
- humidity, sintered alumina and zircon, elec. resistivity rel. to surface area of oxides (*Japanese*) 4-63751
- hygrometer, compact, using thermosensitive capacitor, DIY design (*German*) 4-68235
- interdigitated electrode structures, polymer covered, for CO, CO<sub>2</sub>, CH<sub>4</sub> and H<sub>2</sub>O sensing 4-95401
- IR laser radiation detection using antenna-coupled point contact Schottky diode, responsivity study (*Japanese*) 4-78374
- ISFET, membranes fabrication by ion-beam technique 4-95402
- ISFET pH sensor, surface and buried channel, characterisation 4-72033
- liquid He level indicator, appl. of amorphous supercond. alloys 4-86403
- magnetic sensor, double-diffusion differential amplification type, design and characts. 4-90575
- magnetoresistive Permalloy sensors and magnetometers 4-90615
- MOM detector for optical of submillimetre regions, developments 4-73516
- MOS integrated sensors, electrochem. and charge-imaging effects 4-82786
- multielectrode microprobe for extracellular biopotential recording 4-115320
- neural prostheses, natural and artificial sensors development 4-115275
- optoelectronic magnetic-field-sensitive element 4-106334
- Permalloy thin film sensor, design, construction and appl. 4-111123
- photoelasticity, static and dynamic, data acquisition, photometric meas., sensors 4-86464
- piezoelectric vibrating wire sensor for press. measurement 4-72738
- piezoresistive gauge for press. meas. from short laser pulse 4-111097
- piezoresistive strain sensors in weighing technology, theory and applications (*German*) 4-101825
- PMMA with Cu thermistor, shock loaded, direct temp. meas. 4-106322
- pressure, temperature and mag. field sensors, design and characts. (*French*) 4-111121
- proximity/interruption/reflection detection, IR optoelectronic systems with optical fibres (*French*) 4-111208
- self-detecting light-emitting diode optical sensor for object proximity meas. 4-95411
- semiconductor gas sensor, environmental changes effect on sensitivity 4-62431
- semiconductor gas sensor characts. obs., using fast gas selection valve 4-58840

**electric sensing devices continued**

- silicone composite material, glassy film conversion, humidity-sensing props. rel. to elec. resistance 4-63752  
 solid-state devices and materials, conf., Tokyo, Japan (Aug.-Sept. 1983) 4-82595  
 temperature measurement systems calibration 4-73409  
 temperature sensor characteristics and measurement system design 4-86400  
 thick film hybrid probes, used for liquid or gas flow velocity measurement (*German*) 4-65041  
 thick-film hybrid sensors, design, charact. and meas. appl. (*German*) 4-82789  
 thin film fire sensors, temperature-sensitive resistors, anal. 4-95406  
 unidirectional vacuum gauge by detecting excited neutrals (*Japanese*) 4-63757  
 vibrating capacitor measurement of surface charge 4-11118  
 Wiegand wire sensor charact., use of Co-Fe-V alloy (*German*) 4-101830  
 Al rods impaction on PMMA target, radial displacement meas. method 4-106280  
 AlO<sub>3</sub>/nH<sub>2</sub>O thin films, ageing, elec. struct. and moisture response charact., sensor appls. 4-86393  
 CO<sub>2</sub> electrochemical sensor for high ambient pressures, deep diving appls. 4-106311  
 He level sensor using superconducting wire 4-101808  
 In<sub>2</sub>O<sub>3</sub>-based transparent film temp. sensors, performance under high-density solar fluxes 4-90585  
 O<sub>2</sub> gas sensors using solid electrolyte, miniature rugged design 4-86401  
 O<sub>2</sub> potentiometric sensor based on LaF<sub>3</sub> (*Japanese*) 4-86395  
 O<sub>2</sub> sensors, solid-electrolyte type, review 4-101834  
 Pd MOS structure, H<sub>2</sub> sensitivity over wide press. range 4-63729  
 Si diffusion tensometers, parasitic photosensitivity 4-101829  
 Si diode temp. sensors, stability, 4.2 to 273K 4-68229  
 Si sensors with on-chip signal processing for long-term stability 4-68225  
 Si temperature sensor for microcomputer-based system using SAB 80215 device (*Italian*) 4-86418  
 SnO<sub>2</sub>, elec. props., SO<sub>2</sub> treatment effects, gas sensor appl. 4-92732  
 SnO<sub>2</sub> gas sensors, sintered material, CO sensitivity and response time 4-86394  
 SrFeO<sub>3-x</sub> screen-printed layers for methane detection 4-101832  
 SrTiO<sub>3</sub> detector of liquid <sup>4</sup>He level 4-101833  
 Yb piezoresistance gauges, response to shock front and calibration 4-106314  
 ZnCr<sub>2</sub>O<sub>4</sub>-LiZnVO<sub>4</sub> ceramic sensors, humidity-sensitive props., microstruct. 4-82800  
 ZnO/CuO:Li junctions I-V characteristics, humidity effects, humidity sensor appl. 4-63750

**electric sheet** see iron alloys; silicon alloys

**electric shielding, nuclear** see nuclear screening

**electric sparks** see sparks

**electric steel** see iron alloys; silicon alloys

**electric strain gauges** see strain gauges

**electric strength**

- see also electric breakdown  
 aluminous electrical porcelain, doped with talc, microstruct. and med. props. 4-114674  
 n-perfluorobutane, dielectric strength, press. depend. 4-75220  
 polyethylene, dielec. breakdown at elevated temps. 4-109123  
 polythene, impulse elec. strength, comments 4-109126  
 Weibull statistics, theoretical basis and appls. 4-109121  
 BaTiO<sub>3</sub>, semicond. glass ceramics, oxidation, barrier layer form. 4-114699  
 SO<sub>2</sub>, dielectric strength, press. depend. 4-75220  
 a-Si:H films, anodic oxidation, elec. and optical props. of oxidised films 4-109527

**electric susceptance** see electric admittance

**electric susceptibility** see optical susceptibility

**electric switchgear** see switchgear

**electric transformers** see transformers

**electric utilities** see electricity supply industry

**electric variables control**

- see also electric current control; frequency control; power control; voltage control  
 film transport systems, static control 4-106417  
 film transport systems, static control 4-111223

**electric variables measurement**

- see also attenuation measurement; capacitance measurement; charge measurement; dielectric measurement; electric admittance measurement; electric current measurement; electric field measurement; electric impedance measurement; electric noise measurement; electric reactance measurement; electric resistance measurement; electrical conductivity measurement; frequency measurement; gain measurement; inductance measurement; phase measurement; power factor measurement; power measurement; Q-factor measurement; voltage measurement  
 computerised time-domain EM induction system 4-86442  
 earth station G/T meas., angular extension correction of radio stars 4-105969  
 EHF aplanatic zoned dielectric lens antenna, anal. 4-102998  
 electronic meas. and laboratory practice, book 4-58585  
 errors and uncertainties in electrical measuring techniques (*German*) 4-111148  
 measuring instruments theory, moving coil, bridge and current comparison methods (*German*) 4-58863  
 vacuum-arc cathode spot, current density estimation 4-97902  
 VHF band absorber, improvement (*Japanese*) 4-107492

**electric vehicles**

- see also electric drives; electric propulsion  
 alkaline storage battery aspects of air electrode research, appl. 4-66687  
 batteries for electric vehicles, research and development requirements 4-77082  
 disabled person vehicle, leg muscle propelled 4-93975  
 modular electrochemical storage system for electric road vehicles, development and tests 4-77080  
 secondary cells for electric vehicle propulsion and load levelling applications, progress 4-62338  
 vehicular technology conf. Pittsburgh, PA, USA (May 1984) 4-106118  
 Al-air battery, rapidly refuellable, for electric vehicles, performance evaluation 4-72096  
 Al-battery, rapidly refuellable, for electric vehicles, current development trends 4-72095

**electric vehicles continued**

- Li batteries for electric vehicles, new design project, general overview 4-85363  
 LiAl/FeS cells with molten salt electrolyte for elec. vehicle propulsion (*German*) 4-77076  
 Na-S battery development and appl., Ford Aerospace program, USA 4-66685  
 Ni-Fe batteries for electric vehicles, performance evaluation 4-99960  
 Pb/acid batteries, future outlook in Japan 4-62340  
 Pb/acid batteries, influence on capacity of pulsed discharge, importance for electric vehicles 4-66683  
 Pb/acid cells for electric vehicles, comparison with alternate cells 4-62335  
 Pb-acid batteries for electric vehicles, performance evaluation 4-99960  
 Zn-Br batteries for bulk energy storage, design projections and low cost manufacturing techniques 4-66686  
 ZnCl<sub>2</sub> battery technology, status 1983 4-77075

**electric welding**

- see also arc welding; electron beam welding; resistance welding  
 No entries

**electrical conduction in condensed matter**

- see also carrier density; carrier lifetime; carrier mean free path; carrier mobility; carrier relaxation time; dislocation scattering; electrical conductivity of liquids; electrical conductivity of solids; electrical conductivity transitions; electron density (metals); electron mean free path (metals); electron mobility (metals); electron-phonon interactions; electron relaxation time (metals); high field effects; hopping conduction; impurity scattering; Lorenz number; minimum metallic conductivity; minority carriers; mixed conductivity; negative resistance effects; one-dimensional conductivity; photoconductivity; point defect scattering; size effect; skin effect; small polaron conduction; space-charge-limited conduction; spin disorder resistivity; surface conductivity; surface scattering; thermally stimulated currents; tunnelling  
 Bloch electrons transport in const. elec. or mag. field 4-70768  
 disordered systems, weak localisation and Coulomb interaction 4-104162  
 homogeneous medium with S-type negative differential cond. (*Russian*) 4-88497  
 linear transport coeff., Kubo formula (*Chinese*) 4-92682  
 multilevel spin system, quasi-stationary current distrib. 4-70771  
 percolation conductivity problem, improvement to effective-medium approx. 4-70767  
 quartz sand, aqueous suspension, specific elec. cond., volumetric fraction of sand depend. (*Russian*) 4-85338  
 randomly substituted lattice, long range and nearest neighbour interactions, hopping transport 4-84600  
 transport eqn. for isotropic electron distrib. function and electron relax. (*Russian*) 4-65654  
 Voronoi and regular networks, 3D, percolation and cond., topological disorder theory 4-90539

**electrical conductivity**

- see also electrical conduction in condensed matter; electrical conductivity of gases; electron mobility; ion mobility; space-charge-limited conduction  
 dielectric materials, measurements anal. appls., conf., Lancaster, England (Sept. 1984) 4-106120  
 disordered systems, half flux quanta, Bohm-Aharonov effect 4-90425  
 nonlinear conductors, percolation theory and renormalisation 4-88495  
 random media, dielectric polarisation methods for coeffs. of same generic type 4-99009  
 site-percolation problem, cond., effective-medium theory 4-58798

**electrical conductivity measurement**

- air-deployed oceanographic mooring (AB1034) for current and thermohaline struct. 4-115632  
 air-launched expendable seawater conductivity and temp. profiler 4-115629  
 direct current comparator resistance bridge automation, alloy resistivity appl. 4-90613  
 ferromagnetic materials, relative magnetic permeability and electrical conductivity measurement (*Polish*) 4-90616  
 haemoglobin content of blood, conductimetric procedure for assay 4-85544  
 Hall effect, measuring device (*Chinese*) 4-58870  
 Hall effect meas. in specimens of any shape, automatic system 4-101873  
 Hall voltages changes at high temp. meas., using AC meas. system 4-58866  
 high pressure equipment, two stage nonmagnetic, for studying transport phenomena (*Chinese*) 4-90607  
 high-temperature method 4-86440  
 lecture notes and study guide on process analysers and recorders, book 4-106138  
 liquid semiconductors, automated meas. using fused quartz cell 4-68241  
 material concentration in liq. media, dual freq. monitoring method (*Russian*) 4-81488  
 nervous tissues, diffusely arranged, conductivities and anisotropies, determ. and importance in neurophysiological studies 4-93978  
 nonequilibrium carrier effective lifetime meas. in semiconductor wafers 4-101872  
 oceanographic CTD profilers, measurements contaminated by ocean particulates 4-110303  
 reference specimens of specific elec. cond., eddy current certification 4-95471  
 rod, conducting, AC inspection, contactless method 4-71832  
 sedimentary rocks, frequency dependent dielectric and conductivity response 4-72488  
 semiconductor materials recombination parameters determ. using electrolytic cell with magnetic clamp 4-90612  
 semiconductor thin films, thermopower and conductivity measurements, optical beam deflection technique 4-98786  
 soil water content and elec. cond. meas. technique 4-110307  
 Ge microwave conductivity and recombination radiation obs., <sup>3</sup>He refrigerator construction and test 4-68234  
 W, high-temperature Lorenz number, thermal and elec. cond. meas. (*German*) 4-80564

**electrical conductivity of amorphous metals and alloys**

- see also dislocation scattering; electron density (metals); electron mean free path (metals); electron mobility (metals); electron relaxation time (metals); electronic conduction in metallic thin films; impurity scattering; point defect scattering; surface scattering  
 amorphous alloys, crystallisation, activation energies from elec. resist. meas., review 4-108285

**electrical conductivity of amorphous metals and alloys continued**

- direct current comparator resistance bridge automation, alloy resistivity appl. 4-90613
- electron transport, review 4-75918
- metallic glasses, elec. resist. and sp. ht. due to interaction of cond. electrons with two-level systems 4-92689
- metallic glasses, quasielastic electron scatt. by two-level systems 4-92688
- metals, disordered, elec. cond. and thermoelectric, power computation 4-92686
- metals, elec. resist., phonon ineffectiveness in diff. model 4-113918
- physics of amorphous solids, book 4-90312
- AgCu, conc. layered amorphous thin films, diffusional mixing, elec. resist. meas. 4-92687
- Au-Cu-M metallic glasses, (M=Mg, Si, Sn, Sb), liq.-quenched, form. and low temp. electronic props. 4-75919
- Au<sub>1-x</sub>Si<sub>x</sub>, liq. and amorphous, elec. resist., Ziman theory anal. 4-70774
- Ca-Mg amorphous alloy, low-temp. elec. resist. 4-84603
- Ce<sub>2</sub>Al<sub>100-x</sub>, amorphous, transport and mag. props. 4-108985
- Co-based metallic glasses, low magnetostriction, crystallisation composition depend. 4-84196
- CoNiFe-SiB amorphous zero magnetostrictive alloy, compositional short-range order and ordering kinetics 4-70035
- Co<sub>92</sub>Si<sub>8</sub>Fe<sub>2</sub>B<sub>2</sub>, amorphous alloy, crystn. study using DTA and elec. resist. meas. 4-65181
- Ct<sub>1-x</sub>Mn<sub>x</sub>Ge, amorphous thin films, elec. resist., Hall resist. 4-114049
- Cu<sub>2</sub>Al<sub>1-x</sub>, amorphous, elec. resist. and temp. coeff., pseudopot. theory 4-92692
- Fe amorphous alloys, structural relaxation (*Russian*) 4-104801
- Fe-B amorphous alloys, cryst. and press., elec. resist. study 4-60837
- Fe-Ho-B, metallic glass, mag. props. and crystallisation 4-84793
- Fe<sub>1-x</sub>B<sub>x</sub> glass, crystallisation, elec. cond. study 4-88109
- Fe<sub>2</sub>B<sub>20</sub>-based metallic glasses, struct., small angle X-ray scatt. studies 4-113346
- Fe<sub>2</sub>B<sub>14</sub>, amorphous, thermoelectric power and elec. cond. (*Russian*) 4-65660
- Fe<sub>2</sub>Co<sub>98</sub>Si<sub>2</sub>B<sub>10</sub>, metallic glass, crystn. kinetics 4-65187
- (Fe<sub>1-x</sub>Co<sub>x</sub>)<sub>90</sub>Zr<sub>10</sub> amorphous alloy, elec. resist. minima and mag. props. 4-75922
- Fe<sub>1-x</sub>Cr<sub>x</sub>, short range order inversion, alloy conc. depend. 4-103690
- Fe<sub>30</sub>M<sub>30</sub>B<sub>17</sub> (M=transition metal) metallic glass, elec. resist., transition metal effects 4-108832
- (Fe<sub>1-x</sub>Mn<sub>x</sub>)<sub>75</sub>P<sub>15</sub>C<sub>10</sub> amorphous alloy, transport and mag. props. 4-88498
- Fe<sub>30</sub>Mo<sub>70</sub>, metallic glass, elec. resist., crystallisation and thermoelec. power, annealing effects 4-108831
- (Fe<sub>0.9</sub>Ni<sub>0.1</sub>)<sub>90</sub>-x<sub>10</sub> amorphous alloys, elec. cond. and struct. stability 4-92693
- Fe<sub>40</sub>Ni<sub>60</sub> metallic glass, amorphous-cryst.: transition kinetics, elec. resist. meas. 4-70039
- Fe<sub>40</sub>Ni<sub>60</sub>B<sub>10</sub>Si<sub>3</sub> glassy ribbon, elec. and mag. props. 4-84604
- Fe<sub>40</sub>Ni<sub>38</sub>Mo<sub>18</sub>B<sub>4</sub>, metallic glass, elec. resist., crystallisation and thermoelec. power, annealing effects 4-108831
- Fe<sub>39</sub>Ni<sub>39</sub>Mo<sub>4</sub>Si<sub>8</sub>B<sub>12</sub>, metallic glass, elec. resist., crystallisation and thermoelec. power, annealing effects 4-108831
- Fe<sub>25</sub>Ni<sub>55</sub>Si<sub>10</sub>B<sub>10</sub>, metallic glass, Curie temp. press. depend. 4-84792
- (Fe<sub>2</sub>Ni<sub>1-x</sub>)<sub>70</sub>Si<sub>30</sub>B<sub>14</sub> metallic glass, short range ordering study 4-88108
- (Fe<sub>1-x</sub>Ni<sub>x</sub>)<sub>90</sub>Zr<sub>10</sub> amorphous alloy, elec. resist. minima and mag. props. 4-75922
- Fe<sub>88-x</sub>Si<sub>12</sub> amorphous alloy, crystallisation behaviour 4-75309
- (Fe<sub>1-x</sub>V<sub>x</sub>)<sub>84</sub>B<sub>16</sub> amorphous alloys, mag. and elec. props. (*Chinese*) 4-114094
- Ga thin films, optical props., elec. meas. 4-88800
- La-Ga metallic glasses, elec. cond. meas. 4-98588
- Mg<sub>60</sub>Zn<sub>30</sub>-x<sub>30</sub>Ga, simple metallic glasses, electronic props. 4-75920
- Ni<sub>100-x</sub>B<sub>x</sub>, metallic glasses, elec. props. 4-108830
- Ni<sub>81.5</sub>B<sub>18.5</sub>-x<sub>18.5</sub>P<sub>y</sub>, metallic glasses, elec. props. 4-108830
- Ni<sub>80-x</sub>Fe<sub>20</sub> amorphous alloy, onset of magnetism, magnetisation studies 4-76172
- Ni<sub>24</sub>Zr<sub>76</sub>, sputtered, ordering phenomena during structural relax., elec. resist., shear modulus meas. 4-88102
- Pd<sub>(0.83-x)</sub>Co<sub>0.17</sub> metallic glasses, form., crystallisation and elec. props. 4-92685
- Pd<sub>(0.83-x)</sub>Fe<sub>0.17</sub> metallic glasses, form., crystallisation and elec. props. 4-92685
- Pd<sub>80</sub>Ni<sub>18</sub>Si<sub>2</sub>, amorphous, neutron irradi., elec. resist. meas. 4-70772
- Pd<sub>(0.83-x)</sub>Ni<sub>0.17</sub> metallic glasses, form., crystallisation and elec. props. 4-92685
- Pd<sub>90</sub>Si<sub>10</sub>, amorphous, prep. by ion implantation, proton irradi., damage, elec. resist. meas. 4-103833
- Pd<sub>90</sub>Si<sub>10</sub>, amorphous and annealed, neutron irradi., elec. resist. meas., structural relax. 4-70772
- Si<sub>1-x</sub>Cr<sub>x</sub> amorphous film, metal-semicond. transition, scaling behaviour and min. metallic cond. 4-70885
- U<sub>2</sub>Zn<sub>1</sub>, heavy-electron system, mag. ground state 4-71093
- Zr-Ni(Co) amorphous alloys, crystallisation, DSC and elec. resist. studies (*Chinese*) 4-103658
- Zr-Pd(Ni), amorphous, electronic density of states and superconducting props. 4-70738
- Zr<sub>75</sub>Rh<sub>25</sub>, amorphous alloy, metallic and activation cond. coexistence 4-70773

**electrical conductivity of amorphous semiconductors and insulators**

- see also carrier density; carrier lifetime; carrier mean free path; carrier mobility; carrier relaxation time; dislocation scattering; electrical conductivity transitions; electronic conduction in insulating thin films; high field effects; hopping conduction; impurity scattering; minority carriers; negative resistance effects; photoconductivity; point defect scattering; small polaron conduction; surface scattering
- amorphous semiconductor thin films, trapping and switching 4-113942
- amorphous thin films, switching, at. and electronic processes 4-113941
- chalcogenide glasses, tunnelling relax. in a.c. cond. 4-70812
- cyanooacetylene polymerisation products, struct., elec. cond. 4-113953
- electrothermographic system of leuco malachite green mixed films of acrylonitrile butadiene styrene, electrical properties, obs. 4-98626
- glass/alumina composites, density, crystallisation, elec. cond. 4-113937
- organic polyiodide chain complexes, elec. conduction, press. depend. 4-75962
- physics of amorphous solids, book 4-90312
- PMMA films, containing adsorbed moisture, DC cond., effect of thermal treatment 4-75980
- poly(3-methylthiophene) films, electrochemically prepared, ESR studies and cond. mech. 4-109074

**electrical conductivity of amorphous semiconductors and insulators continued**

- polyacetylene: IrCl<sub>6</sub>, giant dielectric const. 4-92997
- polyacetylene, doped, bipolaron interchain hopping as transport mechanism 4-70810
- polyacrylonitrile thin films, metastable at. deexcitation spectroscopy (*French*) 4-71506
- polyarylate-polyarylenesulphoneoxide block copolymers, transitions and relax. (*Russian*) 4-61087
- polyarylates, carborene-containing, elec. props. of pyrolysis products (*Russian*) 4-62194
- polyethylene<sub>2</sub>, elec. conduction 4-88511
- polyethylene, irradiated, elec. conduction meas., models 4-108866
- polyethylene, low density; radiation induced conductivity 4-84622
- polyimide, electric conduction, residual solvent effects 4-84617
- polymer films, elec. cond. changes induced by pyrolysis and high energy ion irradi. 4-75966
- polymers, branched, topological struct. and transport props. 4-92108
- polymers, electrical cond. and carrier traps, review 4-108854
- polyparaphenylene, doped, bipolaron interchain hopping as transport mechanism 4-70810
- polypyrrole, proton modification, elec. cond., optical absorpt. spectra, XPS 4-75969
- polyvinylidene fluoride, conductivity, constant current corona charging studies 4-108857
- polyvinylidene fluoride, DC cond. and dielec. absorption 4-80588
- porous layers, electrophysical and optical props. 4-65680
- rubber, vulcanised, elec. cond., crystallinity and glass transition 4-113944
- semiconductor, electron transport, Mott-CFO model anal. 4-113939
- semiconductors, DC electronic transport, long-range pot. influence 4-113947
- a-Si:H film, prep. by reactive sputtering, optical and elec. props. 4-71457
- As-Ge-Se, glass, small conc. of Se, elec. cond. rel. to temp. 4-92729
- As<sub>2</sub>Se<sub>3</sub>Ni(Cu)(Fe)(Bi)(Sn), extrinsic cond. and optical const. meas. 4-75971
- As<sub>4</sub>Se<sub>3</sub>Te<sub>3</sub>, amorphous, radiation and thermal induced defects, electrical cond. 4-75528
- As<sub>2</sub>Se<sub>3</sub>Te<sub>x</sub> glasses, DC props., neutron and gamma-ray effects 4-103814
- As<sub>2</sub>Te<sub>3</sub> amorphous films, electronic struct., field effect and time of flight studies 4-113852
- Ba(PO<sub>3</sub>)<sub>2</sub>-AlF<sub>3</sub>-LiF, elec. cond. rel. to struct. 4-92771
- BaTiO<sub>3</sub> amorphous film, elec. and struct. props. 4-80701
- Bi<sub>2</sub>O<sub>3</sub>-B<sub>2</sub>O<sub>3</sub> glasses, memory switching process, role of chem. reduction 4-114002
- C:H amorphous film, H<sub>2</sub> gas reactive RF sputtering prep. on low temp. substrates 4-76673
- C<sub>60</sub>-Si<sub>1-x</sub> amorphous film, elec. and optical props. 4-113962
- CdGe<sub>1-x</sub>Si<sub>x</sub>As<sub>2</sub> glasses, elec. props. and phase stability 4-104202
- CdS:Sb films, vacuum deposited, struct., elec. and optical props., impurity conc. effect 4-98607
- ErF<sub>3</sub> amorphous thin films, AC cond. meas. 4-76059
- Fe<sub>2</sub>O<sub>3</sub>-CaO-SiO<sub>2</sub> glasses, DC cond., Mossbauer and ESR spectra 4-70807
- a-Ge:Fe(Ni) films, cond. and localised states 4-104163
- Ge-Sn(Sb)(Al) amorphous thin films, hopping cond. meas., 130 to 300K, localised state variations 4-92713
- GeO<sub>2</sub> films, amorphous, elec. characterisation in MIS and MIM structs. 4-70816
- GeO<sub>2</sub>-V<sub>2</sub>O<sub>5</sub>-VCl<sub>3</sub> glass, optical absorpt., DC cond. rel. to VCl<sub>3</sub> content 4-65675
- Ge<sub>2</sub>Se<sub>3</sub>-Cu(Ag), glassy, doping effect on elec. and optical props. (*Russian*) 4-98625
- (GeS<sub>2</sub>)<sub>100-x</sub>Bi<sub>x</sub>, glass, photoconductivity meas. 4-98670
- GeSe<sub>2</sub>, cryst. and glassy, photoelec. props. 4-108905
- (GeSe<sub>3</sub>)<sub>100-x</sub>Bi<sub>x</sub>, glass, photoconductivity meas. 4-98670
- (GeSe<sub>3</sub>)<sub>100-x</sub>Bi<sub>x</sub>, struct. and resist. effect of dopants, high press. study 4-103660
- (GeSe<sub>3</sub>)<sub>100-x</sub>Sb<sub>x</sub>, struct. and resist. effect of dopants, high press. study 4-103660
- Ge<sub>1-x</sub>Si<sub>x</sub>Sn amorphous film, elec. cond. and thermoelec. power 4-65678
- Ge<sub>20</sub>Te<sub>80</sub> glass, bulk, elec. transport and high press. studies 4-114003
- Ge<sub>20</sub>Te<sub>80</sub> glass, elec. cond. transition, press. and temp. depend. 4-98619
- InO<sub>3</sub>, amorphous, electron mobility, cond., and supercond. near metal-insulator transition 4-80710
- KP<sub>13</sub>, crystalline and amorphous, semiconducting props. 4-98603
- Li<sub>2</sub>O-SiO<sub>2</sub> glass ceramic systems, density, crystallisation, elec. cond. 4-113937
- Na<sub>2</sub>O-CuO-GeO<sub>2</sub> glass, elec. cond., chem. content depend. 4-98673
- Nb<sub>2</sub>O<sub>5</sub> amorphous film, elec. behaviour study (*Russian*) 4-84722
- Nb<sub>2</sub>O<sub>5</sub>, XPS and optical spectra, low-valence cations and electron props. 4-98623
- a-Sb, elec. resist. and thermoelec. power meas. 4-108886
- Se, amorphous, DC conductivity thickness dependence 4-84620
- a-Se:Bi films, crystallisation, dark cond. and activation energy 4-88104
- Se-Te(Ge)(Sb) amorphous, DC conductivity thickness dependence 4-84620
- Se<sub>1-x</sub>Te<sub>x</sub> glasses, electronic cond. at high press. and low temp. 4-104198
- Se<sub>39</sub>Te<sub>40</sub>As<sub>1</sub>:Li, chemical modification and elec. cond. 4-75970
- a-Si, cond. and thermoelectric power below mobility edge 4-108888
- a-Si, electron transport, photocurrent transit time method 4-65679
- a-Si, electronic and vibr. props., book 4-67878
- a-Si film, RF sputtered, optical absorpt., elec. cond., effect of thermal annealing 4-80583
- a-Si, mobility edge, temp. depend. 4-92723
- Si:Ga sputtered amorphous alloys, thermopower and elec. cond. 4-61403
- Si:H, amorphous, DC triode sputtered, electronic transport 4-61374
- p-Si:H, amorphous, prepared by photo-CVD, electronic and optical props. 4-70959
- Si:H, amorphous films, glow discharge decomposition, Hg(Kr) effects 4-76687
- Si:H, B(P), amorphous CVD layer, impurity doping 4-60941
- a-Si:H, conductivity, localisation and mobility edge 4-70819
- a-Si:H, DC elec. cond. Meyer-Neldel rule and Staebler-Wronski effect 4-113948
- a-Si:H, high-rate deposition from SiH<sub>4</sub> using RF discharge technique, elec. and optical props. 4-85119
- a-Si:H, P(B), dark cond. and photocond., thickness depend. 4-84624
- a-Si:H, prep. by glow discharge of Si<sub>2</sub>H<sub>6</sub>, optical and elec. props. 4-114237

**electrical conductivity of amorphous semiconductors and insulators continued**

- Si:H, RF sputtered amorphous film, dark cond. and photocond., annealing effects 4-70960  
 a-Si:H, time-resolved charge transport and photocond. 4-70871  
 a-Si:H, Li, surface photovolt. and dark conductance, light-induced changes 4-70861  
 a-Si:H, P film, acoustoelectric effect, thickness depend. study 4-104273  
 Si:H amorphous films, glow discharge deposition in cascade reactors 4-76680  
 Si:H amorphous films, laser CVD by ArF excimer laser photodissociation of  $S_2H_2$  4-61859  
 a-Si:H film, complex impedance meas. 4-76055  
 a-Si:H film, high rate prep. by reactive evaporation method, photocond. and dark cond. meas. 4-61248  
 a-Si:H film, produced by magnetron sputtering, ion beam anal. 4-92583  
 a-Si:H films, anodic oxidation, elec. and optical props. of oxidised films 4-109527  
 a-Si:H films, CVD growth, phys. props. 4-92715  
 a-Si:H films, DC planar magnetron reactive sputtering and characterisation 4-93218  
 a-Si:H films, doping effect, RF sputtering and p-n junction form. 4-88973  
 a-Si:H films, reactive sputtering, elec. and optical props. 4-104203  
 a-Si:H films, thickness effects on electrical and photoelectrical properties 4-98484  
 a-Si:H thin films, glow discharge effects on electronic and optical props. 4-75977  
 Si:H wide optical gap binary alloy films, elec. props. 4-113956  
 a-Si/a-Si<sub>3</sub>N<sub>4</sub>/a-SiN<sub>x</sub> superlattices, optical bandgap and elec. resist. 4-114026  
 a-Si-Ge-B alloys, props. and electronic device appls. (Japanese) 4-92728  
 p-Si:C:H, amorphous, prepared by photo-CVD, electronic and optical props. 4-70959  
 a-Si:C:H glow-discharge film, electronic and optical props. 4-84623  
 Si<sub>1-x</sub>Ge<sub>x</sub>:H amorphous films, planar magnetron sputtered, optical and elec. props. 4-98671  
 Si<sub>1-x</sub>Ge<sub>x</sub>:H amorphous planar magnetron sputtered films, elec. and optical props. (Japanese) 4-99312  
 SiO<sub>2</sub> films, RF sputtered, AC cond. mechanisms 4-92721  
 SiO<sub>2</sub> films, RF sputtered, AC cond. mechanisms, single polaron correl. barrier hopping 4-92722  
 SmF<sub>3</sub> thin films, DC elec. cond. 4-113949  
 SnSe-GeSe<sub>2</sub>-AsSe, glass formation, physicochemical props. 4-92365  
 Ta<sub>2</sub>O<sub>5</sub>, amorphous, conductivity changes study during degradation in strong elec. field 4-108872  
 Ta<sub>2</sub>O<sub>5</sub>, XPS and optical spectra, low-valence cations and electron props. 4-98623  
 V<sub>2</sub>O<sub>5</sub> amorphous thin films, props., influence of quenching rate 4-108956  
 V<sub>2</sub>O<sub>5</sub>-As<sub>2</sub>O<sub>3</sub> glasses, semicond. props. 4-80593  
 V<sub>2</sub>O<sub>5</sub>-B<sub>2</sub>O<sub>3</sub> glass, struct., IR spectra and elec. cond. 4-88107  
 WO<sub>3</sub> thick films, elec. cond. and electrochromism 4-65674  
 WO<sub>3-x</sub>H<sub>2</sub>O amorphous films, elec. cond. and thermopower 4-61378  
 ZnO-B<sub>2</sub>O<sub>3</sub> glass, X-ray diff., density and elec. cond. obs. 4-61423
- electrical conductivity of crystalline metals and alloys**  
*see also* dislocation scattering; electron density (metals); electron mean free path (metals); electron mobility (metals); electron relaxation time (metals); electronic conduction in metallic thin films; impurity scattering; point defect scattering; surface scattering  
 alloys, precipitation rel. to elec. resist. 4-114546  
 alloys, residual resist. changes due to clustering, t-matrix anal. 4-98591  
 direct current comparator resistance bridge automation, alloy resistivity appl. 4-90613  
 impurity-containing metals, field effects 4-65670  
 martensite, elec. cond., thermoelectric power and electronic struct. (Russian) 4-65657  
 metallic long wires, quantum particle kinetics, cond. and localisation 4-92669  
 metals, current vortices in inhomogeneous mag. field (Russian) 4-80563  
 metals, electrical contact cond., statistical theory 4-80652  
 pure, cold worked, annealing characts rel. to trace element additions 4-109438  
 rare earth-Cd equiatomic cpds., struct. and mag. phase transitions 4-84795  
 rare earth alloys, RNiGe, R=Y, Yb, Tb, Dy, Ho, Er, Tm, Lu, cryst. struct., mag. and elec. props. (Russian) 4-88134  
 rare earth alloys RCoGe, R=Y, Yb, Tb, Dy, Ho, Er, Tm, Lu, cryst. struct., mag. and elec. props. (Russian) 4-88134  
 recovery and recrystallization, book contrib. 4-109429  
 shielding, clad metals appl. 4-108836  
 short-range ordered alloy, elec. resist., tight-binding calcs. 4-70778  
 single metals elec. resistivity and scatt. theory 4-92694  
 steel, austenitic stainless, electron irradiation-induced struct. phase transformations 4-109418  
 steel, austenitic stainless, gamma-ray induced short-range ordering, point defect influence 4-92123  
 steel, austenitic stainless, thermal and radiation-stimulated ageing, kinetics 4-66354  
 steel, C, powder metallurgical, elec. cond., thermal cond. and thermal expansion, temp. depend. 4-65658  
 steel, low C, Al killed, decomp. of Mn-C dipoles during quench ageing, resist. obs. 4-71661  
 steel, low C, quenched, precip. kinetics 4-99394  
 steel, low-alloy, powder metallurgical, elec. cond., thermal cond. and thermal expansion, temp. depend. 4-65658  
 steel, nonorientated electric, composition effect on loss, elec. cond. and texture 4-81219  
 steel bar sorting, two parametric eddy current method 4-71833  
 thin wires, elec. transport phenomena 4-104181  
 transition metal, electron-phonon coupling and phonon-limited resist. calcs. 4-70799  
 transition metal alloy, disordered, electron-phonon interaction influence on elec. cond. 4-70800  
 Ag-Cu dilute alloys, defect production and annealing 4-75442  
 Ag-Cu dilute alloys, electron irradiation, defect prod. and annealing 4-75441  
 Ag-Mg(Cu), internal oxidation mechanism 4-93305  
 Ag-Zn, conc., electron irradiation, elec. resist., recovery 4-104182  
 α-AgAl, short-range order parameter, determ. from resist. meas. 4-98287  
 Ag<sub>2</sub>MnAl, Silmanal, magnetic phase growth (Russian) 4-109014  
 Ag<sub>2</sub>Pd<sub>1-x</sub>, elec. cond. and thermopower calcs. 4-70776  
 Al, elec. and thermal cond., 400 to 850K 4-75927

**electrical conductivity of crystalline metals and alloys continued**

- Al wires, low cycle fatigue, lattice defects, resist., temp. depend. (Japanese) 4-99508  
 Al-Cu, θ' phase form., departures from Matthiessen's rule, elec. resist. obs. 4-71660  
 Al-Cu alloy, and thermal cond., 400 to 850K 4-75927  
 Al-Cu-Mg, thermomech. treatment, age hardening rel. to Mg/Cu ratio (Japanese) 4-89064  
 Al-Mg, ageing, metastable phases in early stages of precip., DSC and resist. obs. 4-71656  
 Al-Mg, dil., neutron irradiation, internal friction, elastic modulus, recovery stages studied by elec. resist. meas. 4-103876  
 Al-Mg-Bi, Al-Mg-Li and Al-Li-Mg low-activation alloy development for fusion device 4-108460  
 Al-Mg-Si-Sn, ageing, clustering process rel. to Sn addition, elec. resist., TEM obs. 4-114529  
 Al-Mn, polyvalent films, elec. cond. anomaly 4-80688  
 Al-Mn alloy, commercial homogenisation, stability of primary particles, resist. and TEM obs. 4-99408  
 Al-Sc (0.3 at %) alloy, ageing, precipitation obs. (Russian) 4-104786  
 Al-Sc alloys, age hardening kinetics, elec. resist. study 4-61949  
 AlZn, residual resist. of Guinier-Preston zones, pseudopot. approach 4-70779  
 Au-Cd liq. and solid alloy, elec. resist. studies 4-88499  
 AuY(Zr)(Nb)(Rh)(Pd), dil. alloys, thermoelectric power, resistivity, low temp. study, phase-shift anal. 4-113926  
 AuY(Zr)(Nb)(Rh)(Pt)(Pd), dil. alloys, thermoelectric power, resistivity, low temp. studies 4-113925  
 Be, high pressure phase transition, elec. resist. study 4-75663  
 Bi whiskers, longit. magnetoresist. meas. 4-88500  
 Bi<sub>2</sub>Se<sub>3</sub>, electron scatt., low temp. 4-108835  
 CeCu<sub>2</sub>, heavy-fermion system, elec. resist., susceptibility and sp. ht. meas. 4-104402  
 CeCu<sub>2</sub>Si<sub>2</sub>, Kondo lattice substance superconductivity 4-98797  
 Ce(In<sub>1-x</sub>Sn<sub>x</sub>)<sub>3</sub>, intermediate valence study 4-61340  
 Ce<sub>2</sub>La<sub>1-x</sub>Al<sub>2</sub>, dense Kondo state, elec. resist., mag. susceptibility meas. 4-108984  
 Ce<sub>99-x</sub>La<sub>1-x</sub>Th<sub>0.1-x</sub>, γ-α transition, x-P-T phase diagrams 4-76755  
 Co-based heat resisting alloys, radiative and optical props. 4-74847  
 CoSi<sub>2</sub>, formation and Schottky barrier heights 4-108922  
 Cr foil, influence of heat treatment on struct. and props. (Russian) 4-65412  
 Cr, neutron irradiation, internal friction, elastic modulus, recovery stages studied by elec. resist. meas. 4-103875  
 Cr-Co alloys, local electron states, elec. resist. and magnetoresist. studies 4-80550  
 Cr-Ga, dilute, mag. phase diagram, elec. cond. meas. 4-88669  
 Cs, phonon frequencies, Debye temp., Gruneisen parameter, transport props., lattice dynamical model 4-108561  
 Cu, electronic props. of 4d transition metal and sp impurities 4-70731  
 Cu-Al, neutron irradiation, microhardness, resistivity, electron microscopy 4-103811  
 Cu-based shape-memory alloy, mech. and elec. props., sonic studies 4-76773  
 Cu-Be alloy, struct. transform. mechanisms during ageing; internal friction and resist. obs. 4-114536  
 Cu-Be alloys, precipitation, elec. resist. and thermopower 4-114549  
 Cu-Be-Co (2, 0.2 wt %), precip. hardening investigation by microhardness and elec. resist. meas. 4-61947  
 Cu-H, electron irradiation, elec. resist. meas., annealing behaviour 4-92240  
 Cu-Mn, elec. resist. max. and thermo-EMF, short-range antiferromagnetism (Russian) 4-84608  
 Cu-Mn, neutron irradiation, microhardness, resistivity, electron microscopy 4-103811  
 Cu-Ni, neutron irradiation, microhardness, resistivity, electron microscopy 4-103811  
 Cu-Zn, high energy electron irradiation, radiation enhanced diffusion, interstitial mechanism, elec. resist. meas. 4-92239  
 Dy<sub>2</sub>Si<sub>3</sub>, low-temp. phase transitions and mag. ordering 4-71071  
 Fe, pure and C doped, electron irradiation, resistivity recovery 4-108834  
 Fe-Al rapidly quenched cryst. ribbons, mag., elec. and mech. props. 4-76174  
 Fe-B alloys, α-γ transition lines and activity coeffs., conductometric studies 4-103926  
 Fe-based heat resisting alloys, radiative and optical props. 4-74847  
 Fe-Cr-Ni(Si), acoustic emission and resist. variation during cyclic heating 4-81296  
 Fe-Ni-Mn (21.1, 4.0 wt %), athermal martensitic transform. with isothermal component 4-89052  
 Fe-W dilute alloy wires, diffusion coefficients, resistometric methods 4-65427  
 Fe<sub>2</sub>Cr<sub>3</sub>, short range order inversion, alloy conc. depend. 4-103690  
 FeSi-Fe<sub>2</sub>Si<sub>3</sub> eutectic alloy, sintered, annealing, FeSi<sub>2</sub> form., elec. props. 4-109414  
 Ga, size-induced deviations from Matthiessen's rule 4-70775  
 Gd-Y-Lu single cryst., double ferromagnetism, mag., elec. and thermal studies 4-84817  
 GdCu<sub>2</sub>-Zn<sub>2</sub>Si<sub>2</sub>, cryst. struct., mag. and elec. props. 4-92145  
 GdIn, magnetic and electrical props., metamagnetic-ferromagnetic transition, magnetic struct. 4-114138  
 GdIn<sub>2</sub>Sn<sub>2</sub>, elec. resist. below Neel temp. 4-75924  
 Gd<sub>2</sub>Si<sub>3</sub>, low-temp. phase transitions and mag. ordering 4-71071  
 HoPr, mag. and elec. props. meas. (Russian) 4-80784  
 In-Mn, polyvalent films, elec. cond. anomaly 4-80688  
 In-Tl, elec. resist. studies, average phonon energy 4-113920  
 InSb bicrystal, grain boundary barrier height and elec. cond. 4-92216  
 Ir, electron and neutron irradiation, elec. resist. studies 4-108447  
 K, spin-wave excitations, Landau Fermi-liquid parameters 4-114098  
 Mn-Ge, Invar type, antiferromag., transition metal influence on props. (Japanese) 4-65826  
 MnRhAs, antiferromagnetic-ferromagnetic transition, mag. props., elec. resist. meas. 4-104417  
 Na, spin-wave excitations, Landau Fermi-liquid parameters 4-114098  
 Nb, anomaly of elec. cond. temp. depend. 4-70777  
 Nb, thin wires, heat treatment 4-66355  
 Nb, twinning at low temp., elec. effects obs. 4-70168  
 Nb-Ti, thin wires, heat treatment 4-66355  
 Nb-Ti (41.55 wt %), superconductor, elec. resist. 4-92853  
 Nd, solid and liq., elec. resist. studies 4-92691  
 Ni-based heat resisting alloys, radiative and optical props. 4-74847  
 Ni-Cu, anomalous resistivity, 4.2 to 1100K 4-92708

# electrical conductivity of crystalline metals and alloys continued

- Ni-Fe-Cr alloys, extraordinary Hall coeff. sign reversal and DC resist. 4-113922  
 Ni-Fe-V alloys, extraordinary Hall coeff. sign reversal and DC resist. 4-113922  
 Ni-Gd dilute alloys, defect reactions, diffuse X-ray scatt. studies 4-75440  
 Ni-Si dilute alloys, defect reactions, diffuse X-ray scatt. studies 4-75439  
 NiCr films, electrical resistance in freq. range 10-100 MHz 4-80567  
 Ni<sub>3</sub>Cr, ordered state, annealing, elec. resist., electron diffr. obs. 4-109394  
 Ni<sub>2</sub>MnIn Heusler alloy, elec. resist. and magnetisation 4-82695  
 Pb-Mn(Fe), polyvalent films, elec. cond. anomaly 4-80688  
 Pd-Ag-H, struct. and elec. props. (Russian) 4-79981  
 Pd-Cu-Ni alloys, elec. resist., atomic ordering effects (Russian) 4-108833  
 Pr, solid and liq., elec. resist. studies 4-92691  
 PrAg, elec. mag. and struct. props. meas. 4-80566  
 PrAl<sub>2</sub>, elec. resist. dominated by quadrupole scatt., spin correl. effects 4-104191  
 Pt ultrathin drawn wires, struct. and elec. props. 4-92696  
 PtCr, nonmagnetic resist. anomalies 4-113919  
 PtCr<sub>2</sub>Mn<sub>1-x</sub>, elec. cond. and mag. props. 4-104180  
 Si-Fe nonoriented semiprocessed steel, core loss and permeability, elec. resist. effects 4-61556  
 Sm, solid and liq., elec. resist. studies 4-92691  
 Sn, semiconductor-metal transition, press. effects 4-92613  
 Sn, single crystal, lattice defect kinetics (Russian) 4-80029  
 Sn-Gc dilute alloys, semiconductor-metal transition, press. effects 4-92613  
 Sn-Mn, polyvalent films, elec. cond. anomaly 4-80688  
 (Sn<sub>1-x</sub>Cu<sub>x</sub>)<sub>2</sub>H<sub>2</sub>, superconductivity and cond. studies 4-92840  
 Ta, electron-electron scatt., elec. resist. meas. 4-113935  
 Tb, electrical cond. and magnetoresistance anomalies at 90K 4-84606  
 Tb<sub>2</sub>Gd<sub>25</sub>, Hall effect and elec. resist. near Curie point 4-61361  
 Tb<sub>2</sub>Si<sub>3</sub>, low-temp. phase transitions and mag. ordering 4-71071  
 TiNi, martensitic transform, mech. props., struct. rel. to thermomech. treatment 4-66376  
 TiTe<sub>2</sub>, CDW transitions and transport props. 4-80521  
 Ti<sub>2</sub>Fe<sub>2</sub>Te<sub>6</sub>, strongly anisotropic ferromagnetism, first order phase transitions 4-84796  
 UPt<sub>3</sub>, elec. resist., press. depend., spin fluctuation model anal. 4-98589  
 UPt<sub>3</sub>, spin fluctuations, superconductivity and elec. cond. 4-114057  
 V-Ti, thin wires, heat treatment 4-66355  
 V<sub>2</sub>Ge<sub>1-x</sub>Al<sub>x</sub>(Si<sub>1-x</sub>Sb<sub>x</sub>), superconductivity, electron-phonon parameter, electron-atom ratio 4-114058  
 VN<sub>x</sub>, superconducting and normal state props. 4-84731  
 VSe<sub>2</sub>, CDW transitions and transport props. 4-80521  
 W, doped, internal oxidation, elec. resist. study 4-62128  
 W, high-temperature Lorenz number, thermal and elec. cond. meas. (German) 4-80564  
 W powders produced by plasma reduction, gas adsorpt., effect on electron work function and elec. cond. 4-70550  
 W, sintered, resistivity, void size effects 4-75925  
 W-Fe, dil., segregation of Fe to grain boundaries, elec. resist., thermopower, AES meas. 4-103943  
 Y<sub>2</sub>Co<sub>7</sub>, ferromag. inhomogeneous supercond., sample size and meas. power effects 4-76065  
 Zn, single crystal, deformation stress and electrical resistance change due to dislocation 4-60978  
 Zn-Al superplastic alloys, Al atoms redistribution, elec.-resist. and small angle X-ray scatt. study 4-62004  
 Zr, fusion neutron irradiation, damage prod. and recovery, resist. obs. 4-108461  
 Zr, pure, neutron irradiation, annealing, point defect prod. and annihilation, saturation resist. 4-108465  
 Zr, purification by electrotransport processing, resist. ratio obs. 4-85126

# electrical conductivity of crystalline semiconductors and insulators

- see also carrier density; carrier lifetime; carrier mean free path; carrier mobility; carrier relaxation time; dislocation scattering; electronic conduction in crystalline semiconductor thin films; electronic conduction in insulating thin films; high field effects; hopping conduction; impurity scattering; minority carriers; negative resistance effects; photoconductivity; point defect scattering; small polaron conduction; surface scattering  
 alkaline earth niobates, electronic cond. rel. to complex perovskite structs. 4-70821  
 bicrystal semiconductor, elec. cond. for tunnel charge transport 4-88576  
 conference, Alanya, France (June-July 1982) 4-95052  
 coronene layers, elec. cond. and trap distrib. 4-84626  
 deterministic stratification of current and isolated branches of I-V characts. 4-98602  
 diamond, Ohmic conductivity of electrons calc. 4-108864  
 disodium sulphosaltic pyroelec. cryst., elec. props. (Chinese) 4-114212  
 disordered polycrystalline semiconductor, freq. dispersion of elec. cond. 4-70802  
 electro-physical prop. nonuniformity (Russian) 4-65672  
 explosives, PBX and PBXW, elec. resist. and dielec. breakdown meas. 4-108865  
 ferroelectrics, domain struct. influence on elec. cond. 4-99067  
 ferromagnetic semiconductors, elec. resist. reson. rel. under FMR saturation conditions 4-92726  
 GASH single crystal, ferroelec. domain struct., SEM studies 4-71320  
 graphite, electrical resistivity, in-plane, T<sub>2</sub> depend. at very low temps. 4-80845  
 graphite, thermomechanical treatment, neutron irradiation-induced changes in props. 4-108451  
 graphite intercalation compounds containing AsF<sub>6</sub><sup>-</sup> and AsF<sub>6</sub><sup>-</sup>-AsF<sub>3</sub>, NMR 4-114166  
 graphite oxide fibres, produced by oxidation of C-graphite fibres 4-76740  
 hydrogen bis (phthalocyaninato) neodymium (III), iodination effect on elec. cond. 4-70808  
 nonstoichiometric compounds, transport processes, conf., Cracow, Poland (Aug. 1980) 4-95060  
 oxides, binary and ternary, point defects and transport props. 4-98366  
 oxides, chemical diffusion coeff. calcs. 4-98370  
 pentacene layers, dispersive charge carrier transport 4-80703  
 piezoelectrics, even elec. cond. with streaming, separation of shift and ballistic contributions 4-113951  
 polyacetylene:1, cis and trans, DC and microwave cond. 4-92716  
 polyene semicond., compensation effect, I-V characts. 4-61372  
 quartz, elec. cond., relax. dielec. losses, temp. depend. due to electrolysis 4-113959  
 refractory boride thick films, elec. cond. (Russian) 4-76058

# electrical conductivity of crystalline semiconductors and insulators continued

- sapphire, single cryst., high temp. electronic struct., VUV reflectance spectra 4-84556  
 semiconductor, elec. props., appl. of two stage nonmagnetic high press. equipment (Chinese) 4-90607  
 semiconductor superlattices, np-layered, optical absorption, time depend. 4-93034  
 semiconductors, charge carrier transfer and diffusion in strong mag. field (Russian) 4-88520  
 semiconductors, high field quantum transport theory 4-80599  
 semiconductors, polycryst., percolation nonohmic cond. 4-108871  
 semiconductors, thermoelectric, electron electrothermofusion 4-75985  
 n-Si, radiation defect formation, annealing, defect interactions 4-113499  
 TCNQ salt, DEPA(TCNQ)<sub>4</sub>, cryst. struct., elec. cond., mag. susceptibility meas. 4-80027  
 TCNQ salt, DTT-TCNQ, optical props.; cond. and cryst. struct. 4-113435  
 TCNQ salts, Cs<sub>2</sub> (TCNQ)<sub>3</sub>(II), synthesis, anal., novel isomeric struct. 4-114376  
 TCNQ salts, elec. mag. and struct. characterisation 4-88162  
 ternary semiconductors, relationship between physicochemical and electro-physical props. 4-108856  
 THSe, dielec. props., elec. cond., thermodynamical 4-88779  
 (TMTSF)<sub>2</sub>FSO<sub>3</sub>, organic semicond., cond. and cond. transitions 4-113870  
 transition metal carbide and carbonitride solid solns., mag., elec. transport, supercond. props., review 4-80590  
 transition metal molybdates, M<sub>2</sub>Mo<sub>3</sub>O<sub>8</sub> (M=Mn, Fe, Co, Ni), crystal growth, mag. and elec. props. 4-71537  
 triarylmethane: F, cond. transitions 4-70881  
 Ag<sub>2</sub>As<sub>2</sub>S<sub>3</sub>, low temp. elec. cond. anisotropy 4-88509  
 AgTiX (X=S, Se, Te), elec. and crystallographic props. 4-70111  
 Al<sub>2</sub>Ga<sub>1-x</sub>As<sub>x</sub>, graded-gap, effective resistance, temp. dependence 4-113961  
 As, galvanomagnetic props. and current carriers energy spectrum (Russian) 4-98638  
 As<sub>2</sub>Te<sub>3</sub>, cryst., semiconductor-metal transition, elec. resist., thermoelec. power meas. 4-98523  
 β-B, doped, thermoelectric materials, thermal cond. and elec. props. 4-75990  
 Bi<sub>1-x</sub>C<sub>x</sub>, cond. mechanism, elec. cond., Seebeck coeff., and Hall coeff. meas. 4-70811  
 Ba<sub>2</sub>NbNb<sub>2</sub>O<sub>7</sub>, elec. cond., oscillatory and chaotic states 4-98611  
 BaRu<sub>2-x</sub>Mo<sub>2-x</sub>O<sub>10</sub>, M=Rh, Ir, Mn, Fe, Co, Ni, cryst. struct. and elec. cond. (German) 4-84265  
 BaSr<sub>1-x</sub>Nb<sub>2-x</sub>O<sub>7</sub>, defect struct., elec. and ionic cond. 4-98676  
 BaTiO<sub>3</sub>, combined doping, electron-conduction compensation 4-113475  
 BaTiO<sub>3</sub> oxide perovskites, dielec. meas., surface layer effects 4-65962  
 BaTiO<sub>3</sub>, pure and Nb-doped, elec. cond. 600-800°C, defect struct. 4-98604  
 BaTiO<sub>3</sub> thick film, grain boundaries, TEM obs. 4-84300  
 BaTiO<sub>3</sub>:Ca, impurity site occupancy, channelling enhanced microanal. studies 4-108394  
 BaTiO<sub>3</sub>:Nb(Al), donor doped, defect chem. 4-84307  
 Bi whisker crystals, nonlinear conduction props. under phonon generation 4-65687  
 Bi<sub>2</sub>Ge<sub>20</sub>, field and charge distrib. in case of trap thermal ionisation 4-66010  
 Bi<sub>2</sub>Ge<sub>20</sub>, MIS struct., elec. cond. and photoconductivity 4-98776  
 Bi<sub>2</sub>Ge<sub>20</sub>, trap parameter determ. by optical probing 4-88479  
 Bi<sub>2</sub>Mo<sub>2</sub>O<sub>7</sub>, preparation, cryst. struct., elec. and optical props. 4-84266  
 n-Bi<sub>2</sub>Te<sub>3</sub>, free carrier mobility, Hall and Seebeck coeffs., temp. depend. 4-61369  
 Bi<sub>2</sub>Te<sub>3</sub>:Pb(Ge), doping props., elec. cond. and Seebeck measurements 4-75467  
 Bi<sub>2</sub>Te<sub>3</sub>:Sb<sub>2</sub>Te<sub>3</sub>, n-type solid solution, effect of annealing in air on electro-physical props. 4-113945  
 C material, dimensional changes, under compressive stress at high temp. 4-85182  
 Ca<sub>2</sub>NaMg<sub>2</sub>V<sub>2</sub>O<sub>12</sub> garnet, elec. cond. and thermopower 4-70822  
 CaSO<sub>4</sub>:Dy single cryst., cryst. growth and elec. props. 4-113943  
 Ca<sub>3-x</sub>Y<sub>x</sub>Mn<sub>2</sub>Ge<sub>2</sub>O<sub>12</sub>, thermopower and elec. cond., 30 to 1000°C 4-70847  
 CdCr<sub>2</sub>Se<sub>4</sub>:In, static I-V characts. 4-70815  
 p-Cd<sub>2</sub>Hg<sub>1-x</sub>Te, photoconductivity and photomagnetic effect 4-104268  
 n-Cd<sub>2</sub>Hg<sub>1-x</sub>Te single crystals, hot electrons at strong elec. fields (Russian) 4-98628  
 Cd<sub>2</sub>Hg<sub>1-x</sub>Te under uniaxial deform., photoelectric props. 4-70864  
 CdS, dark current and photocurrent in strong elec. field, temp. dependence 4-113998  
 CdS, uniaxially deformed, current saturation and oscill. (Russian) 4-70818  
 CdS<sub>1-x</sub>Se<sub>x</sub>, single cryst., elec. cond. and Hall effect studies 4-113974  
 CdSiAs<sub>2</sub>, single crystal growth by chem. vapor transport, struct. and elec. props. 4-114367  
 CdTe, growth from vapour phase, on substrate out of contact with vapour walls 4-109315  
 CdTe:In, electroconductivity at high temp. 4-61373  
 CdTe-InSb MIS struct., electronic props. 4-98778  
 CeCu<sub>2</sub>Si<sub>2</sub>, superconducting T<sub>c</sub> maximum 4-98800  
 CeM<sub>2</sub>B<sub>2</sub> (M=Co, Ru, Rh, Ir), mixed valence, mag. and elec. props. 4-113905  
 CeO<sub>2</sub>-Y<sub>2</sub>O<sub>3</sub>, nonstoichiometric, electronic conduction, dopant effects 4-92733  
 CeSi<sub>1.86</sub>, elec. cond. and paramagnetism 4-104207  
 CoFe<sub>2-x</sub>Ni<sub>x</sub>O<sub>4</sub>, spinel system, cryst. struct., elec. cond. and mag. susceptibility 4-112121  
 CoMn<sub>2-x</sub>Ni<sub>x</sub>O<sub>4</sub>, spinel system, cryst. struct., elec. cond. and mag. susceptibility 4-70121  
 CoO:Li, pure and doped, elec. cond., carrier mobility and conc. 4-92731  
 Co<sub>2</sub>O<sub>3</sub>, point defects and transport props. 4-98366  
 Cr<sub>2</sub>O<sub>3</sub>, doped, hot pressing, annealing, elec. cond., density, grain size, XPS 4-113946  
 Cr<sub>2</sub>O<sub>3</sub>:Li, elec. cond., O activity depend. 4-61376  
 CrVnNbO<sub>6</sub>, semicond., elec. resist., mag. susceptibility meas. 4-109000  
 CuAlTe<sub>2</sub> single cryst., CVD growth and elec. characterisation 4-114366  
 (CuCr<sub>2</sub>Se<sub>4</sub>)<sub>1-x</sub>(Cu<sub>0.5</sub>Ga<sub>0.5</sub>Cr<sub>2</sub>Se<sub>4</sub>)<sub>x</sub>, semiconducting spin glasses, resistance, magnetoresistance, studies 4-108862  
 (CuCr<sub>2</sub>Se<sub>4</sub>)<sub>1-x</sub>(Cu<sub>0.5</sub>In<sub>0.5</sub>Cr<sub>2</sub>Se<sub>4</sub>)<sub>x</sub>, semiconducting spin glasses, resistance, magnetoresistance, studies 4-108862  
 CuFe<sub>2</sub>O<sub>4</sub>, conduction mechanism, annealing effect, resist. and thermopower meas. 4-104206

**electrical conductivity of crystalline semiconductors and insulators continued**

- CuGaTe<sub>2</sub>, vapour growth, thermodynamics and elec. characts. 4-71536  
 CuInS<sub>2</sub>, defect chemistry, elec. and Mossbauer studies 4-70730  
 n-CuInSe<sub>2</sub>, elec. and thermal conductivity 4-75974  
 CuInSe<sub>2</sub>, radiative recombination and shallow centres 4-109250  
 CuInSe<sub>2</sub>, sintered, grain size, SEM obs., resist., Hall obs. 4-66284  
 CuInTe<sub>2</sub>, vapour growth, thermodynamics and elec. characts. 4-71536  
 Cu<sub>2</sub>O, elec. cond. meas. 4-98624  
 Cu<sub>2</sub>Se, thermal props., elec. cond. and Hall effect 4-88523  
 Cu<sub>2</sub>SnS<sub>4</sub>, CDW transitions, elec. and thermal props. 4-98618  
 CuWO<sub>4</sub>, single cryst., elec. props., photoelectrochem. study 4-65708  
 DyB<sub>6</sub>, antiferromagnet, elec. resist. and thermoelec. power studies 4-113982  
 DyB<sub>6</sub>, low temp. resistivity and mag. props. 4-108859  
 DyMnO<sub>3</sub>, decomposition, O partial press. and elec. cond. 4-85290  
 Er<sub>2</sub>Si<sub>2</sub>, mag. phase transition, elec. cond. and cryst. struct. 4-88675  
 Fe<sub>2</sub>(MoO<sub>4</sub>)<sub>3</sub>, polycrystalline, elec. cond., 370-900K, O partial press. depend. 4-75965  
 α-Fe<sub>2</sub>O<sub>3</sub>, anisotropy of elec. props., mag. order depend. 4-108853  
 Fe<sub>2</sub>O<sub>3</sub>, pure and doped semicond., elec. cond. and Seebeck voltage 4-92759  
 α-Fe<sub>2</sub>O<sub>3</sub>-ZrO<sub>2</sub>, elec. cond. rel. to stoichiometry depend. Zr solubility 4-70820  
 Fe<sub>3</sub>O<sub>4</sub>, magnetite, elec. cond. below Verwey temperature 4-70809  
 Fe<sub>3</sub>O<sub>4</sub>, magnetite, elec. cond. mech. and rel. to mag. after-effects 4-76195  
 Fe<sub>3</sub>O<sub>4</sub>, point defects and transport props. 4-98366  
 FeSb<sub>2</sub>S<sub>4</sub>, berthierite, antiferromag. phase transition 4-65813  
 FeSn, pyrrhotite, elec. cond. meas. 4-80587  
 FeVNO<sub>6</sub>, semicond., elec. resist., mag. susceptibility meas. 4-109000  
 GaAlAs, proton-bombarded, thermal annealing, elec. cond. recovery 4-98146  
 Ga<sub>1-x</sub>Al<sub>x</sub>As, carrier transport under impurity radiative recombination conditions 4-104211  
 GaAs doping superlattices, weak localisation and magnetoresist. 4-98720  
 GaAs, electrical properties and impurity states 4-75963  
 GaAs, electron- and proton-irradiated, elec. props. 4-75975  
 GaAs, growth from melt and elec. props. 4-99300  
 GaAs, LEC grown, improved elec. uniformity by high temp. annealing 4-65684  
 GaAs LEC substrate, characterisation of impurities and microdefects (Japanese) 4-103778  
 GaAs, LPE growth and nonequil. deep centre trapping 4-108744  
 GaAs, n-i-p-i crystals, doping to alter electronic and optical props. (German) 4-98590  
 GaAs, negative differential cond. at transit reson. frequencies 4-84638  
 GaAs, proton-bombarded, thermal annealing, elec. cond. recovery 4-98146  
 GaAs, semi-insulating, deep donor conc., dislocations and elec. resist. 4-103781  
 GaAs semi-insulating substrate, inhomogeneity characterisation, expt. study 4-65759  
 GaAs:Cr, ion irradi. effect on defect thermal annealing 4-98156  
 GaAs:Cr-GaAs epitaxial junction, IR characterisation 4-109170  
 GaAs:Cr(O), electrical properties and impurity states 4-75963  
 GaAs:Si, LEC and horizontal Bridgman growth, elec. uniformity 4-65683  
 GaAs-AlGaAs heterojunction, phonon emission and electron heating 4-70927  
 GaCrSe<sub>3</sub>, antiferromag. semicond., mag. susceptibility, cond., EPR, IR reflection spectrum, Neel temp., energy gap meas. 4-61522  
 GaInAsP alloy semiconductors, book 4-58588  
 GaSb cryst., facet regions and Czochralski growth 4-75348  
 GaSb-InSb, behaviour of Sn in solid solns., elec. props. 4-75967  
 GaSe:Co, injection and thermoelectricalisation currents 4-70833  
 GaSe:Fe, elec. cond. and impurity states 4-113957  
 Ga<sub>2</sub>Te<sub>3</sub>, electrical and optical props. meas. 4-61380  
 GdB<sub>6</sub>, antiferromagnet, elec. resist. and thermoelec. power studies 4-113982  
 GdBi<sub>3</sub>, low temp. resistivity and mag. props. 4-108859  
 GdMnSi, M=first row transition metal, cryst. struct., mag. and elec. props. 4-70083  
 Ge bicrystal p-type inversion layers, anomalous magneto-transport props. 4-98719  
 Ge, deep impurity conc., elec. resist. and Hall coeff. meas. 4-65638  
 p-Ge, nuclear doped, elec. cond., 0.06 to 300K, impurity conc. depend. 4-61382  
 n-Ge:As, conductivity and magnetoresistance, effect of localised states 4-113950  
 Ge:Cu, impurity states, annealing effects 4-104148  
 Ge:Zn, nonohmic hopping cond. in strong elec. fields 4-88515  
 GeS, hole drift mobility anisotropy 4-70814  
 GeSe, cryst. and glassy, photoelec. props. 4-108905  
 (GeTe)<sub>1-x</sub>(AgSbTe)<sub>x</sub>, thermoelec. figure of merit 4-84637  
<sup>74</sup>Ge, neutron doped, low-temp. elec. cond. 4-80594  
 Hg<sub>1-x</sub>Ag<sub>x</sub>Cr<sub>2</sub>Se<sub>4</sub>, mag. semicond., exchange interaction, carrier effects 4-114103  
 Hg<sub>1-x</sub>Cd<sub>x</sub>Te, annealing of radiation defects, electron irradiation 4-108442  
 p-Hg<sub>1-x</sub>Cd<sub>x</sub>Te, elec. resist. and Hall coeffs., low-temp. anomalies 4-108885  
 HgCr<sub>2</sub>Se<sub>4</sub>, ferromagnetic semicond., elec. cond., photocond. meas., temp. depend. 4-61375  
 HgCr<sub>2</sub>Se<sub>4</sub>, mag. semicond., resist. and magnetisation changes and relax. 4-65682  
 Hg<sub>2</sub>Ga<sub>2</sub>□Te<sub>3</sub>, Hg<sub>2</sub>Ga<sub>2</sub>□Te<sub>6</sub>, pressure-induced phase transitions, elec. resistivity meas. 4-80497  
 HgI<sub>2</sub>, optically excited electronic processes 4-104254  
 HgIn□Te<sub>4</sub>, pressure-induced phase transitions, elec. resistivity meas. 4-80497  
 Hg<sub>1-x</sub>Mn<sub>x</sub>Te, transport meas. using the alternating current technique 4-92720  
 α-HgS, conductivity anisotropy and Hall coeffs. 4-92719  
 HgTe, zero-gap, intrinsic cond. theory 4-70813  
 HoMo<sub>2</sub>S<sub>8</sub>, ferromagnet, domain walls, superconductivity obs. 4-80718  
 In<sub>2</sub>MoS<sub>7</sub> (0≤x≤1) intercalation compound, synthesis and characts. 4-104200  
 InP, freq. depend. of negative cond., Gunn effect (Russian) 4-70825  
 InP, localisation of inversion electrons, Fourier transform spectra studies 4-98555  
 InP:He, ion implanted, elec. cond. study 4-80586

**electrical conductivity of crystalline semiconductors and insulators continued**

- InP:Mg(Ca,Zn) crystals grown by synthesis solute diffusion, electrical and optical props. 4-85093  
 InP:Sn(Sn)(Zn)(Fe) single crystals, LEC growth, perfection, carrier conc., TEM obs. 4-71550  
 InP:Se, ion implanted, annealing and transport props. 4-108397  
 InP:Zn crystals, bulk and surface effects of heat treatment 4-84625  
 p-InSb, elec. current which is even in elec. field obs. 4-113952  
 InSb, polycrystalline, thermomagnetic and galvanic props. (German) 4-75987  
 n-InSb, strongly compensated, electron mobility meas. 4-70834  
 InSb, US absorpt., elec. resist., mag. field effects 4-88243  
 p-InSb, ultrasonic attenuation and elec. resistivity at low temps. and high mag. fields 4-80165  
 InSe, elec. props., thickness depend. 4-88507  
 In<sub>2</sub>Se<sub>3</sub>, annealing in Se vapour, physical props. 4-61414  
 In<sub>2</sub>Te<sub>3</sub>, electrical and optical props. meas. 4-61380  
 KH<sub>2</sub>PO<sub>4</sub>, ferroelectric, phase transition at T=110°C 4-76389  
 KI thin films, high-field elec. cond. study 4-80702  
 KInO<sub>3</sub>, ferroelec. semicond., positive temperature resist. coeff. 4-113958  
 KSBF<sub>4</sub>, structural phase transitions, NQR, specific heat, X-ray powder anal., permitt., elec. cond. 4-113605  
 K<sub>2</sub>V<sub>2</sub>S<sub>8</sub>, prep., cryst. struct., and props. 4-84269  
 La<sub>2</sub>Ba<sub>2</sub>Cu<sub>6</sub>O<sub>14+y</sub>, struct., electron transport and mag. props. 4-70110  
 LaMo<sub>2</sub>S<sub>8</sub>, Chevrel phase, resistivity meas. 4-84619  
 LaMo<sub>2</sub>Se<sub>8</sub>, Chevrel phase, resistivity meas. 4-84619  
 LaS<sub>2</sub>, non-stoichiometric, thermoelectric props. 4-75992  
 LiNbO<sub>3</sub> cryst. growth, melt composition effect on props. 4-84227  
 LiNbO<sub>3</sub>, electrooptic cells, γ-irrad. effect on optical inhomogeneity 4-76438  
 LiNbO<sub>3</sub>, single cryst., phys. props. 20-200°C 4-76397  
 Li<sub>1+x</sub>Ti<sub>2-x</sub>O<sub>4</sub> ceramics, elec. and supercond. props. 4-104342  
 Li<sub>1/2</sub>Ti<sub>1/2</sub>O<sub>4</sub>, semicond. props., elec. cond., thermopower meas. 4-108858  
 (Mn<sub>1-x</sub>Cd<sub>x</sub>)<sub>2</sub>Sb<sub>2</sub>O<sub>7</sub>, pyrochlores, synthesis and solid state studies 4-88140  
 MnO, point defects and transport props. 4-98366  
 MnO, self-diffusion studies 4-98344  
 MnO, stabilised and Mn<sub>1-x</sub>Zn<sub>x</sub>O solid solns., elec. props. 4-98605  
 Mn<sub>2</sub>Sb<sub>2</sub>O<sub>7</sub>, pyrochlores, synthesis and solid state studies 4-88140  
 Mo<sub>2</sub>O<sub>6</sub>S<sub>3</sub>, elec. and mag. props. study 4-80595  
 n-MoTe<sub>2</sub>, carrier mobility, thermoelec. power and elec. resist., one-band model anal. 4-98612  
 Na<sub>2</sub>CoO<sub>2</sub>-y electrode material, electronic processes during intercalation 4-76012  
 Na<sub>2</sub>CoO<sub>2</sub>-y, intercalation cpd., transport props. 4-92734  
 Na<sub>2</sub>SO<sub>4</sub>-Ag<sub>2</sub>SO<sub>4</sub>, order-disorder transform., elec. cond., thermal anal., X-ray diff. 4-65382  
 NaX-Te cryst., current flow regime from I-V curves 4-88508  
 NbO<sub>2+x</sub>, phase equilibria and defect struct. 4-98246  
 Nb<sub>2</sub>(Se<sub>4</sub>)<sub>2</sub>(Te<sub>4</sub>), one-dimensional, thermoelectric power 4-70848  
 NbB<sub>6</sub>, low temp. resistivity and mag. props. 4-108859  
 Nd<sub>2-x</sub>Ba<sub>x</sub>Cu<sub>1-y/2</sub>O<sub>5-x</sub>, cryst. struct., mag. susceptibility, elec. cond. (French) 4-75418  
 NiO, interaction with O<sub>2</sub>, H<sub>2</sub>S and SO<sub>2</sub>, surface and vol. processes 4-98372  
 NiO:Li(Al), or undoped, elec. cond. and high temp. defect struct. 4-80617  
 NiO:O<sub>2</sub>, interaction, elec. cond., thermal flux 4-98627  
 NiV<sub>2</sub>Nb<sub>2</sub>O<sub>10</sub>, semicond., elec. resist., mag. susceptibility meas. 4-109000  
 NpBe<sub>13</sub>, mag. and elec. props. meas. 4-98887  
 Np<sub>0.68</sub>U<sub>0.32</sub>Be<sub>13</sub>, mag. and elec. props. meas. 4-98887  
 P, black, electronic props. and elec. cond. (Japanese) 4-92606  
 (Pb<sub>0.76</sub>Ca<sub>0.24</sub>)((Co<sub>1/2</sub>W<sub>1/2</sub>)<sub>0.04</sub>Ti<sub>0.96</sub>)O<sub>3</sub> ceramics, piezoelec. props. MnO addition effects 4-104532  
 (Pb<sub>0.75</sub>Ca<sub>0.25</sub>)(Mg<sub>1/3</sub>Nb<sub>2/3</sub>)<sub>0.0625</sub>Ti<sub>0.9375</sub>O<sub>3</sub>:Mn ceramics, US, elastic and dielec. props. 4-104543  
 Pb<sub>2</sub>Fe(Cn)<sub>6</sub>2H<sub>2</sub>O, with interstitial water impurity mols., electronic cond. activation 4-75972  
 Pb(FeNb)<sub>2</sub>O<sub>3</sub> ceramics and single crystals, prep., struct., X-ray diff., neutron powder diff., dielec. and elec. meas., SEM 4-75412  
 Pb(Fe<sub>1/2</sub>Nb<sub>1/2</sub>)<sub>2</sub>O<sub>3</sub>-Pb(Ni<sub>1/2</sub>Nb<sub>1/2</sub>)<sub>2</sub>O<sub>3</sub> solid soln. system, dielec. props. 4-104517  
 Pb<sub>1-x</sub>Ge<sub>x</sub>Te, ferroelec. phase transition, high press. investigation, DC resist., capacitance meas. 4-71312  
 Pb<sub>1-x</sub>Ge<sub>x</sub>Te, undoped and In-doped, anomalous scatt. of carriers by defects and impurities near ferroelec. phase transition 4-98622  
 Pb<sub>1-x</sub>Ge<sub>x</sub>Te:In, elec. props., band edge struct., impurity effects 4-108880  
 PbMoO<sub>4</sub>, electrical cond. and optical absorpt. study 4-104205  
 PbMoO<sub>4</sub>, stoichiometry deviation, electron transfer, elec. cond. meas. 4-80591  
 PbMo<sub>2</sub>S<sub>8</sub>, Chevrel phase, resistivity meas. 4-84619  
 PbMo<sub>2</sub>Se<sub>8</sub>, Chevrel phase, resistivity meas. 4-84619  
 PbS polycryst. samples, current and photocurrent flow mechanisms 4-104196  
 PbSe<sub>1-x</sub>Te<sub>x</sub>:Ti, energy spectra and elec. cond. 4-70724  
 PbSnTe, negative differential mobility in high elec. fields 4-104216  
 Pb<sub>1-x</sub>Sn<sub>x</sub>Te, ferroelec. phase transition close to band inversion 4-76364  
 Pb<sub>1-x</sub>Sn<sub>x</sub>Te:In, elec. transport props. 4-61371  
 PbTe films, hot wall epitaxy, elec. characts., SEM and X-ray obs. 4-71564  
 PbTe, negative differential mobility in high elec. fields 4-104216  
 PbTe, sintered, elec. cond. and thermoelec. power, annealing effects 4-84621  
 PbTe:Ga, elec. and optical meas. (Russian) 4-84636  
 PbTe(Se)(S), lattice thermal cond. meas. 4-98598  
 (PbTe)<sub>1-x</sub>(SnSe)<sub>x</sub> solid solns., single cryst., phys. props. 4-65673  
 PrB<sub>6</sub>, low temp. resistivity and mag. props. 4-108859  
 PuBe<sub>13</sub>, mag. and elec. props. meas. 4-98887  
 Ru<sub>2</sub>Ti<sub>1-x</sub>O<sub>2</sub>:Cl coatings, solid solution formation 4-70392  
 Sb, phase transitions at hydrostatic press. up to 9 GPa 4-75666  
 Sb<sub>2</sub>Mo<sub>2</sub>O<sub>4</sub>, preparation, cryst. struct., elec. and optical props. 4-84266  
 Sb<sub>2</sub>Mo<sub>2</sub>O<sub>6</sub>, band struct., transport props. 4-108773  
 Sb<sub>2</sub>Te<sub>2</sub>:Pb(Ge), doping props., elec. cond. and Seebeck measurements 4-75467  
 Sb<sub>2</sub>/Zn<sub>2</sub>O<sub>4</sub> sintered spinel, elec. cond. and Seebeck coeff., 400-800°C 4-61368  
 Si (111), 2D hole gas, conductivity, logarithmic corrections 4-98685  
 Si (111), adsorbed Cs, inversion layers, positive and negative magnetoresistance 4-98645  
 Si, carrier lifetime, elec. resist. meas. by contactless method 4-61392  
 n-Si, deformed, drag thermoelectric power anisotropy 4-104247  
 n-Si, electrical conduction, thermodynamic anal. 4-92711

electrical conductivity of crystalline semiconductors and insulators continued  
 Si, electron and  $\gamma$  irradi., influence on defect annihilation 4-98094  
 Si, electron and  $\gamma$ -ray irradiated, efficiency of radiation defect formation 4-92237  
 Si, excitation depend. grain boundary recombination velocity 4-104217  
 Si, fast neutron irradiation effects on resistivity in single crystals 4-98138  
 Si, grain boundary recombination vel., study for different injection levels 4-98633  
 Si,  $\gamma$ -ray irradi., conductivity, eddy current meas. 4-104201  
 Si, heavily doped, built-in elec. field for holes 4-80584  
 n-Si, hot electron conductivity in transverse elec. field, intravalley scatt. obs. 4-80596  
 n-Si, intervalley relax. time, elec. cond. study 4-98621  
 Si inversion layer, 2D, weak localisation and interaction effects 4-98766  
 n-Si, irradiated by  $\gamma$ -rays, changes in carrier lifetime 4-104232  
 Si, n-type, heavily-doped, minority hole mobility, empirical expression, device modelling appl. 4-98608  
 Si, plastically deformed, deep levels, capacitance, reverse current meas. 4-61319  
 Si, polycrystalline, elec. cond. props., small signal theory 4-70804  
 Si, polycrystalline, elec. cond. props., I-V characts. 4-70805  
 Si, polycrystalline, elec. cond. model 4-92712  
 Si, polycrystalline, elec. props. 4-104199  
 Si, polycrystalline, implantation under thermal and laser annealing, sheet resist, and doping profiles 4-75487  
 Si, polycrystalline, mobility and carrier conc. depend. on grain size and doping conc. 4-92730  
 Si, profiling techniques using spreading resistance 4-75498  
 n-Si, proton irradiated, electrophysical props. 4-108861  
 Si:As, high dose ion implanted, As clustering, TEM and SIMS studies 4-70384  
 Si:As, ion implanted, carrier density profiles, elec. meas., annealing behaviour 4-70179  
 Si:As, low-energy ion implantation 4-75466  
 Si:As, P, B, ion implanted, fast isothermal annealing and elec. props. 4-92224  
 Si:Au, donor level, entropy factor, resist, and DLTS meas. 4-70707  
 n-Si:Au, elec. cond. and photoconductivity 4-104213  
 Si:B, implanted, elec. activation and damage annealing by flash lamp irradi. 4-70196  
 Si:B ingots, effective segregation coeff. of B, elec. studies 4-88192  
 p-Si:Fe, conductance along grain boundaries 4-80585  
 Si:H, grown by zone melting, A-centre distrib. study 4-76666  
 a-Si:H film, Staebler-Wronski effect 4-108852  
 Si:Li, phonon scatt., acoustic paramagnetic resonance study 4-71157  
 Si:N(O), microdefect formation during single crystal growth, influence of impurities on nucleation 4-114386  
 Si:O, nonequilibrium cond. and thermal donors 4-104212  
 p-Si:P, elec. activity of P in diffusion zone (Russian) 4-70817  
 Si:Sb, ion implanted, supersaturation, vitreous C strip heater annealing, Rutherford backscattering, elec. meas. 4-92375  
 Si:Te, donor states, Hall effect and cond. meas. 4-104145  
 SiO<sub>2</sub>, electrical conductivity and permittivity of different polymorphs of quartz (Russian) 4-72580  
 SiO<sub>2</sub>, in <sup>60</sup>Cr-SiO<sub>2</sub>-pSi capacitor, conduction and charge storage 4-61474  
 SiO<sub>2</sub>, luminescence study of elec. cond. 4-61756  
 SiO<sub>2</sub>, Si-rich, elec. cond. theory 4-108850  
 p-Si:Te<sub>2</sub>, hygroscopic cryst., elec. cond. anisotropy, vacuum meas. 4-92718  
 Si-H, bonds and H-induced defects study 4-66058  
 SmB<sub>6</sub>, microwave conductivity meas. 4-70851  
 Sm<sub>1-x</sub>Gd<sub>x</sub>S solid soln: single crystals, phase transition during uniaxial compression, elec. cond. and colour change obs. 4-70375  
 SnI<sub>2</sub>, single crystal growth in silica gel in elec. field, elec. cond., mag. props. 4-93209  
 SnI<sub>4</sub>, single crystal growth in silica gel in elec. field, elec. cond., mag. props. 4-93209  
 SnMo<sub>4</sub>S<sub>8</sub>, Chevrel phase, resistivity meas. 4-84619  
 SnMo<sub>4</sub>S<sub>8</sub>, Chevrel phase, resistivity meas. 4-84619  
 SnO<sub>2</sub>, elec. props., SO<sub>2</sub> treatment effects, gas sensor appl. 4-92732  
 SrAs<sub>3</sub>, monoclinic, Fermi surface determ. by Shubnikov-de Haas effect 4-108763  
 SrCa<sub>1-x</sub>Nb<sub>2-x</sub>O<sub>7</sub>, defect struct., elec. and ionic cond. 4-98676  
 SrCeO<sub>3</sub>-SrZrO<sub>3</sub> solid solutions, X-ray characterisation and elec. cond. 4-84239  
 SrFeO<sub>3</sub>, screen-printed layers for methane detection 4-101832  
 SrTiO<sub>3</sub>, equilb. elec. cond. at 1000°C effect of Sr/Ti ratio 4-84618  
 SrTiO<sub>3</sub>, oxide perovskites, dielec. meas., surface layer effects 4-65962  
 SrTiO<sub>3</sub>, V<sup>3+</sup> partial substitution for Ti<sup>4+</sup>, ion-deficient perovskites, elec. and optical props. 4-80589  
 Ta<sub>2</sub>O<sub>5</sub>, effect of CaO addition, ionic transport number 4-98349  
 Ta<sub>2</sub>O<sub>5</sub> films on Si, electrical props. 4-84720  
 TaS<sub>2</sub>-IT, phase transition at 282K, DSC, elec. cond. and Hall effect meas. 4-92349  
 Te, neutron irradi. induced defects, optical props. near fundamental energy gap 4-84318  
 Te-Se, solid solutions, ordering near melting temp. 4-60878  
 TiB<sub>2</sub>, sintering and props. of samples made from powder synthesised in plasma-arc heater 4-76715  
 TiCl<sub>3-x</sub>, x=0.6 to 0.9, recovery of quenched-in vacancies 4-65257  
 TiC<sub>2</sub>, high-temp. supercond. phase near lower bound of homogeneity region 4-114063  
 TiS<sub>2</sub>, semicond.-semimetal transition at 40 kbar 4-84660  
 TiS<sub>2</sub>, elec. cond. and Hall effect 4-65677  
 TiBiTe<sub>2</sub>, growth, elec. and optical props. 4-65676  
 TiCuSe<sub>2</sub>, p-type metal with layer struct. 4-70652  
 UAs<sub>2</sub>Se<sub>1-x</sub>, electronic and mag. struct. determ. 4-61281  
 UM<sub>2</sub>B<sub>2</sub> (M=Co, Ru, Ir), mixed valence, mag. and elec. props. 4-113905  
 U<sub>5</sub>Mn(Bi)(Zr),  $\alpha$ - $\beta$  phase equilibrium and elec. cond. (French) 4-103927  
 V-C, homogeneity region, electrophysical props. 4-80611  
 WO<sub>3</sub> film, electrochromic props. 4-81027  
 WO<sub>3</sub> thick films, elec. cond. and electrochromism 4-65674  
 WO<sub>3-x</sub>, point defects evolution into extended defects, elec. cond. and gravimetric meas. 4-70143  
 WS<sub>2</sub>Br<sub>0.1</sub>, elec. cond. meas. 4-75973  
 WS<sub>2</sub>I<sub>0.1</sub>, elec. cond. meas. 4-75973  
 YIG, doped, for thermistor-bolometers 4-68280  
 Yb sulphides, thermoelectric props. 4-75991  
 Zn<sub>1-x</sub>Co<sub>x</sub>O<sub>3</sub>, solid soln., wurtzite-type struct., elec. cond. 4-92724

electrical conductivity of crystalline semiconductors and insulators continued  
 Zn<sub>1-x</sub>Ga<sub>2x/3</sub>Cr<sub>2</sub>Se<sub>4</sub>, magnetic semiconducting solid solutions study 4-109002  
 ZnGeAs<sub>2</sub>, electron- and proton-irradiated, elec. props. 4-75975  
 ZnO, adsorption sensitive elements, thermal characts. (Russian) 4-65549  
 ZnO, non-stoichiometric, diffusion processes 4-98352  
 ZnO, powdered, freq. dispersion of elec. cond. 4-70802  
 ZnO varistor, polycrystalline, elec. props. 4-104199  
 ZnO varistor ceramics, SEM EBIC studies 4-75981  
 ZnO weak accumulation layers, electron transport and Hall effect 4-98686  
 ZnO-Nb<sub>2</sub>O<sub>5</sub> ceramics, elec. props. and microstruct., wettability additives effect (Japanese) 4-76719  
 ZnS<sub>2</sub>Se<sub>1-x</sub>, deep impurity, trap embedding, luminesc. spectra 4-61321

**electrical conductivity of electrolytic liquids**  
*see also electrochemical analysis; electrolytic ion mobility; Wien effect*  
 alkylammonium salts, elec. cond. of extracts in benzene (nitrobenzene) (German) 4-61123  
 aqueous electrolytes, conductance, conc. depend. 4-84432  
 binary isothermal electrolyte solns., linear vector transport processes (German) 4-108640  
 butyric acid-water mixtures, cond. fluctuations 4-70421  
 decyltrimethylammonium bromides, aq. soln., critical micelle conc., elec. cond. 4-98325  
 hexyltrimethylammonium bromide, aq. soln., critical micelle conc., elec. cond. 4-98325  
 isobutyric acid-water mixtures, cond. fluctuations 4-70421  
 (KSCN, NaSCN)<sub>1-x</sub>0.3(Ca(NO<sub>3</sub>)<sub>2</sub>)<sub>0.7</sub>0.6H<sub>2</sub>O melts, mixed alkali effect 4-108642  
 Li/LiClO<sub>4</sub> in polypropylene carbonate/V<sub>2</sub>O<sub>5</sub>, evolution of AC impedance 4-99954  
 lyotropic mesophase with perforated lamellae, elec. cond. calcs. 4-98322  
 metals, elec. cond. and thermoelectric, power computation 4-92686  
 molten salts, assoc. and mobility isotherms 4-75247  
 polyelectrolyte solns., transport numbers, modified Hittorf method 4-103982  
 AgCl, molten, electrolytic cond. 4-108638  
 AgCl:CaCl<sub>2</sub>, molten, electrolytic cond. 4-108638  
 AgCl:CdCl<sub>2</sub>, molten, electrolytic cond. 4-108638  
 AgCl:CsCl, molten, electrolytic cond. 4-108638  
 AgCl:LiCl, molten, electrolytic cond. 4-108638  
 AlCl<sub>3</sub>-SOCl<sub>2</sub> based electrolytes, transport props. 4-88323  
 CuSO<sub>4</sub> aq. solns., elec. resist. fluctuations 4-75713  
 HCl in glycol mixtures, cond. meas. 4-65425  
 KH<sub>2</sub>PO<sub>4</sub> crystal growth from aqueous solution, in-line bulk supersaturation measurement by electrical conductometry 4-114371  
 KSO<sub>4</sub> ion pairs, dissociation in water at 25°C, press. effect (Japanese) 4-103985  
 LiAlCl<sub>4</sub> solutions conductivity in nitromethane containing SO<sub>2</sub>, concentration and temp. dependence, applicability assessment for Li/SO<sub>2</sub> cells 4-66596  
 LiCl-KCl molten system, internal cation mobilities determ. at 723K 4-92400  
 LiClO<sub>4</sub>-propylene carbonate electrolytic props., additive effects of Li<sup>+</sup> ion solvation compounds 4-65424  
 (Rb-Cs)NO<sub>3</sub> molten binary system, internal mobilities 4-108637

**electrical conductivity of gases**  
*see also space-charge-limited conduction*  
 air, electron beam generated cond. 4-113131  
 electron energy distrib. in gas in electric field, Boltzmann eqn., multiterm soln. 4-79709  
 gas mixtures, electrical cond. for strong fields 4-79764  
 inert gases, electron swarm parameters calc. 4-65145  
 CO<sub>2</sub>, electron transport, Monte Carlo and Boltzmann two-term calcs. 4-113109  
 He HF discharge conductivity in low hybrid resonance range (Russian) 4-92009  
 Hg vapour, slightly ionised, elec. cond., density depend. 4-113108  
 N<sub>2</sub> electron beam generated cond. 4-113131

**electrical conductivity of liquids**  
*see also electrical conductivity of electrolytic liquids*  
 amphiphilic liquid crystals, ionic cond. anisotropy 4-84435  
 benzylneopentate liquid ion injection and Kerr plots 4-80581  
 cholesteryl pelargonate liq. cryst., current flow, relax. processes 4-88770  
 cyanobiphenyl liq. crystals, current flow, relax. processes 4-88770  
 cyclohexane+triethylamine mixtures, keto-enol tautomerism 4-113589  
 dense matter in liq. metal phase, low-temp. quantum corrections to elec. and thermal conds. 4-63040  
 dense molecular fluids, shock wave eqn. of state and elec. cond. 4-108517  
 ester mixture, dynamic scatt. and conductivity anisotropy 4-109161  
 glassy materials, temp. coeffs. of transport props. 4-92409  
 hydrocarbon liquids, elec. conductivity meas. 4-92749  
 liquid binary mixtures, vel. field and self-diffusion, generalised Stokes-Einstein relation 4-61118  
 liquid dielectrics electrical conductivity, role of EHD motion, power capacitor example 4-98326  
 MBBA liq. cryst., current flow, relax. processes 4-88770  
 melts, electrical cond. and Hall coeff. meas. using van der Pauw's method 4-98606  
 metallic melts, electrical cond. and Hall coeff. meas. using van der Pauw's method 4-98606  
 metals, electrical conductivity, effective medium approx. 4-92690  
 methylpyridinium iodides, molten, transport props., <sup>1</sup>H NMR spectra and struct. 4-92966  
 nitrobenzene solns., critical props. study by elec. cond. method 4-113954  
 nitrobenzene solns., elec. resist. anomaly near critical point 4-113955  
 polar liquid dielectrics, temp. depend. of elec. conductance 4-98995  
 polychlorobiphenyl liquid ion injection and Kerr plots 4-80581  
 polystyrene latex suspensions, in electrolyte solns., adsorpt. and elec. cond. props. (Russian) 4-114848  
 PVC-ethylacrylate 4-vinylpyridine copolymers blends, miscibility, interactions, mech. props. 4-103670  
 quantum liqs., inhomogeneous, direct correl. function, appl. to liq. metals 4-60796  
 semiconductors, automated meas. using fused quartz cell 4-68241  
 smectic liq. cryst. thin oriented layers, elec. cond. mechanism 4-113960  
 water, dielec. props., charge injection and transport anal. 4-99023  
 water, high purity, resistivity meas., temp. depend. 4-113940

**electrical conductivity of liquids continued**

- Ag-Au, elec. resist., conc. depend., role of pseudopot. refinements 4-84605
- Ag-TiTe system, molten, elec. and mag. props. 4-104179
- Al, band energies, elec. resist., thermoelec. power, pseudopotential parameters determ. 4-98512
- Al, liq., structural props., elec. resist., X-ray diffr. 4-79925
- Al-Cu, liq., structural props., elec. resist., X-ray diffr. 4-79925
- As-Ge-Se, glass, small conc. of Se, elec. cond. rel. to temp. 4-92729
- As-Cd liq. and solid alloy, elec. resist. studies 4-88499
- Au<sub>1-x</sub>Si<sub>x</sub>, liq. and amorphous, elec. resist., Ziman theory anal. 4-70774
- Co-Ce liq. alloy, Ce valence state determ. 4-61358
- Cu complex, organometallic disc-like cpd., hexagonal columnar mesophase obs. 4-70025
- Cu, liq., structural props., elec. resist., X-ray diffr. 4-79925
- Cu-Au, elec. resist., conc. depend., role of pseudopot. refinements 4-84605
- Fe-Ce liq. alloy, Ce valence state determ. 4-61357
- Ga, supercooled and normal, elec. resist., temp. depend. 4-75921
- Ga<sub>2</sub>Te<sub>3</sub>, electrical cond. and Hall coeff. meas. using van der Pauw's method 4-98606
- Ga<sub>2</sub>Te<sub>3</sub> liquid semicond., elec. transport activation energies 4-88506
- H<sub>2</sub>AlP<sub>2</sub>O<sub>10</sub>·2H<sub>2</sub>O, electrorheological suspensions, disperse phase, charge transport characteristics 4-103426
- KCl-glycerol supercooled liq. solns., ionic mobility and dielec. relax. 4-88326
- KCl<sub>(s)</sub>+Ag<sub>(l)</sub>, disperse phase system, elec. cond., rel. to temp. and particle size 4-98680
- Nd, solid and liq., elec. resist. studies 4-92691
- Ni(II) complex with 1-phenyl-3,5-dimethylpyrazole, cond., electronic and IR spectra, mag. susceptibility meas. 4-76104
- Pr, solid and liq., elec. resist. studies 4-92691
- S<sub>10</sub>+C<sub>60</sub>, disperse phase system, elec. cond., rel. to temp. and particle size 4-98680
- Sm, solid and liq., elec. resist. studies 4-92691
- Sn complexes, cond. behaviour in nonaqueous solvents 4-76466
- Ti complexes, cond. behaviour in nonaqueous solvents 4-76466
- Ti<sub>2</sub>Se<sub>10-x</sub>, elec. cond. and thermopower, temp. depend., ionic and electronic transport 4-80592
- electrical conductivity of one-dimensional systems** *see one-dimensional conductivity*
- electrical conductivity of plasmas** *see plasma transport processes*
- electrical conductivity of solids**  
*see also electrical conductivity of amorphous metals and alloys; electrical conductivity of amorphous semiconductors and insulators; electrical conductivity of crystalline metals and alloys; electrical conductivity of crystalline semiconductors and insulators; electronic conduction in crystalline semiconductor thin films; electronic conduction in insulating thin films; electronic conduction in metallic thin films; ionic conduction in solids; recovery; superconductor*
- anisotropic solids, generalised Ohm and Fourier cond. laws, intrinsic symmetries of material tensors 4-75916
- attapulgite, temp. and freq. variations of elec. props. 4-61616
- bis(ethylenedithiotetrathiofulvalene), elec. props. meas. 4-75917
- carnauba wax, thermoelectric state, charge carrier identification 4-99008
- composites, EM and elastic props., correlation, microgeometries corresponding with effective medium approx. 4-70251
- conducting medium with nonlinearly conducting ellipsoidal inclusions, elec. field, current and Joule energy dissipation 4-108829
- conducting/insulating particulate mixture, elec. cond. model 4-84662
- conducting/insulating sphere mixture, AC cond., percolation approach 4-108911
- conductivity, critical exponents rel. to static exponents 4-95323
- dielectrics, conduction and breakdown, conf., Toulouse, France (July 1983) 4-106109
- dielectrics, conduction and breakdown phenomena, role of electrodes 4-108869
- disordered low-dimensional materials, near DC cond. and anomalous low-freq. dispersion 4-70769
- disordered systems, elec. cond. and diffusion processes, freq. depend. 4-61356
- electron gas, Anderson localisation and elec. cond., self-consistent mode-coupling theory 4-61336
- eutectic two-phase materials, bounds on transport, elastic and thermal expansion parameters 4-92684
- Fermi function, elec. cond., temp. depend., probability density function 4-98586
- glass-metal particulate composites, memory switching obs. 4-104761
- graphite fibres, intercalated, for electrical power transmission appl. 4-80562
- graphite intercalation compounds, c-axis cond. and thermoelec. power 4-80561
- graphite intercalation compounds, modification of material props. 4-60890
- graphite-AsF<sub>5</sub> intercalated foils and compacted flakes, elec. resist. studies 4-92683
- graphite-SbCl<sub>3</sub>-C<sub>12</sub>SbCl<sub>3</sub> intercalation cpd., resistivity and Hall effect (Russian) 4-113917
- impurity containing medium, freq. depend. dielec. const. and cond. 4-109107
- incommensurate SDWs, collective modes and elec. cond. 4-98594
- infinite cluster, percolation, mass fluctuations meas. 4-82759
- inhomogeneous medium, effective cond. in strong mag. fields 4-80559
- interacting disordered electron system, single-particle density of states, renormalisability 4-104115
- ionic lattice, solvated polaron, electronic transport mode 4-80518
- isomorphism of transport phenomena and percolation theory 4-104178
- linear response theory for DC conductivity 4-82744
- low field cond. in condensed matter 4-104177
- metal-insulator transition, kinetic coefficients, DC cond. and diffusion 4-80501
- monoclinic crystals, optical parameters 4-61648
- periodic and almost periodic crystals, oscillatory length-dependent cond. 4-61354
- poly(2,5-seleniénylene), elec. cond., synthesis 4-70886
- poly(2,6-naphthylene), electronic props. calcs. 4-88441
- poly(4-phenylquinoline), electronic props. calcs. 4-88441
- poly(metal-yl), prod. from butadiyne, elec. cond. 4-70782
- poly(p-phenylene):Li(K), electron spin echo studies 4-71155
- poly-yne, prod. from butadiyne, elec. cond. 4-70782

**electrical conductivity of solids continued**

- polyacetylene:1, stability after encapsulation, microwave meas. 4-109112
- polyacetylene, undoped and oxidised, thermal stability 4-89278
- polyfluorocarbon films containing Co(Al) clusters, plasma polymerisation 4-81433
- polyimides, Ag-doped, method for cond. increase 4-88608
- polymers, molded, percolation conductivity for orientation detection 4-92777
- polyquinoline, electronic props. calcs. 4-88441
- random systems, electron localisation and diffusion 4-98572
- resistivity and Hall effect (Russian) 4-113917
- resistivity saturation, self-consistent theory 4-75910
- resolvent method appl. to electronic transport in solids 4-84601
- rock, complex resistivity and dielectric behaviour 4-100538
- semiconductor, polar with anisotropic conduction valleys, high freq. cond. 4-113938
- semiconductor large diameter wafers, process nonuniformities, resistance characterisation 4-113963
- semiconductors, conductivity induced by impinging mol. vibr. to electronic energy transfer 4-84615
- semiconductors, electronic and atomic diffusion, D grad  $\nu$  and grad(D $\nu$ ) descriptions 4-104195
- semiconductors, macroscopic electron transport, Fokker-Planck eqn. soln. 4-98600
- size quantised systems with rough boundaries, electron states, cond. 4-75914
- small-polaron electronic transport in boron carbides 4-75988
- super-normal conductors, conduction in random networks, nonlinearity 4-98584
- Sylgard 184 containing hollow microspherical fillers, high temp. elec. cond. and thermal decomp. 4-92710
- temperature depend. of elec. cond. and probability density function 4-98585
- textured materials, kinetic props., grain interaction effects 4-60938
- TTF-FeOCl intercalation cpd., struct., IR spectra and mag. susceptibility 4-70128
- TTT-FeOCl intercalation cpd., struct., IR spectra and mag. susceptibility 4-70128
- two-dimensional continuum percolation and conduction 4-98583
- two-dimensional disordered electron systems, conductivity, interelectron effects 4-65656
- two-dimensional interacting disordered electron model, spin fluctuations 4-104398
- weak localisation in thin films, review 4-92829
- weakly localised regime, higher order interaction effects, case of repulsive force 4-75908
- AlN/Al cermet, reactive DC planar magnetron sputtering prep., elec. transport props. 4-88607
- Al<sub>2</sub>O<sub>3</sub>, alumina, humidity sensor, elec. resistivity rel. to surface area oxides (Japanese) 4-63751
- As-Sb-Se system, glass-ceramic composites, varistor-like behaviour 4-114009
- Au-SiO<sub>2</sub> composite granular films, conductivity and crossover effects 4-114047
- C fibre epoxy resin composites, conductivity and percolation 4-98679
- C film, elec. cond. changes induced by pyrolysis and high energy ion irradi. 4-75966
- C films, diamondlike, ion beam deposition and props. 4-85113
- C:H amorphous film prep. by H<sub>2</sub> gas reactive RF sputtering of graphite 4-76671
- Co(II) complex with 1-phenyl-3,5-dimethylpyrazole, cond., electronic and IR spectra, mag. susceptibility meas. 4-76104
- Cr-SiO cermet films, composition and sheet resistance effect on strain sensitivity obs. 4-111117
- CsF-UF<sub>6</sub> binary fused mixtures, elec. cond. 4-108847
- CuCl(Al<sub>2</sub>O<sub>3</sub>) composites, elec. cond., particle size effects 4-88548
- Cu(II) complex with 1-phenyl-3,5-dimethylpyrazole, cond., electronic and IR spectra, mag. susceptibility meas. 4-76104
- Cu(II) complex with 1-phenyl-3,5-dimethylpyrazole, cond., electronic and IR spectra, mag. susceptibility meas. 4-76104
- Ir III complexes, <sup>1</sup>H and <sup>13</sup>C NMR, cond. and mag. susceptibility meas. 4-71192
- KF-UF<sub>6</sub> binary fused mixtures, elec. cond. 4-108847
- La<sub>2</sub>CuO<sub>4</sub> with K<sub>2</sub>NiF<sub>4</sub> struct., at displacements, mag. and transport props., anisotropic bonding effects 4-75358
- LaNi<sub>1-x</sub>Mn<sub>x</sub>O<sub>2</sub>, valence states and mag. props. 4-84772
- La<sub>2</sub>NiO<sub>4</sub> with K<sub>2</sub>NiF<sub>4</sub> struct., at displacements, mag. and transport props., anisotropic bonding effects 4-75358
- Li<sub>0.5</sub>Mo<sub>0.5</sub>O<sub>1.7</sub>, quasi-two-dimensional electronic props. 4-104189
- Mo-SAM-E composite, electrophysical props. 4-76742
- Na<sub>2</sub>V<sub>2</sub>Si<sub>2</sub>S<sub>2</sub>, structural, elec., mag., NMR studies (French) 4-75414
- Ni(II) complex with 1-phenyl-3,5-dimethylpyrazole, cond., electronic and IR spectra, mag. susceptibility meas. 4-76104
- Pd II complexes, <sup>1</sup>H and <sup>13</sup>C NMR, cond. and mag. susceptibility meas. 4-71192
- Pt II complexes, <sup>1</sup>H and <sup>13</sup>C NMR, cond. and mag. susceptibility meas. 4-71192
- RbF-UF<sub>6</sub> binary fused mixtures, elec. cond. 4-108847
- Rh III complexes 4-71192
- TaS<sub>2</sub> (1T), commensurate CDW state, electronic cond., Hall coeff. meas. 4-98639
- TiTe<sub>2</sub>, band struct., elec. and mag. props. 4-92595
- Tl<sub>2</sub>VS<sub>4</sub>NMR and topotactic redox reactions 4-84859
- VP<sub>4</sub>, ambient press. synthesis, cryst. struct., mag. and elec. props., bonding 4-75408
- ZrSiO<sub>4</sub>, zircon, humidity sensor, elec. resistivity rel. to surface area oxides (Japanese) 4-63751
- electrical conductivity transitions**  
*see also metal-insulator transition*
- Anderson transition, conductivity and dielectric constant, universal relations 4-75857
- chalcogenide glass thin films, threshold switching and trap filling 4-92770
- chalcogenide glass thin films, threshold switching effects 4-92769
- chalcogenide glasses, switching effects, inhomogeneous model anal. 4-88546
- electrothermographic system of leuco malachite green mixed films of acrylonitrile butadiene styrene, electrical properties, obs. 4-98626
- fast ionic conductors, review 4-70439
- glass-metal particulate composites, memory switching obs. 4-104761

**electrical conductivity transitions continued**

- p-n junction, reverse-biased, switching to high cond. state, computer simulation 4-61452
- rubber, vulcanised, elec. cond., crystallinity and glass transition 4-113944
- semimetallic thin wires, semimetal semicond. transition due to quantum freeze-out of carriers 4-92833
- TCNQ salts, AgTCNQ and CuTCNQ, optical transitions 4-69487
- tetrathiafulvalene-p-chloranil, EPR study of soliton formation 4-109073
- (TMTSF)<sub>2</sub>FSO<sub>3</sub> organic semicond., cond. and cond. transitions 4-113870
- triarylmethane: F, cond. transitions 4-70881
- Ag epitaxial films on Ge (001), superconductivity and electron localisation 4-114062
- Ag thin films, electroformed, humidity memory effect (*Japanese*) 4-61471
- Ag thin films, electroformed, humidity sensitive switching 4-108908
- Ag<sub>2</sub>S, chem. prepared films, mixed conductivity study 4-104277
- As-Ge-Se, glass, small conc. of Se, elec. cond. rel. to temp. 4-92729
- As<sub>2</sub>Te<sub>3</sub>, cryst., semiconductor-metal transition, elec. resist., thermoelec. power meas. 4-98523
- Bi ultrathin aggregated film, cond. transition, classical percolation two-dimensional continuum model 4-104330
- Bi<sub>2</sub>O<sub>3</sub>-B<sub>2</sub>O<sub>3</sub> glasses, memory switching process, role of chem. reduction 4-114002
- CdF<sub>2</sub>:Er<sup>3+</sup>, insulator to semiconductor transition, site selective laser spectroscopy 4-99155
- CdS, optoelectronic switching, laser controlled, photoconductivity meas. (*German*) 4-84646
- CdSe-VO<sub>2</sub> contact, barrier to antibarrier transition during metal-semiconductor phase transition 4-65738
- Fe<sub>2</sub>Mn<sub>1-x</sub>S<sub>x</sub>, metal-insulator transition study 4-98527
- Fe<sub>2</sub>O<sub>3</sub>, heat capacity at Verwey transition 4-70405
- GaAs, growth from melt and elec. props. 4-99300
- GaAs, optoelectronic switching, laser controlled, photoconductivity meas. (*German*) 4-84646
- GaSb:Se, quantum localisation of electrons in metal-insulator transition region 4-70654
- GeSe, glass, bulk, press. induced electronic and structural transformations 4-114004
- Ge<sub>20</sub>Te<sub>80</sub> glass, bulk, elec. transport and high press. studies 4-114003
- Ge<sub>20</sub>Te<sub>80</sub> glass, elec. cond. transition, press. and temp. depend. 4-98619
- HgCr<sub>2</sub>Se<sub>4</sub>, mag. semicond., resist. and magnetisation changes and relax. 4-65682
- InO<sub>x</sub>, amorphous, electron mobility, cond., and supercond. near metal-insulator transition 4-80710
- KSbF<sub>4</sub>, structural phase transitions, NQR, specific heat, X-ray powder anal., permitt., elec. cond. 4-113605
- Na<sub>2</sub>Co<sub>2</sub>-y electrode material, electronic processes during intercalation 4-76012
- Nb-H alloys as electrothermal resistors, switching phenomena 4-98674
- NbSe<sub>3</sub>, CDW depinning, switching 4-75945
- NbSe<sub>3</sub>, chaotic response, evidence for new CDW phase 4-92706
- NiS:transition metals, first-order mag. and elec. transition, impurity effects 4-92909
- Pr-Cu point contacts low temp., high purity, I-V characteristics 4-114018
- Pr-Pr point contacts, low temp., high purity, I-V characteristics 4-114018
- Si, optoelectronic switching, laser controlled, photoconductivity meas. (*German*) 4-84646
- Si, polycrystalline, elec. cond. props., I-V characts. 4-70805
- Si:Sb, possible obs. of electronic phase transition, low temp. magnetoresist. study 4-80633
- Si<sub>1-x</sub>N<sub>x</sub>, amorphous, vapour deposited, struct., resist. characts., density, electron diff. meas. 4-61424
- SmB<sub>6</sub>, compound with intermediate valency, correl. gap, press. effect 4-70882
- Sn, semiconductor-metal transition, press. effects 4-92613
- Sn-Ge dilute alloys, semiconductor-metal transition, press. effects 4-92613
- Sn-Se liq. alloy, thermoelec. power, semicond.-semimetal transition 4-108909
- Ta<sub>2</sub>S<sub>5</sub>, onset of current carrying CDW state, switching, hysteresis, oscill. phenomena 4-75944
- Ta<sub>2</sub>S<sub>5</sub>, orthorhombic, CDW deformation relax. and thermal memory effects 4-104190
- 2H-TaSe<sub>2</sub>, CDW phase transition at low temp. and high press. 4-104276
- TiS<sub>2</sub>, semicond.-semimetal transition at 40 kbar 4-84660
- TiSe<sub>2</sub>:Zr, elec. cond. and phase transitions 4-104278
- VO<sub>2</sub>-WO<sub>3</sub>:H, photoinduction of H into the heterostructure, semiconductor-metal transition studies 4-113478
- ZnTe films, memory switching in MSM structures 4-70883

**electrical contacts**

- see also contact potential; contact resistance; ohmic contacts; point contacts*
- closed contact temp. rise with regard to skin effect, calc. (*Russian*) 4-84671
- contact materials with reduced noble metal content, corrosion behaviour (*German*) 4-99640
- contact resistance measurement for two different metals, allowing for thermal EMF 4-92794
- nonohmic contacts with double injection, theory 4-88563
- nonohmic contacts with double injection 4-88564
- poly base contact etch process 4-71746
- reactive metal contact diffusion barrier, passivation technique 4-104907
- semiconductor/metal contact, potential probe response to nonequilibrium situations 4-92820
- Al, fretting in elec. contacts 4-92798
- Au, acid hard electrodeposits, performance eval. 4-76020
- Au/Al contacts, intermetallic bonds and contact resist. (*Russian*) 4-113819
- Bi<sub>2</sub>GeO<sub>20</sub> cryst., surface-barrier photo-EMF 4-104315
- Bi<sub>2</sub>SiO<sub>20</sub> cryst., surface-barrier photo-EMF 4-104315
- Cd<sub>2</sub>Hg<sub>1-x</sub>Te/In system, current noise in contact regions, defect influences 4-88595
- p-CuInSe<sub>2</sub>-metal contacts, elec. props., solar cell appls. 4-70935
- Aln/Hg-insulator contacts, differential resistance and capacitance characts. 4-92819
- Pd-Ni electrodeposits, performance eval. 4-76020
- Pd<sub>2</sub>Si/Si system, contact growth and elec. characts., dry etching effects 4-104313

**electrical double layers *see electrochemistry; liquid theory***

**electrical engineering**

- see also high-voltage engineering*
- American Power Conference, Chicago, USA (April 1983) 4-86112
- quantum electronics, ideas and stumbling blocks 4-91427
- steel construction material, surface treatment and coating development (*German*) 4-76896
- electrical engineering applications of computers *see electrical engineering computing*
- electrical engineering computing
  - see also computerised control; computerised instrumentation; power system CAD*
  - eddy current computation with EDDYNET 4-59958
  - EM field problems, 3D, soln. on minicomputer 4-59947
  - medium isotropic thermoelectric generator test facilities, software and hardware requirements 4-72138
  - vehicular technology conf., Pittsburgh, PA, USA (May 1984) 4-106118
  - parallel-connected batteries, failure behaviour prediction by computer 4-72082
  - Pb/acid battery lifetime prediction, computerised pattern recognition application to life-cycling test data 4-81530
  - Pb-acid batteries for photovoltaic systems, math. model and computer simulation 4-72092
- electrical fault location *see fault location*
- electrical forming *see electroforming*
- electrical insulation *see insulation*
- electrical noise *see noise*
- electrical power systems *see power systems*
- electrical properties of substances
  - see also dielectric properties of substances; discharges (electric); electrical conductivity; flexoelectricity; thermoelectricity*
  - condensed matter physics, Iberian Symposium, Lisbon, Portugal (Sept. 1983) 4-78036
  - Ag thin films, pure and O covered, photoelec. and elec. props. 4-92831
- electrical resistance measurement *see electric resistance measurement*
- electrical resistivity *see electrical conductivity*
- electrical transport processes *see electrical conductivity*
- electricity
  - see also atmospheric electricity; electric charge; electric current; electrical properties of substances; electromagnetism; terrestrial electricity*
  - electrical and electronic phenomena and devices, book 4-67952
- electricity supply industry
  - advanced molten carbonate and solid oxide fuel cells for utility load levelling appls. 4-72104
  - electric utilities, developments (*Dutch*) 4-89460
  - forecasting system, intermediate future, conf. Washington DC, USA (Aug. 1982) 4-78038
  - Germany, economic and environmentally safe fuel for energy generation, considerations (*German*) 4-93652
  - nuclear power plant computer-aided design and draughting benefits 4-59311
  - solar energy option rating by Florida electric utilities 4-66662
  - solar photovoltaic power systems, electric utility R and D perspective 4-93622
  - Na-S battery development and appl., Ford Aerospace program, USA 4-66685
  - Zn<sub>2</sub>Fe(CN)<sub>6</sub>-Zn<sub>2</sub>Fe(CN)<sub>4</sub> battery system for utility load levelling and solar photovoltaic/wind appls. 4-72055
- electro-oculography *see bioelectric potentials; eye*
- electro-optical devices
  - see also electrochromic devices; liquid crystal devices; optical modulation*
  - aberration studies utilising an opto-electronic coherent microscope 4-83548
  - anisotropic waveguide, acoustooptic and electrooptic guided wave conversion to leaky waves 4-91583
  - bistable devices with short delay times in the feedback bifurcations 4-96980
  - book, optical waves in crystals, laser radiation propag. and control 4-86135
  - cable inspection using electro-optical technique and microprocessing technology 4-106347
  - conference on solid state optical control devices, Los Angeles, USA (Jan. 1984) 4-95024
  - digital optical architecture for performing matrix algebra 4-96815
  - distance measurement, FEN 2000 family of instruments using pulse-timing meas. (*German*) 4-62967
  - electric field strength measurement using electro-optical instrument, sensitivity improvement techniques (*Japanese*) 4-78298
  - fiber depolarizer for monochromatic light 4-79330
  - focusing devices, optimisation 4-74644
  - frequency domain storage, polarisation gated writing of photochem. holes for FM polarisation detection 4-87292
  - guided wave control technology 4-107817
  - high-speed shutter using ns gated image intensifier 4-64762
  - image recognition, optical-electronic system with operational input and preliminary processing of images for recognition (*Russian*) 4-107526
  - industrial applications of electro-opt. instrumentation, conf., Arlington, USA (Apr. 1983) 4-90286
  - infrared radiation thermometers, industrial, design concepts for running in hostile environments 4-106323
  - InGaAsP, linear electro-optic effects and device design 4-88809
  - integrated optical travelling wave switch/modulators, vel.-matching techniques 4-74748
  - intensity modulation system, low distortion, with optical feedback 4-91577
  - intensity-to-spatial frequency transformations in optical signal processing using electro-optical systems 4-79045
  - ion implantation, effects on props. 4-80067
  - Langmuir-Blodgett films, prep. charact. and appls. 4-61245
  - large aperture optical switching devices for inertial confinement fusion lasers 4-96944
  - laser anemometer gas streak vel. meas. electro-optical convertor and photoelectric controller appl. (*Russian*) 4-60564
  - leaky anisotropic waveguides using nematic liq. cryst. overlays 4-97063
  - low light level imaging system field performance estimation, spectral matching considerations 4-73506
  - Mach-Zehnder travelling-wave modulator, 17 GHz bandwidth 4-97058

**electro-optical devices continued**

- microchannel spatial light modulator, materials limitations 4-74697  
mirrors in  $\text{LiNbO}_3$  intersecting channel waveguides, light switching appls. 4-79348  
modulators on the basis of KDP and DKDP crystals 4-112489  
MOS electroabsorption waveguide light modulator, field relax. 4-107815  
multichannel Pockels cell spectropolarimeter for Anglo-Australian Telescope 4-110533  
optical commercial development prospects, the fourth wave 4-112340  
photorefractive laser beamsteering using thick diff. gratings, configurations 4-96968  
piezoelectric films with waveguides for light modulation 4-112488  
Pockels cell driver, Si switch development for optical pulse generation in Nova, Novette fusion lasers 4-107702  
PRIZ light modulator, use of insulating layer, grating hologram recording 4-103007  
PRIZ spatial light modulator, phys. basis of operation 4-83688  
PRIZ-type space time light modulation, increased photosensitivity (*Russian*) 4-69544  
single pulse selector for high repetition rate mode-locked lasers (*Chinese*) 4-87355  
smectic A cells, ferroelectric, preparation for electrooptical microsecond switches appl. 4-75272  
spatial light modulator, integral transform implementation 4-91576  
spatial light modulator, linear array total internal refl., for optical information processing 4-74695  
spatial light modulators, theoretical resolution limitations, fundamental considerations 4-87440  
spatial light modulators, theoretical resolution limitations, effects of crystallographic orientation 4-87441  
switch for unpolarised radiation in  $\text{Nd}^{3+}$ :YAG laser with intracavity SHG in crystals exhibiting aperture effect 4-74574  
thin film optics, appl. of ion implantation 4-74757  
thin film technologies, conf., Geneva, Switzerland (Apr. 1983) 4-73137  
transformations in optical signal processing, conf., Seattle, WA, USA (Feb. 1981) 4-78023  
video-bandwidth ADC using optical techniques for extended precision 4-69594  
 $\text{Bi}_{1-x}\text{Sb}_x\text{Te}$ , electron beam controlled spatial and temporal light modulator 4-60142  
CO<sub>2</sub> laser, Q-switched, electro-optic freq. shifts 4-87377  
GaAlAs electroabsorption modulators, monolithically integrated array 4-103006  
GaAs, optical guided-wave monolithic interferometer 4-112561  
GaAs/GaAlAs quantum well self-electro-optic effect device as hybrid optically bistable switch 4-91522  
InGaAsP/InP gigahertz-bandwidth optical modulators/switches with DH waveguides 4-112585  
InP based integrated optics 4-64796  
 $\text{KD}_2\text{PO}_4$  based shutters, transmission contrast, anomalous biaxiality effects 4-60139  
 $\text{KD}_2\text{PO}_4$ , piezoelectrically induced acoustic waves, strain optic effect 4-66005  
 $\text{KH}_2\text{PO}_4$  with plasma electrodes, electro-optic harmonic conversion switch for large-aperture multipass laser systems 4-97000  
 $\text{LiNbO}_3$  broad-band guided-wave electrooptical modulators 4-97057  
 $\text{LiNbO}_3$  electro-optic modulator for diode laser, design and 600 Mbit/s operation (*German*) 4-79199  
 $\text{LiNbO}_3$  electrooptic cells,  $\gamma$ -irrad. effect on optical inhomogeneity 4-76438  
 $\text{LiNbO}_3$ , Ti diffused optical waveguide, effects of lossy thin plasma film 4-107818  
 $\text{LiNbO}_3$ , Ti diffused waveguide interferometric modulator (*Chinese*) 4-112564  
 $\text{LiNbO}_3$  waveguide bistable devices, blocking oscill., theoretical and expt. study (*Japanese*) 4-87484  
 $\text{LiNbO}_3$  waveguide electro-optic prism beam deflector, bistability obs. 4-103005  
 $\text{LiNbO}_3$  wideband electro-optic modulators 4-97056  
 $\text{LiNbO}_3$ :Ti based optical waveguide devices 4-69555  
 $\text{LiNbO}_3$ :Ti coupled channel waveguides and  $\Delta\beta$  electrodes for electrooptical modulator 4-74699  
 $\text{LiNbO}_3$ :Ti integrated oscillators and multivibrators 4-64795  
 $\text{LiNbO}_3$ :Ti strip waveguide modulators, polarisation insensitive 4-79281  
 $\text{LiNbO}_3$ :Ti strip waveguide integrated optical freq. translator 4-112562  
 $\text{LiNbO}_3$ :Ti travelling wave microwave optical modulator 4-112563  
 $\text{LiNbO}_3$ :Ti waveguide Mach-Zehnder modulator, low drive voltage, fibre-optic sensing appls. 4-91575  
 $\text{LiTaO}_3$ :Ag waveguide based electro-optic Bragg modulator with apodised electrode struct. 4-74700  
 $\text{NH}_4\text{D}_2\text{PO}_4$ , piezoelectrically induced acoustic waves, strain optic effect 4-66005  
 $\text{Si}_3\text{N}_4$  MNOS struct. dielec., built in charge during elec. and optical recording (*Russian*) 4-65746  
Ti:LiNbO<sub>3</sub> travelling-wave optical modulator for  $\lambda = 1.32 \mu\text{m}$  4-69595

**electro-optical effects**

- see also electroabsorption; electrochromism; electroluminescence; electroreflectance; Kerr electro-optical effect; photorefractive effect; Pockels effect; Stark effect  
birefringent crystals, linear and circular, electrooptical field meas. 4-104572  
bond charges extended model, appl. to optical props. of crystals 4-76413  
book, optical waves in crystals, laser radiation propag. and control 4-86135  
1,1,1,4,4,4-butanediol, molten, Raman spectra conformational depend. of Fermi reson. 4-69048  
cholesteric liq. crystals, blue phases, elec. field induced birefringence 4-76426  
cholesteric mixture, compensated liquid crystals, fluorescent guests props. 4-65168  
cholesteric texture change electro-optical effect, two-freq. addressing 4-71347  
cholesteric thin large-pitch films, polar electro-optic effect 4-114246  
constants for crystals, data tables, book 4-58593  
DOBAMBC, liquid cryst., cell thickness effect on elec. props., optical switching and memory 4-98998  
dynamic image selection under nonlinear elec. field conditions; role of injection currents 4-61661  
ester mixture, dynamic scatt. and conductivity anisotropy 4-109161

**electro-optical effects continued**

- esters, nematic eutectic mixtures, electrooptic, dielec. and physical props. 4-108271  
fast processes, electrooptical method study, quantum limitations 4-107585  
ferroelectric liquid crystals, microsecond electro-optic switching using transient light scatt. 4-93052  
ferroelectric liquid crystals, mol. orientation dynamic response 4-98005  
ferroelectric semicond., photorefractive phenomena caused by fluctuations and phonons 4-66009  
HOBACPC, liquid cryst., cell thickness effect on elec. props., optical switching and memory 4-98998  
hydroxypropyl cellulose, nematic polymer, optical props. in elec. field 4-65176  
isotropic media subjected to DC electric field, nonlinear refr. index phenomena 4-64750  
light modulation by electrooptic effect in KDP type crystals. 4-76437  
linear electro-optic effect, crystallographic aspects 4-80905  
liquid crystals, electro-optic display device appls. 4-103651  
MBBA nematic layer, splay  $e_{12}$  flexoelec. coeff., electro-optical studies 4-84180  
methylamine, intensity and electro-optical parameters, CNDO calc. 4-83397  
molecular liquid, single molecule cross-correlation functions using elec. field induced birefringence 4-93056  
molecules, electrooptical parameters physical meaning derived from IR intensities 4-69127  
negative electrooptical feedback lasers, secondary electrooptical effect on lasing 4-79160  
nematic structure, twisted-wedge, domain type, electrooptical behaviour 4-93051  
nematic twisted cells, electro-optic dynamic hysteresis 4-109160  
noncentrosymmetric cubic cryst., induced birefringence anisotropy 4-88812  
nonlinear optical media, electro-optic shock radiation theory 4-112498  
optical devices, effects of ion implantation on props. 4-80067  
photoconducting piezoelectrics, opto-electric conversion during nonlinear optoacoustic interaction 4-109155  
photoconductive ferroelectrics, optical device applications 4-64744  
photorefractive crystals as optical devices, elements, and processors 4-97033  
photorefractive materials, space charge fields 4-99094  
piezoelectric semiconductor with acoustic instability, threshold for controlled Franz-Keldysh stimulated scatt. 4-69507  
PLZT epitaxial thin films, ferroelec. and electrooptical props. 4-104530  
polarisation, definitions and nomenclature, instrument polarisation 4-82604  
polyatomic mols., electro-optical parameters, IR band intensities, semi-empirical theory 4-78844  
polydisperse particle size analysis by pulsed electric birefringence 4-84948  
polyester, aromatic cholesteric polymer, optical props. in elec. field 4-65176  
polysiloxanes, smectic, field induced director reorientation, electro-optic props. 4-76436  
semiconductor, dimensionally quantised, nonlinearly absorbed light in elec. field presence 4-107758  
semiconductors, impurity centres, nonlinear polarisability 4-84589  
smectic A liquid cryst., electrohydrodynamic instability and turbulent motion 4-70030  
thin film technologies, conf., Geneva, Switzerland (Apr. 1983) 4-73137  
triglycine sulphate:  $L\alpha$  alanine ferroelec. cryst., piezooptical props. 4-76431  
tunable diode laser spectroscopy of molecules in solids and on surfaces 4-111210  
AsSe<sub>4</sub>-chiral-liquid-crystal struct., phase boundary effect on electrooptical props. 4-93057  
BaO-TiO<sub>2</sub>-SiO<sub>2</sub> glass-ceramics, ferroelec., depolarisation currents, dielec. and electrooptical props. 4-76317  
Ba<sub>0.8</sub>Si<sub>0.2</sub>Nb<sub>0.8</sub>O<sub>6</sub> ferroelec. cryst., electrooptical coefficients 4-76434  
BaTiO<sub>3</sub>, anisotropic self diffraction 4-107762  
Bi<sub>2</sub>GeO<sub>10</sub>, field and charge distrib. in case of trap thermal ionisation 4-66010  
Bi<sub>2</sub>SiO<sub>20</sub> crystal volume phase holograms, light diff. 4-83539  
Bi<sub>2</sub>SiO<sub>20</sub> crystals, electro-optic coeff. meas., optical activity influence 4-93055  
Bi<sub>2</sub>Si(TiO<sub>2</sub>)<sub>20</sub> gyrotropic crystals, electro-optical and optical props. (*Russian*) 4-93058  
Ca<sub>3</sub>Nb<sub>2</sub>O<sub>7</sub>-CaTiO<sub>3</sub> ferroelectric, crystallochemical props. 4-71288  
Cd<sub>2</sub>Nb<sub>2</sub>O<sub>7</sub>, diffuse and sharp phase transitions, dielec., optical, and electro-optical studies 4-71309  
Cu halides, electron-phonon interaction and optical props., Raman spectra studies 4-66008  
GaInAsP/InP BH injection lasers, network modelling and modulation characts. 4-96890  
H-like ions, reson. doublet spectrum in intense elec. field, laser plasma diagnostics appl. 4-84074  
InGaAsP, linear electro-optic effects and nonlinear optical coeffs., device design appls. 4-88809  
InP, linear electro-optic coeff., Raman scatt. meas. 4-61659  
K<sub>2</sub>CO<sub>3</sub>(SO<sub>4</sub>)<sub>2</sub> ferroelastic, optical props. 4-66000  
La<sub>2</sub>Ti<sub>2</sub>O<sub>7</sub>-CaTiO<sub>3</sub> ferroelectric, crystallochemical props. 4-71288  
 $\alpha$ -LiIO<sub>3</sub>, phase-type gratings induced by electro-optical effect, space charge fluctuation 4-66012  
 $\alpha$ -LiIO<sub>3</sub>, quasi-one-dimensional ionic conductor, light diff. due to space charge fluctuations 4-109156  
 $\alpha$ -LiIO<sub>3</sub>, quasi-one-dimensional ionic conductor, light diff. due to space charge fluctuations 4-109157  
LiNbO<sub>3</sub>, elec. field effect on polariton Raman spectra 4-104575  
LiNbO<sub>3</sub>:Fe crystals, photoelec. and photorefr. prop. control during growth by elec. current 4-80904  
 $\text{N}(\text{D}_2\text{H}_1)_2\text{N}(\text{D}_2\text{H}_1)_2\text{PO}_4$ , dielectric and electro-optical props. meas. 4-76313  
Na<sub>2</sub>O-Nb<sub>2</sub>O<sub>5</sub>-SiO<sub>2</sub> glass-ceramics, ferroelec., depolarisation currents, dielec. and electrooptical props. 4-76317  
Nd<sub>2</sub>Ti<sub>2</sub>O<sub>7</sub>-CaTiO<sub>3</sub> ferroelectric, crystallochemical props. 4-71288  
O<sub>3</sub> dipole moment function, vibrational-transition probabilities 4-69051  
PLZT ceramics, ferroelec. and electrooptic props. 4-76353  
PLZT retardation plates, nonhomogeneity of light modulation 4-61660  
Pb<sub>2</sub>GeO<sub>11</sub> type crystals, electrogyration, dispersive and temp. depend. 4-76433

# electro-optical effects continued

- PbTiO<sub>3</sub> type crysts., electrogyration, dispersive and temp. depend. 4-76433  
 Rb<sub>2</sub>ZnCl<sub>4</sub>, incommensurate and ferroelec. phases, electro-optical props. 4-104574  
 Si, optical phase conjugation, elec. fields effect 4-107756  
 Si-electrolyte interface, elec. field modulated IR internal reflection studies 4-98749  
 ZnS:Mn electroluminesc. thin layers, doping and cryst. struct. 4-75810

# electroabsorption

- CCD spatial light modulator, 1D, signal correlation 4-107542  
 MOS electroabsorption waveguide light modulator, field relax. 4-107815  
 Cd<sub>1-x</sub>Mn<sub>x</sub>Te solid solns., Mn photoionisation detection 4-71349  
 CuCl, excitonic absorpt. edge, IR laser radiation induced electroabsorpt. 4-61287  
 GaAlAs electroabsorption modulators, monolithically integrated array 4-103006  
 InGaAsP-InP DH modulators, electroabsorption, polarisation depend. 4-93054  
 a-Si:H-a-SiN<sub>x</sub>:H heterojunction, lattice mismatch, electroabsorption study 4-76029  
 ZnO:Ni, photoionisation band edge fine struct., electroabsorption studies 4-109162

# electroacoustic effects *see acoustoelectric effects*

# electroacoustic generators *see acoustic generators*

# electrocaloric effects *see pyroelectricity*

# electrocardiogram *see electrocardiography*

# electrocardiography

- see also bioelectric potentials; biomagnetism; cardiology*  
 50 Hz interference subtraction 4-85545  
 arrhythmias, computer detect., historical review 4-89807  
 arrhythmias monitoring on electrocardiogram, digital cardiometer appl. 4-72447  
 atrial strip ECGs in frogs, comparison with theoretical predictions 4-89555  
 autoregressive model with abnormal values, order estimation (*Japanese*) 4-67145  
 body surface multielectrode for inverse problem in electrocardiography and its application (*Japanese*) 4-62621  
 body surface potential mapping system development (*Japanese*) 4-72446  
 breast carcinoma, ECG changes after radiation therapy 4-93845  
 cardiogram signal compression with AZTEC algorithm (*Chinese*) 4-105355  
 colour display 180 electrode ECG-body surface pot. map system derived data 4-85551  
 computerised ECG processing, symptom pattern recognition 4-105372  
 computers for heart, electronics in intensive care 4-109986  
 electrocardiograph functional testing, microprocessor-controlled signal generator 4-115252  
 EMG noise reduction for high resolution ECG 4-85564  
 epicardial mapping in open-heart surgery, practical approach 4-93959  
 epicardial potentials, determ. from body surface pots. 4-115044  
 error analysis in forward ECG problems 4-85553  
 esophageal ECGs interpretation, solid-angle anal. 4-93726  
 estimated action potentials during repolarization phase from the body surface electrocardiogram 4-89817  
 FFT appl. for heart disease diagnosis 4-62618  
 Fourier descriptors for ECG data compression 4-89800  
 HF information, extpt. and clinical investigations 4-93728  
 high resolution ECG 4-85562  
 history, early ECG in medical practice 4-115250  
 IMACC-8001 signal analysis system (*Spanish*) 4-73427  
 inverse recovery of two dipoles using a realistic human torso model 4-85418  
 inverse solutions from human body surface ECG maps 4-85555  
 late potentials as a noninvasive marker for ventricular tachycardia 4-93945  
 localisation of cardiac activity sources 4-93940  
 monitors, evaluation of four machines 4-109982  
 myocardial scintigraphy using <sup>201</sup>Tl, ECG-gated, rel. to imaging time 4-81765  
 nerve or muscle fibre pot. calc. model 4-106143  
 noisy peak recognition 4-93939  
 numerical calculation of the electric field at the heart (*German*) 4-85571  
 pacemaker cardiac spike detect. in ECG signal, encoding in digital ambulatory recorder 4-100353  
 QRS detection in ambulatory monitoring, review 4-85540  
 radioisotope imaging with ECG gating system 4-72413  
 rate variability data, point events series, spectra comparison 4-81793  
 registration and automatic analysis apparatus for electrocardiographic QRS signals (*Bulgarian*) 4-93955  
 signal averaging system for high resolution ECG 4-85563  
 single moving dipole, appl. in man 4-85556  
 surface potential mapping, cardiac statistical imaging problem 4-85552  
 time domain and spectral anal. of electrograms in man 4-81791  
 torso, human, modifiable computer model development for ECG studies 4-85554  
 ventricular depolarisation, calc. of isochrones 4-66930  
 ventricular repolarisation assessment by pot. mapping 4-89806  
 waveform alignment and extrasystoles rejection, cross-correlation function 4-93941

# electrocataphoresis *see electrophoresis*

# electrochemical analysis

- see also electrochemistry; polarography; voltammetry (chemical analysis)*  
 alloy identification kit 4-101823  
 cells for in situ EXAFS 4-99800  
 InP:Zn epitaxial layers, MOCVD grown, doping, Hall effect, SIMS, electrochemical profiling 4-80077  
 interface studied by surface plasmon excitation in focused light 4-71937  
 marine sediment, redox state meas. technique using Pt electrode 4-94262  
 steel, tool, tempered surface layers formed during grinding, thickness determ. using electrochem. method 4-71814  
 Ag electrolyte system, electrochemical interface studied by surface plasmon excitation 4-71938  
 CO<sub>2</sub> electrochemical sensor for high ambient pressures, deep diving appls. 4-106311  
 LiF-KF eutectic melt, oxide ion anodic behaviour at glassy C electrode 4-66594

# electrochemical analysis continued

- Nd(III) trace determ. with methyl thymol blue using dropping Hg electrode 4-114875  
 O<sub>2</sub> electrochemical meter for liquid Na 4-89370  
 Pr(III) trace determ. with methyl thymol blue using dropping Hg electrode 4-114875  
 Si:H, amorphous, Fe<sub>2</sub>O<sub>3</sub>-coated semiconductor electrode by solar cell, XPS, AES and electrochem. meas. 4-66691

# electrochemical batteries *see cells (electric)*

# electrochemical electrodes

## *see also electrochemistry*

- bipolar disc electrode with many holes, network model components 4-109668  
 composite insertion electrodes using solid electrolytes, theory 4-89386  
 electric cells with porous electrochemical electrodes, potential and current density distribution study (*Hungarian*) 4-105098  
 electrodes, electrochemical form. of oxide films, SEM and TEM studies 4-104908  
 fuel cells catalysed by WC in H<sub>3</sub>PO<sub>4</sub>, corrosion resistance and catalytic activity 4-66689  
 graphite, inert, for Ti/Fe redox flow battery 4-81534  
 high surface area nickel electrode testing, for H<sub>2</sub> producing water electrolyser 4-105127  
 iron phthalocyanine film electrodes, anodic dissolution in H<sub>2</sub>SO<sub>4</sub> 4-61453  
 large area woven fibre cathodes 4-99802  
 molten carbonate fuel cell isotropic porous anode model 4-66688  
 Ni electrode development with stable charging and discharging and wide temperature range 4-72063  
 polyacetylene, electrochemistry and aqueous chemistry, rechargeable battery cell fabrication 4-77013  
 polyacetylene electrodes for rechargeable electrochem. cell, investig. 4-104994  
 polyazulene, electropolymerised films, electroactive props. 4-88810  
 porous gas diffusion electrodes prep. and characts. for alkaline low-temp. H<sub>2</sub>-O<sub>2</sub> fuel cells 4-62349  
 power sources, status and development 4-62322  
 pyrographite, electrochemical intercalation of fluorides, for high energy density battery cathodes 4-81444  
 Raney nickel electrode, testing for H<sub>2</sub> producing water electrolyser 4-105127  
 secondary cells, Ni composite electrodes, concept and feasibility study 4-72065  
 secondary cells, Ni electrode performance and degradation 4-72064  
 secondary cells, Ni sinter plates, electrochemical impregnation bath ageing of Ni(OH)<sub>2</sub> 4-72067  
 secondary cells with PTFE bonded Ni(OH)<sub>2</sub> electrodes, structural and electrochemical characts. 4-72061  
 semiconducting photoelectrodes, efficiency of splitting water 4-93635  
 semiconductor electrodes, oxidation, corrosion, elec. double layer model 4-62235  
 sintered alloy nickel electrode, testing, for H<sub>2</sub> producing water electrolyser 4-105127  
 three-layer Raney Ni-H<sub>2</sub> electrode for fuel cells (*Japanese*) 4-89396  
 Ag electrode, roughened, adsorbed 4-benzyl pyridine, surface enhanced Raman bands, voltage induced intensity changes 4-93080  
 Ag high index faces, surface plasmon excitation, photoemission-into-electrolyte study 4-109308  
 Al-air batteries, electrochemical characteristics of air electrode with Fe phthalocyanine 4-93608  
 Br electrodes in Zn/Br and Zn/air batteries, electrochemical calorimetry 4-104995  
 C, glassy, electrode in LiF-KF eutectic melt, oxide ion anodic behaviour 4-66594  
 C, use in electrochem. power sources, improved material characts. 4-62324  
 Cd-Pb composite amalgam cathode for standard cells (*Japanese*) 4-86439  
 n-CdIn<sub>2</sub>Se<sub>4</sub> single cryst. electrodes in polysulphide electrolytes, photoelectrochemical behaviour 4-77117  
 CdS, polycrystalline thin film electrodes photoelectrochemical studies 4-109747  
 CdS/Cu<sub>2</sub>S heterojunction solar cells, electrochemical method for improving spectral response 4-109744  
 n-CdS<sub>0.9</sub>Se<sub>0.1</sub>, photoelectrochemical props. (*Chinese*) 4-81565  
 CdSe, polycrystalline thin film electrodes photoelectrochemical studies 4-109747  
 Cd<sub>1-x</sub>Zn<sub>x</sub>S sprayed film, photoelectrochem. cells, Zn composition effects 4-114912  
 Cu<sub>2</sub>S cathodes in organic electrolyte Li batteries, electrochem. behaviour 4-104996  
 Fe<sub>2-x</sub>O<sub>3</sub>, electrochemical kinetic studies 4-99803  
 p-GaP photoelectrochem. cells, absorpt. coeff. and diffusion lengths, differential photocurrent determ. 4-89455  
 H<sub>2</sub>/O<sub>2</sub> evolution photoelectrocatalysis 4-105112  
 n-InP photoelectrodes, subbandgap response, effect of surface modification 4-88582  
 Ir, activated, potentiometric behaviour in acrylamide and H<sub>2</sub>SO<sub>4</sub> (*French*) 4-62247  
 Li anode cells, primary and secondary, review 4-72054  
 Li batteries, current status and future developments 4-62332  
 Li cell, nonaqueous, electrochemistry 4-62333  
 Li/CF battery, electrochemical characts. 4-99955  
 Li-Al electrode secondary cell, cycling behaviour in LiClO<sub>4</sub>-propylene carbonate solutions 4-72058  
 Li-Al electrode secondary cell at room temp., Li-Al alloy electrochemical formation kinetics 4-72059  
 Li-B/LiNO<sub>3</sub> anode-electrolyte system, potentiostatic studies 4-66676  
 LiAl thin film electrodes for secondary batteries, overpotentials 4-109737  
 Li<sub>1-x</sub>V<sub>x</sub>O<sub>4</sub> solid soln. cathodes for secondary Li batteries 4-109736  
 Mg anode, for dry cell, open-circuit potential-time transient 4-66597  
 MnO<sub>2</sub>/active C as O<sub>2</sub> electrode in alkaline fuel cells (*Japanese*) 4-89397  
 MnO<sub>2</sub>-Zn rechargeable alkaline cells, test cell construction and development, cycling tests 4-81531  
 p-MoS<sub>2</sub>, for photoelectrocatalytic production of H<sub>2</sub> 4-114963  
 MoSe<sub>2</sub> photoanodes, transient photocurrent studies 4-104258  
 n-TiO<sub>2</sub> semiconductor photoanode preparation, photoelectrochemical behavior (*Chinese*) 4-85377  
 NH<sub>4</sub><sup>+</sup> ion selective electrode, electrochem. props. 4-81445  
 Na-S batteries, molten polysulphide electrodes, pot. distrib. and electrochem. reaction rate 4-66678

**electrochemical electrodes continued**

- NaCrS<sub>2</sub> cathode for secondary Li cells, props. and cyclic performance 4-93605  
 Ni electrode sinter, mechanical stress estimation 4-72066  
 Ni/Fe accumulators, new generation, for industrial manufacturing (French) 4-62331  
 Ni-Cd and Ni-H cells, overall efficiency of Ni electrode operation 4-72084  
 Ni-H<sub>2</sub> cell, long-life Ni electrodes, initial performance test 4-72088  
 Ni-S<sub>2</sub> for alkaline electrolysis of water, microscopic and spectroscopic study 4-113766  
 Ni(O) electrode secondary cells, voltammetry of material dispersion and redox behaviour 4-72062  
 Ni(OH)<sub>2</sub> electrode cell technology, past developments and future prospects 4-72060  
 Ni(OH)<sub>2</sub> electrode poisoning by Fe<sup>3+</sup> ions 4-66680  
 Ni(OH)<sub>2</sub>/NiO(OH) electrodes, plastic-bonded, ESCA investigations, for alkaline storage batteries 4-109733  
 O<sub>2</sub> electrochemical meter for liquid Na 4-89370  
 Pb-acid battery, new ideas 4-62329  
 Pb/acid secondary cells, kinetics of PbO<sub>2</sub> growth on electrode 4-109732  
 Pb/graphite accumulator using aqueous HF acid, advantages and disadvantages 4-66682  
 Pb-acid automotive battery, 'precharged' positive plate, incorporation of PbO<sub>2</sub> 4-77070  
 Pb-acid automotive-battery, PbO<sub>2</sub> incorporation into 'precharged' positive plate 4-77069  
 Pb-acid batteries, positive plates cryst. and amorphous components, quantitative phase anal., elec. vehicle appl. 4-77068  
 Pd, adsorpt. of CO, IR refl. spectrosc. obs. 4-107348  
 Pt, adsorpt. of SO<sub>2</sub>, electrooxidation in conc. solns. 4-61219  
 Pt, adsorption of tripeptide, AC admittance meas. 4-92538  
 Pt, adsorption of tripeptide, kinetics and isotherms 4-92539  
 Ru electrodes, electrochemical form. of oxide films, SEM and TEM studies 4-104908  
 Sb electro-oxidation and electro-reduction kinetics in alkaline solns. 4-66681  
 n-Si photoanode stabilisation against photoanodic decomp. with polyacetylene films 4-72123  
 n-SnO<sub>2</sub> electrodes coated with poly-(4-vinyl pyridine) films, photogalvanic effects 4-89454  
 SrTiO<sub>3</sub> photoelectrode for aerobic photoelectrochemical converter of regenerative type 4-93633  
 SrTiO<sub>3</sub> polycrystalline anodes, photoelectrochemical props., influence of mech. polishing 4-75998  
 n-SrTiO<sub>3</sub>/Nb/Fe(CN)<sub>6</sub><sup>3-</sup> (IrCl<sub>6</sub><sup>2-</sup>) interfaces, electroreduction 4-65740  
 n-TiO<sub>2</sub> photoelectrochemical sintered electrodes, hole diffusion length 4-70929  
 WSe<sub>2</sub> photoanodes, transient photocurrent studies 4-104258  
 Zn electrodes in Zn/Br and Zn/air batteries, electrochemical calorimetry 4-104995

**electrochemical machining** see *electrolytic machining*

**electrochemical polishing** see *electrolytic polishing*

**electrochemistry**

- see also *Debye-Huckel theory; electrical conductivity of electrolytic liquids; electrochemical analysis; electrochemical electrodes; electrolysis; electrolytic devices; electrophoresis*  
 adiabatic rate processes in condensed systems and interfaces, quantum model anal. 4-71986  
 anthraquinone radical anions obtained by in situ electrochemical method, ESR study 4-77004  
 4,4'-bipyridine, on Ag electrodes, redox behaviour, Raman and cyclic voltammetry study 4-75778  
 cells for in situ EXAFS 4-99800  
 colloidal systems, conc. elec. double layer interactions 4-114838  
 crystal growth parameters and electrochem. nucleation, integral eqn. anal. 4-66595  
 cyclic water splitting process, evolved H<sub>2</sub> and O<sub>2</sub> measurement by electrochemical method 4-62209  
 decontamination of decommissioned nuclear power station pipework (German) 4-83254  
 double layer dipole orientation at electrodes, polarisation catastrophes anal. 4-98690  
 electric double layer, free energy 4-61436  
 electric double layer, interface potential between diffuse and dense parts 4-81443  
 electric double layers interaction, metal electrolyte interface and the Donnan membrane 4-62449  
 electrical double layer, dissimilar flat, Stern plane, variation of pot. 4-62208  
 electrical double layers, ion density profile calcs. 4-71935  
 electrochemical double layer, dielectric enhancement and electrophoresis 4-71936  
 electrode/electrolyte interface, desorption rates and electrochem. meas. 4-104066  
 electrodes, electrochemical form. of oxide films, SEM and TEM studies 4-104908  
 elemental semiconductors, electrochemical oxidation, surface states (French) 4-76044  
 hydration forces near charged surfaces 4-99841  
 III-V semiconductors, electrochemical oxidation, surface states (French) 4-76044  
 intercalation of fluorides into pyrographite, for high energy density battery cathodes 4-81444  
 interface studied by surface plasmon excitation in focused light 4-71937  
 marine electrochemistry (book) 4-101599  
 3-methylthiophene polymer films, in situ Fourier transform IR spectra, vibronic coupling 4-87115  
 mixed boundary-value problems connected with a limiting electrochemical perforation 4-89306  
 organic dyes, photovoltaic cells, chem. props. 4-84998  
 organic, exchange of O between gas and solid, electrochemical study 4-98357  
 p-n junction GaAs photovoltaic electrolyser for hydrogen production by water electrolysis 4-89451  
 photoelectrochemical energy conversion, review 4-72125  
 poly(3-methylthiophene) films, electrochemically prepared, elec. cond. and <sup>13</sup>C NMR spectrum 4-76275  
 poly(3-methylthiophene) films, I<sub>2</sub> doped, electrochemical prep. 4-80577  
 polyacetylene, electrochemical doping, in situ Raman scatt. 4-74665

**electrochemistry continued**

- polyacetylene, electrochemical doping, reduction potentials meas. 4-65284  
 polyacetylene, electrochemistry and aqueous chemistry 4-77013  
 polypyrrole, conducting polymer, electrochemical prep., battery appl. (Japanese) 4-75942  
 polythiophene:BF<sub>4</sub><sup>-</sup> (Bu<sub>4</sub>N<sup>+</sup>), electrochemical n-type and p-type doping, elec. and optical props. 4-61363  
 polythiophene, conducting polymer, electrochemical prep., battery appl. (Japanese) 4-75942  
 power sources, status and development 4-62322  
 power sources and sinks, electrochemical reactions 4-62339  
 repassivation in alkaline soln., oxidation rates 4-104909  
 secondary cells, Li/LiClO<sub>4</sub> in polypropylene carbonate/V<sub>2</sub>O<sub>5</sub>, evolution of AC impedance 4-99954  
 semiconductor-insulator interface, electrophysical props., general theory 4-76045  
 semiconductors, deep levels and interface states, electrochem. photocapacitance spectroscopy method 4-65635  
 semiconductors, electrochemical carrier conc. profiling, review 4-75495  
 semiconductors, electrolytic Schottky-gated Hall effect profiling 4-75497  
 semiconductors, photoelectrochemistry, book contrib. 4-88585  
 solid electrolyte mixed potential phenomena 4-71939  
 solid surface, chemical and electrochemical treatment, low energy electron induced X-ray spectra 4-76572  
 steel, crevice corrosion electrochemical meas. (Japanese) 4-89201  
 steel, stainless, electrochemical potential, BWR water chemistry variation effects, cracking 4-85262  
 transition metal dichalcogenides, optical anisotropy, photoelectrochem. determ. 4-71335  
 water oxidation processes at n-PtS<sub>2</sub> and n-RuS<sub>2</sub> semicond. surfaces, ns-pulse laser study 4-89308  
 Zircaloy 2, electrochemical potential, BWR water chemistry variation effects, cracking 4-85262  
 Ag-adsorption of SO<sub>2</sub>, surface second harmonic generation 4-65647  
 Ag electrolyte system, electrochemical interface studied by surface plasmon excitation 4-71938  
 Ag surfaces and halide layers protonation of pyridine by adsorbed H<sub>2</sub>O, Raman spectra 4-89322  
 Al-air batteries, electrochemical characteristics of air electrode with Fe phthalocyanine 4-93608  
 Al-Mo alloys, ion implanted, corrosion resist., AES studies 4-99626  
 Al-Zn (Cu)(5 wt.%), with and without Ti, stress corrosion cracking, electrochemical aspects 4-104920  
 n-CdS/electrolyte interface, photoelectrochem. characterisation 4-84689  
 CdS-Cu<sub>2</sub>S heterojunction photocells, Cu<sub>2</sub>S electroplating on CdS 4-99354  
 CdSe/ferro-ferricyanide photoelectrochemical system, I-V behaviour 4-88580  
 CdSe/sulphide-polysulphide photoelectrochemical system, I-V behaviour 4-88580  
 CuCNS photocathodes, dye sensitisation in aq. KCNS 4-104257  
 Cu<sub>2</sub>-PSI<sub>2</sub>, photointercalation and optical information storage 4-79058  
 Cu<sub>2</sub>S cathodes in organic electrolyte Li batteries, electrochem. behaviour 4-104996  
 CuWO<sub>4</sub> single cryst., elec. props., photoelectrochem. study 4-65708  
 Fe alloy surfaces in acid media, H<sub>2</sub> evolution kinetics, metallurgical and electrochem. factors 4-85335  
 Fe, corrosion in molten carbonate, electrochem. studies 4-104917  
 Fe, corrosion in molten chloride, electrochem. studies 4-104915  
 Fe, corrosion in molten sulphate, electrochem. studies 4-104916  
 Fe, passive film form. in borate solns., electrochem. and ellipsometric studies 4-66490  
 Fe-Cu, H permeation in H<sub>2</sub>SO<sub>4</sub> with and without H<sub>2</sub>S, electrochem. and surface anal. studies 4-104898  
 Fe(CN)<sub>6</sub><sup>3-</sup> (n=3,4), Fe-C bond lengths, EXAFS spectroelectrochemistry 4-107364  
 Fe<sub>1-x</sub>O, electrochemical kinetic studies 4-99803  
 Ga<sub>1-x</sub>In<sub>x</sub>P, electrochem. behaviour in aq. and nonaqueous media, common anion rule 4-70928  
 H<sub>2</sub> production, p-Si cathode surface treatment effects on photoelectrochemical kinetics 4-93649  
 H<sub>2</sub> production, by photoelectrochemical decomposition of water (Hungarian) 4-100009  
 H<sub>2</sub> production by electrochemical gasification of coal 4-66814  
 H<sub>2</sub> production by photoelectrocatalysis on p-MoS<sub>2</sub> 4-114963  
 H<sub>2</sub> production by water splitting, using photochemical reaction in concentrated phosphoric acid 4-89470  
 H<sub>2</sub>/electrical power simultaneous production, using carbonaceous fuels and high-temperature nuclear process heat, thermodynamic anal. 4-89472  
 H<sub>2</sub>O<sub>2</sub> evolution photoelectrocatalysis 4-105112  
 In-Bi-Pb, liquid, thermodynamic props., EMF meas., 673 to 873K 4-98310  
 InP photoelectrodes, surface states, photocapacitance spectra studies 4-114010  
 InSe, lamellar, n- and p-type, in aqueous soln., photoelectrochemistry 4-88579  
 La<sub>1-x</sub>Ca<sub>x</sub>FeO<sub>3-y</sub> ferrites, mixed valence and electrochem. props. 4-70752  
 La<sub>1-x</sub>Sr<sub>x</sub>FeO<sub>3-y</sub> ferrites, mixed valence and electrochem. props. 4-70752  
 La<sub>2</sub>Ti<sub>2</sub>O<sub>7</sub>:Cr<sup>3+</sup> and La<sub>2</sub>Y<sub>2</sub>TiO<sub>7</sub>:Cr<sup>3+</sup>, photoelectrochem. props. 4-70874  
 Li cell, nonaqueous, electrochemistry 4-62333  
 Li secondary electrochemical cell, electrochemical, thermodynamic and O<sub>2</sub> pot. quantities 4-77072  
 Li/CF battery, electrochemical characts. 4-99955  
 Li-Al/FeS cell, FeS positive electrode effective conductivities in LiCl-KCl eutectic electrolyte 4-99958  
 LiAlCl<sub>4</sub> solutions conductivity in nitromethane containing SO<sub>2</sub>, concentration and temp. dependence, applicability assessment for Li/SO<sub>2</sub> cells 4-66596  
 LiF-KF eutectic melt, oxide ion anodic behaviour at glassy C electrode 4-66594  
 MoS<sub>2</sub> battery examined by chronopotentiometry, X-ray diffr. and long term cycling 4-89385  
 MoSe<sub>2</sub> photoanodes, transient photocurrent studies 4-104258  
 n-TiO<sub>2</sub> semiconductor photoanode preparation, photoelectrochemical behavior (Chinese) 4-85377  
 NH<sub>4</sub><sup>+</sup> ion selective electrode, electrochem. props. 4-81445  
 Nd<sub>2</sub>Ti<sub>2</sub>O<sub>7</sub>:Cr<sup>3+</sup> and Nd<sub>2</sub>Y<sub>2</sub>TiO<sub>7</sub>:Cr<sup>3+</sup>, photoelectrochem. props. 4-70874  
 Ni alloy surfaces in acid media, H<sub>2</sub> evolution kinetics, metallurgical and electrochem. factors 4-85335  
 Ni, corrosion in molten carbonate, electrochem. studies 4-104917  
 Ni, corrosion in molten chloride, electrochem. studies 4-104915

**electrochemistry continued**

- Ni, corrosion in molten sulphate, electrochem. studies 4-104916  
 Ni, electroless plating on metals, catalytic activity and electro-oxidation 4-66243  
 Ni, repassivation in alkaline soln., oxidation rates 4-104909  
 Ni(OH)<sub>2</sub>/Ni(OH) electrodes, plastic-bonded, ESCA investigations, for alkaline storage batteries 4-109733  
 O, electrochemical meter for liquid Na 4-89370  
 Pb/acid cells, immobilized electrolyte, design limitations 4-81532  
 Pb/acid cells, rotating ring-disc electrode study of impurity effects on lead corrosion in sulphuric acid 4-81533  
 Pb/acid cells for electric vehicles, comparison with alternate cells 4-62335  
 Pb/acid secondary cells, kinetics of PbO<sub>2</sub> growth on electrode 4-109732  
 Pb/graphite accumulator using aqueous HF acid, advantages and disadvantages 4-66682  
 PbO, standard molar Gibbs free energy of form., O conc. cell meas. 4-105010  
 PbO<sub>2</sub>,  $\alpha$  and  $\beta$ , proton localisation, X-ray and neutron diff. studies. (French) 4-88142  
 Pd-Al<sub>2</sub>O<sub>3</sub> catalyst, plug of Pb/acid batteries, deterioration prevention 4-93613  
 Pr<sub>2</sub>Ti<sub>2</sub>O<sub>7</sub>-Cr<sup>3+</sup> and Pr<sub>2</sub>/TiO<sub>3</sub>-Cr<sup>3+</sup>, photoelectrochem. props. 4-70874  
 Pt layer on graphite and RuO<sub>2</sub> substrates, ion bombard., electrocatalytic props. 4-71968  
 Pt surface, Sn underpot. deposition in H<sub>2</sub>SO<sub>4</sub> soln. 4-81480  
 Ru electrodes, electrochemical form. of oxide films, SEM and TEM studies 4-104908  
 n-Si, photoelectrodes, silicide coated, electrochemical and photoelectrochemical behavior 4-88581  
 Si/Sb, electrolytical Sb diffusion in MOS structures 4-80299  
 Si/methanol liquid junction, open circuit volt. and oxide form. 4-114030  
 SiAs electrode, photoelectrochemistry, influence of surface morphology 4-89309  
 SrTiO<sub>3</sub> polycrystalline anodes, photoelectrochemical props., influence of mech. polishing 4-75998  
 n-SrTiO<sub>3</sub>/Nb/Fe(CN)<sub>6</sub><sup>3-</sup>-(IrCl<sub>6</sub><sup>2-</sup>) interfaces, electroreduction 4-65740  
 Ti-Al alloy VT1-0, anodic soln. under potentiostatic conditions (Russian) 4-71778  
 Ti<sub>2</sub>Cu<sub>1-x</sub> alloys, electrochemical and thermal oxidation and electrochemical O<sub>2</sub> evolution 4-93452  
 n-TiO<sub>2</sub> photoelectrochemical sintered electrodes, hole diffusion length 4-70929  
 TiO<sub>2</sub> thin films, plasma-enhanced CVD, photoelectrochemical props. 4-80627  
 TiO<sub>2</sub>/RuO<sub>2</sub>/O<sub>2</sub> biphasic syst. in aq. soln., photoelec. props. 4-84648  
 Ti<sub>2</sub>V<sub>2</sub>S<sub>8</sub>, NMR and topocatic redox reactions 4-84859  
 V<sub>2</sub>W<sub>2</sub>O<sub>8</sub>, Wadsley-Roth phases, electrolytic reduction prep. from molten salts 4-66247  
 WO<sub>3</sub>.x(H<sub>2</sub>O) films, influence of crystallisation as hydration 4-88424  
 WSe<sub>2</sub> photoanodes, transient photocurrent studies 4-104258  
 Zr-Ni alloys in halide media, electrochemical behaviour, influence on corrosion resistance 4-104921  
 Zn anodic dissolution in alkaline electrolytes, three step model 4-103941  
 Zr, electrochem. corrosion protection 4-99634

**electrochromic devices**

- Er complex, Er-dipthalocyanine films, electrochromism for all solid display cells 4-76435  
 In<sub>2</sub>-Sn<sub>2</sub>O<sub>3</sub>/WO<sub>3</sub>/SiO<sub>2</sub>/Au electrochromic devices, electrooptic spectroscopy studies 4-109163  
 Na<sub>2</sub>WO<sub>4</sub> films, optical absorption spectra, electrochromic cell appls. 4-76544  
 WO<sub>3</sub> electrochromic cells, equivalent ccts., AC impedance (Japanese) 4-88808  
 WO<sub>3</sub> electrochromic devices for energy efficient windows, oblique deposition effect on response time 4-112537

**electrochromism**

- 1,1-dialkyl-4,4'-bipyridinium salts, ioneneomeric liq. crystals, mesophase transition temps. and electrochromism 4-88078  
 materials for controlled radiant energy transfer in buildings 4-112536  
 polyazulene, electropolymerised films, electroactive props. 4-88810  
 all-trans retinal in polyethylene and polypropylene matrices, electrochromism in viscous systems 4-96634  
 Er complex, Er-dipthalocyanine films, electrochromism for all solid display cells 4-76435  
 IrO<sub>3</sub> reactively sputtered coatings, electrochromism (Japanese) 4-99095  
 Li<sub>2</sub>WO<sub>6</sub> amorphous film, electrochromism colouring/bleaching processes, Li<sup>+</sup> ion transport 4-114244  
 PbMoO<sub>4</sub>, electrical cond. and optical absorpt. study 4-104205  
 V<sub>2</sub>O<sub>5</sub>, electrochemically coloured, PMR investig. 4-104499  
 V<sub>2</sub>O<sub>5</sub> films, vacuum deposited, electrochromic props. (Japanese) 4-88897  
 WO<sub>3</sub> amorphous films, electrochromic colour centres, Raman scatt. studies 4-113445  
 WO<sub>3</sub> anodic films, electrochromic, TEM, RHEED and Raman studies 4-99114  
 WO<sub>3</sub> electrochromic cells, equivalent ccts., AC impedance (Japanese) 4-88808  
 WO<sub>3</sub> film, electrochromic props. 4-81027  
 WO<sub>3</sub> films, atmospheric evaporated, electrochromism 4-99092  
 WO<sub>3</sub> polycrystalline electrochromic films; Drude model, ellipsometry meas. as direct evidence 4-88799  
 WO<sub>3</sub> thick films, elec. cond. and electrochromism 4-65674  
 WO<sub>3</sub> thin films, electrochromic response modification by O<sub>2</sub> backfilling 4-88892

**electrodeposited coatings** *see electrodeposits***electrodeposited films** *see electrodeposits***electrodeposited layers** *see electrodeposits***electrodeposition**

- see also electrodeposits; electroplating*  
 actinide electrodeposition method for alpha spectrometer source preparation 4-101969  
 compound coatings from electrolyte suspensions, deposition mechanisms, comp. calc. method (Russian) 4-71605  
 metal dendrites, electrocrystallisation rate under galvanostatic conditions 4-61265  
 metal electrodeposition, pulsating current, microthrowing power, SEM obs. 4-93240  
 metals, electrodeposition, pulsating current, spongy deposit prevention 4-93241

**electrodeposition continued**

- metals, electrodeposition after cation-exchange on modified C fibre electrodes 4-76701  
 polyacrylonitrile, electropolymerisation on metal substrate, spectroscopic obs. of film attachment and growth mechanism (French) 4-66191  
 steel, electroerosion alloying with W, C influence on surface layer form. 4-114714  
 thermal ionisation mass spectrometry, microelectrodeposition for sample purification and loading technique 4-68314  
 transient nucleation kinetics under galvanostatic electrolysis conditions 4-60874  
 Ag electrodeposition during diffusion-controlled multisweep voltammetry 4-104743  
 Cd, electrodeposition from acidic chloride baths, morphology and hardness rel. to addition agents 4-93238  
 Cd-Ni, electrodeposition from ammoniacal baths, corrosion resist. 4-66253  
 CdS thin films, electrodeposited in fused salt solns., struct. and morphology rel. to substrate 4-66250  
 p-CdTe, undoped, in situ prep. by cathodic electrochem. deposition 4-61880  
 Co foil making by electrolytic method, for nuclear expts. 4-104742  
 Co-W-Mn thin mag. film deposition, electrocrystallisation (Russian) 4-65592  
 Co<sub>1-x</sub>B<sub>x</sub>, amorphous alloy, electrolytical and chemical prep., struct. 4-70603  
 Cu, dendritic electrodeposits, fractal behaviour 4-75825  
 Cu deposition from cyanide bath, selective case hardening 4-104744  
 Cu electrodeposition on Pt (111), LEED and AES studies 4-66244  
 Cu fine powders, electrodeposition, organic additions influence 4-61888  
 Cu-In-S layers, electrodeposition, photoelectrochemical characterisation 4-99355  
 Ga<sub>1-x</sub>Al<sub>x</sub>As/GaAs solar cell with antirefl. coating, LPE grown, design, fabrication and characts. (Polish) 4-114904  
 InSe, lamellar p-type, photointercalation and photodeposition of Cu 4-93539  
 Mo, electrodeposition in fused salts 4-71607  
 Ni electrodeposited from sulphate and acetate salts, hardness and struct. 4-114431  
 Ni, electrodeposition, hardness, microstruct. 4-66252  
 Ni, electrodeposition from formamide soln. 4-66251  
 Ni-B composites, electroless and electrodeposition 4-88990  
 Ru dendrites, form. by electrolysis of chloride melt, morphology 4-80465  
 RuO<sub>4</sub> thin films, electrochem. deposition from soln. 4-66246  
 Sb electro-oxidation and electro-reduction kinetics in alkaline solns. 4-66681  
 Sn, electrodeposition on Al alloys (Russian) 4-88991  
 Su-Fe, electrodeposition, effect of amino acid surfactants 4-93242  
 V<sub>2</sub>W<sub>2</sub>O<sub>8</sub>, Wadsley-Roth phases, electrolytic reduction prep. from molten salts 4-66247

**electrodeposits***see also electroplated coatings*

- chlorophyll-a, surface cond. in various ambient gases 4-108921  
 Co-W-Mn alloy electrodeposited coatings struct., effect of electrolytes containing Na<sub>2</sub>WO<sub>4</sub>, NaWO<sub>3</sub> (Russian) 4-65593  
 coatings on steel substrate, phys. and mech. props. after pulse shock loading 4-66489  
 internal stress calc. 4-80464  
 metals, electrodeposition, pulsating current, spongy deposit prevention 4-93241  
 polymer film, electropolymerised, spectroscopic studies of electronic props., effect of prep. parameters (French) 4-66192  
 steel, electrodeposited protective Cu/Ni/Cr coatings, corrosion testing 4-66505  
 steel, electrodeposited protective three layer Cu/Ni/Cr coatings, corrosion testing 4-66504  
 Ag electrodeposition on Pt (100) surface, thermal desorption, Auger effect, LEED 4-80449  
 Cd, electrodeposition from acidic chloride baths, morphology and hardness rel. to addition agents 4-93238  
 Cd-Ni, electrodeposition from ammoniacal baths, corrosion resist. 4-66253  
 CdS thin films, electrodeposited in fused salt solns., struct. and morphology rel. to substrate 4-66250  
 CdTe films, electrochem. deposited, optical props. 4-85022  
 Co-P amorphous electrodeposited layers, Barkhausen effect, torsion effects 4-76198  
 Co-P amorphous electrodeposits, elastic props. and struct. relax. 4-92282  
 Co-P amorphous layers, mag. and struct. props. 4-76199  
 Co-P electrodeposited amorphous alloys, reorientation kinetics of induced mag. anisotropy 4-84783  
 Co-P, amorphous alloy characterisation using SEM 4-76937  
 Cr, black, electrodeposits for heliothermic conversion (French) 4-77143  
 Cu coating on ultrahigh strength maraging steels, H embrittlement (Japanese) 4-89114  
 Cu, dendritic electrodeposits, fractal behaviour 4-75825  
 Cu plating for selective case-hardening 4-104744  
 Cu-In-S layers, electrodeposition, photoelectrochemical characterisation 4-99355  
 Fe-Co electrodeposited films, field induced mag. anisotropy 4-92943  
 Fe-P amorphous electrodeposited layers, Barkhausen effect, torsion effects 4-76198  
 Fe-P amorphous electrodeposits, elastic props. and struct. relax. 4-92282  
 Ni coating on ultrahigh strength maraging steels, H embrittlement (Japanese) 4-89114  
 Ni electrodeposited from sulphate and acetate salts, hardness and struct. 4-114431  
 Ni, electrodeposition, hardness, microstruct. 4-66252  
 Ni electrodeposits, struct., X-ray diff. and Mossbauer studies 4-104102  
 Ni electrodeposits, struct., positron lifetime meas. 4-104103  
 Ni-P amorphous electrodeposits, IR reflectivity spectra 4-93078  
 Ni-P electrodeposited alloy struct., X-ray diff. (Chinese) 4-75363  
 Ni<sub>81</sub>Fe<sub>19</sub>-Ni<sub>100-x</sub>Co<sub>x</sub> mag. films, exchange-coupled, mag. reversal characts. 4-76200  
 Ni-P, amorphous alloy characterisation using SEM 4-76937  
 Pb<sub>2</sub>Ti<sub>2</sub>O<sub>7</sub>, electrodeposit, cryst. structure (Japanese) 4-88138  
 Pt electrodeposits, incorporation of organic matter, mass spectra 4-88997  
 Pt group metals, electrodeposited coatings from molten alkali metal cyanide baths 4-93244

## electrodeposits continued

- Zn and Cd coatings, automatic regeneration by ion exchange (*German*) 4-104970  
 Zn leaves grown by electrodeposition fractal struts. 4-98483

## electrodes

- see also anodes; cathodes; earth electrodes; electrochemical electrodes; electron tube components; microelectrodes  
 alkaline fuel cell with matrix and no precious catalyst, new electrode structure development (*French*) 4-77084  
 alkaline storage battery aspects of air electrode research, appl. 4-66687  
 bipolar stimulating electrode, small and atraumatic, for use on fine relatively inaccessible nerves 4-115309  
 body surface multi-electrode for inverse problem in electrocardiography and its application (*Japanese*) 4-62621  
 cardiac pacing electrodes, low threshold 4-85581  
 ceramic electrodes for ELF bioeffects studies 4-115296  
 coated electrodes, current generation efficiency increase by laser light 4-76007  
 coplanar electrode systems, electric-field distribution 4-96748  
 copper II 8-quinolinedithiocarboxylate, liquid membranes, extraction and electrode props. 4-81446  
 corrosion products formed on electrodes subjected to corona discharges 4-76910  
 developer substances oxidation expts. in Ag and Ag<sub>2</sub>S electrodes (*Russian*) 4-68306  
 diagonal MHD channel, problems associated with consolidation of electrode currents 4-85378  
 dielectrics, conduction and breakdown phenomena, role of electrodes 4-108869  
 discharges with electrode evaporated in vacuum 4-87972  
 electrode/electrolyte interface, desorption rates and electrochem. meas. 4-104066  
 electrostatic, precipitator rods, DC corona discharge and ion flow distribution characts. 4-97933  
 EMG, intraluminal electrodes, evaluation for oesophagus and gastrointestinal tract studies 4-115313  
 Faraday MHD generator, finitely segmented, power output characts. 4-77118  
 fast ionic conductors, review 4-70439  
 fluidised bed electrode, charge transfer, bipolar mechanism 4-79654  
 HV electrode systems, post streamer stage of discharge in a nonuniform field (*Russian*) 4-69968  
 HV vacuum electrodes, conditioning using controlled emission current 4-90596  
 hydroquinone developer oxidation expts. in Ag and Ag<sub>2</sub>S electrodes (*Russian*) 4-68306  
 implantable active electrode, design techniques 4-81815  
 integrated optic travelling wave switch/modulators, vel.-matching techniques 4-74748  
 interdigitated electrode structures, polymer covered, for CO, CO<sub>2</sub>, CH<sub>4</sub> and H<sub>2</sub>O sensing 4-95401  
 intracerebral stimulating, cylindrical coordinate Laplace's eqn., numerical soln. 4-89541  
 metal-molten salt interface, capacitance depend. on local density profiles near electrode 4-92797  
 metals evaluation for ultra-high purity p-type Si surface barrier detectors 4-59563  
 mirror electrode for laser initiated discharge channels 4-69932  
 Ni-Cd batteries, construction and electric parameters of plastic bonded cells (*Hungarian*) 4-105102  
 pacemaker electrodes, long-term evaluation by implantable refl. telemetry 4-115267  
 plasma production, RF, parallel plate, sustaining mechanisms 4-79818  
 prebreakdown electron emission currents, switching and other nonlinear phenomena 4-76641  
 pulsed discharge, high-energy, electrode erosion phenomena 4-60772  
 refractory metal base sintered materials, erosion resist. in stationary arc 4-62068  
 semiconductor colloidal electrode particles, photogenerated carrier transport and kinetics 4-65671  
 semiconductor photoanodes in aq. electrolytes, transition metal doped, photoresponse characts. 4-70875  
 skin-surface recording electrodes, practical considerations in use 4-85557  
 Ag, adsorbed 4,4'-bipyridine, redox behaviour, Raman and cyclic voltammetry study 4-75778  
 Ag, adsorp. of KSCN, surfaced enhanced Raman spectra 4-80370  
 Ag adsorption of SO<sub>4</sub><sup>2-</sup>, surface second harmonic generation 4-65547  
 Ag electrode, adsorbed phthalazine, surface enhanced Raman spectra and mol. orientation 4-104585  
 Ag electrode, of NH<sub>3</sub>, surface enhanced Raman scatt., vibr. anal., charge transfer processes 4-93545  
 Ag electrodes, interfacial OH and OD, surface enhanced Raman scatt. 4-93570  
 Ag electrodes, laser damage, surface-enhanced Raman scatt. and Auger emission spectrosc. obs. 4-60955  
 Ag, surface enhanced Raman scatt., contrib. of charge transfer complexes and photochemical effects 4-88841  
 Ag, surface plasmon enhanced second harmonic generation 4-65617  
 AgCl miniature electrodes, electric field intensity meter for oceanographic appl. 4-62974  
 Au electrode, surface oxidation in H<sub>2</sub>SO<sub>4</sub> electrolyte, XPS study 4-93465  
 C fibre fabrics, activated, appl. to electrodes of rechargeable battery and organic electrolyte capacitor 4-99957  
 Cu-W electrodes, arcing phenomena, current density 4-87894  
 InP photoelectrodes, surface states, photocapacitance spectra studies 4-114010  
 InSe, lamellar p-type, photointercalation and photodeposition of Cu 4-93539  
 Li<sub>2</sub>TiS<sub>2</sub>, intercalation study by TEM 4-103953  
 Li<sub>2</sub>V<sub>2</sub>O<sub>7</sub>, intercalation study by TEM 4-103953  
 Mo, afterdischarge electron emission by treatment with glow discharge 4-87987  
 Mo electrodes, selective SiO<sub>2</sub> form. for MOS struts. 4-98467  
 N<sub>2</sub>, compact capacitively coupled laser with new electrode design 4-60067  
 Pt electrodes, chemisorp. of aromatic moles., effect of surface pretreatment with flat oriented intermediates 4-99836  
 n-Si, photoelectrodes, silicide coated, electrochemical and photoelectrochemical behavior 4-88581

## electrodes continued

- SrTiO<sub>3</sub> photoanodes, sensitisation by transition metal ion doping 4-70876  
 TiO<sub>2</sub>, n-type photoanode, dye-sensitized photocurrent spectrum, high press. studies 4-98666

## electrodynamics

- see also electron beams; electron optics; electron tubes; ion beams; ion optics; ion sources; quantum electrodynamics  
 action integral in electrodynamics, general expression, Maxwell eqns. derivation 4-69278  
 atom, electric dipole moment light absorpt., semiclassical radiation theory 4-102651  
 beam charge conc. spreading, electrohydrodynamics 4-96773  
 black holes, Schwarzschild electrodynamics, irregular wavefunctions 4-106022  
 book, kinetic theory of electromagnetic process 4-82601  
 boundary problems, combined orthogonal coordinate systems 4-112334  
 boundary value problems, soln. accuracy improvement 4-78999  
 charged particle, laminar relativistic motion, kinematic invariants and geometrised eqns. 4-96769  
 charged particle in const. mag. field, propagator evaluation 4-69292  
 charged particle in plane wave during transitions from free to trapped states, change in adiabatic invariant 4-96770  
 charged particles in turbulent electric fields, relative diffusion, scaling prop. 4-79020  
 charged-particle energy statistics in stratified elec. field 4-69295  
 classical, unified field theory (*German*) 4-102867  
 classical charged particle with spin in external EM field, projective constrained variational principle 4-64666  
 classical electrodynamics, canonical transformation method 4-74395  
 classical spinning magnetic dipole in classical electrodynamics with classical electromagnetic zero-point radiation 4-74401  
 cosmic grains fluff, effects on field emission, charge and particle levitation 4-94578  
 cross-field runaway electrons, quantum mechanics 4-64669  
 crystals, relativistic particles paths simulation and radiation spectra 4-75591  
 Dirac eqn., elementary derivation, electrodynamic hydrogen field transversality 4-95188  
 distributed generator with retardation, onset of chaos 4-107499  
 effective charge electrodynamics 4-113124  
 EH-EB analogies (*Japanese*) 4-102853  
 elastic dielectrics, variational principle 4-78145  
 electromagnetism in R<sup>3</sup>, teaching 4-78079  
 electron beam-plasma interactions, computer simulation, appl. to SEPAC/SpaceLab 1 mission 4-87887  
 electron beams, relativistic, slipping instability 4-74407  
 electron motion with Coulomb interaction and EM radiation (*Japanese*) 4-83532  
 electron spontaneous emission in relativistic nonneutral electron beam 4-79021  
 electrons, relativistic correlations kinetic eqn. with radiation reaction 4-91391  
 electrostatic electron-optical systems with discontinuous fields 4-74408  
 electrostatic ion trap, operation in uniform mag. field 4-64665  
 EM wave radiation in inhomogeneously and nonstationarily moving media 4-79011  
 equations of motion, axiomatic deduction 4-95190  
 extended classical charged particle in mag. field, self-torque, radiation reaction, H atom appl. 4-90394  
 ferromagnet deformable., undergoing mag. reson., electrodynamics 4-76261  
 Fresnel's drag coeff., photon theory 4-86161  
 gauge theoretical approach to macroscopic electrodynamics 4-73254  
 group of external transformations of electromagnetic field variables 4-68493  
 induction-dynamic systems optimal inductor thickness selection 4-112319  
 ionosphere, energy principle for high-latitude electrodynamics 4-85812  
 Lagrangian theory of the classical spinning electron 4-102868  
 Langevin equation of motion of electrons in slowly time varying electric field 4-59965  
 macroscopic electrodynamics, foundations 4-106198  
 matter-radiation equilibrium for relativistic periodic systems 4-78210  
 Maxwell-Hertz theory, electrodynamic potentials 4-74402  
 metal surface electrodynamics, dielec. responses 4-88552  
 MHD generators, diagonal, electrodynamic parameters determi. (*Chinese*) 4-89457  
 Moll, Gerrit, electromag. expts. 4-63466  
 multiple expansions, toroidal moments, analytical struct., review 4-95960  
 neutron stars, Schwarzschild electrodynamics, irregular wavefunctions 4-106022  
 particle in EM field with memory potential, propagator 4-112333  
 particle in three-dimensional EM field, exact invariants in momentum 4-69291  
 particle radiation reaction dynamics in EM wave and const. E-field 4-83527  
 photon decomposition and polarisation selection rules in moving medium 4-87259  
 plasma, Poisson structure of the equations of ideal multispecies fluid electrodynamics 4-97773  
 pulsar magnetosphere, electrodynamics calcs. 4-106018  
 quantum, unified field theory (*German*) 4-102867  
 radiators carrying electric and mag. currents, infinitely long, comparative anal., geophys. prospecting appls. (*Russian*) 4-102875  
 relativistic electron beam equilibria, radially confined, appl. to longit. wiggler free electron laser 4-112447  
 relativistic electron beam in dielectric medium 4-64663  
 relativistic electron scatt. in EM field, radiation scatt., photon statistics 4-112368  
 relativistic heavy-current beam dynamics in an external mag. field (*Ukrainian*) 4-87258  
 relativistic particles with arbitrary spin in electric and magnetic fields (*Russian*) 4-112335  
 relativistic radiating charge random motion 4-73251  
 relativistic-electron helical trajectories in combined uniform axial and helical mag. fields, instability 4-83529  
 rotating conductor, Schiff's eqns. 4-87261  
 semiconductor cylinder polarization by plane EM wave 4-79016  
 semiparabolic medium, radiation of electrons in uniform motion 4-83530

- electrodynamics** continued  
stationary gravitational systems, electromagnetic field analogy, Killing vector field 4-106214  
three-layer medium, light reflection, electrodynamic Green's functions 4-109150  
TM waves stimulated scatt. by strongly magnetised relativistic ribbon electron beam, nonlinear theory 4-74403  
two-band direct gap semiconductor, electrodynamics, SCF theory 4-98497  
two-body bound-state mass in strongly coupled classical electrodynamics 4-73252  
GaAs thin-film semiconductor structure with negative differential conductivity, EM wave propag. anal. 4-79017
- electrodynamometers** see **dynamometers**
- electroencephalograms** see **electroencephalography**
- electroencephalography**  
see also **bioelectric potentials**; **biomagnetism**; **brain**  
C6 channel telephone transmission system with cassette recording and CRT display (Spanish) 4-62619  
brain, electrical activity, mech. and interpretation 4-100116  
brainstem modulation of hippocampal EEG activity 4-89552  
cerebral blood flow rel. to EEG characs. 4-89557  
coherence of brain 40 Hz rhythm, cat obs. 4-93727  
cortical and hippocampal, sleep-waking profiles and spectral characs. anal. in rats 4-89551  
data reduction technique for EEG and EMG signals 4-85561  
electrocortical activity controlled by lateral hypothalamus, inference of stable dispersion relation 4-93713  
electrocortical activity under lateral hypothalamic control, test for constant natural frequencies 4-93712  
electrophysiological signal techniques to quantify EEG alterations 4-89804  
epileptic seizures, rel. to intracranial press. 4-100190  
epileptic seizures in mongolian gerbils, electro-clinical studies 4-93722  
epileptic spikes, computerised classification method 4-93952  
epileptiform spike activity, comments on parametric and nonparametric detection 4-109983  
evoked potential processing, system identification techniques for noise reduction 4-105357  
global electrocortical activity, linear model, control by lateral hypothalamus 4-93711  
healthy children, longitudinal EEG study, age and sex differences 4-72233  
hippocampal evoked potentials, amplitude changes during avoidance behaviour in cat 4-77218  
hippocampal penicillin spikes, interactions with theta rhythm 4-100113  
hippocampal EEG rel. to spectral anal. of hippocampal unit train 4-67152  
localised discharge, graphic method for estimating equivalent dipole 4-81795  
morphology of partial epileptic seizures 4-93718  
multidimensional scaling for metric information obtaining from nonmetric data (German) 4-72241  
multiparametric asymmetry score, distinction between normal and ischaemic brains 4-93721  
multiprocessor EEG analyser, distrib. system 4-85560  
neonatal herpes simplex encephalitis, EEG obs. 4-66937  
neurophysics of EEG 4-93731  
off-line montage reformatting 4-100335  
olfactory bulb and cortex, spatial organisation of EEGs 4-77268  
olfactory bulb EEG in rats, freq. anal. 4-93768  
olfactory evoked responses, EEG obs. in malnourished rats 4-93767  
posterior rhythmic slow activity in EEG after eye closure 4-66945  
premature neonates with intraventricular haemorrhage, positive rolandic sharp waves 4-105223  
rhombencephalotomised cat, EEG responses after photic and epileptogenic application 4-72238  
rule-based methods for EEG evaluation 4-93951  
scalp potential distrib., on-line source-density computation with a minimum of electrodes 4-67139  
single unit activity rel. to spontaneous EEG waves, computer analysis 4-72236  
spike and shape wave detection, computerised pattern recognition system 4-109987  
square wave spectral estimates, EEG anal. appl. 4-89805  
structural analysis of human EEGs, 1st-order Markov chain model 4-89553  
swept visual evoked pot., spatiotemporal conditions rel. to oblique effect 4-81676  
temporo-spatial patterns of pre-ictal spike activity in human temporal lobe epilepsy 4-66936  
thalamic alpha rhythm pacemaker mechanism 4-89536  
time-scribe: universal time writer for any EEG/polygraph chart recorder 4-93942  
triphasic waves: a reassessment of their significance 4-77223  
visual evoked potential pattern generation, recording, and data analysis with a single microcomputer 4-67137  
Walsh and Fourier anal. comparison, anaesthesia effects tracking appl. 4-115265
- electroendosmosis** see **electrophoresis**
- electrofluidynamics** see **electrohydrodynamics**
- electrofluorescence** see **electroluminescence**
- electroforming**  
polypropylene evaporated thin films in MIM structs., electroforming 4-80686  
Ag thin films, electroformed, humidity sensitive switching 4-108908  
Cu-SiO<sub>2</sub>/GeO<sub>2</sub>-Cu sandwich structures, elec. props. time, temp. press. depend. 4-108949
- electrogasdynamics** see **electrohydrodynamics**
- electrohydrodynamics**  
atmospheric circulation model using EHD stability in quasi-spherical geometry 4-100719  
axisymmetric electric vortex flows (Russian) 4-113045  
axisymmetric electrovortex flow in corrugated tube containing a cylinder 4-108124  
axisymmetric flow between two porous rot. discs in presence of transverse mag. field 4-97576  
beam charge conc. spreading, electrohydrodynamics 4-96773  
convective flow in slip flow regime 4-101128
- electrohydrodynamics** continued  
corona discharge, EGD flow and its influence on motion of dispersed particles 4-103425  
corona discharge effects on gasdynamical flow rate 4-69975  
DC electric field 4-97561  
dielectric fluid vertical layer in horiz. AC elec. field, stability of natural convection 4-79583  
dielectric liq., plane layer, electrothermal convection, cond. model 4-112877  
dielectric liq. layers subjected to electric field, oscillatory convective instability, dielectric constant 4-103427  
EHD pumping in horizontal pipes, temp. induced, finite element method 4-113030  
electrically cond. liq. film flow in mag. field (Russian) 4-113053  
electrically cond. liquids, free jets, reson. breakdown, EM forces, drop form. phases (Russian) 4-113057  
electrically conducting fluid layer, EM interaction process, Rayleigh-Taylor instability 4-108122  
electrovortex flow, periodic, in external mag. fields (Russian) 4-113048  
electrovortex flow in a pipe with nonconducting corrugated walls (Russian) 4-113047  
electrovortex flow in a planar channel (Russian) 4-113049  
ferroliquid in transverse mag. and electric field, nonlinear equilib. form. and waves on surface 4-108130  
fluid interfaces with elec. double layers, coupled longitudinal and transverse wave motion 4-64944  
fluidised bed electrode, charge transfer, bipolar mechanism 4-79654  
forces acting on a solid in a current-carrying liquid (Russian) 4-113046  
Hall effects on heat and mass transfer flow through porous medium 4-101125  
p-n-heptyloxybenzoic acid smectic C liq. cryst., electrohydrodynamic transient instability 4-75270  
HV electrohydrodynamic generator, liquid flow study 4-97705  
hydrocarbon-electrolyte systems in pulsed electric field, hydrodynamic behaviour 4-79675  
hydrodynamic phenomena accompanying solidification of a continuous ingot under conditions of inductive MHD action 4-108138  
hydromagnetic free convection with mass transfer in rotation fluid, effects of Hall current 4-101134  
jet flow in weakly cond. dielectric liquids produced by nonuniform electric field 4-108136  
laser velocimeter, multicomponent, for vel. meas. of gas and liq. currents in strong elec. fields (Russian) 4-69837  
liquid dielectrics electrical conductivity, role of EHD motion, power capacitor example 4-98326  
liquid metal films, electromag. induced breakdown during free flow on surface (Russian) 4-114210  
methoxybenzylidenebutylaniline-cholesterol nonanogate liq. cryst. mixture, electrohydrodynamic instabilities 4-113329  
MHD and EHD waves, incorporation of photons 4-110894  
mixed boundary-value problems connected with a limiting electrochemical perforation 4-89306  
molten metals, EM vibr. treatment under microgravity, hydrodynamic effects 4-97698  
nematic liq. crystals, electric field induced flow, surface forces 4-70528  
nematic liquid crystal, EMD instability anal. by dynamic texture image processing technique 4-92069  
nonNewtonian fluid, laminar radial flow between parallel discs in axial elec. field, inertia effects 4-83930  
nuclear power plants, emergency reactor core cooling system 4-97704  
orthogonal electromagneto-fluid-dynamic flows, classification 4-60556  
plane-parallel flow stability in longitudinal elec. field 4-60557  
plasma, collisionless, energy vars. and elec. fields rel. to convection 4-100868  
plasma, EHD parameters, quantisations eqn. of motion 4-103469  
polydisperse mixtures, electromagnetic separation, conc. effects 4-103424  
power capacitors, electrohydrodynamic motion induced by injection from plane polymer sheets 4-97706  
properties and convective mechanism of current transfer (Russian) 4-113073  
self-similar solutions in the theory of EHD jets 4-108137  
semi-insulating liquids, electrokinetic streaming current, induction sensing 4-65033  
shock waves 4-65031  
smectic A liquid cryst., electrohydrodynamic instability and turbulent motion 4-70030  
squeeze films between spherical planes under periodic motion 4-97699  
stability study for EHD induction pumps 4-97703  
toroidal electric vortex flow in a cylinder (Russian) 4-112912  
tubes, insulating, flow-induced charge accumulation and field generation by semi-insulating liquids 4-65032  
viscous dielectric fluid electrohydrodynamic behaviour and current response to voltage changes 4-97702  
weakly-conducting fluid, isothermal flow in nonuniform elec. field (Russian) 4-83958  
Fe particles in Hg, particle interaction and clumping in an electrically conducting magnetic liquid 4-108623  
H<sub>2</sub>AIP<sub>2</sub>O<sub>10</sub>·2H<sub>2</sub>O, electrorheological suspensions, disperse phase, charge transport characteristics 4-103426  
Pb, electrically cond. liquids, free jets, reson. breakdown, EM forces, drop form. phases (Russian) 4-113057
- electrojets**  
see also **ionosphere**  
auroral electrojet, cond. vars. rel. to correl. between optical and mag. pulsations 4-105789  
auroral electrojet, elec. field and plasma density meas. 4-72783  
auroral electrojet, generation of vertical thermospheric winds during geomag. disturbances 4-105782  
auroral electrojet, hemispherical Joule heating as function of AE indices 4-72788  
auroral electrojet AE index, correl. with magnetosphere-solar wind interactions 4-72802  
auroral electrojet irregularities studied using STARE radar 4-67523  
auroral electrojets, evolution during geomag. disturbances, correl. with polar cap currents developed 4-77682  
auroral electrojets, latit. vars. of Joule heating 4-72784  
eastward auroral electrojet, electron drift vel. rel. to auroral power spectra vars. 4-72777  
equatorial electrojet, local time depend. of response to DP2 and SI disturbances 4-105802

**electrojets continued**

- equatorial electrojet meas. from daily geomag. var., coastal effect in Peruvian and Nigerian zones 4-110044
- ionosphere, aurora and electrojet configuration in early morning sector 4-72789
- radiowave heating expt., signal from modulated equatorial electrojet 4-115654
- reversal of equatorial electrojet during severe magnetic storms 4-105798
- Sq current loop positions over Africa 4-82323
- substorm period global elec. currents 4-67534

**electrokinetic effects**

- see also *electrodynamics*; *electrophoresis*
- glycine- $\text{Al}_2\text{O}_3\cdot\text{nH}_2\text{O}$  mixtures, points of zero charge (German) 4-85314
- membranes, artificial lipid-coated membrane, electrokinetic effects 4-72221
- polyethylenimine, aq. soln., modification of surface props. of solids 4-80334
- quartz, surface properties, modification by polyethylenimine aq. solns. 4-80334
- semi-insulating liquids, electrokinetic streaming current, induction sensing 4-65033
- Teflon, surface props. modification by polyethylenimine aq. solns. 4-80334
- tubes, insulating, flow-induced charge accumulation and field generation by semi-insulating liquids 4-65032
- $\text{AuCl}_4^-$  complexes, adsorption on goethite 4-109678

**electroluminescence**

- see also *phosphors*
- electroluminescent emitters, activated by rare earth elements (Russian) 4-109248
- organoluminophores, solns., elec. generated chemiluminesc. 4-104687
- polyethylene, elec. ageing effects, TSC and electroluminesc. meas. 4-109127
- tourmaline, pyroelectroluminescence during heating and cooling 4-66078
- $\text{Al-Al}_2\text{O}_3\cdot\text{Ag}$  tunnel junctions, surface plasmons and light emission 4-88553
- $\text{AlGaAs}$  heterostructure, photoelectroluminescence study 4-99193
- Ar, cryocrystals, high-energy excitations, hot luminesc. 4-99194
- $\text{BaTiO}_3\cdot\text{Fe}$ , electrolum., elec. field depend. 4-66077
- $\text{CaS}\cdot\text{Cu}$ , Er (Sm) electrolumins., radiation controlled enhancement of electroluminescence 4-76529
- $\text{CaS}\cdot\text{Er}$  phosphor, electrolum. spectrum and  $\text{Er}^{3+}$  ion energy level splitting 4-71446
- $\text{Ga}_{1-x}\text{Al}_x\text{P}$ , epitaxial struct., luminesc. study 4-85011
- GaAs, electroluminescence and photoluminescence in aq. redox electrolyte 4-88584
- GaAs, electroluminescence spectra of free excitons, optical resonances 4-88883
- GaAs:Si, Al p-n structures, radiative recomb., electrolum. characts. (Russian) 4-109249
- p-GaAs:Zn, emission band, electron irradi. and annealing effects 4-88881
- $\text{GaAs}_{1-x}\text{P}_x\text{GaAs}_{1-x}\text{P}_x$  isotype heterojunction electrodes in photoelectrochem. cells, photoluminescent and electroluminescent props. 4-99140
- GaN, polarised luminescence transitions and electroluminescence quenching 4-104670
- GaP diode struct., electroluminescence polarisation study (Russian) 4-88884
- InP:Yb p-n junctions; electroluminescence studies 4-66079
- $\text{LiNbO}_3$  single cryst., electroluminescence obs. 4-99197
- Ne, cryocrystals, high-energy excitations, hot luminesc. 4-99194
- $\text{SiO}_2$ , luminescence study of elec. cond. 4-61756
- $\text{SiO}_2$  MIS struct., electroluminescence emission studies 4-93114
- Xe, cryocrystals, high-energy excitations, hot luminesc. 4-99194
- Xe, electroluminescence, partial excitation and VUV fluoresc. at normal press. 4-83973
- Xe, electroluminescence and electron resonance trapping 4-108158
- ZnO electroluminophor, brightness waves, grain size effects 4-104675
- ZnO electroluminophores, brightness, volt. and freq. depend. 4-104676
- $\text{ZnO:Nd(Yb)}$ , electrolum. brightness, voltage and freq. depend. at liq.  $\text{N}_2$  temp. 4-93113
- $\text{ZnS}\cdot\text{Cu}$ , Cl, Er films, electroluminesc., hot electron energy distribution 4-85012
- $\text{ZnS}\cdot\text{Cu}$ , Er phosphor, electroluminescence and photoluminescence emission spectra 4-76512
- $\text{ZnS:Er(Mn,Er)}$  phosphors, electro- and photo-luminescence props. 4-104652
- $\text{ZnS:Mn}$ , coprecipitated phosphors, photo- and electro-luminescence 4-61739
- $\text{ZnS:Mn}$  ACTFEL electroluminescent devices 4-88882
- $\text{ZnS:Mn}$  electroluminesc. thin layers, doping and cryst. struct. 4-75810
- $\text{ZnS:Mn}$  electroluminescent thin film structures, short pulse excitation 4-76530
- $\text{ZnS:Mn}$  thin films, electrolum., diffusion and trapping 4-104677
- $\text{ZnS:Sm(Cu)}$  electroluminescent phosphors, Alfrey-Taylor relation 4-114331
- $\text{ZnS:SmF}_3$  thin films, red electroluminesc. and crystallinity 4-99195
- $\text{ZnS(Se)}$  phosphor DC electroluminescent cells, self-activated centers, low field recombination 4-99196
- ZnSe photoelectrochemical cells, radiative recombination 4-89456

**electroluminescent devices** see *luminescent devices***electrolysis**

- see also *anodisation*; *electrical conductivity of electrolytic liquids*; *electrodeposition*; *electroforming*; *electrolytic dissociation*; *electrolytic ion mobility*; *electrolytic machining*; *electrolytic polishing*
- Canadian trends in hydrogen energy, review of work at Institut de Recherche d'Hydro-Quebec 4-62401
- double layer dipole orientation at electrodes, polarisation catastrophes anal. 4-98690
- electrolytic  $\text{H}_2$ , economics and potential applications in the future 4-114961
- electrolytic  $\text{H}_2$  production status in USA and abroad 4-62400
- electrolytic hydrogen production market potential in United States northeastern utility service areas 4-105133
- electrolytic water splitting, HTR heat source, possibilities of improving power generation efficiency 4-93532
- laser-beam propagation fundamental mode, optically inhomogeneous electrochem. media with electrochem. species conc. gradients 4-112341
- metallic radwaste, electrochemical decontamination 4-68754
- mild steel  $\text{H}_2$  evolution reaction, in alkaline media 4-93533

**electrolysis continued**

- photovoltaic solar hydrogen plant material and energy requirements 4-72189
  - poly(thiophene) doped films, charge storage, optical study 4-109219
  - polyacetylene, electrochem. doping with  $\text{InCl}_2\text{-LiCl}$  in nitromethane soln. 4-75465
  - power sources, status and development 4-62322
  - quartz:Ag(Cu), X-ray irradi. induced optical absorpt., impurity electrolysis effect 4-70208
  - quartz, elec. cond., relax. dielec. losses, temp. depend. due to electrolysis 4-113959
  - steel, decarburisation in anodic process of elec. heating (Russian) 4-71776
  - steel 40Kh, nitriding kinetics under electrolytic heating conditions (Russian) 4-85253
  - thermomechanical hydrogen production, Co-Br hybrid water-splitting process (Japanese) 4-66806
  - thin-film high temperature water electrolysis cells, for  $\text{H}_2$  production, development advances 4-105126
  - transient nucleation kinetics under galvanostatic electrolysis conditions 4-60874
  - urea and other wastes in uremic canine dialysate canine dialysate, direct electrolytic oxidation 4-89307
  - water, electrolytic disoc. in bipolar ion-exchange membranes 4-62211
  - water, microscopic and spectroscopic study of Ni-S electrodes 4-113766
  - water, pulse discharge, decontaminating factors influence (Russian) 4-84094
  - water, splitting with semicond. photoelectrodes, efficiency 4-93635
  - water photoelectrolysis, electrodes and dopants for solar energy conversion 4-72127
  - Ag thin films, electroformed, humidity sensitive switching 4-108908
  - C black dispersions, charge exchange, electrochemical/ESR studies 4-93562
  - Fe, commercial grade, nitriding kinetics under electrolytic heating conditions (Russian) 4-85253
  - Fe-Ni codeposits,  $\text{H}_2$  evolution reaction, in alkaline media 4-93533
  - $\text{Fe}_2\text{O}_3$ , doped, p-n assembly, water, catalytic photodisoc. 4-62207
  - $\text{H}_2$  evolution, Peltier coeffs. evaluation 4-62210
  - $\text{H}_2$  production, by high temp. high pressure water electrolysis 4-105127
  - $\text{H}_2$  production, from water vapour and  $\text{CO}_2$ , thermoradiation processes 4-93651
  - $\text{H}_2$  production by electrolysis, design and process engineering concepts (German) 4-93644
  - $\text{H}_2\text{S}$  as hydrogen source, obtained as waste product from fossil fuels, methods of use 4-89471
  - I, radioelectrophoretic and chromatographic study (Chinese) 4-71934
  - LiF- $\text{AlF}_3$  cryolite melts, interdiffusion 4-88324
  - Ru dendrites, form. by electrolysis of chloride melt, morphology 4-80465
  - $\text{SO}_2$ , adsorpt. on Pt electrode, electrooxidation in conc. solns. 4-61219
  - $\text{SrTiO}_3$  photoanodes, sensitisation by transition metal ion doping 4-70876
  - T, electrolytic gettering from air using solid proton electrolyte 4-86966
- electrolytes**
- for solid electrolytes see *superionic conducting materials*
  - see also *electrolysis*; *superionic conducting materials*
  - acetonitrile, liq., solvation of  $^{23}\text{Na}^+$ ,  $^{87}\text{Rb}^+$  and  $^{14}\text{N}$ , local symm. demonstration, NMR study 4-78870
  - aqueous 1:1 electrolytes, pair correl. functions from linearised Poisson-Boltzmann eqn. 4-103627
  - aqueous diffusion const., intermolecular dipolar spin relax., microdynamical models 4-88321
  - aqueous electrolytes, conductance, conc. depend. 4-84432
  - aqueous solutions, dielec. effects, kinetic depolarisation, saturation and solvent relax. 4-80859
  - binary isothermal electrolyte solns., linear vector transport processes (German) 4-108640
  - charged hard spheres in electrolyte soln., equil. props., Monte Carlo and integral eqn. results 4-70004
  - Co-W-Mn alloy electrodeposited coatings struct., effect of electrolytes containing  $\text{Na}_2\text{WO}_4$ ,  $\text{NaWO}_3$  (Russian) 4-65593
  - dilute solns., salt effect on surface tension 4-88368
  - Donnan equilibrium of 1-1 electrolyte, osmotic press., electric pot. and conc. 4-105028
  - electrical double layers, ion density profile calcs. 4-71935
  - electrochemical double layer, dielectric enhancement and electrophoresis 4-71936
  - equilibrium statistical mechanics, theories, and appls., book 4-58589
  - glass, corrosion, in weak-acid and weak-alkali solns., effect of electrolyte additions 4-81316
  - ion assoc. reactions, cluster approach 4-99755
  - ion-solvent interactions and activity coeffs. 4-66607
  - junction/hard sphere electrolyte interphase, model for electric double layer 4-70908
  - laser-beam propagation fundamental mode, optically inhomogeneous electrochem. media with electrochem. species conc. gradients 4-112341
  - mass transport in membranes, math. model 4-99832
  - metal-electrolyte boundary, hard core ions at charged surfaces, unrestricted primitive model, HNC/MSA approach 4-88587
  - mixed aqueous electrolytes, local structure, Raman and EXAFS studies 4-60808
  - Nafion polyelectrolytes, luminesc. probe studies 4-88880
  - organoluminophores, solns., elec. generated chemiluminesc. 4-104687
  - poly(ethylene oxide) complex electrolyte,  $\text{PEO}(\text{LiCF}_3\text{SO}_3)_x$ , DSC, NMR studies 4-61047
  - polyelectrolyte chain in d dimensions, config. props., Monte Carlo simulation 4-83505
  - polyelectrolyte chains, length distrib. in reversible thermodynamic equil. 4-59924
  - polyelectrolyte solns., thermodynamic props., ellipsoidal model 4-84137
  - polyelectrolyte solns., transport numbers, modified Hittorf method 4-103982
  - polyelectrolytes (Dutch) 4-91376
  - polystyrene charged spheres in dilute soln., fluorescence labeled, electrolyte friction meas. 4-98323
  - solns. in dipolar aprotic, IR spectra and struct. 4-112175
  - solution, charged aggregates interaction, Monte Carlo simulation 4-97986
  - solutions, US wave propag., pulse-echo technique 4-60990
  - spheres with thin double layers, dilute suspension in asymmetric electrolyte, dielec. response 4-105031
  - statistical mechs. aspects 4-108261

**electrolytes continued**

- surface struct. near critical point, free energy formalism anal. 4-92038  
 suspension, deposition mechanisms of cpd. electrochem. coatings, comp. calc. method (Russian) 4-71605  
 tetramethyl ammonium ion-paramagnetic anion pair, motion in aq. solns., NMR study 4-88735  
 tetramethylammonium chloride, in 1-butanol, viscosity determ. 4-103987  
 thin-film high temperature water electrolysis cells, for H<sub>2</sub> production, development advances 4-105126  
 thiocyanates, sodium, potassium and ammonium in 1-butanol, viscosity determ. 4-103987  
 transport through charge micromosaic membranes 4-105023  
 water, interfacial, in electrolytes, surface enhanced Raman scatt., metal cation effect 4-91268  
 weakly-conducting fluid, isothermal flow in nonuniform elec. field (Russian) 4-83958  
 AgI, molar heat capacity, cationic and anionic contrib. evaluation from thermolec. power data 4-98303  
 $\beta^0$ -Al<sub>2</sub>O<sub>3</sub> electrolyte and Na wick for beta-batteries, development 4-77077  
 B<sub>2</sub>S<sub>3</sub>-Li<sub>2</sub>S-LiI electrolyte for solid state batteries 4-77078  
 Ca(NCS)<sub>2</sub> solns. in dipolar aprotic, IR spectra and struct. 4-112175  
 CuSO<sub>4</sub> aq. solns., elec. resist. fluctuations 4-75713  
 KCl transport through charge micromosaic membranes 4-105023  
 KNCS solns. in dipolar aprotic, IR spectra and struct. 4-112175  
 Li anode batteries high wattour per unit weight, electrolytes 4-93601  
 Li anode cells, primary and secondary, review 4-72054  
 Li/Cu<sub>2</sub>V<sub>2</sub>O<sub>7</sub> battery with 1-M LiClO<sub>4</sub>-propylene carbonate/1,2-dimethoxyethane electrolyte 4-93607  
 Li-Al electrode secondary cell, cycling behaviour in LiClO<sub>4</sub>-propylene carbonate solutions 4-72058  
 Li-Al electrode secondary cell at room temp., Li-Al alloy electrochemical formation kinetics 4-72059  
 Li-Al/FeS cell, FeS positive electrode effective conductivities in LiCl-KCl eutectic electrolyte 4-99958  
 LiAlCl<sub>2</sub> solutions conductivity in nitromethane containing SO<sub>2</sub>, concentration and temp. dependence, applicability assessment for Li/SO<sub>2</sub> cells 4-66596  
 LiAsF<sub>6</sub> in 2-methyltetrahydrofuran, mol. relax., US absorpt. investig. 4-109108  
 LiBF<sub>4</sub> in 2-methyltetrahydrofuran, mol. relax., US absorpt. investig. 4-109108  
 LiCl, transport through charge micromosaic membranes 4-105023  
 LiClO<sub>4</sub> in 2-methyltetrahydrofuran, mol. relax., US absorpt. investig. 4-109108  
 LiClO<sub>4</sub>-propylene carbonate electrolytic props., additive effects of Li<sup>+</sup> ion solvation compounds 4-65424  
 Mn<sub>2</sub>Ca<sub>1-x</sub>(NO<sub>3</sub>)<sub>2</sub>·6H<sub>2</sub>O paramag. solns., conc., muon spin relax. study 4-71244  
 Mn(NO<sub>3</sub>)<sub>2</sub> paramag. solns., conc., muon spin relax. study 4-71244  
 NANCs solns. in dipolar aprotic, IR spectra and struct. 4-112175  
 NH<sub>2</sub>-electrolyte solns., NH stretching and bending vibrs., intermol. coupling, polarised Raman scatt. 4-61700  
<sup>14</sup>N, solvated by liq. acetonitrile, local symm. demonstration, NMR study 4-78870  
 NaCl, mass transport in Nafion membranes, math. model 4-99833  
 NaCl, transport through charge micromosaic membranes 4-105023  
<sup>23</sup>Na<sup>+</sup>, solvated by liq. acetonitrile, local symm. demonstration, NMR study 4-78870  
 Pb/acid cells, immobilized electrolyte, design limitations 4-81532  
 Pb/acid cells, rotating ring-disc electrode study of impurity effects on lead corrosion in sulphuric acid 4-81533  
 Pd-Ni soln. parameters effects on performance of electrodeposits on contacts 4-76020  
<sup>87</sup>Rb, solvated by liq. acetonitrile, local symm. demonstration, NMR study 4-78870  
 tri-n-alkylammonium nitrates, benzene solns., dielec. obs. at 298.15K 4-114196

**electrolytes, solid** *see superionic conducting materials***electrolytic capacitors**

- C fibre fabrics, activated, appl. to electrodes of rechargeable battery and organic electrolyte capacitor 4-99957

**electrolytic conductivity of liquids** *see electrical conductivity of electrolytic liquids***electrolytic deposition** *see electrodeposition***electrolytic devices**

- cell with magnetic clamp, for semiconductor materials recombination parameters determ. 4-90612

**electrolytic dissociation***see also electrolytic ions*

- 160 MW OTEC plantship design for methyl alcohol production 4-114936

**electrolytic ion mobility***see also electrophoresis*

- ion hydration and mobility in soln. 4-62176  
 ionic mobilities, -transference numbers, and self-diffusion coeffs. meas. using NMR pulsed gradient expt. 4-88744  
 radionuclide ion mobility determ. in free electrolyte, meas. method 4-77024  
 redox-flow battery, voltage drop and elec. resist. for ion exchange membranes 4-109681  
 HCl aq. solns., fast H<sup>+</sup>-ion motion, vel. concepts vs. config. description 4-80276  
 HCl aq. solns., fast H<sup>+</sup>-ion motion, NMR determ. 4-80277  
 HCl aq. solns., fast H<sup>+</sup>-ion motion, neutron scatt. study 4-80278  
<sup>131</sup>I<sup>-</sup> ion mobility determ. in free electrolyte 4-77024  
<sup>160</sup>Tb<sup>3+</sup> ion mobility determ. in free electrolyte 4-77024

**electrolytic ions**

- see also electrical conductivity of electrolytic liquids; electrolytic dissociation; electrolytic ion mobility*  
 No entries

**electrolytic machining***see also electrolytic polishing*

- steel, stainless, Cr-Ni, electrochemical treatment of surface bearing photoresist layer (Russian) 4-71773

**electrolytic polishing***see also electrolytic machining*

- amorphous ribbons, electropolishing, power loss and domain struct. 4-76158

**electrolytic polishing continued**

- austenitic stainless steel (German) 4-71771  
 steel tubes, autofrettage, fatigue strength, thermal shock, tempering, electropolishing 4-104865  
 Co-Ta alloy, welded joints, electrolytic polishing investig. (Russian) 4-71777  
 Nb<sub>3</sub>Sn, thick diffusion produced layers, struct. and power losses rel. to electrochemical polishing 4-65781  
 Ni-base superalloy, single cryst., crack tip plastic strain 4-89231  
 TiAl, intermetallic cpd., specimen prep., microcracks obs. on polished surfaces 4-81382  
 W wires, electropolished, struct. changes after thermal treatment rel. to surface state (Polish) 4-85249

**electromagnetic absorption** *see electromagnetic wave absorption***electromagnetic compatibility***see also frequency allocation*

- absorber-lined chambers design for EMC meas., geometrical optics approach 4-112320  
 air-soil interface close-in environments, back emission, backscattering, Klein-Nishina injection effects 4-59945  
 degraded absorber performance effect 4-69646  
 magnification factor for mode stirred chambers 4-69647  
 Maxwell's eqns. in generalised nonorthogonal coords., finite difference soln. 4-59943  
 Maxwell's eqns. solns., total field vs. scatt. field finite difference codes 4-59942  
 switch-mode power supplies, magnetic field emission meas. and prediction models 4-106283  
 TEM cells bandwidth limitations due to resonances 4-72300  
 THREDS, finite-difference time-domain EMP code in 3-D spherical coords. 4-59944

**electromagnetic corrections**

- "electromagnetic corrections" is distinguished in use from "radiative corrections" by application to elementary particle and nuclear interactions  
*see also radiative corrections*

- Abelian gauge fields, IR radiative corrections and zero momentum mode 4-58949  
 Cabibbo angle, radiative corrections in L-R symmetric models 4-111344  
 composite Goldstone supermultiplets, absence of radiative mass corrections,  $\pi^2/\mu^2$  mass difference 4-111459  
 e<sup>+</sup>e<sup>-</sup> annihilation, energy-energy correlations in perturbative QCD 4-59112  
 Higgs boson, neutral and charged mass upper bounds from radiative corrections 4-102021  
 Higgs masses, renormalisation, effective potential in SU(5) to one loop 4-73704  
 pseudoscalar meson semileptonic decays, radiative corrections, model dependence 4-111441  
 Schwinger source theory, 'space-time' structure of radiative corrections 4-102045  
 semileptonic decays, e-e correlations 4-86714  
 spontaneously broken supersymmetry SU(2)×U(1) model, self masses radiative corrections 4-111352  
 SU<sub>c</sub>(2)×SU<sub>R</sub>(3) model, scalar field set addition fermion mass generation, radiative corrections 4-73637  
 SU(2)×U(1) symmetry breaking induced by radiative corrections 4-58996  
 symmetry mass relations Majorana neutrinos, radiative corrections 4-106531  
 vector particles, renorminvariant mass, vacuum struct. in mag. field 4-82900  
 weak decays, one-gluon corrections in QCD 4-86639  
 e<sup>+</sup>e<sup>-</sup> → e<sup>+</sup>e<sup>-</sup>γ, radiative corrections in SU(2)×U(1) 4-111432  
 e<sup>+</sup>e<sup>-</sup> → e<sup>+</sup>e<sup>-</sup>γ, radiative corrections, total cross-section calcs. 4-68589  
 e<sup>+</sup>e<sup>-</sup> → e<sup>+</sup>e<sup>-</sup>γ + pseudoscalar particle, two photon physics, radiative corrections, five point function 4-95798  
 e<sup>+</sup>e<sup>-</sup> → l<sup>+</sup>l<sup>-</sup>γ, electroweak model dependence of electromagnetic corrections 4-73705  
 e<sup>+</sup>e<sup>-</sup> → μ<sup>+</sup>μ<sup>-</sup>γ asymmetry, electroweak radiative corrections in SU(2)×U(1) model 4-68559  
 γe → γeX, radiative corrections in deep inelastic scatt. 4-102109  
 Δ → p e<sup>-</sup>, model independent order and radiative correction 4-86705  
 Σ → Δ e<sup>-</sup>, model independent order and radiative correction 4-86705  
 Σ → n e<sup>-</sup>, model independent order and radiative correction 4-86705  
 Σ → Δ e<sup>-</sup>, model independent order and radiative correction 4-86705  
 Z neutral current flavour changing decay induced by radiative corrections 4-95751  
 e<sup>+</sup>e<sup>-</sup> → γγ, double bremsstrahlung, photon ang. distrib., radiative corrections 4-82953

**electromagnetic decays**

- glueball EM decay in MIT bag model 4-90884  
 glueball model, heavy quarkonium <sup>3</sup>S, state pion cascades, OZI violation 4-95771  
 ground state mesons, radiative decays, covariant quark model, hadron currents 4-90883  
 heavy meson radiative decay in integer charge quark model 4-68537  
 heavy quarkonia, radiative decays, relativistic kinetic energy 4-86713  
 pseudoscalar meson decays in theory with broken chiral symm. (Russian) 4-68569  
 quarkonia radiative decays into Goldstone fermions, SUSY breaking, T appl. 4-73762  
 review, Z 4-67907  
 spinless boson radiative decay, anomalous γll events 4-111440  
 spinless boson radiative decay, possible source of anomalous l<sup>+</sup>l<sup>-</sup>γ in Z searches 4-102148  
 tripositronium decay, yield at electron accelerators (Russian) 4-95795  
 A<sub>1</sub> → π<sup>+</sup>γ, radiative partial width from π<sup>+</sup>N collisions 4-59105  
 A<sub>1</sub> → π<sup>+</sup>γ Coulomb dissociation, decay widths 4-90885  
 A<sub>2</sub> → π<sup>+</sup>γ Coulomb dissociation, decay widths 4-90885  
 B<sup>+</sup> (1235) → π<sup>+</sup>γ Coulomb dissociation, decay widths 4-90885  
 χ → J/ψ γ, radiative decays from charmonium P states 4-106533  
 χ → γγ, small x-gluon distrib. from inclusive ψ cross section 4-106547  
 D → Dγ, P-odd effects in radiative decays, P-invariance violation (Ukrainian) 4-64002  
 D<sup>0</sup> → D<sup>0</sup>γ, decay widths and excited meson props. 4-111443  
 D<sup>+</sup> → D<sup>+</sup>γ, decay widths and excited meson props. 4-111443  
 Δ → Nγ, radiative decay, effect of quark-quark tensor and spin-spin force 4-64003

**electromagnetic decays continued**

- $e^+e^-$  collisions, resonance production and decay estimates from radiative Z decays 4-90903  
 $e^+e^- \rightarrow \gamma\gamma$ , scalar/pseudoscalar boson contributions, masses and coupling constants 4-111436  
 $e^+e^- \rightarrow \mu\mu\gamma(\gamma)$ , cross section, coupling constant, comparison with QED predictions 4-111435  
 $\eta$  and  $\eta'$  radiative decays, light quark mass ratios, vacuum flavour symmetry breaking 4-73761  
 $\eta' \rightarrow \mu^+\mu^-\gamma$ , rare decays, conservation law tests, neutral currents 4-102113  
 $F^0 \rightarrow F\gamma$ , P-odd effects in radiative decays, P-invariance violation (*Ukrainian*) 4-64002  
 $\iota(1440)$ , with glueball, identification in simple quarkonium-glueball mass matrices 4-68534  
 $\iota \rightarrow \gamma\gamma$  decay mode width in QCD framework 4-59033  
 $\rho$  meson, production and decay rates, gluonium component 4-111458  
 $J/\psi \rightarrow \gamma + \text{pseudogluon}$ , pseudomeson glueball component, process width (*Chinese*) 4-102098  
 $J/\psi \rightarrow \gamma\gamma\rho^0$ ,  $Q^2$  state prod., colour-spin structure, potential and bag models 4-106511  
 $K^{*0} \rightarrow K^0\gamma$  Coulomb dissociation, decay widths 4-90885  
 $\mu \rightarrow e\gamma$ , flavour changing suppression in technicolour, pseudo-Goldstone bosons, Cabibbo mixing 4-102075  
 $\omega \rightarrow \pi^0\gamma$ , chiral Lagrangian, nonAbelian anomaly, vector-meson decays 4-106510  
 $\Omega^-$  hadronic and radiative decays, lifetime, branching ratios and decay asymmetry 4-86702  
 $\phi \rightarrow \eta\gamma$ , relative decay probability meas. 4-59085  
 $\phi \rightarrow \eta\gamma$ , VEPP-2M storage ring, width and branching ratios, mixing angle 4-111457  
 $\phi \rightarrow \pi^0\gamma$ , VEPP-2M storage ring, width and branching ratios, mixing angle 4-111457  
 $\pi^0 \rightarrow 2\gamma$ , bag model, decay width calculation (*Chinese*) 4-102097  
 $\pi^0 \rightarrow e^+e^-(e^+e^-e^+e^-)$  ( $e^+e^-\gamma$ ), rare decays, conservation law tests, neutral currents 4-102113  
 $\pi^0 \rightarrow e^+e^-\gamma$ , form factor slope and decay amplitude calc. using quark triangle mechanism 4-59069  
 $\pi^0 \rightarrow \gamma\gamma$ , Jupiter magnetosphere emission 4-101239  
 $\psi \rightarrow \eta(\eta')$ ,  $\pi\eta$ - $\eta'$  mixing model 4-86712  
 $\psi \rightarrow \gamma X$ ,  $\chi(2.22)$  production, properties consistent with  $L=3$  s8 meson. 4-86666  
 $(q\bar{q}) \rightarrow \gamma(\bar{q}q)$ , production and decay rate of gluino bound state 4-102118  
 $\rho^0 \rightarrow \pi^+\pi^-$  Coulomb dissociation, decay widths 4-90885  
 $T^0 \rightarrow T_0\gamma$  effect of Higgs bosons and hyperpions 4-90871  
 $\tau \rightarrow e\mu(\mu\nu\tau)$ , g-value test, radiation zeros 4-86707  
 $\theta(1640)$ , with glueball, identification in simple quarkonium-glueball mass matrices 4-68534  
 $T(\gamma)$  decays, direct photons obs. and QCD scale parameter determ. 4-64004  
 $Z \rightarrow e^+e^-\gamma$ , composite scalars in  $e^+e^-$  collisions and radiative Z decays 4-86694  
 $Z \rightarrow eE(eE) \rightarrow e\gamma$ , cascade decays through new particle, electron mag. moment, coupling constraint 4-102147  
 $Z \rightarrow \eta\gamma\gamma$ , Z mixing with degenerate bound colour quarkonium 4-111486  
 $Z^0$  anomalous radiative decay 4-78579  
 $Z^0 \rightarrow e^+e^-\gamma$ , composite boson coloured constituents, hypercolour binding 4-111425  
 $Z^0 \rightarrow e^+e^-\gamma$ , scalar/pseudoscalar boson contributions to  $e^+e^-$  interactions, masses, decay 4-111436  
 $Z^0 \rightarrow \gamma + \text{squarkonium}$ , production of  $^1S_0$  squarkonium states, gluon jets 4-111487  
 $Z^0 \rightarrow \mu^+\mu^-\gamma$ , anomalous lepton magnetic moments, constraints 4-86750  
 $@ Z^0$  anomalous radiative decay, possible new pseudoscalar particle 4-68577  
 $T \rightarrow \gamma\gamma$ ,  $\chi(8.3 \text{ GeV})$  interpreted as Higgs boson 4-111447

**electromagnetic energy see electromagnetic waves****electromagnetic field theory**

- see also *electromagnetic waves; electromagnetism*  
 action integral in electrodynamics, general expression, Maxwell eqns. derivation 4-69278  
 Ampere tension in electric conductors 4-79001  
 basics of electrotechnology, book (*German*) 4-101595  
 circular cone with longitudinal slits, electric dipole excitation (*Russian*) 4-83523  
 classical electrodynamics, equations of motion, axiomatic deduction 4-95190  
 collisionless plasma, statistical mech. of relativistic charges and radiation 4-75165  
 continuation problems of EM fields 4-110892  
 dipoles, coupling through multilayered shields 4-107488  
 dispersive plane-stratified anisotropic medium, EM field theory 4-78158  
 EH-EB analogies (*Japanese*) 4-102853  
 Einstein's field equations, static, spherically symmetric solutions, massless scalar field 4-95275  
 electrodynamic boundary value problems, soln. accuracy improvement 4-78999  
 free electromagnetic field, conservation laws 4-110891  
 Helmholtz theorem for antisymmetric second-rank tensor fields and electromagnetism with magnetic monopoles 4-63447  
 homogeneous medium bounded by perfectly conducting walls, dyadic Green's function props. 4-64659  
 inhomogeneous compound layers, with lossy particles and fibres, absorption and shielding props. 4-69289  
 liquid dielectric, radiation force and momentum of light 4-102965  
 liquid-metal film stability under electromagnetic field (*Russian*) 4-96755  
 longitudinal EM field, action principle,  $\gamma$  coeff. investigation 4-63948  
 magnetic recording, reciprocity integral, convolution or correlation 4-79002  
 Maxwell EM field eqns. in  $R^6$  six-dimensional space-time 4-73250  
 Maxwell equation solution in case of internal conic refraction 4-87252  
 Maxwell field at null infinity containing IR part, total action 4-101666  
 multitime correlation functions calc. using phase space procedure 4-107486  
 nonAbelian systems, field strength formulation, covariant field equations 4-95677  
 planar thermal source, Maxwell-Langevin theory and radiant intensity 4-78279  
 plane EM wave on rot. circular cylinder of isotropic material, transverse radiation press. and torque 4-59941

**electromagnetic field theory continued**

- plane nonlinear EM field problems anal. (*Russian*) 4-87244  
 quantum unified field theory, enlarged coordinate transformation group, reciprocity and conservation relations 4-107493  
 scalar potentials in multiply connected regions 4-63528  
 spherical media, Casimir stress, EM zero-point field 4-101667  
 square aperture reflector, implementation of stationary phase method (*French*) 4-83518  
 stationary electromagnetic fields uniqueness theorems 4-107494  
 superpotential, Hertz's method 4-63527  
 two-dimensional EM field problems, appl. of boundary-element method 4-83516  
 virial constraint, solitonlike solutions 4-82889
- electromagnetic fields**  
 450-MHz RF exposure of man, specific absorption rate average and distrib. 4-115119  
 anisotropic solids, generalised Ohm and Fourier cond. laws, intrinsic symmetries of material tensors 4-75916  
 ANSI C95.1-1982 standard, human exposure to RF EM fields, safe distances determination 4-109873  
 atmospheric microwave discharges, EM field patterns meas. 4-69959  
 book, optical waves in crystals, laser radiation propag. and control 4-86135  
 charged particle, laminar relativistic motion, kinematic invariants and geometrised eqns. 4-96769  
 charged particle in plane wave during transitions from free to trapped states, change in adiabatic invariant 4-96770  
 computer modelling EM field distribution in lossy dielectrics, clinical appls. 4-109785  
 conducting circular cylinders, EM field and multiple scattering study (*Japanese*) 4-59963  
 conducting surface, small or comparable to wavelength, E-field solution 4-87250  
 conformal mappings using Schwartz-Christoffel integral 4-91382  
 cubical block model of man in specific absorption rate distrib. calc., limitations 4-115118  
 cylinder in mag. dipole field over horizontal interface of media, secondary field (*Russian*) 4-102855  
 dark solitary waves, in optical fibres, wave solution, radial dependence of field 4-107860  
 dosimetry in biomedical investigs. 4-115227  
 Earth, diurnal var. of EM field in N France using ancient recordings 4-110042  
 eddy currents, three-dimens. problems, soln. methods 4-112321  
 electro-explosive devices in EM fields, safe use 4-107487  
 ELF naval communications facilities, health hazards assessment 4-115115  
 Euclidean space, algebraic field description, electromag. field, Lorentz transformations, duality rotations 4-106462  
 exploding wires, EM and thermal fields, numerical anal. 4-60679  
 gas, secondary emission in strong standing EM wave field 4-103464  
 generation in course of electron emission from metal target surfaces subjected to laser radiation 4-81041  
 gyrotropic media, EM field problems, variational formulation 4-96757  
 helicity of the electromagnetic field 4-59957  
 human EM hazard analysis, human body impedance in VLF to MF band 4-115120  
 human exposure, energy deposition and thermal response models 4-115117  
 induction-dynamic systems optimal inductor thickness selection 4-112319  
 infinitely long radiators carrying electric and mag. currents, comparative anal., geophys. prospecting appls. (*Russian*) 4-102875  
 interaction of the near-zone fields of a slot on a conducting sphere with a spherical model of man 4-115123  
 irregular waveguides and open resonators theory, EM fields, variational techniques 4-102852  
 linear induction accelerator, diaphragmed electron beams, stability 4-96301  
 magnetic field analysis, computer graphics using finite element method 4-59956  
 metals, crack-containing, failure mechanism under the effect of electromag. field 4-81274  
 multitime correlation functions calc. using phase space procedure 4-107486  
 NDT, high-strength EM field visualisation method, model defects investig. 4-109607  
 power line, 3-phase, EM fields in vitro simulation 4-109874  
 probe, noise anal. 4-106309  
 probe for EM field meas., of submillimeter dimensions 4-106310  
 quantum statistics of systems interacting with electromagnetic fields 4-95296  
 random static fields in spatial noise, optimum estimation of shift 4-96753  
 regulations and standards in connection with biomedical effects 4-69269  
 RF hazards, specific absorption rate distribution in a full-scale model of man at 350 MHz 4-115122  
 RF human whole-body absorption rates, effect of separation from ground 4-115121  
 secondary planar source generated fields 4-83517  
 shells, deformable, in presence of EM effects, nonlinear theory 4-74864  
 static fields measurements, extrapolation using finite element method 4-83514  
 stationary gravitational systems, electromagnetic field analogy, Newtonian and Machian aspects 4-106214  
 thin-walled cylindrical screens, Fredholm eqn. soln. for two-dimensional EM field, screening efficiency (*Russian*) 4-102856  
 three dimensional EM field problems, soln. on minicomputer 4-59947  
 toroidal shell, current-carrying, EM load, stress state 4-74051  
 wave beam, intensity maxima on axis, properties of focused field 4-69288
- electromagnetic induction**  
 see also *induction*  
 accelerated conductors with frontal compression and rear dilation of mag. flux, theory 4-107485  
 Bitter plate tokamaks, coupled EM and thermal problems, transient nonlinear solns. 4-59412  
 coaxial cable pairs, study of interference arising from radio wave induction (*Chinese*) 4-107484  
 conductor acceleration in pulsed mag. field of a solenoid 4-59961  
 cylinder in mag. dipole field over horizontal interface of media, secondary field (*Russian*) 4-102855

**electromagnetic induction continued**

- detector of conducting objects, time domain response analysis and obs. 4-100790
- Earth, coastal effect at equatorial latits. with appls. to Peruvian and Nigerian zones 4-110044
- Earth, Frechet derivatives of EM induction 4-85622
- Earth, uniqueness theorem for horizontal loop EM freq. soundings 4-67168
- Earth resistivity measurement, EM method 4-62667
- emulsion, destruction under action of elec. field and magnetodynamic layer of granules (*Russian*) 4-71991
- ferromagnetic materials, induction distribution, field calc. 4-96754
- Feynman's Disk Paradox 4-106158
- forceless magnetic fields construction 4-64653
- functional anal. calc. in conductors of various cross sections 4-64652
- induction-dynamic systems optimal inductor thickness selection 4-112319
- magnetic levitation, track currents, lift and drag forces 4-96750
- magnetically soft materials, magnetisation under dynamic conditions, investigation (*Russian*) 4-114136
- multivectors, magnetic force surfaces 4-91384
- perfectly conducting strip on planar interface between semiinfinite half-spaces, induced current determ. 4-69275
- Fe-Si (3 wt.%), coarse-grained anisotropic elec. engineering steel, mag. losses and induction (*Russian*) 4-109036

**electromagnetic interference**

- see also radiofrequency interference*
- air-sol interface close-in environments, back emission, backscattering, Klein-Nishina injection effects 4-59945
- building attenuation enhancement, conductive paint appl. 4-107496
- daily variation of 10 and 27 kHz atmospheric in Germany 4-110205
- daily variation of VLF atmospherics, depend. on meteorological conditions 4-110206
- electro-explosive devices in EM fields, safe use 4-107487
- FELIX facility to study EM effects for first wall, blanket and shield systems 4-111820
- fusion reactors EM anal., status and need 4-111818
- HV laboratory, EMI investigation 4-106165
- ISM (industrial, scientific, and medical) equipment, emissions and interference caused 4-72445
- LF star fields, EM smog (*German*) 4-59971
- Maxwell's eqns. in generalised nonorthogonal coords., finite difference soln. 4-59943
- Maxwell's eqns. solns., total field vs. scatt. field finite difference codes 4-59942
- MIL-STD-461B, RE-01 limit for LF radiated magnetic field emissions 4-107483
- reverberation chambers, design 4-69648
- satellite power systems, terrestrial EM environmental effects (*Japanese*) 4-62930
- THREDS, finite-difference time-domain EMP code in 3-D spherical coords. 4-59944

**electromagnetic lenses *see* magnetic lenses**

**electromagnetic oscillations**

- see also cavity resonators; lasers; masers; ring lasers*
- coupled resonators employing phase-conjugating and ordinary mirrors, calc. of oscillation conditions 4-107795
- double-proton bombarded laser, emission properties, kinks and self-sustained oscillations 4-112437
- rough interface between media, local EM oscills. 4-70899

**electromagnetic pulse *see* electromagnetic compatibility; electromagnetic interference; radiofrequency interference**

**electromagnetic radiation *see* electromagnetic waves**

**electromagnetic theory of light**

No entries

**electromagnetic wave absorption**

- see also electromagnetic wave propagation in plasma; gamma-ray absorption; light absorption; spectra; X-ray absorption*
- aerosol particle, Brownian rotation, EM radiation absorpt. modulation 4-85341
- biological effects (*Japanese*) 4-62524
- building attenuation enhancement, conductive paint appl. 4-107496
- dielectric glasses, nonlinear US and EM relax. absorpt. 4-60995
- E-polarised RF fields, whole-body absorpt. of humans, effect of freq. and grounding 4-100229
- extended boundary condition method (EBCM), soln. stability improvement and freq. range extension 4-64660
- glass, resonant EM and acoustic absorption in alternating field 4-65346
- inhomogeneous compound layers, with lossy particles and fibres, absorpt. and shielding props. 4-69289
- ionosphere, appl. of single-freq. A1 data to test of International Reference Ionosphere 4-90020
- ionosphere, day/night absorpt. ratio in auroral and subauroral zone riometer meas. during auroral absorpt. 4-90018
- equatorial ionosphere, depend. of seasonal var. of radio wave absorpt. on solar activity 4-90022
- maximum achievable ratio of the absorbed and scattered powers 4-79013
- microwave atmospheric attenuation, differential emission meas. at 20.3 and 31.4 GHz by radiometry 4-85751
- microwave transmission, ionospheric effects (*Japanese*) 4-63010
- microwave transmissions, neutral atmosphere effects (*Japanese*) 4-62931
- partially-shielded dielectric sphere, EM absorption cross-section calc. 4-112328
- intense radio waves in upper ionosphere, anomalies attenuation obs. 4-110354
- radiowave attenuation due to rain, errors for prediction (*French*) 4-67377
- rain attenuation measurements, freq. depend. at microwave freqs. 4-67308
- semiconductors, electroacoustic effects due to charged dislocations 4-65717
- Sun tracker atmospheric attenuation meas. at 35 GHz 4-105636
- superconductor, phonon generation during HF EM field absorpt. (*Russian*) 4-84743
- VHF band absorber, improvement (*Japanese*) 4-107492

**electromagnetic wave attenuation *see* electromagnetic wave absorption; electromagnetic wave scattering**

**electromagnetic wave diffraction**

- see also electromagnetic wave propagation in plasma; gamma-ray diffraction; light diffraction; X-ray diffraction*
- circular cone with longitudinal slits, electric dipole excitation (*Russian*) 4-83523
- curved plate, EM scatt. soln. by uniform asymptotic theory of diffr., monostatic radar cross-section 4-64658
- cylinder dimension measuring problem, diffraction eqn. (*Russian*) 4-74392
- E-polarised wave diffraction on plane ship, dual integral eqns. (*Russian*) 4-96758
- equivalent dipole moments of a circular aperture near parallel screen 4-112331
- equivalent edge currents for arbitrary aspects of observation 4-69281
- inclined screen, inhomogeneous EM surface wave conversion (*Ukrainian*) 4-69279
- Kottler line integrals disappearance 4-74399
- lateral waves, HF theory 4-73249
- lossy dielectric slab, EM plane wave diffraction by slit 4-79005
- microwave diffraction tomography for biomedical appls., analytical approach, comments 4-85481
- nonclosed surfaces of revolution, diffraction problems 4-87253
- partially metalised thin gyrotropic cylinder, EM wave diffraction/scattering, two-dimensional problem 4-87257
- perfect arbitrary form conductor, two-dimensional problems (*Chinese*) 4-107489
- perfectly conducting bodies of complex cross section, approx. anal. method (*Russian*) 4-102866
- perfectly conducting half-plane, 3-D diffraction problems, exact soln. and uniform theories testing 4-69282
- physical theory of diffraction, singularities treatment 4-102862
- plasma sphere, diffraction of plane TM wave, spatial dispersion 4-79799
- radiation from planar aperture distributions by evanescent wave and complex ray analysis 4-74398
- slit in thick screen, EM wave diffr. (*Japanese*) 4-96763
- sphere in layered inhomogeneous medium, EM wave diffr. (*Russian*) 4-112332
- TE/TM waves obliquely incident on plasma cylinder, spatial dispersion effects 4-84005
- thin semitransparent cylindrical shell, H-polarised EM wave diffr. 4-79018
- three-dimensional wave diffr. problems, Rayleigh and Sommerfeld approximations 4-79014
- transparent inhomogeneous objects, Kirchoff's approx., extension 4-69285
- wedge, perfectly conducting, uniform geometrical theory of diffraction 4-64657

**electromagnetic wave diffusion *see* electromagnetic wave scattering**

**electromagnetic wave interference**

- see also atmospherics; electromagnetic wave interferometers; electromagnetic wave interferometry; electromagnetic wave propagation in plasma; light interference; Moire fringes*
- Ag thin film, interference fringes intensity of X-ray diffr. line profiles 4-75799

**electromagnetic wave interferometers**

- see also electromagnetic wave interferometry; light interferometers*
- digital sign correlator for a very long baseline radiointerferometer 4-94609
- microwave interferometer system for biological subject displacement meas. (*Japanese*) 4-110019
- MM-wave permittivity and permeability meas., Fabry-Perot interferometer 4-73452
- near-mm wavelength, complex refr. spectra temp. variation determ. of reasonably transparent solids 4-101911
- radio interferometers, appl. of complex FFT processor for image synthesis (*Japanese*) 4-94639
- radioastronomy instruments for space observation (*Japanese*) 4-85876
- two-beam interferometers, for optical constants meas. at near-millimeter wavelengths 4-86474
- two-scanning mirror Fourier transform interferometer for plasma diagnostics 4-103570
- ultrahigh vacuum angular encoder, microradian resolution 4-95624
- VLBI K-3 system, US-Japan test observation 4-78367

**electromagnetic wave interferometry**

- see also light interferometry; Moire fringes*
- diffuse reflectance far IR interferometric spectroscopy 4-78391
- district heating pipeline configurations, design improvements 4-103180
- flow measurement, optical systems, review (book contrib.) 4-79690
- FRX-C field-reversed configs., side-on interferometric investig. 4-69964
- GPS determined attitude, development and appls. 4-73502
- ionospheric refraction, correction of, radioastronomy interferometry observations (*French, English*) 4-67643
- laser heterodyne system for plasma diagnostics 4-84079
- laser measurement interferometry microscope for emulsion telescope in high energy physics 4-96391
- nonrigid molecular liquids orientational motion, depolarised light-scatt. investig. 4-66048
- phase-stable multielement long-baseline interferometric system, use of reference object method 4-94608
- compact planetary nebulae, Arcelbio interferometer obs. 4-82534
- plasma density meas. by microwave interferometry using freq. modulation 4-97898
- plasma gradient phasometry, submillimetre range 4-84084
- radio interferometry, high-sensitivity correl. receiver, cosmic radio source meas. 4-72887
- radio interferometry, ionospheric propag. effects 4-90095
- radio interferometry, self-calibration and isoplanatism 4-115685
- radio sources, extragalactic, in ecliptic region, VLBI obs. 4-73088
- very long baseline radio interferometry use in geodesy 4-72765
- VLBI, hybrid mapping of radio sources using max. entropy method 4-72892
- VLBI in astronomy, theoretical introduction (*Polish*) 4-63084
- X-ray anomalous dispersion meas. by X-ray interferometry 4-61767
- X-ray interferometry applications (*Japanese*) 4-86515
- X-ray interferometry for absorption and dispersion meas. at K-edge of Cu 4-61775
- CO<sub>2</sub> TEA laser, electron density of afterglow of pulsed discharge and UV photoionisation, meas. using microwave interferometer (*Chinese*) 4-87315

**electromagnetic wave interferometry continued**

- H arc plasma, electron density, interferometric and spectrosc. investig. 4-84082  
 HF laser mixtures, electron density of afterglow of pulsed discharge and UV photoionisation, meas. using microwave interferometer (*Chinese*) 4-87315  
 He-F<sub>2</sub>-Kr atmospheric discharge, electron density, streak interferometric method 4-84092  
 Hg plasma, low press., electron density meas. by laser heterodyne method 4-84081

**electromagnetic wave propagation**

- see also *atmospheric electromagnetic wave propagation; atmospheric light propagation; backscatter; electromagnetic wave absorption; electromagnetic wave diffraction; electromagnetic wave interference; electromagnetic wave propagation in plasma; electromagnetic wave reflection; electromagnetic wave refraction; electromagnetic wave scattering; guided electromagnetic wave propagation; light propagation; radiowave propagation*  
 book, optical waves in crystals, laser radiation prop. and control 4-86135  
 cosmic microwave background galaxy cluster gravit. screen model for spatial fluctuations 4-63344  
 electro-magneto-thermo-elastic plane waves in rotating media with thermal relax. 4-91723  
 electrofluidised beds, small wave propagation and reflection analysis 4-97677  
 focusing through a dielectric interface 4-112323  
 hemispherical open resonator, plane mirror long groove, quasi-natural modes anal. 4-96760  
 inhomogeneous isotropic media, propagation by geometrical optics theory 4-83520  
 inhomogeneous media, EM wave dispersion props. 4-91387  
 interplanetary plasma, radio backscatter method for meas. of ion-acoustic turbulence and solar wind vel. 4-110480  
 Kottler line integrals disappearance 4-74399  
 lateral waves, HF theory 4-73249  
 metallic thin slabs, EM field spikes under anomalous skin effect conditions 4-104250  
 nonlinear ferromagnet, EM wave propagation 4-104481  
 packetlike solutions of the homogeneous-wave equation 4-87249  
 periodically corrugated surface, EM wave propagation, plasmons 4-79279  
 plane waves on moving boundary between stationary media, numerical anal. 4-102857  
 ray tracing in absorbing media 4-74423  
 solar power satellite antenna, characts. (*Japanese*) 4-62932  
 stochastic medium, numerical modelling 4-112325  
 transverse-electric surface and leaky waves guided by asymmetric layer configuration, evolution 4-112322  
 water waves propagation, analogy with EM waves 4-115413  
 GaAs thin-film semiconductor structure with negative differential conductivity, EM wave prop. anal. 4-79017

**electromagnetic wave propagation in plasma**

- see also *ionospheric electromagnetic wave propagation; light propagation in plasma; magnetospheric electromagnetic wave propagation*  
 anisotropic Maxwellian plasma, wave absorpt. near electron cyclotron freq. 4-65101  
 anisotropic plasma, EM wave scatt. by periodic surface, Rayleigh hypothesis 4-113152  
 anomalous Thomson scatt. in low- $\alpha$  plasma 4-91937  
 bi-Maxwellian plasma, form factor of radiation scatt. (*Chinese*) 4-91882  
 bounded RF discharge, stimulated ionisational scatt. dynamics 4-103502  
 Bragg resonator excitation in ionospheric plasma containing artificial periodic array 4-115658  
 coherent spontaneous emission from a modulated beam injected in a magnetized plasma 4-103472  
 cold stratified loss free plasma, wave tunnelling, complex ray tracing study 4-77683  
 collisionless plasma, statistical mech. of relativistic charges and radiation 4-75165  
 convective Raman backscatt. thresholds, Thomson scatt., noise, collisions and Landau damping effect 4-97820  
 current startup and quasistationary drive by lower hybrid waves in Tokamak 4-79753  
 decay of an electromagnetic wave into an ion-acoustic wave and a Langmuir mode which is heavily damped 4-65089  
 density fluctuations in semi-infinite plasma-mol. medium, EM wave scatt. effects 4-108173  
 Doublet III diverter discharges, NBI heated, fluctuations and energy loss 4-75129  
 electron beam effects on Brillouin backscatt. of EM wave 4-79807  
 electron beam interaction, reson. excitation, EM wave radiation 4-84028  
 electron distribution function during electron cyclotron heating in a Tokamak 4-87918  
 electron plasma waves parametric excitation by microwave radiation in filled waveguide 4-97802  
 electron transport and laser interaction at INRS-Energie 4-97767  
 EM field absorpt. in turbulent plasma 4-84012  
 EM radiation ellipticity and reson. effect spectrosc. meas. 4-84087  
 energy transfer from electrons and ions when monochromatic EM wave mixes in plasma, collision effects 4-79739  
 expanding plasma, EM wave prop., electrons and ions acceleration 4-108175  
 fluctuations of electromagnetic waves in an anisotropic random plasma (*German*) 4-84014  
 frequency doubling due to electrostatic fluctuations in magnetoactive plasma 4-91935  
 Gaussian EM beam, nonlinear interaction with electron-plasma wave 4-91898  
 glow discharge, millimetre wave EM radiation interaction 4-88001  
 half-space homogeneous warm plasma, EM wave interaction, ion collision effects 4-103506  
 harmonic emission,  $\omega_0/2$  and  $3\omega_0/2$ , from 526 nm laser produced plasmas 4-79840  
 intense radiation transmission along, track of interrupted laser breakdown in gas 4-75167  
 INTOR Tokamak plasma, ICRF wave prop. and absorpt. 4-113197  
 ion-acoustic turbulence in microwave field, hot electron generation and electron acceleration 4-108170  
 ionospheric heating, soliton vs. parametric instabilities params. 4-82334  
 kinetic model for plasmas in a strong high-frequency field 4-60642

**electromagnetic wave propagation in plasma continued**

- kinetic problem treatment (*Chinese*) 4-91869  
 laser beam refl. from dense Xe plasma, refl. coeff. meas. 4-84016  
 laser radiation anomalous interaction with plasma 4-108174  
 laser-beam self-focusing in a moving inhomogeneous plasma 4-102992  
 linear coupling of EM waves in inhomogeneous weakly-ionised media 4-102845  
 lower hybrid wave heating waves, EM wave coherent scatt. detection 4-69923  
 magneto plasma slab, collisional, power reflection, transmission and absorpt. coeffs. 4-113114  
 magneto-static fluctuations in relativistic plasma, parametric generation 4-79834  
 medium with progressive sinusoidal fluctuation, EM wave prop. (*Japanese*) 4-74393  
 methane plasma diagnostics and modelling, use in CVD growth of a-C films 4-104979  
 microwave discharge, energy charact. change by surface-wave ionisational instability 4-87968  
 microwave plasma, nonlinear propagation, solitons and cavities (*Japanese*) 4-75150  
 modulational instability of whistlers and lower hybrid waves with plasma heating 4-103500  
 nonequilibrium electron beam-plasma system (*Russian*) 4-97814  
 nonequilibrium plasma interacting with RF charge density waves in strong mag. fields, emission 4-97811  
 nonlinear generation in magnetoplasma 4-103481  
 nonlinear laser interaction mechanism, instability and chaos 4-97790  
 nonmonotonic radiation of recombining plasma in a shock wave 4-108171  
 nonpreionised gas in cylindrical discharge tube, wave breakdown, electron prod. kinetics 4-60766  
 optimum absorption of electromagnetic waves by bounded plasmas 4-87873  
 p-polarised radiation, total absorpt. in inhomogeneous plasma, self-consistent model 4-75163  
 parametric coupling of a whistler pump with a drift wave 4-97783  
 parametric decay obs. using CO<sub>2</sub> laser scatt. 4-97784  
 plasma-glass boundary layer in T-tube, time development, light refraction 4-60647  
 polarised EM wave coupling to Z mode near critical angle 4-60641  
 profile modification in inhomogeneous isotropic warm plasma with reson. layer 4-91936  
 propagation of intermediate frequency waves in a bounded magnetoplasma 4-65091  
 pulse envelope change with pulse packet in dispersive medium 4-69914  
 pumping wave decay into two lower hybrid waves in magnetised plasma 4-84008  
 radiation problems in stable linear plasma 4-110829  
 radiowaves propagation (book) 4-67900  
 raman and Brillouin scattering, classical reflection, and relativity 4-97799  
 relativistic, EM wave propagation, polarised, in intense mag. field (*Spanish*) 4-75162  
 resonance phenomena in the magnetized semiconductor plasma and their application for the design of the millimeter and submillimeter wave components 4-104249  
 resonant particle nonlinear interactions with HF wave packets 4-84015  
 RF current-driven tokamak plasma, electron cyclotron emission 4-103549  
 saturation of stimulated Brillouin backscatter 4-97800  
 scattering in a plasma in the direction of the incident wave electric vector 4-108172  
 scattering of an electromagnetic wave by an intense magnetized relativistic electron beam in a waveguide 4-87871  
 shock wave generated by trapezoidal laser pulse, streak camera meas. 4-97795  
 space and time evolution of SBS ion waves and harmonics 4-97801  
 sphere, diffraction of plane TM wave, spatial dispersion 4-97999  
 stimulated Brillouin scatt. of EM wave, negative ions effect 4-75164  
 stimulated Brillouin scattering in laser plasma, absolute instability study 4-103534  
 stimulated Brillouin scattering of a laser in a magnetised plasma in the presence of negative ions 4-65090  
 stimulated Raman scattering, two-plasmon decay, and hot electron generation from underdense plasmas at 0.35  $\mu\text{m}$  4-97797  
 strong EM wave, Faraday effect and rot. in magnetised plasma 4-91934  
 supersonic propagation of an ionization wave along a laser beam 4-97931  
 TE/TM waves obliquely incident on plasma cylinder, spatial dispersion effects 4-84005  
 Tokamaks, electron-cyclotron heating, EM and Bernstein waves absorption and prop. 4-69927  
 X-ray energy spectrum from plasma electrons, relativistic effect 4-91977  
 Kr plasma, dense, absorpt. coeff. and thermodynamic props. meas. 4-84017  
 Nd:glass laser discharge supersonic prop. away from region of microsec. breakdown in air in beam direction 4-79823  
 SF<sub>6</sub> plasma, net radiation emission coeffs. 4-87845

**electromagnetic wave reflection**

- see also *electromagnetic wave propagation in plasma; light reflection; X-ray reflection*  
 classical electrodynamics, canonical transformation method 4-74395  
 cylindrical wave from infinite line source, near field behaviour, dielec. interface (*Japanese*) 4-96762  
 inhomogeneous bounded layers with variable refr. Index, geometric optics approx. 4-112330  
 ionosphere, appl. of virtual refl. height data to test of International Reference Ionosphere 4-90020  
 IR surface EM wave reflection on a corrugated metal surface 4-83519  
 L-band multipath fading sea surface reflection, characts. 4-105739  
 lateral EM wave reflection expts. 4-79008  
 lateral EM wave reflection from perpendicular boundaries 4-79007  
 medium with progressive sinusoidal fluctuation, EM wave prop. (*Japanese*) 4-74393  
 nonstationary medium with large-scale inhomogeneities, phase conjugation 4-69286  
 periodic homogeneous multilayered struct. refl. and transmission of 3-D Gaussian beam (*Japanese*) 4-107495  
 radiofrequency imaging for geophysical applications 4-72720  
 RATAN-600 radio telescope, reflecting-surface precision of primary reflector 4-63058

# electromagnetic wave reflection continued

slotted infinite length cylinder, scatt. of H-polarised plane wave 4-83522  
speckle phenomena at 10  $\mu$ m wavelength 4-69317  
square aperture reflector, implementation of stationary phase method (French) 4-83518

# electromagnetic wave refraction

see also *electromagnetic wave propagation in plasma; light refraction*  
atmospheric refraction correction calc. 4-77611  
inhomogeneous EM wave refraction, at boundary surface between isotropic media 4-79010  
ionospheric refraction, correction of radioastronomy interferometry observations (French, English) 4-67643  
Maxwell equation solution in case of internal conic refraction 4-87252  
microwave transmission, ionospheric effects (Japanese) 4-63010  
radiofrequency imaging for geophysical applications 4-72720

# electromagnetic wave scattering

see also *backscatter; electromagnetic wave propagation in plasma; gamma-ray scattering; light scattering; X-ray scattering*  
anisotropic magnetically-oriented inhomogeneities, radiowave scatt., intensity 4-112329  
anisotropic plasma, EM wave scatt. by periodic surface, Rayleigh hypothesis 4-113152  
book, scattering theory for diff. gratings 4-86125  
book, scattering theory of waves and particles 4-67876  
building attenuation enhancement, conductive paint appl. 4-107496  
charge simulation method for anal. of scattering problems (Japanese) 4-83526  
conducting circular cylinders, EM field and multiple scattering study (Japanese) 4-59963  
conducting circular cylinders, multiple scattering anal. 4-102858  
conducting cylinders embedded in lossy medium, EM scatt. 4-112324  
conducting cylinders with rectangular cross-section, EM wave scattering, expt. study (Japanese) 4-83525  
conducting strip above dielec.-clad ground plane, scattering problem anal. (Japanese) 4-83524  
conducting surface, small or comparable to wavelength, E-field solution 4-87250  
curved plate, EM scatt. soln. by uniform asymptotic theory of diff., monostatic radar cross-section 4-64658  
dielectric bodies, homogeneous, integral eqn. for EM scatt. 4-64656  
dielectric body, integral equations for scattered and transmitted fields 4-64655  
dielectric spheres, large, backscattering, reson. component 4-102859  
Earth-space links, digital, effect of ice-induced cross polarisation 4-62904  
electric and mag. type integral eqn. formulations for scatt. by impedance objects 4-87248  
electron beam EM wave induced scatt. with relativistic energy dispersion 4-69294  
extended boundary condition method (EBCM), soln. stability improvement and freq. range extension 4-64660  
generalized ambiguity function of signals with compression in the presence of scattering of waves by bodies of a complex shape 4-79015  
hemispherical open resonator, plane mirror long groove, quasi-natural modes anal. 4-96760  
HF scalar waves scatt. from two-scale surfaces for large distances 4-87254  
HF scattering of plane EM wave by perfectly conducting strip 4-87255  
inclined screen, inhomogeneous EM surface wave conversion (Ukrainian) 4-69279  
incoherent scatter radar meas. spectral estimation, nonlinear MEM 4-100808  
inhomogeneous lossy dielectric slab, EM wave scatt., singularity expansion method 4-74397  
interaction of the near-zone fields of a slot on a conducting sphere with a spherical model of man 4-115123  
interfaces, acoustic and EM wave scattering anal. 4-83754  
inverse electromagnetic algorithm for aspect-limited data 4-102863  
inverse scattering in the first Born approximation 4-68057  
upper ionosphere, glancing angle scatt. of radio waves by artificial turbulence 4-110354  
IR angular scattering by long Cu and brass cylinders 4-107490  
maximum achievable ratio of the absorbed and scattered powers 4-79013  
Maxwell-Bloch equation complex soln., inverse scatt. problem 4-73253  
microwave transmissions, neutral atmosphere effects (Japanese) 4-62931  
Mie scattering theory, angular function calc. 4-87281  
non-Rayleigh scattering statistics model 4-102865  
nonGaussian rough surfaces, scattering cross sections for composite models 4-102860  
nonspherical particles layer active remote sensing, radiative transfer theory appl. 4-87256  
partially metallised thin gyrotropic cylinder, EM wave diffraction/scattering, two-dimensional problem 4-87257  
perfect conducting cylinders, EM wave scatt., discrete singularity method, optimisation (Japanese) 4-96761  
perturbed sinusoidal surface, backscattering coeff., coherent model 4-69284  
plane EM wave incident on closed dielec. shield, numerical anal. 4-74394  
plane H-wave scattering from cylindrical body with edge points, numerical anal. by mode matching method 4-91386  
plane waves, by conducting rectangular cylinders, horizontal polarisation 4-79004  
radiowave attenuation due to rain, errors for prediction (French) 4-67377  
radiowave scattering by rain, received power 4-89974  
Radon transform and appls., book contrib. 4-106172  
random gyrotropic media, ray dispersion 4-91404  
randomly perturbed quasiperiodic surface, EM wave scatt., radar appls. 4-88847  
RATAN-600 radio telescope, retrieval of convolution of scattered background and source pattern 4-63082  
RATAN-600 radio telescope, scattered background determ. from Sun obs. 4-63055  
relativistic electron scatt. in EM field, radiation scatt., photon statistics 4-112368  
relativistic electron-EM wave scatt. Klein-Nishina formula, appl. to plasma and solid-state physics 4-64661  
resistive plate, LF scattering 4-69283  
response of object to excitation waveform, deconvolution methods 4-69280  
scalar wave scattering from rough surfaces, anal. 4-79009

# electromagnetic wave scattering continued

scatterometry, influence of nonlinear wind-wave growth processes 4-105586  
semifinite dielectric layer imbedded in perfectly conducting half space 4-69287  
slotted infinite length cylinder, scatt. of H-polarised plane wave 4-83522  
spheroidal object causing EM wave scatt., for imperfectly conducting objects 4-83521  
square aperture reflector, implementation of stationary phase method (French) 4-83518  
Sun tracker atmospheric attenuation meas. at 35 GHz 4-105636  
three dimensional disordered systems, theory of power spectrum and scatt. props. 4-75244  
TM waves stimulated scatt. by strongly magnetised relativistic ribbon electron beam, nonlinear theory 4-74403  
transition scattering of velocity waves from stationary sources of the electric and magnetic fields 4-112326  
two-dimensional plane EM wave scattering from dielec. cylinders, boundary element method 4-79019  
two-frequency microwave ocean wave scatterometer 4-105773  
unilateral fin lines with dielectric layers, dispersion anal. 4-79006  
variable profile antenna (VPA) of RATAN-600, surface-error scattered background of antenna directional pattern 4-63053  
weakly nonlinear objectives 4-74400

# electromagnetic wave transmission

see also *light transmission*  
classical electrodynamics, canonical transformation method 4-74395  
cylindrical wave from infinite line source, near field behaviour, dielec. interface (Japanese) 4-96762  
dielectric body, integral equations for scattered and transmitted fields 4-64655  
low frequency moment solution for electromagnetic coupling through an aperture of arbitrary shape 4-96756  
medium with progressive sinusoidal fluctuation, EM wave propag. (Japanese) 4-74393  
periodic homogeneous multilayered struct. refl. and transmission of 3-D Gaussian beam (Japanese) 4-107495  
strip gratings, simple formulae for transmittance 4-107809

# electromagnetic waves

see also *bremsstrahlung; channelling radiation; Cherenkov radiation; electromagnetic field theory; electromagnetism; gamma-rays; heat radiation; light; microwaves; solar radiofrequency radiation; sunlight; synchrotron radiation; transition radiation; undulator radiation; whistlers; X-rays*  
cable radiation, evaluation model 4-107497  
charged particle, random motion in const. mag. field in plane EM wave 4-96768  
classical electrodynamics, equations of motion, axiomatic deduction 4-95190  
coal derived energy resources, electromagnetic techniques for remote detection, monitoring and mapping 4-72042  
continuation problems of EM fields 4-110892  
electrodynamic boundary value problems, soln. accuracy improvement 4-78999  
EM-acoustic excitation for radial resonances in metal rods 4-68213  
Fourier synthesis approach 4-95106  
induced interaction of electron beam with superstrong EM radiation at boundary of two media 4-107706  
inhomogeneous media, EM waves variational principles, operator eqns. 4-74396  
inhomogeneous plane waves, appls. 4-86220  
intensity maxima on axis, properties of focused field 4-69288  
inverse black-body radiation, closed form approximations 4-86419  
light waves, Young's attitude towards wave theory 4-63435  
linear coupling of EM waves in inhomogeneous weakly-ionised media 4-102845  
radiation in inhomogeneously and nonstationarily moving media 4-79011  
radio stations, EM radiation meas. 4-106281  
relativistic electron beams parametric interaction with EM waves, polarisation effects 4-96767  
rough interface between media, local EM oscils. 4-70899  
running plane E waves in nonlinear medium, dielec. permittivity rel. to elec. field amplitude 4-112327  
semiconductor cylinder polarization by plane EM wave 4-79016  
singular integral problem in surfaces, comments and reply 4-87251  
spinor eqn. of pure EM field 4-64654  
spinor formalism generalisation to anisotropic media 4-96759  
surface polaritons, Fabry-Perot type interferometer theory 4-75870  
time dependent inverse source problem 4-101659  
transverse EM waves with nonzero E.B. comments and reply 4-59962  
vacuum resonators and transmission lines, EM oscillations, nonlinear effects 4-96779

# electromagnetism

see also *electric fields; electrodynamics; electromagnetic field theory; electromagnetic induction; electromagnetic oscillations; electromagnetism waves; magnetic fields; magnetism*  
accidental degeneracies, Zeeman effect, symmetry groups 4-90785  
air-gap between cylindrical surfaces, reluctance-appliance (French) 4-78997  
air-sol interface close-in environments, back emission, backscattering, Klein-Nishina injection effects 4-59945  
book, kinetic theory of electromagnetic process 4-82601  
circular ring interaction with mag. spin and mag. monopoles 4-96752  
conformally invariant theory of gravitation and electromagnetism 4-86283  
conservation laws, relation to algebra of space-time symmetry group 4-95703  
Dunnington's  $e/m_0$  meas. method, undergraduate expt. 4-106144  
eddy current losses, boundary value and transmission problems, Helmholtz eqn. 4-91385  
electric field eqns. comparison with mechanical material eqns. (German) 4-83512  
electrical and electronic phenomena and devices, book 4-67952  
force on a dielectric slab inserted into a parallel-plate capacitor 4-82627  
Hankel functions, determination of  $v$ -zeros using NUZERO program 4-102844  
Helmholtz eqn. separation in prolate spherical coordinates 4-107491  
inhomogeneous anisotropic medium, variational principle 4-101669  
introductory physics, EM interaction unified presentation 4-95105  
inverse source problems, degree of nonuniqueness 4-101671

**electromagnetism continued**

- laser-beam propagation fundamental mode, optically inhomogeneous electrochem. media with electrochem. species conc. gradients, Maxwell's eqns. 4-112341
- Lorentz transformation of Debye potentials 4-101670
- Lorentz-Dirac equation uniqueness 4-64667
- magnetostrictive effects, numerical simulation by finite elements 4-61359
- magnetostatics, Coulomb gauge conditions 4-106159
- Maxwell's eqns., 3-D time-domain finite differencing in spherical coords. 4-59944
- Maxwell's eqns., in free space, spinor solns. 4-91401
- Maxwell's eqns. in generalised nonorthogonal coords., finite difference soln. 4-59943
- Maxwell's eqns. solns., total field vs. scatt. field finite difference codes 4-59942
- Maxwell's equations and density matrix equations, atomic systems, used to calc. light pulses 4-107695
- Maxwell eqns., source free, on compact space  $S^3 \times S^1$ , eigenfunctions and eigenvalues 4-96744
- Maxwell eqns. in accelerated media, wave-like solns., transparency criterion 4-96743
- Maxwell equation solution in case of internal conic refraction 4-87252
- Maxwell potentials on Hilbert space 4-82690
- Maxwell-Bloch equation complex soln., inverse scatt. problem 4-73253
- MHD system modelling at critical parameter values (*Russian*) 4-91847
- Moll, Gerrit, electromag. expts. 4-63466
- neo-Hertzian electromagnetism, wave eqn. soln. for field detector 4-69267
- optical activity, phenomenological description, other crystal optics problems (*French*) 4-74414
- Poincare and related gauges in EM theory 4-67928
- potential integrals for uniform and linear source distributions on polygonal and polyhedral domains 4-69268
- radiative heat transfer, stationary, macroscopic theory rel. to EM fluctuations 4-64828
- radioactive flow, electric fields from ion recombination effects 4-103435
- second law of thermodynamics in presence of EM effects 4-68191
- slab optical waveguide bending, radiation losses anal. (*Chinese*) 4-97059
- spectral distribution for a nonrelativistic gas of particles with structure 4-64668
- stripe geometry lasers, self-consistent model based on beam propagation method, Maxwell's equations 4-112438
- theory in  $R^{2,1}$ , teaching 4-78079
- waveguide, elastic, circular cylindrical, EM effects 4-102864

**electromagnets**

- see also coils; superconducting magnets
- Advanced Toroidal Facility, helical field coils, design descript. 4-111905
- far IR transmission expts., low temp. cryomagnetic set using pulsed electromagnets 4-73525
- NDT, design parameter of local magnetizers 4-109606
- R-tokamak, low activation coil system 4-111903
- TASKA-M, 17.5 T hybrid choke coils 4-111887
- TFCX, candidate TF coil system options, parametric system studies 4-111899
- two-dimensional electromagnetic pole pieces, external mag. field calc. 4-79000

**electromechanical effects**

- biological cell membranes, electroelastic effects 4-77206
- electromagnetic solid continua, mech. behaviour, conf. Paris, France (July 1983) 4-73163
- metallic materials, electric effects, mech. props. eval. methods, review 4-99673
- quartz, X-cut, SAW temp. stability 4-108693
- semiconductor complex structs., EMF due to dynamic deformation 4-65953
- symmetry breaking and dynamical electromagnetic-elastic couplings 4-76337
- TGS, cryst., phys. props., influence of defects 4-76329
- TGSe, cryst., dielec. and electromechanical props. under high hydrostatic press. 4-76296
- TGSe, cryst., phys. props., influence of defects 4-76329
- triglycine fluoroberyllate, cryst., dielec. and electromechanical props. under high hydrostatic press. 4-76296
- triglycine fluoroberyllate, cryst., phys. props., influence of defects 4-76329
- BaTiO<sub>3</sub>, ferroelec. phase transitions, stress effects 4-71315
- KH<sub>2</sub>PO<sub>4</sub> type crystals, ferroelec. phase transition, stress effects 4-76365
- (Pb,Ln)(Zr,Ti)O<sub>3</sub> ceramics, stress anisotropy induced by polarisation 4-104536
- PbTiO<sub>3</sub>, ferroelec. phase transitions, stress effects 4-71315

**electrometers**

- see also charge measurement
- No entries

**electrometry see electrometers****electromigration**

- metals and alloys, book contrib. 4-113689
- planar microleons distributed-index form. process 4-87487
- $\alpha$ -quartz, electrodiffusion of charge-compensating ions 4-61153
- quartz, vacuum swept, Al and OH<sup>-</sup> defect centres 4-61335
- repassivation in alkaline soln., oxidation rates 4-104909
- semiconductors, heterogeneous anisotropic, electrodiffusion purification 4-71533
- Al alloy conductors (*German*) 4-75737
- Al, electromigration at high current density, phenomenological obs. 4-84470
- Al thin film, effect of vapour contaminants on props. 4-88435
- Al-Cu films, microstructure and electromigration studies 4-88413
- Al-Cu-Si sputtered thin film conductors electromigration resistance 4-88611
- Cu<sub>2-x</sub>S ionic conductor, Cu electromigration 4-88354
- GaAs<sub>1-x</sub>P<sub>x</sub>, internal elec. field-enhanced impurity diffusion and p-n junction form. 4-84469
- In films, electromigration 4-61152
- In-Si (111) interface, charge transfer and surface electromigration 4-108667
- Nb, electromigration of Nb, Fe, Co, Ta and Cr 4-65500
- NbH<sub>x</sub>, H electromigration, multilattice method meas. 4-65501
- Ni, repassivation in alkaline soln., oxidation rates 4-104909
- Pd:H, H diffusion, induced Hall voltage 4-70463

**electromigration continued**

- Si/SiO<sub>2</sub>/Al capacitors, interface trap generation and H electromigration 4-70940
- Sn thin film, tracer study of self-diffusion and electromigration 4-103991
- TiO<sub>2-x</sub>, isothermal electromigration 4-92448
- electromotive force see electric potential
- electromyography see bioelectric potentials; muscle
- electron absorption
- see also beta-ray absorption
- positron absorption in targets, theory 4-88206
- MgO, absorption pots. for low energy electron scatt. 4-93157
- MoS<sub>2</sub> (2H), absorption pots. for low energy electron scatt. 4-93157
- NbSe<sub>2</sub> (2H), absorption pots. for low energy electron scatt. 4-93157
- electron accelerators
- see also betatrons; electron ring accelerators; microtrons
- 80-GW relativistic electron beam accelerator 4-111978
- accelerating gap with mag. quadrupole system, high-current electron gap 4-64266
- Advanced Test Accelerator, beam dynamics 4-112026
- beam-breakup calculations for Los Alamos free-electron laser linac 4-83256
- chromaticity correction in the TRISTAN Phase I main ring version 11 4-102424
- collective free electron lasers 4-112449
- colliding  $\gamma$  e and  $\gamma\gamma$  beams from single-pass  $e^+e^-$  accelerators 4-86984
- depolarizing effects of quantum fluctuations, second-order perturbative theory 4-96319
- DESY storage ring expts. 4-96302
- electron beams for electron-beam lasers 4-74532
- experimental data accelerator, time-resolved beam profile meas. 4-112021
- experimental test accelerator, electron beam propagation in ion focused regime 4-112022
- experimental test accelerator, propagation in air, current enhancement 4-112023
- free electron generators of coherent radiation, conf., Orcas Island, WA, USA (June 1983) 4-82588
- free electron laser, high power, short wavelength, accelerator technology 4-83255
- free electron laser ICF driver, electron accelerator power source 4-107084
- free electron lasers, theory and expt., review 4-112448
- free electron tapered-wiggler laser, large electron-beam energy extraction 4-83588
- frequency ratio, injector linac and electron-position storage ring (*Chinese*) 4-102407
- HERA, design, and possible expts. (*German*) 4-102412
- high gradient linear accelerators, wake field transformation 4-74061
- HV pulse generator for subnanosecond electron accelerators 4-59593
- induced interaction of electron beam with superstrong EM radiation at boundary of two media 4-107706
- KEK NODAL users guide for TRISTAN accelerator (*Japanese*) 4-102565
- laser-driven electron (positron) acceleration 4-107185
- Lawrence Berkeley Laboratory and Lawrence Livermore National Laboratory free electron laser using 4.5 MeV Experimental Test Accelerator 4-83611
- linear accelerators, standing wave accelerating structs. 4-107182
- linear induction accelerator, diaphragmed electron beams, stability 4-96301
- MARK-J at PETRA, expt. results, QED and QCD studies 4-111434
- medical accelerators, high energy, neutron contamination detect. using electrochem. etching 4-72431
- nanosecond accelerator for generating ion and electron beams 4-74076
- nanosecond high-current electron accelerator, 2 MeV design and operation 4-102410
- NBS electron storage SURF-II, direct determ. of stored electron beam current 4-64250
- NIKHEF-K 180° electron-scatt. facility overlapping-scintillator system 4-102450
- PEP and PETRA, single beam stability, computer simulation 4-68843
- PETRA  $e^+e^-$  storage ring, review of experimental investigations 1978-83 4-90851
- pilot CW superconducting electron accelerator design, fabrication and test 4-102409
- plasma, inhomogeneous, electron acceleration by laser driven plasma waves 4-96299
- pulsed high-frequency single resonator electron accelerator, design 4-74058
- quantum fluctuations, depolarizing effects, action of nonlinear wigglers on equilibrium polarization level 4-96318
- sealed-off linear waveguide electron accelerator development 4-86982
- silica aerogel threshold Cherenkov counters, pion detection, intermediate energies 4-102496
- standing-wave electron accelerators, RF electronics 4-107183
- standing-wave linear electron accelerators, multiperiodic struct. adjustment 4-64248
- storage rings, undulator radiation as function of e-beam parameters 4-91132
- synchrotron radiation, undulator trajectories, variational derivation 4-96311
- synchrotron radiation source with arbitrarily adjustable elliptical polarisation 4-64662
- electron affinity
- 3d-metal tetraoxanions, rel. between electronic struct. and electron affinity, discrete variational X $\alpha$  calc. 4-87045
- 4d-metal tetraoxanions, rel. between electronic struct. and electron affinity, discrete variational X $\alpha$  calc. 4-87045
- absolute hardness, companion: parameter to absolute electronegativity 4-59659
- actinides, ground state electron affinities 4-78983
- alkali metal atoms, core polarisation pot., intershell correl. effects, ab initio SCF CI calcs. 4-68970
- alkaline earth metal atoms, core polarisation pot., intershell correl. effects, ab initio SCF CI calcs. 4-68970
- alkenes, linear and cyclic, transmission functions and electron affinities determ. 4-87234
- anions, electronic struct., variational X $\alpha$  calc., electron affinity 4-87044
- aromatic hydrocarbons, solid, positronium form., temp. effects 4-71467

# electron affinity continued

- atomic energy differences, electron correl. coeffs. approximate method 4-83304  
benzene, low energy electron impact, formation and dissociation of negative ions 4-96707  
benzene, polycyano derivatives, electron affinity and ionisation pot., MNDO calcs. 4-68958  
N-benzylquinolinium chloride-diphenylamine hemihydrate . . . complex, cryst. and mol. struct. 4-60908  
chalcophenes, electron affinities,  $X\alpha$  calcs. 4-102823  
elemental electronegativities, electron affinities, ionis. pots. and hardnesses calcs. 4-112099  
fluorobenzenes, low energy electron impact, formation and dissociation of negative ions 4-96707  
hydrocarbons, conjugated, electron affinities calc. using semi-empirical MO theory 4-96720  
MIS and SIS structures, electron affinity and work function, interfacial charge effects 4-70910  
mixed negative ion dimers, dissociation, electron affinities 4-109634  
molecular liquids, anion form., correl. with mol. shape 4-92059  
open-shells, cluster expansion techniques appl., ionisation pot., electron affinity and excitation energy calcs. 4-74129  
poly(2,6-naphthylene), electronic props. calcs. 4-88441  
poly(4-phenylquinoline), electronic props. calcs. 4-88441  
polyquinoline, electronic props. calcs. 4-88441  
unsaturated hydrocarbon, polycyano derivatives, electron affinity and ionisation pot., MNDO calcs. 4-68958  
 $C_1$  vertical electron affinity and ionisation potentials 4-112295  
 $F_2$  dipole polarisability, electron affinity, many-body perturbation theory 4-64363  
GaAs glass-bonded NEA transmission photocathode, XPS study 4-104716  
GaAs, relaxation of hot electron energy, surface plasmons 4-98631  
( $CHO_2$ ) $_n$  struct., ab-initio multiconfig. SCF gradient optimisation method 4-83290  
 $HO_2$ , H-O bond energy, rel. to abstraction reactions 4-102574  
 $He_2^+$ , electronic struct. examined using CI wave functions, electron affinity 4-64396  
Si (111) surface composition and band struct. 4-92778  
a-Si:H-Si n-p amorphous-cryst. heterojunctions, elec. characts. 4-84688  
ZnO surfaces, work function, electron affinity, and band bending, angle-resolved UPS study 4-92792

# electron annihilation see electron-positron interactions

# electron attachment

- air, avalanche breakdown, water vapour effects 4-65144  
benzene, low energy electron impact, formation and dissociation of negative ions 4-96707  
chloroethylene anions, formation and dissociation, electron attachment spectra 4-71876  
discharges, electron beam ionised, with added attaching gases, characts. 4-84118  
fluorobenzenes, low energy electron impact, formation and dissociation of negative ions 4-96707  
ionization/recombination kinetics 4-64613  
molecular anions, dipole coupling channels 4-74333  
perfluoroalkanes, electron attachment rate constants, negative ion form., high-pressure swarm technique appl. 4-87188  
n-perfluorobutane, dielectric strength, press. depend. 4-75220  
polar molecules, dissociation, attachment, ang. depend. calcs. 4-107454  
 $Cl_2$  electron attachment, rate const. 4-107452  
 $^{18}O_2$  thermal electron attachment mechanism, isotope effect studies in inert gases and hydrocarbons 4-102795  
OH, anomalous photodetachment thresholds from electron dipole interactions, rot. doubling effects 4-74298  
 $SO_2$ , dielectric strength, press. depend. 4-75220

# electron avalanches

- air, avalanche breakdown, water vapour effects 4-65144  
electrical streamer propag. in gases, avalanches and space-charge 4-65049  
gases, electron multiplication in nonuniform elec. fields, theory 4-97920  
particles, suspended, detection by laser-induced electron emission 4-90705  
statistical theory and Monte Carlo simulation 4-87959  
transition to corona, temporal characts., electrode radius of curvature effects 4-84104  
 $SF_6$  prebreakdown avalanche pulses under uniform field 4-113244

# electron beam absorption see electron absorption

# electron beam applications

- see also electron beam deposition; electron beam lithography; electron beam machining; electron beam welding; radiation therapy  
absorption spectroscopy using picosec. electron beam and streak camera 4-73531  
Cherenkov microwave generators with relativistic electron beams, plasma form. 4-91960  
crystal surfaces, electron current image diffraction at low energies 4-92014  
excimer lasers with various pumping schemes 4-69385  
gas laser electron beam pumping, energy deposition problems 4-69381  
high energy electron beams, radiobiological and microdosimetric characts., radiotherapy appls. 4-72417  
laser excitation, energy deposition meas. of intense relativistic electron beam 4-69297  
lasers using electron beams 4-74532  
medulloblastoma treatment, modified radiotherapy technique 4-89728  
microwave powered electron linear accelerator, radiotherapy appls. 4-72401  
pattern writer for X-ray masks 4-95562  
plasma diagnostics, Fourier-analyzing coil arrays for pulsed relativistic electron beam experiments 4-113222  
radiotherapy, calibration of high-energy photon and electron beams 4-109920  
radiotherapy, central axis per cent depth dose for 4-29 MeV electrons, beam angulation effect 4-115223  
radiotherapy, intercomparison of absorbed dose by Fricke dosimetry 4-85523  
radiotherapy, low energy electron beams, depth doses improvement 4-89759  
rotational total skin electron irradi., clinical aspects 4-85495  
rotational total skin electron irradi., surface dose calc. 4-109942  
sample heating, multiple sample holder 4-95443

# electron beam applications continued

- scanning electron beam annealing of implanted semiconductors appl., using REM-200 electron microscope 4-93319  
solar cells, minority carrier SEM-EBIC signal and grain boundaries 4-80609  
therapy, central axis depth-dose 4-67124  
therapy, dose enhancement in bone 4-81788  
therapy, dosimetric effects on field shaping and shield positioning 4-72434  
therapy, electron beam isodose distrib., analytic calc. 4-85517  
thermal wave imaging of subsurface structure with IR detection 4-86413  
UV ion laser, continuous, DC electron beam excited (Russian) 4-69367  
X-ray production, depth distrib. 4-63851  
CO row industrial laser, electron beam-controlled with 10 kW output power, energy characts. 4-74492  
CdS laser, electron-beam-pumped, excitation density distrib. 4-79162  
F CW laser action 4-91439  
GaAs laser, electron-beam-pumped, excitation density distrib. 4-79162  
 $H_2$ - $F_2$  pulsed laser, photolysis and electron beam method initiation efficiency 4-74499  
HF electron beam initiated pulsed chem. laser 4-69391  
HgCl lasers, electron-beam pumped 4-69388  
I- $H_2$  laser, electron-beam-controlled 4-74498  
KrF laser, electron beam pumped, high energy, multi atm. 4-60066  
KrF laser, electron beam pumped, for laser fusion appl. 4-79113  
KrF laser, electron-beam pumped 4-69388  
KrF laser, electron-beam pumped, optimisation with Ne buffer gas 4-112384  
KrF lasers, electron beam controlled discharge pumping 4-60018  
KrF lasers, electron-beam-excited, using Ar-free mixtures at 1 atm. 4-112382  
Si, deformed, EBIC/TEM study of defects 4-80045  
Si:B, ion implanted shallow layers, electron beam annealing, expt. study using SIMS 4-98133  
Si-Er interface, ErSi, formation using electron beam heating 4-65494  
Xe IR lasing, effect of pumping conditions in Ar-Xe mixtures 4-107599  
XeCl lasers, electron beam controlled discharge pumping 4-60018  
XeCl, tunable electron-beam-pumped excimer lasers 4-69384  
XeF laser, electron beam pumped, laser parameters determ. 4-96874  
XeF, tunable electron-beam-pumped excimer lasers 4-69384  
ZnO UV laser with longitudinal electron beam pumping 4-79164

# electron beam deposition

- alloy films, submicron, electron probe microanal. 4-75808  
coating deposition by electron-beam evaporation method, unique features 4-74767  
evaporated film, optical props. influence substrate temp. 4-76546  
metallisation, simultaneous evaporation with electron beam guns for semicond. devices (Polish) 4-93221  
MIS solar cells, high open-cct. devices, electron-beam metallisation, surface damage study 4-99968  
optical thin films, ion-assisted deposition, prep. and appls. 4-87402  
protective dielectric coatings produced by ion-assisted deposition 4-69598  
rod-fed evaporation, ternary alloy source material fabrication process, mag. disc manufacture appl. 4-114581  
 $Al_2O_3$  films obtained by electron-beam evaporation 4-74669  
Au film enhanced bonding by ion-assisted electron-beam deposition 4-109324  
Au films deposited by electron beam evaporation or sputtering, Si outdiffusion, annealing ambients effects 4-70459  
Be adherent film production by electron beam evaporation 4-66238  
Co- $Al_2O_3$  coevaporated composite films, solar selectivity 4-72169  
Co-Nb amorphous films, electron beam deposited, ion mixed, FMR, magnetisation meas. 4-71138  
Co-Nb multilayered compositionally modulated films, e-beam deposited, FMR, magnetisation, B-H loop meas. 4-71139  
Cr obliquely deposited films, spectral and angular selectivity 4-112535  
Ge obliquely deposited films, spectral and angular selectivity 4-112535  
GeO $_2$  films, amorphous, elec. characterisation in MIS and MIM structs. 4-70816  
 $In_{2-x}Sn_xO_{3-y}$  coating deposition, three-step process, low sheet resist. 4-81159  
 $In_{2-x}Sn_xO_{3-y}$  films, transparent and heat-reflecting, elec. and optical props., ionised impurity scatt. 4-66087  
 $In_{2-x}Sn_xO_{3-y}$  transparent and heat-reflecting films, optical props. 4-114334  
Nb films and Josephson tunnel junction fabrication by electron beam evaporation (Chinese) 4-76080  
Nb superconducting thin films, electron beam evaporation prep. 4-114401  
Ni- $Al_2O_3$  electron beam evaporated condensates, creep props. 4-93361  
Si solar cell production system, electron beam heating in a vacuum 4-62362  
 $Si_3N_4$  films, electron beam assisted CVD, conformal step coverage 4-61869  
 $SiO_2$  films, electron beam assisted CVD, conformal step coverage 4-61869  
 $SiO_2/TiO_2$  hard multilayers, reactive sputtering (Polish) 4-112554  
 $Ta_2O_5/SiO_2$  antireflection coatings, electron-beam deposited, 1064-nm damage tests, review 4-75525  
ZrO $_2$ - $SiO_2$  thin amorphous film prep. by electron-beam evaporation from multiple sources 4-74674

# electron beam effects

- see also beta-ray effects; cathodochromism; cathodoluminescence; electron impact; plasma-beam interactions  
amorphous alloys, crystn., effect of irradiation particle mass 4-79936  
anthracene, excitons and diffusion effects 4-92617  
axial channelling radiation, mol. type, from MeV electrons 4-75582  
chalcogenide glasses, electron microscopy of reactions with metals and electron beam induced crystn. 4-80315  
channel created by deep penetration, shape and size, electron beam simplified model (Polish) 4-113500  
coherent bremsstrahlung and channelling radiation from kilovolt electrons 4-85030  
composite organic insulators, electron and neutron irradiation effects on mech. props. 4-75533  
crystals, elastic interaction of relativistic electrons 4-65301  
crystals, electron and positron channelled radiation 4-108494  
crystals, electron channelling radiation and Zeeman effect 4-65319  
crystals, interaction pot. of light channelled particles 4-108492

## electron beam effects continued

- damage structures, evolution under 14 MeV neutron, 4 MeV ion and 1.25 MeV electron irradiation 4-108418
- depth-dose and lateral-dose functions, energy and at. number depend. 4-65320
- diamond, type Ia, defect-induced one-phonon absorption 4-84981
- diamond, types Ia and IIa, electron and positron planar channelling radiation spectra 4-75579
- dielectrics, electron irradiated, vol. electrification meas. 4-71270
- dielectrics, fast electron irradiated, space-charge dynamics 4-71279
- dielectrics, radioactive, elec. vol. charge 4-71276
- discharges, electron beam ionised, with added attaching gases, characts. 4-84118
- EM wave emission from electron beam-space plasma interactions 4-87886
- excitation energy distrib., Gaussian models, appl. to X-ray microanal. and solid state electronics 4-65303
- FCC alloys, Suzuki segregation, TEM study 4-89054
- fluorinated hydrocarbon films, electron-stimulated desorption 4-98451
- fusion reactor first wall coatings, gas release under electron impact 4-91097
- gas interaction process, unbalanced states investig. (*Russian*) 4-79816
- glass, electron irradiated, discharge form. 4-71275
- glass, electron-irradiated, discharge phenomena 4-71277
- glass, fast electron irradiated, space-charge dynamics 4-71279
- glow discharge electron gun, cathode geometry rel. to beam spatial distrib. 4-87990
- glutamine synthetase, mols., time-resolved low dose electron microscopy 4-100420
- graphite, relativistic electron beam propag., energy absorpt. 4-70221
- graphite+H reactivity, electron bombardment enhanced 4-93529
- graphite fluoride, electron beam induced decomposition, X-ray C K-emission spectra 4-93144
- graphite fluoride, electron beam induced decomposition, X-ray emission band meas. 4-93524
- HVEM, electron scatt. and energy depend., appl. to chem. anal. 4-66162
- II-VI compounds, irradiation-produced dislocation loops, HVEM study 4-75529
- inelastic electron scatt. in solids, review 4-66151
- insulating thin films, Auger electron spectra, electron and ion beam effects 4-109283
- ionosphere, plasma interaction with STS-3 DC and modulated electron beams, wave emissions 4-90023
- ionosphere, wave-particle interaction prod. by injected electron beam 4-87888
- ionosphere, whistlers generation from STS-3 electron beam-plasma interaction 4-90024
- Kapton, dielectric charging and discharging in spectral electron environments 4-61440
- kinetic cyclotron maser instability associated with a hollow beam of electrons 4-87861
- Kumakhov radiation in axial channelling, general case in classical theory 4-103842
- metallic novel surfaces, directed energy production 4-74775
- metallic thin films, etching with  $\text{CCl}_4$ , electron flux activation 4-93446
- metals, internal friction peaking effect due to electron or  $\gamma$ -ray irradiation 4-103873
- microscopy, microanal., and microlithography aspects, conf., Monterey, CA, USA (April 1982) 4-63394
- microscopy, radiation damage effects 4-79911
- microscopy and anal., conference, Guildford, England (Aug.-Sept. 1983) 4-78034
- MIS solar cells, high open-cct. devices, electron-beam metallisation, surface damage study 4-99968
- molecular cryst., radiation damage morphology, high resolution electron microscopy 4-70219
- NIKHEF-K 180° electron-scatt facility overlapping-scintillator system 4-102450
- optical fibres, MCVD, PCS and DC/TC types, props. in radiation environments 4-80102
- optical fibres, PCS and all  $\text{SiO}_2$ , radiation induced absorpt. 4-80105
- optical fibres in adverse environments, conf., Paris, France (May 1983) 4-78025
- organic compounds, electron irradiation damage in electron microscope, encapsulation effects 4-79912
- organic material, electron microscopy, electron beam irradiation damage rel. by cooling to 4K 4-65158
- organic materials, TEM studies, radiation damage 4-82867
- OSR, dielectric charging and discharging in spectral electron environments 4-61440
- oxides, electron bombardment evaporation, physical model anal. 4-60965
- p-n junctions, electron beam induced short circuit currents, carrier lifetime 4-92806
- p-n shallow junction, electron beam induced current 4-80662
- n-paraffins, electron beam damage quasi-thermal mechanism, electron diffraction studies 4-98135
- plasma interactions, computer simulation, appl. to SEPAC/Spacelab 1 mission 4-87887
- PMMA, fast electron irradiated, space-charge dynamics 4-71279
- polydiacetylene cryst., radiation damage and high resolution electron microscopy 4-80111
- polyethylene, electron irradiation, melting and crystallisation, calorimetric study (*Russian*) 4-84223
- polyethylene, electron irradiated, thermostimulated exoemission and radical recomb. 4-93003
- polyethylene, fast electron irradiated, space-charge dynamics 4-71279
- polyethylene, low density, radiation induced conductivity 4-84622
- polyethylene, thermal characts., electron and gamma-neutron irradiation effects (*Russian*) 4-103977
- polymer dielectrics, fast electron irradiation, space-charge storage 4-71280
- polymers, electron beam modification and form., ESCA investig. 4-99287
- polymers, fracture and emission of electrons, ions and photons 4-98189
- polymers, identification by unsaturated bond form. in electron irradiation 4-79962
- polymers, structure and composition, electron beam damage meas. 4-80110
- polystyrene, fast electron irradiated, space-charge dynamics 4-71279
- polysulphones, electron irradiation, tensile and viscoelastic props. 4-61981
- polythiophene, conducting polymer, electron beam irradiation in  $\text{SF}_6$  gas, elec. and optical props. 4-75531

## electron beam effects continued

- polyvinylalcohol: resists, electron beam chem. and radiation sensitivity study 4-75530
- positron channelling: radiation intensity, influence of multiple scattering 4-75580
- quartz, alpha phase, dielectric charging and discharging in spectral electron environments 4-61440
- quartz, electrical and optical props., neutron,  $\gamma$ , and electron irradiation effects 4-60968
- radiation aging of insulating resins, electrical effects, 4-111621
- radioactive waste glass, simulated, density changes under ion, electron, and gamma irradiation 4-73974
- radiotherapy fraction size rel. to effects on human skin 4-115179
- rubber insulation, charge deposition under electron irradiation 4-111620
- Schottky barrier, EBIC, voltage depend., Gaussian models 4-65303
- Schottky-barrier diode, EBIC contrast from individual surface-parallel dislocations, temp. depend. 4-103749
- SEM, electron beam interaction with target 4-63827
- semiconductors, cathodoluminescence, EBIC and SIMS studies 4-76531
- silicate glasses, electron irradiation, damage mechanism 4-70216
- single crystals, Kumakhov radiation in axial channelling, dipole approx. in classical theory 4-103841
- skin, human, radiotherapy, acute reaction rel. to overall treatment time 4-115180
- SOI structures, recrystallization by electron beam annealing (*Japanese*) 4-88207
- solid, soliton state in wake interaction following ion or positron motion 4-75550
- space charge waves, growth and damping due to nonlinear Landau damping 4-79780
- stainless steel, surface composition, electron bombardment effects, SXAPS obs. 4-108683
- steel, austenitic stainless, cavity formation during electron irradiation, effect of pre-implanted He 4-108444
- steel, austenitic stainless, dual-ion and/or electron irradiation in HVEM, in-situ obs. of cavity growth process 4-98134
- steel, austenitic stainless, electron irradiation-induced structural phase transformations 4-109418
- steel, austenitic stainless, electron irradiation, void swelling, effect of C and N 4-108445
- steel, austenitic stainless, melt layer form. under repetitive electron beam heating, simulation of plasma disruption 4-75535
- steel, austenitic stainless, modified, void suppression, effect of segregation of minor alloying elements 4-104789
- steel, austenitic stainless, thermal and radiation-stimulated ageing, kinetics 4-66354
- steel, austenitic stainless, void swelling, effects of C and N 4-98149
- steel, tool, wear resistance, effect electron irradiation 4-71740
- steel, tool, wear resistance, effect of electron radiation dose 4-62067
- surface melting, rapid solidification microstructures 4-89046
- Teflon, dielectric charging and discharging in spectral electron environments 4-61440
- p-terphenyl, electron and  $\Gamma$ -irradiation, absorpt. spectra (*Russian*) 4-71421
- thick targets, X-ray continuum, Kramer's law modification 4-99234
- thin crystals, electron and positron channelling, radiation intensity 4-108489
- thin film formation under effect of electron and ion bombardment 4-84529
- tokamak first wall/blanket/shield programme, e-beam effects, designs, recent progress 4-111800
- w-tricosenoic acid, Langmuir-Blodgett film, technique for charact. 4-113834
- TTF-TCNQ, strongly irradiated, CDW fluctuations, X-ray diffuse scattering study 4-84611
- two-layer material, irradiation, axially symmetric heating problem soln. (*French*) 4-65302
- weakly ionised gas, discharge threshold and space charge distributions, with electron beam emission 4-84109
- x-ray laser by channeling radiation 4-74541
- Ag films and particles on MgO, surface diffusion under intense electron irradiation 4-98412
- Ag-Cu dilute alloys, electron irradiation, defect prod. and annealing 4-75441
- Ag-Zn, conc., electron irradiation, elec. resist., recovery 4-104182
- $\text{Ag}_{50}\text{Cr}_{50}\text{P}_{50}$ , quasi-one-dimensional antiferromagnet, electron irradiation and substitution induced disorder 4-98866
- Al, cavity formation in samples irradiated with pulsating beam of 225 MeV electrons 4-108443
- Al, clean and  $\text{H}_2$  exposed,  $\text{H}_2$  adsorption, electron stimulated desorption study 4-75792
- Al cylinder, acoustic wave excitation by low energy electrons 4-80168
- Al, electron irradiation, incoherent tunnelling of positive muons and trapping by vacancies, muon spin relax. meas. 4-65909
- Al, oxide formation in presence of  $\text{CO}_2$  and electron irradiation 4-93441
- Al polycrystalline surface, oxidised, interaction with electron beams, AES study 4-93154
- Al, relativistic electron beam propagation, energy absorpt. 4-70221
- Al-Mg-Sc, electron irradiation, precipitation and structure (*Russian*) 4-66339
- AlGaAs-GaAs solar cells for space apps. 4-81543
- Al $_2\text{SiO}_5$ , sillimanite, absorption edge fine structure study using electron channelling 4-80127
- Ar, liq., geminate recombination 4-69207
- Ar solid, electron stimulated desorption, luminescence and exciton creation 4-80381
- Au, photon linear polarization in the elementary process of atomic-field bremsstrahlung 4-91354
- $\text{Au}_2\text{Cd}$ , electron damage, high resolution electron microscopy study 4-92241
- $\text{Au}_3\text{Mn}$ , electron damage, high resolution electron microscopy study 4-92241
- BN, cubic, prep. of small particles by electron irradiation of hexagonal BN in TEM 4-61895
- $\text{BaF}_2 \cdot \gamma^{3+}(\text{Pb}^{2+})$  crystals, electronic excitation decay, impurity effect 4-109209
- $\text{BaMnO}_{3-x}$  system, electron irradiation, phase transform., high resolution electron microscopy 4-65395
- $\text{BaTiO}_3$ , Ca, impurity site occupancy, channelling enhanced microanal. studies 4-108394
- C amorphous thin film, low energy electron attenuation length studies 4-84323
- C, photon linear polarization in the elementary process of electron-electron bremsstrahlung 4-91355
- C, stopping power, zero-energy density effect 4-80129

## Electron beam effects continued

- CO, chemisorbed layer on Ru (001), electron-induced desorption 4-104075  
 CaF<sub>2</sub>, electron irradi., anion voidage and void superlattice 4-108350  
 CaF<sub>2</sub>:Y<sup>3+</sup>(Pb<sup>2+</sup>) crystals, electronic excitation decay, impurity effect 4-109209  
 CaO, lattice defect prod. by electronic excitation 4-70213  
 CdS, electron beam annealing, defects diffusion 4-103801  
 CdS, electron irradi., photoluminescence study 4-99189  
 Cu (110), adsorption of water vapour, electron beam damage to adlayer 4-80396  
 Cu (111), adsorption and chemisorption of water vapour, electron beam damage of adlayer 4-80397  
 Cu anode foils disruption by high-current relativistic electron beams irradi. 4-108195  
 Cu, photon linear polarization in the elementary process of atomic-field bremsstrahlung 4-91354  
 Cu, relativistic electron-beam propag., energy absorpt. 4-70221  
 Cu-Be (1.35 at.%), undersaturated, irradiated, formation of precipitates 4-104791  
 Cu-H, electron irradi., elec. resist. meas., annealing behaviour 4-92240  
 Cu-Ni-Fe alloys, electron irradi., clustering and decomposition, neutron scatt. studies 4-114555  
 Cu-Zn, high energy electron irradi., radiation enhanced diffusion, interstitial mechanism, elec. resist. meas. 4-92239  
 CuInSe<sub>2</sub>, sputtered surface characterisation using AES, O<sub>2</sub> adsorpt. 4-93147  
 (CuZn)S-CuInSe<sub>2</sub> heterojunction solar cell, interface props. 4-89401  
 Fe alloys, dil., electron irradi., muon spin rot. obs. 4-65913  
 Fe, BCC, electron or neutron irradi., induced defects, model 4-65300  
 α-Fe, electron and neutron irradiated, low-temp., mag. relax. spectra 4-84831  
 Fe, electron irradi., internal friction (Polish) 4-92234  
 Fe, pure, irradi. in HVEM, void form. onset temp. 4-103804  
 Fe, pure and C doped, electron irradi., resistivity recovery 4-108834  
 Fe, pure and doped, muon trapping at vacancies 4-65901  
 Fe-Cr-Si(Ti), electron and ion-irradi., void and precip. struct. 4-103802  
 Fe-Ni dilute alloys, electron and neutron irradiated, low-temp., mag. relax. spectra 4-84831  
 GaAs (111), direct electron beam writing of oxide layer 4-92235  
 GaAs, deep centres, electron probe method anal. 4-104158  
 GaAs, defect anisotropy following electron irradiation 4-75534  
 GaAs, E3 centre accumulation, effect of defect charge state 4-60966  
 n-GaAs, electron irradi., dislocation glide, TEM studies 4-92207  
 GaAs, electron irradi., electronic struct. of E3-defects 4-70720  
 GaAs, electron irradi., surface electron energy spectrum, photoemission studies 4-88554  
 GaAs, electron irradiated, carrier-capture cross sections meas. technique 4-61394  
 n-GaAs, electron irradiated, As anti-site defects, IR spectra and EPR 4-84317  
 GaAs, electron- and proton-irradiated, elec. props. 4-75975  
 GaAs solar cells, equivalent electron fluence for space qualification 4-77097  
 GaAs surface structure (110), mech. destruction and electron bombardment effects, XPS obs. (Russian) 4-113772  
 GaAs:B, interstitial centre, radiation induced, cluster-Bethe lattice treatment 4-98090  
 GaAs:Si, localised vibr. mode IR absorpt. meas. 4-104599  
 p-GaAs:Zn, emission band, electron irradi. and annealing effects 4-88881  
 GaAs<sub>1-x</sub>P<sub>x</sub>, internal elec. field-enhanced impurity diffusion and p-n junction form. 4-84469  
 GaN:Zn, cathodoluminesc. anomalous kinetics 4-85015  
 GaP, electron irradi., defect creation, luminescence and elec. studies (Chinese) 4-108441  
 n-GaP, electron irradi., defects, positron annihilation studies 4-109273  
 Ge, electron irradiation and thermal quenching, defects production 4-60962  
 Ge, radiation-induced rod-like defects 4-92238  
 Ge:Cu, impurity states, annealing-effects 4-104148  
 Hg<sub>1-x</sub>Cd<sub>x</sub>Te, annealing of radiation defects, electron irradiation 4-108442  
 Hg<sub>1-x</sub>Cd<sub>x</sub>Te, electron irradi., elec. props., heat treatment effects 4-65713  
 InP, electron irradi., antisite defects, EPR study 4-80816  
 InP, electron irradi., induced deep traps, deep level optical spectroscopy 4-104156  
 InP, electron irradiation induced defects, energy and orientation depend. 4-108810  
 n-InP, self-trapping and metastable M-centre 4-108809  
 InP solar cells, radiation resistant, electron irradi. damage 4-62351  
 InP:Si, electron irradi.-induced deep traps, impurity conc. effects 4-88468  
 InP:Zn, electron irradi. damage, carrier conc. effects, minority carrier diffusion length 4-80107  
 Ir, electron and neutron irradi., elec. resist. studies 4-108447  
 KBr, electron irradi., positron annihilation centre accumulation 4-88902  
 KCl, acoustic wave generation by electron beam, polarisation-optical recording method 4-109154  
 KCl:Na, electron irradi., F-centre generation, absorption spectra studies 4-113444  
 K<sub>0.30</sub>MoO<sub>3</sub>, electron irradi., CDW pinning in Peierls distorted state by induced defects, nonlinear cond. 4-98595  
 KrXe<sup>+</sup> form. and decay in electron beam excited inert gas mixtures 4-83479  
 LiF crystals, fast electron irradiated, space-charge dynamics 4-71279  
 LiF, planar channelling radiation from relativistic positrons and electrons 4-75581  
 LiNbO<sub>3</sub>, crystalline, Nb<sub>2</sub>O<sub>5</sub> precipitates, TEM studies 4-98290  
 LiNbO<sub>3</sub>, electron irradi., point defects, ESR and IR spectra studies 4-70139  
 LiNbO<sub>3</sub>, single cryst., cathodoluminescence emission, surface damage 4-93115  
 LiNbO<sub>3</sub>, thermochemically reduced and electron irradi., positron annihilation, optical absorpt. meas. 4-104697  
 MgF<sub>2</sub>:Li, electron irradi., holelike defects, ESR study 4-60964  
 MgO, electron irradi., point defect kinetics, HVEM study 4-70214  
 MgO, lattice defect prod. by electronic excitation 4-70213  
 Mo, pure, electron and He ion irradi., vacancy loop form. 4-108480  
 N<sub>2</sub>O, chemisorbed layer on Ru (001), electron-induced desorption 4-104075  
 NaAlH<sub>4</sub>, decomposition, Na single cryst. form., electron microscopic study 4-108296

## Electron beam effects continued

- NaCl, electron irradi., appl. to radioactive waste repositories 4-75532  
 Na<sub>2</sub>O-SiO<sub>2</sub> glass, electron irradiated, evidence of enhanced diffusion process 4-80108  
 Na<sub>2</sub>O-SiO<sub>2</sub> glass surface, electron stimulated desorption mechanisms 4-92514  
 Nb, electron irradi., isochronal recovery spectrum, metastable self-interstitial config. 4-70212  
 Nb, electron-irradiated, muon diffusion and trapping by defects 4-65905  
 Nb single crystal, neutron and electron irradi., dislocation sweeping of defects 4-103810  
 NbSe<sub>3</sub>, electron irradi., strandlike domains in CDW states 4-70220  
 Ni, electron axial channelling radiation spectra 4-75583  
 Ni, electron irradi., muon spin rot. obs. 4-65913  
 Ni, high temperature electron induced embrittlement 4-108448  
 Ni/He, preimplanted, electron irradi., 1 MeV, He bubble growth 4-103803  
 Ni-based alloys, HVEM irradi., void form. rel. to γ precipitation 4-108446  
 Ni-Ge dilute alloys, defect reactions, diffuse X-ray scatt. studies 4-75440  
 Ni-Si (12.7 at.%), solute redistrib. under irradi., TEM invest. 4-108416  
 Ni-Si dilute alloys, defect reactions, diffuse X-ray scatt. studies 4-75439  
 Ni-Ti foils, electron irradi., precipitation characs. 4-108625  
 Pb chalcogenides, carrier diffusion length and lifetime, EBIC meas. 4-92748  
 RbMgF<sub>3</sub>:Mn<sup>2+</sup>, electron irradi., vacancy-interstitial pair and F-centre-impurity ion pair form. 4-70215  
 Rb<sub>0.30</sub>MoO<sub>3</sub>, electron irradi., CDW pinning in Peierls distorted state by induced defects, nonlinear cond. 4-98595  
 SF<sub>6</sub>, frozen, sputtering by electron bombardment, mass spectra studies 4-76571  
 Se<sub>2</sub>S<sub>3</sub>, cryst. struct., electron irradi. induced disorder 4-103713  
 Si, axial channelling radiation of MeV electrons 4-92276  
 Si, channelled electrons, axial channelling radiation, temp. depend. 4-75576  
 Si, channelling radiation emitted from 350 MeV planar channelled electrons 4-75578  
 Si, channelling radiation from relativistic positrons, energy eigenvalue calc., self consistent approx. method 4-80128  
 Si, computer simulation, relativistic electrons, multiple scatt., axial channelling 4-108491  
 Si, Czochralski, C in radiation damage centres, luminesc. study 4-93107  
 Si, deformed, EBIC/TEM study of defects 4-80045  
 Si, EBIC imaging of point defects 4-79909  
 Si EFG ribbon solar cells, ion implantation and pulsed electron beam annealing fabrication 4-62364  
 Si, electron and γ irradi., influence on defect annihilation 4-98094  
 Si, electron and γ-ray irradiated, efficiency of radiation defect formation 4-92237  
 Si, electron and positron irradi. effects (Russian) 4-88208  
 Si, electron beam annealing, pulsed, thermal model 4-60963  
 Si, excitation depend. grain boundary recombination velocity 4-104217  
 Si film, ion implanted, electron beam recrystallisation 4-98137  
 Si film on SiO<sub>2</sub> substrate, electron beam recrystallisation 4-98136  
 Si, gettering efficiency of different dislocation types, EBIC, TEM, obs. 4-103787  
 Si, high purity, intercarrier scatt. effects, laser and electron beam excitation 4-92725  
 Si, ion implanted, beam annealing 4-75510  
 Si, ion implanted, laser or electron beam annealing, electronically active defects, DLTS 4-80527  
 Si, ion implanted, laser or electron beam annealing; minority carrier recomb., EBIC, photoluminescence meas. 4-80601  
 n-Si, irradiated, Si-Si centre, optical excitation and relaxation, EPR study 4-109075  
 Si, lateral epitaxy, electron beam annealing 4-99308  
 Si MINP solar cells, reliability under 1 MeV electron irradi. 4-77096  
 Si, mol. type axial channelling radiation from MeV electrons 4-75582  
 Si p-n junctions, electron irradi., differential resist. in avalanche breakdown region, temp. depend. 4-88571  
 p-Si photoresistors, electron irradi., pulsed operation 4-84655  
 Si, polycrystalline, interacting grain boundaries, surface recombination vel., EBIC study 4-70828  
 Si polycrystalline solar cells, struct. defects, TEM/EBIC studies 4-108380  
 Si, positron channelling radiation, photon intensity and polarisation, computer simulation 4-75584  
 Si, radiation-induced rod-like defects 4-92238  
 Si sheets, edge-supported pulling, electron channelling and EBIC studies, rel. to solar cell appls. 4-75695  
 Si solar cell, with induced channel, stability of characs. rel. to irradi. and temp. changes (Russian) 4-109739  
 Si solar cells, electrical microcharacterisation using SEM 4-81560  
 Si:As, ion implanted regions, 2-D shape, etching and EBIC studies 4-88187  
 Si:As(B), ion implanted and electron beam annealed, TEM and HREM studies 4-80058  
 Si:As(Sb)(In), ion implanted, pulsed electron beam annealing, impurity diffusion 4-103984  
 p-Si:B, ion implanted, electron beam annealing 4-60960  
 Si:B solar cell, electron irradi., photon effects 4-93618  
 Si:B solar cell material, EBIC contrast, microstruct. and composition effects 4-108878  
 Si:C, electron irradi., optical absorpt. spectra 4-88861  
 Si:Ge(Sb)(W), electron beam doping, SIMS and RBS studies (Japanese) 4-108401  
 Si:H<sub>2</sub>O, grain boundary impurity effect determ. 4-92214  
 a-Si:H p-i-n devices, EBIC defect 4-92796  
 a-Si:H solar cells, EBIC microcharacterisation of fabrication defects 4-93629  
 Si:Li and Si:Li<sub>2</sub>C, electron irradi., luminesc. decay time, absorpt., isotope splitting, and Zeeman meas. 4-71434  
 Si:Li p-n junction solar cells, electron induced degradation, recovery under space conditions 4-105110  
 Si:Li solar cells, counterdoped, increased radiation resistance to electron irradi. 4-81539  
 Si:Sb, ion implanted, dopant site location and profiles, channelling studies 4-108393  
 Si:Sn, implanted, subthreshold energy electron beam annealing, Mossbauer effect 4-88205  
 SiC, partial dislocation motion under electron irradi. in TEM 4-75453

**electron beam effects continued**

- SiC/Al(Pd) interface form., annealing and oxidation, AES studies 4-80420  
 $\text{Si}_3\text{N}_4$ ,  $\text{Ar}^+$  ion bombarded, electron irradiation effect on surface composition 4-80109  
 $\text{SiO}_2$ , charge neutralisation by electron bombardment 4-98694  
 $\text{SiO}_2$ , electron irradi., IR absorpt. from  $\text{OH}^-$ -related defects 4-104633  
 $\text{SiO}_2$  fibre, plastic clad, radiation induced transient attenuation 4-80106  
 $\text{SiO}_2$  film, ion implanted, electron beam recrystallisation 4-98137  
 $\text{SiO}_2$  films, space charges study with pulsed electron beam 4-88622  
 $\text{SiO}_2$  glass, radiation induced charges 4-70217  
 $\text{SiO}_2$ , lattice defect prod. by electronic excitation 4-70213  
 $\text{SiO}_2$ , vitreous, electron bombarded, stress relaxation 4-70218  
 $\text{SiO}_2\text{N}_x$ ,  $\text{Ar}^+$  ion bombarded, electron irradiation effect on surface composition 4-80109  
 $\text{SrF}_2$ ,  $\text{Y}^{3+}$  ( $\text{Pb}^{2+}$ ) crystals, electronic excitation decay, impurity effect 4-109209  
 $\text{SrTiO}_3$ , lattice defect prod. by electronic excitation 4-70213  
Ta, electron-irradiated, muon diffusion and trapping by defects 4-65905  
Ti-Si interface, Ti-Si<sub>2</sub> formation by wide-area electron beam irradi. 4-92236  
TiO<sub>2</sub>, colour centre accumulation under electron exposure 4-60927  
W (110) with surface adsorbed CO, electronic transitions, low-threshold neutral desorption,  $\alpha$ - $\beta$  conversion, calcs. 4-113785  
W, field ion study of mixed dislocations 4-108369  
ZnGeAs<sub>2</sub>, electron- and proton-irradiated, elec. props. 4-75975  
p-ZnGeP<sub>2</sub>, electron irradi., defects, positron annihilation studies 4-85032  
ZnO varistor ceramics, SEM EBIC studies 4-75981  
ZnSe, luminescence spectra, pulsed irradiation with electrons 4-109230  
Zr, electron irradi., disloc. loops, electron microscopy studies 4-84296  
Zr<sub>3</sub>Al, electron damage, high resolution electron microscopy study 4-92241

**electron beam impact** *see electron impact***electron beam lithography***see also electron resists*

- backscattering from complex struct., rel. to lithography resolution 4-66153  
electron beam interactions with solids, rel. to microscopy, microanal., and microlithography 4-63394  
Fresnel zone plate electron beam fabrication and characterisation for soft X-ray microscopy 4-95587  
high resolution zone plates for soft X-rays, lithographic manufacturing technique 4-63817  
holography, digital, E-beam lithography, algorithms and 3-D display 4-107561  
moiré topography of substrates, IC production appl. 4-101811  
Monte Carlo simulation for electron scatt. in solid targets 4-66155  
optical pattern recognition, use of E-beam written computer generated holography 4-107533  
pattern writer for X-ray masks 4-95562  
soft X-ray zone plate, imaging props., manufacturing inaccuracies effects 4-63844  
warm carrier device with thin film antenna for CO<sub>2</sub> laser detection, fabrication 4-73507  
X-ray zone plates, fabrication by electron beam lithography and reactive ion etching 4-90701  
Au, electroplating and nanometer e-beam lithography for mag. flux quantisation measurements 4-73455  
Nb thin film point contact Josephson junctions, fabrication by magnetron sputtering and electron beam lithography 4-80721  
YIG film artificial anisotropic waveguides, sputter etching 4-83694

**electron beam machining**

No entries

**electron beam welding**

- Mo-Hf-C, electron beam welded joint, tensile strength, ductility, comp. depend. 4-109470  
Mo-Nb-C, electron beam welded joint, tensile strength, ductility, comp. depend. 4-109470  
Mo-Re-C, Z 4-109470  
Ti, pure, electron beam welding, mech. props., fusion reactor appls. 4-109471  
Ti-Al-V (6, 4 wt.%), electron beam welding, mech. props., fusion reactor appls. 4-109471

**electron beams***see also electron impact; electron optics; Schwarz-Hora effect*

- acceleration by laser, dynamics of synchronisation 4-69479  
angular spread of magnetized relativistic electron beam determ., from passage through micro-openings 4-74077  
annular, performance with magnetically insulated splitter 4-59970  
annular, prod. on Gamble II using magnetically insulated splitter 4-59969  
autoaccelerator for ICF 4-60755  
biprism interferences with 1 MeV electrons from monofile Van de Graaff generator 4-107503  
cathode materials for high brightness electron beams 4-71508  
charged particle energy analysers with wedge-shaped electrode 4-91395  
collisionless relaxation of a cold high-current electron beam 4-69298  
current meas., Faraday cage, rotary motion 4-82866  
current modulation in light wave field at interface between two media 4-74409  
diagnostic technique using optical fibres 4-78742  
dielectric lined waveguide, microwaves excitation by relativistic electron beam 4-60718  
differential pumping system for electron beam system 4-86429  
diffusion theory of energy losses of electrons bombarding a target 4-98160  
Doppler-shift dominated cyclotron masers, efficiency, thermal effects 4-74473  
dual-feed low inductance diode development 4-113230  
electron spontaneous emission in relativistic nonneutral electron beam 4-79021  
electrostatic wedge analyzer with a cubic field 4-91396  
EM wave induced scatt. with relativistic energy dispersion 4-69294  
energy deposition meas. of intense relativistic electron beam, gas laser excitation appl. 4-69297  
energy spread and angular scatter in foilless diodes 4-69967  
equations for electron trajectories perturbed by small changes in the initial conditions and geometry of electron-optical systems 4-96780  
fine-focused electron beam profile meas. using semiconductor detector 4-87263

**electron beams continued**

- free electron generators of coherent radiation, conf., Orcas Island, WA, USA (June 1983) 4-82588  
free electron laser, long pulse, driven by linear induction accelerator 4-87348  
free electron laser, MM wave, radiation growth in collective regime, freq. resolved meas. 4-60054  
free electron laser oscillator expt. at Los Alamos electron beam diagnostics 4-83604  
free electron lasers, bright electron beams 4-87347  
free electron tapered-wiggler laser, large electron-beam energy extraction 4-83588  
glow-discharge-created electron beams 4-95560  
high current electron ring dynamics in conventional betatron accelerator 4-74069  
high-current beams formation in modified betatron fields 4-96305  
hose instabilities in rot. electron beams, model 4-69904  
induced interaction of electron beam with superstrong EM radiation at boundary of two media 4-107706  
lasers using electron beams 4-74532  
linear induction accelerator, diaphragmed electron beams, stability 4-96301  
low energy electrons, electron-electron interactions in finely focused beams 4-87262  
low-impedance high power electron beam diodes investigation 4-112012  
magnetic insulation time for coaxial diodes 4-73580  
magnetized high-intensity electron beam, cyclotron resonance of pumping wave, induced rad. 4-69293  
modulated Gaussian beams 4-83531  
nonlinear effects, relativistic electron beams, numerical simulation, inertial fusion 4-107502  
nonlinear implicit code for relativistic electron beam tracking studies 4-102421  
nonlinear theory of the instability of an electron-ion two-beam system 4-87266  
optics, development trends, appls. (*Chinese*) 4-83536  
parametric generation in electron beams 4-102872  
picosecond current pulse formation method using microwave deflector 4-68857  
pinched, axisymmetric instability 4-69905  
pinching electron-ion beam, quasi-equilib. states 4-69941  
potential electrostatic beams, thermoemission conditions at cathode, exact solns. 4-102869  
production with grid plasma emitter, low-pressure arc use 4-69966  
profile meas. of finely focused electron beams, in SEM 4-58919  
pulsed, high-current, uniform, prod. by plasma grid emitter systems 4-68322  
quantum coherence in electron beams 4-112338  
relativistic, high current, transport in dielec. channels 4-102871  
relativistic, propag. in gases, return. current 2-dimens. mapping 4-69301  
relativistic charged particle radiation in crystals, unified theory, quantum mech. treatment 4-96765  
relativistic electron beam, charge-neutralised, steady states in mag. quadrupole system 4-107505  
relativistic electron beam equilibria, radially confined, appl. to longit. wiggler free electron laser 4-112447  
relativistic electron beam in coaxial waveguide, diocotron instability conditions 4-96778  
relativistic electron beam in dielectric medium 4-64663  
relativistic electron beams, confined, diocotron instabilities 4-107506  
relativistic electron beams, neutralised, injection near plasma-filled half-space 4-103517  
relativistic electron beams, slipping instability 4-74407  
relativistic electron beams parametric interaction with EM waves, polarisation effects 4-96767  
relativistic electron scatt. in EM field, radiation scatt., photon statistics 4-112368  
relativistic heavy-current beam dynamics in an external mag. field (*Ukrainian*) 4-87258  
relativistic partly neutralised electron hollow beam, accelerating process 4-86983  
relativistic-electron helical trajectories in combined uniform axial and helical mag. fields, instability 4-83529  
secondary emission multiplication in microwave elec. fields 4-107500  
slow wave cyclotron amplifier, nonlinear efficiency and bandwidth 4-96313  
solar flares, unimportance of beam momentum in electron-heated models 4-101279  
source of HV glow discharge, geometric parameters control (*Russian*) 4-68320  
special relativity, calorimetric test using electron beams 4-63504  
storage ring, transverse electron-ion instability (*Russian*) 4-83258  
student experiments using fine-beam CRT 4-58611  
Thomson-scattering experiment to determine parallel vel. spread in intense relativistic electron beam 4-96776  
TM waves stimulated scatt. by strongly magnetised relativistic ribbon electron beam, nonlinear theory 4-74403  
tomographic technique in relativistic electron beam experiments 4-112029  
transmission of electron beam through wedge-shaped diode 4-107504  
transport in unidirectional field of uniform density beam with nonuniform velocity (*Russian*) 4-79024  
unguided wave Cherenkov amplifier 4-102913  
University of California free electron laser wiggler props. 4-83605  
variable emittance filter for electron laser facility 4-82859  
LaB<sub>6</sub> long-life emitter for electron beam generation 4-86501

**electron bombarded semiconductor devices**

- Si:B solar cell, electron irradi., photon effects 4-93618  
a-Si:H p-i-n devices, EBIC decay 4-92796

**electron capture***see also charge exchange; electron attachment*

- dielectronic recombination, complex-pot. model 4-96695  
fast projectile large-angle scatt., electron capture theory 4-107449  
glass, electron-irradiated, discharge phenomena 4-71277  
hydrogenic ion, electron capture by fully stripped ion, relativistic second Born approx. 4-87209  
inert gas atom-ion electron capture collisions, recoil charge distrib. 4-59892  
ion-atom collisions, electron capture, symmetries -eikonal-type approx. 4-83464

iron capture continued  
 light ion impact, K-shell ionisation cross sections 4-99258  
 multiply charge ion-gas target collision, charge transfer cross sections 4-102789  
 potential model for estimating exchange effects 4-96689  
 relativistic heavy ion-atom collisions, radiative capture obs. 4-96679  
 supernovae, electron capture role 4-63189  
 Ar+Si<sup>13,14+</sup>, single and multiple electron capture, K X-ray production 4-102785  
 Ar<sup>2+</sup>+He(He), electron capture reactions studied by means of double translational spectroscopy 4-96686  
 Ar<sup>3+</sup>+Ar, electron capture reactions studied by means of double translational spectroscopy 4-96686  
 Au<sup>8+</sup>+He, electron capture, ionisation and transfer ionisation cross sections 4-78960  
 C<sup>q+</sup>, (q=6, 5, 4), incident on inert gas atoms, K-Auger electron prod. 4-78818  
 Ca II, reson. electron capture to high Rydberg states 4-112268  
 ClNO<sub>3</sub>, thermal energy electron capture, ECR study 4-91340  
 F<sup>q+</sup>, (q=9, 8, 7), incident on inert gas atoms, K-Auger electron prod. 4-78818  
 F<sup>q+</sup>+He(He), K Auger-electron prod. cross sections, charge-state depend. 4-96693  
 Ga<sub>2</sub>O<sub>3</sub>:Cr crystals, luminesc. parameters, impurity centre electron capture effects 4-81016  
 H atoms, electron capture by fully stripped ions, intrashell mixing and Stark effect 4-59888  
 H+Be<sup>4+</sup>(B<sup>3+</sup>)(C<sup>2+</sup>)(N<sup>7+</sup>)(O<sup>8+</sup>) electron capture cross-sections calcs. 4-102791  
 H+C<sup>2+</sup>(C<sup>3+</sup>) ions, state-selective electron capture, translational energy spectroscopy 4-59891  
 H+C<sup>4+</sup>(N<sup>3+</sup>)(O<sup>6+</sup>) electron capture, 0.25-25 keV amu<sup>-1</sup> 4-69205  
 H+C<sup>q+</sup>(N<sup>q+</sup>)(O<sup>q+</sup>) ions, electron removal cross section 4-83460  
 H+fully stripped ion, final-states mixing following slow collision, electron capture 4-107451  
 H+H<sup>+</sup> collisions, reson. electron transfer from Rydberg atom 4-74329  
 H+He<sup>2+</sup>(Be<sup>3+</sup>)(B<sup>3+</sup>)(C<sup>2+</sup>)(N<sup>7+</sup>)(O<sup>8+</sup>) collisions, electron transfer, at orbital expansion description 4-78962  
 H+Li<sup>2+</sup>(Li<sup>3+</sup>), electron capture by fast ions 4-91343  
 H+X<sup>2+</sup> charge transfer collisions, long-range secondary couplings 4-102790  
 H<sup>+</sup>+H(He), electron capture, symmetries eikonal-type approx. 4-83464  
 H<sup>+</sup>+H(He) Thomas peak in electron capture 4-96692  
 H<sup>+</sup>+H(He) reson. electron capture, T-matrix element calcs. 4-102792  
 H<sup>+</sup>+He, electron capture, coherent excitation, multiple scatt. approach 4-87212  
 H<sup>+</sup>+He(He), electron capture cross sections 4-69200  
 H<sub>2</sub><sup>+</sup> existence investig., rel. to form. by electron capture 4-74331  
 H<sub>2</sub><sup>+</sup> dissociative electron capture, velocity dist., vibrational excitations 4-85207  
 H<sub>2</sub>+C<sup>+</sup>, charge transfer, polarised light emission 4-83463  
 H<sub>2</sub><sup>+</sup> existence investig., rel. to form. by electron capture 4-74331  
 HNO<sub>3</sub>, thermal energy electron capture, ECR study 4-91340  
 He, double ionisation by collisions with fast, fully stripped ions 4-112265  
 He, positron impact electron capture, differential and total cross-sections calcs. 4-107447  
 He<sup>n+</sup> (n=0, 1, 2), electron loss and capture in various media 4-69206  
 He+C<sup>4+</sup>(N<sup>4+</sup>)(O<sup>4+</sup>)(F<sup>4+</sup>)(Ne<sup>4+</sup>)(Kr<sup>4+</sup>), one-electron capture at low energies, Landau-Zener model calcs. 4-96685  
 He+C<sup>4+</sup>(N<sup>4+</sup>)(O<sup>4+</sup>) ions, electron removal cross section 4-83460  
 He+H<sup>+</sup>(e<sup>+</sup>), electron capture, differential and total cross-sections calcs. 4-107447  
 He<sup>+</sup>+neutral ats., charge transfer in low-energy collisions 4-74326  
 Li isoelectronic series, radiative decay following charge exchange on neutral gas targets 4-87069  
 Li+Ar<sup>q+</sup>(Ne<sup>q+</sup>)(Kr<sup>q+</sup>)(Xe<sup>q+</sup>) collisions, q=2 to 10, electron capture cross sections from slow projectiles 4-74328  
 Li+H<sup>+</sup>(He<sup>+</sup>)(He<sup>2+</sup>) collisions, single electron capture 4-74327  
 Li<sup>3+</sup>+neutral ats., charge transfer in low-energy collisions 4-74326  
 Li<sup>2+</sup>+C<sup>2+</sup>(N<sup>3+</sup>)(O<sup>4+</sup>) core-conserving electron capture ion excitation, metastable fraction meas. 4-83465  
 N<sup>-</sup> existence investig., rel. to form. by electron capture 4-74331  
 N<sup>q+</sup>, (q=7, 6, 5), incident on inert gas atoms, K-Auger electron prod. 4-78818  
 N<sup>6+</sup>+He, transfer ionisation and two-electron capture processes at 3-34 keV energies 4-96688  
 N<sup>6+</sup>+He (H<sub>2</sub>), electron capture in autoionising configurations, N<sup>4+</sup> studied by electron spectrometry 4-59889  
 N<sub>2</sub><sup>+</sup> existence investig., rel. to form. by electron capture 4-74331  
 Ne<sup>0</sup>+Br<sup>7+</sup>-Br<sup>n+</sup>+Ne<sup>q+</sup>, contribution of K-capture to Ne<sup>q+</sup> production 4-83466  
 O<sup>q+</sup>, (q=8, 7, 6), incident on inert gas atoms, K-Auger electron prod. 4-78818  
 O+H<sup>+</sup>(H<sup>-</sup>), electron capture, electron loss, excitation 4-64590  
 Xe<sup>+</sup>+Xe collisions using decelerated heavy ions from GSI-UNILAC 4-87207

electron capture, nuclear see nuclear electron capture

electron density  
 see also carrier density; current density; electron density (metals); plasma density  
 acetylene, mag. props. and induced current density, HF calcs. 4-78767  
 Ar I and II systems, collisional radiative coeffs. of 4p groups 4-65059  
 atoms, electronic density of the nucleus, bounds calcs. 4-68935  
 auroral electron density vars., power spectra rel. to electron drift vel. in eastward electrojet 4-72777  
 auroral kilometer radiation-aurora correlation, electron density anal. 4-90039  
 conference on beacon satellite studies of ionosphere, at New Delhi, India (February 1983) 4-86110  
 D-region, electron density profile estimation with VLF refl. coeffs., improved technique (Japanese) 4-85827  
 dense plasma effects on dielectric satellites to the 1:s<sup>2</sup> 1, S<sub>0</sub>-1 s<sup>2</sup> p<sup>1</sup> P<sub>1</sub> line in a laser plasma 4-113193  
 diverted ASDEX discharges, particle balance 4-97855  
 divertor and boundary layer of tokamak, Mach number from probe meas. 4-97866  
 divertor discharges, electron density and temperature meas. 4-97841  
 divertor equilibria, edge particle recycling, improved energy confinements 4-97849  
 divertor plasma D-III, numerical model 4-97860

electron density continued

E-region, EISCAT data rel. to GEOS-2 electron flux vars. 4-100857  
 E-region, electron gas heating due to magnetosphere convection, effect on cond. 4-100847  
 EBT, birth of new folds and competing point attractors 4-65122  
 ECRH, transport simulation in Heliotron E using 1-D code 4-65056  
 electron content irregularities and UHF/SHF scintillation at Ascension Island 4-90030  
 electrostatic stability of nonrelativistic non-neutral electron flow in cylindrical diode 4-91902  
 equatorial spread-F irregularities, control of VHF nighttime scintillations 4-90031  
 ethylene, singularities of mag. field induced electron density 4-78764  
 ethylene positive column electron density from neutral gas temp. (Russian) 4-75118  
 F<sub>1</sub>-layer, electron density var. due to distant plasma instabilities on mag. field lines 4-85817  
 F<sub>2</sub>-layer, electron density modulation by 160-minute solar pulsations rel. to micropulsation amplitudes 4-105803  
 F<sub>2</sub>-layer ionospheric electron content of Wuchang, China, VHF obs. 4-115659  
 F-region, polar, ohmic heating by HF pulses, effects on electron density and temp. 4-85814  
 interstellar scintillation of pulsars emission, electron density var. 4-94919  
 ionic radicals, semiempirical model of exchange polarisation mechanism of transferred hyperfine interaction 4-112105  
 ionosphere, elec. field and plasma density meas. in auroral electrojet 4-72783  
 ionosphere, electron content at low latitudes, day-to-day var. 4-90036  
 ionosphere, electron density depletion at high latitude, EISCAT meas. 4-100858  
 ionosphere, 'electron density' profiles, effects of longitudinal currents 4-94289  
 ionosphere, plasma drift instabilities and auroral rays mechanism 4-94286  
 ionosphere, plasma electron density and vel. near electron-injecting satellite 4-110353  
 ionosphere, test of International Reference Ionosphere using single-freq. AI absorpt. data 4-90020  
 polar ionosphere, UHF scintillation evidence for HF-produced electron density irregularities 4-105794  
 ionosphere, validity of George's method for reducing AI absorpt. data 4-90019  
 ionosphere bubble, radiowave propag. and pulse distortion 4-90032  
 ionosphere electron content determ., use of geodetic Doppler receivers 4-90009  
 ionosphere electron content var. during mag. storms, effect on VHF equatorial scintillations 4-90034  
 ionosphere electron content var. throughout solar eclipses, satellite beacon obs. 4-90038  
 ionosphere F-region, recombination dynamics rel. to electron density 4-110352  
 ionosphere irregularities, VHF/UHF and amplitude scintillation fast Faraday polarisation var. 4-90033  
 ionosphere plasma irregularities anal. from scintillation obs. 4-90029  
 ionosphere total electron content, NAVSTAR L band ionospheric calibration rel. to Faraday rot. meas. 4-90010  
 ionosphere total electron content over E Mediterranean, spatial var., Faraday rot. obs. 4-90037  
 ions, electronic density of the nucleus, bounds calcs. 4-68935  
 methane, mol. electron density, fitting method 4-74143  
 methane plasma diagnostics and modelling, use in CVD growth of a-C films 4-104979  
 molecules, electron density, electrostatic field characts., machine graphics methods 4-84123  
 molecules, fitting method 4-74143  
 neutral system, numerical collisional radiative model 4-91868  
 planetary nebulae, electron density determ. using Si III UV emission line strengths 4-94583  
 plasma density from Fe XVIII-XXIII 8-14 nm lines 4-87927  
 plasma impurity influx in Tokamak 4-65117  
 plasma in Nagoya bumpy torus, heavy ion beam probing 4-60684  
 plasma RF confinement by two cylindrical electrodes 4-108199  
 plasmopause characts. at 6.6 R<sub>E</sub>, GEOS 2 relaxation sounder data 4-67559  
 porphyrin dianions+H<sup>+</sup> donors (alkyl halides), reaction products electron density distrib. 4-107284  
 protonosphere electron content, depletion and recovery during geomag. storms 4-90041  
 scrape-off layer, impurity flux meas. in TCA tokamak 4-97840  
 scrape-off layer of ASDEX plasmas, temporal behaviour of electron density profile 4-97755  
 solar wind electron density determ. from solar radio burst anal. 4-77687  
 spheromak formation and operation 4-65115  
 Sun, sunspots, EUV spectra anal. and plasma characts. 4-94719  
 Tokamak plasma, FT-1, discharge parameters effect on impurity transport 4-69948  
 transition metal carbides, nitrides and oxides, structural defects, influence on character of mutual solubility 4-113643  
 travelling ionospheric disturbances effect on radio interferometry 4-90095  
 UV spectroscopic electron density diagnostics, multidensity plasma effects 4-94574  
 Venus, ionosphere, daytime, radiowave refr. and vertical electron density 4-77744  
 Venus ionosphere, transterminator flow, electron temp. and density models 4-67659  
 whistler mode trapping in magnetospheric ducts 4-105808  
 HF, mol. electron density, fitting method 4-74143  
 H<sub>2</sub>O, mol. electron density, fitting method 4-74143  
 He-like ions, electronic density of the nucleus, bounds calcs. 4-68935  
 NH<sub>3</sub>, electron density, fitting method 4-74143  
 PH<sub>3</sub>, electron density, fitting method 4-74143

electron density (crystallography) see crystallography

electron density (metals)

binary alloys, electronegativity in local density functional formalism 4-70061  
 Al, charge densities, interionic pot., phonon freq., calcs. 4-113856  
 Al-Mg(Ga)(In)(Si)(Ge)(Sn), distribution of electric field gradients around impurities, conduction electron screening lattice strain 4-113910  
 Cu films, CO-covered, optical and elect. props. 4-80693

- electron density (semiconductors and insulators)** *see carrier density*
- electron density of states** *see electronic density of states*
- electron density of states (condensed matter)** *see electronic density of states*
- electron detachment**
- acetaldehyde enolate anion, dipole-band states, photodetachment threshold study 4-87168
  - negative ions, electron detachment in slow collisions with atoms 4-69198
  - $\text{Ar} + \text{H}^-(\text{Li}^+)(\text{Na}^+)(\text{K}^-)$ , electron detachment cross sections 4-78952
  - $\text{Cl}_2 + \text{Cl}^-(\text{Br}^-)(\text{I}^-)$  charge transfer and electron detachment, absolute total cross-sections meas. 4-69202
  - D-, very-low-energy electron detachment 4-91336
  - H-, rare gas collisions, electron detachment 4-102766
  - H-, very-low-energy electron detachment 4-91336
  - $\text{H}^+ + \text{Ar}(\text{He})$ , electron detachment, energy spectra, Born approx. 4-83459
  - $\text{H}^+ + \text{He}$ , electron detachment in slow collisions 4-69198
  - $\text{H}^+ + \text{He}(\text{Ar})(\text{H}_2)(\text{O}_2)(\text{CO}_2)$ , electron detachment and charge exchange to shape resonances 4-69203
  - $\text{He}^+(n=0, 1, 2)$ , electron loss and capture in various media 4-69206
  - $\text{He} + \text{H}^-(\text{Li}^+)(\text{Na}^+)(\text{K}^-)$ , electron detachment cross sections 4-78952
  - $\text{Ne} + \text{H}^-(\text{Li}^+)(\text{Na}^+)(\text{K}^-)$ , electron detachment cross sections 4-78952
  - $\text{SF}_6$  negative ions, electron detachment and its importance in elec. breakdown 4-91337
- electron detection and measurement**
- calorimeter, prototype end plug gas,  $\pi/e$  separation 4-59534
  - CR-39 plastic track detectors, formation of etchable tracks by delta-ray 4-96327
  - detectors, use of microprocessors 4-111999
  - dosimetry associated with the beam scanning technique in linacs, approach to overcome inconveniences 4-100323
  - dosimetry with thermally stimulated exoelectron emission 4-115224
  - EELS spectrometer, detector efficiency 4-63828
  - electron-positron spectrometer using lamphshade magnet 4-68871
  - electrostatic electron spectrometer with electron retarder and double cylindrical mirror analyser 4-74086
  - flight-time detector with KBr as the sensitive substance 4-74097
  - high resolution angle-resolved photoelectron spectrometer system 4-91146
  - hybrid detector telescope, response to monoenergetic positrons and electrons 4-102516
  - incident photon flux monitor for synchrotron radiation 4-91175
  - ion beam image formation in gelatine and various polymers 4-96339
  - ionisation chamber, collection efficiency in a pulsed and mag. swept electron beam 4-109938
  - Kodak CN-85 detectors, dyed track method, electron appl. 4-96340
  - lead glass drift calorimeter design, Monte Carlo studies 4-64275
  - multilayer spherical ring positron emission tomography, mega-channel coincidence circuit 4-74122
  - NBS electron storage SURF-II, direct determ. of stored electron beam current 4-64250
  - NIKHEF-K  $180^\circ$  electron-scatt facility overlapping-scintillator system 4-102450
  - polythiophene, conducting polymer, electron beam irradi. in  $\text{SF}_6$  gas, elec. and optical props., radiation detector appl. 4-75531
  - positron camera, spatial sensitivity and detection efficiency 4-62567
  - potable water in Saudi Arabia, material radioactivity 4-89789
  - proportional counter, electron drift time between electrodes meas. 4-68903
  - proportional electron detector for nuclear gamma-resonance spectroscopy 4-86448
  - QDD spectrometer system, design, performance 4-91140
  - scintillation counter, electron detector with low  $\gamma$ -ray sensitivity 4-91164
  - scintillation glass shower counter, energy resolution of 1-25 GeV positions 4-59529
  - scintillation hodoscope spectrometer for electrons and high-energy photons 4-59487
  - SEM, electron signal and detector strategy 4-63830
  - streamer tracks in Ne obs. under pressure 4-74110
  - tapered cell drift-chamber, prototype development and testing with e beam 4-102539
  - twin BGO detectors for high resolution positron emission tomography 4-74105
  - (e,2e) spectrometer for investigating the spectral momentum density of thin films 4-111257
  - $\pi/e$  discrimination with a Pb-liquid Ar calorimeter, LEP ELECTRA appl. 4-74100
  - Pb scintillator shower counter, Si photodiode readout 4-74102
  - Si detectors, passivated and ion-implanted 4-112038
  - n-Si surface barrier high resolution detectors for  $<20$  keV conversion electrons 4-74103
  - p-Si: P surface-barrier detectors fabrication and appl. 4-87018
  - Xe liquid in ionisation chamber, spectrometry of 1 MeV electrons 4-107263
- electron device noise**
- 1/f noise in semicond. materials and devices, comparison of theories 4-65719
  - avalanche photodiodes with separate absorption, grading and multiplications, excess noise statistics meas. 4-112587
  - coupled cavity semiconductor lasers, detuned loading and quantum noise 4-112418
  - cryogenic broad-band ultra-low-noise Schottky diode mixer receiver from 80 to 115 GHz 4-85875
  - fast photoconductive detector, new minority hole sinked photodetector with 80 ps fall time 4-69592
  - Josephson junction, current-driven, microwave induced steps 4-65772
  - MM-wave superconducting tunnel junction receiver for 2.6 mm 4-77714
  - PIN-FET receiver for fibre optics 4-74744
  - semiconductor device noise, Monte Carlo particle modelling 4-65720
  - R-SQUID, RF-biased, noise thermometer, low freq. impedance, tank circuit influence 4-58849
  - PR-SQUID, RF-biased, noise thermometer, noise props. 4-58850
  - V-channelled substrate inner stripe lasers in single-longitudinal mode, low-noise characs. 4-96910
  - AlGaAs CSP-type lasers, linewidth enhancement estimation method 4-83577
  - AlGaAs laser, 0.8  $\mu\text{m}$ , spectral width with 1/f noise 4-96892
  - AlGaAs laser oscillating in single longit. mode, LF feedback noise 4-96909
  - GaAs JFET low-noise high-speed optical receiver for optical fibre systems 4-74743
  - HgCdTe 0.1 eV photoconductive detector, optimum thickness 4-111204
- electron device noise continued**
- HgI<sub>2</sub> large area photodetectors 4-59562
  - NbN granular Josephson microbridges, noise props., freq. mixer appl. 4-70995
  - $\text{Pb}_{1-x}\text{Sn}_x$  Te diodes, excess noise rel. to I-V characs. 4-61426
  - W field emission gun, emission noise, anode cleanliness effect 4-78437
- electron device testing**
- see also electron tube testing; integrated circuit testing; semiconductor device testing*
  - laser diodes for undersea transmission systems, screening method 4-69477
  - MCP in windowless EUV photon detectors, lifetime testing results 4-64297
- electron diffraction**
- see also electron diffraction crystallography; electron diffraction examination of materials; gas phase electron diffraction; high energy electron diffraction; low energy electron diffraction*
  - amorphous electron microscope objects, elastically and inelastically scattered electrons 4-60790
- electron diffraction crystallography**
- see also crystal atom structure; Debye-Waller factors; electron diffraction examination of materials*
  - analytical electron microscopy, imaging, chem. anal. and microdiffr. 4-108255
  - automatic computer anal. of diffraction patterns 4-60792
  - bent crystal, high resolution structure images around pole pattern 4-113277
  - biological and plastic materials, elastic and inelastic electron scatt., Monte Carlo calcs. 4-97976
  - channelling microscopy technique, obs. of crystallographic contrast in polycrystals (Chinese) 4-60789
  - conference, Hamburg, Germany (Aug. 1984) 4-106107
  - convergent beam diffr., lattice parameter and cryst. symmetry appls. (French) 4-88041
  - convergent beam electron diffr., struct. studies of Ni superalloys 4-88132
  - convergent beam electron diffr. and optical reconstruction, conf., Liege, Belgium (May 1983) 4-86107
  - convergent beam electron diffr. determ. of point and space groups (Japanese) 4-92033
  - convergent beam electron diffraction, cryst. struct. and defect appls. 4-79906
  - convergent beam electron diffraction, recent developments 4-88042
  - convergent beam electron diffraction, struct. refinement 4-79907
  - convergent beam electron diffraction, theory and practice (French) 4-88039
  - convergent beam electron diffraction analysis, use of reciprocal lattice layer spacing 4-113272
  - convergent beam electron diffraction using electron hollow-cone illumination 4-60791
  - crystals, diffuse scatt. and struct. fluctuations (Japanese) 4-113265
  - diffraction spot patterns, computer storage via digitising pad 4-69993
  - double diffraction pattern indexing for decomposing  $\text{CdI}_2$  and  $\text{CdBr}_2$  4-108252
  - electron microscope for convergent beam diffr. and high resolution imaging 4-106432
  - inelastic electron diffr., implications of (e,2e) scatt. 4-103613
  - inelastic electron diffr., implications of (e,2e) scatt. 4-103614
  - JEOL 200CX electron microscope, combined electron diffr. and high resolution imaging 4-95580
  - MEED intensities calc. in 5-10 keV electron energy range 4-79904
  - microscopy and anal., conference, Guildford, England (Aug.-Sept. 1983) 4-78034
  - phase transformation studies, use of electron microscopy, and electron diffraction 4-113281
  - Philips EM400T analytic microscope, combined electron diffr. and high resolution microscopy 4-95581
  - photoelectron diffraction in surface structure determ., review 4-97977
  - polycrystalline specimens, multiple-beam diffr. of fast electrons, calc. of reflected intensities 4-113273
  - positron spectroscopy applied to surface analysis 4-71493
  - proteins, negatively stained, dynamical electron scatt. calcs. 4-100085
  - real space high resolution images, tridimensional effects (French) 4-88040
  - surface, stepped, electron and atom diffr. anal. 4-65530
  - tilted cryst., convergent beam diffraction patterns, asymmetry 4-79905
  - Mo (100), Kikuchi patterns, primary electron localisation 4-84130
  - Ni (001), adsorbed S, core-level azimuthal photoelectron diffr. 4-109306
  - Ni (001), adsorbed S, intermediate energy azimuthal X-ray photoelectron diffr. 4-109307
  - Ti surface, basal plane, low-energy electron current image diffr. 4-65531
- electron diffraction examination of materials**
- see also gas phase electron diffraction; high energy electron diffraction; low energy electron diffraction; reflection high energy electron diffraction*
  - alkaline earth-ferrite glasses, glass forming region and  $\text{Fe}^{3+}$  coordination (Japanese) 4-113348
  - atomic clusters, helical, electron diffr. patterns, computer simulation (French) 4-59940
  - bicrystal model, expansion at large angle grain boundaries, electron diffr. calcs. 4-84519
  - bicrystals, symmetry determ. using convergent beam electron diffr. 4-80431
  - 2-bromo-1,3,2-dioxarsolane, mol. struct. by electron diffr. 4-112292
  - 2-bromo-1,3,2-dithiarsolane, mol. struct. by electron diffr. 4-112292
  - catalyst dispersed particles, stacking faults and struct., electron microdiffr. studies 4-88178
  - 2-chloro-1,3,2-dioxarsolane, mol. struct. by electron diffr. 4-112292
  - chlorotrifluoromethane, stretching and bending anharmonicity, electron diffr. study 4-69042
  - conference on electron crystallography of macromols., Phoenix, USA (Aug. 1983) 4-95054
  - crotonin complex thin cryst., expt. strategy in 3D struct. determ. 4-100416
  - cyclobutanone, mol. struct., electron diffr. and spectrosc. obs. 4-59893
  - cytochrome oxidase, crystalline, selective contrast in electron microscopy 4-100419
  - DNA, electron crystallographic studies 4-100074
  - FCC/BCC interfaces, semicoherent and incoherent, electron diffr. obs. of dislocation arrays 4-70160
  - ferritin, horse-spleen, electron phase-contrast imaging 4-100066

## electron diffraction examination of materials continued

- glycoproteins, variables surface, of *Trypanosoma brucei*,  $\alpha$ -helical coiled-coil struct., 4-115011  
 graphite/metal mixtures, diamond form: under shock compression and flash heating 4-108516  
 p-hydroxybenzoic acid, aromatic polyester PHBA, ordering and topotactic transitions 4-65197  
 IN-738LC, Ni-base superalloy, precip. of  $\beta$  phase in  $\gamma$  particles 4-114559  
 metallic thin films, crystal growth, initial steps, microscopic studies 4-98486  
 methane, clusters, electron diff. patterns 4-74367  
 n-paraffins, electron beam damage quasi-thermal mechanism, electron diff. studies 4-98135  
 phase transformation studies, use of electron microscopy and electron diffraction 4-113281  
 PMMA:Si ion implanted film, struct. anal. using differential etching 4-79951  
 PMMA positive electron resist, crystal. struct. and sensitivity 4-98031  
 poly(cyclopentane- $\beta$ -carboxyamine), crystalline struct., electron diff. study 4-84214  
 polyacetylene, oriented crystalline, Durham prep. in stress field, morphology and struct. 4-66300  
 polyacetylene, single-fibre, prod. and struct. 4-114469  
 polyacetylene, conducting polymer, synthesis by  $\gamma$ -ray polymerisation 4-75958  
 polyvinylidene fluoride-PMMA blends, melting pt., crystalline morphology, light scatt. obs. 4-84217  
 proteins, soluble, specimen prep. methods for electron crystallography 4-100415  
 rare earth metal thin films, struct., effect of ion irradi. 4-70240  
 steel, alloy, secondary hardening mechanisms 4-99396  
 steel, dual-phase, dislocation substruct. as function of strain 4-99435  
 steel, ferritic, low alloy, carbide precip.,  $\text{Mo}_2\text{C} \rightarrow \text{M}_6\text{C}$  transform. 4-66344  
 steel, ferritic stainless, stabilisation breakdown 4-114718  
 thin films, spectral momentum density obs. using ( $e, 2e$ ) spectrometer 4-111257  
 transition metal nitrides, ultrafine particles, growth by reactive gas evaporation technique with electron beam heating 4-61894  
 VA transition metal oxides of V, Nb, and Ta, oxidation mechanism, phase form., cryst. struct., electron microscopy, electron- and X-ray diff. studies 4-62119  
 $\beta^{\text{II}}$ -Mg-Si-Al-O-N system, X-ray and electron diff., rhombohedral struct. 4-65246  
 Ag films and particles on MgO, surface diffusion under intense electron irradiation 4-98412  
 AgInTe<sub>2</sub> thin films, flash evaporation growth, X-ray and electron diff. characterisation 4-114408  
 Ag<sub>2</sub>TaS<sub>3</sub>, Ag intercalation, electron diffraction studies 4-80068  
 Al, liq., chem. reaction with B fibres 4-61891  
 Al, rare gas bubble press. and density, EELS, TEM obs. 4-113508  
 Al thin film, laser induced melting, time resolved picosecond electron diff. study 4-88269  
 Al-Ag(In)<sub>3</sub>Sn systems, mixing behaviour study by Ar ion beam irradiation 4-65402  
 Al-Cu system, metastable states controlled by diffusion 4-65463  
 Al-Cu-Mg-Ag, precipitate struct. and orientation relationship, effect of Ag additions 4-93303  
 Al-Mg-Si alloys, transitional state formation by diffusion 4-61135  
 Al-Mn-Zr, rapidly quenched from melt transform. behaviour 4-81185  
 Al-Ti long-period one-dimensional antiphase structures, electron diff. and microscopy, X-ray diff. 4-113398  
 $\beta^{\text{II}}$ -Al<sub>2</sub>O<sub>3</sub>:MgO, long-period polymorph, microtwins, selected-area electron diff. obs. 4-103770  
 Ar, clusters, electron diff. patterns 4-74367  
 As<sub>2</sub>S<sub>3</sub> chalcogenide films, solvent-cast morphology and thermal props. 4-84530  
 (Au,Ag)Te<sub>2</sub>, krennerite, modulated struct., electron microscopic studies 4-108319  
 Au small particles, crystalline struct., STEM microdiffraction studies 4-108305  
 Au/Cu bilayers, ion-induced solid solutions and ordered cpd. form. 4-108470  
 Au<sub>2</sub>Mn<sub>2</sub>, long period antiphase boundary struct., electron diff., electron microscopy obs. 4-103946  
 B fibres, chem. reaction with liq. Al 4-61891  
 BN, films, interaction with Ni at high temps. 4-70583  
 Ba<sub>3</sub>Cs<sub>2</sub>Ti<sub>18</sub>O<sub>40</sub>, hollandite-related superstructures 4-70085  
 BaFe<sub>2</sub>O<sub>19</sub> ferrite, M phase, superstruct. obs. 4-84275  
 Ba<sub>2</sub>NaNb<sub>2</sub>O<sub>15</sub>, tetragonal bronze-like struct., modulated phases and domain struct. 4-113616  
 BaTiO<sub>3</sub> thin films, crystallisation from amorphous phase, electron microscope study 4-113830  
 C films, diamondlike, ionized deposition from methane gas 4-65586  
 C:H amorphous film, H<sub>2</sub> gas reactive RF sputtering prep. on low-temp. substrates 4-76673  
 C:H amorphous film prep. by H<sub>2</sub> gas reactive RF sputtering of graphite 4-76671  
 CO<sub>2</sub>, thermal averages, effective harmonic oscillator method appl. 4-112153  
 CS<sub>2</sub>, thermal averages, effective harmonic oscillator method appl. 4-112153  
 Ca<sub>2</sub>LaFe<sub>2</sub>O<sub>8+x</sub>, cryst. struct. determ. 4-80014  
 CdI<sub>2</sub>(Br<sub>2</sub>), partially decomposed, electron double diff. pattern indexing 4-108252  
 Cd<sub>1-x</sub>Mn<sub>x</sub>Te, atomic layer epitaxial growth on CdTe(111)B substrates 4-76676  
 CeAl<sub>3</sub>, phonon softening, neutron scatt. studies 4-92318  
 Co-Al<sub>2</sub>O<sub>3</sub> coevaporated composite films, solar selectivity 4-72169  
 Co-base alloy coating, contact fatigue resist. 4-93426  
 Cr films electroplated on (001) Cu substrates, misfit twins and dislocations 4-108748  
 Cu-Be (1.0 wt.%), aged, twinned microstruct. 4-89070  
 Cu-Ni-Sn alloys, spinodal decomposition, applied stress effects 4-114551  
 $\beta$ -Cu-Zn-Al,  $\gamma$ -brass-type precipitates, origin of incommensurate electron diff. pattern 4-76775  
 Cu-Zn-Au, ordered, two-dimensional antiphase struct., electron diff. study 4-113397  
 CuAl, dil. disordered, diffuse size effect scatt. in high voltage electron diff. 4-113395  
 CuGa<sub>1-x</sub>In<sub>x</sub>S<sub>2</sub>, LPE growth on ZnSe substrate 4-80436

## electron diffraction examination of materials continued

- CuNi compositionally modulated foils, electron and X-ray diffraction studies 4-80455  
 CuO-Ta<sub>2</sub>O<sub>5</sub> struct. of Ta<sub>2</sub>O<sub>5</sub>-rich phases, electron-optical and X-ray powder diff. studies 4-108329  
 Cu<sub>2-x</sub>S, long period modulated struct. with continuously variable periodicity 4-113469  
 Cu<sub>2-x</sub>S/CdS heterostruct., misfit accommodation and growth 4-108730  
 Cu<sub>2-x</sub>Te<sub>2-x</sub>, long period modulated struct. with continuously variable periodicity 4-113469  
 Cu<sub>2-x</sub>VS<sub>2-x</sub>, long period modulated struct. with continuously variable periodicity 4-113469  
 Cu<sub>2</sub>Zr<sub>2</sub>, 3D long-period superstructure, electron diff., electron microscopy obs. 4-70068  
 ErH<sub>2</sub> films, epitaxial growth by vacuum deposition 4-70596  
 Fe Z 4-65836  
 Fe-Cr-Ni, martensitic transition and cryst. geometry (*Russian*) 4-66332  
 Fe-Mn-Al-C (15, 8, 2 wt.%), rapidly solidified, phase struct. and morphology 4-114504  
 Fe-Nd-B permanent magnet system, metallurgy 4-109381  
 Fe-Sb-Ce alloys, Ce state at cryst. boundaries, electron diff. studies (*Chinese*) 4-98114  
 Fe<sub>8</sub>B<sub>14</sub>, amorphous layer form. on surface using elec. spark 4-65180  
 Fe<sub>2</sub>N pigments, mag. props. rel. to specific surface area 4-65836  
 Fe<sub>3</sub>O<sub>4</sub> magnetite particles in ferromagnetic colloids, size distrib. anal. 4-109043  
 Fe<sub>3</sub>(PO<sub>4</sub>)<sub>8</sub>, mixed valent, prep., cryst. struct., mag. props., Mossbauer spectra (*French*) 4-88146  
 Fe<sub>2</sub>TiO<sub>3</sub>, cryst. struct., TEM, electron diff., X-ray powder diff. studies 4-103726  
 GaAs (100), reconstructed, electron microscopy and diff. studies 4-108690  
 GaAs, crystal struct. determ. using convergent beam electron diff. 4-103612  
 GaAs/Gc single crystal layers, MBE growth and patterning on Si substrates 4-99315  
 Ge:Te, ion implanted, amorphisation phenomena, electron microscope and electron diff. studies 4-103656  
 H<sub>2</sub>O, thermal averages, effective harmonic oscillator method appl. 4-112153  
 In-Tl, premartensitic phenomena, role of Fermi surface 4-84384  
 InSb, polycrystalline, thermomagnetic and galvanic props. (*German*) 4-75987  
 In<sub>1-x</sub>Sn<sub>x</sub>O<sub>3</sub>/InP solar cells, RF sputtering prep. and device performance 4-99967  
 (In<sub>1-x</sub>Te<sub>x</sub>)<sub>2</sub>Sn<sub>1-x</sub>, obtained by splat cooling, Mossbauer study and electron diff. 4-109101  
 KAlF<sub>4</sub>, struct. phase-transition study 4-113617  
 K<sub>1/3</sub>Mg<sub>11/3</sub>Sb<sub>4/3</sub>O<sub>16</sub>, supercell ordering study 4-80006  
 LiFe phengite, mica, cryst. struct. of di-trioctahedral 1M polymorphic modification, electron diff. study 4-60894  
 Mg-Al spinel, microtwins, selected-area electron diff. obs. 4-103770  
 Mo, FCC needle crystals, Auger and electron diff. studies 4-92584  
 N<sub>2</sub> clusters, electron diff. patterns 4-74367  
 Nb<sub>2</sub>O<sub>5</sub>, P-form, space group symmetry, convergent beam electron diff. study 4-70118  
 NbTe<sub>4</sub>, evidence for deform. modulated struct. 4-113424  
 Ni-Al thin foils, pre-martensitic phase, electron diff. study 4-114518  
 Ni-base superalloys, struct. and space groups by convergent beam electron diff. 4-88132  
 Ni-based amorphous alloys, crystallisation processes, microstruct. anal. 4-84183  
 Ni-based superalloys, precipitate/matrix lattice mismatch, temp. depend. 4-80430  
 Ni-Cr-Mo system, isothermal sections of Ni rich portion, analytical electron microscopy 4-71638  
 Ni-Mo-Al eutectic alloy, unidirectionally solidified composite,  $\gamma/\gamma'$  phases, microstruct. changes 4-114493  
 Ni-P amorphous alloys, crystn. phases, electron diff. study (*Chinese*) 4-113331  
 Ni<sub>2</sub>Al, cold-rolled, recrystn. annealing 4-81213  
 NiCr thin films, Cr<sub>2</sub>O<sub>3</sub> phase appearance, electron microscopy and diff. study 4-81344  
 Ni<sub>3</sub>Cr, ordered state, annealing, elec. resist., electron diff. obs. 4-109394  
 NiO, interaction with O<sub>2</sub>, H<sub>2</sub>S and SO<sub>2</sub>, surface and vol. processes 4-98372  
 Ni<sub>1-x</sub>S, cryst. struct., electron and optical diff. studies 4-88152  
 Ni<sub>3-x</sub>Te<sub>2-x</sub>, long period modulated struct. with continuously variable periodicity 4-113469  
 Ni<sub>3</sub>(Ti<sub>1-x</sub>V<sub>x</sub>) alloys, long period struct., electron diff. studies (*Chinese*) 4-98064  
 PbF<sub>2</sub>-RF<sub>3</sub>, R=La, Nd, Gd, Ho, Yb and Y, synthesis, cryst. struct., electron diff. obs. (*French*) 4-75405  
 Pb<sub>3</sub>NaNb<sub>2</sub>O<sub>15</sub>, tetragonal bronze-like struct., modulated phases and domain struct. 4-113616  
 mpNb<sub>3</sub>-nBi<sub>2</sub>S<sub>3</sub>, long period modulated struct. with continuously variable periodicity 4-113469  
 Pd-Si (111), study by LEED, RHEED and AES 4-113765  
 $\beta$ -PtO<sub>2</sub>, new high-pressure form 4-70081  
 RbAlF<sub>4</sub>, struct. phase-transition study 4-113617  
 SO<sub>2</sub>, thermal averages, effective harmonic oscillator method appl. 4-112153  
 Se<sub>2</sub>S<sub>3</sub>, cryst. struct., electron irradi. induced disorder 4-103713  
 Si (111), reconstructed, electron microscopy and diff. studies 4-108690  
 Si epitaxial single cryst. films, origin of additional electron diff. spots 4-104104  
 Si microtwins, selected-area electron diff. obs. 4-103770  
 Si, polycryst., laser annealed, diff. studies 4-104106  
 Si, polycrystalline films, X-ray and electron diff. anal. 4-61258  
 Si polycrystalline films amorphised by ion implantation, solid phase epitaxial growth 4-108731  
 Si, porous, electron diffraction studies 4-113274  
 SiAs, low-energy ion implantation 4-75466  
 Si:H, Al-covered, solid-state reaction between film and substrate 4-92498  
 SiC cubic single cryst., CVD prep. and elec. props. 4-99345  
 Si<sub>1-x</sub>Sn<sub>x</sub>, amorphous, vapour deposited, struct., resist. characts., density, electron diff. meas. 4-61424  
 Sr<sub>2</sub>KNb<sub>2</sub>O<sub>13</sub>, tetragonal bronze-like struct., modulated phases and domain struct. 4-113616  
 Sr<sub>2</sub>NaNb<sub>2</sub>O<sub>15</sub>, tetragonal bronze-like struct., modulated phases and domain struct. 4-113616

**electron diffraction examination of materials continued**

- TaTe<sub>4</sub>, evidence for deform. modulated struct. 4-113424  
 Ti thin films, struct. and elec. props. 4-80441  
 Ti thin foil, cryst. symmetry, convergent beam electron diffr. studies 4-80456  
 Ti/Ni bilayered thin films, amorphisation and ion beam mixing 4-88408  
 Ti-R, R=Ce, Dy, Er, Gd, La, Nd or Y, rapidly solidified dispersion strengthened, struct. and props. 4-114561  
 Ti-Ni-based alloy, radiation-induced amorphisation 4-103830  
 Ti<sub>1.8</sub>Ni<sub>3.7</sub>Al<sub>1.8</sub>, charge wave density transitions, electron microscopy study 4-98596  
 TiO<sub>2</sub> thin films, struct. and elec. props. 4-80441  
 V<sub>8</sub>N, crystal struct. from 1 MV electron microscopy 4-92161  
 W-Ni-Fe(Cu), liq. phase sintered, interphase boundary precip. 4-99364  
 WO<sub>3</sub>·x(H<sub>2</sub>O) films, influence of crystallisation as hydration 4-88424  
 Y<sub>2</sub>O<sub>3</sub> films, struct. and phys. props. 4-65585  
 Zn chalcogenides, CVD using elemental source materials, struct. props. 4-98481  
 ZnBr<sub>2</sub> in N,N-dimethylformamide soln., complex form. and solvation, electron diffr. and Raman spectra 4-93502  
 ZnS films, RF sputtering prep. and microstruct. props. 4-88417  
 ZnS-type crystal struct. determ. using convergent beam electron diffr. 4-103612  
 Zr, oxide film growth kinetics, interferometry, ellipsometry, X-ray photoelectron spectra obs. 4-66482

**electron-electron double resonance see ELDOR****electron-electron interactions**

see also electron-electron scattering

No entries

**electron-electron scattering**

see also electron-electron interactions

No entries

**electron emission**

see also cathodes; electron field emission; exoelectron emission; photoemission; secondary electron emission; spin polarised electron emission; thermionic electron emission; work function

- charged particle emission in failure of solids 4-99291  
 charged particle emission in failure of solids 4-99292  
 cyclotrimethylenetrinitramine (RDX) explosive single crystals, fractoemission 4-81120  
 epoxide polymers, breakdown, ionisation processes role, mechanoemission mechanism 4-88952  
 ion induced electron ejection, projectile vel. depend. oscills. 4-76578  
 metal/polymer frictional contact, electron emission 4-66198  
 metastable atom-surface interaction, electronic emission (French) 4-76623  
 polybutadiene, fracto-emission, effect of cross-linking 4-66419  
 polymers, fracture and emission of electrons, ions and photons 4-98189  
 styrene-butadiene copolymer, fracto-emission, effect of cross-linking 4-66419  
 sucrose, fracture, electron and positive ion emission, triboluminescence 4-104686  
 sucrose, fracture and emission of electrons, ions and photons 4-98189  
 Wint-o-green Lifesavers, fracture, electron and positive ion emission, triboluminescence 4-104686  
 $\alpha$ -Al<sub>2</sub>O<sub>3</sub>, defect structure, electron emission meas. 4-93145  
 Mo, afterdischarge electron emission by treatment with glow discharge 4-87987  
 SiO<sub>2</sub>, fracture and emission of electrons, ions and photons 4-98189

**electron energy bands see band structure****electron energy loss spectra**

- acetylene decomposition on Pd (111) and (100) surfaces EELS study 4-66582  
 adsorbed atoms and mols., vibr. spectroscopy, overview 4-88837  
 adsorbed layers on metal surfaces, survey of vibr. spectroscopic methods 4-104065  
 angle-resolved single-loss profiles, retrieval 4-99252  
 biological specimen, EELS for quantitative X-ray microanalysis, mass thickness determ. 4-62644  
 trans-1,3-butadiene, C-C bond lengths, K-shell EELS study 4-69229  
 1,3-butadiene, excited states determ. by electron energy loss spectroscopy 4-87131  
 1,3-butadiene anion, electronic struct. vibr. excitation and electron transmission spectra 4-69227  
 2-butene, C-C bond lengths, K-shell EELS study 4-69229  
 conference, X-ray optics and microanalysis, Toulouse, France (Sept. 1983) 4-63389  
 deconvolution of loss features from electron spectra 4-66149  
 diamond, Auger line shape 4-66138  
 diamond, conduction band struct., core electron excitation spectra anal. 4-70647  
 2,3-dimethylbutadiene, NV<sub>2</sub> valence transition, EELS 4-69231  
 EELS technique for bulk and surface studies 4-61788  
 electron beam interactions with solids, rel. to microscopy, microanal. and microlithography 4-63394  
 elemental mapping and Z-contrast imaging 4-79913  
 energy analyser design for electron spectrometry (French) 4-63826  
 ethylene adsorbed on Pt or Pd, EELS and IR spectra studies 4-104065  
 ethylenes, chloro-substituted, electron impact investig. of singlet-triplet transitions 4-102807  
 excitation of mols. and atoms on metal surface and their nonradiative relax. 4-81460  
 foil electron transport, energy loss and straggling due to at. electron collisions and bremsstrahlung 4-70249  
 graphite, conduction band struct., core electron excitation spectra anal. 4-70647  
 hexatriene, Rydberg states, electron impact, energy loss spectra 4-78974  
 high-temperature analysis techniques, surface characteristics 4-99927  
 HVEM, electron scatt. and energy depend., appl. to chem. anal. 4-66162  
 II-VI semiconductors, crystal growth, optical and surface props. (Japanese) 4-88957  
 inelastic electron scatt. in solids, review 4-66151  
 inner-shell electron excitation loss, signal/background ratio, thickness depend. 4-99245  
 instrumental artifacts, elimination and correction 4-68334  
 lens system for surface vibrational spectroscopy at high impact energies 4-111258  
 metal overlayer/metal structures, sputtering, AES and EELS studies 4-76617  
 metal surfaces, electronically excited states of adsorbates, EELS 4-88917  
 metals, adsorbed CO, valence electronic excitations, EELS 4-81052

**electron energy loss spectra continued**

- microanalysis using EELS in high voltage electron microscopy 4-68335  
 microanalysis using EELS ion electron microscope 4-68332  
 microanalysis with high spatial resolution using X-rays and electron energy loss scattering 4-109714  
 microscopy and anal., conference, Guildford, England (Aug.-Sept. 1983) 4-78034  
 microspectroscopy, characterisation of solids 4-66161  
 oxide films grown on Si surface, TEM and EELS study (French) 4-75809  
 parametric partial cross section 4-73602  
 perfluoro-2-butene, C-C bond lengths, K-shell EELS study 4-69229  
 plural scattering removal techniques 4-73601  
 polyethylene, Auger line shape 4-66138  
 positron spectroscopy applied to surface analysis 4-71493  
 quantitative microanalysis, in STEM 4-114872  
 rare earth metals, core level resonances monitored by EELS 4-93156  
 rate earth sesquioxide thin films, fine struct., EELS investig. 4-70247  
 single scattering formulas, deviations 4-93138  
 spectral library, appl. to materials science research 4-68333  
 spectrometer, detector efficiency 4-63828  
 steel, Cr-Mo, anal. of second phase particles, energy dispersive X-ray spectra, EELS obs. 4-81207  
 steel, Low C, AIN precip. identification using EELS (French) 4-76938  
 steel, stainless, microanalysis by EELS, comparison with EDX 4-80248  
 steel, transition metal precipitate elemental anal. using EELS 4-81205  
 steel, V, EELS of small particles 4-104795  
 STEM, computer-controlled analytical microscopy 4-82868  
 surface analysis by low energy SEM with a field emission gun 4-79915  
 surface phonon spectroscopy, recent developments 4-61200  
 tetramethyl silane, valence shell electronic excitation, EELS 4-83480  
 transition metal 3d oxides, L<sub>2</sub>/L<sub>1</sub> white-line intensity ratios in electron energy-loss spectra 4-96621  
 transition metal oxide films, deconvolution of EELS 4-81053  
 transition metals, 3d, autoionisation emission by electron impact 4-81051  
 transition metals, core electron binding energies determ. by XPS, AEAPS and EELS 4-85081  
 transition metals, electron-stimulated autoionisation emission 4-88915  
 X-ray detection and electron energy loss events in time coincidence 4-99919  
 Ag, chemisorption of noble gases, excited states and decay mechanisms 4-98436  
 Ag, thin foil, surface plasmon excitation during electron energy loss 4-70695  
 Al (111), low energy electronic excitations, EELS studies 4-99253  
 Al, chemisorption of noble gases, excited states and decay mechanisms 4-98436  
 Al, rare gas bubble press. and density, EELS, TEM obs. 4-113508  
 Al, surface layer thermal expansion, determ. using plasmon losses in EELS 4-88317  
 Al thick layers, penetration of 24.8 MeV electrons, energy spectra 4-66148  
 Al-Cu alloy, EELS for GP zones and precipitates 4-61786  
 $\alpha$ -Al<sub>2</sub>O<sub>3</sub> (0001), high resolution EELS meas., surface phonons 4-99247  
 Al<sub>2</sub>SiO<sub>5</sub>, sillimanite, absorption edge fine struct. study using electron channelling 4-80127  
 Au (110) and (111), adsorption of O<sub>2</sub>, substrate impurity effects, EELS, AES, and XPS study 4-93160  
 Au, adsorption of O<sub>2</sub>, Au<sub>2</sub>O<sub>3</sub> prod. by DC reactive sputtering, EELS, AES, and XPS study 4-93161  
 Au, chemisorption of noble gases, excited states and decay mechanisms 4-98436  
 Au deposition on H saturated Si (111) surfaces, AES and EELS study 4-108742  
 AuGa<sub>2</sub> (001), surface net characterisation and electronic struct. 4-80642  
 C, glassy, conduction band struct., core electron excitation spectra anal. 4-70647  
 C thick layers, penetration of 24.8 MeV electrons, energy spectra 4-66148  
 CO adsorbed on K precovered Ru (001), EELS scatt. profiles of vibr. overtones and double losses 4-109287  
 CO, adsorbed on metals, bonding, EHT calcs. 4-113800  
 CO, fine struct., K-shell EELS, ab initio methods 4-91346  
 CO, high coverage struct. on metal FCC (111) and HCP (0001) surfaces, LEED, HREELS and IR spectra study 4-65573  
 Ce, core EELS, surface oxidation effects 4-85048  
 Cl<sub>2</sub>, electronic struct., EELS 4-64626  
 Cr (110) with adsorbed O<sub>2</sub>, photon stimulated O<sup>+</sup> desorption 4-98438  
 Cu (100), long-range electron-phonon coupling at metal surfaces, EELS meas. 4-80647  
 Cu (100), surface dynamic processes, excitation of electron-hole pairs 4-70902  
 Cu (111), chemisorbed acetylene, vibr. props., EELS studies 4-65567  
 Cu, chemisorption of noble gases, excited states and decay mechanisms 4-98436  
 Cu clusters on graphite, valence bands and core levels, XPS, Auger and EELS studies 4-113860  
 Cu surface, organic mol. adsorption 4-80409  
 Cu thick layers, penetration of 24.8 MeV electrons, energy spectra 4-66148  
 F<sup>+</sup> molecule, electron detachment and charge exchange to shape reson. 4-96687  
 F<sub>2</sub>, electron energy loss spectroscopy 4-69228  
 Fe, laser irradi., surface structural and electronic props. 4-60956  
 Fe-P alloys, intergranular fracture planes, chemical states, Auger and electron energy loss spectra 4-93385  
 Fe<sub>2</sub>B<sub>2</sub>Si<sub>6</sub>, amorphous and crystallised, UPS, XPS and EELS 4-104122  
 Fe<sub>2</sub>B<sub>2</sub>Si<sub>6</sub>, ferromagnet, spin-flip Stoner excitations, EELS studies 4-104410  
 Fe<sub>2</sub>B<sub>1.5</sub>Si<sub>3</sub>, Si<sub>3</sub> glass, primary crystallisation and  $\alpha$ -Fe dendrites, EELS studies 4-84202  
 FeS<sub>2</sub> (Fe<sub>2</sub>S<sub>3</sub>)(FeS) surfaces, AES and EELS studies 4-114349  
 GaAs (100) 4-70546  
 GaAs (110), O<sub>2</sub> chemisorption, photon simulation, AES and EELS studies 4-113804  
 GaAs:Te, H ion bombarded, free carrier density, EELS studies 4-98632  
 GaAs-Ag, high resolution EELS study 4-99248  
 GaP, volume plasmon dispersion, transmission electron energy loss studies 4-88465  
 Ge (111)-(2X1), dangling bond states, HREELS and photoelectron spectra study 4-65725

## electron energy loss spectra continued

- HCl, ionisation pot. D isotope effect, EELS 4-83467  
 HF, valence shell dipole excitation spectrum, photoabsorption cross section 4-91345  
 InP (100), optical surface phonons obs. using high res. electron energy loss spectroscopy 4-70546  
 InP (100) and (111) surfaces, EELS study, bulk and surface plasmons (*Chinese*) 4-85047  
 InP, volume plasmon dispersion, transmission electron energy loss studies 4-88465  
 InSb (110), surface quenching of surface plasmon, exptl. evidence 4-61310  
 La<sub>2</sub>SrVO<sub>3</sub>, metal-insulator transition, photoemission study 4-84567  
 LiF (100) surface, elastic and inelastic scatt. of slow positrons 4-104704  
 LiF, EELS in band gap region 4-99254  
 MgO (001), IR optical const., EELS meas. 4-71337  
 MgO, absorption pots. for low energy electron scatt. 4-93157  
 Mo, coadsorption of Cs monolayer and O on (100), electronic props., EELS, UPS, work function meas. 4-61787  
 MoS<sub>2</sub> (2H), absorption pots. for low energy electron scatt. 4-93157  
 MoS<sub>2</sub>-2H, layered, low energy electron, reflection intensities, scatt. matrix, calcs. 4-109286  
 N<sub>2</sub> mol., generalised oscillator strength for K-shell near edge struct. 4-64546  
 NO dimeric thin films, vibr. excitation via shape reson. in electron scatt. 4-99250  
 Na<sub>2</sub>WO<sub>3</sub>, surface phonon features in high-resolution EELS 4-93158  
 Nb, polycrystalline, oxidation at room temp., EELS 4-104705  
 NbSe<sub>2</sub>(2H), absorption pots. for low energy electron scatt. 4-93157  
 Ne, electron impact excitation cross sections, EELS 4-64620  
 Ni (001) with chemisorbed pyridine, molecular orientation effects on electronic excitations 4-93551  
 Ni (100), adsorbed O<sub>2</sub>, surface-extended energy loss fine struct. study 4-61790  
 Ni (100), clean and O-covered, surface vibr. dispersion, EELS study 4-109288  
 Ni (100), clean and with adsorbed O, surface vibr. dispersion curves, EELS study 4-80363  
 Ni (100), coadsorption of CO and K, XPS, UPS, work function, and EELS meas. 4-92552  
 Ni (100), Fe adsorption and growth, LEED and EELS studies 4-113808  
 Ni (100), K-dosed, CO and D<sub>2</sub> adsorpt., XPS, UPS, TDS, EELS and work function studies 4-84509  
 Ni (100), long-range electron-phonon coupling at metal surfaces, EELS meas. 4-80647  
 Ni (100), S-covered, adsorption of CO, vibr. spectroscopy study 4-108720  
 Ni (100), surface dynamic processes, excitation of electron-hole pairs 4-70902  
 Ni (100) surface with adsorbed O, surface phonons, EELS study 4-104086  
 Ni (110), ferromagnetic, spin polarised EELS study (*German*) 4-76573  
 Ni (110), H<sub>2</sub>(D<sub>2</sub>) adsorption, EELS study 4-65564  
 Ni (111), adsorbed graphitic C, geometrical struct. EELS study 4-61789  
 Ni (111), chemisorbed acetylene, vibr. props., EELS studies 4-65567  
 Ni (111) with adsorbed graphite and C overlayers, electronic struct. study 4-61213  
 Ni, Stoner excitation spectrum, spin polarised EELS studies 4-104411  
 Ni surface quantum motion of chemisorbed H<sub>2</sub> 4-80385  
 Ni-Al thin film, ion irradi., EELS study 4-88916  
 NiCl<sub>2</sub>(Br<sub>2</sub>)(I<sub>2</sub>), UV reflectance and electronic states 4-71406  
 NiSi<sub>2</sub> epilayers on Si (001), electronic struct. determ. 4-88549  
 Os single crystals, optical props. in VUV region, (E=5-43 eV) 4-109210  
 Pb, oxidation, XPS and EELS obs. 4-88913  
 Pb thick layers, penetration of 24.8 MeV electrons, energy spectra 4-66148  
 Pd (100), adsorpt. and catalytic reaction of H<sub>2</sub>O, O and H, EELS and LEED study 4-71969  
 Pd (100) and (111) with adsorbed acetylene, decomposition, EELS evidence for CCH formation 4-99829  
 Pd (111), chemisorbed acetylene, vibr. props., EELS studies 4-65567  
 Pd (111), O<sub>2</sub> adsorption, AES, EELS, TDS, ESD and work function studies 4-80410  
 Pd, reflection electron energy loss study of electronic and struct. props. 4-70641  
 Pd<sub>1-x</sub>In<sub>x</sub>, optical props. in VUV region, (E=5-43 eV) 4-109210  
 Pt (111), adsorption and decomp. of methyl isocyanide, EELS and thermal desorption study 4-108721  
 Pt (111), cyclopentene adsorpt., cyclopentadienyl obs. by EELS and TDS 4-65558  
 Pt (111), H<sub>2</sub> adsorption, vibr. props., EELS and inelastic neutron scatt. studies 4-113806  
 Pt surface, organic mol. adsorption 4-80409  
 Re (0001), adsorption of acetylene, vibrational electron energy loss spectroscopy (*French*) 4-75774  
 Rh (111), adsorption and decomposition of methanol, EELS and thermal desorption spectroscopy 4-92565  
 Rh (111), CO and K coadsorption, HREELS, TPD, AES and LEED study 4-84508  
 Rh (111) with surface adsorbed HNCO, effects of preadsorbed O 4-113781  
 Ru (001), chemisorbed H<sub>2</sub>O clusters, desorption mass spectra, EELS 4-75786  
 Ru (001) surface, coadsorption of K and CO, thermal desorption vibr. overtone spectroscopy 4-70565  
 Ru (001) surface precovered with K, KOH form. and decomp. 4-93544  
 Ru single crystals, optical props. in VUV region, (E=5-43 eV) 4-109210  
 Se, MBE growth on cleaved Te, RHEED, AES and LEELS characterisation 4-99343  
 Si (001)2×1, K chain monolayer, plasmon dispersion, EELS 4-98446  
 Si (100) 2×1, pre-exposed to O in submonolayer range, chem. shifts of Si-H stretching freqs. 4-80368  
 Si (100) surface, electronic excitations, EELS study 4-108914  
 Si (100)2×1, H adsorpt., coverage and temperature-dependent vibr. spectra, EELS and LEED studies 4-80408  
 Si (100)(2×1), chemisorbed H<sub>2</sub>O and D<sub>2</sub>O, multiple vibr. excitations, high resolution EELS study 4-109289  
 Si (111) (7×7), NO adsorption and reactions, EELS, LEED and AES studies 4-65562  
 a-Si:H, H<sub>2</sub> chemisorption, AES and EELS meas. 4-108715

## electron energy loss spectra continued

- Si<sub>3</sub>N<sub>4</sub>, Ar<sup>+</sup> ion bombarded, electron irradiation effect on surface composition 4-80109  
 SiO<sub>2</sub>N<sub>x</sub>, Ar<sup>+</sup> ion bombarded, electron irradiation effect on surface composition 4-80109  
 Ta, polycrystalline, oxidation at room temp., EELS 4-104705  
 Tc UV photoemission and electron energy loss spectra 4-85087  
 Ti (0001), clean and oxidised, electron emission and ion desorption spectroscopy 4-92561  
 Ti oxidation, Auger and electron energy loss studies 4-109550  
 TiO<sub>2</sub>(N<sub>x</sub>), optical props., EELS study 4-99082  
 TiO<sub>2</sub> (110), surface defects, XPS, X-ray induced AES, EELS study 4-80351  
 V<sub>3</sub> Si, precipitates, EELS anal: using STEM and high-voltage electron microscope 4-81495  
 VC<sub>x</sub>, C/metal ratio, quantitative EELS studies 4-98299  
 VC<sub>x</sub>(N<sub>x</sub>), optical props., EELS study 4-99082  
 W (001), adsorbed H-induced surface reconstruction, LEED and EELS study 4-92492  
 W (001), EELS, elastic and inelastic scatt. of slow electrons 4-114350  
 W (100), adsorption of H, surface reconstruction, symm. effects, refl. EELS study 4-80382  
 W (100), EELS spectrum, effect of adsorption of gas mols. 4-93159  
 W (110), adsorbed O<sub>2</sub>, vibrational modes, EELS study 4-80402  
 WO<sub>3</sub>, surface phonon features in high-resolution EELS 4-93158  
 ZrO<sub>2</sub>-CaO system; directionally solidified eutectic, EELS 4-72009

## electron energy states (condensed matter)

- see also band structure; band theory models and calculation methods; deep levels; defect electron energy states; dopplers; electron energy states of amorphous solids; electron energy states of liquid metals; electron energy states of liquid semiconductors; electron gas; electron traps; electronic density of states; exchange interactions (electron); excitons; Fermi level; Fermi surface; field interactions (condensed matter); heli-cons; hole traps; impurity electron states; Landau levels; localised electron states; magnetic breakdown; magnons; metal-insulator transition; metal theory; plasmons; polar semiconductors; polarons; positron states; ripplons; spin-orbit interactions; spin-phonon interactions; surface electron states; triplet state  
 crystal Green's functions in complex energy plane, analytical tetrahedron method 4-60996  
 density functionals for ground-state energies 4-92589  
 exact density functionals for ground state energies 4-98498  
 graded mixed crystals, quasi-Bloch functions as basis functions 4-92585  
 metals and alloys, conf., Johnsbach, Germany (May 1983) 4-67867  
 periodic ground states, one dimension, Lennard-Jones-type potentials 4-95336  
 s-d model, electronic spectrum and damping with Coulomb interaction 4-92588  
 Wigner-Seitz cells, multiple scatt. problem, convergence props. 4-70612  
 Ar fluid, electron energy bands 4-84645  
 Kr fluid, electron energy bands 4-84645  
 Xe fluid, electron energy bands 4-84645

## electron energy states of amorphous solids

- see also Anderson model  
 Anderson model, 2- and 3-D, density of states, diagonal and off-diagonal disorder effects 4-113846  
 chalcogenide glass thin films, threshold switching effects 4-92769  
 chalcogenide glasses, one-electron density of states 4-84548  
 chalcogenide glasses, two-step optical excitation, rel. to valence band struct. 4-85062  
 disordered systems, 3-D, exponential band tails and localisation 4-113900  
 disordered systems, localised states as bound states in pot. wells 4-113904  
 electronic states, theoretical models 4-70638  
 epoxy resin, two-level states, effect on thermal cond. and sp. ht. 4-70488  
 glass, hyperspherical harmonics, symmetry, Landau theory and polytope models 4-103659  
 glass, spontaneous two-pulse elec. echo-decay 4-70329  
 glassy semiconductors, electronic transitions in mobility gap 4-61275  
 metallic glasses, phonon absorpt. due to two-level systems 4-70327  
 metals, energy spectrum and density of states calcs. (*Russian*) 4-113854  
 one-dimensional disordered binary alloys, cluster mean-field theory 4-92599  
 one-dimensional disordered system, extended states 4-80484  
 organic polyiodide chain complexes, elec. conduction, press. depend. 4-75962  
 physics of amorphous solids, book 4-90312  
 polyacene, ground state electronic struct. 4-70630  
 polyacetylene, cis and trans, electronic states, muon spin resonance studies 4-65922  
 polyacetylene chains, solitons and breathers, Hamiltonian studies 4-108764  
 polyazine, pi system, band props., EHT calcs. 4-108765  
 polyazothene, pi system, band props., EHT calcs. 4-108765  
 polymers, conjugated, electronic struct., extended Huckel cryst. orbital scheme calc. 4-65604  
 polyparaphenylene chains, geometric and electronic struct. 4-92109  
 polypyrrole, band struct., polarons, and optical spectrum 4-98546  
 polypyrrole chains, geometric and electronic struct. 4-92109  
 polythiophene chains, geometric and electronic struct. 4-92109  
 random systems, exponential band tails 4-104167  
 semiconductor, amorphous, electron transport, Mott-CFO model anal. 4-113939  
 semiconductor, amorphous, long-range structural and electronic coherence 4-80485  
 semiconductors, amorphous Husimi cacti alloys, topological disorder 4-104119  
 semiconductors, electron states, multi-electron effects 4-98510  
 semiconductors, transitions from localised states; rel. to density of states meas. 4-84547  
 tetrathiosquarato nickel(II), one dimens. crystal orbital calcs., neighbour-strand interactions 4-113853  
 thin films, threshold switching and trap filling 4-92770  
 topologically disordered systems, localisation, self consistent theory 4-92672  
 transition metal alloys, binary alloys, multiautom interactions, relevance for determ. of stability of ordered structures and short range order 4-88444  
 transition metal-boron alloy, amorphous and cryst., B-K<sub>x</sub> X-ray spectra and electronic struct. 4-71482

**electron energy states of amorphous solids continued**

- transition metal-Fe-B metallic glasses, electronic struct., XPS study 4-75837
- As<sub>2</sub>Te<sub>3</sub> amorphous films, electronic struct., field effect and time of flight studies 4-113852
- CdS amorphous films, optical absorption coeff. and gap state density 4-66088
- Cu complexes, diacetyl-bis(thiosemicarbazone)Cu(II), electronic struct. and intermol. interactions 4-61586
- Cu complexes, methylglyoxal-bis(thiosemicarbazone)Cu(II), electronic struct. and intermol. interactions 4-61586
- Cu-Ni, disordered, positron spatial distrib. effects 4-104170
- Cu<sub>2</sub>Zr<sub>1-x</sub> metallic glass, electronic struct. calcs. 4-104120
- Fe, local density of states via recursion and equation of motion methods, comparative study 4-98505
- Fe<sub>1-x</sub>B<sub>x</sub> amorphous alloys, electronic struct., XPS studies 4-75838
- Fe<sub>2</sub>B<sub>2</sub>Si<sub>6</sub> amorphous and crystallised, UPS, XPS and EELS 4-104122
- GaP amorphous film, local order study and electronic props. 4-70591
- GaSb amorphous film, local order study and electronic props. 4-70591
- a-Ge, localised impurity states 4-104163
- Ge-Si, amorphous, RF sputtered, electronic props. 4-61370
- GeO<sub>2</sub>-B<sub>2</sub>O<sub>3</sub>(SiO) films, opt. absorpt. edge, additions influence 4-71455
- InP amorphous film, local order study and electronic props. 4-70591
- MoS<sub>2</sub>, poorly crystallised, electronic states, UPS study 4-92607
- Ni<sub>40</sub>Fe<sub>40</sub>P<sub>10</sub>Si<sub>10</sub> amorphous, electronic struct., extreme UV photoemission 4-85066
- Pd<sub>2</sub>, Fermi surface imaging effect in D short-range order 4-70633
- Se, amorphous, defect states and photoelec. behaviour 4-113903
- a-Se, electronic and vibr. struct., Raman spectra, cluster method 4-74387
- Se-Te, As glassy films, pure and doped, deep level defects, xerographic spectra studies 4-61339
- Se-Te-As, amorphous, defect states and photoelec. behaviour 4-113903
- a-Si, AC field effect and density of gap states 4-92670
- a-Si alloys, metastable defect states, X<sub>α</sub> scatt. wave calc. 4-113899
- a-Si alloys, photocond., dark Fermi level position depend. 4-113987
- Si, amorphous CVD films, H<sub>2</sub> plasma annealing localized state density 4-61337
- Si, electron structure change during amorphisation, electrorefl. spectra (Russian) 4-98509
- a-Si, electronic and vibr. props., book 4-67878
- a-Si, electronic struct., photoemission and optical props. 4-71522
- a-Si, electronic struct. of defects, cluster Bethe lattice method 4-70739
- a-Si films, localised density of states, electrophotography studies 4-113844
- a-Si films, RF sputtered, photocond. meas. 4-61416
- a-Si, ion implantation form. and optical state characterisation 4-88186
- a-Si, localised electron state spectroscopy 4-70741
- a-Si, long-range structural and electronic coherence in amorphous semiconductors 4-80485
- a-Si, static charge fluctuations, band struct. calcs. 4-70636
- Si-F, amorphous, electronic struct. theory 4-92600
- a-Si:H, absorpt. edge, struct. disorder model for amorphous semiconductor 4-80483
- Si:H, amorphous, light-induced defects, annealing 4-92762
- p-Si:H, amorphous, prepared by photo-CVD, electronic and optical props. 4-70959
- a-Si:H, B, P, electron structure and density of states of B-P pairs, cluster calc. 4-65642
- a-Si:H, broken bonds and electronic density of states, H effects 4-65178
- a-Si:H, conductivity, localisation and mobility edge 4-70819
- a-Si:H, correlated defects and steady-state photoconductivity 4-61417
- a-Si:H, electronic struct., theoretical models 4-70638
- a-Si:H, electronic struct. study using Auger electron spectroscopy (French) 4-75840
- a-Si:H, energy distrib. of light-induced gap states, photocond. meas. 4-76004
- a-Si:H, non-substitutional dopant states and carrier density statistics 4-113902
- a-Si:H, structural and vibr. spectra calcs. 4-98017
- a-Si:H, TSC meas., density of states behaviour 4-98366
- a-Si:H(O/N) alloys, electron trapping states, tight binding formalism calcs. 4-113901
- Si:H amorphous compensated films, xerographic discharge meas. 4-80603
- a-Si:H Schottky diodes and n-in devices, single and double carrier injection 4-114015
- a-Si:H sputtered films, steady-state photocond. and recombination processes 4-108902
- Si:H wide optical gap binary alloy films, elec. props. 4-113956
- a-Si-based field effect transistors, flat-band volt. and surface states 4-92825
- p-SiC:H, amorphous, prepared by photo-CVD, electronic and optical props. 4-70959
- a-Si<sub>1-x</sub>C<sub>x</sub>H<sub>1-x</sub>, luminescence from photo-generated carriers, polarisation memory 4-99186
- Si<sub>1-x</sub>Ge<sub>x</sub>H, amorphous, occupied gap state obs. 4-70637
- Si<sub>3</sub>N<sub>4</sub> amorphous, electronic struct., X-ray, emission and XPS studies 4-75839
- SiNi<sub>2</sub>H, amorphous, localised states at conduction band edge 4-104168
- SiO<sub>2</sub> glass, rotary phonon echoes 4-70328
- SiO<sub>2</sub>, radiation induced charges 4-70217
- Y-Cu-Fe metallic glasses, XPS study of electronic struct. 4-104121
- Y<sub>1-x</sub>Gd<sub>x</sub>Fe<sub>2</sub>O<sub>7</sub>, noncrystalline garnet films, electron transport and thermopower 4-108958
- Zr-Cu, amorphous, sputtered, low-energy excitations, thermal cond., sp. ht. meas. 4-70987
- Zr-Cu<sub>1-x</sub> metallic glass, sp. ht., thermal cond. props. after structural relax. 4-70406
- (ZrF<sub>0.57</sub>)(BaF<sub>2</sub>)<sub>0.33</sub>(ThF<sub>4</sub>)<sub>0.75</sub> (V-52) glass, reson. interaction of acoustic waves with two-level systems 4-70290
- Zr<sub>76</sub>Ni<sub>24</sub> amorphous, low-energy excitations, thermal cond., sp. ht. meas. 4-70987
- Zr-Ni, metallic glass, XES study of electronic states 4-80482
- Zr-Ni-D, metallic glass, XES study of electronic states 4-80482

**electron energy states of glassy solids** *see electron energy states of amorphous solids*

**electron energy states of liquid metals**

- alkali-group IV alloys, liq. and solid, electronic struct. and cluster form. 4-92601
- alloy, partially ionic, screening role in electronic and atomic struct. 4-70635

**electron energy states of liquid metals continued**

- energy spectrum and density of states calcs. (Russian) 4-113854
- Fe, local density of states via recursion and equation of motion methods, comparative study 4-98505

**electron energy states of liquid semiconductors**

- Ga<sub>2</sub>Te<sub>3</sub> liquid semicond. elec. transport activation energies 4-88506
- Si, molten, electronic and bonding props. 4-98503

**electron field emission**

- cathode materials for high brightness electron beams 4-71508
- cosmic grains fluff, effects on field emission, charge and particle levitation 4-94578
- explosive emission, mag. field and initial cathode temp. effects 4-71531
- gun, for high resolution Auger spectroscopy (French) 4-63825
- gun, paraxial rays and aberrations 4-106428
- gun, with mag. accelerator lens 4-112000
- ion bombardment suppression effects of a field-emission cathode 4-114363
- IV-V transition metal nitrides, field emitters 4-93203
- metal/insulator/metal structure formation, upper electrode effects 4-61466
- microprocessor-aided remoulding of field emitters 4-111250
- new field emission gun, electrostatic lens, characs. (Chinese) 4-85091
- oxide cathodes, emission mechanism, semiconductor model 4-61812
- photofield emission, rapid oscills. in applied field 4-71530
- pointed field emission cathodes, model 4-76644
- potential well in an elec. field, nature of electron emission (Russian) 4-78182
- prebreakdown electron emission currents, switching and other nonlinear phenomena 4-76641
- SEM, surface analysis by low energy SEM with a field emission gun 4-79915
- sputtering of field electron emitters by self-generated positive ions 4-76642
- TEM with thermally stabilised field emission gun 4-70000
- visualisation of field emission in microwave field 4-104724
- Ga, liquid, explosive emission study 4-109311
- GaAs-Al contact, semicond. electron field emission props., metal adsorption effect 4-99289
- Mo-Si<sub>3</sub>N<sub>4</sub>-Al structures, electrode surface relief effect on parameters 4-76048
- PbO<sub>2</sub> vacuum evaporated films, electron emission and I-V characs. (Japanese) 4-76643
- W (110) field emitter, diffusion of H at low temp. 4-92549
- W field emission gun, emission noise, anode cleanliness effect 4-78437
- W point cathodes, electron field emission instability, adsorption effects 4-61813
- W, prebreakdown effects and peak current densities in nanosecond field emission pulses 4-66197

**electron gas**

- see also cathode ray tubes; electron optics*
- air, discharge plasma, electron gas, transport coeff., binary collision rates 4-97759
- Anderson localisation and elec. cond., self-consistent mode-coupling theory 4-61336
- density functional theory in electron gas models 4-73341
- density functionals obtained from models of the electron first and second order density matrices 4-73342
- density of states in the presence of a strong magnetic field and random impurities 4-68121
- dielectric function and spin susceptibility, exchange effects 4-70692
- dielectric function of electron liq. local field corrections 4-84578
- electric breakdown waves 4-87836
- finite and infinite, many-body theory, rigorous theorems 4-68124
- fractional quantised Hall states hierarchy, quasiparticle stats., electron gas 4-70837
- GaInAs-InP heterojunction, interface 2-D electron gas props., MOCVD growth and characterisation (French) 4-76685
- interacting closed shell systems, induction and dispersion forces in electron gas theory 4-113880
- interacting non-uniform electron gas energy, density functional exchange part, non-local approx. 4-70691
- inversion layer width, electron-electron interactions, fractional quantum Hall effect 4-75880
- metal clusters, small, ionisation pot., effect of electron statistics 4-108923
- metallic densities, exchange and correlation 4-88464
- metals, superconductivity from nonphonon interactions 4-84737
- nonuniform, struct. factor at small wavelength 4-61309
- p-n-p struct., 2d electron gas, ground subband energy, variational calc. 4-70917
- plasma, Coulomb one-component, variational wavefunctions 4-87846
- positron screening, quadratic response theory 4-99221
- quantum Hall effect in two-dimensional electron systems 4-61398
- quasi two-dimensional electron-hole system, correl. energy 4-84580
- quasi-one-dimensional supercond. under mag. field, spin effects 4-84730
- screened Coulomb exchange energy, density functional theory gradient expansion approx. 4-61312
- screening of moving positive particle 4-70690
- semiconductor superlattice two-dimensional electron gas, sp. ht., magneto-thermal oscils. in quantising mag. field 4-70688
- semiconductors, absorption edge, free carrier Fermi-liq. interaction effects 4-114236
- semiconductors, defect form., electron gas heating effects 4-84284
- semiconductors, Voigt effect and magneto-conductivity in strong elec. field 4-99099
- spatially inhomogeneous samples, de Haas-van Alphen effect 4-113849
- specific heat, determ. for any degree of degeneracy up to order e<sup>4</sup> 4-92636
- thermodynamic and mag. props. in inhomogeneous mag. field Hr<sup>-1</sup> 4-90788
- thermodynamic functs. and Padé approx. 4-65626
- three-dimensional degenerate electron gas, cond. near mobility edge 4-98616
- triple electron collisions effect on photoelectron distribution in ultraquantal mag. field 4-113997
- two dimensional, lifted spectral degeneracy 4-92638
- two dimensional, quantized Hall conductance in a two dimensional periodic potential 4-70770
- two dimensional, quasi-particle Coulomb inelastic lifetime 4-98554
- two-band direct gap semicond., electrodynamics, SCF theory 4-98497

**electron gas continued**

- two-dimensional, crystallisation of incompressible quantum fluid state in strong mag. field 4-108792
- two-dimensional, density of states in random external mag. field 4-68123
- two-dimensional, disordered, resist. in mag. field 4-84634
- two-dimensional, in quantising mag. field, magnetisation, sp. ht., magneto-thermal effect and thermoelec. power 4-98728
- two-dimensional, magnetisation and mag. susceptibility 4-113881
- two-dimensional electron gas, charged particle interaction, transition radiation 4-81033
- two-dimensional electron plasmas, integrals relating dielectric behaviour 4-97751
- two-dimensional electron solid on liquid He, propag. of shear 4-104018
- two-dimensional electron solids, static and dynamic props., effects of anharmonicities and broken time-reversal invariance 4-70689
- two-dimensional electron systems, magnetothermal effect 4-80684
- Al, liquid, struct. factor, influence of electron-gas response junction 4-75265
- Al superconducting films, antisymm. Fermi liq. and Pauli susceptibility renormalisation, spin polarised tunnelling meas. 4-70997
- n-AlGaAs/GaAs selectively doped heterojunctions, high mobility electron gas 4-80657
- AlGaAs/GaAs/AlGaAs single quantum well transistor with 2-D electron gas, logic device appl. 4-61443
- AlGaAs-GaAs heterojunction, two-dimens. electron gas gate control characts., optimum doping (*Chinese*) 4-114021
- AlGaAs-GaAs modulation doped layers, 2-D electron gas, room temp. mobility, parallel conduction effects 4-76027
- Al<sub>0.3</sub>Ga<sub>0.7</sub>As/GaAs heterostructure, selectively doped, transient photocond. obs. 4-70862
- Al<sub>0.3</sub>Ga<sub>0.7</sub>As/GaAs heterojunction FET, 2D electrons, cyclotron resonance studies 4-98743
- GaAs/(GaAl)As two-dimens. electron gas, cyclotron reson. study 4-104297
- GaAs/AlGaAs heterojunction, 2D electron gas, cyclotron resonance studies 4-76032
- GaAs/AlGaAs heterostruct., screening and polaron effects, cyclotron resonance studies 4-98741
- GaAs/N-AlGaAs heterostructures, selectively doped, MBE grown, tungsten-halogen lamp annealing effects 4-61444
- GaAs-Al<sub>0.3</sub>Ga<sub>0.7</sub>As, quantised Hall resistance and 2D electron gas behaviour 4-98724
- GaAs-Al<sub>0.3</sub>Ga<sub>0.7</sub>As heterostructures, 2D electron gas, disorder, fractional quantum Hall effect 4-76033
- GaAs-Al<sub>0.3</sub>Ga<sub>0.7</sub>As heterostructure, thermopower meas. on 2D electron gas 4-98729
- GaAs-AlGaAs, optical activity of plasma oscils. 4-84930
- GaAs-AlGaAs superlattice and interface, acoustic props. 4-80366
- GaAs-GaAlAs heterostructure, electron mobility limits 4-76030
- GaAs-GaAlAs heterostructs., 2-D electron gas, electron mobility, temp. dependence 4-98704
- GaInAs/AlInAs heterojunctions, cyclotron resonance and polaron effects 4-98742
- GaInAs/InP heterojunctions and superlattices, cyclotron resonance and polaron effects 4-98742
- Hg<sub>1-x</sub>Cd<sub>x</sub>Te zero gap MIS struct., size quantisation in accumulation layers 4-65753
- In<sub>0.53</sub>Ga<sub>0.47</sub>As, 2D electron gas, alloy scatt. limited mobility 4-98620
- InP-n-AlInAs heterostructure, magnetotransport study 4-88570
- K, spin-wave excitations, Landau Fermi-liquid parameters 4-114098
- Li, electron dynamic structure factor, inelastic synchrotron X-ray scatt. 4-80524
- N<sub>2</sub>O+Ar collisions, intermol. pot., electron gas model, comparison with mean square torques meas. 4-78923
- Na, spin-wave excitations, Landau Fermi-liquid parameters 4-114098
- Ne solid, surface two-dimensional electron system 4-98683
- Si (111), 2D hole gas, conductivity, logarithmic corrections 4-98685
- Si, anisotropic 2D system, negative magnetoresistance 4-70841
- Si inversion layer, ballistic phonon scatt. and absorption 4-65756
- Si, MIS inversion channel, quantum Hall effect studies 4-104321
- Si MIS struct., relax. time of wave-function phase in two-dimens. electron gas 4-88605
- Si-MOSFET inversion layer, warm electron coeff. calc. for two-dimens. electron gas 4-65748

**electron guns**

- field emission, fitted to electron microscopy, micrograph nonisoplanatism effect 4-68339
- field emission, for high resolution Auger spectroscopy (*French*) 4-63825
- field emission, with mag. accelerator lens 4-112000
- field emission gun, paraxial rays and aberrations 4-106428
- gas electron diffraction, telefocus gun construction 4-112269
- glow discharge electron gun, cathode geometry rel. to beam spatial distrib. 4-87990
- glow-discharge-created electron beams 4-95560
- hybrid electron-ion gun, structural design electron optics and appl. 4-63807
- LEED, high resolution, electron gun and detector 4-90691
- microprocessor-aided remoulding of field emitters 4-111250
- new field emission gun, electrostatic lens, characts. (*Chinese*) 4-85091
- secondary emission electron gun, appl. to gas lasers and plasma chem. reactor 4-90689
- SEM, surface analysis by low energy SEM with a field emission gun 4-79915
- SEM gun brightness at low kV using intermediate extraction electrode 4-95575
- sources, use of microprocessors 4-111999
- W field emission gun, emission noise, anode cleanliness effect 4-78437

**electron-hole avalanches** *see impact ionisation***electron-hole drops**

- anthracene, cryst., carrier pairs prod. and recombination by VUV radiation 4-84571
- exciton condensation kinetics into electron-hole liq. in finite size crysts. 4-70674
- indirect gap semiconductor, recombination in electron-hole droplets 4-70832
- layered electron-hole liq., ground state correlations 4-92620
- long wave plasmon decay into two pairs, probability 4-61313
- rare gas crystal, exciton processes study, synchrotron radiation appl. (*Russian*) 4-98530
- RPA quasiparticle energies, low density approach 4-80526

**electron-hole drops continued**

- semiconductor, excitonic matter 4-75866
- semiconductor crystallites, electron-electron and electron-hole interactions, size depend. of excited electronic state 4-70660
- semiconductors, electron-hole droplets, book 4-101582
- two-photon resonant Raman scattering of light involving free electron-hole pairs 4-66039
- Al<sub>0.3</sub>Ga<sub>0.7</sub>As heteroepitaxial struct., photoluminescence study 4-104673
- CdS, radiative recomb. mechanisms for high density excitons 4-88458
- CdSe, picosecond spectroscopy at high excitation densities 4-81003
- Ga-Al-As, luminescence lineshapes of electron-hole plasma 4-109242
- GaAs, electron-hole plasma density meas. 4-61408
- GaAs, light scatt. nonequilibrium electron-hole plasma 4-104616
- GaP:Te(N)(As), impurity influence on electron-hole plasma 4-75862
- Ge, cyclotron resonance and radiative recombination for excitons, free carriers, electron-hole droplets 4-71183
- Ge, electron-hole liq., relax. kinetics near nucleation threshold, collective decay of small electron-hole drops 4-98541
- Ge, electron-hole liq. droplet destruction in nonuniform deformation field 4-61297
- Ge, electron-hole liquid, phonon-absorpt. imaging 4-61292
- Ge exciton condensation, microwave studies, biexcitons and electron-hole droplets 4-70668
- Ge exciton condensation, microwave breakdown, one- and two-photon carrier excitation luminescence 4-70670
- Ge, exciton condensation, microwave methods using pulsed optical excitation, kinetics 4-70671
- Ge exciton microwave breakdown, exciton and free carrier kinetics with electron-hole drops 4-70669
- Ge, luminescence signal of electron-hole plasma 4-104674
- Ge, stressed, with large electron-hole drop; magnetoacoustic props. 4-98529
- Nal:TI, excitation fluoresc. intensity in VUV 4-84987
- Si, crystalline and amorphous, energy transfer during laser irradi. 4-76412
- Si, laser irradi., influence of electron-hole density profile on reflectivity 4-104559

**electron-hole plasma** *see solid-state plasma***electron-hole recombination**

- see also carrier mobility*
- amorphous materials, transient photocurrent curve scaling 4-104269
- amorphous semiconductors, picosecond electronic relaxations 4-108892
- amorphous semiconductors, transient photocond., effect of repeated carrier trapping 4-61420
- anisotropic lattices, bimol. charge carrier recombination, Monte Carlo study 4-92743
- anthracene, cryst., carrier pairs prod. and recombination by VUV radiation 4-84571
- covalent semiconductors, electron capture cross-section 4-104227
- direct-gap semiconductor, nondegenerate, interband luminesc. and absorpt. coeff. 4-61749
- exactly compensated crystal, donor-acceptor recombination kinetics 4-92751
- geminate electron-hole pair in cryst. lattices, time depend. dissoc., Monte Carlo study 4-98635
- geminate recombination, random walk theory 4-61390
- grain boundary barrier heights, surface state effects 4-92780
- III-V semiconductor lasers, threshold current, temp. dependence 4-79132
- indirect gap semiconductor, recombination in electron-hole droplets 4-70832
- n-InSb, photoconductivity and hole trapping centre capture coeff., press. studies 4-98668
- laser materials, Auger recomb. and intervalence band absorpt. 4-80885
- MOS capacitors, charge variation rel. to voltage step, generation lifetime meas. 4-65755
- nonmetallic solids, amorphisability under heavy ion bombard., covalent-ionic transition 4-80122
- p-n abrupt junctions recombination current in space charge layers 4-65732
- p-n junction diodes, carrier lifetime and surface recomb. vel. determ. using transient responses 4-77093
- p-n junctions, electron beam induced short circuit currents, carrier lifetime 4-92806
- p-n variable gap struct., photoelectric effect characts. 4-65737
- photoelectrochemical solar cells, quantum efficiency, theoretical model anal. 4-114913
- phthalocyanine,  $\beta$ -metal-free, carrier generation, photoconductivity, delayed fluoresc. study 4-70855
- polydiacetylene, transient photoinduced absorpt. spectrum 4-61725
- semiconductor, finite length, magnetoconcentration effects 4-84633
- semiconductor, HF relaxational oscils. in homogeneous electron-hole plasma heated by Auger recomb. 4-108891
- semiconductor, transient photoconductivity spectrum, surface recombination effects 4-65712
- semiconductor colloidal electrode particles, photogenerated carrier transport and kinetics 4-65671
- semiconductor materials recombination parameters determ., using electrolytic cell with magnetic clamp 4-90612
- semiconductor surface regions, ESR techniques and results 4-109059
- semiconductor thin films, minority carrier lifetime and surface recomb. vel. meas., small-signal admittance meas. 4-68239
- semiconductor thin layers, double injection, light and mag. field effects 4-65760
- semiconductor with bipolar photoconduction, recombination parameters determ. in mag. field 4-114000
- semiconductor-metal contacts, Schottky barrier photosensitivity spectra in strong absorption region (*Russian*) 4-65741
- semiconductor-metal variable gap struct., photoelectric effect characts. 4-65737
- semiconductors, amorphous, time-dependent geminate recombination for hopping site energy disorder 4-61395
- semiconductors, large-signal photocond., Shockley-Read recomb. model 4-88537
- semiconductors, multi-valley, Auger processes with energy transfer to bound charge carriers 4-80607
- semiconductors, p-type, impact recombination by deep and shallow acceptors 4-84632
- semiconductors, recombination through deep centers in electron-hole scattering 4-113970

**electron-hole recombination continued**

- semiconductors, small gap, intrinsic photocond., electron and hole heating effects 4-88542  
 triple electron collisions effect on photoelectron distribution in ultraquantal mag. field 4-113997  
 AlGaAs LED; radiative and nonradiative, recombination rates, meas. 4-112434  
 As<sub>2</sub>Se<sub>3</sub> cryst. and amorphous, recomb. and excited-state absorption at photolum. centres 4-99182  
 BaTiO<sub>3</sub>/Fe, electrolum., elec. field depend. 4-66077  
 (Cd,Zn)S-CuInSe<sub>2</sub> Boeing solar cells, current transport 4-81546  
 CdI<sub>2</sub>, soln. grown cryst., photoconductivity, nonlinear behaviour 4-61413  
 CdIn<sub>2</sub>S<sub>4</sub> single cryst., photocond., photoluminescence and non-equilib. carrier recombination 4-65706  
 CdS surface, clean and Au covered, surface recombination vel., photoluminescence studies 4-80600  
 CdS/Cu thin films, photoexcit., field quenching 4-84718  
 GaAs: Mn, spin-depend. recombination, optical pumping studies 4-99183  
 GaAs-Al<sub>0.3</sub>Ga<sub>0.7</sub>As quantum wells, photoluminesc. from spike doped hydrogenic donors 4-104668  
 GaInAsP, nonlinear carrier dynamics, optical bleaching study 4-74625  
 Ga<sub>0.9</sub>In<sub>0.1</sub>P, photolum. dynamics of high density electron-hole plasma and psec. laser excitation 4-109228  
 n-Ge, low temp. breakdown characs. 4-92737  
 Ge, neutron transmutation doped, annealing, DLTS study 4-60942  
 Ge single cryst.,  $\alpha$ -particle irradiat., defects and photoelectromag. effects 4-84654  
 Ge surface, nonequilib. charge carrier recombination, isotopic effects 4-92750  
 Ge/D, plasma treated, D diffusion and interaction with point defects, deep level recombination centres 4-60951  
 GeSe<sub>2</sub>, cryst. and glassy, photoelec. props. 4-108905  
 Hg<sub>0.1</sub>Cd<sub>0.9</sub>Te, LPE grown, photoluminescence study 4-80986  
 InGaAs epilayers, optical studies of carrier dynamics 4-98788  
 In<sub>0.53</sub>Ga<sub>0.47</sub>As LPE layers, high purity, photoluminescence processes 4-99187  
 In<sub>0.53</sub>Ga<sub>0.47</sub>As, laser operation, thermal behaviour 4-87331  
 InGaAsP, 1.3  $\mu$ m bandgap, photoexcited carrier lifetime and Auger recomb. 4-108893  
 InGaAsP epilayers, optical studies of carrier dynamics 4-98788  
 InGaAsP laser, radiative and nonradiative, recombination rates, meas. 4-112434  
 InGaAsP/InP DH, luminescence and laser threshold characs. 4-85008  
 InGaAsP/InP lasers, 4-5  $\mu$ m emissions and excitations in split-off valence band 4-96916  
 InP p<sup>+</sup>-n junctions,  $\gamma$ -ray irradiat., electron trap annealing 4-98748  
 InP, Raman spectra, optically excited carriers, surface recombination vel. 4-71368  
 n-InSb, Auger recombination of holes via deep donors 4-104229  
 InSb, photoconductivity under picosecond illumination (*Russian*) 4-88543  
 PbS<sub>0.9</sub>Se<sub>0.1</sub> small gap semicond., second order Auger recombination 4-80606  
 a-Si alloys, photocond., dark Fermi level position depend. 4-113987  
 Si, carrier lifetime, elec. resist. meas. by contactless method 4-61392  
 Si defected substrates, minority carrier lifetime, injection level depend. 4-92753  
 Si, gamma-irradiated, carrier recombination, dislocation effects 4-75982  
 Si, gamma-irradiated, charge carrier recombination 4-84631  
 Si, grain boundary recombination vel., study for different injection levels 4-98633  
 Si, ion implanted, laser or electron beam annealing, minority carrier recomb., EBIC, photoluminescence meas. 4-80601  
 Si, polycrystalline, interacting grain boundaries, surface recombination vel., EBIC study 4-70828  
 Si, pulsed laser induced recombination centres 4-108873  
 Si solar cells, limiting efficiency, extended detailed balance method 4-81554  
 Si solar cells, open-circuit voltage and efficiency, limits imposed by Auger recomb. processes 4-81549  
 Si solar cells, P precip. effects on open circuit voltage 4-62361  
 Si, stacking faults and nonradiative lifetime, photoacoustic meas. 4-103772  
 Si surface, excess carriers, light-induced recombination 4-76005  
 a-Si:H, F p-n junctions, generation; recombination currents, computer simulation 4-84683  
 a-Si:H, geminate recombination and mobility 4-104223  
 a-Si:H, radiative combination at dangling bonds, quantitative model, expt. study 4-114326  
 a-Si:H, transient photoinduced absorpt. 4-104634  
 a-Si:H pin devices, excess dark currents and diode quality factor 4-114016  
 a-Si:H Schottky barriers, sputtered, freq. depend. capacitance, admittance meas. 4-98693  
 a-Si:H sputtered films, steady-state photocond. and recombination processes 4-108902  
 Si:S, persistent photoconductivity effect obs. 4-113995  
 Si/methanol liquid junction, open circuit volt. and oxide form. 4-114030  
 a-Si-based alloy p-i-n solar cells, elec. field distrib. and open circuit volt. 4-89405  
 a-SiC/c-Si p<sup>+</sup>-n heterostructure, plasma CVD growth and elec. props. 4-80660  
 TiO<sub>2</sub>/Cr, doping effect on elec. and catalytic props. under UV and visible illumination 4-98663  
 ZnSe, photoelectrochemical etching and nonuniform charge flow in Schottky barriers 4-80672

**electron impact**

- see also atomic electron impact excitation; atomic electron impact ionisation; molecular electron impact dissociation; molecular electron impact excitation; molecular electron impact ionisation; secondary electron emission  
 alkali halide surfaces, electronic desorption of excited alkali atoms 4-61236  
 alkali halides, sputtering by electrons 4-61791  
 alkanes, branched, solid, electron stimulated desorption 4-61240  
 backscattering, analytical models 4-66152  
 backscattering diffusion model appls. 4-66154  
 backscattering from complex structs., rel. to lithography resolution 4-66153  
 backscattering from thick layers 4-99249

**electron impact continued**

- beam interactions with solids, rel. to microscopy, microanal., and microlithography 4-63394  
 Boltzmann transport eqn. theory 4-66159  
 covalent systems, models for desorption 4-61230  
 cyclohexane film, photon and electron-stimulated desorption, mech. of ion formation and desorption 4-61241  
 desorption, electron stimulated, mechanisms 4-61227  
 desorption, electronic, mechanisms, overview 4-61229  
 desorption, electronically induced, of ions and neutrals, mechanisms 4-61228  
 desorption, negative ion electron stimulated, and photodesorption 4-61233  
 desorption induced by electronic transitions, workshop, Williamsburg, VA, USA (May 1982) 4-58556  
 electronic transition-induced desorption, laser induced fluorescence studies 4-75780  
 ferromagnet, spin polarised electron elastic scatt., anisotropy, pseudopotential anal. 4-114348  
 films, amorphous and polycryst., plural electron scatt., Monte Carlo calc. 4-66158  
 fusion reactor first wall coatings, gas release under electron impact 4-91097  
 graphite+H reactivity, electron bombardment enhanced 4-93529  
 inelastic and elastic multiple scatt., transport eqn. description 4-66160  
 metal, surface electrons, drift focusing by mag. field 4-92786  
 metal surfaces, nature of electron stimulated desorption active species 4-61232  
 metals, transmission and backscattering coeffs. meas. for monokinetic electrons 4-99251  
 methanol film, photon and electron-stimulated desorption, mech. of ion formation and desorption 4-61241  
 molecular structure at surfaces, determ. using angle resolved electron- and photon-stimulated desorption, review 4-61234  
 Monte Carlo electron trajectory calculations of electron interactions in samples with special geometries 4-66156  
 Monte Carlo simulation, appl. to electron microscopy, microanal., and microlithography 4-66155  
 multicomponent specimen backscattering coeff. 4-93162  
 positron scattering and surface state formation 4-88914  
 semiconductors, electron stimulated desorption and adsorption 4-66150  
 solid surface, chemical and electrochemical treatment, low energy electron induced X-ray spectra 4-76572  
 sputtering by particle bombardment, book 4-95080  
 stimulated desorption spectroscopy 4-61235  
 transition metals, 3d, autoionisation emission by electron impact 4-81051  
 water film, photon and electron-stimulated desorption, mech. of ion formation and desorption 4-61241  
 Ag epitaxial film on Cu (111), interfacial effects in electron transmission 4-114050  
 Al, adsorbed water, electron stimulated desorption, H<sup>+</sup> ion energy distrib. 4-92536  
 Al, electron scatt., X-ray intensity calc. by Monte Carlo simulation (*Chinese*) 4-71480  
 Al polycrystalline surface, oxidised, interaction with electron beams, AES study 4-93154  
 Au, electron scatt., X-ray intensity calc. by Monte Carlo simulation (*Chinese*) 4-71480  
 CO, solid, low temp. electronic sputtering by light ions and electrons 4-71502  
 Cu, electron scatt., X-ray intensity calc. by Monte Carlo simulation (*Chinese*) 4-71480  
 H<sub>2</sub>O, solid, low temp. electronic sputtering by light ions and electrons 4-71502  
 Na<sub>2</sub>O-SiO<sub>2</sub> glass surface, electron stimulated desorption mechanisms 4-92514  
 Ni (100), adsorption of residual gases, electron impact effects 4-65543  
 Ni (110), oxidised, electron stimulated desorption of O<sup>+</sup> ions, role of inner shell excitations 4-108718  
 Ni surface, adsorbed O<sub>2</sub>, electron stimulated desorp. 4-65565  
 Pd (111), O<sub>2</sub> adsorption, AES, EELS, TDS, ESD and work function studies 4-80410  
 W, adsorbed water, electron stimulated desorption, H<sup>+</sup> ion energy distrib. 4-92536  
 YCl<sub>3</sub>:Er<sup>3+</sup> electron impact excitation, level population mechanism 4-74335  
 YF<sub>3</sub>:Er<sup>3+</sup> electron impact excitation, level population mechanism 4-74335

**electron interactions** see elastic scattering of electrons by atoms and molecules; electron attachment; electron beam effects; electron beams; electron-electron interactions; electron-electron scattering; electron impact; electron-nucleon interactions; electron-nucleon scattering; electron-nucleus reactions; electron-nucleus scattering; electron-positron interactions; electron-positron scattering; electron spectra; hadron electroproduction; neutrino-electron interactions; neutrino-electron scattering; secondary emission

**electron ionisation** see electron impact

**electron lenses**

- see also aberrations; electron microscopes; electron optics; electrostatic lenses; magnetic lenses  
 aberration coeffs., dependence on object and aperture position 4-79025  
 asymmetrical, axial magnetic field characs. 4-64671  
 asymmetrical condenser-objective lenses, electron optical props. (*Chinese*) 4-96775  
 double gap objective lens for obs. mag. domains by means of differential phase contrast electron microscopy 4-86506  
 electron microscopy at 4K 4-106426  
 electrostatic lens, five-element, magnification behaviour 4-87264  
 high flux density single polepiece electron lenses 4-79026  
 instrumentation, electron optics and X-ray spectroscopy 4-63818  
 new field emission gun, electrostatic lens, characs. (*Chinese*) 4-85091  
 objective lens, high resolution, for an electron microscope, design procedure 4-95569  
 open rotationally symmetric lenses, computation by coupled finite element and boundary integral methods 4-91392  
 optimisation, spherical aberration minimisation, extended field lens (*Chinese*) 4-83535  
 surface vibrational spectroscopy at high impact energies 4-111258  
 third-order aberrations of electrostatic lenses by nonparaxial electron trajectories (*Chinese*) 4-83534

- electron lifetime (metals) *see* electron relaxation time (metals)
- electron lifetime (semiconductors) *see* carrier lifetime
- electron lithography *see* electron beam lithography
- electron mean free path (metals)
- film, ang. and surface roughness depend. of elec. resist., Cottey theory based model 4-70954
  - film, columnar and polycryst., resist., TCR and Hall coeff. 4-70952
  - film, polycryst./monocryst. struct. assumption checking using Hall coeff. variations, size effect 4-70953
  - film, unlike surfaces effect, Cottey model 4-70951
  - IR absorption coeff., nonlocal theory anal. 4-93042
  - metals, amorphous elec. resist., phonon ineffectiveness in diff. model 4-113918
  - Co films, elec. cond. temp. depend. (Russian) 4-88613
  - Ga amorphous thin films, optical props., elec. meas. 4-88800
  - Nb, thermomodulation optical spectrum and electronic struct. 4-66018
  - Nb-Ge, thin films, electrical resistivity, temp. depend. 4-108963
  - Nb-Si, thin films, electrical resistivity, temp. depend. 4-108963
  - Ti, polycrystalline films, resistivity-thickness depend. study 4-108954
- electron mean free path (semiconductors) *see* carrier mean free path
- electron micrographs *see* electron microscope examination of materials; electron microscopy
- electron microprobe analysers *see* electron probe analysis
- electron microprobes *see* electron probes
- electron microscope applications
- see also* electron microscope examination of materials; scanning electron microscope applications
  - selective image analyser for use in particle metrology employing TV monitor and computer equipment (German) 4-101985
- electron microscope examination of materials
- see also* electron microscope applications; electron microscopy; scanning electron microscope examination of materials; scanning-transmission electron microscope examination of materials; transmission electron microscope examination of materials
  - alloys, amorphous; plastic deform. and failure, in situ electron microscopy 4-93481
  - alloys, ordered, two-dimensional antiphase structures, dark-field high resolution images 4-113662
  - aluminosilicate refractories, creep 4-81242
  - antigrain, microstruct., high resolution electron microscopy study 4-103952
  - breast, human, ultrastructure of mucoid carcinoma (Chinese) 4-115028
  - chalcogenide glasses, electron microscopy of reactions with metals and electron beam induced crystn. 4-80315
  - copolymer system, rubber plasticised, processing influence on morphology-prop. relationships (German) 4-85209
  - copper phthalocyanine, planar polymerised, struct. and form. 4-79963
  - copper phthalocyanines, localised mol. arrangements, electron microscopy study 4-80028
  - damage structures, evolution under 14 MeV neutron, 4 MeV ion and 1.25 MeV electron irradi. 4-104818
  - diamond, natural, platelet defects, electron microscopy study 4-103740
  - EBIC technique using scanning Auger microprobe 4-97981
  - electron irradiated, void swelling, effect of C and N 4-108445
  - enamel hydroxyapatite crystallites, human, high resolution electron microscopy 4-105177
  - fluorescein fluorescent dyes, photoelectron microscopy and photoelectron quantum yields 4-82869
  - glass fibre reinforced polyamide, fracture mechanism, acoustic emission and microscopy obs. 4-66417
  - graphite, catalytic oxidation by FeSO<sub>4</sub>, electron microscopy studies 4-85328
  - human tooth enamel, apatite crystals, carious dissolution, electron microscopy study 4-85599
  - II-IV-V<sub>2</sub> glassy semicond., synthesis, stability and microstruct. 4-70042
  - II-VI compounds, irradiation-produced dislocation loops, HVEM study 4-75529
  - lipid extraction during freeze-substitution of bacterium cells for electron microscopy 4-89862
  - lysozyme interaction with phospholipid bilayer, molecular conformation, M obs. 4-66888
  - metal catalysts, supported, particle distrib. determ. by X-ray small angle scatt. 4-97967
  - metal reinforced plastics, struct. during pressure and temp. changes 4-89088
  - metal-semiconductor heterostructures, transition regions, exam. using electron microscopy and Auger spectroscopy 4-65579
  - metallic films, electron micrographs, computer anal. 4-61259
  - metallic glass, amorphous ribbon, as-cast, crystn. and heat treatment effect (Chinese) 4-84190
  - metallic thin films, crystal growth, initial steps, microscopic studies 4-98486
  - molecular cryst., radiation damage morphology, high resolution electron microscopy 4-70219
  - nickel phthalocyanine, struct. change by I doping 4-84305
  - Pd surface, interaction with low voltage H plasma 4-113160
  - pearlite interlamellar spacing, review of data 4-93293
  - PET-p-hydroxybenzoic acid copolyester fibres microstruct. 4-103672
  - phase transformation studies, use of electron microscopy and electron diffraction 4-113281
  - PMMA, syndiotactic, ordered struct. in soln. solid state 4-65166
  - poly p-xylylene, high temp. phase transform. and struct., EM obs. 4-66330
  - polyarylenesulphonoxide-polybutadiene block copolymer films, morphology (Russian) 4-61100
  - polydiacetylene cryst., radiation damage and high resolution electron microscopy 4-80111
  - polyethylene fibres, strength and elasticity, electron microscopy (Russian) 4-85180
  - polymer electrets, radiation induced charge transport 4-71264
  - polymers, identification by unsaturated bond form. in electron irradi. 4-79962
  - quartz, incommensurate phase, transition to  $\alpha$ -phase 4-80216
  - radioactive waste glass, simulated, density changes under ion, electron, and gamma irradi. 4-73974
  - rare earth metal thin films, struct., effect of ion irradi. 4-70240
  - rhodamine fluorescent dyes, photoelectron microscopy and photoelectron quantum yields 4-82869
  - ribosomes, immunoelectron microscopy, book contrib. 4-93988
- electron microscope examination of materials continued
- SBR-cis-polybutadiene elastomer blends, mechanically dispersed, morphology 4-113354
  - sialon polytypoids, struct. characterisation 4-75426
  - steel, alloy, secondary hardening mechanisms 4-99396
  - steel, austenitic stainless, C or N ion irradi., double peak of voidage depth profile 4-98147
  - steel, austenitic stainless, dual-ion and/or electron irradi. in HVEM, in-situ obs. of cavity growth process 4-98134
  - steel, austenitic stainless, electron irradi.-induced struct. phase transformations 4-109418
  - steel, austenitic stainless, fracture modes under He ion and neutron irradi., temp. depend. 4-104853
  - steel, austenitic stainless, heat resistant, precip. and carbide transform. (German) 4-81196
  - steel, austenitic stainless, modified, void suppression, effect of segregation of minor alloying elements 4-104789
  - steel, austenitic stainless, sensitised, Cr depletion in carbide vicinity rel. to heat treatment 4-71654
  - steel, austenitic stainless, void swelling, effects of C and N 4-98149
  - steel, C redistribution by explosion-thermal treatment 4-71673
  - steel, cast Mn, shock wave loaded, struct. and residual props. 4-93369
  - steel, Cr-Mn-Ti, carburised, struct. and hardness rel. to cyclic heat treatment 4-66406
  - steel, electric, Fe-Si (3 wt.%), grain growth in recrystallised material 4-81217
  - steel, high C, electric spark alloyed with refractory carbides, surface struct. 4-66503
  - steel, ion-nitrided structure, electron microscopic studies (Bulgarian) 4-81354
  - steel, low alloy, cast, thermal-mech. fatigue crack propag., effect of strain wave shape 4-66445
  - steel, low C and low alloy, brittle fracture, fractographic characteristics, test temp. effects (Russian) 4-109495
  - steel, microalloyed, hot-rolled, isothermal decomp. of austenite 4-99409
  - steel, Mn-Al, austenitic precipitation, fine structure after annealing (Russian) 4-104787
  - steel, type Kh17N8, phase transitions during deform. press. effect (Russian) 4-81188
  - styrene ionomers, ampholytic, domain struct., small angle neutron scatt. 4-84220
  - thorium phthalocyanine, high resoln. electron microscopy of struct. defects 4-75429
  - tooth enamel, human, struct., digital Fourier harmonic superposition method 4-89495
  - transmembrane channels of E. coli, 3D reconstruction from electron micrographs 4-100418
  - twin boundary dislocations, determ. of Burgers vector by weak beam method 4-80051
  - VA transition metal oxides of V, Nb, and Ta, oxidation mechanism, phase form., cryst. struct., electron microscopy, electron and X-ray diff. studies 4-62119
  - X-ray microanalysis in electron microscopy, spatial resolution 4-72026
  - X-ray films, structure and resistivity, transverse elec. field effect (German) 4-76052
  - Ag halide layer, particle size distrib. from electron micrographs of ultra-thin sections (German) 4-68300
  - Ag-Cu-Zn, ternary  $\beta$ -phase alloys, ordering and phase separation, EM obs. 4-66310
  - Ag<sub>2</sub>O monolayers on Ag (111) film, atomic struct., electron microscopy studies 4-108691
  - Al film, black Zn-coated, solar collector coatings, optimisation and microstruct. anal. 4-62397
  - Al mirrors, laser irradiated in air, damage study by electron microscopy 4-79203
  - Al single crystal, dislocation multiplication during creep 4-98106
  - Al-Ag(In)(Sn) systems, mixing behaviour study by Ar ion beam irradiation 4-65402
  - Al-Al<sub>2</sub>O<sub>3</sub>, composite anodised layer, spectrally selective, solar collector appl., ESCA studies 4-66789
  - Al-Cu, rapidly solidified, decomp. struct. 4-104775
  - Al-Cu alloys, Guinier-Preston zones and solute clusters, high resolution lattice images 4-114543
  - Al-Cu system, metastable states controlled by diffusion 4-65463
  - Al-Cu-Mg-Ag, precipitate struct. and orientation relationship, effect of Ag additions 4-93303
  - Al-Cu-Si, Al 2014, tensile props., 250 to 500°C 4-76816
  - Al-Mg (5 wt.%), high temp. fatigue, squared-up grain struct. 4-81277
  - Al-Mg-Si alloys, transitional state formation by diffusion 4-61135
  - Al-Sc (0.3 at.%) alloy, ageing, precipitation obs. (Russian) 4-104786
  - Al-Ti long-period one-dimensional antiphase structures, electron diff. and microscopy, X-ray diff. 4-113398
  - Al-Zn-Mg alloys, struct. and mech. props., effect of low-temp. thermomech. treatment 4-66352
  - Al-Cu smoke particles, coalescence, electron microscopy study 4-81483
  - $\gamma$ -Al<sub>2</sub>O<sub>3</sub> spherical particles, cryst. struct. and surface morphology, electron microscopy study 4-92149
  - (Au,Ag)<sub>2</sub>Te<sub>2</sub>, krennerite, modulated struct., electron microscopic studies 4-108319
  - Au (111), direct atomic imaging after in situ C etching 4-113770
  - Au-Mn long-period ordered structures, electron microscopy study 4-113396
  - Au-Mn partially disordered, high resolution electron microscopy images 4-92146
  - Au<sub>2</sub>Cd, electron damage, high resolution electron microscopy study 4-92241
  - Au<sub>2</sub>Mn, electron damage, high resolution electron microscopy study 4-92241
  - Au<sub>2</sub>Mn<sub>2</sub>, long period antiphase boundary struct., electron diff., electron microscopy obs. 4-103946
  - BN, films, interaction with Ni at high temps. 4-70583
  - Ba<sub>2</sub>Cs<sub>2</sub>Ti<sub>12</sub>O<sub>40</sub>, hollandite-related superstructures 4-70085
  - BaFe<sub>2</sub>O<sub>7</sub> ferrite, prep. phase transition study (Chinese) 4-93254
  - BaMnO<sub>3-x</sub> system, electron irradi., phase transform., high resolution electron microscopy 4-65395
  - Ba<sub>2</sub>NaNb<sub>3</sub>O<sub>15</sub>, tetragonal bronze-like struct., modulated phases and domain struct. 4-113616
  - BaP<sub>2</sub>O<sub>8</sub>(WO<sub>3</sub>)<sub>2m</sub>, X-ray diff. and high-temperature electron microscopy study of struct. 4-84250
  - Bi-Mo-Nb oxides, complex phases, struct. determ. by high resolution electron microscopy 4-103950

## electron microscope examination of materials continued

- Bi-Se(Te) thermoelements, eutectic soldering, electron microscopy study (Russian) 4-98652  
 Bi-W bronzes, oxidation, high resolution electron microscopy study 4-89156  
 Bi-W-Mo oxides, complex phases, struct. determ. by high resolution electron microscopy 4-103950  
 Bi-W-Nb oxides, complex phases, struct. determ. by high resolution electron microscopy 4-103950  
 Bi<sub>2</sub>(Mo,Nb)<sub>2</sub>O<sub>10</sub>,  $\gamma/2$ , struct. props., high resolution electron microscope studies 4-84771  
 Bi<sub>2</sub>O<sub>3</sub>-WO<sub>3</sub> layered phases, struct. props., high resolution electron microscopy studies 4-70113  
 Bi<sub>2</sub>(W,Nb)<sub>2</sub>O<sub>10</sub>- $\gamma/2$ , struct. props., high resolution electron microscope studies 4-84771  
 C fibre reinforced plastics, struct. during pressure and temp. changes 4-89088  
 Ca<sub>2</sub>Fe<sub>3-2</sub>Mn<sub>2</sub>O<sub>8+y</sub>, O defect perovskite struct., X-ray diffr. and HREM study 4-92382  
 Ca<sub>2</sub>Nb<sub>2</sub>O<sub>7</sub>-CaTiO<sub>3</sub>, ferroelectric, crystallochemical props. 4-71288  
 Co, HCP, effects of systematic reflections on diffr. contrast 4-92035  
 Co-based metallic glasses, low magnetostriction, crystallisation composition depend. 4-84196  
 Cr films, evaporated, internal stress, struct., substrate temp. depend., electron microscopy obs. 4-98495  
 Cu films, structure and resistivity, transverse elec. field effect (German) 4-76052  
 Cu, plastic flow and dynamic recrystallisation in single crystals 4-66394  
 Al-Ti, internal oxidation, dispersion hardening (Japanese) 4-89065  
 Cu-Be alloys, Guinier-Preston zones and solute clusters, high resolution lattice images 4-114543  
 Cu-Co alloys, Co precipitate coarsening, electron microscope studies 4-114544  
 Cu-H, electron irradi., elec. resist. meas., annealing behaviour 4-92240  
 Cu-Ni, twin boundary dislocations, determ. of Burgers vector by weak beam method 4-80051  
 $\beta$ -Cu-Zn, single cryst., deformed in compression, dislocation struct. 4-70162  
 $\beta$ -Cu-Zn-Al,  $\gamma$ -brass-type precipitates, origin of incommensurate electron diffr. pattern 4-76775  
 Cu<sub>2</sub>O metastable oxide formed in initial Cu oxidation, struct., electron microscope study 4-65228  
 Cu<sub>2-x</sub>S, long period modulated struct. with continuously variable periodicity 4-113469  
 Cu<sub>2-x</sub>Te<sub>2</sub>, long period modulated struct. with continuously variable periodicity 4-113469  
 Cu<sub>65</sub>VS<sub>2</sub>, long period modulated struct. with continuously variable periodicity 4-113469  
 CuZn, antiphase boundary energy, superlattice dislocations, slip systems, weak-beam electron microscopy obs. 4-104792  
 Cu<sub>60</sub>Zr<sub>40</sub> alloy system, amorphous, crystallisation kinetics 4-108279  
 Cu<sub>5</sub>Zr<sub>3</sub>, 3D long-period superstructure, electron diffr., electron microscopy obs. 4-70068  
 Dy<sub>2</sub>O<sub>3</sub> thin films, high resolution CTM images, effect of slight disorientation on image aspect 4-70602  
 Fe, dislocation loop form. by self-ion irradi. at 40K, electron microscopy obs. 4-70242  
 Fe fine particles, prep. from goethite microcrysts., morphology and mag. props. 4-65835  
 Fe-base superalloy,  $\sigma$ -phase, planar faults, domain structures, high resolution electron microscopy obs. 4-104793  
 Fe-Cr-Si(Ti), electron and ion-irrad., void and precip. struct. 4-103802  
 Fe-Cu (2 wt.%), needle-precip. growth directions, invariant line strain 4-66336  
 Fe-Mn-Si (19, 1.2 wt.%), stretched, anomaly of  $\alpha'/\epsilon$  orientation ratio (Russian) 4-93289  
 Fe-Mo, lattice imaging of solute atom clusters, electron microscopy obs. 4-81362  
 Fe-Nb, lattice imaging of solute atom clusters, electron microscopy obs. 4-81362  
 Fe-Nb-C(-B), isothermally transformed, microstruct. 4-114510  
 Fe-Nd-B alloy permanent magnets, domain walls, Lorentz electron microscopy study 4-92934  
 Fe-Ni alloys, Ni redistribution by diffusion precipitation (Russian) 4-104785  
 Fe-Ni-P alloys, growth of intragranular ferrite 4-76777  
 Fe<sub>2</sub>Fe<sub>0.8</sub>Nb<sub>0.2</sub>O<sub>3</sub>, ferromag. material for magnetic recording 4-104464  
 Fe<sub>3</sub>O<sub>4</sub> magnetite particles in ferromagnetic colloids, size distrib. anal. 4-109043  
 Fe<sub>3</sub>O<sub>4</sub> particles of mag. fluid, superparamagnetic behaviour, Mossbauer spectra 4-104466  
 GaAs (110), cleaved, surface steps and dislocations, reflection electron microscopy study 4-65529  
 GaAs, heteroepitaxial growth on (0001) mica by ionised vapour evaporation under elec. field 4-104100  
 GaAs:Te, deformed, precip., defect struct., electron microscopy obs. 4-103752  
 Ga<sub>2/3</sub>Cr<sub>2/3</sub>S<sub>4</sub>, cation deficient chalcogenide spinels, electron microscope study 4-113443  
 Ge, laser-induced periodic surface struct., fluencé regimes, feedback and topography 4-108436  
 Ge, radiation-induced rod-like defects 4-92238  
 Ge, symmetrical tilt grain boundaries,  $\Sigma=9, 11$ , struct., electron microscopy obs. 4-70169  
 Ge, tilt boundaries at struct., HREM obs. 4-103767  
 Ge:Te, ion implanted, amorphisation phenomena, electron microscope and electron diffr. studies 4-103656  
 H(UO<sub>2</sub>)(AsO<sub>4</sub>)<sub>2</sub>H<sub>2</sub>O, phase transition temps. and ferroelec. domain struct. 4-76400  
 Ho-Co sputtered amorphous films with perpendicular mag. anisotropy 4-80796  
 InCr<sub>2</sub>/S<sub>2</sub>, cation deficient chalcogenide spinels, electron microscope study 4-113443  
 KCuNb<sub>2</sub>(Ta<sub>2</sub>)O<sub>8</sub>, pentagonal tunnel structures, X-ray diffr. and electron microscopy studies 4-98069  
 La<sub>2</sub>Ti<sub>2</sub>O<sub>7</sub>-CaTiO<sub>3</sub>, ferroelectric, crystallochemical props. 4-71288  
 MgF<sub>2</sub> films, evaporated, internal stress, struct., substrate temp. depend., electron microscopy obs. 4-98495  
 MgO containing metal precipitates, optical and mech. props. 4-70161  
 MgO, dislocation motion and plasticity 4-80043

## electron microscope examination of materials continued

- MgO, electron irradi., point defect kinetics, HVEM study 4-70214  
 MgO-CaTiO<sub>3</sub>-CaO<sub>2</sub>SiO<sub>2</sub> system, phase equilib. and microstruct., isothermal sections 4-114496  
 Mo, deformation mechanism and dislocation struct., HVEM study 4-71682  
 NH<sub>4</sub>H<sub>2</sub>PO<sub>4</sub>, oriented crystallisation, electron-microscope study 4-65202  
 NaAlH<sub>4</sub>, decomposition, Na single cryst. form., electron microscopic study 4-108296  
 NaNbO<sub>3</sub>, cryst. struct. deduced from HREM images and X-ray powder diffr. data 4-65222  
 Na<sub>2</sub>Nb<sub>2</sub>W<sub>2</sub>O<sub>10</sub>, cryst. struct. determ. 4-108312  
 Na<sub>2</sub>Ti<sub>2</sub>O<sub>7</sub>, electron microscopic study, struct. refinement by lattice energy minimization 4-69996  
 Nb-H, hydrogen embrittlement, electron microscopy study 4-93396  
 Nb/Si, metal-semiconductor heterostructures, exam. using electron microscopy and Auger spectroscopy 4-65579  
 (NbSe<sub>2</sub>)<sub>1</sub>, struct., electron microscopy study, rel. to elec. props. 4-79995  
 Nd<sub>2</sub>Ti<sub>2</sub>O<sub>7</sub>-CaTiO<sub>3</sub>, ferroelectric, crystallochemical props. 4-71288  
 Ni magnetic particles, formation in inert gas, electron microscope studies 4-76192  
 Ni, pure, heavy ion irradi. damage, in situ electron microscopy 4-103828  
 Ni/SiC mixed layers, ion and laser irradi., microstruct. anal. 4-84415  
 Ni-base eutectic composite, deform. and failure, examination in HVEM 4-66382  
 Ni-base superalloy, single cryst., crack tip plastic strain 4-89231  
 Ni-based amorphous alloys, crystallisation processes, microstruct. anal. 4-84183  
 Ni-Cr, conc. FCC alloys, heterogeneous deform. mechanisms 4-81236  
 Ni-Cr base alloys, creep behaviour and microstruct. 4-71705  
 Ni<sub>3</sub>Al, cold-rolled, recryst. annealing 4-81213  
 NiO, dislocation core region in grain boundaries, mean inner pot. charge, electron microscope obs. 4-103755  
 NiO films grown by sputter oxidation 4-99658  
 Ni<sub>3-x</sub>Te<sub>2</sub>, long period modulated struct. with continuously variable periodicity 4-113469  
 Ni<sub>3</sub>Ti<sub>1-x</sub>V<sub>1-x</sub>, polymorphs, ordered struct., stacking sequence, high resolution electron microscopy study 4-79984  
 Ni<sub>40</sub>Zn<sub>50</sub>Cu<sub>10</sub> martensite, tempering, morphology and recovery 4-109404  
 NiZr<sub>2</sub> glasses, quenched, phase separation and supercond. props. 4-60839  
 P<sub>2</sub>O<sub>5</sub>(WO<sub>3</sub>)<sub>2m</sub> bronzes, struct. props., electron microscopy studies 4-103721  
 Pb<sub>2</sub>NaNb<sub>2</sub>O<sub>15</sub>, tetragonal bronze-like struct., modulated phases and domain struct. 4-113616  
 mPbS-nBi<sub>2</sub>S<sub>3</sub>, long period modulated struct. with continuously variable periodicity 4-113469  
 Ru, ion irradi., vacancy loops, electron microscopy obs. 4-80046  
 Se<sub>2</sub>S<sub>3</sub>, cryst. struct., electron irradi. induced disorder 4-103713  
 Si, floating-zone crystals, microdefects, metallographic and electron microscopical anal. 4-103737  
 Si, image contrast from extrinsic stacking faults, quantitative anal. 4-75458  
 Si noncrystalline thin films, struct. props. and impurity content 4-88434  
 Si, radiation-induced rod-like defects 4-92238  
 Si tilt boundaries at struct., HREM obs. 4-103767  
 Si-B microcrystalline films, crystallinity, morphology and elec. cond. 4-108749  
 Si-O, helicoidal dislocations, electron microscopic study 4-92208  
 Si-Al-O-N oxynitride glasses, synthesis, stability and microstruct. 4-70042  
 SiC, lattice imaging of 201R polytype 4-75384  
 SiC, polytype and its intergrowth structures, high resolution electron microscopic studies 4-65231  
 SiC, structural defects and grain boundaries, electron microscope study 4-92217  
 Si<sub>3</sub>N<sub>4</sub>, reaction bonded, sintered, densification kinetics, microstruct. 4-76726  
 Si<sub>3</sub>N<sub>4</sub>, structural defects and grain boundaries, electron microscope study 4-92217  
 SiO<sub>2</sub> glass film, crack tip geometry, water ageing, high resolution electron microscopy 4-71724  
 Si-H, bonds and H-induced defects study 4-66058  
 Sm(Co<sub>0.8</sub>Fe<sub>0.2</sub>Cu<sub>0.2</sub>)<sub>7</sub>, magnets, high resolution electron microscopy study 4-61098  
 SmS, helicoidal dislocations, electron microscopic study 4-92208  
 Sr<sub>2</sub>KNb<sub>2</sub>O<sub>15</sub>, tetragonal bronze-like struct., modulated phases and domain struct. 4-113616  
 Sr<sub>2</sub>NaNb<sub>2</sub>O<sub>15</sub>, tetragonal bronze-like struct., modulated phases and domain struct. 4-113616  
 (TaSe<sub>2</sub>)<sub>1</sub>, struct., electron microscopy study, rel. to elec. props. 4-79995  
 Ti, hydride precipitation, electron microscope study 4-92376  
 Ti, quenched, beta to alpha transition, electron microscopy study (Russian) 4-104776  
 Ti-Cr(V)(Mn)(Fe)(Mo), influence of ageing on incommensurate struct. (Russian) 4-65218  
 Ti-Nb-Ni(-Ge), struct. and supercond. props. (Russian) 4-92143  
 TiAl, cryst. struct. determ. 4-113401  
 TiB<sub>2</sub>, implanted with 1 MeV Ni<sup>+</sup> ions, microstruct. and surface mech. props. 4-70232  
 TiC coatings of cemented carbide tools by halide-activated pack cementation process, props. 4-71600  
 TiO<sub>2</sub>, evaporated films, phase transformations by annealing 4-113615  
 TiO<sub>2</sub>, polymorphic transform. by mech. grinding 4-66328  
 TiO<sub>2</sub>-x, interaction of small and extended defects 4-75443  
 U-Mo, U-Nb and U-Ti alloys, quantitative X-ray microanalysis with analytical electron microscope 4-114870  
 UO<sub>2</sub>, charact. of oxides formed by reaction with water IR and sorption anal. 4-74012  
 V, neutron irradi., hardness, tensile props. 4-103809  
 V-H, hydrogen embrittlement, electron microscopy study 4-93396  
 V<sub>2</sub>Si, precipitates, EELS anal. using STEM and high-voltage electron microscope 4-81495  
 V<sub>2</sub>N, crystal struct. from 1 MV electron microscopy 4-92161  
 V<sub>2</sub>Si, martensitic transition, 1 MV electron microscopy high resolution images 4-92354  
 V<sub>2</sub>Si, perfect, Al<sub>15</sub> supercond., structure imaging by high resolution electron microscopy 4-70065  
 W interaction with Al<sub>2</sub>O<sub>3</sub> and Cr<sub>2</sub>O<sub>3</sub> thin films 4-70576  
 WO<sub>3-x</sub>, interaction of small and extended defects 4-75443  
 WSe<sub>2-x</sub>, zone axis patterns, changes with variations in voltage, thickness, composition and temp. 4-92157

**electron microscope examination of materials continued**

- Zr, electron irradi., disloc. loops, electron microscopy studies 4-84296  
 -Zr, Al, electron damage, high resolution electron microscopy study 4-92241  
 ZrO<sub>2</sub>, glaze coatings, microstruct. effect on whiteness 4-81304
- electron microscopes**  
*see also electron microscopy; field emission electron microscopes; scanning electron microscopes; scanning-transmission electron microscopes; transmission electron microscopes*  
 analytical electron microscope, 400 kV high resolution 4-90690  
 Cliff-Lorimer *k* factors determination by analysis of crystallised microdroplets, EDX calibration 4-62271  
 computer interfaced, control, image processing and struct. anal. 4-106430  
 convergent beam diffr. and high resolution imaging 4-106432  
 interference microscope in electron microprobe, specimen exact focusing 4-82864  
 Philips EM 300 electron microscope, cold stage for biological specimens 4-95579  
 Philips eucentric goniometer stage, extreme-tilt holder 4-73600  
 test object for electron microscopes, use of partially crystallized C 4-90692

**electron microscopy**

- see also electron microscope applications; electron microscope examination of materials; electron microscopes; field emission electron microscopy; metallography; scanning electron microscopy; scanning-transmission electron microscopy; specimen preparation; transmission electron microscopy*  
 amorphous electron microscope objects, elastically and inelastically scatt. electrons 4-60790  
 amplitude contrast, rel. to plural electron scatt., Monte Carlo calc. 4-66158  
 analytical, crystallographic calc. methods used in RAD group of computer programs 4-77040  
 astigmatism in electron micrographs, correction using joint transform 4-90694  
 atomic inelastic electron scatt. cross sections, electron microscopy aspects 4-64623  
 autoradiography, rapid, improved method using En<sup>2</sup>Hance 4-115301  
 bent crystal, high resolution structure images around pole pattern 4-113277  
 biological frozen-hydrated specimens prep. for high resolution studies 4-115318  
 biological objects, image reconstruction from projection 4-85596  
 biological specimen, EELS for quantitative X-ray microanalysis, mass thickness determ. 4-62644  
 Boltzmann transport eqn. theory of electron scatt. 4-66159  
 brass 70/30, oxidised surface, Auger spectrometry and RHEED study 4-69994  
 ceramics, high resolution electron microscopy appls. 4-108257  
 Chromatic change in magnification and rotation for magnetic lenses 4-63820  
 Cliff-Lorimer *k* factors determination by analysis of crystallised microdroplets, EDX calibration 4-62271  
 Cliff-Lorimer *k* factors for quantitative X-ray microanalysis in analytical electron microscope 4-62270  
 condensed matter physics, research facilities in USA 4-69987  
 conference, Boston, USA (Nov. 1983) 4-106124  
 conference, Guildford, England (Aug.-Sept. 1983) 4-78034  
 convergent beam diffr., lattice parameter and cryst. symmetry appls. (French) 4-88041  
 convergent beam electron diffr., struct. studies of Ni superalloys 4-88132  
 convergent beam electron diffr. and optical reconstruction, conf., Liege, Belgium (May 1983) 4-86107  
 convergent beam electron diffraction, recent developments 4-88042  
 convergent beam electron diffraction, theory and practice (French) 4-88039  
 cryogenic storage device, simple and inexpensive, for microscopy specimens 4-95572  
 cryoprotection of organic material rel. to electron beam irradi. damage by cooling to 4K 4-65158  
 crystallography, conf., Hamburg, Germany (Aug. 1984) 4-106107  
 dispersive system, alpha, symmetrical and mag., use in spectrometer or energy filter (French) 4-63822  
 electron beam interactions with solids, rel. to microscopy, microanal., and microlithography 4-63394  
 freeze-dried cryosection preparation, sublimation rates of ice in cryoultramicrotome 4-62647  
 freeze-dried cryosection preparation using section press and low elemental support 4-62645  
 glutamine synthetase, mols., time-resolved low dose electron microscopy 4-100420  
 high resolution electron microscopy, pseudoweak phase object approx. (Chinese) 4-113276  
 high resolution electron microscopy 4-79902  
 high resolution images with small defect contrast in rutile 4-97982  
 high-resolution electron microscopes, crystalline test specimens for calibration 4-11260  
 historical developments 4-95124  
 holograms, electron off-axis, speckled background in reconstructions 4-91393  
 holography, electron Fourier, non-interferometric reconstruction props. 4-91394  
 holography, Fourier, aberrations elimination 4-69345  
 holography, Fourier, scatt. foil choice, resolution limitation 4-69346  
 holography, off-axis, noise contrib. 4-69344  
 holography and electron-transfer theory, conf., Antwerp, Belgium (Sept. 1983) 4-67865  
 HVEM, electron scatt. and energy depend., appl. to chem. anal. 4-66162  
 image processing, Boolean algebra operations using digital frame store 4-101979  
 image processing, quality assurance appl. 4-95563  
 image reconstruction three-dimensional (Japanese) 4-112347  
 imaging, chem. anal. and microdiffr. 4-108255  
 imaging, diffraction, microanalysis and artefacts 4-78428  
 immunoelectron microscopy of ribosomes, book contrib. 4-93988  
 JEOL 200CX electron microscope, combined electron diffr. and high resolution imaging 4-95580  
 low temperature electron microscopy at 4K 4-106426  
 macromolecular complexes, electron micrographs, 3D image reconstruction 4-85597

**electron microscopy continued**

- materials testing, microscopy (German) 4-93492  
 metallic thin films and small particles, structure and topography, electron microscopy techniques, review 4-109576  
 metrological possibilities of the electron microscopy 4-95582  
 microanalysis using EELS in high voltage electron microscopy 4-68335  
 microanalysis using EELS ion electron microscope 4-68332  
 micrometrology, conference, Germany (2-3 November 1983) 4-90299  
 molecular biology, structure determination, image averaging methods comparison 4-100662  
 Monte Carlo simulation for electron scatt. in solid targets 4-66155  
 nonideal system, poorly conducting, beam techniques for surface analysis 4-93575  
 object wavefunction statistical estimation under weak scatt. conditions using low-dose illum. from different directions 4-69296  
 objective lens, high resolution, for an electron microscope, design procedure 4-95569  
 organic compounds, electron irradi. damage in electron microscope, encapsulation effects 4-79912  
 periodic specimen, 3-D reconstruction from single view of an oblique section 4-97984  
 Philips EM400T analytic microscope, combined electron diffr. and high resolution microscopy 4-95581  
 photoelectron spectromicroscopy, resolution and contrast 4-95577  
 quantitative Auger electron spectroscopy and microscopy, review 4-95578  
 radiation damage effects 4-79911  
 radioautographic coating apparatus for monolayer emulsion coating 4-58920  
 scanning Auger electron microscopy, instrumental effects 4-85352  
 scanning tunneling microscopy, theory 4-113280  
 scanning X-ray photoelectron and Auger electron microscopes for surface anal., review 4-85351  
 secondary electron emission, microscopy and microanal. aspects, review 4-66147  
 surfaces, electron microscopy, direct atomic images, image simulation 4-65532  
 texture, determ. in electron microscope 4-81395  
 virus microcrystalline layers, images in electron microscope, digital storage methods 4-85594  
 weak-contrast electron microscopic image restoration (Russian) 4-58918  
 wear mechanisms investigation by microscopy, review 4-114743  
 Young's double hole method in electron microscopy, transverse coherence length determ. 4-90695  
 CaMg(CO<sub>3</sub>)<sub>2</sub>, dolomite, interpretation of high resolution electron micrographs 4-79903  
 Fe-Co-Cr mag. disc., Lorentz microscopy and read/write characts. 4-80746  
 Si, self-interstitial scatt. and imaging 4-80033

**electron mobility**

- see also carrier mobility; electron mobility (metals)*  
 gases, dense, with small polarisability, electron mobility calc. 4-60580  
 n-heptane, electron mobility, diffusion coeff. 4-79711  
 n-hexane, electron mobility, diffusion coeff. 4-79711  
 inert gases, electron swarm parameters calc. 4-65145  
 methane, electron transport calc., Boltzmann eqn. anal. 4-103461  
 negative differential cond., generalised Einstein relation 4-79710  
 n-octane, electron mobility, diffusion coeff. 4-79711  
 n-pentane, electron mobility, diffusion coeff. 4-79711  
 phenomena in ionised gases, conference, Dusseldorf, Germany (Sept. 1984) 4-82598  
 streamer development at large E/P in drift approx. 4-69978  
 Ar, transient electron mobility in pulse irradiated gas under steady field 4-113106  
 CO, electron drift vel. at moderate E/N values 4-79712  
 CO<sub>2</sub>, electron drift vel. at moderate E/N values 4-79712  
 CO<sub>2</sub> laser mixtures, electron mobility, diffusion coeffs. ratio 4-112374  
 F<sub>2</sub>, electron swarm parameters, Boltzmann eqn. calcs. 4-79713  
 He, dense gas, electron localisation by external elec. field 4-75119  
 H<sub>2</sub> vapour, electron charact.-energy and momentum transfer cross-section (Korean) 4-79705  
 N<sub>2</sub>, electron drift vel. at moderate E/N values 4-79712  
 N<sub>2</sub>, electron transmission, drift vel. depend. 4-79714  
 Ne, high density gas, electron mobility 4-75121  
 O<sub>2</sub>, electron drift vel. at moderate E/N values 4-79712  
 Xe gas, dense, drift velocity 4-113110

**electron mobility (metals)**

- noble metal, electron-phonon and electron-electron scatt. investigations on Fermi surface 4-70798  
 transition metal, electron-phonon and electron-electron scatt. investigations on Fermi surface 4-70798  
 AuY(Zr)(Nb)(Rh)(Pt)(Pd), dil. alloys, thermoelectric power, resistivity, low temp. studies 4-113925  
 n-Bi<sub>1-x</sub>Sb<sub>x</sub>, electron scatt., low temp. 4-108835

**electron mobility (semiconductors and insulators) *see carrier mobility*****electron multipliers**

- channel, rejuvenation process, particle detect. appls. 4-87021  
 GIOTTO cometary mission, microchannel plate electron multiplier for mass spectrometer 4-63064  
 incident photon flux monitor for synchrotron radiation 4-91175  
 large-entry-window detector consisting of a microchannel plate and a channel-type electron multiplier 4-87013  
 MCP for X-ray and γ-ray imaging 4-64286  
 MCP in windowless EUV photon detectors, lifetime testing results 4-64297  
 MCP nude type electron multipliers, config. and characts. 4-95412  
 MCP output current saturation and lifetime problems 4-64296  
 MEPSICRON photon counter for high dispersion spectrophotometry 4-94621  
 MOSAIC, Mosaicked Optical Self-Scanned Array Imaging Camera for space UV 4-110522  
 Poisson branching point processes 4-90046  
 secondary electron multipliers, T adsorption and desorption, fusion reactor appl. 4-59413  
 space research appl., lifetime tests of channel multiplier compatible materials 4-72850  
 two-dimensional photon counting system, appl. in astronomy (Japanese) 4-94627

electron nuclear double resonance *see* ENDOR

# electron-nucleon interactions

*see also electron-nucleon scattering; electron-proton interactions*  
deep-inelastic electron scatt., partial quark deconfinement, symm. breaking in nucl. matter 4-111372  
QCD effects in few nucleon systems, high energy electron expts. 4-59027  
ed-enp reaction, relativistic effects in deuteron 4-59086  
eN deep inelastic, covariant formulation for cross-sections 4-64006

# electron-nucleon scattering

*see also electron-nucleon interactions; electron-proton scattering*  
 $\sigma$ - $\omega$  model, electromagnetic interactions in nucl. dynamics, quasielastic scatt. cross section 4-111365  
eN-eN, covariant formulation for cross-sections 4-64006

# electron-nucleus reactions

*for inelastic electron-nucleus scattering, see "electron-nucleus scattering"*  
*see also electron-nucleon interactions; nuclear electron capture*  
deep-inelastic electron scatt., partial quark deconfinement, symm. breaking in nucl. matter 4-111372  
low energy photo- and electrofission 4-102249  
QCD effects in few nucleon systems, high energy electron expts. 4-59027  
very inelastic electro- and photo-nuclear reactions at intermediate energies 4-102258  
Z $\geq$ 90 nuclei, photo and electrofission at intermediate energy 4-102331  
(e,e'N), knockout reactions, coincidence form factors interpretation 4-68677  
(e,e' $\pi^+$ ), longitudinal and transverse spin-isospin modes, photopionic processes 4-68619  
(e,e'X), X=d or NN, two nucleon contrib. to deep inelastic scatt. for light nuclei 4-86823  
(e,X), lowest level energy in quantum mech. system, generalised convexity props. 4-73299  
(e,e' $\pi^+$ ), actinide region, giant resonance fission decay, review 4-73942  
<sup>27</sup>Al(e,e'p), hole state excitation and spectral functions 4-73792  
Al(e, $\pi$ ), E $\pi$ =1.2 GeV, pion yield estimates, optimum target thickness (Chinese) 4-102262  
Be(e, $\pi$ ), E $\pi$ =1.2 GeV, pion yield estimates, optimum target thickness (Chinese) 4-102262  
<sup>209</sup>Bi(e, $\pi$ ), 25-55 MeV, electrofission cross section, fission barriers from stat. anal. 4-73943  
<sup>12</sup>C(e, $\pi^+$ )  $\pi^+$  energy spectra study 4-90998  
<sup>12</sup>C(e,e'X), multiple scatt. series, Wigner transform methods 4-102260  
<sup>12</sup>C(e,eX), quasielastic scatt., rel. nuclear pots. effects, response functions 4-106610  
<sup>12</sup>C(e,e'n), 200, 500 MeV/c, longitudinal and transverse response functions, continuum RPA correlations 4-102261  
<sup>12</sup>C(e,e'p), 200, 500 MeV/c, longitudinal and transverse response functions, continuum RPA correlations 4-102261  
<sup>12</sup>C(e,e'p), hole state excitation and spectral functions 4-73792  
<sup>40</sup>Ca(e,eX), A=40.48, |q| $\leq$ 550 MeV/c, deep inelastic scatt., Coulomb sum rule 4-78628  
<sup>40</sup>Ca(e, $\pi^+$ )  $\pi^+$  energy spectra study 4-90998  
<sup>40</sup>Ca(e,eX), quasielastic scatt., rel. nuclear pots. effects, response functions 4-106610  
C(e, $\pi$ ), E $\pi$ =1.2 GeV, pion yield estimates, optimum target thickness (Chinese) 4-102262  
Cu(e, $\pi$ ), E $\pi$ =1.2 GeV, pion yield estimates, optimum target thickness (Chinese) 4-102262  
<sup>56</sup>Fe(e,eX), |q| $\leq$ 550 MeV/c, deep inelastic scatt., Coulomb sum rule 4-78628  
<sup>2</sup>H(e,NN), large q $^2$  electrodisintegration, total and diff. cross sections 4-86822  
<sup>2</sup>H(e,e'p)n, P $\pi$ =295-500 MeV/c, cross section, isobar configuration influence 4-90996  
<sup>2</sup>H(e,en), electrospallation current, neutron polarisation and form factor 4-95998  
<sup>2</sup>H(e,np), struct. props. from (e,e) 4-59225  
<sup>2</sup>H(e,pn), d quark struct. and relativistic quark dynamics 4-95800  
Pt(e,f), 25-55 MeV, electrofission cross section, fission barriers from stat. anal. 4-73943  
Pt(e, $\pi$ ), E $\pi$ =1.2 GeV, pion yield estimates, optimum target thickness (Chinese) 4-102262  
<sup>28</sup>Si(e, $\pi^+$ )  $\pi^+$  energy spectra study 4-90998  
<sup>51</sup>V(e,e'p), hole state excitation and spectral functions 4-73792  
W(e,f), A=182,184,186, 25-55 MeV, electrofission cross section, fission barriers from stat. anal. 4-73943

# electron-nucleus scattering

*see also electron-nucleon scattering*  
A $\leq$ 4, struct. props. from (e,e) 4-59225  
distorted wave approximation anal. (Spanish) 4-86806  
electric sum rule all-multipolarity validity 4-102180  
experimental aspects, motivation, results 4-64123  
magnetic dipole states, electroexcitation in deformed nucl., isovector K=1 $^+$  state, RPA 4-111532  
magnetic transition, generalised isospin sum rule 4-102179  
quasifree, ang. correlations and missing energy spectrum, DWIA anal. 4-59228  
spin mode study with EM and hadronic probes, stretched excitations 4-68682  
spin-isospin response, transverse and longitudinal channels, intermediate energies 4-90964  
weak neutral-current effects in electron-scattering coincidence experiments 4-68607  
(e,e), highly deformed nuclei, eikonal approx. appl. 4-96007  
(e,e), transverse response function,  $\Delta$ -contrib.,  $\Delta$ -hole approach, dynamical model 4-68668  
(e,e) coherent nucleon density fluctuations, nucleon-nucleon correlations 4-96008  
(e,e'), inelastic scatt., external radial integrals evaluation 4-68676  
(e,e'), inelastic scatt., sum rules and long range dipole correl. 4-64122  
(e,e'), R-function method for radiative corrections (Chinese) 4-111540  
(e,e') Dirac single-particle wave functions in inelastic electron scattering 4-83048  
(e,e') on <sup>54,56</sup>Fe, <sup>60</sup>Ni, Coulomb form factors for 0 $^+$ -4 $^+$  transitions in 2p-1f shell, HFB anal. 4-59143  
(e,e') on Ti, Cr, Fe isotopes, form factors for 2 $^+$  states excitation in 2p-1f shell, HFB anal. 4-59142  
<sup>3</sup>Be(e,e'), electromagnetic form factors, effects of meson exchange currents 4-111539  
<sup>12</sup>C, magnetic multipole excitation by inelastic electron scatt. 4-95899  
<sup>12</sup>C(e,e') deep inelastic scatt., relativistic scaling 4-83047

# electron-nucleus scattering continued

<sup>12</sup>C(e,e') dynamical correlations in sum rules 4-59227  
<sup>40</sup>Ca(e,e'), O $_2^+$  state electroexcitation, form factor, coexistence model verification 4-90948  
<sup>56</sup>Fe(e,e'), 180 $^\circ$  quasielastic scatt. cross sections 4-96011  
<sup>156</sup>Gd(e,e'), form factors, low-lying K $^{\pi}$ =1 $^+$  mode 4-111522  
<sup>2</sup>H(e,e'), d quark struct. and relativistic quark dynamics 4-95800  
<sup>2</sup>H(e,e'), elastic scatt., degrees of freedom, pot. effects, rel. approach, review 4-95799  
<sup>2</sup>H(e,e'), form factors, signatures for QCD in nuclear physics 4-90949  
<sup>3</sup>He(e,e'), charge form factors by nucl. recoil detection 4-68617  
<sup>163</sup>Ho(e,e'), oriented, improved eikonal approx. 4-96006  
<sup>6</sup>Li(e,e'), spin-isospin transitions, momentum transfer depend., cross sections, tensor force 4-78593  
<sup>6</sup>Li(e,e'), electromagnetic form factors, effects of meson exchange currents 4-111539  
<sup>24</sup>Mg(e,e'), 90-280 MeV, negative parity states, transitions, EM form factors 4-73806  
<sup>24</sup>Mg(e,e')<sup>24</sup>Mg, excitation of low-lying isoscalar states 4-96024  
<sup>14</sup>N(e,e'), inelastic scatt., M4 transition based on stretched particle-hole excitation 4-68650  
<sup>14</sup>N(e,e')<sup>14</sup>N, M1 form factors at high momentum transfer 4-68675  
<sup>20</sup>Ne(e,e')<sup>20</sup>Ne, excitation of low-lying isoscalar states 4-96024  
<sup>16</sup>O(e,e') dynamical correlations in sum rules 4-59227  
<sup>208</sup>Pb(e,e'), nuclear twist, DWBA, 2 $^+$  state current transition densities 4-96009  
<sup>32</sup>Si(e,e')<sup>32</sup>Si, low multipolarity mag. transitions, cross section meas. 4-59226  
<sup>28</sup>Si(e,e')<sup>28</sup>Si, excitation of low-lying isoscalar states 4-96024  
<sup>8</sup>Sr(e,e'), 23.7-261.6 MeV, 1 $^+$  3.486 MeV state electroexcitation, B(M1), form factors 4-102182  
<sup>8</sup>Sr(e,e') 1 $^+$  excitation at 3.486 MeV, form factor, B(M1)-value 4-68673  
<sup>90</sup>Zr(e,e'), nuclear twist, DWBA, 2 $^+$  state current transition densities 4-96009

# electron optics

*see also beta-ray spectrometers; electron beams; electrostatic lenses; ion optics; magnetic lenses; particle optics*  
astigmatism in electron micrographs, correction using joint transform 4-90694  
asymmetrical condenser-objective lenses, electron optical props. (Chinese) 4-96775  
asymmetrical electron lenses, axial magnetic field charact. 4-64671  
average characteristics of electron optical systems 4-102870  
beam energy spread and angular scatter in foilless diodes 4-69967  
biprism interferences with 1 MeV electrons from monofilament Van de Graaff generator 4-107503  
charged particle energy analysers with wedge-shaped electrode 4-91395  
current image diffraction from crystal surfaces at low energies 4-92034  
development trends, appls. (Chinese) 4-83536  
diverging lens, problems rel. to conical EM fields 4-102874  
double gap objective lens for obs. mag. domains by means of differential phase contrast electron microscopy 4-86506  
electrode and pole piece reconstruction from optimized axial field distrib. 4-112337  
electrostatic electron-optical systems with discontinuous fields 4-74408  
electrostatic wedge analyzer with a cubic field 4-91396  
equations for electron trajectories perturbed by small changes in the initial conditions and geometry of electron-optical systems 4-96780  
field calculations, for systems with both large and small components 4-102873  
field emission gun, paraxial rays and aberrations 4-106428  
field emission gun, with mag. accelerator lens 4-112000  
guns and detectors, for analytical instruments 4-111999  
Heidelberg proton microprobe, secondary electron imaging 4-101973  
holograms, electron off-axis, speckled background in reconstructions 4-91393  
holography, electron Fourier, aberration compensation 4-69345  
holography, electron Fourier, non-interferometric reconstruction props. 4-91394  
holography, electron off-axis, noise contrib. 4-69344  
holography, Fourier, scatt. foil choice resolution limitation 4-69346  
holography and electron transfer theory, conf., Antwerp, Belgium (Sept. 1983) 4-67865  
hybrid electron-ion gun, structural design electron optics and appl. 4-63807  
instrumentation, electron optics and X-ray spectroscopy 4-63818  
interferometry by electron Fourier holography 4-83537  
low energy electrons, electron-electron interactions in finely focused beams 4-87262  
low temperature electron microscopy at 4K 4-106426  
magnetic round lens and sextupole system, aberration theory (Chinese) 4-96774  
microscope fitted with field emission gun, micrograph nonisoplanatism effect 4-68339  
microscopy and anal., conference, Guildford, England (Aug.-Sept. 1983) 4-78034  
Mollenstedt biprism interferometer interference pattern, effects of chromatic aberration and partial coherence 4-87265  
new field emission gun, electrostatic lens, charact. (Chinese) 4-85091  
object wavefunction statistical estimation in electron microscopy under weak scatt. conditions using low-dose illum. from different directions 4-69296  
parametric generation in electron beams 4-102872  
potential perturbations calc. in problems with weakly broken axisymm. 4-74406  
prism charged-particle energy analysers, matrix calc. of aberrations 4-64670  
profile meas. of finely focused electron beams, in SEM 4-58919  
quadrupole lenses, three dimens., made with permanent magnets 4-107251  
relativistic electron beam, propag. in gases, return. current 2-dimens. mapping 4-69301  
relativistic heavy-current beam dynamics in an external mag. field (Ukrainian) 4-87258  
source of HV glow discharge, geometric parameters control (Russian) 4-68320  
TEM, astigmatic brightfield, image quality azimuthal development 4-106429

- electron optics continued
- third-order aberrations of electrostatic lenses by nonparaxial electron trajectories (*Chinese*) 4-83534
- time resolution analysis, electron transit time calc. 4-96777
- truncated spherical mirror for energy anal. combined with direct meas. of ang. distrib. 4-64259
- two-stage electron energy analyzer for angle-resolved photoemission spectroscopy 4-101986
- ultrahigh vacuum instruments and devices, appls. of high permeable materials in mag. ccts. 4-82809
- Young's double hole method in electron microscopy, transverse coherence length determ. 4-90695
- electron pair annihilation** *see* electron-positron interactions
- electron pair production**
- astrophysical, pair processes in steady mildly relativistic thermal plasmas 4-94582
- cosmic ray muons, electron pair production cross-section, in iron 4-110466
- Dirac equation, strong coupling theory for external time-depend. pot., pair creation 4-111273
- Klein-Gordon equation, bound-state solns. for strong pots. 4-106461
- Schwinger source theory of moving charges in condensed matter 4-86532
- single crystals, creation of electron-positron pairs by high energy photons 4-108439
- vacuum polarisation and tunnel transition, potential well in electric field 4-86635
- $(\gamma, e^+e^-)$ , nuclear excitation during pair prod., transition total cross sections 4-73893
- W, high energy  $\gamma$  quanta-induced polarised electrons and positions 4-80104
- electron pairs**
- see also* electron pair production; positronium
- No entries
- electron paramagnetic resonance** *see* paramagnetic resonance
- electron-phonon interactions**
- see also* phonon drag; strong-coupling superconductors; tunnelling spectra; tunnelling spectroscopy; Umklapp process
- Al<sub>5</sub> compound, phonon dispersion curves and electron-phonon interaction calcs. 4-70313
- A<sup>IV</sup>B<sup>VI</sup> cpds., cubic cryst., vibronic const. calcs. 4-61025
- alkali metals, electron-phonon interaction, exchange effect. (*Chinese*) 4-75872
- alloys, amorphous, thermopower, electron-phonon enhancement 4-108839
- alloys, anisotropic superconducting, time depend. Ginzburg-Landau eqns. 4-88630
- anharmonic cryst., statistical mechanics of phonons and phonon linewidths 4-70309
- bipolarons and superconductivity 4-65620
- bipolarons in disordered media 4-70680
- Bloch electrons transport in const. elec. or mag. field 4-70768
- CDW ground state, effects of impurities, mean field calc. 4-70687
- coherent light emission through vibronic levels 4-76499
- compounds with intermediate valency, polaron density waves (*Russian*) 4-84576
- coronene in n-heptane single cryst., phononless line intensity and shift 4-109238
- crystals, elastic interaction of relativistic electrons 4-65301
- deep charged impurity centres, multiphonon light absorpt. 4-71417
- deformation potentials and electron-phonon scatt. theorems 4-61306
- direct-gap semiconductor, nondegenerate, interband luminesc. and absorpt. coeff. 4-61749
- discrete lattice model, asymptotic behaviour, Maslov's method 4-95349
- excited electron state, vibr. relax. 4-98226
- ferroelectric, permittivity in the field of a strong EM wave 4-92988
- ferroelectrics, electron-phonon interaction and phonon softening, Kristoffel-Konsin mechanism 4-65363
- ferromagnetic semiconductor, electron-phonon interaction, s-d model 4-92326
- gapless supercond. in strong exchange fields, Eliashberg theory (*Chinese*) 4-70977
- graphite intercalation compounds, c-axis cond. and thermoelec. power 4-80561
- heavily doped semiconductors, electron relax. effect on phonon damping 4-70317
- hole mobility anisotropy, temp. depend. 4-65681
- III-V semiconductor quantum well struct., free carrier absorption for polar optical phonon scatt. 4-104551
- impurity centres in two-well adiabatic pots., relax. process effect on luminesc. spectra and burnup 4-109223
- impurity mol. embedded in crystal lattice, electronic circular dichroism lineshapes theory 4-76424
- Jahn-Teller matrix elements,  $\Gamma \times e$ , evolution by group theory method 4-92678
- localized electron-phonon system, analytical model, photon echo theory 4-65364
- metal, superconducting state parameters pseudopotential approach 4-61478
- metal surface, laser induced electron-phonon processes 4-75873
- metallic thermopower, electron-phonon enhancement, appl. to metallic glasses 4-92702
- metals, amorphous elec. resist., phonon ineffectiveness in diff. model 4-113918
- metals, electron relax. effect on phonon damping 4-70317
- metals, electron-electron scatt. amplitude, Coulomb and phonon-exchange interactions 4-113936
- metals, electron-phonon interaction strength, point contact spectroscopy anal. 4-65623
- metals with open Fermi surface, thermoelectromotive force at low temps. (*Russian*) 4-92699
- molecular crystal, one-dimensional electron-phonon system 4-70315
- molecular-crystal model, adiabatic limit and phonon dispersion influence 4-113553
- NaCl layers, monoenergetic electron attenuation length, photoelec. studies 4-70803
- narrow band gap semiconductor, impurity recomb. accompanied by local phonon excitation 4-88516
- noble metal, electron-phonon and electron-electron scatt. investigations on Fermi surface 4-70798
- noble metals, electron-phonon interaction, exchange effect (*Chinese*) 4-75872
- electron-phonon interactions continued
- nonequilibrium phonon distribution in quantising mag. field, phonon generator appl. 4-61008
- normal-superconducting multifilm struct., tunnelling and  $T_c$  (*Chinese*) 4-104368
- one-dimensional molecular chains, ultracold neutron scatt. by Davydov solitons (*Russian*) 4-69992
- organic conductors, correlation effects in IR props. 4-92765
- palladium phthalocyanine, reson. Raman, fluoresc., and phosphorescence spectra in Shpol'skii matrices 4-71426
- Peierls systems, electronic correlations 4-70684
- phonon super-radiance 4-92325
- phosphate glass: Nd<sup>3+</sup>, Yb<sup>3+</sup>, phonon-assisted energy transfer and spectra (*Chinese*) 4-93096
- phosphors, binary compounds, cathodoluminesc. efficiency calc. 4-61754
- polar double heterostructures, interface optic phonons and magnetophonon effects 4-98739
- polar semiconductor, donor-acceptor pair capture cross section highly excited electrons 4-61330
- polar semiconductors, dielectric materials, phase transitions, absorption edge anomalies 4-109146
- polar semiconductors, donor-acceptor pair transition, electron-phonon coupling 4-108566
- polyacetylene, IR phonons and Peierls gap, Raman scatt. study 4-76475
- trans-polyacetylene, vibr. props., resonant Raman scatt., theory 4-66031
- polyacetylene, vibr. spectra calcs. 4-61709
- polyacetylene and related cpds., anisotropy of small-polaron narrowing of electron bands 4-61273
- polymers dielectrics, elec. breakdown rel. to high-mobility states 4-109119
- quantum Hall regime, critical currents 4-98644
- quantum wells, quasi-one-dimensional and quasi-two-dimensional, phonon scatt. of electrons 4-98731
- quasi-2D electron systems, electron-phonon interaction and screening effects 4-98547
- quasi-one-dimensional metal, electron-libron scatt. influence on transport props. 4-70795
- quasi-one-dimensional metal, mutual influence of phase transitions, scatt. and localisation of electrons 4-70796
- quasi-one-dimensional metals, superconductivity and optimal phonon freq., theory 4-76066
- rare earth chalcogenides, intermediate valence, Raman scatt., electron-phonon coupling and charge fluctuations 4-88815
- resistivity saturation, self-consistent theory 4-75910
- ruby, Raman spin-lattice relax. induced by optically generated zone boundary phonons 4-66044
- semiconductor, amorphous, electron transport, Mott-CFO model anal. 4-113939
- semiconductor, optical phonons, carrier-assisted laser pumping under strong mag. fields 4-80182
- semiconductor heterolayers, mobility in Bloch-Grüneisen range 4-108932
- semiconductor quasitwo-dimensional quantum-well struct., electron phonon scatt. 4-70918
- semiconductor superlattice, longitudinal magnetoresist. in strong mag. fields 4-61399
- semiconductor surface, electronic collective modes, instabilities and electron-phonon interactions 4-108797
- semiconductor/metal (*Russian*) 4-70931
- semiconductors, dynamic defect reactions induced by multiphonon nonradiative recomb. of injected carriers at deep levels 4-70316
- semiconductors, electron-phonon interaction, point-contact spectroscopy anal. 4-65621
- semiconductors, high field quantum transport theory 4-80599
- semiconductors, mobility fluctuation  $1/f$  noise parameter and phonons 4-114005
- semiconductors, multivalley polar with impurities, optical absorption by electron plasmas 4-114230
- semiconductors, n-type, galvanomagnetic effects in case of electron scatt. by optical phonons 4-80642
- semiconductors, nonequilibrium electrons, optical phonons and acoustic phonons, transport eqns. 4-108851
- semiconductors, phonon drag in longitudinal quantising mag. field 4-98225
- semiconductors, quasi-one-dimensional, low-field electron transport 4-80605
- semiconductors, tetrahedral, electron-phonon interaction and phonon softening due to heavy doping, Kristoffel-Konsin mechanism 4-65363
- single metals elec. resistivity and scatt. theory 4-92694
- small bipolaron form, by electrons coupling to acoustic phonons 4-70679
- small polaron model with nonlinear electron-phonon interactions 4-61304
- solids and molecules, non-radiative transitions and electron-phonon interactions 4-71432
- soliton energetics in electron-phonon models, Peierls-Hubbard models 4-70678
- solitons, generalised master eqns. and polaron propag. 4-104133
- solitons in condensed media, review 4-61028
- strong coupling superconductors, effects of Kondo impurities 4-92845
- strong-coupling supercond. with Shiba-Rusinov impurities, free energy formula 4-104358
- strong-coupling superconductors, local-phonon model of electron-phonon interactions 4-84739
- superconducting thin films in resistive state, heating of electrons due to EM radiation 4-61487
- superconducting transition temp. in strong electron-phonon coupling limit 4-98802
- superconductivity of deformable solids, influence of EM interaction 4-76078
- superconductor, phonon generation during HF EM field absorpt. (*Russian*) 4-84743
- superconductor, weak coupling anisotropic, functional derivative of  $T_c$  with  $\alpha(\omega)F(\omega)$  4-92847
- superconductor/normal metal point contacts, I-V characts. and electron-phonon interaction (*Russian*) 4-70993
- superconductors, disordered narrow band, spin and density fluctuations 4-104355
- superconductors, lower-dimensional, anomalies of crit. mag. fields 4-65776
- superconductors, phonon anomalies 4-65351
- superconductors, Shiba-Rusinov theory of mag. impurities, beyond s-wave scatt., Eliashberg formalism 4-114060
- tight binding model, electron-phonon coupling 4-75628

## electron-phonon interactions continued

- (TMTSF)<sub>2</sub>ClO<sub>4</sub> organic supercond., polarised far IR reflectivity meas. 4-114279  
 (TMTSF)<sub>2</sub>X and related cpds., anisotropy of small polaron narrowing of electron bands 4-61273  
 transition metal, electron-phonon and electron-electron scatt. investigations on Fermi surface 4-70798  
 transition metal, electron-phonon coupling and phonon-limited resist. calcs. 4-70799  
 transition metal alloy, disordered, electron-phonon interaction influence on elec. cond. 4-70800  
 transition metal alloy, disordered, Eliashberg eqns., CPA calc., supercond. crit. temp. depend. factors 4-70976  
 transition metal compounds, low temperature mag. susceptibility. (Russian) 4-114095  
 transition metals, 5d, electron-phonon interaction, relativistic calcs., Hopfield parameter (Ukrainian) 4-88255  
 transition metals, electron-phonon interactions, acoustic NMR meas. 4-70318  
 triple electron collisions effect on photoelectron distribution in ultraquantal mag. field 4-113997  
 two-dimensional systems, electronic props., conf., Oxford, England (Sept. 1983) 4-95050  
 two-photon resonant Raman scattering of light involving free electron-hole pairs 4-66039  
 zero-phonon impurity lines, thermal broadening in absorpt. and fluoresc. spectra 4-109216  
 Ag, electron-phonon interaction, relativistic calcs., Hopfield parameter (Ukrainian) 4-88255  
 Ag, Pd<sub>1-x</sub>, Hall coeff. and band struct. calcs. 4-70780  
 n-(Al,Ga)As/GaAs heterojunctions, hot-electron mobility study at moderate elec. fields 4-84678  
 Al-Al<sub>2</sub>O<sub>3</sub>-metal junctions, thermally shorted, point contact spectroscopy 4-80687  
 AlGaAs/GaAs heterostruct., 2D magnetotransport, electron heating effects 4-98736  
 Bi whisker crystals, nonlinear conduction props. under phonon generation 4-65687  
 n-Bi<sub>1-x</sub>Sb<sub>x</sub>, electron scatt., low temp. 4-108835  
 Bi<sub>2</sub>Te<sub>3</sub>(Se<sub>3</sub>), weak-field transport, thermoelec., galvano- and thermo-mag. coefficients 4-98613  
 CaF<sub>2</sub>:Dy<sup>3+</sup>, Eu<sup>2+</sup> crystals, electron-excitation relax. kinetics and nonequilibrium acoustic phonons. 4-88256  
 CdGeAs<sub>2</sub>, electron scatt. by optical phonon piezoelec. pot. 4-88257  
 CdS, piezoelec. semicond., stimulated Brillouin scatt. of electromagnetic wave, acoustic amplification 4-114291  
 Co, electronic struct., magnetism and Curie temps. 4-75843  
 Co films, elec. cond. temp. depend. (Russian) 4-88613  
 Cu (100), long-range electron-phonon coupling at metal surfaces, EELS meas. 4-80647  
 Cu halides, electron-phonon interaction and optical props., Raman spectra studies 4-66008  
 DyB<sub>2</sub> antiferromagnet, elec. resist. and thermoelec. power studies 4-113982  
 Fe, electronic struct., magnetism and Curie temps. 4-75843  
 Fe<sub>3</sub>O<sub>4</sub>, magnetite, Verwey transition 4-88447  
 n-GaAs, electron energy relax. due to 2TA phonons 4-92324  
 GaAs heterolayer, low temp. two-dimens. mobility 4-108933  
 GaAs, negative differential cond. at transit reson. frequencies 4-84638  
 GaAs:Mn, phonon scatt. at acceptor ground state 4-70729  
 GaAs:N, isoelectronic traps study by photoluminesc. (Chinese) 4-93098  
 GaAs-Al<sub>0.1</sub>Ga<sub>0.9</sub>As tunnel junctions, sequential single-phonon emission obs. in electron transport 4-80667  
 GaAs-AlGaAs heterojunction, phonon emission and electron heating 4-70927  
 GaInAs/InP(AlInAs) heterojunctions and superlattices, 2-D magnetophonon resonance 4-98740  
 Ga<sub>1-x</sub>In<sub>x</sub>Se single crystals, energy gap, temp. dependence 4-92610  
 GaMo<sub>4</sub>X<sub>8</sub> chalcogenides, electron-phonon contrib. to Stoner enhancement 4-84803  
 GaSe, layer crystals, Jahn-Teller effect 4-108824  
 GdB<sub>2</sub> antiferromagnet, elec. resist. and thermoelec. power studies 4-113982  
 n-Ge, hot electron capture by dipoles at low temps., field depend. 4-75979  
 α-Ge, phonon struct., inelastic electron tunnelling spectra obs. 4-61031  
 Ge, picosecond-pulse laser annealing, phenomenological model 4-88198  
 Ge:Sb, wave-function phase, relax. time, temp. depend. 4-88517  
 Hf-Mo, amorphous, upper critical fields 4-98829  
 In, electron-phonon mass-enhancement parameter anisotropy and cyclotron mass 4-84544  
 In, electronic lifetime anisotropy, pseudopotential model calc. 4-113928  
 In-SrTiO<sub>3-x</sub> contact, tunnelling electron-phonon interaction strength 4-98754  
 In<sub>0.5</sub>Ga<sub>0.5</sub>As, electron mobility, rel. to two-mode lattice vibrs. 4-80582  
 n-InP, electron energy relax. due to 2TA phonons 4-92324  
 InP, LEC grown, photoluminesc. study, 1.8 to 40K (Chinese) 4-84993  
 InSb, photoresistance on electron heating in mag. field, two-phonon oscils. 4-84650  
 p-InSb/i-GaAs, heteroepitaxial struct., quasi-2D electrons, nonequilibrium galvanomagnetic effects 4-70916  
 n-InSe, electron scatt. mechanisms, Hall effect and magnetoresist. meas. 4-80614  
 KCl:Ti, X-irrad., TSEE energy spectra, surface pot. meas. 4-61814  
 KI:TiF<sub>4</sub>, hot luminescence and vibr. relax. 4-85019  
 LaH<sub>2</sub>, electron-phonon interaction and supercond. destruction by H absorption 4-65622  
 LiH, electron-phonon interactions in luminescence spectra 4-71439  
 Li(Y,Eu)F<sub>4</sub>Tm<sup>3+</sup>, laser channels, stimulated emission 4-112444  
 Li(Y,Lu)F<sub>4</sub>Tm<sup>3+</sup>, laser channels, stimulated emission 4-112444  
 LiYF<sub>4</sub>:Nd<sup>3+</sup>, electronic Raman scatt. and two-photon fluorescence (Chinese) 4-104581  
 MgO (100), surface dislocation, secondary electron emission study 4-80345  
 Mn dihalides, d-excitons, vibr. struct., IR and Raman spectra studies 4-113873  
 N<sub>2</sub> crystalline, exciton luminesc. and luminesc. spectrum struct. 4-104641  
 N<sub>2</sub>, matrix isolated, electron-phonon coupling 4-83403  
 Nb, anomaly of elec. cond. temp. depend. 4-70777

## electron-phonon interactions continued

- Nb, electron-phonon interaction, relativistic calcs., Hopfield parameter (Ukrainian) 4-88255  
 Nb, phonon singularities on I-V curves, point contact spectroscopy 4-71000  
 Nb-Ge, thin films, electrical resistivity, temp. depend. 4-108963  
 Nb-Si, thin films, electrical resistivity, temp. depend. 4-108963  
 Nb-Ti (41.55 wt.%), superconductor, elec. resist. 4-92853  
 Nb<sub>3</sub>Al based ternary phases, superconducting T<sub>c</sub> volume depend. (Russian) 4-65765  
 Nb<sub>3</sub>Al(Ge)(Sn), thermodynamic props. calc. 4-84741  
 NbH<sub>2</sub>, electron-phonon interaction and supercond. destruction by H absorption 4-65622  
 Nb<sub>3</sub>Sn and Nb<sub>3</sub>Sb, phonon dispersion curves and electron-phonon interaction calcs. 4-70313  
 Nb<sub>50</sub>Zr<sub>35</sub>Si<sub>15</sub>, Nb<sub>70</sub>Zr<sub>15</sub>Si<sub>15</sub>, amorphous alloys, supercond. and electronic props., cold rolling effect 4-61480  
 Ni (100), long-range electron-phonon coupling at metal surfaces, EELS meas. 4-80647  
 Ni, electronic struct., magnetism and Curie temps. 4-75843  
 Os, electron-phonon interaction, point contact spectra studies (Russian) 4-70676  
 Pb chalcogenides, carrier heating mechanisms 4-92738  
 Pb<sub>1-x</sub>Sn<sub>x</sub>Te, ferroelec. phase transition close to band inversion 4-76364  
 Pd, electron-phonon interaction, relativistic calcs., Hopfield parameter (Ukrainian) 4-88255  
 Pd, X-ray emission spectra, anisotropy of cyclotron masses and many-body effects 4-104700  
 Rh, electron-phonon interaction, relativistic calcs., Hopfield parameter (Ukrainian) 4-88255  
 SbCl<sub>4</sub><sup>3-</sup>, in crystal lattice, intervalence absorpt., IR study 4-61734  
 Sb<sub>2</sub>Te<sub>3</sub>, weak-field transport, thermoelec., galvano- and thermo-mag. coefficients 4-98613  
 Si (111) slab, interface, electron-phonon interaction and broken symm. 4-80517  
 n-Si, deformed, drag thermoelectric power anisotropy 4-104247  
 Si, electron inversion layer, scatt. and adsorption of ballistic phonons, theory and expt. 4-98767  
 Si hole space charge layers, interaction between electronic and phonon Raman scatt. 4-98774  
 n-Si, intervalley relax. time, elec. cond. study 4-98621  
 Si inversion layer, ballistic phonon scatt. and absorption 4-65756  
 n-Si, inversion layers in MOSFET, phonon limited hot-electron temp. 4-70945  
 Si MOSFETs, energy relax. of warm electrons under substrate bias 4-104318  
 Si, picosecond-pulse laser annealing, phenomenological model 4-88198  
 Si:In(B), phonon scatt. at acceptor ground state 4-70729  
 Si-MOSFET inversion layer, warm electron coeff. calc. for two-dimens. electron gas 4-65748  
 Smp, mixed valent, EXAFS and near edge struct., energy threshold determ. 4-66126  
 Sm<sub>1-x</sub>Y<sub>x</sub>S, mixed valent, EXAFS and near edge struct., energy threshold determ. 4-66126  
 SrS:Ce,Sm, luminescence, optical and thermal stimulation 4-99174  
 T<sub>c</sub>-C film, superconducting T<sub>c</sub> and critical fields 4-104353  
 Ta, electron-electron scatt., elec. resist. meas. 4-113935  
 2H-TaSe<sub>2</sub>, CDW phase transition at low temp. and high press. 4-104276  
 Te, superconducting props., energy band struct. calcs. 4-104343  
 Te-Zr, hexagonal close packed, supercond. properties, t-matrix approx. 4-108961  
 Ti-Pd(Mo), amorphous, upper critical fields 4-98829  
 TiN(O), anomalies in surface-phonon dispersion 4-75771  
 TiSe<sub>2</sub>-S, mixed crystals, thermoelec. power 4-70849  
 TmVO<sub>4</sub>, cooperative vibronic system, thermal cond. 4-70485  
 V<sub>2</sub>Ga, thermodynamic props. calc. 4-84741  
 V<sub>2</sub>Ge<sub>1-x</sub>Al<sub>x</sub>(Si<sub>1-x</sub>Sb<sub>x</sub>), superconductivity, electron-phonon parameter, electron-atom ratio 4-114058  
 V<sub>2</sub>O<sub>5</sub>, amorphous thin films, props., influence of quenching rate 4-108956  
 VSi point-contact spectra, singularities 4-108925  
 α-Zr, band structure, APW calcs., optical props., superconducting props. 4-113857  
 Zr-Mo(Pd)(Rh), amorphous, upper critical fields 4-98829  
 Zr-Si, amorphous, upper critical field meas. 4-84754

## electron-positron inclusive interactions

- annihilation, quark flavour separation, appl. to electroweak asymmetries, quark lifetimes 4-95768  
 collective bag quark current, Feynman rules, hadron time-like struct. functions (Chinese) 4-73729  
 conference on particles and fields, Banff, Canada (Aug. 1981) 4-63404  
 DESY storage ring expts. 4-96302  
 e<sup>+</sup>e<sup>-</sup> annihilation, energy-energy correlations in perturbative QCD 4-59112  
 energy-energy correlation function, test of perturbative QCD, pp collider 4-86667  
 fundamental interactions, unity, summer school, Erice, Italy, (July-Aug., 1981) 4-86102  
 hadron production in single photon mechanism 4-86721  
 hadronic jet fragmentation including soft gluon interference, QCD parton model 4-82945  
 hydrodynamic theory, t-mass and quark number restrictions, e<sup>+</sup>e<sup>-</sup> and pp comparison 4-86664  
 jet production and fragmentation at 12-43 GeV 4-73766  
 Majorana particle production signature in e<sup>+</sup>e<sup>-</sup> and pp collisions 4-78547  
 new particle searches, electroweak interference effects 4-86722  
 perturbative QCD, factorisation, soft and collinear divergences, e<sup>+</sup>e<sup>-</sup> appl. 4-63966  
 perturbative QCD, jet Monte Carlo simulation and soft gluon radiation 4-102086  
 QCD cluster model of hadronization for e<sup>+</sup>e<sup>-</sup> annihilation 4-90792  
 supersymmetry, experimental tests using e<sup>+</sup>e<sup>-</sup> and pp 4-73676  
 top quark search in e<sup>+</sup>e<sup>-</sup> annihilation between 39.8 and 45.2 GeV 4-64009  
 transverse polarization effects, perturbation theory, gauge models, scalar resonance parity 4-102110  
 e<sup>+</sup>e<sup>-</sup>, √s=29 GeV, highly ionising particles prod. cross section limit 4-59065  
 e<sup>+</sup>e<sup>-</sup>, multiplicity distribns., KNO moment energy depend., Novorodpredazzi method 4-68588

## electron-positron inclusive interactions continued

- $e^+e^- \rightarrow \gamma^*/Z, \gamma^*/Z$  charged particle production at 29 GeV 4-86734  
 $e^+e^- \rightarrow (q\bar{q})$ , finite-energy sum rules for heavy quarkonia 4-111412  
 $e^+e^-$  annihilation, 14-36.7 GeV, local compensation of baryon number,  $\beta$ - $p$  pair prod. 4-68578  
 $e^+e^-$  annihilation, energy-energy correl. function, higher order QCD corrections 4-59092  
 $e^+e^-$  annihilation, quark mass effects for energy-energy correlations 4-90904  
 $e^+e^-$  annihilation fractionally charged particles at 29 GeV 4-68579  
 $e^+e^-$  annihilation jets at PETRA, 9.4-31.6 GeV CM, transverse particle momenta meas. 4-59091  
 $e^+e^- \rightarrow B, B_s, X_{B\mu}$ , decay of heavy quarks, branching ratios 4-59070  
 $e^+e^- \rightarrow$  beauty, lifetime meas. 4-90898  
 $e^+e^- \rightarrow$  charm, lifetime meas. 4-90898  
 $e^+e^-$  collisions, resonance production and decay estimates from radiative Z decays 4-90903  
 $e^+e^- \rightarrow e^+e^-X$ ,  $e\gamma$  deep inelastic scatt. from virtual photons, structure functions, double tag events 4-95785  
 $e^+e^- \rightarrow e^+e^-X$ , photon structure function,  $x$  depend. QCD scale parameter 4-95796  
 $e^+e^- \rightarrow e^+e^-X$ , radiative corrections, total cross-section calcs. 4-68589  
 $e^+e^- \rightarrow e^+e^-(\gamma\gamma)$ (hadrons), composite scalars in  $e^+e^-$  collisions and radiative Z decays 4-86694  
 $e^+e^- \rightarrow$  exotic particles, fragmentation functions, branching ratios 4-90894  
 $e^+e^- \rightarrow \gamma\gamma\gamma$ , cross section, selection propagator mass calc. 4-102108  
 $e^+e^- \rightarrow$  hadrons, at PETRA, one-photon annihilation and two-photon interactions, review 4-64012  
 $e^+e^- \rightarrow$  hadrons, narrowness of hadronic multiplicity distrib., cell theory, KNO scaling 4-59088  
 $e^+e^- \rightarrow$  hadrons, supersymmetry QCD theory 4-59087  
 $e^+e^- \rightarrow$  hadrons in dynamical phase space; statistical jet evol. 4-73767  
 $e^+e^- \rightarrow$  hadrons( $\gamma\gamma$ )( $\mu\mu$ )( $e^+e^-$ ), 39.79-45.52 GeV, new particle search, toponium,  $e^+$  4-90902  
 $e^+e^- \rightarrow$  heavy quarks, D meson tagging 4-90896  
 $e^+e^-$  in Upsilon region,  $Z$  and  $\Lambda$  prod. from T decay, gluon and quark fragmentation 4-90900  
 $e^+e^- \rightarrow$  jets, 29 GeV, proton prod. characs., momentum and  $p_T$  depends. 4-90901  
 $e^+e^- \rightarrow$  jets, flavour independence of quark-gluon coupling const. 4-59090  
 $e^+e^- \rightarrow$  jets, lepton and quark asymmetries, weak neutral currents 4-90897  
 $e^+e^- \rightarrow \mu^+\mu^-H$ , Higgs mass calcs. in QED 4-86695  
 $e^+e^- \rightarrow \mu^+\mu^-X$ ,  $\sqrt{s}=43.45$  GeV, multiparticle event with 2 isolated muons 4-86719  
 $e^+e^-$  physics at 100 GeV, electroweak tests 4-64011  
 $e^+e^- \rightarrow \phi X$ , 29 GeV,  $\phi$  prod. rate from  $K^+K^-$  invariant mass spectrum 4-86718  
 $e^+e^- \rightarrow q\bar{q}g$ , model depend. of coupling const. in 2nd order QCD 4-59089  
 $e^+e^- \rightarrow q\bar{q}\gamma$ , coloured quark electric charge assignments, expt. implications 4-73765  
 $e^+e^-$  results from CESR, B meson and  $\psi$  bottomonium props. 4-63991  
 $e^+e^-$  results from PETRA, QED and electroweak tests, lepton searches, jets, Higgs 4-64010  
 $e^+e^- \rightarrow$  single jet, QCD branching processes and hadronisation, differential-difference eqn. 4-111374  
 $e^+e^- \rightarrow \tau^+\tau^-X$ ,  $\tau$  lifetime determ. 4-86696  
 $e^+e^- \rightarrow \mu^+hX$ , flavour tagging, multiplicity dist., semileptonic branching ratios 4-90895  
T mass meas. in CESR 4-86720  
 $e^+e^- \rightarrow q\bar{q}X$ , sum over resonances, Thomas-Fermi model, local duality 4-90899

## electron-positron interactions

- see also electron-positron inclusive interactions; electron-positron scattering; positron annihilation in liquids and solids*  
 conference, unification and particle physics, Honolulu, HI, USA (Aug. 1983) 4-95065  
 $e^+e^- \rightarrow T$ , props. of triplet wave ( $b\bar{b}$ ) states 4-90893  
 $e^+e^-$  annihilation, line emission from sources contributing to X-ray background 4-77976  
 $e\bar{e} \rightarrow E\pi^+\pi^-$ , resonance in  $KK\pi$  system 4-90905  
 electro-weak physics in  $e^+e^-$  interactions 4-90852  
 gas atom finite assemblies, positron annihilation 4-59896  
 MARK-J at PETRA, expt. results, QED and QCD studies 4-111434  
 PETRA  $e^+e^-$  storage ring, review of experimental investigations 1978-83 4-90851  
 substructure of leptons, quarks,  $W^\pm$ , Z bosons,  $e^+e^-$  collider tests 4-111428  
 $e^+e^-$ , nonstandard Higgs bosons prod. 4-59066  
 $e^+e^-$  annihilation,  $\gamma\gamma\gamma$  prod. and photino mass 4-68558  
 $e^+e^- \rightarrow BB^*$ , unitarized quark model tests 4-111384  
 $e^+e^- \rightarrow BB^*$ , unitarized quark model tests 4-111384  
 $e^+e^- \rightarrow B^*B^*$ , unitarized quark model tests 4-111384  
 $e^+e^- \rightarrow e^+e^-$  + hadrons, photon structure function, comparison with QCD models 4-111455  
 $e^+e^- \rightarrow e^+e^-$  + pseudoscalar particle, two photon physics, radiative corrections, five point function 4-95798  
 $e^+e^- \rightarrow e^+e^-(\gamma\gamma)(\mu^+\mu^-)(\tau^+\tau^-)$ , 39.8-45.2 GeV, spin-0 boson partial width limits 4-73737  
 $e^+e^- \rightarrow e^+e^-e^+e^-$ , cross section calc. using Feynman diagrams, helicity amps. 4-86693  
 $e^+e^- \rightarrow e^+e^-e^+\pi^0$ ,  $\gamma^*\gamma^*\pi^0$  form factor, QCD sum rule method and perturbative QCD comparison 4-82946  
 $e^+e^- \rightarrow \eta\gamma$ , cross section meas. in the vicinity of  $\phi(1020)$  4-59085  
 $e^+e^- \rightarrow \eta\pi^+\pi^-$ , threshold enhancement of cross section 4-111465  
 $E^+e^-$  fermion-antifermion, electroweak induced asymmetry meas. stats., asymmetric ang. distrib. 4-59068  
 $e^+e^- \rightarrow \gamma^*\gamma$ , scalar/pseudoscalar boson contributions, masses and coupling constants 4-111436  
 $e^+e^- \rightarrow \gamma Z^0$ , neutrino generation counting 4-86754  
 $e^+e^- \rightarrow \gamma\gamma$ , experimental searches for squarks, sleptons and SUSY gauge bosons, mass limits 4-59019  
 $e^+e^- \rightarrow \gamma\gamma$ , scalar/pseudoscalar boson contributions, masses and coupling constants 4-111436  
 $e^+e^- \rightarrow \gamma\gamma\gamma$ , photino production cross-section calcs. 4-90850  
 $e^+e^- \rightarrow \gamma\gamma\gamma\gamma$ , cross section, helicity amplitudes in high energy limit 4-90848  
 $e^+e^- \rightarrow$  hadrons( $\gamma\gamma$ )( $\mu\mu$ )( $e^+e^-$ ), 39.79-45.52 GeV, new particle search, toponium,  $e^+$  4-90902

## electron-positron interactions continued

- $e^+e^- \rightarrow$  jets, QCD Monte Carlo code PARJET 4-78560  
 $e^+e^- \rightarrow \gamma^*\gamma$ , electroweak model dependence of electromagnetic corrections 4-73705  
 $e^+e^- \rightarrow \mu^+\mu^-$ , charge asymmetry, weak single loop corrections,  $\gamma Z$  box 4-59063  
 $e^+e^- \rightarrow \mu^+\mu^-$ , muon forward-backward asymmetry, higher order corrections in Weinberg-Salam model 4-78546  
 $e^+e^- \rightarrow \mu^+\mu^-$  asymmetry, electroweak radiative corrections in  $SU(2) \times U(1)$  model 4-68559  
 $e^+e^- \rightarrow \mu\mu\gamma(\gamma)$ , cross section, coupling constant, comparison with QED predictions 4-111435  
 $e^+e^-$  physics, evidence for theoretical ideas 4-95786  
 $e^+e^- \rightarrow q\bar{q}$ , scalar/pseudoscalar boson contributions, masses and coupling constants 4-111436  
 $e^+e^- \rightarrow W^-W^+$ , single W prod. cross section 4-59064  
 $e^+e^- \rightarrow W^+W^-(Z\gamma)(ZZ)(ZH)$ , muon spectra from W and Z decays 4-73738  
 $\gamma\gamma \rightarrow \eta$  in  $e^+e^- \rightarrow e^+e^- \pi^+\pi^- \gamma$ , transition form factor 4-95867  
 $e^+e^- \rightarrow \gamma\gamma$ , double bremsstrahlung, photon ang. distrib., radiative corrections 4-82953  
**electron-positron scattering**  
*see also electron-positron interactions*  
 $e^+e^- \rightarrow e^+e^+$ , radiative corrections in  $SU(2) \times U(1)$  4-111432  
 $e^+e^- \rightarrow e^+e^-$ , scalar/pseudoscalar boson contributions, masses and coupling constants 4-111436  
 $e^+e^- \rightarrow e^+e^-(\gamma\gamma)(\mu^+\mu^-)(\tau^+\tau^-)$ , 39.8-45.2 GeV, spin-0 boson partial width limits 4-73737  
 $e^+e^- \rightarrow$  hadrons( $\gamma\gamma$ )( $\mu\mu$ )( $e^+e^-$ ), 39.79-45.52 GeV, new particle search, toponium,  $e^+$  4-90902  
 $e^+e^-$  results from PETRA, QED and electroweak tests, lepton searches, jets, Higgs 4-64010  
**electron probe analysers** *see electron probe analysis*  
**electron probe analysis**  
 aerosols, atmospheric, LAMMA and electron microprobe anal. 4-81501  
 Al (111), pure textured polycrystalline, analytical SEM with JAMP-10 Auger microprobe 4-61785  
 alloy films, submicron, electron probe microanal. 4-75808  
 alloys, X-ray production and quantitative electron-probe micro anal., depth distrib. (Chinese) 4-99855  
 austenitic alloys, surface reactions with light elements, EPMA, wavelength-dispersive spectrometry 4-81360  
 biological specimen, EELS for quantitative X-ray microanalysis, mass thickness determ. 4-62644  
 Boltzmann transport eqn. theory of electron scatt. 4-66159  
 borosilicate waste glasses, ion bombard., fracture toughness and leaching behaviour 4-75545  
 $\beta$ -brass, Sn alloyed, Auger/SEM obs. of corrosion 4-89172  
 carbides, quantitative electron probe microanal. using Gaussian  $\phi(\rho z)$  eqn. 4-76930  
 Cliff-Lorimer  $k$  factors determination by analysis of crystallised microdroplets, EDX calibration 4-62271  
 Cliff-Lorimer  $k$  factors for quantitative X-ray microanalysis in analytical electron microscope 4-62270  
 coating thickness measurements, X-ray studies 4-63717  
 detection limit, vol. and surface impurity diffusion effects 4-99918  
 diffraction effects on electron path in recrystallised thin films (French) 4-63816  
 electron beam interactions with solids, rel. to microscopy, microanal., and microlithography 4-63394  
 electron microscopy, analytical crystallographic calc. methods used in RAD group of computer programs 4-77040  
 electron probe X-ray microanalysis, of surface and thin films 4-81507  
 excitation energy distrib., Gaussian models, appl. to X-ray microanal. and solid state electronics 4-65303  
 fluorescence correction procedure for microprobe analysis near phase boundaries 4-63814  
 freeze-dried cryosection preparation, sublimation rates of ice in cryoultramicrotome 4-62647  
 freeze-dried cryosection preparation using section press and low elemental support 4-62645  
 Gaussian curves evaluation, use in electron probe microanalysis 4-99926  
 grain boundary segregation 4-80244  
 Heidelberg proton microprobe, secondary electron imaging 4-101973  
 heterogeneous sample analysis (French) 4-63815  
 history of quantitative electron probe microanalysis 4-63471  
 human skin, proton and electron microprobe analysis 4-105390  
 hybrid electron-ion gun, structural design electron optics and appl. 4-63807  
 in-depth microanalysis, of multi-layered samples 4-114871  
 Incoloy 800, oxidation in moist air containing HCl at 800°C 4-81327  
 Inconel, aluminised, microstruct. characterisation of coating 4-76911  
 inelastic electron scatt. in solids, review 4-66151  
 instrumentation, electron optics and X-ray spectroscopy 4-63818  
 ionic substitution, MEB and X-ray microanal. investig. 4-79889  
 irregular and unusually shaped sample corrections 4-81499  
 light element anal. using energy-dispersive spectrometers 4-66635  
 microanalysis at grazing incidence, correction calcs. (French) 4-63811  
 microanalysis with high spatial resolution using X-rays and electron energy loss scattering 4-109714  
 microanalytical maps, use of colour scales 4-72010  
 mineralogical measuring procedures automation 4-114879  
 monomode optical fibres and preforms, elemental distrib., electron microprobe investig. 4-79318  
 Monte Carlo simulation for electron scatt. in solid targets 4-66155  
 multicomponent specimen backscattering coeff. 4-93162  
 nonideal system, poorly conducting, beam techniques for surface analysis 4-93575  
 nuclear fuel, irradiated particles, fission product localisation using unshielded electron microprobe 4-73981  
 nuclear fuel dissolution residues, microprobe anal. apps. 4-74014  
 optical fibre structures, electron microprobe study (Polish) 4-112576  
 oxide films, characterisation by soft X-ray spectroscopy and microanal. 4-76909  
 particulate material, automated electron microprobe anal. 4-81500  
 phase relationships in alloys, EPMA studies 4-76933  
 polyacenic, pristine and doped, semiconducting props. 4-75949  
 qualitative and quantitative surface microscopy, book contrib. 4-109619  
 quantitative light element electron probe microanalysis, correction procedure evaluation 4-63809

**electron probe analysis continued**

- quantitative microanalysis, matrix effects (*French*) 4-66630  
 rare earth alloys, R-Co, hexagonal phases, abnormal mag. props. and mixed valence states 4-113907  
 scanning Auger microprobe and ion scattering spectrometry combination 4-68336  
 scanning electron microscope microprobe anal. appls. 4-101981  
 secondary electron emission, microscopy and microanal. aspects, review 4-66147  
 specimen preparation, Ga supporting medium 4-111114  
 spherically aberrated probes in STEM, electron density distrib. 4-78427  
 steel, bearing, surface layers, effect of grinding (*Chinese*) 4-99628  
 steel, Cr-Mn austenitic, phase stability and corrosion on exposure to pure Li 4-107061  
 steel, Cr-Mn austenitic, thermally aged, phase instability, precip. reactions 4-109410  
 steel, ferromag., electron beam microanal., stray mag. fields (*German*) 4-66622  
 steel, improved corrosion resist. in water after abrasive blasting with  $\text{Al}_2\text{O}_3$  4-62099  
 steel, seamless tubes, anal. of oxide inclusion responsible for internal defects (*French*) 4-76935  
 steel, sintered, Mn diffusion coatings 4-89186  
 steel, stainless; austenite-ferrite duplex, preferential phase dissolution in  $\text{H}_2\text{SO}_4$ -NaCl soln. rel. to heat treatment and comp. 4-81341  
 steel, stainless, Nb-stabilized, Cr-depleted, oxidation, Cr conc. for healing layer form. 4-81326  
 steel, submerged arc welds, inclusion anal. using EPMA and TEM 4-76744  
 Superprobe JXA-733, application program 4-85344  
 TEM, book contrib. 4-109620  
 thin film electron microprobe analysis, Monte Carlo simulation Mott, scatt. cross sections 4-63810  
 thin films, electron microprobe anal. and SIMS comparison 4-66631  
 thin foils, electron beam spreading in STEM-EDS X-ray micro anal. 4-85279  
 X-ray loss due to electron backscatter 4-63813  
 X-ray microanalysis in analytical TEM, bremsstrahlung-produced fluoresc. effect 4-89365  
 X-ray production, depth distrib. 4-63851  
 Zircaloy-4, SAM determ. of O gradients, deform. modelling 4-88191  
 Al film on Si, thickness determ. by Monte Carlo code with secondary fluorescence correction 4-63716  
 Al-Fe-Mn system, Al-rich corner, phase equilb. and crystn. studies 4-114480  
 Al-Si-Sb, eutectic, struct. rel. to Sb addition, electron beam microanalysis (*German, English*) 4-66314  
 Al-Ti-B alloys, Al-rich, nature and morphology of Ti- and B-rich crysts. (*French*) 4-61919  
 $\text{AlGa}_{1-x}\text{As}$  epitaxial film, XPS study 4-93189  
 AlN, oxynitride bonded ceramics; sintering, microstruct., densification, flexural strength, oxide additions effect 4-76727  
 $\text{Al}_2\text{SiC}_5$  mixed carbide, prep. and struct. studies 4-88144  
 Au-Cu minerals, study using electron probe anal. 4-76934  
 $\text{BaTiO}_3$ - $\text{SrTiO}_3$ , high-temp. reactions, EPMA and SEM investig. 4-80292  
 $\text{BaZrO}_3$ - $\text{BaTiO}_3$ , high-temp. reactions, EPMA and SEM investig. 4-80292  
 CdSe, reaction with Pb and S containing reactive gas phase 4-105016  
 Co-Ti-C system, phase relations, diffusion paths, 1273K 4-109382  
 $\text{Co}_{1-x}\text{O}_x$ -Ni single crystal, Ni impurity diffusion and interaction with vacancies 4-92437  
 Cu/Sn-Cu diffusion couple, electron microprobe anal. (*Chinese*) 4-104008  
 Cu-Pb engine bearings, multilayer diffusion barriers 4-98331  
 Cu-Ti interface, electron probe anal. of diffusion zones 4-62151  
 Cu-Zn-Al (25, 6 wt.%), isothermal decomp. of  $\beta'$  phase 4-99387  
 $\text{DyFe}_2\text{Al}_{2-x}\text{Fe}_{1+x}$  X-ray emission spectra, electron microprobe anal. 4-76563  
 Fe-Cr (26.6 at.%), sulphidation mechanism in  $\text{H}_2\text{S}$ - $\text{H}_2$  atmospheres at temps. of 973 to 1173K and S press.  $10^{-4}$  to  $10^{-6}$  Pa 4-93460  
 $\text{Fe}_{1-x}\text{Co}_x$  single cryst. solid solutions, homogeneity studies 4-75693  
 $\text{Fe}_2\text{GeO}_6$ , mixed valent, prep., struct., mag. props. (*French*) 4-88148  
 $\text{Fe}_{1-x}\text{Ni}_x$  single cryst. solid solutions, homogeneity studies 4-75693  
 $\text{Fe}_2\text{SiO}_4$ , Fayalite sint., segregates or precipitates anal. by electron probe microanal. (*Japanese*) 4-99698  
 GaAs:In, isoelectrical doping, X-ray and electron microprobe anal. 4-75491  
 $\text{Ge}_2\text{Fe}_{1-x}\text{O}_4$ , mixed valent, prep., struct., mag. props. (*French*) 4-88148  
 $\text{MgO}$ - $\text{CaTiO}_3$ - $\text{CaO}$ - $\text{SiO}_2$  system, phase equilb. and microstruct., isothermal sections 4-114496  
 Ni-(Al-Ti)-(Cr-Mo), pseudoternary phase diagram, phase relationship study using EPMA 4-76933  
 Ni-Al-Mo-Ta system, constitution of Ni-rich alloys at 1523K 4-66313  
 $\text{PbTiO}_3$ - $\text{PbZrO}_3$ , high-temp. reactions, EPMA and SEM investig. 4-80292  
 Ru-Rh system, constitution, solid solubility and lattice consts. 4-70390  
 SiC filament reinforced Ti, metal composite, filament microanal. and strength characterisation 4-104753  
 $\text{SiO}_2$ - $\text{V}_2\text{O}_5$  thin films, memory elements, metallic conducting filaments in low resist. state 4-75804  
 Sn, laser alloyed layers on GaAs substrates, elec. props., surface damage 4-99622  
 Th-Co, hexagonal phases, abnormal mag. props. and mixed valence states 4-113907  
 Ti, corrosion in  $\text{H}_2$ - $\text{H}_2\text{S}$  atmospheres, TGA, X-ray diff. 4-109559  
 $\text{TiO}_2$ -based crystalline ceramic nuclear waste forms, processing and microstruct. 4-83150  
 $\text{TlBiTe}_3$ , growth, elec. and optical props. 4-65676  
 U-Mo, U-Nb and U-Ti alloys, quantitative X-ray microanalysis with analytical electron microscope 4-114870  
 $\text{UO}_2$  irradiated thermal reactor fuel, fission products, electron-probe microanal. appls. 4-73980  
 $\text{UO}_2$ , low enriched, Triso coated, post-irradiation electron probe microanal. 4-68769  
 V-MoSe<sub>2</sub> and V-NbSe<sub>2</sub>, volume changes in sintering 4-66271  
 Zn-Al-Si (21, 2 at.%), frictional surface charact. under boundary lubrication 4-66452  
 $\text{Zn}_{1-x}\text{Co}_x\text{S}$ , single cryst. solid solutions, homogeneity studies 4-75693

**electron probe analysis continued**

- ZnS films, RF sputtering prep. and microstruct. props. 4-88417  
 $\text{ZrO}_2$ - $\text{SiO}_2$ - $\text{TiO}_2$  system, phase equilb. and solid solubility, relationship 4-85143  
**electron probe microanalysis** *see electron probe analysis*  
**electron probe microscopy** *see electron probe analysis*  
**electron probes**  
*see also electron probe analysis*  
 grating spectrometer with point source and crossed-grating configuration efficiency 4-63819  
 interference microscope in electron microprobe, specimen exact focusing 4-82864  
 microprobe control program, software system design 4-68327  
 microprobes, automation, software system designed, control program 4-68326  
**electron-proton interactions**  
*see also electron-proton scattering*  
 deep inelastic scatt. deuteron six-quark component from struct. function 4-59047  
 $\text{Sb}_2\text{Te}_3$  single cryst., weak field charge transport 4-108887  
**electron-proton scattering**  
*see also electron-proton interactions*  
 No entries  
**electron radiation**  
 Cherenkov relativistic electron RF sources, cyclotron reson. mode selection 4-69299  
 Cherenkov relativistic electron source for millimetre range, Bragg resonator use 4-69300  
 CT-6 Tokamak, electron cyclotron radiation diagnosis by GaAs Schottky diode heterodyne receiver 4-103541  
 cyclotron emission rates in superstrong mag. fields 4-59967  
 electron spontaneous emission in relativistic nonneutral electron beam 4-79021  
 magnetized high-intensity electron beam, cyclotron resonance of pumping wave, induced rad. 4-69293  
 polarised electrons, spatial asymm. of transition radiation 4-83528  
 Smith-Purcell radiation enhancement from a grating with surface-plasmon excitation 4-87260  
 spatially periodic medium, radiation of electrons in uniform motion 4-83530  
 spectral quantum approach to induced Cherenkov and transition radiation of electrons 4-78193  
**electron relaxation time (metals)**  
 metal, surface state damping in angle resolved photoemission 4-71527  
 metallic films with unlike surfaces, electron scatt. model 4-76051  
 In, electronic lifetime anisotropy, pseudopotential model calc. 4-113928  
 Zn single cryst., transverse electron focusing and specular reflection 4-92707  
**electron relaxation time (semiconductors)** *see carrier relaxation time*  
**electron resists**  
 PMMA positive electron resist, crystal. struct. and sensitivity 4-98031  
 polymers, aromatic, halogenated, negative electron resists, crosslinking reactions 4-89292  
 polyvinylalcohol - resists, electron beam chem. and radiation sensitivity study 4-75530  
 $\text{SrF}_2$ , single cryst., on GaAs (001) electron beam resist. and dielec. for insulator/semicond. struct. 4-98758  
**electron ring accelerators**  
 betatron, RECE-Christa, electron ring acceleration 4-59463  
 electron ring trapping in mirror fields, simulation 4-60715  
 electron-proton collider of European laboratory for particle physics, world's largest particle accelerator (*German*) 4-74064  
 resists for storage ring X-ray lithography 4-95597  
 storage ring design for X-ray lithography 4-96303  
**electron scattering** *see elastic scattering of electrons by atoms and molecules; electron beam effects; electron beams; electron-electron interactions; electron-electron scattering; electron impact; electron-nucleon interactions; electron-nucleon scattering; electron-nucleus reactions; electron-nucleus scattering; electron-positron interactions; electron-positron scattering; electron spectra; hadron electroproduction; neutrino-electron interactions; neutrino-electron scattering; secondary emission*  
**electron solvation** *see solvation*  
**electron spectra**  
*see also Auger effect; conversion electron spectra; electron energy loss spectra; electron impact; electron spectroscopy; photoelectron spectra*  
 24.8 MeV electrons backscattering from C, Al, Cu, and Pb, energy spectra 4-88912  
 2-bromo-1,3,2-dioxarsolane, mol. struct. by electron diff. 4-112292  
 2-bromo-1,3,2-dithiarsolane, mol. struct. by electron diff. 4-112292  
 chemical ionisation mass spectrometry, electron impact mass spectra simulation by charge exchange 4-111241  
 2-chloro-1,3,2-dioxarsolane, mol. struct. by electron diff. 4-112292  
 chloroethylene anions, formation and dissociation, electron attachment spectra 4-71876  
 EELS instrumental artifacts, elimination and correction 4-68334  
 ion sources, collective acceleration, Thomson spectrometer anal. 4-107180  
 noble metals, unoccupied band critical point energies 4-61276  
 selenophene, electron transmission spectra 4-102823  
 tellurophene, electron transmission spectra 4-102823  
 Au/Si<sub>3</sub>N<sub>4</sub>/Si system, elec. effects of Au (*Chinese*) 4-98757  
 $\text{BaTiO}_3$  based solid solns., ferroelec. transition temp. and electron spectra 4-93013  
 Br+Pb(L) collisions,  $\delta$ -electron spectra study 4-74321  
 $\text{CO}_3^{+}$ , C $\Sigma$ g $\Sigma_2^+$  state, photoionis. shape reson., electron spectrosc. obs. 4-112236  
 Cu<sub>2</sub>O, ESCA and Auger spectroscopy determ. of binding energy (*French*) 4-66638  
 D<sup>-</sup>, very-low-energy electron detachment 4-91336  
 $\alpha$ - $\text{Fe}_2\text{O}_3$  and  $\text{Fe}_3\text{O}_4$ , ESCA and Auger spectroscopy determ. of binding energy (*French*) 4-66638  
 $\text{Fe}(\text{OH})_3$  and  $\gamma$ - $\text{FeOOH}$ , ESCA and Auger spectroscopy determ. of binding energy (*French*) 4-66638  
 H<sup>+</sup>, very-low-energy electron detachment 4-91336  
 H<sup>+</sup>+inert gas atom, multiply ionising collisions,  $\delta$ -electron spectra 4-83438  
 I+Pb collisions,  $\delta$ -electron spectra study 4-74321  
 N<sup>6+</sup>+He (H<sub>2</sub>), electron capture in autoionising configurations N<sup>4+</sup> studied by electron spectrometry 4-59889

**electron spectra continued**

- Ni (111), adsorption and decomposition of NO, metastable quenching electron spectroscopy 4-92567  
 NiO, ESCA and Auger spectroscopy determ. of binding energy (French) 4-66638

**electron spectrometers**

- see also beta-ray spectrometers  
 calibrating device 4-101980  
 charged particle spectrometer design using synchrotron radiation 4-82862  
 charged-particle spectrometers, spectrometer functions, optimisation and output current limitations 4-90693  
 conversion electron Mossbauer spectrometer for depth selective spectroscopy 4-74089  
 crossed electric and magnetic fields, rotation of polarisation vector of electron beam 4-86996  
 EELS spectrometer, detector efficiency 4-63828  
 electrostatic electron spectrometer with electron retarder and double cylindrical mirror analyser 4-74086  
 ESCA and AES spectrometer for highly radioactive materials 4-73603  
 high resolution angle-resolved photoelectron spectrometer system 4-91146  
 inelastic electron tunnelling spectroscopy 4-78418  
 inner-shell electron impact spectrometer, for at. and mol. studies 4-69233  
 NIKHEF-K 180° electron-scatt facility overlapping-scintillator system 4-102450  
 prism charged-particle energy analysers, matrix calc. of aberrations 4-64670  
 QDD spectrometer system, design, performance 4-91140  
 retarding-grid electron spectrometer for Mossbauer spectroscopy 4-86514  
 scintillation glass shower counter, energy resolution of 1-25 GeV positions 4-59529  
 scintillation hodoscope spectrometer for electrons and high-energy photons 4-59487  
 time projection chamber, LAMPF spectrometer,  $e^+$  spectrum in  $\mu$  decay 4-59493  
 UV angular photoemission, spectrometer design (French) 4-63824  
 VUV radiation physics, conf., Jerusalem, Israel, 8-12 Aug. (1983) 4-82583  
 X-ray photoelectron spectrometers, energy calibration 4-99284  
 X-ray photoelectron spectrometers, energy calibration 4-99285  
 (e,2e) spectrometer for investigating the spectral momentum density of thin films 4-111257  
 $\mu-e^+e^-e^+$ , search using SINDRUM mag. spectrometer 4-59480  
 p-Si:P surface-barrier detectors fabrication and appl. 4-87018  
 Xe liquid in ionisation chamber, spectrometry of 1 MeV electrons 4-107263

**electron spectroscopy**

- see also electron spectra; photoelectron spectroscopy  
 AES introduction and appls. in materials science (Afrikaans) 4-73598  
 anisotropic electron emission from localised and delocalised sources 4-99244  
 Auger electron energy analyser using a cylindrical mirror with ring-to-axis focusing 4-90696  
 Auger electron spectroscopy, backscattering factors calc. (Chinese) 4-73597  
 calibration, rel. to 1s ionis. energy of Ne 4-78984  
 core-level electron-electron coincidence spectroscopy 4-78420  
 dipole oscillator strengths for mol. photoabsorpt., photoionis. and ionic fragmentation 4-78915  
 EELS spectral library, appl. to materials science research 4-68333  
 electronic energy levels interpretation in solid-state physics (French) 4-66134  
 electrostatic charged particle energy analyzers with a wedge-shaped electrode 4-91395  
 electrostatic wedge analyzer with a cubic field 4-91396  
 energy analyser design for electron spectrometry (French) 4-63826  
 ESCA, radiation damage, bremsstrahlung contribution 4-99915  
 ESCA core binding energies, inductive effects 4-78419  
 ESCA signal acquisition and processing system, ATD 16 (French) 4-66639  
 lens system for surface vibrational spectroscopy at high impact energies 4-111258  
 microanalysis using EELS in high voltage electron microscopy 4-68335  
 microanalysis using EELS ion electron microscope 4-68332  
 multichannel analyser for electron spectroscopy 4-91184  
 polyethylene terephthalate films, photooxidation and ageing, ESCA and contact angle obs. 4-61806  
 positron spectroscopy applied to surface analysis 4-71493  
 quantitative Auger electron spectroscopy and microscopy, review 4-95578  
 surface composition, scanning electron microscopy 4-71505  
 surface phenomena exam. by electron spectroscopy, temperature controller design 4-78304  
 surface quantitative anal. by electron spectroscopy (French) 4-72023  
 VUV radiation physics, conf., Jerusalem, Israel, 8-12 Aug. (1983) 4-82583  
 Ni-Fe, dissoln. and passivation, influence of S adsorp. 4-71757  
 n-Si surface barrier high resolution detectors for <20 keV conversion electrons 4-74103

**electron spin**

- geomagnetic field model involving spinning electrons 4-115333  
 Hund's multiplicity rule, quantum mechanical explanation 4-96418  
 QED 8th order contributions to electron anomaly from vacuum polarization graphs 4-95749  
 spinor chain path integral, Dirac eqn., spin transition amplitudes 4-111271

**electron spin-lattice relaxation**

- euproprium ethylsulfate.Ce<sup>3+</sup>, Ce<sup>3+</sup> EPR spin-lattice relax. rate, press. effects 4-65855  
 free radicals in ion-exchange materials, spin-lattice relax. via excited vibr. states 4-59815  
 imidazole series nitroxide radicals, superslow rot. pulse EPR study 4-80821  
 myoglobin, phonon bottleneck, electron spin relax. study 4-109780  
 nematics, fluctuations, mean fields and order parameters 4-88070  
 nickelocenium cation, electronic struct., Jahn-Teller effect, EPR study 4-64517  
 paramagnetic systems, nuclear spin-lattice and spin-spin relax. for S=3/2 and S=5/2 4-96570  
 phosphate glass:Yb<sup>3+</sup>, electron spin-lattice and phase relax. 4-114158  
 polyacetylene, electron spin-lattice relax. rate meas. 4-61583

**electron spin-lattice relaxation continued**

- ruby, Raman spin-lattice relax. induced by optically generated zone boundary phonons 4-66044  
 spin relaxation and electromagnetic vacuum fluctuations in nonrelativistic quantum mech. 4-101696  
 spin-polarised radicals, ESR, microwave-switched time integration study 4-87143  
 2,2,6,6-tetramethyl-4-piperidone-N-oxyl, liq. solns., spin relax., EPR and ELDOR obs. 4-107373  
 uniaxial ferroelectrics, spin-lattice relax. at phase transitions, effect of relaxing defects, appl. to TGS 4-99059  
 yttrium ethylsulfate.Ce<sup>3+</sup>, Ce<sup>3+</sup> EPR spin-lattice relax. rate, press. effects 4-65855  
 CoNbOF<sub>6</sub>.6H<sub>2</sub>O:Mn(II), host spin-lattice relax. narrowing in EPR, phase transition 4-71162  
 Cr complex, HMBA Cr V radical in 1,2 propylene glycol soln., spectral and relax. time meas. at 150 GHz 4-91289  
 Fe-Ni Invar alloys, Mossbauer spectra 4-88748  
 GaP:Ni, state of impurity centres, EPR, spin-lattice relax. time, spin Hamiltonian parameters 4-88476  
 KH<sub>2</sub>PO<sub>4</sub>:Se, ESR relax. time meas. 4-92957  
 LiNbO<sub>3</sub>:Mn<sup>2+</sup>(Cr<sup>3+</sup>)(Cu<sup>2+</sup>), spin-lattice relax., EPR studies 4-114157  
 Si<sub>3</sub>-Ge<sub>3</sub>P, EPR study and spin-lattice relax. (Russian) 4-71177  
 ZnNbOF<sub>6</sub>.6H<sub>2</sub>O:Mn(II), host spin-lattice relax. narrowing in EPR, phase transition 4-71162

**electron spin polarisation**

- see also CIDEP: spin polarised electron emission  
 alkali metal atoms, optically pumped; electron spin randomisation in spin temp. limit (Chinese) 4-112147  
 benzyl radicals, stationary nutations and CIDEP during methyl benzyl ketone photolysis 4-76252  
 bromomethane, angle- and spin-resolved photoelectron spectroscopy 4-83417  
 diamond, transition from isotropic muonium state to axially symm. anomalous muonium state 4-71237  
 double focusing electron spin polarimeter characts., mag. field shape effects 4-95573  
 ferromagnet, spin polarised electron elastic scatt., anisotropy, pseudopot. method anal. 4-114348  
 ferromagnetic semiconductor, conduction electron spin polarisation 4-88682  
 iodomethane, angle- and spin-resolved photoelectron spectroscopy 4-83417  
 Kondo effect, conduction electron polarisation, absence 4-71021  
 optically pumped atoms, electron polarisation meas., H<sup>-</sup> ion source appl. 4-64258  
 polyacetylene, solitons, Coulomb interactions, Monte Carlo simulation 4-70677  
 rare earth alloys, RCo<sub>2</sub>B<sub>2</sub>, R=Gd-Tm, antiferromag. and paramag. states, NMR spectra 4-109089  
 relativistic spin-polarised scatt. theory, soln. of single-site problem 4-92679  
 two-dimensional spin-polarised fermion lattice gas, Monte Carlo study 4-68177  
<sup>3</sup>He, spin-polarized film on <sup>4</sup>He substrate, superfluidity detection 4-70527  
 Al superconducting films, antisymp. Fermi liq. and Pauli susceptibility renormalisation, spin polarised tunnelling meas. 4-70997  
 Ar atom, (<sup>3</sup>P<sub>2</sub>) state, orientation by laser optical pumping 4-112148  
 Co single crystals, spin polarised Auger electrons 4-85044  
 Fe (110), exchange split empty energy bands inverse photoemission studies 4-84551  
 Fe (110), ferromag., spin-polarised low-energy electron diff., temp. effects 4-104456  
 Fe (110)p(2×2)-S, surface ferromagnetism, chemisorption, absorbate-induced substrate reconstruction effect, spin-polarised LEED calcs. 4-80395  
 Fe single crystals, spin polarised Auger electrons 4-85044  
 Fe<sub>2</sub>B<sub>3</sub>Si<sub>6</sub> ferromagnet, spin-flip Stoner excitations, EELS studies 4-104410  
 GaAs, optical spin orientation of Γ<sub>15</sub> conduction band electrons, photoemission study 4-66188  
 GaAs: Mn, spin-depend. recombination, optical pumping studies 4-99183  
 GdCo amorphous cosputtered film, surface versus bulk magnetisation curves, threshold photoemission and photoelectron spin polarisation 4-71131  
 Ge-Ni(Ce), spin depolarisation study 4-104722  
 H, spin polarised, atomic, condensation on superfluid <sup>4</sup>He 4-104037  
 H, spin polarised atomic, on liquid He, polaronic aspects 4-104034  
 H, spin polarised, collective spin oscillations 4-70525  
 H, spin polarized, three-body recombination rates 4-70526  
 H, spin-polarized, nucl. spin waves, NMR study 4-70524  
<sup>3</sup>He liquid, fully spin polarised, ground state energy and Landau parameters 4-75750  
<sup>3</sup>He-, gaseous, spin rot. effects and spin waves 4-79734  
 I<sub>2</sub>, angle- and spin-resolved photoelectron spectroscopy 4-83417  
 Na, optically pumped atoms, electron polarisation meas., H<sup>-</sup> ion source appl. 4-64258  
<sup>23</sup>Na atomic beam, polarisation by laser optical pumping 4-107467  
 Ni (001), photoemission spectrum struct. reinterpretation 4-71518  
 Ni (110), ferromagnetic, spin polarised EELS study (German) 4-76573  
 Ni single crystals, spin polarised Auger electrons 4-85044  
 Ni, spin-polarised Compton profile, relativistic corrections to classical Hamiltonian 4-71464  
 Ni, Stoner excitation spectrum, spin polarised EELS studies 4-104411  
 Si, magnetic energy states of shallow acceptors, spin depend. luminesc. study 4-104655  
 Si:B(μ<sup>+</sup>), tetrahedral interstitial impurities, electronic struct., spin-polarised calc. 4-65636  
 TmS(Se), exchange-induced plasma edge splitting, magneto-optical study 4-61663  
 Xe, spin polarisation transfer, photoelectron emission 4-83343

**electron spin relaxation** see *electron spin-lattice relaxation*

**electron spin resonance** see *paramagnetic resonance*

**electron states, impurity** see *impurity electron states*

**electron states, surface** see *surface electron states*

**electron streams** see *electron beams*

electron structure of solids (crystallography) *see crystallography*

electron structure of solids and liquids (energy structure) *see electron energy states (condensed matter)*

electron theory

*see also Dirac equation; quantum electrodynamics*

No entries

electron theory of metals *see metal theory*

electron traps

*see also colour centres; hole traps; impurity electron states*

amorphous semiconductor, dispersive transport, multiple-trapping model, effect of energy depend. capture cross section 4-70830

amorphous semiconductors, picosecond electronic relaxations 4-108892

coronene layers, elec. cond. and trap distrib. 4-84626

covalent semiconductors, electron capture cross-section 4-104227

depletion regions, carrier capture from free-carrier tails 4-92746

disordered solids, with continuous trap distrib., dispersive carrier transport 4-108874

dosimeters, solid-state, ionising energy storage, rel. to trapping levels 4-68838

ethylene propylene fluorinated copolymer, positive charge stabilisation 4-65688

glycine, radiothermoluminesc., ESR investig. 4-61758

hydrocarbon glasses,  $\alpha$  irradi., trapped electrons, photoconductivity study 4-65700

LDPE, trapping parameters rel. to morphology, TSC meas. 4-108877

MIS, tunnel capacitor, leakage current effects on DLTS 4-70938

MOS capacitors, field controlled charge trapping in tunnel oxides 4-70939

narrow band gap semicond., impurity recomb. accompanied by local phonon excitation 4-88516

pentacene, electron and hole traps, thermally stimulated current techniques, quadrupolar traps 4-61391

pentacene layers, dispersive charge carrier transport 4-80703

PET-metal contacts, space charge injection under stress 4-108938

polyethylene, electron irradiated, thermostimulated exoemission and radical recomb. 4-93003

polyethylene terephthalate electrets, AC elec. field form. and TSC studies 4-84902

polymers, electrical cond. and carrier traps, review 4-108854

polythene films, space-charge limited charge distrib., discharge currents 4-88621

semiconductor, deep centres, carrier capture cross section meas. method (Chinese) 4-92741

semiconductor struct., vaporisation deposited, light refraction mechanism 4-76542

semiconductors, excited quasistationary states relax. as source of exoelectron emission 4-99290

semiconductors, free carrier capture kinetics by deep traps 4-80536

semiconductors, grain-boundary admittance theory 4-108849

semiconductors, nonradiative multiphonon capture of carriers by deep traps 4-75889

semiconductors, persistent photocond. and charge carrier capture cross sections 4-80608

Ag halide microcrystals, spectroscopic identification of localised electrons and holes 4-114308

Al-SiO<sub>2</sub>-Si MOS structure, X-ray induced interface traps, stress relax. effects 4-98755

Al-SiO<sub>2</sub>-Si struct., X-ray irradi., interface traps. 4-104281

AlGaAs GaAs modulation doped heterostruct., persistent photocond. studies 4-98705

n-AlGaAs, MBE grown, deep electron traps 4-98570

Al<sub>0.7</sub>Ga<sub>0.3</sub>As:Si MBE layers, electron trap conc., DLTS study 4-61317

Al<sub>0.7</sub>Ga<sub>0.3</sub>As, correlation of photoluminescence and deep trapping 4-80537

n-Al<sub>0.7</sub>Ga<sub>0.3</sub>As, MBE grown, deep electron traps, growth conditions and alloy composition influence 4-98558

Al<sub>0.7</sub>Ga<sub>0.3</sub>As/GaAs heterostructure, selectively doped, transient photocond. obs. 4-70862

Al<sub>2</sub>O<sub>3</sub>:Co, thermoluminescence and trap parameters 4-76532

BaTiO<sub>3</sub> ceramics, lanthanide doped, EPR spectra 4-109072

Bi<sub>2</sub>GeO<sub>20</sub>, field and charge distrib. in case of trap thermal ionisation 4-66010

Bi<sub>2</sub>GeO<sub>20</sub>, trap parameter determ. by optical probing 4-88479

CdS, spontaneous oscills. in presence of temp.-electric instability 4-104266

n-CdTe, electron traps, DLTS study 4-80533

n-CdTe:In, electron traps, DLTS study 4-80533

CdTe-ZnTe heterojunction, interface trap depths 4-61442

D<sub>2</sub>, solid, proton irradi., electron trapping, IR absorption studies 4-75751

GaAs, amorphous, high-defect-density, subpicosecond carrier trapping 4-80621

GaAs, EL2 and EL0 midgap levels, electron emission in strong elec. fields 4-88510

GaAs, EL2 defect, technological and physical aspects 4-75891

GaAs, electron irradiated, carrier-capture cross sections meas. technique 4-61394

GaAs, electron traps, midgap, and multimetastable states, photoquenching studies 4-88466

GaAs, electron traps, props. and nature 4-75890

GaAs, LPE growth, deep intrinsic centers, anisotropic capture 4-113897

GaAs, MOCVD grown, deep electron traps, DLTS obs. 4-84585

GaAs, semi-insulating, deep donor conc., dislocations and elec. resist. 4-103781

GaAs, semi-insulating, surface cond. mechanism, space-charge-limited current leakage 4-70901

GaAs, semi-insulating optical photogenerated traps 4-108875

GaAs, trap parameters meas. by photo-excited DLTS (Japanese) 4-80544

GaAs: Mn, spin-depend. recombination, optical pumping studies 4-99183

GaAs:N, isoelectronic traps study by photoluminesc. (Chinese) 4-93098

GaAs:Si, ion implanted, and semi-insulating GaAs, deep levels, photoconductivity study 4-88469

GaAs:Sn/GaAs:Cr interface, electron and hole traps, photovoltaic studies 4-104283

GaAs:Al(Au) Schottky barrier contacts, LEC grown, electron traps, DLTS signals, effect of metal 4-84691

GaAsP strained-layer superlattice structures and their buffer layers, comparison of trapping levels 4-113885

GaP: N epitaxial films, n-type, local cathodolum. kinetics 4-109251

GaSe:Co, injection and thermopolarisation currents 4-70833

electron traps continued

Ge, impurities microinhomogeneities, capture channels, time-amplitude anal. 4-108876

Ge:Cu(Au), nonradiative multiphonon capture of carriers by deep traps 4-75889

GeS film, crystalline and amorphous, photoconductivity study (Russian) 4-70870

GeSe<sub>2</sub>, cryst. and glassy, photoelec. props. 4-108905

HgI<sub>2</sub>, optically excited electronic processes 4-104254

InP, electron irradi. induced deep traps, deep level optical spectroscopy 4-104156

InP p<sup>+</sup>-n junctions,  $\gamma$ -ray irradi., electron trap annealing 4-98748

KBr:In(Tl), light sum slow component characts. in presence of fast component, photoluminescence (Russian) 4-114320

NaYF<sub>4</sub>, polycryst. powder, X-irrad., thermolum. and colour centre obs. 4-61757

PbI<sub>2</sub>, thermally stimulated currents at low elec. fields 4-65689

Pb<sub>1-x</sub>Sn<sub>x</sub>Te, defect states, impurity photoconductivity transient studies 4-80545

Pt-SiO<sub>2</sub>-Si MIS struct., flat-band voltage shift 4-108944

SeTe, As glassy films, pure and doped, deep level defects, xerographic spectra studies 4-61339

Si, amorphous, high-defect-density, subpicosecond carrier trapping 4-80621

Si, amorphous CVD films, H<sub>2</sub> plasma annealing localized state density 4-61337

Si, computer simulation, relativistic electrons, multiple scatt., axial channelling 4-108491

n-Si, electron capture coeff. of quenching centres 4-104159

Si film, LPCVD, elec. props., effect of film thickness 4-88615

Si, grain boundaries, spin-depend. trapping, effects of light and modulation freq. 4-104155

Si,  $\gamma$ -ray irradi., trapping centres, DLTS studies 4-104147

Si, plastically deformed, deep levels, capacitance, reverse current meas. 4-61319

a-Si, space charge limited current rel. to density of states 4-98637

Si:Au, donor and acceptor levels, DLTS meas. 4-88473

Si:B polycrystalline films, activation energy of resist., effects of grain boundary trapping state energy distrib. 4-88616

a-Si:H, glow discharge decomposition prep., electron drift mobility, photocurrent (Chinese) 4-84616

a-Si:H, long-time drift mobility, photocurrent study 4-104221

a-Si:H, radiative combination at dangling bonds, quantitative model, expt. study 4-114326

a-Si:H, transient photoinduced absorpt. 4-104634

a-Si:H:N film, TSC and photoconductivity 4-104222

a-Si:H:O(N) alloys, electron trapping states, tight binding formalism calcs. 4-113901

a-Si:H film, IR quenching of photoluminescence and photoconductivity 4-104656

Si:Mn, Cu, impurity energy levels, DLTS and capacitance studies 4-88471

Si:P,O, trap spectrum of O donor, DLTS study 4-92651

Si:Pd, deep levels, DLTS study (Chinese) 4-113887

Si:S, persistent photoconductivity effect obs. 4-113995

Si:Ti, recombination props., capture rates 4-104149

Si/SiO<sub>2</sub> MOS capacitors, donor state generation rate, anode field depend. 4-92826

Si-SiO<sub>2</sub>, interface traps in diode struct., small signal admittances 4-80678

Si-SiO<sub>2</sub>-Mo MOS diodes, carrier trapping centres and interface states induced by RF sputtering of Mo 4-88603

Si<sub>3</sub>N<sub>4</sub> film MNOS struct., trapped charge profile and relax. currents 4-65749

Si<sub>3</sub>N<sub>4</sub>, high trap density, trapping kinetics 4-104218

Si<sub>3</sub>N<sub>4</sub>:F films, plasma enhanced CVD, insulating props. 4-61865

SiO<sub>2</sub>, charge neutralisation by electron bombardment 4-98694

SiO<sub>2</sub> film traps, microcomputer-based avalanche injection system, area density anal. 4-101870

SiO<sub>2</sub> thin films, nitridation and elec. props. 4-61435

TiO<sub>2</sub>, multiphoton interactions, laser induced photoluminesc. and photocond. 4-93093

V<sub>2</sub>O<sub>5</sub>-P<sub>2</sub>O<sub>5</sub>-ZnO thin film glasses, space charge limited conduction 4-84627

Yb<sub>2</sub>O<sub>3</sub> thin films, trap levels, thermally stimulated method anal. 4-65763

ZnO electrolumiphor, brightness waves, grain size effects 4-104675

ZnO:Gd(Pr), thermoluminesc. under UV,  $\beta$ - and  $\gamma$ -ray irradiations 4-93119

ZnSe:N, acceptor levels, optically excited DLTS study 4-61322

electron tube components

*see also electron guns*

W wires, electropolished, struct. changes after thermal treatment rel. to surface state (Polish) 4-85249

electron tube diodes *see diodes*

electron tube rectifiers *see rectifier tubes*

electron tube testing

image intensifier tube VARO 4215, testing for astronomical appls. 4-72889

electron tubes

*see also cold-cathode tubes; diodes; electron emission; microwave tubes; relativistic electron beam tubes; thermionic tubes; triodes; ultra-high frequency tubes; X-ray tubes*

cyclotron radiofrequency amplifier, requirements 4-111987

light valve projector for large screen display (Japanese) 4-107792

electron tunnelling *see tunnelling*

electron valves *see electron tubes*

electron-wave tubes

*see also klystrons; magnetrons; travelling-wave-tubes*

No entries

electronegativity

absolute hardness, companion parameter to absolute electronegativity 4-59659

alkali metals, adsorption on transition metal surfaces, electronic charge transfer 4-92554

alloy, liq., partially ionic, screening role in electronic and atomic struct. 4-70635

amine-boranes, <sup>14</sup>N nuclear quadrupole double reson. and B-N bond study 4-87145

**Electronegativity continued**  
 amine-trifluoroboranes,  $^{14}\text{N}$  nuclear quadrupole double reson. and B-N bond study 4-87145  
 binary alloys, electronegativity in local density functional formalism 4-70061  
 binary cpds., energy gaps, polarisation and partial metallic valence 4-103697  
 crystal field parameters in a modified point charge model 4-104176  
 discharge onset levels in strongly electroneg. gases and gas mixtures, Paschen's law calcs. 4-79880  
 elemental electronegativities, electron affinities, ionis. pots. and hardnesses calcs. 4-112099  
 elements, electronegativities, density functional theory HF Slater theory 4-96442  
 intermetallic compounds,  $\text{AB}_2$  binary, three-dimens. struct. diagram 4-70080  
 merocyanine dyes, solar photovoltaic cells, performance correl. with mol. struct. 4-85369  
 polymer donor-acceptor systems, one-dimens., band struct., INDO calcs. 4-113847  
 semiconductor-electrolyte junctions, anion electronegativity effects 4-70930  
 semiconductor-metal junctions, anion electronegativity effects 4-70930  
 Al alloys, thermodynamics and struct., solvent-solute interaction 4-113670  
 $\text{AlGa}_{1-x}\text{As}$  epitaxial film, XPS study 4-93189  
 $\text{C}_2\text{O}^+$  cation radical in Ne matrix, ESR investig. 4-78873  
 $\text{Cu}_3\text{TaS}_4(\text{Se}_4)(\text{Te}_4)$ , isomer shifts of 6.2 keV nucl. transition, Mossbauer spectra 4-109104  
 $\text{MoO}_3$ , impurities, defect form. and charge compensation, EPR studies 4-80054  
 $\text{Na}_2\text{Mo}_2\text{O}_7$ , impurities, defect form. and charge compensation, EPR studies 4-80054

#### electronic calculators

for calculator applications see under relevant applications e.g. engineering computing; natural sciences computing  
 spectral analyses of  $\gamma$ -rays (Chinese) 4-68859

#### electronic conduction in crystalline semiconductor thin films

for electronic conduction in amorphous thin films, see "electrical conductivity of amorphous semiconductors and insulators"  
 see also electrical conductivity of amorphous semiconductors and insulators; electrical conductivity of crystalline semiconductors and insulators; electrical conductivity transitions  
 carrier transport in semiconductor magnetic field sensors 4-70844  
 epitaxial high-purity layers, low-pressure MOCVD growth 4-61861  
 $\text{GaInAs-InP}$  heterojunction, interface 2-D electron gas props., MOCVD growth and characterisation (French) 4-76685  
 $\text{InP-Zn}$  epitaxial layers, MOCVD grown, doping, Hall effect, SIMS, electrochemical profiling 4-80077  
 nonlinear conductivity of layers with dimensionally quantized electron energy spectrum 4-114051  
 poly-N-vinylcarbazole layers, cryst., dark cond. meas. 4-76050  
 thermopower and conductivity measurements, optical beam deflection technique 4-98786  
 unipolar films, nonlinear elec. cond. 4-88617  
 $\text{Ag}_2\text{S}$ , chem. prepared films, mixed conductivity study 4-104277  
 $\text{Al}_x\text{-In}_x\text{As}$ , nominally undoped, MBE growth and charact. 4-98472  
 Bi thin films, vacuum deposited, semiconducting props. rel. to annealing 4-65758  
 Bi ultrathin aggregated film, cond. transition, classical percolation two-dimensional continuum model 4-104330  
 $\text{Bi}_2\text{CdS}_4$  film, spray pyrolysis deposited, substrate temp. effect on elec. and opt. props. 4-70962  
 $\text{Bi}_2\text{CdS}_4$  films, spray pyrolysis deposition, elec. and optical props. 4-76669  
 $\text{Bi}_2\text{Sb}_{1-x}\text{Te}_x$  films, strain-resist. effects, struct. effects 4-114052  
 $\text{Cd}_3\text{Hg}_{1-x}\text{Te}$ , epitaxial film growth by chem. transport reactions, elec. props. 4-70965  
 $\text{CdS}$  film, deposited by hot wall technique, characterisation of doped and undoped films 4-114405  
 $\text{CdS}$  films grown by spray pyrolysis in an  $\text{N}_2$  ambient 4-61843  
 $\text{CdS}$  thin film, RF-sputtered, elec. props., effect of temp. and bias 4-80699  
 $\text{CdS}$  thin films prep. by spray deposition, vacuum annealing effect on elec., structural and optical props. 4-70966  
 $\text{CdS-In film}$ , elec. props. meas. 4-104329  
 $\text{CdS-O}_2$  highly photocond. films, spray pyrolysis prep. 4-88533  
 $\text{CdS(In)}$  films chemical bath-deposited, electrical and optical props. 4-92832  
 $\text{CdTe}$  film, composition and elec. props. 4-80696  
 $\text{CdTe}$  films on  $\text{InSb}$ , MBE growth, charact. 4-98470  
 $\text{CdTe}$  thin films, DC cond. rel. to  $\text{H}_2$  exposure 4-76053  
 $\text{CdTe}$  thin films for solar cell appls., deposition and elec. props. 4-76054  
 $\text{CdTe:H-Au}$  contacts, hydrogenation effects 4-80695  
 $\text{Cd}_{1-x}\text{Zn}_x\text{S}$  films, prep. at various  $\text{Cd/Zn:S}$  ion ratios, use in electrochem. photovoltaic cells 4-85099  
 Ce epitaxial layers, plasma enhanced CVD growth of free-standing films 4-81866  
 $\text{Cu}_x\text{Fe}_{1-x}\text{Cr}_2\text{S}_4$  films, elec. and galvanomagnetic props. 4-76056  
 $\text{Ga}_{1-x}\text{Al}_x\text{S:Zn}$ , (Se), doping in MOCVD growth, carrier conc. and cond. 4-88982  
 GaAs epitaxial layers, MOCVD, surface morphology and elec. props. 4-84493  
 GaAs MBE layers, elec. props. of oval defects, FET appl. 4-92574  
 GaAs semi-insulating substrate, inhomogeneity characterisation, expt. study 4-65759  
 GaAs:Cr, epitaxial layers, Cr doping and elec. parameters 4-76683  
 $\text{Ga}_{0.4}\text{In}_{0.6}\text{As}$  layers, MOCVD growth and characterisation (French) 4-76685  
 $\text{GaInAsP}$ , low field carrier mobility, book contrib. 4-61383  
 $\text{Ga}_{1-x}\text{In}_x\text{AsSb}_{1-y}$  epitaxial layers, reflection spectra analysis 4-114340  
 n-Ge:As, growth on Si by MBE, charact. 4-98469  
 Ge:Ga(Sb), film on GaAs, doping and elec. props. study (Russian) 4-70182  
 GeS film, crystalline and amorphous, photoconductivity study (Russian) 4-70870  
 HgS mixed films, elec. and optical props. (French) 4-84715  
 InAs, struct. and electrical cond. behaviour under deposition conditions 4-98787

#### electronic conduction in crystalline semiconductor thin films continued

$\text{InGaAs}$ , high-purity, conventional LPE growth, carrier conc. and mobility 4-99353  
 InP layers, MOCVD growth and characterisation (French) 4-76685  
 $\text{InP:Ge(Sn)}$ , donor identification, photolum. and far IR photocond. in high mag. fields 4-70705  
 $\text{In}_2\text{Se}_3$  films, flash and thermal evaporation growth, struct. and elec. characterisation 4-114409  
 $\text{In}_2\text{-Sn}_2\text{O}_3\text{-Y}$  coating deposition, three-step process, low sheet resist. 4-81159  
 $\text{In}_2\text{-Sn}_2\text{O}_3\text{-Y}$  films, transparent and heat-reflecting, elec. and optical props., ionised impurity scatt. 4-66087  
 $\text{In}_2\text{-Sn}_2\text{O}_3\text{-Y}$  thin films, deposition by reactive ion plating, elec. resist., visible transmittance meas. 4-99348  
 $\text{In}_2\text{-Sn}_2\text{O}_3\text{-Y}$  transparent conducting films, DC reactive sputtering deposition, optical and elec. props. 4-112533  
 $\text{Pb}_{1-x}\text{Eu}_x\text{Te}$ , MBE growth and elec. and optical props. 4-81142  
 $\text{Pb}_{1-x}\text{Hg}_x\text{Se}$  flash-evaporated films, optical and elec. props. 4-114335  
 PbS film, photosensitivity and luminescence studies 4-104679  
 PbS thin films, laser and thermal annealing effects on elec. props. 4-65298  
 PbSe epitaxial film, photoconductivity relax. study 4-104270  
 PbTe thin film, electrophys. props., degradation and recovery 4-88619  
 PbTe thin films, elec. props., effect of boundary layers 4-88618  
 Si film, LPCVD, elec. props., effect of film thickness 4-88615  
 poly-Si interface phenomena at Si grain boundaries 4-70925  
 Si laser recrystallised MOSTs, current cond. mechanism 4-76057  
 SiAs thin films, As fast diffusion during rapid thermal annealing 4-113714  
 Si:B microcrystalline films, crystallinity, morphology and elec. cond. 4-108749  
 Si:B polycrystalline films, activation energy of resist., effects of grain boundary trapping state energy distrib. 4-88616  
 Si:B(As), low resistance ion implanted films 4-108398  
 Si:C layers, CVD growth, microstruct. and resist. 4-70599  
 n-Si:P polycrystalline CVD films, elec. props., grain size and impurity conc. effects 4-70963  
 Si:P(As), ion implanted film, elec. props. 4-61473  
 $\text{SnO}_2\text{-Sb}$  film deposition by sol-gel technique, optical and elec. characts. 4-71604  
 $\text{SnO}_2\text{(Sb)}$  films, resistivity and optical transmittance, annealing effects 4-70967  
 SnTe thin films, elec. cond. and Hall effect 4-84716  
 $\text{TiO}_2$  thin films, struct. and elec. props. 4-80441  
 YIG films, electrical props. 4-80698  
 YIG:Ca epitaxial layers, elec. cond. meas. 4-80694  
 $\text{ZnO:Al}$  films, RF magnetron sputtering, elec. and optical props. 4-85100  
 ZnS conductive film, MBE prep. with single effusion source, luminesc. and elec. props. 4-99323  
 ZnSe films, low press. MOCVD growth and elec. and optical props. 4-93230  
 ZnSe films, MBE growth, elec. cond., Hall effect and photoluminescence studies 4-99344  
 n-ZnSe, OMVPE undoped films, elec. and optical props. 4-93226

**electronic conduction in insulating thin films**  
 see also electrical conductivity of amorphous semiconductors and insulators; electrical conductivity of crystalline semiconductors and insulators  
 hydrocarbon polymer dielectric films, hot-electron transport 4-92837  
 oxides, tunnel, in MOS capacitor, field controlled charge trapping 4-70939  
 PET films, ion implantation with F ions, elec. cond. 4-92717  
 polyacetylene, highly oriented, struct. and cond. (Japanese) 4-92111  
 polymer, electropolymerised, spectroscopic studies of electronic props., effect of prep. parameters (French) 4-66192  
 polystyrene films, underwater, interfacial polaris. in bilamellar struct., dielec. anal. 4-84901  
 polysulphone films, corona charged, surface potential decay characts. determ., expt. 4-92836  
 polythene films, space-charge limited charge distrib., discharge currents 4-88621  
 SIMOX films, Hall mobility and electrical conductivity, temp. dependence 4-80700  
 vinylidene fluoride-trifluoroethylene copolymer, ferroelec. hysteresis 4-99065  
 $\text{AlO}_x\text{-nH}_2\text{O}$  thin films, ageing, elec. struct. and moisture response characts., sensor appls. 4-86393  
 BN gate insulators, CVD growth on InP, ellipsometry, XPS, AES, cond. meas. 4-80443  
 BN:P film in InP, grown by CVD, elec. props. 4-99336  
 $(\text{CH}_3)_x\text{M}$ , (M=C, Si, Ge, Sn) polymer film prod., photocond. 4-104260  
 Cr/SiO<sub>2</sub> thin films, elec. cond. transport props. 4-92830  
 ErF<sub>3</sub> thin films, elec. cond., 323-396K 4-98791  
 FeF<sub>3</sub> thin film, impurity cond. along least resistance paths 4-80705  
 $\text{GeO}_2/\text{SiO}_2$  thin films, ESR rel. to elec. and optical props. 4-65860  
 $\text{LaMo}_6\text{S}_4$  films, supercond. props. and normal state resist. 4-92876  
 (Pb,Zr)TiO<sub>3</sub> thin films, magnetron RF sputtering and dielectric props. 4-88970  
 PbO<sub>2</sub> vacuum evaporated films, electron emission and I-V characts. (Japanese) 4-76643  
 Si oxide films, elec. props. and oxidation characts. 4-65762  
 $\text{Si}_3\text{N}_4$  dielectric film; electron conduction; expt. study 4-114053  
 $\text{Si}_3\text{N}_4$  layers, ion beam synthesised, dielec. breakdown, current density-voltage and capacitance-voltage characts. 4-80706  
 $\text{Si}_3\text{N}_4$  layers formed by ion implantation, elec. props. 4-75484  
 $\text{Si}_3\text{N}_4\text{:F}$  films, plasma enhanced CVD, insulating props. 4-61865  
 Si<sub>3</sub>Ny films, photo-CVD, props. study 4-99338  
 SiO<sub>2</sub>/SnO<sub>2</sub> coevap. films in sandwich struct., high-field cond. and opt. absorpt. 4-108948  
 SiO<sub>2</sub>-V<sub>2</sub>O<sub>5</sub> thin films, memory elements, metallic conducting filaments in low resist. state 4-75804  
 SiO<sub>2</sub> films, current-temp. characts. in metal-insulator-metal struct. 4-84721  
 SiO<sub>2</sub> films, photo-CVD, props. study 4-99338  
 SiO<sub>2</sub> films, thermally nitrided, elec. characts. study 4-88620  
 SiO<sub>2</sub>, RF sputtered, AC cond. mechanisms 4-92721  
 SiO<sub>2</sub>, RF sputtered, AC cond. mechanisms, single polaron correl. barrier hopping 4-92722  
 SiO<sub>2</sub> thin film, elec. cond. meas. using MIS struct. with MOSFET 4-61476  
 SmF<sub>3</sub> amorphous thin films, DC elec. cond. 4-113949

**electronic conduction in insulating thin films continued**

- Ta-N-O films, DC reactive sputtered, elec. resist., microstruct., oxidation 4-80704  
 Ta<sub>2</sub>O<sub>5</sub> amorphous films, leakage current suppression with micro-pinhole growth control 4-84723  
 Ta<sub>2</sub>O<sub>5</sub> gate insulator in MIS struct., electrophys. props. 4-61475  
 TiSi<sub>2</sub> films, sputter deposition at high substrate temps., elec. and struct. props. 4-114393  
 Y<sub>3</sub>-Gd, Fe<sub>2</sub>O<sub>3</sub> noncrystalline garnet films, electron transport and thermopower 4-108958  
 Y<sub>2</sub>O<sub>3</sub> films, struct. and phys. props. 4-65585

**electronic conduction in metallic thin films**

see also *discontinuous metallic thin films; electrical conductivity of amorphous metals and alloys; electrical conductivity of crystalline metals and alloys*

- Ag thin films, electroformed, humidity sensitive switching 4-108908  
 angular and surface roughness dependence, Cotter theory based model 4-70954  
 columnar and polycrystalline, resist., TCR and Hall coeff. 4-70952  
 electrical conductivity of discontinuous thin metal films and conducting filaments 4-98785  
 electron-electron interaction, weak localisation and magnetoconductance 4-114048  
 granular films, relax. phenomena 4-108747  
 Mayadas-Shatzkes conducting model, isotropy limits 4-108953  
 metallic thin films, electrical resistivity, effects of rough surface 4-104327  
 semicontinuous thin films, resist. based on computer model of thin film formation 4-80692  
 size effect, polycryst./monocryst. struct. assumption checking using Hall coeff. variations 4-70953  
 strain coefficients, Fuchs-Sondheimer expression 4-61470  
 superlattices, artificial, struct. and electronic props. 4-84532  
 unlike surfaces, electron scatt. model 4-76051  
 unlike surfaces effect, Cotter model 4-70951  
 weak localisation and magnetoconductivity 4-98784  
 Wiedemann-Franz law expression 4-108951  
 Ag, electroformed, humidity memory effect (*Japanese*) 4-61471  
 Ag film with adsorbed O<sub>2</sub>, CO and ethylene, elec. cond., effect of adsorption 4-108950  
 Ag films, structure and resistivity, transverse elec. field effect (*German*) 4-76052  
 Ag thin films on InP and glass substrates, elec. conductivity and optical transmittance 4-88612  
 Ag-based thin films, ultramicrohardness and internal stresses 4-92582  
 Al film, quantum corrections to resistance above superconducting T<sub>c</sub> 4-84710  
 Al thin film with chemisorbed H, chemisorption effect on elec. cond. 4-88391  
 Al thin superconducting film, quantum effects at T > T<sub>c</sub> 4-80691  
 Al/Mo thin films, reactions 4-61148  
 Al-Cu-Si sputtered thin film conductors electromigration resistance 4-88611  
 Au island film, charge transport and conductance oscill. 4-84712  
 Au semicontinuous thin films, 2D percolation system, conduction and Hall coeffs. 4-70957  
 Au thin films, 2000 Å thick, electron localisation and interaction, electronic cond., dimensionality crossover 4-80689  
 Au thin films, dynamic scaling near percolation threshold, AC cond. and dielectric const. meas. 4-98525  
 Au-based thin films, ultramicrohardness and internal stresses 4-92582  
 Bi discontinuous thin film, electron localisation and conductivity (*Russian*) 4-98780  
 Bi<sub>0.9</sub>Tl<sub>0.1</sub> amorphous film, quantum corrections to resistance above superconducting T<sub>c</sub> 4-84710  
 Co films, elec. cond. temp. depend. (*Russian*) 4-88613  
 CoSi<sub>2</sub> film, elec. transport props., metallic cond. 4-70950  
 CoSi<sub>2</sub> single cryst. films, <sup>4</sup>He irradi., elec. cond. studies 4-98782  
 Cr/SiO<sub>2</sub> thin films, elec. transport props. 4-92830  
 Cr<sub>1-x</sub>Mn<sub>x</sub>Ge amorphous thin films, elec. resist., Hall resist. 4-114049  
 Cu films, CO-covered, optical and elect. props. 4-80693  
 Cu films, structure and resistivity, transverse elec. field effect (*German*) 4-76052  
 Cu thin films, 2000 Å thick, electron localisation and interaction, electronic cond., dimensionality crossover 4-80689  
 ErRh<sub>2</sub>B<sub>4</sub> ferromagnetic superconducting thin film, photoexcitation, nonequilibrium effects 4-114059  
 Fe-Zr amorphous films, elec. and mag. props. 4-75923  
 Mg cylindrical film, resist. oscills. and electron localisation 4-80568  
 Mn, elec. props. characteris., use in thin film resistor fabrication 4-108952  
 Mo films, DC magnetron sputtering with RF substrate bias 4-81126  
 MoSi<sub>2</sub> film, elec. resist. and Hall const. meas., anomalous props. obs. 4-70949  
 Nb ultrathin film, anomalous magnetoresistance 4-84711  
 Nb-Ge, thin films, electrical resistivity, temp. depend. 4-108963  
 Nb-Si, thin films, electrical resistivity, temp. depend. 4-108963  
 Nb-Ti layered ultrathin coherent structures, elec. conduction (*Chinese*) 4-76023  
 Ni-Cr-Al films, highly disordered, temp. depend. resist. 4-80690  
 NiSi<sub>2</sub> film, elec. transport props., metallic cond. 4-70950  
 NiSi<sub>2</sub> single cryst. films, <sup>4</sup>He irradi., elec. cond. studies 4-98782  
 Pb, discontinuous thin films, mass fluctuations meas. 4-82759  
 Pd films, elec. props. rel. to deposition conditions 4-98781  
 Pd thin films, weak localisation, electron-electron interactions 4-84713  
 PdH<sub>2</sub> thin films, weak localisation, electron-electron interactions 4-84713  
 Pt film, sputter deposition, resistivity and struct. 4-104732  
 Rh-Si amorphous alloy film, form. and crystallisation 4-108750  
 Sn film, quantum corrections to resistance above superconducting T<sub>c</sub> 4-84710  
 TaSi<sub>2</sub> film, electronic transport props. and struct. 4-88610  
 Ti, polycrystalline films, resistivity-thickness depend. study 4-108954  
 Ti thin films, struct. and elec. props. 4-80441  
 TiSi<sub>2</sub> film, electronic transport props. and struct. 4-88610  
 TiSi<sub>2</sub> thin films, electronic transport props., classical metallic behaviour 4-70955  
 W CVD films, selectively deposited, elec. props. 4-88609  
 W films, DC magnetron sputtering with RF substrate bias 4-81126  
 WSi<sub>2</sub> film, electronic transport props. and struct. 4-88610

**electronic conduction in metallic thin films continued**

- Y<sub>2</sub> substrate temp., deposition rate and annealing effect on elec. resist. 4-98779  
 Zr<sub>76</sub>Cu<sub>24</sub> amorphous sputtered alloys supercond. critical field and normal state resist. 4-114077  
 Zr<sub>76</sub>Ni<sub>24</sub> amorphous sputtered alloys supercond. critical field and normal state resist. 4-114077
- electronic density of states**  
 alloys, nonrandom, substitutionally disordered, densities of states calcs. 4-113843  
 amorphous metals, energy spectrum and density of states calcs. (*Russian*) 4-113854  
 amorphous semiconductors, electron states, multielectron effects 4-98510  
 amorphous semiconductors, electronic states, transitions from localised states, rel. to density of states meas. 4-84547  
 amorphous solids, energy gap and electronic density of states calcs. 4-88485  
 Anderson model, 2- and 3-D, density of states, diagonal and off-diagonal disorder effects 4-113846  
 asymptotic medium concept and averaged Green function, optical consts. and electronic density of states 4-80472  
 Bethe-lattice approach, cluster size depend. 4-70621  
 binary alloys, order-disorder transitions, electronic theory 4-113572  
 chalcogenide glasses, one-electron density of states 4-84548  
 continued fraction expansion, analytic integration 4-65598  
 crystals, inhomogeneous electron damping and electron states 4-70615  
 CWD superconductors, nonmagnetic impurity effects 4-70683  
 degenerate electronic band, martensitic transition temp., mag. field depend., enhancement by Coulomb and exchange interactions 4-104138  
 density functional theory, book 4-73189  
 density functionals, self-interaction correction method 4-73304  
 diamond, conduction band struct., core electron excitation spectra anal. 4-70647  
 diatomic polymers, Green's function study 4-80552  
 dirty supercond. in weakly localised regime, transition temp., upper crit. field 4-108964  
 disordered binary harmonic chain, renormalisation group decimation technique 4-88489  
 disordered fermion system, interaction driven metal-insulator transition 4-104127  
 disordered systems, 3-D, exponential band tails and localisation 4-113900  
 disordered systems, electron-electron interaction in a self-consistent localisation theory 4-92673  
 electron gas models and density functional theory 4-73341  
 electron glass, electronic props. theory 4-70736  
 empty electronic states, inverse UV photoemission 4-104715  
 ferromagnetic semiconductor, conduction electron spin polarisation 4-88682  
 free-electron solid of submicron dimensions, Fermi energy and density of states, influence of boundary conditions 4-92785  
 glass, hyperspherical harmonics, symmetry, Landau theory and polytope models 4-103659  
 graphite, conduction band struct., core electron excitation spectra anal. 4-70647  
 Green's function calcs., simplification through analytic continuation 4-61274  
 ground-state density and wavefunctions in energy functional theories 4-73301  
 Heusler alloys, band struct., mag. moments, hyperfine fields, local spin density method 4-108767  
 Heusler-type alloy, X-ray spectra and electronic struct., mag. band struct. 4-71465  
 high temp. superconductors, theoretical model (*German*) 4-80716  
 II-IV semiconductor compounds and alloys, cluster-Bethe-lattice approach to electronic struct. 4-70625  
 inhomogeneous metallic polymers, thermoelec. power and elec. cond. 4-70789  
 interacting disordered electron system, single-particle density of states, renormalisability 4-104115  
 intermetallic, recursion method calc. 4-70626  
 liquid metals, energy spectrum and density of states calcs. (*Russian*) 4-113854  
 long range correl. pot., electronic density of localised states 4-98571  
 lowest Landau band in uniform mag. field and white noise potential 4-70620  
 metal-insulator transition, kinetic coefficients, DC cond. and diffusion 4-80501  
 metals, free standing and adsorbed, work functions, quantum size effects 4-92790  
 non-equilibrium diffusive transport 4-70801  
 nonmagnetic metal with mag. impurity, density of states, sp. ht., tridiagonalisation 4-92665  
 nonrandom substitutionally disordered alloys, cluster density of states 4-70737  
 one-dimensional two-block cryst., IR spectrum calc. using Green function method (*Chinese*) 4-71357  
 one-matrix energy functionals, props. 4-73303  
 polyacetylene<sub>1</sub>, cis and trans, DC and microwave cond. 4-92716  
 polyacetylene, doped, bipolaron states calcs. 4-61308  
 polymers, conjugated, electronic struct., extended Huckel cryst. orbital scheme calc. 4-65604  
 polymers, disordered quasi 1D systems, density of states calc. using SCF approach 4-65597  
 polypyrrole, band struct. calcs., ab initio HF study 4-84542  
 quadratic Padé approximant method for calculating densities of states 4-92594  
 quasi-1D solids, band struct. shapes 4-92592  
 random systems, exponential band tails 4-104167  
 recursion coeffs., linear prediction theory, appl. to electronic densities of states of Si and GaAs 4-98502  
 recursion method with plane wave basis, band struct. calc. appls. 4-80471  
 reduced density matrices, geometric study, spin properties 4-73302  
 renormalisation-group decimation technique for spectra, wave functions and density of states 4-104114  
 semiconductor, amorphous, electron transport, Mott-CFO model anal. 4-113939  
 semiconductor quasitwo-dimensional quantum-well struct., electron phonon scatt. 4-70918

electronic density of states continued

- semiconductors, absorption edge, free carrier Fermi-liq. interaction effects 4-114236  
 semiconductors, amorphous Husimi pacts alloys, topological disorder 4-104119  
 semiconductors, deep levels and interface states, electrochem. photocapacitance spectroscopy method 4-65635  
 semiconductors, density of states for position-dependent band struct. 4-61271  
 spin glasses, planar and XY, propagating modes 4-104434  
 superconducting upper critical field, theory for superconductors with energy depend. electronic density of states 4-104379  
 superconductivity, bulk, localisation effects in weakly localised regime 4-92843  
 superlattices, thermopower as probe of density of states distrib. 4-98714  
 symmetric Anderson lattice, ground states calcs. 4-70614  
 tetrahioquarato nickel(II), one dimens. crystal orbital calcs., neighbour-strand interactions 4-113853  
 transition metal alloy, second-order perturbation treatment of correl. and disorder 4-70645  
 transition metal and main group metal systems, L-edge absorpt. systematics, EXAFS obs. 4-66121  
 transition metal monoarsenides, struct. trends, tight binding model anal. 4-92160  
 transition metal silicides, electronic density of states, XPS study 4-61272  
 transition metals, liquid, Muffin-tin model, local density of states, calcs. 4-108755  
 transition metals, magnetism and electronic struct., validity of simple alloy model 4-98865  
 transition metals, paramag. susceptibility, influence of density of states singularities (*Russian*) 4-92889  
 two-band itinerant ferromagnet, discontinuous transition to ferromagnetic phase, band model 4-104397  
 two-dimensional disordered system, electron states and quantum Hall effect 4-104284  
 two-dimensional electron in strong mag. field and random pot., density of states 4-113845  
 two-dimensional electron systems, thermodynamics, shear modulus, mag. moment, in strong mag. fields 4-92637  
 two-dimensional systems, quantum Hall effect and density of states 4-98650  
 Ag-Mn dilute alloys, exchange split virtual bound state 4-92680  
 As, amorphous and polycryst., Compton profile studies 4-99218  
 As<sub>2</sub>Te<sub>3</sub> amorphous films, electronic struct., field effect and time of flight studies 4-113852  
 Au-Cu-M metallic glasses, (M=Mg, Si, Sn, Sb), liq.-quenched, form. and low temp. electronic props. 4-75919  
 AuNi(Co), impurity lineshapes in dilute alloys, UPS study 4-113893  
 Au,Pt<sub>1-x</sub>(Ni<sub>1-x</sub>), substitutionally disordered, electronic struct. calcs. 4-70644  
 BaTiO<sub>3</sub>, cubic to tetragonal transition, covalency effects, band struct. calculations 4-70361  
 Be polarised X-ray emission spectra and partial densities of states calc. 4-66132  
 Bi<sub>1-x</sub>Sb<sub>x</sub>, electronic density of states and its mass 4-88439  
 C, glassy, conduction band struct., core electron excitation spectra anal. 4-70647  
 CaH<sub>2</sub>, bonding and electronic struct., APW calc. and photoemission studies 4-113384  
 Cd-Mg, local electron density of states, Van Hove singularities,  $\mu^+$  Knight shift 4-84887  
 Cd<sub>2</sub>Mg, band struct. and stability (*Russian*) 4-84552  
 Cd<sub>1-x</sub>Mn<sub>x</sub>Se, valence band, Mn 3D electron contrib. 4-75855  
 CdS amorphous films, optical absorption coeff. and gap state density 4-66088  
 CdTe metal-semicond.-metal struct., pot. barriers 4-84708  
 CdTe-InSb MIS struct., electronic props. 4-98778  
 Ce systems, valence fluctuation dynamics, appl. of self consistent perturbation theory 4-70743  
 Co, polycrystalline, ferromagnetic, density of unoccupied states, SXAPS study 4-85039  
 Co-Gd/Al<sub>2</sub>O<sub>3</sub>/Al struct., tunnelling, zero bias anomalies 4-76049  
 CsI, L-edge absorpt. systematics, EXAFS obs. 4-66121  
 Cu-III-VI<sub>2</sub> chalcopyrites, valence bands study, photoemission and X-ray emission spectra, electronic structure calcs. 4-65608  
 Cu-Mn dilute alloys, exchange split virtual bound state 4-92680  
 Cu<sub>2</sub>Au, substitutionally disordered, electronic struct. calcs. 4-70644  
 CuNi impurity lineshapes in dilute alloys, UPS study 4-113893  
 Cu,Zr<sub>1-x</sub>, metallic glass, electronic struct. calcs. 4-104120  
 Eu, BCC, generalised susceptibility and joint density of states 4-76118  
 Fe, BCC, local densities of states, work functions and surface stabilities 4-88443  
 Fe, grain boundary with impurity segregation, atomic and electronic struct., 4-113463  
 Fe, polycrystalline, ferromagnetic, density of unoccupied states; SXAPS study 4-85039  
 FeB BCC alloys, electronic struct., APW calcs. 4-108769  
 Fe<sub>82</sub>B<sub>18</sub>Si<sub>6</sub>, amorphous and crystallised, UPS, XPS and EELS 4-104122  
 (Fe<sub>0.5</sub>Ni<sub>0.5</sub>)<sub>1-x</sub>B<sub>x</sub>, metallic glass, Mossbauer and soft X-ray appearance pot. spectra studies 4-76292  
 GaAs (110), H<sub>2</sub>O chemisorption and Ga and As species-specific densities of states 4-80373  
 GaAs (111), relaxation effects (*Chinese*) 4-70887  
 GaAs, midgap level surface density, heat treatment and capping effects 4-114011  
 GaAs, SAW characterisation of surface and interface states 4-98681  
 GaAs/native oxide interfaces, density of states, C-V meas. 4-88604  
 GaP:O(Zn), size effects and impurity electronic struct. 4-70723  
 GaS, EXAFS spectra and near edge struct. 4-66128  
 GaSb-AlSb, superlattices, light and heavy valence subband reversal, lattice mismatch 4-114103  
 GaSe, EXAFS spectra and near edge struct. 4-66128  
 Ga<sub>2</sub>Te<sub>3</sub> liquid semicond. elec. transport activation energies 4-88506  
 Gd-Tb alloys, magnetisation, temp. depend. 4-84815  
 GdZn, ferromagnetically saturated single crystal, high-field NMR Knight shift, magnetisation studies 4-114176  
 Ge, dislocations, deep electron levels, recursion calc. 4-70716  
 Ge-Sn(Sb)(Al) amorphous thin films, hopping cond. meas., 130 to 300K, localised state variations 4-92713  
 GeS, hole drift mobility anisotropy 4-70814  
 InP, SAW characterisation of surface and interface states 4-98681

electronic density of states continued

- InP:Mn, hopping cond. between deep impurity states 4-104209  
 InSe, EXAFS spectra and near edge struct. 4-66128  
 Ir<sub>2</sub> clusters, electronic struct., X $\alpha$ -SW and EHT calcs. 4-92603  
 KNbO<sub>3</sub>, cubic to tetragonal transition, covalency effects, band struct. calculations 4-70361  
 La, pressure effects on band structure, Fermi surface and super conductivity 4-84553  
 La<sub>1-x</sub>Sr<sub>x</sub>VO<sub>3</sub>, metal-insulator transition, photoemission study 4-84567  
 LiCl crystal, electronic energy bands, density functional calcs., self-interaction-correction theory 4-70651  
 Mg, polarised X-ray emission spectra and partial densities of states calc. 4-66132  
 MnAs, electronic struct. and phase transitions, tight binding calc. 4-108768  
 MnSb, electronic struct., density of states and mag. moments 4-75856  
 MnSi, electronic density of states calcs., paramagnetic susceptibility 4-70622  
 Mo (100), surface states, appl. of quick iterative scheme for transfer matrix calc. 4-76013  
 Mo (110) surface, density of states calcs. 4-70898  
 Mo, BCC, local densities of states, work functions and surface stabilities 4-84443  
 Mo chalcogenides, binary and ternary, Chevrel type, supercond., heat capacity anal. 4-92858  
 Mo<sub>2</sub>Ge, fast neutron irradi., effects on struct. and supercond. props. (*Russian*) 4-92841  
 MoS<sub>2</sub>, electronic struct. and angle depend. X-ray S K-emission bands 4-98521  
 Nb (110)-Pd interface, electronic struct. 4-84674  
 Nb-Ge, thin films, electrical resistivity, temp. depend. 4-108963  
 Nb-Si, thin films, electrical resistivity, temp. depend. 4-108963  
 NbH<sub>2</sub>, electronic struct., NMR study 4-76280  
 Ni, polycrystalline, ferromagnetic, density of unoccupied states, SXAPS study 4-85039  
 Ni-P amorphous electrodeposits, IR reflectivity spectra 4-93078  
 Ni<sub>2</sub>Pt<sub>1-x</sub>, substitutionally disordered, electronic struct. calcs. 4-70644  
 Pd, band struct. approach to X-ray absorpt. and emission spectra 4-71479  
 Pd-H, system, electronic struct. of small clusters, H-metal bonding 4-70624  
 PdH<sub>2</sub>, electronic props. of dilute H 4-88472  
 Pr, band structure, Fermi surface and supercond. under high press. 4-98511  
 Pt-H system, electronic struct. of small clusters, H-metal bonding 4-70624  
 Pt<sub>2</sub> clusters, electronic struct., X $\alpha$ -SW and EHT calcs. 4-92603  
 Ru(NH<sub>3</sub>)<sub>6</sub>Cl<sub>3</sub>, Ru L-edges, EXAFS spectra 4-66122  
 Si (111), electron correlation effects at vacancies 4-98092  
 Si (111), relaxation effects (*Chinese*) 4-70887  
 a-Si, AC field effect and density of gap states 4-92670  
 a-Si alloys, photocond., dark Fermi level position depend. 4-113987  
 Si, dislocations, deep electron levels, recursion calc. 4-70716  
 Si, excitation depend. grain boundary recombination velocity 4-104217  
 a-Si, film, gap density of states determ. 4-80551  
 a-Si films, localised density of states, electrophotography studies 4-113844  
 Si inversion layers, submicron width, quasi 1D effects 4-98765  
 Si MIS struct., amorphous C covered, tunnelling to insulator gap states 4-92824  
 Si, n<sup>+</sup> and p<sup>+</sup> regions, uncertainties about physical electronics, solar cell appls. 4-89428  
 Si, self interstitials, electronic struct. and total energy migration barriers 4-108811  
 a-Si, space charge limited current rel. to density of states 4-98637  
 Si:B, impurity electronic struct. cluster X $\alpha$  calc. 4-65639  
 Si:F, amorphous, electronic struct. theory 4-92600  
 a-Si:H, B, P, electron structure and density of states of B-P pairs, cluster calc. 4-65642  
 a-Si:H, broken bonds and electronic density of states, H effects 4-65178  
 a-Si:H, electronic density of states calcs. (*Russian*) 4-70740  
 a-Si:H, extended state mobility 4-104208  
 a-Si:H, long-time drift mobility, photocurrent study 4-104221  
 a-Si:H, resolution of DLTS energy scale controversy 4-104166  
 a-Si:H, B, doping effect on gap states 4-88488  
 a-Si:H,P, defect states and carrier capture processes 4-104165  
 a-Si:H film, hole mobility model 4-104220  
 a-Si:H film, transient space charge limited cond. study 4-104215  
 a-Si:H Schottky solar cells, gap state density 4-88438  
 Si/SiO<sub>2</sub> interface with gradual chem. transition, electronic density of states 4-708756  
 Si/SiO<sub>2</sub> MOS struct., interface state density and atomic roughness 4-98684  
 Si/SiO<sub>2</sub>/metal struct., electron inversion layers, tunnelling spectra of Landau levels 4-98772  
 Si/ZnO-B<sub>2</sub>O<sub>3</sub>-SiO<sub>2</sub> glass system, surface charges, C-V characteristic meas. 4-65747  
 Si<sub>1-x</sub>Ge<sub>x</sub>H, amorphous, gap state distrib., photoconductivity study 4-108320  
 Si<sub>3</sub>N<sub>4</sub>:H, amorphous, localised states at conduction band edge 4-104168  
 SiO<sub>2</sub>, amorphous, local electronic density of states, influence of Si-Si bonds 4-92671  
 SmB<sub>6</sub>, microwave conductivity meas. 4-70851  
 SmBi<sub>2</sub>, intermediate valence cpds., press.-vol. relationship 4-80554  
 Sn<sub>1-x</sub>Cu<sub>x</sub>, amorphous films, quench-condensed, low temp. sp. ht. 4-70403  
 SnS<sub>2</sub>, electronic struct. and angle depend. X-ray S K-emission bands 4-98521  
 T<sub>c</sub>-C film, superconducting T<sub>c</sub> and critical fields 4-104353  
 T<sub>c</sub>, superconducting props., energy band struct. calcs. 4-104343  
<sup>99</sup>Tc UV photoemission and electron energy loss spectra 4-85087  
 Ti cpds., electronic relax. effects, X-ray absorpt. 4-66114  
 Ti-Pd, specific heat meas. (*Chinese*) 4-75698  
 TiC, electronic density, density of states and chem. binding, APW calc. 4-75356  
 TiC(N<sub>2</sub>), optical props., EELS study 4-99082  
 TiN, nonstoichiometric and hydrogenated, cluster calcs. of electronic states and chem. binding 4-70623  
 TmSe, intermediate valence cpds., press.-vol. relationship 4-80554  
 UBe<sub>13</sub>, electronic struct., XPS study 4-70642  
 U<sub>2</sub>N<sub>7</sub>, heavy-electron system, mag. ground state 4-71093  
 VC(Nx), optical props., EELS study 4-99082

**electronic density of states continued**

- W, BCC, local densities of states, work functions and surface stabilities 4-88443  
 WC (0001), bulk band struct., photoemission studies 4-80496  
 WC, hexagonal, surface and bulk electronic struct., density of states 4-113867  
 YM<sub>2</sub> (M=Mn, Fe, Co, Ni), electronic struct. and mag. props. 4-92602  
 YbO, intermediate valence cpds., press.-vol. relationship 4-80554  
 $\alpha$ -Z, band structure, APW calcs., optical props., superconducting props. 4-113857  
 Zn, polarised X-ray emission spectra and partial densities of states calc. 4-66132  
 ZnNi, impurity lineshapes in dilute alloys, UPS study 4-113893  
 ZnSiP<sub>2</sub>, valence band struct. and chem. binding 4-88445  
 Zr-Pd(Ni), amorphous, electronic density of states and superconducting props. 4-70738  
 (ZrF<sub>4</sub>)<sub>57.5</sub>(BaF<sub>2</sub>)<sub>33.75</sub>(ThF<sub>4</sub>)<sub>8.75</sub> (V-52) glass, reson. interaction of acoustic waves with two-level systems 4-70290  
 ZrH<sub>2</sub>, electronic struct., tetragonal distortion, X-ray diffr. and PMR study 4-84858

**electronic density of states of amorphous solids** *see electron energy states of amorphous solids***electronic density of states of liquid semiconductors** *see electron energy states of liquid semiconductors***electronic desk calculators** *see electronic calculators***electronic engineering computing**

- see also circuit analysis computing; circuit CAD; circuit layout CAD; computerised instrumentation*  
 SAW interdigital transducer pattern masks, computer aided fabrication 4-103168  
 semiconductor doping processes, two-dimensional numerical anal., appl. to MOS processing 4-75470  
 Si solar cell, IBC, two-dimensional anal. of back region 4-77110

**electronic equipment manufacture**

- heat exchangers, open-topped, closed-sided, with vertical fins, heat transfer rates enhancement, for use in electronic equipment cooling 4-79420

**electronic equipment testing**

- high technology electronics exhibition and conference, Detroit, MI, USA, (June, 1983) 4-95014  
 integrated optical broadband, communication system, experimental results and review 4-60170  
 nuclear plant electrical components, aging and seismic qualification correlation 4-59301  
 resistance thermometer testing standardisation in USSR, using GOST 8.461-8.2 standard 4-58851  
 spirometer, experimental evaluation (German) 4-77278  
 spirometer turbine transducer, design (Polish) 4-77279  
 V-converter outlet signal, evaluation (German) 4-77420

**electronic music**

- see also musical acoustics; musical instruments*  
 amplified guitars, infinite sustain through controlled feedback 4-79402  
 BBC Micro, computer music 4-69635  
 electro-acoustic music, proposition for notation system 4-87519

**electronic structure, atomic** *see atomic structure***electronic structure, molecular** *see molecular electronic states***electronics applications of computers** *see electronic engineering computing electronics*

- see also beta-rays; cosmic ray electrons; positrons*  
 charmed meson decay, muon-electron universality verification 4-73745  
 Earth's foreshock boundary, bump-on-tail reduced electron vel. distrib. 4-105804  
 electric neutrality of matter, results summary, quark searches, e-p charge difference 4-59080  
 electromagnetic potential, in non-static gravit. field 4-63873  
 lifetime, decay process 4-90879  
 magnetic moment, line shape 4-78555  
 magnetosphere, evidence for heating of thermal electrons at magnetopause boundary layer 4-105810  
 in magnetosphere, nightside trapping of <40 keV electrons, SCATHA data 4-67554  
 mass, magnetic moment and vacuum energy from field theory finite temp. corrections 4-68346  
 radiation belt high-energy electrons, Interkosmos-Bulgaria 1300 meas. 4-72827  
 scattering cross-section in ionized gases (Chinese) 4-87847  
 solar wind, role of 'core' and 'halo' electrons in ionisation of interstellar wind 4-105863  
 spin polarisation in pulsars, effect on neutrino emission (Russian) 4-67762  
 temperature and density in Venus ionosphere, terminator flow 4-67659  
 wavefunctions and eigenvalues in three-body problem 4-101132  
 $e^+e^-$  → hadrons ( $\gamma\gamma$ ) ( $\mu\mu$ ) ( $e^+e^-$ ), 39.79-45.52 GeV, new particle search, toponium,  $e^+e^-$  4-90902

**electrooptics** *see electro-optical effects***electroosmosis** *see osmosis***electrophoresis***see also electrophoretic coating techniques*

- bacteriology, use of a laser Doppler electrophoresis method 4-115288  
 biological isotachopheric experiments on Salyut-7 orbiting space station, holographic interferometric obs. method 4-74468  
 $\kappa$ -carrageenan, aq. soln., light scatt. investg. 4-104622  
 dielectric liquids, central-symmetry convection in microgravity, simulation 4-97523  
 discharge tubes, cataphoresis, steady-state density profile collapse with large cylindrical end volumes 4-60774  
 DNA separations, sequence-determined, electrophoretic mobility in gels obs., book contrib. 4-93689  
 electrochemical double layer, dielectric enhancement and electrophoresis 4-71936  
 EM fields, interaction with cells, microelectrophoretic effect on ligands and surface receptors 4-100231  
 isotachopheresis, unsteady-state model (Russian) 4-81447  
 isotopic cataphoresis in a crossed-field plasma centrifuge 4-75212  
 liquid suspensions, small electrophoretic mobilities by light scatt. and phase struct. function anal. 4-114844  
 nonuniform medium, motion of near-spherical body 4-109667  
 polystyrene charged spheres in dilute soln., fluorescence labeled, electrophoretic friction meas. 4-98323

**electrophoresis continued**

- Quincke's rotation of spheres in liquid dielectrics with electrostatic field applied 4-96749  
 radionucleic ion mobility determ. in free electrolyte, meas. method 4-77024  
 space environment investigation for pharmaceutical processing 4-72442  
 testosterone-aq. electrolyte interface, electroosmosis, electrophoresis and streaming 4-99838  
 transmission grating velocimeter for particles electric mobility measurements 4-68221  
 yeast cells, static and dynamic dielectrophoresis 4-100105  
<sup>131</sup>I radioelectrophoretic and chromatographic study (Chinese) 4-71934  
<sup>131</sup>I<sup>-</sup> ion mobility determ. in free electrolyte 4-77024  
<sup>161</sup>Tb<sup>3+</sup> ion mobility determ. in free electrolyte 4-77024

**electrophoretic coating techniques**

- deposition kinetics, zetapotential meas. 4-114428

**electrophoretic coatings**

- Cr<sub>3</sub>C<sub>2</sub>-Ni-B electrophoretic coatings, struct. and props. 4-88430

**electrophotography**

- carbazole-containing compounds, ionisation potentials (Russian) 4-83508  
 color imaging process using filter beads (Japanese) 4-95543  
 electrostatic latent image characts., tone improving process, colour reproduction in copier (Japanese) 4-95542  
 organic layers, electrophotographic image contrast, luminesc. effects 4-112540  
 photoreceptor surface pot. decay meas. using X-Y recorder (Japanese) 4-95546  
 pictorial images simulating tone reproduction characteristics of typical electrophotographic photoreceptors (Japanese) 4-95545  
 poly-N-epoxypropylcarbazole electrophotographic layers, photodischarge kinetics 4-112541  
 poly-N-epoxypropylcarbazole, sensitised by dyes and pyrylium salts 4-112542  
 poly-N-vinylcarbazole layers, cryst., SCL current meas. electrophotographic props. 4-75978  
 toner materials, one-component, specific toner charge meas. method 4-68298  
 two-color electrophotography with multilayer photoreceptor (Japanese) 4-95544  
 vinyl polymers with aromatic substituents, photocond. differences w.r.t. charge transfer ease (German) 4-98667  
 xerographic copier, toner concentration control 4-82839  
 CDS binder layers, electrophotographic props. after heat and light treatment 4-79258  
 Se electrophotographic layer parameters, influence of gaseous medium (Russian) 4-68311  
 SeTe, As glassy films, pure and doped, deep level defects, xerographic spectra studies 4-61339  
 a-Si films, localised density of states, electrophotography studies 4-113844  
 Si:H amorphous compensated films, xerographic discharge meas. 4-80603  
 a-Si:H films, reactively RF sputtered, electrophotographic props. (Japanese) 4-81127  
 a-Si:H photoreceptors, electrophotographic imaging process 4-73544  
**electrophotoluminescence** *see electroluminescence; photoluminescence*  
**electrophysiology** *see bioelectric phenomena*  
**electroplated coatings**  
 cavitation erosion of coated steels 4-99611  
 Au, acid hard, on contacts, performance eval. 4-76020  
 CdS-Cu<sub>2</sub>S photocells formed by electroplating, prep. and props. 4-72115  
 Cr films electroplated on (001) Cu substrates, misfit twins and dislocations 4-108748  
 Cu deposition on Fe powder, coating props. 4-89188  
 Cu, electroplated on maraging steel, reduced H embrittlement (Japanese) 4-89113  
 CuO/stainless steel tandem solar absorber converters, optical properties and spectral selectivity 4-99999  
 Cu<sub>2</sub>O/stainless steel tandem solar absorber-converters, optical properties and spectral selectivity 4-99999  
 Ni electrodeposits, interdiffusion coating on mild steel, fretting fatigue 4-114686  
 Ni, electroplated on maraging steel, reduced H embrittlement (Japanese) 4-89113  
 Ni electroplated solar absorber, deposited on Ag-coated glass substrate 4-72175  
 Ni-Co, electrodeposits, interdiffusion coating on mild steel, fretting fatigue 4-114686  
 Ni-Co electroplating, US agitation effect on mech. props. and comp. 4-114430  
 Ni-Cu-Zn alloys, electrodeposition from sulphate bath, effect of additions 4-81163  
 Ni-Fe electroplating, US agitation effect on mech. props. and comp. 4-114430  
 Ni-Pd alloy plating method for H embrittlement in high-strength steel (Japanese) 4-104861  
 Pd-Ni, acid hard, on contacts, performance eval. 4-76020  
 Sn on the Cu alloy, diffusion reaction, effect of additional Fe and Sn 4-71755

**electroplating**

- galvanic bath system, mag. field influence on elec. transfer of metal (Russian) 4-85252  
 heavy metals recovery from waste water 4-99802  
 metal distribution over macroprofiles, electrodeposition from complex salt solns. 4-114432  
 steel, stainless, Ni and Pd filled coloured 4-114949  
 Al plating bath system, <sup>27</sup>Al NMR spectroscopy studies 4-66245  
 Au, electroplating and nanometer e-beam lithography for mag. flux quantisation measurements 4-73455  
 Cd, electroplating from acetic chloride bath, superimposed AC effect 4-93239  
 Cu deposition on Fe powder, coating props. 4-89188  
 Cu plating for selective case-hardening 4-104744  
 Cu selective plating Mo structs. on multilayer ceramic substrates 4-66242  
 Cu-Nb-Sn in situ superconductors, long length, Sn electroplating and processing 4-61878  
 Cu<sub>2</sub>S electroplating on CdS for CdS-Cu<sub>2</sub>S heterojunction photocells 4-99354  
 GaAs:Zn, monolayer surface doping from plated Zn source 4-70172  
 KAu(CN)<sub>2</sub>, electrochem. prep. 4-104741

**Electroplating continued**

- Ni, electroless plating on metals, catalytic activity and electro-oxidation 4-66243  
 Ni electroplating bath control using saccharin additive (*German*) 4-66241  
 Ni-Co electroplating, US agitation effect on mech. props. and comp. 4-114430  
 Ni-Fe electroplating, US agitation effect on mech. props. and comp. 4-114430

**Electropolishing** *see electrolytic polishing***Electroreflectance**

- polydiacetylene crystals, electro-reflectance spectra of 1-dimens. excitons 4-104573  
 semiconductor-liquid junction devices, in situ characterisation 4-99090  
 Ag film, electroreflectance meas. of bulk plasmon dispersion 4-113883  
 CdIn<sub>2</sub>Se<sub>4</sub>, single crystal, electrolyte electroreflectance in photoelectrochemical solar cell 4-89408  
 Cd<sub>1-x</sub>Mn<sub>x</sub>Se(Te) semimagnetic semicond., electroreflection spectra 4-88811  
 Cd<sub>1-x</sub>Mn<sub>x</sub>Te solid solns., Mn photoionisation detection 4-71349  
 p-Ge, anisotropic internal stresses, electroreflectance and photovoltaic effect meas. 4-84947  
 Ge, electroreflectance spectra, oscillations anal. for electron-hole Coulomb interactions 4-66011  
 Ge, surface, electroreflectance and photo EMF (*Russian*) 4-104576  
 In<sub>0.75</sub>Ga<sub>0.25</sub>As<sub>0.56</sub>P<sub>0.44</sub>, electroreflectance spectrum, on InP substrate 4-109158  
 (MnS)<sub>x</sub>(CdSe)<sub>1-x</sub> and (MnS)<sub>x</sub>(CdTe)<sub>1-x</sub> semimagnetic semicond., electroreflection spectra 4-88811  
 (MnSe)<sub>x</sub>(CdTe)<sub>1-x</sub> semimagnetic semicond., electroreflection spectra 4-88811  
 Si, electron structure change during amorphisation, electrorefl. spectra (*Russian*) 4-98509  
 Si-SiO<sub>2</sub>-KOH system, ellipsometric and electroreflectance study 4-99091  
 SnSe, electroreflectance and thermoreflectance 4-71348  
 Ta<sub>2</sub>O<sub>5</sub>/Si, film struct., reflection and electroreflectance spectra 4-109266

**Electroretinography** *see bioelectric potentials; eye***Electrostatic accelerators***see also Van de Graaff accelerators*

- 80-GW relativistic electron beam accelerator 4-111978  
 Doubtlet III neutral injector ion sources, linear optics theory appl. 4-59458  
 free electron laser expt. programme at University of California, Santa Barbara, status report 4-83613  
 high-energy mass spectrometry with large tandem accelerators 4-95557  
 macroparticle projectiles focusing 4-59457  
 multiple electrostatic quadrupole array linear accelerator for negative ion beams 4-107179  
 nanosecond accelerator for generating ion and electron beams 4-74076  
 nuclear physics research appl. 4-107184  
 three-dimensional simulation of the Proto-II convolution 4-111986

**Electrostatic coatings**

No entries

**Electrostatic devices***see also capacitors; dielectric devices; electrostatic accelerators; electrostatic lenses; electrostatic precipitators*

- air-launched expendable seawater conductivity and temp. profiler 4-115629  
 charged particle energy analysers with wedge-shaped electrode 4-91395  
 corona detection by electrostatic probe 4-84061  
 electroseparator, slotted, field strength distrib. calc. (*Russian*) 4-82806  
 ion trap, operation in uniform mag. field 4-64665  
 laser systems, high power, electrostatic technology for dust and hydrocarbon vapour control 4-74533  
 photon stimulated desorption, surface characterization, instrumentation 4-90703  
 space experiments, containerless processing technologies using acoustic and electrostatic levitation 4-95397  
 switch for 600 keV ion implanter 4-73594  
 wedge analyser with cubic field, electron-optical params. 4-91396

**Electrostatic fields** *see electric fields***Electrostatic lenses***see also aberrations; focusing; particle beams*

- diverging lens, problems rel. to conical EM fields 4-102874  
 electrostatic electron-optical systems with discontinuous fields 4-74408  
 five-element lens, magnification behaviour 4-87264  
 new field emission gun, electrostatic lens, characts. (*Chinese*) 4-85091  
 prism charged-particle energy analysers, matrix calc. of aberrations 4-64670  
 quadrupole electron-beam exposure technology for integrated optical device patterns 4-107889  
 rotationally symmetric lens systems, potential and field strength calc. by convergent Fourier-Bessel series 4-96772  
 third-order aberrations of electrostatic lenses by nonparaxial electron trajectories (*Chinese*) 4-83534  
 variable-aperture electrostatic lenses 4-112336

**Electrostatic microphones** *see microphones***Electrostatic precipitation** *see electrostatic precipitators; precipitation (physical chemistry)***Electrostatic precipitators**

- aerosol particle charging by free electrons, charge potential limit model 4-99853  
 DC corona discharge and ion flow distribution characts. of electrostatic precipitator rods 4-97933  
 German steel industry, measures for reduction of dust and noise (*German*) 4-91687  
 isolated collector sphere for charged aerosol collection, electrostatic field direction effect 4-95464  
 (NH<sub>4</sub>)<sub>2</sub>SO<sub>4</sub> conditioning of flue gas for electrostatic precipitator performance improvement 4-62421

**Electrostatics**

- see also electrets; electric charge; electric fields; electrostatic devices; static electrification; triboelectricity*  
 aerosol particles, fibrous, bipolar diffusion charging, elec. mobility and charge meas. 4-89348  
 aerosol particles, fibrous, bipolar diffusion charging, theory 4-89347  
 aerosols, bipolar diffusion charging of monodisperse particles 4-62254  
 atomic ions, electrostatic pot. at nucleus, rel. to chem. pot. 4-68916  
 capacitance of plates, upper bound derivation 4-74390

**Electrostatics continued**

- charged particles, statistics in random elec. fields, quasilinear theory 4-96747  
 cooling by electrostatics, development of flow vel. in boundary layer (*Japanese*) 4-84098  
 corona discharge effects on gasdynamical flow rate 4-69975  
 cubic arrays of nonconducting spheres in uniform elec. field, simulation 4-91380  
 discharge, human body and electronic equipment effects 4-69273  
 discharge simulation, test facility development 4-69274  
 discharges control, geosynchronous spacecraft protection 4-69271  
 electrical double-layer interactions in concentrated colloidal systems 4-114838  
 electrodeless discharges, wall charge variations in 60 Hz fields 4-69981  
 electrolyte solution, charged aggregates interaction, Monte Carlo simulation 4-97986  
 electromagnetism in R<sup>2+1</sup>, teaching 4-78079  
 electron-optical systems with discontinuous fields 4-74408  
 electronic equipment, discharge immunity design 4-69272  
 electrostatic capacity and eigenvalues of the Laplacian 4-87246  
 EMF and potential difference: an illustrative example 4-78078  
 film transport systems, static control 4-111223  
 fluidised bed behaviour under radioactive gas flow conditions 4-97678  
 formamide, mol. electrostatic pots., X $\alpha$  calcs. 4-112113  
 four dimensional, multiple expansions for charge distrib. 4-59953  
 Fredholm's method for determ. of electrostatic fields and equipotentials 4-87245  
 heavy ion beam source, probe appls., mag. field effect on accelerating lens 4-78413  
 image system of a source in no-slip sphere and cylinder 4-64908  
 images by multipole expansion 4-63448  
 liquid scintillation counting, elimination of spurious results due to static elec. 4-87005  
 lunar soil electrostatic erosion 4-94656  
 molecular electrostatic interaction energy anal., separated electronic groups theory (*German*) 4-78927  
 molecular electrostatic potentials, X $\alpha$  calc. methods 4-112113  
 nonspherical charge distrib. and electrostatic interactions 4-80475  
 particle charging by ultraviolet ray exposure 4-99854  
 perfectly conducting cylinder of infinite length, eigenfunction expansion of electric and magnetic dyadic Green's functions 4-102847  
 potential electrostatic beams, thermoemission conditions at cathode, exact solns. 4-102869  
 Radon transform and appls., book contrib. 4-106172  
 rectangular arrays of nonconducting spheres in uniform elec. field, simulation 4-91379  
 self corona discharge of sharp edged ellipsoidal particles in electric field 4-97934  
 semiconductors, nonlinear generation of sum and difference waves by helicon waves 4-80618  
 solids, planar, spherical and cylindrical, dynamical screening and surface excitations 4-78234  
 stimulated radiation of oscillators in weak longitudinal electrostatic field 4-59955  
 surface layers, with spontaneous polarisation, nonhomogeneous dielectrics 4-80654  
 vector potential determ. 4-87247  
 velocity diffusion driven by electrostatic waves, stochastic mag. field effects (*Chinese*) 4-96745  
 weakly conducting fluid, turbulent flow in pipe, boundary current fluctuations 4-108110  
 H<sub>2</sub>O, mol. electrostatic pots., X $\alpha$  calcs. 4-112113  
 He, attractive forces at intermediate distances from metal surface, at matrix element effect 4-80707  
 KNbO<sub>3</sub>, electrostatics, polarisable point-ion model 4-80860

**Electrostriction***see also piezoelectric materials; piezoelectricity*

- constants for crystals, data tables, book 4-58593  
 fluid, electrostriction press. dynamics near spherical electrode 4-93010  
 ions moving through compressible polar solvents, electrostriction and dielectric friction 4-61124  
 linear electro-optic effect, crystallographic aspects 4-80905  
 liquid-filled photoacoustic cells, laser pulse excited, electrostriction effects 4-104538  
 piezoelectric coeff. meas. using electrostriction cell 4-78342  
 piezoelectric semiconductor, free carrier influence on stimulated Brillouin scatt. 4-71399  
 poly(vinylidene fluoride) piezoelec. and pyroelec. props. under high press. 4-99027  
 Rochelle salt, ferroelectric phase transitions, piezoelectric coeffs., electrostrictive coeffs., temp. depend., resonance studies 4-114217  
 solids, transverse acoustic gap waves, parametric excitation by microwave elec. field 4-113774  
 unimode fibre light guide, sound excitation and additional losses occurrence, when transmitting AM optical waves 4-69582  
 volume acoustic wave excitation by electrostrictive effects 4-92767  
 BaTiO<sub>3</sub>, centrosymmetric ceramics, elec. field induced acoustic anisotropy 4-60992  
 KMgF<sub>3</sub>, refr. index, permitt., press. depend. 4-93040  
 MgO, rocksalt-type oxide, electrostrictive coeff. 4-76333  
 PbZr<sub>1-x</sub>Ti<sub>x</sub>O<sub>3</sub> ceramics, electrostrictive coeff., time resolved X-ray diff. studies 4-71282  
 RbHSO<sub>4</sub>, ferroelectric phase transitions, piezoelectric coeffs., electrostrictive coeffs., temp. depend., resonance studies 4-114217

**Electrosynchronisation** *see synchronisation***Electroviscous effect***see also colloids; viscosity*

No entries

**Electroweak model** *see unified field theories***Element origin***see also cosmic ray origin; cosmology*

- Big Bang nucleosynthesis, implications of chemical evolution of light elements 4-67843  
 book 4-78049  
 chemical evolution of galaxies, evidence from element abundances in interstellar medium 4-101459  
 cosmochronology of s- and r-process nucleosynthesis, appl. of <sup>87</sup>Rb/<sup>87</sup>Sr isobaric pair 4-101133  
 cosmology, He and D synthesis in early Universe 4-101548

## element origin continued

- Galaxy chemical evolution, nucleosynthesis constraints form element abundances in metal-poor stars 4-67844
- neutron capture processes, rel. to relative abundances of elements 4-94580
- nucleosynthesis and galactic chem. evolution 4-63293
- pregalactic He and metal enrichment by Population III stars, theory 4-90191
- primeval plasma recombination, supersymm. light-inos, universe expansion rate 4-110794
- solar system, nucleosynthesis time scales rel. to position of Sun in Galaxy 4-94654
- D, possible synthesis by pregalactic massive stars 4-67841
- D, primordial nucleosynthesis 4-63255
- D, synthesis by Population III remnants 4-67842
- He, primordial nucleosynthesis 4-63255
- <sup>7</sup>Li, possible synthesis by pregalactic massive stars 4-67841
- <sup>7</sup>Li, synthesis by Population III remnants 4-67842
- O production by Population I and Population III stars, rel. to O anomaly in metal-poor stars 4-67718
- Os, validity of local approx. for s-process nucleosynthesis and implications for <sup>187</sup>Re-<sup>187</sup>Os cosmochronology 4-115680
- Zr, s-process nucleosynthesis in S-type stars 4-72926

## element relative abundance

- see also isotope relative abundance
- Abell 30, planetary nebula, N/C abundance ratio 4-86011
- basaltoid lavas of continental arches in eastern USSR, distinctive petrochemical features 4-100563
- big bang, element yields, nucl. uncertainties 4-94999
- cerebral atherosclerosis, PIXE investigation 4-105370
- Chainpur meteorite, trace element abundances in rims and interiors of chondrules 4-94693
- Chainpur meteorite (LL-3 chondrite), chondrules comp. rel. to reduced parent rocks and vapour fractionation 4-67705
- chemical elements, origin and abundances (book) 4-78049
- diogenite meteorites, multivariate statistical anal. of orthopyroxene analyses 4-105908
- euclite parent body, mantle comp. and euclites origin 4-77784
- galactic nuclei, spectroscopic obs. of LINERS rel. to element abundances 4-67807
- giant planets, atm. struct. and comp., implications for solar nebular characts. 4-101207
- globular clusters in NGC 5128, stellar content and metallicity from IR photometry 4-86032
- gneiss complexes, Lower Precambrian, of Yenisei Ridge region, USSR, geochemistry 4-100561
- granite from Gabal Mueiliha, Egypt, post-magmatic alteration, trace element distrib. 4-85674
- hair, human, elemental concs., PIXE anal. 4-105364
- halo giant stars, metal abundances determ. 4-115752
- Hawaiian tholeiite, element abundances rel. to metasomatic model for origin 4-85650
- heavy elements, relative abundances rel. to neutron capture nucleosynthesis 4-94580
- heavy ions comp. in solar energetic particle events 4-100939
- interacting galaxies, O abundances and metallicity rel. to star form. rates 4-77926
- interstellar medium, element abundances rel. to chemical evolution of galaxies 4-101459
- interstellar medium, gas-phase abundances form obs. of five stars in Pleiades cluster 4-94904
- kimberlites of Daldyn field, comp. rel. to principal stages of form. 4-100565
- light elements (d, He and Li), abundances rel. to chemical evolution and Big Bang nucleosynthesis 4-67843
- lunar rocks, Zr and Nb partitioning between coexisting opaque phases 4-67651
- M1-7, planetary nebula, plasma characts., element abundances and central star nature 4-115797
- medium energy cosmic nuclei,  $10 \leq Z \leq 26$ , elemental composition 4-94464
- metal abundances in dwarf irregular galaxies, implications for stochastic star form. model 4-67806
- metal-deficient stars, element abundances rel. to nucleosynthesis constraints on early galactic evolution 4-67844
- mobile trace elements in L-chondrites 4-110578
- Mount Isa region, Australia, acid volcanic units geochem. discrimination 4-94033
- nails, human, elemental concs., PIXE anal. 4-105364
- NGC 7385, radio galaxy, metal abundance of blue optical knots 4-90231
- oyster shells, element distrib., environmental and chronological effects PIXE investigation 4-105067
- primordial helium abundance and grand unification schemes 4-110796
- siderophile-rich magnetic spheroids from the Cretaceous-Tertiary boundary in Umbria, Italy, chem. anal. 4-100509
- trace elements in Europe, emission and long-range transport 4-114986
- tumour-related tissue samples, from mice, radioisotope induced X-ray fluorescence anal. 4-105289
- Al, in metal-deficient stars (French) 4-115756
- Ba enhancement in atmospheres of red giant stars 4-63145
- C/He in HD 193793, Wolf-Rayet star 4-67744
- Ca in solar corona, var. in observed abundance in X-ray flare plasmas 4-105925
- Co in Sun and CO I oscillator strengths from Fraunhofer line equivalent widths 4-63125
- Fe and heavy element enrichment of intergalactic medium 4-73083
- Fe meteorites, group IIE resolution from IIBAB, Cu as taxonomic parameter and elemental comp. 4-77787
- He abundance in globular cluster M15, determ. from photographic photometry of RR Lyrae variables 4-101368
- He abundance in  $\mu$  Cassiopeiae, determ. from masses of components 4-72977
- He abundance in RR Lyrae stars, effects on pulsational stability of convective models 4-63158
- Hf/rare earth elements fractionation in sediments, evidence for crustal recycling into mantle 4-110100
- Ir in Cretaceous/Tertiary boundary clays, Bidart section, France 4-105554
- Li in Ba stars, abundance from Li I 670.7 nm resonance doublet 4-67746

## element relative abundance continued

- Mo abundance in Earth mantle, evidence for siderophile elements depletion 4-110099
  - N abundances in disk and halo dwarf stars 4-94755
  - N in open star cluster NGC 6231, B-star spectra 4-90194
  - Nd II, radiative lifetimes and solar Nd abundance meas. 4-78808
  - O anomaly in metal-poor stars, rel. to O prod. by Population I and Population III stars 4-67718
  - O in spiral galaxies rel. to chemical evolution, numerical models 4-77920
  - Ra, occurrence and behaviour in saline formation water of US Gulf Coast region 4-110179
  - <sup>87</sup>Rb/<sup>87</sup>Sr isobaric pair, appl. to cosmochronology of s- and r-process nucleosynthesis 4-101133
  - V concentrations in N Pacific Ocean, profiles of particulate and dissolved 4-77556
  - W abundance in Earth mantle, evidence for siderophile elements depletion 4-110099
  - Xe and noble gases in shales, plastic bag expt. 4-94220
  - Y, localisation behaviour and tumours in nude mice, PIXE investigation 4-105386
- elemental semiconductors**
- $\alpha$ -B<sub>12</sub>, band struct., energy gaps, bonding, cluster approx. 4-70646
  - band struct., semi-empirical tight binding calc. 4-70631
  - Czochralski growth, historical review of technique, impurity conc. and distrib. 4-66213
  - diamagnetism and Van Vleck paramagnetism 4-71019
  - diamond:Fe, electronic struct. calcs. 4-113894
  - diamond, amorphous film deposition using generation/reaction of methylene species 4-104739
  - diamond, cohesive and struct. props., ab initio LCAO calc. 4-60881
  - diamond, conduction band struct., core electron excitation spectra anal. 4-70647
  - diamond, muonium formation, asymmetry and relax. temp. depend. 4-65925
  - diamond, natural, type II, cathodoluminescence from dislocations 4-81012
  - diamond, Ohmic conductivity of electrons calc. 4-108864
  - diamond, semiconducting and insulating natural, picosec. photoconductive switching 4-108895
  - diamond, transition from isotropic muonium state to axially symm. anomalous muonium state 4-71237
  - diamond ionising radiation detector, TSC current and polarisation 4-104230
  - diffusion processes, atomic particle delocalisation effect in disordered media 4-92405
  - EFG ribbon solar cells, ion implantation and pulsed electron beam annealing fabricated 4-62364
  - electrochemical oxidation, surface states (French) 4-76044
  - large-area sheet technology for photovoltaic cells and arrays 4-62352
  - MOS capacitors, charge variation rel. to voltage step, generation lifetime meas. 4-65755
  - muonium, electronic struct. and hyperfine interaction 4-65633
  - nontetrahedrally bonded elements and binary cpds., physical data collection 4-58586
  - physical data, compilation, book 4-63420
  - a-Si:H film, prep. by reactive sputtering, optical and elec. props. 4-71457
  - n-Si, radiation defect formation, annealing, defect interactions 4-113499
  - Si, Schottky-barrier modelling of metal and silicide contacts 4-84693
  - Si IC with ZnO pyroelec. anemometer 4-69846
  - Si solar cells manufacture, technological and economic aspects 4-89403
  - SOI films, laser recrystallisation, Raman microprobe study 4-80462
  - SOI films, recrystallisation by zone melting method, crystallinity study 4-80459
  - SOI technology, laser recrystallisation technique 4-80458
  - solar cell production system, electron beam heating in a vacuum 4-62362
  - SOS, electric props. meas. (Russian) 4-84706
  - SOS, ion implanted, elec. props., effect of heat treatment 4-98759
  - SOS films, carrier mobility, lifetime, ps photocond. meas. 4-80623
  - SOS films, material improvement process by solid phase epitaxial growth 4-81124
  - SOS heteroepitaxial film, surface photovoltage characterisation 4-80697
  - surface, sputtering by N<sup>+</sup> ion beam, excited N<sub>2</sub> mol. rotational states 4-74215
  - X-ray bandpass filter from Ge solid state detector and GeO<sub>2</sub> foil 4-91176
  - Si, ion implantation and laser annealing (Japanese) 4-108404
  - Si amorphous or polycrystalline, epitaxial regrowth and bridging epitaxy by flash lamp irradiation 4-75813
  - $\alpha$ -Sn, semiconducting phase, band structure 4-80489
  - Ag-Ge (100) interface, growth, structural and electronic props. 4-104093
  - Ag-Si, ion beam induced at. mixing, in-situ Rutherford backscattering meas. 4-65404
  - Al/AlN/SiO<sub>2</sub>/Si struct., conduction mechanisms, shallow junction technique study 4-88599
  - Al-SiO<sub>2</sub>-Si MOS structure, X-ray induced interface traps, stress relax. effects 4-98755
  - Al-SiO<sub>2</sub>-Si struct., X-ray irradi., interface traps. 4-104281
  - Au/Si<sub>3</sub>N<sub>4</sub>/Si system, elec. effects of Au (Chinese) 4-98757
  - Au-Ge(:H) interfaces on amorphous Ge, Schottky barrier and cpd. formation 4-84669
  - Au-Si nucl. detectors, gamma-ray effects on rise time 4-59566
  - Au-SiO<sub>2</sub> interface, Au surface-state energy level determ. 4-80640
  - B-based, high temperature, effect of doping 4-75990
  - Bi thin films, vacuum deposited, semiconducting props. rel. to annealing 4-65758
  - C, arc evaporated amorphous film, optical const. study 4-81026
  - Ce-Ag junctions, Schottky barrier form. 4-84694
  - Ce epitaxial layers, plasma enhanced CVD growth of free-standing films 4-61866
  - Cr/Si (100) interface, silicide growth kinetics, cross-sectional TEM 4-61146
  - Cr-SiO<sub>2</sub>-pSi capacitor, conduction and charge storage 4-61474
  - Cu/a-Si:H/a-Si:H(n-type)/Cr Schottky diodes, RF magnetron sputtered 4-88557
  - finas in fluidized bed silane pyrolysis 4-81149
  - GaAs/Ge single crystal layers, MBE growth and patterning on Si substrates 4-99315
  - p-GaSb, heavily doped, low temp. thermal cond. 4-70300
  - Ge 4-97135

## elemental semiconductors continued

- p-Ge, 3.39  $\mu\text{m}$  transmission modulation by tunable CW  $\text{CO}_2$  laser, excitation spectrum 4-79240  
 Ge (001), metal-insulator transition, angle resolved photoemission studies 4-104126  
 Ge (001) substrate for Ag epitaxial film, superconductivity and electron localisation 4-114062  
 Ge (111),  $7\times 7$ ,  $5\times 5$  and  $2\times 8$  struct. models, RHEED intensity distrib. anal. 4-92486  
 Ge (111), deposited ultrathin Sn layers, RHEED study 4-80451  
 Ge (111), electronic structure, temp. dependent UPS study 4-61428  
 Ge (111), shallow donor impurities, variational soln. 4-70893  
 Ge (111) with chemisorbed Sm, photoemission spectra 4-80392  
 Ge (111)-Pb interface form. dynamics and oxidation 4-84518  
 Ge (111)-(2 $\times$ 1), dangling bond states, HREELS and photoelectron spectra study 4-65725  
 Ge (111)2 $\times$ 1, highly dispersive dangling bond band, photoemission study 4-70890  
 Ge, amorphous and crystalline, surface oxidation, photoemission study 4-76880  
 Ge amorphous film, laser enhanced crystallisation, nucleation, growth velocity, recombination enhanced diffusion 4-65295  
 Ge, angular distrib. of annihilation radiation 4-71472  
 p-Ge, anisotropic internal stresses, electroreflectance and photovoltaic effect meas. 4-84947  
 n-Ge, anomalous magnetoresistance study 4-108879  
 Ge, anomalous muonium hyperfine interaction, temp. depend., 5 to 100K 4-71240  
 Ge avalanche photodiode detectors for long-wavelength optical fibre communication systems 4-97134  
 Ge, band calcs., empirically adjusted zone variational method (*Chinese*) 4-75831  
 Ge bicrystal p-type inversion layers; anomalous magneto-transport props. 4-98719  
 Ge bicrystals, anomalous magneto-transport props. of p-type inversion layers (*Japanese*) 4-70842  
 Ge bolometer, neutron-transmutation-doped, resist. meas. 4-106386  
 Ge, book, deposition, growth and technology 4-58579  
 Ge, clean and  $\text{H}_2\text{O}$  adsorbed, scatt. primary and recoiled surface neutrals and ions, TOP spectra 4-63800  
 Ge, compensated, photoresponse to local optical excitation 4-108904  
 Ge, compensated, thermoelec. current instability 4-61404  
 Ge, crystallisation front instability during laser epitaxy (*Russian*) 4-99325  
 Ge crystals, plastically deformed, mag. susceptibility (*Ukrainian*) 4-88644  
 Ge, cyclic loading near yield stress, plastic deform. (*Russian*) 4-113524  
 Ge, cyclotron resonance and radiative recombination for excitons, free carriers, electron-hole droplets 4-71183  
 Ge, deep impurity conc., elec. resist. and Hall coeff. meas. 4-65638  
 Ge, deep level impurities, low temp. passivation techniques 4-59561  
 Ge deposition on Si, reconstructed surface reordering 4-98411  
 Ge, dielectric function, temp. depend. 4-109111  
 Ge, dislocations, deep electron levels, recursion calc. 4-70716  
 Ge, dynamical recovery in high temp. deform. 4-103867  
 Ge, elastic props., ultrasonic meas. 4-98170  
 Ge, electron irradiation and thermal quenching, defects production 4-60962  
 Ge, electron-hole liq., relax. kinetics near nucleation threshold, collective decay of small electron-hole drops 4-98541  
 Ge, electron-hole liq. droplet destruction in nonuniform deformation field 4-61297  
 Ge, electron-hole liquid, phonon-absorpt. imaging 4-61292  
 Ge, electronic and structural props., non-local density functional theory 4-108760  
 Ge, electronically neutral impurities on muonium, low temp. meas. 4-65279  
 Ge, electroreflectance spectra, oscillations anal. for electron-hole Coulomb interactions 4-66011  
 Ge epitaxial growth on GaAs substrate by  $\text{GeH}_4$  thermal decomp. 4-71574  
 Ge, epitaxial growth on Si by ionised cluster beam method (*Chinese*) 4-84522  
 Ge exciton condensation, microwave study 4-68234  
 Ge exciton condensation, microwave studies, biexcitons and electron-hole droplets 4-70668  
 Ge exciton condensation, microwave breakdown, one- and two-photon carrier excitation luminescence 4-70670  
 Ge, exciton condensation, microwave methods using pulsed optical excitation, kinetics 4-70671  
 Ge exciton studies, laser heating effects at liquid He temps. 4-70672  
 Ge, film; RF sputtered, controlled doping 4-80059  
 a-Ge films, laser-beam annealing time resolved TEM studies 4-65297  
 Ge, Frenkel pair component distance distrib. after  $\gamma$  irradi. 4-70142  
 Ge, gamma-irradiated, hole traps 4-103799  
 Ge, grain boundaries, plasma exposure effects, diode studies 4-65276  
 Ge ground surfaces, optical props., refl. matrices appls. 4-84935  
 n-Ge, growth on Si by MBE, charact. 4-98469  
 Ge, high energy LA phonons, anharmonic decay 4-65355  
 Ge, high purity, coaxial detectors performance after fast neutron damage 4-59553  
 Ge, high temp. plasticity, theoretical models 4-98185  
 Ge, high temp. plasticity, anal. of expt. data 4-98186  
 Ge, high-purity, purification, cryst. growth and annealing props. 4-61831  
 Ge, homogeneous CVD growth, review 4-88984  
 n-Ge, hot electron capture by dipoles at low temps., field depend. 4-75979  
 Ge, hot hole submillimetre emission in transverse mag. field 4-71412  
 Ge, IR laser radiation nonlinear absorpt. and self-defocusing due to free carrier generation 4-79248  
 Ge, IR props. of heavily implanted semiconductors 4-104587  
 Ge, impurities microinhomogeneities, capture channels, time-amplitude anal. 4-108876  
 Ge, impurity breakdown kinetics, small-signal anal. 4-113965  
 Ge, injected electron-hole plasma, high-field domains 4-65699  
 Ge, intrinsic, thermoelec. 1/f noise and current 1/f noise 4-61425  
 Ge, inverse dielectric matrix, direct calc. 4-92645  
 Ge, ion channelling, interaction pot., stopping power, ion scatt. spectra 4-75570  
 Ge, irradiated with high-energy heavy ion, induced radioactivities 4-59560  
 Ge island films on insulator, single crystalline, residual strain 4-92573

## elemental semiconductors continued

- Ge island films on insulator, zone melting recrystn. with  $\text{SiO}_2$  capping layers 4-93212  
 Ge, isotopically enriched, low-field anomalous muonium depolarisation 4-71241  
 Ge, laser pulse irradi., plasma and melting kinetics, IR reflectivity studies 4-108594  
 Ge, laser-induced periodic surface struct., fluence regimes, feedback and topography 4-108436  
 Ge lenses, surface struct., veiling glare and image quality in 3 to 10  $\mu\text{m}$  spectral region 4-74648  
 a-Ge, localised impurity states 4-104163  
 n-Ge, low temp. breakdown characts. 4-92737  
 Ge, low temperature muonium depolarisation in transverse fields 4-65928  
 Ge, luminescence signal of electron-hole plasma 4-104674  
 Ge MIS struct., surface irregularity enhanced subband resonance 4-61459  
 Ge, magnetoconcentration effects and current-voltage characts. (*Russian*) 4-98642  
 Ge, magnetoconcentration effect and oscillator oscills. 4-98651  
 Ge, melting, sp. vol. change, semicond.-metal transitions 4-61050  
 Ge microrelief surface, reflecting power and etching form. (*Russian*) 4-64757  
 Ge monocrystalline, K-shell fluoresc. yield 4-85041  
 p-Ge, multiphoton absorption of submillimetre radiation, carrier drag by photons 4-108906  
 Ge, multiple leaky SAW, FFT vel. meas. by line focus-beam acoustic microscope 4-103164  
 Ge, neutron transmutation doped, annealing, DLTS study 4-60942  
 Ge nonequilibrium current carrier microwave absorpt., carrier conc., excitons 4-70852  
 n-Ge, nonlinear thermoelectric effect 4-98654  
 p-Ge, nuclear doped, elec. cond., 0.06 to 300K, impurity conc. depend. 4-61382  
 Ge obliquely deposited films, spectral and angular selectivity 4-112535  
 Ge, p<sup>+</sup>-n junction irradi. with  $\gamma$ -rays, capacitance spectroscopy 4-104287  
 Ge p-i-n photodiode for ultralong optical fibre fault location, S/N improvement study (*Japanese*) 4-60188  
 Ge, phonon dispersion near melting point 4-88250  
 Ge, phonon focusing, imaging by electron-beam scanning 4-61009  
 Ge, phonon pulses detection by fluorescence of deposited  $\text{YF}_3\text{Th}^{3+}$  film 4-113555  
 $\alpha$ -Ge, phonon struct., inelastic electron tunnelling spectra obs. 4-61031  
 Ge photo-induced complex permitt. at 9 GHz, expt. study 4-65703  
 n-Ge, photoconductivity sign dynamic change in intense submillimetre radiation 4-70859  
 Ge photodetector, cryogenic telescope on IRAS appl. 4-110525  
 Ge photodetector reliability testing 4-64706  
 Ge, photoelectron yield curves during X-ray diff. 4-61811  
 Ge, picosecond-pulse laser annealing, phenomenological model 4-88198  
 Ge, plastically deformed, anomalous magnetoresist. 4-113976  
 Ge, positron diffusion const., temp. depend. 4-99222  
 Ge, pulsed laser irradiated, time resolved temp. meas. by thin film thermocouple 4-113494  
 Ge, quenching center form., host interstitial injection by oxidising surface 4-65258  
 Ge, radiation-induced rod-like defects 4-92238  
 Ge, resonant photoemission at 3-p thresholds 4-85070  
 Ge, segmented-electrode detector fabrication, Au mask technique 4-59559  
 Ge, shallow acceptors, ground state calc., allowing for valence band corrugations 4-108817  
 Ge single cryst.,  $\alpha$ -particle irradi., defects and photoelectromag. effects 4-84654  
 Ge single cryst. film growth on  $\text{SiO}_2$  by laterally seeded heteroepitaxy 4-93234  
 Ge single cryst. surface X-ray total external reflection spectra 4-76562  
 Ge, single crystal and amorphous, optical props. meas. 4-95496  
 Ge, spin polarised photoemission 4-88929  
 Ge, sputter etch induced electrically active defects, H passivation 4-108918  
 Ge, stressed, with large electron-hole drop, magnetoacoustic props. 4-98529  
 a-Ge, struct. disorder model, thermodynamic props. 4-75303  
 Ge, submicron layers produced by ion implantation and laser annealing 4-84316  
 Ge, surface, electroreflectance and photo EMF (*Russian*) 4-104576  
 Ge surface, nonequilib. charge carrier recombination, isotopic effects 4-92750  
 Ge surface, periodic struct. form. due to action of intense UV excimer laser light 4-81042  
 Ge surface, phase conjugation, reflecting grating recording by plasma refl. 4-97003  
 Ge, surface periodic structures on intense laser bombardment 4-70201  
 Ge, surface polarization dispersion under intense irradiation 4-113877  
 Ge, symmetrical tilt grain boundaries,  $\Sigma=9$ , 11, struct., electron microscopy obs. 4-70169  
 a-Ge, thermal cond. at low temp. 4-80319  
 Ge, tilt boundaries at struct., HREM obs. 4-103767  
 Ge, US attenuation and nonlinearity const., temp. dependence 4-108552  
 Ge, uniaxially deformed., anisotropy of the oscillator effect (*Russian*) 4-113985  
 Ge with adsorbed  $\text{CaF}_2$ , layer thickness meas. by RBS (*Chinese*) 4-70968  
 Ge:Al, implanted ion projected range distrib. 4-80079  
 Ge:Ar(Sb), neutron-transmutation-doped, defects 4-60967  
 n-Ge:As, conductivity and magnetoresistance, effect of localised states 4-113950  
 n-Ge:Au, deform. influence on deep level position of impurity 4-104160  
 Ge:Au photocells, spectral characts. obs. 4-101919  
 Ge:Be, site distortion of Be acceptor, IR spectra 4-92667  
 Ge:Be IR detectors for low-photon-background IR astronomy 4-101160  
 Ge:Be photoconductor, 30 to 50  $\mu\text{m}$  detector performance and material aspects 4-108899  
 Ge:Cu, impurity contamination reduction by heat treatments above 700°C 4-71535  
 Ge:Cu, impurity states, annealing effects 4-104148  
 Ge:Cu, quenched-in deep acceptors 4-70713  
 Ge:Cu(Au), nonradiative multiphonon capture of carriers by deep traps 4-75889

## elemental semiconductors continued

- Ge:D, plasma treated, D diffusion and interaction with point defects 4-60951  
 a-Ge:Fe(Ni) films, cond. and localised states 4-104163  
 Ge:Ga, crystal growth characs. in vertical Bridgman system 4-70049  
 Ge:Ga, FIR stress induced photoconductivity, broadband meas. 4-70873  
 Ge:Ga, migration of molten inclusion 4-108659  
 Ge:Ga/(Al,Ga)As/GaAs polar semicond. quantum well system, growth and optical props. 4-114314  
 Ge:Ga(Sb), film on GaAs, doping and elec. props. study (Russian) 4-70182  
 a-Ge:H, bond angle disorder and optical absorption edge 4-99083  
 a-Ge:H, photoinduced absorption spectra 4-109220  
 a-Ge:H,P, new paramagnetic centres and impurity states 4-109056  
 a-Ge:H films, planar magnetron sputtering, electronic props. 4-88972  
 Ge:H-based impurity complexes, charge state determ. 4-92663  
 Ge:H(He), ion irradi., structural defect study 4-88164  
 Ge:muonium, anomalous, electronic g-factor anisotropy 4-65927  
 Ge:P, ballistic phonon transport under mag. field 4-70301  
 Ge:Sb, heavily doped, US attenuation, mag. field depend. 4-70283  
 Ge:Sb, intervalley neutral impurity scatt. (Russian) 4-104197  
 Ge:Sb, photoexcited, impurity breakdown and impact ionisation 4-92739  
 n-Ge:Sb, US attenuation, mag. field effects, impurity conc. depend. 4-75618  
 Ge:Sb, wave-function phase, relax. time, temp. depend. 4-88517  
 Ge:Sb(As), impurity state breakdown under uniaxial compression 4-70715  
 Ge:Se, impurity levels, Hall effect study 4-108804  
 Ge:Si, ultrapure and doped, muonium state, positive muon spin precession signals 4-71242  
 Ge:Si(Sn)(Al), thermal cond. meas., impurity conc. effect, temp. depend. 4-80318  
 Ge:Te, ion implanted, amorphisation phenomena, electron microscope and electron diff. studies 4-103656  
 Ge:Zn, far-IR magnetoabsorption of bound excitons 4-114247  
 Ge:Zn, nonohmic hopping cond. in strong elec. fields 4-88515  
 Ge:Zn, Sb, degree of compensation from optical absorption meas. 4-109221  
 Ge/Al interface, chemisorption and metallisation, electronic struct. 4-92527  
 Ge/GaAs heterojunctions, interface struct., TEM and STEM studies 4-108728  
 Ge-Al films, granular, sp. ht., thermal cond. meas., supercond. transitions 4-98809  
 Ge-GaAs interface, electronic struct. 4-84665  
 Ge-GaSe 'Schottky-like' heterojunction 4-108931  
 Ge-Ge<sub>1-x</sub>Si<sub>x</sub> superlattices, interactions of high-freq. EM waves 4-80670  
 Ge-Ni(Ce), spin depolarisation study 4-104722  
 Ge-Si alloys, band calcs., empirically adjusted zone variational method (Chinese) 4-75831  
 Ge-ZnSe (110) interface, ordered and disordered, electronic struct. 4-84666  
<sup>72</sup>Ge, O<sub>2</sub> state lifetime, delayed auto-coincidence of Ge(Li) detector 4-102497  
<sup>74</sup>Ge, neutron doped, low-temp. elec. cond. 4-80594  
 Ge(100)-(2×1), adsorption of Ag, HEED and photoemission study 4-75790  
 Ge(100)-GaAs interfaces, Fermi level position and valence-band edge discontinuity study 4-61450  
 Ge(111)2×1, polarisation depend. of surface-state absorption, photothermal displacement spectroscopy 4-92488  
 In anti-Stokes Raman laser 4-79110  
 In-Hg/Si ohmic contacts, differential resistance and capacitance characs. 4-92819  
 In-Si (111) interface, charge transfer and surface electromigration 4-108667  
 LiNbO<sub>3</sub>-Ge, parametric amplification of SAW 4-108697  
 LiNbO<sub>3</sub>-Ge multilayer structure, nonlinear self-contraction of acoustoelectronic fluctuations spectrum 4-70877  
 Mo-Si system, thin-film reactions and phase diagrams 4-88263  
 Mo-Ti/Si interface, metallisation for self-aligned TiSi<sub>2</sub> process 4-89145  
 Ni-Si (111) interface, Ni<sub>2</sub>Si islands growth, ion scatt. study 4-92444  
 P, black, band struct. and optical props. 4-70650  
 P, black, electronic props. and elec. cond. (Japanese) 4-92606  
 P, black, electronic struct., polarised X-ray emission and absorption studies 4-108771  
 P, black, reson. photoemission theory 4-85088  
 Pd-Al<sub>2</sub>O<sub>3</sub>-SiO<sub>2</sub>-Si MIS struct., flat band voltage shift 4-108945  
 Pd-Si(111) interface, atomic intermixing and electronic interaction 4-70478  
 Pt-SiO<sub>2</sub>-Si MIS struct., flat-band voltage shift 4-108944  
 a-Sb, elec. resist. and thermoelec. power meas. 4-108886  
 Se, amorphous, DC conductivity thickness dependence 4-84620  
 Se, amorphous, defect states and photoelec. behaviour 4-113903  
 Se amorphous film, photo-EMF due to surface barriers 4-88541  
 Se crystal struct. and defects, CDW soliton model 4-70685  
 a-Se, electronic and vibr. struct., Raman spectra, cluster method 4-74387  
 Se electrophotographic layer parameters, influence of gaseous medium (Russian) 4-68311  
 Se, epitaxial crystallisation on linear polyphenyls 4-65590  
 Se, MBE growth on cleaved Te, RHEED, AES and LEELS characterisation 4-99343  
 Se, particle suspensions, electronic processes, microwave probing 4-99852  
 Se single cryst., negative photocond. and IR quenching 4-65709  
 Se, thin film solar, cell. 4-99966  
 a-Se:Bi films, crystallisation, dark cond. and activation energy 4-88104  
 Se:Te, As glassy films, pure and doped, deep level defects, xerographic spectra studies 4-61339  
 Si (001), shallow donor impurities, variational soln. 4-70893  
 Si (001) surface for NiSi<sub>2</sub> epilayers, electronic structs. determ. 4-88549  
 Si (001) wafers, thermally oxidised, P<sub>0</sub> interface centres, ESR study, effect of As<sup>+</sup> ion implantation 4-92960  
 Si (100), adsorbed, In(Sn), superlattice structures, RHEED study 4-113802  
 Si (100), chemisorption of H, TDS study (Chinese) 4-92510  
 Si (100), clean and Cs covered, neutralisation of scattered He ions 4-109294  
 Si (100), energetic He ion scatt., neutralisation, channelling studies 4-76591  
 Si (100), PH<sub>3</sub> and SiH<sub>4</sub> adsorption, saturation coverage 4-88392

## elemental semiconductors continued

- Si (100), surface cleaning, Ag deposition effects, SEM, AES and RHEED studies 4-66471  
 Si (100), surface treatment for Si MBE growth 4-71743  
 Si (100) 2×1, pre-exposed to O in submonolayer range, chem. shifts of Si-H stretching freqs. 4-80368  
 Si (100) 2×1, dissociative adsorption of water, IR spectra obs. 4-93557  
 Si (100) inversion layer, electron mobility, neutral scatt. effects 4-76040  
 Si (100) substrate for Ge<sub>2</sub>Si<sub>1-x</sub> epitaxial film, commensurate and incommensurate struct. 4-108740  
 Si (100) surface, H chemisorbed, work function change, LEED expt. 4-70907  
 Si (100) surface, reconstructed, rainbow atom scattering 4-66174  
 Si (100) surface electronic excitations, EELS study 4-108914  
 Si (100) surface with chemisorbed H, surface states, UVPS study 4-108709  
 Si (100) with adsorbed O<sub>2</sub>, ab initio SCF calcs. 4-98440  
 Si (100)2×1, H adsorpt., coverage and temperature-dependent vibr. spectra, EELS and LEED studies 4-80408  
 Si (100)(2×1), chemisorbed H<sub>2</sub>O and D<sub>2</sub>O, multiple vibr. excitations, high resolution EELS study 4-109289  
 Si (100)(2×1) surface, atomic geometry, elastic LEED intensity anal. 4-92490  
 Si (110), electron subband reson., IR reson. absorpt. 4-61431  
 Si (111), 7×7, 5×5 and 2×8 struct. models, RHEED intensity distrib. anal. 4-92486  
 Si (111), 7×7 reconstruction, strain energy, adatom model anal. 4-108685  
 Si (111), 7×7 surface reconstruction, milk-stool model 4-80353  
 Si (111), (2×1) to (7×7) to (1×1) phase transitions, rel. to defect-phonon interactions 4-108686  
 Si (111), adsorbed Cs, inversion layers, positive and negative magnetoresistance 4-98645  
 Si (111), annealed in high vac., electronic props., surface photovoltage study 4-80628  
 Si (111), benzene bound state vibr. modes and chemisorption bonds 4-108714  
 Si (111), Cs adsorption, Cs valence electron photoemission studies 4-84505  
 Si (111), deposited ultrathin Sn layers, RHEED study 4-80451  
 Si (111), electron correlation effects at vacancies 4-98092  
 Si (111), laser irradi., photoemission of electrons 4-81116  
 Si (111), reconstructed, electron microscopy and diff. studies 4-108690  
 Si (111), relaxation effects (Chinese) 4-70887  
 Si (111), resonant photoemission 4-71514  
 Si (111), surface, far UV laser induced oxidation by bond rearrangement 4-81310  
 Si (111), surface anal. using ultrahigh vacuum SEM 4-68329  
 Si (111), surface phonons and surface reconstruction 4-80364  
 Si (111), surface phonons and reconstruction 4-92509  
 Si (111) 7×7, structural models and scanning tunnelling microscopy data 4-88383  
 Si (111) (7×7), NO adsorption and reactions, EELS, LEED and AES studies 4-65562  
 Si (111) and (100), Cs, K, Na, Li desorption kinetics and surface phase changes, surface ionisation studies 4-65571  
 Si (111) face, thermally agitated electrons, IR reflection obs. 4-93082  
 Si (111) slab, interface, electron-phonon interaction and broken symm. 4-80517  
 Si (111) surface, CoSi<sub>2</sub> epitaxial growth 4-61844  
 Si (111) surface, UPS rare gas titration for surface characteris. 4-88936  
 Si (111) surface chemisorbed Br, X-ray standing wave anal. with synchrotron radiation 4-103607  
 Si (111) surface composition and band struct. 4-92778  
 Si (111) with chemisorbed Sm, photoemission spectra 4-80392  
 Si (111)-Al(Ga)(In) abrupt interfaces, electronic props. 4-84696  
 Si (111)-Mo interfaces, electronic struct., XPS and X-ray excited AES study 4-85085  
 Si (111)-2×1, polarisation depend. reflectivity calc. 4-76496  
 Si (111)-(1×1) total-energy calcs. for 2×1 antiferromag. and 1×1 paramag. states 4-80809  
 Si (111)2×1, identification of surface states as bulk contrib., photoemission spectra 4-88943  
 Si (111)2×1 surface, MeV ion backscattering/channelling studies 4-85051  
 Si, a-Ni<sub>36</sub>W<sub>64</sub> contacts, elec. characs. 4-104311  
 Si, A-centre and thermal donor levels, Hall effect, DLTS meas., press. depend. 4-80529  
 a-Si, AC field effect and density of gap states 4-92670  
 Si, acceptor pairs, hydrogenic, first ionisation energies calc. 4-70710  
 Si, albedo collecting photovoltaic module 4-66711  
 a-Si alloys, metastable defect states, X<sub>α</sub> scatt. wave calc. 4-113899  
 a-Si alloys, photocond., dark Fermi level position depend. 4-113987  
 Si, amorphous, doped, IR and reson. Raman spectrosc. obs. 4-61707  
 Si, amorphous, from ion implantation, refractive index, thermal annealing effect 4-76417  
 Si, amorphous, high-defect-density, subpicosecond carrier trapping 4-80621  
 Si, amorphous, highly doped, MBE grown, epitaxial regrowth 4-98468  
 Si, amorphous, ion implanted, crystn. growth velocities, charged dangling bonds 4-88093  
 Si, amorphous, minority carrier diffusion length, intensity dependence 4-70829  
 Si, amorphous, photovoltaic detector for optical-optical guided-wave modulator 4-103004  
 Si, amorphous and crystalline, surface oxidation, photoemission study 4-76880  
 Si, amorphous CVD films, H<sub>2</sub> plasma annealing localized state density 4-61337  
 Si amorphous film, laser enhanced crystallisation, nucleation, growth velocity, recombination enhanced diffusion 4-65295  
 Si, amorphous films as deep UV lithography masks 4-82837  
 a-Si, amorphous layer effect on lattice images of dislocations 4-79939  
 Si, amplitude depend. of ultrasonic absorpt. 4-70278  
 Si and Ga<sub>1-x</sub>Al<sub>x</sub> solar cells, beam splitting concentrator, optical characterisation 4-66665  
 Si, angular distrib. of annihilation radiation 4-71472  
 Si, anisotropic 2D system, negative magnetoresistance 4-70841  
 Si, anomalous muonium relax., muon spin rot. study 4-71238  
 Si, anomalous thermal props., correlation function method 4-61113  
 Si, atomic diffusion mechanisms theory 4-70430

## elemental semiconductors continued

- Si, axial channelling radiation of MeV electrons 4-92276  
 Si, BC-8 crystal phase, struct. props., phase stability and phase transitions 4-113389  
 Si, band calcs., empirically adjusted zone variational method (*Chinese*) 4-75831  
 Si, bifacial solar cells, comparison of high and low injection cells 4-93627  
 Si, book, deposition, growth and technology 4-58579  
 Si, C and O content determ. by IR spectroscopy 4-113484  
 Si, CMOS active lateral diffusion and linewidth test struct. 4-108665  
 Si, CVD, coupled fluid mechanics and chem. kinetics, math. model 4-61867  
 Si, CVD growth, solid state phase transformations 4-70598  
 Si, CVD in low press. discharge, overview 4-114421  
 Si, carbothermic silica reduction process, computer simulation 4-66200  
 Si, carrier lifetime, elec. resist. meas. by contactless method 4-61392  
 Si, carrier vel. fluctuations in steady-state and transient regimes, Monte Carlo study 4-80637  
 p-Si cathode surface treatment effects on photoelectrochemical kinetics in H<sub>2</sub> production 4-93649  
 Si, channelled electrons, axial channelling radiation, temp. depend. 4-75576  
 Si, channelling electrons, energy band structure, wave functions, calcs. 4-108493  
 Si, channelling radiation emitted from 350 MeV planar channelled electrons 4-75578  
 Si, channelling radiation from relativistic positrons, energy eigenvalue calc., self consistent approx. method 4-80128  
 Si, chemisorption of water on (100), water mol. dissoc., IR spectra study 4-62233  
 Si classical periodic structs., light absorption edge 4-66002  
 Si, clean and SiO<sub>2</sub> covered, picosecond laser heating and evaporation 4-70198  
 Si, cleaved (111) face, X-ray topography study 4-104042  
 Si, clusters of electrically active centres and impurity states 4-70183  
 Si, coated with thin oxide layer, detect. and meas. using high sensitivity depth profiling stationary beam cratering method 4-99711  
 Si, computer simulation, relativistic electrons, multiple scatt., axial channelling 4-108491  
 Si, concentrator solar cells, performance limits, future design speculations 4-89430  
 a-Si, cond. and thermoelectric power below mobility edge 4-108888  
 Si, conference, San Jose, CA, USA (Jan. 1982) 4-110812  
 Si, contamination and near-surface damage caused by reactive ion etching 4-113757  
 Si, crystal growth and processing technology 4-114365  
 Si, crystal growth and wafer prep., book contrib. 4-85098  
 Si, crystal whiskers, cyclically deformed, relaxation spectrum 4-61264  
 Si, crystalline, laser damage by multiple 1.06  $\mu$ m picosec. pulses 4-75515  
 Si, crystalline, production for solar cells (*German*) 4-81121  
 Si, crystalline and amorphous, energy transfer during laser irradi. 4-76412  
 Si, crystalline upgraded metallurgical grade, limiting factors for solar cell appl. 4-77095  
 Si, crystals, Czochralski pulled, O precipitation, diffusion mechanism, etching optical and neutron scatt. obs. 4-65209  
 Si, crystals, interface shape and radial distribution of impurities 4-113371  
 Si, crystals, plastically deformed, mag. susceptibility (*Ukrainian*) 4-88644  
 Si, Czochralski, C in radiation damage centres, luminesc. study 4-93107  
 Si, Czochralski crystal growth, computer controlled 4-66211  
 Si, Czochralski grown compensated thermodons, EPR and Hall studies 4-75898  
 Si, Czochralski growth, impurity clouds, microdefects, scatt. light intensity and etch pit density after annealing 4-84312  
 Si, Czochralski growth, O segregation control by combining mag. field and cryst. rot. 4-104729  
 Si, Czochralski single crystal growth in mag. field (*Japanese*) 4-88959  
 Si, deep impurity levels, cluster method of pseudoatomic orbitals (*Chinese*) 4-84583  
 Si, deep impurity levels, ENDOR and ESR spectra 4-84594  
 Si, deep level impurities, low temp. passivation techniques 4-95951  
 Si, deep level wavefunctions, behaviour in shallow energy region (*Chinese*) 4-92650  
 Si, deep-level wavefunctions with energies near band edges 4-92656  
 Si, defect and carrier lifetime, back-surface damage gettering technique 4-113972  
 Si, defect delineation by chem. etching 4-88171  
 Si, defect states, T<sub>2</sub> symmetric deep level wave functions 4-108801  
 Si, defected substrates, minority carrier lifetime, injection level depend. 4-92753  
 Si, defects and high press. steam oxidation, stacking faults 4-114706  
 n-Si, deformed, drag thermoelectric power anisotropy 4-104247  
 Si, deformed, EBIC/TEM study of defects 4-80045  
 Si, deposition using tetrachlorosilane reactions in Ar-H<sub>2</sub> microwave plasma 4-89268  
 Si, detector structure layers thickness determ., with aid of charged particles 4-102531  
 Si, diaphragm pressure sensor using buried piezoresistors 4-85530  
 Si, diffusion models, enhancements and retardations, book contrib. 4-84467  
 Si, diffusion tensometers, parasitic photosensitivity 4-101829  
 Si, diode temp. sensors, stability, 4.2 to 273K 4-68229  
 Si, dislocation behaviour, review 4-88169  
 Si, dislocation behaviour, X-ray topography study 4-88175  
 Si, dislocation slip planes, EBIC contrast in SEM 4-103754  
 Si, dislocation sources, oxidation induced stacking faults (*Russian*) 4-113457  
 Si, dislocation stress distrib., effects on pendulum fringes 4-60783  
 Si, dislocations, deep electron levels, recursion calc. 4-70716  
 Si, dislocations, isolated, mobility meas. 4-70156  
 Si, disorder profiles at high sputtering dose by oxide growth rate profiling 4-66470  
 Si, dissoln. kinetics in Cr<sub>2</sub>O<sub>3</sub>-HF-H<sub>2</sub>O soln. 4-62082  
 Si, dopant distributions, direct imaging by STEM 4-113481  
 Si, doped, metal-nonmetal transitions 4-80500  
 Si, doped substrate, overetching determ. using combined pulsed capacitance voltage meas. and SIMS 4-85269  
 Si, doping, CVD BN film as B diffusion source 4-98359  
 Si, doping kinetics from atomic beam in vacuum, desorption 4-113479  
 Si, dry etching induced damage 4-81312

## elemental semiconductors continued

- Si, dry oxidation, parabolic kinetic const., stress effects 4-93434  
 Si, dynamical recovery in high temp. deform. 4-103867  
 Si, ESR meas. of chalcogen pairs, theory 4-104493  
 Si, EXAFS study of NiSi formation 4-109277  
 Si, elastic props., ultrasonic meas. 4-98170  
 Si, elastically bent crystals, dechannelling of planar channelled protons 4-75575  
 n-Si, electrical conduction, thermodynamic anal. 4-92711  
 Si, electron and  $\gamma$  irradi., influence on defect annihilation 4-98094  
 Si, electron and  $\gamma$ -ray irradiated, efficiency of radiation defect formation 4-92237  
 Si, electron and positron irradi. effects (*Russian*) 4-88208  
 Si, electron beam annealing, pulsed, thermal model 4-60963  
 n-Si, electron capture coeff. of quenching centres 4-104159  
 Si, electron inversion layer, scatt. and adsorption of ballistic phonons, theory and expt. 4-98767  
 Si, electron structure change during amorphisation, electrorefl. spectra (*Russian*) 4-98509  
 a-Si, electron transport, photocurrent transit time method 4-65679  
 Si, electronic and solar grade, anal. using atomic emission spectroscopy from inductively coupled plasma 4-60948  
 Si, electronic and structural props., non-local density functional theory 4-108760  
 a-Si, electronic and vibr. props., book 4-67878  
 Si, electronic density of states, recursion coeffs., linear prediction theory 4-98502  
 a-Si, electronic struct., photoemission and optical props. 4-71522  
 a-Si, electronic struct. of defects, cluster Bethe lattice method 4-70739  
 Si, elemental composition anal. using SIMS 4-62274  
 Si, energy bands, variational cellular method 4-92598  
 Si, epitaxial, metallic precipitates charact. by etching and TEM 4-98291  
 Si, epitaxial deposition, shallow surface depressions 4-114407  
 Si, epitaxial growth, pyrolysis of SiH<sub>4</sub>, influence of H<sub>2</sub> or Ar carrier gas 4-76682  
 Si, epitaxial growth from SiCl<sub>4</sub>, C contamination, thermodynamic anal. (*Chinese*) 4-113824  
 Si, epitaxial layer, homogeneity and thickness meas. by IR flaw detection method 4-109609  
 Si, epitaxial layer, processing technology and characts. (*Polish*) 4-113827  
 Si, epitaxial layer growth on CaF<sub>2</sub> substrates 4-80448  
 Si, epitaxial layers, formation of transitional conc. regions 4-76678  
 Si, epitaxial layers, thickness meas. by IR reflectance studies 4-111105  
 Si, epitaxial near equilb. growth by CVD, Si-Cl-H system 4-71572  
 Si, epitaxial near equilb. growth by CVD, Si-H-H system 4-71573  
 Si, epitaxial single cryst. films, origin of additional electron diffr. spots 4-104104  
 Si, etching using Ar-ion assisted Cl<sub>2</sub> 4-85054  
 Si, evaporated amorphous film, growth conditions by solid phase epitaxy 4-99307  
 Si, evaporated film, optical props, influence substrate temp. 4-76546  
 p-Si, even photomagnetic effect 4-61421  
 a-Si, excess carrier lifetime and mobility studies 4-104219  
 Si, excess interstitial distribution during thermal oxidation, two-dimensional model 4-84286  
 Si, excitation depend. grain boundary recombination velocity 4-104217  
 Si, extrinsic IR detectors, development status 4-95516  
 Si, far IR transmission from 0.1 to 1 mm wavelength 4-73490  
 Si, far IR transmission spectrum, two-phonon difference band obs. 4-104597  
 Si, fast neutron irradiation effects on resistivity in single crystals 4-98138  
 Si, fast surface-state density determ. using CCD technique 4-76017  
 a-Si film, CVD CO<sub>2</sub> laser deposition process 4-114412  
 a-Si film, elastic and inelastic props. 4-88225  
 a-Si film, epitaxial crystallisation on GaP substrate 4-80452  
 a-Si, film, gap density of states determ. 4-80551  
 Si film, ion implanted, electron beam recrystallisation 4-98137  
 Si film, LPCVD, elec. props., effect of film thickness 4-88615  
 Si film, polycryst., ion implanted, dopant diffusion (*Russian*) 4-108657  
 a-Si film, RF sputtered, optical absorpt., elec. cond., effect of thermal annealing 4-80583  
 Si film, solid, laser heated, Raman scatt. at melting temp. 4-76464  
 poly-Si film CVD deposition, trench coverage characts. 4-114413  
 Si film growth from SiH<sub>4</sub> in CVD and plasma-enhanced CVD systems 4-114419  
 Si film on SiO<sub>2</sub> substrate, electron beam recrystallisation 4-98136  
 Si film plasma enhanced chemical vapour deposition 4-114423  
 Si films, cryst. orientated by metal patterns on planar amorphous substrates 4-66202  
 a-Si films, localised density of states, electrophotography studies 4-113844  
 Si films, monocrystalline and polycrystalline, simultaneous epitaxial growth, struct., elec. props. 4-98488  
 a-Si films, polarisability, refr. index meas. 4-93001  
 a-Si films, RF sputtered, photocond. meas. 4-61416  
 Si films, UHV deposited, crystn. temp. 4-88410  
 Si films and wafers, structural perfection testing using optical scanner 4-96975  
 Si, float zone refining parameter depend. on freq. 4-114387  
 Si, float-zone dislocation-free single crystal, microdefects effect on positron lifetimes (*Chinese*) 4-104694  
 Si, floating-zone crystals, microdefects, metallographic and electron microscopical anal. 4-103737  
 Si, galvanomagneto-combinational effect 4-113980  
 n-Si, gamma and neutron irradi., radiation defect interactions 4-92227  
 Si, gamma-irradiated, carrier recombination, dislocation effects 4-75982  
 Si, gamma-irradiated, charge carrier recombination 4-84631  
 Si, gettering efficiency of different dislocation types, EBIC, TEM obs. 4-103787  
 Si, grain boundaries, spin-depend. trapping, effects of light and modulation freq. 4-104155  
 Si, grain boundary recombination vel., study for different injection levels 4-98633  
 Si, graphoeptitaxy, two-stage artificial epitaxy 4-66229  
 Si, growth of insulating SiO<sub>2</sub> films by oxidation 4-98485  
 Si, growth of ultra-large-area crystals using EFG technique, low cost photovoltaics appl. 4-88961  
 Si,  $\gamma$ -ray irradi., conductivity, eddy current meas. 4-104201  
 Si,  $\gamma$ -ray irradi., trapping centres, DLTS studies 4-104147  
 Si, H<sub>2</sub>O dissociative chemisorption, photoemission studies 4-84514

## elemental semiconductors continued

- Si, Hamiltonian and momentum scaling 4-92593  
 Si hazed polycryst. layers, STEM microanal. studies 4-108692  
 Si, heat treatment influence on dislocation motion kinetics (*Russian*) 4-88173  
 Si, heavily doped, band-gap narrowing study 4-80490  
 Si, heavily doped, built-in elec. field for holes 4-80584  
 Si, heavily doped, intervalley mixing study 4-80491  
 p-Si, heavily doped, low temp. thermal cond. 4-70300  
 Si, heavy ion and particle induced X-ray emission anal. 4-62275  
 Si, heavy-ion induced damage and annealing TEM and channelling studies 4-80115  
 Si, high pressure phase transitions, X-ray diffr. study 4-98272  
 Si, high purity, intercarrier scatt. effects, laser and electron beam excitation 4-92725  
 Si, high temp. plasticity, theoretical models 4-98185  
 Si, high temp. plasticity, anal. of expt. data 4-98186  
 p-Si, highly-purity quenched samples, defect photoluminesc. 4-80979  
 Si, highly doped, intrinsic number and Fermi level modelling for device and process simulation 4-75983  
 Si, highly doped, modeling the intrinsic number and Fermi levels for device and process simulation 4-113966  
 Si, highly undercooled, molten, nucleation and amorphous phase form. 4-70346  
 Si hole space charge layers, interaction between electronic and phonon Raman scatt. 4-98774  
 Si, hole space-charge layers, lifting quasispin degeneracy by surface electric field 4-98516  
 Si, homoepitaxial growth, press. as deposition variable 4-114420  
 Si homoepitaxial structs., LPE growth, power transistor fabrication (*Russian*) 4-109333  
 a-Si, hot carrier thermalisation, picosecond electronic relaxations 4-108892  
 n-Si, hot electron conductivity in transverse elec. field, intravalley scatt. obs. 4-80596  
 Si, IR detector arrays, state-of-the-art review 4-111202  
 Si, IR laser radiation nonlinear absorpt. and self-defocusing due to free carrier generation 4-79248  
 Si, IR props. of heavily implanted semiconductors 4-104587  
 Si, IR radiation absorption from CO<sub>2</sub> laser 4-71367  
 Si, IR spectroscopy characterisation 4-99136  
 Si, ideal vacancy, electronic struct. calcs. 4-70722  
 Si, image contrast from extrinsic stacking faults, quantitative anal. 4-75458  
 Si, implant depth profiles 4-65289  
 Si, implantation doped, elec. and struct. characterisation by IR refl. 4-76476  
 Si, implanted O profiles, model 4-80065  
 Si, implanted oxides, annealing, activation energy 4-75490  
 Si, impurities, activation anal. using charged particle accelerators 4-60946  
 Si, impurity characterisation using neutron activation anal. 4-60947  
 Si, impurity conduction effect of uniaxial compression on p-type Si 4-98617  
 Si, impurity diffusion, fraction of interstitialcy mechanism 4-80308  
 Si, impurity diffusion, impurity conc. doping effects 4-113728  
 Si, impurity incorporation during Czochralski growth 4-114385  
 Si, impurity migration, effect of elastic stresses 4-88349  
 Si, impurity photoabsorption, quantum defect method anal. 4-88858  
 Si induced-inversion layer MOS solar cells, computer anal. 4-77102  
 a-Si, inert gas implantation and sputtering yield enhancement 4-76600  
 Si, inert gas ion bombardment, secondary ion emission, angular depend. 4-76618  
 Si ingots and ribbons, cryst. growth techniques, review 4-93210  
 Si integrated circuits, cross sectioning for SEM, TEM and optical microscopy 4-95400  
 Si intensified photodiode array detector linearity, appl. to coherent anti-Stokes Raman spectroscopy 4-95513  
 poly-Si interface phenomena at Si grain boundaries 4-70925  
 n-Si, intervalley relax. time, elec. cond. study 4-98621  
 Si, intrinsic point defects and diffusion processes 4-108358  
 Si inversion layers, 2D Na impurity band cond. in activated regions, mag. field depend. 4-98769  
 Si inversion layers, de Hass-van Alphen effect obs. 4-98771  
 Si, inversion layers, freq.-induced electron delocalisation and fractional quantisation 4-80681  
 Si inversion layers, impurity band cond. in mag. fields, theory 4-98768  
 Si inversion layers, magnetoconductance and quantised confinement 4-98764  
 Si inversion layers, multiple connected quantised resistance regions 4-98725  
 Si inversion layers, submicron width, quasi 1D effects 4-98765  
 n-Si inversion layers, two-dimensional plasmons and far infrared emission 4-104140  
 n-Si, inversion layers in MOSFET, phonon limited hot-electron temp. 4-70945  
 Si, ion beam etching using chemically assisted technique 4-66493  
 Si, ion bombarded, 14 MeV O ions, non-registered Si produced at metal-Si interface 4-114351  
 Si, ion bombardment, sputtered particles and cascade recoils 4-76621  
 Si, ion etching in CF<sub>4</sub>, modulated ion beam studies 4-85231  
 Si, ion implantation damage profiles, comparison of angle lapping/staining and cross-sectional TEM 4-103775  
 a-Si, ion implantation form. and optical state characterisation 4-88186  
 Si, ion implantation synthesis of SiO<sub>2</sub> 4-70175  
 Si, ion implanted, amorphous surface layer recrystallisation by epitaxial annealing, effect of foreign atoms 4-71553  
 Si, ion implanted, beam annealing 4-75510  
 Si, ion implanted, CO<sub>2</sub> laser annealing, relax. characts. of metastable concentrations 4-75512  
 a-Si, ion implanted, etching in HF soln. and annealing effects 4-80063  
 Si, ion implanted, explosive liq. phase crystallisation by double pulse laser irradi. 4-84188  
 Si, ion implanted, halogen lamp rapid annealing, p-n junction formation 4-88195  
 Si, ion implanted, laser or electron beam annealing, electronically active defects, DLTS 4-80527  
 Si, ion implanted, laser or electron beam annealing, minority carrier recomb., EBIC, photoluminescence meas. 4-80601  
 Si, ion implanted, pulse-laser-induced epitaxial regrowth 4-75511

## elemental semiconductors continued

- Si, ion implanted, pulsed laser and thermal processing, defect anal. 4-70133  
 Si, ion implanted, pyrometric temp. meas. during laser annealing 4-70203  
 Si, ion implanted, rapid thermal arc lamp and pulsed laser annealing, photoluminesc. study 4-93094  
 Si ion implanted film, photoacoustic response study 4-84955  
 n-Si, ion implanted with He<sup>+</sup>, deep donor levels 4-61323  
 Si, ion implanted with noble gases, optical defects, photoluminesc. study 4-71429  
 Si, ion-assisted etching by mol. Cl<sub>2</sub> 4-85228  
 Si, ion-assisted etching by mol. Cl<sub>2</sub>, SIMS study 4-85229  
 Si, ion-implanted, pulsed laser annealing, transient reflectivity studies 4-80086  
 Si, ion-implanted, pulsed laser annealing, reflectivity studies 4-80087  
 Si, irradiated, excitation spectroscopy on 0.79 eV (C) line defect 4-93112  
 n-Si, irradiated, Si-Si centre, optical excitation and relaxation, EPR study 4-109075  
 n-Si, irradiated by  $\gamma$ -rays, changes in carrier lifetime 4-104232  
 Si, irradiated with high-energy heavy ion, induced radioactivities 4-59560  
 Si island growth on amorphous substrates by zone melting recrystallisation 4-65594  
 Si islands, single crystalline, laser recrystn., SOI IC fabrication 4-75798  
 Si LV avalanche photodiode for optical fibre data transmission 4-107877  
 Si large diameter wafers, process nonuniformities, resistance characterisation 4-113963  
 Si, large-diameter Czochralski growth 4-114384  
 Si, laser annealed, polarisation sensitive Raman microprobe studies of local cryst. quality 4-101925  
 Si, laser annealing, advantages over thermal annealing 4-113497  
 Si, laser detection of diatomic products of plasma sputtering and etching 4-114856  
 Si, laser doping by dissociation of metal alkyls 4-80069  
 Si, laser heating, thermal radiation, pyrometric temp. measurements 4-92230  
 p-Si, laser induced changes in surface states 4-104288  
 Si, laser irradi., influence of electron-hole density profile on reflectivity 4-104559  
 Si, laser pulse irradi., plasma and melting kinetics, IR reflectivity studies 4-108594  
 Si laser recrystallised MOSTs, current cond. mechanism 4-76057  
 Si, laser-controlled plasma etching 4-85232  
 Si, laser-induced oxidation for patterned SiO<sub>2</sub> formation 4-99613  
 Si laser-irradiated, instability at melting threshold 4-80094  
 Si, lateral epitaxy, electron beam annealing 4-99308  
 Si, lattice parameter and thermal expansion coeff. between 300 and 1500K 4-88316  
 Si layer growth from melt on graphitised fabric substrates 4-66240  
 a-Si, localised electron state spectroscopy 4-70741  
 Si, localised vacancies, electronic struct. and stability 4-80539  
 a-Si, long-range structural and electronic coherence in amorphous semiconductors 4-80485  
 Si, low energy heavy ion range parameters, Z<sub>1</sub> dependence 4-92248  
 Si, low energy implantation of N<sub>2</sub> and NH<sub>3</sub>, Si<sub>3</sub>N<sub>4</sub> formations 4-75484  
 Si, low energy proton scatt. 4-81087  
 Si, low pressure CVD growth and phys. props. 4-81150  
 Si, low temperature muonium depolarisation in transverse fields 4-65928  
 Si MBE, accelerated ion doping 4-81133  
 Si, MBE, capabilities, materials prospects 4-81144  
 Si MBE, feasibility and appls. 4-81145  
 Si, MBE growth, use of In for surface cleaning 4-99616  
 Si, MBE growth, use of laser processing 4-114406  
 Si MBE layer, Sb adsorption, LEED, AES and TDS study 4-65560  
 Si, MBE technology and appls. (*Japanese*) 4-85104  
 Si MNP solar cells, reliability under 1 MeV electron irradi. 4-77096  
 Si MIS 2D Fermi system, phonon drag of surface charges 4-92812  
 Si, MIS inversion channel, quantum Hall effect studies 4-104231  
 Si MIS struct., amorphous C covered, tunnelling to insulator gap states 4-92824  
 Si MIS struct., magnetoresist. of inversion and accumulation layers 4-61461  
 Si MIS struct., relax. time of wave-function phase in two-dimens. electron gas 4-88605  
 Si MIS struct., surface irregularity enhanced subband resonance 4-61459  
 Si MIS struct., X-ray irradi., interface traps, DLTS studies 4-104282  
 Si MIS structure, fractional quantum Hall effect 4-108947  
 Si MOS inversion layers, complex capacitance in quantised resist. regime 4-98773  
 Si MOS struct., implantation-induced defects, RF annealing using H plasma 4-84308  
 Si MOS structures, donor-like defects 4-61457  
 Si MOS structures, intersubband hole reson. and interaction with two-dimens. plasmons 4-104320  
 Si MOSFET, anal. of quantised Hall resist. at finite temps. 4-98727  
 Si MOSFET, hysteresis phenomena in charging in quantising mag. field 4-104319  
 Si MOSFETs, energy relax. of warm electrons under substrate bias 4-104318  
 Si, magnetic energy states of shallow acceptors, spin depend. luminesc. study 4-104655  
 n-Si, many-valley semicond., impurity states, clustering model 4-80549  
 Si, melting, sp. vol. change, semicond.-metal transitions 4-61050  
 Si, metallic thin film adhesion enhancement by vacuum UV irradi. 4-93498  
 Si microcrystalline films, structure changes on deposition 4-61247  
 Si microrelief surface, reflecting power and etching form. (*Russian*) 4-64757  
 Si, microscopic defects using DTS-1 X-ray topographic spectrometer 4-75362  
 Si microtwins, selected-area electron diffr. obs 4-103770  
 Si, minority carrier diffusion lengths meas. 4-70835  
 Si, minority carrier lifetime meas. using AC surface photovoltages 4-92744  
 a-Si, mobility edge, temp. depend. 4-92723  
 Si, mol. type axial channelling radiation from MeV electrons 4-75582  
 Si, monocrystalline films grown on SiO<sub>2</sub>, defect characterisation 4-61251  
 Si monocrystalline island growth on insulating substrates 4-76670  
 Si multiply implanted targets, range distribns., Rutherford scatt. studies 4-92268

## elemental semiconductors continued

- Si, multiwafer plasma system for anodic nitridation and oxidation 4-85237  
 Si, muon decay channelling positron ang. dist. studies 4-65311  
 Si,  $n^+$  and  $p^+$  regions, uncertainties about physical electronics, solar cell appls. 4-89428  
 Si,  $n$ -type, heavily-doped, minority hole mobility, empirical expression, device modelling appl. 4-98608  
 Si, native oxide form. initial phase, AES study 4-104891  
 Si, negative secondary ion emission, influence of alkali metal implantation 4-104710  
 Si, neutron beam-irradiated single crystals, small angle neutron scatt. study 4-75540  
 Si, neutron irradi., radiation defects and electrophys. parameters 4-84319  
 Si, nitridation in multiwafer plasma system 4-81309  
 Si, noncrystalline, explosive crystallisation 4-98019  
 Si, noncrystalline thin films, struct. props. and impurity content 4-88434  
 Si, nonlinear-optical energy regulation by nonlinear refr. and absorpt. 4-91546  
 Si, normal and oxidised, spectra formation in three-crystal X-ray diffractometry 4-113269  
 p-Si, O low-temp. diffusion coeff. 4-70458  
 Si ohmic contacts, specific contact resistivity from contact end resist. meas. 4-84673  
 Si on insulator form. by O ion implantation 4-80061  
 Si on insulators, CVD single crystal characterisation, heteroepitaxy and epitaxial lateral overgrowth 4-70589  
 Si on sapphire, phonon boundary scatt. at interface 4-104050  
 Si, one-electron excitations, exchange-correlation pot. 4-84579  
 Si optical I/O IC, technology description 4-107888  
 Si, optical phase conjugation, elec. fields effect 4-107756  
 Si optically controlled amorphous photosensitive device 4-108896  
 Si, optoelectronic switching, laser controlled, photoconductivity meas. (German) 4-84646  
 Si overlayer on GaP, heterojunction band discontinuities, synchrotron radiation photoemission 4-81111  
 Si, oxidation, Auger sputter profiling and SIMS study of  $\text{SiO}_2$  4-88924  
 Si, oxidation behaviour, dry, wet, high press. and plasma techniques, book contrib. 4-85240  
 Si, oxidation in  $\text{HCl}/\text{O}_2$  ambient, Cl incorporation at Si/ $\text{SiO}_2$  interface 4-62079  
 Si, oxidation induced stacking faults, dislocations, effects of  $\text{Cl}^+$  and  $\text{F}^+$  implantation, X-ray topography 4-80053  
 Si, oxidation mechanism in dry  $\text{O}_2$ ,  $^{18}\text{O}$  study 4-89153  
 Si, oxidation model, stacking faults and dislocations 4-104888  
 Si, oxidation stacking fault elimination by  $\text{CW CO}_2$  laser annealing (Chinese) 4-113496  
 Si, oxidised surface, localised electronic states 4-88553  
 Si  $p^+$ - $n$ - $n^+$  photodiode, oxide passivated, self-calibration 4-90652  
 Si  $p^+$ - $n$ - $n^+$  solar cells, all-implanted, characts. 4-62355  
 Si  $p$ - $n$  junction contrast in ultra high vacuum SEM 4-95576  
 Si  $p$ - $n$  junctions, electron irradi., differential resist. in avalanche breakdown region, temp. depend. 4-88571  
 Si, partial  $90^\circ$  dislocation, structural and elec. props. 4-108368  
 Si, partial dislocations, glide forces, climb forces, geometrical study 4-113446  
 a-Si, phonon density of states calc., bond angle and length fluctuations 4-75631  
 Si, phonon pulses detection by fluorescence of deposited  $\text{YF}_3\text{:Tb}^{3+}$  film 4-113555  
 n-Si, photo-enhanced etching in dil.  $\text{HCl}$  soln. 4-62072  
 Si photo-induced complex permitt. at 9 GHz, expt. study 4-65703  
 n-Si photoanode stabilisation against photoanodic decomp. with polyacetylene films 4-72123  
 Si photocells, two-film antireflection coating, surface film resist. reduction (Russian) 4-109742  
 Si photocells, violet, construction and operational characts. (Russian) 4-109741  
 Si, photoconductive asymmetries of donor and acceptor impurities 4-70857  
 Si, photocurrent carrier lifetime study during ion implantation 4-75984  
 Si photodetector, cryogenic telescope on IRAS appl. 4-110525  
 Si photoelectric solar energy converters design and efficiency, survey (Russian) 4-66693  
 Si photoelectrochemical cell based on  $p$ -type  $\text{Si/KI}$  saturated soln. in  $\text{NH}_3/\text{K}$  saturated soln. in  $\text{NH}_3/\text{Pt}$  (French) 4-105111  
 n-Si, photoelectrodes, silicide coated, electrochemical and photoelectrochemical behavior 4-88581  
 Si, photoluminescence characterisation of impurities and defects 4-88876  
 p-Si photoresistors, electron irradi., pulsed operation 4-84655  
 Si, photothermally stimulated exoelectron emission, VV centre effects, ESR study 4-88950  
 Si photovoltaic cells, performance evaluation under concentrated sunlight 4-62353  
 Si photovoltaic cells, photogeneration rate, minority carrier lifetime depend. 4-75997  
 Si photovoltaic devices, P implanted, Ar ion implantation gettering influence on props. 4-66703  
 a-Si photovoltaic solar cells, future projections 4-89417  
 a-Si photovoltaic technology, future speculations and forecasts 4-89431  
 Si, picosecond-pulse laser annealing, phenomenological model 4-88198  
 Si, plasma anodic nitridation in  $\text{N}_2\text{-H}_2$  system, struct. and optical props. 4-81307  
 Si, plasma enhanced CVD growth 4-88983  
 Si, plasma etching, spectral fluorescent emission 4-85239  
 Si, plasma etching using  $\text{CF}_4$ , computer simulation and chem. reactions 4-109683  
 Si, plasma etching with  $\text{XeF}_2$  and  $\text{F}$  4-89143  
 Si, plasma oxidation, low temp., microwave plasma stream transport system 4-85230  
 Si, plastically deformed, deep levels, capacitance, reverse current meas. 4-61319  
 Si, plastically deformed, thermostimulated depolarization spectra 4-114199  
 Si, plastically deformed cryst., low freq. internal friction 4-60979  
 Si point contact  $n^+$ - $n$  junction, microwave noise 4-88574  
 Si point contact solar cells 4-81547  
 Si, point defects due to laser annealing, DLTS study (Chinese) 4-84584  
 Si, polycryst., laser annealed, diff. studies 4-104106  
 Si polycryst. layer, grain size and dopant level inspection 4-109529  
 Si, polycrystalline, defect etching 4-81308

## elemental semiconductors continued

- Si, polycrystalline, elec. cond. props., small signal theory 4-70804  
 Si, polycrystalline, elec. cond. props., I-V characts. 4-70805  
 Si, polycrystalline, elec. cond. model 4-92712  
 Si, polycrystalline, elec. props. 4-104199  
 Si, polycrystalline, etching processes 4-61842  
 Si, polycrystalline, implantation under thermal and laser annealing, sheet resist. and doping profiles 4-75487  
 Si, polycrystalline, interacting grain boundaries, surface recombination vel., EBIC study 4-70828  
 Si, polycrystalline, LPCVD by H reduction of dichlorosilane 4-71570  
 Si, polycrystalline, minority carrier diffusion length under solar illum. 4-104225  
 Si, polycrystalline, mobility and carrier conc. depend. on grain size and doping conc. 4-92730  
 Si, polycrystalline, passivated, short term soln. for solar cell appls. 4-89441  
 Si, polycrystalline, recrystallisation by combined CW laser and furnace heating 4-88199  
 Si, polycrystalline, selective plasma etching 4-81311  
 Si, polycrystalline and amorphous substrate for  $\text{RhSi}$  4-80446  
 Si, polycrystalline film deposition processes and plasma assisted deposition, book contrib. 4-85111  
 Si, polycrystalline films, X-ray and electron diffr. anal. 4-61258  
 Si polycrystalline films, grain-driven zone melting 4-93213  
 Si polycrystalline films amorphised by ion implantation, solid phase epitaxial growth 4-108731  
 Si polycrystalline films formed by CVD, surface morphology 4-70588  
 Si, polycrystalline islands on fused  $\text{SiO}_2$ , crack elimination by recrystn. 4-80461  
 Si, polycrystalline  $p^+$ - $n$ - $n^+$  solar cells, diffused junction optimisation by photochemical method 4-72120  
 Si, polycrystalline SOI structures, RF zone melting recrystn. for MOS-FET fabrication 4-88965  
 Si polycrystalline sheet growth by melt spinning, solar cell appl. (Japanese) 4-62368  
 Si polycrystalline sheets for solar cells by improved melt spinning technique 4-81166  
 Si polycrystalline solar cells, struct. defects, TEM/EBIC studies 4-108380  
 Si, porous, electron diffraction studies 4-113274  
 Si porous layers, electrophysical and optical props. 4-65680  
 Si, positron channelling radiation, photon intensity and polarisation, computer simulation 4-75584  
 Si, preparation by plasma technique, thermodynamic calc. of reduction 4-76979  
 Si processing for device fabrication, ion implantation appl. 4-75481  
 Si, product layers formed during etching in  $\text{SF}_6$  4-109682  
 Si production technology, current status for solar cell appls. 4-66723  
 Si, production using rice hulls as raw material 4-99358  
 Si, profiling techniques using spreading resistance 4-75498  
 Si, proton irradi., acceptor level positions of divacancy 4-70725  
 Si, proton irradi., induced defects interaction with surface 4-75564  
 n-Si, proton irradiated, electrophysical props. 4-108861  
 Si, pulse laser irradiated, surface morphology and phase transitions 4-88197  
 Si, pulsed laser induced recombination centres 4-108873  
 a-Si, pulsed laser irradiation, melting temp. and explosive crystallisation 4-88201  
 Si, pulsed microwave annealing, power distribution effects (French) 4-61781  
 Si quantised Hall resistor, two-terminal conductance meas. 4-70942  
 Si, quantum cyclotron reson. 4-108762  
 Si, radiation-induced rod-like defects 4-92238  
 Si radiometer whose response is independ. of operating temp. 4-58882  
 Si, Raman characterisation 4-99106  
 Si, rapid melting and regrowth velocities by UV ps laser pulse heating 4-92232  
 Si reciprocal filter, time of flight neutron spectrometer resolution improvement 4-86997  
 Si reconstructed surface reordering on room temperature Ge deposition 4-98411  
 Si, recrystallized on  $\text{SiO}_2$ , laterally seeded, implantation and annealing studies 4-98121  
 Si, reduced pressure chemical vapour deposition 4-114422  
 Si, relativistic positron channelling,  $\gamma$  ray emission 4-75588  
 Si ribbon growth processes for solar cell/module technology 4-66724  
 Si, ribbon-to-ribbon float zone single crystal growth stabilized by a thin silicon dioxide skin 4-88962  
 Si ribbons, polycrystalline, prep. by fast cooling, for solar cells 4-114508  
 Si ribbons, produced by EFG, comparison of growth characts. 4-66222  
 Si SOI fabrication by zone melting recrystn. (Japanese) 4-88964  
 Si SOI structures, laser annealing, equipment for recrystn. (Japanese) 4-88200  
 Si SOI structures, recrystn. by electron beam annealing (Japanese) 4-88207  
 Si SOS patterned structures, residual stresses, Raman microprobe study 4-92573  
 Si SOS picosecond photoconductors, circuit limits to time resolution 4-98661  
 Si SOS structures, pulse laser irradi., internal stresses, Raman scatt. studies 4-99108  
 Si SOS structures, residual stresses, Raman scatt. studies 4-99107  
 Si, screening energy variations and Auger parameters, XPS studies 4-99275  
 Si, segment analysis in nonhomogeneous illuminated semiconductor solar cells 4-66704  
 Si, selective epitaxy, local loading effect 4-93228  
 Si selective photodetector sensitisation by means of solid-state dye solns. 4-73513  
 Si, self interstitials, electronic struct. and total energy migration barriers 4-108811  
 Si, self-interstitial scatt. and imaging 4-80033  
 Si sensors with on-chip signal processing for long-term stability 4-68225  
 Si, shallow npn bipolar transistors fabrication by triple ion implantation 4-75460  
 Si sheet, EFG in production 4-66221  
 Si, sheet growth at high speeds, stress generation, influence of plastic deform. 4-65211  
 Si sheets, coated, dislocation movement 4-70166

## elemental semiconductors continued

- Si sheets, edge-supported pulling, electron channelling and EBIC studies, rel. to solar cell appls. 4-75693
- Si sheets, large-grain, growth by improved spinning method 4-66223
- Si single cryst., dislocation etching, orientation depend. 4-113454
- Si single cryst., elastically deformed, Pendelosing fringes 4-88035
- Si single cryst., Mossbauer diffr., separation of inelastically and elastically scatt. radiation 4-98984
- Si single crystal, planar channelling studies (*Chinese*) 4-70245
- Si single crystal, unit cell parameters determ. (*German*) 4-79980
- Si single crystal thin film, secondary recrystallisation prep. 4-88421
- Si single crystals, bent, high energy channelled proton deflection 4-75574
- Si solar cell, BSF  $n^+ - n - p^+$  struct. with high low junction emitter, design and characts. (*Korean*) 4-85372
- Si solar cell, EBIC technique using scanning Auger microprobe 4-97981
- Si, solar cell, H passivation of electrically active defects (*French*) 4-62359
- Si solar cell, IBC, two-dimensional anal. of back region 4-77110
- Si solar cell, ion implanted, laser annealed 4-72121
- Si solar cell, pyrene thin film coated, energy transfer between surface pyrene mols. and semiconductor substrate 4-77109
- Si solar cell, V-groove  $n^+ - p$  junction type, design and fabrication using anisotropic etching (*Korean*) 4-85371
- Si solar cell, with induced channel, stability of characts. rel. to irradi. and temp. changes (*Russian*) 4-109739
- Si solar cell fabrication by ion implantation and thermal annealing 4-77089
- Si solar cell junction profiles in ion-implanted texture-etched surfaces 4-93620
- Si, solar cell research and development in Brazil 4-66698
- Si solar cells, 50  $\mu\text{m}$  thick, interconnect welding technology 4-66716
- Si solar cells, carrier lifetime and surface recomb. vel. determ. using transient responses 4-77093
- Si solar cells, crystalline, improved reproducibility in Ni/Sn-Pb metallisation process 4-93626
- Si solar cells, efficiency improvement by surface passivation 4-77094
- a-Si solar cells, efficiency improvement by optical confinement effect using  $\text{TiO}_2/\text{Ag}/\text{SUS}$  back-surface reflector 4-77106
- Si solar cells, electrical microcharacterisation using SEM 4-81560
- Si solar cells, emitter recombination determ. using open-circuit voltage decay 4-99963
- Si solar cells, future R&D problems 4-89415
- Si solar cells, high efficiency, improved version of  $p^+nn^+$  back-surface-field cell 4-72106
- Si solar cells, high temp. stable contact metallisation 4-77098
- Si solar cells, I-V characts. and performance between low- and high-level injection 4-81551
- Si solar cells, influence of base resistivity 4-66705
- a-Si solar cells, Japanese Sunshine Project/solar photovoltaic program 4-66719
- Si solar cells, limiting efficiency, extended detailed balance method 4-81554
- Si solar cells, local area generation characts., elec. field stimulation (*Russian*) 4-109740
- Si solar cells, low-dose ion implanted, optimum flashlamp annealing conditions for fabrication 4-85368
- Si solar cells, majority carrier collection in  $p^+ - p - n^+$  and  $n^+ - p - p^+$  structs. 4-62367
- Si solar cells, minority carrier lifetime meas. 4-77091
- Si solar cells,  $n^+ - p$  and  $n^+ - p - p^+$  spectral sensitivity calcs. 4-89410
- Si solar cells, nonsingle crystal, ion-implanted and thermally diffused, surface damage etching effect on props. 4-77105
- Si solar cells, open-circuit voltage and efficiency, limits imposed by Auger recomb. processes 4-81549
- Si solar cells, optical transfer function, theory and expt. 4-93632
- Si solar cells, P ion implantation emitter tailoring and annealing 4-62366
- Si solar cells, P precip. effects on open circuit voltage 4-62361
- Si solar cells,  $p - n$  junction formation by conventional thermal predeposition processes 4-81562
- Si solar cells, polycrystalline vs. amorphous, photovoltaic appls. 4-89443
- Si solar cells, polycrystalline, high efficiency, substrate characts. and process techniques, future trends 4-89448
- Si solar cells, speculations on efficiency improvement 4-89445
- Si solar cells, speculations on future world market 4-89449
- Si solar cells, thick film metallisation technique, structure and electrical properties analysis 4-62365
- Si solar cells, thin, structural stability using improved wafer etching process 4-81557
- Si solar cells as energy source, economic and technical considerations (*Italian*) 4-62305
- Si solar cells for power supplies to artificial satellites 4-99972
- Si solar cells subjected to intense photoexcitation, nonequilibrium carrier lifetime determ. 4-85374
- Si solar cells with 19.1% efficiency 4-89399
- a-Si solar cells with conversion efficiency  $>9\%$  4-85376
- Si solar cells with high energy conversion efficiencies 4-81550
- Si solar cells with mirror back surface, developments in 1980s 4-89411
- Si, solar grade, spark source mass spectrometry anal. 4-62276
- Si, solar grade versus electronic grade 4-62358
- Si, solar-grade, growth by Zn reduction of  $\text{SiCl}_4$ , morphology 4-66199
- a-Si, solid phase epitaxy, bond rearrangement process, quantitative anal. 4-84534
- a-Si, space charge limited current rel. to density of states 4-98637
- a-Si, space-charge limited currents and photocond. 4-61387
- Si, spectroscopy conf., Cambridge, MA, USA (Nov. 1983) 4-95025
- Si, sputter etch induced electrically active defects, H passivation 4-108918
- Si, sputtering by  $\text{SO}^+$ , yield data 4-88974
- a-Si, static charge fluctuations, band struct. calcs. 4-70636
- a-Si, struct. disorder model, thermodynamic props. 4-75303
- Si submicron epitaxial films, quality 4-88567
- Si, substitutional and interstitial donors, many electron effect 4-113895
- Si substrate, ion implanted and processed, interface characterisation 4-84304
- Si substrate for  $\text{SiO}_2/\text{HCl}(\text{Cl}_2)$  film, impurity distrib. study 4-113485
- Si substrate for P piezoelectric membranes, SAW characts. and transducers 4-104058
- Si substrate for ZnO channel waveguide formation 4-103012
- Si substrates, electro-physical prop. nonuniformity (*Russian*) 4-65672
- p-Si surface,  $^{14}\text{N}_2^+ (\text{H}_2^+)$  bombardment, Raman scatt. obs. 4-114283
- Si surface, (111)- $2\times 1$ , large nonequil. band curvature 4-80644

## elemental semiconductors continued

- Si surface, electronic collective modes and instabilities 4-108796
- Si surface, electronic collective modes, instabilities and electron-phonon interactions 4-108797
- Si surface, excess carriers, light-induced recombination 4-76005
- Si surface,  $\text{F}_2$  plasma etching, synchrotron photoemission study 4-93180
- Si surface, fluorination by  $\text{XeF}_2$  etching, photoeffects 4-77031
- Si surface,  $\text{H}_2\text{O}$  adsorp. effect on charge exchange kinetics of slow electron states 4-84512
- Si surface, interaction with tetrafluoromethane, evidence for parallel etching mechanisms 4-71496
- Si surface, paramag. centre form. during strong cooling 4-65861
- Si surface, phase conjugation, reflecting grating recording by plasma refl. 4-97003
- Si surface, single cryst., fluids influence on microhardness 4-98418
- Si surface, work function changes during thermal oxidation at low  $\text{O}_2$  press. 4-88560
- Si, surface backscattering yield for  $\text{He}^+$  beam energies, 0.5 to 2 MeV 4-81075
- Si, surface band bending variation during thermal oxidation 4-70897
- Si, surface cleaning by ion bombardment 4-88213
- Si, surface disordering by picosecond laser pulses 4-92233
- $n^+ - \text{Si}$ , surface plasmon polaritons, IR studies 4-108788
- n-Si, surface polaritons with DC current and electron thermal press. gradient 4-80516
- Si, surface properties after ion chem. etching 4-66463
- Si, surface struct. generation by laser pulses 4-80358
- Si, surface sub-band calcs. and light scatt. meas. 4-61430
- Si surface two-photon photoemission 4-85076
- Si, swirl defect formation during zone growth 4-71552
- Si switch development for optical pulse generation in Nova, Novette fusion lasers 4-107702
- Si, TEM characterisation 4-97980
- Si TaSi<sub>3</sub> struct., annealing and sheet resistivity 4-108741
- Si temperature sensors, design and characts. (*French*) 4-111121
- Si, thermal oxidation, chemisorption and linear rate const. 4-81458
- Si, thermal oxidation in HCl and trichloroethylene 4-62078
- Si thick film on insulator, zone-melting recrystallisation 4-66225
- Si, thick isolated layers, growth, characterisation and MOSFET props. 4-99309
- Si thin film, formed on insulator by recrystallisation 4-70586
- Si thin films on substrates, Raman study 4-99206
- Si thin layers, double injection, light and mag. field effects 4-65760
- Si, thin layers, ionisation energy losses of highly relativistic charged particles 4-64279
- Si thin single-crystals, anomalous plasticity in the visco-brittle transition temp. range, 500-700°C (*Ukrainian*) 4-88227
- Si tilt boundaries at struct., HREM obs. 4-103767
- Si transducers, design aspects and appl. (*French*) 4-90580
- Si tubes, drawn from melt using wettable shaper 4-61830
- Si, unit cell parameters determ. by precision meas. of Bragg plane spacings 4-113388
- Si VLSI circuit processing, material phenomena 4-103738
- Si, VPE, MBE, Si on insulator structures and doping, book contrib. 4-85106
- Si, vacancy capture cross section by impurity atoms 4-103789
- Si, vacancy energy levels, impurity state pinning, tight-binding calcs., local density theory 4-88470
- Si, vacancy energy spectrum calc. by semiempirical technique using MO approach 4-88478
- a-Si, vacuum deposited, solid-phase epitaxial growth anisotropy 4-75811
- Si vapour deposited cryst. and amorphous films, stresses, X-ray diff., studies 4-75824
- Si wafer, implantation quality monitoring by amorphisation contrast 4-75478
- Si wafer, lapped and polished, surface state evaluation 4-76883
- Si wafer, mechanical properties, effects of laser back-side damage 4-98132
- Si wafer, surface characts. improvement using hydrophilic cleaning 4-109530
- Si wafer bonded to Al, phase-modulated photoacoustics for temp. fluctuation studies 4-103166
- Si wafer props., influence of laser marking 4-113498
- Si wafers, impurity characterisation using IR spectra meas. 4-113486
- Si web growth, thermal stress effects, modelling 4-65210
- Si with adsorbed Ag, growth and diffusion, SEM, study 4-80417
- Si, with structure defects, X-ray scatt. in Laue geometry, dynamical effects 4-75435
- Si with surface chemisorbed F, synchrotron photoemission study 4-108710
- Si, X-ray diff. under specular refl. conditions 4-75239
- Si X-ray optical elements, prod. using diamond turning 4-58924
- Si, zone melting recrystallisation 4-66228
- Si, muonium, anomalous, electronic g-factor anisotropy 4-65927
- Si,  $^{13}\text{C}$ , muon spin rot. and TEM studies 4-71239
- Si,  $^{31}\text{P}$ , implanted, optical refl. changes as function of implantation energy 4-71330
- Si:Al, electronically simulated defect migration 4-113730
- Si:Al epitaxial film, packing defects, growth conditions 4-61255
- Si:Ar, carrier lifetime reduction by Ar ion implantation 4-80604
- Si:Ar Schottky barrier, ion implantation effects on elec. characts. 4-114014
- Si:As, high current density implantation, dynamic self-annealing mechanism 4-65280
- Si:As, high dose ion implanted, As clustering, TEM and SIMS studies 4-70384
- Si:As, implanted (111), twin formation, effect of heating rate and annealing temp. 4-103765
- Si:As, implanted under channelling conditions, impurity spatial distrib., localisation, defect form. characts. 4-84321
- Si:As, ion implantation doses, ellipsometry and spectral reflectance meas. 4-113480
- Si:As, ion implanted, carrier density profiles, elec. meas., annealing behaviour 4-70179
- Si:As, ion implanted, IR radiation annealing of extended defects 4-92228
- Si:As, ion implanted and laser annealed, struct. changes, X-ray diff. study 4-75461
- Si:As, ion implanted channelling Rutherford back-scatt. study (*Chinese*) 4-84324
- Si:As, ion implanted regions, 2-D shape, etching and EBIC studies 4-88187

## elemental semiconductors continued

- Si:As, ion implanted through screen oxide, residual disorder after high temp. anneal 4-113511  
 Si:As, low energy implanted, laser-annealed, channeling and high-resolution backscatt. studies 4-75493  
 Si:As, low-energy ion implantation 4-75466  
 Si:As, P, B, ion implanted, fast isothermal annealing and elec. props. 4-92224  
 Si:As, P, ion implanted, diffusion modelling 4-113729  
 Si:As, segregation to grain boundaries and surface plasmons 4-98289  
 Si:As, shallow implants, depth profiling using SIMS 4-108408  
 Si:As, X-ray standing wave anal. with synchrotron radiation 4-103607  
 Si:As contrast-mode radiometer for AMOS 1.6 m telescope 4-115691  
 Si:As implanted layers, struct., total external reflection spectra studies 4-108330  
 Si:As thin films, As fast diffusion during rapid thermal annealing 4-113714  
 Si:As/Al interface, sintering and diffusion, As dopant effect 4-80427  
 Si:As/Ti interface, As implantation, As out-diffusion during  $\text{TiSi}_2$  formation 4-65493  
 Si:As<sup>+</sup>(BF<sub>3</sub>+), implanted, rapid thermal annealing 4-88181  
 Si:As<sup>+</sup>(Sb<sup>+</sup>), ion implanted and laser annealed, defects, photoluminescence studies 4-75433  
 Si:As(B), ion implanted and electron beam annealed, TEM and HREM studies 4-80058  
 Si:As(Sb), shallow dopant profile production by low-angle ion implantation 4-108396  
 Si:As(Sb)(In), ion implanted, pulsed electron beam annealing, impurity diffusion 4-103984  
 Si:Au, donor and acceptor levels, DLTS meas. 4-88473  
 Si:Au, donor level, entropy factor, resist. and DLTS meas. 4-70707  
 n-Si:Au, doping by laser (*Chinese*) 4-113473  
 Si:Au, effect of mobile dislocations on surface saturation (*Russian*) 4-98107  
 n-Si:Au, elec. cond. and photoconductivity 4-104213  
 Si:Au, electron capture cross section of Au acceptor (*Chinese*) 4-92741  
 Si:Au, photocurrent deep level transient spectra 4-80535  
 Si:Au, solid solution, nuclear-spin lattice relaxation 4-76282  
 Si:Au, transient capacitance of Au acceptor energy level under uniaxial stress (*Chinese*) 4-75888  
 Si:B, (100), shallow junction implants through surface oxide, theoretical and expt. study 4-113476  
 Si:B, deep implanted layers, for IC appl. 4-75482  
 Si:B, deep level impurities at bond centered interstitial site 4-108814  
 Si:B, Fe, exciton photoluminescence study 4-109243  
 Si:B, focused ion beam B<sup>+</sup> implantation 4-92222  
 Si:B, implanted, elec. activation and damage annealing by flash lamp irradi. 4-70196  
 Si:B, impurity electronic struct. cluster  $X\alpha$  calc. 4-65639  
 p-Si:B, ion implanted, electron beam annealing 4-60960  
 Si:B, ion implanted, flash-lamp annealing study 4-108395  
 Si:B, ion implanted shallow layers, electron beam annealing, expt. study using SIMS 4-98133  
 Si:B, lattice const. meas. using X-ray double cryst. method 4-103606  
 Si:B, magnetothermal cond. study 4-71076  
 Si:B, P, compensated semiconductors, coalescence, process, effect and rad. and heat treatment 4-65288  
 p-Si:B, p-type doping in MBE by B coevaporation 4-71561  
 a-Si:B, pure and doped, ion implanted, recrystallisation studies 4-88422  
 Si:B, retardation of B diffusion 4-88346  
 Si:B, thermal cond. resonances of acceptor states 4-104011  
 Si:B,C,O, impurity profiling and analysis by recoil atoms in heavy ion beams 4-108406  
 Si:B,H, neutralisation of shallow acceptor levels by atomic H 4-104153  
 a-Si:B film, optical props. study 4-76540  
 Si:B ingots, effective segregation coeff. of B, elec. studies 4-88192  
 Si:B microcrystalline films, crystallinity, morphology and elec. cond. 4-108749  
 Si:B neck for Josephson bridges 4-98828  
 Si:B polycrystalline films, activation energy of resist., effects of grain boundary trapping state energy distrib. 4-88616  
 Si:B solar cell, electron irradi., photon effects 4-93618  
 Si:B solar cell material, EBIC contrast, microstruct. and composition effects 4-108878  
 Si:B/Ti-W RF sputter-deposited Schottky barrier diodes 4-98691  
 Si:B-SiO<sub>2</sub> MIS struct., ion bombarded, defect annealing study 4-80685  
 Si:B(As), ion implant in-depth error anal., mass interference effects in ion microprobe studies (*Chinese*) 4-111248  
 Si:B(As), low resistance ion implanted films 4-108398  
 Si:B(In), point defects influence on acceptor ground state: splittings 4-70728  
 Si:B(P)(As), dopant diffusion, numerical soln. by solving impurity, vacancy and self-interstitial continuity eqns. 4-80303  
 Si:B( $\mu^+$ ), tetrahedral interstitial impurities, electronic struct. 4-65636  
 Si:C, electron irradi., optical absorpt. spectra 4-88861  
 Si:C, self-interstitial enhanced C diffusion 4-98358  
 Si:C,N, CVD thin films using di-2,2'-bipyridine silicon 4-71586  
 Si:C layers, CVD growth, microstruct. and resist. 4-70599  
 a-Si:Cl, H films, photocond. spectra (*Chinese*) 4-113989  
 Si:Cr(Mn)(Fe)(Co)(Ni), breathing mode relax around tetrahedral interstitial 3d impurities 4-108567  
 Si:Cu, impurity effect on dislocation motion 4-70187  
 Si:D, anomalous muonium atom site determination 4-65277  
 Si:F, amorphous, electronic struct. theory 4-92600  
 Si:F, amorphous and cryst., ion implanted, elec. quadrupole hyperfine interaction at impurity sites 4-92675  
 Si:F, As, ion implanted, defect struct. detection 4-103776  
 p-Si:Fe, conductance along grain boundaries 4-80585  
 n-Si:Fe, impurity bands of Fe clusters, ESR and elec. props. 4-109067  
 Si:Ga, neutron irradi., acceptor level, IR absorpt. spectrum 4-93089  
 Si:Ga sputtered amorphous alloys, thermopower and elec. cond. 4-61403  
 Si:Ge, bulk impurity diffusion, SIMS study 4-70465  
 Si:Ge, Ge diffusion, isotope effects, SIMS studies 4-65491  
 Si:Ge, Ge diffusion and conc. profiles, SIMS studies 4-65490  
 Si:Ge, implantation, pre-amorphisation/rapid thermal annealing procedure for shallow junction formation 4-88188  
 Si:Ge(Sb)(W), electron beam doping, SIMS and RBS studies (*Japanese*) 4-108401  
 a-Si:H, absorpt. edge, struct. disorder model for amorphous semiconductor 4-80483  
 Si:H, Al-covered, solid-state reaction between film and substrate 4-92498

## elemental semiconductors continued

- Si:H, amorphous, CVD growth by Si<sub>2</sub>H<sub>6</sub> pyrolysis in hot wall reactor 4-61864  
 Si:H, amorphous, DC triode sputtered, electronic transport 4-61374  
 Si:H, amorphous, electron mobility meas. using 4-terminal FET structures 4-75964  
 Si:H, amorphous, electron-excited Coster-Kronig transitions 4-88908  
 Si:H, amorphous, Fe<sub>2</sub>O<sub>3</sub>-coated semiconductor electrode by solar cell, XPS, AES and electrochem. meas. 4-66691  
 Si:H, amorphous, glow discharge chemical vapour deposited, X-ray photoelectron spectroscopy 4-93201  
 Si:H, amorphous, glow-discharge deposition, efficiency of gas usage, for solar cells 4-71602  
 Si:H, amorphous, high-rate deposited annealing effects 4-61876  
 Si:H, amorphous, light-induced defects, annealing 4-92762  
 p-Si:H, amorphous, prepared by photo-CVD, electronic and optical props. 4-70959  
 Si:H, amorphous films, glow discharge decomposition, Hg(Kr) effects 4-76687  
 Si:H, amorphous films, optical structure technique 4-91547  
 Si:H, amorphous solar cells, CVD growth 4-66694  
 a-Si:H, As, dispersive transport, trap saturation, transient photocurrent meas. 4-76006  
 a-Si:H, B, P, electron structure and density of states of B-P pairs, cluster calc. 4-65642  
 Si:H, B(P), amorphous CVD layer, impurity doping 4-60941  
 Si:H, B, broken bonds and electronic density of states, H effects 4-65178  
 a-Si:H, conductivity, localisation and mobility edge 4-70819  
 a-Si:H, correlated defects and steady-state photoconductivity 4-61417  
 a-Si:H, DC elec. cond. Meyer-Neldel rule and Staebler-Wronski effect 4-113948  
 a-Si:H, deep recombination centres, luminescence and EPR studies 4-104164  
 Si:H, dislocated, impurity exodiffusion 4-103788  
 a-Si:H, doping and gap states 4-70734  
 Si:H, electron localisation-delocalisation transitions and H<sup>-</sup>-like states 4-92668  
 a-Si:H, electronic density of states calcs. (*Russian*) 4-70740  
 a-Si:H, electronic struct., theoretical models 4-70638  
 a-Si:H, electronic struct. study using Auger electron spectroscopy (*French*) 4-75840  
 a-Si:H, energy distrib. of light-induced gap states, photocond. meas. 4-76004  
 a-Si:H, extended state mobility 4-104208  
 a-Si:H, F p-n junctions, generation; recombination currents, computer simulation 4-84683  
 a-Si:H, geminate recombination and mobility 4-104223  
 Si:H, grown by zone melting, A-centre distrib. study 4-76666  
 a-Si:H, H<sub>2</sub> chemisorption, AES and EELS meas. 4-108715  
 a-Si:H, high-rate deposition from SiH<sub>4</sub> using RF discharge technique, elec. and optical props. 4-85119  
 a-Si:H, high-resolution PMR, high resolution of narrow spectral component 4-104498  
 a-Si:H, homogeneous CVD growth, review 4-88984  
 a-Si:H, IR absorpt., gaseous H<sub>2</sub> and Si-H overtone spectra 4-93075  
 Si:H, lattice state and behaviour of H impurity 4-61095  
 a-Si:H, long-time drift mobility, photocurrent study 4-104221  
 a-Si:H, MIS diode, glow discharge deposited, flat-band capacitance freq. depend. 4-76042  
 Si:H, microcrystalline, IR absorpt. study of Si-H bond formation 4-71416  
 Si:H, microcrystalline, photoinduced free-carrier absorpt. spectra 4-88859  
 n-Si:H, neutron irradiated, deep levels study (*Chinese*) 4-92649  
 a-Si:H, non-substitutional dopant states and carrier density statistics 4-113902  
 a-Si:H, P(B), dark cond. and photocond., thickness depend. 4-84624  
 a-Si:H, photoinduced absorption spectra 4-109220  
 a-Si:H, plasma deposited film, NMR study 4-104502  
 a-Si:H, plasma deposition, two layer struct., surface contribs. 4-70593  
 a-Si:H, plasma-enhanced deposition 4-81160  
 a-Si:H, prep. by glow discharge of Si<sub>2</sub>H<sub>6</sub>, optical and elec. props. 4-114237  
 Si:H, RF sputtered amorphous film, dark cond. and photocond., annealing effects 4-70960  
 a-Si:H, radiative combination at dangling bonds, quantitative model, expt. study 4-114326  
 a-Si:H, resolution of DLTS energy scale controversy 4-104166  
 a-Si:H, structural and vibr. spectra calcs. 4-98017  
 Si:H, study of H-induced defects (*Chinese*) 4-103736  
 a-Si:H, TSC meas., density of states behaviour 4-98636  
 a-Si:H, time-resolved charge transport and photocond. 4-70871  
 a-Si:H, transient photoinduced absorpt. 4-104634  
 a-Si:H, undoped, carrier trapping, picosecond electronic relaxations 4-108892  
 Si:H,B, amorphous, solar cells, deposition from Si<sub>2</sub>H<sub>6</sub> and B doping profiles 4-81540  
 a-Si:H,B, doping effect on gap states 4-88488  
 Si:H,B amorphous CVD films, optical props., B doping effects 4-99086  
 a-Si:H,B film, optical props. study 4-76540  
 a-Si:H,Cl films glow discharge deposition from SiCl<sub>4</sub>-SiH<sub>4</sub> mixtures, elec. and optical characts. 4-71580  
 a-Si:H,F films, F incorporation during glow discharge deposition 4-114426  
 a-Si:H,Li, surface photovolt. and dark conductance, light-induced changes 4-70861  
 a-Si:H,N film, TSC and photoconductivity 4-104222  
 Si:H,O, grain boundary impurity effect determ. 4-92214  
 a-Si:H,O(N) alloys, electron trapping states, tight binding formalism calcs. 4-113901  
 a-Si:H,P, defect states and carrier capture processes 4-104165  
 a-Si:H,P, new paramagnetic centres and impurity states 4-109056  
 a-Si:H,P,B film, drift mobility, photoconductivity meas. 4-104259  
 a-Si:H,P film, acoustoelectric effect, thickness depend. study 4-104273  
 a-Si:H,P(B), ESR and optical props., thickness depend. 4-84853  
 Si:H (100)(2×1), surface IR studies 4-99116  
 Si:H absorbing films, optical const. unambiguous determ. by reflectance and transmittance meas. 4-65997  
 Si:H amorphous compensated films, xerographic discharge meas. 4-80603  
 Si:H amorphous film optical waveguides, propag. characts. 4-107821  
 Si:H amorphous films, glow discharge deposited, electron drift mobility, substrate temp. dependence 4-61393

## elemental semiconductors continued

- Si:H amorphous films, glow discharge deposition in cascade reactors 4-76680  
 Si:H amorphous films, laser CVD by ArF excimer laser photodissociation of  $S_2H_6$  4-61859  
 Si:H amorphous films, prep., characterisation absorpt. and laser-damage resistance 4-74676  
 Si:H amorphous p-n solar cell, design, fabrication and characts. 4-114905  
 a-Si:H film, annealing behaviour of  $g=2.0026$  ESR line 4-109057  
 a-Si:H film, complex impedance meas. 4-76055  
 a-Si:H film, deposition mechanism from plasma 4-114411  
 a-Si:H film, drift mobility, xerographic determ. 4-104224  
 a-Si:H film, high rate prep. by reactive evaporation method, photocond. and dark cond. meas. 4-61248  
 a-Si:H film, hole mobility model 4-104220  
 a-Si:H film, hyperfine interaction, ENDOR study 4-65881  
 a-Si:H film, IR quenching of photoluminescence and photoconductivity 4-104656  
 a-Si:H film, low freq. glow discharge prep. (Japanese) 4-76692  
 a-Si:H film, optical props. meas. 4-76539  
 a-Si:H film, plasma polymerisation and deposition from RF and DC silane plasmas 4-85115  
 a-Si:H film, produced by magnetron sputtering, ion beam anal. 4-92583  
 a-Si:H film, sputtered, elemental anal., STEM study 4-104105  
 a-Si:H film, Staebler-Wronski effect 4-108852  
 a-Si:H film, time resolved photoluminescence and phonon transport 4-71445  
 a-Si:H film, transient space charge limited cond. study 4-104215  
 a-Si:H film for H passivation of implantation defects in Si-SiO<sub>2</sub> MOS struct. 4-71744  
 a-Si:H films, anodic oxidation, elec. and optical props. of oxidised films 4-109527  
 a-Si:H films, CVD growth, phys. props. 4-92715  
 a-Si:H films, DC planar magnetron reactive sputtering and characterisation 4-93218  
 a-Si:H films, doping effect, RF sputtering and p-n junction form. 4-88973  
 a-Si:H films, electron drift mobility, xerographic determination 4-61377  
 a-Si:H films, luminescence fatigue and ODMR studies 4-85005  
 a-Si:H films, planar magnetron sputtering, electronic props. 4-88972  
 a-Si:H films, pot. barriers and photo-EMF 4-88561  
 a-Si:H films, RF sputtering, substrate temp. calibration (Japanese) 4-76672  
 a-Si:H films, reactive sputtering, elec. and optical props. 4-104203  
 a-Si:H films, thickness effects on electrical and photoelectrical properties 4-98484  
 a-Si:H films, transient photocond. meas. 4-88539  
 a-Si:H films reactively RF sputtered, electrophotographic props. (Japanese) 4-81127  
 a-Si:H glow discharge deposited films, morphology, temp. and substrate depend. 4-61260  
 a-Si:H MIS Schottky barrier struct., dark currents 4-104322  
 a-Si:H nip solar cells, B contamination and photoresponse 4-89407  
 a-Si:H optical confinement type solar cell using milky tin oxide on glass 4-81556  
 a-Si:H p-i-n devices, EBIC decay 4-92796  
 a-Si:H p-i-n solar cells, performance, effect of prep. conditions (Korean) 4-114908  
 a-Si:H p-i-n solar cells on SnO<sub>2</sub> on glass, stability and efficiency 4-62354  
 a-Si:H photoceptors, electrophotographic imaging process 4-73544  
 a-Si:H pin devices, excess dark currents and diode quality factor 4-114016  
 a-Si:H pin solar cells, LPCVD growth, transport props. 4-114907  
 a-Si:H reactively sputtered films, H partial press. effects 4-93219  
 a-Si:H Schottky barriers, photocurrent spectral sensitivity 4-65727  
 a-Si:H Schottky barriers, sputtered, freq. depend. capacitance, admittance meas. 4-98693  
 a-Si:H Schottky diodes and nin devices, single and double carrier injection 4-114015  
 a-Si:H Schottky solar cells, gap state density 4-88438  
 Si:H single cryst., defect distrib. and density, X-ray projection topography studies (Chinese) 4-98086  
 a-Si:H solar cells, EBIC microcharacterisation of fabrication defects 4-93629  
 a-Si:H solar cells, photovoltage profiling 4-93617  
 a-Si:H sputtered films, steady-state photocond. and recombination processes 4-108902  
 a-Si:H surface barrier structs., photocurrent, freq. depend. 4-61418  
 a-Si:H thin films, glow discharge effects on electronic and optical props. 4-75977  
 a-Si:H thin films, O distrib. and modifications induced by heavy ion bombard. 4-70233  
 Si:H wide optical gap binary alloy films, elec. props. 4-113956  
 a-Si:H/Si p-n junction, optoelectronic props. 4-114020  
 Si:H/Si<sub>3</sub>N<sub>4</sub> amorphous semiconductor superlattices, charge transfer doping 4-92219  
 a-Si:H/SiO<sub>2</sub>/Pd diodes, H induced Schottky barrier modulation detect. by photoemission 4-70905  
 a-Si:H/a-Ge/H/a-Si<sub>1-x</sub>C<sub>x</sub>/a-SiN<sub>x</sub>/H superlattices, CVD growth and struct. 4-114416  
 a-Si:H/a-Si<sub>1-x</sub>N<sub>x</sub>/H quantum well struct., luminescence and current transport 4-114024  
 a-Si:H/a-SiN<sub>x</sub>/a-SiO<sub>2</sub> multilayer films, struct., elec. and optical props. 4-114025  
 Si:H-Ag junctions, Schottky barrier form. 4-84694  
 a-Si:H-Si n-p amorphous-cryst. heterojunctions, elec. characts. 4-84688  
 a-Si:H-a-SiN<sub>x</sub>/H heterojunction, lattice mismatch, electroabsorption study 4-76029  
 a-Si:H(D) thin films, coupled local mode vibrs., IR absorpt. study 4-88259  
 Si:In, isoelectronic bound excitons, transient photoluminesc. study 4-80507  
 Si:In(B), phonon scatt. at acceptor ground state 4-70729  
 Si:Li, phonon scatt., acoustic paramagnetic resonance study 4-71157  
 Si:Li and Si:Li, C, electron irradi., luminesc. decay time, absorpt., isotope splitting, and Zeeman meas. 4-71434  
 Si:Li p-n junction solar cells, electron induced degradation, recovery under space conditions 4-105110  
 Si:Li solar cells, counterdoped, increased radiation resistance to electron irradi. 4-81539

## elemental semiconductors continued

- Si:Mg, implanted, doping behaviour, elec. props. 4-75485  
 Si:Mg(Al)(S), third-period interstitials, electronic struct. calcs. 4-108808  
 Si:Mn, Cu, impurity energy levels, DLTS and capacitance studies 4-88471  
 Si:Mo doping by recoil implantation, RBS anal. (Chinese) 4-70173  
 Si:muon, spin polarised electron struct. of positive muon, LCAO-Green's function anal. 4-65634  
 Si:muonium, interstitial atom mobility, radiation defect effects 4-65256  
 Si:N, B diffusion profile 4-113726  
 Si:N, ion implanted, optical props. (Chinese) 4-114306  
 Si:N, low energy implant depth profiles, surface peak, Auger studies 4-80074  
 Si:N single cryst., ion implanted, photoluminescence studies 4-114313  
 Si:N(O), microdefect formation during single crystal growth, influence of impurities on nucleation 4-114386  
 Si:Na<sup>+</sup>, two-dimensional hopping cond. in mag. field 4-98687  
 Si:O, buried oxide layers formation by O<sup>+</sup> implantation 4-88180  
 Si:O, C, annealed, photoluminesc. of impurity complexes 4-88866  
 Si:O, Czochralski grown, annealed, impurity precipitates, induced defects, TEM obs. (Chinese) 4-92368  
 Si:O, Czochralski grown, thermally-induced microdefects, high resolution TEM studies 4-108626  
 Si:O, helicoidal dislocations, electron microscopic study 4-92208  
 Si:O, impurity conc. meas. using IR spectra, multiple reflection effects 4-113487  
 Si:O, isotope effects and photoluminescence spectra 4-104661  
 Si:O, nonequilibrium cond. and thermal donors 4-104212  
 Si:O, O thermal donor, symmetry and electronic props., DLTS studies 4-113886  
 Si:O, P, thermal donors, optical absorption spectra studies 4-65637  
 Si:O, piezogalvanomagnetic effects in presence of thermal donor levels 4-104239  
 Si:O, rare earth atoms, impurity interaction and donor accumulation 4-103783  
 Si:O, recombination centres induced by heat treatment at 600 to 800°C 4-104154  
 a-Si:O,H CVD films, struct. model 4-88427  
 Si:O cryst., minority carrier lifetime, O precipitation effects, IR studies 4-113971  
 Si:O Czochralski crystals, O precipitation and microdefects 4-84411  
 Si:O<sub>2</sub>, precipitation at various impurity levels 4-113654  
 Si:O, impurity conc., IR absorption studies 4-113488  
 Si:P, diffusion study, influence of internal electric field 4-108662  
 Si:P, dislocation motion, onset delay times, etching study 4-70163  
 Si:P, EPR study of low-temp. mag. props. 4-84854  
 p-Si:P, elec. activity of P in diffusion zone (Russian) 4-70817  
 Si:P, heavily doped, optical reflectivity spectra 4-61735  
 Si:P, IR absorption spectrum 4-71414  
 Si:P, ion implanted, diffusion during rapid thermal annealing 4-113713  
 a-Si:P, ion implanted, phonon scatt. study 4-70325  
 Si:P, ion implanted, Xe flash lamp annealing, Rutherford backscatt. study 4-88196  
 Si:P, motional narrowing of ESR line 4-104484  
 Si:P, P diffusion from solid source for solar cell fabrication 4-77085  
 Si:P, proton and neutron irradi., impurity composition and defect clustering 4-65291  
 Si:P, Sb, P diffusion, self-interstitial supersaturation and vacancy undersaturation 4-70457  
 Si:P, variable angle submillimeter laser reflection spectroscopy 4-104701  
 Si:P,Cl<sup>+</sup>, Cl<sup>+</sup> implantation effects on oxidation enhanced P diffusion 4-92429  
 Si:P,N, pulsed laser annealing, substitutional N impurities, EPR studies 4-98120  
 Si:P,O, trap spectrum of O donor, DLTS study 4-92651  
 Si:P film, deposition by thermal decomposition of silane 4-114414  
 Si:IR detector field enhanced photoresponse up to 43  $\mu$ m 4-90656  
 Si:IR detectors for low-photon-background IR astronomy 4-101160  
 n-Si:P polycrystalline CVD films, elec. props., grain size and impurity conc. effects 4-70963  
 p-Si:P surface-barrier detectors fabrication and appl. 4-87018  
 Si:P<sup>+</sup>, implanted, dislocation struct. development, effect of cryst. orientation, TEM obs. 4-80040  
 Si:P(As), ion implanted film, elec. props. 4-61473  
 Si:P(As)(Sb), many-valley semicond., shallow donor polarisabilities 4-92666  
 Si:P(B), heavy doping effect on band struct. and optical props. 4-92998  
 Si:P(B), substrate orientation depend. of enhanced epitaxial regrowth 4-108737  
 Si:P(B), thermal wave contrast, dopant conc. depend. 4-103978  
 Si:P(Sb), ion implanted, flash lamp annealing 4-108735  
 Si:Pd, deep levels, DLTS study (Chinese) 4-113887  
 Si:Re, Czochralski grown cryst., thermal stability study 4-109318  
 Si:S, charge states, electronic struct. 4-104152  
 Si:S, deep levels, DLTS meas. 4-84592  
 Si:S, implanted, depth distrib. as function of ion energy, fluence and anneal temp., SIMS meas. 4-80078  
 Si:S, persistent photoconductivity effect obs. 4-113995  
 Si:Sb, electrolytic Sb diffusion in MOS structures 4-80299  
 Si:Sb, implanted-laser irradi., crystn. annealing, time-resolved reflectivity, TEM, Rutherford backscattering anal. 4-80093  
 Si:Sb, ion implanted, dopant site location and profiles, channelling studies 4-108393  
 Si:Sb, ion implanted, supersaturation, vitreous C strip heater annealing, Rutherford backscattering, elec. meas. 4-92375  
 Si:Sb, possible obs. of electronic phase transition, low temp. magnetoresist. study 4-80633  
 Si:Sb single crystals, impurity atom localisation, Rutherford backscatt. yield in planar channelling 4-75489  
 Si:Se, photocapacitance, photocond. and donor levels 4-65714  
 Si:Se<sup>+</sup>, ESR study 4-109071  
 Si:Sn, amorphous vacuum deposited films, impurity states 4-84595  
 Si:Sn, implanted, subthreshold energy electron beam annealing, Mossbauer effect 4-88205  
 Si:Te, donor states, Hall effect and cond. meas. 4-104145  
 Si:Ti, recombination props., capture rates 4-104149  
 Si:Ti, isoelectronic bound excitons, transient photoluminesc. study 4-80507  
 Si:Xe, implanted Xe reemission by He<sup>+</sup> ion bombardment 4-75462  
 Si/a-Si:H,B/metal junctions, current-volt. characts. 4-114033  
 Si/a-Si/metal tunnel rectifier 4-88586

## elemental semiconductors continued

- a-Si/a-SiC<sub>2</sub>/a-SiN<sub>x</sub> superlattices, optical bandgap and elec. resist. 4-114026
- Si/Ag system, atomic mixing using 45 keV Ar<sup>+</sup> ion beam 4-80119
- Si/Al interface, atomic redistributions, XPS studies 4-80311
- n-Si/Al planar Schottky diodes, changes in breakdown characts. 4-88594
- n<sup>+</sup>-Si/Al-Si system, metallisation by fast heat-pulse alloying, hillock elimination 4-114034
- Si/AlGaAs cascade solar cells, sensitivity and efficiency 4-85375
- Si/Au interface, atomic redistributions, XPS studies 4-80311
- Si/Au(Ag) interfaces, reactivity, MeV ion scatt. studies 4-80424
- Si/CaF<sub>2</sub> heterostructure interface, MBE grown, Raman spectra studies 4-98462
- Si/CoSi<sub>2</sub>/Si epitaxial monolithic structures, transistor effect 4-114036
- Si/Ge<sub>1-x</sub>Si<sub>x</sub> strained layer superlattice, MBE growth 4-92576
- Si/insulator/Si structure, VPE growth (*Japanese*) 4-88987
- Si/methanol liquid junction, open circuit volt. and oxide form. 4-114030
- Si/MgO·Al<sub>2</sub>O<sub>3</sub>/SiO<sub>2</sub>/Si SOI struct., epitaxial film quality 4-80460
- Si/Ni interfaces, silicide form., atom-probe study 4-70475
- Si/oxide interface, plasma diagnostics and high contrast end point detection 4-89150
- Si/Pd<sub>2</sub>Si system, contact growth and elec. characts., dry etching effects 4-104313
- Si/Pt (Pd) Schottky contacts, XPS study (*Chinese*) 4-114358
- Si/Pt interface, silicide form., Raman spectra studies 4-80423
- Si/SiO<sub>2</sub> interface, XPS and electron escape depth variation 4-81104
- Si/SiO<sub>2</sub> interface, amorphous Si/cryst. Si facet form. during solid phase epitaxy 4-88423
- Si/SiO<sub>2</sub> interface, Ar annealed, fixed oxide charge density 4-98756
- Si/SiO<sub>2</sub> interface, atomic struct. and elec. props. 4-80677
- Si/SiO<sub>2</sub> interface, defects, high resolution TEM study 4-108386
- Si/SiO<sub>2</sub> interface, ESR techniques and results 4-109059
- Si/SiO<sub>2</sub> interface with gradual chem. transition, electronic density of states 4-108756
- Si/SiO<sub>2</sub> MOS capacitors, donor state generation rate, anode field depend. 4-92826
- Si/SiO<sub>2</sub> MOS struct., interface state density and atomic roughness 4-98684
- Si/SiO<sub>2</sub>/Al capacitor struct., ion beam fluorination and interface state density 4-70176
- Si/SiO<sub>2</sub>/Al capacitors, radiation-induced oxide defects, ESR study, bias effects 4-70205
- Si/SiO<sub>2</sub>/Al capacitors, interface trap generation and H electromigration 4-70940
- Si/SiO<sub>2</sub>/Al struct., internal photoemission, surface band bending effects 4-84705
- Si/SiO<sub>2</sub>/Mo struct., SiO<sub>2</sub> formation by interfacial oxidation method 4-98467
- Si/SiO<sub>2</sub>/Si<sub>3</sub>N<sub>4</sub>, N and O distrib. profiles, Auger studies (*Russian*) 4-65578
- Si/SiO<sub>2</sub>/Si<sub>3</sub>N<sub>4</sub>/Al capacitors, ion/atom beam milling, damage effects 4-70941
- Si/SiO<sub>2</sub>/Si<sub>3</sub>N<sub>4</sub>/electrolyte system, static and dynamic volt-ampere characts. (*Russian*) 4-65739
- Si/SiO<sub>2</sub>/metal struct., electron inversion layers, tunnelling spectra of Landau levels 4-98772
- n-Si/SnO<sub>2</sub> solar cells 4-66702
- Si/Ti interface, ion implanted with As<sup>+</sup>, P<sup>+</sup>, B<sup>+</sup>, TiSi<sub>2</sub> formation 4-88183
- Si/V-Ta(Ti), interaction of alloy films with Si, silicide formation 4-88436
- Si/W-Ti direct contact system, contact resist., heat treatment effects 4-114032
- Si/ZnO-B<sub>2</sub>O<sub>3</sub>-SiO<sub>2</sub> glass system, surface charges, C-V characteristic meas. 4-65747
- Si-Ag interface, nonlinear surface EM waves 4-80892
- Si-Ag junctions, Schottky barrier form. 4-84694
- n-Si-Au, defect characterisation, SEM-CCM studies 4-113278
- Si-Au(Ag)(Al) Schottky barrier diodes, barrier height and hot electron attenuation length meas. 4-98751
- Si-BP-Si double heterojunction, current-voltage characteristics 4-80658
- a-Si-based alloy p-i-n solar cells, performance enhancement rel. to B profiling 4-77087
- a-Si-based alloy p-i-n solar cells, elec. field distrib. and open circuit volt. 4-89405
- a-Si-based alloys, vibr. props. and local modes 4-70323
- a-Si-based field effect transistors, flat-band volt. and surface states 4-92825
- a-Si-based solar cells, high conversion efficiency 4-93619
- Si-CaF<sub>2</sub> epitaxial surface morphology, SEM study 4-113822
- Si-electrolyte interface, elec. field modulated IR internal reflection studies 4-98749
- Si-Er interface, ErSi<sub>2</sub> formation using electron beam heating 4-65494
- Si-H-Cl system, Si condensation, equilibrium calcs., 300 to 3000K 4-61107
- Si-Hg Schottky barrier, crystal damage during CV profiling 4-98753
- Si-MOSFET inversion layer, warm electron coeff. calc. for two-dimens. electron gas 4-65748
- Si-metal and Si-silicide interfaces, electronic and chemical structure 4-104312
- Si-metal interface, dislocation mediated melting 4-103912
- Si-metal struct., scanning-tunnelling microscopy, voltage drop 4-114038
- Si-Mo contacts, ion-beam sputter deposition, defects, DLTS and EBIC studies 4-61848
- Si-Mo interface, silicide form. kinetics induced by ion bombard. 4-61243
- Si-Mo Schottky barriers formation by Mo films CVD growth 4-98695
- Si-Mo-Ni contacts, elec. characts. study 4-80653
- Si-Nb interface, silicide form. kinetics induced by ion bombard. 4-61243
- Si-NiSi<sub>2</sub> grid formation by MBE 4-114044
- Si-on-insulator, Si stripes in SiO<sub>2</sub> grooves, double laser recrystn., orientation control 4-75506
- Si-on-insulator, subgrain boundary free, strip heater recrystn. 4-75796
- Si-on-insulator films, ion implanted, annealing using scanned graphite strip heater 4-80066
- Si-on-insulator films, zone-melting recrystallized, O distribution and sub-boundary formation 4-80433
- Si-PbSe heterojunctions, solution-grown, elec. and photoelec. props. 4-114023
- Si-Pd<sub>2</sub>Si interface, electronic struct. 4-84665
- Si-polyacetylene interface, Auger spectra obs. of Si-C binding, peak shift depend. on adsorp. level (*French*) 4-66141

## elemental semiconductors continued

- Si-Pt interface, silicide formation and chemical reactions 4-92570
- Si-SiO<sub>2</sub> interface cyclotron resonance lineshape distortion (*Chinese*) 4-84701
- Si-SiO<sub>2</sub> interface traps in diode struct., small signal admittances 4-80678
- Si-SiO<sub>2</sub> laser recrystn. of Si films with heat sink struct. 4-60954
- Si-SiO<sub>2</sub> work function and oxidation studies 4-61439
- Si-SiO<sub>2</sub> XPS study of interface states 4-98682
- Si-SiO<sub>2</sub> interface, As<sup>+</sup> implanted, defects, ESR study 4-61591
- Si-SiO<sub>2</sub> interface, B drive diffusion in oxidizing ambients, segregation coeff. determ. 4-75690
- Si-SiO<sub>2</sub> interface, B segregation during neutral anneals 4-70387
- Si-SiO<sub>2</sub> interface, charge fluctuations, MIS cond. freq. depend. 4-114041
- Si-SiO<sub>2</sub> interface, electronic struct. 4-84665
- Si-SiO<sub>2</sub> interface, oxidation, chem. bonding in transition layer, photoemission spectra using synchrotron radiation 4-85062
- Si-SiO<sub>2</sub> interface, shallow donor impurities, variational soln. 4-70893
- Si-SiO<sub>2</sub> interface states, degeneracy and capture cross sections, DLTS studies 4-76039
- Si-SiO<sub>2</sub> interface structure, oxidation of singular and vicinal surfaces of Si 4-104317
- Si-SiO<sub>2</sub> MIS structures, hole traps, trivalent Si centres, EPR meas. 4-80817
- Si-SiO<sub>2</sub> MOS struct., C-V characts. different oxidation process effect 4-92823
- Si-SiO<sub>2</sub> MOS struct., H passivation of implantation defects using a-Si:H film 4-71744
- Si-SiO<sub>2</sub> MOS struct., microstructural variations in oxides, electron spin reson. obs. 4-61590
- Si-SiO<sub>2</sub> multilayer structure, thermal stresses 4-113682
- Si-SiO<sub>2</sub> phase boundary, surface hole mobility 4-104323
- Si-SiO<sub>2</sub> SOI structures, zone melting recrystn., topographic imperfections 4-99303
- Si-SiO<sub>2</sub> structure, transparent layer ellipsometric study in layer-substrate structs. with indistinct transition region 4-86469
- Si-SiO<sub>2</sub>:Ar<sup>+</sup>(As<sup>+</sup>), ion implanted layers, EPR study 4-84849
- Si-SiO<sub>2</sub>:P interface, Auger study of P pile-up 4-103780
- Si-SiO<sub>2</sub>:Al MIS structures, with plasma deposited SiO<sub>2</sub>, alkali ion motion, C-V characts. (*Russian*) 4-114042
- Si-SiO<sub>2</sub>:KOH system, ellipsometric and electroreflectance study 4-99091
- Si-SiO<sub>2</sub>:Mo MOS diodes, carrier trapping centres and interface states induced by RF sputtering of Mo 4-88603
- Si-SiO<sub>2</sub>:Na, Na<sup>+</sup>-induced surface states, DLTS study 4-61463
- Si-SiO<sub>2</sub>:Ta<sub>2</sub>O<sub>5</sub>/Al MIS struct., electrophys. props. of thermal Ta<sub>2</sub>O<sub>5</sub> 4-61475
- Si-SiO<sub>2</sub>:phosphosilicate glass-Al struct., positive charge buildup 4-98777
- Si-Ti interface, TiSi<sub>2</sub> formation by fast radiative processing 4-113731
- Si-Ti(Hf) 4-70906
- n-Si-tunnel oxide-metal struct. with MOSFET for meas. elec. cond. of SiO<sub>2</sub> films 4-61476
- SIB, implanted, impurity depth profiles,  $\alpha$ -particle spectra, Monte Carlo calc 4-80081
- a-SiC/c-Si p<sup>+</sup>n heterostructure, plasma CVD growth and elec. props. 4-80660
- a-Si<sub>1-x</sub>C<sub>x</sub>/H/a-Si(H) heterojunctions, photoemission studies 4-65731
- Si<sub>1-x</sub>Ge<sub>x</sub>:H, amorphous, occupied gap state obs. 4-70637
- Si<sub>1-x</sub>H<sub>2x+1</sub>, defects, molecular cluster studies 4-84586
- SiO<sub>2</sub>/poly-Si/SiO<sub>2</sub> composite filter, reaction ion etching process in single reactor 4-85236
- Si-H, bonds and H-induced defects study 4-66058
- Si(111) surface chain model, optical props. and excitons 4-108916
- Si(111)-2 $\times$ 1, surface geometry, buckled chain model, LEED calc., work function meas. 4-75765
- Si(111)2 $\times$ 1 surface, structure analysis, LEED study 4-113769
- $\alpha$ -Sn, band struct., angular resolved photoemission studies 4-84554
- Sn, semiconductor-metal transition, press. effects 4-92613
- Sn, tetrahedrally bonded, anisotropy of Compton profile 4-99217
- Ta-Si system, thin-film reactions and phase diagrams 4-88263
- Te (0001), weak localisation under lifted spin degeneracy conditions 4-92781
- Te crystal struct. and defects, CDW soliton model 4-70685
- Te, dimensionally quantised accumulation layer, quantum kinetic phenomena 4-88555
- Te, hole mobility anisotropy, temp. depend. 4-65681
- Te, neutron irradi. induced defects, optical props. near fundamental energy gap 4-84318
- Te photo-induced complex permitt. at 9 GHz, expt. study 4-65703
- Ti-Si interface, Ti-Si<sub>2</sub> formation by wide-area electron beam irradi. 4-92236
- Ti-Si system, thin-film reactions and phase diagrams 4-88263
- TiSi<sub>2</sub>/n<sup>+</sup> poly-Si, co-sputter-deposited, rapid lamp heating, MOS device fabrication appl. 4-99311
- W-Si system, thin-film reactions and phase diagrams 4-88263
- WSi<sub>2</sub>/poly-Si/SiO<sub>2</sub>-Si MOS struct., interface reaction and resistivity 4-114040
- Zn,Cd<sub>1-x</sub>S/Si, p-n heterojunction photovoltaic solar cell 4-85366
- ZnSe-Ge heterojunction, valence-band discontinuities 4-84676

## elementary particle coupling constants

- 1<sup>++</sup> QQqq states, bag model, QQ state mixing, hadronic transitions (*Chinese*) 4-102089
- $\lambda(\Phi^2 - \Phi^4)$  lattice Hamiltonian field theory, bound state spectrum 4-90731
- big bang supersymmetric relics, neutral gauge/Higgs fermion mass 4-77988
- CERN-collider Z<sup>0</sup> anomalous decays, conjectured second strong force on heavy quarks 4-106508
- charmed particles, hadronic props. from elastic pion scatt. 4-102128
- chiral symmetry, composite models, scalar and fermion fields, large-N limit 4-106523
- composite fermions, masses and anomalous mag. moments, non-renormalizable supersymm. interactions 4-111421
- Coulomb interaction, string potential, static quarks on random lattice, strong coupling limit 4-111292
- decay constants, pseudoscalar mesons and scalar diquarks 4-90819
- deep inelastic lepton-interactions QCD anal. 4-90887
- Dirac cosmology, var. of fund. interactions coupling consts. 4-82567
- energy dependence at high energy and unified field theory 4-82406
- energy-energy correlation function, test of perturbative QCD, pp collider 4-86667

**elementary particle coupling constants continued**

- fermion-fermion condensation in superconductivity model,  $n\bar{n}$  oscillations and  $\nu$  mass 4-82927  
 glueball model, heavy quarkonium  $^3S_1$  state pion cascades, OZI violation 4-95771  
 GUTs, minimal SU(5) Higgs scalar effects and supersymmetry, p decay 4-90763  
 instanton and meron fields, Dirac Hamiltonian self-adjointness 4-95673  
 lattice gauge theories with Susskind fermions, strong coupling expansion 4-95645  
 lattice QCD, non-zero baryon density, chiral symm. restoration, strong coupling 4-102062  
 mass gap of lattice Q(3) non-linear  $\sigma$ -model with naive and improved actions 4-86553  
 minimal SU(5) model with canonical particle content, proton lifetime, fermion masses 4-73694  
 MIT bag model with broken chiral symmetry, massive quarks and pions 4-59049  
 neutron elec. dipole moment, strong CP violating soft-pion nucleon coupling constant contrib. 4-68407  
 open b-flavour states, hadronic couplings 4-68542  
 perturbative QCD, ambiguity resolution, Stevenson's principle of minimal sensitivity 4-90798  
 proton valence quarks, SU(6) symmetry and quark forces in perturbative QCD 4-86663  
 QCD parameters on lattice and in continuum 4-86645  
 QCD SU(3) deconfining transition, with closed quark loops 4-86644  
 quark axial coupling quenching and nucleon coupling constants 4-82949  
 scalars coupled to fermions in 1+1 dimensions 4-86584  
 Skyrme model, strong-coupling approx., nonstrange baryons, excited states 4-106513  
 SLAC PEP, Bhabha scatt., muon pair prod., supersymm. scalar electrons 4-106502  
 Sp(2,2) coherent states, unstable system geometrized decay model 4-95686  
 spin three self interactions, free field gauge invariance, coupling constant 4-111315  
 SU<sub>c</sub>(3) mass differences and axial vector coupling const., QCD sum rules 4-73679  
 SU(1,1) supergravity models, gravitino and gaugino masses, Yukawa couplings 4-90473  
 SU(2)×U(1) breaking constraints for vacuum misalignment, partially chiral technicolour group 4-111350  
 SU(3)×SU(2)×U(1) interactions, D=10 N=2 supergravity, comparison with strong, electroweak interactions 4-90773  
 SU(3)×SU(2)×U(1) interactions, D=11 supergravity, comparison with strong, electroweak interactions 4-90772  
 SU(5) supersymmetric cosmology, masses and coupling const. 4-78502  
 SU(6) grand unified model, simple Higgs fields, anomalous fermions. (Chinese) 4-102076  
 substructure effects, composite leptons, quarks and W bosons, W couplings 4-111422  
 U(1) lattice gauge theory, 2+1 dimens., string tension and glueball mass 4-86586  
 B $\pi$ →B $\pi$ l, pion decay widths, single quark coupling const. 4-90872  
 $e^+e^- \rightarrow e^+e^-$ , scalar/pseudoscalar boson contributions, masses and coupling constants 4-111436  
 $e^+e^- \rightarrow \gamma^*\gamma$ , scalar/pseudoscalar boson contributions, masses and coupling constants 4-111436  
 $e^+e^- \rightarrow \gamma\gamma$ , scalar/pseudoscalar boson contributions, masses and coupling constants 4-111436  
 $e^+e^-$ -jets, flavour independence of quark-gluon coupling const. 4-59090  
 $e^+e^- \rightarrow \mu^+\mu^-$ , charge asymmetry, weak single loop corrections,  $\gamma Z$  box 4-59063  
 $e^+e^- \rightarrow \mu\mu\gamma(\gamma)$ , cross section, coupling constant, comparison with QED predictions 4-111435  
 $e^+e^- \rightarrow q\bar{q}$ , scalar/pseudoscalar boson contributions, masses and coupling constants 4-111436  
 $e^+e^- \rightarrow q\bar{q}g$ , model depend. of coupling const. in 2nd order QCD 4-59089  
 H+dyon-W $^\pm$ +dyon, zero gauge coupling constant, gauge boson bound states 4-106466  
 NN elastic scatt., polarization data for coupling constants 4-106576  
 $\bar{\nu}N$ , weak hadronic neutral current, right coupling const. 4-90854  
 p charge radius, mag. moment and coupling const. in solution bag model 4-90822  
 $p\bar{p} \rightarrow 2/3$  mesons, quark annihilation model, vector-meson-quark interaction 4-106539  
 $p\bar{p} \rightarrow 3$  mesons, quark rearrangement model, vector-meson-quark interaction 4-106539  
 $\pi NN$  coupling constant, deuteron D/S ratio, nucleon-nucleon interactions 4-106535  
 $\pi NN$  coupling constant, deuteron props., one-pion exchange 4-106536  
 WO<sub>3</sub> amorphous films, colour centres, EPR study 4-84291

**elementary particle decay**

- see also *electromagnetic decays; elementary particle coupling constants; hadron decay; lepton decay; leptonic decays; nonleptonic decays; semileptonic decays*  
 covariant polarisation bases for spin  $1/2$ , 1 and  $3/2$  particles, vector boson decay and prod. 4-64025  
 dyon decay, EM properties 4-73612  
 electroweak SUSY theories; b-lifetime, t-mass and CP violation 4-82918  
 gravitinos, decay and lifetimes, X-ray emission, appl. to galaxy clusters and background radiation 4-101154  
 Higgs boson decay following prod. in lepton+lepton and hadron+hadron collisions 4-106503  
 intermediate vector bosons and neutrino cosmology 4-68485  
 particle properties review, masses, decays and lifetimes 4-67885  
 photinos, decay and lifetimes, X-ray emission, appl. to galaxy clusters and background radiation 4-101154  
 S<sub>4</sub> permutation symmetry, CP nonconservation, rare decays and quark/lepton electric moments 4-86600  
 spinless boson radiative decay, possible source of anomalous  $1^+1^- \gamma$  in Z searches 4-102148  
 weak decays, one-gluon corrections in QCD 4-86639  
 weak quark decays, diagrammatic approach 4-73718  
 weak quark decays, gluonic corrections, leading log summation 4-73724  
 $e^+e^-$  annihilation, quark flavour separation, appl. to electroweak asymmetries, quark lifetimes 4-95768  
 $e^+e^- \rightarrow W^+W^- (Z\gamma)(ZZ)(ZH)$ , muon spectra from W and Z decays 4-73738

**elementary particle decay continued**

- H $^\pm$ W $^\pm$  Higgs branching ratio 4-90938  
 $1^- \rightarrow \gamma\gamma$  decay mode width in QCD framework 4-59033  
 q $\bar{q} \rightarrow q\bar{q}$ , possible decay for  $p\bar{p}$  missing  $p_T$  events 4-102135  
 QQ→gg, gluino production, decay rates 4-86752  
 t-quark, weak prod. and semileptonic decay 4-73728  
 W decay, new composite bound state 4-68602  
 W decay, weak spectral functions and applications 4-64026  
 W decay in QCD and Weinberg model, constraint on N<sub>c</sub> species 4-68467  
 W→heavy lepton→electron decay signature study 4-73788  
 W→ $\nu_\mu$ , heavy unstable neutrinos from weak boson decays 4-86751  
 W→ $\nu_\mu l$ , heavy lepton detection in  $p\bar{p}$  collider 4-68604  
 W→ $\nu_b$ , top particle weak production, mass  $\approx 35$  GeV 4-111482  
 W→ $\nu_b(b)$ , top quark, QCD radiation effects, lepton signatures 4-95827  
 W $^\pm$  decay, experimental searches for squarks, sleptons and SUSY gauge bosons, mass limits 4-59019  
 W $^\pm \rightarrow e^+e^- \nu(e^-\bar{\nu})$ , decay props., comparison with electroweak theory 4-95832  
 W $^\pm \rightarrow Z l H^\pm$ , search for Higgs in left-right symmetric models 4-95865  
 Z decay in QCD and Weinberg model, constraint on N<sub>c</sub> species 4-68467  
 Z→ $e^+e^- \gamma$ , composite scalars in  $e^+e^-$  collisions and radiative Z decays 4-86694  
 Z→ $e^+e^- \gamma$ , interpretations and other tests 4-78578  
 Z→ $e^+e^- \gamma$ , preon theories of particle struct., compositeness scale lower bound 4-106522  
 Z→ $ll\gamma\gamma$ , Z mixing with degenerate bound colour quarkonium 4-111486  
 Z neutral current flavour changing decay induced by radiative corrections 4-95751  
 Z→ $\nu_\mu \bar{\nu}_\mu$ , heavy neutrino explanation for anomalous  $1^+1^- \gamma$  events 4-102149  
 Z-boson decay, effective flavour-changing neutral current 4-82979  
 Z $^0$  anomalous radiative decay 4-78579  
 Z $^0 \rightarrow e^+e^- (e^+e^- \gamma)$ , decay props., comparison with electroweak theory 4-95832  
 Z $^0$  four body decay, heavy flavours 4-68605  
 Z $^0 \rightarrow \gamma^* \gamma^*$  squarkonium, production of  $^1S_0$  squarkonium states, gluon jets 4-111487  
 Z $^0 \rightarrow l^+l^- \gamma$ , anomalous lepton magnetic moments, constraints 4-86750  
 Z $^0 \rightarrow l^+l^- \gamma$ , collinear radiation and lepton universality 4-78577  
 Z $^0 \rightarrow \nu\bar{\nu}$ , heavy unstable neutrinos from weak boson decays 4-86751  
 Z $^0 \rightarrow \nu\bar{\nu}$ , neutrino generation counting 4-86754  
 Z $^0 \rightarrow q\bar{q} l^+l^-$ , Monte Carlo calcs. 4-90936  
 Z $^0 \rightarrow Z l H$ , search for Higgs in left-right symmetric models 4-95865  
 @ W→ $\nu b$ , collinear radiation and lepton universality 4-78577  
 @ Z $^0$  anomalous radiative decay, possible new pseudoscalar particle 4-68577  
 W→heavy fermion→light fermion cascade decay covariant formalism 4-73788  
 Z→ $l^+l^- \gamma$ , excited lepton states 4-78580
- elementary particle electromagnetic interactions**  
 see also *Weinberg model*  
 $\sigma$ - $\omega$  model, electromagnetic interactions in nucl. dynamics, Dirac-based theories 4-111365  
 electro-weak theory, introduction 4-59011  
 electron initiated EM showers in air, radiation dose distrib. close to shower axis 4-59020  
 few nucleon systems, EM and weak interactions 4-59155  
 longitudinal EM field, action principle,  $\gamma$  coeff. investigation 4-63948  
 meson Lagrangians, U(3) group, four-quark interaction model 4-95684  
 spin-1 particle, anomalous moment Hamiltonian exact diagonalisation expression 4-73758
- elementary particle gravitational interactions**  
 see also *supergravity*  
 boson creation in a subquantum lattice 4-73711  
 bosons, spin-0, axion mass and couplings from macroscopic forces 4-90790  
 combined symmetries in curved space-times 4-102081  
 fermion gravitational interactions, chiral Lorentzian anomalies 4-90747  
 massive spinning particle motion in presence of flat metric and vector torsion 4-78216  
 semileptonic interactions, strong gravity and Lorentz non-invariance 4-90789  
 Universe expansion nature, role of gravit. and elementary particles (Russian) 4-82581
- elementary particle inclusive interactions**  
 see also *electron-positron inclusive interactions; elementary particle large momentum transfer interactions; pion-proton inclusive interactions; proton-proton inclusive interactions*  
 baryon exchange processes, pole exchange, duality and broken SU(3), review 4-63987  
 boson charge bunching in high energy collisions, Centauro-like events 4-59114  
 branching models with constant weights, KNO scaling, jets appl. 4-73627  
 cascade model, semi-inclusive sphericity distrib., hadron-hadron collisions 4-102101  
 collective quark tubes and multiplicity distrib. in high energy  $\alpha\alpha$  collisions 4-82948  
 cosmic ray hadron bundles, obs. in Chacaltaya two storey emulsion chamber 4-106553  
 cosmic ray NN fragmentation collisions, EM contrib. 4-86748  
 decay inelastic singlet. struct. functions and scaling violation (Chinese) 4-68573  
 diffractive dissociation in multi TeV hadron-hadron and hadron-nucleus collisions 4-102145  
 Drell-Yan cross section high-moment corrections with alternate parton density 4-86743  
 exotic fireballs in collider expts., Mini-Centauro and Geminion type events 4-106548  
 fire-ball production in inclusive spectra, radial scaling 4-95860  
 gluon and quark jets, particle multiplicity ratios,  $\sqrt{\alpha(Q^2)}$  corrections in QCD 4-86660  
 gluon fragmentation contribs. to small P<sub>T</sub> hadron-hadron inclusive single particle distrib. 4-82944  
 hadron production from low mass clusters, phenomenological model 4-90818  
 hadron-nucleus collisions, inclusive spectra in additive quark model 4-90838  
 hadron-nucleus high energy interactions, projectile indep. of charged particle multiplicity ratio 4-59116

**elementary particle inclusive interactions continued**

- heavy-quark jets and their semi-leptonic fragmentation 4-73721  
 high energy distributions, dynamics and partial distrib. 4-95824  
 hN-X, particle production mechanisms in cosmic ray interactions 4-95862  
 induced angular resolution effect on high energy fixed target expts. 4-73789  
 initial state interactions, factorization, and the Drell-Yan process 4-63967  
 interference correlations of identical particles in models with closely spaced sources 4-78575  
 jet fragmentation, Monte Carlo code BAMJET 4-78518  
 jets, hadronic average multiplicities, QCD predictions 4-111386  
 large  $p_T$  hadronic reactions, jets, lowest order QCD quark/gluon scatt. 4-90812  
 large- $p_T$  single-particle inclusive cross sections and temperatures 4-68598  
 long-range rapidity correlations in hadron-nucleus interactions 4-86742  
 multiparticle clustering in hadron-nucleus collisions at cosmic ray energies 4-102279  
 multiparticle production in quark-gluon model, statistical mechanical interpretation 4-78537  
 multiplicity correlation coefficients, energy depend. in high energy hadron-nucleus collisions 4-102281  
 multiplicity-generating function, hadron-nucleus collisions, QCD and dual topological unitarization 4-111383  
 neutrino charged current inclusive interactions 4-90858  
 parity violating spin asymmetries in high energy inclusive reactions 4-95704  
 partons, multiplicities and correls. in jets taking into account coherence effects, QCD calcs. 4-82951  
 perturbative QCD, jet Monte Carlo simulation and soft gluon radiation 4-102086  
 PETRA  $e^+e^-$  storage ring, review of experimental investigations 1978-83 4-90851  
 proton beam dump experiments, prompt neutrino flux meas. 4-90935  
 pseudorapidity correlation in hadron-nucleus interaction at cosmic ray energies 4-102280  
 QCD hard-scattering-jet effect on the gamma-ray families observed at mountain altitudes 4-110457  
 QCD high  $p_T$  physics, Lund Monte Carlo method 4-78566  
 QCD jet simulation in  $10^{13}$ - $10^{17}$  eV hadron collisions, Monte Carlo approach 4-110458  
 quark fragmentation with different recombination functions, QCD jets 4-68528  
 technijets structure, QCD anal., expt. signals 4-111387  
 two-particle rapidity correl. in  $\alpha\alpha$ ,  $\alpha p$ , and  $pp$  interactions at CERN ISR 4-59118  
 weak charged current interaction, hadronic final states 4-90857  
 $\alpha\alpha$  collisions, multiplicity dist. and coloured strings 4-59122  
 $ed \rightarrow eX$ , high energy inclusive cross section polarisation depend 4-78574  
 $e^+e^-$  - hadrons, at PETRA, one-photon annihilation and two-photon interactions, review 4-64012  
 $g$ -particle multiplicity in  $p$ ,  $p$ ,  $\pi$  and  $K$  collisions with emulsion 4-102132  
 $\gamma\gamma$ , hard processes obs. in collision of two quasi-real photons 4-63996  
 $\gamma\gamma$ ,  $1^+1^+$  resonances,  $(qq)$ ,  $(qq\bar{q}\bar{q})$ ,  $(q\bar{q}g)$ ,  $(gg)$ ,  $(ggg)$  spectroscopy 4-68601  
 $\gamma N$ , 20-70 GeV, in emulsion, neutral charmed meson lifetime and mass 4-73750  
 $\gamma N$ -charm, inclusive cross-section, meson lifetimes 4-90891  
 $\gamma N$  in emulsion, 20-70 GeV,  $D^+$  and  $\Lambda_c^+$  lifetimes 4-73749  
 $\gamma p \rightarrow K_S^0(\Lambda_c^+)X$ , inclusive photoproduction of neutral strange particles at 20 GeV 4-73764  
 $\gamma p \rightarrow VX$  polarization in large- $p_T$  photoproduction of vector mesons 4-90892  
 hd,  $^6$  total cross sections, smearing correction, 50 to 370 GeV 4-90924  
 hh-jets, experimental props., comparison with QCD 4-73774  
 hh-jets, QCD Monte Carlo simulation, COJETs program 4-95763  
 hh-quarks, production cross-sections in cosmic rays 4-95845  
 hh- $W^{\pm}(Z^0)$  in Weinberg model with QCD bremsstrahlung, Monte Carlo program WIZJET 4-95825  
 hh-X, jet structure and transverse energy 4-86737  
 hh-X secondary inclusive spectra in additive quark model 4-95853  
 $h_1h_2 \rightarrow \gamma X$ , direct  $\gamma$ -quanta prod., polarisation phenomena 4-73783  
 $h_1h_2 \rightarrow Xh_2$  process, two-gluon exchange model 4-59113  
 hN, multiparticle production, multiplicities at cosmic ray energies 4-95854  
 hN, multiparticle production at cosmic ray energies, A-dependence 4-95855  
 hN, shower multiplicity studies at cosmic ray energies 4-95856  
 hN cross-section calcs. using Glauber multiple scatt. 4-95846  
 hN-hX, scaling in compound multiplicity 4-95844  
 hN inclusive spectra, scaling violation in fragmentation 4-95852  
 hN- $l\bar{l}X$ , in nuclei, soft and hard quark processes role in dilepton prod., A depend. 4-95820  
 hN-X, simple model 4-95863  
 hN-X inclusive inelastic spectra, effect of Fermi motion 4-95858  
 Kp, secondary inclusive spectra using additive quark model and quark statistics rule 4-82978  
 K  $p \rightarrow hX$ , effect of strange particles on cosmic ray processes and energy dist. 4-95839  
 K  $p \rightarrow \pi$ s, string fragmentation model predictions at 110 GeV 4-59111  
 K $^+$ p, 32 GeV/c,  $K_S^0$ ,  $\Lambda$  and  $\bar{\Lambda}$  prod., total and semi-inclusive cross sections 4-95829  
 K $^+$ p- $\gamma$ 's, inclusive production cross-section 4-86738  
 K $^+$ p-( $R-\Delta^{++}$ )X, production of gluonic long-lived state 4-111481  
 k $^+$ p-jets, planar events, structures, momentum flows 4-95833  
 K $p$ ,  $\leq 20$  GeV/c, charged particle average multiplicities, energy depend. 4-111475  
 $\Lambda_c$ ,  $\Lambda_b$  inclusive nonleptonic decays, bag model, W-exchange contribs. 4-106529  
 $\mu^+N \rightarrow \mu^+X$ , muon interference expts.,  $Z^0$  existence, unification and electroweak reviews (Russian) 4-78557  
 $\mu p \rightarrow X$ , 200 GeV, Bethe-Heitler bremsstrahlung meas. 4-73710  
 Nd-NX, high energy inclusive cross section polarisation depend 4-78574  
 NN, multiparticle production, quark-gluon plasma 4-68593  
 NN cosmic ray interactions, ang. dist., fractional energy spectra 4-101092  
 NN in dd,  $\alpha\alpha$ ,  $\sqrt{s_{NN}}=31$  GeV, central region total neutral energy spectra 4-86735

**elementary particle inclusive interactions continued**

- NN interactions, baryon distribution of quark-gluon plasma 4-64022  
 nN- $\Lambda_c^+X$ , 40-70 GeV,  $\Lambda_c^+$  mass, decays and cross section 4-95830  
 $\bar{p}N$ , neutral current interaction, neutral strange particle prod.,  $K^0$  multiplicity 4-73740  
 $\bar{p}N$  in Ne, semi-inclusive coherent diffractive charged current interactions 4-73741  
 $\bar{p}N \rightarrow K^0X$ , neutral current production of strange particles 4-111437  
 $\bar{p}N \rightarrow X$ , hadron up-down asymmetry 4-111439  
 $\bar{p}p$ -charm, inclusive production results 4-95788  
 $\bar{p}p$ , neutral to charged current cross section ratio determ. 4-63988  
 pd-hX, 70 GeV,  $h=\pi^{\pm}$ ,  $K^{\pm}$ ,  $p$ ,  $\bar{p}$ , invariant cross sections for large  $p_T$  hadron prod. 4-90923  
 pN, 120 GeV, on Be, Ta, inclusive  $\phi$  prod. cross section, A-dependence study 4-59120  
 pN, 200 GeV, multiplicity and rapidity distributions 4-86741  
 pN, 22.6-400 GeV/c, in emulsion, mean normalised shower multiplicity, multiparticle prod. mech. 4-90920  
 pN, 300 GeV/c, in emulsion, dynamical correlation among rel. particles, Monte Carlo calc. 4-90921  
 pN, 400 GeV in emulsion, charged shower multiplicity distrib. scaling 4-73782  
 pN, 400 GeV/c, pseudorapidity and rapidity gap distrib. 4-102140  
 pN- $\chi$ arm, production cross-section from dimuon continuum 4-102138  
 pN- $D(\Lambda_c^+)X$ , upper limit for charm production 4-78567  
 pN-hX, anal. of secondary tracks in  $\phi$ - $\theta$  space 4-95841  
 pN-hX, elasticity, cascade effects 4-95840  
 pN-hX, non-pion production, collision process 4-95843  
 pN inclusive interactions, stopping power of nuclear matter 4-68597  
 pN-jets, 4-momentum transfer between fireballs, multiplicity dependence 4-95842  
 pN-pX, inclusive cross section, stopping power in heavy nuclei 4-86744  
 pN- $\bar{p}p(\bar{p}p)X$ , narrow meson resonance search 4-95810  
 pN- $\pi^+X$ , narrow meson resonance production search 4-95810  
 pN- $\pi^+X$ , large  $p_T$ , soft and hard quark collisions in nuclei,  $\pi$  spectrum 4-95821  
 pN- $Z^0(\Lambda^0)$  inclusive production, cross-section ratios 4-102139  
 pN-X, leading particle spectrum in bremsstrahlung 4-90839  
 $\pi^+ \rightarrow \pi^0X$ , pionisation and fragmentation, inelasticity 4-95857  
 $\pi^-C$ -jets, behaviour of hadrons, average sphericity 4-90932  
 $\pi^-N$ , 50 GeV/c, pseudorapidity and rapidity gap distrib. 4-102140  
 $\pi^-N$ -charm+X, production cross-section from dimuon continuum 4-102138  
 $\pi^-N$ , 278 GeV, on Fe, forward prod. of charm states and prompt single muons 4-64023  
 $\pi^-N$  interactions, leading particle effect 4-95850  
 $\pi^-N-K^+K^0X$ , charge multiplicity, mass distrib., differential cross-sections 4-111479  
 $\pi^-N-\mu^+\mu^-X$ , 225 GeV/c, massive  $\mu$  pair transverse momentum distrib., at mass depend. 4-90925  
 $\pi^-N-pX$ ,  $\sim 16$  GeV/c, in nuclei, inelastic collisions and fast hadron formation zone 4-102133  
 $\pi^-N-\phi\phi X$ , inclusive  $\phi\phi$  production, search for narrow resonances 4-95826  
 $\pi^-N \rightarrow \pi^+X$ , secondary  $\pi^-$  production, space-time characteristics 4-78572  
 $\pi^-N \rightarrow \pi^+X$ , inclusive cross sections in dual parton model 4-111474  
 $\pi^-N \rightarrow \psi\bar{\psi}X$ , cross section calc. in  $O(\alpha_s^4)$  QCD 4-95831  
 $\pi^-N \rightarrow X$ , maximum multiplicity, cluster size determ. 4-90928  
 $\pi^-N$ , 120 GeV, on Be, Ta, inclusive  $\phi$  prod. cross section, A-dependence study 4-59120  
 $\pi^-N \rightarrow \pi^+X$ , inclusive cross sections in dual parton model 4-111474  
 W and Z multiple prod. as strong interaction signal for electroweak symmetry breaking 4-95722  
 pN-X maximum multiplicity, cluster size determ. 4-90928

**elementary particle interaction models**

- see also bootstrapping; composite models of hadrons; diffraction model; duality and dual models; peripheral models; statistical models; vector meson dominance model; Weinberg model  
 boson charge bunching in high energy collisions, Centauro-like events 4-59114  
 deep inelastic scatt.,  $R(\sigma_1/\Sigma_T)$  ratio, meson and diquark contribs. (Chinese) 4-73732  
 Froissaron production mechanisms 4-78541  
 hadron production from low mass clusters, phenomenological model 4-90818  
 hadron scattering theory, field quanta exchange 4-59055  
 interference correlations of identical particles in models with closely spaced sources 4-78575  
 jet fragmentation, Monte Carlo code BAMJET 4-78518  
 leading-logarithm model, QCD, mesons containing one heavy and one light quark 4-106519  
 non-relativistic quark-potential model, nucleon and delta spectra, oscillator variational states 4-106515  
 nucleon-nucleon scattering, total cross sections, spin effects, superhigh energies, quasipotential approach 4-95816  
 partial-wave analysis of a relativistic Coulomb problem 4-86687  
 potential model masses of mesons and baryons 4-78542  
 quark mass scale,  $\theta$  calculation, CP violation, Kobayashi-Maskawa mechanism 4-106504  
 quark potential model, NN scatt. phase shifts, delta cross sections 4-106538  
 schematic model of mesons based on analytic propagators 4-68513  
 semiphenomenological nucleon-nucleon potentials 4-59098  
 small angle, high energy hadron scatt., spin effects, total cross section strength 4-78544  
 statistical bootstrap model, density of states 4-86684  
 string model, revival in four dimensions 4-68526  
 supersymmetric four-fermion interactions, Gross-Neveu and Thirring models 4-106487  
 supersymmetric hadrons,  $\bar{t}Q\bar{Q}$  and  $\bar{g}Q\bar{Q}$ , variational model, resonance wave functions 4-106493  
 b-c quark mass differences, potential model problem 4-78543  
 eld elastic scatt., degrees of freedom, pol. effects, rel. approach, review 4-95799  
 hh-X, jet structure and transverse energy 4-86737  
 NN interaction, combined variable phase off-shell scatt. theory 4-73768  
 NN resonance spectrum in potential model 4-73831  
 pN, 22.6-400 GeV/c, in emulsion, mean normalised shower multiplicity, multiparticle prod. mech. 4-90920

**elementary particle interaction models continued**

- $\pi N$  scattering, parity violating asym., meson exchange potential model, Glauber theory 4-102126  
 $pN \rightarrow X$ , leading particle spectrum in bremsstrahlung 4-90839  
 $pp$  elastic scatt. and Chou-Yang model results, 1. in  $10^{12}$  accuracy 4-64018  
 $pp \rightarrow \pi n$ , differential cross sections, forward dip, comparison with NN potential models 4-111466  
 $\pi$  evolution kernel beyond leading order, QCD correction, exclusive process anal. 4-111385  
 $\pi N \rightarrow \pi N$ , isobar model partial wave anal. 4-111470  
 $\pi N$  t-matrix, dynamical theory for off-shell continuation 4-68583  
 $\pi N$ , pseudorapidity, inelasticity and angular distributions 4-78562  
 $\pi N \rightarrow pX$ ,  $\sim 16$  GeV/c, in nuclei, inelastic collisions and fast hadron formation zone 4-102133  
 $\pi^+ p \rightarrow K^+ \Sigma^+$ , threshold-2.35 GeV, energy depend. partial wave anal., SU(3) breaking 4-82971  
 $Q^2$  state production, colour-spin structure, potential and bag models 4-106511  
 $Q\bar{Q}$  hybrid meson spectroscopy, potential model, excited states 4-102100  
 $T(S) \rightarrow T(4S)$  mass splitting, potential models and unitarized quark model tests 4-111384  
 $e^+e^- \rightarrow q\bar{q}X$ , sum over resonances, Thomas-Fermi model, local duality 4-90899  
 $pp \rightarrow d\pi$ , 578 MeV, relativistic calc., formalism, comp. with expt. 4-59093  
 $\pi N \rightarrow \pi N$ , approx chiral dynamical models,  $(\pi, 2\pi)$  anal. comparison 4-95978

**elementary particle interactions**

- see also cosmic ray effects and interactions; elementary particle coupling constants; elementary particle electromagnetic interactions; elementary particle gravitational interactions; elementary particle inclusive interactions; elementary particle large momentum transfer interactions; elementary particle scattering; elementary particle strong interactions; elementary particle weak interactions; hadron-deuteron interactions; hadron-hadron interactions; high-energy cosmic ray interactions; lepton-deuteron interactions; lepton-hadron interactions; lepton-lepton interactions; photon-deuteron interactions; photon-hadron interactions; photon-lepton interactions; photon-photon interactions; polarisation in elementary particle interactions; quantum field theory of interactions; unified field theories; vertex functions  
amplitude structure of off-shell processes 4-86690  
book on nucleus comp., elementary particles and fields 4-82617  
fundamental interactions, unity, summer school, Erice, Italy, (July-Aug., 1981) 4-86102  
neutron properties, interactions, expt. data review 4-63997  
positive muons trapping by metallic materials, vacancies obs. (Japanese) 4-104515  
quadratic constraints in amplitude analysis 4-86691

**elementary particle large momentum transfer interactions**

- see also elementary particle inclusive interactions  
jet production, at very large transverse momentum at  $pp$  collider 4-64024  
large  $p_T$  hadronic reactions, jets, lowest order QCD quark/gluon scatt. 4-90812  
large  $p_T$  jets observed in Chacaltaya gamma ray families 4-106551  
large- $p_T$  single-particle inclusive cross sections and temperatures 4-68598  
meson-nucleon high  $p_T$  exclusive scatt., perturbative QCD appl. 4-90815  
 $p\bar{p} \rightarrow Z^0 X$ , high  $p_T$  studies 4-73776  
 $Q^2$ -dependent parameterizations of pion parton distribution functions 4-111410  
QCD, hadronic wavefunctions, large momentum transfer interactions, deep inelastic lepton scatt. 4-63975  
QCD, large  $p_T$  hadron prod., effective interaction scale, qq partonic sub-processes 4-95762  
QCD, sum rules and exclusive form factors, review 4-82941  
QCD high  $p_T$  physics, Lund Monte Carlo method 4-78566  
review, Z 4-67907  
 $\gamma\gamma \rightarrow$  baryon+antibaryon, high  $p_T$  exclusive scatt., perturbative QCD appl. 4-90815  
 $\gamma p \rightarrow VX$  polarization in large- $p_T$  photoproduction of vector mesons 4-90892  
 $hh \rightarrow$  jets, experimental props., comparison with QCD 4-73774  
 $hh \rightarrow X$ , jet structure and transverse energy 4-86737  
 $pd \rightarrow hX$ , 70 GeV,  $h = \pi^+, K^+, p, \bar{p}$ , invariant cross sections for large  $p_T$  hadron prod. 4-90923  
 $pN$ , 70 GeV, large  $p_T$  hadron pair prod., A-depend. 4-59107  
 $pN \rightarrow$  mesons at large momentum transfer in QCD 4-90933  
 $pN \rightarrow \pi X$ , large  $p_T$ , soft and hard quark collisions in nuclei,  $\pi$  spectrum 4-95821  
 $pp, \sqrt{s} = 540$  GeV, electron and hard jet prod., large missing  $p_T, W^{\pm}$  prod., QCD processes 4-68595  
 $pp \rightarrow 4$  jets, structure at large momentum transfer 4-73784  
 $pp \rightarrow \gamma(\gamma\gamma)$  large  $p_T$  production, QCD predictions 4-78568  
 $pp$  inclusive and semi-inclusive interactions, relation between KNO scaling and momentum distrib. 4-90927  
 $pp \rightarrow$  jets, particle densities at high  $p_T$  4-73785  
 $pp(pp) \rightarrow \gamma X$ , prompt photon hadronprod. at large  $p_T$  in QCD,  $O(\alpha_s^2)$  calc. 4-73779  
 $pp \rightarrow W^{\pm} X$ , high  $p_T$  production, comparison with electroweak theory 4-95832  
 $pp \rightarrow W^{\pm} X$ , high  $p_T$  studies 4-73776  
 $pp \rightarrow X\bar{X} X$ , high  $p_T \pi^0$  production, momentum distributions 4-95834  
 $pp \rightarrow Z X$ , high  $p_T$  production, comparison with electroweak theory 4-95832  
 $pp \rightarrow Z^0(-Z, \nu\bar{\nu})X$ , neutrino species determ. 4-90930  
 $\pi \rightarrow p\gamma(\gamma\gamma)$  large  $p_T$  production, QCD predictions 4-78568

**elementary particle mass**

- see also baryon mass; lepton mass; mass differences; mass formulae; meson mass  
 $\theta$  dependence of quark condensates, U(1) problem, dynamically generated quark mass 4-111388  
bag model, c.m. motion, chiral symm. influence on hadron masses, electroweak parameters 4-106516  
baryogenesis, CP violation at GUT scale, quark mass matrix 4-111336  
big bang supersymmetric relics, neutral gauge/Higgs fermion mass 4-77988  
composite Higgs mass, confining ultracolour group SU(N),  $N \geq 3$  4-106467  
cosmologically acceptable GUT, SUSY breaking, top quark mass 4-111354

**elementary particle mass continued**

- current and constituent quark masses 4-68517  
electroweak SUSY theories; b-lifetime, t-mass and CP violation 4-82918  
Euclidean lattice field theory, Ising model, particle masses, perturbation theory 4-106473  
extended survival hypothesis and fermion masses 4-73670  
fermion and weak boson masses, composite model of quarks and leptons 4-90826  
fermion mass dynamical generation, u-quark/d-quark mass difference 4-111451  
fermion mass generation in Weinberg-Salam model, lepton sector 4-102067  
fermion masses in potential models of chiral symmetry breaking 4-63903  
flavour changing neutral currents and mass generation in Technicolour theories 4-95741  
flavour mixing and masses of leptons and quarks 4-63981  
gauge-boson masses and mixings in left-right-symmetric models 4-73692  
glueball mass in mixed action SU(2) lattice gauge theory 4-111407  
gluino mass generating mechanisms 4-68462  
gluino production signature,  $pp$  collider, lower limit on gluino mass 4-86740  
gluon effective mass in bag model 4-86676  
gravitino and photino masses in supersymmetric cosmology, galaxy form. 4-67845  
gravitino mass generation in locally supersymmetric grand unified theories 4-73703  
hadron mass inequalities, extended form based on lattice QCD 4-95765  
hadron masses in lattice QCD 4-59061  
hadronic mass spectrum, computer calcs. in lattice QCD 4-59060  
hadronic mass spectrum, Monte Carlo computations 4-68557  
Higgs boson, neutral and charged mass upper bounds from radiative corrections 4-102021  
Higgs masses, renormalisation, effective potential in SU(5) to one loop 4-73704  
Higgs particles, lightest mass upper limit in supersymmetric theories 4-86620  
horizontal interactions as the source of family mixing 4-95742  
hydrodynamic theory, t-mass and quark number restrictions,  $e^+e^-$  and  $pp$  comparison 4-86664  
inos rest mass, lower limit from Galaxy halo data 4-82409  
intermediate bosons, masses, weak mixing angle effects 4-68484  
left-right symmetric composite model, fermion mass relation and t-quark mass 4-73730  
light quark mass renormalisation in lattice gauge theory, strong coupling and crossover regions (Chinese) 4-73644  
low mass second neutral vector boson in SO(10) 4-68475  
Majorana masses, two-component fermions 4-106463  
mass gap of lattice O(3) non-linear  $\sigma$ -model with naive and improved actions 4-86553  
minimal SU(5) model with canonical particle content, proton lifetime, fermion masses 4-73694  
mirror particles, N=2 supersymmetric models, low energy constraints 4-102068  
neutrinos, rest mass rel. to cosmological const. and form. of neutrino halos 4-67817  
non-abelian supersymmetric gauge field theory, monopole mass, one-loop quantum corrections 4-111285  
non-minimal gauge kinetic terms, supergravity models, direct gaugino masses 4-111001  
nonscompact sigma model, dynamical mass generation, composite gauge bosons, supergravity theories 4-111299  
particle properties review, masses, decays and lifetimes 4-67885  
particles and interactions, supersymmetric theories, quarks, leptons, W, Z, Winos, Zinos and Higgs 4-73674  
photino mass and  $\gamma\gamma\gamma$  prod. in  $e^+e^-$  annihilation 4-68558  
photino mass generating mechanisms 4-68462  
photon mass, Doppler effect in Klein-Gordon radio 4-95748  
pseudo-Goldstone boson masses in technicolour model with massive techniquarks 4-73691  
QCD, effective quark mass, spontaneous chiral symmetry breaking dynamics 4-82939  
QCD, external source problem, massless quarks, stability and fluctuations 4-90797  
QCD, light quark masses, model independ. determ. 4-111375  
QCD, quark mass gauge-parameter independence, SU(6) model 4-106512  
QCD, supersymmetry breaking, superpotential production by instantons 4-90796  
QCD in Veneziano limit, elfin theory, string model, baryon dynamics 4-59037  
QCD parameters on lattice and in continuum 4-86645  
QCD picture of broken chiral symmetry, neutral PCAC scheme 4-73715  
quark and lepton mass hierarchy in N=1 supergravity GUTs 4-78224  
quark and lepton mass relations in SO(10)  $\times$  U(1)<sub>PM</sub> model 4-59002  
quark mass scale,  $\bar{b}$  calculation, CP violation, Kobayashi-Maskawa mechanism 4-106504  
quark masses, effect on perturbative thrust in QCD 4-86653  
quark-hadron phase transition, QCD sum rules, quark dynamical mass 4-111393  
quarkless QCD, Monte Carlo mass calculations, lattice gauge dynamics 4-68524  
 $S_4$  permutation symmetry, CP nonconservation, rare decays and quark/lepton electric moments 4-86600  
scalar neutrino mass, effect on intermediate boson, tau lepton and kaon decays 4-90744  
spontaneous symm. breaking, induced physical mass, one-loop approx., massless scalar field 4-106480  
squark/gluino mass ratio, lower bound, low energy supergravity 4-86625  
strange quark mass from  $\phi$ -p mass difference 4-59062  
SU<sub>L</sub>(2)  $\times$  SU<sub>R</sub>(3) model, scalar field set addition fermion mass generation, radiative corrections 4-73637  
SU(1,1) supergravity models, gravitino and gaugino masses, Yukawa couplings 4-90473  
SU(2)<sub>L</sub>  $\times$  U(1) gauge theory, permutation group, top quark mass prediction 45 GeV 4-111342  
SU(3) chiral model, mass gap, Monte Carlo method 4-86603  
SU(3) lattice gauge Monte Carlo simulation results 4-58785  
SU(5)  $\otimes$  SU(8) model, fermion masses and neutrino mixing 4-68473  
SU(8) theory of multigenerational grand unification 4-59000  
Susskind fermions, mass term symmetry properties 4-90816  
top quark mass and B meson lifetime 4-63990

**elementary particle mass continued**

- two-loop finite supersymm. SU(5) GUT, top quark mass prediction 155  
GeV 4-106497  
U(1) lattice gauge theory, 2+1 dims., string tension and glueball mass  
4-86586  
unstable photino mass bound from cosmology 4-78505  
vacuum baryon number, chiral bag model, free quarks with position  
dependent mass 4-102093  
W boson mass constraints in SU(2)<sub>L</sub> × SU(2)<sub>R</sub> × U(1)<sub>V</sub> gauge theories  
4-111310  
b-c quark mass differences, potential model problem 4-78543  
B decay, CP violation, mixing angles, t-quark mass, in six-quark model  
4-82959  
b-u quark mass differences, potential model problem 4-78543  
b-c quark mass differences, potential model problem 4-78543  
η and η' radiative decays, light quark mass ratios, vacuum flavour sym-  
metry breaking 4-73761  
K<sub>L</sub> → μ<sup>+</sup> μ<sup>-</sup>, six-quark scheme tests, limits on top-quark mass 4-111389  
pp → WX → tX, top particle weak production, mass ≈ 35 GeV 4-111482  
q<sup>2</sup> states, bag model mass estimates with pairing effect 4-95772  
W<sup>±</sup> Z<sup>0</sup> mass relation, electroweak higher order effects test, leading log  
corrections 4-82929  
Z boson, second mass in SU(2)<sub>L</sub> electroweak gauge theories 4-90779

**elementary particle scattering**

- see also bootstrapping; elementary particle interactions; hadron-deuteron  
scattering; hadron-hadron scattering; lepton-deuteron scattering; lep-  
ton-hadron scattering; lepton-lepton scattering; Mandelstam representa-  
tion; photon-deuteron scattering; photon-hadron scattering; photon-lepton  
scattering; photon-photon scattering; polarisation in elementary particle  
scattering; Pomeronchuk poles and trajectories; quantum field theory of  
elastic scattering; Regge poles and trajectories; relativistic scattering  
theory; S-matrix theory  
elastic three-body to three-body scattering in the hyperspherical formalism  
4-82906  
hadron scattering theory, field quanta exchange 4-59055  
meson spectrum and automodelity in a dual approach (Russian) 4-82952  
multiple scattering during particle diffusion, Padé approximant calcs.  
4-101126  
strongly interacting particles, elastic scatt. at GeV energies, diffraction  
peak width bound 4-73736  
two-body scattering for Schrödinger operators involving zero-range interac-  
tions 4-63567

**elementary particle strong interactions**

- see also composite models of hadrons; duality and dual models; hadron  
classification schemes; peripheral models; quantum field theory of  
strong interactions  
CERN-collider Z<sup>0</sup> anomalous decays, conjectured second strong force on  
heavy quarks 4-106508  
Dirac equation, strong coupling theory for external time-depend. pot., pair  
creation 4-111273  
fragmentation model comparison, hadronic distributions, 3-jet parton  
events 4-111420  
kaonic hydrogen, atomic ground state interaction, model-independent  
formalism 4-96726  
meson Lagrangians, U(3) group, four-quark interaction model 4-95684  
nucleon-nucleon scattering, total cross sections, spin effects, superhigh  
energies, quasipotential approach 4-95816  
quark-gluon model with conformal symmetry 4-82947  
spontaneous SU(2N) breaking, strongly interacting gauge theories,  
fermion representations 4-111334  
spontaneous symm. breaking, induced physical mass, one-loop approx.,  
massless scalar field 4-106480  
T and strong interaction theories (Russian) 4-95780  
W and Z multiple prod. as strong interaction signal for electroweak sym-  
metry breaking 4-95722

**elementary particle symmetry**

- see also chiral symmetries; conservation laws; discrete symmetries;  
dynamical symmetry; helicity (elementary particles); isotopic spin  
(elementary particles); nonlinear symmetries; spontaneous symmetry  
breaking; SU<sub>N</sub> theory; supersymmetry  
Backlund transformations, infinitesimal, gauge symmetries and conserved  
currents 4-82890  
baryon symmetric cosmology, nature depend. on CP violation type, obs.  
tests 4-78012  
compositeness, dynamical models, in QFT, negative metric ghost fields  
4-95776  
conformal spinors and semispinors, book contrib. 4-58976  
cosmic string produced of Yang-Mills symmetry 4-115840  
infinitesimal symmetries of the kth order 4-68460  
Pecci-Quinn, symmetry as flavour symmetry and grand unification  
4-59001  
quantum symmetries in particle interactions 4-95681  
SO(10) × U(1)<sub>PM</sub> model, mixing angles and CP violation 4-59002  
SU(5) model, proton lifetime and weak angle predictions 4-86602  
three-colour quarks and paraquarks, parastatistics and internal symmetries  
4-95755  
triplet code model of leptons and quarks, composite symmetries from  
SO(4) 4-95778  
NN system, symmetry studies 4-59097  
J muonproduction, spin-spin asymmetries, gluon helicity distribution func-  
tion 4-95803

**elementary particle theory**

- see also Bethe-Salpeter equation; complex angular momentum plane;  
current algebra; dispersion relations; electron theory; elementary particle  
interaction models; elementary particle symmetry; Feynman diagrams;  
form factors (elementary particles); group theoretical schemes; helicity  
(elementary particles); isotopic spin (elementary particles); Lee model;  
mass formulae; quantum field theory; S-matrix theory; scaling phe-  
nomena; structure functions; sum rules; vertex functions  
abelian and nonabelian chiral anomalies, higher dimensions, and differen-  
tial geometry 4-90739  
aesthetic field theory, bounded systems, confluence type topological  
particles 4-95652  
amplitude structure of off-shell processes 4-86690  
book, physics of the atom 4-95094  
conference, few body problems, Karlsruhe, Germany (Aug. 1983)  
4-85553  
Dirac-Miyung-Santilli delta function, extension to field theory, hadronic  
isotopic generalisation 4-68377

**elementary particle theory continued**

- energy-momentum operator four vectors, noncanonical commutation rel.,  
hadronic mechanics 4-78545  
fermion masses in potential models of chiral symmetry breaking 4-63903  
Feynman amplitudes, ε → 0 limit, zero-mass particles 4-86537  
field theory in elementary particles, conf., Coral Gables, FL, USA (Jan.  
1982) 4-67869  
hadron-hadron potentials, distortions of resonance couplings 4-106524  
inflationary Universe, quantum creation in elementary particle theories  
4-77990  
Majorana masses, two-component fermions 4-106463  
mirror particle model, astronomical implications 4-63046  
P matrix analysis of nucleon-nucleon scattering 4-59095  
quadratic constraints in amplitude analysis 4-86691  
quantum field theory for elementary particles, renormalisability, review  
4-68433  
quantum relativistic rotators, contraction limits and expt. justification for  
meson resonances 4-86262  
quarkonium states, spectra, decays, mixing in potential and quark models  
4-63976  
radiation zeros in gauge amplitudes, spin dependent null zone 4-68431  
schematic model of mesons based on analytic propagators 4-68513  
second-order nonlinear ODEs, particle-like solns. with arbitrary specified  
no. of nodes, uniqueness 4-86542  
spin statistics theorem in non-relativistic quantum mechanics, SU(2)  
theory 4-86261  
supersymmetry and fundamental interactions in the region of the Fermi  
scale 4-63919  
toponium, charmonium and bottomium properties in Coulomb linear  
potential model, masses 4-95782  
μ, g-factor by cavity resonance theory 4-59081  
**elementary particle weak interactions**  
see also neutral currents; quantum field theory of weak interactions;  
Weinberg model  
book, weak interactions, formulae, results, derivations 4-110814  
book on nucleus comp., elementary particles and fields 4-82617  
boson creation in a subquark lattice 4-73711  
composite W bosons, ρ-parameter in weak interactions 4-73731  
dispersive medium, weak force long range interaction, Zγ mixing  
4-68498  
effective field theory and weak non-leptonic interactions 4-90804  
electro-weak physics in e<sup>+</sup>e<sup>-</sup> interactions 4-90852  
electro-weak theory, introduction 4-59011  
few nucleon systems, EM and weak interactions 4-59155  
flavour changing suppression in technicolour, pseudo-Goldstone bosons,  
Cabibbo mixing 4-102075  
flavour mixing and masses of leptons and quarks 4-63981  
fundamental particle interactions using supersymmetry and N=1 spon-  
taneously broken supergravity 4-73673  
future accelerators for weak interaction research 4-91123  
gluino production signature, pp collider, lower limit on gluino mass  
4-86740  
Higgs model supersymmetry and random sources 4-73678  
left-right symmetric electroweak model, leptonic charged weak interac-  
tions, ν mass, μ decay 4-86615  
lepton conservation in weak interaction processes 4-90756  
Majorana neutrinos, EM props. and neutral current weak interactions  
4-68482  
massive neutrino gas, transport processes 4-90791  
N=1 supergravity and strong CP violation, axion soln. 4-95279  
parity violation in high energy physics 4-95713  
pion decay, rel. to massive neutrinos 4-111442  
quark mass scale, θ calculation, CP violation, Kobayashi-Maskawa  
mechanism 4-106504  
semileptonic interactions, strong gravity and Lorentz non-invariance  
4-90789  
skyrmions and weak interactions, Weinberg-Salam Higgs field, technicol-  
our 4-86614  
standard electroweak model, neutrino masses, lepton triplets, lepton-  
number-violating currents 4-106498  
weak decays, one-gluon corrections in QCD 4-86639  
K<sup>+</sup> → μ<sup>+</sup> ν<sub>μ</sub> longitudinal polarisation meas. 4-63989  
Λ nonleptonic decays, chiral bag model and weak interactions, s- and  
p-wave amplitudes 4-102119  
μ rare and normal decays, standard model, left-right symmetric theories  
4-102120  
pN scattering, parity violation asymm., meson exchange potential model,  
Glauber theory 4-102126  
t-quark, weak prod. and semileptonic decay 4-73728  
T decay, W couplings 4-90893  
<sup>19</sup>F<sup>+</sup> decay, parity nonconservation, weak meson-nucleon coupling con-  
straints 4-68454

**elementary particles**

- see also bosons; charm particles; composite particles; cosmic rays;  
fermions; gamma-rays; hadrons; hypothetical particles; leptons; quantum  
field theory; strange particles  
cosmology, inflationary Universe 4-78015  
cosmology, rel. to particle physics 4-67820  
dark matter in Universe, implications for particle physics 4-67838  
left hand of creation, book 4-77998  
Universe expansion nature, role of gravit. and elementary particles (Rus-  
sian) 4-82581

**elements (chemical)**

- for specific metals and non-metals see appropriate chemical names  
see also elemental origin; element relative abundance; periodic system of  
elements  
electronegativities, density functional theory HF Slater theory 4-96442  
heavy target elements bombarded with protons in energy range 0.5 MeV  
to MeV, K-shell ionisation 4-96507  
light element anal. using energy dispersive X-ray spectra 4-99922  
light elements, thick targets, H<sup>+</sup> bombardment, continuous X-ray spectra  
4-99214  
thick and thin, x-ray fluorescence analysis with monochromatic X-rays  
4-72020  
total rate imaging with X-rays in a scanning electron microscope  
4-71481  
transplutonium research, accomplishments and practical appl. 4-59661  
X-ray photoelectron cross sections of elements in atomic no. range 11 to  
27 4-59682  
X-ray production cross sections for elements by H<sup>+</sup> impact 4-96648

Eliashberg strong-coupling model *see* strong-coupling superconductors

Elinvar  
dispersion-hardened, mag. and physical props. (*Russian*) 4-104800

## ellipsometers

*see also* ellipsometry

all-fibre ellipsometer 4-68266

automatic ellipsometer, high precision device with rotary disc encoder, design and appl. (*Japanese*) 4-86471

interference, based on Fabry-Perot interferometer 4-86468

## ellipsometry

*see also* ellipsometers; polarimetry

apparent optical figure error meas. caused by coating nonuniformity, ellipsometric meas. technique 4-74778

application in measuring refractive indices and layer thickness of semiconductor materials 4-95495

combined reflection and transmission ellipsometry for optical anal. of absorbing double layers. 4-95494

complex reflection coefficient determ. 4-86470

dichroic elliptic birefringent media, Jones matrix 4-107509

Faraday rotators and modulators design 4-79282

gelatin, interphase adsorptional layers, thickness meas. by internal reflection spectroscopy and ellipsometry (*Russian*) 4-104090

glass, thin film, polished, ellipsometric parameters rel. to incidence angle (*Rumanian*) 4-69519

layered structure in situ ellipsometry, inverse problem soln. 4-107513

leached layers on optical glass, type BaK4, spectrophotometric and ellipsometric study 4-73482

magneto-optic thin-film multilayer system ellipsometry 4-85021

metal surface strain determination 4-74972

metallic thin films, optical props. of grain boundaries (*German*) 4-71461

modulation ellipsometry for absolute gradient-index profile meas. 4-86472

multiple angle measurements, optimisation of angle of incidence (*Russian*) 4-95493

photoelastic modulator for polarimetry and ellipsometry 4-11183

PMMA film on InP, thickness determ. by ellipsometry 4-75821

polyacrylonitrile film, electropolymerisation on metal substrate, spectroscopic obs. of film attachment and growth mechanism (*French*) 4-66191

quartz, lattice vibrs., dielec. function, ellipsometry 4-75627

rotating-analyzer ellipsometry, improved meas. method 4-86467

semiconductors, characterisation by spectroscopic ellipsometry 4-99859

semiconductors, conf., Cambridge, MA, USA (Nov. 1983) 4-95025

stratified anisotropic media, 4x4 matrix formalisms for optics 4-87272

thin film compositional anal. using null or fixed wavelength ellipsometry 4-90645

thin film deposition polarisation monitor 4-73485

transparent layers in layer-substrate structs. with indistinct transition region, ellipsometric study 4-86469

window tilt changing in heated vacuum system 4-101900

Al, polycrystalline, surface strain determination using optical ellipsometry 4-74972

AuSn diffusion produced alloys, optical props. 4-80897

BN gate insulators, CVD growth on InP, ellipsometry, XPS, AES, cond. meas. 4-80443

BiSi, differential polarisability, optical reflectance ellipsometry study 4-88796

C amorphous films, ellipsometric, Raman scatt., and XPS studies 4-88418

Cd, Hg<sub>1-x</sub>Te, ellipsometric studies of interband transitions 4-92999

Cu films, Co-covered, optical and elect. props. 4-80693

Fe, passive film form. in borate solns., electrochem. and ellipsometric studies 4-66490

Fe, passive films, in borate solns., electrochemical and ellipsometric studies, film growth 4-89178

GaAs (100) etch pits and cryst. defects, ellipsometry and reflectivity studies 4-84492

GaAs, implanted layers, elec. props., Si<sub>3</sub>N<sub>4</sub> encapsulation effects, ellipsometry study 4-98609

GaAs:Be, ion implanted, annealing behaviour, spectroscopic ellipsometry and Raman scatt. 4-113482

Ge, dielectric function, temp. depend. 4-109111

Hg<sub>1-x</sub>Cd<sub>x</sub>Te, native oxides and interfaces, spectroscopic ellipsometry studies 4-80426

In films on mica substrates, surface plasmon modes and energy loss function 4-85024

MnZn ferrite, (100) surface, mag. surface props., influence of sputter etching 4-88813

MoSi<sub>2</sub>, dielec. function, spectroscopic ellipsometry 4-93041

Ni (111) with surface adsorbed C and CO, thermal decomposition of ethylene 4-113782

NiO films grown by sputter oxidation 4-99658

PbFe<sub>12-x</sub>Ga<sub>x</sub>O<sub>19</sub>, optical props. 4-93086

SbSi, differential polarisability, optical reflectance ellipsometry study 4-88796

SbSeI, differential polarisability, optical reflectance ellipsometry study 4-88796

p-Si cathode surface film thickness and refractive index measurement 4-93649

Si, contamination and near-surface damage caused by reactive ion etching 4-113757

Si, ion implanted, characterisation by Rutherford backscatt. spectrometry and ellipsometry 4-85043

Si, low energy implantation of N<sub>2</sub> and NH<sub>3</sub>, Si<sub>3</sub>N<sub>4</sub> formation study 4-75484

Si, plasma anodic nitridation in N<sub>2</sub>-H<sub>2</sub> system, struct. and optical props. 4-81307

Si:As, ion implantation doses, ellipsometry and spectral reflectance meas. 4-113480

Si:N, ion implanted, optical props. (*Chinese*) 4-114306

Si:P(B), heavy doping effect on band struct. and optical props. 4-92998

Si-SiO<sub>2</sub> structure, transparent layer ellipsometric study in layer-substrate structs. with indistinct transition region 4-86469

Si-SiO<sub>2</sub>-KOH system, ellipsometric and electroreflectance study 4-99091

SiO<sub>2</sub> film, thickness meas. using automatic ellipsometry (*Japanese*) 4-86471

WO<sub>3</sub> polycrystalline electrochromic films; Drude model, ellipsometry meas. as direct evidence 4-88799

YIG:Bi epitaxial films, refr. index and optical absorption spectra at UV to near IR wavelengths 4-104553

ZnIn<sub>2</sub>S<sub>4</sub>, optical const., ellipsometric determ. 4-76414

## ellipsometry continued

Zr, oxide film growth kinetics, interferometry, ellipsometry, X-ray photoelectron spectra obs. 4-66482

ZrZn<sub>2</sub>, optical props. from 0.6 to 3.8 eV 4-84934

elliptical polarisation *see* polarisation

## elongation

*see also* deformation; thermal expansion

copolyester of lactic and glycolic acid, strain induced crystallisation, optical and X-ray scatt. obs. 4-85186

ferrous laminated composites, steel/Fe, superplasticity 4-81235

materials strain, plastic cracking (*Polish*) 4-84341

measurement apparatus for long optical fibre 4-74734

metals, anisotropic hardening 3D model, sheet metal formability analysis 4-66348

model polyisobutylene networks, strain induced crystallisation 4-75324

optical fibres, Al, hermetically coated, transmission loss reduction 4-97112

PET film, amorphous, extrusion drawn, irreversible spontaneous elongation 4-109440

polyamide 6-6 rubber blends, morphology and mech. props. 4-93344

polycarbonate blends with ABS and SAN, tensile and impact tests, energy absorb. 4-66389

polyethylene, high density, cryst. axes orientation and state of order during elongation FTIR study 4-99111

polyethylene melt, low density, shear and elongational flow data, BKZ model 4-69803

polymer, elongational flow processes modelling, viscometric methods (*German*) 4-71707

polymer solution, dilute, mass transfer to a cylindrical wire 4-108093

polymeric films, biaxial stretching instability, appl. of Swift criterion (*French*) 4-92581

polymers, strength, temp. depend. (*Russian*) 4-104806

polystyrenes of narrow mol. wt. distrib., blending, creep flow and recovery in elongation 4-97454

polysulphones, electron irradi., tensile and viscoelastic props. 4-61981

polyurethane elastomer, MDI/diol-based, hard-segment polymorphism 4-65195

PVC blends, photodegradation by UV irradi., mech. props. 4-81450

steel, austenitic, neutron irradi., high temp. deform. behaviour (*German*) 4-81262

steel, austenitic stainless, cold worked and irradiated, correl. of fracture toughness with tensile props. 4-93376

steel, austenitic stainless, proton irradiation creep of thin foil specimens, thickness effects on mech. props. 4-103820

steel, austenitic stainless, radiation damage, fusion reactor candidate material 4-98140

steel, austenitic stainless, SCC in molten salts 4-71758

steel, austenitic stainless, TiC precipitation, influence on creep rupture strength, ductility and He embrittlement 4-99388

steel, Co eutectoid, mech. props. 4-114629

steel, Cr, m-d superplasticity relation (*Chinese*) 4-81237

steel, dual-phase, Mn-Si, stabilisation of retained austenite, effect on mech. props. (*Korean*) 4-104818

steel, effect on wear resist. in abrasive friction 4-93425

steel, eutectoid, mech. props., effect of Si additions 4-93365

steel, high Cr, impurity redistrib. and mech. props. during 475°C ageing (*Russian*) 4-93317

steel, HSLA, tensile strength and ductility, dependence on microstruct. 4-114603

steel, low C, dual-phase, continuously annealed, effect of prior cold rolling 4-66350

steel, maraging, tensile strength and ductility, dependence on microstruct. 4-114603

steel, martensitic, low C, controlled rolled and quenched, strengthening effects 4-99393

steel, martensitic stainless, HT-9, thermal creep deform., constitutive design eqns. 4-93338

steel, mech. props., effect of laser quenching 4-66356

steel, microduplex stainless, rapidly solidified, superplastic response rel. to ferrite-austenite content 4-99433

steel, Mn, 13 to 19 wt.%, sinter-forged, mech. props. 4-81283

steel, Mn, 13 wt.%, prod. by powder metallurgy method 4-81169

steel, normalised 04G2B, Y additions effects on mech. props. 4-93390

steels, austenitic stainless and high Mn austenitic, neutron irradiated, comparison of tensile props. 4-103807

submarine optical cable, anal. 4-74735

superplastic materials, elongation, grain growth and cavitation effects 4-71711

Al-Cu-Li-Mn-Cd, Al 2020, fatigue crack growth behaviour 4-71728

Al-Cu-Si, Al 2014, punch-stretching behaviour, 250 to 500°C 4-76817

Al-Cu-Si, Al 2014, tensile props., 250 to 500°C 4-76816

Al-glass composite, produced by powder metallurgy route, mech. props. 4-66275

Al-Mg, 5083 alloy plates, mech. props. and stress corrosion cracking, anisotropy effects (*Japanese*) 4-66496

Co-Nb eutectic alloy, comp., microstruct. and tensile strength 4-66320

CsH<sub>2</sub>(SeO<sub>2</sub>)<sub>2</sub>, antiferroelectric, elastic compliance const., anomalies at transition point 4-108500

Cu-Al system, dual-phase, deform. behaviour 4-61993

Cu-Al-Zn system, high damping  $\beta$  alloys, effect of aging in martensite condition on mech. props. 4-114588

Cu-Ni (25 wt.%), sintered and pressed coinage alloy, tensile props., SEM and X-ray obs. 4-71697

Cu-Ni-Sn spinodal alloys, deformation behaviour, ageing treatment effects 4-114628

Fe-Al-Si (20.5 at.%), DO<sub>3</sub>-ordered alloys, tensile behaviour 4-93337

Fe-C, induced mag. moment by tetragonally elongated lattice expansion, magnetisation, Mossbauer spectra meas. 4-98930

Fe-N, induced mag. moment by tetragonally elongated lattice expansion, magnetisation, Mossbauer spectra meas. 4-98930

Fe-Ni-C, induced mag. moment by tetragonally elongated lattice expansion, magnetisation, Mossbauer spectra meas. 4-98930

Fe-Ni-Cr ferritic alloy, soft mag. props. and mech. strength 4-61555

Fe-Si (3 wt.%), electrical engineering steel, anisotropic, mag. losses, annealing and elongation effects (*Russian*) 4-104459

(Fe<sub>2</sub>Co<sub>7</sub>)<sub>8</sub>, v. tensile deforms, 20-1000°C, fracture mode and ductility rel. to order-disorder transform. 4-66427

Fe<sub>3</sub>Si, DO<sub>3</sub>-ordered alloys, tensile behaviour 4-93337

GaAs, plastic deforms, yield stress, photoluminescence, effect of impurity-vacancy complexes 4-70261

## emagitation continued

- Mg-Li-Al-Mn and Mg-Li-Al-Zn-Mn-Ce system alloys, mech. props. and corrosion resist. 4-93455  
 Mo, high temp. neutron irradi., annealing, void form., mech. props. 4-108456  
 Mo, sintered sheet, tensile props., improvement by reducing O impurity levels 4-89132  
 Mo-base alloys, welded joints, long-term strength characs. effect of alloying with N 4-109513  
 Nb, mech. props. at low temp., Ti effect 4-93391  
 Nb single crystal, neutron and electron irradi., dislocation sweeping of defects 4-103810  
 Ni O embrittlement, prevention and reversal 4-71733  
 Ni-B alloys, CVD deposited, microstruct. and mech. props. 4-71581  
 Ni<sub>3</sub>Cr, Ni<sub>3</sub>Cr, high temp. deform., effect of ordering 4-93358  
 Pb<sub>80</sub>Bi<sub>20</sub> superconducting filament, high transition temp., produced by glass-coated melt spinning 4-80712  
 Sn, plastic deformation and elongation, slip systems (*Russian*) 4-109467  
 Ti, plastic flow and fracture at low temps. 4-76803  
 Ti-Al-V (6, 4 wt.%), tensile props. and fracture mode, temp. depend. 4-109488  
 Ti<sub>2</sub>O<sub>3</sub>V<sub>2</sub>O<sub>5</sub>, cryst. struct., X-ray diff. study 4-60892  
 U-Nb (6 wt.%), microstruct., mech. props. and corrosion, effect of quench rate 4-114558  
 V, neutron irradi., hardness, tensile props. 4-103809  
 V-Cr-Ti(Fe-Zr), mech. props. rel. to O contamination, fusion appls. 4-109499  
 $\beta$ -VH<sub>0.5</sub>(D<sub>0.5</sub>), stabilisation mechanism, elastic energy formulation 4-108303  
 Zn sheet, strain-rate sensitivity 4-99438

## m. waves see electromagnetic waves

## embrittlement

- see also ductile-brittle transition; hydrogen embrittlement; liquid metal embrittlement  
 alloys, amorphous, stress relief annealing, mag. props. 4-104797  
 Borsselle reactor vessel, neutron embrittlement Charpy tests 4-96132  
 environmentally-induced embrittlement and pitting, possible role of surface stress 4-62086  
 fusion reactor materials, conf., Albuquerque, NM, USA (Sept. 1983) 4-90290  
 interfacial and surface microchemistry, book contrib. 4-109421  
 intergranular corrosion of steels and alloys, book 4-95084  
 intergranular embrittlement, impurity interactions within grain boundary, MO calcs. 4-80147  
 metal, book contrib. 4-108508  
 nuclear reactor materials neutron irradiation effects 4-103806  
 nuclear reactor vessels, brittle fracture resistance, calc. 4-96143  
 spallation neutron source materials, He embrittlement, thermal fatigue, irradi. creep 4-108464  
 steel, alloy, type 15Kh2NMFA, radiation embrittlement and temper brittleness (*Russian*) 4-66407  
 steel, austenitic stainless, irradiation, fracture toughness, SEM obs. 4-104836  
 steel, austenitic stainless, microstructural design for improved He embrittlement resist. under HFIR irradi. 4-103790  
 steel, austenitic stainless, TiC precipitation, influence on creep rupture strength, ductility and He embrittlement 4-99388  
 steel, austenitic stainless, tubular specimens, endurance and long-term ductility, effect of prior irradi. 4-92243  
 steel, C-Mn, grain boundary segregation of Cu, Sb and Sn at 900°C 4-93300  
 steel, Cr-Mo, temper-embrittled, effects of grain size and hardness 4-99554  
 steel, Cr-Mo-V-W, ferritic, impact props., effect of specimen size and Ni content 4-104848  
 steel, creep damage and embrittlement at high temp., US meas. (*French*) 4-61973  
 steel, Cu-bearing, conf., Luxembourg (May 1983) 4-86106  
 steel, Cu-bearing, hot shortness in controlled rolling process 4-89105  
 steel, ferritic stainless, irradi. embrittlement 4-93392  
 steel, ferritic transformable, specific heat capacity (*German*) 4-80252  
 steel, low alloy, Cr-Mo-V, high temp. low cycle fatigue rel. to softening and embrittlement (*Japanese*) 4-99519  
 steel, low alloy, reversible temper embrittlement, role of microstructure, scanning Auger microscopy study 4-81286  
 steel, low alloy cast, temper embrittlement, microstruct. obs. by Auger electron spectroscopy (*Chinese*) 4-71725  
 steel, Ni-Cr-Mo-V, creep rupture and service properties improvement (*German*) 4-76862  
 steel, Ni-Cr-Mo-V, fracture behaviour effect of S content 4-99601  
 steel, Ni-Mo, martensitic A533B pressure vessel, tempered, brittle fracture and fatigue crack growth, segregation effects, Auger obs. 4-66400  
 steel, pressure vessels, radiation embrittlement and annealing 4-11626  
 steel, stainless, ferritic-austenitic, embrittlement, mag. inspection 4-99704  
 steel, steam turbine casing and rotor, mech. props. rel. to service life (*Japanese*) 4-89119  
 steel, water-water power reactor vessel material, brittle fracture resist. and radiation embrittlement 4-96142  
 topaz, deformation expts. indicating embrittlement by water 4-94101  
 Al-Mg solid solutions, ductility loss at high temps. 4-104857  
 Al-Zn-Mg single crystals, environmentally-assisted cracking 4-71762  
 (Fe,Ni)V, ordered alloy, irradi. in HFIR, microstruct. and bend ductility 4-108454  
 (Fe,Ni)<sub>3</sub>V alloy, long-range ordered, strain rate and ageing effect on mech. props. 4-109501  
 Fe, grain boundary with impurity segregation, atomic and electronic 'structs., 4-113463  
 Fe-base metallic glasses, thermal embrittlement model 4-89098  
 Fe-P, segregated grain boundaries crack propag. mol. dynamics calcs. 4-114663  
 Fe-P-W(Mo)(Mn), grain boundary embrittlement, impurity-induced, influence of alloying elements 4-114654  
 Fe<sub>40</sub>Ni<sub>60</sub>B<sub>20</sub>, metallic glass, melt surface tension and embrittlement, effects of elemental additions and superheat 4-65184  
 Mo, neutron irradiation embrittlement, influence of irradi. temp. and heat treatment 4-108453  
 Mo-Ti-Zr, TZM, neutron irradiation embrittlement, influence of irradi. temp. and heat treatment 4-108453  
 Nb alloy, plastic deform. with subsequent nitriding effect on mech. props. 4-114713

## embrittlement continued

- Ni, high temperature electron induced embrittlement 4-108448  
 Ni O embrittlement, prevention and reversal 4-71733  
 Ti-Al-Mo-Sn-Si, TC<sub>9</sub>, microstruct. change during thermal exposure at 500°C (*Chinese*) 4-61959  
 W, grain boundaries of twist misorientation about (100), direct meas. of work of fracture 4-98116  
 W-Ni-Fe(Cu), liq. phase sintered, interphase boundary precip. 4-99364

## e.m.c. see electromagnetic compatibility

## emergency power supply

- Pb/acid batteries for UPS and telephone system back-up power, acid ageing behaviour of polycarbonates 4-93612  
 Pb/acid sealed recombination cells for standby power 4-93610

## e.m.f. see electric potential

## emission nebulae see nebulae

## emission spectra see spectra

## emissivity

- see also brightness  
 black body, integrated emissivity evaluation 4-60251  
 blackbody radiation from cubes and spheres, solidification of microspheres appl. 4-107998  
 clear sky emissivity 4-62937  
 glass, hard Chinese-built no.95, IR radiation props. (*Chinese*) 4-107771  
 IR thermometry for low emissivity metals, Al hot rolling control appl. 4-82796  
 materials for radiative cooling to low temperatures 4-112683  
 oxide-metal-oxide low-emittance films on glass, industrial realisation 4-112531  
 radiation pyrometry techniques, comparison of alternatives 4-73508  
 solar absorbing surfaces, spectrally selective, charact. parameters, meas. techniques 4-77145  
 solar narrowband absorbers, highly selective, combined with fluoresc. concentrators 4-114953  
 steel, IR emission of overloaded metals during fatigue process (*Chinese*) 4-114636  
 Al film, black Zn-coated, solar collector coatings, optimisation and microstruct. anal. 4-62397  
 a-C:H, low emittance coatings for high temperature solar collectors 4-114950  
 Co<sub>2</sub>O<sub>3</sub>-based selective surfaces prep. by dip-coating process for solar absorber-convertors 4-72172  
 Cr, black, electrodeposits for heliothermic conversion (*French*) 4-77143  
 Cr obliquely deposited films, spectral and angular selectivity 4-112535  
 CrN, DC reactively sputtered layers with surface roughness, as selective absorbers in solar collectors 4-77147  
 Ge obliquely deposited films, spectral and angular selectivity 4-112535  
 MoO<sub>3</sub>, black solar selective absorbers, thermal stability and performance 4-114952  
 Ni-P thin film, selective absorber, for photothermal conversion of solar radiation 4-81589  
 Si, CVD growth, solid state phase transformations 4-70598  
 n-Si inversion layers, two-dimensional plasmons and far infrared emission 4-104140  
 Si, laser heating, thermal radiation, pyrometric temp. measurements 4-92230  
 a-Si<sub>1-x</sub>C<sub>x</sub>-H, low emittance coatings for high temperature solar collectors 4-114950  
 W, spectral emissivity, analytic expressions for 340 nm to 2.6  $\mu$ m spectral region 4-60127

## emitters see television camera tubes

## EMP see electromagnetic compatibility; electromagnetic interference; radiofrequency interference

## employees see personnel

## employment

- see also personnel  
 science and engineering graduate utilisation in energy-related employment 4-66647

## emulsions

- see also nuclear track emulsions; photographic emulsions  
 carbene derived radical pairs in microemulsions, behaviour, mag. field effects, triplet multiplicity 4-62164  
 critical microemulsion system, apparent field, variable, exptl. evidence 4-75646  
 destruction under action of elec. field and magnetodynamic layer of granules (*Russian*) 4-71991  
 droplet sizes in microemulsions 4-77034  
 ferroemulsion, hydrodynamics, effective viscosity and shear flow 4-109693  
 heavy crude oil-in-water emulsions, rheological characteristics 4-60530  
 large particle bubbling fluidised beds, heat transfer 4-113004  
 Micelles and microemulsions, attractive interactions, small angle neutron scatt. 4-105032  
 microemulsion, three-component, struct. in critical region, small-angle neutron scatt. obs. 4-66620  
 microemulsions, percolation and critical points 4-114842  
 microemulsions extractant anions, FTIR studies on hydration 4-99848  
 oil in water microemulsions, fluoresc. probe study 4-89342  
 oil-water microemulsion model 4-99849  
 perfluorotributylamine, FC-43 emulsion blood substitute, spin relax., spin probe and O effect 4-69111  
 shear viscous bubble and drop deform. 4-91835  
 sodium di-2-ethylsuccinate-D<sub>2</sub>O-decane microemulsions, struct., small angle neutron scatt. 4-114847  
 supermolecular liquid-crystalline structures in solutions of amphiphilic molecules, review 4-98010  
 vinylidene fluoride-3-oxaperfluorohexene-1 copolymers, mol. mass distrib. (*Russian*) 4-85309  
 viscosity meas. of gas-oil emulsions, semiautomatic unit based on capillary principle (*German*) 4-103442  
 water-oil microemulsions, DSC, permitt., dielec. loss tangent meas. 4-89343  
 Winsor concentrated microemulsions, X-ray scatt. study 4-79922  
 AgBr, emulsion microcrystals, spectral transmittance reflectance and absorpt. coeff. 4-104556

emulsions (nuclear track) *see nuclear track emulsions*

emulsoids *see emulsions*

## encapsulation

*see also packaging*

- electronics ageing mechanisms, neutron and  $\gamma$ -ray effects, nuclear power plant instrumentation 4-59363
- microparticle feed development for marine suspension feeders 4-114849
- organic compounds, electron irradiation, damage in electron microscope, encapsulation effects 4-79912
- polyacetylene-1,2, stability after encapsulation, microwave meas. 4-109112
- Sylgard 184 containing hollow microspherical fillers, high temp. elec. cond. and thermal decomp. 4-92710
- $Al_0.3Ga_{0.7}As$ , encapsulated with  $Si_3N_4$  films, disorder-activated modes, Raman spectra 4-80916
- GaAs, encapsulated annealing in  $AsH_3$ , surface protection 4-88378
- GaAs, implanted layers, elec. props.,  $Si_3N_4$  encapsulation effects 4-98609
- GaAs:Si, Si diffusion using rapid thermal processing, encapsulant effects 4-65464
- Ge island films on insulator, zone melting recrystn. with  $SiO_2$  capping layers 4-93212
- Ge single cryst. film growth on  $SiO_2$  by laterally seeded heteroepitaxy 4-93234
- Si thick film on insulator, zone-melting recrystallisation 4-66225
- $Si_3N_4$  film deposition by plasma-enhanced CVD, appl. to GaAs LSI 4-71569

## encoding

*see also codes; decoding*

- Anger camera, fast parallel encoding scheme 4-59556
- binary Fourier transform holograms, quantisation and phase encoding errors reduction 4-107557
- cardiogram signal compression with AZTEC algorithm (*Chinese*) 4-105355
- computer-generated holography, performance and appls., conf., San Diego, CA, USA (Aug. 1983) 4-106105
- holography, computer generated and longwave, Lissajous coding 4-107559
- image reconstruction technique from limited sampled data, use of a priori knowledge 4-59994
- image vector quantization with perceptually-based cell classifier 4-102900
- intensity-to-spatial frequency transformations in optical signal processing 4-79045
- multifaceted volume hologram based information encoding systems 4-74462
- optical logical processing in parallel with theta modulation 4-112349
- optics in entertainment, conf., Los Angeles, CA, USA (Jan. 1984) 4-110802
- $\pi$ -phase filtering of zero-freq. spectral component and pseudocolour encoding, contrast reversal condition 4-107540
- photograph enhancement and deblurring, image processing system 4-91413
- psychoacoustic computational models, use in speech processing, coding and objective performance evaluation 4-97217
- real-time density encoder with three primary colours 4-79063
- scintillator hodoscopic systems, optical data encoding 4-59573
- seismic signal compression using adaptive differential pulse code modulation 4-72714
- space-variant processing, 2D white light, for separable point spread function, colour encoding 4-74436
- spatial frequency pseudocolour encoding using coarse gratings 4-74431
- spatial frequency pseudocolour encoding with interference filters 4-59998
- spatial frequency pseudocolouring by interference, texture appl. 4-74432
- speech recognition system, LPC anal. and peripheral auditory system model, comparison 4-105257
- speech signals, digital coding (*Chinese*) 4-60223
- three-dimensional projection with circular polarizers 4-112344
- two-dimensional image processing by one-dimensional filtering of projection data 4-79036
- underwater images compression for transmission on low bit rate acoustic channel 4-103079
- white-light density pseudocolour encoding with three primary colours 4-59997
- Na vapour, CW off-reson. rings and CW on-reson. enhancement 4-102973

end-fire antennas *see antenna arrays*

## ENDOR

- acetone cation,  $\gamma$ -irrad.,  $^{13}C$  ESR and ENDOR investig. 4-69114
- l-asparagine- $H_2O$ , single cryst., X-irrad., free radical ESR-ENDOR study 4-76253
- benzil in bibenzyl, cryst. forces, conformation, ENDOR study 4-88745
- p-benzosemiquinone anion radical, powder ENDOR anal. 4-74275
- caffeine hydrochloride dihydrate, X-ray irrad., free radical ENDOR study 4-112214
- coil, for RF generation 4-63763
- g-tensors and A-tensors, anisotropic and non-coincident, least squares fitting 4-61607
- 6-hydroxypyrido[1,2-c:2',1'-c]-imidazolium iodide radical cation, second order effects, ENDOR, ESR triple reson. 4-107375
- metmyoglobin, N hyperfine interaction ENDOR, EHT calcs. 4-59644
- P700<sup>+</sup> in spinach chloroplasts, ENDOR evidence supporting a monomeric nature 4-77192
- paramagnet, polycrystalline ENDOR patterns, g and hyperfine tensors of arbitrary symm. and relative orientation 4-98979
- paramagnetic complexes, NMR shift ENDOR spectra 4-71210
- phenoxyls, low temp. conform., ESR, ENDOR, and TRIPLE reson. obs. 4-107370
- photosynthetic bacterial reaction centres, struct. of primary donor cation radical 4-77183
- cis-polyacetylene:ReF<sub>6</sub> ENDOR obs. 4-74276
- trans-polyacetylene, ENDOR obs. 4-74276
- polyacetylene, soliton wave-functions, ENDOR study 4-75878
- semiquinone anion radicals, hyperfine tensors, methyl group interaction, ENDOR 4-64520
- spectroscopy, controlled return flux three loop, two-gap microwave resonators 4-86454
- $Al_2O_3$ :Cr<sup>3+</sup>, Cr<sup>3+</sup> electron spin resonance line ENDOR and saturation optical detect. 4-84873
- CHOR radical, in X-irrad. methyl  $\beta$ -D-galactopyranoside, geometry, ESR/ENDOR obs. 4-102712

## ENDOR continued

- CaF<sub>2</sub>:Er<sup>3+</sup>, transferred hyperfine interaction parameters, ENDOR 4-84872
- CaF<sub>2</sub>:Tm<sup>2+</sup>, Tm<sup>2+</sup> electron spin resonance line ENDOR and saturation optical detect. 4-84873
- Cu II complexes, in Ni II host lattice and toluene-d<sub>3</sub> solns., <sup>1</sup>H and <sup>31</sup>P ENDOR spectra 4-91292
- GaAs, deep impurity levels, ENDOR and ESR spectra 4-84594
- GaP, deep impurity levels, ENDOR and ESR spectra 4-84594
- Pb<sub>2</sub>Ge<sub>2</sub>O<sub>7</sub>:Gd<sup>3+</sup>, superhyperfine interaction, ESR and ENDOR studies 4-114159
- Si, deep impurity levels, ENDOR and ESR spectra 4-84594
- a-Si:H film, hyperfine interaction, ENDOR study 4-65881
- energies, molecular dissociation *see molecular dissociation energies*
- energy, binding *see binding energy*
- energy, lattice *see lattice energy*
- energy, surface *see surface energy*
- energy bands *see band structure*
- energy bands, electron *see band structure*
- energy control *see power control*
- energy conversion, direct *see direct energy conversion*
- energy dispersive X-ray analysis *see X-ray chemical analysis*
- energy gap
  - see also superconducting energy gap*
  - amorphous semiconductor, physico-chemical props., review 4-93038
  - amorphous solids, energy gap and electronic density of states calcs. 4-88485
  - $\alpha$ -B<sub>2</sub>, band struct., energy gaps, bonding, cluster approx. 4-70646
  - band gap width, rel. to short-range environment of S atom 4-80493
  - binary cpds., energy gaps, polarisation and partial metallic valence 4-103697
  - conjugated macrocyclic ligands, closed-shell cryst. orbital calcs. on columnar stacks 4-74160
  - DH laser, heterojunction interface energy gap grade width influence on charact. temp. (*Chinese*) 4-112432
  - double heterostructures, electron-hole plasma heating 4-65734
  - glassy semiconductors, electronic transitions in mobility gap 4-61275
  - high speed semiconductor devices, abrupt and graded gap structures anal. 4-76026
  - II-VI semiconductors, crystal growth, optical and surface props. (*Japanese*) 4-88957
  - III-V semiconductors, nonlinear absorpt., coherent radiation-exciton interaction model 4-99078
  - inert gas, solids, conduction band states, excitons, photoemission 4-85057
  - insulators, exchange-correlation potential determ. 4-61279
  - ionic crystals, rocksalt struct., homopolar and heteropolar energy gaps 4-92134
  - MOS solar cells, perform. calcs. at various temps. 4-72117
  - multibandgap photovoltaic receiver using back surface reflectors 4-66726
  - narrow band gap semicond., magnetoabsorption of weak light wave in presence of strong wave 4-84951
  - p-n abrupt junctions recombination current in space charge layers 4-65732
  - p-n junctions, tunnel capture influence on impurity-level recombination of charge carriers (*Russian*) 4-70923
  - Pariser-Parr-Pople and linear Hubbard models, valence bond theory 4-78273
  - piezoelectric semiconductors, transverse acoustoelectric effect charact. (*Russian*) 4-70878
  - polyacrylonitrile, pyrolysed, optical and IR absorpt. spectra, TGA 4-92106
  - polydiacetylene, conducting polymer, synthesis by  $\gamma$ -ray polymerisation 4-75958
  - quantum chains, leading order corrections to the energy gap 4-86345
  - rare earth sesquisulphides, energy band struct., X-ray spectral anal. 4-80492
  - sapphire, single cryst., high temp. electronic struct., VUV reflectance spectra 4-84556
  - semiconductor, elec. props., appl. of two stage nonmagnetic high press. equipment (*Chinese*) 4-90607
  - semiconductor, lightly doped compensated, Coulomb gaps and Hubbard gaps 4-80542
  - semiconductor thin films, dielec., function calc., screening effect 4-70693
  - semiconductors, absorptive optical bistability due to band gap shrinkage 4-69482
  - semiconductors, Auger and impact ionisation processes, calc. of commonly neglected terms in matrix element 4-99237
  - semiconductors, band gap related oxidation-in electron stimulated adsorption 4-66150
  - semiconductors, exchange-correlation potential determ. 4-61279
  - semiconductors, excited quasistationary states relax. as source of exoelectron emission 4-99290
  - semiconductors, thermal contraction of energy gap effect on optical breakdown 4-80910
  - solar cells, amorphous/crystalline tandem structs., conversion efficiency determ. using computer anal. 4-72116
  - SOS, intense-field effects rel. to order of multiphoton processes 4-79225
  - solid heteroepitaxial film, surface photovoltage characterisation 4-80697
  - space charge limited currents, fundamental assumptions and results of theory (*Polish*) 4-65964
  - superconductors, US attenuation, electron drag on dislocations, energy gap meas. 4-92862
  - ternary semiconductors, relationship between physicochemical and electro-physical props. 4-108856
  - thiones, aromatic, radiationless decay of second excited singlet states, energy gap law verification 4-78892
  - two-dimensional strip, quantized Hall cond. and edge states 4-92591
  - Ag<sub>2</sub>S films on Ag, spectrally selective props., for solar absorber convertors 4-99211
  - Al, band struct., pseudopotential coeffs., deform. potentials, piezoreflectance meas. 4-98514
  - Al<sub>0.5</sub>Ga<sub>0.5</sub>As layer waveguides, light absorpt. 4-103011
  - AlGaInPAs lattice matched to GaAs, LPE growth, photolum. obs. 4-70581
  - Al<sub>1-x</sub>In<sub>x</sub>As, nominally undoped, MBE growth and charact. 4-98472
  - As<sub>2</sub>S<sub>3</sub> chalcogenide glass films, photostruct. changes 4-104560
  - AsSI, glassy, optical props. meas. (*Russian*) 4-71340
  - AsSe chalcogenide glass films, photostruct. changes 4-104560

## energy gap continued

- As<sub>2</sub>Se<sub>3</sub>:Ni(Cu)(Fe)(Bi)(Sn), extrinsic cond. and optical const. meas. 4-75971
- As<sub>2</sub>Se<sub>3</sub>:Te film, transient photocurrent study 4-113991
- Au-Ge-Sn structure, capacitance-voltage meas. at liq. N<sub>2</sub> temp. 4-84707
- B<sub>12</sub>As<sub>2</sub>, band struct., energy gaps, bonding, cluster approx. 4-70646
- BN band struct., APW calc. method appl. 4-92608
- BN RF sputter deposited films, struct. and optical props. rel. to sputtering conditions 4-88415
- B<sub>12</sub>P<sub>2</sub>, band struct., energy gaps, bonding, cluster approx. 4-70646
- BaPb<sub>0.7</sub>Bi<sub>0.3</sub>O<sub>3</sub> supercond. thin films for highly sensitive optical detector fabrication 4-82825
- Bas(Se)(Te), band-overlap metallisation, self-consistent augmented-spherical-wave calc. 4-80499
- n-BaTiO<sub>3</sub> electrolyte redox systems, photoelectrochemistry 4-72124
- BaTiO<sub>3</sub>, oxygen-octahedral ferroelectrics, two-photon spectroscopy study 4-114300
- BeO, structural and electronic props., phase transform., pseudopotential calcs. 4-70100
- Bi-Se-Te system, struct. and band gap, X-ray and IR absorpt. obs. 4-104124
- Bi<sub>2</sub>CdS<sub>4</sub> film, spray pyrolysis deposited, substrate temp. effect on elec. and opt. props. 4-70962
- Bi<sub>2</sub>CdS<sub>4</sub> films, spray pyrolysis deposition, elec. and optical props. 4-76669
- C:H amorphous film, H<sub>2</sub> gas reactive RF sputtering prep. on low temp. substrates 4-76673
- Cd<sub>2</sub>Hg<sub>1-x</sub>Te graded energy-gap structures, interf. photoelectromag. effect 4-113992
- CdS amorphous films, optical absorption coeff. and gap state density 4-66088
- CdS film, deposited by hot wall technique, characterisation of doped and undoped films 4-114405
- n-CdS/electrolyte interface, photoelectrochem. characterisation 4-84689
- n-CdS<sub>0.9</sub>Se<sub>0.1</sub> electrode, liquid junction photoelectrochemical cells, props. (Chinese) 4-81565
- CdSe, hot excitons and electron-hole pairs and Raman spectra 4-114285
- CdSe<sub>1-x</sub>Te<sub>x</sub>, hetero-photoconductors, spectral characts. (Russian) 4-66692
- CdTe thin layers, crystal and energy structures for photoelectric transducers 4-98298
- Cd<sub>2</sub>Zn<sub>1-x</sub>Mn<sub>x</sub>Te, lattice parameter and energy gap 4-75847
- Cr and its alloys, SDW, kink lattice struct. 4-104480
- Cs selenogallates, cryst. struct. and abnormal linear oligomeric anions 4-92185
- CsCl crystals., ionic and covalent energy gaps 4-75852
- (Cu<sub>1-x</sub>Ag<sub>x</sub>)(Ga<sub>1-x</sub>In<sub>x</sub>)(Se<sub>1-x</sub>Te<sub>x</sub>), lattice parameter and energy gap 4-75847
- CuIn(S<sub>2</sub>Se<sub>1-x</sub>Te<sub>x</sub>)<sub>2</sub>, solid solubility, optical energy gap values 4-70074
- CuInSe<sub>2</sub>, single cryst. electrode, solar cell performance, surface chemistry 4-66696
- CuInSe<sub>2</sub>, surface photocond. and positive cryst. splitting 4-65649
- Cu<sub>2</sub>P<sub>7</sub>, preparation and cryst. struct. 4-80008
- Cu<sub>2</sub>PS<sub>3</sub>, photointercalation and optical information storage 4-79058
- EuErS<sub>4</sub>, band gap width, rel. to short-range environment of S atom 4-80493
- EuGdS<sub>4</sub>, band gap width, rel. to short-range environment of S atom 4-80493
- EuHoS<sub>4</sub>, band gap width, rel. to short-range environment of S atom 4-80493
- EuLaS<sub>4</sub>, band gap width, rel. to short-range environment of S atom 4-80493
- FeAs<sub>2</sub> films, organo-metal CVD growth from (CO)<sub>2</sub>Fe+AsH<sub>3</sub> on GaAs, optical gap and IR transmission 4-61868
- Ga-Al-As, luminescence lineshapes of electron-hole plasma 4-109242
- Ga<sub>1-x</sub>Al<sub>x</sub>As, carrier transport under impurity radiative recombination conditions 4-104211
- GaAs, k,p interaction and effective mass, band gap depend. 4-113850
- GaAs, p-n junctions, spectral distrib. of avalanche breakdown radiation (Russian) 4-98715
- GaAs p-n-p-n superlattices, LPE growth 4-80665
- GaAs/AlGaAs MQW heterostructure current-injection lasers, carrier-induced energy-gap shrinkage 4-112423
- GaAs-AlGa<sub>1-x</sub>As quantum wells, energy-gap discontinuities and effective masses 4-92623
- (GaAs)<sub>1-x</sub>Ge<sub>2x</sub>, bond and struct. models 4-108772
- GaCrSe<sub>3</sub>, antiferromag. semicond., mag. susceptibility, cond., EPR, IR reflection spectrum, Neel temp., energy gap meas. 4-61522
- Ga<sub>1-x</sub>In<sub>x</sub>Se single crystals, energy gap, temp. dependence 4-92610
- Ga<sub>1-x</sub>In<sub>x</sub>Se system, magneto-optical props. near fundamental band gap 4-109166
- GaP, defect electronic struct. calcs. 4-61326
- GaP:O(Zn), size effects and impurity electronic struct. 4-70723
- GaSb, press. depend. of E<sub>g</sub> gap, reson. Raman technique study 4-76469
- GaSb, Raman freq. depend. on press. 4-109188
- Ga<sub>2</sub>Te, semicond., electronic struct. and bonding 4-84563
- GdInSn<sub>3-x</sub>, elec. resist. below Neel temp. 4-75924
- a-Ge:H, bond angle disorder and optical absorption edge 4-99083
- Ge-Si, amorphous, RF sputtered, electronic props. 4-61370
- GeO<sub>2</sub>-B<sub>2</sub>O<sub>3</sub>(SiO)<sub>2</sub> films, amorphous, opt. absorpt. edge, additions influence 4-71455
- GeS, hole drift mobility anisotropy 4-70814
- Ge<sub>2</sub>S<sub>3</sub>:Cu(Ag), glassy, doping effect on elec. and optical props. (Russian) 4-98625
- Ge<sub>2</sub>S<sub>3</sub>-x glasses, short range order model, optical gap calc., IR band intensity 4-75310
- GeSe, thin film, laser-induced synthesis 4-80095
- GeSe<sub>2</sub>, thin film, laser-induced synthesis 4-80095
- Ge<sub>20</sub>Se<sub>80-x</sub> thin films, optical properties determ., forbidden-band width determ. 4-114337
- Hg<sub>1-x</sub>Cd<sub>x</sub>Te, characterisation using transverse acoustoelectric volt. meas. 4-104275
- Hg<sub>1-x</sub>Cd<sub>x</sub>Te, electric subbands in the limit E<sub>G</sub>→0, for IR reson. study 4-104286
- HgMnTe semimagnetic MIS inversion layers, quantum transport 4-98775
- HgTe-CdTe superlattices, electronic props. 4-84680
- InAs, Raman freq. depend. on press. 4-109188
- InAsSb strained layer superlattices for long wavelength detector, appls. 4-98706
- In<sub>0.53</sub>Ga<sub>0.47</sub>As, epitaxially grown by LPE, VPE, MBE, band gap energy spatial var., photoluminescence spectra 4-104125

## energy gap continued

- In<sub>0.53</sub>Ga<sub>0.47</sub>As LPE layers, high purity, photoluminescence processes 4-99187
- InGaAsP/GaAs, double heterojunctions, photoluminesc. studies 4-76504
- InGaAsP/InP double heterojunctions, photoluminesc. studies 4-76504
- InP, k,p interaction and effective mass, band gap depend. 4-113850
- (InP)<sub>1-x</sub>Ge<sub>x</sub>, energy gap and phase transition 4-80494
- InSb, Raman freq. depend. on press. 4-109188
- InSb, Raman scatt. at high temp., diminishing energy gap near melting point 4-114274
- In<sub>2</sub>Se<sub>3</sub> films, flash and thermal evaporation growth, struct. and elec. characterisation 4-114409
- In<sub>3</sub>Se<sub>70</sub> films, optical absorption, heat treatment effects 4-85027
- K<sub>2</sub>SnTe<sub>5</sub> semicond., electronic struct. and bonding 4-84563
- KTaO<sub>3</sub>, oxygen-octahedral ferroelectrics, two-photon spectroscopy study 4-114300
- LiCl crystal, electronic energy bands, density functional calcs., self-interaction-correction theory 4-70651
- Lif, EELS in band gap region 4-99254
- MgSiP<sub>3</sub>, electronic struct. calcs. 4-108774
- MnO, self-consistent Hartree energy band calcs. 4-92612
- NbN, electronic props., optical study 4-66003
- NiH, optical props. 4-114235
- Pb chalcogenides, resonance absorpt. in indirect transitions (Russian) 4-88855
- Pb<sub>1-x</sub>Eu<sub>x</sub>Te, MBE growth and elec. and optical props. 4-81142
- Pb<sub>1-x</sub>Hg<sub>x</sub>Se flash-evaporated films, optical and elec. props. 4-114335
- Pb<sub>1-x</sub>Sn<sub>x</sub>Te, valence band struct. near phase transition 4-84564
- PbTe:B, absorpt. spectra and impurity states 4-104638
- (PbTe)<sub>1-x</sub>(SnSe)<sub>x</sub>, solid solns., single cryst., phys. props. 4-65673
- PdO cathodes, photoelectrolysis and electronic props. 4-85313
- Re-P system, phase equilibria, cryst. growth, struct. refinements props. 4-88150
- Re<sub>2</sub>Te<sub>5</sub> semicond., electronic struct. and bonding 4-84563
- a-Si, electronic struct. of defects, cluster Bethe lattice method 4-70739
- a-Si, film, gap density of states determ. 4-80551
- Si, heavily doped, intervalley mixing study 4-80491
- Si MIS 2D Fermi system, phonon drag of surface charges 4-92812
- Si, n<sup>+</sup> and p<sup>+</sup> regions, uncertainties about physical electronics, solar cell appls. 4-89428
- Si solar cells, n<sup>+</sup>-p and n<sup>+</sup>-P-P<sup>+</sup> spectral sensitivity calcs. 4-89410
- Si-H, absorpt. edge, struct. disorder model for amorphous semiconductor 4-80483
- Si:H, amorphous, CVD growth by Si<sub>2</sub>H<sub>6</sub> pyrolysis in hot wall reactor, optical gap meas. 4-61864
- p-Si:H, amorphous, prepared by photo-CVD, electronic and optical props. 4-70959
- Si:H, B(P), amorphous CVD layer, impurity doping, optical gap 4-60941
- a-Si:H, energy distrib. of light-induced gap states, photocond. meas. 4-76004
- a-Si:H, prep. by glow discharge of Si<sub>2</sub>H<sub>6</sub>, optical and elec. props. 4-114237
- a-Si:H:B, doping effect on gap states 4-88488
- a-Si:H:Cl films glow discharge deposition from SiCl<sub>4</sub>-SiH<sub>4</sub> mixtures, elec. and optical characts. 4-71580
- a-Si:H:P, defect states and carrier capture processes 4-104165
- a-Si:H:P(B), ESR and optical props., thickness depend. 4-84853
- Si:H amorphous film 4-85115
- Si:H amorphous films, laser CVD by ArF excimer laser photodissociation of Si<sub>2</sub>H<sub>6</sub> 4-61859
- a-Si:H film, low freq. glow discharge prep. (Japanese) 4-76692
- a-Si:H films, CVD growth, phys. props. 4-92715
- a-Si:H films, DC planar magnetron reactive sputtering and characterisation 4-93218
- a-Si:H films, reactive sputtering, elec. and optical props. 4-104203
- a-Si:H thin films, glow discharge effects on electronic and optical props. 4-75977
- Si:H wide optical gap binary alloy films, elec. props. 4-113956
- a-Si:H/a-Si<sub>3</sub>N<sub>4</sub>/a-SiO<sub>2</sub> multilayer films, struct., elec. and optical props. 4-114025
- Si:Mg(Al)(S), third-period interstitials, electronic struct. calcs. 4-108808
- a-Si/a-Si<sub>3</sub>N<sub>4</sub>/a-SiN<sub>x</sub> superlattices, optical bandgap and elec. resist. 4-114026
- p-SiC:H, amorphous, prepared by photo-CVD, electronic and optical props. 4-70959
- a-SiC:H glow-discharge film, electronic and optical props. 4-84623
- Si<sub>1-x</sub>Ge<sub>x</sub>H, amorphous, gap state distrib., photoconductivity study 4-108820
- Si<sub>1-x</sub>Ge<sub>x</sub>H, amorphous, occupied gap state obs. 4-70637
- Si<sub>1-x</sub>Ge<sub>1-x/2</sub>H amorphous sputtered films, optical absorpt. 4-93090
- SiO amorphous films, optical absorpt. edge, temp. depend. 100 to 474K 4-93122
- SiO/SnO<sub>2</sub> coevap. films in sandwich struct., high-field cond. and opt. absorpt. 4-108948
- SiO<sub>2</sub>, amorphous, local electronic density of states, influence of Si-Si bonds 4-92671
- SiO<sub>2</sub> polymorphs, relationship between refr. index and density 4-66001
- SiO<sub>2</sub>, properties of high-pressure fluorite struct. phase 4-110135
- Si<sub>1-x</sub>Sn<sub>x</sub>, (0≤x≤0.3), amorphous RF sputtered film, struct. and elec. props. 4-70956
- Si<sub>1-x</sub>Sn<sub>x</sub>H, (0≤x≤0.3), amorphous RF sputtered film, struct. and elec. props. 4-70956
- SmbB<sub>3</sub>, compound with intermediate valency, correl. gap, press. effect 4-70882
- SmbB<sub>3</sub>, microwave conductivity meas. 4-70851
- Sm<sub>2</sub>Bi<sub>3</sub>, intermediate valence cpds., press.-vol. relationship 4-80554
- SnSe, electroreflectance and thermoreflectance 4-71348
- SrTiO<sub>3</sub>, oxygen-octahedral ferroelectrics, two-photon spectroscopy study 4-114300
- n-SrTiO<sub>3</sub>:Nb, electronic struct., PES and IPES studies 4-108775
- TiO<sub>2</sub> (110), surface defects, XPS, X-ray induced AES, EELS study 4-80351
- TiS<sub>2</sub>, semicond.-semimetal transition at 40 kbar 4-84660
- TmSe, intermediate valence cpds., press.-vol. relationship 4-80554
- W<sub>1-x</sub>Mo<sub>x</sub>Se<sub>2</sub>, x=0-1 fundamental absorpt. edges, optical indirect band gaps 4-99076
- YbO, intermediate valence cpds., press.-vol. relationship 4-80554
- ZnGeP<sub>2</sub>, electronic struct. calcs. 4-108774
- ZnIn<sub>2</sub>S<sub>4</sub> layered cpd., energy gap, temp. depend., optical meas. 4-88803
- Zn<sub>1-x</sub>Mn<sub>x</sub>Te, paramag. phase, excitonic magnetoabsorption, magnetisation meas. 4-71353

## energy gap continued

- ZnO- $P_2O_5$  glasses, optical absorpt. coeffs. 4-84932  
 ZnSiP<sub>2</sub>(As<sub>2</sub>), electronic struct. calcs. 4-108774  
 ZnSnP<sub>2</sub>, electronic struct. calcs. 4-108774

## energy gap, superconducting see superconducting energy gap

## energy level crossing

see also Hanle effect

- alkali metal dimers, crossing states, pot. energy curves; ab initio calcs. 4-68995

- 9,10-anthraquinone triplet state in organic glass at 77K, spin-polarised EPR spectra 4-59848

- (2-anthryl)ethylenes, laser flash photolysis, triplet-related photophysical behaviours 4-99812

- aromatic and heteroaromatic hydrocarbons, adsorbed, inter-system-crossing rate, luminesc. spectra 4-59843

- atom-ion collisions charge transfer, laser assisted, coupled dressed quasi-molecular states approach 4-96684

- avoided crossings, use of effective Hamiltonians, adiabatic pot. curves 4-59681

- avoided crossings, use of effective Hamiltonians, nearly diabatic pot. curves 4-59858

- diatomic mol's, Rydberg-valence vibronic interactions 4-83364

- muon physics, level crossing (French) 4-112304

- naphthaldehydes, picosecond time resolved absorpt. spectra and intersystem crossing kinetics 4-64484

- propene, sigmatropic shifts, MC-SCF STO calcs. 4-104972

- pyrazine with rovibronic level excitation, fluoresc., mag. field effects, intersystem crossing 4-83407

- retinals, isomeric, transient Raman spectra, lowest excited triplet state, cis-trans isomerisation 4-91265

- spin system nonlinear interaction with radio freq. fields in presence in level crossing in a zero field 4-91238

- state multiplets meas. using level-crossing techniques 4-96498

- C+NO(X<sup>2</sup>II), collinear reaction pot. energy barrier, correl. diagram, ab initio calcs. 4-99766

- CS<sub>5</sub>, laser-excited electronic fluorescence, quenching and self-quenching, intersystem crossing 4-69134

- <sup>133</sup>Cs vapour, spin system nonlinear interaction with radio freq. fields in presence of level crossing in a zero field 4-91238

- H, radiative decay, final-state interferences 4-83333

- H, Stark effect level crossings, relativistically enhanced ionisation rates 4-69010

- (H<sub>2</sub>)<sub>p</sub>, (n=2, 3, 5), bound excited state form., CI calcs. 4-96740

- He<sup>+</sup>+H, charge transfer, laser assisted, coupled dressed quasimolecular states approach 4-96684

- KCN, vibr. chaos, quantum and classical calc. comparison 4-102662

- <sup>83</sup>Kr, 5p levels, hyperfine struct. const. meas. (French) 4-78980

- <sup>90</sup>Mo 4d<sup>5</sup> 5p z<sup>2</sup>P<sub>3/2</sub> states, HFS investigation by levelcrossing spectroscopy 4-96499

- <sup>90</sup>Mo 4d<sup>5</sup> 5p z<sup>2</sup>P<sub>3/2</sub> states, HFS investigation by levelcrossing spectroscopy 4-96499

- Na+He(Ne), population transfer, mol. pot. curves, avoided crossings 4-96655

- Ne, level-crossing spectroscopy of atoms dressed by optical photons in degenerate four-wave mixing 4-107299

- UO<sub>2</sub><sup>2+</sup>, excited, photophys. and reversible crossing in aq. soln. 4-112233

- UO<sub>2</sub><sup>2+</sup>, excited, photophys. in aq. soln., solvent exchange and H abstraction 4-112235

- UO<sub>2</sub><sup>2+</sup>, photophys. in aq. soln., acidity effects, pH 0.5-4.0 4-112234

- <sup>131</sup>Xe, hyperfine struct. const. meas. (French) 4-78980

## energy level transitions, atomic see atomic spectra

## energy level transitions, molecular see molecular spectra

## energy level transitions, nuclear see nuclear energy level transitions

## energy levels see energy states

## energy levels, atomic see atomic structure

## energy levels, molecular see molecular energy levels

## energy levels, nuclear see nuclear energy levels

## energy levels in solids and liquids see electron energy states (condensed matter)

## energy loss of particles

see also channelling; electron energy loss spectra; radiation effects

- alkali silicate glasses, ion irradi., glass comp. modification by alkali ion migration 4-70238

- alpha particle lineshape from natural source, ionisation loss formulae anal. 4-96413

- alpha particle thickness gauge by air equivalent method (Chinese) 4-82778

- alpha particles, extrapolated ranges and stopping cross-sections in normal and cyclo-hydrocarbons 4-96414

- alpha particles, extrapolated ranges and stopping cross-sections in liq. hydrocarbons 4-96415

- atomic electronic stopping powers for low projectile vels., shell correction 4-64599

- Bethe electronic stopping power formula, Z<sub>1</sub><sup>3</sup> and Z<sub>2</sub><sup>2</sup> corrections 4-92275

- biological mol's., mol. size effects in fast heavy ion induced desorption 4-66880

- blocking effects and patterns (Japanese) 4-92277

- bremstrahlung studies with conducting and non-conducting radiators 4-59597

- cellulose nitrate track detector, ion beam response 4-59585

- charge exchange of heavy ions in matter, radiation calc. 4-76548

- charged particle in various substances, ionisation energy loss, density effect 4-95073

- Charlesby law, modification for doses below macroscopic sensitivity (French) 4-84327

- Charlesby law, scission density profile calc. (French) 4-84326

- conversion factor C<sub>K</sub> alterations due to 43 MV X-ray filtration (Russian) 4-78749

- cosmic ray muon energy loss by ionisation, track lengths 4-110425

- cosmic ray muons; underwater, depth-intensity curve, sea-level momentum 4-78751

- CR-39 plastic detector for detection and identification of ions with 2≤Z≤5 4-68894

- cross-sections in repulsive power law potentials 4-65312

- crystals with implanted positive pions, study by lattice steering of decay muons 4-75567

- cyclotron trap for muonic atom studies 4-83277

- dechannelling, based on stochastic theory 4-103838

## energy loss of particles continued

- density effect for fast ions 4-64267

- dielectric materials, erosion by high-energy ions 4-61802

- effective stopping power charge of ions in condensed matter 4-92255

- electron beam bombard., excitation energy distrib., Gaussian models, appl. to X-ray microanal. and solid state electronics 4-65303

- electron beam bombardment of semi-infinite target, energy losses, diffusion theory 4-98160

- electron depth-dose and lateral-dose functions, energy and at. number depend. 4-65320

- electron energy loss fluctuations in deterministic streaming ray calcs., Monte Carlo simulation 4-106667

- electron energy-loss straggling algorithm, improved, for Monte Carlo transport codes 4-85499

- electron inelastic and elastic multiple scatt., transport eqn. description 4-66160

- electron initiated EM showers in air, radiation dose distrib. close to shower axis 4-59020

- electron interactions in samples with special geometries, Monte Carlo electron trajectory calc. 4-66156

- equilibrium charge distrib. for B, C, N ions passing through matter 4-75586

- fast electrons, penetration and energy loss through matter, theory 4-88220

- fast ions in solids, excited state populations and charge-exchange 4-80126

- films, amorphous and polycryst., plural electron scatt., Monte Carlo calc. 4-66158

- fission fragments, specific energy losses meas. with back-to-back ionisation chamber-semiconductor detector system 4-87024

- heavy ions, pre-equilibrium energy losses meas. 4-88218

- inelastic energy loss in solids, statistical model anal. 4-92257

- inner-shell ionization and the Z<sub>1</sub><sup>3</sup> and Barkas effects in stopping power 4-99259

- ion beams, electronic stopping cross sections and projected ion-range distribution moments (Chinese) 4-113512

- ion range distrib. calc. using Boltzmann transport eqn. 4-92249

- ion stopping cross-section in solids, effects of electronic struct. 4-92273

- ion stopping in ICF plasmas 4-107149

- ion stopping power, semi-empirical formula 4-59598

- ions, convoy electron velocity and ion velocity correlation 4-81061

- ions, inelastic scattering at surfaces and stopping powers meas. 4-81066

- ions in liquids, stopping power, semi-empirical formula 4-87025

- ions in solids, ranges, analytical formula 4-78750

- ions in solids at nonrelativistic velocities, mean projected ranges, stopping power eqn. 4-65315

- Landau density and distribution functions, asymptotic expansions 4-98157

- Makrofol Polycarbonate plastic track detector, calibration using heavy ions 4-64307

- metal targets, proton irradi., electronic energy loss, impact parameter depend. 4-108485

- metallic foils, ion stopping power and effective charge theorem 4-92254

- metals, heavy particle motion, adiabatic and non-adiabatic approx. 4-60970

- metals; implanted N<sub>2</sub><sup>+</sup> mol. ion range, nuclear reaction anal. 4-92250

- methane (d<sub>4</sub>), electron impact spectra 4-83482

- muons, charge exchange in gases, density operator formalism theory 4-69201

- muons charge exchange in gases, kinetic eqns. appl. to muon spin reson. signals 4-74330

- narrow beam of fast charged particles, passage through matter, particle spectrum 4-75590

- nuclear emulsions, alpha particle tracks, strong ionising events 4-92270

- photon attenuation coefficient meas., effect of scattered photons 4-59596

- plasmas, atomic mean excitation energies for stopping powers from local plasma oscillator strengths 4-97749

- plastic detectors, particle energy losses, explicit temp. depend. 4-102479

- PMMA, ion beam modifications, electronic stopping power 4-84322

- polycrystalline foils, multiply peaked energy loss spectra of heavy ions 4-92272

- polyester films, MeV proton losses, lateral and angular spreads 4-108468

- polyester films, multiple scatt. lateral spread of MeV protons 4-92262

- polyester films, proton irradi., stopping power and energy straggling 4-88215

- position sensitive proportional detector for focal plane of mag. spectrograph 4-59580

- positive muon residual polarisation in water, CS<sub>2</sub>, and organic liqs. under strong decoupling fields 4-71949

- proton and alpha particle stopping power rel. to dosimetry of fast neutrons and actinides 4-68840

- quartz glass track detectors, <sup>56</sup>Fe ion tracks study 4-59586

- scattering angle evaluation in Monte Carlo simulation 4-92251

- slow ion energy losses as function of at. number 4-107436

- solids, at. collisions, conf., Bad Burg, Germany (July 1983) 4-73144

- solids, ion energy loss ang. depend. 4-65313

- solids, nucl. stopping power, binding force effect 4-65316

- solids, proton energy loss and stopping cross sections 4-108469

- SSNTD, finite temp. effect on particle energy losses, track formation implications 4-112047

- stopping power effective charge of energetic ions in metals 4-65321

- stopping power measurement using thick alpha sources 4-102442

- stopping powers of pre-equilibrium heavy ion beams 4-88221

- Teflon,  $\beta$ -decay electrons and positrons energy distrib. parameters (Russian) 4-75592

- thin foils, transmitted particles, nuclear stopping power 4-92267

- e, N<sub>2</sub> collision, rotational excitation, mean fractional energy loss; atmospheric gas 4-113105

- Ag, angle dependent energy loss of 7-MeV protons, stopping powers meas., geometrical effect 4-96658

- Ag, electron backscatt., Monte Carlo calcs. 4-66157

- Ag, electronic stopping power, excitation energy alpha-particle time of flight expt. 4-67916

- Ag film, proton and deuteron stopping cross section 4-92260

- Al, alpha-particle ang. blocking dips, multistring Monte-Carlo simulation and analytical calcs. 4-92274

- Al, angle dependent energy loss of 7-MeV protons, stopping powers meas., geometrical effect 4-96658

- Al,  $\alpha$ -particle stopping power, ang. distrib. 4-83276

- Al,  $\beta$ -decay electrons and positrons energy distrib. parameters (Russian) 4-75592

## energy loss of particles continued

- Al, electron and positron slowing down 4-108486  
 Al, electron backscatt., Monte Carlo calcs. 4-66157  
 Al, electronic stopping power, excitation energy alpha-particle time of flight expt. 4-67916  
 Al foil, inelastic ion energy loss and scatt. angle in transmission expts. 4-92265  
 Al foil target, ion stopping in heated targets 4-112080  
 Al, kV electron scatt. processes, Monte Carlo simulation, rel. to AES 4-66145  
 Al, low energy heavy ion range parameters,  $Z_1$  dependence 4-92248  
 Al, proton stopping power, energy loss straggling, effective-charge fractions and straggling of heavy ions 4-103843  
 Al thick layers, penetration of 24.8 MeV electrons, energy spectra 4-66148  
 Al, thin film, electron transmission, electron NGR spectroscopy study 4-60971  
 Al<sub>2</sub>SiO<sub>5</sub>, sillimanite, absorption edge fine struct. study using electron channelling 4-80127  
 Au, electron and positron slowing down 4-108486  
 Au, electron backscatt., Monte Carlo calcs. 4-66157  
 Au, electronic stopping power, excitation energy alpha-particle time of flight expt. 4-67916  
 Au film, proton and deuteron stopping cross section 4-92260  
 Au, ion channelling, energy stopping power depend., interatomic interaction potentials at high projectile velocities 4-80125  
 Au, proton stopping power, energy loss straggling, effective-charge fractions and straggling of heavy ions 4-103843  
 Au, stopping power of protons, 3 to 8 MeV 4-92258  
 Au, thin film, electron transmission, electron NGR spectroscopy study 4-60971  
 Be, angle dependent energy loss of 7-MeV protons, stopping powers meas., geometrical effect 4-96658  
 Be,  $\beta$ -decay electrons and positrons energy distrib. parameters (Russian) 4-75592  
 Be foil, stopping power of 7 MeV protons, geometrical effects 4-92264  
 Br<sub>2</sub> gas, proton and <sup>4</sup>He stopping cross sections 4-92259  
 C amorphous thin film, low energy electron attenuation length studies 4-84323  
 C foil, specific energy loss of <sup>16</sup>O ions, thickness depend. 4-92261  
 C, proton stopping power, energy loss straggling, effective-charge fractions and straggling of heavy ions 4-103843  
 C, stopping power, zero-energy density effect 4-80129  
 C thick layers, penetration of 24.8 MeV electrons, energy spectra 4-66148  
 C thin foil, pre-equilibrium stopping for <sup>1</sup>H and <sup>4</sup>He ions 4-92253  
 C thin targets, stopping power for He, Li and C ions, charge state depend. 4-92252  
 C very thin foils, energy loss of He<sup>+</sup> beams, nonequilibrium effects 4-103837  
 C<sup>+</sup> inelastic collisions, kinetic energy-loss spectra 4-64568  
 CO, solid, range meas. of keV H ions 4-92263  
 Cd, stopping power for 6.5 MeV protons and mean excitation energies 4-92271  
<sup>235</sup>Cf fission fragments, range and energy losses, LSS theory anal. 4-108490  
 Cl<sub>2</sub> gas, proton and <sup>4</sup>He stopping cross sections 4-92259  
 Cu, angle dependent energy loss of 7-MeV protons, stopping powers meas., geometrical effect 4-96658  
 Cu, electron and positron slowing down 4-108486  
 Cu, electron backscatt., Monte Carlo calcs. 4-66157  
 Cu, electronic stopping power, excitation energy alpha-particle time of flight expt. 4-67916  
 Cu film, proton and deuteron stopping cross section 4-92260  
 Cu foil, stopping power of 7 MeV protons, geometrical effects 4-92264  
 Cu, low energy N atom implantation, profiles, ranges and straggling 4-80062  
 Cu single-crystal films, Na<sup>+</sup>(K<sup>+</sup>)(Rb<sup>+</sup>) ion beams transmission, angular and energy distrib. 4-98159  
 Cu thick layers, penetration of 24.8 MeV electrons, energy spectra 4-66148  
 CuAg alloys, cone form, during Ar<sup>+</sup> ion sputtering 4-75552  
 F<sup>+</sup>+C(X) foils, equil. charge state, particle vel. depend. 4-64594  
 Fe, thin film, electron transmission, electron NGR spectroscopy study 4-60971  
 GaAlAs, proton energy loss straggling meas. for nucl. profiling appl. 4-70246  
 Ge, ion channelling, interaction pot., stopping power, ion scatt. spectra 4-75570  
 H to Ar, stopping powers, mean excitation energies 4-91344  
 H<sup>+</sup>+C(Al) foil, ion energy loss ang. depend. 4-65313  
 H<sup>+</sup>+heavy atom, inelastic scatt. relativistic effects, Born approx. 4-83449  
 H<sub>2</sub><sup>+</sup> mol. ion beam bombard. of solid and gaseous targets 4-76579  
 H<sub>2</sub>O, low-energy, H<sup>+</sup> stopping power, modified local plasma model 4-83485  
 HgCdTe and CdTe, ion implanted with <sup>1</sup>H, <sup>2</sup>H, <sup>4</sup>He, depth distributions, SIMS study 4-88182  
 In, stopping power for 6.5 MeV protons and mean excitation energies 4-92271  
 N<sub>2</sub>, low-energy H<sup>+</sup> stopping power, modified local plasma model 4-83485  
<sup>14</sup>N<sup>+</sup> stopping cross section in Al 4-107266  
 Na<sub>2</sub>O-SiO<sub>2</sub> glass, ion implanted impurities, range and spatial distrib. 4-108287  
 Ni,  $\beta$ -decay electrons and positrons energy distrib. parameters (Russian) 4-75592  
 O<sub>2</sub>, low-energy H<sup>+</sup> stopping power, modified local plasma model 4-83485  
 O<sub>2</sub>, solid, range meas. of keV H ions 4-92263  
 Pb, stopping power for 6.5 MeV protons and mean excitation energies 4-92271  
 Pb thick layers, penetration of 24.8 MeV electrons, energy spectra 4-66148  
 Pd, stopping power for 6.5 MeV protons and mean excitation energies 4-92271  
 Si, ion bombarded, 14 MeV O ions, non-registered Si produced at metal-Si interface 4-114351  
 Si, low energy heavy ion range parameters,  $Z_1$  dependence 4-92248  
 Si multiply implanted targets, range distrib., Rutherford scatt. studies 4-92268

## energy loss of particles continued

- Si, thin layers, ionisation energy losses of highly relativistic charged particles 4-64279  
 SiO<sub>2</sub> radial energy distrib. around ionising particle tracks 4-108487  
 Sn, thin film, electron transmission, electron NGR spectroscopy study 4-60971  
 Ta, angle dependent energy loss of 7-MeV protons, stopping powers meas., geometrical effect 4-96658  
 Ta<sub>2</sub>O<sub>5</sub>, altered layer prod. by He ion sputtering, depth profiling 4-80075  
 Ta<sub>2</sub>O<sub>5</sub> targets, transmitted MeV <sup>4</sup>He ions, multiple scatt. angular distrib. 4-92269  
<sup>23</sup>U, ion track registration characteristics, in polycarbonate Chao Yang No.1 (Chinese) 4-102536  
 W, electron and positron slowing down 4-108486  
 W, range distrib. of Xe ions, expt. and computer simulation studies 4-92256  
 Xe, frozen, sputtering by keV heavy ions 4-71503  
 Xe, lateral multiple scatt. of 15-60 keV ions 4-92266  
 Zr, stopping power for 6.5 MeV protons and mean excitation energies 4-92271

energy measurement *see* power measurementenergy-range relations *see* energy loss of particles

## energy resources

- see also* fuel; geothermal power; hydrogen economy; solar energy concentrators; solar power; wind power  
 1970's energy data and anal. 4-72046  
 alternative energy development in USA, effectiveness of state government incentives 4-99933  
 alternative energy sources, 6th International Conference, Miami Beach, FL, USA (Dec. 1983) 4-63395  
 alternative energy sources and environmental effects, course development 4-63465  
 Antarctica, petroleum prospects and geology and geophysics studies 4-81952  
 biomass energetic utilisation, possibilities and barriers (Hungarian) 4-99978  
 biomass energetic utilisation (Hungarian) 4-99979  
 charcoal as an alternative energy carrier: net energy and cost analyses 4-114882  
 conference, American Nuclear Society annual meeting, New Orleans, LA, USA (June 1984) 4-106112  
 conference on climate and offshore energy resources at London, England (October 1980) 4-78044  
 consumption, pollution and climate (book) 4-90310  
 consumption, pollution and climate (book) 4-90311  
 economic method for studying future conditions and present extraction of natural resources 4-66645  
 EEC, energy priorities and options 4-89372  
 Egypt, hydrocarbon generation and prospects in Western Desert 4-77482  
 emergency energy concepts, promise assessment 4-62279  
 energy from biomass by socio-economic groups—a case study of Bangladesh 4-77134  
 energy generation economics, comparison of various sources (German) 4-66643  
 energy islands, internal logic 4-62283  
 European Communities' medium-term energy modelling, Netherlands results of Reference Case II 4-77046  
 European Communities' medium-term energy modelling, Irish results of Reference Case II 4-72035  
 European geothermal update, third international seminar at Munich, Germany (November-December 1983) 4-58567  
 forecasting system, intermediate future, conf. Washington DC, USA (Aug. 1982) 4-78038  
 forestal biomass, importance as energy resource/raw material, utilisation possibilities (Hungarian) 4-99995  
 fossil fuels, probable future role 4-105090  
 gas deposits of Louisiana continental shelf, USA 4-110103  
 geothermal energy resources, new techniques for exploiting existing resources in Sweden 4-99939  
 Green River oil shale, organic matter chemical structure 4-81516  
 GREPOM, energy policy model 4-81510  
 heat transfer in energy problems, conf., Tokyo, Japan (Sept.-Oct., 1980) 4-82599  
 hydrocarbon prospecting in Western Siberia, first attempt at EM core sounding 4-100448  
 hydrocarbon reserves of North Sea Basin, economically recoverable, estimation 4-99938  
 hydrothermal resources at mid-oceanic ridge axes 4-114893  
 Intermediate Future Forecasting System for energy market modelling 4-81511  
 Intermediate Future Forecasting System implementation and software design 4-81512  
 Jamaican biomass resource assessment, history and prospects 4-66674  
 kelp culturing and utilisation for methane production 4-114887  
 Kentucky oil shale, preferable technologies as defined by bench-scale retorting studies 4-62288  
 Labrador Sea basin, gas deposits existence, drilling and geological obs. (Russian) 4-82058  
 Latin America, energy consumption patterns and problems 4-89373  
 low-grade fuels—Swedish energy option 4-89376  
 macroeconomic energy model EURECA and modifications 4-66646  
 methanol as a viable energy source in today's world 4-62284  
 Minnelusa sands hydrocarbon deposits, Wyoming, USA, seismic exploration 4-109715  
 natural gas, Sweden (Swedish) 4-77044  
 nonfossil energy sources, impact of hydrogen 4-66819  
 nuclear fuel supply system, adequacy for future requirements (German) 4-68753  
 nuclear fusion powered H production 4-62407  
 offshore continental shelf oil and gas development 4-115457  
 oil and gas reserves in recoverable deposits, calculation 4-105093  
 oil recovery from reservoir rocks, use of CO<sub>2</sub> 4-105092  
 oil reserve estimation, saturated growth process appl. Iran 4-62286  
 oil reservoirs evaluation by gamma ray spectral logging and pulsed neutron application 4-62990  
 oil shale combustion retorting 4-62287  
 Penticon Tertiary outcrop, BC, Canada; potential of geothermal energy site 4-72538  
 petroleum asphaltene structure determ. by proton NMR 4-80822

**energy resources continued**

- petroleum prospecting, formulation of geological problem of geophysical regionalisation 4-100827
- power for the future, overview 4-62281
- proceedings of second international symposium on nonconventional energy, Trieste, Italy, August, 1981 4-78040
- quality and equivalence of different energy sources (*Italian*) 4-62280
- reed culms as an energy resource in Sweden 4-77047
- regenerative energy sources, development trends (*German*) 4-81509
- renewable energy sources for power generation, Italian experience 4-81514
- renewable energy sources for rural and urban areas in developing countries 4-81515
- renewable sources of energy and chemicals, photosynthetic plants 4-81569
- science and engineering graduate utilisation in energy-related employment 4-66647
- solar energy technology (*German*) 4-105096
- solar power, new estimates of mean daily diffuse solar radiation in Thailand 4-100697
- solar power, simple statistical model of daily global solar radiation in Thailand 4-100698
- source rocks classification, based on shale resistivity ratio parameter 4-81517
- submerged plate boundaries and pot. mineral and energy resources 4-67192
- swiss energy statistics for 1983 4-99932
- tidal power, renewable energy technologies, contribution to future energy requirements 4-99934
- unconventional, Italian energy projects 4-81513
- underground coal, gasification, cavity growth 4-99985
- underground coal gasification, potential in USA 4-99982
- underground coal gasification, technical feasibility 4-99983
- USA energy plans (*French*) 4-77045
- waste resource recovery and energy generation 4-93585
- WIDCO's program for UCG commercialisation 4-99984
- Yugoslavian hydropower potential, possibilities of utilisation 4-105094
- U nuclear fuel supply, status report (*German*) 4-68751

**energy states**

- see also atomic structure; electron energy states (condensed matter); energy level crossing; molecular energy levels; nuclear energy levels; population inversion
- partition function, Pade approximant method, quartic anharmonic oscillator 4-86326
- partition function, Pade approximant method 4-86325
- semiclassical level spacings when regular and chaotic orbits coexist 4-110909

**energy states in solids and liquids** see electron energy states (condensed matter)**energy storage**

- see also capacitor storage; direct energy conversion; energy storage devices
- active heat pipe solar water heating system 4-72155
- alternative energy sources, 6th International Conference, Miami Beach, FL, USA (Dec. 1983) 4-63395
- aquifer seasonal energy storage—results and simulation of moderate temperature field experiments 4-66795
- Canadian trends in hydrogen energy, review of work at Institut de Recherche d'Hydro-Quebec 4-62401
- concentration difference energy system and engine, developments, heat transfer studies and appls. 4-66786
- concrete utilisation in energy-efficient buildings (*German*) 4-66739
- direct-fired engine driven heat pumps, future developments 4-99987
- domestic solar system instrumentation, long-term stability and performance 4-99989
- domestic space heating using air to water heat pumps, use of floor panel energy storage 4-89462
- electronic controls for solar heating and heat/cool storage systems 4-93642
- ferroelectric polymers, props. and applications 4-65954
- fluorides, organic and inorganic chemistry and energy storage 4-72184
- flywheel energy storage system, peak reducing potential, digital simulation 4-66791
- geothermal energy resources, new techniques for exploiting existing resources in Sweden 4-99939
- ground heat storage with solar in Sweden, experimental projects 4-66798
- ground water pumping for irrigation using wind electric energy 4-114889
- heat accumulators with solid filler, heat transfer by air stream 4-93640
- high temperature fluids, transport system, new pipeline design 4-66803
- high-temperature salt/ceramic thermal storage, phase-change media 4-66797
- hot dry rock geothermal reservoir development 4-62295
- latent heat storage equipment for solar energy, transient heat transfer anal. 4-66792
- low melting materials relevant to energy storage, thermal cond. 4-92450
- LPG bulk storage, New Zealand, town planning appls. 4-109753
- metal hydride storage bed, mass and heat transfer dynamic analysis program 4-66816
- molten-salt thermal storage and heat-pipes for ECA Stirling engines 4-66765
- moving bed thermal energy storage system, appl. to fossil and solar powered boilers 4-105118
- natural gas/hydrogen compressed storage, comparison as vehicle fuels 4-89375
- packed bed for thermal energy storage, transient response 4-114959
- power for the future, overview 4-62281
- recent progress in energy storage technology 4-66790
- residential heating by off-peak thermal storage, field test and assessment 4-66793
- residential solar/electric water heater simulation model development and evaluation 4-72050
- RSG-2 drop-forged steel radiators as heat absorbers for solar water heater 4-93638
- salt gradient solar pond, stability, effective insulation, heat loss 4-105120
- solar, field experiments and thermal use of aquifer 4-66799
- solar energy, chemical storage, demonstration using colour change 4-90334
- solar energy thermal storage physico-mathematical model, for high temperature 4-81595
- solar pond, saturated, laboratory-scale, self-generation 4-62396

**energy storage continued**

- solar ponds, operating at different latitudes, performance characts. 4-105119
  - solar radiation accumulation in organic photoisomers 4-93643
  - solar thermal energy storage system, anal. 4-81596
  - solar total energy experimental facility, operating characts. 4-72183
  - solid state chemistry, conf., Veldhoven, Netherlands (June, 1982) 4-67863
  - solidification around vertical cylinders, thermal energy storage materials 4-100007
  - space power system using Fresnel lenses for solar power utilisation, thermal energy storage 4-72176
  - Stirling engines, coal-burning, large-scale, possible applications 4-72148
  - stratified heat accumulator in solar heating system, design of water distributor 4-93641
  - stratified heat storage with heat pump, optimal loading strategy 4-66794
  - thermal for utility interactive photovoltaic research house 4-66670
  - thermal modelling of a few novel solar collector cum storage units for passive heating 4-77152
  - thermal performance of a heat storage module using calcium chloride hexahydrate 4-114960
  - thermal storage experience at Solar One and the molten salt thermal energy storage subsystem research experiment 4-66796
  - thermosiphon solar domestic hot water system performance 4-62394
  - toroidal energy storage device with relativistically densified electrons, travelling mag. waves 4-60764
  - wind power systems with energy storage, power supply loss probability 4-89377
  - $\text{Na}_2\text{SO}_4 \cdot \text{H}_2\text{O}$  systems, phase transition kinetics 4-98248
- energy storage devices**
- alkaline fuel cells for the regenerative fuel cell energy storage system 4-72102
  - alkaline storage battery aspects of air electrode research, appl. 4-66687
  - Canadian trends in hydrogen energy, review of work at Institut de Recherche d'Hydro-Quebec 4-62401
  - electrochemical storage of solar energy, review 4-89468
  - flywheel energy storage for X-ray machines 4-85506
  - flywheels for energy storage, operation, development and practical applications 4-105125
  - heat pump equipped with PCM heat storage unit (*Japanese*) 4-109752
  - raft thermocline thermal storage system, raft's stability and effectiveness evaluation 4-66802
  - regenerative fuel cell system for orbital energy storage, development status 4-72101
  - solar, thermal energy storage systems, value and cost analyses 4-66800
  - solar total energy systems, development of latent heat storage unit using form-stable high density polyethylene, progress report 4-66801
  - thermal energy storage in aquifers, short-term, system description 4-66804
  - thermochemical energy storage with heat pump system for industrial steam supply, expt. 4-66805
  - Fe/Cr redox battery; mathematical model 4-89469
  - Zn-Br batteries for bulk energy storage, design projections and low cost manufacturing techniques 4-66886
- energy transfer collisions, molecular** see molecular inelastic collisions
- engineering**
- see also biomedical engineering; civil engineering; design engineering; electrical engineering; environmental engineering; maintenance engineering; mechanical engineering; naval engineering
  - mechanics, advances and instruction in France 1800-30 4-63468
  - OCEANS '83, utilisation of sea, conference, San Francisco, CA, USA (Aug.-Sept. 1983) 4-106113
  - Saudi Arabian engineering education, role of physics 4-90329
- engineering applications of computers** see engineering computing
- engineering computing**
- see also aerospace computing; civil engineering computing; communications computing; electrical engineering computing; electronic engineering computing; mechanical engineering computing; nuclear engineering computing
  - automatic plastic design, reliability-based optimisation technique 4-103214
  - heat exchangers, open-topped, closed-sided, with vertical fins, heat transfer rates enhancement, for use in electronic equipment cooling 4-79420
  - Illuminating Engineering Society Annual Conf., Los Angeles, USA (Aug. 1983) 4-90291
  - Maritsa East 2 thermal power station  $\text{SO}_2$  emissions reduction (*Bulgarian*) 4-100042
  - metal hydride hydrogen storage beds 'In-Out' and 'Out-In' hydrogen reaction alternatives using RET 1 computer code 4-66812
  - Stirling engine using two-phase two-component working fluid, computer modelling 4-66784
- engineering facilities**
- see also test facilities
  - United States Naval Civil Engineering Laboratory developments 4-110175
- engineering societies** see societies
- engines**
- see also aerospace engines; heat engines; internal combustion engines; ion engines; propulsion
  - high temp. gas engine driven heat pumps, industrial appls. 4-89463
  - ramjet combustion efficiencies comparison (*German*) 4-99797
  - Stirling analysis code validation using free-piston engine base line data 4-77141
- entertainment** see sports and entertainment
- enthalpy**
- see also heat of
  - alkali metal fluorides and chlorides, solution enthalpies of divalent defects 4-98316
  - alkali metal oxides, binary, high temp. vapourisation behaviour 4-98260
  - alkanois-water systems, thermodynamic props. 4-92388
  - alloys, dilute, free enthalpy of impurity-vacancy binding, solvent diffusion meas. 4-84465
  - alloys, with non-negligible evaporation rates, high temp. calorimetry procedure 4-68232
  - alloys with non-negligible evaporation rates, high temp. calorimetry 4-78320
  - azoxyarylethanes, mesomorphic props., potential stationary phases in gas chromatography 4-113316
  - benzenes, substitutes, in glassy forming solvents,  $\beta$  process study 4-92990

**enthalpy** continued

- bicrystal, grain boundary phase equilib., computer mol. dynamics simulation 4-113461  
 binary alloys, surface comp. profiles, generalised free enthalpy 4-75761  
 carbohydrates, thermal props. heat flow calorimetric obs. 4-78312  
 Cartesian two dimensional phase change, fixed mesh finite element solution 4-112669  
 1,2-chloriodoethane, photodissoc. at 248 and 266 nm, enthalpy of formation 4-114809  
 4,4'-dialkanoyldiphenyldiacetylenes, homologous series, mesomorphic behaviour 4-113310  
 DNA supercoiling, free energy rel. to enthalpy 4-77182  
 energy system productivity, application of Hamilton and Fermat principles 4-68184  
 3-fluoro-4-cyanophenyl 4'-n alkylbenzoates, synthesis, mesomorphic and phys. props. 4-113318  
 glassy materials, temp. coeffs. of transport props. 4-92409  
 heat conduction, phase change, enthalpy formulation, numerical soln. 4-97300  
 n-hexane-n-hexadecane mixtures, excess molar enthalpies 4-103967  
 liquid crystalline ternary mixtures, eutectic compositions, determ. methods 4-113317  
 liquid crystals phase transition, enthalpy and birefringence 4-98277  
 MBBA, metastable solid, dielectric props. under press. 4-80865  
 metallurgical thermodynamics, equilib. states and influencing factors, book contrib. 4-109375  
 metals, relation between self-diffusion, equilib. defect parameters and characts. 4-65445  
 (+)-2-methylbutyl-p((p-methoxy benzylidene)amino) cinnamate, liq. cryst., transitions and texture, enthalpy and entropy 4-113628  
 phase change boundary in two dims., tracking by enthalpy methods 4-87550  
 phase equilibrium, complex model, appl. to systems with asymmetric miscibility gap and two miscibility gaps 4-70397  
 photochemical reactions obs., using tunable pulsed dye laser cryogenic photocalorimeter 4-105005  
 PMMA blends with copolymers of methylmethacrylate and butylmethacrylate, thermodynamic study (*Russian*) 4-77027  
 polyethylenes, linear, heat capacity, enthalpy and crystallinity, DSC study 4-113667  
 polymers, comp.-depend. glass transition, temp.-press.-comp. relationships 4-84398  
 shock loaded solids, thermodynamic props., influence of defects 4-113680  
 steel, ferritic transformable, specific heat capacity (*German*) 4-80252  
 thermodynamic association const. and standard enthalpy of association 4-88047  
 transition metal germanides, heat of formation and enthalpy 4-89321  
 transition metal silicides, heat of formation and enthalpy 4-89321  
 triphenyl aluminium, sublimation press. determ. from mass effusion and torsion recoil rate 4-80207  
 UK Consortium Stirling engine regenerator effectiveness and heater performance 4-66753  
 water vapour, self-deactivation, dimer effect 4-102773  
 water-methane vapour, excess enthalpies up to 698.2K and 12.6 MPa 4-113097  
 Ag-Pb, liq., thermodynamic study of dissolved O 4-92379  
 $\alpha$ -AgAl, short-range order parameter, determ. from resist. meas. 4-98287  
 Al-Ag, solubility of Ag in Al, effect of high press. 4-81179  
 Al-Si system, enthalpies of form. of liq. alloys 4-113679  
 Al<sub>2</sub>O<sub>3</sub> ceramics, subcrit. crack propag., activation enthalpies and mechanisms (*German*) 4-62010  
 BaO, enthalpy and specific heat in high temp. region 1200 to 2200K 4-113672  
 Ce<sub>1-x</sub>Ca<sub>x</sub>O<sub>2-x</sub>, vacancy binding energy, polarisation contrib. 4-88165  
 Ce<sub>1-x</sub>Gd<sub>x</sub>O<sub>2-x</sub>, vacancy binding energy, polarisation contrib. 4-88165  
 CeNi<sub>5-x</sub>Al<sub>x</sub> alloys, H<sub>2</sub> storage props. 4-61206  
 Ce<sub>1-x</sub>Ni<sub>2-x</sub>Cu<sub>2-x</sub> alloys, hyperstoichiometric, H<sub>2</sub> sorption 4-61207  
 Ce<sub>1-x</sub>Y<sub>2-x</sub>O<sub>2-x</sub>, vacancy binding energy, polarisation contrib. 4-88165  
 Cs<sub>2</sub>UO<sub>4</sub> phase, high temp., thermodynamic stability 4-13671  
 Cu-Bi(Sb), liq., Bi and Sb activity meas. by Knudsen effusion method with electrobalance 4-66312  
 $\alpha$ -Fe, positron annihilation expts. in thermal equil., one-interstitial model confirmation 4-109271  
 Ga, heat capacity, enthalpy, melting temp., thermodynamic functions 4-80255  
 HCl-N<sub>2</sub>O liquid mixtures, thermodynamics and densities 4-98311  
 In, deformed, low-temp., recovery activation enthalpy, positron annihilation meas. 4-76556  
 La<sub>1-x</sub>Sr<sub>x</sub>CrO<sub>3-y</sub>, defect struct. and thermodynamic props. 4-98099  
 Li breeder blanket, impure, T. extraction by Y, thermochem. analysis 4-107027  
 MoO<sub>3</sub>, molar heat capacities, 350 to 950K, scanning calorimetry studies 4-98306  
 NH<sub>4</sub>Cl<sub>1-x</sub>Br<sub>x</sub> solid solns., heat capacity near  $\gamma$ - $\beta$  transition 4-103958  
 N<sub>2</sub>O, sublimation press. meas. between 125K and 147K (*French*) 4-70358  
 NaCl, aq. soln., thermodynamic props. 4-98313  
 NbO<sub>2+x</sub>, phase equilibria and defect struct. 4-98246  
 Ni-Cu(Ga)(Ag)(Au), bonding and enthalpy studies 4-79978  
 NiO, cationic self-diffusion and oxidation 4-92419  
 Pd-Cu(Ga)(Ag)(Au), bonding and enthalpy studies 4-79978  
 Pd-Rh-H solid solution, thermodynamics and phase equilib. 4-76748  
 PdTx(D<sub>x</sub>), solubility study and thermodynamic props. 4-70395  
 PrO<sub>2</sub>, vacancy struct., lattice energy calcs. 4-70058  
 Pr<sub>2</sub>O<sub>3</sub>, vacancy struct., lattice energy calcs. 4-70058  
 Pr<sub>2</sub>O<sub>16</sub>, vacancy struct., lattice energy calcs. 4-70058  
 Pt-Cu(Ga)(Ag), bonding and enthalpy studies 4-79978  
 SnBr<sub>4</sub> binary mixtures, molar excess enthalpies and volumes 4-108630  
 W, enthalpy of solid and liquid, heat capacity, levitation calorimetry 4-108632  
 W<sup>3</sup>He, ion implanted, diffusivity study 4-104004  
 Xe+ethyl chloride liquid mixture, thermodynamic props. meas. 4-70408  
 Zr:D, ion implantation, lattice defect trapping, binding enthalpy, migration 4-108400

**entropy**

see also entropy of substances

- 2-state stationary Markov chain, entropy, stat. estimation, limit distrib. (*Russian*) 4-68130  
 adsorption, energy and entropy 4-80412

**entropy** continued

- algorithmic variants of the entropy concept (*Russian*) 4-101796  
 alloys, Thermodynamics and entropy of mixing 4-103935  
 asymptotically non-stationary chaos, 1-dimens. map, generalised entropy 4-90500  
 binary systems, hydrodynamic instability and perturbation system 4-108064  
 bridge functions, universality, rel. to var. perturbation theory and eqns. of state 4-73290  
 chemical process, locally attractive normal modes 4-104962  
 communal entropy in melting and the glass, fast-ion, and superfluid transitions 4-70342  
 compensation effect in diffusion, chem. pot. and entropy 4-65439  
 compressors and turbines, entropic efficiency 4-64830  
 cubic alloy, vibr. entropy due to order-disorder transition 4-113668  
 d-dimensional classical lattice models, exact variational methods and cluster-variation approx. 4-101768  
 data anal., maximal entropy method 4-63487  
 differentiable dynamical systems, dimension, entropy anal. Lyapunov exponents 4-68135  
 entangled polymer, entropy calcs. 4-103969  
 equilibrium states, entropy maxima, superadditivity, simple gas model 4-95362  
 evolution patterns and iterative maps 4-73360  
 expanding Universe, order and entropy increases 4-77991  
 four-dimensional statistical mechanics, Poincare invariant Hamiltonian dynamics. 4-95169  
 functions in Beta functions (*Japanese*) 4-101797  
 gas flow, 1-D, infinite Lie group of symmetry, entropy distributions 4-103358  
 Hamiltonian systems, nonintegrability, Kolmogorov entropy 4-82696  
 hexagonal lattice with boundary, dimer problem soln. 4-68159  
 hypersonic viscous gas flow, boundary layer perturbation propag., entropy layer effect 4-60457  
 ice, cubic crystals, surface energy, entropy and stability 4-98309  
 inert gas crystals, surface energy, entropy and stability 4-98309  
 information entropy and Thomas-Fermi theory 4-91201  
 ionic conductors, nonequilibrium steady states of stochastic lattice gas 4-73385  
 irreversible processes, heterogeneity and stochastic phenomena, gas shock wave ionisation appl. 4-63696  
 Ising antiferromagnet, FCC, hysteresis and free energy, computer simulation 4-114127  
 Josephson junctions, onset of chaos, influence of nonlinear conductance and cos $\phi$  term 4-104375  
 Kaluza-Klein cosmologies, entropy from extra compact dimensions 4-90269  
 liquid crystals, stress, thermal and EM effects, entropy, constitutive theory 4-75271  
 metals, magnetotransport, exactly soluble model 4-75928  
 metals and alloys, liquid, entropy, expansion coeff., sp. ht. and Debye temp. 4-103963  
 naphthalene, solns. in water-ethanol mixtures, thermodynamic props. 4-80264  
 neuronal spike train activity, anal. by various methods 4-100115  
 noise-induced order 4-58742  
 nonequilibrium states, stability criteria and fluctuations 4-101750  
 nonlinear systems far from equilibrium, thermodynamic variational principle 4-86378  
 order-disorder transitions of dipolar relaxations, entropy change 4-93002  
 organic cpds., linear free energy relations 4-109675  
 organic molecules-electrically neutral metal complexes, outer-sphere coordination 4-62228  
 periodic series entropies and complexities, appl. to turbulent transition in logistic map 4-111034  
 physical processes and cosmological advances, entropy 4-82622  
 Potts models, ferromag. and antiferromag., phase transition, Bethe approx. 4-92918  
 quantum logic, entropy of observables 4-82714  
 quantum systems, dynamical maps, mixing enhancing and evolution 4-58685  
 quantum thermodynamic entropy, classical limit 4-82745  
 relativistic heavy ion collisions,  $\pi$  prod., light fragment form., entropy, fluid-dynamical model 4-78645  
 relativistic heavy ion collisions, entropy production 4-68716  
 revised Enskog eqn., local entropy prod., general form. for inhomogeneous fluids 4-58795  
 Riemann solvers, the entropy condition, and difference approximations 4-68192  
 self-consistent maximal-entropy propag., time evolution 4-111092  
 shock-wave generating function, k-shocks within low-shock Mach-numbers 4-97609  
 snowflakes, surface energy, entropy and stability 4-98309  
 spectral estimation for short data sequence, fast algorithm of maximum entropy method 4-63678  
 spin systems, inverse problems, maximum entropy approach 4-98836  
 SU(N) Anderson impurity model, thermodynamic Bethe-ansatz eqns. 4-104110  
 thermodynamics of continuous media using entropy flux of Muller 4-90542  
 topological entropy props. of polyhedron self-mappings 4-63483  
 uncertainty relations, entropic, for angle-ang. momentum and position-momentum 4-90421  
 Universe, locally supersymmetric theory, SUSY breaking sector, energy density, entropy crisis 4-77995  
 Universe, thermal death and entropy (*Japanese*) 4-110795  
 viscous incompressible fluid, characteristic exponents, subjected to time depend. forces 4-69728  
 $\gamma$ -Al<sub>2</sub>O<sub>3</sub>, adsorption of alkanes and aromatic hydrocarbons, thermodynamic props., chromatography (*Chinese*) 4-61210  
 Ga<sub>2</sub>In<sub>1-x</sub>(Sb,As,P), short-range clustering, thermodynamic anal. 4-61093  
 S<sub>2</sub>, orthorhombic crystal, lattice dynamical calcs., non-rigid mol. model 4-98217

**entropy of substances**

- p-n-alkoxybenzylidene-p-aminobenzoic acids, liq. cryst., phase transitions, thermal studies 4-113629  
 4-(trans-4'-n-alkylcyclo hexyl) benzoates, mesomorphic, thermodynamic and dielec. props. 4-84390  
 azoxyarylethanes, mesomorphic props., potential: stationary phases in gas chromatography 4-113316

## entropy of substances continued

- betaine arsenate single cryst., ferroelec.-ferroelastic transition and sp. ht. 4-65415
- binary alloys, BCC and FCC, test of statistical approximations, Monte Carlo simulation 4-113681
- n*-butanol, binary polar mixtures, dielec. props. and excess thermodynamic functions 4-114195
- cholesteryl  $\omega$ -arylalkanoates, liq. cryst., cholesteric-isotropic transitions, thermal props. 4-108615
- creep damage and rupture in three-dimens., strain-dependent thermodynamic foundations 4-75607
- 4,4'-dialkanoxydiphenyldiacetylenes, homologous series, mesomorphic behaviour 4-113310
- distillation, entropy production minimisation 4-87555
- ferrocene- $d_{10}$  cryst., thermodynamic props. 4-88307
- 3-fluoro-4-cyanophenyl 4'-*n* alkylbenzoates, synthesis, mesomorphic and phys. props. 4-113318
- gaseous double molecules, entropies and heat capacities, empirical estimation 4-103459
- glass-forming metallic melts, undercooled, free energy approx. 4-70414
- glassy materials, temp. coeffs. of transport props. 4-92409
- p*-*n*-hexyloxybenzylidene-*p*'-butylaniline, smectic liq. cryst., glass transition 4-84392
- KPb, compound forming liquid alloys, hard sphere system, entropy of mixing calcs. 4-113650
- liquid crystal homologous series with bent linkages, thermal props. 4-75275
- long-period superstructure models, ANNNI model 4-113366
- magnetic alloys, dil., low temp. thermodynamic props., anomalous contrib., in presence of cryst. field 4-84801
- MBBA, metastable solid, dielectric props. under press. 4-80865
- metal-ethanoate hydrates, thermodynamic props., phase transitions 4-98305
- metals, FCC, void nucleation kinetics, mol. dynamics simulation 4-92197
- (+)-2-methylbutyl-*p*-(*p*-methoxy benzylideneamino) cinnamate, liq. cryst., transitions and texture, enthalpy and entropy 4-113628
- multichain athermal lattice systems, entropy 4-113675
- nematics, orthorhombic, isothermal hydrodynamics 4-92080
- phenols, enthalpies, free energies and entropies of transfer from nonpolar solvents to water 4-105009
- 3-phenyl-4-hydroxybenzoic acid liq. cryst. esters, thermodynamic props. 4-84391
- phenylhydroquinone, liq. cryst. esters, thermodynamic props. 4-84391
- PMMA blends with copolymers of methylmethacrylate and butylmethacrylate, thermodynamic study (Russian) 4-77027
- polydimethylsiloxane solns., thermodynamics, solvent activities 4-103960
- polymer melts, surface tension, nonlocal entropy effects 4-104040
- polymers, comp.-depend. glass transition, temp.-press.-comp. relationships 4-84398
- polytetrafluoroethylene, glass transition, thermodynamic props., DSC obs. 220-700K 4-61108
- rare earth-transition metal alloys, magnetic cooling near Curie temperatures above 300K 4-88677
- semiflexible polymer chains, statistics 4-75256
- spin glasses, sp. ht., time-dependent, two-dimensional  $\pm J$ -Ising model 4-65822
- transition metals, HCP, FCC and BCC structs., relative stability and entropy 4-113677
- triphenyl boron, sublimation and bond dissociation enthalpy 4-103919
- water vapour, self-deactivation, dimer effect 4-102773
- Ag-Pb, liq., thermodynamic study of dissolved O 4-92379
- Au-Cd liq. and solid alloy, elec. resist. studies 4-88499
- BaCl<sub>2</sub>, melting, solid-solid transitions at high pressures 4-80195
- Be, temp. and press. induced phase transitions 4-70369
- Bi<sub>2</sub>(SO<sub>4</sub>)<sub>3</sub>= $\alpha$ -Bi<sub>2</sub>O(SO<sub>4</sub>)<sub>2</sub>+SO<sub>3</sub>, equil. press.,  $\alpha$ - $\beta$  transform. study 4-71959
- Br electrodes in Zn/Br and Zn/air batteries, electrochemical calorimetry 4-104995
- C fibre reinforced plastic, damage susceptibility estimation, thermodynamic approach 4-99542
- Cd-Pb, thermodynamic props. at 900°C 4-80263
- CdCl<sub>2</sub>, CdBr<sub>2</sub>, CdI<sub>2</sub>, melting, solid-solid transitions at high pressures 4-80195
- CeNi<sub>2</sub>, Al, alloys, H<sub>2</sub> storage props. 4-61206
- Ce<sub>3</sub>, Ni<sub>2</sub>, Cu<sub>2</sub> alloys, hyperstoichiometric, H<sub>2</sub> sorption 4-61207
- Cu<sub>2</sub>(Se), ionic thermoelectromotive force, rel. to temp. and mobile ion conc. 4-75719
- Cu<sub>2</sub>-Se, superionic transition, DSC study 4-88338
- Fe-Cr  $\alpha$  and  $\sigma$  phase alloys, sp. ht. and entropy of formation 4-103959
- Ga-N<sub>2</sub> system, high pressure thermodynamics, heat and entropy of GaN form. 4-62227
- HCl-N<sub>2</sub>O liquid mixtures, thermodynamics and densities 4-98311
- <sup>4</sup>He II, entropy meas. from 1.6K to  $\lambda$  line 4-70494
- K<sub>0.3</sub>MoO<sub>3</sub>, quasi-one-dimensional cond., CDWs, thermodynamics 4-80257
- KTI, compound forming liquid alloys, hard sphere system, entropy of mixing calcs. 4-113650
- La<sub>1-x</sub>Sr<sub>x</sub>CrO<sub>3-y</sub>, defect struct. and thermodynamic props. 4-98099
- Li breeder blanket, impure, T extraction by Y, thermochem. analysis 4-107027
- Li-Pb(Ag) (Mg) liq. alloys, model, chemical short-range order, heat and entropy of formation 4-75266
- Mg, molten, melting and self-diffusion coeffs., pressure effects (Russian) 4-103908
- MoO<sub>3</sub>, molar heat capacities, 350 to 950K, scanning calorimetry studies 4-98306
- NH<sub>4</sub>BeF<sub>3</sub>, ferroelastic, successive phase transitions, sp. ht., thermal expansion meas. 4-108605
- (NH<sub>4</sub>)<sub>2</sub>H(SeO<sub>4</sub>)<sub>2</sub>, thermal and dielec. studies, 90 to 357K, isotope effects 4-70365
- N<sub>2</sub>O, sublimation press. meas. between 125K and 147K (French) 4-70358
- NaF-AlF<sub>3</sub>, melt, thermodynamic data for reactions from vapour pressure meas. 4-85325
- NaGa, compound forming liquid alloys, hard sphere system, entropy of mixing calcs. 4-113650
- NaHg liquid alloys, entropy of mixing, hard-sphere system calcs. 4-92371
- NaI, vapour press. and evaporation thermodynamics 4-103915
- NbO<sub>2+x</sub>, phase equilibria and defect struct. 4-98246

## entropy of substances continued

- NbVH<sub>3</sub>, monohydride-dihydride equil. and thermodynamic anomalies 4-65419
- Ni (100), N<sub>2</sub> adsorption, thermodynamic meas. 4-92563
- Ni catalysts, alumina supported, particle size distrib., superparamagnetic meas. 4-104465
- PbCl<sub>2</sub>, PbBr<sub>2</sub>, melting, solid-solid transitions at high pressures 4-80195
- Pd-Rh-H solid solution, thermodynamics and phase equil. 4-76748
- Pd<sub>2</sub>, T solubility, partial molar enthalpy and nonconfigurational entropy 4-92372
- PdTx(D<sub>8</sub>), solubility study and thermodynamic props. 4-70395
- SbZn liquid alloys, entropy of mixing, hard-sphere system calcs. 4-92371
- Si:Au, donor level, entropy factor, resist. and DLTS meas. 4-70707
- SrBr<sub>2</sub>, melting, solid-solid transitions at high pressures 4-80195
- Tm intermediate valence cpds., mag. susceptibility and sp. ht. 4-108999
- U dipnictides, mag. props., cryst. field interpretation 4-76146
- UO<sub>2</sub>, high temp. thermolec. power studies 4-104244
- VBr<sub>2</sub>, 2-D triangular Heisenberg antiferromag., heat capacities 4-76156
- VCl<sub>2</sub>, 2-D triangular Heisenberg antiferromag., heat capacities 4-76156
- VL<sub>1</sub>, 2-D triangular Heisenberg antiferromag., heat capacities 4-76156
- Xe in liq. *n*-alkanes, solubility, free energies, entropies and enthalpy of soln. 4-70389
- Yb-Fe dilute alloys, thermodynamics, Henry's Law vaporisation studies 4-92390
- Zn electrodes in Zn/Br and Zn/air batteries, electrochemical calorimetry 4-104995
- Zn, molten, melting and self-diffusion coeffs., pressure effects (Russian) 4-103908
- environmental engineering**  
see also air conditioning; cooling; ergonomics; lighting; safety; space heating; temperature control; ventilation
- artificial reef design, prefabrication and testing 4-114973
- artificial reef module for marine environmental quality enhancements 4-114972
- German electricity supply industry, economic and environmentally safe fuel for energy generation, considerations (German) 4-93652
- Maritsa East 2 thermal power station SO<sub>2</sub> emissions reduction (Bulgarian) 4-100042
- satellite imagery for solving environmental problems 4-93675
- steam power stations, fuel consumption, environmental problems (Hungarian) 4-109761
- environmental requirements** see environmental engineering
- environmental testing**  
see also corrosion testing
- artificial reef design, prefabrication and testing 4-114973
- automobile studded tyres, environmental investigation using PIXE 4-105146
- OTEC cold water GFRP pipe field test 4-114933
- OTEC Keahole Point (Hawaii) test facility extension 4-114934
- physical methods in medicine and environmental sciences 4-115144
- polymers, strength and deform. under artificial weathering (German) 4-89229
- recreational fishing reef construction from coal waste blocks 4-114974
- solar crop drying systems, field performance studies 4-77063
- solar reflective surfaces, environmental responses 4-114896
- AlGaAs/GaAs concentrator solar cells under high temp. and humidity conditions 4-66708
- GaAs solar cells, equivalent electron fluence for space qualification 4-77097
- enzymes** see proteins
- epitaxial growth**  
see also liquid phase epitaxial growth; vapour phase epitaxial growth
- atomic pair correlation function during early stages 4-92577
- carbides, oriented growth possibilities during reaction diffusion 4-61256
- ice surfaces, epitaxial freezing of supercooled droplets 4-98052
- III-V ternary antimonides, material prep., cryst. and epitaxial growth, review 4-98045
- layer-by-layer two-dimensional random growth model, backscattered electron diff. beam profile 4-84535
- metals, BCC and hexagonal, epitaxy on FCC (001) substrates 4-108751
- nucleation and growth of thin films 4-92579
- patterned films, graphoeptitaxy and zone-melting recrystn. 4-66228
- polysilene films, epitaxy on mica substrates 4-84212
- semiconductor advanced multilayer epitaxial structure growth 4-71557
- semiconductors, graphoeptitaxy, two-stage artificial epitaxy 4-66229
- SQS films, material improvement process by solid phase epitaxial growth 4-81124
- spinel films, epitaxial growth by solid state reactions 4-61252
- stratified media technology, conf., Los Angeles, CA, USA (Jan. 1983) 4-82585
- sulphides, oriented growth possibilities during reaction diffusion 4-61256
- VLSI technology, textbook 4-82610
- XPS and Auger-electron forward scatt., tool for studying epitaxial growth and core-level binding-energy shifts 4-109304
- Si amorphous or polycrystalline, epitaxial regrowth and bridging epitaxy by flash lamp irradiation 4-75813
- Al epitaxial growth on Ge (001), first principles calc. of energy 4-92580
- Al<sub>2</sub>SiC<sub>4</sub> mixed carbide, prep. and struct. studies 4-88144
- Co, solid, adsorption of multilayers on Cu (100), epitaxial growth of new cryst. struct., LEED, IR spectra 4-113373
- CoSi<sub>2</sub> epitaxial growth on Si (111) surface 4-61844
- CoSi<sub>2</sub> films, solid-phase epitaxial growth, patterning effects 4-84537
- Cu film, epitaxial growth, effects of low energy ion bombardment 4-98478
- GaAs:Si, implanted, radiation annealing with CW Xe arc lamp 4-75486
- GaInAsP alloy semiconductors, book 4-58588
- KBr:In(Tl) polycrystalline films, luminescent, epitaxial growth (Russian) 4-113833
- KCl crystallites, graphoeptitaxial alignment in presence of water vapour 4-92571
- Ni/Si interfaces, silicide form., atom-probe study 4-70475
- Se, epitaxial crystallisation on linear polyphenyls 4-65590
- Si, epitaxial layer growth on CaF<sub>2</sub> substrates 4-80448
- Si evaporated amorphous film, growth conditions by solid phase epitaxy 4-99307
- Si, ion implanted, amorphous surface layer recrystallisation by epitaxial annealing, effect of foreign atoms 4-71553
- Si, ion implanted, pulse-laser-induced epitaxial regrowth 4-75511
- Si, lateral epitaxy, electron beam annealing 4-99308
- Si monocrystalline island growth on insulating substrates 4-76670

# epitaxial growth continued

- Si, polycrystalline, recrystallisation by combined CW laser and furnace heating 4-88199  
 Si polycrystalline films amorphised by ion implantation, solid phase epitaxial growth 4-108731  
 Si, shallow npn bipolar transistors fabrication by triple ion implantation and solid phase epitaxy 4-75460  
 a-Si, solid phase epitaxy, bond rearrangement process, quantitative anal. 4-84534  
 a-Si, vacuum deposited, solid-phase epitaxial growth anisotropy 4-75811  
 a-Si:B, pure and doped, ion implanted, recrystallisation studies 4-88422  
 Si:P(B), substrate orientation depend. of enhanced epitaxial regrowth 4-108737  
 Si:Sb, implanted laser irr., crystn. annealing, time-resolved reflectivity, TEM, Rutherford backscattering anal. 4-80093  
 Si/SiO<sub>2</sub> interface, amorphous Si/cryst. Si facet form. during solid phase epitaxy 4-88423  
 Xe bubble press. and density, epitaxial growth in Al, EELS, TEM obs. 4-113508  
 ZnS (Se)(Te), chemoepitaxy, reactive diffusion, struct. and growth kinetics 4-80442

# epitaxial layers

- see also magnetic epitaxial layers; metallic epitaxial layers; semiconductor epitaxial layers  
 alkaline earth fluorides, epitaxial growth on semiconductors, Rutherford backscatt./channelling studies 4-80438  
 PLZT epitaxial thin films, ferroelec. and electrooptical props. 4-104530  
 surface, stepped, electron and atom diff. anal. 4-65530  
 two-dimensional random growth model in layer-by-layer epitaxy, backscattered electron diff. beam profile 4-84535  
 zinc phthalocyanine film, charge transfer complex with piperidine, unit cell constr., crystal habit 4-88425  
 (Ba,Sr)TiO<sub>3</sub> heteroepitaxial ferroelec. films, domain struct. 4-65993  
 CaF<sub>2</sub>-Si, epitaxial surface morphology, SEM study 4-113822  
 Ca<sub>1-x</sub>Sr<sub>x</sub>F<sub>2</sub>, epitaxial growth in GaAs/Ca<sub>1-x</sub>Sr<sub>x</sub>F<sub>2</sub>/GaAs (100) lattice-matched MBE structures 4-88562  
 ErH<sub>3</sub> films, epitaxial growth by vacuum deposition 4-70596  
 NiSi<sub>2</sub> epilayers on Si (001), electronic struct. determ. 4-88549  
 Pd-Si(111) interface, atomic intermixing and electronic interaction 4-70478  
 SrF<sub>2</sub>, single cryst., on GaAs (001) electron beam resist. and dielec. for insulator/semicond. struct. 4-98758  
 TiO<sub>2</sub>-V<sub>2</sub>O<sub>5</sub> catalysts, EXAFS study 4-62244

# epitaxy see epitaxial growth

# EPR see paramagnetic resonance

# EPR line breadth

- alkali silicate glass, EPR of trapped hole centres 4-76237  
 antisymmetric exchange chains, ESR linewidth ang. depend. asymmetry 4-71160  
 (BEDT-TTF):ReO<sub>4</sub> salts, comparative study of an organic supercond., Peierls metal and semicond., EPR 4-71172  
 bis[1,2-bis(2-methoxyethoxy)ethane] sodium biphenylide, spin diffusion, mag. props. ESR study 4-71154  
 di-tert butylnitroxide, soln., electron spin exchange, EPR 4-64518  
 di-terbutylnitroxide, spin label for EPR studies in liq. crystals, proton hyperfine tensor 4-84855  
 difluoranthenyolphosphorhexafluoride, Overhauser shift, hyperfine interaction 4-76235  
 EPR, lineshapes, freq. swept and field swept for spin 1/2 4-86451  
 EPR linewidths and exchange integrals 4-76244  
 graphite-MnCl<sub>2</sub> intercalation cpds., first and second stage, mag. props. 4-109058  
 hexaimidazolecadmium (II) nitrate: Cu (II), Jahn-Teller distortion, EPR 4-71165  
 hydrogen copper (II) maleate tetrahydrate, one-dimensional ferromagnetism 4-71051  
 inhomogeneous broadening, saturation of Zeeman subsystem (Russian) 4-92949  
 intrinsic strain determ. from EPR linewidths and spin-strain coupling tensor 4-84850  
 Kevlar 49 fibres, EPR study of stress-induced free radicals 4-109076  
 metallic samples, paramagnetic reson. lineshape anal., appl. to Gd alloys 4-88714  
 nematic-smectic A transition, spin probe mol. dynamics, ESR obs. 4-108614  
 nickelocenium cation, electronic struct., Jahn-Teller effect, EPR study 4-64517  
 poly(p-phenylene) and p-phenylene oligomers, alkali metal doped, EPR study 4-76238  
 polyacetylene, <sup>13</sup>C NMR and ESR, Coulomb effects 4-109087  
 polybenzyl glutamate, rodlike, rot. motion, ESR line-shape anal. 4-59812  
 radicals, spin polarised (CIDEP), continuous wave flash photolysis ESR spectra using time integration spectroscopy 4-74274  
 spin-echo amplitudes, line shapes, slow-motion approach 4-104483  
 TANOL, nitroxide spin labels, very slow motion detect. from double modulation ESR spectra 4-109054  
 TANOL, nitroxide spin probes, line widths and shifts, ESR 4-71181  
 Tempone nitroxide radical, in MBBA liq. cryst., mag. field induced distrib., ESR 4-80820  
 transition metal-polymer composites, superparamagnetic, EPR obs. 4-88716  
 wide line spin generator side band effects in EPR lines 4-95480  
 Al-based dilute foils, conduction electron spin resonance linewidths 4-92961  
 Al<sub>2</sub>O<sub>3</sub>:Cr, photoacoustically detected EPR (Korean) 4-114155  
 Cu, fine particles, CESR 4-76251  
 CoNbOF<sub>6</sub>·6H<sub>2</sub>O:Mn(II), host spin-lattice relax. narrowing in EPR, phase transition 4-71162  
 Cr<sub>2</sub>O<sub>3</sub>, ferromag., Curie point transition, EPR obs. 4-109061  
 Cr<sub>2</sub>TeO<sub>6</sub>, antiferromag. insulator, MM wavelength mag. reson. study 4-80812  
 Cr<sub>2</sub>WO<sub>6</sub>, antiferromag. insulator, MM wavelength mag. reson. study 4-80812  
 CsFeS<sub>2</sub>, quasi 1-D alternating antiferromag., EPR study 4-109062  
 Cu complexes, bis-piperidinium tetrachlorocuprate, ESR linewidth ang. depend. 4-71160  
 Cu complexes, polyamine Cu (II) in soln., ESR hyperfine linewidth anal. 4-83394  
 Fe-Ni-P spin glass alloys, ESR study 4-71153

# EPR line breadth continued

- Fe<sub>2</sub>Ni<sub>80</sub>-P<sub>14</sub>B<sub>6</sub>, amorphous, spin glass alloys, EPR meas. and mag. props. 4-84847  
 FeOHSO<sub>4</sub> superparamagnetic particles, EPR linewidth 4-84820  
 Ge-S glasses, narrow Lorentzian ESR signals 4-65858  
 KBr-KI, Ag atoms behaviour (Russian) 4-76245  
 KCrO<sub>2</sub>, EPR linewidths and exchange integrals 4-76244  
 KTaO<sub>3</sub>:Fe<sup>3+</sup>, EPR spectra, superhyperfine struct., spin Hamiltonian parameters 4-98942  
 LiCrO<sub>2</sub>, EPR linewidths and exchange integrals 4-76244  
 LiNbO<sub>3</sub>:Mn<sup>2+</sup>(Cr<sup>3+</sup>)(Cu<sup>2+</sup>), spin-lattice relax., EPR studies 4-114157  
 Mg, fine particles, CESR 4-76251  
 MnCl<sub>2</sub>·4H<sub>2</sub>O, photoacoustically detected EPR (Korean) 4-114155  
 MnSO<sub>4</sub>·4H<sub>2</sub>O, photoacoustically detected EPR (Korean) 4-114155  
 MnSeO<sub>4</sub>, antiferromag. ordering EPR study 4-92954  
 NH<sub>4</sub>AlF<sub>6</sub>, clusters and critical slowing down near T<sub>c</sub>, EPR study 4-65982  
 NaAl(SO<sub>4</sub>)<sub>2</sub>·12H<sub>2</sub>O:Fe<sup>3+</sup>, single crystal EPR, resonance linewidths, crystal field splittings 4-84851  
 Na<sub>2</sub>O-SiO<sub>2</sub> glass, ferrite precip., ESR and Mossbauer obs. 4-99386  
 Ni (III) complex, dichloro bis-o-phenylene bis-dimethyl arsino nickelate (III) chloride, exchange interaction, EPR 4-71164  
 NiCl<sub>2</sub>-graphite intercalation cpd., two-dimensional ferromagnet, EPR meas. 4-109069  
 O<sub>2</sub>, collisional ESR linewidths 4-91288  
 Rb<sub>2</sub>ZnCl<sub>4</sub>:Mn<sup>2+</sup>, incommensurate phase, quadrupolar cryst. field modulation, EPR study 4-76239  
 Si (001) wafers, thermally oxidised, P<sub>b</sub> interface centres, ESR study, effect of As<sup>+</sup> ion implantation 4-92960  
 Si:P, motional narrowing of ESR line 4-104484  
 Si-SiO<sub>2</sub> interface, As<sup>+</sup> implanted, defects, ESR study 4-61591  
 ThBr<sub>4</sub>, incommensurate phase, Gd<sup>3+</sup> EPR study 4-76246  
 VO<sup>2+</sup> ion impurities in crystalline solids, EPR spectra and spin Hamiltonian parameters 4-104490  
 ZnNbOF<sub>6</sub>·6H<sub>2</sub>O:Mn(II), host spin-lattice relax. narrowing in EPR, phase transition 4-71162
- epsilon meson resonances** see eta meson resonances
- equalisers**  
 digital optical communication, numerical optimisation of equalising filters 4-83721  
 diode-switchable coaxial cable delay system for a synthesis radio telescope 4-101164
- equations**  
 for equations used in specific subjects, see the specific indexing heading  
 see also Bethe-Salpeter equation; differential equations; equations of state; functional equations; integral equations; nonlinear equations  
 No entries
- equations of state**  
 see also equations of state of gases; equations of state of liquids; equations of state of solids; phase transformations; thermodynamics  
 aerosols, gas-solid, Joule-Thomson effect statistical thermodynamics 4-65048  
 compressible two-phase flow, appl. to flow metering 4-97656  
 elastic body with boundary load sources, network model 4-95177  
 fluids, perturbed hard-sphere equations of state of real fluids, effective hard-sphere diameters calc. 4-113566  
 fluids, pure, cubic eqns. of state on crit. isotherms 4-113564  
 gas solubility calcs., new group contrib. eqn. of state appl. 4-88296  
 general relativistic fluid eqns. of motion, beam equilibrium and stability 4-113173  
 hard sphere and disc systems, eqns. of state 4-98233  
 hard sphere fluids, classical and quantum, eqns. of state 4-60793  
 hard-sphere fluid near hard wall, virial approach, superposition approximation calcs. 4-63649  
 hard-sphere suspensions, diffusion investigation 4-114839  
 Ising ferromagnets, three-dimensional, phase transitions in classical vector models 4-61548  
 model equations of state for thermodynamic characteristics 4-68195  
 multiphase equilibrium phenomena calc. using eqn. of state 4-113565  
 neutron stars, rotating, constraints on eqn. of state from gamma-ray freq. shifts and line broadening 4-101398  
 PTFE, eqn. of state up to 80 GPa, phase change, shock-recovery expts. 4-75615  
 quark-gluon plasma, confinement effect on sound vel. 4-68508  
 shear-free perfect fluids with zero mag. Weyl tensor 4-68060  
 supernova matter eqn. of state, neutrino oscill. effects 4-67760  
 supernovae 4-63187  
 suspensions, semiconcentrated fibre, rheological eqn. of state 4-97452  
 Van der Waals eqn. of state 4-63697  
 Van der Waals fluids, saturation and metastable props. 4-61039  
 X-Y model, eqn. of state and quantal crossover in longit. mag. field 4-63682  
 CO<sub>2</sub> hydrocarbon mixtures, Peng-Robinson eqn. of state for vapour-liquid equilib. calc. 4-70334  
 \*He adsorbed monolayer film, effective pot. approx. (Chinese) 4-92471  
 Ne-Kr(O<sub>2</sub>) systems, interaction second initial coeffs. at low temps. 4-98234
- equations of state of gases**  
 acetone-methyl acetate, excess second virial coeff. and critical temp., 4-75109  
 Bose-Einstein gases, expt. eqns. of state (German) 4-95297  
 cyclohexane, vapour, second virial coeff. and viscosity coeff. (German) 4-60577  
 dense gases, second virial coeffs., phase space subdivision 4-97736  
 dense monatomic and molecular fluids and their mixtures, shear viscosity, thermal cond., anal. 4-113688  
 ethanol, second virial coeff. determ. by meas. press. as function of const. vol. and mass (German) 4-83971  
 explosive, RX-26-AF, shock initiation, reactive flow lagrange anal. 4-109661  
 fluids, orthobaric props. of spherical and linear mols., intermol. pot. effect 4-74310  
 HMX explosive, thermal initiation and burning prior to detonation 4-109656  
 ideal Bose gas, magnetised, crit. props. 4-58734  
 imperfect gases, low density expansions, condensed phase prediction 4-97738  
 inert gas mixtures, equilibrium and transport props. at low density 4-97744  
 inert gases, equilibrium and transport props. at low density 4-97744

## equations of state of gases continued

- methane, VIM theory of mol. thermodynamics, analytic eqn. of state 4-113282  
 methanol, second and third virial coefficients determ. from press. meas. (German) 4-83970  
 polar fluids, VIM theory of mol. thermodynamics, analytic eqns. of state 4-113283  
 real gases, differential equation, correlation functions 4-69855  
 second virial coeff. estimation from press. meas. 4-75110  
 unified equation incorporating behaviour in pericritical region 4-79699  
 Ar, high press. PVT meas. 4-97737  
 Ar, third virial coefficient, nonadditive three-particle interactions effects 4-69857  
 Ar<sub>2</sub>, VIM theory of mol. thermodynamics, analytic eqn. of state 4-113282  
 C, thermodynamics of vaporisation and virial eqn. of state 4-103918  
 He bubbles, equation of state for small cavities 4-103824  
 N<sub>2</sub> gas, structural second virial coeff., neutron scatt., meas. 4-69854  
 Ne-Ar, interatomic pot., dilute gas bulk and microscopic props. 4-96638

## equations of state of liquids

- acetic acid, dipole assoc. in nonpolar solvents (German) 4-109116  
 benzene, liquid, shock compression and Hugoniot data 4-108518  
 benzene-cyclohexane, density meas., excess thermodynamic quantities calc., equation of state 4-80261  
 calorim. eqn. of state near crit. point (Russian) 4-84360  
 dense molecular fluids, shock wave eqn. of state and elec. cond. 4-108517  
 dense monatomic and molecular fluids and their mixtures, shear viscosity, thermal cond., anal. 4-113688  
 fluids, orthobaric props. of spherical and linear mols., intermol. pot. effect 4-74310  
 hard convex bodies and hard body eqn. of state, average correl. function 4-60798  
 hard convex mol. fluids, third and fourth virial coeff. 4-60799  
 hard sphere binary mixture, nonadditive parameter, Percus-Yevick results 4-70012  
 hard sphere of eqn. of state, molecular dynamics calcs. 4-103626  
 infinitely thin hard platelets, isotropic-nematic transition, Monte Carlo study 4-108616  
 internal pressure behaviour w.r.t. variations in temp., vol. and cohesive energy density 4-108571  
 Lennard-Jones two dimens. eqn. of state, mol. dynamics study 4-84361  
 liquid state, vapour condensation, canonical partition function, virial expansion 4-97991  
 methane, VIM theory of mol. thermodynamics, analytic eqn. of state 4-113282  
 molecular fluids, effective spherical pot. 4-108267  
 molecular liquids, thermodynamic props. of binary mixtures of weakly nonspherical mols. 4-113563  
 naphthalene, solns. in water-ethanol mixtures, thermodynamic props. 4-80264  
 nitromethane, Raman scatt. temp. meas. behind a shock wave 4-114287  
 nonionic micellar solns., phase diagrams, statistical model, osmotic compressibility, virial coeff. 4-89337  
 polar fluids, VIM theory of mol. thermodynamics, analytic eqns. of state 4-113283  
 polybutene, liquid, shock compression and Hugoniot data 4-108518  
 polymer liquids, equation of state for PVT behaviour 4-75638  
 polymer mixing in aq. soln., second virial coeffs. 4-113649  
 polymer solns., dilute, in viscoelastic fluids, rheological eqns. of state with single relax. time 4-64986  
 polymer solns., non-Newtonian shear viscosity, normal stress coeffs., corresponding states in rheology 4-64899  
 polymer solutions, equation of state theory, polymer-solvent interaction parameter 4-84359  
 polymer solutions, field theoretic renormalisation group and scaling behaviour 4-84134  
 polymer solutions, virial equations, transformation between conc. scales 4-108570  
 polystyrene in toluene and methyl ethyl ketone soln., conc. fluctuation dynamics 4-103637  
 polystyrene solns., expansion coeff. light scatt. (Japanese) 4-97999  
 pyrrhotite (Fe<sub>9</sub>S<sub>8</sub>), eqn. of state at Earth core conditions 4-115395  
 quantum liqs., inhomogeneous, direct correl. function, appl. to liq. metals 4-60796  
 unified equation incorporating behaviour in pericritical region 4-79699  
 virial eqn. conformity condition and compressibility (Russian) 4-70332  
 water, PVT props. in critical region (Japanese) 4-98235  
 Ar<sub>2</sub>, VIM theory of mol. thermodynamics, analytic eqn. of state 4-113282  
 CO<sub>2</sub>+methane liquid mixtures, thermodynamic props. 4-70335  
 Cs, eqn. of state and pVT data up to 2000K and 600 bar 4-103898  
 Fe<sub>9</sub>S<sub>8</sub> (pyrrhotite), eqn. of state at Earth core conditions 4-115395  
 H<sub>2</sub>O-NaOH-SiO<sub>2</sub> system, p-V-T behaviour, rel. to hydrothermal growth of quartz 4-60875  
<sup>3</sup>He-CO<sub>2</sub> mixture, coexisting phases near liquid-vapour transition (Russian) 4-88364  
 N<sub>2</sub> fluid, equation of state near critical points, scaling props. 4-98238  
 NaCl, aq. soln., thermodynamic props. 4-98313  
 Ne fluid, equation of state near critical points, scaling props. 4-98238  
 O<sub>2</sub>+N<sub>2</sub> liquid mixture, Hugoniot states and shock press. 4-108572  
 S, doped liq., polymerisation transition, heat capacity 4-85308  
 ZnCl<sub>2</sub>, aqueous soln., refractive index and eqn. of state under shock 4-114238

## equations of state of solids

- alkali metals, equations of state, shock wave isotherms 4-108573  
 alloys, plastic eqn. of state rel. to scaling behaviour 4-109462  
 benzene, eqn. of state and optical luminosity shocked up to 210 GPa (2.1 Mbar) 4-61041  
 CsCl, Decker equations of state, polynomial representation 4-84362  
 detonation, overdriven expts., product EOS above Chapman Jouguet press. 4-109664  
 Dicke-like models, fluctuations and phase transitions 4-92923  
 explosive, RX-26-AF, shock initiation, reactive flow lagrange anal. 4-109661  
 explosives, Composition B-3 and PBXW-109(I), unreacted Hugoniot and shock ignition 4-109654  
 graphite (0001), adsorption of hydrocarbons, polarisability anisotropy, mol. statistical theory 4-80379

## equations of state of solids continued

- III-V covalent semicond. crystals, equation of state, bulk modulus press. derivative 4-98236  
 metal unsintered powders, Hugoniot meas. using C gauges 4-108578  
 metals, potential at at. boundaries in Thomas-Fermi model and eqns. of states (Chinese) 4-70333  
 nitromethane, shocked, OK isotherm, electronic struct. calc. 4-108579  
 noble metals, Hugoniot curve calc., by pseudopotential method 4-80188  
 one-component plasma liquid, eqn. of state for strongly coupled limit 4-103896  
 polybutene, eqn. of state and optical luminosity shocked up to 210 GPa (2.1 Mbar) 4-61041  
 polyethylene, eqn. of state and optical luminosity shocked up to 210 GPa (2.1 Mbar) 4-61041  
 pyrrhotite (Fe<sub>9</sub>S<sub>8</sub>), eqn. of state at Earth core conditions 4-115395  
 shock wave effects, conf., Santa Fe, USA (July 1983) 4-106116  
 solids, Hugoniot data from nuclear-explosive generated shocks 4-108521  
 two dimensional lattice, virial theorem, lattice dynamics and struct. instability (Russian) 4-68154  
 Al, damage simulation in high velocity impact 4-108529  
 Al, P-V-T relation as press. and temp. scale under very high press. 4-75637  
 Al, shock compressibility in range 0.4 to 4 Gbar, reflection method 4-92294  
 Al, shock impedance match expts., 0.1-2.5 TPa 4-108522  
 Al, sound velocity behind strong shock waves, optical technique anal. 4-108554  
 C powders, Ar(N<sub>2</sub>)(CO<sub>2</sub>) adsorption, second gas-solid virial coeffs., chromatographic determ. 4-114819  
 CoO, eqn. of state and Gruneisen parameters 4-92331  
 CsCaF<sub>3</sub>, parameter free eqn. of state calcs. 4-70336  
 CsCl, eqn. of state used for secondary calibration scale at low temps. 4-103897  
 Fe 4-108576  
 FeO, eqn. of state and Gruneisen parameters 4-92331  
 Fe<sub>9</sub>S<sub>8</sub> (pyrrhotite), eqn. of state at Earth core conditions 4-115395  
 H<sub>2</sub>, solid, adiabatic eqn. of state at 150 kbar 4-113567  
 MgO, static P-T-V meas. and shock wave data 4-108574  
 MnO, eqn. of state and Gruneisen parameters 4-92331  
 Mo, shock impedance match expts., 0.1-2.5 TPa 4-108522  
 Na, equation of state 4-61040  
 NaCl, Anderson-Gruneisen parameter, volume coefficient of thermal expansion, equation of state, calcs. 4-98237  
 NaCl, Decker equations of state, polynomial representation 4-84362  
 NaCl, eqn. of state used for secondary calibration scale at low temps. 4-103897  
 NaCl, equations of state, shock wave isotherms 4-108573  
 Ne, low temp. eqn. of state under megabar press. 4-61042  
 NiO, eqn. of state and Gruneisen parameters 4-92331  
 SiO<sub>2</sub>, properties of high-pressure fluorite struct. phase 4-110135  
 Ta, shock Hugoniot meas. up to 0.78 TPa 4-108523  
 Ta, shocked; rarefaction velocities and high press. melting point 4-108524  
 U, equation of state, self-consistent muffin-tin orbital calc. 4-108575  
 V, Hugoniot meas. using LLNL two stage light gas gun 4-108577  
 Xe, solid, high press. X-ray diffr. study and eqn. of state, rel. to metallisation transition 4-92333  
 YbH<sub>3</sub>, equation of state and high press. X-ray diffr. studies 4-75665
- equilibrium, chemical** *see chemical equilibrium*  
**equilibrium, phase** *see phase equilibrium*  
**equilibrium constants** *see chemical equilibrium*  
**equilibrium diagrams** *see phase diagrams*  
**equivalent circuits**  
*see also network analysis; network synthesis*  
 AC-MHD salient-pole synchronous generator coupled to Tokamak fusion reactor 4-64238  
 acoustic reflection coefficients and transfer functions meas. by cepstral techniques, elec. analogue 4-60236  
 flux gate sensors, capacitively loaded, steady state characts. 4-101876  
 human EM hazard analysis, human body impedance in VLF to MF band 4-115120  
 impedance meter use for dielectric meas. 4-58841  
 magnetic field problems, nonlinear transient, comparison of lumped and distributed solns. 4-59959  
 piezoelectric disc, transient voltage, 2-D equivalent circuit (Chinese) 4-88772  
 piezoelectric transducers, thickness-mode, three-port model 4-97255  
 trans-polyacetylene/Al photodiode, defect-related current transport 4-76002  
 RF human whole-body absorption rates, effect of separation from ground 4-115121  
 shell, elastic, spherical, equivalent circuit 4-91749  
 sonar HF transducers, review of current practice 4-69654  
 US transducers, high-power asymmetric sandwich (Polish) 4-112618  
 WO<sub>3</sub>, electrochromic cells, equivalent ccts., AC impedance (Japanese) 4-88808
- erbium**  
*see also nuclei with .....*  
 antiferromagnetic phase transition, muon-spin-relax. studies 4-65811  
 electronic struct., press induced 4d occupancy enhancement 4-75844  
 films, hydridisation and catalysis 4-71984  
 L-subshell ionisation cross section, projectile atomic number depend. 4-99267  
 magnetic phase transitions, dilatometric study 4-104415  
 specific heat, 0.4-23K 4-76143  
 total and photoelectric cross sections 4-91244  
 UV-visible and IR spectra, radiative transition probabilities for fluoresc. level 4-114309  
 α-Al<sub>2</sub>O<sub>3</sub>:Er(Gd)(Tb) crystals, radiative and thermochem. effects 4-76491  
 Ba(PO<sub>3</sub>)<sub>2</sub>:Er<sup>3+</sup>(Yb<sup>3+</sup>)(Nd<sup>3+</sup>), quenching of Er luminesc., effect of Nd<sup>3+</sup> and OH<sup>-</sup> 4-81006  
 CaF<sub>2</sub>:Er<sup>3+</sup>, transferred hyperfine interaction parameters, ENDOR 4-84872  
 CaF<sub>2</sub>:La(Er), impurity local structural environments, EXAFS determ. 4-66129  
 Ca(NbO<sub>3</sub>)<sub>2</sub>:Er<sup>3+</sup>, stimulated emission and laser channels 4-91480  
 Cs:Cu, Er, europium, radiation controlled enhancement of electroluminescence 4-76529  
 Cs:Er phosphor, electrolum. spectrum and Er<sup>3+</sup> ion energy level splitting 4-71446

ium continued

- CdF<sub>2</sub>:Er<sup>3+</sup>, energy transfer up-conversion 4-99162  
 CdF<sub>2</sub>:Er<sup>3+</sup>, insulator to semiconductor transition, site selective laser spectroscopy 4-99155  
 CsMnBr<sub>3</sub>:Er<sup>3+</sup>, one-dimensional antiferromagnet, energy migration, luminesc. 4-99149  
 CsMnI<sub>3</sub>:Er<sup>3+</sup>, one-dimensional antiferromagnet, energy migration, luminesc. 4-99149  
 Er,Pr:LiYF<sub>4</sub> crystal quasi-continuous lasing at 0.85  $\mu$ m 4-60049  
 Er,Yb: glass lasers, flash-pumped, energy parameter improvement 4-64711  
 Er<sup>3+</sup> electron impact excitation, level population mechanism 4-74335  
 Er<sup>3+</sup> in ionic crystals, nephelauxetic effect and radial expectation values, dielec. screening model 4-61344  
 Er:BaYbF<sub>8</sub> lamp-pumped 2  $\mu$ m range laser, energy characts. 4-69414  
 Er:glass laser, 1.545  $\mu$ m, Q-switched, output-stabilised, high-repetition rate 4-74545  
 Er<sup>3+</sup>:glass laser, 1.55  $\mu$ m Q-switched, 130 km-long fault location for single-mode optical fibre 4-91601  
 Er<sup>3+</sup>:YAG cross-relaxation laser emitting at 2.94  $\mu$  4-60048  
 Er, A=166.168, pionic M X-rays, energies and widths of transitions 4-112305  
 KLa(MoO<sub>4</sub>)<sub>2</sub>:Er<sup>3+</sup>(Ho<sup>3+</sup>), stimulated emission studies 4-84980  
 LaF<sub>3</sub>:Er<sup>3+</sup> high freq. phonon dynamics, optical detection methods 4-65357  
 LiYF<sub>4</sub>:Er, laser emission parameters 4-79158  
 LiYF<sub>4</sub>:Er,Pr crystal quasi-continuous lasing at 0.85  $\mu$ m 4-60049  
 MgO:Er<sup>3+</sup>, strain results, superposition model of orbit-lattice interaction 4-80557  
 RbMnBr<sub>3</sub>:Er<sup>3+</sup>, one-dimensional antiferromagnet, energy migration, luminesc. 4-99149  
 Si-Er interface, ErSi<sub>2</sub> formation using electron beam heating 4-65494  
 Sr<sub>2</sub>Cd<sub>1-x</sub>F<sub>2-x</sub>:Er<sup>3+</sup>, energy transfer up-conversion 4-99162  
 YAG:Er, photoluminescence spectra meas. (Russian) 4-71442  
 YAlO<sub>3</sub>:Er, laser emission parameters 4-79158  
 YCl<sub>3</sub>:Er<sup>3+</sup> electron impact excitation, level population mechanism 4-74335  
 YF<sub>3</sub>:Er<sup>3+</sup> electron impact excitation, level population mechanism 4-74335  
 Yb, Er: glass lasers, possible lamp pumping efficiency improvement 4-87337  
 ZnS:Cu, Cl, Er films, electroluminesc., hot electron energy distribution 4-85012  
 ZnS:Cu, Er phosphor, electroluminescence and photoluminescence emission spectra 4-76512  
 ZnS:Er(Mn,Er), phosphors, electro- and photo-luminescence props. 4-104652

## erbium alloys

- Ag-Er, dil., impurity-induced muon depolarisation, mag. field depend. 4-71228  
 Dy-Er<sub>1-x</sub>Ni<sub>x</sub>, mag. struct. characts. (Russian) 4-92894  
 Er-H, mag. props., H content effects 4-98923  
 ErCo<sub>5</sub>Sn<sub>6</sub>, cryst. struct. and mag. props. (Russian) 4-88135  
 ErFe<sub>2</sub>, intermetallics, SXAPS studies 4-81039  
 ErFe<sub>23</sub>, mag. struct. study 4-108987  
 ErGa<sub>2</sub>, metamagnetic, spin-flip transitions, magnetoresistance anomalies (Russian) 4-98880  
 ErNi<sub>3</sub>, crystal electric field splitting, inelastic neutron scatt. study 4-65648  
 Er<sub>2</sub>NiB<sub>13</sub>, cryst. struct. determ. 4-75376  
 Er<sub>3</sub>Rh<sub>2</sub>, mag. props. meas. 4-61521  
 ErRh<sub>4</sub>B<sub>4</sub>, mag. props. and crystal field effects 4-84767  
 ErRh<sub>4</sub>B<sub>4</sub>, metamagnetism, magnetisation anomaly 4-114144  
 Sc-Er, spin glasses with uniaxial anisotropy 4-71099  
 Ti-Er, rapidly solidified dispersion strengthened, struct. and props. 4-114561  
 Ti-Er, rapidly solidified dispersion strengthened, tensile and creep props. 4-114562  
 Y-Sc, spin glasses with uniaxial anisotropy 4-71099

## erbium compounds

- see also erbium alloys  
 hexa antipyrine tri-iodide:Gd<sup>3+</sup>, soft mode dynamics, phase transition, EPR 4-109068  
 ionic crystals, Er<sup>3+</sup> nephelauxetic effect and radial expectation values, dielec. screening model 4-61344  
 (CaF<sub>2</sub>)<sub>1-x</sub>(ErF<sub>3</sub>)<sub>x</sub> solid soln., superstructure, ODMR and MCD study 4-75401  
 CeO<sub>2</sub>-Er<sub>2</sub>O<sub>3</sub> solid solutions, elec. cond., temp. depend., 400-1200°C 4-61142  
 Er complex, Er-dipthalocyanine films, electrochromism for all solid display cells 4-76435  
 Er<sup>3+</sup> complexes, diglycollate, circular dichroism, optical density 4-80902  
 Er<sup>3+</sup> complexes, pyrogermanate, circular dichroism, optical density 4-80902  
 Er<sub>0.8</sub>Ca<sub>0.2</sub>CrO<sub>3</sub>, ionic cond. and thermal expansion 4-84461  
 Er<sub>2</sub>CoO<sub>4</sub>, Er<sub>2</sub>CoO<sub>4</sub>, synthesis and high-temperature study (French) 4-85095  
 ErCrO<sub>3</sub>, quadrupole splitting and NMR near Morin-type transition 4-80839  
 ErF<sub>3</sub> amorphous thin films, AC cond. meas. 4-76059  
 ErF<sub>3</sub>, thin films, elec. cond., 323-396K 4-98791  
 ErFe<sub>2</sub>B, with struct. of CeCo<sub>2</sub>B type, unit cell parameters determ. 4-65243  
 ErFeO<sub>3</sub>, muon site determ. 4-71227  
 ErFeO<sub>3</sub>, spin reorientation in Landau theory of phase transformations 4-98884  
 ErH<sub>2</sub> films, epitaxial growth by vacuum deposition 4-70596  
 Er<sub>0.4</sub>Ho<sub>0.6</sub>Rh<sub>4</sub>B<sub>4</sub>, reentrant supercond., US attenuation meas., 1.5 to 20K 4-98810  
 Er<sub>2</sub>O<sub>3</sub>, relative concs. in tunnelling barriers, XPS obs., antiferromag. transition 4-88934  
 Er(OH)<sub>3</sub>, relative concs. in tunnelling barriers, XPS obs., antiferromag. transition 4-88934  
 Er(OH)<sub>3</sub>.0.5H<sub>2</sub>O, amorphous, short-range order struct., X-ray diff. 4-75296  
 Er<sub>2</sub>O<sub>3</sub>SO<sub>4</sub>, magnetic phase diagram, magnetisation and susceptibility meas. 4-92912  
 ErRh<sub>4</sub>B<sub>4</sub>, coexistence of superconductivity and mag. order 4-104423  
 ErRh<sub>4</sub>B<sub>4</sub>, coexistence phase of ferromagnetism and supercond., in terms of modulated supercond. state 4-98805

## erbium compounds continued

- ErRh<sub>4</sub>B<sub>4</sub>, ferromagnetic superconductor, d-f interaction 4-98801  
 ErRh<sub>4</sub>B<sub>4</sub>, mag. supercond., muon spin relax. studies 4-65923  
 ErRh<sub>4</sub>B<sub>4</sub>, mixed state and mag. props. 4-98830  
 ErS, energy band struct., X-ray study 4-84565  
 Er<sub>2</sub>S<sub>3</sub>, prep. in high purity powder form from elements 4-108298  
 Er<sub>2</sub>Si<sub>5</sub>, mag. phase transition, elec. cond. and cryst. struct. 4-88675  
 ErTiO<sub>3</sub>, single cryst., magnetisation and mag. susceptibility 4-88652  
 Er<sub>2</sub>V<sub>10</sub>O<sub>28</sub>.25H<sub>2</sub>O, cryst. struct. 4-75387  
 (Er<sub>1-x</sub>Y<sub>x</sub>)<sub>3</sub>Al<sub>5</sub>O<sub>12</sub>, crystals, temp. dependence of phononless f-f transitions 4-71339  
 EuEr<sub>2</sub>S<sub>4</sub>, band gap width, rel. to short-range environment of S atom 4-80493  
 (Gd<sub>1-x</sub>Er<sub>x</sub>)Al<sub>5</sub>O<sub>12</sub> garnet, 3  $\mu$ m stimulated emission, concentrational tuning 4-76498  
 Ho<sub>1-x</sub>Er<sub>x</sub>Mo<sub>6</sub>S<sub>8</sub>, relaxation of ferromagnetic ordering and superconductivity 4-98886  
 K<sub>2</sub>Bi<sub>0.9</sub>Er<sub>0.1</sub>(MoO<sub>4</sub>)<sub>2</sub>, single crystals, Czochralski growth and optical props. (Chinese) 4-114294  
 PbF<sub>2</sub>-GaF<sub>3</sub>-Al(PO<sub>3</sub>)<sub>3</sub>-ErF<sub>3</sub>-based fluoride glasses, fluorescence studies 4-99170

## ergodic theorem see statistical mechanics

## ergonomics

- see also human factors; man machine systems  
 bicycle ergometer for paralysed muscle 4-85573  
 display terminal, eye scanning behaviour 4-81706  
 ergometer, UT-7508, upgrading of automatic physical load control 4-93977  
 exercise efficiency during arm ergometry: effects of speed and work rate 4-93781  
 joint motion in men using electrogoniometers 4-81739  
 perinatal monitoring, ergonomic study 4-85568  
 sunburn, annotated bibliography, historical development 4-58608  
 United States Navy Diving Biomedical R&D Program overview 4-115255  
 upper extremity electro-ergometer 4-89811

## erosion

- Adriatic Sea beaches, erosion and protection (Italian) 4-82028  
 alluvial fan development, book 4-82613  
 Ardeche Submediterranean rangelands, France, surface runoff and sediment yield 4-115462  
 rock avalanches due to earthquakes 4-82059  
 Bahia State, Brazil, rock chem. weathering anal. and salinity 4-100560  
 beach erosion processes 4-94087  
 bedrock weathering and silcrete formation in S Africa 4-62817  
 bottom current changes and sediment erosion during last 5 M years 4-82033  
 SE Brazilian Plateau, hillslope evolution and Quaternary sediments 4-62807  
 continental topography, long-term erosional decay rel. to flexural models of lithosphere 4-67189  
 Earth crust, effects of denudation on evolution of structures formed by vertical movements 4-100504  
 gneiss, frost weathering in intertidal zone 4-115385  
 gravel-lined channels, bank erosion rate investigation 4-82102  
 N Greece, agriculture influences upon erosion and runoff processes 4-115460  
 Hunza River, Karakoram region, sediment load and erosion 4-62874  
 Hunza Valley, Pakistan, Quaternary glacial history, geomorphology and sediments 4-62825  
 Hunza Valley, Pakistan, salt efflorescences and salt weathering 4-62827  
 Idukki reservoir catchment, Kerala, India, valley slumping, sedimentation and reservoir capacity 4-100628  
 intertidal zone, rock weathering due to frost action 4-115385  
 NE Iowa, USA, geology and erosion of Palaeozoic Plateau area 4-77491  
 NE Iowa, USA, karst development in Palaeozoic rocks 4-77518  
 Japan, precipitation causing landslide (Japanese) 4-105635  
 Karakoram region, glacier meltwater runoff, sediment anal. and erosion 4-62869  
 limestone, frost weathering in intertidal zone 4-115385  
 lunar soil electrostatic erosion 4-94656  
 Mediterranean Sea site in Messinian, lakes characts., river flow directions and erosion 4-100625  
 Mojave Desert, California, USA, downhill movement of stones 4-115461  
 Negev desert, erosion cirques triggered by emerging groundwater 4-77516  
 oceans and land erosion 4-81831  
 SW Pacific, bottom current changes and sediment erosion during last 5 M years 4-82033  
 pebble abrasion by wave action on coastal benches 4-115386  
 piedmont junction migration, hillslope and channel processes 4-62808  
 riverbank erosion, failure mechanisms of shallow sandbed stream banks 4-62852  
 rock crack growth during unroofing of crustal rocks 4-94102  
 rock weathering processes at high altitude 4-62821  
 rocks chemical weathering in Hunza region, Karakoram, rock temp. obs. 4-62816  
 scarplike landform evolution model 4-110148  
 schist, frost weathering in intertidal zone 4-115385  
 Sinai, Egypt, erosion cirques triggered by emerging groundwater 4-77516  
 slopes on opposite sides of road cutting, erosion and runoff influenced by rain direction 4-77563  
 soil erosion, book 4-101598  
 soil erosion by water runoff, stochastic model 4-100641  
 Southern Ocean, erosion by bottom currents in Atlantic sector 4-82034  
 mountain stream, en masse removal of stored sediment 4-115459  
 submerged continental margin 4-100534  
 Sussex Downs, England, exceptional rainfall causing soil erosion 4-82207  
 Tatra Mts., Poland aeolian sediment erosion and deposition 4-62818  
 Torlesse mountain stream, New Zealand, stored sediment removal by streamflow 4-115459  
 turbidity currents in glacial lake, occurrence and movement monitoring with three-dimensional sensor network 4-100644  
 weathering of rocks, chemical kinetics 4-94135  
 wind erosion from coal surfaces, computer simulation program 4-82211

## error analysis

- see also error correction; error detection  
 acoustic power/intensity under water, measurement using dual-hydrophone system (Chinese) 4-103091

**error analysis continued**

- astrometric determ. of absolute stellar proper motions, error anal. via Monte Carlo simulation 4-94563  
 camera, high speed, real time error anal. by laser and position sensing system 4-111227  
 crack problems, fully plastic, consistency check appl. 4-97420  
 data smoothing, matrix formulation, least-squares principle 4-102557  
 dispersive optical fibre, channels, digital pulse position transmission anal. 4-60177  
 Fourier transform filtering of two-dimensional fluorescence data 4-101820  
 frequency comparison by pulse coincident method 4-58815  
 heat transfer, unsteady state, in a wall, finite difference anal. (French) 4-60416  
 laser automatic refractometer phase transform. error anal. 4-63776  
 linear algebraic equations, direct and indirect optical solutions, error source modelling 4-96816  
 lunar radio flux data use in broadband antenna system meas., error anal. 4-110549  
 measure of relative error for vectors 4-58625  
 measurement data processing, error analysis (German) 4-101806  
 multiplicity measurements, error analysis, fold patterns 4-102556  
 optics, near-cylindrical, orthonormal surface error descriptor set 4-107911  
 ordinary differential equations numerical integration, global error estimation, stochastic approach, celestial mechanics appl. 4-82401  
 Orr-Sommerfeld equation asymptotic solns., error estimates 4-103419  
 soil heat sounding by ball probe, results interpretation and meas. error anal. 4-94250  
 spectroscopy, measurement optimisation, generalized error anal. (Russian) 4-58892  
 speech, all-zero model for higher pole correction 4-103146  
 stiffness and the automatic selection of ODE codes 4-67968  
 structural elements, stress conc., empirical-numerical methods, accuracy 4-108013  
 weather, large-scale forecast skill rel. to predictability error growth estimates 4-62884

**error compensation**

- see also error correction*  
 analogue meas. channels, design for metrological reliability (Russian) 4-95369  
 marine shallow seismic responses, dispersion compensation 4-110315

**error correction**

- band-limited discrete-time signals interpolation, out-of-band energy minimisation 4-103110  
 microprocessor-controlled remote data acquisition unit for hyperbaric environment 4-109985  
 optical discs systems and applications, conf., Arlington, VA, USA (June 1983) 4-90287  
 turbulent temp. field, temp. fluctuation meas. correction, using cold wires 4-60567  
 TV sets, colorimetric errors correction (Polish) 4-101894

**error correction codes**

- planet photographs transmission to Earth (Afrikaans) 4-77724  
 underwater acoustic telemetry error detection and correction codes 4-112624

**error detection**

- see also error analysis*  
 microprocessor-controlled remote data acquisition unit for hyperbaric environment 4-109985  
 optical discs systems and applications, conf., Arlington, VA, USA (June 1983) 4-90287

**error detection codes**

- planet photographs transmission to Earth (Afrikaans) 4-77724

**error statistics**

- radioactive lifetime estimation with large experimental errors 4-102558

**errors**

- see also measurement errors*  
 algorithm for error adjustment of potential field data along a survey network 4-100438  
 atmospheric band transmittance, approx. of product error during calc. 4-72701  
 balloon measurements of troposphere and stratosphere wind, tracking errors 4-110293  
 basis set error and geometry optimisation in ab initio calc. 4-64357  
 binary Fourier transform holograms, quantisation and phase encoding errors reduction 4-107557  
 coherent optical spectrum analysers, assembly and alignment errors 4-74651  
 dimethyl sulphoxide, basis set error and geometry optimisation in ab initio calc. 4-64357  
 flood discharge meas., error modelling 4-82127  
 Fourier transform spectroscopy, phase error correction 4-101930  
 hydrology, statistical models, estimation theory and errors 4-82128  
 Indo-Asian plate convergence and triangulation surveys anal., errors determ. 4-62788  
 Langmuir probe for ion parameters determ., appl. to ionosphere 4-105731  
 molecular simulation calcs., error estimation 4-88050  
 Pakistan to Soviet Union triangulation connection, error anal. and plate motion 4-62661  
 predictability of atm. and ocean, Lagrangian and Eulerian views 4-62877  
 SEASAT altimeter measurements over English Channel, geoid and tides, error anal. 4-67490  
 shell, circular cylindrical, fluid filled beam-type, fluid filled, bending vs. membrane theory 4-87580  
 Shimadzu multichannel selective stat analyser CL-12, interference factor anal. for precision of quantitative clinical anal. (Japanese) 4-62620  
 stars, microturbulent velocities determ., systematic errors 4-77814  
 two-phase flow, voids fraction meas. by acoustic sounding method, error estimation 4-65006

erythema *see biological effects of ultraviolet radiation*

erythrocytes *see blood; cellular biophysics*

Esaki diodes *see tunnel diodes*

Esaki effect *see tunnelling*

ESCA *see electron spectroscopy; spectrochemical analysis; X-ray photoelectron spectroscopy*

ESR *see paramagnetic resonance*

**estimation theory**

- see also information theory*  
 adaptive satellite orbit estimation scheme 4-82373  
 detector use for unbiased estimation of no. and sizes of arbitrary particles 4-86386  
 hydrology, statistical models, estimation theory and errors 4-82128  
 log-normal quantiles in hydrology, estimation, Monte Carlo results and first order approx. 4-100771  
 noisy speech, optimal estimators for spectral restoration 4-103130  
 orbital lifetime estimation method for near Earth satellites 4-82374  
 orbits, small perturbations determ. via estimation method 4-82403  
 random static fields in spatial noise, optimum estimation of shift 4-96753  
 retardation effect, fast moving sound source motion parameter estimation 4-103160

**eta meson resonances**

- $D^+$  semileptonic decay widths,  $I=0$   $\eta$  and  $\eta'$  final states, QCD sum rules 4-95789  
 $\eta$  and  $\eta'$  radiative decays, light quark mass ratios, vacuum flavour symmetry breaking 4-73761  
 $\eta \rightarrow \phi\phi$  decay obs.,  $\eta$  spin and parity determ. 4-78550  
 $\eta$ ,  $\eta'$  (1275) pseudoscalar  $J^{PC}=0^{-+}$  spectrum in QCD 4-90805  
 $\eta \rightarrow 3\pi$ , isospin violating, branching ratio 4-78551  
 $F^+$  semileptonic decay widths,  $I=0$   $\eta$  and  $\eta'$  final states, QCD sum rules 4-95789  
 $\gamma\gamma \rightarrow \eta'$  in  $e^+e^- \rightarrow e^+e^-\pi^+\pi^-\gamma$ , transition form factor 4-95867  
 $\gamma\gamma \rightarrow \eta\pi^0$ , gluonic contribs. to two photon exclusive processes, gg Fock states 4-59123  
 $\pi^0 \rightarrow \eta\eta$ , 38 GeV/c, glueball search, G(1590) decays 4-78565  
 $\pi^0 \rightarrow \gamma\gamma$ , 13 GeV/c, expt. search for narrow resonances,  $\eta$  prod. 4-73772

**eta mesons**

- pseudoscalar  $J^{PC}=0^{-+}$  spectrum in QCD 4-90805  
 short-range NN repulsion, omega and eta meson exchange, Regge behaviour 4-106576  
 $D^+$  semileptonic decay widths,  $I=0$   $\eta$  and  $\eta'$  final states, QCD sum rules 4-95789  
 $e^+e^- \rightarrow \pi^+\pi^-\pi^0$ , threshold enhancement of cross section 4-111465  
 $\eta \rightarrow 3\pi$ , discrepancies due to departure from chiral symmetry, unitarity and analyticity 4-102116  
 $\eta$  and  $\eta'$  radiative decays, light quark mass ratios, vacuum flavour symmetry breaking 4-73761  
 $\eta$  production in cosmic ray X-ray families 4-106554  
 $\eta \rightarrow \pi^+\pi^-\pi^0$ , current-quark mass ratios, mass-matrix element,  $\rho$ -dominance assumption 4-106528  
 $\eta \rightarrow \mu^+\mu^-\gamma$ , rare decays, conservation law tests, neutral currents 4-102113  
 $F^+$  semileptonic decay widths,  $I=0$   $\eta$  and  $\eta'$  final states, QCD sum rules 4-95789  
 $\pi^0 \rightarrow \eta\eta$ , 38 GeV/c, glueball search, G(1590) decays 4-78565

etalons *see interferometers*

etchants *see etching*

**etching**

- see also crystal defects; dislocation etching; sputter etching*  
 aluminised plastic track detectors, spot development around track- and electric trace-induced perforations 4-102474  
 biotite mica, particle identification by track etch rate meas. as HI residual range function 4-96344  
 brittle fracture, environmentally induced, crystallographic charact. techniques 4-81383  
 cellulose nitrate track detector, ion beam response 4-59585  
 conference on solid state nuclear track detectors, Acapulco, Mexico (Sept. 1983) 4-95027  
 CR-39 damage track detectors for personnel neutron dosimetry, etching processes 4-96377  
 CR-39 detector, proton track etch characts., implications for neutron dosimeter 4-96371  
 CR-39 detectors, p and  $\alpha$  electrochem. etched tracks, pre-etching effects 4-102470  
 CR-39 detectors, pre-irradiation treatments 4-68885  
 CR-39 foil, electrochem. etching, electrostriction effects on track formation 4-102469  
 CR-39 plastic detector, etching conditions and resolution power 4-96330  
 CR-39 plastic detectors, electrolytical meas. for heavy ion identification,  $^{20}\text{Ne}$  appl. 4-96338  
 CR-39 plastic track detector,  $\alpha$ -track registration props., pre-irradiation annealing effect 4-59589  
 CR-39 plastic track detectors, formation of etchable tracks by delta-ray 4-96327  
 CR-39 plastic track detectors, light charged particle registration characts. 4-64306  
 CR-39 thin SSNTD, alpha track etch formation, variable etch rate ratio 4-96329  
 Daicel cellulose nitrate detectors, Fe track etch induction time meas. 4-96334  
 film preparation and etching, vacuum or plasma technology, conf., Brighton, UK (March, 1983) 4-78031  
 graphite, vacancy formation energy, etching and TEM studies 4-92198  
 heteroepitaxial structures, prep. by selective etching 4-99617  
 III-V semiconductor solar cells, anisotropically etched, design and anal. using ray-tracing models 4-72114  
 Kapton films,  $\text{CO}_2$  laser assisted UV ablative photoetching 4-93429  
 laser induced rapid etching of surface relief in solids 4-60100  
 latent-image photoetching mechanism, photochemical reaction (Chinese) 4-85223  
 Lexan, track recording behaviour, mag. field effects 4-59583  
 LR115 coloured cellulose nitrate detectors, etching parameter optimisation for processing 4-96332  
 LR115 SSNTD, bulk and  $\alpha$ -track etch rates 4-96331  
 Magnox alloys, etched, surface anal. by secondary ion mass spectrometry and ion scatt. spectroscopy 4-93456  
 Makrofol Polycarbonate plastic track detector, calibration using heavy ions 4-64307  
 metal-polymer bond, adhesion and durability, review 4-99743  
 metals, polycrystalline and single surfaces, sputtering and topography 4-109322  
 mica, muscovite, ion implanted, defect struct. thermal annealing 4-70177

## ing continued

minerals, nuclear track formation models, etching and annealing, review 4-70235

nuclear track technique using heavy ion beams, potential appls. 4-59607

optical etch-rate monitoring, computer simulation of reflectance 4-89152

optical fibres, etching technique for obs. of cross-sections 4-79332

optical fibres, high  $\text{SiO}_2$ , reaction with HF soln. 4-60164

plastic detectors, electrochemical etching optimisation, irradiation fluence effects 4-102468

plastic detectors, track formation theories, etching rate expt. data 4-96328

plastics, etchable track formation for radiation detection 4-68879

PMMA:Si ion implanted film, struct. anal. using differential etching 4-79951

PMMA films, self-developing photoetching by near UV irr. 4-87403

poly base contact etch process 4-71746

polycarbonate,  $\alpha$  and recoil track electrochem. etching response, energy and track density effects 4-102471

polycarbonate foil electrochem. etching, neutron contamination detect. from high energy medical accelerators 4-72431

polycarbonate neutron personnel dosimeters, track electrochem. etching, etchant optimisation 4-102472

polycarbonate neutron track detectors, electrochem. etching of Makrofol E 4-96398

polyimide films, excimer laser etching, emission spectra 4-89142

polyimide films, thermal props. and etching characteristics 4-85225

polymer film, ablative photodecomposition by far UV radiation, microscopic model 4-71483

polymer gratings preparation, by vacuum-UV photoetching 4-91570

$\alpha$ -quartz, electrodeposition of charge-compensating ions 4-61153

quartz, fission damage, etching studies in NaOH, SSNTD appl. 4-96335

quartz, hydrothermally grown, Q determ., IR meas. and etch channel meas. 4-61627

quartz BT-cut plates, etch figures, asymm. etch rate distrib. 4-114703

quartz glass track detectors,  $^{56}\text{Fe}$  ion tracks study 4-59586

quartz plates, AT, CT and DT-cut, etching investig. (*Japanese*) 4-104885

radioactive waste materials, ion implantation effects on dissolution props., simulation of internal irr. due to  $\alpha$ -decay 4-75544

reactive ion beam etching, for semiconductor production, review 4-81322

SAW devices, Ar and reactive ion beam etching 4-81318

semiconductor-liquid junction devices, in situ characterisation 4-99090

semiconductors, photoelectrochemistry, book contrib. 4-88585

silicates, high energy U ion tracks, struct. and annealing 4-70236

solar highly absorbing coatings using graded refractive indices and textured surfaces 4-77146

solid detectors, single- and multi-track events, chemical track etching 4-96333

solid state nuclear track detection, etched track parameters 4-59511

SSNTD, bulk etch rate, effects of etchant conc. and temp. 4-96345

SSNTD, electrochemically etched, particle fluence effects on track diameter and response 4-102473

SSNTD, use of different Mexican commercial polymers, etching, dosimeters 4-102476

steel, austenitic stainless, metallographic revelation of  $\sigma$ -phase and  $\delta$ -ferrite, etching and mag. techniques (*German, English*) 4-66540

steel, austenitic stainless, precipitation kinetics, selective dissolution methods 4-114527

steel, austenitic stainless, SCC in  $\text{MgCl}_2$  soln., fractography, grain struct., SEM obs. (*Japanese*) 4-99651

steel, austenitic stainless, sorption of gaseous T, etching obs. 4-75788

steel, Cr-Ni, annealed,  $\sigma$ -phase precipitation, potentiostatic etching (*German, English*) 4-71823

steel, ferritic stainless, intergranular corrosion susceptibility, etching method 4-85265

steel, stainless, austenite-ferrite duplex, preferential phase dissolution in  $\text{H}_2\text{SO}_4$ -NaCl soln. rel. to heat treatment and comp. 4-81341

steel, stainless high-alloy, black coatings produced by chem. methods 4-69606

steel, tool, tempered surface layers formed during grinding, thickness determ. using electrochem. method 4-71814

steel, weathering, preetched, electrochemical and corrosion props. 4-62092

submarine optical fibre cable, high strength splicing technique 4-74732

VLSI technology, textbook 4-82610

(Al,Ga)As heterojunctions, laser-induced defects, photochem. etching 4-113439

Al-Cu films deposited by sputtering techniques, microstruct. 4-108733

Al-Cu-Mg, 2017, surface characterisation as vacuum vessel for nuclear fusion devices 4-96266

Al-Si-Cu, reactive ion etching, rel. to film deposition characteristics 4-81357

Al-Zn-Mg-Cu, phase identification, X-ray analysis, sequential etching 4-104950

Au film, deposited on Si, dynamic recoil mixing, parameter optimisation 4-70180

$\text{B}_2\text{O}_3\text{-SiO}_2$  glasses, radiation effects, point defects, microstructural changes, etching, leaching 4-70195

(Ba,Sr)TiO<sub>3</sub> heteroepitaxial ferroelec. films, domain struct. 4-65993

BaMoO<sub>4</sub> single cryst., flux evaporation growth and morphology 4-114369

C-steel etching of with  $\text{FeCl}_3$  4-76970

C-steel with  $\text{Fe}(\text{ClO}_4)_3\text{-HClO}_4$  and with  $\text{Fe}(\text{H}_2\text{O})_6^{3+}$ , etching kinetics 4-76969

$\text{CaCO}_3$ , pentagonal etch pit morphology on cleavage faces 4-75760

CdTe photoelectrodes, photoelectrochemical props., XPS and AES studies 4-88578

Fe, cast, metallographic differences between compacted and vermicular graphite 4-114753

Fe powder, Ni-coated, compacted, phase identification by colour etching 4-114755

GaAs (100), chemical etching and annealing 4-65722

GaAs (100) etch pits and cryst. defects, ellipsometry and reflectivity studies 4-84492

GaAs (100) surfaces, XPS anal. after technology-etchant appl. 4-93196

GaAs, chemical etchants, comparative study 4-114701

GaAs, ductile brittle transition in (001) surface layers in single crystals, effect of medium 4-70266

GaAs, reactive ion etching in  $\text{CCl}_4/\text{H}_2$  and  $\text{CCl}_4/\text{O}_2$ , AES, Raman spectra 4-81306

GaAs wafer, (100) surface, orientation determ. by etching technique 4-99619

## etching continued

GaAs-HCl-H<sub>2</sub> system, phase equilib., dominant reactions for VPE, etching obs. 4-71579

GaAs-Hg Schottky barrier, crystal damage during CV profiling 4-98753

GaNAsP/InP BH laser diodes, fabrication technique 4-74507

GaNAsP/InP BH laser with chemically etched and mass-transported mirror 4-74537

Ge microlens surface, reflecting power and etching form. (*Russian*) 4-64757

Ge, segmented-electrode detector fabrication, Au mask technique 4-59559

$\text{In}_{0.53}\text{Ga}_{0.47}\text{As}$ , epilayer thickness meas. from etched steps 4-62074

InGaAsP oxidised films interface, Auger/ion sputtering anal. 4-104884

InP Z 4-99619

InP:Yb p-n junctions; electroluminescence studies 4-66079

InP/InGaAsP 1.5  $\mu\text{m}$  BH laser with etched cavity 4-83575

InSb surface, chem. etch effect (*Chinese*) 4-109528

$\text{LiNbO}_3$ :Ti waveguide integrated optics processing, uses of EDTA etch soln. 4-112590

Mo electrodes, selective  $\text{SiO}_2$  form. for MOS structs. 4-98467

Mo-Ti/Si interface, metallisation for self-aligned TiSi<sub>2</sub> process 4-89145

$(\text{NH}_4)_2\text{Cr}_2\text{O}_7$  crystals grown from aqueous soln., morphology and charact. 4-103679

Ni-P thin film, selective absorber, for photothermal conversion of solar radiation 4-81589

$\text{PbO-K}_2\text{O-Na}_2\text{O-As}_2\text{O}_3\text{-SiO}_2$ , optical glass, effects of salt additions on specific surface and polishing 4-79257

$\text{PbTiO}_3$  heteroepitaxial ferroelec. films, domain struct. 4-65993

Si CMOS active lateral diffusion and linewidth test struct. 4-108665

Si, Czochralski growth, impurity clouds, microdefects, scatt. light intensity and etch pit density after annealing 4-84312

Si, defect delineation by chem. etching 4-88171

Si, deformed, EBIC/TEM study of defects 4-80045

Si, dissoln. kinetics in  $\text{Cr}_2\text{O}_7\text{-HF-H}_2\text{O}$  soln. 4-62082

Si doped substrate, overetching determ. using combined pulsed capacitance voltage meas. and SIMS 4-85269

Si, epitaxial, metallic precipitates charact. by etching and TEM 4-98291

Si, floating-zone crystals, microdefects, metallographic and electron microscopical anal. 4-103737

Si, ion etching, effect of ion species on bombardment induced topography 4-81320

a-Si, ion implanted, etching in HF soln. and annealing effects 4-80063

Si, low energy implantation of N<sub>2</sub> and NH<sub>3</sub>,  $\text{Si}_3\text{N}_4$  formation study 4-75484

Si microlens surface, reflecting power and etching form. (*Russian*) 4-64757

Si, nitridation in multiwafer plasma system 4-81309

n-Si, photo-enhanced etching in dil. HCl soln. 4-62072

Si polycryst. layer, grain size and dopant level inspection 4-109529

Si, polycrystalline, defect etching 4-81308

Si, polycrystalline, etching processes 4-61842

Si, product layers formed during etching in  $\text{SF}_6$  4-109682

Si solar cell, V-groove  $n^+p$  junction type, design and fabrication using anisotropic etching (*Korean*) 4-85371

Si solar cell junction profiles in ion-implanted texture-etched surfaces 4-93620

Si solar cells, nonsingle crystal, ion-implanted and thermally diffused, surface damage etching effect on props. 4-77105

Si solar cells, thin, structural stability using improved wafer etching process 4-81557

Si substrates, electro-physical prop. nonuniformity (*Russian*) 4-65672

Si surface, fluorination by  $\text{XeF}_4$  etching, photoeffects 4-77031

Si wafer props., influence of laser marking 4-113498

Si:As, ion implanted, IR radiation annealing of extended defects 4-92228

Si:As, ion implanted regions, 2-D shape, etching and EBIC studies 4-88187

a-Si:H CVD films, struct. model 4-88427

$\text{Si}_3\text{N}_4/\text{Si}_3\text{N}_4$ , N and O distrib. profiles, Auger studies (*Russian*) 4-65578

Si-Hg Schottky barrier, crystal damage during CV profiling 4-98753

$\text{Si}_3\text{N}_4$  film MNOS struct., trapped charge profile and relax. currents 4-65749

$\text{Si}_3\text{N}_4$  films, plasma-deposited, prep. and characterisation 4-88986

Si:Si<sub>3</sub>N<sub>4</sub> plasma-enhanced CVD films, anomalously high etch rate, optical props. 4-104108

Si:Ny films, photo-CVD, props. study 4-99338

$\text{SiO}_2$ , dry etching, review of recent developments 4-81319

$\text{SiO}_2$  film, low temp. CVD, etching kinetics 4-99614

$\text{SiO}_2$  films, chemically vapour deposited from  $\text{SiH}_4\text{-O}_2\text{-N}_2$  mixtures 4-76885

$\text{SiO}_2$  films, photo-CVD, props. study 4-99338

$\text{SiO}_2$ , fused silica, broadband reduced refl. using etched nuclear tracks 4-107764

$\text{SiO}_2$  glass, radiation effects, point defects, microstructural changes, etching, leaching 4-70195

$\text{SmCo}_5$  permanent alloys, metallographic study, improved phase and grain boundary etching 4-114754

n-TiO<sub>2</sub> photoelectrochemical, sintered electrodes, hole diffusion length 4-70929

$\text{Y}_2\text{FeO}_{12}$  single cryst., top seeded soln. growth method and mag. props. 4-93207

ZnS, surface morphology after thermal etching 4-80346

ZnSe crystals, etch pits and polarity identification 4-99621

ZnSe, photoelectrochemical etching and nonuniform charge flow in Schottky barriers 4-80672

ZnTe crystals, etch pits and polarity identification 4-99621

ether drift see special relativity

Ettingshausen effect see thermomagnetic effects

## europium

see also nuclei with .....

alkali halides:Eu<sup>2+</sup>, X-irrad. effect on impurity vacancy dipoles and aggregation precipitation state, F-centre production 4-70209

alkali metal rare earth fluorides,  $\text{MR}_3\text{F}_{10}\text{-Eu}^{2+}$  (M=K, Rb, Cs; R=Y, Gd, Lu), Eu<sup>2+</sup> luminesc. 4-66073

atoms, isotope shift, parametric description appl. 4-74191

BCC, generalised susceptibility and joint density of states 4-76118

crystal structure from first principles calcs. 4-70064

evaporated film, oxidation, photoemission study 4-85073

impurities in fluoride deposits study by EPR and neutron activation anal. 4-80815

## europium continued

- ion impurity optical props. in non-metallic cryst. 4-61733  
 rare earth molybdates,  $\text{Eu}^{3+}$  doped, fluorescence studies 4-66072  
 resonance of 4f partial photoionisation cross section 4-93188  
 $\beta\text{-Al}_2\text{O}_3\text{-La}_2\text{O}_3\text{:Eu}^{3+}$  structure, laser excited fluorescence study 4-66071  
 $\text{BaFCl:Eu}$  X-ray phosphor, transparent thin films prep. by evaporation 4-88874  
 $\text{BaFCl:Eu}^{2+}$ ,  $\gamma$ -ray irradi., thermoluminescence glow curves 4-76533  
 $\text{BaSO}_4\text{:Eu}$  thermoluminescent detectors, screening in cosmic ray expts. 4-102523  
 $\text{CaF}_2\text{:Dy}^{3+}$ ,  $\text{Eu}^{2+}$  crystals, electron-excitation relax. kinetics and nonequilibrium acoustic phonons 4-88256  
 $\text{CaF}_2\text{:Eu}$ , phononless impurity-centre line, inhomogeneous broadening under plastic deform. conditions 4-88864  
 $\text{CaF}_2\text{:Eu}^{2+}$ , phononless line profile under random deformations, luminesc. bands 4-70726  
 $\text{CaSO}_4\text{:Eu}$ , thermoluminesc. and radiophotoluminesc. 4-93118  
 $\text{CdF}_2\text{:Eu}$ , deep centre characterisation by thermally controlled EPR 4-71174  
 $\text{CdF}_2\text{:Eu}$ , thermoluminescence processes, photo-ESR studies 4-66085  
 $\text{Eu(III)}$  in silica gel glass, fluoresc., cation binding and cage symm. 4-114835  
 $\text{Eu I, II}$ , electron-impact excitation of 4f electrons 4-83478  
 $\text{Eu I}$ , VUV absorpt. spectrum identification,  $4f^75d^1(^2D)$  np state calc. 4-91215  
 $\text{Eu I}$  spectrum,  $4f^76s6p$  configuration, isotope shift, parametric anal. 4-59678  
 $\text{Eu II}$ , hyperfine structure and isotope shifts 4-87085  
 $\text{Eu(II)}$ , relativistic mode-potential oscillator strengths and transition probabilities for  $4f^6s-4f^6p$  transitions 4-112144  
 $^{155}\text{Eu}$ , atmospheric fallout samples collected in 1981 4-62891  
 $\text{LaF}_3\text{:Eu}^{3+}$ , fine struct. parameters, hyperfine splittings, X-band EPR meas. 4-71176  
 $\text{LiNbO}_3\text{:Eu}^{3+}$ , impurity optical absorpt. 4-66056  
 $\text{Ni}_8(\text{AlO}_2)_3(\text{SiO}_2)_{40-24}\text{H}_2\text{O:Eu}^{2+}$ , adsorption of  $\text{O}_2$ , fluorescence study 4-84511  
 $\text{NaGdTiO}_4\text{:Eu}^{3+}$ , nonradiative relax. by multiphonon emission 4-76507  
 $\text{RbBr:Eu}$ , optical study of  $\text{Eu}$  precipitation 4-80233  
 $\text{RbCl:Eu}$ , optical study of  $\text{Eu}$  precipitation 4-80233  
 $\text{RbGd}_2\text{F}_{10}\text{:Eu}^{3+}$ ,  $\text{Eu}^{3+}$  fluorescence,  $\text{Gd}^{3+}$  effects 4-104663  
 $\text{RbMgF}_2\text{:Eu,Mn}$ ,  $\text{Eu}^{2+}$ -sensitized  $\text{Mn}^{2+}$  luminescence 4-76521  
 $\text{SrF}_2\text{:Eu}^{3+}$ , phonon diffusion and decay, impurity luminesc. study 4-61006  
 $\text{Y}_2(\text{WO}_4)_3\text{:Eu}^{3+}$ , prep. and luminesc. props. 4-81009  
 $\text{Y}_2(\text{WO}_4)_3\cdot n\text{H}_2\text{O:Eu}^{3+}$ , luminescent precipitate prep., photolum. brightness 4-114330  
 $\text{ZrO}_2\text{:Eu}^{3+}$ , monoclinic zirconia, fluoresc. spectra studies (French) 4-99152

## europium alloys

- photoemission, reson., using soft X-ray monochromators at BESSY 4-95583  
 $\text{ErRh}_2\text{B}_4$ , ferromagnetic superconducting thin film, photoexcitation, nonequilibrium effects 4-114059  
 $\text{Eu-Hg}$ , Mossbauer spectra and X-ray diffr. study 4-76290  
 $\text{EuCo}_2\text{Si}_2$ , valence change, X-ray absorpt. study 4-85037  
 $\text{EuCu}_2\text{Si}_2$ , mixed valent, isomer shift, mag. susceptibility 4-98573  
 $\text{EuFe}_2\text{Al}_8$ , X-ray absorpt. near edge struct. study 4-61769  
 $\text{EuFe}_2\text{Si}_2$ , valence change, X-ray absorpt. study 4-85037  
 $\text{EuIr}_7$ , Mossbauer isomer shift, trivalent  $^{151}\text{Eu}$  4-114191  
 $\text{EuNi}_8$ , Mossbauer isomer shift, trivalent  $^{151}\text{Eu}$  4-114191  
 $\text{Eu}_2\text{Ni}_{17}$ , Mossbauer isomer shift, trivalent  $^{151}\text{Eu}$  4-114191  
 $\text{EuNi}_2\text{Si}_2$ , valence change, X-ray absorpt. study 4-85037  
 $\text{EuPd}_3$ , Mossbauer isomer shift, trivalent  $^{151}\text{Eu}$  4-114191  
 $\text{EuPd}_3\text{B}$ , valence behaviour of  $\text{Eu}$ , possible charge ordering in  $\text{EuPd}_3\text{B}$  4-80850  
 $\text{EuPd}_3\text{B}_2(\text{Si}_2)$ , valence state studies 4-70748  
 $\text{EuPd}_3\text{P}_2$ , valence state of  $\text{Eu}$  and unit-cell vol. anomaly 4-104174  
 $\text{EuPd}_3\text{Sb}_2$ , cryst. struct. determ. 4-79985  
 $\text{EuPd}_3\text{Si}_2$ , mixed valence system, high press.  $\text{L}_{III}$  X-ray absorption spectra study 4-61342  
 $\text{EuPd}_3\text{Si}_3$ , alloying effects, XANES study 4-88905  
 $\text{EuPt}_5$ , Mossbauer isomer shift, trivalent  $^{151}\text{Eu}$  4-114191  
 $\text{EuRh}_2$ , Mossbauer isomer shift, trivalent  $^{151}\text{Eu}$  4-114191  
 $\text{EuRh}_2\text{B}_2$ , X-ray absorpt. near edge struct. study 4-61769  
 $\text{EvSb}_2$ , collinear antiferromag. struct., neutron diffr. studies 4-108993

## europium compounds

- see also europium alloys  
 band gap width, rel. to short-range environment of S atom 4-80493  
 ethylsulphate  $\text{Ce}^{3+}$ ,  $\text{Ce}^{3+}$  EPR spin-lattice relax. rate, press. effects 4-65855  
 mixed valence phenomena, phenomenological thermodynamics 4-113906  
 oxide and chalcogenides, exchange interactions, LCAO calculations 4-109009  
 $\text{Ca}_{1-x}\text{Eu}_x\text{Ti}_{1-x}\text{Fe}_2\text{O}_7$ , perovskite solid soln. systems, prep. and charact. 4-70123  
 $\text{CsEuNaNb}_2\text{O}_{15}$ , struct. and ferroelec. props. 4-109141  
 $\text{Eu}$  complex, tris(ethylsulphate) ennehydrate, elec. dipole intensity parameters 4-70756  
 $\text{Eu}$  complexes in soln., electronic spectra modelling for struct. study 4-114245  
 $\text{EuAl}_3(\text{BO}_3)_4$ , UV absorpt., luminesc., circular dichroism spectra, gyrotropic characts. 4-114301  
 $\text{EuAlO}_3$ , perovskite struct., vibr. study, force field calc. 4-113416  
 $\text{EuB}_6$ , absorber materials for fast breeder reactor control rod systems, physical and chemical props. 4-83147  
 $\text{EuB}_6$ , neutron absorber for fast reactors (German) 4-83146  
 $\text{EuBr}_2\text{-EuI}_2$ , preparatory and crystallographic studies using X-ray diffr. 4-88143  
 $\text{Eu}_8\text{Ca}_{20}\text{CrO}_3$ , ionic cond. and thermal expansion 4-84461  
 $\text{EuCl}_2\text{-EuI}_2$ , preparatory and crystallographic studies using X-ray diffr. 4-88143  
 $\text{EuCl}_3$  in soln.,  $\text{Eu}^{3+}$  vibronic spectra of luminesc. excitation 4-104642  
 $\text{EuCl}_3$  solns., optical transitions of  $\text{Eu}^{3+}$  ions 4-114298  
 $\text{EuCoO}_3$ , quadrupole interactions,  $^{151}\text{Eu}$  Mossbauer spectroscopy 4-76295  
 $\text{EuCrO}_3$ , quadrupole interactions,  $^{151}\text{Eu}$  Mossbauer spectroscopy 4-76295  
 $\text{EuCu}_2\text{Si}_2$ , Mossbauer effect, high mag. field influence (German) 4-80851  
 $\text{EuEr}_2\text{S}_4$ , band gap width, rel. to short-range environment of S atom 4-80493  
 $\text{EuF}_3$ , dielectric constant, temp. depend., polarisability 4-92995  
 $\text{EuF}_3$ , permitt., dielec. loss tangent, cond. meas. 4-104523

## europium compounds continued

- $\text{EuFeO}_3$ , muon site determ. 4-71227  
 $\text{EuFeO}_3$ , quadrupole interactions,  $^{151}\text{Eu}$  Mossbauer spectroscopy 4-76295  
 $\text{Eu}_2\text{Fe}_2\text{O}_{12}$ ,  $\text{Eu}^{3+}$  nucleus relax. processes in domains and domain boundaries 4-88739  
 $\text{EuGd}_2\text{S}_4$ , band gap width, rel. to short-range environment of S atom 4-80493  
 $\text{Eu}_2\text{Ge}_2\text{O}_7$ , hydrothermal synthesis and cryst. struct. 4-60900  
 $\text{EuHo}_2\text{S}_4$ , band gap width, rel. to short-range environment of S atom 4-80493  
 $\text{Eu(III)}$  complexes, cryptates, luminesc. and UV spectra 4-80978  
 $\text{Eu}_2\text{Ir}_2\text{S}_4$ , H sites, geometric model 4-88155  
 $\text{EuLa}_2\text{S}_4$ , band gap width, rel. to short-range environment of S atom 4-80493  
 $\text{EuMnO}_3$ , quadrupole interactions,  $^{151}\text{Eu}$  Mossbauer spectroscopy 4-76295  
 $\text{EuMo}_6\text{S}_8$ , bulk superconductivity obs. under pressure 4-71004  
 $\text{EuMo}_6\text{S}_8$ , divalent Chevrel-phase supercond., effect of press. and O defects 4-80711  
 $\text{Eu}(\text{NO}_3)_3$ ,  $\text{EuCl}_3$  and  $\text{Eu}(\text{ClO}_4)_3$ , f-f transitions, oscillator strengths and Judd-Ofelt parameters 4-59856  
 $\text{Eu}(\text{NO}_3)_3$  in soln.,  $\text{Eu}^{3+}$  vibronic spectra of luminesc. excitation 4-104642  
 $\text{EuO}$ , doped, degenerate ferromag. semicond., spin waves at low temps. 4-114096  
 $\text{EuO}$ , Heisenberg ferromag., longitudinal spin wave pumping 4-88661  
 $\text{EuO:Gd}$ , longitudinal Nernst-Ettingshausen effect, temp. and mag. field dependences 4-65697  
 $\text{Eu}_2\text{O}_3$ , absorber materials for fast breeder reactor control rod systems, physical and chemical props. 4-83147  
 $\text{Eu}_2\text{O}_3$ , total gamma-ray cross sections 4-60959  
 $\text{EuPd}_3\text{Si}_2$ , Mossbauer effect, high mag. field influence (German) 4-80851  
 $\text{EuS}$ , doped, degenerate ferromag. semicond., spin waves at low temps. 4-114096  
 $\text{EuS}$ , energy band struct., X-ray study 4-84565  
 $\text{EuS}$ , FIR dielec. energy loss function 4-84895  
 $\text{EuS}$ , ferromagnetic semicond., thermal cond., phonon and magnon contribs. 4-71050  
 $\text{Eu}_2\text{Sc}_2\text{Fe}_2\text{O}_{12}$ , EFG sign at  $^{57}\text{Fe}$  nuclei, Mossbauer spectra 4-84599  
 $\text{EuScO}_3$ , quadrupole interactions,  $^{151}\text{Eu}$  Mossbauer spectroscopy 4-76295  
 $\text{EuSe}$ , chem. transport growth in  $\text{I}_2$  atm. 4-109313  
 $\text{Eu}_2\text{Sn}_{1-x}\text{Mo}_x\text{S}_8$ , mag. field induced supercond. 4-98808  
 $\text{EuSr}_{1-x}\text{S}$  ferromagnetic epitaxial layers, magnetooptic studies (German) 4-76441  
 $\text{EuSr}_{1-x}\text{S}$  spin glass, cryst., phonon scatt. by mag. two-level systems 4-71106  
 $\text{Eu}_2\text{TaO}_7$ , IR and Raman vibr. spectra 4-61679  
 $\text{EuTe}$ , chem. transport growth in  $\text{I}_2$  atm. 4-109313  
 $\text{EuVO}_4$ , stoichiometric, nucl. quadrupole optical hole-burning 4-80969  
 $\text{La}_{1-x}\text{Eu}_x\text{FeO}_3$ , perovskite solid soln. systems, prep. and charact. 4-70123  
 $\text{Li(Y,Eu,Fa,Tm)}^{3+}$ , laser channels, stimulated emission 4-112444  
 $\text{NaEvTiO}_4$ , 2D system, luminescence and energy migration 4-99161  
 $\text{Pb}_{1-x}\text{Eu}_x\text{Se}_{1-y}\text{Te}_y$  diode lasers, wavelength coverage 4-102928  
 $\text{Pb}_{1-x}\text{Eu}_x\text{Se}_{1-y}\text{Te}_{1-y}$  heterojunction stripe geometry lasers grown by MBE 4-112458  
 $\text{Pb}_{1-x}\text{Eu}_x\text{Se}_{1-y}\text{Te}_{1-y}$  long-wavelength laser diodes, fabrication and props. 4-96954  
 $\text{Pb}_{1-x}\text{Eu}_x\text{Te}$ , MBE growth and elec. and optical props. 4-81142  
 $\text{Y}_3\text{-Eu}_2\text{Fe}_5\text{-Ga}_2\text{O}_{12}$  mag. bubble films, LPE growth 4-109332  
 $(\text{YEuTmCa})_2(\text{FeGe})_2\text{O}_{12}$  ferrite-garnet epitaxial films, fine struct. of mag. spectra 4-76206

## eutectic alloys

- $\text{Al-Ni}$  alloy, effects of morphology of  $\text{Al}_3\text{Ni}$  whiskers on tensile strength 4-88133  
 irregular, theoretical basis of grain growth (Polish) 4-93258  
 solidification, eutectic, normal and anomalous 4-89045  
 solidification, microstruct. and phase spacings 4-93284  
 stir cast microstructure 4-89049  
 two-phase materials, bounds on transport, elastic and thermal expansion parameters 4-92684  
 $\text{Al}$  alloy, laser treatment, strengthening and microstruct. (Russian) 4-71665  
 $\text{Al-AlCu}$  thin films, directionally solidified, interlamellar spacing 4-93285  
 $\text{Al-Al}_3\text{Ni}$  eutectic composites, work hardening in stage II, 293-673K (Japanese) 4-89067  
 $\text{Al-Al}_3\text{Ni}$  eutectics, directionally solidified, interfacial microstructures, TEM obs. 4-81187  
 $\text{Al-Cu}$ , columnar crystals, unidirectionally solidified in flowing melt 4-81181  
 $\text{Al-Cu}$ , directional solidification, off-eutectic composite growth, segregation, convection effects 4-71647  
 $\text{Al-Cu}$  eutectic, rapid solidification, with nonhomogeneous thermal contact 4-93276  
 $\text{Al-CuAl}_2$  eutectic alloys, melting mechanism 4-114507  
 $\text{Al-CuAl}_2$  lamellar eutectic composites, high temp. yield strength rel. to microstruct. 4-81247  
 $\text{Al-Ge}$ , binary constitution diagrams at very high press. 4-104766  
 $\text{Al-Sc}$  system, metastable state diagram 4-114485  
 $\text{Al-Si}$ , binary constitution diagrams at very high press. 4-104766  
 $\text{Al-Si}$ , directional solidification, eutectic fibrous struct. rel. to comp. and growth velocity 4-61927  
 $\text{Al-Si}$  eutectic alloy, U centre mechanism for superconductivity enhancement (Chinese) 4-92203  
 $\text{Al-Si}$  system, phase relations up to 5.5 GPa 4-104765  
 $\text{Al-Si-Cu-Mg}$ , strengthening with continuous  $\text{CO}_2$  laser 4-62117  
 $\text{Al-Si-Mg-Sr}$ , hypoeutectic alloys, melting losses of Sr rel. to holding time 4-114498  
 $\text{Al-Si-Sb}$ , eutectic, struct. rel. to Sb addition, electron beam microanalysis (German, English) 4-66314  
 $\text{AlCu}$  eutectic, fine grained superplastic alloys, anelastic strains, grain boundary cavity distrib., sintering 4-66359  
 $\text{Bi-Cd-In}$  system, eutectic alloys, microstruct. 4-93263  
 $\text{Bi-Se(Te)}$  thermoelements, eutectic soldering, electron microscopy study (Russian) 4-98652  
 $\text{Cd-Pb}$  thin films, directionally solidified, interlamellar spacing 4-93285  
 $\text{Co-Al}$ , directionally solidified eutectic, compressive yield stress rel. to lamellar termination density 4-81263  
 $\text{Co-C}$ , hypereutectic alloy, diamond form. at high press. 4-109374  
 $\text{Co-Co}_7\text{Gd}_2$ , off-eutectic, growth by floating zone techniques 4-99304

## eutectic alloys continued

- Co-Ge eutectics, X-ray spectral investigation (*Russian*) 4-76564  
 Co-NbC eutectic alloy, comp., microstruct. and tensile strength 4-66320  
 Co(Cr,Ni)-TaC, eutectic, thermal cycling, calc. of residual stresses and strains 4-66380  
 Cu alloy, laser treatment, strengthening and microstruct. (*Russian*) 4-71665  
 Fe based, coatings, boride and carbide strengthened, laser irradiated, wear resist. (*Russian*) 4-85250  
 Fe-Cr-C, hypereutectic alloys unidirectionally solidified, hot hardness of primary carbides 4-99492  
 Fe-Ge eutectics, X-ray spectral investigation (*Russian*) 4-76564  
 FeSi-Fe<sub>2</sub>Si<sub>3</sub> eutectic alloy, sintered, annealing, FeSi<sub>2</sub> form., elec. props. 4-109414  
 In-Sn and In-Bi-Sn eutectic alloy solders for Josephson packaging, mech. props. 4-71687  
 Ni alloys,  $\gamma$ - $\gamma'$ ,  $\gamma$ - $\alpha$  and  $\gamma'$ - $\alpha$ , yield stress and deform. struct., temp. depend. 4-93346  
 Ni alloys, high-alloy, microstruct. and comp. characts. of eutectic  $\gamma'$  phase (*Russian*) 4-92380  
 Ni superalloy, creep and recovery kinetics, report 4-62000  
 Ni-Al-Mo alloy, unidirectional solidification 4-76765  
 Ni-base eutectic composite, deform. and failure, examination in HVEM 4-66382  
 Ni-Ge eutectics, X-ray spectral investigation (*Russian*) 4-76564  
 Ni-Mo-Al eutectic alloy, unidirectionally solidified composite,  $\gamma/\gamma'$  phases, microstruct. changes 4-11493  
 Ni-Mo-Al unidirectionally solidified eutectic, microstruct. instability 4-61926  
 Ni-Nb-Al  $\gamma$ - $\gamma'$  eutectic composite, prep. and morphology 4-114500  
 Ni-Nb-NbC, eutectic alloys, powder metallurgy, physical props., high temp. use 4-85125  
 Ni-Ni<sub>3</sub>Al-Mo eutectic composite, crystallographic orientation of phases 4-114501  
 Ni-Ni<sub>3</sub>Al-NbC, eutectic, thermal cycling, calc. of residual stresses and strains 4-66380  
 NiAl-Cr quasibinary eutectic, rapidly solidified, microstruct. and phase solubility extension 4-66319  
 Pb-Sn, superplastic eutectic alloy, stress/strain in biaxial tensile system 4-71698  
 Pb-Sn thin films, directionally solidified, interlamellar spacing 4-93285  
 Sb-Cu<sub>2</sub>Sb, eutectic alloys, melting mechanism 4-114507  
 Sb-InSb, eutectic alloys, melting mechanism 4-114507  
 Sn-Bi elastic behaviour near melting point from sound vel. and attenuation meas. 4-75597  
 Sn-Pb (38.1 wt.%), eutectic, fine-grained, accelerated coarsening of microstruct. during superplastic deformation 4-61997  
 Zn-Ge eutectic alloy, (100) textured Ge crystallites, morphology 4-76783  
 ZrC-Co-base eutectic, mech. props. rel. to microstruct. 4-89135

## eutectic structure

- carbon tetrabromide-hexachloroethane phase diagram, determ. using DSC 4-98244  
 IN-100, Ni-base superalloy, cast, microstruct. changes during fractional melting 4-109434  
 Mo-Al<sub>2</sub>O<sub>3</sub>/Cr<sub>2</sub>O<sub>3</sub> eutectic thermionic emitter 4-72141  
 polyurethane, segmental compatibility in block copolymers and oligomeric blends 4-113361  
 refractory oxides, oriented eutectics, microstruct. and related props. 4-71627  
 solidification, eutectic, normal and anomalous 4-89045  
 steady-state columnar and equiaxed growth 4-89044  
 steel, high C, fatigue crack growth retardation by massive eutectic carbides 4-99586  
 Stellite, Co-based wear-resistant alloy, liq. phase sintered, carbide comp. 4-99365  
 thin films, eutectic, growth 4-88995  
 two-phase materials, bounds on transport, elastic and thermal expansion parameters 4-92684  
 Al-Al<sub>3</sub>Cu, eutectic alloy thin films, growth 4-88995  
 Al-Al<sub>3</sub>Ni eutectics, directionally solidified, interfacial microstructures, TEM obs. 4-81187  
 Al-CuAl<sub>3</sub>, eutectic alloys, melting mechanism 4-114507  
 Al-CuAl<sub>3</sub>, lamellar eutectic composites, high temp. yield strength rel. to microstruct. 4-81247  
 Al-CuAl<sub>3</sub>, system, directionally solidified, faceting behaviour 4-76766  
 Al-Fe-Mn system, Al-rich corner, phase equilib. and crystn. studies 4-114480  
 Al-In (17.5 wt.%), monotectic alloy, unidirectional solidification struct. 4-109391  
 Al-In (17.5 wt.%), unidirectional solidification, monotectic struct. 4-109392  
 Al-Mg-La system, Al-rich corner, liquidus invest. (*Chinese*) 4-61917  
 Al-Si, Al halo form. during directional solidification 4-99381  
 Al-Si, directional solidification, eutectic fibrous struct. rel. to comp. and growth velocity 4-61927  
 Al-Si, eutectic solidification 4-89045  
 Al-Si, silumins, permanent modification with Sr and Sb (*Polish*) 4-85145  
 Al-Si (12.4 wt.%), near-eutectic, solid-liq. interface (*German*) 4-81184  
 AuSn-Pb quasibinary section of phase diagram, thermal anal. 4-93265  
 Bi-Cd-In system, eutectic alloys, microstruct. 4-93263  
 Bi-In system, phase diagram and eutectic struct. 4-93264  
 Cd-Pb, eutectic alloy thin films, growth 4-88995  
 CdS, crystallisation kinetics, growth from CdS+CdCl<sub>2</sub> melt 4-114380  
 Co-Al, directionally solidified eutectic, compressive yield stress rel. to lamellar termination density 4-81263  
 Co-NbC eutectic alloy, comp., microstruct. and tensile strength 4-66320  
 Cr<sub>3</sub>C<sub>2</sub>-Ni-B electrophoretic coatings, struct. and props. 4-88430  
 Fe-C eutectic solidification, equil. partition coeff. of third element rel. to graphitization 4-99380  
 Fe-C-Si, irregular eutectic, theoretical basis of grain growth (*Polish*) 4-93258  
 InSb-InTe, spreading of droplets of eutectic melt 4-113752  
 LaB<sub>6</sub>-ZrB<sub>2</sub> system, interaction, phase diagram study 4-89030  
 Mg-Al-Cd, constitution diagram, eutectic transform., X-ray and thermal analysis 4-114487  
 MgO-ZrO<sub>2</sub>, directionally solidified eutectic microstruct., misfit dislocations, TEM obs. (*Japanese*) 4-66324  
 Ni-Al-Hf system,  $\beta$ -(Ni,Al)-Hf<sub>2</sub> eutectic struct., cryst. morphology, struct., stacking faults, TEM, X-ray diff. obs. 4-81182  
 Ni-Al-Mo alloy, unidirectional solidification 4-76765

## eutectic structure continued

- Ni-base creep-resisting alloys, cast, grain boundary relax., effect of struct. of boundary vol. 4-71677  
 NiAl-Cr quasibinary eutectic, rapidly solidified, microstruct. and phase solubility extension 4-66319  
 NiO-CaO eutectic, directionally solidified, crystallography 4-113658  
 NiO-Y<sub>2</sub>O<sub>3</sub> system, composite microstruct. and interface struct. 4-70578  
 Pb-Sn, eutectic alloy thin films, growth 4-88995  
 Pb<sub>2</sub>-PbO system, condensed phase diagram 4-98245  
 Sb-Cu<sub>2</sub>Sb, eutectic alloys, melting mechanism 4-114507  
 Sb-InSb, eutectic alloys, melting mechanism 4-114507  
 Sn-Pb (38.1 wt.%), eutectic, fine-grained, accelerated coarsening of microstruct. during superplastic deform. 4-61997  
 TiC-TiB<sub>2</sub> eutectics, directional solidification 4-76767  
 Ti-Bi, pre-eutectic contact fusion 4-61059  
 Zn-Al, diecasting alloy, fracture 4-89128  
 ZrC-TiB<sub>2</sub> eutectics, directional solidification 4-76767  
 ZrC-ZrB<sub>2</sub> eutectics, directional solidification 4-76767  
 ZrO<sub>2</sub>-CaO system, directionally solidified eutectic, EELS 4-72009
- eutectic transformations** see phase diagrams; phase equilibrium
- eutectoid steel** see carbon steel
- eutectoid transformations** see solid-state phase transformations
- evaporated layer production** see vapour deposition
- evaporation**  
 see also drying; field evaporation  
 acetone droplet, evap., low and high mass flux data, wet bulb temp. 4-80341  
 aerosols, random fluctuations, effects on behaviour 4-82189  
 alloys, steady-state evaporation in vacuum 4-70356  
 alloys, with non-negligible evaporation rates, high temp. calorimetry procedure 4-68232  
 atmosphere, evapotranspiration potential in Belgium, estimation procedure 4-115476  
 Big Quill Lake, Saskatchewan, saline lake, effect of groundwater inflow on evaporation 4-100632  
 bubbling bed with vane separator, suppression of entrainment 4-103184  
 capillary discharge from evaporating wall, magnetohydrodynamic model 4-69973  
 capillary-porous structs., approx. hydrodynamic theory 4-113750  
 carbon tetrachloride droplet, evap., low and high mass flux data, wet bulb temp. 4-80341  
 coal-water mixtures on horizontal brass surface, film boiling of discrete droplets 4-64829  
 dichloromethane droplet, evap., low and high mass flux data, wet bulb temp. 4-80341  
 diffusion coefficients, resistometric methods 4-65427  
 drag of evaporating or condensing droplets in low Reynolds number flow 4-83933  
 dual evaporation installations, exergetic anal. (*Bulgarian*) 4-98253  
 ethanol droplets, evap., and condensation rates deduced from struct. resonances in fluorescence spectra 4-91304  
 ethyl ether droplet, evap., low and high mass flux data, wet bulb temp. 4-80341  
 evapotranspiration from vegetation, uncoupled multi-layer model for latent heat flux density 4-105618  
 evapotranspiration potential in Belgium, estimation procedure 4-115476  
 falling film evaporator, heat transmission meas. for condensation and evaporation (*German*) 4-111126  
 fuel droplet, evaporation dynamics, press. effect 4-103914  
 furan, two-phase bubble, evaporation through immiscible liq., heat transfer 4-87781  
 heat transfer intensification (*German*) 4-112689  
 heat transmission from metal surface to boiling water under atmospheric press. 4-97295  
 heather moorland, transpiration and evaporation meas. 4-105619  
 hot spray, evaporation rate const. laser diff. technique meas. 4-87777  
 interphase layer, mass, momentum and energy conservation law, surface parameters 4-112692  
 liquid droplet on heated surface, evaporation, heat transfer characteristics 4-83804  
 liquid evaporation in small capillaries 4-61171  
 liquid metal surface instability under intense IR laser irradi. 4-80340  
 liquid surface, evaporating, linearised stability anal. 4-103293  
 metal clusters multiply charged, observability, appl. to Pb clusters 4-96742  
 metal heated spikes, evaporation and heat loss 4-107993  
 metals, laser interaction, evaporation influence on melt behaviour 4-76566  
 metals, surface phenomena induced by intense laser irradi. 4-81044  
 microstructure of flow inside minute drops evaporating on a surface 4-60467  
 n-octane droplet, evap., low and high mass flux data, wet bulb temp. 4-80341  
 open solar regenerator performance testing 4-72177  
 OTEC plant sliding-pressure operation evaluation 4-114927  
 oxides, electron bombardment evaporation, physical model anal. 4-60965  
 n-pentane, two-phase bubble, evaporation through immiscible liq., heat transfer 4-87781  
 n-pentane, volatile liq. lens on stagnant liq. surface, evaporation 4-87548  
 phase separation late stage, dynamics in two dimensions 4-98254  
 polar liquid, evaporation, microwave irradi. effects 4-80201  
 polar liquid, evaporation, microwave irradi. effects 4-80202  
 Sierras de Cordoba, Argentina, evapotranspiration and energy balance of surface boundary layer 4-105671  
 slowly evaporating droplet near hot plate 4-97620  
 sprays, evaporating, conc. probability density function. 4-103188  
 Stirling engines with controlled evaporation of a two-phase two-component working fluid 4-66785  
 surface, evaporation and condensation, mass and heat transfer, kinetic anal. 4-88270  
 theory of evaporation and condensation 4-64833  
 time series multiple linear regression models for evaporation from a free water surface 4-82137  
 trichlorofluoropropane, volatile liq. lens on stagnant liq. surface, evaporation 4-87548  
 tropospheric evaporation duct, height evaluation (*French*) 4-82215  
 water, evaporation under an obliquely impinging laminar ducted slot jet - a numerical model. 4-108100  
 water droplet, evap., low and high mass flux data, wet bulb temp. 4-80341

## evaporation continued

- Al-Mg, oxidation, Mg diffusion and surface segregation, AES 4-98293  
 H<sub>2</sub>O clusters, evolution of magic numbers in mass spectra 4-96733  
<sup>4</sup>He, liquid, phonon and roton-induced evaporation 4-65511  
<sup>4</sup>He, liquid, quantum evaporation by rotors and phonons 4-70492  
 Mg, evaporation, effect of gases and vapours 4-84375  
 PrBi, evaporation charact., enthalpy of form., mass spectra analysis 4-88274  
 Si, clean and SiO<sub>2</sub> covered, picosecond laser heating and evaporation 4-70198  
 W (100) with chemisorbed N<sub>2</sub>, diffusion and evaporation study 4-98434  
 ZnS, surface morphology after thermal etching 4-80346

Evershed effect *see* sunspotsevoked potentials *see* bioelectric potentials

## evolution (biological)

- clial cells evolved for vision hyperpolarize 4-93741  
 end-Cretaceous brachiopod extinctions in chalk of Denmark, evidence for impact hypothesis 4-72598  
 terminal Cretaceous extinctions in Hell Creek area, Montana, compatible with catastrophic extinction 4-72587  
 Cretaceous-Tertiary boundary, sharp boundary or gradual transition 4-72589  
 Cretaceous-Tertiary extinctions, Ir anomaly at palynological boundary in Raton Basin 4-72588  
 Late Devonian mass extinction horizon, no geochemical evidence for asteroidal impact 4-62811  
 impacts of large asteroids and comets on Earth, biological implications, conference, Snowbird, Utah (1981 October 19 to 22) 4-100577  
 invertebrate fossil record at Cretaceous-Tertiary boundary, evidence for impact theory of mass extinctions 4-72597  
 marine fossil families, periodicity of extinctions rel. to extraterrestrial forces 4-72596  
 mass extinction of species by periodic comet showers, role of solar companion star 4-72594  
 mass extinctions, evidence from crater ages for periodic impacts on Earth 4-72595  
 mass extinctions, periodicity rel. to Sun's oscillation about galactic plane 4-72592  
 periodic mass extinctions, role of distant solar companion star 4-72593  
 mass extinctions due to cometary impacts, periodicity rel. to Sun's motion perpendicular to galactic plane 4-72591  
 origin of life, conf., Mainz, Germany (July 1983) 4-101569  
 protein tertiary structures role, book contrib. 4-93690  
 terrestrial and extraterrestrial life (book contrib.) 4-73180

## EXAFS

- amorphous alloys and metallurgy, EXAFS results 4-93135  
 amplitude determination, thickness effects 4-66106  
 anisotropic systems, EXAFS anal. 4-66103  
 application to determ. of structural parameters of solns. and catalysts 4-93132  
 bond angle determ. 4-66100  
 broadening of EXAFS arising from K hole finite lifetime 4-99229  
 catalysts, EXAFS and XANES studies 4-62241  
 conference on EXAFS and near edge struct., Frascati, Italy (Sept. 1982) 4-63397  
 database and program library for data reduction and anal. 4-63727  
 Debye-Waller factors in R-space analysis 4-65368  
 electrochemical cells for in situ EXAFS 4-99800  
 graphite 2s level, constant initial state spectroscopy, EXAFSlike modulation 4-81105  
 in situ measurements, sample cell 4-61779  
 inelastic effects role, SCF HF formalism 4-64492  
 inverse problems in spectroscopy, regular methods of soln. 4-66111  
 metal-ion exchanged layer structures, EXAFS studies 4-62196  
 metallic glasses, structural studies using EXAFS and XANES 4-60848  
 metallurgy appls., review 4-66104  
 mixed aqueous electrolytes, local structure., Raman and EXAFS studies 4-60808  
 multi-component oxide glasses, local environment, EXAFS studies 4-60852  
 noise effect on struct. parameters 4-66105  
 oxide glasses, local order, EXAFS studies review 4-60849  
 polyacetylene film, EXAFS study 4-109277  
 porphyrin complexes EXAFS, interference and multiple scatt. effects 4-64493  
 r-space EXAFS data anal. 4-93131  
 radial distrib. function by EXAFS 4-93133  
 real-space analysis, regular methods 4-66110  
 self-scanning photodiode array as position-sensitive X-ray detector 4-111263  
 short-range interatomic correlations, probing using EXAFS 4-93130  
 solutions, aqueous, structural studies using EXAFS and X-ray diff. 4-60807  
 spectrometer, laboratory facilities 4-61776  
 spectrometer for laboratory studies 4-61778  
 spectrometer on beam line 10B at Photon Factory (Japanese) 4-59489  
 statistical noise effect on structural parameters in EXAFS data anal. 4-93134  
 steel, microalloyed, EXAFS invest. 4-109594  
 structural information from EXAFS, reliability of ab initio calcs. 4-66102  
 synchrotron radiation sources, SSRL Beam Line Wunder 4-58928  
 synchrotron X-ray focusing monochromator for EXAFS studies, design, operation 4-95613  
 three-atom system, thermal vibr. effect on EXAFS 4-64491  
 time resolved modulated carrier rapid flow system for EXAFS spectroscopy 4-100377  
 time-resolved technique 4-61777  
 topographic EXAFS 4-76560  
 transition metal and main group metal systems, L-edge absorpt. systematics, EXAFS obs. 4-66121  
 transition region between XANES and EXAFS 4-66099  
 triatomic system, thermal vibr. effect on EXAFS 4-102698  
 TTF-FeOCl intercalation cpd., struct. and EXAFS studies 4-70129  
 TTF-FeOCl intercalation cpd., struct. and EXAFS studies 4-70129  
 TTF-FeOCl intercalation cpd., struct. and EXAFS studies 4-70129  
 X-ray beam line, double focusing for EXAFS 4-95623  
 X-ray filters, large area, fabrication 4-101992  
 X-ray scattering and EXAFS, model comparison 4-66109

## EXAFS continued

- Ag-Mn spin glass, short range order, appl. of EXAFS in metallurgy, review 4-66104  
 AgI, superionic conductor, struct., EXAFS 4-66125  
 (AgI)<sub>1-x</sub>(Ag<sub>2</sub>O-B<sub>2</sub>O<sub>3</sub>)<sub>x</sub> superionic glasses, EXAFS studies 4-60855  
 Al-Zn, EXAFS in dispersive mode for fast microanalysis, use of synchrotron radiation plus photodiode array 4-72019  
 Al-Zn alloys, Guinier-Preston zones, appl. of EXAFS in metallurgy, review 4-66104  
 Al<sub>2</sub>O<sub>3</sub> catalysts, short range order, EXAFS studies 4-62246  
 Al<sub>2</sub>O<sub>3</sub>, supported Rh catalyst, O interaction, EXAFS study 4-66097  
 Ar:Ag solid, EXAFS of Ag particles 4-104699  
 Au thin film, fluorescence detection of surface EXAFS 4-93136  
 B<sub>2</sub>O<sub>3</sub>-SiO<sub>2</sub>-TeO<sub>2</sub> glass, coordination, EXAFS and XANES studies 4-60851  
 Br<sub>2</sub>, EXAFS, ab initio calcs. 4-64492  
 Br<sub>2</sub>O, thermal vibr. effect on EXAFS 4-102698  
 CaF<sub>2</sub>:La(Er), impurity local structural environments, EXAFS determ. 4-66129  
 CaF<sub>2</sub>:Sr<sup>2+</sup> (Y<sup>3+</sup>), lattice relax. around impurities, EXAFS study 4-93140  
 CaO-Al<sub>2</sub>O<sub>3</sub>-SiO<sub>2</sub> glasses, struct. features, EXAFS and XANES studies 4-60850  
 Cd<sub>1-x</sub>Mn<sub>x</sub>Te, struct. props., EXAFS studies 4-60902  
 Cd<sub>1-x</sub>Mn<sub>x</sub>Te, ternary semiconducting random solid solutions, local structure 4-113414  
 Co, HCP, phase transferability of Co atom pairs, EXAFS anal. 4-61771  
 Co<sub>2</sub>-B<sub>2</sub> glasses, local struct., EXAFS studies 4-60854  
 Co<sub>2</sub>Nb, C15 struct., phase transferability of Co atom pairs, EXAFS anal. 4-61771  
 Co<sub>2</sub>Ta, C15 struct., phase transferability of Co atom pairs, EXAFS anal. 4-61771  
 CrH<sub>3</sub>, H lattice site location EXAFS 4-93137  
 CsI, L-edge absorpt. systematics, EXAFS obs. 4-66121  
 Cu-Ag isovalent solid soln., elastic core effects, EXAFS studies 4-60886  
 Cu-Zr, amorphous, local struct., EXAFS study 4-88101  
 Cu(110), adsorbed (2X1)O, azimuthal and polar angle depend. surface EXAFS 4-61770  
 Fe, EXAFS contributions and near neighbour components 4-61774  
 Fe, multiple scattering effects in EXAFS 4-66108  
 Fe<sub>80</sub>B<sub>20</sub> metallic glass, radial distrib. function asymmetry by EXAFS 4-93133  
 Fe(CN)<sub>6</sub><sup>4-</sup> (n=3,4), Fe-C bond lengths, EXAFS spectroelectrochemistry 4-107364  
 Fe<sub>1-x</sub>P, EXAFS contributions and near neighbour components 4-61774  
 Fe<sub>70</sub>P<sub>30</sub>, amorphous alloys, EXAFS contributions and near neighbour components 4-61774  
 GaS, EXAFS spectra and near edge struct. 4-66128  
 GaSe, EXAFS spectra and near edge struct. 4-66128  
 InSe, EXAFS spectra and near edge struct. 4-66128  
 KCl<sub>1-x</sub>Br<sub>x</sub>, lattice relax. and local environment near Br<sup>-</sup> ions, EXAFS studies 4-60903  
 KMnO<sub>4</sub>, XANES multiple scatt. study 4-76561  
 Kr, matrix isolated in solid Kr, Ar and N<sub>2</sub>, EXAFS studies 4-64416  
 La atomic, metallic and in complexes, relaxation effects in inner-shell photoemission and absorption 4-64441  
 LaNiO<sub>3</sub>, reduced phases, Ni oxidation states, XANES and EXAFS studies 4-61343  
 LaNiO<sub>3</sub>, struct. and Ni<sup>2+</sup> local environment, X-ray diff. and EXAFS studies 4-60901  
 Mg-Zn isovalent solid soln., elastic core effects, EXAFS studies 4-60886  
 MgCl<sub>2</sub> supported TiCl<sub>3</sub> catalysts, fluorescence EXAFS 4-62242  
 MnPS<sub>2</sub> layered cpd., disorder effects by cation intercalation, EXAFS studies 4-61773  
 Mo<sub>42</sub>C<sub>58</sub> amorphous sputtered films, EXAFS and anomalous X-ray scatt. 4-61766  
 Na<sub>2</sub>O-SiO<sub>2</sub>-UO<sub>3</sub> glass, struct. EXAFS studies 4-65179  
 NbZr multilayers, EXAFS struct. studies 4-70595  
 Ni<sub>60</sub>B<sub>40</sub>, glassy, Ni-Ni distrib., multishell modelling, EXAFS studies 4-60853  
 NiH<sub>x</sub>, H lattice site location EXAFS 4-93137  
 NiSi formation on Si, EXAFS study 4-109277  
 NiSi<sub>3</sub> nucleation on Si (111), direct struct. determ., SEXAFS meas. 4-99227  
 NiZr<sub>2</sub> metallic glasses, amorphous and cryst., X-ray absorpt. near edge struct. and EXAFS spectra 4-66120  
 Ni<sub>2</sub>Zr<sub>1-x</sub> amorphous alloy, local order, EXAFS studies 4-75302  
 O on Cu, SEXAFS spectra using soft X-ray monochromators at BESSY 4-95583  
 P<sub>2</sub>Se<sub>1-x</sub> glasses, struct., conc. depend. of short-and intermediate-range order 4-113342  
 PbF<sub>2</sub>-M<sup>II</sup>F<sub>2</sub>-M<sup>III</sup>F<sub>3</sub> (M<sup>II</sup>=Mn, Zn; M<sup>III</sup>=Fe, Ga), fluoride glasses, local order, EXAFS studies 4-70036  
 PbO-PbCl<sub>2</sub> glasses, coordination of divalent Pb studied by EXAFS 4-84198  
 PbTiO<sub>3</sub>, amorphous and cryst., bond lengths, annealing effect, Raman spectra, EXAFS study 4-79935  
 Pd, reflection electron energy loss study of electronic and struct. props. 4-70641  
 Pd<sub>80</sub>Ge<sub>20</sub> metallic glasses, amorphous and cryst., X-ray absorpt. near edge struct. and EXAFS spectra 4-66120  
 Pt catalysts, classical and inorganic cluster derived, EXAFS studies 4-62245  
 Rh/Al<sub>2</sub>O<sub>3</sub> catalyst, highly dispersed, CO adsorption, EXAFS study 4-62243  
 Ru(NH<sub>3</sub>)<sub>6</sub>Cl<sub>3</sub>, Ru L-edges, EXAFS spectra 4-66122  
 SbSi ferroelectric, L<sub>III</sub> edge above transition temp., EXAFS study 4-61772  
 SbSi, L absorption edges, EXAFS studies 4-71475  
 SbSi, paraelectric and ferroelec. phases, L-edge XANES and EXAFS obs. 4-88904  
 SnP, mixed valent, EXAFS and near edge struct., energy threshold determ. 4-66126  
 SmS, mixed valent, high press. phase, EXAFS study 4-66127  
 Sm<sub>1-x</sub>Y<sub>x</sub>S, mixed valent, EXAFS and near edge struct., energy threshold determ. 4-66126  
 Ti-Nb-Ta oxides, metamict, alpha-recoil damage study by EXAFS and XANES spectroscopy 4-76559  
 TiFe, EXAFS, multiple scattering effects 4-66108  
 TiO<sub>2</sub>-V<sub>2</sub>O<sub>5</sub> catalysts, EXAFS study 4-62244  
 V<sub>2</sub>O<sub>5</sub>-Ga<sub>2</sub>S<sub>3</sub>-As<sub>2</sub> superconductor, impurity location using EXAFS 4-88190

change forces in nucleus see nuclear forces

change interactions (electron)

- see also antiferromagnetism; ferromagnetism; RKKY interaction; superexchange interactions
- 2D hole gas, conductivity, logarithmic corrections 4-98685
- alkali metals, electron-phonon interaction, exchange effect (Chinese) 4-75872
- antiferromagnetic superconductor, theory of upper crit. field 4-76090
- antiferromagnetic XY chain with impurities, local magnetisation, Green's function calc. 4-98846
- cyclohexylammonium copper trichloride and tribromide, exchange anisotropy study 4-80758
- degenerate electronic band, martensitic transition temp., mag. field depend., enhancement by Coulomb and exchange interactions 4-104138
- dielectric function and spin susceptibility, exchange effects 4-76092
- disordered alloy, magnetisation, susceptibility in cluster-variational method 4-92900
- disordered Hubbard alloys, spin glass behaviour 4-92928
- disordered magnet near the percolation threshold 4-92921
- electron gas, nonuniform, struct. factor at small wavelength 4-61309
- electron gas energy, density functional exchange part, non-local approx. 4-76091
- electron spectroscopy in solid-state physics, electronic energy levels interpret. (French) 4-66134
- electron-hole plasma, exchange-correlation energies and Pade approximants calc. 4-65628
- EPR linewidths and exchange integrals 4-76244
- ferromagnet, exchange anisotropy and plane domain walls 4-80777
- ferromagnetic Ising model, dilute crystalline, amorphisation and high-field magnetisation 4-98911
- ferromagnetic semicond., magnetic excitation theory 4-76128
- ferromagnetic semiconductors, degenerate, spin waves at low temps. 4-114096
- first order mag. phase transitions of the order-disorder type 4-65814
- graphite:Fe, ion implanted, mag. props. 4-61562
- Heisenberg ferromagnet, surface spin wave freqs., temp. variation in exchange-dominated regime 4-80755
- Heisenberg ferromagnetic interface, magnetisation and excitation spectrum 4-80788
- Heisenberg planar ferromag., biquadratic interactions 4-88641
- Heisenberg spin exchange model, CIDEF and relax. 4-88722
- Heisenberg-Ising spin 1/2 chain, quantum domain walls 4-104442
- hexagonal lattice, simple, with competing interactions, modulated phases, Ising model 4-92925
- homogeneously random Ising antiferromagnet, Monte Carlo study 4-61501
- hot electron problem, quantum field theory 4-65685
- hydrogen copper (II) maleate tetrahydrate, one-dimensional ferromagnetism 4-71051
- intermediate valence systems, ferromagnetism stability 4-71061
- ion-induced  $K_L^+$  and  $K_L^-$  multiple vacancy production 4-99262
- ionic radicals, semiempirical model of exchange polarisation mechanism of transferred hyperfine interaction 4-112105
- Ising chain with nearest neighbour and next nearest neighbour exchange interactions, spin-lattice coupling 4-76153
- Ising ferromagnet, amorphisation, high-field magnetisation 4-84762
- Ising ferromagnet, polar states and charge ordering 4-71117
- Ising model, 2-D, local mag. field distrib. and thermodynamic quantities 4-98908
- Ising models for ferroelectric and ferromagnetic transitions 4-65821
- Ising two-dimensional generalised arbitrary spin model, effective Hamiltonian derivation 4-98847
- Kondo effect and magnetoresist. in weakly localised regime 4-108837
- local distortion correlation influence on mag. props. of Jahn-Teller centre pair 4-88646
- local electron pair models for intra- and inter-molecular exchange interactions (German) 4-78774
- long-period superstructure models 4-113366
- magnesium acetate tetrahydrate:  $Mn^{2+}$ , EPR, spin Hamiltonian parameters 4-114156
- magnetic insulator, second quantisation and equivalent two-body operators 4-88642
- magnetic materials with  $S \geq 1$ , exchange interaction and self consistent field method 4-61498
- magnetic superconductor, EM effects theory 4-84745
- magnetic thin films and semi-infinite model, local autocorrelation time, nearest-neighbour Ising model 4-76201
- many-electron systems, ground state energy and X-ray scatt. cross sections 4-114344
- metallic electron system with self-consistent consideration of exchange interaction, elec. susceptibility (Korean) 4-113882
- metals, anomalous antiferromag. structures, by isotropic indirect exchange 4-98860
- metals, antiferromagnetic, magnon relax. study (Russian) 4-80749
- metals, cryst. and amorphous, indirect exchange interaction, computer simulation 4-84779
- metals, ferromagnetic, exchange interactions and spin-wave stiffness 4-84776
- metals, ferromagnetic, non-uniform, mag. susceptibility calcs. 4-109001
- mixed valence compounds, magnetic impurity spin interaction with conduction electrons 4-104173
- mixed valence  $d^1-d^2$  clusters, vibronic reduction effects 4-88490
- multiquantum well heterostructures, magneto-optical studies of two-dimens. electrons 4-104580
- narrow-band mag. semicond., at operator representation 4-75961
- nickel acetate tetrahydrate:  $Mn^{2+}$ , EPR, spin Hamiltonian parameters 4-114156
- noble metals, electron-phonon interaction, exchange effect (Chinese) 4-75872
- noncollinear antiferromagnet, spin-flip transitions 4-104425
- one-dimensional classical planar model with competing interactions 4-107782
- orbitally anisotropic exchange interaction, magnetic ions, creation-annihilation operators 4-109008
- paramagnetic cryst., electron impurity centres (Russian) 4-88483
- Potts models, ferromag. and antiferromag., phase transition, Bethe approx. 4-92918
- quantum quadrupole ordering transition in mag. field 4-98889
- quantum spin systems, low temp. critical behaviour (Russian) 4-71013
- random ferromagnet-spin glass transitions, Heisenberg model 4-84787

exchange interactions (electron) continued

- rare earth alloys,  $R_2Rh_3$ ,  $R$ -Gd, Tb, Dy, Ho, Er, mag. props. meas. 4-61521
- rare earth alloys,  $RCO_2B_4$ ,  $R$ =Gd-Tm, antiferromag. and paramag. states, NMR spectra 4-109089
- rare earth borides,  $RRh_2B_4$ , low-temp. ordered mag. states 4-98859
- ruby, exchange integrals and Hamiltonians 4-98876
- s-f model in zero bandwidth limit, complete analytical soln. 4-76101
- screened Coulomb exchange energy, density functional theory gradient expansion approx. 4-61312
- semi-infinite n-vector model, mag. surface critical behaviour, exchange anisotropy effects 4-98898
- singlet-triplet paramagnet, Curie point vicinity, mode-mode coupling effects 4-98854
- solids with weak random anisotropy, mag. props. 4-98878
- spin glasses, short range three-dimensional nearest-neighbour Ising model, Monte Carlo simulations 4-92926
- spin glasses with uniaxial anisotropy, Monte Carlo simulations 4-61542
- spin-1/2 chain with Ising/Heisenberg/XY exchange, multiple bound states 4-88689
- spinel ferrites Curie point, O param. effect 4-84798
- TMNB, 1-D short range and 3-D long range mag. order, neutron scatt. study 4-108991
- transition metals, inner-core photoelectron spectra, perturbation approach 4-71517
- triangular magnetic configs. at OK in various mag. fields 4-92895
- two-dimensional mag. system, stationary states (Russian) 4-84765
- unordered magnet, competing exchange interactions, microstructure and mag. props. 4-76150
- zinc acetate dihydrate:  $Mn^{2+}$ , EPR, spin Hamiltonian parameters 4-114156
- Ag-Fe interface, electronic struct. and mag. props. 4-80645
- Ag-Mn dilute alloys, exchange split virtual bound state 4-92680
- AgMn, spin-glass, spin correl. decay, muon spin relax. meas. 4-71081
- AlGaAs/GaAs quantum wells, photoluminescence studies 4-93105
- $Al(NO_3)_3Cr^{3+}$ , exchange-coupled  $Cr^{3+}-Cr^{3+}$  pairs, EPR obs. 4-88717
- Ar, solid and liq., excitons, reflection spectra study 4-84570
- Au-Fe dilute alloy, exchange-circulation electron current between Fe atoms (Chinese) 4-114102
- BaMnF<sub>2</sub>, 2D antiferromag., optical magnon sidebands and exciton dynamics 4-98875
- $Cd_{1-x}Mn_xS$ , magnetisation, s-d exchange interaction, spin-flip Raman scatt. 4-76103
- $Cd_{1-x}Mn_xS$ , s-d exchange interaction sign, spin flip Raman scatt. studies 4-71052
- $Cd_{1-x}Mn_xSe$ , far-IR obs. of electric dipole spin resonance 4-92978
- $Cd_{1-x}Mn_xSe$ , Raman scatt., magnetisation and exchange energy 4-80940
- $Cd_3Mn_2O_8$  spin glass, magnon contrib. to mag. sp. ht. 4-98906
- CdTe doped with mag. ions, anomalous optical effects (Russian) 4-99103
- CeBi, type-I antiferromag., hybridisation-mediated exchange, anisotropic excitation behaviour 4-71053
- Co film, Brillouin scatt. from thermal magnons 4-71458
- $CoFe_2O_4$ , small particle ferrites, mag. hyperfine fields 4-61568
- $Co(Si_{1-x}Se_x)_2$ , mag. props. modelling (Russian) 4-80762
- Cr (100), mag. phase transition, angle resolved photoelectron spectra studies 4-98888
- $Cr_2O_3$ , exchange integrals and Hamiltonians 4-98876
- $Cr_2O_3$ , ferromag., Curie point transition, EPR obs. 4-109061
- $(Cr_2O_7RCO_6)_n^+$  clusters, magnetic behaviour, isotropic dynamic distortion model 4-92905
- CrSb, mag. props., mol. field theory 4-108995
- $CsMn_2Mg_{1-x}Br_3$ , biquadratic exchange 4-61531
- $CsNi_2Cd_{1/4}F_3$ , crystal struct. and linear trimers mag. interactions 4-71041
- $Cs_2Ti_2Cl_6$ , exchange interaction in orbitally degenerate binuclear units 4-71054
- Cu (II) complex, CuMn (thioxalato)<sub>2</sub>·7.5H<sub>2</sub>O, quasi-one-dimens. ferrimag. chain, magnetisation and susceptibility study 4-80748
- Cu complex, 2DMSO·CuCl<sub>2</sub>, 1D Heisenberg antiferromag., mag. susceptibility 4-61516
- Cu tetraclusters, adiabatic pot., mag. props., Jahn-Teller effect 4-108823
- Cu, total Compton profile, nonlocal exchange-correlation effects 4-81032
- Cu-Fe dilute alloy, exchange-circulation electron current between Fe atoms (Chinese) 4-114102
- Cu-Mn dilute alloys, exchange split virtual bound state 4-92680
- Cu-Ni interface, electronic struct. and mag. props. 4-80645
- Cu, resonant Raman scatt. in region of edge excitons 4-76472
- $Dy_2(Fe_{1-x}Al_x)_{17}$ , pseudobinary intermetallic cpd., mag. props. 4-71032
- ErTiO<sub>3</sub>, single cryst., magnetisation and mag. susceptibility 4-88652
- Eu oxide and chalcogenides, exchange interactions, LCAO calculations 4-109009
- $EuMo_2S_8$ , bulk superconductivity obs. under pressure 4-71004
- Fe (001) ferromagnetic, spin- and angle-resolved photoemission spectra 4-85063
- Fe (110), exchange split empty energy bands inverse photoemission studies 4-84551
- Fe complex, halobis(diethyliselenocarbamate)iron(III), mag. props. 4-76124
- Fe, electronic struct., exchange splitting, spin- and angle-resolved photoemission spectra 4-88944
- Fe epitaxial films, electronic and mag. states 4-80646
- Fe small clusters, electronic struct., spin density functional theory anal. 4-113859
- Fe surface layer at nonmag. material interfaces, magnetisation, temp. depend. 4-61575
- Fe-Ag(MnF<sub>2</sub>) interface, magnetisation study 4-80789
- Fe-Al-Mo, Mossbauer study, of atomic struct. and mag. polarisation 4-80848
- Fe-Cr-B, metallic glass, mag. props. and density 4-84773
- Fe-Cr-Co-Si-B amorphous alloys, mag. props. and hyperfine interactions (Russian) 4-108994
- Fe-Ni-Mn(Cr) alloys with mixed exchange interactions, mag. phase transitions, sp. ht. study 4-65820
- Fe-W-B, metallic glass, mag. props. and density 4-84773
- $Fe_8B_{17}$ , ferromag., spin polarised  $L_{23}M_{23}M_{23}$  AES 4-104703
- $Fe_{21}B_{15}Si_6$ , ferromagnet, spin-flip Stoner excitations, EELS studies 4-104410
- $Fe_{21}B_{13}Si_3C_2$ , Metglas 3605SC, mag. and hyperfine interactions 4-71223
- $Fe_{0.725}Co_{0.275}Cl_2$ , disordered spin-flop phase obs. 4-104420

## exchange interactions (electron) continued

- $\text{Fe}_{1-x}\text{Co}_x\text{Cl}_2$ , competing anisotropy system,  $\text{Fe}^{2+}$  spin orientation, Mossbauer spectra 4-92906  
 $\text{Fe}_2\text{Co}_{1-x}$  complex, hexa(pyridine-N-oxide)  $(\text{ClO}_4)_2$ , decoupled mag. sub-systems 4-98895  
 $\text{Fe}_{1-x}\text{Ga}_x\text{BO}_6$  boroferite, hyperfine interactions, Mossbauer studies 4-109099  
 $\text{Fe}_{30}\text{M}_2\text{B}_{17}$  based glassy alloys, ferromag. exchange and Curie temp. 4-76129  
 $\text{Fe}_2\text{Mg}_{1-x}\text{Cl}_2$  phase diagram, mag. susceptibility meas. 4-61535  
 $\text{Fe}_2\text{O}_3\text{-B}_2\text{O}_3\text{-PbO}$  glasses, ferric ion distrib., EPR studies 4-109064  
 $(\text{Fe}_2\text{O}_3)_x(\text{B}_2\text{O}_3\text{-PbO})_{1-x}$  glass, mag. props. study 4-88654  
 $(\text{Fe}_3\text{O}(\text{RCOO})_6)^+$  clusters, magnetic behaviour, isotropic dynamic distortion model 4-92905  
 $\text{Fe}_2\text{SnMo}_2\text{S}_6$  Chevrel phase, supercond. crit. temp. meas. 4-84729  
 $(\text{Fe}_{1-x}\text{V}_x)_{16}\text{B}_{16}$  amorphous alloys, mag. and elec. props. (Chinese) 4-114094  
 $\text{Fe}_{0.99}\text{Co}_{0.99}\text{Cl}_2$  magnetoelastic coupling at  $\text{Fe}^{2+}$  ions Mossbauer spectrum 4-92948  
Gd, d-f exchange reson. and j polaron 4-75874  
Gd-Tb alloys, magnetisation, temp. depend. 4-84815  
GdFe/TbFe amorphous double-layer films, magneto-optical characts. 4-61665  
H, spin polarized, collective spin oscillations 4-70525  
H, spin-polarized, nucl. spin waves, NMR study 4-70524  
H three-atom systems, exchange interactions, asymptotic anal. 4-74144  
 $^3\text{He}$ , solid BCC phase, sp. ht. and isochoric press., current four-spin exchange model 4-65516  
 $\text{Hg}_{1-x}\text{Ag}_x\text{Cr}_2\text{Se}_4$  mag. semicond., exchange interaction, carrier effects 4-114103  
 $\text{Hg}_{1-x}\text{Fe}_x\text{Te}$  crystal, negative magnetoresist. and Hall effect 4-65696  
 $\text{Hg}_{1-x}\text{Mn}_x\text{Te}$ , transport meas. using the alternating current technique 4-92720  
HoAlGa, mag. transitions, mag. and cryst. structures, X-ray diffr., thermal expansion meas. 4-114113  
 $\text{HoTiO}_3$ , single cryst., magnetisation and mag. susceptibility 4-88652  
 $\text{KCrO}_2$ , EPR linewidths and exchange integrals 4-76244  
 $\text{KMnCl}_3$ , canted antiferromagnet, mag. props. 4-88655  
La, photoionisation, local density-based random phase approx. calc. 4-102656  
 $\text{LaNi}_{1-x}\text{Co}_x\text{O}_3$ , ferrimagnetic interactions, mag. susceptibility meas. 4-88662  
 $\text{LaNi}_{1-x}\text{Cr}_x\text{O}_3$ , ferrimagnetic interactions, mag. susceptibility meas. 4-88662  
 $\text{LaNi}_{1-x}\text{Fe}_x\text{O}_3$ , antiferromagnetic interactions, mag. susceptibility meas. 4-88662  
 $\text{LiCrO}_2$ , EPR linewidths and exchange integrals 4-76244  
 $\text{Li}_{0.5-2/3}\text{Zn}_{2/3-5/6}\text{O}_4$  ferrites, Curie temp. and mag. moments 4-109013  
 $\text{MnFe}_2\text{O}_4$ , small particle ferrites, mag. hyperfine fields 4-61568  
 $\text{Mn}_2\text{-Cu}$ , pseudo-Zeeman splitting of excited states 4-104579  
MnP, Lifshitz point, spin localised model 4-84810  
MnSb, solid solns., evidence of critical Mn-Mn distance for onset of ferromagnetism 4-84780  
 $\text{NaCl:Mn}^{2+}$ , Suzuki phase, impurity exchange coupling, mag. susceptibility, EPR meas. 4-65788  
Ni (III) complex, dichloro bis-o-phenylene bis-dimethyl arsino nickelate (III) chloride, exchange interaction, EPR 4-71164  
Ni ferrites, mechanical activation effects on mag. props. 4-98882  
Ni, photoemission spectra study of magnetically spin-split electronic states (German) 4-71523  
Ni, Stoner excitation spectrum, spin polarised EELS studies 4-104411  
 $\text{Ni}_2\text{Al}$ , weak itinerant ferromagnet, de Haas-van Alphen effect, Curie temp. 4-113848  
 $\text{NiBr}_2$ , helimag. and antiferromag., mag. excitations, neutron scatt. studies 4-104409  
 $\text{Ni}_{81}\text{Fe}_{19}\text{-Ni}_{100-x}\text{Co}_x$  mag. films, exchange-coupled, mag. reversal characts. 4-76200  
NiO single cryst. and powder, mag. susceptibility and exchange const. 4-84775  
NiS: transition metals, first-order mag. and elec. transition, impurity effects 4-92909  
 $\text{NiSiF}_6\cdot 6\text{H}_2\text{O}$ , singlet ground state ferromag. ordering 4-88657  
 $\text{NiZn}$  ferrite, magnetic permeability, initial, comparison of theory with experiment (Russian) 4-98922  
 $\text{Ni}_{1-x}\text{-xZn}_x\text{Fe}_2\text{O}_4$  ferrite, mag. props.,  $\text{Fe}^{2+}$  ion effects 4-109035  
 $\text{Ni}_2\text{Zn}_{1-x}\text{SiF}_6\cdot 6\text{H}_2\text{O}$ , mag. interactions, paramagnetic Curie temp. studies 4-88645  
Pd-Au interface, electronic struct. and mag. props. 4-80645  
PdMn, dilute ferromagnet, muon spin relax. 4-71251  
 $\text{Rb}_3\text{Co}_{1-x}\text{Mg}_x\text{F}_4$ , 2D mag. alloys, neutron scatt., computer simulation 4-84768  
 $\text{Rb}_3\text{Co}_{0.5}\text{Mn}_{0.5}\text{F}_4$ , 2D mag. alloys, neutron scatt., computer simulation 4-84768  
 $\text{Rb}_3\text{Co}_{0.5}\text{Ni}_{0.5}\text{F}_4$ , 2D mag. alloys, neutron scatt., computer simulation 4-84768  
 $\text{RbMnCl}_3$ , antiferromag. with alternating strong and weak coupling, absorpt. spectra, fluoresc. meas. 4-88659  
 $\text{ScCo}_2$ , exchange enhanced Pauli paramagnet, mag. susceptibility, Knight shift meas. 4-108983  
ScRu, electron struct. and X-ray emission spectra, exchange and correl. effects 4-70697  
Si, anomalous muonium relax., muon spin rot. study 4-71238  
 $\text{TbCo}_3$ , intersublattice exchange parameters (Russian) 4-80743  
Th, photoionisation, local density-based random phase approx. calc. 4-102656  
 $\text{Ti}_2\text{Fe}_6\text{Te}_6$ , strongly anisotropic ferromagnetism, first order phase transitions 4-84796  
 $\text{TmS}(\text{Se})$ , exchange-induced plasma edge splitting, magneto-optical study 4-61663  
 $\text{TmSe}$  mixed valence cpd., soft X-ray resonant photoemission studies 4-108822  
U mononictides, antiferromagnetic transition theory 4-88672  
U, photoionisation; local density-based random phase approx. calc. 4-102656  
W (001), EELS, elastic and inelastic scatt. of slow electrons 4-114350  
 $\text{WV}_2\text{O}_6$ , exchange interaction in orbitally degenerate binuclear units 4-71054  
Y-Fe alloys, exchange interactions, coordination props. studies 4-114104  
 $(\text{Y}_{1-x}\text{Gd}_x)_3\text{Ni}_3$ , mag. props. meas. 4-80785

## exchange interactions (electron) continued

- YIG, amorphous, appl. of hyperfine and exchange field distrib. in amorphous speromagnets 4-104413  
YIG, magnetic permeability, initial, comparison of theory with experiment (Russian) 4-98922  
YIG,  $\text{Me}^{+}$  implanted, mag. props., annealing effects 4-71057  
Zn ferrites, mechanical activation effects on mag. props. 4-98882  
 $\text{ZnFe}_2\text{O}_4$  ferrite, mag. struct. and Neel temp. 4-108986  
 $\text{Zn}_{0.9}\text{Mn}_{0.05}\text{Se}$ , conduction electron exchange energy, Raman and mag. studies 4-104401  
 $\text{Zn}_{1-x}\text{Mn}_x\text{Se}$ , magnetisation and exchange consts. 4-114142  
 $\text{Zn}_{1-x}\text{Mn}_x\text{Te}$ , paramag. phase, excitonic magnetoabsorption, magnetisation meas. 4-71353  
exchange models see peripheral models  
exchanges (chemical) see chemical exchanges  
excimer lasers  
alkali metal dimers, crossing states, pot. energy curves, ab initio calcs. 4-68995  
atmospheric species measurement using excimer lasers 4-110279  
 $\text{Cl}_2$  ( $D^3 \Pi_g - A^3 \Pi_u$ ) transition, improved gain at 258 nm by halogen donor mixing 4-107601  
diatomic molecule light amplification coeff. calc. at electron transitions (Russian) 4-79115  
dimer lasers, review 4-96870  
dye laser, excimer pumped, picosec. pulse amplification (Japanese) 4-83574  
inert gas halide, UV pulse light source appl. (German) 4-112544  
inert gas halide lasers, high repetition rate 4-69383  
inert gas halogen excimer lasers, VUV and EUV generation 4-96863  
laser processing, semiconductor surface processing, materials purification and formation (Japanese) 4-74474  
laser source technology, recent developments 4-87356  
lasers for analytical and industrial chem., conf., Los Angeles, CA, USA (Jan. 1984) 4-106100  
pumping schemes for excimer lasers 4-69385  
rare-gas-halide lasers, X-ray preionisation 4-74488  
short wavelength generation using high spectral brightness  $\text{KrF}^*$  and  $\text{ArF}^*$  excimer lasers 4-107746  
spark gap switch for repetitive excimer lasers (Chinese) 4-107659  
static repetitive excimer lasers, discharge gas heat-expanding model (Chinese) 4-112387  
ultrashort pulse generation using excimer laser based system 4-96934  
X-ray preionisation performance (Chinese) 4-60087  
ArF excimer laser, doubly preionised 4-112398  
ArF, laser action using transverse discharge pumping scheme 4-69382  
ArF, phase conjugation by four wave mixing 4-107613  
HgBr laser system, narrow-band injection locking, B $\rightarrow$ X transition 4-79111  
HgBr, process kinetics meas., radiative lifetimes and quenching rate consts. 4-64701  
HgBr/HgBr dissociation laser, discharged pumped (Japanese) 4-74490  
HgCl lasers, electron-beam pumped 4-69388  
HgI, process kinetics meas., radiative lifetimes and quenching rate consts. 4-64701  
Kr $_2$ , VUV-excimer radiation build-up and decay frequencies, excited by  $\alpha$ -particles 4-91437  
KrCl(F), laser action using transverse discharge pumping scheme 4-69382  
KrF excimer laser, electron beam excited, high efficiency operation 4-74491  
KrF fast discharge excimer laser with symmetric geometry (Chinese) 4-83610  
KrF, injection locking excimer lasers in the UV 4-83608  
KrF laser, electron beam pumped, high energy, multi atm. 4-60066  
KrF laser, electron beam pumped, for laser fusion appl. 4-79113  
KrF laser, electron-beam pumped 4-69388  
KrF laser, electron-beam pumped, optimisation with Ne buffer gas 4-112384  
KrF laser based ultrashort laser pulse generation method 4-96934  
KrF laser drivers for inertial confinement fusion 4-107083  
KrF laser radiation, stimulated Brillouin scatt., in  $\text{SF}_6$  4-107752  
KrF laser system pulse compression, laser drivers for inertial-fusion reactors 4-69464  
KrF laser with automatic preionisation, construction and design 4-96945  
KrF lasers, electron beam controlled discharge pumping 4-60018  
KrF lasers, electron-beam-excited, using Ar-free mixtures at 1 atm. 4-112382  
KrF, process kinetics meas., radiative lifetimes and quenching rate consts. 4-64701  
Kr $_2$ F photochemical laser, active medium bleaching wave optical inhomogeneities, interferometric study 4-60022  
KrF\* laser picosecond gain dynamics 4-60056  
N $_2$  compact capacitively coupled laser with new electrode design 4-60067  
N $_2$  laser, pump and radiation wave spatial and temporal dynamics investigation 4-60020  
N $_2$  laser, TEA, thyatron-switched 4-64721  
N $_2$  laser oscillation-amplifier system, thyatron switched for DFB dye laser 4-69439  
N $_2$  laser with transverse discharge, light source for multichannel system calibration 4-74096  
N $_2$  multimodular laser for diagnostics of plasma formed using relativistic electron beam generators 4-75199  
N $_2$  pulsed-discharge lasers preionised by pulse or CW X-rays 4-69387  
N $_2$  TE helical electrode laser, travelling-wave excitation 4-102926  
Na $_2$  optically pumped laser, freq. control 4-87321  
Na $_2$  violet band laser, gain and fluoresc. spectrum obs. 4-69373  
NaBr gas laser, optically pumped, using electronic transitions 4-107614  
Rn monohalides, laser amplification 4-83567  
TiHg laser, discharge excited 4-69389  
Xe $_2$ , excimer laser, selective multiphoton excitation, VUV emission 4-74262  
XeBr(Cl)(F), laser action using transverse discharge pumping scheme 4-69382  
XeCl excimer laser, aerodynamic device and elec. excitation system description (French) 4-102949  
XeCl excimer laser, IR laser emission 4-96876  
XeCl excimer laser, picosecond-pulse amplification (Japanese) 4-96880  
XeCl laser, discharge constriction effects 4-74489  
XeCl laser, microwave-pumped, active mode locking 4-74487  
XeCl laser, passive mode locking using dye saturable absorbers 4-112485

**excimer lasers** continued

- XeCl laser, self-sustained discharge pumped, theory 4-96875  
 XeCl laser, single longitudinal mode operation 4-112386  
 XeCl laser, spectral composition of radiation (*Russian*) 4-69380  
 XeCl laser, X-ray preionised discharge, small signal gain characts. (*Chinese*) 4-112388  
 XeCl laser based ultrashort laser pulse generation method 4-96934  
 XeCl laser efficient stimulated Raman scatt. in high-pressure H<sub>2</sub> cell 4-96999  
 XeCl laser excited by longit. gas discharge (*Chinese*) 4-107603  
 XeCl laser using liq. as Cl donor (*Chinese*) 4-112390  
 XeCl laser with automatic preionisation, construction and design 4-96945  
 XeCl lasers, effects of diluent gas (*Chinese*) 4-107605  
 XeCl lasers, electron beam controlled discharge pumping 4-60018  
 XeCl, long pulse, generation of 300 psec pulse by direct mode locking using acousto-optic modulator and saturable absorber 4-112490  
 XeCl pulse-periodic laser, reasons for output power fall during operation 4-74494  
 XeCl tunable laser system (*Chinese*) 4-112467  
 XeCl X-ray preionised repetitive pulsed excimer lasers 4-64698  
 Xe<sub>2</sub>Cl<sub>2</sub>, tunable electron-beam-pumped excimer lasers 4-69384  
 XeCl\* laser, discharge stability 4-91441  
 XeCl\* lasing as result of chem. radiative collisions 4-60023  
 XeF<sub>2</sub> (B) excimer form. kinetics in photoexcitation of Xe-F<sub>2</sub> mixture 4-60024  
 XeF (C-A) laser oscill. using electron beam excitation 4-87320  
 XeF excimer laser intermediates, degradation of dielec. films 4-74534  
 XeF fast discharge excimer laser with symmetric geometry (*Chinese*) 4-83610  
 XeF injection locking excimer lasers in the UV 4-83608  
 XeF, injection-locked, quenching of backward stimulated Raman scatt. by broadband forward Raman rad. 4-91535  
 XeF laser, electron beam pumped, laser parameters determ. 4-96874  
 XeF laser output spectrum, XeF(B) to XeF(X) transition, photolytic pumping of XeF<sub>2</sub> 4-79117  
 XeF laser using grating-interferometer-based cavity, single-mode tunable operation 4-102956  
 XeF, process kinetics meas., radiative lifetimes and quenching rate consts. 4-64701  
 XeF pulsed laser transverse mode form. in low-magnification positive-branch unstable resonators 4-73521  
 XeF, tunable electron-beam-pumped excimer lasers 4-69384  
 XeF\* laser radiation stimulated Raman scatt. in H<sub>2</sub> 4-74611

**excimers***see also excimer lasers*

- anthracene-TEA (DMA) complexes formed in supersonic jets, van der Waals and charge transfer states 4-112226  
 9,9'-bianthryl, intramolecular electron transfer, solvent effects. fluoresc. study 4-96598  
 1,4-bis(β-pyridyl-2-vinyl)benzene, anal. mixed cryst., fluoresc. and lifetime meas. 4-104658  
 α, ω-biscarbazolylalkanes, doped in polycarbonate, excimer fluoresc. 4-107382  
 9-cyanoanthracene, lattice distortion, exciton-induced, excimer form. 4-70659  
 1-cyanonaphthalene-triethylamine van der Waals complex, internal, exciplex form. in mol. 4-69164  
 9,10-dibromoanthracene, liq. soln., singlet-triplet energy transfer. fluoresc. quenching 4-112222  
 9,10-dichloroanthracene, liq. soln., singlet-triplet energy transfer. fluoresc. quenching 4-112222  
 9,10-dicyanoanthracene, liq. soln., singlet-triplet energy transfer. fluoresc. quenching 4-112222  
 N,N-dimethylaniline-methyl acrylates, photopolymerisation kinetics and mechanism 4-62199  
 2,5-distyrylpyrazine, anal. mixed cryst., fluoresc. and lifetime meas. 4-104658  
 lattice distortion, exciton-induced, excimer form. 4-70659  
 methyl methacrylate, polymerisation monitoring using excimer fluorescence 4-89293  
 organic molecules, luminescence of excimers and exciplexes 4-104997  
 perylene-TEA (DMA) complexes formed in supersonic jets, van der Waals and charge transfer states 4-112226  
 polyaceneaphthylene and poly(acenaphthylene-co-N-vinylcarbazole), singlet energy migration, quenching, excimer form. 4-83408  
 polymer colloids, fluorescence techniques 4-85342  
 polystyrene, head-to-head, intramol. excimer form. and energy migration 4-114325  
 polystyrene solutions, intramolecular excimer form., solvent viscosity, press. depend. 4-92054  
 polyvinylcarbazole, intramol. exciplex form. 4-68923  
 pyrene, fluoresc. and diffusion on C<sub>18</sub> reversed-phase liq. chromatographic packing 4-112219  
 pyrene, lattice distortion, exciton-induced, excimer form. 4-70659  
 1-(1-pyrene)-3-(dimethylaminophenyl)propane, conformational dynamics, viscosity and temp. depend. 4-62168  
 pyrene-N,N-dimethylaniline complex radical pairs, exciplex luminesc., environment effect on mag. field modulation 4-99147  
 α-pyrenyl-ω-alkylamine exciplexes, electronic struct., substitution pattern and chain length effects 4-112097  
 triatomic excimer kinetics, electron beam-pumped (*Chinese*) 4-62156  
 Ar, relativistic electron beam excitation, fluoresc. and absorpt. 4-69220  
 Ar, solid, excimer-like states, numerically optimised geometries 4-65624  
 Ar<sub>2</sub> excimers, electronic struct., ab initio CI calc. (*French*) 4-78788  
 Hg<sub>2</sub>, pot. energy curves, electronic states, ab initio CI calcs. 4-112124  
 Kr<sub>2</sub> excimers, electronic struct., ab initio CI calc. (*French*) 4-78788  
 Ne+Ne, interaction excimer pots., atomic beam study 4-64563  
 pyrene-diethylaniline exciplexes, in methanol, delayed fluoresc. 4-59845  
 THg, pot. energy curves, electronic states, ab initio CI calcs. 4-112124  
 Xe, VUV laser excited spectra 4-107398  
 XeF (B) excimer form. kinetics in photoexcitation of Xe-F<sub>2</sub> mixture 4-60024  
 Xe<sub>2</sub>\* excimers, photoionisation processes 4-83430

**exciplex lasers** *see excimer lasers***exciplexes** *see excimers***excitonic molecules**

- dephasing relaxation constant, proposed method for meas. 4-70664  
 semiconductor, excitonic matter 4-75866  
 semiconductors, coherent pairing of excitons and biexciton Bose-Einstein condensation 4-88459

**excitonic molecules** continued

- semiconductors, direct-gap, coherent far IR radiation sources on hot excitons 4-109213  
 CdS, laser induced gratings 4-104630  
 CdS, spectral-time characts. of nonlinear emission (*Russian*) 4-104620  
 CuBr, biexciton two-photon absorpt., Raman scatt., perturbation theory calc. 4-75864  
 CuCl, dense exciton-biexciton system, optical bistability 4-64732  
 CuCl exciton-excitonic mol. system, optical bistable behaviour 4-96993  
 CuCl, nonlinear optical props. of biexcitons, degenerate four-wave mixing 4-69488  
 GaAs<sub>1-x</sub>P<sub>x</sub>N, excitons and excitonic mols. bound to impurity, calcs. 4-108785  
 Ge exciton condensation, microwave studies, biexcitons and electron-hole droplets 4-70668  
 HgI<sub>2</sub>, red, two-photon reson. Raman scatt. via excitonic mol. state 4-99113  
 α-O<sub>2</sub>, polarised satellites of biexciton absorpt. vibronic bands 4-98540

**excitons***see also excitonic molecules; phonon-exciton interactions*

- alkali halides, contribution of electronic processes in sputtering 4-61803  
 alkali halides, defect creation mechanisms 4-60915  
 alkali halides, excitonic and impurity-excitonic mechanisms for F,H pair creation (*Russian*) 4-80034  
 alkali halides, fracture-induced luminesc. and crack vel. 4-104685  
 alkali halides, longitudinal excitons and plasmons 4-84569  
 alkali halides, stability and optical props. of self-trapped exciton 4-104129  
 alkali metal halides, F-centre states, hybrid method with floating 1-s Gaussian basis 4-70709  
 anisotropic systems, Wannier exciton energy states 4-88454  
 anthracene, doped and undoped, exciton-polariton luminesc. (*Russian*) 4-99172  
 anthracene, excitons and diffusion effects 4-92617  
 anthracene, isotopically mixed, disordered crysts., exciton transport in rel. correl. functions 4-113872  
 anthracene, luminescence of strong exciton transitions 4-104643  
 anthracene, single cryst., singlet exciton transport transient grating meas. 4-65611  
 antiferromagnetic dielec., hybrid excitations, anal. of mag. and optical props. 4-76233  
 benzophenone glass, nonequilibrium exciton diffusion, phosphorescence studies 4-61290  
 biphenyl cryst. reson. excited defect emission 4-109231  
 biphenyl-naphthalene mixed crystals, delayed fluoresc., role of quadratic terms in kinetics 4-109232  
 1,4-bis(β-pyridyl-2-vinyl)benzene, anal. mixed cryst., fluoresc. and lifetime meas. 4-104658  
 2-bromonaphthalene glassy films, spectral diffusion and triplet exciton localisation 4-98538  
 charge transfer states, electric field assisted dissociation as a photocarrier prod. 4-70744  
 coherent exciton-biexciton system, soliton waves and self-induced transparency 4-60119  
 complex cryst. lattice with Frenkel excitons, 0-99 energy bands (*Japanese*) 4-75865  
 condensation kinetics into electron-hole liq. in finite size crysts. 4-70674  
 crystal optics with spatial dispersion, and excitons, book 4-101583  
 cubic semiconductors, effect of spin-split valence band on exciton energy 4-84855  
 cyanine dye monoclinic cryst., exciton polaritons, reflectivity studies 4-80513  
 9-cyanoanthracene, lattice distortion, exciton-induced, excimer form. 4-70659  
 delocalised surface exciton-impurity states with low binding energy (*Russian*) 4-70900  
 2,5-distyrylpyrazine, anal. mixed cryst., fluoresc. and lifetime meas. 4-104658  
 epitaxial high-purity layers, low-pressure MOCVD growth 4-61861  
 exciton-photon system, soliton creation 4-61640  
 excitonic optical bistability, effects of mirror reflectivity 4-83632  
 ferroelectrics, dipole-dipole mechanism of energy transfer 4-88482  
 Frenkel excitons, Bose-Einstein condensation and superfluidity 4-98537  
 heterojunctions, exciton quenching mechanism (*Russian*) 4-84687  
 highly excited crysts., polariton energy spectra, RPA calc. 4-61302  
 III-V semiconductors, nonlinear absorpt., coherent radiation-exciton interaction model 4-99078  
 III-VI layered semiconductors, electronic and vibrational spectra 4-71390  
 inclusion cpts. reactions, symmetry conservation, electronic energy transfer processes 4-71943  
 incoherent, kinetics of bimolecular quenching 4-70661  
 inert gas, solids, conduction band states, excitons, photoemission 4-85057  
 insulating solid, isolated excitonic transition 4-92993  
 insulator, excitonic, with spatially inhomogeneous gap, spin wave zero sound mode 4-61528  
 ionic crystal, three-channel exciton decay by light emission (*Russian*) 4-99171  
 lattice distortion, exciton-induced, excimer form. 4-70659  
 magnetic materials, anisotropic, optical props. in external mag. field, theory 4-80907  
 N-methylcarbazole/naphthalene transparent glass, microcryst. formation and triplet-triplet energy transfer (*German*) 4-75297  
 molecular crystals, coupled phonon vibr. and dipole plasma quanta (*Russian*) 4-104131  
 molecular crystals, exciton luminesc. 4-109224  
 molecular crystals, mixing Frenkel excitons with charge-transfer excitons 4-108784  
 molecular crystals, solitary wave excitation by coherent EM field 4-98534  
 molecular crystals and aggregates, exciton dynamics calcs. 4-78064  
 molecular luminescence and its applications, conf., Kharkov, USSR (1982) 4-106094  
 naphthalene, absorpt. spectra study of bound exciton states 4-108782  
 naphthalene, isotopically mixed, disordered crysts., exciton transport in rel. correl. functions 4-113872  
 naphthalene, isotopically mixed crysts., triplet states, high resolution optical spectroscopy 4-75863  
 naphthalene, mol. cryst. triplet excited states, spin-lattice relax. 4-98556  
 naphthalene cryst., excitons, defects and intramolecular phonon interactions (*Russian*) 4-98532

## excitons continued

- non-local dielectrics, surface exciton polaritons, dispersion relations 4-92628  
nucleic acids and their components, intrinsic luminesc. 4-105178  
one dimensional electron-exciton model pairing and CDW correlations 4-104137  
optical lineshapes at finite temps., stochastic model 4-61286  
optically-induced drift by resonance illumination 4-61298  
organic crystals, photoemission into gases 4-71511  
organic mol. cryst. in strong mag. fields, low temp. phosphoresc. 4-99142  
organic molecular crystals, excitonic processes (*Russian*) 4-98531  
organic superconductor, one-dimensional, exciton mechanism 4-92857  
polar cryst. plate, exciton state and binding energy, appl. to PbI<sub>2</sub> 4-70673  
poly-N-epoxypropylcarbazole, sensitized, photosensitivity, low mol. cpds., effects 4-113999  
polyacetylene, exciton two-soliton state 4-98528  
polydiacetylene, reson. Raman excitonic profiles, linear susceptibility theory 4-109171  
polydiacetylene crystals, electro-reflectance spectra of 1-dimens. excitons 4-104573  
polydiacetylenes, charge-transfer exciton spectra, Green's function study 4-71405  
polymers, linear chain, localised excitations, resonant energy transfer 4-80505  
polyvinylcarbazole-vinylbenzocarbazole, fluorescence and host-guest energy transfer 4-99166  
pseudoisocyanin, exciton-phonon coupling, vibronic struct., UV spectrum, self-consistent theory 4-70658  
pyrene, lattice distortion, exciton-induced, excimer form. 4-70659  
quantum-well struct., resonant impurity states 4-61327  
quasi, luminescence, ODMR study 4-85001  
quasi-one-dimensional mol. chains, solitons 4-86227  
rare gas crystal, exciton processes study, synchrotron radiation appl. (*Russian*) 4-98530  
rare gas crystals, local optical centres and exciton states 4-98561  
self-energy, many particle system calculations 4-98536  
semiconducting films, excitons, Bose condensation 4-98542  
semiconductor, excitonic matter 4-75866  
semiconductor, quantum well structs., photoluminesc. lineshape, interfacial quality influence 4-71424  
semiconductor alloys, excitonic photoluminesc. linewidth 4-80972  
semiconductor crystallites, electron-electron and electron-hole interactions, size depend. of excited electronic state 4-70660  
semiconductor superlattices, collective excitations theory 4-61451  
semiconductor superlattices, quantum wells, and heterostructs., elec. and optical props. 4-80666  
semiconductor surface, electronic collective modes, instabilities and electron-phonon interactions 4-108797  
semiconductor surface, electronic collective modes and instabilities 4-108796  
semiconductor thin films, Wannier-Mott exciton decay at surface projections 4-65614  
semiconductors, coherent pairing of excitons and biexciton Bose-Einstein condensation 4-88459  
semiconductors, core exciton resons. at inner-shell thresholds, dynamical scanning effects 4-80506  
semiconductors, diamond-like, Frenkel exciton self-localisation 4-61295  
semiconductors, direct gap alloys, free exciton optical absorption, disorder effects 4-65996  
semiconductors, direct-gap, coherent far IR radiation sources on hot excitons 4-109213  
semiconductors, disordered, spatially extended quasiparticles, disorder effects 4-98499  
semiconductors, disordered organic and inorganic, non-equilibrium diffusive transport 4-70801  
semiconductors, excitonic absorption line broadening, strong magnetic field, calcs. 4-108786  
semiconductors, excitons and biexcitons of high density, coherent nonlinear processes 4-102985  
semiconductors, momentum relax. time of Wannier-Mott excitons scatt. by charged impurities 4-61296  
semiconductors, recombination-stimulated phenomena 4-61288  
semiconductors, resonant light scatt. through exciton-polaritons 4-109204  
semiconductors, uncooled, optical bistability rel. to excitons 4-74592  
semiinfinite cryst., exciton-polariton theory 4-70667  
solids, time resolved VUV luminesc. under synchrotron radiation selective excitation 4-84985  
spatially dispersive medium, reson. Brillouin scatt. 4-80953  
squarylium dye, polymorphs, cryst. field influence on UV spectra 4-104626  
stilbene, mol. cryst., triplet exciton  $\alpha$  particle excitation, diffusion coeff. 4-104130  
superconducting pairing condensates, exciton mediated, phonon effect on T<sub>c</sub> 4-70974  
TCNQ salt with triphenyl methyl arsenic cation triplet excitation radical, exchange anomaly resolution 4-70760  
TCNQ salts, quasi-one-dimensional metals and semiconds., mol. excitons, optical props. 4-76494  
p-terphenyl, electron and  $\Gamma$ -irrad., absorpt. spectra (*Russian*) 4-71421  
n-terphenyl, pure and impure crystals, exciton, visible absorpt. and fluorese. spectra 4-99141  
tetracene, delayed fluorese., role of charge transfer states in triplet exciton form. 4-99191  
s-tetrachlorobenzene, triplet exciton scatt. and trapping, electron spin echo 4-108783  
1,2,4,5-tetrachlorobenzene, triplets, exciton trapping, nonexponential luminesc. intensities 4-93101  
topologically disordered systems, localisation, self consistent theory 4-92672  
transition metal compounds, exciton satellites in photoelectron spectra 4-70665  
1,3,5-trioxane, single and mol. crystals, internal phonons ang. dispersion, Raman spectra 4-61687  
two-band direct gap semicond., electrodynamics, SCF theory 4-98497  
vibron solitons in one-dimensional molecular crystals 4-80177  
VUV radiation physics, conf., Jerusalem, Israel, 8-12 Aug. (1983) 4-82583  
AgBr:I, multiphonon emission, excitons, photoluminescence 4-99159  
AgCl(Br), ion polarisability, lattice const. and exciton energies 4-113387

## excitons continued

- (Al,Ga)As/GaAs/Ge:Ga polar semicond. quantum well system, growth and optical props. 4-114314  
AlGaAs/GaAs quantum wells, photoluminescence studies 4-93105  
Al<sub>x</sub>Ga<sub>1-x</sub>As, line broadening in photoluminescence spectra 4-109241  
Al<sub>x</sub>Ga<sub>1-x</sub>As:Si, grown by MBE, photoluminesc. composition depend. 4-84996  
Al<sub>x</sub>Ga<sub>1-x</sub>As:Si, grown by MBE, photoluminesc. spectra, defect-related emissions 4-84997  
Al<sub>x</sub>Ga<sub>1-x</sub>As/GaAs single quantum well, exciton transport 4-88451  
Ar, solid, cathodoluminescence excitation spectra, desorption, exciton creation 4-85013  
Ar solid, electron stimulated desorpt., luminesc. and exciton creation 4-80381  
Ar, solid, electronically excited, sputtering and luminesc. 4-104708  
Ar, solid and liq., excitons, reflection spectra study 4-84570  
As<sub>2</sub>Se<sub>3</sub> cryst. and amorphous, recomb. and excited-state absorption at photolum. centres 4-99182  
B compounds, low energy Auger transitions 4-88909  
BaMnF<sub>2</sub> 2D antiferromag., optical magnon sidebands and exciton dynamics 4-98875  
Ba(NO<sub>3</sub>)<sub>2</sub>·H<sub>2</sub>O, pure and doped single crystals, fluorese. and phosphoresc. study 4-109227  
CO<sub>2</sub>, solid, mol. excitons, UV absorpt. and XPS spectra study 4-65613  
Cd halides, electronic struct., UV reflectivity 4-84974  
CdGa<sub>2</sub>Se<sub>4</sub>, excitonic wavelength modulated reflectance 4-71336  
Cd<sub>x</sub>Hg<sub>1-x</sub>Te, ellipsometric studies of interband transitions 4-92999  
Cd<sub>1-x</sub>Mn<sub>x</sub>Te, piezomodulation study of absorpt. edge and Mn<sup>2+</sup> transition 4-112422  
CdS, cavityless optical bistability due to light-induced absorpt. 4-102971  
CdS, exciton diffusion and exciton momentum scatt. 4-65616  
CdS, exciton-polaritons, resonant Brillouin scatt. studies 4-108789  
CdS, excitons in high mag. fields, gauge-invariant energy variational calc. 4-80508  
CdS, frequency tuning of far-IR radiation on hot excitons 4-69415  
CdS, laser induced gratings 4-104630  
CdS, nonlinear exciton transmission, Maxwell's eqn. anal. 4-98535  
CdS, radiative recomb. mechanisms for high density excitons 4-88458  
CdS, resonant Brillouin scatt. study 4-61721  
CdS, resonant Brillouin spectra calcs. 4-61722  
CdS, thermally stimulated brightening of cryst. boundary in exciton absorption region 4-114234  
CdS, thin plate, reflection spectrum, interference struct. anal. 4-76402  
CdSe, free exciton dynamics study 4-98788  
CdSe, hot excitons and electron-hole pairs and Raman spectra 4-114285  
CdSe, picosecond energy-relax. processes of excitons, luminesc. study 4-109244  
CdSe, picosecond spectroscopy at high excitation densities 4-81003  
CdTe, cooperative processes, spontaneous and stimulated emission 4-104662  
CdTe doped with mag. ions, anomalous optical effects (*Russian*) 4-99103  
CdTe MBE films on InSb, impurity doping and photoluminesc. props 4-88980  
CsI, 60 GPa effects, UV absorpt. spectra 4-76490  
CsI, optical absorpt. spectra, meas. at press. up to 60 GPa 4-76495  
CsNiF<sub>6</sub>, ferromagnet, optical absorption and magneto-optical properties 4-99100  
Cu complexes, Cu-phthalocyanine single cryst., visible absorpt. band, temp. depend. 4-76489  
CuBr<sub>2</sub>·2H<sub>2</sub>O, spin-orbit splitting energy, exciton spectra, disorder effects 4-88457  
CuCl, dense exciton-biexciton system, optical bistability 4-64732  
CuCl, dielec. function, exciton-biexciton transitions and population effects 4-80525  
CuCl exciton-excitonic mol. system, optical bistable behaviour 4-96993  
CuCl, excitonic absorpt. edge, IR laser radiation induced electroabsorpt. 4-61287  
CuCl excitonic optical bistability, effects of mirror reflectivity 4-83632  
CuCl, excitonic polaritons, picosecond spectroscopy (*Japanese*) 4-76403  
CuCl, optical nonlinearity due to Z<sub>1</sub> and Z<sub>1,2</sub> excitons, study by reflected four-wave mixed light generation 4-79217  
CuCl, resonant Raman scatt. in region of edge excitons 4-76472  
CuI, single crystals and thin films, excitons, uniaxial stress effects 4-98539  
Cu<sub>2</sub>O, ortho-exciton states, time-resolved hot luminesc., reson. Raman scatt. 4-71438  
Cu<sub>2</sub>O, para-exciton luminesc. polarisation in mag. field 4-92624  
Cu<sub>2</sub>O thin films on Cu, defect luminesc. 4-66062  
Fe<sub>1-x</sub>Mn<sub>x</sub>F<sub>2</sub>, light scatt. by mag. excitons 4-71388  
GaAs, electroluminescence spectra of free excitons, optical resonances 4-88883  
GaAs, excitonic polaritons in elec. fields at surfaces 4-92633  
GaAs, excitons, self-energy, many particle system calculations 4-98536  
GaAs, SAW characterisation of surface and interface states 4-98681  
GaAs, selectively excited luminesc. 4-104639  
GaAs single quantum wells, low temp. exciton trapping on interface defects, photolum. 4-93111  
GaAs, undoped and Cr doped, exciton region, impurity and illumination effect on photoconductivity 4-61411  
GaAs:N, isoelectronic traps study by photoluminesc. (*Chinese*) 4-93098  
GaAs/Al<sub>x</sub>Ga<sub>1-x</sub>As quantum wells, struct. and optical props. 4-99151  
GaAs/Al<sub>x</sub>Ga<sub>1-x</sub>As quantum wells, Be doped, photoluminescence studies 4-104653  
GaAs/AlGaAs inverted heterojunctions, photoluminescence studies 4-98460  
GaAs/AlGaAs multiple quantum well structures, room temp. excitonic nonlinear absorpt. and refract. 4-74590  
GaAs/AlGaAs single quantum well struct., enhanced luminescence 4-99150  
GaAs-Al<sub>0.3</sub>Ga<sub>0.7</sub>As quantum wells, photoluminesc. from spike doped hydrogenic donors 4-104668  
GaAs-Al<sub>x</sub>Ga<sub>1-x</sub>As quantum well struct., exciton binding energy 4-75868  
GaAs-Al<sub>x</sub>Ga<sub>1-x</sub>As quantum wells, energy-gap discontinuities, and effective masses 4-92623  
GaAs-AlGaAs multiple quantum well heterostruct., delocalised exciton state 4-92621  
GaAs-AlGaAs superlattice grown by MBE, struct. and optical props. 4-84538  
GaAs-Ga<sub>1-x</sub>Al<sub>x</sub>As, binding energy of exciton in GaAs quantum well, magneto-optical determination 4-114027

## excitons continued

- GaAs-GaAlAs double heterostructure, quantisation of excitonic polaritons 4-92634
- GaAs-GaAlAs multiple-quantum-well structures, sharp line photolum. spectra 4-93110
- GaAs-GaAlAs quantum well struct., optical props., review 4-104146
- GaAs-GaAlAs quantum wells, reflectance of two-dimensional excitations 4-109211
- GaAs<sub>1-x</sub>P<sub>x</sub>, localised excitons, luminescence study 4-61291
- GaAs<sub>1-x</sub>P<sub>x</sub>N, exciton tunnelling inhibited by disorder 4-92622
- GaAs<sub>1-x</sub>P<sub>x</sub>N, excitons and excitonic mols. bound to impurity, calcs. 4-108785
- GaAs<sub>1-x</sub>P<sub>x</sub>N<sup>+</sup>Zn<sup>+</sup>, implanted, photoluminescence spectra, impurity conc. depend. (Chinese) 4-93099
- GaAs<sub>1-x</sub>P<sub>x</sub>, fundamental absorpt., optical absorpt. coeff. 4-76408
- Ga<sub>0.9</sub>In<sub>0.1</sub>Se system, magneto-optical props. near fundamental band gap 4-109166
- GaP (110), intrinsic unoccupied surface states and valence band minimum 4-80641
- GaP, press. depend. of bound excitons 4-61293
- GaP:N, exciton transfer, NN<sub>2</sub>-pair luminesc. enhancement, stochastic model 4-104660
- GaP:N,Te,Zn, photolum. under high press. (Chinese) 4-93097
- GaSb-AlSb, superlattices, light and heavy valence subband reversal, lattice mismatch 4-114013
- GaSe, excitons in high mag. fields, gauge-invariant energy variational calc. 4-85058
- GaSe, optical orientation of carriers, optically detected EPR 4-88746
- GaSe single cryst., luminescence spectra, isothermal annealing effects 4-81001
- GaSe, uncooled, optical bistability rel. to excitons 4-74592
- Ge, cyclotron resonance and radiative recombination for excitons, free carriers, electron-hole droplets 4-71183
- Ge, dielectric function, temp. depend. 4-109111
- Ge, electron-hole liq. relax. kinetics near nucleation threshold, collective decay of small electron-hole drops 4-98541
- Ge, electron-hole liq. droplet destruction in nonuniform deformation field 4-61297
- Ge, electroluminescence spectra, oscillations anal. for electron-hole Coulomb interactions 4-66011
- Ge exciton condensation, microwave study 4-68234
- Ge exciton condensation, microwave studies, biexcitons and electron-hole droplets 4-70668
- Ge exciton condensation, microwave breakdown, one- and two-photon carrier excitation luminescence 4-70670
- Ge, exciton condensation, microwave methods using pulsed optical excitation, kinetics 4-70671
- Ge exciton microwave breakdown, exciton and free carrier kinetics with electron-hole drops 4-70669
- Ge exciton studies, laser heating effects at liquid He temps. 4-70672
- Ge nonequilibrium current carrier microwave absorpt., carrier conc., excitons 4-70852
- Ge:Zn, far-IR magnetoabsorption of bound excitons 4-114247
- HBr, cryst., two-exciton spectra 4-104586
- HCl, cryst., two-exciton spectra 4-104586
- HgI<sub>2</sub>, polariton energy relax., thermal barrier effect 4-84573
- InBr, magneto-reflectance of excitons 4-76439
- In<sub>1-x</sub>Ga<sub>x</sub>As, indirect conduction band minima determ. 4-98517
- In<sub>1-x</sub>Ga<sub>1-x</sub>As multi quantum well structs., strained, optical props. 4-104669
- In<sub>1-x</sub>Ga<sub>x</sub>AsP<sub>1-x</sub>, indirect conduction band minima determ. 4-98517
- In<sub>1-x</sub>Ga<sub>x</sub>Sb, indirect conduction band minima determ. 4-98517
- InI, magneto-reflectance of excitons 4-76439
- InP, absence of core exciton induced resonant photoemission 4-114360
- InP epilayers, cathodoluminescence study 4-104678
- InP, excitons bound to neutral acceptors, stress effects, photoluminesc. study 4-61294
- InP, SAW characterisation of surface and interface states 4-98681
- InP:Co, impurities, optical and transport studies 4-71444
- InP:Gd(Yb) epitaxial films, doping effects on low-temp. edge photoluminescence 4-85028
- InSb, photomagnetic effect and photocond. in mag. field, diamag. exciton discrete struct. 4-108903
- n-InSe, photoluminescence and free exciton emission 4-99176
- InSe, polypyrrolin in the exciton absorpt. spectrum (Russian) 4-114304
- KBr:Cl, and undoped crystals, anion Frenkel defect creation, luminesc. study (Russian) 4-80980
- KBr:Cl, X-irradiated, luminesc. study (Russian) 4-80981
- KBr:In, A<sup>2+</sup>, F-centres formed by low-energy excitons, photoluminescence spectra (Russian) 4-113874
- KCl:I, impurity-localised excitons, luminesc. and absorpt. spectroscopy study 4-92625
- KCl:I, luminescence of localised excitons at low temp. 4-80990
- KI, generation of free excitons by optical excitation of self-trapped excitons, luminesc. emission 4-88453
- KI, single cryst., birefringence induced by spatial dispersion 4-76429
- KI, UV irradi., V<sub>K</sub> motion and luminesc. quenching 4-66063
- KI very thin cryst., melt grown, optical absorpt. and refl. spectra 4-93035
- K<sup>15</sup>N<sub>2</sub><sup>14</sup>N<sub>2</sub>O<sub>2</sub>, disordered linear chain, excitation transfer, polarisability effect 4-70662
- K<sub>2</sub>SeO<sub>4</sub>, Raman and for IR spectra, rel. to selenate radical movement at orthorhombic sites 4-76448
- LiH(D), radiation induced defect form. 4-60952
- LiH(D):Na, radiation induced defect form. 4-60952
- MgO:Ca<sup>2+</sup>, coexistence of large- and small-radius excitons bound on defects 4-92619
- Mn dihalides, d-excitons, vibr. struct., IR and Raman spectra studies 4-113873
- MnBr<sub>2</sub>, exciton dispersion, optic d-d transition line shape 4-104629
- MnI<sub>2</sub>, exciton dispersion, optic d-d transition line shape 4-104629
- N<sub>2</sub> crystalline, exciton luminesc. and luminesc. spectrum struct. 4-104641
- N<sub>2</sub>, solid, exciton resonances in VUV spectra (Russian) 4-99134
- NaCl, cryst., X-irrad., F-centre decay during photoannealing 4-80036
- NaCl, F-centre form., excitonic pot. surface, absorpt. spectra 4-71415
- NaCl:Br, impurity-localised excitons, luminesc. and absorpt. spectroscopy study 4-92625
- NaI:Pb, photoluminescence decay temp. and aggregation depend. 4-99177
- NaI:TI, excitation fluoresc. intensity in VUV 4-84987

## excitons continued

- Na<sub>2</sub>O-SiO<sub>2</sub>, vitreous, excitons and localised excitations (Russian) 4-98533
- Nd<sub>3</sub>La<sub>1-x</sub>P<sub>3-x</sub>O<sub>14</sub>, four wave mixing and exciton dynamics 4-83638
- Ne, solid, Ne<sub>2</sub><sup>+</sup> centres, vibr. relax. and hot luminescence 4-99178
- Ne, solid, self-trapped excitons, electronic struct., hybrid method with floating 1-s Gaussian basis 4-70709
- NiO, valence band photoemission spectra 4-61809
- P, black, reson. photoemission theory 4-85088
- PbCl<sub>2-2x</sub>Br<sub>2x</sub>, self-trapped excitons, luminesc. (Russian) 4-80982
- PbI<sub>2</sub>, binding energies of exciton-ionised donor complex and exciton line n=1 4-70666
- PbI<sub>2</sub>:Ag, exciton spectrum, photodoping effects (Russian) 4-92626
- PbO, exciton luminescence under powerful laser excitation 4-109235
- Pr-Cu point contacts low temp., high purity, I-V characteristics 4-114018
- Pr-Pr point contacts, low temp., high purity, I-V characteristics 4-114018
- Rb<sub>2</sub>MnCl<sub>4</sub>, 2D antiferromag., optical absorption and luminesc. 4-80991
- Rb<sub>2</sub>MnCl<sub>4</sub>, mag. moment origins, magnon sidebands, excitons, optical absorpt. spectra, MCD meas. 4-99097
- Rb<sub>2</sub>MnCl<sub>4</sub>, two-dimensional antiferromagnet, IR absorpt., Raman spectra, MCD studies 4-61713
- Rb<sub>2</sub>Mn<sub>2</sub>Cl<sub>7</sub>, 2D antiferromag., optical absorption and luminesc. 4-80991
- Rb<sub>2</sub>Mn<sub>2</sub>Cl<sub>7</sub>, two-dimensional antiferromagnet, IR absorpt., Raman spectra, MCD studies 4-61713
- SC<sub>2</sub>O<sub>3</sub>, ODMR study of exciton trapping 4-80503
- Si (110), electron subband reson., IR reson. absorpt. 4-61431
- Si, substitutional and interstitial donors, many electron effect 4-113895
- Si:Bi, Fe, exciton photoluminescence study 4-109243
- Si:In(Tl), isoelectronic bound excitons, transient photoluminesc. study 4-80507
- Si:Li and Si:Li, C, electron irradi., luminesc. decay time, absorpt., isotope splitting, and Zeeman meas. 4-71434
- Si:P(B), heavy doping effect on band struct. and optical props. 4-92998
- Si, Ge<sub>1-x</sub>, Frenkel core excitons, binding energy 4-75867
- SiO<sub>2</sub>, vitreous and quartz phases, excitons and localised excitations (Russian) 4-98533
- Si(111) surface chain model, optical props. and excitons 4-108916
- SrS, electronic excitations and recomb. luminesc. (Russian) 4-80984
- TbF<sub>3</sub>, fluorescence, exciton diffusion and up conversion mechanisms 4-66075
- TiGaS<sub>2</sub> layer crystals, exciton bands, temp.-induced shift and deformation effects 4-65615
- TlInS<sub>2</sub> crystals, free and bound excitons radiative recombination 4-80504
- YAG:Nd crystals coloured with X-rays, thermoluminesc. 4-76534
- Y<sub>2</sub>O<sub>3</sub>, ODMR study of exciton trapping 4-80503
- Zn<sub>0.972</sub>Cd<sub>0.028</sub>Se, excitation migration between localised excitons, photoluminesc. absorpt. spectra 4-88456
- Zn<sub>0.972</sub>Cd<sub>0.028</sub>Se solid soln., localised exciton migration, pumping intensity effects 4-92618
- Zn<sub>0.972</sub>Mn<sub>0.028</sub>Te, free exciton excited states 4-70663
- Zn<sub>1-x</sub>Mn<sub>x</sub>Te, paramag. phase, excitonic magnetooptical, magnetisation meas. 4-71353
- ZnO films, surface exciton polaritons, ATR mode 4-65618
- ZnO, nonlinear light absorpt., two-photon absorpt. spectra 4-96992
- ZnO:Ni, photoionisation band edge fine struct., electroabsorption studies 4-109162
- ZnSe, VPE growth, photoluminesc. props. 4-61858
- ZnTe, donor bound exciton states, Zeeman spectra 4-88452
- ZnTe polycryst. films, resonant light scatt. spectra 4-99207
- ZnTe:Ni, absorpt. spectra, impurity states (Russian) 4-113898

## exhibitions

- Testekspo-83, nondestructive materials monitoring (Russian) 4-81384

## exobiology see extraterrestrial life

## exoelectron emission

- alkali halides, hole-induced thermo-exoemission 4-85092
- ferroelectric semicond., photoferroelectric phenomena caused by fluctuations and phasons 4-66009
- ionic crystals, exoelectron emission during fracture, energy distrib. function depend. on charge struct. 4-88951
- semiconductors, excited quasistationary states relax. as source of exoelectron emission 4-99290
- surface damage evaluation using exoelectron emission phenomena (Japanese) 4-114742
- thermally stimulated, electron dosimetry, appl. 4-115224
- Al, vacancy migration energy, exoelectron emission meas. 4-65456
- BeO films, laser evaporated, thermally and optically stimulated exoelectron emission 4-88949
- CaF<sub>2</sub> vapour deposited thin films, TSEE, thermolum. meas. 4-81119
- CaSO<sub>4</sub> phosphors, thermoluminescence and exoelectron emission, radical effects 4-93120
- Cd, vacancy migration energy, exoelectron emission meas. 4-65456
- CsBr:TI, V<sub>K</sub> centres, thermostimulated exoelectron emission 4-76645
- Cu, vacancy migration energy, exoelectron emission meas. 4-65456
- KCl:TI, X-irrad., TSEE energy spectra, surface pot. meas. 4-61814
- LIF, exoelectron emission during fracture, energy distrib. function depend. on charge struct. 4-88951
- LIF vapour deposited thin films, TSEE, thermolum. meas. 4-81119
- NaCl:Ag, cleaved before and after X-ray irradi., thermo-exoemission 4-93204
- Ni, vacancy migration energy, exoelectron emission meas. 4-65456
- Si, photothermally stimulated exoelectron emission, VV centre effects, ESR study 4-88950
- Yb<sub>2</sub>O<sub>3</sub> thin films, trap levels, thermally stimulated method anal. 4-65763

## exosphere

- drag on artificial satellites, coupling with Earth oblateness, effect on orbit 4-82375
- drag on near Earth satellites and method orbital lifetime estimation 4-82374
- He 1083 nm airglow at midlatitude, seasonal and solar zenith angle depend. 4-105786
- O<sup>+</sup> escape to magnetosphere, thermospheric control of aurora O<sup>+</sup> source 4-72786

## exotic atoms

- see also hadronic atoms; muonic atoms
- No entries

## expanding universe see cosmology

## expansion, thermal see thermal expansion

## expansion chambers see cloud chambers

expert systems *see artificial intelligence*

exploding foils *see exploding wires and foils*

exploding wires and foils

*see also discharges (electric); plasma production*

cathode processes in exploding electron emission, cyclic nature 4-79872

conductor, luminesc. brightness meas. 4-60768

EM and thermal fields, numerical anal. 4-60679

explosive emission, mag. field and initial cathode temp. effects 4-71531

hydro-spark forming, impulsive hydraulic press. and gas bubble motion

(*Japanese*) 4-103594

metal, impulsive heating by current and electrical explosion of conductors

4-87904

nanosecond electrical explosion of thin Cu wires 4-103539

vacuum gap triggered by exploding wire, delay time 4-87960

vaporised wires, plasma prod., heating and motional impedance 4-75179

Al, forming by underwater Cu wire explosions, bulging expt. 4-75217

Al, picosecond laser induced shock wave press. meas. 4-113259

Al target, laser-driven shock wave evolution 4-113258

C target, collision of laser accelerated discs, high press. shock production

4-113257

C-Si, picosecond laser induced shock wave press. meas. 4-113259

Cu anode foils disruption by high-current relativistic electron beams irradi.

4-108195

Cu, exploding current pause 4-87905

Cu wire explosive emission, MHD processes in the initial stage 4-75226

GaAs, picosecond laser induced shock wave press. meas. 4-113259

explosion bubbles *see bubbles*

explosions

*see also accidents; detonation; nuclear explosions; safety; shock waves*

complex mols., population inversion of electronic-vibr. states during adiabatic thermal explosion 4-102746

Composition B-3 and PBXW-109(I), unreacted Hugoniot and shock ignition

4-109654

container, spherical, surrounded by infinite elastic medium, blast loading

4-97390

cyclohexane, shock wave diagnostics by Raman and IR meas. 4-109712

cylindrical shell containing fluid, explosive deform. 4-108038

decomposition rates, multiple wave effects 4-109663

detonation, overdriven expts., product EOS above Chapman Jouguet press.

4-109664

detonation wave intensity, influence of humidity and air excess, using

gaseous phase spherical detonation mathematical model 4-109652

electro-explosive devices in EM fields, safe use 4-107487

electrostatic discharges, charged insulator minimum potential for incendiary

discharges 4-97936

energetic materials, porous, compaction at deflagration-detonation transition

4-108546

framing high-speed shearing interferography with pulsed He-Ne lasers,

flow, shock, combustion and explosion problem appls. 4-68275

free-falling multicomponent droplets, combustion and microexplosion

4-103388

granular explosive wave growth obs. using velocity interferometer system

for any reflector 4-101907

granular porous explosives, shock sensitivity, grain size effects 4-108548

hemispherical implosion system, diamond synthesis, ultrafast chemical

reaction triggered by shock wave forming C and  $\gamma$ -CuBr from CBr<sub>4</sub> and

Cu 4-114389

heterogeneous explosives, shock-induced initiation, burning topology

4-109660

hexanitrosilbene, explosive, shock sensitivity, grain size effects 4-108514

HMX, melt-phase characterisation by rapid-scan FT-IR spectrosc.

4-109701

HMX explosive, thermal initiation and burning prior to detonation

4-109656

HMX explosive grain burning behaviour, velocity interferometer obs.

4-101908

HNS porous explosive, shock initiation, mixture theory appls. 4-109658

liquid, breakdown under high hydrostatic press., electroexplosive action

(*Russian*) 4-71273

LX-10, LX-1, and RX-26-AF, spherically diverging detonation wave vel.

4-108544

magnetic flux compression by explosion, 1.04 MOe field strength

(*Japanese*) 4-95475

nitroaromatic explosives, C(KVV) Auger line shapes, intra- and intermol.

H bond form. 4-71928

nitroaromatic explosives, molecular electronic props., Auger study

4-93530

nitromethane, chemiluminesc. products form. from ArF laser-induced

decomp., implications to explosive chemistry 4-89302

oblique shock wave incidence on a semi-infinite detonating medium (*Russian*)

4-112957

pattern recognition algorithm for explosives detection 4-96824

PBX and PBXW, elec. resist. and dielec. breakdown meas. 4-108865

pentaerythritol tetrinitrate explosive, shock initiation sensitivity, cryst.

orientation effect 4-70272

pentaerythritol tetrinitrate, shock wave diagnostics by Raman and IR

meas. 4-109712

point explosion in arbitrary atmosphere with radiative heat transfer

4-112955

n-propyl nitrate, chemiluminesc. products form. from ArF laser-induced

decomp., implications to explosive chemistry 4-89302

RDX, melt-phase characterisation by rapid-scan FT-IR spectrosc.

4-109701

reactive explosive mixtures, initiation and growth-to-detonation 4-109657

RX-26-AF, shock initiation, detonation wave propag. and metal acceleration

4-109662

RX-26-AF, shock initiation, reactive flow lagrange anal. 4-109661

shaped explosive charges, detonation wave shaping, computer simulation

anal. 4-108545

shell, cylindrical, explosive destruction, fragment distrib. calc. (*Russian*)

4-74949

shock recovery fixture, two-dimensional simulation 4-108536

slag explosive condensation kinetics in MHD generator channel 4-113025

solid high explosives, detonation front meas. 4-66592

solids, shock-induced mol. excitation 4-109665

stochastic anal., qualitative approach 4-81441

strong explosions in plane stratified media, appl. to supernovae and galactic

jets 4-85871

TEN, explosive density effect on air shock wave parameters 4-99792

thermal explosion theory for partially insulated reactants 4-87746

explosions continued

thermal explosions with simultaneous parallel reactions, theory 4-62205

thin-pulse shock initiation threshold, meas. optimisation 4-108059

transition of none-dimensional flows produced by explosions into one

dimensional flows 4-69781

transitory gaseous film study (*French*) 4-62206

triaminotribenzene, explosive, short-duration shock initiation

4-108543

triaminotribenzene-based explosives, shock initiation, particle size and

temp. depend. 4-109659

underwater electric explosion use in elec. modelling of high-speed deform.

of pipes 4-97336

underwater explosion of ring charge near a free surface 4-87759

vapour-gas bubble ignition in a liq. 4-71924

volcanic explosions, book 4-110823

volcano, time distrib. of Sakurajima explosion occurrence (*Japanese*)

4-72555

Al, forming by underwater Cu wire explosions, bulging expt. 4-75217

Ar, weak imploding shock waves, streak camera obs. 4-112950

CO-O<sub>2</sub> mixtures, population inversion of electronic-vibr. states during

adiabatic thermal explosion 4-102746

H<sub>2</sub>-CO<sub>2</sub> in air, flammability and detonability in radioactive waste process

ing 4-106741

N<sub>2</sub> superheated liqs., explosive flashing in discharge through short nozzles

4-112936

O<sub>2</sub> superheated liqs., explosive flashing in discharge through short nozzles

4-112936

Pb(N<sub>3</sub>)<sub>2</sub>, laser radiation effect on thermal decomposition (explosions)

4-71927

exposure meters *see photometers*

extended Hückel theory calculations *see EHT calculations*

extended X-ray absorption fine structure *see EXAFS*

extensive air showers *see cosmic ray showers and bursts*

extensometers

lateral extensometer long-term accuracy assessment using optical tech-

nique 4-78296

pushrod dilatometers design and error sources (*German*) 4-68210

removable multidirectional extensometer (*French*) 4-82791

external flows

aerodynamic sound generation by turbulent boundary-layer flows along

walls (*German*) 4-112637

air flow from rough to smooth transition under neutral stratification,

mathematical model (*Italian*) 4-91831

axisymmetric electrovortex flow in corrugated tube containing a cylinder

4-108124

circular cylinder, porous, circulatory flow of non-Newtonian fluid, suction

effects 4-87728

concentration profiles near a wall at  $Pr \gg 1$  4-97734

drag reduction studies by compliant surfaces and surface-active substances

4-91796

elastic fluid flow over circular cylinder, complex variables anal. 4-87663

exterior irrotational flow, three dims. boundary layer free interaction

4-112816

flat plate, turbulent boundary layer response to external flow pulsation

4-87695

flow around axisymmetric bodies with three constant-velocity sections

4-87751

flow past blunt obstacles of circular section placed on a plane boundary

(*Japanese*) 4-112823

flow round profile near rectilinear boundary, quasi theoretical profiles

(*Russian*) 4-87749

free stream turbulence effect on flow round bluff bodies 4-64930

gas flow-surface interactions, heat and mass transfer 4-97559

hydrofoil, noncavitating, optimum shape for max. lift 4-103333

hydrofoil, optimum shape giving max. lift in steady two dims. fully-

cavitating flow 4-103334

hypersonic flow past a lift airfoil, Navier-Stokes eqn. soln. 4-108088

impervious sails, two dims. 4-103440

incompressible flows over infinite swept wings, inverse mode boundary

layer calcs. 4-112832

incompressible viscous flow between two rot. spheres, finite difference soln.

4-87725

incompressible viscous fluid, asymptotic expansions for stationary flow

4-87659

infinite domain, steady flow round airfoil, numerical calc., grid size reduction

by higher order far field asymptotics 4-87686

jet-aerodynamic surface interference effects, theoretical model 4-112970

laminar flow past wing body junctions 4-103287

laminar free convection from vertical flat plate 4-75007

longitudinal flow around cylindrical body, heat exchange and friction

(*Russian*) 4-74998

macromolecules, rodlike, in conc. soln., rot. relax., free energy, external

flow effect, isotropic-nematic transition 4-69251

MHD heat transfer in flow past variable temp. semiinfinite plate

4-108116

NASA GA(W)-1 airfoil, separated flow study 4-97490

near-one-dimensional two-phase flow 4-69814

Newtonian fluids, dip coating finite element simulation 4-113088

non-Newtonian fluids, dip coating, finite element simulation 4-112963

nonequilibrium three-dims. viscous shock-layer flows over complex

geometries 4-112930

nonselfsimilar unsteady boundary-layer eqn. soln. 4-60368

poorly streamlined bodies, heat or mass transfer 4-69760

potential flow over circular cylinder in a wind tunnel 4-91787

skin friction meas. by laser interferometer in three dims. flows

4-97505

stationary hypersonic multishocked flow around blunt body with breaks

(*Russian*) 4-112946

steady state flow of a fluid stream with streamline disturbance around an

arbitrary arc (*Russian*) 4-87667

transonic potential external viscous flow over airfoils, boundary layers and

wakes calcs. 4-64972

tube bundles in transverse flows, heat exchange intensification 4-69759

turbulent 4-60471

turbulent shear flow, conf., St. Louis, Missouri, USA, June 1982

4-86119

two dims. viscous flow over cylinders in unsteady motion 4-97482

unsteady flow around airfoil 4-97567

viscoelastic cond. fluid, flow past an oscillating infinite plate 4-112965

viscoelastic fluid, MHD flow past accelerated plate 4-97617

- ernal flows continued  
 viscoplastic fluid, modes of generalised MHD Couette flow 4-108125  
 viscous fluid, small particle motion, circular disk effect 4-65013  
 viscous liquid, nonstationary periodic flow in wake of a cylinder, numerical model (*Russian*) 4-113023  
 viscous-inviscid interactions on axisymmetric bodies of revolution in supersonic flow 4-60367  
 vortex shedding from circular cylinder with step 4-112892
- ernal modes (crystals) *see* lattice dynamics
- traordinary ray *see* birefringence
- trapolation  
 radioactivity standardisation using  $4\pi\beta(\text{PC})-\gamma$  coincidence counting, systematic effects due to increasing self-absorpt. 4-87026  
 static fields measurements, extrapolation using finite element method 4-83514
- traterrestrial atmospheres *see* planetary satellite atmospheres
- traterrestrial life  
 bacterial interstellar grains, spectroscopic identification 4-67780  
 Drake-Sagan equation, implications of planetary orbits in binary star systems (*German*) 4-67607  
 interstellar bacteria, UV absorption and mass density constraints 4-101458  
 interstellar grains as bacteria, discussion meeting, London, England (November 1983) 4-95046  
 Mars, Viking biology experiments explained by  $\text{MnO}_2$  chemistry 4-67662  
 origin and nature (book contrib.) 4-73180  
 origin of life, conf., Mainz, Germany (July 1983) 4-101569  
 search strategy for ETI signals with small duty cycle (*German*) 4-67648  
 Solar Power Satellites as interstellar beacons, theoretical anal. 4-63027
- traterrestrial radiofrequency radiation *see* radiofrequency cosmic radiation
- xtremum control *see* optimal control
- extrusion  
 axisymmetric combined backward-forward, upper-bound solutions (*Chinese*) 4-81212  
 nylon-11 lamellar crystals, boundary face orientation rel. to mech. treatment 4-103668  
 PET film, amorphous, extrusion drawn, irreversible spontaneous elongation 4-109440  
 PET films, extrusion drawn amorphous and semi-crystalline, linear thermal expansion analysis 4-109439  
 PET films, uniaxially drawn, crystallisation kinetics, DSC obs. 4-92103  
 plain strain extrusion, flow patterns for hardening materials with slipline field methods 4-89092  
 poly p-phenylene terephthalamide films, extruded and drawn, tensile strength, void struct. rel. to heat treatment 4-81257  
 poly-para-phenylene, conducting oriented fibres, synthesis, struct. and  $\text{AsF}_5$  doping 4-65666  
 polyethylene, crystal block size change during single axial extension 4-76800  
 polyethylene, linear, low density, characterisation by capillary rheometry 4-80279  
 polyethylene, linear, low density, shear modification in melt 4-80280  
 polyethylene, linear oriented, stiffness, relax., US meas. 4-81232  
 polyethylene films, low-density, imperfection form. during extrusion 4-113353  
 polymer melts, extrusion flow in a plastic net 4-109371  
 polymer melts, extrusion flow in a plastic net 4-109372  
 polypropylene, crystal block size change during single axial extension 4-76800  
 polypropylene, supermol. struct. and mech. props., cooling rate influence (*German*) 4-98032  
 Rene 95, Ni-base superalloy, fatigue, effect of processing and microstruct. 4-104843  
 thermoplastics, cellulosic filler efficiency, processing characts. and mech. props. 4-61913  
 thermoplastics, reinforced, compounding and fabrication, book contrib. 4-66304  
 Al-Fe-Ni-Co, prep. from atomised powder, prod. struct. and props. 4-114446  
 Al-Mg (10 wt.%), extrusion and mech. props. of compacts prep. from rapidly solidified powders 4-66395  
 Al-Mg (5 wt.%), direct hot extrusion of billet, pure Al cladding effect 4-109355  
 Cu, tough-pitch, drawn and extruded, stress/strain props. 4-104824  
 Cu-P alloys, extruded, microstruct. and mech. props. 4-114574  
 Fe-Ag composite sheets, anisotropy of phys. and mech. props. 4-99368  
 NiAl, Ni-rich, extruded, deform. struct., TEM study 4-93341  
 U-Nb (2.4 wt.%),  $\gamma$ -phase comp., effect of extrusion 4-61998  
 U-Nb (2.4 wt.%), linear thermal contraction, tensile strength rel. to extrusion 4-109472
- eye  
*see also* contact lenses; vision  
 accommodation and convergence under high pressure sodium illumination 4-93739  
 accommodative disfacility presenting as intermittent exotropia 4-100131  
 accommodative dysfunction, orthoptic treatment results prediction 4-62471  
 accommodative infacility of school-aged children, rel. To symptoms 4-62470  
 acuity and hyperacuity, physical limits 4-89573  
 albinos, human, eye movements rel. to aberrant anatomical pathways 4-109796  
 aspartate-induced dissociation of proximal from distal retinal activity in the mudpuppy 4-81677  
 astigmatic modulus and its age-dependence 4-100129  
 binocular point spread function dynamic recording 4-100126  
 binocular rivalry, dynamic model 4-81690  
 chest radiographs, eye fixations during diagnostic interpretation, anal. 4-85423  
 ciliary cells evolved for vision hyperpolarize 4-93741  
 computer-based ophthalmotropes 4-81666  
 cone excitations, system of photometry and colorimetry 4-111176  
 cone oil droplets of Emydoidea blandingii: pigment types, densities and concs. 4-81685  
 cone response latency and log sensitivity: proportional changes with light adaptation 4-62479  
 cone retina, vertebrate, electronic simulation of cones, horizontal cells and bipolar cells 4-105231  
 cone retina, vertebrate, influence of amacrine cells on receptive field organisation of ganglion cells 4-105233  
 cones of different spectral types in turtle retina, direct excitatory interactions 4-105236  
 congenital nystagmus, hypothetical explanation 4-93735  
 contrast sensitivity, brightness function anal. 4-100136  
 contrast sensitivity and ocular refr. of rabbits, VECF obs. 4-62472  
 cornea, microscopy using soft contact lens (*Italian*) 4-81818  
 corneal endothelium, rabbit, damage by UV-B 4-109878  
 corneal markers and reflections, translation invariance 4-85421  
 cortical indices of impaired ocular accommodation and associated convergence mechanisms 4-62475  
 $\delta$ -crystallin accumulation in chicken embryo lens, laser light scatt. spectroscopy 4-72229  
 crystalline lens, intact, nondestructive method for refr. index meas. 4-67161  
 display terminal, eye scanning behaviour 4-81706  
 EEG, posterior rhythmic activity after eye closure 4-66945  
 electro-oculogram, gain calibration method using eye optical props. 4-115306  
 electro-oculography data acquisition system, microcomputer-based neurological diagnosis 4-89819  
 ERG, high fidelity extended duration obs. 4-62473  
 ERG, model and effect of vitreous haemorrhage 4-89571  
 eyeball retraction/latency meas. in conscious rabbits, photodiode technique 4-81826  
 eyetracker system for office use, performance 4-62638  
 fovea, 20 ns ruby laser exposure, bioeffects evaluation, by grating visual evoked pots. 4-62476  
 foveal and peripheral sensitivity comparisons, rel. to time discrimination 4-89577  
 foveal line-separation discrimination curve, smooth or segmented? 4-89572  
 GABAergic neurons in catfish proximal retina, identification and some functions 4-109805  
 GABAergic neurons in the distal catfish retina, identification and some functions 4-66951  
 ganglion cells in retina, nonlinear anal. of response characts. (*Japanese*) 4-115051  
 ganglion cells of generalised vertebrate cone retina, electronic simulation 4-105232  
 glaucoma, thermal model for US treatment, rabbit obs. 4-89660  
 green rod pigment of the bullfrog, Rana catesbeiana 4-62484  
 hazard from GaAs lasers and near IR radiation 4-93797  
 horizontal cell bodies in tiger salamander retina, elec. coupling 4-89567  
 horizontal cells in goldfish retina, depolarising, responses under intense chromatic background 4-109804  
 human eye, transmission characts. and link between natural scene and TV viewer (*German*) 4-85422  
 Illuminating Engineering Society Annual Conf., Los Angeles, USA. (Aug. 1983) 4-90291  
 intraocular light scatter 4-93734  
 iris colour rel. to hearing loss 4-62499  
 Japanese characters, readability on CRT and visual fatigue (*Japanese*) 4-93743  
 laser medicine, injurious effects and clinical appls. 4-72341  
 laser safety 4-85524  
 lens, accelerated heavy particle irradi., cataractogenic pot. 4-67036  
 lens, theoretical optical power rel. to refr. index (*Italian*) 4-81667  
 lens alterations after chronic professional exposure to low LET ionising radiation (*Italian*) 4-81741  
 lenses, normal and cataractous, PIXE and microprobe anal. in rats and humans 4-100386  
 microaneurysms in retinopathy fluoro-angiogram, automatic detection 4-100338  
 microwave radiation hazard, metal-framed spectacles effect 4-109877  
 microwaves, X-band, effects on crayfish eye 4-77309  
 monocularly deprived kittens, prevention of ocular dominance changes by cortical activity disruption 4-72246  
 movement anal. system using IR fundus images (*Japanese*) 4-85486  
 movement meas., double mag. induction method 4-81751  
 movement monitor, inexpensive, using the scleral search coil technique 4-81750  
 movement of eye, anal. by computer 4-85537  
 movements, 2D, computer graphics study 4-93740  
 movements, acceleration perceived with dynamic visual noise 4-72256  
 myopia, behavioural treatment, refr. errors and acuity changes 4-62466  
 myopia, progression in military students: effects of plus lens, prism and bifocals 4-62467  
 objective refraction: comparison of retinoscopy and automated techniques 4-62543  
 ocular exposure to infrared radiation in the Swedish iron and steel industry 4-62603  
 ocular plethysmograph evaluation, simple time-series approach 4-81798  
 ophthalmic solutions lubrication props. meas., using strain gauge bridge 4-89797  
 ophthalmologic department instrumentation of municipal polyclinic, automated control system prerequisites 4-93953  
 ophthalmology appls. of red Kr laser and green Ar laser (*French*) 4-89676  
 optic secretions of dolphins, nature and hydrodynamic activity (*Russian*) 4-72283  
 optical defects rel. to human vision 4-100127  
 optokinetic reflex, cat, modelling and computer simulation 4-93736  
 orbit, mag. resonance imaging, preliminary experience 4-62551  
 overaccommodation, underaccommodation, and the clinical phoropter 4-81665  
 pachometry measurements, reliability and variability 4-109792  
 pattern ERG of the cat 4-109803  
 peripheral spatio-temporal, frequency parallel pathway (*Japanese*) 4-115057  
 photocurrents of single retinal rods from Rana pipiens tadpoles 4-109809  
 photoreceptor simultaneous image processing and feature extraction for two-dimensional non-uniform sensors 4-105234  
 photoreceptor terminals, barnacle, localised  $\text{Ca}^{2+}$  and  $\text{Ca}^{2+}$ -activated  $\text{K}^{+}$  conductances 4-72735  
 photoreceptors, hyperpolarising, of giant clam Tridacna, UV sensitivity 4-72738  
 photoreceptors, light-dependent  $\text{Ca}^{2+}$  release, laser micro-mass. anal. 4-72736

## eye continued

- physiology and vision in astronomy 4-62464  
 presbyopia, review of ciliary muscle effort 4-62474  
 primate photoreceptor lattice, quality rel. to spatial vision limits 4-62480  
 primate superior colliculus, shift of auditory receptive fields with eye position changes 4-77261  
 pterygium in Sardinia w.r.t. occupational exposure, epidemiological obs. 4-81740  
 pupil of human eye, solid-state instrument for dynamic changes meas. 4-100294  
 pupil reflex to light, experimental and modelling studies 4-89563  
 refraction, comparison of Dioptron Nova data with conventional data 4-109795  
 refraction, ocular component anal. by vergence contrib. 4-109794  
 refractive error development theories, review and evaluation 4-100128  
 refractive error in dark- and in light-reared kittens, eyelid closure effects 4-77232  
 retina, carp, L-type horiz. cell response,  $Ba^{2+}$  ion effects (*Japanese*) 4-81671  
 retina, isolated, toad, effects of low  $[Ca^{2+}]_o$  upon  $[K^+]_o$  during and after maintained illum. 4-109802  
 retinal chromophores, photoisomerization, adiabatic potential surfaces 4-109807  
 retinal eccentricity, effects on displacement thresholds for unidirectional and oscillatory stimuli 4-109819  
 retinal ganglion cell layer and optic nerve from postmetamorphic *Xenopus laevis*, morphometry 4-66947  
 retinal glial cell membrane, regional specialisation 4-72247  
 retinal light adaptation, evidence for a feedback mechanism 4-100139  
 retinal nerve fibres in primate optic nervehead, axons degeneration obs., glaucoma causes 4-77241  
 retinal rod photoreceptor membranes, enzymatic processes, light scatt. probe 4-72224  
 retinal rods, cation selectivity of light-sensitive conductance 4-77237  
 retinal rods outer segment, Monte Carlo simulation of light absorpt., rhodopsin conc. 4-81680  
 retinotopy and orientation columns in the monkey 4-81670  
 rhodopsin, vertebrate, hydrolysis pathways 4-66950  
 rhodopsin and visual adaptation, anal. of photoreceptor thresholds in the isolated skate retina 4-62481  
 rhodopsin lateral diffusion rel. to rod outer segment disk membrane axial position 4-66944  
 rod outer segment disc membranes, bovine, attached to lecithin bilayer, photoelec. signals generation 4-105237  
 rod outer segment disks, Necturus, barrier to lateral diffusion of porphyropsin 4-66920  
 rod photoreceptor populations in retina of *Xenopus laevis* 4-109800  
 rod-cone interaction, time-course 4-81673  
 saccade-related brain pots. in guessing tasks, late components 4-66946  
 saccadic anomalies, vergence-induced large departures from ball-and-socket behaviour 4-62477  
 saccadic horizontal eye movements model 4-81678  
 smooth eye-movement control with secondary visual feedback 4-89562  
 spatial filtering of retinal images by the human visual system and its consequences for visual thresholds 4-100134  
 spectacle-corrected aphakes, clinical determ. of corrected retinal image size 4-62468  
 spectral sensitivity of single cones in the retina of *Macaca fascicularis* 4-77247  
 sustained discharge of Limulus visual cells, current pulse effect 4-89561  
 t-test, significance when applied to ocular measures. 4-62463  
 tonic accommodation, heuristic model 4-89570  
 US, axially traversing, ray tracing model 4-85458  
 US diagnostics, fast B-scan, in severe trauma situations (*Italian*) 4-81749  
 US echographic methods in ophthalmology (*Italian*) 4-67051  
 vergence eye movements and visual suppression 4-81672  
 vision, daytime variation in steady-state accommodation 4-81668  
 visual accommodation, acquisition of distant targets 4-81681  
 vitamin A<sub>2</sub> aldehyde in crayfish eye 4-109808  
 vitreous humour, modelling by an oscill. viscoelastic sphere 4-105278  
 voluntary eye movements, information potential 4-105375  
 wide-angle optical model 4-62469  
 X-cells in cat, receptive field organisation 4-81674  
 YAG laser appls. in ophthalmology 4-105313

## F-centres

- see also A-centres; M-centres; R-centres; Z-centres  
 alkali halide cryst., Frenkel defect accumulation, temp. and impurity conc. depend. 4-98093  
 alkali halide crystals, colour centre IR luminesc. and stimulated emission 4-80997  
 alkali halides:  $Eu^{2+}(Pb^{2+})(Ca^{2+})(Sr^{2+})$ , X-irrad. effect on impurity vacancy dipoles and aggregation precipitation state, F-centre production 4-70209  
 alkali halides, excitonic and impurity-excitonic mechanisms for F,H pair creation (*Russian*) 4-80034  
 alkali halides, fracture-induced luminesc. and crack vel. 4-104685  
 alkali halides, K band of F-centre 4-60923  
 alkali halides, low temp. processes, reaction-rate theory 4-60925  
 alkali halides, photoconductivity of colour centres, temp. depend. 4-98669  
 alkali halides, with F-centres, hopping-type electronic processes in pre-breakdown elec. fields 4-108868  
 alkali metal halides, F-centre states, hybrid method with floating 1-s Gaussian basis 4-70709  
 alkali metal halides, F-centres, photoacoustic signals 4-80964  
 alkali metal halides, radiolysis process 4-70194  
 continuous model and relaxed excited state problem, self-consistent solns. 4-84290  
 impurity complexes, excites state deactivation, correlated electron tunnelling 4-98559  
 ionic solids, spin-orbit fine struct. of vacancy-trapped electrons, host-lattice effects 4-70147  
 $Al_2O_3$ , X-ray irradiated, F-centre glow peaks spectral emission 4-71452  
 $\alpha-Al_2O_3:Er(Gd)(Tb)$  crystals, radiative and thermochem. effects 4-76491  
 $Al_2O_3-x$  anodic oxide films, paramagnetic centres and optical absorpt. spectra studies 4-104494  
 BaFCl, flux-grown crystals, thermoluminesc., effect of flux 4-104680  
 CaO, IR-stimulated luminesc. due to O vacancies 4-81017  
 CaO spin triplet, g and D values determ. in case of misalignment 4-98508  
 KBr, excited F-centre emission, effect of CO<sub>2</sub> laser light 4-61742

## F-centres continued

- KBr, F-centres, mag. permeab. change, ang. freq. and temp. depend. 4-60922  
 KBr, metastable F-centres perturbed by charged defects 4-70151  
 KBr:Cl, and undoped crystals, anion Frenkel defect creation, luminesc. study (*Russian*) 4-80980  
 KBr:Cl, X-irradiated, luminesc. study (*Russian*) 4-80981  
 KCl powders, coloration stability, particle size depend. 4-60921  
 KCl, with and without F-centres, positive muon spin depolarisation rate 4-65915  
 KCl:Ag, Ca, X-irrad., electron centre form., luminesc., optical absorpt. studies 4-60920  
 KCl:Ag, X-irrad., electron centre form., luminesc., optical absorpt. studies 4-60920  
 KCl:Na, electron irrad., F-centre generation, absorption spectra studies 4-113444  
 KI, F-centre luminesc., mag. circular polarisation, anomalous effect 4-93062  
 LiCl, substitutional defects, molecular cluster-INDO calcs. 4-108806  
 LiF, substitutional defects, molecular cluster-INDO calcs. 4-108806  
 LiF:Mg, OH, room temp. laser action using F-centres 4-91481  
 LiF:OH<sup>-</sup>, gamma-ray irrad., lattice defects, EPR studies 4-75437  
 LiH(D), radiation induced defect form. 4-60952  
 LiH(D):Na, radiation induced defect form. 4-60952  
 Li<sub>2</sub>O, thermal neutron irrad. effects, lattice parameter and expansion changes, F-centres 4-107028  
 MgF<sub>2</sub> windows, spectral transmission change caused by prolonged UV irrad. 4-64752  
 MgO, F<sup>+</sup> centre, electronic point defects with self consistent lattice polarisation 4-93091  
 MgO, polycryst., F-centres initiation by strong isotropic compression 4-70148  
 MgO single cryst., high anion vacancy conc., cathodoluminescence obs. 4-88886  
 MgO, surface  $\gamma$ -conductivity, kinetics and decay, F-centres 4-65726  
 NaCl, cryst., X-irrad., F-centre decay during photoannealing 4-80036  
 NaCl, electron irrad., appl. to radioactive waste repositories 4-75532  
 NaCl, F-centre form., excitonic pot. surface, absorpt. spectra 4-71415  
 NaCl, substitutional defects, molecular cluster-INDO calcs. 4-108806  
 NaF polycrystalline thin films, neutron and X-irrad., photochemical hole burning 4-76518  
 NaF, substitutional defects, molecular cluster-INDO calcs. 4-108806  
 RbCl, first-order Raman scatt. due to F-centres 4-93076  
 RbMgF<sub>2</sub>:Mn<sup>2+</sup>, electron irrad., vacancy-interstitial pair and F-centre-impurity ion pair form. 4-70215  
 Sr(NO<sub>3</sub>)<sub>2</sub>, X-irradiated, colour centres, ESR study 4-61589
- F<sub>2</sub>-centres** see M-centres  
**F<sub>3</sub>-centres** see R-centres  
**F<sub>A</sub>-centres** see A-centres  
**F-layer** see F-region  
**F-region**  
 auroral F-region, expt. evidence of non-isotropic ion temp. distrib. 4-105793  
 chemical modification expt. using rocket exhaust, incoherent scatter obs. 4-67533  
 corpuscular ionisation, latitudinal depend. during Forbush decrease 4-101051  
 dynamic coupling with thermosphere, EISCAT obs. 4-100864  
 effective electron collision rate, empirical altitude depend. 4-94288  
 EISCAT obs. of plasma convection in high-latitude winter 4-100856  
 EISCAT obs. of plasma flows during prolonged northward IMF 4-100855  
 electron density irregularity spectra near auroral acceleration and shear regions 4-110358  
 electron density profiles, effects of longitudinal currents 4-94289  
 electron temperature empirical model for F<sub>2</sub>-layer 4-105795  
 electrons, low energy, in E and F-regions, nonthermal components obs. 4-63008  
 electrostatic drift instability, theory 4-113142  
 equatorial, nonlinear mode coupling theory of the lower-hybrid-drift instability appl. 4-75153  
 equatorial bubbles, artificial triggering and radiowave propag. characts. 4-90035  
 equatorial spread-F duration characteristics 4-100848  
 equatorial spread-F irregularities, control of VHF nighttime scintillations 4-90031  
 $f_oF_2$  dependence on solar activity 4-94290  
 F<sub>2</sub>-layer, electron density var. due to distant plasma instabilities on mag. field lines 4-85817  
 F<sub>2</sub>-layer, electron density modulation by 160-minute solar pulsations rel. to micropulsation amplitudes 4-105803  
 F<sub>2</sub>-layer, statistical model of critical freq. 4-110350  
 F<sub>2</sub>-layer critical frequencies, correl. relations between cyclical increments 4-110351  
 F<sub>2</sub>-layer ionospheric electron content of Wuchang, China, VHF obs. 4-115659  
 F<sub>2</sub>-layer modelling and magnetosphere plasma global convection var. 4-94293  
 heating during intense aurora, EISCAT study 4-100863  
 HF ray tracing at high-latitudes using observed meridional electron density distrib. 4-85823  
 interferometric phase velocity measurements of plasma waves 4-94295  
 ion temperatures, at high latitude 4-72794  
 ionization patches in polar cap nighttime F<sub>2</sub>-layer 4-67539  
 irregularities generated by thermal source, effect of electron-ion collisions 4-82343  
 irregularities in high-latitude lower F-region 4-110360  
 mid-latitude ionospheric trough and ion densities, electron precipitation and 630 nm emission 4-100845  
 neutral winds in high latit. winter F-region, coordinated obs. from ground and space 4-100836  
 parametric plasma heating, turbulent expansion 4-72795  
 plasma density as manifestation of magnetosphere convection 4-72790  
 plasma depletion expts., snowplough effects or plasma recomb. model for depletion core form 4-100851  
 plasma instabilities in equatorial region, role of Coulomb collisions 4-82342  
 plasma instability theory 4-65074  
 plasma interactions with space vehicles and assoc. glows 4-90053  
 plasma vel. meas. method using EISCAT 4-100807

region continued  
 polar region, ohmic heating by HF pulses, effects on electron density and temp. 4-85814  
 radiowave heating expt. using .430 MHz radar, obs. of enhanced plasma lines 4-85825  
 Rayleigh-Taylor instability in the presence of a stratified shear layer 4-83993  
 recombination dynamics in F-region, limit line for phase space trajectories 4-110352  
 spike-like electric field obs. at poleward edge of auroral zone 4-67535  
 equatorial spread F ionisation bubbles and plasma instabilities 4-72799  
 spread F occurrence in evening sector during equinoctial periods 4-110359  
 equatorial spread F-irregularities spectral classification 4-67524  
 equatorial spread-F, evidence for large-scale elec. field gradient at onset 4-82328  
 spread-F and stable auroral red arc, latitudinal distrib. 4-82325  
 spread-F irregularities generated in E-region in post-sunset period 4-82326  
 storm-time ion composition and temperature, theory 4-67527  
 transionospheric scintillation at 4 and 6 GHz, meas. by Asian ground stations 4-85822  
 VHF intensity scintillation of transionospheric signals, due to F- and E-regions 4-115648  
 VHF transequatorial propagation due to scatt. from F-region 4-115646  
 Ba release experiment, study of plasma column density fluctuations 4-110355  
 He<sup>+</sup> distrib. in equatorial ionosphere, neutral wind effects 4-82337  
 NO<sup>+</sup> ionospheric chemistry 4-67528  
 SF<sub>6</sub> release experiments, calc. of chemistry, spectral emissions and plasma instabilities 4-94300

values see oscillator strengths

ices (crystal) see crystal faces

facility location see operations research

facsimile document reproduction see photocopying

facsimile signals see video signals

faculae see Sun

fading

see also radiowave propagation

7.6 GHz Delhi-Sonepat line of sight link 4-67311

L-band multipath fading sea surface reflection, chars. 4-105739

multiple tropospheric paths, statistical model of propagation (French) 4-82214

optical fibre time-domain reflectometry, coherent, fading rates 4-83703

failure (mechanical)

see also fracture; mechanical strength; plastic deformation

anisotropic material response on continuum damage, expt. evaluation 4-99565

automatic plastic design, reliability-based optimisation technique 4-103214

beams, cantilever, elastic, with nonlinear elements, instability, butterfly catastrophe 4-87599

composite material, unidirectional, micromech. finite element anal. incl. longitudinal shear loading 4-91722

elastic body containing a flaw, dimensional analysis 4-103255

failure detection in dynamical systems, hierarchical diagnosis based on linear modelling (Japanese) 4-76957

fastener groups, limit anal. under eccentric load 4-87565

fibre bundles, strength, statistical theory 4-74868

fibre reinforced composite laminated plate, initial failure and ultimate strength theory (Japanese) 4-97417

fibre reinforced materials, failure criterion, macroscopic 4-81266

fracture mechanics parameters, transferability from CT-specimens to tensile specimens 4-86875

glass fibre reinforced epoxy laminate, elastic consts., stress-strain relations, failure stresses (Japanese) 4-99415

ice sheet indentation, limit anal. 4-94179

laminated composites, strength and elastic props., macroscopic description 4-97399

metallographic replica technique, appl. to material exam. and failure anal. 4-109578

perforated casing, finite element anal. of collapse 4-91736

rectangular structures, stress anal. under internal pressure 4-91727

ring stiffened cylindrical shell, buckling under unsymmetrical axial loads 4-81261

steel fibre reinforced mortar, polystyrene impregnated, interfacial failure 4-99571

strain hardening materials, failure assessment diagram under cyclic and monotonic loading 4-93367

unidirectional fibrous composites, time dependent failure, statistical and micromechanical modelling 4-79517

viscoelastic solids, linear, classification based on failure criterion 4-83834

C-C-TiC composite materials obtained by CVI of porous C-C substrates 4-71595

failure analysis

see also wear

boiler waterwall tubes root-cause failure analyses in fossil-fuel-fired power stations 4-89141

CANDU-PHWR ECCS unavailability following small LOCA 4-64232

failure detection in dynamical systems, hierarchical diagnosis based on linear modelling (Japanese) 4-76957

measurement facilities maintenance planning 4-101805

measurement instruments with two types of failure, check-interval determ. 4-90548

PWR in-core detectors fault analysis using time-series models 4-86935

Ni-H<sub>2</sub> cells, cycle life test and failure model 4-72087

Si polycryst. layer, grain size and dopant level inspection 4-109529

fallout

see also air pollution

Columbia River, Oregon, USA, radioactive pollution in sediments 4-66824

nuclides and natural radioactivity accumulation in snails 4-62609

nuclides concentration in animal livers consumed by man 4-62610

Pacific islands, population exposure to Pacific nuclear tests fallout, on Rongelap and Utrik, environmental and personnel monitoring 4-62611

<sup>137</sup>Cs, determ. of conc. in urine samples 4-96290

<sup>137</sup>Cs<sup>+</sup> uptake by plants, long term fallout on grassland, soil parameters effect 4-109967

<sup>155</sup>Eu, atmospheric fallout samples collected in 1981 4-62891

fallout continued

Pu concentration origin in Nyu Bay sediments, Japan 4-62410

<sup>90</sup>Sr, determ. of conc. in urine samples 4-96290

<sup>88</sup>Y, atmospheric fallout samples collected in 1981 4-62891

Faraday effect

diode laser spectroscopy, source noise reduction using Faraday effect 4-90668

ferrite tensor permeability meas., using Faraday rotation 4-58873

fibre Faraday rotator 4-69559

garnet epilayers, remanent domain struct. after planar saturation 4-88708

garnet film, domain nucleation, Faraday contrast modulation 4-76203

helical struct., transverse electronic motion, optical and magneto-optical rot. 4-87161

hexahelicene, transverse electronic motion, optical and magneto-optical rot. 4-87161

ionic crystals, Faraday effect due to mag. moments of optical phonons 4-66017

BL Lacertae, rotation measure determ. 4-73062

magnetic materials, magneto-optical figure of merit, light scatt. meas. 4-61666

MHD generator performance, effects of cathode slag polarisation, expts. 4-72131

partially coherent radiation depolarisation by doubly refracting elements (Russian) 4-79029

rare earth garnets, R<sub>3</sub>Fe<sub>2</sub>O<sub>12</sub>, Faraday effect in strong mag. fields 4-80908

rare earth garnets, R<sub>3</sub>Y<sub>3-x</sub>Fe<sub>2</sub>O<sub>12</sub>, Faraday effect in strong mag. fields 4-80908

rotators and modulators design 4-79282

spectroscopy, Faraday rotation, with colour centre laser, differential detect. scheme 4-95525

strong EM wave, Faraday effect and rot., in magnetised plasma 4-91934

Tokamak plasma electron density and plasma current distrib. meas. 4-87930

volume holograms, mutual EM wave conversion in presence of Faraday effect 4-79081

weakly ferromagnetic rhombohedral antiferromagnets, magneto-optic effects 4-114248

(BiTm)<sub>3</sub>(FeGa)<sub>2</sub>O<sub>12</sub> epitaxial film, mag. bubbles study 4-109049

Cd<sub>1-x</sub>Mn<sub>x</sub>Te, spin glass, dynamic behaviour, Faraday effect study 4-71354

CdSe, magnetopolaritons, dipole forbidden transmission 4-98544

CeF<sub>3</sub>, magnetic susceptibility and Verdet const. 4-61507

Co<sub>3</sub>B<sub>2</sub>O<sub>13</sub>Br, spontaneous birefringence and Faraday effect 4-71351

CsNiF<sub>6</sub> ferromagnet, optical absorption and magneto-optical properties 4-99100

Fe garnet magneto-optic spatial light modulator in optical image processor or display system 4-74696

FeBO<sub>3</sub>, nonlinear optical effects due to influence of optical fields on mag. props. 4-69513

FeBO<sub>3</sub>, single crystal, magneto-optic effects 4-114248

Ga<sub>2</sub>Se<sub>3</sub>, <sup>77</sup>Fe single cryst., Mossbauer effect and mag. susceptibility 4-104513

H, ground state, multipole moments, time derivative fields 4-69021

Hg<sub>1-x-y</sub>Mn<sub>x</sub>Cd<sub>y</sub>Te, spin glass phase transition, interband Faraday rot., mag. susceptibility meas. 4-61545

Hg<sub>1-x</sub>Mn<sub>x</sub>Te, spin glass phase transition, interband Faraday rot., mag. susceptibility meas. 4-61545

Ho<sub>0.9</sub>Y<sub>2.2</sub>Fe<sub>2</sub>O<sub>12</sub>, spin-reorientation phase transition, Faraday effect, magnetisation meas. 4-88814

InSb, compensated, magneto-optic activity meas. using long-wave IR magnetopolarimeter 4-73484

Mn-Cu-Bi, thin film, RF sputtering prep., mag. and magneto-optical props. 4-61847

Mn-Ni-Bi thin film, RF sputtering prep., mag. and magneto-optical props. 4-61847

NdF<sub>3</sub>, magnetic susceptibility and Verdet const. 4-61507

Ni<sub>2</sub>Mg<sub>2-x</sub>GeO<sub>4</sub> spinel solid solutions, mag. props. 4-71017

PbTe:Ga, elec. and optical meas. (Russian) 4-84636

PrF<sub>3</sub>, magnetic susceptibility and Verdet const. 4-61507

Pr<sub>2</sub>Y<sub>3-x</sub>Ge<sub>x</sub>Fe<sub>2-y</sub>O<sub>12</sub> garnet single cryst. magnetisation and Faraday rotation 4-61664

R<sub>3-x-y</sub>Bi<sub>y</sub>Pb<sub>z</sub>Fe<sub>3-2x-2y-2z</sub>O<sub>12</sub> garnet films, mag. and magneto-optical props. 4-80802

Si, high purity, intercarrier scatt. effects, laser and electron beam excitation 4-92725

TiBr-TlI polycrystalline fibre, optical props. at individual CO<sub>2</sub> laser lines, magneto-optic effects 4-109165

Y<sub>1-x-y</sub>Bi<sub>y</sub>Pb<sub>z</sub>Fe<sub>3-2x-2y-2z</sub>O<sub>12</sub> garnet films, magneto-optic prop. meas. using piezobirefr. modulation 4-66013

Zn<sub>0.972</sub>Mn<sub>0.028</sub>Te, free exciton excited states 4-70663

farming

lobster culture development and commercial viability 4-115446

marine recreational facilities, activities, activities and technological advances 4-115001

solar lake-condensation tower system (SL/CT system), application to land irrigation water production 4-72182

fast amplifiers see pulse amplifiers

fast Fourier transforms

acoustic noise suppression using two-point receiving signals (Japanese) 4-91695

acoustic signals, personal computer based signal compression method for sound field meas. in pipes (Japanese) 4-97209

acoustic signals, two-channel FFT analysers 4-103107

acousto-optical processor architectures and techniques 4-87435

algorithm design for real-time audio signal processing 4-103111

architectural acoustic measurements using periodic pseudorandom sequences and FFT 4-112638

complex FFT processor for image synthesis in radio astronomy, appl. to interferometer data (Japanese) 4-94639

continuous speech recognition using dynamic programming, parameters comparison 4-79393

digital signal processing for precision wide-swath bathymetry 4-67432

discrete, improved algorithm 4-110854

double layered plate, eddy current calculations 4-88692

ECG, FFT appl. for heart disease diagnosis 4-62618

flow meas., CCD chirp-Z FFT Doppler signal processor, laser velocimetry, oceanographic appl. 4-87819

high freq. content improvement 4-78112

**fast Fourier transforms** continued

- inverse scattering solns. by sine basis, multiple source, moment method 4-97213
- isolated word recognition, auditory models 4-105256
- lossy dielectric bodies, EM wave specific absorption rate distrib., calc. using FFT method 4-85459
- medical imaging, Fourier transform anal. appl. 4-100262
- multidimensional spectroscopic data array processing 4-106285
- multiple leaky SAW, FFT vel. meas. by line focus-beam acoustic microscope 4-103164
- piezoelectric disc, transient voltage, 2-D equivalent circuit (Chinese) 4-88772
- porous elastic layers, response to moving loads 4-74854
- signal processing IC, use for Doppler blood flow studies 4-93826
- signal processor for 6502 microcomputers 4-106146
- spectral functions estimation for normal random noises 4-68197
- time filtering and fast Fourier transforms in acoustic scatt. and absorption meas. (French) 4-97166
- tomography, first-order diffraction, limitations of imaging 4-115257

**fast ion conductors** *see* **superionic conducting materials****fastening** *see* **joining processes****fatigue**

- for corrosion fatigue see stress corrosion cracking; for thermal fatigue see thermal stress cracking*
- see also fatigue cracks; fatigue testing*
- acrylic bone cement, tensile fatigue failure 4-105379
- acrylonitrile-butadiene rubber C reinforcement, static fatigue, statistical analysis 4-99683
- advanced HTR systems, alloys eval., creep: fatigue, corrosion, neutron effects 4-78699
- aerospace structures, conf., Boston, MA, USA (Nov. 1983) 4-73167
- age-hardened alloy single crystals, fatigue behaviour 4-99563
- Alloy 800, fatigue, high temp., damage mechanics 4-93422
- alloys, fatigue failure curves, centre portion anal. 4-92292
- brass, fatigue life, effect of programmed load spectrum parameters (Polish) 4-62028
- ceramics, N-based, conf., Falmer, England (Aug. 1981) 4-67873
- ceramics, thermal shock resistance and fatigue, acoustic emission study 4-62054
- complex loading, fatigue life estimation method (Chinese) 4-81264
- composite laminates, fatigue damage parameter using stiffness change 4-76864
- composite laminates, fatigue under spectrum loading 4-62021
- composite material analysis, survey 4-74862
- composite materials, fatigue-proof design, reliability-based 4-99604
- composite materials, reliability-based, fatigue-proof 4-99392
- composites, fatigue failure, probabilistic modelling employing Markov process 4-74961
- corrosion fatigue, crack length distrib. 4-104923
- creep prestress effect on fatigue behaviour 4-104856
- cyclic saturation and strain localisation in BCC and FCC metals and alloys, review 4-99533
- damping alloys, noise and vibration control appl., service condition parameters (German) 4-66365
- dislocation concepts appl. in fatigue, book contrib. 4-99564
- elastic-plastic finite element analysis of voids and inclusions 4-92195
- epoxy resin, filler reinforced, impact tensile fatigue strength, statistical analysis (Japanese) 4-99504
- ethylene-propylene elastomers, long-time dynamic compatibility with liq. N<sub>2</sub>H 4-114609
- failure, self-similar nature, damage accumulation 4-79513
- fibre reinforced Al-Mg alloy, fibre/matrix interface effect on fatigue, optimum processing parameters 4-114635
- fibre reinforced plastic, fatigue life estimation under sinusoidal wave loads (Japanese) 4-99505
- fission reactors, SNR-300 mixing devices, stress and fatigue analyses 4-64203
- fracture mechanics, new approaches 4-103266
- fracture toughness characteristics relationship for cyclic and dynamic loadings 4-99536
- fretting wear and fretting fatigue, relationship 4-65339
- fusion reactor materials for INTOR and DEMO, first wall lifetime, effect of material props. and operating conditions variations 4-96265
- glass, fatigue, crack growth and crack tip sharpening models 4-89101
- glass fibre, bending strength, static fatigue rel. to atmosphere 4-99490
- glass fibre reinforced polyester, laminates, residual strength degradation model under repeated tension-compression loading 4-99574
- glass fibre reinforced polyester, short-fibre SMC, shear fatigue degradation and fracture 4-76845
- glass fibre reinforced polyester laminate, residual strength degradation prediction model (Japanese) 4-99503
- grain boundary migration during high temp. deform. 4-98115
- graphite fibre reinforced epoxy laminates, fatigue loading damage accumulation, acoustic emission monitoring 4-81265
- high-tension steel, corrosion fatigue crack growth in NaCl soln. 4-114711
- HSLA, fatigue threshold, thermally activated behaviour of effective stress intensity 4-76853
- impact-tension compression test using split-Hopkinson bar 4-87639
- IN 100, Ni-base superalloy, thermal fatigue 4-93417
- IN 738, high temp. low cycle fatigue models, predictive capability 4-93411
- IN-617, Ni-base superalloy, fatigue, high temp. low cycle 4-66425
- IN-718, Ni-base superalloy for gas turbines, elevated temp. fatigue life estimation 4-66449
- Inconel 718, benchmark cyclic plastic notch strain measurement 4-104956
- Inconel 718 gas turbine disc material, crack initiation from notch under creep fatigue conditions 4-99567
- interaction diagram for time-dependent fatigue 4-104866
- Itamid 25, notch effect on instantaneous, and fatigue strength (Polish) 4-66432
- joints, butt-welded, fatigue crack initiation and propag. at toes (Japanese) 4-93382
- Kevlar 29 braid, bending fatigue life rel. to resin impregnation 4-93394
- Kevlar fibre rope endurance obs. and selection guidelines 4-114676
- materials behaviour at high temperatures 4-99473
- mechanical behaviour of materials, conf., Stockholm, Sweden (Aug. 1983) 4-90297
- metallic composites, endurance of matrix during thermal fatigue loading 4-71722

**fatigue** continued

- metallic sample, fatigued mesoscopic vol. elements, plastic deform. spectrum, X-ray method 4-71708
- metallic systems and structures, book contrib. 4-109514
- metals, cyclic creep, relationship with hysteresis loop energy 4-109456
- metals, fatigued, elastic strain distrib. and X-ray reflex profiles 4-76796
- metals, wear reduction and analysis, surface modification by ion beams 4-81290
- Nimonic PE-16, irradi. in HFIR at 430°C, fatigue performance 4-109497
- nylon fibre rope endurance obs. and selection guidelines 4-114676
- optical fibre fusion splicing induced stress transformation 4-91591
- pitting model for rolling contact fatigue 4-64888
- plate, orthotropic, with circular hole, fatigue failure 4-74953
- polyamide 66 fibre, loading criteria for fatigue failure, acceleration of creep failure 4-62008
- polyester fibre rope endurance obs. and selection guidelines 4-114676
- polyheteroarylene reinforced epoxy composite, long-cycle fatigue, freq. depend. 4-89130
- porcelain, high-alumina, for HV insulators, strength under dynamic and cyclic loads (German, English) 4-76836
- powder metallurgy parts, fatigue design, methods to determ. relevant material props. 4-66436
- pressure vessels, steel, corrosion fatigue, development of engineering codes 4-93406
- reactor primary circuit component fatigue, calc. method and operational meas. (Czech) 4-83237
- reinforced thermoplastic composites, creep resistance, fatigue endurance 4-61994
- Rene 95, Ni-base superalloy, fatigue, effect of processing and microstruct. 4-104843
- semiliptical surface flaws, fatigue life prediction 4-103261
- short cracks effect on fatigue limit, analytical soln. 4-66440
- solid solutions and intermetallics, mech. props. book contrib. 4-109423
- solid surface, thermoelastic action of powerful high repetition rate laser radiation 4-75522
- SPAULRAD-S laminate for fusion reactor appls., irradiation and mech. props. 4-111768
- spotwelded joints, static and fatigue fracture (French) 4-114637
- statistical cumulative damage theory for fatigue life prediction 4-74955
- steam turbine rotor steel crack growth detection and monitoring by acoustic emissions meas. 4-76961
- steel, alloy type, Ca treated resulphurised, mech. props. and machinability, S and sulphide shape effect, report 4-62048
- steel, austenitic stainless, fatigue props. rel. to 20 MeV proton irradi. 4-71737
- steel, austenitic, AM-2, various properties and products of nonmagnetic steels 4-114590
- steel, austenitic and ferritic, for use in fusion reactor liq. metal blankets, compatibility, review 4-107054
- steel, austenitic stainless, Alloy 800, low cycle fatigue at 600°C, influence of dislocation-precip. interaction 4-99529
- steel, austenitic stainless, butt joint, friction welded, fatigue strength and fractographic features (Japanese) 4-114648
- steel, austenitic stainless, creep-fatigue, in high temp. materials, constitutive relationships 4-93353
- steel, austenitic stainless, creep-fatigue studies under biaxial stress state at elevated temps. 4-66409
- steel, austenitic stainless, cumulative fatigue damage at high temps., effect of cyclic strain 4-93414
- steel, austenitic stainless, cyclic creep and life 4-99445
- steel, austenitic stainless, fatigue, high temp., damage mechanics 4-93422
- steel, austenitic stainless, fatigue, initial stage, morphometrical evaluation of surface roughness 4-104840
- steel, austenitic stainless, fatigue strength under varying stress amplitude at high temp. (Japanese) 4-114646
- steel, austenitic stainless, fatigue-oxidation interaction, 550°C, microcrack propag. (Japanese) 4-99520
- steel, austenitic stainless, low cycle fatigue, notch effect in creep-fatigue interaction at elevated temp. 4-66444
- steel, austenitic stainless, low cycle fatigue damage at high temp., X-ray obs. (Japanese) 4-114642
- steel, austenitic stainless, precip. hardening, fatigue crack growth, effect of precip. (Japanese) 4-89122
- steel, austenitic stainless, pressurised tube, ion bombardment, fatigue life, simulated fusion first wall environment 4-104850
- steel, austenitic stainless, radiation damage, fusion reactor candidate material 4-98140
- steel, austenitic stainless, surface observation after thermal shock fatigue fracture (Japanese) 4-99547
- steel, austenitic stainless cumulative damage strain controlled fatigue tests, 20°C 4-104863
- steel, C, annealed, comparison of rotating bending and plane bending fatigue (Japanese) 4-89121
- steel, C, fatigue behaviour, influence of compressive mean stresses (German) 4-81284
- steel, C, fatigue damage under const. amplitude biaxial loading 4-99481
- steel, C and alloy, fatigue strength, statistical analysis of S-N data (Japanese) 4-99500
- steel, carburised, fatigue of steels with internal oxides and non-martensitic microstruct. near surface 4-114655
- steel, cast, fatigue, const. and variable amplitude, room temp. and -45°C 4-99551
- steel, Co eutectoid, mech. props. 4-114629
- steel, constructional, cyclic creep in plane stressed state, life determ. 4-99446
- steel, constructional, near-threshold fatigue, struct. influence 4-93397
- steel, Cr-Mo, cast, corrosion fatigue strength in fresh water, freq. and inhibitor effect (Japanese) 4-99650
- steel, Cr-Mo, fatigue props., effect of intermittent rest periods 4-99588
- steel, Cr-Mo, fatigue strength under varying stress amplitude at high temp. (Japanese) 4-114646
- steel, Cr-Ni-Mo-V, cyclic creep in complex stress state 4-99447
- steel, eutectoid, mech. props., effect of Si additions 4-93365
- steel, eutectoid, rail, fatigue behaviour 4-66412
- steel, fatigue strength of butt welded joints with different plate thickness, stress relief effect 4-62011
- steel, fatigue strength rel. to cold surface rolling press. (Japanese) 4-99514
- steel, ferritic-pearlitic, fatigue, inelastic strain and mag. noise 4-114664
- steel, heat resistant, fatigue resist., cycle asymmetry with long loading bases 4-99545

## fatigue continued

- steel, heat-resistant, crack resist. characts., temp. and loading cycle asymmetry influence 4-99535
- steel, high strength, heat-treatable, fatigue at  $+20^{\circ}\text{C}$  and  $-70^{\circ}\text{C}$  4-93364
- steel, high-speed, hot isostatic pressing, struct. and contact fatigue 4-114440
- steel, HSLA, fatigue fracture surface, X-ray obs. (Japanese) 4-114644
- steel, HSLA, fatigue threshold, effect of strength and surface asperities on closure 4-76852
- steel, HSLA, small fatigue crack initiation and growth, in various environments (Japanese) 4-89124
- steel, IR emission of overloaded metals during fatigue process (Chinese) 4-114636
- steel, low alloy, Cr-Mo-V, high temp. low cycle fatigue rel. to softening and embrittlement (Japanese) 4-99519
- steel, low alloy, creep fatigue and environmental interactions 4-99593
- steel, low alloy, fracture under corrosive environment, high temp. creep, fatigue, creep-fatigue 4-99592
- steel, low C, notched, fatigue threshold prediction 4-99559
- steel, low C, notched fatigue strength rel. to pre-straining and nitriding 4-109489
- steel, low C, rolling contact fatigue rel. to Tufftriding treatment 4-109517
- steel, low-cycle fatigue resist. under nonisothermal loading, kinetic strain criterion 4-66438
- steel, martensitic, high-strength structural, fatigue fracture kinetics, endurance limit and crack resist. 4-99537
- steel, mechanical props. rel. to US detectable discontinuities 4-71713
- steel, medium C, heat treated, fatigue behaviour, overstress effects 4-62007
- steel, mild, fretting fatigue rel. to diffusion coatings from Ni-Co electrodeposits 4-114686
- steel, mild, renitrogenised, cyclically deformed, prep. of thin foils for TEM 4-89233
- steel, Mn pearlitic ferrite, fatigue dislocation structure (Chinese) 4-85201
- steel, Ni type, phase comp. effect on low-cycle impact fatigue resist. 4-93389
- steel, roll type 9Kh, small N and B additions effect on struct. and mech. props. 4-93342
- steel, rolled, initial fatigue fracture surface, laminated struct. effect (Japanese) 4-89118
- steel, stainless, austenitic, plastic deform. symmetrical cyclic bending of different length specimens 4-99442
- steel, stainless, austenitic, type 316, flowing Li environment effect on fatigue and tensile props. 4-107055
- steel, stainless, low cycle fatigue tests, elevated temp. 4-109492
- steel, stainless, transition and martensitic-class, superplasticity 4-61983
- steel, stamping tool, service life, low cycle fatigue, effect of surface roughness 4-114668
- steel, steam turbine rotor type, creep-fatigue damage, report 4-62047
- steel, structural, fatigue fractured surfaces, residual stress, X-ray diff. (Japanese) 4-99513
- steel, structural, fine-grained, low cycle fatigue, influence of cold forming 4-104841
- steel, weld joints, cruciform-welded, mean stress effect on fatigue crack growth under random loading, report 4-66450
- steel 40 Kh, damping capacity and residual life, preliminary cyclic loading influence 4-99544
- steel C45, powder pack cemented test bars, fatigue strength and notch sensitivity study 4-70270
- steel tubes, autofrettage, fatigue strength, thermal shock, tempering, electropolishing 4-104865
- steel tubes, autofrettaged, fatigue strength 4-104864
- steel wire reinforced Al alloy, KAS-1A composite, resources eval. 4-66442
- steels, austenitic stainless, 316 and 253MA, high temp. low cycle fatigue, comparison between mech. props. and microstruct. 4-93410
- steels, fatigue fracture, X-ray fractography (Japanese) 4-89123
- steels, heat-resisting, surface layer fatigue failure, protective effect of alloy coatings 4-93470
- strain hardening materials, failure assessment diagram under cyclic and monotonic loading 4-93367
- striation numerical analysis, crack tip plasticity 4-64883
- structural materials, homogeneous thermal fatigue, rel. to struct. stresses 4-99594
- structural materials, mech. props. at low temps. rel. to stressed state and mode of loading 4-93350
- surface-coated materials, mech. props. 4-99625
- thermally unstable alloy, thermal fatigue 4-93417
- thermoplastics, recovery-induced thermal deform. 4-99469
- Udimet 700, creep-fatigue, in high temp. materials, constitutive relationships 4-93353
- viscoelastic bodies, subcritical growth of microscopic fatigue cracks 4-108048
- X-ray fractography of fatigue fractures in subcrit. crack growth zone 4-114757
- Al alloy, fatigue life, effect of programmed load spectrum parameters (Polish) 4-62028
- Al alloy, high strength, notch fatigue, limits to applicability of LEFM 4-71721
- Al alloy fatigue strength, biaxial plastic prestrain effect 4-104833
- Al alloys, scale removal, improved fatigue strength 4-85263
- Al, fretting in elec. contacts 4-92798
- Al wires, low cycle fatigue, lattice defects, resist., temp. depend. (Japanese) 4-99508
- Al-Ag, age hardened, persistent slip bands, energy dispersive spectra 4-104794
- Al-Cu-Mg, low cycle fatigue, influence of cold forming 4-104841
- Al-Cu-Mg alloy, shot peening effect on fatigue crack initiation by fretting 4-66448
- Al-Mg (5 wt.%), high temp. fatigue, squared-up grain struct. 4-81277
- Al-Mg-Si, age hardened, fatigue crack propag. under two-step loading (Japanese) 4-99518
- Al-Zn (3.5, 5.3 wt.%), GP zones, size distrib. 4-76779
- Al-Zn-Mg, 7075-T6, fatigue strength under combined axial loading and torsion 4-99483
- Al-Zn-Mg, 7075-T651, fatigue crack growth, effect of short-term heating cycles 4-99484
- Al-Zn-Mg, cyclic SCC, crack growth rate (Japanese) 4-99648

## fatigue continued

- Al<sub>2</sub>O<sub>3</sub> fibre reinforced FP alloy, orthotropic plate with circular hole, fatigue failure 4-74953
- Al<sub>2</sub>O<sub>3</sub> fibre reinforced Mg, tensile and fatigue behaviour, fibre fraction and orientation 4-114652
- Al<sub>2</sub>O<sub>3</sub> fibre reinforced Mg alloys, tensile and fatigue behaviour, matrix alloying effects 4-114653
- C fibre reinforced epoxy, unnotched laminates, fatigue and reliability evaluation 4-76846
- C fibre reinforced epoxy laminates, fatigue failure behaviour with edge notch 4-114669
- C fibre reinforced plastic laminates, compression fatigue rel. to anti-buckling guides 4-89099
- C fibre reinforced plastics, generalised fatigue curve parameter estimation 4-89109
- Ca(PO<sub>3</sub>)<sub>2</sub>OH, prestressed ceramics, fatigue props. 4-62052
- Co-base alloy coating, contact fatigue resist. 4-93426
- Co-base superalloy, MAR M509, cast, thermal fatigue 4-93416
- Co-Cr-Mo for hip joint endoprostheses, fatigue strength, remaining lifetime after loosening (German) 4-62627
- Co<sub>7</sub>Si<sub>10</sub>B<sub>15</sub>, amorphous alloys, fatigue props. 4-66424
- Cu, brazed, low cycle fatigue in high vacuum rel. to cold work 4-109500
- Cu, creep fatigue, failure life and microdamage mode rel. to wave shape 4-109508
- Cu, cyclically deformed [001], dislocation struct. 4-108362
- Cu, fatigue of single crystals in air and vacuum, persistent slip bands and dislocation microstruct. 4-99521
- Cu, fatigue of single crystals in air and vacuum, fatigue crack propag. 4-99522
- Cu-Co (2 at.%) single crystals, age hardened, fatigue limit 4-104860
- Cu-Si, dil. alloy, internal oxidation, grain boundary cavitation under creep or fatigue loading 4-71726
- (Fe, Co, Ni)<sub>3</sub>Al, ductile ordered alloys, phys. metallurgy and mech. props. 4-114612
- $\alpha$ -Fe binary alloys, BCC, fatigue, effect of alloying elements 4-66426
- Fe, fatigue crack initiation, Coffin-Manson relations 4-85212
- Fe-Al-Ni-Mo (5.7, 2.5, 2.0 at.%), containing coherent precipitates, effect of plastic deform. on elevated temp. Ostwald ripening 4-85159
- Fe-Cr-Al-Y plasma sprayed coatings, post-treated, mech. props. 4-93471
- Fe-(Si), fatigue threshold, effect of strength and surface asperities on closure 4-76852
- Fe-(Si), fatigue threshold, thermally activated behaviour of effective stress intensity 4-76853
- KCl absorption, reversible and irreversible changes during multiple pulse 10.6  $\mu\text{m}$  irradi. 4-75518
- Mg alloy, cast ML8, surface strain hardening treatment effect on low-cycle fatigue 4-99656
- Mg-Nd-Zr, cyclic strengthening and loss of strength in air and vacuum at 293 and 140K 4-93399
- Mo, cyclic strength and localisation of deform. 4-61999
- Mo, endurance limit in high cycle fatigue rel. to heat treatment and alloying 4-109498
- NaCl absorption, reversible and irreversible changes during multiple pulse 10.6  $\mu\text{m}$  irradi. 4-75518
- Ni and alloys, fatigue lifetimes and fractography in air and liq. Hg 4-99557
- Ni electrode sinter, mechanical stress estimation 4-72066
- Ni, H embrittlement, influence of plastic deform. 4-71729
- Ni, low-cycle fatigue, slip-induced intergranular cavitation at intermediate temp. 4-66402
- Ni, polycryst., slip-induced cavitation, effect of boundary struct. 4-108378
- Ni-base superalloy, DKS, directionally solidified, mech. props., influence of grain orientation 4-93420
- Ni-base superalloy, MAR M002, high temp. low cycle fatigue, importance of initiation and propag. phases 4-93418
- Ni-base superalloy, single cryst., creep-fatigue behaviour, effect of orientation 4-109512
- Ni-base superalloy, Udimet 720; coated and uncoated, low cycle fatigue in air and corrosive environment 4-99657
- Ni-Co, FCC, elastic eigenstrains, X-ray study 4-71716
- Ni<sub>3</sub>Si<sub>2</sub>B<sub>17</sub>, amorphous alloys, fatigue props. 4-66424
- SiC fibre for ICF applic., strength and fatigue analysis 4-109502
- SiC, sintered, fatigue props., effect of different sintering additives 4-62055
- Si<sub>3</sub>N<sub>4</sub>, pressureless sintered, high temp. fatigue failure 4-76867
- Si<sub>3</sub>N<sub>4</sub>, reaction sintered, cyclic fatigue resist. 4-76869
- Si<sub>3</sub>N<sub>4</sub>, sintered, static and cyclic fatigue strength (Japanese) 4-99502
- SiO<sub>2</sub>, silica glass for optical fibres, fatigue anal. 4-103022
- steel, low alloy, cyclic strength, effect of laser irradi. 4-71723
- Ti, fatigue endurance, influence of rest period 4-99486
- Ti-Al-Mo-Sn-Si,  $\alpha/\beta$ , simulated flight fatigue 4-104838
- Ti-ALV, ion implantation effect on fretting fatigue 4-76916
- Ti-ALV (6, 4 wt.%), fatigue strength, influence of adiabatic shear bands 4-99485
- Ti-ALV (6, 4 wt.%), fatigue endurance, influence of rest period 4-99486
- $\alpha+\beta$ Ti-ALV and Ti-Al-Cr-Mo-V, annealed, struct. and mech. props. 4-61988
- TiB<sub>2</sub> powder, pressureless sintered, mech. props. in liq. Al environment, impurity segregation 4-114700
- W, cross-rolled, tensile and low-cycle fatigue meas. at 1505K 4-109503
- W fibre reinforced Ni, mech. props. at elevated temps., diffusion barriers to improve struct. stability 4-93423

## fatigue cracks

- centre cracked tensile panel in net section yield, crack tip opening displacement calc. 4-60335
- compact specimen, fatigue crack closure, finite element analysis 4-97433
- composite laminates, fatigue damage parameter using stiffness change 4-76864
- composite laminates, matrix crack growth, stochastic simulation model 4-74960
- cycle counting for fatigue crack growth anal. 4-104839
- cyclic loading, crack path and elastic energy intensity, taking account of welding stresses 4-114666
- cylinder, thin-walled hollow, fatigue crack growth rate (Japanese) 4-91771
- cylinders, autofrettaged, fatigue crack initiation from holes, R-ratio effect 4-87626
- dislocation concepts appl. in fatigue, book contrib. 4-99564
- flexible samples, cracks, determ. of zones of distrib. 4-60344

**fatigue cracks continued**

- fusion reactor first walls, lifetime calc., creep-fatigue design criteria 4-96254
- general crack opening stress equation 4-60342
- glass, elliptical crack, transient growth, mathematical model 4-104845
- glass fibre reinforced plastics, fatigue crack growth, environmental effect, compliance and moire techniques 4-89200
- growth at high strain amplitudes 4-103265
- growth equations, classical Griffith concept 4-79512
- growth rate and closure in incipient short and elastic-plastic long cracks (Japanese) 4-92291
- growth rate material parameters in fatigue propagation 4-62039
- Inconel 718, fatigue and creep-fatigue crack propag., influence of neutron irradiat. 4-99496
- Inconel 718, time-depend. fatigue crack propag., effect of small scale to large scale creep transition (Japanese) 4-93383
- joints, butt-welded, fatigue crack initiation and propag. at toes (Japanese) 4-93382
- material aspects of crack tip yielding and subcrit. crack growth in eng. alloys 4-93408
- mechanics of fatigue crack propagation by crack-tip plastic blunting 4-71719
- metal fatigue, role of crack growth, book 4-95085
- metallic glasses, fatigue crack propag. and overload effect 4-109511
- metals, fatigue crack propag. rate, correl. with J-integral or crack opening displacement (Japanese) 4-114649
- metals, fatigue-crack growth in vacuum and gaseous media 4-93398
- metals, surface current distrib. around surface flaws 4-60984
- near threshold fatigue crack growth, at elevated temps., oxide wedging effect 4-91775
- plant life prediction at elevated temp., creep-fatigue and thermal shock failure 4-91774
- plate, surface cracks originating at open hole, shape and growth rate meas. 4-87625
- PMMA, fatigue crack closure, dependence on fracture features 4-80149
- PMMA, fatigue crack development 4-93401
- PMMA, fatigue loaded, crack propag., craze zone, optical interference obs. 4-66422
- prestressed lightweight concrete barrier for cryogenic containment vessel 4-114675
- propagation, residual stress distrib., X-ray meas. (Japanese) 4-99685
- PVC, fatigue loaded, crack propag., craze zone, optical interference obs. 4-66422
- PVC, particle filled, fracture mechanism rel. to fatigue crack growth (Japanese) 4-89120
- reliability analysis of fatigue crack propag. life by Markov chain (Japanese) 4-112768
- rocks, fracture toughness under bending rel. to fatigue crack length (Japanese) 4-100557
- semielliptical surface flaws, fatigue life prediction 4-103261
- short cracks effect on fatigue limit, analytical soln. 4-66440
- short fatigue crack behaviour and the concept of absolute and relative fatigue thresholds 4-84344
- shot-peened specimens, fatigue crack propagation due to repeating tensile stresses (Japanese) 4-99548
- steel, austenitic stainless, crack growth under creep-fatigue interaction (Japanese) 4-99501
- steel, austenitic stainless, fatigue crack propag. threshold 4-99590
- steel, austenitic stainless, fatigue crack propagation in specimens subjected to thermal shock 4-93413
- steel, austenitic stainless, fatigue-oxidation interaction, 550°C, microcrack propag. (Japanese) 4-99520
- steel, austenitic stainless, low cycle fatigue, elevated temps., crack propag. and fracture modes (Japanese) 4-89125
- steel, austenitic stainless, low cycle fatigue damage at high temp., X-ray obs. (Japanese) 4-114642
- steel, austenitic stainless, melt layer form. under repetitive electron beam heating, simulation of plasma disruption 4-75535
- steel, austenitic stainless, precip. hardening, fatigue crack growth, effect of precip. (Japanese) 4-89122
- steel, C, crack growth and closure under impact fatigue 4-114630
- steel, C, torsional fatigue crack, nonpropagating phenomena (Japanese) 4-99549
- steel, cast, fatigue, const. and variable amplitude, room temp. and -45°C 4-99551
- steel, corrosion fatigue, Monte Carlo simulation model (Japanese) 4-99647
- steel, Cr, fatigue crack growth under rot., three-point bend loading, tempering temp. influence (Chinese) 4-114631
- steel, Cr-Mo, carbonitride, crack initiation and propag. bending fatigue (Japanese) 4-99509
- steel, Cr-Mo, cast, corrosion fatigue strength in fresh water, freq. and inhibitor effect (Japanese) 4-99650
- steel, Cr-Mo, fatigue crack growth at 525°C, effects of environment and dwell 4-99523
- steel, Cr-Mo, fatigue crack growth at 525°C, prediction of continuous cycling endurance 4-99524
- steel, Cr-Mo, fatigue crack growth at elevated temps., effect of hold periods 4-104867
- steel, Cr-Mo-V, crack growth, influence of cyclic loading 4-93421
- steel, dual phase, fatigue crack growth rel. to prestrain and ageing 4-85213
- steel, dual-phase, fatigue crack propag., effect of microstruct. on crack path morphology 4-99525
- steel, fatigue crack growth rate in aqueous corrosive medium, rel. to crack tip electrochem. conditions 4-93466
- steel, fatigue crack propagation by crack-tip plastic blunting 4-71719
- steel, fatigue strength of butt welded joints with different plate thickness, stress relief effect 4-62011
- steel, fatigue-crack growth in vacuum and gaseous media 4-93398
- steel, high C, fatigue crack growth retardation by massive eutectic carbides 4-99586
- steel, high strength, fatigue crack propag., microfractography (Chinese) 4-62006
- steel, high strength, fatigue crack propag., overload-induced 4-99482
- steel, high strength, fatigue crack retardation in saltwater 4-66446
- steel, high tensile strength, fatigue crack growth and closure in vacuum (Japanese) 4-93381
- steel, IR emission of overloaded metals during fatigue process (Chinese) 4-114636

**fatigue cracks continued**

- steel, low alloy, cast, thermal-mech. fatigue crack propag., effect of strain wave shape 4-66445
- steel, low alloy, fatigue crack propag. in viscous environment 4-99579
- steel, low alloy, small fatigue crack growth behaviour under two-stress level, multiple loading 4-66411
- steel, low alloy ferritic, low cycle fatigue, elevated temps., crack propag. and fracture modes (Japanese) 4-89125
- steel, low C, fatigue crack initiation rel. to annealing and prestressing (Japanese) 4-99517
- steel, low C, fatigue crack retardation in saltwater 4-99552
- steel, low-C cast, cyclic crack resist., heat treatment influence 4-62035
- steel, medium C, short crack fatigue behaviour 4-66410
- steel, mild, plate with small circular hole, fatigue crack propag., fracture mechanisms (Japanese) 4-62025
- steel, Ni-Mo, A533B, fatigue crack growth in simulated PWR loop 4-104834
- steel, Ni-Mo, martensitic A533B pressure vessel, tempered, brittle fracture and fatigue crack growth, segregation effects, Auger obs. 4-66400
- steel, power plant steam pipes, analysis of faults after long term operation 4-76857
- steel, pressure vessel, plated with anticorrosive claddings, fracture behaviour 4-99595
- steel, stainless, claddings, fatigue crack growth rate in air and vacuum at 300°C 4-66413
- steel, stainless, corrosion fatigue crack growth thin type 422, in boiling NaCl soln. 4-66499
- steel, stainless, duplex austenite-ferrite, fatigue crack propag. 4-81287
- steel, stainless, VNS-25, fatigue damage inspection by positron annihilation method 4-81390
- steel, strain meas. near growing fatigue crack tip 4-114651
- steel, surface strain hardening effect on fatigue crack growth 4-66439
- steel plate, explosively bonded stainless clad pressure vessel, fatigue crack growth (Japanese) 4-114643
- steel plates, fatigue crack sizing by double inclination US probe 4-109589
- steel pressure vessels, corrosion fatigue crack growth 4-93405
- steel rails, mixed fatigue-tensile surface crack growth 4-89100
- steels, austenitic stainless, 316 and 253MA, high temp. low cycle fatigue, comparison between mech. props. and microstruct. 4-93410
- stress intensity factors 4-97428
- striation numerical analysis, crack tip plasticity 4-64883
- structural materials, fatigue crack growth and crack closure (Japanese) 4-112767
- threshold stress intensity factor, crit. assessment 4-103264
- viscoelastic bodies, subcrit. growth of microscopic fatigue cracks 4-108048
- Al alloy sheet, flaw inspection, fatigue crack parameter selection in setting specimens 4-109605
- Al alloys, fatigue crack growth, thermoactivation anal. 4-99597
- Al alloys, fatigue-crack growth in vacuum and gaseous media 4-93398
- Al alloys, strain meas. near growing fatigue crack tip 4-114651
- Al-Cu, fatigue crack growth anal., cycle counting 4-104839
- Al-Cu-Li-Mn-Cd, Al 2020, fatigue crack growth behaviour 4-71728
- Al-Cu-Mg, fatigue crack propag., overload-induced 4-99482
- Al-Cu-Mg, fatigue crack propag., statistical characts. (Japanese) 4-99501
- Al-Cu-Mg, near threshold fatigue crack growth, stress intensity factors, crack closure 4-99583
- Al-Cu-Mg alloy D16 plates, struct. strength, chem. comp. and heat treatment effects 4-61986
- Al-Mg-Si, age hardened, fatigue crack propag. under two-step loading (Japanese) 4-99518
- Al-Zn-Mg, fatigue crack advance model, crack tip parameters 4-66401
- Al-Zn-Mg, fatigue crack closure in 7475, microstruct. and ageing effect 4-62032
- Al<sub>2</sub>O<sub>3</sub> fibre reinforced Mg composite, off-axis fracture, critical stress intensity 4-66430
- B<sub>2</sub>C/B fibre reinforced Ti-Al-V, fatigue crack growth behaviour 4-93374
- Co-Cr-Mo for hip joint endoprostheses, fatigue strength, remaining lifetime after loosening (German) 4-62627
- Co-Fe-Mn-B-Si, metallic glass, fatigue crack propag. and overload effect 4-109511
- Co-Fe-Mo-B-Si, metallic glass, fatigue crack propag. and overload effect 4-109511
- Cu, fatigue crack propagation by crack-tip plastic blunting 4-71719
- α-Fe binary alloys, BCC, fatigue, effect of alloying elements 4-66426
- Fe, nodular, cast, fatigue crack growth obs., using bonded-resistance gauges 4-93477
- Fe, pure, annealed, fatigue crack nucleation sites under reversed bending stress (Japanese) 4-99516
- Fe-Cr-Al, oxide dispersion strengthened MA 956, fatigue crack growth 4-62031
- Fe-Si (3 wt.%), single cryst., fatigue crack propag. and crystallographic path, effect of single peak overload 4-99475
- Ni-base superalloy, microstruct. effects of fatigue crack propag., TEM study 4-104871
- Ni-base superalloy, single cryst., crack tip plastic strain 4-89231
- Ni-base superalloys, long and short fatigue crack growth, influence of microstruct. 4-99531
- Ni-Co-W-Cr single crystal superalloy, crack tip plasticity, fatigue crack growth at elevated temp. 4-71727
- Pb(Zr,Ti)O<sub>3</sub> ceramic, fracture mechanics evaluation of acoustic fatigue 4-95416
- SiC fibre reinforced Ti-Al-V, fatigue crack growth behaviour 4-93374
- Ti-Al-Sn-Zr-Mo-Si, H-enhanced fatigue crack growth 4-114640
- Ti-Al-V (6, 4 wt.%), fatigue strength, effect of rest periods during monitoring 4-66414
- Ti-Al-V (6, 4 wt.%), near-threshold fatigue crack growth, effect of corrosive environment 4-81269
- Ti-V, fatigue crack propag. rel. to overload cycling 4-62029
- Zr-Nb, fatigue crack kinetics, tubular, ring and flat samples 4-93400

fatigue failure see fatigue

fatigue fracture see fatigue

fatigue life see fatigue

fatigue testing

for corrosion fatigue testing, see corrosion testing

accelerated tests, methodology, initial curves determ. with min. time expenditure 4-66542

automotive components, random loading in high endurance range, time-reduced performance fatigue test (German) 4-114747

**fatigue testing continued**

- benchmark cyclic plastic notch strain measurement 4-104956
- brittle materials, high-temp. device 4-66527
- composite materials, secant stiffness meas., using peak valley detector 4-66514
- crack propagation, residual stress distrib., X-ray meas. (Japanese) 4-99685
- cycle counting for fatigue crack growth anal. 4-104839
- cyclic bending device in SEM (German, English) 4-71822
- data fitting to Bernstein and inverse normal distributions 4-99672
- endurance limit, accelerated Locati method 4-99702
- glass fibre reinforced plastics, fatigue crack growth, environmental effect, compliance and moire techniques 4-89200
- high-cycle, strain-controlled loading regimes realisation 4-66543
- ice, thermal patterns obs. under dynamic loading 4-106320
- impact fatigue wear testing method 4-89216
- life prediction for complex load vs. time histories 4-104953
- load recording method 4-66526
- loading data computer anal. for fatigue evaluation and testing 4-71816
- metallic systems and structures, book contrib. 4-109514
- metals, fatigue test method for cyclic and pulsating torsional load 4-66525
- metals, fatigue testing methods for critical stage of failure 4-93493
- metals, strain controlled creep-fatigue tests 4-89209
- nonisothermal fatigue tests and analysis 4-93497
- optical fibres, Al-coated, optical, mechanical and radiation perform. at high temp. 4-97111
- optical fibres, double mandrel, technique for studying static fatigue 4-60161
- plastic, creep testing and eval. method in static bending fatigue tests (German) 4-71821
- PMMA, fatigue loaded, crack propag., craze zone, optical interference obs. 4-66422
- prestressed lightweight concrete barrier for cryogenic containment vessel 4-114675
- progressive loading machine for accelerated fatigue test (Japanese) 4-85271
- PVC, fatigue loaded, crack propag., craze zone, optical interference obs. 4-66422
- reliability analysis and design, crack growth model (Japanese) 4-99687
- S-N curves, determ. with pre-cracked specimens 4-99739
- seawater pressure resistant concrete structure test data and trends 4-114760
- servomechanical-fatigue-test machine 4-99667
- shortened test method for creep eval. during static bending fatigue tests (German) 4-71821
- specific work for failure determination 4-93495
- spring materials fatigue strength determ. using hyperbolic method 4-71829
- steel, endurance limit, accelerated Locati method 4-99702
- steel, high strength, endurance limit diagrams, fatigue testing (Japanese) 4-89223
- steel, stainless, fatigue test, IR monitoring 4-109585
- stroboscopic cathetometer attachment 4-89217
- thermal fatigue testing by direct passage of elec. current, appl. to stainless steels 4-93496
- thermoplastics, using computerised machine 4-104934
- tubular, ring and flat samples, crack growth kinetics comparison 4-93400
- wood, creep testing and eval. method in static bending fatigue tests (German) 4-71821
- Al alloy, accelerated tests methodology 4-66542
- Pb(Zr,Ti)O<sub>3</sub>, ceramic, fracture mechanics evaluation of acoustic fatigue 4-95416
- Ti-Al-V (6, 4 wt.%), fatigue strength, effect of rest periods during monitoring 4-66414
- Zr-Nb, fatigue crack kinetics, tubular, ring and flat samples 4-93400

**fault location**

- component fault testing in electro- and cable-technology, nuclear reactor appl. 4-106839
- multimode optical fibre, stimulated Raman scattering appl. 4-74733
- nuclear power plant failure detection and isolation under steady-state conditions by constrained least-squares method 4-86934
- optical fibre, single mode, 1.55  $\mu$ m time-domain-reflectometry, long fault location appl. 4-64797
- optical fibre, single-mode, 130 km-long fault location using 1.55  $\mu$ m Er<sup>3+</sup>-glass laser 4-91601
- optical fibre fracture location using pulse reflectometer (Czech) 4-64802
- optical fibres ultralong, fault location using Ge p-i-n photodiode S/N improvement study (Japanese) 4-60188
- OTDR long-range fibre-optic fault locator 4-73480
- single mode fibres, characterisation and fault location, long wavelength optical time domain reflectometry appl. 4-107838
- thermocouple cct. analysis, gradient approach 4-63743

**fault-tolerant computing**

- spacecraft guidance and control techniques, conf., Florence, Italy (Sept. 1983) 4-73164

**f.d.m. see frequency division multiplexing****feature extraction see pattern recognition****feedback****see also control systems**

- amplified guitars, infinite sustain through controlled feedback 4-79402
- coherent FSK transmitter using a negative feedback stabilised semiconductor laser 4-107875
- diode laser, feedback of light interacting coherently, incoherently with laser cavity field, influence on oscill. spectrum 4-91451
- drift-tearing modes control in Tokamak discharges 4-87867
- electro-optic intensity modulation system, low distortion, with optical feedback 4-91577
- electrooptic bistable devices with short delay times in the feedback bifurcations 4-96980
- fibre-optic gyroscopes, gated phase-modulation feedback approach 4-79324
- graded-index lens external cavity semicond. laser with optical feedback, spectral props. study 4-87371
- injection laser, single-mode, line narrowing due to external optical feedback 4-79142
- injection laser noise properties due to optical feedback 4-79143
- instabilities feedback control in tandem-mirror fusion device 4-87866
- MHD, equilib. bifurcations, automatic control influence 4-113024
- microcomputer DC discharge intensity-stabilization 4-108248

**feedback continued**

- NMR, marginal oscillator, active feedback control 4-95479
- nuclear reactor, suboptimal stochastic control 4-102346
- nuclear reactor optimal feedback control by frequency-domain methods 4-64197
- optical phase measurement instrument, control loop sensor for an optical synthetic aperture 4-106339
- positive feedback amplifier, phase transitions 4-90546
- semiconductor cleaved-coupled-cavity laser, single mode, spectral props., external optical feedback effect 4-69405
- semiconductor single-mode lasers, noise theory in presence of optical feedback 4-79137
- single mode fibre optic recirculating delay line with bandwidth >1 GHz 4-97114
- synchrotron radiation double crystal instruments, feedback control system 4-65152
- unstable heat eqn., feedback stabilisation using auxiliary functional observer 4-78109
- AlGaAs semiconductor laser, frequency stabilization by thermal and current feedback control 4-60071
- BaTiO<sub>3</sub>, self-pumped phase conjugation, optical feedback, wavelength response and interf. effects 4-97004
- GaAlAs laser diode coupled to an external cavity intensity noise suppression and modulation characts. 4-79144
- GaAlAs laser oscillating in single longit. mode, LF feedback noise 4-96909

**feeds, antenna see antenna feeders****FEM see field emission electron microscopy****Fermi-Dirac statistics see quantum statistical mechanics****Fermi gas see fermion systems****Fermi level**

- amorphous RF sputtered film, struct. and elec. props. 4-70956
- disordered systems, electron-electron interaction in a self-consistent localization theory 4-92673
- electron-gas, 2-D, magnetisation and mag. susceptibility 4-113881
- electron gas, cond. near mobility edge 4-98616
- free-electron solid of submicron dimensions, Fermi energy and density of states, influence of boundary conditions 4-92785
- grain boundary barrier heights, surface state effects 4-92780
- heterogeneous surface characterization by photoemission of adsorbed Xe 4-88935
- Heusler alloys, band struct., mag. moments, hyperfine fields, local spin density method 4-108767
- metal surface, laser induced electron-phonon processes 4-75873
- metals, free standing and adsorbed, work functions, quantum size effects 4-92790
- metals, superconductivity from nonphonon interactions 4-84737
- MIS structures, hole traps, trivalent Si centres, EPR meas. 4-80817
- nonmagnetic metal with gap, impurity, density of states, sp. ht., tridiagonalisation 4-92665
- oxide, exchange of O between gas and solid, electrochemical study 4-98357
- oxides, surface props. at high temps., work function studies 4-98697
- proton-surface collisions, charged fractions for low energy protons 4-81084
- quantum Hall regime, critical currents 4-98644
- semiconductor colloidal electrode particles, photogenerated carrier transport and kinetics 4-65671
- semiconductors, amorphous, DC electronic transport, long-range pot. influence 4-113947
- semiconductors, resonant absorpt. of high-intensity light 4-71408
- solar cell contact resist., review 4-81544
- substitutional impurities, indirect interaction in linear at. chain 4-61318
- superlattices, thermopower as probe of density of states distrib. 4-98714
- two-dimensional electron systems, sound propag. in strong mag. fields 4-65718
- two-dimensional strip, quantized Hall cond. and edge states 4-92591
- X-ray absorpt. edges, chemical shift calcs. 4-99228
- Ag (110) unoccupied surface state, inverse photoemission study 4-71515
- Ag, Fermi level excitation threshold, press. depend. 4-80479
- Ag film with adsorbed O<sub>2</sub>, CO and ethylene, elec. cond., effect of adsorption 4-108950
- $\alpha$ -Al<sub>2</sub>O<sub>3</sub>, defect structure, electron emission meas. 4-93145
- As, rhombohedral, electronic band struct., angle-resolved UPS and pseudopot. studies 4-113868
- C-Ag junctions, Schottky barrier form. 4-84694
- CdTe metal-semicond.-metal struct., pot. barriers 4-84708
- Ce<sub>1-x</sub>La<sub>x</sub>Ni<sub>2</sub>, mixed valence, thermopower and band struct. 4-113927
- CeNi<sub>2</sub>, mixed valence, thermopower and band struct. 4-113927
- Cu<sub>2</sub>Zr<sub>1-x</sub>, metallic glass, electronic struct. calcs. 4-104120
- DyFe<sub>2</sub> intermetallics, SXAPS studies 4-81039
- ErFe<sub>2</sub> intermetallics, SXAPS studies 4-81039
- Fe, cast, white, annealing, Fermi energy, thermoEMF obs. rel. to crystallisation in acoustic vibration field 4-76768
- GaAs (100), chemical etching and annealing, Fermi level pinning 4-65722
- GaAs MBE-grown (001) surface, band bending, photoemission studies 4-99276
- GaAs Surface, (110), Fermi level pinning, elec. field induced Raman scatt. 4-88845
- GaAs/Al interface, electronic struct. and bending 4-84700
- GaAs/AlGaAs heterostructures, carrier density, hydrostatic press. control 4-98735
- GaAs-Al<sub>0.3</sub>Ga<sub>0.7</sub>As, quantised Hall resistance and 2D electron gas behaviour 4-98724
- GaAs-Ge(100) interfaces, Fermi level position and valence-band edge discontinuity study 4-61450
- n-GaAs<sub>1-x</sub>P<sub>x</sub>, anodes in aq. Se<sup>2-</sup>/Se<sub>2</sub><sup>2-</sup> solns., characts. 4-104310
- GaAs(1110)-In interface, photoemission study 4-85079
- GaSb<sub>2</sub>Se, quantum localisation of electrons in metal-insulator transition region 4-70654
- GaSb-InAs heterojunction, quantum Hall effect study 4-98726
- GdZn, ferromagnetically saturated single crystal, high-field NMR Knight shift, magnetisation studies 4-114176
- Ge/Al interface, chemisorption and metallisation, electronic struct. 4-92527
- HfS<sub>2</sub>, electronic struct. by high resolved angular photoemission 4-84557
- Hg<sub>1</sub>SCN, thermoelec. power and Fermi level 4-104243
- n-HgTe zero gap semicond., effective electron mass, mag. quantisation effects 4-88442

## Fermi level continued

- InGa<sub>1-x</sub>As-InP heterojunction, quantum Hall effect and hopping cond. 4-98723  
 InP (110)-Cu(Ag)(Au) interface, soft X-ray photoemission study 4-85080  
 InP, surface and interface states 4-92782  
 InP:Mn, hopping cond. between deep impurity states 4-104209  
 InP/Pd interface, In segregation and PdP form., XPS study 4-80422  
 InP:Ag interface, reactions and Schottky barrier form., XPS studies 4-92821  
 InSb, effective electron mass in inversion layers, surface elec. field effect 4-104280  
 K complex, K<sub>2</sub>Pt(CN)<sub>4</sub>Br<sub>0.3</sub>H<sub>2</sub>O, electronic struct., multiple scatt. generalised partitioning mol. cluster model 4-70629  
 La<sub>2</sub>CuO<sub>4</sub>, with K<sub>2</sub>NiF<sub>6</sub> struct., at displacements, mag. and transport props., anisotropic bonding effects 4-75358  
 La<sub>2</sub>NiO<sub>4</sub>, with K<sub>2</sub>NiF<sub>6</sub> struct., at displacements, mag. and transport props., anisotropic bonding effects 4-75358  
 La<sub>1-x</sub>Sr<sub>x</sub>VO<sub>3</sub> metal-insulator transition, photoemission study 4-84567  
 MnO, self-consistent Hartree energy band calcs. 4-92612  
 Mo chalcogenides, binary and ternary, Chevrel type, supercond., heat capacity anal. 4-92858  
 Ni, polycrystalline, inverse photoemission 4-61808  
 Ni, X-ray absorpt. near edge struct. and band struct. 4-114346  
 NiH<sub>0.85</sub>, X-ray absorpt. near edge struct. and band struct. 4-114346  
 NiO:Cr, pure and doped, Seebeck effect and vacancies 4-92775  
 P, black, electronic struct., polarised X-ray emission and absorption studies 4-108771  
 Pb (111), electronic energy bands, angle resolved photoemission and self-consistent field calcs. 4-113858  
 Pd (111) surface inverse photoemission and band struct. 4-104721  
 Pd, X-ray absorpt. near edge struct. spectra, high resolution anal. of L<sub>2,3</sub> white lines 4-66124  
 PdH<sub>x</sub>, electronic props. of dilute H 4-88472  
 PdH<sub>x</sub>, X-ray photoemission study of electronic struct. 4-84561  
 S, highly doped, modeling the intrinsic number and Fermi levels for device and process simulation 4-113966  
 a-Si, AC field effect and density of gap states 4-92670  
 a-Si alloys, photocond., dark Fermi level position depend. 4-113987  
 Si, amorphous, ion implanted, crystn. growth velocities, charged dangling bonds 4-88093  
 a-Si, film, gap density of states determ. 4-80551  
 Si, highly doped, intrinsic number and Fermi level modelling for device and process simulation 4-75983  
 a-Si, mobility edge, temp. depend. 4-92723  
 Si, n<sup>+</sup> and p<sup>+</sup> regions, uncertainties about physical electronics, solar cell appls. 4-89428  
 Si surface two-photon photoemission 4-85076  
 Si:As, P, ion implanted, diffusion modelling 4-113729  
 a-Si:Cl, H films, photocond. spectra (Chinese) 4-113989  
 a-Si:H, energy distrib. of light-induced gap states, photocond. meas. 4-76004  
 a-Si:H, non-substitutional dopant states and carrier density statistics 4-113902  
 a-Si:H, TSC meas., density of states behaviour 4-98636  
 a-Si:H:N film, TSC and photoconductivity 4-104222  
 Si:O, nonequilibrium cond. and thermal donors 4-104212  
 Si/methanol liquid junction, open circuit volt. and oxide form. 4-114030  
 Si/SiO<sub>2</sub>/metal struct., electron inversion layers, tunnelling spectra of Landau levels 4-98772  
 Si-Ag and Si-H-Ag junctions, Schottky barrier form. 4-84694  
 SiN<sub>x</sub>:H, amorphous, electronic struct., photoemission 4-108776  
 a-SiN<sub>x</sub>:H layers, prep. by glow discharge decomp. of N<sub>2</sub>/SiH<sub>4</sub> mixtures, optical and photoelectronic props., effects of doping 4-114001  
 Si<sub>1-x</sub>Sn<sub>x</sub>:H, (0 ≤ x ≤ 0.3), amorphous RF sputtered film, struct. and elec. props. 4-70956  
 Te, neutron irradiat. induced defects, optical props. near fundamental energy gap 4-84318  
 Te/CdS thin film Schottky barrier diodes 4-70909  
 Ti cpds., electronic relax. effects, X-ray absorpt. 4-66114  
 TiSe<sub>2</sub>, electronic struct. by high resolved angular photoemission 4-84557  
 Ti<sub>1-x</sub>V<sub>x</sub>Se<sub>2</sub>, electronic struct. by high resolved angular photoemission 4-84557  
 TiBiTe<sub>2</sub>, growth, elec. and optical props. 4-65676  
 TiCu<sub>2</sub>Se<sub>2</sub>, p-type metal with layer struct. 4-70652  
 Zr-Pd(Ni), amorphous, electronic density of states and superconducting props. 4-70738  
 ZrH<sub>x</sub>, electronic struct., tetragonal distortion, X-ray diffr. and PMR study 4-84858

Fermi liquid *see fermion systems*

## Fermi resonance

- alkali halide: BH<sub>4</sub><sup>-</sup>, IR and Raman spectra, Fermi resonances isotope shift 4-61695  
 all-trans-n-alkanes, cryst. struct. and C-H stretching modes 4-70126  
 5-aminotetrazole monohydrate, Raman spectra, Fermi resonance 4-114266  
 aniline-d<sub>3</sub>, three-level reson. in aminogroup stretching vibr. region 4-107331  
 benzene-d<sub>3</sub>(d<sub>6</sub>), highly excited overtones, classical dynamics 4-102664  
 benzene-d<sub>6</sub>(d<sub>6</sub>), intramolecular vibr. relax., IR overtone spectra 4-102663  
 1,1'-binaphthyl, conform. dynamics, fluoresc. obs. 4-112224  
 bromotrifluoromethane, IR and Raman spectra, cryst. struct. 4-104690  
 1,1,1,4,4,4-butanediol, molten, Raman spectra conformational depend. of Fermi reson. 4-69048  
 carbon tetrachloride, in Kr matrix, orientational ordering, site struct., IR spectra 4-64459  
 1-chloronaphthalene, vapour phase, vibronic state, Fermi-type reson., UV obs. 4-59791  
 1-fluoronaphthalene, vapour phase, vibronic state, Fermi-type reson., UV obs. 4-59791  
 methane-d<sub>3</sub>, CH chromophore spectrosc. and dynamics 4-112167  
 methanol-d<sub>3</sub> laser lines, optically pumped, assignment and correction anal. 4-79120  
 methyl cyanide, laser Stark spectra, Fermi reson., rovibr. transitions 4-59822  
 quinzarin, hot luminesc. spectra in supersonic expansion 4-97747  
 transition metal formate dihydrates, Evans holes, IR spectra 4-66019  
<sup>12</sup>C<sup>18</sup>O<sub>2</sub>, Σ and Π Fermi dyads in 4.5 μm region, wavenumbers, spectrosc. consts. 4-59745

## Fermi resonance continued

- CS<sub>2</sub>, jet-cooled, <sup>13</sup>C(V)-Σ<sub>g</sub><sup>+</sup>(X) transition, excitation and dispersed fluoresc. spectra 4-64527  
 H-bonded crystals, vibr. spectra, anharmonicity and reson. interaction effects 4-61684  
 K<sub>4</sub>Fe(CN)<sub>6</sub>·3H<sub>2</sub>O, cryst. vibr., second order IR spectrum 4-65348  
 (ND<sub>3</sub>)<sub>2</sub>D<sub>2</sub>O, IR spectra and phase transitions between 100 and 15K 4-114258  
 (ND<sub>3</sub>)<sub>2</sub>H<sub>2</sub>O, IR spectra and phase transitions between 100 and 15K 4-114258  
 (NH<sub>3</sub>)<sub>2</sub>D<sub>2</sub>O, IR spectra and phase transitions between 100 and 15K 4-114258  
 (NH<sub>3</sub>)<sub>2</sub>H<sub>2</sub>O, IR spectra and phase transitions between 100 and 15K 4-114258
- Fermi surface**  
 alloys, electronic energy calc., improved perturbation theory 4-65601  
 alloys (Japanese) 4-113391  
 Anderson Hamiltonian, periodic, Fermi liq. description 4-75827  
 brass, momentum density of annihilation photons, one-dimensions. Fourier transform method 4-70634  
 CWD superconductors, nonmagnetic impurity effects 4-70683  
 graphite, thermoelec. power, Kohn phonon drag effect 4-88525  
 heavy particles in metals, Fermi surface effects (Japanese) 4-65603  
 linear interpolation used in analytical tetrahedron method, Fermi surface 4-70617  
 metal plate, electromag. generation of sound in perpendicular mag. field 4-80632  
 metallic elements, homogeneously strained, electron states and Fermi surfaces, data compilation 4-73178  
 metals, interaction forces for charge carriers and bounding surface (Russian) 4-84641  
 metals, magnetotransport, exactly soluble model 4-75928  
 metals, thermodynamic props. when Fermi surface is close to Brillouin zone surfaces 4-70404  
 metals with open Fermi surface, thermoelectromotive force at low temps. (Russian) 4-92699  
 noble metal, electron-phonon and electron-electron scatt. investigations on Fermi surface 4-70798  
 quasi-one-dimensional metallic phase, in mag. fields, stability against spin density wave form. 4-80572  
 RKKY interaction, band structure and matrix element effects 4-98877  
 semiconductors, absorption edge, free carrier Fermi-liq. interaction effects 4-114236  
 transition metal, electron-phonon and electron-electron scatt. investigations on Fermi surface 4-70798  
 Ag, doppleron oscils., carrier reflection influences 4-80481  
 Al, Fermi surface, topological transitions under stress (Russian) 4-108761  
 As, galvanomagnetic props. and current carriers energy spectrum (Russian) 4-89638  
 Au<sub>1-x</sub>Pt<sub>x</sub>(Ni<sub>1-x</sub>), substitutionally disordered, electronic struct. calcs. 4-70644  
 Bi, Shubnikov-de Haas effect, strong anisotropic strains 4-113979  
 Cd, doppleron oscils., carrier reflection influences 4-80481  
 Cd<sub>2</sub>Mg alloys, electronic energy spectrum and de Haas-van Alphen effect (Russian) 4-70639  
 Cr-Mn-V, phase diagram, two-band models, influence of reservoir and Fermi surface 4-114107  
 Cu (100), surface dynamic processes, excitation of electron-hole pairs 4-70902  
 Cu, electronic props. of 4d transition metal and sp impurities 4-70731  
 Cu, phonon anomalies on Fermi surface maps 4-70312  
 Cu-Pd random substitutional alloy, [111] neck radius on the Fermi surface 4-80476  
 Cu<sub>3</sub>Au, substitutionally disordered, electronic struct. calcs. 4-70644  
 Eu, BCC, generalised susceptibility and joint density of states 4-76118  
 Fe, BCC, Fermi surface and energy bands under press., APW calc. 4-80478  
 Hg<sub>1-x</sub>As<sub>x</sub>F<sub>6</sub>, incommensurate, mag. breakdown 4-84543  
 In, electron-phonon mass-enhancement parameter anisotropy and cyclotron mass 4-84544  
 In, electronic lifetime anisotropy, pseudopotential model calc. 4-113928  
 In, Fermi surface, topological transitions under stress (Russian) 4-108761  
 In-Tl, premartensitic phenomena, role of Fermi surface 4-84384  
 K, anisotropic Hall coeff., induced-torque anomaly theory 4-104185  
 KHg<sub>2</sub> graphite intercalation cpd., electronic struct., Shubnikov-de Haas effect 4-92596  
 La, pressure effects on band structure, Fermi surface and super conductivity 4-84553  
 Mo-Nb dilute alloys, thermoelec. props. at low temps. 4-92700  
 Nb-Ge, thin films, electrical resistivity, temp. depend. 4-108963  
 Nb-Si, thin films, electrical resistivity, temp. depend. 4-108963  
 Nb<sub>2</sub>Mo<sub>3</sub> disordered alloy, Fermi surface, positron study 4-80480  
 NbSe<sub>2</sub> quasi-1D metal, Hall effect and sliding Frohlich modes 4-65669  
 Nb<sub>1-x</sub>Ta<sub>x</sub>Se<sub>2</sub> supercond. layered cpd., upper critical fields 4-114078  
 Ni (100), surface dynamic processes, excitation of electron-hole pairs 4-70902  
 Ni<sub>2</sub>Al, weak itinerant ferromagnet, de Haas-van Alphen effect, Curie temp. 4-113848  
 Ni<sub>2</sub>Pt<sub>1-x</sub>, substitutionally disordered, electronic struct. calcs. 4-70644  
 Ni<sub>46.8</sub>Ti<sub>53.2</sub>Fe<sub>2</sub>, phonon softening study 4-84354  
 PbSe, anisotropy of Fermi surface of holes 4-104117  
 Pb<sub>1-x</sub>Sn<sub>x</sub>Te, band struct. changes during struct. and band inversion transitions 4-65607  
 Pb<sub>1-x</sub>Sn<sub>x</sub>Te, Shubnikov-de Haas effect, temp. depend. scatt. parameter 4-113978  
 Pd, X-ray emission spectra, anisotropy of cyclotron masses and many-body effects 4-104700  
 PdD<sub>2</sub>, Fermi surface imaging effect in D short-range order 4-70633  
 Pr, band structure, Fermi surface and supercond. under high press. 4-98511  
 Sb<sub>2</sub>Te<sub>2</sub> single cryst., weak field charge transport 4-108887  
 Si MIS 2D Fermi system, phonon drag of surface charges 4-92812  
 SnTe, low carrier conc., Fermi surface, Shubnikov-de Haas studies 4-98506  
 SrAs<sub>3</sub>, monoclinic, Fermi surface determ. by Shubnikov-de Haas effect 4-108763  
 Te (0001), weak localisation under lifted spin degeneracy conditions 4-92781  
 Ti cpds., electronic relax. effects, X-ray absorpt. 4-66114

**fermi surface continued**

- Ti-Pd, specific heat meas. (*Chinese*) 4-75698
- TiC, Fermi surface, const. energy KKR-GF calc. 4-84545
- TiN, Fermi surface, const. energy KKR-GF calc. 4-84545
- VS, metal-insulator transition and elec. props. 4-84568
- W-Ta dilute alloys, thermoelec. props. at low temps. 4-92700
- WC, hexagonal, surface and bulk electronic struct., density of states 4-113867

**Fermi-Thomas model. see Thomas-Fermi model****fermion systems**

- see also electron gas; liquid helium-3*
- Anderson Hamiltonian, periodic, Fermi liq. description 4-75827
- Boson representation of the antisymmetrizer 4-101746
- Brownian motion, stochastic differential eqns. solns. 4-63664
- collective field treatment of confined fermions and bosons in the large- $N$  approximation 4-58736
- density functional theory, Kohn-Sham eqns. 4-86329
- disordered fermion system, interaction driven, metal-insulator transition 4-104127
- equidensity and pairwise equidensity orbitals for systems of noninteracting fermions 4-90483
- excitonic insulator with spatially inhomogeneous gap, spin wave zero sound mode 4-61528
- extended Thomas-Fermi model at finite temperature, second order gradient corrections 4-90958
- Fermi liquid, cylindrical Poiseuille flow 4-84481
- Fermi liquid, normal, Landau kinetic eqn., nonlinear corrections 4-63650
- few-body techniques in many-body perturbation theory 4-68629
- gas, ground state energy 4-101744
- Hamiltonians, spin-depend., matrix elements 4-78167
- heavy fermion superconductivity, renormalised perturbation theory anal. 4-104354
- heavy ion collisions, coalescence process, Fermi gas simulation in schematic model 4-86861
- Hubbard chain, thermodynamics, temp. extension of ground-state renormalisation for fermions 4-70613
- infinite free Fermion gas, quantum detailed balance 4-101677
- interacting disordered electron system, single-particle density of states, renormalisability 4-104115
- interacting fermion-boson systems, microscopic formulation 4-90959
- many boson and many fermion systems, perturbation theory approach 4-58732
- many-fermion system, generalised mean field expansions (*Chinese*) 4-101742
- many-fermion systems, real coherent state 4-68122
- many-fermion systems, Sturm spectral representation of Green's functions 4-78235
- massive Thirring model, continuum limit of Heisenberg model 4-73336
- meron solutions of Weyl invariant fermionic model, Gursay term 4-95661
- metals, antiferromagnetic, magnon relax. study (*Russian*) 4-80749
- Monte Carlo method, appls. in condensed-matter physics, statistical mechanics and related fields, book 4-101584
- Monte Carlo methods for the many-fermion problem 4-73337
- N interacting fermion system, canonical density operator, single particle approx. 4-63657
- noninteracting, with mag. moments, magnetisation 4-86330
- non-topological solitons, Green's functions and bound states, self-interacting scalar field 4-90831
- nucleus, Fermi liq., surface effects on particle self-energies 4-86786
- one-component plasma, phase diagram 4-90484
- one-dimensional Fermi system, Peierls instability 4-108840
- one-dimensional interacting Fermi system in mag. field, crit. props. 4-63653
- particle particle propagator, higher order approx. in algebraic diagrammatic construction 4-102595
- quantised Hall effect theory 4-98646
- quantum few-body problem, Monte Carlo calc. 4-95293
- relativistic Fermi gas in strong mag. field, thermodynamics 4-58731
- relativistic Fermi system with Bose condensate, at finite temp., thermodynamic props. 4-95688
- relativistic fermion systems, superfluidity and superconductivity, gap equations, free energies 4-90489
- relativistic partition function and polarisation props. 4-106475
- spin-free fermion model, metal-insulator transition and density fluctuations (*Russian*) 4-65610
- spinless fermion model, order-disorder transition 4-78258
- Sturm expansions, perturbation theory 4-63659
- superconductivity and superfluidity, phases 4-82742
- symmetric Anderson lattice, ground states calcs. 4-70614
- tachyon ideal gases, covariant statistical mechanics formalism 4-95295
- Thirring and Schwinger models, two-dimensional curved space-time 4-90734
- Thomas-Fermi eqns. soln. using imaginary time step method 4-68627
- two-charged-component Fermi fluids, many-body variational method 4-75886
- two-component Fermi liq., sound wave propag. 4-61311
- two-dimensional interacting fermions in uniform mag. field 4-70686
- two-dimensional one-component plasma, free energy and correlation functions 4-90485
- two-dimensional spin-polarised fermion lattice gas, Monte Carlo study 4-68177
- two-dimensional system, fractional quantum Hall effect 4-92757

**fermions**

- see also baryons; fermion systems; leptons*
- Abelian Higgs models, nontrivial fixed points, renormalisation group functions 4-95663
- composite models, masses and anomalous mag. moments, non-renormalizable supersymm. interactions 4-111421
- field theory, finite mode regularisations 4-73639
- Goldstone fermions in  $N=1$  supersymmetry 4-73657
- lattice QCD, Monte Carlo calc. of hadron masses, unquenched Wilson fermions 4-111392
- lattice QCD, non-zero baryon density, chiral symm. restoration, Susskind fermions 4-102062
- Majorana masses, two-component fermions 4-106463
- many-particle spin states, group-theoretic property derivation 4-82640
- primeval plasma recombination, supersymm. light-inos, universe expansion rate 4-110794

**fermions continued**

- QCD, extracting hidden fermions from bosonic effective theories 4-111378
- quantum mechanical Hamiltonian lower bound, relativistic kinetic energy 4-90466
- quantum theory, fermionic zero-mode interpretation 4-78161
- quantum-statistical distributions, R-inherent quantum mechanics, four-dimensional symmetry 4-95294
- stochastic quantisation method, superspace formulation 4-73636
- $SU_1(2) \times SU_2(3)$  model, scalar field set addition fermion mass generation, radiative corrections 4-73637
- $SU(2) \times U(1)$  electroweak theory, lattice gauge model using Wilson fermions 4-111356
- $SU(6)$  grand unified model, simple Higgs fields, anomalous fermions. (*Chinese*) 4-102076
- supersymmetric gauge theory vacua and chiral fermions, SUSY breaking 4-82917
- Susskind fermions, mass term symmetry properties 4-90816
- technicolour model, fermion degeneracy, flavour 4-111346
- unified theories, mirror fermions,  $SU(3) \times SU(2) \times U(1)$  gauge symmetry 4-86604

**fermium**

*see also nuclei with .....*

- $^{254}\text{Fm}$ , L-Auger spectra meas. 4-96511

**fermium compounds**

No entries

**ferrimagnetic properties of substances**

- see also ferrimagnetism; ferrites; garnets; magnetic semiconductors*
- metallic glasses, mag. props. 4-114139
- oxides, mag., muon hyperfine interactions, spin rot. studies 4-65917
- rare earth alloys,  $\text{R}_2\text{Fe}_{23}$  intermetallic cpds., magnetisation, mol. field anal. 4-71031
- tetramethylammonium manganese (iron) cyanide octahydrate, chain struct. and magnetism 4-71073
- $\text{BaFe}_{12}\text{O}_{19}$ , magnetic vitroceraics, prep. and props. 4-93256
- $\text{BaFe}_{12}\text{O}_{19}$  permanent magnets, sintering temp. effect on mag. props. and density (*Afrikaans*) 4-76170
- $\text{BaO-B}_2\text{O}_3\text{-Fe}_2\text{O}_3$  glasses, splat cooled, mag. props. 4-71107
- $\text{Cd,Cu}_{1-x}\text{Fe}_x\text{O}_4$  spinel, low temp. Mossbauer obs. of mag. interactions 4-98983
- $\text{Cd,Ni}_{1-x}\text{Fe}_x\text{O}_4$  system, nonlinear spin struct., magnetisation and Mossbauer obs., Yafet-Kittel angles 4-71022
- $\text{CoFe}_2\text{O}_4$  ultra-fine spinel ferrites, prep. and characterisation 4-71130
- $\text{Co,Fe}_{1-x}\text{O}_4$  ceramic ferrite, mag. props. (*Spanish*) 4-88649
- Cu (II) complex,  $\text{CuMn}$  (thioxalato),  $7.5\text{H}_2\text{O}$ , quasi-one-dimens. ferrimag. chain, magnetisation and susceptibility study 4-80748
- $\text{Cu,Fe}_{1-x}\text{O}_4$  oxidation states,  $^{57}\text{Fe}$  Mossbauer study 4-71225
- $\text{Dy}_2(\text{Fe}_{1-x}\text{Al}_x)_4$ , pseudobinary intermetallic cpd., mag. props. 4-71032
- $\text{Er}_2\text{O}_3\text{-SrO}$ , magnetic phase diagram, magnetisation and susceptibility meas. 4-92912
- $\text{Fe}_{1-x}\text{Cu}_x\text{C}_4\text{S}_8$ , ferrimagnetic to ferromagnetic order transition, ion valence states, NMR 4-88670
- $\gamma\text{-Fe}_2\text{O}_3$  microparticle materials, mag. and Mossbauer studies 4-104542
- $\gamma\text{-Fe}_2\text{O}_3$  Co, textural and surface props. rel. to mag. recording appls. 4-65833
- $\text{Fe}_3\text{O}_4$  ceramic ferrite, mag. props. (*Spanish*) 4-88649
- $\gamma\text{-(Fe}_{1-x}\text{O}_x)_2\text{O}_3$  thin films, perpendicular mag. anisotropy 4-84833
- $\text{Fe}_2\text{S}_3$  pyrrhotite type nonstoichiometric cpds., with different vacancy concs., magnetisation 4-61523
- Gd-Fe amorphous films, vacuum deposited, Kerr hysteresis meas. 4-66014
- $\text{Gd}_2\text{Ni}_2\text{Al}_{15}$ , band struct. and ferrimag. moments, APW calc. 4-80487
- $\text{LaNi}_{1-x}\text{Co}_x\text{O}_3$ , ferrimagnetic interactions, mag. susceptibility meas. 4-88662
- $\text{LaNi}_{1-x}\text{Cr}_x\text{O}_3$ , ferrimagnetic interactions, mag. susceptibility meas. 4-88662
- $\text{LaNi}_{1-x}\text{Mn}_x\text{O}_3$ , valence states and mag. props. 4-84772
- $\text{LiFe}_2\text{O}_8$ , magnetic vitroceraics, prep. and props. 4-93256
- $\text{LiMnFeF}_6$ ,  $\alpha$ - and  $\beta$ -phases, magnetisation, Mossbauer and neutron studies 4-88752
- $\text{LiMnMF}_6$  ( $M=\text{Fe, V, Ti, Cr, Ga}$ ), cationic distribution and mag. behaviour 4-71026
- $\text{MgFe}_2\text{O}_4$ , polycryst., elastic behaviour and internal friction in mag. field 4-71143
- $\text{MnFe}_2\text{O}_4$  ultra-fine spinel ferrites, prep. and characterisation 4-71130
- $\text{Mn}_x\text{Fe}_{3-2x}\text{O}_4$  ceramic ferrite, mag. props. (*Spanish*) 4-88649
- $\text{Mn}_{0.75}\text{Mg}_{0.25}(\text{Cr}_{1-y}\text{V}_y)_2\text{O}_4$  mixed spinel systems, spin-glass-like behaviour 4-109024
- $\text{Mn}_{1-x}\text{Mg}_x\text{Fe}_2\text{O}_4$ , elastic behaviour, comp. and mag. field depend.,  $\Delta E$  effect 4-98929
- $\text{Mn}_2\text{Mo}_3\text{O}_{10}$ , crystal growth, mag. and elec. props. 4-71537
- $\text{Mn}_2\text{Zn}_{1-x}\text{Cr}_x\text{O}_4$  mixed spinel systems, spin-glass-like behaviour 4-109024
- $\text{Mn}_{1-x}\text{Zn}_x\text{Fe}_2\text{O}_4$ , hot pressed, prior heat treatment effect on props. 4-89016
- $\text{NdCu}_{3-x}\text{Mn}_{x+1}$ , synthesis, composition and mag. props. 4-108997
- $\text{Ni,Fe}_{1-x}\text{O}_4$  ceramic ferrite, mag. props. (*Spanish*) 4-88649
- $\text{Ni}_2\text{Zn}_{1-x}\text{Fe}_x\text{O}_4$ , Co-substituted, elastic moduli at low temps., mag. anisotropy-energy interpret. 4-61578
- $\text{Pr}_2\text{V}_{2-x}\text{Ge}_x\text{Fe}_{10-x}\text{O}_{12}$  garnet single cryst. magnetisation and Faraday rotation 4-61664
- $\text{TbCo}_2$ , mag. moments, susceptibility meas. 4-61525
- TbFe thin films, amorphous, ageing phenomena, hysteresis cycles 4-71134
- $\text{UAs}_{1-x}\text{Se}_x$ , mag. phase diagram, mag. susceptibility meas. 4-88651
- $(\text{Y}_{1+2x}\text{Zr}_{2-2x})(\text{Fe}_{2x}\text{Zr}_{2-2x})\text{Fe}_3\text{O}_{12}$  mag. atom critical conc., neutron polarisation study 4-61514
- $\text{Y}_2\text{Fe}_2\text{O}_{12}$  garnet film, mode conversion of guided mag. waves 4-92942
- $\text{Y}_2\text{Fe}_2\text{O}_{12}$  single cryst., top seeded soln. growth method and mag. props. 4-93207
- YIG LPE films, birefringence control, magneto-optical waveguide appls. 4-61652
- YIG, magnetic insulator, losses 4-71121
- YIG single cryst. and epitaxial film, sublattice anisotropy and mag. linear dichroism 4-61667

**ferrimagnetic resonance**

- ferrite spheres resonance linewidth meas., using homodyne meas. system 4-58867
- ferrites, polycrystalline, ferrimagnetic resonance losses, computer controlled meas. 4-61595

**ferrimagnetism**

- see also *ferrimagnetic properties of substances*  
 dust samples, remanent magnetism and coercive force meas. using micro-computer controlled magnetometer 4-86447  
 erasable magneto-optical laser disc mass memory 4-91405  
 lung, ferrimagnetic particles, magnetising process 4-66969  
 lung, ferrimagnetic particles, relax. process 4-66970  
 solid state chemistry, correlation between struct. and phys. props. 4-70063  
 two-sublattice systems with quartic repulsion, reentrant behaviour of magnetisation 4-88701

**ferrite applications**

- see also *ferrite devices*  
 No entries

**ferrite devices**

- see also *ferrite applications*  
 No entries

**ferrites**

- see also *ferrimagnetic properties of substances; ferrimagnetism; ferrite applications; ferrite devices*  
 alkaline earth-ferrite glasses, glass forming region and  $\text{Fe}^{3+}$  coordination (Japanese) 4-113348  
 conference, Eger, Hungary (Sept. 1983) 4-78029  
 data collection on oxides and related cpds., mag. and other props. 4-67886  
 domain wall mobility 4-76169  
 film/semiconductor layer structs., surface magnetostatic wave propag. 4-61529  
 FMR linewidth measurement by differential curve method (Chinese) 4-73466  
 garnet epitaxial films, dichroic axis and magnetisation rotation 4-93047  
 garnet films, transition layer study 4-75816  
 garnet-ferrite films, magnetic vortices 4-76197  
 giant magnetostriction, influence of magnetoelastic interaction, review in rare earth and actinide magnetics 4-71151  
 hexaferrite films, prep. and device appls. 4-61883  
 magnetic media, surface parameters for tribology 4-82780  
 magnetic recording heads, toughness evaluation 4-104951  
 magnets, three-dimensional solitons and their stability 4-71010  
 Mg-Mn ferrite, elastic behaviour at room temp. 4-65327  
 muon hyperfine interactions, spin rot. studies 4-65917  
 permeability meas., using Faraday rotation 4-58873  
 polycrystalline, ferrimagnetic resonance losses, computer controlled meas. 4-61595  
 polycrystalline, impulsive reverse-magnetisation of weak-field switching 4-84816  
 polycrystalline, model of initial mag. permeability (Russian) 4-98921  
 powder, form, mechanism in fused salts, SEM studies 4-70399  
 Q-factor meas. and tuning of oscillatory systems 4-101871  
 rare earth orthoferrites, moon site determ. 4-71227  
 rare earth orthoferrites, Rayleigh wave emission and domain wall drag 4-88695  
 rare earth perovskites, flux grown single crystals, microhardness, indentation tests 4-99493  
 semiconductor-ferrite interface, oblique magnetostatic surface waves 4-80752  
 semiconductor-vacuum-ferrite struct., sound interaction with surface helicon-spin oscills. (Russian) 4-88713  
 semiconductor/ferrite thin film struct., electron broadening of ferromag. resonance lines 4-76260  
 single-crystal spheres resonance linewidth meas., using homodyne meas. system 4-58867  
 spin wave parametric excitation by noise modulation of a mag. field 4-92904  
 spin waves, parametrically excited, relax. processes at low temps. (Russian) 4-98867  
 spinel ferrites Curie point, O param. effect 4-84798  
 spinels, Fe-M-O ( $\text{M}=\text{Al}, \text{Cr}, \text{Zn}, \text{Co}, \text{Mn}$ ), vacancy substituted, order-disorder, IR absorpt. spectra (French) 4-76447  
 steel, stainless, duplex austenite-ferrite, fatigue crack propag. 4-81287  
 transition metal ferrites,  $\text{MFe}_2\text{O}_4$ ,  $\text{M}=\text{Co-Cu}$ , stability in reducing atm., TGA, X-ray diff. studies 4-76999  
 waveguide excitation of magnetostatic oscills. and waves 4-109007  
 $\beta$ -Ag ferrite, 2-D metallic aggregates, X-ray diffuse scatt. studies 4-88299  
 $\beta''\text{-Al}_2\text{O}_3\text{-Na}_2\text{O:Fe}$ , decomposition processes, microscopic mechanisms 4-109415  
 $\text{BaFe}_{12}\text{-M}_2\text{O}_{19}$  ( $\text{M}=\text{Al}, \text{Ga}, \text{Sc}$ ) ferrites, anisotropy fields and FMR linewidths 4-71058  
 $\text{BaFe}_{12}\text{-Mn}_2\text{O}_{19}$ , bipyramidal site occupancy, Mossbauer spectra 4-73420  
 $\text{BaFe}_{12}\text{O}_{19}$  ferrite, M phase, superstruct. obs. 4-84275  
 $\text{BaFe}_{12}\text{O}_{19}$  ferrite, prep., phase transition study (Chinese) 4-93254  
 $\text{BaFe}_{12}\text{O}_{19}$  glassy ferrites, effects of mag. quenching 4-61898  
 $\text{BaFe}_{12}\text{O}_{19}$ , magnetic viroceramics, prep. and props. 4-93256  
 $\text{BaFe}_{12}\text{O}_{19}$  permanent magnets, sintering temp. effect on mag. props. and density (Afrikaans) 4-76170  
 $\text{BaSnFe}_2\text{O}_{13}$ , cryst. struct., neutron diff., Mossbauer spectra, magnetisation meas. 4-75406  
 $\text{BaTi}_2\text{Fe}_2\text{O}_{11}$ , cryst. struct., neutron diff., Mossbauer spectra, magnetisation meas. 4-75406  
 $\text{Ba}_2(\text{Zn}_{1-x}\text{Co}_x)_2\text{Fe}_2\text{O}_{22}$  ferrites, first-order magnetisation processes 4-76188  
 $\text{Ca}_2\text{LaFe}_2\text{O}_{8+x}$ , cryst. struct. determ. 4-80014  
 $\text{Cd}_{1-x}\text{Cu}_x\text{Fe}_2\text{O}_4$ , hyperfine field interactions, Mossbauer spectra 4-65885  
 $\text{Cd}_{1-x}\text{Cu}_x\text{Fe}_2\text{O}_4$  spinel, low temp. Mossbauer obs. of mag. interactions 4-98983  
 $\text{CdFe}_2\text{O}_4$ , stability in reducing atm., TGA, X-ray diff. studies 4-76999  
 $\text{Cd}_{1-x}\text{Fe}_x\text{O}_4$  system, nonlinear spin struct., magnetisation and Mossbauer obs., Yafet-Kittel angles 4-71022  
 $\text{Co-Ni-Zn}$  ferrites, microstruct., mag. props., BaO additions effect 4-88302  
 $\text{CoFe}_2\text{O}_4$ , small particle ferrites, mag. hyperfine fields 4-61568  
 $\text{CoFe}_2\text{O}_4$  ultra-fine spinel ferrites, prep. and characterisation 4-71130  
 $\text{Co}_{16}\text{Fe}_{24}\text{O}_{48}$  ferrite, mag. anisotropy, torque meas. 4-114105  
 $\text{Co}_2\text{Fe}_{1-x}\text{O}_4$ , ceramic ferrite, mag. props. (Spanish) 4-88649  
 $\text{Co}_2(\text{NiZn})_{1-x}\text{Fe}_x\text{O}_4$  ferrites, magnetostrictive props. 4-84839  
 $\text{CuFe}_2\text{Al}_2\text{O}_4$ , orthorhombic distortions due to doping 4-70103  
 $\text{CuFe}_2\text{O}_4$ , conduction mechanism, annealing effect, resist. and thermopower meas. 4-104206

**ferrites continued**

- $\text{Cu}_{1-x}\text{Ge}_x\text{Fe}_2\text{O}_4$ , orthorhombic distortions due to doping 4-70103  
 $\text{DySc}_2\text{Fe}_{1-x}\text{O}_3$  orthoferrites, mag. props., Sc substitution effects 4-104463  
 $\text{Fe-Mo-W-C}$ , phase equilib. and diagrams 4-85140  
 $\text{Fe}_2\text{-Ga}_2\text{BO}_6$  boroferrite, hyperfine interactions, Mossbauer studies 4-109099  
 $\gamma\text{-Fe}_2\text{O}_3$  magnetic powder, perpendicular orientation, Mossbauer study 4-65838  
 $\text{Fe}_2\text{O}_3$ , stability in reducing atm., TGA, X-ray diff. studies 4-76999  
 $\gamma\text{-Fe}_2\text{O}_3\text{-Co}$  magnetic powder, perpendicular orientation, Mossbauer study 4-65838  
 $\gamma\text{-Fe}_2\text{O}_3\text{-Fe}_2\text{O}_3\text{-Co}$  thin films, coercivity study 4-114145  
 $\text{Fe}_2\text{O}_3\text{-NiO}$  mixed oxides, phase anal., IR, mag. and X-ray diff. studies 4-98243  
 $\text{Fe}_2\text{O}_3$ , biogenic, mag. props. (Japanese) 4-72277  
 $\text{Fe}_2\text{O}_4$ , ceramic ferrite, mag. props. (Spanish) 4-88649  
 $\text{Fe}_2\text{O}_4$  particles of mag. fluid, superparamagnetic behaviour, Mossbauer spectra 4-104466  
 $\text{Fe}_2\text{O}_3\text{-Ni}$ , self-diffusion, SIMS study 4-98342  
 $\text{Fe}_2\text{O}_3\text{-MgFe}_2\text{O}_4$  system, cation distrib., thermoelec. coeff., 600-1300°C 4-61402  
 $\text{La}_{1-x}\text{Ca}_x\text{FeO}_{3-y}$  ferrites, mixed valence and electrochem. props. 4-70752  
 $\text{La}_{1-x}\text{Ca}_x\text{FeO}_{3-y}$ , high temp. order-disorder transition 4-113618  
 $\text{La}_{1-x}\text{Sr}_x\text{FeO}_{3-y}$  ferrites, mixed valence and electrochem. props. 4-70752  
 $\text{Li}_{10}\text{Fe}_5\text{Al}_5\text{O}_{40}$ , atomically ordered spinel, mag. struct., neutron diff. study 4-61513  
 $\text{LiFe}_2\text{O}_8$ , mag. domain walls interaction with microstruct. features 4-71122  
 $\text{LiFe}_2\text{O}_8$ , magnetic vitroceraics, prep. and props. 4-93256  
 $\text{Li}_{0.5-x}\text{Zn}_{1-x}\text{Fe}_{2.5-x/2}\text{O}_4$  ferrites, Curie temp. and mag. moments 4-109013  
 $\text{MgAl}_2\text{Fe}_{2-x}\text{O}_4$ , Mossbauer study of spin struct. 4-84875  
 $\text{Mg}_{1-x}\text{Cd}_x\text{Fe}_2\text{O}_4$  ferrite, mag. props. Mossbauer studies 4-84878  
 $\text{MgFe}_2\text{O}_4$ , polycryst., elastic behaviour and internal friction in mag. field 4-71143  
 $(\text{Mn}, \text{Zn})\text{Fe}_2\text{O}_4$  ferrite, EDX analysis, digital mapping appls. to channelling effect 4-81508  
 $(\text{Mn}, \text{Zn})\text{Fe}_2\text{O}_4$ , mag. domain walls interaction with microstruct. features 4-71122  
 $\text{Mn-Zn-Ti}$  ferrites, effects of post-sinter cooling 4-85165  
 $\text{MnFe}_2\text{O}_4$ , small particle ferrites, mag. hyperfine fields 4-61568  
 $\text{MnFe}_2\text{O}_4$  ultra-fine spinel ferrites, prep. and characterisation 4-71130  
 $\text{Mn}_2\text{Fe}_2\text{-O}_4$ , ceramic ferrite, mag. props. (Spanish) 4-88649  
 $\text{Mn}_{1-x}\text{Mg}_x\text{Fe}_2\text{O}_4$ , elastic behaviour, comp. and mag. field depend.,  $\Delta E$  effect 4-98929  
 $\text{MnZn}$  ferrite, (100) surface, mag. surface props., influence of sputter etching 4-88813  
 $\text{MnZn}$  ferrite, monocryst., uniaxial tensile stress effect on permeability 4-61579  
 $\text{MnZn}$  ferrite, monocrystalline, anal. of complex permeability 4-88703  
 $\text{MnZn}$  ferrite coprecipitation 4-61091  
 $\text{MnZn}$  ferrites, hot pressed, brittle and strength props by microindentation method 4-62044  
 $\text{MnZn}$  ferrites, hot-pressed, powder particle size distrib. and heterogeneity 4-61907  
 $\text{Mn}_{1-x}\text{Zn}_x\text{Fe}_2\text{O}_4$  ferrite, microstruct. and permeability during sintering 4-109432  
 $\text{Mn}_{1-x}\text{Zn}_x\text{Fe}_2\text{O}_4$ , hot pressed, prior heat treatment effect on props. 4-89016  
 $\text{Mn}_{1-x}\text{Zn}_x\text{Fe}_2\text{O}_4$ , sintering of powders produced by different methods, mechanism and assoc. processes 4-89015  
 $\text{Mn}_2\text{Zn}_2\text{Fe}_2\text{O}_4$  ferrites, mag. and dielec. relax 4-84904  
 $\text{Na}_2\text{O-SiO}_2$  glass, ferrite precip., ESR and Mossbauer obs. 4-99386  
 $\text{Ni}$  ferrites, mechanical activation effects on mag. props. 4-98882  
 $\text{Ni}_{0.98}\text{Co}_{0.02}\text{Mn}_{0.02}\text{Fe}_2\text{O}_4$ , magnetostrictive, magnetomechanical props., hysteresis loop, elastic moduli, internal friction, influence of mag. history 4-76212  
 $\text{Ni}_{0.93}\text{Fe}_{2.07}\text{O}_4$  ferrite, dissol. in EDTA soln. 4-88295  
 $\text{Ni}_1\text{Fe}_{3-x}\text{O}_4$ , ceramic ferrite, mag. props. (Spanish) 4-88649  
 $\text{Ni}_{0.98-x}\text{Mn}_{0.02}\text{Co}_x\text{Cu}_{1-x}\text{Fe}_2\text{O}_4$ , stress sensitivity coeff. 4-76213  
 $\text{Ni}_{0.93}\text{Mn}_{0.07}\text{Co}_{0.02}\text{Fe}_2\text{O}_4$  ferrites,  $\Delta E$  effect 4-76229  
 $\text{NiZn}$  ferrite, magnetic permeability, initial, comparison of theory with experiment (Russian) 4-98922  
 $\text{NiZn}$  ferrites, prod. by shock hot working, props. 4-61905  
 $\text{Ni}_{1-x}\text{Zn}_x\text{Fe}_2\text{O}_4$  ferrite, mag. props.  $\text{Fe}^{2+}$  ion effects 4-109035  
 $\text{Ni}_{0.6}\text{Zn}_{0.4}\text{Fe}_{1.5}\text{Mn}_{0.5}\text{O}_4$ , near-microwave material characterisation using non-dispersive Fourier transform spectroscopy 4-93033  
 $\text{Ni}_{1-x}\text{Zn}_x\text{Fe}_2\text{O}_4$ , hyperfine fields NMR spin echo studies 4-61351  
 $\text{Ni}_2\text{Zn}_{1-x}\text{Fe}_2\text{O}_4$ , Co-substituted, elastic moduli at low temps., mag. anisotropy energy interpret. 4-61578  
 $\text{Sr}_2\text{Nd}_{1-x}\text{Fe}_{3-x}\text{O}_{12}$ , cryst. struct. determ. 4-80013  
 $\text{SrZn}_{1-x}\text{Co}_x\text{Fe}_{10-2x}$  hexaferrite, mag. and crystallographic studies 4-88697  
 $\text{TbFe}_{1-x}\text{Al}_x\text{O}_3$ , magnetic props., influence of mag. vacancies 4-104414  
 $\text{TmMO}_3$  ( $\text{M}=\text{Al}, \text{Fe}, \text{Cr}, \text{V}$ ), mag. and cryst. field props., Mossbauer studies 4-98888  
 $\text{Y}$  orthoferrites, domain-wall motion obs. 4-80778  
 $(\text{YEuTbCa})_2(\text{FeGe})_2\text{O}_{12}$  ferrite-garnet epitaxial films, fine struct. of mag. spectra 4-76206  
 $\text{YFe}_2\text{O}_4$ , two-dimensional spin correl., neutron and X-ray diff. 4-109022  
 $\text{Y}_2\text{Fe}_2\text{O}_{12}\text{-Pb}$ , epitaxial films, Pb effect on optical props. 4-99210  
 $\text{Zn}$  ferrites, mechanical activation effects on mag. props. 4-98882  
 $\text{ZnFe}_2\text{O}_4$ , stability in reducing atm., TGA, X-ray diff. studies 4-76999  
 $\text{Zn}_{0.36}\text{Mn}_{0.59}\text{Fe}_{2.07}\text{O}_4$ , non-stoichiometric ferrite spinel, mag. props. 4-108996  
 $\text{Zn}_{0.25}\text{Ni}_{0.75-x}\text{Ti}_x\text{Fe}_{2-2x}\text{O}_4$ , hyperfine field meas., Mossbauer effect study 4-71224

**ferritic steel see steel****ferroacoustic resonance**

- No entries

**ferroelastic transitions see ferroelasticity; solid state phase transformations ferroelasticity**

- see also *shape memory effects*

- betaine arsenate single cryst., ferroelec.-ferroelastic transition and sp. ht. 4-65415  
 betaine borate, ferroelastic phase transition 4-61072  
 binary cryst., displacement domains caused by defects (Chinese) 4-70254  
 bulk acoustic wave interaction with ferroelastic domain regular struct. 4-108551

**ferroelasticity continued**

- butyloxy phenylnonyl oxybenzoate, ferroelastic smectic A-smectic C transition 4-80229  
 elpasolite struct. single crystals, ferroelastic phase transitions 4-65387  
 ferroic compounds, transition temp. determ. by microhardness meas. 4-71302  
 9-hydroxyphenalene, phase transitions and ferroelasticity 4-113614  
 Jahn-Teller crystals, antiferrodistortive ordering in external mag. field 4-108608  
 polyvinylidene fluoride, ferroelec. and 33 ferroelastic hysteresis 4-99066  
 rare earth niobates,  $\text{RNbO}_4$ , ferroelasticities with the fergusonite type structure 4-75659  
 rare earth niobates and tantalates, schedule structures, ferroelasticity 4-70377  
 structural aspects of phase transitions in  $\text{MM}'\text{Bx}_4$  type crystals 4-65241  
 p-terphenyl, ferroelastic phase transition, elastic constant, Brillouin spectra 4-98180  
 p-terphenyl, improper ferroelastic transition, acoustic anomalies 4-65389  
 viscous phenomena in ferroelectrics and ferroelasticities 4-76367  
 $\text{Ba}_2\text{NaNb}_2\text{O}_7$ , ferroelastic-incommensurate transition, Brillouin scatt. study 4-70362  
 $\text{BiVO}_4$ , ferroelastic, spontaneous birefringence obs. 4-93045  
 $\text{BiVO}_4$ , refractive index temp. depend. 4-71338  
 $\text{Cs}_2\text{BiCl}_6$ , phase transitions, first phase props. 4-75657  
 $\text{CsCa}_2\text{Nb}_2\text{O}_{10}$ , layered ferroelastic perovskite, cryst. struct., X-ray diff. (French) 4-75419  
 $\text{Gd}_2(\text{MoO}_4)_3$ , acoustic wave reflection from ferroelastic domain walls 4-98209  
 $\text{Gd}_2(\text{MoO}_4)_3$ , ferroelectric-ferroelastic, acoustic emission and domain wall dynamics 4-84925  
 $\text{H}(\text{UO}_2)(\text{AsO}_4)_2\text{H}_2\text{O}$ , phase transition: temps. and ferroelec. domain struct. 4-76400  
 $\text{K}_2\text{Cd}_2(\text{SO}_4)_3$  ferroelastic, optical props. 4-66000  
 $\text{KFe}(\text{MoO}_4)_2$ , ferroelastic domain switching 4-92343  
 $\text{KH}_2(\text{SeO}_3)_2$ , ferroelastic domain struct. dynamics, internal friction meas. 4-80156  
 $\text{KH}_2(\text{SeO}_3)_2$ , ferroelastic, light deflection by domain walls 4-104550  
 $\text{KH}_2(\text{SeO}_3)_2$ , normal and deuterated ferroelastic, Raman scatt. studies 4-71393  
 $\text{KIn}(\text{MoO}_4)_2$ , ferroelastic domain switching 4-92343  
 $\text{KLiSO}_4$ , ferroelastic transition, microscopic model 4-75664  
 $\text{KSe}(\text{MoO}_4)_2$ , ferroelastic domain switching 4-92343  
 $\text{LaNbO}_4$ , ferroelastic, spontaneous birefringence obs. 4-93045  
 $\text{LiKSO}_4$  crystals, ferroelasticity and internal friction 4-75612  
 $(\text{ND}_4)_3\text{D}(\text{SO}_4)_2$ , successive phase transitions studied by  $\text{VO}^{2+}$  ion and  $\text{SeO}_3$  radical EPR 4-76388  
 $\text{NH}_4\text{BeF}_3$ , ferroelastic, successive phase transitions, sp. ht., thermal expansion meas. 4-108605  
 $\text{NH}_4\text{BeF}_3$ , ferroelastic, domain struct., polarising microscope obs. 4-108629  
 $(\text{NH}_4)_3\text{H}(\text{SO}_4)_2$ , successive phase transitions studied by  $\text{VO}^{2+}$  ion and  $\text{SeO}_3$  radical EPR 4-76388  
 $(\text{NH}_4)_3\text{H}(\text{SeO}_4)_2$ , thermal and dielec. studies, 90 to 357K, isotope effects 4-70365  
 $\text{NaH}_2(\text{SeO}_3)_2$  biaxial ferroelec., ferroelastic and ferroelec. domains 4-93027  
 $\text{NaH}_2(\text{SeO}_3)_2\text{Cr}^{3+}$ , EPR spectra, temp. and external elec. field effects 4-88715  
 $\text{Na}_5\text{-K}_4\text{W}_3\text{O}_{15}$ , Bridgman-Stockbarger growth, ferroelec. and ferroelastic props., permittivity, birefr. meas. 4-65969  
 $\text{Na}_5\text{-Li}_4\text{W}_3\text{O}_{15}$ , Bridgman-Stockbarger growth, ferroelec. and ferroelastic props., permittivity, birefr. meas. 4-65969  
 $\text{NaNH}_4$  tartrate crystals, refractive index and birefringence 4-76406  
 $\text{Na}_2\text{W}_2\text{O}_7$ , ferroelastic transition and detwinning 4-80226  
 $\text{NdP}_2\text{O}_7$ , acoustic wave reflection from ferroelastic domain walls 4-98209  
 $\text{NdP}_2\text{O}_7$ , domain walls, SAM and SPAM study 4-99064  
 $\text{Ni}_2\text{B}_2\text{O}_7$ , magnetoelastic effect, mag. and elec. meas. 4-71144  
 $\alpha\text{-PbO}$ , low temp. phase obs. by X-ray diff., ferroelastic transitions (French) 4-80211  
 $\text{Pb}_2\text{V}_2\text{O}_8$ , cryst. struct. of ferroelectric  $\alpha$  phase (French) 4-84259  
 $\text{Pb}_2\text{V}_2\text{O}_8$  and  $\text{Pb}_2\text{V}_{2(1-x)}\text{P}_{2x}\text{O}_{13}$ , ferroelastic props. and crystal struct. 4-70264  
 $\text{Pb}_2\text{V}_{2(1-x)}\text{P}_{2x}\text{O}_8$ , ferroelectric transition and acousto-optic props. 4-75660  
 $\text{RbCdF}_3$ , competition between ferroelectricity and ferroelasticity 4-76355  
 $\text{RbHSeO}_4$ , ferroelec. ferroelastic, light deflection 4-80883  
 $\text{RbIn}(\text{MoO}_4)_2\text{Cr}$ , ferroelastic, structural phase transitions, EPR study 4-70372  
 $\text{RbMnCl}_3$ , crystal and mag. structure heterogeneities, ferroelastic transition obs. 4-84276  
 $\text{RbMnCl}_3$  crystals, struct. phase transition, exptl. and group theoretical study 4-75658  
 $\text{Tb}_2(\text{MoO}_4)_3$ , ferroelectric-ferroelastic, acoustic emission and domain wall dynamics 4-84925  
 $\text{TiH}_2\text{PO}_4$ , ferroelastic phase transition, permittivity meas. 4-65393  
 $\text{TiH}_2(\text{SeO}_3)_2$ , dielec. props., phase transitions, cryst. struct. 4-65965  
 W bronze tetragonal struct. non-stoichiometric phases, dielec., ferroelastic and nonlinear optical props. 4-65972

**ferroelectric Curie temperature**

- betaine arsenate and phosphate, deuterated, ferroelectric props. 4-80876  
 DOBAMBC, liquid cryst., cell thickness effect on elec. props., optical switching and memory 4-98998  
 HOBACPC, liquid cryst., cell thickness effect on elec. props., optical switching and memory 4-98998  
 lattice dynamics and phase transitions 4-80169  
 methylammonium mercury trichloride, ferroelec. transition, thermal, dielec., optical meas. (French) 4-76392  
 polarised defects, effects near Curie point 4-70134  
 triglycine sulphate:  $\alpha$ -alanine ferroelec. cryst., piezooptical props. 4-76431  
 tris-sarcosine calcium chloride, ferroelec. phase transitions, IR and Raman studies 4-71296  
 uniaxial ferroelectrics, spin-lattice relax. at phase transitions, effect of relaxing defects, appl. to TGS 4-99059  
 $\text{BaABNb}_2\text{O}_{15}$  ( $\text{A}=\text{Ca}$  or  $\text{Sr}$ ;  $\text{B}=\text{K}$  or  $\text{Ti}$ ) ferroelectric materials, synthesis and characteristics 4-104547  
 $\text{Ba}_{0.5}\text{Sr}_{0.48}\text{Nb}_2\text{O}_{15}$ , pure and  $\text{La}(\text{Ce})$  doped, thermally stimulated electron emission, dielec. charact., impurity effects (Russian) 4-114356  
 $\text{BaTiO}_3$ , powder processing, grain size, ferroelec. props. 4-93253  
 $\text{BaTiO}_3\text{:Yb}$ , dielec. and X-ray diff. study 4-84896

**ferroelectric Curie temperature continued**

- $\text{BaTiO}_3$ -based materials, dielec. props. and chem. inhomogeneity, effect of sintering 4-85128  
 $\text{Bi}_2\text{Pb}_{1/3}\text{Bi}_{2/3}\text{Ti}_{1/3}\text{W}_{2/3}\text{O}_{15}$  perovskite ferroelec., dielec. props. 4-88783  
 $\text{Cd}_2\text{Nb}_2\text{O}_7$ , photoferroelectric phenomena 4-88785  
 $\text{Cs}_2\text{EuNaNb}_2\text{O}_{15}$ , struct. and ferroelec. props. 4-109141  
 $\text{CH}_3(\text{SeO}_3)_2$ , antiferroelectric, elastic compliance consts., anomalies at transition point 4-108500  
 $\text{Cu}_2\text{B}_2\text{O}_7\text{-Cl}$ , ferroelec. and paraelec. phases, optical rot., birefr., optical susceptibilities 4-109151  
 $\text{KD}_2\text{PO}_4$ -type ferroelectrics, static and dynamic props., applicability of mean-field approach 4-93022  
 $\text{KH}_2\text{PO}_4$  type crystals, ferroelec. phase transition, stress effects 4-76365  
 $\text{KH}_2\text{PO}_4\text{:Se}$ , ESR relax. time meas. 4-92957  
 $\text{KNbO}_3$  ferroelec. semicond., positive temperature resist. coeff. 4-113958  
 $\text{Li}_2\text{O-M}_2\text{O-M}'_2\text{O}_4$ ,  $\text{M}=\text{Nb}$ ,  $\text{Ta}$ ,  $\text{M}'=\text{Ti}$ ,  $\text{Zr}$ , non-stoichiometric phases, cryst. chem. and ferroelec. props. 4-65968  
 $\text{MgO}$ , dipolar defect ordering due to dissolved  $\text{CO}_2$  4-71287  
 $\text{Ni}_4\text{AlF}_6$ , clusters and critical slowing down near  $T_c$ , EPR study 4-65982  
 $\text{NH}_4\text{HSeO}_4$ , dielectric, piezoelectric and elastic props. 4-80878  
 $\text{Na}_{1/3}\text{Bi}_{2/3}\text{TiO}_3$  ceramics, pyroelectric props., perspective appl. in pyroelectric radiation detectors 4-88776  
 $\text{Na}_{5-x}\text{K}_x\text{W}_3\text{O}_{15}$ , Bridgman-Stockbarger growth, ferroelec. and ferroelastic props., permittivity, birefr. meas. 4-65969  
 $\text{Na}_{5-x}\text{Li}_x\text{W}_3\text{O}_{15}$ , Bridgman-Stockbarger growth, ferroelec. and ferroelastic props., permittivity, birefr. meas. 4-65969  
 $\text{PLZT}$ , chemically prepared, charact. and props. 4-76712  
 $\text{PLZT}$  piezoelectric ceramic, fabricated by atmospheric sintering, electrical charact. and optical transmittance (Korean) 4-114211  
 $\text{PZT}$  material, high density, prep. by coprecipitation technique 4-76711  
 $(\text{Pb}_{0.75}\text{Ca}_{0.25})(\text{Mg}_{1/3}\text{Nb}_{2/3})_{0.0625}\text{Ti}_{0.9375}\text{O}_3$ :Mn ceramics, US, elastic and dielec. props. 4-104543  
 $\text{Pb}(\text{Fe}_{1/2}\text{Nb}_{1/2}\text{O}_3)\text{-Pb}(\text{Ni}_{1/3}\text{Nb}_{2/3}\text{O}_3)$  solid soln. system, dielec. props. 4-104517  
 $\text{Pb}_2\text{GeO}_{11}$ , soft modes rel. to crit. fluctuations, neutron and Raman scatt. meas. 4-65370  
 $\text{Pb}_2\text{InNbO}_6$ , single crystal, perovskite and pyrochlore modifications, prep. and props. 4-76662  
 $\text{PbO-BaO-TiO}_2\text{-B}_2\text{O}_3$  glass ceramic system, crystal clamping, X-ray diff., dilatometry 4-109386  
 $\text{PbSn}_{1-x}\text{Te}$ , ferroelectric transition temp. and saturation effect (Russian) 4-71318  
 $\text{Pb}_{2-x}\text{Th}_x\text{KTaO}_{15}$ , crystallographic and dielec. props. (French) 4-79987  
 $\text{Pb}_{2-x}\text{Th}_x\text{Ta}_2\text{O}_{15}$ , crystallographic and dielec. props. (French) 4-79987  
 $\text{Rb}_{0.52}(\text{ND}_4)_{0.48}\text{D}_2\text{PO}_4$  cryst., proton glass dielec. behaviour 4-114218  
 $\text{SbSrBr}$ , ferroelec. phase transitions, elec. permittivity studies 4-65981  
 $\text{SbSI}$ , paraelectric and ferroelec. phases, L-edge XANES and EXAFS obs. 4-88904  
 $\text{Sn}_2\text{P}_2\text{S}_6$  ferroelec. semicond., Curie temp. photoinduced shift 4-93017  
 $\text{Sr}_2\text{P}_2\text{S}_6$ , low freq. lattice vibr. in IR spectra 4-71389  
 $\text{Sr}_2\text{KNb}_2\text{O}_7(\text{TiNb}_2\text{O}_7)$ , ferroelectric materials, synthesis and characteristics 4-104547  
 $(\text{Sr}_{0.50}\text{Pb}_{0.25}\text{Ca}_{0.25})\text{TiO}_3$ - $(\text{Bi}_2\text{O}_3\text{-}3\text{TiO}_2)_x$ , dielectric props., HV capacitor application 4-98997  
 $\text{SrTeO}_3$ , dielectric const. dispersion study (Russian) 4-88762  
 W bronze tetragonal struct. non-stoichiometric phases, dielec., ferroelastic and nonlinear optical props. 4-65972

**ferroelectric devices**

- conference, Malaga, Spain (Sept. 1983) 4-63384  
 DOBAMBC, liquid cryst., cell thickness effect on elec. props., optical switching and memory 4-98998  
 HOBACPC, liquid cryst., cell thickness effect on elec. props., optical switching and memory 4-98998

**ferroelectric domains see electric domains****ferroelectric materials**

- see also antiferroelectric materials; electric domain walls; ferroelectric semiconductors; ferroelectric thin films; ferroelectric transitions; lattice dynamics of ferroelectric crystals  
 acoustic-phonon dispersion at incommensurate phase transitions, Brillouin scatt. obs. 4-61724  
 alanine-TGS ferroelectric crystals, pyroelec. props. (Chinese) 4-114213  
 alkali metal phosphates,  $\text{A}'\text{B}'\text{PO}_4$ ,  $\text{A}=\text{Na}$ ,  $\text{K}$ ,  $\text{B}=\text{Ca}$ ,  $\text{Zn}$ ,  $\text{Sr}$ ,  $\text{Cd}$ ,  $\text{Ba}$ ,  $\text{Pb}$ , ferroelec., phys. props. 4-65992  
 ammonium Rochelle salt, deuterated, dielec. and pyroelec. props. 4-114220  
 betaine arsenate, dielec. props. near ferroelec. transition 4-71307  
 betaine arsenate and phosphate, deuterated, ferroelectric props. 4-80876  
 betaine arsenate single cryst., ferroelec.-ferroelastic transition and sp. ht. 4-65415  
 betaine calcium chloride dihydrate, phase transitions, crit. dielec. phenomena and hysteresis effects, probable ferroelec. phase 4-76304  
 ceramics, ferroelectric; switching and hysteresis effects 4-76401  
 ceramics, internal mechanical stresses 4-113530  
 chiral triphenyl esters, columnar mesophases, structure and ferroelectric-antiferroelectric transition 4-60815  
 cholesteric liq. cryst.- $\text{KNO}_3$  mixtures; ferroelec. behaviour 4-109134  
 conference, Kyoto, Japan (May 1983) 4-101564  
 crystals, optical rot., microscopic model 4-65959  
 di(tetramethylammonium) copper tetrabromide, phase transition sequence, phenomenological theory 4-99055  
 di(tetramethylammonium) $\text{MCl}_4$ , ( $\text{M}=\text{Co}$ ,  $\text{Zn}$ ,  $\text{Cu}$ ), incommensurate, phase transitions, free energy phenomenological parameters 4-76378  
 di-(tetramethylammonium- $d_2$ ) cobalt tetrachloride, commensurate-incommensurate transition 4-80023  
 dicalcium barium propionate, symm. change at I-II phase transition, X-ray diff. study 4-108607  
 dicalcium lead propionate, ferroelec. press. induced II-III transition, polarising microscope obs., permitt. meas. 4-80879  
 dicalcium lead propionate, ferroelec.-paraelec. transition, dopant conc. depend. 4-99048  
 dicalcium strontium propionate, ferroelec. press. induced II-III transition, polarising microscope obs., permitt. meas. 4-80879  
 dicalcium strontium propionate, ferroelectric phase transition, X-ray diff. study 4-65988  
 diglycine nitrate, low-temp. dielec. props., freq. depend. 4-76299  
 displacive ferroelectrics, soft mode mechanisms 4-65351  
 DOBA-1-MBC, ferroelec. liq. cryst. with large spontaneous polarisation 4-60813

## ferroelectric materials continued

- DOBAMBC, liquid cryst., cell thickness effect on elec. props., optical switching and memory 4-98998  
 DOBAMBC, smectic liq. cryst., phase diagram in external mag. field, laser light diff. meas. 4-65170  
 DOBAMBC, smectic liq. cryst. structural phase transition, energy-dispersive X-ray diff. 4-75674  
 domain struct. influence on elec. cond. 4-99067  
 electric aging, low freq. polarisation relaxation (*Russian*) 4-99010  
 ferroelectric smectic liquid crystals, struct. and design 4-11307  
 ferroic crystals, non-magnetic, tensorial classification 4-76344  
 ferromagnetoelectrics, spin waves, reson. excitation by external elec. field 4-98871  
 GASH single cryst., ferroelec. domain struct., SEM studies 4-71320  
 guanidinium aluminium sulfate hexahydrate, ferroelectric, cleavage surfaces, spiral patterns 4-108367  
 HOBACPC, liquid cryst., cell thickness effect on elec. props., optical switching and memory 4-98998  
 hysteresis curve tracer using a single-board microcomputer 4-95461  
 liquid crystals, microsecond electro-optic switching using transient light scatt. 4-93052  
 liquid crystals, permittivity 4-76307  
 methylammonium aluminum alum, dielectric props. meas. 4-76312  
 methylammonium mercury trichloride, ferroelec. transition, thermal, dielec., optical meas. (*French*) 4-76392  
 monoaxial ferroelectrics, with second order phase transition, nonlinear pyroelectric response 4-88777  
 organic halides,  $[(CH_3)_4N]_2MX_4$ , ferroelectricity and antiferroelectricity 4-65957  
 oxides, phys. props., phase transitions 4-65974  
 perovskites, phase transition influence on oscillation spectrum 4-76362  
 photoconductive, optical device applications 4-64744  
 photorefractive, nonlinear optical expts., optical device applications, review 4-64744  
 PLZT, ferroelec. films, reactive sputtering prep. and dielec. props. 4-104731  
 PLZT ceramics, polarisation switching chars. 4-99006  
 PLZT epitaxial thin films, ferroelec. and electrooptical props. 4-104530  
 polarisation fluctuations correlation function 4-88766  
 poly(vinylidene fluoride) film, struct. under high elec. fields 4-98029  
 polymers, props. and applications 4-65954  
 polyvinylidene fluoride, ferroelec. and 33 ferroelastic hysteresis 4-99066  
 polyvinylidene fluoride and copolymers, ferroelec. switching, computer simulation 4-99049  
 polyvinylidene fluoride film, piezoelectric and ferroelectric props. under shock wave action 4-109131  
 PZT, electrically excitable mechanical reson. 4-114225  
 rare earth molybdates, ferroelec., soft mode temp. depend., light scatt. anal. 4-71299  
 Rochelle salt, dielectric permittivity low-freq. dispersion, influence of pre-history 4-76298  
 Rochelle salt, ferroelectric phase transitions, piezoelectric coeffs., electrostrictive coeffs., temp. depend., resonance studies 4-114217  
 Rochelle salt, prototype-incommensurate ferroelectric phase transition 4-80880  
 Rochelle salt, Raman spectrum, mode assignments, permitt. meas. 4-93011  
 Rochelle salt, soft modes, piezoelec. props. and ferroelec. transitions 4-76360  
 sitosterol undecylate-KNO<sub>3</sub> mixtures, ferroelec. behaviour 4-109134  
 smectic A cells, ferroelectric, preparation for electrooptical microsecond switches appl. 4-75272  
 smectic C\* liq. crystals, helicoidal struct., field induced processes 4-65171  
 solid soln., superionic phase transition in disordered sublattice 4-84919  
 space charge limited currents, fundamental assumptions and results of theory (*Polish*) 4-65964  
 space-charge limited currents, fundamental assumptions and results of theory (*Polish*) 4-65690  
 surface discharges study 4-84119  
 susceptibility anomalies in the vicinity of a nonpolar commensurate phase 4-114219  
 tetramethylammonium tetrachlorozincate, deuterated, ferroelec., temp.-press. phase diagram 4-76377  
 tetramethylammonium tetrachlorozincate, temp.-press. phase diagram 4-80217  
 tetramethylammonium zinc(cobalt) bromide, ferroelectric, phase transitions, X-ray diff. study 4-114216  
 TGS, and deuterated, ferroelec. crystals, pyroelec. props. (*Chinese*) 4-114213  
 TGS, cryst., phys. props., influence of defects 4-76329  
 TGS, deuterated, pyroelectric coeff., Q-factor, determ. by absolute dynamic method 4-84914  
 TGS, doped cryst., dielec. permittivity nonlinearity, rel. to growth conditions 4-76297  
 TGS, doped single crystals, pyroelec. and dielec. props. meas. 4-76346  
 TGS, ferroelec., Brillouin spectra angular depend. studies 4-71393  
 TGS, ferroelec. switching current, effect of time between polarisation reversals 4-76368  
 TGS, ferroelec. switching current, method of expt. meas. 4-76369  
 TGS, ferroelec. transition, critical behaviour, defect influence 4-65983  
 TGS, L- $\alpha$  alanine doped, polarisation, influence of growth conditions 4-76314  
 TGS, lateral struct. of domains, obs. using laser probe technique with high pyroelectric signal 4-88786  
 TGS, pyroelec. figure of merit and thermodynamic props., elec. field depend. 4-76347  
 TGS, pyroelectric response relax., role of viscous phenomena 4-71284  
 TGS, single cryst., metal ion doped, pyroelec. response relax. 4-76344  
 TGS, universal behaviour of dynamic relax. 4-80863  
 TGS crystal, polarisation current, domain width distrib. 4-71262  
 TGS group ferroelectrics, mean field to critical behaviour crossover (*Japanese*) 4-93012  
 TGSe, cryst., dielec. and electromechanical props. under high hydrostatic press. 4-76296  
 TGSe, cryst., phys. props., influence of defects 4-76329  
 TGSe, ferroelec. transition, critical behaviour, defect influence 4-65983  
 TGSe, phase transition rel. to deuteration 4-76387  
 thiourea, Brillouin scatt. under hydrostatic press., elastic constants study 4-76479

## ferroelectric materials continued

- thiourea, incommensurate phase transitions; phase mode dynamics, neutron and Raman scatt. studies 4-65966  
 thiourea, lock-in transitions, successive, in incommensurate systems 4-76379  
 thiourea, modulated phase study 4-76372  
 THSe, dielec. props., elec. cond., thermodynamical 4-88779  
 triglycine fluoroberyllate, cryst., dielec. and electromechanical props. under high hydrostatic press. 4-76296  
 triglycine fluoroberyllate, cryst., phys. props., influence of defects 4-76329  
 triglycine sulphate-L- $\alpha$  alanine ferroelec. cryst., piezooptical props. 4-76431  
 triglycine sulphate/polymer composites, dielec. const. and pyroelec. props. 4-109132  
 tris sarcosine calcium chloride, ferroelec. transition and soft modes 4-93024  
 tris-sarcosine calcium chloride, ferroelec. phase transitions, IR and Raman studies 4-71296  
 tris-sarcosine calcium chloride (bromide), ferroelec. phase transition, IR and Raman studies 4-93023  
 tris-sarcosine calcium chloride-bromide, soft modes, IR, and Raman spectra studies 4-71290  
 trissarcosine calcium chloride, iodinated, dielec. props., temp. and press. depend. 4-76310  
 trissarcosine calcium chloride (bromide), polarisation reversal 4-88780  
 Ts-TS-19 ceramic, gamma irradi., influence on photovoltaic effects 4-84656  
 TS-TS piezoceramic, dielec. props., influence of 90° domain struct. 4-76396  
 TS-TSN-V ferroelec. ceramic; residual polarisation and piezo effect 4-76316  
 uniaxial ferroelectrics, spin-lattice relax. at phase transitions, effect of relaxing defects, appl. to TGS 4-99059  
 uniaxial ferroelectrics, US absorpt. and vel., order parameter crit. fluctuations anisotropy spectrum, appl. to CsH<sub>2</sub>PO<sub>4</sub> 4-98206  
 vinylidene fluoride-trifluoroethylene copolymer, ferroelec. hysteresis 4-99065  
 vinylidene fluoride-trifluoroethylene copolymer, ferroelec. switching 4-109137  
 vinylidene fluoride-trifluoroethylene copolymer, ferroelec. transition, bulk modulus anomaly, thermal expansion, press. depend. 4-84917  
 vinylidene fluoride-trifluoroethylene copolymer, permittivity near ferroelec. transition 4-99051  
 vinylidene fluoride-trifluoroethylene copolymers, ferroelec. transition and dielec. props. 4-99052  
 vinylidene fluoride-trifluoroethylene copolymers, ferroelec. transition, statistical theory anal. 4-99053  
 vinylidene fluoride-trifluoroethylene copolymers; ferroelec. transition, struct. studies 4-99054  
 vinylidene fluoride/trifluoroethylene copolymer, ferroelec. transitions 4-99050  
 vinylidene fluoride/trifluoroethylene copolymers, piezoelec. and pyroelec. props. 4-99031  
 Ag<sub>3</sub>AsS<sub>3</sub>, proustite, incommensurate phase in region of second-order phase transition, NQR, sp. ht. meas. 4-71314  
 Ag<sub>3</sub>AsS<sub>3</sub>, proustite, noncommensurate phase associated with mode interactions 4-93014  
 AgNbO<sub>3</sub>, ceramic, ferroelec. phase, dielec. props. 4-61631  
 (Ba,Sr)TiO<sub>3</sub> heteroepitaxial ferroelec. films, domain struct. 4-65993  
 (Ba,Sr)TiO<sub>3</sub> polycryst. and heteroepitaxial ferroelec. films, phase transition 4-65977  
 BaABNb<sub>2</sub>O<sub>15</sub> (A=Ca or Sr; B=K or Ti) ferroelectric materials, synthesis and characteristics 4-104547  
 BaBiO<sub>3</sub>-BaPbO<sub>3</sub>, dielec. and supercond. transitions, Mossbauer line isomer shift 4-65973  
 BaMnF<sub>3</sub>, magneto-electric, unsolved problems 4-76255  
 Ba<sub>2</sub>NaNb<sub>2</sub>O<sub>7</sub>, ferroelec. transition, critical narrowing of central peak, Raman studies 4-71291  
 Ba<sub>2</sub>NaNb<sub>2</sub>O<sub>7</sub>, incommensurate, Brillouin spectra meas. 4-76482  
 Ba<sub>2</sub>NaNb<sub>2</sub>O<sub>7</sub>, interaction of incommensurate modulation with mobile and fixed defects 4-75446  
 BaO-TiO<sub>2</sub>-SiO<sub>2</sub> glass-ceramics, ferroelec., depolarisation currents, dielec. and electrooptical props. 4-76317  
 BaPbO<sub>3</sub>-BaBiO<sub>3</sub> system, supercond. and ferroelec. phase transitions 4-76061  
 Ba<sub>2-x</sub>Sr<sub>x</sub>Di<sub>2-x</sub>Na<sub>2x</sub>Nb<sub>2</sub>O<sub>7</sub>, ferroelec. props., dielec. const., piezoelec. and electromechanical coupling coeffs. 4-65958  
 Ba<sub>0.5</sub>Sr<sub>0.5</sub>Nb<sub>2</sub>O<sub>7</sub>, ferroelec. cryst., electrooptical coefficients 4-76434  
 Ba<sub>0.5</sub>Sr<sub>0.5</sub>Nb<sub>2</sub>O<sub>7</sub>, pure and La(Ce) doped, thermally stimulated electron emission, dielec. characs., impurity effects (*Russian*) 4-114356  
 Ba<sub>0.5</sub>Sr<sub>0.5</sub>TiO<sub>3</sub>, soft mode behaviour, ferroelec. transition and IR reflectometry 4-80872  
 BaTiO<sub>3</sub>, band struct. and ferroelec. transition, two-photon spectra studies 4-93016  
 BaTiO<sub>3</sub> based solid solns., ferroelec. transition temp. and electron spectra 4-93013  
 BaTiO<sub>3</sub> centrosymmetric ceramics, elec. field induced acoustic anisotropy 4-60992  
 BaTiO<sub>3</sub> ceramics, analogy between mech. and dielec. strength distrib. 4-61942  
 BaTiO<sub>3</sub> cryst., ferroelec. domain struct., SEM and optical microscopy studies 4-71319  
 BaTiO<sub>3</sub> crystals,  $\gamma$ -irradiated, with equil. domain struct., polarisational state 4-76395  
 BaTiO<sub>3</sub>, cubic to tetragonal transition, covalency effects, band struct. calculations 4-70361  
 BaTiO<sub>3</sub>, displacive type ferroelastic, lattice model 4-76394  
 BaTiO<sub>3</sub>, displacive/order-disorder crossover, soft mode temp. depend., contrib. to low freq. permittivity 4-65369  
 BaTiO<sub>3</sub> doped single cryst., ferroelec. transition, substitutional defect influence 4-65984  
 BaTiO<sub>3</sub>, electron energy struct. of cond. band, X-ray photoemission yield spectra 4-61282  
 BaTiO<sub>3</sub>, ferroelec., permittivity, effect of grain size 4-76306  
 BaTiO<sub>3</sub> ferroelec., sp. ht. at low temps. 4-65416  
 BaTiO<sub>3</sub> ferroelec. cryst., photovoltaic current anal. 4-75994  
 BaTiO<sub>3</sub>, ferroelec. crystal, electrostatic pot. at surface 4-76350  
 BaTiO<sub>3</sub>, ferroelec. phase transitions, stress effects 4-71315  
 BaTiO<sub>3</sub>, ferroelec. phase transition microregion approach 4-76363  
 BaTiO<sub>3</sub>, gamma irradi., influence on photovoltaic effects 4-84656

## ferroelectric materials continued

- BaTiO<sub>3</sub>, lattice deformation induced cryst. field variations, Mossbauer and EPR studies 4-71159  
 BaTiO<sub>3</sub>, liquid phase sintering and composite ceramics with Pb<sub>5</sub>Ge<sub>3</sub>O<sub>11</sub> 4-104746  
 BaTiO<sub>3</sub>, oxide perovskites, dielec. meas., surface layer effects 4-65962  
 BaTiO<sub>3</sub>, oxygen-octahedral ferroelectrics, two-photon spectroscopy study 4-114300  
 BaTiO<sub>3</sub>, PTC ceramic, strength and fracture toughness 4-62051  
 BaTiO<sub>3</sub>, piezoceramic, dielec. props., influence of 90° domain struct. 4-76396  
 BaTiO<sub>3</sub>, poly. and single cryst. dielec. after-effects and domain walls 4-71267  
 BaTiO<sub>3</sub>, polycryst. and heteroepitaxial ferroelec. films, phase transition 4-65977  
 BaTiO<sub>3</sub>, powder processing, grain size, ferroelec. props. 4-93253  
 BaTiO<sub>3</sub>, reverse switching effect 4-76393  
 BaTiO<sub>3</sub>, reversed c-domain patterns and elastic wave velocity surfaces 4-84924  
 BaTiO<sub>3</sub>, soliton physics and ferroelectric transitions 4-80875  
 BaTiO<sub>3</sub>, substituted, ferroelec. phase transitions and phase diagrams 4-65978  
 BaTiO<sub>3</sub>:Fe, soft mode behaviour, ferroelec. transition and IR reflectometry 4-80872  
 BaTiO<sub>3</sub>:Fe(Nb), dielectric relax. meas. 4-80864  
 Bi layer-structured ferroelec. ceramics, pyroelec. props. 4-104540  
 BiFeO<sub>3</sub> single cryst., ferroelec. domains, birefringence, and light absorption 4-71324  
 Bi<sub>2</sub>MoO<sub>6</sub>, kochchilinite, cryst. struct., neutron powder diff. profile refinement 4-88139  
 Bi<sub>2</sub>Pb<sub>1/3</sub>Bi<sub>2/3</sub>Ti<sub>4/3</sub>W<sub>2/3</sub>O<sub>9</sub> perovskite ferroelec., dielec. props. 4-88783  
 CO oxidation over Pd deposited on LiNbO<sub>3</sub> ferroelectrics, adsorptive and catalytic props., polarisation 4-99837  
 CdD<sub>2</sub>PO<sub>4</sub>, disordered crystals undergoing structural phase transitions, at order parameter determ. by cryst. struct. anal. 4-88126  
 Cd<sub>2</sub>Nb<sub>2</sub>O<sub>7</sub>, anharmonicity of thermal vibrs., X-ray diff. 4-65367  
 Cd<sub>2</sub>Nb<sub>2</sub>O<sub>7</sub>, diffuse and sharp phase transitions, dielec., optical, and electro-optical studies 4-71309  
 Cd<sub>2</sub>Nb<sub>2</sub>O<sub>7</sub>, thermo-optic and photochromic effects, phase transitions 4-99104  
 Cd<sub>2</sub>Nb<sub>2</sub>O<sub>7</sub>:Fe(Gd), narrow phase transitions, elec. field and impurity effects 4-71316  
 Cd<sub>2</sub>Nb<sub>2</sub>O<sub>7</sub>:Gd<sup>3+</sup>, ferroelec. transitions, EPR spectra 4-98945  
 CdTiO<sub>3</sub>:Mn<sup>2+</sup>, ferroelec. transitions, EPR studies 4-61588  
 Co<sub>2</sub>B<sub>2</sub>O<sub>7</sub>, spontaneous birefringence and Faraday effect 4-71351  
 Co<sub>2</sub>B<sub>2</sub>O<sub>7</sub>:F(OH), cryst. struct., X-ray diff. 4-65242  
 Cr<sub>2</sub>B<sub>2</sub>O<sub>7</sub>Cl<sub>2</sub> ferroelec. orthorhombic to monoclinic transition 4-71301  
 CsD<sub>2</sub>PO<sub>4</sub>, quasi-one-dimensional, behaviour of thermodynamic quantities near ferroelec. phase transition 4-61634  
 CsEuNaNb<sub>2</sub>O<sub>9</sub>, struct. and ferroelec. props. 4-109141  
 CsH<sub>2</sub>(D<sub>2</sub>)<sub>2</sub>PO<sub>4</sub>, ferroelectric, dielec. relaxation, activation energy, isotope effects 4-65989  
 CsH<sub>2</sub>PO<sub>4</sub> (CsD<sub>2</sub>PO<sub>4</sub>) ferroelectric phase transitions in transverse Ising model 4-93025  
 CsH<sub>2</sub>PO<sub>4</sub>, antiferroelec. fluctuations, Raman spectroscopy studies 4-71297  
 CsH<sub>2</sub>PO<sub>4</sub> ferroelec., domain struct. relax. 4-71322  
 CsH<sub>2</sub>PO<sub>4</sub>, normal and deuterated, ferroelec. phase transition, Raman studies 4-71295  
 CsH<sub>2</sub>PO<sub>4</sub>, paraelec. phase, soft relax. mode, dielec. spectra studies 4-65986  
 CsH<sub>2</sub>PO<sub>4</sub> pseudo-1D ferroelec., thermal cond. 4-65505  
 CsH<sub>2</sub>PO<sub>4</sub>, quasi-one-dimensional, behaviour of thermodynamic quantities near ferroelec. phase transition 4-61634  
 CsH<sub>2</sub>PO<sub>4</sub>, Raman OH stretching band shape and H-bonds, transition moment 4-66024  
 CsH<sub>2</sub>PO<sub>4</sub>, Raman scatt. study 4-71377  
 CsH<sub>2</sub>PO<sub>4</sub>, Slater-Senko model, ferroelec. transition 4-76370  
 CsH<sub>2</sub>PO<sub>4</sub>, thermal expansion, quasi-one-dimensional Ising model 4-80268  
 CsLiMoO<sub>4</sub>, ferroelec. phase transitions, Raman and NMR studies 4-71289  
 CsLiMoO<sub>4</sub>-type crystals, ferroelec. phase transitions 4-65979  
 Cu<sub>2</sub>B<sub>2</sub>O<sub>7</sub>Cl<sub>2</sub> ferroelec. and paraelec. phases, optical rot., birefr., optical susceptibilities 4-109151  
 β-Gd<sub>2</sub>(MoO<sub>4</sub>)<sub>3</sub>, domain walls, SAM and SPAM study 4-99064  
 Gd<sub>2</sub>(MoO<sub>4</sub>)<sub>3</sub>, ferroelectric-ferroelastic, acoustic emission and domain wall dynamics 4-84925  
 Gd<sub>2</sub>(MoO<sub>4</sub>)<sub>3</sub> polydomain ferroelec., quadrupole fields 4-80882  
 HCl-DCI, dipolar correlation times, NQR study 4-80171  
 H(O<sub>2</sub>)(AsO<sub>4</sub>)<sub>2</sub>·4H<sub>2</sub>O, phase transition temps. and ferroelec. domain struct. 4-76400  
 (K-Na)TaO<sub>3</sub>, dynamics of random-site interacting dipoles 4-80170  
 KD<sub>2</sub>PO<sub>4</sub>, photon emission during uniaxial deform., Curie temp. 4-81028  
 KD<sub>2</sub>PO<sub>4</sub>, piezoelectrically induced acoustic waves, strain optic effect 4-66005  
 KD<sub>2</sub>PO<sub>4</sub>-type ferroelectrics, static and dynamic props., applicability of mean-field approx. 4-93022  
 KH<sub>2</sub>AsO<sub>4</sub>, paraelec., quasi-static NMR 4-76286  
 KH<sub>2</sub>PO<sub>4</sub>, acoustic soft mode, piezoelectric obs. 4-71266  
 KH<sub>2</sub>PO<sub>4</sub>, C<sub>33</sub> anomaly near ferroelec. transition, US attenuation studies 4-65325  
 KH<sub>2</sub>PO<sub>4</sub>, doped, TSD in paraelec. phase 4-76321  
 KH<sub>2</sub>PO<sub>4</sub>, far IR reflectivity in 10 to 420K temp. range 4-76477  
 KH<sub>2</sub>PO<sub>4</sub> ferroelec., domain struct., dielec. and loss consts. 4-65994  
 KH<sub>2</sub>PO<sub>4</sub> ferroelec., domain struct. relax. 4-71322  
 KH<sub>2</sub>PO<sub>4</sub> ferroelectric, phase transition at T=110°C 4-76389  
 KH<sub>2</sub>PO<sub>4</sub>, paraelec., quasi-static NMR 4-76286  
 KH<sub>2</sub>PO<sub>4</sub>, photon emission during uniaxial deform., Curie temp. 4-81028  
 KH<sub>2</sub>PO<sub>4</sub>, single cryst. growth from supersaturated boiling solns. 4-66205  
 KH<sub>2</sub>PO<sub>4</sub> single crystal, far IR reflectivity spectra 4-114257  
 KH<sub>2</sub>PO<sub>4</sub> type crystals, low freq. E mode Raman spectra 4-71364  
 KH<sub>2</sub>PO<sub>4</sub> type crystals, ferroelec. phase transition, stress effects 4-76365  
 KH<sub>2</sub>PO<sub>4</sub>, US study near press. induced tricritical point 4-76386  
 KH<sub>2</sub>PO<sub>4</sub>:Ni, EPR spectrum meas. 4-80813  
 KH<sub>2</sub>PO<sub>4</sub>:Se, ESR relax. time meas. 4-92957  
 KH<sub>2</sub>PO<sub>4</sub>-type transition, struct. studies, review 4-76351  
 KIO<sub>3</sub>, low temp. ferroelec. transition under press. NQR studies 4-93019  
 K<sub>2</sub>Li<sub>2</sub>Nb<sub>2</sub>O<sub>7</sub>, ferroelec. props., dielec. const., piezoelec. and electromechanical coupling coeffs. 4-65958  
 K<sub>2</sub>Li<sub>2</sub>Nb<sub>2</sub>O<sub>7</sub>, solid solns., struct. and dielec. props. 4-75381  
 K<sub>1-x</sub>Li<sub>x</sub>TaO<sub>3</sub>, IR reflectivity, two mode behaviour 4-71363

## ferroelectric materials continued

- (K<sub>1-x</sub>Na<sub>x</sub>)<sub>0.4</sub>(Sr<sub>1-y</sub>Ba<sub>y</sub>)<sub>0.6</sub>Nb<sub>2</sub>O<sub>6</sub>, single cryst. growth and phys. props. 4-76352  
 (K<sub>1-x</sub>Na<sub>x</sub>)<sub>0.4</sub>(Sr<sub>1-y</sub>Ba<sub>y</sub>)<sub>0.6</sub>Nb<sub>2</sub>O<sub>6</sub>, ferroelec. single cryst. series, pyroelec. props. 4-76345  
 K<sub>1-x</sub>Na<sub>x</sub>TaO<sub>3</sub>, IR reflectivity, two mode behaviour 4-71363  
 KNbO<sub>3</sub>, cubic to tetragonal transition, covalency effects, band struct. calculations 4-70361  
 KNbO<sub>3</sub>, dispersive/order-disorder crossover, soft mode temp. depend., contrib. to low freq. permittivity 4-65369  
 KNbO<sub>3</sub>, electrostatics, polarisable point-ion model 4-80860  
 KNbO<sub>3</sub>, ferroelec. domain struct., IR spectra anal. 4-71323  
 KNbO<sub>3</sub> ferroelec. films, liquid phase epitaxy growth 4-76695  
 KNbO<sub>3</sub>, lattice dynamics and anomalous Raman spectrum 4-71360  
 KNbO<sub>3</sub>, refractive index and polarisation 4-99081  
 K<sub>2</sub>SeO<sub>4</sub>, acoustic phonon wavevector depend. near commensurate-incommensurate transition, Brillouin spectra 4-71313  
 K<sub>2</sub>SeO<sub>4</sub>, Brillouin spectra, scatt. angle and press. depend. 4-76481  
 K<sub>2</sub>SeO<sub>4</sub>, incommensurate phase, SHF Obs. 4-61635  
 K<sub>2</sub>SeO<sub>4</sub>, incommensurate phase transitions, phase mode dynamics, neutron and Raman scatt. studies, review 4-65966  
 K<sub>2</sub>SeO<sub>4</sub>, incommensurate-ferroelec. transition, struct. study 4-76381  
 K<sub>2</sub>SeO<sub>4</sub>, incommensurate transition, order parameter, EPR lineshape anal. 4-99056  
 K<sub>2</sub>SeO<sub>4</sub>, incommensurately modulated struct., X-ray diff. obs. 4-108318  
 K<sub>2</sub>SeO<sub>4</sub>, incommensurate-ferroelectric transition, structural study 4-109138  
 K<sub>2</sub>SeO<sub>4</sub>, phase transitions, thermal expansion coeffs., thermodynamic anal. of dilatometric and calorimetric data 4-88784  
 K<sub>2</sub>SeO<sub>4</sub>, phase-transition, Raman spectra, uniaxial stress depend. 4-76450  
 KTA<sub>1-x</sub>Nb<sub>x</sub>O<sub>3</sub>, ferroelec. soft mode, hyper-Raman scatt. studies 4-99060  
 KTA<sub>1-x</sub>Nb<sub>x</sub>O<sub>3</sub>, glasslike behaviour and press. effects 4-99058  
 KTA<sub>1-x</sub>Nb<sub>x</sub>O<sub>3</sub> quantum ferroelec., mode softening, neutron scatt. studies 4-71292  
 KTAO<sub>3</sub>, anharmonic interactions, X-ray diff. study 4-61036  
 KTAO<sub>3</sub> incipient ferroelec., mode softening, hyper-Raman spectra studies 4-71366  
 KTAO<sub>3</sub>, oxygen-octahedral ferroelectrics, two-photon spectroscopy study 4-114300  
 KTAO<sub>3</sub>, sintering with the aid of MnO 4-61901  
 KTAO<sub>3</sub>:Li, incipient ferroelec., off-centre impurity induced phase transition 4-76383  
 KTAO<sub>3</sub>:Li single cryst., dielec. dispersion, dielec. spectra studies 4-76322  
 K<sub>2</sub>Th<sub>2</sub>Nb<sub>2</sub>O<sub>9</sub>, tetragonal tungsten bronze phase, cryst. struct., elec. and optical props. 4-70116  
 K<sub>2</sub>ZnCl<sub>4</sub>, commensurate ferroelec. phase, phonon freq., permitt., IR refl. spectra 4-71387  
 K<sub>2</sub>ZnCl<sub>4</sub>, incommensurate ferroelec., phase transitions, lattice dynamics, Raman effect 4-84922  
 K<sub>2</sub>ZnCl<sub>4</sub>, metastable chaotic state close to incommensurate-commensurate transition, <sup>51</sup>Cl NQR obs. 4-76285  
 K<sub>2</sub>ZnCl<sub>4</sub>, noncommensurate ferroelec., lattice dynamics and transitions, Raman studies 4-92313  
 K<sub>2</sub>ZnCl<sub>4</sub>, phase transitions, thermal expansion coeffs., thermodynamic anal. of dilatometric and calorimetric data 4-88784  
 LiH<sub>2</sub>(SeO<sub>4</sub>)<sub>2</sub>, ferroelec., single cryst. growth from soln. (Korean) 4-114375  
 LiKSO<sub>4</sub>, press. effect on phase transitions 4-104546  
 LiNH<sub>4</sub>SO<sub>4</sub>, ferroelec. domain struct., SEM studies 4-71321  
 LiNH<sub>4</sub>SO<sub>4</sub>, phase transitions, X-ray diff. study 4-88277  
 LiNbO<sub>3</sub> amorphous films, dielec. and elec. props. 4-104531  
 LiNbO<sub>3</sub>, ballistic heat pulse propag., effect of piezoelec. 4-76335  
 LiNbO<sub>3</sub>, complex elastoelectric effect 4-80629  
 LiNbO<sub>3</sub> cryst. growth, melt composition effect on props. 4-84227  
 LiNbO<sub>3</sub>, electron irradi., point defects, ESR and IR spectra studies 4-70139  
 LiNbO<sub>3</sub>, ferroelec., band struct. and optical props. in fundamental absorption region 4-75845  
 LiNbO<sub>3</sub>, gamma irradi., influence on photovoltaic effects 4-84656  
 LiNbO<sub>3</sub>, inelastic light scatt. and dielec. anomalies connection 4-84923  
 LiNbO<sub>3</sub>, integrated optical waveguides, fabrication using ion implantation 4-79347  
 LiNbO<sub>3</sub>, laser irradi., photovoltaic effects 4-70868  
 LiNbO<sub>3</sub>, Mossbauer diff., separation of elastically and inelastically scatt. γ-radiation 4-98985  
 LiNbO<sub>3</sub>, Raman scatt. isofrequency temp. depend. 4-76474  
 LiNbO<sub>3</sub>, single cryst., phys. props. 20-200°C 4-76397  
 LiNbO<sub>3</sub>, spontaneous polarisation screening on free surface 4-88767  
 LiNbO<sub>3</sub>, thermoelectrically reduced and electron irradi., positron annihilation, optical absorpt. meas. 4-104697  
 LiNbO<sub>3</sub> type ferroelectrics, dielec. thermal and soft mode behaviour 4-71298  
 LiNbO<sub>3</sub>:C<sup>3+</sup>(Mn<sup>2+</sup>), axial cryst. field parameters, EPR spectra 4-98579  
 LiNbO<sub>3</sub>:Fe, photocurrent jumps due to domain struct. (Russian) 4-75996  
 LiNbO<sub>3</sub>:Fe, Rayleigh scatt., effect of photoref. 4-80957  
 LiNbO<sub>3</sub>:Fe (III) ferroelec., Mossbauer spectra and EPR studies 4-65960  
 LiNbO<sub>3</sub>:Ti, impurity diffusion as a function of stoichiometry 4-80304  
 Li<sub>2</sub>O-LiNbO<sub>3</sub>-B<sub>2</sub>O<sub>3</sub>, new solid electrolyte glass material, electrical conductivity 4-108649  
 Li<sub>2</sub>O-M<sub>2</sub>O<sub>2</sub>-M'<sub>2</sub>O<sub>4</sub>, M=Nb, Ta, M'=Ti, Zr, non-stoichiometric phases, cryst. chem. and ferroelec. props. 4-65968  
 LiTaO<sub>3</sub>, complex elastoelectric effect 4-80629  
 LiTaO<sub>3</sub> crystals, poling using interdigital electrodes, appl. to bulk wave transducers 4-99068  
 LiTaO<sub>3</sub>, ferroelec., band struct. and optical props. in fundamental absorption region 4-75845  
 LiTaO<sub>3</sub>, ferroelec. crystal, electrostatic pot. at surface 4-76350  
 LiTaO<sub>3</sub>, Raman scatt. isofrequency temp. depend. 4-76474  
 LiTaO<sub>3</sub>, reduced photoelec. props., spectral and temp. depend. 4-84657  
 LiTaO<sub>3</sub>, sintering with the aid of MnO 4-61901  
 LiTaO<sub>3</sub>:Fe, photorefraction, photovoltaic effect, photocond., depend. on light intensity (Russian) 4-114226  
 LiTiO<sub>3</sub> ferroelec. cryst., photogalvanic effect anisotropy 4-75995  
 MgO, dipolar defect ordering due to dissolved CO<sub>2</sub> 4-71287  
 Mn<sub>2</sub>B<sub>2</sub>O<sub>7</sub>Cl<sub>2</sub>(Br)(I), cubic-orthorhombic ferroelec. transition, sp. ht. studies 4-104545  
 (ND<sub>4</sub>)<sub>2</sub>D(SO<sub>4</sub>)<sub>2</sub>, successive phase transitions studied by VO<sup>2+</sup> ion- and SeO<sub>3</sub> radical EPR 4-76388

## ferroelectric materials continued

- $N(D_2H_{1-x})_4(D_2H_{1-y})_2PO_4$ , dielectric and electro-optical props. meas. 4-76313
- $(NH_4)_2BeF_4$ , dielectric hysteresis and anomalous temperature 4-93026
- $NH_4AlF_6$ , clusters and critical slowing down near  $T_c$ , EPR study 4-65982
- $(NH_4)_2BeF_4$ , incommensurate phase, SHF Obs. 4-61635
- $(NH_4)_2BeF_4$ , incommensurate phase, in applied elec. field 4-76376
- $NH_4D_2PO_4$ , piezoelectrically induced acoustic waves, strain optic effect 4-66005
- $NH_4H_2PO_4$ , cryst. perfection, flow visualisation expts. 4-65042
- $(NH_4)_2H(SO_4)_2$ , successive phase transitions studied by  $VO^{2+}$  ion and  $SeO_3$  radical EPR 4-76388
- $NH_4HSeO_4$ , deuterated, polymorphous transition, NMR study 4-114215
- $NH_4HSeO_4$ , dielec. nonlinearity, ferroelec. transition 4-76366
- $NH_4HSeO_4$ , dielectric, piezoelectric and elastic props. 4-80878
- $NH_4HSeO_4$ , ferroelec. phase transition mechanisms, NMR studies 4-93015
- $NH_4HSeO_4$ , ferroelec. transitions, Raman scatt. and vibr. props. 4-93066
- $NH_4HSeO_4$ , ferroelec., with varying D content, phase transitions, dielec. anomalies 4-99061
- $(NH_4)_2SO_4$ , proton spin-lattice relax. time, effect of  $^{17}O$  natural abundance 4-109092
- $(NH_4)_2SO_4 \cdot CrO_3$ , phase transitions studied by EPR spectra 4-88723
- $(NH_4)_2SO_4 \cdot K_2SO_4 \cdot CrO_3$ , phase transitions studied by EPR spectra 4-88723
- $(NH_4)_2ZnBr_4$ , ferroelec., Raman scatt. study of phase transitions 4-104589
- $(NH_4)_2ZnCl_4$ , incommensurate phase transition, dielec. props., X-ray diffr. study 4-93021
- $Na_{0.5}Bi_{0.5}TiO_3$ , cryst., birefringence and opalescence, temp. depend. 4-76425
- $Na_{0.5}Bi_{0.5}TiO_3$ , pure and Ba-doped, cryst. struct., ferroelec. props., neutron diffr. 4-70102
- $Na_{0.5}Bi_{0.5}TiO_3$ , soft-modes and central peak, inelastic neutron scatt. studies 4-61037
- $Na_{0.5}Bi_{0.5}TiO_3$ , grain-oriented ferroelectric ceramics, piezoelec. props. (Japanese) 4-61625
- $Na_{1/2}Bi_{1/2}TiO_3$  ceramics, pyroelectric props., perspective appl. in pyroelectric radiation detectors 4-88776
- $NaH_2(SeO_3)_2$  biaxial ferroelec., ferroelastic and ferroelec. domains 4-93027
- $NaH_2(SeO_3)_2$  crystals, ferroelec., existence of interphase between  $\alpha$ - and  $\beta$ -phases 4-104544
- $NaH_2(SeO_3)_2 \cdot Cr^{3+}$ , EPR spectra, temp. and external elec. field effects 4-88715
- $Na_{3-x}K_xW_3O_{15}$ , Bridgman-Stockbarger growth, ferroelec. and ferroelastic props., permittivity, birefr. meas. 4-65969
- $Na_{3-x}Li_xW_3O_{15}$ , Bridgman-Stockbarger growth, ferroelec. and ferroelastic props., permittivity, birefr. meas. 4-65969
- $NaNO_2$ , modulated phase study 4-76372
- $NaNO_2$ , struct. of incommensurate modulated phase 4-103707
- $NaNO_2$ , zero-phonon transition, isotope shifts, UV absorpt. spectra 4-88853
- $NaNO_3$ , paraelectric-ferroelectric transition, isotropy group description 4-84918
- $NaNbO_3$ , bladed crystallisation in  $Na_2O-Nb_2O_5-B_2O_3$  system 4-61061
- $Na_2O-Nb_2O_5-SiO_2$  glass-ceramics, ferroelec., depolarisation currents, dielec. and electrooptical props. 4-76317
- $Na_3Sc_2(PO_4)_3$  and isomorphs, ferroelec.-superionic cond. phase transitions 4-71310
- Nb oxides, synthesis of new materials based on decomp. with  $HF_2$  4-66563
- $(Nd_4Ca_2)Ti_6O_{20}$ , ferroelec. cpd., perovskite-derived, crystal growth and characterisation 4-76657
- $(NH_4)_2HPO_4 \cdot (PO_4)_2Te(OH)_6$ , NMR study of phase transition 4-80877
- $Ni_3B_2O_{13}Br$ , magnetoelec. effect, mag. and elec. meas. 4-71144
- PLZT, ageing and space charge arising in hot poling 4-76327
- PLZT ceramic, coarse-grain light scatt. and elec. hysteresis 4-76399
- PLZT ceramics, ferroelec. and electrooptic props. 4-76353
- PLZT ceramics, poling strategy 4-76319
- PLZT, chemically prepared, charact. and props. 4-76712
- PLZT, ferroelec. ceramic, hot poling, polarisation, ageing rel. to space charge 4-99045
- PLZT ferroelec. films, prep., props. and appls. 4-66230
- PLZT, microscopic characterisation 4-61903
- PLZT retardation plates, nonhomogeneity of light modulation 4-61660
- PLZT, tetragonal ceramic,  $90^\circ$  domains under poling, XRD study 4-76398
- PZT, amorphous, ferroelec. phase transition 4-61637
- PZT, dielec. props. at high press., p-T phase diagrams 4-99062
- PZT, doped, diffuse phase transition, ultrasound meas. 4-76385
- PZT, lattice site of Zn, Se, Fe ions, X-ray anal. 4-75488
- PZT material, high density, prep. by coprecipitation technique 4-76711
- PZT microparticle materials, amorphous state ferroelectricity 4-104542
- PZT, prep. using cupferron 4-61904
- $(PbLa)(Zr,Ti)O_3$  ceramics, stress anisotropy induced by polarisation 4-104536
- $(Pb,Zr)TiO_3$  thin films, magnetron RF sputtering and dielectric props. 4-88970
- $Pb_{1-x}Ba_xNb_2O_6$  ceramics, hot pressed, dielec. and piezoelec. props. 4-104533
- $Pb_{1-x}Ba_xNb_2O_6$  ferroelec. props., dielec. const., piezoelec. and electromechanical coupling coeffs. 4-65958
- $(Pb_{0.22}Ba_{0.78})Ti_3$ , ferroelec., phase-transition, high press. Raman study 4-76451
- $(Pb_{0.76}Ca_{0.24})(Co_{1/2}W_{1/2})_{0.04}Ti_{0.96}O_3$  ceramics, piezoelec. props. MnO addition effects 4-104532
- $(Pb_{0.75}Ca_{0.25})(Mg_{1/3}Nb_{2/3})_{0.0625}Ti_{0.9375}O_3$  Mn ceramics, US, elastic and dielec. props. 4-104543
- $Pb(FeNb)_{0.5}O_3$  ceramics and single crystals, prep., struct., X-ray diffr., neutron powder diffr., dielec. and elec. meas., SEM 4-75412
- $Pb(Fe_{0.5}Nb_{0.5})O_3$ , anharmonicity of thermal vibrs., X-ray diffr. 4-65367
- $Pb(Fe_{0.5}Nb_{0.5})O_3$  ferroelec., mag. and magnetoelec. props. 4-65847
- $Pb(Fe_{1/2}Nb_{1/2})_2O_3$ - $Pb(Ni_{1/3}Nb_{2/3})_2O_3$  solid soln. system, dielec. props. 4-104517
- $Pb(Fe_{0.5}Ta_{0.5})O_3$ , anharmonicity of thermal vibrs., X-ray diffr. 4-65367
- $PbFe_{0.5}Ta_{0.5}O_3$  single cryst., ferroelec./antiferromag., spontaneous birefringence 4-71344
- $Pb_2Ge_2O_{11}$  crystals, Raman scatt. near phase transition, isofrequency temp. depends. 4-66043

## ferroelectric materials continued

- $Pb_2Ge_2O_{11}$ , ferroelec., surface states role in polarisation reversal 4-71325
- $Pb_2Ge_2O_{11}$  ferroelec. thin film, reactive sputtering prep. and props. 4-65961
- $Pb_2Ge_2O_{11}$ , hydrothermally grown crystals, dielec., pyroelectric props., X-ray diffr. 4-84915
- $Pb_2Ge_2O_{11}$ , lattice dynamics near Curie point (Russian) 4-98221
- $Pb_2Ge_2O_{11}$ , pyroelectric coeff., Q-factor, determ. by absolute dynamic method 4-84914
- $Pb_2Ge_2O_{11}$ , soft modes rel. to crit. fluctuations, neutron and Raman scatt. meas. 4-65370
- $Pb_2Ge_2O_{11}$  type crystals, electrogyration, dispersive and temp. depend. 4-76433
- $Pb_2Ge_2O_{11} \cdot Gd^{3+}$ , superhyperfine interaction, ESR and ENDOR studies 4-114159
- $Pb_2Ge_2Si_2O_{11}$  thick films, printing technique prep. and pyroelec. props. 4-104541
- $PbTiO_3$ , ferroelec. transition effects on absorption edges 4-93020
- $Pb_{1-x}In_xNbO_6$ , order-disorder transitions and dielec. props. 4-65980
- $Pb_3(MF_2)_3$  ( $M=Ti, V, Cr, Fe, Ga$ ), ferroelectric phase transitions 4-71311
- $PbMg_{1/3}Nb_{2/3}O_3$ , diffuse phase transition 4-65967
- $PbMg_{1/3}Nb_{2/3}O_3$ , mean square displacements, thermal expansion coeff. in diffuse ferroelec. transition region, X-ray diffr. meas. 4-65971
- $PbMg_{1/3}Nb_{2/3}O_3$ , single cryst., growth by mass crystallisation method, elec. relax. study 4-76315
- $Pb(Mg_{1/3}Nb_{2/3})_2O_3$ - $Pb(Zn_{1/3}Nb_{2/3})_2O_3$  solid solns., ceramic, dielec. charact. 4-76354
- $PbO-BaO-TiO_2-B_2O_3$  glass ceramic system, crystal clamping, X-ray diffr., dilatometry 4-109386
- $Pb_2ScNbO_6$ , order-disorder transitions and dielec. props. 4-65980
- $Pb_{2-x}Th_xKTaO_3$ , crystallographic and dielec. props. (French) 4-79987
- $Pb_{2-x}Th_xTaO_3$ , crystallographic and dielec. props. (French) 4-79987
- $PbTiO_3$ , amorphous, Raman spectra, low wave-number response 4-104590
- $PbTiO_3$ , amorphous and cryst., bond lengths, annealing effect, Raman spectra, EXAFS study 4-79935
- $PbTiO_3$  amorphous films, dielec. and elec. props. 4-104531
- $PbTiO_3$ , delayed phenomena in transient pyroelectric response derived from cylindrical shaped domains 4-61630
- $PbTiO_3$ , electron energy struct. of cond. band, X-ray photoemission yield spectra 4-61282
- $PbTiO_3$ , ferroelec. phase transitions, stress effects 4-71315
- $PbTiO_3$  heteroepitaxial ferroelec. films, domain struct. 4-65993
- $PbTiO_3$ , single crystal, dislocation and domain struct. 4-75452
- $PbTiO_3$ , six sites model for successive transitions 4-80873
- $PbTiO_3$ , substituted, ferroelec. phase transitions and phase diagrams 4-65978
- $PbTiO_3$  thin films, CVD prep. and dielec. props. 4-104736
- $PbTiO_3$  type crystals, electrogyration, dispersive and temp. depend. 4-76433
- $(PbTiO_3)_{0.9}[Pb(Mg_{1/2}W_{1/2})_2O_3]_{0.1}$ , photovoltaic effect and beam intensity sensor 4-98664
- $Pb(Ti_{0.81}Sn_{0.19})_3O_3$ , ferroelec., phase-transition, high press. Raman study 4-76451
- $Pb(Ti_{1-x}Zr_x)_2O_3$ , ferroelec. phase transitions and phase diagrams 4-65978
- $Pb_2V_2O_7$  cryst. struct. of ferroelectric  $\alpha$  phase (French) 4-84259
- $Pb(Zr,Ti)O_3$  ceramics, ageing and ferroelec. props., heterovalent substitution effects 4-99046
- $Pb(Zr,Ti)O_3$  ferroelec. films, reactive sputtering prep. and dielec. props. 4-104731
- $PbZrO_3$ , soft mode in ferroelectric transition 4-99063
- $PbZrO_3$ , with O vacancies, phase transitions, dielec. props. 4-76391
- $PbZrO_3$ , with vacancies, para, ferro and antiferroelectric phase transitions, influence of hydrostatic press. 4-76390
- $Pb(Zr_{0.55}Ti_{0.45})_3O_3$  ceramics, piezoelec. props., porous struct. effects 4-104534
- $Pb(Zr_{1-x}Ti_x)_2O_3$  ceramic strips, width and thickness strain meas. 4-80869
- $PbZr_{1-x}Ti_xO_3$  cryst., T, x, E phase diagram anal. 4-76359
- $PbZr,Ti_{1-x}O_3$  ceramics, electrostrictive coeff., time resolved X-ray diffr. studies 4-71282
- $Pb_{1-x/2}[Zr_{1-(x+y)}Ti_yNb_y]O_3$  ceramic transducers, pyroelec. and mechano-dielec. charact. 4-109136
- $Rb_1(NH_4)H_2PO_4$  mixed crystals, phase transitions in cluster approx., pseudospin model 4-80881
- $RbAlF_4$  ferroelec. phase transitions, EPR studies 4-71158
- $RbCdF_4$ , competition between ferroelectricity and ferroelasticity 4-76355
- $Rb_2Cd(SO_4)_2$ , thermal expansion, 77 to 300K 4-92396
- $RbD_2(SeO_3)_2$  ESR spectra and dielec. const. meas. 4-76305
- $RbD_2(SeO_3)_2$  ferroelectric phase transition, dielec. anomaly 4-65987
- $RbH_2PO_4 \cdot Ti^{2+}$ , paramag. complexes, symmetry lowering, EPR studies 4-65857
- $RbHSO_4$ , ferroelectric phase transitions, piezoelectric coeffs., electrostrictive coeffs., temp. depend., resonance studies 4-114217
- $RbHSeO_4$  ferroelec. ferroelastic, light deflection 4-80883
- $RbHSeO_4$  ferroelec. phase transition mechanisms, NMR studies 4-93015
- $RbH_2(SeO_3)_2$  ESR spectra and dielec. const. meas. 4-76305
- $RbLiMoO_4$  cryst. struct. determ. and phase transition 4-79999
- $Rb_{0.52}(NDa_{0.48}D_2)PO_4$  cryst., proton glass dielec. behaviour 4-114218
- $Rb_{-x}(NH_4)_xH_2PO_4$  ferroelec. pseudo-spin glass state, NMR meas., dynamic cluster freeze-out model 4-65875
- $Rb_{-x}(NH_4)_xH_2PO_4$  single cryst. proton glasses, struct. and dielec. props. 4-76323
- $Rb_{-x}(NH_4)_xH_2PO_4$  glass, H-bonded, NMR relax. study 4-98974
- $(Rb_{1/2}(NH_4)_{1/2})_2SO_4$ , dielectric relax. meas. 4-80862
- $Rb_2ZnBr_4$ , isomorphs, EFG tensor modulation, model calc. 4-75904
- $Rb_2ZnCl_4$  ferroelec., phase transitions, dielec. and DTA studies, rel. to cryst. growth conditions 4-76374
- $Rb_2ZnCl_4$ , incommensurate, modulation wave floating, NMR meas. 4-65991
- $Rb_2ZnCl_4$ , incommensurate-ferroelec. phase transition, X-ray study 4-76373
- $Rb_2ZnCl_4$ , incommensurate ferroelec. phase transitions, lattice dynamics, Raman effect 4-84922
- $Rb_2ZnCl_4$ , incommensurate and ferroelec. phases, electro-optical props. 4-104574
- $Rb_2ZnCl_4$ , incommensurate phase, dynamic dielec. props., pinning effects 4-109140
- $Rb_2ZnCl_4$ , metastable chaotic state with randomly pinned solitons, NMR, permittivity meas. 4-65875

## ferroelectric materials continued

- Rb<sub>2</sub>ZnCl<sub>4</sub>, modulated ferroelec., thermal hysteresis and pinning 4-76380  
 Rb<sub>2</sub>ZnCl<sub>4</sub>, non-dimensional ferroelec., lattice dynamics and transitions, Raman studies 4-92313  
 Rb<sub>2</sub>ZnCl<sub>4</sub>, nucleation processes at commensurate-incommensurate transition 4-80874  
 Rb<sub>2</sub>ZnCl<sub>4</sub>, phase transitions, thermal expansion coeffs., thermodynamic anal. of dilatometric and calorimetric data 4-88784  
 Rb<sub>2</sub>ZnCl<sub>4</sub>, phase-transition, Raman spectra, uniaxial stress depend. 4-76450  
 Rb<sub>2</sub>ZnCl<sub>4</sub>, soft modes rel. to crit. fluctuations, X-ray scatt. meas. 4-65370  
 Sb chalcogenohalide based ACH-2 ferroelectric, soft microwave modes 4-84920  
 SbSBr, ferroelec. phase transitions, elec. permittivity studies 4-65981  
 SbSI ferroelectric, L<sub>III</sub> edge above transition temp., EXAFS study 4-61772  
 Sb<sub>2</sub>Se<sub>3-x</sub>, ferroelec. phase transition, dilatometric study 4-114222  
 SbTeI, cryst. struct., full matrix least squares refinement 4-92168  
 Sn<sub>2</sub>P<sub>2</sub>S<sub>6</sub>, influence of hydrostatic pressure on vibrational spectra 4-109192  
 Sn<sub>2</sub>P<sub>2</sub>S<sub>6</sub>, low freq. lattice vibrs. in IR spectra 4-71389  
 Sn<sub>2</sub>P<sub>2</sub>S<sub>6</sub>(Se<sub>2</sub>), IR spectra of ferroelectric transition splitting 4-84966  
 Sr<sub>8</sub>Al<sub>2</sub>O<sub>24</sub>(CrO<sub>4</sub>)<sub>2</sub>, flux grown, ferroelec. phase transition, domain studies, birefr., polarisation, permittivity, transition enthalpy meas. 4-65970  
 Sr<sub>1-x</sub>Ba<sub>x</sub>Nb<sub>2</sub>O<sub>6</sub>, ferroelec. props., dielec. const., piezoelec. and electromechanical coupling coeffs. 4-65958  
 Sr<sub>1-x</sub>Ca<sub>x</sub>TiO<sub>3</sub>, XY quantum ferroelec. with transition to randomness 4-88781  
 Sr<sub>2</sub>KNb<sub>2</sub>O<sub>15</sub>, ferroelec. props., dielec. const., piezoelec. and electromechanical coupling coeffs. 4-65958  
 Sr<sub>2</sub>KNb<sub>2</sub>O<sub>15</sub>(TiNb<sub>2</sub>O<sub>15</sub>), ferroelectric materials, synthesis and characteristics 4-104547  
 Sr<sub>2</sub>Nb<sub>2</sub>O<sub>7</sub>, ferroelec., incommensurate-polar transition 4-76375  
 ((Sr<sub>0.56</sub>Pb<sub>0.25</sub>Ca<sub>0.25</sub>)TiO<sub>3</sub>)<sub>100-x</sub>(Bi<sub>2</sub>O<sub>3</sub>.3TiO<sub>2</sub>)<sub>x</sub>, dielectric props., HV capacitor application 4-98997  
 Sr<sub>2</sub>Ta<sub>2</sub>O<sub>7</sub>, ferroelec. transition temp. and optical absorption edge, press. depend. 4-93018  
 SrTeO<sub>3</sub>, dielectric const. dispersion study (Russian) 4-88762  
 SrTiO<sub>3</sub>, band struct. and ferroelec. transition, two-photon spectra studies 4-93016  
 SrTiO<sub>3</sub>, intrinsic ferroelectric, sp. ht. in range 0.5 to 6K 4-84420  
 SrTiO<sub>3</sub>, low-freq. noise in alternating elec. field 4-109133  
 SrTiO<sub>3</sub>, O<sub>2</sub> photo-adsorption, ESR study 4-65550  
 SrTiO<sub>3</sub>, oxide perovskites, dielec. meas., surface layer effects 4-65962  
 SrTiO<sub>3</sub>, oxygen-octahedral ferroelectrics, two-photon spectroscopy study 4-114300  
 SrTiO<sub>3</sub>, US attenuation and vel. near ferroelec. transition 4-65345  
 SrTiO<sub>3</sub>, ultrasonic props. near phase transition 4-113544  
 SrTiO<sub>3</sub>; Fe<sup>2+</sup>-V<sub>O</sub> pairs, electronic struct. calcs. 4-113890  
 TGS, ferroelec. transition and domains, positron annihilation, TEM and decoration studies 4-65985  
 TGS, surface layer far IR spectra 4-88828  
 TGS, audiofrequency dielec. dispersion, universal behaviour and temp. depend. 4-76303  
 Ta oxides, synthesis of new materials based on decomp. with HF<sub>2</sub> 4-66563  
 Tb<sub>2</sub>(MoO<sub>4</sub>)<sub>3</sub>, ferroelectric-ferroelastic, acoustic emission and domain wall dynamics 4-84925  
 Te(OH)<sub>6</sub>.2NH<sub>4</sub>H<sub>2</sub>PO<sub>4</sub>.(NH<sub>4</sub>)<sub>2</sub>HPO<sub>4</sub>, cryst. struct., X-ray diffr. study 4-60888  
 Te(OH)<sub>6</sub>.2NH<sub>4</sub>H<sub>2</sub>PO<sub>4</sub>.(NH<sub>4</sub>)<sub>2</sub>HPO<sub>4</sub>, dielec., thermal and optical props. 4-61636  
 Te(OH)<sub>6</sub>.2NH<sub>4</sub>H<sub>2</sub>PO<sub>4</sub>.(NH<sub>4</sub>)<sub>2</sub>HPO<sub>4</sub>, single cryst. growth and morphology 4-61821  
 TiCdF<sub>3</sub>.Gd<sup>3+</sup>.O<sub>2</sub><sup>-</sup>, critical phenomena above and below T<sub>c</sub>, EPR studies 4-65854  
 TiH<sub>3</sub>(SeO<sub>3</sub>)<sub>2</sub>, cryst. struct., phys. props., phase transitions 4-84921  
 TiH<sub>3</sub>(SeO<sub>3</sub>)<sub>2</sub>, dielec. props., phase transitions, cryst. struct. 4-65965  
 TiInS<sub>2</sub>, structural phase transitions, dielec. props. at subMM wavelengths 4-98275  
 Ti<sub>2</sub>SeO<sub>4</sub>, ferroelec. transition, birefringence studies 4-65976  
 Ti<sub>2</sub>SeO<sub>4</sub>, phase transition and lattice const., X-ray diffr. study 4-71294  
 W bronze tetragonal struct. non-stoichiometric phases, dielec., ferroelastic and nonlinear optical props. 4-65972

## ferroelectric phenomena see ferroelectricity

## ferroelectric semiconductor materials see ferroelectric semiconductors

## ferroelectric semiconductors

- controllable variband structs., energy schemes 4-80871  
 EM reception and excitation of SAW 4-80630  
 heavily doped, inhomogeneous state stability conditions and struct., linear approx. 4-71286  
 IV-VI compounds, dynamical properties, book 4-58590  
 IV-VI compounds, electronic and dynamical props., book contrib. 4-61003  
 photoferroelectric phenomena caused by fluctons and phasons 4-70856  
 photoferroelectric phenomena caused by fluctons and phasons 4-66009  
 titanates, Fe doped, point defects and semicond. behaviour 4-70137  
 AgPbSb<sub>2</sub>S<sub>6</sub>, andorite, piezoelec. and phase transition props., acoustic meas. 4-93009  
 BaTiO<sub>3</sub>, birefr., Kerr effect 4-88805  
 BaTiO<sub>3</sub>, combined doping, electron-conduction compensation 4-113475  
 n-BaTiO<sub>3</sub> electrolyte redox systems, photoelectrochemistry 4-72124  
 BaTiO<sub>3</sub>, pure and Nb-doped, elec. cond. 600-800°C, defect struct. 4-98604  
 BaTiO<sub>3</sub>, semicond. glass ceramics, oxidation, barrier layer form. 4-114699  
 BaTiO<sub>3</sub>, surface domains, double Laue pattern topography 4-104548  
 BaTiO<sub>3</sub>, synthesis, polycryst., nonstoichiometry rel. to solid-solid reaction mechanism 4-99305  
 BaTiO<sub>3</sub>, thick film, grain boundaries, TEM obs. 4-84300  
 BaTiO<sub>3</sub>.Co, impurity valence states, EPR 4-75901  
 BaTiO<sub>3</sub>.Fe, electroform., elec. field depend. 4-66077  
 BaTiO<sub>3</sub>.Nb(Al), donor doped, defect chem. 4-84307  
 BaTiO<sub>3</sub>.Yb, dielec. and X-ray diffr. study 4-84896  
 BaTiO<sub>3</sub>-based materials, dielec. props. and chem. inhomogeneity, effect of sintering 4-85128  
 BiSI ferroelec. semicond., energy band struct., X-ray spectral studies 4-65609  
 Cd<sub>2</sub>Nb<sub>2</sub>O<sub>7</sub>, photoferroelectric phenomena 4-88785

## ferroelectric semiconductors continued

- KNbO<sub>3</sub>, ferroelec. semicond., positive temperature resist. coeff. 4-113958  
 KTaO<sub>2</sub>, spin-flip Raman scatt. in mag. fields, obs. of donor states 4-71384  
 KTaO<sub>3</sub>, anharmonicity of thermal vibrs., X-ray diffr. 4-65367  
 KTaO<sub>3</sub>.Fe<sup>3+</sup>, EPR spectra, superhyperfine struct., spin Hamiltonian parameters 4-98942  
 LiNbO<sub>3</sub>.Eu<sup>2+</sup>, impurity optical absorpt. 4-66056  
 LiNbO<sub>3</sub>.Fe, polarisation-anisotropic light-induced light scatt. 4-87395  
 LiNbO<sub>3</sub>.Ni<sup>2+</sup>, cryst. field splitting of impurity levels 4-65647  
 (Pb, Sn, Ge)Te, semicond., dielec. props. and soft modes, review, book contrib. 4-61622  
 Pb<sub>1-x</sub>Ge<sub>x</sub>Te, ferroelec. phase transition, high press. investigation, DC resist., capacitance meas. 4-71312  
 n-Pb<sub>1-x</sub>Ge<sub>x</sub>Te, free carrier mobility, ferroelectric phase transition 4-71317  
 Pb<sub>1-x</sub>Ge<sub>x</sub>Te, rhombohedral phase, energy surfaces and domain struct. 4-76010  
 Pb<sub>1-x</sub>Ge<sub>x</sub>Te, undoped and In-doped, anomalous scatt. of carriers by defects and impurities near ferroelec. phase transition 4-98622  
 Pb<sub>1-x</sub>Sn<sub>x</sub>Te, ferroelec. phase transition close to band inversion 4-76364  
 Pb<sub>1-x</sub>Sn<sub>x</sub>Te system, plasma oscill. freq., temp. depend. 4-88836  
 Pb<sub>1-x</sub>Sn<sub>x</sub>Te, ferroelectric transition temp. and saturation effect (Russian) 4-71318  
 SbSI, differential polarisability, optical reflectance ellipsometry study 4-88796  
 SbSI ferroelec. semicond., energy band struct., X-ray spectral studies 4-65609  
 SbSI, L absorption edges, EXAFS studies 4-71475  
 SbSI, para-ferroelec. phase transition, photoacoustic spectra studies 4-65975  
 SbSI, paraelectric and ferroelec. phases, L-edge XANES and EXAFS obs. 4-88904  
 SbSI type cryst., soft modes, microwave dielec. studies 4-71293  
 SbS<sub>1-x</sub>Se<sub>x</sub> crystal, soft mode in microwave dielec. spectrum 4-76361  
 Sn<sub>2</sub>P<sub>2</sub>S<sub>6</sub>, ferroelec. semicond., Curie temp. photoinduced shift 4-93017  
 p-SnTe, struct. and ferroelec. transitions, review 4-65390  
 SrTiO<sub>3</sub>, equilb. elec. cond. at 1000°C effect of Sr/Ti ratio 4-84618  
 SrTiO<sub>3</sub>, In contact, tunnelling electron-phonon interaction strength 4-98754

## ferroelectric switching

- ceramics, ferroelectric, switching and hysteresis effects 4-76401  
 current, method of expt. meas. 4-76369  
 liquid crystal mol. orientation dynamic response 4-98005  
 liquid crystals, microsecond electro-optic switching using transient light scatt. 4-93052  
 PLZT ceramics, polarisation switching characts 4-99006  
 polyvinylidene fluoride and copolymers, ferroelec. switching, computer simulation 4-99049  
 TGS, ferroelec. switching current, effect of time between polarisation reversals 4-76368  
 TGS, ferroelec. switching current, method of expt. meas. 4-76369  
 TGS crystals, repeated switching-induced fatigue, struct. props. 4-71300  
 trisarcosine calcium chloride (bromide), polarisation reversal 4-88780  
 vinylidene fluoride-trifluoroethylene copolymer, ferroelec. switching 4-109137  
 vinylidene fluoride/trifluoroethylene copolymer, ferroelec. transitions 4-99050  
 viscous phenomena in ferroelectrics and ferroelastics 4-76367  
 BaTiO<sub>3</sub>, reverse switching effect 4-76393  
 BaTiO<sub>3</sub>.Fe, electroform., elec. field depend. 4-66077  
 Gd<sub>2</sub>(MoO<sub>4</sub>)<sub>3</sub>, ferroelectric-ferroelastic, acoustic emission and domain wall dynamics 4-84925  
 Pb<sub>2</sub>Ge<sub>2</sub>O<sub>11</sub>, ferroelec., surface states role in polarisation reversal 4-71325  
 Tb<sub>2</sub>(MoO<sub>4</sub>)<sub>3</sub>, ferroelectric-ferroelastic, acoustic emission and domain wall dynamics 4-84925

## ferroelectric thin films

- conference, Kyoto, Japan (May 1983) 4-101564  
 PLZT, ferroelec. films, reactive sputtering prep. and dielec. props. 4-104731  
 PLZT epitaxial thin films, ferroelec. and electrooptical props. 4-104530  
 poly(vinylidene fluoride) film, struct. under high elec. fields 4-98029  
 vinylidene fluoride-trifluoroethylene copolymer, ferroelec. hysteresis 4-99065  
 (Ba,Sr)TiO<sub>3</sub> heteroepitaxial ferroelec. films, domain struct. 4-65993  
 (Ba,Sr)TiO<sub>3</sub> polycryst. and heteroepitaxial ferroelec. films, phase transition 4-65977  
 BaTiO<sub>3</sub> polycryst. and heteroepitaxial ferroelec. films, phase transition 4-65977  
 BaTiO<sub>3</sub> thin films, crystallisation from amorphous phase, electron microscope study 4-113830  
 LiNbO<sub>3</sub> amorphous films, dielec. and elec. props. 4-104531  
 PLZT ferroelec. films, prep., props. and appls. 4-66230  
 PLZT thin-film waveguides, electrooptic Kerr coeffs. 4-91578  
 (Pb,Zr)TiO<sub>3</sub> thin films, magnetron RF sputtering and dielectric props. 4-88970  
 Pb<sub>2</sub>Ge<sub>2</sub>O<sub>11</sub> ferroelec. thin film, reactive sputtering prep. and props. 4-65961  
 PbTiO<sub>3</sub> amorphous films, dielec. and elec. props. 4-104531  
 PbTiO<sub>3</sub> heteroepitaxial ferroelec. films, domain struct. 4-65993  
 PbTiO<sub>3</sub> thin films, CVD prep. and dielec. props. 4-104736  
 Pb(Zr,Ti)O<sub>3</sub> ferroelec. films, reactive sputtering prep. and dielec. props. 4-104731

## ferroelectric transitions

- see also critical fluctuations; displacive transformations; ferroelectric Curie temperature; order-disorder transformations  
 acoustic-phonon dispersion at incommensurate phase transitions, Brillouin scatt. obs. 4-61724  
 alanine-TGS ferroelectric crystals, pyroelec. props. (Chinese) 4-114213  
 ammonium Rochelle salt, deuterated, dielec. and pyroelec. props. 4-114220  
 behaviour in nonresonance EM wave fields 4-88782  
 betaine arsenate, dielec. props. near ferroelec. transition 4-71307  
 betaine arsenate and phosphate, deuterated, ferroelectric props. 4-80876  
 betaine arsenate single cryst., ferroelec.-ferroelastic transition and sp. ht. 4-65415  
 ceramics, diffuse phase transition, exponent  $\gamma$  determ. 4-76384  
 ceramics, ferroelectric, switching and hysteresis effects 4-76401  
 ceramics, ferroelectric phase transition, thermodynamic model anal. (Russian) 4-99057

## ferroelectric transitions continued

- chiral triphenyl esters, columnar mesophases, structure and ferroelectric-antiferroelectric transition 4-60815  
 crystals, phase transitions, X-ray topography, review 4-65990  
 di(tetramethylammonium) copper tetrabromide, phase transition sequence, phenomenological theory 4-99055  
 di(tetramethylammonium)MCl<sub>4</sub> (M=Co,Zn,Cu), incommensurate, phase transitions, free energy phenomenological parameters 4-76378  
 di-(tetramethylammonium-d<sub>12</sub>) cobalt tetrachloride, commensurate-incommensurate transition 4-80023  
 dicalcium lead propionate, ferroelec. press. induced II-III transition, polarising microscope obs., permitt. meas. 4-80879  
 dicalcium lead propionate, ferroelec.-paraelec. transition, dopant conc. depend. 4-99048  
 dicalcium strontium propionate, ferroelec. press. induced II-III transition, polarising microscope obs., permitt. meas. 4-80879  
 dicalcium strontium propionate, ferroelectric phase transition, X-ray diff. study 4-65988  
 dipole-dipole mechanism of energy transfer 4-88482  
 elastic light scattering near phase transitions 4-71394  
 ferroic compounds, transition temp. determ. by microhardness meas. 4-71302  
 incommensurate phase formation, fluctuation effect mechanism 4-76371  
 using models for ferroelectric and ferromagnetic transitions 4-65821  
 IV-VI compounds, electronic and dynamical props., 'book contrib. 4-61003  
 lattice dynamics and phase transitions 4-80169  
 light scatt. from point defects in crystals near phase transition points 4-88850  
 martensitic transform. mechanisms for improper transitions 4-71304  
 martensitic transform. mechanisms for proper transitions 4-71303  
 martensitic transform. mechanisms for successive transitions 4-71305  
 methylammonium mercury trichloride, ferroelec. transition, thermal, dielec., optical meas. (French) 4-76392  
 monoaixial ferroelectrics, with second order phase transition, nonlinear pyroelectric response 4-88777  
 optical phonons, contribution to electronic transitions 4-65371  
 order-disorder phase transitions, crit. anomalies of vibr. lineshape 4-103893  
 organic halides, [(CH<sub>3</sub>)<sub>4</sub>N]<sub>2</sub>MX<sub>4</sub>, ferroelectricity and antiferroelectricity 4-65957  
 oxides, ferroelec., antiferroelectric, Seignettomagnetic, phys. props., phase transitions 4-65974  
 perovskite ferroelectrics, existence of ferroelectric phases of different symmetries 4-114221  
 perovskites, phase transition influence on oscillation spectrum 4-76362  
 polarisation fluctuations correlation function 4-88766  
 polarised defects, effects near Curie point 4-70134  
 Rochelle salt, ferroelectric phase transitions, piezoelectric coeffs., electrostrictive coeffs., temp. depend., resonance studies 4-114217  
 Rochelle salt, prototype-incommensurate ferroelectric phase transition 4-80880  
 Rochelle salt, soft modes, piezoelec. props. and ferroelec. transitions 4-76360  
 semiconductor, photoferroelectric phenomena caused by fluctuations and phases 4-66009  
 semiconductors, photoferroelectric phenomena caused by fluctuations and phases 4-70856  
 soft modes, dielec. spectroscopy studies 4-109135  
 solid soln., superionic phase transition in disordered sublattice 4-84919  
 soliton physics and ferroelectric transitions 4-80875  
 squaric acid, Ising model, Monte Carlo calc. 4-71306  
 squaric acid, thermal expansion, high resolution meas. along b-axis 4-92393  
 structural aspects of phase transitions in MM'Bx<sub>4</sub> type crystals 4-65241  
 surface distortions near phase transition points, quadrupole moment anomalies 4-88385  
 tetragonal ferroelectric, with defects, crit. fluctuations and phase transitions 4-71308  
 tetramethylammonium tetrachlorozincate, deuterated, ferroelec., temp.-press. phase diagram 4-76377  
 tetramethylammonium tetrachlorozincate, temp.-press. phase diagram 4-80217  
 tetramethylammonium zinc(cobalt) bromide, ferroelectric, phase transitions, X-ray diff. study 4-114216  
 TGS, and deuterated, ferroelec. crystals, pyroelec. props. (Chinese) 4-114213  
 TGS, ferroelec. transition, critical behaviour, defect influence 4-65983  
 TGSe, cryst., dielec. and electromechanical props. under high hydrostatic press. 4-76296  
 TGSe, ferroelec. transition, critical behaviour, defect influence 4-65983  
 TGSe, phase transition rel. to deuterisation 4-76387  
 thermal hysteresis near commensurate-incommensurate phase transition, interpretation 4-76382  
 thiourea, Brillouin scatt. under hydrostatic press., elastic constants. study 4-76479  
 thiourea, deuterated, neutron diff. study under high elec. field 4-109142  
 thiourea, incommensurate phase transitions, phase mode dynamics, neutron and Raman scatt. studies 4-65966  
 thiourea, lock-in transitions, successive, in incommensurate systems 4-76379  
 thiourea, modulated phase study 4-76372  
 p-toluidinium bromide, NQR, phase transition obs. 4-71205  
 p-toluidinium iodide (d<sub>3</sub>), NQR, phase transition obs. 4-71205  
 triglycine fluoroberyllate, cryst., dielec. and electromechanical props. under high hydrostatic press. 4-76296  
 tris sarcosine calcium chloride, ferroelec. transition and soft modes 4-93024  
 tris-sarcosine calcium chloride, dielec. const. and loss meas. in paraelec. phase, behaviour near ferroelec. transition 4-71258  
 tris-sarcosine calcium chloride, ferroelec. phase transitions, IR and Raman studies 4-71296  
 tris-sarcosine calcium chloride (bromide), ferroelec. phase transition, IR and Raman studies 4-93023  
 tris-sarcosine calcium chloride-bromide, soft modes, IR, and Raman spectra studies 4-71290  
 trissarcosine calcium chloride, iodinated, dielec. props., temp. and press. depend. 4-76310  
 uniaxial ferroelectrics, spin-lattice relax. at phase transitions, effect of relaxing defects, appl. to TGS 4-99059

## ferroelectric transitions continued

- uniaxial ferroelectrics, US absorpt. and vel., order parameter crit. fluctuations anisotropy spectrum, appl. to CsH<sub>2</sub>PO<sub>4</sub> 4-98206  
 vinylidene fluoride-trifluoroethylene copolymer, ferroelec. hysteresis 4-99065  
 vinylidene fluoride-trifluoroethylene copolymer, ferroelec. transition, bulk modulus anomaly, thermal expansion, press. depend. 4-84917  
 vinylidene fluoride-trifluoroethylene copolymer, permittivity near ferroelec. transition 4-99051  
 vinylidene fluoride-trifluoroethylene copolymers, ferroelec. transition and dielec. props. 4-99052  
 vinylidene fluoride-trifluoroethylene copolymers, ferroelec. transition, statistical theory anal. 4-99053  
 vinylidene fluoride-trifluoroethylene copolymers, ferroelec. transition, struct. studies 4-99054  
 vinylidene fluoride/trifluoroethylene copolymer, ferroelec. transitions 4-99050  
 Ag<sub>3</sub>AsS<sub>3</sub>, proustite, incommensurate phase in region of second-order phase transition, NQR, sp. ht. meas. 4-71314  
 Ag<sub>3</sub>AsS<sub>3</sub>, proustite, noncommensurate phase associated with mode interactions 4-93014  
 AgPbSb<sub>2</sub>S<sub>6</sub>, andorite, piezoelec. and phase transition props., acoustic meas. 4-93005  
 (Ba,Sr)TiO<sub>3</sub>, polycryst. and heteroepitaxial ferroelec. films, phase transition 4-65977  
 BaBiO<sub>3</sub>-BaPbO<sub>3</sub>, dielec. and supercond. transitions, Mossbauer line isomer shift 4-65973  
 Ba<sub>2</sub>NaNb<sub>2</sub>O<sub>15</sub>, ferroelec. transition, critical narrowing of central peak, Raman studies 4-71291  
 Ba<sub>2</sub>NaNb<sub>2</sub>O<sub>15</sub>, interaction of incommensurate modulation with mobile and fixed defects 4-75446  
 BaPbO<sub>3</sub>-BaBiO<sub>3</sub> system, supercond. and ferroelec. phase transitions 4-76061  
 Ba<sub>2</sub>Sr<sub>1-x</sub>Nb<sub>2</sub>O<sub>6</sub>, pyroelectric efficiency 4-114214  
 Ba<sub>9</sub>Sr<sub>10</sub>IO<sub>3</sub>, soft mode behaviour, ferroelec. transition and IR reflectometry 4-80872  
 BaTiO<sub>3</sub>, band struct. and ferroelec. transition, two-photon spectra studies 4-93016  
 BaTiO<sub>3</sub> based solid solns., ferroelec. transition temp. and electron spectra 4-93013  
 BaTiO<sub>3</sub>, cubic to tetragonal transition, covalency effects, band struct. calculations 4-70361  
 BaTiO<sub>3</sub>, displacive type ferroelastic, lattice model 4-76394  
 BaTiO<sub>3</sub>, displacive/order-disorder crossover, soft mode temp. depend., contrib. to low freq. permittivity 4-65369  
 BaTiO<sub>3</sub> doped single cryst., ferroelec. transition, substitutional defect influence 4-65984  
 BaTiO<sub>3</sub>, ferroelec. phase transitions, stress effects 4-71315  
 BaTiO<sub>3</sub>, ferroelec. phase transition microregion approach 4-76363  
 BaTiO<sub>3</sub>, polycryst. and heteroepitaxial ferroelec. films, phase transition 4-65977  
 BaTiO<sub>3</sub>, soliton physics and ferroelectric transitions 4-80875  
 BaTiO<sub>3</sub>, substituted, ferroelec. phase transitions and phase diagrams 4-65978  
 BaTiO<sub>3</sub>:Fe, soft mode behaviour, ferroelec. transition and IR reflectometry 4-80872  
 Cd<sub>2</sub>Nb<sub>2</sub>O<sub>7</sub>, diffuse and sharp phase transitions, dielec., optical, and electro-optical studies 4-71309  
 Cd<sub>2</sub>Nb<sub>2</sub>O<sub>7</sub>, photoferroelectric phenomena 4-88785  
 Cd<sub>2</sub>Nb<sub>2</sub>O<sub>7</sub>, thermo-optic and photochromic effects, phase transitions 4-99104  
 Cd<sub>2</sub>Nb<sub>2</sub>O<sub>7</sub>:Fe(Gd), narrow phase transitions, elec. field and impurity effects 4-71316  
 Cd<sub>2</sub>Nb<sub>2</sub>O<sub>7</sub>:Gd<sup>3+</sup>, ferroelec. transitions, EPR spectra 4-98945  
 CdTiO<sub>3</sub>:Mn<sup>2+</sup>, ferroelec. transitions, EPR studies 4-61588  
 Cr<sub>2</sub>B<sub>3</sub>O<sub>7</sub>Cl, ferroelec. orthorhombic to monoclinic transition 4-71301  
 Cs<sub>2</sub>PO<sub>4</sub>, quasi-one-dimensional, behaviour of thermodynamic quantities near ferroelec. phase transition 4-61634  
 CsH<sub>2</sub>PO<sub>4</sub> (Cs<sub>2</sub>PO<sub>4</sub>) ferroelectric phase transitions in transverse Ising model 4-93025  
 CsH<sub>2</sub>PO<sub>4</sub>, antiferroelec. fluctuations, Raman spectroscopy studies 4-71297  
 CsH<sub>2</sub>PO<sub>4</sub>, normal and deuterated, ferroelec. phase transition, Raman studies 4-71295  
 CsH<sub>2</sub>PO<sub>4</sub> pseudo-1D ferroelec., thermal cond. 4-65505  
 CsH<sub>2</sub>PO<sub>4</sub>, quasi-one-dimensional, behaviour of thermodynamic quantities near ferroelec. phase transition 4-61634  
 CsH<sub>2</sub>PO<sub>4</sub>, Raman scatt. study 4-71377  
 CsH<sub>2</sub>PO<sub>4</sub>, Slater-Senko model, ferroelec. transition 4-76370  
 CsLiMoO<sub>4</sub>, ferroelec. phase transitions, Raman and NMR studies 4-71289  
 CsLiMoO<sub>4</sub>-type crystals, ferroelec. phase transitions 4-65979  
 H(UO<sub>2</sub>)(AsO<sub>2</sub>)<sub>4</sub>H<sub>2</sub>O, phase transition temps. and ferroelec. domain struct. 4-76400  
 KD<sub>2</sub>PO<sub>4</sub>, photon emission during uniaxial deform., Curie temp. 4-81028  
 KH<sub>2</sub>PO<sub>4</sub>, acoustic soft mode, piezoelectric obs. 4-71266  
 KH<sub>2</sub>PO<sub>4</sub>, C<sub>33</sub> anomaly near ferroelec. transition, US attenuation studies 4-65325  
 KH<sub>2</sub>PO<sub>4</sub>, ferroelectric, phase transition at T=110°C 4-76389  
 KH<sub>2</sub>PO<sub>4</sub>, photon emission during uniaxial deform., Curie temp. 4-81028  
 KH<sub>2</sub>PO<sub>4</sub> type crystals, ferroelec. phase transition, stress effects 4-76365  
 KH<sub>2</sub>PO<sub>4</sub>, US study near press. induced tricritical point 4-76386  
 KH<sub>2</sub>PO<sub>4</sub>-type transition, struct. studies, review 4-76351  
 KIO<sub>3</sub>, low temp. ferroelec. transition under press. NQR studies 4-93019  
 K<sub>2</sub>Li<sub>2</sub>Nb<sub>2</sub>O<sub>10</sub>, solid solns., struct. and dielec. props. 4-75381  
 KNbO<sub>3</sub>, cubic to tetragonal transition, covalency effects, band struct. calculations 4-70361  
 KNbO<sub>3</sub>, displacive/order-disorder crossover, soft mode temp. depend., contrib. to low freq. permittivity 4-65369  
 KNbO<sub>3</sub>, electrostatics, polarisable point-ion model 4-80860  
 K<sub>2</sub>SeO<sub>4</sub>, acoustic phonon wavevector depend. near commensurate-incommensurate transition, Brillouin spectra 4-71313  
 K<sub>2</sub>SeO<sub>4</sub>, Brillouin spectra, scatt. angle and press. depend. 4-76481  
 K<sub>2</sub>SeO<sub>4</sub>, incommensurate phase, SHF Obs. 4-61635  
 K<sub>2</sub>SeO<sub>4</sub>, incommensurate phase transitions, phase mode dynamics, neutron and Raman scatt. studies, review 4-65966  
 K<sub>2</sub>SeO<sub>4</sub>, incommensurate-ferroelec. transition, struct. study 4-76381  
 K<sub>2</sub>SeO<sub>4</sub>, incommensurate transition, order parameter, EPR lineshape anal. 4-99056  
 K<sub>2</sub>SeO<sub>4</sub>, incommensurate-ferroelectric transition, structural study 4-109138

## ferroelectric transitions continued

- K<sub>2</sub>SeO<sub>4</sub>, phase transitions, thermal expansion coeffs., thermodynamic anal. of dilatometric and calorimetric data 4-88784  
 K<sub>2</sub>SeO<sub>4</sub>, phase-transition, Raman spectra, uniaxial stress depend. 4-76450  
 KTa<sub>1-x</sub>Nb<sub>x</sub>O<sub>3</sub>, ferroelec. soft mode, hyper-Raman scatt. studies 4-99060  
 KTa<sub>1-x</sub>Nb<sub>x</sub>O<sub>3</sub>, glasslike behaviour and press. effects 4-99058  
 KTaO<sub>3</sub>:Li, incipient ferroelec., off-centre impurity induced phase transition 4-76383  
 K<sub>4</sub>Th<sub>2</sub>Nb<sub>2</sub>O<sub>15</sub>, tetragonal tungsten bronze phase, cryst. struct., elec. and optical props. 4-70116  
 K<sub>2</sub>ZnCl<sub>4</sub>, incommensurate ferroelec., phase transitions, lattice dynamics, Raman effect 4-84922  
 K<sub>2</sub>ZnCl<sub>4</sub>, metastable chaotic state close to incommensurate-commensurate transition, <sup>51</sup>Cl NQR obs. 4-76285  
 K<sub>2</sub>ZnCl<sub>4</sub>, noncommensurate ferroelec., lattice dynamics and transitions, Raman studies 4-92313  
 K<sub>2</sub>ZnCl<sub>4</sub>, phase transitions, thermal expansion coeffs., thermodynamic anal. of dilatometric and calorimetric data 4-88784  
 LiKSO<sub>4</sub>, press. effect on phase transitions 4-104546  
 LiNH<sub>4</sub>SO<sub>4</sub>, normal and deuterated, II-III phase transition, elec. field effects 4-65396  
 LiNbO<sub>3</sub>, Raman scatt. isofrequency temp. depend. 4-76474  
 LiO-M<sub>2</sub>O<sub>5</sub>-M'<sub>2</sub>O<sub>4</sub>, M=Nb, Ta, M'=Ti, Zr, non-stoichiometric phases, cryst. chem. and ferroelec. props. 4-65968  
 LiTaO<sub>3</sub>, Raman scatt. isofrequency temp. depend. 4-76474  
 Mn<sub>2</sub>B<sub>2</sub>O<sub>7</sub>Cl(Br)(I), cubic-orthorhombic ferroelec. transition, sp. ht. studies 4-104545  
 (ND<sub>4</sub>)<sub>2</sub>D(SO<sub>4</sub>)<sub>2</sub>, successive phase transitions studied by VO<sup>2+</sup> ion and SeO<sub>4</sub> radical EPR 4-76388  
 (NH<sub>4</sub>)<sub>2</sub>BeF<sub>4</sub>, dielectric hysteresis and anomalous temperature 4-93026  
 (NH<sub>4</sub>)<sub>2</sub>BeF<sub>4</sub>, incommensurate phase, SHF Obs. 4-61635  
 (NH<sub>4</sub>)<sub>2</sub>BeF<sub>4</sub>, incommensurate phase, in applied elec. field 4-76376  
 (NH<sub>4</sub>)<sub>2</sub>H(SO<sub>4</sub>)<sub>2</sub>, successive phase transitions studied by VO<sup>2+</sup> ion and SeO<sub>4</sub> radical EPR 4-76388  
 NH<sub>4</sub>HSO<sub>4</sub>, deuterated, polymorphous transition, NMR study 4-114215  
 NH<sub>4</sub>HSO<sub>4</sub>, dielec. nonlinearity, ferroelec. transition 4-76366  
 NH<sub>4</sub>HSO<sub>4</sub>, dielectric, piezoelectric and elastic props. 4-80878  
 NH<sub>4</sub>HSO<sub>4</sub>, ferroelec. phase transition mechanisms, NMR studies 4-93015  
 NH<sub>4</sub>HSO<sub>4</sub>, ferroelec. transitions, Raman scatt. and vibr. props. 4-93066  
 NH<sub>4</sub>HSO<sub>4</sub>, ferroelec., with varying D content, phase transitions, dielec. anomalies 4-99061  
 (NH<sub>4</sub>)<sub>2</sub>SO<sub>4</sub>:CrO<sub>3</sub>, phase transitions studied by EPR spectra 4-88723  
 (NH<sub>4</sub>)<sub>2</sub>SO<sub>4</sub>:K<sub>2</sub>SO<sub>4</sub>:CrO<sub>3</sub>, phase transitions studied by EPR spectra 4-88723  
 (NH<sub>4</sub>)<sub>2</sub>ZnBr<sub>4</sub>, ferroelec., Raman scatt. study of phase transitions 4-104589  
 (NH<sub>4</sub>)<sub>2</sub>ZnCl<sub>4</sub>, incommensurate phase transition, dielec. props., X-ray diff. study 4-93021  
 Na<sub>0.5</sub>Bi<sub>0.5</sub>TiO<sub>3</sub>, soft-modes and central peak, inelastic neutron scatt. studies 4-61037  
 Na<sub>1/2</sub>Bi<sub>1/2</sub>TiO<sub>3</sub> ceramics, pyroelectric props., perspective appl. in pyroelectric radiation detectors 4-88776  
 NaH<sub>2</sub>(SeO<sub>3</sub>)<sub>2</sub> crystals, ferroelec., existence of interphase between  $\alpha$ - and  $\beta$ -phases 4-104544  
 NaNO<sub>2</sub>, modulated phase study 4-76372  
 NaNO<sub>3</sub>, paraelectric-ferroelectric transition, isotropy group description 4-84918  
 Na<sub>3</sub>Sc<sub>2</sub>(PO<sub>4</sub>)<sub>3</sub> and isomorphs, ferroelec.-superionic cond. phase transitions 4-71310  
 (NH<sub>4</sub>)<sub>2</sub>HPO<sub>4</sub>(PO<sub>4</sub>H<sub>2</sub>)<sub>2</sub>Te(OH)<sub>6</sub>, NMR study of phase transition 4-80877  
 PLZT ceramics, ferroelec. and electrooptic props. 4-61633  
 PZT, amorphous, ferroelec. phase transition 4-61637  
 PZT, dielec. props. at high press., p-T phase diagrams 4-99062  
 PZT, doped, diffuse phase transition, ultrasound meas. 4-76385  
 (Pb, Sn, Ge)Te, semicond., dielec. props. and soft modes, review, book contrib. 4-61622  
 (Pb<sub>0.77</sub>Bi<sub>0.23</sub>)Ti<sub>3</sub>, ferroelec., phase-transition, high press. Raman study 4-76451  
 Pb(FeNb)<sub>0.5</sub>O<sub>3</sub> ceramics and single crystals, prep., struct., X-ray diff., neutron powder diff., dielec. and elec. meas., SEM 4-75412  
 PbFe<sub>0.5</sub>Ta<sub>0.5</sub>O<sub>3</sub> single cryst., ferroelec./antiferromag., spontaneous birefringence 4-71344  
 Pb<sub>2</sub>Ge<sub>2</sub>O<sub>11</sub>, lattice dynamics near Curie point (Russian) 4-98221  
 Pb<sub>1-x</sub>Ge<sub>x</sub>Te, ferroelec. phase transition, high press. investigation, DC resist., capacitance meas. 4-71312  
 n-Pb<sub>1-x</sub>Ge<sub>x</sub>Te, free carrier mobility, ferroelectric phase transition 4-71317  
 Pb<sub>1-x</sub>Ge<sub>x</sub>Te, undoped and In-doped, anomalous scatt. of carriers by defects and impurities near ferroelec. phase transition 4-98622  
 PbHfO<sub>3</sub>, ferroelec. transition effects on absorption edges 4-93020  
 PbInNbO<sub>6</sub>, order-disorder transitions and dielec. props. 4-65980  
 Pb<sub>2</sub>(MF<sub>6</sub>)<sub>3</sub> (M=Ti, V, Cr, Fe, Ga), ferroelectric phase transitions 4-71311  
 PbMg<sub>1/3</sub>Nb<sub>2/3</sub>O<sub>3</sub>, diffuse phase transition 4-65967  
 PbMg<sub>1/3</sub>Nb<sub>2/3</sub>O<sub>3</sub>, mean square displacements, thermal expansion coeff. in diffuse ferroelec. transition region, X-ray diff. meas. 4-65971  
 Pb<sub>2</sub>ScNbO<sub>6</sub>, order-disorder transitions and dielec. props. 4-65980  
 Pb<sub>1-x</sub>Sn<sub>x</sub>Te, ferroelec. phase transition close to band inversion 4-76364  
 Pb<sub>2</sub>Sn<sub>1-x</sub>Te, ferroelectric transition temp. and saturation effect (Russian) 4-71318  
 PbTiO<sub>3</sub>, ferroelec. phase transitions, stress effects 4-71315  
 PbTiO<sub>3</sub>, six sites model for successive transitions 4-80873  
 PbTiO<sub>3</sub>, substituted, ferroelec. phase transitions and phase diagrams 4-65978  
 Pb(Ti<sub>0.9</sub>Sn<sub>0.1</sub>)O<sub>3</sub>, ferroelec., phase-transition, high press. Raman study 4-76451  
 Pb(Ti<sub>1-x</sub>Zr<sub>x</sub>)O<sub>3</sub>, ferroelec. phase transitions and phase diagrams 4-65978  
 Pb<sub>2</sub>V<sub>2</sub>O<sub>8</sub>, cryst. struct. of ferroelectric  $\alpha$  phase (French) 4-84259  
 PbZrO<sub>3</sub>, soft mode in ferroelectric transition 4-99063  
 PbZrO<sub>3</sub>, with O vacancies, phase transitions, dielec. props. 4-76391  
 PbZrO<sub>3</sub>, with vacancies, para, ferro and antiferroelectric phase transitions, influence of hydrostatic press. 4-76390  
 PbZr<sub>1-x</sub>Ti<sub>x</sub>O<sub>3</sub> cryst., T, x, E phase diagram anal. 4-76359  
 Pb<sub>(1-y/2)</sub>Zr<sub>(1-x+y/2)</sub>Ti<sub>y</sub>Nb<sub>0.5</sub>O<sub>3</sub> ceramic transducers, pyroelec. and mechano-dielectric charact. 4-109136  
 RB<sub>1-x</sub>(NH<sub>4</sub>)<sub>x</sub>H<sub>2</sub>PO<sub>4</sub> mixed crystals, phase transitions in cluster approx., pseudospin model 4-80881

## ferroelectric transitions continued

- RbAlF<sub>4</sub>, ferroelec. phase transitions, EPR studies 4-71158  
 Rb<sub>2</sub>Cd<sub>2</sub>(SO<sub>4</sub>)<sub>2</sub>, thermal expansion, 77 to 300K 4-92396  
 Rb<sub>1-x</sub>Cs<sub>x</sub>D<sub>2</sub>PO<sub>4</sub>, monoclinic, phase transitions, dielec. studies 4-109139  
 RbD<sub>2</sub>(SeO<sub>3</sub>)<sub>2</sub>, ESR spectra and dielec. const. meas. 4-76305  
 RbD<sub>2</sub>(SeO<sub>3</sub>)<sub>2</sub>, ferroelectric phase transition, dielec. anomaly 4-65987  
 RbHSO<sub>4</sub>, ferroelectric phase transitions, piezoelectric coeffs., electrostrictive coeffs., temp. depend., resonance studies 4-114217  
 RbH<sub>2</sub>(SeO<sub>3</sub>)<sub>2</sub>, ESR spectra and dielec. const. meas. 4-76305  
 RbLiMoO<sub>4</sub>, cryst. struct. determ. and phase transition 4-79999  
 Rb<sub>0.52</sub>(ND<sub>4</sub>)<sub>0.48</sub>D<sub>2</sub>PO<sub>4</sub> cryst., proton glass dielec. behaviour 4-114218  
 Rb<sub>2</sub>ZnCl<sub>4</sub>, ferroelec., phase transitions, dielec. and DTA studies, rel. to cryst. growth conditions 4-76374  
 Rb<sub>2</sub>ZnCl<sub>4</sub>, incommensurate, modulation wave floating, NMR meas. 4-65991  
 Rb<sub>2</sub>ZnCl<sub>4</sub>, incommensurate-ferroelec. phase transition, X-ray study 4-76373  
 Rb<sub>2</sub>ZnCl<sub>4</sub>, incommensurate ferroelec., phase transitions, lattice dynamics, Raman effect 4-84922  
 Rb<sub>2</sub>ZnCl<sub>4</sub>, incommensurate phase, dynamic dielec. props., pinning effects 4-109140  
 Rb<sub>2</sub>ZnCl<sub>4</sub>, modulated ferroelec., thermal hysteresis and pinning 4-76380  
 Rb<sub>2</sub>ZnCl<sub>4</sub>, noncommensurate ferroelec., lattice dynamics and transitions, Raman studies 4-92313  
 Rb<sub>2</sub>ZnCl<sub>4</sub>, phase transitions, thermal expansion coeffs., thermodynamic anal. of dilatometric and calorimetric data 4-88784  
 Rb<sub>2</sub>ZnCl<sub>4</sub>, phase-transition, Raman spectra, uniaxial stress depend. 4-76450  
 Sb chalcogenohalide based ACH-2 ferroelectric, soft microwave modes 4-84920  
 SbSbR, ferroelec. phase transitions, elec. permittivity studies 4-65981  
 SbSi ferroelectric, L<sub>III</sub> edge above transition temp., EXAFS study 4-61772  
 SbSi, para-ferroelec. phase transition, photoacoustic spectra studies 4-65975  
 SbSi type cryst., soft modes, microwave dielec. studies 4-71293  
 SbsSe<sub>1-x</sub>I<sub>x</sub> ferroelec. phase transition, dilatometric study 4-114222  
 Sn<sub>2</sub>P<sub>2</sub>S<sub>6</sub>, influence of hydrostatic pressure on vibrational spectra 4-109192  
 Sn<sub>2</sub>P<sub>2</sub>S<sub>6</sub>(Se<sub>2</sub>), IR spectra of ferroelectric transition splitting 4-84966  
 p-SnTe, struct. and ferroelec. transitions, review 4-65390  
 Sr<sub>2</sub>Al<sub>2</sub>O<sub>7</sub>(CrO<sub>4</sub>)<sub>2</sub>, flux grown, ferroelec. phase transition, domain studies, birefr., polarisation, permittivity, transition enthalpy meas. 4-65970  
 Sr<sub>1-x</sub>Ca<sub>x</sub>TiO<sub>3</sub>, XY quantum ferroelec. with transition to randomness 4-88781  
 Sr<sub>2</sub>Nb<sub>2</sub>O<sub>7</sub>, ferroelec., incommensurate-polar transition 4-76375  
 Sr<sub>2</sub>Ta<sub>2</sub>O<sub>7</sub>, ferroelec. transition temp. and optical absorption edge, press. depend. 4-93018  
 SrTiO<sub>3</sub>, band struct. and ferroelec. transition, two-photon spectra studies 4-93016  
 SrTiO<sub>3</sub>, O<sub>2</sub> photo-adsorption, ESR study 4-65550  
 SrTiO<sub>3</sub>, US attenuation and vel. near ferroelec. transition 4-65345  
 SrTiO<sub>3</sub>, ultrasonic props. near phase transition 4-113544  
 TGS, ferroelec. transition and domains, positron annihilation, TEM and decoration studies 4-65985  
 TGSe, audiofrequency dielec. dispersion, universal behaviour and temp. depend. 4-76303  
 TiCdF<sub>6</sub>:Gd<sup>3+</sup>, O<sup>2-</sup>, critical phenomena above and below T<sub>c</sub>, EPR studies 4-65854  
 TiH<sub>2</sub>(SeO<sub>3</sub>)<sub>2</sub>, cryst. struct., phys. props., phase transitions 4-84921  
 TiH<sub>2</sub>(SeO<sub>3</sub>)<sub>2</sub>, dielec. props., phase transitions, cryst. struct. 4-65965  
 TiInS<sub>2</sub>, structural phase transitions, dielec. props. at subMM wavelengths 4-98275  
 Ti<sub>2</sub>SeO<sub>4</sub>, ferroelec. transition, birefringence studies 4-65976  
 Ti<sub>2</sub>SeO<sub>4</sub>, phase transition and lattice const., X-ray diff. study 4-71294

## ferroelectricity

- see also antiferroelectricity; ferroelectric devices; ferroelectric materials; ferroelectric switching; ferroelectric transitions  
 antiferromagnetic ferroelectric, equilibrium state of mag. subsystem 4-71150  
 ceramics, phase transition, thermodynamic model anal. (Russian) 4-99057  
 conference, Malaga, Spain (Sept. 1983) 4-63384  
 crystal symmetry and ferroelectricity 4-65955  
 crystals, soliton propag. and electroacoustic interactions (French) 4-99047  
 deformable, shock waves 4-76358  
 dipole-dipole mechanism of energy transfer 4-88482  
 domain layer surface wave, dispersion eqns. 4-88787  
 double sine-Gordon chain, damped, uniformly moving domain walls, rel. to A<sub>2</sub>BX<sub>4</sub>-type ferroelec. crystals 4-90391  
 electron-phonon interaction and phonon softening in ferroelectrics, Kristofel-Konsin mechanism 4-65363  
 lattice and spin dynamical theories 4-76357  
 lattice dynamics and phase transitions 4-80169  
 liquid crystal mol. orientation dynamic response 4-98005  
 liquid crystals and ordered fluids, conference, Las Vegas (USA), (March-April 1982) 4-82596  
 liquids, ferroelec. physics 4-76356  
 magnetization phenomena, symmetry aspects 4-66015  
 microcrystals of cooperatively-coupled materials, phys. props. 4-88778  
 nematic liq. cryst., longitudinal domain struct., laser diff. studies 4-60829  
 permittivity in the field of a strong EM wave 4-92988  
 perovskite ferroelectrics, existence of ferroelectric phases of different symmetries 4-114221  
 phonon anomalies in ferroelectrics and supercond. 4-65351  
 photovoltaic effect, review 4-65956  
 photovoltaic effects in piezoelec. and ferroelec. crystals 4-75993  
 polarised defects, effects near Curie point 4-70134  
 polydomain ferroelectrics, uniaxial, soft local vibr. 4-93028  
 polymers, piezoelectric, pyroelec. and ferroelec. props., conf., USA (July 1983) 4-95030  
 pseudo-spin system, isolated point defects and order parameter 4-70138  
 smectic chiral C phases, new systems 4-84916  
 soft modes, dielec. spectroscopy studies 4-109135  
 soliton physics and ferroelectric transitions 4-80875  
 stochastic US signal emission on polarisation initiation (French) 4-109051  
 surface modes, dispersion curves and soft mode temp., Ising model anal. 4-65538

**ferroelectricity continued**

- surface modes in ferroelec. materials 4-61632
- symmetric phases, Raman scatt. spectrum, forbidden lines 4-76444
- symmetrical phase, forbidden Raman lines 4-66026
- weakly ferromagnetic ferroelectrics, static and dynamic props. of mag. domain walls (*Russian*) 4-92936
- X-ray induced metastable photovoltaic centres in ferroelectrics 4-104253

**ferrofluids** *see magnetic fluids***ferromagnetic-antiferromagnetic transitions**

- see also metamagnetism; Morin temperature*
- Heisenberg, magnetic materials, intermediate ordered phases, calcs. 4-114132
- magnetic materials near phase transition, relax. process 4-88671
- rare earth-Cd equiatomic cpds., struct. and mag. phase transitions 4-84795
- unordered magnet, competing exchange interactions, microstructure and mag. props. 4-76150
- CeD<sub>2</sub>, order-disorder transform. and mag. struct. 4-61069
- Er, specific heat, 0.4-23K 4-76143
- ErCrO<sub>3</sub>, quadrupole splitting and NMR near Morin-type transition 4-80839
- ErRh<sub>4</sub>B<sub>4</sub>, coexistence of superconductivity and mag. order 4-104423
- La(Fe<sub>1-x</sub>Al<sub>x</sub>)<sub>13</sub>, metamagnetic transitions and struct. aspects 4-92910
- Mn<sub>2</sub>B<sub>4</sub>, mag. props. under high mag. field 4-84799
- Mn<sub>3</sub>Ge<sub>8</sub>, cryst. struct. and lattice const. temp. depend. 4-103702
- MnRhAs, antiferromagnetic-ferromagnetic transition, mag. props., elec. resist. meas. 4-104417
- Tb<sub>0.5</sub>Y<sub>0.5</sub>Ni, metamagnetism and coercivity 4-71070
- V<sub>2</sub>Fe<sub>1-x</sub>S<sub>x</sub>, crystallographic and spin rotation transitions, Mossbauer studies 4-98270

**ferromagnetic Curie temperature** *see Curie temperature***ferromagnetic-paramagnetic transitions**

- see also Curie temperature*
- ferromagnetic materials, phase transitions, 2nd order near Curie point 4-98890
- intermediate valence systems, ferromagnetism stability 4-71061
- Ising model, two-dimensional random, domain-wall renormalisation group study 4-71113
- ising models for ferroelectric and ferromagnetic transitions 4-65821
- metallic glasses, mag. props. 4-114139
- transition metals, ferromagnetic-paramagnetic phase transformations and collective phenomenon (*German*) 4-71068
- CoTi<sub>1-x</sub>Al<sub>x</sub>, transition from nonmag.-ferromag. state, magnetisation and NMR meas. 4-76133
- $\alpha$ -Fe, Co diffusion, effect of mag. transition 4-65481
- FeCo(Mn)(V), coupling between chemical and mag. interactions, NMR study 4-114173
- Fe<sub>2</sub>P, metamagnetic transitions, magnetisation studies 4-98883
- Fe<sub>2</sub>P, metamagnetic transitions, PT diagram studies 4-114111
- FePCr(Cr), structural and mag. coherence lengths 4-88100
- Fe<sub>2</sub>P<sub>1-x</sub>Si<sub>x</sub>, hexagonal-orthorhombic transition, Mossbauer studies 4-109102
- Fe<sub>90</sub>Zr<sub>10</sub> glass, H induced mag. phase transform., Mossbauer spectroscopy study 4-61536
- Mn<sub>2</sub>Ge<sub>8</sub>, thermal expansion meas., 4.2-800K, Curie point, press. shifts 4-98320
- MnRhAs, antiferromagnetic-ferromagnetic transition, mag. props., elec. resist. meas. 4-104417
- Ni, stress effects on mag. phase transitions 4-114106
- Ni-Si-B metallic glasses, Hall effect, mag. ordering near resist. minimum 4-75933

**ferromagnetic properties of substances**

- see also ferromagnetic relaxation; ferromagnetic resonance; ferromagnetism; magnetic semiconductors*
- alloys, amorphous, extended freq. anal. of permeability aftereffect 4-84822
- Alnico magnets, microstruct., comp., atom probe field ion microscopy 4-71828
- amorphous alloys, zero-magnetostrictive, struct. approach to permeability aftereffect 4-84832
- amorphous ribbon, simultaneous magnetic meas. and torsional creep 4-111163
- bis[1,2-bis(2-methoxyethoxy)ethane] sodium biphenylide, spin diffusion, mag. props. ESR study 4-71154
- bulk metal, parallel configuration of FMR, surface impedance, calcs. 4-98953
- components, quality control by coercive field strength meas. 4-93475
- cyclohexylammonium copper trichloride, magnon bound state excitations 4-80751
- cyclohexylammonium copper trichloride and tribromide, exchange anisotropy study 4-80758
- degenerate ferromagnetic semiconductors, spin waves at low temps. 4-114096
- dilute ferromagnet, phase transitions, from Grassmann path integrals 4-92911
- dirty nearly ferromagnetic metallic films, triplet supercond., weak localisation effect 4-98798
- ferromagnetic emulsion, hydrodynamics, effective viscosity and shear flow 4-109693
- ferromagnetoelectrics, spin waves, reson. excitation by external elec. field 4-98871
- garnet thin films, ferromagnetic, microwave props., review 4-80803
- graphite:Fe, ion implanted, mag. props. 4-61562
- hydrogen copper (II) maleate tetrahydrate, one-dimensional ferromagnetism 4-71051
- intermediate valence systems, ferromagnetism stability 4-71061
- linear Ising model, crystal field effect, ferromag. and antiferromag. susceptibilities 4-98845
- metal, ferromag., spin polarisation of Auger photoelectrons 4-71528
- metallic glasses, mag. aftereffects, induced anisotropy and role of two-level systems 4-84821
- metallic glasses, Metglas 2605S-3 and 2705M, mag. permeability, effects of neutron irradiation 4-71125
- metallic glasses, thermoelec. power, elec. resist., spin-disorder model 4-75935
- metals, crystalline and amorphous, shear magnetostriction theory 4-98931
- metals, ferromagnetic, exchange interactions and spin-wave stiffness 4-84776

**ferromagnetic properties of substances continued**

- metals, muon hyperfine fields, influence of lattice relax. and zero-point motion 4-65919
- metals and alloys, book contrib. 4-114093
- metals spin-polarised AES, theory 4-104703
- NpAsTe, mag. props. (*French*) 4-84766
- Permalloy, mag. permeability, effects of neutron irradiation 4-71125
- Permalloy, surface layer, light irradi., magnetoelectric phenomena 4-76218
- Permalloy evaporated films, coercive force and mag. domains (*Japanese*) 4-104474
- Permalloy film, on antiferromag. substrate, FMR freqs., effect of domain struct. 4-92965
- Permalloy films, mag. anisotropy and domain struct. patterning effects 4-88707
- Permalloy polycrystal, spin polarisation of electron-excited secondary electrons, surface magnetism effects 4-61784
- Permalloy thin films, micron size, magnetisation dynamics 4-61573
- rare earth-Cd equiatomic cpds., struct. and mag. phase transitions 4-84795
- rare earth alloys, R<sub>3</sub>Rh<sub>2</sub>, R-Gd, Tb, Dy, Ho, Er, mag. props. meas. 4-61521
- rare earth alloys, R-Fe-based metallic glasses, anomalous mag. hysteresis and coercive force 4-114140
- rare earth intermetallics, RFe<sub>2</sub>H<sub>2</sub> (R=Gd, Ho, Er, Tm, Lu), mag. props. and cryst. struct., absorbed H<sub>2</sub> effects (*Russian*) 4-104458
- rare earth-Co intermetallics, RCo<sub>2</sub> type, domain struct. 4-114133
- relative magnetic permeability and electrical conductivity measurement of ferromagnetic materials (*Polish*) 4-90616
- semiconductors, elec. resist. reson. rel. under FMR saturation conditions 4-92726
- semiconductors, nonequilibrium system of electrons and magnons, fluctuations in strong elec. fields 4-98870
- static characteristics, automatic meas. and recording, HISTEREZOGRAF BH-1 4-106333
- steel, electric, coating effect on domain struct. 4-80775
- steel, Fe-Si (3 wt.%), grain oriented, compression effects on domain struct. 4-80774
- steel, ferromag., electron beam microanal., stray mag. fields (*German*) 4-66622
- steel, NDT, residual magnetic field above surface, tangential component distrib. 4-71843
- steel, rotor, mag. induction, cooling rate depend 4-76184
- steel, stainless, ferritic-austenitic, embrittlement, mag. inspection 4-99704
- steels, ferromagnetic components used in magnetic fusion reactors, anal. of forces 4-91110
- thin films, high vac. evaporation, prod. technology for mag. tapes 4-66234
- thin films, perpendicular hysteresis models 4-71132
- TMNB, 1-D short range and 3-D long range mag. order, neutron scatt. study 4-108991
- transition metal fluorides, ionic and mag. ordering 4-70096
- transition metal-Fe-B amorphous alloys, magnetisation reversal, mech. stress effects 4-76171
- transition metal-metalloid amorphous ferromagnets, mag. moment distrib. and temp. depend. of reduced hyperfine fields 4-92899
- transition metals, magnetism and electronic struct., validity of simple alloy model 4-98865
- water-based ferromagnetic solns. parametric transformation 4-66727
- Ag<sub>5</sub>MnAl, Silmanal, magnetic phase growth (*Russian*) 4-109014
- Au-Fe dilute alloy, exchange-circulation electron current between Fe atoms (*Chinese*) 4-114102
- Bi oxides, sillenite phase form. mag., EPR and IR studies 4-88137
- CdCr<sub>2</sub>Se<sub>4</sub>, surface magnetostatic wave obs. 4-84778
- Ce-Co-Cu, magnetically hard alloys, isostructural precipitation and atomic ordering (*Russian*) 4-104784
- CeD<sub>2</sub>, order-disorder transform. and mag. struct. 4-61069
- Ce<sub>1-x</sub>Hf<sub>x</sub>Co<sub>2</sub>, anomalous mag. behaviour 4-88664
- CeM<sub>2</sub>B<sub>2</sub> (M=Co, Ru, Rh, Ir), mixed valence, mag. and elec. props. 4-113905
- Ce<sub>1-x</sub>Zr<sub>x</sub>Co<sub>2</sub>, anomalous mag. behaviour 4-88664
- Co alloy amorphous sputtered films, mag. props. 4-84836
- Co, electronic struct., magnetism and Curie temps. 4-75843
- Co, polycrystalline, approach to saturation at intermediate fields, role of internal demagnetising fields 4-76183
- Co, polycrystalline, ferromagnetic, density of unoccupied states, SXAPS study 4-85039
- Co single crystals, spin polarised Auger electrons 4-85044
- Co-(Fe, Mn)-Nb system, amorphous sputtered films, magnetostriction and HF permeability 4-71147
- Co-Ag-Pd, transient fields, g-factor, gyromagnetic ratios 4-113914
- Co-Cr ferromagnetic thin films, high rate magnetron sputtering 4-66232
- Co-Cr layers, mag. orientation, effect of RF sputter parameters 4-65840
- Co-Cr sputtered thin films, surface and vol. coercive fields 4-65841
- Co-Ir sputtered films, mag. props. 4-71141
- Co-Nb-Ti system, amorphous sputtered films, magnetostriction and HF permeability 4-71147
- Co-Ni-P, amorphous thin films, small planar domains, nucleation and equil. conditions 4-71123
- Co-O perpendicular magnetic film by evaporation 4-92941
- Co-P amorphous alloys, NMR enhancement factor and multiple echoes 4-76270
- Co-P amorphous electrodeposited layers, Barkhausen effect, torsion effects 4-76198
- Co-P amorphous layers, mag. and struct. props. 4-76199
- Co-Sb multilayered films, cpd. form., interface magnetism, <sup>59</sup>Co NMR obs. 4-109095
- Co-Si-B (-Fe) metallic glasses, mag. props., annealing effects 4-109039
- Co-W-Mn thin mag. film deposition, electrocrystallisation (*Russian*) 4-65592
- Co<sub>100-x</sub>B<sub>x</sub> amorphous alloys, mag. anisotropy, mag. annealing effects 4-76131
- Co<sub>75</sub>B<sub>25</sub> amorphous alloys, mag. relax. processes 4-84825
- Co<sub>2</sub>B<sub>2</sub>O<sub>7</sub>Br, spontaneous birefringence and Faraday effect 4-71351
- Co<sub>1-x</sub>Ni<sub>x</sub> amorphous alloys, magnetic moments, Friedel's model 4-76123
- CoNiFe-SiB amorphous zero magnetostrictive alloy, compositional short-range order and ordering kinetics 4-70035
- Co<sub>55</sub>Ni<sub>35</sub>Fe<sub>10</sub>Si<sub>16</sub> amorphous; mag. aftereffects after field annealing 4-84823

## ferromagnetic properties of substances continued

- Co<sub>9</sub>Ni<sub>1-x</sub>Fe<sub>1-x</sub>B<sub>10</sub>, amorphous, mag. hysteresis loops after heat treatment below Curie point 4-80781
- Co<sub>9</sub>Ni<sub>1-x</sub>MnGe, magnetic transforms., effect of external press. 4-104418
- Co<sub>95-x</sub>Si<sub>5-x</sub>B<sub>x</sub>, amorphous alloys, mag. aftereffects 4-84824
- CoTi, amorphous thin films, small planar domains, nucleation and equilib. conditions 4-71123
- Co<sub>100-x</sub>Ti<sub>x</sub> thin films, field induced anisotropy 4-71133
- Co<sub>100-x</sub>Al<sub>x</sub>, transition from nonmag. ferromag. state, magnetisation and NMR meas. 4-76133
- Co<sub>92</sub>Zr<sub>8</sub>Nb<sub>10</sub>SiO<sub>2</sub> multilayered struct. amorphous films, mag. props. 4-104462
- Cr (100), mag. phase transition, angle resolved photoelectron spectra studies 4-98888
- Cr, magnetic moment fluctuations and magnetovol. variations 4-109026
- CrBr<sub>3</sub>, optical spectra near mag. transition temp. 4-61729
- Cr<sub>2</sub>Mn<sub>1-x</sub>As, thermal and mag. props., 100 to 500K 4-92922
- CrO<sub>2</sub> particles prod. for mag. tape appls. 4-65831
- CrO<sub>2</sub> powders, hydrothermal synthesis and charact., mag. recording appl. 4-89000
- Cr<sub>2</sub>O<sub>3</sub>, ferromag., Curie point transition, EPR obs. 4-109061
- Cs<sub>2</sub>Ni<sub>2</sub>CdF<sub>12</sub>, hexagonal perovskites, intra-and intercluster mag. interactions 4-104405
- Cs<sub>2</sub>Ni<sub>4</sub>CdF<sub>15</sub> hexagonal perovskites, intra-and intercluster mag. interactions 4-104405
- CsNiF<sub>3</sub>, failure of classical approx. for magnetisation calcs. 4-71126
- CsNiF<sub>3</sub> ferromagnet, optical absorption and magneto-optical properties 4-99100
- CsNiF<sub>3</sub>, model, sp. ht. of classical easy-plane ferromag. chain 4-104452
- Cu-Fe (1.59 wt.%),  $\alpha$ - $\gamma$  martensitic transform. of Fe particles, magnetisation obs. 4-66335
- Cu-Fe dilute alloy, exchange-circulation electron current between Fe atoms (Chinese) 4-114102
- (CuCr<sub>2</sub>Se<sub>4</sub>)(Cu<sub>0.5</sub>Ga<sub>0.5</sub>Cr<sub>2</sub>Se<sub>4</sub>)<sub>1-x</sub>, semiconducting spin glasses, resistance, magnetoresistance, studies 4-108862
- (CuCr<sub>2</sub>Se<sub>4</sub>)(Cu<sub>0.5</sub>In<sub>0.5</sub>Cr<sub>2</sub>Se<sub>4</sub>)<sub>1-x</sub>, semiconducting spin glasses, resistance, magnetoresistance, studies 4-108862
- Cu<sub>2</sub>MnAl, Heusler alloy, decomposition during isochronal annealing, mag. props. 4-61916
- CuRb<sub>2</sub>Br<sub>4</sub>·2H<sub>2</sub>O, mag. props. meas. 4-89925
- DyAl<sub>2</sub>, ferromag., magnetisation, NMR studies 4-80787
- DyCu<sub>2</sub>Ge<sub>2</sub>, mag. and cryst. struct., neutron diff. studies 4-65794
- Dy<sub>2</sub>Er<sub>1-x</sub>Ni<sub>x</sub>, mag. struct. charact. (Russian) 4-92894
- (Dy<sub>0.7</sub>Tb<sub>0.3</sub>)<sub>2</sub>Fe<sub>20</sub>, mechanostress strain as a function of magnetic field and mechanical elastic stresses 4-113523
- Er<sub>0.6</sub>Ho<sub>0.6</sub>Rh<sub>0.8</sub>B<sub>4</sub>, reentrant supercond., US attenuation meas., 1.5 to 20K 4-98810
- ErRh<sub>4</sub>B<sub>4</sub>, coexistence phase of ferromagnetism and supercond., in terms of modulated supercond. state 4-98805
- ErRh<sub>4</sub>B<sub>4</sub>, ferromagnetic superconductor, d-f interaction 4-98801
- ErRh<sub>4</sub>B<sub>4</sub>, ferromagnetic superconducting thin film, photoexcitation, nonequilibrium effects 4-114059
- ErRh<sub>4</sub>B<sub>4</sub>, mag. supercond., muon spin relax. studies 4-65923
- ErRh<sub>4</sub>B<sub>4</sub>, mixed state and mag. props. 4-98830
- Eu oxide and chalcogenides, exchange interactions, LCAO calculations 4-109009
- EuO, Heisenberg ferromag., longitudinal spin wave pumping 4-88661
- EuO:Gd, longitudinal Nernst-Ettingshausen effect, temp. and mag. field dependences 4-65697
- EuS, ferromagnetic semicond., thermal cond., phonon and magnon contr. 4-71050
- Eu<sub>2</sub>Sr<sub>1-x</sub>S<sub>x</sub> ferromagnetic epitaxial layers, magnetooptic studies (German) 4-76441
- Fe (001), electronic struct., magnetism, muon spin relax. 4-70888
- Fe (001), magnetic domains obs. by SEM using spin polarised secondary electrons 4-61549
- Fe (001) ferromagnetic, spin- and angle-resolved photoemission spectra 4-85063
- Fe (110), exchange split empty energy bands inverse photoemission studies 4-84551
- Fe (110), ferromag., spin-polarised low-energy electron diff., temp. effects 4-104456
- Fe (110)p(2×2)-S, surface ferromagnetism, chemisorption, adsorbate-induced substrate reconstruction effect, spin-polarised LEED calcs. 4-80395
- Fe, BCC, electron or neutron irradi. induced defects, model 4-65300
- $\alpha$ -Fe, Co diffusion, effect of mag. transition 4-65481
- Fe complex, halobis(diethylselenocarbamate)iron(III), mag. props. 4-76124
- Fe, electronic struct., exchange splitting, spin- and angle-resolved photoemission spectra 4-88944
- Fe, electronic struct., magnetism and Curie temps. 4-75843
- Fe epitaxial films, electronic and mag. states 4-80646
- Fe, ferromagnetic, even magnetooptic effect, spectral thermal emission linear polarisation 4-99096
- Fe, ferromagnetic, high purity, magnetomechanical damping, influence of struct. defects 4-76226
- Fe ferromagnetic, magneto-optic effect on thermal IR spectra, expt. study 4-76442
- Fe, ferromagnetic, wave-vector depend. temp. behaviour of empty bands 4-104123
- Fe ferromagnetic thin films, high rate magnetron sputtering 4-66232
- Fe film and single cryst., microwave generation of 9.4 GHz phonons 4-61422
- Fe films, organo-metal CVD growth from (CO)<sub>2</sub>Fe+AsH<sub>3</sub> on GaAs 4-61868
- Fe fine particles, prep. from goethite microcrysts., morphology and mag. props. 4-65835
- Fe fully relativistic band struct. calcs. 4-113855
- Fe, Gilbert damping, critical fluctuation effects, ferromag. resonance study 4-61539
- Fe, impurity hyperfine fields and adiabatic pot., self-consistent calc. 4-65632
- Fe, mag. Compton profile meas. using circularly polarised  $\gamma$ -rays from oriented <sup>191</sup>Ir nuclei 4-71462
- Fe, muon, uniaxially stress-induced freq. shifts 4-65918
- Fe, muon precession, var. with magnetisation angle 4-65920
- Fe, polycrystalline, ferromagnetic, density of unoccupied states, SXAPS study 4-85039
- $\alpha$ -Fe, positron annihilation expts. in thermal equil., one-interstitial model confirmation 4-109271

## ferromagnetic properties of substances continued

- Fe powders, chem. instability and corrosion, mag. tape appls. (Chinese) 4-98982
- Fe single crystals, spin polarised Auger electrons 4-85044
- Fe, sintered, mag. suscept. and porosity, semi-empirical rel. 4-84774
- Fe, spin polarised positron annihilation and enhancement effects 4-93126
- Fe surface layer at nonmag. material interfaces, magnetisation, temp. depend. 4-61575
- Fe, thick foil, mag. domain wall obs. 4-80780
- Fe whisker, Barkhausen jump field distrib., temp. depend. 4-76182
- Fe wires, Barkhausen jumps, deform. effects 4-76187
- Fe Z 4-65836
- Fe/Fe<sub>3</sub>O<sub>4</sub>, high magnetisation material with alternate layer struct., HF mag. core appl. 4-104470
- Fe-Ag-Pd, transient fields, g-factor, gyromagnetic ratios 4-113914
- Fe-Al (48 at.%), mag. props. rel. to heat treatment 4-109003
- Fe-Al rapidly quenched cryst. ribbons, mag., elec. and mech. props. 4-76174
- Fe-B amorphous alloys, mag. anisotropy, thermal treatment effects 4-65805
- Fe-based amorphous alloys, magnetoelastic props., X-ray diff. studies 4-76209
- Fe-C, induced mag. moment by tetragonally elongated lattice expansion, magnetisation, Mossbauer spectra meas. 4-98930
- Fe-Co alloys, magnetostriction, recryst., heat treatment, and strain texture effects (Russian) 4-104476
- Fe-Co based metallic glasses, nearly magnetostrictive, disaccommodation 4-84828
- Fe-Co disordered alloys, magnetisation, tight-binding calc. 4-98924
- Fe-Co electrodeposited films, field induced mag. anisotropy 4-92943
- Fe-Cr-Co (12 wt.%) permanent magnet alloys, mag. props., effect of alloying 4-84771
- Fe-Cr-Co alloy, Ti effect on rate of high-coercivity transform. 4-93296
- Fe-Cr-Co-Si-B amorphous alloys, mag. props. and hyperfine interactions (Russian) 4-108994
- Fe-graphite system, carbide form. high press. and temp., mag. props. 4-99371
- Fe-Hf based amorphous alloys, crystallisation and hyperfine fields 4-71030
- Fe-Mo-B, amorphous, hyperfine fields mag. props. 4-92933
- Fe-N, induced mag. moment by tetragonally elongated lattice expansion, magnetisation, Mossbauer spectra meas. 4-98930
- Fe-Nb-Si-B amorphous alloys, mag. props. 4-71145
- Fe-Nd-B alloy permanent magnets, domain walls, Lorentz electron microscopy study 4-92934
- Fe-Nd-Ti films with perpendicular mag. anisotropy, RF sputtering 4-61570
- Fe-Ni austenitic alloys, crack growth and plasticity, influence of mag. ordering (Russian) 4-93368
- Fe-Ni Elinvar alloys, dispersion-hardened, mag. and physical props. (Russian) 4-104800
- Fe-Ni Invar alloys, Mossbauer spectra 4-88748
- Fe-Ni layered films, ferromagnetic, appl. of phase resolved photoacoustic microscopy 4-79406
- Fe-Ni wires, Barkhausen jumps, deform. effects 4-76187
- Fe-Ni-C, induced mag. moment by tetragonally elongated lattice expansion, magnetisation, Mossbauer spectra meas. 4-98930
- Fe-Ni-Co film, mag. domain walls, dynamic props. 4-88705
- Fe-Ni-Cr ferritic alloy, soft mag. props. and mech. strength 4-61555
- Fe-Ni-Mn(Cr) alloys with mixed exchange interactions, mag. phase transitions, sp. ht. study 4-65820
- Fe-Ni-P-B amorphous alloys, mag. props., proton implantation effects 4-104416
- Fe-Ni-P-B-(Si) metallic glasses, magnetoelastic effects in ferromag. resonance 4-61581
- Fe-Ni-Ti(Cr)(Al), nitrided layer, Mossbauer studies (Russian) 4-109555
- Fe-P amorphous electrodeposited layers, Barkhausen effect, torsion effects 4-76198
- Fe-Si, saturation magnetisation, mag. anisotropy, g-factor determ., FMR, ferromagnetic antiresonance obs. 4-76258
- Fe-Si (3 wt.%), coarse-grained anisotropic elec. engineering steel, mag. losses and induction (Russian) 4-109036
- Fe-Si (3 wt.%), electrical engineering steel, anisotropic, mag. losses, annealing and elongation effects (Russian) 4-104459
- Fe-Si (3 wt.%), reversible magnetisation curve at any angle to rolling direction 4-61558
- Fe-Si (6.5 wt.%) rapidly quenched ribbon, texture and mag. props. 4-104455
- Fe-Si alloys, mag. domains, stroboscopic study using SEM 4-68323
- Fe-Si laser scribed gain oriented steel, stacked transformer core appls. 4-61552
- Fe-Si multilayered films, mag. props. and domain struct. 4-61574
- Fe-Si sheets, Bitter patterns, ferrofluid birefringence studies 4-76202
- Fe-Si sheets, magnetisation processes, grain boundary effects 4-76180
- Fe-Si steel, magnetisation, thermodynamic pot. model 4-61557
- Fe-Si steel, magnetostriction and magnetocrystalline energy anisotropy, texture effects 4-61532
- Fe-W-B glasses, mag. aftereffect, effect of W 4-84827
- Fe-Zr amorphous films, elec. and mag. props. 4-75923
- Fe<sub>1-x</sub>B<sub>x</sub> amorphous films, crystallisation kinetics and mag. props. 4-75807
- Fe<sub>1-x</sub>B<sub>x</sub> amorphous films, magnetostriction, strain-modulated FMR study 4-76217
- Fe<sub>100-x</sub>B<sub>x</sub> amorphous alloys, mag. anisotropy, mag. annealing effects 4-76131
- Fe<sub>80</sub>B<sub>20</sub> amorphous, mag. hysteresis loops after heat treatment below Curie point 4-80781
- Fe<sub>80</sub>B<sub>20</sub> amorphous foil, sputtered ductile, mag. and structural study 4-80782
- Fe<sub>83</sub>B<sub>17</sub>, ferromag., spin polarised L<sub>23</sub>M<sub>23</sub>M<sub>23</sub> AES 4-104703
- (Fe<sub>82</sub>B<sub>18</sub>)<sub>0.18</sub>(La<sub>0.90</sub>La<sub>0.05</sub>La<sub>0.05</sub>)<sub>0.05</sub> amorphous metal alloys, ferromag. reson. and g-factor 4-71188
- Fe<sub>82</sub>B<sub>18</sub>Si<sub>6</sub> ferromagnet, spin-flip Stoner excitations, EELS studies 4-104410
- Fe<sub>81</sub>B<sub>13</sub>Si<sub>5</sub>C<sub>2</sub>, Metglas 3605SC, mag. and hyperfine interactions 4-71223
- FeCo based alloys, strength and mag. props. rel. to cold rolling and heat treatment 4-98918
- Fe<sub>2</sub>Co<sub>7</sub>B<sub>20</sub> amorphous, mag. aftereffects after field annealing 4-84823
- Fe<sub>2</sub>Co<sub>1-x</sub>Cr<sub>2</sub>S<sub>4</sub>, magnetisation and Curie point meas. 4-104461

## ferromagnetic properties of substances continued

- FeCo(Mn)(V), coupling between chemical and mag. interactions, NMR study 4-114173  
 (Fe<sub>100-x</sub>Co<sub>x</sub>)<sub>76</sub>Pr<sub>16</sub>O<sub>8</sub>, thermal effects of Co moderate substitutions 4-71124  
 Fe<sub>60</sub>Si<sub>40</sub>B<sub>10</sub>, amorphous, mag. permeability, annealing in transverse mag. field (*Russian*) 4-104467  
 Fe<sub>60</sub>Si<sub>40</sub>B<sub>10</sub>, zero magnetostrictive amorphous alloy, permeability and field-induced anisotropy 4-71056  
 Fe<sub>60</sub>Co<sub>40-x</sub>Si<sub>15</sub>B<sub>15</sub>, magnetostrictive amorphous alloys, stress-induced anisotropy and permeability 4-71055  
 (Fe<sub>1-x</sub>Co<sub>x</sub>)<sub>90</sub>Zr<sub>10</sub> amorphous alloy, elec. resist. minima and mag. props. 4-75922  
 (Fe<sub>1-x</sub>Cr<sub>x</sub>)<sub>100-x</sub> metallic glasses, onset of magnetism, Mossbauer spectra 4-71217  
 (Fe<sub>1-x</sub>Cr<sub>x</sub>)<sub>100-x</sub>Mn<sub>1-y</sub>, <sup>55</sup>Mn and <sup>57</sup>Fe NMR, comp. depend. 4-98960  
 (Fe<sub>1-x</sub>Cr<sub>x</sub>)<sub>100-x</sub>Mn<sub>1-y</sub>, impurity mag. state, <sup>55</sup>Mn and <sup>57</sup>Fe NMR study 4-98961  
 Fe<sub>1-x</sub>Cu<sub>x</sub>C<sub>4</sub>S<sub>4</sub>, ferrimagnetic to ferromagnetic order transition, ion valence states, NMR 4-88670  
 Fe<sub>70</sub>Fe<sub>30</sub>Sn<sub>0.4</sub>Ni<sub>0.7</sub>O<sub>0.3</sub>, ferromag. material for magnetic recording 4-104644  
 Fe<sub>80</sub>M<sub>20</sub>B<sub>17</sub> (M=transition metal) metallic glass, elec. resist., transition metal effects 4-108832  
 Fe<sub>80</sub>M<sub>20</sub>B<sub>17</sub> based glassy alloys, ferromag. exchange and Curie temp. 4-76129  
 (FeMn)CP alloys, amorphous, ferromag. reson. and mag. ordering 4-71187  
 (Fe<sub>1-x</sub>Mn<sub>x</sub>)<sub>75</sub>P<sub>15</sub>C<sub>10</sub> amorphous alloy, transport and mag. props. 4-88498  
 Fe<sub>2</sub>N pigments, mag. props. rel. to specific surface area 4-65836  
 FeNi, neutron irradi. effect on mag. props. 4-92907  
 FeNi(Si,Cr,Mo), neutron irradi. effect on mag. props. 4-92907  
 Fe<sub>0.66</sub>Ni<sub>0.34</sub>, Curie point at ultrahigh press. 4-88676  
 (Fe<sub>0.5</sub>Ni<sub>0.5</sub>)<sub>1-x</sub>B<sub>x</sub> amorphous alloys, mag. moments, temp. variation 4-76122  
 Fe<sub>40</sub>Ni<sub>40</sub>B<sub>20</sub>, amorphous, mag. hysteresis loops after heat treatment below Curie point 4-80781  
 Fe<sub>40</sub>Ni<sub>40</sub>B<sub>20</sub>, amorphous alloys, neutron irradi., mag. props. isotope effects 4-75541  
 Fe<sub>40</sub>Ni<sub>40</sub>B<sub>20</sub> amorphous alloy, ferromag. resonance and antiresonance studies 4-76256  
 Fe<sub>40</sub>Ni<sub>40</sub>B<sub>20</sub>, amorphous alloys, as-quenched, mag. aftereffect 4-84826  
 Fe<sub>80-x</sub>Ni<sub>x</sub>B<sub>20</sub> amorphous sputtered films, ferromag. saturation 4-61520  
 Fe<sub>2</sub>Ni<sub>80-x</sub>B<sub>19</sub>Si<sub>1</sub> metallic glasses, absolute thermoelec. power meas. 4-92701  
 FeNiCo thin film, multiple spin echo study 4-84870  
 Fe<sub>65</sub>Ni<sub>35-x</sub>Cr<sub>x</sub>, magnetostrict. and ferromag. spin glass transitions 4-113924  
 Fe<sub>80-x</sub>Ni<sub>x</sub>Cr<sub>20</sub>, mag. phase diagram, neutron diffr. study 4-71069  
 FeNiCrMoBSi amorphous ribbons, magnetostriction, capacitance studies 4-61580  
 (Fe<sub>1-x</sub>Ni<sub>x</sub>)<sub>2</sub>Ge, magnetisation, Curie temp., mag. moments, X-ray diffr. studies 4-98862  
 (Fe<sub>1-x</sub>Ni<sub>x</sub>)<sub>3</sub>Ge, magnetisation, Curie temp., mag. moments, X-ray diffr. studies 4-98862  
 (Fe<sub>1-x</sub>Ni<sub>x</sub>)<sub>1</sub>M, M=P, B, Si or Al, metallic glass, Mossbauer study of high press. 4-84880  
 Fe<sub>2</sub>Ni<sub>80-x</sub>Mn<sub>20</sub>, specific heat determ. (*Russian*) 4-65414  
 Fe<sub>39</sub>Ni<sub>39</sub>Mo<sub>2</sub>Si<sub>6</sub>B<sub>12</sub> metallic glass, mag. props., Mossbauer studies 4-109012  
 Fe<sub>40</sub>Ni<sub>40</sub>P<sub>16</sub>B<sub>6</sub>, amorphous isotropic ferromag., mag. excitations 4-71043  
 Fe<sub>40</sub>Ni<sub>40</sub>P<sub>16</sub>B<sub>6</sub> amorphous ribbons, mag. props. and struct., influence of laser annealing 4-88663  
 Fe<sub>40</sub>Ni<sub>40</sub>P<sub>16</sub>B<sub>6</sub> metallic glass, dynamical power loss annealing effects 4-76175  
 Fe<sub>40</sub>Ni<sub>40</sub>P<sub>16</sub>B<sub>6</sub> metallic glass, mag. permeability with AC and DC currents 4-76176  
 Fe<sub>2</sub>Ni<sub>80-x</sub>P<sub>16</sub>B<sub>6</sub>, amorphous ferromag. and reentrant alloys, ferromag. reson. study 4-84856  
 (Fe<sub>1-x</sub>Ni<sub>x</sub>)<sub>90</sub>Zr<sub>10</sub> amorphous alloy, elec. resist. minima and mag. props. 4-75922  
 FeO-Fe<sub>2</sub>O<sub>3</sub>, magnetite, magnetostriction isotherms at low temps. 4-61582  
 Fe<sub>2</sub>O<sub>3</sub> magnetite particles in ferromagnetic colloids, size distrib. anal. 4-109043  
 Fe<sub>2</sub>Pd<sub>80-x</sub>Si<sub>10</sub>B<sub>10</sub> metallic glasses, mag. props. and chemical short-range order 4-114109  
 FeSi grain oriented laminations, local correl. effects between Bloch walls 4-76167  
 FeSi tape wound cores, specific Bloch wall area 4-76165  
 Fe<sub>91</sub>Si<sub>8</sub>B<sub>15</sub> metallic glass, Young's modulus, internal friction, mag. hysteresis loop 4-76215  
 Fe<sub>91</sub>Si<sub>8</sub>B<sub>15</sub> metallic glass, stress pattern mag. domains 4-76161  
 Fe<sub>2</sub>Si<sub>90-x</sub>B<sub>10</sub> metallic glasses, mag. props., chem. composition depend. 4-76135  
 (Fe<sub>1-x</sub>V<sub>x</sub>)<sub>84</sub>B<sub>16</sub> amorphous alloys, mag. and elec. props. (*Chinese*) 4-114094  
<sup>57</sup>Fe film, spectral analysis of spin-echo signals 4-104510  
<sup>57</sup>Fe thin film system, surface and interface magnetism, Mossbauer spectra studies 4-104468  
 FeSi strips, mag. props. and domain struct., laser scribing effects 4-61550  
 Ga<sub>0.3</sub>Mo<sub>0.7</sub>S<sub>2</sub> spinel, cryst. struct., mag. props., temp. depend. 4.2-300K 4-114110  
 GaMo<sub>2</sub>X<sub>2</sub> chalcogenides, electron-phonon contrib. to Stoner enhancement 4-84803  
 Gd, magnetostriction, temp. depend. 4-76220  
 Gd, positron lifetime near ferromag. transition temp. 4-93127  
 Gd-Fe amorphous alloy films, crystallisation and ferromag. reson. behaviour 4-71189  
 Gd-Tb, magnetostriction, temp. depend. 4-76220  
 Gd-Y-Lu single cryst., double ferromagnetism, mag., elec. and thermal studies 4-84817  
 Gd<sub>1-x</sub>La<sub>x</sub>Al<sub>2</sub>, loss of ferromagnetism 4-98885  
 Gd<sub>1-x</sub>Tb<sub>x</sub>Al<sub>2</sub>, loss of ferromagnetism 4-98885  
 Gd<sub>1-x</sub>U<sub>x</sub>Al<sub>2</sub>, loss of ferromagnetism 4-98885  
 GdAl<sub>2</sub>, ferromag., magnetisation, NMR studies 4-80787  
 Gd<sub>2</sub>Au<sub>2</sub>Al<sub>1-x</sub>, pseudobinary cpd., mag. behaviour 4-76136  
 GdCo amorphous co-sputtered film, surface versus bulk magnetisation curves 4-71131  
 GdCu<sub>1-x</sub>Zn<sub>x</sub>Si, cryst. struct., mag. and elec. props. 4-92145  
 Gd<sub>1-x</sub>Dy<sub>x</sub>Al<sub>2</sub>, NMR spectra, dipole field rot. 4-109084

## ferromagnetic properties of substances continued

- Gd<sub>2</sub>In, magnetic and electrical props., metamagnetic-ferromagnetic transition, magnetic struct. 4-114138  
 GdZn, ferromagnetically saturated single crystal, high-field NMR Knight shift, magnetisation studies 4-114176  
<sup>3</sup>He, liq., surface-induced ferromagnetism, review (*Japanese*) 4-70512  
 Hg<sub>1-x</sub>Ag<sub>x</sub>Cr<sub>2</sub>Se<sub>4</sub>, mag. semicond., exchange interaction, carrier effects 4-114103  
 HgCr<sub>2</sub>Se<sub>4</sub> ferromag. semiconductor, luminesc. study with quantum energy exceeding the forbidden band gap 4-80992  
 HgCr<sub>2</sub>Se<sub>4</sub>, ferromagnetic semicond., elec. cond., photocond. meas., temp. depend. 4-61375  
 HgCr<sub>2</sub>Se<sub>4</sub> mag. semicond., resist. and magnetisation changes and relax. 4-65682  
 Ho-Co amorphous films, with perpendicular anisotropy, planar Hall effect 4-75932  
 HoMo<sub>2</sub>S<sub>8</sub>, ferromagnet, domain walls, superconductivity obs. 4-80718  
 Ho<sub>1-2-x</sub>R<sub>x</sub>Mo<sub>0.8</sub>S<sub>8</sub>, R=Er, Tb, relaxation of ferromagnetic ordering and superconductivity 4-98886  
 K<sub>2</sub>FeO<sub>4</sub>, mag. ordering and critical slowing down, Mossbauer studies 4-76148  
 La(Fe<sub>1-x</sub>Al<sub>x</sub>)<sub>13</sub>, metamagnetic transitions and struct. aspects 4-92910  
 LaNi<sub>1-x</sub>Mn<sub>x</sub>O<sub>3</sub>, valence states and mag. props. 4-84772  
 Mn-Al(Bi) hard magnets formed by rapid quenching 4-80794  
 MnAs, electronic struct. and phase transitions, tight binding calc. 4-108768  
 MnAs, mag. struct. under high press., powder neutron diffr. studies 4-108988  
 Mn<sub>0.90</sub>Fe<sub>0.10</sub>P, mag. phases, Mossbauer spectroscopy study 4-88753  
 Mn<sub>2</sub>Ge<sub>2</sub>, thermal expansion meas., 4.2-800K, Curie point, press. shifts 4-98320  
 MnP, Lifshitz point, spin localised model 4-84810  
 MnSb, solid solns., evidence of critical Mn-Mn distance for onset of ferromagnetism 4-84780  
 MnSb-based solid solns., recording media in optical memory appls. 4-61572  
 MnSi itinerant ferromag., neutron scattering and muon spin rotation collaborations 4-65890  
 Mo/Ni superlattices, magnetisation, Curie temp. and magnon spectra, Brillouin scatt. study 4-61560  
 Nd, Fe<sub>2</sub>B, single crystal, mag. props. study 4-114143  
 Nd, Sm<sub>1-x</sub>Fe<sub>x</sub>, Laue phase spin-reorientation temp., mag. anisotropy, Mossbauer spectra (*Japanese*) 4-61533  
 Nd, Sm<sub>1-x</sub>Ni<sub>x</sub>, mag. struct. charact. (*Russian*) 4-92894  
 Ni (001), electronic struct., magnetism, muon spin relax. 4-70888  
 Ni (110), ferromagnetic, spin polarised EELS study (*German*) 4-76573  
 Ni, anisotropy constants, temp. depend., universal function descript. 4-71059  
 Ni, bulk magnetisation and magnetocryst. anisotropy 4-76189  
 Ni, Curie point at ultrahigh press. 4-88676  
 Ni, electronic struct., magnetism and Curie temps. 4-75843  
 Ni, ferromagnet, critical phenomena, muon spin relax. study 4-71252  
 Ni ferromagnetic film, FMR imaging using photothermal deflection 4-88725  
 Ni film, on LiNbO<sub>3</sub>, SAW attenuation in mag. field, strain and temp. depend. 4-98421  
 Ni film and single cryst., microwave generation of 9.4 GHz phonons 4-61422  
 Ni fully relativistic band struct. calcs. 4-113855  
 Ni, inner-shell photoelectron spectroscopy, many-body effects 4-88930  
 Ni, mag. small-angle neutron scatt. by dislocations 4-84299  
 Ni magnetic particles, formation in inert gas, electron microscope studies 4-76192  
 Ni, magnetoelastic anomalies at US freqs. 4-104479  
 Ni,  $\mu$  spin precession and giant hyperfine anomaly 4-71254  
 Ni, photoemission spectra study of magnetically spin-split electronic states (*German*) 4-71523  
 Ni, polycrystalline, ferromagnetic, density of unoccupied states, SXAPS study 4-85039  
 Ni single crystals, spin polarised Auger electrons 4-85044  
 Ni, Stoner excitation spectrum, spin polarised EELS studies 4-104411  
 Ni surface, sputter-cleaned, work function meas. 4-114017  
 Ni, thermoelectric power and sp. ht. near Curie temp., AC method meas. 4-75934  
 Ni wires, Barkhausen jumps, deform. effects 4-76187  
 Ni, yield point, temp. depend., mag. field effects 4-80807  
 Ni/Cu (001) interface, electronic struct., magnetism, muon spin relax. 4-70888  
 Ni-base alloys, ferromagnetic, domain wall mobility 4-76169  
 Ni-Co-Nb, damping capacity, mag. and mech. props. 4-61564  
 Ni-Cu, anomalous resistivity, 4.2 to 1100K 4-92708  
 Ni-Cu, thermoelectric power and sp. ht. near Curie temp., AC method meas. 4-75934  
 Ni-Fe-Co-Ti, Incalloy, domain struct. study by differential phase contrast Lorentz microscopy, max. specimen thickness 4-65825  
 Ni-Fe-Cr alloys, extraordinary Hall coeff. sign reversal and DC resist. 4-113922  
 Ni-Fe-V alloys, extraordinary Hall coeff. sign reversal and DC resist. 4-113922  
 Ni-Mn disordered alloys, magnetostrict. of spin glass and ferromag. states 4-61360  
 Ni-Mo-Fe ternary alloys, mag. props. and ferromag. shielding at cryogenic temps. 4-109038  
 Ni-Pd, anomalous Hall effect rel. to mag. anisotropy (*Russian*) 4-92697  
 Ni-Rh alloys, magnetism and atomic short range order 4-98899  
 Ni-Si-B metallic glasses, Hall effect, mag. ordering near resist. minimum 4-75933  
 Ni-Ti, forced vol. magnetostriction, press. coeffs. 4-88711  
 Ni-V, forced vol. magnetostriction, press. coeffs. 4-88711  
 Ni<sub>2</sub>B<sub>2</sub>O<sub>3</sub>Br, magnetoelc. effect, mag. and elec. meas. 4-71144  
 NiCl<sub>2</sub>-graphite intercalation cpd., two-dimensional ferromagnet, EPR meas. 4-109069  
 Ni<sub>100-x</sub>Co<sub>x</sub>Ni<sub>81</sub>Fe<sub>19</sub> mag. films, exchange-coupled, mag. reversal charact. 4-76200  
 NiCr alloys, mag. struct. amplitudes, polarised neutron studies 4-108989  
 NiCuM (M=Zn, Al, Si) alloys, spontaneous magnetisation, thermal variation 4-65796  
 Ni<sub>60-x</sub>Fe<sub>20</sub> amorphous alloy, onset of magnetism, magnetisation studies 4-76172  
 Ni<sub>78-x</sub>Fe<sub>22</sub>Si<sub>2</sub>B<sub>10</sub> amorphous alloys, mag. props. 4-84794

**magnetic properties of substances continued**

- NiMg<sub>0.6</sub>H<sub>2</sub>O (M=Zr,Si,Ti,Sn) easy axis ferromagnets, transverse susceptibility 4-61515  
 NiMn, magnetisation, phase diagrams and metamagnetism 4-98920  
 Ni<sub>2</sub>MnGa, ferromagnetic order and martensitic transformations 4-61512  
 Ni<sub>2</sub>MnIn Heusler alloy, elec. resist. and magnetisation 4-92695  
 Ni<sub>2-x</sub>MnSb, chemical order and mag. props. 4-88666  
 Ni<sub>1-x</sub>Ru<sub>x</sub>, mag. struct. amplitudes, pol. neutron data reanal., projection operator form. 4-92896  
 NiSiF<sub>6</sub>H<sub>2</sub>O, singlet ground state ferromag. ordering 4-88657  
 Ni<sub>1-x</sub>V<sub>x</sub> alloys, bulk magnetisation and magnetocryst. anisotropy 4-76189  
 Ni(100) films, electronic struct. and magnetism 4-70640  
 Pb-Zn host granular supercond., frustration and disorder 4-98799  
 Pd-Fe, ion implanted, ferromagnetism study 4-71137  
 Pd-Fe alloy, transition temp. determ. using SQUID magnetometer combined with ion implantation 4-58877  
 PdCuSiM alloys, (M=Fe, Co, Mn), spin glasses, exptl. evidence for mag. two level systems 4-71082  
 Pd<sub>67</sub>Cu<sub>33</sub>M<sub>0.05</sub> (M=Fe or Mn), glasses, ferro- and antiferromagnetism study 4-71063  
 PdMn, dilute ferromagnet, muon spin relax. 4-71251  
 PdMn, thermoelectric power, phonon drag effect 4-104187  
 Pr-Fe-Co alloy sheets, rapid quenching, magnetic properties (*Japanese*) 4-114141  
 Pr<sub>2</sub>Sm<sub>1-x</sub>Fe<sub>2</sub>, Laue phase, spin-reorientation temp., mag. anisotropy, Mossbauer spectra (*Japanese*) 4-61533  
 Pt-Co dilute alloys, resistance thermometers with low magnetoresistive effects 4-111132  
 Pt-Fe alloys, mag. props. 4-84842  
 PtMnSb, magneto-optical props. and electronic struct. 4-61662  
 Rb<sub>2</sub>CrCl<sub>4</sub>, ferromagnet, CI NMR study (*Japanese*) 4-98967  
 Rb<sub>2</sub>Mn<sub>1-x</sub>Cr<sub>x</sub>Cl<sub>4</sub> mixed insulating ferromag. and antiferromag., ferromag. resonance studies 4-65863  
 ribbon, 6.5%, rapidly quenched, mag. props. stability (*Japanese*) 4-76196  
 Sc<sub>2</sub>In weak itinerant electron ferromag., negative magnetoresistance 4-75931  
 Sc<sub>1-x</sub>Ti<sub>x</sub>Fe<sub>2</sub>, itinerant electron system, coexistence of ferro- and antiferromagnetism 4-98857  
 Si-Fe, Bloch wall motion, surface EMF meas. 4-76168  
 Si-Fe nonoriented semiprocessed steel, core loss and permeability, elec. resist. effects 4-61556  
 Si-Fe oriented sheets, mag. interactions and domain struct., Mossbauer study 4-76163  
 Si-Fe sheets, quenching destabilisation of domain struct., effect on mag. props. 4-76166  
 Si-Fe-Sn(Cu) high permeability ribbon oriented steel, recrystallisation and grain sizes 4-61953  
 SiFe, polycrystalline, approach to saturation at intermediate fields, role of internal demagnetising fields 4-76183  
 Sm-Co alloy, powder particles and agglomerates, individual mag. props. and particle size effect 4-88702  
 Sm-Co amorphous films, mag. props. 4-65842  
 Sm-Co ferromagnetic thin films, high rate magnetron sputtering 4-66232  
 Sm-Fe-Co alloy sheets, rapid quenching, mag. props. (*Japanese*) 4-114141  
 Sm(Co<sub>0.8</sub>Fe<sub>0.2</sub>Cu<sub>0.2</sub>Zr<sub>0.2</sub>)<sub>7.5</sub> magnets, high resolution electron microscopy study 4-61098  
 SmCo<sub>5</sub> magnets, thermal remagnetisation, domain rearrangement 4-71074  
 Sm(Co<sub>1-x</sub>Cu<sub>x</sub>)<sub>2</sub> cellular permanent magnets, coercivity 4-76191  
 SmFe<sub>2</sub>, mechanostriuctive strain as a function of magnetic field and mechanical elastic stresses 4-113523  
 Sm<sub>2</sub>Fe<sub>17-2x</sub>Co<sub>x</sub>, magnetic cooling near Curie temperatures above 300K 4-88677  
 Tb, magnetostriction, temp. depend. 4-76220  
 Tb-Ce, dil., intermediate valent, time depend. hyperfine fields, TDPAC study 4-75907  
 Tb<sub>75</sub>Gd<sub>25</sub>, Hall effect and elec. resist. near Curie point 4-61361  
 TbCo amorphous films, perpendicular mag. anisotropy 4-61569  
 TbFe<sub>2</sub>, mag. and magnetomech. hysteresis 4-76219  
 Tb<sub>2</sub>Fe<sub>2x</sub>, mechanostriuctive strain as a function of magnetic field and mechanical elastic stresses 4-113523  
 TiBe<sub>2-x</sub>Cu<sub>x</sub>, onset of ferromagnetism, neutron small angle scatt. study 4-84797  
 Ti<sub>1-x</sub>Mn<sub>1.8</sub>D<sub>3</sub>, structure and mag. props., neutron diffr. study 4-75368  
 Ti<sub>2</sub>Fe<sub>6</sub>Te<sub>6</sub>, strongly anisotropic ferromagnetism, first order phase transitions 4-84796  
 Tm intermediate valence cpds., mag. susceptibility and sp. ht. 4-108999  
 UAs<sub>1-x</sub>Se<sub>x</sub>, mag. phase diagram, mag. susceptibility meas. 4-88651  
 UH<sub>3</sub>B<sub>2</sub>, proton NMR study 4-84865  
 UM<sub>2</sub>B<sub>2</sub> (M=Co, Ru, Ir), mixed valence, mag. and elec. props. 4-113905  
 U<sub>2</sub>Th<sub>1-x</sub>Se solid solns. mag. props. 4-104419  
 V/Fe compositionally-modulated struct., mag. props. and superconductivity 4-61561  
 WC, sintered, Co inclusions, magnetisation curves 4-109040  
 Y-Fe alloys, exchange interactions, coordination props. studies 4-114104  
 Y<sub>90</sub>Co<sub>10</sub> ferromag. inhomogeneous supercond., sample size and meas. power effects 4-76065  
 Y(Fe<sub>2</sub>Al<sub>2</sub>)<sub>2</sub> alloys, mag. behaviour 4-76116  
 Y<sub>2</sub>Fe<sub>14</sub>B, single crystal, mag. props. study 4-114143  
 Y<sub>2</sub>Fe<sub>17-2x</sub>Co<sub>x</sub>, magnetic cooling near Curie temperatures above 300K 4-88677  
 YIG ferromagnetic films, spin-wave solitons obs. 4-71135  
 YM<sub>2</sub> (M=Mn, Fe, Co, Ni), electronic struct. and mag. props. 4-92602  
 Y(Mn<sub>1-x</sub>Co<sub>x</sub>)<sub>12</sub>, mag. struct., neutron diffr. study (*Chinese*) 4-92892  
 ZrCrFe-based hyperstoichiometric alloys and hydrides, mag. props. 4-109025  
 ZrZn<sub>2</sub>, ferromag. and paramag. phases, magnetisation density and mag. struct. 4-76114

**ferromagnetic relaxation**

- see also *ferromagnetic resonance*  
 amorphous ribbon, simultaneous magnetic meas. and torsional creep 4-111163  
 ferrofluids, magnetostatic props., effect of anisotropy-controlled Neel relax. 4-76194

**ferromagnetic resonance**

- see also *ferromagnetic relaxation*  
 cyclohexylammonium copper trichloride, magnon bound state excitations 4-80751

**ferromagnetic resonance continued**

- cyclohexylammonium copper trichloride and tribromide, exchange anisotropy study 4-80758  
 deformable ferromagnet, undergoing mag. reson., electrodynamics 4-76261  
 ferrite, linewidth measurement by differential curve method (*Chinese*) 4-73466  
 ferrite/semicond. thin film struct., electron broadening of ferromag. resonance lines 4-76260  
 ferromagnetic bulk metal, parallel configuration of FMR, surface impedance, calcs. 4-98953  
 garnet films, anisotropy fields 4-114147  
 garnet thin films, ferromagnetic, microwave props., review 4-80803  
 insulating thin films, homogeneous, effective spin-pinning, critical angles, surface modes 4-98896  
 linewidth measurement by differential curve method (*Chinese*) 4-73466  
 metal, cubic, FMR and FMAR, low temp. meas. 4-76257  
 metallic thin films, spin wave resonance, surface mode obs. 4-98954  
 parametric optical phenomena in magnetically ordered media, occurring in conditions of ferromag. reson. (*Russian*) 4-80906  
 Permalloy film, on antiferromag. substrate, FMR freqs., effect of domain struct. 4-92965  
 photoacoustic signal meas. using piezoelec. detector 4-109282  
 semiconductors, elec. resist. reson. rel. under FMR saturation conditions 4-92726  
 tapes, layered ferromag., ferromag. reson. depth profiles using photoacoustic detect. 4-71186  
 BaFe<sub>12-x</sub>M<sub>x</sub>O<sub>19</sub> (M=Al, Ga, Sc) ferrites, anisotropy fields and FMR linewidths 4-71058  
 Co-Nb amorphous films, electron beam deposited, ion mixed, FMR, magnetisation meas. 4-71138  
 Co-Nb multilayered compositionally modulated films, e-beam deposited, FMR, magnetisation, B-H loop meas. 4-71139  
 Fe, Gilbert damping, critical fluctuation effects, ferromag. resonance study 4-61539  
 Fe-Ni layered films, ferromagnetic, appl. of phase resolved photoacoustic microscopy 4-79406  
 Fe-Ni-P-B-(Si) metallic glasses, magnetoelastic effects in ferromag. resonance 4-61581  
 Fe-Ni-based metallic glasses, fracture and annealing, ferromag. resonance studies 4-109078  
 Fe-Si, saturation magnetisation, mag. anisotropy, g-factor determ., FMR, ferromagnetic antiresonance obs. 4-76258  
 Fe<sub>1-x</sub>B<sub>x</sub> amorphous films, magnetostriction, strain-modulated FMR study 4-76217  
 (Fe<sub>0.82</sub>B<sub>0.18</sub>)<sub>0.90</sub>La<sub>0.05</sub>R<sub>0.05</sub> amorphous metal alloys, ferromag. reson. and g-factor 4-71188  
 Fe<sub>1-x</sub>Co<sub>x</sub>Cl<sub>2</sub>, random mixture with competing spin anisotropies, AFMR, FMR obs. 4-76259  
 (FeMn)CP alloys, amorphous, ferromag. reson. and mag. ordering 4-71187  
 Fe<sub>40</sub>Ni<sub>60</sub>B<sub>20</sub> amorphous alloy, ferromag. resonance and antiresonance studies 4-76256  
 Fe<sub>2</sub>Ni<sub>80</sub>-P<sub>14</sub>B<sub>6</sub> amorphous ferromag. and reentrant alloys, ferromag. resonance study 4-84856  
 Gd-Fe amorphous alloy films, crystallisation and ferromag. reson. behaviour 4-71189  
 GdFe<sub>2</sub>H<sub>3</sub> films, ferromag. resonance and mag. props. 4-61594  
 HfCr<sub>2</sub>Se<sub>4</sub> mag. semicond., resist. and magnetisation changes and relax. 4-65682  
 Ni ferromagnetic film, FMR imaging using photothermal deflection 4-88725  
 Rb<sub>2</sub>Mn<sub>1-x</sub>Cr<sub>x</sub>Cl<sub>4</sub> mixed insulating ferromag. and antiferromag., ferromag. resonance studies 4-65863  
 Y<sub>2</sub>Fe<sub>17-2x</sub>Co<sub>x</sub> single cryst., top seeded soln. growth method and mag. props. 4-93207  
 Y<sub>2</sub>Fe<sub>17-2x</sub>Co<sub>x</sub>H<sub>3</sub><sup>++</sup>, ferromagnetic resonance study 4-84857  
 YIG, Me<sup>+</sup> implanted, mag. props., annealing effects 4-71057

**ferromagnetism**

- see also *ferromagnetic properties of substances*; *ferromagnetic relaxation*; *ferromagnetic resonance*; *Ising model*; *spin waves*  
 (1+1)-dimensional Ashkin-Teller model, phase diagram and critical props. 4-68162  
 AC magnetising process, hysteresis and losses, industrial diagnostic appls. 4-76177  
 amorphous and polycrystalline, microeddy currents with point defects (*Russian*) 4-109037  
 amorphous ribbons, magnetisation reversal, neutron depolarisation studies 4-98919  
 bars, electromagnetoelectric excitation of elastic longit. cylindrical waves 4-79003  
 beam with elliptic cross section, magnetoelastic buckling 4-112737  
 chain, classical Heisenberg model, magnetisation, sp. ht., crossover between two regimes 4-104441  
 classical ferromagnets with complex external field 4-61502  
 conductor, cylindrical, with weak nonlinearity in harmonic quasistationary regime, weak skin effect (*French*) 4-65698  
 cores, cyclic mag. reversals, laws for harmonic magnetisation components 4-80793  
 cubic, critical behaviour, Potts model anal. 4-61546  
 cubic ferromagnet with fourth- and sixth-order anisotropy, crit. behaviour, Potts models 4-98897  
 cubic ferromagnet with induced uniaxiality, mag. phase diagrams and domain structs. 4-65809  
 cubic single-domain-crystallites, skew-symmetric stresses 4-76228  
 cylinders, partially saturated, magnetostatics 4-59949  
 deformable ferromagnet, undergoing mag. reson., electrodynamics 4-76261  
 degenerate electronic band, martensitic transition temp., mag. field depend., enhancement by Coulomb and exchange interactions 4-104138  
 dilute magnets, phase transitions, critical behaviour, percolation, random fields 4-88690  
 diluted ANNNI models, modulated phases, conc. depend., spin configs., percolation 4-80770  
 disordered, spin excitation spectrum, fluctuation limits with competing anisotropy (*Russian*) 4-109021  
 disordered spin system with frustration, phase transitions (*Russian*) 4-104427  
 domain structure, neutron optical study 4-84812

**ferromagnetism continued**

- domain wall dynamics, influence of magnetoelastic interaction (*Russian*) 4-92935
- domain walls, modified finite-element method for calculation 4-88709
- domain walls, sine-Gordon approx., validity limits 4-84813
- dust samples, remanent magnetism and coercive force meas. using micro-computer controlled magnetometer 4-86447
- Dyson chains, with discrete spins, crit. props. 4-76154
- Dyson chains with discrete spins, critical props. 4-104443
- easy-plane ferromagnetic chain, dynamical correl. functions due to solitons, ideal gas phenomenology 4-92916
- elastic beam, soft ferromag., magnetoelastic buckling 4-74913
- elastic ferromagnetics, Bloch wall oscillations 4-76230
- EM-acoustic transform. by superimposed transducers 4-109613
- enhanced domain struct. imaging techniques using pigmented coatings 4-58874
- exchange anisotropy and plane domain walls 4-80777
- excitonic insulator with spatially inhomogeneous gap, spin wave zero sound mode 4-61528
- ferrofluids, magnetostatic props., effect of anisotropy-controlled Neel relax. 4-76194
- ferrohydrodynamic shock waves and their evolution (*Russian*) 4-80772
- ferromagnetic colloids, anisotropic theory 4-93563
- ferromagnetic film with local excitation, spin wave decay-instability threshold 4-80801
- ferromagnetic liquid, capillary waves and spontaneous magnetisation (*Russian*) 4-113031
- ferromagnetic semiconductor, conduction electron spin polarisation 4-88682
- ferromagnetic semiconductors, magnetisation simulation by HF field pulses 4-71046
- ferromagnetic slab, power spectra and localised retarded modes 4-80736
- ferromagnetic thin film, charged Neel domain walls (*Russian*) 4-80804
- ferromagnetoelectrics, electronic-type, mag. polaritons 4-71148
- ferromagnets, spin wave excitation by EM field pulses (*Russian*) 4-65797
- film, 360° neel wall form., role of mag. suspension (*Russian*) 4-92945
- films, magnetic bubble formation in nonuniform mag. fields 4-92947
- fine particle colloid dispersions, mag. props., Monte Carlo calc. 4-109044
- frustrated Ising zigzag chains, dilution and boundary condition effects, 2 spin correls. 4-71109
- garnet films, magnetic vortex dynamics using the optical Cotton-Mouton effect 4-92986
- Heisenberg ferromagnet, amorphous, short-range order and mag. props. 4-76157
- Heisenberg ferromagnet, gauge formulation of generating operator, Zakharov-Shabat system 4-90419
- Heisenberg ferromagnet, one-dimensional anisotropic classical, with in-plane field, sp. ht. 4-104452
- Heisenberg ferromagnet, semi-infinite, quasilocalised surface excitations under action of random surface pot. 4-80756
- Heisenberg ferromagnet, spin Green's functions 4-104394
- Heisenberg ferromagnet, spin wave damping theory 4-80754
- Heisenberg ferromagnet, surface spin wave freqs., temp. variation in exchange-dominated regime 4-80755
- Heisenberg ferromagnetic chain, anharmonic solitary clusters of spin deviations and lattice deform. 4-92930
- Heisenberg ferromagnetic interface, magnetisation and excitation spectrum 4-80788
- Heisenberg Hamiltonian in spin wave theory, dynamical interactions 4-98874
- Heisenberg model, anisotropic, low-temp. behaviour, symm. props. 4-61503
- Heisenberg model, correlation theory, dimension, field and temp. depend. 4-114086
- Heisenberg model, kinematical interactions and magnon excitation spectrum 4-114130
- Heisenberg model, spectral density method anal. 4-114087
- Heisenberg model with planar anisotropy, ferromag. and antiferromag., ground state magnetisation transitions 4-71120
- hierarchical vector model, Lee-Yang theorem 4-104391
- Hubbard, ferromagnet, narrow-band, carriers in spin wave range of temps. 4-92887
- Hubbard model, inverse degeneracy expansions 4-104396
- hysteresis, mathematical theory 4-61551
- incommensurate magnetic structures formation, exchange integrals 4-114088
- induction distribution, field calc. 4-96754
- Ising ferromagnet, amorphisation, high-field magnetisation 4-84762
- Ising ferromagnet, bond-diluted, bond percolation on the pentagon lattice 4-114083
- Ising ferromagnet, correl. functions in two-dimens. narrow strips at phase coexistence, Monte-Carlo calcs. 4-104439
- Ising ferromagnet, diluted, amorphisation, effective field theory with correl. 4-80771
- Ising ferromagnet, finite-size scaling at first-order phase transitions 4-104448
- Ising ferromagnet, polar states and charge ordering 4-71117
- Ising ferromagnet, pure and dil. reaction fields 4-114082
- Ising ferromagnets, three-dimensional, phase transitions in classical vector models 4-61548
- Ising model, 2-D, universality, Monte Carlo renormalisation group studies 4-114085
- Ising model, anisotropic, thermodynamical props., correlated-effective-field treatment 4-98910
- Ising model, dilute crystalline, amorphisation and high-field magnetisation 4-98911
- Ising model, ferromag., on triangular lattice, renormalisation group study 4-104450
- Ising model decorated hypercubic lattice with multiple transitions, transition point location 4-109034
- Ising model of surfaces, phase separation, critical temp. 4-88636
- Ising random field model on Bethe lattice, spin-flip ferromag. transitions 4-98909
- Ising spin-1/2 model, appl. to Li-Mg short range order 4-113664
- Ising square, two-dimens., cluster variation method calcs. of crit. temp. (*Turkish*) 4-114126
- Landau-Lifschitz eqn., inverse scatt. problem, boundary problem for spin waves in ferromagnet 4-92903
- lattice tubes for pair correlation in uniaxial ferromagnet 4-111308
- linear Ising ferromagnet with antiferromagnetic impurities ground state 4-71118

**ferromagnetism continued**

- local-band theory anal. of spin polarised, angle-resolved photoemission spectroscopy 4-92886
- magnetisation process and magnetomechanical effects 4-80786
- magnetoacoustic effects, ferromagnets and antiferromagnets, symmetry breaking for mag. ordering 4-84844
- magnetoacoustics of ferro- and antiferromagnets 4-76224
- magnetoelastic buckling, interaction of two nearby ferromag. panels 4-74911
- magnetoresistive Permalloy sensors and magnetometers 4-90615
- material inspection, harmonic analysis of hysteresis loops 4-71127
- mean spherical model, random external field, replica method for free energy 4-95303
- metallic jellium and Wigner cryst., cooperative magnetism and transitions 4-76149
- metals, non-uniform, mag. susceptibility calcs. 4-109001
- microcrystals of cooperatively-coupled materials, phys. props. 4-88778
- mixed valence d<sup>1-d2</sup> clusters, vibronic reduction effects 4-88490
- mixed valence dimeric unit, electronic and vibronic coupling, mag. aspects 4-92674
- neutron star matter, mag. susceptibility and ferromagnetic transition 4-94579
- nonlinear effects, soliton excitations 4-104385
- nonlinear ferromagnet, EM wave propagation 4-104481
- nonlinear ferromagnet, magnetisation, interaction of EM solitons 4-109042
- nonlinear ferromagnet, multisoliton struct. of EM field 4-71104
- one-dimensional classical planar model with competing interactions 4-80767
- one-dimensional system, magnetisation switching 4-80792
- p-state chiral clock model, low temp. phase diagram, mean-field approx. 4-92917
- phase transitions, 2nd order-near Curie point 4-98890
- planar, kink dynamics and static soliton spin structures 4-76141
- planar chain, sound propag. and magnetostriiction 4-98932
- planar ferromagnet, mag. vortex dynamics 4-104386
- planar Heisenberg model, biquadratic interactions 4-88641
- planar Ising ferromagnets, magnetisation and phase transitions 4-71067
- planar magnetron system for ferromagnetic targets, magnetic field distrib. near target surface 4-109321
- planar with random anisotropy, mag. soliton dynamics 4-71042
- plane nonlinear EM field problems anal. (*Russian*) 4-87244
- Potts model, three-component ferromagnetic, Yang-Lee zeros 4-101769
- Potts model of magnetism, critical dimensionalities and props. 4-61499
- Potts model on a closed Cayley tree 4-61497
- Potts model partition function, location of the phase transition 4-86346
- Potts models, ferromag. and antiferromag., phase transition, Bethe approx. 4-92918
- q-state Potts model on BCC and FCC lattice, critical points 4-80734
- quantum quadrupole ordering transition in mag. field 4-98889
- quasione-dimensional ferromagnet, soliton dynamics (*Russian*) 4-65823
- random ferromagnet-spin glass transitions, Heisenberg model 4-84787
- ribbons with negative magnetoelastic const., induced mag. anisotropy 4-104475
- s-f model in zero bandwidth limit, complete analytical soln. 4-76101
- semi-infinite n-vector model, mag. surface critical behaviour, exchange anisotropy effects 4-98898
- semiconductor, electron-phonon interaction, s-d model 4-92326
- semiconductor, magnetic excitation theory 4-76128
- semiconductor, relax. time, Green's function calc. 4-88660
- sheets, magnetic anisotropy, static zeroing method meas. 4-73465
- soft ferromagnetic elastic solids, finite deform. theory 4-97312
- solid state chemistry, correlation between struct. and phys. props. 4-70063
- solids with weak random anisotropy, mag. props. 4-98878
- spherical model, Weierstrassian and Levy random walks 4-61538
- spherical model in random external field, free energy 4-88634
- spin glass, bound rotator model, upper bound on correlation function decay 4-114116
- spin polarised electron elastic scatt., anisotropy, pseudopot. method anal. 4-114348
- spin wave spectrum and scatt. amplitudes 4-114099
- spin waves, low energy excitation spectrum on percolating network, effective medium approx. 4-71044
- spontaneous magnetisation, surface anisotropy effects 4-61518
- stochastic US signal emission (*French*) 4-109051
- superconductivity under ferromagnetic mol. field, one-dimensional electron-band model, appl. to ErRh<sub>4</sub>B<sub>4</sub> 4-98805
- superconductors, ferromag., superconductors, field depend. of spin-spiral phase 4-61483
- superparamagnetism of ferromagnets with thermodynamically unstable long-range mag. order 4-71128
- susceptibility, transfer matrix in plane-rotator model 4-114084
- texture polycryst., magnetisation, thermodynamic pot. model 4-61557
- thin ferromagnetic film, mag. bubble domain stretching (*Russian*) 4-65844
- thin films, amorphisation of regular domain structures at second-order phase transitions, dislocation-disclination mechanism 4-98928
- thin layers, saturation magnetisation (*German*) 4-84837
- three-dimensional Heisenberg ferromagnet, instantons 4-92885
- transverse Ising model with disordered surface, surface magnetism 4-88688
- tricritical points in ferromagnets with cubic single-ion anisotropy 4-88679
- two-band itinerant ferromagnet, discontinuous transition to ferromagnetic phase, band model 4-104397
- two-dimensional, anisotropy and magnetisation 4-109010
- two-dimensional ferromagnets, dynamic topological solitons 4-65801
- two-dimensional Ising ferromagnet, energy variable, scaling limit 4-11041
- weak ferromagnetic linear chains, solitons 4-80769
- F ion bombardment of ferromagnetic surface, polarization pick-up detection 4-81062

**ferromagnets** see *ferromagnetic properties of substances; ferromagnetism*

**ferrous alloys** see *iron alloys*

**Feshbach resonances** see *atomic resonant states; molecular resonant states*

**f.e.t.** see *field effect transistors*

**few-nucleon reactions** see *nuclear reactions involving few nucleon systems*

**n-nucleon scattering** see *nuclear scattering involving few nucleon systems*  
**n-nucleon systems** see *nuclei with mass number 1 to 5*  
**Feynman diagrams**  
 cluster propagator and multiparticle prod. in nonlocal quantum field theory, hadron masses 4-73653  
 four-point vertex, convergence of crossing-symmetric perturbation series 4-63866  
 hydrodynamics, fluctuation effects in 2-D systems 4-112804  
 Josephson array, microscopic formulation using Feynman diagrams 4-92868  
 quantum mechanics, formulation of phase space of \* products 4-78474  
 string formation in gas of Feynman diagrams 4-68545  
 supergraphs, background field method 4-101736  
 UV and IR divergences, corrected R\* operation 4-111295  
 $e^+e^- \rightarrow e^+e^-e^+e^-$ , cross section calc. using Feynman diagrams, helicity amps. 4-86693  
**T** see *fast Fourier transforms*  
 **fibre optics**  
 Used for fibre optic instruments and their components e.g. fibre optic gyroscopes, endoscopes and fibre lasers. For optical fibre waveguides used in telecommunications, see optical fibres  
 see also optical fibres  
 absorption cell with variable path length for meas. of extinction in liquids 4-63765  
 acoustic transducers, surface displacement, fibre optic meas. 4-97261  
 acousto-optical frequency shifting in birefringent fibre 4-91600  
 advances in instrumentation, conf. Houston, Texas, USA (Oct. 1983) 4-106121  
 adverse environment effects, conf., Paris, France (May 1983) 4-78025  
 all-PANDA-fibre gyroscope with long-term stability 4-79298  
 analogue fibre loops using long-wavelength devices 4-74741  
 astronomical instrument appl. (Russian) 4-110537  
 astronomical spectrograph for high resolution spectra of point sources (French) 4-82419  
 attenuator, tension adjusted, in-line 4-112581  
 biomedical optical fibres, conf., Paris, France (May 1983) 4-82587  
 bloodstream, local velocity meas., laser method based on two or three light guides (Russian) 4-72323  
 Bridgman-anvil press. chambers, press. meas., fibre optic imaging 4-90609  
 broadband networks, instrumentation and urban and industrial environment appls., conf., Paris, France (May 1983) 4-78024  
 catheter, fibre optic laser tunnelling device, for thromboembolic disease therapy 4-72343  
 coiled-birefringent-fibre polarisers 4-91599  
 colorimetric analyzer of transmitted, reflected and diffused light, using optical fibres (French) 4-82813  
 coupled heterodyne-detection at 10  $\mu$ m 4-64787  
 couplers for spectrophotometry prospects for in situ, in-line and remote meas. 4-78382  
 coupling efficiency to IR fibre optics in focal plane, radiometric analysis 4-106380  
 curved fibre light pipe, optical losses, heating effects 4-69580  
 delay line signal processing, overview 4-97093  
 device for projected particle vel. meas. (Japanese) 4-78297  
 distance sensor with optical-fibre-array spatial filter (Japanese) 4-78309  
 Doppler velocimeter, mixed-fibre interferometric sensor with microretroreflectors 4-91613  
 edge sensor with arrayed optical fibres, characts. and performance (Japanese) 4-86387  
 electron beam diagnostics using optical fibers 4-78742  
 ellipsometer, all-fibre, using polarisation-maintaining single-mode fibre 4-68266  
 endoscopic fibre optic surgery and therapy, appls. in USA 4-85473  
 enlarged taper ended, for laser radiation delivery systems, construction, surgical appls. 4-85472  
 Fabry-Perot resonator for intensity-independent freq. stabilisation of semiconductor laser 4-91458  
 Faraday rotator using single-mode fibre 4-69559  
 film lenses analysis, with complex source point method 4-64792  
 Fizeau interferometer for minute biological displacements meas., tympanic membrane appl. 4-89853  
 flames, propagating, temp. distrib. meas., fibre optics appl. 4-97115  
 fluid distribution measurement system, application in nuclear reactor loss-of-coolant experiment 4-106315  
 fluorimeter system, limitations due to background fluorescence 4-97083  
 fluorometer, absorption corrected, microcomputer controlled, appls. 4-78376  
 fluorometer for endoscopic diagnosis of tumors 4-109899  
 Fluoroptic thermometry, temp. sensing using optical fibres 4-78314  
 fluoroptic thermometry use in hyperthermia treatment of cancer 4-85470  
 focon use combined with luminaance amplifiers 4-69579  
 focon/optical waveguide systems design guidelines 4-93592  
 gamma irradiation effects (French) 4-80103  
 gas sensor for remote absorpt. meas. of low-level methane in near-IR 4-99865  
 gyroscope, all-fibre-optic phase-reading, using optical phase and amplitude modulation 4-97088  
 gyroscope, drift stability improvement by ratio recording 4-106306  
 gyroscope, pseudo-heterodyne detection scheme, phase swept 4-69568  
 gyroscope with linearised scale factor, gated phase-modulation approach 4-97087  
 gyroscope with passive quadrature detection 4-69570  
 gyroscopes, gated phase-modulation feedback approach 4-79324  
 gyroscopes, review 4-74713  
 gyroscopes with high-birefringent fibre and broadband sources, polarizer requirements 4-91612  
 gyroscopes with imperfect polariser/depolariser phase error bounds study 4-63732  
 illuminance distribution produced by fibre bundle 4-112570  
 image fibre, transmission characts. anal. 4-107848  
 in-line fibre-polarisation-rotating rotator and filter 4-91597  
 integrated and fibre optics in Germany, national review 4-64788  
 integrated-optic gyro chip 4-91613  
 interference reactions in optical fibre sensors (Polish) 4-112578  
 interferometer, demonstration of gravitationally induced phase shift of optical waves (Japanese) 4-101739  
 interferometer with a monochromatic-light depolariser 4-78370  
 interferometers, polarisation fading elimination, passive technique 4-64778

## fibre optics continued

interferometers, thermal phase compensation 4-73494  
 interferometric detection of slow temperature change using unlimited phase compensation 4-107862  
 interferometry for vibration and velocity measurements (Japanese) 4-87462  
 IR fibre sensors, polarisation, press. sensitivity 4-78371  
 JET Tokamak  $H_\alpha$  light monitoring using optical fibres in high-radiation environment 4-79837  
 laser Doppler anemometry device for gas/liquid flow and solid surface velocity meas. 4-108152  
 laser Doppler velocimeter using external-cavity semiconductor laser 4-97096  
 laser Doppler vibration amplitude meas. with optical fibre probe (Japanese) 4-112781  
 laser endoscopic resections in bronchology, technical problems 4-85475  
 laser therapy in tissue contact using quartz fibres 4-85476  
 low-loss single-mode WDM with etched fibre arrays 4-103024  
 macrobend tapped delay lines for high-speed signal processing 4-97094  
 magnetic-field sensor detect. scheme free from ambiguity due to material mag. hysteresis 4-78303  
 magnetometer, phase shift nulling DC field type with metallic glass sensor 4-86445  
 matching methods for integrated-optics devices and fibre-optic communication lines, review 4-60184  
 measurement applications using fibre sensors 4-64785  
 mechanical quantity sensor converter using fibre optics 4-78307  
 medical optoelectronics: laser appls., fibre-optic instrumentation and IR thermography (Japanese) 4-89678  
 metallic glass, magnetostrictive props. meas. using fibre optic interferometer 4-90618  
 Michelson high resolution thermometer 4-97105  
 micro pressure transducer for medical appls. 4-85531  
 microbend fiber optic sensor 4-112584  
 microbend sensors, sensitivity as a function of distortion wavelength 4-79323  
 micro lenses terminated optical fibres, fabrication, biomedical appls. 4-83737  
 Mitsubishi fiber-optic laser Doppler velocimeter 4-106279  
 monomode fibre optic vortex shedding flowmeter 4-97711  
 monomode fibres, characts., loss and appl. (French) 4-83714  
 NRL Optical Sciences Division research and development program 4-107849  
 optical gyroscopes 4-68276  
 optimised microbend displacement sensor 4-91617  
 organic translucent thin films, optical microscopy, visibility enhancement using fibre-optic cables 4-106378  
 OTDR long-range fibre-optic fault locator 4-73480  
 photo radiation therapy involving hematoporphyrin derivative, laser-fiber optic system appl. 4-85478  
 planar monolithic fiber optic receiver chip on a GaAs semi-insulating substrate 4-97142  
 plasma temperature fluctuation meas. using optical fibre luminosity probe 4-87926  
 polarimetric sensor using polarisation rot. in low birefr. monomode fibres 4-107859  
 polarisation maintaining fibres, update 4-91605  
 polarisation-preserving fibres, high birefringence, characterisation and performance 4-91604  
 polariser, in-line birefr. fibre 4-91606  
 polarising directional coupler 4-74726  
 proximity/interruption/reflection detection, IR optoelectronic systems with optical fibres (French) 4-111208  
 pyrometer using light guides, high temp. monitoring appls. 4-58857  
 radiation pyrometers with light conductors to solve access difficulties (Russian) 4-101920  
 radiometer in remote sensing instrumentation 4-82247  
 refractometer using tapered optical fibre 4-82818  
 remote fibre fluorimetry for on-stream analysis 4-72007  
 remote fibre fluorimetry of process and product and waste streams 4-99929  
 remote spectroscopic sensing of chem. adsorption using single multimode optical fibre 4-89355  
 review of optical fibres in the industrial and commercial environment 4-79292  
 ring interferometer with a multimode waveguide 4-73498  
 ring resonator for rotation sensing, passive 4-112580  
 ring resonator for rotation sensing 4-91611  
 semiconductor laser diodes, longitudinal mode stabilisation by extremely short optical waveguides 4-91474  
 sensing with  $\text{LiNbO}_3$  electro-optic modulator 4-91575  
 sensor, spectrophotometric appls. (Polish) 4-95490  
 sensor, twin-core, for simultaneous temp. and strain meas. 4-91619  
 sensor for distance and velocity meas., laser speckle pattern motion appl. (Japanese) 4-58845  
 sensor readout, output linearisation 4-91595  
 sensor telemetry, branch couplers construction (Japanese) 4-87461  
 sensors, metrological parameters assessment (German) 4-86409  
 sensors, recent advances 4-91610  
 sensors, review (Japanese) 4-87459  
 sensors, review 4-91609  
 sensors, technology and appls. (German) 4-95409  
 sensors for biomedical appls. 4-89682  
 signal processing using fibre and integrated optical devices 4-64794  
 single mode fibre optic recirculating delay line with bandwidth >1 GHz 4-97114  
 single mode fibres, high-birefringence, polarisation quality meas. 4-69573  
 single mode fused tapered fibre couplers, fabrication and anal. 4-97082  
 single-mode fibre saturable absorber 4-91543  
 single-mode fibre-optic holography 4-60004  
 SIR heterodyning using Ag halide fibres 4-107854  
 solid state dosimeter appls. 4-78738  
 spherical dipole probe system, 30 Hz 1 MHz EM fields meas. 4-106282  
 stabilised fibre-end retroreflecting interferometer 4-106357  
 stellar interferometer with fibre optic synthetic aperture 4-110524  
 step index fibres, angular aperture, light power transmission 4-83698  
 step-index fibre, power transmitted by different modes 4-79317  
 strain and vibration meas. sensor 4-64786  
 stress concentration measurement in a rectangular plate using an array of embedded optical fibers 4-108057  
 surface defect, acoustic wave scatt., fibre optic detection 4-85275

**fibre optics continued**

- tandem Van de Graaff accelerator using plastic clad SiO<sub>2</sub> fibres 4-78740  
 taper-polarisers, highly birefringent, finite cladding effects 4-69569  
 temperature sensor, use of optical fibre refl. two-wave interferometer 4-107852  
 therapeutic applications of lasers, review 4-85471  
 thermometer for medical use 4-100292  
 thermometer with GaAs sensor, temp. meas. by photolum. (*Danish*) 4-78315  
 twisted optical fibres as strain sensor, tensile strain conversion to optical loss 4-97086  
 two-mode fibre modal coupler 4-74705  
 underwater sound detection using optical interference in optical fibres (*Japanese*) 4-112621  
 United States fibre optics market overview 4-107879  
 US characterization of edge cracks using near-field acoustic displacement amplitude and fibre optics 4-99725  
 vibration analyser, low-freq., using fibre-optic interferometer (*French*) 4-78293  
 viewing systems, spectral prism design 4-74682  
 viscometer, semi-automatic, for specific viscosity meas., using fibre optics 4-87821  
 waveguides, time domain optical spectrometric appls. 4-86483  
 Ag halide fibres, transmission meas. in 1-11  $\mu\text{m}$  wavelength region 4-69575  
 Al-coated, optical, mechanical and radiation perform. at high temp. 4-97111  
 Ar laser therapy using fibre optics transmission 4-85474  
 D<sub>2</sub> gas-in-SiO<sub>2</sub> fibre Raman laser, synchronously pumped, operating at 1.56  $\mu\text{m}$  4-79181  
 InGaAsP 1.3  $\mu\text{m}$  optical amplifier-modulator integrated with a fibre-resonator mode-locked laser 4-91491  
 Nd:YAG laser-fibre optic system, surgical coagulation appls. 4-85477  
 O<sub>2</sub> partial pressure meas. in vivo, fibre-optic probe method 4-62633  
 SiO<sub>2</sub> low-loss high-resolution image fibre fabrication, imaging optics method 4-97095  
 SiO<sub>2</sub>/GeO<sub>2</sub> low-loss high-resolution image fibre fabricated by multiple-fibre method 4-97159

**fibre reinforced composites**

- see also carbon fibre reinforced composites; glass fibre reinforced plastics  
 anisotropic continua, tensor representation of energy dissipation characts. (*Ukrainian*) 4-64839  
 anisotropic layered, singularities at tip of crack normal to interface 4-74952  
 antisymmetrically laminated composites, thermal residual stresses, finite element anal. 4-97306  
 cement paste, mortar and concrete, mech. props. and fabrication, book contrib. 4-66298  
 ceramic matrix, fabrication and mech. props., book contrib. 4-66297  
 critical length of reinforcing fibres 4-71695  
 cross-reinforced, heat conduction anal. using double periodic harmonic functions (*Ukrainian*) 4-87537  
 cylinder, multilayer, wave propag. rel. to anisotropy and viscosity 4-108040  
 damping composite materials development 4-76797  
 discontinuous, strength, probabilistic theory 4-81244  
 dynamic loading of fibre reinforced beams 4-99454  
 effective axial shear modulus and transverse thermal cond. 4-97323  
 elastic constants of composites containing anisotropic fibres 4-75596  
 elastic materials, stability, finite plane strain 4-87579  
 elastic matrix with nonuniform subcritical state, fibre stability 4-108031  
 elastic props., rule of mixtures 4-109448  
 elastoplastic response, finite element micromechanical analysis 4-87581  
 epoxy optical alignment tube, thermal structural deform. optimisation 4-87415  
 epoxy-graphite fibre reinforced plate, anticlastic curvature suppression 4-83832  
 epoxy-impregnated C fibre panel fabrication and testing for submm telescope use 4-103033  
 failure criterion, macroscopic 4-81266  
 fatigue-proof design, reliability-based 4-99604  
 fibre reinforced composites, fibre-matrix bond form. kinetics during rolling 4-71674  
 hybrid composite sheet, stress concs. due to fibre breakage 4-97426  
 hybrid fibre reinforced epoxide composite, environmental response of flexural props. 4-76809  
 inelastic, delayed failure 4-97434  
 inelasticity, effect on strength in static loading 4-71678  
 insulating materials, electron and neutron irradi. effects on mech. props. 4-75533  
 intermingled hybrid composites, stress conc. rel. to fibre vol. and strength 4-108020  
 Kevlar fibre-reinforced epoxy resin composites, fracture toughness rel. to controlled interfacial bonding 4-66423  
 laminated plates, design for max. stiffness 4-75599  
 laminated plates, initial failure and ultimate strength theory (*Japanese*) 4-97417  
 laminated plates, optimum design 4-97367  
 laminated plates and beams, fibre vol. fraction, dynamic mech. props. 4-89078  
 laminated symmetric beams, damping and dynamic moduli 4-80154  
 laminates, delamination, fracture mechanics 4-97431  
 laminates, fatigue damage parameter using stiffness change 4-76864  
 laminates, fracture toughness meas. using three-point bend and compact-tension specimen 4-99735  
 laminates, material design with required flexural stiffness 4-99391  
 laminates, matrix crack growth, stochastic simulation model 4-74960  
 laminates, onset of delamination, expt. and analytical study 4-76847  
 laminates, thermal expansion, effect of microcracks 4-80270  
 laminates, with circular holes, interlaminar stresses, effect of geometry 4-79447  
 laminates plates, inelastic, constitutive relations 4-103200  
 mechanical behaviour of materials, conf., Stockholm, Sweden (Aug. 1983) 4-90297  
 metal matrix, directionally solidified, book contrib. 4-66277  
 metal matrix composites, fabrication, book contrib. 4-66276  
 metal matrix composites, stress-strain and failure behaviour 4-76831  
 metallic, generalised classif., book contrib. 4-109357

**fibre reinforced composites continued**

- metallic glass ribbon reinforcement characts., pull-out tests in different matrices 4-71717  
 microstress redistrib. due to time-depend. processes 4-97329  
 multilayered composites, delamination stress determ., iterative approach 4-112702  
 NDT techniques, vibrational 4-81367  
 NDT with acoustic flaw detector (*German*) 4-76941  
 new materials technology 4-88953  
 nondestructive evaluation, design philosophy 4-99734  
 organic matrix, mech. props. at elevated temps., model for prediction 4-81240  
 organic plastic, damage cumulation in quasistatic and cyclic loading 4-89090  
 organic plastic, unidirectionally reinforced, creep strain prediction 4-89234  
 orthotropic, elastic and photoelastic calibration, appl. of least squares, method 4-69717  
 plasma spraying on fibres, thermal characts. 4-66254  
 plastic matrix, fatigue life estimation under sinusoidal wave loads (*Japanese*) 4-99505  
 plastic matrix, plates, stresses around partial contact pin-loaded holes 4-79520  
 plastic matrix, stable crack growth, influence of fibre orientation 4-99570  
 plate, orthotropic, with circular hole, fatigue failure 4-74953  
 plates, laminated composite, mixed finite element anal. 4-74904  
 Plexiglas-stee interface, US transmission at subcrit. angles 4-69641  
 polyethylene fibrillated tape reinforced cement, mech. props. 4-109493  
 polyheteroarylene reinforced epoxy composite, long-cycle fatigue, freq. depend. 4-89130  
 polymer matrix, mechanics of winding, book contrib. 4-66303  
 polymer-based, thermal testing of struct. and mech. props. 4-85268  
 polypropylene fibre reinforced mortar, thin slabs, fracture toughness under flexural or impact loading 4-99576  
 porous metallic matrix, stresses at fibre/matrix boundaries 4-93335  
 pressure vessel, elastic-plastic solns. (*Chinese*) 4-112725  
 quasi-isotropic laminates, thermal expansion behaviour, surface anisotropy 4-80269  
 residual stresses during thermal cycling 4-71634  
 resin matrix high-performance composites, book contrib. 4-66302  
 semi-infinite composite with long reinforced phase, edge crack analysis 4-97400  
 shear anomalies of high-modulus fibrous materials 4-108014  
 shells of revolution, laminated, vibration, numerical analysis 4-108036  
 short fibre composites, mech. behaviour 4-98173  
 short fibre composites, strength, probabilistic theory 4-76830  
 short fibre composites, stress distrib., effect of fibre-end geometry 4-74869  
 short fibre composites, stress distrib. under axial load, finite element analysis 4-108009  
 short fibre reinforced ceramics, mech. aspects of failure (*French*) 4-81280  
 steel fibre reinforced Al alloy, prep. by explosion techniques, mech. props. at low temp. 4-114634  
 steel fibre reinforced cement, fibre debonding and pullout, adhesional interfacial shear strength 4-66388  
 steel fibre reinforced cement, free shrinkage, theoretical model 4-93255  
 steel fibre reinforced epoxy beams, dynamic loading 4-99454  
 steel fibre reinforced monolithic refractories, selection and service life 4-109458  
 steel fibre reinforced mortar, polystyrene impregnated, interfacial failure 4-99571  
 steel fibre reinforced mortar, thin slabs, fracture toughness under flexural or impact loading 4-99576  
 steel fibre reinforced Pb-Sn beams dynamic loading 4-99454  
 steel fibre reinforced refractories, fibre-matrix bonding rel. to brazing 4-109367  
 steel wire reinforced Al alloy, KAS-1A composite, resources eval. 4-66442  
 stiffness reduction due to fibre breakage 4-80136  
 structural materials, homogeneous thermal fatigue, rel. to struct. stresses 4-99594  
 tensile tests, at cryogenic temps., acoustic emission 4-76804  
 thermal expansion coefficients 4-70418  
 thermoplastics, reinforced, compounding and fabrication, book contrib. 4-66304  
 time dependent failure, statistical and micromechanical modelling 4-79517  
 tube, circular cylindrical, reinforced by fibres lying along helices, rotation 4-60263  
 uniaxially reinforced composite, stress distrib. near cracks, shear lag theory 4-79518  
 unidirectional, with initially deformed components, corrected elastic props. 4-74861  
 unidirectional composites, matrix cracking 4-74962  
 unidirectional metal matrix composites, thermoplasticity 4-97348  
 Al-Ca-Zn superalloy, composite, fibre reinforced, hot pressing, tensile props. 4-99369  
 Al<sub>2</sub>O<sub>3</sub> fibre reinforced FP alloy, orthotropic plate with circular hole, fatigue failure 4-74953  
 Al<sub>2</sub>O<sub>3</sub> fibre reinforced Mg composite, off-axis fracture, critical stress intensity 4-66430  
 Al<sub>2</sub>O<sub>3</sub> fibre reinforced Mg, tensile and fatigue behaviour, fibre fraction and orientation 4-114652  
 Al<sub>2</sub>O<sub>3</sub> fibre reinforced Mg alloys, tensile and fatigue behaviour, matrix alloying effects 4-114653  
 B fibre reinforced Al, chem. reaction of B fibres with liq. Al 4-61891  
 B fibre reinforced Al, fibre-matrix bond form. kinetics during rolling 4-71674  
 B fibre reinforced Al, rolling in direction of reinforcement 4-66353  
 B fibre reinforced Al, stress-strain and failure behaviour 4-76831  
 B fibre reinforced Al composite, fracture mode and shear strength rel. to interface strength 4-62022  
 B fibre reinforced Al-Mg, interaction between B and matrix 4-70577  
 B fibre reinforced Al-Mg alloy, fibre/matrix interface effect on fatigue, optimum processing parameters 4-114635  
 B fibre reinforced epoxy, orthotropic disk, thermal stresses due to rotating heat source 4-60289  
 B<sub>4</sub>C/B fibre reinforced Ti-Al-V, fatigue crack growth behaviour 4-93374  
 Be fibres reinforced Al alloy, stress-strain and failure behaviour 4-76831

**fibres reinforced composites continued**

- SiC fibre reinforced Al alloy, fabrication and mech. props. (*Korean*) 4-104755
- SiC fibre reinforced Al alloy, composite strengthening, influence of microstruct. 4-99398
- SiC fibre reinforced Al alloy, squeeze cast, thermal expansion, elastic to plastic deform. transition 4-108635
- SiC fibre reinforced Ti-Al-V, fatigue crack growth behaviour 4-93374
- SiC fibre/platelet reinforced Al-Mg-Si, magnitude and mechanism of strengthening 4-76710
- SiC fibres, tensile strength, struct. and phase comp., effect of isothermal annealing 4-66381
- SiC filament reinforced Ti, model composite, filament microanal. and strength characterisation 4-104753
- SiC filament reinforced Ti, model composite, fibre-matrix chem. reaction at high temps. 4-104754
- Ti matrix, fabrication and mech. props., review 4-81170
- UC<sub>2</sub> fuel particles, TRISO-coated, fission product release during post-irrad. annealing 4-111606
- UCO fuel particles, TRISO-coated, fission product release during post-irrad. annealing 4-111606
- W fibre reinforced Cu composite, fracture, acoustic emission obs. (*Japanese*) 4-62024
- W fibre reinforced stainless steel, residual stresses during thermal cycling 4-71634

**fibres**

- see also carbon fibres; composite materials; fibre reinforced composites; glass fibres; optical fibres*
- aerosol particles, fibrous, bipolar diffusion charging, elec. mobility and charge meas. 4-89348
- aerosol particles, fibrous, bipolar diffusion charging, theory 4-89347
- bundles, strength, statistical theory 4-74868
- cellulose fibres, pineapple, mech. and dielec. props. 4-104807
- cotton, mol. dynamics, spin label method investig. (*Russian*) 4-59937
- Fibrillar biopolymers, diffraction from variable sign helix 4-66854
- intervertebral disks rel. to fibre stabilisation of bent cylinders 4-77298
- Kevlar 29 braid, bending fatigue life rel. to resin impregnation 4-93394
- Kevlar fibre rope endurance obs. and selection guidelines 4-114676
- metallophthalocyanine stacks as conducting polymers, fabrication 4-75957
- micromechanical test machine for high temperatures 4-89218
- muscle, rabbit psoas, de-membranised fibre bundles, rigor tension, soln. ionic strength depend., X-ray obs. 4-89610
- nylon 66 fibre, drawn, microstruct. rearrangement during heat treatment, tensile modulus, SAXS obs. 4-76791
- nylon fibre rope endurance obs. and selection guidelines 4-114676
- PET filaments, orientational stretching, intermolecular interaction energy (*Russian*) 4-109460
- PET yarn, oriented, deform., melting-recrystallisation mechanism, SAXS using synchrotron radiation 4-71691
- polyacetylene, single-fibre, prod. and struct. 4-114469
- polyamide 66, loading criteria for fatigue failure, acceleration of creep failure 4-62008
- polyaramid fibres, compressive buckling, mech. model 4-97362
- polycarbonate, oriented, Young's modulus, temp. depend., IR spectra, Gruneisen parameter (*Russian*) 4-109445
- polyester fibre rope endurance obs. and selection guidelines 4-114676
- polyester textile fibres, friction meas. 4-89137
- polyester yarn, spin-oriented, differential scanning calorimetry, obs. 4-79952
- polyester yarn, spun and drawn, differential scanning calorimetric obs. 4-79953
- polyethylene fibres, strength and elasticity, electron microscopy (*Russian*) 4-85180
- polyethylene fibres, tensile props. rel. to morphology 4-104819
- polyethylene fibres, ultrahigh strength fracture process 4-62015
- polyimide, oriented, Young's modulus, temp. depend., IR spectra, Gruneisen parameter (*Russian*) 4-109445
- polymer, elongational flow processes modelling, viscometric methods (*German*) 4-71707
- polymer fibres, orientational drawing termination rel. to supermolecular struct., X-ray obs. 4-75316
- polymers, rigid-rod, high performance materials, review of theoretical investigations 4-81208
- polypropylene, hollow fibres, strain induced porosity, gamma quanta angular correlation (*Russian*) 4-109097
- polypropylene fibres, crystallinity meas. by X-ray diff. curves (*Russian*) 4-84224
- refractory materials, fibrous, specific thermal cond. rel. to temp. and apparent density 4-98379
- sound absorbing materials, struct. and acoustical props. 4-91688
- transparent fibres, weakly anisotropic, sizing using light scatt., correction factors 4-63714
- Al<sub>2</sub>O<sub>3</sub> fibres, polycryst., prod. 4-71618
- Al<sub>2</sub>O<sub>3</sub>-SiO<sub>2</sub> fibres, cristobalite form. at elevated temp. (*German, English*) 4-81197
- B fibres, chem. reaction with liq. Al 4-61891
- B fibres, elastic energy absorpt. mechanism 4-66366
- SiC fibres, mech. props. and struct. (*French*) 4-62003
- SiC fibres, strength degradation after heat treatment above 1200°C 4-66385
- SiC fibres, tensile strength, struct. and phase comp., effect of isothermal annealing 4-66381
- SiC, for ICF applic., strength and fatigue analysis 4-109502
- fibrinogen** *see proteins*
- field, crystal internal** *see crystal field interactions*
- field effect devices**  
*see also field effect integrated circuits; field effect transistors; metal-insulator-semiconductor devices*
- a-Si:H photoreceptors, electrophotographic imaging process 4-73544
- field effect integrated circuits**  
*see also charge-coupled device circuits*
- CMOS active lateral diffusion and linewidth test struct. 4-108665
- CMOS LSI circuit for an implantable cardiac pacemaker 4-77428
- DC monolithic accelerometer design and fabrication 4-11122
- FET humidity sensor incorporates temperature sensor 4-73443
- NMOS fading memory local plane processor 4-107871
- SOI three-dimensional ICs fabrication by laser recryst. of Si islands 4-75798
- ZnO on Si pyroelectric anemometer 4-69846

**field effect integrated circuits continued**

- GaAs semi-insulating single crystal growth by LEC method, IC appls. (*Japanese*) 4-104728
- TiSi<sub>2</sub>/n<sup>+</sup> poly-Si, co-sputter-deposited, rapid lamp heating, MOS device fabrication appl. 4-99311
- field effect transistor circuits**  
*Used for general papers and papers where the use of field effect transistors is significant*
- voltage clamp expts., simulation with FET analogue circuits 4-85591
- field effect transistors**  
*see also field effect integrated circuits; insulated gate field effect transistors; junction gate field effect transistors; Schottky gate field effect transistors*
- high dose MOS dosimeter for space use, design criteria 4-63026
- modulation doped, MOS formalism modelling 4-76041
- MOS integrated sensors, electrochem. and charge-imaging effects 4-82786
- signal design for optical communication 4-83724
- (AlGa)As/GaAs modulation-doped heterostruct., optimisation for TEG-FET operation at room temp. 4-92804
- AlGaAs/GaAs/AlGaAs single quantum well transistor with 2-D electron gas, logic device appl. 4-61443
- AlGaAs-GaAs heterojunction, two-dimens. electron gas gate control charact., optimum doping (*Chinese*) 4-114021
- Al<sub>0.1</sub>Ga<sub>0.9</sub>As/GaAs heterojunction FET, 2D electrons, cyclotron resonance studies 4-98743
- GaAlAs/GaAs selectively doped heterojunction, electron conc., FET appl. 4-98703
- GaAs FET microwave refractometer for tropospheric studies (*French, English*) 4-63778
- GaAs MBE superlattices, elec. props. of oval defects, FET appl. 4-92574
- GaAs p-n-p-n layers, electrical, LPE growth 4-80665
- InGaAs PIN-FET receivers for long-wavelength optical communication systems 4-97133
- Si:H, amorphous, electron mobility meas. using 4-terminal FET structures 4-75964
- a-Si-based field effect transistors, flat-band volt. and surface states 4-92825
- field electron microscopy** *see field emission electron microscopy*
- field emission, electron** *see electron field emission*
- field emission, ion** *see field ion emission*
- field emission electron microscopes**  
*see also field emission electron microscopy*
- gun fitted to electron microscope micrograph nonisoplanatism effect 4-68339
- W imaging, electric field induced surface atomic displacements obs. 4-68337
- field emission electron microscopy**  
*see also field emission electron microscopes*
- electrostatic field emission microscope for Auger electrons spectroscopic microanalysis 4-72021
- energy spread measurement in field electron microscopy 4-65156
- steel, alloy, solute redistribution at pearlite growth front, field emission STEM X-ray chem. microanalysis obs. 4-81191
- TEM with thermally stabilised field emission gun 4-70000
- Ag clusters in Si matrix, Auger anal. using electrostatic field emission microscope 4-72021
- C fiber, field emission microscopy and mass spectrometry anal. 4-66196
- W (111), work function and local field strengths calc. from FEM data 4-66195
- W imaging, electric field induced surface atomic displacements obs. 4-68337
- W, surface diffusion of adsorbed Pd across steps, FEM study 4-92558
- W surface polycryst., chemisorption of NO desorption, FEM and work function meas. 4-92564
- field emission ion microscopes**  
*see also field emission ion microscopy*
- No entries
- field emission ion microscopy**  
*see also atom probe field ion microscopy; field emission ion microscopes*
- adsorption kinetics of gas atoms of mols. 4-92541
- field electron emitters sputtering by self-generated positive ions 4-76642
- field ionisation, of gas at metal surface, review (*Polish*) 4-88948
- Co-Al<sub>2</sub>O<sub>3</sub> coevaporated composite films, solar selectivity 4-72169
- CuAu, microstructure, field ion microscopy study 4-88177
- Fe<sub>40</sub>Ni<sub>60</sub>B<sub>20</sub>, metallic glass, field ion microscopic study at liq. H temp. 4-75311
- Pd-W(Ir)(Cu)(Ag), field ion imaging of surface atoms 4-88384
- Rh, phase transition, field ion microscopy study (*Russian*) 4-81189
- W (110), adsorbed Re, three-body interactions, field ion microscopy study 4-70564
- W (211), lattice steps and adatom binding, FIM study 4-108687
- W, field ion study of mixed dislocations 4-108369
- W, interstitial atom interaction with grain boundaries (*Russian*) 4-65293
- W, proton irrad. induced defects, FIM obs. 4-108483
- W surface, interstitial atom interactions, field-ion microscopy studies 4-61798
- field evaporation**
- alkali halide, cleaved crystal surfaces, ledge struct., evaporation, electric field effect 4-66194
- liquid metal ion source, shape dynamic model 4-81117
- small molecules, laser pulse-induced field desorption 4-80418
- Al<sub>2</sub>O<sub>3</sub>, thermal dissolution of layers on W and Mo substrates in elec. field 4-80405
- C fiber, field emission microscopy and mass spectrometry anal. 4-66196
- Rh, bonding distance and vibr. freq. determ. 4-93202
- W (011), field evaporated ions, charge states distrib., atom probe FIM study 4-81118
- W, field ion study of mixed dislocations 4-108369
- W ion field evaporation, activation energy meas. 4-71529
- field intensity patterns (antenna)** *see antenna radiation patterns*
- field interactions (condensed matter)**  
*see also crystal field interactions; hyperfine field interactions (condensed matter)*
- CaO-B<sub>2</sub>O<sub>3</sub>-Al<sub>2</sub>O<sub>3</sub>-Fe<sub>2</sub>O<sub>3</sub> glass system, photoacoustic spectra of Fe 4-99130
- FeF<sub>3</sub>, amorphous, Mossbauer-Zeeman spectrum study 4-76294

**field ion emission**

- cosmic grains fluff, effects on field emission, charge and particle levitation 4-94578
- field ionisation, of gas at metal surface, review (*Polish*) 4-88948
- high adherence coatings, deposition techniques 4-81161
- Ga, liquid, ion source, construction and technology (*Chinese*) 4-82858
- W ion field evaporation, activation energy meas. 4-71529

**field ion microscopy, atom-probe** *see atom probe field ion microscopy***field ionisation**

- foil-excited Rydberg states in atoms+ion collisions, elec. field ionisation 4-102784
- gas, at metal surface, reviews (*Polish*) 4-88948
- low-temperature attachment to the field ionization source in the MI-1201 mass spectrometer 4-101963
- methyl butyl ether, field ionisation mass spectra 4-59902
- methyl butyl ketone, field ionisation mass spectra 4-59902
- methyl propyl ether, field ionisation mass spectra 4-59902
- methyl propyl ketone, field ionisation mass spectra 4-59902
- unimolecular rate const. functions from field ionisation data conversion, numerical approach 4-93516
- C fiber, field emission microscopy and mass spectrometry anal. 4-66196
- H, Stark effect level crossings, relativistically enhanced ionisation rates 4-69010
- N atom recombination at Pd surface, field ionization evidence of excited molecules 4-99288
- Na, Rydberg levels, microwave field ionisation 4-96710
- Rb+N<sub>2</sub>, thermal energy collision, Rb total depopulation cross sections 4-102783

**field measurement, electric** *see electric field measurement***field measurement, magnetic** *see magnetic field measurement***field plotting**

- see also field strength measurement*
- 3-dimensional magnetic field calculation, modified scalar potential (*Chinese*) 4-101877
- probing EM fields in lossy spheres and cylinders simulating biological objects 4-115295

**field strength measurement**

- see also electric field measurement; magnetic field measurement*
- absorber-lined chamber, correlation of theoretical and measured site attenuation 4-69645
- cable radiation, evaluation model 4-107497
- EMC, degraded absorber performance effect 4-69646
- FCC Part 18 standards for radio equipment 4-69930
- magnification factor for mode stirred chambers 4-69647
- probing EM fields in lossy spheres and cylinders simulating biological objects 4-115295

**field theories, unified** *see unified field theories***field theory, classical** *see classical field theory***field theory, crystal** *see crystal field interactions***field theory, electromagnetic** *see electromagnetic field theory***field theory, meson** *see meson field theory***field theory, quantum** *see quantum field theory***fields, electric** *see electric fields***fields, magnetic** *see magnetic fields***filament lamps**

- halogen lamp, cycle operation under microgravity conditions using sound-ing rocket 4-60128
- Illuminating Engineering Society Annual Conf., Los Angeles, USA (Aug. 1983) 4-90291
- lumen, expt. realisation (*Japanese*) 4-63766
- W halogen tubular lamps, TiO<sub>2</sub>-SiO<sub>2</sub> multilayer IR reflective filter 4-112534
- W, spectral emissivity, analytic expressions for 340 nm to 2.6  $\mu$ m spectral region 4-60127

**file management** *see file organisation***file organisation**

- see also data handling; data structures; database management systems; virtual storage*
- standard data file format for USA synchrotron sources 4-90568

**filled polymers**

- acrylonitrile-butadiene copolymer, glass-filled, thermal cond. meas. to high temp. using line-source technique 4-108668
- acrylonitrile-butadiene rubber C reinforcement, static fatigue, statistical analysis 4-99683
- elastomers, glass bead filled, failure processes near rigid spherical inclusion 4-76841
- epoxide composite, alumina particle filled, fractography (*Japanese*) 4-99512
- epoxide resin, glass bead filled, fracture, yield strength rel. to struct. 4-66416
- epoxy, Fe filled, particulate composite, dynamic mech. props. 4-76794
- epoxy resin, filler reinforced, impact tensile fatigue strength, statistical analysis (*Japanese*) 4-99504
- film, two phase, structural changes during heat treatment 4-80435
- furfuroil acetate binder, mech. props. 4-89080
- highly filled concept criteria (*Russian*) 4-79949
- metal reinforced plastics, struct. during pressure and temp. changes 4-89088
- organic plastic, damage cumulation in quasistatic and cyclic loading 4-89090
- organic plastic, unidirectionally reinforced, creep strain prediction 4-89234
- phase transition between matrix and inclusions in polymeric composites 4-114474
- phenolic resin, talc- or glass-filled, thermal cond. meas. to high temp. using line-source technique 4-108668
- polybutadiene, reinforcement with inorganic fillers, mech. characts. 4-61914
- polyethylene-Pb(Zr,Ti)O<sub>3</sub> composite, pyroelectric effect study 4-99044
- polypropylene, mica-filled, mech. props. influence of particle size 4-81279
- polystyrene, glass bead filled, craze form., microscopic in situ obs., interfacial adhesion 4-62073
- polyurethane foam, compressive creep rel. to particulate reinforcement 4-89084
- PVC, particle filled, fracture mechanism rel. to fatigue crack growth (*Japanese*) 4-89120
- PVC matrix, deform. thermodynamics 4-89089
- rubber, filled pairs, frictional props. (*German*) 4-66454

**filled polymers continued**

- rubber, filler reinforcement, available fillers and behaviour 4-76741
- rubber, silica filled EPDM, network struct., fracture mode rel. to vulcanisation conditions 4-109373
- rubber vulcanisates, carbon-black-filled, stress relax. at moderate strains 4-81233
- silicate filler, tridecylamine coating treatment, ang. depend. XPS obs. 4-109526
- Sylgard 184 containing hollow microspherical fillers, high temp. elec. cond. and thermal decomp. 4-92710
- syntactic foams, three phase, mech. props., dielec. const. 4-89077
- thermoplastics, cellulosic filler efficiency, processing characts. and mech. props. 4-61913
- thermoplastics, glass bead reinforced, creep resistance, fatigue endurance 4-61994
- thermoplastics, reinforced, compounding and fabrication, book contrib. 4-66304
- transition metal-polymer composites, superparamagnetic, EPR obs. 4-88716
- Mo-SAM-E composite, electrophysical props. 4-76742

**film badges** *see dosimeters***films**

- see also adsorbed layers; coatings; foils; helium films; Langmuir films; liquid films; monolayers; optical films; polymer films; replicas; thick films; thin films*
- No entries

**filtering and prediction theory**

- see also information theory; Kalman filters; random processes; Walsh functions*
- acoustic noise cancellation, adaptive, digital filter implementation using modified Widrow-Hoff algorithm 4-103114
- audio filter design, appl. of simple hearing model 4-105260
- audio signal processing, digital, CMOS-VLSI rate conversion digital filter appl. 4-103121
- automatic glottal inverse filtering 4-103143
- continuous speech recognition using dynamic programming, parameters comparison 4-79393
- digital radiographic imaging, appls. of median filter 4-105336
- formant tracking and glottal inverse filtering, two channel (speech and FGG) anal. 4-103144
- frequency domain optimal inverse convolution filtering of noise data 4-105735
- image restoration using Hunt's method, inverse filter effects 4-91411
- image sequence processing, relationships between temporal and spatial dimensions 4-79049
- laser gyro performance, quantisation reduction using moving average filter 4-102970
- linear prediction theory of a homogeneous random field with discrete parameters (*Chinese*) 4-58623
- mammalian reflex dynamics prediction by complementary filtering theory 4-105229
- maximum entropy method, generalisation for processing nonstationary multichannel complex valued data 4-110297
- measurements treated by filtering, redundancy and error considerations (*German*) 4-106258
- noise reduction by nonlinear digital filtering, estimation method 4-91694
- optical communications, conditional probability and conditional expectation in quantum mech., expressions 4-74445
- optimal quantum-mechanical multiparameter estimation fundamental theorem, proof 4-74444
- radio sources detection against set-noise background, errors in coordinates and fluxes 4-63080
- sea-level survey data, digital filtering (*Chinese*) 4-85680
- seismic deconvolution using lattice processors, new results 4-105767
- speech, all-zero model for higher pole correction 4-103146

**filters**

- see also active filters; band-pass filters; crystal filters; digital filters; high-pass filters; Kalman filters; low-pass filters; matched filters; microwave filters; optical filters; passive filters; spatial filters*
- bulk-acoustic-wave-beam filters, effects of diffraction on freq. response 4-60232
- digital optical communication, numerical optimisation of equalising filters 4-83721
- motion picture lighting compensation filters (*Russian*) 4-73552
- noisy images, adaptive estimation procedure comparison 4-102902
- semiconductor detector, spectrometric meas. and signal processing module 4-68908
- spectral analysis of short-time biomedical data using adaptive filters 4-72453
- speech, all-zero model for higher pole correction 4-103146
- variable emittance filter for electron laser facility 4-82859
- X-ray filters and laser targets, thickness variations 4-111262

**filters, optical** *see optical filters***filtration**

- $\nabla \cdot (\nabla \phi) = 0$  equation boundary-value problems 4-103216
- aerosols, blackness (light absorbing ability) rel. to filter blackening 4-62252
- axial-symmetric flow through porous media with free and seepage surfaces, Volterra boundary value problems 4-113002
- blood filtration pressure and erythrocyte deformability meas., evaluation of the Erythrothrom 4-115248
- blood serum proteins, PIXE anal. using gel filtration 4-105367
- blood treatment using ultrafiltration processes 4-81732
- coffer dams, porous orthotropically inhomogeneous, filtration study 4-79665
- deposited layer stability in ultrafiltration (*German*) 4-112690
- erythrocyte deformability, assessment by constant flow filtration technique 4-115282
- erythrocyte deformability, leukocyte removal prior to study, improved method 4-115285
- erythrocyte filterability and anticoagulants 4-115097
- erythrocyte filtration resistance at constant press., technique for continuous meas. 4-115283
- $\beta$ -galactosidase, ultrafiltration induced by pulsatile flow in variable vol. hollow-fiber enzyme reactor 4-77270
- gas-condensate mixture, filtration, asymptote-combination method 4-103406
- heat conduction and filtration in porous bodies, related problems 4-79663
- Hemorrhometre, automated apparatus for filtration initial flow rate meas. 4-115284

## filtration continued

- lipoprotein solns., conc., osmotic press., rel. to ultrafiltration 4-114826
- local pore cooling, steady-state problem 4-79664
- metal phthalocyanines, mol. wt. determ., gel filtration method 4-112307
- metallic gauze porous materials, pore size distrib. 4-66261
- myocardium microcirculation, indirect determ. of fluid filtration and reabsorp. 4-93771
- O-nitrophenyl- $\beta$ -D-galactopyranoside, ultrafiltration induced by pulsatile flow 4-77270
- nonlinear filtration, difference schemes 4-87789
- oil, soluble, ultrafiltration, conc., polaris., membrane fouling and cleaning 4-89330
- phase separation surfaces and rheological characteristics 4-103405
- protein solns., conc., osmotic press., rel. to ultrafiltration 4-114826
- reactor coolant, high temperature EM filtration, radioactive corrosion prod. removal 4-96188
- stationary gravity filtration, mass transfer model, numerical soln. (Ukrainian) 4-65021
- N<sub>2</sub> liquid, solubility of halogen hydrocarbons at 77.4K, filtration study 4-70385

## IM see field emission ion microscopy

## IM, atom-probe see atom probe field ion microscopy

## in lines

dielectric layers, dispersion anal. 4-79006

ne structure, atomic see atomic fine structure

ne structure, molecular see molecular fine structure

## nite automata

cellular automata, reversible, time invariant quantity for subclass 4-78251

## nite element analysis

- 2-D magnetostatic program TRIM converted into RIPS, accuracy of computation (Japanese) 4-64648
- acoustics, integral equations, numerical methods 4-83748
- advanced X-ray astrophysics facility technology mirror assembly epoxy shrinkage effects 4-86512
- advection-diffusion equations, space-time least-square finite element scheme 4-64903
- aerospace structures, conf., Boston, MA, USA (Nov. 1983) 4-73167
- axially symmetric incompressible viscous flow, with perturbations, numerical stability anal. 4-83874
- axisymmetric and 3-dimens. convection anal. using penalty finite elements, computer code (Japanese) 4-64193
- beam, thin, transient finite elastic-viscoplastic deform., numerical simulation 4-97341
- beam with unilateral supports, optimal design 4-106189
- beams, nonlinear vibrations, Lagrange-type formulation for finite element anal. 4-91755
- beams with material and geometric nonlinearities, simple element for static and dynamic response 4-78141
- bilinear-constant velocity-pressure finite elements stability 4-101655
- Bitter plate tokamaks, coupled EM and thermal problems, transient nonlinear solns. 4-59412
- boundary function approximation, Lagrangian, spline and weighted finite difference methods 4-64848
- boundary value problems, multi-grid method numerical soln. 4-101628
- boundary-element methods for transient response analysis, book contrib. 4-60298
- burn injury in blood-perfused skin, finite element model 4-77200
- C<sup>0</sup> triangular plate element with one-point quadrature 4-78140
- cavities, acoustic wave propag., finite element techniques 4-83749
- central crack element in fracture mechanics 4-60338
- channel expansion, laminar flow, spectral element method 4-87797
- classical solutions guiding finite element strategies, examples 4-87423
- collocation procedure for determining fracture mechanics parameters at a corner 4-60340
- compact specimen, fatigue crack closure, finite element analysis 4-97433
- composite laminate elasticity problems with singularities, hybrid finite element approach 4-97324
- composite material, unidirectional, micromech. finite element anal. incl. longitudinal shear loading 4-91722
- composite materials, symmetric rail shear test, mode II fracture toughness, finite element analysis 4-109582
- composites, antisymmetrically laminated, thermal residual stresses, finite element anal. 4-97306
- compressible laminar and turbulent flow, time-split finite element method 4-112932
- computational aspects, book 4-110821
- computational methods for transient analysis, book 4-58594
- computationally uncoupled numerical schemes in linear thermoelasticity 4-87568
- contact friction forces, effect in compressive tests of specimens 4-109596
- convection, natural, in vertical channels, finite element analysis 4-75023
- cost-effective eigen solution method for large systems with Rockwell NASTRAN 4-83128
- crack problems, fully plastic, penalty method solns. 4-97419
- crack problems, solution using finite difference technique 4-69710
- crack tip concordant displacement, finite element method employing singular element 4-69711
- crack tip singularity modeling by quarter point quadrilateral element 4-103252
- creep, crack growth, comparison of finite element predictions with expt. data 4-97410
- crystal growth, finite-element simulation of .Czochralski bulk flow 4-65207
- cylinder, cracked, under internal pressure, finite element calc. evaluation by speckle photography 4-97450
- defect sizes in plant at elevated temp. 4-91773
- deformation and fracture at isolated holes in plane-strain tension 4-61976
- disc, gas turbine, nonstationary temp. fields, finite element method 4-107987
- discs, bladed, blade shear center effects, finite element dynamic anal. 4-87613
- dispersion of semidiscretized and fully discretized systems, book contrib. 4-58626
- distributed source corona photoionization calculations applicable to finite element computer models 4-96506
- duct flow, near sonic, sound propagation, finite difference soln. 4-60197
- ductile materials, crack blunting and initiation, microvoid nucleation 4-60981

## finite element analysis continued

- dynamic analysis of elastic-plastic structures by mode-superposition and equivalent plastic load 4-97350
- dynamic elasticity, finite element simulation 4-106192
- dynamically side-loaded frames, rigid-plastic and simplified elastic-plastic solns. 4-97358
- echocardiograms of left ventricle, computerized 3-D finite element reconstruction 4-100272
- EHD pumping in horizontal pipes, temp. induced, finite element method 4-113030
- elastic bodies working against rigid supports, contact effects (German) 4-82675
- elastic-plastic finite element analysis of voids and inclusions 4-92195
- elasticity, finite element method, appl. of displacement function (Chinese) 4-79449
- elasticity, resolvent finite element eqns., divergence-curl scheme 4-106193
- elastoplastic stress calculation in finite element anal. 4-91734
- elastoplasticity, displacement, equilibrium and hybrid finite element models, unified approach 4-103215
- electron lenses, open, computation by coupled finite element and boundary integral methods 4-91392
- electrostatic rotationally symmetric lens systems, potential and field strength calc. by convergent Fourier-Bessel series 4-96772
- EM field problems, 3D, soln. on minicomputer 4-59947
- engineering problems, numerical soln. based on finite elements 4-110857
- epicardial potentials, determ. from body surface pots. 4-115044
- epitaxial Schottky-barrier diodes, current-voltage characts. 4-88592
- Euler equations, design and implementation of multigrid code 4-60454
- extended surfaces array, heat transfer anal. 4-75008
- factorised vorticity-stream function eqns., finite element method soln. 4-64901
- femur, stress distrib., three-dimensional finite element anal. (Italian) 4-81723
- fibre reinforced composite, elastoplastic response, finite element micromechanical analysis 4-87581
- fibre reinforced composite laminates, thermal expansion, effect of microcracks 4-80270
- fibre reinforced composite laminates, with circular holes, interlaminar stresses, effect of geometry 4-79447
- fibre reinforced composites, short fibres, stress distrib., effect of fibre-end geometry 4-74869
- fibre reinforced plastic, plates, stresses around partial contact pin-loaded holes 4-79520
- fin array, transient finite element analysis of coupled radiation 4-79431
- finite plane domain fracture problem anal. using surface integral finite element hybrid method 4-79501
- finite strain plasticity problem, finite element anal. 4-83835
- fluid motion in a cavity, Benard problem, finite element study 4-65025
- fluid-structure interactions, fluid dynamics, arbitrary Lagrangian-Eulerian finite element methods, book contrib. 4-59392
- fracture mechanics, microscopic, appl. of J-integral concept 4-97435
- fractured-porous rock masses, difficulties of modelling fluid flow by finite-element techniques 4-97665
- frames, plane elastic-plastic, influence of discretisation density 4-79460
- frictional contact, finite-element stress anal. iterative procedure 4-87632
- fusion reactor components, dynamic deform. due to EM forces, finite element anal. 4-74050
- gas centrifuge flow problems, finite element method 4-64952
- glass fibre reinforced plastic, sheet moulding cpd., impact damage 4-76829
- glass fibre reinforced plastic laminates, interlaminar shear strength 4-99575
- graphite fibre reinforced epoxy laminates, three dimensional thermal stress distrib. 4-61943
- graphite fibre reinforced epoxy laminates containing pin loaded holes; failure prediction 4-109583
- head conduction, three-dimensional unsteady, boundary fitted finite-difference calcs., 2D Navier-Stokes eqns. 4-97266
- heat conduction, linear and nonlinear, quadrilateral elements 4-79417
- heat transfer in porous media, presence of phase change, numerical problems, soln. 4-112682
- high energy laser optical elements, cooled finite element modelling 4-87416
- hip, natural adult, contact-coupled finite element anal. 4-100207
- homogeneous conductors, eddy currents calc., boundary Galerkin's approach 4-59960
- human torso, modifiable computer model development for ECG studies 4-85554
- hybrid finite element boundary element solutions using half-space Green's functions 4-59951
- hydrodynamic mass with nonstationary fluid, finite element method 4-103437
- incompressible flow, reference press. location, finite element anal. 4-64909
- inelastic solids and structures, plasticity and creep methods, reactor appls. 4-102339
- interface phenomena at Si grain boundaries in poly-Si 4-70925
- interface surfaces, characteristics modelling using finite element method 4-79521
- inviscid and viscous flow computations, multiple-grid convergence acceleration 4-60455
- isotropic cube, finite element analysis of elasticity 4-86217
- joints, adhesively bonded, geometrically nonlinear anal. 4-99744
- KUBIK program, user manual 4-101631
- laminar boundary layer, Dorodnitsyn finite element formulation 4-112809
- Laplace and Poisson problems, finite element matrix condition 4-87417
- lossy dielectric optical waveguides, approx. scalar finite element anal. (Japanese) 4-87476
- lossy diffused optical waveguide, partially metal-clad, dielectric overlay, anal. (Japanese) 4-60156
- loudspeakers, sound-pressure responses effect of acoustic field in enclosure 4-64815
- magnetic domain walls, modified finite-element method for calculation 4-88709
- magnetic field analysis, computer graphics using finite element method 4-59956
- magnetic field computation using Delaunay triangulation and complementary finite element methods 4-59946
- magnetic field problems, nonlinear transient, comparison of lumped and distributed solns. 4-59959

## finite element analysis continued

- magnetic field problems, three-dimensional, infinite element method 4-59952  
 magnetic rods magnetised by coils, magnetisation characts., numerical anal. 4-65827  
 magnetoresistive effects, numerical simulation by finite elements 4-61359  
 Marangoni thermal convection, numerical anal. of microgravity expts. 4-97526  
 mass with a vertical incline, elastic-plastic problem 4-79468  
 materials parameters estimation in electrodynamic medium 4-90610  
 mechanical space frame structures, nonlinear anal. of plasticity (*German*) 4-83839  
 medical US transducers, narrow piezoelectric parallelepiped vibr., finite element anal. 4-100280  
 mesh generation in 3-D using KUBIK program 4-101630  
 metal hot or warm forming model using deform. mechanism maps 4-83830  
 metals, polycrystalline, elastic deform., X-ray strain analysis (*Japanese*) 4-114598  
 MHD equilibria, numerical approx. of free boundary problem 4-69875  
 MHD generator, cathode wall nonuniformities on electrical characteristics, analytical models 4-77119  
 mirror mount design for cryogenic environments 4-87413  
 mirror optical surface evaluation 4-87418  
 miscible displacement in porous media, time stepping procedure 4-97675  
 mixed mode crack propag. studies, double nodding technique 4-79502  
 moving conductor system, eddy-currents, variational formulation 4-74391  
 moving contact in mechanically fastened joints, finite element anal. 4-83866  
 multi-dimensional nonlinear Schrodinger eqns., numerical calc. 4-63571  
 multiphase two-dimensional flow, finite element study, five-spot problem 4-103389  
 Navier-Stokes eqns., combined finite element and spectral approximation 4-103281  
 Navier-Stokes equations, three-dimensional, nonsteady, finite element method 4-97464  
 neutron transport eqn., finite element method appl., FELICIT program 4-91032  
 Newtonian fluid steady laminar flows, between a ball and a spherical cavity 4-97470  
 Newtonian fluids, dip coating finite element simulation 4-113088  
 nodal forces in elements under surface and body loads in axisymmetric and planar elasticity theory problems 4-95176  
 non-Newtonian fluids, dip coating, finite element simulation 4-112963  
 nonlinear structural stability, finite element method appls. (*Polish*) 4-60310  
 nonstationary plastic-rigid transition, finite element anal. (*German*) 4-83837  
 nuclear engineering computational aspects, conf., Chicago, IL, USA (Aug. 1983) 4-82589  
 nuclear reactor cracked reinforced concrete containments under seismic loads, displacements and stresses 4-96112  
 nuclear reactor design, computational techniques 4-111598  
 nuclear reactors, reinforced concrete double cantilevers testing and finite element verification anal. 4-96113  
 oblong hole in uniaxially loaded plate, stress distrib. 4-97333  
 ocean sound channels, irregular, finite-difference anal. 4-103076  
 optical ray tracing in finite element models, space telescope appls. 4-87425  
 optical structural modelling using finite element method 4-87412  
 optical waveguide, anisotropic, off-diagonal elements in permittivity tensor, scalar finite-element anal. 4-97065  
 orthotropic flat sandwich plates, thick faces theory 4-69692  
 perforated casing, finite element anal. of collapse 4-91736  
 Permalloy films, mag. anisotropy and domain struct. patterning effects 4-88707  
 photovoltaic modules, method for calculating multidimensional elec. fields 4-77104  
 piezoelectric ceramic plate, partially electroded, high resolved vibrs. 4-99036  
 piezoelectric transducer, vibration and acoustic radiation, finite element method-equivalent circuit anal. 4-60241  
 pipe, longit. crack, finite element analysis of leak areas using ADINA program 4-103254  
 plane specimens under biaxial loading, stress/strain state, finite element anal. 4-74867  
 plasma MHD axisymmetric equilibria with flow, finite element computation 4-69881  
 plastic buckling load approx., eigenvalue problem soln. 4-83847  
 plastic deformation, material inhomogeneity and surface roughening 4-99458  
 plasticity, nonassociated, finite elements axisymm. necking in void containing materials 4-79462  
 plate, circular, cylindrically orthotropic, post-buckling behaviour 4-91745  
 plate, circular, isotropic, thermal post-buckling 4-91744  
 plate, crack problems, weight function appl., stress intensity factors using FE calcs. (*German*) 4-83862  
 plate, notched, cyclic elastoplastic strain fields, endochronic analysis 4-97342  
 plate, rhombic, finite element analyses, h- and p-versions 4-112701  
 plate, tensile, small scale, with centre crack tensile test, elastic-plastic FEM computation 4-114737  
 plate and shell finite elements, Hellinger-Reissner principles 4-63514  
 plate bending, comparative analysis of boundary methods and finite element methods 4-112727  
 plates, C and glass fibre reinforced laminates, vibr. damping parameters, prediction and meas. 4-80155  
 plates, elastic, stress intensity factors at sharp notches, path-independent integrals 4-87562  
 plates, elastic-plastic anal., triangular assumed-stress finite element (*Chinese*) 4-79457  
 plates, laminated, anal. using mixed shear flexible finite element 4-103193  
 plates, laminated, anisotropic, natural vibr., finite element model 4-74930  
 plates, laminated, composite, shear-flexible triangular finite element model 4-64840  
 plates, laminated composite, mixed finite element anal. 4-74904  
 plates, thin, viscoelastic, finite element anal. 4-112721  
 potential and viscous flows, numerical method, fundamental solns. 4-64902  
 potential flow over circular cylinder in a wind tunnel 4-91787

## finite element analysis continued

- pressure loads, displacement dependent, nonlinear finite element anal. 4-91742  
 projection-mesh diagrams construction using softened-mixed approx. 4-63508  
 PWR once-through and recirculating steam generators, multidimensional model and THEDA-2 computer code 4-59309  
 quantum field theory, finite element approximation 4-68388  
 radioisotope diffusion in metal grain textures, finite element formulation 4-73399  
 revolution shells, fibre wound composite material, strength using finite element method (*Chinese*) 4-60271  
 rotors, large, quenching stresses calc. using finite-element technique 4-83829  
 scalar potentials in multiply connected regions, complex EM field problem appls. 4-63528  
 seismic sounding, discrete wavenumber/finite element method for synthetic seismograms 4-67175  
 semiconductor plates, current-carrying, in magnetic field, electric field anal. 4-107482  
 shape optimal design using B-splines 4-106190  
 shell, composite, conical, ring-reinforced, optimisation under external press. 4-103197  
 shell, cylindrical, coiled, loaded by internal press., elastoplastic deform. analysis 4-97335  
 shell, cylindrical, contact problem, primary and dual formulation 4-64889  
 shell, slit circular cylindrical, torsion 4-95156  
 shell, thin, self-oscill. problem numerical soln. (*Ukrainian*) 4-69693  
 shell and plate analysis, large rotation, optimal, stable and invariant hybrid elements 4-74865  
 shell elements, bilinear, quadrilateral, bending, exact inextensional solns. 4-112730  
 shell system, spherical, thin, nonaxisymmetrically loaded, nonlinear behaviour and stability (*Russian*) 4-64868  
 shell-plate structures, axially symm., numerical anal. by finite element methods 4-83816  
 shells, thin, arbitrary, effective nonlinear, anal. using simple finite elements 4-60273  
 shells of revolution, laminated, vibration, numerical analysis 4-108036  
 short fibre composites, stress distrib. under axial load, finite element analysis 4-108009  
 simulation of welding and quenching processes in steels with phase transform. 4-99412  
 single polarisation fibres, stress anal. 4-64783  
 skin, human, temp. distrib., blood flow, perspiration and metabolic heat generation effects 4-62446  
 soil-structure interaction, far field representation, boundary element anal. 4-83817  
 soil-structure wave propag., silent boundary methods for transient anal., book contrib. 4-60323  
 solid mechanics large-deform. anal. using mixed Eulerian-Lagrangian displacement model 4-79461  
 sonar ring-shell projectors, perform. and finite-element modelling 4-69652  
 Space Shuttle Orbiter, thermal stresses, anal. versus test 4-83818  
 spinal section, patient-specific computer model 4-100227  
 static fields measurements, extrapolation using finite element method 4-83514  
 steel, dynamic flow curve, symmetric rod impact test 4-109486  
 steel, heat-resistant, static and dynamic fracture toughness, influence of microstruct. and temp. 4-99600  
 steel, low alloy, reheat cracking during stress relief annealing, numerical approach 4-93412  
 steel, mild, sheet, axisymmetric deform., thickness effect 4-99449  
 Stefan problem, computing without the free boundary 4-64939  
 stepped finite element analysis for elastic thin plate equations (*Chinese*) 4-106191  
 Stirling engine reciprocating rod seals thermal and elastohydrodynamic anal. 4-66768  
 Stokesian flow, stability of some mixed finite element methods 4-79540  
 stress analysis of a beveled diamond anvil 4-101869  
 stress concentrations determ. using expt-numerical methods 4-97445  
 stress frame specimens, thermo-elastic-plastic anal. of dynamic stress (*Chinese*) 4-60349  
 structural elements, stress conc., empirical-numerical methods, accuracy 4-108013  
 structural mechanics, role of finite elements 4-87419  
 structural mechanics of optical systems, conf., Cambridge, MA, USA (Nov. 1983) 4-86104  
 structure linear equation system soln. by node oriented sparse matrix operation 4-83129  
 structures composed of composite rev. shells and axisymmetric solids, finite element anal. (*Chinese*) 4-60272  
 tectonics, Signorini problem without friction in linear thermoelasticity 4-67199  
 thermal boundary layers, finite-element formulation 4-103305  
 thermoelasticity problems, dynamic coupled, with relax. times, finite element analysis 4-97322  
 thermoelasticity problems, Reissner type variational principle formulation (*Ukrainian*) 4-69679  
 thin meniscus mirror support system design, testing appls. 4-87421  
 thin planes and shell structs., stress hybrid element anal. (*Chinese*) 4-60270  
 thin wavy film, vertical flow, simulation by finite element method 4-74984  
 three dimensional crack problem, crack front elastic stress state 4-97403  
 three dimensional transonic potential flows, multi-grid calculation 4-60452  
 three-point bend specimen, effect of inclusion or hole on approaching crack 4-91767  
 three-point bending fracture toughness specimens, side groove effects, finite element anal. 4-113519  
 tidal flow analysis using improved explicit finite element method 4-115412  
 tongue shape, characterisation from US image data by numerical methods 4-100271  
 transient parallel fluid flows, finite element anal. 4-74986  
 transient structural responses, implicit finite element methods, time integration, book contrib. 4-60276

## finite element analysis continued

- tubes, hollow, stress conc. due to axial loading appl. to axisymm. internal projections 4-91724
- tubes, straight and curved, conveying fluid, vibrations, finite element anal. 4-60319
- turbulent flow, finite-element calc. using  $k-\epsilon$  model 4-97498
- two dimensional elastic crack, fracture mechanics analysis using localised finite element method 4-87624
- two dimensional spatial deterministic model for prediction of wind characteristics 4-85729
- two dimensional transonic flow, solution of Euler equations by multigrid method 4-60453
- two dimensional transonic flows, embedded mesh multigrid treatment 4-60456
- two-dimensional continuum percolation and conduction 4-98583
- two-equation turbulence modelling using finite elements 4-97499
- two-phase immiscible flow, numerical analog, finite element scheme 4-108106
- type contact problem in three dims., finite element soln. 4-83867
- unsteady change-of-phase conduction problem, finite element/Green's function method appl. 4-107986
- US horns, solid, stepped, free vibrations, finite element anal. and expt. (Japanese) 4-103157
- US shear mode piezoelectric ceramic transducer, characteristics and anal. (Japanese) 4-103169
- vibrations, large amplitude 4-91750
- viscoelastic solids of revolution under cyclic loading, thermomech. behaviour, finite-element method 4-108025
- wave motion, finite element analysis 4-90380
- waveguides, elliptical and parabolic, propag., finite element approach 4-64770
- wedge opening loaded specimens, applied crack tip stress intensity effect of loadline shift 4-79530
- welding residual stress fields, crack problems, linear elastic fracture mechanics 4-104878
- Co-base superalloy, MAR M509, cast, thermal fatigue 4-93416
- GaAs crystal, numerical simulation of horizontal Bridgman growth 4-66212
- Si and sapphire ribbons, produced by EFG, comparison of growth characteristics 4-66222
- Si, sheet growth at high speeds, stress generation, influence of plastic deform. 4-65211
- SiO<sub>2</sub> fused glass mirror, thin, low expansion, thermal distortion, analytical approach to error determ. 4-87414
- zr NS IR dome, mortar launched, structural mechanics 4-87433
- finite impulse response filters** *see digital filters*
- finite state automata** *see finite automata*
- inlay-Freundlich red-shift hypothesis** *see gravitational red shift*
- IR filters** *see digital filters*

## fission

- see also accidents; combustion; flames; safety*
- airborne radioactive releases from burning contaminated combustibles 4-106891
- atmosphere wave disturbances due to large fires in USSR 4-72642
- containership holds, forced ventilation anal. 4-79695
- Quebec, relation between dunes, fire and climate recorded in Holocene deposits 4-85753
- sensors, thin film temperature-sensitive resistors, anal. 4-95406
- Li pool fires in fusion reactor safety anal., comp. with Na and Li-Pb, LITFIRE code 4-111787
- Na surface fires in reactor containment, convection current computation, KONVEC 4-91083
- see also fission of plutonium; fission of uranium; photofission; spontaneous fission*
- actinide region, giant resonance fission decay, review 4-73942
- analytical model for the calculation of fission rate (Chinese) 4-111560
- book on nucleus comp., elementary particles and fields 4-82617
- compound nucleus fission following <sup>235</sup>U + <sup>16</sup>O(<sup>27</sup>Al) fission 4-102299
- compressed nuclei, surface tension, fission barriers, vibr. nucleus calcs., excited nuclear matter 4-102184
- conference on nuclear physics at large tandem accelerators, Padova, Italy (March 1983) 4-86108
- conference on semiclassical methods in nuclear physics, Grenoble, France, (Mar. 1984) 4-101567
- fission processes, liquid-drop model, nuclear proximity energy, barrier heights 4-95999
- fluctuations in the nuclear dynamics 4-96002
- Fokker-Planck eqn., relaxation to Kramers stationary solution, application to fission dynamics 4-96003
- fragment angular distributions in rotating liq. drop model 4-73892
- fragmentation dynamics in shell model 4-96060
- fragmentation of nuclei by particles and nuclei of intermediate and high energies 4-95997
- group state props. in semiclassical HF, deformation energy surfaces, fission barriers 4-102172
- heavy ion collisions, dynamical model for fission, fusion and damped oscillations 4-96056
- heavy ion induced fission, fragment ang. distrib., stat. scission model 4-91030
- heavy ion induced fission, pre-equilib. neutron emission, mean field approach, review 4-86849
- heavy ion reactions, fusion-fission ang. distrib. 4-68733
- heavy-ion reactions, charged-particle evaporation, GANES program simulation 4-59279
- (HI.f), fast fission and compound nucleus form. contribs. 4-59278
- hot high spin nuclei decay following heavy ion collisions 4-73802
- low energy photo- and electrofission 4-102249
- neutron multiplicities when viewed as diffusion process 4-59292
- nuclear and solid state phys., symposium, Mysore, India (Dec. 1983) 4-63403
- polarised neutron induced, parity violation effects 4-64183
- proton pairing in fission yields, delayed neutron yields versus proton, neutron and mass numbers 4-96084
- saddle to scission potential energy landscape 4-96001
- scission neck rupture in deep inelastic collisions 4-78624
- statistical nucleon pair breaking 4-96000
- tunneling and quantisation in multidimensional hamiltonian systems 4-96083
- unchanged charged density and fragmentation theory 4-96004

## fission continued

- $Z \geq 90$  nuclei, photo and electrofission at intermediate energy 4-102331
- <sup>237</sup>Np( $\mu$ ,f), prompt and delayed muon induced fission 4-83123
- <sup>108</sup>Ag(<sup>18</sup>O,X), 86 MeV/N, multifragment emission, fission and total cross sections using SSNTD 4-96050
- <sup>108</sup>Ag(p,X) fission and spallation cross-section meas. 4-83119
- Ag(p,f), 1 GeV, binary fission, fragment energies and correls., mass distrib., stat. anal. 4-102329
- <sup>244</sup>Am(n,fission) cross-section meas. 4-83118
- (<sup>40</sup>Ar,X) on <sup>197</sup>Au, <sup>209</sup>Bi, <sup>238</sup>U product mass distribution, ang. momentum 4-86855
- <sup>40</sup>Ar(<sup>18</sup>O,X) A=165 to 208, fusion-fission and neutron evaporation residue cross-sections 4-73922
- <sup>212</sup>At, compound nucleus fission, mean fragment kinetic energy, Fokker-Planck eqn. 4-96003
- <sup>197</sup>Au(<sup>16</sup>O,f), 31 MeV/ $\mu$ , fission fragments in coincidence with quasi-projectile, linear momentum transfer 4-59267
- <sup>197</sup>Au(<sup>18</sup>O,X), 86 MeV/N, multifragment emission, fission and total cross sections using SSNTD 4-96050
- <sup>197</sup>Au(<sup>40</sup>Ar,f), E=44 MeV/u, linear momentum transfer to fissioning nucleus 4-102328
- <sup>197</sup>Au(p,X) fission and spallation cross-section meas. 4-83119
- Au(p,f), 1 GeV, binary fission, fragment energies and correls., mass distrib., stat. anal. 4-102329
- <sup>209</sup>Bi(<sup>30</sup>Ti,X) fusion-fission and neutron evaporation residue cross-sections 4-73922
- <sup>209</sup>Bi(e,f), 25-55 MeV, electrofission cross section, fission barriers from stat. anal. 4-73943
- <sup>209</sup>Bi(p,X) fission and spallation cross-section meas. 4-83119
- Bi(p,f), 1 GeV, binary fission, fragment energies and correls., mass distrib., stat. anal. 4-102329
- <sup>12</sup>C(<sup>238</sup>U,X), 2.38, 3.97 GeV, ang. distrib. and branching ratios using SSNTD, fission 4-96047
- <sup>A</sup>Cm(n,X), A=246,247, neutron data evaluation 4-102276
- <sup>59</sup>Co(<sup>25</sup>S,X), evaporation residue, fissionlike fragments, cross sections, transitional dissipative mech. 4-106628
- <sup>59</sup>Co(<sup>25</sup>S,X), fission-fusion like processes, intermediate mechs., dynamical model anal. 4-111548
- <sup>59</sup>Co(<sup>25</sup>S,X), fragment mass distrib., cross sections, dynamical fission and transitional mechs. 4-86868
- <sup>A</sup>Es, A=255, 256, fission after p, d, t, <sup>3</sup>He and  $\alpha$  induced reactions, fragments, mechanisms 4-106637
- <sup>A</sup>Fm, A=255,257, fission after p, d, t, <sup>3</sup>He and  $\alpha$  induced reactions, fragments, mechanisms 4-106637
- <sup>76</sup>Ge(<sup>25</sup>S,X), fission-fusion like processes, intermediate mechs., dynamical model anal. 4-111548
- <sup>76</sup>Ge(<sup>25</sup>S,X), fragment mass distrib., cross sections, dynamical fission and transitional mechs. 4-86868
- <sup>165</sup>Ho(p,X) fission and spallation cross-section meas. 4-83119
- <sup>165</sup>Ho, fission after p, d, t, <sup>3</sup>He and  $\alpha$  induced reactions, fragments, mechanisms 4-106637
- Ni(p,f), 1 GeV, binary fission, fragment energies and correls., mass distrib., stat. anal. 4-102329
- <sup>237</sup>Np(n, fission), integral cross-section meas. 4-111544
- <sup>237</sup>Np(n,f), 2.6, 8.5, 14.5 MeV, cross sections statistical anal. 4-106639
- <sup>237</sup>Pa(n,f), fragment ang. distrib., Makrofol detector 4-96386
- <sup>208</sup>Pb(<sup>16</sup>O,X), near barrier energies, quasielastic and fusion simultaneous descript. 4-96065
- <sup>208</sup>Pb(<sup>30</sup>Ti,X) fusion-fission and neutron evaporation residue cross-sections 4-73922
- <sup>208</sup>Pb(<sup>36</sup>Fe,X), dynamics, mass drift of reaction products 4-96085
- <sup>208</sup>Pb(p,X) fission and spallation cross-section meas. 4-83119
- Pt(e,f), 25-55 MeV, electrofission cross section, fission barriers from stat. anal. 4-73943
- Sb(p,f), 1 GeV, binary fission, fragment energies and correls., mass distrib., stat. anal. 4-102329
- <sup>228</sup>Th(n, fission), cross-section meas., fragment ang. dist. 4-73944
- <sup>228</sup>Th(n,fission), charge distribution meas. 4-102327
- <sup>230</sup>Th(d,pf), obs. of new states in the third well 4-106636
- <sup>230</sup>Th( $\alpha$ ,f), 50 MeV, total kinetic energy release, mass yield distrib. 4-59291
- <sup>230</sup>Th(n,f), fragment ang. distrib., Makrofol detector 4-96386
- <sup>232</sup>Th(<sup>16</sup>O,f), 31 MeV/ $\mu$ , fission fragments in coincidence with quasi-projectile, linear momentum transfer 4-59267
- <sup>232</sup>Th( $\alpha$ , fission) fission fragment ang. distribution, momentum transfer 4-86869
- <sup>232</sup>Th(d, fission) fission fragment ang. distribution, momentum transfer 4-86869
- <sup>232</sup>Th(n, fission), integral cross-section meas. 4-111544
- <sup>232</sup>Th(p, fission) fission fragment ang. distribution, momentum transfer 4-86869
- <sup>A</sup>W(e,f), A=182,184,186, 25-55 MeV, electrofission cross section, fission barriers from stat. anal. 4-73943
- <sup>184</sup>W(<sup>18</sup>O,X), 86 MeV/N, multifragment emission, fission and total cross sections using SSNTD 4-96050
- <sup>184</sup>W(p,X) fission and spallation cross-section meas. 4-83119
- W(p,f), 1 GeV, binary fission, fragment energies and correls., mass distrib., stat. anal. 4-102329
- <sup>168</sup>Yb, compound nucleus fission, mean saddle-to-scission time, Fokker-Planck eqn. 4-96003

## fission counters

- albedo and incident neutron effects in fission and track detectors (Hungarian) 4-87023
- CANDU, computer controlled: travelling flux detector system using miniature fission chamber 4-59368
- double ionisation chamber for fission fragment detection 4-64284
- fragment energy loss meas., back-to-back ionisation chamber-semiconductor detector system 4-87024
- noble gas-fluoromethane filled counters, radiation stability 4-59554
- parallel plate avalanche detectors for electrofission and photofission expts. 4-64283
- position sensitive fission counter for LWR in-core flux profile monitoring 4-59365
- <sup>235</sup>U(<sup>238</sup>U) fission counter assembly detection efficiency calc. and meas. 4-68897

## fission of plutonium

- activity measurement of spontaneously fissile Pu mixture 4-102326
- <sup>A</sup>Pu( $\mu$ ,f), A=242, 244, prompt and delayed muon induced fission 4-83123

## fission of plutonium continued

- <sup>239</sup>Pu(n,f), A=239, 242, 2.6, 8.5, 14.5 MeV, cross sections statistical anal. 4-106639  
<sup>240</sup>Pu(n,f), A=239, 241, cross sections for thermal neutrons 4-83051  
<sup>240</sup>Pu(n,f), A=239, 242, <sup>135</sup>Xe and <sup>135</sup>Xe isomer yields 4-96086  
<sup>239</sup>Pu(n, fission), integral cross-section meas. 4-111544  
<sup>239</sup>Pu(n,f), electron spectra from fission products 4-64184  
<sup>239</sup>Pu(n,f), fragment energy and mass characteristics compared to <sup>240</sup>Pu spontaneous fission 4-96087  
<sup>240</sup>Pu analytical model for the calculation of fission rate (Chinese) 4-111560  
<sup>240</sup>Pu fission probability calc. including equilibration process, viscosity role (Chinese) 4-83116  
<sup>240</sup>Pu, neutron multiplication corrections applying the shift register technique 4-83117

## fission of uranium

- <sup>235</sup>U(n,f), TRISTAN mass separator thermal ion source, rare-earth products 4-102414  
<sup>48</sup>Ca(<sup>238</sup>U,X), dynamics, mass drift of reaction products 4-96085  
<sup>50</sup>Ti(<sup>238</sup>U,X), dynamics, mass drift of reaction products 4-96085  
<sup>UO<sub>2</sub></sup> fissile kernel/ThO<sub>2</sub> fertile kernel system, high temp. reactor tests 4-106779  
<sup>U</sup>(<sup>238</sup>U,f), 16.7 MeV/n, five-pronged fission events obs. using mica SSNTD 4-96082  
<sup>U</sup>(<sup>238</sup>U,f), 9.03 MeV/u, heavy fragment correlations, sequential fission, cross sections 4-64186  
<sup>A</sup>U, A=236, 238, spontaneous fission characteristics meas. 4-106638  
<sup>A</sup>U(α,f), A=235, 238, fissionable nuclei lifetime meas. 4-78654  
<sup>A</sup>U(γ, fission) A=235, 238, cross-sections 40-105 MeV 4-68742  
<sup>A</sup>U(γ, fission) A=235, 238, absolute cross-section meas. in GDR region 4-83120  
<sup>A</sup>U(γ,f), A=235, 238, 12-30 MeV, isomeric yield ratios, primary angular momenta 4-73895  
<sup>A</sup>U(γ,f), A=235, 238, 12-30 MeV, elemental product yields, isotopic distributions 4-73896  
<sup>A</sup>U(n, fission) A-233, 235, alignment effects 4-91031  
<sup>A</sup>U(n,f), A=233, 235, 238, 2.6, 8.5, 14.5 MeV, cross sections statistical anal. 4-106639  
<sup>A</sup>U(n,f), A=233, 235, cross-sections for thermal neutrons 4-83051  
<sup>A</sup>U(n,f), A=233, 235, 238, <sup>135</sup>Xe and <sup>135</sup>Xe isomer yields 4-96086  
<sup>232</sup>U(n,fission), charge distribution meas. 4-102327  
<sup>232</sup>U, isomeric level excitation by positrons (Russian) 4-71474  
<sup>232</sup>U(μ,f), prompt and delayed muon induced fission 4-83123  
<sup>232</sup>U(n,f), electron spectra from fission products 4-64184  
<sup>232</sup>U(n,f), fission to capture cross section ratio, intermediate struct. anal. 4-96034  
<sup>232</sup>U(n,f), oriented nuclei, neutron ang. distrib. 4-64185  
<sup>236</sup>U(n,f), unchanged and charged density and fragmentation theory 4-96004  
<sup>238</sup>U(α,α'X), X=p or fission fragment, 172 MeV, direct N knockout, precompound emission 4-83084  
<sup>238</sup>U fission fragments, muon attachment probability after prompt fission 4-102828  
<sup>238</sup>U(<sup>238</sup>U,f), ternary fission dynamics in three centre model 4-64181  
<sup>238</sup>U(<sup>238</sup>U,f), ternary fission dynamics liquid drop model 4-64182  
<sup>238</sup>U(<sup>25</sup>Cl,X), 240-350 MeV, fast fission 4-91028  
<sup>238</sup>U(<sup>40</sup>Ar,X) <sup>4</sup>He emission for fusion-fission and sequential fission identification 4-83108  
<sup>238</sup>U(<sup>40</sup>Ar,f), E=44 MeV/u, linear momentum transfer to fissioning nucleus 4-102328  
<sup>238</sup>U(<sup>56</sup>Fe,f), α and p emission from pre- and post-fission sources 4-102304  
<sup>238</sup>U(μ,f), muon fate after prompt fission 4-83122  
<sup>238</sup>U(n, fission), integral cross-section meas. 4-111544  
<sup>238</sup>U(n, fission), product yield (A=131-135) 4-68741  
<sup>238</sup>U(p,X) fission and spallation cross-section meas. 4-83119  
<sup>238</sup>U(x, fission) cross-section meas., charge-mass-energy spectra 4-68724  
<sup>U</sup>(p, fission), high energy model 4-91027

## fission products

- <sup>272</sup>112 prod. and spontaneous fission from Hg(HI,X), secondary reaction 4-86870  
 aluminised plastic track detectors, spot development around track- and electric tree-induced perforations 4-102474  
 beta decay data on short-lived nuclides for JNDC FP Decay Data File 4-59209  
 CR-39 plastic detector, response to γ-radiation, effect on track registration 4-96346  
 CR-39 Track Profile Technique, alpha and fission fragment range and energy meas. 4-96336  
 energy loss meas. with back-to-back ionisation chamber-semiconductor detector system 4-87024  
 fission reactor LWR, fission product transport anal., class 9 accident 4-106933  
 fission reactor PWR, parametric study of aerosol behavior during AB and TMLB accidents 4-106934  
 Fort St. Vrain HTGR, plateau probe anal. 4-111661  
 fragment angular distributions in rotating liq. drop model 4-73892  
 ground level air, radionuclide conc. in N Germany and N. Norway, 1980-3 4-77164  
 heavy ion induced fission, fragment ang. distrib., stat. scission model 4-91030  
 HTGR, fission product plateau, linear time-depend. isothermal laminar flow soln. 4-96192  
 HTGR, spatial fission product behaviour within pebble bed, math. treatment (German) 4-68749  
 HTGR fission product plateau, linear time-depend. multiregion isothermal slug flow soln. 4-96193  
 HTGR under hypothetical accident conditions, reactivity behaviour study 4-68780  
 HTR modular fuel element, fission product release under accident conditions, calc. 4-96247  
 HTR under accident conditions, fission product retention in core and fuel (German) 4-64231  
 identification from photofission by delayed neutron and gamma emission 4-109709  
 level density parameters, resonances, neutron cross sections 4-59150  
 LMFBRs, Na aerosols and puddles, fuel, fission products and Na release 4-91084  
 LWR fuel rods, transient fission gas release and microstruct. variations during power ramping 4-96161

## fission products continued

- Makrofol detector for fission fragment ang. distrib. studies 4-96386  
 mixed carbide reactor fuels, irradi., defect struct., fission gas bubbles, precipitates, TEM obs. 4-83145  
 muscovite SSNTDs, optical efficiency for fission fragment track recording 4-96382  
 nuclear fuel, fission product behaviour under normal and accident conditions, improved model 4-74032  
 nuclear fuel, irradiated particles, fission product localisation using unshielded electron microprobe 4-73981  
 pressurised water reactor, severe fuel damage tests, fission product effects 4-106777  
 reactors, LWR, containment failure mode influence on fission product source term 4-106932  
 spectroscopy with large surface barrier detectors, TOF and pulse height 4-74087  
 SSNTD, use of different Mexican commercial polymers, etching, dosimeters 4-102476  
 thermal neutron induced fission fragments of <sup>235</sup>U and <sup>239</sup>Pu, beta spectrum meas. 4-64320  
 TIBSO-TC program system, prod. and transfer of radionuclides, nuclear reactors 4-106669  
 TRISO fuel pellet, fission product transport through cladding layers, model 4-107003  
 VHTR fuel compacts, fission product diffusion in matrix graphite 4-73976  
 VIPER reactor expts. on fission gas release from mixed oxide fuel pins 4-64216  
 Zircaloy fuel cans, stress corrosion cracking with multiple fission product intrusion 4-96160  
 (n,γ) effect on radiative characteristics of fission product mixtures in fuel rods 4-106661  
 (p,f), on Z=28 to 83, 1 GeV, binary fission, fragment energies and correls., mass distrib., stat. anal. 4-102329  
<sup>235</sup>U(n,f), TRISTAN mass separator thermal ion source, rare-earth products 4-102414  
 (<sup>40</sup>Ar,X) on <sup>197</sup>Au, <sup>209</sup>Pb, <sup>238</sup>U product mass distribution, ang. momentum 4-86855  
<sup>197</sup>Au(<sup>16</sup>O,f), 31 MeV/u, fission fragments in coincidence with quasi-projectile, linear momentum transfer 4-59267  
<sup>197</sup>Au(<sup>40</sup>Ar,f), E=44 MeV/u, linear momentum transfer to fissioning nucleus 4-102328  
<sup>148</sup>Ba, mass-separated short-lived fission products, half-life meas. 4-59204  
<sup>7</sup>Be concentration and deposition in lower atmosphere over Kaohsiung City, Taiwan 4-62418  
<sup>25</sup>Cr fission fragments, range and energy losses, LSS theory anal. 4-108490  
<sup>59</sup>Co(<sup>25</sup>S,X), fragment mass distrib., cross sections, dynamical fission and transitional mechs. 4-86868  
<sup>137</sup>Cs, determ. of conc. in urine samples 4-96290  
<sup>A</sup>Es, A=255, 256, fission after p, d, t, <sup>3</sup>He and α induced reactions, fragments, mechanisms 4-106637  
<sup>A</sup>Fm, A=255, 257, fission after p, d, t, <sup>3</sup>He and α induced reactions, fragments, mechanisms 4-106637  
<sup>76</sup>Ge(<sup>25</sup>S,X), fragment mass distrib., cross sections, dynamical fission and transitional mechs. 4-86868  
<sup>4</sup>He emission for fusion-fission and sequential fission identification in <sup>238</sup>U(<sup>40</sup>Ar,X) 4-83108  
 Kr fission product, beneficial uses 4-109930  
<sup>23</sup>Md, fission after p, d, t, <sup>3</sup>He and α induced reactions, fragments, mechanisms 4-106637  
 Mo diffusion through graphite in HTGR 4-111631  
<sup>99m</sup>Mo, fission prod. on tech. scale from <sup>235</sup>U fuel elements 4-77386  
<sup>208</sup>Pb(<sup>16</sup>O,X), near barrier energies, quasiclastic and fusion simultaneous descript. 4-96065  
<sup>239</sup>Pu(n,f), electron spectra from fission products 4-64184  
<sup>239</sup>Pu(n,f), fragment energy and mass characteristics compared to <sup>240</sup>Pu spontaneous fission 4-96087  
<sup>A</sup>Sr, A=93, 94, mass-separated short-lived fission products, half-life meas. 4-59204  
<sup>90</sup>Sr, determ. of conc. in urine samples 4-96290  
<sup>228</sup>Th(n, fission), cross-section meas., fragment ang. dist. 4-73944  
<sup>229</sup>Th(n, fission), charge distribution meas. 4-102327  
<sup>230</sup>Th (d,pf), obs. of new states in the third well 4-106636  
<sup>230</sup>Th(α,α'), 50 MeV, total kinetic energy release, mass yield distrib. 4-59291  
<sup>232</sup>Th(<sup>16</sup>O,f), 31 MeV/u, fission fragments in coincidence with quasi-projectile, linear momentum transfer 4-59267  
<sup>232</sup>Th(α, fission) fission fragment ang. distribution; momentum transfer 4-86869  
<sup>232</sup>Th(d, fission) fission fragment ang. distribution, momentum transfer 4-86869  
<sup>232</sup>Th(p, fission) fission fragment ang. distribution, momentum transfer 4-86869  
 U-rich crystals, radiation damage using nuclear track and thermoluminescence methods 4-98130  
 UO<sub>2</sub> fissile kernel/ThO<sub>2</sub> fertile kernel system, kernel swelling, fast neutron effects 4-106779  
 UO<sub>2</sub> irradiated thermal reactor fuel, fission products, electron-probe microanal. appls. 4-73980  
 UO<sub>2</sub>, microstruct. during ramping, transient fission gas release (German) 4-83136  
<sup>U</sup>(<sup>238</sup>U,f), 9.03 MeV/u, heavy fragment correlations, sequential fission, cross sections 4-64186  
<sup>A</sup>U(α,f), A=235, 238, fissionable nuclei lifetime meas. 4-78654  
<sup>A</sup>U(γ, fission) A=235, 238, cross-sections 40-105 MeV 4-68742  
<sup>A</sup>U(γ,f), A=235, 238, 12-30 MeV, isomeric yield ratios, primary angular momenta 4-73895  
<sup>A</sup>U(γ,f), A=235, 238, 12-30 MeV, elemental product yields, isotopic distributions 4-73896  
<sup>232</sup>U(n,fission), charge distribution meas. 4-102327  
<sup>232</sup>U(n,f), electron spectra from fission products 4-64184  
<sup>238</sup>U fission fragments, muon attachment probability after prompt fission 4-102828  
<sup>238</sup>U(<sup>40</sup>Ar,f), E=44 MeV/u, linear momentum transfer to fissioning nucleus 4-102328  
<sup>238</sup>U(n, fission), product yield (A=131-135) 4-68741  
 Xe, fission product, beneficial uses 4-109930  
 Xe, production, presence and significance in environment 4-109931  
 Xe, A=133, 135, g and m isomers, yield from U and P fission 4-96086

## fission reactor cooling and heat recovery

see also *cooling; fission reactor core control and monitoring* ;  
 annular air-water flow, liquid mass transport 4-96182  
 AST-500 reactor, coolant circulation stability 4-106855  
 AVR expts., LEU spherical fuel elements, induced transients 4-86939  
 axisymmetric and 3-dimens. convection anal. using penalty finite elements, computer code (*Japanese*) 4-64193  
 blowdown jet forces on containment structures 4-86944  
 boiling noise in a two-region 1-D reactor with feedback 4-73951  
 burst fuel can rewetting in LOCA conditions 4-86947  
 BWR, 1300 MW class, pipe fracture accident, thermal behaviour simulation 4-91087  
 BWR, crud deposits on fuel rod surfaces, sampling and examination 4-86956  
 BWR, flow stability in fuel element channels 4-86889  
 BWR, instantaneous pipe rupture, void fraction measurement using gamma-ray densitometer 4-86931  
 BWR, thermohydraulic parameters, noise-analytic meas. and interpretation, review 4-91070  
 BWR digital feedwater controller conceptual design 4-59379  
 BWR feedwater manifold operating characts. 4-86945  
 BWR jet discharge experiment, DRIX-2D code anal. 4-86881  
 BWR LOCA, jet discharge test results 4-86880  
 BWR piping, IGSCC countermeasure implementation in USA 4-111644  
 BWR pressure suppression system, press. propagation following steam bubble collapse 4-96178  
 BWR recirculation loop piping, improved pipe components manufacturing 4-111642  
 BWR refill-reflood program, final report 4-83241  
 CANDU-PHWR ECCS unavailability following small LOCA 4-64232  
 circular tube cooled by dissociating  $N_2O_4$ , unsteady heat transfer for turbulent flow (*Russian*) 4-74022  
 conference, American Nuclear Society annual meeting, New Orleans, LA, USA (June 1984) 4-106112  
 conference, nuclear technology, Frankfurt, Germany (May 1984) 4-90301  
 conference on multiphase processes in LMFBR safety analysis, Ispra, Italy (Mar.-Apr. 1982) 4-78042  
 containment heat removal recovery 4-111682  
 coolant, high temperature EM filtration, radioactive corrosion prod. removal 4-96188  
 cooling system efficiency, atomic power plant, WWER reactors (*Bulgarian*) 4-96177  
 critical heat flux, reduction mechanism in subcooled flow boiling 4-86930  
 Cylindrical Core Test Facility, C1-1, reflood phase loop flow resistance test 4-59396  
 DWR fresh steam safety cut-out valve function props. under operating and fault conditions 4-106878  
 emergency decay heat removal systems of nuclear ships under accident conditions 4-96196  
 entrainment effects in rapidly expanding gas bubbles 4-86949  
 fast reactor, unevenly heated, gas-cooled fuel element, mech. calc., PRORT program (*Russian*) 4-74021  
 FBR, delayed heat removal using natural convection and boiling 4-86950  
 FBR, heat transfer channel adaptive modeling 4-74017  
 FBR, radial power shifts in heterogeneous fast reactor calculations 4-106935  
 FBR modular steam generator, dynamic loads from leaking water/steam-sodium reaction (*Russian*) 4-68783  
 fin, annular, const.-width, with variable thermal cond. and internal heat generation, temp. field 4-78713  
 FLASH-4 technique for compressible two-phase flow in BWR pipe network, Edwards problem 4-106893  
 fluid fueled marine nuclear reactor, convection and heat dissipation, numerical anal. 4-86938  
 fresh steam valves, dimensioning and function proving for pipe failure, simulation 4-107005  
 fuel element temp. and rewetting, pellet-can gap effect 4-86946  
 GERDA experimental facility for the investigation of PWR small break LOCAs 4-96228  
 GERDA test rig, two-phase coolant conditions, conductivity measuring probes 4-86948  
 HDR blowdown expts., DAISY simulation program for fracture size 4-86962  
 heat exchangers, fretting-wear damage 4-106877  
 heat transfer research, safety aspects, Japanese research 4-83243  
 heated channels, hydrodynamics and heat transfer, vibr. field effects (*Russian*) 4-74023  
 HTGR, fission product plateout, linear time-depend. isothermal laminar flow soln. 4-96192  
 HTGR, spatial fission product behaviour within pebble bed, math. treatment (*German*) 4-68749  
 HTGR fission product plateout, linear time-depend. multiregion isothermal slug flow soln. 4-96193  
 HTR, coolant circuit simulation, heat transfer anal. 4-86952  
 HTR, effective thermal conductivity in packed beds of spheres (*German*) 4-78712  
 HTR, heat transfer in gas pipes 4-86953  
 HTR, pressure drop, spacer arrangement in fuel bundles, effects 4-86954  
 HTR cooling breakdowns, temp. rises and safety margins 4-96241  
 HTR gas circulation, press. fluctuations 4-86951  
 HTR He/He heat exchanger, design and semitechnical testing, coal gasification 4-78711  
 HTR hot gas ducts, design status and testing 4-78663  
 hybrid reactor, design and safety study, fast fission blanket safety performance 4-96274  
 in-pile LMFBR accident simulations anal. by Kalman filter methods 4-86936  
 ion exchange resin, volume reduction system, nuclear reactors 4-106750  
 JAERI reactor engineering department annual report (April 1, 1982 - March 31, 1983) 4-59302  
 KONVOI pipelines, preliminary and quality testing of catalogue components 4-106842  
 KORI-1 PWR, very small LOCA, decay heat removal and operator intervention calcs. 4-102375  
 LMFBR, acoustic imaging of vapor bubbles through optically non-transparent media 4-59364  
 LMFBR, core disruptive accident, expansion phase, scoping anal. 4-91081  
 LMFBR, correlation for downward melt penetration into a miscible low-density substrate 4-106946

## fission reactor cooling and heat recovery continued

LMFBR, fuel and cladding relaxation during LOF accidents 4-106938  
 LMFBR, TOP and LOF accidents, post-clad failure phenomena 4-78721  
 LMFBR accident, core bubble/Na pool interface phenomena, SIMMER modification 4-78727  
 LMFBR accident, multiphase flow, heat and momentum transfer, phase change modelling 4-78724  
 LMFBR accident multiphase flow, hydrodynamical eqns., SIMMER-II code 4-78725  
 LMFBR accidents, upper struct. transient thermohydraulics, SIMMER-II anal. 4-78733  
 LMFBR HCDA and LOF accidents, core expansion phase models with Na entrainment 4-78728  
 LMFBR hypothetical accidents, fuel propagation through interwrapper gaps 4-91036  
 LMFBR JOYO, natural circulation evaluation 4-96186  
 LMFBR local core anomaly detection using temperature and flow fluctuations 4-91071  
 LMFBR LOF accident simulation in Sodium Loop Safety Facility 4-83230  
 LMFBR loss of heat sink accidents, core coolability limits 4-106945  
 LMFBR safety anal., basic multiphase flow eqns. and physics 4-78723  
 LMFBR safety anal., stability anal. and numerical procedures for SIMMER-II code 4-78726  
 LMFBR SIMMER-II calculations of COVA experiments 4-91035  
 LOCA, electrical insulation degradation for chem. sprays 4-68799  
 LOCA, heat conduction of coolant in flow direction (*Chinese*) 4-83885  
 LOCA, hydrodynamic loading and structural response in PWR and HDR, STEALTH/WHAMSE anal. 4-68786  
 LOCA, REWET-II reflood expt. project 4-106867  
 LOCA, two-phase flow through a small horizontal branch in a pipe with stratified flow 4-91079  
 LOCA anals., water stable, metastable and unstable states, fundamental eqn. 4-59394  
 LOCA safety anal., counter-current flow through vertical path study 4-97642  
 low power HTRs, design principles, siting and core inserts 4-86892  
 LWR, containment failure mode influence on fission product source term 4-106932  
 LWR, containment heat transfer coeffs. during LOCA 4-106929  
 LWR, coolant pump seizure and sheared shaft accidents 4-106869  
 LWR, fission product transport anal., class 9 accident 4-106933  
 LWR, methyl iodide removal efficiency of charcoal bed 4-107171  
 LWR, preexisting containment leakage areas for severe accident conditions 4-106930  
 LWR, severe fuel damage scoping test, degraded core cooling accident 4-106776  
 LWR, steam-air mixture, air absorption during condensation 4-106874  
 LWR large break LOCA, clad deform. and heat transfer, azimuthal effects modelling 4-102377  
 LWR large-break LOCA, thermal-hydraulic response, COBRA/TRAC results 4-106925  
 LWR low-pressure steam turbines, corrosive salt solubility in dry steam 4-111692  
 LWR pipe rupture accident, two-phase jet impingement, numerical anal. 4-74031  
 LWR pressurised thermal shock problem, 3-dimens. temperature prediction scheme 4-106894  
 LWR primary circuits, Co release from component wear, radiation field buildups 4-102383  
 LWR structural integrity, EPRI research 4-68784  
 medium enriched core for TR-2 based on average burnup 4-59306  
 molten salt converter reactors, neutronic and burnup characts. 4-78661  
 Nine Mile Point Unit 1, recirculation piping replacement 4-111643  
 Obrigheim nuclear power station, steam generator replacement, personnel exposure 4-86960  
 pebble bed reactors, thermohydraulic behaviour, natural convection flow expts. (*German*) 4-106875  
 PFR steam generator experience, leaks, design basis, remedial actions 4-59357  
 PFR superheater and reheater replacement and evaporator repair 4-68776  
 pipe mechanical welding using pincer welding technique 4-106844  
 pipe welded seams, stress estimation for internal forces and pipeline forces 4-106843  
 pipeline components prod., manufacturing technologies and processes 4-106841  
 pipeline design and layout, use of published regulations 4-106670  
 PNP He/He heat exchanger, welding construction techniques 4-106879  
 power plant, commercial, appl. of advanced instrumentation and control technology 4-102373  
 primary circuit component fatigue, calc. method and operational meas. (*Czech*) 4-83237  
 primary coolant radioactivity monitoring under postaccident conditions 4-107169  
 PWR, departure from nucleate boiling ratio, sensitivity to operating parameter variation 4-64226  
 PWR, inadequate core cooling detection using thermocouples 4-106870  
 PWR, KWU-type, pipework design, leak-before-break criterion appl. 4-96123  
 PWR, parametric study of aerosol behavior during AB and TMLB accidents 4-106934  
 PWR, probabilistic risk assessment of containment fan cooler 4-106931  
 PWR, prototype residual heat removal pump, behaviour during sharp pressure decrease 4-91091  
 PWR, pump seal failure calcs. 4-106868  
 PWR, radionuclide dispersion in primary cooling circuits (*Russian*) 4-78709  
 PWR, severe fuel damage in degraded core cooling accident 4-106775  
 PWR, steam, two-phase and subcooled discharge flows, coupled valve dynamic model 4-96211  
 PWR, transient thermal mixing in full-height cold leg and downcomer 4-96205  
 PWR, water polisher systems performance at Plant Bowen, Georgia 4-59380  
 PWR and PHWR steam generator tube performance, experience during 1981 4-111651  
 PWR blocked four rod bundle, single and two-phase heat transfer for ECC 4-96210  
 PWR cold leg and downcomer, fluid and thermal mixing, COMMIX-1A anal. 4-96219

## fission reactor cooling and heat recovery continued

PWR coolant, chemical additive role in corrosive impurity transport in steam 4-96189  
 PWR cores, statistical thermal design review, DNB protection, design margins 4-102376  
 PWR feedwater corrosive species conc. models, water chemistry changes 4-59378  
 PWR fuel pin failure determination by coolant radioactivity meas. 4-73961  
 PWR LOCA, 163-rod bundle flow blockage data from FLECHT-SEASET 4-102382  
 PWR LOCA, core reflooding, multi-dimens. and two phase flow, ARAMIS code 4-96209  
 PWR LOCA, decay heat removal expts. in U-tube steam generator test facility 4-83239  
 PWR LOCA, mass-flow-weighted skew upwind differencing scheme implementation in COMMIX-1A 4-83242  
 PWR LOCA, pump performance under two-phase flow conditions, anal. model 4-96212  
 PWR LOCA, reflood heat transfer, grid spacers effects 4-74029  
 PWR LOCA, reflood phase, saturated film boiling heat transfer, turbulent boundary layer model 4-74030  
 PWR LOCA decay heat removal in steam generator, condensation in single inverted U-tube 4-96206  
 PWR pipework, unstable crack propagation and stoppage behaviour 4-96225  
 PWR power plant radioactivity, effect of coolant chemistry 4-68800  
 PWR pressure vessel loads due to cold-line leak, DAISY anal. 4-96226  
 PWR pressurised thermal shock, eval. for B&W designed NSS plants 4-106924  
 PWR pressuriser, transient response model expt. 4-102384  
 PWR primary coolant pipe leak failure using probabilistic mechanics 4-64215  
 PWR primary coolant pumps, long-term inspection requirements 4-96187  
 PWR primary loop, radiation field effects of shutdown-cooldown techniques 4-83224  
 PWR small break LOCA, heat transfer, lower plenum break, parametric study 4-96195  
 PWR small-break LOCA, ECC tests at GERDA expt. facility 4-96229  
 PWR steam generator chemical cleaning database 4-83225  
 PWR steam generator denting, magnetite-producing contaminant threshold tests 4-64205  
 PWR steam generator transient analysis computer code 4-59310  
 PWR steam generator units, transient modelling 4-64220  
 PWR steam generators, corrosion products under typical operating conditions 4-102371  
 PWR steam generators, denting causes, nonprotective magnetite prod. on carbon steel 4-104924  
 PWR steam generators, dilute reagent decontamination, oxide film removal 4-102385  
 PWR steam generators, simulation of FRIGG heated rod bundle expt. by ATHOS and FLOW3 4-96190  
 PWR temperature transients leading to core hypercriticality, simulation (German) 4-59358  
 PWR thermal-hydraulic anal., automatic controllers effects in TRAC-PF1/MOD1 4-106895  
 PWR U-tube steam generator transient simulation studies 4-68779  
 PWR-LOCA, ECC water downcomer penetration, parameter effects 4-59388  
 reactor core heat transfer crisis, quasistationary method calcs. 4-74034  
 reflood test, initial clad temp. effects 4-96208  
 reflooding and core uncover, heat transfer, safety aspects 4-83228  
 ROSA II recirculation pump discharge line break, test run 961 4-102370  
 rotating fluidised bed reactor, thermal-hydraulic design concepts 4-96106  
 safety-relief valves flow capacity measurement 4-91077  
 safety/relief valve diagram in steam flow transients, PISCES-PIPE code 4-91080  
 severe core damage accident, particle bed height and composition 4-106872  
 Sizewell B PWR steam generator design 4-86874  
 SNR-300, operation and fault transient simulation 4-86890  
 steam, high press. high temp., convection-radiation interaction 4-74018  
 steam generator heating pipe testing and repair, tele-operated manipulator 4-86959  
 steam generator tubesheet crevices cleaning using amine borane compounds 4-111662  
 steam generator with pre-heat chambers, thermohydraulic performance and operational characs. 4-106880  
 steam-water jet effects, design estimates 4-83131  
 steel, austenitic stainless, WWER steam generator tubes, hardening and intergranular corrosion cracking (Czech) 4-85257  
 steel, stainless, tube bundles subjected to blockages, heat transfer 4-68758  
 stream-line method to remove cross numerical diffusion, Navier-Stokes appl. in reactors 4-102368  
 Swedish BWRs' water chemistry to prevent stress corrosion cracking 4-91055  
 TMI-1, OTSG unplugged tubes, mechanical integrity analysis using linear elastic fracture mechanics 4-86877  
 two-fluid model for nuclear reactors, general conservation eqns. and jump conditions 4-102367  
 two-phase flow, pipe boundary conditions, numerical treatment, safety anal. 4-106892  
 VHTR test facility HENDEL, construction, technical problems (Japanese) 4-96180  
 void fraction distribution in water filled pipes,  $\gamma$ -ray computed tomography meas. 4-96135  
 VVER neutron physical characteristics precision improvement using BIPR-5K program (Russian) 4-78659  
 water layer stability over hot tin melt, core-melt accident simulation, ECC effects 4-96235  
 Winfrith primary circuit filtration by high-temp EM filter 4-83223  
 Wurgassen BWR power station, steam and feedwater pipelines replacement 4-86955  
 $N_2O_4$  coolant reactor loop, radioiodine behaviour, decontamination (Russian) 4-74035  
 Na boiling following contact with molten fuel 4-91082  
 Na, liquid,  $O_2$  electrochemical meter 4-89370  
 (Th,Pu) $UO_2$  fuel bundle expts. in ZED 2 4-74024

## fission reactor cooling and heat recovery continued

$Y_2O_3$ , wear resistant layers for use in high temp. reactor heat exchanger 4-106845  
 $ZrO_2$ , wear resistant layers for use in high temp. reactor heat exchanger 4-106845

fission reactor core control and monitoring  
 see also fission reactor safety; fission research reactors; nuclear engineering; nuclear reactor instrumentation  
 active zone temp. field meas., using computer-based system (Slovak) 4-83221  
 adaptive predictive control strategy for nuclear reactors (Spanish) 4-96176  
 AGR, reactivity and channel power effects of burnable poisons, predictive methods validation 4-91073  
 ASEAT-ATOM control rods, experience and development 4-91053  
 automated system for carrying out overpower loop tests in VVR-SM reactors 4-106856  
 AVR expts., LEU spherical fuel elements, induced transients 4-86939  
 Biblis power plant, fuel element maintenance, BSN failed fuel element detection system 4-96159  
 boiling noise in a two-region 1-D reactor with feedback 4-73951  
 BWR, adaptive core simulation 4-86888  
 BWR, FNR program for core, Xe and I monitoring, safety measures 4-86964  
 BWR, thermohydraulic parameters, noise-analytic meas. and interpretation, review 4-91070  
 BWR, traversing incore probe automatic scanning operation system 4-59376  
 BWR cell, collision probabilities for non-uniform neutron sources 4-96174  
 BWR control blade for long cycle operations, conceptual design, lifetime extension 4-106864  
 BWR control rod replacement, improved method development 4-83227  
 BWR core design and operational data collection 4-59381  
 BWR core performance calculation program for on-line management 4-106865  
 BWR core-fuel design, status and future perspectives (Japanese) 4-83127  
 BWR cores adaptive simulation using 3-D coarse-mesh neutron diffusion theory 4-86933  
 BWR extended range start-up monitor, in-core neutron flux meas. 4-59366  
 BWR neutron noise, transport theory anal. using TWOTRAN-II, detector reading interpretation 4-102372  
 BWR symptom oriented emergency operating procedures, human factors enhancement 4-111673  
 CANDU, computer controlled travelling flux detector system using miniature fission chamber 4-59368  
 CANDU reactors, self-powered flux detectors, dynamic response degradation 4-106876  
 conference, American Nuclear Society annual meeting, New Orleans, LA, USA (June 1984) 4-106112  
 conference, nuclear technology, Frankfurt, Germany (May 1984) 4-90301  
 control panel enhancement in power plants, safety 4-83220  
 control rod insertion to arbitrary distance, scram distribution 4-111680  
 control room improvement project, design review, operator acceptance 4-111660  
 control room operator performance research, safety related operator actions and simulators 4-111676  
 control room personnel training and entry level qualifications, eval. methods 4-111675  
 coupled-core reactors, time-optimal control, computational aspects 4-96104  
 critical function monitoring system algorithm development 4-59374  
 critical reactor, neutron count variance and covariance divergence 4-96173  
 digital control of power transients in a nuclear reactor, integrated closed-loop system 4-59360  
 fast critical assemblies, effects of fission neutron spectra on reactor calcs. (Korean) 4-64195  
 fast critical assembly, Na void worth, leakage and nonleakage components, sensitivity coeffs. 4-96185  
 fast reactor hexagonal assemblies, diffusion coeffs. calc. model, ASDIC program 4-96184  
 FBR, fast neutron fluence spectra and integral reaction rates determined with nuclear research emulsions 4-96370  
 FBR, radial power shifts in heterogeneous fast reactor calculations 4-106935  
 FBR control rod systems, adsorbent materials 4-83147  
 FBR cover-gas monitor using charcoal-Ge  $\gamma$ -ray spectrometer combination 4-59370  
 fuel assembly placing and reload, gradient projection method for automation 4-106866  
 fuel element planning for enhanced fuel utilisation efficiency 4-86886  
 fuel performance evaluation, simplified power history 4-106771  
 gamma thermometer for PWR reactor, heat density behaviour (French) 4-64214  
 HTGR, graphite structural material (German) 4-68755  
 HTR-500 core heating incident, reactivity anal. using ASTERIX-2 4-91089  
 human initiated problems, diagnosis and mitigation, MAU decision making model 4-111570  
 irradiation expt. evaluation, burn up coeff. determ. (German) 4-73960  
 JAERI reactor engineering department annual report (April 1, 1982 - March 31, 1983) 4-59302  
 KNK-II, defective fuel pin detection, fission gas release 4-96164  
 light water moderated  $UO_2$  and  $PuO_2$  loaded cores, power distrib. calc. 4-64194  
 LIMCOM, limiting conditions of operation monitor, automated system for power plants 4-111568  
 LMFBR, fuel pin failure, temp. oscillations 4-106942  
 LMFBR spectrum using SAND 2 and differential and integral spectrometers (Czech) 4-68778  
 low power HTRs, design principles, siting and core inserts 4-86892  
 LWR, degraded core events, core and containment transient anal. 4-106873  
 LWR cell anal., resonance shielding procedures validation, fuel cycle optimisation 4-96118  
 LWR reactivity control, control rods and burnable absorbers, review 4-91075

# fission reactor core control and monitoring continued

- LWR safety, contribution of control systems 4-59390
- matched activation detectors method for reactor neutron fields, statistical anal. 4-106857
- MAXI-LILLIPUT: a simplified model of a French pressurized water reactor power plant 4-83222
- measuring systems for fault conditions, operating efficiency improvements 4-107004
- medium enriched core for TR-2 based on average burnup 4-59306
- MTR-II 5-MWt nuclear reactor digital control schemes, experimental evaluation 4-86932
- molten salt converter reactors, neutronic and burnup charact. 4-78661
- MULTICELL 3D code for CANDU reactivity device simulation 4-86883
- MVPACK, package for computer aided design of multivariable control systems 4-86882
- neutron absorber spheres for spherical fuel reactor control 4-86941
- neutron coupling coefficient evaluation in nodal/modal anal. 4-73948
- neutron current control apparatus for VVER-440 during refuelling (*Russian*) 4-78708
- neutron density fluctuations in point reactor systems with dichromatic reactivity noise 4-91034
- neutron multiplication and compound interest 4-73952
- neutron noise measurement by travelling air bubbles in research reactors 4-64212
- neutron sensor, analytical response model for dynamic response and degradation 4-59367
- neutron sensors, testing by high voltage perturbation technique 4-59362
- NRC control room design review audits: a contractor's perspective 4-111659
- nuclear power stations, monitoring and fault diagnosis system for early fault detection (*German*) 4-59384
- optimal feedback control by frequency-domain methods 4-64197
- pebble bed AVR, core physical descript. for multiple recycling process, 3D simulation method (*German*) 4-64196
- pebble bed reactors, HEU/LEU equilib. combined cores, AVR appl. (*German*) 4-102345
- PFR, B,C control rod pin performance, cladding compatibility, 4-91076
- plant diagnosis through knowledge about systems descriptions, preliminary study 4-111567
- point reactor model, internal fluctuations and parametric noise theory 4-96103
- position sensitive fission counter for LWR in-core flux profile monitoring 4-59365
- power plant, commercial, appl. of advanced instrumentation and control technology 4-102373
- power plant control room design, function allocation for man or machine 4-111565
- power plant symptoms oriented operating procedures in control room, emergency procedures 4-111665
- probabilistic method for evaluating reactivity margin of nuclear reactors 4-96105
- PWR, axial Gd burnable poison optimisation using conjugate gradients 4-106863
- PWR, fuel sharing strategy to reduce costs 4-86887
- PWR, gamma thermometer as local power monitor in reactor thimble tube 4-59369
- PWR, load following capability extension by optimal control 4-86929
- PWR core and fuel element distribution, computer programming system 4-86942
- PWR in-core detectors fault analysis using time-series models 4-86935
- PWR in-core instrumentation, functions and performance, review 4-59371
- PWR linear-time-invariant systems monitoring and sensor placement, output uniformity index 4-86937
- PWR spatial power oscillations, Xe-induced, time optimal control 4-111652
- PWR temperature transients leading to core hypercriticality, simulation (*German*) 4-59358
- radiation effect in coolant and core spaces,  $S_N$  calcs. 4-86884
- random neutron sensor fluctuations, instrumentation channel surveillance for power plant protection 4-59361
- reactivity control in power reactors, spectral displacement, fuel cells, PHWR appl. (*Spanish*) 4-96175
- review of control and instrumentation for large nuclear power station 4-111654
- SGHWR, Winfrith, reactivity control, moderator and rapid shutdown systems 4-91074
- shutdown reactivity meas, using improved source jerk technique 4-91072
- Smorn-Ill benchmark test on reactor noise analysis methods 4-96119
- SNR-300, operation and fault transient simulation 4-86890
- SNR-300 PWR, core disruptive accident anal. 4-96203
- starting range neutron monitor system 4-59375
- suboptimal stochastic control 4-102346
- Superphenix FBR plant clad failure detection systems 4-111656
- SVEA BWR fuel, large scale introduction 4-91051
- THTR, fuel charging expts. and calcs. 4-86940
- TMI-2 postaccident core configuration, ultrasonic mapping 4-106871
- uncollied point flux estimator, track length estimation 4-96183
- VVER neutron physical characteristics precision improvement using BIPR-5K program (*Russian*) 4-78659
- Gd<sub>2</sub>O<sub>3</sub>, fuel charging strategy changes, leakage reduction 4-86943
- N<sub>2</sub>O<sub>4</sub> cooled reactor, fuel envelope diagnostics by  $\gamma$ -spectroscopy (*Russian*) 4-74019
- <sup>241</sup>Pu, neutron absorption in 1 eV resonance, scatt. data effect on result 4-68767
- (Th,Pu)O<sub>2</sub> fuel bundle expts. in ZED 2 4-74024

# fission reactor decommissioning

- see also fission reactor safety; radiation protection; radioactive waste
- cost estimates, updating 4-111975
- decontamination and remedial actions for decommissioned facilities 4-107178
- decontamination processes, sandblasting, OZOX A, and electrochemical methods 4-86981
- electrochemical decontamination of decommissioned nuclear power station pipework (*German*) 4-83254
- Elk river reactor, experiences 4-107175
- environmental and health implications of chemical wastes, during decommissioning operations 4-107177
- FRN research reactor shut-down and decontamination 4-86979

# fission reactor decommissioning continued

- Gundremmingen BWR power station, shut-down, decommissioning and scrap decontamination 4-86980
- hazardous materials control in decommissioning nuclear facilities 4-107176
- health and environmental aspects of DOE's remedial action program 4-107174
- IAEA technical committee report 4-73153
- radioactive waste management in EEC 4-106813
- radwaste treatment and disposal (*German*) 4-59320
- Three Mile Island unit 2, tests for waste hazard potential, decontamination, decommissioning 4-106754

# fission reactor fuel

- see also claddings; fission of plutonium; fission of uranium; fission reactor fuel preparation and reprocessing; isotope separation; radioactive waste
- <sup>238</sup>Pu production ability of fusion breeders 4-106854
- actinide fuel materials, fissile and fertile, nuclear data, resonances and cross sections 4-73955
- activation anal. for N, O, F content determ. 4-102358
- advanced light water prebreeder/breeder conceptual reactor systems, comparison of two Th fuel cycles 4-68805
- advanced PWR, Pu enrichment effects on reaction rates 4-86928
- AGR fuel management, discharge irradiation increase 4-91049
- alpha spectroscopy for nuclear data meas. 4-102348
- AVR expts., LEU spherical fuel elements, induced transients 4-86939
- Barnwell Nuclear Fuel Plant as Pu storage facility 4-73965
- Biblis power plant, fuel element maintenance, BSN failed fuel element detection system 4-96159
- BWR, advanced fuel assembly designs, comparison with standard designs 4-96144
- BWR 9X9 fuel assemblies for improved reliability and reduced costs 4-102365
- BWR core design and operational data collection 4-59381
- BWR core-fuel design, status and future perspectives (*Japanese*) 4-83127
- BWR cores adaptive simulation using 3-D coarse-mesh neutron diffusion theory 4-86933
- BWR low-leakage refueling, General Electric experience, core designs 4-106696
- CANDU MOX rods, NDA working standards, destructive/nondestructive comparison, safeguards 4-106985
- CCTV solid state storage system for nuclear material safeguards 4-106976
- CETAMA, French organisation for nuclear safeguards development and quality insurance 4-111699
- channels between fuel plates of KUCA, void reactivity coeff. expt. study 4-59313
- conference, nuclear technology, Frankfurt, Germany (May 1984) 4-90301
- conference on safeguards and nuclear materials management, Venice, Italy, (May 84) 4-106114
- criticality accidents review for European Community, Saclay, Mol and Windscale 4-106919
- criticality safety audit/appraisal system improvement 4-106897
- criticality safety audits, USA Nuclear Regulatory Commission overview 4-106901
- criticality safety audits and subsequent action response program at Rockwell Hanford Operations 4-106905
- criticality safety audits by USA DOE Albuquerque Operations Office of fissile material 4-106899
- criticality safety audits in France, procedures and organisations 4-106902
- cryptographic safeguard seals for surveillance and containment of nuclear materials 4-106975
- cylindrical fuel lattices, improved intermediate resonance approximation in heterogeneous system 4-91033
- damage due to cooling circulation failure, asymmetric power distrib. effects 4-96227
- damaged nuclear fuel rods from CABRI distortion expts., quantitative radiography 4-106836
- dissolution of fuel samples, methods and apparatus survey (*Czech*) 4-59331
- DoD method for standard deviations in nuclear safeguards, stat. anal. 4-111737
- DWR cladding tubes, props. above annealing temp., mech. props. after thermal shock 4-106835
- electronic seals for nuclear safeguards, potential appls. 4-106974
- element simulation to determine limit operating values 4-59339
- ENDF/B IV data file, cross section verification for PWR fuel 4-86885
- EURATOM'S role in international nuclear safeguards collaboration 4-106954
- extended fuel burnup, advantages of fuel reinsertion, FCYCLS code calcs. 4-106682
- fabrication plant, weighing scales accuracy and precision for nuclear safeguards 4-111701
- FAID ultrasonic fuel assembly sealing system, test at Kahl BWR, safeguards 4-106968
- fast coincidence nondestructive assay, geometry and matrix effects reduction 4-73971
- fast critical assembly, safeguards implementation using C/S and NDA 4-106965
- fast reactor, unevenly heated, gas-cooled fuel element, mech. calc., PRORT program (*Russian*) 4-74021
- FBR, CAMEL II intra-pin fuel injection test, transient overpower accident 4-106937
- FBR, fuel pin failure modeling 4-106936
- FBR, He bonding concept for carbide fuel pins, test results 4-96172
- FBR fuel rod behaviour under steady-state/transient conditions, FARST computer code 4-111611
- FBR mixed carbide fuel rods, post-experimental results 4-106834
- FCA fast critical facility, portal and penetration monitoring system for international safeguards 4-106970
- FIDES automated U-enrichment meter for nuclear safeguards inspection 4-106992
- fissile material accountancy and evaluation for safeguards, corrections for balance periods 4-111726
- fission gas release from solid fuel at high temp., TRAFIC and NEFIG code anal. 4-102344
- fission product behaviour under normal and accident conditions, improved model 4-74032

## fission reactor fuel continued

- Fort Calhoun PWR, extended burn-up fuel design, economic goals 4-106681
- Fort Calhoun PWR, low-leakage fuel management implementation 4-106694
- fuel cycle back end, revitalization 4-78703
- fuel cycle facilities, inspection goals for safeguards 4-106955
- fuel element cans, production planning using BEKA, BIEG and NAVO programs 4-96157
- fuel element planning for enhanced fuel utilisation efficiency 4-86886
- fuel pin transient deformation, cladding strains, MOX fuel appl., creep 4-102378
- gas centrifuge enrichment plant, cascade area, NDA meas. for safeguards 4-106993
- gas centrifuge nuclear plant, U enrichment meas. in pipework by  $\gamma$ -spectrometry 4-111706
- heterogeneous water moderated systems, criticality accident experience 4-106918
- HEU detection in  $UF_6$  centrifuge process piping,  $\gamma$ -meas., safeguards appl. 4-106994
- holdup study in large processing facilities 4-74008
- HTR unirradiated coated particle fuel, U contamination in coating 4-91045
- HTR fuel elements, spherical, behaviour under accident conditions 4-83236
- HTR fuel particles, HRB, GA, and CEGB fission gas release models 4-91052
- HTR fuel pellets with LEU, irradiation testing reference data 4-96162
- HTR irradiated spherical fuel elements with MOX-BISO particles, failure simulation at 1400-2500°C 4-96245
- HTR modular fuel element, fission product release under accident conditions, calc. 4-96247
- HTR under accident conditions, fission product retention in core and fuel (*German*) 4-64231
- hybrid reactor, design and safety study, fast fission blanket safety performance 4-96274
- IAEA's Safeguards Information System, 3 years of experience 4-111724
- IAEA nuclear safeguards support by national programmes coordination 4-111696
- IAEA safeguards implementation in European community, EURATOM involvement 4-106962
- ICT improvements, five year development consequences, nuclear safeguards 4-111721
- IDA-80 meas. eval. programme for U and Pu mass spectrometric isotope dilution anal. 4-111719
- Idaho Chemical Processing Plant, criticality safety audit system and philosophy 4-106896
- international nuclear safeguards, IAEA system problems and prospects 4-106963
- international nuclear safeguards, optimal allocation of inspection resources 4-106961
- international nuclear safeguards, practical implications, international agreement 4-106959
- international nuclear safeguards, problems and further developments 4-106956
- international nuclear safeguards, role of Italy, R&D programmes 4-96223
- irradiated coated fuel particles, stress anal. models 4-64207
- irradiated particles, fission product localisation using unshielded electron microprobe 4-73981
- irradiated reactor fuel monitoring using Cherenkov methodology, safeguards surveillance 4-106977
- JAERI computerised nuclear material accountability system, safeguards 4-111728
- Japanese Pu fuel facility, safeguards samples, preparation for laboratory anal. 4-111720
- K-edge densitometer for nuclear safeguards 4-111709
- KNK-II, defective fuel pin detection, fission gas release 4-96164
- laser holographic-interferometry measurements, sensitivity of fringe-interpretation technique 4-69719
- LEU fuel, non-destructive assay using photoneutron interrogation, safeguards appl. 4-106990
- LEU samples, active well coincidence counter meas. for safeguards assay 4-106991
- Livermore criticality accident, 1963, nuclear criticality safety aspects 4-106921
- LMFBR, fuel and cladding relaxation during LOF accidents 4-106938
- LMFBR, fuel freezing mechanism in rod bundle in HCDA 4-106939
- LMFBR, fuel pin failure, temp. oscillations 4-106942
- LMFBR fuel bundle distortion characterization using neutron tomography and potting 4-86893
- LMFBR LOF accident simulation in Sodium Loop Safety Facility 4-83230
- LMFBR multiaxial ductile tests for irradiation in FFTF 4-111632
- LMFBRs, Na aerosols and puddles, fuel, fission products and Na release 4-91084
- long term away-from-reactor water pool fuel storage, safeguards appls. 4-106958
- Los Alamos Critical Assembly Facility, initiatives in training, safety and design eval. 4-106912
- Los Alamos criticality safety audit practices, risk control 4-106898
- LWR, severe fuel damage scoping test, degraded core cooling accident 4-106776
- LWR, slow fission gas dilution behaviour on fuel rods 4-106765
- LWR fuel, increased burnup with Exxon designs, burnup capabilities 4-106683
- LWR fuel bundle design for extended burnup 4-106764
- LWR fuel element maintenance, operating procedure with repaired fuel elements 4-96158
- LWR fuel rod, irradiated induced I pressure 4-106676
- LWR fuel rod behaviour evaluation under operational transient conditions 4-111612
- LWR fuel rods, transient fission gas release and microstruct. variations during power ramping 4-96161
- LWR fuels, low temp. swelling and densification 4-102352
- LWR fuels, reprocessing input balance using non-destructive measurements 4-111715
- LWR large break LOCA, clad deform. and heat transfer, azimuthal effects modelling 4-102377
- LWR low-leakage fuel management, Babcock and Wilcox experience 4-106693

## fission reactor fuel continued

- LWR low-leakage fuel management, utility perspective 4-106691
- LWR low-leakage fuel management, Westinghouse experience, loading pattern designs 4-106695
- LWR overpower transients, fuel pellet-cladding interaction, safety analysis record review 4-96218
- LWR severe fuel damage accidents, NRC research program 4-106774
- management, safeguards, INMM annual meeting, Vail, CO, USA, (July 1983) 4-78021
- mixed carbide fuel performance modeling using SPECKLE-III code 4-106664
- mixed carbide reactor fuels, irradiat., defect struct., fission gas bubbles, precipitates, TEM obs. 4-83145
- MOX fuel fabrication plant, observed MUF as function of throughput 4-106964
- near-real-time nuclear material accountability for reprocessing facility, test procedures comparison 4-111740
- near-real-time nuclear materials accountability retrospective testing/statistical tests comparison 4-111739
- Neutron Coincidence Collar in prototype FBR, fuel loading verification for safeguards 4-111708
- neutron multiplicity counter, absolute calibration technique for spontaneous fission sources, safeguards 4-111712
- new and spent fuel storage criticality safety, optimum moderation, 3D modelling 4-106913
- NRC safety/safeguards relations 4-74025
- Nuclear Criticality Information System, status, plans and capabilities 4-106911
- nuclear criticality inspection, audit and appraisal programme at Westinghouse Hanford Co. 4-106906
- nuclear criticality safety audit at Westinghouse Hanford Co., 1970-81 review 4-106907
- nuclear criticality safety audits within the Babcock & Wilcox Company 4-106904
- nuclear criticality safety calcs., benchmarking with subcritical expts. 4-106908
- nuclear criticality safety oversight program at the Rocky Flats Plant 4-106903
- nuclear facility design, impact of potential for criticality, safety, doses 4-106923
- nuclear fuel cycle cost, current data and developments (*French*) 4-91064
- nuclear installation inspection for safeguards, in-field computer support 4-111727
- nuclear material, computer-based control, accounting and reporting system in Finland 4-111730
- nuclear material, near real time accountability in a large commercial reprocessing facility 4-111732
- nuclear material balance data, verification tests, MUF, safeguards 4-111738
- nuclear material batch designation and follow-up in Euratom safeguards 4-111729
- nuclear material large bulk handling facilities, tag inventory, physical inventory verification 4-106966
- nuclear materials, destructive assay uncertainties, 1983 target values, safeguards 4-107001
- nuclear materials meas., assay design and meas. interpretation for safeguards 4-106955
- nuclear materials transit control by Euratom safeguards 4-111725
- nuclear reactor fuel rod performance, adjoint sensitivity anal. 4-111610
- nuclear safeguards, automated procedure for performing computer security risk analysis 4-111735
- nuclear safeguards, automatic identification in containment and surveillance 4-106972
- nuclear safeguards, isotropic correlation technique procedure test by ESARDA 4-111702
- nuclear safeguards, neutron sensitive swinging door monitor 4-106973
- nuclear safeguards, radiation fields as barrier to SUM diversion at non-power reactors 4-111695
- nuclear safeguards, signature comparison system 4-106971
- nuclear safeguards, software, data structs. and data eval. for verification system 4-111700
- nuclear safeguards, tank calibration data eval. in RITCEX, errors 4-111703
- nuclear safeguards and international Cooperation, European Community R&D 4-106999
- nuclear safeguards reporting system using mobile word-processor, operational experience 4-111733
- nuclide composition and burnup in VVER-440 4-102360
- on-line state estimation and indirect measurement in safeguards systems 4-73992
- ONION cell code for Gd bearing PWR fuel 4-102343
- optical surveillance for international safeguards present and future 4-73968
- Pacific Northwest Lab., criticality safety audit and review practices 4-106900
- pebble bed HTGR spherical fuel elements, core heat-up simulation for accident conditions (*German*) 4-64230
- pebble bed HTR,  $ThO_2$  and  $UO_2$  spherical fuel elements 4-78698
- pebble bed reactors, HEU/LEU equilb. combined cores, AVR appl. (*German*) 4-102345
- performance evaluation, simplified power history 4-106771
- PERLA Laboratory at Ispra for nuclear safeguards performance, calibration and training 4-111697
- Pickering nuclear power station, retubing of units 1 and 2 4-78696
- power plants, safeguards concepts, optimisation problems, basic conditions 4-106957
- PWR, fuel management for extended burn-up, safety anal. 4-106680
- PWR, fuel sharing strategy to reduce costs 4-86887
- PWR, severe fuel damage in degraded core cooling accident 4-106775
- PWR, severe fuel damage tests, fission product effects 4-106777
- PWR core and fuel element distribution, computer programming system 4-86942
- PWR fuel pin failure determination by coolant radioactivity meas. 4-73961
- PWR low-leakage fuel management, Florida Power and Light Company experience 4-106692
- RA-2 critical assembly, prompt critical excursion accident, causes and consequences 4-106916
- RA-2 criticality accident, yield and quench mech. anal. 4-106917
- radiation testing facility using reactor spent fuel 4-107255

# fission reactor fuel continued

radioactive waste from fast-neutron reactor fuel cycle, management in France 4-106812

reactivity control in power reactors, spectral displacement, fuel cells, PHWR appl. (*Spanish*) 4-96175

recycled U fuel rods, monitoring and testing for viability 4-91066

reprocessing, improved computer modelling for safeguards 4-111734

rod anal. using NUFAP code 4-106773

rod evaluation system using FREY code 4-106663

rod performance, FRAPCON-2, TACO-2, COMETHE-3L codes 4-106665

safeguards, access denial systems, delay element interaction 4-78692

safeguards, accountability using intelligent microprocessor vision system 4-78690

safeguards, analysis of material accounting data 4-73993

safeguards, analysis of MUF time series 4-73997

safeguards, Augmented Automated Material Accounting Statistics System (AMASS) 4-78679

safeguards, bar code usage in nuclear materials accountability 4-78689

safeguards, bar codes for ease of accounting 4-78686

safeguards, calibration problem, regression anal. 4-73991

safeguards, data acquisition system for the NLO error propagation exercise 4-78687

safeguards, decision anal. 4-73994

safeguards, DYMCA computerized accountability program 4-78683

safeguards, efficient estimation of material loss 4-73998

safeguards, equipment development by IAEA 4-78670

safeguards, error propagation statistics 4-78681

safeguards, estimation of measurement error models 4-73988

safeguards, evaluating measurement errors from inter-laboratory comparisons 4-73989

safeguards, game theoretic analysis of inventory verification 4-74002

safeguards, guard tower structural design concept for perimeter security systems 4-73969

safeguards, IAEA inspection effort allocation and distrib. in 1982 4-106960

safeguards, IAEA principles 4-78664

safeguards, IAEA research programme for isotopic correlation techniques appl. 4-78671

safeguards, INEL central alarm monitoring and assessment system 4-73970

safeguards, INMACS program, materials accounting and control system 4-78706

safeguards, insider threat, NRC perspective 4-78676

safeguards, Interactive Measurement Evaluation and Control System at Rocky Flats 4-73972

safeguards, inventory verification using the inspector's sufficient statistics 4-74003

safeguards, licensee practices in error propagation 4-78680

safeguards, material accountability and data verification 4-74001

safeguards, materials accounting, statistical methodology evolution 4-73986

safeguards, mathematical and statistical methods, lecture course, Ispra, Italy (Nov.-Dec., 1981) 4-73132

safeguards, mathematical statistical techniques 4-73987

safeguards, meas. real time accountability data verification 4-78685

safeguards, MUF time series variance matrix deviation 4-73995

safeguards, near-real time material accountability 4-78667

safeguards, nonconstant bias correction propagation in accounting 4-78682

safeguards, on-line accountability system 4-78666

safeguards, operational concerns in addressing insider protection 4-78677

safeguards, physical protection elements for insider actions 4-78714

safeguards, physical protection methods against unauthorised insider acts 4-78678

safeguards, physical protection systems, reliability tests 4-78693

safeguards, process component inventory in a large commercial reprocessing facility 4-78684

safeguards, real time loss detection based on sequential partial inventory verification 4-74004

safeguards, real-time accountability and verification, gaming simulation 4-74005

safeguards, Rocky Flats plant Safeguards Accountability Network 4-78668

safeguards, sampling plans for inventory verification 4-74000

safeguards, Sandia Labs. bar code system for control and inventory system 4-78688

safeguards, unconventional applications of conventional intrusion detection sensors 4-73967

safeguards, vehicle monitors, evaluation test 4-78691

safeguards, verification of materials accounting data 4-73999

safeguards 4-73996

safeguards as confidence building measures in the nuclear field 4-106953

safeguards effectiveness criteria and safeguards efficiency 4-78669

safeguards measurement variance estimation and hypothesis testing 4-73990

safeguards systems development 4-78665

sequential probability ratio controllers for nuclear safeguards radiation monitors 4-111694

Simultaneous Calorimetric Assay System, transportable device for Pu meas. in safeguards 4-106984

smarter radiation monitors for safeguards and security 4-73966

space vehicles, thermionic fuel element technology status 4-106759

special nuclear materials, gamma spectrometric and absorpt. meas. for safeguards 4-111717

spent fuel measurement system 4-74007

spent fuel storage alternatives, United States 4-86897

spent nuclear reactor fuel management, present state 4-102350

spent reactor fuel dry-storage techniques, probabilistic risk assessment 4-59337

stainless steel clad fuel, fuel performance code 4-106772

SVEA BWR fuel, large scale introduction 4-91051

Swedish joint nuclear fuel, chemistry and materials research and development program 4-91054

swelling and transient behaviour, scanning transmission electron microscopy examination 4-73982

Taiwan Research Reactor, irradiated fuel rod testing 4-59326

ternary carbide systems, actinides with 4th-8th group transition metals, phase relations (*German*) 4-85142

THTR, fuel charging expts. and calcs. 4-86940

# fission reactor fuel continued

THTR-300 reactor, fuel feeding system construction and commissioning experience 4-106847

TMI-2 fuel debris location in cooling system, SSNTD neutron dosimetry appl. 4-96194

Tokai Reprocessing Plant, leached fuel hull monitoring system, <sup>137</sup>Cs indicator for safeguards 4-106980

transient melting in nuclear combustion 4-96129

TRISO coated fuel particles, irradiat., failure during high temp. annealing 4-73979

TRISO fuel pellet, fission product transport through cladding layers, model 4-107003

URENCO centrifuge enrichment plant, cascade hall neutron area monitoring for safeguards 4-106969

USSR, nuclear material export/import information, computerization for safeguards purposes 4-111723

VAK-III fuel assembly sealing process, recent progress and results from Kahl BWR 4-106967

VHTR fuel compacts, fission product diffusion in matrix graphite 4-73976

VHTR reference fuels, irradiation expts., weight and dims. changes, failure fraction (*Japanese*) 4-64201

VIPER reactor expts. on fission gas release from mixed oxide fuel pins 4-64216

VVER-440, burnup and isotopic composition determ. 4-102355

WIS computerized information system for a waste processing facility, nuclear safeguards 4-111731

Zircaloy fuel rod cladding, strain rate sensitivity 4-64202

(n,γ) effect on radiative characteristics of fission product mixtures in fuel rods 4-106661

Am-Pu simultaneous determination in plutonium nitrate solns. 4-74006

<sup>232</sup>Cf nuclear parameters of safeguards interest, half-life, neutron multiplicity 4-106986

<sup>232</sup>Cf source driven neutron noise anal., spatial effect corrections to sub-criticality meas. 4-106909

Cs<sub>2</sub>UO<sub>4</sub> phase, high temp., thermodynamic stability 4-113671

Ge detector array for nuclear safeguards 4-74098

<sup>131</sup>I release from defective LWR fuel rods at temps. up to 1100°C, LOCA appl. 4-96233

N<sub>2</sub>O<sub>4</sub> cooled reactor, fuel envelope diagnostics by γ-spectroscopy (*Russian*) 4-74019

Nb tubes internal protective coating, fuel pin accidental behaviour 4-68771

Pu active facility, automatic batch identification using laser bar code reader, safeguards 4-111736

Pu, alpha particle spectrometry 4-102347

Pu assay sample masses from neutron coincidences, induced fission correction, safeguards appl. 4-111705

Pu assays, neutron signal pulse train anal. methods for safeguards 4-111714

Pu confinement and surveillance for safeguards, thermal fluxmetry appl. 4-111693

Pu content verification by calorimetry for nuclear safeguards of high burnup samples 4-111704

Pu imaging through heavy shielding using pinhole, safeguards appl. 4-106989

Pu, isotopic composition, gamma-spectrometric determ., safeguards appl. 4-106978

Pu isotopic composition determ. by high res. γ-ray spectrometry, safeguard appl., PLUTO code 4-106979

Pu nuclear parameters of safeguards interest, half-life, neutron multiplicity 4-106986

Pu safeguards standards, Euratom time correlation analyser for passive assay 4-111716

Pu samples from processing plants, safeguards assay using scintillator neutron coincidence counter 4-111713

Pu solution characterisation by γ-spectrometry, densitometry and isotopic anal., safeguards 4-111707

Pu storage, proposed alternatives 4-73964

Pu storage, purpose and objectives 4-73962

Pu storage, status and options 4-73963

Pu-bearing irradiated fuels, examination using scanning electron microscope (*French*) 4-73604

PuO<sub>2</sub> assay variations, sample representative control and analysis accuracy, safeguards 4-106998

PuO<sub>2</sub> nuclear material reference sample preparation in sealed glass containers for safeguards appl. 4-106987

<sup>238</sup>Am, A=239.241, thermal neutron constants 4-83051

<sup>238</sup>Am, α-activity fraction in NBS Pu standard reference materials 946 and 947, safeguards 4-107000

<sup>240</sup>Pu, neutron absorption in 1 eV resonance, scatt. data effect on result 4-68767

<sup>240</sup>Pu, neutron multiplication corrections applying the shift register technique 4-83117

SiC coatings of nuclear fuel particles, characterisation (*German*) 4-78702

<sup>232</sup>Th(n,X), total neutron cross section meas. in off-resonance region below 300 eV 4-96013

(Th,Pu)O<sub>2</sub> fuel bundle expts. in ZED 2 4-74024

Th fuel cycles for CANDU reactors 4-68768

ThC, molten nuclear fuel, optical consts., 450-750 nm (*German*) 4-84933

<sup>232</sup>Th use in nuclear reactors, design recommendations 4-96125

<sup>232</sup>Th(n,X), 24 keV, relationship between Doppler and self-shielding effects 4-73975

(U,Ce)O<sub>2</sub> cation redistribution in thermal gradient (*French*) 4-73978

(U,Pu)C fuel, swelling, densification and creep under irradiation 4-83144

(U,Pu)C mixed carbide, fast reactor fuel development in Germany, 1969-84, pin irradiat. experience 4-83143

(U,Pu)C, mixed carbide fuel, irradiat., X-ray diff. study 4-83138

(U,Pu)O<sub>2</sub>, diffusion meas., effects of chem. surface gradient, mechanical polishing 4-98354

(U,Pu)O<sub>2</sub> MOX fuels comparison in fast reactor, thermal cond. and other characts. 4-91059

(U,Pu)O<sub>2</sub>, mixed oxide fuel, temporal stoichiometry drift, control 4-83135

(U,Pu)O<sub>2</sub> mixed oxide fuel, irradiat., X-ray diff. study 4-83138

(U,Pu)O<sub>2-x</sub> substoichiometric mixed oxide fuel, O pot., struct. models 4-106671

(U,Pu)O<sub>2-x</sub> mixed oxide fuel, irradiat., O pot. meas. 4-83137

(U,Th)O<sub>2</sub> HTR fuel elements, spherical, behaviour under accident conditions 4-83236

**fission reactor fuel continued**

- (u,Pu) $O_{2+x}$  nuclear fuel oxide, diffusion processes, surface effects 4-98353  
 U and Pu analytical assessments in reprocessing plant laboratory, guaranteed accuracy 4-111722  
 U burnup improvement by 50% or more, benefits 4-74015  
 U demand projections for USA and western world 4-62312  
 U, isotopic composition, gamma-spectrometric determ., safeguards appl. 4-106978  
 U, medium enriched, KUCA expts. anal. using ANL code system 4-59305  
 U nuclear fuel supply, status report (German) 4-68751\*  
 U nuclear fuel supply system, adequacy for future requirements (German) 4-68753  
 U-Nb (2.4 wt.%),  $\gamma$ -phase comp., effect of extrusion 4-61998  
 U-Nb (2.4 wt.%), linear thermal contraction, tensile strength rel. to extrusion 4-109472  
 UC, fast reactor fuel, critical constants, sensitivity anal. 4-68757  
 UC fuel pin experience for space nuclear power 4-106760  
 UC, molten nuclear fuel, optical consts., 450-750 nm (German) 4-84933  
 UC $O_{2.013}$ , failed HTGR fuel, oxide kernel migration 4-111630  
 UF<sub>6</sub> gas phase sampling for safeguards 4-78672  
 UN fuel pin experience for space nuclear power 4-106760  
 UO<sub>2</sub>, containing simulated fission product elements, high temp. vap. press. 4-102351  
 UO<sub>2</sub>, creep deform. behaviour, 2100 to 2600°C 4-76814  
 UO<sub>2</sub>, elimination of small voids during irradi. 4-103813  
 UO<sub>2</sub>, fast reactor fuel, critical constants, sensitivity anal. 4-68757  
 UO<sub>2</sub>, fissile kernel/ThO<sub>2</sub> fertile kernel system, fuel particle irradiation tests 4-106779  
 UO<sub>2</sub> fuel particles, TRISO-coated, fission product release during post-irrad. annealing 4-111606  
 UO<sub>2</sub> fuel pellets, sintering, grain growth rel. to S content 4-85134  
 UO<sub>2</sub> fuel pin experience for space nuclear power 4-106760  
 UO<sub>2</sub>, indentation creep before and after irradiation, sintered pellets 4-61977  
 UO<sub>2</sub>, irradi., densification algorithm 4-59329  
 UO<sub>2</sub> irradiated thermal reactor fuel, fission products, electron-probe microanal. appls. 4-73980  
 UO<sub>2</sub>, low enriched, Triso coated, post-irradiation electron probe microanal. 4-68769  
 UO<sub>2</sub>, microstruc. during ramping, transient fission gas release (German) 4-83136  
 UO<sub>2</sub>, molten nuclear fuel, optical consts., 450-750 nm (German) 4-84933  
 UO<sub>2</sub>, O Frenkel disorder obs., neutron scatt. study 4-60917  
 UO<sub>2</sub> pellets, gravimetric U determs., repeatability and reproducibility, safeguards 4-111718  
 UO<sub>2</sub> powder and pellets containing Gd<sub>2</sub>O<sub>3</sub>, Gd and U determ. for nuclear safeguards 4-107002  
 UO<sub>2</sub> spheres quenched in Na, fragmentation time calc. 4-111609  
 UO<sub>2</sub>/Zircaloy 4 reaction layer sequence, total interfacial energy 4-83142  
 UO<sub>2</sub>/Zircaloy-4, diffusion couple, interfacial energy and work of adhesion 4-83141  
 UO<sub>2</sub>/Zircaloy-4 chemical interaction 4-83140  
 UO<sub>2</sub>-PuO<sub>2</sub> reaction kinetics with Na, fission products effects, LMFBR appl. 4-106673  
 UO<sub>2+x</sub> nuclear fuel oxide, diffusion processes, surface effects 4-98353  
<sup>235</sup>U, A=233,235, thermal neutron constants 4-83051  
<sup>235</sup>U abundance determ. by  $\gamma$ -spectrometry, certified ref. materials for enrichment standards 4-111698  
<sup>235</sup>U, isomeric level excitation by positrons (Russian) 4-71474

**fission reactor fuel preparation and reprocessing**

- see also isotope separation; radioactive waste  
<sup>235</sup>Pu production ability of fusion breeders 4-106854  
 accelerator breeder applications 4-59435  
 accelerator breeders and fission converter reactors, need and implementation scale 4-59436  
 accelerator spallation reactors for breeding fissile fuel and transmuting fission products 4-59434  
 actinide waste transmutation concept 4-59350  
 aerosol filters for nuclear process plants 4-64211  
 AGR fuel management, discharge irradiation increase 4-91049  
 airborne radionuclides, recovery and storage, dose commitments versus costs 4-106808  
 Barnwell Nuclear Fuel Plant as Pu storage facility 4-73965  
 BWR low-leakage refueling, General Electric experience, core designs 4-106696  
 BWR spent fuel, <sup>137</sup>Cs  $\gamma$ -spectrometry for burn-up verification and isotopic comp., safeguards 4-106983  
 caustic waste tank, Pu build-up and recovery, nuclear criticality safety 4-106922  
 commercial reprocessing prospects in USA 4-78704  
 criticality accidents review for European Community, Saclay, Mol and Windscale 4-106919  
 criticality safety audit/appraisal system improvement 4-106897  
 criticality safety audits and subsequent action response program at Rockwell Hanford Operations 4-106905  
 criticality safety audits by USA DOE Albuquerque Operations Office of fissile material 4-106899  
 cumulative error models for the tank calibration problem 4-74009  
 decision time 4-81524  
 decommissioning of nuclear facilities, IAEA technical committee report 4-73153  
 decontamination, examination and fuel element monitoring procedures (German) 4-64217  
 decontamination plant at Almelo, Netherlands, for UF<sub>6</sub> containers and equipment 4-96169  
 dissolution residues, microprobe anal. appls. 4-74014  
 economics of fusion breeders 4-59353  
 economics of reprocessing, discounted cash flow anal. 4-106849  
 fabrication plant, weighing scales accuracy and precision for nuclear safeguards 4-111701  
 FBR, He bonding concept for carbide fuel pins, test results 4-96172  
 FBR fuel reprocessing, current status and future trends in USA 4-68775  
 fissile material assays for crated nuclear waste, PACC counter for safeguards 4-111711  
 fluidized-bed volume reduction system, radioactive waste, economic analysis 4-106749  
 Fort Cathoun PWR, low-leakage fuel management implementation 4-106694

**fission reactor fuel preparation and reprocessing continued**

- fuel cycle back end, revitalization 4-78703  
 fuel cycle facilities, inspection goals for safeguards 4-106955  
 fuel element fabrication workers, U in urine determ. 4-105348  
 fuel reprocessing tank vol. determ., use of U and Mg as isotopic dilution tracers, safeguards 4-106997  
 fuel rod cutting, oxide fuel contrib. to mech. props., tool design 4-91068  
 fuel-cladding separation by cladding-tube heating (German) 4-83218  
 fusion breeder, development pathways 4-107101  
 fusion breeder, fission suppressed, safety studies 4-107103  
 fusion breeder design review 4-107099  
 fusion breeder economics, systems analysis, and market penetration 4-107100  
 gas centrifuge enrichment plant, cascade area, NDA meas. for safeguards 4-106993  
 gas centrifuge enrichment plant, leak detection using SALT cart 4-90598  
 gas centrifuge enrichment plants, international safeguards, LFUA mode 4-91069  
 gas centrifuge nuclear plant, U enrichment meas. in pipework by  $\gamma$ -spectrometry 4-111706  
 Hanford Pulser, criticality accident in Pu scrap recovery building 4-106920  
 HEU detection in UF<sub>6</sub> centrifuge process piping,  $\gamma$ -meas., safeguards appl. 4-106994  
 high power spallation neutron source, FRG project 4-59478  
 HLW and spent fuel disposal repositories, Nuclear Waste Policy Act implementation 4-106684  
 holdup study in large processing facilities 4-74008  
 hot impact densification for producing ceramic fuel pellets (German) 4-83215  
 HTGR unirradiated coated particle fuel, U contamination in coating 4-91045  
 HTR for process heat, accident response, Th fuel cycle for pebble bed design 4-78718  
 HTR fuel, alpha spectrometric anal. 4-102444  
 HTR fuel, aqueous chemical reprocessing, PUREX/THOREX process 4-74016  
 hybrid blankets, time depend. performance characts. 4-59428  
 IDA-80 meas. eval. programme for U and Pu mass spectrometric isotope dilution anal. 4-111719  
 Idaho Chemical Processing Plant, criticality safety audit system and philosophy 4-106896  
 interim spent fuel storage using rod consolidation 4-106703  
 intermediate level radwaste from reprocessing operations, management 4-59323  
 irradiated coated fuel particles, stress anal. models 4-64207  
 Japanese Pu fuel facility, safeguards samples, preparation for laboratory anal. 4-111720  
 Los Alamos criticality safety audit practices, risk control 4-106898  
 LWR, feasibility study of fuel recycling 4-106853  
 LWR cell anal., resonance shielding procedures validation, fuel cycle optimisation 4-96118  
 LWR fuel reprocessing, world-wide status and outlook in United States 4-68774  
 LWR fuels, reprocessing input balance using non-destructive measurements 4-111715  
 LWR low-leakage fuel management, Babcock and Wilcox experience 4-106693  
 LWR low-leakage fuel management, utility perspective 4-106691  
 LWR low-leakage fuel management, Westinghouse experience, loading pattern designs 4-106695  
 LWR MOX fuel homogeneity setting during prod. by COM process 4-91067  
 LWR spent fuel shipments, burnup credit eval. for nuclear criticality safety 4-106914  
 management, safeguards, INMM annual meeting, Vail, CO, USA, (July 1983) 4-78021  
 molten salt fusion breeder, blanket materials compatibility 4-107102  
 MOX fuel fabrication plant, observed MUF as function of throughput 4-106964  
 MTR fuel elements, production of dense U<sub>3</sub>O<sub>8</sub> by special crystal growth 4-96171  
 MTR spent fuel, high res. gamma spectrometry verification for safeguards 4-106982  
 near-real-time materials accountancy, appl. to reprocessing facility safeguards 4-68772  
 near-real-time nuclear material accountancy for reprocessing facility, test procedures comparison 4-111740  
 new and spent fuel storage criticality safety, optimum moderation, 3D modelling 4-106913  
 nuclear criticality inspection, audit and appraisal programme at Westinghouse Hanford Co. 4-106906  
 nuclear criticality safety audit at Westinghouse Hanford Co., 1970-81 review 4-106907  
 nuclear criticality safety audits within the Babcock & Wilcox Company 4-106904  
 nuclear criticality safety oversight program at the Rocky Flats Plant 4-106903  
 nuclear criticality safety research program at JAERI 4-68797  
 nuclear fuel cycle cost, current data and developments (French) 4-91064  
 nuclear fuel reprocessing plant safety and health physics experience, 25 years (French) 4-74054  
 nuclear material, near real time accountancy in a large commercial reprocessing facility 4-111732  
 nuclear safeguards, isotopic correlation technique procedure test by ESARDA 4-111702  
 Nuclear Waste Policy Act, utility/USA DOE cooperative R&D on spent fuel storage 4-106697  
 on-site spent fuel storage options, cost comparisons 4-102364  
 parametric anal. of economics, DCF techniques 4-106850  
 pellet production by heat application compaction by continuously operating pelletisers 4-96170  
 PFR fuel reprocessing, SNM analytical quality control, safeguards 4-106996  
 poison tube tank containing UO<sub>2</sub>(NO<sub>3</sub>), criticality expts. 4-106910  
 PWR low-leakage fuel management, Florida Power and Light Company experience 4-106692  
 PWR spent fuel shipping cask, thermal anal. 4-64247  
 radioactive waste, conditioning and treatment at nuclear fuel reprocessing plants in USA 4-106794

**fission reactor fuel preparation and reprocessing continued**

- radioactive waste from Tokai nuclear reprocessing plant, treatment, conditioning and storage 4-106799
- radioactive wastes from nuclear reprocessing facilities, treatment and conditioning in India 4-106798
- radioactive wastes from nuclear reprocessing plants, management in UK 4-106797
- radioactive wastes from nuclear reprocessing plants, treatment and conditioning in FRG 4-106796
- radioactive wastes from reprocessing facilities, treatment and packaging in France 4-106795
- REA-2023 storage cask, effects of extended burnup and consolidated fuel use, shielding 4-106700
- recycled U fuel rods, monitoring and testing for viability 4-91066
- reprocessing, improved computer modelling for safeguards 4-111734
- reprocessing gaseous wastes management,  $^3\text{H}$ ,  $^{14}\text{C}$ ,  $^{85}\text{Kr}$  and  $^{129}\text{I}$  emissions 4-59438
- safeguards, IAEA research programme for isotopic correlation techniques appl. 4-78671
- safeguards, INMACS program, materials accounting and control system 4-78706
- safeguards, near real-time inventory and accountability within a uranium enrichment plant 4-78705
- safeguards, process component inventory in a large commercial reprocessing facility 4-78684
- safeguards, Rocky Flats plant Safeguards Accountability Network 4-78668
- spent fuel, Carolina Power & Light at-reactor dry storage demonstration programme 4-106698
- spent fuel consolidation technology, NUSCO/industry programme 4-106701
- spent fuel element transitional storage at Creys-Malville FBR power plant 4-91062
- spent fuel measurement system 4-74007
- spent fuel processing, policy and public attitudes 4-59356
- spent fuel reprocessing methods and economics (*Hungarian*) 4-78707
- spent fuel storage pool water, radioactivity, positively charged ions predominance 4-111650
- spent reactor fuel storage, installation description, thermal and thermomech. calcs. 4-96149
- symbiotic molten-salt systems coupled with accelerator molten salt breeder or ICF hybrid molten salt breeder 4-59352
- TBP and Dodecane extraction materials, dispersion from aqueous process streams in mixer 4-96168
- Tokai Reprocessing Plant, leached fuel hull monitoring system,  $^{137}\text{Cs}$  indicator for safeguards 4-106980
- tokamak fusion breeder, fission suppressed blanket, nuclear anal. 4-107104
- transmutation of waste, assessment of feasibility 4-59351
- UK commercial nuclear fuel reprocessing, review of developments 4-59354
- URENCO centrifuge enrichment plant, cascade hall neutron area monitoring for safeguards 4-106969
- US-DOE fusion breeder program, blanket design and system performance 4-59426
- VEPCO interim spent fuel storage program 4-106702
- VEPCO/DOE/EPRI dry cask spent fuel storage cooperative demonstration programme 4-106699
- volatile radionuclides from nuclear fuel reprocessing, treatment and disposal of  $^3\text{H}$ ,  $^{14}\text{C}$ ,  $^{85}\text{Kr}$ ,  $^{129}\text{I}$  (*German*) 4-59318
- volatile radionuclides in reprocessing plant, modular dissolver off-gas purification system design 4-106810
- WAK reprocessing plant,  $\text{H}_2$  radiolysis in cooling system,  $\text{H}_2$  concs., safety 4-91065
- Waste Experimental Reduction Facility description and progress report 4-106752
- WIS computerized information system for a waste processing facility, nuclear safeguards 4-111731
- WVER-440 spent fuel, nondestructive anal. using gamma and neutron meas., safeguards 4-106981
- Am-Pu simultaneous determination in plutonium nitrate solns. 4-74006
- Be in fusion breeder blanket assemblies, neutron multiplication calcs. 4-107105
- CsF-UF<sub>6</sub> binary fused mixtures, elec. cond. 4-108847
- D-cycle Tokamaks integration with decentralised small fusion and fission reactors 4-59406
- $^3\text{H}$ -bearing wastes and effluents, management at nuclear facilities 4-106793
- $^{129}\text{I}$  management from fuel reprocessing plants, air and water discharges 4-91115
- KF-UF<sub>6</sub> binary fused mixtures, elec. cond. 4-108847
- $^{99m}\text{Tc}$ , fission prod. on tech. scale from  $^{235}\text{U}$  elements 4-77386
- Np, in-line determ. in process streams by EDXRF 4-74010
- Pu determination in MOX fuel fabrication plant wastes by passive neutron assay 4-111710
- Pu drop deposited source for alpha spectrometric assay 4-101971
- Pu, in-line determ. in process streams by EDXRF 4-74010
- Pu pricing mechanisms, midterm future nuclear power growth scenario 4-106852
- Pu waste arisings and glove box hold-up, nondestructive assay techniques for safeguards 4-106988
- Pu-U mixed nitrate solns., direct denitration by microwave heating (*Japanese*) 4-96165
- $\text{Pu}$ , A=238, 239, 240, content in tobacco crop near nuclear fuel separation facility 4-115237
- $^{238}\text{Pu}$ , determ. in irradiated fuel by alpha-spectrometry 4-102366
- RbF-UF<sub>6</sub> binary fused mixtures, elec. cond. 4-108847
- (Th, U)<sub>2</sub>O<sub>7</sub>, mixed oxide fuel, dissoln. in conc. HNO<sub>3</sub> 4-83217
- Th fuel cycles for CANDU reactors 4-68768
- U and Pu analytical assessments in reprocessing plant laboratory, guaranteed accuracy 4-111722
- U enrichment, present technology and future prospects, review 4-91063
- U extraction from seawater, present status 4-59355
- U, in-line determ. in process streams by EDXRF 4-74010
- U mine, underground radiation protection design 4-96166
- U mine decommissioning, radiological critical pathways, ALARA considerations 4-96167
- U production conversion and enrichment assessment and future developments in nuclear fuel markets 4-68773
- U utilities holding, price dependent strategy 4-106851
- UF<sub>6</sub>, cryogenic deposits, thermal cond. coeff. 4-106848

**fission reactor fuel preparation and reprocessing continued**

- UF<sub>6</sub>, mechanical booster pump for dangerous gases 4-86432
- UF<sub>6</sub>-UF<sub>3</sub> system, vaporisation, high temp. reduction and disproportionation 4-114770
- U<sub>6</sub>Fe, low enrichment dispersion fuels for research and test reactor 4-83216
- UO<sub>2</sub>, charact. of oxides formed by reaction with water IR and sorption anal. 4-74012
- UO<sub>2</sub> fissile kernel/ThO<sub>2</sub> fertile kernel system, fuel particle irradiation tests 4-106779
- UO<sub>2</sub> fuel, conversion into U<sub>3</sub>O<sub>8</sub> at head-end of HTR reprocessing 4-74013
- UO<sub>2</sub> fuel pellets, sintering characts. 4-66288
- UO<sub>2</sub> fuel pellets, sintering, grain growth rel. to S content 4-85134
- UO<sub>2</sub>-U<sub>2</sub>O<sub>3</sub> vapour reaction, kinetics and mechanisms 4-74011
- U<sub>2</sub>Si<sub>2</sub>, U<sub>3</sub>Si<sub>2</sub>, low enrichment dispersion fuels for research and test reactor 4-83216
- $^{232}\text{U}$ , determ. in irradiated fuel by alpha-spectrometry 4-102366

**fission reactor instrumentation see nuclear reactor instrumentation**
**fission reactor materials**

- see also claddings; fission reactor fuel; fusion reactor materials; materials handling; moderators; radioactive waste
- advanced HTR systems, alloys eval., creep, fatigue, corrosion, neutron effects 4-78699
- AGR, pressure vessels, pressure tests 4-59391
- blanket sector and T breeding for INTOR/NET 4-111830
- brittle fracture resistance, calc. 4-96143
- BWR, containment pressure suppression under LOCA 4-59389
- BWR coolant pressure boundary piping, cracking, material selection, processing guidelines 4-111635
- BWR pipe cracking, heat-sink welding, corrosion resistant cladding 4-111639
- BWR pipe cracking, last pass heat-sink welding, field procedure development 4-111636
- BWR pipe cracking in weld heat affected zones 4-111634
- BWR pipe cracking induction heating stress improvement, qualification scheme 4-111637
- BWR piping, IGSCC countermeasure implementation in USA 4-111644
- BWR piping welds, flaw characts. using US satellite pulses 4-85272
- BWR recirculation loop piping, improved pipe components manufacturing 4-111642
- BWR water electrochemical pots., in-plant meas., stress corrosion cracking indication 4-96191
- cladding repairs, manual, numerical assessment of tolerance 4-66549
- component fault testing in electro- and cable-technology, nuclear reactor appl. 4-106839
- component support materials, Unresolved Safety Issue A-12, integrity assessment 4-106780
- concrete, thermophysical and transport props. 4-111613
- concrete containment structures, load anal. with ABAQUS-EPGEN code 4-68794
- concrete containment wall elements, reinforced and prestressed tension tests 4-68793
- concrete walls, reinforced, turbine missile impact effects 4-68789
- conference, American Nuclear Society annual meeting, New Orleans, LA, USA (June 1984) 4-106112
- conference, nuclear technology, Frankfurt, Germany (May 1984) 4-90301
- control materials and light coolants, cross section data 4-73956
- dosimetry, gas prod. and activation cross-section data 4-73958
- endochronic theory, application to dynamic viscoplasticity 4-86878
- ferro-concrete structures for nuclear facilities, computer simulation for impact loadings 4-107006
- fluorides, organic and inorganic chemistry and energy storage 4-72184
- Fort St. Vrain HTRG, plateout probe anal. 4-111661
- fracture mechanics parameters, transferability from CT-specimens to tensile specimens 4-86875
- graphite, laser localised emission spectroscopic anal., discharge gas effects (*German*) 4-64206
- graphite composites in reactors, influence of neutron and  $\alpha$ -particle bombardment 4-96141
- graphite radiation damage in fission and fusion reactor systems 4-96263
- graphite short bars with hemispherical seats failure mechanism 4-78694
- graphite structural material for HTGR (*German*) 4-68755
- Hastelloy XR for HTGR,  $\text{H}_2$  permeation in simulated reactor environment 4-75732
- HDR blowdown expts., DAISY simulation program for fracture size 4-86962
- heat resistant alloy sheets, corrosion props. in He environment (*Japanese*) 4-96136
- heavy coolants, structural and shielding materials, cross section data 4-73957
- HTGR, equilib. comp. in C-H-O system, calc. method 4-91047
- HTGR, primary circuit component carburisation protection 4-68770
- Incoloy 802,  $\text{H}_2$  permeation inhibition by corrosion oxide layers (*German*) 4-66506
- Inconel 617, surface crack form. and propag., effect of temp. reactor primary circuit He 4-114641
- Inconel 750, Co release rates in oxidising and reducing water environments 4-66476
- Inconel X750, in BWR primary system, corrosion products release rates meas. using radiotracer technique 4-91040
- inelastic design anal., constitutive eqns. 4-91737
- instrumentation electronics, radiation testing 4-111625
- KONVOI pipelines, preliminary and quality testing of catalogue components 4-106842
- liner construction for pre-stressed concrete reactor pressure vessels, anchors 4-106840
- LMFBR fuel element materials, swelling resist. (*German*) 4-83148
- LMFBR safety anal., Na-concrete reaction data appl. 4-83231
- LMFBRs, Na aerosols and puddles, fuel, fission products and Na release 4-91084
- LOCA, hydrodynamic loading and structural response in PWR and HDR, STEALTH/WHAMSE anal. 4-68786
- LWR, overcooling, pressure vessel cracking 4-64204
- LWR primary circuits, Co release from component wear, radiation field builds up 4-102383
- LWR stainless steel clad fuel, fuel performance code 4-106772
- LWR structural integrity, EPRI research 4-68784

## fission reactor materials continued

machine components manufacture, use of nondestructive testing in quality control, review 4-106837  
 Magnox alloys, etched, surface anal. by secondary ion mass spectrometry and ion scatt. spectroscopy 4-93456  
 Nine Mile Point Unit 1, recirculation piping replacement 4-111643  
 organic insulator for radiation-resistant and flame retardant electric cable 4-111623  
 organic insulators, radiation thresholds by thermogravimetric anal. 4-111622  
 organic materials, accelerated ageing tests for radiation degradation prediction 4-83233  
 organic materials, radiation effects data compilation 4-111624  
 pebble bed reactors, thermohydraulic behaviour, air and helium coolants (German) 4-106875  
 Pickering nuclear power station, retubing of units 1 and 2 4-78696  
 pipe impact on rigid restraints and concrete slabs 4-68791  
 pipe mechanical welding using pincer welding technique 4-106844  
 pipe welded seams, stress estimation for internal forces and pipeline forces 4-106843  
 pipeline components prod., manufacturing technologies and processes 4-106841  
 piping, stiff and flexible, anal. and test correlation 4-68765  
 piping extreme dynamic response studies 4-68795  
 PISC 1 Programme DDT plates 1 and 2, destructive examination 4-102363  
 polymeric insulation cable materials, radiation induced degradation in nuclear power plants 4-111619  
 polymers, thermal ageing kinetics, thermogravimetric testing 4-71859  
 post-accident primary coolant sampling systems 4-96204  
 pressure vessel nozzle, crack indications in pressurised eddy current testing, spatial resolution of probe coil (German) 4-76942  
 pressurised thermal shock analysis, materials behaviour prediction techniques 4-111628  
 pressurised thermal shock evaluation, singular shift correlation approach 4-111627  
 pressurised thermal shock fracture mechanics anal., mechanical props. role 4-111629  
 primary circuit component fatigue, calc. method and operational meas. (Czech) 4-83237  
 PWR, axial Gd burnable poison optimisation using conjugate gradients 4-106863  
 PWR pipework, unstable crack propagation and stoppage behaviour 4-96225  
 PWR power plant radioactivity, effect of coolant chemistry 4-68800  
 PWR pressurised thermal shock, eval. for B&W designed NSS plants 4-106924  
 PWR primary coolant pipe leak failure using probabilistic mechanics 4-64215  
 PWR stainless steel pipe SCC obs. and countermeasures 4-59335  
 PWR steam generator corrosion denting, nonprotective magnetite formation, acid vs. neutral chloride tests 4-59333  
 PWR steam generator denting, magnetite-producing contaminant threshold tests 4-64205  
 R and D reactor research laboratory, hall type, working activities (Czech) 4-83151  
 radiation aging of insulating resins, electrical effects 4-111621  
 RBMK-1000, surface states of constructional materials 4-102356  
 reactivity modulator for periodically pulsed fast reactor, optimisation study 4-68756  
 rubber insulation, charge deposition under electron irradi. 4-111620  
 safeguards, mathematical and statistical methods, lecture course, Ispra, Italy (Nov.-Dec., 1981) 4-71312  
 seismic fragilities, nuclear power plant risk studies 4-86879  
 SNR-300 mixing devices, stress and fatigue analyses 4-64203  
 space reactor fuel-cladding chemical compatibilities 4-106763  
 SSNTD autoradiography appls. in nuclear industry, weld inspection, Pu distrib. 4-99665  
 stainless steel,  $^{60}\text{Co}$  content control in fission reactors 4-64198  
 stainless steel, deformation and failure from neutron irradiation 4-102357  
 standard neutron cross section data for nuclear reactor materials 4-73954  
 steam-water jet effects, design estimates 4-83131  
 steel,  $\text{Cr-Mo-V-W}$ , HT-9, austenitising and microstruct. 4-93320  
 steel, austenitic, Cr-Ni type, reactor irradi. effect on refractory characts. 4-66398  
 steel, austenitic, neutron irradi., high temp. deform. behaviour (German) 4-81262  
 steel, austenitic, Ti stabilised type DN 1.4970, irradiation, induced  $\gamma'$ -phase form. 4-98144  
 steel, austenitic stainless,  $^{60}\text{Co}$  tracer diffusion 4-75731  
 steel, austenitic stainless, Alloy 800 H, surface crack form. and propag., effect of temp. reactor primary circuit He 4-114641  
 steel, austenitic stainless, BWR pipe cracks, weld overlay repair 4-111638  
 steel, austenitic stainless, BWR piping, induction heating stress improvement method (Japanese) 4-96137  
 steel, austenitic stainless, Co release rates in oxidising and reducing water environments 4-66476  
 steel, austenitic stainless, corrosion rate in liquid Na environment (Japanese) 4-96138  
 steel, austenitic stainless, fast reactor fuel cladding, sigma phase form. rel. to liquid Na exposure 4-106672  
 steel, austenitic stainless, Incoloy 800,  $\text{H}_2$  permeation inhibition by corrosion oxide layers (German) 4-66506  
 steel, austenitic stainless, irradiation, fracture toughness, SEM obs. 4-104836  
 steel, austenitic stainless, microhardness changes under fast neutron irradiation and cold deformation (Russian) 4-76861  
 steel, austenitic stainless, oxide layer structure, formed in simulated LWR conditions 4-76893  
 steel, austenitic stainless, stress rupture in-reactor creep cavity form. model 4-104854  
 steel, austenitic stainless, WWER steam generator tubes, hardening and intergranular corrosion cracking (Czech) 4-85257  
 steel, austenitic stainless in BWR primary system, corrosion products release rate, radiotracer obs. 4-91040  
 steel, carbon, in PWR steam generators, denting causes, nonprotective magnetite prod. 4-104924  
 steel, Cu-Ni-Cr, compact and surface-flawed specimens, fracture toughness meas. comp. 4-104858  
 steel, H and D diffusion under fission reactor radiation 4-113503

## fission reactor materials continued

steel, Ni-Mo, A533B, fatigue crack growth in simulated PWR loop 4-104834  
 steel, Ni-Mo, martensitic A533B pressure vessel, tempered, brittle fracture and fatigue crack growth, segregation effects, Auger obs. 4-66400  
 steel, nuclear structural, A-203D, low temp. deform., effect of microstructure 4-66386  
 steel, pressure vessel, A 508 2 and A 533 B, comparison of stress relief cracking 4-109510  
 steel, pressure vessel, statistical distrib. of mech. props., study of outlier 4-76780  
 steel, pressure vessel, unstable ductile fracture under combined load of thermal shock and tension (Japanese) 4-93380  
 steel, pressure vessels, radiation embrittlement and annealing 4-111626  
 steel, reactor pressure vessel, A533B, environmentally-assisted cyclic crack growth 4-99627  
 steel, stainless, claddings, fatigue crack growth rate in air and vacuum at  $300^\circ\text{C}$  4-66413  
 steel, stainless, electrochemical potential, BWR water chemistry variation effects, cracking 4-85262  
 steel, stainless, extruded type 316 production 4-111640  
 steel, stainless, fuel cladding failures in Connecticut Yankee PWR, stress corrosion cracking 4-99659  
 steel, stainless, Rb contamination in reactor pressure vessels, stress corrosion problems 4-96148  
 steel, stainless, thermophysical and transport props. 4-111613  
 steel, stainless, tube bundles subjected to blockages, heat transfer 4-68758  
 steel, stainless, type 316, pipe production 4-111641  
 steel, stainless 4-109564  
 steel, steam turbine rotor type, creep-fatigue damage, report 4-62047  
 steel, type A533B, fractographic study 4-83154  
 steel, water-water power reactor vessel material, brittle fracture resist. and radiation embrittlement 4-96142  
 steel casing, turbine missile impact effects 4-68788  
 steel pressure vessels, corrosion fatigue crack growth 4-93405  
 steel structures in nuclear power plants, lamellar tearing 4-104870  
 structural integrity anal. with ABAQUS/EPGEN finite element code 4-68787  
 structural materials, neutron irradiation effects 4-103806  
 structure optimisation problems under creep conditions, math. models, plates appl. 4-102354  
 Superphenix FBR plant clad failure detection systems 4-111656  
 Swedish BWRs' water chemistry to prevent stress corrosion cracking 4-91055  
 Swedish joint nuclear fuel, chemistry and materials research and development program 4-91054  
 test plate destructive examination in defect detection trials 4-83153  
 TIBSO-TC program system, prod. and transfer of radionuclides, nuclear reactors 4-106669  
 TMI, radioisotope dist. from contamination of leadscrew 4-59336  
 TMI-2 debris, absence of pyrophoric characteristics 4-106778  
 TMI-2 leadscrew, decontamination barrier 4-111633  
 US-1000 computer controlled US test system, reactor component appl. 4-109621  
 viscoelastic-plastic material behaviour, intermediate configs., strains, reactor appls. 4-102337  
 void fraction distribution in water filled pipes,  $\gamma$ -ray computed tomography meas. 4-96135  
 water distillation columns, computer aided simulation 4-96134  
 Zircaloy, fracture, influence of environment on form. of fluting microstruct. 4-104911  
 Zircaloy, HF impurity monitoring by sequential plasma emission spectrometry 4-73984  
 Zircaloy, textured, creep modelling under biaxial stressing 4-93354  
 Zircaloy-2, electrochemical potential, BWR water chemistry variation effects, cracking 4-85262  
 Zircaloy-4, plane strain compression testing, plastic flow rel. to texture (German) 4-85270  
 Zircaloy cladding, chemical model for cadmium liquid-metal embrittlement 4-106770  
 Zircaloy cladding tubes, ductile fracture anal. 4-106768  
 Zircaloy fuel cans, stress corrosion cracking with multiple fission product intrusion 4-96160  
 Zircaloy fuel cladding, numerical simulation of plastic deformation 4-106767  
 Zircaloy fuel rod cladding, strain rate sensitivity 4-64202  
 Zircaloy membrane, D transport kinetics, surface oxides influence 4-89325  
 Zircaloy-2 cladding, localised stress-strain influence on SCC behaviour 4-106769  
 Zircaloy-2 cladding tube I-induced stress corrosion cracking time anal. 4-109549  
 Zircaloy-2 cladding tubes, stress corrosion cracking 4-106766  
 Zircaloy-4, anodic behaviour in conc.  $\text{H}_2\text{SO}_4$ , form. of two surface films 4-76899  
 Zircaloy-4, creep at 673K, texture evolution 4-114613  
 Zircaloy-4, microstruct. after air cooling from high temp.  $\beta$ -phase, effect of P impurity content 4-89071  
 Zircaloy-4, SAM determ. of O gradients, deform. modelling 4-88191  
 Zircaloy-4, SCC in neutral aq. chloride soln. 4-66478  
 Zircaloy-4 claddings, SCC at elevated temps., relevance to transient LWR fuel rod behaviour 4-104912  
 Al, self-ion damage and comparison of ion damage rates with neutron damage rates 4-113506  
 $^{10}\text{B}$  control rods, burnup characteristics 4-102361  
 Be, neutron wave propag., space and angle depend. study 4-73947  
 C material, dimensional changes, under compressive stress at high temp. 4-85182  
 Cu, D $^+$  irradi., two-level fracture in blistering 4-75560  
 Cu, irradi., stored energy, calorimetric determ. 4-103829  
 Fe spheres, neutron leakage spectra, meas. and calc. 4-68837  
 He atmosphere effects on machine components, bearings, lubricants, sliding surfaces, contacts, HTGR appl. 4-106838  
 Li isotope separation by cryptand ( $2n,2,1$ ) polymer 4-74039  
 MgO bricks lined ex-vessel cavity, PAHR, thermophysical props. 4-111613  
 Mo diffusion through graphite in HTGR 4-111631  
 Mo-alloys, space nuclear reactor primary heat transfer materials 4-106761  
 Na boiling following contact with molten fuel 4-91082

## fission reactor materials continued

- Na reaction with  $\text{UO}_2\text{-PuO}_2$  kinetics, fission product effects 4-106673  
Na surface fires in reactor containment, convection current computation, KONVEC 4-91083  
Na, thermophysical and transport props. 4-111613  
Nb-Zr-C alloys for space nuclear appls. 4-106762  
 $^{93}\text{Nb}(\text{n},\text{p})$ , 14 MeV, proton pre-equilib. emission, ang. distrib., stat. model anal. 4-96019  
Ni, high temperature electron induced embrittlement 4-108448  
 $^{64}\text{Ni}(\text{n},\gamma)$ , capture widths for s-wave resonances,  $\gamma$ -ray spectra 4-96021  
Pd-Al alloys, T mobility and permeability, influence of struct. of segregation on overlayers 4-70472  
SiC coatings of nuclear fuel particles, characterisation (German) 4-78702  
steel, Mn-Mo-Ni, for reactor pressure vessels, neutron irradiation effects on mech. props. 4-108467  
Ta-W-Hf alloys for space nuclear appls. 4-106762  
Ta-W-Re-Hf-C alloys for space nuclear appls. 4-106762  
TiN-TiC multilayer coatings on Nb tubes, nucl. reactor fuel pin accidental behaviour 4-68771  
TiNi-based alloy, radiation-induced amorphisation 4-103830  
 $\text{UO}_2$  fissile kernel/ $\text{ThO}_2$  fertile kernel system, fuel particle and interlayer tests 4-106779  
 $\text{UO}_2$ , thermophysical and transport props. 4-111613  
V, T-charged, obs. of cylindrical cavities at dislocations 4-60913  
W-alloys, space nuclear reactor primary heat transfer materials 4-106761  
W-Re (10 at.%), neutron irradi., homogeneous rad.-induced precip., atomic resoln. study 4-108449  
 $\text{Y}_2\text{O}_3$ , wear resistant layers for use in high temp. reactor heat exchanger 4-106845  
Zr alloys, oxidation kinetics,  $\text{H}_2$ -pickup and  $\text{O}_2$  dissolution 4-99641  
 $\alpha$ -Zr, hydride form., an  $\alpha$ -phase, pendulum technique investig. 4-70398  
Zr membrane, D transport kinetics, surface oxides influence 4-89325  
Zr proton irradiation and thermal creep at elevated temps. under stress 4-75559  
Zr, purification by electrotreatment processing, resist. ratio obs. 4-85126  
Zr-D, ion implantation, lattice defect trapping, binding enthalpy, migration 4-108400  
Zr-base alloys, oxidation rate transitions at reactor operating temps. 4-109568  
Zr-Nb, nuclear reactor pressure tubes, fracture micromechanisms, use of  $J_R$  curves 4-99582  
Zr-Nb (20 wt.%),  $\beta$ -phase decomp. rel. to thermal treatment 4-109411  
Zr-Nb (2.5 wt.%), CANDU pressure tubes, high temp. creep model for loss of coolant accident 4-109473  
Zr-Nb alloys, size changes under high fluence in SM-2 reactor 4-108466  
Zr-Sn (0.1-1.5 wt.%), neutron irradi., effect of tin on growth of polycryst. Zr 4-75537  
 $\text{ZrO}_2$ , wear resistant layers for use in high temp. reactor heat exchanger 4-106845

## fission reactor operation

- see also fission reactor cooling and heat recovery; fission reactor core control and monitoring; fission reactor safety  
330 MWe HTGR experience base at Fort St. Vrain, United States 4-68806  
900 MW PWR operators post-accident support display system 4-111670  
artificial intelligence based operator aid, NRC eval. 4-111566  
AVR facility, progress report, concept and components, operation, radiation protection 4-78710  
BWR in-service pipeline changes, flange seal use for greater utilisation 4-86957  
BWR power plant computerised surveillance test guide system 4-59373  
BWR symptom oriented emergency operating procedures, human factors enhancement 4-111673  
CANDU-PHW nuclear steam generating system, performance and essential characts. 4-68808  
commercial instrumentation, research and development projects at EPRI 4-102374  
conference, American Nuclear Society annual meeting, New Orleans, LA, USA (June 1984) 4-106112  
high-temperature experimental nuclear reactor, with combined cycle operation (German) 4-83219  
historical data storage and retrieval systems for plant operator assistance 4-59372  
HTR nuclear process heat plant, safety concept and operational criteria 4-78719  
HTR-500, layout design and risk assessment, safety anal., PWR comparison 4-96243  
human initiated problems, diagnosis and mitigation, MAU decision making model 4-111570  
in-pile LMFBR accident simulations anal. by Kalman filter methods 4-68936  
LIMCOM, limiting conditions of operation monitor, automated system for power plants 4-111568  
LWR fuel element maintenance, operating procedure with repaired fuel elements 4-96158  
maintenance training development 4-106862  
MAPPS, maintenance personnel performance simulation model for nuclear power plants, PRA anal. 4-111569  
NRC control room design review audits: a contractor's perspective 4-111659  
Obrigheim nuclear power station, emergency plant additions during normal operation 4-86963  
operating personnel training in Czechoslovakia, nuclear safety (Czech) 4-68782  
operator diagnostic ability training using knowledge based CAI 4-106883  
operator personnel, nuclear technology nonresidential degree option 4-106861  
organised documentation for information retrieval at nuclear power stations 4-86958  
plant diagnosis through knowledge about systems descriptions, preliminary study 4-111567  
power plant control room design, function allocation for man or machine 4-111565  
power plant symptoms oriented operating procedures in control room, emergency procedures 4-111665  
prioritizing plant modifications and projects using safety significance measures 4-111677  
PWR steam generator, Tricastin 1 power plant, saturation press., circulation ratio and carry-under 4-111657

## fission reactor operation continued

- PWR Tricastin 1 steam generator, steady state thermal meas. on secondary side 4-111658  
relief valves, acoustic testing of operation 4-59377  
shutdown problems, energy optimal control with maintenance time (Japanese) 4-106660  
systematic human action reliability procedure, probabilistic risk assessment, nuclear plant systems 4-106952  
technical staff training 4-106860  
THTR breakdowns, operational experience, failure nature and response action 4-96242  
THTR-300 reactor, fuel feeding system construction and commissioning experience 4-106847  
US power reactors, operation during September and October 1983 4-64213  
USA nuclear power unit operating experience, 1980 to 1982 4-83226  
Wurgassen BWR power station, steam and feedwater pipelines replacement 4-86955
- fission reactor safety  
see also fission reactor cooling and heat recovery; fission reactor core control and monitoring  
900 MW PWR operators post-accident support display system 4-111670  
ABAQUS code for struct. response and thermal stresses, introductory course 4-111597  
accidents, off-site consequence modelling review, evacuation time significance 4-106888  
accidents, off-site consequence modelling using Monte-Carlo method 4-106887  
AGR, pressure vessels, pressure tests 4-59391  
AGR cores with longer moderator life, expt. 4-107008  
airborne radioactive releases from burning contaminated combustibles 4-106891  
ALARA application to normal radioactive emissions from nuclear facilities 4-96222  
ALARA in CANDUs, LWRs, station doses and dose reduction 4-96221  
anisotropic creep damage in the framework of continuum damage mechanics, reactor appls. 4-102338  
annular air-water flow, liquid mass transport 4-96182  
ANO-2 turbine trip test, computer anal. 4-59382  
aseismic design method for equipment and piping 4-59308  
AST-500 reactor, coolant circulation stability 4-106855  
auxiliary hoist evaluation, generic and experience data comparison 4-111679  
AVR, water ingress accident, whole facility behaviour, numerical simulation (German) 4-96215  
AVR expts., LEU spherical fuel elements, induced transients 4-86939  
blowdown jet forces on containment structures 4-86944  
boundary seismic PRA analysis 4-111689  
burst fuel can rewetting in LOCA conditions 4-86947  
BWR, 1300 MW class, pipe fracture accident, thermal behaviour simulation 4-91087  
BWR, containment pressure suppression under LOCA 4-59389  
BWR, crud deposits on fuel rod surfaces, sampling and examination 4-86956  
BWR, FNR program for core, Xe and I monitoring, safety measures 4-86964  
BWR, instantaneous pipe rupture, void fraction measurement using gamma-ray densitometer 4-86931  
BWR control rod replacement, improved method development 4-83227  
BWR coolant pressure boundary piping, cracking, material selection, processing guidelines 4-111635  
BWR cores adaptive simulation using 3-D coarse-mesh neutron diffusion theory 4-86933  
BWR feedwater manifold operating characts. 4-86945  
BWR LOCA, instantaneous pipe rupture, void fraction meas. with X-ray densitometer 4-74036  
BWR LOCA, jet discharge test results 4-86880  
BWR LOCA, radiolytic gas generation in pressure suppression containment, calc. 4-111664  
BWR loose parts location by impact sound sources, pattern recognition appl. 4-74028  
BWR low-leakage refueling, General Electric experience, core designs 4-106696  
BWR pipe crack repairs, weld overlays, design and development 4-96198  
BWR pipe cracking, heat-sink welding, corrosion resistant cladding 4-111639  
BWR pipe cracking, last pass heat-sink welding, field procedure development 4-111636  
BWR pipe cracking in weld heat affected zones 4-111634  
BWR pipe cracking induction heating stress improvement, qualification scheme 4-111637  
BWR piping, IGSCC countermeasure implementation in USA 4-111644  
BWR pressure suppression system, press. propagation following steam bubble collapse 4-96178  
BWR refill-reflood program, final report 4-83241  
BWR symptom oriented emergency operating procedures, human factors enhancement 4-111673  
BWR water electrochemical pots., in-plant meas., stress corrosion cracking indication 4-96191  
BWRs, austenitic stainless steel piping systems, intergranular stress corrosion cracking, experience 4-96197  
CANDU LOCA, high temp. creep model for Zr-Nb pressure tubes 4-109473  
CANDU reactors, self-powered flux detectors, dynamic response degradation 4-106876  
CANDU-PHW ECCS unavailability following small LOCA 4-64232  
Category I structures, probability based load combinations, research results overview 4-96109  
Clinch River Breeder Reactor licensing, struct. research needs for plant safety 4-96200  
commercial instrumentation, research and development projects at EPRI 4-102374  
component fault testing in electro- and cable-technology, nuclear reactor appl. 4-106839  
component support materials, Unresolved Safety Issue A-12, integrity assessment 4-106780  
computer security, assessment for safe operation 4-106950  
concrete containment structures, load anal. with ABAQUS-EPGEN code 4-68794

**fission reactor safety continued**

concrete containment wall elements, reinforced and prestressed tension tests 4-68793  
 conference, American Nuclear Society annual meeting, New Orleans, LA, USA (June 1984) 4-106112  
 conference, nuclear technology, Frankfurt, Germany (May 1984) 4-90301  
 conference on multiphase processes in LMFBF safety analysis, Ispra, Italy (Mar.-Apr. 1982) 4-78042  
 conference on nuclear track registration, Richland, WA, USA (Jul. 1982) 4-67851  
 conference on structural and mechanical engineering for nuclear power plants, Chicago, IL, USA (Aug. 1983) 4-95044  
 containment building, H<sub>2</sub> combustion and control 4-111666  
 containment heat removal recovery 4-111682  
 containment vessels, limit anal. and design, plasticity, stress, fracture 4-102340  
 containment-like cylindrical geometries under combined shear and bending, buckling 4-96116  
 containments, buckling design research 4-96117  
 containments, integrated leakage rate test duration criteria 4-59393  
 control panel enhancement in power plants, safety 4-83220  
 control rod insertion to arbitrary distance, scram distribution 4-111680  
 control room operator performance research, safety related operator actions and simulators 4-111676  
 control room personnel training and entry level qualifications, eval. methods 4-111675  
 coolant, high temperature EM filtration, radioactive corrosion prod. removal 4-96188  
 core heat-up accidents, inherently forgiving reactors, design considerations 4-91037  
 core melt accidents, reactor safety goal compatibility using uncertain prob. risk anal. 4-111663  
 core melt-concrete foundations interaction, gas outflow 4-96237  
 core seismic design, vibr. anal., using flow path network approximation 4-111668  
 core seismic design, vibr. anal., using flow-path network approximation 4-111667  
 cracked reinforced concrete containments under seismic loads, displacements and stresses 4-96112  
 CRACOME code for reactor accidents, containment, meteorology and evacuation consequences 4-106886  
 Cylindrical Core Test Facility, C1-1 reflood phase loop flow resistance test 4-59396  
 damped discrete-type structures, bounding technique for dynamic plastic deform., reactor appl. 4-102341  
 de minimis concept appl. in risk management 4-107161  
 de minimis dose limits acceptance, implications on nuclear radiation practice 4-107162  
 de minimis level criteria for radiation protection and risk assessment 4-107160  
 decontamination, decommissioning and remedial actions of nuclear facilities 4-107178  
 deep penetration problems, expectation estimator, importance biasing scheme for 1D slab shields 4-96275  
 digital control of power transients in a nuclear reactor, integrated closed-loop system 4-59360  
 dosimetry, gas production, and activation cross-section data 4-73958  
 Duane Arnold integrated plant for plant modifications 4-111595  
 DWR fresh steam safety cut-out valve function props. under operating and fault conditions 4-106878  
 earthquake hazard at nuclear facilities in the Eastern United States 4-111688  
 earthquakes, conservatism in structure design calcs. for reactors 4-91090  
 electrical equipment, qualification aging, German philosophy and practice 4-86961  
 electronics ageing mechanisms, neutron and  $\gamma$ -ray effects, nuclear power plant instrumentation 4-59363  
 emergency decay heat removal systems of nuclear ships under accident conditions 4-96196  
 emergency preparedness drill in Brazil, degraded core scenarios 4-106928  
 energy education in power station emergency planning zone 4-109729  
 extreme wind hazard analysis in nuclear power plant PRA studies 4-111686  
 FBR, CAMEL II intra-pin fuel injection test, transient overpower accident 4-106937  
 FBR, fuel pin failure modeling 4-106936  
 FBR, HCDA anal. of axially heterogeneous core 4-106944  
 FBR, radial power shifts in heterogeneous fast reactor calculations 4-106935  
 FBR fuel rod behaviour under steady-state/transient conditions, FARST computer code 4-111611  
 FBR modular steam generator, dynamic loads from leaking water/steam-sodium reaction (Russian) 4-68783  
 ferro-concrete structures for nuclear facilities, computer simulation for impact loadings 4-107006  
 fire detection rates modeling 4-111684  
 fire risk methodology 4-111685  
 FLASH-4 technique for compressible two-phase flow in BWR pipe network, Edwards problem 4-106893  
 fluid-structure interaction in curved pipes, two-dimensional model 4-111563  
 fluid-structure interactions, fluid dynamics, arbitrary Lagrangian-Eulerian finite element methods, book contrib. 4-59392  
 Fort Calhoun PWR, low-leakage fuel management implementation 4-106694  
 fracture mechanics parameters, transferability from CT-specimens to tensile specimens 4-86875  
 fresh steam valves, dimensioning and function proving for pipe failure, simulation 4-107005  
 fuel element damage due to cooling circulation failure, asymmetric power distrib. effects 4-96227  
 fuel element temp. and rewetting, pellet-can gap effect 4-86946  
 fuel motion, cineradiography appl. to nuclear reactor safety studies 4-111672  
 fuel pin transient deformation, cladding strains, MOX fuel appl., creep 4-102378  
 fuel transient melting in nuclear combustion 4-96129  
 GERDA experimental facility for the investigation of PWR small break LOCAs 4-96228  
 German Safety Commission recommendations 4-96207

**fission reactor safety continued**

GESSAR II seismic event risk analysis 4-111691  
 HDR blowdown expts., DAISY simulation program for fracture size 4-86962  
 heat transfer research, safety aspects, Japanese research 4-83243  
 historical method of seismic hazard analysis 4-83130  
 historical data storage and retrieval systems for plant operator assistance 4-59372  
 HTGR, fission product plateout, linear time-depend. isothermal laminar flow soln. 4-96192  
 HTGR, graphite structural material (German) 4-68755  
 HTGR, spatial fission product behaviour within pebble bed, math. treatment (German) 4-68749  
 HTGR fission product plateout, linear time-depend. multiregion isothermal slug flow soln. 4-96193  
 HTGR under hypothetical accident conditions, reactivity behaviour study 4-68780  
 HTR cooling breakdowns, temp. rises and safety margins 4-96241  
 HTR for process heat, accident response, Th fuel cycle for pebble bed design 4-78718  
 HTR fuel elements, spherical, behaviour under accident conditions 4-83236  
 HTR graphitic component corrosion in operating and accident conditions 4-96163  
 HTR irradiated spherical fuel elements with MOX-BISO particles, failure simulation at 1400-2500°C 4-96245  
 HTR modular fuel element, fission product release under accident conditions, calc. 4-96247  
 HTR nuclear process heat plant, safety concept and operational criteria 4-78719  
 HTR pressure relief incident, long-term air entry effects, simulation expt. 4-91092  
 HTR under accident conditions, fission product retention in core and fuel (German) 4-64231  
 HTR-500, behaviour during failures leading to core heating, safety assessment 4-96244  
 HTR-500, layout design and risk assessment, safety anal., PWR comparison 4-96243  
 HTR-500 core heating incident, reactivity anal. using ASTERIX-2 4-91089  
 human initiated problems, diagnosis and mitigation, MAU decision making model 4-111570  
 hybrid reactor, design and safety study, fast fission blanket safety performance 4-96274  
 hypothetical core-melt through in concrete foundations, core-concrete interactions 4-91088  
 in-pile LMFBF accident simulations anal. by Kalman filter methods 4-86936  
 in-plant post-accident radiation transport, computer model 4-83240  
 inelastic solids and structures, plasticity and creep methods, reactor appls. 4-102339  
 integrated planning for plant modifications 4-111596  
 JAERI reactor engineering department annual report (April 1, 1982 - March 31, 1983) 4-59302  
 KNK-II, defective fuel pin detection, fission gas release 4-96164  
 Koerber power station in S Africa, safe commissioning aspects (Afrikaans) 4-74027  
 KORI-1 PWR, very small LOCA, decay heat removal and operator intervention calcs. 4-102375  
 KUCA, void reactivity coeff. expt. study 4-59313  
 legislation, Nuclear Technical Committee work review (German) 4-111669  
 liner construction for pre-stressed concrete reactor pressure vessels, anchors 4-106840  
 liquid flow continuity determ. apparatus, two-phase flow in reactor appl. (Russian) 4-74020  
 LMFBF, accident post-disassembly phase, event sequence and processes 4-78722  
 LMFBF, acoustic imaging of vapor bubbles through optically non-transparent media 4-59364  
 LMFBF, core disruptive accident, expansion phase, scoping anal. 4-91081  
 LMFBF, correlation for downward melt penetration into a miscible low-density substrate 4-106946  
 LMFBF, failure to scram accident, reactor shutdown unavailability 4-106949  
 LMFBF, fire safety 4-106881  
 LMFBF, fuel and cladding relaxation during LOF accidents 4-106938  
 LMFBF, fuel freezing mechanism in rod bundle in HCDA 4-106939  
 LMFBF, fuel pin failure, temp. oscillations 4-106942  
 LMFBF, HCDA, containment problems 4-106941  
 LMFBF, intersubassembly gap plugging in HCDA 4-106940  
 LMFBF, multicomponent phase transition modeling 4-106943  
 LMFBF, TOP and LOF accidents, post-clad failure phenomena 4-78721  
 LMFBF accident, core bubble/Na pool interface phenomena, SIMMER modification 4-78727  
 LMFBF accident, multiphase flow, heat and momentum transfer, phase change modelling 4-78724  
 LMFBF accident multiphase flow, hydrodynamical eqns., SIMMER-II code 4-78725  
 LMFBF accidents, upper struct. transient thermohydraulics, SIMMER-II anal. 4-78733  
 LMFBF HCDA, core expansion, UK expts. and calcs., review 4-78730  
 LMFBF HCDA, expansion phase phenomena, scale model expts., SIMMER-II and SOLA-VOF verification 4-78732  
 LMFBF HCDA and LOF accidents, core expansion phase models with Na entrainment 4-78728  
 LMFBF hypothetical accidents, fuel propagation through interwrapper gaps 4-91036  
 LMFBF JOYO, natural circulation evaluation 4-96186  
 LMFBF local core anomaly detection using temperature and flow fluctuations 4-91071  
 LMFBF LOF accident, transition phase anal., recirculation, review 4-78731  
 LMFBF LOF accident simulation in Sodium Loop Safety Facility 4-83230  
 LMFBF loss of heat sink accidents, core coolability limits 4-106945  
 LMFBF safety anal., basic multiphase flow eqns. and physics 4-78723  
 LMFBF safety anal., core expansion studies, CARAVELLE expts. and IRIS code 4-78729  
 LMFBF safety anal., Na-concrete reaction data appl. 4-83231

## fission reactor safety continued

LMFBR safety anal., stability anal. and numerical procedures for SIMMER-II code 4-78726  
 LMFBR SIMMER-II calculations of COVA experiments 4-91035  
 LMFBRs, Na aerosols and puddles, fuel, fission products and Na release 4-91084  
 LOCA, electrical insulation degradation for chem. sprays 4-68799  
 LOCA, heat conduction of coolant in flow direction (*Chinese*) 4-83885  
 LOCA, hydrodynamic loading and structural response in PWR and HDR, STEALTH/WHAMSE anal. 4-68786  
 LOCA, REWET-II reflood expt. project 4-106867  
 LOCA, two-phase flow through a small horizontal branch in a pipe with stratified flow 4-91079  
 LOCA anals., water stable, metastable and unstable states; fundamental eqn. 4-59394  
 LWR, containment failure mode influence on fission product source term 4-106932  
 LWR, containment heat transfer coeffs. during LOCA 4-106929  
 LWR, coolant pump seizure and sheared shaft accidents 4-106869  
 LWR, degraded core events, core and containment transient anal. 4-106873  
 LWR, fission product transport anal., class 9 accident 4-106933  
 LWR, KWU-type, radioactive releases from air exhaust and waste water 4-96234  
 LWR, methyl iodide removal efficiency of charcoal bed 4-107171  
 LWR, overcooling, pressure vessel cracking 4-64204  
 LWR, preexisting containment leakage areas for severe accident conditions 4-106930  
 LWR, severe fuel damage scoping test, degraded core cooling accident 4-106776  
 LWR containment, H<sub>2</sub> behaviour during accidents, production, mixing, combustion 4-64221  
 LWR core-melt interaction with concrete foundations, crust form., long-time behaviour 4-96236  
 LWR fuel rod behaviour evaluation under operational transient conditions 4-111612  
 LWR fuel rods, transient fission gas release and microstruct. variations during power ramping 4-96161  
 LWR kinetics benchmark anal. using 2-dimens. space-time kinetics model 4-59383  
 LWR large break LOCA, clad deform. and heat transfer, azimuthal effects modelling 4-102377  
 LWR large-break LOCA, thermal-hydraulic response, COBRA/TRAC results 4-106925  
 LWR LOCA, blowdown thrust force under pipe rupture accident, expt. eval., decompression 4-102379  
 LWR LOCA, blowdown thrust force under pipe rupture accident, partial and ramped opening breaks 4-102380  
 LWR low-leakage fuel management, Babcock and Wilcox experience 4-106693  
 LWR low-leakage fuel management, utility perspective 4-106691  
 LWR low-leakage fuel management, Westinghouse experience, loading pattern designs 4-106695  
 LWR low-pressure steam turbines, corrosive salt solubility in dry steam 4-111692  
 LWR overpower transients, fuel pellet-cladding interaction, safety analysis record review 4-96218  
 LWR pipe rupture accident, two-phase jet impingement, numerical anal. 4-74031  
 LWR pressure vessel surveillance dosimetry, solid state track recorders, appl. 4-68884  
 LWR pressure vessel surveillance dosimetry, use of SSNTD 4-96365  
 LWR pressurised thermal shock problem, 3-dimens. temperature prediction scheme 4-106894  
 LWR primary circuits, Co release from component wear, radiation field buildups 4-102383  
 LWR probabilistic risk assessment adequacy, quality assurance matrix 4-64229  
 LWR safety, contribution of control systems 4-59390  
 LWR severe fuel damage accidents, NRC research program 4-106774  
 LWR structural and mechanical engineering research at US NRC, status 4-96108  
 LWR structural integrity, EPRI research 4-68784  
 MADEC mobile decontamination plant for machine parts and tools 4-86965  
 MAPPS, maintenance personnel performance simulation model for nuclear power plants, PRA anal. 4-111569  
 material safeguards, containment and surveillance techniques 4-68796  
 materials, pressurised thermal shock evaluation, singular shift correlation approach 4-111627  
 measuring systems for fault conditions, operating efficiency improvements 4-107004  
 modular HTRs for electricity and process steam, advantages, safety, costs 4-78717  
 MITSU nuclear ship, shielding anal. method evaluation (*Japanese*) 4-83235  
 neutron sensors, testing by high voltage perturbation technique 4-59362  
 Nine Mile Point unit 1, liquid radwaste storage capacity modifications, decontamination planning 4-106753  
 Nine Mile Point Unit 1, recirculation piping replacement 4-111643  
 nozzle corner crack, three-dimens. J-integral evaluation under thermal transient loading (*Japanese*) 4-91772  
 NRC safety/safeguards relations 4-74025  
 nuclear criticality safety research program at JAERI 4-68797  
 nuclear facility building concepts against aircraft crash, vibrs. effects 4-102381  
 nuclear facility unplanned release, in situ noble gas radionuclide spectrometric meas. 4-106889  
 nuclear fuel, fission product behaviour under normal and accident conditions, improved model 4-74032  
 nuclear power plant equipment seismic qualification, recent methodology research review 4-96202  
 nuclear power plant personnel nuclear safety, progress (*French*) 4-74033  
 nuclear power stations, decontamination, examination and fuel element monitoring procedures (*German*) 4-64217  
 nuclear power stations, monitoring and fault diagnosis system for early fault detection (*German*) 4-59384  
 nuclear power stations, successes, failures and perspectives (*German*) 4-74026  
 Obrigheim nuclear power station, emergency plant additions during normal operation 4-86963

## fission reactor safety continued

off-site dose rates estimation using BWR containment high range monitor after accident 4-106890  
 operating personnel training in Czechoslovakia, nuclear safety (*Czech*) 4-68782  
 operator diagnostic ability training using knowledge based CAI 4-106883  
 organic materials, accelerated ageing tests for radiation degradation prediction 4-83233  
 PAHR in hypothetical LMFBR core disassembly accident, release of molten core debris 4-111613  
 pebble bed HTR spherical fuel elements, core heat-up simulation for accident conditions (*German*) 4-64230  
 PFR steam generator experience, leaks, design basis, remedial actions 4-59357  
 physical protection elements for insider actions 4-78714  
 physical protection methods against unauthorised insider acts 4-78678  
 pipe impact on rigid restraints and concrete slabs 4-68791  
 pipe whip, nonlinear dynamic anal. with ABAQUS-EPGEN code 4-68792  
 piping, stiff and flexible, anal. and test correlation 4-68765  
 piping extreme dynamic response studies 4-68795  
 post-accident primary coolant sampling systems 4-96204  
 potentially damaging failure modes of high- and medium-voltage electrical equipment 4-83234  
 power plant, commercial, appl. of advanced instrumentation and control technology 4-102373  
 power plant alarm systems, procedure for reviewing and improving 4-68798  
 power plant buildings, stresses due to aircraft impact using 3-dimens. shell model 4-96230  
 power plant maintenance training/qualification programmes, safety related problems 4-111674  
 power plant pipework system behaviour during earthquakes, comparison with calcs. 4-96231  
 power plant symptoms oriented operating procedures in control room, emergency procedures 4-111665  
 power plants, turbine casing missiles impact code calcs., nonlinear code comparison 4-96214  
 power station optimal design, load reduction of dynamic strains by plasticising 4-91039  
 PRA, event classification and systems modeling of common cause failures 4-106947  
 PRA, event tree anal. code 4-106948  
 PRA application to NRC Systematic Evaluation Program 4-111678  
 PRA of external events 4-111683  
 pressure vessels, statistical distrib. of mech. props., study of outliers 4-76780  
 pressurised thermal shock analysis, materials behaviour prediction techniques 4-111628  
 pressurised thermal shock fracture mechanics anal., mechanical props. role 4-111629  
 pressurised vessels, operational behaviour, probabilistic assessment 4-91086  
 primary circuit component fatigue, calc. method and operational meas. (*Czech*) 4-83237  
 primary coolant radioactivity monitoring under postaccident conditions 4-107169  
 prioritizing plant modifications and projects using safety significance measures 4-111677  
 probabilistic risk assessment, engineering aspects 4-91078  
 probabilistic risk assessment documentation design 4-106951  
 PWR, cooling of core debris and impact on containment transient pressure during accident 4-64227  
 PWR, departure from nucleate boiling ratio, sensitivity to operating parameter variation 4-64226  
 PWR, fuel management for extended burn-up, safety anals. 4-106680  
 PWR, heavy load drop consequences, critical and radiological anal., safety 4-106915  
 PWR, inadequate core cooling detection using thermocouples 4-106870  
 PWR, KWU-type, pipework design, leak-before-break criterion appl. 4-96123  
 PWR, parametric study of aerosol behavior during AB and TMLB accidents 4-106934  
 PWR, probabilistic risk assessment of containment fan cooler 4-106931  
 PWR, prototype residual heat removal pump, behaviour during sharp pressure decrease 4-91091  
 PWR, pump seal failure calcs. 4-106868  
 PWR, severe fuel damage in degraded core cooling accident 4-106775  
 PWR, severe fuel damage tests, fission product effects 4-106777  
 PWR, steam, two-phase and subcooled discharge flows, coupled valve dynamic model 4-96211  
 PWR, thermal mixing in lower plenum and core, power distrib. effects, safety 4-96213  
 PWR, transient thermal mixing in full-height cold leg and downcomer 4-96205  
 PWR and PHWR steam generator tube performance, experience during 1981 4-111651  
 PWR blocked four rod bundle, single and two-phase heat transfer for ECC 4-96210  
 PWR cold leg and downcomer, fluid and thermal mixing, COMMIX-1A anal. 4-96219  
 PWR containment vessel mechanical behaviour during core-melt accidents and earthquakes ROTMEM code 4-96240  
 PWR coolant, chemical additive role in corrosive impurity transport in steam 4-96189  
 PWR cores, statistical thermal design review, DNB protection, design margins 4-102376  
 PWR hypothetical core-melt accident, H<sub>2</sub> risks and containment 4-96239  
 PWR LOCA, 163-rod bundle flow blockage data from FLECHT-SEASET 4-102382  
 PWR LOCA, core reflooding, multi-dimens. and two phase flow, ARAMIS code 4-96209  
 PWR LOCA, decay heat removal expts. in U-tube steam generator test facility 4-83239  
 PWR LOCA, mass-flow-weighted skew upwind differencing scheme implementation in COMMIX-1A 4-83242  
 PWR LOCA, pump performance under two-phase flow conditions, anal. model 4-96212  
 PWR LOCA, reflood heat transfer, grid spacers effects 4-74029  
 PWR LOCA, reflood phase, saturated film boiling heat transfer, turbulent boundary layer model 4-74030

## fission reactor safety continued

- PWR LOCA decay heat removal in steam generator, condensation in single inverted U-tube 4-96206  
 PWR low-leakage fuel management, Florida Power and Light Company experience 4-106692  
 PWR overpressure protection with Sebim valves by Electricité de France 4-78716  
 PWR pipework, unstable crack propagation and stoppage behaviour 4-96225  
 PWR pressure vessel loads due to cold-line leak, DAISY anal. 4-96226  
 PWR pressurised thermal shock, eval. for B&W designed NSS plants 4-106924  
 PWR pressurised, transient response model expt. 4-102384  
 PWR primary coolant pipe leak failure using probabilistic mechanics 4-64215  
 PWR primary coolant pumps, long-term inspection requirements 4-96187  
 PWR small break LOCA, core inventory history and operator time margin, TMI-2 appl. 4-64224  
 PWR small break LOCA, heat transfer, lower plenum break, parametric study 4-96195  
 PWR small-break LOCA, ECC tests at GERDA expt. facility 4-96229  
 PWR stainless steel pipe SCC obs. and countermeasures 4-59335  
 PWR steam generator chemical cleaning database 4-83225  
 PWR steam generator units, transient modelling 4-64220  
 PWR steam generators, dilute reagent decontamination, oxide film removal 4-102385  
 PWR steam generators, simulation of FRIGG heated rod bundle expt. by ATHOS and FLOW3 4-96190  
 PWR thermal-hydraulic anal., automatic controllers effects in TRAC-PF1/MOD1 4-106895  
 PWR U-tube steam generator transient simulation studies 4-68779  
 PWR waste gas system anal., O<sub>2</sub> concentrations for safe operation 4-78720  
 PWR-LOCA, ECC water downcomer penetration, parameter effects 4-59388  
 qualified life equipment in safety related equipment 4-59385  
 R and D reactor research laboratory, hall type, working activities (Czech) 4-83151  
 radiation effect in coolant and core spaces, S<sub>N</sub> calcs. 4-86884  
 radioactive aerosol formation due to coolant leaks 4-106882  
 random neutron sensor fluctuations, instrumentation channel surveillance for power plant protection 4-59361  
 reactor core heat transfer crisis, quasistationary method calcs. 4-74034  
 reactor core with spherical fuel elements, earthquake behaviour using SAMSON vibr. test bed 4-96246  
 reactor pressure vessel, quality assurance, NDT, human reliability models 4-68781  
 real-time assessment system for reactor accidents 4-111671  
 redundant system with dependent human error, common mode failures anal. 4-64225  
 reflood test, initial clad temp. effects 4-96208  
 reflooding and core uncover, heat transfer, safety aspects 4-83228  
 regulations and safety approval procedures, deterministic and probabilistic approaches 4-96224  
 regulatory standards, summary and comparison of USA and world standards 4-96201  
 reinforced concrete containment design, allowable stresses to limit shearing deformation 4-96111  
 reinforced concrete containments, tangential shear design, research results and appls. 4-96110  
 reinforced concrete double cantilevers testing and finite element verification anal. 4-96113  
 relief valves, acoustic testing of operation 4-59377  
 replacement parts quality control for class 1E equipment 4-59387  
 reports, standards, and safety guides 4-64223  
 RETRAN, reactivity transient anal. 4-111580  
 risk analysis method with fixed barrier models, radioactive leaks 4-91085  
 ROSA III recirculation pump discharge line break, test run 961 4-102370  
 safety parameter display system, effective implementation programme, guidelines 4-83232  
 safety related equipment, aging and seismic performance 4-59386  
 safety-relief valves flow capacity measurement 4-91077  
 safety/relief valve diagram in steam flow transients, PISCES-PIPE code 4-91080  
 seismic capacities for structure and equipment for PRA 4-111690  
 seismic design criteria, double earthquake approach 4-86876  
 seismic fragilities, nuclear power plant risk studies 4-86879  
 seismic risk models, sensitivity studies for power plants 4-96220  
 Seismic Safety Margins Research Programme, status report, NRC reports 4-96199  
 seismic shock effects on nuclear installations, mech. system dynamic behaviour in plastic regime 4-96232  
 seismic soil-structure interaction by the superposition method 4-64228  
 severe accident risk benchmarking and cost-benefit analysis 4-111681  
 severe core damage accident, particle bed height and composition 4-106872  
 severe reactor accident consequences, early evacuation, shelter and relocation effectiveness 4-106885  
 severe reactor accident consequences, NRC modelling using CRAC code 4-106884  
 SNR-300, operation and fault transient simulation 4-86890  
 SNR-300 mixing devices, stress and fatigue analyses 4-64203  
 SNR-300 prototype FBR, risk oriented anal., accident consequences 4-64219  
 SNR-300 PWR, core disruptive accident anal. 4-96203  
 soil-structure interaction of nuclear containments, SIMQUAKE II explosive test 4-68785  
 solid state track recorder neutron dosimetry, appl. to TMI-2 recovery 4-68878  
 spontaneous evacuation during radiological emergency, planning 4-83229  
 SSNTD autoradiography appls. in nuclear industry, weld inspection, Pu distrib. 4-96665  
 steam, high press. high temp., convection-radiation interaction 4-74018  
 steam-water jet effects, design estimates 4-83131  
 steel, austenitic stainless, BWR pipe cracks, weld overlay repair 4-111638  
 steel, stainless, electrochemical potential, BWR water chemistry variation effects, cracking 4-85262  
 steel, stainless, tube bundles subjected to blockages, heat transfer 4-68758

## fission reactor safety continued

- steel containment buckling research-program [for nuclear plant] 4-96114  
 steel containment models, pneumatic pressure tests, recent developments 4-90115  
 steel structures in nuclear power plants, lamellar tearing 4-104870  
 structural integrity anal. with ABAQUS/EPGEN finite element code 4-68787  
 Superphenix FBR plant clad failure detection systems 4-111656  
 Swedish joint nuclear fuel, chemistry and materials research and development program 4-91054  
 Swedish policy and practice for reactor safety, waste management and radiation protection 4-64218  
 systematic human action reliability procedure, probabilistic risk assessment, nuclear plant systems 4-106952  
 Three Mile Island unit 2, tests for waste hazard potential, decontamination, decommissioning 4-106754  
 THTR breakdowns, operational experience, failure nature and response action 4-96242  
 THTR-300 MW, construction status, 500 MW follow-on plant design 4-78662  
 TMI, radioisotope dist. from contamination of leadscrew 4-59336  
 TMI-1, OTSG unplugged tubes, mechanical integrity analysis using linear elastic fracture mechanics 4-86877  
 TMI-2, TRU waste management programme, characterisation, removal and storage 4-106709  
 TMI-2 debris, absence of pyrophoric characteristics 4-106778  
 TMI-2 fuel debris location in cooling system, SSNTD neutron dosimetry appl. 4-96194  
 TMI-2 leadscrew, decontamination barrier 4-111633  
 TMI-2 leadscrew section decontamination, use of pressurised water 4-96216  
 TMI-2 postaccident core configuration, ultrasonic mapping 4-106871  
 TMI-2 reactor building polar crane repair procedures 4-59395  
 TMI-2 recovery operations, waste management, decontamination, defueling, review 4-64222  
 TMI-2 special wastes from accident and cleanup, treatment 4-106787  
 TMI-2 underhead area, loose fuel debris flushing using high-pressure water systems 4-96217  
 tornado wind speed threshold, excess probability 4-111687  
 TRISO fuel pellet, fission product transport through cladding layers 4-107003  
 turbine missile impact effects on reinforced concrete walls 4-68789  
 turbine missile impact effects on steel casing 4-68788  
 turbine missile risk anal., probabilistic TURMIS code 4-68790  
 two-fluid model for nuclear reactors, general conservation eqns. and jump conditions 4-102367  
 two-phase flow, pipe boundary conditions, numerical treatment, safety anal. 4-106892  
 unavailability due to common cause failure, beta factor, multiple dependent failure fraction 4-78715  
 US Rayleigh critical angle method to meas. metal surface properties 4-97235  
 V-1 reactor protection struct. system, probabilistic reliability eval. (Czech) 4-83238  
 VHTR fuel compacts, fission product diffusion in matrix graphite 4-73976  
 VHTR reference fuels, irradiation expts., weight and dimensions changes, failure fraction (Japanese) 4-64201  
 vibration isolation and large piles for nuclear building concepts; aircraft crashes 4-107007  
 void fraction distribution in water filled pipes,  $\gamma$ -ray computed tomography meas. 4-96135  
 water layer stability over hot tin melt, core-melt accident simulation, ECC effects 4-96235  
 Zircaloy 2, electrochemical potential, BWR water chemistry variation effects, cracking 4-85262  
 Zircaloy fuel cans, stress corrosion cracking with multiple fission product intrusion 4-96160  
 H combustion test program in nuclear pressure vessel 4-106927  
 H flame propagation model in 1-D, pressure transients 4-106926  
 H<sub>2</sub> distribution in reactor containment following serious accidents, WAVCO anal. 4-96238  
<sup>131</sup>I release from defective LWR fuel rods at temps. up to 1100°C, LOCA appl. 4-96233  
<sup>131</sup>I thyroid uptake blocking by RI, nuclear accidental appl., review 4-115232  
 N<sub>2</sub>O<sub>4</sub> coolant reactor loop, radioiodine behaviour, decontamination (Russian) 4-74035  
 N<sub>2</sub>O<sub>4</sub> cooled reactor, fuel envelope diagnostics by  $\gamma$ -spectroscopy (Russian) 4-74019  
 Na boiling following contact with molten fuel 4-91082  
 Na surface fires in reactor containment, convection current computation, KONVECS 4-91083  
 Nb tubes internal protective coating, fuel pin accidental behaviour 4-68771  
<sup>235</sup>TH(n,X), total neutron cross section meas. in off-resonance region below 300 eV 4-96013  
 UO<sub>2</sub> containing simulated fission product elements, high temp. vap. press. 4-102351  
 UO<sub>2</sub>-PuO<sub>2</sub>, reaction kinetics with Na, fission products effects, LMFBR appl. 4-106673

## fission reactor theory and design

- see also fission reactors; fission research reactors; neutron transport theory  
 actinide fuel materials, fissile and fertile, nuclear data, resonances and cross sections 4-73955  
 actinides, neutron data eval., coupled channel method, optical parameters, reactor appl. (Russian) 4-73913  
 adaptive predictive control strategy for nuclear reactors (Spanish) 4-96176  
 adjoint equations and operators terminology for neutron transport 4-96096  
 advanced PWR, Pu enrichment effects on reaction rates 4-86928  
 AGR, reactivity and channel power effects of burnable poisons, predictive methods validation 4-91073  
 air,  $\gamma$ -ray Kerma buildup factors, Monte Carlo calcs. and anal. approx. 4-96292  
 albedo boundary condition for neutron transport, extended variational principle 4-96091

## ion reactor theory and design continued

alpha spectroscopy for nuclear data meas. 4-102348  
 anisotropic creep damage in the framework of continuum damage mechanics, reactor appls. 4-102338  
 ANO-2 turbine trip test, computer anal. 4-59382  
 ASEA-ATOM control rods, experience and development 4-91053  
 aseismic design method for equipment and piping 4-59308  
 asymptotically stable solutions of 1-D space-time kinetics in the presence of delayed neutrons 4-64192  
 AVR, water ingress accident, whole facility behaviour, numerical simulation (German) 4-96215  
 AVR facility, progress report, concept and components, operation, radiation protection 4-78710  
 boiling noise in a two-region 1-D reactor with feedback 4-73951  
 burst fuel can rewetting in LOCA conditions 4-86947  
 BWR, adaptive core simulation 4-86888  
 BWR, flow stability in fuel element channels 4-86889  
 BWR, instantaneous pipe rupture, void fraction measurement using gamma-ray densitometer 4-86931  
 BWR cell, collision probabilities for non-uniform neutron sources 4-96174  
 BWR control blade for long cycle operations, conceptual design, lifetime extension 4-106864  
 BWR core design and operational data collection 4-59381  
 BWR core performance calculation program for on-line management 4-106865  
 BWR core-fuel design, status and future perspectives (Japanese) 4-83127  
 BWR cores adaptive simulation using 3-D coarse-mesh neutron diffusion theory 4-86933  
 BWR jet discharge experiment, DRIX-2D code anal. 4-86881  
 BWR LOCA, jet discharge test results 4-86880  
 BWR low-leakage refueling, General Electric experience, core designs 4-106696  
 BWR neutron noise, transport theory anal. using TWOTRAN-II, detector reading interpretation 4-102372  
 BWR symptom oriented emergency operating procedures, human factors enhancement 4-111673  
 Category I structures, probability based load combinations, research results overview 4-96109  
 cell analysis, ENDF/B-V multigroup cross-section library 4-59312  
 circular tube cooled by dissociating  $N_2O_4$ , unsteady heat transfer for turbulent flow (Russian) 4-74022  
 Clinch River Breeder Reactor licensing, struct. research needs for plant safety 4-96200  
 coarse-mesh transport theory response matrix method 4-111573  
 computational techniques 4-111598  
 computer security, assessment for safe operation 4-106950  
 conference, American Nuclear Society annual meeting, New Orleans, LA, USA (June 1984) 4-106112  
 conference, nuclear technology, Frankfurt, Germany (May 1984) 4-90301  
 conference on multiphase processes in LMFBF safety analysis, Ispra, Italy (Mar.-Apr. 1982) 4-78042  
 conference on structural and mechanical engineering for nuclear power plants, Chicago, IL, USA (Aug. 1983) 4-95044  
 containment vessels, limit anal. and design, plasticity, stress, fracture 4-102340  
 containment-like cylindrical geometries under combined shear and bending, buckling 4-96116  
 containments, buckling design research 4-96117  
 control materials and light coolants, cross section data 4-73956  
 control rod fall into thimble under earthquake conditions, simulation 4-97372  
 control room improvement project, design review, operator acceptance 4-111660  
 cooling system efficiency, atomic power plant, WWER reactors (Bulgarian) 4-96177  
 core heat-up accidents, inherently forgiving reactors, design considerations 4-91037  
 core seismic design, vibr. anal., using flow path network approximation 4-111668  
 core seismic design, vibr. anal., using flow-path network approximation 4-111667  
 cost-effective eigen solution method for large systems with Rockwell NASTRAN 4-83128  
 coupled-core reactors, time-optimal control, computational aspects 4-96104  
 cracked reinforced concrete containments under seismic loads, displacements and stresses 4-96112  
 critical heat flux, reduction mechanism is subcooled flow boiling 4-86930  
 critical reactor, neutron count variance and covariance divergence 4-96173  
 criticality Monte Carlo calcs., systematic errors 4-102342  
 cylindrical fuel lattices, improved intermediate resonance approximation in heterogeneous system 4-91033  
 cylindrical geometry, neutron transport calcs., integral transform. and  $F_N$  method 4-96094  
 cylindrical Milne problem in one- and two-group transport theory, extrapolation distance 4-96093  
 damped discrete-type structures, bounding technique for dynamic plastic deform., reactor appl. 4-102341  
 deep penetration problems, expectation estimator, importance biasing scheme for 1D slab shields 4-96275  
 dosimetry, gas prod. and activation cross-section data 4-73958  
 Duane Arnold integrated plan for plant modifications 4-111595  
 dynamic behaviour of reactor structures subjected to impulse loads 4-73959  
 earthquakes, conservatism in structure design calcs. for reactors 4-91090  
 electron energy loss fluctuations in deterministic streaming ray calcs., Monte Carlo simulation 4-106667  
 electron transport, Spencer-Lewis eqn., upwind finite difference approx., discretisation error 4-106668  
 electron transport models, semi-empirical, generation and use 4-111579  
 electron/photon/Cherenkov cascades in generalised geometry, Monte Carlo simulation 4-106666  
 emerging nuclear energy system, conf., Helsinki, Finland (June 1983) 4-58546  
 ENDF/B IV data file, cross section verification for PWR fuel 4-86885  
 endochronic theory, application to dynamic viscoplasticity 4-86878  
 engineering status reports for effective management of engineering work 4-111594

## fission reactor theory and design continued

fast critical assemblies, effects of fission neutron spectra on reactor calcs. (Korean) 4-64195  
 fast critical assembly, Na void worth, leakage and nonleakage components, sensitivity coeffs. 4-96185  
 fast flux test facility nuclear reactor, transient turbulent flow, simulation model 4-97503  
 fast flux test facility nuclear reactor turbulent flow, simulation model 4-97502  
 fast reactor, unevenly heated, gas-cooled fuel element, mech. calc., PRORT program (Russian) 4-74021  
 fast reactor hexagonal assemblies, diffusion coeffs. calc. model, ASDIC program 4-96184  
 FBR, CAMEL II intra-pin fuel injection test, transient overpower accident 4-106937  
 FBR, fuel pin failure modeling 4-106936  
 FBR, HCDA anal. of axially heterogeneous core 4-106944  
 FBR, heat transfer channel adaptive modeling 4-74017  
 FBR fuel rod behaviour under steady-state/transient conditions, FARST computer code 4-111611  
 few group two-dimens. HEXAB-II-30K, outer iteration convergence acceleration (Russian) 4-78660  
 finite element method, computational aspects, conf., Chicago, IL, USA (Aug. 1983) 4-82589  
 fission gas release from solid fuel at high temp., TRAFIC and NEFIG code anal. 4-102344  
 fission product nuclei, level density parameters, resonances, neutron cross sections 4-59150  
 fluid fueled marine nuclear reactor, convection and heat dissipation, numerical anal. 4-86938  
 fluid-structure interaction in curved pipes, two-dimensional model 4-111563  
 fluid-structure interactions, fluid dynamics, arbitrary Lagrangian-Eulerian finite element methods, book contrib. 4-59392  
 Fort Calhoun PWR, extended burn-up fuel design, economic goals 4-106681  
 fracture mechanics parameters, transferability from CT-specimens to tensile specimens 4-86875  
 fresh steam valves, dimensioning and function proving for pipe failure, simulation 4-107005  
 fuel, mixed carbide fuel performance modeling using SPECKLE-III code 4-106664  
 fuel assembly placing and reload, gradient projection method for automation 4-106866  
 fuel element planning for enhanced fuel utilisation efficiency 4-86886  
 fuel element temp. and rewetting, pellet-can gap effect 4-86946  
 fuel performance evaluation, simplified power history 4-106771  
 fuel rod evaluation system using FREY code 4-106663  
 fuel rod performance, FRAPCON-2, TACO-2, COMETHE-3L codes 4-106665  
 group structure variation, propag. of neutron flux and cross section covariances 4-96107  
 HDR blowdown expts., DAISY simulation program for fracture size 4-86962  
 heat exchangers, fretting-wear damage 4-106877  
 heated channels, hydrodynamics and heat transfer, vibr. field effects (Russian) 4-74023  
 heavy coolants, structural and shielding materials, cross section data 4-73957  
 historical method of seismic hazard analysis 4-83130  
 HTGR, equilib. comp. in C-H-O system, calc. method 4-91047  
 HTGR, fission product plateout, linear time-depend. isothermal laminar flow soln. 4-96192  
 HTGR, graphite inner reflector design, dimensional criteria (German) 4-96120  
 HTGR, spatial fission product behaviour within pebble bed, math. treatment (German) 4-68749  
 HTGR fission product plateout, linear time-depend. multiregion isothermal slug flow soln. 4-96193  
 HTGR under hypothetical accident conditions, reactivity behaviour study 4-68780  
 HTR, coolant circuit simulation, heat transfer anal. 4-86952  
 HTR, effective thermal conductivity in packed beds of spheres (German) 4-78712  
 HTR for process heat, accident response, Th fuel cycle for pebble bed design 4-78718  
 HTR fuel particles, HRB, GA, and CEBG fission gas release models 4-91052  
 HTR gas circulation, press. fluctuations 4-86951  
 HTR hot gas ducts, design status and testing 4-78663  
 HTR-500, layout design and risk assessment, safety anal., PWR comparison 4-96243  
 hybrid reactor, design and safety study, fast fission blanket safety performance 4-96274  
 improved generalized Benoist formalism for homogenized neutron transport analysis 4-111575  
 inelastic solids and structures, plasticity and creep methods, reactor appls. 4-102339  
 integrated planning for plant modifications 4-111596  
 irradiation expt. evaluation, burn up coeff. determ. (German) 4-73960  
 JAERI reactor engineering department annual report (April 1, 1982 - March 31, 1983) 4-59302  
 $k_{eff}$  variation as a function of multigroup lifetimes 4-111582  
 KUCA MEU fuel expts. anal. using ANL code system 4-59305  
 laser pellet, Tokamak and hybrid reactors, review 4-59422  
 light water moderated  $UO_2$  and  $PuO_2$  loaded cores, power distrib. calc. 4-64194  
 linear characteristic-nodal transport method for arbitrary triangular meshes in (x,y) geometry 4-106658  
 LMFBF, core disruptive accident, expansion phase, scoping anal. 4-91081  
 LMFBF, correlation for downward melt penetration into a miscible low-density substrate 4-106946  
 LMFBF, failure to scram accident, reactor shutdown unavailability 4-106949  
 LMFBF, fire safety 4-106881  
 LMFBF, fuel freezing mechanism in rod bundle in HCDA 4-106939  
 LMFBF, fuel pin failure, temp. oscillations 4-106942  
 LMFBF, HCDA, containment problems 4-106941  
 LMFBF, intersubassembly gap plugging in HCDA 4-106940  
 LMFBF, multicomponent phase transition modeling 4-106943

**fission reactor theory and design continued**

LMFBR design, cost reduction potential 4-68750  
 LMFBR HCDA, core expansion, UK expts. and calcs., review 4-78730  
 LMFBR HCDA and LOF accidents, core expansion phase models with Na entrainment 4-78728  
 LMFBR hypothetical accidents, fuel propagation through interwrapper gaps 4-91036  
 LMFBR LOF accident, transition phase anal., recriticality, review 4-78731  
 LMFBR loss of heat sink accidents, core coolability limits 4-106945  
 LMFBR safety anal., basic multiphase flow eqns. and physics 4-78723  
 LMFBR safety anal., Na-concrete reaction data appl. 4-83231  
 LMFBR SIMMER-II calculations of COVA experiments 4-91035  
 LMFBR spectrum using SAND 2 and differential and integral spectrometers (Czech) 4-68778  
 LOCA anals., water stable, metastable and unstable states, fundamental eqn. 4-59394  
 Los Alamos Critical Assembly Facility, initiatives in training, safety and design eval. 4-106912  
 low power HTRs, design principles, siting and core inserts 4-86892  
 LWBR, advanced design concept for 1000 MWe unit 4-68804  
 LWR, containment failure mode influence on fission product source term 4-106932  
 LWR, containment heat transfer coeffs. during LOCA 4-106929  
 LWR, fission product transport anal., class 9 accident 4-106933  
 LWR, preexisting containment leakage areas for severe accident conditions 4-106930  
 LWR empirical burnup, linear variation of reactivity 4-111581  
 LWR fuel, increased burnup with Exxon designs, burnup capabilities 4-106683  
 LWR fuel rod behaviour evaluation under operational transient conditions 4-111612  
 LWR kinetics benchmark anal. using 2-dimens. space-time kinetics model 4-59383  
 LWR large break LOCA, clad deform. and heat transfer, azimuthal effects modelling 4-102377  
 LWR LOCA, blowdown thrust force under pipe rupture accident, expt. eval., decompression 4-102379  
 LWR LOCA, blowdown thrust force under pipe rupture accident, partial and ramped opening breaks 4-102380  
 LWR low-leakage fuel management, Westinghouse experience, loading pattern designs 4-106695  
 LWR pipe rupture accident, two-phase jet impingement, numerical anal. 4-74031  
 LWR power plants, standardisation in design process 4-96121  
 LWR structural and mechanical engineering research at US NRC, status 4-96108  
 materials, pressurised thermal shock evaluation, singular shift correlation approach 4-111627  
 medium enriched core for TR-2 based on average burnup 4-59306  
 modular HTRs for electricity and process steam, advantages, safety, costs 4-78717  
 molten salt converter reactors, neutronic and burnup characts. 4-78661  
 MULTICELL 3D code for CANDU reactivity device simulation 4-86883  
 multigroup diffusion modeling of at-power neutron noise 4-59303  
 MUTSU nuclear ship, shielding anal. method evaluation (Japanese) 4-83235  
 MYPACK, package for computer aided design of multivariable control systems 4-86882  
 neutron coupling coefficient evaluation in nodal/modal anal. 4-73948  
 neutron density fluctuations in point reactor systems with dichotomic reactivity noise 4-91034  
 neutron diffusion coeff., self-consistent evaluation method 4-59304  
 neutron entrainment by moving coolant 4-102334  
 neutron flux calcs., boundary perturbation of ratios of linear functionals 4-111578  
 neutron multiplication and compound interest 4-73952  
 neutron shielding, series expansion approach in Monte Carlo method 4-73949  
 neutron transport eqn., finite element method appl., FELICIT program 4-91032  
 neutron transport equation, multigroup finite-element soln. on X-Y geometry 4-73950  
 neutronic and thermal design considerations for heat pipe reactors, SABRE 4-68809  
 Nine Mile Point unit 1, liquid radwaste storage capacity modifications, decontamination planning 4-106753  
 nodal power-buckling method for Generation of consistent one-dimensional cross sections 4-111574  
 nonlinear neutron diffusion with poisoning effects 4-111564  
 NRC control room design review audits: a contractor's perspective 4-111659  
 NRC perspective of quality assurance 4-111584  
 nuclear data for nuclear reactor anals., overview 4-73953  
 nuclear facility building concepts against aircraft crash, vibrs. effects 4-102381  
 nuclear facility design, impact of potential for criticality, safety, doses 4-106923  
 nuclear power plant equipment seismic qualification, recent methodology research review 4-96202  
 nuclear reactor fuel rod performance, adjoint sensitivity anal. 4-111610  
 one-dimensional diffusion eqn., anal. soln. 4-111576  
 ONION cell code for Gd bearing PWR fuel 4-102343  
 optimal feedback control by frequency-domain methods 4-64197  
 Organic Rankine Cycle for district heating reactor 4-91038  
 particle transport, Monte Carlo variance comparison for expected value versus sampled splitting 4-106659  
 pebble bed AVR, core physical descript. for multiple recycling process, 3D simulation method (German) 4-64196  
 pebble bed reactors, HEU/LEU equilb. combined cores, AVR appl. (German) 4-102345  
 perturbation theory within the framework of a higher order nodal method 4-111572  
 PFR steam generator experience, leaks, design basis, remedial actions 4-59357  
 pipe whip, nonlinear dynamic anal. with ABAQUS-EPGEN code 4-68792  
 pipeline design and layout, use of published regulations 4-106670  
 piping, stiff and flexible, anal. and test correlation 4-68765  
 piping system buckling anal. 4-112746

**fission reactor theory and design continued**

plant computer-aided design and draughting benefits 4-59311  
 point reactor model, internal fluctuations and parametric noise theory 4-96103  
 power plant buildings, stresses due to aircraft impact using 3-dimens. shell model 4-96230  
 power plant control room design, function allocation for man or machine 4-111565  
 power station optimal design, load reduction of dynamic strains by plasticising 4-91039  
 PRA, event classification and systems modeling of common cause failures 4-106947  
 PRA, event tree anal. code 4-106948  
 PRA application to NRC Systematic Evaluation Program 4-111678  
 pressure vessels, steel, corrosion fatigue, development of engineering codes 4-93406  
 pressurised thermal shock analysis, materials behaviour prediction techniques 4-111628  
 pressurised thermal shock fracture mechanics anal., mechanical props. role 4-111629  
 pressurised vessels, operational behaviour, probabilistic assessment 4-91086  
 primary circuit component fatigue, calc. method and operational meas. (Czech) 4-83237  
 probabilistic method for evaluating reactivity margin of nuclear reactors 4-96105  
 proton pairing in fission yields, delayed neutron yields versus proton, neutron and mass numbers 4-96084  
 PWR, axial Gd burnable poison optimisation using conjugate gradients 4-106863  
 PWR, fuel management for extended burn-up, safety anals. 4-106680  
 PWR, fuel sharing strategy to reduce costs 4-86887  
 PWR, KWU-type, pipework design, leak-before-break criterion appl. 4-96123  
 PWR, load following capability extension by optimal control 4-86929  
 PWR, parametric study of aerosol behavior during AB and TMLB accidents 4-106934  
 PWR, probabilistic risk assessment of containment fan cooler 4-106931  
 PWR blocked four rod bundle, single and two-phase heat transfer for ECC 4-96210  
 PWR core and fuel element distribution, computer programming system 4-86942  
 PWR cores, statistical thermal design review, DNB protection, design margins 4-102376  
 PWR LOCA, pump performance under two-phase flow conditions, anal. model 4-96212  
 PWR LOCA, reflood phase, saturated film boiling heat transfer, turbulent boundary layer model 4-74030  
 PWR small break LOCA, core inventory history and operator time margin, TMI-2 appl. 4-64224  
 PWR steam generator transient analysis computer code 4-59310  
 PWR steam generator units, transient modelling 4-64220  
 PWR-LOCA, ECC water downcomer penetration, parameter effects 4-59388  
 qualified life equipment in safety related equipment 4-59385  
 quality assurance, cost reduction 4-111589  
 quality assurance, issues and outlook from industry's perspective 4-111585  
 quality assurance, legal implications 4-111588  
 quality assurance, survival of an industry 4-111587  
 quality costs in perspective 4-111591  
 quality improvement, practical approach 4-111590  
 quality improvement without cost increases 4-111593  
 radiation effect in coolant and core spaces,  $S_N$  calcs. 4-86884  
 radiation transfer, statistical corrections 4-106662  
 RAPAS module for nuclear plant layout and pipeline planning 4-86891  
 recursive discrete ordinates method, accuracy 4-111577  
 redundant system with dependent human error, common mode failures anal. 4-64225  
 regulatory standards, summary and comparison of USA and world standards 4-96201  
 reinforced concrete containment design, allowable stresses to limit shearing deformation 4-96111  
 reinforced concrete containments, tangential shear design, research results and appls. 4-96110  
 reinforced concrete double cantilevers testing and finite element verification anal. 4-96113  
 RETRAN, reactivity transient anal. 4-111580  
 rod anal. using NUFRAP code 4-106773  
 rotating fluidised bed reactor, thermal-hydraulic design concepts 4-96106  
 seismic design criteria, double earthquake approach 4-86876  
 seismic fragilities, nuclear power plant risk studies 4-86879  
 Seismic Safety Margins Research Programme, status report, NRC reports 4-96199  
 seismic shock effects on nuclear installations, mech. system dynamic behaviour in plastic regime 4-96232  
 shielding problems, transport calculation methods utilising cross section sensitivity coeffs. 4-96291  
 shutdown problems, energy optimal control with maintenance time (Japanese) 4-106660  
 shutdown reactivity meas. using improved source jerk technique 4-91072  
 Sizewell B PWR steam generator design 4-86874  
 Smorn-III benchmark test on reactor noise analysis methods 4-96119  
 SNR-300, operation and fault transient simulation 4-86890  
 SNR-300 prototype 'FBR, risk oriented anal., accident consequences 4-64219  
 SNR-300 PWR, core disruptive accident anal. 4-96203  
 St. Lucie unit 2, construction, quality assurance program 4-111586  
 stainless steel clad fuel, fuel performance code 4-106772  
 standard neutron cross section data for nuclear reactor materials 4-73954  
 steam, high press. high temp., convection-radiation interaction 4-74018  
 steam-water jet effects, design estimates 4-83131  
 steel containment buckling research-program [for 'nuclear plants'] 4-96114  
 steel containment models, pneumatic pressure tests, recent developments 4-96115  
 stochastic structural dynamics methods, critical review of reactor appls. 4-102336  
 stochastic time series anal., negative real root phenomena 4-111583  
 stream-line method to remove cross numerical diffusion, Navier-Stokes appl. in reactors 4-102368

# nuclear reactor theory and design continued

- structure linear equation system soln. by node oriented sparse matrix operation 4-83129
- structure optimisation problems under creep conditions, math. models, plates appl. 4-102354
- suboptimal stochastic control 4-102346
- SVEA BWR fuel, large scale introduction 4-91051
- Swedish policy and practice for reactor safety, waste management and radiation protection 4-64218
- thermal stability control 4-59421
- THERMIX-2D model, pebble bed reactors, thermohydraulic behaviour, expt. verification (*German*) 4-106875
- THTR, fuel charging expts. and calcs. 4-86940
- THTR-300 MW, construction status, 500 MW follow-on plant design 4-78662
- THTR-300 reactor, fuel feeding system construction and commissioning experience 4-106847
- TIBSO-TC program system, prod. and transfer of radionuclides, nuclear reactors 4-106669
- time dependent monoenergetic neutron flux in infinite medium, reconstruction from moments 4-106657
- TMI-1, OTSG unplugged tubes, mechanical integrity analysis using linear elastic fracture mechanics 4-86877
- total quality control leads to lower quality costs 4-111592
- TRISO fuel pellet, fission product transport through cladding layers, model 4-107003
- two-fluid model for nuclear reactors, general conservation eqns. and jump conditions 4-102367
- UKCNDNC data libraries, evaluated decay data 4-102335
- uncertainties minimisation in reactor theory and nuclear data 4-96102
- V-1 reactor protection struct. system, probabilistic reliability eval. (*Czech*) 4-83238
- variational coarse-mesh methods 4-111571
- vibration isolation and large piles for nuclear building concepts, aircraft crashes 4-107007
- viscoelastic-plastic material behaviour, intermediate configs., strains, reactor appls. 4-102337
- VVER neutron physical characteristics precision improvement using BIPR-5K program (*Russian*) 4-78659
- ZPPR-9 fast critical assembly, asymmetric cells, drift and diffusion coeffs. calc. 4-59307
- (n,  $\gamma$ ) effect on radiative characteristics of fission product mixtures in fuel rods 4-106661
- Fe spheres, neutron leakage spectra, meas. and calc. 4-68837
- <sup>240</sup>Pu, neutron absorption in 1 eV resonance, scatt. data effect on result 4-68767
- <sup>232</sup>Th use in nuclear reactors, design recommendations 4-96125
- <sup>232</sup>Th(n, X), 24 keV, relationship between Doppler and self-shielding effects 4-73975
- UO<sub>2</sub> spheres quenched in Na, fragmentation time calc. 4-111609

## fission reactors

- see also fission reactor decommissioning; fission reactor materials; fission reactor operation; fission reactor theory and design; fission research reactors; hybrid reactors; nuclear engineering; nuclear physics; nuclear power stations
- accelerator breeder applications 4-59435
- accelerator breeders and fission convertor reactors, need and implementation scale 4-59436
- accelerator spallation reactors for breeding fissile fuel and transmuting fission products 4-59434
- advanced light water prebreeder/breeder conceptual reactor systems, comparison of two Th fuel cycles 4-68805
- AGR system, progress 4-91093
- alloy evaluation for reactor heat pipes 4-72157
- Arizona State University research related to thermionic energy conversion 4-59399
- fast breeder reactors, technological readiness and role in world nuclear future 4-62318
- fast critical assemblies, space depend. neutron spectra study at core-blanket boundary 4-68777
- high power spallation neutron source, FRG project 4-59478
- HTGR advanced process heat plant, 2240 MWt nuclear heat source design 4-68803
- HTR, BBC/HRB concept of nuclear process heat for coal gasification 4-81526
- HTR, high temp. process heat appls. 4-81525
- HTR modular reactor for the generation of process heat 4-89381
- HTR nuclear process heat, technical assessment and future perspectives 4-81529
- in-core thermionic space reactors, overview 4-77121
- LMFBR steam cycle selection factors 4-68807
- low specific mass space power supply using nuclear thermophotovoltaics, conceptual design 4-77111
- modular HTR, nuclear process heat appls., commercial utilisation 4-81527
- nuclear reactor space power systems, gas-cooled and liquid-metal-cooled, comparison 4-72149
- nuclear thermionic conversion, ultrallloys 4-77127
- oil shale gasification, optimal yield using HTR for process heat (*German*) 4-105115
- organic Rankine cycle power conversion systems for space applications 4-72150
- pebble bed reactors, thermohydraulic behaviour, natural convection flow expts. (*German*) 4-106875
- PWR secondary water chemistry and damage 4-68802
- PWR steam generators tubes denting reduction by boric acid 4-68801
- self-sustaining systems of reactors 4-59430
- small MEU/HEU reactors for district heating 4-89382
- small reactors in a neutron-abundant world 4-62317
- space nuclear reactor heat pipe design, high power, performance demonstration 4-72156
- space-nuclear-reactor ultrallloys, thermionic-energy-conversion implications 4-59398
- sustainable energy system, nuclear technology, conf., Laxenburg, Austria (May, 1981) 4-58577
- sustainable minireactors, decentralised nuclear energy systems framework 4-62316
- synergistic nuclear energy options, spectrum of choices 4-59429
- US space nuclear reactors 4-59397
- VHTR development in Japan, process heat appl. 4-74038

## fission reactors continued

- water splitting, thermochemical processes using HTR, status and outlook 4-81576
- H<sub>2</sub> production, thermochemical processes, coupling with HTGR 4-66808
- fission research reactors
  - see also fission reactor core control and monitoring; fission reactor theory and design; nuclear reactor instrumentation
  - advanced PWR, Pu enrichment effects on reaction rates 4-86928
  - automated system for carrying out overpower loop tests in VVR-SM reactors 4-106856
  - AVR expts., LEU spherical fuel elements, induced transients 4-86939
  - Berlin Experimental Reactor, BER II, charact., expansion and future planning (*German*) 4-102386
  - criticality accidents review for European Community, Sclay, Mol and Windscale 4-106919
  - Cylindrical Core Test Facility, C1-1 reflood phase loop flow resistance test 4-59396
  - FRN research reactor shut-down and decontamination 4-86979
  - GERDA test rig, two-phase coolant conditions, conductivity measuring probes 4-86948
  - HENDEL M<sub>1</sub> loop performance tests (*Japanese*) 4-96181
  - heterogeneous water moderated systems, criticality accident experience 4-106918
  - ionising radiation appls. and technology, research reactor role 4-74037
  - JAERI reactor engineering department annual report (April 1, 1982 - March 31, 1983) 4-59302
  - Livermore criticality accident, 1963, nuclear criticality safety aspects 4-106921
  - Los Alamos Critical Assembly Facility, initiatives in training, safety and design eval. 4-106912
  - monochromatic thermal neutrons from IRT-2000 horizontal channel (*Russian*) 4-78741
  - MTR fuel elements, production of dense U<sub>3</sub>O<sub>8</sub> by special crystal growth 4-96171
  - neutron absorber spheres for spherical fuel reactor control 4-86941
  - neutron flux unfolding codes for appl. to research reactors and neutron generators in developing countries 4-68748
  - neutron noise measurement by travelling air bubbles in research reactors 4-64212
  - neutron source reactor YAYOI radiation beam, RBE meas. 4-77301
  - R and D reactor research laboratory, hall type, working activities (*Czech*) 4-83151
  - RA-2 critical assembly, prompt critical excursion accident, causes and consequences 4-106916
  - RA-2 criticality accident, yield and quench mech. anal. 4-106917
  - ROSA III recirculation pump discharge line break, test run 961 4-102370
  - SEFOR <sup>252</sup>Cf irradiation facility 4-106859
  - SO-2M subcritical assembly, fast neutron spectra meas. 4-106858
  - Taiwan Research Reactor, irradiated fuel rod testing 4-59326
  - VHTR test facility HENDEL, construction, technical problems (*Japanese*) 4-96180
  - VIPER reactor expts. on fission gas release from mixed oxide fuel pins 4-64216
- fissures see cracks
- flame sprayed coatings
  - steel substrate, abrasive and erosion wear resist. 4-93428
  - Al flame sprayed coating on CO, bonding, emission Mossbauer spectroscopy study 4-92979
- flame spraying
  - powder particle deposition rate rel. to flame vel. profile 4-85110
  - Fe-Ni amorphous alloys, flame spray quenching, coating on metal substrates 4-71797
  - SiO<sub>2</sub>-TiO<sub>2</sub> glass planar optical waveguides, flame hydrolysis deposition on Si 4-64769
  - WC-Co powders, hypersonic flame spraying, particle vel. meas. by laser Doppler velocimetry 4-81353
- flames
  - see also chemically reactive flow; combustion; fires
  - acetylene, turbulent diffusion flames, sooting, parametric effects 4-89295
  - acetylene/O<sub>2</sub> flame, three-photon-excited fluoresc. detect. 4-81440
  - aliphatic flames, aromatic compounds formation mechanism 4-89297
  - bimodal cellular flames bifurcation in vertical channels, flame propag. 4-99796
  - CARS, broadband rot. and vibr., N<sub>2</sub> temp. determ. 4-102983
  - combustible media, two dims. nonstationary flow, visualisation study 4-69836
  - cylindrical stretched flame, ignition-extinction behaviour 4-109650
  - deflection mapping using moiré effect 4-106355
  - diffusion laminar flames, spatially resolved soot-absorpt. meas. using laser vapourisation of particle 4-79211
  - electrical discharges and combustion, colloquium, London, England (April 1984) 4-67870
  - electrical fields application to combustion systems 4-69985
  - enclosed deflagrations, one dims. homogeneous and heterogeneous, numerical modelling 4-89300
  - ethylene-air diffusion flames, N<sub>2</sub> CARS thermometry 4-77008
  - flat-plate with diffusion flame, boundary layer turbulent props. 4-97507
  - fuel-air homogeneous mixture, turbulence effects on combustion 4-97497
  - gas jet, low-calorific value, combustion in cross-flow, flame stability problem 4-75096
  - gas turbine combustion chambers, flame radiation 4-114798
  - gases/solids ignition by electrical discharges 4-69986
  - heat transfer between hot combustion gases and cold wall in narrow channels 4-99789
  - heat transfer in flames 4-83808
  - hydrocarbon flames, ion current calc., temp. depend. 4-89296
  - ions in flames, origin and props. 4-71932
  - laminar, thickness, definition 4-108141
  - laser-enhanced ionisation, theory 4-64638
  - liquid-fuel spray in jet-type burner 4-104991
  - methane-air flame, OH molecule photoacoustic detect. 4-77036
  - methane-air flame CO detect. using two-photon absorpt. 4-62261
  - methane-air premixed turbulent flames time resolved density meas. 4-99787
  - methane-H<sub>2</sub> flames, ion current calc., temp. depend. 4-89296
  - methane-N<sub>2</sub>O-N<sub>2</sub>, O atom flame detection 4-109673
  - methane-O<sub>2</sub> flame, OH meas. using photoacoustic deflection spectroscopy 4-62204

**flames continued**

- methane/O<sub>2</sub>/N<sub>2</sub> flame, N<sub>2</sub> coherent anti-Stokes Raman spectra, accurate convolutions 4-79236  
 nonpremixed turbulent flame, vel. and scalars, laser Doppler velocimetry and Raman scatt. 4-75101  
 open and closed vessels, turbulent combustion, flame propag. 4-89301  
 oxy-fuel, H and OH radicals distrib. determ. 4-99798  
 plane and curved flame stability 4-99795  
 PMMA, limiting combustion regimes in free convection absence 4-71921  
 porous powdered fuel, nonstationary convective combustion regimes 4-81442  
 premixed flames, spatially resolved soot-absorpt. meas. using laser vaporisation of particle 4-79211  
 premixed fuel-oxidiser flames, microwave effects 4-109649  
 premixed jet flame, flow field struct. meas. 4-97628  
 propagating, temp. distrib. meas., fibre optics appl. 4-97115  
 propagation, stirred percolation, contact propag. regime, propag. rel. scaling 4-111036  
 propagation and sooting at rich limit of flammability, plasma jet ignition effect 4-89299  
 propane cylindrical flame temp. meas. using speckle photography 4-68228  
 propane-O<sub>2</sub> premixed flame, OH radical recomb. kinetics of quartz wall 4-109627  
 propane-propylene fuel, C particle effect on radiation spectrum in test furnace 4-96530  
 RDX decomposition, CARS probe study 4-99788  
 resonance fluorescence flame atomic detection, polarisation rejection of scatt. laser light 4-109707  
 soot particles formation, growth and oxidation, sonic sampling technique and flat flames 4-104990  
 soot particles formation, growth and oxidation 4-104989  
 soot particles in flame, laser vaporisation obs. with CW probe laser 4-93528  
 stability inside refractory tube 4-103430  
 swirling flow in closed vessels, flame development 4-75029  
 temperature in intermittent-combustion chamber 4-85312  
 time-dependent elec. currents 4-71929  
 turbulent, stability, coalescence/dispersion model 4-81437  
 turbulent combustion, in premixed flame, theory and expt. 4-103429  
 turbulent gas flame, sound radiation mechanism 4-71919  
 turbulent nonpremixed combustion, stretched laminar flamelet model 4-103431  
 H<sub>2</sub> flame propagation model in 1-D, pressure transients in reactor vessel 4-106926  
 H<sub>2</sub>-O<sub>2</sub>, with excited species mag. quenching of emission intensities 4-78891  
 OH laser-induced fluorescence in a flame, rapidly sequenced pair of two-dimens. images 4-79212  
 OH spatially resolved meas. in flame using cross-beam saturated absorpt. spectroscopy 4-77006  
 TiBr<sub>4</sub> and argon passed through microwave discharge, emission band systems, vibrational analysis 4-87130

**flares, solar see solar flares****flash lamps**

- dye laser UV source, flashlamp driven, integrating system for energy meas. 4-67158  
 high power vortex gas flow stabilized flashlamp for dye laser pumping 4-64718  
 photographic electronic flash sequencer 4-58900  
 Xe linear flashlamp time resolved spectroscopy, solar radiation simulator appls. 4-73518  
 Xe-filled large bore flash lamps, optical and electrical characteristics 4-97941

**flash photolysis see photolysis****flashover**

- HV generator breakdown, flashover model (French) 4-65949  
 low-current arcs on insulating surface, expt. investigation 4-75229  
 particles, suspended, detection by laser-induced electron emission 4-90705  
 surface flashover of conical insulators in vacuum 4-108234  
 SiO<sub>2</sub>, vitreous, flashover model (French) 4-65949

**flaw detection see crack detection****flexoelectricity**

- cholesteric thin large-pitch films, polar electro-optic effect 4-114246  
 MBBA, nematic liq. cryst., flexoelectric coeffs., bend curvature elastic const. meas. 4-65169  
 MBBA nematic layer, splay  $e_{12}$  flexoelec. coeff., electro-optical studies 4-84180  
 nematic liq. cryst. hybrid aligned cell, Fredericksz transition 4-92073  
 nematic liquid crystal, order parameter depend. of flexoelectric coeff. 4-103647  
 nematic liquid crystals, flexoelectric instability anal. 4-65173  
 p-n-octyloxy-p-cyanobiphenyl, nematic liq. cryst., flexoelectric coeffs., bend curvature elastic const. meas. 4-65169

**flexural strength see bending strength****flicker noise see random noise****flight control see aerospace control****flip-chip devices**

see also thin film circuits

No entries

**flip-flops**

- logic system design for RISK spectrometer, using event preselector 4-86998

**floating zone method (crystal growth) see zone melting****floating zone refining see zone refining****flocculation**

see also colloids; sedimentation

- CdS, periodic precipitation in lyophilic colloid, diffusion-controlled autocatalytic growth 4-71993

**floppy discs see magnetic disc and drum storage****flow**

see also boundary layers; chemically reactive flow; compressible flow; Couette flow; electrohydrodynamics; external flows; flow instability; flow measurement; flow through porous media; Knudsen flow; laminar flow; magnetohydrodynamics; multiphase flow; non-Newtonian flow; pipe flow; plasma flow; Poiseuille flow; pulsatile flow; rotational flow; shear flow; stratified flow; supersonic flow; transonic flow

**flow continued**

- associated binary mixtures, viscosity and thermodynamics of viscous flow (German) 4-84439  
 free-piston Stirling engine/linear compressor system parametric testing and evaluation 4-66779  
 image system of a source in no-slip sphere and cylinder 4-64908  
 reciprocating gas-handling machinery, heat transfer during compression and expansion 4-64821  
 relaxation flow for high cell Peclet number flow simulation 4-79539  
 Stirling machines analysis using second-order mathematical mode 4-66758  
**flow birefringence**  
 cellulose nitrate solns., polydispersity parameters, flow birefr. obs. (Russian) 4-84942  
 polymer fluids, channel flow, unsteady, birefringence obs. 4-113018  
 polymer melts, hole pressure, flow birefringence obs. 4-113019  
 polymer melts, rheology and flow birefringence, book 4-69727  
 polymer solutions, conformational dynamics, conc. depend., flow birefringence meas. 4-112311  
 polyoxyphenylbenzoxazol terephthalamide in soln., macromolecular hydrodynamics and conformation (Russian) 4-79919  
 polyoxyphenylbenzoxazoleterephthalamides, para- and meta-isomers in H<sub>2</sub>SO<sub>4</sub>, flow birefringence and conformational characts. (Russian) 4-84944  
 terephthalic acid aromatic polyesters solns., conformational props. 4-103636  
 xanthan polysaccharide, mol. viscoelasticity, light scatt., electric and flow birefringence 4-115005  
 xanthan solutions, rheology, molecular association and aggregation, liq. cryst. domains 4-112798

**flow charts see flowcharting****flow control**

- adjustable fixed-flow restrictor with wide turndown ratio 4-87825  
 fluidic flowmeter for low flow rate electronic calorimeters for air conditioning systems 4-91854  
 heat exchangers, flow reversible, temp.-entropy bond graph modelling 4-112938  
 petroleum flow metering requirement and methods used 4-108145  
 resonant molecules flow through metal capillary, laser control 4-69800  
 steam metering comparison of various methods 4-108146  
 valve stroking using dynamic programming control waterhammer transients 4-97696

**flow diagrams see flowcharting****flow instability**

- 1-D transonic flow, multiple steady states 4-64973  
 ablatively accelerated slab, vortex shedding, compressibility, Rayleigh-Taylor stabilisation 4-65083  
 acoustic vibrations of heat releasing medium in confined space, nonlinear stabilisation 4-69756  
 aquatic animals, actively-moving, boundary layer stability (Russian) 4-72280  
 V1343 Aquilae (SS 433), jet instabilities rel. to nonthermal emission 4-72948  
 asymmetric instabilities in buoyancy-driven flow in a tall vertical annulus 4-83877  
 atmosphere, barotropic nondivergent flow, instability 4-62903  
 axially symmetric incompressible viscous flow, with perturbations, numerical stability anal. 4-83874  
 axisymmetric flow in infinitely long cylinder, 3D instability excited by rot. mag. field (Russian) 4-113034  
 Benard-Marangoni problem, nonlinear stability analysis 4-112863  
 Benard-Von Karman instability, expt. study near threshold 4-74989  
 bimodal cellular flames bifurcation in vertical channels, flame propag. 4-99796  
 binary fluid mixture, anisotropic spinodal decomposition under shear flow 4-69738  
 binary fluid mixtures, Benjamin-Feir instability convection onset 4-64948  
 binary systems, hydrodynamic instability and perturbation system 4-108064  
 bi-periodic flow, transition to chaos 4-95305  
 body of revolution in liq. with jet separation, unsteady weakly perturbed motion 4-112896  
 boiling channel, press-drop and density-wave instability thresholds 4-79598  
 boiling channel, vertical, two-phase flow instabilities, effect of heater surface configs. 4-79597  
 boundary layers, three dimensional, instabilities excitation and development 4-87679  
 Burgers stretched vortices, stability and struct., Navier-Stokes eqn. soln. 4-97582  
 capillary waves in nonuniformly heated liquid, instability under effect of lower radiation 4-64961  
 catastrophe theory, nonelementary, appl. to imperfect bifurcation problems 4-58649  
 columnar vortices instability 4-112908  
 columnar vortices stability 4-112905  
 combustion of low-calorific value gas jet in cross-flow, flame stability problem 4-75096  
 compressible flow, shock waves and wakes, numerical prediction 4-97483  
 compressible laminar boundary layers along curved walls, suction, cooling, instability 4-64912  
 conduits and channels, transient free surface flow, numerical methods, TRAN6 program (Chinese) 4-108108  
 continuous spectrum in differentially rotating perfect fluids, effect of gravit. radiation reaction 4-101149  
 continuous wave motion in rough inclined channel 4-112924  
 convection boiling, forced, flow oscillations, finite difference analysis of density-wave oscillations 4-79595  
 convection in liquids, book 4-82606  
 convective sheath, oscillations and bifurcations in 2-D 4-91794  
 crystal-melt interfaces, coupled convective instabilities 4-88120  
 cylinder, Couette spiral forming disturbances and Poiseuille flow, instabilities (German) 4-83954  
 dielectric fluid vertical layer in horiz. AC elec. field, stability of natural convection 4-79583  
 dielectric liq., plane layer, electrothermal convection, cond. model 4-112877  
 dielectric liq. layers subjected to electric field, oscillatory convective instability, dielectric constant 4-103427  
 drops, slender, tip streaming in nonlinear extensional flow 4-103278

## flow instability continued

duct, circular, abrupt expansion, self-excited flow oscillation 4-103412  
 EHD stability in quasi-spherical geometry, model of atmospheric circulation 4-100719  
 electrically cond. liq. film flow in mag. field (*Russian*) 4-113053  
 electrically conducting fluid layer, EM interaction process, Rayleigh-Taylor instability 4-108122  
 elliptical vortex in straining field, three dims.: linear stability 4-79556  
 extensional flow and extending viscoelastic fluid sheets, stability 4-87670  
 exterior irrotational flow, three dims.: boundary layer free interaction 4-112816  
 falling thin liquid film, flows, wave instability (*Rumanian*) 4-69778  
 ferrofluids, mag. microconvection on diffusion front 4-108129  
 fibres, slender, viscous, stability, effects of boundary conditions 4-97487  
 film boiling, instability 4-112691  
 flame, turbulent, stability, coalescence/dispersion model 4-81437  
 flame stability inside refractory tube 4-103430  
 flat plate, boundary layer flow stability for small disturbances (*German*) 4-83883  
 flat plate boundary layers, wave packet calcs. from Navier-Stokes eqns. (*German*) 4-83884  
 fluid agitation in rotating cavities, approx. soln. method 4-75044  
 fluid flow through rigid porous medium, stability 4-113003  
 fluid interface, Richtmyer-Meshkov instability 4-108091  
 gas, gravitational instability, thermal radiation, uniform rot. and mag. field (*Italian*) 4-69736  
 gas flow into vacuum through a perforated plate 4-60373  
 gas-liquid flow, horizontally and vertically separated, large disturbance wave initiation 4-60494  
 gravity waves, rotational, hydrodynamic stability calcs. 4-75049  
 gravity waves, Zakharov eqns. modifications 4-87744  
 gyroscope, instabilities prod. by rapidly rot. highly viscous liquid 4-112894  
 heat transfer in unsteady stagnation-point flow with variable wall temperature 4-87721  
 heated chimney under conditions of natural convection, dynamic stability (*German*) 4-83902  
 Hele-Shaw cells, two-phase displacements, viscously driven instabilities 4-75074  
 heterogeneous rot. fluid layer with free boundaries, thermal instability 4-75032  
 horizontal line heat source, laminar natural convection flow, stability characteristics 4-75013  
 hydrodynamic flows with steady vorticity, reduction theorem 4-91815  
 hydrodynamic stability 4-97488  
 hydrodynamic stability of shear flows 4-74991  
 hypersonic flow unsteady three dims.: boundary layer interaction 4-112943  
 immiscible fluids with different viscosities, flow, nonuniqueness and configuration stability 4-75064  
 immiscible liquids with different viscosities in pipe, instability anal. 4-74988  
 incompressible flow with const. vorticity in elliptic cylinder, stability 4-87669  
 interfaces with elec. double layers, coupled longitudinal and transversal wave motion 4-64944  
 Kelvin-Helmholtz instability for relativistic particle beams, stability anal. for vortex sheet flows 4-85870  
 Kelvin-Helmholtz interface instability in interstellar environment, appl. to Corona Austrina dark cloud complex 4-82535  
 laminar, axisymmetric thermal plume linear stability eqns. 4-79549  
 laminar incompressible fluid flow over rotating disk with applied mag. field 4-75033  
 lifting surfaces in unsteady flow, aerodynamic press., integral eqns. 4-64922  
 linear Görtler instability of boundary layer flow over concave wall, heating effect 4-64920  
 liquid surface, evaporating, linearised stability anal. 4-103293  
 liquid-metal jet, hollow, stabilisation of Rayleigh instability by mag. field 4-108132  
 liquids, unsteady flow under heat exchange conditions (*Russian*) 4-64919  
 lunate-tail swimming propulsion, curved lifting line in unsteady flow, asymptotic theory 4-87750  
 magnetic liquid drop, singly connected axisymmetrical forms, numerical simulation 4-108131  
 magnetic liquid drop, trapped, MHD instability in free surface, numerical simulation 4-108127  
 marginal stability curve and linear growth rate for rotating Couette-Taylor flow and Rayleigh-Bénard convection 4-64921  
 Maxwell-Cattaneo fluid, Benard-Marangoni instability 4-112864  
 MHD, conference, Riga, Latvian SSR 4-106123  
 MHD instability and two-dimensional turbulence in the general hydrodynamic problem (*Russian*) 4-113032  
 mixtures, binary, phase separating, turbulence anal. 4-64923  
 multitubular polymerisation reactors, uniform flow distrib. stability 4-99786  
 natural convection in inclined water layer, thermal instability and heat transfer, interferometric study 4-112855  
 natural gaseous inhomogeneities evolution 4-79619  
 nematic liq. cryst. flow stability down an inclined plane 4-112819  
 nighttime drainage winds, observational study of instability and turbulence 4-105620  
 non-local dissipative fluid obeying non-local constitutive equations, small amplitude waves 4-112914  
 nonaxisymmetric flow between parallel rot. disks, visualisation 4-60436  
 nonequilibrium fluid undergoing planar Poiseuille-Couette flow, light scatt. 4-112520  
 nonlinear boundary-layer stability nonparallelism, three dimensionality and mode interaction effects 4-97515  
 nonlinear convection in high vertical channels 4-87716  
 nonlinear instabilities of slowly divergent shear flow, spectral theory 4-103294  
 nonlinear stability of 3D stratified flow, Richardson number 4-87671  
 nonlinear stability of a diffusion equation 4-110884  
 nonlinear symmetric baroclinic waves 4-79604  
 nonNewtonian fluid, relax. props. and stability 4-97469  
 nonNewtonian fluids, extensional flow, hydrodynamic instability 4-60465  
 nonNewtonian liquids, surface-instability phenomenon 4-97486  
 nonselfsimilar unsteady boundary-layer eqn. soln. 4-60368  
 nonsimilar stratified flow over vertical flat plate unsteady incompressible laminar free convection boundary layer 4-97639

## flow instability continued

nonuniform compressible fluid, shear flow, wave theory 4-60449  
 ocean, thermal internal forcing rel. to linear baroclinic instability of non-zonal flow 4-62840  
 oscillating bluff bodies, separated flow, vortex shedding 4-91816  
 partially filled unsteady pipe flow, frictional losses, Colebrook-White formula 4-97684  
 particle-fluid mixture with temp. gradient, oscills., thermal convection instability 4-87697  
 pebble bed reactors, thermohydraulic behaviour, natural and forced convection flow (*German*) 4-106875  
 periodically fluctuating flow generated with rot. cylinder row, wake profile meas. 4-97568  
 periodically fluctuating flow in cascade, unsteady boundary layer 4-97510  
 planar metal jet, Rayleigh instability stabilisation by mag. field and by heat flow (*Russian*) 4-112820  
 plane and curved flame stability 4-99795  
 plane self-similar flow in expanding regions, stability 4-112817  
 plane-parallel flow stability in longitudinal elec. field 4-60557  
 Poiseuille flow, laminar to shear turbulent transition, stability study 4-60546  
 Poiseuille flow stability of a conducting liquid in a longitudinal magnetic field (*Russian*) 4-113042  
 polyethylene, high and low density blends, melt mixed, capillary flow instability 4-83871  
 polymer liquid crystals, macroscopic phenomena, Frederiks transition 4-75284  
 primary laminar flow stability (*Russian*) 4-112977  
 quasi-harmonic capillary-gravity waves, modulational instability, mag. field effect 4-91845  
 radiogalaxy jets luminosity, contrib. of turbulent cascades and instability effects 4-105870  
 Rayleigh-Bénard convection, externally modulated, Lorenz eqns. 4-91809  
 Rayleigh-Bénard convection, symmetries and pattern selection 4-87672  
 Rayleigh-Bénard convection in vertical rotation and mag. field, stability 4-79591  
 Rayleigh-Taylor instability in astrophysical fluids 4-77704  
 Rayleigh-Taylor instability of thin layer, 3D nonlinear evolution 4-97485  
 recirculating flow, three dims., shear driven, visualisation study 4-87829  
 Rivlin-Ericksen fluid, unstable plane motion of Poiseuille type 4-60371  
 roll waves down an open inclined channel 4-97685  
 rotation symmetric vortex in laminar flow, stability and break-up location (*German*) 4-83915  
 rotational flow instability in azimuthal mag. field w.r.t. azimuthal perturbations, semicircle theorem 4-79674  
 salt-finger convection in shear flow 4-64947  
 second order fluid, flow stability down inclined plane 4-91795  
 second order fluid, unsteady laminar flow due to flat plate movement 4-97484  
 self-similar flow behind cylindrical shock wave, thermal radiation, MHD 4-75060  
 self-similar flow stability, Primakoff soln. 4-87668  
 shear driven 3D recirculating flow, visualisation studies, Taylor-type instabilities vortices 4-103346  
 shearing fluids, instability mechanism at interface 4-103291  
 shock localisation, unsteady problems, optimisation procedures 4-112948  
 skin friction meas. using hot element gauges (*French*) 4-65045  
 smectic A liquid cryst., electrohydrodynamic instability and turbulent motion 4-70030  
 stellar accretion discs, mag. field instabilities 4-63132  
 stratified fluid, internal gravity waves, modal struct. bifurcations, stability parameter variation 4-75048  
 stratified plane Couette flow, stability 4-97638  
 stratified shear flow, Howard-Kocher-Jain theorem, parallel flow stability 4-60477  
 stratified shear flow, radiation instability 4-60372  
 streamwise corner, laminar boundary layer stability 4-60374  
 superposed fluids with lower fluid having finite depth, Taylor instability, nonlinear theory 4-103290  
 supersonic unsteady lifting surfaces, aerodynamic force, doublet point method 4-64975  
 swirling flow above infinite rot. disc, similarity soln. stability 4-103340  
 swirling flow in azimuthal mag. field rel. to axisymmetric disturbances, semi-ellipse theorem 4-91846  
 swirling Poiseuille flow, inviscid centre-modes and wall-modes, stability theory 4-60542  
 Taylor columns over topography, temporal evolution 4-62843  
 Taylor vortices in small-gap limit, evolution eqns. 4-75043  
 thermal convection, influence of vertical vorticity 4-60396  
 thermal stability of natural convection of vertical layer with uniform volumetric heat source 4-75019  
 thermocapillary convection in a two-layer system 4-69758  
 thermohaline columns, layered, wave motion at boundaries 4-87742  
 thin liquid films, flow, stabilisation length 4-69737  
 thin liquid jets in air, dynamics, instability condition 4-60473  
 time-dependent natural convection in Hele-Shaw cells, boundary layer instability (*German*) 4-83901  
 transient fluid instabilities, acoustic noise, natural monopoles 4-108067  
 transient two-component flow, modelling using four-point implicit method 4-97691  
 transitory gaseous film study (*French*) 4-62206  
 transonic separated flows, viscous-inviscid interaction, semi-implicit and numerical methods (*French*) 4-64974  
 transverse axisymmetric flow rotating in axial mag. field, stability 4-108121  
 turbulent, burner, thermal-acoustic efficiency spectrum 4-97518  
 turbulent shear flows, aeroacoustics 4-91805  
 two component solid mixture-fluid suspensions, sedimentation, instabilities 4-79555  
 two dims., viscous flow over cylinders in unsteady motion 4-97482  
 two-dimensional unsteady compressible flows, computational technique 4-112931  
 two-layer spin-up and frontogenesis 4-87729  
 two-phase flow, instabilities in horizontal boiling channel 4-97661  
 two-phase flow, instabilities in vertical boiling channel, nonlinear description 4-97660  
 unsteady flow from source in rot. fluid 4-108080  
 unsteady flow through channel with permeable walls, solute dispersion, vel. distrib. 4-113020

**flow instability continued**

- unsteady free convection near a forward stagnation point at small Prandtl number 4-75012
- unsteady laminar and turbulent boundary layers characts. 4-60365
- unsteady Newton-Busemann theory for flow past three dimens. bodies 4-97481
- unsteady separated flow around square prism, numerical anal. by vortex shedding model 4-60435
- unsteady turbulent boundary layers, near wall region behavior, press. grad. 4-87691
- vaporiser systems, two-phase flow, periodic instability (*French*) 4-60504
- viscous correction method for unsteady transonic flow about airfoils 4-112940
- viscous incompressible fluid, 2D linear flows, stability, vorticity growth 4-74990
- viscous liquid between rotating coaxial cylinders, pointwise nonlinear stability 4-79603
- vortex, linear with deformed core, stability study 4-91813
- vortex motions, stability in presence of mag. fields 4-65030
- wake, incompressible 2D, stability 4-112884
- wall confinement effects for spheres in the Reynolds number range of 30-2000 4-103348
- weakly conducting fluid, turbulent flow in pipe, boundary current fluctuations 4-108110
- <sup>4</sup>He, liq., convection in rot. cell, stability and heat transfer study 4-113736
- Hg, chaotic phases, mag. order and Rayleigh-Benard convection 4-69761
- Hg flow in circular pipe, instability development, longitudinal mag. field effect (*Russian*) 4-113038

**flow measurement**

- see also *anemometers; flow visualisation; flowmeters; laser velocimeters*
- acoustic Doppler current profiling systems, sea-truth expts. 4-110166
- acoustic flowmeter, long-wave, fluid flow meas. in pipe for single-phase 4-83965
- aerosols, liquid, instrument for meas. mass median diameter and total quantity in gas stream 4-60571
- air, jet impinging on inclined adjacent wall, flow characts. 4-87770
- air-deployed oceanographic mooring (AB1034) for current and thermohaline struct. 4-115632
- air-water two-phase downward annular flow config. (*Japanese*) 4-97654
- airflow perturbation device for measuring airways resistance of humans and animals 4-115297
- anemometers for wind speed measurement (*French*) 4-75102
- annular two-phase flow, entrained liq., laser tomographic meas. 4-60527
- arterial system, clinical parameters indirect determ. method using velocimetric data (*French*) 4-67154
- asymmetric flowfield development on slender body, laminar boundary layer separation 4-64951
- axially rotating pipe, three dimens. turbulent boundary layer development 4-87690
- axisymmetrical discontinuous flow, interference method study 4-60461
- Benard-Von Karman instability, exptl. study near threshold 4-74989
- blood flow and vel. meas. in vivo by EM induction 4-77357
- blood flow determination, validation of a CT method 4-81775
- blood flow meas. using digital angiography and parametric imaging 4-67098
- blood flow measurement using multichannel pulsed Doppler US, repeatability 4-72319
- blood flow monitor, diode laser source and detection in probe 4-115154
- book, measurement of turbulent fluctuations 4-63422
- book 4-78050
- brain blood flow meas. by intravenous H<sub>2</sub><sup>15</sup>O, emission CT, theory and error anal. 4-72373
- brain blood flow meas. by intravenous H<sub>2</sub><sup>15</sup>O, emission CT, implementation and validation 4-72374
- buildings, flow metering systems, on-site calibration 4-97726
- cavitation, physical modelling using optical meas. techniques 4-60469
- cavitation inception meas. using electrostatic technique 4-103377
- cerebral blood flow, regional, accuracy of stable Xe/CT meas. 4-67073
- channel-type solar energy air heaters with corrugated plates, design parameters 4-114941
- chemical reactors, meas. of dwell time (*Spanish*) 4-75099
- chemically reactive flow, holographic interferometry method study 4-69833
- cochlear blood flow meas. technique combining microspheres with surface prep. dissection 4-93981
- continuous flow anal. system, microcomputer-controlled, matching colorimeter output to A/D convertor 4-97717
- corrosion testing, rotating cylinder electrode for velocity sensitivity testing 4-89197
- curved duct flow, secondary motion, turbulent and laminar flow, vel. meas. 4-87805
- delay time correlation method, volume and mass flows (*German*) 4-69839
- direct-flow rotameters, calibration and checking by flowmeter test system 4-91853
- directional pressure probe for complex flow fields, design, calibration and testing 4-69843
- Doppler flow meas. and processing, signal-to-noise ratio enhancement 4-100286
- echo-Doppler angle determination for noninvasive transmittal blood velocity calculations in normal and porcine bioprosthetic mitral valves 4-100192
- electromagnetic flowmeter with insulated electrodes of large surface area 4-87820
- ethylene measurement in ethylene-N<sub>2</sub> flow stream using photothermal deflection spectroscopy 4-81487
- fast gas injection system for plasma physics experiments 4-103477
- feet of diabetic patients, blood flow, meas. with MWPC positron camera and C<sup>13</sup>O<sub>2</sub> 4-100316
- fibre optic laser Doppler anemometry device for gas/liquid flow and solid surface velocity meas. 4-108152
- flat plate, turbulent boundary layer response to external flow pulsation 4-87695
- flat-plate collectors with phase-changing fluids, testing 4-114940
- flat-plate with diffusion flame, boundary layer turbulent props. 4-97507
- flow and temperature profile independence of flow measurements using long acoustic waves 4-103445
- flow with const. vel. shift. in longitudinal mag. field (*Russian*) 4-113036
- fluid mechanics, physical laws, appl. to meas. techniques book contrib. 4-79685

**flow measurement continued**

- fluid mechanics research, data acquisition system, minicomputer-based 4-69845
- fluid velocity measurement, two-dimens., case of digital-speckle correl techniques 4-87815
- fluid velocity measurement in convection flows, thermistor anemometer appl. 4-97729
- fluidic flowmeter for low flow rate electronic calorimeters for air conditioning systems 4-91854
- fluidised bed, laser Doppler meas. of flow in freeboard 4-75077
- foetal blood flow meas. by Doppler US, methodology and basic problems 4-89662
- framing high-speed shearing interferography with pulsed He-Ne lasers, flow, shock, combustion and explosion problem appls. 4-68275
- fuel-air homogeneous mixture, turbulence effects on combustion 4-97497
- gas, pulsation damping criteria, freq. limits 4-103447
- gas flow metering, flowmeters, meas. and control systems using microelectronics (*Dutch*) 4-91855
- gas mass flow measurement by bubble method, measurement errors anal. 4-103441
- gas-liquid system, two-phase flow meas. techniques; review (book contrib.) 4-79692
- gasdynamic focusing for sample concentration in ultrasensitive analysis 4-93567
- heated cylinder in crossflow in cylinder array, heat transfer, turbulence meas. 4-112869
- helical boiler tube, full scale modelling 4-60574
- Hemorrhometre, automated apparatus for filtration initial flow rate meas. 4-115284
- hydraulic flow calculations, consideration of bottom region turbulence 4-83964
- hydrodynamic mass with nonstationary fluid, finite element method 4-103437
- industrial measurements of small flow rate by capacitance method (*Polish*) 4-113083
- laminar flow velocity determ. using photon correlator, systematic errors (*Russian*) 4-108142
- laser beam appl. to flow meas., CCD chirp-Z FFT Doppler signal processor, laser velocimetry, oceanographic appl. 4-87819
- laser diagnostics, techniques and appls. 4-65039
- laser Doppler anemometry, burst mode, flow related data processing (*German*) 4-103375
- laser dual focus velocimetry in high turbulent intensity and particle density fluid 4-108147
- laser speckle photography and particle image velocimetry, photographic film noise 4-113076
- Laval nozzle for absolute humidity of air determ. 4-65046
- lecture notes and study guide on basic instrumentation, book 4-106137
- liquid atomising jets, spray angle meas. 4-97657
- liquid flow continuity determ. apparatus, two-phase flow in reactor appl. (*Russian*) 4-74020
- liquid hold-up fluctuations meas. using technique based on microwave radiation absorpt. 4-60572
- liquid velocity measuring system with two delay line oscillators 4-69844
- magnetic flowmeters for liquid flow meas., design and appls. 4-103449
- mean flow field and heat transfer along cooled supersonic diffuser 4-113077
- metastable liquids, transient thermodynamic props. meas. by Brillouin scatt. 4-97712
- methane-air premixed turbulent flames time resolved density meas. 4-99787
- micropipeller for measurement of water speed fluctuations 4-67446
- miniature fluid parameter sensor (*Chinese*) 4-69838
- mixed-layer entrainment, annulus study 4-79565
- motored model engine, flow meas. and calcs. 4-87827
- myocardial perfusion, <sup>82</sup>Rb positron emission CT, extraction fraction and flow meas. 4-72378
- natural convection in inclined water layer, thermal instability and heat transfer, interferometric study 4-112855
- NMR flow imaging method 4-100298
- nonNewtonian fluid, free convection motion studied by interferograms 4-103326
- nonNewtonian fluids, fluid mechanics meas., review (book contrib.) 4-79691
- nonpremixed turbulent flame, vel. and scalars, laser Doppler velocimetry and Raman scatt. 4-75101
- ocean, current meter, bottom mounted Doppler acoustic equipment 4-115620
- ocean current profiling with 1.15 kHz shipboard Doppler acoustic backscatter system 4-110314
- on-axis velocity measurement by laser Doppler anemometry 4-87818
- optical systems, review (book contrib.) 4-79690
- optical temperature gradient measurements using speckle photography 4-87554
- particles in two-phase flows velocity and size meas. using laser interferometer technique 4-79679
- Permalloy thin film sensor, design, construction and appl. 4-111123
- petroleum flow metering requirement and methods used 4-108145
- physical modelling of multi-phase flow, conference, Coventry, England (April 1983) 4-58559
- polyethylene oxide, rheological meas., flow curves, shear thinning region 4-97455
- premixed jet flame, flow field struct. meas. 4-97628
- pressure measurement, differential, instrumentation, book contrib. 4-78289
- pulsed laser measurement of fluid flow, scatt. particle characts., speckle velocimetry vs. particle image velocimetry 4-83963
- pulsed-probe anemometer for meas. of vel. and flow direction in slowly moving air 4-100337
- PWR supply pipe flow meas. using US flowmeter (*Japanese*) 4-111655
- reattaching separated flow, 2D, spanwise struct. studied using multisensor hot-wire anemometry 4-87734
- recirculating region in flow past surface-mounted obstacle 4-97516
- recirculating two dimens. turbulent flow meas., transient case 4-97503
- recirculating two dimens. turbulent flow meas. 4-97502
- regional blood flow, first-pass positron emission tomography with external detectors, modelling 4-72388
- rough surface boundary layer behaviour in turbulent wake presence 4-87724
- separation nozzles, flow and diffusion processes, appls. 4-75068

- w measurement continued  
 shear flow, laser velocimeter sampling bias and its correction, expt. verification 4-103444  
 shear stress turbulent fluctuations at wall, hot-wire anemometry study 4-112834  
 sidewall effects on airfoil tests 4-65040  
 slurry flow in shell and tube heat exchangers, flow rate meas. 4-79666  
 soft tissue tumour of rabbit, regional blood flow meas. with positron imaging 4-72289  
 solid component consistometry in volume flow-rate measurement 4-91833  
 speckle photography in fluid flows, signal recovery with two-step processing 4-69834  
 spherical magnetic-discharge cell 4-86433  
 splenic blood flow and platelet transit time, meas. methods using  $^{111}\text{In}$ -labelled platelets 4-81773  
 starch rich materials, glutinisation behaviour studied using rot. viscometer 4-97721  
 steam metering comparison of various methods 4-108146  
 steam turbine-generator, acceptance test demonstration and verification 4-87826  
 stream structure study by MHD method 4-108133  
 swirling annular-mist two-phase flow, liq. film characts. 4-97571  
 swirling annular-mist two-phase flow, liq. film flowrate along tube 4-97570  
 swirling annular-mist two-phase flow, torque and swirler efficiency 4-97569  
 Tee junction, one- and two-phase flow, vel. meas. using press and flow visualisation photographs 4-60570  
 temperature fluctuation meas. correction, using cold wires 4-60567  
 theory, applications and choice of parameters (book contrib.) 4-79684  
 thermostat capillary rheometer, design and use 4-87816  
 thick film hybrid probes, used for liquid or gas flow velocity measurement (German) 4-65041  
 thick-film hybrid sensors, design, characts. and meas. appl. (German) 4-82789  
 thin fluid layer undergoing end-compression, buckling 4-103452  
 three-dimensional flow field anal. using image processing techniques 4-97719  
 throttling in capillary tubes, laboratory equipment (Bulgarian) 4-97682  
 tomoflow system for intracardiac blood flow information display, Doppler US appl. 4-85469  
 transient conditions, differential pressure transducer appl. 4-97731  
 triple free jet, mixing process, coherent struct., laser meas. 4-87771  
 turbofan mixer nozzle three dims. flowfield study 4-87773  
 turbulent boundary layers, streamwise vel. fluctuations hot wire meas. 4-79570  
 turbulent flow over large-amplitude wavy surfaces, vel. meas. 4-60380  
 turbulent shear flow, conf., St. Louis, Missouri, USA, June 1982 4-86119  
 two-phase flow, voids fraction meas. by acoustic sounding method, error estimation 4-65006  
 two-phase flow, with Herschel venturis 4-97730  
 two-phase flow pressure and void fraction fluctuations meas. using rapid response time instruments 4-60529  
 ultrasonic, industrial flowmeter design problems 4-108144  
 unseparated shock wave/turbulent boundary-layer interaction, hot wire meas. 4-97506  
 unsteady fluid flow measurement by partial flowmeter (Bulgarian) 4-97714  
 unsteady reacting muzzle exhaust flow, flow field and vel. meas. 4-60563  
 vehicle wake characts., hot film probe and pitot tube meas. 4-87723  
 velocity distrib. meas. by laser beam, appls., aerosol introduction into fluid 4-97718  
 venous occlusive RN plethysmography: comparison with electrical admittance plethysmography 4-62581  
 ventilatory impedance meas., flow transducer transfer function modelling 4-81792  
 volume, (book contrib.) 4-79688  
 volume transformer for flowmeters with frequency-analogue output signal (German) 4-69840  
 vortex flowmeter behaviour in liquid-liquid two-phase flow 4-60573  
 wall shear stress meas., review (book contrib.) 4-79693  
 wall shear stress measurements in annular two-phase flow 4-60526  
 water tunnel for aerodynamical studies 4-83920  
 water-kerosene two-phase flow, vortex flowmeter behaviour 4-60573  
 zigzag flow cells for meas. of liq. and air flow 4-77727  
 Ni-H battery cells, heat rate and coulombic efficiency during simulated geosynchronous orbit cycling 4-72074  
 SF<sub>6</sub> puffer circuit breaker hot circulation, laser Schlieren visualisation following fault interruption 4-113078
- flow process charts** see flowcharting  
**flow resistance** see viscosity  
**flow separation**  
 airfoil undergoing dynamic stall, laser holographic interferometry 4-97591  
 arterial pressure wave propagation, theory and model 4-72296  
 asymmetric flowfield development on slender body, laminar boundary layer separation 4-64951  
 asymptotic theory of turbulent separation 4-69745  
 axisymmetric Couette flow at large Taylor numbers 4-103296  
 body of revolution in liq. with jet separation, unsteady weakly perturbed motion 4-112896  
 boundary layers, three dims., separation criteria calc. 4-97491  
 boundary-layer interaction theory 4-97479  
 cavitation in vapour and gas, simulation 4-97623  
 cavitation phenomena within regions of flow separation 4-60468  
 centrifuges, separability of highly dispersive liquids (Russian) 4-112901  
 channel expansion, laminar flow, spectral element method 4-87797  
 circular pipe bends, two-phase flow, flow struct. and press. loss 4-103402  
 component pressure loss during two-phase flow 4-60510  
 compressible laminar and turbulent flow, time-split finite element method 4-112932  
 cross-flow around roughened circular cylinders universal wake numbers 4-97565  
 cylinder, rotating, in crossflow at two turbulence level, aerodynamic forces, separation 4-103357  
 delta wings with leading-edge separation, lateral aerodynamics, unsteady vortex lattice method 4-79614  
 drops, cylindrical, differentially rotated at moderate Reynolds number 4-103397
- flow separation continued**  
 flow about Savonius rotor, calcs. using singularity method and discrete vortex method 4-103446  
 flow around blunt bodies, press. fluctuations 4-60451  
 forced oscillation experiments in supercritical diffuser flows 4-97626  
 gas-liquid flows, conf., Grenoble, France (Sept. 1983) 4-58558  
 heat transfer in separated flow region created by abrupt circular pipe expansion 4-60419  
 heat transfer model for separated flows in tubes 4-60428  
 horizontal square cylinder, natural convection, temp. inversions 4-87702  
 hydroelastic fluctuations in two-phase flow in tube bundles 4-103336  
 impervious sails, two dims., 4-103440  
 incompressible flows over infinite swept wings, inverse mode boundary layer calcs. 4-112832  
 incompressible fluid boundary layer on moving surface of cylinder 4-112810  
 instability waves generation in flows separating from smooth surfaces 4-112921  
 internal gravity waves generation and evolution 4-112922  
 interstitial flow intensification in packed granular bed filters 4-97668  
 inviscid and viscous flow computations, multiple-grid convergence acceleration 4-60455  
 laminar and incompressible boundary layer flow induced by an airfoil (German) 4-64916  
 laminar flow, separated forced convection in cavities, finite difference anal. 4-112812  
 laminar steady flow in sinusoidal channels 4-87798  
 mean flow field and heat transfer along cooled supersonic diffuser 4-113077  
 NASA GA(W)-1 airfoil, separated flow study 4-97490  
 oscillating bluff bodies, separated flow, vortex shedding 4-91816  
 packed spheres beds, heat transfer, local aerodynamics 4-97543  
 potential and viscous flows, numerical method, fundamental solns. 4-64902  
 profiles, boundary layer calc. with laminar transition and turbulent flow zones 4-74999  
 pulsatile flowfield in the vicinity of an abrupt circular channel expansion 4-103421  
 reattached and separated flows, turbulence near-wall model appl. 4-79567  
 reattaching separated flow, 2D, spanwise struct. studied using multisensor hot-wire anemometry 4-87734  
 recirculating region in flow past surface-mounted obstacle 4-97516  
 rectangular diffuser, low flow detachment visualisation in corner region 4-87828  
 rotating and translating cylinder, time-dependent boundary layer flow 4-75042  
 shear flow, laser velocimeter sampling bias and its correction, expt. verification 4-103444  
 skin friction meas. using hot element gauges (French) 4-65045  
 steam-water separation using cyclones 4-60533  
 Stokes flow, fine struct. near central hole of torus 4-79628  
 subsonic laminar separation from discontinuity edge of profile 4-108063  
 subsonic turbulent flow over a rearward facing segmented step 4-60388  
 supersonic impulse turbine blade cascade, flow and losses in blade passage and design criteria 4-103335  
 supersonic laminar flow past flat plate, boundary layer separation 4-97603  
 thermosphon, countercurrent flow, heat and mass transfer 4-97547  
 three-dimensional separation, rel. to vortex skeletons (German) 4-112909  
 three-dimensional separation, streamwise bifurcations, vorticity and press. derivatives (German) 4-97725  
 transonic separated flows, viscous-inviscid interaction, semi-implicit and numerical methods (French) 4-64974  
 tube bundles, laminar flow, vortices separation, heat transfer, vel. fluctuations 4-97542  
 turbulent boundary layer, intermittent separation mechanism studied by flow visualisation 4-87687  
 turbulent boundary layers, shock wave effects, form. of separation region, geometrical characteristics 4-112836  
 turbulent boundary-layer interaction with shock wave at compression corner 4-87676  
 turbulent flow over large-amplitude wavy surfaces, vel. meas. 4-60380  
 turbulent fluctuations, separability into coherent and chaotic time depend. 4-83880  
 turbulent separated flows, three-dims., finite difference calc. procedure 4-91786  
 turbulent shear flow, conf., St. Louis, Missouri, USA, June 1982 4-86119  
 two dims. hydrofoil, press. distrib. and drag reduction in dil. polymer solns. 4-87763  
 two-phase flow, with Herschel venturis 4-97730  
 unsteady measurements in a separated and reattaching flow 4-103439  
 unsteady separated flow around square prism, numerical anal. by vortex shedding model 4-60435  
 unsteady separation from circular cylinder, mathematical simulation 4-69852  
 viscous flow over circular cylinder, turbulence effect on heat transfer coeff. 4-97537  
 viscous fluid flow hydrodynamic params. in convective problems for flow separation in channels 4-79587  
 viscous-inviscid interactions computing in internal flows 4-103314  
 vortex tube, temp. separation characts., estimation method 4-97573  
 water flow in rot. channel of square section, visualisation and separation meas. 4-112898
- flow through porous media**  
 acetylene diffusion through a capillary, nonthermal effect of incoherent IR light 4-79671  
 air saturated porous media in short cylinder, transient heat transfer 4-108073  
 aromatic substances, separation from aq. soln. by reverse osmosis with membrane 4-99840  
 axial-symmetric flow through porous media with free and seepage surfaces, Volterra boundary value problems 4-113002  
 binary fluid mixtures, Benjamin-Feir instability convection onset 4-64948  
 book 4-78053  
 capillary porous bodies, transport processes, laser monitoring 4-112999  
 chemically reacting gas in granular bed, mass transfer 4-79678  
 circular cylinder, porous, circulatory flow of nonNewtonian fluid, suction effects 4-87728

## flow through porous media continued

coffer dams, porous orthotropically inhomogeneous, filtration study 4-79665  
 combined natural and forced convection in horizontal porous channel 4-75004  
 connectivity transitions 4-90532  
 convection, cellular in fluid layer between horizontal porous plates with nonuniform heat source 4-75082  
 convection, oscillatory region (French) 4-112998  
 convection cellular, in fluid layer between horizontal porous plates with nonuniform heat source 4-75082  
 convection-diffusion problem porous medium, strong solns. in 3D case (French) 4-87698  
 convective flow in slip flow regime 4-101128  
 Couette flow in space partly filled with porous medium 4-87790  
 Darcy-Brinkman viscous flow through permeable membrane, microscopic theory 4-83946  
 diffusion-limited aggregation and two-fluid displacements 4-69820  
 diphasic flow, nonlinear partial differential eqns. (French) 4-60538  
 dispersion of a soluble matter in a porous medium channel with homogeneous and heterogeneous chemical reaction 4-69823  
 evaporative heat transfer in channel filled with porous highly conductive metal 4-83895  
 evaporative process in capillary-porous structs., approx. hydrodynamic theory 4-113750  
 fibrous material of a random array of parallel infinite-cylindrical rods, permeability 4-79660  
 film condensation with lateral mass flux about a body of arbitrary shape in a porous medium 4-108598  
 filtration and heat conduction in porous bodies, related problems 4-79663  
 flow of vapour in channel with porous filler, condensation process, analytic model 4-83942  
 fluid flow through rigid porous medium, stability 4-113003  
 fluid layer overlying layer of porous medium, vel. and temp. distrib. 4-103410  
 fluid-saturated porous thermoelastic solid, acoustic perturbations (French) 4-79356  
 fluid-solid heat exchange, transient single-blow responses, numerical prediction 4-97662  
 foam, fluid displacement in porous media 4-91837  
 foaming agents, mixed, flow through porous media, chain length and surface props. effects 4-97670  
 fractured-porous rock masses, difficulties of modelling fluid flow by finite-element techniques 4-97665  
 free convection and mass transfer through porous medium, rot. and Hall currents effect 4-108074  
 gas motion in porous medium for quadratic drag law, 1D self-similar problems soln. 4-103407  
 gas transient flow through tight sand core samples, measurement and anal. 4-60539  
 gas transport through polyethylene membranes 4-112992  
 gas-flow in tubes, with mass transfer through walls, anal., application to steam turbine control valves 4-75091  
 gas-foam and foam-gas interfaces, shock wave refraction 4-69791  
 gaseous phase permeability in capillary network 4-103409  
 heat and mass transfer in flow through porous medium, effects of Hall current 4-101125  
 heat emitting surface, influence of porous coating on heat transfer during boiling, calc. and obs. 4-108070  
 heat transfer for turbulent flow in a circular tube with uniform suction or injection 4-103319  
 heat transfer in a corner flow with suction 4-112937  
 heat-releasing apparatus inlet, hydromechanics 4-79669  
 heated pipe flow, turbulence statistics, suction effects 4-65023  
 heated vertical wall in porous medium, induced flow 4-69821  
 horizontal unsaturated flow in porous media, wetting front 4-97667  
 hydromagnetic free convection with mass transfer in rotation fluid, effects of Hall current 4-101134  
 immiscible fluids, homogeneous porous material 4-97674  
 immiscible fluids flow in porous media, displaced phase, capillary blocking, end effect 4-112996  
 interstitial flow intensification in packed granular bed filters 4-97668  
 laminar flow in a porous tube 4-103411  
 laminar flow of two phases through a capillary tube with variable square cross-section 4-60548  
 liquid bubble motion in vertical porous tubes 4-60487  
 liquid evaporation in small capillaries 4-61171  
 liquid in differentially heated porous slab, free surface 4-75078  
 liquids containing suspended and emulsified substances, filtration, mass transfer 4-69818  
 local pore cooling, steady-state problem 4-79664  
 macromolecules, membrane rejection coeffs., conc. and charge effects 4-89333  
 magnetisable fluid flow in elec. cond. porous media 4-109694  
 membrane, porous, separation quality determ. (German) 4-81482  
 membrane nonzero thickness effect on diffusion through membranes 4-72225  
 MHD flow and heat transfer in channel with porous walls 4-87808  
 MHD flow through porous medium bounded by oscillating porous plate 4-113026  
 MHD free-convection oscillatory flow past porous limiting surface; effects of Joule heating and viscous dissipation 4-67616  
 MHD free-convective oscillatory flow past porous limiting surface, effects of Joule heating and viscous dissipation 4-67615  
 mica, fine-pore, toluene diffusion under resonant laser beam irradi. 4-91840  
 miscible displacement, time stepping procedure for mixed finite element approx. 4-97675  
 miscible fluid flows in porous medium, acoustic studies 4-97672  
 mixed convection about horizontal heated surface in fluid-saturated porous medium, non-similar boundary layer anal. 4-69752  
 mobile bed contactor with low-density packing particles, hydrodynamics 4-60536  
 model heat exchanger, velocity distributions, measured and predicted values 4-69767  
 moving interface dynamics in porous media, for power law fluids with yield stress 4-91838  
 natural convection in porous media in rectangular cavity, transient characts. 4-60397  
 natural convection in saturated porous layers with internal heat sources 4-87705

## flow through porous media continued

Navier-Stokes eqns., spatial stability of a class of similarity solutions 4-74983  
 nonDarcy regime for vertical boundary layer natural convection in a porous medium 4-87709  
 oil displacement by polymer solution, influence of inaccessible pore volume 4-112997  
 oscillatory flow past infinite porous vertical plate, suction and free convection effects 4-75081  
 packed beds at low gas flow rates, steady-state meas., corrs. of axial effective thermal cond. 4-113000  
 packed column, combined state and parameter estimation 4-65017  
 parallel rotating porous disks, heat transfer study 4-64953  
 percolation model of immiscible displacement in the presence of buoyancy forces 4-91839  
 permeable plate with blown gas, limiting relative friction law 4-69819  
 polar fluid, MHD flow through porous medium 4-79673  
 pool boiling heat transfer on porous surfaces, electrolytic surface prod. (Chinese) 4-107997  
 porous channel and tube flow development 4-75079  
 porous flat plate, isothermal turbulent flow in wake downstream of injection segment 4-75028  
 porous materials, geometric and mass transfer parameters determ. 4-66518  
 random walks, transport and dispersion 4-60535  
 recirculation of fluid in porous layer heated from below 4-97673  
 regularity of solutions of the equation of porous mediums in a space dimension (French) 4-97664  
 rocks, fluid flow through crack network 4-100570  
 rotating porous layer, thermal convection 4-60429  
 saturated porous medium, thermal convective instabilities, temp. distrib. 4-112878  
 second grade incompressible fluid flow past an infinite porous plate, exact soln. 4-108096  
 second grade non-Newtonian fluid injection/suction through long vertical channel 4-97614  
 second order fluid flow past infinite wall with periodic suction 4-69822  
 seepage and membrane contact problems 4-65016  
 separation extent in single permeation stages 4-71982  
 solute transport in heterogeneous porous formations 4-113001  
 sphere packing, capillary hysteresis, blob movement meas. 4-61175  
 spherical particles, lateral migration in porous flow channel, appl. to membrane filtration 4-65020  
 spout-fluid beds, hydrodynamics (German) 4-103403  
 stationary gravity filtration, mass transfer model, numerical soln. (Ukrainian) 4-65021  
 subterranean water dynamics in multilayer percolation medium (Russian) 4-115473  
 thermal convection in a porous medium with horizontal cracks 4-97551  
 thermal ignition in porous media, convection effects 4-79657  
 transient film condensation on a vertical surface in a porous medium, heat transfer 4-87713  
 transient heat transfer behaviors in cylindrical porous beds at relatively large Reynolds numbers 4-64950  
 turbulent heat transfer in accelerated flows on permeable surfaces 4-103320  
 two dimens. plane jet issuing in porous medium Brinkman eqn. soln. 4-97633  
 two-phase cooling film on adiabatic wall 4-83943  
 unsteady flow in porous media, temp. fields 4-69817  
 unsteady flow through channel with permeable walls, solute dispersion, vel. distrib. 4-113020  
 unsteady gas flow into vacuum through a perforated plate 4-60373  
 variational inequalities solns. (French) 4-73209  
 viscous liquid, flow through porous bed, analogy with unsteady MHD convective diffusion 4-75080  
 water movement in concrete when it freezes 4-103408  
 water permeability with incomplete water saturation 4-97676  
 Br<sub>2</sub> gas diffusion through capillaries, laser control, energy efficiency 4-75113  
 K<sub>2</sub>SO<sub>4</sub>-methane, mass transfer in granular bed 4-79678  
 N<sub>2</sub> diffusion through a capillary, nonthermal effect of incoherent IR light 4-79671

**flow visualisation**  
 airfoil undergoing dynamic stall, laser holographic interferometry 4-97591  
 axial flow pump, entrained air effect on performance 4-97722  
 buildings boundary-layer flows, near-wake parameters 4-79599  
 circular cylinder in stratified fluids, vortex wakes from flow visualisation expt. 4-112886  
 circular pipe flow complexities arising from sudden expansion and coiling 4-69830  
 cowlings jets and wakes, 3D vortex motions, flow visualisation meas. 4-75038  
 combustible media, two dimens. nonstationary flow, visualisation study 4-69836  
 convective heat transfer visualisation 4-60425  
 coronary grafts, blood flow visualisation by US method 4-100264  
 direct injection methods, review (book contrib.) 4-79689  
 dispersion of gases into liquids by mixed flow agitators 4-60531  
 elastoid-inertia oscillations of rigidly rot. fluid in cylindrical vessel 4-112893  
 enclosed concentric vertical cylinders natural convection, laminar flow pattern visualisation 4-97531  
 fan, cross-flow, aerodynamics and performance 4-97597  
 fluid mechanics review, book 4-90314  
 foam, fluid displacement in porous media 4-91837  
 gas-liquid flow in slotted disks centrifuge extractor, struct. investigation 4-103395  
 hydraulic flow calculations, consideration of bottom region turbulence 4-83964  
 impervious soils, two dimens. 4-103440  
 inward melting in horizontal tube, heat transfer 4-87708  
 jet, incipient round, visual obs. of evolution 4-75067  
 jets, submerged of nonNewtonian fluid, laminar length meas. by flow visualisation technique 4-64997  
 laminar-turbulent boundary layer transition, thermal imaging system 4-112814  
 laser Doppler velocimeter using electro-optic modulator 4-103443

# flow visualisation continued

- laser-produced plasma, density and temp. profile, tracer and visualisation meas. techniques 4-103581
- modern optical techniques, review 4-91856
- natural convection, 3D, in inclined cylindrical annulus, flow visualisation 4-87710
- natural convection in inclined air layer 4-103317
- neutrally buoyant anisotropic particles for flow visualization 4-65015
- nonaxisymmetric flow between parallel rot. disks, visualisation 4-60436
- nonrectangular inclined enclosure, convective fluid motion and heat transfer 4-64941
- physical modelling of multi-phase flow, conference, Coventry, England (April 1983) 4-58559
- planar free shear layers, flow visualisation technique 4-79680
- polymer solutions, stratified two-component flow 4-75061
- pressure driven three dimens. boundary layers, direct force wall shear meas. 4-87689
- pulse Doppler flow imaging using a SAW CZT processor 4-97728
- recirculating flow, three dimens., shear driven, visualisation study 4-87829
- rectangular diffuser, low flow detachment visualisation in corner region 4-87828
- resistance coefficient of a solid sphere approaching plane and curved boundaries 4-60569
- road vehicles, drag, wake struct. flow visualisation study 4-97564
- rotating disk, boundary layer transition, spiral vortices 4-83910
- Savonius rotor, vortex shedding in wake (French) 4-103338
- shear driven 3D recirculating flow, visualisation studies, Taylor-type instabilities vortices 4-103346
- sheetlike plumes near a heated bottom plate at large Rayleigh number 4-64943
- skin friction meas. by laser interferometer in three dimens. flows 4-97505
- spark-ignition engine, combustion, flame photographs 4-87811
- standing surface gravity wave, horizontal cellular streaming, visualisation 4-112926
- Stokes flow, visualisation of cellular struct. flow, by rotation of circular cylinder (French) 4-112900
- stroboscopic illumination with unambiguous record of direction 4-113080
- subsonic turbulent flow over a rearward facing segmented step 4-60388
- supersonic laminar flow past flat plate, boundary layer separation 4-97603
- swirl combustor flow meas. with and without combustion 4-103436
- Tee junction, one- and two-phase flow, vel. meas. using press and flow visualisation photographs 4-60570
- thermohaline columns, layered, wave motion at boundaries 4-87742
- three-dimensional flow field anal. using image processing techniques 4-97719
- three-dimensional flow visualisation, computer graphics techniques 4-103450
- tube-bank type crossflow heat exchanger, heat transfer, press. drop and flow visualisation expt. 4-112680
- turbulent boundary layer, intermittent separation mechanism studied by flow visualisation 4-87687
- turbulent flame fronts, visualisation via planar laser-induced fluoresc. 4-97492
- turbulent flow heat transfer, press. drop in converging-diverging tubes 4-113022
- turbulent mixing layer, wakes, vortices, visualisation study 4-79566
- two component solid mixture-fluid suspensions, sedimentation, instabilities 4-79555
- two-dimensional recirculating flows, prediction of flow characts. 4-113082
- two-phase critical flow, boundary layers, visualisation study 4-60498
- unsteady measurements in a separated and reattaching flow 4-103439
- velocity gradient measurement, using photochromic dyes (French) 4-75097
- viscous gas flowing from slit or cylindrical channels into region of lower press., interferometric study 4-113021
- vortex shedding from circular cylinder with step 4-112892
- wall confinement effects for spheres in the Reynolds number range of 30-2000 4-103348
- water, natural convection in inclined rectangular cavity at density extremum 4-112874
- water, superheat, natural convection effect on freezing around isothermal, horizontal cylinder 4-108588
- water flow in rot. channel of square section, visualisation and separation meas. 4-112898
- wave tank flow region, US images of jets and wakes, oceanographic appls. 4-113085
- N<sub>2</sub> low-pressure gas jet, multipass dark-ground photography 4-91851
- NH<sub>4</sub>H<sub>2</sub>PO<sub>4</sub> cryst. perfection, flow visualisation expts. 4-65042
- SF<sub>6</sub> puffer circuit breaker hot circulation, laser Schlieren visualisation following fault interruption 4-113078

# flowcharting

- see also programming; systems analysis
- VISAR, data reduction method 4-111191

# flowmeters

- see also anemometers; flow measurement; laser velocimeters
- acoustic flowmeter, long-wave, fluid flow meas. in pipe for single-phase 4-83965
- advances in instrumentation, conf. Houston, Texas, USA (Oct. 1983) 4-106121
- biological flowmeter for slow-flowing physiological liquids 4-115311
- blood flow measurement by NMR and transcutaneous EM flowmeters 4-77362
- buildings, flow metering systems, on-site calibration 4-97726
- compressible two-phase flow, appl. to flow metering 4-97656
- direct-flow rotameters, calibration and checking by flowmeter test system 4-91853
- directional pressure probe for complex flow fields, design, calibration and testing 4-69843
- Doppler velocimeters, coded, signal-to-clutter ratio limitation, cardiology appls. 4-100285
- electromagnetic, with two-coil magnet structs., readings, vel. profile depend. 4-108148
- electromagnetic flow velocity meter with W-type core, 2D mathematical model (Russian) 4-113087
- electromagnetic flowmeter for oceanographic work 4-69847
- electromagnetic flowmeter in two-phase air-water upward flow 4-60528

# flowmeters continued

- electromagnetic flowmeter with insulated electrodes of large surface area 4-87820
- electronic flow meters calibration (German) 4-60566
- EM flowmeter, compact design with integral detector/converter unit 4-79683
- EM flowmeter with zero-error-eliminating bipolar pulse operation 4-91852
- fluidic flowmeter for low flow rate electronic calorimeters for air conditioning systems 4-91854
- gas flow metering, flowmeters, meas. and control systems using microelectronics (Dutch) 4-91855
- ion deflection air flow meter with constant deflection 4-87824
- laser Doppler tissue flowmeters, signal processor 4-85484
- magnetic flowmeters for liquid flow meas., design and appls. 4-103449
- MHD, conference, Riga, Latvian SSR 4-106123
- micropipette for measurement of water speed fluctuations 4-67446
- monomode fibre optic vortex shedding flowmeter 4-97711
- NBS long-wave acoustic flowmeter, evaluation 4-97720
- partial flowmeter for unsteady fluid flow measurement (Bulgarian) 4-97714
- pulsating stream, mean flow rate meas. using float type flowmeter, pulsation error (Japanese) 4-75106
- pulse Doppler flow imaging using a SAW CZT processor 4-97728
- spherical EM ocean current meter 4-115625
- steam metering comparison of various methods 4-108146
- transverse Doppler acoustic current profiler design and operation 4-115626
- turbine, performance handling water and water-solid mixture 4-97732
- turbine, vortex and electromagnetic flowmeters, test results compared with published data 4-75100
- ultrasonic industrial flowmeter design problems 4-108144
- US Doppler velocity meter for quantitative flow meas. and turbulence anal. 4-85464
- volume transformer for flowmeters with frequency-analogue output signal (German) 4-69840
- vortex flowmeters, unsteady characts. in oscill. flow 4-103438
- vortex shedding flowmeters, for cryogenic liquids, operating principles, performance, calibration, applications 4-108151
- zigzag flow cells for meas. of liq. and air flow 4-97727

# fluctuations

- see also Brownian motion; critical fluctuations; current fluctuations; noise; random processes
- 1/f noise studies, theory 4-98677
- acoustic instability conditions, Brillouin scatt., width and line profile 4-61723
- aerosols, random fluctuations, effects on behaviour 4-82189
- air cross flow, vel. fluctuations in space between tubes in bundles 4-83892
- aircraft in wind tunnel, wall press. fluctuations 4-108150
- alloys, short-range order fluctuations and Fermi surface effects (Japanese) 4-113391
- amorphous polymer density fluctuation theory in a glass transition region and photon correlation spectroscopy 4-98026
- anharmonic effects on the dynamics of two-dimensional anisotropic melting 4-92339
- atmospheric optical propagation, uniqueness of statistics derived from moments of irradi. fluctuations 4-74425
- axisymmetric Couette flow at large Taylor numbers 4-103296
- balanced vane pump pressure pulsation, fluidborne noise generation characts. 4-112843
- bistable nonequilibrium systems, plane front propag., fluctuation effect 4-63660
- blue phase liq. cryst., lattice spacing fluctuations, refl. microscopy obs. 4-103649
- boundary conditions for high-shear grain flows 4-112991
- Brusselator chem. reaction, fluctuations stochastic simulation, ensemble statistics 4-114766
- t-butyl alcohol, aq. solns., conc. fluctuations, light scatt. study 4-76484
- classical charged systems, pot. and field fluctuations 4-60587
- Coleman-Weinberg GUT model, phase transitions and fluctuation in inflationary universe 4-115838
- dielectric breakdown, Weibull statistics, theoretical basis and appls. 4-109121
- domain growth, temp. depend., Ising model Monte Carlo simulation 4-58761
- drift waves in rotating plasmas 4-113144
- dye laser, intensity corrs. for laser with fluctuating pump 4-69400
- dynamical electric fields in strongly coupled equilibrium plasmas 4-91870
- dynamical systems, discrete, linear and nonlinear response, chaotic attractors 4-68128
- easy-plane ferromagnetic chain, dynamical correl. functions due to solitons, ideal gas phenomenology 4-92916
- EM wave dispersion props. in unsteady-state inhomogeneous media 4-91387
- explosive behaviour, stochastic anal., qualitative approach 4-81441
- ferromagnetic semicond., nonequilibrium system of electrons and magnons, fluctuations in strong elec. fields 4-98870
- first order mag. phase transitions of the order-disorder type 4-65814
- flat-plate with diffusion flame, boundary layer turbulent props. 4-97507
- fluctuating plasma, electron plasma waves, localisation theory 4-60626
- fluidised bed, particle size effect on press. fluctuations and slugging 4-112993
- fluorescein in boric acid glass, thermoluminesc. study of biphotonic systems sensitivity to light fluctuations 4-114810
- fractals, percolation, mass fluctuations meas. 4-82759
- free electron laser, coherence and fluctuations, fully quantum mech. approach 4-87345
- glycerol, normal and metastable supercooling liq., fluctuating voltage spectrum, crystn. process 4-92991
- hard disk systems, two-dimens., long-range corrs., nonequilib. mol. dynamics calcs. 4-103633
- harmonic oscillator, damped, quantum theory 4-73256
- HBAc smectic liq. cryst., nuclear spin-lattice relax., NMR studies 4-84868
- Heisenberg antiferromag. and ferromag., correlation theory, dimension, field and temp. depend. 4-114086
- holographic interference fringes recorded from diffusely illuminated objects, amplitude-phase characts. fluctuations effect 4-91425

**Fluctuations continued**

- homogeneous axisymmetric turbulence, appl. of modified zero-fourth-cumulant approx. 4-79564  
 hybrid bistable optical devices fluctuations 4-107734  
 hydrodynamic systems, 2-D, nonthermodynamic fluctuations 4-90375  
 hydrodynamics, fluctuation effects in 2-D systems 4-112804  
 incommensurate phase formation, fluctuation effect mechanism 4-76371  
 incompressible fluid, turbulent flow, vel. and press. fluctuations 4-91804  
 infinite cluster, percolation, mass fluctuations meas. 4-82759  
 inhomogeneous, cryst., local phase transition points, fluctuation enhancement 4-65373  
 inviscid shear flow, flat eddy evolution near a wall 4-60392  
 isothermal chemical reactions, coupling of density and internal energy fluctuations 4-71962  
 isotropic turbulence response to spectrally local disturbance 4-112830  
 kinetic model for plasmas in a strong high-frequency field 4-60642  
 lattice gas interface, field dependence of eigenvalues of correlation function matrices 4-78253  
 linear oscillator, statistical fluctuations 4-90488  
 linear study of the fluctuating field in a channel (*French*) 4-69824  
 magnetic fluctuations in high- $\beta$  tokamak plasmas 4-60589  
 metallic glass formation, conc. fluctuations effects 4-84195  
 metallic glasses, quasielastic electron scatt. by two-level systems 4-92688  
 MHD channel, fluctuation summation and estimation 4-114915  
 monochromatic particle beam, acceleration effect due to thermal fluctuations 4-74404  
 nematics, fluctuations, mean fields and order parameters 4-88070  
 nonequilibrium hydrodynamic fluctuations, Langevin formalism 4-112805  
 nonequilibrium states, stability criteria and fluctuations 4-101750  
 nonequilibrium steady states, critical fluctuations 4-78100  
 nonlinear Langevin equation, numerical soln. 4-73346  
 nuclear fluid dynamical calcs., effects of fluctuations 4-78620  
 ocean floor, viscous sublayer and buffer layer, turbulence spectra 4-82067  
 oil-water microemulsion model 4-99849  
 optical bistable systems, wide-aperture, fluctuation effects 4-83634  
 optical fibre mode-power fluctuations between polarisation states 4-97085  
 2,3,5,6-paradeuterobenzene overtone lineshapes, pure-dephasing model 4-91309  
 periodically fluctuating flow generated with rot. cylinder row, wake profile meas. 4-97568  
 periodically fluctuating flow in cascade, unsteady boundary layer 4-97510  
 permanent magnets, magnetic field fluctuations, spin wave theory 4-61565  
 plasma, magnetic turbulence during mag. field line reconnection expts. 4-84011  
 plasma chemical reaction rates, fluctuation anal. and correl. spectrosc. investig. 4-87943  
 poloidal divertor Tokamak plasma, H-model regime, fluctuation phenomena 4-103468  
 polymer solutions, stratified two-component flow 4-75061  
 premixed jet flame, flow field struct. meas. 4-97628  
 quantum small system, dynamics with weak coupling to reservoir, reservoir fluctuations and self-reaction 4-58733  
 quantum theory, ergodicity and mixing 4-90428  
 random variables, probability distributions with given multivariate marginals 4-95302  
 random walks of a particle on fractal lattices with traps 4-73359  
 Rayleigh piston, transport eqn., nonlinear fluctuations 4-111083  
 reactive components, fluctuation thermodynamic props., species correl. function integrals 4-71965  
 ring laser, freq. fluctuation meas. 4-87382  
 second-order pair-correlation function for multicomponent plasmas 4-91871  
 self-gravitating system, random fluctuations in general relativity 4-110945  
 semiconductor, quantum well structs., photoluminesc. lineshape, interfacial quality influence 4-71424  
 shear stress turbulent fluctuations at wall, hot-wire anemometry study 4-112834  
 solids, photoacoustic pulse generation, microscopic theory 4-84348  
 spin glass phase, random anisotropy model, 1/N expansion, replica-symmetry breaking soln. 4-104436  
 statistical mechanics, temp. fluctuations, polythermal ensemble 4-86152  
 stimulated Raman scatt., fluctuations in nonlinear regime 4-91531  
 stratifying solns., acoustic wave dispersion and absorption by conc., fluctuations 4-80164  
 temperature and heat flux from nonequilib. state, coupled fluctuations 4-112681  
 thermal field interference from line sources in grid turbulence 4-103297  
 tube bundles, laminar flow, vortices separation, heat transfer, vel. fluctuations 4-97542  
 turbulent atmosphere, light beam intensity fluctuations, effect of initial degree of spatial coherence 4-107522  
 turbulent boundary layers, streamwise vel. fluctuations hot wire meas. 4-79570  
 turbulent bursts, statistical props. 4-91797  
 turbulent flow, higher level simulation 4-103304  
 unsteady measurements in a separated and reattaching flow 4-103439  
 viscoelastic liquids, Rayleigh-Brillouin spectroscopy 4-114288  
 weakly conducting fluid, turbulent flow in pipe, boundary current fluctuations 4-108110  
 whistler scatt. from density fluctuations 4-79792  
 C fibre epoxy resin composites, conductivity and percolation 4-98679  
 $\text{CsH}_2\text{PO}_4$ , antiferroelec. fluctuations, Raman spectroscopy, studies 4-71297  
 $\text{CsH}_2\text{PO}_4$ , Raman scatt. study 4-71377  
 Na-Cs liquid alloys, conc. fluctuations 4-92063  
 $\text{NiBr}_2$ , helimag. and antiferromag., mag. excitations, neutron scatt. studies 4-104409  
 Pb, discontinuous thin films, mass fluctuations meas. 4-82759  
 W point cathodes, electron field emission instability, adsorption effects 4-61813

**Fluctuations in superconductors**

- used only for thermal (thermodynamic) fluctuations around the order parameter near the critical point  
 disordered narrow band, spin and density fluctuations 4-104355  
 inhomogeneous condensate state, phase transition, Lagrangian model 4-61044

**Fluctuations in superconductors continued**

- inhomogeneous superconductors, correlation length and fluctuations 4-65770  
 Josephson junction chain, quantum fluctuations 4-98812  
 Josephson tunnel junction, overdamped, I-V charac., capacitance effects 4-108976  
 metallic weak links, quantum stability and screening 4-76085  
 nonequilibrium superconductors, new instability toward inhomogeneous states 4-70979  
 proximity effect sandwiches, local spin fluctuations, renormalisation group anal. 4-114073  
 superconductor-normal metal weak links, fluctuation and nonlinear props. 4-80726  
 (TMTSF) $_2\text{ClO}_4$ , NMR study and fluctuations 4-80834  
 (TMTSF) $_2\text{PF}_6$  quasi-1D superconductor, fluctuation conductivity 4-61490  
 (TMTSF) salt, (TMTSF) $_2\text{PF}_6$  and (TMTSF) $_2\text{ClO}_4$ , thermal transport props. 4-104362  
 Al, metallic granular, three-dimensional, magnetoresist., localisation and electron-interaction contribs. 4-113923  
 Al, superconducting fluctuation regime of cylindrical films, quantum oscils. 4-114068  
 Cu-Pb thin proximity layers, electron localisation and superconductivity 4-76083  
 $\text{ErRh}_4\text{B}_4$ , ferromagnetic superconductor, d-f interaction 4-98801  
 $\text{ErRh}_4\text{B}_4$ , mixed state and mag. props. 4-98830  
 $\text{UBe}_{13}$ , p-wave supercond., sp. ht., spin fluctuation parameter 4-76073  
 $\text{Zr}_{0.1}\text{Ti}_{0.9}$ , superconducting amorphous alloy, elec. resist. meas., fluctuations obs. 4-65768
- fluctuations of cross sections** see statistical theory of nuclear reactions and scattering
- fluid composition control** see chemical variables control
- fluid composition measurement** see chemical variables measurement
- fluid dynamics**  
 see also aerodynamics; biological fluid dynamics; drag reduction; flow; hydrodynamics; liquid oscillations; Navier-Stokes equations; rarefied fluid dynamics; relativistic fluid dynamics; surface waves (fluid); turbulence; wakes  
 Bernoulli eqns., n coupled class, linearisation 4-105167  
 bilinear-constant velocity-pressure finite elements stability 4-101655  
 Boltzmann equation, fluid dynamics relations, flows, layers and shocks 4-69730  
 book syncretics, concepts, mathematical tools 4-63411  
 combined finite element and spectral approximation of the Navier-Stokes equations 4-103281  
 compressible fluid dynamics, second-order Godunov scheme 4-86219  
 computational methods for transient analysis, book 4-58594  
 computational methods for turbulent, transonic and viscous flows, book 4-101597  
 computer extended series, appl. to fluid flow 4-91858  
 conference on fluid motions, atm. and oceanographic appl., at San Diego, USA (February 1983) 4-58543  
 conference on mathematical physics, Boulder, CO, USA (Aug. 1983) 4-67856  
 contact-line problems in fluid mechanics 4-98409  
 continuum mechanics, spatial variational principles 4-87650  
 converse topological stability theorem for flows on surfaces 4-110880  
 coordinate generation method based on mapping technique 4-103283  
 cusp-like free-surface flow due to a submerged source or sink 4-97466  
 data acquisition system, minicomputer-based 4-69845  
 equations solving, computer model 4-91785  
 Euler flow, nonlinear evolution eqns. 4-82683  
 Eulerian flow machines, operating point determ. 4-64906  
 exact decay of correlations for infinite range continuous systems 4-58648  
 fibre spinning, dynamical regimes 4-113092  
 fishing trawl net design, hydrodynamic testing facility development 4-115639  
 five-component Benard system, stochastic perturbations 4-110882  
 fluid motion in a cavity, Benard problem, finite element study 4-65025  
 fluid transient analysis, numerical methods, conf., Houston, Texas, USA (June 1983) 4-95061  
 fluid-structure interactions, fluid dynamics, arbitrary Lagrangian-Eulerian finite element methods, book contrib. 4-59392  
 four-dimensional dissipative dynamical system, global bifurcation structure 4-95181  
 frost layers on cold surfaces, growth rate and props. 4-60259  
 gun exhaust plumes, ignition 4-81438  
 high temperature fluids, transport system, new pipeline design 4-66803  
 ice sheets, plane steady flow, nonuniform temp. distrib. influence 4-60407  
 incompressible flow, boundary-element methods for transient response analysis, book contrib. 4-60298  
 incompressible flows, two-dimens. new mixed formulation 4-64904  
 incompressible fluid flow, limit for vanishing viscosity 4-97735  
 incompressible fluid flow prediction using SIMPLE method 4-108062  
 incompressible second order fluid flow over stretching sheet 4-97460  
 inhomogeneous gas, moving, two-dimens. discharge into vac. 4-108098  
 invertible maps for chaotic behaviour 4-90377  
 inviscid fluid flows, book 4-69733  
 IR telescopes, purging flow protection 4-101158  
 jet washers, absorption efficiency, liquid distrib. influence (*German*) 4-112699  
 longitudinal flow around a cone with a source (*Russian*) 4-69849  
 microcontinuum fluid mechanics, boundary-value problems 4-110883  
 mixing system for gas flow based on vortices produced by special vortex generator 4-83911  
 modern optical techniques, review 4-91856  
 multiphase mixtures of fluids, constitutive eqns. 4-79642  
 natural interpolation formula for Prandtl's singular integrodifferential equation 4-79538  
 Navier-Stokes equations, three-dimensional, nonsteady, finite element method 4-97464  
 Newtonian fluid flow simulation, Lagrangian finite element method 4-112801  
 non-local dissipative fluid obeying non-local constitutive equations, small amplitude waves 4-112914  
 non-stationary flows, one- and two-dimens., boundary conditions, numerical treatment (*German*) 4-83872  
 nonequilibrium gas-surface solid relax. gasdynamics 4-60562  
 nonlinear Schrödinger eqn., long-wave solns. 4-63526

- fluid dynamics** continued  
 nonuniform gas flow, constraints on averaging of total press. 4-64905  
 numerical methods, book 4-110817  
 Oldroyd-B fluid, plane and axisymmetric stagnation flows 4-97476  
 one-dimensional identical elastic hard rods, hydrodynamics 4-70013  
 open-end outflow boundary approx. for soln. of unsteady 1D gas flow eqn. by Lax-Wendroff method 4-64907  
 perfect gas three-dimens. stream free expansion 4-108102  
 planar automodelling problem of the flow of a viscous liquid through a zone with moving boundaries (*Russian*) 4-86218  
 plane pot. flow past finite amplitude sinusoidal wall 4-108060  
 plane stick-slip problem soln. appl. to Newtonian jet swell 4-97467  
 plate in fluid, waveform vibr. flow vels. field (*Russian*) 4-69851  
 pole condensation and the Riemann surface associated with a shock in Burger's equation 4-106195  
 process flow rate reconciliation by matrix projection 4-75107  
 radiation transport eqns. in solving 2D radiation-gasdynamic problems, averaging methods 4-103434  
 regular waves in articulated cylinder, mean drift 4-97589  
 rotating gas centrifuges, flow field, curvature effects 4-60440  
 rotation ellipsoid, pressure distrib. in incompressible potential flow (*German*) 4-83873  
 sailwings, single membrane, various airfoil shape modes and steady state stability 4-112802  
 self gravitating fluid mass, Liapunov's theorem generalisation 4-90376  
 shallow water free surface gravity flows, stationary points, variational formulation 4-108153  
 shells, cylindrical, eigen vibrs. in pot. flow with liq. coupling (*German*) 4-74936  
 simple fluid, Noll's definition 4-87654  
 simple fluid, Noll's definition 4-87655  
 slender body, incompressible flow at stagnation point 4-91857  
 solid bodies floating on free surface of liq. in vortex funnel, submergence problems (*Russian*) 4-87727  
 solid vibrating profile, press. distrib. (*Russian*) 4-69850  
 soliton dynamics in 2-D flows, wake developments 4-69772  
 spreading of a paraboloid elevation of liquid over a horizontal base 4-115470  
 stable mass-flow-weighted two-dimensional skew upwind scheme 4-60410  
 Stokesian, stability of some mixed finite element methods 4-79540  
 thin fluid layer undergoing end-compression, buckling 4-103452  
 three-dimensional grid generation using elliptic equations with direct grid distribution control 4-79537  
 transition of nonone-dimensional flows produced by explosions into one-dimensional flows 4-69781  
 turning flow in pin-fin configuration, heat transfer coeff. and press. drops 4-97553  
 two-dimens. Stokes flow between indefinite parallel plates (*French*) 4-83966  
 UK Consortium Stirling engine regenerator effectiveness and heater performance 4-66753  
 unidirectional solidification and related fluid parameters, in microgravity optical obs. 4-80194  
 unsteady flow eqn. as basis for extrapolation of stream flow data 4-65028  
 unsteady processes in neighbourhood of well, nonlinear flow law, stratum parameters determ. 4-72585  
 variational inequalities solns., (*French*) 4-73209  
 variational principles in Eulerian and Lagrangian descriptions 4-95180  
 viscous film flow with free boundaries, one-dimensional approx. 4-87831  
 LiBr film flowing down adiabatic wall, mass transfer in absorpt. of water 4-64831  
 N<sub>2</sub> liquid, flow through N-sequential orifice inlet configurations, critical mass flux and axial press. profile data 4-103451
- fluid flow** *see* flow
- fluid instability** *see* flow instability
- fluid mechanics**  
*see also* capillarity; cavitation; compressibility of gases; compressibility of liquids; fluid dynamics; hydrostatics; Mach number  
 8th Australasian Fluid Mechanics Conference, Newcastle, NSW, Australia (Nov.-Dec. 1983) 4-67858  
 chaotic behaviour of deterministic systems, reprint selection 4-101759  
 computer-extended series, bad behaviour and counter measures 4-6981  
 Garfield Thomas Water Tunnel, hydrodynamics and fluid mechanics research progress 4-65044  
 inhomogeneous plasmas and fluids, fluctuations spectrum 4-91901  
 non-Newtonian fluids, fluid mechanics meas., review (book contrib.) 4-79691  
 physical laws, appl. to meas. techniques book contrib. 4-79685
- fluid rheology**, *see* rheology
- fluid theory, dense** *see* liquid theory
- fluid valves** *see* valves
- fluid amplifiers**  
*see also* hydraulic amplifiers  
 low press. bubble with jet attachment, transient response 4-87780
- fluidic devices**  
 flowmeter for low flow rate electronic calorimeters for air conditioning systems 4-91854  
 micrometer for vacuum chamber, pressure-related transfer characteristics 4-111144  
 pulsating fluid signal, transmission characteristics improvement, rarefied gas use (*Japanese*) 4-87762  
 CO<sub>2</sub> conc. in air, meas. using fluidic oscillator (*Italian*) 4-114862
- fluidic logic**  
 low press. bubble with jet attachment, transient response 4-87780
- fluidised beds**  
 atmospheric fluidized-bed coal combustion for electric utility applications 4-109717  
 bubble size measurement and correlation in beds at high temperatures 4-112983  
 combustion of solid fuels 4-99935  
 electrode, charge transfer, bipolar mechanism 4-79654  
 electrostatic fluidised bed behaviour under radioactive gas flow conditions 4-97678  
 fine-grain material eruptions from nonuniform fluidised bed 4-79655  
 fuel-air combustion in fluidised bed model 4-87787  
 gas bubble rise vel. in liq. fluidised beds, Davies-Taylor eqn. 4-87785  
 gas burner for dust laden air in lime kiln 4-97666  
 gas fluidisation, segregation mechanisms 4-87784
- fluidised beds** continued  
 gas-solid, transient axial solid and gas temp. profiles in grid zones 4-97669  
 gas-solid fluidised beds, bubble- to dense-pulse mass transfer (*German*) 4-112994  
 gas-solid fluidised beds, mixing, lateral dispersion coeffs. 4-87783  
 heat exchange between unsecured model particle and fluidised bed 4-79662  
 heat exchanger, fluidised bed, wall to bed heat transfer in vertical tube 4-60398  
 heat transfer between fluidised beds of large particles and horizontal tube bundles at high pressures 4-103404  
 horizontal tube arrangement optimisation, heat transfer 4-60537  
 horizontal tube heat transfer surface roughness effect in gas fluidised beds 4-113005  
 large particle bubbling fluidised beds, heat transfer 4-113004  
 laser Doppler meas. of flow in freeboard 4-75077  
 liquid fluidised beds, mechanistic description of unsteady state expansions 4-79656  
 liquid in bubble bed apparatus, large scale circulatory motion (*Russian*) 4-60442  
 local heat transfer coefficients for a horizontal tube in a large-particle fluidised bed at elevated temperature 4-112846  
 low-grade fuels—Swedish energy option 4-89376  
 minimum fluidisation velocity, pressure effect 4-65002  
 mixed particle size gas, void fraction and minimum fluidisation velocity 4-97679  
 mixing, packet mechanism 4-112995  
 nonuniform fluidised bed, press. pulsation mechanism 4-79661  
 packed beds, heat transfer, thermal cond. 4-64936  
 particle size effect on press. fluctuations and slugging 4-112993  
 pressure and vel. meas. methods (*Hungarian*) 4-65043  
 single particle combustion calc. 4-71925  
 small signal wave propagation and reflection analysis for electrofluidised beds 4-97677  
 solid particle distrib. in liq. fluidised beds 4-79659  
 solid particles circulation in spouted bed (*Bulgarian*) 4-97671  
 solid-fuel combustion in fluidised bed, two-phase model 4-71926  
 spout-fluid beds, hydrodynamics (*German*) 4-103403  
 spouting, processes with phase transform. 4-69812  
 suspended solid layer, expansion at critical impeller speed turbulence 4-87778  
 three dimensional and 2D beds, high-pressure, high-speed photographs, bubbling behaviour 4-65018  
 tubular flow, twisted tape heat transfer augmentation 4-97530  
 viscoelastic fluid flow study 4-79658  
 C continuous adsorp. process 4-97651  
 H<sub>2</sub> production in autothermal fluidized gasifier 4-72187
- fluidised powders** *see* powders
- fluidity** *see* viscosity
- fluids**  
*see also* bubbles; classical theories of fluid structure; disperse systems; fluid mechanics; fluidised beds; gases; gravity waves; liquids; non-Newtonian fluids; quantum fluids; quantum theories of fluid structure  
 No entries
- fluorescence**  
*see also* atomic fluorescence; fluorescent lamps; fluorescent screens; molecular fluorescence; nonradiative transitions; X-ray fluorescence analysis  
 2-acetylthianthracenes, luminesc. and coplanar conformations, temp. depend. 4-104648  
 alkali halide:CN<sup>-</sup>, vibrational fluoresc., nonradiative luminesc. quenching 4-81005  
 anthracene, cryst., carrier pairs prod. and recombination by VUV radiation 4-84571  
 anthracene, excitons and diffusion effects 4-92617  
 anthracene, fluoresc. excitation spectra 4-84990  
 anthracene, fluoresc. excitation spectrum beyond first ionisation pot., photoelectron spectra 4-84989  
 anthracene cryst., fluoresc. excitation and absorpt. spectra relationship for photon energies up to 10 eV 4-84988  
 aromatic hydrocarbons, polynuc., liq. solns.,  $\beta$ -induced fluoresc. spectra 4-88879  
 bacteria, photosynthetic, picosecond spectrochronography study 4-100098  
 p-benzoquinone, fluid soln., phosphoresc. and fluoresc. spectrum 4-66065  
 3,4-benzpyrene, multiplets in the Shpol'skii spectra 4-99188  
 9,9'-bianthryl, viscous solvents, intramolecular electron transfer luminesc., high press. study 4-80977  
 biological systems, concentration meas., continuous, optical fluorescence sensors 4-85584  
 biphenyl cryst. reson. excited defect emission 4-109231  
 biphenyl-naphthalene mixed crystals, delayed fluoresc., role of quadratic terms in kinetics 4-109232  
 1,4-bis( $\beta$ -pyridyl-2-vinyl)benzene, anal. mixed cryst., fluoresc. and lifetime meas. 4-104658  
 cancer cells, laser-excited microscopic fluorescence measurement method (*Japanese*) 4-115315  
 cholesteric mixture, compensated liquid crystals, fluorescent guests props. 4-65168  
 colour penetrant system, new method (*German*) 4-89228  
 coronene in n-heptane single cryst., phononless line intensity and shift 4-109238  
 4-cyano-4'-alkoxybiphenyls, liq. cryst., energy transfer and migration 4-76516  
 cyclohexane, electron scavenger effect on positronium form. and fluoresc. intensities 4-105002  
 1,2-di-(1-naphthyl)ethylenes, cis-trans-photoisomerisation, luminesc. and X-ray studies 4-93540  
 differential pulse fluorometry using matched photomultipliers 4-64639  
 diphenyl with fluoranthene impurity, mol. crystals, sensitised and delayed fluoresc. kinetics 4-104647  
 2,5-diphenylloxazole, in liq. mesitylene, far vacuum UV excitation spectrum, fluoresc. 4-84991  
 2,5-distyrylpyrazine, anal. mixed cryst., fluoresc. and lifetime meas. 4-104658  
 DPA-TCNB complexes, triplet-triplet annihilation, reson. microwave field effect 4-76287  
 dyes adsorbed in Langmuir-Blodgett films, selectively laser excited, persistent spectral hole burning 4-88878

## fluorescence continued

- electronic transition-induced desorption, laser induced fluorescence studies 4-75780
- europium benzoyl-trifluoroacetate solns., fluorescence quenching by applied voltage effect of transparent insulating films (*Japanese*) 4-99175
- fluorescent fluorescent dyes, photoelectron microscopy and photoelectron quantum yields 4-82869
- fluorimeter, fibre optic, absorption corrected, microcomputer controlled, appls. 4-78376
- fluorimetry, multifreq. phase and modulation, in biophys., book contrib. 4-93985
- fluorophosphate glass:  $\text{Ti}^{3+}$ , fluorescence and oscillator strengths 4-99165
- Gaussian laser lineshape in resonance fluorescence 4-69363
- n-heptane, multiplets in the Shpol'skii spectra 4-99188
- heterogeneous emissions, meas. by multifreq. phase and modulation fluorimetry, review 4-101922
- hydrophilic solid, adsorpt. of nonionic surfactant, fluoresc. decay obs. 4-108679
- impurity centres in two-well adiabatic pots., relax. process effect on luminesc. spectra and burnup 4-109223
- inner shell ionisation by light ions, conf., Linz, Austria (Aug. 1983) 4-95035
- ionic micelle soln., counterion fluoresc. quenching 4-81485
- K-fluorescence yield in K and L shells, multiple ionisation effects 4-99232
- laser-induced fluorescence spectroscopy (*Japanese*) 4-111217
- liquids and liq. cryst., fluorescence depolarisation intensity deconvolution 4-93103
- low temperature spectra, empirical method for eliminating background prod. by diffuse reflection 4-96482
- luminescence spectrometer, computer-controlled, for relative fluoresc. quantum yield meas. 4-106400
- membrane, fluorescence emission anisotropy, orientational dynamics contrib. to depolarisation 4-107478
- membranes, fluorescence depolarisation intensity deconvolution 4-93103
- 2-(4-methoxyphenyl)-5-(2-naphthyl)-1,3,4-oxadiazole, liq. scintillator, energy transfer quenching 4-104651
- naphthalene, isotopically mixed cryst., delayed fluoresc. study 4-84999
- NPL spectrophotometer, for fluoresc. meas. of opaque materials 4-106354
- oil in water microemulsions, fluoresc. probe study 4-89342
- optical fibre fluorimeter system, limitations due to background fluorescence 4-97083
- organic dyes, photovoltaic cells, chem. props. 4-84998
- oxazine dyes, solvent deuteration effects, fluoresc., laser efficiency 4-79127
- palladium phthalocyanine, reson. Raman, fluoresc., and phosphorescence spectra in Shpol'skii matrices 4-71426
- penetrant fluorescent measurement 4-66530
- pentacene, in benzoic acid, photostatic photon echo study 4-64745
- percolating systems, fluoresc. line narrowing 4-96486
- phenanthrene, fluoresc. excitation spectra 4-84990
- phthalocyanine,  $\beta$ -metal-free, carrier generation, photoconductivity, delayed fluoresc. study 4-70855
- picosecond spectroscopy by single photon counting method (*Japanese*) 4-73527
- polydiacetylene solns. and glasses, absorpt., fluoresc. and emission spectra 4-71425
- polymers, bulk, mol. viscoelasticity determ. by neutron scatt., IR dichroism and fluoresc. polarisation 4-114596
- polystyrene, head-to-head, intramol. excimer form. and energy migration 4-114325
- polystyrene charged spheres in dilute soln., fluorescence labeled, electrolyte friction meas. 4-98323
- polystyrene films, doped,  $\alpha$ -particles irradi., delayed specific luminesc. 4-61753
- polystyrene spheres on Ag substrates, structural resonances observed in the fluoresc. emission 4-84984
- polystyrene-polyvinylmethylether blends, phase separation, fluoresc. emission anal. 4-114324
- polyvinylcarbazole-vinylbenzocarbazole, fluorescence and host-guest energy transfer 4-99166
- pulse fluorimetry using simultaneous acquisition of fluorescence and excitation 4-11219
- pyrene, fluoresc. excitation spectra 4-84990
- Raman-fluorescence discrimination, time resolved picosecond interferometry 4-11215
- rare earth molybdates,  $\text{Eu}^{3+}$  doped, fluorescence studies 4-66072
- rare earths in amorphous media and on high surface area supports, fluorescence and nonradiative relax 4-99156
- rhodamine fluorescent dyes, photoelectron microscopy and photoelectron quantum yields 4-82869
- smectic mesophases, rank order parameters, angle resolved fluoresc. depolarised meas. 4-62443
- solar fluorescent concentrators combined with highly selective narrowband absorbers 4-114953
- solar fluorescent planar concentrator, energy conc. factor 4-114895
- spectroscopy, apparatus design and factors affecting fluorescence 4-106397
- synchronous fluorescence spectrometry, rapid scanning, const. energy, flow cell evaluation 4-78380
- p-terphenyl, cryst., UV absorpt. and fluoresc. obs. 4-61744
- p-terphenyl, fluoresc. excitation spectra 4-84990
- n-terphenyl, pure and impure crystals, exciton, visible absorpt. and fluoresc. spectra 4-99141
- tetracene, delayed fluoresc., role of charge transfer states in triplet exciton form. 4-99191
- thin film microanalysis, X-ray absorpt. and fluoresc. 4-72029
- total internal reflection fluorescence in biophysics, book contrib. 4-93987
- two-level system in biharmonic field, resonance fluorescence spectra 4-96853
- vinyl chloride-vinyl acetate vapour-swollen polymers, fluoresc. probe for microenvironments, solvent vapour effect 4-81002
- xanthene dyes, solvent deuteration effects, fluoresc., laser efficiency 4-79127
- zero-phonon impurity lines, thermal broadening in absorpt. and fluoresc. spectra 4-109216
- $\beta\text{-Al}_2\text{O}_3\text{-La}_2\text{O}_3\text{:Eu}^{3+}$ , structure, laser excited fluorescence study 4-66071
- Au thin film, fluorescence detection of surface EXAFS 4-93136
- $\text{BaClF:Sm}^{2+}$ , impurity states in mag. field, fluoresc. study 4-108805

## fluorescence continued

- $\text{Ba}(\text{NO}_3)_2\cdot\text{H}_2\text{O}$ , pure and doped single crystals, fluoresc. and phosphoresc. study 4-109227
- Be,  $1s$  binding energy, core levels, state-specific many-electron theory 4-75887
- $\text{BeAl}_2\text{O}_4\text{:Cr}^{3+}$ , alexandrite, resonant  $40\text{ cm}^{-1}$  phonons, lifetime and line-width 4-65356
- $\text{BeAl}_2\text{O}_4\text{:Cr}^{3+}$ , alexandrite, fluorescence of inversion site  $\text{Cr}^{3+}$  ions 4-107647
- $\text{CaF}_2\text{:Na}$ , photochemical conversion of  $\text{M}_A$ -centres, identification of  $\text{M}_A$ -centre, absorpt. and fluoresc. spectra 4-76501
- $\text{CdF}_2\text{:Er}^{3+}$ , insulator to semiconductor transition, site selective laser spectroscopy 4-99155
- $\text{CdS}$ , colloidal crystallites, excited electronic states, size effects, optical props., Raman spectra 4-71334
- $\text{CdSnO}_3$  and  $\text{Cd}_2\text{SnO}_4$ , EPR signals due to vacancies, comparison with  $\text{CdO}$ , yellow fluorescence phenomenon 4-71179
- $\text{CsCaCl}_3\text{:Mn}^{2+}(\text{Ni}^{2+})(\text{Co}^{2+})$ , fluoresc. emission, excitation, IR absorpt. spectra studies 4-99153
- $\text{Cs}_2\text{NaScCl}_6\text{:Cr}^{3+}$  cryst., dopant fluoresc. props. 4-61745
- $\text{Cs}_2\text{TaOCl}_5$ , prep., fluoresc. spectra 4-108299
- $\text{Cs}_2\text{TaCl}_5$ , prep., fluoresc. spectra 4-108299
- $\text{DyF}_3$ , optically excited, fluorescent excitation and absorpt. spectra 4-99154
- Fe II fluorescence in stellar atmospheres, UV triplet lines 4-63154
- $\text{GdCl}_3\text{:Pr}^{3+}$ , crystal field levels, coord. geometry depend. 4-70755
- $\text{Gd}_3\text{Ga}_2\text{O}_{12}$ , fluorescence radiation due to X-ray standing waves 4-71437
- $\text{Gd}_3\text{Sc}_2\text{Al}_3\text{O}_{12}\text{:Cr}^{3+}$ , tunable room temp. CW laser action 4-74518
- Ge monocrystalline, K-shell fluoresc. yield 4-85041
- Ge, phonon pulses detection by fluorescence of deposited  $\text{YF}_3\text{:Tb}^{3+}$  film 4-113555
- $\text{HgI}_2$ , optically excited electronic processes 4-104254
- $\text{KClO}_2$ , fluoresc. time depend. study 4-109239
- $\text{KNO}_3\text{:Tm}^{3+}$  soln., optical absorpt. spectra 4-84957
- $\text{KNDP:O}_2$ , radiative transition probabilities 4-80973
- $\text{KNDP:O}_2$ -based cryst., laser time resolved selective excitation 4-99163
- $\text{La}_{0.7}\text{Pr}_{0.2}\text{Nd}_{0.03}\text{F}_3$ , fluorescence decay characts. 4-71436
- $\text{LaCl}_3\text{:Nd}^{3+}$ , isotope shifts, laser-induced fluoresc. 4-71428
- $\text{LaCl}_3\text{:Pr}^{3+}$ , crystal field levels, coord. geometry depend. 4-70755
- $\text{LiF}$ ,  $\text{R}'$ -centre aggregate, spectral linewidths, depend. on irradiat. method 4-70193
- $\text{Li}_2\text{O-Nd}_2\text{O}_3\text{-GeO}_2(\text{SiO}_2)$  ternary systems, subsolidus phase equil. and fluorescence activity 4-113596
- $\text{LiPrP}_2\text{O}_{12}$ , absorption and fluoresc. intensity anal. of  $\text{Pr}^{3+}$  4-104654
- $\text{LiYF}_6\text{:Nd}^{3+}$ , electronic Raman scatt. and two-photon fluorescence (*Chinese*) 4-104581
- $\text{MgNO}_3\cdot 6\text{H}_2\text{O:Tm}^{3+}$  soln., optical absorpt. spectra 4-84957
- $\text{MgO:Ce}^{3+}$ , fluoresc., thermoluminesc. and decay 4-93117
- $\text{NH}_4\text{NO}_3\text{:Tm}^{3+}$  soln., optical absorpt. spectra 4-84957
- $\text{Na}_2(\text{AlO}_2)_6(\text{SiO}_2)_{40}\cdot 24\text{H}_2\text{O:Eu}^{2+}$ , adsorption of  $\text{O}_2$ , fluorescence study 4-84511
- $\text{NaCl:Ag}^+$ ,  $\text{Ag}^+$  ion dimer centres, optical props. 4-66076
- $\text{Na}_2\text{Eu}(\text{MO}_4)_4$ ,  $\text{M}=\text{Mo, W}$ , cryst. field effect, mag. susceptibility, fluoresc. study 4-88867
- $\text{NaF}$  polycrystalline thin films, neutron and X-irrad., photochemical hole burning 4-76518
- $\text{NaF:Cu}$ , fluorescence kinetics, three-level model anal. 4-99184
- $\text{Na:Ti}$ , excitation fluoresc. intensity in VUV 4-84987
- $\text{Na}_1\text{+xMg}_x\text{Al}_{1-x}\text{O}_2\text{:Nd}^{3+}$  platelet laser absorpt. spectra, fluoresc. lifetime, laser-pulse shape and peak emission wavelength 4-60044
- $\text{NaNO}_3\text{:Tm}^{3+}$  soln., optical absorpt. spectra 4-84957
- Nd laser glasses, gain saturation modelling, broadband and laser excited fluorescence spectroscopy 4-112443
- $\text{Nd:SiO}_2$  glasses prep. by axial injection plasma torch CVD 4-93229
- $\text{Nd}_2\text{O}_3\cdot\text{WO}_3\cdot\text{GeO}_2(\text{MO: M=Ca, Sr, Ba, Mg, Zn})$ , subsolidus phase equil. and fluorescence activity 4-113597
- $\text{PbF}_2\text{-GaF}_3\text{-Al(PO}_3)_3\text{-ErF}_3$ -based fluoride glasses, fluorescence studies 4-99170
- $\text{RbGd}_2\text{F}_{10}\text{:Eu}^{3+}$ ,  $\text{Eu}^{3+}$  fluorescence,  $\text{Gd}^{3+}$  effects 4-104663
- $\text{RbMnCl}_3$ , antiferromag. with alternating strong and weak coupling, absorpt. spectra, fluoresc. meas. 4-88659
- $\text{Si}$ , phonon pulses detection by fluorescence of deposited  $\text{YF}_3\text{:Tb}^{3+}$  film 4-113555
- $\text{TbF}_3$ , fluorescence, exciton diffusion and up conversion mechanisms 4-66075
- $\text{TiHBr}_4\text{:Pa}^{4+}$ , incommensurate phase, single cryst.,  $\text{Pa}^{4+}$  optical spectroscopy 4-71422
- $\text{Tm}(\text{NO}_3)_3\cdot 5\text{H}_2\text{O}$  soln., optical absorpt. spectra 4-84957
- Xe, electroluminescence, partial excitation and VUV fluoresc. at normal press. 4-83973
- $\text{XeF}(\text{C-A})$  laser oscill. using electron beam excitation 4-87320
- $\text{Y}_2\text{Ga}_2\text{O}_7\text{:Nd}$  thin film waveguide, RF sputtering growth, fluoresc. spectrum, optical amplifier appl. 4-60146
- Zn tetraphenylporphyrin, spectral-fluoresc. props., aggregate state and temp. effects 4-78906
- $\text{ZrO}_2\text{:Eu}^{3+}$ , monoclinic zirconia, fluoresc. spectra studies (*French*) 4-99152
- fluorescence of atoms** see *atomic fluorescence*
- fluorescence of molecules** see *molecular fluorescence*
- fluorescent lamps**
- lumen depreciation due to ion bombardment 4-99157
- performance characteristics, effect of ballast combinations, photometric testing 4-90642
- photosensitivity tests, fluorescent lamp apparatus 4-115172
- fluorescent screens**
- see also *electroluminescence*
- electro-optical systems, moiré phenomena appl. to modulation transfer function 4-79334
- radiographic intensifying screens, preferred image characts. of various types 4-109909
- radiography using photographic paper with different thickness of lumino-phore of fluorescent screen 4-73548
- X-ray intensifying, energy imparted from primary and scatt. radiation, screen, thickness and comp. effects 4-67109
- fluorimetry** see *spectrochemical analysis*
- fluorine**
- see also *nuclei with .....*
- adsorption by  $\text{SiO}_2$  during sputtering by  $\text{Ar}^+$  ions and  $\text{XeF}_2$  4-93177
- atom, absolute transition probability of visible lines in  $\text{Ar-F}$  arc 4-79856
- atoms, 3p state radiative lifetimes 4-107311

## fluorine continued

- atoms, IR intensities and charge flux param. and transferability in  $\text{BF}_3$ ,  $\text{NF}_3$  and  $\text{CF}_4$  4-69072  
chemisorbed on Si, synchrotron photoemission study 4-108710  
determination, in near-surface region of solids using  $^{19}\text{F}(\text{p},\text{p}')^{19}\text{F}$  reson. reaction 4-85348  
doping in consolidation process of VAD soot preform for single mode fibres 4-97154  
element analysis using charged-particle induced prompt  $\gamma$  rays 4-89362  
fission reactor fuel, activation anal. for  $\text{N}$ ,  $\text{O}$ ,  $\text{F}$  content determ. 4-102358  
gas, electron swarm parameters, Boltzmann eqn. calcs. 4-79713  
ion bombardment of ferromagnetic surface, polarization pick-up detection 4-81062  
laser action, CW 4-91439  
molecular fluid, orthobaric props., intermol. pot. effect 4-74310  
molecule, electron energy loss spectroscopy 4-69228  
molecule, electron momentum density distrib. 4-78763  
molecule, total energies calc. using electron cloud displacement model (Chinese) 4-74136  
molecules, electron scatt. cross sections, CI calcs. 4-91348  
molecules, electrons elastic scatt., cross sections, polarisation effects 4-78963  
particle excitation mechanisms  $\text{F}$ ,  $\text{Ar}$ ,  $\text{O}$ ,  $\text{N}_2$ ,  $\text{CO}$  and perfluoromethyl radical in glow discharge 4-79860  
triarylmethane:  $\text{F}$ , cond. transitions 4-70881  
X-ray meas. of anomalous dispersion correction 4-87090  
Ar-F arc, spectroscopic anal. in case of two emitting layers 4-79856  
 $\text{F}^-$ , dipole polarisability, electron affinity, many-body perturbation theory 4-64363  
 $\text{F}_2$  solvation, geometrical features, pattern recognition anal. 4-114781  
 $\text{F}^{q+}$ , ( $q=9, 8, 7$ ), incident on inert gas atoms, K-Auger electron prod. 4-78818  
 $\text{F-Xe}$ , two-state collision problems for exponential coupling 4-74315  
 $\text{F+D}_2$ , reactive infinite order sudden approx. calc., cross-sections and vibr. branching ratios 4-66571  
 $\text{F+DBr}$ , collinear H-transfer reactions, dominant reaction probabilities evaluation 4-89245  
 $\text{F+H}_2$ , BKLT eqn. for reactive scatt. of collinear nonsymm. systems 4-114787  
 $\text{F+H}_2$ , reactive scatt. resonances 4-99780  
 $\text{F+H}_2$  reaction, quantum dynamics, energy partitioning and entropy anal. of collision complex 4-114782  
 $\text{F+H}_2$  reaction, quantum dynamics, scatt. wave function density and flux analysis 4-114783  
 $\text{F+H}_2$  reactions, MRD-CI pot. surfaces using balanced basis sets 4-93521  
 $\text{F+H}_2$  reactions, reson. periodic orbits, semiclassical theory 4-114788  
 $\text{F+H}_2$  reactions, semiclassical adiabatic theory 4-114786  
 $\text{F+H}_2\text{O}$ ,  $\text{HO}_2$  prod., vibr. band strength for  $\nu_2$  band meas. 4-74220  
 $\text{F+H}_2(\text{HD})(\text{D}_2)$ , collinear exchange reactions, probability densities, stabilisation calcs. 4-81415  
 $\text{F+H}^+$ , two-state collision problems for exponential coupling 4-74315  
 $\text{F+HF}$ , vibr. level deactivation 4-96666  
 $\text{F+I}_2(\text{HI})(\text{ICN})$ , exchange reaction, pot. surface,  $\text{I}^2(\text{P}_{1/2})$  two photon laser induced fluoresc. 4-76982  
 $\text{F}^-$  methyl fluoride, activation barriers, fourth order MB RSPT calcs. 4-62167  
 $\text{F}^-$  molecule, electron detachment and charge exchange to shape reson. 4-96687  
 $\text{F}^+ + \text{C}(\text{X})$  foils, equilib. charge state, particle vel. depend. 4-64594  
 $\text{F}^+ + \text{He}$ , one-electron capture at low energies, Landau-Zener model calcs. 4-96685  
 $\text{F}^+ + \text{He}(\text{Ne})$ , K Auger-electron prod. cross sections, charge-state depend. 4-96693  
 $\text{F}_2^+$ , high resolution UV PES 4-112228  
 $\text{F}_2$ -Kr-He atmospheric discharge, electron density, streak interferometric method 4-84092  
 $\text{F}_2 + \text{Ca}$  reactions, crossed laser mol. beam studies and  $\text{CaF}$  prod. mol. rot. polarisation 4-91364  
 $\text{F}_2 + \text{O}_2$ , chemical reactions in red spectral range, excitation spectrum, low-energy pathways 4-85318  
 $\text{F}_2 + \text{Si}$  collision, time-resolved at. reson. absorpt. spectrosc. investigation 4-102765  
 $^{19}\text{F}$ , 197 keV  $3/2$  state, g factor measurement from hyperfine frequencies 4-96712  
 $\text{F}^*$  laser, discharge-pumped, intense laser generation 4-60062  
 $\text{H}_2\text{-F}_2$  pulsed laser, photolysis and electron beam method initiation efficiency 4-74499  
 $\text{He-F}_2(\text{SF}_6)$  mixtures, elec. breakdown 4-79720  
 $\text{Si-F}$ , amorphous, electronic struct. theory 4-92600  
 $\text{Si-F}$ , amorphous and cryst., ion implanted, elec. quadrupole hyperfine interaction at impurity sites 4-92675  
 $\text{Si-F}$ , As, ion implanted, defect struct. detection 4-103776  
 $\text{a-Si:H}$ , F p-n junctions, generation; recombination currents, computer simulation 4-84683  
 $\text{a-Si:H:F}$  films, F incorporation during glow discharge deposition 4-114426  
 $\text{Si}_3\text{N}_4$ -F films, plasma enhanced CVD, insulating props. 4-61865  
 $\text{SiO}_2\text{-F}_2$  fibre manufacture by outside vapour deposition 4-91645  
 $\text{SnO}_2\text{-F}$  conducting glass film for SIS solar cells, optical props. 4-88894

## fluorine compounds

- fluorides, perovskite-type, wide band gap expts., excitation of thermally stimulated luminesc. and conductivity 4-85018  
fluorite deposits, Gd, Ce and Eu impurities study by EPR and neutron activation anal. 4-80815  
photonuclear activation ratios as index of bremsstrahlung quality, radiology appl. 4-109913  
 $\text{BaF}_2\text{-GdF}_3\text{-ZrF}_4$  optical fibre, preparation 4-103045  
 $\text{D+FD}$  reactive reson., partial widths and isotope effects calc. by reaction path Hamiltonian model 4-71890  
 $\text{FH}$ , RHF, NDDO and MOM mol. one-electron expectation values calc. using minimum basis sets 4-102598  
 $\text{FH+Li}$ , collinear reaction, quasi-classical versus quantum calcs. 4-66556  
 $\text{FH}_2$  reaction energies, pot. energy surfaces, ab initio calcs. 4-114789  
 $\text{HFH}^-(\text{FDF}^-)$  isolated in alkali halides crystals, IR and Raman spectra, temp. depend. 4-59760  
 $\text{FNO}$ ,  $\nu_2$  and  $\nu_3$  fundamentals, high resolution Fourier transform spectroscopy 4-59749  
 $\text{FO}_2$ , FIR laser mag. reson. detection from  $\text{F+O}_2(\text{O}_3)$  reactions 4-59811

## fluorine compounds continued

- $\text{FO}_2$  radical,  $\nu_2$  band, IR diode laser spectra 4-74237  
 $\text{F}_2\text{O}$ , oxidation number, electron distrib., ab initio MO wave functions 4-107276  
 $\text{F}_2\text{O}_2$ , oxidation number, electron distrib., ab initio MO wave functions 4-107276  
 $\text{FONO}_2$ , gas phase struct., rigid asymmetric rotor theory, IR transitions 4-112172  
 $\text{H+FH}$  reactive reson., partial widths and isotope effects calc. by reaction path Hamiltonian model 4-71890  
**fluoroscopy** see radiography  
**flux (magnetic)** see magnetic flux  
**flux (neutron)** see neutron flux  
**flux creep**  
see also flux pinning  
No entries  
**flux crystal growth** see crystal growth from solution  
**flux flow**  
see also flux pinning  
microbridges, long, current-induced resistive state, optical radiation influence 4-98816  
type I superconducting microbridge, flux flow voltage, time dependent, high resolution recording 4-76084  
wide films, new resistive state and vortices (Russian) 4-71003  
 $^4\text{He}$ , superfluid vorticity nucleation by ions 4-88360  
Nb-Nb oxide-Pb well-damped Josephson transmission line, fluxon propagation 4-65771  
Pb/Nb oxide/Nb resistively coupled Josephson transmission line, fluxon threshold props. 4-70989  
**flux-line lattice**  
curved flux line near the edge of a type II superconductor 4-92878  
superconductor, dynamic response to external rotating moment in transverse mag. field (Russian) 4-84744  
two-vortex interactions and elastic constants in type II superconductors 4-92877  
type II superconductors, deformed flux-line lattice, mag. field distrib. 4-71007  
type II superconductors, vortex motion and effect of controllable defects 4-84757  
Nb, effective volume of voids for flux pinning 4-84758  
Nb-Ta, global pinning force density saturation 4-80730  
V, effective volume of voids for flux pinning 4-84758  
**flux line motion** see flux flow  
**flux pinning**  
see also flux creep; flux flow  
hexagonal to quadratic vortex lattice transition, pinning on surfaces and large grain boundaries 4-80729  
multifilamentary superconductors, coupling current losses calc. 4-71006  
plane flux pinning model of type II superconductors (Chinese) 4-76091  
superconducting broad films, resistive state, vortex changes 4-65780  
superconductor, dynamic response to external rotating moment in transverse mag. field (Russian) 4-84744  
type II supercond., elemental-flux pinning pot. 4-76093  
type II superconductor, curved flux line pinning by macroscopic inclusions 4-65778  
type II superconductors, vortex motion and effect of controllable defects 4-84757  
type-II superconductors, mechanism and fundamental theory of superconductors (Japanese) 4-65777  
Nb, effective volume of voids for flux pinning 4-84758  
Nb film, supercond. crit. current in weak mag. field (Russian) 4-92880  
Nb, superconducting, flux pinning mechanism of grain boundaries (Japanese) 4-76094  
Nb, superconducting, surface oxidised and neutron irradi., flux pinning 4-76095  
Nb superconducting films, flux line pinning by grain boundaries (Russian) 4-84756  
Nb-Sn supercond. wires, processed, electromag. props., stress effects (Japanese) 4-84759  
Nb-Ta, global pinning force density saturation 4-80730  
Nb-Ti supercond. wires, electromag. props., stress effects (Japanese) 4-84759  
Nb-Ti superconductors, flux pinning by gas bubbles (Russian) 4-104381  
NbN film, supercond. crit. current in weak mag. field (Russian) 4-92880  
NbTi, pinning force, upper critical field (Chinese) 4-76092  
 $\text{Nb}_3\text{Zr}_3\text{Si}_5$ ,  $\text{Nb}_{30}$ ,  $\text{Zr}_{15}\text{Si}_{15}$ , amorphous alloys, supercond. and electronic props., cold rolling effect 4-61480  
V, effective volume of voids for flux pinning 4-84758  
V, superconducting, surface oxidised and neutron irradi., flux pinning 4-76095  
Zr-Si, amorphous, upper critical field meas. 4-84754  
**flux vortex flow** see flux flow  
**flux vortex lattice** see flux-line lattice  
**fluxmeters**  
see also magnetic field measurement; magnetic flux  
No entries  
**fluxoid array** see flux-line lattice  
**FMR** see ferromagnetic resonance  
**foams**  
see also bubbles  
acoustic properties of rigid closed-cell foams (Chinese) 4-85337  
fluid displacement in porous media 4-91837  
foaming agents, mixed, flow through porous media, chain length and surface props. effects 4-97670  
ocean surf zone, bubble size spectra in foam patches 4-115406  
PU rigid foam, elastic props. at low temp. (Chinese) 4-105030  
swirled foam beds, heat and mass transfer 4-60401  
**focused collision sequences** see sputtering  
**focusing**  
see also self-focusing  
acceleration column, laminar flow quadrupole-focused, design 4-107212  
acoustic focusing gain of liquid-filled spheres (Chinese) 4-87523  
acoustic lens design using geometrical theory of diffraction 4-74833  
charged particle beam focusing devices, quantum mech. anal. 4-59470  
conference, polarised proton ion sources, Vancouver, BC, Canada (May 1983) 4-106092  
confocal images, edge enhancement by defocusing 4-102894  
criterion for best focusing based on image pixel intensity 4-107528

**focusing continued**

- electrostatic lenses, five-element, magnification behaviour 4-87264  
 electrostatic prism for microparticle beam steering, on 2-MV Van der Graaf dust accelerator 4-64263  
 EM wave focusing through dielectric interface 4-112323  
 film lenses analysis, with complex source point method 4-64792  
 free electron tapered wiggler lasers, emittance acceptance 4-83589  
 Fresnel-type IDT for underwater focusing ultrasonic wave (*Japanese*) 4-83797  
 gradient-index lens for laser-diode beam, focusing props. 4-87411  
 grazing incidence spectroscopy focusing, by elastic deformation of the grating 4-82834  
 half-symmetric unstable resonator with internal axicon, reflexicon deforms effect on geom. parameters 4-69524  
 interference microscope in electron microprobe, specimen exact focusing 4-82864  
 laser beam, higher-order mode, waist location and Rayleigh range 4-91508  
 low energy electrons, electron-electron interactions in finely focused beams 4-87262  
 magnetized high-intensity electron beam, cyclotron resonance of pumping wave, induced rad. 4-69293  
 metal, surface electrons, drift focusing by mag. field 4-92786  
 microscopes, fine focusing mechanism (*Russian*) 4-73503  
 multimode optical fibres, image transmission characts. study (*Japanese*) 4-87475  
 negative ion clusters, collimated beam from plasma focus source 4-107210  
 neutron scattering instrumentation at reactor based installations 4-102465  
 neutron spectrometer resonance detector, time focusing effect 4-102462  
 parametric focusing source, sound field calc. 4-74831  
 photochronographic camera imprecise focusing rel. to subpicosecond laser pulse shape distortions 4-64729  
 plasma lens, oscillations effect on focused ion beams 4-113229  
 plasma lenses, necessary conditions for strong elec. field form. 4-103585  
 point diffraction interferometry appl. 4-58887  
 pupil misfocus tolerance seen by inspection of ambiguity function 4-107530  
 quasimonochromatic light beam, spectral broadening by focusing 4-91400  
 RATAN-600 radio telescope, energy characts. of focusing system 4-63056  
 receiving telescope focal plane light intensity fluctuations caused by round-trip propag. through turbulent atm. 4-62952  
 scintillation blocks amplitude-time characts. improvement 4-87016  
 single mode fibre core alignment by focusing method 4-91622  
 space-time focused light plasma beams for ICF fusion 4-107147  
 spectrograph with holographic lens as dispersing/focusing element (*Chinese*) 4-73523  
 Strehl ratio symmetries and periodicities 4-96832  
 superconducting solenoidal coil, focusing props. 4-102461  
 superposed converging spherical wave focus, three-dimens. intensity distrib. 4-59973  
 synchrotron radiation, toroidal grating monochromator, nonstigmatic optics 4-97052  
 synchrotron X-ray focusing monochromator for EXAFS studies, design, operation 4-95613  
 synchrotron X-ray microprobe, focusing optics 4-95608  
 three-dimensional intensity distribution near the focus in systems of different Fresnel numbers 4-102878  
 two-stage sector mass analyzers, first order double focusing anal. 4-73558  
 US beam, focusing by piezoelectric annular array 4-97219  
 wave beam, intensity maxima on axis, properties of focused field 4-69288  
 X-ray imaging with UIS baseline 4-95598  
 X-ray synchrotron radiation focusing, using Si ribbed crystal, fabrication 4-101993  
 X-ray zone plates, fabrication by electron beam lithography and reactive ion etching 4-90701  
 D<sup>+</sup> ribbon beams, focusing by transverse electric fields 4-107211  
 H atomic beam, spin polarised, focusing and optics 4-107228  
 H atomic beam source for ion production 4-107234  
 H polarised atomic beam source, feasibility study 4-107468  
 H<sup>+</sup> extraction and acceleration from mag. multipole source 4-107206  
 H<sup>+</sup> polarised ion source at Munich 4-107240  
<sup>4</sup>He collimated beams from plasma focus source 4-107210  
 He-Ne laser emission power stabilisation; using gas-discharge lens 4-102938

**focusing, particle see focusing; particle optics****fog**

- attenuation of IR radiation 4-115480  
 Bering Sea, longitudinal rolls and steam fog in boundary layer 4-72641  
 blue-green propagation through clouds (*French, English*) 4-67399  
 electric parameters var. 4-67313  
 NE England, 1983 July heatwave, fog occurrence effect on sunshine totals 4-100717  
 Madras airport, India, Brunt's formula for fog 4-67343  
 remote sensing of fog cover by satellite IR radiometry method (*German*) 4-82276  
 spatial distribution of fog droplets, investigation by holographic method 4-62979  
 steam fog occurring in condensation nuclei free air 4-80200  
 terminal velocity of droplets and optical extinction coeffs. in fog models 4-82151  
 transmittance measurements using variable angular field-of-view transmissometer 4-100813

**foils**

- diatomic mols., interactions with thin foils, multiple scatt. and wake effects 4-76629  
 electron transport through foils, energy loss and straggling due to at. electron collisions and bremsstrahlung 4-70249  
 medical foil filters for equalised chest radiography 4-81779  
 metal foils, thermolec. power 4-84609  
 micromechanical test machine for high temperatures 4-89218  
 steel, stainless, nitrided, TEM specimen prep. from surface layers 4-103619  
 thickness meas. using alpha particle thickness gauge by air equivalent method (*Chinese*) 4-82778  
 thin foils, shock wave generation using lasers and light ion beams 4-103877

**foils continued**

- X-ray foil filters, numerical design 4-86509  
 Ag, thin foil, surface plasmon excitation during electron energy loss 4-70695  
 Ag-Pd composition modulated foil, interdiffusion coeffs. 4-70477  
 Ag-Pd-Ag multilayered films, microstructure changes rel. to layer spacing, TEM obs. 4-80432  
 Au-Ag-Au multilayered films, microstructure changes rel. to layer spacing, TEM obs. 4-80432  
 C, implanted with T, prep. and analysis w.r.t. fusion reactor safety 4-91100  
 C, very thin, energy loss of He<sup>+</sup> beams, nonequilibrium effects 4-103837  
 Co foil making by electrolytic method, for nuclear expts. 4-104742  
 Co<sub>85</sub>Ni<sub>15</sub>Fe<sub>10</sub>Si<sub>6</sub> foil, thermal expansion coeff. and isothermal compressibility (*Russian*) 4-65421  
 Cr foil, influence of heat treatment on struct. and props. (*Russian*) 4-65412  
 Cu, neutron irradi., damage prod. rate meas. at liq. He temp. 4-65307  
 Fe, magnetic hyperfine fields determ. by Mossbauer spectroscopy, using internal standard 4-114185  
 Fe thin foils, STEM energy dispersive X-ray microanalysis 4-69999  
 Fe<sub>80</sub>B<sub>20</sub> amorphous foil, sputtered ductile, mag. and structural study 4-80782  
 Fe<sub>40</sub>Ni<sub>40</sub>B<sub>20</sub> foil, thermal expansion coeff. and isothermal compressibility (*Russian*) 4-65421  
 Mo foil and films preparation, by decomposing MoCl<sub>5</sub> vapour 4-93231  
 Ni-Fe-Co-Ti, Incalloy, domain struct. study by differential phase contrast Lorentz microscopy, max. specimen thickness 4-65825  
 Pd-Fe, ion implanted, ferromagnetism study 4-71137

**Fokker-Planck equation**

- acousto-optic bistability with fluctuations, nonlinear Fokker-Planck eqn. 4-83636  
 asymptotic properties near crit. points, Hopf bifurcation 4-101785  
 asymptotic properties near Hopf bifurcation 4-101784  
 bacteria chemotaxis, nonlinear Fokker-Planck equation, stochastic computer simulation 4-95304  
 beam-beam interaction in electron storage rings, renormalised Fokker-Planck eqn. 4-59466  
 bistable flow driven by coloured Gaussian noise, critical study 4-111018  
 Brownian motion, extremely underdamped, eigenvalues in inclined periodic pot. 4-68125  
 collective mode damping in DIC, random-matrix model, Fokker-Planck eqn. 4-102246  
 conservative difference systems (*Russian*) 4-86377  
 conservative nonlinear dynamical system with a few degrees of freedom, chaos, irreversibility 4-63671  
 dense plasma, open mag. trap calc. using computer 4-103540  
 diffusion, inertial corrections using Fokker-Planck eqn. 4-78280  
 diffusion coefficient, polymer chain, dynamic exponent in good solvents 4-86375  
 discrete ordinate method of soln. for eqn. with bistable pot. 4-106234  
 double-well pot., Fokker-Planck and BGK operators, eigenvalues 4-58790  
 environmental noise and vibr., random level distrib. prediction 4-103094  
 euclidean field theory stochastic quantization with fermions 4-68359  
 first-order phase transitions, nucleation-growth processes, scaling laws (*Japanese*) 4-113568  
 fission dynamics, relaxation to Kramers stationary solution, inverted oscillator 4-96003  
 functional integrals for degenerate diffusion matrix 4-101627  
 highly excited phonon mode decay, master eqn. anal. 4-65362  
 ICRF enhancement of beam driven currents, Fokker-Planck treatment 4-74042  
 Lagrangian representation of Fokker-Planck dynamics, non-renormalised description 4-68137  
 Lagrangian representation of Fokker-Planck dynamics, renormalised description 4-68138  
 metastable system, integration soln. method 4-106249  
 monoenergetic charged particle transport, Fokker-Planck eqn. soln. 4-68181  
 nonequilibrium hydrodynamic fluctuations, Langevin formalism 4-112805  
 nonequilibrium phase transition existence, sufficient intrinsic conditions 4-73405  
 nonequilibrium statistical mech., projection operator techniques, book 4-78797  
 nonlinear Fokker-Planck eqns: spectral density in high freq. limit 4-111084  
 nonlinear Langevin equation, numerical soln. 4-73346  
 nonlinear laser model with multiplicative coloured noise, distrib. function 4-78312  
 nonlinear system in stationary field statistical approach to bistable behaviour 4-95193  
 nuclear magnetisation vector; stochastic motion; Fokker-Planck eqn. study 4-61600  
 one-dimensional Heisenberg systems with random anisotropies, low-temp. props. 4-76100  
 phase transformation threshold analogy, effects of finite damping 4-111031  
 quantum mechanical diffusion coeff., fundamental constraint 4-101698  
 quantum small system, dynamics with weak coupling to reservoir, reservoir fluctuations and self-reaction 4-58733  
 random gyrotropic media, ray dispersion 4-91404  
 ray dispersion in gyrotropic stratified media 4-107521  
 ray dispersion in random isotropic media 4-73306  
 reformulation in terms of Riemann-Christoffel tensor 4-82769  
 road traffic noise in Hiroshima 4-103095  
 SADI numerical scheme for two dims. Fokker-Planck eqn. 4-60665  
 semi-infinite medium, 1-dimens. Fokker-Planck eqn., half range completeness, orthogonality 4-95359  
 semiconductor surface, rate of capture of minority carriers 4-92754  
 semiconductors, macroscopic electron transport, Fokker-Planck eqn. soln. 4-98600  
 single crystals, Kumakhov radiation in axial channelling, dipole approx. in classical theory 4-103841  
 stationary diffusion over multidimensional pot. barrier, Kramers' formula generalisation 4-58792  
 stochastic differential eqn. with exponential noise; Fokker-Planck approach 4-101756  
 stochastic processes, master equation, Fokker-Planck eqn. by scaling expansion method 4-95140

**Fokker-Planck equation continued**

- supersymmetric field theory, stochastic quantisation, Parisi-Wu method 4-90742  
 supersymmetry and the bistable Fokker-Planck equation 4-73402  
 temperature and heat flux, from nonequilibrium state, coupled fluctuations 4-112681  
 thermally activated crossing of a sharp potential barrier 4-114765  
 three-level atom dynamics in resonant light field 4-83361  
 tokamak hot ion plasma, two component ion distrib. 4-79827  
 two-photon laser with injected signal, theory 4-91431  
 two-photon lasers, theory, Fokker-Planck eqn. treatment 4-91430  
 weak-noise limit of Fokker-Planck models 4-11025  
 $\alpha$ -particles distribution function and diffusion in DT fusion plasma 4-102394

**Food processing industry**

- Industrial Temperature Booster, a waste-heat-powered heat pump, industrial applications 4-72160  
 low-level microwave treatment of mountain pine beetle and darkling beetle 4-115125  
 raw water treatment-using stratified-bed cation-exchange filter systems 4-71915  
 salmon ranching technology and utilisation of waste heat and food 4-115447  
 seafood processing waste management and disposal in oceans 4-114965  
 waste utilisation for biogas and fertilizer production 4-66735

**Forbidden gap see energy gap****Orbush decreases see cosmic ray variations**

- Force**  
 see also atomic forces; coercive force; Coriolis force; force control; force measurement; molecular force constants; nuclear forces  
 generic field theory, definition of force 4-58966  
 nodal forces in elements under surface and body loads in axisymmetric and planar elasticity theory problems 4-95176

**Force constants see lattice dynamics; molecular force constants**

- Force control**  
 ergometer, UT-7508, upgrading of automatic physical load control 4-93977

**Force measurement**

- see also dynamometers  
 calibration and standards 4-95417  
 capacitive transducer for continuous measurement of vertical foot force 4-85541  
 dynamic force measurement with a hydraulic force balance valve 4-86405  
 EC comparison between PTB (Braunschweig) and TNO (Delft) 4-63737  
 feedback dynamometers with differential scale conversion 4-90581  
 muscle force estimation from intramuscular total press. 4-115114  
 peristalsis, strain gauge transducer for in vivo meas. (Japanese) 4-77284  
 quartz crystals as mechanical sensors 4-95407  
 sensors, for small values, precise meas., dist. meas., direct conversion and zero defl. sensor types 4-82785  
 standard machines of National Institutes for metrology 4-106318  
 transducer calibrations and measurements 4-73431  
 transducers calibration, EC comparison between PTB (Braunschweig) and MD/SM (Brussels) 4-63738  
 transducers calibration, EC comparison between PTB (Braunschweig) and NPL (Teddington) 4-63739  
 transducers calibration, EC comparison between PTB (Braunschweig) and IMGC (Turin) 4-63740

**Force meters see force measurement****Forecasting, technological see technological forecasting****Forecasting theory**

- flood forecast response systems, concept 4-110181

**Forging**

- cold forging, materials testing 4-99714  
 Rene 95, Ni-base superalloy, fatigue, effect of processing and microstruct. 4-104843  
 steel, microalloyed eutectoid, austenite recrystn. and pearlite colony size, effect of Nb 4-114572  
 steel, Mn, 13 to 19 wt.%, sinter-forged, mech. props. 4-81283  
 steel, Ni-Cr-Mo-V, fracture behaviour effect of S content 4-99601  
 steel, Ni-Cr-Mo-V, fracture toughness, overheating, effect of S content (Japanese) 4-93377  
 Mo-V(Zr)(Ti)(Nb)(Ru)(Cr), interstitial-free, workability and ductility, effect of alloying element 4-93345  
 Zn-Al (22wt.%), superplastic, closed die forging 4-104817

**Form factors, atomic see atomic structure****Form factors (elementary particles)**

- see also form factors (nuclear)  
 Altarelli-Parisi eqns., jet-calculus propagators, transverse-momentum calcs. 4-106518  
 bag model, nucleon and pion form factors 4-78530  
 Majorana particles from CPT invariance, constraints on interactions 4-59006  
 mesons, EM form factor behaviour in small and intermediate  $Q^2$ , rel. quark model 4-82963  
 neutron properties, interactions, expt. data review 4-63997  
 nucleon axial form factor and axial vector meson dominance 4-59084  
 nucleon mass and pionic form factor 4-78554  
 pion form factor and the Klein-Gordon equation 4-95797  
 pion form factor in the vorton-quark model 4-78531  
 pion radiative decay, vector and axial-vector form factors and modified bag model 4-59048  
 pion-surrounded nucleon bag recoil and axial form factors 4-59054  
 QCD, sum rules and exclusive form factors, review 4-82941  
 weak currents, supersymmetry,  $\beta$ -decay form factors, gluino exchange, scalar-quark masses 4-106505  
 $\gamma^* \rightarrow \pi^0$  in  $e^+e^-$ , form factor, QCD sum rule method and perturbative QCD comparison 4-82946  
 $\gamma \rightarrow \pi$  in  $e^+e^-e^+e^-$ ,  $\pi^0\pi^0$ , transition form factor 4-95867  
 $K \rightarrow \pi\pi$ ,  $K_{12}$  form factors in bag model 4-82954  
 KN inverse scatt. problem, interaction form factor 4-111471  
 N- $\Delta$  quadrupole transition amplitude in quark models, form factors 4-111405  
 pp-2/3 mesons, quark annihilation model, vector-meson-quark interaction 4-106539  
 pp-3 mesons, quark rearrangement model, vector-meson-quark interaction 4-106539  
 $\pi$  form factor measurement in time-like region 4-64001

**Form factors (elementary particles) continued**

- $\pi$  mass, elastic form factors, cavity approx., to bag model 4-111416  
 $\pi^0 \rightarrow e^+e^- \gamma$  ( $e^+e^-$ ), form factor slope and decay amplitude calc. using quark triangle mechanism 4-59069  
 $\pi$ NN form factor, pion electroproduction, chiral SU(2)  $\times$  SU(2) symm. breaking 4-111462  
 $\Sigma^-$ -new, electron energy spectrum and asymmetry meas. 4-90877

**Form factors (nuclear)**

- A=3 system, ground state energy, wave function and form factor, variational calc. 4-106566  
 A $\leq$ 4, struct. props. from (e,e) 4-59225  
 even-even nuclei, effective form parameters for large ang. momenta states, microscopic calc. 4-95894  
 friction form factor, one-body energy dependence 4-59145  
 inverse scatt., S-wave rank-one, reformulation and analytic solution 4-59215  
 magnetic dipole states, electroexcitation in deformed nuclei, isovector  $K=1^+$  state, RPA 4-111532  
 meson exchange currents, soft pions to spin excitations, review 4-64037  
 nuclear bound nucleons, structure functions, nuclear effects 4-73760  
 nucleon folding potentials for deformed nuclei, and exchange effects 4-78614  
 one-body nuclear friction, form factor, microscopic calc. 4-59263  
 P-wave neutron strength functions in nuclear vibrational region 4-95895  
 quantum tunneling in multidimensional systems 4-83036  
 two particle transfer form factors, depend. on single particle states 4-90950  
 (e,e) on  $^{54,56}\text{Fe}$ ,  $^{60}\text{Ni}$ , Coulomb form factors for  $0^+ \rightarrow 4^+$  transitions in 2p-1f shell, HFB anal. 4-59143  
 (e,e) on Ti, Cr, Fe isotopes, form factors for  $2^+$  states excitation in 2p-1f shell, HFB anal. 4-59142  
 (e,e'N), knockout reactions, coincidence form factors interpretation 4-68677  
 $^{48}\text{Ca}$ , M1 form factor, spin-isospin polarization 4-86770  
 $^{26}\text{Be}(e,e')$ , electromagnetic form factors, effects of meson exchange currents 4-111539  
 $^{12}\text{C}$ , magnetic multipole excitation by inelastic electron scatt. 4-95899  
 $^{12}\text{C}(^{12}\text{C}, ^{12}\text{C})^{12}\text{C}$ , second order processes, form factors 4-59271  
 $^{12}\text{C}(p,p)$ , E=0-18 MeV, l=0-5 phase shifts, single-channel RGM, charge form factor 4-106583  
 $^{40}\text{Ca}(e,e')$ ,  $0^+ \rightarrow 2^+$  state electroexcitation, form factor, coexistence model verification 4-90948  
 $^{A}\text{Cr}$ , A=50, 52, form factors for  $0^+ \rightarrow 2^+$  transitions in 2p-1f nuclei 4-83025  
 (d, $^6\text{Li}$ ) microscopic cluster form factor in DWBA calcs. 4-64161  
 $^{20}\text{D}$ , EM form factors from wave functions 4-102170  
 $^2\text{H}$ , nucleon form factor, enhanced sea-quark distrib. anal. 4-59146  
 $^4\text{He}$ , A=54, 56, form factors for  $0^+ \rightarrow 2^+$  transitions in 2p-1f nuclei 4-83025  
 $^{156}\text{Gd}(e,e')$ , form factors, low-lying  $K^{\pi}=1^+$  mode 4-111522  
 $^2\text{H}$ , EM form factors and tensor force, non-relativistic calc. 4-90951  
 $^2\text{H}$ , nucleon form factor, enhanced sea-quark distrib. anal. 4-59146  
 $^2\text{H}(e,e)$ , form factors, signatures for QCD in nuclear physics 4-90949  
 $^2\text{H}(e,e'n)$ , electrosplallation current, neutron polarisation and form factor 4-95998  
 $^2\text{H}(e,np)$ , struct. props. from (e,e) 4-59225  
 $^2\text{H}(k^+X)$ ,  $X=\Sigma^0$  or  $\Lambda$ , disintegration with two-body final states, cross sections, form factors 4-102321  
 $^2\text{H}$ , magnetic form factors, current conservation, meson exchange currents 4-86768  
 $^3\text{He}$ , charge form factors by nucl. recoil detection 4-68617  
 $^3\text{He}$  form factor and large transfer momenta, six quark admixture 4-102176  
 $^3\text{He}$ , magnetic form factors, current conservation, meson exchange currents 4-86768  
 $^4\text{He}$ , two and 3-body forces, E0 energy weighted sum rule 4-106592  
 (Li,d) microscopic cluster form factor in DWBA calcs. 4-64161  
 $^4\text{Li}$ , charge form factor in Born approx., single particle model 4-111500  
 $^6\text{Li}$  ground state, cluster struct. in three body model, principal parameters 4-59186  
 $^6\text{Li}(e,e')$ , electromagnetic form factors, effects of meson exchange currents 4-111539  
 $^7\text{Li}$ , t- $\alpha$  system, orthogonality-condition model, dust 4-95943  
 $^{24}\text{Mg}$ , e and p scatt., excitation of low-lying isoscalar states 4-96024  
 $^{24}\text{Mg}(e,e')$ , 90-280 MeV, negative parity states, transitions, EM form factors 4-73806  
 $^{14}\text{N}$  levels electroexcitation, 12-21 MeV 4-68650  
 $^{14}\text{N}(e,e')^{14}\text{N}$ , M1 form factors at high momentum transfer 4-68675  
 $^{20}\text{Ne}$ , e and p scatt., excitation of low-lying isoscalar states 4-96024  
 $^{28}\text{Si}$ , e and p scatt., excitation of low-lying isoscalar states 4-96024  
 $^{28}\text{Si}$  oblate-prolate deform., form factors, open shell RPA limitations, comparison with  $^{24}\text{Mg}$  4-78591  
 $^{88}\text{Sr}$ , M1 form factor, spin-isospin polarization 4-86770  
 $^{88}\text{Sr}(e,e')$ , 23.7-261.6 MeV, 1 $^+$  3.486 MeV state electroexcitation, B(M1), form factors 4-102182  
 $^{88}\text{Sr}(e,e')$  1 $^+$  excitation at 3.486 MeV, form factor, B(M1)-value 4-68673  
 $^{A}\text{Ti}$ , A=46, 48, 50, form factors for  $0^+ \rightarrow 2^+$  transitions in 2p-1f nuclei 4-83025

**Formation, heat of see heat of formation****Forming processes**

- see also casting; electroforming  
 deep-drawing forming limits, three-dimens. ductile damage model 4-99596  
 experimental and theoretical forming limit diagrams, comparison 4-93348  
 hydro-spark forming, impulsive hydraulic press. and gas bubble motion (Japanese) 4-103594  
 mechanical behaviour of materials, conf., Stockholm, Sweden (Aug. 1983) 4-90297  
 metal hot or warm forming model using deform. mechanism maps 4-83830  
 metal sheets, rate-sensitive, formability limits 4-93349  
 metals, anisotropic hardening 3D model, sheet metal formability analysis 4-66348  
 metals, formability, max. uniform strain, effect of matrix and second phase 4-99465  
 metals, plastic behaviour, torsion tests on solid and tubular specimens 4-93473  
 metals, strain hardening exponent 4-99406

**forming processes continued**

- plane-isotropic sheets, anisotropic plasticity 4-97346
- plastic deformation, material inhomogeneity and surface roughening 4-99458
- plastic instability in sheet-metal forming 4-99462
- sheet formability and plastic instability, effect of geometry and materials props. 4-99351
- sheet metals, anisotropic, forming limit diagrams, prediction 4-99466
- steel, dual-phase, Al-killed, forming props., influence of microstruct. and texture 4-99459
- steel, dual-phase, law of mixtures, relevance to sheet formability 4-99470
- steel, HSLA, sheet, press forming problems 4-99471
- steel, low C, deep drawing cold-rolled sheet prod. by continuous annealing, control of steel chem. 4-114565
- steel, low C, deep-drawing, prod. by continuous annealing 4-114566
- steel, plastic properties, effect of non-linear strain path 4-99463
- steel, plastic properties, effect of nonlinear strain paths 4-99474
- steel, structural, fine-grained, low cycle fatigue, influence of cold forming 4-104841
- steel sheet, hot rolled, test methods for formability 4-99736
- steel tubes, autofrettage, fatigue strength, thermal shock; tempering, electropolishing 4-104865
- steel tubes, autofrettaged, fatigue strength 4-104864
- thermoplastics, recovery-induced thermal deform. 4-99469
- Al, forming by underwater Cu wire explosions, bulging expt. 4-75217
- Al sheets, square cup drawing characts. 4-61941
- Al-Cu (10 wt.%), prod. by rheocasting, rel. between struct. and mech. props. 4-99467
- Al-Cu-Mg, low cycle fatigue, influence of cold forming 4-104841
- Al-Cu-Si, Al 2014, punch-stretching behaviour, 250 to 500°C 4-76817
- Al-Cu-Si, Al 2014, tensile props., 250 to 500°C 4-76816
- Fe, pure, orthogonally planed surface layer, X-ray lattice strains rel. to texture (Japanese) 4-114567
- Nb<sub>3</sub>Sn-Cu, superconducting wire, welded annular region of Nb<sub>3</sub>Sn filaments 4-99363
- Ti sheet, forming limit curves 4-99464
- W, powder metallurgy rods, swaging process workability rel. to texture (Japanese) 4-89068
- Zn-Al, review of commercial alloys 4-88954

**FORTAN**

- programming and computer simulation teaching by diffusion in percolative lattice 4-78076

**Foucault currents** *see eddy currents***fountain effect** *see superfluid helium-4***Fourier analysis**

- see also Fourier transforms; harmonic analysis; waveform analysis*
- abelian groups, Fourier anal. on multiplier representation 4-58616
- atrial flutter, gated blood-pool study, Fourier anal. 4-72371
- coil arrays for pulsed relativistic electron beam expts., plasma diagnostics appl. 4-113222
- EEG, Walsh and Fourier anal. comparison, anaesthesia effects tracking appl. 4-115265
- ileum, rat, pendular movements of longit. musculature, computer aided Fourier spectral analysis (German) 4-62505
- interferogram analysis, frequency domain description 4-112343
- local magnetisation and mag. viscosity, stochastic characts. and meas. methods 4-73456
- mixed aqueous electrolytes, local structure., Raman and EXAFS studies 4-60808
- Navier-Stokes eqns., combined finite element and spectral approximation 4-103281
- plasma equilibria calcs., appl. of implicit Fourier expansion method in 3-D 4-69883
- Rayleigh-Benard convection onset, nonlinear pattern formation 4-91810
- scanning photoacoustic microscope, imaging and resolution, Fourier anal. 4-112654
- seismology, calc. of synthetic seismograms for complex subsurface geometries 4-105457
- semi infinite solid with heat supply, three-dimens. thermoelastic analysis 4-112715
- soft magnetic materials, magnetisation and losses, microprocessor controlled system 4-73457
- surface roughness problems, fractal dimension and minimal yardstick range 4-98410
- tooth enamel, human, struct., digital Fourier harmonic superposition method 4-89495
- transmission electron microscopy, time shared television digital image processing system 4-106431
- trigonometric Fourier coeff. calc. for seismological appl. 4-72507
- ventricular performance in congenital left-to-right shunt: temporal Fourier analysis of gated blood-pool data 4-72376
- Al, grain boundary struct., computer simulation studies 4-113459
- Cd<sub>1-x</sub>Mn<sub>x</sub>Te, struct. props., EXAFS studies 4-60902
- Cs<sub>2</sub>Ca(Nb<sub>2</sub>)<sub>2</sub>H<sub>2</sub>O, cryst. struct., X-ray diff. studies 4-92164
- Cs<sub>9</sub>K<sub>13</sub>Si<sub>3</sub>Al<sub>32</sub>O<sub>192</sub> zeolites, normal and deuterated, cryst. struct. 4-92169
- GaS<sub>2</sub>, charge density wave depinning and nonlinear transport 4-70790
- G<sub>2</sub>C<sub>4</sub>(N<sub>2</sub>)<sub>15</sub>, cryst. struct., single cryst. X-ray diff. studies 4-108332
- Ni-Cr-Co-Al-Ti-Nb-W-Mo-V-Hf, cryst. lattice periods mismatch determ. 4-65219
- Ni<sub>60</sub>B<sub>40</sub> glassy, Ni-Ni distrib., multishell modelling, EXAFS studies 4-60853
- Si<sub>92-x</sub>Al<sub>x</sub>O<sub>384</sub> Linde Y-zeolites, struct., neutron diff. studies 4-113403
- ZnSiP<sub>2</sub>, valence band struct. and chem. binding 4-88445

**Fourier series** *see series (mathematics)***Fourier transform optics**

- see also Fourier transform spectroscopy*
- autocorrelation unfolding 4-79054
- band-limited optical systems, discrete close points at output at any given intensity 4-69327
- binary Fourier transform holograms, quantisation and phase encoding errors reduction 4-107557
- centro-symmetry and partial coherence 4-102881
- coherent optical techniques for diagonalization and inversion of circulant matrices and circulant approximations to Toeplitz matrices 4-59989
- coherent-optical matched filters, increased light efficiency 4-74684
- complex Fourier spectrum phase meas. method 4-79061
- continuous Fourier transforms of real signals obtained using a bulk acoustic signal processor 4-74428
- cosinusoidal transforms in white light 4-59987

**Fourier transform optics continued**

- current trends in optical and hybrid processing methods 4-74434
- electron Fourier holography, non-interferometric reconstruction props. 4-91394
- electron holography, Fourier, aberrations elimination 4-69345
- electron holography, Fourier, scatt. foil choice, resolution limitation 4-69346
- filters, production by computer controlled scanning interferometric pattern system 4-107801
- folded spectrum analysis 4-79047
- grating-based interferometric processor for real-time optical Fourier transformation 4-95500
- holograms, computer generated, efficiency and versatility 4-107556
- holograms, computer-generated, interpolation approach 4-107558
- holographic image subtraction based on Fourier plane recording and spatial filtration 4-96848
- hybrid optical implementation of a real formalism of discrete Fourier transform in terms of circular correlations 4-107534
- image reconstruction from frequency-offset Fourier data 4-96835
- incoherent optical two-dimensional Fourier transform using the chirp-z algorithm 4-79064
- interferogram analysis, freq. domain description 4-107516
- interferogram analysis, frequency domain description 4-112343
- interferograms, speckle and holographic, produced by recording object light field in Fourier plane 4-83554
- inversion of deficient data 4-79056
- laser speckle photography with cross-slit aperture (Chinese) 4-107520
- lens, test signal image appl. for computation of focal length and aberration (Russian) 4-107776
- matched filtering in white light illumination 4-74685
- microscopic image formation, Abbe's theory, formal representation 4-102893
- multidimensional hybrid signal processing architectures 4-79042
- multidimensional signal processing, projection theorem appls. 4-79037
- photograph enhancement and deblurring, image processing system 4-91413
- processor architectures and techniques 4-87435
- rainbow holographic process, point spread and transfer functions 4-79076
- reconstruction and synthesis applications of an iterative algorithm 4-79050
- solid-state Fourier-transform ring laser, good-quality beam 4-69453
- surface finish, precision meas. and characterisation 4-106265
- synthetic aperture propag., point spread function, computer model 4-96813
- Talbot and Lau effects, a parametrical approach 4-69322
- texture classification, optical preprocessing using specialised binary black and white pseudocolouring masks 4-74440
- time-frequency interrelationships in optical information processing 4-79044
- tomographic imaging, non-iterative, limited-angle, using eigenfunctions adapted to space-limited objects 4-69326
- transformations in optical signal processing, conf., Seattle, WA, USA (Feb. 1981) 4-78023
- two-photon-resonant image upconvertors using Fourier mode optical systems, chromatic aberrations (Japanese) 4-60116
- two-scanning mirror Fourier transform interferometer for plasma diagnostics 4-103570
- two-stage spatial filtering for diff. pattern anal., processor digital simulation using cytogenetic data 4-59986
- visibility magnitudes, phase estimation 4-59985
- white-light signal processor, noise performance, temporally partially coherent illum. 4-69320

**Fourier transform spectroscopy**

- absolute radiometry with Fourier transform spectrometers 4-101944
- absorbing materials, vacuum compatible, submm and mm refl. spectroscopy 4-108214
- allene-d<sub>4</sub>, C-C stretching band  $\nu_c$  4-64468
- L-amino acids and related mol., FIR FT spectra 4-96531
- anisotropic phases, multiple-quantum NMR, projections of two dimens. MQNMR spectra 4-104497
- array-processor-based Fourier-transform ion cyclotron resonance mass spectrometer 4-101965
- atmosphere remote sensing using Fourier transform spectroscopy method 4-110269
- atom-probe FIM composition profile, spectral anal. using Fourier techniques 4-89232
- automated interferometer for Fourier transform spectroscopy at near-mm wavelengths 4-101914
- bacterial cells, intact and living ultrastructural information from FTIR 4-100094
- 2-bromopropene, internal rot. anal. of ground state microwave spectrum 4-96717
- 1,3-butadiene, adsorbed on silica surface, Fourier transform IR spectra 4-78843
- carbohydrates, aq. solns., mutarotation FT IR spectrosc. investig. 4-78833
- Cardiothane 51, quantitative surface anal. by FT attenuated total reflection IR spectroscopy 4-103662
- Cary 82 laser Raman spectrometer, computer enhanced spectroscopy 4-58894
- complex hydrocarbon mixtures separation using mixed fused silica columns, GC/FT-IR considerations 4-105037
- conference, Durham, England (Sept. 1983) 4-101566
- cryogenic IR radiance instrument for shuttle CIRRIS telescope 4-94614
- cyclohexane, liq., dielec. loss in millimetre and submillimetre wavelength region 4-99015
- diethylamine, gaseous, overtone absorpt. spectra, conformationally non-equivalent C-H and N-H local mode oscillators 4-96528
- diffuse reflectance far IR interferometric spectroscopy 4-78391
- dimethylamine, gaseous, overtone absorpt. spectra, conformationally non-equivalent C-H and N-H local mode oscillators 4-96528
- dipolar gases, stark effect measured by microwave Fourier transform spectroscopy 4-74278
- dispersive, optical const. determ. of solids in visible 4-101934
- display system, array-mapped, for Fourier transform IR spectroscopy 4-101945
- double cat's eye small interferometer for rapid-scanning Fourier transform spectroscopy 4-101913
- dual beam interferometry and double chopping for scintillation free measurements 4-106368

## Fourier transform spectroscopy continued

- EELS, plural scattering removal techniques 4-73601  
 EPR spectra simulation recorded using phase-sensitive detection at any modulation freq. harmonic 4-86452  
 far IR, high efficiency polarising interferometer 4-106407  
 far IR, microcomputer expt. control and data analysis 4-106406  
 far IR, solid sampling techniques review 4-101941  
 far IR Fourier matrix-isolation spectroscopy, state-of-the-art report 4-102677  
 formaldehyde,  $X^1A_1$  state, vibr. const., stimulated emission spectra 4-87111  
 FT-IR absorbance subtraction from mixtures, automated procedure 4-105036  
 FT-IR-PAS spectra, particle size effect 4-105035  
 gases, dispersive Fourier transform spectroscopy in visible region 4-101935  
 n-heptane, liq., dielec. loss in millimetre and submillimetre wavelength region 4-99015  
 hexahydro-1,3,5-trinitro-s-triazine, mol. struct. in vapour. soln. and solid phases, IR obs. 4-69064  
 n-hexane, liq., dielec. loss in millimetre and submillimetre wavelength region 4-99015  
 high background noise operation 4-90661  
 high resolution molecular spectroscopy in submillimetre wavelength region 4-90669  
 history 4-101615  
 HMX, melt-phase characterisation by rapid-scan FT-IR spectrosc. 4-109701  
 hydraulic high precision moving mirror drive for Fourier transform spectroscopic appls. 4-11213  
 ICP, near-IR spectral emission characts. 4-78390  
 ICP, temp. determ. using Fourier transform spectrometer 4-108220  
 inorganic thin coatings on metals, Fourier transform IR spectra 4-104688  
 interferometer, switched-field-of-view, for complex refl. spectra determ. of heavily-absorbing solids 4-101912  
 interferometer for complex refl. spectra temp. variation determ. of reasonably transparent solids at near-mm wavelength 4-101911  
 ion cyclotron mass spectrometry using pseudo-random noise excitation 4-93571  
 IR photoacoustic spectroscopy, conformation probe technique 4-95533  
 IR spectroscopic cell for FTIR meas. at press. up to 100 MPa 4-86491  
 IR specular reflection spectroscopy of surfaces, appl. to plasma sprayed  $Cr_2O_3$  deposits 4-101942  
 light interferometry and assoc. Fourier spectrometer (*Japanese*) 4-94628  
 linear dichroism using polarisation modulation FT-IR technique 4-104566  
 low-cost Fourier transform spectrometer using a Burleigh Inchworm covering visible and MM wavelengths 4-73532  
 mass spectrometry using random-noise excitation 4-90684  
 methane gas, refr. index, dispersive Fourier transform spectroscopy in visible region 4-101935  
 methanol, high-resolution FIR and IR spectroscopy 4-96533  
 methanol C-O stretch band, IR obs. 4-78853  
 methanol laser line assignments, IR spectra study 4-79119  
 methylamine, gaseous, overtone absorpt. spectra, conformationally non-equivalent C-H and N-H local mode oscillators 4-96528  
 methyleneimine,  $\nu_8$  band, high-resolution IR spectra in 10  $\mu m$  region 4-96534  
 3-methylthiophene polymer films, in situ Fourier transform IR spectra, vibronic coupling 4-87115  
 microcomputers in Fourier transform spectroscopy 4-101928  
 microemulsions extractant anions, FTIR studies on hydration 4-99848  
 molecular spectroscopy progress (*Chinese*) 4-11212  
 MOS device, IR FT spectroscopy of two dimens: space charge layers 4-99109  
 multiple pulse and 2 dimens. Fourier transform NMR computer simulation 4-78352  
 NMR, high resolution powder spectra for dipole-dipole interaction determ. 4-65867  
 NMR spectra, automatic phase correction, lineshape anal. 4-68246  
 obtained using Fourier transform spectrometer 4-91257  
 n-octane, liq., dielec. loss in millimetre and submillimetre wavelength region 4-99015  
 perfluorotributylamine, Fourier transform ion cyclotron mass spectrometry using pseudo-random-noise excitation 4-93571  
 phase correcting an emission line spectrum 4-101927  
 phase error correction 4-101930  
 phenanthrene, oriented single crystals, far-IR spectra, temp. depend. 4-114262  
 photoacoustic IR spectroscopy, depth profiling, cell reson. effect 4-101943  
 photoacoustic spectroscopy and thermal wave imaging, tutorial review 4-106391  
 photothermal beam deflection spectroscopy for IR studies of materials 4-106403  
 poly(2,6-dimethyl 1,4-phenylene oxide)-atactic polystyrene blends, orientation and relax. 4-79955  
 poly( $\gamma$ -benzyl glutamate),  $\alpha$ -helical conformation, Fourier transform IR photoacoustic spectra 4-95533  
 polyethylene, FT-IR study of soln. grown crystals. 4-108343  
 polyethylene, high density, cryst. axes orientation and state of order during elongation FTIR study 4-99111  
 polymer deformation studies by FT-IR spectroscopy, mechanical stretcher interface 4-103850  
 polymer deformation studies by time-resolved FT-IR spectroscopy 4-103851  
 polymer degradation on refl. metal films, Fourier transform IR refl. absorpt. obs. 4-112539  
 polymers, Fourier transform IR spectroscopy, theory and appl. 4-76458  
 polypropylene, mech. deform., Fourier transform IR obs. 4-66363  
 polysaccharides, FIR FT absorpt. spectra 4-96532  
 polystyrene, cross-linked, near-mm wave material characterisation using non-dispersive Fourier transform spectroscopy 4-93033  
 polytetrafluoroethylene, glass-loaded 4-93033  
 polyvinylalcohol-chitosan blends, intermolecular interactions, mech. props., Fourier transform IR spectra 4-84409  
 polyvinylidene fluoride films, piezoelec. effect at high temp., Fourier transform IR spectra 4-76334  
 polyvinylidene fluoride films, poled semicrystalline, FIR Fourier spectra, X-ray obs. 4-60858

## Fourier transform spectroscopy continued

- portable FTIR spectrometer using a rotating refractor, JANOS 1000 series 4-105040  
 proteins, two dimensional  $^{13}C$  chemical shift correlated spectroscopy at natural abundance 4-89504  
 quartz, near-mm wave material characterisation using non-dispersive Fourier transform spectroscopy 4-93033  
 rapid-scanning Fourier transform spectroscopy, source of problem 4-73536  
 RDX, melt-phase characterisation by rapid-scan FT-IR spectrosc. 4-109701  
 saccharides, mono- and di-, FIR FT absorpt. spectra 4-96532  
 soda-lime-silica glass, complex refl. spectra determ. using switched-field-of-view interferometer 4-101912  
 sodium dodecyl sulphate-water system, phase transitions, FT IR obs. 4-84389  
 solid surfaces, FT-IR, diffuse reflectance and photoacoustic spectrum 4-61706  
 submillimetre FT spectrometer for stratosphere spectra and chem. composition 4-110268  
 tetramethyldioxetane, vibr. freq. Fourier transform IR and Raman spectra 4-64478  
 TFR tokamak diagnostic system using Fourier spectrometer 4-75201  
 thermal radiation problem 4-95520  
 time-domain dielectric spectroscopy, use with lossy dielectrics, precautions in use 4-85592  
 time-resolved, stretched polymer film changes obs. appl. 4-101940  
 time-resolved FTS of molecular and atomic IR emission 4-96473  
 tobacco samples, FT-NIR diffuse reflectance spectroscopy anal. 4-105034  
 trimethylchlorosilane polymorphism, FIR study 4-61685  
 two-beam interferometer for dispersive refl. spectroscopy of solids in far IR 4-106405  
 two-dimension method for high resolution solids NMR spectroscopy of homonuclear broadened spins 4-61597  
 two-dimensional fluorescence data filtering 4-101820  
 vibrational circular dichroism meas. of single enantiomer on FT-IR spectrometers 4-102816  
 vibrational circular dichroism measurements by optical subtraction FT-IR spectrometry 4-101938  
 visible light spectrometer using Michelson interferometer 4-101936  
 $Al_2O_3$  surface with adsorbed HCN, far IR Fourier spectroscopy 4-104593  
 $BF_3 \cdot CO(N_2)$ , weakly bound complexes, Fourier transform IR spectra 4-87125  
 C, determ. in organic cpds., FT near-IR spectrometric method using Ar ICP 4-72008  
 $C^+$ , branching ratios of  $2s^2 3p^2$  term, Fourier transform and VUV spectroscopy 4-87066  
 $CO_2$ , vibr. rot. bands in 540 to 890  $cm^{-1}$  region 4-64466  
 $^{13}C$  FT NMR spectra, why it cannot be phased 4-86453  
 $^{14}CO$ , vibr.-rot., pot. energy curves, IR spectra 4-59754  
 $Cr_2O_3$  plasma-sprayed deposits, IR Fourier transform specular reflection spectroscopy of surfaces 4-101942  
 $CS_2$ , first two excited  $^1\Sigma_g^+$  states, IR fluoresc. study 4-64525  
 Cu film, optical const. meas. in visible using dispersive Fourier transform spectroscopy 4-101934  
 $D^+NO_3$ , D hyperfine struct. microwave Fourier transform spectroscopy study 4-96719  
 GaAs, far IR optical props. at 6, 300K, amplitude and phase refl. spectra 4-104594  
 H, determ. in organic cpds., FT near IR spectrometric method using Ar ICP 4-72008  
 $H_2$  isotopic molecules adsorbed in NaCa zeolites, induced IR overtone and fundamental bands 4-102678  
 $(HF)_n$  in solid Ar matrix, FT IR spectra 4-69066  
 $H_2O$  in liq. crystal, polarised FT-IR spectra 4-64473  
 $H_2O$  isolated in solid gas matrices, far IR Fourier spectroscopy 4-102677  
 $H_2O$ , matrix isolated in  $D_2O$  cubic ice, vibr. data 4-69045  
 $H_2S-HCl$ , H bonded complex, rot. const., Fourier transform microwave obs. 4-59732  
 $H_2S-HF$ , hyperfine coupling const., rot., pulsed-nozzle Fourier transform microwave spectra 4-107333  
 InP, far IR optical props. at 6 and 300K 4-109174  
 InP, localisation of inversion electrons, Fourier transform spectra studies 4-98555  
 $KZn_{1-x}Co_xF_3$ , Fourier transform IR spectroscopy of  $Co^{2+}$  excitations 4-104596  
 Mo catalysts supported on  $Al_2O_3$  or  $SiO_2$ , Fourier transform IR spectroscopy of sulphidation 4-105014  
 N, solid,  $NH_3$  rotation, FTIR study 4-79964  
 $N_2$ , temp. depend. collision induced IR absorpt. 4-69058  
 $N_2$ -DF, rot., hyperfine and quadrupole coupling const., 4-112195  
 $NH_3$  isolated in solid gas matrices, far IR Fourier spectroscopy 4-102677  
 $N_2H_4$ , gaseous, overtone absorpt. spectra, conformationally non-equivalent C-H and N-H local mode oscillators 4-96528  
 $N_2O$ , IR vibr. rot. spectrum in lowest fundamental  $\nu_2$  region 4-64465  
 $N_2O$  line strengths meas. from high resolution Fourier transform spectra 4-59748  
 $^{14}N^{16}O_2$ ,  $\nu_1$  band, line positions and intensities, Fourier transform IR spectra 4-59755  
 $Na_2$ , double minimum state, IR fluoresc. spectra 4-91305  
 $Na_2O-CaO-SiO_2-Si_3N_4$  glass, prep., Fourier transform IR spectra, XPS 4-84192  
 $Ni_{0.6}Zn_{0.4}Fe_{0.3}Mn_{0.1}O_4$ , near-mm wave material characterisation using non-dispersive Fourier transform spectroscopy 4-93033  
 OC-HCN, weakly bound complex, rot. spectrum investig. by pulsed nozzle, FT microwave spectroscopy 4-74228  
 OCS, rot. transitions and  $T_2$  relax. 4-96525  
 OCS, Stark effect measured by microwave Fourier transform spectroscopy 4-74278  
 OCS, vibr. rot. bands in 540 to 890  $cm^{-1}$  region 4-64466  
 S, determ. in organic cpds., FT near IR spectrometric method using Ar ICP 4-72008  
 $SO_2$ , Fourier transform absorption spectrum, analysis 4-112165  
 $SO_2$ , rot. transitions and  $T_2$  relax. 4-96525  
 Si, far IR transmission spectrum, two-phonon difference band obs. 4-104597  
 $SiF_4$ , ion-molecule reactions, FT mass spectra 4-93518

**Fourier transform spectroscopy continued**

SiO<sub>2</sub> surface with adsorbed HCN, far IR Fourier spectroscopy 4-104593  
U III, wavelength and energy level meas. using Fourier-transform spectrometer 4-102623

**Fourier transforms**

*see also fast Fourier transforms; Fourier analysis; Fourier transform optics*  
acoustic diffraction, Fourier integral transforms appl. to theory 4-103048  
acoustic imaging system, synthetic focus, Fourier domain reconstruction 4-97210  
attenuative subsurface layered media parameter estimation, frequency-domain approach 4-107941  
brass, momentum density of annihilation photons, one-dimens. Fourier transform method 4-70634  
degenerate functional integral, functional delta-functions and Fourier transforms 4-58619  
electron micrograph astigmatism correction using joint transform 4-90694  
electrooptic spatial light modulators, theoretical resolution limitations, fundamental considerations 4-87440  
ESR Bruker spectrometer, using digital phase-sensitive detection and Aspect 2000 minicomputer 4-68253  
fast Walsh and Fourier transforms for bones mechanical integrity meas. 4-72458  
four-dimensional symmetry, uncertainty relations, R-inherent quantum mechanics 4-95226  
Fourier domain techniques for digital angiography of the heart 4-109905  
geophysical inverse problem soln. for gamma-ray well logging 4-77636  
hydrophone arrays, collinear, hybrid time-delay/phase-shift digital beam-forming 4-83777  
Josephson tunnel junctions, current density distrib. (German) 4-84750  
lattice sums, rapid convergence by use of Fourier transforms 4-79973  
liquids and liq. cryst., fluorescence depolarisation intensity deconvolution 4-93103  
Lorentz group, Heisenberg picture and Fourier transform 4-90441  
lossy dielectric slab, EM plane wave diffraction by slit 4-79005  
membranes, fluorescence depolarisation intensity deconvolution 4-93103  
momentum representation of Dirac relativistic wave functions for hydrogen like atoms 4-112129  
N-dimensional free-particle, harmonic oscillator and Coulomb problems, Green's functions, propagators from integral representations 4-63542  
nonrelativistic Coulomb problem, Sturmian propagator 4-63561  
plate, orthotropic, thermoelastic problem of uniform heat flow disturbed by central crack 4-79511  
polypropylene and polycarbonate, study of dielectric relaxation in polymer blends - transient current approach 4-99021  
proton recoil spectra evaluation including inverse filtering in Fourier domain 4-64314  
quantum mechanical two-level system in applied elec. field Fourier transform treatment 4-101673  
SEM-microcomputer system for quantitative morphological analysis, single object case 4-111251  
SEM-microcomputer system for quantitative morphological analysis, complex images case 4-111252  
slit in thick screen, EM wave diffr. (Japanese) 4-96763  
spectral estimation for short data sequence, fast algorithm of maximum entropy method 4-63678  
test object for electron microscopes, use of partially crystallized C 4-90692  
US imaging through an inhomogeneous layer by least-mean-square error fitting 4-60234  
Weibull-distributed weather clutter, frequency domain anal. 4-100688  
wideband ocean noise and propagation loss, real-time digital signal processing algorithms 4-107938  
Wightman functional, integral representation, positive definiteness condition, Fourier transform 4-111270  
wing aerodynamics in supersonic shear flow 4-97602  
CN adsorbed on Ag electrode, Fourier transform IR spectra studies 4-93067  
Fe, EXAFS contributions and near neighbour components 4-61774  
Fe<sub>17</sub>P, EXAFS contributions and near neighbour components 4-61774  
Fe<sub>2</sub>P<sub>2</sub>, amorphous alloys, EXAFS contributions and near neighbour components 4-61774  
KAl<sub>3</sub>(Si<sub>4</sub>)O<sub>8</sub> monoclinic feldspars, crystal growth, PBC vector analysis 4-92119  
Mn dihalides, d-excited, vibr. struct., IR and Raman spectra studies 4-113873  
Ne, FCC, high press. eqn. of state, Gaussian orbital techniques 4-92332  
ZrZn<sub>2</sub>, ferromag. and paramag. phases, magnetisation density and mag. struct. 4-76114

**fractionation** *see distillation***fracture**

*see also brittle fracture; crack-edge stress field analysis; cracks; creep fracture; ductile-brittle transition; ductile fracture; embrittlement; fatigue; fracture toughness; stress corrosion cracking*  
3D fracture mechanics, boundary integral equation-boundary element method appls. (Chinese) 4-97398  
adhesive joints, mode I and II fracture 4-93387  
alkali borosilicate glass rods, partially leached, abraded and unabraded strength rel. to heat treatment 4-89144  
alkali halides, fracture-induced luminesc. and crack vel. 4-104685  
aluminous electrical porcelain, doped with talc, microstruct. and med. props. 4-114674  
anisotropic creep damage in the framework of continuum damage mechanics, reactor appls. 4-102338  
ankle joint biomechanics, effects of fibular shortening 4-100226  
bars, round, loaded in mode III, fracture and procedure for fracture toughness determ. 4-69709  
bauxite brick, lower temp. firing, microanalyses and SEM fractographs, K<sub>2</sub>O content 4-61892  
beams, reinforced, failure in combined loading 4-87629  
biaxial fields, higher order approx. for T-criterion 4-79495  
brass, microfractography, SEM study (Polish) 4-93363  
brittle materials, lifetime and rationalised load 4-69712  
brittle materials, slow crack growth resistance testing with double torque method 4-81375  
cast Fe, SG, fracture mechanics, cracks, elasticity anal., microtension tests (Chinese) 4-62027  
ceramics, cracking behaviour, microprocessor-controlled meas. 4-62056

**fracture continued**

ceramics, fracture energy, elastic anisotropy and grain size dependence 4-60983  
ceramics, heterogeneous, fracture, acoustic emission and sub-crit. events 4-62050  
ceramics, surface damage, strength degradation, erosion and wear, acoustic NDT 4-76872  
charged particle emission in failure of solids 4-99291  
charged particle emission in failure of solids 4-99292  
composite materials, biaxially stressed, inconsistency in max. strain theory of failure 4-112769  
composite materials, delamination, fracture mechanics 4-97431  
composite organic insulators, electron and neutron irradi. effects on mech. props. 4-75533  
composite plates, delamination growth during impact, fracture mechanics analysis 4-79526  
composite sheet, hybrid, stress concs. due to fibre breakage 4-97426  
composites, inelastic, delayed failure 4-97434  
crack growth kinetics, method for determ. under cyclic loading 4-89215  
crack micromechanics, thermodynamic approach 4-88234  
crystal in prefracture state, acoustic emission theory 4-80166  
crystalline materials, characteristic deformation temperatures 4-70258  
cyclotrimethylenetrinitramine (RDX) explosive single crystals, fractoemission 4-81120  
detaching elastic body motion, boundary value problem 4-87569  
drawing techniques for high-strength long-length optical fibers 4-74736  
elastic-plastic fracture, energy flux into process region 4-69705  
elastomers, glass bead filled, failure processes near rigid spherical inclusion 4-76841  
environmentally assisted, atomistic models using transition rate theory 4-83855  
epoxide polymers, breakdown, ionisation processes role, mechanoemission mechanism 4-88952  
epoxide resin, glass bead filled, fracture, yield strength rel. to struct. 4-66416  
femoral bone, human, work-of-fracture obs. 4-62515  
fibre reinforced composites, stiffness reduction due to fibre breakage 4-80136  
fibre reinforced composites model, acoustic emission evaluation 4-81380  
fibre reinforced metal composites, stress-strain and failure behaviour 4-76831  
fibre reinforced plastics, tensile tests, at cryogenic temps., acoustic emission 4-76804  
fibre reinforced Ti matrix composites, fabrication and mech. props., review 4-81170  
films, compressed, delamination and spalling mechanics 4-79500  
finite plane domain fracture problem anal. using surface integral finite element hybrid method 4-79501  
geological materials, subcritical crack growth, review 4-94096  
glass, soda-lime silicate, Vickers indented, delayed fracture in deionised water 4-81268  
glass fibre reinforced epoxy resin, fracture initiation under impact compression 4-76863  
glass fibre reinforced epoxy resins, curing conditions effect on mech. props. 4-99487  
glass fibre reinforced plastic laminates, interlaminar shear strength 4-99575  
glass fibre reinforced polyamide, fracture mechanism, acoustic emission and microscopy obs. 4-66417  
glass-C hybrid reinforced plastics, mech. props. 4-93407  
granite from Japan, microcrack growth in aqueous environments 4-94100  
graphite, nuclear, fracture, acoustic emission and sub-crit. events 4-62050  
graphite fibre reinforced epoxy laminates, damage accumulation, final fracture rel. to ply thickness 4-81288  
graphite fibre reinforced epoxy laminates, pin loaded holes, sizing methods, failure load 4-109507  
graphite fibre reinforced epoxy laminates, tensile failure, delamination fracture surfaces, SM obs. 4-66418  
graphite fibre reinforced epoxy laminates containing pin loaded holes, failure prediction 4-109583  
graphite fibre reinforced polyimide, fracture and elastic props., influence of 4-99572  
graphite fibre reinforced polyimide panels, high temp. fracture rel. to buffer strip use 4-62023  
graphite short bars with hemispherical seats failure mechanism 4-78694  
hard coating flaking under shear stress, fracture mech. anal. 4-69713  
ice fracture mechanics 4-62866  
ice sheet indentation, limit anal. 4-94179  
impulse radar for fracture detection in rocks 4-72732  
Inconel X-750, Ni-base superalloy, creep and fracture, prior deform. effects 4-114656  
internal stress energy and fracture characteristics of inhomogeneous solids (German) 4-83861  
ionic crystals, exoelectron emission during fracture, energy distrib. function depend. on charge struct. 4-88951  
irreversible systems obeying max. dissipation principle, bifurcation and stability (French) 4-78139  
linear thermoelasticity conservation law (French) 4-78138  
mechanics of material behaviour 4-95069  
mechanics parameters, transferability from CT-specimens to tensile specimens 4-86875  
metal, book contrib. 4-108508  
metallic materials, creep, determ. for long-service lives by multistage process 4-114624  
metals, crack-containing, failure mechanism under the effect of electro-mag. field 4-81274  
metals, fracture mechanism, energetic anal. (Spanish) 4-70269  
metals, fracture surfaces fractal charact. 4-71734  
metals, sheet, deep drawing, influence of temp. 4-66399  
metals, surfaces, impurities and defects, embedded atom method 4-92590  
microscopic fracture mechanics, appl. of J-integral concept 4-97435  
mixed mode fracture studies, evaluation of compact shear specimen 4-103277  
mixed-mode break mechanics, crack ductility level and deflection angle (German) 4-83864  
new approaches in fracture mechanics 4-103266  
nonlinear fracture mechanics, phenomenological theory, fundamentals 4-97429  
nonlinear viscoelastic media, deform., fracture analysis, generalised J integral, correspondence principles 4-103253

## acture continued

- ordered alloys, long-range, phys. metallurgy and struct. appl., review 4-114638  
 organic plastic, damage-cumulation in quasistatic and cyclic loading 4-89090  
 PET filaments, orientational stretching, intermolecular interaction energy (Russian) 4-109460  
 pipe, gas-pressurised, break opening times for axial rupture 4-62040  
 pipelines, catastrophic fracture 4-95122  
 plane strain dynamic crack bifurcation 4-83857  
 plasticity and fracture, deform. modes 4-98177  
 plate, spalling fracture under shock loading 4-89112  
 plate with a moving slit and heat source, thermoelastic state 4-108016  
 PMMA, secondary cracks, form. mechanism, X-ray microanal. and acoustic emission 4-66421  
 poly(1,4-dimethylene-trans-cyclohexyl suberate), crack propag. and morphology 4-114662  
 polybutadiene, fracto-emission, effect of cross-linking 4-66419  
 polycrystalline materials, cumulative damage estimation 4-64894  
 polyester unsaturated resin, surface markings in brittle plastic plate, two dims. anal. 4-113527  
 polyethylene, fracture, simple model for chain scission 4-76849  
 polyethylene, high-density, moulded sheets tear strength 4-104846  
 polyethylene, ultra high mol. wt., crosslinking with dicumylperoxide, tensile props. 4-81436  
 polyethylene fibres, ultrahigh strength fracture process 4-62015  
 polyethylene film, yield and fracture in liq. environment 4-62077  
 polyimide films, fracture-crack resist. by high mol. weight incorporation 4-89108  
 polymer, oriented, homogeneous fracture under irradiation, kinetics (Russian) 4-103797  
 polymer macromol. degradation in elec. fields and under mech. loading (Russian) 4-104869  
 polymers, computer simulation, fracture mechanism, two coupled anharmonic chains with strong interaction 4-113531  
 polymers, fracture and emission of electrons, ions and photons 4-98189  
 polymers, fracture micromechanisms, direct obs. in SEM 4-99578  
 polymers, fracture velocity in transient stages, US fractography study 4-99732  
 polymers, notched, deform. and fracture, effect of temp. 4-81276  
 polymethylmethacrylate, evolution of fractures, prolonged action of electric field 4-108507  
 polypropylene, mech. future, ionic product form. 4-114660  
 polystyrene, chain scission and mech. degradation 4-93395  
 polystyrene, evolution of fractures, prolonged action of electric field 4-108507  
 porous solids, strength, rel. to pore vol. and max. pore length 4-71714  
 prefracture zone, influence of local hardening on plastic deform. 4-70262  
 pressurised thermal shock fracture mechanics anal., mechanical props. role 4-111629  
 PVC, craze development and breakdown during cyclic loading 4-66465  
 PVC, particle filled, fracture mechanism rel. to fatigue crack growth (Japanese) 4-89120  
 pyrophyllite, shear cracks and seismic conditions in specimens containing low-strength inclusions 4-100554  
 quartz, crack propagation affected by chem. environment 4-94097  
 quartz, diffusional crack healing in aqueous environment 4-94098  
 quartz, fracture surface and interface free energies 4-94091  
 quartz glass, triboluminesc. during frictional sliding 4-105547  
 reactor containment vessels, limit anal. and design, plasticity, stress, fracture 4-102340  
 Reichert-Jung freeze fracture apparatus, anticontamination device modification 4-89863  
 research review over period 1965 to 1983 4-99568  
 resorcinol crystals, mechanoluminesc. at low temp. 4-93121  
 rocks, appl. of fracture mechanics to hydraulic fracturing stress meas. 4-77509  
 rocks, crack growth during unroofing of crustal rocks 4-94102  
 rocks, fracture mechanics and acoustic emission of anti-plane shear cracks 4-77507  
 rocks, microfractures and fracture criterion rel. to earthquake premonitory phenomena 4-77459  
 rocks, subcritical crack growth and influence of aqueous environment 4-94099  
 rubber, silica filled EPDM, network struct., fracture mode rel. to vulcanisation conditions 4-109373  
 salt rocks, acoustic emission props. during failure processes 4-77510  
 shell, cylindrical, explosive destruction, fragment distrib. calc. (Russian) 4-74949  
 shock wave effects, conf., Santa Fe, USA (July 1983) 4-106116  
 snow, fracture under tensile stress 4-100629  
 solid mechanics large-deform. anal. using mixed Eulerian-Lagrangian displacement model 4-79461  
 solids, dilation mechanism for strength 4-88235  
 spall fracture models, kinetic relation 4-98192  
 steam turbine, low-pressure cylinder welded rotor, damage build-up evaluation 4-93404  
 steel, austenitic stainless, low cycle fatigue, elevated temps., crack propag. and fracture modes (Japanese) 4-89125  
 steel, austenitic stainless, nitrided, microstructure, optical microscopy, TEM obs. 4-81359  
 steel, austenitic stainless, SCC in MgCl<sub>2</sub> soln., fractography, grain struct., SEM obs. (Japanese) 4-99651  
 steel, austenitic stainless, stress-rupture under increasing stress, time-temp. parameter 4-66447  
 steel, C, fracture form., shock wave exit angle effect on free surface 4-99498  
 steel, C, tempered, radial direction fracture surface, SEM obs. (Japanese) 4-89115  
 steel, C-Mn, hot-rolled, ductility and anisotropy of sulphide inclusion spacings, effect of inclusion shape 4-99437  
 steel, Cr-Mo, temper-embrittled, effects of grain size and hardness 4-99554  
 steel, dual phase, necking and tensile fracture, void distrib. 4-99580  
 steel, dual-phase, C-Mn, mech. props. and fracture mechanism, influence of martensite morphology 4-99530  
 steel, dual-phase, Mn-C, tensile behaviour and fracture characteristics 4-99598  
 steel, dual-phase, tempered, fracture behaviour 4-89127  
 steel, high strength structural, stress relief cracking susceptibility 4-109509

## fracture continued

- steel, high tensile strength, fatigue crack growth and closure in vacuum (Japanese) 4-93381  
 steel, low alloy, crack branching 4-109490  
 steel, low alloy, fracture under corrosive environment, high temp. creep, fatigue, creep-fatigue 4-99592  
 steel, low alloy, reversible temper embrittlement, role of microstructure, scanning Auger microscopy study 4-81286  
 steel, low alloy ferritic, low cycle fatigue, elevated temps., crack propag. and fracture modes (Japanese) 4-89125  
 steel, maraging, ultrahigh strength, delayed failure 4-93402  
 steel, mech. props., influence of pressurised H<sub>2</sub> 4-109494  
 steel, medium and low strength, ductile behaviour, computer simulation 4-104832  
 steel, microalloyed, rel. between microstruct. and H embrittlement 4-99605  
 steel, Ni-Cr-Mo, H embrittlement susceptibility, delayed failure time, effect of specimen geometry 4-85204  
 steel, pressure vessel, plated with anticorrosive claddings, fracture behaviour 4-99595  
 steel, rotor forgings, unstable fracture, effect of small clustered flaws (Japanese) 4-93378  
 steel, spalling resistance, effect of system scale 4-99538  
 steel, spheroidized 1090, dislocation density distrib. in tensile specimens, H effect 4-84298  
 steel, type A533B, fractographic study 4-83154  
 steel structures in nuclear power plants, lamellar tearing 4-104870  
 stress intensity factors 4-97428  
 styrene-butadiene copolymer, fracto-emission, effect of cross-linking 4-66419  
 sucrose, fracture, electron and positive ion emission, triboluminescence 4-104686  
 sucrose, fracture and emission of electrons, ions and photons 4-98189  
 superalloy, IN 100, crack growth under sustained load, statistics 4-99555  
 surface motion excited by acoustic emission from a buried penny-shaped crack 4-97423  
 surface scratching in abrasive or erosive processes, effect of brittleness index and sliding speed 4-71741  
 tartaric acid crystals, mechanoluminesc. at low temp. 4-93121  
 thermal protection system of space shuttle, fracture behaviour 4-85208  
 thermoelastic body, crack growth, contour invariants in fracture theory 4-108042  
 thermoelastic crack fracture problem (German) 4-83824  
 TRISO coated fuel particles, irradiation, failure during high temp. annealing 4-73979  
 unified theory, book 4-63426  
 viscoplastic materials, advanced deformations and fracture initiation, constitutive modelling 4-103856  
 Wint-o-green Lifesavers, fracture, electron and positive ion emission, triboluminescence 4-104686  
 Zircaloy, fracture, influence of environment on form. of fluting microstruct. 4-104911  
 Al, fracture form., shock wave exit angle effect on free surface 4-99498  
 Al, microfractography, SEM study (Polish) 4-93363  
 Al-Cu-Li-Mg-Zr, splat-quenched, microstruct. and tensile props. 4-114620  
 Al-glass composite, produced by powder metallurgy route, mech. props. 4-66275  
 Al-Mg (7 wt.%), hot-rolled, prep. from rapidly solidified powder, fracture mechanism 4-71731  
 Al-Zn-Mg (4.25, 2.75 wt.%), SCC by slow strain-rate method 4-66495  
 Al-Zn-Mg-Cu, V95, microstruct. at early stages of spalling 4-114665  
 AlMg fracture form., shock wave exit angle effect on free surface 4-99498  
 Al<sub>2</sub>O<sub>3</sub> tubes, multiaxial loading fracture 4-62016  
 Al<sub>2</sub>O<sub>3</sub> tubes, multiaxial loading fracture, Weibull statistical predictions 4-62017  
 Au films, vacuum evaporated, compressive-type fracture (Japanese) 4-75822  
 Au films, vacuum evaporated, compressive-type fracture (Japanese) 4-75823  
 B fibre reinforced Al composite, fracture mode and shear strength rel. to interface strength 4-62022  
 C fibre reinforced epoxy composite, tensile stress appl. parallel to fibres, elastic constants, failure (Japanese) 4-85199  
 C fibre reinforced epoxy composite, tension appl. perpendicular to fibres, elastic constants, failure stresses (Japanese) 4-85200  
 C fibre reinforced plastic laminates, rigidity and strength (Japanese) 4-99431  
 C-fibre reinforced plastics, under uniaxial tension, failure behaviour, stress-strain diagram (Japanese) 4-99550  
 Cu, D<sup>+</sup> irradiation, two-level fracture in blistering 4-75560  
 Cu, fracture form., shock wave exit angle effect on free surface 4-99498  
 Cu, fracture strain and flow stress, invest. by tension and torsion methods (Polish) 4-93362  
 Cu, fracture stresses time depend. during spall 4-99499  
 Cu, microfractography, SEM study (Polish) 4-93363  
 Cu, spall fracture, models applicability 4-98192  
 Cu-Al<sub>2</sub>O<sub>3</sub>, dispersion hardened, tensile failure, temp. depend., grain boundary fracture 4-66405  
 Cu-P alloys, extruded, microstruct. and mech. props. 4-114574  
 Fe, cast, grey, profilometric characteris. of microstruct. (French) 4-71820  
 Fe-Cr-Mo Ti heat-resisting alloy, Chi phase strengthened 4-71800  
 Fe-Nb, nitrided, void form., mech. props., optical microscopy, SEM, TEM obs. 4-81361  
 Fe-Ni-based metallic glasses, fracture and annealing, ferromag. resonance studies 4-109078  
 Fe-P, segregated grain boundaries crack propag., mol. dynamics calcs. 4-114663  
 Fe-Si (3.25 at.%) alloy, mechanisms of crack origin and twins role in dynamic loading, 77-573K 4-99539  
 Fe-Si-C, cast, fracture micromechanism 4-62036  
 LiF bicrystals, fracture at plastic deform. 4-75609  
 LiF, exoelectron emission during fracture, energy distrib. function depend. on charge struct. 4-88951  
 Li<sub>2</sub>O-Al<sub>2</sub>O<sub>3</sub>-SiO<sub>2</sub> glass-ceramic, superplastic ductility, rel. to hydrostatic press. and humidity 4-109474  
 Mg, H embrittlement and environmentally-induced cracking 4-71718  
 MgO containing metal precipitates, optical and mech. props. 4-70161  
 MgO, resin-bonded, C-bearing magnesia, mech. props. 4-114673  
 MgO-graphite, C-bearing magnesia, mech. props. 4-114673

**fracture continued**

- Mo single crystals, low temp. bend props.; surface effect 4-99561  
 Mo, sintered sheet, tensile props., improvement by reducing O impurity levels 4-89132  
 Mo-base alloys, welded joints, long-term strength characts. effect of alloying with N 4-109513  
 $\text{Na}_2\text{O}-\text{B}_2\text{O}_3$  glass, prep., mech., thermal and optical props. rel. to N content 4-60845  
 Nb, Pd- and Ni-coated, hardening and fracture initiation, resulting from  $\text{H}_2$  adsorpt.-desorpt. cycling 4-81282  
 Ni, fracture stresses time depend. during spall 4-99499  
 Ni O embrittlement, prevention and reversal 4-71733  
 Ni/Cu/(001)/Ni triple layer films, tensile props. 4-99324  
 Ni-base eutectic composite, deform. and failure, examination in HVEM 4-66382  
 a-Si:H glow discharge deposited films, morphology, temp. and substrate depend. 4-61260  
 SiC ceramics interfaces, contact stresses distrib. rel. to geometry 4-76873  
 SiC fibre reinforced Al alloy, fabrication and mech. props. (Korean) 4-104755  
 $\alpha$ -SiC, sintered, phenomenology of fracture 4-93372  
 $\text{Si}_3\text{N}_4$  ceramics interfaces, contact stresses distrib. rel. to geometry 4-76873  
 $\text{Si}_3\text{N}_4$  polycrystalline materials, high temp. deform. and fracture 4-76866  
 $\text{Si}_3\text{N}_4$ , reaction-bonded, flaw populations, effect of oxidation 4-62059  
 $\text{Si}_3\text{N}_4$ -MgO, hot pressed, fracture stress, temp. and strain rate depend. 4-85207  
 $\text{SiO}_2$ , fracture and emission of electrons, ions and photons 4-98189  
 Sn-Cd (5 wt.%), plasticity rel. to eutectoid transform 4-114605  
 Ti, fracture stresses time depend. during spall 4-99499  
 Ti, plastic flow and fracture at low temps. 4-76803  
 W bicrystals, dynamic fracture resist., effect of crack vel. 4-99528  
 W fibre reinforced Cu composite, fracture, acoustic emission obs. (Japanese) 4-62024  
 W, grain boundaries of twist misorientation about (100), direct meas. of work of fracture 4-98116  
 W polycrystals, dynamic fracture resist., effect of crack vel. 4-99528  
 W single crystals, dynamic fracture resist., effect of crack vel. 4-99527  
 WC-(Co-Ni) hardmetals, mech. props., variation with Ni/Co ratio 4-114462  
 WC-C, mechanical behaviour, room temp. to 1000°C 4-62002  
 WC-Co cemented carbide, liq. phase sintering, origins of discontinuous grain growth 4-104759  
 ZnO triode sputtered films, stress relax. study 4-104109  
 ZnS, multispectral chemically vapour-deposited, initial characterisation 4-76418  
 Zr-Al, ordered alloy, flow and fracture, review 4-114639  
 $\text{ZrO}_2$ , MgO partially stabilised, Weibull modulus 4-61972  
 $\text{ZrO}_2\text{-Y}_2\text{O}_3$ , domain boundaries generated by cubic-tetragonal transition, TEM study, rel. to fracture behaviour 4-70378

**fracture strength** *see fracture toughness***fracture strength testing** *see fracture toughness testing***fracture toughness**

*see also notch brittleness; notch ductility; notch strength*

- acrylic plastic, strength under complex stress state 4-99543  
 acrylic polymers, fracture in water 4-76881  
 axial beltline flaws, pseudo-elastic anal. 4-97406  
 bars, round, loaded in mode III, fracture and procedure for fracture toughness determ. 4-69709  
 bone, long, deform. rate rel. to flexural fracture behaviour 4-77276  
 borosilicate waste glasses, ion bombard., fracture toughness and leaching behaviour 4-75545  
 brittle materials, microcracking, crack-growth resist. 4-83858  
 brittle solid, indenter loading, fracture mechanisms, flaws, Hertzian cracks 4-97432  
 brittle surface in sliding contact with spherical indenters, strength degradation 4-104881  
 ceramic, high-performance, materials characterisation role 4-66279  
 ceramic composite, tough, capabilities and design issues 4-66292  
 ceramic-polymer composite biomaterials, fracture 4-76844  
 ceramics, microstructure, fracture toughness and thermal shock resist. relationships 4-62049  
 ceramics, nondestructive failure prediction, fracture models 4-76964  
 ceramics, transformation-toughened, fracture toughness; crack-size depend. 4-93373  
 concrete beam, rectangular reinforced, behaviour and ultimate strength under combined torsion, bending and shear 4-62046  
 copolymer system, rubber plasticised, processing influence on morphology-prop. relationships (German) 4-85209  
 corundum single crystals, cracking resist. rel. to dislocation density 4-93370  
 cyclic and dynamic loadings, fracture toughness characts. relationships 4-99536  
 cylindrical specimens, fatigue precracked, fracture under combined mode I and III loading configs. 4-79510  
 diamond dispersed alumina composite, very high press. sintered, fracture toughness, phase transform. 4-99372  
 elastic-plastic analysis of rel. between  $K_{Ic}$  and CTOD 4-103267  
 fibre reinforced Al alloy, prep. by explosion technique, mech. props. at low temp. 4-114634  
 fibre reinforced ceramics, mech. aspects of failure (French) 4-81280  
 fibre reinforced composites, short fibres, mech. behaviour 4-98173  
 fibre reinforced plastics, stable crack growth, influence of fibre orientation 4-99570  
 flow localisation and plastic instability, microstruct. aspects 4-85192  
 glass and glass ceramic, brittle, disturbed surface layer parameters effect on struct. strength 4-99541  
 glass fibre reinforced epoxy, stable crack growth, influence of fibre orientation 4-99570  
 glass fibre reinforced epoxy, unidirectional, fracture toughness in mode II 4-93366  
 glass fibre reinforced epoxy resin laminates, transverse cracking rel. to mech. props. of matrix 4-99489  
 glass fibre reinforced polyurethane, dynamic fracture toughness rel. to void and fibre content (Japanese) 4-99506  
 glass fibre reinforced thermoplastic alloy, mech. props. at elevated temps. 4-76855  
 graphite, polycrystalline rods, single impact stress calc. 4-76840  
 graphite fibre reinforced epoxy, delamination and transverse fracture 4-99577

**fracture toughness continued**

- graphite fibre reinforced epoxy, mixed mode fracture 4-99569  
 hardmetal, creation of stable cracks using bridge indentation 4-66434  
 Kevlar fibre-reinforced epoxy resin composites, fracture toughness rel. to controlled interfacial bonding 4-66423  
 materials with cracks, stress intensity rel. to fracture toughness 4-79507  
 mechanical behaviour of materials, conf., Stockholm, Sweden (Aug. 1983) 4-90297  
 metal plate, spalling fracture under shock loading 4-89112  
 metallic glass ribbon, pull-out test in different matrices, charact. of fibre reinforcement 4-71717  
 metallic glass ribbon reinforced epoxy resin, fracture strength and ribbon shape effects 4-99479  
 metallic glass ribbon reinforced epoxy resin, strengthening by fibre prestressing 4-99480  
 metals, spalling, microdamage initiation; critical loading conditions 4-89111  
 metals and alloys, stress-rupture strength in complex stressed state, criteria development 4-99540  
 microstructure, influence on brittle fracture toughness 4-93388  
 mullite-cordierite composites, sintering, hot pressing, microstruct., mech. and thermal props. 4-89017  
 mullite-zirconia composites, microstruct. and mech. props. 4-114672  
 nuclear reactor pressure tubes, fracture micromechanisms, use of  $J_R$  curves 4-99582  
 nuclear reactor vessels, brittle fracture resistance, calc. 4-96143  
 nuclear waste glasses, fracture toughness, hardness, elastic recovery, indentation testing 4-104844  
 panel, centre cracked, plane stress tensile deform., J integral estimation 4-103262  
 polyamide 6-rubber blends, morphology and mech. props. 4-93344  
 polyethylene fibrillated tape reinforced cement, mech. props. 4-109493  
 polypropylene, mica-filled, mech. props., influence of particle size 4-81279  
 polypropylene fibre reinforced mortar, thin slabs, fracture toughness under flexural or impact loading 4-99576  
 porcelain, high-alumina, for HV insulators, strength under dynamic and cyclic loads (German, English) 4-76836  
 powder metallurgy parts, fatigue design, methods to determ. relevant material props. 4-66436  
 pressure vessel, strength criterion in presence of prod. and service defects 4-64887  
 $\alpha$ -quartz, electrodiffusion of charge-compensating ions 4-61153  
 quartz, ST cut, tensile fracture strength 4-71739  
 rocks, fracture toughness under bending rel. to fatigue crack length (Japanese) 4-100557  
 sialon, fracture toughness, effect of deform. 4-76868  
 spotwelded joints, static and fatigue fracture (French) 4-114637  
 steam turbines, last-stage blades, efficiency and reliability improvements 4-89061  
 steel, alloy, fracture strain and characteristic fracture distance, microstruct. interpretation 4-85211  
 steel, alloy, mech. props. and precip. hardening response 4-89107  
 steel, alloy type, Ca treated resulphurised, mech. props. and machinability, S and sulphide shape effect, report 4-62048  
 steel, austenitic, AM-2, various properties and products of nonmagnetic steels 4-114590  
 steel, austenitic, neutron irradiat., high temp. deform. behaviour (German) 4-81262  
 steel, austenitic stainless, cold worked and irradiated, correl. of fracture toughness with tensile props. 4-93376  
 steel, austenitic stainless, irradiation, fracture toughness, SEM obs. 4-104836  
 steel, C, fracture toughness, stretch zone, ductility, transition region 4-99468  
 steel, C, plate, projectile impact strength critical fracture energy 4-99477  
 steel, C-Mn, fracture toughness studies in different regions of weld heat affected zone 4-76838  
 steel, cast, fracture toughness, Charpy V notch test 4-99560  
 steel, constructional, fracture resist., method of stress raiser appl. influence 4-62037  
 steel, constructional, strengthening using thermomech. treatment and deform. in intercrit. temp. range 4-114585  
 steel, Cr, fracture toughness and mech. props., effect of tempering 4-76854  
 steel, Cr-Mo, fracture toughness degradation after long-term service in petroleum refining (Japanese) 4-89126  
 steel, Cr-Mo, fracture toughness in transition region, interpretation of scatter and thickness effect 4-99603  
 steel, Cr-Mo-V, fracture toughness for steam turbine rotor appl. 4-104868  
 steel, Cr-Ni ferritic, rapidly solidified, struct. and mech. props. 4-109388  
 steel, Cu-bearing, conf., Luxembourg (May 1983) 4-86106  
 steel, Cu-Ni-Cr, compact and surface-flawed specimens, fracture toughness meas. comp. 4-104858  
 steel, ductile, static resistance to cracking calc. under ductile fracture conditions (Russian) 4-66415  
 steel, ductile fracture and fracture toughness, effect of stress triaxiality and temp. (Japanese) 4-93379  
 steel, effect on wear resist. in abrasive friction 4-93425  
 steel, failure predictions, tearing instability and limit load 4-99589  
 steel, ferritic stainless, welds,  $\gamma$ - $\alpha$  transform temp., direct determ. method 4-114752  
 steel, fracture toughness, quasi-state and impact, effect of different thermal treatments 4-99599  
 steel, fracture toughness as function of temp. 4-66403  
 steel, heat-resistant, crack resist. characts., temp. and loading cycle asymmetry influence 4-99535  
 steel, heat-resistant, static and dynamic fracture toughness, influence of microstruct. and temp. 4-99600  
 steel, high Cr, impurity redistrib. and mech. props. during 475°C ageing (Russian) 4-93317  
 steel, high strength, SCC, growth mechanisms 4-81333  
 steel, HSLA, crack resist. of differently alloyed steels 4-104877  
 steel, hypereutectoid, Mode III fracture initiation toughness, depend. on strength and microstruct. 4-71720  
 steel, impact fracture toughness rel. to anti-tuffriding coating (Japanese) 4-99515  
 steel, line-pipe, high toughness, abnormal fracture appearance from drop weight tear test (German) 4-114748  
 steel, low alloy, high-temp. brittle fracture, review 4-99562

## acture toughness continued

- steel, low alloy, low C weld metal, transform. behaviour and toughness 4-114670  
 steel, low alloy, mech. props. rel. to second phase particle size 4-99591  
 steel, low alloy mild, ductile fracture, rel. between J-integral and COD 4-104842  
 steel, low and medium strength, crack resist. 4-62034  
 steel, low-C cast, cyclic crack resist., heat treatment influence 4-62035  
 steel, maraging, Ni, fracture toughness, effect of treatment condition 4-76856  
 steel, martensitic, high-strength structural, fatigue fracture kinetics, endurance limit and crack resist. 4-99537  
 steel, martensitic, low C, controlled rolled and quenched, strengthening effects 4-99393  
 steel, martensitic, press. vessel, cleavage fracture 4-71730  
 steel, martensitic hyperferritic, rapid heat hardening using incomplete homogenisation effect 4-71671  
 steel, martensitic stainless, crack opening displacement, stretched zone size and  $J_{IC}$  4-104875  
 steel, martensitic stainless, HT-9, weldments, microstruct., hardness and fracture toughness, effect of preheat 4-99495  
 steel, microalloyed, cast, microstruct. and mech. props., influence of phase charges (French) 4-81278  
 steel, microalloyed, fracture micromechanics 4-99602  
 steel, mild, C-Mn, Charpy V transition temp. rel. to various material parameters 4-66431  
 steel, Mn-Mo-Al, transform. of austenite and cryogenic mech. props., effect of intercrit. heat treatment (Chinese) 4-85152  
 steel, Ni-Cr-Mo-V, fracture behaviour effect of S content 4-99601  
 steel, Ni-Cr-Mo-V, fracture toughness, overheating, effect of S content (Japanese) 4-93377  
 steel, Ni-Cu-Mo, sintered Ancoloy SA powder, fracture toughness rel. to pore size and heat treatment 4-76843  
 steel, Ni-Mo, martensitic A533B pressure vessel, tempered, brittle fracture and fatigue crack growth, segregation effects, Auger obs. 4-66400  
 steel, normalised 04G2B, Y additions effects on mech. props. 4-93390  
 steel, rolled, impact toughness and transition temp., effect of delamination (Korean) 4-76848  
 steel, rotor forgings, unstable fracture, effect of small clustered flaws (Japanese) 4-93378  
 steel, spalling resistance, effect of system scale 4-99538  
 steel, stainless, Rb contamination in reactor pressure vessels, stress corrosion problems 4-96148  
 steel, steam turbine casing and rotor, mech. props. rel. to service life (Japanese) 4-89119  
 steel, structural, weldability, effect of residual elements 4-85214  
 steel, water-water power reactor vessel material, brittle fracture resist. and radiation embrittlement 4-96142  
 steel, weld metal, heat-affected-zone toughness, influence of Cu 4-89106  
 steel fibre reinforced mortar, thin slabs, fracture toughness under flexural or impact loading 4-99576  
 steel plates, high-toughness, commercial production by reheating of slabs 4-114589  
 steel rails, mixed fatigue-tensile surface crack growth 4-89100  
 steels, low alloy, fracture toughness studies 4-109491  
 styrene-butadiene block copolymers, deform. rel. to pretreatment, impact strength 4-93331  
 thermoplastics, cellulosic filler efficiency, processing charact. and mech. props. 4-61913  
 three-point bending fracture toughness specimens, side groove effects, finite element anal. 4-113519  
 X-ray fractography of fatigue fractures in subcrit. crack growth zone 4-114757  
 Al-Cu (10 wt.%), prod. by rheocasting, rel. between struct. and mech. props. 4-99467  
 Al-Cu-Li-Cd, 2020, microstruct., fracture toughness and SCC 4-76851  
 Al-Cu-Li-Mn-Cd, Al 2020, fatigue crack growth behaviour 4-71728  
 Al-Cu-Mg, 2024 sheets, plastic energy dissipation and toughness, size effect 4-89102  
 Al-Cu-Mg alloy D16 plates, struct. strength, chem. comp. and heat treatment effects 4-61986  
 Al-Cu-Mg wrought alloy 1163, props. 4-62038  
 AlN ceramic, thermal shock resist. 4-81289  
 $Al_2O_3$ , bend specimens, crack resistance curves, influence of grain size 4-62058  
 $Al_2O_3$  ceramic, strength rel. to microstructure 4-62060  
 $Al_2O_3$  fibre reinforced Mg composite, off-axis fracture, critical stress intensity 4-66430  
 $Al_2O_3$ , polycrystalline, strength rel. to flow distrib. 4-109505  
 $Al_2O_3$ , sintered, fracture strength, effect of surface condition 4-62057  
 $\beta$ - $Al_2O_3$ , sintering, microstruct. and mech. props. 4-85136  
 $Al_2O_3$ :MgO:CaO, translucent, fracture, influence of temp. and CaO 4-92290  
 $Al_2O_3$ :AlN spinel, fabrication, thermomech. props. 4-89097  
 $Al_2O_3$ :AlON composite ceramic, hot pressing reaction sintering, mech. props., high temp. appls. 4-62062  
 $Al_2O_3$ :PMMA (PBMA), composite biomaterials, fracture 4-76844  
 $\beta$ - $Al_2O_3$ :ZrO<sub>2</sub>, slip cast transform. toughened composites, mech. props., ionic cond. 4-103995  
 $Al_2O_3$ :ZrO<sub>2</sub>, ceramics, high press. sintered, fracture toughness rel. to phase transform. 4-76839  
 $Al_2O_3$ :ZrO<sub>2</sub>, powders, prep. by evaporative decomp. of sols. 4-85137  
 B<sub>2</sub>C, hardness and fracture toughness rel. to stoichiometry 4-62019  
 B<sub>2</sub>C, struct. and mech. props., hot pressing conditions effect 4-61906  
 BaTiO<sub>3</sub>, PTC ceramic, strength and fracture toughness 4-62051  
 C fibre/glass fibre reinforced polyester, hybrid composites, flexural and fracture props. (Japanese) 4-99429  
 Ca<sub>3</sub>Ga<sub>2</sub>Ge<sub>2</sub>O<sub>12</sub>, garnet single crystals, microhardness, brittle fracture 4-65337  
 (Fe,Ni)<sub>3</sub>V alloy, long-range ordered, strain rate and ageing effect on mech. props. 4-109501  
 Fe, cast, ductile, fracture toughness, X-ray diff. obs. of fracture surface 4-99581  
 Fe, cast, flake graphite, fracture toughness 4-104872  
 Fe, sintered, crack propag. and processes near crack tip 4-66435  
 Fe-Ni-C, fracture toughness rel. to transform. induced plasticity and grain boundary segregation 4-99585  
 Fe<sub>90</sub>Zr<sub>10</sub> amorphous alloy, struct. and mech. props. rel. to heat treatment 4-75305  
 Gd<sub>3</sub>Ga<sub>5</sub>O<sub>12</sub>, garnet single crystals, microhardness, brittle fracture 4-65337

## fracture toughness continued

- Mo, endurance limit in high cycle fatigue rel. to heat treatment and alloying 4-109498  
 Na<sub>1-x</sub>Zr<sub>x</sub>P<sub>2</sub>-Si<sub>2</sub>O<sub>7</sub> ceramics, prep., ionic cond., durability and strength 4-113711  
 Nb alloy, plastic deform. with subsequent nitriding effect on mech. props. 4-114713  
 Nb, mech. props. at low temp., Ti effect 4-93391  
 Ni-Cr-Co (22, 9 wt.%) superalloy, solid solutions strengthened, development, weldability, oxidation resist. 4-61975  
 (Pb,Lu)(Zr,Ti)O<sub>3</sub> ceramics, stress anisotropy induced by polarisation 4-104536  
 SiC fibre for ICF applic., strength and fatigue analysis 4-109502  
 Si<sub>3</sub>N<sub>4</sub>, fracture toughness, effect of deform. 4-76868  
 Si<sub>3</sub>N<sub>4</sub>, hot pressed, fracture toughness, mech. props. rel. to comp. and microstruct. 4-76870  
 Si<sub>3</sub>N<sub>4</sub> powder, shock induced densification study 4-109352  
 Si<sub>3</sub>N<sub>4</sub>, sintered, static and cyclic fatigue strength (Japanese) 4-99502  
 Si<sub>3</sub>N<sub>4</sub>, thermal props. and thermal shock resist. rel. to microstruct. and processing parameters 4-76871  
 Si<sub>3</sub>N<sub>4</sub>-Y<sub>2</sub>O<sub>3</sub> based ceramics, sintering, densification, oxidation, strength and porosity 4-76835  
 Si<sub>3</sub>N<sub>4</sub>O ceramic, thermal shock resist. 4-81289  
 Ti-Al-Nb-Ta-Mo, welds and castings, impact roughness, segregation and influence of B 4-114658  
 Ti-Al-V (6, 4 wt.%), tensile props. and fracture mode, temp. depend. 4-109488  
 Ti-Al-V (6.4 wt.%), laminated plate, damage tolerance life 4-104862  
 $\alpha$ / $\beta$ Ti-Al-V and Ti-Al-Cr-Mo-V, annealed, struct. and mech. props. 4-61988  
 TiB<sub>2</sub> powder, pressureless sintered, mech. props. in liq. Al environment, impurity segregation 4-114700  
 TiB<sub>2</sub>, sintering and props. of samples made from powder synthesised in plasma-arc heater 4-76715  
 Ti(C,N)-Ni-Mo, hard metal, fracture toughness rel. to microstruct. 4-104873  
 V-Cr-Ti(Fe-Zr), mech. props. rel. to O contamination, fusion appls. 4-109499  
 W, cross-rolled, tensile and low-cycle fatigue meas. at 1505K 4-109503  
 W, powder metallurgy, fracture toughness and short-term strength, quantitative correl. 4-89133  
 WC-Co, cemented carbide, hot isostatic pressing 4-66293  
 WC-Co, hardmetal, creation of stable cracks using bridge indentation 4-66434  
 WC-Co-P, wear resist., P addition influence 4-66458  
 Zn-Al, diecasting alloy, fracture 4-89128  
 ZrO<sub>2</sub> ceramics, process zone toughening by microcracking 4-62020  
 ZrO<sub>2</sub>, sintered stabilized powders, cracking resist. rel. to pore struct. 4-93371
- fracture toughness testing**  
 see also notch testing  
 adhesive bonded joint, strength tests using acoustic emission method 4-109614  
 bending test, defect position rel. to strength variance 4-99661  
 brittle fracture resistance, calc. using crit. brittleness 4-104936  
 ceramics, failure probability, Weibull modulus estimation 4-104928  
 ceramics, flexure strength, Weibull fracture statistics 4-104954  
 ceramics clay-based, fracture props., practical technique using diamond indentation 4-62144  
 compact specimen, crack arrest toughness validation 4-99715  
 composite materials, losipescu shear test 4-71807  
 composite materials, symmetric rail shear test, mode II fracture toughness, finite element analysis 4-109582  
 composites, cement-based, modified instrumented Charpy test 4-89204  
 concrete, impact testing, meas. device effect on curve shape (German) 4-66535  
 concrete specimen in multiaxial compression finite element failure analysis (Japanese) 4-99686  
 crack growth under rolling contact, defect installing technique 4-85284  
 critical brittleness temperatures determined on specimens with different stress raisers 4-104937  
 ductile-brittle transition temperature, determ. using criterion of meeting plane strain conditions 4-104935  
 elastic-plastic fracture toughness, Japanese standard test method 4-99737  
 elastic/plastic indentation fracture, indenter geometry effects 4-60346  
 energy criterion  $J_{IC}$  expt. determ. 4-66523  
 ferrites for recording heads, toughness evaluation 4-104951  
 fibre reinforced composite laminates, fracture toughness meas. using three-point bend and compact-tension specimen 4-99735  
 glass, strength testing, time of failure, incremental loading, step size effect 4-62145  
 glass, toughened, thin thermally polished, strength asymmetry 4-89103  
 hybrid composite, unidirectional fibre, amplitude distrib. AE signatures 4-89198  
 $J_{IC}$  test on Charpy size specimens (Japanese) 4-93487  
 $J_{IC}$  test procedures in transition temp. region (Japanese) 4-93486  
 J-integral, method for determ. 4-66524  
 metals, mixed mode fracture testing 4-89202  
 microtome, instrumented for improved histological sections and fracture toughness meas. 4-62637  
 PMMA, dynamic fracture toughness, determ. by impact bending test (Japanese) 4-93488  
 shearable elements, of circular cross section, limiting strength evaluation 4-99703  
 sheet metals, equipment for fracturing at given crack propag. rate 4-99677  
 single edge notched bend specimens, deflection meas. test setup 4-76929  
 solar mirror glass, crack growth, strength, lifetime prediction 4-89194  
 steel, alloy, arc shaped specimens of pipe, errors in J-integral determ. 4-62142  
 steel, alloy, J-integral determ. 4-66524  
 steel, as-rolled, tensile tests in mixed fracture range (German) 4-66511  
 steel, austenitic stainless, stress rupture strength, statistical prediction 4-99701  
 steel, C, impact bending test, specimen shape and dimensions effect (Japanese) 4-99689  
 steel, C, laser glazed hot rolled Charpy samples, impact testing 4-81377  
 steel, C, plate, projectile impact strength critical fracture energy 4-99477  
 steel, Charpy V notch impact testing with laser glazing pre-cracking 4-99681

**fracture toughness testing continued**

- steel, constructional, fracture toughness indirect determ., energy approach 4-99676
- steel, Cr-Mo-V-W, ferritic, impact props., effect of specimen size and Ni content 4-104848
- steel, dynamic toughness, drop weight nil ductility transition test 4-99679
- steel, ferritic, impact testing, classification of absorbed energy-temperature curves 4-89230
- steel, fracture toughness meas. using specimen strength ratio 4-81371
- steel, fracture toughness tests; scatter of results, statistical model 4-81370
- steel, HSLA, shear failure, development of fractographic features 4-76837
- steel, H780 weldments, fracture toughness evaluation of heterogeneous bond region 4-99713
- steel,  $J_{IC}$  test on Charpy size specimens, evaluation of heat-affected zone fracture toughness (Japanese) 4-93487
- steel, sintered, fracture mechanics behaviour, influence of specimen size 4-81372
- strain hardening materials, toughness meas.,  $J$ -estimation formulae 4-81378
- stress intensity factor formula of four point bending 4-62143
- stress intensity factors for curved crack fronts in compact tension specimens 4-99680
- superhard materials, crack resist. determ., samples and loading 4-93494
- thermoplastics, using computerised machine 4-104934
- Fe, cast, flake graphite, fracture toughness 4-104872
- Fe-base alloys, dynamic fracture toughness, results from instrumented impact machine 4-81373
- Mo-base alloy, dynamic fracture toughness, results from instrumented impact machine 4-81373
- Ni-base alloys, dynamic fracture toughness, results from instrumented impact machine 4-81373
- W, high-temperature cracking resistance determination 4-89213
- WC-Co cemented carbide, defect position in bending test rel. to strength variance 4-99661

**francium**

- see also nuclei with .....
- atom, hyperfine struct. intervals, relativistic many-body calcs. 4-68986

**francium compounds**

No entries

**Frank-Condon factors**

- acetaldehyde- $d_0$ -( $d_1$ )-( $d_3$ )-( $d_4$ ), jet cooled electronic spectrum at rot. resolution 4-112225
- alkali halide crystals, colour centre IR luminesc. and stimulated emission 4-80997
- benzene, mol. Rydberg states, vibronic coupling, Franck-Condon spectrum, Jahn-Teller ion core 4-87096
- 1,1'-binaphthyl, conform. dynamics, fluoresc. obs. 4-112224
- cytochrome c, Stokes and anti-Stokes reson. Raman scatt. 4-74360
- diamole molecules spectra, quantum and classical methods, efficiency and accuracy study 4-78830
- diamole mols., Franck-Condon distrib., reflection and interference struct. 4-59854
- dihaloethylenes, photoelectron spectra, vibr. fine struct., Franck-Condon factor calcs., geometries 4-96619
- dimethylated metal alkyl mols., photodissoc., analytic theory 4-99808
- 1,2-dimethylnaphthalene, n-hexane matrix, vibr. struct., IR and fluoresc. obs. 4-78903
- dimolybdenum tetracetate, metal-metal bond, vibr. fine struct. photoelectron band 4-102739
- formaldehyde, photoelectron spectra, vibronic anal., ab initio SCF CI calcs. 4-112121
- formulation of Franck-Condon principle, errors through Heisenberg uncertainty principle violation 4-96625
- multidimensional optimization of structural changes of molecules upon ionization in Franck-Condon factor calculations 4-59853
- cis,trans-1,3,5,7-octatetraene in n-alkane matrices, one-photon fluoresc. spectra, vibr. resolved 4-64529
- phenylacetylene excited mol., quantum mech. calc. of vibr. freq. 4-112155
- polar media, bound two-electron quasi-mol. autolocalised impurity centres, energy states and optical props. 4-84590
- polyatomic molecules, linear symm., photodissoc., analytic theory 4-99808
- pyrazine, vibronically coupled excited states, spectra, multimode effects 4-96517
- reactive processes in condensed systems, quasideadabatic models, rel. to Franck-Condon separation (German) 4-81430
- AlO, blue-green band, transition moment, Franck-Condon factors, perturbed simple harmonic model 4-59852
- $Ar^+ + CS(PN)$  radicals, emission spectra prod. from thermal energy charge transfer reactions 4-74325
- $B_2O_3$ , geometrical struct., photoelectron spectra, ab initio MO calcs. 4-68932
- $Br_2 + N_2$ , quenching, energy exchange; rate const.; Franck-Condon factors 4-64530
- $CO^+ + CS_2$ , in flowing afterglow, charge-transfer excitation, energy reson. and Franck-Condon criteria 4-93500
- $CO^+ + He$ , electronically excited  $CO^+$  collisional deactivation 4-64580
- $CS_2$ , jet-cooled,  $B_2(V) - \Sigma_g^+(X)$  transition; excitation and dispersed fluoresc. spectra 4-64527
- $CS_2^+$ , ( $A^+ - X^+$ ) emission prod. in  $Ar_2^+ + CS_2$  charge transfer reactions in Ar afterglow 4-96552
- $HIS_3$ , IR, Raman, and reson. Raman spectra, valence force field 4-93077
- InP, electron irradi. induced deep traps, deep level optical spectroscopy 4-104156
- $Li_2$ , isotope separation, sequential two-photon ionisation 4-87167
- $Li_2$ , isotope separation using different laser wavelengths for excitation and ionisation processes 4-69235
- $N_2$ , dissoci. photoionisation from threshold to 29 eV 4-96631
- $NH_3$ , reson. rovibronic Raman scatt., Franck-Condon factors, line-shape anal. 4-96550
- $Na_2$ , rotational const., Franck-Condon factors 4-69050
- $O + HCN$  reaction dynamics, laser fluoresc. spectroscopy 4-114785
- $Sr_2$  laser induced bound-bound and bound-continuum emission of  $A^+ \Sigma_v^+ - X^+ \Sigma_g^+$  system 4-107388
- Frank-Read sources**
- Cu-Ni-Zn,  $Li_1$  and  $Li_2$  alloys, order-disorder transitions, microstructure obs. 4-114511
- Fe-Si, compression test, ordering heat treatment 4-89095
- Fraunhofer lines** see solar spectra
- free-electron approximation**
- Fermi energy and density of states in free-electron solid of submicron dimensions, influence of boundary conditions 4-92785
- liquid metals, Hall effect theory, mass renormalisation corrections 4-113921
- AuY(Zr)(Nb)(Rh)(Pd), dil. alloys, thermoelectric power, resistivity, low temp. study, phase-shift anal. 4-113926
- free electron lasers**
- acousto-optic output coupler for free electron lasers 4-83601
- amplifier design, energy spread reduction at high laser intensities using phase space displacement 4-83592
- amplifier performance in Compton regime 4-87338
- analytical wave analysis 4-69420
- bright electron beams 4-87347
- broadly-tunable oscillator capabilities 4-107653
- Cerenkov lasers in the Compton regime 4-96856
- chaotic optical modes 4-87343
- coherence and fluctuations, fully quantum mech. approach 4-87345
- collective free electron lasers 4-112449
- collective instabilities and high-gain regime 4-91483
- Compton laser, non-collinear, effects of saturation and inhomogeneous broadening 4-60052
- computer simulation of lasers with variable Wigglers 4-102935
- conference, Orcas Island, WA, USA (June 1983) 4-82588
- description of free electron laser in moving frame 4-87349
- development and advantages, theory and expts: 4-69427
- dispersive FEL, a hybrid optical klystron-free electron laser 4-96927
- electron beams for electron-beam lasers 4-74532
- EM radiation production by accelerated charge and early developments 4-69419
- far-IR radiation of UCSB free electron laser 4-74529
- finite-length free electron laser gain, velocity spread effect 4-107655
- Frascati-ADONE laser, gain meas. and energy extraction optimisation from electrons 4-87341
- gain enhancement by external laser 4-83597
- gain mechanism calc. 4-79169
- gain optimisation for gaussian beam 4-87342
- gas-loaded laser 4-96928
- harmonic Raman-Nath eqn., non-trivial perturbative soln. 4-60051
- high gain laser amplifier expt. 4-60855
- high gain tapered-wiggler free electron laser 4-112451
- high intensity, for inertial confinement fusion 4-96931
- high power, millimeter wave laser, gain, bandwidth, tunability 4-112452
- high-gain laser amplifier, radially resolved simulation 4-83594
- high-gain lasers, small signal gain spectrum 4-83593
- high-power coherent radiation sources at mm to UV wavelengths 4-60053
- inertial confinement fusion, free electron laser driver, numerical model 4-107084
- injection locking by  $BeAl_2O_3:Cr^{3+}$  (alexandrite) laser 4-83587
- instabilities and quantum initiation 4-87351
- IR, broadband optical cavities 4-112479
- IR medium power FEL SHG conversion efficiency anal. 4-83643
- $K_\alpha$ -band Ubitron 4-112450
- klystron experiments for ACO storage ring free electron lasers 4-96920
- laser source technology, recent developments 4-87356
- lasers for analytical and industrial chem., conf., Los Angeles, CA; USA (Jan. 1984) 4-106100
- lateral injection, momentum balance and axial shift of electrons 4-96932
- Lawrence Berkeley Laboratory and Lawrence Livermore National Laboratory free electron laser status 4-83611
- Lawson-Penner limit and single passage laser performance, supermode theory 4-91482
- linear gain and stable pulse propag. 4-83586
- long pulse laser driven by linear induction accelerator 4-87348
- long-pulse, high-current free electron laser with no external focusing 4-69421
- Los Alamos laser linac, beam-breakup calcs. 4-83256
- Los Alamos laser oscillator expt., electron beam diagnostics 4-83604
- Los Alamos laser oscillator expt., plans and present status 4-83612
- Los Alamos laser oscillator expt. using subharmonic buncher 4-83603
- low-gain, low-voltage laser, mode struct. 4-96942
- magnetic crystal, channelled particle radiation, appl. to laser gain 4-113513
- magnetised free electron lasers and auto resonance cyclotron masers, non-linear efficiency 4-96921
- maser, expt. study 4-107587
- media free electron lasers for VUV and X-ray radiation production 4-96925
- MM wave, radiation growth in collective regime, freq. resolved meas. 4-60054
- MM-wave ubitron experimental design 4-69426
- multiphoton transitions in free electron lasers 4-69422
- nonlinear orbits with linear mag. wiggler and strong axial mag. guide field 4-74527
- orbitron maser 4-69357
- orotron free electron laser, quantum model anal. 4-87350
- oscillation stability of electron near quasioptical minimum 4-91484
- oscillator, noise to coherence, photon noise and electron shot noise theory 4-87344
- oscillator mirror alignment tolerance scaling laws 4-83602
- parametric generation in electron beams 4-102872
- particle motion stochastic instability 4-74525
- permanent magnetic wiggler design and simulation device with a few periods (Chinese) 4-112462
- photon statistics quantum mechanical calc. 4-69418
- power output performance, superradiation generation (Chinese) 4-107654
- pulse propag., two-dimensional, semi-analytical formulation 4-83585
- pulse propagation, model for noise introduction into computer simulations 4-87346
- quantum coherence in electron beams 4-112338
- quantum kinetic theory of free-electron lasers in external fields of arbitrary amplitude 4-79168
- quantum theory, Glauber coherence antibunching and squeezing 4-83596
- Raman free electron laser, tunable, spectral meas. 4-96929

**free electron lasers continued**

- Raman laser, three-dimens. theory 4-96924  
 Raman lasers with axial guide fields, nonlinear simulation 4-96923  
 Raman type, two-dimensional hollow beam, optimum thickness (*Japanese*) 4-107714  
 rectangular waveguide resonator, cylindrical Gaussian eigenmodes, gain per mode 3D calc. 4-87368  
 relativistic electron beam equilibria, radially confined, appl. to longit. wiggler free electron laser 4-112447  
 relativistic-electron helical trajectories in combined uniform axial and helical mag. fields, instability 4-83529  
 review 4-96930  
 simplified small signal gain calculations in free electron lasers 4-69423  
 single particle dynamics and gain, Lorentz force eqn. 4-79167  
 single-mode efficiency in free-electron lasers 4-74528  
 single-pass device operation, Lawson-Penner limit considerations 4-83591  
 small signal gain simplified calcs. 4-107656  
 Stanford superconducting 3.2  $\mu\text{m}$  FEL optical beam quality meas. 4-83626  
 stationary pulse solutions (*Chinese*) 4-102934  
 stimulated Compton free electron lasers, expt., theoretical and design concepts 4-96943  
 stimulated undulator radiation of electrons in waveguide and free electron lasers 4-79022  
 storage ring free electron laser oscillator at ACO storage ring 4-79165  
 storage ring free electron laser oscillator operation at 6500 Å 4-87340  
 storage ring free electron lasers, macro-temporal struct. anal. 4-79166  
 superradiant mm-wave laser operating in collective regime radiation growth and emission spectrum 4-96922  
 tapered wiggler laser, long pulse evolution 4-83584  
 tapered wiggler laser gain displacement effects 4-83595  
 tapered wiggler lasers, emittance acceptance 4-83589  
 tapered-wiggler laser, large electron-beam energy extraction 4-83588  
 tapered-wiggler laser amplifier expt. at Los Alamos, optical gain results 4-83590  
 theoretical analysis 4-107652  
 theory and applications 4-64714  
 theory and expt., review 4-112448  
 Thirteenth international quantum electronics conf., Anaheim, CA, USA (Jun. 1984) 4-86105  
 transverse modes evolution, appl. to Orsay expt. 4-87339  
 TRW/Stanford tapered wiggler oscillator expt. status 4-83614  
 two stage laser with EM wiggler 4-96941  
 two-stage, low loss quasi-optical cavity 4-87369  
 two-stage free electron laser, cavity design 4-69424  
 two-stage laser programme at KMS Fusion Inc., review 4-83615  
 ubitron, three-dimensional theory 4-69425  
 undulator and Cherenkov free electron lasers, preliminary comparison 4-102936  
 University of California, Santa Barbara, laser expt. programme, status report 4-83613  
 University of California laser wiggler props. 4-83605  
 unstable resonators beam quality and small mode area 4-87370  
 variable emittance filter for electron laser facility 4-82859  
 wiggler periodic length choice and freq. variations (*Chinese*) 4-112446  
 wiggler variable spatial periodic length, energy conversion efficiency 4-64713  
 X-ray free electron laser, proposal 4-74526  
 X-ray free electron laser prospects, review 4-96926

**free energy**

- acetonitrile-pentyl acetate (n-butanol) (n-propanol) (carbon tetrachloride), excess Gibbs function determ. 4-80262  
 adenosine diarsenate, deuterated, dielectric relax. meas. 4-93004  
 adsorbed solid films, incomplete wetting 4-92530  
 alkali metal oxides, binary, high temp. vapourisation behaviour 4-98260  
 alkali metals, BCC, thermodynamic props. at high temps. 4-92392  
 alkali metals, liquid, thermodynamic props. using classical plasma reference system 4-60810  
 9-alkylfluorene + (9-alkylfluorenyl)lithium,  $\text{H}^+$  transfer reactions, Bronsted coeffs. 4-99754  
 alloys, binary, free energy, high temp. calc. (*Russian*) 4-92389  
 alloys, magnetisation and phase decomposition, structural diagrams 4-76138  
 alloys, ordering kinetics accompanying phase separation 4-113653  
 alloys, Thermodynamics and entropy of mixing 4-103935  
 ANNNI model, low temp. anal. in external mag. field 4-58774  
 benzene, liq., residual Helmholtz energies between 390 and 465K and up to 60 MPa 4-88309  
 binary systems, demixing, stable long-period comp. variations 4-84406  
 binary systems, demixing, stable long-period comp. variations 4-84407  
 Blume-Capel model, two spin cluster approx., expansion of free energy, tricritical point 4-95343  
 cluster free energy, interfacial contribs., Ising model Monte Carlo method calc. 4-11073  
 cluster variation method, consistent relations in method of reducibility 4-58776  
 colloidal suspensions, aq., phase separation induced by dissolved polymer 4-114840  
 correlation function and free energy of two-component two-dimensional plasma 4-87842  
 crack micromechanics, thermodynamic approach 4-88234  
 critical wetting in systems with long-range forces 4-88374  
 crystal stability and shape, mol. motion effect 4-113375  
 crystalline sphere in fluid, thermodynamic equilibrium 4-98321  
 crystals in external stress field, phase form. thermodynamics 4-84386  
 curved interfaces in simple fluids, generalised van der Waals theory 4-113753  
 cyclohexanol, vapour press. and excess Gibbs free energies 4-98312  
 cyclohexanol-n-heptane mixtures, vapour press. and excess Gibbs free energies 4-98312  
 defect solids, free energy, lattice spectrum contrib. 4-75630  
 diamond, vacancy formation energy, crystallisation studies 4-108354  
 Dicke maser model, infinite-mode, with  $A^2$ -term, approximating Hamiltonian method 4-74472  
 dimers, directional attractive forces, single mol. site, thermodynamic perturbation theory 4-95290  
 dipolar fluids, coexistence curve, orientation correls., effective pair pot. 4-88055  
 disordered Hubbard alloys, spin glass behaviour 4-92928  
 disordered magnet near the percolation threshold 4-92921

**free energy continued**

- DNA supercoiling, free energy rel. to enthalpy 4-77182  
 DOBAMBC, liquid cryst., cell thickness effect on elec. props., optical switching and memory 4-98998  
 elastic-plastic fracture, energy flux into process region 4-69705  
 electric double layer, free energy 4-61436  
 embrittlement and pitting, environmentally-induced, possible role of surface stress 4-62086  
 excess Gibbs energy and vap. press. of associated systems 4-88048  
 ferromagnetic Heisenberg Hamiltonian in spin wave theory, dynamical interactions 4-98874  
 finite-size scaling, universal critical amplitudes and free energy 4-95365  
 first order phase transitions, physical kinetics, quantum nucleation and tunnelling 4-90543  
 glass, thermodynamics of grain boundary crystallisation 4-75314  
 glass-forming metallic melts, undercooled, free energy approx. 4-70414  
 glycine, aq. soln., conformational energy, ab initio LCAC-MO-SCF calcs. 4-96449  
 grain boundary model, impurity effects, cluster variation method calcs. 4-113465  
 graphite with adsorbed methane, commensurate-incommensurate transition model 4-70572  
 hard spheres near soft repulsive wall, thermodynamics, variational approach 4-60800  
 Heisenberg anisotropic spin  $1/2$  model, thermodynamic props. in transverse field 4-98913  
 Helmholtz, Poisson-Boltzmann eqn. derivation using variational principle 4-58804  
 n-heptane, vapour press. and excess Gibbs free energies 4-98312  
 hierarchical lattice spin systems, phase transition phenomena 4-95364  
 HOBACPC, liquid cryst., cell thickness effect on elec. props., optical switching and memory 4-98998  
 incommensurate magnetic structures formation, exchange integrals 4-114088  
 incommensurate structures superspace symmetry and Landau theory 4-103689  
 incommensurate systems, phase diagrams 4-113571  
 inert gas adsorbed films on graphite, incomplete wetting 4-92530  
 inert gas crystal, ideal, vibr. thermodynamic props., anharmonic contrib. 4-98307  
 inhomogeneous, cryst., local phase transition points, fluctuation enhancement 4-65373  
 inhomogeneous ordered binary alloys, stationary states, long-period superlattices 4-113399  
 inner-sphere reorganisation in optical electron transfer 4-83420  
 interacting systems, thermodynamic props., Monte Carlo method using Fourier representations of path integrals 4-82743  
 internal variables handling in thermodynamic calculations 4-103964  
 ionic crystals, electronic Mott-Hubbard transition 4-92615  
 Ising antiferromagnet, FCC, hysteresis and free energy, computer simulation 4-114127  
 Ising model, two-dimensional random, domain-wall renormalisation group study 4-71113  
 Josephson array, microscopic formulation using Feynman diagrams 4-92868  
 lamellar lyotropic mesophase, neutron scatt. study of structural defects 4-103646  
 Landau-Ginzburg-Wilson model, renormalisation scheme 4-111091  
 Lennard-Jones diatomic fluid, perturbation theory, thermodynamic and quasithermodynamic props. 4-97990  
 linear relationships, information theoretic view (*German*) 4-78287  
 lipid bilayer vesicles, giant neutral, free energy pot. for aggregation by Van der Waals attraction 4-115026  
 liquid crystal bistable cell, Clausius eqn. and thermodynamics 4-88065  
 liquid crystal-isotropic transition temperature depression by a mag. field 4-98281  
 liquid drops, spherical fluid-vapour interfaces, surface tension, curvature corrections 4-88372  
 liquid metal mixtures, intermolecular forces, excess Gibbs energy 4-65418  
 liquid state, perturbation theory, approximate free energy functional minimisation 4-88054  
 liquid theory, linear integral equations and renormalization group 4-103634  
 long-period superstructure models, ANNNI model 4-113366  
 macromolecules, rodlike, in conc. soln., rot. relax., free energy, external flow effect, isotropic-nematic transition 4-69251  
 magnetic alloys, dil., low temp. thermodynamic props., anomalous contrib. in presence of cryst. field 4-84801  
 MBBA, metastable solid, dielectric props. under press. 4-80865  
 MBRA8 liquid crystal, smectic A-chiral-smectic C transition, Landau free energy 4-92358  
 mean spherical model, random external field, replica method for free energy 4-95303  
 metallurgical thermodynamics, equilib. states and influencing factors, book contrib. 4-109375  
 metals, crystn., initial stages 4-114505  
 metals, FCC, interfacial free energy between dislocation core and bulk material 4-65262  
 metals, FCC, void nucleation kinetics, mol. dynamics simulation 4-92197  
 metastability and analyticity in drop-like model 4-58805  
 methane adsorbed on graphite, model of commensurate-incommensurate transitions 4-80394  
 microemulsions, droplet sizes 4-77034  
 molecular fluids, equilib. props. in semiclassical limit 4-103632  
 molecular structural changes, macroscopic description 4-68941  
 multicomponent systems, mixing effects, subregular eqn. 4-84401  
 naphthalene, solns. in water-ethanol mixtures, thermodynamic props. 4-80264  
 $\alpha$ -naphthylamine-diphenylamine, phase diagram (*German*) 4-108587  
 nematic liq. crystals, isotropic phase, orientational correlation function 4-92071  
 nematic liquid crystals, anisotropy induced director refraction inside inversion walls 4-103644  
 nematic liquid crystals, variational approach to theory and phase transitions (*Russian*) 4-88074  
 nematics, orthorhombic, isothermal hydrodynamics 4-92080  
 nucleation kinetic theory, pot. energy barrier 4-85326  
 oil-water microemulsion model 4-99849  
 one-dimensional Heisenberg systems with random anisotropies, low-temp. props. 4-76100

## free energy continued

- one-dimensional nonlinear lattice, critical props. and hadron phys. 4-59032  
 organic cpds., linear free energy relations 4-109675  
 original-incommensurate-commensurate phase transition sequence 4-88285  
 p-state chiral clock model, low temp. phase diagram, mean-field approx. 4-92917  
 perovskites, structural transitions with soft rot. modes 4-61038  
 phase equilibrium, complex model, appl. to systems with asymmetric miscibility gap and two miscibility gaps 4-70397  
 phenols, enthalpies, free energies and entropies of transfer from nonpolar solvents to water 4-105009  
 3-phenyl-4-hydroxybenzoic acid liq. cryst. esters, thermodynamic props. 4-84391  
 phenylhydroquinone, liq. cryst. esters, thermodynamic props. 4-84391  
 planar spin models, specific heat and free energy, XY model anal. 4-58801  
 PMMA blends with copolymers of methylmethacrylate and butylmethacrylate, thermodynamic study (*Russian*) 4-77027  
 polar molecular fluids, interaction sites, critical points 4-70011  
 polarising liquid, perturbation theory 4-68194  
 polaron, free energy and effective mass at finite temps. 4-113879  
 polyethylene, cryst., growth kinetics and lateral. growth habits 4-88123  
 polyethylene oxides, solution-gas interface, adsorption characs. 4-79921  
 polyimide, cured, interfacial reaction during metallisation, XPS obs., chem. bond form. 4-88932  
 polymer melts, surface tension, nonlocal entropy effects 4-104040  
 polymers, entangled, elastic response 4-98168  
 polystyrene spheres in mixtures, miscibility and glass forming 4-70382  
 Potts model, q-state, free energy critical amplitude 4-73394  
 Potts spin glass, mean field theory 4-104429  
 quantum crit. behaviour, quenched impurity influence 4-63656  
 quantum Langevin eqn. soln., return to thermal equilibrium 4-58675  
 random magnets, crossover effects induced by lattice compressibility 4-76140  
 rippled commensurate state, new type of incommensurate state 4-65372  
 shock loaded solids, thermodynamic props., influence of defects 4-113680  
 sine-Gordon systems, statistical mechanics props., boundary condition effects 4-63529  
 smectic B and E phases, disclinations and ovals near clearing temp. 4-75268  
 solid on solid interface model, free energies of surface steps 4-113780  
 solid-liquid interface, wetting by gas, free energy functional 4-88373  
 solutions, optical electron transfer, dispersion spectroscopy 4-80854  
 solvation and solvatochromism, statistics 4-85327  
 spatially inhomogeneous samples, de Haas-van Alphen effect 4-113849  
 spherical model in random external field, free energy 4-88634  
 spin glass, quenched and annealed free energies 4-104428  
 spin glass phase, random anisotropy model, 1/N expansion, replica-symmetry breaking soln. 4-104436  
 spin glasses, scaling model, transverse freezing and correlation lengths 4-114118  
 spin glasses, singularities of free energy near freezing temp. 4-104430  
 spin systems, quasichiral approx., spin coherent states (*Russian*) 4-114124  
 steel, austenitic stainless, recrystn., grain boundary diffusion and free energy 4-114569  
 steel, crystallisation, initial stages 4-114505  
 strong-coupling supercond. with Shiba-Rusinov impurities, free energy formula 4-104358  
 surface, light scatt. near phase transition point 4-99128  
 surface energy, contact angle meas., spreading press. effects 4-61173  
 surface struct. near critical point, free energy formalism anal. 4-92038  
 surfaces, light scatt. near phase transition points 4-66049  
 surfaces, roughening transition 4-113569  
 tetrachloromethane +  $\alpha,\omega$ -dichloroalkane, vapour pressure, vapour-liquid equilb. 4-98256  
 TGSe, phase transition rel. to deuteration 4-76387  
 thermodynamics of continuous media using entropy flux of Muller 4-90542  
 thiourea, modulated phase study 4-76372  
 tunnelling units, interacting, density of states in absence of long-range order, thermodynamic props. 4-80185  
 two-dimensional aqueous solution-like system, conc. fluctuations, Monte Carlo study 4-70008  
 two-dimensional one-component plasma, free energy and correlation functions 4-90485  
 two-dimensional square-well fluid, thermodynamic props. 4-111093  
 two-phase interface, planar, free energy study 4-92478  
 vesicles, mixed phosphatidylcholine/phosphatidylserine lipid, free energy pot. for aggregation 4-66897  
 vinylidene fluoride/trifluoroethylene copolymer, ferroelec. transitions 4-99050  
 water, fluid phase thermophys. props. 4-98314  
 water-methane vapour, excess enthalpies up to 698.2K and 12.6 MPa 4-113097  
 X-Y one-dimensional S=1 model with single-ion anisotropy, crit. behaviour 4-104454  
 Ag-Sn(In) dilute alloys, correlated impurity diffusion jump processes, isotope effect 4-84446  
 AgBrO<sub>3</sub>, preferential solvation in methanol-dimethylsulphoxide mixtures 4-93515  
 Al biaxial creep behaviour, thermodynamic aspects (*French*) 4-85187  
 Al, melting curve study at high press. 4-103911  
 $\gamma$ -Al<sub>2</sub>O<sub>3</sub>, adsorption of alkanes and aromatic hydrocarbons, thermodynamic props., chromatography (*Chinese*) 4-61210  
 Au-Ni (40 at.%), chem. and elastic contrib. to free energy above miscibility gap 4-76747  
 Be, temp. and press. induced phase transitions 4-70369  
 Bi-In, liq., activity coeff. of O 4-80242  
 Bi-Sb, liq. alloys, activities and free energy of form., EMF obs. (*Japanese*) 4-61920  
 C fibre reinforced plastic, damage susceptibility estimation, thermodynamic approach 4-99542  
 C filaments, tubular growth 4-93245  
 $\alpha$ -CO, librational motion, anharmonic effects 4-103892  
 CO<sub>2</sub>, librational motion, anharmonic effects 4-103892  
 Ca-Mg melts, excess partial Gibbs energies 4-61079  
 Ce, valence under high press., free energy depend. 4-92676

## free energy continued

- Co-Fe-Mo-Ni, phase equilb., Gibbs energy and activity coeff., SOLGAS-MIX program 4-84369  
 Cu-Zn-Al, shape memory alloys, ageing and stabilisation of martensite 4-109441  
 D<sub>2</sub> mol. fluid, equilb. props. in semiclassical limit 4-103632  
 DyMnO<sub>3</sub>, decomposition, O partial press. and elec. cond. 4-85290  
 ErRh<sub>2</sub>B<sub>2</sub>, coexistence of superconductivity and mag. order 4-104423  
 Fe-Al alloys, segregation to static and migrating diffuse antiphase boundaries 4-114541  
 Fe-B alloys,  $\alpha$ - $\gamma$  transition lines and activity coeffs., conductometric studies 4-103926  
 Fe-C eutectic solidification, equilb. partition coeff. of third element rel. to graphitization 4-99380  
 Fe-Ni binary alloy, massive transform. study using DTA (*Korean*) 4-104778  
 Fe-Ni Invar alloys, phase transforms. 4-70373  
 FeO, temp.-press. stability fields at high press., thermodynamic calc. 4-103965  
 Ga-N<sub>2</sub> system, high pressure thermodynamics, heat and entropy of GaN form. 4-62227  
 H<sup>+</sup> transfer reactions theory, adiabaticity effect on free energy relations 4-81406  
 H<sub>2</sub> mol. fluid, equilb. props. in semiclassical limit 4-103632  
 HCl-N<sub>2</sub>O liquid mixtures, thermodynamics and densities 4-98311  
<sup>3</sup>He, superfluid, A-phase, rot., analytic vortices and mag. resonances 4-98393  
<sup>3</sup>He, superfluid, core structure and vortex calcs. 4-75749  
<sup>3</sup>He, superfluid A phase, nonanalytic free energy 4-80325  
<sup>3</sup>He, superfluid A phase, nonanalytic props. and normal current 4-92462  
<sup>4</sup>He liquid film, strongly-coupled ripplonic polarons in high magnetic fields 4-98388  
<sup>4</sup>He, solid, surface free energy, faceting and phase transition 4-88361  
<sup>4</sup>He, superfluid, third sound, healing, relax. thermal cond. and viscosity effect 4-88359  
 Hf-Ni films, amorphisation by thin film solid state reaction 4-80428  
 Ho<sub>1-x</sub>R<sub>x</sub>Mo<sub>2</sub>S<sub>8</sub>, R=Er, Tb, relaxation of ferromagnetic ordering and superconductivity 4-98886  
 In-Bi-Pb, liq., thermodynamic props., EMF meas., 673 to 873K 4-98310  
 K-Rb, free energy, high temp. calc., phase diagram (*Russian*) 4-92389  
 KClF<sub>3</sub>, phase transitions and cryst. struct. 4-84379  
 K<sub>2</sub>SeO<sub>4</sub>, phase-transition, Raman spectra, uniaxial stress depend. 4-76450  
 La<sub>2</sub>CoO<sub>4</sub>, standard Gibbs energy of form. and high temp. thermodynamic stability 4-71958  
 LaCrO<sub>3</sub>/Mg, defect struct., model and thermogravimetric meas. 4-75434  
 Li breeder blanket, impure, T extraction by Y, thermochem. analysis 4-107027  
 $\alpha$ -N<sub>2</sub>, librational motion, anharmonic effects 4-103892  
 NH<sub>4</sub>Br, third order elastic consts. near  $\lambda$ -point 4-88223  
 N<sub>2</sub>O, librational motion, anharmonic effects 4-103892  
 Na, martensitic nucleation and growth, mol. dynamics simulation studies 4-114520  
 NaCl ion pair interaction in water, computer simulation 4-60795  
 NaF-AlF<sub>3</sub>, melt, thermodynamic data for reactions from vapour pressure meas. 4-85325  
 (NaI)<sub>2</sub> and (NaI)<sub>3</sub>, thermochemistry, free energy, dimerisation and trimerisation entropy 4-80205  
 NaI, vapour press. and evaporation thermodynamics 4-103915  
 NaNO<sub>2</sub>, modulated phase study 4-76372  
 Na<sub>2</sub>O, phase transitions, phenomenological theory 4-92348  
 Np compounds, thermodynamic behaviour in water and groundwater, pH and Gibbs energy, radwaste appl. 4-78701  
 PbO, standard molar Gibbs free energy of form., O conc. cell meas. 4-105010  
 PbO-CO<sub>2</sub>-H<sub>2</sub>O solid systems, stability and solubility rels. 4-84399  
 Rb<sub>2</sub>ZnCl<sub>4</sub>, incommensurate and ferroelec. phases, electro-optical props. 4-104574  
 Rb<sub>2</sub>ZnCl<sub>4</sub>, phase-transition, Raman spectra, uniaxial stress depend. 4-76450  
 Si, dry oxidation, parabolic kinetic const., stress effects 4-93434  
 Si-H-Cl system, Si condensation, equilibrium calcs., 300 to 3000K 4-61107  
 Si<sub>3</sub>N<sub>4</sub>-based systems, phase equilb. calcs. 4-71645  
 Sn-S-O system, high temp. study of oxide-sulphide equilb. 4-66315  
 Ta<sub>2</sub>S, vapourisation, enthalpy of reaction, free energy functions 4-88311  
 Ta<sub>2</sub>S, vapourisation, enthalpy of reaction, free energy functions 4-88311  
 IT-Ta<sub>2</sub>(Se<sub>2</sub>), CDW states, three-dimensional orderings 4-65625  
 TiC-N<sub>1-x</sub> solid solns., theoretical CVD conditions 4-61857  
 Tm intermediate valence cpds., mag. susceptibility and sp. ht. 4-108999  
 W-Ni alloys, liq. phase sintering, chem. induced migration of molten Ni films between W grains 4-114435  
 Xe in liq. n-alkanes, solubility, free energies, entropies and enthalpy of soln. 4-70389  
 Xe+methyl chloride liquid mixture, thermodynamic props. meas. 4-70408  
 Yb-Es dilute alloys; thermodynamics, Henry's Law vaporisation studies 4-92390  
 Zn anodic dissolution in alkaline electrolytes, three step model 4-103941

## free field rooms see anechoic chambers

## free induction decay (optical) see optical coherent transients

## free radical reactions

- benzene mixtures, muonium substituted free radical form. 4-71886  
 benzene-styrene mixtures, muonium radical form., MSR study 4-71951  
 sec-butyl radical, chem. activated unimol. reactions, weak collisions and steady states 4-81405  
 carbene derived radical pairs in microemulsions, behaviour, mag. field effects, triplet multiplicity 4-62164  
 carbene-type cation radicals, gas-phase chem. 4-114791  
 chlorodifluoromethyl radical + HCl, reaction rate, vibr. excitation influence 4-93507  
 CIDEP, polarisation, time evolution, oscillatory pattern 4-102711  
 p-cyanonitrobenzene anion radical, H bonding, kinetic parameters 4-102713  
 cyclohexadienyl radical, muonium substituted +2, 3-dimethyl-1,3-butadiene, rate const. 4-71887  
 cyclohexadienyl radicals+quinones, rate consts., muon spin rot. study 4-71888

## free radical reactions continued

- flavin radicals, form. and UV-vis. spectra, effects of pH and presence of  $\beta$ -mercaptoethanol 4-83384  
 formyl radical + NO( $O_2$ ) reaction, collision complex form. 4-71899  
 formyl radicals, vibr. excited, reactions and relax. 4-71898  
 laser-induced, IR and CARS spectroscopy (*German*) 4-81431  
 liquid phase chem., radical structs. and reaction rates using positive muon probes 4-71885  
 magnetic and spin effects, paramagnetic impurities influence 4-89252  
 methoxy + NO<sub>2</sub>, gas phase kinetics studies using fluoresc., vacuum UV and mass spectrometry 4-62172  
 methyl radical + Cl<sub>2</sub>(Br<sub>2</sub>), rate consts., product vibr. excitation and hot radical reactions 4-71893  
 onium salts, reduction by stable radicals and radical anions, kinetics 4-109644  
 2-propanone, pure and in aq. soln., muonic radical form.,  $\mu$ SR study 4-71950  
 radical rearrangements in liqs., rate const. obtained by muon spin rot. 4-89282  
 radical-radical reactions, products, vel. consts., far IR LMR study (*German*) 4-71913  
 tetrachlorosilane reactions in Ar-H<sub>2</sub> microwave plasma 4-89268  
 1,1,2-trichloroethane, acid-catalysed and radical chain transforms. 4-109641  
 triphenyl verdazyl radical + HgCl<sub>2</sub>, reaction, adiabatic and nonadiabatic events 4-109639  
 unsaturated organic liquids, muon substituted free radicals 4-83498  
 4-vinylcyclohexene cation radical, retro-Diels-Alder reaction mechanism 4-81408  
 CN + H<sub>2</sub>(O<sub>2</sub>)(CO)(CO<sub>2</sub>)(N<sub>2</sub>)(HCN)(methane)(cyanogen), vibr. energy effect on reaction, laser meas. 4-99769  
 HS + NO + M  $\rightarrow$  HSNO + M, (M = He, Ar, N<sub>2</sub>), rate coeffs: in temp. range 250 to 445K 4-71895  
 N<sub>2</sub><sup>+</sup> + N<sub>2</sub> + M  $\rightarrow$  N<sub>4</sub><sup>+</sup> + M, ion-molecule association reaction for M = N<sub>2</sub>, Ne and He 4-99764  
 N<sub>2</sub> + NO reactions, rate consts. determ. at 295K 4-71863  
 NH<sub>2</sub> radicals, vibr. excitation studied by laser-induced fluoresc., reaction rate and relax. processes 4-89274  
 NH<sub>2</sub> + NO, gas phase kinetics studies using fluoresc., vacuum UV and mass spectrometry 4-62172  
 NH<sub>3</sub><sup>+</sup> + H<sub>2</sub>S reaction, depend. on translational and internal energy of NH<sub>3</sub><sup>+</sup> 4-71891  
 NO<sub>2</sub> radical nighttime reactions with biogenic organic cpds. 4-89975  
 NO<sub>2</sub> + Cl(ClO), kinetic growth and decay meas. using time resolved absorpt. 4-89247  
 OH radicals, recombination kinetics on quartz wall in propane-O<sub>2</sub> flame 4-109627  
 OH + ethene (propene), reaction rate consts., laser photolysis/resonance fluoresc. study 4-83598  
 OH + methanol, temp. depend. and branching ratio meas. by mass spectrometry and LIF method 4-62169  
 SO<sub>2</sub> + OH, prod. of HOSO<sub>2</sub> radical, IR detection 4-78835

## free radicals

- see also *free radical reactions; paramagnetic resonance of free radicals*  
 acetamides,  $\beta$ -halo substituted radical anions in X-irrad. crystals, INDO calcs., EPR obs. 4-102714  
 acetone cation,  $\gamma$ -irrad., <sup>13</sup>C ESR and ENDOR investig. 4-69114  
 alkyl radicals, ionisation pot., oscillator strength, UV spectra 4-96561  
 alkyl radicals, UV spectra, ab initio SCF and CI calcs. 4-96560  
 alkylamines and cation radicals, electronic and spatial struct., CNDO/2 calcs. 4-59647  
 p-aminophenoxy radical, aq. soln. fundamental vibr. reson. Raman study 4-102690  
 aniline <sup>2</sup>B<sub>1</sub> radical cation, jet cooled, two colour photoionisation spectra, vibr. 4-64547  
 2-anthracene carboxylic acid alkyl ester cation radicals, charge transfer, photolysis obs. 4-102788  
 aromatic radical dimer cations, charge reson. energies 4-87230  
 benzodithiazolyl free radicals, ESR spectrosc., stability and spin probe props. 4-69118  
 benzophenone + aromatic amines photochem. reactions, transiently prod. spin polarised radical pairs 4-99806  
 p-benzosemiquinone anion radical, powder ENDOR anal. 4-74275  
 p-benzosemiquinone radical anion, vibr. struct., isotope effects, reson. Raman and MO investig. 4-59780  
 benzyl radicals, stationary nutations and CIDEP during methyl benzyl ketone photolysis 4-76252  
 benzylperoxy radical, dipole meas. by microwave dielect. absorpt. 4-59915  
 sec-butyl radical, chem. activated unimol. reactions, weak collisions and steady states 4-81405  
 caffeine hydrochloride dihydrate, X-ray irrad., free radical ENDOR study 4-112214  
 carbene-type cation radicals, gas-phase chem. 4-114791  
 carbon tetrachloride, solids containing acetals, gamma-irrad., <sup>13</sup>Cl radical prod. 4-93504  
 chalcogeno triphenylarsoranyl radicals, matrix isolated, ESR, obs. 4-91290  
 chlorofluoromethyl cations and radicals, ground state, photoelectron spectrosc. obs. 4-64541  
 chloromethyl cations and radicals, ground state, photoelectron spectrosc. obs. 4-64541  
 chlorophyll and pheophytin radicals, Mn mag. dipole interaction at photo-system II reaction centres 4-66846  
 collisional dissoc. form. of H<sub>3</sub><sup>+</sup> 4-66555  
 p-cyanonitrobenzene anion radical, H bonding, kinetic parameters 4-102713  
 cyclohexadienyl radical, muonium substituted +2, 3-dimethyl-1,3-butadiene, rate const. 4-71887  
 cyclohexadienyl radicals, muonium substituted, isomer distrib., radiolytical processes, muon spin rot. 4-92984  
 cyclohexadienyl radicals + quinones, rate consts., muon spin rot. study 4-71888  
 di-tertbutylnitroxide, spin label for EPR studies in liq. crystals, proton hyperfine tensor 4-84855  
 dibenzanthracenes radical cations, optical electronic spectra correl. with PES 4-96615  
 dibenzochrysene radical cations, optical electronic spectra correl. with PES 4-96615  
 dibenzocycloheptadienyldiene, laser flash photolysis 4-62212

## free radicals continued

- dichloromethyl cations and radicals, ground state, photoelectron spectrosc. obs. 4-64541  
 2,6-difluoropyridine radical cations, EPR investig. 4-107372  
 disodium anthraquinone-2,6-disulphonate, radical anion, time-resolved reson. Raman spectra 4-91266  
 disulphenimidylyl free radicals, ESR spectrosc., stability and spin probe props. 4-69118  
 dithiadiazolyl free radicals, ESR spectrosc., stability and spin probe props. 4-69118  
 dithiazolyl free radicals, ESR spectrosc., stability and spin probe props. 4-69118  
 doublet state radicals, ordering of modified virtual orbitals 4-68973  
 electronic transition moments, MCSCF-SCEP wave functions calc. 4-74166  
 ethyl radical, direct adiabatic channel computation for excited state relax. to give H + ethylene 4-96433  
 flames, oxy-fuel, H and OH radicals distrib. determ. 4-99798  
 2-fluoropyridine, radical cations, EPR investig. 4-107372  
 formaldehyde diradical, adsorption on MgO (001), ab initio MO calcs., lattice defect methods 4-81476  
 formyl radical + NO( $O_2$ ) reaction, collision complex form. 4-71899  
 formyl radicals, adsorption on MgO (001), ab initio MO calcs., lattice defect methods 4-81476  
 formyl radicals, vibr. excited, reactions and relax. 4-71898  
 Heisenberg spin exchange model, CIDEP and relax. 4-88722  
 hydroxymethyl radical, adsorption on MgO (001), ab initio MO calcs., lattice defect methods 4-81476  
 iodoacetamide, X-irrad.,  $\sigma^*$  radical anion struct., EPR and INDO calc. 4-69119  
 ionic radicals, semiempirical model of exchange polarisation mechanism of transferred hyperfine interaction 4-112105  
 maleic anhydride radical, EPR hyperfine struct. coupling const., temp. depend., vibr. effects (*German*) 4-91285  
 methoxy radical, <sup>2</sup>E ground state, rot. mol. consts., microwave spectrum 4-107334  
 methoxy radical, A' and A'' states, structs. and vibr. freqs. 4-112095  
 methoxy radical, adsorption on MgO (001), ab initio MO calcs., lattice defect methods 4-81476  
 methyl radical, IR laser line absorpt. and emission at elevated temps. 4-112171  
 methyl radical + Cl<sub>2</sub>(Br<sub>2</sub>), rate consts., product vibr. excitation and hot radical reactions 4-71893  
 methyl-d<sub>3</sub> free radicals, electron impact ionisation and dissociative ionisation 4-102810  
 methylene, dipole moments, ab initio rot.-vibr. transition moments 4-59688  
 methylene, singlet,  $\nu_1$  and  $\nu_3$  spectra, IR flash kinetic method obs. 4-59737  
 methylene-d<sub>3</sub>, free radicals, electron impact ionisation and dissociative ionisation 4-102810  
 methylpyrazines radical, triplet state, photophysics and photochemistry, CIDEP 4-69115  
 1,4-naphthoquinone radical anion intramol. charge transfer complexes, ESR investig. 4-107374  
 nitroxide free radicals, local spin density theory 4-68933  
 nitroxide radicals in soln., superhyperfine struct., ESR spectra, computer simulation 4-96578  
 olefin radical cation optical spectra, hyperconjugation transitions 4-74259  
 organic radicals, heat of form. from appearance energies 4-89318  
 pentafluoroethyl free radical, matrix isolation IR spectrum 4-69069  
 pentafluoropyridine radical cations, EPR investig. 4-107372  
 phenoxy radicals and ions, vibr. spectra and struct., reduction, oxidation and H<sup>+</sup> transfer 4-59806  
 phenoxy radical-d<sub>6</sub>-(d<sub>5</sub>)-(d<sub>3</sub>), aq. solns., vibr. modes, reson. Raman obs. 4-107352  
 phosphonyl radicals, optical absorption spectra 4-74257  
 polyenes, linear, radicals and ions, correlated states, transition moment, spin densities, PPP VB theory 4-68962  
 polymers, conjugated, doped, transport props., role of organic radicals and ions 4-75956  
 propylene radical cations, twisted struct., EPR investig. 4-83393  
 proteins, radical formation under pulsed picosec. laser radiation action 4-109777  
 pyrene-N,N-dimethylaniline complex radical pairs, exciplex luminesc., environment effect on mag. field modulation 4-99147  
 radical pair mechanism electron spin polarisation, CIDEP 4-87142  
 semiquinone anion radicals, hyperfine tensors, methyl group interaction, ENDOR 4-64520  
 semiquinones-Mn<sup>2+</sup>(Cu<sup>2+</sup>)(Gd<sup>3+</sup>) interaction in aq. solns. relax. and complex formation 4-99777  
 spectral line detect. using double modulation laser mag. reson. spectrometer 4-73467  
 spectroscopy, Faraday rotation, with colour centre laser, differential detect. scheme 4-95525  
 spectroscopy using colour centre lasers of small free radicals 4-64479  
 spin polarised (CIDEP) radicals, continuous wave flash photolysis ESR spectra using time integration spectroscopy 4-74274  
 spin trapping of radicals produced by glow discharge on low-density polyethylene 4-61592  
 spin-lattice relax. in free radicals in ion-exchange materials, via excited vibr. states 4-59815  
 spin-polarised radicals, ESR, microwave-switched time integration study 4-87143  
 TCNQ salt with triphenyl methyl arsenic cation triplet excitation radical, exchange anomaly resolution 4-70760  
 Tempone in glycerol, mol. motion, two dims. electron spin echo spectra 4-109055  
 N,N,N',N'-tetramethylbenzidine cation radicals, photoproduced, lifetime distrib., reactivity 4-7018  
 tetramethylene diradical intermediate, singlet state, ab initio MC SCF geom. optimisation 4-96432  
 thiophenoxy radicals, emission spectra and emission lifetimes at 77K 4-96593  
 three-body assoc. reactions with Kr and Ar at 80K 4-71883  
 TMTSeF, and radical cation, superconductors, vibr. IR and Raman obs. 4-88821  
 TMTTF, and radical cation 4-88821  
 trimethylene diradical, force consts. two config. SCF and HF wave functions 4-59618  
 trimethylethylene, radical cations, twisted struct., EPR investig. 4-83393

## free radicals continued

- triphenyl verdazyl radical +  $\text{HgCl}_2$ , reaction, adiabatic and nonadiabatic events 4-109639  
 triphenylmethylsulphane radical pairs, ESR study 4-88724  
 unsaturated organic liquids, muon substituted free radicals 4-83498  
 vinyl radicals, electronic struct., VB and CI calcs., quantum chem. with attached processor 4-68963  
 4-vinylcyclohexene cation radical, retro-Diels-Alder reaction mechanism 4-81408  
 $\text{Al}_2\text{O}_3$ -x anodic oxide films, paramagnetic centres and optical absorpt. spectra studies 4-104494  
 Ar triplet and cold radical prod. with pulsed elec. discharge in pulsed supersonic flow 4-84090  
 $\text{Ar}^+ + \text{CO}(\text{N}_2)$  collisions, integral cross section meas. 4-78929  
 $\text{Br}_2^+$  radical in aq. soln. harmonic freq., anharmonicity const., reson. Raman spectra 4-74247  
 $\text{C}_2$ , elementary gas phase processes, laser kinetic spectroscopy 4-69054  
 CCl triplet and cold radical prod. with pulsed elec. discharge in pulsed supersonic flow 4-84090  
 CH radical, energetics, laser induced fluoresc. 4-114777  
 $\text{CH}^+$ , A II state shape resons., exterior complex scaling calcs. 4-74307  
 $\text{C}_2\text{H}_3\text{N}^+$ , mobilities in He at 293K 4-79706  
 CHOR radical, in X-irrad. methyl  $\beta$ -D-galactopyranoside, geometry, ESR/ENDOR obs. 4-102712  
 $[\text{C}_2\text{H}_2\text{O}]^+$  isomerisation, ab initio SCF calc. in gas phase (French) 4-71880  
 CN, collisional vibr. relax. in A II state 4-69035  
 CN radical evolution in  $\text{N}_2$ -ethanol mixture pulsed discharge 4-81428  
 $\text{C}_2\text{N}_2^+$ , mobilities in He at 293K 4-79706  
 $\text{C}_2\text{NH}_2^+$  isomers, struct., relative energies ab initio MO STO calcs. 4-102572  
 $\text{C}_2\text{NH}_2^+$  isomers, struct., relative energies ab initio MO STO calcs. 4-102572  
 CO triplet and cold radical prod. with pulsed elec. discharge in pulsed supersonic flow 4-84090  
 $\text{CO}^+$ , isolated ions, IR spectra quantitative prediction 4-69075  
 $\text{CO}^+$ , cation radical in Ne matrix, ESR investig. 4-78873  
 $\text{CO}_2^+$ , isolated ions, IR spectra quantitative prediction 4-69075  
 $\text{CO}_2^+$  radical, metastable states, unimolecular dissoc. 4-76972  
 $\text{CO}_2^+$  cation radicals, matrix isolated, EPR and ab initio investig. 4-74273  
 $\text{CS} + \text{Ar}^+$ , emission spectra prod. from thermal energy charge transfer reactions 4-74325  
 $\text{CS}_2^+$ , isolated ions, IR spectra quantitative prediction 4-69075  
 $\text{Cl}_2^+$  radical in aq. soln. harmonic freq., anharmonicity const., reson. Raman spectra 4-74247  
 CsO, hyperfine interactions and bonding, semiempirical valence bond model 4-112120  
 $\text{FO}_2$ , FIR laser mag. reson. detection from  $\text{F} + \text{O}_2(\text{O}_3)$  reactions 4-59811  
 $\text{FO}_2$  radical,  $\nu$  band, IR diode laser spectra 4-74237  
 $\text{HCN}^+$ , mobilities in He at 293K 4-79706  
 $\text{H}_2\text{NO}$  free radicals, local spin density theory 4-68933  
 $\text{HO}_2$  dimer, cyclic, two-hydrogen-bond form 4-91360  
 $\text{HO}_2$  vibr. band strength for  $\nu_3$  band meas. 4-74220  
 $\text{HOSO}_2$  radical, Ar matrix isolated, IR spectra 4-78835  
 $\text{HS} + \text{NO} + \text{M} \rightarrow \text{HSNO} + \text{M}$ , (M=He, Ar,  $\text{N}_2$ ), rate coeffs. in temp. range 250 to 445K 4-71895  
 $\text{He}^+ + \text{N}_2$  thermal charge transfer reaction,  $\text{N}_2^+$  predissoc. channel 4-91317  
 IO radical, A II $_{3/2}$ -X $^2$ II $_{3/2}$  system, laser-RF spectrosc. obs. 4-59819  
 $\text{N}_2^+$  predissociative channel in low energy  $\text{He}^+ + \text{N}_2$  charge transfer 4-91317  
 $\text{N}_2^+ + \text{N}_2 + \text{M} \rightarrow \text{N}_4^+ + \text{M}$ , ion-molecule association reaction for M=Ne, Ne and He 4-99764  
 $\text{N}_2 + \text{NO}$  reactions, rate consts. determ. at 295K 4-71863  
 NF radicals, electronically excited, prod. in  $\text{NH}_3\text{-F-O}_2(\text{a}^1\Delta)$  system 4-83309  
 $\text{NF}_2(\text{X}^2\text{B}_1)$ ,  $\nu_3$  band, IR laser spectroscopy 4-69082  
 NH metastable, radiative lifetimes, transition moments 4-74292  
 NH radical, A II $^+$ -X $^2\Sigma^+$  system, lifetimes, laser-induced fluoresc. 4-78890  
 $\text{NH}_3^+ + \text{H}_2\text{S}$  reaction, depend. on translational and internal energy of  $\text{NH}_3^+$  4-71891  
 $\text{N}_2\text{H}_4$  radical cation optical spectra, hyperconjugation transitions 4-74259  
 $\text{N}_2\text{O}$  radical, gas phase, far-IR LMR study 4-102718  
 $\text{NH}_2(\text{X}^2\text{B}_1)$  detection by CARS spectroscopy 4-62262  
 $\text{NO}$  vibr. overtone band, colour centre laser spectroscopy of small free radicals 4-64479  
 $\text{NO}_3$  in atmosphere, nighttime reactions with biogenic organic cpds. 4-89975  
 $\text{NO}_3$  radical, in nighttime atmosphere of S California, USA 4-100028  
 NS radical, far IR LMR study 4-91286  
 OH, anomalous photodetachment thresholds from electron dipole interactions, rot. doubling effects 4-74298  
 OH conc. at ground level, optical absorption meas. 4-72666  
 OH, electronic transition moments, MCSCF-SCEP wave functions calc. 4-74166  
 OH, fundamental vibr. spectrum, colour centre laser spectroscopy of small free radicals 4-64479  
 OH internal state distrib., prod. from O+cyclic hydrocarbons, laser induced fluoresc. study 4-77000  
 OH molecule photoacoustic detect. in methane-air flame 4-77036  
 OH, photoionisation cross sections UV spectra 4-112237  
 OH, pulse discharge, VUV photoabsorption cross sections 4-107362  
 OH radical, fragment from  $\text{H}_2\text{O}_2$  photodissociation, fluoresc. study 4-109674  
 OH radical detect. using sequential two-photon laser-induced fluoresc. technique 4-93566  
 OH radicals, recombination kinetics on quartz wall in propane- $\text{O}_2$  flame 4-109627  
 P-centred radical cations, EPR of dil. solns. 4-83395  
 PH radicals, term energy, bond lengths, vibr. freq., visible obs. 4-87095  
 PH(D), X $^2\Sigma^+$  vibronic state, far-IR laser mag. reson. 4-59814  
 $\text{PN} + \text{Ar}^+$ , emission spectra prod. from thermal energy charge transfer reactions 4-74325  
 RbO, hyperfine interactions and bonding, semiempirical valence bond model 4-112120  
 SiCl radical, ground vibronic state, spin states, mol. const., microwave spectra 4-59727  
 SiH radicals, A $^2\Delta$  state, radiative lifetime meas. by laser induced fluoresc. 4-96622

## free radicals continued

- SiH $_2$  radical, laser-induced fluoresc., lifetimes, bending vibr. spacing 4-59827  
 SiH $_3$  radical, pot. surface and rot. vib. energies, ab initio calc. 4-96457
- freezing  
 see also refrigeration  
 alloy, bicomponent, liquid mixtures separation in a freezing-out process 4-103185  
 alloy, binary, freezing, periodic growth rate effect on morphological stability 4-98039  
 aqueous solutions of clathrate forming gases, freezing-nucleation 4-75647  
 aromatic cpds., dil. solns., dielectric behaviour on freezing 4-88759  
 biological specimen, liq. He cooled slam freezing device 4-115299  
 Cartesian two dimensional phase change, fixed mesh finite element solution 4-112669  
 clusters, melting and freezing behaviour 4-108593  
 clusters, unequal freezing and melting temps. 4-75639  
 coal liquids, vap. press. incorporating renormalisation group formulations with corresponding state principle 4-88271  
 density wave theory with crystal symmetry 4-70350  
 ethanol coolant for rapid freezing of biological material 4-89860  
 ice nucleation in supercooled water sample, laboratory expts. 4-115545  
 ice surfaces, epitaxial freezing of supercooled droplets 4-98052  
 lipid extraction during freeze-substitution of bacterium cells for electron microscopy 4-89862  
 metals and alloys, solidification, book contrib. 4-109393  
 monocytes, human, liq. propane jet-freezing, freeze-drying and rotary replication of cytoskeleton and membrane assoc. struct. 4-89861  
 optical microscope stage, low-temp., for solidification studies in aqueous soln. 4-111199  
 phospholipid-water systems, calorimetric studies of water behaviour 4-66900  
 planar or radial freezing with solid-solid transitions and convective heating at the solid-liquid interface 4-80198  
 Reichert-Jung freeze fracture apparatus, anticontamination device modification 4-89863  
 salol, solid-liq. interface props., dynamic light scatt., thermal diffusivity, lattice const. 4-109203  
 sea ice, freezing process, flow model for brine expulsion 4-85694  
 small sample storage under liq.  $\text{N}_2$ , rapid-access system 4-73428  
 solid liquid interface, freezing solutions, motion of interface 4-108592  
 thylakoid membranes, isolated, inactivation during freezing 4-105195  
 two-dimensional problems anal. by finite element method 4-97291  
 water, superheat, natural convection effect on freezing around isothermal, horizontal cylinder 4-108588  
 water droplets supercooling 4-97294  
 water movement in concrete when it freezes 4-103408  
 $\text{C}_3\text{S}_4$  hydration products, obs. using cryo stage in SEM 4-71874  
 $\text{K}_2\text{K}_3$ , freezing temperature, crit. points 4-70349  
 Kr layer on graphite in one-to-two layer regime, phase diagram, freezing transitions 4-103910  
 $(\text{MnO})_2(\text{Al}_2\text{O}_3)_2(\text{SiO}_2)_2$ , spin glass, amorphous, crit. behaviour, field expansion and scaling, susceptibility, magnetisation meas. 4-92920  
 Pd, calibration of thermocouples and pyrometers 4-80196
- Frenkel defects  
 accumulation at low temp., computer simulation by Monte Carlo method (Russian) 4-113442  
 accumulation kinetics, irradi. induced, similar defect aggregation (Russian) 4-113493  
 alkali halide cryst., Frenkel defect accumulation, temp. and impurity conc. depend. 4-98093  
 alkali halides, excitonic and impurity-excitonic mechanisms for F,H pair creation (Russian) 4-80034  
 crystals, accumulation kinetics of Frenkel defects 4-70141  
 high concentrations, explosive annealing 4-108356  
 ionic crystal, three-channel exciton decay by light emission (Russian) 4-99171  
 phase transitions, Coulomb effects, Debye-Huckel approx. anal. 4-61074  
 quartz, luminescence, ODMR study 4-85001  
 unstable, metastable, and separated Frenkel pair defects in solids 4-75444  
 Ag halides, halide ion and  $\text{Ag}^+$  adsorption, interaction pot. 4-75785  
 Ag-Cu dilute alloys, defect production and annealing 4-75442  
 AgBr, role of Frenkel defects in radiation stimulated processes 4-98095  
 $\text{Ba}_{0.78}\text{Al}_{1.05}\text{O}_{17.14}$ , hexaaluminate phase I, cryst. struct. and nonstoichiometry 4-70087  
 $\text{Ba}(\text{NO}_3)_2 \cdot \text{K}$ , d.c. ionic cond. meas. 4-84456  
 $\text{CaF}_2$ , electron irradi., anion voidage and void superlattice 4-108350  
 $\text{CaF}_2$ , thermally induced anion disorder, neutron scatt. meas. 4-98338  
 Cu, single Frenkel-pair production by neutrino recoil 4-98089  
 $\text{Fe}_{1-x}\text{S}$ , self-diffusion coeffs., Mossbauer spectroscopy 4-98351  
 Ge, Frenkel pair component density distrib. after  $\gamma$  irradi. 4-70142  
 Ir, electron and neutron irradi., elec. resist. studies 4-108447  
 KBr, unstable, metastable, and separated Frenkel pair defects 4-75444  
 KBr:Cl, and undoped crystals, anion Frenkel defect creation, luminesc. study (Russian) 4-80980  
 KCl:Ti, lattice defects creation and corrosion during annihilation of electronic excitations (Russian) 4-80035  
 $\text{La}_{0.82}\text{Al}_{1.9}\text{O}_{10.09}$ , cryst. struct., single cyst. X-ray diffr. studies 4-103723  
 LiH(D), radiation induced defect form. 4-60952  
 LiH(D):Na, radiation induced defect form. 4-60952  
 Ni-Ge dilute alloys, defect reactions, diffuse X-ray scatt. studies 4-75440  
 Ni-Si dilute alloys, defect reactions, diffuse X-ray scatt. studies 4-75439  
 $\text{PbF}_2$ , thermally induced anion disorder, neutron scatt. meas. 4-98338  
 $\text{PbMoO}_4$ , stoichiometry deviation, electron transfer, elec. cond. meas. 4-80591  
 Si, electron and  $\gamma$  irradi., influence on defect annihilation 4-98094  
 Si, electron and  $\gamma$ -ray irradiated, efficiency of radiation defect formation 4-92237  
 $\text{SrCl}_2$ , thermally induced anion disorder, neutron scatt. meas. 4-98338  
 $\text{SrF}_2$ , interstitial atom hopping by electronic excitation of Frenkel pairs 4-70140  
 $\text{SrF}_2$ , photo-induced transform. of close Frenkel pairs, absorption and luminesc. props. 4-76500  
 $\text{Sr}(\text{NO}_3)_2$ , d.c. ionic cond. meas. 4-84456  
 $\text{Sr}(\text{NO}_3)_2 \cdot \text{Na}(\text{Al})$ , d.c. ionic cond. meas. 4-84456  
 $\text{UO}_2$ , O Frenkel disorder obs., neutron scatt. study 4-60917

- quency agility**  
see also *information theory*  
two-frequency microwave ocean wave scatterometer 4-105773
- quency allocation**  
Earth-space links, digital, effect of ice-induced cross polarisation 4-62904
- quency changers** see *frequency converters*
- quency control**  
passive atomic frequency standards, improved vibr. performance by servo-loop control 4-68216  
H maser frequency standards, NR series microprocessor monitor and control system 4-68202
- quency converters**  
see also *frequency multipliers; mixers (circuits); optical frequency conversion*  
lateral photo effect and position-frequency converter, anal. (Japanese) 4-105108
- quency division multiplexing**  
Atlanta single-mode experiment, optical technology appl. 4-107840  
low-loss single-mode WDM with etched fibre arrays 4-103024  
monofrequency optical carrier, modulated by frequency multiplexed voice channels, spectral anal. 4-102889  
multimode fibre optic wavelength division multiplexing, state-of-the-art survey 4-79339  
multimode wavelength multiplexer for 850-1300 nm, fabrication 4-91658  
multiple multiplexers, shared optical function components (French) 4-79340  
optical fibre 3 Gbit/s close-spaced WDM at 1.5 micron 4-103014  
optical multiplexer/demultiplexer for subscriber loop system (Japanese) 4-79342  
optical single-mode fibres for WDM communication systems, crosstalk due to stimulated Raman scatt. 4-107857  
optical subscriber loop for business premises and local area appls. (Japanese) 4-79304  
optical subscriber loop system for local area appl. (Japanese) 4-79307  
optical subscriber system for business premises appl. (Japanese) 4-79306
- quency-domain analysis**  
see also *frequency-domain synthesis*  
adaptive optics systems, control servo designs 4-87431  
analogue data recording and processing, for high-resolution frequency analysis 4-63725  
attenuative subsurface layered media parameter estimation, frequency-domain approach 4-107941  
bat's sonar signal, wideband ambiguity function computation and numerical anal. 4-109845  
concatenated cabled optical fibres, pulse dispersion meas. at 1.3  $\mu$ m 4-64774  
seismology, time-shift estimation and alignment of discrete time signals, frequency domain method 4-105772  
time series, freq. and time domain anal., approaches for use in hydrology 4-82307  
Weibull-distributed weather clutter, frequency domain anal. 4-100688  
He speech unscrambling, frequency-domain algorithm 4-107960
- quency-domain synthesis**  
see also *frequency-domain analysis*  
nuclear reactor optimal feedback control by frequency-domain methods 4-64197
- quency doublers** see *frequency multipliers*
- quency measurement**  
see also *atomic clocks*  
atomic frequency standards, history 4-68200  
atomic frequency standards using laser beam (technology (Japanese) 4-58821  
bandwidth of far-IR radiation of UCSB free electron laser 4-74529  
comparison by pulse coincident method, errors analysis 4-58815  
development of frequency and time standards (Japanese) 4-58816  
instrumentation for time and frequency standards (Japanese) 4-58818  
international time transfer expt. 4-68218  
maser time and frequency standards, status and appl. (Italian) 4-86389  
mean square relative random frequency variation calc. 4-95393  
meas. methods for frequency and time (Japanese) 4-58817  
measurement chain to 30 THz using FIR Schottky diodes and submm. backward wave oscillator 4-73414  
microwave helix waveguide absorption cell for passive frequency standard 4-95391  
microwave passive frequency source, 24 GHz, microwave absorption in  $^{14}\text{NH}_3$  gas, operation (French) 4-111108  
microwave spectrometer, broadband, mm-to-cm range 4-78373  
national and international time and frequency comparisons 4-68217  
NTT's standard RF facility, appl. (Japanese) 4-58830  
passive atomic frequency standards, improved vibr. performance by servo-loop control 4-68216  
pulsars, potential applications as time standards 4-72970  
satellites appl., time service system development (Japanese) 4-58833  
secondary frequency standard based IR synthesizer programmable, using tunable Pb-salt diode lasers 4-111107  
standard broadcast station JG2AS/JJF-2 time service, LW radio appl. (Japanese) 4-58832  
standard frequency and time services, development (Japanese) 4-58829  
standard frequency and time services, review (Japanese) 4-58828  
standard signals errors estimation, systematic linear frequency variation 4-95392  
 $^9\text{Be}^+$  ions laser cooled, appl. in freq. standard 4-68204  
Cs atomic frequency standard, appl. (Japanese) 4-58819  
Cs beam frequency standard cavity phase shift analysis 4-101814  
Cs beam frequency standard, pulling by neighbouring transitions 4-101815  
H compact maser, performance 4-69353  
H maser atomic frequency standard, appl. (Japanese) 4-60006  
H maser frequency standards, NR series microprocessor monitor and control system 4-68202  
 $^3\text{He}$ -Ne laser locked to methane E-line, accurate freq. meas. 4-96868  
 $^{199}\text{Hg}$  trapped ion freq. standards, exptl. and theoretical results 4-68203  
Rb atomic frequency standard, development (Japanese) 4-58820  
Rb vapour cell freq. standards, compact rectangular cavity 4-68201
- quency meters**  
8 digit meter, kit design using CMOS devices (French) 4-95408
- quency meters continued**  
power frequency meter, analog indication, low cost high-resolution cct. design 4-111150  
timer-counters and freq. meters, configs. and performance characts. (German) 4-106328
- quency modulation**  
see also *frequency shift keying*  
coherent optical communication systems, based on polarisation-preserving fibres, bandwidth-limiting effects 4-69587  
differential-modulation correlator for extracting 4-74441  
frequency domain storage, polarisation gated writing of photochem. holes for FM polarisation detection 4-87292  
linear prediction vocoder, gain errors 4-81717  
plasma density meas. by microwave interferometry using freq. modulation 4-97898  
scanning acoustic microscope in interference mode using frequency modulation method 4-97231  
semiconductor lasers, direct FM and FM noise 4-69463  
semiconductor lasers, injection locking characts. 4-64707  
spectroscopy, freq. modulation polarisation,  $\text{I}_2$  vapour saturation holes 4-111218  
GaInAsP cleaved coupled-cavity laser, tunable design, FM operation for communication appl. 4-69451
- quency multipliers**  
microwave passive frequency source, 24 GHz, microwave absorption in  $^{14}\text{NH}_3$  gas, operation (French) 4-111108  
 $\text{H}_2$  maser frequency standards, limitations due to receiver noise 4-96854
- quency regulation** see *frequency control*
- quency response**  
bulk-acoustic-wave-beam filters, effects of diffraction on freq. response 4-60232  
dielectric loss measurement, frequency response analyser system, minicomputer-controlled, errors and calibration technique 4-111159  
spatial dynamic structure of combustion zone, frequency charact. matrix determ. 4-85311  
synergistic control system for paralyzed extremity joint 4-100359
- quency shift keying**  
coherent FSK transmitter using a negative feedback stabilised semiconductor laser 4-108755  
semiconductor laser, direct FSK by acoustic waves 4-91507
- quency stability**  
see also *frequency control; laser frequency stability*  
mean square relative random frequency variation calc. 4-95393  
meas. methods for frequency and time (Japanese) 4-58817  
microwave passive frequency source, 24 GHz, microwave absorption in  $^{14}\text{NH}_3$  gas, operation (French) 4-111108  
quartz oscillator, very low temperature design (Japanese) 4-58860  
 $\text{H}_2$  maser, freq. stability improvement by new state selection 4-96855  
 $\text{H}_2$  maser frequency standards, limitations due to receiver noise 4-96854
- quency synthesizers**  
see also *frequency converters*  
microwave passive frequency source, 24 GHz, microwave absorption in  $^{14}\text{NH}_3$  gas, operation (French) 4-111108
- quency synthesizers** see *frequency synthesizers*
- quency triplers** see *frequency multipliers*
- friction**  
see also *internal friction; lubrication*  
ablation by frictional heating 4-97440  
alloys, friction and wear, appl. of dislocation concepts, book contrib. 4-98103  
beam, self-excited vibr. with dry friction, parametric reson. 4-87604  
beam, self-excited vibr. with dry friction in parametric reson. region 4-87605  
boundary of elastic materials, subsonic propag. of shear displacement edge with friction 4-108049  
brittle surface in sliding contact with spherical indenters, strength degradation 4-104881  
ceramics, friction wear, theoretical and expt. studies 4-62069  
ceramics and cemented carbide, friction with superhard abrasive grains 4-109522  
coefficient measurement, mech. sensor/indicator device 4-86411  
cold incoherent dust, braking effect on relativistic motion of a sphere 4-95168  
compressive tests of specimens, effect of contact friction forces 4-109596  
contact, finite-element stress anal. iterative procedure 4-87632  
crystalline solids and geomaterials, finite plastic flow 4-98184  
diffusion in surface layers in friction of solids 4-65338  
elasticity, Signorini and friction free boundary problems using boundary elements, Trefftz approach 4-63513  
ellipsoid motion on rough surface with slippage 4-60261  
elliptical contact, numerical soln. for thermoelastohydrodynamic problem (Chinese) 4-97437  
explosive, single crystal, shear strength determ., modified junction growth eqn. appl. 4-98195  
flat rectangular duct, heat transfer response to periodic disturbances at one principal wall 4-60418  
fluorides, organic and inorganic chemistry and energy storage 4-72184  
gas mixtures, barodiffusion 4-69856  
granite fault with gauge, frictional sliding rate sensitivity 4-94105  
granular material rapid flow, kinetic model 4-60484  
heat flux gauge calibration for skin friction meas. 4-97723  
heat transfer and friction effect on cylinder in longitudinal turbulent air flow with variable physical props. 4-83891  
incompressible fluid, turbulent flow, vel. and press. fluctuations 4-91804  
incompressible internal flows, inverse problem 4-87684  
Invar pin-tool steel couple, crit. thickness of protective films 4-109519  
irreversible systems obeying max. dissipation principle, bifurcation and stability (French) 4-78139  
junction growth equation and applic. to explosive cryst. 4-98195  
laminar and incompressible boundary layer flow induced by an airfoil (German) 4-64916  
longitudinal flow around cylindrical body, heat exchange and friction (Russian) 4-74998  
magnetic tape, friction coefficient meas. rel. to test parameters 4-85221  
mechanical systems with dry friction, nonlinear oscillations 4-74939  
metal-polymer pair, probabilistic model analysis of contact and friction 4-108513  
metal/polymer frictional contact, electron emission 4-66198  
metallic glasses, sliding friction and struct. relax. 4-99606

## friction continued

- metals, sheet, deep drawing, influence of temp. 4-66399  
 metals, wear reduction and analysis, surface modification by ion beams 4-81290  
 non-Newtonian fluids, turbulent friction factors prediction in noncircular ducts 4-108092  
 noncircular duct, peripheral temp. variation in wall, heat transfer calc. 4-97552  
 nylon, humidity effect on friction, hardness and shear strength 4-62064  
 one dimensional gas flow with internal heating 4-97692  
 ophthalmic solutions lubrication props. meas., using strain gauge bridge 4-89797  
 partially filled unsteady pipe flow, frictional losses, Colebrook-White formula 4-97684  
 permeable plate with blown gas, limiting relative friction law 4-69819  
 planar collisions, particle and rigid body, friction, restitution and energy loss 4-101646  
 plane contact problem formulation with wear of interacting bodies 4-74965  
 plane cut in elastic medium with slip and adhesion of surfaces, 3D mixed problems 4-60326  
 plane die in brittle half-plane, crack form: at edge 4-112770  
 polycarbonate, sliding against graphite fibre reinforced epoxy composite, tribological behavior 4-89136  
 polyester textile fibres, friction meas. 4-89137  
 polyethylene, high density, deform. in split Hopkinson bar, interfacial friction effect 4-114627  
 polyethylene, ultrahigh mol. wt., sliding against graphite fibre reinforced epoxy composite, tribological behavior 4-89136  
 polymer solutions, dynamical properties and perturbation theory near four dims. 4-92401  
 polymeric materials, rolling friction coeff. meas. apparatus (Japanese) 4-95120  
 quartz glass, triboluminesc. during frictional sliding 4-105547  
 rectangular ducts, fully-developed flow, vel. distrib. and skin friction resistance 4-83948  
 rigid indenter, interaction with near-surface void or inclusion 4-74966  
 rock, velocity-depend. friction in humid environment 4-94104  
 rod of elastoplastic material, dynamics of buckling, friction properties and hysteresis 4-112743  
 rolling contact fatigue, pitting model 4-64888  
 rolling friction torque, determ. as function of speed (Rumanian) 4-79522  
 rough surface boundary layer behaviour in turbulent wake presence 4-87724  
 rubber, filled pairs, frictional props. (German) 4-66454  
 Schlichting's surface roughness expt. 4-103303  
 Signorini problems with friction, existence of solns. 4-91777  
 single degree of freedom elastic system with rate and state depend. friction, slip motion and stability 4-64890  
 skin friction meas. using hot element gauges (French) 4-65045  
 sliding surfaces, dynamical friction, perturbation and mol. dynamics calcs. 4-115333  
 sliding surfaces, friction coeff., wear debris, metal trans 4-85218  
 slip steady state for frictional contact under moving loads 4-97442  
 slug flow in vertical ducts, wall friction mechanism 4-60490  
 solid mechanics large-deform. anal. using mixed Eulerian-Lagrangian displacement model 4-79461  
 steady state sliding, upper bound approach to ridge and sublayer deform. 4-85219  
 steel, constructional, carburised case relax. props. influence on antigalling resist. 4-114684  
 steel, contact zone under friction, X-ray and Auger electron microanal. 4-75763  
 steel, Cr-Ni, tribological characts. after complex thermochem. treatment 4-93427  
 steel, friction and wear of hardened, nitrided and borided couples in air and vacuum 4-109523  
 steel, high-speed, hot isostatic pressing, struct. and contact fatigue 4-114440  
 steel, low-C, structural changes during damage by surface friction 4-93424  
 steel, stainless and bearing, surface analysis, ion implantation and tribological processes 4-99607  
 steel, tool, wear resistance, effect electron irradi. 4-71740  
 steel fibre reinforced cement, free shrinkage, theoretical model 4-93255  
 steel-PTFE pair, steel microtopography influence on tribology 4-108513  
 Stirling engine performance predictions, effects of pressure-drop correlations 4-66752  
 theory of friction, general 4-112776  
 turbomachine cascade profile, friction and heat transfer calcs. 4-112833  
 turbulent flow heat transfer, press. drop in converging-diverging tubes 4-113022  
 two-phase flow in horizontal pipe, turbulence 4-64926  
 unlubricated sliding, interaction between dynamic normal and frictional forces 4-64892  
 vibrating circular cylinder, elastic rod collision appl. to nuclear reactor 4-97372  
 vibratory conveyor, vel-depend. function coeff. (Japanese) 4-103229  
 viscoplastic materials, rate effects in steady forming processes 4-83831  
 Ag, tribological behaviour, influence of temp. and atm. press. (German) 4-114683  
 Al alloy, plastic deformation, sliding contact with wedge, friction-wear relations 4-89139  
 Al bronze on steel, sliding friction break-in curves, effect of flat-on-ring sample alignment 4-81294  
 Al-Sb, ion implanted, hardness, friction and wear props. 4-66451  
 Al-Cu-Mg alloy, shot peening effect on fatigue crack initiation by fretting 4-66448  
 Al-Si alloy, cast, graphite additions influence on wear characts. 4-109520  
 Al-Zn-base alloys, tribological props. (Polish) 4-85216  
 Cu-Su filled crystalline glass composite, frictional and strength props. 4-66456  
 Fe, cast, tribological behaviour in inert and reducing gas media 4-71742  
 Fe-Si (3 wt.%) alloy pin-tool steel couple, crit. thickness of protective films 4-109519  
 Fe-Ti alloys, ion implanted, C<sup>+</sup> implantation effects on surface mech. props. 4-114707  
 Mg alloys, structure and physicochemical props. different methods of Stepanov crystallisation effect 4-99297  
 Ni-S-Fe (Mo)(Nb), friction and wear modification by sulphide form. 4-66460

## friction continued

- SiC ceramics interfaces, contact stresses distrib. rel. to geometry 4-76877  
 Si<sub>3</sub>N<sub>4</sub> ceramics interfaces, contact stresses distrib. rel. to geometry 4-76873  
 Ti-N, abrasion resistance, homogeneity region 4-114681  
 Zn-Al-Si (21, 2 at.%), frictional surface charact. under boundary lubrication 4-66452
- friction, internal** see *internal friction*
- frictional electricity** see *triboelectricity*
- FSK** see *frequency shift keying*
- fuel**  
 see also *coal; fission reactor fuel*  
 160 MW OTEC plantship design for methyl alcohol production 4-114936  
 alcohol-fueled engine cold starting 4-62292  
 automotive engine, H<sub>2</sub>-fueled, design database 4-62403  
 bioenergy conversion by crop and forest residues utilisation, environmental risks 4-62374  
 bioenergy conversion processes and economics 4-81518  
 biogas installations using farm animal waste, design and costs (Italian) 4-77048  
 biogas plant economics in developing countries 4-66651  
 biogas production by solid fermentation in Chinese rural areas 4-66736  
 biomass conversion to methane and fertiliser slurry 4-66733  
 coal-liquid mixtures, possibilities and expectations as fuel for boiler installations (Dutch) 4-89374  
 coal-natural gas fuel mixture, combustion characts. and viability 4-77052  
 coal-oil mixtures, production process 4-72037  
 complex mixture charact., IR and photoionisation detector eval. 4-85349  
 dielectric properties of New Brunswick oil shale 4-72043  
 diesel engine fuel displacement by biomass producer gas 4-66652  
 diesel-cycle engine, H<sub>2</sub>-fueled, two-stroke, performance improvements 4-62404  
 dissociated methanol engine testing results using H<sub>2</sub>-CO mixtures 4-62290  
 distillate liquid fuels, chemical and physical properties during combustion in gas turbine 4-114884  
 droplet, evaporation dynamics, press. effect 4-103914  
 electromagnetic heating techniques for the in situ recovery of heavy oils 4-72039  
 electrothermic system for recovery of heavy viscosity oil 4-72044  
 energy balance in Hungarian agriculture, present and future role (Hungarian) 4-109750  
 energy conversion engineering conference, Orlando, Florida, USA, August, 1983 4-67861  
 ethanol-water separation by novel extraction process 4-62293  
 ethyl alcohol production from waste bananas 4-66730  
 flames, oxy-fuel, H and OH radicals distrib. determ. 4-99798  
 food waste utilisation for biogas and fertilizer production 4-66735  
 fossil fuel industries and energy policy, 1973-83 4-77050  
 fossil fuels, probable future role 4-105090  
 fuel-air combustion in fluidised bed model 4-87787  
 German electricity supply industry, economic and environmentally safe fuel for energy generation, considerations (German) 4-93652  
 heavy oil residue utilisation, chemical aspects 4-62289  
 hydrocarbons from Calotropis procera in Northern Australia 4-99936  
 industrial cellulosic waste conversion to diesel fuel 4-72143  
 mooring oil shale kerogen, extraction by supercritical gas process, chemical structure determ. 4-78837  
 metal hydride hydrogen storage in automobiles, technio-economic aspects 4-105130  
 methane fueled engine performance and emissions characteristics [automobile engine] 4-66653  
 methane production, by fermentation of agricultural/organic waste, applications (French) 4-99981  
 methanol fuel production from municipal solid waste 4-66732  
 microcrystalline cellulose aqueous digestion process evaluation 4-66731  
 microwave energy interaction for upgrading fuel precursors, chemical product analysis 4-72040  
 microwave heating for fuel recovery, heating process and chromatographic analysis 4-72041  
 natural gas/hydrogen compressed storage, comparison as vehicle fuels 4-89375  
 Nepalese biogas developments and prospects 4-66650  
 palm oil processing for fuel augmentation and substitution 4-66649  
 peat fuel for district heating in Finland 4-93584  
 petroleum-based fuel for transportation appls. 4-85353  
 radiofrequency heating process for fuel recovery from oil shale and tar sand 4-72038  
 reformed methanol vehicle system considerations 4-62291  
 refuse-derived, processes, combustion, costs (Italian) 4-105091  
 solid propellant, composite, catalyst role in ignition mechanism 4-77011  
 solid propellant, thermal behaviour obs. using shock tube, ignition delay 4-77010  
 stationary combustion systems, overview of research requirements 4-72045  
 Swedish residential energy use and conservation (1963-80) 4-66644  
 thermal analysis appls. 4-89210  
 USA hydrogen fuel industry 4-66815  
 gasification of rice hulls and straw O<sub>2</sub> 4-66737  
 H<sub>2</sub> for closed-cycle diesel engines, use of Ar, He and CO<sub>2</sub> as working fluids instead of N<sub>2</sub>, effects on performance 4-66743  
 H<sub>2</sub> fuel comparison with synthetic fossil fuels, economic and environmental aspects 4-66648  
 H<sub>2</sub> fueled engine for underground mining vehicle, with ultra-low emissions 4-62406  
 H<sub>2</sub> production and use for rural Alaskan community, programme design and planning 4-89473  
 H<sub>2</sub> production in autothermal fluidized gasifier 4-72187  
 H<sub>2</sub> thermochemical production using nuclear process heat, developments in West Germany 4-114962  
 H<sub>2</sub>/electrical power simultaneous production, using carbonaceous fuels and high-temperature nuclear process heat, thermodynamic anal. 4-89472  
 H<sub>2</sub>S as hydrogen source, obtained as waste product from fossil fuels, methods of use 4-89471  
 NH<sub>4</sub>HCO<sub>3</sub> augmentation of rural biogas digester yield 4-66734
- fuel batteries** see *fuel cells*
- fuel cells**  
 acidic H<sub>2</sub>-O<sub>2</sub> fuel cells, hydrogen-electrode processes investig. 4-105106

**cells continued**  
 advanced batteries and fuel cells, conference, Talence, France, April, 1983 4-73161  
 advanced molten carbonate and solid oxide fuel cells for utility load levelling appls. 4-72104  
 alkaline fuel cell with matrix and no precious catalyst, new electrode structure development (*French*) 4-77084  
 alkaline fuel cells for the regenerative fuel cell energy storage system 4-72102  
 alkaline low temperature  $H_2$ - $O_2$ , prep. and characts. of  $H_2$  and  $O_2$  gas diffusion electrodes 4-62349  
 batteries and fuel cells, handbook 4-67891  
 batteries and fuel cells for traction appls., research and development requirements 4-77083  
 electrochemical power sources, expected development 4-62330  
 electrochemical power sources, progress review 4-62334  
 electrochemical reactions in power sources and sinks 4-62339  
 ion conducting ceramic electrolytes, with enhanced oxygen surface exchange kinetics 4-61141  
 molten carbonate fuel cell isotropic porous anode model 4-66688  
 nuclear power stations, fuel cell effects on reactor embrittlement and fuel cycle optimisation 4-72100  
 phosphoric acid fuel cell development program, EPRI and GRI, USA. 4-62348  
 regenerative fuel cell system for orbital energy storage, development status 4-72101  
 research and development requirements for batteries and fuel cells 4-77081  
 solid alkaline electrolyte fuel cell with matrix (*French*) 4-114902  
 three-layer Raney Ni- $H_2$  electrode for fuel cells (*Japanese*) 4-89396  
 C electrode, use in electrochem. power sources, improved material characts. 4-62324  
 $H_2PO_4$  fuel cells, reactions at high temp. and press. rotating disk electrode apparatus 4-89398  
 $H_2PO_4$  pressurised fuel cell stacks, gas-cooled, performance evaluation 4-72103  
 $MnO_2$ /active C as  $O_2$  electrode in alkaline fuel cells (*Japanese*) 4-89397  
 WC in  $H_2PO_4$ , corrosion resistance and catalytic activity 4-66689

**efugacity**  
 see also kinetic theory of gases  
 benzene-cyclodextrin inclusion complexes aq. soln., vapour press.-solubility meas. 4-99823  
 classical fluids, dimers and s-mers, highly directional forces, statistical thermodynamics 4-95289  
 O efugacity of mafic rock minerals and oxidation state determ. 4-100519

**full wave rectification** see rectification

**function approximation**  
 see also Chebyshev approximation; interpolation  
 boundary function approximation, Lagrangian, spline and weighted finite difference methods 4-64848  
 cryogenic temperature, subroutine for natural logarithm computation on K 1510 microcomputer (*German*) 4-90595  
 engineering problems, numerical soln. based on finite elements 4-110857

**function evaluation**  
 FFT algorithm improvement 4-110854

**functional analysis**  
 see also harmonic analysis  
 $1/r$  function, nth gradient tensor, partial derivatives 4-101621  
 algebras of unbounded operators and quantum dynamics 4-73279  
 bifurcation theory of the time-dependent von Karman equations 4-112720  
 boundary problems in generalised analytical functions, variational-difference method (*Russian*) 4-63490  
 density functional theory, book 4-73189  
 density functional theory, recent developments 4-73210  
 density functionals, self-interaction correction method 4-73304  
 density functionals obtained from models of the electron first and second order density matrices 4-73342  
 electron gas models and density functional theory 4-73341  
 exact Wigner functions of biconical unitary transformations 4-58661  
 free energy density functionals for non-uniform classical fluids 4-75122  
 ground-state density and wavefunctions in energy functional theories 4-73301  
 hyperspherical quantum gauge field models, harmonic functions and matrix elements 4-63870  
 inverse problem of calculus of variations, functional analytic and finite dimensional methods 4-95137  
 JWKB approximations, quartic oscillator, effective potential method 4-110913  
 JWKB approximations, radial problems, modification of the effective potential 4-110912  
 Lagrangian systems on graded manifolds, independence theorem 4-67961  
 mixing layer, 3-dimens., eqns. of motion, numerical soln. for blunt bodies (*Russian*) 4-64915  
 nonseparable Sturm-Liouville operator, deficiency indices and spectrum (*Russian*) 4-95136  
 one-matrix energy functionals, props. 4-73303  
 orthogonal decompositions of finite dimens. vector spaces 4-63477  
 partial difference eqns. with constant coeffs. and appl., system decoupling 4-86182  
 periodic functions, interpolation, differentiation and soln. of eigenvalue problems 4-73207  
 recursion method basic vectors for periodic Hamiltonians, asymptotic form 4-111049  
 reduced density matrices, geometric study, spin properties 4-73302  
 rigged Hilbert space construction describing resonances and virtual states 4-73208  
 second order functional invariance, rots. transformations 4-67962

**functional equations**  
 circle homeomorphisms with golden ratio rotation number, functional eqns. 4-58633  
 one-dimensional maps, symmetries and stable periodic orbits 4-63493

**functionals** see functional equations

**functions**  
 see also Bessel functions; Boolean functions; Green's function methods; random functions; recursive functions; transfer functions; vertex functions; Walsh functions  
 analytic functions, zeros determ., generalisation 4-95138  
 anharmonic oscillators and generalized hypergeometric functions 4-95220

## functions continued

degenerate functional integral, functional delta-functions and fourier transforms 4-58619  
 distribution functions in physics, review 4-90348  
 Hankel functions, determination of  $\nu$ -zeros using NUZERO program 4-102844  
 Lagrangians, singular, regularisation method 4-95219  
 Lie algebras, Kostant partition function 4-95134  
 Lowdin's alpha-function calc. 4-68010  
 luminance efficiency function, anal. (*Japanese*) 4-106350  
 mapping, logarithmic link between growth and quadratic mapping 4-63479  
 orthonormal basis functions, special-purpose, for motor unit action pots. 4-81660  
 periodic Ljapunov functions (*German*) 4-82668  
 plasma cross-field diffusion problems, shape functions for separable solutions 4-97761  
 $Sp(2d, R)$  symplectic group, partially coherent states 4-95133

**fundamental constants** see constants

**fundamental law tests**  
 neutron interferometry and its relation to fundamental phys. 4-68011

**fundamental particles** see elementary particles

**fundamental physics concepts** see physics fundamentals

**fundamentals of physics** see physics fundamentals

**furnaces**  
 see also electric furnaces; refractories  
 annealing vacuum furnaces AC power supply, temp. controller 4-106297  
 casting unit, heat exchange, inverse heat cond. calcs. 4-107982  
 double cyclone furnace 4-86424  
 fast jet furnace with top-mounted burners, heat exchange 4-97629  
 glass-melting, monitoring method for corrosion of refractories 4-89208  
 glass-melting, vertical honeycomb resist. of refractories, stat. testing method 4-89207  
 multifaceted concentrator solar furnace, simple model for predicting flux distribution through focal plane 4-114958  
 one-dimensional, radiative heat transfer 4-64827  
 propane-propylene fuel, C particle effect on radiation spectrum in test furnace 4-96530

**Furry theorem** see quantum electrodynamics

**fusion** see melting

**fusion, nuclear** see nuclear fusion

**fusion-fission reactors** see hybrid reactors

**fusion reactor fuel**  
 advanced fuel cycles for improving the commercial attractiveness of fusion reactors 4-59417  
 advanced fuel fusion synergism 4-59424  
 advanced fuels, selection criteria, performance studies 4-91113  
 Alcator C tokamak, energy confinement pellet fueling expts. 4-97894  
 conference on fusion engineering, Philadelphia, PA, USA (Dec. 1983) 4-110807  
 electrolytic gettering of T from air 4-86966  
 glass microballoon laser target, nondestructive fuel assay 4-102387  
 ICF target fabrication using polystyrene mandrels, plastic coated metal shells prep. 4-91962  
 ignition of self-sustained fusion reaction in dense DT plasma 4-102395  
 INTOR tokamak engineering test reactor, impurity control studies 4-107070  
 magnetized fuel targets: fuels other than D-T? 4-59420  
 safe-handling apparatus for D-T in muon catalyzed fusion expts. 4-107136  
 self-cooled liquid-metal blanket concepts, tritium breeding ratio, neutronics analyses 4-107097  
 target capsules for muon catalyzed fusion expts. 4-107137  
 tokamak reactor studies, impurity control, RF heating and confinement 4-107074  
 tritiated water, T recovery by reaction with U 4-86967  
 tritiated water, T removal system using isotopic exchange reaction, expt. eval. 4-111812  
 Tritium Systems Test Assembly, control logic specification, structured flowcharts 4-111851  
 TSTA, U beds design and performance for pumping T-D 4-86968  
 D-D catalysed fuel ignition in high-field OMITRON type Tokamaks 4-59405  
 D-T spin-polarised fuel, fusion gains using homogeneous ignition and central ignition model 4-59409  
 T breeding and activation in cascade reactor 4-111814  
 T breeding and electricity generating blanket sector for INTOR/NET 4-111830  
 T breeding in He cooled fusion blankets, nuclear data library comparison 4-111779  
 T control and activation in Pulse\*Star ICF reactor 4-111815  
 T enrichment in metallic Li, distillation column design, fusion fuel appl. (*German*) 4-64237  
 T extraction facility for T conc. in neutron irradiation Li metal, calibrations 4-111811  
 T in-situ recovery results from TRIO-01 expt. 4-111817  
 T inventories, breeding requirements in power reactors 4-107113  
 T isotopic enrichment using host-guest chemistry 4-59414  
 T pellet injection sequences for TFTR 4-111878  
 T permeation through steam generator-tubes at CANDU stations 4-111813  
 T production-rate distrib. in simulated fusion blanket assemblies at FNS 4-74048  
 T recovery expt. TRIO-01, gas anal. system design, fabrication and testing 4-111816

**fusion reactor ignition**  
 see also fusion reactor materials; plasma heating; plasma production  
 ablation accelerator design for impact fusion 4-83245  
 Antares facility for inertial fusion 4-96957  
 ASDEX tokamak, LHRH amplifiers and transmitters, wave propag. 4-87897  
 autocatalytic fusion-fission implosions, thermonuclear energy appl. 4-59410  
 beam-beam fusion device (*Korean*) 4-111767  
 beamline for light ion fusion demonstration reactor 4-102390  
 conference on fusion engineering, Philadelphia, PA, USA (Dec. 1983) 4-110807  
 cryogenic hollow shell target irradiated by light ion beam, optimisation 4-111965

**fusion reactor ignition continued**

current startup and quasistationary drive by lower hybrid waves in Tokamak 4-79753  
 Delfin-1 laser facility, spherical target irradiation, temporal uniformity determination 4-74045  
 Delfin-1 laser installation, heating and compression of high aspect ratio target 4-102392  
 Doublet III, fault protection in electron cyclotron heating system 4-111868  
 Doublet III neutral injector ion sources, linear optics theory applied 4-59458  
 dual energy heavy ion target concepts 4-59419  
 EBT-S, microwave launchers, mixed-mode, design 4-111865  
 energy production enhancement during neutral beam injection 4-107110  
 fast charged particle interaction with high density ICF plasma targets 4-111963  
 field-reversed, use of neg. ion beam sources 4-107223  
 free electron generators of coherent radiation, conf., Orcas Island, WA, USA (June 1983) 4-82588  
 free electron laser ICF driver, two-dimensional numerical model 4-107084  
 free electron lasers, high intensity, for inertial confinement fusion 4-96931  
 Fusion Power Demonstrator, tandem mirror test reactor, ignited central cell 4-107073  
 fusion power demonstrator program, alpha heating for D-T burning 4-107072  
 GEKKO MII glass laser 20 cm aperture, interferometric wavefront meas. 4-102933  
 glass gas-filled microspheres irradiated in Sokol laser facility, X-ray images 4-75177  
 heavy ion accelerators as drivers for inertial confinement fusion 4-107086  
 heavy ion beam fusion, target study 4-102388  
 Helios CO<sub>2</sub> laser, high-density implosion expts. 4-68828  
 high aspect ratio targets, heating and compression with Delfin-1 4-102392  
 high heat flux target for neutral beams at ORNL 4-111866  
 high power particle beam conf., San Francisco, CA, USA, (Sept. 1983) 4-110808  
 high-power laser system development for laser-fusion research in China 4-68825  
 ICF, dense plasma-particle beam interaction, electrostatic fields and double layers 4-113171  
 ICF, ignition of isobarically compressed D-T targets, burn propagation anal. 4-68813  
 ICF, implosion concepts by particle beams and lasers 4-111966  
 ICF, muonic or polarised fusion for ignition 4-59400  
 ICF intense ion beam research 4-112003  
 ICF photocurrent target 4-68811  
 ICF target, ion stopping in heated targets 4-112080  
 ICF target burn, fusion product energy loss effects 4-107112  
 ICF targets, heavy ion driven, irradiation, symmetry 4-64235  
 ICF targets, heavy ion pulse shape optimization, quasi-isentropic compression 4-107087  
 ICF targets, ion beam interactions 4-107148  
 ICRF heating generators for ASDEX and W VII 4-111937  
 ICRF launcher, slow wave structure 4-103524  
 ICRF transmission system for D-III fusion reactor 4-111863  
 ICRH, high power tetrode, design and testing 4-111862  
 ICRH antenna design for tokamaks and stellarators 4-111871  
 ICRH in ASDEX tokamak and W-VII stellarator 4-87896  
 impact fusion using ablation accelerator as driver 4-96248  
 implosion experiment status at LLL 4-68822  
 inertial confinement fusion, energy transfer 4-102391  
 inertial confinement fusion, KrF excimer laser drivers 4-107083  
 inertial confinement fusion target compression, use of strong shock waves 4-111968  
 inertial effects in laser-driven ablation 4-111969  
 inertial fusion commercial applications, driver cost and performance effects 4-107089  
 inertial fusion research at Los Alamos scientific laboratory 4-68823  
 intense ion beam diode, anode heating with CO<sub>2</sub> laser 4-112011  
 intense ion beam stopping power in partially ionised material 4-113167  
 intense pulsed ion beams for fusion reactors, generation and transportation (Japanese) 4-74078  
 inverse pinch ion diode characteristics, for ICF appl. 4-112019  
 ion beam driven cannonball target for fusion reactor ignition 4-60650  
 ion diode research overviews 4-112009  
 ISX-B tokamak, preionisation and start-up using electron cyclotron heating at 28 GHz 4-97892  
 JIPP T-II, ICRF heating expts., power balance anal. 4-103523  
 laser driven, cavity type target and scaling laws 4-84036  
 laser driven D-T fusion targets, thermonuclear particle study using CR-39 4-96249  
 laser drivers for inertial-fusion reactors, KrF laser system pulse compression 4-69464  
 laser fusion and isotope separation research and development at Lawrence Livermore National Lab., review 4-90324  
 laser fusion pellet, absorpt. rate and uniformity 4-78735  
 laser fusion research at ILE Osaka 4-68824  
 laser fusion targets; neutron energy spectrum meas. with CR-39 SSNTD 4-96368  
 laser fusion using e-beam pumped KrF laser 4-79113  
 laser-plasma interaction and target compression 4-69936  
 laser-plasma interaction expts. rel. to ablatively driven fusion processes 4-69935  
 laser-plasma interactions and related plasma phenomena, conf., Monterey, CA, USA (Oct. 1982) 4-95063  
 laser-produced plasma ion source for heavy ion inertial fusion 4-102389  
 light ion beam fusion 4-111959  
 light ion beam fusion studies in ETIGO project 4-111962  
 light ion beam ICF, review 4-107144  
 light ion beam inertial confinement fusion 4-107146  
 light ion beam prod. by applied Br magnetically insulated annular diode for ICF appl. 4-112013  
 light ion beam reactor driver, D-T ignition, inertial confinement fusion 4-107085  
 light ion beam system 4-111964  
 LLL laser-fusion-programme overview and future directions in laser fusion systems 4-68821

**fusion reactor ignition continued**

magnetic compression generator, collapsing shell instability suppression 4-75182  
 magnetic confinement fusion plasmas, appl. of lasers 4-108218  
 microinstabilities of light ion beams in fusion target chambers 4-112004  
 muon catalyzed fusion, power reactor concepts 4-107139  
 muon induced fusion, design considerations 4-107143  
 muon production colliding beam system for muon catalyzed fusion reactor 4-107140  
 muon production costs for fusion catalysis 4-107142  
 neutral injection with long pulses, water cooled grids for ion removal 4-87899  
 neutral particle injectors RIG for fusion reactors 4-60657  
 neutron-feedback ICF reactors, laser blanket design 4-107088  
 Nova, Novette fusion lasers, Si switch development for optical pulse generation 4-107702  
 Novette short wavelength laser-target interaction system 4-96956  
 nuclear-pumped lasers theory, ICF reactor driver appls., review 4-96958  
 OLION code for ion beam diode simulation 4-102399  
 OMITRON type high-field Tokamaks, ignition of D-<sup>3</sup>He and catalysed D-D fuels 4-59405  
 one-dimensional Cannonball target, hot electron energy distrib. 4-113191  
 particle beam ICF research at ILE Osaka 4-111961  
 particle-beam fusion, pulsed-power technology 4-68826  
 pellet acceleration with railgun for mag. fusion device refuelling 4-91099  
 PLT tokamak, ICRF heating, changes in impurity radiation 4-103526  
 power-balance analysis of muon-catalyzed fusion-fission hybrid reactor systems 4-107141  
 quasi-steady operation, OH coil recharging optimization 4-96251  
 radiative plasma in lasers for exciting thermonuclear fusion reactions (Russian) 4-97770  
 relativistic electron beams, nonlinear effects, numerical simulation, inertial fusion 4-107502  
 self-sustained fusion reaction in dense DT plasma 4-102395  
 soft X-ray driven ablation processes 4-84041  
 solid-state laser driver technology for inertial confinement fusion 4-107082  
 space-time focused light plasma beams for ICF fusion 4-107147  
 spheromak plasma heating concepts for reactor operation 4-111835  
 stabilization of propagating light ion beam by its rotating motion 4-112005  
 system concepts for muon-catalyzed fusion 4-107138  
 tandem mirrors, density profile calcs. fueled by pellets 4-113216  
 target capsules for muon catalyzed fusion expts. 4-107137  
 target implosion, nonuniformity effect on ICF parameter 4-111967  
 target preheating suppression, laser irradiation, and electrostatic field effects investig. 4-113190  
 terawatt pulse generators for ICF research 4-111960  
 tokamak plasma ignition, compatibility with sputtering, JET-like discharge 4-96270  
 tokamak reactor studies, possibility of very long burn times 4-107074  
 transport and focusing considerations for light-ion ICF 4-112008  
 W-VII A stellarator, ECRH, fusion plasma generation and heating 4-87898  
 zone plate coded imaging, theory and appls., book contrib. 4-107501  
 $\alpha$ -particles distribution function and diffusion in DT fusion plasma 4-102394  
 CO<sub>2</sub> laser-target interaction expts. 4-68827  
 D beam species meas. by D-D fusion product anal. 4-107247  
 D-<sup>3</sup>He fusion plasmas, nuclear elastic scatt. effects 4-103543  
 D-D fusion plasmas, nuclear elastic scatt. effects 4-103543  
 D-T spin-polarised fuel, fusion gains using homogeneous ignition and central ignition model 4-59409

**fusion reactor instrumentation** *see nuclear reactor instrumentation***fusion reactor materials**

*see also fission reactor materials; fusion reactor fuel; radioactive waste activation product aerosol formation during accidents* 4-111783  
 activation product transport in fusion reactors, radiation fields calc. around plant components 4-107153  
 activation products impact on fusion reactor safety 4-111780  
 aerosols characterisation from fusion energy systems 4-107016  
 alloy system, irradiation, constrained equilib. thermodynamics 4-103793  
 blanket comparison and selection study, decision analysis methodology 4-107091  
 blanket comparison and selection study overview 4-107090  
 blanket expts. and data 4-59408  
 blanket high temp. heat transfer 4-111822  
 blanket materials, candidate, for fusion reactor appl. 4-91107  
 blanket structures, activation product release, safety research 4-111781  
 blanket thermal requirements for testing in fusion devices 4-107119  
 blankets, liquid metal corrosion product transfer, MHD effects, safety 4-111786  
 blankets, neutronic testing requirements in fusion devices 4-107118  
 blankets, stress distrib., influence of irradiation and thermal creep 4-91111  
 Blankets for tritium catalyzed deuterium fusion reactors 4-107117  
 Borsselle reactor vessel, neutron embrittlement Charpy tests 4-96132  
 brazing of bulk graphite/solid T breeder materials to metal substrates 4-111753  
 breeder blanket materials, solid, development advances 4-107020  
 breeder materials, solid, irradiation, retained He and T meas., technique 4-107021  
 Cascade solid breeder blanket microspheres, design and fabrication 4-107127  
 ceramic materials for fusion reactor applications 4-111758  
 conference, Albuquerque, NM, USA (Sept. 1983) 4-90290  
 conference on fusion engineering, Philadelphia, PA, USA (Dec. 1983) 4-110807  
 current density phenomena of tokamak high-current contact materials 4-107133  
 damage structures, evolution under 14 MeV neutron, 4 MeV ion and 1.25 MeV electron irradiation 4-108418  
 DEMO, first wall lifetime, effect of material props. and operating conditions variations 4-96265  
 deposited and redeposited materials, review 4-107065  
 design studies and R&D, reacting-plasma project (Japanese) 4-111764  
 disruption heat load simulations using electron beams 4-111911  
 Doublet III, modification for large D-shaped vacuum vessel, materials use 4-107053  
 Doublet III tokamak, limiter damage, over-heat load due to plasma disruptions 4-96252

## ion reactor materials continued

Doublet III vacuum vessel, field installed brazed thermocouple feed-throughs 4-111947  
 energy deposition on the walls of the ohmically and neutral-beam-heated ASDEX tokamak 4-108180  
 Fe-cermet, Fe-Cr-Al, D permeation 4-111754  
 ferromagnetic components used in magnetic fusion reactors, anal. of forces 4-91110  
 first wall, bremsstrahlung energy deposition in mag. confinement systems 4-107121  
 first wall, crit. flaw size prediction methodology 4-96268  
 first wall, magnetically guided flow obs. (Japanese) 4-102397  
 first wall connectors in Tokamak devices, high current contact material design constraints 4-113227  
 first wall material properties depend. of depolarisation rates of D-T plasmas 4-91096  
 first walls, lifetime calc., creep-fatigue design criteria 4-96254  
 first-wall protection through falling solid particles 4-107125  
 fluorides, organic and inorganic chemistry and energy storage 4-72184  
 fusion breeder, fission suppressed, safety studies 4-107103  
 Fusion Materials Irradiation Test Facility, design and objectives 4-107036  
 fusion reactor components, dynamic deform. due to EM forces, finite element anal. 4-74050  
 graphite, pyrolytic, ls binding energy shift under deuterium ion bombardment 4-91103  
 graphite+H reactivity, electron bombardment enhanced 4-93529  
 graphite armor tile, contact thermal conductance meas. on Doublet III 4-111930  
 graphite limiter tiles, 3-D anal. of contact conditions for TFTR 4-111928  
 graphite radiation damage in fission and fusion reactor systems 4-96263  
 He-Li test loop for two-phase flow (Japanese) 4-91102  
 high flux irradiation, test facility, development review 4-107048  
 high heat flux components, materials requirements 4-91109  
 high-energy multiplication blankets for Cat-D fusion reactors 4-107106  
 ICF facility FIRST STEP, blanket struct., fuel assembly design 4-107123  
 ICF targets, heavy ion pulse shape optimization, quasi-isentropic compression 4-107087  
 impurity control, candidate materials 4-91108  
 impurity elements in JIPP T-II fusion device, PIXE anal. 4-105073  
 Incoloy 800, compatibility with flowing Li 4-107062  
 Inconel 625 as tokamak wall material, hydrogen recycling model calcs. 4-97870  
 inertial confinement fusion, progress and perspective, review 4-74044  
 INTOR, first wall lifetime, effect of material props. and operating conditions variations 4-96265  
 ion impact desorption mechanisms, substrate role, fusion device relevance 4-93164  
 irradiated structural materials in situ regeneration and approach to their development 4-111762  
 irradiation damage simulation, induced radioactivity by 16 MeV, protons and 30 MeV  $\alpha$ -particles 4-107038  
 irradiation facilities, neutron dosimetry and radiation damage calc. developments 4-107043  
 JET first wall coatings, gas release under electron impact 4-91097  
 JT-60 metal gate valves, ceramic breaks, reliability tests 4-111922  
 JT-60 Tokamak device, materials aspects 4-107051  
 JT-60 vacuum vessel, evaluation of mechanical strength of welded bellows 4-111920  
 LAMPF irradiation facility for fusion materials, radiation environment characteris. 4-107041  
 limiter damage in mag. field error region of ZT-40M expt. 4-108179  
 liquid breeders, compatibility of structural materials 4-111750  
 low pressure blanket concepts, nitrate/nitrite molten salt-cooled blanket 4-107095  
 low-activation diagnostic equipment and auxiliary heating components for fusion 4-107134  
 low-pressure boiling lithium as a first-wall coolant 4-107120  
 magnetic fusion reactors, surface melting and evaporation due to plasma disruptions 4-96255  
 MARS, liquid  $\text{Li}_2\text{Pb}$  cooled fusion reactor blanket, corrosion product cleanup system 4-111785  
 MARS blanket, three dims. neutronics anal. 4-107115  
 material property uncertainty, projection, anal. approach 4-96267  
 materials data base for fusion reactors 4-96262  
 materials needs for compact fusion reactors 4-91106  
 metal, neutron irradi., localised plastic flow characterisation with indentation hardness 4-109581  
 metallic, glasses, ion irradi., damage, He and Ar, bubble form., blistering, exfoliation 4-108481  
 metals, dislocation loop punching by He bubbles 4-103748  
 metals, He bubbles, equation of state for small cavities 4-103824  
 microstructural evolution of irradiated materials, effects of gas and precipitates 4-108412  
 mirror advanced reactor study, fusion technology development 4-107071  
 mirror and tokamak upgrade reactors, activation anal. for safety 4-111784  
 molten salt fusion breeder, blanket materials compatibility 4-107102  
 neutron-feedback ICF reactors, laser blanket design 4-107088  
 Nimonic PE-16, irradi. in HFIR at 430°C, fatigue performance 4-109497  
 nucleation of voids and precipitates under cascade damage 4-103794  
 organic materials for fusion reactor applications 4-111757  
 plasma-material interactions and high heat flux component design 4-91098  
 R-tokamak, first wall design 4-96261  
 R-tokamak, first wall design from low activation Al alloy, cooling 4-111802  
 R-tokamak, low activation Al alloy vacuum vessel, EM forces, stress anal. 4-111801  
 radiation damage, D-T neutrons, defect struct. 4-103812  
 radiation damage, pulse ion irradi. microstruct. 4-103821  
 radiation damage calc., nuclear model codes 4-107045  
 radiation damage microstructure, microcomputer system for quantitative image analysis 4-103617  
 reacting plasma project, low-activation materials 4-111946  
 reflow test, initial clad temp. effects 4-96208  
 refractory coatings thermal performance exposed to a tokamak plasma 4-108202  
 RIGGATRON tokamak, material and design aspects 4-107052

## fusion reactor materials continued

self-cooled liquid-metal blanket concepts, tritium breeding ratio, neutronics analyses 4-107097  
 self-cooled liquid-metal breeder/coolant blanket, D-T fusion reactor 4-107093  
 SPAULRAD-S laminate for fusion reactor appls., irradiation and mech. props. 4-111768  
 stainless steel, thermal hydraulic testing for fusion reactor first wall 4-111932  
 STARFIRE first wall, element activation calcs., waste disposal implications 4-107046  
 steel, aluminised, irradi. with He ions, erosion resist. 4-66488  
 steel, austenitic, AM-2, various properties and products of nonmagnetic steels 4-114590  
 steel, austenitic, Cr-Ni type, reactor irradi. effect on refractory characts. 4-66398  
 steel, austenitic, fusion reactor candidate first-wall materials 4-111799  
 steel, austenitic and ferritic, corrosion behaviour in eutectic Pb-Li environment 4-107056  
 steel, austenitic and ferritic, for use in fusion reactor liq. metal blankets, compatibility, review 4-107054  
 steel, austenitic and ferritic stainless, crack growth modelling 4-104851  
 steel, austenitic stainless, C or N ion irradi., double peak of voidage depth profile 4-98147  
 steel, austenitic stainless, cavity formation during electron irradi., effect of pre-implanted He 4-108444  
 steel, austenitic stainless, crit. flaw size prediction methodology 4-96268  
 steel, austenitic stainless, D permeation, plasma-driven, effect of surface comp. 4-113718  
 steel, austenitic stainless, dual-ion and/or electron irradi. in HVEM, in-situ obs. of cavity growth process 4-98134  
 steel, austenitic stainless, dual-ion irradi., microstruct. evolution under various He injection schedules 4-98150  
 steel, austenitic stainless, electron irradiated, void swelling, effect of C and N 4-108445  
 steel, austenitic stainless, first wall lifetime, impact of swelling 4-96269  
 steel, austenitic stainless, fracture modes under He ion and neutron irradi., temp. depend. 4-104853  
 steel, austenitic stainless, ion-irradiated, depth-dependent microstruct. 4-98151  
 steel, austenitic stainless, irradiated, void swelling, He bubbles 4-103792  
 steel, austenitic stainless, irradiation, fracture toughness, SEM obs. 4-104836  
 steel, austenitic stainless, irradiation creep, light ion simulation 4-104815  
 steel, austenitic stainless, melt layer form. under repetitive electron beam heating, simulation of plasma disruption 4-75535  
 steel, austenitic stainless, microstruct. and tensile props., rad.-induced changes, depend. on displacement rate 4-103808  
 steel, austenitic stainless, microstructural design for improved He embrittlement resist. under HFIR irradi. 4-103790  
 steel, austenitic stainless, microstructural evolution in PCA, dual ion irradi., effect of He 4-103819  
 steel, austenitic stainless, modified, void suppression, effect of segregation of minor alloying elements 4-104789  
 steel, austenitic stainless, PCA, unirradi., tensile props. from room temp. to 700°C 4-104812  
 steel, austenitic stainless, pressurised tube, ion bombardment, fatigue life, simulated fusion first wall environment 4-104850  
 steel, austenitic stainless, proton irradiation creep of thin foil specimens, thickness effects on mech. props. 4-103820  
 steel, austenitic stainless, radiation damage, fusion reactor candidate material 4-98140  
 steel, austenitic stainless, stress rupture in-reactor creep cavity form. model 4-104854  
 steel, austenitic stainless, swelling and cavity microstruct. development, irradi. in EBR-II and HFIR 4-98131  
 steel, austenitic stainless, swelling and precip. behaviour during irradi., effect of P 4-103818  
 steel, austenitic stainless, swelling behaviour, neutron-induced 4-98141  
 steel, austenitic stainless, swelling incubation, effect of microchem., microstruct. and environmental mechanisms 4-108413  
 steel, austenitic stainless, swelling resistance in fusion reactors 4-107012  
 steel, austenitic stainless, swelling resistance under HFIR irradi., improvement through microstruct. control 4-103791  
 steel, austenitic stainless, thermal creep and stress-affected precip. 4-99428  
 steel, austenitic stainless, Ti modified, prep. by rapid solidification processing, dual-ion irradi. 4-98155  
 steel, austenitic stainless, Ti- and Si-modified, microstruct. evolution, effects of pulsed and/or dual ion irradi. 4-98154  
 steel, austenitic stainless, Ti-modified, irradi. response in specimens prep. by rapid solidification processing 4-103816  
 steel, austenitic stainless, TiC precipitation, influence on creep rupture strength, ductility and He embrittlement 4-99388  
 steel, austenitic stainless, void swelling, effects of C and N 4-98149  
 steel, austenitic stainless, Path A-type alloys, neutron irradi., mech. props. 4-98139  
 steel, Cr, martensitic, impurity level rel. to fusion reactor first wall appl. 4-107013  
 steel, Cr-Mn austenitic, thermally aged, phase instability, precip. reactions 4-109410  
 steel, Cr-Mo-V-W; ferritic, impact props., effect of specimen size and Ni content 4-104848  
 steel, Cr-Mo-V-W, ferritic-martensitic; reduction of ductile-brittle transition temp. 4-104849  
 steel, Cr-Ni ferritic, rapidly solidified, struct. and mech. props. 4-109388  
 steel, ferritic, Cr-Mo-V-Nb, microstruct. after irradi. to 36 dpa at elevated temps. in HFIR 4-98153  
 steel, ferritic, D and He trapping at TiC particles 4-98152  
 steel, ferritic, fusion reactor candidate first-wall materials 4-111799  
 steel, ferritic and type 316, exposed to static Pb-Li, corrosion reactions, surface analysis 4-107064  
 steel, ferritic and type 316, transmutation and activation effects in fusion neutron spectrum 4-107040  
 steel, G-Mn austenitic, phase stability and corrosion on exposure to pure Li 4-107061  
 steel, H and D diffusion under fission reactor radiation 4-113503  
 steel, martensitic stainless, cleavage fracture, micromech. mechanisms 4-104855  
 steel, martensitic stainless, HT9, first wall/blanket module, magnetically-induced forces 4-96264

## fusion reactor materials continued

- steel, martensitic stainless, HT-9, thermal creep deform., constitutive design eqns. 4-93338  
 steel, martensitic stainless, HT-9, weldments, microstruct., hardness and fracture toughness, effect of preheat 4-94945  
 steel, stainless, austenitic, modified PCA, mass transfer behaviour in Li 4-107063  
 steel, stainless, austenitic, type 316, flowing Li environment effect on fatigue and tensile props. 4-107055  
 steel, stainless, ferritic and austenitic, P segregation, radiation-induced 4-98148  
 steel, stainless, H transport 4-113722  
 steel, stainless, radiation erosion by  $H^+$  and  $He^+$  simultaneous bombardment 4-107066  
 steel, stainless, type 316, chem. compatibility with  $Li_2O$  breeder 4-107060  
 steel, stainless, type 316, corrosion by liq. Li using LILLO-7 thermoconvection loops 4-107059  
 steel, stainless, type 316, D-T neutron induced activities 4-68820  
 steel, stainless, type 316, with TiC coating, void form. near interface by diffusion annealing 4-109557  
 steel, Ti-modified, prep. by rapid solidification processing, microstruct. response to neutron irradi. 4-98143  
 steel shell wall design of cascade reactor, T breeding and activation 4-111814  
 steels, austenitic stainless and high Mn austenitic, neutron irradiated, comparison of tensile props. 4-103807  
 structural, strategic planning issues for irradi. programme 4-107035  
 structural alloys, austenitic, T permeation barrier development 4-113717  
 structural component lifetime evaluation using SMILE code 4-111743  
 superconducting D3 magnet for tokamak, design development (*Chinese*) 4-91095  
 superconducting structures, magnetoclastic buckling and Earnshaw's theorem 4-74049  
 surface composition changes of Inconel 625 during RG and ECR discharge cleaning of TEXTOR at 300°C 4-108203  
 swelling resistance of commercial alloys neutron irradi. to high fluence 4-98142  
 tandem mirror experiment-upgrade, TMX-U, surface area meas. of the first-wall 4-108201  
 tandem mirror reactors, materials engng. 4-91105  
 TASKA-M, compact fusion technology test facility, design 4-107037  
 TASKA-M, liquid metal test blanket design 4-111944  
 TEM disc specimens, shear punch tests 4-104944  
 TEXTOR first wall charact. w.r.t. H recycling 4-91968  
 TEXTOR liners and limiters surface conditioning by plasmachemical C deposition 4-108183  
 TFCX limiter and first wall, thermal shock considerations 4-111933  
 TFTR, materials problems in design and construction 4-107050  
 TFTR vacuum vessel, pre-assembly, testing 4-111921  
 TFTR vacuum vessel bellows, eddy current testing of Inconel 625 4-111810  
 thermionic diode materials selection and performance 4-107018  
 tokamak first wall/blanket/shield programme, e-beam effects, designs, recent progress 4-111800  
 tokamak fusion breeder, fission suppressed blanket, nuclear anal. 4-107104  
 Tokamak reactors, European communities design studies 4-111741  
 toroidal field coil support structures of INTOR-NET 4-111749  
 toroidal shell, current-carrying, EM load, stress state 4-74051  
 transition metal, chem. compatibility with  $Li_2O$  breeder 4-107060  
 TRIO-01 heat transfer results on solid breeder blanket designs 4-107098  
 tritium release from irradiated Li compounds obs. (*Japanese*) 4-102396  
 wall materials, activated, waste disposal, NRC regulation and limit setting 4-107039  
 water-cooled liquid and solid breeder blanket concepts 4-107092  
 Zircaloy, oxide film cracking on fuel cladding tubes, strain anal. 4-91046  
 Al, cavity formation in samples irradi. with pulsating beam of 225 MeV electrons 4-108443  
 Al, cavity nucleation and growth, relative role of gas generation and displacement rates 4-108473  
 Al, cyclic irradi., void growth and swelling at low temp. 4-103795  
 Al, He bubble nucleation on dislocations during 600 MeV proton irradi. 4-113504  
 Al powder, sintered, protective coatings for in-vessel fusion devices 4-111751  
 Al, pure, 600 MeV proton irradi., H and He bubble form. at grain boundaries 4-108479  
 Al vacuum vessel, low radioactivity fusion device, R-tokamak design 4-96253  
 Al, void and bubble form., 600 MeV proton irradi., temp. depend., 130-430°C 4-108482  
 Al/Si protective coatings for in-vessel fusion devices 4-111751  
 Al-Cu-Mg, 2017, surface characterisation as vacuum vessel for nuclear fusion devices 4-96266  
 Al-Mg-Bi, Al-Mg-Li and Al-Li-Mg low-activation alloy development for fusion device 4-108460  
 Al-Mg-V alloys for nonbreeding blanket in fusion reactor 4-111744  
 Al-Zn(Mg), neutron irradi., radiation damage 4-80112  
 $Al_2O_3$  protective coatings for in-vessel fusion devices 4-111751  
 $Al_2O_3$  windows, neutron-induced RF loss meas. and thermal stress calcs. 4-113501  
<sup>27</sup>Al( $n, 2n$ )<sup>26</sup>Al reaction cross section, fusion reactor appls. 4-107049  
<sup>10</sup>B coatings in NPL devices, power deposition in cylindrical geometry 4-60600  
<sup>10</sup>B slab and spherical sources, charged particle spectra 4-60599  
 Be, advantages and limitations for use in mag. fusion devices 4-107017  
 Be as surface tile material in DCT-8 pumped limiter design 4-96259  
 Be, health risk implications 4-107015  
 Be in fusion breeder blanket assemblies, neutron multiplication calcs. 4-107105  
 Be limiters, heavy impurity contamination reductions 4-86969  
 Be, neutron irradi. at various temps., compression props. and swelling 4-108458  
 Be-D, retention and thermal release of implanted D 4-113477  
 BeO, surface tile material for fusion reactor DCT-8 pumped limiter design 4-96259  
 C, trapping of sub-eV H and D atoms 4-111761  
 C-graphite materials, He ion irradi., surface erosion 4-80120  
 C-SiC alloy coated armor/limiter tiles in Doublet III 4-108178

## fusion reactor materials continued

- C-SiC alloy coating for limiter-armor tiles on Doublet III fusion reactor test results 4-111924  
 C-SiC coating on graphite tiles for Doublet III armour/limiters, process evaluation and characterisation 4-111755  
<sup>12</sup>C( $n, \gamma$ ), 14.1 MeV,  $\alpha$ -spectra and ang. distrib., kerma factor for fusion reactors 4-96020  
 Cr-Mn austenitic stainless steels, props. for fusion reactor appls. 4-111746  
 Cu alloys, dil., chem. redistrib. under simulation irradi. 4-108478  
 Cu and alloys, neutron irradi., microhardness, resistivity, electron microscopy 4-103811  
 Cu and alloys for fusion reactor appls., DOE-OFE workshop report 4-107014  
 Cu, brazed, low cycle fatigue in high vacuum rel. to cold work 4-109500  
 Cu, neutron cross sections for defect prod. by high energy displacement cascades 4-108462  
 Cu, stabiliser materials, magnetoresistivity, fusion neutron effect 4-113502  
 Cu, thermal neutron irradi., defect production efficiencies 4-108463  
 Cu-Ag alloy plate, thermal fatigue behaviour 4-111931  
 Cu-Li alloy, surface material for fusion devices 4-97888  
 (Fe,Ni)V, ordered alloy, irradi. in HFIR, microstruct. and bend ductility 4-108454  
 (Fe,Ni)<sub>3</sub>V alloy, long-range ordered, strain rate and ageing effect on mech. props. 4-109501  
 Fe, BCC crystal, irradiation creep, stress induced edge dislocation/interstitial atom interaction 4-104814  
 Fe, pure, irradi. in HVEM, void form, onset temp. 4-103804  
 Fe, radiation damage calc. by NJOY nuclear data, processing system 4-107044  
 Fe-Cr-Ni, austenitic alloy, He bubbles at grain boundaries 4-108471  
 Fe-Cr-Ni (15.15 wt.%), weak beam imaging of He bubbles 4-103618  
 Fe-Cr-Ni-Mo, austenitic alloy, void swelling, effect of pulsed irradi. 4-108474  
 Fe-Cr-Ni-Mo, austenitic alloy, pulsed ion irradi., temp. aspects 4-108476  
 Fe-Cr-Si(Ti), electron and ion-irradi., void and precip. struct. 4-103802  
 Fe-Ni-Cr, austenitic, neutron irradiated, swelling and creep 4-108452  
 Fe-Ni-Cr (16, 15 wt.%), void swelling, effect of C and Nb additions 4-103817  
 Fe-Ni-Cr-B-C, swelling behaviour, influence of Li shell effect on microscopy determ. 4-109580  
 Fe-Ni-Cr-C, Ti-modified, void swelling, pre-irradi. ageing effects 4-104798  
 Fe<sub>40</sub>Ni<sub>38</sub>B<sub>18</sub>Mo<sub>4</sub>, Metglas 2826 MB 5 keV He implantation, bubble growth, free vol. relax. model 4-103822  
 (Fe<sub>0.49</sub>Ni<sub>0.51</sub>)<sub>3</sub>V, ordered alloys, microstruct. and creep rel. to implanted He 4-108399  
 H isotope permeation in structural alloys 4-113720  
 H recycling constant of TEXTOR liner, in situ meas. 4-108182  
 He-cooled blanket, pressurized module design, reliability and neutronics performance 4-107094  
 Hf-Al-N ternary system, phase equilib. invest. rel. to fusion reactor materials 4-76759  
 K, liq. metal for D-T, D-D and T-T fusion sources, energy deposition 4-68810  
 Li breeder blanket, impure, T extraction by Y, thermochem. analysis 4-107027  
 Li CTR blanket performance parameters, discrepancies between meas. and calcs. 4-59407  
 Li isotope separation by cryptand (2q,2,1) polymer 4-74039  
 Li limiter effects on <sup>3</sup>H breeding in compact tokamak without inboard breeding 4-107114  
 Li, liq., tokamak fusion reactor-liq. metal blankets; mag. field penetration 4-111824  
 Li, liq. metal for D-T, D-D and T-T fusion sources, energy deposition 4-68810  
 Li metal, T conc. from neutron irradiation, extraction facility calibration 4-111811  
 Li pool fires in fusion reactor safety analys., comp. with Na and Li-Pb, LITFIRE code 4-111787  
 Li self-cooled blankets, <sup>3</sup>H breeding-energy multiplication plots 4-107116  
 Li-Al, T release on heating or NaOH dissolving rel. to Li conc. 4-75733  
 Li-Pb alloy, liq., breeder blanket materials, thermodynamic investig. of dil. solns. of H 4-107033  
 Li-Pb alloy, liq., breeder blanket materials, interaction of H isotopes investigated 4-107034  
 $\gamma$ -LiAlO<sub>2</sub> breeder material, TRIO-01 expt. for in-situ T recovery 4-107023  
 $\gamma$ -LiAlO<sub>2</sub>, solid breeder, in-situ T recovery and heat transfer performance 4-111817  
 LiF and LiF-PbF<sub>2</sub> pellets, thermal neutron irradiated, T release behaviour, fusion reactor appl. 4-74040  
 Li<sub>2</sub>O, activity coeff. of dissolved LiOH, water press.-temp. regime, breeder material 4-107029  
 Li<sub>2</sub>O breeder, chem. compatibility with transition metals 4-107060  
 Li<sub>2</sub>O breeder, blanket pellet, water vapour adsorption in He sweep gas stream 4-107032  
 Li<sub>2</sub>O breeder material, neutron irradi., T release expts. 4-107030  
 Li<sub>2</sub>O breeder material, neutron irradi. behaviour and compatibility testing 4-107031  
 Li<sub>2</sub>O, Li<sub>2</sub>ZrO<sub>3</sub>, Li<sub>2</sub>SiO<sub>4</sub> and  $\gamma$ -LiAlO<sub>2</sub> breeder blanket material developments 4-107020  
 Li<sub>2</sub>O, LiAlO<sub>2</sub>, Li<sub>2</sub>SiO<sub>4</sub> and Li<sub>2</sub>ZrO<sub>3</sub> breeder materials, fast neutron irradi. expts. 4-107024  
 Li<sub>2</sub>O pellet, T recovery, assay techniques 4-107022  
 Li<sub>2</sub>O pellet breeder materials, in-situ T recovery expt. 4-107026  
 Li<sub>2</sub>O single crystal, breeder material, D<sub>2</sub> solubility 4-107025  
 Li<sub>2</sub>O slab assemblies, angle depend. neutron spectra by time-of-flight method 4-74047  
 Li<sub>2</sub>O, thermal neutron irradi. effects, lattice parameter and expansion changes, F<sup>-</sup> centres 4-107028  
 Li<sub>2</sub>O, vapourisation, effect of H<sub>2</sub>O vapour in the carrier gas 4-75650  
 Li<sub>17</sub>Pb<sub>33</sub> alloy blanket concept for tritium breeding in INTOR-NET 4-111747  
 Li<sub>17</sub>Pb<sub>33</sub> alloy blanket material, T recovery 4-111745  
 Li<sub>17</sub>Pb<sub>33</sub> liquid alloy, physical and chemical props. for fusion reactors 4-111748  
 Mo, cyclic irradi., void growth and swelling at low temp. 4-103795  
 Mo, endurance limit in high cycle fatigue rel. to heat treatment and alloying 4-109498

## fusion reactor materials continued

- Mo, He cavity growth and nucleation at 300K, expt. HDS and TEM studies 4-108348  
 Mo, He trapping at low-angle tilt boundary 4-113505  
 Mo, high temp. neutron irradi., annealing, void form., mech. props. 4-108456  
 Mo, neutron irradiation embrittlement, influence of irradi. temp. and heat treatment 4-108453  
 Mo, pulse ion irradi., void nucleation 4-103826  
 Mo, pulsed irradiation, theory of depleted zone annealing 4-108417  
 Mo, pure, electron and He ion irradi., vacancy loop form. 4-108480  
 Mo, thermal neutron irradi., defect production efficiencies 4-108463  
 Mo, tokamak wall material, hydrogen recycling model calcs. 4-97870  
 Mo-Hf-C, electron beam welded joint, tensile strength, ductility, comp. depend. 4-109470  
 Mo-Nb-C, electron beam welded joint, tensile strength, ductility, comp. depend. 4-109470  
 Mo-Re-C, electron beam welded joint, tensile strength, ductility, comp. depend. 4-109470  
 Mo-Ti-Zr, TZM, neutron irradiation embrittlement, influence of irradi. temp. and heat treatment 4-108453  
 Na, liq. metal for D-T, D-D and T-T fusion sources, energy deposition 4-68810  
 Na-K, liq. metal for D-T, D-D and T-T fusion sources, energy deposition 4-68810  
 Nb, H permeation, surface effects 4-113723  
 Nb single crystal, neutron and electron irradi., dislocation sweeping of defects 4-103810  
 Nb<sub>2</sub>O<sub>3</sub> radiation hardening by 14 MeV neutrons rel. to O content. 4-104852  
 Nb<sub>3</sub>Sn supercond. wires, neutron irradiation effect on T<sub>c</sub> 4-61477  
 Ni (100), He ion irradiation, He precipitate nucleation at point defects 4-103823  
 Ni, D implanted, reemission and permeation 4-113721  
 Ni, dislocation/obstacle interaction during low dose D irradi., creep 4-104813  
 Ni foils, He injected, self-ion irradi., annealing, voids, TEM obs. 4-103827  
 Ni, He prod. calcs. and meas. comparison using neutron cross sections for <sup>58</sup>Ni 4-107042  
 Ni, He<sup>+</sup> ion irradiated, bubble growth, microstruct. contrib. 4-108472  
 Ni, pure, heavy ion irradi. damage, in situ electron microscopy 4-103828  
 Ni, radiation damage calc. by NJOY nuclear data processing system 4-107044  
 Ni, void formation during ion bombardment, conditions for suppression 4-108477  
 Ni-He, preimplanted, electron irradi., 1 MeV, He bubble growth 4-103803  
 Ni-Au films, ion-induced comp. change, role of grain boundary diffusion at elevated temps. 4-108475  
 Ni-based alloys, HVEM irradi., void form. rel to  $\gamma'$  precipitation 4-108446  
 Ni-Cr-Ti-Mo(Nb), precipitation strengthened, HFIR irradi., ductility, microstruct. 4-108457  
 Ni-Si (12.7 at.%), solute redistrib. under irradi., TEM invest. 4-108416  
 Pb, liq. metal for D-T, D-D and T-T fusion sources, energy deposition 4-68810  
 Pb(n,2n), 14 MeV, neutron multiplication in fusion blanket 4-64234  
 Si chemical behaviour in fusion reactor liq. Li systems 4-107058  
 Si, low Z shielding materials, implanted H effects at high conc. 4-111760  
 SiC, CVD coating, permeation of H 4-92403  
 SiC fibre for ICF applic., strength and fatigue analysis 4-109502  
 SiC, first wall material, radiation erosion 4-80120  
 SiC, fusion reactor first wall appl., thermal and mech. props. (German) 4-83244  
 SiC shell wall design of cascade reactor, T. breeding and activation 4-111814  
 SiC, sintered and siliconised, microstruct. of neutron irradi. induced defects 4-108459  
 SiC, surface tile material for fusion reactor DCT-8 pumped limiter design 4-96259  
 steel, Cr-Mo and 316 types, compatibility with flowing Li 4-107062  
 T containment problems, blanket comparison and selection study 4-107096  
 T inventories, breeding requirements in power reactors 4-107113  
 Ta, blister formation by 30 MeV alpha particles bombardment 4-113507  
 Ta film, first wall in ICF chamber, chem. reactions with pellet debris 4-107057  
 Ta protective coatings for in-vessel fusion devices 4-111751  
 Ti, pure, electron beam welding, mech. props., fusion reactor appls. 4-109471  
 Ti, thermal cycling in D<sub>2</sub> atmosphere 4-99497  
 Ti-Al-Sn-Zr-Mo-Si, H-enhanced fatigue crack growth 4-114640  
 Ti-Al-V (6, 4 wt.%), electron beam welding, mech. props., fusion reactor appls. 4-109471  
 TiC as tokamak wall material, hydrogen recycling model calcs. 4-97870  
 TiC co-deposited with Ar gas, props. 4-111752  
 TiC limiter surface analysis exposed to JIPP-II stellarator/tokamak hybrid device 4-108177  
 TiC, low Z films, correl. of residual stress with microstruct. 4-114695  
 TiC, low Z films, PVD coated, residual stresses 4-114696  
 TiC, low Z films, residual stress measurement by X-ray diffractometry 4-114694  
 TiC protective coatings for in-vessel fusion devices 4-111751  
 TiC, surface studies by impact-collision ion scattering spectroscopy 4-93163  
 TiC-coated graphite limiters improved performance by surface texturing 4-108181  
 TiC-graphite, thermal cycling tests, surface damage study 4-111756  
 TiC-stainless steel interface, reaction zone struct. produced by vacuum annealing 4-104918  
 TiN, low Z films, correl. of residual stress with microstruct. 4-114695  
 TiN, low Z films, PVD coated, residual stresses 4-114696  
 TiN, low Z films, residual stress measurement by X-ray diffractometry 4-114694  
 UO<sub>2</sub> slab and spherical sources, charged particle spectra 4-60599  
 V alloys, fusion reactor candidate first-wall materials 4-111799  
 V and V-Cr-Ti alloy, fusion reactor blanket use, analysis of attack by O and water vapour 4-107019  
 V, neutron irradi., hardness, tensile props. 4-103809

## fusion reactor materials continued

- V, neutron irradi., temp. depend. of damage microstruct. 4-108455  
 V, T charged, <sup>3</sup>He bubble formation, TEM obs. 4-103825  
 V, T-charged, obs. of cylindrical cavities at dislocations 4-60913  
 V-B<sub>2</sub>C, neutron irradi., temp. depend. of damage microstruct. 4-108455  
 V-base alloys, candidate materials for fusion appl., weldability 4-99494  
 V-base alloys, corrosion and oxidation 4-109556  
 V-Cr-Ti, fusion reactor blanket material, neutron activation cross sections 4-107047  
 V-Cr-Ti Path C alloy for fusion reactors, V volatility, safety anal. 4-111782  
 V-Cr-Ti(Fe-Zr), mech. props. rel. to O contamination, fusion appls. 4-109499  
 W, cross-rolled, tensile and low-cycle fatigue meas. at 1505K 4-109503  
 W, proton irradi. induced defects, FIM obs. 4-108483  
 Y, H diffusivity, 960 to 1160K 4-113716  
 Y, H trapping in low temp. Li 4-111759  
 Y-Nb, H diffusivity, 960 to 1160K 4-113716  
 Y-Nb alloy-H<sub>2</sub> system, isothermal equilib. press. 4-70557  
 Y-Th, H diffusivity, 960 to 1160K 4-113716  
 Zr, fusion neutron irradi., damage prod. and recovery, resist. obs. 4-108461  
 Zr, pure, neutron irradi., annealing, point defect prod. and annihilation, saturation resist. 4-108465  
 Zr tritides, ageing, TEM study 4-75503  
 Zr-V-Fe alloys, bulk getters, H and D diffusion 4-113719
- fusion reactor theory and design**  
*see also fusion reactor ignition; fusion reactor materials; plasma confinement; plasma heating; plasma production*  
<sup>238</sup>Pu production ability of fusion breeders 4-106854  
 AC-MHD salient-pole synchronous generator coupled to Tokamak fusion reactor 4-64238  
 activation product aerosol formation during accidents 4-111783  
 activation product transport in fusion reactors, radiation fields calc. around plant components 4-107153  
 activation products impact on fusion reactor safety 4-111780  
 advanced fuel burning nucl. reactors, feasibility study 4-59403  
 advanced physics tokamak, max. toroidal mag. field impact on performance and cost 4-111793  
 Advanced Toroidal Facility, helical field coils, design descript. 4-111905  
 Advanced Toroidal Facility, superconducting magnet, preliminary design and test 4-111891  
 Alcator DCT, heat removal and impurity control 4-96260  
 alternative fusion concepts, reactor systems studies 4-107075  
 ambipolar reactor, effect on characteristics of <sup>4</sup>He retention 4-102398  
 Argonne Pulsed Cable Test Facility, tests and progress for tokamak coils 4-111890  
 ASDEX divertor tokamak, ohmic heating phase results 4-107080  
 ASDEX Upgrade project, machine parameters 4-96256  
 ATF, computer simulation of mag. field circuits 4-111874  
 atomic plasma physics in inertial fusion 4-102762  
 autocatalytic fusion-fission implosions, thermonuclear energy appl. 4-59410  
 beam dump panel design, performance and failure mode 4-111915  
 beam fusion, historical remarks 4-96273  
 beamline for light ion fusion demonstration reactor 4-102390  
 Big Dee tokamak, poloidal coil design and construction 4-111883  
 Bitter plate tokamaks, coupled EM and thermal problems, transient non-linear solns. 4-59412  
 blanket comparison and selection study, decision analysis methodology 4-107091  
 blanket comparison and selection study overview 4-107090  
 blanket expts. and data 4-59408  
 blanket high temp. heat transfer 4-111822  
 blanket optimisation, nonlinear simplex method 4-107124  
 blanket structures, activation product release, safety research 4-111781  
 blankets, liquid metal corrosion product transfer, MHD effects, safety 4-111786  
 blankets, neutronic testing requirements in fusion devices 4-107118  
 Blankets for tritium catalyzed deuterium fusion reactors 4-107117  
 book, magnetic fusion confinement, physics and technology 4-110815  
 CAD, program systems development (Japanese) 4-111766  
 Cascade reactor, mechanical and thermal design, stress anal. 4-111855  
 cascade reactor, T breeding and activation 4-111814  
 Cascade solid breeder blanket microspheres, design and fabrication 4-107127  
 Cat-d tandem mirror fusion reactor, comparison to dt reactor, plugs, heating 4-111807  
 charged particle fusion cross sections, data status for reactor design 4-111772  
 charged particles fusion (French) 4-91112  
 commercial high  $\beta$  tokamaks, systems anal. 4-107130  
 compact fusion reactors availability analysis, for pinch and tokamaks 4-111856  
 compact magnetic fusion reactor concepts, review (Korean) 4-113207  
 compact reversed field pinch reactor, plasma engineering design 4-111901  
 conceptual <sup>3</sup>He breeder reactor 4-107132  
 conceptual design of fusion reactor, road to commercialisation 4-59402  
 conference on fusion engineering, Philadelphia, PA, USA (Dec. 1983) 4-110807  
 Coulombic large energy transfer collisions, effects in fusion grade plasma 4-75172  
 cycle operation by adiabatic compression in mag. confinement reactor 4-59411  
 DCT-8 pumped limiter design, Be, BeO, SiC as surface tile materials 4-96259  
 design considerations for achieving high vacuum integrity in fusion devices 4-91101  
 diagnostic systems, radiation hardening, critical issues 4-111849  
 direct drive laser fusion 4-97830  
 direct illumination spherical target experiments 4-97824  
 disruption heat load simulations using electron beams 4-111911  
 Doublet III, neutral beam data archiving for offline analysis and access 4-111841  
 Doublet III, noncircular plasmas, divertor configuration, reactor-like temp. values 4-107081  
 Doublet III beam heated, cold-dense plasma obs. with single-null poloidal divertor 4-74043

## fusion reactor theory and design continued

Doublet III Big-Dee upgrade, diagnostic data acquisition computer system 4-111842  
 Doublet III design and capabilities in large dee config. 4-111831  
 Doublet III limiter and wall protective armour, design and operational performance 4-111912  
 Doublet III tokamak, limiter damage, over-heat load due to plasma disruptions 4-96252  
 Doublet III vacuum vessel, field installed brazed thermocouple feed-throughs 4-111947  
 dual energy heavy ion target concepts 4-59419  
 dynamo effect in sustained Reversed-Field Pinch discharges 4-75183  
 EBT-P control/interlock/display system using commercially available equipment 4-111848  
 EBT-S, microwave launchers, mixed-mode, design 4-111865  
 economics of fusion breeders 4-59353  
 EDDYTRAN program for tokamak eddy current, EM force and structural anal. 4-111791  
 electron storage between cathode and anticathode in axial mag. field 4-107250  
 EM anal. for fusion reactors, status and needs 4-111818  
 EM mass-accelerator development, impact fusion 4-107135  
 emerging nuclear energy system, conf., Helsinki, Finland (June 1983) 4-58546  
 energy deposition on the walls of the ohmically and neutral-beam-heated ASDEX tokamak 4-108180  
 energy deposition uniformity for laser driven fusion 4-97826  
 energy production enhancement during neutral beam injection 4-107110  
 ETR-INTOR tokamak design, all-remote operation and maintenance config. 4-111770  
 exhaust plasma, interface with imperfect conductor, boundary conditions 4-65069  
 fast charged particle interaction with high density ICF plasma targets 4-111963  
 FED-A, advanced performance fusion eng. device based on low safety factor and current drive 4-111852  
 field-reversed, use of neg. ion beam sources 4-107223  
 first wall, bremsstrahlung energy deposition in mag. confinement systems 4-107121  
 first wall lifetime, impact of swelling 4-96269  
 first walls, lifetime calc., creep-fatigue design criteria 4-96254  
 first-wall protection through falling solid particles 4-107125  
 fluid dynamic stabilized high gain magnetic inertial fusion target 4-60701  
 fusion breeder, development pathways 4-107101  
 fusion breeder, fission suppressed, safety studies 4-107103  
 fusion breeder, potential role and prospects 4-59431  
 fusion breeder design review 4-107099  
 fusion breeder economics, systems analysis, and market penetration 4-107100  
 Fusion Experimental Reactor, steady and quasi-steady, lower hybrid wave current drive, design 4-68819  
 Fusion Power Demonstrator, tandem mirror test reactor, ignited central cell 4-107073  
 fusion power demonstrator program, tandem mirror expt. test reactor 4-107072  
 fusion technology, measurement assurance with MIL STD 45662, quality assurance 4-111798  
 fusion torch appls., review 4-60749  
 heavy ion accelerators as drivers for inertial confinement fusion 4-107086  
 HIBLIC-1 heavy ion fusion reactor, conceptual design using  $^{208}\text{Pb}$  beams 4-68816  
 high heat flux target for neutral beams at ORNL 4-111866  
 high wall loading compact tokamak reactors 4-107107  
 high-energy multiplication blankets for Cat-D fusion reactors 4-107106  
 high-temperature low-activation design for the Cascade reactor 4-107126  
 hybrid blankets, time depend. performance characts. 4-59428  
 hybrid reactor, design and safety study, fast fission blanket safety performance 4-96274  
 ICF, ignition of isobarically compressed D-T targets, burn propag. anal. 4-68813  
 ICF, muonic or polarised fusion for ignition 4-59400  
 ICF facility FIRST STEP, blanket struct., fuel assembly design 4-107123  
 ICF facility FIRST STEP 4-107122  
 ICF reactor, diagnostic techniques for transient meas. 4-111945  
 ICF target burn, fusion product energy loss effects 4-107112  
 ICF targets, heavy ion driven, irrads. symmetry 4-64235  
 ICF targets, heavy ion pulse shape optimization, quasi-isentropic compression 4-107087  
 ICRF enhancement of beam driven currents, Fokker-Planck treatment 4-74042  
 ignition of self-sustained fusion reaction in dense DT plasma 4-102395  
 ignitor plasma chamber, thermal and structural anal. 4-111929  
 implosion process, theoretical and computational investig. 4-97829  
 impurity control, candidate materials 4-91108  
 Inconel 625 as tokamak wall material, hydrogen recycling model calcs. 4-97870  
 inertial confinement fusion, progress and perspective, review 4-74044  
 inertial confinement fusion target compression, use of strong shock waves 4-111968  
 inertial confinement reactor options technical risks identification and classification 4-68817  
 inertial effects in laser-driven ablation 4-111969  
 inertial fusion commercial applications, driver cost and performance effects 4-107089  
 inertial fusion reaction chamber, magnetically guided flow obs. (Japanese) 4-102397  
 inertially stabilized thermo-nuclear Z-pinch 4-60680  
 intense ion beam stopping power in partially ionised material 4-113167  
 INTOR magnetics and electromagnetics, phase IIA results for TF system 4-111900  
 INTOR reactor, TF-ripple losses from a non-circular tokamak 4-103544  
 INTOR tokamak engineering test reactor, critical issues studies 4-107070  
 INTOR workshop status, technical issues for engineering test reactor 4-111857  
 INTOR-NET mechanical configuration, systems integration, assembly, disassembly, maintenance 4-111742  
 INTOR/NET, T breeding and electricity generating blanket sector 4-111830

## fusion reactor theory and design continued

ion stopping in ICF plasmas 4-107149  
 irradiation sources for struct. materials development and testing programmes 4-107035  
 ISX-B tokamak, preionisation and start-up using electron cyclotron heating at 28 GHz 4-97892  
 JAERI, fusion research and development, present status 4-111789  
 JET, commissioning tests, plasma operation and discharge 4-107077  
 JET, impurity control studies 4-96258  
 JET heating system components by neutral beam injection (French) 4-103583  
 JET internal windings, construction, insulation and cooling, for plasma confinement (French) 4-96271  
 JET project, status and perspectives 4-111790  
 JET toroidal field coils, design, manufacture, performance 4-111881  
 JFT-2M tokamak, coil system design and fabrication 4-111880  
 JFT-2M tokamak, design, fabrication and testing of noise prevention and grounding system 4-111847  
 JFT-2M tokamak, poloidal coil power supply system, construction and design 4-111958  
 JT-60, charge exchange neutral particle mass and energy analyser 4-111843  
 JT-60, communications in control systems, D-port 4-111846  
 JT-60, diagnostics data management facility 4-111850  
 JT-60 evaluation and operation region of first wall, heat flux related 4-111914  
 JT-60 tokamak, divertor research 4-96257  
 JT-60 tokamak, eddy current anal. using EDDYMULT program 4-68818  
 JT-60 vacuum vessel, evaluation of mechanical strength of welded bellows 4-111920  
 JT-60 vacuum vessel fabrication 4-111917  
 KARIN-I moving ring reactor, review 4-68815  
 Large Coil Test Facility, pulse coil coolant system design 4-111884  
 Large Coil Test Facility, two coil test, struct. anal. 4-111906  
 large fusion systems, superconducting magnet qualification, TPCX and Alcator DCT 4-111904  
 large tokamaks,  $\alpha$ -particle confinement, lower hybrid wave heating effects 4-75170  
 large toroidal field coil winding, shear stress peaks in superconducting cable 4-111892  
 laser controlled fusion, numerical simulations 4-68814  
 laser driven, cavity type target and scaling laws 4-84036  
 laser implosion fusion experiments at ILE Osaka 4-97828  
 Lawrence Livermore nuclear data libraries used for fusion reactor calcs. 4-111773  
 LCTF superconducting pulse coils, design, fabrication, testing 4-111882  
 LIBRA ICF conceptual reactor, first wall tubes, mech. anal. 4-111826  
 light ion beam reactor driver, D-T ignition, inertial confinement fusion 4-107085  
 limiter damage in mag. field error region of ZT-40M expt. 4-108179  
 LITE device, engineering aspects 4-111819  
 Los Alamos nuclear data libraries for fusion neutronics calcs. 4-111774  
 low pressure blanket concepts, nitrate/nitrite molten salt-cooled blanket 4-107095  
 low-activation diagnostic equipment and auxiliary heating components for fusion 4-107134  
 low-pressure boiling lithium as a first-wall coolant 4-107120  
 magnetic data assessment for commercialisation 4-111832  
 magnetic fusion energy research, centralized supercomputer support, computer codes 4-59415  
 magnetic mirror fusion, vacuum technology developments 4-111860  
 magnetic mirror fusion reactor, history of evolution 4-86168  
 MARS, liquid  $\text{Li}_2\text{Pb}$  cooled fusion reactor blanket, corrosion product cleanup system 4-111785  
 MARS, tandem mirror research, status and prospects 4-111788  
 MARS blanket, three dimens. neutronics anal. 4-107115  
 MARS end plasma system design 4-111821  
 materials needs for compact fusion reactors 4-91106  
 MCFR magnets, irradiation effects on superconducting materials 4-111888  
 MCNP fusion neutronics code, sensitivity method development and appl. 4-111778  
 MCNP transport code, capabilities for fusion neutronics appls. 4-111776  
 MFTF yin-yang coils, switching transient in large superconducting coils 4-111894  
 MFTF yin-yang magnet displacement, mag. field calcs. and meas., review 4-111907  
 MFTF-3, superconducting trim coils and magnet alignment 4-111895  
 MFTF- $\alpha$ +T, 18 T superconducting choke coil 4-111897  
 MFTF- $\alpha$ +T, end plug magnet design, shielding 4-111889  
 MFTF- $\alpha$ +T end cell vacuum vessel and nuclear shield trade studies 4-107131  
 MFTF-B, end-cell vacuum vessel and shielding installation design 4-111909  
 MFTF-B axicell, vacuum vessel and cryopumping, design features 4-111859  
 MFTF-B neutral beam accel. DC power supply, computer model 4-111955  
 MFTF-B plasma diagnostics, data acquisition and control system 4-111838  
 MFTF-B vacuum vessel, static and dynamic calcs. 4-111804  
 microwave kinoform for magnetic fusion 4-107571  
 mirror advanced reactor study, fusion technology development 4-107071  
 mirror and tokamak upgrade reactors, activation analcs. for safety 4-111784  
 Mirror Engineering Test Reactor, fusion power demonstration concept 4-111853  
 Mirror Fusion Test Facility upgrade, config. issues and evolution 4-111836  
 molten salt flowing mixtures, mag. field, polarisation 4-87806  
 molten salt fusion breeder, blanket materials compatibility 4-107102  
 muon catalyzed fusion, power reactor concepts 4-107139  
 muon induced fusion, design considerations 4-107143  
 muon production colliding beam system for muon catalyzed fusion reactor 4-107140  
 muon production costs for fusion catalysis 4-107142  
 neutral atoms kinetics near fusion reactor wall kinetics 4-103513  
 neutral beam developments for MFTF  $\alpha$ +T system 4-91947  
 Neutral Beam Engineering Test Facility, design fabrication and operation of mechanical systems 4-111943

## fusion reactor theory and design continued

- neutral beam heating and plasma impurity control for tokamak fusion reactors 4-60664  
neutral beam heating system, water flow calorimeter, calibration system 4-111837  
neutron-feedback ICF reactors, laser blanket design 4-107088  
NPL plasma, charged particle spectra from  $^{10}\text{B}$  and  $\text{UO}_2$  slab and spherical sources 4-60599  
NPL plasma, power deposition in cylindrical geometry using  $^{10}\text{B}$  coatings 4-60600  
nuclear data measurement program for fusion energy development 4-111771  
OMITRON type high-field Tokamaks, ignition of  $\text{D}^3\text{He}$  and catalysed D-D fuels 4-59405  
one-dimensional Cannonball target, hot electron energy distrib. 4-113191  
PAFEC as preprocessor for MSC/NASTRAN for fusion reactor stress anal. 4-111794  
PDX dissipation of magnetic energy during disruptive current termination 4-75148  
pellet acceleration with railgun for mag. fusion device refuelling 4-91099  
plasma-material interactions and high heat flux component design 4-91098  
plasmas, inertially confined, ion density correlations, thermonuclear reaction rate 4-91974  
power-balance analysis of muon-catalyzed fusion-fission hybrid reactor systems 4-107141  
primary heat transfer loop design for the Cascade ICF reactor 4-107129  
Princeton large torus, current drive and RF heating expts. 4-107079  
Pulse-Star ICF reactor, T control and activation 4-111815  
pulsed and steady-state tokamak reactors, burn cycle requirements comparison 4-111808  
pulsed reactors, thermal storage systems and thermomech. effects 4-111956  
quality assurance, lessons learned in nuclear power industry 4-111796  
quasi-steady operation, OH coil recharging optimization 4-96251  
R-tokamak, first wall design 4-96261  
R-tokamak, first wall design from low activation Al alloy, cooling 4-111802  
R-tokamak, low activation Al alloy vacuum vessel, EM forces, stress anal. 4-111801  
R-tokamak, low activation coil system 4-111903  
Rayleigh-Taylor instability and resulting failure modes of ablatively imploded inertial fusion targets 4-97789  
Rayleigh-Taylor instability of thin layer, three dimens., nonlinear evolution 4-113148  
reacting plasma project, low-activation materials 4-111946  
reactivity enhancement by fast waves in advanced fuel tokamaks 4-107109  
refractory coatings thermal performance exposed to a tokamak plasma 4-108202  
relativistic electron beam propag. through a plasma region into vacuum 4-97808  
relativistic electrons, linear gyrokinetic eqn., fusion research 4-65130  
reliability, availability and maintainability, practical insight 4-111797  
reverse field pinch expt., mag. circuit study with U-D model 4-111877  
reversed field pinch mag. config., driven dynamo for maintenance 4-113215  
RFC reactor including cusp field, alpha particle heating 4-59416  
RFX, closed loop control of plasma current and toroidal field 4-111844  
RFX air core conceptual design 4-111941  
selection logistics of fusion options and R&D programs 4-111769  
self-cooled liquid-metal breeder/coolant blanket, D-T fusion reactor 4-107093  
SENRI ICF reactor design, pellet gain scaling 4-107151  
spatial coherence reduction of fusion lasers for uniform acceleration of fusion targets 4-60677  
SPAU LRAD-S laminate for fusion reactor appls., irradiation and mech. props. 4-111768  
spheromak plasma, engineering feasibilities for tilt and shift stabilisations 4-111875  
spheromak plasma heating concepts for reactor operation 4-111835  
stellarator helical vacuum vessel design 4-111916  
stellarator W VII, engineering details for modular design 4-111951  
stellarators, energy confinement time 4-75184  
streaming matrix hybrid method use for discrete ordinates fusion reactor calcs., ICF appl. 4-111777  
structural component lifetime evaluation using SMILE code 4-111743  
structural material, dynamic deform. due to EM forces, finite element anal. 4-74050  
suppressed fission ICF hybrid, neutronics aspects 4-111858  
surface composition changes of Inconel 625 during RG and ECR discharge cleaning of TEXTOR at  $300^\circ\text{C}$  4-108203  
surface exposed to fusion reactor plasmas, steady state H transport 4-74041  
surface melting and evaporation due to plasma disruptions, magnetic fusion reactors 4-96255  
system concepts for muon-catalyzed fusion 4-107138  
system design studies and R&D, reacting-plasma project (Japanese) 4-111764  
tandem mirror experiment-upgrade, TMX-U, surface area meas. of the first-wall 4-108201  
tandem mirror fusion power demonstrator, config. and layout 4-111834  
tandem mirror reactor,  $\alpha$ -particle distribution function, thermalised fraction 4-107111  
tandem mirror reactor, drift-pump coil design 4-111827  
tandem mirror reactor, initial start-up study 4-111823  
tandem mirror reactors, materials engng. 4-91105  
tandem mirrors, density profile calcs. fueled by pellets 4-113216  
target implosion, nonuniformity effect on ICF parameter 4-111967  
TASKA-M, 17.5 T hybrid choke coils 4-111887  
TASKA-M, compact fusion technology test facility, design 4-107037  
TASKA-M, liquid metal test blanket design 4-111944  
TASKA-M, plasma engineering considerations 4-111902  
TENTOK reactor, plasma engineering anal. 4-111876  
TEXTOR: research programme on plasma wall interaction 4-108200  
TEXTOR first wall characs. w.r.t. H recycling 4-91968  
TEXTOR liners and limiters surface conditioning by plasmachemical C deposition 4-108183  
TEXTOR plasma edge impurity meas. using deposition probe techniques 4-108205

## fusion reactor theory and design continued

- TFCX, candidate TF coil system options, parametric system studies 4-111899  
TFCX, tokamak reactor plasma engineering studies 4-111805  
TFCX device, configurational studies and project definition 4-111854  
TFCX limiter and first wall, thermal shock considerations 4-111933  
TFCX poloidal field coil and current distrib. study 4-111806  
TFM/TFTR vacuum vessel stress analysis 4-111803  
TFTR, configuration management during final fabrication, assembly and installation 4-111795  
TFTR, design and fabrication of moveable limiter 4-111919  
TFTR, structural support design for detectors, actuators, shielding, diagnostic equipment 4-111942  
TFTR, universal diagnostic probe system 4-111939  
TFTR, X-ray crystal spectrometer, mech. design 4-111949  
TFTR bumper limiter design 4-111925  
TFTR graphite limiter tiles, 3-D anal. of contact conditions 4-111928  
TFTR moveable limiter installation 4-111926  
thermionic diode materials selection and performance 4-107018  
thermonuclear dynamo 4-59418  
thermonuclear magneto-acoustic cone instability, quasilinear theory 4-65082  
thermonuclear reaction rates in dense plasma, screening pot. and enhancement 4-64236  
TMX-U thermal barrier tandem mirror expts., end-plug ion microstability 4-107078  
TMX-Upgrade, computer control of Ti getter system 4-111845  
TMX-Upgrade, systems control, small computer appl. 4-111840  
TMX-Upgrade, X-ray detection system development, hardware and software 4-111839  
tokamak, long pulse commercial reactor design aspects 4-111833  
tokamak as a candidate for a D-T fusion reactor 4-59423  
Tokamak de Varennes, control of rapid plasma motion, radial position feedback system 4-111809  
Tokamak de Varennes, vacuum vessel EM characteristics and loadings 4-111913  
tokamak development, peak toroidal flux density 4-96272  
Tokamak discharge chamber, H interaction 4-103512  
tokamak fusion breeder, fission suppressed blanket, nuclear anal. 4-107104  
tokamak fusion core experiment, configuration review, superconducting and copper toroidal-field designs 4-107068  
tokamak fusion core experiment, project definition studies 4-107067  
tokamak fusion reactor liq. metal blankets, mag. field penetration 4-111824  
tokamak fusion test reactor, energy confinement time, adiabatic compression of plasma 4-107076  
Tokamak Fusion Test Reactor, internal windings, construction, insulation and cooling, for plasma confinement (French) 4-96271  
tokamak plasma ignition, compatibility with sputtering, JETlike discharge 4-96270  
tokamak pulsed reactors, first wall and limiter lifetime 4-111918  
tokamak reactor, swimming-pool type, radiation shielding for repair and maintenance 4-96250  
tokamak reactor plasmas, bean-shaped, magnet systems 4-111825  
tokamak reactor studies, operation reliability improvements 4-107074  
Tokamak reactors, European communities design studies 4-111741  
tokamak reactors, high-performance copper toroidal field magnet design 4-107069  
tokamak reactors, smaller coil systems by ripple reduction 4-111893  
tokamak structural anal., coupling of magnetodynamics and elastomechanics, modeling 4-111792  
toroidal fusion device, circular magnets, stress model 4-111879  
toroidal reverse field 2-pinch, electrical design 4-111940  
TRIO-01 heat transfer results on solid breeder blanket designs 4-107098  
US-DOE fusion breeder program, blanket design and system performance 4-59426  
VITAMIN-E cross-section library for fusion neutronics calcs. 4-111775  
vertex shedding and the Rayleigh-Taylor instability in laser ablation 4-60636  
water-cooled liquid and solid breeder blanket concepts 4-107092  
Westinghouse LCP coil, He leak testing, test sensitivity 4-111886  
Westinghouse LCP coil, header region joints, design, testing and fabrication 4-111885  
Westinghouse LCP coil winding 4-111896  
 $\alpha$ -particles distribution function and diffusion in DT fusion plasma 4-102394  
Al vacuum vessel, low radioactivity fusion device, R-tokamak design 4-96253  
Be in fusion breeder blanket assemblies, neutron multiplication calcs. 4-107105  
C-SiC alloy coated armor/limiter tiles in Doublet III 4-108178  
 $^{12}\text{C}(\text{n},\gamma)$ , 14.1 MeV,  $\alpha$ -spectra and ang. distrib., kerma factor for fusion reactors 4-96020  
D- $^3\text{He}$  fusion, neutronisation as a function of ion temp. and confinement quality 4-59404  
D-cycle Tokamaks integration with decentralised small fusion and fission reactors 4-59406  
D-T plasma depolarisation by recycling in material walls 4-91096  
D-T spin-polarised fuel, fusion gains using homogeneous ignition and central ignition model 4-59409  
DT burn dynamic expt. in scaled up field reversed theta pinch 4-107108  
DT muon catalysed fusion, energy production approaches 4-59401  
H recycling constant of TEXTOR liner, in situ meas. 4-108182  
He cryopumping in fusion power systems, charcoal sorbents development 4-111861  
He-cooled blanket, pressurised module design, reliability and neutronics performance 4-107094  
 $^3\text{He}$ -AFILINT self-sufficient target ICF reactor 4-107150  
Li CTR blanket performance parameters, discrepancies between meas. and calcs. 4-59407  
Li limiter effects on  $^3\text{H}$  breeding in compact tokamak without inboard breeding 4-107114  
Li pool fires in fusion reactor safety anal., comp. with Na and Li-Pb, LITFIRE code 4-111877  
Li self cooled blankets,  $^3\text{H}$  breeding-energy multiplication plots 4-107116  
LiF and LiF-PbF<sub>2</sub> pellets, thermal neutron irradiated, T release behaviour, fusion reactor appl. 4-74040  
Li<sub>2</sub>O slab assemblies, angle depend. neutron spectra by time-of-flight method 4-74047  
Mo, tokamak wall material, hydrogen recycling model calcs. 4-97870

## fusion reactor theory and design continued

- T breeding in He cooled fusion blankets, nuclear data library comparison 4-111779  
 T inventories, breeding requirements in power reactors 4-107113  
 T issues in solid-breeder Cascade reaction chamber study 4-107128  
 T production-rate distrib. in simulated fusion blanket assemblies at FNS 4-74048  
 TIC as tokamak wall material, hydrogen recycling model calcs. 4-97870  
 TIC-coated graphite limiters improved performance by surface texturing 4-108181  
 V-Cr-Ti Path C alloy for fusion reactors, V volatility, safety anal. 4-111782

## fusion reactors

- see also fusion reactor ignition; fusion reactor materials; fusion reactor theory and design; hybrid reactors; plasma heating  
 advanced fuel fusion synergism 4-59424  
 aerosols characterisation from fusion energy systems 4-107016  
 ASDEX, divertor reactor expt. for nuclear fusion 4-86971  
 ASDEX long pulse neutral injection, watercooled grid performance 4-111936  
 ASDEX UPGRADE, divertor-tokamak expt. for fusion reactor conditions 4-86972  
 atomic spectra and oscillators, conf., Lund, Sweden, 17-19 Aug. (1983) 4-86109  
 book, magnetic fusion confinement, physics and technology 4-110815  
 cold stratified loss free plasma, wave tunnelling, complex ray tracing study 4-77683  
 conference, American Nuclear Society annual meeting, New Orleans, LA, USA (June 1984) 4-106112  
 conference on fusion engineering, Philadelphia, PA, USA (Dec. 1983) 4-110807  
 confinement concepts and commercial power prod., comparison of mainline and alternative approaches 4-111828  
 cryopumpings, fusion research appl. 4-95453  
 digital control and power supply system (Japanese) 4-111765  
 Doublet III, gas-fed system for ion sources 4-111869  
 ECE diagnostic system on TEXTOR 4-103579  
 FELIX facility to study EM effects for first wall, blanket and shield systems 4-111820  
 HIBLIC-I heavy ion fusion reactor, conceptual design using  $^{208}\text{Pb}$  beams 4-68816  
 highly-ionized atoms in fusion research plasmas, diagnostic techniques 4-87915  
 ICF, stability and symm. implications anal. 4-97823  
 ICF diagnostics 4-97904  
 ion source components, fabrication 4-111867  
 JAERI, fusion research and development, present status 4-111789  
 JAERI Fusion Research Centre, annual report 1982-3 4-74046  
 JET, assembly, commissioning and first operation 4-111898  
 JET, large cryopump systems construction 4-95456  
 JET, vacuum meas. and control 4-86970  
 JET project, status and perspectives 4-111790  
 JET thermonuclear fusion reactor 4-78734  
 light atom beams of neutralised neg. ions, fusion applications 4-107224  
 light ion inertial fusion research at US Naval Research Lab., Washington, DC 4-107145  
 magnetic booster target inertial confinement fusion driver 4-69938  
 MARS tandem mirror reactor, neutral beam injector system 4-107221  
 MFTF-B, impurity separator/neutralizer 4-111864  
 MHD flow with free surface in thermonuclear reactors with mag. plasma confinement (Russian) 4-113135  
 mirror reactors, pellet fueling, physical requirements 4-111872  
 muon catalysed fusion, conf., Jackson Hole, WY, USA (June 1984) 4-106119  
 neutral beam plasma heating for mag. fusion energy 4-107010  
 neutral beam sources, overcurrent protection device 4-111957  
 neutral beam systems, negative-ion-based, tokamak and mirror confinement device requirements 4-107219  
 neutral beam test stand for reacting plasma project 4-111938  
 neutron flux unfolding codes for appl. to research reactors and neutron generators in developing countries 4-68748  
 nuclear fusion power prospects (Korean) 4-91104  
 pinch plasmas, high beta, for nuclear fusion reactors (Japanese) 4-75188  
 plasma confinement, high frequency (Japanese) 4-75189  
 plasma targets for high energy neg. ions, neutralisation efficiency 4-107217  
 power generation and breeding, MeV and GeV prospects for producing large ion layer config. 4-60681  
 reversed field pinch approach to magnetic fusion 4-79825  
 RF test facility as multipurpose development tool 4-111935  
 secondary electron multipliers, T adsorption and desorption, fusion reactor appl. 4-59413  
 secondary emission electron gun, appl. to gas lasers and plasma chem. reactor 4-90689  
 small fusion reactor concepts, economy of scale 4-111829  
 sustainable energy system, nuclear technology, conf., Laxenburg, Austria (May, 1981) 4-58577  
 synergistic nuclear energy options, spectrum of choices 4-59429  
 TASKA-M, an optimized tandem mirror device for fusion technology tests 4-111952  
 technology status, Tokamak testing devices, overview (Japanese) 4-111763  
 TEXTOR, data processing and acquisition system (German) 4-102400  
 TEXTOR nuclear fusion project, improved performance (Japanese) 4-113201  
 TFTR, laser beam diagnostic system, mech. design 4-111954  
 TFTR, TF and PF coils, electrical test, test results eval. 4-111908  
 TFTR MM-wave measurements of line integrated density and electron temp. 4-75208  
 TFTR movable limiter instrumentation and controls 4-111953  
 TFTR neutral beam lines, mech. installation 4-111950  
 TFTR vacuum system operational experience and performance 4-111927  
 thermonuclear laser-heated plasma, ionic temp., direct meas. by neutrons 4-65134  
 thermonuclear reactors, Tokamak type, research and development problems 4-107011  
 thermonuclear synthesis expts., target position monitoring using TV systems 4-102393  
 TMX-U, neutral beam test stand for quality assurance 4-111934

## fusion reactors continued

- TMX-U vacuum system configuration and operating parameters 4-111923  
 Tokamak fusion expt., soft X-ray and VUV spectroscopic diagnostics 4-87928  
 tokamak magnetics, effects of aspect ratio 4-111873  
 vacuum systems for lithium coolant system 4-111910  
 Wendelstein VII-AS, modular stellarator with non-planar coils, supercond. coil description 4-86967  
 X-ray diagnostic instruments for TFTR fusion reactor 4-111948  
 H arc discharge with bulk cathodes 4-111870  
 T implanted in C, foil prep. and analysis w.r.t. to fusion device safety 4-91100

## fuzzy set theory

- energy exchange models, fuzzy identification 4-107976

## g-factor

- see also gyromagnetic ratio; Zeeman effect  
 acetone cation,  $\gamma$ -irrad.,  $^{13}\text{C}$  ESR and ENDOR investig. 4-69114  
 antiferromagnetic XY chain with impurities, local magnetisation, Green's function calc. 4-98846  
 atomic systems, hyperfine interactions of excited nuclei, review, book contrib. 4-68950  
 axial-vector coupling const., model dependence, g-factor sensitivity 4-68621  
 chalcogeno triphenylarsoranyl radicals, matrix isolated, ESR obs. 4-91290  
 conference on nuclear physics at large tandem accelerators, Padova, Italy (March 1983) 4-86108  
 diamagnetic crystal with paramag. ions, nuclear relax. rates 4-65789  
 dipole moment operator, renormalized, in 2p-1f shell, effective operator anal. 4-59149  
 dodecamethylferrocene, paramag., electronic and mag. props., Mossbauer meas. and MO calcs. 4-80845  
 DPPH free radical, EPR, local demagnetisation field meas. for FMR and FMAR of cubic metals 4-76257  
 ENDOR and EPR, g-tensors and A-tensors, anisotropic and non-coincident, least squares fitting 4-61607  
 ferric complexes, quantum mixed-spin, EPR param. 4-92951  
 fluorophosphate and phosphate glasses,  $\gamma$ -ray irradi., colour centres, EPR studies 4-103747  
 graphite-MnCl<sub>2</sub> intercalation cpds., first and second stage, mag. props. 4-109058  
 heavy and light holes, dynamical features on principal trajectories in crossed fields 4-113851  
 4-hydroxy-2,2,6,6-tetramethylpiperidine-1-oxyl, (TANOL), nitroxide radical, ESR 4-71182  
 linear chain compounds, moving CDW, Josephson-type oscillations 4-92644  
 magnesium acetate tetrahydrate:  $\text{Mn}^{2+}$ , EPR, spin Hamiltonian parameters 4-114156  
 manganese(II) protoporphyrin IX myoglobin, powder single cryst. EPR at various microwave freqs. 4-89503  
 neptunium tetrakisethylborohydride, diluted in Zr cpd., distortion effect on EPR 4-88719  
 nickel acetate tetrahydrate:  $\text{Mn}^{2+}$ , EPR, spin Hamiltonian parameters 4-114156  
 paramagnet, polycrystalline ENDOR patterns, g and hyperfine tensors of arbitrary symm. and relative orientation 4-98979  
 perovskite struct. crystals, spin-orbit interaction in  $\text{ns}^1$  clusters 4-61349  
 poly(3,4-dimethylthiophene): sulphur trioxide trifluoromethyl ions, electrochemically generated, EPR, g-factor 4-98946  
 poly(3-methylthiophene): sulphur trioxide trifluoromethyl ions, electrochemically generated, EPR, g-factor 4-98946  
 radical pair mechanism electron spin polarisation, CIDEP 4-87142  
 semiquinone cations, g values,  $\pi$  electron spin density distrib. 4-69116  
 spin glasses, macroscopic dynamical theory above  $T_g$  4-109028  
 (TMTSF)<sub>2</sub>ClO<sub>4</sub> single cryst., ESR g-factors, rel. to mol. orbital calc. 4-76236  
 (TMTSF)<sub>2</sub><sup>+</sup> cations in solns., ESR g-factors, rel. to mol. orbital calc. 4-76236  
 Z=54-78, g-factors and collective M1 transitions in neutron-proton IBA 4-90953  
 zinc acetate dihydrate:  $\text{Mn}^{2+}$ , EPR, spin Hamiltonian parameters 4-114156  
 $\mu$ , g-factor by cavity resonance theory 4-59081  
 $\tau$ -equiv( $\mu\text{B}^2/h\nu$ ), g-value test, radiation zeros 4-86707  
 Al<sub>2</sub>O<sub>3</sub>:Cr, photoacoustically detected EPR (Korean) 4-114155  
 Bi<sub>2</sub>Ti<sub>2</sub>O<sub>7</sub> ceramics, grain orientation, ESR and thermal expansion studies 4-104482  
 C<sub>60</sub><sup>+</sup> cation radicals, matrix isolated, EPR and ab initio investig. 4-74273  
 (CaF<sub>2</sub>)<sub>1-x</sub>(ErF<sub>3</sub>)<sub>x</sub>, solid soln., superstructure, ODMR and MCD study 4-75401  
 CaO spin triplet, g and D values determ. in case of misalignment 4-98508  
<sup>48</sup>Ca, M1 strength distrib., shell model study 4-59201  
 Cd, muon Knight shift, spin rot. meas. 4-65916  
 Ca<sub>2</sub>-Mn<sub>2</sub>Se<sub>2</sub>, far-IR obs. of electric dipole spin resonance 4-92978  
<sup>134</sup>Ce level structure study using  $\gamma$  and  $e^-$  spectroscopic methods 4-59127  
 Co-Ag-Pd, transient fields, g-factor, gyromagnetic ratios 4-113914  
 Cr complex, of tris(acetylacetonato), lowest doublet excited states, optical Zeeman spectra 4-66061  
<sup>57</sup>Cr, M1 strength distrib., shell model study 4-59201  
 Cu (II) complexes, correl. of EPR parameters with thermodynamic stability 4-98937  
 (Cu<sub>2</sub>(diethylenetriamine)<sub>2</sub>Cl<sub>2</sub>)(ClO<sub>4</sub>)<sub>2</sub>, cryst. and mol. struct. 4-75431  
 DyAg, EPR at far IR wavelengths 4-76249  
<sup>151</sup>Dy, A=153-156, spin precession of unresolved high-spin states 4-111494  
<sup>152</sup>Dy, s-band antialignment and low-spin struct., g-factors, cranked HFB calc. 4-111493  
<sup>158</sup>Dy yrast states g-factors, transient field technique meas. 4-86772  
<sup>159</sup>Er, A=154,155, high spin state g-factors, 13/2<sup>+</sup> neutron quasispin state 4-95901  
<sup>157</sup>Er, 197 keV  $\gamma$  state, g factor measurement from hyperfine frequencies 4-96712  
 Fe complex, halobis(diethyldiselenocarbamate)iron(III), mag. props. 4-76124  
 Fe-Ag-Pd, transient fields, g-factor, gyromagnetic ratios 4-113914

- factor continued  
 Fe-Ni-P-B-(Si) metallic glasses, magnetoelastic effects in ferromag. resonance 4-61581  
 Fe-Si, saturation magnetisation, mag. anisotropy, g-factor determ., FMR, ferromagnetic antiferromagnetic obs. 4-76258  
 (Fe<sub>0.82</sub>Co<sub>0.18</sub>)<sub>99</sub>La<sub>0.05</sub>Ru<sub>0.05</sub> amorphous metal alloys, ferromag. reson. and g-factor 4-71188  
 Fe<sub>40</sub>Ni<sub>40</sub>B<sub>20</sub> amorphous alloy, ferromag. resonance and antiresonance studies 4-76256  
<sup>54</sup>Fe, M1 strength distrib., shell model study 4-59201  
<sup>215</sup>Fr, in-beam  $\alpha$ , e and  $\gamma$ -spectroscopy 4-68647  
 GaAs, shallow acceptors, ground state calc., allowing for valence band corrugations 4-108817  
 GdFe<sub>2</sub>H<sub>3</sub> films, ferromag. resonance and mag. props. 4-61594  
 Ge, shallow acceptors, ground state calc., allowing for valence band corrugations 4-108817  
 Gemuonium, anomalous, electronic g-factor anisotropy 4-65927  
 Ge-S glasses, narrow Lorentzian ESR signals 4-65858  
 Hg, A=189-198, two and three quasiparticle states in IBM 4-82981  
 InP, electron irradi., antisite defects, EPR study 4-80816  
 Ir, A=191, 193, nuclear mag. dipole moments, direct meas. using atom beam mag. resonance 4-73824  
 KBr-KI, Ag atoms behaviour (Russian) 4-76245  
 Li in inert gas matrices, mag. circular dichroism, study of <sup>2</sup>S-<sup>3</sup>P transition 4-59670  
 Li<sub>2</sub> clusters, matrix isolated, g-value, HF coupling, EPR spectra 4-74266  
 LiF:Ni<sup>2+</sup>, Ni<sup>2+</sup>-F<sup>-</sup> distance for square planar and linear Ni<sup>2+</sup>-centres from isotropic superhyperfine const. 4-98581  
 LiNbO<sub>3</sub>:Cu<sup>2+</sup>, EPR and optical absorption spectra, Jahn-Teller effects 4-71166  
 MgO:Co<sup>2+</sup>, g value, Jahn-Teller effect 4-88492  
<sup>24</sup>Mg g-factors, transient field technique meas. 4-86772  
 MnCl<sub>2</sub>·4H<sub>2</sub>O, photoacoustically detected EPR (Korean) 4-114155  
 MnI<sub>2</sub>:Cu, pseudo-Zeeman splitting of excited states 4-104579  
 MnSO<sub>4</sub>·4H<sub>2</sub>O, photoacoustically detected EPR (Korean) 4-114155  
 Mo, hyperfine struct., RF, at beam mag. reson. and laser spectroscopic investig. 4-64410  
 MoO<sub>3</sub>, impurities, defect form. and charge compensation, EPR studies 4-80054  
<sup>95</sup>Mo, gyromagnetic ratios of 3/2<sup>+</sup> vibrational states 4-82988  
 NH<sub>4</sub>I:Cu<sup>2+</sup>, anomalous positive g-shift 4-92952  
 NaF:Ni<sup>2+</sup>, Ni<sup>2+</sup>-F<sup>-</sup> distance for square planar and linear Ni<sup>2+</sup>-centres from isotropic superhyperfine const. 4-98581  
 Na<sub>2</sub>Mo<sub>2</sub>O<sub>7</sub>, impurities, defect form. and charge compensation, EPR studies 4-80054  
 Na<sub>2</sub>O-SiO<sub>2</sub> glass, ferrite precip., ESR and Mossbauer obs. 4-99386  
 Na<sub>2</sub>UO<sub>2</sub>, anomalies of ESR and mag. susceptibility 4-92958  
<sup>20</sup>Ne g-factors, transient field technique meas. 4-86772  
<sup>22</sup>Ne, transient field g-factor meas. of first 4<sup>+</sup> state 4-68622  
 Ni (III) complex, dichloro bis-o-phenylene bis-dimethyl arsino nickelate (III) chloride, exchange interaction, EPR 4-71164  
<sup>16</sup>O, 6.13 MeV 3<sup>+</sup> state, g factor measurement from hyperfine frequencies 4-96712  
<sup>16</sup>Os A=188, 190, 192, gyromagnetic ratios, B(E2) rates in IBA models 4-68649  
<sup>195</sup>Pt, <sup>3</sup>D<sub>3/2</sub> states, magnetic dipole hyperfine interaction 4-102622  
 RbIn(MoO<sub>4</sub>)<sub>2</sub>:Cr, ferroelastic, structural phase transitions, EPR study 4-70372  
 Rh complexes, tetrakis(triisopropylphosphite)rhodium, zero valent, EPR at X- and Q-band freqs. 4-98944  
<sup>101</sup>Ru, gyromagnetic ratios of 3/2<sup>+</sup> vibrational states 4-82988  
 Si I, meas. of 3<sup>3</sup>P<sub>0</sub>-3<sup>3</sup>P<sub>1</sub> fine-struct. interval and g<sub>J</sub>-factor by laser mag. reson. 4-85866  
 Si, magnetic energy states of shallow acceptors, spin depend. luminesc. study 4-104655  
 Si: muonium, anomalous, electronic g-factor anisotropy 4-65927  
 Si:Se<sup>2+</sup>, ESR study 4-109071  
 Si(SiO<sub>2</sub>)<sub>2</sub> interface, As<sup>+</sup> implanted, defects, ESR study 4-61591  
 Sr(NO<sub>3</sub>)<sub>2</sub>, X-irradiated, colour centres, ESR study 4-61589  
 TiS<sub>2</sub>, intercalation cpd. with Mn, chemical vapor growth and EPR studies 4-66201  
<sup>50</sup>Ti, M1 strength distrib., shell model study 4-59201  
 TmVO<sub>4</sub> EPR using optically pumped far IR laser 4-76250  
 V<sub>2</sub>O<sub>5</sub>-Sb<sub>2</sub>O<sub>3</sub>, nonstoichiometric rutile-type phase, ESR and X-ray diff. studies 4-71163  
<sup>146</sup>Xe, A=122-130, positive parity states, extended IBA calc. 4-102161  
 YbF<sub>3</sub> (n=6,8), mol. hyperfine interactions, Dirac scatt. wave calcs. 4-68982  
<sup>157</sup>Yb, high spin state g-factors, 13/2<sup>+</sup> neutron quasiparticle state 4-95901  
 Zn, muon-Knight shift, spin rot. meas. 4-65916  
 ZnS:Ni<sup>2+</sup>, ESR, optical absorption and luminescence studies 4-92955  
 ZrSiO<sub>4</sub>:Pr<sup>4+</sup>, ESR, hyperfine interactions and g-values 4-71175

## gadolinium

see also nuclei with .....

- 5d to 4f intensity ratio in inverse photoemission 4-109269  
 atom, L-shell X-ray prod. cross sections for protons of energy 1-2 MeV 4-96656  
 d-f exchange reson. and j polaron 4-75874  
 electric field gradient at Gd nucleus, integral perturbed angular correlation studies 4-98991  
 erbium hexa antipyrine tri-iodide:Gd<sup>3+</sup>, soft mode dynamics, phase transition, EPR 4-109068  
 films, hydridisation and catalysis 4-71984  
 impurities in fluoride deposits study by EPR and neutron activation anal. 4-80815  
 lanthanum ethyl sulphate:Gd<sup>3+</sup>, zero field splitting of Gd<sup>3+</sup> 4-96713  
 magnetostriction, temp. depend. 4-76220  
 paramagnetic, acoustic relax. time, mag. field effects 4-113548  
 positron lifetime near ferromag. transition temp. 4-93127  
 PWR, axial Gd burnable poison optimisation using conjugate gradients 4-106863  
 s-p impurities, hyperfine field systematics 4-70758  
 thin films, struct., effect of ion irradi. 4-70240  
 total and photoelectric cross sections 4-91244  
 ytterbium hexa antipyrine tri-iodide:Gd<sup>3+</sup>, soft mode dynamics, phase transition, EPR 4-109068  
 $\alpha$ -Al<sub>2</sub>O<sub>3</sub>:Gd, crystals, radiative and thermochem. effects 4-76491  
 BaF<sub>2</sub>:GdF<sub>3</sub>-ZrF<sub>4</sub> optical fibre, preparation 4-103045  
 BaFCl:Gd flux grown crystal., thermoluminescence studies 4-66081

## gadolinium continued

- CdF<sub>2</sub>:Gd<sup>3+</sup>, EPR, anomalous high elec. field effect 4-71173  
 Cd<sub>2</sub>Nb<sub>2</sub>O<sub>7</sub>:Gd, narrow phase transitions, elec. field and impurity effects 4-71316  
 Cd<sub>2</sub>Nb<sub>2</sub>O<sub>7</sub>:Gd<sup>3+</sup>, ferroelec. transitions, EPR spectra 4-98945  
 EuO:Gd, longitudinal Néron-Ettingshausen effect, temp. and mag. field dependences 4-65697  
 Gd<sup>3+</sup>-semiquinones interaction in aq. solns. relax. and complex formation 4-99777  
 Gd<sub>2</sub>(MoO<sub>4</sub>)<sub>3</sub>, lattice parameters, thermal expansion, DSC and X-ray investig. 4-108315  
 Gd, heavy charged particle impact, K-shell ions. 4-69195  
<sup>155</sup>Gd/<sup>157</sup>Gd, neutron fluence determ. for isotopic variation meas. 4-91186  
 InP:Gd epitaxial films, doping effects on low-temp. edge photoluminescence 4-85028  
 NaCl:Gd, microhardness, influence of Gd impurity 4-103868  
 Pb<sub>2</sub>Ge<sub>2</sub>O<sub>7</sub>:Gd<sup>3+</sup>, superhyperfine interaction, ESR and ENDOR studies 4-114159  
 PrAlO<sub>3</sub>:Gd<sup>3+</sup>, order parameter behaviour, EPR study 4-70076  
 RbCaF<sub>2</sub>:Gd, O, first order phase transition, EPR of Gd<sup>3+</sup>+O<sup>2-</sup> centre 4-84378  
 RbCaF<sub>2</sub>:Gd<sup>3+</sup>+O<sup>2-</sup> local fluctuations above and below T<sub>c</sub>, EPR study 4-76247  
 Sc-Gd, spin glasses with uniaxial anisotropy 4-71099  
 Si:Gd-SiO<sub>2</sub> interface, negative elec. effects produced by Gd impurities 4-108940  
 SrF<sub>2</sub>:Gd<sup>3+</sup>, phosphors, thermostimulable, center-center transitions, luminesc. 4-80996  
 ThBr<sub>4</sub>:Gd, incommensurate phase, Gd<sup>3+</sup> EPR study 4-76246  
 ThBr<sub>4</sub>:Gd<sup>3+</sup>, incommensurate, phase fluctuations near transition temp., phase pinning, EPR meas. 4-92956  
 ThS<sub>2</sub>:Gd<sup>3+</sup>, cryst. struct., single cryst. diffractometric obs. 4-108316  
 TlCdF<sub>2</sub>:Gd<sup>3+</sup>+O<sup>2-</sup>, critical phenomena above and below T<sub>c</sub>, EPR studies 4-65854  
 ZnO:Gd, thermoluminesc. under UV,  $\beta$ - and  $\gamma$ -ray irradiations 4-93119

## gadolinium alloys

- Ag-Gd, dil., impurity-induced muon depolarisation, mag. field depend. 4-71228  
 Ag-Gd, solid solubility, metastable extension (Chinese) 4-61918  
 Au-Gd, dil., impurity-induced muon depolarisation, mag. field depend. 4-71228  
 Co-Co<sub>2</sub>Gd<sub>3</sub>, off-eutectic, growth by floating zone techniques 4-99304  
 Co-Gd amorphous films, tunnelling, zero bias anomalies 4-76049  
 Gd-Co amorphous films, spontaneous Hall effect in vicinity of the composition composition 4-75929  
 Gd-Fe amorphous alloy films, crystallisation and ferromag. reson. behaviour 4-71189  
 Gd-Fe amorphous films, vacuum deposited, Kerr hysteresis meas. 4-66014  
 Gd-Fe composition-graded thin films, mag. meas. device appl. 4-88710  
 Gd-Fe evaporated films, crystn. behaviour 4-80445  
 Gd-Fe-Co amorphous film, struct. and mag. props. 4-80434  
 Gd-Fe-Ni amorphous film, struct. and mag. props. 4-80434  
 Gd-Ni-Co amorphous film, struct. and mag. props. 4-80434  
 Gd-Pd, effect of H<sub>2</sub> absorpt. on mag. and cryst. props. 4-104412  
 Gd-Sn phase diagram, intermetallic cpds. and peritectic and eutectic reactions (Chinese) 4-114476  
 Gd-Tb, magnetostriction, temp. depend. 4-76220  
 Gd-Tb alloy crystal magnetostriction meas., using 13 T superconducting solenoid, microcomputer-controlled system 4-58876  
 Gd-Tb alloys, magnetisation, temp. depend. 4-84815  
 Gd-Y-Lu single crystal., double ferromagnetism, mag., elec. and thermal studies 4-84817  
 Gd<sub>1-x</sub>La<sub>x</sub>Al<sub>2</sub>, loss of ferromagnetism 4-98885  
 Gd<sub>1-x</sub>Tb<sub>x</sub>Al<sub>2</sub>, loss of ferromagnetism 4-98885  
 Gd<sub>1-x</sub>U<sub>x</sub>Al<sub>2</sub>, loss of ferromagnetism 4-98885  
 GdAl<sub>2</sub>, ferromag., magnetisation, NMR studies 4-80787  
 GdAl<sub>2</sub>,  $\mu$ SR spectroscopy 4-84894  
 Gd<sub>2</sub>AuAl<sub>1-x</sub>, pseudobinary cpd., mag. behaviour 4-76136  
 GdCo amorphous computered film, surface versus bulk magnetisation curves 4-71131  
 Gd<sub>2</sub>Co, crystn., cryst. struct. and mag. props. in microgravity 4-98915  
 GdCo<sub>2-x</sub>Al<sub>x</sub>, magnetoelastic interactions (Russian) 4-65845  
 Gd(Co<sub>0.9</sub>Ni<sub>0.1</sub>)<sub>2</sub>, paramagnetic reson. lineshape anal. 4-88714  
 GdCo<sub>2</sub>Si<sub>2</sub>, charge transfer, X-ray absorpt. spectra study 4-81037  
 GdCu<sub>2</sub>Ge<sub>2</sub>, charge transfer, X-ray absorpt. spectra study 4-81037  
 GdCu<sub>2</sub>Si<sub>2</sub>, charge transfer, X-ray absorpt. spectra study 4-81037  
 GdCu<sub>1-x</sub>Zn<sub>x</sub>Si<sub>2</sub>, cryst. struct., mag. and elec. props. 4-92145  
 Gd<sub>1-x</sub>Dy<sub>x</sub>Al<sub>2</sub>, NMR spectra, dipole field rot. 4-109084  
 GdFe film, oxidation by overlaid SiO<sub>2</sub> film, Kerr enhancement 4-84949  
 GdFe/TbFe amorphous double-layer films, magneto-optical characs. 4-61665  
 GdFeGe<sub>2</sub>, charge transfer, X-ray absorpt. spectra study 4-81037  
 GdGe<sub>6</sub>, constitution diagram, thermodynamic properties, EMF obs. 4-89024  
 Gd<sub>2</sub>In, magnetic and electrical props., metamagnetic-ferromagnetic transition, magnetic struct. 4-114138  
 GdInSn<sub>3-x</sub>, elec. resist. below Neel temp. 4-75924  
 GdMn<sub>2</sub>Ge<sub>2</sub>, charge transfer, X-ray absorpt. spectra study 4-81037  
 GdNi<sub>2</sub>, paramagnetic reson. lineshape anal. 4-88714  
 Gd<sub>2</sub>Ni<sub>3</sub>Al<sub>15</sub>, band struct. and ferromag. moments, APW calc. 4-80487  
 Gd<sub>2</sub>Rh<sub>2</sub>, mag. props. meas. 4-61521  
 Gd<sub>2</sub>Si<sub>3</sub>, low-temp. phase transitions and mag. ordering 4-71071  
 (Gd<sub>0.2</sub>Tb<sub>0.8</sub>)<sub>3</sub>Co, crystn., cryst. struct. and mag. props. in microgravity 4-98915  
 GdTbFe amorphous sputtered films, mag. props. 4-65843  
 Gd<sub>2</sub>Y<sub>1-x</sub>Co<sub>2</sub> cluster glasses, mag. props. and magnetovolume effects 4-76207  
 GdZn, ferromagnetically saturated single crystal, high-field NMR Knight shift, magnetisation studies 4-114176  
 Tb<sub>2</sub>-Gd<sub>3</sub>, Hall effect and elec. resist. near Curie point 4-61361  
 Ti-Gd, rapidly solidified dispersion strengthened, struct. and props. 4-114561  
 Y-Gd, spin glasses with uniaxial anisotropy 4-71099  
 (Y<sub>1-x</sub>Gd<sub>x</sub>)Ni<sub>3</sub>, mag. props. meas. 4-80785

## gadolinium compounds

see also gadolinium alloys

- (BiPrGdYb)<sub>3</sub>(FeAl)<sub>2</sub>O<sub>12</sub> garnet single crystal, films for ring laser gyroscopes (Chinese) 4-60123

## gadolinium compounds continued

- Ce<sub>1-x</sub>Gd<sub>x</sub>O<sub>2-x</sub>, vacancy binding energy, polarisation contrib. 4-88165  
 CeO<sub>2</sub>-Gd<sub>2</sub>O<sub>3</sub> solid solutions, elec. cond., temp. depend., 400-1200°C 4-61142  
 EuGd<sub>2</sub>S<sub>4</sub>, band gap width, rel. to short-range environment of S atom 4-80493  
 (Gd<sub>2</sub>Sc)<sub>2</sub>Ga<sub>2</sub>O<sub>12</sub>:Nd<sup>3+</sup>, Cr<sup>3+</sup> laser operating in pulse-periodic regime, output characs. 4-74521  
 Gd complexes, pyridoxine-Gd(III) in aq. soln., PMR study of struct. 4-114179  
 Gd-Ga garnet, absorpt. coeff. and refractive index determ. 4-80895  
 Gd-Ni-Si, X-ray phase anal. of compounds formed 4-114494  
 GdAl<sub>3</sub>(BO<sub>3</sub>)<sub>4</sub>, polymorphic relationships with other rare earth borates 4-84279  
 GdB<sub>2</sub>, antiferromagnet, elec. resist. and thermoelec. power studies 4-113982  
 GdB<sub>2</sub>, low temp. resistivity and mag. props. 4-108859  
 Gd<sub>0.5</sub>Ca<sub>0.5</sub>CrO<sub>3</sub>, ionic cond. and thermal expansion 4-84461  
 GdCl<sub>3</sub>Pr<sup>3+</sup>, crystal field levels, coord. geometry depend. 4-70755  
 Gd<sub>2</sub>CoO<sub>4</sub>, Gd<sub>2</sub>CoO<sub>3</sub>, synthesis and high-temperature study (French) 4-85095  
 GdCrO<sub>3</sub>, NQR and spin-flip transition 4-104509  
 (Gd<sub>1-x</sub>Er<sub>x</sub>)Al<sub>2</sub>O<sub>3</sub> garnet,  $\lambda$   $\mu$ m stimulated emission, concentrational tuning 4-76498  
 GdFe<sub>2</sub>H<sub>3</sub> films, ferromag. resonance and mag. props. 4-61594  
 Gd<sub>2</sub>Ga<sub>2</sub>O<sub>12</sub>, fluorescence radiation due to X-ray standing waves 4-71437  
 Gd<sub>2</sub>Ga<sub>2</sub>O<sub>12</sub> garnet,  $\gamma$  and neutron irradiat., effect on optical props. 4-99135  
 Gd<sub>2</sub>Ga<sub>2</sub>O<sub>12</sub>, garnet single crystals, microhardness, brittle fracture 4-65337  
 Gd<sub>2</sub>Ga<sub>2</sub>O<sub>12</sub>, hypersonic wave attenuation 4-75620  
 Gd<sub>2</sub>Ga<sub>2</sub>O<sub>12</sub>:Nd,Cr, laser props., modified Czochralski growth (Chinese) 4-112441  
 Gd<sub>2</sub>Ga<sub>2</sub>O<sub>12</sub>:Pr(Bi) garnet epitaxial layers, site selectivity, dichroism studies 4-84533  
 Gd<sub>2</sub>Ga<sub>2</sub>SnO<sub>7</sub>, pyrochlore prep., cryst. struct., X-ray diff. 4-75400  
 GdMSi, M=first row transition metal, cryst. struct., mag. and elec. props. 4-70083  
 Gd<sub>2</sub>(MoO<sub>4</sub>)<sub>3</sub>, acoustic wave reflection from ferroelastic domain walls 4-98209  
 $\beta$ -Gd<sub>2</sub>(MoO<sub>4</sub>)<sub>3</sub>, domain walls, SAM and SPAM study 4-99064  
 Gd<sub>2</sub>(MoO<sub>4</sub>)<sub>3</sub>, ferroelectric-ferroelastic, acoustic emission and domain wall dynamics 4-84925  
 Gd<sub>2</sub>(MoO<sub>4</sub>)<sub>3</sub>, polydomain ferroelec., quadrupole fields 4-80882  
 GdNbO<sub>4</sub>, photochromic coloration enhancement by doping 4-61639  
 Gd<sub>2</sub>O<sub>3</sub> in UO<sub>2</sub> fuel, Gd determ. for safeguards 4-107002  
 Gd<sub>2</sub>O<sub>3</sub>-Ga<sub>2</sub>O<sub>3</sub>, binary phase diagram and melting 4-88264  
 GdP<sub>2</sub>O<sub>14</sub>, sp. ht. anomalies, 0.4 to 20K 4-92386  
 GdS, energy band struct., X-ray study 4-84565  
 Gd<sub>2</sub>Sc<sub>2</sub>Al<sub>2</sub>O<sub>12</sub>:Cr<sup>3+</sup>, tunable room temp. CW laser action 4-74518  
 GdTbO<sub>4</sub>:Tb<sup>3+</sup>, energy transfer phenomena, photoluminescence 4-109234  
 GdT<sub>2</sub>Li<sub>2</sub>O<sub>12</sub>, photoluminesc. and energy transfer in rare earth activated garnets (German) 4-76508  
 KGd(WO<sub>4</sub>):Nd<sup>3+</sup>, struct., morphological and optical characs. 4-69518  
 NaGdTlO<sub>4</sub>:Eu<sup>3+</sup>, nonradiative relax. by multiphonon emission 4-76507  
 RbGdF<sub>10</sub>:Eu<sup>3+</sup>, Eu<sup>3+</sup> fluorescence, Gd<sup>3+</sup> effects 4-104663  
 Sm<sub>1-x</sub>Gd<sub>x</sub>S solid soln. single crystals, phase transition during uniaxial compression, elec. cond. and colour change obs. 4-70375  
 Y<sub>1-x</sub>Gd<sub>x</sub>Fe<sub>2</sub>O<sub>4</sub>, noncrystalline garnet films, electron transport and thermopower 4-108958  
 Y<sub>1-x</sub>Gd<sub>x</sub>H<sub>1.98</sub>, diffusion constants and pulsed NMR 4-80840  
 (Y<sub>1-x</sub>Gd<sub>x</sub>)<sub>2</sub>O<sub>3</sub>:Sb luminesc. study 4-81013  
 (YGdYbBi)<sub>2</sub>(FeAl)<sub>2</sub>O<sub>12</sub> films, magnetostrictive vibr. study 4-98927

## gain (amplification) see amplification

## gain measurement

- linear prediction vocoder, gain errors 4-81717  
 GaAlAs diode laser, picosecond gain meas. 4-107638

## gait analysis see biomechanics

## galactic cosmic rays

- abundances of unstable cosmic-ray isotopes 4-94485  
 acceleration and propagation, HEAO-3 meas. implications 4-94347  
 acceleration and transport in stellar winds with terminal shocks 4-100897  
 acceleration by diffusive shocks and cut-off energy 4-94525  
 acceleration by supernova remnant shock 4-73049  
 acceleration in interplanetary medium, associated solar wind disturbances 4-94378  
 active galaxies nuclei,  $\gamma$ -ray and relativistic particles prod. and spectra anal. 4-100891  
 anisotropies during solar cycle 20 4-94437  
 anisotropy in high velocity solar wind fluxes 4-100976  
 anisotropy of cosmic rays of superhigh energies 4-94515  
 anomalous low-energy component, origin 4-94361  
 antiprotons in primary cosmic rays, characs. (French) 4-105817  
 baryon symmetric cosmology testing on a supergalactic scale 4-100920  
 black holes, mass accretion and plasma processes,  $\gamma$ -ray emission model, 3C 273 appl. 4-101536  
 CG 195+04,  $\gamma$ -ray line emission search 4-101521  
 2CG 195+4, gamma ray flux periodicity and energy spectra, EAS obs. 4-101527  
 CG 195+4, gamma-ray var., obs. of Cherenkov radiation due to air showers 4-101528  
 composition of low-energy cosmic rays from stellar X-ray sources 4-101512  
 Crab Nebula, search for  $\gamma$ -ray lines 4-101462  
 cross section uncertainties effect on source composition derivations 4-94344  
 Cygnus X-3,  $\gamma$ -ray emission, period from EAS data anal. 4-101531  
 Cygnus X-3,  $\gamma$ -ray emission var., small air showers arrival directions obs. 4-101529  
 Cygnus X-3, gamma ray var., Cherenkov radiation due to air showers 4-101528  
 daily variation harmonics of galactic cosmic rays 4-100991  
 Davis' experiment, galactic cosmic rays, solar neutrino flux 4-101096  
 density distribution in heliosphere, quasistationary asymmetry 4-67573  
 diffuse  $\gamma$ -ray background origin 4-100891  
 diffuse  $\gamma$ -ray emission, bremsstrahlung component spectra and cosmic ray electrons energy spectra 4-100889  
 diffuse galactic gamma-ray emission and cosmic ray-interstellar matter interactions 4-100890  
 diffusive shock acceleration of energetic electrons subject to synchrotron losses 4-115661

## galactic cosmic rays continued

- diurnal effect on galactic ray intensity, from stratospheric meas. 4-100985  
 electron acceleration in supernova remnants, evolution as radio sources 4-63246  
 electron density near galactic centre from gamma ray emission 4-63300  
 electron energy spectrum from radio loop III 4-94516  
 electron-photon interactions, EM cascade showers initiation 4-101537  
 electron-positron component and lepton prod. in black hole accretion discs 4-82500  
 electrons, distrib. and diffusion,  $\gamma$ -ray anal. 4-101487  
 electrons, energy spectra characs. from bremsstrahlung component of gamma ray emission anal. 4-90042  
 electrons, energy spectrum meas. rel. to cosmic ray confinement 4-94460  
 electrons, spectral index variations in the galactic radio continuum emission 4-94335  
 electrons distribution in face-on spiral galaxies 4-110749  
 electrons producing diffuse galactic  $\gamma$ -ray bremsstrahlung component energy spectra 4-100889  
 energetic hysteresis of galactic cosmic ray intensity during solar mag. field inversion 4-94406  
 energy spectra from HEAO-3 meas. 4-94469  
 extragalactic cosmic rays, sources characs. and intergalactic propag. 4-100926  
 flux constancy from <sup>22</sup>Na and <sup>26</sup>Al lunar sample meas. 4-100917  
 flux variation deduced from <sup>22</sup>Na-<sup>26</sup>Al data of lunar samples 4-67577  
 Forbush decreases, technique to study anisotropy 4-94439  
 Forbush decreases, variations in IMF and solar wind velocity 4-94456  
 galactic anticenter direction  $\gamma$ -ray sources, obs. 4-101524  
 galactic centre, 2-20 MeV gamma-ray map and energy distrib. 4-101523  
 galactic plane cosmic ray event excess 4-85845  
 galaxy clusters, Coma-type radio halos form., role of galactic cosmic ray electrons 4-90248  
 Galaxy corona supported by cosmic rays, model 4-82550  
 gamma ray burst sources, distance model 4-101518  
 gamma ray burst sources observed by Hinotori satellite, energy spectra, time history and origin 4-101513  
 gamma ray imaging via detect. of atm. Cherenkov radiation due to air showers 4-101176  
 gamma ray sources, excess fluxes search, EAS data anal. 4-101533  
 gamma-ray burst of 1978 March 25, absorpt. feature characs. 4-101522  
 gamma-ray bursters, assoc. X-ray emission, neutron star model 4-101517  
 gamma-ray bursts, high time resolution  $\gamma$ -ray spectral obs. with Solar Maximum Mission 4-101514  
 gamma-ray diffuse component meas., by high-altitude balloon 4-100888  
 gamma-ray discrete sources (E>10<sup>15</sup> eV), search in EAS data 4-101530  
 gamma-ray emission from interstellar clouds 4-100892  
 gamma-ray sources, absorpt. features, effects of emitted photons-interstellar photon interactions 4-101535  
 gamma-ray sources at E=10<sup>15</sup> eV, search, EAS data anal. 4-101534  
 gamma-ray sources emission, Cherenkov radiation obs. 4-101532  
 gamma-ray-photon interactions, EM cascade showers initiation 4-101537  
 gamma-rays from interstellar H<sub>2</sub> and H I, energy spectra anal. 4-101486  
 global modulation in interplanetary space 4-94430  
 global radio continuum of nearby galaxies 4-94334  
 gradient and modulation effects obs. by Voyager and Pioneer spacecraft 4-94415  
 heliolongitudinal asymmetry of solar activity and cosmic ray distribution 4-101003  
 heliosphere, galactic cosmic ray propag., electric field effects, modulation 4-94400  
 heliosphere, long term cosmic ray modulation, 1-25 AU, Pioneer, Voyager, ISEE-3 and Helios data 4-94421  
 hypothetical particles, decay, UV and X-ray emission 4-101154  
 inner heliosphere, galactic cosmic ray modulation by solar flare disturbances 4-94419  
 intensity depression, effect of solar wind disturbances 4-94451  
 intensity transient decreases, solar wind stream interfaces 4-94449  
 intensity variation, effect of equatorial coronal holes 4-94450  
 intensity variations, relation to solar mag. field 4-94370  
 interactions with comet nuclei and formaldehyde form. 4-94682  
 interactions with galactic matter and photons, diffuse  $\gamma$ -ray background origin 4-77975  
 intergalactic photons, zero-point field accel. and energy spectra 4-100887  
 interplanetary propagation, effect of convection on charged particle transport in random mag. fields 4-94569  
 interplanetary propagation of galactic cosmic rays 4-72838  
 interstellar cloud accretion and evaporation, implication for cosmic ray and  $\gamma$ -ray emission 4-100892  
 interstellar clouds acceleration, role of cosmic rays 4-110727  
 interstellar H I interactions, diffuse  $\gamma$ -ray emission 4-100890  
 interstellar interactions and  $\gamma$ -ray emission in outer Galaxy 4-86049  
 interstellar interactions and galactic X-ray emissivity 4-100886  
 interstellar interactions and gamma ray emission 4-101525  
 interstellar interactions and nucleosynthesis 4-63293  
 interstellar photons-gamma-ray source photon interactions, absorpt. features origin 4-101535  
 ionization effects shaping the elemental cosmic-ray source composition 4-100914  
 LMC, cosmic rays origin, models and expected radio and  $\gamma$ -ray emission 4-101485  
 localized nature of the galactic cosmic rays 4-94340  
 massive black holes, 511 keV annihilation line, origin due to tidally disrupting stars 4-101405  
 massive stars winds as energy sources for locally accel. cosmic rays 4-94730  
 mean lifetime in dynamical halo model 4-94341  
 modulation, solar mag. field effects 4-94432  
 modulation by solar activity processes, shock wave steady-state model 4-94413  
 modulation by solar wind, subsonic streaming transition in nonlinear model 4-94404  
 modulation by solar wind in spherically symmetric nonstationary diffusive model 4-94402  
 modulation during 1970-4, anomalous phenomena due to coronal holes 4-94422  
 molecular clouds, gamma-ray line emission and cosmic ray interactions 4-101463  
 multiple supernova I galactic source of ultra high energy particles 4-94350  
 nuclei, age and source characs., isotopic comp. anal. 4-94357

**galactic cosmic rays continued**

- nuclei, comp. and nucleosynthesis 4-94356
- nuclei, mean masses of C, N, Ne, Mg, Si, S, Fe, HEAO-3 meas. 4-94482
- nuclei elemental composition from Be to Ni 4-94468
- nuclei propagation and accel., energy spectra anal. 4-94355
- OB association, upper mass limit, cosmic ray implication and cosmic abundances 4-101208
- OB associations, mechanical energy output, cosmic ray accel. at wind shocks 4-101447
- origin, composition and energy spectra 4-94354
- origin and acceleration characts. 4-94363
- origin in extragalactic sources, role of radioastronomy 4-105816
- outer Galaxy, electrons and nuclei distrib., H I maps and  $\gamma$ -ray distrib. 4-90237
- photino-dominated Universe, cosmic-ray antiprotons 4-105818
- photon damping in cosmic ray acceleration in active galactic nuclei 4-94349
- plerions, pulsar dominated evolution, mag. field, relativistic particles and luminosity 4-90201
- positrons and electrons, propag. and energy spectra anal. 4-94358
- power spectra variations, correlation with Sun's activity 4-94436
- primary cosmic rays, zonal modulation rel. to solar mag. field 4-94396
- production in quasars and active galactic nuclei, radiowave and  $\gamma$ -ray emission 4-100929
- propagation analysis and solar modulation, use of matrix methods 4-100927
- propagation and reson. diffusion 4-94362
- propagation in interplanetary medium, estimate of cosmic ray latit. gradient (1981-1982) 4-85849
- propagation in nested leaky box model 4-94343
- protons Cherenkov radiation and extrasolar planets IR detect. 4-77725
- PSR 0531+21, 1-20 MeV pulsed  $\gamma$ -ray emission anal. 4-101391
- PSR 0531+21,  $\gamma$ -ray flux and energy spectra, Cherenkov radiation obs. 4-101393
- PSR 0531+21, gamma ray emission, possible sporadicity, Cherenkov radiation anal. 4-101392
- PSR 0531+31 and 1937+214 (millisecond pulsar),  $\gamma$ -ray emission, Cherenkov radiation obs. 4-101394
- PSR 0532+31,  $\gamma$ -ray periodicity, EAS data anal. 4-101534
- PSR 0833-45, 1-20 MeV pulsed gamma-rays obs. 4-101390
- PSR 0833-45, possible transient  $\gamma$ -ray emission obs. 4-101395
- PSR 0833-45 and 0950+08,  $\gamma$ -ray emission, Cherenkov radiation anal. 4-101396
- pulsars,  $\gamma$ -ray luminosity anal. and distrib. in Galaxy 4-101526
- quasars,  $\gamma$ -ray and relativistic particles prod. and spectra anal. 4-100891
- radial gradients, Pioneer 10 meas. at 1 to 29 AU through solar maximum 4-94418
- radiosources, electron energy spectra produced by turbulent reson. accel. 4-94978
- radiosources, visible-IR spectra cutoff due to cosmic ray electrons energy spectra evolution 4-106073
- secondary galactic antiprotons, flux from propag. models and origin anal. 4-94359
- secondary/primary ratio and energy-dependent truncation of the path-length distribution 4-94346
- Seyfert galaxies nuclei, cosmic ray accel. and energy spectra, photons and neutrinos as probes 4-100925
- sidereal daily variation, seasonal variation due to heliomagnetosphere 4-101008
- solar modulation, long-term intensity vars. rel. to different indices of solar activity 4-110398
- solar modulation effects including interplanetary shocks and Forbush decrease 4-67566
- solar modulation of cosmic ray electrons (1978 to 1983) 4-85851
- solar modulation of intensity from anal. of tree ring  $^{14}\text{C}$  dating 4-94423
- solar modulation var. and terrestrial atm.  $^{14}\text{C}$  prod. 4-94424
- source abundance determ. effects of nucl. cross-section uncertainties 4-100928
- source of ultra-high energy cosmic rays in galactic centre (*Russian*) 4-85847
- spectra distribution in galactic diffusion model 4-94517
- star types for dominant cosmic ray injectors 4-100913
- statistical acceleration of electrons in the galactic halo 4-100911
- supernova remnants, radio emission and electrons accel. at various evolutionary stages 4-73025
- supernova remnants, radioemission evolution, role of relativistic electrons accel. by MHD turbulence 4-73026
- supernova remnants, radiosources, mag. field amplification and particle accel. (*Russian*) 4-67786
- ultra-heavy nuclei, particle identification using SSNTD 4-101070
- ultra-high energy cosmic rays, propag. and origin 4-94360
- variations in heliosphere from radioactivity meas. of meteorites 4-94369
- weak modulation a few million years ago 4-100916
- e.p., and He spectra 1965-79 as modulation theory tests 4-94407
- Mn isotopes, cosmic ray age determ. method 4-94487

**galactic nuclei**

- 0241+622, low-redshift quasar, spectrophotometry and image anal. of assoc. nebulosity 4-90253
- 2021+614, narrow-line radiogalaxy, dust content, core luminosity and visible spectra 4-86045
- accretion disk, viscous transonic flow around inner edge 4-115772
- active galactic nuclei, catapult model for narrow-line region in Seyferts and radio galaxies 4-101477
- active galactic nuclei, emission spectra due to accretion onto massive black holes 4-106063
- active galactic nuclei, observational props. and interpretation 4-63289
- active galactic nuclei, X-ray and gamma-ray prop. (*Polish*) 4-63340
- active galactic nuclei, X-ray spectral signatures of accreting black holes 4-72973
- active galaxies,  $\gamma$ -ray and relativistic particles prod. and spectra anal. 4-100891
- active galaxies, black hole accretion discs, emission contrib. to high energy background radiation 4-77985
- active galaxies, cosmic rays prod., radiowave and  $\gamma$ -ray emission 4-100929
- active galaxies, line continuum luminosity ratio 4-90226
- active galaxies, role of central massive black holes 4-106020
- active galaxies nuclei, gamma-ray emission characts. due to cosmic ray interactions 4-101537

**galactic nuclei continued**

- active nuclei,  $\gamma$ -ray data as test of black hole accretion models 4-101484
- active nuclei, evolution 4-106062
- active nuclei, radio jets rel. to mass outflow from newly-forming stars 4-67719
- black hole, numerical study of nonspherical accretion 4-63195
- black holes form. 4-106021
- Centaurus A (NGC 5128), high-resolution obs. of gamma-ray spectrum between 70 keV and 8 MeV 4-86031
- Circinus galaxy, infrared activity of galaxy containing luminous  $\text{H}_2\text{O}$  masers 4-94990
- classification for galaxies with active nuclei 4-73101
- conference on QSOs, at Padova; Italy (March 1983) 4-101568
- 3CR radio galaxies, X-ray survey of complete sample 4-63269
- Cygnus A, nucleus struct. and dust distrib. 4-82551
- dissipative dynamical evolution, influence of binary stars 4-63212
- dissipative dynamical evolution of stellar systems, cooling and heating of system by binary stars 4-63211
- elliptical galaxies, nucl. activity correl. with supernova occurrence 4-82548
- elliptical galaxies, survey of forbidden O II emission 4-77927
- emission line galaxies, extinction and use of 10  $\mu\text{m}$  dust emission features 4-86018
- galaxies with UV continuum, RATAN-600 obs. 4-94940
- Galaxy, 2-20 MeV gamma-ray map and energy distrib. 4-101523
- Galaxy, CO struct. with strong positional and kinematic gradients 4-63310
- Galaxy, OH large-scale survey 4-63311
- Galaxy, OH-IR stars distrib. and kinematics 4-63312
- Galaxy, radio, X-ray and IR characts. 4-94970
- H II regions in galaxies with emission lines 4-110721
- high-velocity emission and absorpt. line clouds, accel. mechanisms 4-110727
- IC 4553, peculiar galaxy, VLA-A obs. of OH megamaser 4-86036
- IC 5135, mini-Seyfert galaxy with starburst characts., UV spectral anal. 4-110734
- interacting galaxies, star form. rates from spectrophotometric obs. 4-77926
- interacting spirals, induced nuclear emission-line activity 4-90242
- Kazaryan 163, new Seyfert galaxy, spectrophotometric obs. and direct photography 4-94938
- BL Lacertae objects, continuum spectral energy distrib. of X-ray observed sample 4-82546
- BL Lacertae objects, nuclei X-ray emission, origin and anal. 4-77940
- BL Lacertae type objects, interpretation of optical spectrum 4-101469
- low-ionisation nuclear emission-line regions (LINERS), spectroscopic obs. rel. to abundances in galactic nuclei 4-67807
- M31, centre and 10 kpc annulus, continuum emission 4-77915
- M33, stellar population, UV obs. 4-115817
- M82, far IR forbidden O I and III emission 4-90241
- M82, luminous SNR candidates anal. 4-77911
- M87(NGC 4486), nucl. struct. 4-77914
- M87 (Virgo A), two-component star cluster models 4-115823
- Markarian 266, double Seyfert nucleus, UV spectra obs. and anal. 4-90239
- Markarian 348 (NGC 262), core dominated Seyfert, sub-arcsecond radiostruct. 4-94966
- Markaryan 141, Seyfert component of double system, multicolour surface photometry 4-106059
- Markaryan 201 (NGC 4194), spectroscopic evidence for star form. burst in nucleus 4-94936
- Markaryan galaxies, effects of nuclei on photometric parameters compared with normal spiral galaxies 4-94937
- MR 2251-178, nearby quasar, obs. of assoc. [O III] emission 4-101496
- NGC 1068, NGC 4151, Seyfert galaxies, obs. of IR H I recomb. line emission 4-86039
- NGC 1097, VLA obs. of optical jets and nucleus 4-63288
- NGC 1275, 20-year spectral evolution of radio nucleus (3C 84) 4-86029
- NGC 1275, nucleus radio and IR emission anal. 4-94963
- NGC 1510, centre condensations struct. and nature 4-63278
- NGC 1667 and 5135, mini-Seyfert galaxies, H I Lyman  $\alpha$  anal. 4-110734
- NGC 253 edge-on spiral galaxy, props. of central radio source 4-115814
- NGC 2782, starburst galaxy obs. at radio, IR, optical, UV and X-ray freqs. 4-110754
- NGC 3379, elliptical galaxy, evidence for central spike of light 4-94967
- NGC 3448, interacting galaxy, discovery of UV source in galactic nucleus 4-73065
- NGC 4151, Seyfert galaxy, HEAO 1 obs. from 2 keV to 2 MeV 4-86038
- NGC 4151 and 7469, IUE UV spectra of nuclei of Seyfert galaxies 4-63319
- NGC 4945, infrared activity of galaxy containing luminous  $\text{H}_2\text{O}$  masers 4-94990
- NGC 5128 (Centaurus A), radio obs. of gas within peculiar giant elliptical galaxy 4-106065
- NGC 7172, nucleus activity obs. 4-73074
- optical monitoring of radio sources, B-band light curves 4-110763
- PKS 0634-20, radiogalaxy, O III forbidden line emission along radio axis 4-86059
- PKS 2155-304, BL Lacertae object, optical redshift and implications for X-ray absorpt. feature 4-86057
- PKS 2155-304, BL Lacertae object, sharp X-ray absorpt. feature obs. 4-86056
- quasars, direct imaging obs. of host galaxies assoc. with galaxy clusters 4-86078
- quasars, emission-line ratios rel. to X-ray heating in broad-line region 4-90254
- radio cores search in distant galaxies 4-77931
- radio galaxies, dipole mag. field model for radio configurations 4-94941
- radio jets and strong explosions in plane stratified media 4-85871
- radiogalaxies, alternating-side ejection 4-86044
- radiogalaxies, extended, search for cores at 5 GHz 4-63272
- radiogalaxies, multifrequency one-dimensional radio brightness distrib. in centimetre band 4-63282
- radiogalaxies as cosmic ray sources 4-100926
- Seyfert 1 nuclei, X-ray to optical luminosity ratio 4-86058
- Seyfert 2 galaxies, spectral properties assoc. with ionisation of nuclear region by starlight 4-94951
- Seyfert galaxies, contrib. to Seyfert galaxies nuclei 4-82562
- Seyfert galaxies, dynamics of narrow line regions 4-86034

## galactic nuclei continued

- Seyfert galaxies, emission-line ratios rel. to X-ray heating in broad-line region 4-90254  
 Seyfert galaxies, gravit. lensed, origin for QSO phenomenon 4-77968  
 Seyfert galaxies, nuclei extinction, colours and axial ratios anal. 4-106061  
 Seyfert galaxies, nuclei X-ray emission, origin and anal. 4-77940  
 Seyfert galaxies, research at Royal Observatory, Edinburgh 4-106079  
 Seyfert galaxies, spectral characts., visible and UV anal. 4-63322  
 Seyfert galaxies, X-ray emission and evolution 4-67812  
 Seyfert galaxies as cosmic ray sources 4-100926  
 Seyfert galaxies in Markarian lists, radioemission characts. 4-90225  
 Seyfert galaxies nuclei, cosmic ray accel. and energy spectra, photons and neutrinos as probes 4-100925  
 Seyfert galaxies nuclei, gravitationally lensed QSO phenomenon: origin 4-77967  
 Seyfert nuclei, envelopes cloud form. and line emission 4-101480  
 spectral emission of active nuclei, H-line ratios 4-110753  
 spinars in double radio sources, theory 4-63330  
 spiral galaxies, nucleus radio source origin, starburst or accretion mechanisms 4-94945  
 spiral galaxies, obs. of IR H I recomb. line emission 4-86039  
 steep-spectrum compact sources, peculiar radio struct. of quasar (3C 380) 4-63338  
 superluminal separation velocities of extragalactic object components 4-86076  
 supermassive black holes and active galactic nuclei, book 4-58601  
 The Galaxy, radio lobe above galactic centre 4-106067  
 The Galaxy, radioemission from large scale structures 4-106066  
 unified Yang-Mills theory, topological strings, massive black holes in galactic nuclei 4-101727  
 wind-type model for the generation of astrophysical jets, appl. to active galactic nuclei 4-101139  
 Fe<sup>9+</sup> region in active nuclei 4-77919  
 H<sub>2</sub>O maser emission from galactic nuclei, 22.235 GHz obs. 4-101478

## galactic radio waves see radiofrequency cosmic radiation

## galaxies

- see also *BL Lacertae-type objects; clusters of galaxies; galactic nuclei; H I regions; H II regions; intergalactic matter; Magellanic Clouds; Markarian galaxies; nebulae; radiogalaxies; Seyfert galaxies; The Galaxy*  
 0241+622, low-redshift quasar, spectrophotometry and image anal. of assoc. nebulousity 4-90253  
 Abell 1142, poor galaxy cluster, redshift survey 4-73085  
 Abell 1795 cD galaxy, star form. characts. and UV spectral obs. 4-90236  
 adiabatic formation theory, protogalactic gas thermochemical evolution 4-63291  
 Anon 1336-27, SN discovery position and magnitude (1984 March) 4-67756  
 anonymous galaxy in Hydra, supernova discovery, approximate position, and photographic magnitude 4-72962  
 Arakelian galaxies, space density 4-77916  
 ARP 220, H<sub>2</sub> detection in IR luminous merging galaxies 4-115821  
 Arp 220, H<sub>2</sub> emission from distributed galaxy, IR obs. 4-101474  
 Arp 91 (NGC 5953-4) 4-90230  
 barred galaxies, 1/1 reson. 4-63280  
 barred galaxies, three-dimens. dynamics 4-94947  
 Bibliography of Astronomical Objects 4-94902  
 binary spiral galaxies, mass-light distrib. and massive haloes 4-73075  
 blue compact galaxies, near-IR photometry rel. to nature, stellar populations, and age 4-94957  
 blue galaxies, large scale distrib., red shift anal. (Russian) 4-67830  
 blue galaxies in distant clusters, nature from spectral obs. 4-77933  
 Bootes void survey, 231 galaxies red shift obs. 4-77936  
 Centre for Astrophysics redshift survey anal. 4-77935  
 chemical evolution, evidence from element abundances in interstellar medium 4-101459  
 chemical evolution and N/O versus O/H relationship 4-86063  
 chemical evolution and nucleosynthesis 4-63293  
 chemical evolution of spirals, numerical models 4-77920  
 Circinus galaxy, infrared activity of galaxy containing luminous H<sub>2</sub>O masers 4-94990  
 classification system and illustrated atlas of dwarfs in Virgo cluster 4-115827  
 cluster central galaxy, growth due to star form. from cooling gas flows 4-110759  
 colliding galaxies, stellar vel. perturbations 4-82530  
 collisionless Boltzmann eqn. for spherical stellar systems, integration 4-72990  
 colour distribution of faint galaxies and their evolution 4-77932  
 companion galaxies to low-z quasars, CCD spectra 4-115828  
 conference on star bursts in galaxies, at London, England (May 1983) 4-73148  
 conference on Universe struct. and galaxies form. and evolution at La Plagne, France (March 1983) 4-63401  
 correlation hierarchy in perturbation theory 4-86033  
 counts and determination of cosmological parameters 4-73120  
 deceleration of nearby galaxies 4-73080  
 density wave theory, Bessel products summation, closed forms 4-87884  
 diffuse low-energy gamma-ray background, contrib. of normal galaxies 4-82561  
 disc dynamics, stabilising and destabilising effects of haloes 4-73070  
 disc galaxies, distance moduli from H I 21 cm line widths 4-101198  
 disc galaxies, numerical study of relaxation of one-dimensional gravit. systems 4-106044  
 disc galaxies formation, neutrino accretion effects 4-67840  
 discs, mass distrib. 4-94946  
 discs thickness, role of transient spiral wave heating 4-67802  
 disk bending, optical meas. (Japanese) 4-115810  
 disk galaxies; intrinsic shape of ring structures 4-67789  
 disk galaxies, absolute (blue) luminosity/21 cm linewidth relation 4-63276  
 dissipationless collapse and initial conditions 4-110731  
 dissipative structures form. 4-86042  
 most distant galaxies, Christmas lecture of British Astronomical Association 4-73073  
 distribution function, from statistical thermodynamics of gravitationally interacting bodies 4-67801

## galaxies continued

- disturbed galaxies, stability of continuum models for interstellar gas 4-63270  
 double, UVB obs. 4-110747  
 Draco dwarf spheroidal galaxy, chem. inhomogeneity, red giants spectra anal. 4-110737  
 dust content rel. to obscuration of cosmologically distant objects, test using quasars 4-86025  
 dusty spiral galaxies, 1-millimetre continuum obs. 4-115834  
 dwarf galaxies, 1405 MHz continuum survey 4-63274  
 dwarf galaxies in M81/M82 group, luminosity profiles 4-94953  
 dwarf irregular galaxies, stochastic self propagating star form. model 4-67806  
 dwarf irregulars, mass-to-light ratios for binary pairs 4-90243  
 dwarf spheroidal galaxies on Palomar Sky Survey prints, new discoveries 4-77903  
 dynamical friction and rotation, merger effects 4-77923  
 dynamical friction in spherical stellar system, theory for bar or satellite galaxy 4-101476  
 E and S0 galaxies (NGC 1052, 2749, 3998 and 4125); stellar and gaseous kinematics 4-73066  
 E galaxies, metal abundance spread 4-105978  
 early Universe, locally supersymmetric model, primordial inflation and supercosmology 4-67831  
 early-type galaxies in clusters, bright end of colour-magnitude relation from UBVR photometry 4-86026  
 elliptical galaxies, form. and dynamics of optical shells 4-86041  
 elliptical galaxies, form. and evolution (Japanese) 4-63275  
 elliptical galaxies, periodic orbits. characts. 4-90192  
 elliptical galaxies, rot. axis 4-101482  
 elliptical galaxies, rotation-surface brightness relation rel. to dissipation during form. 4-67805  
 elliptical galaxies, survey of forbidden O II emission 4-77927  
 elliptical galaxies in Coma-type compact clusters, rot. origin mechanisms 4-101481  
 elliptical systems, stellar dynamical models 4-115813  
 ellipticals, N-body simulations of evolution 4-115822  
 envelopes, unseen matter existence as substellar bodies 4-77942  
 ESO 131147-4224.7, Sc-type galaxy, supernova discovery, approximate position, and magnitudes 4-77857  
 ESO 308-G05, supernova discovery, approximate position, and photographic magnitude 4-77856  
 ESO-323-G 99, supernova spectral obs. 4-77858  
 ESO-Uppsala survey of ESO (B) Atlas, suspected planetary nebulae identification as galaxies 4-101454  
 evolution and classical cosmology tests 4-73121  
 face-on spiral galaxies, radio emission characts. 4-110749  
 faint galaxy obs., optimum signal-noise ratios 4-106057  
 Fairall 71, M87-like jet features, CCD images 4-90245  
 filaments in galaxy counts, reality anal. 4-78005  
 finite rotating universe, null geodesics, caustics and galaxies apparent motion 4-67822  
 formation, dynamical constraints during violent relaxation and effects on final state 4-94956  
 formation, effects of ionisation by Population III stars 4-90191  
 formation, role of dark matter in Universe 4-67838  
 formation, role of missing matter (Japanese) 4-110790  
 formation, role of pregalactic activity and hidden mass 4-67797  
 formation and evolution (book contribution) 4-63352  
 formation and low-mass collisionless particles in expanding Universe 4-67622  
 formation and strings evolution within GUT 4-78017  
 formation and structure growth in Universe 4-73127  
 formation in matter and radiation dominated universes 4-73082  
 formation in neutrino dominated universes, adiabatic theory 4-78006  
 formation in neutrino dominated Universe 4-95005  
 formation in relativistic cosmology (book) 4-82609  
 formation model, hierarchical 4-67839  
 formation of galaxies and globular star clusters, role of dark matter 4-90262  
 formation via adiabatic fluctuations and pancake collapse, microwave background problem 4-78004  
 G-variable cosmologies, galaxy form. in Hoyle-Narlikar and Brans-Dicke theories 4-101547  
 generalised Mestel disc and truncated Toomre discs, exact solns. 4-72865  
 giant elliptical in front of broad absorption-line QSO 4-63332  
 global radio continuum of nearby galaxies 4-94334  
 gravitational lenses and QSOs nature 4-77967  
 gravitino and photino masses in supersymmetric cosmology, galaxy form. 4-67845  
 halo formation, mathematical soln. of MHD equations 4-101468  
 haloes, dark matter, evidence for non-baryonic nature 4-67795  
 halos, role of massive neutrinos and photinos 4-63375  
 He 2-10, structure and physical conditions 4-67788  
 Holmberg IX, dwarf galaxy, colour-magnitude diagram for brightest red and blue stars 4-101466  
 Horologium region, spectroscopic and photometric data 4-110757  
 hydraulic jumps in viscous accretion discs, appl. to neutron stars and galaxies 4-90081  
 hydrodynamical jets with inhomogeneous viscosity, structure 4-67619  
 IC 121, supernova discovered in 1984, astrometric obs. 4-115771  
 IC 121, supernova discovery position and magnitude (1984 August) 4-110637  
 IC 2153, shock-induced star formation in colliding galaxy pair 4-110739  
 IC 4553, peculiar galaxy, VLA-A obs. of OH megamaser 4-86036  
 inflationary Universe, primordial sound waves and galaxy formation 4-78015  
 inflationary Universe scenario in supersymmetric models without unnatural fine-tuning 4-63363  
 interacting galaxies, evidence from JHKL photometry for recent star form. 4-94959  
 interacting galaxies, star form. rates from spectrophotometric obs. 4-77926  
 interacting galaxies groups, morphological features investigation 4-94939  
 interacting spirals, induced nuclear emission-line activity 4-90242  
 interstellar chemical composition from supernova remnants spectrophotometry 4-77905  
 interstellar clouds sweeping from rot. galaxy by intergalactic medium, dynamics 4-94943  
 intervening galaxies, rel. to low-excitation absorpt. line systems in QSOs 4-73096

## axies continued

- intervening galaxies mol. clouds as origin for QSO, absorpt. lines 4-77965
- intervening galaxies rel. to absorption lines with small redshifts in quasars spectra, absorpt. lines identifications 4-94984
- intervening galaxies towards quasars, absorpt. in continuum energy distrib. 4-110765
- intervening galaxies towards quasars, absorpt. lines origin 4-106081
- intervening galaxy towards BL Lac object 0215+015 as origin for absorpt. struct. 4-77941
- intervening galaxy towards QSO 0957+561 A,B 4-110772
- intervening galaxy towards QSO 2345+007A,B, interstellar clouds characts. 4-110769
- intervening galaxy towards quasar pairs, absorpt. lines anal. and nature of intervening objects 4-77966
- intrinsic shapes, kinematic tests 4-94962
- invisible axions, domain walls, energy crisis and galaxy form. 4-59018
- IR galaxies in IRAS minisurvey 4-86054
- IRAS point sources, unidentified, optical counterparts are IR luminous galaxies 4-77970
- isolated elliptical galaxies, X-ray cooling flows 4-73078
- isolated galaxies, H I content UHF obs. 4-110736
- isolated galaxies, rotation and masses (*Russian*) 4-86060
- jet phenomena (*Japanese*) 4-115679
- Kazaryan 163, new Seyfert galaxy, spectrophotometric obs. and direct photography 4-94938
- kinematics from stellar spatial velocities 4-85991
- Local Group galaxies, Einstein Observatory obs. of X-ray sources 4-101510
- low surface brightness galaxies in region 1046+65, photometric obs. 4-94952
- luminosity function and cosmological tests  $N(z)$  and  $N(m)$  4-82564
- M101, spiral galaxy, photometry of images in rocket UV 4-90234
- M31, 33, 83 and 101, chemical evolution, numerical models 4-77920
- M31, 610 MHz obs., data reduction and 36W radio source catalogue 4-77915
- M31, colour-magnitude and two-colour diagrams of globular clusters 4-63233
- M31, ellipticities of five globular star clusters on B-plate (*Russian*) 4-85992
- M31, H I structures and holes 4-63317
- M31, high resolution H I survey 4-63316
- M31, IR emission, IRAS obs. 4-86052
- M31, M33, IUE and ground-based obs. of Hubble-Sandage variables 4-85941
- M31 (Andromeda galaxy), extragalactic source of 1000 GeV gamma rays 4-101470
- M31 globular clusters, metallicity parameters, comparison with Galaxy 4-101479
- M33, Cepheids photometry and periods 4-94806
- M33, orientation of galactic plane from surface photometry and spiral arm shapes 4-73069
- M33 globular clusters, ages and metallicities, spectral obs. 4-110695
- M51, spiral galaxy SHF radio maps 4-94979
- M81, colour-magnitude diagram for brightest red and blue stars 4-101466
- M82, central H I and OH content, VLA obs. 4-110740
- M82, distrib. and kinematics of interstellar CO 4-101471
- M82, far IR forbidden O I and III emission 4-90241
- M87, Virgo cluster galaxy, 2 novae, February 1984 discovery 4-110623
- mass distrib. from gravitational light deflection 4-115820
- masses, cosmological implications 4-73081
- massive black holes in clusters and galaxies nuclei, relativistic dynamics 4-77883
- massive haloes, baryonic nature 4-67794
- MCG 3-22-14, SN discovery and photographic magnitudes (1984 Jan.-Feb.) 4-67757
- MCG 8-15-47, supernova discovery, approximate position, and photographic magnitude 4-63184
- MCG 9-19-19, supernova discovery, approximate position, and photographic magnitude 4-67752
- microphysical cosmology, foundations and working pictures, galaxies and microwave background 4-73117
- missing mass problem 4-90268
- molecular clouds distrib. 4-82544
- monopole dominated universe, galaxy formation, clusters, perturbation growth 4-115844
- morphological type correl. with globular clusters occurrence, size and shape 4-106069
- morphology-density relation 4-110732
- MR 2251-178, nearby quasar, obs. of assoc. [O III] emission 4-101496
- multiple imaging of quasars by galaxies and rich clusters 4-94988
- neutrino halos formation, role of cosmological const. 4-67817
- neutrino mass and possible role in galaxy formation 4-115826
- NG 4594 (Sombrero galaxy), globular cluster system struct. 4-63273
- NGC 1058, nearly face-on spiral galaxy, H I distrib. and vel. field 4-94946
- NGC 1097, VLA obs. of optical jets and nucleus 4-63288
- NGC 1559, supernova discovery, position and magnitude (July 1984) 4-101382
- NGC 1559, supernova observations 4-101383
- NGC 1559, supernova of type II at centre of galaxy 4-110635
- NGC 1600 and 4261, early-type galaxies, isophotal struct. 4-115816
- NGC 185, emission nebular near dwarf elliptical core, probable SNR 4-115802
- NGC 205, dwarf elliptical galaxy, red giant branch population obs. 4-90228
- NGC 2403, colour-magnitude diagram for brightest red and blue stars 4-101467
- NGC 2403, H II region spectrophotometry and Cepheid extinction 4-63247
- NGC 253 edge-on spiral galaxy, large-scale radio continuum struct. 4-115814
- NGC 2684, isolated galaxy ultraviolet excess due to young stars 4-94950
- NGC 2782, starburst galaxy obs. at radio, IR, optical, UV and X-ray freqs. 4-110754
- NGC 3079, water maser discovery in infrared emitting galaxy 4-115805
- NGC 3169, SN astronomy, spectra and magnitudes 4-67758
- NGC 3169, SN discoveries, positions and mags. (1984 March) 4-63186
- NGC 3227, supernova visual magnitude estimate (1983 December 3) 4-63185

## galaxies continued

- NGC 3256, far IR obs. of peculiar galaxy indicating starburst 4-94969
- NGC 3379, elliptical galaxy, geometry anal. 4-90240
- NGC 3384, lenticular galaxy, photometric study of inner struct. 4-110748
- NGC 3448, interacting galaxy, combined optical, radio and UV investigation 4-73065
- NGC 3557, elliptical galaxy, rot., luminosity and shape 4-90238
- NGC 3622, isolated galaxy ultraviolet excess due to young stars 4-94950
- NGC 3682, isolated galaxy ultraviolet excess due to young stars 4-94950
- NGC 4244, 4565 and 5907, edge-on spiral galaxies, radio continuum obs. 4-73067
- NGC 4246, possible discovery of supernova 4-67754
- NGC 4419, SN visual magnitude estimates 4-67759
- NGC 4419, supernova during 1984, IR behaviour of Type I object 4-67753
- NGC 4419, supernova IR magnitudes (29 February 1984) 4-67755
- NGC 4449, irregular galaxy, SNR in H II region, UV spectra anal. 4-90195
- NGC 4449 supernova remnant, models and age from X-ray, UV and visible obs. 4-77910
- NGC 4566, isolated galaxy ultraviolet excess due to young stars 4-94950
- NGC 4650A, spindle-like galaxy, rot. of diffuse stellar component 4-90232
- NGC 4736, spiral galaxy bulge dispersion velocity meas. (*Spanish*) 4-90244
- NGC 4753, SN 1983h, spectra obs. 4-82496
- NGC 4945, infrared activity of galaxy containing luminous H<sub>2</sub>O masers 4-94990
- NGC 5128, stellar content and metallicity of globular clusters 4-86032
- NGC 5128 (Centaurus A), radio obs. of gas within peculiar giant elliptical galaxy 4-106065
- NGC 5266, NGC 3108, early-type galaxies with ionised gas discs, struct. and kinematics 4-86030
- NGC 6166 and 7720, brightest cluster galaxies and their multiple nuclei, orbit anal. 4-86066
- NGC 6240, H<sub>2</sub> detection in IR luminous merging galaxies 4-115821
- NGC 6240, ultraluminous interacting galaxy, identification with IRAS source (1650+024PO4) 4-77925
- NGC 6240 H<sub>2</sub> emission from distributed galaxy, IR obs. 4-101474
- NGC 628, NGC 1566, spiral galaxies, vertical velocity dispersion of stars in galactic discs 4-86028
- NGC 6822, discovery, photometry and spectrum of C star 4-63168
- NGC 6850, supernova discovery and confirmation 4-106013
- NGC 6907, discovery position and magnitude of possible supernova 4-82497
- NGC 6946, massive star form. characts. and H I and H<sub>2</sub> distrib. correl. 4-90227
- NGC 7013, H I distrib. and motions in lenticular galaxy 4-67787
- NGC 7184, supernova discovery, July 1984 observations 4-101381
- NGC 891, 3079, 3556, 4631 and 7331, edge-on galaxies, 2.8 cm obs. 4-73068
- NGC 991, supernova discovered in 1984, astrometric obs. 4-115771
- NGC 991, supernova discovery, position and magnitudes 4-110636
- NGC 991, supernova of type II 4-115770
- NGC 991, supernova UVB photometry, astrometry and spectrometry 4-110637
- nonlinear gravitational clustering 4-94975
- nonstationary viscous gaseous discs 4-63323
- Nordic Optical Telescope observing projects 4-63321
- normal galaxies as cosmic ray sources 4-100926
- one millimetre wavelength infrared sources 4-94989
- optical positions of active galaxies from PSS plates 4-63287
- optically variable QSOs near bright galaxies, statistical anal. 4-77969
- pancake theory of galaxy form., role of massive neutrinos 4-110791
- periodic orbits in a rotating triaxial potential 4-77881
- physical cosmology, Les Houches Session XXXII, France (July 1979) 4-67874
- PKS 2155-304, BL Lacertae object, optical redshift of assoc. nebulosity 4-86057
- polar rings, orbital characts. 4-115808
- Population II stars, form. via thermal instability 4-67717
- properties in voids and in clusters, comparison 4-77937
- protogalactic eddies, structure 4-63290
- Q1101-264, red shift systems anal., intervening galaxies or intergalactic clouds 4-90250
- Q 0957+561, twin QSO, UBVR<sub>IJK</sub> magnitudes of lensing galaxy 4-90251
- in quasar fields, catalogue of objects discovered in imaging survey 4-94644
- quasars host galaxies, direct imaging obs. and assoc. with galaxy clusters 4-86078
- red shift survey of very faint field galaxies and their evolution 4-77934
- red shifts not assoc. with Universe expansion, evidence 4-77928
- relativistic stellar dynamics 4-77883
- relaxation time of stellar systems 4-72989
- ring galaxies and polar rings (*Japanese*) 4-115811
- ring galaxy 1008-3814 in Vela, TAURUS obs. 4-77922
- ring structure in galaxies, stellar dynamical model rel. to ring stability 4-94944
- rotating self-gravitating gaseous disk; nonlinear disturbances (*Russian*) 4-86061
- rotation curves of normal galaxies 4-63292
- rotation in binary galaxies, tidal effects (*Russian*) 4-67793
- rotation of galaxies and clusters, prod. by tidal torques 4-67804
- SO galaxies with polar rings, intrinsic orientation determ. 4-101465
- Sc I galaxies, distances and props., visible and IR anal. 4-90220
- scale free models, oblate E<sub>0</sub> set. 4-110692
- Sculptor Group, brightest galaxies, photoelectric UBVR<sub>I</sub> sequences 4-110690
- secular dynamical evolution, effects on galactic and evolution 4-67800
- Shapley-Ames galaxies, IRAS obs. 4-86053
- shock waves with energy supply and release 4-115825
- SIMBAD data base, astronomical contents 4-94901
- southern binary galaxies, dynamical analysis, mass distrib. 4-67809
- southern compact bright-nuclear galaxies, spectral obs. 4-110750
- spatial distribution and clustering 4-77943
- spatial distribution in neighbouring superclusters 4-77950
- spherical galaxies, construction of analytical models 4-72992
- spherical stellar system, numerical study of gravit. collapse 4-101438
- spheroidal gravitational lenses 4-77703

## galaxies continued

- spiral galaxies, discs luminosity-depend. line ratios 4-110745  
 spiral galaxies, four-colour photometry and comparison with Markaryan galaxies 4-94937  
 spiral galaxies, mag. field struct. 4-101475  
 spiral galaxies, mass to light ratios and haloes nature 4-67796  
 spiral galaxies, mol. clouds and star form., CO obs. 4-63318  
 spiral galaxies, molecular clouds, star formation and galactic structure 4-90219  
 spiral galaxies, obs. of IR H I recomb. line emission 4-86039  
 spiral galaxies, struct. and star form., particle hydrodynamics simulation 4-86050  
 spiral galaxies, two dominant dimensions in objective classification scheme 4-86027  
 spiral galaxies and companions, mag. fields anal. 4-106052  
 spiral galaxies in clusters, radial gradients in Coma and (Abell 1367) 4-82553  
 spiral galaxies rot. curves, effects of Newtonian gravit. modification 4-105869  
 spiral normal mode deformation to bar patterns 4-115824  
 spiral patterns excitation in responsive density wave theory 4-63213  
 spiral structure, influence of bar strength and pattern speed 4-94958  
 spiral structure formation in galaxies with accreted matter drifting within the corotation resonance region (*Russian*) 4-94972  
 spirals, part star formation rates 4-110738  
 stellar discs heating by massive objects, theory 4-67803  
 stellar orbits in angle variables, numerical theory 4-85990  
 stellar velocity dispersions in galactic discs, massive gas cloud effects 4-77882  
 string in Universe seeded for galaxy formation 4-115840  
 supernovae, constraints on masses of progenitors from star form. rates 4-63183  
 supernovae detection in distant galaxies, automatic system developments 4-67642  
 surface photometry, digital processing techniques (*Russian*) 4-115695  
 thermodynamic history of the Universe 4-86096  
 tidal interactions modelling 4-94955  
 time-dependent galactodetonation waves in galactic discs, propag. and stability 4-90235  
 topologically stable strings, grand unification phase transition; galaxy formation 4-95264  
 triaxial galaxies, fitting of N-body potentials to Eddington pot. 4-67799  
 triaxial galaxies, second integral of motion in bisymmetrical pot. field 4-73072  
 triaxial galaxies, struct. and evolution 4-67798  
 triple galaxies, isolated, electrophotometry 4-110758  
 Tully-Fisher relation, errors 4-106087  
 UGC 7576, spindle-like galaxy, mapping in H I, UHF obs. 4-73076  
 UV excess galaxies, Kiso survey 4-101196  
 UV radiation, obs. from Astron UV telescope (*Russian*) 4-67630  
 very early Universe, astrophysical scale, isotropy and baryonic and non-baryonic content 4-63355  
 very early Universe, strings, GUTs and galaxy form. 4-63359  
 Virgo cluster, meas. of four photoelectric UBVR sequences near cluster galaxies 4-94741  
 Virgo cluster and field galaxies, H I and optical diameters 4-77939  
 Virgo cluster spiral galaxies, evidence for low dust content 4-101464  
 VV 371 (UGC 9274), study of peculiar galaxy and nearby companion 4-67792  
 wave-particle duality in quantised red-shifts of galaxies 4-101697  
 young galaxies, gas ionisation characts. 4-82557  
 young luminous optical pulsars in extragalactic SNRs, search 4-86007  
 Z 0902+36, isolated galaxy ultraviolet excess due to young stars 4-94950  
 II Zw 73, spindle-like galaxy, mapping in H I, UHF obs. 4-73076  
 H I contents, search for optimal means of comparative H I anal. 4-90233

## gallium

- see also nuclei with .....  
 amorphous, radial distrib. function and struct. factor, quasi-cryst. model 4-84186  
 amorphous thin films, optical props., elec. meas. 4-88800  
 atom, photoionisation saturation by reson. ionisation 4-64434  
 atoms,  $K\beta_5/K\beta_2$  and  $K\beta_2/K\beta_1$  radiative transition rates meas. 4-91231  
 coating on Ge-Cu, impurity contamination reduction by heat treatments above 700°C 4-71535  
 diffusion in Au, isotope effect meas. 4-65476  
 gallium trimethyl, visible multiphoton dissociation, time-resolved multiphoton ionisation of Ga atoms 4-87164  
 heat capacity, enthalpy, melting temp., thermodynamic functions 4-80255  
 isoelectronic sequence from  $Rb^{6+}$  to  $In^{18+}$ ,  $4s^2 4p^2$  intervals, fine struct. splitting meas. 4-64400  
 liquid, explosive emission study 4-109311  
 liquid, interface with glass, phonons, Brillouin scatt. study 4-80955  
 liquid, ion source, construction and technology (*Chinese*) 4-82858  
 liquid, mechanisms and kinetics of dissolution of Cd 4-114530  
 liquid, radial distrib. function and struct. factor, quasi-cryst. model 4-84186  
 liquid, supercooled and normal, elec. resist., temp. depend. 4-75921  
 liquid, ultrasonic vel., temp. depend., elastic moduli, vol. depend. 4-60989  
 liquid struct. determ. 4-98000  
 local-field enhancement of rough surface 4-104047  
 SAW excitation and magnetoacoustic effects 4-70545  
 single atoms detection in atomic beams 4-107321  
 size-induced deviations from Matthiessen's rule 4-70775  
 supporting medium for specimen prep. 4-111114  
 surface acoustic waves and de Haas-van Alphen meas. 4-70540  
 trivalent ion, position-depend. antishielding factors 4-70762  
 YIG:Ga(La) magneto-optical waveguide, TE to TM mode conversion by alternating-coupling coeff. 4-69545  
 Au/Ga thin film couples, room temp. interdiffusion 4-61149  
 $Bi_2SiO_{20}$ , Ga, optical absorp. spectra, photochromism (*Russian*) 4-114311  
 Ga I, autoionising levels studied by photo-ionisation expts. 4-78810  
 Ga XXX, X-ray spectra excited by low-inductance spark plasma 4-74181  
 Ga-Au, excess enthalpies meas. using heat flow calorimeter 4-80237  
 Ga-N<sub>2</sub> system, high pressure thermodynamics, heat and entropy of GaN form. 4-62227  
 GaAs:Cr, eval. of Cr conc. by optical absorpt. 4-104635  
 GaSe<sub>2</sub>/Ga, glassy semiconductor, doping effect, positron annihilation 4-61764

## gallium continued

- Ge-Ga, crystal growth characts. in vertical Bridgman system 4-70049  
 Ge-Ga, FIR stress induced photoconductivity, broadband meas. 4-70873  
 Ge-Ga, migration of molten inclusion 4-108659  
 Ge-Ga film on GaAs, doping and elec. props. study (*Russian*) 4-70182  
 Ge-Ga/(Al,Ga)As/GaAs polar semicond. quantum well system, growth and optical props. 4-114314  
 InP:Ga,Sb crystals, dislocation density reduction by isoelectronic double doping 4-60940  
 InSe-Ga, dopant segregation and distrib. study 4-103940  
 PbTe-Ga, elec. and optical meas. (*Russian*) 4-84636  
 Si (111)-Ga abrupt interfaces, electronic props. 4-84696  
 Si-Ga, neutron irradi., acceptor level, IR absorpt. spectrum 4-93089  
 Si-Ga sputtered amorphous alloys, thermopower and elec. cond. 4-61403  
 Si-Ga(Sb), amorphous, highly doped, MBE grown, epitaxial regrowth 4-98468
- gallium alloys**  
 see also gallium compounds  
 rare earth alloys,  $R_{80}Ga_{20}$ -based metallic glasses, mag. props. 4-114139  
 Al-Ga, distribution of electric field gradients around impurities, conduction electron screening lattice strain 4-113910  
 Al-Ga equilibrium diagrams, thermodynamic anal., appl. of modified sub-regular soln. model 4-92387  
 AuGa<sub>2</sub> (001), surface net characterisation and electronic struct. 4-80642  
 Ce<sub>2</sub>Ga<sub>7</sub>Ni<sub>2</sub>, cryst. struct. determ. 4-75375  
 Cr-Ga, dilute, mag. phase diagram, elec. cond. meas. 4-88669  
 Cu-Ga/V, multifilamentary superconductors, brittle fracture, acoustic emission anal. 4-71715  
 ErGa<sub>2</sub>, metamagnetic, spin-flip transitions, magnetoresistance anomalies (*Russian*) 4-98880  
 Ga-As-Sn system, phase diagram and LPE growth rates 4-93237  
 Ga-Sn-Zn alloy, electrovortex flow in a planar channel (*Russian*) 4-113049  
 Ga-Te, molten, at. arrangement of Ga<sub>2</sub>Te<sub>3</sub> associates, metallic-like bonding, neutron scatt. obs. 4-103639  
 (GaSb)<sub>1-x</sub>(Ge<sub>2</sub>)<sub>x</sub> semicond. alloys, phase transforms. 4-92347  
 Ge-Ga, freezing, periodic growth rate effect on morphological stability 4-98039  
 HoAlGa, mag. transitions, mag. and cryst. structures, X-ray diffr., thermal expansion meas. 4-114113  
 In-Ga-Sb alloys, liq., phase diagram calc., Krupkowski's eqn. (*Polish*) 4-85139  
 In-Ga-Sn, natural convection, mag. field orientation influence (*Russian*) 4-113061  
 In-Ga-Sn liq. alloy in pipe, degenerate turbulence behind grid in mag. field (*Russian*) 4-113040  
 La-Ga metallic glasses, elec. cond. meas. 4-98588  
 La<sub>2</sub>Ga, amorphous, superconductivity obs. (*Chinese*) 4-104338  
 Li-Ga, cryst. struct. determ. 4-79986  
 Mg<sub>0.9</sub>Zn<sub>0.1</sub>-Ga, simple metallic glasses, electronic props. 4-75920  
 Mo-Ga phase diagram, binary Mo<sub>3</sub>Ga<sub>4</sub> cpd. 4-76753  
 NaGa, compound forming liquid alloys, hard sphere system, entropy of mixing calcs. 4-113650  
 Nb-Al-Ga, vacuum deposited films, struct. and supercond.-transition temp. rel. to heat treatment 4-65764  
 Nd<sub>2</sub>Ga<sub>3</sub>Ni<sub>2</sub>, cryst. struct. determ. 4-75375  
 Ni-Ga, bonding and enthalpy studies 4-79978  
 NiGa, vacancy controlled  $\gamma$ -brass phase, struct. determ. 4-60885  
 Ni<sub>2</sub>MnGa, ferromagnetic transition and martensitic transformations 4-61512  
 Pd-Ga, bonding and enthalpy studies 4-79978  
 Pt-Ga, bonding and enthalpy studies 4-79978  
 RGA<sub>2</sub>Ni<sub>2-x</sub> ( $1 \leq x \leq 2$ , R=La-Lu), phase form. struct., comp., X-ray analysis 4-114488  
 UGaCo, mag. props., temp. depend. 4-71033  
 V<sub>3-x</sub>Fe<sub>x</sub>Ga, NMR Knight shift and paramagnetism 4-65873  
 V<sub>3</sub>Ga, A15 cpd., <sup>48</sup>V and <sup>67</sup>Ga self-diffusion, tracer study 4-75718  
 V<sub>3</sub>Ga A15 intermetallic cpd., <sup>48</sup>V diffusion 4-65454  
 V<sub>3</sub>Ga composite superconductors, in situ, prep. by external diffusion, microstruct. and supercond. props. 4-92844  
 V<sub>3</sub>Ga composite superconds., prep. and high field supercond. props. 4-92881  
 V<sub>3</sub>Ga superconducting wires, multifilamentary, specimen prep. technique for TEM 4-76921  
 V<sub>3</sub>Ga, thermodynamic props. calc. 4-84741  
 V<sub>3</sub>Ga wire, supercond. props. and modified jelly roll prep. 4-104749  
 V<sub>7</sub>Ge<sub>2</sub>Ga<sub>5</sub> A-15 superconductor, impurity location using EXAFS 4-88190  
 YbGa<sub>8</sub>Co<sub>2</sub>, cryst. struct., X-ray diffr. 4-84237
- gallium arsenide**  
 (100), laser irradi., photoemission of electrons 4-81116  
 (100) surface, optical surface phonons obs. using high res. electron energy loss spectroscopy 4-70546  
 (100) surfaces, XPS anal. after technology-etchant appl. 4-93196  
 (110) with adsorbed H, H<sub>2</sub>, temp. programmed desorption study 4-92528  
 A surface (111), contact with In-Ga-As-P saturated liq., Auger anal. 4-104046  
 acceptor level, 78 meV, luminescence and Raman scatt. studies 4-70704  
 adsorption of H on (110) surface, EHM method calc. (*Chinese*) 4-113787  
 adsorption of O on (111) surface, XPS study (*Chinese*) 4-85077  
 alloying behaviour of Au and Au-Ge(-Ni) on GaAs 4-80454  
 amorphous, high-defect-density, subpicosecond carrier trapping 4-80621  
 amorphous, MBE grown, local struct., EPR and NMR studies 4-104492  
 amorphous thin films, transient annealing, Raman scatt. study 4-80926  
 ballistic large-wavevector phonon propag., direct obs. 4-61013  
 ballistic photocurrents, mag. field influence 4-70866  
 Bridgman ingots, photocond., 80-300K, CR and O. impurity effects 4-65705  
 carrier vel. fluctuations in steady-state and transient regimes, Monte Carlo study 4-80637  
 cleaved, work function var. rel. to cooling 4-88556  
 compensation resulting from N ion implantation 4-104150  
 concentrator solar cells, resistance effects and cell performance 4-77086  
 conduction band splitting for k along [110] 4-108777  
 conduction bands, strain-induced splitting 4-75854  
 contour maps of EL2 deep level, dislocations 4-80530  
 crystal, numerical simulation of horizontal Bridgman growth 4-66212  
 crystal and amorphous, pulsed laser irradi. under O<sub>2</sub> and silane atmospheres, O incorporation and losses 4-80091  
 crystal struct. determ. using convergent beam electron diffr. 4-103612

- lium arsenide** continued
- crystallisation by nonequilibrium electroliq. epitaxy, molten soln. parameter determ. 4-75817
  - crystallisation from melt, rate, elec. current effects 4-71551
  - CVD, low press., in Ga-HCl-AsH<sub>3</sub>-H<sub>2</sub>-H<sub>2</sub>S system, modelling of S doping 4-99333
  - deep acceptor, Hall effect obs. and photoluminescence 4-80532
  - deep centre point defect introduction 4-108819
  - deep centres, electron probe method anal. 4-104158
  - deep impurity levels, ENDOR and ESR spectra 4-84594
  - deep level wavefunctions, behaviour in shallow energy region (*Chinese*) 4-92650
  - deep levels associated with vacancy-impurity pairs 4-92662
  - deep-level wavefunctions with energies near band edges 4-92656
  - defect anisotropy following electron irradiation 4-75534
  - defect visualisation by oxidation in water 4-92194
  - dielectric constant meas. in 100 GHz range (*Japanese*) 4-106330
  - diode lasers, variable-resolution data collection 4-69428
  - dislocations and point-defect complex formations, thermal stability 4-103758
  - DLTS and deep level optical spectroscopy, appl. to E<sub>1</sub> and E<sub>2</sub> in GaAs 4-108815
  - donor transition anomalous line broadening in high-purity samples in mag. fields 4-109214
  - doped, cond. electron spin relax. times, precession mechanism, spin splitting 4-98948
  - doping superlattices, bipolar cond., tunability 4-70914
  - doping superlattices, weak localisation and magnetoresist. 4-98720
  - doping to alter electronic and optical props. (*German*) 4-98590
  - double heterojunction injection laser, constructional details (*Dutch*) 4-83609
  - double heterostructure laser (*German*) 4-83620
  - dry etching induced damage 4-81312
  - ductile brittle transition in (001) surface layers in single cryst., effect of medium 4-70266
  - EL2 and EL0 midgap levels, electron emission in strong elec. fields 4-88510
  - EL2 defect, technological and physical aspects 4-75891
  - electrical properties and impurity states 4-75963
  - electroluminescence and photoluminescence in aq. redox electrolyte 4-88584
  - electroluminescence spectra of free excitons, optical resonances 4-88883
  - electron irradi., dislocation glide, TEM studies 4-92207
  - electron irradi., electronic struct. of E3-defects 4-70720
  - electron irradi., surface electron energy spectrum, photoemission studies 4-88554
  - electron irradiated, carrier-capture cross sections meas. technique 4-61394
  - electron traps, midgap, and multimetastable states, photoquenching studies 4-88466
  - electron traps, props. and nature 4-75890
  - electron- and proton-irradiated, elec. props. 4-75975
  - electron-hole plasma density meas. 4-61408
  - electronic density of states, recursion coeffs., linear prediction theory 4-98502
  - electronic structure of (100) and (111) faces, angle resolved photoemission 4-84559
  - emission band at 1.35 eV, doping and temp. variations 4-76519
  - encapsulated annealing in AsH<sub>3</sub>, surface protection 4-88378
  - epitaxial diode struct., nonequilibrium carrier lifetimes 4-70920
  - epitaxial film, MBE grown, capture of accidental impurities, influence of growth conditions 4-108743
  - epitaxial films, 1/f noise under conditions of strong geometric magnetoresist. 4-61427
  - epitaxial films, line impurity photocond. spectra, fine-struct. splitting 4-65761
  - epitaxial growth, plasma-assisted, in H<sub>2</sub> plasma, elec. props. 4-104740
  - epitaxial high-purity layers, low-pressure MOCVD growth 4-61861
  - epitaxial layer, homogeneity and thickness meas. by IR flaw detection method 4-109609
  - epitaxial layer, processing technology and characts. (*Polish*) 4-113827
  - epitaxial layer growth in multiwafer VPE system, IMPATT device fabrication 4-104738
  - epitaxial layers, MOCVD, surface morphology and elec. props. 4-84493
  - epitaxial selective regions in Si substrate windows, struct. perfection 4-75812
  - epitaxial short wavelength visible laser diodes 4-107628
  - epitaxial structs., photomemory effect, influence of deep levels 4-104261
  - equation of state, bulk modulus press. derivative 4-98236
  - excitonic polaritons in elec. fields at surfaces 4-92633
  - excitons, self-energy, many particle system calculations 4-98536
  - far IR optical props. at 6; 300K, amplitude and phase refl. spectra 4-104594
  - far IR radiation subnanosecond optical switching using method laser irradiation of Si and GaAs 4-74575
  - FET microwave refractometer for tropospheric studies (*French, English*) 4-63778
  - film growth on insulators by artificial epitaxy 4-61873
  - flash annealing of Mg implants, using incoherent radiation 4-84306
  - free carrier lifetime from photoluminescence studies 4-80988
  - GaAs fast supercomputer circuits (*Swedish*) 4-65282
  - GaInAs-InP heterojunction, interface 2-D electron gas props., MOCVD growth and characterisation (*French*) 4-76685
  - gas phase epitaxy, doping and impurity trapping 4-108745
  - glass-bonded NEA transmission photocathode, XPS study 4-104716
  - growth from melt and elec. props. 4-99300
  - growth using OMVPE, electronic and optical props. 4-114402
  - heteroepitaxial growth on (0001) mica by ionised vapour evaporation under elec. field 4-104100
  - heterojunctions and homojunctions, deep levels, tunnel spectra meas. 4-84685
  - heterolayer, low temp. two-dimens. mobility 4-108933
  - high field transport of holes 4-80598
  - high-field transport, model 4-88512
  - hot carrier transient response, vel. overshoot 4-92736
  - hot photoluminescence polarisation and spectrum 4-61743
  - impact-ionized plasma instability, delay time estimation, Monte Carlo technique 4-70853
  - implanted layers, elec. props., Si<sub>3</sub>N<sub>4</sub> encapsulation effects 4-98609
  - impurities identification by magneto-optical photoluminescent spectroscopy 4-60945
- gallium arsenide** continued
- impurity photocurrent and deep level spectroscopy 4-70865
  - injection laser pulse duration meas. 4-64728
  - injection lasers, short pulse excitation, threshold current temp. dependence 4-74506
  - integrated optical device fabrication, Cl<sub>2</sub>-Ar reactive ion etching technique 4-87483
  - integrated optoelectronic devices for high-speed IC interconnects 4-97139
  - interrupted MBE growth, epitaxial InAs protection layer 4-114400
  - inverse dielectric matrix, direct calc. 4-92645
  - ion beam assisted etching using focused ion beam 4-93431
  - ion bombarded heated specimens, surface comp., AES and SIMS anal. 4-113510
  - ion implanted, ion implanted, diffusion of Be and Mn during damage recovery 4-104002
  - ion implanted, photolum. after laser annealing 4-76525
  - ion implanted, transient capless annealing appl. to IC fabrication 4-103779
  - IR properties of heavily implanted semiconductors 4-104587
  - irradiated, E3 centre accumulation, effect of defect charge state 4-60966
  - isotope scatt. of large wave vector phonons 4-108564
  - JFET low-noise high-speed optical receiver for optical fibre systems 4-74743
  - k.p interaction and effective mass, band gap depend. 4-113850
  - laser, electron-beam-pumped, excitation density distrib. 4-79162
  - laser alloyed Sn layers, elec. props., surface damage 4-99622
  - laser diode and LED, coaxial transverse junction struct., design and characts. 4-87357
  - laser-enhanced reactive ion etching in CCl<sub>4</sub>-H<sub>2</sub> mixture 4-71747
  - laser-induced Si diffusion from deposited Si<sub>3</sub>N<sub>4</sub> film 4-60958
  - laser-induced sputtering and damage 4-71485
  - lasers, homo- and single heterostructure, time delay characts. 4-107633
  - lateral growth over W gratings by CVD, application to FET transistors 4-81148
  - lattice dynamics, local Heine-Abarenkov model pot. 4-98222
  - layers, MBE grown on Ge islands on insulator, zone melting recrystallisation, grain boundaries, photoluminescence obs. 4-84524
  - LEC crystal growth in mag. field (*Japanese*) 4-88960
  - LEC grown, EPR identification of As<sub>2</sub> antisite defects 4-71178
  - LEC grown, improved elec. uniformity by high temp. annealing 4-65684
  - LEC growth in vertical mag. field, homogeneity anal. 4-76661
  - LEC substrate, characterisation of impurities and microdefects (*Japanese*) 4-103778
  - LEC wafers, undoped, defect characterisation by electron-beam-induced charge collection microscopy 4-60932
  - light scatt. nonequilibrium electron-hole plasma 4-104616
  - liquid encapsulated Czochralski growth, deep level study 4-98569
  - LPE growth, deep intrinsic centers, anisotropic capture 4-113897
  - LPE growth and nonequilib. deep centre trapping 4-108744
  - LPE growth rates 4-93237
  - LPE layers, residual impurities, growth soln. baking effects 4-92226
  - LPE layers, space-charge scatt. and mobility killers 4-84714
  - LPE layers, surface morphology, effect of substrate misorientation (*Chinese*) 4-84521
  - magnetic circular dichroism-ODMR study of EL2 defect 4-104151
  - material and devices, thermal wave imaging 4-75711
  - MBE, extrinsic effects in RHEED 4-98476
  - MBE, thermodynamics of O incorporation 4-61253
  - MBE films, growth and elec. props. (*Chinese*) 4-84523
  - MBE grown, surface defects obs. 4-61246
  - MBE growth, As source 4-99321
  - MBE growth, dynamic RHEED obs. 4-92572
  - MBE growth, free of oval defects 4-98475
  - MBE growth, role of As and As<sub>2</sub> in controlling quality, theoretical studies 4-98477
  - MBE growth in diffusion pumped systems 4-85105
  - MBE growth of high purity layers, photolum. charact. 4-98474
  - MBE growth on Si (100), optical props. 4-88975
  - MBE growth using trimethylgallium as a Ga source 4-81138
  - MBE layers, elec. props. of oval defects, FET appl. 4-92574
  - MBE layers, spatially-resolved luminescence at oval defects 4-75803
  - MBE-grown (001) surface, band bending, photoemission studies 4-99276
  - melting in Au contacts, in situ X-ray diff. study 4-88593
  - metal/AlGaAs/GaAs modulation-doped structs., physical correspondence with MOS struct. 4-76041
  - midgap level surface density, heat treatment and capping effects 4-114011
  - MIS solar cells, I-V characts. under illum., ideality factor and barrier height 4-93625
  - MOCVD grown, deep electron traps, DLTS obs. 4-84585
  - MOCVD growth, doping profiles, H<sub>2</sub>Se memory effects 4-81152
  - MOCVD growth 4-99329
  - MOS structures with anodic oxides, defect states, DLTS study 4-114043
  - muonium states, positive muon depolarisation 4-71243
  - n<sup>+</sup>-p-n<sup>+</sup> ballistic struct., I-V charact. calc. (*Chinese*) 4-80659
  - n<sup>+</sup>-n-n<sup>+</sup> structures, high field reson. magnetotransport meas. 4-104295
  - n-type, anodic oxidation, surface treatment effects 4-114702
  - n-type, conduction band struct. in 2 and 3 valley band models 4-70649
  - n-type, electron energy relax. due to 2TA phonons 4-92324
  - n-type, electron irradiated, As anti-site defects, IR spectra and EPR 4-84317
  - n-type, free-carrier absorption, quantum mechanical perturbation theory 4-80893
  - n-type, hopping cond. freq. depend. 4-70806
  - n-type, metallic, inelastic scatt. time, temp. depend. 4-98630
  - n-type, power broadening and nonlinear far IR magnetophotocond. 4-108897
  - n-type, ring structure, self-excited oscillations, microwave generation 4-70948
  - n-type, thin films, field-assisted photomagneto-elec. effect 4-80626
  - n-type, Z 4-80970
  - negative differential cond. at transit reson. frequencies 4-84638
  - negative magnetoresist. associated with quantum localisation correction to cond. 4-61400
  - neutral impurity scatt., far-IR cyclotron reson. study 4-92964
  - neutral impurity scatt., far-IR cyclotron resonance study 4-71185
  - neutron irradi., antisite defects, associated defect model, ESR studies 4-88166
  - neutron irradi., defect form., EPR obs., comparison with Cu halides 4-70224
  - neutron irradi., optical absorption coeff., spectral depend. 4-99137

**gallium arsenide continued**

ohmic contact brazing using apparatus for pulsed light heat treatment 4-81313  
 ohmic contacts formation obs., high-temperature substage for a scanning electron microscope 4-101989  
 optical bistability, physics and appls. (*Italian*) 4-107729  
 optical bistable device, all-optical data switching in optical fibre link 4-91529  
 optical guided-wave monolithic interferometer 4-112561  
 optical spin orientation of  $\Gamma^{15}$  conduction band electrons, photoemission study 4-66188  
 optical waveguide modulator with low-loss and high speed, fabrication by RIE 4-60148  
 optoelectronic switching, laser controlled, photoconductivity meas. (*German*) 4-84646  
 p-n junction GaAs photovoltaic electrolyser for hydrogen production by water electrolysis 4-89451  
 p-n junctions, spectral distrib. of avalanche breakdown radiation (*Russian*) 4-98715  
 p-n-p doped submicron structures, LPE grown, n-channel conductivity modulation 4-61447  
 p-n-p-n superlattices, LPE growth 4-80665  
 p-type, laser materials, Auger recomb. and intervalence band absorpt. 4-80885  
 phonon frequencies 4-75626  
 phonons, long-lived short wavelength TA phonons propag., Monte Carlo simulation 4-61015  
 photoacoustic absorpt. meas. by laser heterodyning (*Chinese*) 4-58893  
 photoacoustic signal meas. by laser heterodyne at high temps. 4-106388  
 photoemission, monochromatic electron intense source 4-71510  
 photoenhanced oxidation, AES and work function meas. 4-81302  
 photoexcited, heat pulse propag., large k-vector phonons obs. 4-61014  
 photoexcited, phonon transport 4-92322  
 photoexcited carriers, femtosecond orientational relax. 4-98634  
 photoexcited cond. electron spin polarisation precession in band-bending region 4-88945  
 photoluminescence characterisation of impurities and defects 4-88876  
 photoluminescence intensities, computer-controlled mapping 4-104650  
 photon-assisted dry etching using ArF laser 4-114689  
 physical data, compilation, book 4-63420  
 picosecond laser induced shock wave press. meas. 4-113259  
 picosecond photoconductors, circuit limits to time resolution 4-98661  
 plasma enhanced epitaxy, low temp. 4-99330  
 plastic deform., yield stress, photoluminescence, effect of impurity-vacancy complexes 4-70261  
 proton-bombarded, thermal annealing, elec. cond. recovery 4-98146  
 pulsed laser-assisted MBE technique 4-104733  
 quantum well lasers, visible, grown by MBE 4-91454  
 quantum well structs., reson. tunnelling 4-104299  
 Raman probe of Brillouin zone for nonequib. phonons 4-66045  
 Raman scatt. and two-phonon density of states 4-66046  
 Raman scatt. study of phonon-surface polaritons 4-80931  
 reactive ion etching, H mixing effects in Cl-containing gases 4-89148  
 reactive ion etching in  $\text{CCl}_4/\text{H}_2$  and  $\text{CCl}_4/\text{O}_2$ , AES, Raman spectra 4-81306  
 relaxation of hot electron energy, surface plasmons 4-98631  
 SAW characterisation of surface and interface states 4-98681  
 scanning DLTS investig. 4-75892  
 Schottky barrier photodetectors for microwave fibre optic links 4-101918  
 Schottky barrier photodetectors for microwave fibre optic links 4-92793  
 Schottky barrier photodiode, planar struct., ultrahigh speed 4-111200  
 Schottky barrier struct., defects and elec. props. 4-108924  
 Schottky contacts, elec. props. and interface chem., sputtering effects 4-80674  
 Schottky diodes, deep levels, photocapacitance spectra 4-61410  
 Schottky diodes, transport mechanism, deep centre effects 4-88558  
 selectively excited luminesc. 4-104639  
 semi-insulating, 0.635 eV photoluminescence band, EL2 level 4-114315  
 semi-insulating, deep donor conc., dislocations and elec. resist. 4-103781  
 semi-insulating, elec. and photoelectric props., book contrib. 4-88544  
 semi-insulating, elec. props. for microwave electronics 4-108846  
 semi-insulating, surface, photoexcited 2D electron system, reson. Raman spectra 4-109190  
 semi-insulating, surface cond. mechanism, space-charge-limited current leakage 4-70901  
 semi-insulating, undoped and low Cr doped, LEC grown, photoluminescence props., whole ingot annealing effects 4-84994  
 semi-insulating LEC grown, impurity distribution, cathodoluminesc. study 4-88885  
 semi-insulating single crystal growth by LEC method, IC appls. (*Japanese*) 4-104728  
 semi-insulating substrate, inhomogeneity characterisation, expt. study 4-65759  
 semi-insulating substrate monolithically integrated laser diode, photo monitor and electric cts. 4-60179  
 sensor in fibre-optic thermometer, temp. meas. by photoluminescence (*Danish*) 4-78315  
 shallow acceptors; ground state calc., allowing for valence band corrugations 4-108817  
 short  $n^+n^-$  section, hot electron effects 4-61385  
 single cryst. growth by liquid encapsulated Czochralski method 4-114377  
 single cryst. growth of large size, vertical mag. field appl. LEC apparatus 4-85094  
 single domain growth on Ge (100) by MOCVD 4-99342  
 single quantum wells, low temp. exciton trapping on interface defects, photolum. 4-93111  
 solar cells, equivalent electron fluence for space qualification 4-77097  
 solar cells, fabrication using plasma-deposited  $\text{Si}_3\text{N}_4$  as oxidation mask 4-89409  
 solar cells, improved performance design for space appl. 4-81552  
 solar cells, short-circuit current red. caused by proton irradi. damage 4-72108  
 solar cells, state-of-the-art review 4-81543  
 solar cells for power supplies to artificial satellites 4-99972  
 solar photovoltaic cell technologies 4-72109  
 spectra of quantum yields and photoemission (*Polish*) 4-93190  
 spectroscopy conf., Cambridge, MA, USA (Nov. 1983) 4-95025  
 spin polarised photoemission 4-88929  
 sputter etch induced electrically active defects, H passivation 4-108918  
 stoichiometry, X-ray intensity meas. of quasi-forbidden reflections 4-84416

**gallium arsenide continued**

substrate, annealing as gettering technique prior to MBE growth 4-99615  
 substrate, organo-metal CVD growth of Fe and  $\text{FeAs}_2$  films, AES study 4-61868  
 substrate for  $\text{Ge:Sb(Ga)}$  films, doping and elec. props. study (*Russian*) 4-70182  
 substrate for  $\text{SrF}_2$  single cryst., electron beam resist. and dielec. for insulator/semiconductor struct. 4-98758  
 substrate for Zn piezoelectric membranes, SAW characts. and transducers 4-104058  
 substrates for GaAs ICs, growth processes 4-99299  
 surface, (100), chemical etching and annealing 4-65722  
 surface, (110), and GaAs/Au(Pd) interfaces, high energy ion channelling studies 4-65318  
 Surface, (110), Fermi level pinning, elec. field induced Raman scatt. 4-88845  
 surface, (110),  $\text{H}_2\text{O}$  adsorption, TDS and LEED studies 4-65568  
 surface, (110), initial oxidation, core-level photoemission study 4-93195  
 surface, (110),  $\text{O}_2$  chemisorption, photon simulation, AES and EELS studies 4-113804  
 surface, (110), randomly stepped, ordering kinetics, LEED study 4-84495  
 surface, (111)  $2 \times 2$ , multilayer reconstruction model 4-84497  
 surface, (111), direct electron beam writing of oxide layer 4-92235  
 surface, (111), vacancy-induced  $2 \times 2$  reconstruction 4-75764  
 surface, phase conjugation, reflecting grating recording by plasma refl. 4-97003  
 surface (100), etch pits and cryst. defects, ellipsometry and reflectivity studies 4-84492  
 surface (100), reconstructed, electron microscopy and diff. studies 4-108690  
 surface (100) prep. using  $\text{Ar}^+$  ion bombard. 4-104886  
 surface (110),  $^{20}\text{Ne}^+$  ion yield and neutralisation, 300-1200 eV 4-76581  
 surface (110), cleaved, surface steps and dislocations, reflection electron microscopy study 4-65529  
 surface (110),  $\text{H}_2\text{O}$  chemisorption and Ga and As species-specific densities of states 4-80373  
 surface (111), relaxation effects (*Chinese*) 4-70887  
 surface (111)( $2 \times 2$ ), struct., vacancy buckling model, LEED study 4-70533  
 surface atomic geometry, photoemission spectroscopy determ. for (110) surface 4-108684  
 surface cleaning by ion bombardment 4-88213  
 surface disordering by picosecond laser pulses 4-92233  
 surface electronic structure, angle resolved photoemission spectra 4-93185  
 surface preparation, chemical etchants, comparative study 4-114701  
 surface structure (110), mech. destruction and electron bombardment effects, XPS obs. (*Russian*) 4-113772  
 tetrahedrally bonded, anisotropy of Compton profile 4-99217  
 thermal cond., hydrostatic press. depend. 4-61157  
 thick-film silk-screen deposition technique 4-109320  
 thin-film semiconductor structure with negative differential conductivity, EM wave propag. anal. 4-79017  
 transient hole transport, Monte Carlo study 4-80602  
 transistors and ICs using GaAs, advantages and characts. (*German*) 4-98678  
 trap parameters meas. by photo-excited DLTS (*Japanese*) 4-80544  
 undoped, beam coupling at  $1.06 \mu\text{m}$  using photorefractive effect 4-96987  
 undoped and Cr doped, exciton region, impurity and illumination effect on photoconductivity 4-61411  
 vacancy energy levels, impurity state pinning, tight-binding calcs., local density theory 4-88470  
 VPE, Cl desorption by  $\text{H}_2$ , quantum chemistry 4-70553  
 wafer, (100) surface, orientation determ. by etching technique 4-99619  
 wafer production, crystal fabrication device using supercond. mag. field 4-114379  
 wide band-gap, deep levels, review, book contrib. 4-88484  
 XANES spectra, k-edge region 4-109278  
 (Al,Ga)As heterojunctions, laser-induced defects, photochem. etching 4-113439  
 (Al,Ga)As, interrupted MBE growth, epitaxial InAs protection layer 4-114400  
 (Al,Ga)As, proton-bombarded, thermal annealing, elec. cond. recovery 4-98146  
 n-(Al,Ga)As/GaAs heterojunctions, hot-electron mobility study at moderate elec. fields 4-84678  
 (Al,Ga)As/GaAs/Ge/Ga polar semicond. quantum well system, growth and optical props. 4-114314  
 (Al,Ga)As-GaAs double heterostructure laser technology 4-74539  
 Al/n $^+$ GaAs/n-GaAs Schottky contacts, MBE grown, field-enhanced tunnelling and barrier lowering study 4-114037  
 Al-GaAs Schottky diodes, barrier height modification using MBE 4-70937  
 AlAs-GaAs superlattice, MBE growth and luminescence 4-114403  
 AlGaAs CSP high-power laser diodes under modulation, freq. stabilisation using short guides 4-79190  
 AlGaAs CSP semiconductor laser, negative feedback stabilised for coherent FSK transmitter 4-107875  
 AlGaAs CSP-type lasers, linewidth enhancement estimation method 4-83577  
 AlGaAs, crystal growth by MOCVD (*Japanese*) 4-76684  
 AlGaAs DH diode lasers fabricated on monolithic GaAs/Si substrate 4-112408  
 AlGaAs DH semiconductor diode laser, passive mode locking, subpicosec. coherent pulse generation (*Japanese*) 4-60060  
 AlGaAs, epitaxial short wavelength visible laser diodes 4-107628  
 AlGaAs GaAs modulation doped heterostruct., persistent photocond. studies 4-98705  
 (AlGa)As heterolasers with distrib. feedback, polarisation effects 4-64708  
 AlGaAs heterostructure laser with distributed feedback 4-74538  
 AlGaAs heterostructure, photoelectroluminescence study 4-99193  
 (AlGa)As heterostructure laser diodes, psec. pulse generation 4-107632  
 AlGaAs high power TJS laser diodes, mech. stress compensation 4-96914  
 AlGaAs injection laser with external dispersion resonator using returning mirror 4-107641  
 AlGaAs injection laser, dispersion of linewidth enhancement factor 4-112425

## gallium arsenide continued

- AlGaAs LED, radiative and nonradiative, recombination rates, meas. 4-112434
- AlGaAs laser, 0.8  $\mu\text{m}$ , spectral width with 1/f noise 4-96892
- AlGaAs laser, modulation freq. characts. for FM direct modulation 4-69463
- AlGaAs laser amplifiers for fibre transmission, device characts. 4-69578
- n-AlGaAs, MBE grown, deep electron traps 4-98570
- AlGaAs, MBE growth of high purity layers, photolum. charact. 4-98474
- AlGaAs mode locked laser, subpicosecond pulse generation 4-107697
- AlGaAs nonabsorbing mirror constricted DH large-optical cavity diode lasers 4-83579
- AlGaAs p/n graded band-gap solar cells grown by organometallic VPE 4-99961
- AlGaAs phase-locked injection laser arrays with nonuniform stripe spacing 4-107672
- AlGaAs quantum well lasers, threshold currents 4-79136
- AlGaAs semiconductor laser, frequency stabilization by thermal and current feedback control 4-60071
- AlGaAs single- and multiple-stripe quantum-well heterostruct. laser diodes in external grating cavity 4-96902
- AlGaAs TJS external cavity laser for fibre optic laser Doppler velocimeter 4-97096
- AlGaAs:Si MBE layers, donor levels anal. 4-61316
- AlGaAs/GaAs, single quantum well heterostruct. on  $\text{Al}_{0.30}\text{Ga}_{0.70}\text{As}$  buffers, MBE grown, electron mobility study 4-114029
- AlGaAs/GaAs concentrator solar cells under high temp. and humidity conditions 4-66708
- AlGaAs/GaAs heterostruct., 2D magnetotransport, electron heating effects 4-98736
- (AlGa)As/GaAs modulation-doped heterostruct., optimisation for TEG-FET operation at room temp. 4-92804
- AlGaAs/GaAs modulation-doped heterostructures, anomalous photomagnetoresist. 4-98702
- AlGaAs/GaAs quantum wells, photoluminescence studies 4-93105
- n-AlGaAs/GaAs selectively doped heterojunctions, high mobility electron gas 4-80657
- AlGaAs/GaAs single quantum well structs., MBE grown, photoluminesc. props. 4-61863
- AlGaAs/GaAs/AlGaAs single quantum well transistor with 2-D electron gas, logic device appl. 4-61443
- p-AlGaAs/p-GaAs/n-GaAs solar cells, high efficiency 4-114910
- AlGaAs/Si cascade solar cells, sensitivity and efficiency 4-85375
- AlGaAs-GaAs heterojunction interfaces, deep levels, forward I-V and DLTS meas. 4-70915
- AlGaAs-GaAs CW DH long-lifetime laser operated at room temp. 4-69474
- AlGaAs-GaAs DH, photoluminescence efficiency 4-85006
- AlGaAs-GaAs DH LED, efficiency for optical communications (*Spanish*) 4-69586
- AlGaAs-GaAs heterojunction, two-dimens. electron gas gate control characts., optimum doping (*Chinese*) 4-114021
- AlGaAs-GaAs laser with external dispersive cavity multimode rate-eqn. soln. of mode selection and tuning props. (*Chinese*) 4-91462
- AlGaAs-GaAs modulation doped layers, 2-D electron gas, room temp. mobility, parallel conduction effects 4-76027
- AlGaAs-GaAs short-cavity laser and its monolithic integration using microcleaved facets process 4-60064
- AlGaAs-GaAs solar cells for space appls. 4-81543
- AlGaAs-GaAs superlattice optical cavity multiple-quantum-well lasers, MBE grown, struct. and fabrication 4-64719
- AlGaAs-GaAs superlattices, magnetisation meas., de Haas-van Alphen oscils. 4-98734
- $\text{Al}_{0.2}\text{Ga}_{0.8}\text{As}$ :Si MBE layers, electron trap conc., DLTS study 4-61317
- $\text{Al}_{0.3}\text{Ga}_{0.7}\text{As}$ , encapsulated with  $\text{Si}_3\text{N}_4$  films, disorder-activated modes, Raman spectra 4-80916
- $\text{Al}_{0.3}\text{Ga}_{0.7}\text{As}$ -GaAs distributed feedback surface emitting laser diode 4-112424
- $\text{Al}_{0.3}\text{Ga}_{0.7}\text{As}$ -GaAs heterojunction, selectively doped, persistent photocond. effect 4-98717
- $\text{Al}_{0.85}\text{Ga}_{0.15}\text{As}$ /GaAs:Zn diffused superlattice, X-ray rocking curve and backscatt. studies 4-113818
- $\text{Al}_x\text{Ga}_{1-x}\text{As}$  avalanche diodes, heat- and radiation-resistant, elec. props. 4-65728
- $\text{Al}_x\text{Ga}_{1-x}\text{As}$ , cathodoluminescence study 4-71449
- $\text{Al}_x\text{Ga}_{1-x}\text{As}$ , correlation of photoluminescence and deep trapping 4-80537
- n-Al $_x\text{Ga}_{1-x}\text{As}$  epilayers, photoluminescence study 4-114316
- $\text{Al}_x\text{Ga}_{1-x}\text{As}$  epitaxial film, XPS study 4-93189
- $\text{Al}_x\text{Ga}_{1-x}\text{As}$ , Fourier anal. of optical spectra 4-99131
- $\text{Al}_x\text{Ga}_{1-x}\text{As}$ , graded-gap, effective resistance, temp. dependence 4-113961
- $\text{Al}_x\text{Ga}_{1-x}\text{As}$  heteroepitaxial struct. photoluminescence study 4-104673
- $\text{Al}_x\text{Ga}_{1-x}\text{As}$  layers, Rutherford backscatt. using 30 MeV  $^{16}\text{O}$  ions 4-93170
- $\text{Al}_x\text{Ga}_{1-x}\text{As}$ , line broadening in photoluminescence spectra 4-109241
- n-Al $_x\text{Ga}_{1-x}\text{As}$ , MBE grown, deep electron traps, growth conditions and alloy composition influence 4-98558
- $\text{Al}_x\text{Ga}_{1-x}\text{As}$  MBE growth, Ga desorpt., AES and photoluminesc. studies 4-93220
- $\text{Al}_x\text{Ga}_{1-x}\text{As}$  MBE layers, free carrier conc., Raman scatt. study 4-84970
- $\text{Al}_x\text{Ga}_{1-x}\text{As}$  MBE layers, persistent photocond. centre (*Chinese*) 4-88529
- $\text{Al}_x\text{Ga}_{1-x}\text{As}$  p-n junctions, organometallic VPE, anomalous light sensitivity 4-92817
- $\text{Al}_x\text{Ga}_{1-x}\text{As}$  pulsed DH laser, emission characts., influence of longit. mode carrier-depend. shifts and gain profile 4-87335
- $\text{Al}_x\text{Ga}_{1-x}\text{As}$ , Si donor behaviour, effect of Al comp. 4-98709
- $\text{Al}_x\text{Ga}_{1-x}\text{As}$  solar cell structs., photoluminescence and spectral response 4-89404
- $\text{Al}_x\text{Ga}_{1-x}\text{As}$ :Be, conference, Charlotte, NC, USA (Nov. 1983) 4-73146
- $\text{Al}_x\text{Ga}_{1-x}\text{As}$ :Be, radiative recombinations 4-76515
- $\text{Al}_x\text{Ga}_{1-x}\text{As}$ :Si, grown by MBE, photoluminesc. composition depend. 4-84996
- $\text{Al}_x\text{Ga}_{1-x}\text{As}$ :Si, grown by MBE, photoluminesc. spectra, defect-related emissions 4-84997
- $\text{Al}_x\text{Ga}_{1-x}\text{As}$ :Si MOCVD layers, transport props. 4-92834
- $\text{Al}_x\text{Ga}_{1-x}\text{As}$ :Te(Sn) epitaxial films, carrier density changes due to band struct. modifications 4-61381
- $\text{Al}_x\text{Ga}_{1-x}\text{As}$ :Zn, CVD deposited, luminescence study 4-80985
- $\text{Al}_x\text{Ga}_{1-x}\text{As}$ /GaAs heterostructure, selectively doped, transient photocond. obs. 4-70862

## gallium arsenide continued

- $\text{Al}_x\text{Ga}_{1-x}\text{As}$ /GaAs heterojunction FET, 2D electrons, cyclotron resonance studies 4-98743
- $\text{Al}_x\text{Ga}_{1-x}\text{As}$ /GaAs heterojunction, subband struct. at low temp. 4-104298
- $\text{Al}_x\text{Ga}_{1-x}\text{As}$ /GaAs single quantum well, exciton transport 4-88451
- $\text{Al}_x\text{Ga}_{1-x}\text{As}$ -GaAs concentrator solar cells, efficient circular contact grid design 4-72113
- $\text{Al}_x\text{Ga}_{1-x}\text{As}$ -GaAs double heterostructure optically pumped laser 4-96888
- $\text{Al}_x\text{Ga}_{1-x}\text{As}$ -GaAs heterostructures, 1/3 and 2/3 fractional quantum Hall effect, activation energies 4-92811
- $\text{Al}_x\text{Ga}_{1-x}\text{As}$ -GaAs heterojunction, EMF due to dynamic deform. 4-98746
- $\text{Al}_x\text{Ga}_{1-x}\text{As}$ -GaAs heterostruct., growth conditions effect in organometallic-AsH<sub>3</sub>-H<sub>2</sub> systems on solar cell param. 4-113838
- $\text{Al}_x\text{Ga}_{1-x}\text{As}$ -GaAs injection lasers, longitudinal mode selection obs. 4-79153
- $\text{Al}_x\text{Ga}_{1-x}\text{As}$ -GaAs injection laser self-modulation associated with external optical feedback 4-112440
- $\text{Al}_x\text{Ga}_{1-x}\text{As}$ -GaAs multiple well quantum well lasers, wavelength modification 4-64705
- $\text{Al}_x\text{Ga}_{1-x}\text{As}$ -GaAs multiple quantum well laser structures, MBE growth conditions 4-91465
- $\text{Al}_x\text{Ga}_{1-x}\text{As}$ -GaAs twin-channel substrate mesa guide laser with antiref. coatings, single longit. mode operation 4-83619
- $\text{Al}_x\text{Ga}_{1-x}\text{As}$  layer waveguides, light absorpt. 4-103011
- $\text{Al}_x\text{Ga}_{1-x}\text{As}$ /Sb<sub>1-y</sub>/GaSb heterostruct., conditions for LPE growth 4-114429
- $\text{Al}_x\text{Ga}_{1-x}\text{As}$ /Sb<sub>1-y</sub>/Sb<sub>2</sub> heterojunction photocells, LPE fabrication 4-81559
- AlGaInPAs lattice matched to GaAs, LPE growth, photolum. obs. 4-70581
- AlInAs/GaInAs avalanche photodiodes and AlInAs electroabsorption p-i-n photodiodes grown by MBE 4-69591
- $\text{Al}_{0.48}\text{In}_{0.52}\text{As}$ /Ga<sub>0.47</sub>In<sub>0.53</sub>As avalanche photodiode for long wavelength fibre optic communication, MBE growth 4-79337
- $\text{Al}_{0.48}\text{In}_{0.53}\text{As}/\text{n}^+\text{-Ga}_{0.47}\text{In}_{0.53}\text{As}$ , low resist. alloyed ohmic contacts 4-84692
- CaAs: Cr LEC wafer, Cr<sup>2+</sup> distribution, EPR studies 4-98124
- (Ga,Al)As/GaAs double heterostructures, LPE, struct. and lasing characts. rel. to As vapour press. 4-66249
- (Ga,In)(As,P), adducts in MOVPE 4-71575
- (Ga,In)As, adducts in MOVPE 4-71575
- Ga-Al-As, luminescence lineshapes of electron-hole plasma 4-109242
- Ga-Al-As system, MOVPE, current status for optoelectronic appls. 4-104737
- Ga-Al-As/GaAs, liq. epitaxy capillary effect 4-98408
- Ga-In-As-P system, VPE of mixed III-V compounds 4-71578
- Ga-In-P-As system, LPE, growth kinetics 4-88426
- Ga-In-P-As system, MOVPE, current status for optoelectronic appls. 4-104737
- GaAs/Ni reactive interface, soft X-ray photoemission spectra studies 4-113820
- GaAlAs BH 100 Mbit/s laser diode terminal with optical gain for fibre-optic LANs 4-112586
- GaAlAs BH window lasers, 11 GHz direct modulation bandwidth 4-112410
- GaAlAs bright visible-range injection laser development 4-69441
- GaAlAs buried multi-quantum-well laser fabricated by diffusion induced disordering 4-74547
- GaAlAs buried multi-quantum well lasers fabricated by diffusion-induced disordering 4-91452
- (GaAl)As cleaved coupled-cavity laser anal. 4-96900
- (GaAl)As cleaved-coupled-cavity lasers, coupling strength study 4-91459
- GaAlAs diode laser, picosecond gain meas. 4-107638
- (GaAl)As diode lasers, spectral characteristics at 1.7K 4-112411
- GaAlAs electroabsorption modulators, monolithically integrated array 4-103006
- (GaAl)As heterojunction laser, optically controlled two-component 4-107640
- GaAlAs laser, MESFET and photodiode, monolithic optoelectronic integration 4-74747
- GaAlAs laser, picosecond pulse generation by optoelectronic feedback 4-96885
- GaAlAs laser, simultaneous wavelength and power stabilisation using single detector scheme 4-91456
- GaAlAs laser, wavelength stabilisation using integrated optic Fabry-Perot interferometer 4-91457
- GaAlAs laser diode coupled to an external cavity intensity noise suppression and modulation characts. 4-79144
- GaAlAs laser diode optical switches, isolation characteristics 4-107680
- GaAlAs laser oscillating in single longit. mode, LF feedback noise 4-96909
- GaAlAs laser picosecond pulse temporal coherence props., directly modulated and freq. stabilised optical communication system appls. 4-74509
- GaAlAs lasers, catastrophic and latent damage due to elec. transients 4-79146
- GaAlAs lasers, transverse-mode stabilised MOCVD grown, with embedded-confining layer on optical waveguide 4-69443
- GaAlAs light sources, radiative coeffs., carrier dependence 4-64703
- GaAlAs, MBE, thermodynamics of O incorporation 4-61253
- GaAlAs material epitaxial growth, devices for optical communications 4-74746
- GaAlAs, optical communication through low-visibility atmosphere using a CW diode laser 4-112589
- GaAlAs, proton energy loss straggling meas. for nucl. profiling appl. 4-70246
- GaAlAs semiconductor laser fabrication, integration with fibre V-groove alignment struct. 4-96948
- GaAlAs single quantum well size effect modulation light sources 4-97014
- (GaAl)As transverse-mode stabilised laser diodes, MOCVD growth 4-96912
- GaAlAs V-groove lasers, 4 ps light pulses generation 4-69407
- GaAlAs very high speed lasers and detectors for integrated optoelectronic devices 4-96889
- GaAlAs/GaAs quantum-well lasers, organometallic VPE and MBE grown, developments and expt. study 4-69442
- GaAlAs/GaAs selectively doped heterojunction, electron conc., FET appl. 4-98703
- GaAlAs/GaAs surface-emitting injection laser, pulsed oscill. 4-79175

## gallium/arsenide continued

- GaAlAs/GaAs surface emitting injection laser, room-temp. pulsed operation 4-112416
- GaAlAs/GaAs twin channel laser with high CW power and low beam divergence 4-74548
- (GaAl)As-GaAs DH lasers,  $D_2^+$  bombardment isolated stripe geometry (Chinese) 4-112431
- GaAlAs-GaAs DH lasers, narrow-channelled substrate stripe-type, characts. meas. and anal. (Chinese) 4-112433
- GaAlAs-GaAs heterostructure, nuclear profiling of Al 4-98123
- GaAlAs-GaAs integrated optical repeater 4-97143
- GaAlAs-GaAs modulation doped heterostruct., self-consistent variational calcs. and alloy scatt. 4-98733
- Ga<sub>0.4</sub>Al<sub>0.6</sub>GaAs heterostructures, LPE growth, layer height profiles rel. to convection and cooling rates 4-66248
- Ga<sub>1-x</sub>Al<sub>x</sub>Si(Se), dopant incorporation during MBE growth 4-99320
- Ga<sub>1-x</sub>Al<sub>x</sub>As, carrier transport under impurity radiative recombination conditions 4-104211
- Ga<sub>1-x</sub>Al<sub>x</sub>As, crystalline struct., two-phonon Raman spectra study 4-71385
- Ga<sub>1-x</sub>Al<sub>x</sub>As, spatial dielec. functions, site and comp. depend. 4-104136
- Ga<sub>1-x</sub>Al<sub>x</sub>As superlattices, acoustic modes, Brillouin and Raman scatt. study 4-80928
- p-Ga<sub>1-x</sub>Al<sub>x</sub>As:Be-p-GaAs:Be-n-GaAs:Si heterojunction LPE growth for solar cells 4-109334
- Ga<sub>1-x</sub>Al<sub>x</sub>As:Zn, (Se), doping in MOCVD growth, carrier conc. and cond. 4-88982
- Ga<sub>1-x</sub>Al<sub>x</sub>As/GaAs solar cell with antiref. coating, LPE grown, design, fabrication and characts. (Polish) 4-114904
- Ga<sub>1-x</sub>Al<sub>x</sub>As-GaAs, Raman scatt. theory 4-76460
- Ga<sub>1-x</sub>Al<sub>x</sub>As-GaAs heterostructure, LPE grown, dislocation extension and density distrib. (Chinese) 4-113449
- Ga<sub>1-x</sub>Al<sub>x</sub>As-GaAs interface, fractional quantum Hall effect in a two-dimensional hole system 4-108930
- Ga<sub>1-x</sub>Al<sub>x</sub>As-GaAs/GaAs (001) superlattices, structural parameters, X-ray diffr. 4-84257
- Ga<sub>0.4</sub>Al<sub>0.6</sub>As and Si solar cells, beam splitting concentrator, optical characterisation 4-66665
- Ga<sub>0.4</sub>Al<sub>0.6</sub>As/GaAs system, elastic surface waves, Green's function anal. 4-108695
- GaAlSbAs-GaSb injection laser, operation and luminescence study 4-74508
- Ga<sub>1-x</sub>Al<sub>x</sub>Sb<sub>1-x</sub>As<sub>x</sub>/GaSb epitaxial films As segregation coeff. and distrib. over thickness 4-75692
- Ga<sub>1-x</sub>Al<sub>x</sub>Sb<sub>1-x</sub>As<sub>x</sub>/GaSb, LPE, phase equilib. rel. to lattice mismatch strain 4-93236
- GaAs (110)-Al interface form. at low temp., electronic and struct. props. 4-84695
- GaAs (110)-ZnSe interface, LEED and AES characterisation 4-84517
- GaAs, semi-insulating optical photogenerated traps 4-108875
- GaAs, spin doublet, mag. field depend., photocond. obs. 4-104255
- GaAs: Mn, spin-depend. recombination, optical pumping studies 4-99183
- GaAs:B, existence of B<sub>A</sub> impurity antisite centres, IR absorption lines study 4-71413
- GaAs:B, interaction between B and defects 4-80082
- GaAs:B, interstitial centre, radiation induced, cluster-Bethe lattice treatment 4-98090
- GaAs:Be, ion implanted, reduced damage generation 4-113474
- GaAs:Be, ion implanted, annealing behaviour, spectroscopic ellipsometry and Raman scatt. 4-113482
- GaAs:C(Si), impurity and defect anal. by IR absorpt. spectra 4-75893
- GaAs:Cr, Cr-related complex, photoluminesc. studies 4-88467
- GaAs:Cr, epitaxial layers, Cr doping and elec. parameters 4-76683
- GaAs:Cr, impurities, optical and transport studies 4-71444
- GaAs:Cr, impurity photocond., internal quantum efficiency 4-88540
- GaAs:Cr, ion implanted, Cr redistribution 4-88194
- GaAs:Cr, ion irradi. effect on defect thermal annealing 4-98156
- GaAs:Cr, ionisation processes by upper conduction band electrons, mag. field effects 4-65640
- GaAs:Cr, LEC growth, mag. field effect on impurity conc. 4-114378
- GaAs:Cr, photolum. at 0.839 eV, polarisation of Zeeman spectra 4-71427
- GaAs:Cr, photoluminescence excitation spectra, Cr<sup>2+</sup> internal luminesc. 4-81004
- GaAs:Cr, semi-insulating, inhomogeneities, optical obs. 4-60944
- GaAs:Cr, semi-insulating, Four-wave mixing using photorefractive effect, optical processing appl. 4-74585
- GaAs:Cr, US attenuation and vel. meas. 4-98212
- GaAs:Cr picosecond optoelectronic switches, pulse modulation of GaAs-(GaAl)As DH diode laser 4-107701
- GaAs:Cr-GaAs epitaxial junction, IR characterisation 4-109170
- n-GaAs:Cr<sup>2+</sup>, acoustic paramagnetic resonance study 4-71171
- GaAs:Cr<sup>2+</sup>, comparison of static and dynamic Jahn-Teller models 4-61345
- GaAs:Cr<sup>2+</sup>, trigonal symmetry sites, photoluminescence spectra anal. 4-108391
- GaAs:Cr(Ni), deep impurity charact., photoluminescence study 4-98557
- GaAs:Cr(O), electrical properties and impurity states 4-75963
- GaAs:Fe, Cu, epilayers, deep states, DLTS study 4-108802
- GaAs:Ge(Si), LEC grown, dislocation structure etching rel. to dopant conc. 4-113451
- GaAs:Ge(001), MBE grown, TEM image contrast from antiphase domains 4-104098
- GaAs:In, isoelectric doping, X-ray and electron microprobe anal. 4-75491
- GaAs:Mn, charge state of Mn impurities, mag. susceptibility ESR and Hall effect meas. 4-108982
- GaAs:Mn, Mn redistribution, interstitial-substitutional model anal. 4-92433
- GaAs:Mn, phonon scatt. at acceptor ground state 4-70729
- GaAs:Mn, thermal cond. resonances of acceptor states 4-104011
- GaAs:N, isoelectronic traps study by photoluminesc. (Chinese) 4-93098
- GaAs:O p-n structs., magnetically sensitive, elec. characts. (Russian) 4-65729
- GaAs:Si(Si), implant sublattice site determ., PIXE studies 4-98119
- GaAs:Se, deep acceptor, photoluminescence study 4-80534
- n-GaAs:Se, free electron optical absorpt. theory 4-104637
- GaAs:Se<sup>+</sup>, implanted, amorphous-cryst. interface, high resolution struct. charact. 4-70171
- GaAs:Si, (100), vacuum annealed, free carrier reduction 4-98610

## gallium arsenide continued

- GaAs:Si, Al p-n structures, radiative recomb., electrolum. characts. (Russian) 4-109249
- n-GaAs:Si,  $\alpha$ -irrad., positron annihilation study 4-104696
- GaAs:Si, crystal growth by horizontal gradient-freeze technique, carrier and dislocation density 4-66216
- GaAs:Si, implanted, elec. props., pulse laser annealing effects 4-60953
- GaAs:Si, implanted, radiation annealing with CW Xe arc lamp 4-75486
- GaAs:Si, ion implantation, ion beam purity and mass spectra 4-99864
- GaAs:Si, ion implanted, and semi-insulating GaAs, deep levels, photoconductivity study 4-88469
- GaAs:Si, LEC and horizontal Bridgman growth, elec. uniformity 4-65683
- GaAs:Si, local vibr. modes and elec. activation, Raman study 4-84357
- GaAs:Si, localised vibr. mode IR absorpt. meas. 4-104599
- GaAs:Si, planar channelling of Si implants 4-75483
- GaAs:Si, Si diffusion using rapid thermal processing, encapsulant effects 4-65464
- GaAs:Si, Si doping from Si<sub>3</sub>H<sub>8</sub> in MOCVD growth 4-75459
- GaAs:Si MOCVD films, free carrier profile synthesis by atomic plane doping 4-92221
- GaAs:Si p-n structures, degree of compensation, photoluminesc. study 4-65736
- GaAs:Si/AlGaAs DH TJS lasers grown by MBE 4-107671
- GaAs:Sn,Te, dual implanted damage and annealing, challenging studies 4-80116
- GaAs:Sn with SiO<sub>2</sub> cap, thermal diffusion, doping mechanism 4-104006
- GaAs:Sn/GaAs:Cr interface, electron and hole traps, photovoltaic studies 4-104283
- GaAs:Te, deformed, precip., defect struct., electron microscopy obs. 4-103752
- GaAs:Te, H ion bombarded, free carrier density, EELS studies 4-98632
- GaAs:transition metals, electronic struct. of bulk centres 4-108818
- GaAs:V, semi-insulating, V redistribution during heat treatment 4-80070
- GaAs:Zn, monolayer surface doping from plated Zn source 4-70172
- p-GaAs:Zn, emission band, electron irradi. and annealing effects 4-88881
- GaAs:Zn, reproducible leaky tube Zn diffusion with submicron junction depths 4-98361
- GaAs:Zn, thermal pulse diffusion of Zn from elemental source 4-98360
- GaAs/(AlGa)As selectively doped heterostruct., transport props. 4-70913
- GaAs/(GaAl)As two-dimens. electron gas, cyclotron reson. study 4-104297
- GaAs/Al interface, electronic struct. and bonding 4-84700
- GaAs/Al interface, low temp. form. and structure, LEED, AES and work function meas. 4-80425
- GaAs/Al<sub>1-x</sub>Ga<sub>x</sub>As superlattices and heterojunctions, elec. props., numerical solns. 4-70924
- GaAs/Al<sub>1-x</sub>Ga<sub>x</sub>As heterostructures, 2D electron localisation 4-98718
- GaAs/Al<sub>1-x</sub>Ga<sub>x</sub>As heterostruct., photocond. studies 4-98744
- GaAs/Al<sub>1-x</sub>Ga<sub>x</sub>As quantum well struct., low temp. electron mobility, alloy disorder scatt. contrib. 4-92808
- GaAs/Al<sub>1-x</sub>Ga<sub>x</sub>As quantum wells, struct. and optical props. 4-99151
- GaAs/Al<sub>1-x</sub>Ga<sub>x</sub>As quantum wells, Be doped, photoluminescence studies 4-104653
- GaAs/AlAs multiple quantum well struct., electron-hole plasma, picosecond dynamics 4-92803
- GaAs/AlAs-GaAs superlattice/GaAs superlattice barrier capacitor: a structure for the investigation of heterojunction interfaces 4-84679
- GaAs/AlGaAs, MOCVD growth and homogeneous nucleation 4-99340
- GaAs/AlGaAs DH laser, LPE fabricated, design optimisation for entertainment electronics (German) 4-102948
- GaAs/AlGaAs heterointerfaces, struct. evaluation, TEM studies 4-84516
- GaAs/AlGaAs heterojunction, 2D electron gas, cyclotron resonance studies 4-76032
- GaAs/AlGaAs heterostructures, 2D electron plasma, optical processes 4-76523
- GaAs/AlGaAs heterostructures, carrier density, hydrostatic press. control 4-98735
- GaAs/AlGaAs heterostruct., screening and polaron effects, cyclotron resonance studies 4-98741
- GaAs/AlGaAs heterostruct., organometallic VPE growth and characterisation 4-99341
- GaAs/AlGaAs inverted heterojunctions, photoluminescence studies 4-98460
- GaAs/AlGaAs MQW heterostructure current-injection lasers, carrier-induced energy-gap shrinkage 4-112423
- GaAs/AlGaAs multi-quantum-well lasers, polarization-dependent gain 4-112412
- GaAs/AlGaAs multiple quantum well structures, room temp. excitonic nonlinear absorpt. and refract. 4-74590
- GaAs/AlGaAs multiple quantum well structs., photoexcited carriers intraband relax., femtosecond studies 4-88565
- GaAs/AlGaAs single quantum well struct., enhanced luminescence 4-99150
- GaAs/AlGaAs solar cell battery-on Venera spacecraft, optical and metrological characts. 4-93615
- GaAs/AlGaAs three-dimensional optical waveguides, anal. of characts. (Chinese) 4-83689
- GaAs/AlGaAs/GaAs heterojunction barrier, MOCVD grown, electron transport 4-80661
- GaAs/Au contacts, Schottky barrier photosensitivity spectra in strong absorption region (Russian) 4-65741
- GaAs/Au interface struct., XPS, RHEED and ion scatt./channelling studies 4-80421
- n-GaAs/Au Schottky contacts, elec. props. and interface chem., sputtering effects 4-80674
- n-GaAs/Au-Ge Ohmic contact fabrication by IR lamp alloying 4-84690
- GaAs/Au-Ge-Ni ohmic contacts, CO<sub>2</sub> laser alloying 4-76038
- GaAs/Au-Ti(Au) Schottky contacts, damage-induced degradation 4-84699
- GaAs/AuGe ohmic contact, Ge and Au profiles, SIMS studies 4-103782
- GaAs/Ca<sub>1-x</sub>Sr<sub>x</sub>F<sub>2</sub>/GaAs (100) lattice-matched MBE structures 4-88562
- GaAs/Ga<sub>1-x</sub>Al<sub>x</sub>As quantum well wires, hydrogenic impurity states 4-92815
- GaAs/GaAlAs, antiref. coated twin DH diode external cavity ring laser, optical bistability study 4-91460
- GaAs/GaAlAs DH stripe geometry lasers, Be-implanted, MOCVD growth 4-107635
- GaAs/GaAlAs integrated optoelectronics for optical interconnect applications 4-97140

## Ilium arsenide continued

- GaAs/GaAlAs lasers, synchronous mode locking by picosecond optoelectronic switch 4-96965
- GaAs/GaAlAs monolithically Peltier-cooled laser diodes 4-74540
- GaAs/GaAlAs multiple-quantum-well semicond., optical bistability due to increasing absorpt. 4-74598
- GaAs/GaAlAs quantum well self-electro-optic effect device as hybrid optically bistable switch 4-91522
- GaAs/GaAlAs quantum well structs., oscillatory magnetoresist. studies 4-98738
- GaAs/GaAlAs single mode laser diodes, free space optical communication, design and system requirements 4-79176
- GaAs/GaAlAs subthreshold DH twin stripe laser, interstripe coupling and current spreading 4-79139
- GaAs/GaAlAs twin stripe lasers, current rise time effect on beam stability, expt. study 4-91510
- GaAs/GaAlAs waveguide phase modulator, MBE grown heterostruct., design for PSK optical fibre systems 4-83685
- GaAs/Ge single crystal layers, MBE growth and patterning on Si substrates 4-99315
- GaAs/Ge(Al)As heterojunctions, interface struct., TEM and STEM studies 4-108728
- GaAs/metal contacts, interface struct., TEM and STEM studies 4-108728
- GaAs/metal interface, Schottky barrier heights meas. 4-76018
- GaAs/N-AlGaAs heterostructures, selectively doped, MBE grown; tungsten-halogen lamp annealing effects 4-61444
- GaAs/nAlGaAs superlattice devices, high speed electrons and hot electron effects appls. (Japanese) 4-61449
- GaAs/native oxide interfaces, density of states, C-V meas. 4-88604
- GaAs/Ni film system, interfacial reactions, TEM and X-ray diff. studies 4-108729
- GaAs/Ni-Ta interfacial reactions, metallisation appl. 4-98367
- i-GaAs/p-InSb, heteroepitaxial struct., quasi-2D electrons, nonequilibrium galvanomagnetic effects 4-70916
- GaAs/Pt, ion beam mixing and ohmic contact form. 4-92244
- p-GaAs/Ti-Pt ohmic contact (Chinese) 4-88589
- GaAs-(Al,Ga)As superlattices, MBE grown, growth temp. influence 4-81139
- GaAs-(AlGa)As large optical cavity lasers 4-107631
- GaAs-(AlGa)As lasers, passive waveguide coupled, mode behaviour 4-91499
- GaAs-(AlGa)As modulation-doped heterostructs., reson. inelastic light scatt. studies 4-84973
- GaAs-(AlGa)As strip geometry laser diodes, dynamical thermal props. 4-79206
- GaAs-(AlGa)As twisted DH laser, composite cavity config., design and longit./transverse mode operation 4-69456
- GaAs-(AlGa)As two-dimens. electron plasma, optical emission and excitation processes 4-104666
- GaAs-(GaAl)As DH diode laser, pulse modulation by picosecond optoelectronic GaAs:Cr switches 4-107701
- GaAs-Ag, high resolution EELS study 4-99248
- GaAs-Al contact, semicond. electron field emission props., metal adsorption effect 4-99289
- GaAs-Al interface, IR surface second harmonic generation and characts. (Chinese) 4-74606
- GaAs-Al<sub>0.3</sub>Ga<sub>0.7</sub>As, quantised Hall resistance and 2D electron gas behaviour 4-98724
- GaAs-Al<sub>0.3</sub>Ga<sub>0.7</sub>As quantum wells, photoluminesc. from spike doped hydrogenic donors 4-104668
- GaAs-Al<sub>0.3</sub>Ga<sub>0.7</sub>As DH laser with two sections in a common cavity (Chinese) 4-112466
- GaAs-Al<sub>0.3</sub>Ga<sub>0.7</sub>As abrupt heterojunctions grown by MBE, Auger composition profiles 4-80429
- GaAs-Al<sub>0.3</sub>Ga<sub>0.7</sub>As quantum well structs., Raman scatt. study 4-93079
- GaAs-Al<sub>0.3</sub>Ga<sub>0.7</sub>As heterostructures, 2D electron gas, disorder, fractional quantum Hall effect 4-76033
- GaAs-Al<sub>0.3</sub>Ga<sub>0.7</sub>As heterostructure, low temp. fractional quantum Hall effect 4-98722
- GaAs-Al<sub>0.3</sub>Ga<sub>0.7</sub>As heterostructure, anal. of quantised Hall resist. at finite temps. 4-98727
- GaAs-Al<sub>0.3</sub>Ga<sub>0.7</sub>As heterostructure, thermopower meas. on 2D electron gas 4-98729
- GaAs-Al<sub>0.3</sub>Ga<sub>0.7</sub>As heterostructure, quantum Hall resistance, temp. depend. 4-114028
- GaAs-Al<sub>0.3</sub>Ga<sub>0.7</sub>As multiple quantum well struct., magneto-Raman characterisation 4-104577
- GaAs-Al<sub>0.3</sub>Ga<sub>0.7</sub>As quantum well struct., exciton binding energy 4-75868
- GaAs-Al<sub>0.3</sub>Ga<sub>0.7</sub>As quantum wells, energy-gap discontinuities and effective masses 4-92623
- GaAs-Al<sub>0.3</sub>Ga<sub>0.7</sub>As superlattices, Raman probing of phonons and interfaces 4-80927
- GaAs-Al<sub>0.3</sub>Ga<sub>0.7</sub>As stripe geometry lasers, spectral behaviour, lateral hole-burning effects, numerical investigation 4-87334
- GaAs-Al<sub>0.3</sub>Ga<sub>0.7</sub>As tunnel junctions, sequential single-phonon emission obs. in electron transport 4-80667
- GaAs-AlAs heterojunction barriers, inelastic tunnelling characts. 4-98710
- GaAs-AlAs heterostructures, photoacoustic spectroscopy by piezoelec. transducers 4-61448
- GaAs-AlAs multiple quantum well struct., Raman scatt. and luminescence study 4-99105
- GaAs-AlAs semiconductor superlattices, MOCVD prep., interface struct. study 4-108726
- GaAs-AlAs:Zn superlattice, Zn impurity diffusion, X-ray study 4-75729
- GaAs-AlGaAs, optical activity of plasma oscils. 4-84930
- GaAs-AlGaAs GRIN-SCH lasers, MBE grown for optoelectronic integrated circuit appl. 4-96894
- GaAs-AlGaAs heterojunction, phonon emission and electron heating 4-70927
- GaAs-AlGaAs injection lasers (Dutch) 4-87329
- GaAs-AlGaAs monolithically integrated optical circuit fabrication 4-69597
- GaAs-AlGaAs multiple quantum well heterostruct., delocalised exciton state 4-92621
- GaAs-AlGaAs superlattice and interface, acoustic props. 4-80366
- GaAs-AlGaAs superlattices, MBE grown, direct obs. of lattice arrangement 4-84528
- GaAs-AlGaAs superlattice grown by MBE, struct. and optical props. 4-84538

## gallium arsenide continued

- GaAs-AlGaAs transverse junction stripe laser, Si doped, MBE fabrication 4-96893
- GaAs-AlGaAs window-stripe multi-quantum well heterostruct. laser fabrication 4-69436
- GaAs-Al(Au) Schottky barrier contacts, LEC grown, electron traps, DLTS signals, effect of metal 4-84691
- GaAs-Au tunnel structs., differential cond. characts. 4-61455
- GaAs-Ga<sub>1-x</sub>Al<sub>x</sub>As, lateral superlattice struct. 4-92816
- GaAs-Ga<sub>1-x</sub>Al<sub>x</sub>As, binding energy of exciton in GaAs quantum well, magneto-optical determination 4-114027
- GaAs-Ga<sub>1-x</sub>Al<sub>x</sub>As heterojunction, electron energy level calcs. 4-108915
- GaAs-Ga<sub>1-x</sub>Al<sub>x</sub>As multilayer struct. masked and selective and thermal oxidation, technology for stripe-geometry DH lasers and integrated optics 4-69610
- GaAs-Ga<sub>1-x</sub>Al<sub>x</sub>As multiple quantum well structs., Hall mobility, electron conc. and buffer width depend. 4-80668
- GaAs-GaAlAs channelled-substrate lasers, single longit. mode, grown by MBE 4-69403
- GaAs-GaAlAs double heterostructure, quantisation of excitonic polaritons 4-92634
- GaAs-GaAlAs heterojunction, freq. enhanced fractional quantisation, quantum Hall effect 4-80664
- GaAs-GaAlAs heterostructures, hot photoluminescence polarisation and spectrum 4-61743
- GaAs-GaAlAs heterostructs., 2-D electron gas, electron mobility, temp. dependence 4-98704
- GaAs-GaAlAs heterostructures, interband scatt. in mobility 4-98732
- GaAs-GaAlAs interface, 2D electron gas, cyclotron reson. 4-109077
- GaAs-GaAlAs multiple-quantum-well structures, sharp line photolum. spectra 4-93110
- GaAs-GaAlAs pnnp negative-resistance laser with low threshold current density 4-69448
- GaAs-GaAlAs quantum well lasers tunable by long wavelength radiation 4-69404
- GaAs-GaAlAs quantum well struct., optical props., review 4-104146
- GaAs-GaAlAs quantum wells, coupled, photoluminesc. and excitation spectroscopy 4-104667
- GaAs-GaAlAs quantum wells, reflectance of two-dimensional excitations 4-109211
- GaAs-GaAlAs superlattices, third order nonlinear optical susceptibility 4-74586
- GaAs-GaAlAs superlattice, Raman study of folded modes 4-80929
- GaAs-GaAlAs system, superlattices, quantum wells, and heterostructs., review 4-80666
- GaAs-Ge interface, electronic struct. 4-84665
- GaAs-Ge(100) interfaces, Fermi level position and valence-band edge discontinuity study 4-61450
- GaAs-HCl-H<sub>2</sub> system, phase equilb., dominant reactions for VPE, etching obs. 4-71579
- GaAs-Hg Schottky barrier, crystal damage during CV profiling 4-98753
- GaAs-In<sub>0.3</sub>Ga<sub>0.7</sub>As MOCVD strained-layer superlattices, lattice distortion, TEM study 4-88406
- p-GaAs-KCl electrolyte interface, photoemission rate law 4-71513
- GaAs-metallic glass contacts, TEM obs. 4-104094
- GaAs-nAlGaAs structures, modulation doped, elec. props., effect of IR flash lamp annealing 4-98712
- GaAs-NiSi thermal stability ohmic contact 4-88590
- n-GaAs-p-GaAs:Si-p-Al<sub>0.3</sub>Ga<sub>0.7</sub>As, solar heterophotocells with increased p-n junction depth 4-77103
- n-GaAs-polyisiloxane-metal struct., elec. props. (French) 4-61460
- GaAs-Si interface, nonlinear surface EM waves 4-80892
- GaAs-thin Au/Cr bilayer structure, interfacial chemical reactions and drive-out diffusion, AES study 4-80313
- (GaAs)<sub>1-x</sub>(Ge)<sub>2x</sub> bond and struct. models 4-108772
- GaAsP p-n junctions, avalanche multiplication and ionisation rates, SEM studies 4-65733
- GaAsP strained-layer superlattice structures and their buffer layers, comparison of trapping levels 4-113885
- n-GaAs<sub>1-x</sub>P<sub>x</sub> anodes in ac. Se<sup>2-</sup>/Se<sup>2-</sup> solns., characts. 4-104310
- GaAs<sub>1-x</sub>P<sub>x</sub>, EL2 metastable state, photocapacitance quenching study 4-70717
- GaAs<sub>1-x</sub>P<sub>x</sub>, Fourier anal. of optical spectra 4-99131
- GaAs<sub>1-x</sub>P<sub>x</sub>, internal elec. field-enhanced impurity diffusion and p-n junction form. 4-84469
- GaAs<sub>1-x</sub>P<sub>x</sub>, localised excitons, luminescence study 4-61291
- GaAs<sub>1-x</sub>P<sub>x</sub>, N, exciton tunnelling inhibited by disorder 4-92622
- GaAs<sub>1-x</sub>P<sub>x</sub>, N, excitons and excitonic mols. bound to impurity, calcs. 4-108785
- GaAs<sub>1-x</sub>P<sub>x</sub>, N<sup>+</sup>, Zn<sup>+</sup>, implanted, photoluminescence spectra, impurity conc. depend. (Chinese) 4-93099
- GaAs<sub>1-x</sub>P<sub>x</sub>-GaAs<sub>1-y</sub>P<sub>y</sub> isotype heterojunction electrodes in photoelectrochem. cells, photoluminescence and electroluminescent props. 4-99140
- GaAsP<sub>1-x</sub> mixed cryst., long-wavelength optical phonons (Chinese) 4-108559
- GaAsP<sub>1-x</sub> phonon modes, Raman scatt. study 4-108563
- GaAsP<sub>1-x</sub>Cu, LEDs, Cu impurities, thermal redistribution 4-80080
- GaAsP<sub>1-x</sub>/GaP strained-layer superlattices, Be-implantation doping 4-80057
- GaAsP<sub>1-x</sub>/GaP superlattices, strain depth profiles, misfit dislocations obs 4-104095
- GaAs<sub>1-x</sub>P<sub>x</sub>, fundamental absorpt., optical absorpt. coeff. 4-76408
- GaAs<sub>1-x</sub>Sb<sub>x</sub>, electron irradi., electronic struct. of E3-defects 4-70720
- GaAs(001)-Au interface, formation by MBE and thermal stability 4-99328
- GaAs(110)-In interface, photoemission study 4-85079
- GaInAs epitaxial layers, thickness and uniformity by automated scanning double axis X-ray diff. 4-65589
- GaInAs, MBE, thermodynamics of O incorporation 4-61253
- GaInAs-InP double heterostructure, epitaxial low press. MO-CVD growth for device appl., book contrib. 4-61875
- GaInAs-InP heterostructure emitters, 1.3-1.55 μm 4-104308
- GaInAs-InP IR detectors, applications of electron microscope techniques to semiconductors 4-103622
- GaInAs-InP quantum-well lasers, gain and intervalence band absorpt. 4-96899
- Ga<sub>0.47</sub>In<sub>0.53</sub>As, hot electron velocity overshoot 4-70823
- Ga<sub>0.47</sub>In<sub>0.53</sub>As, ion implanted, annealing, TEM obs. 4-70228
- Ga<sub>0.47</sub>In<sub>0.53</sub>As layers, MOCVD growth and characterisation (French) 4-76685

## gallium arsenide continued

- Ga<sub>0.47</sub>In<sub>0.53</sub>As, MBE planar doped barriers in InP, elec. characts. 4-98708
- Ga<sub>0.47</sub>In<sub>0.53</sub>As photoconductive detector prepared by VPE 4-86478
- Ga<sub>0.47</sub>In<sub>0.53</sub>As/Al<sub>0.48</sub>In<sub>0.52</sub>As heterojunction, conduction band discontinuity, photoluminescence study 4-76028
- Ga<sub>0.47</sub>In<sub>0.53</sub>As-InP, Raman scatt. theory 4-76460
- Ga<sub>1-x</sub>In<sub>x</sub>As based materials, recrystallisation in temp. gradient 4-114390
- Ga<sub>1-x</sub>In<sub>x</sub>As, bond lengths, virtual crystal approx. 4-75385
- GaInAsP 1.5  $\mu$ m laser diode, Raman amplification in low fiber loss region 4-96955
- GaInAsP alloy semiconductors, book 4-58588
- GaInAsP BH laser, low-threshold, multiple-cavity, longit.-mode stabilised 4-91468
- GaInAsP cleaved coupled-cavity laser, tunable design, FM operation for communication appl. 4-69451
- GaInAsP, defect motion and growth of extended non-radiative defect structs., book contrib. 4-60914
- (GaIn)(AsP) epilayers, growth, optical communication requirements, review 4-61833
- GaInAsP, epitaxial layers, thickness and uniformity by automated scanning double axis X-ray diffr. 4-65589
- GaInAsP heterostructure laser with distributed feedback 4-74538
- (GaIn)(AsP) heterostructure laser diodes, psec. pulse generation 4-107632
- GaInAsP, high field transport meas., review, book contrib. 4-61389
- GaInAsP, high purity, charact., growth, back contrib. 4-61334
- GaInAsP inner stripe laser diodes on p-InP substrate 4-96886
- GaInAsP, ion implantation, book contrib. 4-60943
- GaInAsP, LPE growth on InP, review, book contrib. 4-61882
- GaInAsP lattice matched to InP, electronic struct., book contrib. 4-61284
- GaInAsP, low field carrier mobility, book contrib. 4-61383
- GaInAsP, low field transport calcs., book contrib. 4-61384
- GaInAsP, n-type, lattice matched to InP, hot electron transport, book contrib. 4-61388
- GaInAsP, nonlinear carrier dynamics, optical bleaching study 4-74625
- GaInAsP, photolum., and optical gain spectra, book contrib. 4-61752
- GaInAsP picosecond optical absorption saturation 4-91541
- GaInAsP, VPE growth, review, book contrib. 4-61874
- GaInAsP/InP 1.3  $\mu$ m distributed feedback lasers, LPE growth 4-96913
- GaInAsP/InP BH laser diodes, fabrication technique 4-74507
- GaInAsP/InP BH laser with chemically etched and mass-transported mirror 4-74537
- GaInAsP/InP BH injection lasers, network modelling and modulation characts. 4-96890
- GaInAsP/InP DFB laser, 1.5  $\mu$ m range, longitudinal mode behaviour 4-74512
- GaInAsP/InP DFB lasers, 1.3  $\mu$ m, monolithic integrated struct., WDM optical communication appl. 4-83618
- GaInAsP/InP hetero-multilayers, LPE fabrication and reflectivity 4-99357
- GaInAsP/InP laser, single-mode, low-temp. single-step LPE growth 4-112407
- GaInAsP/InP phase adjusted active distributed reflector laser, 1.5  $\mu$ m, for dynamic single mode operation 4-69437
- GaInAsP/InP BH but-jointed built-in integrated, lasers, 1.5-1.6  $\mu$ m operation, static characts. 4-60065
- GaInAsP-InP DH lasers, review, book contrib. 4-60037
- GaInAsP-InP DH lasers, temp. depend. of laser threshold current, book contrib. 4-60038
- GaInAsP-InP DH lasers, carrier leakage current estimation using high mag. fields 4-91453
- GaInAsP-InP double heterostructure, epitaxial low press. MO-CVD growth for device appl., book contrib. 4-61875
- GaInAsP-InP lasers, applications of electron microscope techniques to semiconductors 4-103622
- GaInAsP-InP mass-transported BH lasers, fabrication, characterization and analysis 4-112473
- Ga<sub>0.33</sub>In<sub>0.67</sub>As<sub>0.70</sub>P<sub>0.30</sub> (100) oriented, electron and hole ionisation coeffs. 4-98662
- Ga<sub>1-x</sub>In<sub>x</sub>AsP<sub>1-y</sub> solid solutions, LPE, conc. profiles 4-93233
- Ga<sub>1-x</sub>In<sub>x</sub>AsP<sub>1-y</sub> layer on InP:Sn substrate, linear thermal expansion coeff. meas. 4-75709
- Ga<sub>1-x</sub>In<sub>x</sub>AsSb<sub>1-y</sub>, epitaxial layers, reflection spectra analysis 4-114340
- GaInP/AlGaAs double heterostructures, LPE, lasing, 77-230K 4-71606
- Ga<sub>1-x</sub>In<sub>x</sub>PyAs<sub>1-y</sub>, gas source MBE growth 4-81140
- Ga<sub>1-x</sub>In<sub>x</sub>(Sb,As,P), short-range clustering, thermodynamic anal. 4-61093
- GaP/GaAsP<sub>1-y</sub> strained layer superlattices, minority carrier diffusion lengths 4-76025
- Ga<sub>1-x</sub>As<sub>x</sub>, crystalline struct., two-phonon Raman spectra study 4-71385
- GaP<sub>2</sub>As<sub>1-x</sub>N<sub>x</sub>, covalent, localised states of negative ions stabilised by enhanced correl. effects 4-104157
- GaP<sub>2</sub>As<sub>1-x</sub>Sb<sub>1-y</sub> epitaxial layers, luminescence studies 4-76505
- GaSb-GaAlAsSb injection heterolaser, emitted radiation characts. 4-79152
- Ge, US attenuation and nonlinearity const., temp. dependence 4-108552
- H ion implanted, range and damage distrib. 4-103774
- (In,Ga)As/InP n-p-n heterojunction bipolar transistors grown by LPE with high gain 4-85097
- InGaAs, 1.6  $\mu$ m, radiative and nonradiative minority carrier lifetimes 4-70826
- InGaAs epilayers, optical studies of carrier dynamics 4-98788
- InGaAs epitaxial layer, LPE growth and carrier mobility, dopant effects 4-84717
- InGaAs, high-parity, conventional LPE growth, carrier conc. and mobility 4-99353
- InGaAs, LPE using novel graphite boat 4-88994
- InGaAs planar photodiodes, reliability 4-91635
- InGaAs:Mg on INP, LPE-grown, MgO-free surface 4-76699
- InGaAs/GaAs strained layers superlattices, molecular beam growth conditions and characterisation 4-70585
- InGaAs/GaAs strained layer superlattices, high quality p-n junctions 4-98707
- InGaAs/InGaAlAs/InAlAs/InP separate confinement heterostruct. multi-quantum-well-laser diodes, MBE grown 4-83617
- InGaAs-InP injection laser, operation and luminescence study 4-74508
- InGaAs-InP modulation doped heterostruct., self-consistent variational calcs. and alloy scatt. 4-98733
- InGaAs-InP superlattices, chloride VPE growth, struct. and optical props. 4-81158

## gallium arsenide continued

- In<sub>0.7</sub>Ga<sub>0.8</sub>As/GaAs strained-layer superlattice, ion implanted, struct. integrity 4-113821
- In<sub>0.53</sub>Ga<sub>0.47</sub>As 1.6- $\mu$ m lasers, temp. sensitive operation 4-96903
- In<sub>0.53</sub>Ga<sub>0.47</sub>As, 2D electron gas, alloy scatt. limited mobility 4-98620
- In<sub>0.53</sub>Ga<sub>0.47</sub>As, carrier energy relax., picosecond luminesc. studies 4-114312
- In<sub>0.53</sub>Ga<sub>0.47</sub>As, electron mobility, rel. to two-mode lattice vibrs. 4-80582
- In<sub>0.53</sub>Ga<sub>0.47</sub>As, epilayer thickness meas. from etched steps 4-62074
- In<sub>0.53</sub>Ga<sub>0.47</sub>As, epitaxially grown by LPE, VPE, MBE, band gap energy spatial var., photoluminescence spectra 4-104125
- In<sub>0.53</sub>Ga<sub>0.47</sub>As, LPE growth on InP (100) substrate (Chinese) 4-85121
- In<sub>0.53</sub>Ga<sub>0.47</sub>As LPE layers, high purity, photoluminescence processes 4-99187
- In<sub>0.53</sub>Ga<sub>0.47</sub>As, laser operation, thermal behaviour 4-87331
- In<sub>0.53</sub>Ga<sub>0.47</sub>As, MIS diode anodic oxidation, interface characteristics 4-104324
- In<sub>0.53</sub>Ga<sub>0.47</sub>As planar diodes, fabrication using open tube method for Zn diffusion 4-95519
- In<sub>0.53</sub>Ga<sub>0.47</sub>As, shallow donors, submillimeter wave photocond. 4-104256
- In<sub>1-x</sub>Ga<sub>x</sub>As, indirect conduction band minima determ. 4-98517
- In<sub>1-x</sub>Ga<sub>1-x</sub> multi quantum well structs., strained, optical props. 4-104669
- In<sub>1-x</sub>Ga<sub>1-x</sub>As/GaAs strained layer superlattice, MBE growth, strain and layer thickness effects 4-99319
- In<sub>1-x</sub>Ga<sub>1-x</sub>InP quantum well struct., low temp. electron mobility, alloy disorder scatt. contrib. 4-92808
- In<sub>1-x</sub>Ga<sub>1-x</sub>As-GaAs strained-layer superlattices, phonon frequencies, Raman scatt. meas. 4-99121
- In<sub>1-x</sub>Ga<sub>1-x</sub>InP heterojunction, quantum Hall effect and hopping cond. 4-98723
- InGaAsP, 1.3  $\mu$ m bandgap, photoexcited carrier lifetime and Auger recomb. 4-108893
- InGaAsP 1.3  $\mu$ m optical amplifier-modulator integrated with a fibre-resonator mode-locked laser 4-91491
- InGaAsP 1.3  $\mu$ m real-index-guided lasers, leakage current anal. 4-96895
- InGaAsP 1.53  $\mu$ m DFB lasers made by mass transport 4-102947
- InGaAsP (InGaP), LPE layers on GaAs (001), composition modulated structures 4-76698
- InGaAsP and InGaP LPE layers, dislocation loops, TEM studies 4-92206
- InGaAsP and InP epitaxial layers, MOVPE at atmospheric press. 4-81154
- InGaAsP BH 1.3  $\mu$ m lasers, anomalous polarisation characts. 4-69402
- InGaAsP crescent mesa substrate BH lasers at 1.55  $\mu$ m 4-112429
- InGaAsP double-channel BH lasers, short-cavity, HF small-signal modulation characts. 4-69462
- InGaAsP double-channel buried-hetero structure lasers, 1.55  $\mu$ m, high-temp. operation, LPE 4-79174
- InGaAsP epilayers, optical studies of carrier dynamics 4-98788
- InGaAsP etched mesa BH lasers, 1.3  $\mu$ m, threshold current, active layer placement effects 4-112414
- InGaAsP film laser, optically pumped, chirp, passive pulse compression in optical fibres 4-107700
- (InGa)(AsP) heterolayers with distrib. feedback, polarisation effects 4-64708
- InGaAsP heterostructure laser with distributed feedback 4-74538
- InGaAsP injection-lasers, short pulse excitation, threshold current temp. dependence 4-74506
- InGaAsP LPE layers on InP, refractive index in transparent wavelength region 4-71333
- InGaAsP, LPE-grown, high-uniformity,  $\lambda=1.3 \mu$ m 4-76700
- InGaAsP, laser, radiative and nonradiative, recombination rates, meas. 4-112434
- InGaAsP laser diode optical switches, isolation characteristics 4-107680
- InGaAsP laser diode switch, BH type, 1.3  $\mu$ m operation; design and fibre optic communication appl. 4-112461
- InGaAsP laser-diode optical switch module 4-83616
- InGaAsP lasers, gain- and index-guided, spectral linewidth 4-112417
- InGaAsP lasers for 1.52 operation, linewidth and FM-noise spectrum meas. 4-83580
- InGaAsP, lattice matched to GaAs, lattice dynamics, Raman scatt. study 4-61673
- InGaAsP light sources, radiative coeffs., carrier dependence 4-64703
- InGaAsP, linear electro-optic effects and nonlinear optical coeffs., device design appls. 4-88809
- InGaAsP long-wavelength 1.0-1.6  $\mu$ m detectors 4-91634
- InGaAsP, MBE growth IR reflectivity, diode laser source/detector 4-71391
- InGaAsP material epitaxial growth, devices for optical communications 4-74746
- InGaAsP, optically pumped, tunable CW mode locked laser action 4-107699
- InGaAsP, quadratic electro-optic Kerr effects, dispersion 4-109159
- InGaAsP ridge lasers,  $\lambda \approx 1.5 \mu$ m, grown by gas source MBE 4-112413
- InGaAsP separate confinement heterostructure lasers, 1.5  $\mu$ m, electron leakage 4-96904
- InGaAsP, theoretical design of single-layer antireflection coatings on laser facets 4-69409
- InGaAsP three-channel buried crescent lasers, 1.51  $\mu$ m, high-speed analog and digital modulation 4-112409
- InGaAsP tunable DFB laser pumped by heterostructure injection laser 4-96907
- InGaAsP:Zn highly reliable 1.3  $\mu$ m surface emitting LEDs for high speed optical communication systems 4-97137
- InGaAsP/GaAs, double heterojunctions, photoluminesc. studies 4-76504
- InGaAsP/GaAs, LPE grown, defects, TEM and STEM studies 4-108387
- InGaAsP/InGaP lasers, low threshold, 810 nm, LPE growth 4-69435
- InGaAsP/InGaP lasers, LPE growth on GaAs, room temp. CW lasing at 727 nm 4-79133
- InGaAsP/InGaP/GaAs DH lasers, low threshold pulsed and CW operation 4-87336
- InGaAsP/InP 1.3  $\mu$ m buried crescent lasers using short external optical cavity, single-mode operation 4-74511
- InGaAsP/InP 1.3  $\mu$ m buried crescent lasers, single transverse-mode conditions 4-96897
- InGaAsP/InP 1.3  $\mu$ m buried crescent laser diode, degradation mechanism 4-96915
- InGaAsP/InP amplifier-modulator integrated with a cleaved-coupled-cavity injection laser 4-91505

- alium arsenide continued
- InGaAsP/InP buried crescent lasers, 1.3  $\mu\text{m}$ , high temp., and long life operation 4-69444
- InGaAsP/InP buried crescent laser, dynamic characts., computer simulation method (*Chinese*) 4-96887
- InGaAsP/InP buried crescent laser diode emitting at 1.3  $\mu\text{m}$ , high temp. CW operation 4-112427
- InGaAsP/InP channelled-substrate BH lasers, VPE base struct. and LPE regrowth 4-96905
- InGaAsP/InP DFB laser diodes, cleaved facet, grating phase effects 4-60063
- InGaAsP/InP DFB laser diodes, lasing characts., at 1.5  $\mu\text{m}$ , effect of mirror facets 4-74513
- InGaAsP/InP DFB ridge-waveguide laser, 1.2 Gbit/s optical fibre transmission over 113.7 km 4-107847
- InGaAsP/InP DH, luminescence and laser threshold characts. 4-85008
- InGaAsP/InP DH stripe lasers fabricated by O ion implantation 4-96906
- InGaAsP/InP double heterojunctions, photoluminesc. studies 4-76504
- InGaAsP/InP GRIN rod external coupled-cavity BH lasers, single longit. mode operation 4-91473
- InGaAsP/InP gigahertz-bandwidth optical modulators/switches with DH waveguides 4-112585
- InGaAsP/InP heterostructure waveguides integrated with optical devices 4-97146
- InGaAsP/InP injection lasers, LPE grown, three-layer-waveguide DH design 4-91490
- InGaAsP/InP lasers, 4-5  $\mu\text{m}$  emissions and excitations in split-off valence band 4-96916
- InGaAsP/InP laser diode, monolithic integration with heterojunction bipolar transistors 4-102927
- InGaAsP/InP lasers, failure modes due to adhesives 4-107678
- InGaAsP/InP lateral p-n-p transistor fabrication using open diffusion technique 4-104003
- InGaAsP/oxidised films interface, Auger/ion sputtering anal. 4-104884
- InGaAsP-Au contacts, X-ray study of Au interactions 4-80675
- InGaAsP-InGaP rapidly degraded DH laser grown by LPE, dark-line defects 4-69406
- InGaAsP-InP 1.3  $\mu\text{m}$  BH lasers, improved linearity criterion, high-bit-rate fibre communication system appls. 4-74510
- InGaAsP-InP 1.55  $\mu\text{m}$  DH ridge waveguide laser, optimum design 4-102955
- InGaAsP-InP BC laser diode emitting at 1.3  $\mu\text{m}$ , fabrication, design, characteristics 4-112474
- InGaAsP-InP DH, photoluminescence efficiency 4-85006
- InGaAsP-InP DH modulators, electroabsorption, polarisation depend. 4-93054
- InGaAsP-InP planar buried DH, LPE growth, melt-carry-over effect 4-99352
- InGaAsP-InP single-longitudinal-mode 1.3  $\mu\text{m}$  DFB-DC-PBH diodes 4-91467
- In<sub>0.75</sub>Ga<sub>0.25</sub>As<sub>0.56</sub>P<sub>0.44</sub>, electroluminescence spectrum, on InP substrate 4-109158
- In<sub>0.79</sub>Ga<sub>0.21</sub>As<sub>0.44</sub>P<sub>0.56</sub>, luminescence study of binding energy variation 4-71435
- In<sub>1-x</sub>Ga<sub>x</sub>As<sub>1-y</sub>P<sub>y</sub>, composition depend. of microhardness anisotropy 4-108506
- In<sub>1-x</sub>Ga<sub>x</sub>As<sub>1-y</sub>P<sub>y</sub>, indirect conduction band minima determ. 4-98517
- In<sub>1-x</sub>Ga<sub>x</sub>As<sub>1-y</sub>P<sub>y</sub>, laser material, intervalence band absorpt. and Auger recomb. 4-80885
- InGaP/GaAs, LPE grown, defects, TEM and STEM studies 4-108387
- In<sub>1-x</sub>Ga<sub>x</sub>P<sub>1-2</sub>As<sub>2</sub>, solid solution, LPE, crystn. and optical props. 4-108736
- InP/InGaAsP 1.5  $\mu\text{m}$  BH laser with etched cavity 4-83575
- InP/InGaAsP DFB double-channel PBH laser diode, 1.55  $\mu\text{m}$ , single longit. mode operation 4-87358
- InP/InGaAsP DH, LPE grown, misfit dislocations, TEM study 4-113826
- InP/InGaAsP optoelectronic integrated device with optical bistability, design, fabrication and characts. study 4-83726
- InP/InGaAsP p-type substrate and mass transported doubly BH laser 4-112428
- InP/InGaAsP stripe geometry lasers, design and fabrication using D<sup>+</sup> bombardment 4-83622
- InP/InGaAsP/InGaAs high-speed avalanche photodiodes 4-69590
- InP-In<sub>0.5</sub>Ga<sub>0.47</sub>As-InP DH wafers, LPE grown, misfit dislocations, X-ray and photoluminescence topography 4-80042
- InP-InGaAsP-InP DH, photoluminescence intensity 4-61738
- LSI, Si<sub>3</sub>N<sub>4</sub> film deposition by plasma-enhanced CVD 4-71569
- Si<sub>3</sub>Ge<sub>1-x</sub>Ga<sub>x</sub>As heterojunction, interface carrier recombination velocity determ. 4-104304

## alium compounds

- see also gallium alloys; gallium arsenide
- III-V semiconductors, phys. data, compilation, book 4-63420
- AgGaS<sub>2</sub>, high-power difference-freq. generation at 5-11  $\mu\text{m}$  4-96997
- AgGaS<sub>2</sub>-Cr<sup>3+</sup>, EPR study, spin-Hamiltonian parameters 4-104488
- Al<sub>1-x</sub>Ga<sub>x</sub>As<sub>1-y</sub>Sb<sub>1-y</sub>/GaSb heterostruct., conditions for LPE growth 4-114429
- AlGaInP/GaInP DH visible light lasers, MOCVD grown, room temp. pulsed operation 4-69445
- AlGaInPAs lattice matched to GaAs, LPE growth, photolum. obs. 4-70581
- Al<sub>1-x</sub>Ga<sub>x</sub>In<sub>1-y</sub>Sb<sub>1-y</sub> epitaxial layers, luminescence studies 4-76505
- AlGaSb, LPE, substrate treatment optimisation, carrier conc., Raman spectra, photoluminesc. 4-93235
- Al<sub>0.17</sub>Ga<sub>0.83</sub>Sb/GaSb multi-quantum well lasers, room-temp. operation, MBE growth 4-60033
- Al<sub>1-x</sub>Ga<sub>x</sub>Sb multilayer heterostructures, coherent light polarisation props. 4-71460
- Al<sub>1-x</sub>Ga<sub>x</sub>Sb-InAs<sub>1-y</sub>Sb<sub>1-y</sub> heterostructures, LPE growth 4-104097
- As<sub>2</sub>Te<sub>3</sub>-GaSb superlattice, MBE growth and luminescence 4-114403
- As<sub>2</sub>Te<sub>3</sub>-GaSb, phase diagram, peritectic reaction 4-61046
- Ca<sub>3</sub>Ga<sub>2</sub>Ge<sub>2</sub>O<sub>12</sub>Cr<sup>3+</sup>, EPR spectra 4-71170
- CaGa<sub>2</sub>S<sub>4</sub>, effective ionic charges, optical phonon spectra 4-103894
- CdGa<sub>2</sub>(S<sub>2</sub>Se<sub>2</sub>)<sub>4</sub>, mixed defect cryst., Raman scatt. 4-61688
- CdGa<sub>2</sub>Se<sub>4</sub>, effective ionic charges, optical phonon spectra 4-103894
- Cs-Ga-Se phase diagrams, ternary cpds. obs. 4-71644
- (Cu<sub>1-x</sub>Ag<sub>x</sub>)(Ga<sub>1-y</sub>In<sub>y</sub>)(Se<sub>1-z</sub>Te<sub>z</sub>)<sub>2</sub>, lattice parameter and energy gap 4-75847
- (CuCr<sub>2</sub>Se<sub>4</sub>)(Cu<sub>0.5</sub>Ga<sub>0.5</sub>Cr<sub>2</sub>Se<sub>4</sub>)<sub>1-x</sub>, semiconducting spin glasses, resistance, magnetoresistance, studies 4-108862

## gallium compounds continued

- CuGa<sub>2</sub>In<sub>1-x</sub>Se<sub>2</sub> chalcopyritic semicond., ESR studies 4-109070
- CuGa<sub>2</sub>Se<sub>2</sub>, thermal expansion, 301-958K 4-80266
- CuS-Ga<sub>2</sub>S<sub>3</sub> system, phase diagram and CuGaS<sub>2</sub> phase field range 4-71640
- Fe<sub>2-x</sub>Ga<sub>2x</sub>BO<sub>6</sub> boroferrite, hyperfine interactions, Mossbauer studies 4-109099
- (Ga<sub>1-x</sub>In<sub>x</sub>)(As<sub>1-y</sub>P<sub>y</sub>), adducts in MOVPE 4-71575
- Ga hexacoordination complexes, <sup>19</sup>F NMR, second coordination sphere 4-81410
- Ga-In-P system, phase diagram calcs. near growth temp. and comp., Ga<sub>1-x</sub>In<sub>x</sub>-P LPE (*Chinese*) 4-114427
- Ga-In-P-As system, LPE, growth kinetics 4-88426
- Ga-In-P-As system, MOVPE, current status for optoelectronic appls. 4-104737
- Ga-In-Sb phase diagram, thermodynamic data, associated soln. model, book contrib. 4-89031
- Ga-P solution-melt system, diffusion coeff. determ. by X-ray microanalysis 4-88320
- Ga-Te, vapour composition, mass spectroscopic investigation of sublimation 4-108601
- Ga<sub>1-x</sub>Al<sub>x</sub>P, epitaxial structs., luminesc. study 4-85011
- Ga<sub>1-x</sub>Al<sub>x</sub>P p-n structures, epitaxially grown, plastically and elastically deformed, quantum efficiency spectra 4-84651
- Ga<sub>1-x</sub>Al<sub>x</sub>Sb, phonon dispersion calcs. 4-88252
- GaAlSbAs-GaSb injection laser, operation and luminescence study 4-74508
- Ga<sub>1-x</sub>Al<sub>x</sub>Sb<sub>1-y</sub>As<sub>y</sub>/GaSb epitaxial films As segregation coeff. and distrib. over thickness 4-75692
- Ga<sub>1-x</sub>Al<sub>x</sub>Sb<sub>1-y</sub>As<sub>y</sub>/GaSb, LPE, phase equilb. rel. to lattice mismatch strain 4-93236
- GaAs-Al<sub>1-x</sub>Ga<sub>x</sub>As heterostructures, electron mobility, temp. depend. from 1-10K 4-80669
- GaAs-GaAlAs heterostructure, electron mobility limits 4-76030
- GaAsP strained-layer superlattice structures and their buffer layers, comparison of trapping levels 4-113885
- GaAs<sub>1-x</sub>P<sub>x</sub>, EL2 metastable state, photocapacitance quenching study 4-70717
- GaAs<sub>1-x</sub>P<sub>x</sub>N, exciton tunnelling inhibited by disorder 4-92622
- GaAsP<sub>1-x</sub>GaP superlattices, strain depth profiles, misfit dislocations obs 4-104095
- GaCl<sub>3</sub> in vapour phase, IR spectra, valence force fields 4-74244
- Ga<sub>2</sub>/Cr<sub>2</sub>Se<sub>4</sub> cation deficient chalcogenide spinels, electron microscope study 4-113443
- GaCrSe<sub>2</sub>, antiferromag. semicond., mag. susceptibility, cond., EPR, IR reflection spectrom., Neel temp., energy gap meas. 4-61522
- GaGeTe<sub>2</sub>, Raman spectrum and lattice dynamics 4-80941
- GaInAs/AlInAs heterojunctions, cyclotron resonance and polaron effects 4-98742
- GaInAs/InP heterojunctions and superlattices, cyclotron resonance and polaron effects 4-98742
- GaInAs/InP(AlInAs) heterojunctions and superlattices, 2-D magnetophonon resonance 4-98740
- GaInAsP alloy semiconductors, book 4-58588
- GaInAsP, defect motion and growth of extended non-radiative defect structs., book contrib. 4-60914
- (GaIn)(AsP) heterostructure laser diodes, psec. pulse generation 4-107632
- GaInAsP, high field transport meas., review, book contrib. 4-61389
- GaInAsP, high purity, charact., growth, back contrib. 4-61334
- GaInAsP, ion implantation, book contrib. 4-60943
- GaInAsP, LPE growth on InP, review, book contrib. 4-61882
- GaInAsP lattice matched to InP, electronic struct., book contrib. 4-61284
- GaInAsP, low field carrier mobility, book contrib. 4-61383
- GaInAsP, low field transport calcs., book contrib. 4-61384
- GaInAsP, n-type, lattice matched to InP, hot electron transport, book contrib. 4-61388
- GaInAsP, photolum. and optical gain spectra, book contrib. 4-61752
- GaInAsP, VPE growth, review, book contrib. 4-61874
- GaInAsP/InP heterostructure lasers, gas source MBE growth 4-69401
- GaInAsP/InP phase adjusted active distributed reflector laser, 1.5  $\mu\text{m}$ , for dynamic single mode operation 4-69437
- GaInAsP-InP DH lasers, review, book contrib. 4-60037
- GaInAsP-InP DH lasers, temp. depend. of laser threshold current, book contrib. 4-60038
- GaInAsP-InP double heterostructure, epitaxial low press. MO-CVD growth for device appl., book contrib. 4-61875
- GaInAsP-InP lasers, applications of electron microscope techniques to semiconductors 4-103622
- GaInAsP-InP mass-transported BH lasers, fabrication, characterization and analysis 4-112473
- GaInP/AlGaAs double heterostructures, LPE, lasing, 77-230K 4-71606
- Ga<sub>2</sub>In<sub>0.5</sub>P<sub>0.5</sub>, photolum. dynamics of high density electron-hole plasma under psec. laser excitation 4-109228
- Ga<sub>1-x</sub>In<sub>x</sub>P, phonon modes, Raman scatt. study 4-108563
- Ga<sub>1-x</sub>In<sub>x</sub>P, electrochem. behaviour in aq. and nonaqueous media, common anion rule 4-70928
- Ga<sub>1-x</sub>In<sub>x</sub>P, LPE growth on GaAs substrates, cathodoluminesc. and photoluminesc. spectra (*Chinese*) 4-113825
- Ga<sub>1-x</sub>In<sub>x</sub>(Sb<sub>1-y</sub>As<sub>y</sub>)P, short-range clustering, thermodynamic anal. 4-61093
- Ga<sub>1-x</sub>In<sub>x</sub>Se single crystals, energy gap, temp. dependence 4-92610
- Ga<sub>1-x</sub>In<sub>x</sub>Se, optical phonons, far-IR reflectivity spectra 4-104583
- Ga<sub>1-x</sub>In<sub>x</sub>Se system, magneto-optical props. near fundamental band gap 4-109166
- Ga<sub>2</sub>Mo<sub>2</sub>S<sub>4</sub> spinel, cryst. struct., mag. props., temp. depend. 4-2-300K 4-114110
- GaMo<sub>2</sub>X<sub>2</sub> chalcogenides, electron-phonon contrib. to Stoner enhancement 4-84803
- GaN crystal growth, vapor-liquid-solid mechanism, NH<sub>3</sub> reaction with Ga 4-61823
- GaN, crystals, high pressure soln. growth, equilb. N<sub>2</sub> press. over Ga-GaN mixtures 4-61822
- GaN, heat and entropy of form. under high press. 4-62227
- GaN, polarised luminescence transitions and electroluminescence quenching 4-104670
- GaN:Zn, cathodoluminesc. anomalous kinetics 4-85015
- Ga<sub>2</sub>O<sub>3</sub>, UPS, DV-X $\alpha$  method 4-83413
- $\beta$ -Ga<sub>2</sub>O<sub>3</sub>:Cr crystals, luminesc. parameters, impurity centre electron capture effects 4-81016
- Ga<sub>2</sub>O<sub>3</sub>-CaO glass, form. density, refr. index, crystn. temp., hardness, IR spectra 4-113635

## gallium compounds continued

- GaP, 3d impurity excitation spectra, separation of one- and many-electron effects 4-75900  
 GaP (110), intrinsic unoccupied surface states and valence band minimum 4-80641  
 GaP (110), surface structure, atomic geometries, R-factor minimization 4-84494  
 GaP amorphous film, local order study and electronic props. 4-70591  
 GaP, crystal growth under microgravity in SALYUT-6 space station 4-98035  
 GaP crystal quality in soln. growth P press. effects 4-103685  
 GaP crystals, Raman light scatt. from polaritons using reflection scheme 4-66042  
 GaP, deep impurity levels, ENDOR and ESR spectra 4-84594  
 GaP, defect electronic struct. calcs. 4-61326  
 GaP diode struct., electroluminescence polarisation study (*Russian*) 4-88884  
 GaP, donor wave functions and band struct. 4-98519  
 GaP, electron irradi., defect creation, luminescence and elec. studies (*Chinese*) 4-108441  
 n-GaP, electron irradi., defects, positron annihilation studies 4-109273  
 GaP epitaxial layer, processing technology and characs. (*Polish*) 4-113827  
 GaP, Hall meas. anal., influence of thermal impurity activation energy temp. depend. 4-104238  
 GaP, large single crystals, LEC growth, LEDs 4-99301  
 GaP, laser-induced sputtering and damage 4-71485  
 GaP, lattice dynamics, local Heine-Abarenkov model pot. 4-98222  
 GaP, localised vacancies, electronic struct. and stability 4-80539  
 GaP microcrystals, electromagnetic surface modes, optical response 4-98543  
 GaP, molecular beam epitaxial growth on Si 4-70587  
 GaP, optical phonon lifetimes, temp. dependence, optical meas. 4-61016  
 GaP p-n junctions, avalanche multiplication and ionisation rates, SEM studies 4-65733  
 GaP, phase transformations at ultrahigh press., X-ray diff. obs. 4-98273  
 p-GaP photoelectrochem. cells, absorpt. coeff. and diffusion lengths, differential photocurrent determ. 4-89455  
 GaP powders, surface phonons, Raman scatt. 4-109193  
 GaP, press. depend. of bound excitons 4-61293  
 GaP prism couplers, optical characs. (*Chinese*) 4-60134  
 GaP, Raman scatt. by surface EM waves 4-80930  
 GaP, Raman scatt. efficiency, press. effect 4-76462  
 GaP, Raman scatt. study of phonon-surface polaritons 4-80931  
 GaP, scanning DLTS investig. 4-75892  
 GaP single crystals, muonium decoupling in high transverse mag. field 4-92985  
 GaP, spinodal decomp.,  $^{31}\text{P}$  NMR spectra, chem. shifts 4-76279  
 GaP substrate for a-Si film, epitaxial crystallisation 4-80452  
 GaP, symm. deep level wavefunction for defect pairs (*Chinese*) 4-104144  
 GaP, thermal oxidation, surface topography and oxide interface struct. 4-80342  
 GaP, thick sample, optical absorpt. coeff. determ. using photoacoustic spectroscopy 4-106402  
 GaP, volume plasmon dispersion, transmission electron energy loss studies 4-88465  
 GaP, wide band-gap, deep levels, review, book contrib. 4-88484  
 n-GaP with adsorbed organics, monolayer influence on Schottky barrier height 4-104290  
 GaP: N epitaxial films, n-type, local cathodolum. kinetics 4-109251  
 GaP: transition metal, impurity electron states calcs. 4-70711  
 GaP:Cr, EPR study of  $\text{Cr}^{2+}$  centre 4-104487  
 GaP:N, electron-hole plasma under resonant free exciton excitation 4-71430  
 GaP:N, exciton transfer,  $\text{NN}_2$ -pair luminesc. enhancement, stochastic model 4-104660  
 GaP:N, photothermal capacitance meas. 4-84647  
 GaP:N, Te VPE layers, minority carrier lifetime, photoluminesc. decay study 4-76520  
 GaP:N,Te,Zn, photolum. under high press. (*Chinese*) 4-93097  
 GaP:Ni, state of impurity centres, EPR, spin-lattice relax. time, spin Hamiltonian parameters 4-88476  
 GaP:Ni $^{2+}$ , Jahn-Teller coupling forces, self consistent LCAO calc. 4-98577  
 GaP:O, electronic impurity states calcs. 4-80547  
 GaP:O, electronic struct. of single neutral ideal P vacancy 4-92657  
 GaP:O(Zn), size effects and impurity electronic struct. 4-70723  
 GaP:Te(N)(As), impurity influence on electron-hole plasma 4-75862  
 GaP:Zn, O LEDs, centre responsible for capacitance slow relax. 4-65735  
 GaP:Zn,O, LPE layers, cleaved surfaces photoluminesc., macrosteps and grooves 4-65588  
 GaP/GaAs $\text{P}_{1-x}$  strained layer superlattices, minority carrier diffusion lengths 4-76025  
 GaP-Si heterojunction band discontinuities, synchrotron radiation photoemission 4-81111  
 GaP $_{1-x}\text{As}_x$ , crystalline struct., two-phonon Raman spectra study 4-71385  
 GaS, amorphous, short range order (*Russian*) 4-98015  
 GaS, EXAFS spectra and near edge struct. 4-66128  
 Ga $_2\text{S}_3$ -CdS, phase diagram, crystallographic study, DTA, X-ray diff. 4-109387  
 GaS $_{1-x}\text{Se}_x$ , layer solid solns., Raman scatt. spectra, effect of substitution-type disorder 4-99115  
 0.69Ga $_2\text{S}_3$ .0.31 La $_2\text{O}_3$ :Nd $^{3+}$ , glass spectral luminesc. props. 4-76511  
 GaSb (110) surface, ion beam crystallography 4-80343  
 GaSb amorphous film, local order study and electronic props. 4-70591  
 GaSb, conduction bands, strain-induced splitting 4-75854  
 GaSb cryst., facet regions and Czochralski growth 4-75348  
 GaSb epitaxial films, photoluminescence spectra 4-88896  
 GaSb, equation of state, bulk modulus press. derivative 4-98236  
 p-GaSb, heavily doped, low temp. thermal cond. 4-70300  
 GaSb, lattice dynamics, local Heine-Abarenkov model pot. 4-98222  
 GaSb, oxidation and interfacial chem. reactions, XPS study 4-85226  
 GaSb, phonon-phonon interactions, lattice thermal cond. 4-80320  
 GaSb, plasma-assisted epitaxial growth in  $\text{H}_2$  plasma, elec. props. 4-104740  
 GaSb, press. depend. of  $E_g$  gap, reson. Raman technique study 4-76469  
 GaSb, Raman freq. depend. on press. 4-109188  
 GaSb substrates, LEC growth, optical communication requirements, review 4-61833  
 GaSb:Se, quantum localisation of electrons in metal-insulator transition region 4-70654

## gallium compounds continued

- GaSb:Zn epitaxial films, photoluminescence spectra 4-88896  
 GaSb-AlSb, superlattices, light and heavy valence subband reversal, lattice mismatch 4-114013  
 GaSb-GaAlAsSb injection heterolaser, emitted radiation characs. 4-79152  
 GaSb-InAs heterojunction, quantum Hall effect study 4-98726  
 GaSb-InAs $_{1-x}\text{Sb}_x$  heterostructures, LPE growth 4-104097  
 GaSb-InSb, behaviour of Sn in solid solns., elec. props. 4-75967  
 GaSb(110) surface atomic geometry and dynamics 4-70537  
 GaSe, EXAFS spectra and near edge struct. 4-66128  
 GaSe, excitons in high mag. fields, gauge-invariant energy variational calc. 4-80508  
 GaSe, ground state energies of shallow donors 4-92654  
 GaSe, layer crystals, Jahn-Teller effect 4-108824  
 GaSe, optical orientation of carriers, optically detected EPR 4-88746  
 GaSe, phonon inelastic scatt. from He atom impact 4-98426  
 GaSe, Raman scatt. study of phonon-surface polaritons 4-80931  
 GaSe single cryst., luminescence spectra, isothermal annealing effect 4-81001  
 p-GaSe, space charge limited current behaviour 4-80597  
 GaSe, surface pot.,  $\text{Ar}^+$  sputtering effects, XPS obs. 4-81103  
 GaSe, uncooled, optical bistability rel. to excitons 4-74592  
 GaSe:Co, injection and thermodepolarisation currents 4-70833  
 GaSe:Fe, elec. cond. and impurity states 4-113957  
 GaSe:Yb single cryst., photocond. and photoluminescence studies 4-84649  
 p-GaSe/n-Cu $_2\text{In}_2\text{S}_3$  heterojunctions, elec. and photoelec. props. 4-88573  
 GaSe/SnO $_2$  heterojunctions, energy struct., reflectivity studies 4-66053  
 GaSe-Ge 'Schottky-like' heterojunction 4-108931  
 GaSe-metal interface, chem. reactivity 4-71973  
 GaSe $_2$  single crystals, visible reflection spectra 4-80965  
 GaSe $_2$ :Ag, photodoping physics study 4-75464  
 GaSe $_3$ ,  $^{57}\text{Fe}$  single cryst., Mossbauer effect and mag. susceptibility 4-104513  
 GaTe, single crystals, visible reflection spectra 4-80965  
 GaTe, amorphous films, elec. breakdown in pulsed fields 4-114209  
 Ga $_2\text{Te}_3$ , electrical and optical props. meas. 4-61380  
 Ga $_2\text{Te}_3$ , electrical cond. and Hall coeff. meas. using van der Pauw method 4-98606  
 Ga $_2\text{Te}_3$  liquid semicond. elec. transport activation energies 4-88506  
 Ga $_2\text{Te}_3$  semicond., electronic struct. and bonding 4-84563  
 Gd-Ga garnet, absorpt. coeff. and refractive index determ. 4-80895  
 Gd $_2\text{O}_3$ -Ga $_2\text{O}_3$ , binary phase diagram and melting 4-88264  
 HgGa $_2\text{Se}_4$ , crystal growth and refinement (*French*) 4-75380  
 Hg $_2\text{Ga}_2\text{QTe}_6$ , Hg $_2\text{Ga}_2\text{QTe}_6$ , pressure-induced phase transitions, elec. resistivity meas. 4-80497  
 InAs/GaSb superlattices, Landau levels and magneto-optical props. 4-98737  
 InAs/GaSb superlattices, electronic collective modes 4-104134  
 InAs-GaSb system, superlattices, quantum wells, and heterostructs., review 4-80666  
 InGaAsP 1.3  $\mu\text{m}$  optical amplifier-modulator integrated with a fibre resonator mode-locked laser 4-91491  
 InGaAsP double-channel BH lasers, short-cavity, HF small-signal modulation characs. 4-69462  
 InGaAsP film laser, optically pumped, chirp, passive pulse compression in optical fibres 4-107700  
 InGaAsP, laser, radiative and nonradiative, recombination rates, meas. 4-112434  
 InGaAsP/InGaP lasers, low threshold, 810 nm, LPE growth 4-69435  
 InGaAsP/InP amplifier-modulator integrated with a cleaved-coupled cavity injection laser 4-91505  
 InGaAsP/InP buried crescent lasers, 1.3  $\mu\text{m}$ , high temp. and long life operation 4-69444  
 InGaAsP/InP lateral p-n-p transistor fabrication using open diffusion technique 4-104003  
 InGaAsP-InGaP rapidly degraded DH laser grown by LPE, dark-line defects 4-69406  
 InGaAsP-InP BC laser diode emitting at 1.3  $\mu\text{m}$ , fabrication, design, characteristics 4-112474  
 InGaAsP-InP DH modulators, electroabsorption, polarisation depend. 4-93054  
 In $_{1-x}\text{Ga}_x\text{As}_{1-y}\text{P}_y$ , composition depend. of microhardness anisotropy 4-108506  
 In $_{1-x}\text{Ga}_x\text{As}_{1-y}\text{P}_y$ , laser material, intervalence band absorpt. and Auger recomb. 4-80885  
 InGaP LED/optical fibre system for optical remote detection of propane gas 4-105155  
 InGaP/GaAs, LPE grown, defects, TEM and STEM studies 4-108387  
 InGaP/AlInP quantum well structures for visible region, MBE growth 4-99314  
 In $_2\text{Ga}_2\text{P}_2$ , spinodal decomp., phase segregation,  $^{31}\text{P}$ -NMR spectra; chem. shifts 4-76279  
 In $_{1-x}\text{Ga}_x\text{Sb}$ , indirect conduction band minima determ. 4-98517  
 In $_2\text{Ga}_2\text{O}_3$ -Ga $_2\text{O}_3$ -CuO(CoO), phase relations and cryst. structures 4-98242  
 LaGaO $_2$ Se $_2$ , cryst. struct., X-ray diff. study (*French*) 4-65234  
 NdGa $_2\text{O}_7$ , phase diagram, crystal growth by floating zone method 4-76665  
 PbF $_2$ -GaF $_3$ -Al(PO $_3$ ) $_3$ -ErF $_3$ -based fluoride glasses, fluorescence studies 4-99170  
 PbF $_2$ -M $^{III}\text{F}_3$ -M $^{III}\text{F}_3$  (M $^{III}$ =Mn, Zn; M $^{III}$ =Fe, Ga), fluoride glasses, local order, EXAFS studies 4-70036  
 PbF $_2$ -MnF $_2$ -GaF $_3$ , fluoride glasses, vibrational spectroscopy 4-114261  
 PbF $_2$ -Ga $_2\text{O}_3$ , optical props. 4-93086  
 PbO-B $_2\text{O}_3$ -Bi $_2\text{O}_3$ -Y $_2\text{O}_3$ -Ga $_2\text{O}_3$ -Fe $_2\text{O}_3$ , phase diagram invest. 4-93208  
 Sm-GaSe barrier structures, elec. and photoelec. props. 4-84698  
 Sm $_2\text{O}_3$ -Ga $_2\text{O}_3$ , binary phase diagram and melting 4-88264  
 TiGa $_2$ -Nd $_2\text{S}_3$ , TiGa $_2$ -Nd $_2\text{S}_3$ , interactions, solubility, optical props. 4-109385  
 TiGaSe $_2$ , negative photoelec. effects 4-61419  
 (YBi) $_2$ (FeGa) $_2\text{O}_{12}$  garnet, cryst. growth from flux and LPE 4-93208  
 YGa $_2\text{O}_{12}$ :Nd thin film waveguide, RF sputtering growth, fluoresc. spectrum, optical amplifier appl. 4-60146  
 YbGa $_2\text{S}_4$ , cryst. struct., polymorphic modifications, X-ray diff. study 4-60893  
 Zn $_{1-x}\text{Ga}_{0.667x}\text{Cr}_x\text{Se}_4$ , mag. phase transitions induced by strong mag. fields, magnetisation meas. 4-109018  
 Zn $_{1-x}\text{Ga}_{2x/3}\text{Cr}_x\text{Se}_4$ , magnetic semiconducting solid solutions study 4-109002

- lanising *see surface treatment*  
 lanoluminescence *see luminescence*  
**lanomagnetic effects**  
*see also Hall effect; magnetoresistance; Suhl effect; thermomagnetic effects*  
 dielectric crystal, photogalvanomagnetic phenomena 4-65702  
 linear response theory for DC conductivity 4-82744  
 magnetocapacitance origin in Anderson-localised regime 4-61285  
 semiconductors, magnetically induced photogalvanic effect 4-84653  
 semiconductors, n-type, galvanomagnetic effects in case of electron scatt. by optical phonons 4-80612  
 two-dimensional disordered system in strong mag. field, N-orbital model 4-98641  
 $\text{Bi}_2\text{Te}_3(\text{Se}_3)$ , weak-field transport, thermoelec., galvano- and thermo-mag. coefficients 4-98613  
 n- $\text{Cd}_3\text{As}_2$ , degenerate, Debye screening length under influence of arbitrary mag. quantisation 4-70836  
 GaAs, electrical properties and impurity states 4-75963  
 n-GaAs, metallic, inelastic scatt. time, temp. depend. 4-98630  
 GaAs:Cr(O), electrical properties and impurity states 4-75963  
 Ge bicrystals, anomalous magneto-transport props. of p-type inversion layers (Japanese) 4-70842  
 Ge, electron-hole lik. droplet destruction in nonuniform deformation field 4-61297  
 InSb-based magnetosensitive elements, operating principles at high and low temps., survey (Russian) 4-65691  
 Sb<sub>2</sub>Te<sub>3</sub> single cryst., weak field charge transport 4-108887  
 Sb<sub>2</sub>Te<sub>3</sub>, weak-field transport, thermoelec., galvano- and thermo-mag. coefficients 4-98613  
 Si, galvanomagnetocombinational effect 4-113980  
**lanomagnetism** *see electromagnetism*  
**lanometers**  
 electrical measuring instruments theory, moving coil, bridge and current comparison methods (German) 4-58863  
 forced simple harmonic motion 4-90335  
**lanothermoelectric effects** *see thermomagnetic effects*  
**ame theory**  
*see also information theory*  
 differential games, basic optimal strategies 4-106238  
**amma fission reaction** *see photofission*  
**amma radiation** *see gamma-rays*  
**amma-ray absorption**  
 cylindrical sample,  $\gamma$ -ray self-absorption, correction factors 4-109267  
 elements and compounds, photon cross-section meas. 30 to 660 keV 4-59680  
 energy-absorption coefficients for  $\gamma$ -rays in compounds or mixtures 4-100324  
 tissue attenuation correction in gastric emptying studies 4-109902  
 whole-body determ. of  $^{57}\text{Co}$   $\text{B}_{12}$  absorpt., attenuation correction 4-72379  
**amma-ray angular distribution**  
*see also gamma-ray spectra*  
 $^{37}\text{Cl}$  levels,  $J^\pi$ ,  $T_{1/2}$  and  $\gamma$ -ang. distrib. from  $^{36}\text{S}(p,\gamma)$  4-90941  
 $e^+e^- \rightarrow \gamma\gamma$ , double bremsstrahlung, photon ang. distrib., radiative corrections 4-82953  
 $^{81}\text{Sr}$ , high-spin states and shape change 4-64030  
 $^{199}\text{Tl}$  rotational states,  $J^\pi$  and transitions from  $^{197}\text{Au}(\alpha,2n)$  (Chinese) 4-82980  
 $^{172}\text{Yb}$  multipole mixing ratios, energy levels, from  $^{172}\text{Lu}$  decay 4-95955  
 $^{61}\text{Zn}$ , gamma ray spectroscopy from  $^{58}\text{Ni}(\alpha,n\gamma)$  4-102223  
**amma-ray applications**  
*see also radiation therapy*  
 BWR LOCA, instantaneous pipe rupture, void fraction meas. with X-ray densitometer 4-74036  
 cancer treatment, medical appl. of  $\gamma$ -emitting radioisotopes. (Chinese) 4-62566  
 imaging techniques, Int. Workshop, Southampton, England (July 1983) 4-63386  
 intracavitary  $\gamma$ -therapy, methods of dose distrib. form. (Russian) 4-89749  
 laryngeal tumours, gamma ray treatment, phantom dosimetry obs. 4-72407  
 NDT and imaging, gamma-ray scatt. techniques 4-63834  
 oil reservoirs evaluation by gamma ray spectral logging and pulsed neutron application 4-62990  
 radiation therapy, shield block use for field form. (Russian) 4-72352  
 radiometric survey equipment for seabed investigations 4-77671  
 Shimadzu automated multigamma counter RAW-1600 for radioimmunoassay in clinical chem. laboratories (Japanese) 4-59578  
 therapeutic  $\gamma$ -ray units, radiation field sizes determ. (Russian) 4-93848  
 welded joints in ship hulls; radiographic inspection by  $\gamma$ -flaw detector 4-109603  
 Sm intestinal marker, prompt  $\gamma$  and neutron activation anal. 4-105078  
**amma-ray astronomical observations**  
 at  $E=10^{15}$  eV, search, EAS data anal. 4-101534  
 background  $\gamma$ -ray spectrum balloon-borne spectrometer meas. 4-59482  
 burst of 1978 March 25, absorpt. feature characts. 4-101522  
 burst sources, optical counterparts detect. methods 4-101516  
 burst sources observed by Hinotori satellite, energy spectra, time history and origin 4-101513  
 bursts, high time resolution  $\gamma$ -ray spectral obs. with Solar Maximum-Mission 4-101514  
 3C 120,  $\gamma$ -ray emission fluxes 4-101524  
 Centaurus A (NGC 5128), high-resolution obs. of gamma-ray spectrum between 70 keV and 8 MeV 4-86031  
 CG 195+04,  $\gamma$ -ray line emission search 4-101521  
 2CG 195+4, gamma ray flux periodicity and energy spectra, EAS obs. 4-101527  
 CG 195+4, gamma-ray var., obs. of Cherenkov radiation due to air showers 4-101528  
 cosmic gamma-ray background, meas. at balloon altitudes above Beijing area (Chinese) 4-82355  
 Crab Nebula,  $\gamma$ -ray emission fluxes 4-101524  
 Crab nebula, gamma radiation spectrum in  $10^{13}$  eV energy range 4-73006  
 Crab Nebula, search for  $\gamma$ -ray lines 4-101462  
 Cygnus X-3, gamma ray var., Cherenkov radiation due to air showers 4-101528  
 galactic anticentre direction  $\gamma$ -ray sources, obs. 4-101524  
 galactic centre, 2-20 MeV gamma-ray map and energy distrib. 4-101523  
 galactic plane cosmic ray event excess 4-85845  
**gamma-ray astronomical observations continued**  
 gamma-ray burst of 1978 March 25, spectral characts. and neutron star fireball model 4-110784  
 gamma-ray bursts, obs. in X-rays and  $\gamma$ -rays 4-110785  
 Hercules X-1, obs. of a  $\gamma$ -ray pulsar 4-86090  
 M31 (Andromeda galaxy), extragalactic source of 1000 GeV gamma rays 4-101470  
 molecular clouds, gamma-ray line emission and cosmic ray interactions 4-101463  
 NGC 1275,  $\gamma$ -ray line emission search 4-101521  
 NGC 4151, Seyfert galaxy, HEAO 1 obs. from 2 keV to 2 MeV 4-86038  
 PSR 0531+21, 1-20, MeV pulsed  $\gamma$ -ray emission anal. 4-101391  
 PSR 0531+21,  $\gamma$ -ray flux and energy spectra, Cherenkov radiation obs. 4-101393  
 PSR 0531+21, Crab pulsar, HEAO 3 gamma-ray obs. 4-94843  
 PSR 0531+21, Crab pulsar, search for periodic low-energy gamma-ray emission 4-106019  
 PSR 0531+21, gamma ray emission, possible sporadicity, Cherenkov radiation anal. 4-101392  
 PSR 0531+31 and 1937+214 (millisecond pulsar),  $\gamma$ -ray emission, Cherenkov radiation obs. 4-101394  
 PSR 0532+31,  $\gamma$ -ray periodicity, EAS data anal. 4-101534  
 PSR 0833-45, 1-20 MeV pulsed gamma-rays obs. 4-101390  
 PSR 0833-45, possible transient  $\gamma$ -ray emission obs. 4-101395  
 PSR 0833-45 4-94996  
 PSR 0833-45 and 0950+08,  $\gamma$ -ray emission, Cherenkov radiation anal. 4-101396  
 solar flare gamma-ray events, temporal evolution, ISEE 3 data 4-90123  
 solar flares, gamma-ray obs., energy spectra 4-105968  
 sources emission, Cherenkov radiation obs. 4-101532  
 supernovae, search for  $\gamma$ -ray emission, upper limits 4-101384  
**gamma-ray astronomy**  
*see also gamma-ray sources (astronomical)*  
 altazimuth mountings of a gamma-ray telescopes, choice of astatic system for controlling DC motor speed 4-105886  
 artificial satellite missions 4-63089  
 background radiation, contrib. of black hole accretion discs in active galaxies nuclei 4-77985  
 background radiation, contrib. of zero-point field accel. in intergalactic medium 4-100887  
 background radiation as obs. test for baryon symm. cosmology 4-78012  
 balloon borne  $\gamma$ -ray telescope, background induced by neutron-payload interactions 4-101171  
 balloon mounted  $\gamma$ -spectrometers,  $\gamma$ -ray background induced by atmospheric neutrons 4-67512  
 balloon-borne detector, background  $\gamma$ -ray spectra origin 4-100720  
 coded aperture  $\gamma$ -ray telescope, statistical anal. 4-67635  
 coded aperture cameras, performance of practical designs, computer simulations 4-67638  
 coded masks telescopes, numerical method for virtual image recognition 4-67639  
 COMPTEL imaging Compton telescope on the Gamma Ray Observatory 4-63061  
 conference on Southern Galaxy Surveys at Leiden, Netherlands (August 1982) 4-58565  
 COS-B, gamma-ray astronomy operation 4-67813  
 diffuse  $\gamma$ -ray background origin 4-100891  
 diffuse background, contrib. of Seyfert galaxies nuclei 4-82562  
 diffuse background radiation at low-energy, contrib. of normal galaxies 4-82561  
 diffuse background spectra, model involving positronium annihilation 4-63045  
 diffuse component meas. by high-altitude balloon 4-100888  
 diffuse galactic  $\gamma$ -ray background, origin 4-77975  
 diffuse galactic emission, bremsstrahlung component at MeV energies, constraints on cosmic rays 4-90042  
 diffuse galactic gamma-ray emission and cosmic ray-interstellar matter interactions 4-100890  
 diffuse galactic radiation, bremsstrahlung component spectra and cosmic ray electrons energy spectra 4-100889  
 galactic  $\gamma$ -ray emission, correl. with interstellar gas distrib. 4-63300  
 galactic cosmic ray electrons, distrib. and diffusion,  $\gamma$ -ray anal. 4-101487  
 galactic emission, radial distrib. 4-86049  
 galactic emission correlation with local interstellar gas distrib. 4-63304  
 galactic emission distrib. rel. to CO and H I distrib. 4-63301  
 galactic emission from cosmic ray and positrons 4-94358  
 galactic gamma-ray-photon interactions, EM cascade showers initiation 4-101537  
 galactic plane  $\gamma$ -ray flux and  $\text{H}_2$  density in mol. ring 4-63302  
 galactic radial distrib., H I maps and cosmic rays distrib. 4-90237  
 high-energy astrophysics and gamma-ray astronomy, review 4-106084  
 imaging device for telescope, using rotating coded mask 4-63062  
 imaging systems for low energy range 4-72881  
 imaging techniques, Int. Workshop, Southampton, England (July 1983) 4-63386  
 interstellar  $\text{H}_2$  distrib., correl. with  $\gamma$ -ray emission intensity and energy spectra anal. 4-101486  
 interstellar medium, energy depend. of cosmic gamma-ray intensity of H and  $^{12}\text{CO}$  4-110409  
 Jupiter, magnetosphere gamma ray prod. and process involving trapped protons and electrons 4-101239  
 LMC, cosmic rays origin, models and expected radio and  $\gamma$ -ray emission 4-101485  
 radial distribution in outer Galaxy from H I kinematics anal. 4-63303  
 review (French) 4-115836  
 SIGMA, high resolution space observatory project for gamma-ray sources 4-105875  
 space-borne studies, review 4-77972  
 spectrometer for balloon or space operation, using n-type Ge detector 4-63060  
 supernovae, search for  $\gamma$ -ray emission, upper limits 4-101384  
 telescope with arc minute resolution, image reconstruction 4-72882  
 two-dimensional imaging of atm.-Cherenkov light, appl. to  $\gamma$ -ray astronomy 4-101176  
 ultrahigh-energy photons, high-precision system for meas. of arrival time 4-105885  
 ZEBRA,  $\gamma$ -ray telescope, evaluation of background introduced from coded aperture mask 4-67629  
 Ge position-sensitive detector for  $\gamma$ -ray astronomy 4-63078

**gamma-ray detection and measurement**

- see also gamma-ray spectrometers; radioactivity measurement
- aberrations in gamma-ray imaging systems 4-67084
- acrylic scintillation counter, attenuation length, time resolution 4-102522
- among upgrading plants, external radiation levels 4-62602
- Anger camera, coded aperture gamma ray optics studies 4-112065
- Anger gamma-camera systems 4-63835
- ascorbic acid, aq. solns., chemical dosimetry appls. by UV spectrophotometry 4-74118
- balloon mounted  $\gamma$ -spectrometers,  $\gamma$ -ray background induced by atmospheric neutrons 4-67512
- BDEG-6931-20 large volume scintillator, intrinsic background meas. 4-107262
- BGO detector with photomultiplier, fast time resolution for  $\gamma$ -rays 4-74106
- BGO scintillators for photon detection 4-107260
- bone mineral content measurement using dual photon absorptiometry, prototype apparatus (French) 4-67155
- bulk TRU waste, high sensitivity assay systems using neutron and gamma methods 4-111615
- charged-particle induced prompt  $\gamma$ -rays in elemental analysis 4-89362
- coded aperture  $\gamma$ -ray telescope, statistical anal. 4-67635
- Compton suppression  $\gamma$ -counting, count-rate effect on efficiency 4-102448
- cosmic rays, high-precision system for meas. of arrival time of ultrahigh-energy photons 4-105885
- CR-39 as a gamma ray dosimeter, bulk etch rates 4-102475
- direct-charging detector with dielectric scatterer 4-87014
- dose buildup factors of collimated gamma radiation behind steel and aluminum plates 4-107154
- dose equivalent rate estimates due to natural radioactivity sources in Saudi Arabia 4-72433
- dosimeter calibration in equivalent dose units 4-62599
- dwellings in the Republic of Ireland,  $\gamma$ -radiation levels 4-93880
- exposure dose rate meas. instrument for intense pulsed X-ray and gamma rays 4-87020
- fast-response radiation-identifying instrument with separate integration of the signal components 4-102559
- film badge accuracy determ. 4-62591
- fusion reactor breeder materials, solid, irradiated, retained He and T meas. technique 4-107021
- gas centrifuge nuclear plant, U enrichment meas. in pipework by  $\gamma$ -spectrometry 4-111706
- high resolution PET detection system, small detectors geometrical study 4-72363
- high-resolution gamma spectrometer using HPGe coaxial detectors and time-variant filters 4-64270
- imaging probes for tumor detection 4-62571
- imaging techniques, Int. Workshop, Southampton, England (July 1983) 4-63586
- incident photon flux monitor for synchrotron radiation 4-91175
- indoor exposure rates to gamma and cosmic rays, Ge spectrometer and ionisation chamber obs. 4-93893
- indoor exposure to natural radiation, conf., Anacapri, Italy (Oct. 1983) 4-90285
- indoor gamma exposure measurements in Italy 4-93881
- integral scatt. cross-sections of gamma-rays at small angles 4-102686
- ionisation chambers exposed to  $^{60}\text{Co}$   $\gamma$ -rays, calc. response and wall correction factors 4-64304
- lead glass drift calorimeter design, Monte Carlo studies 4-64275
- low power radiation survey instruments 4-59440
- luminescent glass neutron/gamma detectors design 4-59555
- LWR fuels, reprocessing input balance using non-destructive measurements 4-111715
- MCP for X-ray and  $\gamma$ -ray imaging 4-64286
- modular scintillation camera for use in nuclear medicine 4-72366
- MTR spent fuel, high res. gamma spectrometry verification for safeguards 4-106982
- multi-isotopic gamma-ray assay system for alpha-contaminated waste 4-78673
- multireaction activation detectors, particle flux spectra determ. 4-91150
- MWPC, X-ray and  $\gamma$ -ray imaging 4-64287
- MWPC arrays, two dimensional imaging of  $\gamma$ -rays 4-68889
- NDT and imaging, gamma-ray scatt. techniques 4-63834
- NE213 liq. scintillation counter, digital discrimination unit for neutron-gamma discrimination 4-64312
- NE213 liquid scintillator, temp. dependence of pulse shape discrimination 4-102541
- nuclear reactor cover-gas monitor using charcoal-Ge  $\gamma$ -ray spectrometer combination 4-59370
- nuclear safeguards, software, data structs. and data eval. for verification system 4-111700
- plastics, etchable track formation for radiation detection 4-68879
- portable detectors for  $^{125}\text{I}$ -insulin absorption measurement during subcutaneous infusion with portable pumps 4-67157
- proportional tube photon position detector, performance 4-102512
- PWR, gamma thermometer as local power monitor in reactor thimble tube 4-59369
- radiation monitors, hand held, various materials 4-59443
- radioactivity standardisation using  $4\pi(\text{PC})\gamma$  coincidence counting, systematic effects due to increasing self-absorpt. 4-87026
- scintillation hodoscope spectrometer for electrons and high-energy photons 4-59487
- scintillation reson. detectors for time expts. 4-64272
- self-powered flux detectors, bibliography 4-73195
- sensitive gamma detector using MCP photomultiplier, characterisation 4-64293
- sequential probability ratio controllers for nuclear safeguards radiation monitors 4-111694
- Shimadzu automated multigamma counter RAW-1600 for radioimmunoassay in clinical chem. laboratories (Japanese) 4-59578
- special nuclear materials, gamma spectrometric and absorpt. meas. for safeguards 4-111717
- spent fuel measurement system 4-74007
- terephthalate dosimeter for X,  $\gamma$  and  $\beta$ -radiation 4-74117
- TESSA, Total Energy Suppression Shield Array, Daresbury, props. and first results 4-86795
- thermoluminescent dosimetry, comparative parameters of  $\text{MgB}_4\text{O}_7:\text{Dy}$  sintered pellets and  $\text{CaSO}_4:\text{Dy}$  Teflon discs 4-89757
- thermoluminescent dosimetry, photon energy depend. of sensitised LiF phosphor 4-89758

**gamma-ray detection and measurement continued**

- thermometer for PWR reactor, heat density behaviour (French) 4-64214
- Tokai Reprocessing Plant, leached fuel hull monitoring system,  $^{137}\text{Cs}$  indicator for safeguards 4-106980
- TRU material meas. in TMI-2 demineraliser, n and  $\gamma$  meas. system 4-111618
- TRU nuclides, in vivo meas. using high purity Ge detector,  $\gamma$  and X-ray meas. 4-115194
- vacuum UV region, detect. using microchannel laminar 4-86479
- WVER-440 spent fuel, nondestructive anal. using gamma and neutron meas., safeguards 4-106981
- ZEBRA,  $\gamma$ -ray telescope, evaluation of background introduced from coded aperture mask 4-67629
- n- $\gamma$  dose rate, NDK 601 instrument dosimetric characts. 4-59454
- $\text{BaSO}_4:\text{Dy}$ , thermoluminesc. detectors response functions to  $\gamma$ -radiation 4-112037
- $\text{Bi}_4\text{Ge}_2\text{O}_{12}$  anti-Compton spectrometer design and appl. in nucl. spectroscopy 4-64269
- $\text{Bi}_4\text{Ge}_2\text{O}_{12}$  detector efficiency for monoenergetic  $\gamma$ -rays and  $\gamma$  cascades 4-68896
- $\text{Bi}_4\text{Ge}_2\text{O}_{12}$  detector role in  $\gamma$ -ray spectroscopy 4-59551
- $\text{Bi}_4\text{Ge}_2\text{O}_{12}$  gamma-ray detector system for fast neutron-induced reactions 4-64280
- $\text{Bi}_4\text{Ge}_2\text{O}_{12}$  scintillator efficiency, Monte Carlo calcs. comparison with meas. 4-64294
- $\text{Bi}_4\text{Ge}_2\text{O}_{12}$  scintillator efficiency 4-68895
- $\text{CaSO}_4:\text{Dy}$  thermoluminesc. detectors response functions to  $\gamma$ -radiation 4-112037
- $^{252}\text{Cf}(\text{sf})$  use in vivo, environmental and radiocological lab. expts. prompt photon detection 4-89790
- $^{60}\text{Co}$   $\gamma$ -rays, fatal accidental exposure, dose estimation from watch jewel thermolum. 4-89754
- D(T) plasma diagnostics by spectrometry of radiative capture reaction 4-69951
- Ge detector array for nuclear safeguards 4-74098
- Ge detectors, segmentation and pulse shape discrimination techniques for background rejection 4-64291
- Ge HP closed ended detectors charge collection time, Monte Carlo simulation 4-59569
- Ge low background detectors, characterization meas. techniques 4-102488
- Ge position-sensitive detector for  $\gamma$ -ray astronomy 4-63078
- Ge, segmented n-type detector development, appl. to astron.  $\gamma$ -ray spectroscopy 4-63060
- Ge spectrometer, background reduction, material selection, geometry shielding 4-102489
- Ge(Hp)  $\gamma$ -ray spectrometer with NaI(Tl) anticoincidence shield 4-59482
- $^{76}\text{Ge}$ ,  $0_1^+$  state lifetime, delayed auto-coincidence of Ge(Li) detector 4-102497
- HgI<sub>2</sub> detectors, energy resolution enhancement 4-59565
- HgI<sub>2</sub> large area photodetectors 4-59562
- $^{125}\text{I}$  dosimetry using LiF 4-72432
- Li-Si disilicate glasses with Nd-U contents, response to  $\gamma$ -rays and neutrons 4-96399
- NaI modularised  $\gamma$ -ray spectrometer 4-91142
- NaI(Tl)  $3''\text{O} \times 3''$  detector, response functions, data and method assessment 4-74104
- Pu solution characterisation by  $\gamma$ -spectrometry, densitometry and isotopic anal., safeguards 4-111707
- $^{238}\text{Pu}$ , decay  $\alpha$ -particle and  $\gamma$ -ray emission probabilities 4-102434
- Rn, indoor meas. using activated C collectors 4-89771
- Rn, measurement in dwellings using activated charcoal 4-93897
- Si planar diffused diodes for dosimetry of irradiation of pourable bulk materials (German) 4-68832
- Tl halide crystal cond. counters, appl. to  $\alpha$ -particle and  $\gamma$ -ray detection 4-69577
- gamma-ray diffraction**
- crystals,  $\gamma$  and X-ray modulation by US vibrs. 4-88903
- Mossbauer cryst. diffr. at low temp. 4-88749
- single crystals, degree of perfection, gamma-ray and neutron diffraction methods 4-65155
- solids,  $\gamma$ -ray scatt. and diffr. due to thermal vibrs. of atoms (Japanese) 4-113275
- $\text{FeBO}_3$ , Mossbauer transmission spectra at pure nucl. dynamical diffr. in Bragg geometry 4-71218
- $\text{FeBO}_3$ , nuclear resonance diffraction in Bragg geometry, anomalous high reflectivity obs. 4-69995
- $\text{LiNbO}_3$ , Mossbauer diffr., separation of elastically and inelastically scatt.  $\gamma$ -radiation 4-98985
- Si single cryst., Mossbauer diffr., separation of inelastically and elastically scatt. radiation 4-98984
- gamma-ray effects**
- see also biological effects of gamma-rays; radiolysis
- acetone cation,  $\gamma$ -irrad.,  $^{13}\text{C}$  ESR and ENDOR investig. 4-69114
- acetone in  $\text{CCl}_4\text{F}$  crystals,  $\gamma$ -ray irradiation; ESR study 4-91287
- aluminated surfaces, radiation-induced, modification toward blood compatibility 4-62630
- alkali borate mixed glasses containing Ni, induced optical absorpt. rel. to  $\gamma$ -ray exposure 4-76502
- alkali halide,  $\gamma$ -irrad., luminescence characts. (Chinese) 4-76526
- alkane mixtures, comparison of  $\gamma$ -radiolysis in glassy and polycryst. states 4-62215
- anthracene, excitons and diffusion effects 4-92617
- bacterial spores, anoxic, modification of radiation sensitivity by alcohols 4-72308
- carbon tetrachloride, solids containing acetals, gamma-irrad.,  $\cdot\text{CCl}_3$  radical prod. 4-93504
- cycloaliphatic epoxy resin,  $\gamma$ -irrad. under vacuum, phys. props., ageing 4-103800
- cylindrical sample,  $\gamma$ -ray self-absorption, correction factors 4-109267
- dielectrics, gamma-irradiated, elec. charge form. 4-71278
- dimethylcyclohexane, ring decomp., skeletal conform. conservation 4-114806
- electronics ageing mechanisms, neutron and  $\gamma$ -ray effects, nuclear power plant instrumentation 4-59363
- fibre optic behaviour in gamma radiation (French) 4-80103
- fluorophosphate and phosphate glasses,  $\gamma$ -ray irradi., colour centres, EPR studies 4-103747
- gelation of chains, gamma-radiation induced, exptl. study 4-77033
- glass:Cr, dominant visible absorpt. rel. to  $\gamma$ -ray irradi. 4-76503

gamma-ray effects continued  
 hydrocarbon glasses,  $\alpha$  irradi., trapped electrons, photoconductivity study 4-65700  
 inclusion cpds. reactions, symmetry conservation, electronic energy transfer processes 4-71943  
 landfill leachate,  $\gamma$ -irrad. conditions required in combined radiation-microbial process 4-93677  
 metals, internal friction peaking effect due to electron or  $\gamma$ -ray irradi. 4-103873  
 nuclear power station cables, gamma radiation and thermal ageing of polyethylene insulation 4-75526  
 nuclear waste storage materials, radiation effects 4-73973  
 nylon-6 membranes, grafted, permeability of KCl, selectivity 4-114832  
 nylon-6 membranes, grafted, permeability of urea and KCl, selectivity 4-114831  
 optical fibres, Al-coated, optical, mechanical and radiation perform. at high temp. 4-97111  
 optical fibres, heated, real-time attenuation in a nuclear reactor 4-80101  
 optical fibres, MCVD, PCS and DC/TC types, props. in radiation environments 4-80102  
 optical fibres, step index and graded index, induced attenuation during steady state and pulsed irradi. 4-80098  
 optical fibres in adverse environments, conf., Paris, France (May 1983) 4-78025  
 optoelectronic component behaviour in gamma radiation (*French*) 4-80103  
 organic materials for fusion reactor applications 4-111757  
 pentane-2-methylpentane mixtures,  $\gamma$ -irrad., energy transfer 4-76254  
 photomultipliers, amplitude distrib. of output pulses obs. 4-87015  
 polyacetylenes and polydiacetylenes, solid state reactivity and props. under  $\gamma$ -irradiation 4-75318  
 polyamides, aliphatic, chem. conversion under  $\gamma$ -irrad., spectrosc. investig. 4-85320  
 polyethylene,  $\gamma$ -irrad., environmental stress relax., effect of ketones, temp. depend. 4-109450  
 polyethylene, linear,  $\gamma$ -irrad., NMR and mech. relax. In  $\gamma$ -loss band 4-80832  
 polyethylene, thermal characts., electron and gamma-neutron irradi. effects (*Russian*) 4-103977  
 polyethylene-isotactic polypropylene blends,  $\gamma$ -irrad., tensile props. 4-76818  
 polymers, conducting, polymerisation from diacetylene, thermal and  $\gamma$ -ray induced doping 4-66589  
 polyolefins,  $\gamma$ -ray radiation degradation, isomer yields for butanes and butenes 4-77015  
 polypropylene, radiation sterilised, tensile props. 4-108440  
 porous polymers, pore struct. rel. to irradi. temp. 4-66301  
 quartz, electrical and optical props., neutron,  $\gamma$ , and electron irradi. effects 4-60968  
 quartz, synthetic, irradi. induced coloration (*Turkish*) 4-114307  
 radiation testing facility using reactor spent fuel 4-107255  
 radioactive waste, intermediate level, bitumen encapsulation, radiation swelling 4-106674  
 radioactive waste glass, simulated, density changes under ion, electron, and gamma irradi. 4-73974  
 rock salt, gamma irradi., thermomech. props., rel. to radioactive waste disposal 4-75527  
 ruby,  $\gamma$ -irradiated, X-ray and optical spectra of Cr ions 4-114345  
 n-Si, radiation defect formation, annealing, defect interactions 4-113499  
 silica core optical fibres,  $\gamma$ -ray induced absorpt. band at 770 nm 4-79296  
 single crystals, creation of electron-positron pairs by high energy photons 4-108439  
 SPAULRAD-S laminate for fusion reactor appls., irradiation and mech. props. 4-111768  
 statistical model with random displacement energy 4-88204  
 steel, austenitic stainless, gamma-ray induced short-range ordering, point defect influence 4-92123  
 styrycyanine dye solns., radiation dosimetry appls. 4-68836  
 p-terphenyl, electron and  $\Gamma$ -irrad., absorpt. spectra (*Russian*) 4-71421  
 TGS, cryst., phys. props., influence of defects 4-76329  
 TGSe, cryst., phys. props., influence of defects 4-76329  
 triglycine fluoroberyllate, cryst., phys. props., influence of defects 4-76329  
 Ts-TS-19 ceramic, gamma irradi., influence on photovoltaic effects 4-84656  
 AgBr, role of Frenkel defects in radiation stimulated processes 4-98095  
 Al<sub>2</sub>Ga<sub>1-x</sub>As avalanche diodes, heat- and radiation-resistant, elec. props. 4-65728  
 Al<sub>2</sub>O<sub>3</sub>, strongly coupled mag. ions, obs. by low temp. thermal expansion meas. 4-70419  
 $\alpha$ -Al<sub>2</sub>O<sub>3</sub>:Er(Gd)(Tb) crystals, radiative and thermochem. effects 4-76491  
 As<sub>2</sub>Se<sub>3</sub>Te<sub>2</sub>, amorphous, radiation and thermal induced defects, electrical cond. 4-75528  
 As<sub>2</sub>Se<sub>3</sub>Te<sub>2</sub>, glasses, DC props., neutron and gamma-ray effects 4-103814  
 Au-Si nucl. detectors, gamma-ray effects on rise time 4-59566  
 B<sub>2</sub>O<sub>3</sub>-Na<sub>2</sub>O-Nd<sub>2</sub>O<sub>3</sub> glasses, thermoluminescent props. 4-66086  
 Ba(ClO<sub>4</sub>)<sub>2</sub>·3H<sub>2</sub>O,  $\gamma$ -irrad., ClO<sub>4</sub> radical, ESR temp. depend. 4-98950  
 BaCl<sub>2</sub>·2H<sub>2</sub>O,  $\gamma$ -ray interaction in energy range 30-660 KeV 4-80096  
 BaFCl, flux-grown crystals, thermoluminesc., effect of flux 4-104680  
 BaFCl:Eu<sup>2+</sup>,  $\gamma$ -ray irradi., thermoluminescence glow curves 4-76533  
 BaSO<sub>4</sub>, barytes single crystals,  $\gamma$  irradi., optical absorpt., thermolum. 4-66080  
 BaTiO<sub>3</sub> crystals,  $\gamma$ -irradiated, with equil. domain struct., polarisational state 4-76395  
 BaTiO<sub>3</sub>, gamma irradi., influence on photovoltaic effects 4-84656  
 Bi<sub>2</sub>SiO<sub>20</sub>, single crystal, effect of doping with Al, Ga and Cr on props. 4-76407  
 CaF<sub>2</sub>:rare earth doped, gamma irradi. induced dielec. relax. 4-70210  
 CaF<sub>2</sub>:Sm crystal, gamma-irradiated, optical study 4-81015  
 CdS,  $\gamma$ -irrad., photoelectron spectra and photoconductivity (*Russian*) 4-71521  
 CsBr, total gamma-ray cross sections 4-60959  
 CsI, irradiated single crystals, intrinsic hole colour centres 4-114332  
 Dy<sub>2</sub>O<sub>3</sub>, total gamma-ray cross sections 4-60959  
 Eu<sub>2</sub>O<sub>3</sub>, total gamma-ray cross sections 4-60959  
 GaAs, E3 centre accumulation, effect of defect charge state 4-60966  
 Gd<sub>3</sub>Ga<sub>5</sub>O<sub>12</sub>, garnet,  $\gamma$  and neutron irradi., effect on optical props. 4-99135  
 Ge, Frenkel pair component distance distrib. after  $\gamma$  irradi. 4-70142  
 Ge, gamma-irradiated, hole traps 4-103799  
 Ge, p<sup>+</sup>-n junction irradi. with  $\gamma$ -rays, capacitance spectroscopy 4-104287

## gamma-ray effects continued

H<sub>2</sub>, gamma-ray double photoionis., electron correls. 4-64548  
 InP p<sup>+</sup>-n junctions,  $\gamma$ -ray irradi., electron trap annealing 4-98748  
 InP single crystals and solar cells,  $\gamma$ -irrad. damage 4-62356  
 KBr:Cr<sup>2+</sup>,  $\gamma$ -irrad., thermally stimulated depolarisation currents 4-71263  
 KCl, gamma irradiation of single crystal, shift in  $K_{\alpha 1}$  line, EPR study 4-114163  
 KNO<sub>3</sub>,  $\gamma$ -ray interaction in energy range 30-660 KeV 4-80096  
 K<sub>2</sub>O-SiO<sub>2</sub> glass, gamma-irrad., defect centre struct., EPR obs. 4-70211  
 K<sub>2</sub>SO<sub>4</sub>,  $\gamma$ -ray interaction in energy range 30-660 KeV 4-80096  
 LiF, ballistic phonon interaction with defects, heat-pulse technique study 4-98228  
 LiF cryst.,  $\gamma$ -ray irradi. effects on dislocation damping coeff. 4-65267  
 LiF F<sub>2</sub> centre laser, relationship between F<sub>2</sub> centre density and laser stability (*Chinese*) 4-91477  
 LiF:H,  $\gamma$ -irrad. and mechanically loaded, H atom localisation 4-88179  
 LiF:OH<sup>-</sup>, gamma-ray irradi., lattice defects, EPR studies 4-75437  
 LiNbO<sub>3</sub>, electrooptic cells,  $\gamma$ -irrad. effect on optical inhomogeneity 4-76438  
 LiNbO<sub>3</sub>, gamma irradi., influence on photovoltaic effects 4-84656  
 MgO, surface  $\gamma$ -conductivity, kinetics and decay, F<sub>2</sub>-centres 4-65726  
 MgO, thermoluminescence charge transfer mechanism 4-71450  
 MgSO<sub>4</sub>·7H<sub>2</sub>O,  $\gamma$ -ray interaction in energy range 30-660 KeV 4-80096  
 (NH<sub>4</sub>)<sub>2</sub>SO<sub>4</sub>,  $\gamma$ -ray interaction in energy range 30-660 KeV 4-80096  
 NaCl, cryst., X-irrad., F-centre decay during photoannealing 4-80036  
 NaCl,  $\gamma$  and laser irradi., internal friction and dislocation damping 4-80153  
 NaCl,  $\gamma$ -irrad., aqualuminesc. in presence of metal ions 4-114317  
 NaCl,  $\gamma$ -irrad., interstitial dislocation loops (*Russian*) 4-113455  
 NaCl,  $\gamma$ -ray interaction in energy range 30-660 KeV 4-80096  
 NaCl:Ba, post  $\gamma$ -irradiation thermolum., effect of plastic deform. 4-104682  
 NaClO<sub>3</sub>,  $\gamma$ -ray interaction in energy range 30-660 KeV 4-80096  
 NaNO<sub>3</sub>,  $\gamma$ -ray interaction in energy range 30-660 KeV 4-80096  
 Na<sub>2</sub>O-CaO-SiO<sub>2</sub>,  $\gamma$  radiation colouring in 600-1000 nm region 4-80948  
 Na<sub>2</sub>O-SiO<sub>2</sub> glass, nature of dissolved water, effect on phys. props. 4-109180  
 Ni-Co matrix, ThO<sub>2</sub> particles, oxide growth inhibition 4-104796  
 RbD<sub>2</sub>(SeO<sub>3</sub>)<sub>2</sub>, ESR spectra and dielec. const. meas. 4-76305  
 RbH<sub>2</sub>(SeO<sub>3</sub>)<sub>2</sub>, ESR spectra and dielec. const. meas. 4-76305  
 Si, electron and  $\gamma$  irradi., influence on defect annihilation 4-98094  
 Si, electron and  $\gamma$ -ray irradiated, efficiency of radiation defect formation 4-92237  
 n-Si, gamma and neutron irradi., radiation defect interactions 4-92227  
 Si, gamma-irradiated, carrier recombination, dislocation effects 4-75982  
 Si, gamma-irradiated, charge carrier recombination 4-84631  
 Si,  $\gamma$ -ray irradi., conductivity, eddy current meas. 4-104201  
 Si,  $\gamma$ -ray irradi., trapping centres, DLTS studies 4-104147  
 n-Si, irradiated by  $\gamma$ -rays, changes in carrier lifetime 4-104232  
 Si solar cell, with induced channel, stability of characts. rel. to irradi. and temp. changes (*Russian*) 4-109739  
 Si:B, P, compensated semiconductors, coalescence process, effect and rad. and heat treatment 4-65288  
 Si-SiO<sub>2</sub>, MIS structures, hole traps, trivalent Si centres, EPR meas. 4-80817  
 Si-SiO<sub>2</sub> MOS struct., microstructural variations in oxides, electron spin reson. obs. 4-61590  
 $\beta$ -Si<sub>3</sub>N<sub>4</sub>, Mossbauer spectra, effect of heat treatment and  $\gamma$ -irrad. 4-80846  
 SiO<sub>2</sub>, amorphous, X- and gamma-irrad., E'-centre variants, EPR obs. 4-70207  
 SiO<sub>2</sub> core polymer coated optical waveguides low temp. gamma irradi. response 4-80100  
 SiO<sub>2</sub> fibers, irradi. and photobleaching at low temps. 4-80099  
 SiO<sub>2</sub> fibres, effect of irradi. up to 10<sup>5</sup> rads, comparison with PCS fibres and massive samples between 0.4 and 2.5  $\mu$ m 4-80097  
 SrCl<sub>2</sub>·6H<sub>2</sub>O,  $\gamma$ -ray interaction in energy range 30-660 KeV 4-80096  
 Sr(NO<sub>3</sub>)<sub>2</sub>,  $\gamma$ -ray interaction in energy range 30-660 KeV 4-80096  
 W, high energy  $\gamma$  quanta-induced polarised electrons and positions 4-80104  
 Y<sub>3</sub>Al<sub>5</sub>O<sub>12</sub>:Nd<sup>3+</sup>, garnets,  $\gamma$ -ray irradi., colour centres and optical props. 4-114310  
 Y<sub>2</sub>O<sub>3</sub>, total gamma-ray cross sections 4-60959  
 ZnO:Gd(Pr), thermoluminesc. under UV,  $\beta$ - and  $\gamma$ -ray irradiations 4-93119  
 ZrSiO<sub>4</sub>, swelling induced by alpha and gamma irradi. 4-75543

**gamma-ray interactions**  
 see also gamma-ray scattering  
 No entries

**gamma-ray lasers**  
 inverse Compton scattering in high freq. region, coherent effects 4-96764  
 planar channelling particle sine-squared pot. and Kumakhov radiation for charged particles,  $\gamma$ -ray laser appls. (*Chinese*) 4-91390

**gamma-ray polarisation**  
 spectra intensity differences in linearly polarised experiments 4-102460

**gamma-ray production**  
 hot facility, low-cost, for high Ci gamma-source processing 4-74084  
 radiation testing facility using reactor spent fuel 4-107255  
 pp annihilation at rest, monoenergetic  $\gamma$ -ray search, mixed qq+NN model 4-68581  
<sup>241</sup>Am/ $\beta$  source, high 4.4 MeV  $\gamma$ -ray output rel. to total neutron output, shield design calcs. 4-59469

**gamma-ray scattering**  
 see also Compton effect; gamma-ray interactions  
 crystal, X-ray and Mossbauer radiation scatt., effect of forced vibrs. 4-76558  
 inhomogeneous media, scatt. of collimated  $\gamma$  radiation 4-99708  
 inverse Compton interaction, cosmic-ray electrons with interstellar photons 4-101088  
 solids,  $\gamma$ -ray scatt. and diff. due to thermal vibrs. of atoms (*Japanese*) 4-113275  
 two-layered systems, photon backscattering, Monte Carlo treatment 4-76565

**gamma-ray sources** see gamma-ray production

**gamma-ray sources (astronomical)**  
 1979 March 5  $\gamma$ -ray burst link with LMC SNR N49, obs. 4-77909  
 1979 March 5 burst, neutron star corequake and shock heating model 4-101519  
 1979 March 5 burst source,  $\gamma$ -rays absorpt. and distance determ. 4-94994

**gamma-ray sources (astronomical) continued**

- absorption features, effects of emitted photons-interstellar photon interactions 4-101535  
 active galactic nuclei,  $\gamma$ -ray data as test of black hole accretion models 4-101484  
 active galaxies nuclei,  $\gamma$ -ray and relativistic particles prod. and spectra anal. 4-100891  
 active galaxies nuclei, gamma-ray emission characts. due to cosmic ray interactions 4-101537  
 background  $\gamma$ -ray spectrum balloon-borne spectrometer meas. 4-59482  
 black holes, mass accretion and plasma processes,  $\gamma$ -ray emission model, 3C 273 appl. 4-101536  
 burst of 1978 March 25, absorpt. feature characts. 4-101522  
 burst of 1978 March 25, spectral characts. and neutron star fireball model 4-110784  
 burst sources, 1983 review 4-110780  
 burst sources, distance model 4-101518  
 burst sources, Franco-Soviet and Soviet results, obs. overview 4-110781  
 burst sources, neutron star thermonuclear runaway model 4-101502  
 burst sources, obs. by Hakucho 4-110786  
 burst sources, optical counterparts detect. methods 4-101516  
 burst sources, spectral props. review 4-110782  
 burst sources observed by Hinotori satellite 4-101513  
 bursters, archival search for optical counterparts 4-101515  
 bursters, neutron star model involving interior neutrons bombarding crust 4-101401  
 bursters model, thermonuclear runaway on neutron stars accreting interstellar matter 4-101520  
 bursts, associated X-ray emission, model involving neutron star emission 4-101517  
 bursts, high time resolution  $\gamma$ -ray spectral obs. with Solar Maximum Mission 4-101514  
 bursts, obs. in X-rays and  $\gamma$ -rays 4-110785  
 3C 120,  $\gamma$ -ray emission fluxes 4-101524  
 3C 273,  $\gamma$ -ray emission model 4-101536  
 catalogue from SAS II data 4-101525  
 Centaurus A (NGC 5128), high-resolution obs. of gamma-ray spectrum between 70 keV and 8 MeV 4-86031  
 CG 195+04,  $\gamma$ -ray line emission search 4-101521  
 CG 195+4, detect. of quasar 0630+180 inside error box 4-101500  
 2CG 195+4, gamma ray flux periodicity and energy spectra, EAS obs. 4-101527  
 CG 195+4, gamma-ray var., obs. of Cherenkov radiation due to air showers 4-101528  
 CG 195+4 (Geminga), proposed identification with quasar (QS 0630+180) 4-90252  
 2CG 353+16, in  $\rho$  Ophiuchi dark cloud, high-resolution radio obs. of nearby nonthermal sources 4-72995  
 conference on high-energy transients, at Santa Cruz, United States (July 1983) 4-106091  
 COS-B, gamma-ray astronomy operation 4-67813  
 Crab Nebula,  $\gamma$ -ray emission fluxes 4-101524  
 Crab nebula, gamma radiation spectrum in  $10^{13}$  eV energy range 4-73006  
 Crab Nebula, search for  $\gamma$ -ray lines 4-101462  
 Cygnus X-1, review of X-ray and gamma-ray object 4-115785  
 Cygnus X-3,  $\gamma$ -ray emission, period from EAS data anal. 4-101531  
 Cygnus X-3,  $\gamma$ -ray emission var., small air showers arrival directions obs. 4-101529  
 Cygnus X-3, clues from photonuclear time scale on nature of particle accelerators 4-101503  
 Cygnus X-3, distance and  $\gamma$ -ray absorpt. 4-72979  
 Cygnus X-3, gamma ray var., Cherenkov radiation due to air showers 4-101528  
 Cygnus X-3, magnetic pair production and  $\gamma$ -ray. spectrum cut-off 4-72985  
 Cygnus X-3, periodic  $\gamma$ -ray emission anal. throughout orbit (Russian) 4-94879  
 discrete sources ( $E > 10^{15}$  eV), search in EAS data 4-101530  
 discrete sources ( $E > 10^{15}$  eV), search in Kiel EAS data 4-94991  
 distribution in Galaxy and nature 4-101526  
 $E = 10^{15}$  eV sources search, EAS data anal. 4-101534  
 emission due to cosmic ray-interstellar matter interactions 4-101525  
 excess fluxes search, EAS data anal. 4-101533  
 extragalactic, emission mechanism involving cosmic rays prod. at massive black holes 4-100929  
 extragalactic sources, X-ray and gamma-ray prop. (Polish) 4-63340  
 fast narrow burst, freq. and burst classification 4-110783  
 galactic and extragalactic gamma-ray sources, review 4-106084  
 galactic anticentre direction  $\gamma$ -ray sources, obs. 4-101524  
 galactic centre, 2-20 MeV gamma-ray map and energy distrib. 4-101523  
 galactic plane cosmic ray event excess 4-85845  
 galaxy clusters,  $\gamma$ -ray emission, contrib. to background 4-82554  
 Geminga, Xosats obs. of candidate X-ray counterpart 4-101505  
 Geminga, search for radio counterpart at 21 cm 4-90257  
 Geminga, X-ray evidence for increasing 59 s period 4-101504  
 Hercules X-1, obs. of a  $\gamma$ -ray pulsar 4-86090  
 interstellar cloud accretion and evaporation, implication for cosmic rays and  $\gamma$ -ray emission 4-100892  
 M31 (Andromeda galaxy), extragalactic source of 1000 GeV gamma rays 4-101470  
 magnetic flare model of  $\gamma$ -ray bursts 4-94850  
 massive black holes, 511 keV annihilation line, origin due to tidally disrupting stars 4-101405  
 MeV emission spectrum, role of pair processes in steady mildly relativistic thermal plasmas 4-94582  
 molecular clouds, gamma-ray line emission and cosmic ray interactions 4-101463  
 neutron stars, rotating, gamma-ray freq. shifts and line broadening 4-101398  
 NGC 1275,  $\gamma$ -ray line emission search 4-101521  
 NGC 4151, Seyfert galaxy, HEAO 1 obs. from 2 keV to 2 MeV 4-86038  
 OB associations, time depend. energetics and  $\gamma$ -ray emission 4-101447  
 PSR 0531+21, 1-20 MeV pulsed  $\gamma$ -ray emission anal. 4-101391  
 PSR 0531+21,  $\gamma$ -ray flux and energy spectra; Cherenkov radiation obs. 4-101393  
 PSR 0531+21, Crab pulsar, HEAO 3 gamma-ray obs. 4-94843  
 PSR 0531+21, Crab pulsar, search for periodic low-energy gamma-ray emission 4-106019

**gamma-ray sources (astronomical) continued**

- PSR 0531+21, gamma ray emission, possible sporadicity, Cherenkov radiation anal. 4-101392  
 PSR 0531+31 and 1937+214 (millisecond pulsar),  $\gamma$ -ray emission; Cherenkov radiation obs. 4-101394  
 PSR 0532+31,  $\gamma$ -ray periodicity, EAS data anal. 4-101534  
 PSR 0833-45, 1-20 MeV pulsed gamma-rays obs. 4-101390  
 PSR 0833-45, possible transient  $\gamma$ -ray emission obs. 4-101395  
 PSR 0833-45 4-94996  
 PSR 0833-45 and 0950+08,  $\gamma$ -ray emission, Cherenkov radiation anal. 4-101396  
 pulsars, distrib. and  $\gamma$ -ray luminosity anal. 4-101526  
 quasars,  $\gamma$ -ray and relativistic particles prod. and spectra anal. 4-100891  
 quasars, gamma-ray emission characts. due to cosmic ray interactions 4-101537  
 Seyfert galaxies nuclei, cosmic ray characts. from photons and neutrinos as probes 4-100925  
 statistical analysis of gamma-ray obs. 4-73102  
 statistical reliability of detection 4-101190  
 steady  $\gamma$ -ray emission, Cherenkov radiation obs. 4-101532  
 switched-off pulsars,  $\gamma$ -ray and X-ray emission mechanism 4-77863  
 switched-off pulsars, X-ray and  $\gamma$ -ray emission 4-94845  
 Vela X-1 (4U 0900-40), clues from photonuclear time scale on nature of particle accelerators 4-101503

**gamma-ray spectra**

- see also gamma-ray angular distribution; gamma-ray spectra of liquid, and solids; nuclear decay theory  
 bulk TRU waste, high sensitivity assay systems using neutron and gamma methods 4-111615  
 BWR spent fuel,  $^{137}\text{Cs}$   $\gamma$ -spectrometry for burn-up verification and isotopic comp., safeguards 4-106983  
 CANDU MOX rods, NDA working standards, destructive/nondestructive comparison, safeguards 4-106985  
 curve fitting, least squares and utmost correl. methods comparison 4-67967  
 dental calculus, human, major and trace element determ. by instrumental NAA 4-105371  
 escape peaks, more accurate evaluation of gamma-ray intensity 4-96323  
 FIDES automated U-enrichment meter for nuclear safeguards inspection 4-106992  
 gas centrifuge enrichment plant, cascade area, NDA meas. for safeguards 4-106993  
 gas centrifuge nuclear plant, U enrichment meas. in pipework by  $\gamma$  spectrometry 4-111706  
 HEU detection in  $\text{UF}_6$  centrifuge process piping,  $\gamma$ -meas., safeguards appl. 4-106994  
 intensity differences in linearly polarised experiments 4-102460  
 LWR fuels, reprocessing input balance using non-destructive measurements 4-111715  
 moments of inertia,  $\gamma$ -ray studies, high spin 4-95882  
 MTR spent fuel, high res. gamma spectrometry verification for safeguards 4-106982  
 neutron activation analysis, net peak area computation method 4-77039  
 nuclear spectral data, resolution improvement using arithmetic operation 4-74125  
 positronium, gamma-ray energy spectra from 3-gamma decay (Chinese) 4-112306  
 prompt gamma-ray spectroscopy for fundamental const. meas. 4-63847  
 random sum peak use in resolving time determ. of NaI(Tl) scintillation detectors 4-87004  
 Simultaneous Calorimetric Assay System, transportable device for Pu meas. in safeguards 4-106984  
 special nuclear materials, gamma spectrometric and absorpt. meas. for safeguards 4-111717  
 spectrometry baseline estimation, computer program comparison 4-74090  
 TRU material meas. in TMI-2 demineraliser, n and  $\gamma$  meas. system 4-111618  
 TRU waste nondestructive assay systems at Los Alamos Nat. Lab. 4-106713  
 WWER-440 spent fuel, nondestructive anal. using gamma and neutron meas., safeguards 4-106981  
 $\beta$ - $\gamma$  spectroscopic method for determ. of delayed neutron emission probability 4-59595  
 $^{137}\text{Au}$ ,  $\beta^+$ /EC decay,  $\gamma$ -ray identification 4-95971  
 B detection limit from capture gamma-ray meas. after preconcentration 4-105086  
 $^{137}\text{B}(\gamma)$ ,  $\gamma$ -spectra, direct-semidirect anal., ang. distrib., anal. power 4-106615  
 $^{137}\text{C}(\gamma)$ ,  $\gamma$ -spectra, direct-semidirect anal., ang. distrib., anal. power 4-106615  
 $^{106}\text{Cd}$ ,  $A=106, 108$ , levels study from  $\beta^+$ /EC decay of  $^{106}\text{In}^{m+8}$  and  $^{108}\text{In}^{m+8}$  4-68645  
 $^{134}\text{Ce}$  level structure study using  $\gamma$  and  $e^-$  spectroscopic methods 4-59127  
 $^{160}\text{Dy}$ ,  $\gamma\gamma$  directional correl. coeff. meas. 4-59197  
 $^{164}\text{Dy}(n,\gamma)^{165}\text{Dy}$ , 580-2200 keV, decay scheme of 'excited' state 4-91000  
 $^A\text{Hg}(d,pn\gamma)$ ,  $A=202, 204, 205$  MeV, gamma ray and conversion electron spectra, yrast state population 4-102162  
 $^A\text{Hg}(n,p)^A\text{Au}$ ,  $A=202, 204$ , gamma-ray spectroscopy, coincidence methods 4-95956  
 $^{202}\text{Au}$ ,  $^{202}\text{Au}$  decay 4-95956  
 $^{202}\text{Hg}$  isomeric state and  $\gamma$ -emission probabilities from  $^{202}\text{Tl}$  decay 4-86802  
 $\text{H}^+$  induced  $\gamma$ -ray emission (PIGE) analysis, external beam technique 4-99883  
 $^{165}\text{Ho}$   $\mu$  capture, neutron and X-ray spectra 4-59207  
 $^{166}\text{Ho}$ , 1.776 MeV first-forbidden beta transition, gamma-ray spectra 4-59205  
 $^{39}\text{K}$ , I-forbidden Gamow-Teller transition 4-59206  
 $^{41}\text{K}$  spectroscopy from  $^{40}\text{K}(n,\gamma)$  4-59195  
 $^{173}\text{Lu}$  decay, X-ray and soft  $\gamma$ -ray spectra 4-95966  
 $\text{N}_2\text{O}$  cooled reactor, fuel-envelope diagnostics by  $\gamma$ -spectroscopy (Russian) 4-74019  
 $^A\text{Nd}$ ,  $A=143, 145$ , Coulomb excitation of levels 4-68646  
 $^{151}\text{Nd}$ , low-lying levels decay props. 4-73853  
 $^{64}\text{Ni}(n,\gamma)$ , capture widths for s-wave resonances,  $\gamma$ -ray spectra 4-96021  
 $^{103}\text{Pd}$ , gamma-ray spectroscopy 4-59196  
 $^{151}\text{Pm}$  level scheme in high excitation energy region up to 2 MeV 4-59194

**gamma-ray spectra continued**

- <sup>210</sup>Pt(d,pn<sub>γ</sub>), A=196, 198, 25 MeV, gamma ray and conversion electron spectra, yrast state population 4-102162
- Pu imaging through heavy shielding using pinhole, safeguards appl. 4-106989
- Pu, isotopic composition, gamma-spectrometric determ., safeguards appl. 4-106978
- Pu isotopic composition determ. by high res. γ-ray spectrometry, safeguard appl. PLUTO code 4-106979
- Pu solution characterisation by γ-spectrometry, densitometry and isotopic anal., safeguards 4-111707
- Pu waste arisings and glove box hold-up, nondestructive assay techniques for safeguards 4-106988
- <sup>152</sup>Sm(<sup>32</sup>S, X), 214 MeV, ang. momentum alignment 4-73938
- <sup>152</sup>Sm, low-lying levels decay props. 4-73853
- <sup>181</sup>Ta γ-rays from <sup>181</sup>W EC decay 4-95968
- <sup>98</sup>Tc, high-spin states 4-73816
- <sup>4</sup>Th, A=228, 230, rotational levels from (α,α'2n) reactions 4-68609
- <sup>212</sup>Th(d,pn<sub>γ</sub>), 25 MeV, gamma ray and conversion electron spectra, yrast state population 4-102162
- <sup>205</sup>Tl, 3291 keV J<sup>π</sup>=25/2<sup>+</sup> level 4-68611
- U, isotopic composition, gamma-spectrometric determ., safeguards appl. 4-106978
- <sup>235</sup>U abundance determ. by γ-spectrometry, certified ref. materials for enrichment standards 4-111698
- <sup>176</sup>Yb(d,pn<sub>γ</sub>), 25 MeV, gamma ray and conversion electron spectra, yrast state population 4-102162
- <sup>61</sup>Zn, gamma ray spectroscopy from <sup>58</sup>Ni(α,n<sub>γ</sub>) 4-102223

**gamma-ray spectra of liquids and solids**

- see also Mossbauer effect
- electron shell effect on gamma ray emission by nuclei in laser irradiation 4-88755
- hyperfine interactions, study by nucl. methods, book contrib. 4-70763
- hyperfine interactions of radioactive nuclei, condensed matter studies, book 4-67877
- metals, defects, hyperfine interaction studies, review, book contrib. 4-70135
- metals, noncubic, elec. quadrupole interaction studies, review, book contrib. 4-70764
- metals, point defects obs. and dynamics, perturbed γγ angular correl. method 4-88757
- PIXE anal., sample uniformity and surface contamination, Al X-ray yield ratio 4-109704
- polypropylene, hollow fibres, strain induced porosity, gamma quanta angular correlation (Russian) 4-109097
- rare earth trifluoride single cryst., electric field gradient at Gd nucleus, integral perturbed angular correlation studies 4-98991
- Ag, radiation damage, O decoration and <sup>111</sup>In TDPAC studies 4-75555
- Ag-Pt-In dilute alloys, In migration, PAC studies 4-65460
- Al-In, dil., He, localised diffusion around In impurities, PAC obs. 4-65470
- AuFe alloys, spin glass freezing, PAC study 4-71216
- α-Ce, local mag. susceptibility meas., TDPAD study 4-65792
- CsBr, total gamma-ray cross sections 4-60959
- Cu, single Frenkel-pair production by neutrino recoil 4-98089
- Cu-In, dil., channelling effect of conversion electrons emitted from radioactive impurities 4-75569
- Cu-In (0.1 at.%), vacancy trapping, PAC and ion channelling study 4-84876
- Dy<sub>2</sub>O<sub>3</sub>, total gamma-ray cross sections 4-60959
- Eu<sub>2</sub>O<sub>3</sub>, total gamma-ray cross sections 4-60959
- Fe<sub>3</sub>B<sub>12</sub>Si<sub>2</sub>C<sub>2</sub>, amorphous, mag. anisotropy meas. (Russian) 4-65804
- Fe<sub>2</sub>O<sub>3</sub>, hematite, quadrupole shifts, temp. depend., γ-ray spectra anal. 4-65888
- GaAlAs-GaAs heterostructure, nuclear profiling of Al 4-98123
- Gd, electric field gradient at Gd nucleus, integral perturbed angular correlation studies 4-98991
- InSe, electric field gradients, nuclear quadrupole freqs., anomalous temp. behaviour 4-71221
- La, depend. of <sup>140</sup>Ce recoil motion on phonon spectrum, nucl. reson. fluorescence study 4-98216
- LaF<sub>3</sub>, depend. of <sup>140</sup>Ce recoil motion on phonon spectrum, nucl. reson. fluorescence study 4-98216
- PdFeCd dilute alloys, hyperfine field at Cd, PAC spectroscopy studies 4-92681
- PdIn, constitutional and thermally created lattice defects, TDPAC study 4-103745
- Si:F, amorphous and cryst., ion implanted, elec. quadrupole hyperfine interaction at impurity sites 4-92675
- V-Si, electron momentum distrib. and charge transfer, γ-ray Compton scatt. study 4-70059
- Y<sub>2</sub>O<sub>3</sub>, total gamma-ray cross sections 4-60959
- Zn, single cryst., level crossing reson. on <sup>68</sup>Ge 4 μs (9/2)<sup>+</sup> isomer, in-beam study 4-76289
- Zn-Ag, higher order level mixing resonances of oriented nuclei 4-92982

**gamma-ray spectrometers**

- see also gamma-ray spectra
- background determ. in quantitative gamma-resonance spectroscopy 4-74094
- beta-gamma coincidence spectrometer for low radioactivity measurements (Russian) 4-74093
- Compton suppression γ-counting, count-rate effect on efficiency 4-102448
- computerised acquisition system 4-59484
- dead-time correction method, short-lived radioisotopes, gamma-ray spectrometry 4-102543
- electrodynamic drive for a Mossbauer spectrometer 4-101996
- geological sample gamma-ray spectrometer with underground detector 4-105765
- high-resolution gamma spectrometer using HPGe coaxial detectors and time-variant filters 4-64270
- Mossbauer spectrometer for in situ low temperature studies of ion-bombarded metals 4-73608
- Mossbauer spectrometer in pulse height modulation mode (Chinese) 4-68860
- nuclear reactor cover-gas monitor using charcoal-Ge γ-ray spectrometer combination 4-59370
- portable gamma ray spectrometer/computer 4-59485
- radioactivity meas. of large-volume samples, calibration coeff. determ. 4-74095

**gamma-ray spectrometers continued**

- scintillation hodoscope spectrometer for electrons and high-energy photons 4-59487
- TESSA, Total Energy Suppression Shield Array, Daresbury, props. and first results 4-86795
- Bi<sub>2</sub>Ge<sub>2</sub>O<sub>12</sub> anti-Compton spectrometer design and appl. in nucl. spectroscopy 4-64269
- Bi<sub>2</sub>Ge<sub>2</sub>O<sub>12</sub>, Compton suppression spectrometer 4-91135
- Bi<sub>2</sub>Ge<sub>2</sub>O<sub>12</sub> detector role in γ-ray spectroscopy 4-59551
- Ge detector array for nuclear safeguards 4-74098
- Ge gamma-ray spectrometer, collimator geometries 4-102459
- Ge low background spectrometer 4-59486
- Ge, segmented n-type detector development, appl. to astron. γ-ray spectroscopy 4-63060
- Ge spectrometer, background reduction, material selection, geometry, shielding 4-102489
- Ge(Hp) γ-ray spectrometer with NaI(Tl) anticoincidence shield 4-59482
- Ge(Li) detector system with massive shielding, chem. samples anal. for environmental radioactivity levels 4-66843
- HgI<sub>2</sub> large area photodetectors 4-59562
- NaI modularised γ-ray spectrometer 4-91142
- NaI plastic shielded γ-ray spectrometer, performance 4-91136
- NaI(Tl) γ-ray scintillator, spectral anal. by programmable calculator (Chinese) 4-68859

**gamma-ray transport see photon transport theory****gamma-rays**

- atmospheric gamma rays, due to cosmic ray interactions 4-110400
- radiation protection, accumulation factor, effect of collimation of γ-rays 4-102405
- shielding geometry, dose factors of γ-ray build up 4-102406
- tomography, medical appl. of imaging methods 4-72451
- tomography for nondestructive evaluation 4-71809
- tomography for nondestructive evaluation 4-71810

**gamma transition see glass transition (polymers)****Gamow-Teller transitions see beta-decay****garnets**

- includes ferrimagnetic insulators, M<sub>3</sub>Fe<sub>2</sub>O<sub>12</sub>; for rock-type garnets, MM'(SiO<sub>3</sub>)<sub>2</sub>, see minerals
- see also ferrimagnetic properties of substances
- bubble garnet film, domain wall stationary motion in presence of in-plane mag. field 4-84838
- bubble garnet implantation, review 4-80064
- conference, Eger, Hungary (Sept. 1983) 4-78029
- epitaxial layers, remanent domain structure, after planar saturation 4-88708
- epitaxial layers, coercivity phenomena 4-76204
- ferrite epitaxial films, dichroic axis and magnetisation rotation 4-93047
- ferrite garnet films, transition layer study 4-75816
- ferrite-garnet films, magnetic vortices 4-76197
- film, domain nucleation, Faraday contrast modulation 4-76203
- films, ferromagnetic, microwave props., review 4-80803
- films, ion implanted, induced mag. anisotropy 4-76205
- films, mag., structural props. 4-80805
- giant magnetostriction, influence of magnetoelastic interaction, review 4-71151
- ion implanted film, strain distrib. (Japanese) 4-108753
- laser light deflector using garnet film with submicron domains 4-103002
- magnetic vortex dynamics using the optical Cotton-Mouton effect 4-92986
- monocrystalline cathodoluminescent garnet layers 4-81010
- multilayer bubble films, domain wall dynamics and interface pinning 4-92946
- polycrystalline, ferrimagnetic resonance losses, computer controlled meas. 4-61595
- rare earth garnets, R<sub>3</sub>Fe<sub>2</sub>O<sub>12</sub>, Faraday effect in strong mag. fields 4-80908
- rare earth garnets, R<sub>3</sub>Y<sub>3</sub>-Fe<sub>2</sub>O<sub>12</sub>, Faraday effect in strong mag. fields 4-80908
- structure prediction using energy-minimisation techniques 4-84244
- thin films, amorphisation of regular domain structures at second-order phase transitions, dislocation-disclination mechanism 4-98928
- thin layers, trace amounts of Pt, polarographic determ. 4-99914
- YAG:Nd<sup>3+</sup> crystal generation characs., relation to their passive optical parameters (Russian) 4-79161
- YIG:Ga(La) magneto-optical waveguide, TE to TM mode conversion by alternating-coupling coeff. 4-69545
- YIG permeability meas., using Faraday rotation 4-58873
- YIG surface obs., proportional electron detector for nuclear gamma-resonance spectroscopy 4-86448
- 3Y<sub>2</sub>O<sub>3</sub>:5Fe<sub>2</sub>O<sub>3</sub>, solid state reaction study, IR and mag. props. 4-85301
- Bi-TmFeGa garnet films, anisotropy fields 4-114147
- Bi-YIG garnet films, anisotropy fields 4-114147
- Bi<sub>3</sub>Fe<sub>3</sub>-Ga<sub>2</sub>O<sub>12</sub> layer growth by LPE, review 4-80453
- (BiPrGdYb)<sub>3</sub>(FeAl)<sub>2</sub>O<sub>12</sub> single cryst. films for ring laser gyroscopes (Chinese) 4-60123
- (BiTm)<sub>3</sub>(FeGa)<sub>2</sub>O<sub>12</sub> epitaxial film, mag. bubbles study 4-109049
- Ca<sub>3</sub>Cr<sub>2</sub>Si<sub>2</sub>O<sub>12</sub>, synthetic garnets, Cr coordination and vibr. props., IR study 4-65249
- Ca<sub>3</sub>Ga<sub>2</sub>Ge<sub>2</sub>O<sub>12</sub>, garnet single crystals, microhardness, brittle fracture 4-65337
- Ca<sub>3</sub>Ga<sub>2</sub>Ge<sub>2</sub>O<sub>12</sub>:Cr<sup>3+</sup> EPR spectra 4-71170
- Ca<sub>3</sub>NaMg<sub>2</sub>V<sub>2</sub>O<sub>12</sub> garnet, elec. cond. and thermopower 4-70822
- Ca<sub>3</sub>-Y<sub>2</sub>Mn<sub>2</sub>Ge<sub>2</sub>O<sub>12</sub> thermopower and elec. cond., 30 to 1000°C 4-70847
- DyAG, EPR at far IR wavelengths 4-76249
- Dy<sub>3</sub>Al<sub>2</sub>O<sub>12</sub>, far IR EPR study 4-71214
- (Er<sub>1</sub>Y<sub>1-2</sub>)Al<sub>2</sub>O<sub>12</sub>, crystals, temp. dependence of phononless f-f transitions 4-71339
- Eu<sub>3</sub>Fe<sub>2</sub>O<sub>12</sub>, <sup>151</sup>Eu nucleus relax. processes in domains and domain boundaries 4-88739
- Eu<sub>3</sub>Sc<sub>2</sub>Fe<sub>2</sub>O<sub>12</sub>, EFG sign at <sup>57</sup>Fe nuclei, Mossbauer spectra 4-84599
- Fe garnet magneto-optic spatial light modulator in optical image processor or display system 4-74696
- (Gd,Sc)<sub>3</sub>Ga<sub>2</sub>O<sub>12</sub>:Nd<sup>3+</sup> Cr<sup>3+</sup> laser operating in pulse-periodic regime, output characs. 4-74521
- Gd-Ga garnet, absorpt. coeff. and refractive index determ. 4-80895
- (Gd<sub>1-x</sub>Er<sub>x</sub>)Al<sub>2</sub>O<sub>12</sub> garnet, 3 μm stimulated emission, concentrational tuning 4-76498
- Gd<sub>3</sub>Ga<sub>2</sub>O<sub>12</sub>, fluorescence radiation due to X-ray standing waves 4-71437
- Gd<sub>3</sub>Ga<sub>2</sub>O<sub>12</sub> garnet, γ and neutron irradi., effect on optical props. 4-99135

## garnets continued

- Gd<sub>3</sub>Ga<sub>5</sub>O<sub>12</sub>, garnet single crystals, microhardness, brittle fracture 4-65337  
 Gd<sub>3</sub>Ga<sub>5</sub>O<sub>12</sub>, hypersonic wave attenuation 4-75620  
 Gd<sub>3</sub>Ga<sub>5</sub>O<sub>12</sub>:Nd,Cr, laser props., modified Czochralski growth (*Chinese*) 4-112441  
 Gd<sub>3</sub>Ga<sub>5</sub>O<sub>12</sub>:Pr(Bi) garnet epitaxial layers, site selectivity, dichroism studies 4-84533  
 Gd<sub>3</sub>Sc<sub>2</sub>Al<sub>3</sub>O<sub>12</sub>:Cr<sup>3+</sup>, tunable room temp. CW laser action 4-74518  
 Gd<sub>3</sub>Ti<sub>2</sub>Li<sub>3</sub>O<sub>12</sub>, photoluminesc. and energy transfer in rare earth activated garnets (*German*) 4-76508  
 Ho<sub>3</sub>Fe<sub>5</sub>O<sub>12</sub>, mag. and thermodynamic props., anisotropic mol. field approx. 4-88656  
 Ho<sub>3</sub>Fe<sub>5</sub>O<sub>12</sub>, umbrella mag. struct. thermal evolution, neutron diff. study 4-92893  
 Ho<sub>0.8</sub>Y<sub>2.2</sub>Fe<sub>5</sub>O<sub>12</sub>, spin-reorientation phase transition, Faraday effect, magnetisation meas. 4-88814  
 Lu<sub>3</sub>Al<sub>5</sub>O<sub>12</sub>:Cr<sup>3+</sup>,Tm<sup>3+</sup>, Ho<sup>3+</sup>, stimulated emission of Tm<sup>3+</sup> and Ho<sup>3+</sup>, cross-cascade generation 4-71411  
 NaCa<sub>2</sub>Cu<sub>2</sub>V<sub>3</sub>O<sub>12</sub> garnet, mag. props. study 4-61563  
 Nd:YAG crystals, Czochralski, vertical distrib. conc. determ. of Nd ion (*Chinese*) 4-84310  
 Nd<sub>3</sub>Ga<sub>5</sub>O<sub>12</sub>, single cryst. growth 4-66206  
 Pr<sub>3</sub>Y<sub>3-x</sub>G<sub>x</sub>Fe<sub>5-3x</sub>O<sub>12</sub> garnet single cryst. magnetisation and Faraday rotation 4-61664  
 R<sub>3-x-y</sub>Bi<sub>x</sub>Pb<sub>y</sub>Fe<sub>5-2x-y</sub>M<sub>2</sub>O<sub>12</sub> films, mag. and magneto-optical props. 4-80802  
 (Y, Lu, Sm, Ca)<sub>3</sub>(Fe, Ge)<sub>5</sub>O<sub>12</sub> garnet system, distrib. coeffs. 4-61881  
 YAG cryst., impurity distrib. and Bridgman-Stockbarger growth 4-60950  
 YAG crystals, antirefl. coatings based on Ge-As(Sb)-S(Se), CdGa<sub>2</sub>Se<sub>4</sub> and CaF<sub>2</sub> (*Russian*) 4-97012  
 YAG, hypersonic wave attenuation 4-75620  
 YAG refractories, heat transfer during growth 4-76664  
 YAG:Ce<sup>3+</sup>, defect emission, photoluminesc. decay time measurements 4-80971  
 YAG:Fr, photoluminescence spectra meas. (*Russian*) 4-71442  
 YAG:Nd, Cr, Ce, laser props., gain coeffs. 4-79156  
 YAG:Nd crystals coloured with X-rays, thermoluminesc. 4-76534  
 YAG:Nd<sup>3+</sup>, planar optical waveguide fabrication by ion implantation 4-69552  
 YAG:Nd<sup>3+</sup> single cryst., interconfiguration 4f<sup>2</sup>-4f<sup>2</sup>5d<sup>1</sup> transitions 4-93087  
 YAG:R (R=rare earth), thermal conductivity, phonon scattering obs. 4-98374  
 Y<sub>3</sub>Al<sub>5</sub>O<sub>12</sub>:Nd<sup>3+</sup> garnets,  $\gamma$ -ray irradi., colour centres and optical props. 4-114310  
 (YBi)<sub>3</sub>Fe<sub>5</sub>O<sub>12</sub> film, growth induced anisotropy 4-114146  
 (YBiPb)<sub>3</sub>(FeAlPt)<sub>5</sub>O<sub>12</sub> LPE layers, lattice site determ. by channelling 4-80440  
 Y<sub>1-x</sub>Bi<sub>x</sub>Pb<sub>1-x</sub>Fe<sub>5-x</sub>Pt<sub>x</sub>O<sub>12</sub> films, magneto-optic prop. meas. using piezobirefr. modulation 4-66013  
 Y<sub>1-x</sub>Ca<sub>x</sub>Fe<sub>5-x</sub>Ti<sub>x</sub>O<sub>12</sub> garnets, hyperfine fields and Mossbauer spectra 4-109098  
 (Y<sub>1-2x</sub>Ca<sub>2x</sub>-<sub>2x</sub>)(Fe<sub>2x</sub>Zr<sub>2x-2x</sub>)Fe<sub>5</sub>O<sub>12</sub> mag. atom critical conc., neutron depolarisation study 4-61514  
 Y<sub>1-x</sub>Eu<sub>x</sub>Fe<sub>5-x</sub>Ga<sub>x</sub>O<sub>12</sub> mag. bubble films, LPE growth 4-109332  
 (YEuTmCa)<sub>3</sub>(FeGe)<sub>5</sub>O<sub>12</sub> ferrite-garnet epitaxial films, fine struct. of mag. spectra 4-76206  
 Y<sub>3</sub>Fe<sub>5</sub>O<sub>12</sub> garnet, cryst. growth 4-61818  
 Y<sub>3</sub>Fe<sub>5</sub>O<sub>12</sub> garnet film, mode conversion of guided mag. waves 4-92942  
 Y<sub>3</sub>Fe<sub>5</sub>O<sub>12</sub> ionic structure, neutron induced transformation, calcs. 4-113415  
 Y<sub>3</sub>Fe<sub>5</sub>O<sub>12</sub> single cryst., top seeded soln. growth method and mag. props. 4-93207  
 Y<sub>3</sub>Fe<sub>5</sub>O<sub>12</sub>:Ho<sup>3+</sup>, ferromagnetic resonance study 4-84857  
 Y<sub>3</sub>Fe<sub>5</sub>O<sub>12</sub>:Pb, epitaxial films, Pb effect on optical props. 4-99210  
 Y<sub>3</sub>Fe<sub>5</sub>O<sub>12</sub> garnet epitaxial layers, ion implantation-induced strain and damage profiles 4-75558  
 Y<sub>3</sub>Ga<sub>5</sub>O<sub>12</sub>:Nd thin film waveguide, RF sputtering growth, fluoresc. spectrum, optical amplifier appl. 4-60146  
 Y<sub>3-x</sub>Gd<sub>x</sub>Fe<sub>5</sub>O<sub>12</sub> noncrystalline garnet films, electron transport and thermopower 4-108958  
 (YGdYbBi)<sub>3</sub>(FeAl)<sub>5</sub>O<sub>12</sub> films, magnetostrictive vibr. study 4-98927  
 YIG, acoustic mag. reson. obs. 4-61615  
 YIG, amorphous, appl. of hyperfine and exchange field distrib. in amorphous speromagnets 4-104413  
 YIG containing magnetic glass-ceramics, prep. using colloidal Bi as nucleation catalyst, characts. 4-71628  
 YIG, crystal growth by floating zone method 4-76665  
 YIG, doped, for thermistor-bolometers 4-68280  
 YIG, effect of diffusion relax. on domain walls 4-80773  
 YIG epitaxial films, magnetostatic echo study 4-61576  
 YIG ferromagnetic films, spin-wave solitons obs. 4-71135  
 YIG film, parametric amplification of surface magnetostatic waves 4-109046  
 YIG film, remagnetisation of isolated strip domain (*Russian*) 4-88706  
 YIG film magnetostatic-volume-wave mode conversion at a region of bias-field discontinuity 4-98933  
 YIG films, electrical props. 4-80698  
 YIG, influence of pre-sintering on mag. props. 4-84789  
 YIG LPE films, birefringence control, magneto-optical waveguide appls. 4-61652  
 YIG, magnetic insulator, losses 4-71121  
 YIG, magnetic permeability, initial, comparison of theory with experiment (*Russian*) 4-98922  
 YIG, magnetostatic forward volume wave propag., finite width 4-84770  
 YIG, Me<sup>+</sup> implanted, mag. props., annealing effects 4-71057  
 YIG, microparticle materials, magnon scatt. 4-104542  
 YIG multipin echo phenomena in double exciting pulse sequence 4-71208  
 YIG, nonlinear soliton waves and Bloch walls 4-114097  
 YIG plates and epitaxial films, reson. interaction between magnetostatic and Lamb waves 4-61577  
 YIG, seed and unseeded, growth from high temp. solns., studied by growth striations 4-76656  
 YIG single cryst. and epitaxial film, sublattice anisotropy and mag. linear dichroism 4-61667  
 YIG single crystal spheres, dissoln. forms in H<sub>3</sub>PO<sub>4</sub> and HBr 4-75687  
 YIG, solubility and growth kinetics on (111) substrates, influence of excess iron oxide 4-75802  
 YIG, spin wave excitation by EM field pulses (*Russian*) 4-65797

## garnets continued

- YIG, surface magnon polaritons, ATR spectra calcs. 4-61299  
 YIG triple-layered films, magnetostatic band suppression technique, microwave device appl. 4-84834  
 YIG:Bi epitaxial films, refr. index and optical absorption spectra at UV near IR wavelengths 4-104553  
 YIG:Bi thin films, photoelastic birefringence, phase matching (*Japanese*) 4-80909  
 YIG:Ca epitaxial layers, elec. cond. meas. 4-80694  
 YIG:Ca films, charge compensation mechanism, annealing effects, behaviour on treatment with oxidising and reducing solns. 4-80799  
 YIG:Ca films, surface layer contraction, X-ray diff. and magneto-optic studies 4-61262  
 YIG:H, H diffusion, optical absorption and mag. circular dichroism studies 4-61144  
 YIG:Si, spin reorientation mechanism 4-98892  
 (Y<sub>1-x</sub>Lu<sub>x</sub>)<sub>3</sub>Al<sub>5</sub>O<sub>12</sub>, anharmonicity const., longit. acoustic wave absorp. 4-88248  
 Y<sub>2</sub>O<sub>3</sub>:Fe<sub>2</sub>O<sub>3</sub>, solid state reaction for garnet formation by sintering 4-85302  
 (YSmCa)<sub>3</sub>(FeGe)<sub>5</sub>O<sub>12</sub> garnet films, Ne<sup>+</sup> implanted, cylindrical magnetic domains obs. 4-114148  
 Y<sub>1-x</sub>Sm<sub>x</sub>Fe<sub>5-x</sub>Ga<sub>x</sub>O<sub>12</sub> mag. bubble films, LPE growth 4-109332  
 YSmLuCaFeGe garnet film, mag. anisotropy study 4-88704  
 (YSmLuCa)<sub>3</sub>(GeFe)<sub>5</sub>O<sub>12</sub> epitaxial film, clouddike charged wall, bubble propagation 4-104473  
 Y<sub>1-x</sub>Sm<sub>x</sub>Lu<sub>1-x</sub>Fe<sub>5</sub>O<sub>12</sub> thin film, rare earth site occupation 4-108392
- gas** *see gases*  
**gas analysis** *see chemical analysis*  
**gas blast circuit breakers**  
 SF<sub>6</sub> puffer circuit breaker: Schlieren visualisation of hot circulation following fault interruption 4-113078  
**gas breakdown** *see electric breakdown of gases*  
**gas bubbles** *see bubbles*  
**gas-discharge displays**  
 AC plasma display, transient phenomena 4-91999  
**gas discharge lamps** *see discharge lamps*  
**gas-discharge tubes**  
*see also gas-discharge displays; ion sources; thytrons*  
 nanosecond currents in a gas discharge device 4-79863  
 transducers, gas discharge, brightness and dose sensitivity 4-73512
- gas discharges** *see discharges (electric)*  
**gas dynamic lasers** *see gasdynamic lasers*  
**gas dynamics** *see aerodynamics*  
**gas ionisation** *see ionisation of gases*
- gas lasers**  
*see also chemical lasers; excimer lasers; gasdynamic lasers; ion lasers*  
 Antares facility for inertial fusion 4-96957  
 carbon tetrafluoride optically pumped laser, press. depend. of laser oscill. and superfluoresc. emission 4-69377  
 chlorofluoromethane, optically pumped far IR laser action 4-112395  
 coherent IR radar systems and appls., conf., Arlington, VA, USA (Apr. 1983) 4-95019  
 copper acetylacetonate, vapour, laser action and fluoresc. (*Japanese*) 4-60019  
 DFB helical far IR laser, theory, realisation and mode characts. 4-79186  
 dichlorofluoromethane far IR CW lasing lines, optically pumped, free mecs. 4-102925  
 1,1-difluoroethane new far IR laser lines, CO<sub>2</sub> laser pumping 4-91440  
 difluoromethane 889  $\mu$ m laser, optically pumped, absolute two photo. light shift heterodyne meas. 4-91442  
 difluoromethane far-IR laser, optically pumped, self-pulsing instability 4-91444  
 electron beam pumping, energy deposition meas. of intense relativistic electron beam 4-69297  
 electron beam pumping methods, energy deposition problems 4-69381  
 far IR laser, pulsed, optically pumped effects of pumping pulse width (*Chinese*) 4-112391  
 fast-flow lasers, current flow mechanism in glow discharge positive column 4-113249  
 fluoromethane, CW far IR optically pumped open-cavity laser (*Chinese*) 4-112392  
 fluoromethane 1.60 THz (187  $\mu$ m) optically pumped laser emission free mecs. 4-96873  
 fluoromethane far IR laser, pulsed, optically pumped effects of pumping pulse width (*Chinese*) 4-112391  
 fluoromethane grazing-incidence far-IR laser 4-96949  
 fluoromethane laser, optically pumped 496  $\mu$ m, linear DFB, helical DFB and grazing-incidence types (*Chinese*) 4-107677  
 fluoromethane tunable far IR laser pumped by CO<sub>2</sub> TE laser 4-112472  
 fluoromethane tunable FIR laser, frequency trimming (*Chinese*) 4-69374  
 fluoromethane-<sup>13</sup>C tunable Raman FIR laser, optically pumped, tunability study 4-79122  
 fluoromethane-C<sub>2</sub> far IR laser lines, energy-level structure 4-112394  
 formic acid, CW far IR optically pumped open-cavity laser (*Chinese*) 4-112392  
 formic acid FIR laser active medium refr. index variations induced by interacting microwave field 4-79109  
 formic acid laser freq. determ. by mixing expts. between submillimeter lasers using heterodyne system with Schottky barrier diode 4-102923  
 generalized formula for absorption and stimulated emission of light 4-60011  
 grazing incidence far IR gas laser, config. and characts. 4-79187  
 He-Cd laser with lateral HF discharge, different design comparative characts. (*Russian*) 4-69372  
 He-Ne-methane bichromatic Zeeman laser with nonlinear absorption (*Russian*) 4-69433  
 high power laser industrial applications 4-102966  
 industrial applications of high power lasers, conf., Linz, Austria (Sept. 1983) 4-101561  
 inert gases, electrical discharge, externally maintained, preionised, IR radiation generation, laser efficiency 4-64695  
 intensity perturbation transverse distribution investigation by probing gaseous lens-like media with He-Ne laser radiation 4-79207  
 line shapes of sensitive gas lasers 4-91435  
 metal vapour, high strobe-rate lasers for high-speed holographic testing 4-102903  
 methanol, CW far IR optically pumped open-cavity laser (*Chinese*) 4-112392

## lasers continued

- methanol bromide optically pumped far-IR lasing in multigas mixture 4-102924
- methanol laser, high-power 119  $\mu\text{m}$  operation, water-cooled cavity design, electron density meas. appl. 4-79185
- methanol laser, optically pumped, far IR, emission, torsional transition obs. and assignment 4-107607
- methanol laser, optically pumped, new laser lines in 27.7 to 61.7  $\mu\text{m}$  wavelength range 4-91438
- methanol laser far IR radiation, subnanosecond optical switching 4-74575
- methanol laser for  $^{\circ}\text{SO}_2$  pure rotational spectroscopy using fixed line far IR lasers 4-74246
- methanol laser freq. determ. by mixing expts. between submillimeter lasers using heterodyne system with Schottky barrier diode 4-102923
- methanol optically pumped far-IR lasing in multigas mixture 4-102924
- methanol pumped by  $^{13}\text{C}^{18}\text{O}$  pump laser, sub-MM laser line obs. and assignments 4-69375
- methanol- $\text{d}_3$  laser, optically pumped, far IR line assignments 4-107608
- methanol- $\text{d}_3$  laser, optically pumped, new laser lines in 27.7 to 61.7  $\mu\text{m}$  wavelength range 4-91438
- methanol-methyl bromide-methyl iodide optically-pumped multigas far-IR laser 4-102924
- methyl fluoride,  $\text{CO}_2$  pumped far IR laser line assignment using IR diode laser spectroscopy 4-107610
- methyl iodide optically pumped far-IR lasing in multigas mixture 4-102924
- optically pumped far IR lasers, efficiency improvement 4-107611
- organic compound based lasers, active medium stimulated emission charact. calc. 4-74482
- photon recyclers, optically pumped NMMW lasers 4-87317
- picosecond pulse generation using acoustooptic modulator (Japanese) 4-74558
- POPOP vapour laser, laser bleaching mechanism 4-79114
- rare-gas-halide lasers, X-ray preionisation 4-74488
- receiver concepts for data transmission at 10 microns 4-107884
- repair service selection 4-83599
- review of solid-state and gas laser characts. 4-60008
- ring laser, freq. fluctuation meas. 4-87382
- ring laser, medium, excitation spatial-temporal coherence effect on statistical characts. 4-107590
- ring laser, nonlinear resonance characts., influence of flight effects (Russian) 4-96961
- ring laser with absorbing cell, mag. field effect on competing reson. characts. 4-87376
- ring laser with circularly anisotropic resonator, nonreciprocal effects, transverse mag. field 4-79195
- secondary emission electron gun, appl. to gas lasers and plasma chem. reactor 4-90689
- self-locking of two modes, stable operation 4-74561
- static fill TEA lasers, high repetition rate, gas density perturbations 4-91443
- steady state synchronisation of lateral modes (Russian) 4-60079
- submillimeter lasers, optically pumped, appl. of optoacoustic effect 4-87363
- submillimetre laser, optical pump absorpt. efficiency (Chinese) 4-107606
- submillimetre lasers, power level stabilisation with optical excitation (Russian) 4-79088
- TEA and multiatmosphere  $\text{CO}_2$  lasers, remote sensing appl. 4-110332
- tetrafluoromethane laser, 16  $\mu\text{m}$ , high repetition rate 4-87362
- tetrafluoromethane tunable laser, 16  $\mu\text{m}$ , optically pumped (Chinese) 4-87359
- vinyl bromide,  $\text{CO}_2$  laser pumped, 47 CW far IR laser lines 453 to 2356  $\mu\text{m}$  4-96869
- vinyl bromide far-IR laser action, optically pumped by CW  $\text{N}_2\text{O}$  laser 4-112397
- vinyl chloride far-IR laser action, optically pumped by CW  $\text{N}_2\text{O}$  laser 4-112397
- vinyl fluoride far-IR laser action, optically pumped by CW  $\text{N}_2\text{O}$  laser 4-112397
- Ar, electrical discharge, externally maintained, preionised, IR radiation generation, laser efficiency 4-64695
- Ar mode synchronised laser amplifier system, high-power pulse prod. at high repetition freq. (Russian) 4-69369
- Ar<sup>+</sup> passively mode-locked laser, output light energy characts. 4-64696
- CO CW industrial laser, electron beam-controlled with 10 kW output power, energy characts. 4-74492
- CO CW laser two-mode multiline stabilisation using Fabry-Perot filter under analog and digital computer control 4-60092
- CO cryogenic electroionisation laser, energy characts. 4-69379
- CO electroionisation laser, power and time characts. of light pulses, pump power depend. 4-64700
- CO laser, branch selected, spectral characts. at room temp., Fabry-Perot etalon meas. (Chinese) 4-112389
- CO laser, high-power room-temp. 4-112385
- CO laser appls. in surgery 4-77371
- CO laser gas discharge plasma, oscillatory instability 4-64699
- CO line-tunable laser, appl. to  $\text{H}_2\text{O}$  reson. absorpt. study (Chinese) 4-67398
- CO waveguide laser with selective resonator, emission freq. wide tuning range 4-60069
- $\text{CO}_2$  1000-Hz mini-TEA laser, remote sensing appls. 4-107662
- $\text{CO}_2$  amplifier, light pulse coherent amplification 4-79101
- $\text{CO}_2$  CW, appl. of IR presentation photography 4-111229
- $\text{CO}_2$  CW far IR lasers, optically pumped, using new stabilisation system 4-102954
- $\text{CO}_2$  CW high power transverse flow laser type J16A working gas determ. and catalytic purification (Chinese) 4-112463
- $\text{CO}_2$  CW IR lasers, dynamics, investigation using tunable diode lasers 4-112375
- $\text{CO}_2$  CW industrial ionisation lasers, service life increase using 5-component mixtures 4-112379
- $\text{CO}_2$  CW laser, features 4-107885
- $\text{CO}_2$  CW laser, gain profile, opto-voltaic representation 4-83562
- $\text{CO}_2$  CW laser, radiatively pumped 4-91494
- $\text{CO}_2$  CW RF-pumped IR laser using transverse gas flow 4-74544
- $\text{CO}_2$  CW steady-state laser model 4-112373
- $\text{CO}_2$  CW transverse flow laser, quasi two-dimens. gain distrib. (Chinese) 4-112376
- $\text{CO}_2$  cascade laser, 4.4 micron, resonator design 4-87313

## gas lasers continued

- $\text{CO}_2$  chirp-modulated CW heterodyne laser rangefinder/velocimeter based on acousto-optic modulator 4-96963
- $\text{CO}_2$  commercial technological laser prod. of power 1 to 10 kW 4-107663
- $\text{CO}_2$  compact hybrid single mode TEA laser, stabilisation 4-91495
- $\text{CO}_2$  fast axial flow laser with 1000 watt output power 4-102945
- $\text{CO}_2$  grating selected freq. laser, mode corrugated pipe design (Chinese) 4-87360
- $\text{CO}_2$  Helios laser, high-density implosion expts. 4-68828
- $\text{CO}_2$  high energy pulsed lasers, catalyst evaluation for closed cycle operation 4-96939
- $\text{CO}_2$  high power laser optics 4-102937
- $\text{CO}_2$  high power laser plasma investigation 4-102917
- $\text{CO}_2$  high power laser technology overview 4-107668
- $\text{CO}_2$  high power laser transmissive optics, failure phenomena (Japanese) 4-74530
- $\text{CO}_2$  high power laser with folded resonator, computer simulation 4-102916
- $\text{CO}_2$  high power lasers, multi-kilowatt, for use in industrial production 4-102946
- $\text{CO}_2$  high pressure, absorption of light by  $\text{SF}_6$  4-107420
- $\text{CO}_2$  high-power technological gas elec. discharge laser based on air- $\text{CO}_2$  mixture 4-107664
- $\text{CO}_2$  IR laser, freq. synthesized and continuously tunable in 9-11  $\mu\text{m}$  range 4-96947
- $\text{CO}_2$  injection-locked TEA laser, tunable single-mode design for  $\text{D}_2\text{O}$  laser pumping 4-79184
- $\text{CO}_2$  intracavity plasma shutter for transversely excited  $\text{CO}_2$  lasers 4-103584
- $\text{CO}_2$  laser, 4.3  $\mu\text{m}$ , gain dynamics 4-79180
- $\text{CO}_2$  laser, appl. to strengthening of Al-Si-Cu-Mg 4-62117
- $\text{CO}_2$  laser, gaseous medium temp., influence of high-mol. compound impurities 4-79103
- $\text{CO}_2$  laser, hybrid oscillator/electron-beam preionized amplifier config. for  $\text{D}_2\text{O}$  laser pumping 4-79183
- $\text{CO}_2$  laser, hybrid TE-TEA sealed-off with corona preionisation 4-69430
- $\text{CO}_2$  laser, Q-switched, electro-optic freq. shifts 4-87377
- $\text{CO}_2$  laser, rel. to non-self-sustained discharge with a plasma cathode 4-84114
- $\text{CO}_2$  laser bands, freq. tables, rovibr. consts. 4-60015
- $\text{CO}_2$  laser beam power measurement of high-power lasers, calorimeter development (Japanese) 4-64715
- $\text{CO}_2$  laser development and applications at MIT Lincoln Lab. 4-90325
- $\text{CO}_2$  laser drilling of multilayer PCBs 4-87384
- $\text{CO}_2$  laser for surgical appls. 4-72342
- $\text{CO}_2$  laser frequency stabilisation for sub-MM laser pumping by Stark modulated Lamb dip signal in methanol (Japanese) 4-74485
- $\text{CO}_2$  laser heterodyne bias freq.-locking (Chinese) 4-91512
- $\text{CO}_2$  laser industrial processing facility, Rayleigh range for Hermite-Gaussian modes 4-91508
- $\text{CO}_2$  laser intersatellite data link system, low IF translation loop concept 4-107552
- $\text{CO}_2$  laser mixtures, electron mobility, diffusion coeffs. ratio 4-112374
- $\text{CO}_2$  laser polarimeter 4-78363
- $\text{CO}_2$  laser processing induced plasma, optical absorption prop. development 4-108189
- $\text{CO}_2$  laser produced plasma, harmonic generation study 4-102920
- $\text{CO}_2$  laser pulse shapes determ. using methyl-methacrylate plate 4-91509
- $\text{CO}_2$  laser pumped vinyl bromide, 47 CW far IR laser lines 4-96869
- $\text{CO}_2$  laser radiation detection using antenna-coupled point contact Schottky diode, responsivity study (Japanese) 4-78374
- $\text{CO}_2$  laser spectrometer,  $\text{ClO}_2$  absorption coefficients at  $^{12}\text{C}^{16}\text{O}_2$  and  $^{13}\text{C}^{18}\text{O}_2$  laser wavelengths, appl. to remote monitoring 4-114997
- $\text{CO}_2$  laser system producing single mode microsecond pulses, use in ion-temp. meas. 4-102953
- $\text{CO}_2$  laser transceiver with Gbit/s capability, space-to-space communication appl. 4-107883
- $\text{CO}_2$  laser with plasma electrodes 4-91434
- $\text{CO}_2$  laser with variable output pulse duration 4-60070
- $\text{CO}_2$  lasers, pulsed, damage thresholds for large irradiated spots 4-107595
- $\text{CO}_2$  mirror electrode for laser initiated discharge channels 4-69932
- $\text{CO}_2$  mixing lasers, plasma injection controlled discharge characts. 4-83563
- $\text{CO}_2$  precision calibrating equipment for laser power 4-96969
- $\text{CO}_2$  pulse periodic lasers, appl. to industrial welding 4-107660
- $\text{CO}_2$  pulse-periodic laser, wave-driven gas circulation in a gas chamber with pulse-periodic energy supply 4-60068
- $\text{CO}_2$  pulsed amplifiers, pumping process modelling in elec. discharges 4-83564
- $\text{CO}_2$  pulsed and CW laser, heterodyne freq. offset locking technique 4-96951
- $\text{CO}_2$  pulsed gas lasers, high power 4-96865
- $\text{CO}_2$  pulsed miniature, with sealed-off electron source 4-102950
- $\text{CO}_2$  pump laser freq. controlling method 4-96950
- $\text{CO}_2$  quasi-CW tunable 1-sec pulse laser for optical pumping 4-74536
- $\text{CO}_2$  RF excited lasers, electron energy distrib. and transport coeffs. 4-102919
- $\text{CO}_2$  sealed TEA lasers, high peak power and sustained long life operation 4-87365
- $\text{CO}_2$  single-mode etalon-tuned TEA laser, optimised design for  $\text{NH}_3$  laser pumping 4-79182
- $\text{CO}_2$  TEA and continuous high power laser research and development at Battelle-Frankfurt 4-102944
- $\text{CO}_2$  TEA laser, beam expanding grating plane cavity (Chinese) 4-107689
- $\text{CO}_2$  TEA laser, electron density of afterglow of pulsed discharge and UV photoionisation, meas. using microwave interferometer (Chinese) 4-87315
- $\text{CO}_2$  TEA laser, fine-tuned, high power, optical pumping, methanol FIR laser lines obs. 4-102918
- $\text{CO}_2$  TEA laser, injection locking studies for stable high-power operation 4-60014
- $\text{CO}_2$  TEA lasers, injection locked, transient freq. shift induced by electron density 4-102915
- $\text{CO}_2$  TEA lasers, miniature type, self modulation props. study 4-79202
- $\text{CO}_2$  TEA lasers, multipass-prism interferometer for fine-freq.-turning, single-mode operation 4-107683
- $\text{CO}_2$  TEA repetitive tunable laser, long lifetime, without He (Chinese) 4-112377

## gas lasers continued

- CO<sub>2</sub> technological lasers, materials for optical transmission elements 4-107658  
 CO<sub>2</sub>, temp. and flow distrib. in self-sustained discharge, laser characts. 4-79104  
 CO<sub>2</sub> transverse flowing laser, gain coeff. meas. (Chinese) 4-60013  
 CO<sub>2</sub> transverse-flow laser, 2.5 kW output 4-69446  
 CO<sub>2</sub> transverse-flow laser vibrational and translational temp. determ. (Chinese) 4-112378  
 CO<sub>2</sub> tunable double wavelength laser study (Chinese) 4-91513  
 CO<sub>2</sub> tunable high pressure RF excited laser 4-96938  
 CO<sub>2</sub> tunable high-power CW laser using compound cavity, individual transition selection 4-69366  
 CO<sub>2</sub> two-wave high-power laser 4-107684  
 CO<sub>2</sub> waveguide laser, continuously tunable, RF excited, high-press. 4-74542  
 CO<sub>2</sub> waveguide laser, freq. sweep stabilisation using inverted Lamb dip in NH<sub>3</sub>D 4-79098  
 CO<sub>2</sub> waveguide laser, RF discharge excited, freq. depend. 4-79099  
 CO<sub>2</sub> waveguide laser, RF discharge striations 4-79100  
 CO<sub>2</sub> waveguide laser design for max. output power at specified freq. offset 4-107679  
 CO<sub>2</sub> waveguide lasers, RF-excited sealed-off operation, Xe effects 4-96866  
 CO<sub>2</sub>/OsO<sub>4</sub> waveguide laser with freq. stability of 10<sup>-13</sup> 4-79102  
 CO<sub>2</sub>-CO universal technological elec. ionisation laser 4-107665  
 CO<sub>2</sub>-TEA laser, injection locking, effect of unstable resonator 4-87375  
<sup>12</sup>C<sup>18</sup>O<sub>2</sub> and isotopic mols., laser transition intensity calc. 4-107593  
<sup>13</sup>CH<sub>3</sub>F far IR laser for microturbulence studies on TEXT Tokamak 4-75160  
<sup>13</sup>CO<sub>2</sub> laser frequency measurement chain to 30 THz using FIR Schottky diodes and summm. backward wave oscillator 4-73414  
 Cu halide, burst-mode, interdependence of buffer gas press. and optimum interpulse delay 4-112396  
 Cu halide vapour long-lived sealed-off lasers, operating characts. and projected lifetimes 4-69386  
 Cu oscillator-amplifier system, negative image characts. formed using Cu green and yellow lines 4-79335  
 Cu, pulsed, use in high-speed video 4-112494  
 Cu vapour laser, picosecond pulses amplification 4-96952  
 Cu vapour laser, self-heating, numerical anal. of parameters 4-112393  
 Cu vapour laser, wall temp. meas. using optical pyrometer 4-102951  
 Cu vapour laser pumped dye laser for spectroscopic appl., conversion efficiency 4-107666  
 Cu vapour laser with 230 kHz pulse repetition rate 4-69378  
 Cu vapour lasers with unstable cavities and short inversion times, kinetics 4-96877  
 CuBr, whole heated sealed-off laser, lifetime 4-107681  
 Cu laser with supraoptimal wall temp. metastable Cu atom conc. relax. in afterglow 4-60021  
 D<sub>2</sub> gas-in-SiO<sub>2</sub> fibre Raman laser, synchronously pumped, operating at 1.56  $\mu$ m 4-79181  
 DCN CW waveguide laser operating at 195, 190  $\mu$ m, quartz tube cavity (Chinese) 4-107604  
 D<sub>2</sub>O 385  $\mu$ m laser for Thomson scattering from ion thermal fluctuations in Tokamak plasma, obs. 4-75209  
 D<sub>2</sub>O laser, TEA CO<sub>2</sub> laser pumped, development, plasma in temp. meas. appl. 4-79184  
 D<sub>2</sub>O optically pumped laser with unstable resonator, high-energy design for plasma diagnostics 4-79183  
 D<sub>2</sub>O submm laser for single shot ion temp. meas. by Thomson, scatt. 4-103569  
 F CW laser action 4-91439  
 F\* laser, discharge-pumped, intense laser generation 4-60062  
 H-Ne 633 nm laser, I<sub>2</sub> stabilised, freq. stability and reproducibility 4-91436  
 H<sub>2</sub> optical quenching and energy extraction involving metastable and dissociative states 4-79112  
 HCN CW laser, RF excited, capacitive coupling (Japanese) 4-96879  
 HCN waveguide laser and HCN laser-excited oversized hollow dielec. waveguide submm radiation pattern study 4-107709  
 H<sub>2</sub>O laser interferometer, 28  $\mu$ m, for plasma diagnostics 4-108213  
 H<sub>2</sub>O monomode CW 119  $\mu$ m laser, output beam polarisation improvement 4-112471  
 He-Cd long lifetime laser using continuously tunable He replenisher (Chinese) 4-60089  
 He-Cd-Hg system three-colour hollow cathode laser (Russian) 4-69371  
 He-Ne and Ar\* laser low-freq. beat noise (Chinese) 4-91511  
 He-Ne highly stable laser at 1.15  $\mu$ m (Chinese) 4-112469  
 He-Ne intracavity laser, magnetic field induced beat noise (Chinese) 4-60017  
 He-Ne intracavity laser, polarisation behaviour at 632.8 nm (Chinese) 4-107597  
 He-Ne laser, 0.63  $\mu$ m, effect of an external modulation signal 4-79108  
 He-Ne laser, freq. stabilisation with modular electronic system 4-112476  
 He-Ne laser, high power (Rumanian) 4-96953  
 He-Ne laser, internal mirror, output- and frequency-stabilisation by discharge current control 4-79105  
 He-Ne laser, mode struct. optical spectrum analyser study, undergraduate expt. 4-106152  
 He-Ne laser, stabilisation on absorpt. saturation in <sup>127</sup>I 4-79106  
 He-Ne laser, wavelength variations meas. using Twyman-Green interferometer (Polish) 4-86477  
 He-Ne laser appl. to intracavity dispersion meas. 4-112478  
 He-Ne laser emission power stabilisation, using gas-discharge lens 4-102938  
 He-Ne laser excitation using lateral discharge VHF pumping resonators (Russian) 4-69431  
 He-Ne laser interferometry, small amplitude vibr. meas. (Rumanian) 4-68212  
 He-Ne laser locked to methane E-line, accurate freq. meas. 4-96868  
 He-Ne lasers, active element striation freq. shifts 4-107598  
 He-Ne lasers, design (German) 4-107674  
 He-Ne lasers, excitation mechanisms anal. (Japanese) 4-79116  
 He-Ne lasers, small, striation-onset condition investigation 4-64694  
 He-Ne low breakdown voltage lasers, capillary gas breakdown modelling (Chinese) 4-112380  
 He-Ne ring laser with gain greatly exceeding losses, counterpropag. circularly polarised wave interaction 4-74557

## gas lasers continued

- He-Ne ring laser with selective losses, counter-propag. wave competition and emission spectrum produced by reson. phase-polarisation method 4-79107  
 He-Ne sensitive gas laser, line shapes 4-91435  
 He-Ne small bore discharge, radial optical gain distrib. 4-102921  
 He-Ne transverse Zeeman laser, theoretical anal., beat freq. tuning curve (Chinese) 4-91429  
 He-Ne/methane laser, freq.-modulated resonances (Russian) 4-102961  
 I pulsed gas lasers, high power 4-96865  
 I-H<sub>2</sub> laser, electron-beam-controlled 4-74498  
 I-H<sub>2</sub> laser, nuclear-generation of O<sub>2</sub> by photolysis of O<sub>3</sub> 4-62222  
 K vapour laser, optically pumped tunable far-IR radiation from Rydberg transitions 4-87318  
 KrF pulsed gas lasers, high power 4-96865  
 Mn vapour laser, MnCl<sub>2</sub> lasant, 7 green laser lines (Chinese) 4-107602  
 N<sub>2</sub> discharge laser, model calc. and expts. 4-83568  
 N<sub>2</sub> laser, 1 MW, construction and test parameters (German) 4-96946  
 N<sub>2</sub> TEA laser, intensity distrib. and time behaviour of radiation (German) 4-96871  
 NH<sub>3</sub> far IR lasers, Lorenz instability obs. 4-107612  
 NH<sub>3</sub> IR lasers, dynamics, investigation using tunable diode laser 4-112375  
 NH<sub>3</sub> laser, 16-21  $\mu$ m line tunable, two-step optical pumping 4-112381  
 NH<sub>3</sub> laser, optically pumped, 10-W CW 12- $\mu$ m output 4-64697  
 NH<sub>3</sub> laser, TEA CO<sub>2</sub> laser pumped, high-power pulsed operation at 257/281  $\mu$ m transitions 4-79182  
 NH<sub>3</sub>, pure MW Raman laser emission in superradiant mode, CO<sub>2</sub> laser line pumping 4-69376  
 NH<sub>3</sub>, two-photon optical pumping in multipass cell, lasing lines 16 to 3  $\mu$ m 4-74495  
 NH<sub>3</sub>-N<sub>2</sub> laser amplifier in 800-870 cm<sup>-1</sup> range 4-69440  
 O<sub>2</sub>-I<sub>2</sub> laser, use of O<sub>2</sub> generated by nuclear pumping in flowing Ar-CO<sub>2</sub> mixture 4-60025  
 O<sub>3</sub> laser, optically pumped, CW obs. and assignment of 7 lines 4-107600  
 Pb vapour 4-69386  
 TII, self-induced dynamic stark shifting, intensity depend. 4-74279  
 Xe IR lasing, effect of pumping conditions in Ar-Xe mixtures 4-107599  
 XeCl laser, discharge constriction effects 4-74489  
 XeCl laser, spectral composition of radiation (Russian) 4-69380
- gas permeability** see permeability
- gas phase electron diffraction**  
 2-bromo-3-chloro-1-propene, gas phase mol. struct. and conformation composition determ. by electron diff. 4-69212  
 1-bromo-bipropargyl, gas phase electron diff., conformation and mol. struct. 4-69216  
 p-bromonitrobenzene, mol. struct., internal rot. barrier, gas phase electron diff. 4-112274  
 2-bromopropene, mol. struct., gas-phase electron diff. and microwave spectra 4-112273  
 carbon tetrafluoride, electron diff., mol. vibr., anharmonicity effects, pot. consts. 4-69215  
 cis-1-chloro-3-fluoropropene, electron diff., mol. struct. and conformation 4-69213  
 3-chloro-bicyclo(3,1,0)hexane, gas phase electron diff., struct. 4-64604  
 1-chloropropene, mol. struct. and conform., gas electron diff. and microwave spectrosc. obs. 4-107335  
 2-chloropropene, mol. struct., gas-phase electron diff. and microwave spectra 4-112273  
 cyanocyclopentane, gas phase electron diff., struct. and pseudorotation 4-64602  
 densitometry, multichannel, gas phase electron diffraction pattern intensities investig. 4-79901  
 2,3-dibromo-1-propene, mol. struct. mechanics, electron diff. study 4-112272  
 dicyclobutylidene, struct. from electron diff. data and mol. mechanics 4-59894  
 2,5-dihydrofuran, mol. struct., gas-phase electron diff. meas. 4-64600  
 dimethylindinoromethane, electron diff. study of struct. in gas phase 4-59895  
 fluorobenzene, mol. struct., ring distortion electron diff. study 4-112277  
 1,5-hexadiene-3-yne, gas phase electron diff. and mol. mechanics calculations and struct. 4-64605  
 isoprene, struct. and conformations by vibr. spectroscopy and gas phase electron diff. 4-64606  
 methylenecyclobutane, struct. from electron diff. data and mol. mechanics 4-59894  
 cis-pent-2-ene, vibr., mol. mechanics, electron diff. 4-112277  
 penta-1,4-diene, vibr., mol. mechs., electron diff. 4-112278  
 perchloro-1,5-hexadiene-3-yne, gas phase electron diff. and mol. mechanics calc., conformation and struct. 4-64605  
 phenylmethylsulphone, gas phase, mol. struct., electron diff. study 4-87216  
 propanal, struct. studied by electron diff., microwave and IR spectroscopy 4-64603  
 propionyl chloride, struct. and conformation determ. by electron diff. microwave spectra, force const. 4-69214  
 silaalkanes, halosubstituted, mol. struct., electron diff. study 4-87217  
 telechalcogen construction 4-112269  
 1,3,5-trichlorobenzene, gas phase electron diff., mol. struct. 4-64607  
 1,3,5-trifluorobenzene, gas phase electron diff., mol. struct. 4-64607  
 trifluoromethyl hypochlorite, electron diff. study 4-87215  
 trifluoromethylisocyanide, gas phase struct., electron diff. and microwave spectra 4-69238  
 Cu(NO<sub>2</sub>)<sub>2</sub>, gas phase, mol. struct., electron diff. 4-78965  
 SF<sub>6</sub> laser pumped mols., electron diff. study 4-96626  
 SeF<sub>6</sub>, struct., charge redistribution model, electron diff. study 4-112277  
 SiF<sub>4</sub>, electron diff., mol. vibr., anharmonicity effects, pot. consts. 4-69215
- gas-surface interactions** see sorption
- gas technology, natural** see natural gas technology
- gas turbine power stations**  
 LNG cold energy thermoelectric generator system, conceptual design (Japanese) 4-89458
- gas turbines**  
 see also gas turbine power stations; turbogenerators  
 aircraft, ceramic technology for powerplant 4-104758  
 Allison 501-KB gas turbine engine, Brayton cycle, Cheng dual-fluid cycle effects on power and thermal efficiency 4-66744  
 American Power Conference, Chicago, USA (April 1983) 4-86112

- turbines continued  
 blades surface protection by plasma spray (*German*) 4-99639  
 distillate liquid fuels, chemical and physical properties during combustion in gas turbine 4-114884  
 high temperature gas turbines, heat transfer, film and impingement cooling 4-83905  
 Inconel 718 gas turbine disc material, crack initiation from notch under creep fatigue conditions 4-99567  
 nozzle blades, leading and trailing edges, heat transfer 4-97546
- dynamic lasers**  
 photon recyclers, optically pumped NMMW lasers 4-87317  
 Br<sub>2</sub> recombination gas dynamic laser, electron transitions (*Russian*) 4-96881  
 CO<sub>2</sub> Fabry-Perot resonator, mode struct. 4-60072  
 CO<sub>2</sub> gasdynamic 16  $\mu$ m laser, boundary layer effects on laser gain 4-87314  
 CO<sub>2</sub> gasdynamic laser, regenerative elect. gas heater 4-79179  
 CO<sub>2</sub> gasdynamic laser, radiation intensification in boundary layer on Laval nozzle cooled walls (*Russian*) 4-96867  
 CO<sub>2</sub> gasdynamic lasers with high temp. regenerative heat-exchanger heater, generation params. 4-79178  
 CO<sub>2</sub> laser, gasdynamic, nuclear pumped heat pipe design 4-60016  
 CO<sub>2</sub>, thermally excited cascade laser, calc. of energy parameters, practical recommendations 4-107594  
 H<sub>2</sub>-HF high power pure rotational laser due to vibrational excitation 4-87319  
 H<sub>2</sub>-HF pure rotational laser based on far IR transitions, theoretical study 4-79118  
 S<sub>2</sub> recombination gas dynamic laser, electron transitions (*Russian*) 4-96881
- gaseous insulation**  
 SF<sub>6</sub>, breakdown voltage and time to breakdown under impulse voltage, insulator support effect 4-65150  
 SF<sub>6</sub>, compressed, leader development in short point-plane gaps 4-69972
- gases**  
 see also aerodynamics; compressibility of gases; density of gases; dielectric properties of gases; diffusion in gases; electric breakdown of gases; electrical conductivity of gases; equations of state of gases; ionisation of gases; kinetic theory of gases; liquefaction of gases; luminescence of gases; Scott effect; Senftleben-Beenakker effect; specific heat of gases; thermal conductivity of gases; thermal diffusion in gases; viscosity of gases  
 coherent optics of gaseous media, collisional integral 4-69861
- gate turn-off devices** see thyristors
- gauge field theory**  
 see also Weinberg model; Yang-Mills theory  
 $\lambda(\phi^6 - \phi^4)_2$ , lattice Hamiltonian field theory, bound state spectrum 4-90731  
 $(\phi^2)^2$  theory, gap eqn. and effective action from inverse scatt. transformation 4-86568  
 $(\phi^2)^2$  theory, instantons and 1/N series, vacuum decay rate, inverse scatt. transform. 4-86569  
 $\phi^4$  field theories, random walk appls., survey 4-68391  
 't Hooft loop operator, perimeter law, U(N) and SU(N) lattice gauge theory 4-111291  
 Abelian antisymmetric quantum field theory in any gauge, transformed operator Lorentz covariance 4-78457  
 Abelian gauge field interacting with fermion, gauge invariant effective action, book contrib. 4-63634  
 Abelian gauge fields, IR radiative corrections and zero momentum mode 4-58949  
 abelian Higgs model with mixed action, phase struct., Coulomb confinement 4-102001  
 Abelian Higgs models, nontrivial fixed points, renormalisation group functions 4-95663  
 anomaly cancellation in high dimensions 4-63884  
 anomaly problem, geometrical nature and analysis, Chern-Weil theorem 4-90712  
 arbitrary lattices with arbitrary SU(N) actions, perturbation theory without Feynman diagrams, Wilson loops 4-68417  
 asymptotically euclidean instantons in conformal gravity 4-82737  
 axion and mag. monopole theories 4-59010  
 background field method 4-86587  
 Backlund transformations, infinitesimal, gauge symmetries and conserved currents 4-82890  
 backward hierarchy model coupled to N=1 supergravity, double missing partner mech. 4-110993  
 baryon spectrum in quenched QCD on 16<sup>4</sup> lattice 4-68555  
 Baxter type model fermionisation, U(1) invariance emergence 4-68402  
 Bogomolny-type equations, curved spacetime, Yang-Mills-Higgs system 4-95676  
 book, elementary primer in gauge theory 4-63429  
 book, gauge theories in construction QFT and stat. mechanics 4-63413  
 book, lattice gauge theories and Monte Carlo simulations 4-63414  
 BRs algebra representations for gauge theory canonical formulation, colour confinement 4-82874  
 CERN-collider, obs. interpreted as: Higgs boson prod., SU(3)×SU(2)×U(1) model 4-106468  
 charge-monopole duality, Coulomb phase of gauge theories 4-111298  
 charges in spacelike cones 4-102000  
 Chern-Simons topological Lagrangians, odd dimensions, Kaluza-Klein reduction 4-95262  
 chiral symm. restoration transition, octet and sextet quarks, SU(3) gauge theory 4-111300  
 chiral symmetry, composite models, scalar and fermion fields, large-N limit 4-106523  
 chiral two-loop finite supersymmetric theories, classification 4-90771  
 classical nonabelian gauge field dynamics, review 4-95651  
 Coleman-Weinberg type  $\lambda\phi^4$  theory, Casimir energy of Higgs field configs. 4-68416  
 collective field theory 4-68440  
 collinear photon bremsstrahlung, finite mass effect, gauge theories at high energies 4-90786  
 compact circumferences and gauge couplings calc. from self-consistent dims. reduction 4-63858  
 complex Grassmannian and CP<sup>N-1</sup> nonlinear sigma models, classical and exact solution 4-102047  
 composite bifermion condensates in gauge theories without scalar Higgs fields, symmetry breaking 4-82902  
 composite gluons and scalar fields in 4-D, renormalisation 4-82885
- gauge field theory continued**  
 composite Higgs mass, confining ultracolor group SU(N), N≥3 4-106467  
 composite quarks and leptons, lower and upper bounds on radius 4-63984  
 conference, Corfu, Greece (Sept. 1982) 4-95015  
 conference, gravity, gauge theories, supergravity, Caracas, Venezuela (Dec. 1982) 4-86117  
 conference on higher energy physics, Austin, TX, USA (Nov. 1982) 4-67857  
 conference on particles and fields, Banff, Canada (Aug. 1981) 4-63404  
 conference on quark matter in rel. nucleus-nucleus collisions, Long Island, NY, USA (Sept. 1983) 4-67855  
 confinement, classical models involving one abelian gauge field, scaling law 4-63979  
 conformal invariance, unitarity, and critical exponents in two dimensions 4-68189  
 constant gauge field configurations and Galilean gauge theories 4-58950  
 construction, Abelian Higgs model, UV cutoffs, (QED)<sub>2</sub> and lattice regularisation 4-68387  
 cosmological constant as a canonical variable in grav. field coupled to gauge field 4-110973  
 Coulomb-gauge Gribov horizon, non-Abelian gauge model, colour charge terms 4-95674  
 covariant polarisation bases for spin 1/2, 1 and 3/2 particles, vector boson decay and prod. 4-64025  
 CP<sup>1</sup> model in 2-dimens., fermion effect on instantons, instanton quarks 4-68378  
 CP<sup>N-1</sup> models at large N, lattice to continuum transition 4-95646  
 CP<sup>N-1</sup> supersymmetric model, 1/N expansion 4-102044  
 CP<sup>N-1</sup> supersymmetric models, instantons and condensates 4-111268  
 CP nonconservation, gauge model, GUT constraints, strong CP, Kobayashi-Maskawa model, review 4-63921  
 D=10, N=1 supergravity, nontrivial vacuum state 4-68114  
 d=11 supergravity, homogeneous 7-manifolds, SU(3)×SU(2)×U(1) compactifications 4-90474  
 d=11 supergravity, lagrangian geometrical form, 3-index gauge pot. 4-110989  
 d=11 supergravity, vanishing quantum vacuum energy, round seven-sphere, one-loop order 4-106226  
 d=11 supergravity compactification on S<sup>4</sup>, linearized field eqns., transformation rules 4-95281  
 De Donder-Weyl Hamilton-Jacobi theory appl. to relativistic field theories 4-68374  
 de Sitter space-time, masslessness and gauge invariance 4-73611  
 decoupling and conserving full gauge symmetries, subtraction scheme 4-68395  
 decoupling renormalization, field theoretic solution to hierarchy problem, unified field theory 4-90782  
 density perturbations, evolution through cosmological phase transitions, gauge invariant formalism 4-95010  
 dielectric lattice gauge theory 4-68365  
 dimensional reduction, general formulae 4-110969  
 dimensional reduction of fermions, generalized grav., modification of Riemannian geometry 4-95273  
 Dirac's generalised mechanics and canonical quantisation, gauge invariance 4-73268  
 Dirac eqn. formulation on Schouten space-time 4-68397  
 Dirac fermions coupled to gauge and grav. fields, chiral anomalies, path integral derivation 4-86575  
 Donaldson's moduli space for SU(2) instantons, possible quantum gravity model, book contrib. 4-63629  
 duality and large N limit in non-abelian gauge theories 4-78466  
 dynamical symmetry breaking and particle mass generation in gauge field theories 4-82899  
 dyon charge conjugation, Weinberg-Salam SU(2)×U(1) gauge symm. 4-106449  
 dyon decay, EM properties 4-73612  
 effective field theory and weak non-leptonic interactions 4-90804  
 effective pot. in de Sitter space 4-63370  
 effective spin model for Eguchi-Kawai model comparison with Monte Carlo data 4-102042  
 Einstein's  $\lambda$ -transformation generalisation, gauge field and gravitational copies 4-110962  
 Einstein-Mayer unified theory, 5-D origin of massless scalar field 4-68085  
 electro-weak theory, introduction 4-59011  
 electrodynamics, macroscopic, gauge theoretical approach 4-73254  
 electromagnetically induced nuclear beta decay in electric-field gauge 4-73857  
 electroweak interactions, gauge unification 4-102070  
 electroweak theories and GUTs, flavour mixing and unification 4-63947  
 energy scales in GUTs, QCD, technicolor and SU(2)×U(1) breaking 4-68477  
 Euclidean gauge theories, behaviour in strong fields, functional determinants 4-68413  
 Euclidean gauge theories, self dual instanton solns., SU(2) monopole, reciprocity 4-68348  
 extended supergravity theories, infinite symmetry algebras 4-106223  
 extended supersymmetry partial breaking 4-63876  
 fermion bound states by the method of stationary phase 4-90736  
 fermion determinants, chiral symmetry, and the Wess-Zumino anomaly 4-68355  
 fermion field theory, finite mode regularisations 4-73639  
 fermion gravitational interactions, chiral Lorentzian anomalies 4-90747  
 fermion mass dynamical generation, u-quark/d-quark mass difference 4-111451  
 fermion-rotor system, monopole catalysis, two spacetime dimensions 4-95642  
 fermionic gauge fields, common origin of leptons and quarks 4-86521  
 fermionic path-integral and chiral rotations 4-63879  
 fermionic quark boundaries, surface description of QCD 4-82937  
 field theories without fundamental gauge symmetries 4-58981  
 fine structure constants for gauge couplings, Kaluza-Klein theory appl. 4-58707  
 finite fermion density on the lattice 4-58961  
 finite size scaling test of an SU(2) gauge-spin system 4-86550  
 finite temp. gauge systems, Z<sub>2</sub> and Z<sub>3</sub>, mean field approach 4-95690  
 finite temperature QCD, strong coupling lattice model, chiral symmetry 4-86652  
 finite-action fields, topological charges conservation 4-95636

## gauge field theory continued

- SU<sub>c</sub>(2)×SU<sub>R</sub>(3) model, scalar field set addition fermion mass generation, radiative corrections 4-73637
- SU(16)<sub>c</sub> GUT, spontaneously broken local Pauli-Gursey invariance and constraints on proton decay 4-59003
- SU(1,1) supergravity models, Higgs-fermion Yukawa coupling, CP violation 4-90473
- SU(2)<sub>L</sub>×SU(2)<sub>R</sub>×U(1)<sub>Y</sub> gauge theories, W boson mass constraints 4-111310
- SU(2)<sub>L</sub>×U(1) model, neutrino charge in linear R<sub>c</sub> gauge 4-59005
- SU(2)<sub>L</sub> gauged nonlinear  $\sigma$ -model, ghost confinement 4-68398
- SU(2)×U(1)×U(1) unified models, rel. to electroweak interactions of leptons 4-95716
- SU(2)×U(1) electroweak theory, lattice gauge model using Wilson fermions 4-111356
- SU(2) euclidean lattice gauge theories, Rayleigh-Ritz variational techniques 4-95648
- SU(2) gauge theory, constant fields and invariants 4-90754
- SU(2) gauge theory, mag. monopole interactions, baryon number violation 4-68457
- SU(2) gauge theory, O(3) symmetric solutions, Backlund transformations 4-86522
- SU(2) gauge theory, q-instanton solutions 4-106455
- SU(2) gauge theory, scale of chiral symmetry breaking 4-58954
- SU(2) lattice gauge theories, chiral symmetry breaking absence at high temps. 4-78494
- SU(2) lattice gauge theories, variant action independence of phys. quantities 4-58968
- SU(2) lattice gauge theory, 4-dimens., stochastic confinement and dimensional reduction 4-58979
- SU(2) lattice gauge theory, deconfinement, spontaneous global symm. breaking 4-111379
- SU(2) lattice gauge theory, Hamiltonian variational study 4-78497
- SU(2) lattice gauge theory, Monte Carlo renormalisation group,  $\beta$ -function 4-102029
- SU(2) lattice gauge theory, Monte Carlo renormalisation group improved action 4-102030
- SU(2) lattice gauge theory, stochastic confinement and dimensional reduction in 4-D 4-106458
- SU(2) lattice gauge theory, strings in 3-D 4-102038
- SU(2) lattice gauge theory, universality in 4-D 4-73671
- SU(2) lattice gauge theory in three dims., obs. of string 4-58980
- SU(2) lattice gauge theory with disordered trial wave function, vacuum state estimate 4-68419
- SU(2) lattice theory, Monte Carlo calcs. with dynamical fermions 4-106453
- SU(2) magnetic monopole, electric charge in field theories with fermions 4-102026
- SU(2) mass gap with Symanzik's tree level improved action on 8<sup>4</sup> lattice 4-63889
- SU(2) ordered potentials, stochastic limit 4-90746
- SU(2) string tension from large Wilson loops 4-63881
- SU(2) supersymmetric gauge model, SUSY breaking, 1-loop effective pot. under mag. field and high temp. 4-73680
- SU(2) t'Hooft-Polyakov monopole, quantum fluctuations, U(1) radial Schwinger model 4-102048
- SU(2) theory, monopole interaction with fermions in higher representations 4-78500
- SU(2) Yang-Mills theory, colour screening 4-78498
- SU(3)×SU(2)×U(1) gauge group, baryon number non-conservation, low mass scale 4-111363
- SU(3)×SU(2)×U(1) gauge theory, coupling constant ratios in Kaluza-Klein theory 4-58704
- SU(3)×SU(2)×U(1) interactions, D=10 N=2 supergravity, comparison with strong, electroweak interactions 4-90773
- SU(3)×SU(2)×U(1) interactions, D=11 supergravity, comparison with strong, electroweak interactions 4-90772
- SU(3)⊗SU(2)⊗U(1) gauge spectrum in N=2 supergravity in 11-D 4-110985
- SU(3) adjoint Higgs model, Monte Carlo study 4-63941
- SU(3) flux-tube quark model of hadrons 4-63951
- SU(3) gauge theory, on 8<sup>4</sup> lattice, correlation length 4-63888
- SU(3) gauge theory, unit charge monopole soln. 4-58971
- SU(3) gauge theory with next-to-nearest neighbour interactions on 12<sup>4</sup> lattice, Monte Carlo study 4-111288
- SU(3) lattice gauge Monte Carlo simulation results 4-58785
- SU(3) lattice gauge theory, computation by computer array 4-86544
- SU(3) lattice gauge theory, deconfinement phase transition, influence of quarks 4-68383
- SU(3) lattice gauge theory, finite temp. phase transition 4-102058
- SU(3) lattice gauge theory, hadron mass calcs. 4-106459
- SU(3) lattice gauge theory, heavy quark potential calcs. 4-86545
- SU(3) lattice gauge theory, phase transition of pure glue, Monte Carlo calcs. 4-68384
- SU(3) lattice gauge theory, QCD simulation using 1080 element subgroup 4-106456
- SU(3) lattice gauge theory, renormalisation group improved action, string tension, Wilson loops 4-111287
- SU(3) lattice gauge theory, string tension and glueball masses 4-58956
- SU(3) lattice gauge theory, string tension coeff., Monte Carlo calcs. 4-68503
- SU(3) lattice gauge theory, vectorised Monte Carlo code 4-86523
- SU(3) lattice gauge theory, Z(3) flux loop density in 4-D 4-58972
- SU(3) lattice gauge theory in 3+1-D, Hamiltonian variational approach 4-78453
- SU(3) lattice gauge theory Monte Carlo calc., matrix multiplier/accumulator 4-90713
- SU(4) lattice gauge theory, deconfining transition at strong coupling, Monte Carlo study 4-86574
- SU(4) lattice gauge theory, finite temp. confinement phase transition 4-86543
- SU(4) lattice gauge theory, first order deconfinement phase transition, Monte Carlo calcs. 4-111294
- SU(5)×SU(3) theory, flavour interactions of Goldstone bosons 4-68480
- SU(5) GUTs, proton decay, electroweak mixing angle, gauge hierarchy problem 4-95737
- SU(6) SUSY GUT with dynamical generation of gauge hierarchy 4-82928
- SU(8) supersymmetric nonlinear sigma models, non-compact manifold, gauge boson dynamics 4-111316
- SU(8) theory of multigenerational grand unification 4-59000

## gauge field theory continued

- SU(N)<sub>c</sub> lattice gauge theory, quark-gluon partition function 4-95712
- SU(N)<sub>c</sub>×SU(N)<sub>c</sub> chiral, chiral symmetry breaking of non-abelian gauge 4-58984
- SU(N)<sub>c</sub>×SU(N)<sub>c</sub> chiral model, improved lattice action, Symanzik improvement procedure 4-95708
- SU(N) colour gauge theory, P and CP violation with massive fermions 4-78496
- SU(N) gauge fields in 3-D, parity violation, gauge noninvariance 4-78499
- SU(N) gauge theories, fractional charge and automatic U(1) symmetry without domain walls 4-86525
- SU(N) gauge theories with Higgs scalars, symmetry breaking patterns, antisymm. and symm. 4-86526
- SU(N) gauge theory, colour screening at finite temp. 4-68382
- SU(N) gauge theory, deconfinement transition, Monte Carlo techniques 4-106460
- SU(N) lattice gauge theories, deconfining transitions, mean field analysis 4-73613
- SU(N) lattice gauge theory, block mean field method 4-78463
- SU(N) lattice gauge theory, phase diagrams in 4-D 4-78456
- SU(N) lattice QCD, non-zero baryon density, hamiltonian formalism, Susskind fermions 4-102062
- SU(N) theory, Wilson loops and constant gauge fields 4-58970
- SU(N) twisted fields at high temp., Monte Carlo simulations 4-106484
- super Kobayashi-Maskawa C P-violation 4-86621
- superfield N=4 'superextension of Liouville eqn., gauge SU(2)×SU(2)<sub>c</sub> symm. 4-111322
- supergravity, gauge symmetry breaking, dimensional transmutation 4-110977
- supergravity, instability of parallelized seven-sphere in 11-D 4-86313
- supergravity, spontaneous compactification in 11-D, geometrical interpretations 4-58715
- supergravity gauge theories, quantum effects and SU(2)×U(1) breaking, renormalisation 4-63641
- supergravity UV divergences, auxiliary fields, no-go theorems N=3 barrier, lightcone gauge, book contrib. 4-63646
- superstring theories, props. of covariant formulation 4-106454
- superstrings, covariant, light-cone anal. 4-59056
- supersymmetric (1+1) dims. models with restricted supersymmetry on lattice, hamiltonian Monte Carlo study 4-63880
- supersymmetric CP<sub>N-1</sub> model, gauge-invariant currents 4-111279
- supersymmetric field theory, stochastic quantisation, Parisi-Wu method 4-90742
- supersymmetric gauge models, mag. field effects 4-78484
- supersymmetric gauge theories, nonrenormalisation theorem 4-73641
- supersymmetric gauge theories, two-loop, the chiral anomaly 4-58955
- supersymmetric gauge theory vacua and chiral fermions, SUSY breaking 4-82917
- supersymmetric gauge-invariant interaction, nonchiral superfield, U<sub>1</sub> gauge transformation 4-90745
- supersymmetric GUTs, gauge hierarchy stability 4-78511
- supersymmetric models, CP problem and generation of mass term 4-63939
- supersymmetric QCD, non-renormalisation theorem, non-perturbative breakdown 4-63960
- supersymmetric string theories, spontaneous supersymmetry breaking 4-63861
- supersymmetric SU<sub>c</sub>(3)×SU<sub>R</sub>(2)×U<sub>Y</sub>(1)×U<sub>1</sub>(1) model consistent with low energy phenomena 4-68468
- supersymmetric SU(2)<sub>L</sub>×U(1) models, electroweak  $\rho$ -parameter 4-58999
- supersymmetry and fundamental interactions in the region of the Fermi scale 4-63919
- SUSY GUTs, low energy behaviour 4-58992
- symmetry breaking patterns, unitary group gauge theoretic model 4-111321
- symmetry restoration by magnetic field, theory with spontaneously broken gauge symm. 4-111293
- T<sub>4</sub> theory, BRS and BRS\* transformations, geometric formulation 4-68396
- technijets structure, QCD anal., expt. signals 4-111387
- temporal gauge quantisation, comment on eigenvectors 4-86579
- temporal gauge quantisation, comment on validity 4-86576
- temporal gauge quantisation, comments, on canonical commutation relations, Gauss's law 4-86578
- temporal gauge quantisation, comments, on QED 4-86577
- tetrad, broken symmetries, and the gravitational constant 4-95278
- topological singularities, supersymmetry breaking, Aharonov-Bohm effect, incompatibility with supersymmetry 4-90751
- topologically massive gauge theories, self-duality 4-78515
- topology, geometry and gauge theories, book contrib. 4-58975
- topology and saddle points in field theories 4-63885
- triplet code model of leptons and quarks, modification to electroweak gauge theory 4-95778
- twisted Eguchi-Kawai model, finite temp., deconfining phase transition 4-82876
- twisted Eguchi-Kawai model, heat bath method 4-111289
- twisted Eguchi-Kawai model, numerical study of Langevin eqn. 4-106457
- twisted reduced chiral models at large N 4-95647
- twistor connection, gauge invariant principle 4-68092
- two-dimensional CP<sup>1</sup> models, instantons and condensates 4-63878
- two-loop corrections to the  $\Lambda$  parameters of one-plaquette action 4-68360
- U(1) chiral supergravities, unconstrained conformal superfields 4-90478
- U(1) gauge theory, Hamiltonian and Lagrangian formalisms 4-86566
- U(1) gauge-Higgs system with a radial degree of freedom 4-86552
- U(1) lattice, monopole-antimonopole potential, Monte Carlo simulation 4-111301
- U(1) lattice gauge theory, 2+1 dims., string tension and glueball mass 4-86586
- U(1) lattice gauge theory, linked cluster expansions in 2+1 and 3+1-D 4-82881
- U(1) lattice gauge theory, mean field in Feynman gauge 4-82880
- U(1) lattice gauge theory, mean field perturbation 4-106457
- U(1) lattice gauge theory with long range gauge invariant interactions, Wilson parameter behaviour 4-102003
- U(1) symmetry breaking, soln. to domain wall problem 4-58930
- U(2) four-dimensional simplicial lattice gauge theory, Monte Carlo simulations 4-111318
- U(N) invariant matrix  $\phi^4$  theories, exact solns. in zero dims. 4-102005

- uge field theory continued  
 U(N) lattice gauge theories, gauge symmetry spontaneous breakdown at infinite N 4-68399  
 U(N) lattice gauge theories; loop dynamics, Monte Carlo calcs. 4-78450  
 unified gauge theories approach using generalised Dirac eqn., symmetry breaking to general relativity 4-111357  
 unified theories, renormalisation group evolution of scalar mass term 4-78510  
 unitary flavor unification through higher dimensionality 4-78464  
 vector particles, renorminvariant mass, vacuum struct. in mag. field 4-82900  
 wave function, phase considerations, gauge invariance 4-63551  
 Wentzel pair theory, massless scalar field, renormalised self-energy, radiative corrections 4-95775  
 Wess-Zumino action equivalence to Free Fermi theory in two dims. 4-86548  
 Wess-Zumino model, two-loop effective potential 4-90741  
 Wess-Zumino-Witten effective action, gauge invariance,  $SU(3)_L \times SU(3)_R$  (Chinese) 4-73645  
 Weyl invariant theories, flat space-time stability, cosmological constant term 4-106218  
 Wilson loop-plaquette correlations for four-dimens., compact U(1) gauge theory 4-86585  
 Yang-Mills eqn., pseudoparticle soln. 4-68370  
 Yang-Mills field, Green's functions and observable processes 4-111272  
 Yang-Mills theories struct. in temporal gauge, instanton sector 4-63859  
 Yang-Mills-Einstein supergravity, 5-dimens., gauge coupling constant quantisation 4-95282  
 $Z_2$ -asymmetric gauge theory, mean field anal. 4-95689  
 $Z_N$  lattice gauge theories,  $D=1+2$  phase diagram, variational method 4-111317  
 $Z(2)$  Higgs model, vortex free energy in screening phase 4-68361  
 $Z(2)$  Higgs model and lattice gauge theories, nonlocal order parameters for phase tests 4-82905  
 $Z(4)$  model, phase diagrams for square lattice in whole parameter space 4-90521  
 $Z(N)$  clock model, deconfinement transition 4-78471  
 Zakharov-Shabat system, hamiltonian struct. from gauge transformations 4-73632  
 $e^-$  mass, magnetic moment and vacuum energy from field theory finite temp. corrections 4-68346  
 $e^+e^- \rightarrow \gamma\gamma\gamma$ , cross section, helicity amplitudes in high energy limit 4-90848  
 $\gamma e^-$ , cross-sections from QED on lattice 4-90849  
 hh at extreme energies, light-cone QCD with axial-vector anomaly current 4-59039  
 $\pi^+p$ , high energy cusp search, mag. monopole model of hadrons 4-78569  
 qq long range potential, relativistic corrections and area law 4-59023  
 Gaussian noise *see random noise*  
 Gaussian orbital calculations *see GO calculations*  
 Gaussian-type orbital calculations *see GTO calculations*  
 Ge-Si alloys  
 amorphous, RF sputtered, electronic props. 4-61370  
 band calcs.; empirically adjusted zone variational method (Chinese) 4-75831  
 epitaxial films on Si (100), commensurate and incommensurate struct. 4-108740  
 freezng, periodic growth rate effect on morphological stability 4-98039  
 Frenkel core excitons, binding energy 4-75867  
 lattice vibr. props., Raman spectra, alloying and press. depend. 4-108562  
 solar cells, amorphous, optical loss mechanisms 4-77108  
 solid solutions, local and band mode freqs. 4-70307  
 substitutionally sp<sup>3</sup>-bonded defects, deep energy levels 4-108813  
 surface (111), (5 $\times$ 5) LEED pattern, growth conditions 4-65596  
 thermoelectric materials/devices, high temp., sublimation meas. and anal. 4-77129  
 vibrational modes and phase transition 4-88253  
 Ge diffusion, isotope effects, SIMS studies 4-65491  
 Ge diffusion and conc. profiles SIMS studies 4-65490  
 Ge<sub>1-x</sub>Si<sub>x</sub>Sn amorphous film, elec. cond. and thermoelec. power 4-65678  
 Ge<sub>1-x</sub>Si<sub>x</sub>Ge, superlattices, interactions of high-freq. EM waves 4-80670  
 Ge<sub>1-x</sub>Si<sub>x</sub>/Si strained layer superlattice, MBE growth 4-92576  
 a-Si-Ge-B alloys, props. and electronic device appls. (Japanese) 4-92728  
 Si<sub>1-x</sub>Ge<sub>x</sub>H, amorphous, gap state distrib., photoconductivity study 4-108820  
 Si<sub>1-x</sub>Ge<sub>x</sub>H, amorphous, occupied gap state obs. 4-70637  
 Si<sub>1-x</sub>Ge<sub>x</sub>H amorphous films, planar magnetron sputtered, optical and elec. props. 4-98671  
 Si<sub>1-x</sub>Ge<sub>x</sub>H amorphous planar magnetron sputtered films, elec. and optical props. (Japanese) 4-99312  
 Si<sub>1-x</sub>Ge<sub>x</sub>P, EPR study and spin-lattice relax. (Russian) 4-71177  
 Si<sub>1-x</sub>Ge<sub>x</sub>H amorphous sputtered films, optical absorpt. 4-93090  
 Si<sub>1-x</sub>Ge<sub>x</sub>P(As)(Sb), paired donor impurities energy levels 4-61315  
 Si<sub>1-x</sub>Ge<sub>x</sub>GaAs heterojunction, interface carrier recombination velocity determ. 4-104304  
 Regenschlein *see zodiacal light*  
 Geiger counters  
 organic-quenched Geiger-Muller counter, method of increasing counts for random source 4-59512  
 portable detectors for <sup>125</sup>I-insulin absorption measurement during subcutaneous infusion with portable pumps 4-67157  
 vacuum UV radiation detector, 10 eV, Geiger-Muller counter appl. 4-101937  
 Al Geiger tube planes, trigger for nucleon decay expt. 4-91151  
 Geiger Muller counters *see Geiger counters*  
 Gelatin  
*see also gels*  
 aqueous solution, phase transitions, aliphatic alcohols effect, NMR study 4-109773  
 dichromated gelatin, hologram copying with spectral filtered sunlight 4-74455  
 dichromated undeveloped gelatin film holographic characs., appls. 4-91416  
 molecular weight distribution, relative effects on soln. props. (German) 4-71996  
 partial collagen hydrolyzate gelatin, in aqueous soln., aging, water struct. and helical conformation 4-115012  
 gels  
 agarose, gel saturated with binary liq. mixtures, critical behaviour 4-93565  
 agarose gels, mol. wt., rheological props. 4-60357  
 connectivity transitions 4-90532  
 diacyl phosphatidylcholines, ice melting induced phase transition 4-61676  
 diisocyanates, polycyclotrimerisation, gel form. and rheology (Russian) 4-62203  
 dimyristoyl phosphatidylcholine-water system, phase transitions, high press. study 4-113624  
 distearoyl phosphatidylcholine bilayers, low temp. gel-gel transition, Raman spectra detect. 4-113576  
 DNA separations, sequence-determined, electrophoretic mobility in gels obs., book contrib. 4-93689  
 elastomers, end-linked, bulk cured tetrafunctional networks 4-66585  
 fibrin gels as biological filters and interfaces 4-105269  
 gelation of chains, gamma-radiation induced, exptl. study 4-77033  
 hyaluronate gels, macromolecules, diffusion, methods and preliminary results 4-100366  
 kinetic gelation model and sol-gel transition, solvent effects 4-82773  
 lipid bilayers, mixed, phase transition props. rel. to those of covalent analogues 4-85408  
 mucus glycoprotein gels, cation effects, SEM studies 4-89493  
 mucus glycoprotein gels, purified, cation induced changes in rheological props. 4-105275  
 non-ionic gel, vol. phase transition 4-71989  
 oil, soluble, ultrafiltration, conc. polaris., membrane fouling and cleaning 4-89330  
 oxide coating deposition using sol-gel technology 4-76697  
 oxide gels, electronic props. and appls. 4-71997  
 phase transitions of binary mixtures in porous media 4-70337  
 phospholipid dispersions, thermotropic and high-press. phases, Raman spectroscopy, book contrib. 4-93701  
 physics and chemistry of porous media, conf., Ridgefield, CT, USA (Oct. 1983) 4-67847  
 polyacrylamide gel saturated with binary liq. mixtures, critical behaviour 4-93565  
 polydiacetylene solns., rod-to-coil transition and gelation, light scatt. study 4-64645  
 polydimethylsiloxane, trifunctional cross linkers, computer simulation 4-66584  
 polymers, conjugated, in gels, electric field coupling to slow elastic modes 4-98198  
 silica gel saturated with binary liq. mixtures, critical behaviour 4-93565  
 sodium dodecyl sulphate-water system, phase transitions, FT IR obs. 4-84389  
 soft gels, shear wave propagation 4-97379  
 tetramethoxysilicon sol-gel process, polymerisation kinetics, press. effects 4-114465  
 trioxyethylene glycol monohexadecyl ether-D<sub>2</sub>O system, gel. and liq. cryst. phase structs. 4-84145  
 two dimensional system, obs. of gelation process 4-62257  
 water in clay gels below freezing point, microdynamic behaviour, NMR meas. 4-66618  
 Al<sub>2</sub>O<sub>3</sub>-SiO<sub>2</sub> system, diphasic xerogel prep., DTA and powder X-ray diffr. 4-114846  
 CuSO<sub>4</sub> gel medium electrolyte-diffusion and self-diffusion, transition state theory 4-89339  
 Eu (III) in silica gel glass, fluoresc., cation binding and cage symm. 4-114835  
 MnCl<sub>2</sub> and MnSO<sub>4</sub> gel medium electrolyte-diffusion and self-diffusion, transition state theory 4-89339  
 Na<sub>2</sub>O-B<sub>2</sub>O<sub>3</sub>-SiO<sub>2</sub> graded-index antirefl. coatings deposited by sol-gel process, laser damage thresholds, high power laser appls. 4-74673  
 SiO<sub>2</sub> gels, synthesis by hypercritical solvent evaporation 4-66257  
 SiO<sub>2</sub>-AgCl, diphasic photosensitive xerogel prep. method 4-71990  
 SiO<sub>2</sub>-B<sub>2</sub>O<sub>3</sub> glasses, sol-gel processing 4-70038  
 SiO<sub>2</sub>-B<sub>2</sub>O<sub>3</sub>-Na<sub>2</sub>O gel-derived glasses, microhomogeneity light scatt. meas. 4-114290  
 ZrO<sub>2</sub> gels, pure and MgO-doped, decomposed in vacuo, neutron and X-ray diffr. study 4-61900  
 general relativity  
*see also cosmology; gravitation; gravitational red shift; Schwarzschild metric; space-time configurations; unified field theories*  
 1-form Finsler space from osculating Riemannian space 4-82729  
 (2+1) space-time vacuum field solutions in general relativity 4-67825  
 algebraic extension of general relativity and higher dimensions 4-110941  
 Belinsky-Zakharov method, higher-order poles, Einstein equations 4-95256  
 Bianchi type I vacuum, Brans-Dicke-Kasner solution 4-86267  
 Bianchi type-I models, solution to Einstein's eqns. 4-90447  
 Bianchi type-VI<sub>0</sub> cosmologies, isotropic singularities and isotropization 4-101732  
 black hole, rotating distorted, axisymmetric stationary metric 4-101404  
 black holes, axisymmetric with parallel spins, extrinsic curvature 4-110943  
 black holes, dynamics of N-collisions in nonsingular, asymptotically flat 3-geometry 4-68070  
 black holes, rotating, pseudostationary, Kerr-Newman soln., SU(1,2) group 4-63585  
 black holes and warped spacetime, book 4-58601  
 Bond energy positivity 4-68062  
 canonical formalism and invariant single-particle distrib. function 4-73310  
 charged spinning fluid, mag. dipole moment 4-110946  
 colliding self-gravitating plane waves, metaphysics, Einstein eqns. solns. 4-68071  
 comment on general relativity primer 4-63450  
 conference on mathematical physics, Boulder, CO, USA (Aug. 1983) 4-67856  
 cosmic baldness, relaxation to de Sitter space, early Universe appl. 4-63365  
 cosmological heterogeneous model, macroscopic gravitational eqn. soln. (Russian) 4-101558  
 cosmological solutions of the Einstein equation with heat flow 4-101720  
 cosmology, metrics for spherically symmetric solns. 4-101550  
 cosmology, spacetime thermodynamics and inflationary Universe 4-90263  
 cosmology (book) 4-82609  
 curvature of space-time significance in general relativity 4-82724

## general relativity continued

- diffeomorphisms, rel. to diverging spacetimes and event points (*Italian*) 4-63577
- Dirac equation of free particles in Friedmann space-time, spinor null tetrad formalism (*Chinese*) 4-86095
- dust cloud, cosmic censorship violation 4-72863
- Earth's general relativistic gravitomagnetic field, Foucault pendulum expt., at South Pole 4-111010
- Einstein's equations with cosmological constant, higher dimensional vacuum solns. 4-90451
- Einstein's equivalence principle, gravitational redshift of gravitational clocks 4-90083
- Einstein's equivalence principle and experiments 4-90449
- Einstein's field eqns., iterative solution for radiative gravitational fields (*French*) 4-78201
- Einstein's field equations, static, spherically symmetric solutions, massless scalar field 4-95275
- Einstein's general relativity, derivation of Regge's action in D-dimensions 4-95252
- Einstein's gravitation, energy problem, Hamiltonian approach 4-63597
- Einstein's gravity, quantizable form 4-90467
- Einstein's theory, electrodynamic origins 4-95254
- Einstein's theory energy problem from space-time manifold 4-63596
- Einstein electrovac field eqns., principal Riemann-Hilbert problem and N-fold charged Kerr solution 4-86269
- Einstein eqns., inhomogeneous solutions, de Sitter space-time generalisation 4-90450
- Einstein eqns. solns. taking into account vacuum effects of quantised field 4-73312
- Einstein equation, 2D, parameterized by arbitrary functions,  $O(2,1)$ -model generates soln. 4-110947
- Einstein equation, space-time with Killing tensor with Segre characteristic  $\{[(1)(1)]\}$  (*French*) 4-78203
- Einstein field eqns., many parameter solns. construction, noniterative method 4-86271
- Einstein gravitational field in arbitrary background space-time, exact theory 4-95251
- Einstein tensor, bilinear and trilinear extensions 4-68061
- Einstein universe, closed cosmology with massive mag. field 4-77997
- Einstein-Maxwell eqn., gyroscopic precession on Earth surface, existence of mag. type gravit. 4-94587
- Einstein-Maxwell eqns., exact solns. 4-67815
- Einstein-Maxwell eqns., scalar density concomitants of metric and bivector 4-63482
- Einstein-Maxwell eqns., spherical charged fluid dist. 4-82734
- Einstein-Maxwell equations, symmetric space property and inverse-scatt. formulation 4-82735
- Einstein-Maxwell  $N=2$  supergravity, geometry and Jordan algebras 4-95263
- Einstein-Maxwell waves, scattering by Ellis geometry 4-63603
- Einstein-Mayer unified theory, 5-D origin of massless scalar field 4-68085
- Einstein-Weyl field equations in a Bianchi type-IX space-time 4-90454
- Einstein-zero-mass scalar theory, gravitational repulsion 4-90445
- electromagnetic mass models in general relativity 4-95261
- electrovac type D solutions with cosmological constant 4-101717
- embedding for general relativity with variable rest mass 4-63584
- Euler's eqn. of harmonic maps, soln. and appl. to general relativity (*Chinese*) 4-90444
- exact solutions, global struct., singular behaviour, cosmic censorship 4-73309
- exact solutions of plane symmetric cosmological models 4-101719
- extended bodies, generalisation of Dixon's description mass tensor 4-90446
- extended model of the electron, general relativity, Kerr-Newman field 4-90455
- extended scalar-tensor theory of gravitation and Einstein's theory 4-110951
- field equations of massless particles with arbitrary spin in spinor null tetrad formalism (*Chinese*) 4-82569
- finite rotating universe, null geodesics, caustics and galaxies apparent motion 4-67822
- fluid distributions, exact solutions in general relativity 4-101723
- fourth-order gravity as general relativity plus matter 4-110974
- frequency and time meas., relativistic effects (*Japanese*) 4-58700
- Friedmann eqns. with A-term, exact solns. for dust-radiation Universe 4-63350
- Friedmann universe, closed, with scalar field as source 4-101543
- geodesic equation, Kaluza-Klein theory, 5-dimensional relativity 4-101728
- geometric unification of gravity and EM 4-82733
- $GL_4 \times SO_3 \times SU_2$  dilatation-invariant gravity, unification by proliferation method 4-110963
- global time in the general theory of relativity 4-95257
- Godel cosmological model, nonstationary generalisation, Einstein eqn. soln. 4-82572
- Gowdy  $T^3$  cosmology, stress-energy tensor, combined system symm. bounce 4-101546
- gravitation as an averaged theory 4-95255
- gravitation field, nonlinear eqns. 4-73234
- gravitation of point particle with nonlinear invariant scalar field (*Russian*) 4-110952
- gravitation theory, general relativity gauge group extn. to  $GL(4, R)$  4-90468
- gravitational collapse, spherically symm. shell, Casimir effect 4-110956
- gravitational deflection of radioisotopes by Sun, VLBI obs. 4-101738
- gravitational field dynamic props., classical general theory of relativity 4-58697
- gravitational light deflection in the solar system 4-94585
- gravitational waves on the back of an envelope 4-67917
- gravitationally repulsive domain wall, Einstein's eqns. exact solns. 4-110950
- group covariance without torsion in general relativity, Kaluza-Klein theory, book contrib. 4-63598
- Hamiltonian approach, grav. field space of states 4-82728
- Hamiltonian approach, physical meaning of energy 4-63595
- Hamiltonian description review, time translations, canonical quantisation 4-68069
- hamiltonian formalism, asymptotic anti-de Sitter spaces 4-101724
- Hamiltonian formulation of gravitating perfect fluid and Newtonian limit 4-68063
- general relativity continued
- Hamiltonians, phase-space simplification 4-82727
- Hawking radiation and the back reaction—a first approach 4-110942
- heat conducting fluid, thermal nonequilibrium general relativity 4-110949
- Hermitean relativity dynamical eqns. (*German*) 4-82718
- Higgs scalar field, gravitational collapse 4-115683
- ideal liquid, homogeneous soln. of Einstein eqns. (*Russian*) 4-110953
- inhomogeneous cosmological model in gen. rel., perfect solution 4-115831
- Jordan-Thiry theory, nonsymmetric, nonabelian, gravitation and Yang-Mills unification 4-68094
- Kaluza-Klein theories, one-loop stability of toroidally compact manifold 4-106216
- Kaluza-Klein theory, Einstein Lagrangian with de Sitter structure 4-68084
- Kaluza-Klein theory, linear connection on fibre bundle 4-63607
- Kaluza-Klein theory and the positive energy theorem 4-63608
- Kerr metric, characterisations in general relativity 4-82721
- Kerr metric, timelike vortical trajectories, latitudinal and radial motion 4-95266
- Kerr metric in de Sitter space-time 4-68072
- Kerr-Newman metric, total effective mass 4-63592
- Kerr-Newman metric derivation from Einstein-Maxwell eqns. (*Chinese*) 4-110937
- Killing vectors in algebraically special space-times 4-101721
- kinetic eqns. for inelastically interacting particles in gravit. 4-73311
- Lie admissible gravity, exterior forms, geometrical structure 4-90448
- local black holes, toroidal and spherical 4-77868
- Lorentz manifolds, metric completions and b-completions, Friedmann model appl. 4-68068
- magnetohydrodynamics, centre of mass and far field metric 4-82719
- magnetohydrostatic models of cylindrical symmetry 4-82725
- manifestly positive energy expression in classical general relativity, derivation from supergravity 4-86273
- maximal indecomposable past sets and event horizons 4-58698
- Mercury perihelion precession 4-110552
- Moller's tetrad theory, open or closed Universe, energy density dependence 4-86097
- motion, space-time description, Hamiltonian approach to relativistic particle dynamics, review 4-95258
- multipolar radiation reaction theory 4-101725
- neutrino and Dirac eqns., separation of variables and symmetry operators 4-68064
- neutron stars in supernova remnants, evolution and cooling theories 4-77865
- neutron stars in X-ray binaries shell flashes, core interactions, role of accretion rate 4-110647
- Newtonian-like formulation for Einstein's relativity and rel. quantum mech. 4-68058
- nonequilibrium statistical mechanics, linear fields in kinetic approx. 4-58696
- nonstatic charged fluid spheres in general relativity, Einstein-Maxwell solns. 4-78206
- null geodesic motion, conformal dynamical symmetry 4-63589
- null string congruences, Cauchy-Kovalevski-like problems 4-101715
- null string optics 4-101714
- null symmetries of EM field interacting with gravitational field 4-86285
- planar numerical cosmology, difference eqns. and numerical tests 4-95001
- plane-symmetric Einstein-Dirac cosmology containing classical spinor field, exact nonghost soln. 4-90267
- Poincare group, complete gauge theory 4-63591
- positive energy theorem relating mass and electromagnetic charges 4-110939
- power asymptote singularities, orthogonal spatially homogeneous cosmologies, Einstein field eqns. 4-101711
- present state of gravitational theory, experimental confirmation 4-68074
- principles and manifestation in nature (book) 4-63417
- PSR 1913+16, binary pulsar, post-Newtonian timing effects obs. 4-63192
- quantum conformal cosmology, vanishing likelihood of a space-time singularity 4-82570
- quantum gravity, quantum nondomolition meas. 4-63609
- quantum unified field theory, enlarged coordinate transformation group, relativity principle 4-90463
- quantum-statistical distributions, R-inherent quantum mechanics, four-dimensional symmetry 4-95294
- quasi-Newtonian fluid, null infinity 4-101722
- Rastall prototype theory of gravity, variational principle 4-68067
- Raychaudhuri's eqn., geodesic spray, space-time manifold metric connection 4-101712
- relativistic gravitational fields, geodesic distance and invariants 4-95250
- Riemann tensor, peeling-off property of gravity 4-95007
- Riemannian manifolds, vol. and curvature defects 4-95249
- Riemannian space-time, quantum field theory, principle of local definiteness 4-95272
- Robertson-Walker universe, causal cosmological perturbations, Sachs-Wolfe effect in microwave background 4-73114
- rotating black hole, max. temp. of thermal radiation 4-101148
- rotating charged dust as symmetric electrovac source 4-95260
- rotating homogeneous universe with an electromagnetic field 4-82573
- rotating mass, gravitational effect, Sun angular momentum appl. 4-78204
- scalar tensor theory, axisymmetric stationary vacuum fields 4-101135
- Schwarzschild metric, bound geodesic orbits, singular perturbation soln., precession 4-63583
- self-consistent Kaluza-Klein structures, Einstein eqn. soln. 4-86291
- self-dual Yang-Mills and general relativity Einstein eqns., R gauge parametrisation 4-110948
- self-gravitating system, random fluctuations in general relativity 4-110945
- shear-free perfect fluids, algebraic solutions 4-82726
- shear-free perfect fluids with zero mag. Weyl tensor 4-68060
- singular coordinate transformations 4-63594
- singularity avoided oscillating bouncing cosmological model 4-63351
- $SL_2$  gauge theory, conserved currents 4-63593
- $SL(2, C)$  gauge theory of gravit., conservation laws, general relativity theory 4-110968
- soliton, gravitational, classical and quantum bound states 4-63604
- solitonic gravitational waves, Einstein eqn. soln. 4-78209

- neral relativity continued**  
solitonlike solutions for interacting fields with consideration of gravitation 4-68073  
space-time theories and symmetry groups 4-63578  
spherically symmetric gravitational fields, classical inversion algorithm in general rel. 4-73314  
spherically symmetric perfect fluid distrib. 4-73308  
spinning particles, two, gravitational interaction in general relativity 4-63586  
spontaneous soldering,  $O(k)$  Yang-Mills field, Higgs mechanism, n-dimensional space-time 4-106217  
stability properties of gravitational theories and three dimensional gravities 4-86294  
static relativistic stellar models family, grav. pots. 4-72930  
stationary Einstein-gauge and self-dual Yang-Mills field equations 4-95678  
stationary Einstein-Maxwell fields, multipole expansion 4-68065  
stationary gravitational systems, electromagnetic field analogy, Newtonian and Machian aspects 4-106214  
stellar dynamics 4-77883  
superfluid interferometer for Earth's rot. detection using Josephson effect 4-58728  
superluminal travel, theoretical possibility 4-63579  
Szekeres space-time class with cosmological const. 4-86274  
tensors in Riemann normal coordinates, computer calc. 4-63580  
test bodies under influence of external fields, eqns. of relative motion 4-73313  
test particle in geometric fields, complete multipole expansion 4-68066  
thermodynamical equilibrium of self-gravitating plasma with scalar interaction (Russian) 4-97897  
three-dimensional cosmological gravity: dynamics of constant curvature 4-63345  
time-asymmetric initial data for N black hole problem in general relativity 4-72974  
two-spinning particles, Dietz-Hoenselaers soln., geodesics 4-86270  
type D vacuum and electrovac field equations for nonsingular aligned Maxwell field 4-101718  
unified gauge theories approach using generalised Dirac eqn., symmetry breaking to general relativity 4-111357  
Universe, quantum metrics and matter field configurations 4-78202  
Universe expansion rate 4-95004  
vacuum Bianchi models, types III, IV and  $V$ , inhomogeneous generalisations, exact solns. 4-68059  
vacuum bubble collisions in false background vacuum, general relativity 4-63366  
vacuum C-metric in Weyl form 4-63588  
vacuum Einstein's field eqns., prolongation struct. and Backlund transform. 4-58699  
vacuum Einstein eqns., stationary axisymmetric soln. 4-63587  
vacuum energy in a squashed Einstein universe, book contrib. 4-63618  
vacuum solutions, type-D with cosmological const. 4-82720  
viscous fluid collapse, Einstein's field eqns. solns., interior soln. 4-86272  
vorticity and shear-free space-time in general relativity 4-63590  
wave equations with backscatter approx. causal solutions 4-101716  
wave fields in Weyl spaces, pseudo-Riemannian structure 4-110938  
weighing of energy, principle of equivalence, red-shift formula 4-110944  
Weyl invariant theories, flat space-time stability, cosmological constant term 4-106218  
Weyl tensor and energy-momentum tensor struct. from space-time curvature 4-110940  
wormhole solutions, extended particle interpretation in 5-D 4-82723  
wormhole solutions axisymmetric regular in 5-D 4-82722  
wormhole solutions to higher-dimens. general relativity 4-63581
- generator coordinate method**  
*see also nuclear structure theory*  
 $\hat{p}$  and  $\hat{q}$  systems, exactness of generator coordinate method 4-73835  
collective mass parameters and linear response techniques in three-dimensional grids 4-102202  
collective motion, overcompleteness in generator coordinate method, SU(6) group 4-64027  
collective motions, generator coordinate method, symmetry prop. preservation (Chinese) 4-73813  
collective states, IBM, Bohr-Mottelson model, generator coord. method 4-95934  
Hamiltonian quantisation in curved space nuclear collective motion in GCM appl. 4-102150  
interacting boson model and Bohr-Mottelson model comparison, generator coordinate method. (Chinese) 4-102200  
isoscalar giant vibrations, quantized time-dependent deformed oscillator model 4-102196  
nucleon-meson vertex function, nonrel. quark model, meson probability distrib. from qq interaction (Chinese) 4-82942  
quark potential model, NN scat. phase shifts, delta' cross sections 4-106538  
<sup>36</sup>Ar, collective dilatational and quadrupole vibr., generator coordinate approach 4-59177  
<sup>8</sup>Be, resonance analysis using polarised  $\alpha$ -particles, cluster model 4-90990  
<sup>12</sup>C+<sup>12</sup>C quasimolecule, transitions, moments, RMS radii, energies and widths, GCM method 4-73879  
<sup>12</sup>C(p,p), E=0.18 MeV,  $\gamma$ =0-5 phase shifts, single-channel resonating group method 4-106583  
<sup>3</sup>He(<sup>3</sup>He, <sup>3</sup>He), elastic scat. cross sections, polarisations, generator-coordinate with semirealistic NN pot. 4-73916  
<sup>16</sup>O+<sup>16</sup>O quasimolecule, transitions, moments, RMS radii, energies and widths, GCM method 4-73879  
<sup>208</sup>Pb quadrupole moment E3 transition of 3<sup>-</sup> state using generator coordinate method (Chinese) 4-111521
- generators, acoustic** *see acoustic generators*  
**generators, electric** *see electric generators*  
**genetics** *see cellular biophysics*
- geochemistry**  
*see also Earth structure; geology*  
acid Adirondack lake, New York, short-term changes in base neutralising capacity 4-100643  
Adamello complex, N Italy, country rock assimilation into magma body 4-62734  
NE Africa, Proterozoic crustal evolution from model Nd ages 4-89900  
NW Africa continental margin, geology (book) 4-78059  
Alabama Piedmont, USA, amphibolite petrography, geochem. and tectonic significance 4-94024  
Amazon River system, Ra isotope activity and U, Th and Ba concs. 4-67193  
Andes volcanic rock petrogenesis, geochemical considerations 4-62741  
Antarctica, major structural provinces and metallogenic provinces 4-81951  
Antarctica, metallogenic provinces 4-81950  
Antarctica, petroleum prospects and geology and geophysics studies 4-81952  
apatite, Durango, nucl. microprobe PIXE anal. 4-100787  
Southern Appalachian Piedmont, USA, gabbro-metagabbro assoc. geology 4-94025  
Southern Appalachians, USA, mafic-ultramafic complex geology 4-94027  
Appalachians of USA, mafic complex origin, isotope geochem. evidence 4-94021  
Archean mantle fractionation, evidence from Nd isotopic ratios in igneous rocks 4-100499  
ash-flow tuffs of Macusani, Peru, geochem. of peraluminous tuffs (French) 4-72556  
assimilation of country rock into intruded magma body 4-62734  
Mid-Atlantic Ridge basalt, Ne isotopic var. and mantle component 4-110095  
Bahia State, Brazil, rock chem. weathering anal. and salinity 4-100560  
Baltic Sea, As, Sb and Ge biogeochemistry 4-77154  
basaltic magma, oxidation state, effects of degassing 4-100519  
basaltoids of continental arches in eastern USSR distinctive petrochemical features 4-100563  
bauxite deposits in S America, Africa, India, formed in Early Tertiary 4-77483  
Big Soda Lake, Nevada, hydrogeochemistry 4-77564  
biogeochemical processes, effect on climate 4-82227  
Bishop Tuff, California, USA, Nd, Sr, O isotope study of zoned volcanic rocks 4-89891  
Blake River Group, Abitibi volcanic belt, Quebec, geochemistry and geology 4-72539  
book 4-73192  
book 4-86130  
borehole Eh and pH simultaneous measurement instrument 4-94246  
Bowers Supergroup volcanics, geochemistry rel. to Early Palaeozoic tectonic evolution of N Victoria Land, Antarctica 4-67215  
Britain, provenance and crustal residence ages of sediments in rel. to palaeogeographic reconstructions 4-89895  
British Tertiary Volcanic Province, crustal contamination and granite problem 4-62745  
Caledonian intrusion of Scotland and N England, geochem. and magma sources 4-62743  
Cantal, France, coexisting alkaline magma series, isotope geochemistry and magma chamber characts. 4-110098  
Cape Smith komatiite sulphide deposits, Quebec, <sup>187</sup>Re-<sup>187</sup>Os geochemistry 4-81881  
central Hoggar, Eburnean and pan-African U/Pb ages (French) 4-100501  
clay surficial deposits in Athabasca Tar Sands area, Canada, mineralogy and O isotopes 4-62726  
coal, elemental conc. determ. using synchrotron radiation 4-100785  
conference on arc volcanism at Tokyo and Hakone, Japan (August-September 1981) 4-95032  
continental crust elemental composition, empirical estimate 4-105491  
Cook-Austral islands chain, geochem., geochronology and hot spot origin 4-62746  
cosmic radiation fossil record by <sup>10</sup>Be accelerator mass spectrometry 4-90047  
cosmic spherules in deep-sea sediments, with Pt group nuggets 4-85900  
cretaceous dyke rocks, Pyrenees, geochemical characts. and relation to Sillon Houlier (French) 4-82043  
Crimean continental slope, geology of lower Cretaceous dredged rocks 4-94052  
crustal recycling, mean life of continents is not constrained by Nd and Hf isotopes 4-94047  
Dead Sea surface water, trace element determ. by neutron activation 4-105604  
deep fault zones, fluid regimes, geochemical evidence and <sup>18</sup>O/<sup>16</sup>O ratio 4-94072  
diamond origin from old enriched mantle and age of encapsulated garnets 4-94050  
diamonds from Mbuji Mayi kimberlite district, Zaire, C, N isotopes 4-89893  
East Pacific Rise, hydrothermal vents, graphite crystals anal. 4-94086  
Egypt, hydrocarbon generation and prospects in Western Desert 4-77482  
Eiao Island, Marquesas Archipelago, rock sample petrography and geochemistry (French) 4-81875  
environmental geochemistry and soil and water pollution, book 4-67901  
equilibration in core and upper mantle 4-110106  
equilibria, nonequilibrium and natural waters (book) 4-106133  
estuaries, Ni and Cu separation, role of sediments and seawater 4-82093  
estuaries, suspended trace metals in particulate forms, comp., transport and dimensions 4-82083  
estuarine trace metals, adsorption, role of freshwater-seawater mixing 4-82090  
Explorer Ridge area of NE Pacific, basalt geochemistry 4-72536  
felsic magmas, extreme fractionation through liq.-state diffusion or fractional crystallisation 4-67217  
Fiji, oceanic island-arc magma origin, isotope geochemical evidence 4-89894  
Forsyth area, Queensland, Australia, heavy metal mineralisation survey by helicopter 4-94037  
Freemans Cove volcanic suite, Bathurst Island, petrochemistry and tectonic setting rel. to rifting 4-94124  
French Alps (Briançonnais zone), high press.-low temp. metamorphic evolution 4-81888  
gas and hot spring gush out of sea bottom at coastal area of Taketomijima 4-82084  
gas in rock inclusions, N<sub>2</sub> and H<sub>2</sub>O and influence on estimated mineralization press. and temperature 4-105562  
Gironde Estuary, trace element content assoc. with sediments, var. 4-82091  
gneiss complexes, Lower Precambrian, of Yenisei Ridge region, USSR, geochemistry 4-100561  
gneisses of Georgia Inner Piedmont, scale of Sr isotopic diffusion during post-metamorphic cooling 4-67216  
granite, mineralised, element distrib., neutron activation and particle track anal. 4-81889

## geochemistry continued

- granite from Gabal Mueilha, Egypt, post-magmatic alteration, trace element distrib. 4-85674  
 granitoid magma origin and influence of mantle 4-105498  
 groundwater, dissolved O<sub>2</sub> concs. as indicator of hydrological struts. (French) 4-82098  
 groundwater (book) 4-95083  
 Gulf of Mexico, seawater trace metal and Ra enrichment due to rivers and sediments 4-105594  
 Hawaiian tholeiite magma, metasomatic model for origin 4-85650  
 Herring Bay and Commonwealth Bay, Antarctica, geochronology, petrology and tectonics 4-82016  
 hydrothermal alteration of basalt, B and Li geochemical cycles 4-67191  
 ice shelves meltwater, isotopic tracers and salinity used for shelf charact. determ. 4-67440  
 igneous rocks, phase equilib. controls on tholeiitic and calc-alkaline differentiation trends 4-85651  
 inert gas geochemistry, book 4-82611  
 inversion voltammetry for metal content in river water, seawater and bottom sediments 4-100816  
 island arc magma sources, geochemical study 4-62740  
 Ivrea Zone, NW Italy, amphibolites, chem. comp., petrogenesis and tectonic anal. 4-110146  
 Japan Trench, noncalcareous clay, Fe and Mg anal. 4-105536  
 kaersutite, from New Zealand and USA, inert gas, H<sub>2</sub>O and C isotope geochemistry 4-105477  
 SE Kerguelen, volcanic activity, chrono-spatial evolution and petrochemistry 4-81973  
 kimberlites from USA and S Africa, element distrib. in perovskite 4-105480  
 komatiite magmas, petrogenesis and evolution 4-100564  
 Lachlan Fold Belt, SE Australia, source rocks of granites 4-62742  
 limnology (book) 4-73193  
 Loihi Seamount, Hawaii, Pb, Nd, Sr isotope ratios of basalts 4-105508  
 Louisiana continental shelf, USA, gas deposits extent 4-110103  
 Luni River, India, salinity and water quality 4-100638  
 magma chambers, vertical comp. stratification 4-110114  
 magma genesis, geochemical indications 4-62736  
 magma source identification for basaltic rocks, geochem. aspects 4-62735  
 magma source identification isotope geochemistry, review 4-58607  
 magma sources of crust rocks, constraints imposed by experimental petrology 4-62733  
 magmas assoc. with subduction zones, Nb, Ta, Ti, V anomalies and petrogenesis 4-81886  
 Mahabaleshwar area, Deccan Traps, India, flood basalt, magma origin 4-62738  
 Malaita, Solomon Islands, isotope geochemistry of volcanics and xenoliths and mantle stratigraphy 4-72543  
 mantle 400 km discontinuity and Mg orthosilicate elastic props. 4-100558  
 uppermost mantle along midocean ridge, mineralogic variability 4-105478  
 mantle composition, large-scale SR and Pb isotope anomaly in Southern Hemisphere 4-89899  
 upper mantle composition, petrological models 4-100498  
 mantle convection, constraints placed by isotope and geophysical data 4-115376  
 mantle convective mixing of passive heterogeneities 4-81890  
 mantle mixing, implications of inverse relationship between Sr isotope diversity and rate of oceanic volcanism 4-77490  
 marine electrochemistry (book) 4-101599  
 Mealy dykes, Labrador, petrology, chem. charact., age and tectonic events 4-94125  
 Western Melville Peninsula, NW Territories, Canada, Precambrian geology 4-78068  
 metallogenic maps using new realistic format 4-94247  
 methyl iodide in ocean, comparison of photolysis and substitution decomposition rates 4-100626  
 midocean basaltic glass C isotope composition and origin 4-105476  
 minerals (book) 4-67906  
 minerals in hydrothermal environment, point defect chemistry and deformation 4-94092  
 Minnelusa sands hydrocarbon deposits, Wyoming, USA, seismic exploration 4-109715  
 Mount Isa Inlier, Australia, batholiths geochemistry and age, implications for magmatism 4-94032  
 Mount Isa region, Australia, acid volcanic units geochem. discrimination 4-94033  
 Mount Ontake volcano, Japan, <sup>3</sup>He emissions rel. to volcanic activity 4-89902  
 Mount S. Helens, Washington, USA, SO<sub>2</sub> content of volcanic ash 4-115368  
 Mount S. Helens, 1980 eruptions effect on surface and groundwater quality 4-105616  
 Mount S. Helens, 1980 May eruptions, ash and magma, comp.-chem. 4-105513  
 Mount S. Helens, Washington, USA, radioactive <sup>210</sup>Pb, <sup>210</sup>Po in volcanic ash 4-115367  
 Mozambique Belt, N Tanzania, petrochemistry of geotectonic evolution 4-77475  
 mylonitization, Santa Rosa Mylonite Belt cooling event rel. to uplift 4-94045  
 Nanling region, China, granitic bodies and crust transform., petrochemistry NSF triangular diagram (Chinese) 4-72710  
 natural waters and minerals (book) 4-95093  
 W Nazca plate, dredged basalts and E Pacific Rise evolution 4-81988  
 neutron occurrence in Earth crust, of cosmic ray and radioactivity origin 4-110142  
 New Quebec, Canada, ice lenses in peat bogs, geochemistry, isotope content and genesis 4-100637  
 SW Nigeria, metavolcano-sedimentary sequence east of Ife and Ilesha and metal deposits 4-115353  
 Oahu, Hawaii, geochemistry of Koolau Range lavas rel. to volcanism 4-105509  
 ocean, <sup>18</sup>O gradients rel. to dynamics of meltwater discharge from ice sheets during deglaciation 4-105613  
 ocean chemical speciation and cycling rel. to position on periodic table 4-85722  
 ocean chemistry, carbonate dissolution rate rel. to growth and comp. of Co-rich ferromanganese crusts 4-67206

## geochemistry continued

- ocean chemistry, model for role of oceans in determ. of atmospheric CO<sub>2</sub> conc. 4-62908  
 ocean chemistry, water column anomalies assoc. with hydrothermal activity in Guaymas Basin, Gulf of California 4-67218  
 ocean chemistry and circulation, changes rel. to rapid atmospheric CO<sub>2</sub> vars. 4-62909  
 oceanic basalt geochemistry in vicinity of transform faults 4-105479  
 oil and gas reserves in recoverable deposits, calculation 4-105093  
 Oklo natural fission reactor, Gabon, fission product transport 4-81885  
 Ontong Java Plateau, isotope geochem. and stratigraphy of mantle 4-72543  
 circum-Pacific arc magmas, H<sub>2</sub>O content and phenocryst assemblage 4-81968  
 Pacific Ocean, Hg source 4-105599  
 S Peru, Pb isotope study of magma-crust interaction in Andes 4-105475  
 petroleum and gas prospecting in Oklahoma, USA, by soil gas radioactivity method 4-110104  
 Phanerozoic basalt volcanism of Transbaikai, USSR, comp. evolution 4-100515  
 Philippine Sea island arcs, magmatic evolution and tectonics 4-81969  
 Pine Creek Geosyncline, Australia, realistic metallogenic map 4-94247  
 PIXE analysis of Pt group elements preconcentrated from geological samples 4-100784  
 PIXE-PIGE thick-target anal., accuracy and precision determ. with geological standards 4-99881  
 pond sediments comp. anal. 4-100046  
 Possession Island, Indian Ocean, volcanology, tectonics, geochemistry, geochronology and petrology 4-81974  
 Precambrian granitoid rocks, origin of magma 4-62737  
 Prince Olav Coast, Earth Antarctica, geology and petrology 4-81925  
 pyrrhotite (Fe<sub>9</sub>S<sub>8</sub>), eqn. of state at Earth core conditions 4-115395  
 quartz, O diffusion between quartz and surrounding water, laboratory expts. 4-94093  
 Queen Maud Batholith, central Transantarctic Mts., geology and Rosetta Orogeny 4-81936  
 Queen Maud Land, Antarctica, Sr isotope studies of Ahlmann Ridge and Annandagstoppane 4-81927  
 radioactive waste disposal, granite mine, hydrogeology and heat effect 4-83169  
 radioactivity measurement of geological samples, gamma ray spectrometry with underground detector 4-105765  
 Rainy Lake region, Ontario, Canada, geochem. of mantle-derived Archaean rocks 4-94051  
 Riiser-Larsenisen Ice Shelf, Antarctica, snow chem. comp., marine and non-marine sources 4-100024  
 rivers, chem. elements transport from land to ocean, significance of river input 4-82147  
 rock varnish microchemical laminations 4-110144  
 rock weathering processes at high altitude 4-62821  
 Russian platform, seismic boundary velocities of basement 4-100466  
 N Saskatchewan, Canada, Pb isotope composition in U deposits 4-115348  
 N Saskatchewan, Canada, U/Pb geochronology of Midwest U deposits 4-115347  
 Saudi Arabia, groundwater chem. 4-82104  
 seawater, chemical species of Sn, Sb, As and Ge 4-82313  
 seawater sampling devices for determ. of trace metals, intercomparison 4-82316  
 Setouchi volcanic belt, Japan, high magnesian andesites prod. rel. to Shikoku Basin evolution 4-81970  
 Shikotan, Minor Kuril Islands, magmatic rocks features 4-100568  
 Siberia, lead ore deposits, Pb isotope study 4-105499  
 W Siberian Platform, USSR, salt deposit distrib. 4-105496  
 siderophile-rich magnetic spheroids from the Cretaceous-Tertiary boundary in Umbria, Italy, chem. anal. 4-100509  
 Singbhum granite batholithic complex, India, geochemical evolution and struct. setting 4-81902  
 Snake River Plain, Idaho, USA, origin of flood basalts 4-62739  
 softwater lakes, H<sup>+</sup> conc. determ., use of CO<sub>2</sub> equilibria 4-77169  
 South Shetland Islands, Lesser Antarctica, geochem. and igneous activity due to subduction 4-81948  
 spectrochemical analysis of geochem. samples using two-jet plasmatron 4-110308  
 subsurface contaminant transport from liquid radwaste disposal area groundwater, T data 4-78700  
 sulphide deposits in submarine depression, sub-sill source fluid, dynamic model of brine pools 4-62838  
 Talaud Islands, Indonesia, ophiolites and assoc. volcanic rocks, petrology and geochemistry 4-82051  
 N Tanzania, high fluoride content of rivers, lakes, springs 4-115467  
 Tanzania, xenolith isotope geochem. and mantle origin 4-81882  
 titanomagnetite, aqueous oxidation in submarine basalts and thermomagnetism 4-100497  
 Togo, magnetite and haematite mineralisation of atacamite series rocks (French) 4-77477  
 tonalite from Lakeview Mountains, USA, Fe content anal. 4-100811  
 trace element quantitative analysis, relativistic electrons to induce X-ray emission (REIXE) appl. 4-100786  
 trace metals in Arctic Ocean, conc. 4-82087  
 trace metals in Arctic seawater and snow, differential pulse anodic stripping voltammetry anal. 4-82315  
 trace metals in coastal waters, transfer from water column to sediment 4-82094  
 trace metals in Gulf of Elefsis, conc. 4-82095  
 trace metals in seawater, conf. at Erice, Italy (March-April 1981) 4-78046  
 Trinity peridotite, California, USA, Nd-Sr isotope study and mantle evolution 4-89890  
 upper mantle inhomogeneity parameter and implications for thermally driven processes 4-72542  
 upper mantle rheology and grain-size distribution 4-62747  
 western USA, origin of Mesozoic and Tertiary granitic rocks 4-62744  
 N Vermont, USA, metamorphic schists of Ordovician and Devonian ages 4-94023  
 Vestfold Block, E Antarctica, Sr-Nd isotopes, lithology and crust evolution 4-81929  
 N Victoria Land, Antarctica, airborne gamma-ray survey 4-81953  
 Wadi Natash Volcanic series, Eastern Desert, Egypt, geology and geochemistry 4-115352  
 water and sediment environment geochemistry, book 4-82614

## chemistry continued

- S Wyoming, Early Proterozoic volcanic are succession, tectonic setting and origin, geochemical modelling 4-94123  
 X-ray fluorescence analysis method for rock composition 4-115595  
 Xigaze ophiolite, Tibet, magmatites and tectonites, Pb isotopic anal. and geochronology 4-110139  
 York Canyon, New Mexico, USA, organic matter isotopes across Cretaceous-Tertiary boundary 4-89892  
 Ar loss predictors in basic rocks, test of two alteration indices 4-110140  
 Au prospecting methods for use at Salair, USSR 4-100828  
<sup>10</sup>Be in soil, concentrations and possible <sup>10</sup>Be radioactive dating method 4-81880  
 C flux from mantle to midocean ridge 4-105476  
 C-N cycles, denitrification rates and availability of organic matter in marine environments 4-67282  
 Cl, isotopic variations in nature, determ. method 4-77651  
 Co, Cu, Ni, Mn resources in Pacific seafloor Mn crusts 4-110107  
 Cu concentrations in sub-Arctic waters of NW Pacific, fluxes and origin 4-82088  
 Fe ore deposit, prospecting in Goa, India, Landsat MSS method 4-67427  
 Fe vertical distrib. in Arctic Ocean rel. to Cd and Al profiles and hydrography 4-82089  
 Fe-H<sub>2</sub>O interaction in geochemical evolution of Earth (Japanese) 4-94056  
 Hf/rare earth elements fractionation in sediments, evidence for crustal recycling into mantle 4-110100  
 Hg, air-sea exchange 4-82092  
 Hg annual flux from Kilauea main vent, estimate from Hg/SO<sub>2</sub> ratio 4-72559  
 K-rich volcanic rocks, <sup>18</sup>O/<sup>16</sup>O and chem. relationships, mantle implications 4-110094  
 Mn crust containing Co on seafloor of USA Pacific economic zones 4-110107  
 Mn deep-sea nodule, chem. composition study (French) 4-82025  
 Mn nodule chemical deposition, radiotracer uptake expt. in Pacific 4-110126  
 Mn nodules from Pacific seabed, radioactivity obs. (Chinese) 4-72564  
<sup>231</sup>Pa measurement, appl. to U series geochemical transport model 4-105738  
 Pb geochronological dating method; calc. of isotope growth curves 4-90004  
 Pb isotope geochemistry, inversion of data from worldwide deposits 4-89898  
 Pb ore deposits in Siberia, isotope geochemistry study 4-105499  
<sup>210</sup>Pb, activities and conc. factors in estuarine sediments of rivers in Gujarat, India 4-82103  
 Pu geochemical association in Caithness environment 4-105134  
 Ra fluxes from salt marsh, meas. in Bly Creek, South Carolina 4-77557  
 Ra, occurrence and behaviour in saline formation water of US Gulf Coast region 4-110179  
<sup>222</sup>Ra, activities and conc. factors in estuarine sediments of rivers in Gujarat, India 4-82103  
<sup>222</sup>Rn conc. meas. in natural gas prod., using scintillation chambers 4-64322  
 S-rich volcanic eruptions, contrib. to stratospheric H<sub>2</sub>SO<sub>4</sub> aerosols 4-105511  
 SO<sub>2</sub> in volcanic ash from Mt St Helens May 1980 eruption 4-115368  
 Sb speciation and content in Saanich Inlet water column and interstitial waters 4-82314  
 Se IV and VI dissolved in oceans, distrib. rel. to physical and biological processes 4-82086  
 Si geochemical processes (book) 4-78057  
 Si isotopes use in geochemistry 4-81903  
 SiO<sub>2</sub>, existence and properties in Earth core 4-110135  
 Th isotope distrib. in E equatorial Pacific 4-82096  
 Ti, determ. in geological materials, neutron activation by reactor induced (n, p) reactions 4-82257  
 U, induced fission track method quantitative determ. in neutral waters (Rumanian) 4-100822  
 U, levels in marine waters and biota, using SSNTD 4-100052  
 V concentrations in N Pacific Ocean, profiles of particulate and dissolved 4-77556

## geochronology

## see also radioactive dating

- Aberdeen Newer Gabbros, Scotland, slow post-organic cooling, palaeomagnetic signature 4-77489  
 Afar nascent passive margin, palaeomag. and geochronological evidence for episodic spreading and rift propag. 4-85655  
 NE Africa, Proterozoic crustal evolution from model Nd ages 4-89900  
 Aigurande Plateau, French Massif Central, Pb isotopes indicating Upper Biverian age (French) 4-81877  
 SW Alaska, relations between plate motions and Late Cretaceous to Palaeogene magnetism 4-94131  
 Allan Hills, meteorites distrib., implications for climatology 4-82230  
 Antarctic granulite-facies rocks, ages, metamorphism and mineralogy 4-82049  
 Antarctic Peninsula, Rb-Sr constraints on basement rock ages 4-81949  
 Antarctic Peninsula region, age of post-Gondwana calc-alkaline volcanism 4-81947  
 apatite, fission track annealing, anisotropy using track-in-track length meas. 4-100485  
 apatite, fission track length and density relationship 4-100768  
 apatite, fission-track temperature ages 4-100487  
 apatite; optical studies of fission tracks, alternative dating method 4-100484  
 Appalachians of USA, mafic complex origin, isotope geochem. evidence 4-94021  
 Apuseni Mountains, Cretaceous tectono-magnetic evolution, K-Ar dating 4-77492  
 Archean mantle fractionation, evidence from Nd isotopic ratios in igneous rocks 4-100499  
 Arctic Ocean, palaeosedimentation rate var. from amino acid epimerization 4-110130  
 Arunta Inlier, Australia, Proterozoic crustal events, Rb-Sr geochronology 4-94034  
 South Atlantic coasts, Late Tertiary shorelines evidence, dating and review 4-105563  
 Atlantic continental slope off USA, seafloor morphology and sediment ages 4-67210

## geochronology continued

- Atlas Mountains, Morocco, Tertiary and Quaternary volcanism and tectonic events dating 4-100517  
 basalt from Atlantic and Pacific oceans, mag. characts. rel. to age 4-62800  
 Beringia, sea-level data for Bering-Chukchi shelves, 19000 to 10000 <sup>14</sup>C yr BP 4-94165  
 Blake-Bahama outer ridge, Atlantic, lithosphere heat flow and thermal state, age depend. 4-105487  
 Briançonnais Carboniferous, subsidence of NS groove (French) 4-77473  
 Britain, provenance and crustal residence ages of sediments in rel. to palaeogeographic reconstructions 4-89895  
 Bulth Volcanic Series, Wales, Permo-Carboniferous and Ordovician palaeomagnetic remanence and pole position var. 4-110038  
 central California, correl. between geological record and computed plate motions 4-94127  
 Canadian Arctic Islands, sea floor spreading chronology and sedimentation 4-110124  
 Canary Islands, dating of lava flows by palaeomagnetic method 4-89878  
 western Caribbean, marine tephra sediment chronology 4-62795  
 cave sediments in Norway, palaeomagnetism and magnetic fabric 4-89876  
 central Hoggar, Eburnean and panAfrican U/Pb ages (French) 4-100501  
 Chuckanut Formation, NW Washington, USA, stratigraphy, age and palaeogeography 4-62727  
 clastic sedimentary sequences, quantification in time series anal. 4-94042  
 Columbia Plateau, Washington, palaeomag. study of post 12 Myr clockwise rot. 4-94130  
 conodonts, O isotopic comp., use for palaeoclimate and palaeoceanography anal. 4-110283  
 continental crust, mean life of continents is not constrained by Nd and Hf isotopes 4-94047  
 continental crust formation, geochemistry of Lower Precambrian gneiss complexes of Yenisei Ridge region, USSR 4-100561  
 Cook-Austral islands chain, geochem., geochronology and hot spot origin 4-62746  
 Corella Formation, Mount Isa Inlier, Queensland, stratigraphic review 4-94118  
 cosmic radiation fossil record by <sup>10</sup>Be accelerator mass spectrometry 4-90047  
 terminal Cretaceous extinctions in Hell Creek area, Montana, compatible with catastrophic extinction 4-72587  
 Cretaceous-Tertiary boundary, sharp boundary or gradual transition 4-72589  
 Cretaceous-Tertiary boundary, shocked mineral evidence for impact 4-110149  
 Deer Lake Group, Newfoundland, Early Carboniferous palaeomagnetism, tectonic implications 4-110037  
 last deglaciation, dynamics of meltwater discharge from Northern Hemisphere ice sheets 4-105613  
 diamond origin from old enriched mantle and age of encapsulated garnets 4-94050  
 southwest Egypt, geology of migmatite and metamorphic units 4-77480  
 Enderby Land, Antarctica, geological history of Napier Complex 4-81921  
 ESR dating of geological samples, review 4-63434  
 NW Europe, evidence for pre-Weichselian glaciation, stratigraphy 4-110176  
 Farallon plate subduction beneath North America, determ. from relative plate motions 4-94061  
 fission track dating with low track counts, confidence bounds 4-100488  
 fluorapatite, natural, high temperature fission track annealing, track dating 4-100486  
 Fyfe Hills-Khmara Bay region of Enderby Land, Antarctica, geology 4-81922  
 Gangdese plutonism, Lhasa-Xigaze region, Tibet, U-Pb geochronology and assoc. tectonics 4-110097  
 Gavarnie nappe, France, struct. and thrust sheets emplacement ages 4-105470  
 geomagnetic intensity variations in Egypt and W Asia during second millennium BC, archaeomag. meas. 4-100443  
 geomagnetic secular variation in W United States, AD 750 to 1450, congruent palaeomag. and archaeomag. records 4-100446  
 geothermic source searching by fission track dating of volcanic glasses 4-100765  
 Glacier Peak, Washington, tephrochronology of Late Wisconsin deglaciation and Holocene glacier fluctuations 4-94177  
 Glacier Peak volcano, Washington, USA, tephrochronology and eruption history 4-62768  
 gneisses of Georgia Inner Piedmont, Rb-Sr isochron age and scale of Sr isotopic diffusion 4-62716  
 granitic, orbicular, of French Massif Central, age determ. (French) 4-105555  
 Great Barrier Reef, inaugural conference, Townsville, Australia (1983 August 29 to September 2) 4-90284  
 SW Greenland, Archean crust evolution, review based on Buksefjorden region 4-81899  
 West Greenland, geochronology of Akilia association and Isua supracrustal belt 4-81883  
 Heard and McDonald islands, Indian Ocean, sedimentation record, microfossil evidence 4-82037  
 Heard and McDonald islands, Indian Ocean volcano-tectonic evolution and geochronology 4-81972  
 Herring Bay and Commonwealth Bay, Antarctica, geochronology, petrology and tectonics 4-82016  
 NW Himalaya (N Pakistan), <sup>39</sup>Ar/<sup>40</sup>Ar ages of Alpine tectonometamorphic events 4-94043  
 Hot Springs Ophiolite, age, struct., time for closure of oceanic basin (French) 4-81977  
 Hunza Valley, Pakistan, Quaternary glacial history, geomorphology and sediments 4-62825  
 Iceland, tephrochronology of postglacial eruptions 4-62754  
 impure carbonates, dating using decay series isotopes 4-105736  
 India, Phanerozoic palaeomagnetism, implications for India-Asia collision 4-81997  
 E Indian Ocean, geomag. anomalies due to seafloor spreading and age of crust 4-94007  
 SW Japan, crust struct. and Mesozoic orogeny (French) 4-115373  
 Japan, tephrochronology and Quaternary studies 4-62750  
 Karokoram glaciers, fluctuations anal. techniques 4-62864

## geochronology continued

- Karoo volcanism onset in E Botswana, discovery of Early Jurassic pillow lavas and palynomorphs 4-100506
- SE Kerguelen, volcanic activity, chrono-spatial evolution and petrochemistry 4-81973
- Kerguelen plutonism, petrology, geochronology and geology 4-82052
- Komati Formation, South Africa, age of mag. remanence rel. to early Archaean geomag. field 4-94004
- S Kootenay Arc, SE British Columbia, geochronology and tectonic implications of magmatism and metamorphism 4-105473
- Ladinian-Carnian stage boundary, relation in Triassic sea level change 4-62812
- Laramide orogeny, chronology of subduction of aseismic ridge on Farallon plate 4-94063
- Long Island Sound, Connecticut, chronologies of sedimentary processes in sediments of FOAM site 4-100535
- Lower Rhine Basin, Germany, Plio-Pleistocene deposits, palaeomagnetism and biostratigraphy 4-110036
- Luan County, China metamorphic rock form., K-Ar isochronous age and geological significance (*Chinese*) 4-85640
- Lutzw-Holm Bay region, E Antarctica, tectonic and metamorphic history 4-81926
- Madeira, palaeomag. evidence for Early Cretaceous origin 4-105422
- magnetic reversal time scales, implications for lower mantle convection 4-85620
- Marie Byrd Land, Antarctica, Cretaceous volcanic rocks, palaeomagnetism and palaeopole position anal. 4-81963
- Marie Byrd Land, Antarctica, glacial and tectonic events, chronology recorded by rocks 4-82024
- marine fossil families, periodicity of extinctions rel. to extraterrestrial forces 4-72596
- mass extinctions, periodicity rel. to Sun's oscillation about galactic plane 4-72592
- mass extinctions due to cometary impacts, periodicity rel. to Sun's motion perpendicular to galactic plane 4-72591
- Mealy dykes, Labrador, petrology, chem. charact., age and tectonic events 4-94125
- Western Melville Peninsula, NW Territories, Canada, Precambrian geology 4-78068
- meteorite craters ages, evidence for periodic impacts on Earth 4-72595
- methods (book) 4-73182
- Michipicoten plutonic-volcanic terrain, Ontario, volcanism, tectonics evolution 4-94059
- Midlands, England, Wolstonian stage of British Pleistocene, age 4-72534
- Mount Isa, Queensland, geology of Proterozoic rift zone and implications for mineralisation 4-94117
- Mount Isa Inlier, Australia, batholiths geochemistry and age, implications for magmatism 4-94032
- Nevada, glacial chronology of Ruby Mountains-East Humboldt Range 4-94176
- west-central Nevada, palaeomag. assessment of oroflexural deform. 4-94128
- S New Zealand, overriding of Indian-Antarctica ridge rel. to migration of Late Cainozoic volcanism 4-94082
- N Nigeria, anorogenic ring complexes age migration 4-62753
- southeast Nigeria, Rb-Sr dating and age of Pan-African orogenesis 4-77485
- Ninmaroo Formation, Australia, late diagenetic history and products 4-94120
- Norilsk area, NW Siberian platform, comp. and age of crystalline basement and overlying sedimentary rocks 4-100514
- Normandy loess deposits, thermoluminescence dating 4-100510
- North America, plate motions correl. with continental tectonics during Laramide to Basin-Range period 4-94062
- SW North America, rel. to mid-Tertiary extensional orogeny 4-94129
- North Wadi Kareim area, Egypt, radioactivity distrib. correl. with age and geology 4-100559
- oceanic lithosphere, age rel. to lithosphere flexure seaward of ocean trenches 4-85653
- oceanic lithosphere, cooling trends, geotectic data anal. 4-100508
- oceanic lithosphere stability, with variable viscosity charact. time for amplification of disturbances 4-105492
- oceanic trench-seamount interaction, time-scale determ. via numerical simulation 4-105526
- oolitic goethite transformation to haematite, dating of transformation by palaeomagnetic study 4-62664
- W Oregon-Washington, volcano-tectonic evolution rel. to Cainozoic plate motions 4-94065
- W Pacific, depth anomalies over Mesozoic crust and age determ. 4-81911
- Central Pacific, Mn crust  $^{10}\text{Be}$  dating, implications for palaeocirculation determ. 4-85757
- W Pacific, submarine rocks, ages 4-81915
- palaeoclimate, evidence for enhanced atmospheric circulation over North America during Early Holocene 4-100712
- palaeoclimate (book) 4-95070
- palaeoclimatic change chronology at end of last glaciation 4-115562
- palaeomagnetism, physical model for palaeosecular variation 4-110041
- Pangano Nunatak and Hart Hills area, Antarctica geology 4-81943
- Patia Valley, SW Colombia, geochronology of basic rocks and emplacement 4-105506
- Pedroches Batholith, Spain, geochronology study and Pangaea break up 4-81884
- NE Peninsular Ranges, California, uplift from fission-track dating 4-94045
- Late Pleistocene climate at Marsworth, UK, evidence of two temperate episodes 4-89989
- Possession Island, Indian Ocean, volcanology, tectonics, geochemistry, geochronology and petrology 4-81974
- pottery age determination of thermoluminesc., method for determ. radioactive dose rate 4-82273
- Potwar Plateau, Pakistan, Pleistocene and Holocene sequences dating 4-62751
- Late Quaternary varved clay, remanent magnetism, stress induced var. 4-110133
- Quebec, relation between dunes, fire and climate recorded in Holocene deposits 4-85753
- Queen Maud Land, Antarctica, Sr isotope studies of Ahlmann Ridge and Annandagstoppane 4-81927
- Querigut, France, granite-grandiorite complex genesis, recycling processes, Nd-Sr isotopic systematics 4-110096
- geochronology continued
- radiocarbon dating in Antarctica, problems and significance 4-81954
- Rajasthan, India, Precambrian rocks geochronology and acid magmatism periods determ. 4-81900
- Riukiu limestone, dating 4-105472
- Saharan Pan-African belt, Precambrian age of pre-tectonic magmatic suite (*French*) 4-77476
- Santa Rosa Mylonite Belt, uplift from fission-track dating 4-94045
- Santorini, volcanic eruptions and late Minoan civilisation fired destruction levels, archaeomagnetic dating 4-85647
- N Saskatchewan, Canada, Pb isotope composition in U deposits 4-115348
- N Saskatchewan, Canada, U/Pb geochronology of Midwest U deposit 4-115347
- sedimentation rates in Atlantic ocean, glacial to interglacial vars. from Th meas 4-110129
- sediments as historical record of heavy metals air pollution 4-100046
- Seychelles, granites and xenoliths, dating and parental magma mantle origin with crustal interactions 4-110102
- Shackleton Range, Antarctica, Rb-Sr ages and geological history 4-81937
- Shackleton Range, Antarctica, tectonics and Precambrian struct. stages 4-81938
- Shikoku Basin, Pacific, evolution rel. to high magnesian andesites in Setouchi volcanic belt, Japan 4-81970
- Singhbhum granite batholithic complex, India, geochemical evolution and struct. setting 4-81902
- Sivalik red beds, polarity transition stratigraphy and remanence lock-in times 4-110043
- sphere, fission-track temperature ages 4-100487
- stratigraphic correlation by means of ordinal scales 4-94041
- International Stratigraphic Scale, for Cainozoic 4-105495
- stratigraphy, unitary associations method, graph theory and computer algorithm appls. 4-94040
- northwest Sudan, geology of migmatite and metamorphic units 4-77480
- Sukinda Valley chromites, India, palaeomagnetism, ages and setting 4-77513
- tephra deposit dating by approximate methods 4-62993
- tephra deposit dating by radioactivity methods 4-62992
- tephra deposits in Iceland, tephrochronology by geochem. obs. 4-62748
- tephra layer dating by combined magnetostratigraphy and tephrochronology method 4-62994
- tephra layers as geochronological markers over long distances 4-62995
- Tertiary volcanism of Hocheifel, age and palaeomag. study 4-105419
- Tethys, European margin, distensional movements during Jurassic (*French*) 4-115354
- tidal evolution of Earth's gravit. field and figure, theory 4-105399
- topographic erosion, time const. rel. to flexural models of continental lithosphere 4-67189
- Transbaikal, USSR, Phanerozoic basite volcanism, comp. evolution 4-100515
- tree-ring chronology and dendroclimatology, average value of correlated time series 4-100665
- Trinity peridotite, California, USA, Nd-Sr isotope study and mantle evolution 4-89890
- Tulemalu dykes (Early Proterozoic), Northwest Territories, Canada, age of magnetisation and palaeomagnetism 4-105407
- Umanak Island, Aleutians, Alaska, geology and geochronology 4-72537
- SW United States, chronology of asthenospheric intrusion rel. to thermal regime of lithosphere 4-94058
- W United States, kinematics of plate convergence from Mesozoic structs. in western Cordillera 4-94064
- W United States, tectonic reconstructions from palaeomag. results from Sierra Nevada 4-93998
- W United States, tephrochronology and Quaternary geology 4-62749
- Valle Ricca Pits, Italy, Plio-Pleistocene deposits, palaeomagnetism and biostratigraphy 4-110036
- post-Variscan molasses, Catalanian Pyrenees, Spain, stratigraphy and ages (*French*) 4-105557
- N Vermont, USA, metamorphic schists of Ordovician and Devonian age 4-94023
- Vestfold Block, E Antarctica, Sr-Nd isotopes, lithology and crust evolution 4-81929
- Vesuvian samples, fission-track temperature ages 4-100487
- N Victoria Land, Antarctica, age of Bowers Supergroup 4-81933
- S Victoria Land, Antarctica, provenance and dating of glacial deposits 4-81955
- Villefranche-de-Rouergue fault, France, Tertiary sedimentary deposits evidence for fault motion (*French*) 4-100482
- Wadi Natash Volcanic series, Eastern Desert, Egypt, geology and geochemistry 4-115352
- Williston Basin, USA, mechanical and thermal model for tectonic evolution 4-94067
- Windmill Metamorphics, Casey area, Antarctica, geochronological study 4-81928
- Xigaze ophiolite, Tibet, magmatites and tectonites, Pb isotopic anal. and geochronology 4-110139
- Zacatecas, Mexico, mid-Tertiary felsic volcanism, rock dating and magma origin 4-110113
- $^{40}\text{Ar}$ - $^{39}\text{Ar}$  dating of basalt, containing incompletely degassed xenoliths 4-85764
- $^{10}\text{Be}$  activity in deep-sea sediments, temporal vars. over past 1 Myr 4-110128
- $^{10}\text{Be}$  in soil, concentrations and possible  $^{10}\text{Be}$  radioactive dating method 4-81880
- K-Ar dating of basic rocks, test of two alteration indices as predictors of Ar loss 4-110140
- Pb radioactive dating method, calc. of Pb isotope growth curves 4-90004
- U-Pb dating for case of common Pb with unknown isotopic composition 4-110285
- U-rich crystals, radiation damage using nuclear track and thermoluminescence methods 4-98130
- geodesic lenses see aspherical lenses; integrated optics; lenses
- geodesy
- see also gravity
- Ada County, Idaho, USA, mapping by photogrammetric method 4-110025
- Ada County Project, Idaho, USA, photogrammetric survey 4-110026
- adjustment principle calc. method for set of observations 4-105403

- desy continued  
adjusted theory, using tensor struct. applied to least-squares method 4-72474
- Alpine-Mediterranean region, geodetic models for monitoring regional kinematics 4-100425
- North America, combined correlation anal. of geophys. fields 4-72541
- Antarctic shelf ice, gravity meas. possibilities 4-72624
- Antarctica, gravity and geomagnetic studies between 45 and 65 degrees East 4-81959
- Asal-Ghoubet rift, Djibouti, Africa, strain accumulation study 4-115380
- astrometric and geodetic reference systems, linking from space 4-72856
- NW Atlantic, gravimetric models and surface currents satellite remote sensing 4-67163
- SE Australia, crustal deformation from geodetic evidence? 4-89871
- Baja California, Mexico, geodetic obs. of fault motions 4-72483
- Benue Trough, SE Nigeria, tectonic and sedimentation history 4-77479
- S California, USA, regional deformation near Palmdale 4-72562
- Chattolane Baltimore Gneiss Dome, Maryland, USA, gravity survey 4-81834
- conference, Hamburg, W Germany (1983) 4-106108
- conference on geodesy, at Hamburg, West Germany (August 1983) 4-86111
- crust deformation, use of space/airborne laser ranging systems 4-110324
- datum development and positional errors 4-72484
- deformation anal. of geodetic network, use of pre-zero-epoch covariance matrix 4-72477
- deformations of an elastic Earth, book 4-86133
- distance meas. with Mekometer laser instrument, atmos. corrections and data reduction 4-89998
- Djibouti, satellite positioning obs. of tectonic displacements 4-72476
- downward continuation of gravity and geomag. data, solved as inverse theory 4-85802
- dynamic Earth geoid anomalies 4-110024
- earthquake fault associated gravity anomalies 4-81866
- Ekstrom Ice Shelf, strain meas. geodetic obs. (German) 4-72622
- Filchner-Ronne Ice Shelf, strain meas. geodetic obs. (German) 4-72622
- geodetic networks, numerically efficient soln. of second-order design problem 4-72478
- geoid heights and lithospheric stresses for a dynamic Earth 4-100495
- geoid one degree global models 4-72475
- geoid shape, correl. with seismic surface wave vels. and convection in mantle 4-100529
- geoid shape, effect of large-scale density inhomogeneities on gravity fields 4-62657
- geoid undulations from Doppler satellite positioning and gravimetric techniques, comparison 4-85607
- geoidal undulation patterns in NW Pacific Ocean, resemblance to free-air gravity anomalies 4-105397
- geopotential coefficients of order 29, determ. from orbit of satellite 1967-104B 4-105398
- geopotential field derivatives, computation procedure for coeffs. 4-85605
- Global Positioning System (GPS) appl. to geodesy, estimation and large-scale multiple hypothesis testing 4-77656
- Global Positioning System (NAVSTAR) in differential mode for precise position determ. 4-72713
- Gorringe Ridge, North Atlantic Ocean, interpretation of geoid anomalies 4-67162
- GPS geodetic receiver system testing 4-72735
- gravitational field, modification of point mass model (Russian) 4-115332
- gravity and geomagnetic anomalies due to subsurface struct., computation method 4-85604
- gravity anomaly automatic fitting using 2-D models 4-67421
- gravity field models and the triple correlation function 4-81837
- gravity field represented by point mass system (Russian) 4-77443
- gravity inverse problem theory for multiple density boundary prospecting 4-100431
- gravity potential of buried object, 3-D Fourier transforms theory (Chinese) 4-62651
- Greece, Atalanti region, microgravity network, crustal movements and precursors to earthquakes 4-77440
- ground tilt, correl. with tectonic stress and earthquake occurrence 4-81998
- gyrotheodolite constant calculation from calibration measurements 4-85602
- Imperial Valley, California, 1940 earthquake rel. to vertical movements 4-94079
- inversion of geophysical data by least-squares techniques 4-67423
- isostatic model of Earth's shape 4-100428
- Izu Peninsula, Japan, geodetic strain obs. and tectonics (Japanese) 4-72480
- S Kanto District, Honshu, Japan strain buildup after 1923 Kanto earthquake 4-85630
- Karakorum gravity measurements 4-62652
- Kilauea volcano, Hawaii, eruption forecasting 4-85648
- Laksefjord Nappe, Finnmark, finite strain patterns generation and modification by progressive thrust faulting 4-110031
- laser altimetry by Starlette satellite, effects of orbital perturbations by ocean tides (Chinese) 4-82362
- laser ranging use 4-72765
- least squares collocation in digital terrain modelling 4-81836
- least squares method using tensor struct. approach 4-72474
- levelling system of new design 4-89999
- Los Angeles region, California, Earth model regional deform., seismic, tectonic and geodetic meas. 4-110032
- Louisiana-Mississippi, USA, modern uparching of coastal plain 4-115381
- Lutzw-Holm Bay, Antarctica, gravity, geomag. intensity anomalies and crust tilt 4-81841
- mantle convection, lag and related geoid anomalies and mantle struct. 4-105520
- mantle wave velocities anal. and correl. with heat flow and non-hydrostatic geoid 4-105488
- marine geoid, Seasat obs. of lithosphere flexure seaward of ocean trenches 4-85653
- matrix development of potential and attraction at exterior points rel. to inertia tensors 4-81832
- E Mediterranean, geodetic satellite laser ranging method for crustal motion 4-100770
- E Mediterranean, satellite laser tracking technique for geodynamics 4-100426
- Miura and Boso peninsulas, Kanto, Japan, geodetic survey obs. (Japanese) 4-72481
- geodesy continued  
Mount St. Helens, Washington, USA, seismicity and crust strain before May 1980 eruption 4-85649
- mountain isostatic equilibrium calc. method 4-105529
- Nankai Trough, SW Japan, earthquake deformation cycle 4-85629
- 3-D network adjustment method for spatial and gravity measurements 4-105401
- network adjustment model for long extended traverse nets and gyrotheodolite orientation meas. 4-85601
- network analysis, bivariate interpolation using triangular elements with fifth order polynomials 4-105402
- network theory, exactness and reliability (German) 4-62654
- network theory, sequential equilibrium of free networks (German) 4-62655
- Niue Island atoll, SW Pacific, volcanic core struct. from geophys. obs. 4-94035
- North Sea, geoid, gravity measurement anomalies and SEASAT sea surface heights 4-81840
- North Sea gravity field observations 4-81839
- oblateness, effect on artificial satellite orbits; coupling to exosphere drag effects 4-82375
- ocean surface circulation from satellite altimetry and geoid model anal. 4-67280
- oceanic lithosphere, cooling trends, geodetic data anal. 4-100508
- Pacific, geoid, gravity map, plate age and fracture zones 4-115331
- South Pacific geoid, satellite altimetry obs. 4-85606
- W Pacific margin, extensional basins form, mantle flow and gravimetric data anal. 4-82002
- plate tectonic related geoid undulations 4-100527
- plate tectonics, useful geodetic methods 4-100427
- POPSAT satellite, center of mass correction and statistical confidence 4-110034
- potential field data, 3-D automatic interpretation using Hilbert transforms 4-110289
- potential field data analysis, continuation between arbitrary surfaces 4-110039
- Pratt-Welker seamount chain, Gulf of Alaska, flexure and subsidence, geoid obs. 4-105523
- realistic projections of sphere or rotational ellipsoid fundamental eqns. 4-85603
- reference ellipsoid, formulae for great elliptic line 4-72479
- rheology, isostasy and eustasy conf., Stockholm (July-August 1977) 4-101580
- San Andreas fault near Monarch Peak, California, creep rate geodetic meas. 4-110116
- satellite altimetry, accuracy of altimetric surfaces 4-110022
- satellite Doppler tracking applications in geodesy and geophys. (Spanish) 4-94273
- satellite geodesy applications to geosciences 4-110023
- satellite in 12-hour orbit around Earth, orbit evolution (Russian) 4-115678
- satellite photography, statistical characts. of obs. (Chinese) 4-82242
- SEASAT altimeter measurements over English Channel, geoid and tides, error anal. 4-67490
- SEASAT satellite orbit determ. by laser ranging 4-82299
- SEASAT satellite orbit tracking over Europe 4-82298
- Singhbhum area, India, gravity field, geology, tectonic history 4-89907
- solid Earth tides, geodetic boundary value problem calc. 4-89873
- space laser applications in geophysics 4-110319
- space laser systems for geodetic appls. accuracy requirements 4-110322
- spherical harmonic analysis, coordinate system rotation effects 4-93991
- spherical harmonic model coefficients, for orders 15 and 30 4-93993
- subduction zone geoid anomalies and mantle rheology 4-115330
- subduction zone large-scale gravity anomalies indicating mantle convection 4-100526
- Sudan region, geoid shape 4-89872
- tectonic deformation meas. by photogrammetric method 4-82255
- tectonic displacement, topographic amplification, implications for geodetic meas. of strain changes 4-85642
- tectonic displacement meas. by satellite Doppler positioning method 4-72476
- tidal deformation (Chinese) 4-110548
- tidal evolution of Earth's gravit. field and figure, theory 4-105399
- tilt determ. from US levelling data base, characts. 4-110033
- Tokai region, Japan, vertical crustal movements and tectonic stress, levelling data anal. 4-81999
- TOPEX satellite project, end-to-end ground data system 4-77657
- Turkey, review of geodetic work in Turkey (German) 4-62656
- USSR Far East, mountain areas isostatic equilibrium 4-105529
- Valence hills, Hungary, gravity and geomagnetic anomaly interpretation 4-62728
- very long baseline radio interferometry 4-72765
- Wasatch Front, Utah, horizontal strain, geodetic obs., 4-85608
- geodetics see geodesy
- geolectricity see terrestrial electricity
- geography  
Cambro-Ordovician beds characts. in Italy, palaeogeographical relationships and struct. consequences (French) 4-72584
- Cretaceous and foreland paleogeography, obduction of Hokkaido Ophiolite during late Jurassic (French) 4-81981
- Cretaceous climate model sensitivity, geographic variables effect 4-72692
- Sea of Japan, palaeogeography from  $^{18}\text{O}/^{16}\text{O}$  foraminiferal tests 4-105598
- geology  
see also geomorphology; rocks; topography (Earth)
- Adamello complex, N Italy, country rock assimilation into magma body 4-62734
- central Adriatic Sea, sediments near Tremiti Islands indicating uplift 4-82030
- southern Africa, crustal evolution (book) 4-78052
- northeast Africa, Pan-African crustal accretion 4-77481
- NE Africa, Proterozoic crustal evolution from model Nd ages 4-89900
- NW Africa continental margin, geology (book) 4-78059
- African geology, conf., Nairobi, Kenya (Dec. 1982) 4-73141
- African-Adriatic promontory, geological and tectonic anal. (Italian) 4-81985
- Agua Blanca fault, Baja California, geology and seismology 4-94010
- Aigurande Plateau, French Massif Central, Pb isotopes indicating Upper Brioverian age (French) 4-81877
- Alabama Appalachians, polyphase Late Palaeozoic deform. 4-105516

**geochronology continued**

- Karoo volcanism onset in E Botswana, discovery of Early Jurassic pillow lavas and palynomorphs 4-100506
- SE Kerguelen, volcanic activity, chrono-spatial evolution and petrochemistry 4-81973
- Kerguelen plutonism, petrology, geochronology and geology 4-82052
- Komati Formation, South Africa, age of mag. remanence rel. to early Archaean geomag. field 4-94004
- S Kootenay Arc, SE British Columbia, geochronology and tectonic implications of magmatism and metamorphism 4-105473
- Ladinian-Carnian stage boundary, relation in Triassic sea level change 4-62812
- Laramide orogeny, chronology of subduction of aseismic ridge on Farallon plate 4-94063
- Long Island Sound, Connecticut, chronologies of sedimentary processes in sediments of FOAM site 4-100535
- Lower Rhine Basin, Germany, Plio-Pleistocene deposits, palaeomagnetism and biostratigraphy 4-110036
- Luan County, China metamorphic rock form., K-Ar isochronous age and geological significance (*Chinese*) 4-85640
- Lutzow-Holm Bay region, E Antarctica, tectonic and metamorphic history 4-81926
- Madeira, palaeomag. evidence for Early Cretaceous origin 4-105422
- magnetic reversal time scales, implications for lower mantle convection 4-85620
- Marie Byrd Land, Antarctica, Cretaceous volcanic rocks, palaeomagnetism and palaeopole position anal. 4-81963
- Marie Byrd Land, Antarctica, glacial and tectonic events, chronology recorded by rocks 4-82024
- marine fossil families, periodicity of extinctions rel. to extraterrestrial forces 4-72596
- mass extinctions, periodicity rel. to Sun's oscillation about galactic plane 4-72592
- mass extinctions due to cometary impacts, periodicity rel. to Sun's motion perpendicular to galactic plane 4-72591
- Mealy dykes, Labrador, petrology, chem. charact., age and tectonic events 4-94125
- Western Melville Peninsula, NW Territories, Canada, Precambrian geology 4-78068
- meteorite craters ages, evidence for periodic impacts on Earth 4-72595
- methods (book) 4-73182
- Michipicoten plutonic-volcanic terrain, Ontario, volcanism, tectonics evolution 4-94059
- Midlands, England, Wolstonian stage of British Pleistocene, age 4-72534
- Mount Isa, Queensland, geology of Proterozoic rift zone and implications for mineralisation 4-94117
- Mount Isa Inlier, Australia, batholiths geochemistry and age, implications for magmatism 4-94032
- Nevada, glacial chronology of Ruby Mountains-East Humboldt Range 4-94176
- west-central Nevada, palaeomag. assessment of oroflexural deform. 4-94128
- S New Zealand, overriding of Indian-Antarctica ridge rel. to migration of Late Cainozoic volcanism 4-94082
- N Nigeria, anorogenic ring complexes age migration 4-62753
- southeast Nigeria, Rb-Sr dating and age of Pan-African orogenesis 4-77485
- Nimmaroo Formation, Australia, late diagenetic history and products 4-94120
- Norilsk area, NW Siberian platform, comp. and age of crystalline basement and overlying sedimentary rocks 4-100514
- Normandy loess deposits, thermoluminescence dating 4-100510
- North America, plate motions correl. with continental tectonics during Laramide to Basin-Range period 4-94062
- SW North America, rel. to mid-Tertiary extensional orogeny 4-94129
- North Wadi Kareim area, Egypt, radioactivity distrib. correl. with age and geology 4-100559
- oceanic lithosphere, age rel. to lithosphere flexure seaward of ocean trenches 4-85653
- oceanic lithosphere, cooling trends, geodetic data anal. 4-100508
- oceanic lithosphere stability, with variable viscosity charact. time for amplification of disturbances 4-105492
- oceanic trench-seamount interaction, time-scale determ. via numerical simulation 4-105526
- oolitic goethite transformation to haematite, dating of transformation by palaeomagnetic study 4-62664
- W Oregon-Washington, volcano-tectonic evolution rel. to Cainozoic plate motions 4-94065
- W Pacific, depth anomalies over Mesozoic crust and age determ. 4-81911
- Central Pacific, Mn crust  $^{10}\text{Be}$  dating, implications for palaeocirculation determ. 4-85757
- W Pacific, submarine rocks, ages 4-81915
- palaeoclimate, evidence for enhanced atmospheric circulation over North America during Early Holocene 4-100712
- palaeoclimate (book) 4-95070
- palaeoclimatic change chronology at end of last glaciation 4-115562
- palaeomagnetism, physical model for palaeosecular variation 4-110041
- Pangano Nunatak and Hart Hills area, Antarctica geology 4-81943
- Patia Valley, SW Colombia, geochronology of basic rocks and emplacement 4-105506
- Pedroches Batholith, Spain, geochronology study and Pangaea break up 4-81884
- NE Peninsular Ranges, California, uplift from fission-track dating 4-94045
- Late Pleistocene climate at Marsworth, UK, evidence of two temperate episodes 4-89989
- Possession Island, Indian Ocean, volcanology, tectonics, geochemistry, geochronology and petrology 4-81974
- pottery age determination of thermoluminesc., method for determ. radioactive dose rate 4-82273
- Potwar Plateau, Pakistan, Pleistocene and Holocene sequences dating 4-62751
- Late Quaternary varved clay, remanent magnetism, stress-induced var. 4-110133
- Quebec, relation between dunes, fire and climate recorded in Holocene deposits 4-85753
- Queen Maud Land, Antarctica, Sr isotope studies of Ahlmann Ridge and Annandagstoppane 4-81927
- Querigut, France, granite-granodiorite complex genesis, recycling processes, Nd-Sr isotopic systematics 4-110096

**geochronology continued**

- radiocarbon dating in Antarctica, problems and significance 4-81954
- Rajasthan, India, Precambrian rocks geochronology and acid magmatism periods determ. 4-81900
- Rukui limestone, dating 4-105472
- Saharan Pan-African belt, Precambrian age of pre-tectonic magmatic suite (*French*) 4-77476
- Santa Rosa Mylonite Belt, uplift from fission-track dating 4-94045
- Santorini, volcanic eruptions and late Minoan civilisation fired destruction levels, archaeomagnetic dating 4-85647
- N Saskatchewan, Canada, Pb isotope composition in U deposits 4-115348
- N Saskatchewan, Canada, U/Pb geochronology of Midwest U deposit 4-115347
- sedimentation rates in Atlantic ocean, glacial to interglacial vars. from  $^{210}\text{Th}$  meas 4-110129
- sediments as historical record of heavy metals air pollution 4-100046
- Seychelles, granites and xenoliths, dating and parental magma mantle origin with crustal interactions 4-110102
- Shackleton Range, Antarctica, Rb-Sr ages and geological history 4-81937
- Shackleton Range, Antarctica, tectonics and Precambrian struct. stages 4-81938
- Shikoku Basin, Pacific, evolution rel. to high magnesian andesites in Setouchi volcanic belt, Japan 4-81970
- Singhbhum granite batholithic complex, India, geochemical evolution and struct. setting 4-81902
- Sivalik red beds, polarity transition stratigraphy and remanence lock-in times 4-110043
- sphere, fission-track temperature ages 4-100487
- stratigraphic correlation by means of ordinal scales 4-94041
- International Stratigraphic Scale, for Cainozoic 4-105495
- stratigraphy, unitary associations method, graph theory and computer algorithm appls. 4-94040
- northwest Sudan, geology of migmatite and metamorphic units 4-77480
- Sukinda Valley chromites, India, palaeomagnetism, ages and setting 4-77513
- tephra deposit dating by approximate methods 4-62993
- tephra deposit dating by radioactivity methods 4-62992
- tephra deposits in Iceland, tephrochronology by geochem. obs. 4-62748
- tephra layer dating by combined magnetostratigraphy and tephrochronology method 4-62994
- tephra layers as geochronological markers over long distances 4-62995
- Tertiary volcanism of Hoheifel, age and palaeomag. study 4-105419
- Tethys, European margin, distensional movements during Jurassic (*French*) 4-115354
- tidal evolution of Earth's gravit. field and figure, theory 4-105399
- topographic erosion, time const. rel. to flexural models of continental lithosphere 4-67189
- Transbaikial, USSR, Phanerozoic basite volcanism, comp. evolution 4-100515
- tree-ring chronology and dendroclimatology, average value of correlated time series 4-100665
- Trinity peridotite, California, USA, Nd-Sr isotope study and mantle evolution 4-89890
- Tulemalu dykes (Early Proterozoic), Northwest Territories, Canada, age of magnetisation and palaeomagnetism 4-105407
- Umnak Island, Aleutians, Alaska, geology and geochronology 4-72537
- SW United States, chronology of asthenospheric intrusion rel. to thermal regime of lithosphere 4-94058
- W United States, kinematics of plate convergence from Mesozoic struts. in western Cordillera 4-94064
- W United States, tectonic reconstructions from palaeomag. results from Sierra Nevada 4-93998
- W United States, tephrochronology and Quaternary geology 4-62749
- Valle Ricca Pits, Italy, Plio-Pleistocene deposits, palaeomagnetism and biostratigraphy 4-110036
- post-Variscan molasses, Catalanian Pyrenees, Spain, stratigraphy and ages (*French*) 4-105557
- N Vermont, USA, metamorphic schists of Ordovician and Devonian age 4-94023
- Vestfold Block, E Antarctica, Sr-Nd isotopes, lithology and crust evolution 4-81929
- Vesuvius samples, fission-track temperature ages 4-100487
- N Victoria Land, Antarctica, age of Bowers Supergroup 4-81933
- S Victoria Land, Antarctica, provenance and dating of glacial deposits 4-81955
- Villefranche-de-Rouergue fault, France, Tertiary sedimentary deposits evidence for fault motion (*French*) 4-100482
- Wadi Natash Volcanic series, Eastern Desert, Egypt, geology and geochemistry 4-115352
- Williston Basin, USA, mechanical and thermal model for tectonic evolution 4-94067
- Windmill Metamorphics, Casey area, Antarctica, geochronological study 4-81928
- Xigaze ophiolite, Tibet, magmatites and tectonites, Pb isotopic anal. and geochronology 4-110139
- Zacatecas, Mexico, mid-Tertiary felsic volcanism, rock dating and magma origin 4-110113
- $^{40}\text{Ar}$ - $^{39}\text{Ar}$  dating of basalt, containing incompletely degassed xenoliths 4-85764
- $^{10}\text{Be}$  activity in deep-sea sediments, temporal vars. over past 1 Myr 4-110128
- $^{10}\text{Be}$  in soil, concentrations and possible  $^{10}\text{Be}$  radioactive dating method 4-81880
- K-Ar dating of basic rocks, test of two alteration indices as predictors of Ar loss 4-110140
- Pb radioactive dating method, calc. of Pb isotope growth curves 4-90004
- U-Pb dating for case of common Pb with unknown isotopic composition 4-110285
- U-rich crystals, radiation damage using nuclear track and thermoluminescence methods 4-98130

**geodesic lenses** see *aspherical lenses; integrated optics; lenses*

**geodesy**

see also *gravity*

- Ada County, Idaho, USA, mapping by photogrammetric method 4-110025
- Ada County Project, Idaho, USA, photogrammetric survey 4-110026
- adjustment principle calc. method for set of observations 4-105403

- deasy continued  
adjustment theory, using tensor struct. applied to least-squares method 4-72474
- Alpine-Mediterranean region, geodetic models for monitoring regional kinematics 4-100425
- North America, combined correlation anal. of geophys. fields 4-72541
- Antarctic shelf ice, gravity meas. possibilities 4-72624
- Antarctica, gravity and geomagnetic studies between 45 and 65 degrees East 4-81959
- Asal-Ghoubbet rift, Djibouti, Africa, strain accumulation study 4-115380
- astrometric and geodetic reference systems, linking from space 4-72856
- NW Atlantic, gravimetric models and surface currents satellite remote sensing 4-67163
- SE Australia, crustal deformation from geodetic evidence? 4-89871
- Baja California, Mexico, geodetic obs. of fault motions 4-72483
- Benue Trough, SE Nigeria, tectonic and sedimentation history 4-77479
- S California, USA, regional deformation near Palmdale 4-72562
- Chattolance Baltimore Gneiss Dome, Maryland, USA, gravity survey 4-81834
- conference, Hamburg, W Germany (1983) 4-106108
- conference on geodesy, at Hamburg, West Germany (August 1983) 4-86111
- crust deformation, use of space/airborne laser ranging systems 4-110324
- datum development and positional errors 4-72484
- deformation anal. of geodetic network, use of pre-zero-epoch covariance matrix 4-72477
- deformations of an elastic Earth, book 4-86133
- distance meas. with Mekometer laser instrument, atmos. corrections and data reduction 4-89998
- Djibouti, satellite positioning obs. of tectonic displacements 4-72476
- downward continuation of gravity and geomag. data, solved as inverse theory 4-85802
- dynamic Earth geoid anomalies 4-110024
- earthquake fault associated gravity anomalies 4-81866
- Ekstrom Ice Shelf, strain meas. geodetic obs. (German) 4-72622
- Filchner-Ronne Ice Shelf, strain meas. geodetic obs. (German) 4-72622
- geodetic networks, numerically efficient soln. of second-order design problem 4-72478
- geoid heights and lithospheric stresses for a dynamic Earth 4-100495
- geoid one degree global models 4-72475
- geoid shape, correl. with seismic surface wave vels. and convection in mantle 4-100529
- geoid shape, effect of large-scale density inhomogeneities on gravity fields 4-62657
- geoid undulations from Doppler satellite positioning and gravimetric techniques, comparison 4-85607
- geoidal undulation patterns in NW Pacific Ocean, resemblance to free-air gravity anomalies 4-105397
- geopotential coefficients of order 29, determ. from orbit of satellite 1967-104B 4-105398
- geopotential field derivatives, computation procedure for coeffs. 4-85605
- global Positioning System (GPS) appl. to geodesy, estimation and large-scale multiple hypothesis testing 4-77656
- Global Positioning System (NAVSTAR) in differential mode for precise position determ. 4-72713
- Gorringe Ridge, North Atlantic Ocean, interpretation of geoid anomalies 4-67162
- GPS geodetic receiver system testing 4-72735
- gravitational field, modification of point mass model (Russian) 4-115332
- gravity and geomagnetic anomalies due to subsurface struct., computation method 4-85604
- gravity anomaly automatic fitting using 2-D models 4-67421
- gravity field models and the triple correlation function 4-81837
- gravity field represented by point mass system (Russian) 4-77443
- gravity inverse problem theory for multiple density boundary prospecting 4-100431
- gravity potential of buried object, 3-D Fourier transforms theory (Chinese) 4-62651
- Greece, Atalanti region, microgravity network, crustal movements and precursors to earthquakes 4-77440
- ground tilt, correl. with tectonic stress and earthquake occurrence 4-81998
- gyrotheodolite constant calculation from calibration measurements 4-85602
- Imperial Valley, California, 1940 earthquake rel. to vertical movements 4-94079
- inversion of geophysical data by least-squares techniques 4-67423
- isostatic model of Earth's shape 4-100428
- Izu Peninsula, Japan, geodetic strain obs. and tectonics (Japanese) 4-72480
- S Kanto District, Honshu, Japan strain buildup after 1923 Kanto earthquake 4-85630
- Karakorum gravity measurements 4-62652
- Kilauea volcano, Hawaii, eruption forecasting 4-85648
- Laksefjord Nappe, Finnmark, finite strain patterns generation and modification by progressive thrust faulting 4-110031
- laser altimetry by Starlette satellite, effects of orbital perturbations by ocean tides (Chinese) 4-82362
- laser ranging use 4-72765
- least squares collocation in digital terrain modelling 4-81836
- least squares method using tensor struct. approach 4-72474
- levelling system of new design 4-89999
- Los Angeles region, California, Earth model regional deform., seismic, tectonic and geodetic meas. 4-110032
- Louisiana-Mississippi, USA, modern uparching of coastal plain 4-115381
- Lutzw-Holm Bay, Antarctica, gravity, geomag. intensity anomalies and crust tilt 4-81841
- mantle convection, lag and related geoid anomalies and mantle struct. 4-105520
- mantle wave velocities anal. and correl. with heat flow and non-hydrostatic geoid 4-105488
- marine geoid, Seasat obs. of lithosphere flexure seaward of ocean trenches 4-85653
- matrix development of potential and attraction at exterior points rel. to inertia tensors 4-81832
- E Mediterranean, geodetic satellite laser ranging method for crustal motion 4-100770
- E Mediterranean, satellite laser tracking technique for geodynamics 4-100426
- Miura and Boso peninsulas, Kanto, Japan, geodetic survey obs. (Japanese) 4-72481
- geodesy continued  
Mount St. Helens, Washington, USA, seismicity and crust strain before May 1980 eruption 4-85649
- mountain isostatic equilibrium calc. method 4-105529
- Nankai Trough, SW Japan, earthquake deformation cycle 4-85629
- 3-D network adjustment method for spatial and gravity measurements 4-105401
- network adjustment model for long extended traverse nets and gyrotheodolite orientation meas. 4-85601
- network analysis, bivariate interpolation using triangular elements with fifth order polynomials 4-105402
- network theory, exactness and reliability (German) 4-62654
- network theory, sequential equilibrium of free networks (German) 4-62655
- Niue Island atoll, SW Pacific, volcanic core struct. from geophys. obs. 4-94035
- North Sea, geoid, gravity measurement anomalies and SEASAT sea surface heights 4-81840
- North Sea gravity field observations 4-81839
- oblateness, effect on artificial satellite orbits; coupling to exosphere drag effects 4-82375
- ocean surface circulation from satellite altimetry and geoid model anal. 4-67280
- oceanic lithosphere, cooling trends, geodetic data anal. 4-100508
- Pacific, geoid, gravity map, plate age and fracture zones 4-115331
- South Pacific geoid, satellite altimetry obs. 4-85606
- W Pacific margin, extensional basins form, mantle flow and gravimetric data anal. 4-82002
- plate tectonic related geoid undulations 4-100527
- plate tectonics, useful geodetic methods 4-100427
- POPSAT satellite, center of mass correction and statistical confidence 4-110034
- potential field data, 3-D automatic interpretation using Hilbert transforms 4-110289
- potential field data analysis, continuation between arbitrary surfaces 4-110039
- Pratt-Welker seamount chain, Gulf of Alaska, flexure and subsidence, geoid obs. 4-105523
- realistic projections of sphere or rotational ellipsoid fundamental eqns. 4-85603
- reference ellipsoid, formulae for great elliptic line 4-72479
- rheology, isostasy and eustasy conf., Stockholm (July-August 1977) 4-101580
- San Andreas fault near Monarch Peak, California, creep rate geodetic meas. 4-110116
- satellite altimetry, accuracy of altimetric surfaces 4-110022
- satellite Doppler tracking applications in geodesy and geophys. (Spanish) 4-94273
- satellite geodesy applications to geosciences 4-110023
- satellite in 12-hour orbit around Earth, orbit evolution (Russian) 4-115678
- satellite photography, statistical characts. of obs. (Chinese) 4-82242
- SEASAT altimeter measurements over English Channel, geoid and tides, error anal. 4-67490
- SEASAT satellite orbit determ. by laser ranging 4-82299
- SEASAT satellite orbit tracking over Europe 4-82298
- Singhbhum area, India, gravity field, geology, tectonic history 4-89907
- solid Earth tides, geodetic boundary value problem calc. 4-89873
- space laser applications in geophysics 4-110319
- space laser systems for geodetic appls. accuracy requirements 4-110322
- spherical harmonic analysis, coordinate system rotation effects 4-93991
- spherical harmonic model coefficients, for orders 15 and 30 4-93993
- subduction zone geoid anomalies and mantle rheology 4-115330
- subduction zone large-scale gravity anomalies indicating mantle convection 4-100526
- Sudan region, geoid shape 4-89872
- tectonic deformation meas. by photogrammetric method 4-82255
- tectonic displacement, topographic amplification, implications for geodetic meas. of strain changes 4-85642
- tectonic displacement meas. by satellite Doppler positioning method 4-72476
- tidal deformation (Chinese) 4-110548
- tidal evolution of Earth's gravit. field and figure, theory 4-105399
- tilt determ. from US levelling data base, characts. 4-110033
- Tokai region, Japan, vertical crustal movements and tectonic stress, levelling data anal. 4-81999
- TOPEX satellite project, end-to-end ground data system 4-77657
- Turkey, review of geodetic work in Turkey (German) 4-62656
- USSR Far East, mountain areas isostatic equilibrium 4-105529
- Velence hills, Hungary, gravity and geomagnetic anomaly interpretation 4-62728
- very long baseline radio interferometry 4-72765
- Wasatch Front, Utah, horizontal strain, geodetic obs. 4-85608
- geodetics see geodesy
- geolectricity see terrestrial electricity
- geography  
Cambro-Ordovician beds characts. in Italy, palaeogeographical relationships and struct. consequences (French) 4-72584
- Cretaceous and foreland paleogeography, obduction of Hokkaido Ophiolite during late Jurassic (French) 4-81981
- Cretaceous climate model sensitivity, geographic variables effect 4-72692
- Sea of Japan, palaeogeography from  $^{18}\text{O}/^{16}\text{O}$  foraminiferal tests 4-105598
- geology  
see also geomorphology; rocks; topography (Earth)
- Adamello complex, N Italy, country rock assimilation into magma body 4-62734
- central Adriatic Sea, sediments near Tremiti Islands indicating uplift 4-82030
- southern Africa, crustal evolution (book) 4-78052
- northeast Africa, Pan-African crustal accretion 4-77481
- NE Africa, Proterozoic crustal evolution from model Nd ages 4-89900
- NW Africa continental margin, geology (book) 4-78059
- African geology, conf., Nairobi, Kenya (Dec. 1982) 4-73141
- African-Adriatic promontory, geological and tectonic anal. (Italian) 4-81985
- Agua Blanca fault, Baja California, geology and seismology 4-94010
- Aigurade Plateau, French Massif Central, Pb isotopes indicating Upper Brioverian age (French) 4-81877
- Alabama Appalachians, polyphase Late Palaeozoic deform. 4-105516

## geology continued

- Alabama Piedmont, USA, amphibolite petrography, geochem. and tectonic significance 4-94024  
 SW Alaska, relations between plate motions and Late Cretaceous to Palaeogene magmatism 4-94131  
 S Alpine tectonic deformation (*Italian*) 4-81982  
 W Alps, profiles and tectonic struct. 4-85665  
 Alps, West and Central, mechanistic view of thrust tectonics 4-94057  
 Amnin massif, Cottian Alps, diversity of breccia-rich series (*French*) 4-115398  
 W Anabar area, USSR, paragenesis of rocks and facies and palaeogeographic features 4-105497  
 Anadarko Basin, S Oklahoma, USA, thermal and tectonic evolution 4-105504  
 Central Andes, plate tectonics, volcanism and continental crust 4-105530  
 Andes volcanic rock petrogenesis, geochemical considerations 4-62741  
 SW Angola, vertical crust movement from Pleistocene marine deposits 4-115370  
 Annual Review of Earth and Planetary Sciences, Vol.12 (book) 4-101586  
 Antarctic Earth science, conf., Adelaide, Australia (Aug. 1982) 4-78045  
 Antarctic Earth science remote sensing using Landsat 3 RBV images 4-82312  
 East Antarctic metamorphic shield, Precambrian geological evolution, review 4-81920  
 N Antarctic Peninsula, evolution of Late Mesozoic sedimentary basins 4-81946  
 Antarctic Peninsula, Rb-Sr constraints on basement rock ages 4-81949  
 Antarctic Peninsula region, age of post-Gondwana calc-alkaline volcanism 4-81947  
 West Antarctica, geomag. anomalies and subglacial geology 4-81853  
 Antarctica, gravity and geomagnetic studies between 45 and 65 degrees East 4-81959  
 Antarctica, major structural provinces and metallogenic provinces 4-81951  
 Antarctica, metallogenic provinces 4-81950  
 Antarctica, petroleum prospects and geology and geophysics studies 4-81952  
 Antarctica between Ellsworth Mts. and Antarctic Peninsula, subglacial morphology 4-81945  
 Antarctica Peninsula, active plate margin geological history 4-82021  
 E Antarctica-W Antarctica boundary region, geology and tectonics 4-81930  
 antineutrino production by Earth-interior and possibility of observing them 4-94136  
 Appalachian orogen, Alabama, geodynamic transect geology 4-85677  
 Appalachian orogen, N Newfoundland, geotransverse tectonic characts. 4-85668  
 S Appalachian Piedmont, geophysical anomalies along strike rel. to crustal struct. and tectonics 4-93990  
 Southern Appalachian Piedmont, USA, gabbro-metagabbro assoc. geology 4-94025  
 Appalachian Plateau (New York and Pennsylvania), surface morphology on cross-fold joints of sedimentary rocks 4-94116  
 N Appalachian traverses, Canada, geology and tectonic evolution 4-85675  
 S Appalachians, USA, mafic rock geology, review 4-90319  
 Southern Appalachians, USA, mafic-ultramafic complex geology 4-94027  
 Appalachians of USA, mafic complex origin, isotope geochem. evidence 4-94021  
 Arabian platform, regional joint sets as indicators of intraplate processes 4-94132  
 Archaean-Proterozoic boundary, geological characts. 4-82048  
 Pre-Archaeon times, existence of surface water, palaeoclimate and plate tectonics 4-105564  
 Arctic Ocean, 65 Myr sediment record from Alpha Ridge 4-115388  
 ash-flow tuffs of Macusani, Peru, geochem. of peraluminous tuffs (*French*) 4-72556  
 Ashe Metamorphic Suite, N Carolina, USA, metamorphism and tectonic history 4-94022  
 Central Asia, surface relief and orogenesis rel. to lateral inhomogeneities of upper mantle 4-100505  
 assimilation of country rock into intruded magma body 4-62734  
 North Atlantic, explosive volcanism in Cainozoic and marine sediments 4-62759  
 Atlantic continental slope off USA, seafloor morphology and sediment ages 4-67210  
 Mid-Atlantic Ridge, initiation and collapse of active circulation in hydrothermal system 4-85670  
 Avalonian terrain of Rhode Island region, USA, geology and tectonic characts. 4-85676  
 W Baikal area, USSR, interruptions in Riphean (Precambrian) sedimentation 4-105494  
 Baikal megasearch, USSR, overthrust struct., form. mechanism 4-100567  
 bauxite deposits in S America, Africa, India, formed in Early Tertiary 4-77483  
 Bay of Islands ophiolite complex, Newfoundland, Canada, geology 4-115358  
 Bay of Islands ophiolite suite, mag. props. rel. to magnetisation of oceanic crust 4-85673  
 Belize barrier and atoll reefs, Late Quaternary history 4-67211  
 Benue Trough, SE Nigeria, tectonic and sedimentation history 4-77479  
 Benue-Chad Basin, Cretaceous rift valley system 4-115371  
 Bishop Tuff, California, USA, Nd, Sr, O isotope study of zoned volcanic rocks 4-89891  
 Blake River Group, Abitibi volcanic belt, Quebec, geochemistry and geology 4-72539  
 Blue Ridge Province, N Carolina, USA, compositional layering of Precambrian rocks 4-67188  
 book, general introduction 4-58602  
 borehole in salt, deformation observations 4-64200  
 E Botswana, discovery of Early Jurassic pillow lavas and palynomorphs in Karoo Sequence 4-100506  
 Briançonnais Carboniferous, subsidence of NS groove (*French*) 4-77473  
 Bristol Channel area, SW Britain, seismic study of deep geological struct. 4-110141  
 Britain, provenance and crustal residence ages of sediments in rel. to palaeogeographic reconstructions 4-89895  
 British Isles, geological evolution, book 4-58597  
 British Tertiary Volcanic Province, crustal contamination and granite problem 4-62745

## geology continued

- Broken Hill District, regional magnetic and gravity field characteristics and interpretation 4-62814  
 Broken Hill Field geology, mining and metallurgy, conference, Broken Hill, NSW, Australia (July, 1983) 4-58562  
 Buchan area, Scotland, Caledonides, major shear zones and autochthonous Dalriadan 4-110143  
 Bureau of Mineral Resources (BMR), 11th. symposium, Canberra, Australia (1982 May 4 to 5) 4-90282  
 Caledonian intrusion of Scotland and N England, geochem. and magmatism sources 4-62743  
 central California, correl. between geological record and computed plate motions 4-94127  
 Cambro-Ordovician beds characts. in Italy, palaeogeographical relationships and struct. consequences (*French*) 4-72584  
 Campanian Apennines, Italy, neotectonics and crust struct. (*French*) 4-81878  
 Canada, Lithoprobe seismic and drilling project to study crust 4-11557  
 Cape Fold Belt, South Africa, geodynamics, review 4-85660  
 carbonate sediments and rocks from deep-sea, calcite fabric and acoustic anisotropy 4-82047  
 western Caribbean, marine tephra sediment chronology 4-62795  
 Northern Carpathians, geological evolution of flysch basin 4-89905  
 Carrara Range region, N.T., Australia, preserved Proterozoic landform 4-94038  
 Catalonian Pyrenees, Spain, post-Variscan molasses, stratigraphy and age (*French*) 4-105557  
 Caucasus Alpine cycle; geology, crustal movements and magmatism evolution 4-85666  
 Chara sheet nappe zone, Irtysh-Zaisan fold region, tectonic struct. 4-77494  
 Chuckanut Formation, NW Washington, USA, stratigraphy, age and palaeogeography 4-62727  
 S Chukchi Sea, oil and gas content and geological struct. 4-100575  
 clastic sedimentary sequences, quantification in time series anal. 4-94042  
 clay minerals, conf., London, England (Nov. 1983) 4-95048  
 clinometer for teaching purposes 4-101606  
 coal measure rocks of Pennsylvania, USA, rock elec. props. and radiation attenuation props. 4-72582  
 Columbia Plateau, Washington, palaeomag. study of post 12 Myr clockwise rot. 4-94130  
 computer techniques in geology (book) 4-85793  
 conglomerate pebble previous strain history from pebble microstructure 4-62813  
 continental arches in eastern USSR 4-100563  
 continental tectonic geology, use of earthquake studies 4-72552  
 continental tectonics correl. with plate motions, Laramide orogeny to Basin and Range province 4-94062  
 Corella Formation, Mount Isa Inlier, Queensland, stratigraphic review 4-94118  
 cosmic spherules in deep-sea sediments, with Pt group nuggets 4-85900  
 Coso Range, California, ground mag. survey rel. to faulting and hydrothermal alteration 4-85618  
 crack growth during unroofing of crustal rocks 4-94102  
 subcritical crack growth in geologic materials, review 4-94096  
 crack growth in rocks and influence of aqueous environment 4-94099  
 cracks in glasses and ceramics, growth influenced by chem. environment 4-94095  
 cratonization of continental crust throughout geologic time 4-105493  
 cretaceous dyke rocks, Pyrenees, geochemical characts. and relation to Sillon Houlier (*French*) 4-82043  
 Cretaceous-Tertiary boundary, sharp boundary or gradual transition 4-72589  
 Cretaceous-Tertiary boundary, shocked mineral evidence for impact 4-110149  
 Cretaceous-Tertiary boundary geochem. at York-Canyon, New Mexico, USA 4-89892  
 Cretaceous-Tertiary boundary impact, end-Cretaceous brachiopod extinctions in chalk of Denmark 4-72598  
 Cretaceous-Tertiary boundary sites, nonmarine, Raton Basin, geological framework 4-72588  
 Cretaceous/Tertiary boundary clays, Ir-rich layer in Bidart section, France 4-105554  
 Crimean continental slope, geology of lower Cretaceous dredged rocks 4-94052  
 crust stress field changes due to hydraulic pressure applied to a borehole (*Chinese*) 4-85678  
 Daldyn kimberlite field, USSR, struct., comp. and principal stages of form. 4-100565  
 Damara orogen, model 4-85661  
 deep fault zones, fluid regimes, geological evidence 4-94072  
 Deer Lake basin, Newfoundland, Canada, gravity and magnetic interpretation 4-62653  
 desert region bedrock imaging below sand layer, by satellite radar method 4-100793  
 Late Devonian mass extinction horizon, no geochemical evidence for asteroid impact 4-62811  
 diamond origin from old enriched mantle and age of encapsulated garnet 4-94050  
 Dickenson gold mine, Red Lake, Ontario, metamorphism, mineralisation and alteration 4-62725  
 Dinantian anhydrite form., Hercynian domain, tectonics, palaeogeography (*French*) 4-82044  
 diopside, mineral elastic const. at pressures up to 2 GPa 4-72577  
 Donnybrook Anticline, Australia, seismic-gravity interpretation and tectonic settings 4-94121  
 Earth surface deformation approximation from long buried kinked cracks or intrusive body, simple method 4-94283  
 East Pacific Rise intersection with Tamayo Transform, tectonics and geology 4-67205  
 EFe oil shale deposit, S Israel, geostatistical thickness analysis 4-94134  
 southwest Egypt, geology of migmatite and metamorphic units 4-77480  
 Egypt, hydrocarbon generation and prospects in Western Desert 4-77482  
 Egypt and Sudan, bedrock below sand layer in desert, satellite radar observations 4-100793  
 Eiao Island, Marquesas Archipelago, rock sample petrography and geochemistry (*French*) 4-81875  
 El Salvador, Quaternary tephra and volcanic eruptions 4-62755  
 Ellsworth Mts., W Antarctica, structural and metamorphic history 4-81944  
 encyclopedia (book) 4-95078

## geology continued

- Enderby Land, Antarctica, geological history of Napier Complex 4-81921
- Enderby land, Antarctica, metamorphism of Napier Province 4-81924
- NW Europe continental shelf, petroleum geology, conf. at London, England (March 1980) 4-101579
- evolution of structures formed by vertical movements, mathematical model 4-100504
- Eye-Dashwa pluton, Ontario, Canada, geology of radioactive waste disposal site 4-81919
- Fari'a Anticline, structural evolution in Central Israel 4-94068
- fault zone modifications due to fracturing, water circulation and chem. alteration 4-110082
- felsic magmas, extreme fractionation through liq.-state diffusion or fractional crystallisation 4-67217
- Fiji, oceanic island arc magma origin, isotope geochemical evidence 4-89894
- foredeep basins of Apennine and Carpathian Mountains, flexure of continental lithosphere 4-72563
- Forsyth area, Queensland, Australia, heavy metal mineralisation survey by helicopter 4-94037
- Freemans Cove volcanic suite, Bathurst Island, petrochemistry and tectonic setting rel. to rifting 4-94124
- French Alps (Briançonnais zone), high press.-low temp. metamorphic evolution 4-81888
- Fyfe Hills-Khmara Bay region of Enderby Land, Antarctica, geology 4-81922
- gas flow through cracked rock strata, theory 4-100570
- gas in rock inclusions, N<sub>2</sub> and H<sub>2</sub>O and influence on estimated mineralization press. and temperature 4-105562
- Gavarnie nappe, France, struct. and thrust sheets emplacement ages 4-105470
- Gebel El Mueilha, Egyptian Central Eastern Desert, crust radioactivity and lineaments 4-77486
- general laws 4-100569
- George V continental margin, Antarctica, marine geology and glaciology 4-82035
- Georgia Inner Piedmont, scale of Sr isotopic diffusion during post-metamorphic cooling of gneisses 4-67216
- glacial geology for engineers and Earth scientists, book 4-58596
- Grado lagoon, N Adriatic Sea, origin and development 4-82029
- Gran Paradiso, Italian Alps., hectometric sheath folds (French) 4-82045
- granite, orbicular, of French Massif Central, age determ. (French) 4-105555
- granitoid magma origin and influence of mantle 4-105498
- graywacke, petrofabrics tests of viscous folding theory 4-89915
- Great Barrier Reef, inaugural conference, Townsville, Australia (1983 August 29 to September 2) 4-90284
- Great Barrier Reef, rainfall and river runoff record in coral fluorescent bands 4-105673
- West Greenland, geochronology of Akilia association and Isua supracrustal belt 4-81883
- Guatemala, Quaternary tephra and volcanic eruptions 4-62755
- Gundah Complex, New England Fold Belt, Australia, tectonic melange form. 4-105471
- Haddat Ash Sham sedimentary sequence, Saudi Arabia, primary sedimentary struct. deposition 4-82046
- Heard and McDonald islands, Indian Ocean, volcano-tectonic evolution and petrology 4-81972
- Hell Creek area, Montana, stratigraphy of terminal Cretaceous extinctions compatible with catastrophe 4-72587
- helvetic thrust belt of Switzerland, crustal strain partitioning 4-67184
- Hercynian Europe, Late Palaeozoic plate and intraplate processes 4-105532
- Herring Bay and Commonwealth Bay, Antarctica, geochronology, petrology and tectonics 4-82016
- Highland Border Fracture Zone, Scotland, ophiolite rock tectonic history 4-89904
- NW Himalaya (N Pakistan), <sup>39</sup>Ar/<sup>40</sup>Ar ages of Alpine tectonometamorphic events 4-94043
- N Himalayan foredeep, sequential structural disruption in late-Cainozoic 4-115383
- Ibero-Armorican Variscan arc, W Europe, geotransverse characts. 4-85664
- Iceland, tephra layer 'a' due to Kverkfjöll 1477 AD eruption 4-62761
- ignimbrite eruptions, two-stage model rel. to caldera form. 4-105512
- ignimbrite facies model for large explosive silic eruptions 4-62766
- impact theory of mass extinctions, evidence from invertebrate fossil record at Cretaceous-Tertiary boundary 4-72597
- impacts of large asteroids and comets on Earth, geological implications, conference, Snowbird, Utah (1981 October 19 to 22) 4-100577
- E Indonesia collision zone, tectonic, bathymetric, seismic, volcanic and paleomagnetic features 4-82012
- NE Iowa, USA, geology and erosion of Palaeozoic Plateau area 4-77491
- Iowa, USA, geology of Driftless Area, conf., Decorah, IA, USA (April 1983) 4-73149
- NE Iowa, USA, karst development in Palaeozoic rocks 4-77518
- N Irian Jaya, melange production through shale diapirism in accretionary terrains 4-72586
- Irtysk lineament, USSR, structural metamorphic zoning 4-115362
- island arc magma sources, geochemical study 4-62740
- Italy continental shelf next to Tyrrhenian Sea, tectonic struct. from seismic obs. 4-115351
- Ivrea Zone, NW Italy, amphibolites, chem. comp., petrogenesis and tectonic anal. 4-110146
- Japan, tephrochronology and Quaternary studies 4-62750
- Jurassic volcanism, Aspro Vrissi unit, Greek Macedonia (French) 4-77499
- kaersutite, from New Zealand and USA, inert gas, H<sub>2</sub>O and C isotope geochemistry 4-105477
- South Karakoram synclinorium, geology and tectonic development 4-62723
- W Karakorum, Pakistan, geological struct. and tectonics 4-62722
- Karakorum and Kashmir Himalayas, geology and tectonics 4-62720
- western Kenya, kimberlite pipes in greenstone belt 4-77444
- Kerguelen plutonism, petrology, geochronology and geology 4-82052
- kimberlites from USA and S Africa, element distrib. in perovskite 4-105480
- Ko-Osaka group of Nara City, Japan, Plio-Pleistocene stratigraphy (Japanese) 4-105561
- Kohistan island arc, N Pakistan, geological evolution 4-62721

## geology continued

- komatiite lava emplacement, cooling and spinifex texture development 4-72558
- S Kootenay Arc, SE British Columbia, geochronology and tectonic implications of magmatism and metamorphism 4-105473
- Krakatau, 1883 eruption and effects (book) 4-101587
- Labrador, Canada, Grenville lithotectonic regions and with Sweden 4-115349
- Lachlan Fold Belt, SE Australia, source rocks of granites 4-62742
- Ladinian-Carnian stage boundary, relation in Triassic sea level change 4-62812
- Lake Malawi, Africa, structural evolution 4-62732
- Laramide orogeny, magmatic lull assoc. with subduction of aseismic ridge on Farallon plate 4-94063
- last interglacial ocean study by CLIMAP project 4-77548
- palaeo-latitude determination technique using vertical drill core samples 4-100821
- Lawn Hill Platform Cover, NW Queensland, geological evolution, tectonic style, and economic potential 4-94119
- Lebanon-Syria area, geologic interpretation of SIR-A radar obs. from space (French) 4-62965
- Lesser Antilles, pyroclastic flows and surges 4-62764
- Lesser Antilles arc, marine tephra deposits and explosive volcanism 4-62758
- Limousin, France, Late Carboniferous leucogranites and Himalayan model (French) 4-105558
- lithospheric flexure due to thrust loading, sedimentologic effects 4-100532
- Lorraine coal basin, France, appl. of method for quantifying deform. of given faulted volume (French) 4-105556
- Louisiana continental shelf, USA, gas deposits extent 4-110103
- Lower Palaeozoic of Middle East, Africa and Antarctica, book 4-63415
- Luan County, China metamorphic rock form., K-Ar isochronous age and geological significance (Chinese) 4-85640
- Lutzow-Holm Bay region, E Antarctica, tectonic and metamorphic history 4-81926
- Lutzow-Holm Bay region, E Antarctica, tectonic history and relevance to Gondwanaland 4-82015
- Madeira, palaeomag. evidence for Early Cretaceous origin 4-105422
- magma chamber convection with stagnant layer at bottom 4-62810
- magma chamber evolution fluid dynamics, review 4-58606
- magma chamber location techniques, review 4-58605
- magma genesis, geochemical indications 4-62736
- magma source identification for basaltic rocks, geochem. aspects 4-62735
- magma source identification isotope geochemistry, review 4-58607
- magma sources of crust rocks, constraints imposed by experimental petrology 4-62733
- Mahabaleswar area, Deccan Traps, India, flood basalt, magma origin 4-62738
- Maine Appalachians, USA, Acadian synorogenic mafic intrusions 4-94026
- uppermost mantle along midocean ridge, mineralogical variability 4-105478
- marine fossil families, periodicity of extinctions rel. to extraterrestrial forces 4-72596
- marine geology, morphology of continental margin off W Provence, France (French) 4-105540
- marine geology, tectonic model for ridge-transform-ridge plate boundaries 4-94081
- marine geology rel. to ocean bottom seismic noise, experimental study 4-105458
- marine sediment thermoluminescence profile showing Sun's 11 year activity cycle 4-110131
- mass extinction of species by periodic comet showers, role of solar companion star 4-72594
- mass extinctions, periodicity rel. to Sun's oscillation about galactic plane 4-72592
- periodic mass extinctions, role of distant solar companion star 4-72593
- mass extinctions due to cometary impacts, periodicity rel. to Sun's motion perpendicular to galactic plane 4-72591
- Mayor Island volcano, New Zealand, peralkaline ignimbrite sequences 4-62762
- McArthur Basin, Australia, struct., trends and magnetotelluric profiles 4-93996
- Mealy dykes, Labrador, petrology, chem. characts., age and tectonic events 4-94125
- Mediterranean, continental margin of Israel, bathymetry, crust struct., seafloor topography 4-72567
- Mediterranean region, deep sea tephra deposits and Quaternary volcanism 4-62757
- eastern Mediterranean Sea, tephra sediment distrib. and redeposition 4-62794
- Western Melville Peninsula, NW Territories, Canada, Precambrian geology 4-78068
- Mesozoic geology of the world, book 4-73187
- Messinian compression, tectonics, Rif, Morocco (French) 4-77500
- metalogenic maps using new realistic form 4-94247
- meteorite craters ages, evidence for periodic impacts on Earth 4-72595
- microstructures and fabrics due to rock deformation, conf., Zurich, Switzerland (August-September 1982) 4-63382
- midocean basaltic glass C isotope composition and origin 4-105476
- migratory bird, transequatorial, mag. orientation and mag. sensitive material 4-72276
- mine geology, design and survey applications of computer graphics 4-62815
- mineralogy encyclopaedia 4-95087
- minerals in hydrothermal environment, point defect chemistry and deformation 4-94092
- Minnelusa sands hydrocarbon deposits, Wyoming, USA, seismic exploration 4-109715
- Mirny kimberlite field, USSR, deep seismic sounding studies 4-100513
- Moine thrust zone, NW Scotland, Assynt region tectonics 4-67186
- Mongolia, genetic features of Vendocambrian ophiolites 4-100562
- Morrow formation, New Mexico, USA, seismic profiling of natural gas deposits 4-100457
- Mount Isa, Queensland, geology of Proterozoic rift zone and implications for mineralisation 4-94117
- Mozambique Belt, N Tanzania, petrochemistry of geotectonic evolution 4-77475
- Mozambique Channel, sedimentary cover struct. 4-94054

## geology continued

- Mugodzhir region of Urals, parallel dike intrusion, rock magnetism study 4-100503
- Mukaiyama volcano, Nii-jima Island, Japan, base surge deposits 4-62765
- Nakagusuku Bay of Okinawa-jima, sonic survey 4-82027
- Nanling region, China, granitic bodies and crust transform., petrochemistry NSF triangular diagram (*Chinese*) 4-72710
- Napier and Rayner complexes, Enderby Land, Antarctica, metamorphism and tectonism 4-81923
- W Nazca plate, dredged basalts and E Pacific Rise evolution 4-81988
- neutrino tomography of Earth interior, feasibility of method 4-72721
- neutron occurrence in Earth crust, of cosmic ray and radioactivity origin 4-110142
- west-central Nevada, palaeomag. assessment of oroflexural deform. 4-94128
- New Caledonia, geological characts. (*French*) 4-94126
- S New Zealand, overriding of Indian-Antarctica ridge rel. to migration of Late Cainozoic volcanism 4-94082
- New Zealand, pyroclastic studies of Taupo Volcanic Zone 4-62760
- New Zealand, subduction regression and volcanism oceanward migration 4-85657
- central Nigeria, geological interpretation of Landsat images 4-77478
- SE Nigeria, hydrology and chemistry of water resources of Agwata area 4-115466
- SW Nigeria, metavolcano-sedimentary sequence east of Ife and Ilesha and metal deposits 4-115353
- southeast Nigeria, Rb-Sr dating and age of Pan-African orogenesis 4-77485
- eastern Nigeria, upper mantle character inferred from ultramafic xenoliths 4-77484
- Nimmaroo Formation, Australia, late diagenic history and products 4-94120
- Nordvik dome, Yuryung-Tumus peninsula, USSR, Devonian form. geology 4-77515
- Norilsk area, NW Siberian platform, comp. and age of crystalline basement and overlying sedimentary rocks 4-100514
- SW North America, rel. to mid-Tertiary extensional orogeny 4-94129
- North Himalayan Belt, Tibet, metamorphism and deformation 4-110101
- North Sea basin, Holocene sedimentation, book 4-86134
- Northwest Territories, Canada, palaeomagnetism of Tulemalu dykes 4-105407
- Norwegian Caledonides, detect. of coesite in clinopyroxene and implications for geodynamics 4-105560
- ocean bottom sedimentation due to deep-sea storms 4-77504
- oceanic basalt geochemistry in vicinity of transform faults 4-105479
- Oceanographer Transform area of Atlantic, geology 4-67194
- oil and gas reserves in recoverable deposits, calculation 4-105093
- oil fields, formulation of geological problem of geophysical regionalisation 4-100827
- oil flow underground, book 4-67904
- oil or water flow in neighborhood of a drill-hole 4-72585
- Omsukchan basin, NE, USSR, struct. and geological nature 4-115361
- NW Ontario, Canada, gravity profile across English River Subprovince 4-72482
- oolitic goethite transformation to haematite, dating of transformation by palaeomagnetic study 4-62664
- ophiolite rock formation, origin from oceanic crust of island arcs 4-105502
- ophiolite rock origin, importance of magma in forearcs 4-105503
- W Oregon-Washington, volcano-tectonic evolution rel. to Cainozoic plate motions 4-94065
- orogenic belt profiles (book) 4-82602
- orogenic granitoids, French Hercynian, typology (*French*) 4-77472
- orogeny, theories and petrology (book) 4-63430
- Orville Coast and E Ellsworth Land, Antarctica, geology and plate tectonics 4-82017
- SW Pacific porphyry Cu deposits, geochem. of submarine formation and uplift 4-81887
- East Pacific Rise, hydrothermal vents and sulphides, geological study 4-105538
- E Pacific Rise, submarine hot springs, heat and water flow rate obs 4-105537
- E Pacific Rise, sulphide deposit accumulation rate in hot springs area 4-105537
- Pamirs and S Tien Shan, crust struct. and tectonics 4-62719
- Pamirs Syntaxis poorly correlated with surface geology and orogenic belts 4-62776
- Pamirs-Himalayas syntaxis, geological lineaments seen by LANDSAT 4-62724
- Pangano Nunatak and Hart Hills area, Antarctica geology 4-81943
- Pas-de-Calais coal basin, Hercynian direct faults, dextral wrenchings (*French*) 4-100530
- Patia Valley, SW Colombia, geochronology of basic rocks and emplacement 4-105506
- Pedroches Batholith, Spain, geochronology study and Pangaea break up 4-81884
- Permian island arc in eastern Klamath, lava flows and pyroclastic layers (*French*) 4-82042
- S Peru, Pb isotope study of magma-crust interaction in Andes 4-105475
- petroleum and gas prospecting in Oklahoma, USA, by soil gas radioactivity method 4-110104
- Philippine Sea island arcs, magmatic evolution and tectonics 4-81969
- Phyllites nappes, S Peloponnese, Greece, Alpine metamorphism and deform. geodynamic implications 4-62731
- Pine Creek Geosyncline, Australia, realistic metallogenic map 4-94247
- Pleistocene sediments of Arctic and N Canada, correlation of marine and continental glacial sediments 4-115335
- podzolised sand planes use for palaeoclimatic indicators for weathered cratons 4-110275
- Poodyea Formation, Georgina Basin, Australia, possible Tertiary fluvial unit 4-94122
- Port Hacking estuary, Sydney, Australia, bedrock depth and sediment geology 4-77498
- Portuguese margin, diapiric intrusion of Caidas da Rainha and Jurassic halokinetic movement (*French*) 4-105559
- Possession Island, Indian Ocean, volcanology, tectonics, geochemistry, geochronology and petrology 4-81974
- Precambrian granitoid rocks, origin of magma 4-62737
- Prince Olav Coast, Earth Antarctica, geology and petrology 4-81925
- Proterozoic landforms preserved in Carrara Range region, Australia 4-94038

## geology continued

- pyroclastic deposit terminology 4-62769
- quartz, O diffusion between quartz and surrounding water, laboratory exps. 4-94093
- quartz, O self-diffusion under hydrothermal conditions 4-94094
- quartz rock, flow strength rel. to grain size, press. effects, H<sub>2</sub>O content 4-94111
- quartzite, deformation props. influenced by Na content 4-94110
- quartzite, petrofabric tests of viscous folding theory 4-89915
- quartzite, plasticity props. altered by water content 4-94109
- Queen Maud Batholith, central Transantarctic Mts., geology and Ross Orogeny 4-81936
- Queen Maud Land, Antarctica, Sr isotope studies of Ahlmann Ridge and Annandagstoppane 4-81927
- radioactive waste, geological disposal, thermal loading effects on granite, clay and salt 4-83176
- radioactive waste disposal, granite mine, hydrogeology and heat effect 4-83169
- radioactive waste disposal, site evaluation, geotechnical research 4-83171
- radionuclide transport in geologic media, math. models, INTRACOIN comparison 4-83203
- Rainy Lake region, Ontario, Canada, geochem. of mantle-derived Archean rocks 4-94051
- Rajasthan, India, Proterozoic Delhi and pre-Delhi rock groups. struct. history 4-82050
- Ramshorn Peak area, Idaho-Wyoming thrust belt, United States, fault related folding 4-105517
- remote sensing techniques 4-115613
- rock porosity meas. technique for in-situ rocks, EM tomography method 4-110292
- rock props. influenced by water, conf., Carmel, California, USA (June 1982) 4-90289
- rockbursts in mines and tunnels, conf., London, England (October 1983) 4-58555
- rocks, extensional deformation due to crack growth 4-94103
- E Rouergue, French Massif Central, thrust tectonics and metamorphics (*French*) 4-81876
- Saharan Pan-African belt, Precambrian age of pre-tectonic magmatic suite (*French*) 4-77476
- salt geotechnical behaviour under radwaste repository conditions 4-83180
- San Andreas fault zone materials, California, USA, geological model 4-110110
- N Saskatchewan, Canada, Pb isotope composition in U deposits 4-115348
- N Saskatchewan, Canada, U/Pb geochronology of Midwest U deposit 4-115347
- Saskatchewan, evidence for Proterozoic plate margin from crustal elec. cond. meas. 4-105406
- Scandinavian Caledonides, geotransverse characts. 4-85663
- Sea of Okhotsk, plate tectonics and geology 4-82004
- Seal Nunataks, W Antarctica, active volcanism and heat flow 4-81971
- SEASAT-SAR, imagery for land use and geology appl. 4-82294
- Sede Zin, Negev, Quaternary geology and hydrology of alluvial plain 4-94133
- sediment record of last interglacial climate 4-85754
- sedimentary structures, book, second volume 4-101600
- sedimentary structures, character and physical basis, book 4-90315
- sedimentology, book 4-82612
- Shackleton Range, Antarctica, Rb-Sr ages and geological history 4-81937
- Shackleton Range, Antarctica, tectonics and Precambrian struct. stages 4-81938
- Shackleton Range, Coats Land, Antarctica, Precambrian and Early Proterozoic history 4-81939
- shale compaction process and exponential porosity-depth relation 4-89914
- shatter cones due to meteorite craters 4-115405
- Shelleng-Numan area, Nigeria, geology remote sensing by radar 4-100483
- Shikotan, Minor Kuril Islands, major structural-material complexes 4-100568
- shoreslines and isostasy (book) 4-67903
- SE Siberia, Early Precambrian crustal development, role of endogenous processes 4-85667
- W Siberia, EM core sounding rel. to hydrocarbon deposits 4-100448
- W Siberian Platform, USSR, salt deposit distrib. 4-105496
- Skye, Scotland, relation between alteration indices and Ar loss in basic igneous rocks 4-110140
- Snake River Plain, Idaho, USA, origin of flood basalts 4-62739
- soil properties remote sensing in grassland areas, using Thematic Mapper 4-82269
- solid Earth and ocean tide energy dissipation, review 4-100432
- South Shetland Islands, Lesser Antarctica, geochem. and igneous activity due to subduction 4-81948
- Southern Apennines, Italy, geological evolution of flysch basin 4-89905
- Southern Province, Lake Huron, regional cross section, implications for Murray Fault Zone tectonics 4-94039
- stratigraphic correlation by means of ordinal scales 4-94041
- International Stratigraphic Scale, for Cainozoic 4-105495
- stratigraphy, unitary associations method, graph theory and computer algorithm appls. 4-94040
- Talau Islands, Indonesia, ophiolites and assoc. volcanic rocks, petrology and geochemistry 4-82051
- Tanna fault, Izu, Japan, trenching study of previous fault activity 4-105445
- Tarr Complex, Sinai Peninsula, folding, thrusts and melanges 4-77487
- Tasman orogen, Australia, fault struct. 4-85659
- tephra deposits in Iceland, tephrochronology by geochem. obs. 4-62748
- tephra layers as geochronological markers over long distances 4-62995
- Tertiary volcanism of Hoheifel, age and palaeomag. study 4-105419
- Thorsmork ignimbrite of S Iceland, geology of volcanic deposits 4-62763
- Tien Shan, USSR, pattenite rebed formations of intermontaine basins 4-115364
- titanomagnetite, aqueous oxidation in submarine basalts and thermomagnetism 4-100497
- Togo, magnetite and haematite mineralisation of atacorian series rocks (*French*) 4-77477
- Earth Transbaikai, USSR, injection relief structures 4-115360
- Trinity peridotite, California, USA, Nd-Sr isotope study and mantle evolution 4-89890
- tropical time lines use for palaeoclimatic indicators for weathered cratons 4-110275

- ology continued  
turbidity current deposits in Quebec Appalachians, showing reflected flow 4-115359  
Umbria, Italy, siderophile rich mag. spheroids at Cretaceous-Tertiary boundary 4-100509  
Umbrian Maiolica Formation, Italy, palaeomagnetic and biostratigraphical study 4-105408  
Umnak Island, Aleutians, Alaska, geology and geochronology 4-72537  
W United States, Mesozoic strata, in western Cordillera rel. to kinematics of plate convergence 4-94064  
W United States, tephrochronology and Quaternary geology 4-62749  
Uppington Geotraverse, South Africa, tectonic features 4-85662  
US Gulf Coast region, Ra occurrence and behaviour in saline formation water 4-110179  
western USA, origin of Mesozoic and Tertiary granitic rocks 4-62744  
E USSR, distinctive petrochemical features of basaltoid lavas of continental arches 4-100563  
Velece hills, Hungary, gravity and geomagnetic anomaly interpretation 4-62728  
Vendee eclogites, France, tectonic dispersion during continent-continent collisions (*French*) 4-67214  
N Vermont, USA, metamorphic schists of Ordovician and Devonian age 4-94023  
Vermont and Massachusetts, USA, tectonic emplacement of pre-Silurian eugeoclinal belt 4-94028  
Vestfold Block, E Antarctica, Sr-Nd isotopes, lithology and crust evolution 4-81929  
N Victoria Land, Antarctica, age of Bowers Supergroup 4-81933  
N Victoria Land, Antarctica, airborne gamma-ray survey 4-81953  
N Victoria Land, Antarctica, geochemistry of Cambrian volcanics to Early Palaeozoic tectonic evolution 4-67215  
N Victoria Land, Antarctica, geology of pre-Beacon bedrocks 4-81931  
S Victoria Land, Antarctica, granite geology and orogenesis 4-81935  
S Victoria Land, Antarctica, provenance and dating of glacial deposits 4-81955  
N Victoria Land, Antarctica, tectonics of Robertson Bay Group deformations 4-81932  
N Victoria Land, post-Ross orogeny cratonisation 4-81934  
Wadi Kid metamorphic complex, SE Sinai, stratigraphy and tectonic history 4-72540  
Wadi Natash Volcanic series, Eastern Desert, Egypt, geology and geochemistry 4-115352  
weathering of rocks, chemical kinetics 4-94135  
S Weddell Sea Basin, crust struct. and geologic history 4-81940  
Weller Coal Measures, Victoria Land, Antarctica, geological study 4-81942  
Williston Basin, USA, mechanical and thermal model for tectonic evolution 4-94067  
Windmill Metamorphics, Casey area, Antarctica, geochronological study 4-81928  
S Wyoming, Early Proterozoic volcanic arc succession, tectonic setting and origin, geochemical modelling 4-94123  
Yenisei Ridge region, USSR, geochemistry of Lower Precambrian gneiss complexes 4-100561  
Yucca Mountain, Nevada, USA, sorptive barriers, HLW long term isolation appl. 4-83179  
Zimbabwe, regolith and bedrock rel. to morphological characts. of dambo features 4-100576  
zircon crystals, from Puttetti, S India, microtopography 4-100537  
Al<sub>2</sub>O<sub>3</sub> in geological samples, neutron activation determ. 4-66628  
C flux from mantle to midocean ridge 4-105476  
Mn crust containing Co on seafloor of USA Pacific economic zones 4-110107  
Mn nodule chemical deposition, radiotracer uptake expt. in Pacific 4-110126  
Mn nodules from Pacific seabed, radioactivity obs. (*Chinese*) 4-72564  
SiO<sub>2</sub> in geological samples, neutron activation determ. 4-66628

#### geomagnetic storms *see* magnetic storms

#### geomagnetic variations

*see also micropulsations*

- 500-600 year variations, nature 4-94001  
1969 impulse and Backus' mantle filter theory 4-105413  
AD 1981 observations made at Geomag. Observatory in Czechoslovakia 4-62672  
AE indices, relation to hemispherical Joule heating by auroral electrojets 4-72788  
Alaska, geomag. vars. rel. to Joule heating due to auroral electrojets 4-72784  
auroral ionosphere, mag. data rel. to aurora and electrojet configuration in early morning sector 4-72789  
Czechoslovakian Observatory observations during 1980 AD 4-62671  
daily variation due to ionospheric currents, coastal effect at equatorial latits. 4-110044  
dipole moment deviations from short-term mean dipole moment 4-72489  
dynamo model of geomagnetic non-dipole field variations 4-105415  
estimation methods for use during high-precision aeromagnetic surveys 4-100829  
field response to solar disturbance, solstitial and hemispherical asymmetry 4-72808  
N France, study of diurnal var. of EM field using ancient recordings 4-110042  
geophysical observatory at Hel, Poland, instrumentation and methods in AD 1932 to 1982 period 4-77637  
Greece, archaeomagnitudes evaluation, secular var. 4-110300  
ground level var. and ring current characts. determ. 4-94306  
heliomagnetic cycle of geomag. and ionospheric disturbances and interplanetary activity 4-110369  
HF path between Japan and Germany, geomagnetic disturb. effects on usable freq. bands 4-82331  
induced diurnal variation at Peruvian dip equator, effect of depth of non-conducting layer 4-62668  
induced magnetic field at Peruvian dip equator, effect of depth of non-conducting layer 4-62668  
intensity variations in Egypt and W Asia during second millennium BC, archaeomag. meas. 4-100443  
interplanetary magnetic field sector structure effects 4-100449  
ionosphere, latit. profile and magnetosphere convection elec. field from mag. and radar data 4-72787  
ionosphere, local time depend. of response of equatorial electrojet to DP2 and SI disturbances 4-105802

#### geomagnetic variations continued

- lower Jaramillo polarity transition, Crozet basin sediment core anal. 4-85615  
Jurassic and Cretaceous polar wander from Italian palaeomag. obs. 4-105408  
Jurassic magnetic stratigraphy from Umbrian (Italian) land sections 4-81842  
long-period variations, calc. of shielding effects on source current system 4-105416  
long-period variations, effect of oceans 4-105412  
low-latitude field, effects of solar wind interaction region passage 4-67541  
lunar daily variation elec. currents in ionosphere, multi-layer model 4-82341  
lunar daily variations, rel. to seasonal vars. of ionospheric L equivalent current systems 4-72785  
magnetosphere, ISEE 1 and 2 obs. of oscillating outward moving current sheet near midnight 4-85832  
magnetosphere, magnetic turbulence during mag. field line reconnection 4-84011  
magnetosphere, obs. of resonant Alfvén waves excited by sudden impulse 4-85834  
magnetosphere, relation between ground-level disturbances and struct. of dayside polar cusps 4-110373  
magnetosphere, second harmonic geomag. field line reson. at inner edge of plasma sheet 4-85833  
magnetosphere flux erosion events, identification with flux transfer events 4-72828  
main geomagnetic field and its secular var., representation by Magsat Mount St. Helens, Washington, USA, geomag. field changes of Oct. and Nov. 1981 eruptions 4-100518  
Oahu lavas, Hawaii, geomag. palaeointensities from excursion sequences 4-85616  
Pacific deep-sea cores, geomagnetic polarity transition durations, latitudinal dependency 4-100444  
palaeosecular variation, physical model 4-110041  
palaeosecular variations (last 40000 years) from Japanese volcano palaeomag. observations 4-105418  
periodicity throughout 20th solar cycle 4-94539  
polarity transition durations, latitudinal dependency in Pacific cores 4-100444  
research carried out in Poland in the period 1978 to 1982 AD 4-72486  
reversal sequences analysis, statistical methods 4-85621  
reversal time scales, implications for lower mantle convection 4-85620  
S<sub>p</sub> (ΔH) variation, appl. to anal. of variability of ionospheric dynamo currents 4-90021  
Saskatchewan, geomag. vars. meas. rel. to crustal elec. cond. and Proterozoic plate margin 4-105406  
secular acceleration, impulses and jerks reexamined 4-94005  
secular variation, new model of non-dipole geomag. field 4-62669  
secular variation from Canary Islands volcanic rocks of historical age 4-89878  
secular variation in North America in historical times 4-89877  
secular variation in W United States, AD 750 to 1450, congruent palaeomag. and archaeomag. records 4-100446  
secular variations, implications of <sup>10</sup>Be measurements in deep-sea sediments 4-110128  
secular variations affecting location of conjugate magnetospheric stations to Siple Station 4-110385  
secular variations and perfectly conducting core nature 4-77446  
secular variations and resolvability of fluid upwelling at core-mantle boundary 4-105486  
secular variations d dipolarity of ancient fields 4-100441  
short-period geomagnetic secular variations and core dynamics 4-94000  
South Magnetic Pole, secular motion and core struct. 4-81856  
Sq observations in Africa, and position of Sq current loops 4-82323  
structural var. associated with storm ring current injection, cosmic ray penetration use in anal. 4-94303  
thermosphere, generation of vertical winds and gravity waves during geomag. disturbances 4-105782  
thermosphere, geomag. disturbances rel. to vertical winds and gravity waves generation at auroral latits. 4-105783  
Triassic magnetostratigraphy and palaeomagnetism of Chugwater Formation, Wyoming, USA 4-81846

#### geomagnetism

*see also geomagnetic variations; magnetic storms*

- aeromagnetic data inversion method for single mag. boundary in freq. domain (*Chinese*) 4-85758  
aeromagnetic surveying, method for estimating body remanent magnetization 4-67419  
algorithm for error adjustment of potential field data along a survey network 4-100438  
North America, combined correlation anal. of geophys. fields 4-72541  
anomalies, Magsat obs. of small-scale features 4-85617  
anomalies of oceanic crust in presence of nonuniform spreading, energy density spectrum 4-93999  
anomalous field due to subsurface struct., computation method 4-85604  
anomaly data reduction to common level, use of inverse theory 4-85802  
anomaly field of buried object, 3-D Fourier transforms theory (*Chinese*) 4-62651  
West Antarctica, geomag. anomalies and subglacial geology 4-81853  
Antarctica, gravity and geomagnetic studies between 45 and 65 degrees East 4-81959  
Antarctica and Southern Ocean mag. anomalies from MAGSAT obs. 4-81855  
S Appalachian Piedmont, geophysical anomalies along strike rel. to crustal struct. and tectonics 4-93990  
early Archean geomag. field, palaeomag. study of Komati Formation, South Africa 4-94004  
Australia-Antarctic Discordance zone, plate boundary evolution, aeromagnetic anal. 4-81857  
Australian Antarctic Territory, Davis-Mawson stations region, sedimentation anal. 4-82036  
Bangui anomaly, Central Africa, reduction of satellite mag. anomaly data 4-105421  
book 4-73186  
Broken Hill District, regional magnetic and gravity field characteristics and interpretation 4-62814

## geomagnetism continued

- Canadian Arctic Islands, sea floor spreading anomalies and chronology 4-110124  
 core dynamo, slow hydromagnetic oscils. in outer core 4-77449  
 core dynamo 4-105483  
 Coso Range, California, ground mag. survey 4-85618  
 Deer Lake basin, Newfoundland, Canada, gravity and magnetic interpretation 4-62653  
 direct problem soln. in modelling complex geological media 4-77442  
 dynamo action in a stably stratified core 4-105410  
 Earth's general relativistic gravitomagnetic field, Foucault pendulum expt., at South Pole 4-111010  
 electromagnetic induction in variably conductive sheet in layered Earth 4-89874  
 EM core sounding in Western Siberia, appl. to hydrocarbons prospecting 4-100448  
 EM frequency sounding, uniqueness theorem for horizontal loop soundings 4-67168  
 EM induction in multi-layered spherical medium (and shielding effect) 4-105416  
 EM induction problem, coastal effect at equatorial latits. 4-110044  
 EM induction sounding, Fréchet derivatives 4-85622  
 EM sounding, use of visualisation method in interpreting data obtained by method of transitional processes 4-100826  
 EM sounding using power line harmonic fields, appl. to Earth resistivity meas. 4-62667  
 excitation of quasistatic magnetic fields with axial structure 4-100447  
 field due to dipoles surface distrib. (Chinese) 4-110035  
 field generation via battery effects 4-101138  
 fine-beam cathode ray tube for meas. Earth's mag. field 4-63463  
 N France, study of diurnal var. of EM field using ancient recordings 4-110042  
 geomagnetism and core dynamo, review 4-93997  
 geophysical observatory at Hel, Poland, instrumentation and methods in AD 1932 to 1982 period 4-77637  
 horizontal loop EM response of thin plate in conductive Earth, computational method 4-100434  
 horizontal loop EM response of thin plate in conductive Earth, computational results 4-100435  
 Humboldt's magnetic Verein (1829-34) and his Russian journey (1829) (German) 4-63467  
 India, lithosphere, elec. cond. struct. and magnetometer anal. 4-81850  
 N India, model study for proposed magnetotelluric traverse 4-81851  
 E Indian Ocean, geomag. anomalies due to seafloor spreading and age of crust 4-94007  
 SE Indian Ocean, geomagnetic survey carried out between 1979 and 1982 AD 4-81854  
 Indian shield and Himalaya, lithosphere mag. anomalies 4-81849  
 intensity variations in Egypt and W Asia during second millennium BC, archaeomag. meas. 4-100443  
 inverse problem solution by regularisation method, algorithm 4-105732  
 ionosphere, topside, nighttime, mag. declination rel. to  $O^+$  density depressions 4-63009  
 Jemez volcanic zone, New Mexico, detailed magnetotelluric and audio-magnetotelluric study 4-85619  
 Karakorum mountain range geomagnetic profiles 4-62663  
 western Kenya, kimberlite pipes in greenstone belt 4-77444  
 Kuril-Kamchatka deep-sea trench, tectonics, magnetic anomalies, bathymetry and seismic struct. 4-82006  
 Lake Ladoga-Bothnian Bay zone, Finland, audiomagnetotelluric meas. 4-105411  
 linear anomalies in oceanic crust 4-81848  
 Lutzow-Holm Bay, Antarctica, gravity, geomag. intensity anomalies and crust tilt 4-81841  
 magnetic induction vector components determ., algorithms accuracy 4-94002  
 magnetometer for palaeomagnetic and rock magnetism studies, superconducting instrument 4-90006  
 magnetometer with nonconducting sensor enclosure in conducting fluid, calc. of instrumental corrections 4-100789  
 magnetosphere, dynamo, model of field-aligned currents in polar cap 4-110372  
 magnetosphere, mag. field geometry rel. to  $B_y$ -component in geomag. pulsation data 4-105809  
 magnetosphere, magnetic field in cavity of perfect diamagnetic material 4-105811  
 magnetosphere, scale size and interior struct. of flux transfer events 4-94313  
 magnetosphere flux erosion events, identification with flux transfer events 4-72828  
 magnetotail, mag. neutral lines and average plasma flow between 70 and 220 Earth radii 4-100880  
 magnetotail, magnetic structure from 60-220  $R_E$ , ISEE-3 obs. 4-94308  
 magnetotail structure at 220  $R_E$  rel. to geomagnetic activity 4-94309  
 magnetotelluric response functions, estimation, use of singular value decomposition 4-77445  
 McArthur Basin, Australia, struct., trends and magnetotelluric profiles 4-93996  
 MHD dynamos in planetary interiors, theory 4-105894  
 Niue Island atoll, SW Pacific, volcanic core struct. from geophys. obs. 4-94035  
 non-dipole field, calc. of core dynamo source currents 4-105415  
 non-dipole field model, rel. to geomag. secular variation 4-62669  
 non-dipole magnetic field, physical model rel. to geomag. palaeosecular var. 4-110041  
 oceanic crust mag. anomalies, palaeomagnetic interpretation with lithospheric plate theory 4-100445  
 oceanic crust magnetisation, implications of mag. props. of Bay of Islands ophiolite suite 4-85673  
 oceanic magnetic anomalies and importance of doleritic basalt 4-100551  
 Pacific Ocean, geodynamic features and geomag. anomalies anal. 4-77493  
 potential field data, 3-D automatic interpretation using Hilbert transforms 4-110289  
 potential field data analysis, continuation between arbitrary surfaces 4-110039  
 Princes Elizabeth Land, Antarctica, gravity and mag. anomalies anal. 4-89889  
 N Pyrenean mag. anomaly and crustal current channel nature 4-100433  
 remote reference magnetotellurics, noise correlation lengths 4-100436  
 research carried out in Poland in the period 1978 to 1982 AD 4-72486

## geomagnetism continued

- secular acceleration, impulses and jerks reexamined 4-94005  
 spinning electrons in dynamo model of geomagnetism 4-115333  
 surface field, radio noise spectral characs., few hertz to 50 kHz., expt. data-review 4-89879  
 tectonomagnetic effect, calc. for faulting of Earth crust 4-105404  
 thin bounded bed in high resist. medium, parameters determ. 4-77450  
 Velence hills, Hungary, gravity and geomagnetic anomaly interpretation 4-62728  
 Washington State, tectonic study from magnetotelluric profiles 4-94075  
 Yermak Plateau (Arctic Ocean), mag. anomalies rel. to form, at triple junction 4-85669
- geometrical optics  
 anisotropic media, propag. and interaction of transversely-confined beams (Russian) 4-96794  
 Cartesian sign convention for numerical ray tracing 4-107507  
 Cassegrain-type spectrographic cameras, near axis ray tracing, aberrations and their correction (Japanese) 4-94617  
 complex rays and diffraction by smooth object 4-102882  
 concentration limits in physical optics and wave mechanics 4-96788  
 concentration limits in physical optics and wave mechanics 4-96795  
 coupling between DH laser and fibre 4-69475  
 curved cylinder, light beam eqns. anal., specular reflection (Russian) 4-83543  
 DIFPD parameters influence on final image symmetry of optical systems 4-60130  
 EM wave refl., inhomogeneous bounded layers with variable refr. Index, geometric optics approx. 4-112330  
 evanescent field tracking and generalised ray representation in optics, interconnection, preliminary results 4-102880  
 film lenses analysis, with complex source point method 4-64792  
 Fokker-Planck equation for ray dispersion in gyrotropic stratified media 4-107521  
 free electron laser oscillator mirror alignment tolerance scaling laws 4-83602  
 frequency correlation of optical radiations propagating in a medium with large-scale random inhomogeneities 4-96805  
 Gaussian beam incident on parabolic inhomogeneous slab, transmission and reflection characs. (Japanese) 4-96806  
 Gaussian beam optical system anal. and synthesis 4-82725  
 Gaussian Schell-model fields, propag. characteristics through first-order optical systems 4-83541  
 gradient-index optical imaging systems, conf., Monterey, CA, USA (April 1984) 4-95057  
 grazing incidence spectroscopy focusing, by elastic deformation of the grating 4-82834  
 half-symmetric unstable resonator with internal axicon, reflexicon deforms effect on geom. parameters 4-69524  
 halo phenomena, Monte Carlo simulation, sun ray path tracing through ice crystals 4-72699  
 imaging quality limitations (German) 4-112346  
 inhomogeneous isotropic media, propagation theory 4-83520  
 integral photography, foreshortening change mechanism (Russian) 4-68308  
 IR chopping secondary of Cass telescope, determ. of image aberration 4-107777  
 IR ray path visualisation 4-87269  
 laser beam, higher-order mode, waist location and Rayleigh range 4-91508  
 laser fusion pellet, absorpt. rate and uniformity 4-78735  
 laser radiation directivity pattern axis instability meas. 4-74571  
 lenses, spherical and orthogonal cylindrical, mixed systems, matrix optical analysis of skew rays 4-107779  
 millimeter wave imaging lens antenna 4-91560  
 modulated Gaussian beams 4-83531  
 nonimaging and imaging optics design, connections and transitions 4-96789  
 nonimaging concentrator, relative merits compared with imaging optical systems 4-96792  
 nonimaging concentrators, conf., San Diego, CA, USA (Aug. 1983) 4-95021  
 nonimaging concentrators, etendue theorem conservation appl. for phase space 2-D subdomains 4-91399  
 nonimaging concentrators, ray tracing, generalised algorithm 4-96790  
 nonimaging optic theory for photovoltaic applications 4-99945  
 nonimaging optics development 4-96791  
 nonimaging solar concentrators with flat mirrors 4-99947  
 nonspherical aerosol particles, light scatt. props. 4-96801  
 nonsymmetrical optical systems, matrix theory 4-74645  
 paraxial ray trace for rotationally symmetric homogeneous and inhomogeneous media 4-102879  
 perfect reflecting diffuser refl. indicatrix, geometric conditions influence, gonioreflectometric meas. (German) 4-101902  
 photometric arrangement dimensioning, appl. of optics of Gaussian bundles (German) 4-95489  
 picosecond rotating-mirror autocorrelator, optimisation study 4-107793  
 power series, generic behaviour 4-112350  
 power series, generic behaviour 4-112351  
 power-law hardening material, optical shadow spot method for tensile crack 4-97449  
 prisms, right-angle, use in total internal reflection and interference meas. 4-63458  
 radial gradient lenses compared to homogeneous lenses, first-order props. 4-107778  
 radiation from planar aperture distributions by evanescent wave and complex ray analysis 4-74398  
 random gyrotropic media, ray dispersion 4-91404  
 random phase screen model in thermal self-action of light problem 4-102979  
 ray tracing in absorbing media 4-74423  
 reflecting specimens colours with 45°/0° illumination and observation conditions 4-90644  
 relativistic phase invariance, Lorentz transformations 4-110872  
 resonators with nonuniform magnification 4-87373  
 ripple tank, optical caustics and diff. study 4-95102  
 rotationally distributed-index media, paraxial theory by means of Gaussian const. 4-83544  
 signal description by means of a local frequency spectrum 4-79043  
 size calculations of optical systems, use of Gaussian brackets 4-64753  
 solar concentrators, planar-sectioned, polygon reflectors 4-79260

**ometrical optics continued**

- step index fibres, angular aperture, light power transmission 4-83698
- structural mechanics of optical systems, conf., Cambridge, MA, USA (Nov. 1983) 4-86104
- synthetic aperture arrays, physical understanding via simple models 4-97017
- synthetic aperture propag., point spread function, computer model 4-96813
- synthetic apertures, multiline, performance and phasing 4-97019
- Talbot and Lau effects, a parageometrical approach 4-69322
- three-mirror anastigmat with main mirror and third mirror coincident, theory (*Russian*) 4-101168
- toric unstable resonators, geometrical, diffractive and asymptotic theory 4-91501
- two-photon-resonant image upconverters using type I optical system, thickness aberrations (*Japanese*) 4-79336
- two-photon-resonant image upconverters using Fourier mode optical systems, chromatic aberrations (*Japanese*) 4-60116
- vignetting effect in one-lens and two-lens optical systems for rainbow holography 4-69336
- Wigner distribution function and optical geometrical transformation 4-79028
- zoom system for Gaussian beam, general paraxial theory 4-91562

**ometry**

- see also space time configurations*
- conformal coordinate and point transformation, invariance 4-110855
- dynamical systems with time depend. constraints and Hamiltonian, approach towards quantisation 4-63544
- gauge fields in multidimens. universe 4-68379
- gauge theories, topology and geometry, book contrib. 4-58975
- generalised supermanifolds,  $p$ -supermanifolds 4-63913
- generalised supermanifolds, anal. on superspaces 4-63912
- generalised supermanifolds, superspaces and linear operators 4-63911
- Lagrangian mechanics and second order eqns. 4-90372
- mechanics, affinely-connected manifolds theory and Lie theory 4-63492
- orthogonal, association schemes with 1-D non-isotropic subspaces construction (*Chinese*) 4-95139
- quantum theory, groups, fields and particles, book 4-58592
- S-bends and geometry, teaching using computers 4-101607
- spherical coordinate geometry, complex and appl., appl. to astronomy 4-105890
- SU(2,2)×SU(m) physical symmetry group, geometrical consequences 4-86179
- superpregeometry, implications of supersymmetry breaking and higher order corrections 4-78495
- unification of gravity and EM in general relativity 4-82733

**geomorphology**

- see also topography (Earth)*
- Adriatic Sea and crustal struct., conf. at Trieste, Italy (September 1983) 4-78027
- Adriatic Sea beaches, erosion and protection (*Italian*) 4-82028
- alluvial fan development, book 4-82613
- Andes, glaciers, glaciation and landforms, review 4-67285
- E Antarctica, perennially frozen lakes at glacier/rock margins 4-82144
- Ardeche Submediterranean rangelands, France, surface runoff and sediment yield 4-115462
- South Atlantic coasts, Late Tertiary shorelines, sedimentary and morphological evidence 4-105563
- rock avalanches due to earthquakes 4-82059
- Baikal-Amur trunk railway line, geomorphology of Khani and Katugin areas rel. to seismic risk 4-100479
- beach erosion processes 4-94087
- bedrock weathering and silcrete formation in S Africa 4-62817
- SE Brazilian Plateau, hillslope evolution and Quaternary sediments 4-62807
- Lake Burullos, in Nile delta, Egypt, sediment mineralogy and sources 4-115468
- Carrara Range region, N.T., Australia, preserved Proterozoic landforms 4-94038
- channels, flow and sediments (book) 4-90317
- coastal bars, maintenance by wave interactions 4-67241
- dambo features in Zimbabwe, morphological characts. 4-100576
- desert landform and sand dune remote sensing by SIR-A radar and Landsat (*French*) 4-62964
- discordant river junctions and Playfair's law 4-62819
- NW Europe, evidence for pre-Weichselian glaciation, stratigraphy 4-110176
- geophysical predictions (book) 4-90308
- glacial geology, depositional processes, sediments and landforms, book 4-58596
- glacial moraines of Ruby Mountains-East Humboldt Range, Nevada, morphology and weathering rel. to glacial chronology 4-94176
- glaciated valley cross-section represented by parabola 4-115404
- Glen Rosa, Isle of Arran, Scotland, cross-section of glaciated valley 4-115404
- Grado lagoon, N Adriatic Sea, origin and development 4-82029
- N Greece, agriculture influences upon erosion and runoff processes 4-115460
- Hunza Valley, Karakoram region, Pakistan 4-62824
- Hunza Valley, Pakistan, Quaternary glacial history, geomorphology and sediments 4-62825
- Hunza Valley, Pakistan, salt efflorescences and salt weathering 4-62827
- Hunza Valley, rockfall scree slope model, particle sizes 4-62826
- Idukki reservoir catchment, Kerala, India, valley slumping, sedimentation and reservoir capacity 4-100628
- intertidal zone, rock weathering due to frost action 4-115385
- NE Iowa, USA, geology and erosion of Palaeozoic Plateau area 4-77491
- NE Iowa, USA, karst development in Palaeozoic rocks 4-77518
- Karakoram glaciers, glacial and proglacial debris, sedimentological anal. 4-62868
- Karakoram Mountains, geomorphology of high magnitude-low freq. events 4-62822
- Karakoram Mountains, glacier var. 4-62859
- Karakoram region, glacier meltwater runoff, sediment anal. and erosion 4-62869
- Karakoram glaciers, fluctuations anal. techniques 4-62864
- Lincolnshire area, eastern England, pre-Devensian glaciation, review 4-62786
- Marion Island, Quaternary glaciation of island near Antarctic convergence 4-82142

**geomorphology continued**

- Mojave Desert, California, USA, downhill movement of stones 4-115461
  - Mojave Desert, piedmont junction migration, hillslope and channel processes 4-62808
  - mountain mass denudation in Mojave and Sonoran Deserts 4-62808
  - Negev desert, erosion cirques triggered by emerging groundwater 4-77516
  - central Nigeria, geological interpretation of Landsat images 4-77478
  - Nile delta, Egypt, sedimentation of Lake Burullos 4-115468
  - Nile delta beach sediments and past position of Canopic Nile branch 4-115465
  - North Sea basin, Holocene sedimentation, book 4-86134
  - Ohau River, New Zealand, river channel response to lowering of Lake Benmore 4-62855
  - Pamirs, USSR, Quaternary vertical tectonic movement from geomorphological obs. 4-62772
  - pebble abrasion by wave action on coastal benches 4-115386
  - permafrost marine sediments of N Alaska coast, thawing and brine transport 4-67290
  - piedmont junction migration, hillslope and channel processes 4-62808
  - Proterozoic landforms preserved in Carrara Range region, Australia 4-94038
  - Quaternary vertical tectonic movement from geomorphological obs. 4-62772
  - Rheidol river, Wales, channel change of regulated river 4-62853
  - river basin, geomorphology rel. to alluvium accumulation dynamics and placer deposits 4-100646
  - river bed sand wave spectra, for steady-state and flood flow 4-105615
  - River Derwent, N Yorkshire, England, river channel changes 4-62854
  - riverbank erosion, failure mechanisms of shallow sandbed stream banks 4-62852
  - Riviere aux Outardes estuary, Quebec, Canada, sedimentology after dam construction (*French*) 4-62792
  - rock crack growth during unroofing of crustal rocks 4-94102
  - rock weathering processes at high altitude 4-62821
  - scarplike landform evolution model 4-110148
  - sediment transport, conf. at Istanbul, Turkey (July 1982) 4-78047
  - shore equilib. profile, physical model 4-105543
  - Sinai, Egypt, erosion cirques triggered by emerging groundwater 4-77516
  - slope steepness dependence on rock mass strength 4-62820
  - slopes on opposite sides of road cutting, erosion and runoff influenced by rain direction 4-77563
  - soil erosion, book 4-101598
  - soil erosion by water runoff, stochastic model 4-100641
  - Sonoran Desert, piedmont junction migration, hillslope and channel processes 4-62808
  - Tatra Mts., Poland aeolian sediment erosion and deposition 4-62818
  - topographic information processing, appl. (*Japanese*) 4-85609
  - Earth Transbaikai, USSR, injection relief structures 4-115360
  - valley slumping and soil erosion in catchment of Idukki reservoir, Kerala, India 4-100628
  - Vestfold Hills, E Antarctica, ice movements during Late Quaternary 4-82143
- geons** *see gravitons*
- geophones** *see seismometers*
- geophysical aspects of cosmic rays**
- accelerator neutrino beams, particle production, trajectories in Earth's mag. field 4-101028
  - albedo electrons, source under radiation belts 4-101040
  - altitude and latitude variations obs. by airborne detectors 4-101024
  - altitude variation of the derived electron photon intensity 4-105852
  - annual cosmic ray variations at various atmospheric levels 4-101061
  - applications in hydrology and atm. physics 4-100966
  - arrival direction effects from HEAO-3 expts. 4-101025
  - asymptotic direction change due to cutoff rigidity alteration 4-101022
  - atmosphere  $^{14}\text{C}$  prod. var. and solar modulation of galactic cosmic rays 4-94424
  - atmosphere Cherenkov light emission due to small air showers, imaging 4-101176
  - atmosphere gamma-ray background, meas. at balloon altitudes above Beijing area (*Chinese*) 4-82355
  - atmospheric gamma-ray flux,  $E > 30$  MeV, characteristics in near-Earth cosmic space 4-101035
  - atmospheric neutrino fluxes, effects of oscillations 4-90775
  - atmospheric propagation, geomagnetic field effect 4-101050
  - atmospheric propagation and energy deposition detectors 4-105856
  - atmospheric temperature vertical profile from cosmic ray components 4-101026
  - charged particles telescope to observe proton albedos 4-101039
  - cosmic ray access to satellites from large zenith angles 4-101027
  - cosmic ray asymptotic direction changes in geomagnetic storms 4-101021
  - cosmic ray equator using Epoch 1980.0 reference field 4-101020
  - current sheet passage, cosmic ray modulation 4-101063
  - Cygnus X-3,  $\gamma$ -ray emission and air showers arrival directions anal. 4-101529
  - distant terrestrial magnetosphere, protons, He and heavy ion obs. with ISEE-3 4-94323
  - DUMAND site, photon collection rel. to light transmission in clear seawater 4-62828
  - Elbrus spectrograph detectors, coupling function, meteorological coeffs. 4-101055
  - electrical conductivity of thermosphere and low and middle atmosphere, solar activity effects 4-85826
  - electron aureole with energies of hundred of MeV, mechanism of form. 4-110399
  - electron flux,  $E > 30$  MeV in equatorial region 4-101041
  - electron fluxes at 500 km in equatorial region 4-67569
  - electrons density spectrum at sea level 4-72891
  - emulsion chamber design for cosmic ray expts. at balloon altitudes 4-72890
  - energetic particles in magnetosphere, dynamics 4-67567
  - equator-pole anisotropy, semi-annual variation 4-94443
  - Forbush decrease, anisotropic intensity waves 4-94445
  - Forbush decrease July 13/14 1983, intensity periodicities 4-100973
  - Forbush decreases, effect on atmospheric elec. field and air-Earth current 4-89970
  - fossil record by  $^{10}\text{Be}$  accelerator mass spectrometry 4-90047
  - free air pressure estimation after correcting for cosmic ray barometer effect 4-101037

**geophysical aspects of cosmic rays continued**

- galactic cosmic ray density distribution in heliosphere, quasistationary asymmetry 4-67573  
 gamma rays in atmosphere, due to cosmic ray interactions 4-110400  
 gamma-ray diffuse component meas. by high-altitude balloon at two geomag. latitudes 4-100888  
 gamma-ray flux at balloon altitudes, approximate analytical representation 4-100964  
 geomagnetic disturbances, effect on ground based monitor response 4-101023  
 geomagnetic storm effect on trapped protons at 500 km, 4-67568  
 geomagnetic transmission functions for a 400 km altitude satellite 4-101019  
 hadron energy spectra, atmospheric depth depend. 4-105836  
 high energy cosmic rays, solar and meteorological effects 4-101033  
 high energy electron fluxes in radiation belt 4-101043  
 high energy electrons and photons, intensity-depth relation 4-105854  
 horizontal muon spectrum, charge ratio, atmos. propagation 4-101042  
 integral and differential response functions 4-101056  
 intensity increases during geomagnetic storms 4-94448  
 ionospheric F-region, corpuscular ionisation, latitudinal depend. during Forbush decrease 4-101051  
 Johnstown meteorite, hypersthene grains, nuclear track annealing study device 4-100769  
 latitude observations with lead free neutron monitor 4-101046  
 long term variations, Earth's mag. field effects 4-101030  
 lower atmosphere asymmetry, time variations 4-101032  
 magnetosphere cosmic rays penetration, use in ring current characts. determ. 4-94303  
 measurement stations for cosmic ray variation studies, necessary geographic distrib. 4-110539  
 measurements in deep-sea sediments 4-110128  
 median primary energies for hadrons in the atmosphere 4-101059  
 meteorological coefficients from Musala neutron supermonitor results 4-101045  
 methodical principles in studying cosmic ray variations 4-101060  
 multiplicity response function of the double neutron monitor at Turku 4-101058  
 muon flux at different zenith angles and from east and west 4-72891  
 muon multiple events, simulation calcs. 4-110465  
 muon north-south anisotropy, high rigidities, 27-day recurrence 4-94459  
 muon spectra, derivation at large zenith angles from primary flux 4-110389  
 muon underwater intensities depth range, momentum spectrum 4-110406  
 muons, depth-intensity relation, Monte Carlo simulation 4-110404  
 muons, sea level intensity at Mt. Blanc underground expt., primary nucleon spectrum determ. 4-82356  
 muons characts. anal. and primary cosmic rays characts. determ. 4-94524  
 neutrino atmospheric fluxes, effects of oscillations 4-110408  
 neutrino flux calcs. in atmos. 4-110407  
 neutron coupling coefficients, expt. determ. 4-101054  
 neutron intensity observations by Pb-less counters 4-101047  
 neutron monitor data, Seoul and Tokyo, critical comparisons 4-101048  
 neutron monitors on board r/v Akademichn Aleksander Nesmeyanov 4-101049  
 neutron occurrence in Earth crust, of cosmic ray and radioactivity origin 4-110142  
 nucleon energy distribution, Ottawa large zenith angle muon telescope array 4-101057  
 preferred solar longitude zones in affecting solar activity and geophysical parameters 4-101053  
 prompt lepton production, atmos. muon and neutrino spectra 4-110403  
 propagation in magnetosphere, 4-101029  
 proton, bidirectional opposite streamings in noon low latitude magnetosheath 4-67570  
 protons, penetration of solar particles into magnetosphere 4-100975  
 protons modulation diffusion, stochastic instability in inner radiation belt 4-101038  
 PSR 0531+21,  $\gamma$ -ray emission, air shower arrivals anal. 4-101393  
 radiation belt, high energy particle flux excess 4-101036  
 radionuclide size dependence determ. in marine sediments 4-101101  
 relativistic electron observation expt. in upper atmosphere 4-101044  
 rigidity spectrum, spatial anisotropy May 7, 1978 ground level event meas. 4-101066  
 secondary electron and proton fluxes near Hyderabad at 35-40 km altitude 4-101042  
 sediment thermoluminescent meas., supernovae explosion detection 4-101107  
 soft muon intensity variations, geophysical effects 4-110405  
 solar cosmic ray flux structure at polar caps 4-101034  
 solar proton events, north-south asymmetries of upper stratospheric O<sub>3</sub> depressions 4-110229  
 solar proton spectrum dynamics, time evolution 4-105944  
 solar protons, flux at polar caps 4-67576  
 solar protons, high-latitude profiles in Earth magnetosphere 4-100965  
 solar protons, nuclear interactions in atmosphere rel. to determ. of absolute fluxes above E=100 MeV 4-110397  
 solar protons and electrons, magnetosphere boundary penetration 4-67575  
 space distribution in lower atmosphere 4-101031  
 stratosphere, anomalous C, N and O cosmic ray component after 1972 4-94411  
 stratospheric soundings, 240 day variation dynamics 4-101062  
 sudden storm commencement and Forbush decreases, correlation to solar wind and IMF 4-94447  
 tracks in minerals and cosmic ray comp. determ. 4-101098  
 vertical cutoff rigidities, world grid for Epoch 1980.0 4-101018  
 vertical cutoff rigidities for selected cosmic ray stations for Epoch 1980.0 4-101017  
 zonal modulation, north-south asymmetry, energy selectivity 4-101052  
<sup>10</sup>B/<sup>11</sup>B ratio in saline lakes of Qinghai-Xizang Plateau, <sup>11</sup>B(n, $\alpha$ )/Li influence 4-110401  
<sup>10</sup>Be abundance in ice cores, cosmic ray intensity variation obs. 4-101099  
<sup>10</sup>Be, conc. in deep sea sediments, intensity variation meas. 4-101100  
<sup>14</sup>C dating in tree rings, determ. of cosmic ray solar mod. cycle 4-94423  
He<sup>+</sup> and He<sup>2+</sup> in Earth's outer radiation belts, temporal and spatial variations 4-94324  
<sup>81</sup>Kr production rate in the atmosphere 4-101105  
<sup>6</sup>Li/<sup>7</sup>Li ratio in saline lakes of Qinghai-Xizang Plateau, <sup>6</sup>Li(n, $\alpha$ )/<sup>3</sup>H influence 4-110401

**geophysical equipment**

- see also atmospheric measuring apparatus; data loggers; geophysical prospecting; geophysical techniques; meteorological instruments; oceanographic equipment; seismometers  
 2 MV tandem accelerator mass spectrometer for <sup>10</sup>Be detect. 4-109702  
 borehole Eh and pH simultaneous measurement instrument 4-94246  
 borehole volume strainmeter, data correction for atmospheric pressure changes (Japanese) 4-72711  
 cartographic accuracy of Landsat-4 instruments 4-82267  
 cartography, computer applications (book) 4-90306  
 clinometer for teaching purposes 4-101606  
 computer-assisted stereocopying system 4-94258  
 Dicke-type radiometers for remote sensing of Earth from satellite, resolution aspects 4-67431  
 differential pulse anodic stripping voltammetry anal. for trace metals in seawater and snow 4-82315  
 DZT 90x120 digital plotting table 4-94257  
 electronic inertial seismometers, design principles 4-72763  
 EM frequency sounding equipment for study of sedimentary formations (Hungarian) 4-62975  
 ES-1030, data acquisition, processing and storage system at Obninsk Central Seismological Observatory, USSR 4-100752  
 fibre optical radiometer in remote sensing instrumentation 4-82247  
 geodetic distance meas. with Mekometer laser instrument, atmos. corrections and data reduction 4-89998  
 geoelectric induced polarisation method for time domain studies 4-62666  
 geophone ground coupling, results of laboratory expts. 4-110286  
 GPS geodetic receiver system testing 4-72735  
 gravimeter and horizontal pendulum design with capacitive transducers 4-85759  
 groundwater movement meas. instruments (Slovak) 4-85760  
 heat flow measurement in marine sediments, thermistor based equipment 4-81958  
 high-pressure cell with BeO transparent anvils for Earth mantle studies 4-110291  
 imaging spectrometer, HgCdTe IR focal plane arrays 4-100758  
 impulse radar for fracture detection in rocks 4-72732  
 induced polarisation equipment and methods for time-domain studies 4-67420  
 integrated DC SQUID magnetometer with a high slew rate 4-105761  
 IOZ-1 miniature underwater irradiance meter for lake studies 4-72729  
 IR airborne imaging spectrometer 4-115585  
 IR technology and appl., conf., San Diego, CA, USA (Aug. 1983) 4-110800  
 IRCCD sensors, Schottky barrier, Earth resources features appls. 4-100759  
 Johnstown meteorite, hypersthene grains, nuclear track annealing study device 4-100769  
 Landsat Multispectral Scanner and Thematic Mapper effective bandwidths 4-82272  
 Landsat-4 imaging processing techniques and map making 4-82260  
 Landsat-4 MSS and Thematic Mapper data quality and information content 4-82261  
 Landsat-4 MSS and Thematic Mapper image quality 4-82053  
 Landsat-4 Thematic Mapper, radiometric calibration technique 4-82263  
 Landsat-4 Thematic Mapper and Multispectral Scanner, information contents 4-82266  
 Landsat-4 Thematic Mapper geometric accuracy 4-82268  
 large spaceborne microwave radiometers, mission planning 4-94552  
 large-size coaxial waveguide time domain reflectometry unit for dielec. props. meas. 4-110294  
 laser deformographs for Earth natural oscils. meas. 4-62969  
 geo-magnetic field observing history of Geophys. Observatory at Hel. Poland 4-77637  
 marine magnetic gradiometer, accuracy of ship surveys 4-110288  
 magnetic observatory instrumentation made in Poland 4-72486  
 magnetometer, 3-axis, high stability, for geomagnetic field observation (Japanese) 4-100825  
 magnetometer for palaeomagnetic and rock magnetism studies, superconducting instrument 4-90006  
 magnetometer with nonconducting sensor enclosure in conducting fluid, calc. of instrumental corrections 4-100789  
 metal detector for finding objects such as artillery shells, EM induction coil equipment 4-100790  
 metal ore X-ray fluorescence chem. anal. equipment 4-59564  
 microwave reflectometer for mm wavelength meas. of materials of Earth's surface (Chinese) 4-82244  
 mm wave imaging radiometer for airborne applications 4-77665  
 nuclear microprobes, PIXE anal., appl. to Durango apatite 4-100787  
 ocean bottom seismometer, clock, correction system for clock calibration 4-82280  
 ocean bottom seismometer, description and initial results 4-110277  
 Oceanography International 84, conf. at Brighton, England (March 1984) 4-73157  
 optical fiber sensors applied to geophysics 4-110280  
 photogrammetric camera mounting on light aircraft cabin door, retractable 4-82256  
 photogrammetry; digitization of aerial stereo photos using interactive computer graphics system 4-62659  
 photographic processing equipment, mobile system for air survey films 4-82254  
 PIXE's analytic appls., conference, Heidelberg, Germany (July 1983) 4-95034  
 pneumatic radiator in seismology, seismic transmission expt. 4-62970  
 portable data logger for severe environments 4-100738  
 propane-O<sub>2</sub> detonator for shallow seismic reflections 4-77645  
 radioactivity measurement of geological samples, gamma ray spectrometer with underground detector 4-105765  
 Radon Analyser Model FD125 for <sup>222</sup>Rn meas. in natural gas 4-64322  
 remote sensing from satellites, IR instrumentation for SPOT satellites 4-100761  
 remote sensor, electrooptical airborne imaging scanner, MEIS II push-broom design 4-100760  
 rock core samples, acoustoelastic consts., interferometric meas. using pulsed phase-locked US instrument 4-97237  
 seafloor imaging and turbidity meas. system using laser equipment 50 m above ocean bottom 4-82275  
 marine sediment, thermal conductivity meas., cooling probe method 4-94264  
 seismic instrumentation and meas. techniques, for phenomena preceding seismic events (Italian) 4-67170

**physical equipment continued**

- seismic vibrator equipment control and downgoing P-wave 4-110287
- seismic vibrator source for prospecting, calc. of far field radiation pattern 4-100777
- self-surfacing fluxgate system three axis seafloor magnetometer (*Japanese*) 4-100823
- SIR-A mission, planning and characts. 4-94284
- snow mechanical characteristics measurement method and apparatus 4-105764
- snow pressure gauges for mountain slope snow, characts. (*Japanese*) 4-105609
- soil moisture radar remote sensing calibration using ground truth instrument 4-100794
- soil wet density meas. using ND-A densimeter (*Chinese*) 4-72715
- sonar scene matching in the abandoned limestone mineworkings of the West Midlands 4-67509
- sonar side-scan device for mapping sea-floor topography 4-72737
- space laser systems for geodetic appls. accuracy requirements 4-110322
- SQUID magnetometers for undersea geomagnetic field meas. (*Japanese*) 4-100824
- technology impact in geophysics (book) 4-90307
- Tellurometer MA 100, horizontal crustal movements detection 4-94252
- tire rig for glacier ice fracture toughness determ. 4-62999
- thematic mapper, second-generation Earth resources sensor, overview and preliminary results 4-115586
- thematic mapper in LANDSAT 4 Earth resources satellite, oscillating scan mirror assembly 4-115667
- Thematic Mapper of Landsat, ground stations of ESA Earthnet programme 4-82270
- Thematic Mapper of Landsat, ground stations of ESA Earthnet programme 4-82271
- Thematic Mapper on Landsat-4, comparison with Multispectral scanner 4-82055
- Thematic Mapper on Landsat-4, image quality study 4-82265
- Thematic Mapper on Landsat-4, in-flight radiometric calibration 4-82264
- timekeeping at high Arctic latitude field stations using GOES satellite signal 4-82274
- unattended explosion observation recorder (*Chinese*) 4-110274
- well logging using focused-current instruments, accuracy of control systems 4-100782
- Pu detection in soil, design of Si(Li) X-ray detecting apparatus 4-62427
- Rn portable measurement system, appl. to Rn meas. in Austrian springs 4-93671
- Sn content of minerals, X-ray chem. anal. method (*Chinese*) 4-72716

**geophysical prospecting**

- see also minerals
- AC geoelectric sounding, Schlumberger method, effects on soil resistivity (*Croatian*) 4-67165
- acromagnetic surveying, method for estimating body remanent magnetization 4-67419
- bauxite bearing formations, electrical prospecting method (*Hungarian*) 4-62976
- borehole acoustic array data processing 4-67418
- borehole acoustic logging, influence of invaded zone on wavetrain 4-110290
- S' Chukchi Sea, oil and gas content and geological struct. 4-100575
- coal measure rock probing with radar 4-72582
- coal seam prospecting in N Bohemia, computer well-log evaluation methods 4-100780
- cybernetic system for direct exploration of mineral deposits 4-72708
- cybernetic system for mineral deposit exploration 4-72709
- direct problem in gravimetry and magnetometry, soln. in modelling complex geological media 4-77442
- electrical prospecting of offshore sedimentary basins, using vertical bipolar AC source in sea 4-100776
- EM frequency sounding, uniqueness theorem for horizontal loop soundings 4-67168
- EM frequency sounding equipment for study of sedimentary formations (*Hungarian*) 4-62975
- EM prospecting, survey design for multicomponent EM systems 4-67417
- EM prospecting of thin tabular conductor, transient response 4-85788
- airborne EM prospecting of two-layer crust, wheel curve calc. 4-67429
- EM sounding, use of visualisation method in interpreting data obtained by method of transitional processes 4-100826
- transient EM sounding of ground, influence of superparamagnetic layer at surface 4-100439
- European geothermal update, third international seminar at Munich, Germany (November-December 1983) 4-58567
- gamma logging, resolving power, estimation method 4-110310
- gamma-ray logging of borehole radioactivity, two-step deconvolution method 4-100778
- gamma-ray well logging, discrete Fourier transform applied to inverse problem 4-77636
- gamma-ray well logging method, calibration procedure 4-100779
- geochemical methods for Au prospecting at Salair, USSR 4-100828
- geoelectric induced polarisation method for time domain studies 4-62666
- geoelectric sounding by focused-field surface method 4-62968
- geoelectric sounding results for inhomogeneous soil, statistical interpretation (*Croatian*) 4-67166
- geothermic source searching by fission track dating of volcanic glasses 4-100765
- graphite in Balangir District, Orissa, India, geoelectric prospecting 4-77448
- gravity anomaly inverse problem for multiple density boundary case 4-100431
- groundwater 4-67430
- groundwater prospecting, inverse coefficient problems: formulation 4-105606
- horizontal loop EM response of thin plate in conductive Earth, computational method 4-100434
- horizontal loop EM response of thin plate in conductive Earth, computational results 4-100435
- hydraulic fracturing techniques for tight gas sands stimulation 4-62988
- hydrocarbon prospecting in Western Siberia, first attempt at EM core sounding 4-100448
- Indian remote sensing satellite, programme overview 4-115614
- induced polarisation and relax. phenomena 4-77447
- induced polarisation equipment and methods for time-domain studies 4-67420

**geophysical prospecting continued**

- induced polarisation method, interpretation of complex resistivity 4-62665
- infinitely long radiators carrying electric and mag. currents, comparative anal., geophys. prospecting appls. (*Russian*) 4-102875
- inverse gravimetric problem solution by regularisation method, algorithm 4-105732
- inverse kinematic problem, soln. for borehole seismic exploration 4-77655
- inversion of geophysical data by least-squares techniques 4-67423
- Labrador Sea basin, gas deposits existence, drilling and geological obs. (*Russian*) 4-82058
- magnetotelluric sounding, generalisation and optimisation of finite-difference method (*French*) 4-67167
- magnetotelluric sounding, high-freq. response of heterogeneous ground 4-100442
- marine seismology, estimation of bubble pulse wavelets for seismograms deconvolution 4-67173
- oil reservoirs evaluation by gamma ray spectral logging and pulsed neutron application 4-62990
- oilfield seismic prospecting, statistical structs. of wavefield above an oilfield 4-100468
- ore deposit prospecting in rel. with concealed leucogranitic cupolas using remote sensing (*French*) 4-82246
- petroleum and gas prospecting in Oklahoma, USA, by soil gas radioactivity method 4-110104
- petroleum exploration, applied hydrodynamics, book 4-106131
- petroleum prospecting, formulation of geological problem of geophysical regionalisation 4-100827
- placer deposits exploration appl. of quantitative characts. of alluvium accumulation dynamics 4-100646
- placer mineral exploration and development on United States continental shelves 4-115391
- radiofrequency imaging for geophysical applications 4-72720
- remote sensing by reflectance spectroscopy, quantitative analysis techniques 4-115604
- seismic data migration, influence of amplitude and phase errors 4-100462
- seismic deconvolution using max-likelihood deconvolution algorithm 4-100775
- seismic exploration, calc. of synthetic seismograms for complex subsurface geometries 4-105457
- seismic exploration, formal power series and iterative methods for wave vectors 4-67179
- seismic exploration using surface torque source 4-67424
- seismic method for gas reservoir mapping using interactive interpretation system 4-110103
- seismic profiling using detectors in borehole, 2-D dip estimation 4-67416
- seismic prospecting, vibration signals superposition during source movement at constant vel. 4-100478
- seismic refl. profiling, migration of common midpoint slant stacks 4-67415
- seismic refl. profiling, simulation of true amplitude reflections by stacking shot records 4-67422
- seismic refl. profiling method, optimum suppression of coherent signals with linear moveout 4-67413
- seismic reflection profiling, 3-D velocity inverse problem soln. using travel time like variables 4-110062
- seismic reflection profiling, amplitude data used in slant stack domain inversion method 4-100460
- seismic reflection profiling, method for spectrum equalisation (*French*) 4-67426
- seismic reflection profiling method for lateral stratigraphic changes 4-100457
- seismic reflection profiling method using P- to S-wave mode conversion 4-100456
- seismic sounding, discrete wavenumber/finite element method for synthetic seismograms 4-67175
- seismic sounding, interval velocity analysis by wave extrapolation 4-100463
- seismic sounding, matrix methods in synthetic seismograms computation 4-67176
- seismic sounding, poststack estimation of 3-D crossline statics 4-67414
- seismic soundings, comparison of US and synthetic seismograms for laterally varying struct. 4-67178
- seismic survey streamer/airgun tracking using Simrad transducers 4-77667
- marine seismic surveying, equalization of transformerless seismic streamer response 4-67425
- seismic vibrator source for prospecting, calc. of far field radiation pattern 4-100777
- seismology, vertical seismic profiling (VSP) method with phase distortion due to absorpt. 4-100461
- sulphide ore bodies on mid-ocean ridges, resistivity meas. 4-77675
- thematic mapper, second-generation Earth resources sensor, overview and preliminary results 4-115586
- thematic mapper in LANDSAT 4 Earth resources satellite, oscillating scan mirror assembly 4-115667
- thin bounded bed in high resist. medium, parameters determ. 4-77450
- Turam EM exploration system, modified mode for deep prospecting 4-67428
- vertically varying conductivity profiles, inversion from surface potential meas. 4-67164
- well logging of sand-shale complex, statistical anal. method for incomplete sets of logs 4-100781
- well logging using focused-current instruments, accuracy of control systems 4-100782
- well-to-well tomography for enhanced recovery surveillance 4-62989
- Au content in ores, automated neutron activation anal. method 4-110312
- Fe ore deposit prospecting in Goa, India, Landsat MSS method 4-67427
- <sup>220</sup>Rn discrimination in soil gas using solid state nuclear track detectors 4-100767
- U determination in mineral rocks by CR-39 SSNTD 4-100766
- U ore prospecting, use of radioactivity searches (*Russian*) 4-100819

**geophysical techniques**

- see also atmospheric techniques; hydrological techniques; ionospheric techniques; oceanographic techniques
- 2 MV tandem accelerator mass spectrometer for <sup>10</sup>Be detect. 4-109702
- acoustic well logging in fluid-filled borehole, study of resonance modes (*Chinese*) 4-62962
- active microwave instrument (AMI), development 4-85863

## geophysical techniques continued

- aerial-triangulation methods for earthquake fault displacement detection 4-110282  
 aeromagnetic surveying, method for estimating body remanent magnetization 4-67419  
 airborne synthetic aperture radar, digital processing (*Japanese*) 4-77650  
 algorithms for full-waveform sonic logging 4-72734  
 anomaly data reduction to common level, use of inverse theory 4-85802  
 Antarctic glaciology remote sensing using Landsat 3 RBV images 4-82312  
 antineutrino production by Earth interior and possibility of observing them 4-94136  
 apatite, fission track length and density relationship 4-100768  
 apatite, fission-track temperature ages 4-100487  
 $^{40}\text{Ar}/^{39}\text{Ar}$  dating of a basite from the Western Antarctic 4-85763  
 asymptotic method for near-field accelerograms modelling 4-105434  
 bauxite bearing formations, electrical prospecting method (*Hungarian*) 4-62976  
 beam-steered vertical seismic arrays for wave classification 4-105768  
 borehole acoustic array data processing 4-67418  
 borehole acoustic logging, influence of invaded zone on wavetrain 4-110290  
 bottom seismograph recordings in ocean deep seismic sounding, computer processing 4-100814  
 cartographic accuracy of Landsat-4 instruments 4-82267  
 cartography, computer applications (book) 4-90306  
 chemical analysis of rocks by X-ray fluorescence analysis 4-115595  
 coal analysis, IR microspectroscopy, specimen prep. technique, computer-controlled microspectrophotometer 4-93572  
 coal measure rock probing with radar 4-72582  
 coal seam prospecting in N Bohemia, computer well-log evaluation methods 4-100780  
 coastal seafloor photogrammetry, orientation problems due to ocean waves 4-77441  
 complex seismic trace analysis of thin beds 4-100773  
 computer techniques in geology (book) 4-85793  
 core sample computer logging system using ROCKDISC code 4-62972  
 correlated time series averaging, appls. in dendroclimatology and hydrometeorology 4-100665  
 cosmic ray variation studies, necessary geographic distrib. for meas. stations 4-110539  
 cosmic rays applications in hydrology and atm. physics 4-100966  
 crop type discrimination with Landsat Thematic Mapper 4-82057  
 cross-borehole seismic tomography, resolving power 4-94011  
 crustal stress measurement, appl. of fracture mechanics to hydraulic fracturing stress meas. 4-77509  
 crystalline rock formations, geological assessment for radwaste disposal, groundwater 4-64208  
 data spikes elimination by median filtering and application to oceanic data 4-94261  
 data technique, method of editing time series observations 4-100736  
 dating by  $^{14}\text{C}$  method in Antarctica, problems and significance 4-81954  
 dating methods for Late Tertiary shorelines 4-105565  
 desert landform and sand dune remote sensing by SIR-A radar and Landsat (*French*) 4-92964  
 desert region bedrock imaging below sand layer, by satellite radar method 4-100793  
 distance measurement method using ultrasonic waves 4-103153  
 Doppler satellite system for Earth surface position meas. 4-63001  
 Earth's ground roughness and dielectric const., microwave radiometry study 4-110309  
 Earth exploration from satellites, ground stations features (*German*) 4-110284  
 Earth interior mapping by neutrino tomography, feasibility of method 4-72721  
 earth radiation budget experiment design and development 4-72853  
 Earth resistivity measurement, EM method 4-62667  
 Earth surface deformation approximation from long buried kinked crack or intrusive body, simple method 4-94283  
 earthquake double couple focal mechanisms obtained by linear moment inversion method 4-81864  
 earthquake fault length and rupture vel. determ. by Love and Rayleigh wave method (*Spanish*) 4-94274  
 earthquake hypocentre and seismic velocity struct. simultaneous inversion, theory and method (*Chinese*) 4-85623  
 earthquake prediction, amplitude changes and seismic activity before earthquakes in Himachal Himalayas, India 4-94019  
 earthquake prediction, estimation of parameters in statistical prediction theory 4-100475  
 earthquake prediction, groundwater level meas. rel. to hydrodynamic earthquake precursors 4-100471  
 earthquake prediction, instrumentation and meas. techniques for phenomena preceding seismic events (*Italian*) 4-67170  
 earthquake prediction, shear cracks and seismic conditions in specimens containing low-strength inclusions 4-100554  
 earthquake prediction method and epicentres migration (*Russian*) 4-62708  
 earthquakes location procedure 4-105728  
 electrical prospecting of offshore sedimentary basins, using vertical bipolar AC source in sea 4-100776  
 ELF antenna site choice, geophys. methods for testing ground properties 4-115602  
 EM core sounding in Western Siberia, appl. to hydrocarbons prospecting 4-100448  
 EM distance meas. instruments, atmospheric refraction effects determ. 4-110313  
 EM frequency sounding, uniqueness theorem for horizontal loop soundings 4-67168  
 EM frequency sounding equipment for study of sedimentary formations (*Hungarian*) 4-62975  
 EM induction sounding, Frechet derivatives 4-85622  
 EM prospecting, survey design for multicomponent EM systems 4-67417  
 EM prospecting of thin tabular conductor, transient response 4-85788  
 airborne EM prospecting of two-layer crust, wheel curve calc. 4-67429  
 EM sounding, use of visualisation method in interpreting data obtained by method of transitional processes 4-100826  
 transient EM sounding of ground, influence of superparamagnetic layer at surface 4-100439  
 ERS-1 satellite, mission objectives 4-85861  
 ESR dating of geological samples, review 4-63434

## geophysical techniques continued

- estuarine suspended sediment determ., atmospheric correction to LANDSAT MSS data 4-100741  
 fine-beam cathode ray tube for meas. Earth's mag. field 4-63463  
 fission track dating with low track counts, confidence bounds 4-100488  
 fluorapatite, natural, high temperature fission track annealing, track dating 4-100486  
 food store disturbances use for earthquake intensity var. determ. 4-110276  
 Fourier method for seismic wave calcs. 4-110053  
 frequency domain optimal inverse convolution filtering of noise data 4-105735  
 gamma logging, resolving power, estimation method 4-110310  
 gamma-ray logging of borehole radioactivity, two-step deconvolution method 4-100778  
 gamma-ray well logging, discrete Fourier transform applied to inverse problem 4-77636  
 gamma-ray well logging method, calibration procedure 4-100779  
 geochemical methods for Au prospecting at Salair, USSR 4-100828  
 geochronological dating method using  $^{10}\text{Be}$  in soil 4-81880  
 satellite geodesy applications to geosciences 4-110023  
 geodetic distance meas. with Mekometer laser instrument, atmos. corrections and data reduction 4-89998  
 geodetic levelling system of new design 4-89999  
 geodetic methods useful for plate tectonic research 4-100427  
 geodetic network adjustment model for long extended traverse nets and gyrotheodolite orientation meas. 4-85601  
 geodetic positioning using the Global Positioning System in a differential mode 4-72713  
 geodetic satellite laser ranging method for E Mediterranean tectonics 4-100770  
 geoelectric induced polarisation method for time domain studies 4-62666  
 geoelectric sounding by focused-field surface method 4-62968  
 geoid undulations from Doppler satellite positioning and gravimetric techniques, comparison 4-85607  
 geology remote sensing by radar, applicability to N Nigeria 4-100483  
 geomagnetic anomaly data inversion method for single mag. boundary in freq. domain (*Chinese*) 4-85758  
 geomagnetic field var. determ. in ancient Athens 4-110300  
 geomagnetic field var. estimation during high-precision aeromagnetic surveys 4-100829  
 geomagnetic micropulsations, data acquisition procedures used at L'Aquila, Italy 4-110301  
 geomagnetic reversal sequences analysis, statistical methods 4-85621  
 geopotential field derivatives, computation procedure for coeffs. 4-85605  
 geostatistical analysis of oil shale deposit thickness 4-94134  
 geothermic source searching by fission track dating of volcanic glasses 4-100765  
 granitic rocks, near IR spectrochemical analysis method and obs. 4-72719  
 gravity anomaly automatic fitting using 2-D models 4-67421  
 gravity anomaly inverse problem for multiple density boundary case 4-100431  
 groundwater prospecting 4-67430  
 gyrotheodolite constant calculation from calibration measurements 4-85602  
 hazard monitoring and assessment in Mediterranean region, appl. of METEOSAT system 4-94251  
 heat flow measurement in marine sediments, thermistor based equipment 4-81958  
 high-pressure cell with BeO transparent anvils for Earth mantle studies 4-110291  
 horizontal crustal movements detection using MA 100 Tellurometer 4-94252  
 hydraulic fracturing techniques for tight gas sands stimulation 4-62988  
 hydrogeology, inverse coefficient problems formulation 4-105606  
 image processing, data anal. 4-115611  
 Indian remote sensing satellite, programme overview 4-115614  
 induced polarisation equipment and methods for time-domain studies 4-67420  
 induced polarisation method, interpretation of complex resistivity 4-62665  
 integrated resources survey and applications 4-114881  
 interactive image processing in geophysical analysis 4-77674  
 interactive interpretation of seismic data 4-100774  
 inverse gravimetric problem solution by regularisation method, algorithm 4-105732  
 inverse kinematic problem, soln. for borehole seismic exploration 4-77655  
 inverse methods in geophysics, conf., London, England (May 1984) 4-82600  
 inverse problem soln. by maximum entropy method 4-85800  
 inverse problem soln. using Backus-Gilbert approach 4-85799  
 inversion of geophysical data by least-squares techniques 4-67423  
 near IR reflectance spectroscopy for granitic rock chem. analysis 4-72719  
 IR technology and appl., conf., San Diego, CA, USA (Aug. 1983) 4-110800  
 land surface and air temperature, remote sensing of seasonal variations 4-100743  
 land surface passive microwave remote sensing 4-100791  
 land surface remote sensing for climate model application 4-77677  
 land surface temp. and roughness measurement by microwave radiometry (*Russian*) 4-100788  
 Landsat data and database approach, appls. 4-77658  
 Landsat-4 imaging processing techniques and map making 4-82260  
 Landsat-4 MSS and Thematic Mapper data quality and information content 4-82261  
 Landsat-4 MSS and Thematic Mapper image quality 4-82053  
 Landsat-4 Thematic Mapper, radiometric calibration technique 4-82263  
 Landsat-4 Thematic Mapper and Multispectral Scanner, information contents 4-82266  
 Landsat-4 Thematic Mapper geometric accuracy 4-82268  
 Landsat-4 Thematic Mapper radiometric and geometric correction methods 4-82262  
 laser interferometry in space, future prospects 4-110323  
 laser light telemetry, high precision 4-107716  
 laser ranging use in geodesy 4-72765  
 light rock forming elemental analysis using laser neutron generator 4-110311  
 Lithoprobe, seismic and drilling project to study Canadian crust 4-115576

geophysical techniques continued

low level measurements of natural radionuclides in soil samples around a coal-fired power plant 4-105160

magma chamber location techniques, review 4-58605

geo-magnetic field observing history of Geophys. Observatory at Hel. Poland 4-77637

scalar audio-magnetotelluric method, as used in Hungary 4-100440

magnetotelluric sounding, generalisation and optimisation of finite-difference method (French) 4-67167

magnetotelluric sounding, high-freq. response of heterogeneous ground 4-100442

mantle viscosity determ. from Lageos obs. of gravity anomalies due to postglacial rebound 4-85641

marine seismology, estimation of bubble pulse wavelets for seismograms deconvolution 4-67173

mathematical model for determ. of ground surface deform. 4-110092

maximum entropy method, generalisation for processing nonstationary multichannel complex valued data 4-110297

maximum entropy principle for earthquake recurrence relationships determ. 4-105729

maximum entropy spectral analysis of artificial sinusoidal signals, appl. of Burg's algorithm 4-72718

E Mediterranean, satellite laser tracking technique for geodynamics 4-100426

metal detector for finding objects such as artillery shells, EM induction coil equipment 4-100790

metal ore X-ray fluorescence chem. anal. equipment 4-59564

metallogenic maps using new realistic format 4-94247

micropulsation data acquisition and primary processing at Adolf Schmidt Observatory (German) 4-72704

microwave dielectric constants meas. method for substances of Earth's surface (Chinese) 4-77638

microwave sensors, past and present 4-115609

mini-Sosie method (book) 4-86126

mise-a-la masse anomalies, calc. method for high cond. contrast case 4-77644

modulus method for mag. field components determ., algorithm choice 4-94002

Monterey Fan expt., coherent recombination of sediment borne and water path acoustic signals 4-105770

Mossbauer effect, environmental and geochemical appls., review 4-89484

multisensor images for Earth science appls. 4-77659

multispectral imaging systems, summary 4-77660

natural radionuclides near a coal-fired power station 4-105161

near-IR reflectance used for minerals geochem. var. determ. 4-100811

near-zone seismic techniques in USSR 4-100747

neutrino, geophysics, Earth's projected mass density meas. 4-77642

normal-mode theory for seismic sources parameters determ. 4-72762

nuclear explosion yield estimation by teleseismic waveform intercorrelation 4-89886

oceanic crust heat flow meas., techniques comparison 4-105487

oil reservoirs evaluation by gamma ray spectral logging and pulsed neutron application 4-62990

oilfield seismic prospecting, statistical structs. of wavefield above an oilfield 4-100468

palaeo-climate from marine sediment core foraminifera method, choice of correct mesh size 4-72690

palaeomagnetic analysis incorporating declination-only data 4-105414

palaeomagnetic transitional data display and analysis method 4-115603

palaeomagnetism, estimate of confidence in palaeomag. derived from mixed remagnetisation circle and direct observational data 4-105420

palaeomagnetism technique for drill core sample palaeolatitude determ. 4-100821

particle track techniques, and neutron activation anal., appl. to element distrib. determ. in mineralised graphite 4-81889

pattern recognition techniques, remote sensing data anal. 4-115612

petrochemistry NSF triangular diagram, Nanling region, China, granitic bodies and crust transform. (Chinese) 4-72710

petroleum and gas prospecting in Oklahoma, USA, by soil gas radioactivity method 4-110104

petroleum prospecting, formulation of geological problem of geophysical regionalisation 4-100827

photogrammetric camera calibration, US Geological Survey report 4-110028

photogrammetric camera mission on Spacelab 1, using Zeiss instrument 4-105400

photogrammetry, conf., conference, Washington, DC, USA (March 1984) 4-82593

photogrammetry, digitization of aerial stereo photos using interactive computer graphics system 4-62659

photogrammetry, oblique photograph rectification using ORI/SORA-PR system 4-110029

terrestrial photogrammetry by photo-radiation method 4-81835

PIXE's analytic appls., conference, Heidelberg, Germany (July 1983) 4-95034

PIXE analysis of Pt group elements preconcentrated from geological samples 4-100784

PIXE-PIGE thick-target anal., accuracy and precision determ. with geological standards 4-99881

ploughed field, microwave emissivity calc. for remote sensing application 4-100792

potential field data, 3-D automatic interpretation using Hilbert transforms 4-110289

potential field data analysis, continuation between arbitrary surfaces 4-110039

pottery age determination of thermoluminesc., method for determ. radioactive dose rate 4-82273

probability approach to the separation of potential fields 4-62971

radiation budget of Earth, determ. from NIMBUS-7 satellite ERB expt. obs. 4-105712

radiation budget of Earth, measurement by NIMBUS-7 IR radiometry 4-105713

radioactive waste repositories, geoscientific investigations for site assessment 4-83156

radioactivity measurement of geological samples, gamma ray spectrometer with underground detector 4-105765

radioisotope dilution analyses of geological samples using  $^{236}\text{U}$  and  $^{229}\text{Th}$  4-105737

recursive digital filters, IIR design for velocity selection/rejection in seismic signals 4-115592

reflectivity meas. at mm wavelengths (Chinese) 4-82244

geophysical techniques continued

relative elevation determination from Landsat imagery 4-100833

remote reference magnetotellurics, noise correlation lengths 4-100436

remote sensing, computer program package 4-101114

remote sensing, digital image processing techniques, book 4-86132

remote sensing, influenced by atmospheric haze 4-100746

remote sensing, international scene 4-115616

remote sensing, introduction 4-115608

remote sensing, research problems 4-115615

remote sensing, space appl. 4-85860

remote sensing by reflectance spectroscopy, quantitative analysis techniques 4-115604

remote sensing from satellites, IR instrumentation for SPOT satellites 4-100761

remote sensing of agricultural crops and forest types with Landsat Thematic Mapper 4-82056

remote sensing of Earth from satellite using Dicke-type radiometers, resolution aspects 4-67431

remote sensing of land surface, image analysis techniques 4-77519

remote sensing of land surface, influence of surface optical contrast 4-77632

remote sensing pattern recognition and image processing anal. 4-115610

remote sensing satellites, design of advanced sensor systems 4-110305

remote sensing techniques, geological appls. 4-115613

remote sensing using airborne 92/183 GHz imaging radiometer 4-77520

remote sensing using airborne thematic mapper 4-100744

remote sensing using Landsat instrumentation effective bandwidths 4-82272

remote sensor, electrooptical airborne imaging scanner, MEIS II push-broom design 4-100760

rock magnetism, demagnetization factor determined by multidomain hysteresis method 4-82041

rock mineralization temperature determ. from  $\text{N}_2$  and  $\text{H}_2\text{O}$  in rock inclusions 4-105562

rock parameter determ. allowing for specimen size effect 4-77505

rock porosity meas. technique for in-situ rocks, EM tomography method 4-110292

rock subcritical crack growth meas. technique 4-94096

SAR speckle, nature 4-82285

satellite altimetry, accuracy of altimetric surfaces 4-110022

satellite Doppler tracking applications in geodesy and geophys. (Spanish) 4-94273

satellite geodesy applications to geosciences 4-110023

satellite magnetic anomaly data reduction, theory and appl. 4-105421

satellite photography, statistical characts. of obs. (Chinese) 4-82242

seafloor imaging and turbidity meas. system using laser equipment 50 m above ocean bottom 4-82275

SEASAT SAR images, quality assessment methods 4-82288

SEASAT satellite orbit determ. by laser ranging 4-82299

SEASAT satellite orbit tracking over Europe 4-82298

SEASAT-SAR, imagery for land use and geology appl. 4-82294

SEASAT-SAR imagery of Netherlands, visual interpretation and discrimination 4-82295

marine sediment, redox state meas. technique using Pt electrode 4-94262

marine sediment, thermal conductivity meas., cooling probe method 4-94264

marine sediment seismic profiling method for thinly laminated sediments 4-94260

sediment suspended in coastal waters, airborne thematic mapper remote sensing method 4-100745

seismic activity map compilation methods (Russian) 4-62996

seismic background noise measurements reduction to common representation 4-94270

seismic data, pulse estimation and deconvolution, adaptive least-squares for parametric spectral estimation 4-105766

seismic data interpretation 4-100748

seismic data migration, influence of amplitude and phase errors 4-100462

seismic deconvolution using lattice processors, new results 4-105767

seismic deconvolution using max-likelihood deconvolution algorithm 4-100775

seismic event detection computer algorithms (Spanish) 4-115618

seismic exploration, formal power series and iterative methods for wave vectors 4-67179

seismic exploration, full reconstruction of layered elastic medium from P-SV slant-stack data 4-110069

seismic exploration, inversion of refr. wavefield by imaging in p-x and u-z planes 4-110067

seismic exploration method applied to Minnelusa sands, Wyoming, USA 4-109715

seismic exploration using surface torque source 4-67424

seismic geohistory anal., appl. to Canning Basin, Western Australia 4-100772

seismic Kirchhoff method for finite-freq. body wave synthetic seismograms computation 4-105448

seismic low-freq. Rayleigh waves use for large earthquakes parameters determ. 4-105727

seismic magnitudes determ. method, for Greek earthquakes 4-110058

seismic marine refl. profiling systems, response characts. 4-90005

seismic method for gas reservoir mapping using interactive interpretation system 4-110103

seismic migration, solns. of scalar and elastic wave eqns. 4-100459

seismic optimum data editing technique for noise reduction in multichannel data 4-110278

seismic phase velocity determination by cross-correlation of data from 2 seismic stations 4-105444

seismic predictive deconvolution and the zero-phase source 4-100454

seismic profiling using detectors in borehole, 2-D dip estimation 4-67416

seismic prospecting, vibration signals superposition during source movement at constant vel. 4-100478

seismic recording stations, technical improvement of data assembly and transmission (Russian) 4-100737

seismic refl. profiling, migration of common midpoint slant stacks 4-67415

seismic refl. profiling, simulation of true amplitude reflections by stacking shot records 4-67422

seismic refl. profiling method, optimum suppression of coherent signals with linear movement 4-67413

seismic reflection profiling, 3-D velocity inverse problem soln. using travel time like variables 4-110062

## geophysical techniques continued

- seismic reflection profiling, amplitude data used in slant stack domain inversion method 4-100460  
 seismic reflection profiling, dip-moveout by Fourier transform 4-110061  
 seismic reflection profiling, method for spectrum equalisation (*French*) 4-67426  
 seismic reflection profiling, use of nonlinear fan filtering for data processing 4-94269  
 seismic reflection profiling method for lateral stratigraphic changes 4-100457  
 seismic reflection profiling method using P<sub>s</sub> to S-wave mode conversion 4-100456  
 seismic reflection profiling of boundary depths and seismic velocities 4-72490  
 seismic reflection profiling of horizontal boundary, amplitude data for density characts. 4-105464  
 seismic reflection profiling of pipe-like structures 4-105465  
 seismic reflection techniques for lithosphere anal., appl. in Australia 4-82278  
 seismic signal compression using adaptive differential pulse code modulation 4-72714  
 seismic signals, freq. compression use for undistorted recording 4-100749  
 seismic sounding, discrete wavenumber/finite element method for synthetic seismograms 4-67175  
 seismic sounding, interval velocity analysis, by wave extrapolation 4-100463  
 seismic sounding, poststack estimation of 3-D crossline statics 4-67414  
 seismic sounding of crust, discrepancies between surface and borehole methods 4-100467  
 seismic soundings, comparison of US and synthetic seismograms for laterally varying struct. 4-67178  
 marine seismic surveying, equalization of transformerless seismic streamer response 4-67425  
 seismic tomographic 4-85801  
 seismic velocity anomalies used to determine bedding depth and cross section heterogeneities 4-100830  
 seismic velocity monitoring along fault before earthquake 4-110298  
 seismic vibrator source for prospecting, calc. of far field radiation pattern 4-100777  
 seismic waveforms inversion method 4-72764  
 seismology, calc. of synthetic seismograms for complex subsurface geometries 4-105457  
 seismology, explosion in solid-plugged borehole, seismic radiation field 4-115346  
 seismology, time-shift estimation and alignment of discrete time signals, frequency domain method 4-105772  
 seismology, vertical seismic profiling (VSP) method with phase distortion due to absorpt. 4-100461  
 Shuttle imaging spectrometer experiment for the late 1980s 4-77695  
 signal processing, algorithm for accurate freq. determination 4-94244  
 singular value decomposition use for magnetotelluric response functions estimation 4-77445  
 Siple Station conjugate areas' in N Hemisphere in AD 1975 to 1990 period 4-110385  
 SIR-A radar imaging capabilities for geologic struct. in Beirut-Damascus region (*French*) 4-62965  
 snow, microwave emission properties of snowpack and passive remote sensing, review 4-110184  
 snow mechanical characteristics measurement method and apparatus 4-105764  
 soil heat sounding by ball probe, results interpretation and meas. error anal. 4-94250  
 soil microwave remote sensing, for water content and matrix pot. 4-100795  
 soil moisture radar remote sensing calibration using ground truth instrument 4-100794  
 soil properties remote sensing in grassland areas, using Thematic Mapper 4-82269  
 soil water content and elec. cond. meas. technique 4-110307  
 soil wet density meas. using ND-A densimeter (*Chinese*) 4-72715  
 sonar bottom sounding processing, model 4-105769  
 source parameters of small earthquakes, determ. method (*Chinese*) 4-110273  
 space laser applications in geophysics 4-110319  
 space laser apps. and technology, conf., Les Diablerets, Switzerland (March 1984) 4-106122  
 space-borne optical imagers for Earth observation, large IR detector arrays 4-94248  
 space/airborne laser ranging system for geodesy and crust deform. anal. 4-110324  
 spectrochemical analysis of geochem. samples using two-jet plasmatron 4-110308  
 sphere, fission-track temperature ages 4-100487  
 surface fitting by pseudo-potential functions 4-110296  
 survey techniques for moving terrain, appl. to glaciology and tectonics 4-63000  
 synchrotron radiation for elemental concentration determ. in coal 4-100785  
 synthetic aperture radar, devel. in Canada 4-82290  
 synthetic seismograms computation, matrix methods 4-67176  
 TAMS technique for radiocarbon dating, graphite target prep. 4-86989  
 technology impact in geophysics (book) 4-90307  
 tectonic deformation meas. by photogrammetric method 4-82255  
 tectonic deformation quantification, method for given faulted volume (*French*) 4-105556  
 tectonic displacement meas. by satellite Doppler positioning method 4-72476  
 tectonic strain history determ. for conglomerate pebble 4-62813  
 tephra deposit dating by approximate methods 4-62993  
 tephra deposit dating by radioactivity methods 4-62992  
 tephra layer dating by combined magnetostratigraphy and tephrochronology method 4-62994  
 tephra layers as geochronological markers over long distances 4-62995  
 Thematic Mapper of Landsat, ground stations of ESA Earthnet programme 4-82270  
 Thematic Mapper of Landsat, ground stations of ESA Earthnet programme 4-82271  
 Thematic Mapper on Landsat-4, comparison with Multispectral scanner 4-82055  
 Thematic Mapper on Landsat-4, data analysis method 4-82054  
 Thematic Mapper on Landsat-4, image quality study 4-82265

## geophysical techniques continued

- Thematic Mapper on Landsat-4, in-flight radiometric calibration 4-82264  
 Thematic Mapper simulation, conf., Swindon, England (May 1983) 4-95017  
 three-dimensional seismic survey positioning 4-72722  
 time sequence anal. of geophys. data, book 4-82615  
 timekeeping at high Arctic latitude field stations using GOES satellite signal 4-82274  
 TLD, calibration techniques for low level meas. 4-105347  
 topography mapping by satellite radar method 4-90012  
 trace element quantitative analysis, relativistic electrons to induce X-ray emission (REIXE) appl. 4-100786  
 transuranic speciation in geosphere, assessment using alpha spectrometry 4-105053  
 units used in geophysics (*Spanish*) 4-111096  
 vegetation microwave dielec. props. for remote sensing application 4-100574  
 vegetation remote sensing, radiance indices recorder by NOAA AVHRR satellite instrumentation 4-110147  
 very long baseline radio interferometry use in geodesy 4-72765  
 Vesuvian samples, fission-track temperature ages 4-100487  
 volcano calderas, LANDSAT imaging 4-94060  
 waveform inversion of mantle Love waves, Born seismogram approximation 4-110064  
 well casing cathodic protection levels prediction 4-72733  
 well logging by ultrasonic echography (*French*) 4-67444  
 well logging of sand-shale complex, statistical anal. method for incomplete sets of logs 4-100781  
 well-to-well tomography for enhanced recovery surveillance 4-62989  
<sup>40</sup>Ar-<sup>39</sup>Ar dating of basalt containing incompletely degassed xenoliths 4-85764  
 Au content in ores, automated neutron activation anal. method 4-110312  
 Cl isotopic variations determ. in nature 4-77651  
 Fe ore deposit prospecting in Goa, India, Landsat MSS method 4-67427  
 Fe-Ar dating of basic rocks, test of two alteration indices as predictors of Ar loss 4-110140  
<sup>235</sup>Pa measurement, appl. to U series geochemical transport model 4-105738  
 Pb geochronological dating method, calc. of isotope growth curves 4-90004  
 Sn content of minerals, X-ray chem. anal. method (*Chinese*) 4-72716  
 Ti, determ. in geological materials, neutron activation by reactor induced (n, p) reactions 4-82257  
 U determination in mineral rocks by CR-39 SSNTD 4-100766  
 U ore prospecting, use of radioactivity searches (*Russian*) 4-100819  
 U oxidation state determ. in natural waters 4-105054  
 U-Pb dating for case of common Pb with unknown isotopic composition 4-110285
- geophysics**  
 see also Earth; erosion; geochronology; geodesy; geology; geomagnetism; geophysical aspects of cosmic rays; geophysical techniques; hydrology; meteorology; oceanography; radiation belts; rocks; seismology; solar-terrestrial relationships; space research; terrestrial atmosphere; time and latitude; upper atmosphere  
 12th BMR Symposium, at Canberra, Australia (May 1983) 4-90283  
 Annual Review of Earth and Planetary Sciences, Vol.12 (book) 4-101586  
 antineutrino production by Earth interior and possibility of observing them 4-94136  
 Bureau of Mineral Resources (BMR), 11th symposium, Canberra, Australia (1982 May 4 to 5) 4-90282  
 conference, Hamburg, W Germany (1983) 4-106108  
 encyclopedia (book) 4-95078  
 estuarine geophysics, book 4-106132  
 fluid dynamics of rotating atmosphere and planetary interiors 4-110208  
 fluid dynamics variational principle 4-62847  
 ice-mineral mixtures, spectra and remote sensing implications 4-115682  
 International Karakoram Project, conf. at Islamabad, Pakistan (June 1980) 4-58574  
 International Karakoram Project, conf. at London, England (September 1981) 4-58575  
 neutron occurrence in Earth crust, of cosmic ray and radioactivity origin 4-110142  
 regionalisation of oil fields 4-100827  
 remote sensing, computer program package 4-101114  
 units used in geophysics (*Spanish*) 4-111096
- geophysics computing**  
 see also computerised instrumentation  
 air pollution point source, gaussian eqn. Basic computer program 4-66831  
 air pollution transport and diffusion calcs. over uneven terrain, microcomputer model 4-66829  
 aquifer layers, subterranean, data processing and representation (*Italian*) 4-82099  
 atmospheric light scattering, computing aspects 4-67391  
 bottom seismograph recordings in ocean deep seismic sounding, computer processing 4-100814  
 cartography, computer applications (book) 4-90306  
 clastic sedimentary sequences, quantification in time series anal. 4-94042  
 cloud shape recognition in satellite remote sensing, computer programming 4-72707  
 clouds and aerosol vertical distribution, computer study 4-110330  
 coal seam prospecting in N Bohemia, computer well-log evaluation methods 4-100780  
 colour display and analysis system for hydrographic surveying 4-67452  
 core sample computer logging system using ROCKDISC code 4-62972  
 digital tape formats, recommended standards, book 4-110257  
 directional terrain textures invariant under translation rotation and change of scale, optical digital processing 4-67412  
 DIGT 90x120 digital plotting table 4-94257  
 eigenvector decomposition method, shallow water bearing estimation 4-103080  
 environmental problem solving using satellite imagery 4-93675  
 ES-1030, data acquisition, processing and storage system at Obninsk Central Seismological Observatory, USSR 4-100752  
 HIPAS, interactive image processing in geophysical analysis 4-77674  
 hydrology, nonlinear surface runoff system identification 4-110178  
 interactive interpretation of seismic data 4-100774  
 Landsat data and database approach, apps. 4-77658

**physics computing continued**

- longhole open stope stability assessment using computer models 4-62806  
 meteorology, GARP level III data processing 4-72728  
 micropulsation data acquisition and primary processing at Adolf Schmidt Observatory (*German*) 4-72704  
 minewide 2000-channel data acquisition system 4-62956  
 NOAA satellite sea ice image analysis using ice-breaker Shirase's meteorological data processing systems 4-85762  
 ocean storm surge forecasting using marigraph network with automatic control software 4-82250  
 ocean wave image spectra extraction from SAR data, digital processing efficiency improvement 4-67434  
 oceanographic data acquisition, analysis and presentation standards 4-77676  
 oceanographic data processing 4-63725  
 oceanographic remotely operated submersible vehicle computerised survey and data processing package 4-72746  
 oceanography, digital signal processing for precision wide-swath bathymetry 4-67432  
 photogrammetry, digitization of aerial stereo photos using interactive computer graphics system 4-62659  
 photogrammetry, height interpolation by finite elements using computer program 4-62658  
 PLACES ionospheric plasma testing, rocket vehicle targeting 4-62954  
 relative elevation determination from Landsat imagery 4-100833  
 remote sensing, digital image processing techniques, book 4-86132  
 satellite exploration, ground stations features (*German*) 4-110284  
 sea-level survey data, digital filtering (*Chinese*) 4-85680  
 SEASAT SAR images, quality assessment 4-82288  
 seismic data, digital processing of analogue high-freq. data 4-77673  
 seismic data sets, faulted, automatic contouring 4-100735  
 seismic event detection computer algorithms (*Spanish*) 4-115618  
 seismic exploration, data processing 4-67169  
 sonar side-scan device for mapping sea-floor topography 4-72737  
 stratigraphic correlation by means of ordinal scales 4-94041  
 stratigraphy, unitary associations method, graph theory and computer algorithm appls. 4-94040  
 TAUP program, seismic data interpretation in P-Tau and P-X domains 4-100450  
 techniques in geology (book) 4-85793  
 three-dimensional terrain corrections in resistivity surveys 4-100437  
 volcano calderas, LANDSAT imaging 4-94060  
 weather analysis, based on interactive cooperation between forecaster and computers 4-105672  
 weather data, laser printing 4-100734  
 weather forecasting, numerical prediction model implementation on Cray-1 supercomputer, computational aspects 4-62912  
 weather forecasting by CRAY-1 supercomputer 4-77592  
 weather radar simulator, for pilot training 4-85794  
 weather station using BBC microcomputer for online data acquisition 4-110256  
 wind erosion from coal surfaces, computer simulation program 4-82211

**geopotential see geodesy****geothermal power**

- application, European projects (*Dutch*) 4-66656  
 Atlantic and Indian Ocean floor 'spreading centres' with hydrothermal mineralisation 4-115441  
 commercialisation chances after Department of Environment 4-62296  
 deep high-temperature geothermal reservoirs, exploration 4-93587  
 direct-use geothermal systems, life cycle cost anal. 4-99940  
 Dixie Valley geothermal energy project, development 4-62297  
 down hole steam generator—the boiler 4-62294  
 East Pacific Rise hydrothermalism and sulphide deposits 4-115392  
 energy conversion engineering conference, Orlando, Florida, USA, August, 1983 4-67861  
 energy resources, new techniques for exploiting existing geothermal resources in Sweden 4-99939  
 equipment used in direct heat projects 4-109725  
 ethanol production, use of geothermal energy, optimisation 4-77056  
 European geothermal update, third international seminar at Munich, Germany (November-December 1983) 4-58567  
 extraction from hot dry rocks, thermoelastic analysis of cracklike reservoir 4-114892  
 flashed brine geothermal system scale control 4-62298  
 geothermic source searching by fission track dating of volcanic glasses 4-100765  
 greenhouse heating with low temperature geothermal water 4-99941  
 ground water source heat pumps for space heating, economic and comparative analysis 4-62384  
 Gulf Coast geopressure geothermal wells operational testing 4-62299  
 heat exchangers, tube enhancement evaluation 4-114891  
 hot dry rock geothermal reservoir development 4-62295  
 hydrothermal resources at mid-oceanic ridge axes 4-114893  
 Imperial County of California geothermal development summary report. Activities 1979-82. Part I 4-93590  
 Juan de Fuca ridge sulphide deposit formation from seawater and hydrothermal fluid 4-115401  
 Juan de Fuca ridge axial seamount hydrothermal vents and sulphide deposits 4-115440  
 low-grade geothermal energy conversion by organic Rankine cycle turbine generator 4-77140  
 Mokai 5 geothermal well discharge predictions verification by measurements 4-93588  
 renewable energy technologies, contribution to future energy requirements 4-99934  
 seamount hydrothermal sulphide mineral abundances 4-115399  
 United States national programmes promoting renewable energy business development 4-93589  
 volcanic eruption patterns along submarine rift zones 4-115369

**geothermal power stations**

- Imperial County of California geothermal development summary report. Activities 1979-82. Part I 4-93590  
 low-grade geothermal energy conversion by organic Rankine cycle turbine generator 4-77140  
 sea-thermal power generation, field expt. at station off Shimone, Western Japan Sea (*Japanese*) 4-93586  
 sieve tray direct contact heat exchanger thermal and hydraulic performance 4-60249  
 turbine hydrocarbon vapour expansions condensation behaviour 4-60250

**germanate glasses**

- alkali germanate binary glasses, structure, Raman spectra meas. (*Japanese*) 4-113347  
 multi-component oxide glasses, local environment, EXAFS studies 4-60852  
 $\text{GeO}_2\text{-B}_2\text{O}_3(\text{SiO})$  films, opt. absorpt, edge, additions influence 4-71455  
 $\text{GeO}_2\text{-Sb}_2\text{O}_3$  optical fibres fabricated by vapour-phase axial deposition method 4-107855  
 $\text{GeO}_2\text{-SiO}_2$  optical fibres, CVD, gas phase equilib., thermodynamics calcs. 4-109329  
 $\text{GeO}_2\text{-V}_2\text{O}_5\text{-VCl}_3$  glass, optical absorpt., DC cond. rel. to  $\text{VCl}_3$  content 4-65675  
 $\text{GeO}_2\text{-ZnO-K}_2\text{O}$  glass, cladding of hollow-core fibres, laser diode self-coupling 4-107630  
 $\text{Na}_2\text{O-CuO-GeO}_2$  elec. cond., chem. content depend. 4-98673  
 $\text{SiO}_2\text{-GeO}_2$  core graded index fibres, mode attenuation at 1.39  $\mu\text{m}$ , OH absorption study 4-91590  
 $\text{SiO}_2\text{-GeO}_2\text{-P}_2\text{O}_5$  glass fibres,  $\text{H}_2$ -treated, long-wavelength losses 4-103013  
 $\text{SiO}_2\text{-GeO}_2\text{-P}_2\text{O}_5$  optical fibres, H and D absorption losses, expt. study 4-91589  
 $\text{SiO}_2\text{-GeO}_2\text{-OD}$  4-64779  
 $\text{V}_2\text{O}_5\text{-GeO}_2$ , sp. heat, thermal cond. and diffusivity coeff. 4-92384  
 $\text{V}_2\text{O}_5\text{-SeO}_2(\text{TeO}_2)(\text{GeO}_2)$  glass, ESR and photoacoustic spectra 4-104491

**germanium**

see also nuclei with .....

- $\text{O}_2$  state lifetime, delayed auto-coincidence of Ge(Li) detector 4-102497  
 (111) with chemisorbed Sm, photoemission spectra 4-80392  
 amorphous, phonon struct., inelastic electron tunnelling spectra obs. 4-61031  
 amorphous, struct. disorder model, thermodynamic props. 4-75303  
 amorphous, thermal cond. at low temp. 4-80319  
 amorphous and crystalline, surface oxidation, photoemission study 4-76880  
 amorphous film, laser enhanced crystallisation, nucleation, growth velocity, recombination enhanced diffusion 4-65295  
 amorphous-crystalline transition, stability anal. 4-103686  
 angular distrib. of annihilation radiation 4-71472  
 anisotropic internal stresses, electroreflectance and photovoltaic effect meas. 4-84947  
 anomalous muonium hyperfine interaction, temp. depend., 5 to 100K 4-71240  
 atoms,  $\text{K}\beta_1/\text{K}\beta_2$  and  $\text{K}\beta_2/\text{K}\beta_1$  radiative transition rates meas. 4-91231  
 band calcs., empirically adjusted zone variational method (*Chinese*) 4-75831  
 bicrystal p-type inversion layers, anomalous magneto-transport props. 4-98719  
 bicrystals, anomalous magneto-transport props. of p-type inversion layers (*Japanese*) 4-70842  
 biogeochemistry in Baltic Sea 4-77154  
 bolometer, neutron-transmutation-doped, resist. meas. 4-106386  
 book, deposition, growth and technology 4-58579  
 charge carrier transfer and diffusion in strong mag. field (*Russian*) 4-88520  
 clean and  $\text{H}_2\text{O}$  adsorbed, scatt. primary and recoiled surface neutrals and ions, TOF spectra 4-63800  
 compensated, photoresponse to local optical excitation 4-108904  
 compensated, thermoelec. current instability 4-61404  
 crystal surface struct. determ. 4-92487  
 crystallisation front instability during laser epitaxy (*Russian*) 4-99325  
 cyclic loading near yield stress, plastic deform. (*Russian*) 4-113524  
 deep impurity conc., elec. resist. and Hall coeff. meas. 4-65638  
 deep level impurities, low temp. passivation techniques 4-59561  
 deposition on Si, reconstructed surface reordering 4-98411  
 desorption, IR laser stimulated, of carbon tetrachloride from Ge substrate, time of flight distrib. 4-61203  
 dielectric function, temp. depend. 4-109111  
 dislocations, deep electron levels, recursion calc. 4-70716  
 dynamical recovery in high temp. deform. 4-103867  
 elastic props., ultrasonic meas. 4-98170  
 electrical properties, two stage nonmagnetic high press. equipment appl. (*Chinese*) 4-90607  
 electron irradiation and thermal quenching, defects production 4-60962  
 electron-hole liq. relax. kinetics near nucleation threshold, collective decay of small electron-hole drops 4-98541  
 electron-hole liq. droplet destruction in nonuniform deformation field 4-61297  
 electron-hole liquid, phonon-absorpt. imaging 4-61292  
 electronic and structural props., non-local density functional theory 4-108760  
 electronically neutral impurities on muonium, low temp. meas. 4-65279  
 electroreflectance spectra, oscillations anal. for electron-hole Coulomb interactions 4-66011  
 epitaxial growth on GaAs substrate by  $\text{GeH}_4$  thermal compend. 4-71574  
 epitaxial growth on Si by ionised cluster beam method (*Chinese*) 4-84522  
 epitaxial layers, plasma enhanced CVD growth of free-standing films 4-61866  
 exciton condensation, microwave breakdown, one- and two-photon carrier excitation luminescence 4-70670  
 exciton condensation, microwave methods using pulsed optical excitation, kinetics 4-70671  
 exciton condensation, microwave studies, biexcitons and electron-hole droplets 4-70668  
 exciton condensation, microwave study,  $^3\text{He}$  refrigerator, construction and test 4-68234  
 exciton microwave breakdown, exciton and free carrier kinetics with electron-hole drops 4-70669  
 exciton studies, laser heating effects at liquid He temps. 4-70672  
 film, obliquely deposited, spectral and angular selectivity 4-112535  
 film, RF sputtered, controlled doping 4-80059  
 Frenkel pair component distance distrib. after  $\gamma$  irradi. 4-70142  
 gamma-irradiated, hole traps 4-103799  
 gamma-ray spectrometer, collimator geometries 4-102459  
 grain boundaries, plasma exposure effects, diode studies 4-65276  
 ground surfaces, optical props., refl. matrices appls. 4-84935  
 high energy LA phonons, anharmonic decay 4-65355  
 high purity, coaxial detectors performance after fast neutron damage 4-59553  
 high-press. structural phase transitions and cryst. struct. 4-92350

## germanium continued

- homogeneous CVD growth, review 4-88984  
 hot hole submillimetre emission in transverse mag. field 4-71412  
 impurities microinhomogeneities, capture channels, time-amplitude anal. 4-108876  
 impurity breakdown kinetics, small-signal anal. 4-113965  
 injected electron-hole plasma, high-field domains 4-65699  
 intrinsic, thermoelec. 1/f noise and current 1/f noise 4-61425  
 inverse dielectric matrix, direct calc. 4-92645  
 ion channelling, interaction pot., stopping power, ion scatt. spectra 4-75570  
 IR laser radiation nonlinear absorpt. and self-defocusing due to free carrier generation 4-79248  
 IR properties of heavily implanted semiconductors 4-104587  
 irradiated with high-energy heavy ion, induced radioactivities 4-59560  
 island films on insulator, single crystalline, residual strain 4-92573  
 island films on insulator, zone melting recrystn. with SiO<sub>2</sub> capping layers 4-93212  
 isotopically enriched, low-field anomalous muonium depolarisation 4-71241  
 laser pulse irradi., plasma and melting kinetics, IR reflectivity studies 4-108594  
 laser-induced periodic surface struct., fluence regimes, feedback and topography 4-108436  
 lenses, surface struct., veiling glare and image quality in 3 to 10  $\mu$ m spectral region 4-74648  
 liquid, structural study by thermal neutron scatt. 4-108266  
 local-field enhancement of rough surface 4-104047  
 low temperature muonium depolarisation in transverse fields 4-65928  
 luminescence signal of electron-hole plasma 4-104674  
 magnetoconcentration effect and oscillator oscills. 4-98651  
 magnetoconcentration effects and current-voltage characts. (Russian) 4-98642  
 melting, sp. vol. change, semicond.-metal transitions 4-61050  
 microrelief surface, reflecting power and etching form. (Russian) 4-64757  
 MIS struct., surface irregularity enhanced subband resonance 4-61459  
 monocrystalline, K-shell fluoresc. yield 4-85041  
 multiple leaky SAW, FFT vel. meas. by line focus-beam acoustic microscope 4-103164  
 n-type, anomalous magnetoresistance study 4-108879  
 n-type, growth on Si by MBE, charact. 4-98469  
 n-type, low temp. breakdown characts. 4-92737  
 n-type, nonlinear thermoelectric effect 4-98654  
 n-type, photoconductivity sign dynamic change in intense submillimetre radiation 4-70859  
 neutron transmutation doped, annealing, DLTS study 4-60942  
 nonequilibrium current carrier microwave absorpt., carrier conc., excitons 4-70852  
 p<sup>+</sup>-n junction irradi. with  $\gamma$ -rays, capacitance spectroscopy 4-104287  
 p-i-n photodiode for ultralong optical fibre fault location, S/N improvement study (Japanese) 4-60188  
 p-type, 3.39  $\mu$ m transmission modulation by tunable CW CO<sub>2</sub> laser, excitation spectrum 4-79240  
 p-type, multiphoton absorption of submillimetre radiation, carrier drag by photons 4-108906  
 p-type, nuclear doped, elec. cond., 0.06 to 300K, impurity conc. depend. 4-61382  
 phonon dispersion near melting point 4-88250  
 phonon focusing, imaging by electron-beam scanning 4-61009  
 phonon pulses detection by fluorescence of deposited YF<sub>3</sub>Tb<sup>3+</sup> film 4-113555  
 photo-induced complex permitt. at 9 GHz, expt. study 4-65703  
 photodetector, cryogenic telescope on IRAS appl. 4-110525  
 photodetector reliability testing 4-64706  
 photoelectron yield curves during X-ray diffr. 4-61811  
 physical data, compilation, book 4-63420  
 picosecond-pulse laser annealing, phenomenological model 4-88198  
 plastically deformed, anomalous magnetoresist. 4-113976  
 plastically deformed, mag. susceptibility (Ukrainian) 4-88644  
 plasticity at high temperatures, anal. of expt. data 4-98186  
 plasticity at high temperatures, theoretical models 4-98185  
 positron diffusion const., temp. depend. 4-99222  
 pulsed laser irradiated, time resolved temp. meas. by thin film thermocouple 4-113494  
 purification, cryst. growth and annealing props. 4-61831  
 quenching centre form., host interstitial injection by oxidising surface 4-65258  
 radiation-induced rod-like defects 4-92238  
 resonant photoemission at 3-p thresholds 4-85070  
 segmented-electrode detector fabrication, Au mask technique 4-59559  
 semiconductor materials, theoretical anal. (Italian) 4-65721  
 shallow acceptors, ground state calc., allowing for valence band corrugations 4-108817  
 single cryst.,  $\alpha$ -particle irradi., defects and photoelectromag. effects 4-84654  
 single cryst. film growth on SiO<sub>2</sub> by laterally seeded heteroepitaxy 4-93234  
 single cryst. surface X-ray total external reflection spectra 4-76562  
 single crystal and amorphous, optical props. meas. 4-95496  
 speciation in seawater 4-82313  
 spin polarised photoemission 4-88929  
 sputter etch induced electrically active defects, H passivation 4-108918  
 stressed, with large electron-hole dop, magnetoacoustic props. 4-98529  
 submicron layers produced by ion implantation and laser annealing 4-84316  
 substrate for Ag epitaxial film, superconductivity and electron localisation 4-114062  
 surface, (100)-(2 $\times$ 1), adsorption of Ag, HEED and photoemission study 4-75790  
 surface, (111)2 $\times$ 1, highly dispersive dangling bond band; photoemission study 4-70890  
 surface, (111), 7 $\times$ 7, 5 $\times$ 5 and 2 $\times$ 8 struct. models, RHEED intensity distrib. anal. 4-92486  
 surface, (111), deposited ultrathin Sn layers, RHEED study 4-80451  
 surface, (111), electronic structure, temp. dependent UPS study 4-61428  
 surface, (111), lattice gas model of (7 $\times$ 7), (5 $\times$ 5) and (2 $\times$ 8) structures 4-75767  
 surface, (111) 2 $\times$ 1, polarisation depend. of surface-state absorption, photothermal displacement spectroscopy 4-92488

## germanium continued

- surface, crosslinking of epoxy resins, internal refl. spectrosc. obs. 4-104988  
 surface, electroluminescence and photo EMF (Russian) 4-104576  
 surface, nonequilib. charge carrier recombination, isotopic effects 4-92750  
 surface, periodic struct. form. due to action of intense UV excimer laser light 4-81042  
 surface, phase conjugation, reflecting grating recording by plasma refl. 4-97003  
 surface (001), metal-insulator transition, angle resolved photoemission studies 4-104126  
 surface (111), shallow donor impurities, variational soln. 4-70893  
 surface (111)-(2 $\times$ 1), dangling bond states, HREELS and photoelectron spectra study 4-65725  
 surface periodic structures on intense laser bombardment 4-70201  
 surface polariton dispersion under intense irradiation 4-113877  
 symmetrical tilt grain boundaries,  $\Sigma=9, 11$ , struct., electron microscopy obs. 4-70169  
 textured optical storage media, threshold laser writing powers 4-107769  
 tilt boundaries at struct., HREM obs. 4-103767  
 uniaxially deformed., anisotropy of the oscillator effect (Russian) 4-113985  
 US attenuation and nonlinearity const., temp. dependence 4-108552  
 X-ray bandpass filter from Ge solid state detector and GeO<sub>2</sub> foil. 4-91176  
 Ag-Ge (100) interface, growth, structural and electronic props. 4-104093  
 Au-Ge-Sn structure, capacitance-voltage meas. at liq. N<sub>2</sub> temp. 4-84707  
 Au-Ge(H) interfaces on amorphous Ge, Schottky barrier and cpd. formation 4-84669  
 Bi<sub>2</sub>Te<sub>3</sub>/Pb(Ge), doping props., elec. cond. and Seebeck measurements 4-75467  
 cyclotron resonance and radiative recombination for excitons, free carriers, electron-hole droplets 4-71183  
 GaAs: Si, Ge, Si and Ge codiffusion using rapid thermal processing 4-65464  
 GaAs:Ge, LEC grown, dislocation structure etching rel. to dopant conc. 4-113451  
 GaAs:Ge(001), MBE grown, TEM image contrast from antiphase domains 4-104098  
 GaAs/Ge single crystal layers, MBE growth and patterning on Si substrates 4-99315  
 Ge (111)-Pb interface form. dynamics and oxidation 4-84518  
 Ge, clusters, electronic struct. and props. 4-74374  
 a-Ge films, laser-beam annealing time resolved TEM studies 4-65297  
 n-Ge, hot electron capture by dipoles at low temps., field depend. 4-75979  
 a-Ge, localised impurity states 4-104163  
 Ge with adsorbed CaF<sub>2</sub>, layer thickness meas. by RBS (Chinese) 4-70968  
 Ge XXXI, X-ray spectra excited in low-inductance spark plasma 4-74181  
 Ge<sup>4+</sup> ionic pseudopotentials, atomic number depend., general theory 4-83292  
 Ge:Al, implanted ion projected range distrib. 4-80079  
 Ge:Ar(Sb), neutron-transmutation-doped, defects 4-60967  
 n-Ge:As, conductivity and magnetoresistance, effect of localised states 4-113950  
 n-Ge:Au, defect. influence on deep level position of impurity 4-104160  
 Ge:Au photocells, spectral characts. obs. 4-101919  
 Ge:Be, site distortion of Be acceptor, IR spectra 4-92667  
 Ge:Be IR detectors for low-photon-background IR astronomy 4-101160  
 Ge:Be photoconductor, 30 to 50  $\mu$ m detector performance and material aspects 4-108899  
 Ge:Cu, impurity contamination reduction by heat treatments above 700°C 4-71535  
 Ge:Cu, impurity states, annealing effects 4-104148  
 Ge:Cu, quenched in deep acceptors 4-70713  
 Ge:Cu(Au), nonradiative multiphonon capture of carriers by deep traps 4-75889  
 Ge:D, plasma treated, D diffusion and interaction with point defects 4-60951  
 a-Ge:Fe(Ni) films, cond. and localised states 4-104163  
 Ge:Ga, crystal growth characts. In vertical Bridgman system 4-70049  
 Ge:Ga, FIR stress induced photoconductivity, broadband meas. 4-70873  
 Ge:Ga, migration of molten inclusion 4-108659  
 Ge:Ga/(Al,Ga)As/GaAs polar semicond. quantum well system, growth and optical props. 4-114314  
 Ge:Ga(Sb), film on GaAs, doping and elec. props. study (Russian) 4-70182  
 a-Ge:H, bond angle disorder and optical absorption edge 4-99083  
 a-Ge:H, photoinduced absorption spectra 4-109220  
 a-Ge:H:P, new paramagnetic centres and impurity states 4-109056  
 a-Ge:H films, planar magnetron sputtering, electronic props. 4-88972  
 Ge:H-based impurity complexes, charge state determ. 4-92663  
 Ge:H(He), ion irradi., structural defect study 4-88164  
 Ge:Hg, h.c. capture cross section 4-98567  
 Ge:muonium, anomalous, electronic g-factor anisotropy 4-65927  
 Ge:P, ballistic phonon transport under mag. field 4-70301  
 Ge:Sb, heavily doped, US attenuation, mag. field depend. 4-70283  
 Ge:Sb, intervalley neutral impurity scatt. (Russian) 4-104197  
 Ge:Sb, photoexcited, impurity breakdown and impact ionisation 4-92739  
 n-Ge:Sb, US attenuation, mag. field effects, impurity conc. depend. 4-75618  
 Ge:Sb, wave-function phase, relax. time, temp. depend. 4-88517  
 Ge:Sb(As), impurity state breakdown under uniaxial compression 4-70715  
 Ge:Se, impurity levels, Hall effect study 4-108804  
 Ge:Si, ultrapure and doped, muonium state, positive muon spin precession signals 4-71242  
 Ge:Si(Sn)(Al), thermal cond. meas., impurity conc. effect, temp. depend. 4-80318  
 Ge:Te, ion implanted, amorphisation phenomena, electron microscope and electron diffr. studies 4-103656  
 Ge:Zn, far-IR magnetooptical of bound excitons 4-114247  
 Ge:Zn, nonohmic hopping cond. in strong elec. fields 4-88515  
 Ge:Zn, Sb, degree of compensation from optical absorption meas. 4-109221  
 Ge/Al interface, chemisorption and metallisation, electronic struct. 4-92527

## germanium continued

- Ge/GaAs heterojunctions, interface struct., TEM and STEM studies 4-108728  
 Ge-Al films, granular, sp. ht., thermal cond. meas., supercond. transitions 4-98809  
 Ge-GaAs interface, electronic struct. 4-84665  
 Ge-GaSe 'Schottky-like' heterojunction 4-108931  
 Ge-Ge<sub>1-x</sub>Si<sub>x</sub> superlattices, interactions of high-freq. EM waves 4-80670  
 Ge-Ni(Ce), spin polarisation study 4-104722  
 Ge-scintillation camera coincidence detection, characteristics 4-59567  
 Ge-ZnSe (110) interface, ordered and disordered, electronic struct. 4-84666  
 Ge<sub>2</sub> ground state props., HF and CI calcs. 4-83289  
 Ge(Hp)  $\gamma$ -ray spectrometer with NaI(Tl) anticoincidence shield 4-59482  
 Ge(Li) detector, time resolution improvements by compensation (Chinese) 4-68874  
 GeO<sub>2</sub> films, amorphous, elec. characterisation in MIS and MIM structs. 4-70816  
 GeO<sub>2</sub> scatt. primary and recoiled surface neutrals and ions, TOF spectra 4-63800  
<sup>76</sup>Ge, neutron doped, low-temp. elec. cond. 4-80594  
 Ge(100)-GaAs interfaces, Fermi level position and valence-band edge discontinuity study 4-61450  
 InP/Ge, donor identification, photolum. and far IR photocond. in high mag. fields 4-70705  
 InP:S(Sn)(Ge), (100), vacuum annealed, free carrier reduction 4-98610  
 InSb/Ge, impurity solubility, role of acceptor and donor states 4-60949  
 LiNbO<sub>3</sub>-Ge, parametric amplification of SAW 4-108697  
 LiNbO<sub>3</sub>-Ge multilayer structure, nonlinear self-contraction of acoustoelectronic fluctuations spectrum 4-70877  
 Pb-Ge sandwich targets on Si matrix, PIXE anal. signal enhancement, matrix effects 4-99869  
 Sb<sub>2</sub>Te<sub>3</sub>/Pb(Ge), doping, props., elec. cond. and Seebeck measurements 4-75467  
 Si:Ge, bulk impurity diffusion, SIMS study 4-70465  
 Si:Ge, Ge diffusion, isotope effects, SIMS studies 4-65491  
 Si:Ge, Ge diffusion and conc. profiles, SIMS studies 4-65490  
 Si:Ge, implantation, pre-amorphisation/rapid thermal annealing procedure for shallow junction formation 4-88188  
 Si:Ge(Sb)(W), electron beam doping, SIMS and RBS studies (Japanese) 4-108401  
 a-Si:H/a-Ge:H/a-Si<sub>1-x</sub>C<sub>x</sub>/a-Si<sub>2-x</sub>H<sub>2</sub> superlattices, CVD growth and struct. 4-114416  
 TeO<sub>2</sub>/Sn/Ge film as optical erasable medium 4-91550  
 ZnP<sub>2</sub>/Ge, induced absorption and bleaching under laser irradi. 4-64747  
 ZnP<sub>2</sub>/Ge, induced absorpt. and transmission (Russian) 4-96984  
 ZnSe-Ge heterojunction, valence-band discontinuities 4-84676

## germanium alloys

## see also Ge-Si alloys

- Al-Ge, binary constitution diagrams at very high press. 4-104766  
 Al-Ge, distribution of electric field gradients around impurities, conduction electron screening lattice strain 4-113910  
 Al-Si-Ge, Si<sup>+</sup> ion implantation effects on supercond. temp. (Chinese) 4-76062  
 As<sub>2</sub>Se<sub>4</sub>Ge<sub>3</sub> glassy semicond., photostructural transformations 4-61076  
 Au-Ge bilayers, ion beam mixing, amorphous and metastable phases formation 4-80113  
 Au-Ge/Au ohmic contact struct., grain boundary diffusion of Ge through Au, Auger anal. 4-88344  
 Au-Ge-Ni ohmic contacts on GaAs, CO<sub>2</sub> laser alloying 4-76038  
 Au-Ge(Ni) on GaAs, alloying behaviour 4-80454  
 AuGe/GaAs ohmic contact, Ge and Au profiles, SIMS studies 4-103782  
 Co-Ge eutectics, X-ray spectral investigation (Russian) 4-76564  
 Co-Ni<sub>1-x</sub>MnGe, magnetic transforms., effect of external press. 4-104418  
 Cl<sub>1-x</sub>MnGe, amorphous thin films, elec. resist., Hall resist. 4-114049  
 Cu-Ge, shock loaded, dislocations and plastic response 4-108370  
 DyCu<sub>2</sub>Ge<sub>2</sub>, mag. and cryst. struct., neutron diff. studies 4-65794  
 Fe-Ge eutectics, X-ray spectral investigation (Russian) 4-76564  
 (Fe<sub>1-x</sub>Ni<sub>x</sub>)<sub>2</sub>Ge, magnetisation, Curie temp., mag. moments, X-ray diff. studies 4-98862  
 (Fe<sub>1-x</sub>Ni<sub>x</sub>)<sub>2</sub>Ge, magnetisation, Curie temp., mag. moments, X-ray diff. studies 4-98862  
 n-GaAs/Au-Ge Ohmic contact fabrication by IR lamp alloying 4-84690  
 (GaSb)<sub>1-x</sub>(Ge)<sub>x</sub>, semiconductor alloys, phase transforms. 4-92347  
 GdCu<sub>2</sub>Ge<sub>2</sub>, charge transfer, X-ray absorpt. spectra study 4-81037  
 GdFe<sub>2</sub>Ge<sub>2</sub>, charge transfer, X-ray absorpt. spectra study 4-81037  
 GdGe<sub>1.63</sub>, constitution diagram, thermodynamic properties, EMF obs. 4-89024  
 GdMn<sub>2</sub>Ge<sub>2</sub>, charge transfer, X-ray absorpt. spectra study 4-81037  
 Ge-Al amorphous thin films, hopping cond. meas., 130 to 300K, localised state variations 4-92713  
 Ge-Ga, freezing, periodic growth rate effect on morphological stability 4-98039  
 Ge-Sb amorphous thin films, hopping cond. meas., 130 to 300K, localised state variations 4-92713  
 Ge-Sn alloy, semiconducting phase, band structure 4-80489  
 Ge-Sn amorphous thin films, hopping cond. meas., 130 to 300K, localised state variations 4-92713  
 Ge<sub>1-x</sub>Te<sub>x</sub>, melting and crystn. 4-113584  
 Ge<sub>2</sub>Te<sub>3</sub> glass, elec. cond. transition, press. and temp. depend. 4-98619  
 LaPtGe, superconductivity and superconducting T<sub>c</sub> 4-61484  
 Mn-Ge, Invar type, antiferromag., transition metal influence on props. (Japanese) 4-65826  
 Mn-Ge, liquid, struct. determ. (Russian) 4-103640  
 Mn<sub>2</sub>Ge<sub>8</sub>, cryst. struct. and lattice const. temp. depend. 4-103702  
 Mn<sub>3</sub>Ge<sub>2</sub>, cryst. struct., X-ray diff. 4-65216  
 Mn<sub>3</sub>Ge<sub>3</sub>, thermal expansion meas., 4.2-800K, Curie point, press. shifts 4-98320  
 Mo-Ge amorphous ultrathin supercond. films, localisation and interaction effects 4-65766  
 Mo<sub>2</sub>Ge, fast neutron irradi., effects on struct. and supercond. props. (Russian) 4-92841  
 MoGe<sub>1-x</sub> amorphous sputtered films, supercond. transition temp. (Chinese) 4-98794  
 Nb-Ge, thin films, electrical resistivity, temp. depend. 4-108963  
 Nb-Ge films, X-ray diff. study 4-65584  
 Nb<sub>2</sub>Ge, CVD grown via heteroepitaxial process, growth morphology, cryst. struct., supercond. transition temp. 4-88624  
 Nb<sub>2</sub>Ge superconducting films, bias sputtered, film growth process 4-98804

## germanium alloys continued

- Nb<sub>2</sub>Ge, thermodynamic props. calc. 4-84741  
 Nb<sub>2</sub>Ge:Mg<sup>+</sup>, supercond. film, implantation effect on resistance anomaly (Chinese) 4-92872  
 Nb<sub>2</sub>Ge-a-Si-Pb Josephson tunnel junction 4-104374  
 Nb<sub>2</sub>Ge<sub>2</sub> hexagonal phase, X-ray diff. study 4-76751  
 Ni-Ge dilute alloys, defect reactions, diffuse X-ray scatt. studies 4-75440  
 Ni-Ge eutectics, X-ray spectral investigation (Russian) 4-76564  
 Ni-Ge-Au-Ag low resist. alloyed ohmic contacts to Al<sub>0.48</sub>In<sub>0.52</sub>As/n<sup>+</sup>-Ga<sub>0.47</sub>In<sub>0.53</sub>As 4-84692  
 NiFe-Ge amorphous and cryst. films, planar Hall effect and magnetisation reversal 4-75930  
 Pd<sub>80</sub>Ge<sub>20</sub> metallic glasses, amorphous and cryst., X-ray absorpt. near edge struct. and EXAFS spectra 4-66120  
 Rh<sub>2</sub>MnGe<sub>2</sub>Sn<sub>1-x</sub>P<sub>x</sub> superhyperfine films, Mossbauer study 4-71215  
 Si<sub>63.5</sub>Ge<sub>36.5</sub>P, Hall voltages changes at high temp. meas., using AC meas. system 4-58866  
 Sn-Ge dilute alloys, semiconductor-metal transition, press. effects 4-92613  
 Sn-Ge dilute alloys, semiconductor-metal transition under press. 4-113871  
 Te-Ge, amorphous, compaction process, stability, DSC obs. 4-114448  
 Te-Ge film optical recording media, writing and degradation characs., subbing layer surface energy effects 4-91552  
 Te-Ge thin films for optical data storage, optical props. and stability 4-91553  
 Ti-Ge, plastic deform. induced polymorphic transform., positron annihilation obs. 4-66093  
 Ti-Nb-Ni-Ge, struct. and supercond. props. (Russian) 4-92143  
 U<sub>2</sub>Ge<sub>2</sub>, intermetallics, cryst. growth from melt 4-66219  
 V<sub>3</sub>Ge<sub>1-x</sub>Al<sub>x</sub>(Si<sub>1-x</sub>Sb<sub>x</sub>), superconductivity, electron-phonon parameter, electron-atom ratio 4-114058  
 V<sub>3</sub>Ge<sub>2</sub>Ga<sub>3</sub>, A-15 superconductor, impurity location using EXAFS 4-88190  
 Zn-Ge eutectic alloy, (100) textured Ge crystallites, morphology 4-76783  
 Zr<sub>2</sub>Nb<sub>3</sub>Ge<sub>4</sub>, crystal struct., X-ray diff. studies 4-113393

## germanium compounds

## see also germanium alloys

- cryst., laser Raman spectra 4-114252  
 oxides, resonant photoemission at 3-p thresholds 4-85070  
 X-ray bandpass filter from Ge solid state detector and GeO<sub>2</sub> foil. 4-91176  
 As-Ge-Se, glass, small conc. of Se, elec. cond. rel. to temp. 4-92729  
 As-Ge-Se system, compound form., diagrams, DTA and X-ray investigation (Russian) 4-113587  
 Cu<sub>1.2</sub>Ge<sub>0.2</sub>Fe<sub>1.6</sub>O<sub>4</sub>, orthorhombic distortions due to doping 4-70103  
 (GaAs)<sub>1-x</sub>(Ge)<sub>x</sub>, bond and struct. models 4-108772  
 GaGeTe, Raman spectrum and lattice dynamics 4-80941  
 GaSe<sub>2</sub>Ga, glassy semiconductor, doping effect, positron annihilation 4-61764  
 Ge-As-S-I glasses, chemical bonding and mag. susceptibility (Russian) 4-70041  
 Ge-As(Si)Se vitreous chalcogenide based multilayer reflecting systems for IR lasers 4-69532  
 Ge-As(Sb)-Si-Se, antireflection coatings for YAG crystals (Russian) 4-97012  
 Ge-P-S, semiconductor glass, paramagnetic centres, ESR study 4-80819  
 Ge-S glasses, narrow Lorentzian ESR signals 4-65858  
 Ge-Sb-Se glasses, dilatometric studies 4-108634  
 Ge-Sb-Se vitreous chalcogenide based multilayer reflecting systems for IR lasers 4-69532  
 Ge-Se glasses, microstructure, electron microscopy obs. 4-88305  
 Ge-Se<sub>2</sub>-Se system, liq. and amorphous, phase diagram and short range order 4-103905  
 GeCl, rot. const., high resolution study 4-96523  
 Ge<sub>2</sub>Fe<sub>3</sub>O<sub>4</sub>, mixed valent, prep., struct., mag. props. (French) 4-88148  
 GeH, IR spectra, geometries 4-69078  
 GeH<sup>+</sup>,  $\alpha$ -X transition, vibr. and rot. const., visible spectra 4-59789  
 Ge<sub>2</sub>H<sub>4</sub>, charge iterative relativistic extended Huckel theory and its appl. 4-59643  
 GeH<sub>2</sub>F, excited vibr. states Coriolis reson., MM wave spectra 4-59719  
 GeNi<sub>2</sub>O<sub>4</sub>, mag. hyperfine interaction, <sup>61</sup>Ni Mossbauer spectra 4-98986  
 GeO, obliquely evaporated film, influence of moisture on surface morphology 4-113761  
 GeO<sub>2</sub>, behaviour in dehydration and consolidation processes of VAD method, optical fibre fabrication 4-97155  
 GeO<sub>2</sub> in Cu-SiO<sub>2</sub>/GeO<sub>2</sub>-Cu sandwich structures, elec. props. time, temp. press. depend. 4-108949  
 GeO<sub>2</sub> surface, crosslinking of epoxy resins, internal refl. spectrosc. obs. 4-104988  
 GeO<sub>2</sub>, vitreous, local environment, EXAFS studies 4-60852  
 GeO<sub>2</sub>/SiO<sub>2</sub>-thin films, ESR rel. to elec. and optical props. 4-65860  
 GeO<sub>2</sub>-P<sub>2</sub>O<sub>5</sub>-SiO<sub>2</sub> glass fibre, transient stimulated Raman scatt. (Chinese) 4-91532  
 GeO<sub>2</sub>-P<sub>2</sub>O<sub>5</sub>-SiO<sub>2</sub> single-mode optical fibres, preliminary report 4-69585  
 GeO<sub>2</sub> films, optical const., random bonding model 4-85025  
 GeS film, crystalline and amorphous, photoconductivity study (Russian) 4-70870  
 GeS, hole drift mobility anisotropy 4-70814  
 GeS, hyperfine and isotopically invariant parameters, microwave spectra 4-59728  
 GeS layered monocrystals, photoluminescence spectra, pol. plane orientation change effects 4-66069  
 GeS single crystal, reflectance and thermoreflectance studies 4-71356  
 GeS<sub>2</sub> glass, struct. factor, temp. depend. 4-79944  
 GeS<sub>2</sub>-Ag photosensitive system, holographic grating recording (Russian) 4-96843  
 Ge<sub>2</sub>S<sub>3</sub> glass, undoped and metal doped, impurity surroundings, nature of defects, positron annihilation study 4-79943  
 Ge<sub>2</sub>S<sub>3</sub>:Cu(Ag), glassy, doping effect on elec. and optical props. (Russian) 4-98625  
 Ge<sub>2</sub>S<sub>3</sub>-x glasses, short range order model, optical gap calc., IR band intensity 4-75310  
 (GeS<sub>1/2</sub>)<sub>100-x</sub>Bi<sub>x</sub> glass, photoconductivity meas. 4-98670  
 GeSe, crystal growth from GeSe-I vapour, complex equilibria anal. 4-81122  
 GeSe, thin film, laser-induced synthesis 4-80095  
 GeSe<sub>2</sub>, amorphous thin film, light induced transmittance oscillation 4-76538  
 GeSe<sub>2</sub>, cryst. and glassy, photoelec. props. 4-108905

**germanium compounds continued**

- GeSe<sub>2</sub> glass, bulk, press. induced electronic and structural transformations 4-114004  
 GeSe<sub>2</sub> glass, tunnelling relax. in a.c. cond. 4-70812  
 GeSe<sub>2</sub> thin film, laser-induced synthesis 4-80095  
 Ge<sub>0.1</sub>Se<sub>0.9</sub>:Ag, photodoping physics study 4-75464  
 Ge<sub>2</sub>Se<sub>7</sub>:Ag layers, amorphous, photodoped impurity lateral diffusion 4-70464  
 GeSe<sub>1-x</sub> glass, photoluminescence characts. 4-76513  
 (GeSe<sub>3.3</sub>)<sub>100-x</sub>Bi<sub>x</sub> glass, photoconductivity meas. 4-98670  
 (GeSe<sub>3.3</sub>)<sub>100-x</sub>Bi<sub>x</sub> struct. and resist. effect of dopants, high press. study 4-103660  
 (GeSe<sub>3.3</sub>)<sub>100-x</sub>Sb<sub>x</sub> struct. and resist. effect of dopants, high press. study 4-103660  
 Ge<sub>20</sub>Se<sub>80-x</sub> thin films, optical properties determ. 4-114337  
 GeTe, heats of polymorphic transitions 4-61065  
 GeTe, solubility of ZnTe and CdTe, effects of temp. 4-108622  
 GeTe-Ag<sub>2</sub>Te-Sb<sub>2</sub>Te system, solid soln., fabrication technology 4-75682  
 GeTe-InTe, phase transformations, 300-900K 4-108602  
 Ge<sub>20</sub>Te<sub>80</sub> glass, bulk, elec. transport and high press. studies 4-114003  
 (GeTe)<sub>1-x</sub>(AgSbTe)<sub>x</sub>, thermolec. figure of merit 4-84637  
 Li<sub>2</sub>O-Nd<sub>2</sub>O<sub>3</sub>-GeO<sub>2</sub>(SiO<sub>2</sub>) ternary systems, subsolidus phase equil. and fluorescence activity 4-113596  
 Li<sub>1-x</sub>Zn(GeO<sub>4</sub>) thin films, for solid state batteries, preparation and characteristics 4-93224  
 Nd<sub>2</sub>O<sub>3</sub>-WO<sub>3</sub>-GeO<sub>2</sub> (MO: M-Ca, Sr, Ba, Mg, Zn), subsolidus phase equil. and fluorescence activity 4-113597  
 (Pb, Sn, Ge)Te, semicond., dielec. props. and soft modes, review, book contrib. 4-61622  
 Pb<sub>1-x</sub>Ge<sub>x</sub>Te, ferroelec. phase transition, high press. investigation, DC resist., capacitance meas. 4-71312  
 n-Pb<sub>1-x</sub>Ge<sub>x</sub>Te, free carrier mobility, ferroelectric phase transition 4-71317  
 Pb<sub>1-x</sub>Ge<sub>x</sub>Te, rhombohedral phase, energy surfaces and domain struct. 4-76010  
 Pb<sub>1-x</sub>Ge<sub>x</sub>Te, synthesis and cryst. struct. 4-84261  
 Pb<sub>1-x</sub>Ge<sub>x</sub>Te, undoped and In-doped, anomalous scatt. of carriers by defects and impurities near ferroelec. phase transition 4-98622  
 Pb<sub>1-x</sub>Ge<sub>x</sub>Te:In, elec. props., band edge struct., impurity effects 4-108880  
 Pb<sub>1-x</sub>Ge<sub>x</sub>Te:In, solid solns., impurity photocond., spectra and kinetics 4-113994  
 PdGe formation on Ge, thin film reaction investigation by W marker 4-104964  
 Se-Ge amorphous, DC conductivity thickness dependence 4-84620  
 SiO<sub>2</sub>-GeO<sub>2</sub> low-loss high-resolution image fibre fabricated by multiple-fibre method 4-97159  
 SiO<sub>2</sub>-GeO<sub>2</sub> multimode fibres, H<sub>2</sub> effects on IR absorpt. characts. 4-97106  
 SiO<sub>2</sub>-GeO<sub>2</sub> thin film deposition using sol-gel technology 4-76697  
 SiO<sub>2</sub>-GeO<sub>2</sub> birefringent single mode fibre, optical Kerr coeff. meas. at 1.15  $\mu$ m 4-74629  
 SiO<sub>2</sub>-GeO<sub>2</sub> optical fibres fabricated by vapour deposition techniques, uniform waveguide dispersion segmented-core designs 4-91607  
 SnSe-GeSe<sub>2</sub>-AsSe, glass formation, physicochemical props. 4-92365  
 Te-Ge-Pb(Sn) alloys, glass stability, cryst. struct. effect 4-60836  
 V<sub>2</sub>O<sub>5</sub>-GeO<sub>2</sub> glass, ESR and photoacoustic spectra 4-104491  
 ZnGeAs<sub>2</sub>-CdGeAs<sub>2</sub>, semiconducting alloys, melt quenched, phase stability, glass form., TEM obs. 4-71641  
 ZnGeAs<sub>2</sub>-ZnSnAs<sub>2</sub>, semiconducting alloys, melt quenched, phase stability, glass form., TEM obs. 4-71641  
 ZnGeP<sub>2</sub>, electronic struct. calcs. 4-108774

**getters***see also vacuum techniques*

- fusion devices, use of getters 4-90605  
 ion implantation, dose control, annealing and gettering 4-84309  
 pumping speed meas. in range 10<sup>-2</sup> to 10<sup>7</sup> l per s 4-90604  
 TMX-Upgrade, computer control of Ti getter system 4-111845  
 Be-HfO, Hf<sup>+</sup> implanted, O gettering 4-92218  
 GaAs substrate, annealing as gettering technique prior to MBE growth 4-99615  
 Si photovoltaic devices, P implanted, Ar ion implantation gettering influence on props. 4-66703  
 Si VLSI circuit processing, material phenomena 4-103738  
 SiO<sub>2</sub>:HCl(Cl<sub>2</sub>) film on Si, impurity distrib., SIMS study 4-113485  
 T, electrolytic gettering from air using solid proton electrolyte 4-86966  
 T extraction by gettering with Y for impure Li blanket case 4-107027  
 Ti film, adsorbed O<sub>2</sub>, Ti gettering, surface chem. 4-108707  
 Ti film, characterisation in TMX-U 4-93579  
 Ti film getter pump, gas sticking coeffs. 4-82803  
 Zr with surface adsorbed H, sticking coefficients, binding states, desorption studies 4-113784

**GFRP** *see glass fibre reinforced plastics***giant pulsations (earth)** *see micropulsations***giant resonances** *see nuclear collective states and giant resonances***giant stars***see also supergiant stars*

- AM-1, outer halo cluster, metallicity, giant branch and horizontal branch characts. 4-115788  
 $\alpha$  Andromedae, chemical comp. of red giant atmosphere 4-105988  
 Z Andromedae, symbiotic star, March 1984 brightening 4-67741  
 Z Andromedae, symbiotic star, visual magnitude estimates (1984 March 30 to April 9) 4-67743  
 EG Andromedae, UV spectral changes in symbiotic star, IUE obs. 4-115761  
 asymptotic giant branch, He shell flash, surface luminosity increase and mass ejection 4-72941  
 asymptotic giant branch stars, evolution rel. to He-burning planetary nebulae nuclei 4-63143  
 $\alpha$  Aurigae, He II 30.4 nm line search, interstellar medium implications 4-85924  
 $\alpha$  Aurigae (Capella), magnitude obs. for possible variability 4-94763  
 B-type stars, characts. 4-67880  
 Cool Ba stars, abundances and model atm. anal. 4-63164  
 BD+37°443 shown to be non-variable, AAB obs. 4-67720  
 Y Canum Venaticorum, light and radial vel. changes in C star 4-77844  
 RS Canum Venaticorum stars, UV photometry of five bright new variables 4-101361  
 $\zeta$  Capricorni, Nb and Rb abundances in Ba star 4-67745  
 $\beta$  Capricorni, orbital elements from lunar occultation obs. 4-101407  
 R and S Carinae,  $\alpha$  Cet stars, BV and DDO photometry 4-82477  
 giant stars continued  
 $\nu^2$  Cassiopeiae, chemical comp. of red giant atmosphere 4-105988  
 TU Cassiopeiae, multimode Cepheid, search for chromospheric emission lines 4-77854  
 cataclysmic binaries, evolution and spectral characts. rel. to planetary nebulae 4-110722  
 $\alpha$  Ceti, infalling matter characts. from inverse P Cyg profiles 4-72946  
 circumstellar cyanoacetylene, obs. and anal. 4-85907  
 FK Comae Berenices, light curve vars. and Ho flaring 4-67747  
 FK Comae Berenices, UBVR1 and Ho photometry 4-72945  
 FK Comae Berenices, binary star model involving mass transfer, UV spectral obs. 4-85964  
 FK Comae Berenices, UBVR1 and Ho photometry 4-85963  
 conference on cool stars, stellar systems and Sun, at Cambridge, United States (October 1983) 4-95064  
 cool evolved stars, outer atm. struct., models and mass loss 4-85935  
 cool giant stars, atm. line emission, var. with evolution and structure 4-90144  
 V1016 Cygni, emission lines, geometric implications for eruptive symbiotic stars 4-67727  
 V1016 Cygni, protoplanetary nebula, electron density determ. from Si III UV emission line strengths 4-94583  
 CH Cygni, spectrophotometric obs. red giant with hot spot and dust shell 4-94796  
 V 1329 Cygni (HBV 475), chromospheric event and violet shifted absorpt. and emission lines detect. 4-72957  
 degenerate C core form., mass limit rel. to masses of supernova progenitors 4-63183  
 UY Draconis, light and radial vel. var. in C star 4-77843  
 extreme He stars, UBVR1JKL obs. 4-90158  
 $\delta$  Geminorum, RS CVn star containing red giant, UV lines anal. 4-85911  
 IS Geminorum, SRD-type variable, spectral characts. 4-101354  
 globular cluster giant branch, temp. index rel. to metal abundance index 4-110696  
 globular cluster giant stars, model atm., spectra and mass loss 4-110608  
 $\beta$  Gruis, late-type giant, S I emission lines in EUV spectrum 4-85939  
 $\beta$  Gruis (M3 II), Fe II fluorescence in atmosphere, UV obs. 4-63154  
 GX 1+4, symbiotic X-ray binary star, optical emission lines obs. 4-63201  
 halo giant stars, metal abundances determ. 4-115752  
 HD 110281, 165195 and 232078, metal deficient red giants, chromospheres, spectral obs. 4-85937  
 HD 207739, BV photometry and search for variability 4-94800  
 HD 35155, S-type star, emission lines interpretation 4-85971  
 HD 81817, 'hybrid' K-type giant, discovery of white dwarf companion from IUE obs. 4-101326  
 Herbig Ae stars CD-44°3318 and UX Ori, evolutionary status, obs. 4-94792  
 Hyades giants, UV continua var. between stars and spectral obs. 4-85934  
 HV Hydrate, red variable star, polarimetric obs. 4-85950  
 IRC+10216, C star, C<sub>2</sub>H detect. in shell 4-77834  
 IRC+10216, CN and C<sub>2</sub>H in C star 4-94787  
 irregular variables among zenith tube stars, photometry 4-67735  
 AR Lacertae, eclipsing RS CVn star, Ho obs. 4-82504  
 AR Lacertae, RS CVn star, VLA obs. 4-72976  
 late-type giants and supergiants, Fe II emission and excitation 4-110516  
 late-type giants, atm. excitation mechanisms and UV spectra 4-85940  
 late-type stars, atlas of IR spectra, 2400-2778 cm<sup>-1</sup> 4-94735  
 R Leonis, long-period variable, OH conc. anal., deviation from thermodynamic equilib. 4-94808  
 LMC bar, population struct. and star form., red giants colour-magnitude diagram anal. and construction 4-90229  
 LMC intermediate age star clusters, ages from red giants luminosities anal. in evolution models 4-90193  
 long period variables, intrinsic polarisation var. due to flare effects on circumstellar material 4-94779  
 long-period and semiregular variables, 1984 max./min. predictions 4-77845  
 long-period and semiregular variables in 1984, schematic mags. 4-77846  
 long-period variable stars, photometric colours, effects of radius, temp. and TiO absorpt. bands 4-94809  
 long-period variables, bolometric corrections 4-67725  
 long-period variables discovery in field at  $l=78^\circ$ ,  $b=-6^\circ$ , positions, finding charts and elements 4-67733  
 long-period variables in Baade's Window, 1-12  $\mu$ m photometry 4-115757  
 T Lynxis, UV continuum in N-type C star near max. 4-105994  
 in M67, old open cluster, photometry and comp. 4-82531  
 M-type giant stars in Baade's Window, spectral classifications, positions and apparent I magnitudes 4-101325  
 M-type giants, Li abundance determ., effects of mol. lines [Russian] 4-101331  
 magnetic field observations of evolved stars 4-110605  
 Mira variable stars, spectral classification with phenomenological photometric procedure 4-82476  
 Mira variables in southern hemisphere, spectral classification, catalogue 4-110628  
 SY Muscae, symbiotic star, periodic light vars. due to refl. effect and eclipses 4-77855  
 N-type C stars, Mg II and C II spectra, semi-empirical chromospheric models 4-85966  
 in NGC 205, dwarf elliptical galaxy, red giant branch population obs. 4-90228  
 NGC 2158, open cluster, clump giants spectral obs. 4-63217  
 OH 32.8-0.3, OH-IR star with absorpt. features of pure water ice, IR spectrum 4-110764  
 OH-IR stars distrib. and kinematics in Galaxy centre region 4-63312  
 open clusters red giants and dwarfs, radial vel. anal. 4-63222  
 $\omega$  Orionis, Be star, mass loss episode anal. 4-90156  
 AG Pegasi, symbiotic star, new determ. of photometric period from visual and photoelectric obs. 4-67734  
 SZ Piscium, eclipsing RS CVn star, Ho obs. 4-82504  
 planetary nebula progenitor, wind-planetary nebula Stromgren sphere interaction 4-106046  
 L<sub>2</sub> Puppis, SRB star, BV and DDO photometry 4-82477  
 RX Puppis, symbiotic system with Mira component, visible and IR emission 4-72955  
 R-type stars, chem. comp. and evolutionary state 4-105993  
 radiative processes in cool star chromospheres 4-90152  
 radiative transfer in spherically-extended stellar atmospheres, appl. of integral eqns. 4-94601

# giant stars continued

- red giant and planetary nebulae form. 4-110722
- red giant stars in globular clusters, discovery of intrinsic polarisation 4-82470
- red giant-black dwarf system, dwarf inside giant envelope spiralling in 4-110685
- red giants, circumstellar shells and mass loss 4-85936
- red giants, flare like activity and surface mag. fields 4-94776
- red giants, grains form. and growth 4-77706
- red giants, mass loss rates determ. 4-85938
- red giants, shell flashes, two-zone accreting model 4-77813
- red giants in Draco dwarf spheroidal galaxy, abundance anal. 4-110737
- red giants in old open clusters, evolution and luminosity distrib. 4-105981
- red giants with planetary systems, mass transfer and evolution to cataclysmic binaries 4-85951
- S stars in LMC globular clusters 4-77886
- S-type stars, s-process nucleosynthesis of Zr 4-72926
- S-type stars in galactic globular clusters, photometric and spectroscopic search in M22, NGC 6723, and 47 Tucanae 4-101369
- HM Sagittae, circumstellar shell struct. and wind interactions, SHF/UHF obs. 4-85910
- HM Sagittae, emission lines, geometric implications for eruptive symbiotic 4-67727
- HM Sagittae, X-ray emission from eruptive symbiotic system 4-67728
- single stars, low-, intermediate- and high mass stars evolution 4-90140
- southern late type giants and semiregular variables, radial vel. 4-101333
- symbiotic stars, IUE low dispersion obs. 4-67731
- symbiotic stars, spectral characts. 4-101373
- symbiotic stars, synthetic spectra rel. to binary models 4-94786
- symbiotic stars, X-ray to radio obs. 4-82480
- $\alpha$  Tauri, occultation ang. diameters 4-72936
- RR Telescopii, symbiotic star, periodic light vars. due to Mira-type pulsation 4-77855
- 47 Tucanae, globular cluster, upper giant branch pulsational instability 4-77884
- 47 Tucanae giant branch, CN and methylidyne spectral obs. 4-85921
- PU Vulpeculae, 1979-82 optical variability, UVB photometry 4-63179
- PU Vulpeculae, spectral vars. obs. rel. to expanding circumstellar envelope 4-101356
- X-ray binaries, comparison stars spectral characts. 4-110674
- yellow giants in open clusters, behaviour and cluster evolutionary status 4-63223
- Ba in atmospheres of red giants, selective enhancement 4-63145
- Ba stars, Li abundance from Li I 670.7 nm resonance doublet 4-67746
- Ba stars, search for hot white dwarf companions 4-94784
- C star at 120 kpc and high galactic latitude, nature 4-63160
- C star in NGC 6822, discovery, photometry and spectrum 4-63168
- C stars, C and neutron rich isotopes prod. and distrib. in star 4-85965
- C stars, rapid computational method for graphite condensation in stellar winds 4-72927
- C stars contrib. to M33 intermediate age globular clusters light 4-110695
- C-stars, atm., polyatomic mol. IR opacities 4-77831
- He I D<sub>3</sub> line in G and K stars 4-67724
- OH/IR stars, IRAS obs. 4-85948
- OH/IR stars, VLBI obs. of circumstellar shells 4-77849
- OH-IR stars, circumstellar shell struct. from OH maser emission anal. 4-85970
- OH-IR stars, IR counterparts detect. by IRAS 4-86088
- OH-IR stars (Type II OH masers), radio and IR obs. 4-73089

# Gibbs free energy see free energy

# Gibbs function see free energy

# Ginzburg-Landau theory

- alloys, anisotropic superconducting, time depend. Ginzburg-Landau eqns. 4-88630
- disordered superconductor,  $T_c(p)$  theory 4-84732
- ferromagnetic superconductors, field depend. of spin-spiral phase 4-61483
- generalised Ginzburg-Landau eqn., exact solns. 4-78150
- inhomogeneous condensate state, phase transition, Lagrangian model 4-61044
- inhomogeneous superconductors, correlation length and fluctuations 4-65770
- kinetic depinning transitions 4-70338
- Landau-Ginzburg-Wilson model, renormalisation scheme 4-111091
- liquid drops, spherical fluid-vapour interfaces, surface tension, curvature corrections 4-88372
- liquid-vapour phase transitions, Ginzburg-Landau functional 4-103917
- nonequilibrium dynamics of N-component Ginzburg-Landau fields in zero and one dimensions 4-108965
- nonlinear waves in nonequilibrium oscillator systems 4-73237
- one-dimensional nonlinear lattice, critical props. and hadron phys. 4-59032
- relativistic fermion systems, superfluidity and superconductivity, Ginzburg-Landau free energies 4-90489
- strong-coupling superconductors, non-BCS behaviour of gap edge near  $T_c$  4-70980
- superconducting ring, nonuniform, with dangling side branches 4-84735
- superconducting-normal-superconducting sandwiches with nonmagnetic impurities near critical temp. 4-65775
- superconductor-normal metal-superconductor junction, critical field 4-98821
- surface sheath of superconductivity, diamagnetism calcs. 4-84736
- thiouraea, memory effect, defect density, waves in modulated systems 4-88163
- type II supercond., elemental-flux pinning pot. 4-76093
- type II superconductors, deformed flux-line lattice, mag. field distrib. 4-71007
- <sup>3</sup>He, superfluid, nonunitary vortex struct., stability, orientational effects, and temp. depend. 4-104025
- NbSe<sub>2</sub>H<sub>2</sub>, supercond., crit. parameters, and resist. temp. depend. (Russian) 4-92873

# glaciology

- Allan Hills, meteorites distrib., implications for climatology 4-82230
- Allan Hills meteorite icefield, triangulation network meas. and meteorites collection 4-82145
- Allan Hills meteorites, winter 1981-2 meteorite searches, recovery and distrib. 4-82146
- Amery Ice Shelf, E Antarctica, topography from SEASAT satellite obs. 4-82141

# glaciology continued

- Central Andes, ancient ice islands in salt lakes 4-94178
- Andes, glaciers, glaciation and landforms, review 4-67285
- Antarctic glacier movements, use of Doppler satellite meas. (German) 4-72731
- Antarctic glaciology, conference, Columbus, USA (September 1981) 4-58548
- Antarctic ice shelves, German research stations positions and movements (German) 4-72623
- Antarctic shelf ice, gravity meas. possibilities 4-72624
- West Antarctica, ice stream E dynamics and interaction with ocean 4-85725
- E Antarctica, perennially frozen lakes at glacier/rock margins 4-82144
- Balt Bare Glacier, Karakoram region, surging advance, topographic mapping 4-62862
- Batura Glacier, Karakoram, surface var. mapping, stereophotogrammetric surveys 4-62867
- Batura Glacier, Karakoram Mountains, topographic map and photogrammetry 4-62860
- bottom crevasses in floating ice shelves 4-82108
- Chimborazo, Ecuador, climate record in glacier ice core 4-115560
- climatology, role of seasonal snow, sea ice, ice sheets, mountain glaciers and permafrost 4-82223
- climatology and glaciology, conf., Evanston, Illinois, USA (June-July 1983) 4-110803
- Earth climate model, thermohydrodynamic eqns. for atmosphere, ocean, and ice cover 4-62948
- Ekstrom Ice Shelf, strain meas. geodetic obs. (German) 4-72622
- NW Europe, evidence for pre-Weichselian glaciation, stratigraphy 4-110176
- Filchner-Ronne Ice Shelf, strain meas. geodetic obs. (German) 4-72622
- Flood Lake, Canada, glacier outburst and sudden discharge of 1979 August 4-94174
- George V continental margin, Antarctica, marine geology and glaciology 4-82035
- Ghulkin Glacier, impulse radar ice-depth sounding 4-62871
- glacial geology for engineers and Earth scientists, book 4-58596
- Glen Rosa, Isle of Arran, Scotland, cross-section of glaciated valley 4-115404
- Greenland and Canadian Arctic Holocene precipitation rate from ice core obs. 4-110306
- Hazard Glacier, Yukon, Canada, temp. and thickness of surging glacier 4-72617
- Hispar Glacier, impulse radar ice-depth sounding 4-62870
- Huascaran, Peru, climate record in glacier ice core 4-115560
- Hudson Bay, heat budget and freshwater content, runoff and ice cover effects 4-94139
- ice age climate, European/Atlantic correlations during last interglacial 4-85754
- ice covers, combination radiophysical studies 4-100645
- ice from Roslin Glacier, Greenland, fracture toughness 4-62999
- ice in saline water, mixed convection melting, heat and mass transfer 4-87701
- ice sheet flow theory, thermomechanical balances 4-115472
- ice sheets growth 4-115469
- ice shelves meltwater, isotopic tracers and salinity used for shelf characts. determ. 4-67440
- ice-depth radio echo-sounding techniques, appl. on Hispar and Ghulkin glaciers 4-63002
- impulse radar ice-depth sounding system, use on Vatnajökull ice-cap (1977), performance 4-62998
- inland ice sheet buttressing by floating ice shelves 4-82108
- Jakobshavn Glacier, Greenland, ice flow balance 4-67289
- James Bay, heat budget and freshwater content, runoff and ice cover effects 4-94139
- Karakoram glaciers, glacial and proglacial debris, sedimentological anal. 4-62868
- W Karakoram Mountains, glacier fluctuations 4-62872
- Karakoram Mountains, glacier var. 4-62859
- Karakoram region, glacier meltwater runoff, sediment anal. and erosion 4-62869
- Karakoram glaciers, fluctuations anal. techniques 4-62864
- Landat 3 RBV imagery for remote sensing of Antarctica 4-82312
- Lincolnshire area, eastern England, pre-Devensian glaciation, review 4-67286
- Manatee Glacier, BC, Canada, cryoconite hole thermodynamics 4-72615
- Marie Byrd Land, Antarctica, glacial and tectonic events, chronology recorded by rocks 4-82024
- Marion Island, Quaternary glaciation of island near Antarctic convergence 4-82142
- meltwater discharge dynamics from Northern Hemisphere ice sheets during last deglaciation 4-105613
- Midlands, England, Wolstonian stage of British Pleistocene, age 4-72534
- Milankovitch theory tested using 3-D seasonal energy balance climate model 4-62947
- near-surface flow in glaciers obeying Glen's law 4-72619
- Nevada, glacial chronology of Ruby Mountains-East Humboldt Range 4-94176
- polar ice sheet dynamics model showing two stable flow regimes 4-89952
- polar ice-trapped air age difference at Siple Station 4-115475
- Qinghai-Xizang Plateau, China, glaciers, distrib.-rel. to atm. circulation 4-62863
- Quelccaya Ice Cap, Peru, climate record in glacier ice core 4-115560
- radiocarbon dating in Antarctica, problems and significance 4-81954
- Ross Ice Shelf, recent changes in dynamic conditions 4-82105
- Ross Ice Shelf buttressing inland ice sheet 4-82108
- Ross Ice Shelf grounding line, numerical model of dynamics 4-85725
- NW Scotland, Late Devensian ice-free area of Isle of Lewis 4-85727
- sea ice cover, freq. locking in periodically forced thermal two-phase oscillator 4-62841
- sediments of Arctic Ocean and Banks Island, correlation of marine and continental glacial sediments 4-115335
- surface energy balance with atm. 4-94197
- surges, causes and mechanisms, appl. to Roslin Glacier, Greenland 4-62861
- survey techniques for moving terrain, appl. to glaciology and tectonics 4-63000
- theoretical glaciology, book 4-58591
- Trapridge Glacier, Yukon, Canada, flow, temp., subglacial conditions 4-72616
- valley cross-section represented by parabola 4-115404

**glaciology continued**

- Vatnajökull ice cap, Iceland, impulse radar ice depth sounding 4-62865  
 Vatnajökull ice depth sounding expedition 1977, survey and anal. systems 4-62997  
 Vestfold Hills, E Antarctica, ice movements during Late Quaternary 4-82143  
 Washington, tephrochronology of Late Wisconsin deglaciation and Holocene glacier fluctuations near Glacier Peak 4-94177  
 O isotopes in glacier ice cores, atmospheric model for isotopes in falling snow 4-115522

**glass**

- for semiconductor glasses see *amorphous semiconductors and chalcogenide glasses*  
 see also *aluminosilicate glasses; amorphous semiconductors; borate glasses; chalcogenide glasses; germanate glasses; glass fibre reinforced plastics; glass fibres; glass industry; glass-metal seals; optical glass; phosphate glasses; phosphosilicate glasses; vitreous state; vitrification*  
 acoustic emission signal characteristics of Hertzian and unloading cracks 4-75617  
 alkali, cond. polarization characts. and comparison with halide cryst. 4-99003  
 alkali glasses, ionic elec. cond., temp. depend. 4-113703  
 alkali lime silicate glass, structural relax., viscosity, Adam-Gibbs eqn. 4-113633  
 alkali silicate glass, EPR of trapped hole centres 4-76237  
 alkali silicate glass, thermal expansion, Gruneisen parameter 4-80272  
 alkali silicate glasses, ion bombard., alkali depletion, ion beam mixing 4-70239  
 alkali silicate glasses, ion irradi., glass comp. modification by alkali ion migration 4-70238  
 alkaline earth-ferrite glasses, glass forming region and  $\text{Fe}^{3+}$  coordination (Japanese) 4-113348  
 anharmonic oscillators system state density 4-80184  
 anomalous thermal, acoustic and dielec. props. at low temp. 4-60994  
 ballotini, flow through orifices 4-64999  
 bead filled polystyrene, craze form., microscopic in situ obs., interfacial adhesion 4-62073  
 brittle surface in sliding contact with spherical indenters, strength degradation 4-104881  
 cells adhesivity to glass, change for unchanged density of surface charges 4-66904  
 ceramic, brittle, disturbed surface layer parameters effect on struct. strength 4-99541  
 ceramic, composite rod struct., glued joint, strength evaluation 4-99546  
 ceramic materials, structure-property relationships of the vitreous state 4-75312  
 collinear beam-mixing by amplitude modulated US wave 4-98211  
 corroded, by  $\text{H}_2\text{SO}_4$ , low-energy electron induced X-ray spectrometry, surface characterisation 4-113767  
 corrosion, in weak-acid and weak-alkali solns., effect of electrolyte additions 4-81316  
 cracks in glasses and ceramics, growth influenced by chem. environment 4-94095  
 dielectric glasses, nonlinear US and EM relax. absorpt. 4-60995  
 dielectric relax., Levy distrib. and Williams-Watts model 4-61623  
 electron irradiated, discharge form. 4-71275  
 electron-irradiated, discharge phenomena 4-71277  
 elliptical crack, transient growth, mathematical model 4-104845  
 enamel used in heat energetics, abrasive wear 4-81291  
 fast atom bombard. mass spectroscopy for appl. surface anal. 4-82857  
 fast electron irradiated, space-charge dynamics 4-71279  
 fatigue, crack growth and crack tip sharpening models 4-89101  
 fictive temp., calc. algorithm 4-84395  
 fission fragment tracks, healing time 4-108422  
 fluoride, containing rare earth ions, fluorescence and nonradiative relax., review 4-99156  
 fluorozirconate glasses, thermal cond. meas., 1.5 to 100K 4-84474  
 fused silica, high temp. intrinsic defects 4-75306  
 $0.69\text{Ga}_2\text{S}_3 \cdot 0.31\text{La}_2\text{O}_3 \cdot \text{Nd}^{3+}$  4-76511  
 glass: rare earth ions, low temp. optical depolarizing rate 4-88789  
 glass:Cr, dominant visible absorpt. rel. to  $\gamma$ -ray irradi. 4-76503  
 glass: $\text{Yb}^{3+}$ , statistical modelling, luminescence and absorpt. spectra 4-109247  
 glass-glass contact, influence of brittle quartz particles 4-103271  
 glass-ionomer dental cement, prep. and compressive strength 4-99373  
 glass-plastic plates, deform. during static loading and interaction with a shock 4-79533  
 glass/liquid interface, laser beam induced holographic bubble grating form. 4-83683  
 grinding damage, single- and multi-point comparison 4-85206  
 halide glasses, thermal and elastic props., molecular dynamics calc. 4-109455  
 high-power glass laser system, rel. to X-ray generation 4-96919  
 high-silica, vol. resist. depend. on temp. and leaching parameters 4-70880  
 hyperspherical harmonics, symmetry, Landau theory and polytope models 4-103659  
 insulation, self heating and surface resist. 4-70903  
 ion implanted, SAW propagation velocity 4-113776  
 laser induced crystallisation kinetics, Raman scatt. studies 4-108288  
 low-energy excitations in anharmonic atomic local pots. 4-108568  
 matrix composite, Cu-Su filled, frictional and strength props. 4-66456  
 NBS standard reference materials for microanalysis 4-81498  
 nuclear spin-lattice relax., homogeneous and inhomogeneous averaging 4-114178  
 nuclear waste glass, simulated, thermal shock resist. under water quenching conditions 4-96126  
 nuclear waste glass-bentonite interfaces after one year burial in STRIPA 4-111605  
 nuclear waste glass-glass interfaces after one year burial in STRIPA 4-111604  
 nuclear waste glasses, fracture toughness, hardness, elastic recovery, indentation testing 4-104844  
 optical impurity depahsing, homogeneous linewidths 4-71328  
 oxide, containing rare earth ions, fluorescence and nonradiative relax., review 4-99156  
 oxide, structure, vibr. spectroscopy 4-79945  
 oxide glasses, hyper-Raman and Raman spectra, vibr. excitations 4-76456  
 oxide glasses, local order, EXAFS studies review 4-60849

**glass continued**

- oxide glasses, local symm. effects, X-ray absorpt. near edge struct. spectra 4-66116  
 oxide glasses and ceramics, low temp. prep. from metal alkoxide solns. 4-109369  
 oxynitride glasses, prep. and props. 4-76737  
 phonon localisation and anharmonicity 4-98230  
 photochromic, darkening, temp. depend., role of compositional variables 4-84928  
 polycarbonate-glass interface, Brillouin spectra and photoelastic props. 4-80952  
 polystyrene (polyballs) colloidal crystals and glasses, solidification 4-89353  
 porous with adsorbed rhodamine 6G, photostability study 4-99816  
 preparation for elec. use based alkoxide and unidirectional solidification methods 4-104760  
 pseudo-Brillouin zone boundaries, mol. dynamics simulations 4-80470  
 quartz, ablation, boundary layer, nonequilib. physicochemical process 4-71967  
 quartz, synthesis from gas phase, struct. form. on surface 4-70040  
 radiation effects in insulators, conf., Albuquerque, NM, USA (May-June 1983) 4-73143  
 radioactive waste, leaching glass in porous media, test method 4-83133  
 radioactive waste, medium level, powder technological vitrification by in-can hot pressing 4-83139  
 radioactive waste glass, simulated, density changes under ion, electron, and gamma irradi. 4-73974  
 radwaste forms, leaching backfill materials effects, glass powder backfill 4-59328  
 reactivity in aqueous solutions, leaching of simulated radioactive waste glass 4-93548  
 relaxation theory 4-98021  
 resonant EM and acoustic absorption in alternating field 4-65346  
 rigid networks, excited atom as a gauge for void calibration 4-75307  
 ruby silica, colouring process study by optical and EPR spectroscopy 4-65859  
 semiconductor doped glasses, optical nonlinearities, phenomenological theory 4-102984  
 silica glasses, radiation-induced defects, mol. dynamics study (French) 4-88113  
 silica glasses, diffusion of water at low temp. 4-84464  
 silicate glass: $\text{Nd}^{3+}$ , accumulated photon echo study 4-64746  
 silicate glass system containing  $\text{SrO} \cdot \text{TiO}_2$ , dielectric props., low temp. meas. 4-65940  
 silicate glasses, binary systems, glass data, handbook 4-58584  
 silicate glasses, electron irradi. damage mechanism 4-70216  
 silicate glasses, Nd laser glasses, gain saturation modelling 4-112443  
 silicate glasses, thermotransport, at migration process under effect of temp. gradient 4-80283  
 silicate glasses containing  $\text{TiO}_2$ , refractive index, density, thermal expansion and IR spectra 4-84199  
 SIMS, static, in appl. surface anal. 4-82857  
 simulated nuclear waste, leaching in radiation environment 4-106677  
 simulated nuclear waste glass, Cm doped, radiation damage, annealing, short term leach test 4-83149  
 slow crack growth resistance testing with double torque method 4-81375  
 soda-lime silicate, Vickers indented, delayed fracture in deionised water 4-81268  
 soda-lime silicate glass, stress relax. and ion exchange 4-108284  
 soda-lime-silica glass, complex refl. spectra determ. using switched-field-of-view interferometer 4-101912  
 solid surface, chemical and electrochemical treatment, low energy electron induced X-ray spectra 4-76572  
 spontaneous two-pulse elec. echo decay 4-70329  
 strength testing, time of failure, incremental loading, step size effect 4-62145  
 stressed nuclear waste glass, hydration in saturated water vapour 4-66554  
 structural model of defect melting 4-60846  
 studio, design, effects of glass 4-97201  
 substrates for metallic films, laser damage study 4-108433  
 surface analysis, beam techniques for poorly cond. materials 4-93575  
 surface damage, effect of hardness and thermal cond. of damaging material 4-85234  
 surface thermoelectric deformations caused by a laser 4-103798  
 tellurite-halide ternary systems, glass-forming region, density and thermal expansion 4-80273  
 thermal conductivity, high temp., theoretical anal. of experiments 4-84471  
 thermodynamics of grain boundary crystallisation 4-75314  
 thin films, phonon dispersion meas. 4-70326  
 toughened, thin thermally polished, strength asymmetry 4-89103  
 two-level systems, nonideal Frenkel Kontorova model anal. 4-113345  
 Vycor, superfluidity for  $^4\text{He}$  using helicity moduli calcs of dil. XY models 4-93833  
 Vycor glass with liquid  $^3\text{He}$  and superfluid  $^4\text{He}$ , effects on two-level systems 4-75745  
 willemite glass ceramic, partially crystallised, struct. and comp. 4-61910  
 Al-glass composite, produced by powder metallurgy route, mech. props. 4-66275  
 $\text{BaF}_2 \cdot \text{LaF}_3 \cdot \text{ZrF}_4 \cdot \text{AlF}_3$  glass, crystallisation, devitrification on reheating 4-84194  
 $\text{BaF}_2 \cdot \text{ZrF}_4$  glasses, Raman spectra interpretation 4-84960  
 $\text{BaO} \cdot \text{SiO}_2$  cryst. nucleation kinetics, effect of amorphous phase separation 4-65185  
 $\text{BaO} \cdot \text{TiO}_2 \cdot \text{SiO}_2$  glass-ceramics, ferroelec., depolarisation currents, dielec. and electrooptical props. 4-76317  
 $\text{Ba}_2\text{TiGe}_2\text{O}_8$  glass ceramics, grain oriented, hydrostatic piezoelec. props. and appls. 4-84913  
 $\text{Ba}_2\text{TiSi}_2\text{O}_8$  glass ceramics, grain oriented, hydrostatic piezoelec. props. and appls. 4-84913  
 BeO glass ion beam etching, optical waveguide appls. 4-62071  
 $\text{CaAl}_2\text{Si}_2\text{O}_8$  glass, shock compressed, optical emission spectra 4-114305  
 $\text{CaO} \cdot \text{Fe}_2\text{O}_3 \cdot \text{SiO}_2$  glass formation and props. 4-79946  
 $\text{CaO} \cdot \text{SiO}_2 \cdot \text{TiO}_2$  glasses, struct. analysis, XPS 4-108286  
 $\text{CaTiSiO}_5 \cdot \text{La}$  sphere-based glass-ceramics, La partitioning, Auger studies 4-88112  
 $\text{Ce}_2\text{O}_3$  scintillating glass fiber-optic plate detectors, tracking appls. 4-59533  
 $\text{Cs}_2\text{O} \cdot \text{Na}_2\text{O} \cdot 5\text{SiO}_2$  glass, vibr. spectra 4-109179  
 $(\text{Fe,C,Mg})_2\text{Si}_2\text{O}_6$  ion bombard. effect, XPS 4-84320  
 $\text{FeF}_3$ -based fluoride glasses, Mossbauer studies 4-114192

- glass continued
- Fe<sub>2</sub>O<sub>3</sub>-CaO-SiO<sub>2</sub> glasses, DC cond., Mossbauer and ESR spectra 4-70807
- Ga<sub>2</sub>O<sub>3</sub>-CaO glass, form. density, refr. index, crystn. temp., hardness, IR spectra 4-113635
- H depth profiling using <sup>15</sup>N beam 4-64249
- KAlSi<sub>3</sub>O<sub>8</sub>, amorphous, glass transitions and thermodynamic props. 4-65400
- K<sub>2</sub>O-MgO-PbO-SiO<sub>2</sub> glass, Rayleigh scatt. loss coeffs. 4-114289
- K<sub>2</sub>O-SiO<sub>2</sub>, gamma-irrad., defect centre struct., EPR obs. 4-70211
- LaF<sub>3</sub>-BaF<sub>2</sub>-ZrF<sub>4</sub> fluoride glass, surface crystals. formed by reaction with water 4-81298
- Li silicate glass doped with Ce<sup>3+</sup>, neutron/gamma detectors design 4-59555
- Li-Si disilicate glasses with Nd-U contents, response to γ-rays and neutrons 4-96399
- (LiCl)<sub>2</sub>(H<sub>2</sub>O)<sub>3</sub> glass, hypersonic velocity and attenuation, Brillouin scatt. 4-70286
- Li<sub>2</sub>O-Nb<sub>2</sub>O<sub>5</sub> amorphous dielectrics, crystallisation, elastic and dielec. props. 4-104518
- Li<sub>2</sub>O-SiO<sub>2</sub> glass and glass-ceramic, hydrothermal corrosion 4-85235
- Li<sub>2</sub>O-SiO<sub>2</sub> glass ceramic systems, density, crystallisation, elec. cond. 4-113937
- Li<sub>2</sub>O-SiO<sub>2</sub> glasses, struct., <sup>29</sup>Si NMR studies 4-98964
- Li<sub>2</sub>O-SiO<sub>2</sub> system, glass forming regions rel. to cooling rate, liquidus viscosity obs. (Japanese) 4-75680
- Li<sub>2</sub>SiO<sub>3</sub> glass ceramics, grain oriented, hydrostatic piezoelec. props. and appls. 4-84913
- Li<sub>2</sub>Si<sub>2</sub>O<sub>5</sub>-Li<sub>2</sub>SiO<sub>4</sub> glass, ionic cond. meas. 4-84457
- Mg-Si-O-N glass, crystallisation and microstruct. 4-75313
- Na<sup>+</sup> ion conducting glasses, activation energy and conductivity 4-113707
- NaAlSi<sub>3</sub>O<sub>8</sub>+2, amorphous, glass transitions and thermodynamic props. 4-65400
- Na<sub>2</sub>CO<sub>3</sub>-SiO<sub>2</sub> melts, dissolution of SiO<sub>2</sub> 4-84402
- Na<sub>2</sub>O-BaO-SiO<sub>2</sub> glass transition temp. and devitrification behaviour 4-98285
- Na<sub>2</sub>O-CaO-SiO<sub>2</sub>, γ radiation colouring in 600-1000 nm region 4-80948
- Na<sub>2</sub>O-CaO-SiO<sub>2</sub>, interaction with chloride melts, including MgCl<sub>2</sub> or ZnCl<sub>2</sub>, IR spectroscopic study 4-80949
- Na<sub>2</sub>O-CaO-SiO<sub>2</sub> glass, stress corrosion characts., bending test 4-109535
- Na<sub>2</sub>O-CaO-SiO<sub>2</sub> glasses, ion implanted, mech. props. 4-75542
- Na<sub>2</sub>O-CaO-SiO<sub>2</sub>-Si<sub>3</sub>N<sub>4</sub> glass, prep., Fourier transform IR spectra, XPS 4-84192
- Na<sub>2</sub>O-MO-SiO<sub>2</sub> glass, (M=Ca, Mg, Zn), leaching kinetics, effect of divalent cations 4-109533
- Na<sub>2</sub>O-MgO-SiO<sub>2</sub>, interaction with chloride melts, including MgCl<sub>2</sub> or ZnCl<sub>2</sub>, IR spectroscopic study 4-80949
- Na<sub>2</sub>O-MgO-SiO<sub>2</sub> glass, dielec. relax. and dispersion 4-114204
- Na<sub>2</sub>O-NaF-SiO<sub>2</sub> glass, mol. dynamics simulation 4-98023
- Na<sub>2</sub>O-Nb<sub>2</sub>O<sub>5</sub>-SiO<sub>2</sub> glass-ceramics, ferroelec., depolarisation currents, dielec. and electrooptical props. 4-76317
- Na<sub>2</sub>O-SiO<sub>2</sub>, interaction with chloride melts, including MgCl<sub>2</sub> or ZnCl<sub>2</sub>, IR spectroscopic study 4-80949
- Na<sub>2</sub>O-SiO<sub>2</sub> glass, electron irradiated, evidence of enhanced diffusion process 4-80108
- Na<sub>2</sub>O-SiO<sub>2</sub> glass, ferrite precip., ESR and Mossbauer obs. 4-99386
- Na<sub>2</sub>O-SiO<sub>2</sub> glass, ion implanted impurities, range and spatial distrib. 4-108287
- Na<sub>2</sub>O-SiO<sub>2</sub> glass, nature of dissolved water, effect on phys. props. 4-109180
- Na<sub>2</sub>O-SiO<sub>2</sub> glass disc surfaces disturbed by ion-beam induced absorpt. currents, Na conc. changes 4-93173
- Na<sub>2</sub>O-SiO<sub>2</sub> glasses, struct., <sup>29</sup>Si NMR studies 4-98964
- Na<sub>2</sub>O-SiO<sub>2</sub> melts, Na self diffusion under microgravity, 1200°C 4-84433
- Na<sub>2</sub>O-SiO<sub>2</sub> surface, electron stimulated desorption mechanisms 4-92514
- Na<sub>2</sub>O-SiO<sub>2</sub>-H<sub>2</sub>O glass, hygroscopicity study 4-76997
- Na<sub>2</sub>O-SiO<sub>2</sub>-UO<sub>2</sub> glass, struct. EXAFS studies 4-65179
- Na<sub>2</sub>O-ZnO-SiO<sub>2</sub> glass, struct., Raman spectra 4-71376
- Na<sub>2</sub>O-SiO<sub>2</sub> glass, self-diffusion of Na<sup>+</sup> ions near glass transition temp. 4-88337
- P<sub>2</sub>S<sub>5</sub>-Li<sub>2</sub>S glass, ionic cond. meas. 4-84457
- Pb glass shower counters, pulse height, energy resolution 4-59535
- Pb-glass drift collection calorimeter, design 4-59532
- PbF<sub>2</sub>-MF<sub>2</sub>-MF<sub>3</sub> glass, struct. and props. 4-79948
- PbF<sub>2</sub>-MnF<sub>2</sub>-GaF<sub>3</sub> fluoride glasses, vibrational spectroscopy 4-114261
- PbO-containing glass, XPS study of angular dependence of preferential sputtering 4-88926
- PbO-PbCl<sub>2</sub> glasses, coordination of divalent Pb studied by EXAFS 4-84198
- Rb<sub>2</sub>O-SiOP<sub>2</sub> glass and melt, structure, Raman spectra meas. (Japanese) 4-113349
- Si-Al-O-N<sup>+</sup> oxynitride glasses, synthesis, stability and microstruct. 4-70042
- SiO<sub>2</sub> 4-61145
- SiO<sub>2</sub>, alpha-particle induced damage, vibr. Raman spectra 4-70237
- SiO<sub>2</sub>, amorphous, glass transitions and thermodynamic props. 4-65400
- SiO<sub>2</sub> film, crack tip geometry, water ageing, high resolution electron microscopy 4-71724
- SiO<sub>2</sub> glass, anomalous diffusion behaviour of Na 4-98362
- SiO<sub>2</sub> glass, crack growth under dynamic loading, temp. and humidity effects 4-62018
- SiO<sub>2</sub> glass, NMR study of Si-O-Si bond angle distrib. 4-61599
- SiO<sub>2</sub> glass, struct. model, intermediate range order 4-75308
- SiO<sub>2</sub> glass data, handbook 4-58584
- SiO<sub>2</sub> glass rod, viscosity meas. by rapid torsion method 4-68226
- SiO<sub>2</sub>, radiation effects, point defects, microstructural changes, etching, leaching 4-70195
- SiO<sub>2</sub>, radiation induced charges 4-70217
- SiO<sub>2</sub>, rotary phonon echoes 4-70328
- SiO<sub>2</sub>, vitreous, electron bombarded, stress relaxation 4-70218
- SiO<sub>2</sub>, vitreous, flashover model (French) 4-65949
- SiO<sub>2</sub>, vitreous, low-freq. elastic loss at low temp. 4-70289
- SiO<sub>2</sub>-CaO-Na<sub>2</sub>O glass, plastic processes 4-75602
- 5SiO<sub>2</sub>-M<sub>2</sub>O glass, (M=Li, Na, K, Rb, Cs), vibr. spectra 4-109179
- SiO<sub>2</sub>-MgO-CaO-Na<sub>2</sub>O(K<sub>2</sub>O), glass, surface alkali metals Auger anal. (French) 4-76568
- SiO<sub>2</sub>-Na<sub>2</sub>O-CaO-Fe<sub>2</sub>O<sub>3</sub> glasses, EPR study of behaviour and effect of Fe 4-88111
- SiO<sub>2</sub>-Na<sub>2</sub>O-Fe<sub>2</sub>O<sub>3</sub> glasses, radiation damage, EPR spectra 4-84200
- SiO<sub>2</sub>-Na<sub>2</sub>O(K<sub>2</sub>O), glass, surface alkali metals Auger anal. (French) 4-76568
- glass continued
- Sr<sub>2</sub>TiSi<sub>2</sub>O<sub>8</sub> glass ceramics, grain oriented, hydrostatic piezoelec. props. and appls. 4-84913
- TbO<sub>3</sub> scintillating glass fiber-optic plate detectors, tracking appl. 4-59533
- (ThF<sub>4</sub>)<sub>0.2</sub>(BaF<sub>2</sub>)<sub>0.1</sub>(MnF<sub>2</sub>)<sub>0.5</sub>(AlF<sub>3</sub>)<sub>0.2</sub> glass, low temp. ultrasonic behaviour 4-70285
- Ti<sub>2</sub>S-B<sub>2</sub>S<sub>3</sub> glass, NMR study and struct. 4-88726
- V<sub>2</sub>O<sub>5</sub>-As<sub>2</sub>O<sub>3</sub> glasses, semicond. props. 4-80593
- V<sub>2</sub>O<sub>5</sub>-SeO<sub>2</sub> (TeO<sub>2</sub>)(GeO<sub>2</sub>) glass, ESR and photoacoustic spectra 4-104491
- V<sub>2</sub>O<sub>5</sub>-As<sub>2</sub>O<sub>3</sub> glasses, IR study 4-104614
- Y-Si-Al-O-N glasses, viscosity, glass transition, microhardness rel. to comp. 4-70383
- YIG containing magnetic glass-ceramics, prep. using colloidal Bi as nucleation catalyst, characts. 4-71628
- ZrF<sub>4</sub>-BaF<sub>2</sub>-based fluorozirconate glasses, crystallisation, X-ray diffr. and DSC studies 4-84197
- (ZrF<sub>4</sub>)<sub>57.5</sub>(BaF<sub>2</sub>)<sub>33.75</sub>(ThF<sub>4</sub>)<sub>8.75</sub> (V-52), reson. interaction of acoustic waves with two-level systems 4-70290
- glass fibre reinforced plastics
- acrylonitrile-butadiene copolymer matrix, thermal cond. meas. to high temp. using line-source technique 4-108668
- cloth reinforced polyester panels, elastic props. under low velocity impact 4-89079
- design, reliability-based, fatigue-proof 4-99392
- electrical insulator components, damage in combined elec., mech. and chemical environments 4-66466
- epoxide matrix, hybrid composite, environmental response of flexural props. 4-76809
- epoxy laminate, elastic consts., stress-strain relations, failure stresses (Japanese) 4-99415
- epoxy laminates, orthotropic, birefringent, prep. and photoelasticity 4-89022
- epoxy matrix, acoustic emission evaluation 4-81380
- epoxy matrix, curing conditions effect on mech. props. 4-99487
- epoxy matrix, fracture initiation under impact compression 4-76863
- epoxy matrix, laminated plates, design for max. stiffness 4-75599
- epoxy matrix, laminated symmetric beams, damping and dynamic moduli 4-80154
- epoxy matrix, stable crack growth, influence of fibre orientation 4-99570
- epoxy matrix, stress wave propag. in plates, study by dynamic photoelasticity 4-108037
- epoxy matrix, thick laminates thermoelastic behaviour 4-75706
- epoxy matrix, thin-walled tubes, deform. and failure after transverse indentation 4-99573
- epoxy matrix, unidirectional, fracture toughness in mode II 4-93366
- epoxy matrix, vibr. damping parameters, prediction and meas. 4-80155
- epoxy resin laminates, transverse cracking rel. to mech. props. of matrix 4-99489
- epoxy resin matrix, amine cured, flexural props. and char. yields 4-99425
- fatigue crack growth, environmental effect, compliance and moire techniques 4-89200
- filament wound pipes, acoustic emission under long-term loading 4-99457
- hybrid composite, unidirectional fibre, amplitude distrib. AE signatures 4-89198
- laminates, interlaminar shear strength 4-99575
- mechanics of winding, book contrib. 4-66303
- metallic glass ribbon epoxy resin, fracture strength and ribbon shape effects 4-99479
- metallic glass ribbon reinforced epoxy resin, strengthening by fibre prestressing 4-99480
- metallic glass ribbon reinforcement characts., pull-out tests in different matrices 4-71717
- NDT, remote testing by photothermal anal. of thermal waves 4-81374
- OTEC cold water GFRP pile field test 4-114933
- panel, three-layer, with cellular filler, deform. under static and shock loads 4-64880
- PET matrix, strength, effect of temp. and strain rate 4-93375
- phenolphoromalehyde matrix, laminate plates, shrinkage strains 4-61915
- polyamide matrix, fracture mechanism, acoustic emission and microscopy obs. 4-66417
- polycarbonate matrix, subsurface imaging of fibres by acoustic microscopy 4-76924
- polyester laminate, residual strength degradation prediction model (Japanese) 4-99503
- polyester matrix, elastic consts. rel. to fibre orientation and matrix microcracking 4-109447
- polyester matrix, hybrid composites, flexural and fracture props. (Japanese) 4-99429
- polyester matrix, hybrid composites, interlaminar shear strength (Japanese) 4-99430
- polyester matrix, laminated hybrid, crack growth resist., flexural strength 4-62012
- polyester matrix, laminates, creep characts. (Japanese) 4-114615
- polyester matrix, laminates, residual strength degradation model under repeated tension-compression loading 4-99574
- polyester matrix, orthotropic, elastic and photoelastic calibration, appl. of least squares method 4-69717
- polyester matrix, panels, surface damage due to projectile impact 4-76865
- polyester matrix, short-fibre SMC, shear fatigue degradation and fracture 4-76845
- polyester matrix 4-99456
- polyester molding materials, end-use appls. 4-71632
- polyethylene melts, glass- and vinylon-fibre reinforced, shear viscosity, stress, rheological props. 4-69804
- polymer composites, fluid absorpt., NMR imaging 4-109584
- polypropylene matrix, injection molded bars, residual stress distrib., distortion, annealing temp. gradient 4-81256
- polyurethane foam matrix, flexural strength and modulus, thermal and photodegradation (Japanese) 4-99623
- polyurethane foam matrix, thermal expansion and cond., Young's modulus (Japanese) 4-98318
- polyurethane matrix, dynamic fracture toughness rel. to void and fibre content (Japanese) 4-99506
- reinforced in three directions with variable placement angle with depth, mech. props. 4-89081
- resin matrix high-performance composites, book contrib. 4-66302

**glass fibre reinforced plastics continued**

- roving cloth reinforced, strength in flatwise direction, temp. depend. (Japanese) 4-89087  
 seawater intake canal antifoulant material test results 4-114705  
 sheet moulding compound, impact damage 4-76829  
 shells, three-layer, stress-strain state 4-89091  
 stress corrosion of glass fibre in acidic environments 4-109524  
 thermal testing of struct. and mech. props. 4-85268  
 thermoplastic alloy matrix, mech. props. at elevated temps. 4-76855  
 thermoplastic matrix, creep resistance, fatigue endurance 4-61994  
 thermoplastics, reinforced, compounding and fabrication, book contrib. 4-66304  
 urethane polymers, reaction injection molded, stress relax., DSC, hard segment content 4-89076  
 wound, transverse thermoelastic characts. 4-89082  
 C-glass hybrid fibre reinforced plastics, mech. props. 4-93407

**glass fibres**

- see also fibre optics; optical fibres  
 alkali silicate and aluminosilicate, Young's modulus, effect of vol. and struct. 4-85170  
 basalt glass fibres, microhardness and microbrittleness 4-84342  
 bending strength, static fatigue rel. to atmosphere 4-99490  
 E-glass fibres, tensile props. rel. to acid and post heat treatment 4-104799  
 metallic glass ribbon, pull-out tests in different matrices, characts. as fibre reinforcement 4-71717  
 optical transmission systems appls., industrial control, traffic, telecommunications (German) 4-107876  
 radiation characteristics comparison between various fibres (Polish) 4-74737  
 SEM study of leaching and local comp. 4-81303  
 sensors, technology and appls. (German) 4-95409  
 silica optical fibers, high-strength long-length, drawing study 4-74762  
 slag glass fibres, microhardness and microbrittleness 4-84342  
 GeO<sub>2</sub>-P<sub>2</sub>O<sub>5</sub>-SiO<sub>2</sub> glass fibre, transient stimulated Raman scatt. (Chinese) 4-91532  
 GeO<sub>2</sub>-SiO<sub>2</sub> optical fibres, CVD, gas phase equilb., thermodynamics calcs. 4-109329  
 NaPO<sub>3</sub>, alpha-particle induced damage, vibr. Raman spectra 4-70237  
 SiO<sub>2</sub>, alpha-particle induced damage, vibr. Raman spectra 4-70237  
 SiO<sub>2</sub> CVD preform for optical fibre production OH conc. profiles 4-112579  
 Y(PO<sub>3</sub>)<sub>3</sub>, alpha-particle induced damage, vibr. Raman spectra 4-70237

**glass formation** see vitrification**glass industry**

- furnace linings, monitoring method for corrosion of refractories 4-89208  
 furnace linings, vertical honeycomb resist. of refractories, stat. testing method 4-89207  
 induction heater power control for optical glass melting in Pt container system 4-69608

**glass-metal seals**

No entries

**glass structure** see glass; noncrystalline state structure**glass transition (glasses)**

see also vitrification

- alkali alkaline earth phosphate glasses, He migration, thermal expansion, glass transition temp. 4-108661  
 alkali lime silicate glass, structural relax., viscosity, Adam-Gibbs eqn. 4-113633  
 amorphous solids, physics, book 4-90312  
 communal entropy in melting and the glass, fast-ion, and superfluid transitions 4-70342  
 1-cyano adamantane, mol. reorientation, glass transition, <sup>14</sup>N-NQR, stimulated thermocurrents (French) 4-98284  
 dynamics of glass-like transitions, oscillator model 4-75677  
 fictive temp., calc. algorithm 4-84395  
 halide glasses, thermal and elastic props., molecular dynamics calc. 4-109455  
 hard sphere glass, linear excitations and stability 4-70412  
 II-IV-V<sub>2</sub> glassy semicond., synthesis, stability and microstruct. 4-70042  
 liquid-glass transition, dynamical model 4-75679  
 oxynitride glasses, prep. and props. 4-76737  
 phosphate glasses, containing fluorides of Group I-IV elements, optical and spectral props. rel. to struct. 4-92098  
 smectic-A and -C phases, glassy behaviour 4-98007  
 temperature-time dependences, chem. equilb. theory 4-92366  
 AgI-Ag<sub>2</sub>O-B<sub>2</sub>O<sub>3</sub> system, stable and metastable phases 4-113343  
 As<sub>2</sub>S<sub>3</sub> chalcogenide glass films, photostruct. changes 4-104560  
 As<sub>2</sub>S<sub>3</sub>-x glass, X-ray struct. factor, temp. depend. near glass transition 4-60847  
 As<sub>2</sub>S<sub>3</sub> chalcogenide glass films, photostruct. changes 4-104560  
 As<sub>2</sub>Se<sub>3</sub> glass, X-ray struct. factor, temp. depend. near glass transition 4-60847  
 B<sub>2</sub>O<sub>3</sub>, vitreous, transition, struct., low freq. Raman spectra 4-66028  
 Ba(PO<sub>3</sub>)<sub>2</sub>-CdF<sub>2</sub>, high refractive index glass, optical constants, density and atomic refraction rel. to struct. 4-93043  
 Bi<sub>2</sub>Fe<sub>2</sub>O<sub>9</sub> glass, IR study 4-70381  
 Eu (III) in silica gel glass, fluoresc., cation binding and cage symm. 4-114835  
 Fe<sub>40</sub>Ni<sub>40</sub>P<sub>14</sub>B<sub>6</sub>, of thin film on substrate 4-92367  
 KAlSi<sub>3</sub>O<sub>8</sub>, amorphous, glass transitions and thermodynamic props. 4-65400  
 Li<sub>2</sub>O-Al<sub>2</sub>O<sub>3</sub>-B<sub>2</sub>O<sub>3</sub> glass, form. and transition temp. 4-113634  
 NaAlSi<sub>3</sub>O<sub>8</sub>+x, amorphous, glass transitions and thermodynamic props. 4-65400  
 Na<sub>2</sub>O-Al<sub>2</sub>O<sub>3</sub>-B<sub>2</sub>O<sub>3</sub> glass, form. and transition temp. 4-113634  
 Na<sub>2</sub>O-B<sub>2</sub>O<sub>3</sub> glass, prep., mech., thermal and optical props. rel. to N content 4-60845  
 Na<sub>2</sub>O-BaO-SiO<sub>2</sub> glass system, glass transition temp. and devitrification behaviour 4-98285  
 Na<sub>2</sub>O-SiO<sub>2</sub> glass, self-diffusion of Na<sup>+</sup> ions near glass transition temp. 4-88337  
 PbF<sub>2</sub>-MF<sub>2</sub>-MF<sub>3</sub> glass, struct. and props. 4-79948  
 PbO-BaO-TiO<sub>2</sub>-B<sub>2</sub>O<sub>3</sub> glass ceramic system, crystal clamping, X-ray diffr., dilatometry 4-109386  
 Si-Al-O-N oxynitride glasses, synthesis, stability and microstruct. 4-70042  
 SiO<sub>2</sub>, amorphous, glass transitions and thermodynamic props. 4-65400  
 SnSe-GeSe<sub>2</sub>-AsSe, glass formation, physicochemical props. 4-92365

**glass transition (glasses) continued**

- Ti-Zr-Si system sput coated, glass forming ability, temp.-comp. map 4-71639  
 V<sub>2</sub>O<sub>5</sub>-B<sub>2</sub>O<sub>3</sub> glass, struct., IR spectra and elec. cond. 4-88107  
 Y-Si-Al-O-N glasses, viscosity, glass transition, microhardness rel. to comp. 4-70383  
 Zr<sub>2</sub>Cu<sub>1-x</sub> metallic glass, sp. ht., thermal cond. props. after structural relax. 4-70406

**glass transition (polymers)**

- acrylonitrile-butadiene copolymers,  $\alpha$  relax. kinetics near glass transition temp. 4-81231  
 amorphous polymer density fluctuation theory in a glass transition region and photon correlation spectroscopy 4-98026  
 amorphous solids, physics, book 4-90312  
 aromatic polyester-chlorinated polymer blends, miscibility, morphology, small angle light scatt. 4-84412  
 block copolymers of styrene and vinyltrimethyl silane, optical and mech. props. (Russian) 4-81227  
 composition-dependent glass transition 4-84398  
 copolyester of lactic and glycolic acid, strain induced crystallisation, optical and X-ray scatt. obs. 4-85186  
 dense polymer systems, liq. glass-type transition, dynamic Monte Carlo simulation 4-98286  
 divinyl oligoester polymers, relax. transitions (Russian) 4-81226  
 epoxide resin coatings, internal stress, network struct., glass transition temp., rel. to curing process (Japanese) 4-89866  
 epoxy, Fe filled, particulate composite, dynamic mech. props. 4-76794  
 epoxy polymer, amine cured, dynamic mech. props. rel. to processing conditions 4-89075  
 epoxy resins, interaction with water, glass transition temp. depression 4-89157  
 epoxy resins, oligomeric, zero-shear melt viscosity, temp. depend. 4-80281  
 epoxy-diene networks having high degree of phase separation, glass transition (Russian) 4-103933  
 Gibbs theory of glass transition, quantitative evaluation 4-88294  
 Gibbs-DiMarzio theory, applicability 4-113637  
 graphite fibre enforced epoxy composites, thermomech. props., glass transition 4-92364  
 heterogeneous polymer systems having high degree of phase separation, glass transition (Russian) 4-103933  
 p-n-hexyloxybenzylidene-p'-butylaniline, smectic liq. cryst., glass transition 4-84392  
 isoprene-propylene copolymer, regularly alternating, thermodynamic props., stereoisomerism effects (Russian) 4-103970  
 lignin/paper composites, temp. depend. of tensile props. 4-109451  
 linear flexible macromolecules, thermotropic mesophases and mesophase transitions 4-98011  
 liquid crystalline polymers with amphiphilic and nonamphiphilic side chains, phase behaviour 4-88080  
 PET films, extrusion drawn amorphous and semi-crystalline, linear thermal expansion analysis 4-109439  
 petroleum pitches, fractionated and blended, creep and glass transition, influence of mol. wt. distrib. 4-103864  
 PMMA-fluorescent dyes, glass transition and liq.-liq. transition modification 4-113636  
 PMMA, atactic, glass transition temp. determ. method 4-75678  
 PMMA, glass transition, Gibbs-DiMarzio theory, applicability 4-113637  
 PMMA, stress-orientation-strain relationships, glassy deform. model 4-76812  
 PMMA films, containing adsorbed moisture, DC cond., effect of thermal treatment 4-75980  
 PMMA-Novolac resin mixtures, glass transition temps., H bonding effects 4-103932  
 poly(ethylene oxide) complex electrolyte, PEO(LiCF<sub>3</sub>SO<sub>3</sub>)<sub>x</sub>, DSC, NMR studies 4-61047  
 poly(ethylene terephthalate), viscoelastic props. on homogeneous and plastic deformations 4-114593  
 poly(vinylidene fluoride), mech. and phys. props. at high press. and temp. 4-98167  
 poly(vinylidene fluoride), stress and dielec. relax. studies 4-99014  
 poly- $\alpha$ -methylstyrene, glass transition, Gibbs-DiMarzio theory, applicability 4-113637  
 poly-p-phenylene oxides, chlorinated, solid, dielec., mech. and thermal props. 4-88769  
 polyarylate-polyarylenesulphonoxide block copolymers, transitions and relax. (Russian) 4-61087  
 polybutyleneglycol adipate, thermodynamic props. (Russian) 4-84421  
 polyester carbonate-polyethylene terephthalate alloys, phase props. 4-113357  
 polyethylene, thermally stimulated creep 4-84339  
 polyethylene glycol-plasticised polyvinyl alcohol binder system for Al<sub>2</sub>O<sub>3</sub> powders, granule compaction rel. to binder glass transition temp. 4-85129  
 polyethylene-polypropylene copolymers and blends, thermally stimulated creep 4-84339  
 polymer blends, conf., Ottawa, Ontario, Canada (April 1983) 4-82591  
 polymer melts, viscoelastic function shift factors rel. to apparent activation energy of viscous flow 4-74979  
 polymer side chain liquid crystals, struct., optical and phase transition props. 4-98013  
 polymers, amorphous, vol. structural relax. theory 4-84396  
 polymers, strength, temp. depend. (Russian) 4-104806  
 polymers flexible chain in region of shear rates and stresses, rheological behaviour, elastic state 4-69721  
 polypropylene, thermally stimulated creep 4-84339  
 polystyrene, glass transition, Gibbs-DiMarzio theory, applicability 4-113637  
 polystyrene spheres in mixtures, miscibility and glass forming 4-70382  
 polystyrene/tetramethylpolycarbonate compatible blends, viscoelastic behaviour 4-114594  
 polytetrafluoroethylene, glass transition, thermodynamic props., DSC obs. 220-700K 4-61108  
 polyvinyl acetate, structural-relax. near glass transition, modelling 4-65192  
 polyvinylidenefluoride, transition props. rel. to thermal and mech. history, DSC, 200-500K 4-84397  
 PVC, glass transition, Gibbs-DiMarzio theory, applicability 4-113637  
 PVC, thermally stimulated currents, tacticity and mol. wt. influence 4-113668

# ass transition (polymers) continued

PVC film, segmental mobility, antistatic additives effect, thermally stimulated depolarisation method (*Russian*) 4-109114  
 PVC-CPE blends, mech., dynamical and rheological props., third component influence (*German*) 4-99390  
 rubber, vulcanised, elec. cond., crystallinity and glass transition 4-113944  
 transition temp. determ. method 4-75678  
 vinyl acetate-ethyl  $\alpha$ -cyanocinnamate copolymers, IR,  $^1\text{H}$  and  $^{13}\text{C}$  NMR spectra 4-84208

## lasses see glass

assy state see vitreous state

de, dislocation see slip

## obular star clusters

AM-1, outer halo cluster, cluster and stars characts., BV photometry 4-115788  
 analytical models of globular clusters, construction 4-72992  
 close binaries formation in globular clusters and X-ray sources numbers 4-63219  
 brightness distribution from narrow-slit scanning method 4-63227  
 $\omega$  Centauri, BV photometry of dwarf Cepheids 4-67729  
 collapse of spherical stellar system, numerical study 4-101438  
 collisionless Boltzmann eqn. for spherical stellar systems, integration 4-72990  
 core collapse and post-collapse evolution, role of binary stars 4-101442  
 cores surface photometry and implications for dynamics 4-101443  
 dissipative dynamical evolution, influence of binary stars 4-63212  
 dissipative dynamical evolution of stellar systems, cooling and heating of system by binary stars 4-63211  
 E 3, peculiar star cluster, colour-magnitude diagram 4-110704  
 evolution, effect of binary stars form. 4-63226  
 evolution characts. 4-63229  
 evolution of stars allowing for energy loss due to axion particles 4-115748  
 evolutionary aspects rel. to open clusters 4-63217  
 formation and stellar dynamics (*Russian*) 4-63225  
 formation model, hierarchical 4-67839  
 formation of galaxies and globular star clusters, role of dark matter 4-90262  
 giant stars, model atm., spectra and mass loss 4-110608  
 Hodge 11 in LMC, globular cluster, electronographic stellar photometry 4-94623  
 in NGC 5128, stellar content and metallicity from IR photometry 4-86032  
 Liller 1, no IR burst during type I X-ray burst from Rapid Burster (MXB 1730-335) 4-90190  
 LMC globulars, spectroscopy of M and S stars 4-77886  
 M15, Arecibo interferometer obs. of compact planetary nebula (K648) 4-82534  
 M15, photographic BV photometry of RR Lyrae variables 4-101368  
 M28, Carnegie Southern Observatory plate study of variable stars 4-115758  
 in M31, colour-magnitude and two-colour diagrams 4-63233  
 in M31, ellipticities of five objects on B-plate (*Russian*) 4-85992  
 M31 globular clusters, metallicity parameters, comparison with Galaxy 4-101479  
 M33 globular clusters, ages and metallicities, spectral obs. 4-110695  
 M3, interstellar absorpt. lines obs. rel. to halo gas inflow from galactic North Pole 4-101450  
 M3, M13, discovery of intrinsic polarisation in red giant stars 4-82470  
 M3 (NGC 5272), distance determ. using variable stars (*Russian*) 4-101445  
 M3 (NGC 5272), positions, space distrib. and number of variable stars (*Russian*) 4-101202  
 M4, deep CCD photometry of main sequence stars 4-63215  
 M4, metallicity of blue horizontal-branch stars 4-85918  
 M71 (NGC 6838), photometric anal. of foreground interstellar reddening 4-101441  
 metal abundances anal. 4-110696  
 metallicities and radial velocities, spectral obs. 4-106045  
 NG 4594 (Sombrero galaxy), globular cluster system struct. 4-63273  
 NGC 2808, NGC 6388, southern globular clusters, Reticon BVRI profiles 4-101439  
 NGC 2808, southern globular cluster, main-sequence photometry 4-72991  
 NGC 288, age and abundance from BV photometry obs. 4-110697  
 NGC 288, age from electronographic BV photometry study 4-77888  
 NGC 288, colour-magnitude diagram and peculiarity 4-63214  
 NGC 288, colour-magnitude diagram from BV photographic photometry 4-110702  
 NGC 3201, cluster characts. from RR Lyr stars anal. 4-63216  
 NGC 5466, absolute vel. and perigalactic distance 4-63228  
 NGC 5466, stars, colours, positions and magnitudes 4-67776  
 NGC 6273, possible membership by FK Ophiuchi Cepheid variable 4-110621  
 NGC 6397, metallicity of blue horizontal-branch stars 4-85918  
 NGC 6752, globular cluster, electronographic stellar photometry 4-94623  
 post-collapse evolution and gravothermal oscillation 4-77887  
 relativistic stellar dynamics 4-77883  
 S-type stars in galactic globular clusters, photometric and spectroscopic search in M22, NGC 6723, and 47 Tucanae 4-101369  
 shape, size and numbers correl. with galaxy type 4-106069  
 stellar dynamics and X-ray binaries origin via tidal capture 4-110674  
 surface brightness profiles, electronic camera obs. 4-67777  
 thermodynamic equilibrium hard binary models 4-63236  
 47 Tucanae, binary freq. and kinematic parameters 4-77884  
 47 Tucanae giant branch, CN and methylidyne spectral obs. 4-85921  
 UBVR1 half-light integrated photometry of 72 southern clusters 4-110703  
 X-ray globular clusters, UV obs. 4-101446  
 X-ray sources, Einstein Observatory obs. 4-101509  
 X-ray sources in globular clusters and burst sources, neutron star binary model 4-101508

## lossaries

geology and geophysics 4-95078  
 NMR terms, medical appl. 4-105319  
 polarisation, definitions and nomenclature, instrument polarisation 4-82604  
 surface analysis techniques review and glossary 4-78063  
 vision, glossary of terms and laws (*Italian*) 4-72243

glow curves see thermoluminescence

glow discharge deposition see plasma deposition

glow discharge lamps see discharge lamps

glow discharge microphones see microphones

## glow discharges

anodic instabilities rel. to surface processes at inner wall 4-87993  
 cathode, particle energy distrib., Monte Carlo calc. 4-84101  
 cathode glow, sputtered atom light emission, interferometry 4-87981  
 current column plasma parameters meas. 4-113234  
 DC, temp. and electron density meas. 4-79835  
 electrical fields application to combustion systems 4-69985  
 electrical oscillations, longit. mag. field effects 4-87994  
 electrode treatment, afterdischarge electron emission 4-87987  
 electron beam technique for reactive ion plating 4-114424  
 electron gun, cathode geometry rel. to beam spatial distrib. 4-87990  
 electron source of HV glow discharge, geometric parameters control (*Russian*) 4-68320  
 electron source using glow-discharge-created electron beams 4-95560  
 electron temperature in hollow cathode glow discharge, optogalvanic determ. 4-84073  
 enhancement by shock waves 4-97919  
 fast electron distrib. function in uniform elec. field 4-87970  
 hollow anode discharge spectroscopy 4-75216  
 hollow cathode magnetron discharge, characts. 4-84115  
 hollow-cathode cell for a pulsed vapor laser 4-102939  
 inert gas glow discharge, doubly ionised metal ions, mass spectroscopic anal. 4-97923  
 inert gas glow-discharge plasmas, noise 4-113254  
 inert gases, flowing, in hollow cathode discharge, vac. UV radiation invest. 4-91988  
 laser amplifier, rel. to effect of quantum modulation of electron beams by lasers 4-96864  
 low pressure, plasma throbs and oscillations in cathode and anode regions 4-87992  
 millimetre wave EM radiation interaction 4-88001  
 molecular vibr. excitation 4-60561  
 neutron source from glow discharges in deuterium 4-102423  
 nonlinear ionisation wave packets excited in glow discharge 4-97925  
 optical detection sensitivity of glow discharge in mag. field 4-84091  
 particle excitation mechanisms F, Ar, O, N<sub>2</sub>, CO and perfluoromethyl radical in glow discharge 4-79860  
 pinpoint discharge diagnostic with two-step optogalvanic effect using intersecting laser beams 4-87964  
 plasma temperature, spectroscopic meas. in hollow cathode discharge 4-113117  
 positive column of glow discharge, current flow mechanism in fast flow lasers 4-113249  
 positive glow corona in atmospheric air, simple theoretical model 4-97935  
 RF glow discharges, spectral line shapes, optical emission actinometry 4-87931  
 self sustained, initiation 4-84113  
 self-sustained, cathode-directed ionisation wave instability 4-92019  
 silanes, decomposition kinetics in glow discharge 4-62180  
 slotted hollow cathode discharge, current distrib. 4-84116  
 spectrometry of S diffusion in  $\alpha\text{-Al}_2\text{O}_3$  (*French*) 4-80300  
 spectroscopic light source with continuous sample delivery, characterisation 4-106394  
 spin trapping of radicals produced by glow discharge on low-density polyethylene 4-61592  
 vacuum discharge cathode spot, cyclicity processes 4-87980  
 volume glow discharge in nitrogen, electrode partitioning effect on pinching 4-108239  
 Ar glow discharge plasma, diagnostics 4-87944  
 Ar<sup>+</sup> pulsed hollow cathode discharge laser, operational characteristics 4-83565  
 Ar-NH<sub>3</sub> glow discharges, Ar metastable densities meas. 4-87059  
 CF<sub>4</sub>/O<sub>2</sub> emission, plasma etching systems, spatially resolved optical spectroscopy 4-79852  
 CO, fast flow laser plasma, electron temp. meas. 4-103466  
 Cl<sub>2</sub>-N<sub>2</sub> mixtures, ion dynamics of glow discharge plasmas 4-65142  
 Cu II slotted hollow cathode discharge laser, Cu at. diffusion meas. 4-83569  
 Cu-Ne hollow cathode glow discharge at intermediate currents 4-75224  
 D, glow discharge, high voltage, planar 1D model 4-60767  
 H, emission line shapes in hollow-cathode discharge 4-102645  
 H nonequilibrium positive columns, state transitions, two-temp. model 4-92007  
 H<sub>2</sub> thyratrons, high power plasma switches, plasma props. 4-65135  
 H<sub>2</sub> thyratrons, high power plasma switches, atoms and ion prod. 4-65136  
 H<sub>2</sub>O vapour dissociation in hollow cathode glow discharges 4-89289  
 He capillary glow discharge, collisional radiative model with atomic collisions 4-60773  
 He glow discharge, atm. press., positive column contraction mechanism 4-87996  
 He-Cd<sup>+</sup> hollow cathode laser, population inversion mechanism 4-83570  
 N<sub>2</sub> molecule, C<sup>II</sup>, state vibr. populations in glow discharge 4-87991  
 N<sub>2</sub>-H<sub>2</sub> glow discharges, emission spectroscopy for metal surface nitriding 4-75222  
 N<sub>2</sub>-O<sub>2</sub>, inhomogeneous positive column, electron-energy distrib. and inelastic processes 4-79858  
 Ne neutral level population, time evolution in glow discharge 4-88008  
 O<sub>2</sub> positive column space-charge dipole layer movement 4-92021  
 SiH<sub>4</sub> and Si<sub>2</sub>H<sub>6</sub> glow discharges, SiH<sub>2</sub> detection by freq. modulation absorpt. spectroscopy 4-88981  
 SiH<sub>4</sub> glow discharge, Si atoms conc. profiles meas. by laser-induced fluorescence 4-92004

glueballs see colour model; quark confinement

gluonia see colour model; quark confinement

## GO calculations

see also GTO calculations

basis sets, diffuse s and p supplementary functions 4-68930  
 Huckel model, nonlinear eqns. 4-91198  
 local electron pair models for intra- and inter-molecular exchange interactions (*German*) 4-78774  
 methane elastic electron scatt. cross sections, GO and HF wave function calcs. 4-64334  
 tetrafluoroethane, elastic electron scatt. cross sections, GO and HF wave function calcs. 4-64334  
 transition metal atoms, fourth-row, Gaussian basis sets 4-96447

## GO calculations continued

- $\text{H}_2\text{O}^+$  in crystals, struct. anal., SCF-LCGO calcs. 4-96450  
 HeH, van der Waals, mol., ground state, complete CI calcs. 4-112122  
 $\text{N}_2$ , basis sets, diffuse s and p supplementary functions 4-68930  
 $\text{N}_2\text{--HF(HCl)(HBr)}$ , H bonded complexes, ab initio GO SCF MO calcs. 4-64369  
 $\text{P}_2\text{--HF(HCl)(HBr)}$ , H bonded complexes, ab initio GO SCF MO calcs. 4-64369  
 $\text{S}_2\text{H}_2$ , lone-pair interactions, rot. barriers, ab initio Gaussian basis set calcs. 4-64339

## gold

see also nuclei with .....

- (111) reconstructed surface struct. study 4-80357  
 absorptivity of 10.6  $\mu\text{m}$ , temp. depend., computed from Drude theory 4-76405  
 adatom on NaCl stepped surface, pot. energy calc. 4-80372  
 adsorbed on W (110), work function meas. 4-98692  
 adsorption of Cu, on (111) surface, underpotential region, LEED and RHEED investig. 4-108702  
 adsorption of  $\text{O}_2$ , AES, XPS, and thermal desorption study 4-92556  
 adsorption of  $\text{O}_2$  on (110) and (111) surfaces, substrate impurity effects, EELS, AES, and XPS study 4-93160  
 alloying behaviour on GaAs 4-80454  
 atom, 4f binding energies, Auger effect 4-78817  
 atom, optically excited, in inert gas matrices, radiative lifetimes 4-102642  
 Auger electron spectra 4-81050  
 average M-shell fluorescence yield meas. 4-87071  
 backscattering of  $\text{He}^+$  ions, excitations, optical spectrometry study 4-78944  
 backscattering of  $\text{N}_2^+$  ions at  $180^\circ$ , enhanced surface yield 4-81073  
 band structure and direct transitions, ARUPS studies 4-75842  
 chemisorption of noble gases, excited states and decay mechanisms 4-98436  
 colloids, aqueous, fractal structures formed by kinetic aggregation 4-62258  
 contacts with InP and InGaAsP, X-ray study of interactions 4-80675  
 deposition on H saturated Si (111) surfaces, AES and EELS study 4-108742  
 diffusion of He 4-65488  
 discontinuous films, epitaxial deposition on mica substrates 4-70597  
 elastic collision spikes in sputtering at normal and oblique incidence 4-76602  
 electrical conductivity of discontinuous thin metal films and conducting filaments 4-98785  
 electrode, surface oxidation in  $\text{H}_2\text{SO}_4$  electrolyte, XPS study 4-93465  
 electrodeposits, acid hard, performance eval. on contacts 4-76020  
 electron and positron slowing down 4-108486  
 electron backscatt., Monte Carlo calcs. 4-66157  
 electronic stopping power, excitation energy alpha-particle time of flight expt. 4-67916  
 electroplating and nanometer e-beam lithography for mag. flux quantisation measurements 4-73455  
 film, deposited on Si, dynamic recoil mixing, parameter optimisation 4-70180  
 film, field emission deposition, high adherence coatings 4-81161  
 film, proton and deuteron stopping cross section 4-92260  
 film, structure and topography, electron microscopy techniques 4-109576  
 film, surface state obs. by electron tunnelling spectra of MIM tunnel junctions 4-88606  
 film deposition, using plasma evaporator design with heated needle cathode 4-88989  
 film enhanced bonding by ion-assisted electron-beam deposition 4-109324  
 films, amorphous and polycryst., plural electron scatt., Monte Carlo calc. 4-66158  
 films, growth on Ni as function of substrate temp., AES study (French) 4-65581  
 films, polycrystalline, ion sputtering depth profiles, surface roughness contributions, SEM obs., 4-98487  
 films, reactive ion beam etching, mol. ion dissoc. upon impact 4-71772  
 films, vacuum evaporated, compressive-type fracture (Japanese) 4-75822  
 films, vacuum evaporated, compressive-type fracture (Japanese) 4-75823  
 films deposited by electron beam evaporation or sputtering, Si outdiffusion, annealing ambients effects 4-70459  
 fine grained target, sputtering by heavy multicharged ions 4-109296  
 Forsyth area, Queensland, Australia, heavy metal mineralisation survey by helicopter 4-94037  
 granular films, relax. phenomena 4-108747  
 implanted  $^3\text{He}$  depth profiles,  $^3\text{He}$  post-bombardment effects 4-80073  
 impurity contaminations, PIXE anal. 4-99874  
 impurity diffusion, isotope effect meas. 4-65476  
 ion channelling, energy stopping power depend., interatomic interaction potentials at high projectile velocities 4-80125  
 ion impact L-shell ionisation, higher order processes 4-99265  
 ion-induced secondary electron emission projectile incident angle depend. 4-76596  
 island film, charge transport and conductance oscill. 4-84712  
 isolated microspheroid distrib. effect on surface enhanced Raman scatt. 4-66027  
 K-shell ionisation induced by low energy  $\text{H}^+$  4-96508  
 L shell X production cross sections,  $\text{H}^+$  induced 4-96649  
 L X-ray emission probabilities by 70 MeV Ar ion impact 4-78949  
 L-shell ionisation by Si and S ions, cross sections and alignment 4-99263  
 L-subshell ionisation cross section, projectile atomic number depend. 4-99267  
 L-substrate ionisation cross sections, projectile depend. 4-99264  
 local-field enhancement of rough surface 4-104047  
 mechanisms and kinetics of dissolution in liquid Na 4-114530  
 Meissner effect in Au of Au clad Nb wire induced by Nb proximity effect 4-108970  
 molecule, relativistic electronic struct. calc. using SCF Xalpha Dirac scatt. wave programs 4-59636  
 nuclear spin-lattice relaxation rates, relativistic APW calc. 4-71204  
 optical length determ. in diamond-anvil cell 4-68237  
 overlayer deposition on (Hg,Cd)Te, interactions and diffusion 4-80439  
 oxide-metal-oxide low-emittance films on glass, industrial realisation 4-112531  
 particle array, surface enhanced optical processes 4-87397  
 particles in amorphous silicon matrix, grain growth and twin formation 4-113340  
 gold continued  
 photoacoustic spectra, reflectance effects 4-80961  
 photon linear polarization in the elementary process of atomic-field bremsstrahlung 4-91354  
 physisorbed CO, high resolution C 1s and O 1s core excitation spectroscopy 4-93125  
 plating of stainless steel wall for suppression of T permeation 4-61261  
 point contacts for high freq. phonon generation 4-61007  
 polycrystalline, XPS spectra, background intensities 4-114362  
 potential at at. boundaries in Thomas-Fermi model and eqns. of state (Chinese) 4-70333  
 prospecting at Salair, USSR, geochemical methods use 4-100828  
 proton stopping power, energy loss straggling, effective-charge fraction and straggling of heavy ions 4-103843  
 radioactive isotope, high-temp. resonance cell for laser spectroscopy 4-102648  
 reconstructed (110) surface, struct. study 4-70536  
 recontamination of laser-cleaned metallic surfaces 4-104913  
 reflecting layer, parasitic photosensitivity avoidance in Si diffusion tentometers 4-101829  
 reinforced probes for conductivity profiling of semicond. wafers 4-99712  
 selective optical coating prod. on plastic sheet as heat reflecting film 4-112555  
 self-diffusion, effect of hydrostatic pressure 4-65451  
 self-diffusion, equilib. defect parameters and characts. 4-65445  
 semicontinuous thin films, 2D percolation system, conduction and Hall coeffs. 4-70957  
 small particles, crystalline struct., STEM microdiffraction studies 4-108305  
 small particles suspended in gas, photoelectron yield 4-104713  
 soft surface vibr. of fine particles 4-61201  
 solids, heavy ion charge states and charge transfer 4-76589  
 sputtering, atomic excitations and level populations 4-76590  
 stopping power of protons, 3 to 8 MeV 4-92258  
 submonolayer film, optical absorption,  $\epsilon_{\text{bound}}$  size depend. in small islands 4-66089  
 superthin surface films, waveguide modes as sensitive probe of optical props. 4-61762  
 surface, (100), image pot. surface states identification, inverse photoemission 4-76015  
 surface, (111), direct atomic imaging after in situ C etching 4-113770  
 surface, (111), electronic band struct., photoemission spectra determination, cryst. symm. effect 4-84549  
 surface, (111), reconstruction, high resolution TEM images 4-84500  
 surface, (111), surface potential, STM study 4-84670  
 surface, (111) and (100), at. vibrs., phonon dispersion, interatomic force constants 4-92506  
 surface, adsorption and thermal decomposition of trichlorophosphate, XPS studies 4-98428  
 surface, ion-induced kinetic electron emission; Z $_1$  oscils. 4-76595  
 surface, ion-induced secondary electrons, energy spectra, mol. effect 4-76586  
 surface, low energy  $\text{He}^+$  ion scatt., inelastic loss energy study 4-81081  
 surface, (110)-(1 $\times$ 2), atomic displacements,  $\text{He}^+$  backscatt. studies 4-65533  
 surface (111), band struct., synchrotron radiation study 4-85074  
 surface atom core level shifts, photoemission obs. 4-93183  
 surface backscattering yield for  $\text{He}^+$  beam energies, 0.5 to 2 MeV 4-81075  
 surface periodic gratings, light scattering, field enhancement and SER 4-114292  
 target, impact craters due to glass pellets 4-108689  
 thermodynamics, kinetics and props. of gases and C in metals, data collection 4-73174  
 thermoelectromotive force of metals with open Fermi surface at low temperatures (Russian) 4-92699  
 thin film, Ag $_2$ O monolayers, 4-108691  
 thin film, electron transmission, electron NGR spectroscopy studies 4-60971  
 thin film, fluorescence detection of surface EXAFS 4-93136  
 thin film, optical props. of grain boundaries (German) 4-71461  
 thin film deposits on Ag, struct. study by ATR method 4-84520  
 thin films, 2000 Å thick, electron localisation and interaction, electronic cond., dimensionality crossover 4-80689  
 thin films, agglomerated, phys. and optical props. 4-76545  
 thin films, diffusion of Fe, Ni and Co, XPS study 4-81115  
 thin films, nucleation, epitaxial growth and coalescence on bicryst. substrates of NaCl 4-75814  
 thin films, thermal expansion coeffs., transmission HEED 4-75705  
 tilt boundary energy and segregation, computer simulation studies 4-114540  
 trilayer with island metal film recording layer as optical data disk 4-91548  
 twist boundaries (100), calc. energy and struct., effect of interatomic potential 4-65272  
 two-hole core-level satellite obs. 4-70896  
 ultrahigh-pressure laser-driven shock-wave experiments at 0.26  $\mu\text{m}$  wavelength 4-75180  
 VUV optical mirrors, contamination effect study 4-83666  
 wire, vapourisation, plasma prod., heating and motional impedance 4-75179  
 X-ray anomalous scattering and specular reflection in M, photoabsorption regions 4-93129  
 Ag, band struct., photoemission spectroscopy meas. 4-70643  
 Al-Au(Cu) thin film bilayers, ion beam bombarded, interfacial phase formation 4-70241  
 Al-I-Au tunnel junction, fast light emission, plasmon polaritons (French) 4-80998  
 Au, adsorption of  $\text{O}_2$ , Au $_2\text{O}_3$  prod. by DC reactive sputtering, EELS, AES, and XPX study 4-93161  
 Au, electron scatt., X-ray intensity calc. by Monte Carlo simulation (Chinese) 4-71480  
 Au 1, low-lying transitions, vol. isotope shifts 4-64409  
 Au thin films, dynamic scaling near percolation threshold, AC cond. and dielectric const. meas. 4-98525  
 $^{79}\text{Au}$ , electron wavefunctions, momentum-space representation, relativistic effects calcs. 4-107288  
 Au/Al contacts, intermetallic bonds and contact resist. (Russian) 4-113819  
 Au/ $\text{Al}_2\text{O}_3$  cermets, optical props. and dielec. const., quantum size effects 4-65942

- and continued
- Au/Al<sub>2</sub>O<sub>3</sub> cermets, optical props. and dielec. const., quantum size effects 4-65941
- Au/CdS, surface recombination vel., photoluminescence studies 4-80600
- Au/Cr bilayers on GaAs, interfacial chemical reactions and drive-out diffusion, AES study 4-80313
- Au/Cu bilayers, ion-induced solid solutions and ordered cpd. form. 4-108470
- Au/Fe interface boundary, interdiffusion 4-65497
- Au/Ga thin film couples, room temp. interdiffusion 4-61149
- Au/GaAs (001) interface struct., XPS, RHEED and ion scatt./channelling studies 4-80421
- Au/GaAs contacts, Schottky barrier photosensitivity spectra in strong absorption region (*Russian*) 4-65741
- Au/GaAs Schottky contacts, damage-induced degradation 4-84699
- Au/n-GaAs (100) Schottky contacts, elec. props. and interface chem., sputtering effects 4-80674
- Au/n-InP Schottky diodes with intermediate layer, longitudinal photoelec. effect 4-65743
- Au/Ni, superlattices, dynamical props., computer simulations 4-113777
- Au/Si interface, atomic redistributions, XPS studies 4-80311
- Au/Si interfaces, reactivity, MeV ion scatt. studies 4-80424
- Au/Si/Cu Schottky diode, stress effects, photoelec. meas. 4-88591
- Au/Si<sub>3</sub>N<sub>4</sub>/Si system, elec. effects of Au (*Chinese*) 4-98757
- Au-SiO<sub>2</sub>, metallisation technology comparative study of Nb and TiW barrier layers 4-88969
- Au-Ag-Au multilayered films, microstructure changes rel. to layer spacing, TEM obs. 4-80432
- Au-As<sub>2</sub>S<sub>3</sub>-Al MIM struct., bias voltage depend. of capacitance 4-104325
- Au-CdTe:H contacts, hydrogenation effects 4-80695
- Au-chalcogenide glass-Al sandwich struct., Schottky barrier form. 4-104291
- Au-Fe<sub>3</sub>Au structure, localised electronic state spatial distrib., polarisation study 4-104334
- Au-GaAs Schottky barrier contacts, LEC grown, electron traps, DLTS signals, effect of metal 4-84691
- Au-Ga(In), excess enthalpies meas. using heat flow calorimeter 4-80237
- Au-Ge/Au ohmic contact struct., grain boundary diffusion of Ge through Au, Auger anal. 4-88344
- Au-Ge-Sn structure, capacitance-voltage meas. at liq. N<sub>2</sub> temp. 4-84707
- Au-Ge(H) interfaces on amorphous Ge, Schottky barrier and cpd. formation 4-84669
- Au-InP junction 4-84625
- Au-InP Schottky barriers, semicond. LEC growth, deep level defects (*Chinese*) 4-61320
- Au-kapton-Au resistor bolometer for meas. UV and soft X-ray radiation 4-63783
- Au-M=Au sandwiches, M-Pd,Cr,V, superconducting and mag. props. 4-80709
- Au-n-InP:Fe diode struct., photocurrent amplification 4-70934
- Au-p-CuInSe<sub>2</sub> contacts, elec. props., solar cell appls. 4-70935
- Au-Pd interface, electronic struct. and mag. props. 4-80645
- Au-polymer, film, prep. by plasma polymerisation 4-81162
- Au-Sb<sub>2</sub>S<sub>3</sub>-Al MIM struct., bias voltage depend. of capacitance 4-104325
- Au-Si nucl. detectors, gamma-ray effects on rise time 4-59566
- Au-Si Schottky barrier diodes, barrier height and hot electron attenuation length meas. 4-98751
- Au-Si-SiO<sub>2</sub> interface, Au surface-state energy level determ. 4-80640
- Au-SiO<sub>2</sub> composite granular films, conductivity and crossover effects 4-114047
- Au-Sn surface diffusion in air at room temp. 4-98459
- Au+H<sup>+</sup>, K-shell ionisation cross sections 4-78953
- Au<sup>3+</sup>+He, electron capture, ionisation and transfer ionisation cross sections 4-78960
- CdTe:Ag(Cu), deep levels, pulsed admittance spectroscopy and capture cross sections 4-92653
- GaAs-Au(Pd) interface, high energy ion channelling studies 4-65318
- GaAs-Au tunnel structs., differential cond. characts. 4-61455
- GaAs(001)-Au interface, formation by MBE and thermal stability 4-99328
- n-Ge:Au, deform. influence on deep level position of impurity 4-104160
- Ge:Au, nonradiative multiphonon capture of carriers by deep traps 4-75889
- Ge:Au photocells, spectral characts. obs. 4-101919
- Ge-S<sub>2</sub>:Au glass, impurity surroundings, nature of defects, positron annihilation study 4-79943
- InP (110)-Cu(Ag) interface, soft X-ray photoemission study 4-85080
- Nb/Au/Nb Josephson tunnel junction, ESR study 4-92871
- Si:Au, donor and acceptor levels, DLTS meas. 4-88473
- Si:Au, donor level, entropy factor, resist. and DLTS meas. 4-70707
- n-Si:Au, doping by laser (*Chinese*) 4-113473
- Si:Au, effect of mobile dislocations on surface saturation (*Russian*) 4-98107
- n-Si:Au, elec. cond. and photoconductivity 4-104213
- Si:Au, electron capture cross section of Au acceptor (*Chinese*) 4-92741
- Si:Au, photocurrent deep level transient spectra 4-80535
- Si:Au, solid solution, nuclear-spin lattice relaxation 4-76282
- Si:Au, transient capacitance of Au acceptor energy level under uniaxial stress (*Chinese*) 4-75888
- Si:Au, tunnelling: negative U-centres and photo-induced reactions 4-108816
- n-Si:Au, defect characterisation, SEM-CCM studies 4-113278
- gold alloys**
- see also gold compounds
- alkali metal alloys, MAu (M=Li, Na, K, Rb, Cs), electronic props., self-consistent relativistic band struct. calcs. 4-92604
- dilute, interaction of trivalent solutes with vacancies 4-65259
- thermodynamics, kinetics and props. of gases and C in metals, data collection 4-73174
- Ag-Au surface segregation, modelling, low index planes, steps, kinks, and chemisorption 4-92495
- Au-Ag thin film, grain boundary diffusion coeff. from Ag surface coverage, AES 4-92430
- Au-Ag/Si interfaces, reactivity, MeV ion scatt. studies 4-80424
- Au-based thin films, ultrahardness and internal stresses 4-92582
- Au-Cd liq. and solid alloy, elec. resist. studies 4-88499
- Au-Cu, real crystals with several sublattices, proton planar channelling, ang. depend. 4-70248
- Au-Cu minerals, study using electron probe anal. 4-76934
- gold alloys continued**
- Au-Fe, positron lifetimes in vacancies and vacancy-Fe clusters 4-109274
- Au-Fe alloys, chemical interdiffusion at interface with Au 4-65497
- Au-Fe alloys, evidence against metastable phase separation 4-80239
- Au-Fe alloys, metastable phase separation 4-80238
- Au-Fe dilute alloy, exchange-circulation electron current between Fe atoms (*Chinese*) 4-114102
- Au-Ga from melting in Au contacts to GaAs, in situ X-ray diffr. study 4-88593
- Au-Gd, dil., impurity-induced muon depolarisation, mag. field depend. 4-71228
- Au-Ge bilayers, ion beam mixing, amorphous and metastable phases formation 4-80113
- Au-Ge/Au ohmic contact struct., grain boundary diffusion of Ge through Au, Auger anal. 4-88344
- Au-Ge-Ni ohmic contacts on GaAs, CO<sub>2</sub> laser alloying 4-76038
- Au-Ge(Ni) on GaAs, alloying behaviour 4-80454
- Au-In, dil., channelling effect of conversion electrons emitted from radioactive impurities 4-75569
- Au-Mn long-period ordered structures, electron microscopy study 4-113396
- Au-Mn partially disordered, high resolution electron microscopy images 4-92146
- Au-Ni (40 at.%), chem. and elastic contrib. to free energy above miscibility gap 4-76747
- Au-Pt surface segregation, modelling, low index planes, steps, kinks, and chemisorption 4-92495
- Au-Sn solder, Au-rich for InGaAsP/InP laser 4-107678
- Au-Ti/GaAs Schottky contacts, damage-induced degradation 4-84699
- Au<sub>2</sub>Cd, electron damage, high resolution electron microscopy study 4-92241
- Au<sub>2</sub>Cr, cryst. struct. determ., lattice modulation 4-103703
- AuFe alloys, spin glass freezing, PAC study 4-71216
- AuFe, dilute alloy spin glass, susceptibility, neutron scatt. and muon spin rot. 4-71249
- AuFe, spin glass dynamics, muon spin relax., neutron spin echo meas. 4-71080
- AuGa<sub>2</sub> (001), surface net characterisation and electronic struct. 4-80642
- AuGe/GaAs ohmic contact, Ge and Au profiles, SIMS studies 4-103782
- AuMn, electron damage, high resolution electron microscopy study 4-92241
- AuMn crystal, antiphase boundaries, high resolution TEM image simulation 4-97985
- AuMn<sub>2</sub>, long period antiphase boundary struct., electron diffr., electron microscopy obs. 4-103946
- AuNi(CO), impurity lineshapes in dilute alloys, UPS study 4-113893
- AuPt<sub>1-x</sub>(Ni<sub>1-x</sub>), substitutionally disordered, electronic struct. calcs. 4-70644
- Au<sub>1-x</sub>Si<sub>x</sub>, liq. and amorphous, elec. resist., Ziman theory anal. 4-70774
- AuSn diffusion produced alloys, optical props. 4-80897
- AuSn-Pb quasibinary section of phase diagram, thermal anal. 4-93265
- AuY(Zr)(Nb)(Rh)(Pd), dil. alloys, thermoelectric power, resistivity, low temp. study, phase-shift anal. 4-113926
- AuY(Zr)(Nb)(Rh)(Pt)(Pd), dil. alloys, thermoelectric power, resistivity, low temp. studies 4-113925
- Cu-Au, liquid, elec. resist., conc. depend., role of pseudopot. refinements 4-84605
- Cu-Au alloys, (100) surface; order-disorder transitions and segregation 4-98268
- Cu-Zn-Au, ordered, two-dimensional antiphase struct., electron diffr. study 4-113397
- CuAu, microstructure, field ion microscopy study 4-88177
- Cu<sub>3</sub>Au (100), keV Ne scatt., atom layer effects 4-76580
- Cu<sub>3</sub>Au alloy, first-order phase transitions, nucleation-growth processes, scaling laws (*Japanese*) 4-113568
- Cu<sub>3</sub>Au, displacement cascade collapse at low temps. 4-103835
- Cu<sub>3</sub>Au, substitutionally disordered, electronic struct. calcs. 4-70644
- Cu<sub>3</sub>Au, Zener relax. anisotropy 4-103874
- n-GaAs/Au-Ge Ohmic contact fabrication by IR lamp alloying 4-84690
- Gd<sub>2</sub>Au/Al<sub>1-x</sub> pseudobinary cpd., mag. behaviour 4-76136
- La<sub>80-x</sub>Ru<sub>20-x</sub> (R=Nd, Pr), universal response of EM, acoustic, and mech. influences 4-92851
- Ni-Au, bonding and enthalpy studies 4-79978
- Ni-Au, electronic structure and surface comp., ion etching, X-ray photoelectron spectra 4-66187
- Ni-Au films, ion-induced comp. change, role of grain boundary diffusion at elevated temps. 4-108475
- Ni-Ge-Au-Ag low resist. alloyed ohmic contacts to Al<sub>0.48</sub>In<sub>0.52</sub>As/n<sup>+</sup>-Ga<sub>0.47</sub>In<sub>0.53</sub>As 4-84692
- Pb-Au dil. solutions, bulk equil. lattice parameters, neutron diffr. meas. 4-75372
- Pb-Au dilute solutions, single cryst., struct. in quenched state, X-ray and neutron diffr. studies 4-75371
- Pd-Au, bonding and enthalpy studies 4-79978
- Pd-Au, electronic structure and surface comp., ion etching, X-ray photoelectron spectra 4-66187
- (Pd<sub>1-x</sub>Au<sub>x</sub>)<sub>2</sub>Fe, hyperfine mag. field study 4-88493
- Pd<sub>76</sub>Au<sub>24</sub>Si<sub>18</sub>, amorphous alloy, crystn., SAXS study 4-65186
- Ti-Au, amorphisation, pulsed ion beam annealing study 4-103831
- gold compounds**
- see also gold alloys
- Ag<sub>2</sub>Ga, from melting in Au contacts to GaAs, in situ X-ray diffr. study 4-88593
- (Au<sub>2</sub>Ag)<sub>2</sub>Te<sub>3</sub>, krennerite, modulated struct., electron microscopic studies 4-108319
- Au (I) complexes, bis(N-methyl)-dithioformamidinium, IR spectra 4-66032
- AuCl<sub>3</sub> complexes, adsorption on goethite 4-109678
- Au<sub>2</sub>Ru<sub>4</sub>(μ-H)(CO)<sub>12</sub>(PPh)<sub>3</sub>, synthesis, mol. and cryst. struct. 4-104969
- p-Au<sub>2</sub>Te-n-CdTe heterojunction, deep levels, photocapacitance spectra 4-61410
- KAu(CN)<sub>2</sub>, electrochem. prep. 4-104741
- goniometers**
- optical fibre braids, light transmission coeff. meas. using goniometer 4-87458
- Philips eucentric goniometer stage, extreme-tilt holder 4-73600
- Philips X-ray wide angle goniometer heater attachment 4-95627
- US goniometric method for elastic constants meas. (*French*) 4-60229
- Weissenberg rheogoniometer based biorheological methods, blood appl. 4-110010

## goniometers continued

X-ray goniometer of meas. in temp. range 10 to 293K 4-69988  
 $\text{LaCl}_3\text{-KCl}(\text{NaCl})/(\text{CaCl}_2)$  mixtures, refr. index, goniometric meas.  
 4-109147

## government data processing

see also *police data processing; town and country planning*  
 offshore waste discharge data acquisition and permit preparation acceleration 4-115442

## GP zones see Guinier-Preston zones

## grain boundaries

for grain boundary diffusion, see *diffusion in solids*; for grain boundary segregation, see *segregation*

see also *bicrystals; subboundary structure; twin boundaries*  
 alkali halide bicrystals, high-angle (001) twist grain boundaries 4-103768  
 alkali metal halides, diffusion along grain boundaries and dislocations 4-92439

alloys, microstructure, classification, overview 4-66309

Astrolay, Ni-base superalloy, creep fracture, effect of wavy grain boundaries (Chinese) 4-62005

austenitic alloys, He bubbles at grain boundaries 4-108471

barrier heights, surface state effects 4-92780

bicrystal, grain boundary phase equilib., computer mol. dynamics simulation 4-113461

bicrystal, grain boundary slip at high temp., dislocation model (Russian) 4-92211

bicrystal model, expansion at large angle grain boundaries, electron diffraction 4-84519

bicrystal semiconductor, elec. cond. for tunnel charge transport 4-88576

bicrystals, symmetry determ. using convergent beam electron diffraction 4-80431

brass, Cu-Zn-Pb, precipitation and coarsening of Pb particles 4-109413

brittle fracture toughness, influence of microstruct. 4-93388

Carrara Marble, high temp. flow, grain boundary sliding model 4-110132

carrier recombination velocity on grain boundary, direct meas. 4-70827

cell wall form. mechanism 4-80038

ceramics, bicrystal grain boundaries, orientational relationships 4-70579

ceramics, fine grained, containing liq. phase, superplastic flow mechanism 4-109475

ceramics, grain and phase boundary struts. 4-108381

chemical driving force, role in discontinuous coarsening 4-113651

convergent beam electron diffraction, cryst. struct. and defect appls. 4-79906

copper phthalocyanines, localised mol. arrangements, electron microscopy study 4-80028

creep voids, mechanism of sintering out during subsequent annealing 4-92213

creeping body containing macroscopic crack, constrained grain boundary cavitation 4-92289

crystallites, expansion during appearance of stresses in thin films 4-8479

deformation of grains 4-76745

diffusion, struct. props. and point defect mobility, mol. dynamics simulations 4-80305

diffusion in metals and alloys, conf., Tihany, Hungary (Aug.-Sept. 1982) 4-63405

dislocations, two-dimensional systems, melting, Monte Carlo simulation studies 4-113586

elastic discontinuities, acoustic microscopy 4-60237

FCC crystal, low-angle [001] twist boundary, Volterra-type dislocation model 4-75454

FCC grain boundary, diffusion and struct., mol. dynamics studies 4-113691

ferrites, polycrystalline, model of initial mag. permeability (Russian) 4-98921

film, ion implanted, electron beam recrystallisation 4-98137

fracture mechanics, microscopic, appl. of J-integral concept 4-97435

glass, thermodynamics of grain boundary crystallisation 4-75314

glass, two-level systems, nonideal Frenkel Kontorova model anal. 4-113345

hexagonal to quadratic vortex lattice transition, pinning on surfaces and large grain boundaries 4-80729

impurity effects, cluster variation method calcs. 4-113465

IN-100, Ni-base superalloy, cast, microstruct. changes during fractional melting 4-109434

IN-617, Ni-base superalloy, fatigue, high temp. low cycle 4-66425

IN-738 LC, Ni-base superalloy, creep fracture, effect of grain boundary chem. and segregation 4-81285

Inconel X-750, Ni-base superalloy, creep and fracture, prior deform. effects 4-114656

interaction stress meas. using neutron diffraction, texture effects 4-85282

interaction stress meas. using time of flight neutron diffraction, texture effects 4-85281

interfacial and surface microchemistry, book contrib. 4-109421

interfacial dislocation structures, characterisation using TEM 4-108371

intergranular corrosion of steels and alloys, book 4-95084

intergranular embrittlement, impurity interactions within grain boundary, MO calcs. 4-80147

ionic crystal, space charge regions around dipolar grain boundaries 4-104194

magnetism conference, Eger, Hungary (Sept. 1983) 4-78029

metal film, Mayadas-Shatzkes conducting model, isotropy limits 4-108953

metallic film growth, development of grain struct. 4-65580

metallic materials, polycryst., grain boundaries model effect of mech. props. 4-113458

metallic thin films, optical props. of grain boundaries (German) 4-71461

metals, fracture mechanism, energetic anal. (Spanish) 4-70269

metals, grain boundaries, diffusion mechanisms, review 4-65492

metals, high temp. oxidation, cation diffusing scales form. 4-93457

metals, oxidation, high temp., cation diffusing scale form., SEM obs. 4-71791

metals, stir cast microstructure 4-89049

metals, vacancy-twin boundary interactions, computer simulation studies 4-113491

metals, wedge disclination systems, elastic interaction with grain boundaries 4-65292

metals and alloys grain boundaries and cryst. defects, interatomic pots. 4-113464

migration during high temp. deform. 4-98115

## grain boundaries continued

MIS solar cells, photovoltaic props., grain boundary effects modelling 4-81553

notched bar, creep rupture, continuum damage 4-71735

olivine-basalt partially molten aggregates, diffusion creep during hot pressing 4-110137

oxides and carbides, diffusion along grain boundaries and dislocations 4-92439

oxides and carbides, segregation at surface and grain boundaries 4-92377

oxynitride glasses, prep. and props. 4-76737

p-n junctions, electron beam induced short circuit currents, carrier lifetime 4-92806

polycrystalline materials, creep at low stresses and intermediate temp., diffusion flow mechanism 4-71701

polycrystalline solids, grain-boundary diffusion study (Russian) 4-80309

polycrystals, strong and ductile, grain boundary design, overview 4-65336

radiation damage microstructure, microcomputer system for quantitative image analysis 4-103617

segregation, STEM EDS X-ray microanal., electron probe size effects 4-80244

semiconductors, grain-boundary admittance theory 4-108849

semiconductors, polycryst., percolation nonohmic cond. 4-108871

shape of grain boundary pinned by spherical particle 4-84302

sialon ceramics, thermal diffusivity, effect of crystn. of grain boundary phase 4-88355

solar cells, minority carrier SEM-EBIC signal and grain boundaries 4-80609

solar cells, polycrystalline MIS devices, diode Q-factor 4-109743

solid/solid interfaces, computer simulations, conf., Philadelphia, USA (Oct. 1983) 4-110806

steel, alloy, reheat cracking, scanning Auger and electron microscopy study 4-71490

steel, alloy, secondary hardening mechanisms 4-99396

steel, alloy, type 15Kh2NMFA, radiation embrittlement and temper brittleness (Russian) 4-66407

steel, austenitic, neutron irradiation, high temp. deform. behaviour (German) 4-81262

steel, austenitic stainless, containing Ti and Al, grain boundary precip. 4-99385

steel, austenitic stainless, creep, applicability of creep J-integral to microscale propag. (Japanese) 4-93384

steel, austenitic stainless, fracture modes under He ion and neutron irradiation, temp. depend. 4-104853

steel, austenitic stainless, H attack, TEM study 4-114657

steel, austenitic stainless, high temp. creep rel. to carbide precipitates 4-76802

steel, austenitic stainless, microstructural design for improved He embrittlement resist. under HFIR irradiation 4-103790

steel, austenitic stainless, precip. hardening, fatigue crack growth, effect of precip. (Japanese) 4-89122

steel, austenitic stainless, recrystn., grain boundary diffusion and free energy 4-114569

steel, austenitic stainless, SCC in  $\text{MgCl}_2$  soln., fractography, grain struct., SEM obs. (Japanese) 4-99651

steel, austenitic stainless, sensitised, Cr depletion in carbide vicinity rel. to heat treatment 4-71654

steel, B, hardenability and B segregation (Chinese) 4-61945

steel, C-Mn, grain boundary segregation of Cu, Sb and Sn at 900°C 4-93300

steel, Cr-Mn austenitic, phase stability and corrosion on exposure to pure Li 4-107061

steel, Cr-Mo, intergranular H stress-cracking rel. to grain boundary segregation of P 4-62112

steel, Cr-Ni, precipitation and recrystn. processes (Russian) 4-93299

steel, Fe-Si (3 wt.%), power loss and flux density of neighbouring grains 4-80776

steel, ferritic stainless, recrystn. and deform. inhomogeneities, effect of twinning (Polish) 4-93309

steel, ferritic stainless, stabilisation breakdown 4-114718

steel, H embrittlement by cathodic charging 4-66420

steel, low alloy, low C weld metal, transform. behaviour and toughness 4-114670

steel, low alloy, reversible temper embrittlement, role of microstructure, scanning Auger microscopy study 4-81286

steel, low C, Mn, austenite form-mechanism during annealing 4-85151

steel, Mn-Al, austenitic precipitation, fine structure after annealing (Russian) 4-104787

steel, Mn-Mo-Al, transform. of austenite and cryogenic mech. props., effect of intercrit. heat treatment (Chinese) 4-85152

steel, Mn-Mo-Ni, creep fracture and rupture life (Japanese) 4-114647

steel, Nb-V, low C, controlled-rolled, transform. textures 4-99405

steel, Ni-Cr-Mo, crack paths and H assisted crack growth in  $\text{H}_2$  and  $\text{H}_2\text{S}$ , temp. and press. depend. 4-66429

steel, Ni-Cr-Mo-V, fracture toughness, overheating, effect of S content (Japanese) 4-93377

steel, Ni-Mo-Si, 300M, occurrence of blocky martensite 4-114582

steel, pearlite growth, by combined vol. and phase boundary diffusion 4-114470

steel, rolled, initial fatigue fracture surface, laminated struct. effect (Japanese) 4-89118

steel, stainless, influence of Mo on mechanical props. (Russian) 4-81271

steel, stainless, US inspection, flaw visibility, split spectrum processing, grain size effect 4-89226

steel, steam turbine casing and rotor, mech. props. rel. to service life (Japanese) 4-89119

steel, transformer, effect of Sb additions on texture 4-81216

structure and diffusion, mol. dynamics simulation study 4-65437

structures, temp. ranges for stability 4-98117

textured materials, kinetic props., grain interaction effects 4-60938

three component solid soln., equilib. competitive segregation 4-66338

tilt boundaries, (001) and (111), computer simulations, multiplicity of struts. 4-98112

tilt boundaries, (110), asymm.,  $\Sigma_9$ ,  $\Sigma_{27a}$  and  $\Sigma_{81d}$ , dissociation 4-65273

tilt boundary struct., struct. unit/grain boundary dislocation model anal. 4-113460

Udimet 700, Ni-base superalloy, creep fracture, effects of wavy grain boundaries 4-93415

Zircaloy-4, microstruct. after air cooling from high temp.  $\beta$ -phase, effect of P impurity content 4-89071

Ag, twist boundaries (100), calc. energy and struct., effect of interatomic pot. 4-65272

## in boundaries continued

- Al bicrystals, grain boundaries diffusivity 4-65485  
 Al, cavity formation in samples irradiated with pulsating beam of 225 MeV electrons 4-108443  
 Al, FCC tilt boundary, vacancy migration, computer simulation studies 4-113694  
 Al, grain boundary structure, computer simulation studies 4-113459  
 Al, He bubble nucleation on dislocations during 600 MeV proton irradiation 4-113504  
 Al, high purity, polygonised, TEM, internal friction peak 4-113534  
 Al, internal friction, time measurement technique with torsion pendulum 4-112778  
 Al, internal friction originated by grain boundaries 4-103872  
 Al, plastic deformation at high strain rates 4-84337  
 Al, pure, 600 MeV proton irradiation, H and He bubble form. at grain boundaries 4-108479  
 Al, with small Sn additions, microstructure and corrosion behaviour 4-99630  
 Al-Al<sub>2</sub>O<sub>3</sub>-(Si), creep deform., stress and temp. depend. 4-81246  
 Al-Cr thin film couple, diffusion barriers, Auger study 4-88407  
 Al-Cu films, microstructure and electromigration studies 4-88413  
 Al-Cu-Li-Mg-Zr, splat-quenched, microstructure and tensile props. 4-114620  
 Al-Li, nucleation, growth and coarsening of precipitates 4-81202  
 Al-Mg (5 wt.%), high temp. fatigue, squared-up grain structure 4-81277  
 Al-Mn-Zr, rapidly quenched from melt transform. behaviour 4-81185  
 Al-Zn, cellular decomposition, TEM, DSC obs. 4-114528  
 Al-Zn system, diffusion along grain boundaries and precipitation reactions 4-113697  
 Al-Zn-Mg-Cu, ERGAL 7075, plastic deformation at high strain rates 4-84337  
 AlCuZr, AlCu eutectic, fine grained superplastic alloys, anelastic strains, grain boundary cavity distrib., sintering 4-66359  
 Al<sub>2</sub>O<sub>3</sub> ceramics, subcritical crack propagation, activation enthalpies and mechanisms (German) 4-62010  
 α-Al<sub>2</sub>O<sub>3</sub>, defect structure, electron emission meas. 4-93145  
 Al<sub>2</sub>O<sub>3</sub>, doped, mixed cond. and impurity electron states 4-92773  
 Al<sub>2</sub>O<sub>3</sub>, faceted grain boundaries 4-84301  
 α-Al<sub>2</sub>O<sub>3</sub> growth from transition Al<sub>2</sub>O<sub>3</sub> matrix 4-84380  
 Al<sub>2</sub>O<sub>3</sub>, polycrystalline, strength rel. to flow distrib. 4-109505  
 Al<sub>2</sub>O<sub>3</sub>, translucent sintered tubes, thermophysical stability rel. to impurities and dopants 4-61937  
 Al<sub>2</sub>O<sub>3</sub>:Cr, grain boundary diffusion, anisotropy and doping effects 4-92443  
 Al<sub>2</sub>O<sub>3</sub>-glass composite, hot isostatically pressed, macropore structure 4-71629  
 Al<sub>2</sub>O<sub>3</sub>-ZrO<sub>2</sub> composites, grain growth hindrance by ZrO<sub>2</sub> inclusions 4-76743  
 Au particles in amorphous silicon matrix, grain growth and twin formation 4-113340  
 Au thin films 4-75814  
 Au, tilt boundary energy and segregation, computer simulation studies 4-114540  
 Au, twist boundaries (100), calc. energy and structure, effect of interatomic potential 4-65272  
 BaTiO<sub>3</sub> thick film, grain boundaries, TEM obs. 4-84300  
 Be, neutron irradiation at various temps., compression props. and swelling 4-108458  
 Bi<sub>2</sub>Sb<sub>2</sub>Te<sub>3</sub> films, strain-resist. effects, structure effects 4-114052  
 CaTiO<sub>3</sub>, polycryst., viscous creep deform. at elevated temps. 4-103863  
 CdTe, dislocations and subboundaries, etching studies 4-75451  
 CdTe thin layers, crystal and energy structures for photoelectric transducers 4-98298  
 (CeO<sub>3</sub>)<sub>0.99</sub>-(CaO)<sub>0.11</sub> solid solution, bulk cond. and grain boundary resist., effect of SiO<sub>2</sub> (French) 4-80295  
 Co films, elec. cond. temp. depend. (Russian) 4-88613  
 Co-Ni-Zn ferrites, microstructure, mag. props., BaO additions effect 4-88302  
 CoO, surface morphology changes during vacancy relax. processes 4-75445  
 Cr films, evaporated, mechanical stresses 4-75819  
 Cu, brazed, low cycle fatigue in high vacuum rel. to cold work 4-109500  
 Cu, creep cavitation, grain boundary void growth, small angle neutron scattering obs. 4-85197  
 Cu, diffusivity of In along stationary and migrating grain boundaries 4-65484  
 Cu, Ni diffusion along grain boundaries 4-70428  
 Cu, tilt boundary energy and segregation, computer simulation studies 4-114540  
 Cu, twist boundaries (100), calc. energy and structure, effect of interatomic potential 4-65272  
 Cu-Al<sub>2</sub>O<sub>3</sub>, dispersion hardened, tensile failure, temp. depend., grain boundary fracture 4-66405  
 Cu-Bi, segregation, grain boundary structure and structure transformations 4-113462  
 Cu-Ni-Si, cellular precip., effect of B and P additions 4-66342  
 Cu-Sb (1 wt.%), creep rupture life, effects of pre-existing grain boundary cavities 4-62042  
 Cu-Sb alloys, grain boundary segregation and cracking, Monte Carlo studies 4-114542  
 Cu-Si, dil. alloy, internal oxidation, grain boundary cavitation under creep or fatigue loading 4-71726  
 Cu-Si (6 at.%), tilt boundaries, (110), asymm., Σ9, Σ27a and Σ81d, dislocation 4-65273  
 Cu-Zn-Al (25, 6 wt.%), isothermal decomposition of β' phase 4-99387  
 Fe, BCC, grain boundary diffusion, mol. dynamics simulation studies 4-80287  
 Fe, fatigue crack initiation, Coffin-Manson relations 4-85212  
 Fe, ferromagnetic, high purity, magnetomechanical damping, influence of structure defects 4-76226  
 Fe, grain boundary with impurity segregation, atomic and electronic structures, 4-113463  
 Fe powder, Ni-coated, compacted, phase identification by colour etching 4-114755  
 Fe, pure, annealed, fatigue crack nucleation sites under reversed bending stress (Japanese) 4-99516  
 Fe thin foils, STEM energy dispersive X-ray microanalysis 4-69999  
 Fe-Al-Si, Sendust, brittleness, effect of solidification and heat treatment 4-81281  
 Fe-C, high purity, forced vel. pearlite, expt. 4-93294  
 Fe-C-Si alloys, positron lifetime, trapping and diffusion 4-88901

## grain boundaries continued

- Fe-Co-Ni-Al, Alnico 5, hot workability, microstructure 4-114626  
 Fe-Cr (26.6 at.%), sulphidation props. in H<sub>2</sub>S-H<sub>2</sub> atmospheres at temps. 973 to 1173K and S press. 10<sup>-10</sup>-10<sup>-6</sup> Pa 4-93459  
 Fe-Cr (8 wt.%), ferrite-austenite, isothermal transform. kinetics, grain boundary nucleation 4-109396  
 Fe-Cr-Ni (15, 15 wt.%), He bubble form. during dual beam irradiation 4-75562  
 Fe-Cu (10 wt.%), powder compacts, liq. phase sintering, dimensions changes 4-66267  
 Fe-Mo (6.3 at.%), high temp. creep, stress exponent and substructure 4-76821  
 Fe-Nb, nitrided, void form., mech. props., optical microscopy, SEM, TEM obs. 4-81361  
 Fe-Nb-C-P alloys, grain boundary segregation of P rel. to C content 4-85156  
 Fe-Ni-C, fracture toughness rel. to transform. induced plasticity and grain boundary segregation 4-99585  
 Fe-Ni-C(7.6, 0.48 wt.%) alloys, bainite formation kinetics, effect of step quenching 4-114514  
 Fe-Ni-Cr-C, Ti-modified, void swelling, pre-irradiation, ageing effects 4-104798  
 Fe-Ni-Cr-C(3.6, 1.45, 0.5 wt.%) alloys, bainite formation kinetics, effect of step quenching 4-114514  
 Fe-Ni-Cr-Mo-N, weld metal, annealing, precipitation, metallographic analysis 4-109417  
 Fe-Ni-P alloys, growth of intragranular ferrite 4-76777  
 Fe-Ni-P alloys, nucleation of intragranular ferrite 4-76776  
 Fe-P, segregated grain boundaries crack propagation, mol. dynamics calc. 4-114663  
 α-Fe-P-C solid solns., grain boundary brittleness, low-temp. reversibility (Russian) 4-104835  
 Fe-P-W(Mo)(Mn), grain boundary embrittlement, impurity-induced, influence of alloying elements 4-114654  
 Fe-Sb-Ce alloys, Ce state at crystal boundaries, electron diffraction studies (Chinese) 4-98114  
 Fe-Si sheets, magnetisation processes, grain boundary effects 4-76180  
 Fe-Si-Al, Sendust, hot workability, microstructure 4-114626  
 α-Fe-C, H-induced grain boundary fracture, effect of C 4-93403  
 (Fe<sub>0.49</sub>Ni<sub>0.51</sub>)<sub>3</sub>V, ordered alloys, microstructure and creep rel. to implanted He 4-108399  
 GaAs layers, MBE grown on Ge islands on insulator, zone melting recrystallisation, grain boundaries, photoluminescence obs. 4-84524  
 Ge bicrystal p-type inversion layers, anomalous magneto-transport props. 4-98719  
 Ge, grain boundaries, plasma exposure effects, diode studies 4-65276  
 Ge, symmetrical tilt grain boundaries, Σ=9, 11, structure, electron microscopy obs. 4-70169  
 Ge, tilt boundaries at structure, HREM obs. 4-103767  
 He liquid surface Wigner solid, topological defects and melting 4-98389  
 InSb bicrystal, grain boundary barrier height and elec. cond. 4-92216  
 InSe Bridgman grown crystals, growth parameters, improvement rel. to defects 4-98043  
 KCl, grain boundary influence on motion of crystal inclusions 4-75455  
 LaCrO<sub>3</sub>-Cr cermet, high-temp. creep 4-71693  
 Li<sub>2</sub>CO<sub>3</sub>, single crystal, sub-boundaries on (002) cleavages 4-103751  
 LiF bicrystals, fracture at plastic deformation 4-75609  
 LiFeO<sub>2</sub>, mag. domain walls interaction with microstructure features 4-71122  
 Mg alloy, strain induced grain boundary migration 4-85198  
 MgAl<sub>2</sub>O<sub>4</sub>, grain boundary diffusion, anisotropy and doping effects 4-92443  
 MgO, energy and structure of coincident-site twist boundaries and free (001) surface, computer code 4-60937  
 MgO-Cr, grain boundary diffusion, anisotropy and doping effects 4-92443  
 (Mn,Zn)Fe<sub>2</sub>O<sub>4</sub>, mag. domain walls interaction with microstructure features 4-71122  
 Mn-Zn-Ti ferrites, effects of post-sinter cooling 4-85165  
 Mo, activated sintering, retarded grain boundary mobility 4-99366  
 Mo, cyclic strength and localisation of deformation 4-61999  
 Mo, endurance limit in high cycle fatigue rel. to heat treatment and alloying 4-109498  
 Mo, He trapping at low-angle tilt boundary 4-113505  
 Mo, high temp. neutron irradiation, annealing, void form., mech. props. 4-108456  
 Mo, sintered sheet, tensile props., improvement by reducing O impurity levels 4-89132  
 Mo, tilt grain boundary structure, computer simulation studies 4-113459  
 Nb, superconducting, flux pinning mechanism of grain boundaries (Japanese) 4-76094  
 Nb superconducting films, flux line pinning by grain boundaries (Russian) 4-84756  
 Nb<sub>3</sub>Sn, multifilamentary bronze composites, diffusion reaction growth kinetics, superconduct. critical temp. 4-76064  
 Ni, D segregation, surface and grain boundary SIMS study 4-76774  
 Ni, grain boundaries, Σ distrib., in polycrystals, prep. by strain annealing 4-108377  
 Ni, light purity, reaction mechanism with O<sub>2</sub>+SO<sub>2</sub>, grain boundary diffusion in scale 4-109561  
 Ni, low-cycle fatigue, slip-induced intergranular cavitation at intermediate temp. 4-66402  
 Ni, O assisted intergranular H embrittlement, effects of B, P, Sn and Sb additions 4-62030  
 Ni, polycryst., slip-induced cavitation, effect of boundary structure 4-108378  
 Ni powder, low-temp. diffusion, positron annihilation study 4-98365  
 Ni thick films, grain structure, variation with temp. 4-88412  
 Ni, tilt boundary energy and segregation, computer simulation studies 4-114540  
 Ni-Al thick films, grain structure, variation with temp. 4-88412  
 Ni-Au films, ion-induced comp. change, role of grain boundary diffusion at elevated temps. 4-108475  
 Ni-base creep-resisting alloys, cast, grain boundary relax., effect of structure of boundary vol. 4-71677  
 Ni-Cr-Fe, alloy X-750, SCC resist. in deaerated high temp. water rel. to solution heat treatment (Japanese) 4-62110  
 Ni-Cr-Ti-Mo(Nb), precipitation strengthened, HFIR irradiation, ductility, microstructure 4-108457  
 Ni-Cu alloys, grain boundary segregation and cracking, Monte Carlo studies 4-114542

## grain boundaries continued

- Ni-Sb, retardation of grain boundary self-diffusion 4-84447  
 Ni-Si alloys, intergranular segregation in grain boundaries, X-ray STEM investig. (French) 4-70393  
 Ni-Sn, retardation of grain boundary self-diffusion 4-84447  
 NiO, dislocation core region in grain boundaries, mean inner pot. charge, electron microscope obs. 4-103755  
 NiO:CeO<sub>2</sub>, oxidation and grain boundary diffusion 4-92441  
 Ni<sub>1-x</sub>O ceramic, grain boundaries, TEM studies 4-108382  
 NiSi, Ni<sub>3</sub>Si, thin films, metal silicide form., AES and SIMS study 4-75795  
 Ni<sub>40</sub>Zn<sub>60</sub>Cu<sub>10</sub> martensite, tempering, morphology and recovery 4-109404  
 PLZT, microscopic characterisation 4-61903  
 PbI<sub>2</sub>:Ag, exciton spectrum, photodoping effects (Russian) 4-92626  
 PbMg<sub>1/3</sub>Nb<sub>2/3</sub>O<sub>3</sub> ceramics, dielec. props., microstruct. rel. to sintering temp. and comp. 4-84897  
 PtSi, Pt<sub>3</sub>Si, thin films, metal silicide form., AES and SIMS study 4-75795  
 Si defected substrates, minority carrier lifetime, injection level depend. 4-92753  
 Si, excitation depend. grain boundary recombination velocity 4-104217  
 Si films, monocrystalline and polycrystalline, simultaneous epitaxial growth, struct., elec. props. 4-98488  
 Si, grain boundaries, spin-depend. trapping, effects of light and modulation freq. 4-104155  
 Si, grain boundary recombination vel., study for different injection levels 4-98633  
 Si, polycrystalline, elec. cond. props., small signal theory 4-70804  
 Si, polycrystalline, elec. cond. props., I-V characs. 4-70805  
 Si, polycrystalline, elec. cond. model 4-92712  
 Si, polycrystalline, interacting grain boundaries, surface recombination vel., EBIC study 4-70828  
 Si, polycrystalline, minority carrier diffusion length under solar illum. 4-104225  
 Si, polycrystalline, mobility and carrier conc. depend. on grain size and doping conc. 4-92730  
 Si polycrystalline islands on fused SiO<sub>2</sub>, crack elimination by recrystn. 4-80461  
 Si, polycrystalline ribbon and ingots, grain boundary struct., TEM obs. 4-65275  
 Si single crystal thin film, secondary recrystallisation prep. 4-88421  
 Si tilt boundaries at. struct., HREM obs. 4-103767  
 Si:As, segregation to grain boundaries and surface plasmons 4-98289  
 Si:As/Al interface, sintering and diffusion, As dopant effect 4-80427  
 Si:B polycrystalline films, activation energy of resist., effects of grain boundary trapping state energy distrib. 4-88616  
 p-Si:Fe, conductance along grain boundaries 4-80585  
 Si:H, Al-covered, solid-state reaction between film and substrate 4-92498  
 Si:H<sub>2</sub>O, grain boundary impurity effect determ. 4-92214  
 Si<sub>1-x</sub>Al<sub>x</sub>O<sub>2</sub>N<sub>8-2x</sub>,  $\beta$ -sialon, hot pressed, flexural strength, phase struct., comp. depend. (Japanese) 4-76828  
 SiC, structural defects and grain boundaries, electron microscope study 4-92217  
 Si<sub>3</sub>N<sub>4</sub>, structural defects and grain boundaries, electron microscope study 4-92217  
 Si<sub>3</sub>N<sub>4</sub>-SiO<sub>2</sub>-AlN-Al<sub>2</sub>O<sub>3</sub>-Y<sub>2</sub>O<sub>3</sub> system, phase relations, solid-liq. reactions 4-76762  
 SiO<sub>2</sub> film, ion implanted, electron beam recrystallisation 4-98137  
 SmCo<sub>5</sub> permanent alloys, metallographic study, improved phase and grain boundary etching 4-114754  
 Sn thin film, tracer study of self-diffusion and electromigration 4-103991  
 Sn-Bi (0.5 at.%), creep rate, grain dia. depend. 4-81259  
 ThO<sub>2</sub>-based electrolytes, ionic cond., 300 to 2000K 4-92416  
 Ti alloys, plasticity of coarse grained type VT30 alloy in  $\beta$ -region (Russian) 4-81241  
 $\beta$ -Ti alloys, technique for revealing deformed and recrystallised structs. 4-114571  
 Ti-Al-Nb-Ta-Mo, welds and castings, impact roughness, segregation and influence of B 4-114658  
 Ti-Al-V (6, 4 wt.%), superplasticity rel. to grain struct. and deform. temp. 4-109459  
 TiB<sub>2</sub> powder, pressureless sintered, mech. props. in liq. Al environment, impurity segregation 4-114700  
 V, neutron irradi., temp. depend. of damage microstruct. 4-108455  
 V-B<sub>2</sub>C, neutron irradi., temp. depend. of damage microstruct. 4-108455  
 W, bicrystal, intrinsic grain boundary brittleness (French) 4-99476  
 W bicrystals, dynamic fracture resist., effect of crack vel. 4-99528  
 W bicrystals, oriented, brittle-ductile transition temp. rel. to O and C content, AFS 4-104859  
 W, brittle fracture, impurity effects, Auger electron and scanning electron spectroscopy (French) 4-70268  
 W, grain boundaries of twist misorientation about {100}, direct meas. of work of fracture 4-98116  
 W, interstitial atom interaction with grain boundaries (Russian) 4-65293  
 W, Ni activated sintering, redistrib. of Ni 4-66273  
 W polycrystals, dynamic fracture resist., effect of crack vel. 4-99528  
 W, powder metallurgy, fracture toughness and short-term strength, quantitative correl. 4-89133  
 W-Fe, dil., segregation of Fe to grain boundaries, elec. resist., thermopower, AES meas. 4-103943  
 W-Ni-Fe, fracture behaviour, effect of substitutional impurity elements 4-89134  
 WC-Co composites, carbide-carbide grain boundaries, microanal. 4-80052  
 Zn bicrystals, (10 $\bar{1}$ 0)-tilt, grain boundary struct. transform. effect on sliding 4-103769  
 Zn bicrystals, grain boundary sliding and cryst. slip relationship 4-80048  
 ZnAl eutectoid, fine grained superplastic alloys, anelastic strains, grain boundary cavity distrib., sintering 4-66359  
 ZnO varistor ceramics, SEM EBIC studies 4-75981  
 Zr, grain boundaries, annealing structures 4-92215  
 ZrO<sub>2</sub> ceramic, grain boundaries, TEM studies 4-108382  
 ZrO<sub>2</sub>-Al<sub>2</sub>O<sub>3</sub> ceramic, grain boundaries, TEM studies 4-108382  
 ZrO<sub>2</sub>-based electrolytes, ionic cond., 300 to 2000K 4-92416  
 ZrO<sub>2</sub>-CaO, partially stabilized, grain boundary chem., Auger analysis 4-109409  
 ZrO<sub>2</sub>-Y<sub>2</sub>O<sub>3</sub>, polycryst. and single cryst. elec. cond. 4-80290  
 ZrO<sub>2</sub>-Y<sub>2</sub>O<sub>3</sub>-Bi<sub>2</sub>O<sub>3</sub> solid electrolyte, prep. and elec. props. 4-84452

## grain boundary diffusion see diffusion in solids

## grain growth

- compacts, homogeneously packed, intermediate-stage sintering 4-76702  
 computer simulation of grain growth, grain size distrib., topology and local dynamics 4-66306  
 Coroneze 638, strain-enhanced grain growth during superplastic flow 4-71686  
 eutectics, irregular, theoretical basis of grain growth (Polish) 4-93258  
 kinetic exponent estimation 4-109426  
 kinetics, computer simulation 4-66305  
 metallic film growth, development of grain struct. 4-65580  
 metals, fracture mechanism, energetic anal. (Spanish) 4-70269  
 metals and alloys, book contrib. 4-109429  
 polycrystalline aggregates, grain growth, computer simulation studies 4-113665  
 refractory materials, recrystn., grain growth kinetics 4-76789  
 sintering, liquid phase, pore-filling process 4-99361  
 steel, austenitic stainless, claddings, ring test of tubes oxidised in high temp. steam 4-104816  
 steel, austenitic stainless, Nb-stabilised, hot deformed, grain coarsening 4-93329  
 steel, electric, effective grain growth inhibition 4-81218  
 steel, electric, Fe-Si (3 wt.%), grain growth in recrystallised material 4-81217  
 steel, low C, abnormal grain growth, decarburization treatment 4-71663  
 steel, roll type 9Kh, small N and B additions effect on struct. and mech. props. 4-93342  
 strain-enhanced grain growth phenomenon during superplastic flow 4-71686  
 superplastic materials, elongation, grain growth and cavitation effects 4-71711  
 Al, subgrain growth during static annealing 4-114573  
 Al-Cu (4.3 wt.%), randomly nucleated two-dimens. grain struct., effect of grain growth anisotropy 4-104774  
 Al-Zn-Mg-Cu, cold working, recovery and recrystn. (German) 4-71670  
 Al<sub>2</sub>O<sub>3</sub> compacts, homogeneously packed, intermediate-stage sintering 4-76702  
 Al<sub>2</sub>O<sub>3</sub> powders, with bimodal particle size distrib., sintering 4-85127  
 $\beta$ -Al<sub>2</sub>O<sub>3</sub>, sintering, microstruct. and mech. props. 4-85136  
 $\beta$ -Al<sub>2</sub>O<sub>3</sub>-ZrO<sub>2</sub>, slip cast transform. toughened composites, mech. props., ionic cond. 4-103995  
 Al<sub>2</sub>O<sub>3</sub>-ZrO<sub>2</sub> composites, grain growth hindrance by ZrO<sub>2</sub> inclusions 4-76743  
 BaFe<sub>2</sub>O<sub>19</sub> permanent magnets, sintering temp. effect on mag. props. and density (Afrikaans) 4-76170  
 BaTiO<sub>3</sub>:Sb(Nb), sintering, microstruct. 4-89012  
 Bi<sub>2</sub>TiO<sub>5</sub> ceramics, grain orientation by cold uniaxial method 4-104757  
 $\alpha$ -Ca<sub>3</sub>(PO<sub>4</sub>)<sub>2</sub>, sintering behaviour at 1200 to 1600°C 4-114458  
 Cu-Sn-Cu-Nb composite, reaction annealing, Nb<sub>3</sub>Sn layer growth conditions 4-61886  
 Cu-(Al), cold-worked, recrystn., effect of stacking fault energy 4-81221  
 Fe-C-Si, irregular eutectic, theoretical basis of grain growth (Polish) 4-93258  
 Fe-Ni, single particle martensitic growth, computer simulation studies 4-114521  
 Fe-Si (3 wt.%), thin sheets, development of {110}[001] texture, effect of S content in coating 4-114575  
 Fe-Si (6.5 wt.%), rapidly quenched, grain growth and texture form. by annealing 4-81214  
 Li<sub>2</sub>O, LiAlO<sub>2</sub>, Li<sub>2</sub>SiO<sub>4</sub> and Li<sub>2</sub>ZrO<sub>3</sub> breeder materials, fast neutron irradi. expts. 4-107024  
 Mg alloy, strain induced grain boundary migration 4-85198  
 MgO powder, hot pressing, densification, dislocation creep mechanism 4-114455  
 Mo, activated sintering, retarded grain boundary mobility 4-99366  
 Mo sheet, MgO and CaO-doped, secondary recrystn. kinetics 4-71668  
 Mo-Ni, liq. phase sintering, elimination of pores 4-114445  
 Nb<sub>3</sub>Sn, multifilamentary bronze composites, diffusion reaction growth kinetics, superconduct. critical temp. 4-76064  
 Ni-B alloys, CVD deposited, microstruct. and mech. props. 4-71581  
 Ni<sub>3</sub>Al, cold-rolled, recrystn. annealing 4-81213  
 Si hazed polycryst. layers, STEM microanal. studies 4-108692  
 Si single crystal thin film, secondary recrystallisation prep. 4-88421  
 Si:As thin films, As fast diffusion during rapid thermal annealing 4-113714  
 SiC fibres, strength degradation after heat treatment above 1200°C 4-66385  
 $\beta$ -Ti alloys, technique for revealing deformed and recrystallised structs. 4-114571  
 Ti-Al-V (6, 4 wt.%), evolution of  $\alpha$ + $\beta$  struct. rel. to thermomech. treatment 4-109431  
 TiC-Ti, reactive liq. phase sintering 4-61896  
 TiC-Ti, reactive solid-state hot pressing 4-61897  
 UO<sub>2</sub> fuel pellets, sintering, grain growth rel. to S content 4-85134  
 W, Ni activated sintering, redistrib. of Ni 4-66273  
 WC-Co cemented carbide, liq. phase sintering, origins of discontinuous grain growth 4-104759  
 WC-Co hardmetal, grain growth rate sintering, influence of C content 4-114463  
 Zn-Al eutectoid, strain-enhanced grain growth during superplastic flow 4-71686

## grain refinement

- metallurgical systems, mechanisms and kinetics of dissolution 4-114530  
 steel, Cr-Ni ferritic, rapidly solidified, struct. and mech. props. 4-109388  
 steel, martensitic, precip. and mech. props., influence of high temp. thermomechanical treatment 4-114522  
 steel, strengthening effects of Cu 4-89062  
 steels, grain refinement by Ti inoculation during submerged arc welding 4-85138  
 Al alloy, laser treatment, strengthening and microstruct. (Russian) 4-71665  
 Al alloys, solidification, grain refinement, pseudosurface nucleation mechanisms 4-114497  
 Al-Cu, rheocasting, grain refinement rel. to stirrer rotation velocity (Japanese) 4-89036  
 Al-Ti-(B), impurity distrib. 4-114538  
 Cu alloy, laser treatment, strengthening and microstruct. (Russian) 4-71665  
 Fe-Cu, strengthening effect of Cu 4-89062

## in size

see also grain growth; grain refinement  
 aluminosilicate refractories, creep 4-81242  
 brass, Cu-Zn-Pb, precipitation and coarsening of Pb particles 4-109413  
 $\alpha$ -brass, work hardening in polycrystals 4-61956  
 brittle fracture toughness, influence of microstruct. 4-93388  
 ceramics, fine grained, containing liq. phase, superplastic flow mechanism 4-109475  
 ceramics, fracture energy, elastic anisotropy and grain size dependence 4-60983  
 cermets, optical props. and dielec. const., quantum size effects 4-65941  
 elastic sedimentary sequences, quantification in time series anal. 4-94042  
 computer simulation of grain growth, grain size distrib., topology and local dynamics 4-66306  
 forming limit diagrams, comparison between expt. and theoretical 4-93348  
 germination, of solid on powdery solid, statistical model (French) 4-114816  
 granular porous explosives, shock sensitivity, grain size effects 4-108548  
 heterogeneous materials, large-grained, step-heating technique for thermal diffusivity meas. 4-75738  
 hexanitrostilbene, explosive, shock sensitivity, grain size effects 4-108514  
 metallic film growth, development of grain struct. 4-65580  
 metals, polycryst., inhomogeneous and anisotropic, stress-strain relations (Polish) 4-85179  
 MIS solar cells, photovoltaic props., grain boundary effects modelling 4-81553  
 mullite, influence of  $\text{TiO}_2$  on sintering and microstruct. evolution 4-114457  
 olivine-basalt partially molten aggregates, diffusion creep during hot pressing 4-110137  
 Permalloy, mag. domain struct., complex permeability meas. 4-76164  
 Perminvar, mag. domain struct., complex permeability meas. 4-76164  
 photographic emulsions, film grain noise, optical density model 4-90671  
 polycrystalline plasticity, self consistent relation with nonuniform matrix 4-112729  
 Rene 95, Ni-base superalloy, fatigue, effect of processing and microstruct. 4-104843  
 sintered compacts, grain size, internal strain, photoluminesc. spectra 4-99160  
 sintering, liquid phase, pore-filling process 4-99361  
 solar cells, polycrystalline MIS devices, diode Q-factor 4-109743  
 steel, Cr-Mo-V-W, HT-9, austenitising and microstruct. 4-93320  
 steel, austenitic stainless, dynamic strain ageing, serrated flow rel. to strain rate, temp. and grain size 4-114604  
 steel, austenitic stainless, low temperature yield strength modelling 4-104825  
 steel, austenitic stainless, proton irradiation creep of thin foil specimens, thickness effects on mech. props. 4-103820  
 steel, austenitic stainless, work hardening rel. to grain size 4-81220  
 steel, carburising, core hardenability calcs. 4-99395  
 steel, constructional, near-threshold fatigue, struct. influence 4-93397  
 steel, Cr-Mo, temper-embrittled, effects of grain size and hardness 4-99554  
 steel, Cr-Mo-V, creep recovery by reheat treatment, carbide distrib., X-ray analysis 4-66392  
 steel, Cr-Ni ferritic, rapidly solidified, struct. and mech. props. 4-109388  
 steel, dual-phase, fatigue crack propag., effect of microstruct. on crack path morphology 4-99525  
 steel, electric, Fe-Si (3 wt.%), grain growth in recrystallised material 4-81217  
 steel, H embrittlement by cathodic charging 4-66420  
 steel, having preferred orientation, residual stress evaluation with X-rays 4-114749  
 steel, high-speed, hot isostatic pressing, struct. and contact fatigue 4-114440  
 steel, high-speed, W-Mo, sintered, heat treatment 4-66357  
 steel, HSLA, fatigue threshold, effect of strength and surface asperities on closure 4-76852  
 steel, HSLA, Mn, bearing, strengthening mechanisms rel. to treatment and microstruct. 4-81209  
 steel, low alloy, low C weld metal, transform. behaviour and toughness 4-114670  
 steel, low alloy, mech. props. rel. to second phase particle size 4-99591  
 steel, low and medium strength, crack resist. 4-62034  
 steel, low C, deep drawing cold-rolled sheet prod. by continuous annealing, control of steel chem. 4-114565  
 steel, low C, dual-phase, continuously annealed, effect of prior cold rolling 4-66350  
 steel, low C, strain hardening behaviour, statistical anal. 4-99403  
 steel, martensitic, low C, controlled rolled and quenched, strengthening effects 4-99393  
 steel, martensitic, press. vessel, cleavage fracture 4-71730  
 steel, martensitic stainless, cleavage fracture, micromech. mechanisms 4-104855  
 steel, microalloyed, hot-rolled, isothermal decomp. of austenite 4-99409  
 steel, microalloyed, structural, yield comp., influence of dislocation density and precip. 4-114601  
 steel, mild, C-Mn, Charpy V transition temp. rel. to various material parameters 4-66431  
 steel, Mn-Mo-Al, transform. of austenite and cryogenic mech. props., effect of intercrit. heat treatment (Chinese) 4-85152  
 steel, Nb, strengthening mechanisms, influence of rolling variables 4-71666  
 steel, Nb-V, Nb- and V-carbonitride precipitates, fine struct. (Chinese) 4-61929  
 steel, nonorientated electric, composition effect on loss, elec. cond. and texture 4-81219  
 steel, spheroidized 1090, dislocation density distrib. in tensile specimens, H effect 4-84298  
 steel, stainless, shock loaded, residual struct. and props. 4-109516  
 steel, stainless, US inspection, flaw visibility, split spectrum processing, grain size effect 4-89226  
 steel, structural, fine-grained, low cycle fatigue, influence of cold forming 4-104841  
 steel, structural analysis by ultrasonic backscattering (German) 4-76962  
 steels, hardenability, effect of hot working 4-81211  
 US meas. methods appl. in science and industry 4-104932  
 US measurement of grain size, estimation of scatterer spacing using non-linear least-squares technique 4-99726

## grain size continued

Zircaloy-4, microstruct. after air cooling from high temp.  $\beta$ -phase, effect of P impurity content 4-89071  
 $3\text{V}_2\text{O}_5\cdot 5\text{Fe}_2\text{O}_3$  solid state reaction study, IR and mag. props. 4-85301  
 Ag-based thin films, ultramicrohardness and internal stresses 4-92582  
 Ag-Sn alloys, rapidly quenched, TEM study of struct. defects, depend. on internal residual stresses 4-88172  
 Al, creep substructure effect on stress exponent following stress reductions 4-104820  
 Al, diffusion of H, desorption study 4-65489  
 Al, high purity, polygonised, TEM, internal friction peak 4-113534  
 Al thin film, effect of vapour contaminants on props. 4-88435  
 Al- $\text{Al}_2\text{O}_3$ -(Si), creep deform., stress and temp. depend. 4-81246  
 Al-Cu (4 wt.%), polycryst., containing  $\theta'$  precipitates, cyclic deform., grain size depend. and correl. with single crystals 4-66379  
 Al-Li, precipitate-matrix interfacial energy 4-85160  
 Al-Mg solid solutions, ductility loss at high temps. 4-104857  
 Al-Zn-Mg, fatigue crack closure in 7475, microstruct. and ageing effect 4-62032  
 AlCuZr, AlCu eutectic, fine grained superplastic alloys, anelastic strains, grain boundary cavity distrib., sintering 4-66359  
 $\text{Al}_2\text{O}_3$ , bend specimens, crack resistance curves, influence of grain size 4-62058  
 $\text{Al}_2\text{O}_3$  ceramic, strength rel. to microstructure 4-62060  
 $\text{Al}_2\text{O}_3$  powders, with bimodal particle size distrib., sintering 4-85127  
 $\text{Al}_2\text{O}_3$ , sintered, microstructure and optical props. 4-61649  
 $\text{Al}_2\text{O}_3$ , strength characts. using controlled flaws, microstruct. effects 4-85205  
 $\text{Al}_2\text{O}_3$ /Au cermets, optical props. and dielec. const., quantum size effects 4-65942  
 $\text{Al}_2\text{O}_3$ -ZrO<sub>2</sub> composites, grain growth hindrance by ZrO<sub>2</sub> inclusions 4-76743  
 Au-based thin films, ultramicrohardness and internal stresses 4-92582  
 $\text{B}_4\text{C}$  struct. and mech. props., hot pressing conditions effect 4-61906  
 BN based polycrystalline materials, thermophys. props. 4-61159  
 BaO-TiO<sub>2</sub>-SiO<sub>2</sub> glass-ceramics, ferroelec., depolarisation currents, dielec. and electrooptical props. 4-76317  
 BaTiO<sub>3</sub>, ferroelec., permittivity, effect of grain size 4-76306  
 BaTiO<sub>3</sub>, powder processing, grain size, ferroelec. props. 4-93253  
 BaTiO<sub>3</sub>:Yb, dielec. and X-ray diffr. study 4-84896  
 Be, microplasticity, grain size and heat treatment effects (Russian) 4-104809  
 C films, diamondlike, ionized deposition from methane gas 4-65586  
 CaTiO<sub>3</sub>, polycryst., viscous creep deform. at elevated temps. 4-103863  
 Co-ir sputtered films, mag. props. 4-71141  
 Cr<sub>2</sub>O<sub>3</sub>, doped, hot pressing, annealing, elec. cond., density, grain size, XPS 4-113946  
 Cu, dynamically deformed, annealing-induced struct. variations 4-71667  
 Cu, fracture strain and flow stress, invest. by tension and torsion methods (Polish) 4-93362  
 Cu, recrystallisation, effect of prior cold work on the influence of elec. current pulses 4-61957  
 Cu, work hardening in polycrystals 4-61956  
 Cu-Al-Fe (10, 1 wt.%), corrosion and mech. props., effect of solidification struct. 4-85243  
 Cu-Fe (1.59 wt.%),  $\alpha$ - $\gamma$  martensitic transform. of Fe particles, magnetisation obs. 4-66335  
 Cu-Ni (25 wt.%), sintered and pressed coinage alloy, tensile props., SEM and X-ray obs. 4-71697  
 Cu-Ni-Fe alloys, decomposition neutron scatt. studies 4-114539  
 Cu-P alloys, extruded, microstruct. and mech. props. 4-114574  
 Cu-Sb (1 wt.%), creep rupture life, effects of pre-existing grain boundary cavities 4-62042  
 Cu-Sn-Cu-Nb composite, reaction annealing, Nb<sub>3</sub>Sn layer growth conditions 4-61886  
 Cu(-Al), cold-worked, recrystn., effect of stacking fault energy 4-81221  
 CuInSe<sub>2</sub>, sintered, grain size, SEM obs., resist., Hall obs. 4-66284  
 Al-Fe, creep-induced dislocation subgrain arrangement in ferrite, effect of stress changes 4-76799  
 Fe sintered materials, coercive force, influence of microstruct. 4-66461  
 Fe, strain hardening behaviour, statistical anal. 4-99403  
 Fe-Al rapidly quenched cryst. ribbons, mag., elec. and mech. props. 4-76174  
 Fe-C-Si alloys, positron lifetime, trapping and diffusion 4-88901  
 Fe-Mn alloys,  $\gamma$ - $\delta$  martensitic transformations, recrystn. (Russian) 4-109398  
 Fe-Ni-C alloys, martensitic transformations and primary struct. parameters (French) 4-104781  
 Fe-Si (6.5 wt.%), rapidly quenched, grain growth and texture form. by annealing 4-81214  
 Fe-Si multilayered films, mag. props. and domain struct. 4-61574  
 Fe-(Si), fatigue threshold, effect of strength and surface asperities on closure 4-76852  
 (GaSb)<sub>1-x</sub>(Ge)<sub>x</sub> semicond. alloys, phase transforms. 4-92347  
 In<sub>2</sub>MoS<sub>4</sub> (0  $\leq$  x  $\leq$  1) intercalation compound, synthesis and characts. 4-104200  
 LaCrO<sub>3</sub>-Cr cermets, high-temp. creep 4-71693  
 LaNi<sub>3</sub>-NdNi<sub>3</sub>(CeNi<sub>3</sub>), phase diagrams, grain size anisotropy, H absorpt. characts. (Chinese) 4-93261  
 Mg, hot rolled, texture, grain size and yield strength 4-114579  
 MgO powder, hot pressing, densification, dislocation creep mechanism 4-114455  
 MgO-Cr<sub>2</sub>O<sub>3</sub> granular ceramic, sintering and phase comp. 4-81174  
 Mn<sub>1-x</sub>Zn<sub>x</sub>Fe<sub>2</sub>O<sub>4</sub>, hot pressed, prior heat treatment effect on props. 4-89016  
 Mn<sub>1-x</sub>Zn<sub>x</sub>Fe<sub>2</sub>O<sub>4</sub>, sintering of powders produced by different methods, mechanism and assoc. processes 4-89015  
 Mo, activated sintering, retarded grain boundary mobility 4-99366  
 Mo powder, shock induced densification study 4-109348  
 Na<sub>2</sub>O-Nb<sub>2</sub>O<sub>5</sub>-SiO<sub>2</sub> glass-ceramics, ferroelec., depolarisation currents, dielec. and electrooptical props. 4-76317  
 NbH<sub>3</sub>, H permeability and struct. (Russian) 4-65406  
 Nb<sub>3</sub>Sn, cryst. site determ. of dilute alloying elements, TEM studies 4-88131  
 Nb<sub>3</sub>Sn, multifilamentary bronze composites, diffusion reaction growth kinetics, supercond. critical temp. 4-76064  
 Ni electrodeposited from sulphate and acetate salts, hardness and struct. 4-114431  
 Ni, grain boundaries,  $\Sigma$  distrib., in polycryst. prep. by strain annealing 4-108377  
 Ni, recrystn. after initial recovery (Russian) 4-85162

**grain size continued**

- Ni thick films, grain struct. variation with temp. 4-88412  
 Ni-Al thick films, grain struct. variation with temp. 4-88412  
 Ni-Al<sub>2</sub>O<sub>3</sub> electron beam evaporated condensates, creep props. 4-93361  
 Ni-B alloys, CVD deposited, microstruct. and mech. props. 4-71581  
 Ni-base superalloys, long and short fatigue crack growth, influence of microstruct. 4-99531  
 Ni-Cr base alloys, creep behaviour and microstruct. 4-71705  
 Ni<sub>3</sub>Al, cold-rolled, recrystn. annealing 4-81213  
 NiO:CeO<sub>2</sub>, oxidation and grain boundary diffusion 4-92441  
 PLZT ceramic, coarse-grain light scatt. and elec. hysteresis 4-76399  
 PZT material, high density, prep. by coprecipitation technique 4-76711  
 Pb<sub>80</sub>Bi<sub>20</sub> superconducting filament, high transition temp., produced by glass-coated melt spinning 4-80712  
 (Pb<sub>0.75</sub>Ca<sub>0.25</sub>)(Mg<sub>1/3</sub>Nb<sub>2/3</sub>0.0625Ti<sub>0.9375</sub>)O<sub>3</sub>:Mn ceramics, US, elastic and dielec. props. 4-104543  
 PbMg<sub>1/3</sub>Nb<sub>2/3</sub>O<sub>3</sub> ceramics, dielec. props., microstruct. rel. to sintering temp. and comp. 4-84897  
 Pb(Zr,Ti)O<sub>3</sub> ceramics, spray dried, piezoelec. props. 4-109130  
 Pt ultrathin drawn wires, struct. and elec. props. 4-92696  
 RhSi on polycrystalline and amorphous Si, struct. and growth kinetics 4-80446  
 Si films, monocrystalline and polycrystalline, simultaneous epitaxial growth, struct., elec. props. 4-98488  
 Si, low pressure CVD growth and phys. props. 4-81150  
 Si, polycrystalline, elec. cond. model 4-92712  
 Si, polycrystalline, minority carrier diffusion length under solar illum. 4-104225  
 Si, polycrystalline, mobility and carrier conc. depend. on grain size and doping conc. 4-92730  
 Si, polycrystalline SOI structures, RF zone melting recrystn. for MOS-FET fabrication 4-88965  
 Si polycrystalline sheets for solar cells by improved melt spinning technique 4-81166  
 Si sheets, large-grain, growth by improved spinning method 4-66223  
 Si:B(As), low resistance ion implanted films 4-108398  
 a-Si:H optical confinement type solar cell using milky tin oxide on glass 4-81556  
 n-Si:P polycrystalline CVD films, elec. props., grain size and impurity conc. effects 4-70963  
 Si-Fe nonoriented semiprocessed steel, core loss and permeability, elec. resist. effects 4-61556  
 Si-Fe-Sn(Cu) high permeability grain oriented steel, recrystallisation and grain sizes 4-61953  
 $\beta$ -SiC powders, sintering, hot pressing, densification and mech. props. rel. to prep. 4-109366  
 SiC reinforced Al alloy, fibres and particles, composite strengthening, influence of microstruct. 4-99398  
 Si<sub>3</sub>N<sub>4</sub>, reaction-bonded, strength-porosity relationship 4-76734  
 Si<sub>3</sub>N<sub>4</sub>-Y<sub>2</sub>O<sub>3</sub>, isostatically hot pressed, strength and microstruct. rel. to sintering additives 4-85132  
 Sn thin film, tracer study of self-diffusion and electromigration 4-103991  
 Sn-Bi (0.5 at.%), creep rate, grain dia. depend. 4-81259  
 Sn-Pb (38.1 wt.%), eutectic, fine-grained, accelerated coarsening of microstruct. during superplastic deform. 4-61997  
 Ti, structural recrystallisation,  $\alpha$ - $\beta$  transition (*Russian*) 4-109427  
 Ti-Al-Sn (5, 2.5 wt.%), internal stress, deform. at 300K 4-71700  
 Ti-Al-V (6, 4 wt.%), superplasticity rel. to grain struct. and deform. temp. 4-109459  
 TiB<sub>2</sub> electric spark alloy coating of C steel, TiB<sub>2</sub> struct. influence 4-62121  
 TiB<sub>2</sub> powder, pressureless sintered, mech. props. in liq. Al environment, impurity segregation 4-114700  
 TiB<sub>2</sub>, sintering and props. of samples made from powder synthesised in plasma-arc heater 4-76715  
 Ti(C,N)-Ni-Mo, hard metal, fracture toughness rel. to microstruct. 4-104873  
 Ti-C-Ti, reactive liq. phase sintering 4-61896  
 Ti-C-Ti, reactive solid-state hot pressing 4-61897  
 TiNi single crystals, shape memory alloys, deform. behavior 4-76819  
 TiSi<sub>2</sub> films, sputter deposition at high substrate temps., elec. and struct. props. 4-114393  
 V-Al rapidly quenched alloys, struct. and supercond. props., alloying addition effects 4-70400  
 W, AKS-doped wire, high-temp. creep behaviour, effect of gas bubbles (*German*) 4-81243  
 W-Ni-Fe, dynamic strength calcs. based on grain deform. 4-108511  
 WC powders, particle size distrib., metallography 4-109591  
 WC, sintered, Co inclusions, magnetisation curves 4-109040  
 WC-(Co-Ni) hardmetals, mech. props., variation with Ni/Co ratio 4-114462  
 WC-Co, cemented carbide, hot isostatic pressing 4-66293  
 WC-Co cemented carbide, liq. phase sintering, origins of discontinuous grain growth 4-104759  
 WC-Co hard metals, strengthening by ultrasonic vibrs. 4-62122  
 WC-Co hardmetal, grain growth rate sintering, influence of C content 4-114463  
 Y<sub>2</sub>O<sub>3</sub>-Fe<sub>2</sub>O<sub>3</sub>, solid state reaction for garnet formation by sintering 4-85302  
 Zn-Al (21 wt.%), lamellar, superplastic and cast dendritic, water vapour corrosion 4-62097  
 Zn-Al superplastic alloys, Al atoms redistribution, elec.-resist. and small angle X-ray scatt. study 4-62004  
 ZnO electroluminescent, brightness waves, grain size effects 4-104675  
 ZnO varistor, high-field fine-grained, fabrication by sol-gel processing 4-66282  
 ZnS:Mn electroluminesc. thin layers, doping and cryst. struct. 4-75810  
 ZrAl eutectoid, fine grained superplastic alloys, anelastic strains, grain boundary cavity distrib., sintering 4-66359

**grain structure** *see crystal microstructure***grain subboundaries** *see subboundary structure***grammars***see also context-free grammars*

syntactic patterns clustering anal. using array grammars 4-107546

**graphophones**

No entries

**Granato-Lucke theory** *see dislocation damping***grand unified theory** *see unified field theories***granular materials***see also granular structure*

- composites, fluid saturated, US propagation 4-79357  
 fluidisable cracking catalyst, flow through orifices 4-64999  
 glass ballotini, flow through orifices 4-64999  
 granulation, dynamic conditions models 4-71613  
 non-cohesive solids, flow through orifices 4-64999  
 rapid flow of granular materials, kinetic model 4-60484  
 static equation exact soln. 4-97303  
 superconductors, frustration and disorder, appl. to Pb in Zn host 4-9875  
 volume determ. by mercury pycnometry 4-63713  
 Al-Ge films, granular, sp. ht., thermal cond. meas., supercond. transition 4-98809  
 NbN granular Josephson microbridges, noise props., freq. mixer anal. 4-70995

**granular metallic thin films** *see discontinuous metallic thin films***granular structure***see also granular materials*

granulation, dynamic conditions models 4-71613

**graph theory***see also directed graphs; trees (mathematics)*

- algebraic methods in graph theory conf., Szeged, Hungary (Aug. 1979) 4-78033  
 Coniglio's lemma 4-68163  
 polyhex graphs, operator technique for recursion formulas of charact. a matching polynomials 4-64332  
 rigid body system, 3D, dynamic simulation using vector-network techniques 4-106180  
 simultaneous generation of trees and of sign factors through orientational numbers 4-110851  
 SO(D-1,1) irreducible representations, N=1 superfields, decomposition into higher dimensionalities 4-95696  
 stratigraphy, unitary associations method, graph theory and computational algorithm appls. 4-94040  
 streamflow synthetic models, validation, use of graphical techniques 4-82129

**graphic equipment, computer** *see computer graphic equipment***graphics, computer** *see computer graphics***graphite**

- 2s level, constant initial state spectroscopy, EXAFSlike modulation 4-81105  
 adsorbed H<sub>2</sub>O, adsorption depend. on substrate struct. 4-92515  
 adsorbed inert gas films, incomplete wetting 4-92530  
 adsorbed Kr domain growth, Monte Carlo simulations 4-98444  
 adsorbed Kr monolayer, commensurate-incommensurate transition, X-ray scatt. study 4-61215  
 adsorbed methane, commensurate-incommensurate transition model 4-70572  
 adsorbed methane, intermol. pot. and lattice sums 4-80393  
 adsorbed methane, model of commensurate-incommensurate transition 4-80394  
 adsorbed methane, orientational transition calcs. 4-70573  
 adsorbed methane, two-dimens. liq.-vapour crit. point exponent, sp. study 4-92341  
 adsorbed N<sub>2</sub>, order-disorder herringbone transition kinetics 4-70570  
 adsorbed on Ni (111), geometrical struct., EELFS study 4-61789  
 AGR cores with longer moderator life, expt. 4-107008  
 Balangir District, Orissa, India, geoelectric prospecting 4-77448  
 brazing of bulk graphite/solid Ti breeder materials to metal substrates 4-111753  
 catalytic oxidation by FeSO<sub>4</sub>, electron microscopy studies 4-85328  
 charge density wave and magnetoresistance anomaly 4-92639  
 composites in reactors, influence of neutron and  $\alpha$ -particle bombardment 4-96141  
 condensation in stellar winds, rapid computation method for dust formation 4-72927  
 conduction band struct., core electron excitation spectra anal. 4-70647  
 conjugated bonds, reson. energies and bond orders (*Chinese*) 4-84555  
 deformation under hydrostatic states 4-103859  
 detection method for interstellar and circumstellar environments 4-101187  
 East Pacific Rise, hydrothermal vents, graphite crystals anal. 4-94086  
 electrical resistivity, in-plane, T<sup>2</sup> depend. at very low temps. 4-108845  
 electrochemical electrodes for Ti/Fe redox flow battery 4-81534  
 electron momentum distrib., Compton profile 4-109268  
 electronic phase transition in strong mag. field (*Japanese*) 4-92616  
 enhanced sputtering yield at elevated temps., time of flight mass spectrometry studies 4-76610  
 epoxy laminates, pulsed photothermal evaluation 4-88818  
 far IR magneto-reflection and dielec. const. under high mag. field 4-66016  
 fibres, benzene derived, transverse magnetoresistance study 4-108844  
 fibres, intercalated, for electrical power transmission appl. 4-80562  
 fluoride, electron beam induced decomposition, X-ray emission band measurements 4-93524  
 fluoride, X-ray C K-emission spectra 4-93144  
 fusion reactor graphite limiter tiles, 3-D anal. of contact conditions 4-111928  
 Grafoil, adsorbed O<sub>2</sub>-Ar(N<sub>2</sub>) systems, mag. and thermal props., 3 to 70 K 4-61214  
 Grafoil, positive muon Knight shifts and relax. rates 4-71234  
 graphite-Fe, ion implanted, mag. props. 4-61562  
 graphite hydrogen sulphate, stacking disorder during oxidation, X-ray diff. obs 4-108383  
 graphite-diamond polymorphic transitions at high press. and temp. 4-113380  
 graphite-FeCl<sub>3</sub> interstitial cpds., isobaric thermal anal. 4-81425  
 graphite-NiCl<sub>2</sub> intercalation cpd., two-dimensional ferromagnet, EPR meas. 4-109069  
 graphite/nickel sulphide radioactive fuel cladding matrix materials, long-term disposal (*German*) 4-64210  
 graphite/sulphur radioactive fuel cladding matrix materials, long-term disposal (*German*) 4-64210  
 hexagonal to cubic transition 4-60891  
 HTGR, graphite inner reflector design, dimensional criteria (*German*) 4-96120

## phite continued

- HTR graphitic component corrosion in operating and accident conditions 4-96163  
 intercalated, stage depend. of mag. susceptibility 4-104400  
 intercalated with  $\text{AsF}_5$ , foils and compacted flakes, elec. resist. studies 4-92683  
 intercalated with  $\text{AsF}_5$ , X-ray absorpt. near edge struct. meas. 4-66115  
 intercalated with  $\text{FeCl}_3$  and  $\text{CoCl}_2$ , mag. order, neutron diff. studies 4-61511  
 intercalated with K and  $\text{NH}_3$ ,  $\text{K}(\text{NH}_3)_x\text{C}_{24}$ , tuneable sandwich thickness, cryst. struct. 4-70101  
 intercalated with Li, electron momentum distrib., Compton profile 4-109268  
 intercalated with Li,  $\text{LiC}_6$ , Compton profile, X-ray scatt. meas. 4-61765  
 intercalated with  $\text{SbCl}_5$ , ultrasonic velocity meas. 4-70284  
 intercalated with  $\text{SbCl}_5\text{-C}_{125}$ , resistivity and Hall effect (*Russian*) 4-113917  
 intercalation compound,  $\text{KHgC}_4$ , compressibility and phonon spectra 4-80183  
 intercalation compound with  $\text{FeCl}_3$ , thermal anal. 4-80223  
 intercalation compound with K, liq.-solid transitions, in-plane liq. K density 4-70348  
 intercalation compounds, c-axis cond. and thermolec. power 4-80561  
 intercalation compounds, low stage, Shubnikov-de Haas oscils. (*Russian*) 4-98592  
 intercalation compounds, modification of material props. 4-60890  
 intercalation compounds, theory of press-induced staging transitions 4-75696  
 intercalation compounds, ultramicrostruct. 4-84417  
 intercalation compounds containing  $\text{AsF}_6^-$  and  $\text{AsF}_6^-\text{-AsF}_3$ , NMR 4-114166  
 intercalation compounds with  $\text{CuCl}_2(\text{CoCl}_2)$ , sp. ht. and thermal expansion 4-80260  
 intercalation compounds with Li,  $\text{LiC}_6$ , optical spectra, ab initio calc., origins of plasmons 4-88802  
 intercalation cpd., domain walls, elastic plates model anal. 4-113660  
 intercalation cpd. with alkali metals, stage-one, Thomas-Fermi density functional theory 4-92131  
 intercalation cpd. with  $\text{ICl}$ ,  $\text{C}_6\text{I}_6\text{ICl}$ , press. induced change in intercalation step 4-61397  
 intercalation cpd. with  $\text{SbCl}_5$ , lattice expansion, phase transition effects, X-ray diff. studies 4-98076  
 intercalation cpds. with K, Rb,  $\text{K}_{1-x}\text{Rb}_x\text{C}_8$ , phonon softening, inelastic neutron scatt. 4-92319  
 intercalation cpds. with K and  $\text{SbCl}_5$ , absolute spin susceptibility, orbital paramagnetism 4-76105  
 intercalation cpds. with  $\text{MnCl}_2$ , first and second stage, mag. props. 4-109058  
 ion damaged, annealed, 2-D ordering, Raman study 4-70535  
 ion stopping cross-section in solids, effects of electronic struct. 4-92273  
 laser localised emission spectroscopic anal., discharge gas effects (*German*) 4-64206  
 layer deposited on photographic film, IR pulsed laser radiation field recording appls. 4-78400  
 localised behaviour in Auger spectra 4-93148  
 metal/graphite mixtures, diamond form. under shock compression and flash heating 4-108516  
 multilayer adsorption of solid  $^4\text{He}$ , two-dimensional crit. temp. increase. 4-88366  
 neutron irradiated, relationship between strength-cha. 4-66443  
 neutron irradiated, restoration of dynamic modulus of elasticity in annealing 4-65304  
 nuclear, fracture, acoustic emission and sub-crit. events 4-62050  
 nuclear-grade, mech. and phys. props., influence of prehydrostatic loading 4-102353  
 overlayers on Ni (111), electronic struct. study 4-61213  
 oxidised graphite fibres, produced by oxidation of C-graphite fibres 4-76740  
 physisorbed Kr and Xe monolayers, modulation of at. positions, anharmonicity 4-92531  
 physisorbed  $\text{O}_2$ , f phase struct., LEED determ. 4-108712  
 physisorbed  $\text{O}_2$ , phase transitions, LEED studies 4-88396  
 plasma limiter on PDX, conditioning and power handling 4-97880  
 polycrystalline rods, single impact stress calc. 4-76840  
 positive muon Knight shifts and relax. rates 4-71234  
 pyrographite, electrochemical intercalation of fluorides, for high energy density battery cathodes 4-81444  
 pyrolytic, ls binding energy shift under deuterium ion bombardment 4-91103  
 radiation damage in fission and fusion reactor systems 4-96263  
 radiation dimensional stability 4-102359  
 reactivity with H, electron bombardment enhanced 4-93529  
 relativistic electron beam propag., energy absorpt. 4-70221  
 restructuring, diamond formation, martensitic mechanism, in colloidal systems 4-80212  
 short bars with hemispherical seats failure mechanism 4-78694  
 stagnation-point boundary layers, injection induced turbulence 4-64932  
 structural material for HTGR (*German*) 4-68755  
 structural theory using pseudopotential local-density-functional approach 4-92135  
 substrate for active Pt layer, ion bombard., electrocatalytic props. 4-71968  
 substrate growth, resistance to molten Si in RAD process (*French*) 4-61835  
 surface, (0001), adsorbed ethane monolayers, collective excitations 4-104061  
 surface, adsorbed methane submonolayer, commensurate-incommensurate transition, neutron diff. study 4-65559  
 surface, chemisorbed  $\text{N}_2$ , island growth kinetics, computer simulation studies 4-113813  
 surface,  $\text{D}_2^+$  trapping and reflection coeffs. at oblique incidence 4-61793  
 surface, ethylene absorption, layering, prewetting and wetting 4-98450  
 surface, H chemisorpt., MINDO/3 cryst. orbital LCAO SCF calc. 4-98430  
 surface (0001), adsorbed benzene, orientation, Penning ionisation electron spectroscopy 4-87197  
 surface (0001) adsorption of hydrocarbons, polarisability anisotropy, mol. statistical theory 4-80379  
 surface adsorbed ethylene, molecular dynamics calcs. 4-104079  
 surface adsorbed ethylene, surface diffusional and vibr. motion study 4-104078

## graphite continued

- surface adsorbed ethylene, thermodynamic props. study 4-104068  
 surface adsorbed noble gases, lateral variation of physisorption potential 4-92529  
 surface adsorbed submonolayer Ar, melting transition, specific heat study 4-104077  
 suspensions, aggregation processes, conductometric study 4-109691  
 target preparation for radiocarbon dating by TAMS technique 4-86989  
 thermal conductivity of armor plates in Doublet III fusion reactor 4-111930  
 thermionic diode materials selection and performance for fusion reactor systems 4-107018  
 thermodynamic props., pulse laser melting, ion channelling 4-98315  
 thermoelectric power, Kohon phonon drag effect 4-88525  
 thermomechanical treatment, neutron irradiation-induced changes in props. 4-108451  
 thin layer, compression testing method 4-104939  
 tiles for Doublet III armour/limiters, C-Si-C coatings, process evaluation and characterisation 4-111755  
 trapping of sub-eV H and D atoms 4-111761  
 vacancy formation energy, etching and TEM studies 4-92198  
 VHTR fuel compacts, fission product diffusion in matrix graphite 4-73976  
 $\text{Al}_2\text{O}_3\text{-Al}$  plasma coatings on graphite, oxidation resist., bonding strength and elec. cond. 4-66462  
 C bond-network defects with ring size from 3 to 9, graph theory anal. 4-92138  
 C films, amorphous and graphitic, growth by ion bombardment in RF plasma 4-85116  
 C, graphitised, adsorpt. of sodium dodecyl sulphate (octyltetraethylene glycol), enthalpy determ. 4-70560  
 C-graphite materials, He ion irradi., surface erosion 4-80120  
 $\text{C}_{50}\text{SnC}_6$  layer cpd.,  $^{13}\text{C}$  NQR spectra 4-114180  
 $\text{C}(n,\gamma)$ , 14.1 MeV,  $\alpha$ -spectra and ang. distrib., kerma factor for fusion reactors 4-96020  
 Cu-Ti/graphite interface, struct. microanal. (*Chinese*) 4-61242  
 CuO/C physical mixture thermal behaviour anal. using thermogravimetry and X-ray diffraction 4-99784  
 $\text{CuSO}_4/\text{C}$  physical mixture thermal behaviour anal. using thermogravimetry and X-ray diffraction 4-99784  
 Fe-graphite, sintering, C absorpt. by Fe 4-114437  
 Fe-graphite, sintering, mechanism of C absorpt. by Fe 4-114438  
 $\text{KHg}_x$ -graphite intercalation cpd., electronic struct., Shubnikov-de Haas effect 4-92596  
 MgO-graphite, C-bearing magnesia, mech. props. 4-114673  
 Mo diffusion through graphite in HTGR 4-111631  
 Pb/graphite accumulator using aqueous HF acid, advantages and disadvantages 4-66682  
 $\text{SbCl}_5$ -graphite intercalation cpd., de Haas-van Alphen effect meas. 4-88440  
 TiC-graphite, thermal cycling tests, surface damage study 4-111756  
**graphitic steel** see carbon steel  
**graphitisation**  
 C strip, graphitised, wetting by melts of Al and Al-Si 4-92476  
**graphitising**  
 Fe, cast, graphite morphology, appl. of secondary ion mass spectrometry 4-66343  
 Fe, cast, Mg treated, graphite nodularisation and graphitisation during solidification under 145 atm. Ar pressure 4-66325  
 Fe, cast, white, 4-104790  
 Fe, cast, white, annealing, Fermi energy, thermoEMF obs. rel. to crystallisation in acoustic vibration field 4-76768  
 Fe-C eutectic solidification, equilib. partition coeff. of third element rel. to graphitization 4-99380  
 Fe-Si-C powder compacts, sintered and carburised, graphite growth 4-93306  
**graphs**  
 see also nomograms  
 algebraic structure count, recursion rels. 4-107269  
 ANSI C95.1-1982 standard, human exposure to RF EM fields, safe distances determination 4-109873  
 plotting, best straight line, BASIC programs for BBC Microcomputer 4-82647  
 surface deformation determination from sag of shot-blasted testpiece, grapho-analytical procedure (*Russian*) 4-66519  
 symmetric unimodal distribution dispersion, graph-analytic determ. 4-63699  
**gratings (diffraction)** see diffraction gratings  
**gratings (optical)** see diffraction gratings  
**gratings (spectra)** see diffraction gratings  
**gravimeters**  
 see also geodesy  
 capacitive transducers for gravimeters, construction principles 4-85759  
 laser accelerometer of aviation gravimetric system (*Russian*) 4-96976  
 laser gravimetric measurement accuracy, effect of Gaussian struct. of beam (*Russian*) 4-60099  
**gravimetric instruments** see gravimeters  
**gravimetry** see density measurement; weighing  
**gravitation**  
 see also general relativity; gravitational collapse; gravitational lenses; gravitational red shift; gravitational waves; quantum field theory of gravitation; Schwarzschild metric; unified field theories  
 $\sigma$ -model coupled to gravity, space-time compactification 4-90461  
 adiabatic particle definitions, normal form independence 4-78213  
 algebraic extension of general relativity and higher dimensions 4-110941  
 axially symmetric Reissner-Nordstrom solns. from complexification technique 4-78215  
 Bianchi type-I models, solution to Einstein's eqns. 4-90447  
 Bianchi-Brans-Dicke-Maxwell field eqns., mag. radiation solns. 4-72862  
 black hole, rotating distorted, axisymmetric stationary metric 4-101404  
 black holes, dynamics of N-collisions in nonsingular, asymptotically flat 3-geometry 4-68070  
 black holes, rotating, pseudostationary, Kerr-Newman soln., SU(1,2) group 4-63585  
 Brans-Dicke theory, exact perfect fluid solns. 4-67611  
 Brans-Dicke theory, exact stiff matter solns. for Bianchi type H, VIII and IX models 4-67614  
 Brans-Dicke-Bianchi type II models, exact solns. 4-78217  
 Cartan differential forms (*Rumanian*) 4-78222

## gravitation continued

- Casimir effect and gravitational collapse 4-63602  
 Casimir effect in grav. collapse of spherically symm. shell 4-110956  
 charged dust distribution, geometry under own gravit. field, eqns. of motion 4-90457  
 classical localized solutions in a two-dimensional supersymmetric model 4-86610  
 conference, gravity, gauge theories, supergravity, Caracas, Venezuela (Dec. 1982) 4-86117  
 conformally invariant theory of gravitation and electromagnetism 4-86283  
 constrained system transform., generalised Killing's eqns. (Chinese) 4-90351  
 cosmology, spacetime thermodynamics and inflationary Universe 4-90263  
 coupled electromagnetic and gravitational linearized perturbations of the Kerr-Newman metric 4-101726  
 curved space-time, supersymmetry spontaneous breaking 4-90740  
 differentially rotating charged dust with force-free EM field, Lorentz force 4-86278  
 dimensional reduction and nonAbelian isometries 4-86287  
 Dirac cosmology, gravitational theory in atomic scale units 4-73106  
 dynamic properties of gravitational fields, classical general theory of relativity 4-58697  
 Earth's general relativistic gravitomagnetic field, Foucault pendulum expt., at South Pole 4-111010  
 Einstein's  $\lambda$ -transformation generalisation, gauge field and gravitational copies 4-110962  
 Einstein's equivalence principle, gravitational redshift of gravitational clocks 4-90083  
 Einstein's field eqns., iterative solution for radiative gravitational fields (French) 4-78201  
 Einstein's gravitation, energy problem, Hamiltonian approach 4-63597  
 Einstein's theory energy problem from space-time manifold 4-63596  
 Einstein eqns., inhomogeneous solutions, de Sitter space-time generalisation 4-90450  
 Einstein tensor, bilinear and trilinear extensions 4-68061  
 Einstein-Cartan-Sciama-Kibble, time-dependent gravitational coupling and torsion 4-73320  
 Einstein-Maxwell eqn., gyroscope precession on Earth surface, existence of mag. type gravit. 4-94587  
 Einstein-Maxwell eqns., scalar density concomitants of metric and bivector 4-63482  
 Einstein-Maxwell eqns., spherical charged fluid dist. 4-82734  
 Einstein-Maxwell eqns., transcendent axisymmetric stationary soln. 4-73318  
 Einstein-Maxwell equations, symmetric space property and inverse scatt. formulation 4-82735  
 Einstein-Maxwell waves, scattering by Ellis geometry 4-63603  
 Einstein-Mayer unified theory, 5-D origin of massless scalar field 4-68085  
 Einstein-Yang-Mills system, stability of instanton induced compactification in 8-D 4-110965  
 Einstein-zero-mass scalar theory, gravitational repulsion 4-90445  
 electron, electromag. potential in non-static gravit. field 4-63873  
 exact Brans-Dicke-Bianchi type-V solutions 4-86098  
 exact Brans-Dicke-Bianchi type-V<sub>1</sub> solutions 4-68080  
 Finsler spaces, field theory, intrinsic behaviour of internal vector 4-110936  
 fluid distributions, exact solutions in general relativity 4-101723  
 Friedmann cosmology and hadron properties, unified approach 4-82575  
 G-variable cosmologies, galaxy form. in Hoyle-Narlikar and Brans-Dicke theories 4-101547  
 general relativity, magnetohydrostatic models of cylindrical symmetry 4-82725  
 general scalar-tensor gravitation theory, field of charged particle 4-86289  
 geometric unification of gravity and EM 4-82733  
 $GL_4 \times SO_2 \times SU_2$  dilatation-invariant gravity, unification by proliferation method 4-110963  
 gravitational instability in the presence of a magnetic field in the expanding universe 4-90275  
 Hamiltonian approach, physical meaning of energy 4-63595  
 Hamiltonian formulation of gravitating perfect fluid and Newtonian limit 4-68063  
 Hamiltonian structure with  $R + T^2$  Lagrangian 4-63605  
 heat conducting fluid, thermal nonequilibrium general relativity 4-110949  
 induced gravity theories 4-63606  
 inflationary Universe, Minkowski space candidate for primeval config. 4-82571  
 instability and space-time curvature at finite temp. 4-78220  
 interaction of bodies immersed in fluids, theory 4-101124  
 inverse square law at 0.1 m, deviation 4-86321  
 isometries and dimensional reduction 4-101729  
 Kaluza-Klein cosmologies at late times, equilibrium solution 4-101730  
 Kaluza-Klein cosmology, dimensional reduction 4-58705  
 Kaluza-Klein manifolds, coupling const. ratios 4-110966  
 Kaluza-Klein model, status, formalism, spontaneous compactification 4-86280  
 Kaluza-Klein theories, one-loop stability of toroidally compact manifolds 4-106216  
 Kaluza-Klein theories, recent developments 4-73317  
 Kaluza-Klein theory, Einstein Lagrangian with de Sitter structure 4-68084  
 Kaluza-Klein theory, G and H invariant metrics, colour and Higgs charges 4-110960  
 Kaluza-Klein theory, linear connection on fibre bundle 4-63607  
 Kaluza-Klein theory, mag. monopole solutions 4-110959  
 Kaluza-Klein theory in 6-D, monopole solutions 4-78219  
 Kaluza-Klein vacuum, generating functional 4-90462  
 Kerr metric, timelike vortical trajectories; latitudinal and radial motion 4-95266  
 Kerr metric in de Sitter space-time 4-68072  
 Kerr space-time, imaginary Weyl coordinates 4-95267  
 Lie admissible gravity, exterior forms, geometrical structure 4-90448  
 light deflection in solar system 4-94585  
 Mach-Einstein-universes, equilib. statistical mech. 4-67816  
 magnetohydrodynamics, centre of mass and far field metric 4-82719  
 massive spinning particle motion in presence of flat metric and vector torsion 4-78216  
 massless scalar particles, gravitational creation by vacuum bubble 4-73111

## gravitation continued

- molecular clouds, clump collisions, gravitational instability 4-94911  
 Moller's tetrad theory of gravity and Universe open or closed state 4-86097  
 N=1 light-front supergravity, Ogievetsky-Sokatchev, superspace, Yang-Mills theory 4-111005  
 Newton's inverse square law, const. determ. 4-106199  
 Newton's world model, physical meaning if graviton has mass 4-86292  
 Newton-Cartan theory of gravitation, variational principle, fluids app. 4-95265  
 Newtonian and Machian aspects of stationary gravitational systems, electromagnetic field analogy 4-106214  
 Newtonian gravit. modification, appl. to cosmological and astrophysical situations 4-105869  
 Newtonian gravitation, generalised, minimal grav. coupling and covariance 4-78214  
 nonlinear eqns. of gravit. field 4-73234  
 nonlinear gravitation, effect on characteristic scale of galaxy cluster 4-94975  
 nonlinear photons, anisotropic case 4-86279  
 nonsymmetric gravity, Lie admissible algebra 4-68447  
 null symmetries of EM field interacting with gravitational field 4-86285  
 one-dimensional gravitational system, relax. processes 4-110957  
 optical fibre interferometer demonstration of gravitationally induced phase shift of optical waves (Japanese) 4-101739  
 oscillating universe, dust-like model, one-loop approximation 4-94998  
 physical space topology, breakdown of connectedness 4-73322  
 Poincare gauge theory of gravitation, spontaneous compactification 4-78218  
 Poincare group, complete gauge theory 4-63591  
 positive energy theorem relating mass and electromagnetic charge 4-110939  
 primordial Coleman-Weinberg inflation, energy density fluctuations 4-90459  
 primordial inflation, fluctuations in cosmological models 4-90460  
 principles and manifestation in nature (book) 4-63417  
 pure radiation fields admitting nontrivial null symmetries, Einstein-Maxwell appl. 4-95269  
 quantised multidimensional Einstein-Cartan gravitation, torsion dynamics 4-73321  
 radiating C-metric in Einstein-Maxwell theory, Ricci collineation 4-68086  
 radiation damping effects, model calc. using energy balance method 4-95268  
 radioisignal deflection by Sun's gravitational field, VLBI observations 4-101738  
 Rastall prototype theory of gravity, variational principle 4-68067  
 relativistic cosmology (book) 4-82609  
 rigidly rotating gaseous disks with mag. field, gravit. instability, dispersion relation 4-72866  
 rotating black hole, max. temp. of thermal radiation 4-101148  
 rotating charged dust as symmetric electrovac source 4-95260  
 rotating fluid spheres, slow rotation eqn., mass density eqn. of state 4-68078  
 scalar field condensation in a gravitational field of a massive object 4-90456  
 scalar tensor theory, axisymmetric stationary vacuum fields 4-101135  
 scalar-tensor theory, cosmological model 4-77989  
 scale covariant gravitation; variable G and cosmology 4-72876  
 self gravitating fluid mass, Liapunov's theorem generalisation 4-90376  
 self-dual Yang-Mills and general relativity Einstein eqns., R gauge parametrisation 4-110948  
 self-gravitating system, random fluctuations in general relativity 4-110945  
 shear-free perfect fluids with zero mag. Weyl tensor 4-68060  
 similarity mechanics, application to gravit. 4-110961  
 $SL_2$  gauge theory, conserved currents 4-63593  
 $SL_2(C)$  gauge theory of gravit., conservation laws, Lagrangian densities 4-110968  
 solar system, gravitational boundary for direct and retrograde orbits 4-115696  
 soliton, gravitational, classical and quantum bound states 4-63604  
 solitonic solutions for interacting fields with consideration of gravitation 4-68073  
 spherically symmetric gravitational fields, classical inversion algorithm general rel. 4-73314  
 spinning particles, two, gravitational interaction in general relativity 4-63586  
 spontaneous soldering, O(k) Yang-Mills field, Higgs mechanism, dimensional space-time 4-106217  
 stability properties of gravitational theories and three dimensional gravitation 4-86294  
 stationary Einstein-Maxwell fields, multipole expansion 4-68065  
 SU(5) GUT, inflation with gravity coupling 4-78212  
 supersymmetry, hierarchy problem and GUTs 4-68087  
 symplectic geometry of null infinity and two-surface twistors 4-86281  
 thermogravitational and thermocapillary flows in a horizontal liquid layer under the conditions of a horizontal temperature gradient 4-103415  
 three-dimensional cosmological gravity: dynamics of constant curvature 4-63345  
 time transformations in post-Newtonian Lagrangians 4-86288  
 time-asymmetric initial data for N black hole problem in general relativity 4-72974  
 uncoupled fluids, gauge invariant cosmological fluctuations, early Universe axions 4-67819  
 Universe, quantum metrics and matter field configurations 4-78202  
 Universe expansion nature, role of gravit. and elementary particles (Russian) 4-82581  
 vacuum C-metric in Weyl form 4-63588  
 vacuum Einstein eqns., stationary axisymmetric soln. 4-63587  
 vacuum solutions, type-D with cosmological const. 4-82720  
 vacuum stress tensor in conformally flat spacetime 4-78221  
 vorticity and shear-free space-time in general relativity 4-63590  
 weighing of energy, principle of equivalence, red-shift formula 4-110944  
 Wetterich mechanism for Kaluza-Klein type ground state in high dimensions gravity 4-110964  
 Weyl invariant theories, flat space-time stability, cosmological constant term 4-106218  
 Yukawa potential in a Schwarzschild background 4-68079  
<sup>64</sup>Zn distrib. in zinc during zone recrystallisation, gravitational forces effects 4-76667

- gravitational acceleration** *see gravitation*
- gravitational collapse**  
*see also black holes; cosmology*  
 antineutrino fluxes from collapsing stars 4-110426  
 Casimir effect and gravitational collapse 4-63602  
 Casimir effect in grav. collapse of spherically symm. shell 4-110956  
 dust cloud, cosmic censorship violation 4-72863  
 electron capture in stellar collapse 4-86803  
 galaxies dissipationless collapse and initial conditions 4-110731  
 globular clusters, core collapse and post-collapse evolution; role of binary stars 4-101442  
 globular star clusters, post-collapse evolution and gravothermal oscillation 4-77887  
 Gowdy  $T^3$  cosmology, stress-energy tensor, combined system symm. bounce 4-101546  
 Higgs scalar field, gravitational collapse 4-115683  
 interstellar clouds, fragmentation and collapse 4-77913  
 interstellar rotating isothermal clouds, criteria for collapse and fragmentation 4-85908  
 massive gas cloud, star form. and mag. field interactions 4-101452  
 molecular cloud collapse to protostar 4-101322  
 molecular clouds collapse and fragmentation, protostars form. 4-63138  
 neutrino flux profile 4-72869  
 neutrino-trapping supernovae, iron core temp. and mass effects on mass ejection 4-85972  
 new inflationary universe, Higgs scalar field fluctuation, black-hole formation 4-90452  
 OB association, upper mass limit, cosmic ray implication and cosmic abundances 4-101208  
 oscillating universe, dust-like model, one-loop approximation 4-94998  
 pre-main sequence stars collapse, assoc. ang. momentum loss 4-101342  
 presupernova core, gravitational collapse, rot. and mag. field characts. 4-106015  
 protogalaxies, dynamical constraints during violent relaxation and effects on final state 4-94956  
 protostars dynamic gas-dust envelopes struct. and evolution and massive star form. 4-101335  
 protostellar formation in rot. interstellar clouds, nonisothermal collapse 4-94729  
 quantum mechanical Hamiltonian lower bound, relativistic kinetic energy 4-90466  
 quasinormal modes, black-hole oscillations, stability and late-time behaviour of radiation 4-90453  
 self-similar gravitational collapse in an expanding Universe 4-110788  
 spherical stellar system, numerical study of gravit. collapse 4-101438  
 stars, collapse instability of rapidly rotating presupernova cores with finite entropy 4-63139  
 stars, low-mass Fe core collapse, nucl. and pulsations onset (*Russian*) 4-94743  
 stellar evolution and stability, review 4-72932  
 supernova matter eqn. of state, neutrino oscill. effects 4-67760  
 supernova models, rot. and nonrotating, hydrodynamic collapse calcs. 4-63188  
 viscous fluid collapse, Einstein's field eqns. solns., interior soln. 4-86272  
 white dwarfs, solid, thermonuclear ignition rel. to Type I supernovae and low-mass X-ray binaries 4-77827
- gravitational constant**  
 correction to vacuum, theory of gravit. interaction of bodies immersed in fluids 4-101124  
 energy dependence at high energy and unified field theory 4-82406  
 Kaluza-Klein theories, quantum effective action, cosmological evolution, curved spacetime 4-90465  
 Newton's inverse square law, const. determ. 4-106199  
 oscillating universe, dust-like model, one-loop approximation 4-94998  
 scale invariant quantum gravity renormalizability and Newton's constant calculability 4-106221  
 stress tensor, scalar quantum field, curved space-time, scaling behaviour 4-101733  
 variable G, scale covariant gravitation and cosmology 4-72876
- gravitational experiments**  
 detection of gravity waves 4-95111  
 finite vertical cylinder for gravity detection, reverse problem 4-106230  
 gravitational radiation detector, Lagrangian formalism for reson. capacitive transducers 4-106232  
 gravitational radiation detector, with transducer imperfectly tuned to antenna 4-106231  
 inverse square law at 0.1 m, deviation 4-86321  
 Michelson interferometer in a gravitational Length-Thirring field (*Russian*) 4-68120  
 present state of gravitational theory, experimental confirmation 4-68074  
 PSR 1913+16, binary pulsar, post-Newtonian timing effects obs. 4-63192  
 radio signal deflection by Sun's gravitational field, VLBI observations 4-101738  
 resonance band width, gravitational-wave antennas 4-86320  
 Rochester gravitational wave detector 4-95287  
 superfluid interferometer for Earth rot. detection using Josephson effect 4-58728  
 torsional type antenna for low temp. expts. 4-68119
- gravitational lenses**  
 1E 01042+3153, QSO-galaxy, possible transient lensing candidate 4-63332  
 galaxies, mass distrib. from gravitational light deflection 4-115820  
 galaxy clusters, gravit. screen model rel. to spatial fluctuations of cosmic microwave background 4-63344  
 galaxy superclusters, gravit. imaging theory 4-86069  
 intensity gain studied using plane wave scatt. soln. 4-63454  
 light rays in Schwarzschild and Reissner-Nordstrom space, spherical symmetric models (*German*) 4-85865  
 multiple imaging of quasars by galaxies and rich clusters 4-94988  
 optically selected QSOs in field centred at  $01^h39^m, -55^\circ$ , gravit. lens evidence 4-94986  
 optically variable QSOs near bright galaxies, statistical anal., lensing evidence 4-77969  
 Q 0957+561, twin QSO, CCD brightness monitoring 4-90251  
 QSO 0957+561, gravitational lens B component brightening 4-77960  
 QSO 0957+561 A,B, gravit. lens model incorporating VLBI features 4-110772  
 QSO 2345+007A,B, spectral characts. 4-110769  
 quasar research and gravitational lenses 4-82559
- gravitational lenses continued**  
 quasars nature from gravit. lens anal. 4-77967  
 Seyfert galaxies, gravit. lensed, origin QSO phenomenon 4-77968  
 spheroidal lenses 4-77703  
 transparent lenses, image numbers and locations 4-110513
- gravitational radiation** *see gravitational waves*
- gravitational red shift**  
*see also cosmology*  
 Einstein's equivalence principle, gravitational redshift of gravitational clocks 4-90083  
 neutron stars, nonrotating stellar surface redshift limits 4-90173  
 neutron stars, rotating, gamma-ray freq. shifts and line broadening 4-101398  
 neutron stars in X-ray binaries, red shift var. assoc. with outbursts. 4-101411  
 quasar redshifts, neutrino objects—lack of effect, cosmological significance 4-73097  
 Segal's chronometric theory, physical measurement, red shift, critique 4-78133  
 Segal's chronometric theory, reply to critique 4-78134  
 weighing of energy, principle of equivalence, red-shift formula 4-110944  
 white dwarfs, gravit. and press. red shifts 4-82474
- gravitational waves**  
*see also gravitons*  
 accreting neutron stars, X-ray emission modulation 4-90171  
 antenna for gravitational radiation, coupling of oscillation modes 4-90479  
 antennas, resonance band width 4-86320  
 back-action-evading measurement of optical fields with the use of a four-wave mixer 4-106233  
 black body problem for grav. radiation, quantisation of microscopic and macroscopic world 4-73315  
 continuous spectrum in differentially rotating perfect fluids, effect of gravit. radiation reaction 4-101149  
 cylindrical, source with counter-rotating particles 4-86277  
 detection, expt. verification of single transducer back-action evading meas. scheme 4-111008  
 detection, obs. of  $4 \times 10^{-17}$  cm harmonic displacement using 10 GHz supercond. parametric converter 4-111009  
 detection of gravity waves 4-95111  
 detection using a cylindrical active antenna (*Chinese*) 4-68118  
 detector for gravitational radiation, Lagrangian formalism for reson. capacitive transducers 4-106232  
 detector of gravitational radiation, with transducer imperfectly tuned to antenna 4-106231  
 detectors, squeezed state techniques (*German*) 4-82741  
 freely falling oscillating bar in grav. wave, motion and matter tensor 4-78208  
 general relativity, multipolar radiation reaction theory 4-101725  
 Gowdy  $T^3$  cosmology, stress-energy tensor, combined system symm. bounce 4-101546  
 Hawking radiation and the back reaction—a first approach 4-110942  
 Hawking radiation from black holes, non-thermal nature, contrib. to cosmic rays 4-106023  
 Hawking radiation of Dirac particles in four-dimensional static Riemann spacetime 4-106213  
 isotropic elastic sphere, grav. radiation, grav. luminosity 4-68075  
 laser interferometry in space, future prospects 4-110323  
 MXB 1916-053 (4U 1915-05), gravit. radiation rel. to mass transfer and X-ray bursts 4-63198  
 nonsteady state axisymmetrical surface gravitational waves propag. (*Russian*) 4-86276  
 oblique rotator, gravit. radiation spectra, mag. hydrodynamical model 4-94586  
 oscillating universe, dust-like model, one-loop approximation 4-94998  
 particle plunging into Kerr black hole, gravit. radiation 4-68076  
 particle scatt. by Schwarzschild black hole, gravit. radiation emission 4-68077  
 Poincare gauge theory, massless torsion fields,  $\alpha+2a/3 \neq 0$  case 4-82730  
 positive energy theorem relating mass and electromagnetic charges 4-110939  
 PSR 1937+214, millisecond pulsar, pulse timing and gravit. waves anal. 4-101387  
 QCD, first order phase transition, gravitational signal 4-90803  
 quantum-counting quantum nondemolition meas., state reduction 4-95259  
 quasi-Newtonian fluid, null infinity 4-101722  
 radiation calc. using Newtonian gravity and special relativity 4-67917  
 resonant-mass gravitational wave detector, wideband sensitivity 4-78227  
 Rochester gravitational wave detector 4-95287  
 Schwarzschild black hole free oscill. excitation by gravit. waves from scatt. test particle 4-94851  
 sensitive detectors, responses 4-95286  
 solitonic gravitational waves, Einstein eqn. soln. 4-78209  
 SQUID EM response to gravitational waves, Einstein-Maxwell linear approx. 4-110954  
 string in Universe, gravitational interactions, gravitational radiation and Yang-Mills symmetry breaking 4-115840  
 surface gravitation wave scattering by elliptical inhomogeneities (*Ukrainian*) 4-86275  
 terrestrial gravitational noise on a gravitational wave antenna 4-111011  
 thermodynamics of gravitational radiation 4-63599  
 vibration isolation for broadband gravitational wave antennas 4-111012
- gravitons**  
 minimal supergravity from global supersymm., sliding gravitino mass, spontaneous supersymm. breaking 4-111003  
 N=1 supergravity models, B-violating phenomena discrepancies, gravitino decay 4-111002  
 N=2 extended supergravity, Killing spinor supersymmetry transformation, gravitino solution 4-90477  
 supersymmetric standard model, gravitino regeneration and decay 4-110975  
 thermodynamics of gravitational radiation 4-63599
- gravity**  
*see also gravitation*  
 algorithm for error adjustment of potential field data along a survey network 4-100438  
 North America, combined correlation anal. of geophys. fields 4-72541  
 anomalies due to postglacial rebound, Lagoos obs., lower mantle effective viscosity determ. 4-85641  
 anomalous field due to subsurface density distrib., computation method 4-85604

## gravity continued

- Antarctic shelf ice, gravity meas. possibilities 4-72624  
 Antarctica, gravity and geomagnetic studies between 45 and 65 degrees East 4-81959  
 S Appalachian Piedmont, geophysical anomalies along strike rel. to crustal struct. and tectonics 4-93990  
 asteroid belt, gravit. perturbations on celestial bodies and spacecraft 4-90098  
 asteroid families, collisional origin, effects of target's gravity 4-90104  
 astrophysical gravitating magnetised gaseous disc, equilb. 4-101152  
 NW Atlantic, gravimetric models and surface currents-satellite remote sensing 4-67163  
 Benue Trough, SE Nigeria, tectonic and sedimentation history 4-77479  
 Benue-Chad Basin, Cretaceous rift valley system 4-115371  
 Broken Hill District, regional magnetic and gravity field characteristics and interpretation 4-62814  
 Chattoanee Baltimore Gneiss Dome, Maryland, USA, gravity survey 4-81834  
 conference on geodesy, at Hamburg, West Germany (August 1983) 4-86111  
 Deer Lake basin, Newfoundland, Canada, gravity and magnetic interpretation 4-62653  
 Donnybrook Anticline, Australia, seismic-gravity interpretation and tectonic settings 4-94121  
 Earth, field representation by finite grid of mascons, approx. 4-93995  
 Earth, perturbations in gravit. field and satellite orbits due to rot. vars. 4-101212  
 Earth, tidal evolution of gravit. field and figure 4-105399  
 Earth gravity field, represented by point mass system (*Russian*) 4-77443  
 Earth gravity field models and the triple correlation function 4-81837  
 earthquake fault associated gravity anomalies 4-81866  
 NW Europe continental shelf, petroleum geology, conf. at London, England (March 1980) 4-101579  
 Fennoscandian uplift and glacial isostasy, gravity and seismicity anal. 4-81994  
 free-air gravity anomalies in NW Pacific Ocean, resemblance to pattern of geoidal undulations 4-105397  
 gas-liquid critical point, gravity perturbation effects 4-68190  
 gasdynamics with gravity allowance, operator-difference scheme stability 4-87753  
 geodesy, spherical harmonic model coefficients, for orders 15 and 30 4-93993  
 geodesy downward continuation of gravity data, solved as inverse theory 4-85802  
 geoid gravity anomalies in one degree global model 4-72475  
 geoid shape, correl. with seismic surface wave vels. and convection in mantle 4-100529  
 geoid undulations from Doppler satellite positioning and gravimetric techniques, comparison 4-85607  
 geophysical gravity anomaly automatic fitting 4-67421  
 geophysical prospecting of gravity anomalies for multiple density boundary case 4-100431  
 geopotential coefficients of order 29, determ. from orbit of satellite 1967-1048 4-105398  
 geopotential field derivatives, computation procedure for coeffs. 4-85605  
 geopotential of buried object, 3-D Fourier transforms theory (*Chinese*) 4-62651  
 Gorrings Ridge, North Atlantic Ocean, geoid and gravity anomalies interpretation 4-67162  
 gravimetry, direct problem soln. in modelling complex geological media 4-77442  
 GRAVSAT signal over tectonic features 4-93992  
 Greece, Atalanti region, microgravity network, crustal movements and precursors to earthquakes 4-77440  
 Gulf of Aden, lithosphere flexure and isostatic compensation, bathymetry and gravity profiles anal. 4-105484  
 Imperial Valley, California, seismic refr. and gravity survey 4-85644  
 Indian lithosphere, gravity anomalies and compensation 4-81901  
 intergalactic gas of rich galaxy clusters, He separation from D (*Russian*) 4-94971  
 inverse problem solution by regularisation method, algorithm 4-105732  
 Japan, cross sections of topography, gravity anomalies and heat flow 4-81917  
 Karakorum gravity measurements 4-62652  
 Kuril-Kamchatka deep-sea trench, heat flow and gravity anomalies 4-82006  
 Lutzow-Holm Bay, Antarctica, gravity, geomag. intensity anomalies and crust tilt 4-81841  
 mantle convection, lag and related geoid anomalies and mantle struct. 4-105520  
 mantle convection in layered spherical shell, admittance of gravity over topography 4-67204  
 marine geoid, Seasat obs. of lithosphere flexure seaward of ocean trenches 4-85653  
 matrix development of potential and attraction at exterior points rel. to inertia tensors 4-81832  
 McMurdo Sound are of Antarctica, crust and upper mantle struct. 4-81941  
 Mendocino Fracture Zone, lithosphere thickness and plate horizontal driving force 4-72545  
 Moon, gravity field charact., lunar artificial satellites orbits anal. 4-101209  
 Moon, tidal deformation (*Chinese*) 4-110548  
 Newton's inverse square law, const. determ. 4-106199  
 Niue Island atoll, SW Pacific, volcanic core struct. from geophys. obs. 4-94035  
 North Sea, geoid, gravity measurement anomalies and SEASAT sea surface heights 4-81840  
 North Sea gravity field observations 4-81839  
 NW Ontario, Canada, gravity profile across English River Subprovince 4-72482  
 Pacific, geoid, gravity map, plate age and fracture zones 4-115331  
 W Pacific margin, extensional basins form., mantle flow and gravimetric data anal. 4-82002  
 planets, rot. vars. rel. to perturbations in gravit. fields and satellite orbits 4-101212  
 potential, second degree harmonic coeffs., effect of large-scale density inhomogeneities 4-62657  
 potential fields separation, probability approach 4-62971  
 Princes Elizabeth Land, Antarctica, gravity and mag. anomalies anal. 4-89889

## gravity continued

- principles and manifestation in nature (book) 4-63417  
 quasar as massive black hole, self-gravitation in spherically symmetric accretion 4-63196  
 Quebec Appalachians, seismic profile, gravity and crust struct. 4-72502  
 Singhbhum area, India, gravity field, geology, tectonic history 4-89907  
 spherical harmonic analysis, coordinate system rotation effects 4-93991  
 subduction zone large-scale gravity anomalies indicating mantle convection 4-100526  
 Sun, quadrupole moment 4-94712  
 Velence hills, Hungary, gravity and geomagnetic anomaly interpretation 4-62728  
 Venus, Ishtar positive gravity anomaly 4-105895  
 Venus, long-wave features rel. to tectonics, terrestrial contrasts 4-94660
- gravity meters** see *gravimeters*
- gravity waves**  
 atmosphere, inertial-gravity waves rel. to convective cloud echo bands and heavy rain (*Chinese*) 4-67369  
 atmosphere, inertial-internal gravity waves, hydrostatic and nonhydrostatic eqns. 4-100654  
 atmosphere, measurement network 4-115582  
 atmosphere, VHF Doppler radar obs. of buoyancy waves assoc. with thunderstorms 4-72659  
 atmospheric internal gravity waves (*Russian*) 4-82170  
 capillary gravitational waves at homogeneous liq.-liq. interface 4-112925  
 deep water, periodic capillary-gravity wave instability 4-75053  
 deep-water nonGaussian gravity waves and spectra 4-110167  
 Earth core, kinematic dynamo model driven by inertial gravity waves 4-105410  
 gravity waves, Zakharov eqns. modifications 4-87744  
 hydromagnetic planetary-gravity waves in zonal wind-magnetic shears, instability 4-62940  
 inhomogeneous plane waves, appls. 4-86220  
 intermediate long wave eqn., limit to Benjamin-Ono eqn. 4-63522  
 internal gravity waves from localised sources, propag. (*Russian*) 4-112920  
 internal gravity waves generation and evolution 4-112922  
 internal wave theory 4-67274  
 ionosphere travelling disturbances, dispersion relations rel. to determ. of thermospheric wind vectors 4-90015  
 Kelvin-Helmholtz waves, reson. triads and direct reson. 4-60447  
 lakes, acoustic wave generation by low freq. gravity modes 4-82109  
 linear random gravity wave propag. in variable depth water 4-75051  
 magneto-acoustic-gravity waves, on Sun, theory of running penumbral waves 4-72918  
 modified intermediate long wave eqn., Backlund transformation and scatt. problem 4-63523  
 nonlinear effects on shoaling surface gravity waves 4-60446  
 nonlinear gravity waves, algorithm for dispersion relation 4-72772  
 ocean surface gravity waves, sheltering by islands, model and expt. off S California 4-72599  
 ocean waves, two-freq. microwave scatterometer meas. 4-67471  
 open-channel flow, gravity current upstream of buoyant influx 4-60550  
 quasi-harmonic capillary-gravity waves, modulational instability, mag. field effect 4-91845  
 rotational, hydrodynamic stability calcs. 4-75049  
 sea ice flexural gravity waves, ocean waves role in origin 4-89944  
 small-amplitude free-surface waves generated by moving oscillatory disturbances 4-112923  
 standing surface gravity wave, horizontal cellular streaming, visualisation 4-112926  
 stratified fluid, internal gravity waves, modal struct. bifurcations, stability parameter variation 4-75048  
 stratified fluids, turbulence decay, gravity waves effect 4-60379  
 in sunspots, resonance oscillations and magnetoacoustic gravity wave transform. 4-63123  
 surface gravity-capillary waves, blocking effect by inhomogeneous flow 4-83917  
 thermocline, internal gravity waves generation 4-103350  
 thermosphere, generation of vertical winds and gravity waves at auroral latitudes 4-105782  
 thermosphere, internal gravity waves, parametric instabilities, Doppler spectra 4-100837  
 thermosphere, numerical modelling of vertical winds and gravity waves generation at auroral latitudes 4-105783  
 turbulent conducting fluid, internal Alfvén-gravity wave propag. 4-91820  
 waveguide properties of an atmosphere with a monotonically varying temperature 4-63047
- greasing** see *lubrication*
- Green's function methods**  
 see also *CPA calculations; KKR calculations*  
 $\lambda\phi^4$  theory in curved spacetime and varying background fields, effective Lagrangian, quasiloal approx. 4-111302  
 $\phi^4$  theory, skeleton inequalities and asymptotic nature of perturbation theory 4-68351  
 acoustic pseudo-Rayleigh waves at fluid/solid interface, Green's function anal. 4-60189  
 acoustic wave scattering, null field method and modified Green functions 4-87498  
 alloys, anisotropic superconducting, time depend. Ginzburg-Landau eqns. 4-88630  
 alloys, Auger spectra, partial long range order effects 4-99238  
 anharmonic cryst., isotopically disordered, thermal cond. for phonon scatt. by impurities and anharmonicities 4-98375  
 anharmonic oscillator, eigenvalues and Green's functions, 1/N series 4-63533  
 antiferromagnetic Heisenberg linear chain in mag. field, Green's function approach 4-114129  
 antiferromagnetic superconductor, theory of upper crit. field 4-76090  
 antiferromagnetic XY chain with impurities, local magnetisation, Green's function calc. 4-98846  
 asymptotic medium concept and averaged Green function, optical consts. and electronic density of states 4-80472  
 axisymmetric conductor, current-carrying, magnetostatic field calcs. using eigenfunction expansion, effects of Fe 4-59948  
 Bethe lattice, Coulomb potential problem, random walk Green's function 4-86365  
 binary alloys, order-disorder transitions, electronic theory 4-113572  
 binding with a core models in Green's function method, 1p1h configs., quasiparticle-phonon model 4-95889

## Green's function methods continued

bis(pentadienyl)iron, INDO calcs. photoelectron spectra 4-68960  
 body of revolution in liq. with jet separation, unsteady weakly perturbed motion 4-112896  
 book, Green's functions in quantum theory 4-63423  
 computational mol. physics, conf., Bad Wildsheim, Germany, Aug. 1982 4-58561  
 conducting cylinders embedded in lossy medium, EM scatt. 4-112324  
 conducting strip above dielec.-clad ground plane, scattering problem anal. (Japanese) 4-83524  
 convergent methods for calculating thermodynamic Green functions 4-106254  
 coupled-channel equations, stabilisation of solns. and Green's function, at. and mol. appls. 4-101703  
 crystal Green's functions in complex energy plane, analytical tetrahedron method 4-60996  
 crystal growth problems 4-60871  
 crystal with impurity, LCAO calc. of excess orbitals 4-98568  
 crystal/overlayer system, elastic surface waves, Green's function anal. 4-108695  
 cylinder, elastic circular finite, torsion by annular rigid stamp, stress anal. 4-97310  
 decoupling renormalization, field theoretic solution to hierarchy problem, unified field theory 4-90782  
 density of states, effective medium approx., percolation networks spectral dims. 4-95333  
 diatomic polymers, Green's function study 4-80552  
 diffusion processes and random walks, localised partial traps 4-58793  
 Dirac eqn. solns. and Green's electron function in external EM field 4-73648  
 Dirac-Coulomb problem, exact path-integral soln. 4-90426  
 dislocation-point defect interaction, lattice dynamics model 4-103786  
 disordered transport, high and low density expansions, Green's function 4-73393  
 dispersive plane-stratified anisotropic medium, EM field theory 4-78158  
 drop in partial contact with solid support, free vibrations 4-75757  
 dynamical system stochastic vibrs., Green's multi-dimens. function appl. 4-90352  
 eddy current density, boundary-element computation in contiguous domains 4-64650  
 electromagnetically induced nuclear beta decay calculated by a Green's function method 4-83031  
 electron lenses, open, computation by coupled finite element and boundary integral methods 4-91392  
 electron liquids, correlation energy plasmon dispersion, static and dynamic form factors 4-75885  
 electronic density of localised states in long range correl. pot. 4-98571  
 EM mass splittings in QCD 4-68572  
 EM wave diffraction by nonclosed surfaces of revolution 4-87253  
 energy-dependent quantities, Green's function calcs., simplification through analytic continuation 4-61274  
 excited donor molecule, direct energy transfer 4-96662  
 Fermi liquid, normal, Landau kinetic eqn., nonlinear corrections 4-63650  
 fermion systems, Sturm expansions, perturbation theory 4-63659  
 ferromagnetic semicond., magnetic excitation theory 4-76128  
 ferromagnetic semiconductor, conduction electron spin polarisation 4-88682  
 ferromagnetic semiconductor, electron-phonon interaction, s-d model 4-92326  
 ferromagnetic semiconductor, relax. time, Green's function calc. 4-88660  
 ferromagnetic semiconductors, degenerate, spin waves at low temps. 4-114096  
 ferromagnets, local-band theory anal. of spin polarised, angle-resolved photoemission spectroscopy 4-92886  
 four fermion nonlinear spinor model, renormalisation and Ward identities 4-111264  
 gases, dense, with small polarisability, electron mobility calc. 4-60580  
 gauge symmetries, decoupling and conservation, subtraction scheme 4-68395  
 geminate recombination, random walk theory 4-61390  
 geminate recombination on a lattice 4-11042  
 gravitational effective action, gauge dependence, one-loop order 4-95679  
 Green's electron function in quantised plane EM wave field 4-73709  
 Green's-function Monte-Carlo method in few-body calculations 4-58735  
 hadron energy eigenvalues and coupling strengths determ. with duality, Shifman-Vainshtein-Zakharov method 4-59059  
 Hamiltonian XY model, Green's function Monte Carlo method appl. 4-68418  
 harmonic oscillator, Feynman's formula for Green's function 4-95203  
 harmonic oscillator, temperature Green's function, generating functional 4-90406  
 harmonic oscillators, random masses, exact solutions for spectra and Green's functions 4-78185  
 Heisenberg antiferromagnet, susceptibility, spin-wave Hamiltonian 4-104393  
 Heisenberg ferromagnet, spectral density method anal. 4-114087  
 Heisenberg ferromagnet, spin Green's functions 4-104394  
 Heisenberg ferromagnet, spin wave damping theory 4-80754  
 Heisenberg ferromagnetic interface, magnetisation and excitation spectrum 4-80788  
 Heisenberg model, anisotropic, low-temp. behaviour, symm. props. 4-61503  
 homogeneous medium bounded by perfectly conducting walls, dyadic Green's function props. 4-64659  
 Hubbard, ferromagnet, narrow-band, carriers in spin wave range of temps. 4-92887  
 hybrid finite element boundary element solutions using half-space Green's functions 4-59951  
 infinite crystal with charged point defects, total energy, Green's function calc. 4-108812  
 inhomogeneous media, EM waves variational principles, operator eqns. 4-74396  
 integral representation for the product of two Jacobi functions with different order and arguments 4-86264  
 ionic crystals, surface dynamics, surface Green function matching method 4-108700  
 ionisation spectra, outer and inner valence region, Green's function method 4-59706  
 Ising model, Green function ansatz for K-space pair correl. function 4-58763

## Green's function methods continued

KRSV supersymmetric theories with false vacua, extension to three space dims. 4-58986  
 laser materials, Auger recomb. and intervalence band absorpt. 4-80885  
 light polarisation change in turbulent atmosphere, Green function scalar form 4-107525  
 Liouville string field theory, scatt. amplitudes, Green's functions 4-73617  
 liquid surface and interface waves 4-79613  
 localisation, self-consistent theory 4-98501  
 Lorentz gas, time asymptotics of velocity autocorrelation function 4-106236  
 macroscopic dielectric tensor at crystal surfaces 4-70894  
 macroscopic two-level system, conversion time, resonator free superradiative laser appl. 4-74484  
 magic nuclei, microscopic model for 2p2h config. inclusion, giant resonances 4-86814  
 magnetic rods magnetised by coils, magnetisation characts., numerical anal. 4-65827  
 magnetic thin films, law of approach to saturation, Green's function calc. 4-71136  
 many boson and many fermion systems, perturbation theory approach 4-58732  
 many-body Green's functions of composed systems 4-106580  
 many-fermion system, generalised mean field expansions (Chinese) 4-101742  
 many-fermion systems, Sturm spectral representation of Green's functions 4-78235  
 Mellin transforms associated with Julia sets and phys. appls. 4-58775  
 membrane nonzero thickness effect on diffusion through membranes 4-72225  
 metal surface, randomly rough, enhanced SHG due to localised surface polaritons 4-69500  
 metallic solids, Debye-Waller factor for substitutional Mossbauer impurity 4-75633  
 metallic solids with small conc. of impurities, Mossbauer oscillator strengths, Debye-Waller factor 4-75634  
 metals; crystalline and amorphous, shear magnetostriction theory 4-98931  
 metals, electron spectrum, changes under press. (Russian) 4-108766  
 Mohapatra-Senjanovic model at finite temp., elementary excitation spectra, SU(2)XU(1) (Chinese) 4-73698  
 molecular valence ionisation spectra, ionisation pot. calcs. 4-69140  
 Monte Carlo methods, lattice gauge theories, path integrals in quantum mechanical problems 4-95292  
 moving boundary diffusion problems, pseudo-steady state approx. 4-65004  
 N-dimensional free-particle, harmonic oscillator and Coulomb problems, Green's functions, propagators from integral representations 4-63542  
 Navier-Stokes eqns., steady, anal. based on Green's function approach 4-79541  
 Navier-Stokes eqns., unsteady, anal. based on Green's function approach 4-79542  
 nonlinear surface wave generation in a planar waveguide structure 4-79231  
 nonrandom substitutionally disordered alloys, cluster density of states 4-70737  
 nonrelativistic Coulomb problem, Sturmian propagator 4-63561  
 nontopological solitons, Green's functions and bound states, self-interacting scalar field 4-90831  
 O(N) spin system in 1+1 dims., Green's function method 4-68415  
 one-dimensional lattice, random, dilute, one-particle Green function 4-90524  
 one-dimensional two-block crystal, IR spectrum calc. using Green function method (Chinese) 4-71357  
 one-particle Green's function, computational methods review 4-78108  
 optical fibres, anisotropic, fundamental mode field derivation using Green's function method 4-97075  
 particle particle propagator, higher order approx. in algebraic diagrammatic construction 4-102595  
 perfectly conducting cylinder of infinite length, eigenfunction expansion of electric and magnetic dyadic Green's functions 4-102847  
 periodically ribbed elastic structures under fluid loading, energy transmission 4-97380  
 piezoelectric crystals with thin overlayers, SAW 4-80359  
 piezoelectric cubic crystals, surface and interface Bleustein-Gulyaev waves 4-65537  
 piezoelectric surface waves in layered media 4-108696  
 planar crack of arbitrary shape at interface of two anisotropic elastic half spaces 4-79508  
 plate, elastic thick circular, torsion by annular rigid stamp, stress anal. 4-97310  
 point impurities, generalised Green's function anal. 4-98566  
 polaron electrical conductivity from functional integration, effective mass, lifetime 4-75915  
 polydiacetylenes, charge-transfer exciton spectra, Green's function study 4-71405  
 pore interactions and distrib., effects on diffusion and permeation in membranes 4-98332  
 QED, one-loop corrections, temperature effect on electron charge, mass, wave function 4-86636  
 quantum field theory, infinite temperature limit,  $\phi_2^4$  QED, QCD 4-90706  
 reduced Dirac Green function for Coulomb pot. 4-68009  
 relativistic Coulomb Green function, Sturmian expansion rel. to finite size of nucleus (Russian) 4-111501  
 renormalisation in massless theories and infrared divergencies 4-63892  
 renormalisation-scheme dependence problem, effective charges method for QCD and QED 4-78526  
 Robertson-Walker universe, causal Green function 4-86307  
 s-d model, electronic spectrum and damping with Coulomb interaction 4-92588  
 Schrodinger eqn., linear bound operator, 1-D study with nonlocal potential 4-78197  
 Schwinger source theory, space-time structure of radiative corrections 4-102045  
 semiconductor, deep centre problem, analytic soln. by method of continued fractions 4-61333  
 semiconductor surface, electronic collective modes and instabilities 4-108796  
 semiconductors, core exciton resons. at inner-shell thresholds, dynamical scanning effects 4-80506

## Green's function methods continued

- semiconductors, electronic excitations, variational Green's function approach 4-108759  
 semiconductors, high field quantum transport theory 4-80599  
 semicylindrical concave rigid wall, high freq. acoustical fields (*Japanese*) 4-97203  
 semiinfinite solid, melting with viscous heating, closed-form soln. 4-97299  
 shallow water waveguide characterization using the Hankel transform 4-103069  
 Sierpinski gasket in mag. field, spectrum study 4-78274  
 simple nonpolynomial lagrangian theories, finite Green's functions 4-86556  
 SO(2,1) coherent state path integral, Coulomb Green function 4-102061  
 solids, Auger CVV line shapes, dynamical screening effects 4-93152  
 spatially periodic struct. theory, Bose excitation Green's functions 4-73340  
 spin 1/2 linear array with anisotropic X-Y coupling 4-92931  
 spin systems, quasiclassical approx., spin coherent states (*Russian*) 4-114124  
 statistical, derivation of set of coupled eqns. for order parameter (*Chinese*) 4-90482  
 stratified fluid media, wave field calcs. 4-103071  
 stratified media, dyadic Green's functions (*Ukrainian*) 4-87560  
 Sturmian representation of optical model pot. due to coupling to inelastic channels 4-68659  
 SU(2) theory, monopole interaction with fermions in higher representations 4-78500  
 SU(N)×SU(N) chiral model, mass gap by Green's function method, 2D lattice 4-95707  
 sub-surface crack, elastic wave diff. 4-74926  
 superconducting under critical field, theory for superconductors with energy depend. electronic density of states 4-104379  
 superconductive tunnelling, microwave irradiation effects, Green's function calc. (*Chinese*) 4-104369  
 surface, light scatt. near phase transition point 4-99128  
 surfaces, light scatt. near phase transition points 4-66049  
 thermal cond. of solids, Callaway model, Green's function study 4-98378  
 thermo field dynamics of a quantum algebra 4-102022  
 thermo-piezoelectric continua, moving dislocations and disclinations, mechanical electrical and thermal fields 4-98102  
 three-layer medium, light reflection, electrodynamic Green's functions 4-109150  
 transient heat cond. problems, Green's function soln. 4-103176  
 transient optoacoustic pulse generation and detection 4-69656  
 transition metal complexes, orbital relax. and correl. in photoelectron spectra, INDO calcs. 4-102740  
 transition metals, liquid, Muffin-tin model, local density of states, calcs. 4-108755  
 two-band model, One-Particle Green's functions analytical props. 4-84541  
 two-dimensional velocity/vortex flow characterisation 4-69729  
 U(N) invariant matrix  $\phi^4$  theories, exact solns. in zero dims. 4-102005  
 underground structures, transient response to SH-waves 4-112607  
 vibroacoustic fields compensation by acoustic radiators, optimum distribution calc. 4-103055  
 viscoelastic cond. fluid, flow past an oscillating infinite plate 4-112965  
 viscous fluid, small particle motion, circular disk effect 4-65013  
 weak quark decays, diagrammatic approach 4-73718  
 Wentzel pair theory, massless scalar field, renormalised self-energy, radiative corrections 4-95775  
 Wess-Zumino model, supersymmetry at finite temp. 4-78453  
 Wigner-Seitz cells, multiple scatt. problem, convergence props. 4-70612  
 Yang-Mills field, Green's functions and observable processes 4-111272  
 Yang-Mills super self-dual background, Green functions 4-78449  
 $e^+e^- \rightarrow \mu^+\mu^-$  asymmetry, electroweak radiative corrections in SU(2)×U(1) model 4-68559  
 $(\gamma, N)$  preequil. emission and quantum 4-83043  
 $\pi\pi$  scattering, low energy theorems corrections, QCD tests with current algebra 4-82940  
 Al (001) surface electronic struct. calcs., embedding approach 4-61429  
 CO, Auger spectra, Green's function calcs. 4-64389  
 $^{44}\text{Ca}$ , A=40, 48, M1 resonance calc. including 1 phonon configuration 4-102159  
 CdSe-type uniaxial cryst., excitonic absorpt. band formation (*Russian*) 4-71409  
 CdTe doped with mag. ions, anomalous optical effects (*Russian*) 4-99103  
 CoCl<sub>2</sub>·6H<sub>2</sub>O, paramagnetic phase boundary of antiferromagnet at low temp. 4-88668  
 Cu, electronic props. of 4d transition metal and sp impurities 4-70731  
 Cu-Ni, disordered, positron spatial distrib. effects 4-104170  
 Fe (110), spin-dependent bremsstrahlung 4-88898  
 GaP, defect electronic struct. calcs. 4-61326  
 GaP, symm. deep level wavefunction for defect pairs (*Chinese*) 4-104144  
 Ge:H-based impurity complexes, charge state determ. 4-92663  
 H atoms multiphoton transitions, above-threshold, Coulomb Green function calc. 4-112151  
 H, phase-space formulation, nonrelativistic quantum mechanics 4-102590  
 He<sup>+</sup>, low energy electron impact, Schwinger's variational principle 4-74339  
 Hg<sub>1-x</sub>Cd<sub>x</sub>Te, CPA calcs., Green's function calcs., simplification through analytic continuation 4-61274  
 In<sub>0.3</sub>Ga<sub>0.7</sub>As, laser operation, thermal behaviour 4-87331  
 KCl:Ti<sup>3+</sup>, impurity-level ground and excited states, Green's function calc. 4-98563  
 LiNbO<sub>3</sub>, Y-cut, SAW generation, simplified Green's function allowing for leaky surface wave 4-92500  
 Mo (100), surface states, appl. of quick iterative scheme for transfer matrix calc. 4-76013  
 NaF (001), inelastic He scatt., eikonal approx., surface dynamics 4-109300  
 NbC, C vacancy electronic struct., tight binding calculations 4-92661  
 Ni (001) surface electronic struct. calcs., embedding approach 4-61429  
 NiCl<sub>2</sub>·6H<sub>2</sub>O(4H<sub>2</sub>O), paramagnetic phase boundary of antiferromagnet at low temp. 4-88668  
 NiO single cryst. and powder, mag. susceptibility and exchange const. 4-84775  
<sup>208</sup>Pb, M1 resonance calc. including 1 phonon configuration 4-102159  
 RbCl, first-order Raman scatt. due to F-centres 4-93076  
 Si (100) inversion layer, electron mobility, neutral scatt. effects 4-76040  
 Si (111), surface phonons and reconstruction 4-92509

## Green's function methods continued

- Si (111) slab, interface, electron-phonon interaction and broken symm. 4-80517  
 Si, atomic diffusion mechanisms theory 4-70430  
 Si, defect states, T<sub>2</sub> symmetric deep level wave functions 4-108801  
 Si, ideal vacancy, electronic struct. calcs. 4-70722  
 Si:B( $\mu^+$ ), tetrahedral interstitial impurities, electronic struct., LCAO-Green's function calc. 4-65636  
 Si:muon, spin polarised electron struct. of positive muon, LCAO-Green's function anal. 4-65634  
<sup>232</sup>Th(<sup>16</sup>Ar,X), quasi-elastic multistep heavy ion processes, random matrix model 4-91013  
 TiN (001), anomalies in surface-phonon dispersion 4-75771  
<sup>90</sup>Zr, M1 resonance calc. including 1 phonon configuration 4-102159
- grinding**  
 Broken Hill Field geology, mining and metallurgy, conference, Broken Hill, NSW, Australia (July, 1983) 4-58562  
 burns revealing using opt. differential structurescope 4-109616  
 corundum single crystals, surface structure and deform., chem. med. effect 4-81314  
 diamond, wear for grinding ceramics 4-99609  
 glass, grinding and hole boring of optical glass—a comparison (*German*) 4-74771  
 glass, optical, surface treatment resulting in min. surface roughness and max. beam surface penetration 4-79351  
 glass grinding damage, single- and multi-point comparison 4-85206  
 ground surfaces, inspection of quality by X-ray sliding beam method 4-71813  
 optical aspheric surface generation methods 4-87489  
 optical component surfaces, equipment for preliminary shaping 4-69609  
 optical fabrication technology, present and future 4-107897  
 optical glass, fine diamond grinding, lubricating-cooling liquid rol. 4-69607  
 optical manufacturing and testing, conf., San Diego, CA, USA (Aug. 1983) 4-106104  
 optical precision machining application and technology, overview and perspective 4-107902  
 optical quality lapping and polishing with flexible bound diamond materials 4-103031  
 polystyrene, chain scission and mech. degradation 4-93395  
 prostheses, spherical surface grinding phenomena 4-115274  
 steel, bearing, surface layers, effect of grinding (*Chinese*) 4-99628  
 steel, high-alloy, quenched, residual austenite transformation, high temp. X-ray study (*Russian*) 4-104777  
 steel, low alloys heat treated, grinding residual stress, hardness (*Japanese*) 4-89117  
 steel, tool, tempered surface layers formed during grinding, thickness determ. using electrochem. method 4-71814  
 Al<sub>2</sub>O<sub>3</sub>, sintered, fracture strength, effect of surface condition 4-62057  
 Cu, Bauschinger effect, influence of surface removal 4-114616  
 $\gamma$ -FeOOH powder, grinding, lepidocrocite to hematite transform., morphology and mag. props., Mossbauer obs. 4-66329  
 LiF single crystals, grinding, surface layer, strain hardening, dislocation density, microhardness 4-93312  
 Mg alloy, cast ML8, surface strain hardening treatment effect on low cycle fatigue 4-99656  
 MnB<sub>2</sub> alloy, spontaneous magnetisation changes due to amorphisation (*Russian*) 4-104407  
 TiO<sub>2</sub>, polymorphic transform. by mech. grinding 4-66328
- grinding mills see grinding**  
**ground electrodes see earth electrodes**  
**grounding see earthing**  
**groundwater**  
 Alberta, Canada, geothermal gradient rel. to groundwater flow and topography 4-105490  
 Alberta, Canada, terrestrial heat flow variations and groundwater 4-89901  
 aquifer flow velocity model, for aquifer with recharge and extraction points 4-115479  
 aquifer layers, subterranean, data processing and representation (*Italian*) 4-82099  
 aquifer pollution protection measures necessary around borehole 4-85722  
 axisymmetric elevation spreading 4-115470  
 Big Quill Lake, Saskatchewan, saline lake, effect of groundwater inflow on evaporation 4-100632  
 book, computation simulation of subsurface flow 4-67904  
 Bowser Basin, N British Columbia, effects of groundwater flow on geothermal meas. 4-105474  
 Canberra, Australia, petrol from filling station infiltrating aquifer 4-93653  
 coal mining in Great Britain, groundwater control methods 4-77566  
 coal-fired power stations fly ash/slag wasteyards, surface and groundwater pollution (*Polish*) 4-85390  
 commercial low level radwaste disposal site, radionuclide charact., migration and monitoring 4-83204  
 contaminant transport modelling 4-100010  
 crystalline rock formations, geological assessment for radwaste disposal groundwater 4-64208  
 cyanide detection in surface groundwater by flow injection anal. 4-62411  
 Denmark, natural radioactivity of water from boreholes 4-94173  
 discharges, correl. with tectonic stress and earthquake occurrence 4-81998  
 Earth tide response of confined deep aquifers 4-82107  
 estuaries comparisons, conf. at Gleneden Beach, USA (November 1981) 4-86122  
 Eye-Dashwa pluton, Ontario, Canada, geology of radioactive waste disposal site 4-81919  
 fault gouge permeability to water, effect of confining press. 4-85724  
 fault zone modifications due to fracturing, water circulation and chemical alteration 4-110082  
 fertilizer contaminant plume dynamics 4-100011  
 flow characteristics from borehole temp. meas. 4-105602  
 flow induced by heated vertical wall in a porous medium 4-69821  
 flow through porous media, book 4-78053  
 geysers (*Russian*) 4-82110  
 Ghaggar River basin, India, water table rise under irrigated conditions and quality 4-100639  
 high level radwaste repository, backfill as barrier to radionuclide migration 4-59349

## groundwater continued

- hydraulic head, distribution form, artificial recharge and exploitation effects (*Chinese*) 4-62857  
 hydrogeology, inverse coefficient problems formulation 4-105606  
 ice sheets growth 4-115469  
 India, groundwater, irrigation and water supply, book 4-95090  
 karstic aquifers, hydrological struct. dissolved  $O_2$  indicator (*French*) 4-82098  
 landfill leachate,  $\gamma$ -irrad. conditions required in combined radiation-microbial process 4-93677  
 Larissa plain, Greece, aquifer pollution protection measures necessary around borehole 4-85723  
 Leninabad Region, Tadzhikistan, groundwater level meas. rel. to hydrodynamic earthquake precursors 4-100471  
 low level radwaste shallow burial site, environmental pathways anal. 4-83193  
 measurement of groundwater speed and direction (*Slovak*) 4-85760  
 Mount St. Helens, 1980 eruptions effect on surface and groundwater quality 4-105616  
 Mount St. Helens, 1980 May eruptions, hydrothermal system above magma, chem. 4-105513  
 multi-layer percolation system, groundwater flow model (*Russian*) 4-115473  
 Muromi River Basin, Japan, aquifer storage and transmissivity (*Japanese*) 4-85728  
 Nevada Test Site, radionuclide migration from underground nuclear explosion, review 4-83206  
 New Quebec, Canada, ice lenses in peat bogs, geochemistry, isotope content and genesis 4-100637  
 Nigeria, groundwater prospecting using Landsat images 4-77562  
 SE Nigeria, hydrology and chemistry of water resources of Agwata area 4-115466  
 nitrate concentration in aquifers, numerical model 4-115478  
 nonlinear diffusion with linearly varying diffusivity 4-100640  
 oil or water flow in neighborhood of a drill-hole 4-72585  
 East Pacific Rise, hydrothermal vents and sulphides; geological study 4-105538  
 E Pacific Rise, submarine hot springs, heat and water flow rate obs 4-105537  
 Penitction Tertiary outlier, BC, Canada, potential of geothermal energy site 4-72538  
 permeability and bulk modulus of rocks, pore space model 4-82106  
 permeability of crystalline rocks, new in situ meas. 4-94114  
 physical and chemical properties (book) 4-95083  
 pollution in sandy soil, effects of N fertilisers and rainfall 4-77156  
 pollution migration in aquifer, theory for adsorbable pollutants 4-93655  
 potable water in Saudi Arabia, material radioactivity 4-89789  
 radioactive liquid effluents, release limits and health consequences, water pollution (*French*) 4-83198  
 radioactive waste, geological disposal, thermal loading effects on granite, clay and salt 4-83176  
 radioactive waste, radionuclide time-dependent mass transfer into groundwater 4-106720  
 radwaste disposal sites in USA, geohydrological problems 4-83188  
 recharge problems, appl. of filtration theories 4-77565  
 remote sensing 4-67430  
 reservoir rocks, pore geometries 4-72570  
 rock porosity meas. technique for in-situ rocks, EM tomography method 4-110292  
 rocks, elec. resist. during crack form. rel. to pore water surface cond. 4-62801  
 saline formation water of US Gulf Coast region, Ra occurrence and behaviour 4-110179  
 saline intrusion in coastal aquifer, salt-fresh water interface motion 4-115477  
 salt dome radwaste repository, radiation exposure due to radioactive releases 4-83205  
 Saudi Arabia, groundwater chem. 4-82104  
 Schrendwellerbach drainage basin, Luxembourg, storm runoff, soil characteristics and water table 4-100635  
 soil, seepage water flow, finite element calculation 4-100642  
 soil hydrology, two-layer model 4-115463  
 soil water capacity determ. 4-67295  
 solid LLW shallow land burial, 30 years experience at Savannah River Plant 4-83185  
 solidified TRU-contaminated incinerator ash, leach rates and Pu releases 4-106714  
 subsurface contaminant transport from liquid radwaste disposal area, groundwater, T data 4-78700  
 N Tanzania, high fluoride content of rivers, lakes, springs 4-115467  
 two-layered geologic media, radionuclide migration, radwaste disposal appl. 4-73977  
 Usu Volcano, Japan, seismicity and hot spring temp. prior to 1977 eruption 4-105510  
 Valencia, Spain, groundwater flow for saline intrusion 4-115477  
 Valencia province, Spain, nitrate concentration in aquifers, numerical model 4-115478  
 water supply from groundwater, book 4-95089  
 As pollution, environmental assessment 4-66820  
 Cl, isotopic var. 4-77651  
 Np compounds, thermodynamic behaviour in water and groundwater, pH and Gibbs energy, radwaste appl. 4-78701  
<sup>226</sup>Ra occurrence and  $\alpha$ -particle activity in United States drinking water supplies 4-62411

## group theoretical schemes

- path integrals, group theoretical derivation 4-106496  
 QCD, exotic comutators and ideal mixing 4-68500  
 U(1) problem, pseudoscalar mass spectrum 4-86591

## group theory

- see also Clebsch-Gordan coefficients; crystal symmetry; elementary particle theory; group theoretical schemes; Lie groups; renormalisation;  $SU_n$  theory  
 3-body problems, six-D oscillator based on O(6) 4-82700  
 A15 type struct., mag. symmetry, group theoretical method anal. 4-108990  
 abelian groups, Fourier anal. on multiplier representation 4-58616  
 branching rules for  $E_6/SO_{16}$  4-68000  
 Calogero-Moser many body system, hierarchy of flows 4-101641  
 CI methods, group theory appls. 4-59609  
 Clifford algebras and Cayley-Dickson algebras, construction 4-95132

## group theory continued

- Clifford algebras and finite groups relationship 4-63538  
 coefficients of fractional parentage for  $U(m+p/n+q) \supset U(m/n) \times U(p/q)$  and  $U(m/n) \supset U(m) \times U(n)$  4-90346  
 computational mol. physics, conf., Bad Wildsheim, Germany, Aug. 1982 4-58561  
 conference on collective states in nuclei, Suzhou, China (Sept. 1983) 4-95043  
 conservation laws, relation to algebra of space-time symmetry group 4-95703  
 cubic groups, quantisation on order 4 axis 4-78486  
 $C_{60}$  and  $C_{59}$  symmetry groups, 3jm factors and basis functions 4-78102  
 EM spinor formalism generalisation to anisotropic media 4-96759  
 exponential operator expansion, recursive algorithm 4-78184  
 functional composition, renormalisation group analysis, review 4-73629  
 Hermitian operators using SO(2,1) group unitarily invariant decomp. 4-78165  
 IBM, s-d-g bosons, group theoretical study, subgroup chains 4-95929  
 icosahedral group, quantisation on order 5 axis 4-78487  
 incommensurate crystal phases, superspace groups and representations 4-113376  
 Jahn-Teller matrix elements,  $\Gamma \times e$ , evolution by group theory method 4-92678  
 lattice degeneracies of fermions 4-102006  
 magnetic point groups of infinite order, projective corepresentations, unified theory 4-86177  
 microscopic collective states, dynamical group, coherent state representations 4-102192  
 molecules, vibr. eigenvalues, G-matrix redundant conditions 4-59700  
 $N=2$  supersymmetric theories, representations of classical semisimple groups  $G_2, X_{2,2}$  4-111329  
 $N=4$  supergravity with global SO(4) symmetry 4-68103  
 noncompact symplectic algebra, analytic expressions of matrix elements 4-78098  
 nonequilibrium statistical mechanics, algebraic formulation, dynamical semigroups 4-63647  
 noninvariance groups for many-particle systems: coupled harmonic oscillators 4-90408  
 nonlinear Schrodinger eqn., generalised, group theoretical approach to symmetries 4-106208  
 nuclear collectivity and geometry, 2-D Sp(4) chain 4-83012  
 nuclear collectivity and geometry, subgroup selection 4-83011  
 nuclear multiple quadrupole excitations, U(6) representation matrices 4-95876  
 $O^+(2,2)$  group, representation matrix elements, isomorphisms 4-86178  
 O(1) supergravity, exact plane wave solutions 4-82740  
 one-body coeff. of fractional parentage for group chains  $U(mn) \supset U(m) \times U(n)$  and  $U(mp+nq/mq+np) \supset U(m/n) \times U(p/q)$  4-68020  
 orthogonal scalar operator complete set for config.  $f^3$  4-74141  
 particles, dynamics and covariance, book contrib. 4-58690  
 path integrals, group theoretical derivation 4-106496  
 Poincare group, helicity representations, sharp momentum states, differentiable vectors 4-102053  
 Poincare group, spinor representation in 8-D 4-63503  
 quantum correlation functions from dynamical semigroups 4-78159  
 quantum mechanics, functional integrals on noncompact groups 4-82699  
 quantum theory, groups, fields and particles, book 4-58592  
 quaternion group and modern physics 4-78081  
 relativistic density-functional theory, quantum fluid dynamic, many-electron systems 4-110881  
 rotation-vibration spectra symmetry using U(5) group (*Chinese*) 4-111553  
 rotational mechanics, spinor descriptions devel. from Euler's rigid body displacement theorem 4-78126  
 rotational symmetry systems, bifurcation equation gradient prop. 4-101617  
 Schwinger functionals Borchers's tensor algebra 4-68394  
 SO(10) model, low energy gauge group, proton lifetime 4-90770  
 SO(10) model with  $54+126+10$  Higgs, scalar particle spectrum 4-106482  
 SO(10) theory, CP-violation parameters in a left-right-symmetric model 4-111361  
 SO(1,1)  $\times$  SO(d-2) model, nonlinear string eqns. in d-dimensional space-time, gauge description 4-63898  
 SO(2,1) coherent state path integral, Coulomb Green function 4-102061  
 SO(2) electrostatics, mean curvature and radiation field 4-78492  
 SO(2n)  $\rightarrow$  SO(2n-2)  $\otimes$  U(1) branching multiplicity, evaluation algorithm proof 4-86180  
 SO(3,2) geometry, bag models, Dirac eqn. and solutions for confined quarks 4-111414  
 SO(4) reduction of Yang-Mills eqns. in Minkowski space 4-82888  
 SO(7) irreducible spinor representations 4-78488  
 SO(N) multispinor representations 4-78489  
 Sp(2,2) coherent states, unstable system geometrized decay model 4-95686  
 Sp(2d,R) generator matrix elements, determ. through boson mapping 4-78099  
 Sp(2d,R) symplectic group, partially coherent states 4-95133  
 Sp(6) group, matrix elements of generators for nuclear collective models 4-78600  
 spinor chain path integral, Dirac eqn., Feynman's checkerboard rule 4-111271  
 spinor structure of superspaces 4-73665  
 spinor superfield equations of motion 4-95711  
 SU(1,1) Clebsch-Gordan coeffs., Racah coefficients, Poschl-Teller wavefunctions 4-95208  
 subduccible group, explicit matrix representations 4-78096  
 superkinematics, SUSY groups with one Majorana bispinor generator 4-102050  
 symmetric groups, irreducible characters, Murnaghan's rule 4-78097  
 symmetry transformations, group representations in indefinite metric spaces 4-78490  
 $U_6 \supset U_3$  chain, symmetrical representations, isofactors 4-111341  
 $U(n) \times U(2)$  generators, reduced matrix elements derivation 4-78167  
 U(1) lattice gauge theory, linked cluster expansions in 2+1 and 3+1-D 4-82881  
 U(1) lattice gauge theory, mean field in Feynman gauge 4-82880  
 U(1) lattice gauge theory, mean field perturbation 4-106457  
 U(1) symmetry breaking, soln. to domain wall problem 4-58930  
 U(6/12) group, interpretation of Casimir operators 4-102059

## group theory continued

- U(N) groups, character expansion 4-102054  
 U(N/M) supergroups, character expansion 4-102054  
 U(N) integrals in large N limit 4-111332  
 U(N) lattice gauge theories, loop dynamics, Monte Carlo calcs. 4-78450  
 U(N/M) supergroup, characters dimensions and branching rules 4-78485  
 Wigner-Racah algebra of arbitrary group 4-68055  
 Yang-Mills theory, instantons and geometric invariant theory 4-78446  
 Yukawa potential ground states estimate from Bogoliubov inequality 4-58667  
 BeB<sub>2</sub>H<sub>8</sub>, microcomputer-aided instruction and research in group theory 4-102584  
 CuInSe<sub>2</sub>, sphalerite-chalcopyrite order-disorder transitions, group theory anal. 4-84383  
 TeO<sub>2</sub> crystal, vibr. spectra, group theoretical anal. (Russian) 4-80176

## Grüneisen coefficient

- alkali borate glass, rel. to atomic vibr. in glassy networks 4-80272  
 alkali metal halides, short-range repulsive pot. anal. 4-75361  
 alkali silicate glass, rel. to atomic vibr. in glassy networks 4-80272  
 anharmonic crystals, lattice temp., pressure effects 4-113559  
 characteristic frequency and Grüneisen coeff. calc. for solids (Chinese) 4-113558  
 cohesive energy, elastic const. and Grüneisen coeff. calcs. 4-84230  
 dielectrics, amorphous, kinetic processes, multiphonon theory anal. 4-80186  
 halide glasses, thermal and elastic props., molecular dynamics calc. 4-109455  
 ice, hexagonal, translational lattice vibrs. and permittivity, temp. and press. 4-76309  
 ice, stretching vibrs. of O-H and O-D, Raman spectrum, press. and temp. depend. 4-98218  
 ice clathrate, normal and deuterated, O-H and O-D stretching and vibr., Raman studies 4-61001  
 ionic cryst., lattice and thermodynamic props., overlap repulsion pot. 4-92327  
 phonon localisation and anharmonicity 4-98230  
 PMMA, glassy, low-temp. thermoelastic effects 4-98166  
 poly(vinylidene fluoride) piezoelec. and pyroelec. props. under high press. 4-99027  
 polycarbonate, oriented, Young's modulus, temp. depend., IR spectra, Grüneisen parameter (Russian) 4-109445  
 polyethylene, isotropic and oriented, thermal expansion, Grüneisen parameters, crystallinity 4-75708  
 polyimide, oriented, Young's modulus, temp. depend., IR spectra, Grüneisen parameter (Russian) 4-109445  
 AgCl(Br)(I), anharmonic props., interionic pot. model 4-98056  
 Al, shock impedance match expts., 0.1-2.5 TPa 4-108522  
 Al<sub>2</sub>O<sub>3</sub>:V(Mn), low-temp. thermal expansion meas. 4-61112  
 Ar, liquid, thermodynamic Grüneisen parameter, mol. compressibility and sound speed 4-60974  
 B<sub>2</sub>O<sub>3</sub>, vitreous, transition, struct., low freq. Raman spectra 4-66028  
 Ba(NO<sub>3</sub>)<sub>2</sub>, cohesive energy, elastic const. and Grüneisen coeff. calcs. 4-84230  
 α-CO, librational motion, anharmonic effects 4-103892  
 CO<sub>2</sub>, librational motion, anharmonic effects 4-103892  
 CoO, eqn. of state and Grüneisen parameters 4-92331  
 Cs, Grüneisen parameters, pseudopot. calc. 4-61032  
 Cs, phonon frequencies, Debye temp., Grüneisen parameter, transport props., lattice dynamical model 4-108561  
 Cs, solid and liq., Grüneisen parameter at high press., nature of isostructural electronic transition 4-61035  
 Cs, thermal expansion first-principles calcs. 4-98319  
 CuCl(Br)(I), anharmonic props., interionic pot. model 4-98056  
 CuInTe<sub>2</sub>, thermal expansion coeffs., 30 to 300K 4-103974  
 D<sub>2</sub>O ice, hexagonal, translational lattice vibrs. and permittivity, temp. and press. 4-76309  
 FeO, eqn. of state and Grüneisen parameters 4-92331  
 Gd<sub>3</sub>Ga<sub>5</sub>O<sub>12</sub>, hypersonic wave attenuation 4-75620  
 Ge, elastic props., ultrasonic meas. 4-98170  
 Ge-Si, vibrational modes and phase transition 4-88253  
 H<sub>2</sub>, solid, specific heat and Grüneisen relation 4-92474  
 InAs, lattice dynamics, phonon dispersion curves 4-61019  
 KTaO<sub>3</sub>, anharmonic interactions, X-ray diff. study 4-61036  
 MnO, eqn. of state and Grüneisen parameters 4-92331  
 MnSb<sub>2</sub>O<sub>4</sub>, antiferromagnetic, structural and vibr. studies, anisotropic effects 4-113561  
 Mo, shock impedance match expts., 0.1-2.5 TPa 4-108522  
 α-N<sub>2</sub>, librational motion, anharmonic effects 4-103892  
 NH<sub>4</sub>Br, continuous and discontinuous phase transitions, Raman modes 4-61070  
 NH<sub>4</sub>Br(Cl)(I), cohesion and thermodynamic props. calcs. 4-92126  
 NH<sub>4</sub>Cl, continuous and discontinuous phase transitions, Raman modes 4-61070  
 (NH<sub>4</sub>)<sub>2</sub>PdCl<sub>6</sub>, press. depend. of rot. states 4-60999  
 N<sub>2</sub>O, librational motion, anharmonic effects 4-103892  
 Na, martensitic BCC-HCP transformation, pretransitional phenomena 4-114519  
 NaCl, Anderson-Grüneisen parameter, volume coefficient of thermal expansion, equation of state, calcs. 4-98237  
 NiO, eqn. of state and Grüneisen parameters 4-92331  
 NiSb<sub>2</sub>O<sub>4</sub>, antiferromagnetic, structural and vibr. studies, anisotropic effects 4-113561  
 PbCl<sub>2</sub>, Raman-active modes, anharmonic effects 4-71381  
 Rb, solid and liq., Grüneisen parameter at high press., nature of isostructural electronic transition 4-61035  
 Rb, thermal expansion first-principles calcs. 4-98319  
 RbBr, acoustic-mode Grüneisen parameters, inelastic neutron scatt. study 4-80187  
 Si, elastic props., ultrasonic meas. 4-98170  
 SiO<sub>2</sub>, vitreous, low-temp. thermoelastic effects 4-98166  
 Sr(NO<sub>3</sub>)<sub>2</sub>, cohesive energy, elastic const. and Grüneisen coeff. calcs. 4-84230  
 ThCl(Br)(I), anharmonic props., interionic pot. model 4-98056  
 YAG, hypersonic wave attenuation 4-75620

## GTO calculations

- see also GO calculations  
 computational mol. physics, conf., Bad Wildsheim, Germany, Aug. 1982 4-58561  
 diatomic molecules, anisotropic electronic intracule densities calcs. 4-96422

## GTO calculations continued

- molecular integrals for Gaussian type functions 4-59631  
 Al, crystallographic transitions and equilib. props., Gaussian-orbitals calcs. 4-92353  
 CaOH, dissoc. energy calc., HF and GTO methods 4-64347  
 Fe small clusters, electronic struct., spin density functional theory anal. 4-113859  
 H<sub>2</sub>, X<sup>2</sup>Σ<sup>+</sup> ground state anisotropic electronic intracule densities calcs. 4-96422  
 LiOH, dissoc. energy calc., HF and GTO methods 4-64347  
 MnO, self-consistent Hartree energy band calcs. 4-92612  
 N<sub>2</sub>, X<sup>1</sup>Σ<sup>+</sup> ground state anisotropic electronic intracule densities calcs. 4-96422  
 Ne, FCC, high press. eqn. of state, Gaussian orbital techniques 4-92332

## GTO devices see thyristors

## Gudden-Pohl effect see electroluminescence

## guided electromagnetic wave propagation

- see also guided light propagation; waveguides  
 irregular waveguides and open resonators theory, EM fields, variational techniques 4-102852  
 medium with progressive sinusoidal fluctuation, EM wave propag. (Japanese) 4-74393  
 nonlinear surface wave generation in a planar waveguide structure 4-79231  
 waveguide, elastic, circular cylindrical, EM effects 4-102864  
 whistlers, propag. characs. in high-density magnetospheric ducts in near-equatorial region 4-110371  
 VO<sub>2</sub>, thermally controllable film in slot transmission line, microwave propag. near semiconductor-metal transition 4-70964

## guided light propagation

- see also optical waveguides  
 anisotropic planar waveguides with bent optical axes, wave propag. anal. 4-83691  
 bilayer systems, p-polarised guided wave phonon-polaritons and guided wave surface phonon-polaritons 4-92629  
 circular metallic dielectric-coated waveguides for IR transmission, design theory 4-74704  
 dielectric thin films with bounding media, guided nonlinear waves, dispersion relations 4-69483  
 EM wave field distrib. at open end of microstrip waveguide 4-107825  
 fibre, sharply bent, radiation interaction with absorbing medium 4-79328  
 fibre, single mode, anisotropic, degree and state of polarisation 4-60165  
 fibres, monomode, attenuation as a function of curvature 4-87478  
 fibres, single mode, graded-core, W-type, fundamental mode scalar variational anal. 4-87464  
 fibres, single-mode, guided propag. characts. (French) 4-87468  
 fibres, single-mode, highly twisted, Gaussian pulse splitting and nonsplitting condition 4-97078  
 gradient-index conical rod, transmittance function and modal propag. 4-69546  
 holographic correction of light polarisation at exit of fibre light guides (Russian) 4-87480  
 inhomogeneous anisotropic waveguides, quantitative propag. anal. 4-60154  
 intensity-dependent guided wave obs. 4-79220  
 microlenses, two-dimens., propagating-beam-method anal. 4-87447  
 moving medium with thermal nonlinearity, wave beam propag. 4-74632  
 multimode optical fibre analogue transmission, harmonic distortion, direct laser-diode modulation 4-83700  
 nonlinear dispersive dielectric fibre, exact radial field depend., bright pulse solns. 4-79321  
 nonlinear guided waves, dispersion relations 4-60151  
 planar layer mode propag. const. and cut off freq. computation using reson. technique 4-97068  
 regular multimode lightguides, amplitude-freq. characts. 4-60152  
 single-frequency cleaved-coupled cavity and DFB laser, direct modulation transient chirping study 4-83627  
 taper structures, three-dimens., propagating-beam-method anal. 4-87447  
 thin film guided-wave optical spectroscopy 4-63787  
 waveguides, elliptical and parabolic, propag., finite element approach 4-64770  
 waveguides, elliptical core, propag. characts., perturbation approach 4-87453  
 AlGa<sub>1-x</sub>As layer waveguides, light absorpt. 4-103011  
 LiNbO<sub>3</sub> waveguides, proton exchanged, theoretical anal. 4-64768  
 LiNbO<sub>3</sub> + Ti waveguide, acousto-optical conversion study 4-107827  
 MgO-SiO<sub>2</sub> thin films, refr. index, thickness and birefr. meas. using guided waves 4-76421  
 Si:H amorphous film optical waveguides, propag. characts. 4-107821  
 SiO<sub>2</sub> single-mode fibre dispersion and propag.-delay meas., using freq.- and amplitude modulated C<sup>+</sup> semicond. lasers 4-74725  
 ZnO channel waveguide formation on Si substrates 4-103012

## Guinier-Preston zones

- alloys, precipitation rel. to elec. resist. 4-114546  
 alloys, residual resist. changes due to clustering, t-matrix anal. 4-98591  
 steel, austenitic stainless, electron irradiation-induced struct. phase transformations 4-109418  
 Al alloys, positron annihilation determ. of Guinier-Preston zones (Russian) 4-114342  
 Al-Cu, θ phase form., departures from Matthiessen's rule, elec. resist. obs. 4-71660  
 Al-Cu (2 to 5 wt.%), precip. effects on thermopower 4-99384  
 Al-Cu (4 wt.%), plastically deformed, stability of GP zones 4-61992  
 Al-Cu alloy, EELS for GP zones and precipitates 4-61786  
 Al-Cu alloys, Guinier-Preston zones and solute clusters, high resolution lattice images 4-114543  
 Al-Mg, ageing, metastable phases in early stages of precip., DSC and resist. obs. 4-71656  
 Al-Zn (3.5, 5.3 wt.%), GP zones, size distrib. 4-76779  
 Sr(Zn) alloys, Guinier-Preston zones, appl. of EXAFS in metallurgy, review 4-66104  
 Al-Zn dilute alloys, α<sub>2</sub>'Zn rich precipitate shape, small angle neutron scatt. studies 4-114547  
 Al-Zn-Mg, 7075, heat-treated, acoustic emission during deform. 4-93343  
 Al-Zn-Mg alloys, struct. and mech. props., effect of low-temp. thermomech. treatment 4-66352  
 AlZn, residual resist. of Guinier-Preston zones, pseudopot. approach 4-70779  
 Cu-Be (1.0 wt.%), aged, tweed microstruct. 4-89070

**Guinier-Preston zones continued**

- Cu-Be alloy, struct. transform. mechanisms during ageing, internal friction and resist. obs. 4-114536  
 Cu-Be alloys, Guinier-Preston zones and solute clusters, high resolution lattice images 4-114543  
 Cu-Be alloys, precipitation, elec. resist. and thermopower 4-114549  
 Cu-Be-Co (2, 0.2 wt.%), precip. hardening investigation by microhardness and elec. resist. meas. 4-61947  
 Fe-Nb, nitrided, void form., mech. props., optical microscopy, SEM, TEM obs. 4-81361

**Yul'yaev-Bleustein waves** *see surface acoustic waves***Gunn devices**

*see also Gunn diodes*

No entries

**Gunn diodes**

No entries

**Gunn effect**

- see also limited space charge accumulation; negative resistance effects*  
 InP, freq. depend. of negative cond., Gunn effect (*Russian*) 4-70825  
 Pb<sub>1-x</sub>Sn<sub>x</sub>Te:In, Gunn effect, threshold field rel. to cond. band struct. 4-88513

**Gunn effect devices** *see Gunn devices***Gunn oscillators**

No entries

**Guns, plasma** *see plasma guns***Gyratation** *see rotation***Gyromagnetic effect**

- see also gyromagnetic ratio; magnetic resonance*  
 magnetoelasticity, gyromagnetic phenomena 4-76225

**Gyromagnetic ratio**

- see also g-factor; magnetic resonance*  
 actinide deformed nuclei, yrast states, cranking model 4-90940  
 alkaline earth metals, NMR props. 4-74180  
 electromagnetic operators, fixed-JT averages 4-90952  
 proteins, metal binding, <sup>25</sup>Mg and <sup>43</sup>Ca NMR study 4-77195  
 Co-Ag-Pd, transient fields, g-factor, gyromagnetic ratios 4-113914  
 Fe-Ag-Pd, transient fields, g-factor, gyromagnetic ratios 4-113914  
 KTaO<sub>3</sub>, spin-flip Raman scatt. in mag. fields, obs. of donor states 4-71384  
<sup>95</sup>Mo, gyromagnetic ratios of 3/2<sup>+</sup> vibrational states 4-82988  
<sup>101</sup>Ru, gyromagnetic ratios of 3/2<sup>+</sup> vibrational states 4-82988  
<sup>61</sup>Ti, A=201, 203, 205, effective gyromagnetic ratio calcs. 4-82994

**Gyroscopes**

*see also navigation*

- all-PANDA-fibre gyroscope with long-term stability 4-79298  
 cinematography appl., motion parameters of pan-head meas. using gyroscopic sensor (*Russian*) 4-90678  
 dynamically tuned gyroscope interaction on an elastic platform (*Ukrainian*) 4-86189  
 fibre gyros, bias modulation frequency second harmonic signal, response 4-106317  
 fibre gyroscope, drift stability improvement by ratio recording 4-106306  
 fibre gyroscopes with high-birefringent fibre and broadband sources, polarizer requirements 4-91612  
 fibre optic gyroscope, phase-reading, using optical phase and amplitude modulation 4-97088  
 fibre optic gyroscope, pseudo-heterodyne detection scheme, phase swept 4-69568  
 fibre optic gyroscope with linearised scale factor, gated phase-modulation approach 4-97087  
 fibre optic gyroscope with passive quadrature detection 4-69570  
 fibre optic sensor readout, output linearisation 4-91595  
 fibre-optic gyroscopes, gated phase-modulation feedback approach 4-79324  
 fibre-optic gyroscopes, review 4-74713  
 fibre-optic gyroscopes with imperfect polariser/depolariser phase error bounds study 4-63732  
 fibre-optic ring resonator for rotation sensing, passive 4-112580  
 Filtered Attitude Determination System for spacecraft measurement and control 4-73434  
 gimballess dynamite, dynamic principles (*Chinese*) 4-95415  
 Goryachev-Chaplygin gyrostat in quantum mech. 4-68006  
 instabilities of a gyroscope produced by rapidly rotating, highly viscous liquids 4-112894  
 integrated-optic gyro chip 4-91613  
 integrodifferential equations of motions soln. (*Russian*) 4-90356  
 Lagrangian gyroscopes, connected by spherical hinge, motion exact solns. (*Russian*) 4-90357  
 laser gyro performance, quantisation reduction using moving average filter 4-102970  
 laser gyroscope beat freq. correction (*Chinese*) 4-86399  
 Magnus problem in balanced gimbal-mounted gyros, Rodrigues-Hamilton parameters (*Ukrainian*) 4-86188  
 nonperturbable gyroscopic system mechanics 4-79442  
 optical gyroscopes 4-68276  
 oscillation of rotating axisymmetric elastic rods (*Russian*) 4-90362  
 precession on Earth surface, existence of mag. type gravit. 4-94587  
 ring gyroscopes: an application of adiabatic invariance, inertial rotation sensing 4-58632  
 ring laser gyroscope using (BiPrGdYb)<sub>3</sub>(FeAl)<sub>2</sub>O<sub>12</sub> garnet mag. mirrors (*Chinese*) 4-60123  
 rotor dynamical nonsymmetry influence on stationary motion (*Russian*) 4-90359  
 space groups, current activities of Ferranti UK 4-73433  
 spacecraft guidance and control techniques, conf., Florence, Italy (Sept. 1983) 4-73164
- Gyrotrons** *see microwave tubes*
- Gyrotropy (optical)** *see optical rotation*
- H-centres**
- alkali halide cryst., Frenkel defect accumulation, temp. and impurity conc. depend. 4-98093  
 alkali halides, excitonic and impurity-excitonic mechanisms for F,H pair creation (*Russian*) 4-80034  
 alkali halides, sputtering by electrons 4-61791  
 alkali metal halides, interstitial atomic H centres in mixed config., unrelaxed excited states, MCD optical absorpt. 4-70747  
 alkali metal halides, radiolysis process 4-70194  
 KBr, H centres, low temp. pair associates 4-70149  
 KBr:Cl, X-irradiated, luminesc. study (*Russian*) 4-80981

**H-centres continued**

- KBr:In, radiation storage of activator light sums, role of surface effect, photoluminescence (*Russian*) 4-114322  
 KCl:Ti, lattice defects creation and corrosion during annihilation of electronic excitations (*Russian*) 4-80035  
 NaCl, F-centre form., excitonic pot. surface, absorpt. spectra 4-71415

**H I regions**

- clouds in solar neighbourhood, kinematics 4-106051  
 in external galaxies, H I IR recomb. line emission obs. 4-86039  
 galactic centre, radioemission from large scale structures 4-106066  
 galaxies H I contents, search for optimal means of comparative H I anal. 4-90233  
 heating by supernova remnants 4-73049  
 high-velocity H I clouds, contrib. to absorption lines with small redshifts in spectra of quasars 4-94984  
 inflow towards galactic centre 4-86006  
 latitude struct. of galactic H I on small ang. scales, 21 cm survey 4-94924  
 in NGC 3448, interacting galaxy, kinematics of massive H I clouds 4-73065  
 Pleiades cluster, H I obs. rel. to cloud-cluster collision 4-101449  
 Scorpius X-1, model involving supernova in H I cloud and neutron star form. 4-101410  
 in Seyfert galaxies, single-dish survey 4-63268  
 shells and supershells, obs., effects of artificial boundaries in sky 4-63259  
 in spiral galaxies in clusters, H I radial gradients in Coma and (Abell 1367) 4-82553  
 warm H I medium, ionisation rates from radio recomb. line obs. towards radio source (3C 123) 4-101448

**H II regions**

- Compact H II regions, form. and expansion 4-63138  
 compact H II regions, He I 10830 Å line obs. 4-72998  
 distribution in outer Galaxy 4-86048  
 30 Doradus, IUE obs. of stars rel. to UV extinction and stellar continua 4-85996  
 30 Doradus Nebula, low density envelope, radio obs. 4-67781  
 DR 4, spectrophotographic obs. of former SNR candidate 4-86023  
 dusty H II regions, 1-millimetre continuum obs. 4-115834  
 element abundances, implications for chemical evolution of galaxies 4-101459  
 evolution, mathematical model 4-63245  
 in external galaxies, near-IR photometry and comparison with blue compact galaxies 4-94957  
 Fabry-Perot visible region spectrometer for H II region line profiles 4-110536  
 G333.6-0.2, line-of-sight IR extinction, spectral obs. 4-94917  
 G34.3+0.2, arc second resolution maps of compact radio sources 4-63238  
 G35.2-0.74, molecular cloud, assoc. H II regions characts. 4-110728  
 heavy elements radio recomb. lines obs. 4-90197  
 Herbig Ae-Be stars, IR spectroscopy rel. to circumstellar H II regions 4-77830  
 in galactic nuclei, spectral line intensities rel. to element abundances 4-67807  
 far-IR sources in southern galactic disc, large-scale space distrib. 4-115833  
 level population of H ions 4-101136  
 line surveys for southern galactic hemisphere 4-63297  
 M17, high resolution study at 1.3, 2, 6 and 21 cm wavelength 4-101451  
 M42, visual and photographic magnitude estimates for new variable star (NSV 2229) 4-72952  
 in M82, far IR forbidden O I and III emission 4-90241  
 M8, nebula and assoc. stars observed with S201 far-UV camera 4-106070  
 M8E, radio obs. of H II region assoc. with star form. 4-85994  
 magnetic fields in assoc. C II regions, upper limits 4-86003  
 N44, H II region in LMC, obs. of high-vel. component within small shell 4-115815  
 in NGC 1510, centre condensations struct. and nature 4-63278  
 NGC 1714, spectrophotometric observations 4-110719  
 NGC 2024, interstellar CO absorpt. lines in IR spectrum of IR source (IRS 2) 4-86000  
 in NGC 2403, spectrophotometry and extinction of Cepheids 4-63247  
 in NGC 4449, SNR in H II region 4-90195  
 in NGC 4650A, spindle galaxy, H II ring dynamics rel. to rot. of diffuse stellar component 4-90232  
 NGC 6334/6357 region, polarimetric and new photometric obs. 4-115792  
 NGC 7538 molecular cloud, dust absorpt. in ultracompact H II region 4-85998  
 nuclear H II regions in galaxies with emission lines 4-110721  
 OB associations, environment dynamical evolution 4-63230  
 OB/H II complexes in M101, photometry of images in rocket UV 4-90234  
 obscured compact H II regions, models and exciting stars model atm. 4-110709  
 one millimetre wavelength infrared sources 4-94989  
 Orion Nebula, H<sub>2</sub> infrared emission at 1.064 microns 4-94920  
 Orion Nebula, historical evidence for recent brightening 4-63249  
 Orion Nebula, large-scale internal motions 4-115800  
 Sagittarius B2, arc second resolution maps of compact radio sources 4-63238  
 Sagittarius spiral arm at *l*=305° near-IR study 4-63277  
 Sharpless 106, bipolar nebula and central star, radio, visible and IR obs. 4-94922  
 Sharpless 142, interferometric study 4-67631  
 shell structure in ultracompact H II regions, SHF VLA obs. 4-63237  
 shell-like H II regions, prod. by high-power stellar winds 4-94914  
 stellar wind bubbles, photoionised, in cloudy medium, evolution 4-86017  
 The Galaxy, radio lobe above galactic centre 4-106067  
 W28 region, sources photometry; mapping and star form. evidence 4-73004  
 W31, VLA obs. of ionisation ridge, containing embedded OB cluster in G102-0.3 H II region 4-94930  
 W3, CO J=6-5 691 GHz transition, heterodyne detection 4-90218  
 W3 IRS 4, aperture synthesis map of HCN emission 4-115804  
 W3/W4 region, BV magnitudes of 1150 OBA stars (*Russian*) 4-101330  
 W51, <sup>12</sup>CO J=1-0 obs., maps and cloud vels. 4-115806  
 W51, core submillimetre continuum emission mapping and complex characts., THF obs. 4-82542

**H II regions continued**

- W5, massive star formation along ionization front, IR and mm obs. 4-94908
- young southern compact IR sources, Brackett-alpha emission obs. 4-77904
- CO J=2-1 obs. 4-63260
- CO observations in southern galactic hemisphere H II regions 4-63263
- N/O versus O/H relationship and galactic chemical evolution 4-86063

**Hadfield steel see alloy steel****hadron classification schemes**

- No entries

**hadron current**

- see also *current algebra*
- mass inequalities among hadrons, extended form based on lattice QCD 4-95765
- vector current decay, effective Lagrangian technique 4-90757

**hadron decay**

- see also *baryon decay; meson decay*
- vector current decay, effective Lagrangian technique 4-90757

**hadron-deuteron interactions**

- see also *hadron-deuteron scattering; hyperon-deuteron interactions; meson-deuteron interactions; proton-deuteron interactions*
- total cross sections, smearing correction, 50 to 370 GeV 4-90924
- Nd $\rightarrow$ NX, high energy inclusive cross section polarisation depend 4-78574
- nd $\rightarrow$ nnp, breakup amplitude, Faddeev calc., comparison with pd amplitude 4-106613
- nd $\rightarrow$ nnp, three nucleon force calc. 4-64142

**hadron-deuteron scattering**

- see also *hadron-deuteron interactions; hyperon-deuteron scattering; meson-deuteron scattering; proton-deuteron scattering*
- nd, differential cross sections, tensor polarisations, pole extrapolation 4-96029
- Nd, weak scattering theory 4-64015
- nd scattering, six-quark bag effect on low-energy parameters (Russian) 4-82970

**hadron electroproduction**

- $e^+e^- \rightarrow T$ , props. of triplet wave (b5) states 4-90893
- perturbative QCD, factorisation, soft and collinear divergences,  $e^+e^-$  appl. 4-63966
- pion electroproduction, PCAC representation, chiral SU(2) $\times$ SU(2) symm. breaking 4-111462
- quark-quark scatt., duality, flavour SU(3) $\otimes$  colour SU(3) algebra, polarised electroprod. appl. 4-73722
- $e^+e^-$ , multiplicity distrib., KNO moment energy depend., Noviero-Predazzi method 4-68588
- $e^+e^-$  annihilation, 14-36.7 GeV, local compensation of baryon number,  $p$ - $p$  pair prod. 4-68578
- $e^+e^-$  annihilation, energy-energy correl. function, higher order QCD corrections 4-59092
- $e^+e^-$  annihilation, hadron production in single photon mechanism 4-86721
- $e^+e^-$  annihilation, quark flavour separation, appl. to electroweak asymmetries, quark lifetimes 4-95768
- $e^+e^-$  annihilation jets at PETRA, 9.4-31.6 GeV CM, transverse particle momenta meas. 4-59091
- $e^+e^-$  collisions, resonance production and decay estimates from radiative Z decays 4-90903
- $e^+e^- \rightarrow e^+e^-X$ , photon structure function, x depend. QCD scale parameter 4-95796
- $e^+e^- \rightarrow \gamma\gamma$ , cross section meas. in the vicinity of  $\phi(1020)$  4-59085
- $e^+e^- \rightarrow$ hadrons, at PETRA, one-photon annihilation and two-photon interactions, review 4-64012
- $e^+e^- \rightarrow$ hadrons, narrowness of hadronic multiplicity distrib., cell theory, KNO scaling 4-59088
- $e^+e^- \rightarrow$ hadrons, supersymmetry QCD theory 4-59087
- $e^+e^- \rightarrow$ hadrons in dynamical phase space; statistical jet evol. 4-73767
- $e^+e^- \rightarrow$ hadrons( $\gamma\gamma$ )( $\mu\mu$ )( $e^+e^-$ ), 39.79-45.52 GeV, new particle search, toponium,  $e^+$  4-90902
- $e^+e^-$  in Upsilon region,  $\Xi$  and  $\Lambda$  prod. from T decay, gluon and quark fragmentation 4-90900
- $e^+e^- \rightarrow$ jets, 29 GeV, proton prod. characts., momentum and  $p_T$  depends. 4-90901
- $e^+e^- \rightarrow \phi X$ , 29 GeV,  $\phi$  prod. rate from  $K^+K^-$  invariant mass spectrum 4-86718
- $e^+e^- \rightarrow q\bar{q}g$ , model depend. of coupling const. in 2nd order QCD 4-59089
- $e^+e^- \rightarrow q\bar{q}\gamma$ , coloured quark electric charge assignments, expt. implications 4-73765
- $e^+e^-$  results from CESR, B meson and  $\psi$  bottomonium props. 4-63991
- $e^+e^-$  results from PETRA, QED and electroweak tests, lepton searches, jets, Higgs 4-64010
- $e^+e^- \rightarrow$ single jet, QCD branching processes and hadronisation, differential-difference eqn. 4-111374
- $\rho(1600)$ , hadronic and leptonic decay, electroprod., photoprod. and  $\pi$  interaction prod. 4-90873
- $e^+e^- \rightarrow q\bar{q}X$ , sum over resonances, Thomas-Fermi model, local duality 4-90899

**hadron-hadron interactions**

- see also *baryon-baryon interactions; hadron-hadron scattering; meson-baryon interactions; meson-meson interactions*
- book, hadron interactions, current theories, expt. results 4-110822
- cascade model, semi-inclusive sphericity distrib., hadron-hadron collisions 4-102101
- chromomagnetic vacuum fields, influence on high energy hadron-hadron reactions 4-111484
- diffractive dissociation in multi TeV hadron-hadron and hadron-nucleus collisions 4-102145
- dilepton production phenomena in high energy hadronic collisions 4-68590
- Drell-Yan cross section high-moment corrections with alternate parton density 4-86743
- gluon fragmentation contribs. to small  $p_T$  hadron-hadron inclusive single particle distrib. 4-82944
- hadron elastic scatt. amplitude in Reggeon field theory, REGGEON program 4-102106
- hadron-nucleus collisions, inclusive spectra in additive quark model 4-90838
- hadron-nucleus high energy interactions, projectile independ. of charged particle multiplicity ratio 4-59116

**hadron-hadron interactions continued**

- hadronic compound-systems in cumulative production processes, clusters, colour confinement 4-102130
  - Higgs boson production, collisional, effect of decay 4-106503
  - hN $\rightarrow$ X, particle production mechanisms in cosmic ray interactions 4-95862
  - muon pair production, P-odd interaction 4-73770
  - open b-flavour states, hadronic couplings 4-68542
  - QCD jet simulation in  $10^{12}$ - $10^{17}$  eV hadron collisions, Monte Carlo approach 4-110458
  - soft hardware interactions, colliding component (Chinese) 4-102088
  - very high energy, semi-hard processes, fragmentation of highly virtual quarks 4-95813
  - hh at extreme energies, light-cone QCD with axial-vector anomaly current 4-59039
  - hh $\rightarrow$ jets, QCD Monte Carlo simulation, COJETS program 4-95763
  - hh $\rightarrow$ quarks, production cross-sections in cosmic rays 4-95845
  - hh $\rightarrow$ sleptons, production cross-section limits in cosmic rays 4-101079
  - hh $\rightarrow$ W $^{\pm}$ (Z $^0$ ) in Weinberg model with QCD bremsstrahlung, Monte Carlo program WIZJET 4-95825
  - hh $\rightarrow$ X, exclusive multistring fragmentation model 4-73734
  - hh $\rightarrow$ X, jet structure and transverse energy 4-86737
  - hh $\rightarrow$ X secondary inclusive spectra in additive quark model 4-95853
  - h $_1$ h $_2 \rightarrow X$ , direct  $\gamma$ -quanta prod., polarisation phenomena 4-73783
  - h $_1$ h $_2 \rightarrow X$ b $_2$  process, two-gluon exchange model 4-59113
  - hN, multiparticle production, multiplicities at cosmic ray energies 4-95854
  - hN, multiparticle production at cosmic ray energies, A-dependence 4-95855
  - hN, shower multiplicity studies at cosmic ray energies 4-95856
  - hN cross-section calcs. using Glauber multiple scatt. 4-95846
  - hN $\rightarrow$ hX, scaling in compound multiplicity 4-95844
  - hN $\rightarrow$ inclusive spectra, scaling violation in fragmentation 4-95852
  - hN $\rightarrow$ lX, in nuclei, soft and hard quark processes role in dilepton prod., A depend. 4-95820
  - hN total cross section, SU(3) pomeron octet component, dynamical origin 4-73735
  - hN $\rightarrow$ X, simple model 4-95863
  - hN $\rightarrow$ X inclusive inelastic spectra, effect of Fermi motion 4-95858
- hadron-hadron scattering**
- see also *baryon-baryon scattering; hadron-hadron interactions; meson-baryon scattering; meson-meson scattering*
  - elastic, high energy and low momentum transfer, review 4-111473
  - high-energy, unitarity, U-matrix approach 4-95815
  - small angle, high energy hadron scatt., spin effects, total cross section strength 4-78544
- hadron interactions see hadron-deuteron interactions; hadron-hadron interactions; lepton-hadron interactions; photon-hadron interactions**
- hadron leptonproduction**
- see also *baryon production; hadron electroproduction; meson production*
  - accelerator neutrino beams, particle production, trajectories in Earth's mag. field 4-101028
  - $e^+e^- \rightarrow e^+e^-$ +hadrons, photon structure function, comparison with QCD models 4-111455
  - $\mu N \rightarrow hX$ , hadroproduction by cosmic rays, cross-sections 4-110473
  - J muonproduction, spin-spin asymmetries, gluon helicity distribution function 4-95803
- hadron-nucleus reactions**
- see also *hadron-hadron interactions; hyperon-nucleus reactions; meson-nucleus reactions; nucleon-nucleus reactions*
  - conference on quark matter in rel. nucleus-nucleus collisions, Long Island, NY, USA (Sept. 1983) 4-67855
  - cosmic ray hadron-nucleus collision process, expt. data 4-102277
  - diffractive dissociation in multi TeV hadron-hadron and hadron-nucleus collisions 4-102145
  - fragmentation of nuclei by particles and nuclei of intermediate and high energies 4-95997
  - high energy data review, fragmentation, extrapolation to ultrarelativistic heavy ion collisions 4-68685
  - highly inelastic processes, GeV particle energy deposition mech. 4-68686
  - multiparticle clustering in hadron-nucleus collisions at cosmic ray energies 4-102279
  - multiplicity correlation coefficients, energy depend. in high energy hadron-nucleus collisions 4-102281
  - multiplicity-generating function, hadron-nucleus collisions, QCD and dual topological unitarization 4-111383
  - nucleon emission from high energy cosmic hadron-nucleus interaction 4-102278
  - pseudorapidity correlation in hadron-nucleus interaction at cosmic ray energies 4-102280
  - self induced nuclear transparency in mult TeV hadronic interactions 4-102319
- hadron-nucleus scattering**
- see also *hadron-hadron scattering; hyperon-nucleus scattering; meson-nucleus scattering; nucleon-nucleus scattering*
  - No entries
- hadron photoproduction**
- see also *baryon photoproduction; meson photoproduction*
  - charm particle lifetimes and production 4-68566
  - $e^+e^- \rightarrow$ hadrons, at PETRA, one-photon annihilation and two-photon interactions, review 4-64012
  - $\gamma\gamma$  collisions, QCD test through parton-parton scatt., jet prod. 4-111376
  - $\gamma p \rightarrow K_S^0(\Lambda)X$ , inclusive photoproduction of neutral strange particles at 20 GeV 4-73764
- hadron production**
- see also *baryon production; hadron leptonproduction; hadron photoproduction; meson production*
  - beautiful particles, production in neutrino interactions 4-90856
  - charmed particles, production in neutrino interactions 4-90856
  - cosmic ray nucleon-nucleus collisions, multihadron production, collective mechanism 4-102313
  - cosmic ray nucleon-nucleus collisions, multihadron production, collective mechanism 4-102313
  - heavy flavour production at CERN ISR energies 4-86746
  - heavy hadron production, diffraction dissociation 4-90842
  - heavy quark productions in super high cosmic ray interaction 4-102146
  - multiparticle production in quark-gluon model, statistical mechanical interpretation 4-78537
  - NN $\rightarrow$ hX, total hadron cross-section calcs. 4-68599

hadron production continued  
phenomenological model for hadron production from low mass clusters  
4-90818  
QCD, large  $P_T$  hadron prod., effective interaction scale, qq partonic sub-  
processes 4-95762  
weak charged current interaction, hadronic final states 4-90857  
 $\gamma\gamma$ , hard processes obs. in collision of two quasi-real photons 4-63996  
 $\pi N \rightarrow hX$ , scaling in compound multiplicity 4-95844  
 $\nu N \rightarrow X$ , hadron up-down asymmetry 4-111439  
 $\pi\pi$ -charm, inclusive production results 4-95788  
 $pN$ , 70 GeV, large  $P_T$  hadron pair prod., A-depend. 4-59107  
 $\pi N \rightarrow hX$ , anal. of secondary tracks in  $\phi$ - $\theta$  space 4-95841  
 $\pi N \rightarrow hX$ , elasticity, cascade effects 4-95840  
pp, multiplicity distrib., KNO moment energy depend., Novero-Predazzi  
method 4-68588  
 $\bar{p}p$  collisions, toponium production cross sections, two-gluon fusion  
4-90926  
pp-hX, inclusive cross-section calcs., Feynmann scaling 4-95838  
pp-hX, invariant differential, cross sections, new scaling variable  
4-95837  
pp-hX, KNO scaling violation 4-86733  
pp-hX, scaling violation in statistical model 4-95836  
pp soft interactions, multiparticle hadronic systems production,  $e^+e^-$  com-  
parison 4-86747  
Al( $p,X$ ),  $X=\pi^+K^+$ , p.p. high  $P_T$  hadron prod. at 70 GeV 4-111545  
C( $p,X$ ),  $X=\pi^+K^+$ , p.p. high  $P_T$  hadron prod. at 70 GeV 4-111545  
Cu( $p,X$ ),  $X=\pi^+K^+$ , p.p. high  $P_T$  hadron prod. at 70 GeV 4-111545  
Pb( $p,X$ ),  $X=\pi^+K^+$ , p.p. high  $P_T$  hadron prod. at 70 GeV 4-111545  
Su( $p,X$ ),  $X=\pi^+K^+$ , p.p. high  $P_T$  hadron prod. at 70 GeV 4-111545  
hadron scattering see hadron-deuteron scattering; hadron-hadron scattering;  
photon-hadron scattering  
hadronic atoms  
see also mesic atoms  
 $^6\text{Li}$ ,  $A=6.7$ , antiprotonic atoms, strong interaction effects on X-ray transi-  
tions 4-59921  
hadrons  
see also baryon resonances; baryons; hadron classification schemes;  
hadron current; hadron decay; meson resonances; mesons  
EAS high energy hadrons, energy spectrum, possible heavy particle  
4-82360  
hadronic wave functions in QCD 4-63974  
QCD, hadronic wavefunctions, large momentum transfer interactions, deep  
inelastic lepton scatt. 4-63975  
QCD, sum rules and exclusive form factors, review 4-82941  
quark model, numerical structure 4-111401  
quark rel. center-of-mass motion in bags, mass and mag. moment correc-  
tions 4-102091  
quark-antiquark charge distributions and confinement, hadronic structure,  
2 dims. QCD 4-102094  
quark-gluon plasma, characteristics of hadronic phase transition 4-68505  
SL(N,C) gauge interactions, linear descript., cosmological implications,  
hadrons made from vector bosons 4-111284  
SUSY QCD, coloured scalar quarks and hadrons, cosmological implica-  
tions 4-111371  
 $\gamma$  hadron from  $\gamma/\ell$  events 4-111391  
haemodynamics  
see also blood  
ambulatory long-term blood press., recording and computerised anal.  
(Finnish) 4-89798  
aorta blood flow, viscous fluid steady flow in curved tube 4-89617  
aortic bifurcation casts of humans, steady and pulsatile flow comparison  
4-100221  
aortic pulse wave velocity analysis 4-66979  
aortic valve bioprotheses in a model human aorta, pulsatile flow obs.  
4-115108  
aortic valve prostheses, comparative study of backflow 4-100355  
aortic valve prostheses, in vitro wall shear meas. 4-72462  
arterial pressure wave propagation, theory and model 4-72296  
arterial system, clinical parameters indirect determ. method using velo-  
cimetric data (French) 4-67154  
arterial wall distensibility rel. to flow distrib. 4-115112  
arterial wall mass transport to viscous fluid flow 4-89609  
arteries, elastic props. and their influence on the cardiovascular system  
4-109870  
arterioles, blood flow study 4-100216  
artery, constant radioactivity requirement in the  $C^{15}O_2$  steady-state  
blood-flow model 4-72386  
blood pressure behaviour after treadmill test, hybrid simulation 4-100224  
bloodstream, local velocity meas., laser method based on two or three light  
guides (Russian) 4-72323  
brain blood flow meas. by intravenous  $H_2^{15}O$ , emission CT, theory and  
error anal. 4-72373  
brain blood flow meas. by intravenous  $H_2^{15}O$ , emission CT, implementa-  
tion and validation 4-72374  
cardiac output, single thermistor system for continuous meas. 4-81809  
cardiac output, thermal dilution technique for continuous meas. 4-81794  
cardiac outputs and indices, radioculicide determ. 4-67081  
cardiac volumes and outputs, quantitative evaluation by  $^{99m}\text{Tc}$  labelled  
erythrocytes 4-77379  
cardiopulmonary resuscitation, blood flow, thoracic and abdominal press.  
waves effect 4-115100  
cardiopulmonary resuscitation mechanisms: a computer model 4-89641  
cardiovascular response to lower body negative press. and phys. fitness  
4-89628  
cardiovascular system exercise adaptation in pilots breathing  $O_2$ -poor gas  
mixture, haemodynamic parameters 4-66972  
cardiovascular system exercise adaptation in pilots breathing  $O_2$ -poor gas  
mixture, polycardiographic parameters 4-66973  
central haemodynamics, age-associated features, radiocardiographic obs.  
(Russian) 4-93770  
cerebral blood flow, regional, accuracy of stable Xe/CT meas. 4-67073  
cerebral blood flow, regional, dynamic emission tomography 4-115214  
cerebral blood flow rel. to EEG characs. 4-89557  
cerebral blood flow-metabolism relationship, positron emission tomography  
studies, review 4-115213  
cerebrovascular disease patients, haemodynamic effects of arterial by-pass,  
angiostimulatory study 4-115088  
circulation parameters rel. to electronic oscillography (German) 4-67133  
cochlea, rodent, computerised reconstruction of regional blood flow  
4-115293

haemodynamics continued  
cochlear blood flow meas. technique combining microspheres with surface  
prep. dissection 4-93981  
coronary arteries imaging using FASTBUS based data acquisition system  
4-62570  
coronary artery casting of man, flow resistance, effect of mild atheroscle-  
rosis 4-100218  
coronary circulation, flow dynamics (Japanese) 4-62517  
coronary grafts, blood flow visualisation by US method 4-100264  
coronary venous system, dog, dynamics 4-62513  
cutaneous vascular tone during heat load modified by exercise intensity  
4-81633  
dehydration, effect on circulation and temp. regulation during exercise  
4-81631  
digital radiography of flow patterns in phantoms and canine arteries  
4-89711  
disk-type prosthetic heart valve, turbulent flow through 4-77293  
echo-Doppler angle determination for noninvasive transmittal blood velo-  
city calculations in normal and porcine bioprothetic mitral valves  
4-100192  
end-tidal Xe conc. meas. by mass spectrometry and thermoconductivity,  
CT blood flow meas. appl. 4-67142  
exercising muscles, blood flow meas. by Xe clearance and microsphere  
trapping 4-89620  
feet of diabetic patients, blood flow, meas. with MWPC positron camera  
and  $C^{15}O_2$  4-100316  
femoral artery branch casting, human, press. difference-flow rate variation  
4-77292  
FFT signal processing IC, use for Doppler blood flow studies 4-93826  
flow, max. vel., noninvasive CW Doppler haemodynamic data, intracar-  
diac jets 4-85467  
flow and vel. meas. in vivo by EM induction 4-77357  
flow determination, validation of a CT method 4-81775  
flow disturbance effect on ultrasonic scatt. 4-72287  
flow meas., ultrasonic Doppler effect appl. 4-105265  
flow meas. using digital angiography and parametric imaging 4-67098  
flow measurement by NMR and transcutaneous EM flowmeters 4-77362  
flow measurement using multichannel pulsed Doppler US, repeatability  
4-72319  
flow waveforms reproduction in vitro, digitally controlled system 4-77433  
foetal blood flow meas. by Doppler US, methodology and basic problems  
4-89662  
foetal descending aorta, blood flow rel. to breathing movements and  
cardiac arrhythmia 4-89638  
foeto-placental circulation, assessment with CW Doppler 4-89663  
forearm blood flow control during exercise in the heat, effect of mild  
essential hypertension 4-100196  
gamma-variate relationship, derivation for tracer dilution curves 4-72288  
hand blood flow in hypertensive and normal subjects 4-89644  
heart, total artificial, development, pulsatile vs. nonpulsatile flow, control  
algorithm 4-93972  
heart rate-pressure prod. computer, microprocessor based 4-81808  
high-blood-pressure-associated disease, development risk, cost-effective pot.  
classifiers 4-85457  
impedance of curved artery models 4-77295  
intraaortic balloon pumping as cardiac assistance: simple, closed loop  
model 4-89827  
laser blood Doppler velocimeter, temporal resolution estimation with opti-  
cal fiber 4-66989  
laser Doppler tissue flowmeters, signal processor 4-85484  
laser-Doppler blood flow monitor, diode laser source and detection in  
probe 4-115154  
left ventricular ejection, dynamical relations: flow rate, momentum, force  
and impulse 4-100219  
left-ventricular ejection fractions from gate equilb. blood pool scintigrams,  
automated computation 4-72384  
leukocyte uptake and release by dog lung, effect of pulmonary blood flow  
4-100198  
liver, scintigraphic estimation of arterial and portal blood supplies, online  
computer system 4-72385  
lung, extravascular thermal volume, effect of oedema and haemodynamic  
changes 4-100087  
LV ejection and relaxation, coupling, dog expts. 4-85455  
magnetic resonance signal intensity patterns obtained from continuous and  
pulsatile flow models 4-81722  
myocardial blood flow and metabolism, digital film autoradiography and  
electronic multitracer techniques 4-77377  
myocardial capillaries, anisotropic, length and surface density estimation  
method 4-115302  
myocardial perfusion changes imaging, double-dose technique, evaluation  
in dogs 4-100312  
myocardium microcirculation, indirect determ. of fluid filtration and reab-  
sorption 4-93771  
NMR flow imaging method 4-100298  
nonlinear pulse wave reflection at an arterial stenosis 4-105282  
ocular plethysmograph evaluation, simple time-series approach 4-81798  
paraplegic men, attenuated skin blood flow response to hyperthermia  
4-100202  
perfusometer: an instrument for assessing the condition of critically ill  
patients 4-81799  
photoplethysmograph, pulsed multifreq., skin blood press. appl. 4-77366  
physiological flow, wave phenomena 4-60541  
pneumatic artificial ventricle, haemodynamic models 4-93971  
pole-zero extraction by nonlinear regression of discrete-time arterial  
blood-flow waveforms 4-77277  
pressure, comparison of 2 noninvasive monitors 4-85565  
pressure, indirect meas. by pulse wave vel. method (Japanese) 4-100336  
pressure evaluation using screening programs 4-89795  
pressure measurement, circulation parameters made visible by electronic  
oscillography (German) 4-77272  
prosthetic aortic valve, orientation rel. to arterial flow distrib. 4-109869  
prosthetic heart valves, haemodynamic modelling 4-100356  
prosthetic heart valves, in vitro press. drop results comparison 4-81814  
prosthetic heart valves, pulsatile press. drop and regurgitative characs.,  
online method for evaluation 4-81813  
pulmonary arterial tree numerical simulator 4-81738  
pulmonary circulation fluid mechanics 4-62509  
pulsatile blood flow, time depend., contaminant dispersion 4-79548  
regional blood flow, first-pass positron emission tomography with external  
detectors, modelling 4-72388

**haemodynamics continued**

- RF hyperthermia of deep-seated tumours, dipole array applicator performance study using blood flow simulator (*Japanese*) 4-85406  
 right atrium contractility, nonlinear model for estimation 4-89642  
 shunt haemodynamics and extracorporeal dialysis, elec. resistance network anal. 4-66986  
 shunt-dilution curves, interpretation as bimodal distrib. functions 4-85452  
 soft tissue tumour of rabbit, regional blood flow meas. with positron imaging 4-72289  
 spinal cord thermal stimulation in rabbit, ear-skin and renal blood flow changes 4-81725  
 splenic blood flow and platelet transit time, meas. methods using  $^{111}\text{In}$ -labelled platelets 4-81773  
 stenosed curved artery, flow, math. model 4-77275  
 stenoses and bifurcations, flow through, effect of unsteadiness 4-81726  
 thermal sensation, skin blood flow and freq. anal. of cutaneous vasomotor rhythms 4-105188  
 thermoregulation, cranial vasodilator control of lingual arteriovenous anastomoses 4-81630  
 thrombi, haemodynamic forces, from incipient attachment of single cells to maturity and embolisation 4-72293  
 tomoflow system for intracardiac blood flow information display, Doppler US appl. 4-85469  
 trileaflet heart valve prosthesis, Abiomed, in vitro fluid dynamic characts. 4-105378  
 umbilical vein blood flow in human fetuses 4-89640  
 umbilical venous flow in normal and complicated pregnancy 4-89639  
 US blood flow meas., freq. estimator for sampled Doppler signals 4-62538  
 US Doppler techniques and their diagnostic appl., conf., London, England (June 1983) 4-67849  
 US Doppler velocity meter for quantitative flow meas. and turbulence anal. 4-85464  
 US imaging techniques for diagnostics, blood flow and unborn babies appl. 4-77418  
 valvular calcification and press. drops across malfunctioning heart valves, quantitative determ. 4-81801  
 vascular cells, living, effects of fluid flow 4-100102  
 vascular tree function optimisation by wall shear stress adaptive regulation 4-66980  
 venous occlusive RN plethysmography: comparison with electrical admittance plethysmography 4-62581  
 ventricular performance in congenital left-to-right shunt: temporal Fourier analysis of gated blood-pool data 4-72376  
 ventrolateral medullary surface blood flow,  $\text{H}_2$  clearance determ., cat. obs. 4-89629  
 viscoelastic arteries, wave front propag. 4-109864  
 warm-up behaviour of human extremities after cold-water immersion, model for analysis (*German*) 4-62445  
 wave propagation in a thin-walled liquid-filled initially stressed tube 4-77274  
 $^{239}\text{Pu}$  submicron dioxide inhalation, haemodynamics and heart mass parameters in dogs (*Russian*) 4-67014

**haemoglobin see proteins****haemorrhology see biorheology; blood****hafnium**

- see also nuclei with*.....  
 evaporated film, oxidation, photoemission study 4-85073  
 lattice vibrs., seven parameter model anal. 4-70306  
 muonic atom,  $A=176-180$ , X-ray meas. and anal. 4-95957  
 phonon density of states determ. from sp. ht. (*Russian*) 4-92314  
 powder metallurgy production of refractory metals and alloys 4-66264  
 Zircaloy, HF impurity monitoring by sequential plasma emission spectrometry 4-73984  
 Hf/rare earth elements fractionation in sediments, evidence for crustal recycling into mantle 4-110100  
 $^{176}\text{Hf}$ , pionic M X-rays, energies and widths of transitions 4-112305  
 $^{176}\text{Hf}/^{177}\text{Hf}$  ion Earth crust, no constraints on mean life of continents 4-94047  
 Si-Hf Schottky barriers, interface effects 4-70906

**hafnium alloys**

- see also hafnium compounds*  
 ultralloys for nuclear thermionic conversion 4-77127  
 Be-HfO,  $\text{Hf}^+$  implanted, O gettering 4-92218  
 $\text{Ce}_2\text{HfCo}_5$ , anomalous mag. behaviour 4-88664  
 Fe-Hf based amorphous alloys, crystallisation and hyperfine fields 4-71030  
 Hf-Mo, amorphous, upper critical fields 4-98829  
 Hf-Ni films, amorphisation by thin film solid state reaction 4-80428  
 HfRe<sub>2</sub>, refractory, thermal expansion meas. 4-75710  
 HfW<sub>3</sub>, refractory, thermal expansion meas. 4-75710  
 Mo-Hf-C, electron beam welded joint, tensile strength, ductility, comp. depend. 4-109470  
 Ni-Al-Hf superalloys, thermally activated deform., mech. 4-93327  
 Ni-Al-Hf system,  $\beta + (\text{Ni}, \text{Al})_2\text{Hf}_2$  eutectic struct., cryst. morphology, struct., stacking faults, TEM, X-ray diffr. obs. 4-81182  
 Ni-Co-Cr-Nb-Hf, Ni-base superalloy, MERL 76, powder metallurgy hot isostatic pressing, effect of Ar contamination 4-114447  
 Ni-Cr-Co-Al-Ti-Nb-W-Mo-V-Hf, cryst. lattice periods mismatch determ. 4-65219  
 Ti-Hf (5 wt.%), oxidation from 550 to 800°C, influence of Hf (*French*) 4-71789  
 W-HfC, produced by powder metallurgy, mech. props. 4-71694  
 Zr-Hf (2.2 wt.%), high temp. oxidation rate calc. 4-109536

**hafnium compounds**

- see also hafnium alloys*  
 hydrides, mag. susceptibility, temp. depend. 4-65784  
 silicides and germanides with FeB and ZrSi<sub>2</sub> structures, texture in diffusion-grown layers 4-61147  
 $\text{EuHo}_2\text{S}_4$ , band gap width, rel. to short-range environment of S atom 4-80493  
 Hf-Al-N ternary system, phase equilb. invest. rel. to fusion reactor materials 4-76759  
 HfC, cathode material for high brightness electron beams 4-71508  
 HfC, X-ray Debye temps. and mean square atomic displacements 4-88260  
 $\text{HfF}_2\text{-BaF}_2\text{-LaF}_3\text{-AlF}_3$  glass, IR transparent, stability in humid air, AES study 4-109534  
 HfN, ultrafine particles, growth by reactive gas evaporation technique with electron beam heating 4-61894

**hafnium compounds continued**

- $\text{HfO}_2$ , optical coatings, laser induced damage, spot size scaling 4-79209  
 $\text{HfO}_2$ , optical films and antirefl. coatings deposited from solns. mech. strength 4-74670  
 $\text{HfO}_2\text{-In}_2\text{O}_3$  fluoride solid soln., elect. cond. study 4-80297  
 $\text{HfO}_2\text{-Y}_2\text{O}_3$ , partially stabilised, transformation-toughened, fracture toughness, crack-size depend. 4-93373  
 $\text{HfO}_2\text{-Yb}_2\text{O}_3$  system, phase equilibria and ordering, X-ray diffr. and thermal expansion obs. 4-66317  
 $\text{HfS}_2$ , electronic struct. by high resolved angular photoemission 4-84557  
 $\text{HfS}_3$ , IR, Raman, and reson. Raman spectra, valence force field 4-93077  
 HfTe<sub>2</sub>, lattice dynamics calc., Raman data 4-75623  
 $\text{Na}_2\text{Hf}_2\text{Si}_2\text{P}_2\text{O}_{13}\text{-O}_3$ ,  $\text{Na}^+$  ion cond. and crystallographic cell characterisation 4-113706  
 $\text{H-Ta}_2\text{O}_5\text{-TiO}_2\text{(HfO}_2\text{)(Cr}_2\text{O}_3\text{)}$ , ionic conductivity 4-75722  
 $\text{ZrO}_2\text{-Y}_2\text{O}_3\text{-HfO}_2$  ceramic powders, laser sintering 4-88998

**half adsorption see adlers****half-lives (radioactive) see radioactive decay periods****half wave rectification see rectification****halides**

- see also compounds of individual elements, e.g. "tungsten compounds" and "organic compounds"*  
*see also alkali metal halides; halogens*  
 anion-organic acid (alcohol) complexes, binding energies, struct. effects, equilb. meas. 4-85293  
 group IV halides, liq. phase, vibr. hyper-Raman spectra intensities, bond hyperpolarisability theory 4-69148  
 ion adsorption on Ag halide surface, interaction pot. 4-75785  
 radiation effects in insulators, conf., Albuquerque, NM, USA (May-June 1983) 4-73143  
 transition metal halides, ionic compounds photo-induced covalency 4-88931  
 Cu halides, ionic compounds photo-induced covalency 4-88931  
 Rn monohalides, laser amplification 4-83567

**Hall constant see Hall effect****Hall effect**

- $\sigma$ -model with  $\theta$ -term, localisation in quantised Hall Effect,  $\theta$ -vacuum 4-68368  
 adiabatic charge transport, substrate disorder, many-body interaction quantised Hall effect 4-111078  
 Alfvén wave propag. in incompressible elec. conducting fluid 4-103423  
 anomalous quantum Hall effect, particle-hole symm. 4-75881  
 anomalous quantum Hall effect and 2D classical plasma 4-104241  
 anomalous quantum Hall effect and generalised plasmas 4-88460  
 canonical quantum systems, appl. to quantised Hall effect, coherent-state Langevin eqns. 4-63655  
 carrier transport in semiconductor magnetic field sensors 4-70844  
 chalcogenide glasses, Hall effect studies, temperature dependence of carrier mobility 4-92756  
 conduction electron concentration in nonideal plasma, Hall EMF meas. 4-83979  
 dynamic quantum Hall effect in 2-d electron impurity system 4-113975  
 electron gas, 2-dimens., quantised Hall conductance in a two dimensional periodic potential 4-70770  
 extended-state band levitation in strong mag. field 4-88486  
 finite conducting magnetised Hall medium, gravitational instability, finite Larmor radius 4-113141  
 first-order longitudinal Hall effect 4-108884  
 fractional quantised, ground state energy 4-80663  
 fractional quantised Hall effect, ground states 4-98648  
 fractional quantised Hall states hierarchy, quasiparticle stats., electron gas 4-70837  
 fractional quantized Hall effect, alternating diamagnetism and paramagnetism, magnetoresistance and Hall resistance studies 4-113977  
 fractional quantum, and liq.-solid transition 4-104240  
 fractional quantum Hall effect, role of reversed spins in correlated ground state 4-92758  
 fractional quantum Hall effect and gauge invariance 4-108883  
 fractional quantum Hall effect and mag. symm. 4-108881  
 graphite-SbCl<sub>2</sub>-C<sub>12</sub>SbCl<sub>3</sub> intercalation cpd., resistivity and Hall effect (*Russian*) 4-113917  
 implanted samples, applicability of van der Pauw-Hall meas. technique 4-88521  
 inhomogeneous medium, effective cond. in strong mag. fields 4-80559  
 InP:Zn epitaxial layers, MOCVD grown, doping, Hall effect, SIMS, electrochemical profiling 4-80077  
 inversion layer width, electron-electron interactions, fractional quantum Hall effect 4-75880  
 isomorphism of transport phenomena and percolation theory 4-104178  
 liquid metals, Hall effect theory, mass renormalisation correction 4-113921  
 many-body electron system, Hall cond. gauge invariant form 4-75911  
 measurement of Hall voltages changes at high temp., using AC meas. system 4-58866  
 measurement of specimens of any shape, automatic system 4-101873  
 measuring device for Hall effect (*Chinese*) 4-58870  
 melts, electrical cond. and Hall coeff. meas. using van der Pauw's method 4-98606  
 metal film, columnar and polycryst., resist., TCR and Hall coeff. 4-70952  
 metal film, polycryst./monocryst. struct. assumption checking using Hall coeff. variations size effect 4-70953  
 metallic bicrystal, galvanomagnetic props. 4-84675  
 metallic melts, electrical cond. and Hall coeff. meas. using van der Pauw's method 4-98606  
 metals, amorphous, electron transport, review 4-75918  
 metals, amorphous non-transition, superconductivity and phonon spectra (*Chinese*) 4-98793  
 metals, magnetotransport, exactly soluble model 4-75928  
 metals and alloys, superconducting transition temp. correlation with electronic struct. 4-88627  
 MHD generator interelectrode breakdown obs. 4-66728  
 MHD generator performance, effects of cathode slag polarisation, experimental 4-72131  
 modulation-doped heterostructures, two-dimensional phenomena 4-98721  
 PbTe:Bi, Hall study of self-compensation of donor effect 4-104242  
 polymer films, elec. cond. changes induced by pyrolysis and high energy ion irradi. 4-75966  
 porous layers, electrophysical and optical props. 4-65680

all effect continued  
 quantised, ground state of 2D electrons in strong mag. field 4-98647  
 quantised Hall conductance plateau widths 4-75912  
 quantised Hall effect, critical fluctuations in disordered electronic system, field theory 4-104235  
 quantised Hall effect, field theoretic approach, extended states 4-104234  
 quantised Hall effect, phase transition in nonlinear  $\sigma$ -model in instanton and duality anal. 4-104236  
 quantised Hall effect theory 4-98646  
 quantised Hall resistance, at finite temps., anal. in Si MOSFET and GaAs-AlGaAs heterostruct. 4-98727  
 quantum electrodynamic Hall effect in one time and two space dims. 4-61362  
 quantum Hall effect, anomalous ground state degeneracy and fractionally charged excitations 4-108882  
 quantum Hall effect, sum rule 4-98649  
 quantum Hall effect formalism, Hilbert space of analytic functions 4-80613  
 quantum Hall effect in two-dimensional electron systems 4-61398  
 quantum Hall regime, critical currents 4-98644  
 quantum Hall regime critical non-dissipative current 4-98762  
 rationally quantised Hall effect, chiral anomaly equivalence to QED 4-70838  
 semiconductor, elec. props., appl. of two stage nonmagnetic high press. equipment (*Chinese*) 4-90607  
 semiconductor, multivalley, anomalous Hall effect and multivalued Sasaki effect 4-80615  
 semiconductor heterostruct., fractional statistics and the quantum Hall effect 4-104237  
 semiconductor polycrystalline thin films, with pot. barriers, Hall mobility 4-104331  
 semiconductor purity, Hall effect measurements 4-75986  
 semiconductor superlattices, quantum wells, and heterostructs., elec. and optical props. 4-80666  
 semiconductors, electrolytic Schottky-gated Hall effect profiling 4-75497  
 semiconductors, Hall effect in strong mag. field, percolation theory 4-88522  
 n-Si, radiation defect formation, annealing, defect interactions 4-113499  
 SIMOX films, Hall mobility and electrical conductivity, temp. dependence 4-80700  
 topological charge density renormalisation 4-110915  
 transition metal alloys, amorphous, Hall coeff., temp. depend. 4-92698  
 transition metal carbide and carbonitride solid solns., mag., elec. transport, supercond. props., review 4-80590  
 two dims. systems, Hall cond. quantisation 4-75909  
 two-dimensional disordered system, electron states and quantum Hall effect 4-104284  
 two-dimensional lattice, transverse Hall cond. in Landau subbands 4-104233  
 two-dimensional metals, inhomogeneous, Hall coeff. and magnetoresist. 4-104382  
 two-dimensional random electron system under strong mag. fields, dynamical diffusion coeff., self-consistent treatment 4-98640  
 two-dimensional strip, quantized Hall cond. and edge states 4-92591  
 two-dimensional system, fractional quantum Hall effect 4-92757  
 two-dimensional systems, electronic props., conf., Oxford, England (Sept. 1983) 4-95050  
 two-dimensional systems, quantum Hall effect and density of states 4-98650  
 Ag<sub>2</sub>Pd<sub>1-x</sub>, Hall coeff. and band struct. calcs. 4-70780  
 Ag<sub>2</sub>Te, electronic-ionic cond. calcs. 4-98675  
 Al single crystals, Hall coeff., size effect 4-104183  
 AlGaAs:Si MBE layers, donor levels anal. 4-61316  
 AlGaAs/GaAs heterostruct., 2D magnetotransport, electron heating effects 4-98736  
 AlGa<sub>1-x</sub>As<sub>x</sub>:Si donor behaviour, effect of Al comp. 4-98709  
 AlGa<sub>1-x</sub>As<sub>x</sub>:Si MOCVD layers, transport props. 4-92834  
 AlGa<sub>1-x</sub>As<sub>x</sub>-GaAs heterostructures, 1/3 and 2/3 fractional quantum Hall effect, activation energies 4-92811  
 AlN/Al cermets; reactive DC planar magnetron sputtering prep., elec. transport props. 4-88607  
 As, galvanomagnetic props. and current carriers energy spectrum (*Russian*) 4-98638  
 Au semiconducting thin films, 2D percolation system, conduction and Hall coeffs. 4-70957  
 Bi<sub>1-x</sub>C<sub>x</sub>, cond. mechanism, elec. cond., Seebeck coeff., and Hall coeff. meas. 4-70811  
 n-Bi<sub>1-x</sub>Sb<sub>x</sub>, electron scatt., low temp. 4-108835  
 n-Bi<sub>2</sub>Te<sub>3</sub>, free carrier mobility, Hall and Seebeck coeffs., temp. depend. 4-61369  
 C film, elec. cond. changes induced by pyrolysis and high energy ion irradi. 4-75966  
 CdGe<sub>1-x</sub>Si<sub>x</sub>As<sub>2</sub> glasses, elec. props. and phase stability 4-104202  
 CdHg<sub>1-x</sub>Te, epitaxial film growth by chem. transport reactions, elec. props. 4-70965  
 CdHg<sub>1-x</sub>Te, galvanomagnetic effects in quantising mag. field (*Russian*) 4-70843  
 CdHg<sub>1-x</sub>Te under uniaxial deform., photoelectric props. 4-70864  
 CdS film, deposited by hot wall technique, characterisation of doped and undoped films 4-114405  
 CdS-In film, elec. props. meas. 4-104329  
 CdS<sub>1-x</sub>Se<sub>x</sub> single crystal, elec. cond. and Hall effect studies 4-113974  
 CdSiAs<sub>2</sub> single crystal growth by chem. vapor transport, struct. and elec. props. 4-114367  
 CdTe:Cl, native acceptor defects, Hall effect study 4-75899  
 Cd<sub>1-x</sub>Zn<sub>x</sub>Te alloys, growth, elec. props., photoluminesc. 4-66207  
 Co<sub>90</sub>P<sub>10</sub>, galvanomagnetic characteristics, temp. depend. 4-84635  
 Ct<sub>1-x</sub>Mn<sub>x</sub>Ge, amorphous thin films, elec. resist., Hall resist. 4-114049  
 Cu<sub>2</sub>Fe<sub>1-x</sub>Cr<sub>x</sub>S<sub>4</sub> films, elec. and galvanomagnetic props. 4-76056  
 CuGaTe<sub>2</sub>, vapour growth, thermodynamics and elec. characts. 4-71536  
 CuInS<sub>2</sub>, defect chemistry, elec. and Mossbauer studies 4-70730  
 CuInSe<sub>2</sub>, sintered, grain size, SEM obs., resist., Hall obs. 4-66284  
 CuInTe<sub>2</sub> MIS struct., field effect studies 4-80679  
 CuInTe<sub>2</sub>, vapour growth, thermodynamics and elec. characts. 4-71536  
 Cu<sub>2</sub>SnS<sub>4</sub>, thermal props., elec. cond. and Hall effect 4-88523  
 Fe-Zr amorphous films, elec. and mag. props. 4-75923  
 (Fe<sub>1-x</sub>Mn<sub>x</sub>)<sub>2</sub>P<sub>15</sub>C<sub>10</sub> amorphous alloy, transport and mag. props. 4-88498  
 Ga<sub>1-x</sub>Al<sub>x</sub>GaAs interface, fractional quantum Hall effect in a two-dimensional hole system 4-108930  
 GaAs, deep acceptor, Hall effect obs. and photoluminescence 4-80532  
 GaAs doping superlattices, bipolar cond., tunability 4-70914

## Hall effect continued

GaAs, ion implanted, transient capless annealing appl. to IC fabrication 4-103779  
 GaAs LPE layers, residual impurities, growth soln. baking effects 4-92226  
 GaAs, plasma-assisted epitaxial growth in H<sub>2</sub> plasma, elec. props. 4-104740  
 GaAs, semi-insulating, elec. and photoelectronic props., book contrib. 4-88544  
 GaAs:Cr, epitaxial layers, Cr doping and elec. parameters 4-76683  
 GaAs:Cr, impurities, optical and transport studies 4-71444  
 GaAs:Mn, charge state of Mn impurities, mag. susceptibility ESR and Hall effect meas. 4-108982  
 GaAs:Si, ion implanted, and semi-insulating GaAs, deep levels, photoconductivity study 4-88469  
 GaAs:Si, LEC and horizontal Bridgman growth, elec. uniformity 4-65683  
 GaAs/Al<sub>0.3</sub>Ga<sub>0.7</sub>As heterostructures, 2D electron localisation 4-98718  
 GaAs/AlGaAs heterostructures, carrier density, hydrostatic press. control 4-98735  
 GaAs/N-AlGaAs heterostructures, selectively doped, MBE grown, tungsten-halogen lamp annealing effects 4-61444  
 GaAs-Al<sub>0.3</sub>Ga<sub>0.7</sub>As, quantised Hall resistance and 2D electron gas behaviour 4-98724  
 GaAs-Al<sub>0.3</sub>Ga<sub>0.7</sub>As heterostructures, 2D electron gas, disorder, fractional quantum Hall effect 4-76033  
 GaAs-Al<sub>0.3</sub>Ga<sub>0.7</sub>As heterostructure, low temp, fractional quantum Hall effect 4-98722  
 GaAs-Al<sub>0.3</sub>Ga<sub>0.7</sub>As heterostructure, quantum Hall resistance, temp. depend. 4-114028  
 GaAs-Ga<sub>1-x</sub>Al<sub>x</sub>As multiple quantum well structs., Hall mobility, electron conc. and buffer width depend. 4-80668  
 GaAs-GaAlAs heterojunction, freq. enhanced fractional quantisation, quantum Hall effect 4-80664  
 GaAs<sub>1-x</sub>P<sub>x</sub>/GaP strained-layer superlattices, Be-implantation doping 4-80057  
 GaInAsP, high purity, charact., growth, back contrib. 4-61334  
 GaInAsP, low field carrier mobility, book contrib. 4-61383  
 GaP, Hall meas. anal., influence of thermal impurity activation energy temp. depend. 4-104238  
 GaSb, plasma-assisted epitaxial growth in H<sub>2</sub> plasma, elec. props. 4-104740  
 GaSb-InAs heterojunction, quantum Hall effect study 4-98726  
 Ga<sub>2</sub>Te<sub>3</sub>, electrical cond. and Hall coeff. meas. using van der Pauw's method 4-98606  
 Ga<sub>2</sub>Te<sub>3</sub> liquid semicond. elec. transport activation energies 4-88506  
 Gd-Co amorphous films, spontaneous Hall effect in vicinity of the compensation composition 4-75929  
 Ge, deep impurity conc., elec. resist. and Hall coeff. meas. 4-65638  
 Ge, neutron transmutation doped, annealing, DLTS study 4-60942  
 p-Ge, nuclear doped, elec. cond., 0.06 to 300K, impurity conc. depend. 4-61382  
 Ge:Ar(Sb), neutron-transmutation-doped, defects 4-60967  
 n-Ge:As, growth on Si by MBE, charact. 4-98469  
 n-Ge:Au, defect. influence on deep level position of impurity 4-104160  
 Ge:Ga(Sb), film on GaAs, doping and elec. props. study (*Russian*) 4-70182  
 Ge:Se, impurity levels, Hall effect study 4-108804  
 Hg<sub>1-x</sub>Ag<sub>x</sub>Cr<sub>2</sub>Se<sub>4</sub> mag. semicond., exchange interaction, carrier effects 4-114103  
 Hg<sub>1-x</sub>Cd<sub>x</sub>Te, annealing of radiation defects, electron irradiation 4-108442  
 p-Hg<sub>1-x</sub>Cd<sub>x</sub>Te, elec. resist. and Hall coeffs., low-temp. anomalies 4-108883  
 Hg<sub>1-x</sub>Cd<sub>x</sub>Te, electron irradi., elec. props., heat treatment effects 4-65713  
 Hg<sub>1-x</sub>Cd<sub>x</sub>Te epitaxial layers, organometallic growth and elec. props. 4-71566  
 Hg<sub>1-x</sub>Fe<sub>x</sub>Te cryst., negative magnetoresist. and Hall effect 4-65696  
 Hg<sub>1-x</sub>Mn<sub>x</sub>Te, transport meas. using the alternating current technique 4-92720  
 HgS mixed films, elec. and optical props. (*French*) 4-84715  
 Ho-Co amorphous films, with perpendicular anisotropy, planar Hall effect 4-75932  
 InAs evaporated films, Hall mobility and carrier conc. 4-70961  
 InAs:Si(Te), VPE growth, morphology and elec. props. 4-109326  
 InGa<sub>1-x</sub>As<sub>x</sub>-InP heterojunction, quantum Hall effect and hopping cond. 4-98723  
 InP, ion implanted, elec. activation by CW laser annealing 4-80088  
 InP:Co, impurities, optical and transport studies 4-71444  
 InP:Se, ion implanted, annealing and transport props. 4-108397  
 InP:Sn films, LPE grown, carrier saturation, Hall meas. 4-98789  
 n-InSb nonlinear optical props. photoelectronic investigation 4-96986  
 n-InSb, strongly compensated, electron mobility meas. 4-70834  
 InSb, two-photon reson. photo-Hall effect 4-70863  
 p-InSb, ultrasonic attenuation and elec. resistivity at low temps. and high mag. fields 4-80165  
 InSb:Ge(Si), impurity solubility, role of acceptor and donor states 4-60949  
 InSe, elec. props., thickness depend. 4-88507  
 n-InSe, electron scatt. mechanisms, Hall effect and magnetoresist. meas. 4-80614  
 In<sub>2</sub>Se<sub>3</sub>, annealing in Se vapour, physical props. 4-61414  
 K, anisotropic Hall coeff., induced-torque anomaly theory 4-104185  
 Mg<sub>0.7</sub>Zn<sub>0.3-x</sub>Ga<sub>x</sub> simple metallic glasses, electronic props. 4-75920  
 Mo<sub>2</sub>Se<sub>3</sub>, elec. and mag. props. study 4-80595  
 MoSi<sub>2</sub> film, elec. resist. and Hall const. meas., anomalous props. obs. 4-70949  
 NbSe<sub>2</sub> quasi-1D metal, Hall effect and sliding Frohlich modes 4-65669  
 Ni-Fe-Cr alloys, extraordinary Hall coeff. sign reversal and DC resist. 4-113922  
 Ni-Fe-V alloys, extraordinary Hall coeff. sign reversal and DC resist. 4-113922  
 Ni-Pd, anomalous Hall effect rel. to mag. anisotropy (*Russian*) 4-92697  
 Ni-Pd alloys, monocrystals, anomalous Hall effect anisotropy 4-84607  
 Ni-Si-B metallic glasses, Hall effect; mag. ordering near resist. minimum 4-75933  
 NiFe-Ge amorphous and cryst. films, planar Hall effect and magnetisation reversal 4-75930  
 Pb<sub>1-x</sub>Ge<sub>x</sub>Te, undoped and Fe-doped, anomalous scatt. of carriers by defects and impurities near ferroelec. phase transition 4-98622  
 Pb<sub>1-x</sub>Ge<sub>x</sub>Te:In, elec. props., band edge struct., impurity effects 4-108880

**Hall effect continued**

- Pb<sub>1-x</sub>Sn<sub>x</sub>Te:In, elec. transport props. 4-61371  
 PbTe films, hot wall epitaxy, elec. characts., SEM and X-ray obs. 4-71564  
 PbTe, sintered, elec. cond. and thermoelec. power, annealing effects 4-84621  
 PbTe thin film, electrophys. props., degradation and recovery 4-88619  
 PbTe thin films, elec. props., effect of boundary layers 4-88618  
 PbTe:Ga, elec. and optical meas. (*Russian*) 4-84636  
 PbTe-Bi system, anomalous transport props. 4-88588  
 (PbTe)<sub>1-x</sub>(SnSe)<sub>x</sub>, solid solns., single cryst., phys. props. 4-65673  
 Pd:H, H diffusion, induced Hall voltage 4-70463  
 Sb<sub>2</sub>Mo<sub>2</sub>O<sub>6</sub>, band struct., transport props. 4-108773  
 Si,  $\alpha$ -centre and thermal donor levels, Hall effect, DLTS meas., press. depend. 4-80529  
 Si, Czochralski grown compensated thermodonors, EPR and Hall studies 4-75898  
 Si, electron and  $\gamma$  irradi., influence on defect annihilation 4-98094  
 Si, electron and  $\gamma$ -ray irradiated, efficiency of radiation defect formation 4-92237  
 Si, high purity, intercarrier scatt. effects, laser and electron beam excitation 4-92725  
 Si, inversion layers, ferri-induced electron delocalisation and fractional quantisation 4-80681  
 Si inversion layers, multiple connected quantised resistance regions 4-98725  
 Si, MIS inversion channel, quantum Hall effect studies 4-104321  
 Si MIS structure, fractional quantum Hall effect 4-108947  
 Si, proton irradi., acceptor level positions of divacancy 4-70725  
 Si, proton irradi., induced defects interaction with surface 4-75564  
 n-Si, proton irradiated, electrophysical props. 4-108861  
 Si quantised Hall resistor, two-terminal conductance meas. 4-70942  
 Si, recrystallized on SiO<sub>2</sub>, laterally seeded, implantation and annealing studies 4-98121  
 Si:As, ion implanted, carrier density profiles, elec. meas., annealing behaviour 4-70179  
 Si:As, P, B, ion implanted, fast isothermal annealing and elec. props. 4-92224  
 Si:B ingots, effective segregation coeff. of B, elec. studies 4-88192  
 a-Si:H, conductivity, localisation and mobility edge 4-70819  
 a-Si:H, DC elec. cond. Meyer-Neldel rule and Staebler-Wronski effect 4-113948  
 Si:Mg, implanted, doping behaviour, elec. props. 4-75485  
 Si:O, nonequilibrium cond. and thermal donors 4-104212  
 Si:O, piezocalvanomagnetic effects in presence of thermal donor levels 4-104239  
 Si:O, rare earth atoms, impurity interaction and donor accumulation 4-103783  
 Si:P, proton and neutron irradi., impurity composition and defect clustering 4-65291  
 n-Si:P polycrystalline CVD films, elec. props., grain size and impurity conc. effects 4-70963  
 Si:Sb, ion implanted, supersaturation, vitreous C strip heater annealing, Rutherford backscattering, elec. meas. 4-92375  
 Si:Te, donor states, Hall effect and cond. meas. 4-104145  
 Si/SiO<sub>2</sub>, MOSFET, elec. props. and atomic struct. 4-80677  
 SnTe thin films, elec. cond. and Hall effect 4-84716  
 SrAs<sub>2</sub>, monoclinic, Fermi surface determ. by Shubnikov-de Haas effect 4-108763  
 SrAs<sub>2</sub>, semimetallic, first-order longitudinal Hall effect 4-108884  
 SiTiO<sub>2</sub>, variable colour centre density, Raman spectra studies (*Chinese*) 4-109169  
 TaS<sub>2</sub> (1T), commensurate CDW state, electronic cond., Hall coeff. meas. 4-98639  
 TaS<sub>2</sub>-IT, phase transition at 282K, DSC, elec. cond. and Hall effect meas. 4-92349  
 TaS<sub>3</sub>, Hall effect, contrib. of moving CDW 4-113931  
 TaS<sub>3</sub>, Peierls transition, Hall const. temp. depend. 4-75937  
 Tb<sub>1-x</sub>Gd<sub>x</sub>, Hall effect and elec. resist. near Curie point 4-61361  
 Te, dimensionally quantised accumulation layer, quantum kinetic phenomena 4-88555  
 TiS<sub>2</sub>, semicond.-semimetal transition at 40 kbar 4-84660  
 TiS<sub>3</sub>, elec. cond. and Hall effect 4-65677  
 TiSi<sub>2</sub> thin films, electronic transport props., classical metallic behaviour 4-70955  
 TiTe<sub>2</sub>, band struct., elec. and mag. props. 4-92595  
 TiTe<sub>2</sub>, CDW transitions and transport props. 4-80521  
 TiBiTe<sub>2</sub>, growth, elec. and optical props. 4-65676  
 TiCu<sub>2</sub>Se<sub>2</sub>, p-type metal with layer struct. 4-70652  
 TiInTe<sub>2</sub>, electrophysical props., as function of temp. 4-61401  
 V-C, homogeneity region, electrophysical props. 4-80611  
 VSe<sub>2</sub>, CDW transitions and transport props. 4-80521  
 W CVD films, selectively deposited, elec. props. 4-88609  
 Zn<sub>1-x</sub>Ga<sub>2x/3</sub>Cr<sub>2x/3</sub>Se<sub>4</sub>, magnetic semiconducting solid solutions study 4-109002  
 ZnO weak accumulation layers, electron transport and Hall effect 4-98686  
 ZnS conductive film, MBE prep. with single effusion source, luminesc. and elec. props. 4-99323  
 ZnSe films, MBE growth, elec. cond., Hall effect and photoluminescence studies 4-99344

**Hall effect devices**

- accelerator, electron distrib. function evolution 4-91998  
 displacement sensors: which technologies? (*French*) 4-63710  
 $\alpha$ -HgS, conductivity anisotropy and Hall coeffs. 4-92719

**Hall effect transducers**

- carrier transport in semiconductor magnetic field sensors 4-70844  
 DC ammeter appl., clamp-on design 4-111120  
 magnetic sensor, double-diffusion differential amplification type, design and characts. 4-90575  
 magnetic thickness gauge, temp. stability improvement 4-68214

**Hall generators see Hall effect devices****halogens**

- see also *astatine; bromine; chlorine; fluorine; halides; iodine*  
 atoms, compact contracted Gaussian type basis sets 4-102583  
 battery, Zn-halogen, development trends 4-62345  
 closed shell ions, repulsive interactions with Ar, Kr and Xe, beam and transport meas. comparison 4-96653  
 molecules+Ar(Kr)(Xe) metastable atom quenching cross-section calcs. 4-107304

**halogens continued**

- quadrupolar nuclei, NMR spectroscopy 4-73476  
 tetraza porphyrin polygermyloxane:halogen, band struct. studied by crystal orbital formalism and CNDO approx. 4-65606  
 tetraza porphyrin polysiloxane:halogen, band struct. studied by crystal orbital formalism and CNDO approx. 4-65606  
 H+XY and X+HY where X and Y are Cl, Br or I, 3D DIM-3C pot. energy surfaces 4-66572  
**Hamidashi effect** see *ferroelectricity*  
**handling, materials** see *materials handling*  
**Hanle effect**  
 Ag+He, collisional depolarisation cross section, Hanle effect meas. 4-64585  
 Ar I, 2p level lifetime determ. 4-107310  
 Ar<sup>+</sup> ion beam, optical pumping study 4-87072  
 Ba, time-differential ground-state Hanle effect in fast-beam laser spectroscopy 4-78800  
 Cs+Cs(He), absolute polarisation meas., natural lifetime in Cs 7S<sub>1/2</sub> state 4-83448  
 NO<sub>2</sub>, excited state, fluoresc. light polarisation inversion, light-induced stabilisation 4-96605  
<sup>83</sup>Rb, 5P<sub>1/2</sub> level, lifetime determ. using Hanle effect 4-64428

**hard soldering see brazing****hard-sphere fluids see classical theories of fluid structure; liquid theory; quantum theories of fluid structure; statistical mechanics****hardening**

- see also *dispersion hardening; quench hardening; radiation hardening; solid solution hardening; surface hardening; work hardening*  
 anisotropic hardening in finite-deform. plasticity, stress anal. 4-74900  
 axially loaded crystals in n-fold symmetry, first and second order anal. 4-88233  
 $\alpha$ -brass, anneal-hardening, change in mechs. props. 4-99397  
 critical resolved shear stress and dislocation glide obstacles 4-80049  
 cyclic hardening in BCC and FCC metals and alloys, review 4-99532  
 diamines, aromatic, hardening activity rel. to spectrosc. characts. of primary amino group 4-83372  
 elastic-plastic materials, isotropic, Bauschinger effect model for large computer codes 4-108504  
 elastoplastic strain, large, kinematic hardening and induced anisotropy (*French*) 4-79463  
 hypoelasticity and elastoplasticity, with isotropic or kinematic hardening constitutive relations at finite strain 4-79459  
 kinematic hardening of large plastic deforms., corotational rates 4-74901  
 metals, mechanical instability of cellular dislocation structure 4-65268  
 metals, polycrystalline, finite elastic-plastic deformation 4-89093  
 metals, with memory of maximal prestress, creep-hardening rule 4-76806  
 metals and alloys, plastic deformation, mech. props. and struct. (*Russian*) 4-109468  
 multilite-zirconia composites, microstruct. and mech. props 4-114672  
 nonsymmetric anisotropic hardening for composite materials 4-87592  
 photoresists, plasma induced hardening using various gases 4-71662  
 plasticity, unified framework provided by mathematical programming 4-97354  
 plastics, limit hardening modulus determ. (*Bulgarian*) 4-66368  
 power-law hardening material, optical shadow spot method, for tensile crack 4-97449  
 pure, cold worked, annealing characts rel. to trace element addition 4-109438  
 steel, austenitic stainless, WWER steam generator tubes, hardening and intergranular corrosion cracking (*Czech*) 4-85257  
 steel, B, hardenability and B segregation (*Chinese*) 4-61945  
 steel, cast Mn, shock wave loaded, struct. and residual props. 4-93369  
 steel, hardening in high vacuum furnaces, heat transfer processes, mathematical model 4-85169  
 steel, high strength, high temp. sintering 4-89005  
 steel, low alloy, Cr-Mo-V, high temp. low cycle fatigue rel. to softening and embrittlement (*Japanese*) 4-99519  
 steel, low and medium strength, crack resist. 4-62034  
 steel, low-C, cast, cyclic crack resist., heat treatment influence 4-62035  
 steel, martensitic hypereutectoid, rapid heat hardening using incomplete homogenisation effect 4-71671  
 steel, Nb microalloyed, nonisothermal static softening after hot working 4-114578  
 steel, stainless, hardenable, microstruct.-strength relationship 4-114560  
 steel, structural, cast, strength toughness rel. to intercritical treatment (*French*) 4-81222  
 surface quality in finishing-hardening treatment by plastic deform.; controlling thermophys. fundamentals 4-66383  
 viscoplastic materials, advanced deformations and fracture initiation, constitutive modelling 4-103856  
 Cu plating for selective case-hardening 4-104744  
 Cu, polycrystalline, cyclic creep accel. and retardation, threshold stress temp. depend. 4-66372  
 Cu, single crystal, strain bursts in cyclic creep at ambient temp. 4-66371  
 Cu single crystals, cyclically strained, dislocation microstruct. rel. to plastic strain amplitude 4-66373  
 Fe, cast, high-strength, mech. props. after prior heat treatment and isothermal hardening 4-93321  
 Fe-Mn alloys,  $\gamma$ - $\epsilon$ - $\gamma$  martensitic transformations, recrystn. (*Russian*) 4-109398  
 Mg-Nd-Zr, cyclic strengthening and loss of strength in air and vacuum at 293 and 140K 4-93399  
 Nb, Pd and Ni-coated, hardening and fracture initiation, resulting from H<sub>2</sub> adsorpt.-desorpt. cycling 4-81282  
 SiC fibre/platelet reinforced Al-Mg-Si, magnitude and mechanism of strengthening 4-76710  
 Ti, fatigue endurance, influence of rest period 4-99486  
 Ti-Al-V (6, 4 wt.%), fatigue endurance, influence of rest period 4-99486  
 ZrO<sub>2</sub> ceramics, process zone toughening by microcracking 4-62020

**hardness**

- see also *abrasion; hardness testing*  
 alkali halide mixed crystals, growth and characterisation, microhardness colour centres, radiation hardening 4-70152  
 basalt glass fibres, microhardness and microbrittleness 4-84342  
 boronised alloys, types VK6, TSK10, T15K6, distrib. of B, W, Ti and Cu (*Russian*) 4-80071  
 $\alpha$ -brass, anneal-hardening, change in mechs. props. 4-99397  
 brittle surface in sliding contact with spherical indenters, strength degradation 4-104881

## hardness continued

- coating for tools and sliding elements, acoustic microscopy studies 4-104957  
 coatings on steel substrate, phys. and mech. props. after pulse shock loading 4-66489  
 copolymer system, rubber plasticised, processing influence on morphology-prop. relationships (*German*) 4-85209  
 crystals, mechanoluminescence, microhardness and disloc. density depend. 4-85020  
 cubic single crystals, microhardness and interatomic binding 4-113528  
 diamond dispersed alumina composite, very high press. sintered, fracture toughness, phase transform. 4-99372  
 ferroic compounds, transition temp. determ. by microhardness meas. 4-71302  
 ferromagnetic components quality control by coercive field strength meas. 4-93475  
 glasses, crystn. and props., prep. from Illinois coal fly ash 4-79940  
 hardmetal, creation of stable cracks using bridge indentation 4-66434  
 implant method for determining hardenability of small specimens 4-76919  
 materials selection under erosive wear conditions (*German*) 4-62065  
 metal spheres, plastic compression between smooth parallel platens 4-69715  
 metals, shock wave treatment, texture anal. (*Russian*) 4-103878  
 metals, spalling microdamage initiation, critical loading conditions 4-89111  
 metals, wear reduction and analysis, surface modification by ion beams 4-81290  
 nuclear waste glasses, fracture toughness, hardness, elastic recovery, indentation testing 4-104844  
 nylon, humidity effect on friction, hardness and shear strength 4-62064  
 organic explosive, dislocation etching, microhardness, primary slip systems 4-65266  
 polyamide-6, blending with copolymers, effect on props. (*Polish*) 4-66433  
 polybutadiene, reinforcement with inorganic fillers, mech. characts. 4-61914  
 polyethylene, surface hardening by exposure to  $H_2SO_4$  4-76894  
 pure, cold worked, annealing characts. rel. to trace element additions 4-109438  
 quartz, hardness properties influenced by high-temp. and impurities 4-94107  
 rare earth perovskites, flux grown single crystals, microhardness, indentation tests 4-99493  
 reactive ion plating coatings charact. 4-114424  
 rubber, hardness-Young's modulus relations 4-81228  
 sapphire:Cr(Ti) crystals, hardness 4-93393  
 sialon metalcutting tools, props. and appl. 4-66283  
 slag glass fibres, microhardness and microbrittleness 4-84342  
 steel, alloy, secondary hardening mechanisms 4-99396  
 steel, austenitic, explosion hardened high Mn, residual stress distribution (*Japanese*) 4-114645  
 steel, austenitic stainless, claddings, ring test of tubes oxidised in high temp. steam 4-104816  
 steel, austenitic stainless, microhardness changes under fast neutron irradiation and cold deformation (*Russian*) 4-76861  
 steel, austenitic stainless, surface alloying with Ta using powerful monochromatic radiation 4-71782  
 steel, B, hardenability and B segregation (*Chinese*) 4-61945  
 steel, bearing, surface layers, effect of grinding (*Chinese*) 4-99628  
 steel, C, boronising, electrolytic, boride phase form. kinetics 4-71781  
 steel, C, strain aging equivalent rule, hardness obs. 4-76790  
 steel, C, surface hardening by laser treatment 4-81337  
 steel, C-Mn, low temp. creep crack growth, effect of cold work 4-76850  
 steel, carburisation, sintering, mech. props. rel. to Cu and P alloying 4-89069  
 steel, carburising, core hardenability calcs. 4-99395  
 steel, cast Mn, shock wave loaded, struct. and residual props. 4-93369  
 steel, Cr, fracture toughness and mech. props., effect of tempering 4-76854  
 steel, Cr, ledeburitic cold work, microstruct. and abrasive wear 4-114679  
 steel, Cr-Mn-Ti, carburised, struct. and hardness rel. to cyclic heat treatment 4-66406  
 steel, Cr-Mo, temper-embrittled, effects of grain size and hardness 4-99554  
 steel, die, mech. props. after low-temp. mech. treatment 4-61962  
 steel, dual-phase, cold-rolled sheet, recrystn. kinetics 4-93310  
 steel, dual-phase, martensite-ferrite, tensile strength, shear-lag anal. 4-71704  
 steel, dual-phase, tempered, fracture behaviour 4-89127  
 steel, dynamic flow curve, symmetric rod impact test 4-109486  
 steel, effect on wear resist. in abrasive friction 4-93425  
 steel, electric spark alloying with TiN-Cr, reinforced layer microhardness and comp. 4-89192  
 steel, fracture toughness, quasi-state and impact, effect of different thermal treatments 4-99599  
 steel, hardening by high-velocity intensive plasma treatment 4-114717  
 steel, high strength, H cracking parameters for predicting safe welding conditions 4-66404  
 steel, high strength structural, stress relief cracking susceptibility 4-109509  
 steel, hot rolled, hardness response, estimation by simulating cooling cycles via Jominy bar testing 4-114750  
 steel, hypereutectoid, Mode III fracture initiation toughness, depend. on strength and microstruct. 4-71720  
 steel, low alloy, Cr-Mo-V, high temp. low cycle fatigue rel. to softening and embrittlement (*Japanese*) 4-99519  
 steel, low alloys heat treated, grinding residual stress, hardness (*Japanese*) 4-89117  
 steel, low C, nitrocarburising, annealing, yield stress, brittle-ductile fracture transition 4-66384  
 steel, low C, quenched, precip. kinetics 4-99394  
 steel, maraging, ultrahigh strength, delayed failure 4-93402  
 steel, martensitic stainless, HT-9, weldments, microstruct., hardness and fracture toughness, effect of preheat 4-99495  
 steel, mech. props., effect of laser quenching 4-66356  
 steel, N ion implanted, wear and friction 4-66459  
 steel, Ni-Cr, carburised case depth and hardness, electromag. obs. 4-71830  
 steel, plain C, dual-phase, ferrite-martensitic struct., strength law 4-99399  
 steel, powder, shock induced densification, mechanical props. 4-109347

## hardness continued

- steel, sintered, Mn diffusion coatings 4-89186  
 steel, stainless, shock loaded, residual struct. and props. 4-109516  
 steel, stainless, texture development during annealing and rolling 4-76786  
 steel, structural, deform. mechanisms using high temp. tests 4-109481  
 steel, surface hardening by laser, technological control of surface condition parameters 4-71779  
 steel, tool, tempered surface layers formed during grinding, thickness determ. using electrochem. method 4-71814  
 steel plate, laser melted surface, microstruct., hardness, residual stress 4-71794  
 steel powder, rapidly solidified, shock consolidation 4-109353  
 steels, corrosion-resistant, surface strengthening by laser irradiation (*Russian*) 4-81340  
 steels, hardenability, effect of hot working 4-81211  
 Taiwan Research Reactor, irradiated fuel rod testing 4-59326  
 ternary semiconductors, relationship between physicochemical and electro-physical props. 4-108856  
 thin films, hardness meas. 4-75610  
 thin films, mechanical characterisation using ultramicroindentation apparatus 4-91781  
 ultrasonic 4-89236  
 Vickers hardness measurement, influence of residual stress 4-99691  
 Ag-based thin films, ultramicrohardness and internal stresses 4-92582  
 Al, shock loaded, microstructure and hardness 4-109515  
 Al:Sb, ion implanted, hardness, friction and wear props. 4-66451  
 Al-Cu (10 wt.%), prod. by rheocasting, rel. between struct. and mech. props. 4-99467  
 Al-Cu (4 wt.%), dissoln. kinetics of  $\theta$  phase using thermoelec. power meas. 4-114533  
 Al-Cu system, metastable states controlled by diffusion 4-65463  
 Al-Fe-misch metal, rapidly solidified, microstruct. characterisation 4-114442  
 Al-glass composite, produced by powder metallurgy route, mech. props. 4-66275  
 Al-Mg (10 wt.%), extrusion and mech. props. of compacts prep. from rapidly solidified powders 4-66395  
 Al-Mg-Si alloy, effect of Fe on precipitation 4-104783  
 Al-Mg-Si alloys, transitional state formation by diffusion, microhardness study 4-61135  
 Al-Sc (0.3 at.%) alloy, ageing, precipitation obs. (*Russian*) 4-104786  
 Al-Sc alloys, age hardening kinetics, hardness study 4-61949  
 Al-Si-Mg-Sr, struct. and props., comp. and Sr addition effects 4-61987  
 Al-Zn(Mg), neutron irradi., radiation damage 4-80112  
 AlN powder, hot pressing kinetics, oxidation, mech. props. 4-76731  
 $Al_2O_3$ , strength characts. using controlled flaws, microstruct. effects 4-85205  
 Au-based thin films, ultramicrohardness and internal stresses 4-92582  
 B<sub>2</sub>C, hardness and fracture toughness rel. to stoichiometry 4-62019  
 B<sub>2</sub>C, struct. and mech. props., hot pressing conditions effect 4-61906  
 C, amorphous hard films, growth from hydrocarbon RF plasma 4-85117  
 C coating, diamond-like, development, prep. and uses 4-109525  
 C:H amorphous film prep. by H<sub>2</sub> gas reactive RF sputtering of graphite 4-76671  
 a-C:H hard thin films, RF plasma deposition 4-76681  
 Ca<sub>2</sub>Ge<sub>2</sub>O<sub>12</sub>, garnet single crystals, microhardness, brittle fracture 4-65337  
 Cd, electrodeposition from acidic chloride baths, morphology and hardness rel. to addition agents 4-93238  
 CdTe, dislocations and subboundaries, etching studies 4-75451  
 Co-base alloy coating, contact fatigue resist. 4-93426  
 Co<sub>100-x</sub>B<sub>x</sub>, metallic glass, mag. and mechanical props. 4-84841  
 Cr<sub>3</sub>Cr<sub>2</sub>Ni-B electrophoretic coatings, struct. and props. 4-88430  
 Cu, creep fatigue, failure life and microdamage mode rel. to wave shape 4-109508  
 Cu-Al, neutron irradi., microhardness, resistivity, electron microscopy 4-103811  
 Cu-Al-Fe (10, 1 wt.%), corrosion and mech. props., effect of solidification struct. 4-85243  
 Cu-Al-Ti, internal oxidation, dispersion hardening (*Japanese*) 4-89065  
 Cu-Be-Co (2, 0.2 wt.%), precip. hardening investigation by microhardness and elec. resist. meas. 4-61947  
 Cu-Mn, neutron irradi., microhardness, resistivity, electron microscopy 4-103811  
 Cu-Ni, neutron irradi., microhardness, resistivity, electron microscopy 4-103811  
 Cu-Ni-Cr (30.5 wt.%), quenching, ageing, spinodal decomp., hardness, X-ray diffr. obs. 4-114526  
 Cu-Ni-Sn system, supersaturated solid soln. decomposition 4-81210  
 Cu-Sn-Al<sub>2</sub>O<sub>3</sub>, abrasive composite, physicochem. props., effect of premoulding press. in elec. discharge sintering 4-89020  
 Cu-Ti/diamond interface, struct. microanal. (*Chinese*) 4-61242  
 Cu-Ti/graphite interface, struct. microanal. (*Chinese*) 4-61242  
 Cu-Zn-Al, sliding contact with steel, micro-indentation hardness gradients of worn surface 4-76842  
 Cu-(Al), cold-worked, recrystn., effect of stacking fault energy 4-81221  
 Cu<sub>60</sub>Zr<sub>40</sub> alloy system, amorphous, crystallisation kinetics 4-108279  
 Fe, cast, high-strength, mech. props. after prior heat treatment and isothermal hardening 4-93321  
 Fe, gray and nodular cast, laser surface hardening, erosion resist., near surface microstructure 4-66453  
 Fe, sintered compacts, alloying element effect on carburising response 4-99642  
 Fe-Cr-C, hypereutectic alloys unidirectionally solidified, hot hardness of primary carbides 4-99492  
 Fe-Nd-B permanent magnet system, metallurgy 4-109381  
 Fe-Zn system, formation and growth of  $\delta$  phase, cracks 4-89026  
 Fe<sub>100-x</sub>B<sub>x</sub>, metallic glass, mag. and mechanical props. 4-84841  
 Fe<sub>88</sub>B<sub>12</sub>, amorphous layer form. on surface using elec. spark 4-65180  
 Fe<sub>40</sub>Ni<sub>60</sub>B<sub>10</sub>Si<sub>10</sub>, glassy ribbon, elec. and mag. props. 4-84604  
 Ga<sub>2</sub>O<sub>3</sub>-CaO glass, form. density, refr. index, crystn. temp., hardness, IR spectra 4-113635  
 Gd<sub>3</sub>O<sub>5</sub>Ca<sub>2</sub>O<sub>12</sub>, garnet single crystals, microhardness, brittle fracture 4-65337  
 In<sub>1-x</sub>Ga<sub>x</sub>As<sub>1-y</sub>P<sub>y</sub>, composition depend. of microhardness anisotropy 4-108506  
 LaB<sub>6</sub>-ZrB<sub>2</sub> system, interaction, phase diagram study 4-89030  
 LiF single crystals, grinding, surface layer, strain hardening, dislocation density, microhardness 4-93312  
 Mg-Nd-Zr, cyclic strengthening and loss of strength in air and vacuum at 293 and 140K 4-93399

**hardness continued**

- MgO crystals, microhardness indentation cracks, energy dissipation, X-ray topography 4-75608  
 Mn-Ge, Invar type, antiferromag., transition metal influence on props. (Japanese) 4-65826  
 Mo alloys, dispersion hardened, strength and elasticity, effect of heating 4-114600  
 Mo, deformed, mechanical props. anisotropy under cross rolling, texture 4-66378  
 Mo powder, shock induced densification study 4-109348  
 $\text{NH}_4\text{HCO}_3$ , relations between crystallographic characts. and cryst. struct. (Chinese) 4-75378  
 NaCl:Ca(Pb), plastic deform. parameters, impurity conc. effect, low temp. anomaly 4-88229  
 NaCl:Gd, microhardness, influence of Gd impurity 4-103868  
 NaCl:Tb, quenched, microhardness meas., impurities effect 4-98190  
 $\text{Na}_2\text{O-B}_2\text{O}_3$  glass, prep., mech., thermal and optical props. rel. to N content 4-60845  
 $\text{Na}_2\text{O-B}_2\text{O}_3\text{-Al}_2\text{O}_3\text{-SiO}_2$  transparent glazes, with enhanced chem. and thermal shock-resist. 4-81305  
 Nb alloy, plastic deform. with subsequent nitriding effect on mech. props. 4-114713  
 Nb, Pd- and Ni-coated, hardening and fracture initiation, resulting from H<sub>2</sub> adsorpt.-desorpt. cycling 4-81282  
 Ni detonated coatings, metastable phase form. in Ni-C system 4-71554  
 Ni electrodeposited from sulphate and acetate salts, hardness and struct. 4-114431  
 Ni, electrodeposition, hardness, microstruct. 4-66252  
 Ni-Al-Mo alloy, unidirectional solidification 4-76765  
 Ni-B alloys, CVD deposited, microstruct. and mech. props. 4-71581  
 Ni-Co electroplating, US agitation effect on mech. props. and comp. 4-114430  
 Ni-Fe electroplating, US agitation effect on mech. props. and comp. 4-114430  
 Ni-Nb-NbC, eutectic alloys, powder metallurgy, physical props., high temp. use 4-85125  
 $\text{Ni}_3\text{Al}$  powders, rapidly solidified and annealed 4-93278  
 $\text{Ni}_{80}\text{P}_{20}$  amorphous powder, warm pressing consolidation kinetics 4-81168  
 Pd-Pr-Ir(Rh), phase equilb. of Pt metals at 1400°C 4-71637  
 Pt-Pd-Rh-Ir, phase equilb. of Pt metals at 1400°C 4-71637  
 Pt-Rh-Pd(Ir), phase equilb. of Pt metals at 1400°C 4-71637  
 Rh-Ru-Pd(Ir), phase equilb. of Pt metals at 1400°C 4-71637  
 Ru-Rh system, constitution, solid solubility and lattice consts. 4-70390  
 Si surface, single cryst., fluids influence on microhardness 4-98418  
 a-Si:H CVD films, struct. model 4-88427  
 $\beta$ -SiC powders, sintering, hot pressing, densification and mech. props. rel. to prep. 4-109366  
 $\alpha$ -SiC, sintered, phenomenology of fracture 4-93372  
 $\text{Si}_3\text{N}_4$  powder, shock induced densification study 4-109352  
 $\text{Si}_3\text{N}_4$ -based metalcutting tools, props. and appl. 4-66283  
 $\text{SnI}_2$  single cryst., Vicker's microhardness studies 4-113529  
 $\text{SnI}_4$  single cryst., Vicker's microhardness studies 4-113529  
 Ti alloy OT4, cold rolling, texture and elastic modulus anisotropy change 4-93314  
 Ti, pure, electron beam welding, mech. props., fusion reactor appls. 4-109471  
 Ti-Al-V (6, 4 wt.%), electron beam welding, mech. props., fusion reactor appls. 4-109471  
 $\text{TiB}_2$ , implanted with 1 MeV  $\text{Ni}^{+}$  ions, microstruct. and surface mech. props. 4-70232  
 TiC-Ti, reactive liq. phase sintering 4-61896  
 $\text{TiC}_{1-x}$ , solubility of metals, microhardness, flow stress rel. to C content 4-61931  
 TiN-Ti coatings, reactive pulse plasma deposited, struct. and props. 4-76688  
 TiN-TiC solid soln. powder, shock compaction study 4-109341  
 TiNi, martensitic transform., mech. props., struct. rel. to thermomech. treatment 4-66376  
 U-Nb (6 wt.%), microstruct., mech. props. and corrosion, effect of quench rate 4-114558  
 V, neutron irradi., hardness, tensile props. 4-103809  
 V-Re-C alloy system, isothermal section at 1950°C (Ukrainian) 4-89023  
 $\text{V}_2\text{CrAl}_{1-x}\text{B}_x$ , melt spinning and phase transforms 4-114450  
 W-Ni-Fe (5, 5 wt.%) heavy alloy, precipitation hardening 4-114564  
 W-Re, prep., sintering, phase comp., microhardness, SEM obs. 4-89010  
 WC, indented, dislocation interactions, crack nucleation, TEM obs. 4-80039  
 WC-(Co-Ni) hardmetals, mech. props., variation with Ni/Co ratio 4-114462  
 WC-Co, cemented carbide, hot isostatic pressing 4-66293  
 WC-Co, hardmetal, creation of stable cracks using bridge indentation 4-66434  
 WC-Co hard metals, strengthening by ultrasonic vibrs. 4-62122  
 WC-Co-P, wear resist., P addition influence 4-66458  
 Y-Si-Al-O-N glasses, viscosity, glass transition, microhardness rel. to comp. 4-70383  
 Zn-Al-Sn alloys, quench-aged, phase transforms., rel. to hardness 4-114515  
 Zr, oxide film growth kinetics, interferometry, ellipsometry, X-ray photoelectron spectra obs. 4-66482  
 ZrC-Co-base eutectic, mech. props. rel. to microstruct. 4-89135  
 $\text{ZrO}_2\text{-Y}_2\text{O}_3\text{-HfO}_2$  ceramic powders, laser sintering 4-88998

**hardness testing**

- calcite, cleavages, Knoop and Vickers hardness numbers 4-110136  
 ceramics clay-based, fracture props., practical technique using diamond indentation 4-62144  
 ferrites for magnetic recording heads, toughness evaluation 4-104951  
 indentation fracture, indenter geometry effects 4-60346  
 Jominy end-quench testing, computer-controlled hardness tester 4-99666  
 materials testing, microscopy (German) 4-93492  
 metal, neutron irradi., localised plastic flow characterisation with indentation hardness 4-109581  
 Rockwell hardness testing machine (German) 4-66534  
 steel, quenched and tempered, hardness, X-ray diff. peak, Gaussian curve fitting method 4-76926  
 steel, with impact action standard-fee instruments 4-99675  
 thin films, hardness meas. 4-75610

**hardness testing continued**

- universal hardness tester with electronic data processing (German) 4-66533  
 Vickers hardness measurement, influence of residual stress 4-99691  
**harmonic analysis**  
*see also waveform analysis*  
 ferromagnetic material inspection, harmonic analysis of hysteresis loop 4-71127  
 hydrology, annual runoff and precipitation series, search for periodicity 4-82125  
 ocean tides anal., methods involving time series 4-82310  
 spherical harmonic analysis, coordinate system rotation effects 4-93991  
 St. Lawrence estuary, tidal currents, harmonic and admittance anal. 4-82076

**harmonic generation**

- see also optical harmonic generation*  
 acoustic transducer, large, nearfield, second harmonic and sum freq. radiation 4-74830  
 microwave SHG in plasma-filled waveguide, in static mag. field 4-113157  
 organ pipes, harmonic generation mechanism 4-87522  
 plasma, laser produced harmonic emission generated by reson. absorptio (Chinese) 4-91881  
 quartz, nonlinear acoustic props. and third-order elastic consts. 4-74793  
 Rayleigh waves, nonlinear, harmonic generation, parametric amplification and thermoviscous damping 4-64806  
 US studies of phase transitions in crystals 4-60993  
 BiSB, acoustical nonlinearity near electronic topological transition 4-113547  
 $\text{LiNbO}_3$ , nonlinear acoustic props. and third-order elastic consts. 4-74793

**harmonic oscillators**

- 3-body problems, six-D oscillator based on  $O(6)$  4-82700  
 $\alpha^2 + \beta x^2$  oscillator, analytic treatment 4-63543  
 action-angle variables, ambiguity spin and duplication spin 4-90395  
 anharmonic oscillator, bound state energies, perturbation theory 4-63570  
 anharmonic oscillator, chaotic motion, inversion-symmetric limit cycle 4-90363  
 anharmonic oscillator, covergent renormalized perturbation series 4-86254  
 anharmonic oscillator, ground state eigenvalue, summation of divergent power series 4-95216  
 anharmonic oscillator, quartic and sextic, operator method and eigenvalue 4-78162  
 anharmonic oscillator eigenvalues and Green's functions,  $1/N$  series 4-63533  
 anharmonic oscillator eigenvalues from variational functional method 4-63545  
 anharmonic oscillator one-dimens. model, overtone absorpt. 4-96606  
 anharmonic oscillators, coupled, thermal averages, effective harmonic oscillator method appl. 4-112153  
 anharmonic oscillators, geometric approach to the semiclassical bound state energies of quantum-mechanical models 4-82695  
 anharmonic oscillators, Hamiltonian systems, nonintegrability, Kolmogorov entropy 4-82696  
 anharmonic oscillators and generalized hypergeometric functions 4-9522  
 anisotropic harmonic oscillator, energy variational principle for systems in mag. fields 4-96427  
 bound-state energies calc. using variational functional method 4-78765  
 Calogero-Moser system, solvability in external potentials 4-106207  
 charged particle in const. mag. field, caustics 4-111366  
 classical anharmonic oscillators, perturbation series rescaling 4-101702  
 coherent dynamics of three coupled oscillators, stationary phase approximation 4-96995  
 coherent states for many-body system of harmonic oscillators 4-110931  
 coupled anharmonic oscillators, algebraic models relation 4-90403  
 coupled oscillation, generic behaviour 4-101704  
 D-dimensional isotropic anharmonic oscillator, renormalised perturbation theory 4-68003  
 damped, quantum theory 4-73256  
 discrete mechanics, oscillator evolution operator 4-110928  
 eigenvalues obtained using algebraic technique 4-63444  
 energy dissipation, time-dependent formalism, coupled oscillator model 4-95975  
 exact propagator for damped time-dependent harmonic oscillator 4-7815  
 Feynman's formula for Green's function 4-95203  
 Feynman-Trotter approximations, simple harmonic osc., low temp. quantum systems 4-101707  
 forced harmonic oscillator, diagrammatic representation 4-67943  
 forced magnetic oscillator bifurcations near reson. points 4-95308  
 galvanometer, forced simple harmonic motion 4-90335  
 generalised anharmonic oscillator, energy eigenvalues 4-58663  
 generalised Bargmann inequalities, Schrodinger operators, harmonic oscillators 4-63569  
 geodesic flow perturbations, surfaces with constant negative curvature mixing props. 4-110898  
 Green's functions, propagators from integral representations 4-63542  
 hadron energy eigenvalues and coupling strengths determ. with dualities Shifman-Vainshtein-Zakharov method 4-59059  
 incommensurate harmonic chain, 1-D, dynamics 4-95348  
 integral representation for the product of two Jacobi functions with different order and arguments 4-86264  
 JWKB approximations, quartic oscillator, effective potential method 4-110913  
 JWKB approximations, radial problems, modification of the effective potential 4-110912  
 Kepler orbits, quaternion transformation to 4-D harmonic oscillator 4-95210  
 localized Gaussian wave packet methods for inelastic collisions involving anharmonic oscillators 4-64569  
 minimum-uncertainty coherent states, identity resolution, charged boson coherent states example 4-110932  
 modulated damping or growth model in classical or quantum mechanics 4-68015  
 molecular vibrational energy transfer, regular and chaotic dynamic transition 4-107437  
 Morse oscillator, diatomic RKR pots., vibr.-rot. levels 4-64450  
 Morse oscillator seatt. matrix, algebraic calc. 4-90402  
 Morse oscillator systems, coupled, energy transfer between bonds; quantum dynamics 4-102774

**harmonic oscillators continued**

- Morse-type oscillator, self-consistent maximal-entropy propag., time evolution 4-111092
- multiphoton optical bistability and phase conjugacy, oscillator models 4-69509
- N-dimensional anharmonic oscillator with arbitrary anharmonicity,  $1/N$  expansion, perturbation theory 4-73297
- non-Markovian stochastic differential eqns., dynamical props. 4-68134
- nondemolition, noise reduction with Hermitian operators 4-68053
- noninvariance groups for many-particle systems: coupled harmonic oscillators 4-90408
- nonlinear quantum oscillator, coordinate continuous meas. 4-95241
- nonrelativistic Coulomb problem, Sturmian propagator 4-63561
- offset impact oscillator 4-86245
- optimized harmonic reference system for the evaluation of discretized path integrals 4-67997
- orbits, quantisation of periodic motions, accidental degeneracy of spectral lines 4-95198
- oscillator coupled to one-dimensional extended mechanical field, UV divergence 4-101699
- oscillator-cum-generalised anharmonic potential, Klein-Gordon eqn. soln. 4-106526
- oscillators coupled to a two-level system, variational principle 4-86255
- parametric resonator, simple, quantal description, continuous versus discrete quasi-energy spectrum 4-95230
- partition function, Pade approximant method, quartic anharmonic oscillator 4-86326
- partition function, Pade approximant method 4-86325
- path integral quantization of the damped harmonic oscillator 4-101686
- path integral with memory kernel 4-101681
- path integration, with two-time quadratic action 4-95231
- periodic motion anharmonicity oscils. 4-86148
- plane rotators, Nernst quantisation procedure 4-86252
- potentials, Coulomb and ring-shaped, nonbijective canonical transformations 4-63573
- propagator of the time-dependent forced harmonic oscillator with constant damping 4-101684
- quantum dissipative system, damped harmonic oscillator, Caldirola-Kanai Hamiltonian 4-110911
- quantum equations of motion, finite-difference approach 4-86253
- quantum Langevin eqn., noise spectrum 4-68007
- quantum Langevin eqn. soln., return to thermal equilibrium 4-58675
- quantum mechanical diffusion coeff., fundamental constraint 4-101698
- quantum nondemolition continuous observables, general soln., harmonic oscillator appl. 4-68032
- quantum-mechanical oscillator, simultaneous monitoring of two signals 4-79070
- quantum-statistical distributions, R-inherent quantum mechanics, four-dimensional symmetry 4-95294
- quark-gluon model with conformal symmetry 4-82947
- quartic anharmonic oscillator, continued fractions and quantum mechanical perturbation theory 4-110929
- quartic oscillator, minimal sensitivity optimisation of perturbative wavefunctions 4-90410
- quasiprobability operator defined quantisation procedure, properties 4-90435
- random masses, exact solutions for spectra and Green's functions 4-78185
- rotating harmonic oscillator: violation of an equipartition theorem 4-90111
- Schrodinger eqn., harmonic oscillator, exact soln. for time- and coordinate-dependent mass 4-63536
- Schrodinger equation, hyperviral-Pade scheme, energy eigenvalues of general potential 4-95197
- Schrodinger equation, periodic, with nonperiodic boundary conditions, eigenvalues, semiclassical anal. 4-73259
- Schrodinger-Langevin eqn. solns. and nonexistence of solitary waves 4-63540
- single quantum oscillator with  $|x|^2$ -type pot., specific heat 4-73289
- SL(3,R) realisations, damped harmonic oscillator 4-86595
- spinless bosons, degeneracy splitting 4-86236
- spontaneous radiation, zero-point oscillations 4-95242
- strangled harmonic oscillator, decaying Hamiltonian for damping 4-82706
- strongly anharmonic oscillator and oscillator with double-well pot., analytical formulae for eigenenergies 4-68004
- temperature Green's function, generating functional 4-90406
- three-dimensional, recurrent formulae and some exact relations for radial integrals with Dirac and Schrodinger waves functions (Russian) 4-90442
- time dependent, forced, extended Feynman formula 4-63556
- time-dependent harmonic oscillator, cubic and quartic invariants 4-67973
- vibrational partition functions calculated for limited information 4-58666
- H, 3-dimens. atom, rel. to harmonic oscillator, zero-energy case 4-74132
- H atom in uniform EM field as anharmonic oscillator 4-73266
- KCN, ab initio dipole surfaces, vibr. averaged dipole moments and IR transition intensities 4-64461
- LiCN, ab initio dipole surfaces, vibr. averaged dipole moments and IR transition intensities 4-64461
- SF<sub>6</sub>, multiphoton absorpt. study as function by initial rot. state 4-59866

**harmonics**

- see also harmonic analysis
- Euler's eqn. of harmonic maps, soln. and appl. to general relativity (Chinese) 4-90444
- FCC Part 18 standards for radio equipment 4-69930
- fibre gyros, bias modulation frequency second harmonic signal, response 4-106317
- interfering speech, harmonic magnitude suppression for intelligibility enhancement 4-103133
- magnetostriiction harmonics measurement using double piezoelectric transducer technique 4-88712
- random processes with finite energy, expansions into harmonic components (Russian) 4-101755
- solids, nonlinear Rayleigh waves, far-field soln. (French) 4-98420
- three-dimensional wave diff. problems, Rayleigh and Sommerfeld approximations 4-79014

lartmann lines see Luder's bands

lartree calculations see SCF calculations

lartree-Fock approximation see HF calculations

lartree-Fock calculations see HF calculations

Hasiguti relaxation see anelastic relaxation; dislocation damping

Hastelloy see iron alloys; molybdenum alloys; nickel alloys

He see helium

**headphones**

- see also earphones
- acoustic quality evaluation using manikin equipped with artificial ear (French) 4-107973
- acoustics (German) 4-97202
- acoustics and stereophonics (German) 4-107961

**health care**

- used for systems approach only
- see also patient care
- Am, medical course after accidental exposure 4-109890

health effects of radiation see biological effects of radiation

**health hazards**

- see also biological effects of radiation
- 450-MHz RF exposure of man, specific absorption rate average and distrib. 4-115119
- biomedical optical fibres, conf., Paris, France (May 1983) 4-82587
- blood-brain barrier, microwave energy effects, review 4-115127
- building materials, radiation from, methods of evaluation 4-93869
- building materials, radioactivity concs. limitation based on a practical calc. model 4-93935
- cement industry raw materials and products, natural radioactivity 4-93676
- coal fly ash, elemental particle size distrib. in thick samples, PIXE anal. 4-105069
- concrete, radioactivity induction in constituents by high energy particle irradi. 4-115230
- cosmic rays, indoor exposure rate, NaI:Ti scintillation counter, building material perturbation 4-109936
- CT examinations, energy imparted rel. to radiation risk 4-115225
- cytogenetic aspects of human exposure to transuranics 4-109891
- diver decompression sickness, heart and lung injury evaluation 4-109871
- diver decompression sickness and air embolism therapies 4-109990
- diver decompression sickness prevention 4-109989
- diver noise exposure and hearing conservation standards 4-109844
- diving biomedical research of US Navy 4-109789
- diving operations, regulation and safety organisation 4-106169
- dosimetry, radioecological calcs., reliability, parameter variability 4-115233
- ELF naval communications facilities, health hazards assessment 4-115115
- EM dosimetry and energy deposition, RF and microwave exposure (Japanese) 4-62524
- EM field distribution in lossy dielectrics, clinical appls., computer modelling 4-109785
- EM field dosimetry in biomedical investigs. 4-115227
- EM fields, cubical block model of man in specific absorption rate distrib. calc., limitations 4-115118
- EM fields human exposure, energy deposition and thermal response models 4-115117
- external radiation exposure from aquatic pathways, simple models for prediction 4-105338
- eye, pterygium in Sardinia w.r.t. occupational exposure, epidemiological obs. 4-81740
- eyes, microwave radiation hazard, metal-framed spectacles effect 4-109877
- fallout from Pacific nuclear tests, Rongelap and Utirik Atolls experience 4-62611
- female atomic radiation workers, potential occupational exposure, foetal risk 4-89779
- fusion energy systems, potential aerosols characterisation 4-107016
- gamma background, natural, in Poland, exposure of urban populations 4-100320
- gamma radiation, indoor exposure meas. in Italy 4-93881
- gamma radiation, levels in dwellings in the Republic of Ireland 4-93880
- gamma ray exposure in wooden houses, indoor rel. to outdoor 4-93874
- genetic effects of radiation 4-109872
- hair, trace element anal. of workers using CS<sub>2</sub> (Chinese) 4-72000
- hazardous chemical waste mobilization during decommissioning of chemical plants 4-109771
- hazardous radioactive and chemical wastes, impact on man and environment 4-83196
- heavy ion cyclotron central region, radioactivation 4-91116
- high-blood-pressure-associated disease, development risk, cost-effective pot. classifiers 4-85457
- HLW deep ocean disposal, seafood critical pathway assessment 4-91042
- human EM hazard analysis, human body impedance in VLF to MF band 4-115120
- human exposure to natural radiation 4-93889
- human mononuclear leukocytes exposure to pulse modulated microwaves 4-115126
- in-plant aerosols, PIXE anal. 4-105071
- indoor dose in Milan 4-93878
- indoor environments, radiation aspects, related radioecological problems, Netherlands situation 4-93884
- indoor exposure in a region of central Italy 4-93875
- indoor exposure rates to gamma and cosmic rays, Ge spectrometer and ionisation chamber obs. 4-93893
- indoor exposure to natural radiation, conf., Anacapri, Italy (Oct. 1983) 4-90285
- indoor exposure to natural radiation, models 4-93910
- indoor living, long life and radiation risk 4-93890
- indoor measurements of airborne natural radioactivity in Italy 4-93931
- industrial electric/magnetic fields, effects on health (French, German) 4-72299
- laser radiation hazards 4-77396
- laser safety in medical appls. 4-85524
- leakage and scattered dose equivalent during 25-MV radiation treatments 4-89756
- LF stray fields, EM smog (German) 4-59971
- low level exposure to radioactive pollutants, health risk assessment 4-109965
- low level radwaste sea disposal, NEA research and environmental surveillance programme 4-83210
- low level radwaste shallow burial site, environmental pathways anal. 4-83193
- mammographic screening, low dose, benefit/risk ratios 4-89693

## health hazards continued

- marine environment, radwaste effects, national policy guidelines for USA 4-83212
- microwave oven leaks, interaction of the near-zone fields of a slot on a conducting sphere with a spherical model of man 4-115123
- microwave-induced post-exposure hyperthermia: involvement of endogenous opioids and serotonin 4-115129
- military helicopter flight, disorientation, psychology of visual perception 4-85528
- military helicopter flight associated hearing loss; comparative tests on pilots 4-85529
- military helicopter operations, aeromedical support, 'conf.', Soesterberg, Netherlands, (June 1984) 4-82597
- military helicopter operations, visual problems 4-85527
- milk produced in Channel Islands,  $^{90}\text{Sr}$  and  $^{137}\text{Cs}$  concs. 4-105353
- Misasa Spa, Japan, radioactivity of air and water, chromosome aberrations 4-93927
- natural indoor gamma background in an urban environment of Southern Poland 4-93873
- natural irradiation in dwelling places in France:  $\gamma$ -rays, Rn and Rn daughters obs. 4-93882
- natural radiation in an urban district of West Germany, population exposure 4-93877
- natural radiation in Belgian houses 4-93876
- natural radioactivity of building materials in Austria 4-93905
- neutrons from high-energy X-ray medical accelerators, risk to radiotherapy patient 4-85498
- NMR imaging, pot. hazards, mag. fields rel. to cardiac function in animals obs. 4-105317
- NMR imaging facility, architectural design, shielding requirements 4-89672
- nuclear medical procedures, dose and risk to patients in the GDR 4-89752
- Nuclear Medicine Department, radiation safety program 4-115234
- nuclear plant personnel and neighbouring population radiation protection problems (French) 4-74053
- nuclear power industry, radiation protection and its legal objectives, general overview (German) 4-64239
- nuclear power industry radionuclide emissions; environmental aspects 4-83252
- nuclear power stations, radiation protection planning and management during revision stages (German) 4-64240
- nuclear waste deep ocean disposal, long-lived radionuclide behaviour 4-83213
- ocular exposure to infrared radiation in the Swedish iron and steel industry 4-62603
- ocular hazard from GaAs lasers and near IR radiation 4-93797
- Ontario Hydro's nuclear power stations, radiological impact 4-89791
- organ transformation calc. after radioactive aerosol inhalation 4-62593
- personal noise dosimeter for hazard eval. in industry 4-91701
- potable water in Saudi Arabia, material radioactivity 4-89789
- power line, 3-phase, EM fields in vitro simulation 4-109874
- power lines, 50 Hz elec. field, physiological effects 4-62520
- protective actions, off-site nuclear response considerations 4-107163
- public radiation exposure impact of TRU nuclides from Sellafield liquid wastes 4-83211
- radiation, film badge, accuracy determ. 4-62591
- radiation doses and biological effects of cosmic rays 4-100261
- radiation emission, mandatory performance standards of US Food and Drug Administration 4-89869
- radiation exposure and radioactive emissions from United States DoE operations 4-83202
- radiation exposure rate and distrib. in rooms, determ. 4-93871
- radiation exposures, Sieverts and safety 4-115228
- radiation medical exposure and occupational exposure in AEE of Egypt, intercomparison 4-77401
- radiation protection in medicine, conf., Jodhpur, Rajasthan, India (Feb. 1984) 4-73156
- radiation protection in modern nuclear medicine and brachytherapy departments 4-77402
- radiation protection instrumentation for medical and biochemical radionuclide laboratories 4-77403
- radioactive effluent discharges, transfrontier environmental protection, Euratom Treaty article 37 appl. 4-83200
- radioactive emissions and radiation exposures from nuclear power prod., collective dose 4-83250
- radioactive emissions from nuclear plants, permitted levels, ICRP-26 effects 4-91120
- radioactive high level waste disposal, potential health and safety impacts 4-106745
- radioactive liquid effluents, release limits and health consequences, water pollution (French) 4-83198
- radioactive waste dumping area survey in Massachusetts Bay, USA 4-83214
- radioactive waste sea dumping, oceanographic model and radiological basis for radionuclide release control 4-83209
- radiological consequences of use of building materials containing fly ash, Greece 4-93892
- radionuclide releases, environmental impact, release limits, assessment principles 4-83201
- radionuclide transport, human exposure, health risk calc. 4-109952
- RF hazards, specific absorption rate distribution in a full-scale model of man at 350 MHz 4-115122
- RF human whole-body absorption rates, effect of separation from ground 4-115121
- RF power absorbed by biological samples meas., using high-power network analyser 4-85600
- salt dome radwaste repository, radiation exposure due to radioactive releases 4-83205
- sheltering as protective action in nuclear accidents 4-107164
- short wave diathermy equipment, stray mag. fields and power outputs using tissue equivalent phantoms 4-89755
- skin tumors, work-related distrib. in Sardinia, epidemiological obs. 4-81742
- spent reactor fuel dry-storage techniques, probabilistic risk assessment 4-59337
- standard mortality ratios for CRNL long-term employees in relation to lifetime occupational dose 4-89780
- sunburn, annotated bibliography, historical development 4-58608
- N Tanzania, high fluoride content of rivers, lakes, springs 4-115467
- UV laser radiation, max. permissible exposure estimates 4-62526

## health hazards continued

- walls of buildings, math. models of emitted  $\gamma$ -rays, congruence of mea. 4-93868
- walls of room, radioactivity inhomogeneities rel. to external  $\gamma$ -dose 4-93870
- work environment aerosols, PIXE anal. 4-105070
- working environment aerosols in lead battery factory, toxicity monitoring by PIXE and AAS 4-105072
- X-ray installations in Bangladesh, radiation exposure level assessment for protection 4-77400
- xeromammography, absorbed dose and image quality 4-89695
- <sup>241</sup>Am, medical course after accidental exposure 4-109890
- Be, advantages and limitations for use in mag. fusion devices 4-107017
- Be use in fusion reactors, health risk implications 4-107015
- <sup>3</sup>H exposure risks, conf., Mol, Belgium (Nov. 1982) 4-90294
- <sup>129</sup>I in waterfowl muscle, collection from radioactive leaching pond, S. Idaho 4-115231
- <sup>137</sup>I, thyroid uptake blocking by RI, nuclear accidental appl., review 4-115232
- NO<sub>x</sub> pollutants in atm., conf. at Maastricht, Netherlands (May 1982) 4-101576
- <sup>237</sup>Np, potential toxicity in high-level waste 4-106758
- Pb concentration at roadside, effects on human and animal health 4-100044
- <sup>210</sup>Pb, precipitation exchange separation and detection technique 4-109951
- <sup>210</sup>Po in environment around radioactive disposal area and phosphate of processing plant, Idaho 4-89785
- Pu isotopes in surface air, Japan (1979-82) 4-115239
- <sup>238</sup>Pu, A=238, 239, 240, content in tobacco crop near nuclear fuel separation facility 4-115237
- <sup>238</sup>Pu, A=239, 240, body burden in Lapps, comparison with southern Finl. 4-62590
- <sup>240</sup>Pu/<sup>239</sup>Pu ratio in environmental samples, Lx/ $\alpha$ -ray activity ratio mea. 4-115238
- <sup>226</sup>Ra and bone seeking radionuclides, carcinogenicity; beagle studies 4-115221
- <sup>226</sup>Ra content in drinking water, Denmark 4-94173
- Rn and daughters concs. indoors, mathematical model 4-93916
- Rn and decay prods., equilib. factor meas., method using passive track detectors 4-105352
- Rn and Rn daughter concs. in Swedish homes 4-93930
- Rn and Tn, dosimetry and monitoring, public exposure to natural radiation, OECD/NEA programme 4-93865
- Rn concentration in a basement, variation with barometric pressure 4-67132
- Rn concentrations in residential buildings in Maryland and Pennsylvania, USA 4-93926
- Rn concentrations indoors, temporal variations 4-93924
- Rn control programme in theory and practice 4-93936
- Rn daughter, particle size meas. 4-93913
- Rn daughter, removal by filtration and elec. field 4-93934
- Rn, daughter activities, meas. instrumentation 4-93867
- Rn, daughter activity concs. indoors, approx. meas. technique 4-93866
- Rn daughter attachment, indoor aerosol size distrib., automatic measurement system 4-93914
- Rn daughter collection and passive monitors calibration 4-93673
- Rn daughter conc. in room air, continuous spectrometry by twin channel device 4-93672
- Rn, daughter concentrations in northern part of Netherlands 4-93925
- Rn daughter dose: environmental vs. underground exposure 4-93887
- Rn daughter product, passive detection rel. to plateau 4-93863
- Rn daughter products in indoor air 4-93912
- Rn daughters, deposition rates on indoor surfaces 4-93917
- Rn daughters, indoor concs., soil sources for Swedish houses 4-93903
- Rn daughters, indoor exposure, design and interpretation of large surveys 4-93879
- Rn daughters, indoor exposure, dosimetric approaches to risk assessment 4-93886
- Rn daughters; population exposure, annual dose assessment problem 4-93885
- Rn daughters, respiratory tract deposition in humans 4-93932
- Rn daughters, turbulent plateau in rooms and mines 4-93920
- Rn daughters aerosol, activity size distrib. in buildings, cascade impactor meas. 4-93918
- Rn daughters in indoor air, aerosol and activity size distrib. 4-93915
- Rn daughters in indoor air, aerosol particle conc. rel. to ventilation system 4-93922
- Rn daughters suspended in air, alpha activity, working level in U mines and houses 4-109966
- Rn detection in Finnish dwellings, film detectors calibration 4-93895
- Rn emanation meas. by activated charcoal canisters, counting efficiency 4-109950
- Rn, environmental impact on buildings, mining dumps sources 4-93906
- Rn, exhalation and diffusion from building materials 4-93908
- Rn exhalation from concrete rel. to flyash additives and porosity 4-93907
- Rn exhalation from concrete and alum shale bearing soil, moisture and temp. effect 4-93904
- Rn exhalation from Finnish building materials, room air ventilation rate 4-115236
- Rn, exhalation transients rel. to ventilation and atmospheric pressure 4-93909
- Rn in dwellings, location and limiting 4-93933
- Rn in Finnish houses, geographical distrib. and temporal variation of 4-93929
- Rn, indoor concentration in Swiss dwellings rel. to weather-stripping matched pair anal. 4-93928
- Rn, indoor concs., sources and movement 4-93891
- Rn, indoor exposure rel. to way of living; methodological study 4-93872
- Rn, indoor meas. using activated C collectors 4-89771
- Rn, measurement in dwellings using activated charcoal 4-93897
- Rn, portable meas. systems appl. to conc. in gases 4-93671
- Rn transport into houses, theoretical evaluation 4-93923
- <sup>222</sup>Rn, A=220, 222, daughters in indoor aerosols, particle size distribution 4-93921
- <sup>222</sup>Rn, A=220, 222, diffusion and exhalation from building materials 4-93901
- <sup>222</sup>Rn, A=220, 222, emanating power and specific surface area of building materials 4-93907
- <sup>222</sup>Rn and daughter product concs. in dwellings and open air, equilibrium factor 4-93919

health hazards continued

- <sup>222</sup>Rn and decay products, active and passive dosimetry, international intercomparison 4-93864
- <sup>222</sup>Rn concs. in dwelling, seasonal variation 4-109968
- <sup>222</sup>Rn content in drinking water, Denmark 4-94173
- <sup>222</sup>Rn exhalation from porous materials, diffusion-transport theory 4-93911
- <sup>222</sup>Rn exhalation rate from surface of building materials or soil, meas. apparatus 4-93896
- <sup>222</sup>Rn, indoor concs. in energy efficient homes, NY, USA 4-109963
- Si radiometer for laser hazard meas. appls. 4-58882
- T distrib. and excretion after intratracheal installation of glass microballoon fragments in rats 4-62594
- T, internal contamination of radiological workers at two Netherlands universities, urinalysis dosimetry 4-62597
- T<sub>2</sub>, airborne plume, oxidation rate rel. to release height and atmospheric stability 4-115241
- <sup>95m</sup>Tc in Japanese quail eggs, chronic feeding study 4-62612
- <sup>95m</sup>Tc, in soil, net uptake in plants, field and greenhouse expts. 4-62409
- Th daughter radioactivity released from burning gas lantern mantles 4-89787
- Th, processing plant, airborne radioactivity monitoring 4-109964
- <sup>228</sup>Th retention and dosimetry in beagles 4-93937
- UO<sub>2</sub>, subcutaneous implantation in rats, deposition pattern and toxicity 4-62606
- <sup>133</sup>Xe containing syringes, storage and disposal, radiation hazards 4-109969
- <sup>133</sup>Xe, personnel exposure in nuclear medicine laboratories, instrument evaluation 4-62596
- <sup>135</sup>Xe, released effluent, sector averaged plume, gamma dose rate from side sectors 4-115240

health physics see dosimetry; health hazards; radiation monitoring; radiation protection

hearing

see also bioacoustics; ear; hearing aids; speech

- acoustics conference, Paris, France (July 1983) 4-78035
- adaptation, long-term, in hearing impaired ears, cat obs. 4-93755
- adult cross-language speech perception, phonemic and phonetic factors 4-85445
- albino guinea pigs, rel. to auditory research 4-105251
- AM tones, detect. by frogs, implications for temporal processing mechanisms 4-93746
- amplified pop music and hearing level meas. 4-105254
- amplitude modulation thresholds in chinchillas with high-frequency hearing loss 4-72262
- anteroventral cochlear nucleus neurons responses, Wiener kernel anal. 4-93747
- audio filter design, appl. of simple hearing model 4-105260
- audiogram, microstructure of quiet and masked thresholds 4-109842
- audiometer screening instrument, calibration 4-85432
- auditory discrimination, functional anal. 4-85430
- auditory evoked brainstem responses, signal processing technique 4-85429
- auditory filter dynamic range and asymmetry 4-115065
- auditory nervous system, neuro-synaptic model of bilateral interaction 4-66963
- behaviour patterns, noise sensitivity as function of task complexity 4-81707
- binaural anal., role of monaural freq. selectivity 4-115067
- binaural masking-level difference rel. to masker and test-signal duration 4-89590
- binaural masking-level differences: effects of bandwidth, noise level and signal duration 4-93748
- binaural masking-level differences in nonsimultaneous masking 4-89591
- binaural masking-level differences with tones masked by noises of various bandwidths and levels 4-93749
- binaural measurement system, microcomputer-based 4-100407
- body sensation of low freq. noise for deaf and normal hearing subjects 4-105262
- brain damage assessment in malnourished infants; use of visual and auditory evoked pots. 4-89821
- brain stem auditory evoked potentials, lesions location, computer analysis 4-72258
- brainstem auditory evoked pot. amplitude, latency and waveform: effects of high-pass filter freq. 4-105242
- brainstem auditory evoked pots., human, 3-channel Lissajous' trajectory 4-67135
- brainstem auditory evoked pots., latency rel. to click phase and rate 4-100158
- brainstem auditory evoked responses, constituent components extraction 4-85433
- brainstem auditory evoked responses in chronic renal failure patients 4-100157
- brainstem response and temperature: relationship in guinea pigs 4-77252
- brainstem responses, averaged, quality estimation 4-115082
- brainstem responses, effects of stimulus rise-time and polarity 4-85440
- brainstem responses and behavioural thresholds, stimulus duration effects 4-115071
- brainstem responses recording, artifact rejection criteria efficiency comparison 4-85546
- bullfrog, *Rana catesbeiana*, auditory system, nerve fibre responses, adaptation patterns 4-62502
- central auditory pathway of the gerbil, deoxyglucose study 4-115062
- children, hearing-impaired, auditory-visual vowel perception 4-85431
- click detection, interaural differences of time intensity dependence 4-77260
- cochlea, single fibre responses in guinea pigs with long-term endolymphatic hydrops 4-93759
- cochlea generated distortion, ear canal acoustic and round window elec. correlates 4-109828
- cochlea of Mongolian gerbil, auditory function development 4-89596
- cochlear function in guinea pigs with long-term endolymphatic hydrops, electrophysiological meas. 4-93760
- cochlear hair cell density, guinea pig, rel. to freq. discrimination 4-100166
- cochlear nerve and nucleus, single units, noise masking of tone responses and crit. ratios 4-93757
- cochlear nonlinearities, inference from 2-tone distortion prods. in alligator lizard ear canal 4-105247
- cochlear nucleus neurons, tone-evoked activity reduction by baclofen 4-105244
- hearing continued
- cochlear nucleus of deaf quivering mouse, single unit responses 4-109830
- cochlear potentials, gross, rel. to hair cell pathology in waltzing guinea pig 4-115060
- cochlear shunts in birds, comparative mechs. of hearing 4-109832
- compound action pot. recordings 4-100159
- compound action pots. and single unit responses to 1 kHz haversine 4-100164
- concurrent minimum audible angle, auditory spatial acuity 4-72266
- cortical evoked potentials, interaction to electric and acoustic stimuli 4-115070
- crickets, ventral cord neurones, two-tone interactions and song coding 4-105240
- cubic-difference-tone generation and suppression 4-100167
- Deutsch's dichotic octave illusion experiments (*German*) 4-85428
- dichotic listening, signal detect. theory appl., nonsense syllables obs. 4-115075
- diotic and dichotic perception of sound fluctuations 4-93744
- directional hearing in grass frogs, tympanic membrane vibrs. 4-93751
- discrimination of fundamental frequency of synthesized vowel sounds in a noise background 4-115066
- diver noise exposure and hearing conservation standards 4-109844
- dynamic interaural intensity differences, discrimination 4-100171
- ear acoustic props., short-time power spectra parametric representation 4-103141
- electric response audiometry, slow vertex response discriminator 4-81709
- electric response audiometry, theory and appl. of weighted averaging 4-105241
- electrically stimulated auditory nerve, single fibre recordings 4-100160
- electrically-evoked responses in animals with progressive spiral ganglion degeneration 4-109841
- endocochlear potential and auditory nerve fibre tuning curves in cats 4-100165
- evoked brainstem responses 4-85441
- evoked potentials, auditory and visual, in Huntington's disease 4-72244
- evoked potentials, computer reconstructed, high pass filters effect 4-72449
- evoked potentials, dissociation from perception by bilateral lesions 4-77251
- evoked potentials, objective response detect. 4-85559
- evoked potentials, simultaneous recording 4-85435
- evoked potentials in people with perfect pitch, tone processing without P300 prod. 4-81708
- evoked response in young children, middle components 4-85436
- evoked response of cat brain stem, hypothermia effects 4-72259
- forward masked tuning curves, delay-time and probe level manipulations 4-77257
- forward masking, combined effect of two suppressors 4-77256
- frequency and rate modulation detection by chinchilla 4-72263
- frequency dependence of directional amplification at the cat's pinna 4-93754
- frequency following response in the cat, anal. 4-109838
- frequency threshold curves and simultaneous masking functions in guinea pig auditory nerve 4-100161
- frequency-following responses in the cat 4-109836
- hair-cell neurons, discharges simulation by pseudo-random sequences 4-85444
- human classification of complex sounds 4-115078
- human head, bone and air conducted impulse signals, phase relationships 4-100175
- impedance audiometers, laboratory and commercial, clinical comparison 4-115261
- individual noise, audiometric database 4-109766
- infants, discrimination of intensity variations in multisyllabic stimuli 4-100179
- infants, perceptual reality of tone chroma 4-100169
- infants, speech perception of nasal consonants 4-77263
- inferior colliculus, cat, responses to low intensity tones 4-105248
- inferior colliculus, cat, stimulus intensity effects 4-105249
- interaural intensity discrimination in humans, insensitivity at 1000 Hz 4-72264
- interaural octave phase-shift detection and aural harmonic distortion 4-115064
- interaural phase shift detection between audible and subaudible tones 4-115063
- interaural time differences detect. for clicks and tone pips, effects of interaural signal disparity 4-115061
- ipsilateral acoustic reflex thresholds in neonates and pre-school children 4-85442
- iris colour rel. to hearing loss 4-62499
- isolated word recognition, auditory models 4-105256
- lateral difference in hearing sensitivity 4-89588
- lateralization and frequency selectivity in normal and impaired hearing 4-100172
- level difference thresholds meas., acoustic neuroma detect. appl. 4-62536
- linear frequency modulated sweeps, selective adaptation 4-77259
- loss of hearing in cats and hypersensitivity to elec. stimulation of auditory nuclei 4-89593
- mammalian cochlea, sensitivity modulation by LF tones, basilar membrane motion 4-109826
- mammalian cochlea, sensitivity modulation by LF tones, inner hair cell receptor pots. 4-109825
- mammalian cochlea, sensitivity modulation by LF tones, primary afferent activity 4-109824
- masked normal ears, temporal gap resolution 4-100170
- masking, critical masking interval meas. (*Japanese*) 4-89599
- medial superior olivary neurons, responses rel. to binaural masking and unmasking 4-109839
- military helicopter flight associated hearing loss, comparative tests on pilots 4-85529
- minimum detectable delay of speech and music 4-105259
- monaural localisation, psychophysical basis 4-93750
- nerve action potential, adaptation and recovery 4-77254
- nerve fibres, response to consonant-vowel syllables 4-100176
- nerve impulse cross-correlation model for mixed speech separation (*Japanese*) 4-85443
- neural auditory processing, computational models 4-103139
- noise, temporal averaging of subjective magnitude and proposed rating scale for fluctuating noise 4-83764
- noise effects on detection, spectro-temporal pattern anal. 4-100168

**hearing** continued

- organ of Corti, intercellular elec. coupling obs. 4-93752
- periodicity pitches, strength, influence of temporal cues 4-77258
- personal noise dosimeter for hazard eval. in industry 4-91701
- physical principles in hearing theory, review 4-85434
- pitch of computer-generated complex tones, circularity, paired comparison expt. (*Japanese*) 4-100177
- pitch of multicomponent inharmonic tones, central optimal processor 4-115059
- pitch perception for FM-AM tones, psychoacoustical expts. 4-89600
- primate superior colliculus, shift of auditory receptive fields with eye position changes 4-77261
- profile anal., critical bands and duration 4-72260
- profile analysis and level variation 4-89595
- protection device effectiveness at industrial facility with 107 dB 4-112633
- protection devices, compendium 4-109767
- protectors, international standards 4-62424
- protectors for hearing conservation purposes 4-83769
- psychoacoustical measurements, new methods (*Japanese*) 4-115072
- psychophysical tuning curves in normal-hearing listeners: test reliability and probe level effects 4-115073
- quasi free-field audiometry, modified transducer system 4-85462
- relative loudness discrimination 4-105252
- residual auditory function assessment, use of articulation index 4-72273
- rise time identification and discrimination 4-72261
- sensorineural deafness in the case of functional disorders of the middle ear 4-62500
- sensorineural tinnitus, postmasking effects 4-115077
- shock-proof ear, comparative mechs. of hearing 4-109831
- Shrapnell's membrane, comparative mechs. of hearing 4-109833
- sound localisation, influence of pinnae-based spectral cues 4-72265
- sound pressure level measurement and spectral analysis of brief acoustic transients 4-72257
- sound quality measurements of audio systems based on models of auditory perception 4-105258
- speech, articulation index anal. 4-74815
- speech, pitch and spectral estimation, auditory synchrony model based 4-103140
- speech, pitch perception algorithm 4-83782
- speech, vowel monitoring in isolation and in consonantal contexts 4-100181
- speech, vowels, timbre perception, spectral resolution (*German*) 4-60222
- speech perception, silent intervals role 4-83784
- speech perception, voiced-voiceless contrast in syllable-final stops 4-100180
- speech processing, 1-Bark bandwidth auditory filter 4-83783
- speech recognition in noise, effects of age and mild hearing loss 4-100182
- speech recognition in the case of low-freq. hearing loss 4-72267
- speech recognition system, LPC anal. and peripheral auditory system model, comparison 4-105257
- stapedius reflex and brainstem auditory evoked responses in multiple sclerosis patients 4-85439
- stereo sound/video image interaction (*Japanese*) 4-109843
- stereophonic sound perception, interaural phase anomaly (*Russian*) 4-93761
- stimulus polarity indicator device construction 4-67136
- subjective component of the fidelity of sound reproduction (*Italian*) 4-72268
- swimbladder, carp, responses to sound stimulation, auditory appl. 4-93796
- temporal difference in speech perception by adults, effects of age and intensity 4-115083
- temporal gap detection in sensorineural and simulated hearing impairments 4-115076
- Tennessee tonality test for speech discrimination by hard-of-hearing 4-100178
- tensor tympani acoustic reflex in humans 4-85438
- tone-glide discrimination: normal and hearing-impaired listeners 4-115074
- tone-on-tone masked thresholds, correlates in chinchilla auditory nerve 4-89597
- US, focused, for stimulation of nerve structures 4-72320
- voice pitch representation in discharge patterns of auditory nerve fibres 4-100162
- warning sound perception and attention demand, hearing protector effects 4-105253
- wave propagation and dispersion in the cochlea 4-105243
- word recognition with segmented-alternated CVC words, listeners with normal hearing study 4-115085

**hearing aids**

- acoustics conference, Paris, France (July 1983) 4-78035
- cochlear implants, multiple-channel, acoustic model 4-100173
- cochlear implants, multiple-channel, speech processing, acoustic model 4-100174
- cochlear prosthesis, unit responses of cochlear nucleus to elec. stimulation through prosthesis 4-93753
- fittings for aids, anal. using insertion gain meas. 4-115273
- multichannel cochlear prosthesis for profound-to-total hearing loss 4-109993
- performance of hearing aids from the pre-electronic era 4-62628
- preferred hearing aid gain and bass-cut rel. to prescriptive fitting 4-115081
- Schafer cortical hearing aid 4-85583
- simulated in situ measurement system 4-89833
- tactile aids for deaf people, review 4-77253
- tactile hearing aid, tactile perception of phonemic code 4-109846

**heart** see *cardiology***heart valves** see *cardiology; prosthetics***lava**

- see also *heat transfer; heating; latent heat; specific heat; temperature; terrestrial heat; thermal variables control; thermal variables measurement; thermodynamic properties; thermodynamics*
- nonequilibrium steady states, reversibility, work and heat 4-101803

**heat capacity** see *specific heat***heat conduction**

- see also *thermal conductivity*
- Benard convection and the Cattaneo law of heat conduction 4-69665
- blow-up regimes calc. (*Russian*) 4-112671

**heat conduction** continued

- bounded region, nonlinear heat conduction eqn. with non-powered cool (*Russian*) 4-69661
- calculation formulae selection for solving inverse problems 4-112665
- Cartesian two dimensional phase change, fixed mesh finite element solution 4-112669
- ceramics, brittle, thermal stress fracture on liquid quenching rel. to the mat and mech. props. 4-109504
- composite materials, thermal conductivity, nonlinear inverse problem accuracy of soln. anal. 4-97277
- composite wall, heat cond. 4-112693
- coolant heat conduction in flow direction (*Chinese*) 4-83885
- counterflowing fluids separated by heat conducting plate; heat transfer 4-97522
- crystal growth in Bridgman-Stockbarger config., heat transfer analysis radial temp. variations 4-114381
- cylinder, 3D, transient heat conduction, spatial decay estimates 4-91717
- Darcian free convection boundary layer flow about semi-infinite vertical plate 4-112879
- deformed solids, correl. between solutions of generalised and classical thermomechanics 4-103178
- differential equation modification 4-79416
- disc, circular, non-Fourier thermal stresses 4-97307
- eigenvalue method for solving transient heat conduction problem 4-60245
- electro-magneto-thermo-elastic plane waves in rotating media with therm relax. 4-91723
- electron gas, electric breakdown waves 4-87836
- ferroelectrics, monoaixial, with second order phase transition, nonlinear pyroelectric response 4-88777
- fibrous cross-reinforced materials, heat conduction anal. using double periodic harmonic functions (*Ukrainian*) 4-87537
- filtration and heat conduction in porous bodies, related problems 4-79606
- fin, annular, const.-width, with variable thermal cond. and internal heat generation, temp. field 4-78713
- fluid, thermal nonequilibrium general relativity 4-110949
- freezing, two-dimensional problems anal. by finite element method 4-97291
- furnace, casting unit, heat exchange, inverse heat cond. calcs. 4-107982
- furnace, thermal processes, numerical study 4-107985
- gas-solid nonstationary heat transfer, determ. by inverse heat cond. calc. 4-107994
- green's function solution for transient heat conduction problem 4-103176
- heat exchanger surfaces, testing using selected point matching technique heat cond. effect 4-97296
- heat exchangers, open-topped, closed-sided, with vertical fins, heat transfer rates enhancement, for use in electronic equipment cooling 4-79420
- inhomogeneous anisotropic materials, plane thermostatic problem 4-97318
- inhomogeneous medium, flow and conduction theory 4-79630
- inverse (retrospective) problems, numerical soln. 4-97273
- inverse boundary-value problem, numerical formulation, soln. 4-97276
- inverse boundary-value problem, soln. by iteration algorithm 4-97275
- inverse heat conduction problem, convergence of iteration method 4-97274
- inverse heat conduction problems, soln. methods 4-97270
- inverse heat conduction problem, descriptive soln. in B-spline basis 4-97272
- inverse heat conductivity problems, thermophysical characteristics identification 4-103177
- inverse problem, two-dimens., soln. in cylindrical coord. system 4-97271
- inverse problems, analog computer calcs., instrument error 4-107981
- laminar incompressible permanent flow through circular pipe with axial cond. and viscosity, temp. calc. 4-103284
- linear and nonlinear heat conduction with a quadrilateral element 4-79417
- local heat transfer parameters, statistical identification 4-107979
- magnetic fusion reactors, surface melting and evaporation due to plasma disruptions 4-96255
- materials testing, high temp. inverse heat cond. problem investigation 4-99684
- melting process, coupling of natural convection and phase change (*French*) 4-112854
- multilayer wall heat conduction system, approximate transfer function calcs. 4-79419
- multilayer wall heat transfer, successive state transition method dynamic calcs. 4-87542
- multiple hypergeometric functions 4-87539
- nonlinear heat conduction problems, anal. using hybrid/analog simulation 4-97267
- nonlinear inverse heat conduction problem with radiation boundary condition 4-87538
- nonlinear one-dimens. heat conduction problem in certain temp. range approx. soln. 4-112666
- nonlinear steady-state thermal anal., reduction methods 4-91714
- nonlinear thermal anal., hybrid perturbation/Bubnov-Galerkin technique 4-64818
- nucleate pool boiling, bubble growth rates and departure vols. 4-97649
- phase change, enthalpy formulation, numerical soln. 4-97300
- planar bodies, initial state of heat conduction 4-69662
- plane wall subject to periodic temp. changes, heat and eqn. soln. 4-64806
- plasma spraying on fibres, thermal characts. 4-66254
- plate, nonlinear heat cond. and self-similar solns. 4-74837
- porous body, internal heat transfer coeffs., inverse problem calculation 4-107980
- PVC, deform., shape recovery rel. to temp. distribution (*Japanese*) 4-114614
- reduced order approximation of heat conduction equation (*Japanese*) 4-83798
- semitransparent media, coupled radiation-cond. heat transfer, Monte Carlo finite difference method 4-60247
- single-brain solar still coupled to flat-plate collector, water flow over glass cover, transient anal. 4-99994
- solidification, directional, inverse problem of heat conductivity 4-93272
- solidification, rapid, with nonhomogeneous thermal contact 4-93276
- stellar interiors, heat conduction by neutrinos during core collapse 4-101313
- thermal loads determ. from data of temp. meas. in a solid 4-112667
- thermal pulse, growth and decay predicted by hyperbolic heat cond. eqn. 4-60246

# heat conduction continued

- thermally protective materials, thermophys. characts., inverse heat cond. problem calcs 4-97269
- thermodynamics of continuous media using entropy flux of Muller 4-90542
- thermoelasticity problems, Reissner type variational-principle formulation (Ukrainian) 4-69679
- thermophysical parameters, automated identification of inverse heat cond. calcs. 4-106321
- thermophysics, expl. data processing, hardware and software struct. 4-95420
- three-dimensional unsteady, boundary fitted finite-difference calcs., 2D Navier-Stokes eqns. 4-97266
- transient algorithms anal. for mechanics and heat conduction, stability, book contrib. 4-60248
- transient heat cond. problems, complex two-dimensional, numerical modelling techniques 4-91715
- transient nonlinear heat conduction theory, analytical and numerical methods (Italian) 4-107989
- transient radiation-conduction heat transfer in a finite cylinder filled with an absorbing radiating medium 4-79415
- transition from conduction to convection around a horizontal cylinder experiencing a ramp excursion in internal heat generation 4-97268
- two-layered plate, heat conduction problem with plane heat source between layers 4-79418
- two-phase medium, thermal conductivity tensor, with anisotropic phase distrib., variational estimate 4-79650
- uniqueness in certain inverse problems of the theory of heat conduction 4-74836
- unsteady natural convection in a cavity with internal heating and cooling 4-60408
- vacuum-shield heat insulation, multilayer, radiative-molecular-conductive heat transfer 4-112684
- viscous gas, heat conducting, difference schemes, stability and convergence (Russian) 4-69660
- wedge-shaped regions with moving heat source, effect of heat exchange on form. of temp. field 4-69663
- Si, clean and SiO<sub>2</sub> covered, picosecond laser heating and evaporation 4-70198

# heat content see enthalpy

# heat convection see convection

# heat dissipation see cooling

# heat engines

- 1 kW free-piston Stirling engine alternator unit, development 4-66782
- air-water Stirling engine construction and testing 4-66762
- Allison 501-KB gas turbine engine, Brayton cycle, Cheng dual-fluid cycle effects on power and thermal efficiency 4-66744
- automotive Stirling engine development program—overview and status report 4-66777
- closed-cycle diesel engines, use of Ar, He and CO<sub>2</sub> as working fluids instead of N<sub>2</sub>, effects on performance 4-66743
- concentration difference energy system and engine, developments, heat transfer studies and appls. 4-66786
- cyclic heat transfer phenomena in closed spaces, simplistic model 4-64820
- direct-fired engine driven heat pumps, future developments 4-99987
- DOE/NASA Automotive Stirling Engine Project—Overview 83 4-66749
- ECA Stirling engine, indirectly heated, design features, for small submarine propulsion 4-66774
- energy conversion engineering conference, Orlando, Florida, USA, August, 1983 4-78861
- for submarines ECA Stirling engine combined molten-salt thermal storage and sodium heat pipes 4-66765
- free displacer back-to-back gamma type Stirling engine 4-66783
- free piston Stirling engine: 20 years of development 4-66750
- free-piston Stirling engine, single-cylinder, 1 kW, test results with dashpot load 4-66781
- free-piston Stirling engine/linear compressor system parametric testing and evaluation 4-66779
- gamma-type Stirling engine, with back-to-back free displacer, closed-form anal. 4-66763
- gas absorption power cycle, CO<sub>2</sub> working fluid and K<sub>2</sub>CO<sub>3</sub> solutions as carrier fluids, thermodynamic calcs. 4-66745
- liquid-piston Stirling engine dynamic anal. using vector or phasor method 4-66772
- low-grade geothermal energy conversion by organic Rankine cycle turbine generator 4-77140
- miniature Stirling engines for artificial heart power 4-67150
- MOD I automotive Stirling engine development 4-66776
- nuclear reactor space power systems, gas-cooled and liquid-metal-cooled, comparison 4-72149
- organic Rankine bottoming cycles waste heat recovery 4-66748
- organic Rankine cycle power conversion systems for space applications 4-72150
- organic Rankine cycles, performance characts. with various working fluids 4-99986
- Rankine-cycle heat engine, low-temp., technical and economic study 4-66747
- RE 1-11 rotary expander engine testing and analysis 4-66746
- reciprocating gas-handling machinery, heat transfer during compression and expansion 4-64821
- reciprocating solar heated engine utilizing direct absorption by small particles, thermodynamic efficiency 4-114924
- Ringbom Stirling engines first-order analysis 4-66761
- Ringbom-Stirling air engine, design and operational experience with water as lubricant 4-66770
- Ringbom-Stirling air engine design aspects 4-66769
- Ringbom-Stirling engine, free displacer dynamics determ. 4-66771
- shape memory heat engines 4-81245
- solar heat pump Rankine cycle, development, test and evaluation 4-72153
- Stirling cycle machine anal. methods review 4-66751
- Stirling cycle simulation method, experimentally validated 4-66757
- Stirling engine, free-piston, design and optimisation using non-linear state space stability anal. 4-66759
- Stirling engine, use of back-to-back pumping ring as a rod seal 4-66767
- Stirling engine's torque characts., identification 4-72147
- Stirling engine analysis insights derived from sixteen years of artificial heart power source development 4-66760
- Stirling engine analysis using mathematical model 4-66754

# heat engines continued

- Stirling engine heat-actuated heat pump, progress report 4-66787
- Stirling engine performance predictions, effects of pressure-drop correlations 4-66752
- Stirling engine power conversion system, second generation, design and testing 4-62388
- Stirling engine reciprocating rod seals thermal and elastohydrodynamic anal. 4-66768
- Stirling engine using two-phase two-component working fluid, computer modelling 4-66784
- Stirling engine-generator sets development for the US Army 4-66780
- Stirling engines, coal-burning, large-scale, possible applications 4-72148
- Stirling engines, small, three types, experimental studies 4-66773
- Stirling engines availability criteria 4-66764
- Stirling engines computer-aided design 4-66755
- Stirling engines isothermal anal. 4-66756
- Stirling engines with controlled evaporation of a two-phase two-component working fluid 4-66785
- Stirling machines analysis using second-order mathematical model 4-66758
- terrestrial Stirling engine R and D efforts of Air Force Wright Aeronautical Laboratories 4-66766
- tidal flow heat exchangers for Stirling engines 4-86417
- UK Consortium Stirling engine regenerator effectiveness and heater performance 4-66753
- United Stirling 4-95/4-275 heat engines for underwater use, characts. 4-66775
- waste heat recovery in industry with turbomachines using organic fluids (Rumanian) 4-66738
- Zimmerman-Stirling cryogenic cooler, construction and operation 4-72146
- Ni-Ti (45 at.%), shape memory heat engines 4-81245

# heat exchange see heat transfer

# heat exchangers

## see also cooling towers

- alternate ventilation strategies, comparisons 4-72168
- circular pipe flow complexities arising from sudden expansion and coiling 4-69830
- coal-fired boiler exhaust gas heat recovery 4-64826
- counterflow heat exchanger dynamics calc. using difference equations, errors 4-91719
- design, economic aspects (German) 4-112677
- ECA Stirling engine, indirectly heated, design features, for small submarine propulsion 4-66774
- fabrication and leak-tight furnace brazing of intricate objects 4-78301
- finned tube, cross flow, convection heat transfer and press. drop 4-103329
- finned tube, microbial cell accumulation 4-60400
- finned tube staggered-array banks, in transverse arrays, heat transfer and hydraulic resistance 4-112679
- flow reversible, temp.-entropy bond graph modelling 4-112938
- flow twisting, energy spectra of turbulence 4-112841
- flooded bed, wall to bed heat transfer in vertical tube 4-60398
- fouling and scaling, causes and effects on heat transfer surfaces (German) 4-112678
- geothermal power generation, tube enhancement evaluation 4-114891
- geothermal power station turbine hydrocarbon vapour expansions condensation behaviour 4-60250
- heat and mass transfer on filament-type packing in contact-type exchangers 4-83894
- horizontal finned tubes in cylindrical container, free convection heat transfer 4-103330
- independently heated heat exchanger dynamic, heat flux density nonuniform axial distrib. 4-97282
- Jamaican 1 MWe OTEC pilot plant 4-114929
- laminar flow inversion, coiled configuration and effect on residence time distrib. 4-112806
- laser mirrors, high intensity, heat carrier use in powder and felt porous structs. 4-74659
- link up systems open fire water heating to supplement principle heating system 4-62383
- liquid-liquid direct-contact, immiscible fluids heat exchanger analysis, for energy extraction from solar pond 4-72178
- microminiature Joule-Thomson refrigerators, fine channel heat exchangers, gas flow anal. 4-101851
- microminiature refrigeration, fabrication, design and appl. 4-78324
- model heat exchanger, velocity distributions, measured and predicted values 4-69767
- open-topped, closed-sided, with vertical fins, heat transfer rates enhancement, for use in electronic equipment cooling 4-79420
- organic Rankine cycles, performance characts. with various working fluids 4-99986
- OTEC heat exchanger biofouling, corrosion and heat resistive expts. 4-114935
- OTEC Keahole Point (Hawaii) test facility extension 4-114934
- overall heat exchanger made of paper, performance 4-83589
- parallel flow multichannel heat exchangers 4-75011
- performance simulation using programmable calculator 4-111127
- phase separator for zero-g environment, design and test 4-73442
- plate heat exchangers, U-type arrangement, flow distrib. and press. drop 4-87793
- plate heat exchangers, Z-type arrangement, flow distrib. and press. drop 4-87794
- regenerative heat exchangers for low temp. refrigeration, theory 4-111140
- residential earth coupled heat pump in New York, field test 4-72152
- shell and tube slurry heat exchangers, slurry concentration and flow rates meas. 4-60554
- shell-and-tube type, fouling comparison in tubes with annular turbulence promoters and smooth tubes 4-83893
- sieve tray direct contact heat exchanger thermal and hydraulic performance 4-60249
- single tube with forced crossflow, correl. for heat transfer during subcooled boiling 4-64940
- slurry flow in shell and tube heat exchangers, flow rate meas. 4-79666
- solar air conditioning system, with liquid desiccant, performance computer simulation 4-114944
- solar desiccant air-conditioner using heat exchangers and humidifiers 4-72164

**heat exchangers continued**

- solar energy absorber heat transfer and system behaviour (*German*) 4-81586  
 solar energy thermal storage physico-mathematical model, for high temperature 4-81595  
 spacecraft Heat Rejection System design and manufacture for advanced thermal control 4-83802  
 Stirling engine analysis insights derived from sixteen years of artificial heart power source development 4-66760  
 surfaces, testing using selected point matching technique, heat cond. effect 4-97296  
 thermoconvection loop, LIL-O-7, for studying corrosion behaviour of stainless steel in liq. Li 4-107059  
 thermosiphons, heat transfer study 4-83888  
 thermosiphons, two-phase, max. heat transfer capability 4-83889  
 tidal flow heat exchangers for Stirling engines 4-86417  
 tube bundles in transverse flows, heat exchange intensification 4-69759  
 tube-bank type crossflow heat exchanger, heat transfer, press. drop and flow visualisation expt. 4-112680  
 unsteady state mixing of the heat transport medium in a heat exchanger with twisted tubes 4-108069  
 Ag plugs, sintered, for cryogenic heat exchangers 4-101852  
 Ag powders, sintered, appl. in mK heat exchangers 4-11139  
 He cooling heat exchangers, comparison of Cu, Ag and Pd 4-95433  
 LiBr-water double effect absorption cooling cycle modelling 4-72159  
 Ti heat flux tubes for OTEC, design and appl. 4-81583

**heat flow** *see* **heat transfer****heat insulation** *see* **thermal insulation****heat losses***see also* **thermal insulation**

- 5 MW, cavity receiver, convection heat loss, obs. 4-114956  
 current heating coefficient M and its application (*Polish*) 4-112670  
 district heating pipeline configurations, design improvements 4-103180  
 flat-plate collectors, charged with phase-changing working fluids, performance anal. 4-105121  
 heat exchangers, open-topped, closed-sided, with vertical fins, heat transfer rates enhancement, for use in electronic equipment cooling 4-79420  
 heat pumps, series-connected, thermodynamic analysis 4-85384  
 honeycomb structure transparent insulation rel. to solar energy use, heat loss mechanisms 4-114946  
 residential energy conservation potentials in Connecticut 4-72036  
 salt gradient solar pond, stability, effective insulation, heat loss 4-105120  
 solar collector, flat plate performance with axial cond. and end losses, general soln. 4-81591  
 solar ponds, operating at different latitudes, performance characts. 4-105119  
 solar water heating system, flat plate, parameters effect on performance 4-81593  
 Stirling engines isothermal anal. 4-66756  
 Swedish residential energy use and conservation (1963-80) 4-66644  
 turbulent temp. field, temp. fluctuation meas. correction, using cold wires 4-60567  
 Cr, black, solar selective coatings thermal emittance estimation from stagnation temp. study 4-62393  
 Ni selective coatings thermal emittance estimation from stagnation temp. study 4-62393

**heat measurement** *see* **thermal variables measurement****heat of adsorption**

- adsorption on solid surfaces, vibrational, electronic and struct. props., book 4-78067  
 atoms and mols., adsorbed, core-level binding energy shift anal. 4-61217  
 charcoal, activated, adsorption isotherms and heats of adsorption of  $H_2(Ne)(N_2)$  4-114821  
 entropy and energy of adsorption 4-80412  
 graphite (0001), adsorption of hydrocarbons, polarisability anisotropy, mol. statistical theory 4-80379  
 multicomponent systems, surface adsorption 4-98457  
 semiconductor substrates, with adsorbed metallised atom submonolayers, cooperative phenomena 4-70556  
 thiourea, adsorption on mild steel electrodes in  $H_2SO_4$  4-88390  
 $\gamma-Al_2O_3$ , adsorption of alkanes and aromatic hydrocarbons, thermodynamic props., chromatography (*Chinese*) 4-61210  
 C, graphitised, adsorpt. of sodium dodecyl sulphate (octyltetraethylene glycol), enthalpy determ. 4-70560  
 C surface, benzene adsorption equilibria 4-92512  
 $Li_2O$  breeder blanket pellet, water vapour adsorption in He sweep gas stream 4-107032  
 Ni (100),  $N_2$  adsorption, thermodynamic meas. 4-92563  
 Ni (111), dissociative adsorption and recomb. of CO,  $N_2$ , SO, and  $O_2$  4-93559  
 Ni (111) with surface adsorbed C and CO, thermal decomposition of ethylene 4-113782  
 Ni surface, (111), adsorbed  $H_2$ , phase diagram 4-104083  
 $WS_2$ , adsorption props., gas chromatography 4-80371

**heat of combustion**

- coal-fired boiler exhaust gas heat recovery 4-64826

**heat of crystallisation**

- polybutyleneterephthalate+polyamide interchain exchange reaction, DSC obs. of copolymers produced (*Russian*) 4-77005  
 $(GaSb)_{1-x}(Ge_2)_x$  semicond. alloys, phase transforms. 4-92347

**heat of dissociation**

- adsorbed atoms and mols., adsorbed, core-level binding energy shift anal. 4-61217  
 organic ions, solvation and H bonds, correl. between dissoc. energy and  $H^+$  affinity 4-104973  
 water vapour, self-deactivation, dimer effect 4-102773  
 $Na_2$  vapour, thermal conductivity and temp. discontinuity in dissociating gases at low press. 4-113099

**heat of formation**

- acetonitrile, autoassociation, supersonic mol. beam mass spectrometer study 4-81411  
 alkali metal alloys, MAu ( $M=Li, Na, K, Rb, Cs$ ), electronic props., self-consistent relativistic band struct. calcs. 4-92604  
 alkali metal fluorides and chlorides, solution enthalpies of divalent defects 4-98316  
 alkali metal oxides, binary, high temp. vapourisation behaviour 4-98260  
 alloys, chem. bonding and heat of form., core level shift calorimetry method 4-104714

**heat of formation continued**

- alloys, disordered binary, role of excess vol. of form., virtual cryst. model 4-92133  
 alloys, molten, mixing enthalpies, interchange energies, equilb. const., association model 4-88301  
 alloys, molten, mixing enthalpies, interchange energies, equilb. const., association model 4-89060  
 alloys, thermodynamics and entropy of mixing 4-103935  
 benzene-cyclodextrin inclusion complexes aq. soln., vapour press.-solubility meas. 4-99823  
 binary alloys, charge transfer and energy of formation, CsCl intermetallic cpds. 4-77026  
 2,3'-bipyridyl-1 charge transfer complex, vibr., IR spectra 4-64476  
 3-bromo-1-propene, heat of form. determ. 4-89319  
 carbene-type cation radicals, gas-phase chem. 4-114791  
 3-chloro-1-propene, heat of form. determ. 4-89319  
 1,2-chloriodoethane, photodissoc. at 248 and 266 nm, enthalpy of formation 4-114809  
 conjugated hydrocarbons, enthalpy of formation calc.,  $\pi$ -electron approx. of MO LCAO SCF method 4-62229  
 meta-cyclophanes, conform. anal., mol. mech. calcs. 4-68937  
 diamond, vacancy formation energy, crystallisation studies 4-108354  
 dilanthanum carbides, thermodynamic study by high temp. mass spectrometry 4-69859  
 fluoroethane radical cation, generation from methyl fluoroacetate enthalpy 4-64625  
 formaldehyde dication, form. and decomposition, mass spectra 4-76971  
 graphite, vacancy formation energy, etching and TEM studies 4-92198  
 group equivalents for converting ab initio energies to enthalpies of formation 4-102586  
 hydroxymethylene dication, form. and decomposition, mass spectra 4-76971  
 3-iodo-1-propene, heat of form. determ. 4-89319  
 nitrobenzene-( $d_5$ ), metastable ions, dissoc. ionisation, heat of form. 4-71878  
 nitroso cpds., closed and open forms, relative ionicity, XPS, NDO calcs. 4-107402  
 organic molecules-electrically neutral metal complexes, outer-sphere coordination 4-62228  
 organic onium ions, solvation, H bond,  $H^+$  affinity, enthalpies 4-104974  
 organic radicals, heat of form. from appearance energies 4-89318  
 polybutyleneglycol adipate, thermodynamic props. (*Russian*) 4-84421  
 propionitrile, autoassociation, supersonic mol. beam mass spectrometer study 4-81411  
 rare earth mixed valence cpds., struct. props. 4-70751  
 transition intermetallic alloys, heats of form. 4-99818  
 transition metal borides, thermochemical and phase diagram data, couple pair pot. 4-85324  
 transition metal germanides, heat of formation and enthalpy 4-89321  
 transition metal silicides, heat of formation and enthalpy 4-89321  
 Al-Co, sputtering, surface comp., quantitative AES anal. 4-104045  
 Al-Si system, enthalpies of form. of liq. alloys 4-113679  
 Bi-Sb, liq. alloys, activities and free energy of form., EMF obs. (*Japanese*) 4-61920  
 Br containing compounds, ground states, MNDO calcs. 4-64378  
 $Cl_2$  inert gases, spectroscopic and kinetic study with VUV synchrotron radiation excitation 4-85289  
 $CS_2$ ,  $O_2$ ,  $V_2O_5$ , phase ratios, enthalpy of formation of vanadates 4-76758  
 Cu base liquid alloys, enthalpies of mixing, intermetallic compound form. 4-92374  
 $DyMnO_3$ , decomposition, O partial press. and elec. cond. 4-85290  
 Fe-Cr  $\alpha$  and  $\sigma$  phase alloys, sp. ht. and entropy of formation 4-103959  
 FeO, temp.-press. stability fields at high press., thermodynamic calcs. 4-103965  
 Ga- $N_2$  system, high pressure thermodynamics, heat and entropy of GaN form. 4-62227  
 GdGe<sub>1.63</sub>, constitution diagram, thermodynamic properties, EMF obs. 4-89024  
 $(H_2CN)^+$ , generation, heat of form. and dissoc. characts. 4-109633  
 $(H_2CN)^+$ , generation, heat of form. and dissoc. characts. 4-109633  
 $KAlSiO_4$ , amorphous, glass transitions and thermodynamic props. 4-65400  
 $La_2CoO_4$ , standard Gibbs energy of form. and high temp. thermodynamic stability 4-71958  
 Li secondary electrochemical cell, electrochemical, thermodynamic and pot. quantities 4-77072  
 Li-Pb(Ag) (Mg) liq. alloys, model, chemical short-range order, heat and entropy of formation 4-75266  
 Mn-P, thermal stability in high temp. solid-state galvanic cells 4-89394  
 $(NO)_2$ , dimer heat of form., low temp. near IR study (*French*) 4-69057  
 NaAlF<sub>4</sub>(l), from vapour pressure meas. 4-85325  
 NaAlSi<sub>3</sub>O<sub>8</sub>, amorphous, glass transitions and thermodynamic props. 4-65400  
 $Na_2O-V_2O_5$  melts, thermodynamic props., electrochem. study 4-88310  
 Nb oxides, heat of form. meas. using Tian-Calvet type calorimeter 4-81454  
 Ni, thermodynamics, kinetics and props. of gases and C, data table 4-73173  
 $NiAl_3O_4-Ni_2SiO_4$  spinellites, stability, calorimetric study 4-81456  
 PbO, standard molar Gibbs free energy of form., O conc. cell meas. 4-105010  
 PbO-CO- $H_2O$  solid systems, stability and solubility rels. 4-84399  
 PdH<sub>x</sub>, non-stoichiometric, heat of form., cluster-Bethe lattice approx. 4-75355  
 PrBi, evaporation characts., enthalpy of form., mass spectra analysis 4-88274  
 PtF<sub>6</sub>, gaseous, enthalpies of formation, quasi-equilibrium model of Pt-F system 4-89320  
 PtF<sub>6</sub>, gaseous, enthalpies of formation, quasi-equilibrium model of Pt-F system 4-89320  
 SiC- $^{11}B$  nitride solid soln. electrophys. parameter determ. 4-80241  
 SiO<sub>2</sub>, dimerisation, ab initio quantum chemical study 4-76995  
 SiO<sub>2</sub>, amorphous, glass transitions and thermodynamic props. 4-65400  
 YPd, gaseous, dissoc. energy, Knudsen-effusion mass spectrometry 4-99910  
 ZnTe, growth forms, chem. transport reactions 4-109314  
 Zr-Ni cryst. and amorphous alloys, enthalpies of form. and crystallisation 4-88097

- heat of fusion**  
cesium alkanoates, temp. and enthalpy changes meas. by thermal anal., liq. crystal region 4-70022  
copolymers of tetrafluoroethylene and hexafluoropropylene, heat of fusion rel. to crystallinity 4-103909  
glass-forming metallic melts, undercooled, free energy approx. 4-70414  
graphite, thermodynamic props., pulse laser melting, ion. channelling 4-98315  
ice, enthalpy of fusion and heat capacity, calorimeter studies 4-95425  
integral melting enthalpy of high-melting materials 4-99820  
photovoltaic solar panel optimal coupling to compression cold room with  $\text{ZnSO}_4$  energy storage 4-63749  
poly(1,6 hexamethylene adipate), synthesis and characterisation by dilatometry and X ray diff. 4-79956  
poly(1,6 hexamethylene sebacate), synthesis and characterisation by dilatometry and X ray diff. 4-79956  
poly(2,5 hexamethylene adipate), synthesis and characterisation by dilatometry and X ray diff. 4-79956  
poly(pentamethylene pimelate), synthesis and characterisation by dilatometry and X ray diff. 4-79956  
poly L-lactic acid, isothermal melting behaviour, hot stage microscopy, heat of fusion rel. to annealing time 4-65377  
polybutylene terephthalate + polyamide interchain exchange reaction, DSC obs. of copolymers produced (Russian) 4-77005  
PTFE, heat of fusion rel. to crystallinity 4-103909  
tetrahydrofuran hydrate, enthalpy of fusion and heat capacity, calorimeter studies 4-95425  
trans 1,4-polyisoprene, crystallisation from solution, melting endotherm, heat of fusion, density 4-75315  
water-oil microemulsions, DSC, permitt., dielec. loss tangent meas. 4-89343  
Au-Cd liq. and solid alloy, elec. resist. studies 4-88499  
 $\text{KAlSiO}_6$ , amorphous, glass transitions and thermodynamic props. 4-65400  
Na-ethanoate hydrate, thermodynamic props., phase transitions 4-98305  
 $\text{NaAlSi}_3\text{O}_8$ , amorphous, glass transitions and thermodynamic props. 4-65400  
Ne adsorbed layer on exfoliated graphite, 2-D press.-temp. phase diagram 4-92523  
 $\text{SiO}_2$ , amorphous, glass transitions and thermodynamic props. 4-65400
- heat of mixing**  
alloys, molten, mixing enthalpies, interchange energies, equil. const., association model 4-88301  
alloys, molten, mixing enthalpies, interchange energies, equil. const., association model 4-89060  
alloys, Thermodynamics and entropy of mixing 4-103935  
n-butanol, binary polar mixtures, dielec. props. and excess thermodynamic functions 4-114195  
epoxide-rubber blends, mixing, thermodynamic functions (Russian) 4-103944  
hexan-1-ol-pyridine base mixtures, molar excess enthalpies 4-113647  
KPB, compound forming liquid alloys, hard sphere system, entropy of mixing calcs. 4-113650  
phase equilibrium, complex model, appl. to systems with asymmetric miscibility gap and two miscibility gaps 4-70397  
PMMA blends with copolymers of methylmethacrylate and butylmethacrylate, thermodynamic study (Russian) 4-77027  
polystyrene-poly(2,6-dimethyl 1,4-phenylene oxide) and brominated derivatives mixtures, compatibility and neutron scatt. 4-79957  
primary parameters, group contrib. models 4-88298  
tetrachloromethane +  $\alpha,\omega$ -dichloroalkane, vapour pressure, vapour-liquid equil. 4-98256  
Au-Ga(In), excess enthalpies meas. using heat flow calorimeter 4-80237  
 $\text{CO}_2$ -hexane, excess molar enthalpies meas. 4-80236  
Cu base liquid alloys, enthalpies of mixing, intermetallic compound form. 4-92374  
In-Ga-Sb alloys, liq., phase diagram calc., Krupkowski's eqn. (Polish) 4-85139  
KTI, compound forming liquid alloys, hard sphere system, entropy of mixing calcs. 4-113650  
NaGa, compound forming liquid alloys, hard sphere system, entropy of mixing calcs. 4-113650  
 $\text{Na}_2\text{O-V}_2\text{O}_5$  melts, thermodynamic props., electrochem. study 4-88310  
 $\text{Ti}_2\text{Se-TiX}$  (X=Cl, Br, I), phase diagram and  $\text{Ti}_2\text{Se}_2\text{I}$  cryst. struct. 4-71643
- heat of reaction**  
see also heat of combustion; heat of dissociation; heat of formation  
diatomic cryst., equilibrium chem. reaction kinetics 4-109676  
dilanthanum carbides, thermodynamic study by high temp. mass spectrometry 4-69859  
N,N-dimethylaniline heat of transfer from  $\text{H}_2\text{O}$  to  $\text{H}_2\text{O}$  plus hexamethyl phosphotriamide (French) 4-81422  
nitroaniline, heat of transfer from  $\text{H}_2\text{O}$  to  $\text{H}_2\text{O}$  plus hexamethyl phosphotriamide (French) 4-81422  
oxides, defect energetics and nonstoichiometry 4-92201  
oxides, surface exchange reactions, oxygen transport characteristics 4-98355  
polybutylene terephthalate + polyamide interchain exchange reaction, DSC obs. of copolymers produced (Russian) 4-77005  
 $\text{Bi}_2(\text{SO}_4)_3$ - $\alpha,\beta$ - $\text{Bi}_2\text{O}_3(\text{SO}_4)_2 + \text{SO}_3$ , equil. press.,  $\alpha$ - $\beta$  transform. study 4-71959  
Br electrodes in Zn/Br and Zn/air batteries, electrochemical calorimetry 4-104995  
 $^{222}\text{Cs}^+$  cryptates, in water, stability consts. 4-114817  
GaAs-HCl- $\text{H}_2$  system, phase equil., dominant reactions for VPE, etching obs. 4-71579  
 $^{223}\text{Li}$  cryptates, in water, stability consts. 4-114817  
( $\text{N}_2$ ) $_2$ , electron impact ionisation, appearance energies of  $\text{N}_3^+$  and  $\text{N}_4^+$ , mass spectra. 4-64627  
Na clusters under equil. conditions with Knudsen cell, mass spectra study 4-74379  
NaF-AlF $_3$ , melt, thermodynamic data for reactions from vapour pressure meas. 4-85325  
 $\text{NbVH}_2$ , monohydride-dihydride equil. and thermodynamic anomalies 4-65419  
 $\text{NiSi}$  growth kinetics on (100) and (111) Si 4-75805  
 $\text{O}_4^+ + \text{N}_2$ , three-body reactions,  $\text{O}_4^+(\text{N}_2)_n$  formation with  $n \leq 4$  4-89291  
 $\text{O}_2\text{D}^+ + \text{D}_2$ , forward and reverse rate coeff., enthalpy and entropy changes 4-62165
- heat of reaction continued**  
 $\text{O}_2\text{H}^+ + \text{H}_2$ , forward and reverse rate coeff., enthalpy and entropy changes 4-62165  
Pt, black, catalyst/pyroelectric gas sensor using heat of reaction 4-66564  
 $\text{Ta}_2\text{S}_3$ , vaporisation, enthalpy of reaction, free energy functions 4-88311  
 $\text{Ta}_2\text{S}_3$ , vaporisation, enthalpy of reaction, free energy functions 4-88311  
Zn electrodes in Zn/Br and Zn/air batteries, electrochemical calorimetry 4-104995
- heat of solution**  
alcohol-water mixtures, heat of solubility flow calorimetry study 4-78318  
N-alkylamides, enthalpies of vaporisation and solvation 4-80203  
benzene-water mixtures, heat of solubility flow calorimetry study 4-78318  
glycine, aq. soln., conformational energy, ab initio LCAC-MO-SCF calcs. 4-96449  
hexamethylphosphotriamide-water mixtures, heat of dilution, sp. heat and ultrasonic vel. calc. (French) 4-80250  
microcalorimeter for heat of solution determ., of slightly soluble gases in water 4-78319  
naphthalene, solns. in water-ethanol mixtures, thermodynamic props. 4-80264  
phenols, enthalpies, free energies and entropies of transfer from nonpolar solvents to water 4-105009  
statistics of solvation and solvatochromism 4-85327  
tetra-n-alkylammonium tetraphenylborates, heats of soln. in water 4-105011  
Al-Fe alloys, Fe precipitation and dissolution, thermolec. study 4-61938  
BaF:He, interstitial diffusion, solubility of He, dissolution energy 4-113727  
 $\text{CaCl}_2$  in aq. mixtures of alcohols, enthalpies of soln. at 298.15K 4-103942  
CaF:He, interstitial diffusion, solubility of He, dissolution energy 4-113727  
Cd-Pb, thermodynamic props. at 900°C 4-80263  
Cu base liquid alloys, enthalpies of mixing, intermetallic compound form. 4-92374  
NaCl aq. soln., enthalpy of dilution and excess thermodynamic props. 4-80234  
 $\text{NiAl}_2\text{O}_3$ - $\text{Ni}_2\text{SiO}_4$  spineloids, stability, calorimetric study 4-81456  
PdTi $_3$ , T solubility, partial molar enthalpy and nonconfigurational entropy 4-92372  
RbNO $_3$  in water, heat of soln. meas. at 298K using LKB calorimeter 4-80235  
SrF:He, interstitial diffusion, solubility of He, dissolution energy 4-113727  
Xe in liq. n-alkanes, solubility, free energies, entropies and enthalpy of soln. 4-70389
- heat of sublimation**  
stearic acid, intermolecular potential and surface energies of crystalline polymorph 4-113379  
triphenyl boron, sublimation and bond dissociation enthalpy 4-103919  
(CsI) $_2$ , vaporisation, mass spectrometric study 4-80204  
Ga-Te, vapour composition, mass spectroscopic investigation of sublimation 4-108601  
NaF-AlF $_3$ , natural cryolite, vaporisation and high temp. thermodynamics, mass spectra 4-77025  
Ne adsorbed layer on exfoliated graphite, 2-D press.-temp. phase diagram 4-92523  
Yb-Es dilute alloys, thermodynamics, Henry's Law vaporisation studies 4-92390
- heat of transformation**  
see also heat of crystallisation; heat of fusion; heat of sublimation; heat of vaporisation  
4-(trans-4'-n-alkylcyclo hexyl) benzoates, mesomorphic, thermodynamic and dielec. props. 4-84390  
bis-(4-(4'-n-heptyloxybenzylidene)-1,4-phenylenediamine, liq. cryst., phase behaviour under press. 4-113627  
cholesteryl  $\omega$ -arylalkanoates, liq. cryst., cholesteric-isotropic transitions, thermal props. 4-108615  
diamond, vacancy formation energy, crystallisation studies 4-108354  
ferrocene-d $_0$  cryst., thermodynamic props. 4-88307  
p-gauge Potts model, phase transitions, Monte Carlo calcs. 4-73381  
n-hexyloxybenzylidene-p'-butylaniline, smectic liq. cryst., glass transition 4-84392  
liquid crystal homologous series with bent linkages, thermal props. 4-75275  
low molecular wt. cpds. with rigid group-flexible spacer struct., liq. cryst. behaviour 4-75282  
metal-ethanoate hydrates, thermodynamic props., phase transitions 4-98305  
metallocenes, heat capacity, 10 to 300K, low temp. thermodynamic study of stable and metastable phases 4-98304  
n-pentylphenyl cyano-thiobenzoates, cryst. struct. and nematic phases 4-84281  
phospholipid bilayers, latent heat, meas. by adiabatic compression 4-85407  
polytetrafluoroethylene, glass transition, thermodynamic props., DSC obs. 220-700K 4-61108  
terephthalylidene-bis-(4-n-decylaniline), liq. cryst., phase behaviour under press. 4-113627  
vinylidene fluoride-trifluoroethylene copolymers, ferroelec. transition and dielec. props. 4-99052  
 $\text{Ca}_2\text{Sr}_3\text{Al}_2\text{O}_3(\text{WO}_4)_2$ , phase transition characs., role of cage cation substitution 4-65386  
GeTe, heats of polymorphic transitions 4-61065  
 $\text{Sr}_2\text{Al}_2\text{O}_7(\text{CrO}_4)_2$ , flux grown, ferroelec. phase transition, domain studies, birefr., polarisation, permittivity, transition enthalpy meas. 4-65970
- heat of vaporisation**  
alkali halide crystals, heat of vaporisation 4-113593  
alkanes,  $\text{C}_9$  to  $\text{C}_{11}$ , cohesive energies 4-98257  
n-alkanois, free vol. temp. depend. and intermol. forces study using energy of vaporisation 4-84374  
N-alkylamides, enthalpies of vaporisation and solvation 4-80203  
coal liquids, vap. press. incorporating renormalisation group formulations with corresponding state principle 4-88271  
Darcian half-space, fully saturated, heating, press. generation, phase change 4-97648  
ionic crystals, heat of vaporisation 4-113593  
organic cpds., heat capacities for vaporisation, additivity method calcs. 4-65378

**heat of vapourisation continued**

- C, thermodynamics of vapourisation and virial eqn. of state 4-103918
- Cu-Bi(Sb), liq. Bi and Sb activity meas. by Knudsen effusion method with electrobalance 4-66312
- Na clusters under equilb. conditions with Knudsen cell, mass spectra study 4-74379
- NaI, vapour press. and evaporation thermodynamics 4-103915
- Ne adsorbed layer on exfoliated graphite, 2-D press.-temp. phase diagram 4-92523

**heat of wetting** *see wetting***heat pipes**

- active heat pipe solar water heating system 4-72155
- alloy evaluation for reactor heat pipes 4-72157
- commercial heat pipes under operational conditions 4-97281
- controlled heat pipes, thermodynamic anal. 4-79435
- ECA Stirling engine combined molten-salt thermal storage and sodium heat pipes 4-66765
- film condensation in vertical tube with closed top 4-75009
- forced convective boiling in uniformly heated tubes, critical heat flux 4-112698
- gas-loaded variable conductance heat pipe performance uniaxial model, effects of vapour flow friction and inertia, use in spacecraft thermal modelling 4-74846
- gravity assisted, with internal two-phase parallel flow, design and characteristics 4-79436
- insulation in vacuum steel-jacket pipe systems 4-103181
- L-SAT Telecommunication Satellite thermal design 4-74844
- neutronic and thermal design considerations for heat pipe reactors, SABRE 4-68809
- OTEC cold water GFRP pipe field test 4-114933
- solar water heater heat pipes design 4-62392
- space nuclear reactor heat pipe design, high power, performance demonstration 4-72156
- spacecraft heat pipe processing and testing facility, design and activation 4-72158
- Stirling engines, coal-burning, large-scale, possible applications 4-72148
- thermo-fluid dynamics, use in space station thermal control 4-74845
- Ti heat flux tubes for OTEC, design and appl. 4-81583

**heat pumps**

- 4 U tube heat operated heat pump test results 4-66778
- absorption cycle, fluid pairs selection methods and data requirements 4-72162
- absorption heat pump, for upgrading industrial waste heat to process steam temperatures 4-72163
- absorption heat pump, state of the art and future development 4-62381
- administrative building heating and hot water (French) 4-105122
- air to water heat pumps for domestic space heating, use of floor panel energy storage 4-89462
- air-to-air heat pumps for domestic heating, refrigeration compressor development 4-89461
- air-to-water, heat generating plants for oil or gas (German) 4-114919
- alternate ventilation strategies, comparisons 4-72168
- applications in commercial buildings 4-72144
- community solar heating system performance in southern Finland 4-62302
- compressor-type, series connected, thermodynamic computations and practical applications 4-105116
- computerised simulation using STASAN program for absorption heat pumps (German) 4-114920
- concrete utilisation in energy-efficient buildings (German) 4-66739
- direct-fired engine driven heat pumps, future developments 4-99987
- district heating power stations with heat pump using refrigerant, market opportunities (German) 4-85382
- domestic, control systems 4-114918
- domestic heating in Austria, economic aspects and use of heat pumps (German) 4-81578
- electric, recovering outlet air as heat source for indoor swimming pool heating (German) 4-99988
- energy conservation in buildings—the consequences for heat supply (German) 4-85383
- energy saving potential of heat pump-boiler systems for district heating 4-72154
- future development prospects 4-77135
- gas driven heat pumps in public buildings (German) 4-81580
- gas heat-pumps, operational experiences (German) 4-81581
- gas-motor type, sub-soil water as heat source, for indoor swimming pool heating (German) 4-99988
- ground source heat pumps for air conditioning, operation and characts. 4-114939
- ground water source heat pumps for space heating, economic and comparative analysis 4-62384
- high temp. gas engine driven heat pumps, industrial appls. 4-89463
- Industrial Temperature Booster, a waste-heat-powered heat pump, industrial applications 4-72160
- installations with gas motors in residential buildings, cost effectiveness (German) 4-81579
- metal hydride heat pump operation, effects of dynamic hydrogen sorption 4-105131
- modularised short-distance heat systems using heat pumps, applications to space heating 4-105117
- MW range, present possibilities and limitations (German) 4-81577
- operational results from solar energy absorber installations (German) 4-81588
- optimum arrangement and use of heat pumps in recovering waste heat 4-77137
- passive solar heater-refrigerator 4-81582
- planning an installation of heat pumps with solar energy absorbers (German) 4-81587
- power gain from aerobic sedimentators, practical application (Hungarian) 4-85386
- residential earth coupled heat pump in New York, field test 4-72152
- residential gas absorption heat pump, using R123a/ETFE absorption pair 4-72161
- reversed Carnot cycles, single and multistaged 4-89464
- series-connected, thermodynamic analysis 4-85384
- solar energy absorber heat transfer and system behaviour (German) 4-81586
- solar heat pump Rankine cycle, development, test and evaluation 4-72153
- solar heat pumps for room and water heating (Japanese) 4-85385

**heat pumps continued**

- space heating, developments and economics of heat pumps, general overview 4-62382
- space heating, economic comparison of heat pumps and gas/oil boiler systems (German) 4-72145
- space heating, energy and cost savings with air/air heat pumps 4-62387
- space heating using ground water/water heat pumps, design and operational experience 4-62385
- space heating using latent heat thermal storage heat pumps 4-62386
- stationary model of an electrically driven heat pump 4-66742
- Stirling engine heat-actuated heat pump, progress report 4-66787
- Stirling engines availability criteria 4-66764
- Stirling engines isothermal anal. 4-66756
- storage applications, heat pump equipped with PCM heat storage unit (Japanese) 4-109752
- stratified heat storage with heat pump, optimal loading strategy 4-66799
- temperature and heat flow effects on heat pump performance and running costs (Swedish) 4-77136
- thermochemical energy storage with heat pump system for industrial steam supply, expt. 4-66805
- thermoelectric residential heat pump, solar driven, feasibility 4-72151

**heat radiation**

- alloys, radiative properties at high temp. 4-84952
- atmospheric heat plume characteristic parameter determ. by lidar (Spanish) 4-89483
- averaging the radiation transport equations in solving two-dimensional radiation-gasdynamic problems 4-103434
- black body radiation, non-quantum approach 4-95223
- blackbodies, angle factors between singular points (Chinese) 4-112685
- blackbody radiation distrib. meas. spectral analysis (Chinese) 4-111172
- blackbody radiation from cubes and spheres, solidification of microsphere appl. 4-107998
- coal-dust flame, coke particles, radiative characteristics 4-75014
- conical surfaces, radiation view factors 4-79422
- cooling with selectively IR emitting gases 4-87834
- double-beam optical-null spectrophotometer meas. error due to sample natural thermal radiation 4-58898
- earth radiation budget experiment design and development 4-72853
- electrochromic materials for controlled radiant energy transfer in building 4-112536
- endothermic gasification of a solid by thermal radiation absorbed in dep. 4-103187
- fast jet furnace with top-mounted burners, heat exchange 4-97629
- fin array, transient finite element analysis of coupled radiation 4-79431
- fin geometry optimisation, simultaneous, convective and radiative heat transfer 4-97280
- finite solid radiant cooling 4-107978
- Fourier transform spectroscopy, thermal radiation problem 4-95520
- furnace, thermal processes, numerical study 4-107985
- gas, gravitational instability, thermal radiation, uniform rot. and mag. field (Italian) 4-69736
- glass, molten, thermal conductivity, high temp., theoretical anal. of experiments 4-84471
- honeycomb structure transparent insulation rel. to solar energy use, heat loss mechanisms 4-114946
- hypersonic flow around blunt bodies, shock layer, radiant heat transfer (Russian) 4-83923
- hypersonic flow past flat body, intense radiative heat transfer 4-112944
- initial heating period for a massive body in a high-temperature oven 4-74838
- inverse black-body radiation, closed form approximations 4-86419
- inverse problems solution with unknown model of the process 4-79429
- laminar duct flow development with external radiation and convection 4-97468
- laminar-turbulent boundary layer transition, thermal imaging systems 4-112814
- materials for radiative cooling to low temperatures 4-112683
- maximum temperature possible for thermal radiation, black hole arguments 4-101148
- metal heated spikes, evaporation and heat loss 4-107993
- metals, radiative properties at high temp. 4-84952
- multiple scatt. in 3D cylindrical geometry, exact formalism 4-79427
- nonlinear thermal anal., hybrid perturbation/Bubnov-Galerkin technique 4-64818
- one-dimensional furnaces 4-64827
- optical radiation measurements, temperature inference 4-95488
- plasmatron, local gas blowing, Navier-Stokes eqn. 4-65138
- point explosion in arbitrary atmosphere with radiative heat transfer 4-112955
- polyester fibre insulation, optical props. and radiative heat transfer 4-80896
- polymer fibres, cooling during melt spinning process 4-60258
- radiation fluxes calc. in rectangular channels 4-113013
- radiative heat transfer equilb. approx. 4-112687
- radiative heat-transfer calcs., selectivity allowance 4-112686
- rectangular enclosure, 2D, with grey participating media, radiative transfer, finite element soln. 4-60252
- segregated media, combined convection-radiation anal. 4-64934
- self-similar flow behind cylindrical blast wave, radiation heat flux 4-97608
- self-similar flow behind cylindrical shock wave, thermal radiation, MH 4-75060
- semitransparent dispersive materials nonsteady heat exchange, influence radiation flux characts. and optical props. (Russian) 4-79424
- semitransparent media, coupled radiation-cond. heat transfer, Monte Carlo finite difference method 4-60247
- specular reflection in radiant heat transport across a spherical void 4-87544
- stationary radiative heat transfer, macroscopic theory rel. to EM fluctuations 4-64828
- steam, high press. high temp., convection-radiation interaction 4-74018
- subband method for calc. for radiational heat transfer in surfaces at scatt. media 4-79423
- surfaces at 80K and above ambient, radiative-thermal exchange measurements 4-97284
- transient radiation-conduction heat transfer in a finite cylinder filled with an absorbing radiating medium 4-79415
- two-phase droplet flow, convective and radiative heat transfer 4-75073
- USA research 4-83811

## at radiation continued

- vacuum-shield heat insulation, multilayer, radiative-molecular-conductive heat transfer 4-112684
- workplace thermal radiation meas., sensor design and operation (German) 4-86410
- CO<sub>2</sub> radiation convection heat transfer problem plane channel, turbulence 4-60378
- Co-based heat resisting alloys, radiative and optical props. 4-74847
- Fe-based heat resisting alloys, radiative and optical props. 4-74847
- Ni-based heat resisting alloys, radiative and optical props. 4-74847

## at sinks

- coherent laser arrays, improved heat-sink design 4-102929

## at systems

## see also boilers; heating

- administrative building heating and hot water (French) 4-105122
- analysis of a black liquid flat plate solar collector 4-77138
- domestic heat pump control systems 4-114918
- domestic solar system instrumentation, long-term stability and performance 4-99989
- electronic controls for solar heating and heat/cool storage systems 4-93642
- experimental solar house providing 960 W peak power in Saudi Arabia 4-77064
- free-piston Stirling engine/linear compressor system parametric testing and evaluation 4-66779
- link up systems open fire water heating to supplement principle heating system 4-62383
- performance study of solar water pump using packed-bed collectors 4-77139
- solar water heating system, flat plate, parameters effect on performance 4-81593
- water heating, solar energy adoption patterns in United States 4-109726

## at transfer

## see also condensation; convection; cooling; evaporation; heat conduction;

## heat radiation; radiative transfer; thermal diffusivity

## ablation by frictional heating 4-97440

## acoustic vibrations of heat releasing medium in confined space, nonlinear

## stabilisation 4-69756

## advanced power system problems 4-83809

## advanced power systems, heat transfer problems 4-85388

## advection-diffusion equation, finite difference schemes, stability anal.

## 4-68183

## affluxed bodies, temp. depend. props. with heat transfer, dimensionless

## groups (German) 4-64823

## air cross flow, vel. fluctuations in space between tubes in bundles

## 4-83892

## air refrigeration, transient natural convection heat and mass transfer

## 4-75006

## air saturated porous media in short cylinder, transient heat transfer

## 4-108073

## air-water vapour mixture in greenhouse environment, thermal behaviour

## 4-87545

## annular flow in tubes, crit. heat flux, rel. to crit. liq. film thickness

## 4-75085

## asymmetric instabilities in buoyancy-driven flow in a tall vertical annulus

## 4-83877

## atmosphere, energy balance models incorporating transport of thermal and

## latent energy 4-82181

## benard convection with time-periodic heating 4-64946

## binary gas mixture in nearly free mol. state, aerosol particles, thermo-

## phoresis 4-60483

## boiling heat transfer, research needs 4-83907

## boundary layer, thermal, along semi-infinite plate with variable surface

## temp. similar solns. 4-75021

## building materials, effect on energy conservation 4-89486

n-butanol-N<sub>2</sub>, heat and mass transfer in a laminar boundary layer under

## mist formation (Japanese) 4-97477

## capillary waves in nonuniformly heated liquid, instability under effect of

## lower radiation 4-64961

## circular pipe placed in air jet and corona wind, heat transfer coeff.

## 4-97527

circular tube cooled by dissociating N<sub>2</sub>O<sub>4</sub>, unsteady heat transfer for

## turbulent flow (Russian) 4-74022

## circulating high Prandtl number fluid, rotating agitator effect on heat

## transfer 4-87720

## coal, drying, Stefan model comparison with two-phase model 4-103186

## coal-fired boiler exhaust gas heat recovery 4-64826

## coated films, IR drying, internal heating effect 4-97293

## collisionless plasma flow, total heat transfer to cylindrical collectors

## 4-60604

## combined heat and mass transfer in natural convection on a horizontal

## surface 4-87718

## combustion, pulsed, phase relationships 4-104992

## complex systems, stage-by-stage modelling of thermal conditions

## 4-103179

## complex variable boundary-element method expansion into finite series of

## analytic functions 4-107992

## composite media heat transfer, solns. of transcendental eqn. 4-63691

## compound bodies with contact thermal resistance, appl. of beam method

## 4-91718

## compressible fluid, with weak diffusion, Rayleigh problem (Russian)

## 4-112672

## concentration difference energy system and engine, developments, heat

## transfer studies and appls. 4-66786

## conference on thermal sciences, Miami, USA (Apr. 1982) 4-73165

## convective heat transfer, physical and computational aspects, book

## 4-86128

## corner flow with suction, heat transfer 4-112937

## Couette flow in space partly filled with porous medium 4-87790

## counterflow heat exchanger dynamics calc. using difference equations, errors

## 4-91719

## counterflowing fluids separated by heat conducting plate, heat transfer

## 4-97522

## coupled heat-mass transfer in natural convection under flux condition

## along vertical cone 4-69754

## coupled-field dynamical system, partitioned anal., review, book contrib.

## 4-60359

## critical heat flux, reduction mechanism is subcooled flow boiling 4-86930

## critical heat flux condition in high quality boiling systems 4-83803

## cryogenic heat transfer 4-82799

## heat transfer continued

- cryogenic liquids flowing in tubes, heat transfer during boiling 4-69749
- crystal growth from melt, height, horizontal directional crystn. 4-71544
- cyclic heat transfer phenomena in closed spaces, simplistic model 4-64820
- cylinder, long two layer, temp. field, Newton's law appl. 4-107988
- DC electric field heat transfer during condensation of nonconducting fluids 4-97561
- dessicant dehumidifier cooling system, sorption props. effect on performance 4-88404
- desuperheaters, injection-type operation 4-97549
- dielectrics with low cond., heated in EM field, Stefan problem 4-107999
- diffusion eqn. soln. using 3D method based on superposition principle 4-107984
- direct contact condensation of vapor to falling cooled droplets 4-112697
- disc, gas turbine, nonstationary temp. fields, finite element method 4-107987
- dispersive moist materials with surfaces, heat transfer rate, effect of vibr. (Russian) 4-79425
- double-layered medium, different thermal conds., temp. drop. anal. 4-74842
- dropwise condensation on upper surface of horizontal tube, heat transfer 4-97292
- ducts, slotted with coplanar channels, heat exchange and hydraulic resistance (Russian) 4-79426
- ducts with const. wall temp., heat transfer coeff. 4-60421
- dynamic stresses in elastic regions formed in interaction of powerful heat flows with solid bodies 4-64842
- electrically conducting liq., flow in tube in longit. mag. field, heat exchange 4-108079
- energy exchange models, fuzzy identification 4-107976
- energy problems, conf., Tokyo, Japan (Sept.-Oct., 1980) 4-82599
- ethanol-gasoline mixtures, nucleate boiling 4-87549
- ethyl alcohol vertical layer with thermogravitational convections, temp. fluctuations spectra 4-79580
- evaporative heat transfer in channel filled with porous highly conductive metal 4-83895
- extended Graetz problem 4-60243
- extended irreversible thermodynamics of heat and mass transfer, variational approach 4-101800
- extended surfaces array, heat transfer anal. 4-75008
- external heating of a flat plate in a convective flow 4-97555
- falling film evaporator, heat transmission meas. for condensation and evaporation (German) 4-111126
- falling liquid films with surfactants, thermocapillary breakdown 4-60545
- film boiling, instability 4-112691
- film boiling heat transfer, radiation effect, on plane wall parallel to upward vertical flow 4-112676
- film boiling in laminar boundary-layer flow along a horizontal plate surface 4-97473
- film condensation, heat and mass transfer, mathematical modelling 4-107996
- finite-element model of the heat flow in billets during the transfer and after upsetting in the extrusion container 4-87719
- fission reactors, containment heat transfer coeffs. during LOCA 4-106929
- flame combustion intensity, heat transfer effects 4-83808
- flame temperature in intermittent-combustion chamber 4-85312
- flames, heat transfer between hot combustion gases and cold wall in narrow channels 4-99789
- flat rectangular duct, heat transfer response to periodic disturbances at one principal wall 4-60418
- flat-plate collectors, charged with phase-changing working fluids, performance anal. 4-105121
- flow boiling, correl. for heat transfer 4-79593
- flow in heated channels, two-fluid model eqns. nonlinear eqns. soln. by numerical method 4-108112
- flow induced by heated vertical wall in a porous medium 4-69821
- flow of vapour in channel with porous filler, condensation process, analytic model 4-83942
- flow through periodic assemblage of spheres in duct, heat transfer periodic soln. 4-97558
- fluid, measurement of heat transported by fluid (German) 4-63747
- fluid-solid, transient single-blow responses, numerical prediction 4-97662
- fluidised beds, horizontal tube arrangement optimisation, heat transfer 4-60537
- fluidised beds, pressure and vel. meas. methods (Hungarian) 4-65043
- fluidised beds of large particles and horizontal tube bundles at high press., heat transfer 4-103404
- forced convection heat transfer through self-similar thermal boundary layers on plane and axisymmetric bodies 4-64914
- fouling and scaling, causes and effects on heat transfer surfaces (German) 4-112678
- fouling of heat transfer surfaces 4-88405
- friction and heat transfer effect on cylinder in longitudinal turbulent air flow with variable physical props. 4-83891
- fruit-solar drying, optical characts. of fruit 4-93595
- fuel-element assemblies, cooled with N<sub>2</sub>O<sub>4</sub> dissoci., thermophysical transients cal. 4-83887
- Fulks measures in the heat equation theory (French) 4-95351
- full coverage film cooling studies 4-83906
- fully developed laminar flow and heat transfer in an arbitrarily shaped triangular duct 4-64911
- uran, two-phase bubble, evaporation through immiscible liq., heat transfer 4-87781
- furnace, casting unit, heat exchange, inverse heat cond. calcs. 4-107982
- fusion blanket high temp. heat transfer 4-111822
- gamma-type Stirling engine, with back-to-back free displacer, closed-form anal. 4-66763
- gas, confined, shock wave generation due to rapid heat addition at boundary 4-69796
- gas, convective motion resulting from propag. of heat wave along lower boundary of closed region 4-87717
- gas, inert, shock wave generation due to rapid heat addition at boundary 4-69797
- gas flow-surface interactions, heat and mass transfer 4-97559
- gas fluidised bed, horizontal tube heat transfer, surface roughness effect 4-113005
- gas jet impinging onto a liq. surface, heat transfer study 4-83890
- gas turbine, low flow, nozzle blades, leading and trailing edges, heat transfer 4-97546

## heat transfer continued

- gas vibrations, nonlinear, in closed pipe, rel. to thermoacoustic effects 4-69853
- gas-liquid two-phase annular flow in horizontal circular tube, flow config. (Japanese) 4-75092
- gas-loaded variable conductance heat pipe performance uniaxial model, effects of vapour flow friction and inertia, use in spacecraft thermal modelling 4-74846
- gas-saturated coolant, forced flow, critical heat flux 4-97550
- gas-solid nonstationary heat transfer, determ. by inverse heat cond. calcs. 4-107994
- gas-solid suspensions, flowing, turbulently in vertical pipe, heat transfer 4-97663
- geothermal power generation, heat exchangers, tube enhancement evaluation 4-114891
- geothermal power station turbine hydrocarbon vapour expansions condensation behaviour 4-60250
- Giotto spacecraft thermal design 4-74635
- grains, pneumatic drying, const. rate, mathematical anal. 4-76965
- grains, pneumatic drying, falling rate, mathematical anal. 4-76966
- ground source heat pumps for air conditioning, operation and characts. 4-114939
- half-space, elastic, thermal stresses 4-97408
- He-Cd laser with lateral HF discharge, different design comparative characts. (Russian) 4-69372
- heat emitting surface, influence of porous coating on heat transfer during boiling, calc. and obs. 4-108070
- heat exchangers, shell-and-tube type, fouling comparison in tubes with annular turbulence promoters and smooth tubes 4-83893
- heat flux gage calibration for skin friction meas. 4-97723
- heat pipe, gravity assisted, with internal two-phase parallel flow, design and characteris. 4-79436
- heat pipe thermo-fluid dynamics, use in space station thermal control 4-74845
- heat pipes under operational conditions 4-97281
- heat sources, three dimens. heat flow, temp. calcs. 4-97290
- heat transmission from metal surface to boiling water under atmospheric press. 4-97295
- heat-releasing apparatus inlet, hydromechanics 4-79669
- heated channels, hydrodynamics and heat transfer, vibr. field effects (Russian) 4-74023
- heated cylinder in crossflow in cylinder array, heat transfer, turbulence meas. 4-112869
- heated wire at high subsonic gas velocities 4-83897
- helical boiler tube, full scale modelling 4-60574
- helical coils, critical heat flux and post-dryout temp. regime 4-103416
- n-heptane, forced turbulence flow in tubes, heat transfer coeff. 4-97535
- high flux heat transfer in gaseous solid suspension flow 4-83909
- high flux transfer, power and propulsion system appls. 4-83807
- high performance heat transfer surfaces for boiling and condensation 4-83806
- high temperature gas turbines, heat transfer, film and impingement cooling 4-83905
- hydrodynamic and thermal development in square duct 4-60415
- hydroelastic fluctuations in two-phase flow in tube bundles 4-103336
- ice, superheated, optical homogeneity, elastic light scatt. 4-113578
- ice formation in water flow between two horizontal parallel plates, transition phenomenon 4-64834
- ice sheets, plane steady flow, nonuniform temp. distrib. influence 4-60407
- in-pile LMFBR accident simulations anal. by Kalman filter methods 4-86936
- incompressible fluid steady flow between coaxial cylinders, MHD heat transfer 4-97697
- industrial flow circuits, jet system appls. for heat transfer 4-83936
- inert compressible gas confined between infinite parallel planar walls, response to rapid boundary heating 4-87541
- integrated roof air heater for passive solar space heating of non air conditioned building, thermal modelling 4-77060
- intensification of heat transfer (German) 4-112689
- interacting boundary layers and heat transfer 4-87665
- interfaces, gaseous heat transfer between solid surfaces, photoacoustic expts. 4-83801
- interphase layer, mass, momentum and energy conservation law, surface parameters 4-112692
- inverse nonlinear contact heat transfer in rectangular plate problem, soln 4-97283
- inverse problem, soln., basis of terminology and algorithm 4-107983
- inverse problems solution with unknown model of the process 4-79429
- inward melting in horizontal tube, heat transfer 4-87708
- ion-acoustic turbulent plasma, laser heated, heat transfer due to fast electrons 4-65110
- isopropanol, boiling burnout during crossflow over horizontal cylinders, subcooling effect 4-79594
- isothermal cylinder in conditions of natural convection, heat transfer 4-79579
- Japanese research 4-83903
- jet impingement heat transfer, entrainment temp. effect 4-112867
- jets, round, heat and momentum transport calc. 4-69806
- L-SAT Telecommunication Satellite thermal design 4-74844
- laminar flow and heat transfer of air in in-line tube bank 4-79551
- laminar flow in periodically converging-diverging tube, heat transfer 4-60412
- laminar flow in rotating non-aligned straight pipe 4-103418
- laminar liquid film falling over horizontal cylinders, heat transfer 4-97545
- laminar three-dimensional flow, temp. profiles and heat transfer rates, matched asymptotic solns. 4-75001
- large particle bubbling fluidised beds, heat transfer 4-113004
- large-scale structural effects in developed turbulent flow through closely-spaced rod arrays 4-112861
- latent heat storage equipment for solar energy, transient heat transfer anal. 4-66792
- layered bodies, heat transfer calc. 4-74839
- linear Görtler instability of boundary layer flow over concave wall, heating effect 4-64920
- liquid crystal heat switch, elec. field controlled 4-108272
- liquid droplet on heated surface, evaporation, heat transfer characteristics 4-83804
- liquid film, vaporising, laminar and turbulent boundary layers, momentum, heat and mass transfer 4-60414
- heat transfer continued
- liquid film flow over reducer surface model 4-91790
- liquid in differentially heated porous slab, free surface 4-75078
- liquid metals, flow in pipe in longitud. mag. field of solenoid, heat exchange 4-108117
- liquid-liquid direct-contact, immiscible fluids heat exchanger analysis, energy extraction from solar pond 4-72178
- liquid-piston Stirling engine dynamic anal. using vector or phasor methods 4-66772
- local heat transfer coefficients for a horizontal tube in a large-particle fluidised bed at elevated temperature 4-112846
- local heat transfer parameters, statistical identification 4-107979
- local heat transport from heated cylinder, sound effect 4-112857
- longitudinal flow around cylindrical body, heat exchange and friction (Russian) 4-74998
- marangoni effect in the Couette flow 4-64945
- mass and heat transfer, interrelated, soln. of three-dimensional nonlinear nonstationary problems (Russian) 4-112668
- mass and heat transfer on filament-type packing in contact-type exchangers 4-83894
- Maxwell-Stefan eqns. solns. for multicomponent film model 4-79421
- mean flow field and heat transfer along cooled supersonic diffusers 4-113077
- mesh packet, heat transfer coeff., design relationships (Russian) 4-64822
- metal hydride hydrogen storage beds 'In-Out' and 'Out-In' hydrogen reaction alternatives using RET 1 computer code 4-66812
- metal hydride storage bed, mass and heat transfer dynamic analysis program 4-66816
- metal thin plate, heating and ignition by axisymmetric heat source 4-99794
- metallic melts, numerical treatment of rapid solidification 4-93288
- methane flames, high temp., laminar flow, stagnation point heat transfer 4-65037
- methanol, boiling burnout during crossflow over horizontal cylinders, subcooling effect 4-79594
- MHD flow and heat transfer in channel with porous walls 4-87808
- MHD heat transfer in flow past variable temp. semiinfinite plate 4-108116
- microbiological fouling and scaling meas. with flow cell array 4-115436
- microthermosiphon, boiling heat transfer to water 4-97548
- model heat exchanger, velocity distributions, measured and predicted values 4-69767
- model particle and fluidised bed heat transfer study 4-79662
- moving drop with variable surface tension, diffusion 4-80339
- multicomponent mixtures, tray-column rectification, heat and mass transfer, quasilinear model 4-60402
- nonequilibrium states, heat fluctuation distrib. 4-90544
- non-Newtonian fluid flow, heat and mass transfer, power function velocity profiles 4-60464
- non-Newtonian liquid, flow and heat transfer in arbitrary shape channels, conformal mapping theory (German) 4-97618
- non-Newtonian viscoelastic fluid, conjugated heat transfer in flat duct 4-79627
- noncentrosymmetric crystals, photothermal effects 4-61117
- noncircular duct, peripheral temp. variation in wall, heat transfer calc. 4-97552
- nonequilibrium axial flow model for the calculation of transient behavior in two-phase flow 4-60514
- nonequilibrium three-dimens. viscous shock-layer flows over complex geometries 4-112930
- nonlinear heat diffusion eqn., homology, Backlund transformation 4-69664
- nonlinear steady-state thermal anal., reduction methods 4-91714
- nonNewtonian fluid with variable physical props., channel flow, heat transfer 4-79581
- nonrectangular inclined enclosure, convective fluid motion and heat transfer 4-64941
- nonstationary regimes, internal heat and mass transfer coeffs., explicit function calcs. 4-97278
- nonsteady heat and mass transfer in drying by reduced pressure 4-74844
- nucleate boiling heat transfer, augmentation by prepared surface 4-83805
- nucleate boiling heat transfer, surface configuration effect 4-112695
- nucleate pool boiling, freq. effect on bubble departure diameter 4-97644
- n-octadecane, melting from cavity wall, heat transfer meas. 4-112865
- n-octane, inward solid-liquid phase-change heat transfer in a rectangular cavity with conducting vertical walls 4-97554
- one dimensional gas flow with internal heating 4-97692
- one-dimensional classical many-body system having a normal thermal conductivity 4-73401
- OTEC heat exchanger biofouling, corrosion and heat resistive expts. 4-114935
- packed bed for thermal energy storage, transient response 4-114959
- packed beds, heat transfer, thermal cond. 4-64936
- packed spheres beds, heat transfer, local aerodynamics 4-97543
- parallel rotating porous disks, heat transfer study 4-64953
- particles in pulsatile flow, heat and mass transfer 4-79582
- passive solar heat-refrigerator 4-81582
- pebble bed reactors, thermohydraulic behaviour, natural convection flow expts. (German) 4-106875
- n-pentane, two-phase bubble, evaporation through immiscible liq., heat transfer 4-87781
- n-pentane, volatile liq. lens on stagnant liq. surface, evaporation 4-87544
- phase change transfer problems, useful relations 4-108075
- phase conversions under action of intense energy fluxes 4-103191
- pipe wall temperature effect on nucleate to film boiling transition 4-83947
- pipes of variable cross section, heat exchange between three streams 4-75015
- planar metal jet, Rayleigh instability stabilisation by mag. field and heat flow (Russian) 4-112820
- plane channel with semicylindrical projections, heat transfer 4-103325
- plasma ion-acoustic turbulence, amplification of heat transfer suppression 4-69894
- plate, circular, heat flux, symmetric nonlinear response 4-64825
- plate, orthotropic, thermoelastic problem of uniform heat flow disturbance by central crack 4-79511
- polydisperse liq. fuel diffusional combustion, self-similar conditions kinetics 4-81439
- polymer melts, laminar, three-dimensional flow, temp. profiles and heat transfer rates, matched asymptotic solns. 4-75001

at transfer continued  
 pool boiling heat transfer on porous surfaces, electrolytic surface prod. (Chinese) 4-107997  
 poorly streamlined bodies, heat or mass transfer 4-69760  
 porous body, internal heat transfer coeffs., inverse problem calcs. 4-107980  
 porous heater, temp., transient conditions 4-79434  
 porous media, presence of phase change, numerical problems, soln. 4-112682  
 porous medium, film boiling, lateral mass flux effect 4-87551  
 power cable trenches moisture and heat transfer, physical principles and calculation methods, cable continuous loadability calc. (German) 4-69666  
 propane gas flow around heated cylinders, heat transfer, temp. and pyrolysis effects 4-75005  
 pulsed heat flows, thermal convertor 4-60255  
 PWR small break LOCA, heat transfer, lower plenum break, parametric study 4-96195  
 quartz glass, ablation, boundary layer, nonequilib. physicochemical processes 4-71967  
 radial heat flow in gas, rot. effects 4-64835  
 reactive surface, oxidation in liq. flow, film boiling 4-97707  
 reactor, modelling and numerical simulation 4-109335  
 reactor core heat transfer crisis, quasistationary method calcs. 4-74034  
 reattached and separated flows, turbulence near-wall model appl. 4-79567  
 reciprocating gas-handling machinery, heat transfer during compression and expansion 4-64821  
 recirculating turbulent flow, two-pass procedure for heat transfer calc. 4-60411  
 rectangular flow section downstream from mixing junction, heat transfer characteristics 4-97529  
 reflux condensation in a two-phase closed thermosyphon 4-112688  
 rewetting of a hot surface by a falling liquid film—effects of liquid sub-cooling 4-98403  
 Ringbom Stirling engines first-order analysis 4-66761  
 rods, plane assembly, heat transfer, elastic deform., coupled thermoelastic kinematic problem (French) 4-74878  
 roll rotating at high speed, heat transfer, finite-difference solns. 4-79589  
 RSG-2 drop-forged steel radiators as heat absorbers for solar water heater 4-93638  
 sea surface, drag, heat and moisture transfer coeffs. 4-82164  
 seminfinitesimal body with nonlinear heat liberation from surface, cooling 4-103190  
 semitransparent dispersive materials nonsteady heat exchange, influence of radiation flux characts. and optical props. (Russian) 4-79424  
 separated flow region created by abrupt circular pipe expansion, heat transfer 4-60419  
 separated flows in tubes, heat transfer model appl. 4-60428  
 shear flow turbulence modelling, buoyancy effects 4-79575  
 sieve tray direct contact heat exchanger thermal and hydraulic performance 4-60249  
 single moving fibre, drying kinetics in longitudinal or transverse hot air flow 4-83896  
 single phase flow across high performance heat transfer surfaces 4-83908  
 single tube with forced crossflow, correl. for heat transfer during sub-cooled boiling 4-64940  
 skewed inlet flow in tube, heat transfer coeff. meas. 4-60420  
 soils, moist, unsaturated, heat and mass transfer coeff., diffusion coeff. 4-97556  
 solar collector, flat plate, optimum, heat transfer problem soln. 4-81592  
 solar collector, flat plate performance with axial cond. and end losses, general soln. 4-81591  
 solar energy absorber heat transfer and system behaviour (German) 4-81586  
 solar hothouse transparent film shielding, comparison of heat engineering qualities 4-93594  
 solar pond, effect of wind gusts on flow conditions 4-89467  
 solar power plants, tower-type, thermal optimisation, effect of heat exchange factors 4-91717  
 solar thermionic power plant, central receiver type, optimisation 4-109749  
 solar water heating system, flat plate, parameters effect on performance 4-81593  
 solid body heat transfer and ablation, calc. method (Russian) 4-74843  
 solid propellant, thermal behaviour obs. using shock tube, ignition delay 4-77010  
 solid-fluid countercurrent moving beds heated externally, axial temp. distrib. 4-97645  
 solidification, modelling of heat flow 4-88266  
 solidification, transport processes and growth morphology under microgravity 4-89051  
 solidification around vertical cylinders, thermal energy storage materials 4-100007  
 spacecraft Heat Rejection System design and manufacture for advanced thermal control 4-83802  
 spacecraft thermal control using Giotto shutter 4-83810  
 spontaneous gas oscillation induced in tube with steep temp. gradients, heat transfer 4-60422  
 spot radiometers for direct estimates of heat flow and thermal resist. 4-90638  
 spreader performance, quantitative calcs. 4-74841  
 stable mass-flow-weighted two-dimensional skew upwind scheme 4-60410  
 stagnation-point boundary layers, injection induced turbulence 4-64932  
 star shaped bodies, 3D, in rarefied gas, aerodynamic and thermal characteristics 4-69782  
 steady axis-symmetrical thermocapillary motion of a short melting column 4-83950  
 steam turbine-generator, acceptance test demonstration and verification 4-87826  
 steam-air mixture, air absorption during condensation in nuclear reactor 4-106874  
 steel, stainless, tube bundles subjected to blockages, heat transfer 4-68758  
 Stefan's measurement of the thermal conductivity of air 4-78077  
 Stefan problem, computing without the free boundary 4-64939  
 Stefan problem, free boundary analytical properties (Russian) 4-69668  
 Stefan problem, multidimensional single phase soln. stabilisation (Russian) 4-69669  
 Stefan problem, numerical soln. 4-87543  
 Stefan type free boundary problem soln. in cylindrical symm. 4-108077

## heat transfer continued

Stirling cycle simulation method, experimentally validated 4-66757  
 Stirling engine, free-piston, design and optimisation using non-linear state space stability anal. 4-66759  
 Stirling engine analysis using mathematical model 4-66754  
 Stirling engine using two-phase two-component working fluid, computer modelling 4-66784  
 Stirling engines, coal-burning, large-scale, possible applications 4-72148  
 Stirling engines isothermal anal. 4-66756  
 Stirling engines with controlled evaporation of a two-phase two-component working fluid 4-66785  
 Stirling machines analysis using second-order mathematical model 4-66758  
 stratified heat accumulator in solar heating system, design of water distributor 4-93641  
 strip inserted in boundary layer, effects on plane surface heat transfer 4-87699  
 suction effects on turbulence statistics in a heated pipe flow 4-65023  
 Sun, photospheric heat flow, photometric study 4-110584  
 Sunshine and Moonlight projects, heat transfer research 4-85361  
 supersonic flow past oscillating cone, boundary layer, blowing influence 4-69784  
 surface, evaporation and condensation, mass and heat transfer, kinetic anal. 4-88270  
 surface heat exchange, bottom geometry effects on water body thermal structure 4-103328  
 surface heat flow density meas. (Hungarian) 4-64824  
 surface temp. rel. to heat flux, boundary condition recalculation algorithms 4-107995  
 swirled foam beds, heat and mass transfer 4-60401  
 swirling annular-mist two-phase flow, liq. film characts. 4-97571  
 temperature and heat flux from nonequilib. state, coupled fluctuations 4-112681  
 thermal energy resources 4-85387  
 thermal explosion theory for partially insulated reactants 4-87746  
 thermal flux determination from temperature measurements within a sensor 4-103183  
 thermal performance of a heat storage module using calcium chloride hexahydrate 4-114960  
 thermally nonisolated flowing metal vapours, parameter calc. in closed cycle (Russian) 4-75003  
 thermochemical energy conversion system of inorganic aqueous salt solns., heat transfer 4-85381  
 thermogravitational and thermocapillary flows in a horizontal liquid layer under the conditions of a horizontal temperature gradient 4-103415  
 thermosiphon, countercurrent flow, heat and mass transfer 4-97547  
 thermosiphons, heat transfer study 4-83888  
 thermosiphons, two-phase, max. heat transfer capability 4-83889  
 thin wavy film, vertical flow, simulation by finite element method 4-74984  
 transient boiling heat transfer from small diameter wire and thin film flat surface 4-103321  
 transient film condensation on a vertical surface in a porous medium, heat transfer 4-87713  
 transient flow and heat transfer in natural circulation loop, 2D anal., laminar flow conditions 4-64949  
 transient heat transfer behaviors in cylindrical porous beds at relatively large Reynolds numbers 4-64950  
 trichlorotrifluoropropane, volatile liq. lens on stagnant liq. surface, evaporation 4-87548  
 tube banks, optimum tube arrangement and spacing, heat transfer meas. 4-97532  
 tube bundles, heat transfer coeff. and hydraulic drag 4-97540  
 tube bundles, laminar flow, vortices separation, heat transfer, vel. fluctuations 4-97542  
 tube bundles in transverse flows, heat exchange intensification 4-69759  
 tube-bank type crossflow heat exchanger, heat transfer, press. drop and flow visualisation expt. 4-112680  
 turbomachine cascade profile, friction and heat transfer calcs. 4-112833  
 turbulence, heat transfer influence in stagnation point 4-112853  
 turbulence flow with heat transfer in plane and curved wall jets 4-112862  
 turbulent and transitional boundary layers on convexly curved wall 4-60417  
 turbulent boundary layer, heat transfer, temp. depend. physical props. influence 4-103312  
 turbulent boundary layer, local heat transfer coeff. 4-103308  
 turbulent boundary layers, wall heat flux, double-step change effect 4-60395  
 turbulent boundary layers over rough surfaces with transpiration; heat transfer prediction 4-75010  
 turbulent falling liquid films with or without interfacial shear, heat transfer 4-75000  
 turbulent filmwise condensation on vertical plate, heat transfer 4-97534  
 turbulent flow, steady-state heat transfer of liq. through plane slot with mech. energy dissipation 4-79586  
 turbulent flow heat transfer, press. drop in converging-diverging tubes 4-113022  
 turbulent flow in circular tube with uniform suction or injection, heat transfer 4-103319  
 turbulent heat transfer coeff. in isothermal-walled tube for either built-in or free inlet 4-87704  
 turbulent heat transfer in accelerated flows on permeable surfaces 4-103320  
 turbulent heat transport in circular ducts with varying heat flux 4-112870  
 turbulent wakes, interaction, conditional sampling study, heat transfer 4-60384  
 turning flow in pin-fin configuration, heat transfer coeff. and press. drops 4-97553  
 twisted oval tube bundles in crossflow, hydraulic drag and heat transfer 4-97539  
 twisted tube bank heat exchanger, energy spectra of turbulence 4-112841  
 two dimens. circular jet impingement with crossflow, heat transfer characts. 4-112868  
 two-dimensional impinging jet, heat transfer augmentation technique (Japanese) 4-103379  
 two-phase cooling film on adiabatic wall 4-83943  
 two-phase system, reflection of sound at an interface, taking into account mass and heat transport across it 4-97646

## heat treatment continued

- UK Consortium Stirling engine regenerator effectiveness and heater performance 4-67553  
 underground pipelines, nonsteady state heat exchange, math. models 4-107977  
 unfixed solid phase change material inside horizontal tube, melting, heat transfer 4-87553  
 uniqueness problem, conditions for complex determination of heat-exchange parameters 4-108071  
 unstable heat eqn., feedback stabilisation using auxiliary functional observer 4-78109  
 unsteady change-of-phase conduction problem, finite element/Green's function method appl. 4-107986  
 unsteady heat transfer from a single sphere in Stokes flow 4-87706  
 unsteady stagnation point flow with variable wall temperature 4-87721  
 unsteady stagnation-point heat transfer for a variable freestream temperature 4-60404  
 unsteady state, in a wall, finite difference anal. (French) 4-60416  
 unsteady state mixing of the heat transport medium in a heat exchanger with twisted tubes 4-108069  
 unsteady-state extraction from a falling droplet with nonlinear dependence of distribution coefficient on concentration 4-103374  
 USA research 4-83904  
 vacuum solar collectors, heat transfer model eqns. 4-105123  
 vapour-liquid two-phase flow and heat transfer, Soviet and Chinese research 4-79596  
 view factor for radiant heat transfer between the wall and end of a cylinder 4-63690  
 viscoelastic fluids, eddy diffusivities of momentum and heat 4-112828  
 viscoelastic solids of revolution under cyclic loading, thermomech. behaviour, finite-element method 4-108025  
 viscoelastic thermodiffusion, coupled problems, reciprocity theorem 4-83812  
 viscous flow over circular cylinder, turbulence effect on heat transfer coeff. 4-97537  
 viscous fluid flow over tube bundles heat transfer coeff. 4-97538  
 viscous gas flow, heat transfer terms 4-113095  
 viscous swirling jets, heat and mass transfer, excess temp. distrib. 4-75065  
 water, droplet on heated surfaces, behaviour heat transfer characteristics 4-87711  
 water, flow in rough tube, heat transfer coeff. 4-97541  
 water, nucleate to film boiling transition in pipes 4-97536  
 water, subcooled, falling liq. turbulent films, critical heat fluxes 4-97544  
 wave propagation in inhomogeneous atm., weak mag. field perturbation 4-108089  
 wear, oxidation, origins and development at low ambient temps. 4-81293  
 wet steam, transient thermal processes, interphase transfer influence 4-60509  
 wind-driven waves, spray field, droplet size meas. heat and mass exchange calc. 4-67306  
 woodburning stoves, turbulent shear flow, two-dimens. anal. soln. 4-87688  
 Al-Cu, droplet solidification on chill block, predendrite form. rel. to supercooling 4-89037  
 CO<sub>2</sub> gasdynamic laser, regenerative elect. gas heater 4-79179  
 Cr, black, solar selective coatings thermal emittance estimation from stagnation temp. study 4-62393  
 Fe<sub>40</sub>Ni<sub>40</sub>B<sub>20</sub>, metallic glass, melt surface tension and embrittlement, effects of elemental additions and superheat 4-65184  
 H<sub>2</sub>O-N<sub>2</sub>, heat and mass transfer in a laminar boundary layer under mist formation (Japanese) 4-97477  
 He I, superheated, soil interface, light induced nucleation of vapour bubbles, photoemission model 4-61163  
 He II, flowing, heat transport, transition heat flux limitations 4-80323  
 He II to He I transition in presence of heat flow, forced flow influence 4-61164  
 He, liq. pool boiling, crit. heat flux, heater thermophys. props. effects 4-69667  
<sup>4</sup>He, liq., phase change and heat flow near  $\lambda$  point 4-92455  
<sup>4</sup>He, superfluid, Kapitza resistance effect on standing surface waves 4-84478  
 In film, supercond., surface heat transfer from self-heating hotspots 4-104361  
 InSb, Czochralski: pulling, numerical modelling of elec. current induced growth layers 4-88121  
 K<sub>2</sub>SO<sub>4</sub>, deposition rate and heat transfer on single tube in cross flow 4-99350  
 LiBr film, water vapour absorpt., heat and mass transfer 4-64937  
 LiBr film flowing down adiabatic wall, mass transfer in absorpt. of water 4-64831  
 N<sub>2</sub> dusty gas reactive flow, relax. zone behind normal shock waves 4-60460  
 N<sub>2</sub> gas flow around heated cylinders, heat transfer, temp. difference effects 4-75005  
 N<sub>2</sub> superheated liqs., explosive flashing in discharge through short nozzles 4-112936  
 Na<sub>2</sub>SO<sub>4</sub>-H<sub>2</sub>O systems, phase transition kinetics 4-98248  
 Ne, liq., limiting superheat (Russian) 4-98252  
 Ni selective coatings thermal emittance estimation from stagnation temp. study 4-62393  
 Ni-H battery cells, heat rate and coulombic efficiency during simulated geosynchronous orbit cycling 4-72074  
 NiO-O<sub>2</sub>, interaction, elec. cond., thermal flux 4-98627  
 Ni<sub>2</sub> superheated liqs., explosive flashing in discharge through short nozzles 4-112936  
 Pb film, supercond., surface heat transfer from self-heating hotspots 4-104361  
 Si ribbons, polycrystalline, prep. by fast cooling, for solar cells 4-114508  
 Sn film, supercond., surface heat transfer from self-heating hotspots 4-104361  
 YAG refractories, heat transfer during growth 4-76664

## heat treatment

- see also annealing; normalising; quenching (thermal); spheroidizing; tempering; thermomagnetic treatment; thermomechanical treatment  
 alkali borosilicate glass rods, partially leached, abraded and unabraded strength rel. to heat treatment 4-89144  
 barium stearate, Langmuir films, structure 4-108734  
 corundum monocrystals, polished surfaces structure and thermal treatment 4-113763

## heat treatment continued

- corundum single crystals, cracking resist. rel. to dislocation density 4-93370  
 ferromagnetic components quality control by coercive field strength meas. 4-93475  
 fibre reinforced composites, residual stresses during thermal cycling 4-71634  
 glass fibre, bending strength, static fatigue rel. to atmosphere 4-99490  
 glass fibre reinforced plastic, roving cloth reinforced, strength in flatwise direction, temp. depend. (Japanese) 4-89087  
 glass fibre reinforced polyurethane foam, flexural strength and modulus (thermal and photodegradation (Japanese) 4-99623  
 E-glass fibres, tensile props. rel. to acid and post heat treatment 4-104799  
 IN-100, Ni-base superalloy, cast, microstruct. changes during fractional melting 4-109434  
 Inconel X-750, environmental, stress-state and section-size synergisms during creep 4-61995  
 Lexan, track recording behaviour, mag. field effects 4-59583  
 metals, technological laser development and appl. at Physics Institute, AS USSR 4-107657  
 nylon 66 fibre, drawn, microstruct. rearrangement during heat treatment tensile modulus, SAXS obs. 4-76791  
 phosphosilicate glass film, void formation and IR absorpt. after heat treatment in H<sub>2</sub> atmosphere 4-60840  
 PMMA films, containing adsorbed moisture, DC cond., effect of thermal treatment 4-75980  
 polyarylates, carbonane-containing, elec. props. of pyrolysis products (Russian) 4-62194  
 polymer film, two-phase, structural charges during heat treatment 4-80435  
 polymeric materials, cure behaviour monitoring, dynamic mech. anal. technique 4-109579  
 pyrene, adsorbed on silica gel, singlet quenching of fluoresc. 4-80369  
 quartz, electrical and optical props., neutron,  $\gamma$ , and electron irradi. effects 4-60968  
 quartz mirrors, Zerodur and ULE, dimens. stability under thermal cycling 4-74658  
 Rene 95, Ni-base superalloy, fatigue, effect of processing and microstruct. 4-104843  
 sapphire, neutron irradi. and thermomech. treated, colour centres, visible luminescence study 4-81000  
 semiconductor materials, Hall voltages changes at high temp. meas. 4-58866  
 semiconductor structures, apparatus for pulsed heat treatment with flash-lamp sources 4-81313  
 steel, ° Cr-Mo-V-W, HT-9, austenitising and microstruct. 4-93320  
 steel, alloy, high C, optimisation of heat treatment (French) 4-81224  
 steel, austenitic, AM-2, various properties and products of nonmagnetic steels 4-114590  
 steel, austenitic stainless, high Cr, surface hardening with  $\sigma$ -phase form., effect on wear resist. 4-62115  
 steel, austenitic stainless, modified, void suppression, effect of segregation of minor alloying elements 4-104789  
 steel, austenitization, component redistribution in intercritical temp. range (Russian) 4-109436  
 steel, C, strain aging equivalent rule, hardness obs. 4-76790  
 steel, construction, P/M, thermal and thermomech. treatment, review 4-89072  
 steel, Cr-Mo, fatigue crack growth at 525°C, effects of environment and dwell 4-99523  
 steel, Cr-Mo-V, creep recovery by reheat treatment, carbide distrib., X-ray analysis 4-66392  
 steel, decarburisation in anodic process of elec. heating (Russian) 4-71776  
 steel, dual-phase, fatigue crack propag., effect of microstruct. on crack path morphology 4-99525  
 steel, electric, high-quality automated heat treatment of laminations in small batch quantities 4-81223  
 steel, ferritic stainless, intergranular corrosion susceptibility, etching method 4-85265  
 steel, hardening in high vacuum furnaces, heat transfer processes, math. model 4-85169  
 steel, HSLA, Mn, bearing, strengthening mechanisms rel. to treatment and microstruct. 4-81209  
 steel, HSLA, shear failure, development of fractographic features 4-76837  
 steel, laser heat treatment, hardening 4-76792  
 steel, low alloy, Cr-Mo-V, high temp. low cycle fatigue rel. to softening and embrittlement (Japanese) 4-99519  
 steel, low alloy, mech. props. rel. to second phase particle size 4-99591  
 steel, low alloy, reheat cracking during stress relief annealing, numerical approach 4-93412  
 steel, managing, influence of carbide formation on fracture struct. (Russian) 4-81273  
 steel, martensitic, precip. and mech. props., influence of high temp. thermomechanical treatment 4-114522  
 steel, martensitic hypereutectoid, rapid heat hardening using incomplete homogenisation effect 4-71671  
 steel, martensitic stainless, HT-9, weldments, microstruct., hardness and fracture toughness, effect of preheat 4-99495  
 steel, microalloyed, cast, microstruct. and mech. props., influence of phase charges (French) 4-81278  
 steel, microalloyed, structural, yield props., influence of dislocation density and precip. 4-114601  
 steel, mild, fretting fatigue rel. to diffusion coatings from Ni-Co electrodeposits 4-114686  
 steel, mild, SCC in NaH<sub>2</sub>PO<sub>4</sub> soln., effect of heat treatment and C 4-89167  
 steel, Mn-Mo-Al, transform. of austenite and cryogenic mech. props., effect of intercrit. heat treatment (Chinese) 4-85152  
 steel, Mn-V-Cu austenitic, microstructure rel. to heat treatment and alloying additions 4-89066  
 steel, Ni-Cr-Mo-V, free surface segregation, Mn content effect, Auger spectra 4-66345  
 steel, Ni-Cu-Mo, sintered Ancoloy SA powder, fracture toughness rel. to pore size and heat treatment 4-76843  
 steel, Ni-Mo-Si, 300M, occurrence of blocky martensite 4-114582  
 steel, stainless, austenite-ferrite duplex, preferential phase dissolution in H<sub>2</sub>SO<sub>4</sub>-NaCl soln. rel. to heat treatment and comp. 4-81341  
 steel, stainless, hardenable, microstruct.-strength relationship 4-114560

## t treatment continued

steel, stainless, transition and martensitic-class, superplasticity 4-61983  
 steel, stainless, US inspection, flaw visibility, split spectrum processing, grain size effect 4-89226  
 steel, strain meas. near growing fatigue crack tip 4-114651  
 steel, structural 45, boronisation, B diffusion processes (*Russian*) 4-93311  
 steel, tool alloy, magnetographic inspection, flaw image rel. to heat treatment 4-71834  
 steel, type G20, influence of V, Nb, Ti additions and phase transition (*Russian*) 4-66327  
 steel castings, large-scale, cylindrical, hardening after gradient heating 4-114584  
 structural materials, homogeneous thermal fatigue, rel. to struct. stresses 4-99594  
 surface quality in finishing-hardening treatment by plastic deform., controlling thermophys. fundamentals 4-66383  
 thermoplastics, cellulosic filler efficiency, processing characts. and mech. props. 4-61913  
 Ag-Al (10 at.%), transient creep, effect of  $\mu$  phase precip. 4-114618  
 Al alloys, homogenising ingots, struct. changes 4-61961  
 Al alloys, strain meas. near growing fatigue crack tip 4-114651  
 Al, high purity, polygonised, TEM, internal friction peak 4-113534  
 Al-Cu (3.76 wt.%), Rheocast, ageing characts. rel. to incomplete homogenisation 4-109444  
 Al-Li-Zr (2.34, 1.07 wt.%), composite precipitates 4-85154  
 Al-Mg, kinetics of Mg loss during melting and holding 4-114499  
 Al-Mg alloys, heat treated and cold rolled, oxidation, AES study 4-66474  
 Al-Mn alloy, commercial homogenisation, stability of primary particles, resist. and TEM obs. 4-99408  
 Al-Si-Mg-Sr, hypoeutectic alloys, melting losses of Sr rel. to holding time 4-114498  
 Al-Zn-Mg, 7075-T651, fatigue crack growth, effect of short-term heating cycles 4-99484  
 AlGaSb, LPE, substrate treatment optimisation, carrier conc., Raman spectra, photoluminesc. 4-93235  
 AlMnFeSi particles in Al alloys, STEM study 4-76920  
 Al<sub>2</sub>O<sub>3</sub>-SiO<sub>2</sub>, struct. and surface comp. X-ray diff. and SIMS investigation 4-113764  
 Al<sub>2</sub>O<sub>3</sub>-SiO<sub>2</sub> fibres, cristobalite form. at elevated temp. (*German, English*) 4-81197  
 Al<sub>2</sub>O<sub>3</sub>-x anodic oxide films, paramagnetic centres and optical absorpt. spectra studies 4-104494  
 As<sub>2</sub>S<sub>3</sub> chalcogenide films, solvent-cast morphology and thermal props. 4-84530  
 Au/Cu bilayers, ion-induced solid solutions and ordered cpd. form. 4-108470  
 Au/Si<sub>3</sub>N<sub>4</sub>/Si system, elec. effects of Au (*Chinese*) 4-98757  
 Au-InP junction 4-84625  
 B<sub>4</sub>C/B fibre reinforced Ti-Al-V, fatigue crack growth behaviour 4-93374  
 BaF<sub>2</sub>-LaF<sub>3</sub>-ZrF<sub>4</sub>-AlF<sub>3</sub> glass, crystallisation, devitrification on reheating 4-84194  
 BaO-Al<sub>2</sub>O<sub>3</sub>-SiO<sub>2</sub> thick film crossover dielec.-compositions, dielec. props. rel. to multiple refiring 4-109113  
 BaO-VO<sub>2</sub>-PO<sub>2</sub>, semiconductor glass, crystallisation rel. to composition, temp. and duration of heat treatment 4-92096  
 BaTiO<sub>3</sub> thin films, crystallisation from amorphous phase, electron microscope study 4-113830  
 Bi<sub>2</sub>Fe<sub>2</sub>O<sub>7</sub> glass, IR study 4-70381  
 C material, dimensional changes, under compressive stress at high temp. 4-85182  
 Ca(OH)<sub>2</sub> single cryst., precalcination transformations, Raman studies 4-98266  
 CdGe<sub>1-x</sub>Si<sub>x</sub>As<sub>2</sub> glasses, elec. props. and phase stability 4-104202  
 p-Cd<sub>0.8</sub>Hg<sub>0.2</sub>Te, hopping cond. between intrinsic defects 4-104210  
 CdS binder layers, electrophotographic props. after heat and light treatment 4-79258  
 Co base amorphous ribbon, as-cast, crystn. and heat treatment effect (*Chinese*) 4-84190  
 Co-P amorphous layers, mag. and struct. props. 4-76199  
 Co(Cr,Ni)-TaC, eutectic, thermal cycling, calc. of residual stresses and strains 4-66380  
 Cu-based shape-memory alloy, mech. and elec. props., sonic studies 4-76773  
 Cu-Ga/V multifilamentary superconductors, brittle fracture, acoustic emission anal. 4-71715  
 Cu-Ni-Fe alloys, short-range clustering and decomposition, dynamic scaling props. 4-114554  
 Cu-Sn (14.8%), austenitic and martensitic phase, thermally activated processes, kinetics 4-61963  
 Cu-Ti(P)(Si), Portevin-Le Chatelier effects 4-66374  
 Cu<sub>2</sub>O/CuO selective surface optical props. and surface composition 4-72170  
 Fe base amorphous ribbon, as-cast, crystn. and heat treatment effect (*Chinese*) 4-84190  
 Fe, cast, high-strength, mech. props. after prior heat treatment and isothermal hardening 4-93321  
 Fe, cast, with vermicular graphite, struct. and heat treatment 4-114471  
 Fe-B based metallic glasses, amorphous, mag. hysteresis loops after heat treatment below Curie point 4-80781  
 Fe-base austenitic alloys, high strength evaluation for generator retaining rings 4-99448  
 Fe-Co alloys, magnetostriction, recrystn., heat treatment, and strain texture effects (*Russian*) 4-104476  
 Fe-Ho-B, metallic glass, mag. props. and crystallisation 4-84793  
 Fe-Mo-Ni, magnetisation reversal study (*Russian*) 4-80783  
 Fe-Nd-B permanent magnet system, metallurgy 4-109381  
 Fe-Ni alloy,  $\alpha$ - $\gamma$  transformation, austenite grain growth (*Russian*) 4-109402  
 Fe-Ni-Cr ferritic alloy, soft mag. props. and mech. strength 4-61555  
 Fe-Ni-Cr-W amorphous alloys, corrosion resist. 4-99632  
 Fe-Ni-Mn (21, 4 wt.%), isothermal lath martensite growth at -80°C, cinemicrophotography 4-81193  
 Fe-Si (3 wt.%), deformation and heat treatment, C content effects (*Russian*) 4-109437  
 Fe-Si (6.5 wt.%) rapidly quenched ribbon, texture and mag. props. 4-104455  
 Fe(-C), SCC in NaH<sub>2</sub>PO<sub>4</sub> soln., effect of heat treatment and C 4-89167  
 Fe<sub>3</sub>Al, neutron irradi., at. ordering, Mossbauer spectra, X-ray diff. 4-65306

## heat treatment continued

Fe<sub>40</sub>Ni<sub>60</sub>P<sub>14</sub>B<sub>6</sub>, Metglas 2826, struct. factor, influence of cold rolling 4-61953  
 Fe<sub>2</sub>O<sub>3</sub> metastable transformation, simultaneous thermomag. and dilatometric meas. 4-113602  
 $\alpha$ -Fe<sub>2</sub>O<sub>3</sub>-ZrO<sub>2</sub>, elec. cond. rel. to stoichiometry depend. Zr solubility 4-70820  
 Fe<sub>81.5</sub>Si<sub>18.5</sub>B<sub>14.5</sub> metallic glass, stress pattern mag. domains 4-76161  
 Fe<sub>90</sub>Zr<sub>10</sub> amorphous alloy, struct. and mech. props. rel. to heat treatment 4-75305  
 GaAs, deep acceptor, Hall effect obs. and photoluminescence 4-80532  
 GaAs, deep centre point defect introduction 4-108819  
 GaAs LPE layers, residual impurities, growth soln. baking effects 4-92226  
 GaAs, midgap level surface density, heat treatment and capping effects 4-114011  
 GaAs:Si, Si diffusion using rapid thermal processing, encapsulant effects 4-65464  
 GaAs:P<sub>1-x</sub>Cu, LEDs, Cu impurities, thermal redistribution 4-80080  
 Ga<sub>0.47</sub>In<sub>0.53</sub>As, MBE planar doped barriers in InP, elec. characts. 4-98708  
 Ge, quenching centre form., host interstitial injection by oxidising surface 4-65258  
 Ge:Cu, impurity contamination reduction by heat treatments above 700°C 4-71535  
 Ge-P-S, semiconductor glass, paramagnetic centres, ESR study 4-80819  
 In-pyrrole-N-methylpyrrole contact, XPS study of Schottky barrier 4-104289  
 InP:Cd crystals, bulk and surface effects of heat treatment 4-84625  
 InP:Fe, semi-insulating, with phosphosilicate glass encapsulation heat treatment, photoluminesc. and Raman scatt. characterisation 4-84995  
 InP:Zn crystals, bulk and surface effects of heat treatment 4-84625  
 In<sub>30</sub>Se<sub>70</sub> films, optical absorption, heat treatment effects 4-85027  
 LaB<sub>6</sub>-ZrB<sub>2</sub> system, interaction, phase diagram study 4-89030  
 MgF<sub>2</sub> windows, spectral transmission change caused by prolonged UV irradi. 4-64752  
 Mn<sub>1-x</sub>Zn<sub>x</sub>Fe<sub>2</sub>O<sub>4</sub>, hot pressed, prior heat treatment effect on props. 4-89016  
 Mo, neutron irradiation embrittlement, influence of irradi. temp. and heat treatment 4-108453  
 Mo, pure and alloyed, cold deformed, softening by fast heating (*Russian*) 4-93316  
 Mo-Ti/Si interface, metallisation for self-aligned TiSi<sub>2</sub> process 4-89145  
 Mo-Ti-Zr, TZM, neutron irradiation embrittlement, influence of irradi. temp. and heat treatment 4-108453  
 Na<sub>2</sub>O-B<sub>2</sub>O<sub>3</sub> glass, oxide substituted, alkali resist., porous, heat treatment, leaching, phase decomp. 4-66299  
 Nb, superconducting, flux pinning mechanism of grain boundaries (*Japanese*) 4-76094  
 Nb, thin wires, heat treatment 4-66355  
 Nb-Al-Ga, vacuum deposited films, struct. and supercond. transition temp. rel. to heat treatment 4-65764  
 Nb-H, internal friction, hydride precip. peak, cooling rate and freq. depend. 4-66360  
 Nb-Sn Al<sub>5</sub> alloys, struct. and supercond. props. 4-104344  
 Nb-Ti, thin wires, heat treatment 4-66355  
 Nb-Ti multifilamentary supercond. composites, cold drawn, heat treatment, precip. morphology, TEM obs. 4-71657  
 Nb<sub>2</sub>O<sub>5</sub>, XPS and optical spectra, low-valence cations and electron props. 4-98623  
 Nb<sub>3</sub>Sn, thick diffusion produced layers, struct. and power losses rel. to electrochemical polishing 4-65781  
 Ni electrodeposits, struct., positron lifetime meas. 4-104103  
 Ni-based alloys, HVEM irradi., void form. rel. to  $\gamma'$  precipitation 4-108446  
 Ni-Co matrix, ThO<sub>2</sub> particles, oxide growth inhibition 4-104796  
 Ni-Co-Cr-Nb-Hf, Ni-base superalloy, MERL 76, powder metallurgy hot isostatic pressing, effect of Ar contamination 4-114447  
 Ni-Fe-V, thin sheets, effective mag. permeability and its stress sensitivity, effect of heat treatment and comp. 4-104883  
 Ni-Mo-Al unidirectionally solidified eutectic, microstruct. instability 4-61926  
 Ni-Ni<sub>3</sub>Al-NbC, eutectic, thermal cycling, calc. of residual stresses and strains 4-66380  
 Pb<sub>1-x</sub>Ge<sub>x</sub>Te, undoped and In-doped, anomalous scatt. of carriers by defects and impurities near ferroelec. phase transition 4-98622  
 Pb<sub>2</sub>InNbO<sub>6</sub>, single crystal, perovskite and pyrochlore modifications, prep. and props. 4-76662  
 PbS film, photosensitivity and luminescence studies 4-104679  
 PbTe thin film, electrophys. props., degradation and recovery 4-88619  
 Si, clusters of electrically active centres and impurity states 4-70183  
 Si, Czochralski grown compensated thermodonors, EPR and Hall studies 4-75898  
 Si, plasma anodic nitridation in N<sub>2</sub>-H<sub>2</sub> system, struct. and optical props. 4-81307  
 Si-O, nonequilibrium cond. and thermal donors 4-104212  
 p-Si:P, elec. activity of P in diffusion zone (*Russian*) 4-70817  
 Si<sub>3</sub>/SiO<sub>2</sub>/Si<sub>3</sub>N<sub>4</sub>, N and O distrib. profiles, Auger studies (*Russian*) 4-65578  
 Si-Mo-Ni contacts, elec. characts. study 4-80653  
 SiO<sub>2</sub> interface, negative elec. effects produced by Gd and La impurities 4-108940  
 SiC fibre reinforced Ti-Al-V, fatigue crack growth behaviour 4-93374  
 SiC fibres, strength degradation after heat treatment above 1200°C 4-66385  
 SiO<sub>2</sub>-B<sub>2</sub>O<sub>3</sub>-Al<sub>2</sub>O<sub>3</sub>-Na<sub>2</sub>O glass, porous, precipitation of colloidal silica and pore size distrib. 4-109412  
 SiO<sub>2</sub>-GeO<sub>2</sub>-OD 4-64779  
 Ta-H, internal friction, hydride precip. peak, cooling rate and freq. depend. 4-66360  
 Ta<sub>2</sub>O<sub>5</sub>, XPS and optical spectra, low-valence cations and electron props. 4-98623  
 Ti alloy, damping capacity, energy scatt. mechanism,  $\beta \rightleftharpoons \alpha''$  transform. by twinning 4-93326  
 Ti alloy, two-phase  $\alpha + \beta$ , hardening heat treatment in furnaces with protective atm. 4-114586  
 Ti alloys, phase transitions in VT3-1 alloy during accelerated cooling (*Russian*) 4-66326  
 Ti-Al-V plate, residual stresses after localised heat treatment, US eval. 4-99728

**heat treatment continued**

- TiAl intermetallic, ductility, strength and microstruct., Ag addition effect (*Japanese*) 4-66391  
 TiO<sub>2</sub> (110), surface defects, XPS, X-ray induced AES, EELS study 4-80351  
 TiO<sub>2</sub>, hydrated, porous struct. and mech. strength, hydrothermal treatment temp. influence 4-71696  
 TiO<sub>2</sub>-Cr<sup>3+</sup>, dopant incorporation rel. to calcination temp., EPR obs. 4-104486  
 TiSi<sub>2</sub>/n<sup>+</sup> poly-Si, co-sputter-deposited, rapid lamp heating, MOS device fabrication appl. 4-99311  
 U-Nb (2.4 wt.%), linear thermal contraction, tensile strength rel. to extrusion 4-109472  
 V-H, internal friction, hydride precip. peak, cooling rate and freq. depend. 4-66360  
 V-Ti, thin wires, heat treatment 4-66355  
 W fibre reinforced stainless steel, residual stresses during thermal cycling 4-71634  
 W wires, electropolished, struct. changes after thermal treatment rel. to surface state (*Polish*) 4-85249  
 W-Ti/Si direct contact system, contact resist., heat treatment effects 4-114032  
 Zn-Al superplastic alloys, Al atoms redistribution, elec.-resist. and small angle X-ray scatt. study 4-62004  
 ZnO varistor, high-field fine-grained, fabrication by sol-gel processing 4-66282  
 ZnSe, mechanically polished, oxidation on heating in air 4-62076  
 Zr-Ba-La-Al-F glass, crystn. kinetics 4-70037

**heated cathodes see thermionic cathodes****heating**

- see also electric heating; induction heating; ovens; plasma heating; refractories; space heating*  
 absorption heat pump, state of the art and future development 4-62381  
 air saturated porous media in short cylinder, transient heat transfer 4-108073  
 boundary layer natural convection regime in rectangular cavity 4-112872  
 channel-type solar energy air heaters with corrugated plates, design parameters 4-114941  
 Darcian half-space, fully saturated, heating, press. generation, phase change 4-97648  
 dielectrics with low cond., heated in EM field, Stefan problem 4-107999  
 electron bombardment heating of samples, multiple sample holder 4-95443  
 fast jet furnace with top-mounted burners, heat exchange 4-97629  
 hot-water heating with vacuum collectors (*German*) 4-114943  
 hydromagnetic free convection past on impulsively started vertical plate in rot. fluid 4-108114  
 indoor swimming pool heating using gas and electric heat pumps (*German*) 4-99988  
 interstellar dust grains, transient heating rel. to identification of 'unidentified' IR emission features 4-115790  
 metal reinforced plastics, struct. during pressure and temp. changes 4-89088  
 metal thin plate, heating and ignition by axisymmetric heat source 4-99794  
 metals, heating by laser rad. in oxidising atmos., calc. 4-65503  
 neurosurgery, soft heating method for stereotaxic operations 4-72460  
 ocean, thermal internal forcing rel. to linear baroclinic instability of non-zonal flow 4-62840  
 plasmatron, high freq. induction, heating of porous wall, math. modelling 4-60742  
 relativistic electron beam, propag. in gases, return. current 2-dimens. mapping 4-69301  
 semiinfinite solid, melting with viscous heating, closed-form soln. 4-97299  
 shock wave generation in solid laser targets 4-84345  
 solar concentrator, Fresnel reflecting, optical and thermodynamic study 4-109751  
 solar-energy stimulated, open-looped thermosyphonic air heaters 4-114942  
 stable compositional gradient, heating and cooling from one side 4-97733  
 thermoacoustic heating at the closed end of an oscillating gas column 4-113101  
 C fibre reinforced plastics, struct. during pressure and temp. changes 4-89088  
 He, liq. pool boiling, crit. heat flux, heater thermophys. props. effects 4-69667  
 Ti plate, shock wave-induced temp. rise, thermoviscoplastic model anal. 4-108527

**heating, buildings see space heating****heavily doped semiconductor materials see heavily doped semiconductors****heavily doped semiconductors**

- see also degenerate semiconductors; superconducting semiconductors*  
 absorption edge, free carrier Fermi-liq. interaction effects 4-114236  
 diffusion layers, surface resist. eddy current meter for non-contact meas. (*Russian*) 4-111155  
 electron relax. effect on phonon damping 4-70317  
 n<sup>+</sup>-n-p structure, SEM-EBIC signals, influence of heavily doped regions 4-104309  
 p-type, phonon attenuation 4-70300  
 p-type, phonon attenuation 4-84349  
 CdCr<sub>2</sub>Se<sub>4</sub>In, static I-V characts. 4-70815  
 EuO:Gd, longitudinal Nernst-Ettingshausen effect, temp. and mag. field dependences 4-65697  
 GaAs:Zn, thermal pulse diffusion of Zn from elemental source 4-98360  
 GaAs-Al<sub>x</sub>Ga<sub>1-x</sub>As tunnel junctions, sequential single-phonon emission obs. in electron transport 4-80667  
 p-GaSb, heavily doped, low temp. thermal cond. 4-70300  
 n-Ge:As, conductivity and magnetoresistance, effect of localised states 4-113950  
 Ge:Sb, heavily doped, US attenuation, mag. field depend. 4-70283  
 (GeSe<sub>3</sub>)<sub>100-x</sub>Bi<sub>x</sub>, struct. and resist. effect of dopants, high press. study 4-103660  
 (GeSe<sub>3</sub>)<sub>100-x</sub>Sb<sub>x</sub>, struct. and resist. effect of dopants, high press. study 4-103660  
 In-Sb, strongly compensated, electron mobility meas. 4-70834  
 nSb:Ge(Si), impurity solubility, role of acceptor and donor states 4-60949  
 PbSe<sub>1-x</sub>Te<sub>x</sub>, energy spectra and elec. cond. 4-70724  
 Si, heavily doped, band-gap narrowing study 4-80490  
 Si, heavily doped, built-in elec. field for holes 4-80584

**heavily doped semiconductors continued**

- Si, heavily doped, intervalley mixing study 4-80491  
 p-Si, heavily doped, low temp. thermal cond. 4-70300  
 Si, highly doped, intrinsic number and Fermi level modelling for device and process simulation 4-75983  
 Si, highly doped, modeling the intrinsic number and Fermi levels for device and process simulation 4-113966  
 Si, n<sup>+</sup> and p<sup>+</sup> regions, uncertainties about physical electronics, solar cell appls. 4-89428  
 Si, n-type, heavily-doped, minority hole mobility, empirical expression for device modelling appl. 4-98608  
 n<sup>+</sup>-Si, surface plasmon polaritons, IR studies 4-108788  
 Si:P, heavily doped, optical reflectivity spectra 4-61735  
 Si:P film, deposition by thermal decomposition of silane 4-114414  
 Si:P(B), heavy doped effect on band struct. and optical props. 4-92998  
 Si<sub>63</sub>Ge<sub>36</sub>S<sub>1</sub>P, Hall voltages changes at high temp. meas., using AC meas. system 4-58866  
 ZnSe:In<sup>+</sup>, ion implanted, high electron mobility obs. 4-108863

**Heaviside layer see E-region****heavy ion excited X-ray emission see ion microprobe analysis****heavy ion-nucleus reactions**

- for inelastic heavy ion-nucleus scattering, see "heavy ion-nucleus scattering"*  
 angular localisations and approximations to deformed potential 4-73931  
 angular momentum transfer and orientation, review 4-86860  
 anomalon search using plastic track detectors and automatic measuring technique 4-96051  
 anomalous relativistic ion interactions, cosmic rays in photoemulsions, nucl. pionisation model 4-110429  
 average angular distribution of emitted particles in multi-step compound processes 4-64117  
 boson charge bunching in high energy collisions, Centauro-like events 4-59114  
 Brookhaven CBA use for rel. heavy-ion collisions, quark matter research 4-68844  
 cascade calcs., causality and relativistic effects 4-83100  
 cascade model calc. of pion multiplicity 4-64115  
 central collisions of heavy nuclei, soliton solns. 4-102317  
 CERN programme for rel. heavy ion physics, <sup>16</sup>O ion acceleration in PS 4-68715  
 charged-particle evaporation, GANES program simulation 4-59279  
 coalescence process, Fermi gas simulation in schematic model 4-86861  
 coherent effects in pion production by ions on nuclei 4-102320  
 cold breakup of spectator residues in nucleus-nucleus collisions at high energy 4-59577  
 conference on nuclear physics at large tandem accelerators, Padova, Italy (March 1983) 4-86108  
 conference on quark matter in rel. nucleus-nucleus collisions, Long Island, NY, USA (Sept. 1983) 4-67855  
 conference on semiclassical methods in nuclear physics, Grenoble, France (Mar. 1984) 4-101567  
 cosmic ray anomalous nuclei events observed in the JACEE emulsion chambers 4-102312  
 cosmic ray collisions, multihadron production, collective mechanisms 4-102313  
 cosmic ray collisions, phase transition simulation 4-102314  
 cosmic ray high energy nuclei interactions in emulsion 4-102309  
 cosmic ray nuclei, 20 GeV/nuc., balloon expt. 4-102310  
 cosmic ray nucleus-nucleus interactions above 1 TeV/n in the JACEE emulsion chamber 4-102311  
 cosmic ray relativistic central collisions on heavy targets 4-102315  
 cosmic ray ultra-relativistic heavy ion collisions, high multiplicity events 4-102316  
 cross-section calcs., interaction radius approach 4-83107  
 deep inelastic collisions, average polarisation for planar and pure-statistical reactions 4-102248  
 deep inelastic collisions, fluctuations, dynamical eqns. 4-106624  
 deep inelastic collisions, statistical and nonstatistical effects from tandem 4-86846  
 diabatic interaction potential 4-68726  
 dissipation, model study of two colliding Fermi gases 4-111551  
 dynamical model for fission, fusion and damped oscillations 4-96056  
 elastic scatt. and fusion cross-sections 4-86844  
 entrance channel effects, one-dimens. model 4-68711  
 equilibration of a three component nuclear system in heavy-ion collision 4-91017  
 fast low density nucleonic jets, promptly emitted particles in TDH 4-102305  
 fast nuclei collisions with potential internucleon interactions, microscopic model 4-78610  
 fast nucleon coherent production, preequilibrium emissions 4-83093  
 fission, fragment ang. distribts., stat. scission model 4-91030  
 fission, pre-equilib. neutron emission, mean field approach, review 4-86849  
 fractionally charged relativistic fragment search 4-64167  
 fragmentation, parton description 4-68717  
 fragmentation; stopping power, multiparticle production, transparency 4-68721  
 fragmentation dynamics in shell model 4-96060  
 fragmentation of nuclei by particles and nuclei of intermediate and high energies 4-95997  
 friction form factor, energy-dependent 4-59145  
 fusion, role of dynamics, fusion barriers and cross sections calculated 4-111562  
 fusion barriers, folding optical potential for heavy systems with 1000 < Z<sub>1</sub>Z<sub>2</sub> < 3000 4-96053  
 fusion cross sections, mean field approach, review 4-86849  
 fusion limitation from level density at high energy 4-73935  
 fusion reactions, isovector giant dipole resonances,  $\pi$ -prod. 4-102288  
 fusion reactions in tandem energy region, cross sections, crit. ang. momentum, review 4-86871  
 fusion-fission ang. distrib. 4-68733  
 generalised critical distance model for heavy ion fusion 4-73860  
 giant resonances, multiphonon excitations 4-68727  
 hydrochemical composition, analytic scheme, heavy ion collisions, fireball model 4-102247  
 heavy nuclei, entropy prod. in p and HI induced reactions, rapidity depend., stat. anal. 4-73846  
 (HI,f), fast fission and compound nucleus form. contribs. 4-59278

## heavy ion-nucleus reactions continued

high energy excitations, RPA descript., heavy ion collisions, reaction mechs. 4-73872  
 high energy nucleus-nucleus collisions, dual parton model, quark-gluon plasma 4-68843  
 high-energy collisions, partial-transparency effects 4-68665  
 high-energy collisions, three-step analytic model 4-64160  
 high-precision studies with large tandem accelerators 4-68852  
 hot, dense nuclear matter research in nucleus-nucleus collisions, low energy data 4-68639  
 hot high spin nuclei decay following heavy ion collisions 4-73802  
 hot nuclear systems, semiclassical treatment, entropy, RMS radii, liquid drop model 4-68642  
 hydrodynamical model of heavy-ion reactions, scaling props., inclusive cross sections 4-106626  
 hydrodynamics of hadronic matter in heavy ion collisions 4-68640  
 incomplete fusion, break-up and sum-rules models anal. 4-59277  
 ion-ion optical pot., vol. contrib. from realistic complex NN interaction, magic nuclei 4-64109  
 Lawrence Berkeley Lab., future high energy machine for nuclear beams 4-68845  
 light particle emission and transfer, exactly solvable model 4-83109  
 low energy, light particle emission mechanism 4-96046  
 medium energy reactions, preequilib. nucleon emission, exciton number 4-86847  
 molecular configs. form., rotating liq. drop model anal. 4-59276  
 multifragmentation-evaporation model for intermediate energy nuclear collisions 4-96068  
 N/Z-equilibration and nucleon exchange in dissipative heavy-ion collisions 4-91018  
 Newtonian dynamics of time-dependent mean field theory 4-83097  
 non-equilibrium momentum distrib. systems, thermodynamical formalism 4-82775  
 nonlinear effects in nuclear matter in heavy ion interactions 4-102318  
 nuclear matter boiling under heavy ion bombardment (French) 4-59191  
 nuclear matter transition to quark-gluon plasma, hydrodynamical model 4-111552  
 nuclear potentials from fusion excitation functions 4-95981  
 nuclear response function, temp. depend., random phase approx. 4-96044  
 nucleon transfer, independ. particle model 4-73927  
 nucleus-nucleus collisions, medium mass fragment apparent temp., hot spots 4-106608  
 one-body nuclear friction, form factor, microscopic calc. 4-59263  
 pairing phase transitions in rotating deformed nuclei, two nucleon transfer 4-86862  
 peripheral heavy-ion collisions, pion prod. via isobar giant reson. formation and decay 4-64159  
 peripheral heavy-ion reactions, angular correlations between light fragments 4-68712  
 potential decay. from generalised critical distance model 4-111529  
 QCD deconfining phase transition, supersaturated pion vapour, ultrarelativistic heavy ion collisions 4-102095  
 quark-gluon matter in heavy ion collisions, thermodynamics, finite temp. field theory 4-68637  
 quark-gluon plasma, hydrodynamic evolution, in ultrarelativistic nuclear collisions 4-86674  
 quark-gluon plasma, meson radiation using chromoelectric flux tube model 4-64082  
 quark-gluon plasma, strangeness prod., perturbative QCD anal. 4-68531  
 quark-gluon plasma, Vlasov eqn., Wigner transform. to nonAbelian Yang-Mills symmetries 4-102285  
 quark-gluon plasma formation, energies and mass numbers for heavy ion collisions 4-95766  
 quark-gluon plasma in ultra-relativistic nucleus-nucleus collisions, hydrodynamics, review 4-68638  
 quark-gluon plasma-nuclear matter transition in heavy ion collisions 4-83020  
 quark-matter formation in the fragmentation rapidity region of ultrarelativistic heavy-ion collisions 4-73847  
 quasi-elastic heavy ion reactions,  $SU_4$ -invariant model 4-102303  
 quasi-elastic reactions, DWBA diffractive model, direct cross sections,  $\alpha$ -transfer 4-86851  
 random walk versus discrete master equation for heavy-ion collisions 4-95994  
 relativistic collisions, limiting fragmentation and transparency, hydrodynamical anal. 4-59274  
 relativistic collisions, pion fluctuations and pol.,  $\pi^-$ /proton ratio 4-83098  
 relativistic collisions, quark-gluon plasma temp. meas. using director meson resonances 4-64157  
 relativistic collisions, quark-matter form., spectator temp. signature 4-90966  
 relativistic heavy ion collider, 10 GeV on 10 GeV, baryon rich region research 4-68846  
 relativistic heavy ion collisions,  $\pi$  prod., light fragment form., entropy, fluid-dynamical model 4-78645  
 relativistic heavy ion collisions, entropy production 4-68716  
 relativistic heavy ion collisions, hydrodynamics 4-68718  
 relativistic heavy-ion collision, initial density of quark-gluon plasma 4-111395  
 relativistic heavy-ion collisions, baryon distribution 4-111396  
 relativistic heavy-ion collisions, contribution of NY-NNK in kaon production,  $Y=\Sigma A$  4-83101  
 relativistic heavy-ion collisions, hydrodynamical model 4-91020  
 relativistic heavy-ion collisions, production and detect. of strange quark droplets 4-111399  
 relativistic nuclei in peripheral collisions, EM dissociation, virtual photon spectrum 4-86853  
 resonating group method, equiv. local pots., Perey factors, orthogonality condition model 4-83008  
 rotation-vibration spectra symmetry using  $U(5)$  group (Chinese) 4-111553  
 RPA modes, microscopic description 4-102227  
 self induced nuclear transparency in mult. TeV hadronic interactions 4-102319  
 shock wave characteristics 4-59281  
 shower particles production in heavy ion collisions 4-102308  
 strongly damped collisions, dissipation and relaxation, mean field approach, review 4-86849  
 sub-barrier fusion, coupled channels effect, approx. treatment 4-78655  
 subbarrier fusion cross-section, transfer channel correction 4-73932  
 subthreshold  $K^-$  production, final state interactions effect 4-64106

## heavy ion-nucleus reactions continued

subthreshold pion production in heavy ion reactions, thermodynamic model 4-95996  
 sum rules study and a scaling property of fragmentation mass yield curves 4-64116  
 surface friction model, comparison with TDHF 4-95993  
 TDHF with collisions in heavy ion dynamics 4-95945  
 thermal models for heavy ion reactions, similarities and contrasts 4-64118  
 thermodynamic model approach to pion production in relativistic heavy ion collisions 4-95995  
 time-dependent optical potential for the Schrodinger solution in a truncated subspace 4-73288  
 total reaction cross sections, direct measurements 4-83094  
 transfer reaction polarisation pot., channel nonorthogonality correction 4-68667  
 ultra high energy nuclear interaction producing multiple large  $P_T$  components (Chinese) 4-77685  
 ultra-relativistic collisions, quark-gluon plasma form. in central rapidity region, finite size effects 4-95767  
 ultra-relativistic heavy ion collisions, hydrodynamical space-time evol. of central rapidity region 4-64156  
 ultra-relativistic heavy-ion collision, thermal equilibration 4-59265  
 ultrarelativistic heavy ion central collisions, energy densities, quark-gluon plasma 4-96045  
 ultrarelativistic heavy ion collisions, colour plasma and QCD descriptions 4-68719  
 ultrarelativistic nuclear collisions, new phenomena signatures, quark-gluon plasma 4-68713  
 very high energy heavy ion collisions, quark matter form., review 4-68636  
 wave packet scatt. model with quantum friction 4-59260  
 zero-angle finite-range approx., coupled reaction channels involving nucleon transfer 4-106955  
<sup>12</sup>(<sup>12</sup>C,Be), 2.4-6.4 MeV, subbarrier cross section meas. using plastic detectors 4-96048  
 AGd(<sup>32</sup>S, 4n) A=156, 154, <sup>182,184</sup>Hg ground state shape and crossing of spherical and deformed bonds 4-68730  
 Ag(<sup>40</sup>Ar,X), 27 MeV/u, heavy products, particle emission deexcitation, transferred momentum 4-64173  
 Ag(<sup>40</sup>Ar,X), 285 MeV,  $\alpha$ -particle form., cross-sections, energy and ang. distrib. 4-78650  
 Ag(<sup>40</sup>Ar, X), 8.5 MeV/u,  $\alpha$  evap., multiplicities, composite nucleus spin and lifetime expectancy 4-64172  
 Ag(<sup>56</sup>Fe, X), 8.5 MeV/u,  $\alpha$  evap., multiplicities, composite nucleus spin and lifetime expectancy 4-64172  
 Ag(<sup>14</sup>N, X), 35 MeV/u, Li and Be distrib., fireball, hadronic thermometry and final state interactions 4-106629  
 Ag(Si,X), ultrarelativistic, pseudorapidity distrib. fluctuations, power spectrum anal. 4-96067  
<sup>106</sup>Ag(<sup>18</sup>O,X), 86 MeV/N, multifragment emission, fission and total cross sections using SSNTD 4-96050  
<sup>109</sup>Ag(<sup>7</sup>Li,4n)<sup>111</sup>Sn, excited states, in-beam spectroscopic methods, shell model predictions 4-102221  
<sup>27</sup>Al(<sup>14</sup>N, H1+light particles), 30 MeV/N, projectile fragmentation processes, multifragmentation 4-59264  
<sup>27</sup>Al(<sup>18</sup>O,X) 80 MeV, N isotope identification by Bragg curve spectroscopy 4-96324  
<sup>27</sup>Al(<sup>18</sup>F,<sup>32</sup>Ar)<sup>54</sup>Sc, <sup>44</sup>Sc excited state lifetime meas. 4-68654  
<sup>27</sup>Al(<sup>32</sup>S, <sup>32</sup>Cu), ang. momentum induced deformations,  $\alpha$ -spectra, rot. liq. drop model 4-102175  
<sup>27</sup>Al(<sup>37</sup>Cl,X), 100-200 MeV, cross sections, spectra and ang. distrib., composite system scission 4-86848  
<sup>40</sup>Ar(X), 2 GeV/u, He, Li and Be fragment mass free paths 4-59261  
<sup>40</sup>Ar(X) on <sup>197</sup>Au, <sup>209</sup>Bi, <sup>238</sup>U product mass distribution, ang. momentum 4-86855  
<sup>40</sup>Ar (<sup>40</sup>Ar,X), E=1.8 GeV/N, search for fractionally charged nucl.,  $1 \leq Z \leq 18$  4-106567  
<sup>40</sup>Ar (fragmentation) anomalous search using nuclear emulsions 4-64164  
<sup>40</sup>Ar on Ag, two  $\alpha$ -particle correlations 4-91019  
<sup>40</sup>Ar(<sup>4</sup>Pb, xn), A=204-208, Fm evaporation residues meas., sub-barrier fusion and extra-push probing 4-73939  
<sup>40</sup>Ar(<sup>4</sup>X,X) A=165 to 208, fusion-fission and neutron evaporation residue cross-sections 4-73922  
<sup>40</sup>Ar(<sup>7</sup>Li,Be), <sup>40</sup>Cl mass and low lying level determ. 4-64163  
<sup>197</sup>Au(<sup>12</sup>C,X), 25 GeV, <sup>37</sup>Ar and <sup>127</sup>Xe fragment ang. distrib. and fragmentation mechs. 4-96066  
<sup>197</sup>Au(<sup>12</sup>C,X), x=p,d,t, <sup>4</sup>He, <sup>6</sup>He, <sup>6</sup>He particle spectra, cross-sections 4-59273  
<sup>197</sup>Au(<sup>14</sup>N,X), 115, 168 MeV, incomplete fusion, ang. momentum depend. 4-59268  
<sup>197</sup>Au(<sup>14</sup>N,X), nonequilibrium particle emission in reaction plane 4-73925  
<sup>197</sup>Au(<sup>16</sup>O, 2p), 400 MeV, form. and decay of localised region of high excitation, comments and reply 4-86857  
<sup>197</sup>Au(<sup>16</sup>O,X), 4 MeV/N, projectile Coulomb breakup,  $\alpha$  inclusive meas. 4-73937  
<sup>197</sup>Au(<sup>16</sup>O), 31 MeV/u, fission fragments in coincidence with quasi-projectile, linear momentum transfer 4-59267  
<sup>197</sup>Au(<sup>18</sup>O,X), 86 MeV/N, multifragment emission, fission and total cross sections using SSNTD 4-96050  
<sup>197</sup>Au(<sup>238</sup>U,X), 2.38, 3.97 GeV, ang. distrib. and branching ratios using SSNTD 4-96047  
<sup>197</sup>Au(<sup>40</sup>Ar,F), E=44 MeV/u, linear momentum transfer to fissioning nucleus 4-102328  
<sup>197</sup>Au(<sup>84</sup>Kr, X), 35 MeV/u, high energy relaxed products, expt. evidence 4-73941  
<sup>10</sup>B(<sup>5</sup>Li,d)<sup>14</sup>N, transfer reaction studies 4-102292  
<sup>10</sup>B(<sup>7</sup>Li,p)<sup>16</sup>N, 16.0 MeV, states up to 6.61 MeV 4-73929  
<sup>11</sup>B(<sup>5</sup>Li,<sup>3</sup>e)<sup>14</sup>C, transfer reaction studies 4-102292  
<sup>11</sup>B(<sup>5</sup>Li,t)<sup>14</sup>N, transfer reaction studies 4-102292  
<sup>11</sup>B(<sup>7</sup>Li,e)<sup>14</sup>C, transfer reaction studies 4-102292  
<sup>209</sup>Bi(<sup>30</sup>Ti,X) fusion-fission and neutron evaporation residue cross-sections 4-73922  
 Br(Si,X), ultrarelativistic, pseudorapidity distrib. fluctuations, power spectrum anal. 4-96067  
 C(Ar,X), fragmentation, accelerator test of semi-empirical cross-sections 4-91023  
 C(<sup>197</sup>Au,X), 200 GeV, fragmentation charge peaks 4-91024  
 C(<sup>12</sup>C,p,X), collisions with various target nuclei at 3.6 GeV/nucleon, moving source formation 4-102297

## heavy ion-nucleus reactions continued

- (Ca,X), ultrarelativistic, pseudorapidity distrib., fluctuations, power spectrum anal. 4-96067  
 C(<sup>20</sup>Ne,X), 500 MeV/nuc fragmentation, charge and isotropic cross sections, cosmic ray propagation appl. 4-91022  
 C(<sup>16</sup>O,X), 500 MeV/nuc fragmentation, charge and isotropic cross sections, cosmic ray propagation appl. 4-91022  
 (<sup>12</sup>C,  $\alpha$ X) anomalous interaction mean free path of relativistic  $\alpha$ -particles 4-96077  
 (<sup>12</sup>C,X), 4.1 GeV/c per nucleon, on photographic emulsion, search for anomalous interactions 4-68710  
 (<sup>12</sup>C,X), on emulsion, relativistic nuclei fragmentation, azimuthal effects 4-68709  
 (<sup>12</sup>C, $\alpha$ ), 4.2 GeV/nuc., dissociation in emulsion 4-102307  
 (<sup>12</sup>C, $\pi^+$ X), 86 MeV/nucleon, cross section saturation effect on <sup>6</sup>Li, <sup>12</sup>C, <sup>21</sup>Al, Cd, Pb 4-91011  
<sup>12</sup>C projectile fragmentation in emulsion, Z=2 fragment anomalous mean free path 4-73926  
 (<sup>12</sup>C,  $\pi^0$ X), 60-84 MeV/u, cooperative effects, pion source vel., short-distance phenomena 4-59262  
 (<sup>12</sup>C,<sup>11</sup>B,X), <sup>23</sup>Na compound nucleus formation 4-96072  
 (<sup>12</sup>C(<sup>12</sup>C,  $\pi^-$ ), 60-85 MeV/N, cross sections,  $\pi^-/\pi^+$  ratio and yields 4-102289  
 (<sup>12</sup>C(<sup>12</sup>C, X), 4.2 GeV/nucleon, inclusive characteristics, differential cross section 4-78653  
 (<sup>12</sup>C(<sup>12</sup>C,X), 4.2 GeV per nucleon, secondary particles, collective props. 4-68734  
 (<sup>12</sup>C(<sup>12</sup>C,X), molecular state cluster study 4-59185  
 (<sup>12</sup>C(<sup>12</sup>C, $\alpha$ ), <sup>20</sup>Ne, 13-15 MeV CM, cross section, dominance of l=10 partial wave 4-68732  
 (<sup>12</sup>C(<sup>12</sup>C, $\gamma$ ), radiative capture, <sup>12</sup>C+<sup>12</sup>C, quasimolecule, transitions, moments, RMS radii, energies and widths, GCM method 4-73879  
 (<sup>12</sup>C(<sup>12</sup>C,p), 39 MeV, <sup>23</sup>Na high spin states, J<sup>π</sup>, ang. distrib., and cross sections 4-106562  
 (<sup>12</sup>C(<sup>12</sup>C, $\pi$ ), subthreshold pion production, statistical compound decay theory 4-64166  
 (<sup>12</sup>C(<sup>16</sup>O,X) fusion cross-sections, evaporation residue yields 4-73934  
 (<sup>12</sup>C(<sup>16</sup>O, $\alpha$ ) dominance of <sup>20</sup>Ne\* and <sup>16</sup>O\* resonances 4-59272  
 (<sup>12</sup>C(<sup>18</sup>O,<sup>14</sup>C), 82 MeV, <sup>18</sup>O sequential breakup, DWBA anal. 4-83095  
 (<sup>12</sup>C(<sup>18</sup>O, $\alpha$ ), 10-15 MeV, resonances, excitation functions, ang. distrib. 4-106603  
 (<sup>12</sup>C(<sup>19</sup>F,<sup>19</sup>F), 7.4-24.4 MeV, elastic and inelastic, backward angle excitation function enhancement 4-102295  
 (<sup>12</sup>C(<sup>238</sup>U,X), 2.38, 3.97 GeV, ang. distrib. and branching ratios using SSNTD, fission 4-96047  
 (<sup>12</sup>C(<sup>6</sup>Li, $\alpha$ ), <sup>14</sup>N, transfer reaction studies 4-102292  
 (<sup>12</sup>C(<sup>6</sup>Li,d), <sup>16</sup>O( $\alpha$ ),  $\alpha$ -d ang. correl. functions, optical pot. determ. 4-86859  
 (<sup>12</sup>C(<sup>6</sup>Li,<sup>6</sup>Li), <sup>13</sup>C, ang. dist. and vector analysing power 4-64162  
 (<sup>12</sup>C(<sup>6</sup>Li, $\alpha$ ), excitation functions, energy dist., hot spots 4-86858  
 (<sup>12</sup>C(<sup>16</sup>B,X), <sup>23</sup>Na compound nucleus formation 4-96072  
 (<sup>12</sup>C(<sup>7</sup>Li,<sup>6</sup>He), <sup>14</sup>N, transfer reaction studies 4-102292  
 (<sup>12</sup>C(<sup>7</sup>Li,<sup>6</sup>Li), <sup>14</sup>C, transfer reaction studies 4-102292  
 (<sup>12</sup>C(<sup>6</sup>Li,<sup>6</sup>He), <sup>14</sup>N, charge exchange with spin flip 4-78651  
 (<sup>12</sup>C(<sup>6</sup>Li,d), <sup>18</sup>O,  $\alpha$ -cluster study 4-64078  
 Ca(Ca,X), 400 MeV/N, collective flow in rel. collisions, fragment side splash, global anal. 4-68722  
 Ca(Ca,X), 400 MeV/N, freezeout density in rel. collisions from p-p corrs. 4-102294  
 (<sup>40</sup>Ca(<sup>16</sup>O, $\gamma$ ), extended time-dependent Hartree-Fock theory, one-dimensional collision model 4-111516  
 (<sup>40</sup>Ca(<sup>12</sup>S,X), 320 MeV, scission configurations 4-91014  
 (<sup>40</sup>Ca(<sup>40</sup>Ca, X), E/A=400 and 1050 MeV, thermalisation in symmetric collisions 4-91015  
 (<sup>40</sup>Ca(<sup>6</sup>Li, X), 156 MeV, fusion and nonfusion phenomena, cross sections, <sup>6</sup>Li breakup 4-59299  
 (<sup>40</sup>Ca(<sup>6</sup>Li,<sup>6</sup>Li), angular dist., DWBA calcs. 4-102291  
 (<sup>40</sup>Ca(<sup>16</sup>O,<sup>18</sup>O), <sup>16</sup>O, <sup>18</sup>O simultaneous two-nucleon transfer cross-section 4-78649  
 (<sup>48</sup>Ca(<sup>238</sup>U,X), dynamics, mass drift of reaction products 4-96085  
 (<sup>48</sup>Ca(<sup>12</sup>C,<sup>3n</sup>), 65 MeV, <sup>48</sup>Fe  $\beta$ -delayed proton spectra, cross sections (Chinese) 4-73858  
 (<sup>114</sup>Cd(<sup>13</sup>C,<sup>3n</sup>), <sup>132</sup>Xe band, superbands, J<sup>π</sup>, backbending and  $\gamma$ -transitions 4-102167  
 (<sup>114</sup>Cd(<sup>48</sup>Ca,4n), <sup>158</sup>Er, prolate-oblate shape change in Er 4-102222  
 Cl(Ar,2 $\pi^+$ X) two-pion correlations in heavy ion collisions 4-83102  
 Co(<sup>62</sup>S,X), evaporation residue, fissionlike fragments, cross sections, transitional dissipative mech. 4-106628  
 (<sup>59</sup>Co(<sup>32</sup>S,X), fission-fusion like processes, intermediate mechs., dynamical model anal. 4-111548  
 (<sup>59</sup>Co(<sup>32</sup>S,X), fragment mass distrib., cross sections, dynamical fission and transitional mechs. 4-86868  
 (<sup>59</sup>Co(<sup>32</sup>S,X), intermediate mechanisms, fragment distrib., XTU Tandem results 4-86845  
 A(Cr(<sup>20</sup>Ne,X), A=50, 54, kinetic energy, charge distributions, strongly damped components 4-83105  
 Cu(<sup>12</sup>C,pX), collisions with various target nuclei at 3.6 GeV/nucleon, moving source formation 4-102297  
 (<sup>63</sup>Cu(<sup>27</sup>Al,X), 13.4 MeV/N, projectile-like fragments at grazing angle, reaction mech. 4-83099  
 (<sup>168</sup>Er (<sup>20</sup>Ne, fragmentation) deep-inelastic, multiplicity, anisotropy and circular polarisation 4-64165  
 (<sup>170</sup>Er(<sup>76</sup>Ge,X) fusion-fission cross-section, mass and charge distributions 4-83106  
 (<sup>153</sup>Eu(<sup>16</sup>O, 4n), <sup>165</sup>Lu, proton configuration, transition probabilities 4-86796  
 F(Ne, K<sup>+</sup>X), 2.1 GeV/N, K<sup>+</sup> inclusive diff. cross section in rel. collisions from transport theory 4-102290  
 F(Ne,X), K<sup>+</sup> production, cascade model 4-91012  
 F(Ne,2 $\pi^+$ X) two-pion correlations in heavy ion collisions 4-83102  
 (Fe,X), 710 and 1050 MeV/nuc, fragmentation, cosmic ray propagation appl. 4-91021  
 (<sup>54</sup>Fe(<sup>28</sup>Si,3pn), 103.5, 108 MeV, <sup>78</sup>Rb high spin states, isomers, rot. bands, moment of inertia parameter 4-106563  
 (<sup>56</sup>Fe,X), 2 GeV/u, He, Li and Be fragment mean free paths 4-59261  
 (<sup>56</sup>Fe,X), fragmentation anal. in CR-39 track detector and emulsion 4-102306  
 (<sup>56</sup>Fe,X), on emulsion, relativistic nuclei fragmentation, azimuthal effects 4-68709  
 (<sup>56</sup>Fe(<sup>28</sup>Si,apn), 103.5, 108 MeV, <sup>78</sup>Rb high spin states, isomers, rot. bands, moment of inertia parameter 4-106563  
 heavy ion-nucleus reactions continued  
 (<sup>159</sup>Gd(<sup>48</sup>Ti,X), evaporation decay and gamma multiplicity for <sup>204</sup>Rn v fusion channel 4-64170  
 (<sup>160</sup>Gd(<sup>16</sup>O,xn), 80-134 MeV; ang. momenta, stat. anal., Hf  $\gamma$ -transitions multiplicity and spin distrib. 4-95953  
 (<sup>72</sup>Ge(<sup>40</sup>p,2n), E=48-60 MeV, yrast high-spin states of <sup>86</sup>Y 4-106559  
 (<sup>74</sup>Ge(<sup>48</sup>Kr, Xn), fusion process, impact parameter influence 4-111561  
 (<sup>76</sup>Ge(<sup>14</sup>N, 4n), E=38-56 MeV, yrast high-spin states of <sup>86</sup>Y 4-106559  
 (<sup>76</sup>Ge(<sup>22</sup>S,X), fission-fusion like processes, intermediate mechs., dynamical model anal. 4-111548  
 (<sup>76</sup>Ge(<sup>32</sup>S,X), fragment mass distrib., cross sections, dynamical fission and transitional mechs. 4-86868  
 (<sup>115</sup>H(<sup>15</sup>N, $\alpha$ ), <sup>12</sup>C reson. reaction, appl. to H determ. in Si(SiO<sub>2</sub>) 4-85347  
 (<sup>115</sup>H(<sup>19</sup>F, $\alpha$ ), <sup>16</sup>O\*, g factor measurement, hyperfine frequency of <sup>16</sup>O 6.1 MeV 3<sup>+</sup> state 4-96712  
 (<sup>115</sup>H(<sup>19</sup>F, $\alpha$ ), <sup>16</sup>O reson. reaction, appl. to H determ. in Si(SiO<sub>2</sub>) 4-85347  
 (<sup>115</sup>H(<sup>19</sup>F, $\pi^+$ ), <sup>16</sup>O\*, g factor measurement, hyperfine frequency of <sup>19</sup>F 197 k 5/2<sup>+</sup> state 4-96712  
 Hg(HI,X), secondary reaction, <sup>272</sup>112 prod. and spontaneous fission 4-86870  
 K(Ar,2 $\pi^+$ X) two-pion correlations in heavy ion collisions 4-83102  
 (<sup>36</sup>Kr, X), 1.52 GeV/N, Z $\geq$ 15 projectile fragments, anomalous behaviour 4-86856  
 (<sup>139</sup>La(<sup>63</sup>Cu,X), evaporation decay and gamma multiplicity for <sup>204</sup>Rn v fusion channel 4-64170  
 (<sup>6</sup>Li,d), selectivity, O<sup>+</sup> state excitation, relative cross-sections 4-96062  
 (<sup>6</sup>Li,d) microscopic cluster form factor in DWBA calcs. 4-64161  
 (<sup>6</sup>Li(<sup>14</sup>N, 2 $\alpha$ d), 4-body breakup in PWIA with two spectators (Chinese) 4-83091  
 (<sup>6</sup>Li(<sup>6</sup>Li, $\alpha$ ), 2.4, 4.2 MeV, direct mechanism, quasifree effects 4-106607  
 (<sup>7</sup>Li(<sup>12</sup>C,  $\pi^+$ ), 60-85 MeV/N, cross sections,  $\pi^-/\pi^+$  ratio and yield 4-102289  
 (<sup>24</sup>Mg(<sup>12</sup>C,<sup>3n</sup>), 65 MeV, <sup>33</sup>Ar, half-life (Chinese) 4-73858  
 (<sup>24</sup>Mg(<sup>13</sup>C,<sup>12</sup>C), <sup>25</sup>Mg\*, intermediate stage in <sup>24</sup>Mg\* (2<sup>+</sup>, 1.37 MeV) production 4-102301  
 (<sup>24</sup>Mg(<sup>16</sup>O, <sup>16</sup>O),  $\alpha$ -transfer process, nuclear molecular orbital model 4-106627  
 A(<sup>20</sup>Ne,X), A=92, 100, kinetic energy, charge distributions, strongly damped components 4-83105  
 (<sup>90</sup>Mo(<sup>13</sup>C,<sup>3n</sup>), <sup>108</sup>Cd level struct and lifetimes, cranking and shell model anal. 4-95872  
 (<sup>90</sup>Mo(<sup>81</sup>Br,X), evaporation residue cross-sections for complete fusion 4-73933  
 (<sup>98</sup>Mo(<sup>6</sup>Li,4n), 35-45 MeV, <sup>100</sup>Rh high spin states, isomers, J<sup>π</sup>, T<sub>1/2</sub> and transitions 4-86762  
 (<sup>100</sup>Mo(<sup>14</sup>N, <sup>12</sup>B), 90, 125 MeV, <sup>12</sup>B polarisation meas. from beta-ray asymmetry 4-64318  
 (<sup>100</sup>Mo(<sup>32</sup>S,X), 150 MeV, fragment distrib., ang. distrib. width, spin depolarising modes contrib. 4-73920  
 (<sup>100</sup>Mo(<sup>32</sup>S,X), deep inelastic scatt., statistical effects, XTU Tandem results 4-86845  
 (<sup>14</sup>N,X), on emulsion, relativistic nuclei fragmentation, azimuthal effects 4-68709  
 (<sup>14</sup>N,p), pre-equilibrium light particle emission 4-73888  
 (<sup>14</sup>N(<sup>12</sup>C,X), E $\geq$ 18 MeV/N, fusion cross sections, yields, stat. anal., comparison with <sup>16</sup>B + <sup>16</sup>O 4-73945  
 (<sup>14</sup>N(<sup>6</sup>Li, X), 36 MeV, X=<sup>3</sup>H, <sup>3</sup>He, three particle transfer, shell anal., DWBA anal., A=17, struct. 4-78647  
 (<sup>14</sup>N(<sup>9</sup>Be,X), <sup>23</sup>Na compound nucleus formation 4-96072  
 (<sup>15</sup>N(<sup>6</sup>Li,d), population of negative parity  $\alpha$  clusters in <sup>19</sup>F 4-73823  
 Na(Ne, K<sup>+</sup>X), 2.1 GeV/N, K<sup>+</sup> inclusive diff. cross section in rel. collisions from transport theory 4-102290  
 Na(Ne,X), K<sup>+</sup> production, cascade model 4-91012  
 Na(Ne,X) on NaF, 2.1 GeV/A, K<sup>+</sup> cross section, cascade model 4-102300  
 Na(Ne,2 $\pi^+$ X) two-pion correlations in heavy ion collisions 4-83102  
 Nb(Nb,X), 400 MeV/N, collective flow in rel. collisions, fragment side splash, global anal. 4-68722  
 Nb(Nb,X), 400 MeV/N, freezeout density in rel. collisions from p-corrs. 4-102294  
 Nb(Nb,X), collective flow calcs., short-range nature of nucl. force 4-111507  
 (<sup>93</sup>Nb(<sup>12</sup>C,X), 132-208 MeV, nonequilibrium, p, d, t, <sup>3</sup>He and  $\alpha$  emission statistical anal. 4-111549  
 (<sup>93</sup>Nb(<sup>16</sup>O, X), E=204 MeV, pre-equilibrium nucleon emission, Fermi-gas model 4-96043  
 (<sup>93</sup>Nb(<sup>16</sup>O,X), fast nucleon emission in time-depend. external field model 4-86808  
 (<sup>93</sup>Nb(<sup>93</sup>Nb, fragmentation), fluid dynamical model 4-68720  
 (<sup>93</sup>Nb(<sup>93</sup>Nb, X), E/A=400 and 650 MeV, thermalization in symmetric collisions 4-91015  
 (<sup>93</sup>Nb(<sup>93</sup>Nb,X), 400 MeV/N, kinetic energy flow, nuclear matter hydrodynamic compression 4-68723  
 (<sup>142</sup>Nd(<sup>12</sup>C,<sup>7n</sup>), <sup>142</sup>Dy beta delayed proton activity, half-life 4-106594  
 (<sup>146</sup>Nd(<sup>15</sup>N,4n), <sup>157</sup>Ho, E=74 MeV, signature dependence of M1 and E2 transition probabilities 4-95961  
 (<sup>148</sup>Nd(<sup>16</sup>O, <sup>166</sup>Er\*) compound state,  $\gamma$ -decay of GDR modes 4-68729  
 (<sup>150</sup>Nd(<sup>16</sup>O, <sup>166</sup>Er\*) compound state,  $\gamma$ -decay of GDR modes 4-68729  
 Ne(F,X) hadron production, relativistic model 4-91016  
 Ne(Na,X) hadron production, relativistic model 4-91016  
 (<sup>20</sup>Ne, $\alpha$ ), 9 MeV/nuc., breakup expt. 4-96074  
 (<sup>22</sup>Ne,X), 4.1 GeV/c per nucleon, on photographic emulsion, search for anomalous interactions 4-68710  
 (<sup>22</sup>Ne,X) in emulsion, 4.1A GeV/c, mean free path, anomalous search 4-111547  
 (<sup>58</sup>Ni(<sup>14</sup>N,<sup>2</sup>C $\alpha$ ), 148 MeV, sequential ejectile decay, HI- $\alpha$  coincidence cross sections 4-96069  
 (<sup>58</sup>Ni(<sup>28</sup>S,X), 320 MeV, scission configurations 4-91014  
 (<sup>58</sup>Ni(<sup>28</sup>S,X), 355 MeV, light particle emission and fragmentation process kinematic anal. 4-111550  
 (<sup>58</sup>Ni(<sup>58</sup>Ni,X), coupled-channels fusion calcs. 4-64188  
 (<sup>58</sup>Ni(<sup>58</sup>Ni,X), subbarrier fusion in direct reaction technique 4-73930  
 (<sup>58</sup>Ni(<sup>58</sup>Ni,X), subbarrier fusion in direct reaction technique 4-73930  
 (<sup>16</sup>O,<sup>12</sup>C), selectivity, O<sup>+</sup> state excitation, relative cross-sections 4-96062  
 (<sup>16</sup>O, $\alpha$ ), 9 MeV/nuc., breakup expt. 4-96074  
 (<sup>16</sup>O, compressed nucleus, dense system disassembly, TDHF study, clusterisation, collective flow 4-59190  
 (<sup>16</sup>O,p), pre-equilibrium light particle emission 4-73888  
 (<sup>16</sup>O, X), 2.1 GeV/A, in emulsion, evidence of dynamical correlation 4-96052

## ion-nucleus reactions continued

- <sup>18</sup>O(<sup>10</sup>B,X), E=18 MeV/N, fusion cross sections, yields, stat. anal., comparison with <sup>12</sup>C+<sup>14</sup>N 4-73945
- <sup>16</sup>O(<sup>16</sup>O, <sup>12</sup>C), nonlocal coupling pot. eval., Dini expansion method appl. 4-78646
- <sup>16</sup>O(<sup>16</sup>O,X), complex optical pot., exchange contribs., density matrix approach 4-73928
- <sup>16</sup>O(<sup>16</sup>O,X) fusion and elastic scatt. cross sections, near Coulomb barrier 4-86873
- <sup>16</sup>O(<sup>7</sup>Li,X), Na compound nucleus formation 4-96072
- <sup>16</sup>O(X,Y) X=<sup>27</sup>Al, <sup>48</sup>Ti, <sup>58,62</sup>Ni spin polarisation 4-86854
- Pb(Ar,X), 0.8 GeV/N, nuclear matter stopping power and collective flow 4-102296
- Pb(<sup>12</sup>C,p,X), collisions with various target nuclei at 3.6 GeV/nucleon, moving source formation 4-102297
- Pb(Ne,X), K<sup>+</sup> production, cascade model 4-91012
- Pb(Pb, K<sup>+</sup>X), K<sup>+</sup> inclusive diff. cross section in rel. collisions from transport theory 4-102290
- <sup>208</sup>Pb(<sup>12</sup>C,  $\pi^{\pm}$ ), 60-85 MeV/N, cross sections,  $\pi^{-}/\pi^{+}$  ratio and yields 4-102289
- <sup>208</sup>Pb(<sup>11</sup>B, 4n), E=66 MeV, high-spin states in <sup>215</sup>Fr, particle-hole analysis 4-106560
- <sup>208</sup>Pb(<sup>16</sup>O,X), near barrier energies, quasielastic and fusion simultaneous descript. 4-96065
- <sup>208</sup>Pb(<sup>20</sup>Ne,X), 30 MeV/N, fragment energy spectra, high excitation energy structs. 4-73870
- <sup>208</sup>Pb(<sup>238</sup>U,X), 2.38, 3.97 GeV, ang. distrib. and branching ratios using SSNTD 4-96047
- <sup>208</sup>Pb(<sup>28</sup>Si,X), 225 MeV, quasielastic processes 4-96071
- <sup>208</sup>Pb(<sup>36</sup>Ar,X), 11 MeV/N, fragment energy spectra, high excitation energy structs. 4-73870
- <sup>208</sup>Pb(<sup>30</sup>Ti,X) fusion-fission and neutron evaporation residue cross-sections 4-73922
- <sup>208</sup>Pb(<sup>56</sup>Fe,X), dynamics, mass drift of reaction products 4-96085
- <sup>208</sup>Pb(<sup>58</sup>Fe,n), <sup>26</sup>108 formation, identification from  $\alpha$ -decay chain 4-86863
- <sup>208</sup>Pb(<sup>86</sup>Kr, <sup>87</sup>Kr) <sup>207</sup>Pb, ang. distributions, differential cross-sections, DWBA calcs. 4-83104
- <sup>100</sup>Pb(<sup>19</sup>F,p2n), <sup>128</sup>Xe band, superbands, J<sup>+</sup>, backbending and  $\gamma$ -transitions 4-102167
- <sup>141</sup>Pr(<sup>18</sup>O,4n) <sup>155</sup>Ho, E=85 MeV, signature dependence of M1 and E2 transition probabilities 4-95961
- <sup>101</sup>Ru(<sup>81</sup>Br,X) evaporation residue cross-sections for complete fusion 4-73933
- As(<sup>27</sup>Al,X), 3.5 MeV/N, A=32, 34, fusion evaporation residues, XTU Tandem results 4-86845
- <sup>92</sup>Sr(X), on Ru, Rh, Pd, Mo, sub-Coulomb fusion cross sections, Munich Recoil Spectrometer results 4-86872
- <sup>96</sup>Zr(X), on Ru, Rh, Pd, Mo, sub-Coulomb fusion cross sections, Munich Recoil Spectrometer results 4-86872
- <sup>28</sup>Si(<sup>28</sup>Si, X), extended time-dependent Hartree-Fock theory, one-dimensional collision model 4-111516
- <sup>28</sup>Si(<sup>28</sup>Si,X), excitation functions, statistical anal. 4-73887
- <sup>28</sup>Si(<sup>32</sup>S,X), 320 MeV, scission configurations 4-91014
- <sup>28</sup>Si(<sup>7</sup>Li,<sup>1</sup>Li), angular dist., DWBA calcs. 4-102291
- <sup>4</sup>Sm(<sup>14</sup>N, xn $\gamma$ ), A=152-154, <sup>162-164</sup>Tm yrast band studies 4-82987
- <sup>144</sup>Sm(<sup>12</sup>C,7n), <sup>147</sup>Er beta delayed proton activity, half-life 4-106594
- <sup>144</sup>Sm(<sup>144</sup>Sm,X), deep inelastic collisions, shell struct. influence, N=82 neutron shell 4-64158
- <sup>144</sup>Sm(<sup>144</sup>Sm,X), deep inelastic collisions, shell struct. influence, N=82 neutron shell 4-64158
- <sup>144</sup>Sm(<sup>15</sup>S,X), 214 MeV, ang. momentum alignment 4-73938
- <sup>118</sup>Sn(<sup>12</sup>C,p,X), collisions with various target nuclei at 3.6 GeV/nucleon, moving source formation 4-102297
- <sup>118</sup>Sn(<sup>16</sup>O,3n), <sup>129</sup>Ce band crossing and triaxiality,  $\gamma$ -decay study 4-78583
- <sup>118</sup>Sn(<sup>16</sup>O,4n), <sup>129</sup>Ce band crossing and triaxiality,  $\gamma$ -decay study 4-78583
- <sup>118</sup>Sn(<sup>40</sup>Ar, Xn), fusion process, impact parameter influence 4-111561
- <sup>128</sup>Sn(<sup>28</sup>Si,xn), fusion evaporation reaction,  $\gamma$ -ray emission, high ang. momentum behaviour 4-86793
- <sup>128</sup>Sn(<sup>40</sup>Ar,X), distrib. of ang. momentum adsorbed by compound nuclei 4-59266
- (Sr, X), on A~180 targets, prospects of superheavy element prod. 4-86870
- <sup>139</sup>Ba(<sup>16</sup>N, X), sequential decay probabilities of projectile-like fragments, X-ray coincidence meas. 4-102302
- <sup>139</sup>Ba(<sup>16</sup>O,f), 31 MeV/u, fission fragments in coincidence with quasi-projectile, linear momentum transfer 4-59267
- <sup>232</sup>Th(<sup>40</sup>Ar,X), quasi-elastic multiplet heavy ion processes, random matrix model 4-91013
- <sup>41</sup>Ti(<sup>27</sup>Al,X), 3.5 MeV/N, A=46, 48, fusion evaporation residues, XTU Tandem results 4-86845
- <sup>41</sup>Ti(<sup>16</sup>O,X), 100-200 MeV, cross sections, spectra and ang. distrib., composite system scission 4-86848
- <sup>41</sup>Ti(<sup>16</sup>O,X), 101 MeV, peripheral collisions, light particle-reaction fragment ang. correls. 4-96061
- <sup>50</sup>Ti(<sup>238</sup>U,X), dynamics, mass drift of reaction products 4-96085
- <sup>160</sup>Tm(<sup>35</sup>Cl,X), evaporation decay and gamma multiplicity for <sup>204</sup>Rn via fusion channel 4-64170
- U(<sup>238</sup>U,f), 16.7 MeV/N, five-pronged fission events obs. using mica SSNTD 4-96082
- U(<sup>238</sup>U,f), 9.03 MeV/u, heavy fragment correlations, sequential fission, cross sections 4-64186
- <sup>238</sup>U(<sup>238</sup>U,X), 2.38, 3.97 GeV, ang. distrib. and branching ratios using SSNTD 4-96047
- <sup>238</sup>U(<sup>16</sup>O,X), compound nucleus fission 4-102299
- <sup>238</sup>U(<sup>238</sup>U,X), classical treatment including deformation degrees of freedom 4-96059
- <sup>238</sup>U(<sup>238</sup>U,X), ultra-relativistic collisions, possible vacuum catastrophic phase transition 4-68714
- <sup>238</sup>U(<sup>238</sup>U,f), ternary fission dynamics in three centre model 4-64181
- <sup>238</sup>U(<sup>238</sup>U,f), ternary fission dynamics liquid drop model 4-64182
- <sup>238</sup>U(<sup>27</sup>O,X), compound nucleus fission 4-102299
- <sup>238</sup>U(<sup>35</sup>Cl,X), 240-350 MeV, fast fission 4-91028
- <sup>238</sup>U(<sup>40</sup>Ar,X), 8.5 MeV/u,  $\alpha$  evap., multiplicities, composite nucleus spin and lifetime expectancy 4-64172
- <sup>238</sup>U(<sup>40</sup>Ar,X) <sup>4</sup>He emission for fusion-fission and sequential fission identification 4-83108
- <sup>238</sup>U(<sup>40</sup>Ar,f), E=44 MeV/u, linear momentum transfer to fissioning nucleus 4-102328
- <sup>238</sup>U(<sup>56</sup>Fe,X), 8.5 MeV/u,  $\alpha$  evap., multiplicities, composite nucleus spin and lifetime expectancy 4-64172

## heavy ion-nucleus reactions continued

- <sup>238</sup>U(<sup>56</sup>Fe,X), nonequilibrium excitation energy division 4-73924
- <sup>238</sup>U(<sup>56</sup>Fe,f),  $\alpha$  and p emission from pre- and post-fission sources 4-102304
- <sup>238</sup>U(X, fission) cross-section meas., charge-mass-energy spectra 4-68724
- <sup>51</sup>V(<sup>12</sup>C,X) 36-100 MeV, complete and incomplete fusion 4-96073
- <sup>184</sup>W(<sup>16</sup>O,X), 86 MeV/N, multifragment emission, fission and total cross sections using SSNTD 4-96050
- <sup>70</sup>Zn(<sup>14</sup>C, <sup>16</sup>O) <sup>86</sup>Ni\*, half-life of <sup>88</sup>Ni first excited state 4-106573
- (Zr,X), on A~180 targets, prospects of superheavy element prod. 4-86870
- <sup>4</sup>Zr(<sup>81</sup>Br,X) A=90.94 evaporation residue cross-sections for complete fusion 4-73933
- <sup>4</sup>Zr(<sup>20</sup>Zr,X) A=90.94 evaporation residue cross-sections for complete fusion 4-73933
- <sup>90</sup>Zr(<sup>20</sup>Zr,X), cross sections for compound residues 4-68743

## heavy ion-nucleus scattering

- Coulomb excitation, first-order relativistic corrections, nuclear electromagnetic props. 4-102293
- elastic scatt., absorption and refraction using WKB method 4-86842
- elastic scatt. and fusion cross-sections 4-86844
- elastic scattering, energy storing in compressed nuclear matter 4-102287
- elastic scattering, modified Newton method for inverse scatt. problem 4-83096
- energy dissipation, time-dependent formalism, coupled oscillator model 4-95975
- nuclear rainbows and heavy-ion scattering 4-59259
- quasi-elastic scatt. mass and charge transport coeffs. 4-96055
- resonances and surface waves in complex ang. momentum plane 4-78648
- resonant heavy-ion collisions, nucl. time delay 4-73940
- S-matrix in terms of nucl. matter distrib. and nucleon-nucleon interaction 4-59275
- semiclassical concept application, optical pots. 4-102286
- sub-barrier heavy ion elastic scatt., giant multipole resonance excitation effects 4-96075
- wave packet scatt. model with quantum friction 4-59260
- Al(Ne,Ne), cross section as function of mass number 4-78652
- <sup>197</sup>Au(<sup>238</sup>U,<sup>238</sup>U), 10 MeV/N, elastic scatt., total cross-section, mica SSNTD appl. 4-96049
- <sup>136</sup>Ba(<sup>16</sup>O, <sup>16</sup>O $\gamma$ ) <sup>136</sup>Ba, A=135,137, E=35-45 MeV, study of low-lying states 4-95904
- <sup>136</sup>Ba(<sup>14</sup>N, <sup>14</sup>N $\gamma$ ) <sup>136</sup>Ba, E=40 MeV, study of low-lying states 4-95904
- <sup>136</sup>Ba(<sup>16</sup>O,<sup>16</sup>O), first 2<sup>+</sup> state, quadrupole moment and Coulomb excitation probability, reorientation effect 4-73825
- <sup>99</sup>Bi(<sup>236</sup>Xe, <sup>136</sup>Xe), TDHF collisions, bombarding energy depend. 4-64168
- C(Ne,Ne), cross section as function of mass number 4-78652
- <sup>12</sup>C+<sup>12</sup>C mol. states, intraband  $\gamma$  transitions 4-64169
- <sup>12</sup>C(<sup>12</sup>C, <sup>12</sup>C), E=360 and 1016 MeV, optical model and DWBA analysis 4-96064
- <sup>12</sup>C(<sup>12</sup>C, <sup>12</sup>C)<sup>12</sup>C, second order-processes, form factors 4-59271
- <sup>12</sup>C(<sup>12</sup>C, <sup>12</sup>C)<sup>12</sup>C, nuclear refractive effects at intermediate energies 4-96054
- <sup>12</sup>C(<sup>13</sup>C, <sup>13</sup>C), covalent nuclear molecule formation 4-83092
- <sup>12</sup>C(<sup>16</sup>O, <sup>16</sup>O)<sup>12</sup>C, classical trajectory concepts 4-86156
- <sup>12</sup>C(<sup>24</sup>Mg, <sup>24</sup>Mg)<sup>12</sup>C, coherent component of elastic scatt. cross section 4-59269
- <sup>12</sup>C(<sup>6</sup>Li, <sup>6</sup>Li), 5.8-90 MeV, Regge formalism anal. 4-73936
- <sup>12</sup>C(<sup>6</sup>Li, <sup>6</sup>Li)<sup>12</sup>C, semiclassical and quantum mechanical treatments 4-96057
- <sup>12</sup>C(<sup>6</sup>Li, <sup>6</sup>Li)<sup>12</sup>C ang. dist. and vector analysing power 4-64162
- <sup>12</sup>C(<sup>12</sup>C, <sup>12</sup>C), coupled-reaction-channel approach, molecular orbital phenomena of valence nucleons 4-96063
- <sup>12</sup>C(<sup>12</sup>C, <sup>12</sup>C), molecular core-particle coupling model failure 4-86809
- <sup>40</sup>Ca(<sup>32</sup>S, <sup>32</sup>S), 100-151.5 MeV, ang. distrib., folding model energy depend. reorg. coeffs. 4-73921
- <sup>40</sup>Ca(<sup>40</sup>Ca, <sup>40</sup>Ca), elastic and inelastic, relative motion effect, microscopic potentials anal. 4-59280
- Cu(Ne,Ne), cross section as function of mass number 4-78652
- <sup>19</sup>F(<sup>12</sup>C, <sup>12</sup>C), phase anomaly, ang. distrib. 4-68728
- <sup>54</sup>Fe(<sup>6</sup>Li, <sup>6</sup>Li)<sup>54</sup>Fe, diff. cross-sections for elastic and inelastic scatt. 4-106625
- <sup>160</sup>Ho(<sup>238</sup>U, <sup>238</sup>U), 10 MeV/N, elastic scatt., total cross-section, mica SSNTD appl. 4-96049
- <sup>6</sup>Li(<sup>16</sup>O,<sup>16</sup>O), 18.7 MeV, 3<sup>+</sup>(2.18) MeV state excitation 4-102298
- <sup>24</sup>Mg(<sup>16</sup>O,<sup>16</sup>O)<sup>24</sup>Mg, semiclassical diffraction model 4-96058
- <sup>24</sup>Mg(<sup>13</sup>C,<sup>13</sup>C)<sup>24</sup>Mg\* (2<sup>+</sup>, 1.37 MeV) population probability, spin-independent potentials 4-102301
- <sup>140</sup>Nd(<sup>16</sup>O,<sup>16</sup>O), A=143, 145, Coulomb excitation of levels 4-68646
- <sup>20</sup>Ne(<sup>16</sup>O,<sup>16</sup>O), ang. distrib., elastic  $\alpha$ -transfer, LCNO and DWBA comparison (Chinese) 4-83090
- <sup>58</sup>Ni(<sup>7</sup>Li, <sup>7</sup>Li), 20.3 MeV, optical pot. spin depend., cross section, anal. powers 4-111530
- <sup>16</sup>O(<sup>16</sup>O,X) fusion and elastic scatt. cross sections, near Coulomb barrier 4-86873
- <sup>16</sup>O(<sup>28</sup>Si, <sup>28</sup>Si)<sup>16</sup>O, coherent component of elastic scatt. cross section 4-59269
- <sup>16</sup>O(<sup>6</sup>Li, <sup>6</sup>Li)<sup>16</sup>O, projectile excitation effects in single folding model 4-59270
- Pb(Ne,Ne), cross section as function of mass number 4-78652
- <sup>208</sup>Pb(<sup>104</sup>Ru, <sup>104</sup>Ru), collective and single particle degrees of freedom 4-73923
- <sup>208</sup>Pb(<sup>12</sup>C, <sup>12</sup>C) Coulomb excitation of 3<sup>+</sup> and 2<sup>+</sup> states, branching ratios of E3 and E2 4-59192
- <sup>208</sup>Pb(<sup>13</sup>C, <sup>13</sup>C), E=390 MeV, optical model analysis, nucl. surface transparency 4-96064
- <sup>208</sup>Pb(<sup>16</sup>O, <sup>16</sup>O) Coulomb excitation of 3<sup>+</sup> and 2<sup>+</sup> states, branching ratios of E3 and E2 4-59192
- <sup>208</sup>Pb(<sup>16</sup>O,<sup>16</sup>O), 350, 400 MeV, giant multipole resonance excitation, cross sections 4-73866
- <sup>208</sup>Pb(<sup>16</sup>O,<sup>16</sup>O), 350, 400 MeV, inelastic excitation of giant reson. 4-64171
- <sup>208</sup>Pb(<sup>17</sup>O,<sup>17</sup>O), 380 MeV, giant quadrupole resonance gamma decay 4-73866
- <sup>208</sup>Pb(<sup>20</sup>Ne, <sup>20</sup>Ne), 30 MeV/n, high excitation energy structs., direct excitation process 4-102239
- <sup>208</sup>Pb(<sup>20</sup>Ne, <sup>20</sup>Ne), elastic scatt., radius anomaly in diff. model 4-68731
- <sup>208</sup>Pb(<sup>36</sup>Ar, <sup>36</sup>Ar), 11 MeV/n, high excitation energy structs., direct excitation process 4-102239

**heavy ion-nucleus scattering continued**

- <sup>208</sup>Pb(<sup>7</sup>Li, <sup>7</sup>Li), (<sup>7</sup>Li, <sup>7</sup>Li), 68 MeV, <sup>7</sup>Li excitation, Coulomb and nucl. contrib. 4-68725
- <sup>208</sup>Pb(<sup>84</sup>Kr, <sup>84</sup>Kr), elastic scatt., radius anomaly in diff. model 4-68731
- <sup>28</sup>Si(<sup>16</sup>O, <sup>16</sup>O), 21.1, 22.7 MeV, elastic ang. distrib. backward rise, microscopic descript. 4-68850
- <sup>28</sup>Si(<sup>16</sup>O, <sup>16</sup>O), potential models and resonances 4-96076
- <sup>28</sup>Si(<sup>16</sup>O, <sup>16</sup>O) elastic scatt. excitation functions 4-83103
- <sup>28</sup>Si(<sup>28</sup>Si, <sup>28</sup>Si), excitation functions, statistical anal. 4-73887
- <sup>28</sup>Si(<sup>6</sup>Li, <sup>6</sup>Li)<sup>28</sup>Si, projectile excitation effects in single folding model 4-59270
- <sup>230</sup>Th(<sup>142</sup>Nd, <sup>142</sup>Nd), 447 MeV, level-scheme, ground and octupole bands, transitions 4-86757
- <sup>230</sup>Th(<sup>32</sup>S, <sup>32</sup>S), 135 MeV, rot. and vibr. band excitation,  $\gamma$ -transitions, branching ratio 4-73807
- <sup>230</sup>Th(<sup>32</sup>S, <sup>32</sup>S), 135 MeV, level scheme, ground and octupole bands, transitions 4-86757
- <sup>230</sup>Th(<sup>84</sup>Kr, <sup>84</sup>Kr), 440 MeV, level scheme, ground and octupole bands, transitions 4-86757
- <sup>232</sup>Th(<sup>84</sup>Kr, <sup>84</sup>Kr), elastic scatt., radius anomaly in diff. model 4-68731
- <sup>235</sup>U(<sup>20</sup>Ne, <sup>20</sup>Ne), elastic scatt., radius anomaly in diff. model 4-68731
- <sup>238</sup>U, ion track registration characteristics, in polycarbonate ChaoYang No.1 (Chinese) 4-102536
- <sup>90</sup>Zr(<sup>16</sup>O, <sup>16</sup>O), 350, 400 MeV, inelastic excitation of giant reson. 4-64171
- <sup>90</sup>Zr(<sup>16</sup>O, <sup>16</sup>O), 350, 400 MeV, giant multipole resonance excitation, cross sections 4-73866

**heavy leptons**

- dileptonic system, mass bounds from cosmology, cosmic mass density 4-67625
- neutral heavy leptons, mass and mixing limit extensions 4-86626
- neutrinos, massive, cosmological bounds 4-95008
- tau lepton, lifetimes, review 4-73751
- $\tau \rightarrow 3\pi^0 \pi^+ \nu_\tau$ ,  $\nu_\tau$  mass upper limit determ. 4-73754
- $\tau$  anomalous magnetic moment limits in composite model 4-68548
- $\tau \rightarrow e \nu \gamma$  ( $\mu \nu \gamma$ ), g-value test, radiation zeros 4-86707
- $\tau \rightarrow K_S^0 (K_S^0 \pi^0)$ , Cabibbo suppressed decay, branching fractions 4-73755
- $\tau$  lifetime determ. from  $e^+e^- \rightarrow \tau^+\tau^- X$  4-86696
- $\tau \rightarrow \nu + X$  pions, branching ratios for  $X \geq 2$  4-73756
- $\tau^-$  lepton, leptonic decays, finite  $\nu_\tau$  mass and effects of mass mixing 4-59078
- W-L  $\nu_\tau$ , heavy lepton detection in pp collider 4-68604
- $Z^0 \rightarrow \tau^+\tau^-$  limits on composite structure, CP violation 4-90937
- $\tau^- \rightarrow h \nu_\tau$ , hadronic decays in virtuo-quark model 4-111450

**heavy water**

- Brillouin scattering at press. up to 34 GPa 4-80958
- chemisorbed on Si (100)(2 $\times$ 1), multiple vibr. excitations, high resolution EELS study 4-102929
- distillation columns, computer aided simulation 4-96134
- electron impact disoc., D\* emission cross section 4-107462
- ice, vap. press. below 273K 4-113595
- molecule, local mode pot. function 4-74223
- molecule, OD group vibr. freqs., intermol. interactions and matrix effects 4-102665
- solid films, photon-stimulated ion desorption 4-61239
- US velocity, anomalous temp. dependence 4-103882
- D mass spectroscopic determ. 4-109706
- (D<sub>2</sub>O)<sub>n</sub> clusters, mass spectra 4-74382

**HEED** see high energy electron diffraction**height measurement**

- digital differential depth meter 4-72724
- satellite altimetry, accuracy of altimetric surfaces 4-110022
- sea height variability, expendable bathythermograph and satellite altimeter meas. 4-105582

**Heisenberg model**

- alkali metals, lattice props., Heisenberg Hamiltonian studies 4-108501
- anisotropic, low-temp. behaviour, symm. props. 4-61503
- anisotropic, S=1/2 chain, transfer matrix in plane-rotator model 4-114084
- anisotropic spin 1/2 model, thermodynamic props. in transverse field 4-98913
- antiferromagnet, percolating, spin excitation waves, effective medium approx. anal. 4-114131
- antiferromagnet, two-dimensional classical isotropic model, phase diagram in mag. field 4-109031
- antiferromagnet susceptibility, spin-wave Hamiltonian 4-104393
- antiferromagnetic and ferromagnetic, correlation theory, dimension, field and temp. depend. 4-114086
- antiferromagnetic chain, anisotropic, degenerate ground states and excited states 4-61506
- antiferromagnetic Heisenberg linear chain in mag. field, Green's function approach 4-114129
- antiferromagnetic Heisenberg model, 1-D isotropic, ground state props. 4-98851
- antiferromagnetic linear chain, spin-Peierls instabilities, antiferromag. transitions and phonon dynamics 4-65824
- antiferromagnetic quantum Heisenberg spin systems, Monte Carlo soln. 4-104453
- chain, solitary solns. 4-95342
- classical chain, one-dimensional anisotropic, excitations 4-80735
- classical chain with two anisotropies, low temp. thermodynamics and correlation functions 4-92929
- current algebra, Lie algebra over physical space 4-58990
- dilute antiferromag. chain, critical dynamic response 4-71119
- dilute magnets, phase transitions, critical behaviour, percolation, random fields 4-88690
- dynamics of the Heisenberg-Mattis model with an external magnetic field 4-84763
- ferromagnet, amorphous, short-range order and mag. props. 4-76157
- ferromagnet, gauge formulation of generating operator, Zakharov-Shabat system 4-90419
- ferromagnet, kinematical interactions and magnon excitation spectrum 4-114130
- ferromagnet, one-dimensional anisotropic classical, with in-plane field, sp. ht. 4-104452
- ferromagnet, semi-infinite, quasilocalised surface excitations under action of random surface pot. 4-80756
- ferromagnet, spectral density method anal. 4-114087
- ferromagnet, spin wave damping theory 4-80754

**Heisenberg model continued**

- ferromagnet, surface spin wave freqs., temp. variation in exchange-dominated regime 4-80755
- ferromagnet interface, magnetisation and excitation spectrum 4-80788
- ferromagnetic chain, anharmonic solitary clusters of spin deviations and lattice deform. 4-92930
- ferromagnetic chain, classical model, magnetisation, sp. ht., crossover between two regimes 4-104441
- ferromagnetic Heisenberg Hamiltonian in spin wave theory, dynamical interactions 4-98874
- ferromagnetic spin waves, low energy excitation spectrum on percolating network, effective medium approx. 4-71044
- graphite-FeCl<sub>3</sub> and CoCl<sub>3</sub> intercalation cpd., mag. order, neutron diff. studies 4-61511
- Heisenberg ferromagnet, spin Green's functions 4-104394
- Heisenberg-Ising spin 1/2 chain, quantum domain walls 4-104442
- incommensurate magnetic structures formation, exchange integrals 4-114088
- isotropic spin chain, linearizing integral transform 4-90387
- magnetic materials, intermediate ordered phases, calcs. 4-114132
- massive Thirring model, continuum limit of Heisenberg model 4-73336
- mean field renormalisation, critical temp. 4-98850
- microcanonical renormalisation group, Monte Carlo techniques, O(3) 4-114088
- Heisenberg model 4-111282
- narrow-band mag. semicond., at operator representation 4-75961
- noble metals, lattice props., Heisenberg Hamiltonian studies 4-108501
- one-dimensional classical antiferromagnetic, equivalence at low temp. between mag. field and anisotropy 4-98912
- one-dimensional Heisenberg systems with random anisotropies, low-temp. props. 4-76100
- perturbation expansions and series acceleration procedures 4-71011
- planar anisotropy, ferromag. and antiferromag., ground state magnetisation transitions 4-71120
- planar ferromag., biquadratic interactions 4-88641
- polynes, even and odd, molecular PPP correlations, optical excitations 4-114088
- Heisenberg antiferromagnet 4-74362
- quantum chains, axially anisotropic, ground state props. 4-61505
- quantum spin glass behaviour within Heisenberg model, RPA theory (German) 4-92932
- quasi-one dimensional condensed matter models, nonlinear effects, review 4-65668
- quasione-dimensional ferromagnet, soliton dynamics (Russian) 4-65823
- random ferromagnet-spin glass transitions, Heisenberg model 4-84787
- spin 1/2 anisotropic Heisenberg model in infinite lattice dims., time depend. behaviour 4-68172
- spin exchange model, CIDEF and relax. 4-88722
- spin glasses, irreversible and reversible behaviour, broken ergodicity 4-114125
- spin systems with random fields, crit. dynamics 4-98893
- spin-1 antiferromagnetic chain, ground-state props. calcs. 4-71102
- spin-1 antiferromagnetic Heisenberg-Ising chain 4-71101
- spin-1 chain, critical props., finite-size scaling studies 4-98914
- spin-1/2 chain with Ising/Heisenberg/XY exchange, multiple bound states 4-88689
- spin-Peierls ground state energy, logarithmic corrections 4-104392
- SU(N) Heisenberg model, higher dimensional representations 4-111066
- surfaces, roughening transition 4-113569
- susceptibility using exponents far from T<sub>c</sub> 4-88635
- TCNQ salt with quinolinium, mag. props. and electron-nuclear interaction 4-76126
- three-dimensional Heisenberg ferromagnet, instantons 4-92885
- uniform magnetic chain with second-neighbour interactions at finite temperatures 4-61504
- waves values, weak convergence 4-58683
- XXZ chain of arbitrary spin, ground state and spin waves 4-104451
- Cd<sub>2</sub>MnO<sub>3</sub>Te spin glass, magnon contrib. to mag. sp. ht. 4-98906
- CsNiF<sub>3</sub>, failure of classical approx. for magnetisation calcs. 4-71126
- Cu complex, 2DMSCuCl<sub>2</sub>, 1D Heisenberg antiferromag., mag. susceptibility 4-61516
- Cu tetraclusters, adiabatic pot., mag. props., Jahn-Teller effect 4-108823
- EuO, Heisenberg ferromag., longitudinal spin wave pumping 4-88661
- VBr<sub>2</sub>, 2-D triangular Heisenberg antiferromag., heat capacities 4-76156
- VCl<sub>2</sub>, 2-D triangular Heisenberg antiferromag., heat capacities 4-76156
- Vl<sub>2</sub>, 2-D triangular Heisenberg antiferromag., heat capacities 4-76156

**Heising modulation** see amplitude modulation**helical dislocations** see screw dislocations**helicity (elementary particles)**

- neutrinos, massless, spin 3/2, with nonmaximal helicity states and leptonic decays 4-95794
- nucleon-nucleon scattering, total cross sections, spin effects, superhigh energies, quasipotential approach 4-95816
- Poincare group, helicity representations, sharp momentum states, differentiable vectors 4-102053
- spin-1 fields, Lorentz invariance, helicity and gauge transformation 4-58939
- $e^+e^- \rightarrow e^+e^-e^+e^-$ , cross section calc. using Feynman diagrams, helicity amps. 4-86693
- $e^+e^- \rightarrow \gamma\gamma\gamma\gamma$ , cross section, helicity amplitudes in high energy limit 4-90848
- hp-de  $e^+e^-$ , neutral current effects on asymm. param. and lepton helicity 4-59102
- $\pi^+ \rightarrow \mu^+ \nu_\mu$  helicity, P<sub>ES</sub>/p meas. in muon decay 4-73746
- $\mu$  muoproduction, spin-spin asymmetries, gluon helicity distribution function 4-95803

**helicons****see also solid-state plasma**

- modulation instability of helicons in conductors (Russian) 4-92760
- multivalley conductors, helicon instability and drift EM waves (Russian) 4-84642
- piezoelectric semicond. magnetised plasma; high-power helicon wave parametric decay 4-98657
- semiconductor-ferri-ferite interface, oblique magnetostatic surface wave 4-80752
- semiconductor-vacuum-ferri-ferite struct., sound interaction with surface helicon oscills. (Russian) 4-88713
- semiconductors, nonlinear generation of sum and difference waves by helicon waves 4-80618
- solid state magnetised plasma, Gaussian helicon beam self-focusing 4-113984

## ions continued

- Ag, doppleron oscills., carrier reflection influences 4-80481  
 n-InSb, magnetoactive piezoelec. semiconductor, helicon waves, modulational instability 4-61407

## scopeters

- military, disorientation in flight, psychology of visual perception 4-85528  
 military flight associated hearing loss, comparative tests on pilots 4-85529  
 military operations, aeromedical support, conf., Soesterberg, Netherlands (June 1984) 4-82597  
 military operations, visual problems 4-85527

## lutron see plasma devices

## liports see airports

## lium

- see also nuclei with .....  
 see also helium atoms; helium films; liquid helium; solid helium  
 acoustic anal. of forment bandwidths and frequencies 4-103145  
 airglow, 1083 nm emission at midlatitude 4-105786  
 Bianchi type V cosmological model with tilt, He form., D abundances 4-90265  
 binding limit in Hartree approx 4-102569  
 bubble, dislocation loop punching in metals 4-103748  
 bubble form. in 600 MeV proton irradi., Al 4-108479  
 bubble form. in 600 MeV proton irradi. of pure Al foils 4-108482  
 bubble form. in dual beam irradi. Fe-Cr-Ni alloy 4-75562  
 bubble formation in T charged V, obs. of cylindrical cavities at dislocations 4-60913  
 bubbles, equation of state for small cavities 4-103824  
 bubbles at grain boundaries in austenitic alloys 4-108471  
 bubbles generated during irradiation, growth by coalescence, effect of immobilisation 4-108414  
 bubbles in Al, nucleation on dislocations during 600 MeV proton irradi. 4-113504  
 bubbles in austenitic alloy, void swelling, effect of pulsed irradi. 4-108474  
 bubbles in austenitic stainless steel, in-reactor stress rupture model 4-104854  
 bubbles in austenitic stainless steel, swelling resistance in fusion reactors 4-107012  
 bubbles in Fe-Cr-Ni alloy, weak beam imaging 4-103618  
 bubbles in HFIR irradiated precipitation strengthened Ni-base alloys 4-108457  
 bubbles in irradi. austenitic stainless steel, void swelling 4-103792  
 bubbles in Zr tritides, TEM study of ageing 4-75503  
 buffer gas, interdependence of buffer gas pressure and optimum interpulse delay in a burst-mode copper halide laser 4-112396  
 capillary glow discharge, collisional radiative model with atomic collisions 4-60773  
 cavities containing Van der Waals gas, crit. radius and crit. no. of gas atoms 4-108347  
 cavity growth and nucleation in Mo at 300K, expt. HDS and TEM studies 4-108348  
 cavity growth mechanisms, thermal and athermal processes 4-108349  
 charged particle radiolysis of He-buffered CO<sub>2</sub> to produce CO 4-62216  
 cryogenic liquids flowing in tubes, heat transfer during boiling 4-69749  
 cryopumping in fusion power systems, charcoal sorbents development 4-111861  
 DC discharge anode plasma, propag. phenomena 4-92020  
 dense gas, electron delocalisation by external elec. field 4-75119  
 diffraction from metal surfaces 4-104709  
 diffusion and solubility in SrF<sub>2</sub>, trivalent impurity effect 4-108663  
 diffusion in Au 4-65488  
 electron collision frequency, resonant determ. method 4-69223  
 fusion materials testing, He prod. calcs. and meas. comparison using neutron cross sections for <sup>58</sup>Ni 4-107042  
 fusion reactor breeder materials, Li<sub>2</sub>O, neutron irradi., T and He retention 4-107031  
 fusion reactor cooling He-Li test loop for two-phase flow (Japanese) 4-91102  
 gas, 35 nm coherent radiation generation using KrF laser 4-107744  
 gas, mag. birefr. meas. 4-103465  
 gas breakdown threshold near metal target by laser heating 4-69933  
 gas flow-type cryostat, adsorbed layers of gases obs., under ultrahigh vacuum 4-68224  
 glow discharge, atm. press., positive column contraction mechanism 4-87996  
 glow discharge plasma, ArH<sup>+</sup> Doppler shift ion mobility meas. using diode laser spectroscopy 4-113217  
 He-Cd laser with lateral HF discharge, different design comparative characts. (Russian) 4-69372  
 He-Ne-methane bichromatic Zeeman laser with nonlinear absorption (Russian) 4-69433  
 He/H<sub>2</sub> ratios in Jupiter and Saturn atm., implications for solar nebula 4-77757  
 HF discharge, anomalous plasma resistance in transverse mag. field 4-92023  
 HF discharge conductivity in low hybrid resonance range (Russian) 4-92009  
 high-voltage discharge in hollow cathode 4-103591  
 HTGR components, He atmosphere effects 4-106838  
 implantation in (Fe<sub>40</sub>Ni<sub>60</sub>)V ordered alloy, microstruct. and creep 4-108399  
 impurities in metals, theoretical studies 4-70706  
 Infrared Space Observatory dual liquid H<sub>2</sub>, superfluid He coding system thermal design 4-73441  
 injection in Ni foils, self-ion irradi., voids, TEM obs. 4-103827  
 intergalactic gas of rich galaxy clusters, He separation from D (Russian) 4-94971  
 interstellar He flow in Solar System, obs. at 58.4 nm (by Prognos 6) 4-77767  
 ion irradi. of pure Mo, vacancy loop form. 4-108480  
 ionosphere, equatorial region He<sup>+</sup> distrib. affected by neutral winds 4-82337  
 isoelectronic sequence, two-electron ions, QED, radiative corrections of order  $\alpha(\alpha Z)^3$  mc<sup>2</sup> 4-96466  
 kaersutite, from New Zealand and USA, inert gas, H<sub>2</sub>O and C isotope geochemistry 4-105477  
 leak detection using closed loop system 4-95449  
 light-induced detonation, thermodynamic props. 4-97796  
 low press. plasma, 4713 Å line, electron collisional broadening, CO<sub>2</sub> laser enhancement 4-97908

## helium continued

- low pressure breakdown, stepwise voltage drop 4-69976  
 magnetic monopoles, energy loss from elastic collision with H, He atoms 4-68464  
 Mount Ontake volcano, Japan, <sup>3</sup>He emissions rel. to volcanic activity 4-89902  
 multisphere neutron spectrometer using a central <sup>3</sup>He detector 4-102457  
 plasma, discharge column, low-press., nonlinear behaviour, density changes 4-60771  
 plasma, lines at low electron densities by variation of perturber mass, ion dynamic effects 4-97907  
 plasmasphere of Earth, He<sup>+</sup> diffusive equilibrium distrib. 4-82340  
 radioactive waste transport packages, leakage expts. 4-106740  
 removal by metal deposition in plasma limiter 4-97887  
 spark discharge formation time, discharge gap ionisation depend. 4-69974  
 speech unscrambling, frequency-domain algorithm 4-107960  
 superfluid He dewar use in Infrared Astronomical Satellite cryogenic system 4-77718  
 swelling incubation in austenitic stainless steels, microchem., microstruct. and environmental effects 4-108413  
 weakly ionised plasma, EM shock breakdown wave struct. 4-91932  
 working fluid for closed-cycle diesel engines, effects on performance 4-66743  
 working fluid for Zimmerman-Stirling cryogenic cooler 4-72146  
 Al-In, dil., He localised diffusion around In impurities, PAC obs. 4-65470  
 Ar-He mixtures in microwave capillary discharges 4-87999  
 BaF:He, interstitial diffusion, solubility of He, dissolution energy 4-113727  
 CO-He gas mixtures, thermal conductivity meas. 4-113102  
 CaF:He, interstitial diffusion, solubility of He, dissolution energy 4-113727  
 D-<sup>3</sup>He fusion plasmas, nuclear elastic scatt. effects 4-103543  
 Fe<sub>40</sub>Ni<sub>60</sub>Mo<sub>4</sub>, Metglas 2826 MB 5 keV He implantation, bubble growth, free vol. relax. model 4-103822  
 Ge:He, ion irradi., structural defect study 4-88164  
 H-Ne 633 nm laser, I<sub>2</sub> stabilised, freq. stability and reproducibility 4-91436  
 He flow in horizontal channel, two-phase, hydraulic resistance calc. and obs. 4-108107  
 He I, broadening parameters of  $\lambda=447.15$  nm line in laser prod. plasma 4-78803  
 He I and He II in solar chromosphere active regions, line widths 4-77799  
 He I in solar flares, plasma characts. determ. 4-77798  
 He<sup>+</sup> direct production from He(2S<sub>1/2</sub>) metastable state 4-96316  
 He<sup>+</sup> ions backscattering from Au(Tl)(Pb) targets, excitations, optical spectrometry study 4-78944  
 He-Ar, binary gas mixture, nonisothermal motion through plane channel, kinetic phenomena 4-103368  
 He-buffered CO<sub>2</sub> system, radiolytic dynamics 4-62217  
 He-CO<sub>2</sub>-N<sub>2</sub>, electron-ion recombination 4-102794  
 He-Cd discharge, current disturbances, Cd<sup>+</sup> inversion density, dynamic response 4-108237  
 He-Cd long lifetime laser using continuously tunable He replenisher (Chinese) 4-60089  
 He-Cd-Hg system three-colour hollow cathode laser (Russian) 4-69371  
 He-Cd<sup>+</sup> hollow cathode laser, population inversion mechanism 4-83570  
 He-Cd<sup>+</sup>(Zn<sup>+</sup>)(Ne) lasers, excitation mechanisms anal. (Japanese) 4-79116  
 He-ethene, H<sup>+</sup> spin lattice relax. 4-64504  
 He-F<sub>2</sub>-Kr atmospheric discharge, electron density, streak interferometric method 4-84092  
 He-F<sub>2</sub>(SF<sub>6</sub>) mixtures, elec. breakdown 4-79720  
 He-H Penning ionisation formula 4-91338  
 He-H plasma, ion Bernstein wave heating expt. on JIPPT-II-U device 4-60662  
 He-H<sub>2</sub>O mixtures, gas discharges, metastable He atom density 4-97922  
 He-Hg high press. discharge, electron loss rate meas. 4-65143  
 He-Kr<sup>+</sup> hollow cathode discharge laser, electron energy distrib. function 4-84117  
 He-Ne, binary gas mixture, nonisothermal motion through plane channel, kinetic phenomena 4-103368  
 He-Ne and Ar<sup>+</sup> laser low-freq. beat noise (Chinese) 4-91511  
 He-Ne gas discharge cell, He-Ne probe laser intensity perturbation transverse distribution investigation 4-79207  
 He-Ne highly stable laser at 1.15  $\mu$ m (Chinese) 4-112469  
 He-Ne intracavity laser, magnetic field induced beat noise (Chinese) 4-60017  
 He-Ne intracavity laser, polarisation behaviour at 632.8 nm (Chinese) 4-107597  
 He-Ne laser, 0.63  $\mu$ m, effect of an external modulation signal 4-79108  
 He-Ne laser, freq. stabilisation with modular electronic system 4-112476  
 He-Ne laser, high power (Rumanian) 4-96953  
 He-Ne laser, internal mirror, output- and frequency-stabilisation by discharge current control 4-79105  
 He-Ne laser, mode struct. optical spectrum analyser study, undergraduate expt. 4-106152  
 He-Ne laser, stabilisation on absorpt. saturation in <sup>127</sup>I 4-79106  
 He-Ne laser emission power stabilisation, using gas-discharge lens 4-102938  
 He-Ne laser excitation using lateral discharge VHF pumping resonators (Russian) 4-69431  
 He-Ne laser locked to methane E-line, accurate freq. meas. 4-96868  
 He-Ne lasers, active element striation freq. shifts 4-107598  
 He-Ne lasers, design (German) 4-107674  
 He-Ne lasers, small, striation-onset condition investigation 4-64694  
 He-Ne low breakdown voltage lasers, capillary gas breakdown modelling (Chinese) 4-112380  
 He-Ne mixture purifying system, for 8 m streamer chamber 4-102524  
 He-Ne positive column, laser gain distrib. determ. 4-84111  
 He-Ne ring laser with gain greatly exceeding losses, counterpropag. circularly polarised wave interaction 4-74557  
 He-Ne ring laser with selective losses, counter-propag. wave competition and emission spectrum produced by reson. phase-polarisation method 4-79107  
 He-Ne sensitive gas laser, line shapes 4-91435  
 He-Ne small bore discharge, radial optical gain distrib. 4-102921  
 He-Ne transverse Zeeman laser, theoretical anal., beat freq. tuning curve (Chinese) 4-91429

**helium continued**

- He-Nc/methane laser, freq.-modulated resonances (*Russian*) 4-102961  
 He-O<sub>2</sub> mixtures, breakdown characts. meas. using improved microwave cavity design 4-95465  
 He-Xe mixture, pulse discharge, nonequilib. plasma, electron energy distrib. 4-79874  
 He-Zn-Cd, hollow cathode laser, simultaneous laser oscillation by Cd II and Zn II lines (*French*) 4-112399  
 He<sub>2</sub>, critical binding, pots., quantum parameters 4-69169  
 He<sub>2</sub><sup>+</sup>, electronic struct. examined using CI wave functions, electron affinity 4-64396  
 He<sub>2</sub><sup>+</sup> afterglow, Rydberg dissociative recombination 4<sup>2</sup>-81421  
<sup>3</sup>He and <sup>4</sup>He, relative abundance in cosmic radiation 4-101072  
<sup>3</sup>He bubble formation in T charged V, TEM obs. 4-103825  
<sup>3</sup>He cooled bolometer system for 1 mm continuum obs., astron. appls. 4-105882  
<sup>3</sup>He gas, nuclear polarisation by optical pumping 4-108675  
<sup>3</sup>He-CO<sub>2</sub> mixture, <sup>3</sup>He numerical density on liquid-vapour boundary curve 4-70357  
<sup>3</sup>He-D fuel ignition in high-field OMITRON type Tokamaks 4-59405  
<sup>3</sup>He-fluoromethane filled counters, radiation stability 4-59554  
<sup>3</sup>He—, gaseous, spin rot. effects and spin waves 4-79734  
<sup>4</sup>He, chemical evolution of cosmic abundance rel. to Big Bang nucleosynthesis 4-67843  
<sup>4</sup>He retention in ambipolar reactor, effect on characteristics 4-102398  
 He\*(a), electron beam excited, transient absorpt. in UV and VUV 4-78796  
 InP:He, ion implanted, elec. cond. study 4-80586  
 Mo, proton irradi., He accumulation in 15-30 MeV region 4-80124  
 N<sub>2</sub>-He gas mixture, investigation of viscometric diffusion flux 4-112960  
 N<sub>2</sub>-He mixtures, viscous diffusion in mag. field 4-112959  
 Ni (100), He ion irradiation, He precipitate nucleation at point defects 4-103823  
 Ni:He, preimplanted, electron irradi., 1 MeV, He bubble growth 4-103803  
 O<sub>2</sub>-O<sub>2</sub>-He mixture photolysis by UV light, O<sub>2</sub> <sup>1</sup>Δ generation for I laser operation 4-112401  
 SiO<sub>2</sub>:He, vitreous, thermal props. meas. 4-88306  
 SiF<sub>4</sub>:He, interstitial diffusion, solubility of He, dissolution energy 4-113727

**helium, liquid** *see liquid helium***helium, solid** *see solid helium***helium-3 interactions** *see helium 3-nucleus reactions***helium 3-nucleus reactions**

- for inelastic helium 3-nucleus scattering, *see "helium 3-nucleus scattering"*  
 cold breakup of spectator residues in nucleus-nucleus collisions at high energy 4-95977  
<sup>4</sup>He(d), inner and outer subshell investigation 4-73883  
<sup>4</sup>He\*(He,n), A=107, 109, particle-hole coupling with proton pairing vibration 4-95886  
<sup>27</sup>Al(<sup>3</sup>He,α) excitation functions, differential cross-section, (2l+1) rule 4-68366  
<sup>9</sup>Be(<sup>3</sup>He,p), 3-6 MeV, ang. distrib., DWBA anal. 4-83081  
<sup>12</sup>C(<sup>3</sup>He,π<sup>+</sup>), 235 MeV, differential cross sections and reaction mech. 4-106623  
<sup>18</sup>Ca(<sup>3</sup>He,t)<sup>18</sup>Ca coupled reaction channel calcs. 4-78641  
<sup>110</sup>Cd(<sup>3</sup>He,3n)<sup>111</sup>Sn, excited states, in-beam spectroscopic methods, shell model predictions 4-102221  
<sup>63</sup>Cu(<sup>3</sup>He,t) reaction Q value meas., solar neutrino detector calibration 4-83088  
<sup>19</sup>F(<sup>3</sup>He,d), 15 MeV, <sup>20</sup>Ne 2<sup>+</sup> level, γ and highly retarded α-decay partial widths 4-59211  
<sup>71</sup>Ga(<sup>3</sup>He,t) reaction Q value meas., solar neutrino detector calibration 4-83088  
<sup>4</sup>Gd(<sup>3</sup>He,α) A=156,157 strength functions, levels, comparison with particle rotor model 4-64155  
<sup>1</sup>H(<sup>3</sup>He,d), evidence from missing mass for B=2, T=1 system 4-78642  
<sup>1</sup>He(A), A=p,d,p,p,d, on <sup>12</sup>C, <sup>28</sup>Si, <sup>58</sup>Ni, reaction mechanisms, total cross sections 4-106622  
<sup>3</sup>He(X) on C, Cu, Pb, neutron energy spectra, anal. 4-73908  
<sup>3</sup>He(X) on C, Fe, Cu, Pb, neutron and photon prod., expt., Monte Carlo calcs. 4-73907  
<sup>3</sup>He(df), on A=255-258, fission fragments and mechanisms 4-106637  
<sup>3</sup>He(pf), on A=255-258, fission fragments and mechanisms 4-106637  
<sup>3</sup>He(t), A=12-40, 197 MeV, levels, transitions, giant dipole resonance analogue, DWA anal. 4-86758  
<sup>3</sup>He(t), broad structure in t spectra, breakup-pickup reaction mechanism 4-59253  
<sup>3</sup>He(t) charge exchange reactions, spin-isospin modes 4-68681  
<sup>3</sup>He(t) isovector ΔL=1 strength in self-conjugate nuclei 4-68699  
<sup>3</sup>He(X), cross-section oscillation damping in quasi-elastic processes (*Ukrainian*) 4-86837  
<sup>4</sup>He(<sup>3</sup>He,γ), astrophysical low energies, resonating group calc., S(0) factor, comments 4-96042  
<sup>4</sup>He(<sup>3</sup>He,π<sup>+</sup>), A=3,4, coherent π prod., reaction mech. 4-78639  
<sup>4</sup>In(<sup>3</sup>He,n), A=113, 115, particle-hole coupling with proton pairing vibration 4-95886  
<sup>71</sup>Li(<sup>3</sup>He,π<sup>+</sup>), 235 MeV, differential cross sections and reaction mech. 4-106623  
<sup>16</sup>O(<sup>3</sup>He,t), isovector charge exchange excitations and decays 4-83083  
<sup>16</sup>Pd(<sup>3</sup>He,xn) A=108, 110 neutron ang. correlations, dσ<sup>2</sup>/dE<sub>n</sub>dΩ<sub>n</sub> meas. 4-86839  
<sup>32</sup>S(<sup>3</sup>He,n)<sup>34</sup>Ar, interference between direct and compound reactions, excitation curves 4-59251  
<sup>4</sup>Sb(<sup>3</sup>He,n), A=121, 123, particle-hole coupling with proton pairing vibration 4-95886  
<sup>4</sup>Sn(<sup>3</sup>He,xn) A=118<sup>+</sup>, 124 neutron ang. correlations, dσ<sup>2</sup>/dE<sub>n</sub>dΩ<sub>n</sub> meas. 4-86839  
<sup>126</sup>Te(<sup>3</sup>He,α)<sup>125</sup>Te pick-up reactions, nucl. level struct. investig. 4-78637  
<sup>171</sup>Yb(<sup>3</sup>He,α) strength functions, levels, comparison with particle rotor model 4-64155

**helium 3-nucleus scattering**

- <sup>40</sup>Ca(<sup>3</sup>He,<sup>3</sup>He), 197 MeV, levels, transitions, giant dipole resonance analogue, DWA anal. 4-86758  
<sup>3</sup>He(<sup>3</sup>He,<sup>3</sup>He), elastic scatt. cross sections, polarisations, generator-coordinate with semirelativistic NN pot. 4-73916

**helium-3 scattering** *see helium 3-nucleus scattering***helium atoms**

- 1s2p<sup>2</sup>P<sub>1</sub>-1s2p<sup>2</sup>P<sub>1</sub> transition energy, radiative correction 4-64399  
 1s2p states, isotope shifts and energies 4-74199  
 2<sup>1</sup>P state, electron impact excitation, orbital angular momentum transfer 4-64614  
 2<sup>1</sup>S state, electron impact excitation, intermediate and high energies 4-69218  
 accurate oscill. strengths using var. wave functions 4-78807  
 atom+isoformyl ion, metastability and isomerisation, interstellar appl. 4-91327  
 attractive forces at intermediate distances from metal surface, at matrix element effect 4-80707  
 autoionisation reson. by complex coordinate method with Hermitian Hamiltonian 4-102653  
 autoionisation states, single configuration approx., orthogonality conditions 4-107318  
 coincidence electron impact ionisation, absolute triplet differential cross sections 4-102799  
 collisional hyperfine line shifts of H in He, calc. using exchange perturbation theories 4-64401  
 correlation energies with explicitly correlated Gaussian geminals 4-91204  
 correlation satellites for K-shells, gas-phase photoemission with soft X-rays 4-96614  
 Coulomb and exchange interaction energy, HF calcs. 4-112245  
 dielectronic recombination study 4-107459  
 double ionisation by collisions with fast, fully stripped ions 4-112265  
 doubly excited states, electron correls. 4-87052  
 dynamic polarisability, Cauchy moments, coupled HF calc. 4-74147  
 elastic electron and positron scatt., model pot. method study 4-78967  
 electron impact 2S singlet state excitation, field theoretic approach 4-91350  
 electron impact in supersonic beam, reson. and metastable states (*French*) 4-78971  
 electron impact ionisation, triple differential cross section 4-87220  
 electron impact ionisation cross-section meas., by fast crossed beams 4-107457  
 electron scattering, 11-state r-matrix calcs. 4-69210  
 electronic density of the nucleus, bounds calcs. 4-68935  
 excited state lifetimes, inelastic electron-photon delayed coincidence technique 4-102644  
 excited state radiative lifetimes, regularities (*Russian*) 4-112145  
 fast electron impact ionisation, differential cross section 4-74338  
 geocoronal He airglow obs., contamination by radiation belt particles and O II emissions 4-105787  
 heavy targets, l subshell X-ray production by 1 to 3 MeV protons and He<sup>+</sup> ions 4-96651  
 HF discharge, param. investig. at intermediate press. by spectroscopic methods 4-84099  
 impact on NaF, Ag (111) and GaSe, phonon inelastic scatt. determined 4-98426  
 impact on Ni and Cu, interaction potentials 4-99256  
 inelastic scatt. from Ag (001) and Ag (001) with adsorbed Cl 4-99257  
 interchannel reson. coupling, photo- and Auger emission 4-83356  
 interstellar H and He in heliosphere, ionisation by 'core' and 'halo' solar wind electrons 4-105863  
 ionisation coeff. and total excitation cross section 4-92011  
 ionisation yield of low-energy electrons, statistical fluctuations 4-59899  
 isoelectronic series, atomic electronic density of the nucleus, bounds calcs. 4-68935  
 isoelectronic series, autoionis. states and widths 4-69024  
 isoelectronic series, poorly convergent perturbation expansions via shifted origin series: atomic 1/Z expansions 4-112089  
 laser induced cascade ionisation, secondary ionisation processes 4-83355  
 line-shape parameters for P Feshbach resonances 4-64433  
 metastable atoms in plasma, density meas. by laser-induced fluorescence method 4-60722  
 metastable state electron impact excitation 4-102802  
 multiple props., time depend. CHF method 4-87040  
 muonic, X-ray yield following muon catalysed DD fusion 4-107473  
 muonic He, 2S metastable state, lifetime and quenching rate meas. 4-83497  
 nonlinear optical props., ab initio calcs., freq. depend. dipole polarisabilities, susceptibilities 4-102608  
 parity-violating elec. dipole transitions, electron-electron neutral weak interaction 4-64407  
 photoionisation above N=2 threshold 4-69027  
 photoionisation cross sections, oscillator strengths, polarised orbital method 4-64438  
 photoionisation cross sections for photon energies 59-67 eV, autoionising reson., Rydberg series 4-64437  
 photoionisation in <sup>1</sup>S<sub>0</sub> ground state, photoelectron and photon decay 4-59683  
 primordial nucleosynthesis and interstellar He 4-63255  
 principle series transition energies 4-83321  
 quantum electrodynamic corrections of order α<sup>2</sup>mc<sup>2</sup> 4-78769  
 relativistic SCF calc. with squared Dirac operator 4-78790  
 scattering from W (110) semiclassical perturbation approx. 4-85052  
 Schrödinger eqn. soln. 4-112112  
 solar flare <sup>3</sup>He particles, heating in atm. and characts. 4-101302  
 spectra and struct. in strong mag. field, spherical basis (*French*) 4-68927  
 Stark broadening, electron and H<sup>+</sup> impact line width and shift 4-69009  
 superstrong mag. fields effect 4-74148  
 symmetric (e, 2e) momentum profile meas. 4-78976  
 two-electron atomic model 4-67921  
 H<sup>+</sup>+He, electron detachment in slow collisions 4-69198  
 HF+He, collisional roto-vibrational energy transfer, quantum calc. 4-69182  
 He I, 3p <sup>1</sup>P and 4d <sup>1</sup>D levels alignment and orientation, foil tilt angle depend. 4-102780  
 He I, electron excitation rate coeffs. for transitions from ground state to excited states 4-94571  
 He I, principal series spectral line excitation in electro-atom collision 4-91352  
 He I, Stark broadening params., semiclassical calc. 4-91224  
 He I astrophysical lines, Stark broadening 4-102638  
 He I autoionisation rate determ. by optical emission spectroscopy 4-87087  
 He I D<sub>3</sub> line in G and K stars 4-67724

## um atoms continued

- He I solar flare of 1982 September 4, nature, IR and X-ray emission 4-101299
- He II, principal series spectral line excitation in electro-atom collisions 4-91352
- He II 2p level excitation by electron impact, resonance states (Russian) 4-112283
- He II 30.4 nm line search in  $\alpha$  Aur, interstellar medium implications 4-85924
- He<sup>+</sup> (1s2s2s)<sup>3</sup>S reson., saddle-point complex-rot. method appl. 4-64404
- He<sup>+</sup> autoionisation states, single configuration approx., orthogonality conditions 4-107318
- He<sup>+</sup> dominance regions in high-latit. topside ionosphere, role of plasma convection 4-110363
- He<sup>+</sup> electron impact excitation, 1s-2p transition, modified Glauber approx. 4-112280
- He<sup>+</sup> electron impact excitation in dense plasma 4-112281
- He<sup>+</sup> H-like, elastic positron scatt., polarised orbital method 4-102798
- He<sup>+</sup> low energy electron impact, Schwinger's variational principle 4-74339
- He<sup>n+</sup> (n=0, 1, 2), electron loss and capture in various media 4-69206
- He-HO<sub>2</sub>, collisional energy transfer in low-press. limit unimol. dissoc. 4-83451
- He-like ions, 1s2s <sup>3</sup>S<sub>1</sub>-1s2p <sup>3</sup>P<sub>J</sub> transition freq., two-electron Lamb shifts 4-59675
- He-like ions, asymptotic eigenvalues and wave functions for restricted quantum-mechanical three-body problems 4-101132
- He-like ions, X-ray spectra excited in low-inductance spark plasma 4-74181
- He-N<sub>2</sub>, pot. energy surfaces 4-83315
- He<sup>+</sup> e<sup>-</sup>, reson. energy levels, vibr. modes, semiclassical calcs. 4-87235
- He<sup>+</sup> rich solar particle events, ionic charge state meas. 4-110587
- He<sup>+</sup> Ag(5P<sub>1/2</sub>), collisional depolarisation cross section, Hanle effect meas. 4-64585
- He<sup>+</sup> aniline (S<sub>0</sub>), state to state vibr. excitation, kinetic energy depend. 4-69184
- He<sup>+</sup> Ar<sup>2+</sup>, charge transfer processes studied by crossed-beam expt. 4-91339
- He<sup>+</sup> Ar<sup>2+</sup>(<sup>4</sup>), electron capture reactions studied by means of double translational spectroscopy 4-96686
- He<sup>+</sup> Au<sup>+</sup>, electron capture, ionisation and transfer ionisation cross sections 4-78960
- He<sup>+</sup> Cu<sup>+</sup> (N<sup>4+</sup>) (O<sup>4+</sup>) (F<sup>4+</sup>) (Ne<sup>4+</sup>) (Kr<sup>4+</sup>), one-electron capture at low energies, Landau-Zener model calcs. 4-96685
- He<sup>+</sup> Cu<sup>+</sup>(N<sup>4+</sup>)(O<sup>4+</sup>) ions, electron removal cross section 4-83460
- He<sup>+</sup> CO<sup>+</sup>, electronically excited CO<sup>+</sup> collisional deactivation 4-64580
- He<sup>+</sup> Cr, intramultiplet mixing collisions, fluoresc. 4-64588
- He<sup>+</sup> Cs, absolute polarisation meas., natural lifetime in: Cs 7S<sub>1/2</sub> state 4-83448
- He<sup>+</sup> Cu surface, time-depend. wavepacket scatt. calcs., isolated impurities effect 4-61794
- He<sup>+</sup> cyclopropane, vibr. energy transfer rate consts. calcs. 4-78935
- He<sup>+</sup> F<sup>4+</sup>, K Auger-electron prod. cross sections, charge-state depend. 4-96693
- He<sup>+</sup> H, rate const. meas. for orientation transfer 4-107435
- He<sup>+</sup> H<sub>2</sub>, energy sudden scaling relations, off-energy-shell effects incorporation method 4-69161
- He<sup>+</sup> H<sub>2</sub><sup>+</sup>, exchange reaction, ab initio pot. energy surface, quasiclassical trajectory study 4-76996
- He<sup>+</sup> H<sub>2</sub><sup>+</sup> (D<sub>2</sub><sup>+</sup>) (HD<sub>2</sub><sup>+</sup>), three body dissoc. absolute cross section meas. 4-104984
- He<sup>+</sup> H<sub>2</sub><sup>+</sup>, collisional dissoc., form. of H<sub>2</sub><sup>+</sup> 4-66555
- He<sup>+</sup> H<sub>2</sub>, electron detachment and charge exchange to shape resons. 4-69203
- He<sup>+</sup> H<sup>-</sup>, electron detachment, energy spectra, Born approx. 4-83459
- He<sup>+</sup> H<sup>-</sup> (Li<sup>-</sup>) (Na<sup>-</sup>) (K<sup>-</sup>), electron detachment cross sections 4-78952
- He<sup>+</sup> H<sup>+</sup>, autoionising reson. excited at small ejection angles 4-96681
- He<sup>+</sup> H<sup>+</sup>, elastic scatt., Glauber approx. 4-83447
- He<sup>+</sup> H<sup>+</sup>, electron capture, coherent excitation, multiple scatt. approach 4-87212
- He<sup>+</sup> H<sup>+</sup>, electron capture cross sections 4-69200
- He<sup>+</sup> H<sup>+</sup>, Thomas peak in electron capture 4-96692
- He<sup>+</sup> H<sup>+</sup>, autoionising state excitation cross section 4-59886
- He<sup>+</sup> H<sup>+</sup>, electron capture, symmetries eikonal-type approx. 4-83464
- He<sup>+</sup> H<sup>+</sup>(e<sup>-</sup>), electron capture, differential and total cross-sections calcs. 4-107447
- He<sup>+</sup> HCO<sup>+</sup> (HCS<sup>+</sup>), collision cross sections and rate coeffs. for rot. excitation 4-110514
- He<sup>+</sup> HF, energy transfer, differential cross sections, pot. energy surfaces 4-76992
- He<sup>+</sup> H(D), H(D) 2s and 2p excitation, integral cross sections 4-102786
- He<sup>+</sup> He multiple polarisabilities, dispersion forces, many-body theory 4-87192
- He<sup>+</sup> high-Rydberg atoms in circular states; collisional props. using free electron model 4-96654
- He<sup>+</sup> I<sub>2</sub>, state-to-state rot. transfer-rates, induced fluoresc. 4-91333
- He<sup>+</sup> I<sup>+</sup>, kinetic energy loss, double-focussing mass spectrometer meas. 4-64567
- He<sup>+</sup> inert gas atom, single and double electron loss cross sections of He metastable and ground states 4-59884
- He<sup>+</sup> Li, Li(2s-3d) excitation, D state scatt. amplitudes 4-64570
- He<sup>+</sup> Li<sub>2</sub>, collision-induced dissoc., reaction mechanism, rate const. 4-76976
- He<sup>+</sup> LiH rotationally inelastic collisions, quasi-classical dynamics of atom-rigid rotor trajectories 4-112260
- He<sup>+</sup> methane, exchange interactions, crossed-beam expt. (German) 4-96670
- He<sup>+</sup> methane ion, collision-induced dissoc., beam scatt. study 4-89263
- He<sup>+</sup> Mg, fine struct. transitions, close coupled transitions 4-78951
- He<sup>+</sup> Mg(<sup>3</sup>P) interaction calcs. using SA-MCSCF ICF-CI wavefunctions 4-74314
- He<sup>+</sup> N<sub>2</sub>, collision, rot. energy transfer 4-59879
- He<sup>+</sup> N<sup>4+</sup>, electron capture in autoionising configurations N<sup>4+</sup> studied by electron spectrometry 4-59889
- He<sup>+</sup> N<sup>6+</sup>, transfer ionisation and two-electron capture processes at 3-34 keV energies 4-96688
- He<sup>+</sup> NH, quenching, radiative lifetimes, transition moments 4-74292
- He<sup>+</sup> NO<sub>2</sub>, fluoresc. quenching cross sections, time resolved spectra 4-96603
- He<sup>+</sup> Na, emitted monochromatic light reson. scatt. 4-69022
- He<sup>+</sup> Na, population transfer, mol. pot. curves, avoided crossings 4-96655

## helium atoms continued

- He<sup>+</sup> Na, two-state collision problems for exponential coupling 4-74315
- He<sup>+</sup> Na<sup>+</sup>, excited Na states, collisional depopulation cross-sections 4-83456
- He<sup>+</sup> O<sub>2</sub>, in Ar shock tube, O<sub>2</sub> vibr. relax. study 4-96668
- He<sup>+</sup> OCS, IR linewidth meas., rot. levels, intermol. pot. 4-59764
- He<sup>+</sup> OCS, rot. relax. rates for J=0-1 pure rot. transition 4-69185
- He<sup>+</sup> SF<sub>6</sub>, multiproperty empirical anisotropic intermol. pots. 4-74308
- He<sup>+</sup> Xe, collision induced absorpt. coeff., quantum mech. and classical approach 4-91330
- He<sup>+</sup> Al KL<sup>1</sup> vacancy production cross sections, projectile depend. 4-96676
- He<sup>+</sup> H, excitation cross sections calc. using Vainshtein Presnyakov-Sobel'man approx. 4-64586
- He<sup>+</sup> He, double excitation 4-96677
- He<sup>+</sup> inert gas atoms, charge transfer and direct ionisation channels, electron prod. 4-87191
- He<sup>+</sup> Li collisions, single electron capture 4-74327
- He<sup>+</sup> N II collisions, N II reson. line excitation in VUV region in cathode sheath of hollow cathode discharge 4-87203
- He<sup>+</sup> N<sub>2</sub><sup>+</sup>, N<sup>+</sup> ions prod. in dissoc. double ionisation, ang. correl. 4-102779
- He<sup>+</sup> Na<sup>+</sup>, laser and ion beam excitation, autoionisation 4-69196
- He<sup>+</sup> N<sub>2</sub><sup>+</sup> thermal charge transfer reaction, N<sub>2</sub><sup>+</sup> predissoc. channel 4-91317
- He<sup>2+</sup> H, charge transfer, laser assisted, coupled dressed quasimolecular states approach 4-96684
- He<sup>2+</sup> H collisions, electron transfer, at. orbital expansion description 4-78962
- He<sup>2+</sup> He collisions, Coriolis coupling effect in time depend. HF calcs. 4-91342
- He<sup>2+</sup> Li collisions, single electron capture 4-74327
- He<sup>2+</sup> neutral ats., charge transfer in low-energy collisions 4-74326
- He<sup>+</sup> Ag(Sn)(Sb)(Te)(Ho)(Ta)(W)(Pt)(Bi), L-shell X-ray prod. cross-sections 4-107305
- He<sub>2</sub>, van der Waals pot. model 4-69166
- He<sub>2</sub><sup>+</sup>, electron impact dissociation 4-102812
- HeNe<sup>+</sup> radial nonadiabatic coupling determ. 4-68944
- He<sup>+</sup> ethene, vibr. modes, relax. and excitation, rate consts., vibr.-translation energy transfer 4-59881
- He<sup>+</sup> rich solar particle events, ionic charge distrib., ISEE 3 meas. 4-110586
- He I 1snl energy levels, ionisation energies and Lamb shift 4-64427
- He<sup>+</sup> HD, vibr. relax., mechanisms and rate consts. 4-96669
- He<sup>+</sup> ethene, vibr. modes, relax. and excitation, rate consts., vibr.-translation energy transfer 4-59881
- He<sup>+</sup> He, pot. energy curves obtained by combining scatt., spectroscopy and ab initio theory 4-74177
- He<sup>+</sup> Ne, electronic energy transfer in nozzle-beam scatt. cell expt., visible emission, odd-J levels 4-64578
- He<sup>+</sup> (S), electron beam excited, transient absorpt. in UV and VUV 4-78796
- Li<sub>3</sub><sup>+</sup>/He, rotationally inelastic transfer, scaling of state multipoles 4-87198
- O<sup>4+</sup> + He, charge transfer at thermal energies, cross sections and rate coeff. 4-76991
- W<sup>3+</sup> He, ion implanted, diffusivity study 4-104004

## helium compounds

- HeH, pot. energy curves of ground and excited states, MRD-CI calcs. 4-64393
- HeH, van der Waals, mol., ground state, complete CI calcs. 4-112122
- HeH<sup>+</sup>, IR transition probabilities, calc., equilib. pot. energy and dipole moment functions 4-69061
- HeH<sup>+</sup>, partial photodissoc. cross-sections, wavelength depend. 4-64551
- HeH<sup>+</sup> quasimolecules, autoionisation states 4-64550
- HeH<sup>2+</sup>, Dirac eqn., two dimens. numerical soln. 4-112093
- HeH<sub>2</sub>, analytic ab initio pot. energy surfaces for ground and first singlet excited states 4-96456
- HeSF<sub>6</sub>, multiproperty empirical anisotropic intermol. pots. 4-74308

## helium films

- dimers and trimers, unified framework anal. 4-104013
- superfluid, interaction with spin polarised atomic H, polaronic aspects 4-104034
- two-dimensional electron system above He film, obs. of polaronic transition 4-61305
- <sup>3</sup>He, adsorbed on fluorocarbon microspheres, dynamic polarisation effects, EPR study 4-80324
- <sup>3</sup>He-He film, ions localised near interface, low temp. mobility (Russian) 4-92452
- <sup>3</sup>He-He mixture film, third sound studied 4-92469
- <sup>3</sup>He-He mixture films, superfluid onset temp., third sound vel. 4-88365
- <sup>3</sup>He-He mixture thin films, phase separation study 4-104030
- He, adsorbed layer on Y-zeolite, semiquantum liquid and ordered phases obs. 4-65515
- He adsorbed monolayer film, effective pot. approx. (Chinese) 4-92471
- He adsorbed on Grafoil, multilayer growth 4-104033
- He films with <sup>3</sup>He, binding energy calcs. 4-70514
- He liquid, adsorbed on solid Ne, electron density 4-98683
- He liquid film, electron mobility, polaronic transition 4-98399
- He liquid film, polaronic state of surface two-dimensional electrons 4-98390
- He liquid film, strongly-coupled ripplonic polarons in high magnetic fields 4-98388
- He liquid film adsorbed on solid Ne, surface trapped two-dimensional electrons 4-98387
- He liquid film adsorbed on packed powder, Kosterlitz-Thouless superfluid transition 4-104019
- He, sound velocity temp. variation calcs. 4-70496
- He, superfluid, US third sound scatt. from substrate surface defects 4-104017
- He, superfluid film, theory of localised surface excitations (Russian) 4-92454
- He, superfluid films, third-sound phenomena studied by thin-film oscillator 4-61168
- He superfluid thin films, vortex pinning 4-92458
- He thin film on sapphire, desorption studies 4-98398

## helium I see liquid helium-4

## helium II see superfluid helium-4

## helium nuclei see nuclei with mass number 1 to 5; nuclei with mass number 6 to 19

- Hellman-Feynman theorem** *see quantum theory*
- Helmholtz free energy** *see free energy*
- hemoglobin** *see proteins*
- hemorheology** *see biorheology; blood*
- Hertzprung-Russell diagram** *see stellar evolution*
- heterodyne detection** *see demodulation*
- heuristic programming**  
*see also artificial intelligence*  
 five body problem, model for singularity without collisions, 4-86192
- HEXFET** *see insulated gate field effect transistors*
- HF calculations**  
*see also Alpha calculations*  
 $3s^2 3p^n$  ground configurations, (ionised Cu to Mo), magnetic-dipole transition predicted wavelengths and transition rates 4-68969  
 $\gamma$ -ray internal conversion interdisciplinary appls. and HF calcs. 4-78607  
 acetylene, mag. props. and induced current density, HF calcs. 4-78767  
 actinide and far from closed shell nuclei, symmetry conserving mean field theory 4-95932  
 actinide atomic and cryst. energy levels, f-shell config. parametric model, effective-operator Hamiltonian 4-74165  
 adiabatic TDHF theory with Skyrme interaction 4-59187  
 alkali metal atoms, excited states, photoionisation, initial wave functions 4-83438  
 alkylamines and cation radicals, electronic and spatial struct., CNDO/2 calcs. 4-59647  
 annulene, anions and derivatives, elec. polarisability, CHF-CNDO calcs. 4-64373  
 asymmetric magnetic impurities coupling, phase diagrams, HF approx. 4-80761  
 atomic 4f and 5d shells, elec. quadrupole moment, semiempirical Sternheimer shielding factors 4-102615  
 atomic elastic electron scatt. cross sections, classical and quantum mechanical calcs. 4-64612  
 atomic energy level distributions, HF calc. 4-64333  
 atomic Hartree-Fock wavefunctions, reduced local energy using computer program 4-96421  
 atomic M-shell vacancies, radiative transition rates, X-ray emission, DF approx. 4-96445  
 atomic many-body theory 4-78066  
 atomic orbital interacting configuration determ. using computer code 4-78753  
 atomic positive ions, chem. pot., density functional theory 4-96437  
 atomic spectra, superposition of configurations calc. 4-112128  
 atomic systems, level shifts, Dirac-HF eqns. 4-101700  
 atoms, electron ionization cross-sections for K, L and M shells 4-96705  
 atoms, ionisation and excitation energies, HF and HF-Slater calcs. 4-102723  
 atoms, Slater-type basis functions, iteration procedure 4-68920  
 atoms, valence minimising orbitals, Roothaan-like matrix eqn. 4-68919  
 atoms and ions, electron densities, ionisation pots., X-ray scatt. 4-96441  
 benzene dimer, interaction and dispersion effects, ab initio HF calcs. 4-102579  
 benzene-s-tetrazine mixed dimer, interaction and dispersion effects, ab initio HF calcs. 4-102579  
 biologically important cpds., mol. ions, fragmentation, MO and mass spectrosc. investigation 4-81426  
 bound electrons, bremsstrahlung in field, differential cross sections calcs. 4-69221  
 n-butane, configs., rot. pot. surface, basis set and CI calcs. 4-96460  
 carbanions and dianions, elec. susceptibilities, extended basis CNDO calc. using coupled HF perturbation energy 4-64380  
 carbonyl fluoride anion, struct. and vibr. spectrum, ab initio SCF MO theory 4-87038  
 Cauchy moments for at. and mol. dynamic polarisabilities, coupled HF calc. 4-74147  
 charge exchange in HF approx. of time depend. Anderson model 4-107448  
 CM motion in DDHF calcs., improved approx. treatment 4-86780  
 collective mass parameters and linear response techniques in three-dimensional grids 4-102202  
 collective submanifold, adiabatic TDHF method 4-68632  
 conference on semiclassical methods in nuclear physics, Grenoble, France, (Mar. 1984) 4-101567  
 continuum fluid dynamics and RPA for giant resonances 4-83005  
 cyclohexane-1,4 isomers, IR and Raman spectra, vibr. anal., ab initio HF calcs. 4-59770  
 cycloocta-1,5-diene, anions and derivatives, elec. polarisability, CHF-CNDO calcs. 4-64373  
 cyclopentadienylmanganese(I), mixed valence state stabilisation, cryst. orbital formalism anal. 4-104172  
 degenerate electronic band, martensitic transition temp., mag. field depend. enhancement by Coulomb and exchange interactions 4-104138  
 density fluctuations, shell model and HF method descriptions 4-64041  
 derivative HF theory to all orders 4-107272  
 diamond, one-electron excitations, exchange-correlation pot. 4-84579  
 diatomic hydrides, Hartree-Fock-Roothaan wavefunctions (Chinese) 4-96428  
 dielectric function and spin susceptibility, exchange effects 4-70692  
 electron density energy in external potential, ionisation dependence 4-78776  
 electron spectroscopy in solid-state physics, electronic energy levels interpret. (French) 4-66134  
 elements, electronegativities, density functional theory HF Slater theory 4-96442  
 ethene, adsorbed on transition and noble metals, electronic struct. and conform. 4-92784  
 ethyl radical, direct adiabatic channel computation for excited state relax. to give H+ethylene 4-96433  
 ethylene, elastic electron scatt. cross section, ab initio SCF HF calcs. 4-112270  
 ethylene, IR vibr. freqs. and intensities, NDO HF SCF calcs. 4-64387  
 ethylene, twisted, force consts. two config. SCF and HF wave functions 4-59618  
 EXAFS, inelastic effects role, SCF HF formalism 4-64492  
 extended Hubbard model with half-filled band, ground state beyond the HF approx. 4-76147  
 Fermi liq., two-component, sound wave propag. 4-61311  
 first-row homonuclear diatomic mols., electron momentum-density distrib. 4-78763
- HF calculations continued**  
 formaldehyde, O 1s vacancy ions, saddle point var. method 4-68936  
 formaldehyde+O(OH), H abstraction, pot. energy surface, ab initio HF CI calcs. 4-99770  
 formaldehyde IR vibr. freqs. and intensities, NDO HF SCF calcs. 4-64387  
 formaldehyde oxidation, H at. migration channel study 4-71897  
 formic acid dimer, struct., ab initio MO calcs. 4-102578  
 giant resonances, fluid-dynamical description, first sound and zero sound interaction 4-102238  
 graphite, charge density wave and magnetoresistance anomaly 4-92639  
 ground state correlations, RPA, sum rule approx. to giant resonance 4-102210  
 group state props. in semiclassical HF, deformation energy surfaces, fission barriers 4-102172  
 guanidium-carboxylate interaction, ab initio SCF HF calcs. 4-96436  
 Hartree-Fock-Slater wave function, discrete variational calc. of overlap integrals and dipole matrix elements 4-96429  
 heavy ion collisions, fast low density nucleonic jets, promptly emitted particles in TDHF 4-102305  
 heavy ion collisions, Newtonian dynamics of time-dependent mean field theory 4-83097  
 Heisenberg antiferromagnetic linear chain, spin-Peierls instabilities, antiferromag. transitions and phonon dynamics 4-65824  
 hydrides, first- and second-row, sp hybridisation, ab initio MO studies 4-102575  
 $i_{3/2}$  model, finite temp. Hartree-Fock-Bogoliubov cranking eqn., static fluctuations 4-73837  
 inert gas ions, electron-impact double ionisation 4-64618  
 inertial parameters of collective modes in adiabatic Hartree-Fock model 4-86755  
 inner shell ionisation, wave function effects 4-99235  
 internal conversion coeffs., Wigner-Seitz boundary conditions effects 4-73854  
 inverse mean field method, static and dynamic problems appls. 4-102207  
 iodooacetamide, X-irrad.,  $\sigma^*$  radical anion struct., EPR and INDO calcs. 4-69119  
 ionic mols., dissoc. energy: HF STO calcs. 4-112092  
 isoscalar giant vibrations, quantized time-dependent deformed oscillator model 4-102196  
 $K^{\pi}=1^{+}$  mode, deformed nuclei, Hartree-Bogoliubov and RPA calculations 4-106586  
 lanthanide atomic and cryst. energy levels, f-shell config. parametric model, effective-operator Hamiltonian 4-74165  
 large amplitude collective motion, coupling with intrinsic degrees of freedom, submanifold generalisation 4-90943  
 large amplitude collective motion, eqn. of motion method, semiclassical limit and closed theory 4-102152  
 Lipkin model, occupation renormalised Hartree-Fock approximation (Chinese) 4-102212  
 many-fermion system, generalised mean field expansions (Chinese) 4-101742  
 mean field theories, time-dependent, nuclear dynamics using HF calculations 4-86782  
 mean field theory, functional integral formulation of Brueckner-Hartree-Fock theory 4-73843  
 mean square radii, zero-point motion effect of nucl. surface 4-68618  
 metal clusters and chemisorption on metals, LDF,  $X_{\alpha}$ , Hartree-Fock, CI and valence band calcs. 4-88397  
 metals, potential at at. boundaries in Thomas-Fermi model and eqns. of states (Chinese) 4-70333  
 metals, total energy gradient 4-70698  
 methane, localised second-order elec. props., Hartree Fock calcs. 4-68944  
 methane elastic electron scatt. cross sections, GO and HF wave functions calcs. 4-64334  
 methoxy, electronic spin-orbit splitting calc. using UHF and RHF wave functions 4-59703  
 methyl chloride, anharmonic force field, ab initio MO calcs. 4-112125  
 methyl fluoride, anharmonic force field, ab initio MO calcs. 4-112125  
 methylenebis(ox), H at. migration reaction channel, formed in formaldehyde oxidation 4-71897  
 molecular collision, reactive, HF calcs., self-consistent time-dependent 4-77002  
 molecular interaction energies calc. using pseudopot. Hartree-Fock-Slater-LCAO method 4-96639  
 multiple-vacancy production in the independent-Fermi-particle model 4-81093  
 muon capture in nuclei, schematic model 4-90982  
 1-nitronaphthalene, second hyperpolarisability electronic contrib., CHF-PT-EB-CNDO calcs. 4-68959  
 nuclear dynamics, effect of two-body collisions 4-64114  
 nuclear forces, HF approx., unified theory of dissipation mechanisms 4-59157  
 nuclear HF theory, time dependent, adiabatic limit for collective motion 4-86781  
 nuclear many-body grand partition function, integral representation 4-73844  
 nuclear matter, collective excitations in adiabatic TDHF, density oscillations 4-86787  
 nuclear matter and finite nuclei properties, nonlinear relativistic mean field approach 4-90965  
 nuclear spherical single particle level shifts, HFB calcs. 4-82982  
 nucleus Hartree-Fock-Bogoliubov problem soln. in canonical representation 4-83016  
 one-body Wigner distrib. functions, mean field approx., harmonic oscillator wave functions 4-102208  
 oxetane, adiabatic correction to ring puckering pot. 4-96430  
 pairing-plus-quadrupole-quadrupole force for s-d shell region, cranked HFB anal. 4-59159  
 particle-hole excitation in deformed ground state 4-82986  
 perturbation-dependent basis sets, response props., second-quantisation anal. 4-96424  
 polyacetylenes, ab initio Hartree-Fock calcs. 4-96728  
 polyphenyls, electron spectra of conjugate systems in the  $\pi$ -electron approximation 4-102571  
 polypyrrole, band struct. calcs., ab initio HF study 4-84542  
 porphyrinatonicikel(II) polymer, band struct., semiempirical INDO crystal-orbital approach 4-75829  
 pyridine, vibr. spectra, force field HF calcs. 4-107327  
 rare earth metal atoms, M-shell X-ray emission rates, relativistic HF calculations 4-64413

## F calculations continued

- relativistic calculations 4-87041  
 relativistic Hartree theory of finite nuclei, role of quantum vacuum 4-78621  
 rotational band-level energies, moments of inertia and band crossing freqs., quadrupole pairing influence 4-73798  
 s-d model, electronic spectrum and damping with Coulomb interaction 4-92588  
 second order properties, eqns. of motion approach 4-91199  
 second-row homopol, diatomic mol., pot. curves, spectrosc. consts. and dissoc. energies 4-74309  
 semiconductor, doped, excitation spectrum in nonmetallic regime, concentration-fluctuation model 4-61328  
 semiconductor, electronic struct. and hyperfine interaction of muonium 4-65633  
 semiconductor surface, electronic collective modes and instabilities 4-108796  
 single particle density matrix, Wigner transform, semiclassical calc., semiclassical Hartree-Fock 4-102211  
 single-particle mag. moments in relativistic shell model 4-64071  
 Slater transition-state calculation of one-photon-two-electron excitation energies 4-96465  
 slow ion energy losses as function of at. number 4-107436  
 static nuclear properties, HF and semiclassical extended Thomas-Fermi model links 4-102209  
 static nuclear properties and the parametrisation of Skyrme forces 4-83017  
 TDHF extension for many-fermion systems, path integral approach 4-106587  
 TDHF heavy ion collisions, comparison with surface friction model 4-95993  
 TDHF method for collective motion description, canonical formulation 4-68633  
 TDHF solns., symmetry projection influence on phase transition 4-59188  
 TDHF with collisions in heavy ion dynamics 4-95945  
 tetracyanonickelate(II), mixed valence state stabilisation, cryst. orbital formalism anal. 4-104172  
 tetracyclohexane, struct., complete harmonic force field, vibr. spectra and IR intensities 4-87233  
 tetrafluoromethane, elastic electron scatt. cross sections, GO and HF wave function calcs. 4-64334  
 tetraza porphyrin crystal (II), one-dimensional, electronic struct., solid state props., SCF HF nickel-orbital approach based on semiempirical Hamiltonian 4-70627  
 s-tetrazine dimer, interaction and dispersion effects, ab initio HF calcs. 4-102579  
 thioacetamide, cryst. struct., rotamers, neutron diff. study, ab initio MO MF calcs. 4-103734  
 Thomas-Fermi calculations of hot dense matter 4-64084  
 transition metal atoms, Bauche-Arnoult hyperfine struct. parameters, discrete spectrum contributions 4-59652  
 transition metal sandwich metallocenes, correl. effects, ab initio HF calc. 4-68921  
 trifluoromethoxide anion, struct. and vibr. spectrum, ab initio SCF MO theory 4-87038  
 trimethylene diradical, force consts. two config. SCF and HF wave functions 4-59618  
 trivalent ion, position-depend. antishielding factors 4-70762  
 Waller-Hartree-Fock spatial wave function derivation 4-64331  
 water clusters, neutral and protonated, struct. calc. with mol. graphics 4-96734  
 (e.e.) on  $^{54}\text{Fe}$ ,  $^{60}\text{Ni}$ , Coulomb form-factors for  $0^+ \rightarrow 4^+$  transitions in 2p-1f shell, HFB anal. 4-59143  
 (e.e.) on Ti, Cr, Fe isotopes, form factors for  $2^+$  states excitation in 2p-1f shell, HFB anal. 4-59142  
 Al, positive muon pot., self-consistent cluster calc. 4-71236  
 Al,  $\text{Li-L}_{2,3}\text{M}_{11}$  Coster-Kronig spectrum, exchange, electron correl., and relax. effects 4-74172  
 Ar-HCl(HF), intermolecular forces, HF plus damped dispersion calcs. 4-87039  
 AsF<sub>6</sub> (n=3, 5, 6), cage mol., K-edge excitonic fine struct. 4-83287  
 B cluster surfaces, chemisorption of H<sub>2</sub> ab initio RHF calc. 4-92555  
 Ba, nonlinear ionisation, influence of self-ionisation states 4-107324  
 Ba<sup>+</sup>, critical double-well, many-body approach by g-Hartree method 4-59870  
 Be isoelectronic sequence, transition energy calc. using multiconfig. Dirac Fock and RPA calcs. 4-64364  
 Be-like ion, isoelectronic series, oscillator strengths, wavelengths, energy levels 4-67881  
 Be-like isoelectronic series, oscillator strengths, transition wavelengths, HF relativistic calcs. 4-106127  
 BeF, vibr. excitation of triplet core-ionised states 4-74175  
 Be  $\Lambda$  and  $\Delta_c$  hypernuclei binding energies,  $\Delta_c\text{N}$  interaction, HF calcs. (Chinese) 4-73848  
 $^{90}\text{Bi}$  ( $^{236}\text{Xe}$ ,  $^{136}\text{Xe}$ ), TDHF collisions, bombarding energy depend. 4-64168  
 C, gaseous, stopping power, zero-energy density effect 4-80129  
 CN<sup>-</sup> e<sup>-</sup>, electronic/positronic struct. examined using Hartree-Fock-Roothaan theory 4-64352  
 C<sub>2</sub>NH<sub>2</sub>, isomers, struct., relative energies ab initio MO STO calcs. 4-102572  
 C<sub>2</sub>NH<sub>2</sub><sup>+</sup>, isomers, struct., relative energies ab initio MO STO calcs. 4-102572  
 CO, hyperpolarisability function, derivative HF theory to all orders 4-107272  
 CO, RHF, NDDO and MOM mol. one-electron expectation values calc. using minimum basis sets 4-102598  
 CO-H<sup>+</sup>(Li<sup>+</sup>)(Na<sup>+</sup>)(K<sup>+</sup>) structs., binding energies, ab initio HF calcs. 4-112096  
 CO<sub>2</sub>, binding and correl. effects, gas X-ray diff. investig. 4-102697  
 CO<sub>2</sub>, ground state, photoionisation cross sections, linear algebraic method 4-64549  
 $^{12}\text{C}$ ,  $\pi^0$  condensation, short range correlations, Hartree approx. validity 4-82998  
 Ca, HFS, field isotope shift, multiconfigurational HF method 4-102594  
 CaOH, dissoc. energy calc., HF and GTO methods 4-64347  
 Ca, spherical finite-temp. Hartree-Fock approx., A-dependent effects, thermodynamic props. 4-111515  
 Ca, vibrational excitations, spin distrib., HF and RPA calcs. 4-90942  
 $^{40}\text{Ca}$  ( $^{16}\text{O}$ , X), extended time-dependent Hartree-Fock theory, one-dimensional collision model 4-111516

## HF calculations continued

- Cr binuclear complexes, triple metal bond HF-Slater transition state method 4-59619  
 Cs hyperfine struct. intervals, relativistic many-body calcs. 4-68986  
 Cs, isoelectronic series, ionis. pots., relativistic effects, core polaris. and relax. 4-68985  
 Cu, positive muon pot., self-consistent cluster calc. 4-71236  
 Cu-like ions,  $\text{Ge}^{3+}\text{-Mo}^{3+}$ , 3d-4p transitions, anal. 4-69001  
 $^{154}\text{Dy}$ , deformed shell closure, deformed HF calc. 4-59172  
 $^{158}\text{Dy}$ , s-band antialignment and low-spin struct., g-factors, cranked HFB calc. 4-111493  
 Eu I, VUV absorpt. spectrum identification,  $4f^7 5d^1 2D$  np state calc. 4-91215  
 F, electron momentum density distrib. 4-78763  
 FH, RHF, NDDO and MOM mol. one-electron expectation values calc. using minimum basis sets 4-102598  
 Fe, ab initio hyperfine struct. parameter calcs. 4-78981  
 Fr hyperfine struct. intervals, relativistic many-body calcs. 4-68986  
 Ge<sub>2</sub> ground state props., HF and CI calcs. 4-83289  
 H<sup>+</sup>, binding limit in Hartree approx. 4-102569  
 H<sub>2</sub>, electron elastic scatt. and rot. excitation at 10 to 100 eV, optical pot. model 4-96697  
 H<sub>2</sub>, ground state, photoionisation cross sections, linear algebraic method 4-64549  
 H<sub>2</sub>, multipole props., time depend. CHF method 4-87040  
 H<sub>2</sub>, linear, Hartree-Fock eqns., numerical solns. 4-74142  
 H<sub>2</sub>O, dipole moment derivatives, coupled HF calc. 4-91361  
 H<sub>2</sub>O, localised second-order elec. props., Hartree Fock calcs. 4-68947  
 H<sub>2</sub>S, dipole moment derivatives, coupled HF calc. 4-91361  
 He binding limit in Hartree approx. 4-102569  
 He Coulomb and exchange interaction energy, HF calcs. 4-112245  
 He, multipole props., time depend. CHF method 4-87040  
 He<sup>+</sup>+He collisions, Coriolis coupling effect in time depend. HF calcs. 4-91342  
<sup>3</sup>He liquid, fully spin polarised, ground state energy and Landau parameters 4-75750  
<sup>5</sup>He  $\Lambda$  and  $\Delta_c$  hypernuclei binding energies,  $\Delta_c\text{N}$  interaction, HF calcs. (Chinese) 4-73848  
 KCl, gamma irradiation of single crystal, shift in  $\text{K}\alpha_1$  line, EPR study 4-114163  
 Li clusters 4-98500  
 Li isoelectronic series, Rydberg energy levels determ. by relativistic quantum defect interpretation 4-107278  
 Li, muon interactions with lattice defects, mol. cluster calcs. 4-65255  
 Li<sup>+</sup>, doubly excited quintet states, fine and hyperfine struct., many-body calcs. 4-102609  
 Li-like ions principal series, oscillator strengths, photoionisation cross section calc. 4-83332  
 Li<sub>2</sub> cluster, H<sub>2</sub> impact, Raman enhancement mechanism assoc. with Raman scatterer interaction 4-61675  
 LiCl crystal, electronic energy bands, density functional calcs., self-interaction-correction theory 4-70651  
 LiCl, substitutional defects, molecular cluster-INDO calcs. 4-108806  
 LiCl<sub>2</sub>, excited state electronic struct., RHF calcs. 4-74176  
 LiF, substitutional defects, molecular cluster-INDO calcs. 4-108806  
 LiF<sub>2</sub>, excited state electronic struct., RHF calcs. 4-74176  
 LiH, ground-state props., LCAO HF study using polarisable basis set 4-60882  
 LiH, RHF, NDDO and MOM mol. one-electron expectation values calc. using minimum basis sets 4-102598  
 Li<sub>3</sub>N, electronic struct., Hartree-Fock studies 4-98522  
 LiNO<sub>3</sub>, force and vibr. spectrum, ab initio study 4-112110  
 LiOH, dissoc. energy calc., HF and GTO methods 4-64347  
 Mg, atom-metal XPS and Auger shifts, excited atom model using  $\Delta\text{SCF}$  HF calcs. 4-93191  
 Mo binuclear complexes, triple metal bond HF-Slater transition state method 4-59619  
 N<sub>2</sub>, elastic electron scatt., HF and multiconfiguration SCF CI calcs. 4-102796  
 N<sub>2</sub>, ground state, photoionisation cross sections, linear algebraic method 4-64549  
 N<sub>2</sub>, multipole props., time depend. CHF method 4-87040  
 N<sub>2</sub>, symmetry restricted and unrestricted HF calc. at ab initio LCAO-MO-SCF level 4-87043  
 N<sub>2</sub>, valence ionisation energies, correl. effects, generalised-valence bond interpretation 4-64385  
 N<sub>2</sub><sup>+</sup>, valence-hole state, ab initio LCAO-MO-SCF level HF calcs. 4-68957  
 N<sub>2</sub>-H<sup>+</sup>(Li<sup>+</sup>)(Na<sup>+</sup>)(K<sup>+</sup>) structs., binding energies, ab initio HF calcs. 4-112096  
 N<sub>2</sub>-e<sup>-</sup>, electronic/positronic struct. examined using Hartree-Fock-Roothaan theory 4-64352  
 NH<sub>3</sub>, localised second-order elec. props., Hartree Fock calcs. 4-68947  
 [(NH<sub>3</sub>)<sub>2</sub>Ru]pyrazine<sup>2+</sup>, electronic struct., Hartree-Fock-Slater study 4-96451  
 NO, ground state, photoionisation cross sections, linear algebraic method 4-64549  
 N<sub>2</sub>O+Ar collisions, intermol. pot., electron gas model, comparison with mean square torques meas. 4-78923  
 NaBr.2H<sub>2</sub>O, total lattice pot. energy calc. 4-103696  
 NaCl, substitutional defects, molecular cluster-INDO calcs. 4-108806  
 NaCl<sub>2</sub>, excited state electronic struct., RHF calcs. 4-74176  
 NaF, lattice dynamics, perturbation-theoretical-model calc. in Watson pot. approx. 4-61020  
 NaF, substitutional defects, molecular cluster-INDO calcs. 4-108806  
 NaF<sub>2</sub>, excited state electronic struct., RHF calcs. 4-74176  
 $^{93}\text{Nb}$  ( $^{16}\text{O}$ , X), E=204 MeV, preequilibrium nucleon emission, Fermi-gas model 4-96043  
 Ne, high Rydberg states and autoionising resons., centrifugal 4-68989  
 Ne, lowest <sup>2</sup> particles-two holes' reson. calc., diagonalisation approx. 4-83310  
 Ne, multipole props., time depend. CHF method 4-87040  
 Ni(CN)<sub>4</sub><sup>2-</sup> system, symm. isolations in partially oxidised one dimens. transition metal polymers 4-98524  
 Ni(CO)<sub>4</sub>, geometry optimisation, relativistic corrections, HF approx. 4-78762  
 OH<sup>-</sup>e<sup>-</sup>, electronic/positronic struct. examined using Hartree-Fock-Roothaan theory 4-64352  
 OH<sup>-</sup>(CO<sub>2</sub>)<sub>n</sub> clusters, (n=1, 2), ab initio investig. 4-96737  
 $^{16}\text{O}$ , compressed nucleus, dense system disassembly, TDHF study, clusterisation, collective flow 4-59190

**HF calculations continued**

- <sup>16</sup>O, spherical finite-temp. Hartree-Fock approx., A-dependent effects, thermodynamic props. 4-111515
- <sup>16</sup>O( $\pi^+$ , p), free pion absorption followed by proton emission 4-91026
- P-like ions, energy levels, transition probabilities, multiconfiguration DF study 4-106126
- <sup>208</sup>Pb, neutron single-particle energies, HF calcs. 4-78586
- <sup>208</sup>Pb, vibrational excitations, spin distribs., HF and RPA calcs. 4-90942
- Pd<sub>2</sub>, electronic struct. and bonding, mass spectrosc. and ab initio HF-CI investig. 4-74167
- (Pd<sub>1-x</sub>Au<sub>x</sub>)<sub>2</sub>Fe, hyperfine mag. field study 4-88493
- Rb, isoelectronic series, ionis. pos., relativistic effects, core polaris. and relax. 4-68985
- RbF, lattice dynamics, perturbation-theoretical-model calc. in Watson pot. approx. 4-61020
- SH<sup>-</sup>e<sup>+</sup>, electronic/positronic struct. examined using Hartree-Fock-Roothaan theory 4-64352
- Se crystal struct. and defects, CDW soliton model 4-70685
- Se IX, UV spectrum 100 to 140 Å, HF calc. 4-59667
- Si (111) slab, interface, electron-phonon interaction and broken symm. 4-80517
- n-Si, many-valley semicond., impurity states, clustering model 4-80549
- Si, mol. type axial channelling radiation from MeV electrons 4-75582
- Si, one-electron excitations, exchange-correlation pot. 4-84579
- Si, substitutional and interstitial donors, many electron effect 4-113895
- Si<sub>n</sub>H<sub>2n+2</sub>, defects, molecular cluster studies 4-84586
- <sup>28</sup>Si( $\pi^+$ , X), extended time-dependent Hartree-Fock theory, one-dimensional collision model 4-111516
- <sup>84</sup>Sn, A=100-176, HFB descript. near neutron-drip line, Skyrme interactions 4-86776
- Sr levels, config. mixing and isotope shifts 4-68978
- SrV, spectrum, struct. 4-107295
- <sup>88</sup>Sr, A=80, 82, 84, high-spin yrast spectra, variation-after-projection and HFB anal. 4-59131
- T crystal struct. and defects, CDW soliton model 4-70685
- W binuclear complexes, triple metal bond HF-Slater transition state method 4-59619
- Xe, isoelectronic series, 3d photoabsorpt. in near-threshold region, HF approx. 4-83349
- Xe<sub>2</sub>, model pot. method, SCF and dispersion energy calcs. 4-107426
- Zn isotopes, single-particle orbits and low-lying spectra, microscopic structure calc. 4-59132

**Higgs particles see intermediate bosons****high-energy cosmic ray interactions**

- ANI expt., 10<sup>3</sup>-10<sup>5</sup> TeV hadronic interactions, project theory 4-110462
- ANI installation for 10<sup>3</sup>-10<sup>5</sup> TeV hadron interaction studies 4-110464
- anomalous nuclei events observed in the JACEE emulsion chambers 4-102312
- anomalous relativistic ion interactions, cosmic rays in photoemulsions, nucl. pionisation model 4-110429
- azimuthal effects in hadron and photon families 4-110448
- binuclear gamma-families and large P<sub>t</sub> jets production 4-110445
- boson charge bunching in high energy collisions, Centauro-like events 4-59114
- Centauro and Mini-Centauro events 4-105860
- Centauro events, fireball model, SU(2)×U(1) vacuum 4-101089
- Chiron and Geminion production processes 4-105858
- Chiron type events, Pamir search 4-110443
- Chirons, Centauros, Geminions, pion production, anal. 4-110461
- cluster analysis of gamma-ray families 4-110444
- conference on quark matter in rel. nucleus-nucleus collisions, Long Island, NY, USA (Sept. 1983) 4-67855
- diffractive dissociation in multi TeV hadron-hadron and hadron-nucleus collisions 4-102145
- double core event,  $\Sigma E_{\gamma} \approx 1000$  TeV, particle distribution (Chinese) 4-102143
- E>1000 TeV families,  $\gamma$ -ray and hadron distribution 4-105859
- EAS, K<sub>s</sub>/K distribution in nucleon interactions 4-101087
- EAS, long flying component investigation 4-101084
- EAS hadron, role in muon pair production 4-101091
- emulsion chamber experiment at Mt. Kanbala 4-110435
- exotic event 'C19547117' and Chiron 4-106555
- exotic families, statistics 4-106550
- exotic fireballs in collider expts., Mini-Centauro and Geminion type events 4-106548
- extremely high energy gamma-ray and hadron family with halo 4-106552
- fire-ball production in inclusive spectra, radial scaling 4-95860
- galactic electron-photon interactions, EM cascade showers initiation 4-101537
- galactic gamma-ray-photon interactions, EM cascade showers initiation 4-101537
- galactic nuclei (E≥1 GeV/nucleon), interstellar interactions 4-94355
- gamma-ray sources, absorpt. features, effects of emitted photons-interstellar photon interactions 4-101535
- hadron bundles, obs. in Chacaltaya two storey emulsion chamber 4-106553
- hadronic interactions around 10<sup>15</sup> eV 4-110433
- halo events observed by Mt. Fuji emulsion chamber experiment 4-110431
- halo phenomena in emulsion chambers, Monte Carlo calcs. 4-110432
- halo production by superhigh-energy  $\gamma$ -ray and hadron families 4-110450
- heavy ion relativistic central collisions on heavy targets 4-102315
- heavy primary induced  $\gamma$ -ray families 4-110434
- heavy quark productions in super high cosmic ray interaction 4-102146
- hN-X, particle production mechanisms in cosmic ray interactions 4-95862
- interstellar H I-cosmic ray interactions, diffuse  $\gamma$ -ray emission 4-100890
- large p<sub>t</sub> jets observed in Chacaltaya gamma ray families 4-106551
- leptons, search for 4/3.e charge 4-101078
- long-lived particles produced in extensive air showers 4-94533
- metastable quark matter fireballs with free charm, role in very high energy interactions 4-106557
- Mini-Centauro type events in Pamir experiment 4-110460
- multiparticle clustering in hadron-nucleus collisions at cosmic ray energies 4-102279
- multiplicity correlation coefficients, energy depend. in high energy hadron-nucleus collisions 4-102281
- narrow groups of hadrons in X-ray emulsion chambers 4-110446
- NN fragmentation collisions, EM contrib. 4-86748
- nonsymmetrical double core event 4-110430
- high-energy cosmic ray interactions continued**
- nuclear interactions in photoemulsions 4-100924
- nuclei interactions in emulsion 4-102309
- nucleon interaction cross-sections at 10<sup>15</sup> eV 4-110440
- nucleon-nucleon interactions at high-energies, short- and long-range, correls. 4-78576
- nucleon-nucleus collisions, multihadron production, collective mechanism 4-102313
- nucleon-nucleus collisions, scaling violation 4-105857
- nucleus-nucleus collisions, multihadron production, collective mechanism 4-102313
- nucleus-nucleus collisions, phase transition simulation 4-102314
- nucleus-nucleus interactions above 1 TeV/n in the JACEE emulsion chamber 4-102311
- nucleus-nucleus reactions, 20 GeV/nuc., balloon expt. 4-102310
- Pamir expt.,  $\gamma$ -ray energy spectra and ang. distrib. 4-110438
- particle production, cosmic ray and accelerator data 4-102144
- photon damping in cosmic ray acceleration in active galactic nuclei 4-94349
- proton relativistic central collisions on heavy targets 4-102315
- pseudorapidity correlation in hadron-nucleus interaction at cosmic ray energies 4-102280
- QCD hard-scattering-jet effect on the gamma-ray families observed at mountain altitudes 4-110457
- QCD jet simulation in 10<sup>15</sup>-10<sup>17</sup> eV hadron collisions, Monte Carlo approach 4-110458
- quark flux estimation at sea level 4-101082
- scaling violation in fragmentation region at 10<sup>15</sup>-10<sup>16</sup> eV 4-110439
- scaling violation in fragmentation region of pp collisions 4-105834
- single hadron fraction, inelasticity coeff. at 10<sup>15</sup>-10<sup>16</sup> eV 4-110441
- septon production cross-section limits in hadron-nucleus collisions 4-101079
- statistical analysis methods development 4-110463
- superfamilies in Pamir multilayer X-ray chamber 4-110442
- telescope neutrino events, correlation with acceleration pulses 4-101097
- transverse momenta flow in 10-1000 TeV interactions 4-110453
- ultra high energy nuclear interaction producing multiple large P<sub>t</sub> components (Chinese) 4-77685
- ultra-relativistic heavy ion collisions, high multiplicity events 4-102316
- very high energy cosmic ray events, primary spectral changes, anomalous interactions 4-72842
- $\eta$  production in cosmic ray X-ray families 4-106554
- $\gamma$ -ray big family events observed at Mt. Kanbala 4-110437
- $\gamma$ -ray families, CERN collider data influence on anal. 4-110456
- $\gamma$ -ray families, fluctuations, correlations, scaling violation 4-110447
- $\gamma$ -ray families, Pamir expt., Monte Carlo anal. 4-110454
- $\gamma$ -ray families, with and without haloes, characteristics 4-110452
- $\gamma$ -ray families from  $\pi$ A and NA interactions 4-110449
- $\gamma$ -ray families in Mt. Kanbala emulsion chamber expt. 4-106556
- $\gamma$ -ray family events obs. at Mt. Kanbala 4-110436
- $\gamma$ -ray superfamilies, characteristics with and without halo 4-110451
- $\gamma$ -ray-hadron families, model depend. features 4-110459
- hh-quarks, production cross-sections in cosmic rays 4-95845
- hh-X secondary inclusive spectra in additive quark model 4-95853
- hN, multiparticle production, multiplicities at cosmic ray energies 4-95854
- hN, multiparticle production at cosmic ray energies, A-dependence 4-95855
- hN, shower multiplicity studies at cosmic ray energies 4-95856
- hN cross-section calcs. using Glauber multiple scatt. 4-95846
- hN-hX, scaling in compound multiplicity 4-95844
- hN inclusive spectra, scaling violation in fragmentation 4-95852
- hN-X, simple model 4-95863
- hN-X inclusive inelastic spectra, effect of Fermi motion 4-95858
- NN cosmic ray interactions, ang. dist., fractional energy spectra 4-101092
- NN-jets, production mechanism 4-95861
- NN-X, inelasticity dist. for multiplicity, KNO scaling 4-95847
- $\bar{\nu}$ -charm, inclusive production results 4-95788
- pN-cosmic ray cascades, nuclear target effects 4-95859
- pN-hX, anal. of secondary tracks in  $\phi$ -space 4-95841
- pN-hX, elasticity, cascade effects 4-95840
- pN-hX, non-pion production, collision process 4-95843
- pN inclusive interactions, mean elasticity of leading nucleon 4-95848
- pN-jets, 4-momentum transfer between fireballs, multiplicity dependence 4-95842
- pN- $\pi^+$ X, pionisation and fragmentation, inelasticity 4-95857
- pN-X inelastic charge exchange dependence on production cross-section 4-95851
- pp-hX, effect of strange particles on cosmic ray processes and energy dist. 4-95839
- pp-hX, inclusive cross-section calcs., Feynmann scaling 4-95838
- pp-hX, invariant differential cross sections, new scaling variable 4-95837
- pp-hX, scaling violation in statistical model 4-95836
- pp interactions, effect of isobar formation on recoil nuclei 4-95849
- $\pi^+$ - $\pi^+$ X, pionisation and fragmentation, inelasticity 4-95857
- $\pi^+$ N interactions, leading particle effect 4-95850
- <sup>31</sup>Cl neutrino counting rate, P-P chain reactions, quasi-non-degenerate distrib. 4-101090
- Fe( $\mu,\mu$ ), cosmic ray muon scatt., virtual photon shadowing 4-85852
- Fe(p,X) 0.5-5.0 TeV, cosmic ray hadron component composition at mountain altitudes 4-102325
- Fe( $\pi,X$ ), 0.5-5.0 TeV, cosmic ray hadron component composition at mountain altitudes 4-102325
- $\gamma$ -ray families, emulsion chamber expt. compared to Monte Carlo simulation 4-110455
- high energy electron diffraction**
- see also reflection high energy electron diffraction
- biprism interferences with 1 MeV electrons from monofile Van de Graaff generator 4-107503
- transition metal dichalcogenides, zone-axis patterns for HEED rel. to cryst. pot. 4-103615
- Au thin films, thermal expansion coeffs., transmission HEED 4-75705
- Ge(100)-(2×1), adsorption of Ag, HEED and photoemission study 4-75790
- TaSe<sub>2</sub>, 1T- and 2H-, angle-resolved XPS, azimuthal orientations 4-104718

high-energy nuclear reactions and scattering *see nuclear reactions and scattering*

high fidelity amplifiers *see audio-frequency amplifiers*

high field effects

*see also Gunn effect; hot carriers; impact ionisation; limited space charge accumulation; Poole-Frenkel effect; Schottky effect; Zener effect*  
alkali halides, with F-centres, hopping-type electronic processes in pre-breakdown elec. fields 4-108868

disordered lattice, cond. in strong elec. fields 4-61367  
disordered systems, hopping cond. and weak localisation in strong elec. field 4-75976

electron-impurity systems in strong elec. field, theory of nonlinear transport 4-108870

nematic liq. cryst., high electric field effects and walls 4-84164  
oil, aged transformer, DC cond. under nonuniform high fields 4-88771  
piezoelectrics, even elec. cond. with streaming, separation of shift and ballistic contributions 4-113951

poly(vinylidene fluoride),  $\beta$ -phase, polar axis rotation under high elec. field 4-99007

poly(vinylidene fluoride) film, struct. under high elec. fields 4-98029

polyethylene, low-density, anomalous discharge current 4-114206

semiconductors, high field quantum transport theory 4-80599

semiconductors, magnetically induced photogalvanic effect 4-84653

semiconductors, small gap, intrinsic photocond., electron and hole heating effects 4-88542

semiconductors, submicron thickness, nonsteady-state quasiballistic 4-61472

semiconductors, Voigt effect and magneto-conductivity in strong elec. field 4-99099

Al<sub>0.4</sub>Ga<sub>0.6</sub>As:Si MOCVD layers, transport props. 4-92834

BaTiO<sub>3</sub>:Fe, electrolum., elec. field depend. 4-66077

CdF<sub>2</sub>:Gd<sup>3+</sup>, EPR, anomalous high elec. field effect 4-71173

CdS, dark current and photocurrent in strong elec. field, temp. dependence 4-113998

GaAs, carrier vel. fluctuations in steady-state and transient regimes, Monte Carlo study 4-80637

GaAs, high field transport of holes 4-80598

GaAs high-field transport, model 4-88512

n-GaAs, metallic, inelastic scatt. time, temp. depend. 4-98630

GaAs n<sup>+</sup>-p-n<sup>+</sup> ballistic struct., I-V charact. calc. (Chinese) 4-80659

GaAs n<sup>+</sup>-n-n<sup>+</sup> structures, high field reson. magnetotransport meas. 4-104295

GaAs-Al<sub>0.4</sub>Ga<sub>0.6</sub>As tunnel junctions, sequential single-phonon emission obs. in electron transport 4-80667

Ga<sub>0.47</sub>In<sub>0.53</sub>As, hot electron velocity overshoot 4-70823

GaInAsP, high field transport meas., review, book contrib. 4-61389

GaInAsP, n-type, lattice matched to InP, hot electron transport, book contrib. 4-61388

Ge, compensated, photoresponse to local optical excitation 4-108904

Ge:Si(Bs), impurity state breakdown under uniaxial compression 4-70715

Ge:Zn, nonohmic hopping cond. in strong elec. fields 4-88515

InAs high-field transport, model 4-88512

InP, high field transport of holes 4-80598

InP high-field transport, model 4-88512

InSb MIS structures, photoresponse enhancement in strong elec. field 4-65751

KI thin films, high-field elec. cond. study 4-80702

Si, carrier vel. fluctuations in steady-state and transient regimes, Monte Carlo study 4-80637

Si point contact n<sup>+</sup>-n junction, microwave noise 4-88574

Si/SiO<sub>2</sub> MOS capacitors, donor state generation rate, anode field depend. 4-92826

SiO/SnO<sub>2</sub> coevap. films in sandwich struct., high-field cond. and opt. absorpt. 4-108948

SiO<sub>2</sub> MOS struct., tunnelling current in high field regime 4-88598

SiO<sub>2</sub>, strong elec. field heating of cond. band electrons 4-61386

Ta<sub>2</sub>O<sub>5</sub>, amorphous, conductivity changes study during degradation in strong elec. field 4-108872

Ta<sub>2</sub>S<sub>3</sub>, orthorhombic, CDW state, nonlinear field-effect (Chinese) 4-92735

W imaging in field ion microscope, electric field induced surface atomic displacements obs. 4-68337

high-frequency discharges

air, microwave discharge with preexcitation of neutral mols. 4-103597

air, RF corona discharge, pulsed, spatiotemporal spectrosc. obs. 4-79846

air pulsed RF corona, ns. image intensifier investigation 4-84105

anomalous plasma resistance in transverse mag. field 4-92023

atmospheric microwave discharges, EM field patterns meas. 4-69959

bounded RF discharge, stimulated ionisational scatt. dynamics 4-103502

capacitive RF discharge, electrode layers model 4-108243

capacitively coupled high frequency discharges 4-108246

capacitively coupled radio-frequency discharges 4-84120

CW arc pluming at high-power aerials, scale-model studies 4-69971

instability, kinetic study 4-92008

methane plasma diagnostics and modelling, use in CVD growth of a-C films 4-104979

microwave breakdown threshold lowering in periodic-pulse operation 4-87967

microwave capillary discharge, Ar plasma prod., spectral line intensities 4-88000

microwave discharge, energy charact. change by surface-wave ionisational instability 4-87968

microwave discharge, plasma halo and ionising radiation 4-79871

microwave discharge in waveguide, self-excitation of standing wave 4-103598

microwave discharges, energy balance 4-87998

microwave plasma, prod. by surface waves, characts. 4-69958

pentafluoroethyl free radical, matrix isolation IR spectrum 4-69069

perfluoroalkane-H<sub>2</sub> mixtures, RF plasma decomp. during plasma etching or fluoropolymer deposition 4-108230

perfluoropropane-H<sub>2</sub> RF discharge, chem. mechanisms 4-108231

pulsed RF plasmas obs., CW arc pluming at high-power aerials 4-69970

pulsed surface discharge, light-initiated, high-current stage 4-97927

RF glow discharges, spectral line shapes, optical emission actinometry 4-87931

RF ion sources, breakdown behaviour 4-78417

single channel HF discharge bursts, elec. params. 4-88030

tetrafluoromethane-tetrafluoroethylene mixtures, RF plasma decomp. during plasma etching or fluoropolymer deposition 4-108230

high-frequency discharges continued

transverse capacitative medium press. HF discharge, plasma parameters investigation 4-88002

UHF discharge into waveguide, instability, surface waves, nonlinear model 4-92024

UHF low press. discharge, surface wave self-excitation, electron density study 4-92025

Ar, HF and d.c. low press. discharges 4-79865

Ar-He mixtures in microwave capillary discharges 4-87999

CO<sub>2</sub> waveguide laser, RF discharge striations 4-79100

He HF discharge conductivity in low hybrid resonance range (Russian) 4-92009

He, HF discharge, param. investig. at intermediate press. by spectroscopic methods 4-84099

N<sub>2</sub> microwave discharge, vibr. energy relaxation 4-108249

N<sub>2</sub> pulsed RF corona, ns. image intensifier investigation 4-84105

N<sub>2</sub>, RF corona discharge, pulsed, spatiotemporal spectrosc. obs. 4-79846

NO<sub>x</sub> synthesis in low press. plasma, energy cost improvement 4-85305

Ne, HF plasma, electron kinetics, Fourier expansion technique 4-113242

O<sub>2</sub>, low density discharge, bimolecular processes 4-75225

Xe plasma column, LF-turbulence, ionisation wave, microwave diagnostics 4-92022

high-frequency effects

*see also helicons; hot carriers; skin effect; solid-state plasma*  
bis(ethylene)dithioteatratrifluorvalene), elec. props. meas. 4-75917

metal films, inhomogeneous, 1-2 mm radiation, geometric thickness, impedance model 4-108955

metals, radio wave irradiation, effect on current states, rectification 4-104252

microwave AC cond. of superionic conductors 4-88527

polyacetylene: I<sub>2</sub>, cis and trans, DC and microwave cond. 4-92716

polyacetylene: I<sub>2</sub> (AsF<sub>6</sub>), millimeter-wave and far IR cond. 4-70850

semiconductor, HF relaxational oscils. in homogeneous electron-hole plasma heated by Auger recomb. 4-108891

semiconductor, polar with anisotropic conduction valleys, high freq. cond. 4-113938

semiconductor size-quantised films, nonlinear high freq. props. 4-104332

semiconductor superlattices, high-frequency props. theory 4-70922

semiconductor-electrolyte interfaces, photoeffects, time-resolved microwave cond. 4-88583

solid-state plasma, collision-dominated, surface wave excitation 4-104248

superlattice quantum state transfer device, negative differential resistance at 300K 4-80656

GaAs, negative differential cond. at transit reson. frequencies 4-84638

Ge, cyclotron resonance and radiative recombination for excitons, free carriers, electron-hole droplets 4-71183

Ge exciton condensation, microwave study 4-68234

Ge exciton condensation, microwave studies, biexcitons and electron-hole droplets 4-70668

Ge exciton condensation, microwave breakdown, one- and two-photon carrier excitation luminescence 4-70670

Ge, exciton condensation, microwave methods using pulsed optical excitation, kinetics 4-70671

Ge exciton microwave breakdown, exciton and free carrier kinetics with electron-hole drops 4-70669

Ge exciton studies, laser heating effects at liquid He temps. 4-70672

Ge nonequilibrium current carrier microwave absorpt., carrier conc., excitons 4-70852

Ge-Ge<sub>1-x</sub>Si<sub>x</sub> superlattices, interactions of high-freq. EM waves 4-80670

InP, localisation of inversion electrons, Fourier transform spectra studies 4-98555

n-InSb:Cr, Mn, impact ionis. in 2-mm microwave field 4-70824

n-Si:Fe, impurity bands of Fe clusters, ESR and elec. props. 4-109067

SbM<sub>6</sub>, microwave conductivity meas. 4-70851

(TMTSF)<sub>2</sub>BrO<sub>4</sub>, DC and microwave conductivity and thermoelec. power 4-75950

high-frequency electronic transport *see high-frequency effects*

high-frequency heating *see radiofrequency heating*

high-pass filters

evoked potentials, computer reconstructed, high pass filters effect 4-72449

X-ray bandpass filter from Ge solid state detector and GeO<sub>2</sub> foil. 4-91176

high-pressure effects in solids

*see also high-pressure solid-state phase transformations; piezo-optical effects*

alkali metals, equations of state, shock wave isotherms 4-108573

n-alkanes, solid odd numbered, thermal conductivity at high press., C<sub>9</sub>H<sub>20</sub> to C<sub>19</sub>H<sub>40</sub> 4-61154

aluminosilicate refractories, compressive stress influence on thermal cond. 4-65506

anharmonic crystals, lattice temp., pressure effects 4-113559

binary alloys, press. influence on precipitation (Russian) 4-80232

detonation, overdriven expts., product EOS above Chapman Jouguet press. 4-109664

diffusion under high pressures, rel. to defect mech. 4-65435

diopside, mineral elastic const. at pressures up to 2 GPa 4-72577

europium ethylsulphate:Ce<sup>3+</sup>, Ce<sup>3+</sup> EPR spin-lattice relax. rate, press. effects 4-65855

graphite intercalation compounds, theory of press-induced staging transitions 4-75696

graphite intercalation cpd. with ICl, C<sub>16</sub>I<sub>2</sub>Cl, press. induced change in intercalation step 4-61397

graphite/metal mixtures, diamond form. under shock compression and flash heating 4-108516

ice 1, amorphous phase formed at 77K and 10 kbar 4-98016

lanthanum ethylsulphate:Ce<sup>3+</sup>, energy level shift under hydrostatic press. (Russian) 4-84598

magnesian refractories, compressive stress influence on thermal cond. 4-65506

MBBA, metastable solid, dielectric props. under press. 4-80865

metal unsintered powders, Hugoniot meas. using C gauges 4-108578

metals, electron spectrum, changes under press. (Russian) 4-108766

metals, potential at, boundaries in Thomas-Fermi model and eqns. of states (Chinese) 4-70333

organic polyiodide chain complexes, elec. conduction, press. depend. 4-75962

oxide powders, shear strength up to 600°C and 4 GPa 4-104811

perforated viscoelastic elastomers, press. effects on dynamic props. 4-103879

## high-pressure effects in solids continued

- poly(vinylidene fluoride) piezoelec. and pyroelec. props. under high press. 4-99027  
 polyethylene, high press. extended chain crystallisation kinetics, NMR obs. 4-65191  
 polymer, press. effect on mech. props., glassy parameters substitution for occupied vol. parameters 4-61964  
 pyrrhotite ( $\text{Fe}_0.9\text{S}$ ), eqn. of state at Earth core conditions 4-115395  
 quartz, diffusional crack healing in aqueous environment 4-94098  
 quartz powders, shock-loaded, deform., X-ray line 'broadening' obs. 4-65324  
 rare earth compounds, pressure effect on Curie temp. 4-114108  
 solids, dynamic compression, thermodynamic props. 4-70409  
 solids, Hugoniot data from nuclear-explosive generated shocks 4-108521  
 steel, carbon, strain ageing, influence of high press. (*Russian*) 4-85168  
 styrene-butadiene rubber, mechanochem. reaction at high temp. (*Japanese*) 4-88238  
 TGS, stabilisation of polar states with impurities 4-75468  
 (TMTSF) salt, (TMTSF) $_2\text{PF}_6$  and (TMTSF) $_2\text{ClO}_4$ , thermal transport props. 4-104362  
 toluene sulphonate diacetylene, 2 eV electronic transition, press. depend. 4-114296  
 transition metal compounds, pressure effect on Curie temp. 4-114108  
 yttrium ethylsulfate,  $\text{Ce}^{3+}$ ,  $\text{Ce}^{4+}$  EPR spin-lattice relax. rate, press. effects 4-65855  
 Ac, superconducting transition temp. under high press., vol. depend. 4-84728  
 Al, diffusion of  $^{65}\text{Zn}$ , effects of hydrostatic press. 4-65483  
 Al, Fermi surface, topological transitions under stress (*Russian*) 4-108761  
 Al, melting curve study at high press. 4-103911  
 Al single crystal, dislocation multiplication during creep 4-98106  
 Al, ultrahigh-pressure laser-driven shock-wave experiments at 0.26  $\mu\text{m}$  wavelength 4-75180  
 Al/Ag system, react diffusion, effect of high press. 4-108666  
 Al-Ag, solubility of Ag in Al, effect of high press. 4-81179  
 Al-Ge, binary constitution diagrams at very high press. 4-104766  
 Al-Si, binary constitution diagrams at very high press. 4-104766  
 Al-Si system, phase relations up to 5.5 GPa 4-104765  
 $\text{Al}_2\text{Ga}_{1-x}\text{Al}_x$ -GaAs heterojunction, EMF due to dynamic deform. 4-98746  
 $\text{Al}_2\text{O}_3$ , spray-dried, compaction behaviour 4-76714  
 Ar, solid, volume and isothermal bulk modulus, press. depend. 4-92278  
 Au, optical length determ. in diamond-anvil cell 4-68237  
 Au, self-diffusion, effect of hydrostatic pressure 4-65451  
 Au, ultrahigh-pressure laser-driven shock-wave experiments at 0.26  $\mu\text{m}$  wavelength 4-75180  
 $\text{B}_2\text{O}_3$ -Li $_2\text{O}$  (Li halides), fast ion cond., press. effects 4-88336  
 $\text{BaPb}_2\text{BiO}_7$ ,  $\text{O}_3$  films, supercond. props., high press. study 4-84733  
 Be, strength effect on determ. of high press. 4-65344  
 $\text{Bi}_{1-x}\text{Sb}_x$ , composition influence on electron scatt. intensity 4-88518  
 $\text{CdF}_2$ , alkali metal dopd., association and bound motion 4-80294  
 Ce, electronic struct., press induced 4f occupancy enhancement 4-75844  
 Ce, valence under high press., free energy depend. 4-92676  
 $\text{CeCu}_2\text{Si}_2$ , superconducting  $T_c$  maximum 4-98800  
 $\text{Ce}(\text{In}_{1-x}\text{Sn}_x)_3$ , intermediate valence study 4-61340  
 $\text{CrRu}_{1-x}\text{O}_2$ , high press. distortion, cryst. struct. study 4-80012  
 $\text{CrTi}_{1-x}\text{O}_2$ , high press. distortion, cryst. struct. study 4-80012  
 CsCl, eqn. of state used for secondary calibration scale at low temps. 4-103897  
 CsI, 60 GPa effects, UV absorpt. spectra 4-76490  
 CsI, optical absorpt. spectra, meas. at press. up to 60 GPa 4-76495  
 CsI, optical transmittancy, xenon high pressure transmitting, band closing 4-114299  
 Cu, ultrahigh-pressure laser-driven shock-wave experiments at 0.26  $\mu\text{m}$  wavelength 4-75180  
 Cu-Zn, interdiffusion coeffs., high press. effect 4-88353  
 $\text{CuRb}_2\text{Br}_2\cdot 2\text{H}_2\text{O}$ , mag. props. meas. 4-89925  
 D, solid, rot. excitation under high press., anharmonic theory 4-108674  
 Er, electronic struct., press induced 4f occupancy enhancement 4-75844  
 $\text{EuMo}_6\text{S}_8$ , bulk superconductivity obs. under pressure 4-71004  
 $\text{EuMo}_6\text{S}_8$ , divalent Chevrel-phase supercond., effect of press. and O defects 4-80711  
 Fe 4-108576  
 Fe, BCC, Fermi surface and energy bands under press., APW calc. 4-80478  
 Fe-B amorphous alloys, cryst., and press., elec. resist. study 4-60837  
 Fe-Ni-P-(B-Si) metallic glasses, magnetoelastic effects in ferromag. resonance 4-61581  
 $\text{Fe}_{0.66}\text{Ni}_{0.34}$ , Curie point at ultrahigh press. 4-88676  
 $(\text{Fe}_{1-x}\text{Ni}_x)_m$ ,  $M=\text{P, B, Si}$  or Al, metallic glass, Mossbauer study of high press. 4-84880  
 $\text{Fe}_2\text{Ni}_{55}\text{Si}_{10}\text{B}_{10}$ , metallic glass, Curie temp. press. depend. 4-84792  
 FeO, temp.-press. stability fields at high press., thermodynamic calc. 4-103965  
 $\text{Fe}_2\text{O}_3$ , magnetite, Verwey transition 4-88447  
 $\text{Fe}_0.9\text{S}$  (pyrrhotite), eqn. of state at Earth core conditions 4-115395  
 GaP, press. depend. of bound excitons 4-61293  
 GaSb, Raman freq. depend. on press. 4-109188  
 Ge, elastic props., ultrasonic meas. 4-98170  
 $(\text{GeSe}_3)_{100-x}\text{Bi}_x$ , struct. and resist. effect of dopants, high press. study 4-103660  
 $(\text{GeSe}_3)_{100-x}\text{Sb}_x$ , struct. and resist. effect of dopants, high press. study 4-103660  
 $\text{H}_2\text{O}$  vapour, high temp. and press., CARS spectra rot. diffusion model appl. 4-69085  
 $\text{Hg}_{1-x}\text{Cd}_x\text{Te}$ ,  $\Gamma_6\text{-}\Gamma_8$  band crossover under press., phase transform., thermoelec. power meas. 4-88524  
 $\text{HgTe}$ ,  $\Gamma_6\text{-}\Gamma_8$  band crossover under press., phase transform., thermoelec. power meas. 4-88524  
 In, Fermi surface, topological transitions under stress (*Russian*) 4-108761  
 InAs, Raman freq. depend. on press. 4-109188  
 InSb, Raman freq. depend. on press. 4-109188  
 InSb, shallow donors in high mag. fields and hydrostatic press. 4-80540  
 InSb, thermal oxidation method, XPS study, resistivity 4-114690  
 $\text{KBrLi}^+$ , paraelec. reson. absorption, decomposition under hydrostatic press. 4-104549  
 $\text{KD}_2\text{PO}_4$ , photon emission during uniaxial deform., Curie temp. 4-81028  
 $\text{KH}_2\text{PO}_4$ , photon emission during uniaxial deform., Curie temp. 4-81028  
 La, superconducting transition temp. under high press., vol. depend. 4-84728  
 $\text{La}_2\text{Ga}$ , amorphous, superconductivity obs. (*Chinese*) 4-104338

## high-pressure effects in solids continued

- $\text{Li}_{16-2x}\text{Zn}_x(\text{GeO}_4)_8$ , LISICON, and  $\text{Li}_{3+x}\text{Ge}_2\text{V}_{1-x}\text{O}_4$ , solid electrolyte prep. props. and appl. 4-103998  
 $\text{MgO}$ , static P-T-V meas. and shock wave data 4-108574  
 $\text{Mg}_2\text{SiO}_4$ , elasticity at Earth mantle pressures, Brillouin spectra study 4-100558  
 MnAs, mag. struct. under high press., powder neutron diff. study 4-108988  
 NaCl, eqn. of state used for secondary calibration scale at low temp. 4-103897  
 Ne, FCC, high press. eqn. of state, Gaussian orbital techniques 4-92332  
 Ne, low temp. eqn. of state under megabar press. 4-61042  
 Ni, Curie point at ultrahigh press. 4-88676  
 Ni-Cu, Cu diffusion after dynamic and static deformation (*Russian*) 4-108658  
 Ni-Ti, forced vol. magnetostriction, press. coeffs. 4-88711  
 Ni-V, forced vol. magnetostriction, press. coeffs. 4-88711  
 PZT, dielec. props. at high press., p-T phase diagrams 4-99062  
 $\text{PbCl}_2$ , Raman-active modes, anharmonic effects 4-71381  
 $\text{PbMo}_6\text{S}_8$ , divalent Chevrel-phase supercond., effect of press. and defects 4-80711  
 Pr, band structure, Fermi surface and supercond. under high press. 4-98511  
 $\beta$ - $\text{PtO}_2$ , new high-pressure form 4-70081  
 $\text{Rh}_2\text{Ru}_{1-x}\text{O}_2$ , high press. distortion, cryst. struct. study 4-80012  
 Sc, elastic props. under static compression up to 6 GPa (*Russian*) 4-108515  
 $\text{Se}_{1-x}\text{Te}_x$  glasses, electronic cond. at high press. and low temp. 4-10419  
 Si, elastic props., ultrasonic meas. 4-98170  
 Si, superconductivity at high press. 4-98803  
 $\text{SiO}_2$ , properties of high-pressure fluorite struct. phase 4-110135  
 Sm, electronic struct., press induced 4f occupancy enhancement 4-75844  
 $\text{SmbB}_6$ , compound with intermediate valency, correl. gap, press. effect 4-70882  
 $\text{SmbB}_6$ , galvanomagnetic props., press. effect 4-70840  
 $\text{SmbB}_6$ , defect single crystals, galvanomagnetic props., press. effect 4-70840  
 $\text{SmBi}_2$ , intermediate valence cpds., press.-vol. relationship 4-80554  
 $\text{SnMo}_6\text{S}_8$ , divalent Chevrel-phase supercond., effect of press. and defects 4-80711  
 Ta, shocked, rarefaction velocities and high press. melting point 4-109424  
 $\text{TiO}_2$ , n-type photoanode, dye-sensitized photocurrent spectrum, high press. studies 4-98666  
 $\text{Ti}_2\text{Ru}_{1-x}\text{O}_2$ , high press. distortion, cryst. struct. study 4-80012  
 $\text{TiS}_2$ , semicond.-semimetal transition at 40 kbar 4-84660  
 TmSe, intermediate valence cpds., press.-vol. relationship 4-80554  
 U, equation of state, self-consistent muffin-tin orbital calc. 4-108575  
 V, Hugoniot meas. using LNL two stage light gas gun 4-108577  
 V-H, normal and deuterated, shock compression to 135 GPa 4-92295  
 WC-Co, cemented elements of high press. apparatus, strength safety factors 4-109482  
 Xe, solid, high press. X-ray diff. study and eqn. of state, rel. to metallisation transition 4-92333  
 Yb, electronic struct., press induced 4f occupancy enhancement 4-75844  
 $\text{YbH}_2$ , equation of state and high press. X-ray diff. studies 4-75665  
 $\text{YbO}$ , intermediate valence cpds., press.-vol. relationship 4-80554  
 ZnO oriented crystal, crystal violet dye adsorpt., press. effect 4-98442

## high-pressure phenomena and effects

see also high-pressure effects in solids

- acetone, aq. solution, vapour-liquid equilibrium at 101.325 kPa 4-11359  
 alcohol-water mixtures, density and viscosity, press. depend. (*Japanese*) 4-98327  
 benzene, US vels., density, high press. (*Japanese*) 4-98203  
 benzene liq., C-C bond length, high press. compressibility study 4-65323  
 9,9'-bianthryl, intramolecular electron transfer, solvent effects, fluorescence study 4-96598  
 9,9'-bianthryl, viscous solvents, intramolecular electron transfer luminescence study 4-80977  
 charcoal, activated, adsorpt. from binary solns. at high press. 4-104070  
 charcoal, activated, organic liq. adsorpt. at high press. interfacial phase props. 4-104069  
 chemical equilibrium, thermodynamics at high pressures 4-81453  
 chlorobenzene+nitrobenzene, US speed under high pressure 4-98201  
 cholesterol N-alkanoates, ternary system press. induced reentrant cholesteric phase 4-98002  
 convection with press. and temp. dependent non-Newtonian rheology 4-67203  
 crustaceans, bubble form. following decompression from hyperbaric exposures 4-93784  
 diamond formation in presence of Ni, high press. and temp., rel. to starting C crystallinity 4-66256  
 dibromomethane, molecular solid, pressure tuning resonance 4-113552  
 2,2-dimethylpropane, melting and self-diffusion, press. depend. 4-108589  
 2,2-dimethylpropionitrile, melting and self-diffusion, press. depend. 4-108589  
 dimyristoyl phosphatidylcholine-water system, phase transitions, high press. study 4-113624  
 ethylene, high press. polymerisation, IR and near IR region spectroscopy 4-71917  
 fluidisation, 3D and 2D beds, high-pressure, high-speed photographs, bubbling behaviour 4-65018  
 ice X, high press. form occurring at 44 GPa, Brillouin scatt. 4-61057  
 liquid, breakdown under high hydrostatic press., electroexplosive action (*Russian*) 4-71273  
 liquid crystalline transitions, high pressure studies 4-88288  
 2-methylpropan-2-ol-d $_2$ , melting and self-diffusion, press. depend. 4-108589  
 nematic liquid crystals, high pressure props., perturbation theory for axially symmetric mols. 4-92084  
 oceanic lithosphere, convective stability with temp. and press. dependence, viscosity 4-105492  
 PET, crystallisation, struct. and props. 4-103666  
 polyethylene, high density, high press. injection molded, birefringence 70.5 microns, tensile modulus, press. depend. 4-61655  
 polyphenylmethyl siloxane, relax. processes, polarised photon correlation spectra under high press. 4-104624  
 pressure loads, displacement dependent, nonlinear finite element analysis 4-91742

**high-pressure phenomena and effects continued**

- quasi-isentropic compression wave generation method 4-108539  
 rare earth alloys,  $R_4Cu_{23}$ , high pressure crystn. 4-75369  
 steam, high press. high temp., convection-radiation interaction 4-74018  
 TBAA liquid crystals, phase behaviour at high press., DTA studies 4-98282  
 tetramethoxysilicon sol-gel process, polymerisation kinetics, press. effects 4-114465  
 $(TMTSF)_2FSO_3$ , diamagnetism and superconductivity 4-98855  
 toluene, US vels., density, high press. (*Japanese*) 4-98203  
 Al, P-V-T relation as press. and temp. scale under very high press. 4-75637  
 Cs melting curve, high pressure calcs. 4-113583  
 Fe, cast, Mg treated, graphite nodularisation and graphitisation during solidification under 145 atm. Ar pressure 4-66325  
 Fe-graphite system, carbide form. high press. and temp., mag. props. 4-99371  
 $Fe_9S$  (pyrrhotite), eqn. of state at Earth core conditions 4-115395  
 Ga-N<sub>2</sub> system, high pressure thermodynamics, heat and entropy of GaN form. 4-62227  
 GaN, crystals, high pressure soln. growth, equilib. N<sub>2</sub> press. over Ga-GaN mixtures 4-61822  
 H, metallic, ground state energy in Wigner-Seitz approx. 4-80469  
 KSO<sub>4</sub> ion pairs, dissociation in water at 25°C, press. effect (*Japanese*) 4-103985  
 melting curve, high pressure calcs. 4-113583  
 Mg, molten, melting and self-diffusion coeffs., pressure effects (*Russian*) 4-103908  
 Na melting curve, high pressure calcs. 4-113583  
 Os-Sn, intermediate phases, effects of high pressure on crystn. 4-75366  
 Rb melting curve, high pressure calcs. 4-113583  
 Si, defects and high press. steam oxidation, stacking faults 4-114706  
 Zn, molten, melting and self-diffusion coeffs., pressure effects (*Russian*) 4-103908  
 Zn, tensile deformation testing with a high press. apparatus (*Japanese*) 4-62147

**high-pressure solid-state phase transformations**

- Al-Al<sub>2</sub>O<sub>3</sub>-H<sub>2</sub>O, two high-pressure Al(OH)<sub>3</sub> phases 4-85141  
 binary cryst., displacement domains caused by defects (*Chinese*) 4-70254  
 t-butylchloride, dielec. permittivity and pVT data 4-84898  
 calcite single cryst., elasticity at calcite I-calcite II transition 4-105549  
 cholesterol 1,2,3,3-tetrafluoropropanate, dielec. props. under hydrostatic press., commensurate-incommensurate transition obs. 4-80853  
 diamond dispersed alumina composite, very high press. sintered, fracture toughness, phase transform. 4-99372  
 dicalcium lead propionate, ferroelec. press. induced II-III transition, polarising microscope obs., permitt. meas. 4-80879  
 dicalcium strontium propionate, ferroelec. press. induced II-III transition, polarising microscope obs., permitt. meas. 4-80879  
 dynamic material response to shock wave propagation 4-108531  
 elements, FCC or HCP to BCC transitions, at high press. interatomic distance contraction 4-80215  
 $\alpha$ -KCr(SO<sub>4</sub>)<sub>2</sub>·12H<sub>2</sub>O alum, high pressure mag. resonance study of crystal fields 4-70757  
 melting, solid-solid transitions at high pressures 4-80195  
 methane, solid, high press. transitions 4-88281  
 polyethylene, high press. high temp. transition to amorphous phase 4-84381  
 polymorphic transformations, pressure-induced, kinetics data 4-88275  
 PTFE, eqn. of state up to 80 GPa, phase change, shock-recovery expts. 4-75615  
 quartz, fused, shock loading behaviour 4-108530  
 steel, type Kh17N8, phase transitions during deform. press. effect (*Russian*) 4-81188  
 tetrahedrally bonded cpds., press. induced phase transition to NaCl-phase 4-61073  
 TGSe, cryst., dielec. and electromechanical props. under high hydrostatic press. 4-76296  
 transformations due to shock loading, temp. and deform. 4-113611  
 triglycine fluoroberyllate, cryst., dielec. and electromechanical props. under high hydrostatic press. 4-76296  
 X-ray absorpt. near edge struct. spectra 4-66119  
 Al, crystallographic transitions and equilib. props., Gaussian-orbitals calcs. 4-92353  
 Al, P-V-T relation as press. and temp. scale under very high press. 4-75637  
 Al<sub>2</sub>O<sub>3</sub>-ZrO<sub>2</sub> ceramics, high press. sintered, fracture toughness rel. to phase transform. 4-76839  
 AlP(As)(Sb), high-pressure phase transition 4-88283  
 BaMnF<sub>4</sub>, incommensurate phase, neutron scatt. study, press. effect 4-75654  
 BaTe, band-overlap metallisation, energy-dispersive X-ray diffr. 4-98526  
 Be, high pressure phase transition, elec. resist. study 4-75663  
 Be, temp. and press. induced phase transitions 4-70369  
 C, BC-8 crystal phase, struct. props., phase stability and phase transistors 4-113389  
 C, polymorphic transitions at high press. and temps. 4-113380  
 CdCl<sub>2</sub>, CdBr<sub>2</sub>, CdI<sub>2</sub>, melting, solid-solid transitions at high pressures 4-80195  
 Co-C, hypereutectic alloy, diamond form. at high press. 4-109374  
 Co<sub>80</sub>B<sub>20</sub>, amorphous, high press. and temp. phase stability (*Chinese*) 4-103923  
 Co<sub>2</sub>Ni<sub>1-x</sub>MnGe, magnetic transforms., effect of external press. 4-104418  
 Cs, struct. above s-d transition, LMTO calc. 4-75669  
 CsBr, press. induced struct. transition 4-113607  
 CsCuCl<sub>3</sub>, Jahn-Teller induced phase transition, hydrostatic press. effects 4-65392  
 CsI, press. induced struct. transition 4-113607  
 Cu halides, superionic, phase transition and soft mode behaviour 4-92330  
 Fe, BCC-HCP transition, neutron diffr. expts. using diamond anvils at ultrahigh pressures 4-88038  
 Fe<sub>2</sub>P, metamagnetic transitions, PT diagram studies 4-114111  
 GaP, phase transformations at ultrahigh press., X-ray diffr. obs. 4-98273  
 Ge, high-pressure structural phase transitions and cryst. struct. 4-92350  
 GeSe<sub>3</sub> glass, bulk, press. induced electronic and structural transformations 4-114004  
 Ge<sub>20</sub>Te<sub>80</sub> glass, bulk, elec. transport and high press. studies 4-114003  
 He adsorbed on Grafoil, multilayer growth 4-104033  
 Hg(CN)<sub>2</sub>, stretching vibr. band, press. induced splitting in Raman spectra 4-88819

**high-pressure solid-state phase transformations continued**

- Hg<sub>2</sub>Ga<sub>2</sub>□Te<sub>6</sub>, Hg<sub>3</sub>Ga<sub>2</sub>□Te<sub>6</sub>, elec. resistivity meas. 4-80497  
 Hg<sub>2</sub>, phase relations, red-yellow transition <0.7 GPa, DTA obs. 4-113603  
 HgIn<sub>2</sub>□Te<sub>4</sub>, elec. resistivity meas. 4-80497  
 K, struct. above s-d transition, LMTO calc. 4-75669  
 $\alpha$ -KAl(SO<sub>4</sub>)<sub>2</sub>·12H<sub>2</sub>O alum, high pressure mag. resonance study of crystal fields 4-70757  
 KH<sub>2</sub>PO<sub>4</sub>, US study near press. induced tricritical point 4-76386  
 KTa<sub>1-x</sub>Nb<sub>x</sub>O<sub>3</sub>, glasslike behaviour and press. effects 4-99058  
 LiKSO<sub>4</sub>, press. effect on phase transitions 4-104546  
 N<sub>2</sub>, solid, press. induced struct. phase transitions and internal mode freq. 4-108610  
 $\alpha$ -NH<sub>4</sub>Al(SO<sub>4</sub>)<sub>2</sub>·12H<sub>2</sub>O alum, high pressure mag. resonance study of crystal fields 4-70757  
 $\alpha$ -NH<sub>4</sub>Cr(SO<sub>4</sub>)<sub>2</sub>·12H<sub>2</sub>O alum, high pressure mag. resonance study of crystal fields 4-70757  
 Na<sub>2</sub>WO<sub>3</sub>, compressibilities and high-pressure phase transitions 4-88276  
 $\alpha$ -O<sub>2</sub>, solid, high press. props. 4-61066  
 PZT, dielec. props. at high press., p-T phase diagrams 4-99062  
 PbCl<sub>2</sub>, PbBr<sub>2</sub>, melting, solid-solid transitions at high pressures 4-80195  
 Pb<sub>1-x</sub>Ge<sub>x</sub>Te, ferroelec. phase transition, high press. investigation, DC resist., capacitance meas. 4-71312  
 PbZrO<sub>3</sub>, with vacancies, para, ferro and antiferroelectric phase transitions, influence of hydrostatic press. 4-76390  
 Rb, struct. above s-d transition, LMTO calc. 4-75669  
 RbAg<sub>5</sub>I<sub>3</sub>, high press. superionic phase, NMR study 4-111164  
 ReO<sub>3</sub>, struct. above 'compressibility collapse' transition 4-70099  
 Sb, phase transitions at hydrostatic press. up to 9 GPa 4-75666  
 Si, BC-8 crystal phase, struct. props., phase stability and phase transistors 4-113389  
 Si, high pressure phase transitions, X-ray diffr. study 4-98272  
 Si, high-pressure structural phase transitions and cryst. struct. 4-92350  
 SiO<sub>2</sub>, properties of high-pressure fluorite struct. phase 4-110135  
 Sm<sub>1-x</sub>Gd<sub>x</sub>S solid soln. single crystals, phase transition during uniaxial compression, elec. cond. and colour change obs. 4-70375  
 SmS thin film phase transition material, optical switching, CVD fabrication 4-112538  
 Sn, semiconductor-metal transition under press. 4-113871  
 Sn-Ge dilute alloys, semiconductor-metal transition under press. 4-113871  
 Sn<sub>2</sub>P<sub>2</sub>S<sub>6</sub>, influence of hydrostatic pressure on vibrational spectra 4-109192  
 SrBr<sub>2</sub>, melting, solid-solid transitions at high pressures 4-80195  
 2H-TaSe<sub>2</sub>, CDW phase transition at low temp. and high press. 4-104276  
 ThS, high press. transitions and bulk modulus, X-ray diffr. study 4-70371  
 Ti<sub>8</sub>Si<sub>20</sub>, amorphous, crystallisation study (*Chinese*) 4-103922  
 U<sub>3</sub>, high press. bulk modulus and phase transitions, X-ray diffr. studies 4-70370  
 Yb, pressure-volume relations up to 9 GPa, FCC-BCC transition obs. 4-103925  
 ZrO<sub>2</sub>, high pressure phase transitions, microscopic obs. (*Japanese*) 4-101865  
 ZrO<sub>2</sub>, powder under shock compression, phase transformation 4-108611  
 ZrO<sub>2</sub>, shock modified, energy release and phase transform. 4-108612

**high-pressure techniques**

- AC calorimetric technique for specific heat of solids meas. 4-86423  
 Bridgman-anvil press., chambers, press. meas., fibre optic imaging 4-90609  
 bulkhead strain-gauge cable penetration, pressure vessels appl. 4-63759  
 chamber with transparent BeO anvils for Earth mantle studies 4-110291  
 cryogenic liquids, calorific props. meas. at low temps. and high press. 4-95428  
 diamond anvil pressure cell, lever-arm type, and laser micro-optic system for press. meas. (*Japanese*) 4-101865  
 diamond-anvil cell, optical length determ. 4-68237  
 diamond-anvil high-pressure cell 4-86438  
 energy dispersive X-ray diffr. expts., high press., synchrotron beam heating effects 4-101995  
 energy-dispersive X-ray diffraction with synchrotron radiation at cryogenic temperatures 4-103608  
 EPR meas. of aqueous samples, biomolecules dynamics exam. appl. 4-86458  
 gaseous uptake meas. for organic polymers, quantitative method at high press. 4-86437  
 high press. jet vacuum pumps theory, simulation and design 4-58861  
 IR spectroscopic cell for FTIR meas. at press. up to 100 MPa 4-86491  
 isotope enrichment by high press. ion exchange displacement chromatography 4-59905  
 leak detection, common problems and solutions 4-90597  
 MASS OB-8 mechanism of pressure-generating system 4-78341  
 microprocessor-controlled remote data acquisition unit for hyperbaric environment 4-109985  
 neutron diffr. expts. using diamond anvils at ultrahigh pressures 4-88038  
 NMR probe head for low temp., RbAg<sub>5</sub>I<sub>3</sub> superionic conductor phase study appls. 4-111164  
 optical window based on light guides for a pressure chamber 4-101868  
 piston sealing in a high-pressure apparatus 4-90608  
 polarization scrambling by the glass windows of a Raman cell up to 18 kbar 4-112187  
 pressure generation, multiple-anvil sliding system, with X-ray diffraction 4-82804  
 sealed silica pressure ampoules for crystal growth 4-88955  
 shear strength measurement, to 500°C 4-81376  
 stress analysis of a beveled diamond anvil 4-101869  
 thermal conductivity, apparent, lattice and radiative, 300-1500K, up to 5.6 GPa 4-78322  
 toroidal high-pressure devices with combined pistons, development 4-101867  
 two stage nonmagnetic high press. equipment for studying transport phenomena (*Chinese*) 4-90607  
 up-down toroid device for high press. generation 4-101866  
 vapour-liquid equilibria and saturated densities determ., hydrocarbon-CO<sub>2</sub> mixture meas. appl. 4-103916  
 vapour-liquid equilibrium measurement, high pressure-high temp. chromatographic apparatus 4-70355  
 CO<sub>2</sub> electrochemical sensor for high ambient pressures, deep diving appls. 4-106311  
 H<sub>2</sub> gas, pressurised, storage and transport, safety (*German*) 4-109754

**high-pressure techniques continued**

- $\text{Si}_3\text{N}_4$ , dense compact, gas phase sintering process 4-76730  
 $\text{Si}_3\text{N}_4$ , reaction bonded, sintered, densification kinetics, microstruct. 4-76726  
 Zn, tensile deformation testing with a high press. apparatus (*Japanese*) 4-62147

**high speed steel** *see tool steel***high spin states (nuclear)** *see nuclear collective states and giant resonances***high-temperature phenomena and effects**

- see also refractories*  
 convection with press. and temp. dependent non-Newtonian rheology 4-67203  
 glass, molten, thermal conductivity, high temp., theoretical anal. of experiments 4-84471  
 Harper-Dorn creep, artifact of low-amplitude temp. cycling 4-94089  
 Inconel sheathed Nicrosil, thermocouples, failure mode, SIMS anal. 4-111125  
 limit concept to high temperature design 4-97352  
 low expansion glass mirrors, effect of thermal cycling on dimensional stability, film coating operations 4-112547  
 materials behaviour at high temperatures 4-99473  
 mechanical behaviour of materials, conf., Stockholm, Sweden (Aug. 1983) 4-90297  
 metals, FCC, high temp. plasticity, anal. of expt. data 4-98186  
 metals, FCC, high temp. plasticity, theoretical models 4-98185  
 Nicrosil, stainless steel sheathed, failure mode, SIMS anal. 4-111125  
 Nisil, Inconel sheathed, thermocouples, failure mode, SIMS anal. 4-111125  
 Nisil, stainless steel sheathed, thermocouples, failure mode, SIMS anal. 4-111125  
 noble metals, Hugoniot curve calc., by pseudopotential method 4-80188  
 nonstoichiometric compounds, transport processes, conf., Cracow, Poland (Aug. 1980) 4-95060  
 oceanic lithosphere, convective stability with temp. and press. dependent viscosity 4-105492  
 oxides, deviation from stoichiometry, control and meas. 4-98078  
 oxides, non-stoichiometry at high temp., thermal emission of electrons 4-99273  
 oxides, surface props. at high temps., work function studies 4-98697  
 piezoceramics, high temp. effects on props. 4-99038  
 polymer composites, thermal cond. meas. to high temp. using line-source technique 4-108668  
 quartz, hardness properties influenced by high-temp. and impurities 4-94107  
 seawater, critical point and two-phase boundary, 200 to 500°C 4-67219  
 semiconductors, high temp. plasticity, anal. of expt. data 4-98186  
 semiconductors, high temp. plasticity, theoretical models 4-98185  
 steam, high press. high temp., convection-radiation interaction 4-74018  
 steel, creep damage and embrittlement at high temp., US meas. (*French*) 4-61973  
 steels, austenitic stainless, 316 and 253MA, high temp. low cycle fatigue, comparison between mech. props. and microstruct. 4-93410  
 steels, high temp. behaviour, simulation of welding and quenching processes 4-99412  
 surface characterisation techniques 4-99927  
 welded joints, high temp. deform. and failure 4-93409  
 $\text{BaO}$ , enthalpy and specific heat in high temp. region 1200 to 2200K 4-113672  
 Be, temp. and press. induced phase transitions 4-70369  
 C material, dimensional changes, under compressive stress at high temp. 4-85182  
 C, polymorphic transitions at high press. and temps. 4-113380  
 $\text{CuGaSe}_2$ , thermal expansion, 301-958K 4-80266  
 $\beta\text{-CuZn}$ , single crystal, yield point phenomenon, high temp. 4-113521  
 Fe-graphite system, carbide form. high press. and temp., mag. props. 4-99371  
 Fe-O, work function, determination of phase transitions 4-98698  
 $\text{H}_2\text{O}$  vapour, high temp. and press., CARS spectra rot. diffusion model appl. 4-69085  
 LiF, transparent melts, thermal conductivity 4-113732  
 NaCl, transparent melts, thermal conductivity 4-113732  
 Ni-Al, internal oxidation, O transport at high temps. 4-92442  
 Ni-Cr, internal oxidation, O transport at high temps. 4-92442  
 Ni-Nb-NbC, eutectic alloys, powder metallurgy, physical props., high temp. use 4-85125  
 $\text{Ni}_3\text{Cr}$ ,  $\text{Ni}_3\text{Cr}$ , high temp. deform., effect of ordering 4-93358  
 $\text{R}_2\text{CoO}_3$ ,  $\text{R}_2\text{CoO}_3$ , synthesis and high-temperature study (*French*) 4-85095  
 $\text{UO}_2$ , high temp. thermolec. power studies 4-104244  
 $\text{UO}_2$ , O Frenkel disorder obs., neutron scatt. study 4-60917  
 W, AKS-doped wire, high-temp. creep behaviour, effect of gas bubbles (*German*) 4-81243  
 W-O, work function, determination of phase transitions 4-98698

**high-temperature techniques**

- see also pyrometers; refractories*  
 AC high-stability microprocessor-based temperature controller for use at high temperatures 4-111119  
 conductivity measurement, elec. and thermal, of W, 300-1300K (*German*) 4-80564  
 cyclic-loading stage for SEM 4-78422  
 electrical conductivity test method 4-86440  
 gas-cooled reactor development in Japan, process heat appl. 4-74038  
 light-guide pyrometer for monitoring high temperatures 4-58857  
 materials testing, high temp. inverse heat cond. problem investig. 4-99684  
 molten liquids, density measurement, high temp. techniques 4-95389  
 resonance cell for laser spectroscopy, on low vapour pressure elements 4-102648  
 sealing using elastic metallic joints 4-95447  
 shear strength measurement, to 500°C 4-81376  
 solidification point determ. by specular reflection and centrifugal methods (*Japanese*) 4-76770  
 spectral ratio peak intensity meter, appl. of A/D linear colour-temp./freq. converter (*Russian*) 4-101847  
 spectral ratio peak intensity meter converter, transformation function table dimension reduction (*Russian*) 4-101846  
 thermal conductivity, apparent, lattice and radiative, 300-1500K, up to 5.6 GPa 4-78322  
 thermocouple, calibration, freezing point determ. of Pd 4-80196

**high-temperature techniques continued**

- vapour-liquid equilibrium measurement, high pressure-high temp. chromatographic apparatus 4-70355  
 VUV spectrometers, high temp. 4-82835  
 $\alpha\text{-Al}_2\text{O}_3$ , high-temperature thermal expansion standard, neutron diff. meas. 4-103972  
 GaAs, photoacoustic signal meas. by laser heterodyne at high temps. 4-106388  
 $\text{Si}_3\text{N}_4$ , dense compact, gas phase sintering process 4-76730  
 $\text{Si}_3\text{N}_4$ , reaction bonded, sintered, densification kinetics, microstruct. 4-76726  
**high vacuum gauges** *see vacuum gauges*  
**high-voltage engineering**  
*see also high-voltage techniques*  
 electrohydrodynamic behaviour of viscous dielectric fluid and current response to voltage changes 4-97702  
 flashover model for HV generator breakdown (*French*) 4-65949  
 laser triggered spark-gap mechanism in HV switching 4-79869  
 solid laser pumping, HV pulse generator, 20 kV, design and operation (*Bulgarian*) 4-87352

**high-voltage techniques**

- HV pulse generator for subnanosecond electron accelerators 4-59593  
 laboratory, EMI investigation 4-106165  
 liquid flow study of HV electrohydrodynamic generator 4-97705  
 porcelain, high-alumina, for HV insulators, strength under dynamic and cyclic loads (*German, English*) 4-76836

**hip joint replacements** *see prosthetics***history**

- American Vacuum Society, history 4-78089  
 atomic clocks, at. and mol. time and freq. standards 4-63470  
 atomic frequency standards, history 4-68200  
 bertrand Russell and the foundations of physics 4-110848  
 boundary layers flow noises, review (*Chinese*) 4-95123  
 cardiac arrhythmias, computer detect., historical review 4-89807  
 clouds merging, historical perspective 4-67297  
 colour metrics, historical survey 4-110846  
 crystallography in North America 4-67951  
 Einstein's first paper 4-82639  
 electrical and electronic phenomena and devices, book 4-67952  
 electron microscopy, historical developments 4-95124  
 engineering mechanics, advances and instruction in France 1800-30 4-63468  
 Euler's foundation of continuum mechanics (*German*) 4-110847  
 fossil fuel industries and energy policy, 1973-83 4-77050  
 Fourier transform spectroscopy, early history 4-101615  
 Galilean satellite eclipses (1652-1982), manuscripts anal. 4-90109  
 hearing aids from the pre-electronic era, performance 4-62628  
 Hippolyte Fizeau and the movement of the Earth: a tentative misunderstanding (*French*) 4-110844  
 Humboldt's magnetic Verein (1829-34) and his Russian journey (1829-34) (*German*) 4-63467  
 intelligence constant for scientific research effort and achievement comparison 4-67955  
 Io, eclipse observations collected by Delambre (1775 to 1802) 4-101229  
 Keplero preceded by Maurolico's optics? (*Italian*) 4-78088  
 magnetic mirror fusion reactor, history of evolution 4-86168  
 mathematics, history, international studies approach 4-101616  
 medicine, the early ECG 4-115250  
 metallurgy, physical, historical development, book contrib. 4-110849  
 metals, nonmetals and metal-nonmetal transitions, historical review 4-101614  
 Moll, Gerrit, electromag. expts. 4-63466  
 native American astronomy 4-94653  
 nineteenth century physics development, book 4-95077  
 NPL, a brief history 4-90342  
 optical fibre research, present state and future problems 4-103021  
 Orion Nebula, historical evidence for recent brightening 4-63249  
 physics towards absolute zero (*French*) 4-90343  
 plasma diagnostics, millimeter wave, 1958-83 4-73204  
 quantitative electron probe microanalysis 4-63471  
 Raman scattering discovery 4-86169  
 semiconductor band structure calculations in 1950s, effect on science 4-92597  
 sidescan sonar, review, history and appls. 4-69616  
 soliton history 4-95125  
 sound film, development (*German*) 4-82838  
 sunburn, annotated bibliography, historical development 4-58608  
 superconductivity, history, methodological aspects, 1911-57 4-110845  
 surface science, historical review 4-78093  
 Tambora, 1815 April eruption, reconstruction and analysis 4-110115  
 University of Maryland computer vision research, 20-year retrospective study 4-107543  
 vacuum applications, from Aristotle to Langmuir 4-78090  
 vacuum pressure measurement, historical review 4-78335  
 vacuum pumps, history 4-78091  
 vacuum systems, valves, connectors and traps, development during 20th century 4-78092  
 valency, electronic theory, 1916-1983, role of quantum mechanics (*French*) 4-63469  
 Vienna school of statistical thought, history 4-58614  
 wave mechanics, ghost fields and matter waves, historical perspective (*German*) 4-67950
- HIXE** *see ion microprobe analysis; X-ray chemical analysis*  
**HMO calculations**  
 alternant hydrocarbons, Huckel rule 4-74158  
 conjugated macrocyclic ligands, closed-shell cryst. orbital calcs. on columnar stacks 4-74160  
 ethane-like fragments, 1,2-disubstituted, NMR spin-spin coupling consts. extended HMO calc. 4-112199  
 Gaussian Huckel model, nonlinear eqns. 4-91198  
 hydrocarbon systems, momentum distribution of Huckel  $\pi$  electrons 4-74159  
 nickelocenium cation, electronic struct., Jahn-Teller effect, EPR study 4-64517  
 polyacenes, charge stripping mass spectrometry of mol. ions and HMO theory 4-96673  
 trans-polyacetylene, electronic struct. studied by transfer matrix technique localised state 4-87243  
 polymers, conjugated, electronic struct., extended Huckel cryst. orbital scheme calc. 4-65604

## MO calculations continued

- torsional vibr., internal rot., Huckel-Mobius concept appl. 4-64382  
 Fe, BCC, local densities of states, work functions and surface stabilities 4-88443  
 Ge<sub>2</sub>H<sub>4</sub>, charge iterative relativistic extended Huckel theory and its appl. 4-59643  
 H<sub>2</sub>, linear, Hartree-Fock eqns., numerical solns. 4-74142  
 Mo, BCC, local densities of states, work functions and surface stabilities 4-88443  
 Pb<sub>2</sub>H<sub>4</sub>, charge iterative relativistic extended Huckel theory and its appl. 4-59643  
 Sn<sub>2</sub>H<sub>4</sub>, charge iterative relativistic extended Huckel theory and its appl. 4-59643  
 W, BCC, local densities of states, work functions and surface stabilities 4-88443

O<sup>+</sup> see hydroxonium ion

## obby computing see personal computing

## odoscopes see cosmic ray apparatus

## ole mobility see carrier mobility

## ole theory of liquids see liquid theory

## ole traps

## see also electron traps

- alkali silicate glass, EPR of trapped hole centres 4-76237  
 amorphous semiconductors, transient photocond., effect of repeated carrier trapping 4-61420  
 chalcogenide glass thin films, threshold switching and trap filling 4-92770  
 coronene layers, elec. cond. and trap distrib. 4-84626  
 depletion regions, carrier capture from free-carrier tails 4-92746  
 disordered materials, transient photoconductivity due to step-function excitation 4-88536  
 disordered solids, with continuous trap distrib., dispersive carrier transport 4-108874  
 dosimeters, solid-state, ionising energy storage, rel. to trapping levels 4-68838  
 ethylene propylene fluorinated copolymer, positive charge stabilisation 4-65688  
 inert gas solids, self-trapped holes calcs. 4-84582  
 n-InSb, photoconductivity and hole trapping centre capture coeff., press. studies 4-98668  
 LDPE, trapping parameters rel. to morphology, TSC meas. 4-108877  
 MIS, tunnel capacitor, leakage current effects on DLTS 4-70938  
 MOS capacitors, field controlled charge trapping in tunnel oxides 4-70939  
 organic/inorganic semicond. contact barrier diodes, I-V characts. 4-92810  
 pentacene, electron and hole traps, thermally stimulated current techniques, quadrupolar traps 4-61391  
 pentacene layers, dispersive charge carrier transport 4-80703  
 poly-N-epoxypropylcarbazole electrophotographic layers, photodischarge kinetics 4-112541  
 poly-N-epoxypropylcarbazole, sensitised by dyes and pyrylium salts 4-112542  
 poly-N-epoxypropylcarbazole, sensitized, photosensitivity, low mol. cpds., effects 4-113999  
 RF sputter-deposited Schottky barrier diodes 4-98691  
 semiconductor surface, rate of capture of minority carriers 4-92754  
 semiconductors, free carrier capture kinetics by deep traps 4-80536  
 semiconductors, grain-boundary admittance theory 4-108849  
 semiconductors, nonradiative multiphonon capture of carriers by deep traps 4-75889  
 semiconductors, persistent photocond. and charge carrier capture cross sections 4-80608  
 Ag halide microcrystals, spectroscopic identification of localised electrons and holes 4-114308  
 Al-SiO<sub>2</sub>-Si struct., X-ray irradi., interface traps. 4-104281  
 AlGaAs GaAs modulation doped heterostr., persistent photocond. studies 4-98705  
 Al<sub>0.5</sub>Ga<sub>0.5</sub>As, correlation of photoluminescence and deep trapping 4-80537  
 Al<sub>0.5</sub>Ga<sub>0.5</sub>As p-n junctions, organometallic VPE, anomalous light sensitivity 4-92817  
 Al<sub>2</sub>O<sub>3</sub>-Co, thermoluminescence and trap parameters 4-76532  
 Bi<sub>2</sub>GeO<sub>20</sub>, field and charge distrib. in case of trap thermal ionisation 4-66010  
 GaAs, amorphous, high-defect-density, subpicosecond carrier trapping 4-80621  
 GaAs, impurity photocurrent and deep level spectroscopy 4-70865  
 GaAs, scanning DLTS investig. 4-75892  
 GaAs:Si, ion implanted, and semi-insulating GaAs, deep levels, photoconductivity study 4-88469  
 GaAs:Sn/GaAs:Cr interface, electron and hole traps, photovoltaic studies 4-104283  
 GaP, scanning DLTS investig. 4-75892  
 p-GaSe, space charge limited current behaviour 4-80597  
 GaSe:Co, injection and thermodepolarisation currents 4-70833  
 Ge, gamma-irradiated, hole traps 4-103799  
 Ge, neutron transmutation doped, annealing, DLTS study 4-60942  
 Ge:Cu, quenched in deep acceptors 4-70713  
 Ge:Cu(Au), nonradiative multiphonon capture of carriers by deep traps 4-75889  
 GeS film, crystalline and amorphous, photoconductivity study (Russian) 4-70870  
 InP, electron irradi. induced deep traps, deep level optical spectroscopy 4-104156  
 InP-Si, electron irradi.-induced deep traps, impurity conc. effects 4-88468  
 InP-Zn, grown-in defects, annealing effects, DLTS studies 4-84287  
 MgO phosphor, thermolum., and trapping kinetics 4-88887  
 PbI<sub>2</sub>, thermally stimulated currents at low elec. fields 4-65689  
 Pb<sub>1-x</sub>Sn<sub>x</sub>Te, defect states, impurity photoconductivity transient studies 4-80545  
 Pt-SiO<sub>2</sub>-Si MIS struct., flat-band voltage shift 4-108944  
 SC<sub>2</sub>O<sub>3</sub>, ODMR study of exciton trapping 4-80503  
 Se:Te, As glassy films, pure and doped, deep level defects, xerographic spectra studies 4-61339  
 Si, amorphous, high-defect-density, subpicosecond carrier trapping 4-80621  
 Si, amorphous CVD films, H<sub>2</sub> plasma annealing localized state density 4-61337  
 Si film, LPCVD, elec. props., effect of film thickness 4-88615

## hole traps continued

- Si, gamma-irradiated, carrier recombination, dislocation effects 4-75982  
 Si,  $\gamma$ -ray irradi., trapping centres, DLTS studies 4-104147  
 Si, ion implanted, laser or electron beam annealing, electronically active defects, DLTS 4-80527  
 Si, point defects due to laser annealing, DLTS study (Chinese) 4-84584  
 a-Si:H, long-time drift mobility, photocurrent study 4-104221  
 a-Si:H, radiative combination at dangling bonds, quantitative model, expt. study 4-114326  
 a-Si:H, transient photoinduced absorpt. 4-104634  
 a-Si:H,N film, TSC and photoconductivity 4-104222  
 a-Si:H film, IR quenching of photoluminescence and photoconductivity 4-104656  
 a-Si:H Schottky diodes and nin devices, single and double carrier injection 4-114015  
 Si:Mn, Cu, impurity energy levels, DLTS and capacitance studies 4-88471  
 Si:Ti, recombination props., capture rates 4-104149  
 Si-SiO<sub>2</sub>, interface traps in diode struct., small signal admittances 4-80678  
 Si-SiO<sub>2</sub> MIS structures, hole traps, trivalent Si centres, EPR meas. 4-80817  
 Si<sub>3</sub>N<sub>4</sub> film MNOS struct., trapped charge profile and relax. currents 4-65749  
 Si<sub>3</sub>N<sub>4</sub>, high trap density, trapping kinetics 4-104218  
 SiO<sub>2</sub>, charge neutralisation by electron bombardment 4-98694  
 SiO<sub>2</sub> gate oxide breakdown, expt. study 4-114207  
 TiO<sub>2</sub>, multiphoton interactions, laser induced photoluminesc. and photocond. 4-93093  
 Y<sub>2</sub>O<sub>3</sub>, ODMR study of exciton trapping 4-80503  
 Yb<sub>2</sub>O<sub>3</sub> thin films, trap levels, thermally stimulated method anal. 4-65763  
 ZnO electrolumiphor, brightness waves, grain size effects 4-104675  
 ZnSe:N, acceptor levels, optically excited DLTS study 4-61322

## hollow cathodes see cathodes

## holmium

## see also nuclei with .....

- K-shell ionisation induced by low energy H<sup>+</sup> 4-96508  
 L-shell X-ray prod. cross sections, H<sup>+</sup> induced, ratios 4-66131  
 BaCeO<sub>3</sub>:Ho, mixed elec. cond., dopant effects 4-108910  
 Ho (XXXIX), laser produced plasma, Cu-like lines in X-ray spectra 4-84053  
 Ho+<sup>4</sup>He<sup>+</sup>, L-shell X-ray prod. cross-sections 4-107305  
 Ho(II), relativistic mode-potential oscillator strengths and transition probabilities for 4f<sup>6</sup>-4f<sup>6</sup> transitions 4-112144  
 KLa(MoO<sub>4</sub>)<sub>2</sub>:Er<sup>3+</sup>(Ho<sup>3+</sup>), stimulated emission studies 4-84980  
 LiYF<sub>4</sub>:Ho, laser emission parameters 4-79158  
 Lu<sub>2</sub>Al<sub>2</sub>O<sub>12</sub>:Cr<sup>3+</sup>-Tm<sup>3+</sup>, Ho<sup>3+</sup>, stimulated emission of Tm<sup>3+</sup> and Ho<sup>3+</sup>, cross-cascade generation 4-71411  
 YAlO<sub>4</sub>:Ho, laser emission parameters 4-79158  
 Y<sub>3</sub>Fe<sub>5</sub>O<sub>12</sub>:Ho<sup>3+</sup>, ferromagnetic resonance study 4-84857

## holmium alloys

- Fe-Ho-B, metallic glass, mag. props. and crystallisation 4-84793  
 Ho-Co amorphous films, with perpendicular anisotropy, planar Hall effect 4-75932  
 Ho-Co sputtered amorphous films with perpendicular mag. anisotropy 4-80796  
 HoAlGa, mag. transitions, mag. and cryst. structures, X-ray diffr., thermal expansion meas. 4-114113  
 HoCo thin amorphous films, perpendicular anisotropy near compensation temp. 4-84835  
 HoCo<sub>7</sub>, intermetallics, cryst. growth from melt 4-66219  
 HoCo<sub>2</sub>Sn<sub>6</sub>, cryst. struct. and mag. props. (Russian) 4-88135  
 HoPr, mag. and elec. props. meas. (Russian) 4-80784  
 HoRh<sub>3</sub>, mag. props. meas. 4-61521  
 HoXGe X=Ni, Co, cryst. struct., mag. and elec. props. (Russian) 4-88134  
 MoRh<sub>2</sub>B<sub>4</sub>, mag. props. and crystal field effects 4-84767

## holmium compounds

## see also holmium alloys

- Er<sub>0.4</sub>Ho<sub>0.6</sub>Rh<sub>0.4</sub>B<sub>4</sub>, reentrant supercond., US attenuation meas., 1.5 to 20K 4-98810  
 HoC<sub>2</sub>, tetragonal cryst. struct., neutron diff. studies 4-108322  
 Ho<sub>0.8</sub>Ca<sub>0.2</sub>CrO<sub>3</sub>, ionic cond. and thermal expansion 4-84461  
 HoFeO<sub>3</sub>, muon site determ. 4-71227  
 Ho<sub>2</sub>Fe<sub>2</sub>O<sub>12</sub>, mag. and thermodynamic props., anisotropic mol. field approx. 4-88656  
 Ho<sub>2</sub>Fe<sub>2</sub>O<sub>12</sub>, umbrella mag. struct. thermal evolution, neutron diffr. study 4-92893  
 HoMo<sub>6</sub>S<sub>8</sub>, ferromagnet, domain walls, superconductivity obs. 4-80718  
 Ho<sub>2</sub>O<sub>3</sub>-Nb<sub>2</sub>O<sub>5</sub> system, cubic solid soln. region 4-76772  
 HoP<sub>2</sub>O<sub>14</sub> crystal, spectra and struct. (Chinese) 4-60887  
 Ho<sub>1-2-x</sub>R<sub>x</sub>Mo<sub>6</sub>S<sub>8</sub>, R=Er, Tb, relaxation of ferromagnetic ordering and superconductivity 4-98886  
 HoTiO<sub>3</sub>, single cryst., magnetisation and mag. susceptibility 4-88652  
 HoVO<sub>4</sub>, hyperfine-enhanced nuclear spin ordering, neutron diffr. studies (Japanese) 4-92898  
 Ho<sub>0.8</sub>Y<sub>0.2</sub>Fe<sub>2</sub>O<sub>12</sub>, spin-reorientation phase transition, Faraday effect, magnetisation meas. 4-88814  
 Rb<sub>2</sub>NaHoF<sub>6</sub>(TmF<sub>6</sub>), struct. phase transition 4-75651  
 Y<sub>2</sub>Ho<sub>1-x</sub>C<sub>2</sub>, tetragonal cryst. struct., neutron diffr. studies 4-108322

## holograms see holography

## holographic gratings

- aberration-containing lens, design for post-objective holographic deflector 4-102907  
 binary gratings for laser radar beam control 4-107720  
 binary optical elements, developments in fabrication 4-107808  
 coma aberration correction, concave holographic diffr. grating 4-107805  
 composite grating recorded with a nonlinearity, optical differentiation (Chinese) 4-87300  
 computer-generated holographic tandem component with optimum light efficiency, combination of lens and phase filters 4-79077  
 demultiplexer, HOE, for IR wavelengths 4-107554  
 dichromated gelatin holographic mirrors, diff. efficiency 4-107578  
 dynamic holograms, nonstationary recording by spatially nonuniform light beams 4-91424  
 efficient noise gratings in Ag halide emulsions 4-87304  
 glass/liquid interface, laser beam induced holographic bubble grating form. 4-83683  
 grazing-incidence grating for longit. pumped laser, stimulated emission characts. 4-74504

**holographic gratings continued**

- holens, multifocus, for optical 'matrix-matrix' multiplication method 4-102896
- image formation using high efficiency multifacet holographic optical elements 4-107570
- ion etching production for fibre appls. 4-91420
- large scale replication of holograms, laser button 4-74451
- lens imaging quality evaluation, use of classical OTF (Chinese) 4-87301
- lenses for optical correlators 4-107576
- matched filtering in white light illumination 4-74685
- monochromator, stigmatic coma free grazing incidence 4-83678
- monochromator, wide-band scanning, with concave grating, for optical thin film deposition monitoring 4-69600
- multifacet holographic field lens for diffr. pattern sampling 4-96844
- multifaceted volume hologram based information encoding systems 4-74462
- multiple exposure for HOE with large space-bandwidth product 4-74456
- mutual EM wave conversion in presence of Faraday effect 4-79081
- Newport Button, large scale replication of combined three- and two-dimens. holographic images, advertising premium item 4-112358
- nonclassical concave gratings in fixed-slit monochromators, parameter calc. 4-74491
- phase gratings diffraction, coupled wave method determ. 4-91573
- plastic, dyed, transient interference gratings and holograms 4-91419
- polygonal scanner using flat-field linearised scans with reflection dichromated gelatin holographic grating 4-91418
- PRIZ light modulator, use of insulating layer, grating hologram recording 4-103007
- production in photoresist for IR spectral range, diffr. efficiency 4-91423
- recording in  $\text{Bi}_2\text{SiO}_2$  monocrystals, photoelectret state 4-79079
- spectrograph for educational purposes utilising a holographic transmission grating 4-67948
- spectrograph with holographic lens as dispersing/focusing element (Chinese) 4-73523
- stigmatic conditions for normal incidence mounts 4-83681
- synthetic digital-phase gratings—design, features, applications 4-107563
- three-dimensional phase microholograms, diffr. efficiency 4-83555
- toroidal holographic gratings: efficiency and optical configuration design problem for XUV instrumentation 4-83680
- transmission hologram N gratings, diffr. efficiency changes induced by coupling effects 4-91422
- volume amplitude-phase hologram recording in PLZT ceramic 4-107579
- volume and phase grating characterisation, comment 4-87298
- volume phase holograms in  $\text{Bi}_2\text{SiO}_2$ , light diffr. 4-83539
- volumetric phase gratings, TM-component suppression during polarised-light diffraction (Russian) 4-59974
- $\text{As}_2\text{S}_3$ - $\text{As}_2\text{S}_3$ -Ag, holographic diffr. grating recording (Russian) 4-69341
- CdS, HF holographic diffr. grating recording on surface 4-69339
- GaAs surface, phase conjugation, reflecting grating recording by plasma refl. 4-97003
- Ge surface, phase conjugation, reflecting grating recording by plasma refl. 4-97003
- $\text{GeS}_2$ -Ag photosensitive system, holographic grating recording (Russian) 4-96843
- InSb surface, phase conjugation, reflecting grating recording by plasma refl. 4-97003
- $\text{LiNbO}_3$  different cuts, photorefractive effect in optical waveguides, holographic grating form. 4-74708
- $\text{LiNbO}_3$  planar lightguides, hologram writing 4-79082
- $\text{LiNbO}_3$ :Cu holographic refl. gratings, angular and spectral selectivities 4-74692
- $\text{LiNbO}_3$ :MgO, increased optical damage resist., holographic diffr. meas. of photorefr. 4-69521
- Si surface, phase conjugation, reflecting grating recording by plasma refl. 4-97003
- XeF laser using grating-interferometer-based cavity, single-mode tunable operation 4-102956

**holographic instruments**

- see also *holography*
- auto-stereoscopic display devices 4-74459
- camera, use as design and testing tool 4-107581
- computer generated holographic laser scanner for 2D graphics 4-69332
- high-resolution holography at a very long distance, flying object visualisation appls. 4-74463
- holoconcentrators, wideband angular spectrum aberrations-free 4-96840
- interferometer, common-path, for simple heterodyne interferometry 4-79073
- microscope objective, small spherical aberration and coma 4-106379
- polygonal scanner using flat-field linearised scans with reflection dichromated gelatin holographic grating 4-91418
- thermic fluid velocity sensor, interferometrical temperature field measurement (German) 4-68230
- universal holographic camera 4-64686

**holographic interferometry**

- absolute retardation fringe separation using polarisation holography 4-69343
- airfoil undergoing dynamic stall, laser holographic interferometry 4-97591
- angular displacement meas. using holographic interferometry 4-90336
- aspheric surface testing with interference type, computer-generated holograms (Chinese) 4-87427
- automated system, microprocessor control/data acquisition, real-time signal processing, NDT appl. 4-73501
- biological electrophoresis experiments on Salyut-7 orbiting space station, holographic interferometric obs. method 4-74468
- book 4-95081
- chemically reactive flow, holographic interferometry method study 4-69833
- cracked specimens, elastic and plastic anal., use of lower holographic interferometry (Chinese) 4-83854
- CVD cold wall reactor, temp. field determ. by holographic interferometry 4-71590
- diffusion coefficients determ. from interference fringes 4-81459
- diffusion in liqs., holographic interferometry student expts. 4-106151
- displacement pattern optical differentiation using sandwich-double exposure holograms 4-96847
- electroacoustic transducers, vibration distrib. at diaphragms, quantitative determ. by holographic interferometry methods (German) 4-74829
- electron Fourier holography based interferometry 4-83537
- fluid mechanics, modern optical techniques, review 4-91856

**holographic interferometry continued**

- fringe carrier method for displacement derivative determ. in hologram interferometry 4-79078
  - fringe pattern analysis by image processing using personal computer (Japanese) 4-111197
  - fringe-interpretation technique, sensitivity in laser holographic interferometry techniques 4-69719
  - gases, corrosive, thermal conductivity meas. by holographic interferometry 4-87546
  - gases, corrosive, thermal conductivity meas. by holographic interferometry 4-87547
  - heterodyne interferometry, using holographic common-path interferometer 4-79073
  - high energy laser techniques in industrial measurements 4-102967
  - high strobe-rate lasers for high-speed holographic testing 4-102903
  - holographic interference fringes recorded from diffusely illuminated objects, amplitude-phase characts. fluctuations effect 4-91425
  - human whole-body vibr. meas. by double-pulsed holographic interferometry 4-100398
  - image subtraction based on Fourier plane recording and spatial filtration 4-96848
  - interior warping measurement by holographic interferometry 4-95383
  - laser fusion experiments, image enhancement for fringe patterns tracing 4-96821
  - laser interferometer for testing rubber tyres (Chinese) 4-112363
  - macroscopic self-focusing effects, low density plasma 4-113192
  - mirror testing methods, astron. appl. (Japanese) 4-91642
  - mirrors, deformable, primary, holographic figure sensing 4-74759
  - moire deflectometer for stiff density fields anal. 4-64684
  - molecular gases in self-sustained pulse discharge, holographic interferometric investigation 4-79845
  - multipulse illumination system, controllable synchronised, for electron speckle pattern interferometry and holography 4-101909
  - nonsymmetrical plasmas, holographic interferometric diagnostics 4-84080
  - optical glass refractive index distrib. meas. using holographic interferometric technique (Chinese) 4-91421
  - particle velocity meas.: using double, multiple exposure hologram 4-102904
  - phase measurement two-wavelength holographic interferometry for coarse aspherical surface contouring 4-102905
  - photographic glass plate positioner, liquid gate, design and appl. 4-102941
  - plate, steel, round, forced oscill. study using holographic interferometric method (Russian) 4-79484
  - propellant grains, holographic NDT 4-109586
  - residual welding stress determ. using holographic interferometry 4-73493
  - resonators of frequency pressure transducers interference-holographic inspection 4-78369
  - sandwich holography, ultrahigh resolution of surface deform. 4-79074
  - spatial carrier-fringe-pattern anal. 4-101917
  - speckle and holographic interferograms prod. by recording object light field in Fourier plane 4-83554
  - speckle movement, effect on fringe contrast in holographic interferometry 4-112364
  - speckle shear interferometry, multiplexing 4-101915
  - thermic fluid velocity sensor, interferometrical temperature field measurement (German) 4-68230
  - TM-component suppression during polarised-light diffraction by volumetric phase lattices (Russian) 4-59974
  - tomography by iterative convolution, empirical study and appl. to interferometry 4-95503
  - two-dimensional temp. field in water obs. 4-103189
  - vibration analysis by time-average holographic interferometry (Korean) 4-112365
- holographic optical elements** see *holographic gratings*
- holographic storage**
- binary images in holographic memory units using laser diodes (Russian) 4-107553
  - introduction, data storage and non-destructive testing appls. (German) 4-60003
  - multiple embossment for hologram recording, holographic memory for information retrieval (Japanese) 4-107580
  - optimisation of holographic information devices (Russian) 4-74469
  - PMMA thick films for volume-type multiple hologram memory 4-83550
  - quasi-one-dimensional volume-type hologram memory 4-87299
  - three-dimensional phase microholograms, diffr. efficiency 4-83555
- holography**
- see also *acoustic holography*; *computer-generated holography*; *holographic gratings*; *holographic instruments*; *holographic interferometry*; *holographic storage*; *microwave holography*
  - aberration coefficients in holography, general form 4-87302
  - AC phase measurement technique for moire interferograms 4-106365
  - angular selectivity of holograms, effects of recording and reconstruction conditions 4-107575
  - applications review 4-69334
  - BEBC bubble chamber model, tests of two-beam holography 4-64274
  - birefringent elements, holographic simulation 4-97040
  - colour reflection hologram recording, modulation mechanisms 4-74450
  - correction of light polarisation at exit of fibre light guides (Russian) 4-87480
  - correlation with spherical wave illumination 4-74439
  - damped oscillations, holographic subtraction (Chinese) 4-112362
  - deployable optical systems, conf., Los Angeles, CA, USA (Jan. 1983) 4-73138
  - dichromated gelatin, hologram copying with spectral filtered sunlight 4-74455
  - dye laser, distributed feedback, picosecond pulses generation using gratings 4-112405
  - dynamic holograms, nonstationary recording by spatially nonuniform light beams 4-91424
  - dynamic picosecond holography prod. by photochemical hole burning 4-69335
  - efficient noise gratings in Ag halide emulsions 4-87304
  - electron, off-axis, noise contrib. 4-69344
  - electron Fourier holography, non-interferometric reconstruction properties 4-91394
  - electron Fourier holography based interferometry 4-83537
  - electron holography, Fourier, aberrations elimination 4-69345
  - electron holography, Fourier, scatt. foil choice, resolution limitation 4-69346

## holography continued

- electron holography and electron transfer theory, conf., Antwerp, Belgium (Sept. 1983) 4-67865  
 electron off-axis holograms, speckled background in reconstructions 4-91393  
 electronic display using holograms 4-107566  
 endoscopy using gradient-index optical systems 4-83549  
 energy exchange between waves during recording and reconstruction in holographic media with a lasing response 4-60005  
 falling raster in optical signal processing, analogy with incoherent holography 4-79040  
 far-field in-line holography, image-to-background irradiance ratio optimisation 4-91417  
 fog, holographic investigation of spatial distrib. of droplets 4-62979  
 high speed photography, videography and photonics, conf., San Diego, CA, USA (Aug. 1983) 4-106102  
 holographic interference fringes recorded from diffusely illuminated objects, amplitude-phase characts. fluctuations effect 4-91425  
 image quality, influence of spatial and temporal coherence 4-74457  
 image recognition, optical-electronic system with operational input and preliminary processing of images for recognition (Russian) 4-107526  
 image reconstruction from frequency-offset Fourier data 4-96835  
 image recording in multielement system, coherent reception 4-74465  
 image recording system hologram area reduction 4-83552  
 integral-holographic three-dimensional image, quality of system 4-83556  
 interference pattern location instability effect on hologram quality 4-74464  
 introduction, data storage and non-destructive testing appls. (German) 4-60003  
 joint transform real time optical correlator using  $As_2S_3$  noncrystalline film 4-74461  
 large format holograms in entertainment applications 4-112355  
 large scale replication of holograms, laser button 4-74451  
 lenses for optical correlators 4-107576  
 light-in-flight recording, compensation for limited speed of light used for obs. 4-79075  
 light-sensitive material fabrication 4-74466  
 magneto-optical space-time light modulator, transfer function and pulse response, appls. 4-107816  
 matched holographic filtering in FTIROS 4-79080  
 matrix-matrix multiplication method using multifocus hololens 4-102896  
 microprojection system having a holographic screen 4-79266  
 multi-images of holograms (Chinese) 4-112360  
 multicolour holography of animated scenes by motion synthesis using multiplexing technique 4-74454  
 multicolour holography with single freq. laser utilising triethanolamine as pre-exposure agent 4-112356  
 multicolour periodic stimulated-Raman-scatt. laser, appl. as source for colour holographic motion pictures 4-107682  
 multifacet holographic field lens for diff. pattern sampling 4-96844  
 multifacet lens with parallel axes (Chinese) 4-112359  
 multiple exposure for HOE with large space-bandwidth product 4-74456  
 multiport optical fibre switch 4-91636  
 mutual EM wave conversion in presence of Faraday effect 4-79081  
 natural colour holographic stereograms by superimposing three rainbow holograms 4-112357  
 NDT as mech. design aid 4-114739  
 Newport Button, large scale replication of combined three- and two-dimens. holographic images, advertising premium item 4-112358  
 objects, one dimensional, imagery and microholography at large distances, two wave illum. (French) 4-69324  
 one-shot X-ray holography using optical klystron harmonic generator 4-97001  
 Optics in Australia conference, Sydney, Australia (May 1983) 4-95047  
 optics in entertainment, conf., Los Angeles, CA, USA (Jan. 1984) 4-110802  
 photoanisotropic medium reaction, polarisation-holographic recording 4-74467  
 photoconductive ferroelectrics, optical device applications 4-64744  
 photographic film with dye substituted Ag, phase hologram recording 4-79083  
 photometry in the scheme of holographic spectroscopy 4-82815  
 photorefractive material, transient hologram as high capacity optical switching device 4-64685  
 photorefractive materials, transient energy transfer 4-107774  
 pictorial holography developments, review 4-69333  
 picture segmentation, use of speckle statistics in real hologram reconstructions (German) 4-69342  
 plastic, dyed, transient interference gratings and holograms 4-91419  
 polarisation recording, diff. efficiency and selectivity 4-96845  
 polyvinyl alcohol films, IR hologram recording 4-112366  
 rainbow holographic process, point spread and transfer functions 4-79076  
 rainbow holography, vignetting effect in one-lens and two-lens optical systems 4-69336  
 rainbow-holographic technique for two-dimens. transparencies 4-107577  
 real-time holography with undeveloped dichromated gelatin films, appls. 4-91416  
 recording and readout in  $As_2S_3$  planar waveguide 4-83553  
 recording in  $Bi_{12}SiO_{20}$  monocrystals, photoelectret state 4-79079  
 recording of three-dimensional IR hologram at 10.6  $\mu m$  4-102909  
 reflection mounts for transmission holograms, format compatibility issues 4-112354  
 review 4-107574  
 review of holography and other 3 D techniques, developments and impact on business 4-74449  
 sandwich-double exposure holograms for displacement pattern optical differentiation 4-96847  
 setup using planoconvex lens having short focal length 4-82645  
 single-mode fibre-optic holography 4-60004  
 skeletal muscle, polysarcomeric unit of activation, microdifferential holography 4-66998  
 soft X-ray holographic microscopy experiments at the Brookhaven Synchrotron Light Source 4-96841  
 spatial three-dimensional hologram and object projection system 4-74458  
 stereograms for three-dimens. imaging 4-74453  
 techniques and applications 4-107581  
 telescope analysis of intensity holograms, angular resolution 4-64687  
 thin amplitude holograms, film nonlinearities variations rel. to reconstruction wavelength 4-69337  
 thin meniscus mirror support system design, testing appls. 4-87421  
 three dimensional display fundamentals 4-74448

## holography continued

- three-dimensional, developed photographic film, refractive index calc. 4-112543  
 three-dimensional imaging, conf., Geneva, Switzerland (April 1983) 4-73140  
 three-dimensional phase hologram, wavefront reconstruction in spatial freq. representation 4-112367  
 timer smear corrected multiplex holographic display of computerized tomography data 4-74460  
 two-shutter controller for investigation of the kinetics of the recording of dynamic holograms 4-87303  
 volume phase holograms in  $Bi_{12}SiO_{20}$ , light diff. 4-83539  
 volume phase holograms reconstructed by the object wave 4-87305  
 volume vector holograms using countermoving reference beams 4-83551  
 X-ray microholography of biological specimens 4-72471  
 X-ray transmission gratings and zone plates, free-standing fabrication using UV holography and X-ray lithography 4-97147  
 AgCl emulsion, polarisation holographic study (Chinese) 4-112361  
 $BaTiO_3$ , anisotropic self diffraction 4-107762  
 $Bi_{12}TiO_{20}(SiO_{20})$  photorefractive crystals, hologram formation, optical activity effects 4-60002  
 H, atomic spectroscopy and holography, laboratory expt. 4-67927  
 $LiNbO_3$  planar lightguides, hologram writing 4-79082  
 Nd:glass high power laser rod amplifier, thermal distortion and thermal aberration reproduction time meas. (Chinese) 4-87353  
 homogenising see heat treatment  
 homopolar generators  
 power supply of toroidal-field coil in SNUT-79 Tokamak (Korean) 4-113228  
 homopolymers see polymers  
 hopping conduction  
 alkali halides, with F-centres, hopping-type electronic processes in pre-breakdown elec. fields 4-108868  
 alkaline earth niobates, electronic cond. rel. to complex perovskite structs. 4-70821  
 amorphous RF sputtered film, struct. and elec. props. 4-70956  
 biopolymer systems, electron and hole transport mechanisms 4-108855  
 chalcogenide glasses, tunnelling relax. in a.c. cond. 4-70812  
 cyanoacetylene polymerisation products, struct., elec. cond. 4-113953  
 DC conductivity tensor in mag. field 4-80558  
 disordered lattice, cond. in strong elec. fields 4-61367  
 disordered one-dimensional lattice, low freq. hopping cond. 4-61355  
 disordered system, diagrammatic approach to hopping transport 4-88496  
 disordered systems, diagrammatic two-particle locator theory, Anderson Hamiltonian 4-70765  
 disordered systems, diagrammatic two-particle locator theory, Anderson transition and role of hopping processes 4-70766  
 disordered systems, hopping cond. and weak localisation in strong elec. field 4-75976  
 double tunnel jumps in activationless hopping conductivity 4-84614  
 graphite intercalation compounds, c-axis. cond. and thermoelec. power 4-80561  
 Hall resistance, quantised, at finite temps., anal. in Si MOSFET and GaAs-AlGaAs heterostruct. 4-98727  
 inhomogeneous metallic polymers, thermoelec. power and elec. cond. 4-70789  
 nonmetallic crystals, optically stimulated electron jumps between local electron centres 4-65641  
 one-dimensional bond-percolation model, hopping, cond. in const. field 4-68182  
 one-dimensional disordered classical systems, freq. depend. hopping cond. 4-75936  
 organic polyiodide chain complexes, elec. conduction, press. depend. 4-75962  
 percolation conductivity problem, improvement to effective-medium approx. 4-70767  
 poly-N-vinylcarbazole, charge carrier transport study 4-75999  
 poly-N-vinylcarbazole, nonpolar crosslinking agent effect on relax. processes, hopping mechanism of transport (Polish) 4-65948  
 polyacetylene:  $I_2$ , cis and trans, DC and microwave cond. 4-92716  
 polyacetylene:  $I_2$ ,  $[CH(I_2)]_x$ , hopping and band conduction and thermopower meas. 4-65665  
 polyacetylene, doped, bipolaron interchain hopping as transport mechanism 4-70810  
 polyacetylene, hopping cond. freq. response calcs. 4-61379  
 polyacetylene, nearly metallic, solitons, disorder and charge conduction 4-75954  
 polymer film, electropolymerised, spectroscopic studies of electronic props., effect of prep. parameters (French) 4-66192  
 polyparaphenylene, doped, bipolaron interchain hopping as transport mechanism 4-70810  
 polypyrrole, proton modification, elec. cond., optical absorpt. spectra, XPS 4-75969  
 porphyrinatonicke(II) polymer, band struct., semiempirical INDO crystal-orbital approach 4-75829  
 quasideimensional trapping system, excess carrier hopping current relax. 4-70793  
 random systems, electron localisation and diffusion 4-98572  
 randomly substituted lattice, long range and nearest neighbour interactions, hopping transport 4-84600  
 semiconductors, amorphous, hopping cond., freq. and temp. depend., extended pair approx. 4-98615  
 semiconductors, amorphous, time-dependent geminate recombination for hopping site energy disorder 4-61395  
 semiconductors, anomalous electron tunnelling in mag. fields near surfaces 4-92802  
 semiconductors, hopping conduction, multiple scatt. theory, continuous time random walks and CPA approx. 4-61366  
 semiconductors, positive magnetoresistance in the variable-range hopping region 4-65695  
 site-disordered system, hopping dispersive transport 4-84602  
 small polaron model with nonlinear electron-phonon interactions 4-61304  
 structurally disordered Hubbard model, temp. depend. spin susceptibility 4-71014  
 TCNQ salt,  $(NMP)_{0.54}(Phen)_{0.46}(TCNQ)$ , intersoliton hopping transport of electrons 4-92704  
 two dimensional random lattice hopping model, diffusion and conduction 4-90492  
 $AlCl_3 \cdot SOCl_2$  based electrolytes, transport props. 4-88323  
 $BaSr_{1/3}Nb_{2/3}O_3$ , defect struct., elec. and ionic cond. 4-98676

## hopping conduction continued

- Ca<sub>2</sub>NaMg<sub>2</sub>V<sub>2</sub>O<sub>12</sub> garnet, elec. cond. and thermopower 4-70822  
 p-Cd<sub>0.2</sub>Hg<sub>0.8</sub>Te, hopping cond. between intrinsic defects 4-104210  
 CeO<sub>2</sub>-Y<sub>2</sub>O<sub>3</sub>, nonstoichiometric, electronic conduction, dopant effects 4-92733  
 CuFe<sub>2</sub>O<sub>4</sub>, conduction mechanism, annealing effect, resist. and thermopower meas. 4-104206  
 ErF<sub>3</sub> amorphous thin films, AC cond. meas. 4-76059  
 FeF<sub>3</sub> thin film, impurity cond. along least resistance paths 4-80705  
 Fe<sub>2</sub>O<sub>3</sub>, magnetite, elec. cond. mech. and rel. to mag. after-effects 4-76195  
 n-GaAs, hopping cond. freq. depend. 4-70806  
 Ge bolometer, neutron-transmutation-doped, resist. meas. 4-106386  
 p-Ge, nuclear doped, elec. cond., 0.06 to 300K, impurity conc. depend. 4-61382  
 Ge-Zn, nonohmic hopping cond. in strong elec. fields 4-88515  
 Ge-Si, amorphous, RF sputtered, electronic props. 4-61370  
 Ge-Sn(Sb)(Al) amorphous thin films, hopping cond. meas., 130 to 300K, localised state variations 4-92713  
 GeO<sub>2</sub> films, amorphous, elec. characterisation in MIS and MIM structs. 4-70816  
 In<sub>0.4</sub>As<sub>0.6</sub>-InP heterojunction, quantum Hall effect and hopping cond. 4-98723  
 InP:Mn, hopping cond. between deep impurity states 4-104209  
 KI thin films, high-field elec. cond. study 4-80702  
 Nb<sub>2</sub>N<sub>5</sub> DC cond., supercond. and hopping mechanisms 4-98795  
 NbSe<sub>3</sub>, negative differential resist., dynamic instability 4-88502  
 NiO:Li(Al), or undoped, elec. cond. and high temp. defect struct. 4-80617  
 a-Sb, elec. resist. and thermoelec. power meas. 4-108886  
 Se, amorphous, DC conductivity thickness dependence 4-84620  
 Se-Te(Ge)(Sb) amorphous, DC conductivity thickness dependence 4-84620  
 a-Si, cond. and thermoelectric power below mobility edge 4-108888  
 a-Si film, RF sputtered, optical absorpt., elec. cond., effect of thermal annealing 4-80583  
 Si, impurity conduction effect of uniaxial compression on p-type Si 4-98617  
 Si inversion layers, 2D Na impurity band cond. in activated regions, mag. field depend. 4-98769  
 a-Si:H films, reactive sputtering, elec. and optical props. 4-104203  
 Si:Na<sup>+</sup>, two-dimensional hopping cond. in mag. field 4-98687  
 Si:P, motional narrowing of ESR line 4-104484  
 a-SiC:H glow-discharge film, electronic and optical props. 4-84623  
 SiO<sub>2</sub> films, RF sputtered, AC cond. mechanisms 4-92721  
 SiO<sub>2</sub> films, RF sputtered, AC cond. mechanisms, single polaron correl. barrier hopping 4-92722  
 Si<sub>1-x</sub>Sn<sub>x</sub>, amorphous, vapour deposited, struct., resist. characts., density, electron diff. meas. 4-61424  
 Si<sub>1-x</sub>Sn<sub>x</sub>:H, (0 ≤ x ≤ 0.3), amorphous RF sputtered film, struct. and elec. props. 4-70956  
 SrCa<sub>1/3</sub>Nb<sub>2/3</sub>O<sub>3</sub>, defect struct., elec. and ionic cond. 4-98676  
 SrTeO<sub>3</sub>, dielectric const. dispersion study (Russian) 4-88762  
 (TMTSF)<sub>2</sub>BrO<sub>4</sub>, DC and microwave conductivity and thermoelec. power, variable range hopping obs. 4-75950  
 TaO<sub>2</sub>, amorphous film, electrode state relax. 4-88765  
 TaSi<sub>2</sub>, cosputtered, props., effect of O contamination 4-114046  
 UO<sub>2</sub>, high temp. thermoelec. power studies 4-104244  
 V<sub>2</sub>O<sub>5</sub>-SeO<sub>2</sub> (TeO<sub>2</sub>)(GeO<sub>2</sub>) glass, ESR and photoacoustic spectra 4-104491  
 (V<sub>2</sub>O<sub>5</sub>)(P<sub>2</sub>O<sub>5</sub>)<sub>100-x</sub> glasses, V mixed valence state, X-ray absorpt. near edge struct. determ. 4-65645  
 WO<sub>3-x</sub>H<sub>2</sub>O amorphous films, elec. cond. and thermopower 4-61378  
 Y<sub>3-x</sub>Gd<sub>x</sub>Fe<sub>2</sub>O<sub>12</sub> noncrystalline garnet films, electron transport and thermopower 4-108958  
 Zn<sub>1-x</sub>Ga<sub>2x/3</sub>Cr<sub>2</sub>Se<sub>4</sub>, magnetic semiconducting solid solutions study 4-109002  
 ZnO, powdered, freq. dispersion of elec. cond. 4-70802
- horn antennas** see *directive antennas; waveguide antennas*
- horology** see *time measurement*
- hospital administration** see *medical administrative data processing*
- hospital engineering** see *biomedical engineering*
- hospital information systems** see *medical administrative data processing*
- hot carrier conduction** see *hot carriers*
- hot carriers**  
 amorphous semiconductors, picosecond electronic relaxations 4-108892  
 double heterostructures, electron-hole plasma heating 4-65734  
 hydrocarbon polymer dielectric films, hot-electron transport 4-92837  
 III-V semiconductors, hot carrier transient response, vel. overshoot 4-92736  
 magnetic field expulsion by hot-electron cloud 4-84630  
 nonequilibrium phonon distribution in quantising mag. field, phonon generator appl. 4-61008  
 phosphors, binary compounds, cathodoluminesc. efficiency calc. 4-61754  
 polar semicond., donor-acceptor pair capture cross section highly excited electrons 4-61330  
 polymers dielectrics, elec. breakdown rel. to high-mobility states 4-109119  
 prebreakdown electron emission currents, switching and other nonlinear phenomena 4-76641  
 quantum field theory, hot electron problem 4-65685  
 semiconductor, ballistic hole photocurrents and surface photogalvanic effect 4-84652  
 semiconductor plasma, longitudinal phonon-plasmon interactions 4-98658  
 semiconductor/metal (Russian) 4-70931  
 semiconductors, hot carriers, Boltzmann eqn. stationary solns. 4-104214  
 semiconductors, inversion of sign of transverse hot electron thermo-emf 4-104246  
 semiconductors, nonradiative multiphonon capture of carriers by deep traps 4-75889  
 semiconductors, small gap, intrinsic photocond., electron and hole heating effects 4-88542  
 semiconductors, surface carrier heating, electron temp. striations and current filaments 4-84629  
 subpicosecond hot electron transport, many-body effects for high carrier density 4-108867  
 warm carrier device with thin film antenna for CO<sub>2</sub> laser detection 4-73507  
 n-(Al,Ga)As/GaAs heterojunctions, hot-electron mobility study at moderate elec. fields 4-84678

## hot carriers continued

- AlGaAs/GaAs heterostruct., 2D magnetotransport, electron heating effects 4-98736  
 n-CdHg<sub>1-x</sub>Te single crystals, hot electrons at strong elec. fields (Russian) 4-98628  
 CdSe, hot excitons and electron-hole pairs and Raman spectra 4-114285  
 GaAs, relaxation of hot electron energy, surface plasmons 4-98631  
 GaAs, short n<sup>+</sup>n<sup>+</sup> section, hot electron effects 4-61385  
 GaAs:O p-i-n structs., magnetically sensitive, elec. characts. (Russian) 4-65729  
 GaAs/AlGaAs multiple quantum well structs., photoexcited carrier intraband relax., femtosecond studies 4-88565  
 GaAs/nAlGaAs superlattice devices, high speed electrons and hot electron effects appls. (Japanese) 4-61449  
 Ga<sub>0.47</sub>In<sub>0.53</sub>As, hot electron velocity overshoot 4-70823  
 GalnAsP, n-type, lattice matched to InP, hot electron transport, book contrib. 4-61388  
 n-Ge, hot electron capture by dipoles at low temps., field depend. 4-75979  
 Ge, hot hole submillimetre emission in transverse mag. field 4-71412  
 Ge, picosecond-pulse laser annealing, phenomenological model 4-88198  
 Ge:Cu(Au), nonradiative multiphonon capture of carriers by deep trap 4-75889  
 In<sub>0.53</sub>Ga<sub>0.47</sub>As 1.6-μm lasers, temp. sensitive operation 4-96903  
 n-InSb, current-induced anisotropy of refractive index 4-104564  
 InSb, photoresistance on electron heating in mag. field, two-phonon oscillations 4-84650  
 n-InSb, refractive index, influence of electron drift and heating 4-104561  
 Pb chalcogenides, carrier heating mechanisms 4-92738  
 PbSnTe, negative differential mobility in high elec. fields 4-104216  
 PbTe, negative differential mobility in high elec. fields 4-104216  
 n-Si, hot electron conductivity in transverse elec. field, intravalley scattering obs. 4-80596  
 n-Si, inversion layers in MOSFET, phonon limited hot-electron transport 4-70945  
 Si, picosecond-pulse laser annealing, phenomenological model 4-88198  
 Si/SiO<sub>2</sub>, MOS capacitors, donor state generation rate, anode field dependence 4-92826  
 Si-Au(Ag)(Al) Schottky barrier diodes, barrier height and hot electron attenuation length meas. 4-98751  
 Si-MOSFET inversion layer, warm electron coeff. calc. for two-dimensional electron gas 4-65748  
 ZnS:Cu, Cl, Er films, electroluminesc., hot electron energy distribution 4-85012
- hot cathode tubes** see *thermionic tubes*
- hot cathodes** see *thermionic cathodes*
- hot electrons** see *hot carriers*
- hot pressing**  
 borosilicate glass, nuclear waste, hot isostatic pressing 4-59330  
 ceramics, hot isostatic pressing, shaped part production 4-76736  
 ceramics, isothermal hot pressing temp., effectiveness prediction 4-88999  
 ceramics, stress assisted hot form. 4-76728  
 diffusion bonding, hot isostatic pressing 4-89239  
 fibre reinforced Al-Mg alloy, fibre/matrix interface effect on fatigue, optimum processing parameters 4-114635  
 fibre reinforced ceramics, fabrication and mech. props., book contrib. 4-66297  
 kinetics, semilogarithmic law 4-85123  
 metal matrix composites, fabrication, book contrib. 4-66276  
 metal powder, hot isostatic pressing, energy expenditure, plant design calcs. 4-89008  
 metal powders, densification kinetics in hot pressing in porous shells 4-61885  
 metal powders, densification kinetics in hot pressing in porous shells 4-66260  
 metals, diffusion welding of hot isostatically pressed powders, metallurgical obs. (German, English) 4-66265  
 mica, synthetic, sintering using hydrothermal equipment 4-89013  
 multite-cordierite composites, sintering, hot pressing, microstruct., mech. and thermal props. 4-89017  
 new materials technology 4-88953  
 nuclear fuel pellets, ceramic, new hot impact densification method (German) 4-83215  
 olivine-basalt partially molten aggregates, diffusion creep during hot pressing 4-110137  
 radioactive waste, medium level, powder technological vitrification by hot pressing 4-83139  
 refractory materials, recrystn., grain growth kinetics 4-76789  
 Si<sub>3</sub>N<sub>4</sub>, normally sintered, hot isostatic pressing in N<sub>2</sub> gas as pressure medium 4-114459  
 α-sialon ceramics, hot pressing, thermal expansion, 40°-1040°C 4-88315  
 sialon ceramics, thermal diffusivity, effect of crystn. of grain boundaries phase 4-88355  
 β-sialons, microstruct. evaluation by TEM, correl. to mech. props. 4-76732  
 sintering processes, book contrib. 4-109340  
 steel, Cr-Mo-V, hot work, powder metallurgically produced by hot isostatic pressing 4-93248  
 steel, high-speed, hot isostatic pressing, struct. and contact fatigue 4-114440  
 steel, powder metallurgy, prod. by dynamic hot pressing, design strength 4-89011  
 steels, tool, hot isostatic pressing powder metallurgy fabrication methods 4-89004  
 Al-Ca-Zn superplastic alloy, composite, fibre reinforced, hot pressing, tensile props. 4-99369  
 AlN powder, hot pressing kinetics, oxidation, mech. props. 4-76731  
 AlN powder, shock effects, TEM study 4-109345  
 AlN transparent ceramics, powder and sintering characts. 4-81171  
 β-Al<sub>2</sub>O<sub>3</sub>, sintering, microstruct. and mech. props. 4-85136  
 Al<sub>2</sub>O<sub>3</sub>-Al<sub>2</sub>O<sub>3</sub> composite ceramic, hot pressing reaction sintering, mech. props., high-temp. appls. 4-62062  
 Al<sub>2</sub>O<sub>3</sub>-BN(AION) composite ceramics, mech. props. (French) 4-81177  
 Al<sub>2</sub>O<sub>3</sub>-glass composite, hot isostatically pressed, macropore structure 4-71629  
 Al<sub>2</sub>TiO<sub>5</sub> ceramics, stabilisation by cation substitution, sintering and hot pressing 4-109362  
 B<sub>4</sub>C based materials, resist. to corrosion by H<sub>2</sub>SO<sub>4</sub> soln. 4-62087  
 B<sub>4</sub>C, struct. and mech. props., hot pressing conditions effect 4-61906

## hot pressing continued

- Cr<sub>2</sub>O<sub>3</sub>, doped, hot pressing, annealing, elec. cond., density, grain size, XPS 4-113946
- Cu powder compacts, rel. between compacting press., green density and green strength 4-114444
- Fe-Cr-Al-Y plasma sprayed coatings, post-treated, mech. props. 4-93471
- LaCrO<sub>3</sub>-Cr cermet, high-temp. creep 4-71693
- Li<sub>1-x</sub>Ti<sub>2-x</sub>O<sub>4</sub> ceramics, elec. and supercond. props. 4-104342
- MgO powder, hot pressing, densification, dislocation creep mechanism 4-114455
- MnZn ferrites, hot pressed, brittle and strength props by microindentation method 4-62044
- MnZn ferrites, hot-pressed, powder particle size distrib. and heterogeneity 4-61907
- Mn<sub>1-x</sub>Zn<sub>x</sub>Fe<sub>2</sub>O<sub>4</sub> ferrite, microstruct. and permeability during sintering 4-109432
- Mn<sub>1-x</sub>Zn<sub>x</sub>Fe<sub>2</sub>O<sub>4</sub>, hot pressed, prior heat treatment effect on props. 4-89016
- MoSi<sub>2</sub> based materials, resist. to corrosion by H<sub>2</sub>SO<sub>4</sub> soln. 4-62087
- Na<sub>1-x</sub>P<sub>1-x</sub>Si<sub>2</sub>O<sub>12</sub> ceramics, prep., ionic cond., durability and strength 4-113711
- Ni-Co-Cr-Nb-Hf, Ni-base superalloy, MERL 76, powder metallurgy hot isostatic pressing, effect of Ar contamination 4-114447
- Ni-Nb-NbC, eutectic alloys, powder metallurgy, physical props., high temp. use 4-85125
- Ni<sub>80</sub>P<sub>20</sub>, amorphous powder, warm pressing consolidation kinetics 4-81168
- PZT, sintered, densification by hot isostatic pressing 4-66286
- Si<sub>3</sub>N<sub>4</sub>-Al<sub>2</sub>O<sub>3</sub>-N<sub>2</sub> β-sialon, hot pressed, flexural strength, phase struct., comp. depend. (Japanese) 4-76828
- Si<sub>3</sub>N<sub>4</sub>-Al<sub>2</sub>O<sub>3</sub>-N<sub>2</sub> β-sialon synthesis from Si<sub>3</sub>N<sub>4</sub> and Al alkoxides (Japanese) 4-114461
- SiC fibre reinforced Al<sub>2</sub> alloy, fabrication and mech. props. (Korean) 4-104755
- β-SiC powders, sintering, hot pressing, densification and mech. props. rel. to prep. 4-109366
- SiC-BN composites, thermal diffusivity anisotropy 4-84472
- Si<sub>3</sub>N<sub>4</sub> based materials, resist. to corrosion by H<sub>2</sub>SO<sub>4</sub> soln. 4-62087
- Si<sub>3</sub>N<sub>4</sub>, hot isostatic pressing, densification, bending strength rel. to additives (Japanese) 4-76721
- Si<sub>3</sub>N<sub>4</sub>, hot pressed, fracture toughness, mech. props. rel. to comp. and microstruct. 4-76870
- Si<sub>3</sub>N<sub>4</sub>, hot pressed, strength rel. to high temp.-oxidation 4-114697
- Si<sub>3</sub>N<sub>4</sub>, hot pressing, densification and microstruct. rel. to MgO and Y<sub>2</sub>O<sub>3</sub> additions 4-76729
- Si<sub>3</sub>N<sub>4</sub>, hot-pressed, oxidation kinetics 4-76890
- Si<sub>3</sub>N<sub>4</sub>, hot-pressed, transient creep parameters, determ. by dynamic bending tests 4-81381
- Si<sub>3</sub>N<sub>4</sub>, microstruct. development during fabrication 4-76733
- Si<sub>3</sub>N<sub>4</sub> powder, shocked, hot isostatic processing 4-71617
- Si<sub>3</sub>N<sub>4</sub>, reaction-bonded, strength-porosity relationship 4-76734
- Si<sub>3</sub>N<sub>4</sub>-based ceramics, phase relations 4-76762
- Si<sub>3</sub>N<sub>4</sub>-MgO, hot pressed, fracture stress, temp. and strain rate depend. 4-85207
- Si<sub>3</sub>N<sub>4</sub>-Y<sub>2</sub>O<sub>3</sub>, isostatically hot pressed, strength and microstruct. rel. to sintering additives 4-85132
- SiO<sub>2</sub>, hydrothermal hot pressing, aggregate form., shrinkage 4-109370
- SmCo<sub>5</sub> permanent alloys, metallographic study, improved phase and grain boundary etching 4-114754
- Ti-Nd, rapidly solidified dispersion strengthened, tensile and creep props. 4-114562
- TiC-Ti, reactive solid-state hot pressing 4-61897
- TiO<sub>2</sub>-based crystalline ceramic nuclear waste forms, processing and microstruct. 4-83150
- WC-Co, cemented carbide, hot isostatic pressing 4-66293
- WC-Co-P, wear resist., P addition influence 4-66458
- ZnO varistor, high-field fine-grained, fabrication by sol-gel processing 4-66282

## hot rolling

- analytical rolling model, including through-thickness shear stress distrib. 4-99411
- metal hot or warm forming model using deform. mechanism maps 4-83830
- steel, C, cast and wrought, H induced ductility losses, annealing effects 4-85193
- steel, C, laser glazed hot-rolled Charpy samples, impact testing 4-81377
- steel, C-Mn, hot-rolled, ductility and anisotropy of sulphide inclusion spacings, effect of inclusion shape 4-99437
- steel, Cu-bearing, hot shortness in controlled rolling process 4-89105
- steel, dual-phase, Al-killed, forming props., influence of microstruct. and texture 4-99459
- steel, hardness response, estimation by simulating cooling cycles via Jominy bar testing 4-114750
- steel, HSLA, tensile strength and ductility, dependence on microstruct. 4-114603
- steel, low alloy, quenched directly from hot-deform. temp., influence of austenite substruct. on final struct. and props. 4-99439
- steel, low C, deep-drawing, prod. by continuous annealing 4-114566
- steel, maraging, tensile strength and ductility, dependence on microstruct. 4-114603
- steel, martensitic, low C, controlled rolled and quenched, strengthening effects 4-99393
- steel, mechanical props. rel. to US detectable discontinuities 4-71713
- steel, microalloyed, hot-rolled, isothermal decomp. of austenite 4-99409
- steel, Mn, controlled hot rolling and intercrit. annealing, time-temp.-reaction diagrams 4-66351
- steel, Nb, strengthening mechanisms, influence of rolling variables 4-71666
- steel, Nb-V, low C, controlled-rolled, transform. textures 4-99405
- steel, Nb-V, Nb- and V-carbonitride precipitates, fine struct. (Chinese) 4-61929
- steel, Ni-Co-Mo-Ti, controlled hot rolling and intercrit. annealing, time-temp.-reaction diagrams 4-66351
- steel, stainless, texture development during annealing and rolling 4-76786
- steel plates, high-toughness, commercial production by reheating of slabs 4-114589
- steel sheet, hot rolled, test methods for formability 4-99736
- steels, hardenability, effect of hot working 4-81211
- Al hot rolling control, IR thermometry 4-82796

## hot rolling continued

- Al-Mg(7 wt.%), hot-rolled, prep. from rapidly solidified powder, fracture mechanism 4-71731
- Cu, plastic flow and dynamic recrystallisation in single crystals 4-66394
- Fe-Al-Si, Sendust, brittleness, effect of solidification and heat treatment 4-81281
- Fe-Si (3.4 wt.%), cold workability, effect of struct. and texture (Chinese) 4-61950
- Fe-Si (3 wt.%), deformation and heat treatment, C content effects (Russian) 4-109437
- Fe-Si (3 wt.%), hot rolled, texture formation (Russian) 4-109435
- Fe-Si-Al, Sendust, hot rolling rel. to alloy comp. and mag. props. 4-93322
- Mg, hot rolled, texture, grain size and yield strength 4-114579
- Mo-V(Zr)(Ti)(Nb)(Ru)(Cr), interstitial-free, workability and ductility, effect of alloying element 4-93345
- Ni-Cr-Co (22.9 wt.%) superalloy, solid solutions strengthened, development, weldability, oxidation resist. 4-61975
- Ti-Al-V (6.4 wt.%), evolution of α+β struct. rel. to thermomech. treatment 4-109431
- W, dislocation struct. after rolling, TEM obs. 4-99440
- hot shortness *see* brittleness
- hot strength *see* tensile strength
- hot working
- see also* hot rolling
- high-speed compression testing at constant true strain rates for hot working studies 4-76928
- metal hot or warm forming model using deform. mechanism maps 4-83830
- metals, cubic, fibre texture, quantitative representation (Korean) 4-104946
- metals, plastic behaviour, torsion tests on solid and tubular specimens 4-93473
- steel, austenitic stainless, Nb-stabilised, hot deformed, grain coarsening 4-93329
- steel, C-Mn, grain boundary segregation of Cu, Sb and Sn at 900°C 4-93300
- steel, Cr-Mo-V, hot work, powder metallurgically produced by hot isostatic pressing 4-93248
- steel, HSLA, Cu-bearing, hot shortness 4-89104
- steel, Nb microalloyed, nonisothermal static softening after hot working 4-114578
- steel, quasilamellar and quasimonolithic, character of fracture 4-114659
- steels, tool, hot isostatic pressing powder metallurgy fabrication method 4-89004
- Al-Mg solid solutions, ductility loss at high temps. 4-104857
- Al-Mg-Mn, hot deform. and dynamic recryst. 4-109479
- Cu, fracture strain and flow stress, invest. by tension and torsion methods (Polish) 4-93362
- Fe-Co-Ni-Al, Alnico 5, hot workability, microstruct. 4-114626
- Fe-Si-Al, Sendust, hot workability, microstruct. 4-114626
- NiZn ferrites, prod. by shock hot working, props. 4-61905
- Si, dynamical recovery in high temp. deform. 4-103867
- Ti alloys, plasticity of coarse grained type VT30 alloy in β-region (Russian) 4-81241
- household appliances *see* domestic appliances
- HSLA steel *see* alloy steel
- Hubbard model
- anisotropic 2D, SDW wave vector shift in transient region 4-98853
- chain, thermodynamics, temp. extension of ground-state renormalisation for fermions 4-70613
- disordered Hubbard alloys, spin glass behaviour 4-92928
- extended Hubbard model with half-filled band, ground state beyond the HF approx. 4-76147
- FCC lattice, Curie temp., specific heat, single band Hubbard model high temp. series 4-84764
- ferromagnet, narrow-band, carriers in spin wave range of temps. 4-92887
- four-centre tetrahedral cluster, Hubbard model, eigenvalue calc. 4-113841
- inverse-degeneracy expansions for the Hubbard model 4-104396
- ionic crystals, electronic Mott-Hubbard transition 4-92615
- magnetic and Mott transitions 4-88673
- narrow-band mag. semicond., at operator representation 4-75961
- one-dimensional extended Hubbard model, finite-cell scaling method 4-80738
- one-dimensional extended Hubbard model, real-space renormalisation group method 4-80737
- one-dimensional Hubbard model, use of finite-cell-scaling method 4-70616
- one-dimensional model, 2p<sub>F</sub> and 4p<sub>F</sub> instabilities 4-80467
- Pariser-Parr-Pople and linear Hubbard models, valence bond theory 4-78273
- polyenes, even and odd, molecular PPP correlations, optical excitations 4-74362
- polyenes, infinite, monoexcited CI spectrum, Hubbard approx. 4-68965
- semiconductor, lightly doped compensated, Coulomb gaps and Hubbard gaps 4-80542
- soliton energetics in electron-phonon models, Peierls-Hubbard models 4-70678
- structurally disordered Hubbard model, temp. depend. spin susceptibility 4-71014
- transition metal, local spin fluctuations—CPA model of mag. 4-71016
- transition metal alloy, second-order perturbation treatment of correl. and disorder 4-70645
- transition metal compounds, low temperature mag. susceptibility (Russian) 4-114095
- transition metals, inner-core photoelectron spectra, perturbation approach 4-71517
- transition metals and cpds., weak band magnetism theory of paramag. susceptibility (Russian) 4-108980
- Cr (001), photoemission spectra interpretation, effect of correlations 4-76635
- NiCr alloys, mag. struct. amplitudes, polarised neutron studies 4-108989
- Ni, doped, metal-nonmetal transitions 4-80500
- W (110) with surface adsorbed CO, electronic transitions, low-threshold neutral desorption, α-β conversion, calcs. 4-113785
- Hubble model *see* cosmology
- Huckel molecular orbital calculations *see* HMO calculations
- hue *see* colour

Hugoniot diagrams *see* equations of state

human engineering *see* ergonomics

# human factors

*see also* biocybernetics; ergonomics; man-machine systems

- achromatic images, high contrast, perceptual models, filtering 4-109814
- computer generated imagery, terrain perspectives, exaggerated vertical scale 4-81703
- CRT display, human colour discrimination under ambient illumination 4-81686
- digital image enhancement/restoration efficiency meas. by human performance 4-81704
- display terminal, eye scanning behaviour 4-81706
- joint motion in men using electrogoniometers 4-81739
- power plant alarm systems, procedure for reviewing and improving 4-68798
- reactor pressure vessel, quality assurance, NDT, human reliability models 4-68781
- speech digitization, real-time, evaluation methodology 4-79399
- vision, daytime variation in steady-state accommodation 4-81668
- visual accommodation, acquisition of distant targets 4-81681
- visual contrast sensitivity, psychophysical techniques 4-81682
- visual contrast sensitivity, target detection field performance 4-81683
- visual recognition performance, computer simulation 4-81684
- visual symbol structure effects on information processing 4-81705
- way of living rel. to indoor exposure from Rn: methodological study 4-93872

human-machine systems *see* man-machine systems

# humanities

*see also* archaeology; history; linguistics; music

- Wilhelm Busch, influence on physics instruction 4-106166

# humidity

*see also* atmospheric humidity; hygrometers

- air-water vapour mixture in greenhouse environment, thermal behaviour 4-87545
- atmospheric humidity, effect on NaCl and KBr surface, thickness and refractive index changes (Russian) 4-75783
- atmospheric humidity effect on surface thickness and refractive index (Russian) 4-75783
- grains, pneumatic drying, falling rate, mathematical anal. 4-76966
- hybrid fibre reinforced epoxide composite, environmental response of flexural props. 4-76809
- liquid desiccant heating and cooling system, operational experience in residential use 4-72167
- multilayer 3.8  $\mu$ m coatings, pulsed damage and optical characts., influence of cleaning solvents, sunlight, humidity and HF gas 4-75523
- porous alumina, sintered, impedance humidity sensitivity (Japanese) 4-66642
- porous alumina-boria, sintered, impedance humidity sensitivity (Japanese) 4-66642
- rod-rod gap, sparkover, impulse voltage induced stress and humidity effects 4-79716
- solar desiccant air-conditioner using heat exchangers and humidifiers 4-72164
- sphere-plane gaps in dry air, impulse breakdown, 0.25 to 2 atm. 4-79718
- Ag thin films, electroformed, humidity sensitive switching 4-108908
- AlGaAs/GaAs concentrator solar cells under high temp. and humidity conditions 4-66708
- $\text{Li}_2\text{O}_2\text{-ZnO}$ , ceramics system, ionic and mixed cond. rel. to comp. and humidity 4-98339
- $\text{Na}_2\text{O-SiO}_2\text{-H}_2\text{O}$  glass, hygroscopicity study 4-76997

# humidity control

- desiccant dehumidifier cooling system, sorption props. effect on performance 4-88404
- hybrid desiccant air conditioning systems for commercial buildings, performance influencing factors 4-72166
- hybrid desiccant vapor compression cooling system 4-86416
- solar desiccant residential cooling system high performance dehumidifier 4-72165

# humidity measurement

*see also* hygrometers

- alumina humidity sensor, moisture effect on dielectric props. analysis 4-95442
- calibration of instruments 4-63753
- capacitive humidity metering circuit with digital displays of the relative humidity and limiting value transducers (German) 4-101856
- direct insertion type zirconia oxygen analyzer hygrometer, Fuji Electric 4-111142
- domestic solar system instrumentation, long-term stability and performance 4-99989
- FET humidity sensor incorporates temperature sensor 4-73443
- generator, for establishment of humidity standard (Japanese) 4-111143
- high frequency digital granules hygrometer, appl. (German) 4-86425
- hygrometer, compact, using thermosensitive capacitor, DIY design (German) 4-68235
- IR sounder for moisture and temp. meas., design requirements 4-62959
- Laval nozzle for absolute humidity of air determ. 4-65046
- lecture notes and study guide on process analysers and recorders, book 4-106138
- sensors, sintered alumina and zircon, elec. resistivity rel. to surface area of oxides (Japanese) 4-63751
- silicone composite material, glassy film conversion, humidity-sensing props. rel. to elec. resistance 4-63752
- thick-film hybrid sensors, design, characts. and meas. appl. (German) 4-82789
- $\text{ZnCr}_2\text{O}_4\text{-LiZnVO}_4$  ceramic sensors, humidity-sensitive props., microstruct. 4-82800
- $\text{ZnO/CuO:Li}$  junctions I-V characteristics, humidity effects, humidity sensor appl. 4-63750

h.v. engineering *see* high-voltage engineering

HVEM *see* electron microscopy

hybrid computer methods *see* hybrid simulation

# hybrid integrated circuits

*see also* flip-chip devices; microwave integrated circuits

- cryogenic sensor-amplifier interfaces, hybrid circuit freq. compensation modules 4-90573
- optical fibre receiver, development 4-69589
- PIN-FET receiver for fibre optics 4-74744
- thick-film hybrid sensors, design, characts. and meas. appl. (German) 4-82789

# hybrid reactors

- dense plasma focus based device, role in energy complexes 4-59433
- design and safety study, fast fission blanket safety performance 4-96274
- fusion breeder, potential role and prospects 4-59431
- fusion breeders, economics 4-59353
- fusion-fission hybrid blankets, time depend. performance characts. 4-59428
- fusion-fission hybrid systems evaluation 4-59425
- fusion-fission hybrids based on Tokamak concept (Korean) 4-111970
- laser pellet, Tokamak and hybrid reactors, review 4-59422
- LOTUS fusion-fission hybrid facility, present status 4-59427
- neutron economy with plasma focus source 4-59432
- power-balance analysis of muon-catalyzed fusion-fission hybrid reactor systems 4-107141
- suppressed fusion ICF hybrid, neutronics aspects 4-111858
- sustainable energy system, nuclear technology, conf., Laxenburg, Austria (May, 1981) 4-58577
- symbolic molten-salt systems coupled with ICF hybrid molten salt breeder 4-59352
- synergistic nuclear energy options, spectrum of choices 4-59429
- technological readiness and role in world nuclear future 4-62318
- US-DOE fusion breeder program, blanket design and system performance 4-59426
- D-cycle Tokamaks integration with decentralised small fusion and fission reactors 4-59406

# hybrid simulation

- blood pressure behaviour after treadmill test 4-100224
- heat conductivity problems by Monte Carlo methods (Russian) 4-82767

hydrated electrons *see* solvated electrons

hydration *see* solvation

# hydraulic amplifiers

- dynamic force measurement with a hydraulic force balance valve 4-86405

# hydraulic systems

- pressure transients, errors in simulation 4-83952

hydroacoustics *see* underwater sound

# hydrodynamics

*see also* jets; liquid waves; viscosity of liquids

- barred galaxies, 1/1 reson. 4-63280
- barred galaxies, three-dimens. dynamics 4-94947
- binary systems, hydrodynamic instability and perturbation system 4-108064
- black holes, nonspherical accretion, finite differencing and code calibration 4-110650
- body-fluid system, combined spatial motion problems, direct soln. method 4-74850
- Brownian coagulation kinetics, weak hydrodynamic field 4-79638
- capillary flow, hydrodynamics, no-slip boundary condition 4-60549
- cavitation, physical modelling using optical meas. techniques 4-60469
- charge stabilised dispersions, concentrated, self-diffusion, Brownian dynamics simulation 4-99851
- cholesteric liquid crystals, hydrodynamics in coarse-grained limit 4-87700
- collisions in systems of non-identical particles, numerical simulations, planetary ring appl. 4-101214
- cosmic-ray-mediated shocks with variable compression ratio, theory 4-63021
- diatomic gas, dissociating, coeffs. of additional terms of hydrodynamic eqns. 4-113075
- differentially rot. discs with const. specific ang. momentum, dynamical stability 4-85869
- dynamical meteorology, non-hydrostatic eqns. in pressure and sigma coordinates 4-82202
- evaporative process in capillary-porous structs., approx. hydrodynamic theory 4-113750
- expanding stars, thermal equilb. departures, mass loss 4-90136
- expendable bathythermograph (XBT), bulk dynamics 4-82248
- ferromagnetic emulsion, hydrodynamics, effective viscosity and shear flow 4-109693
- finite amplitude spherical waves in ideal gas, renormalisation calc. 4-83755
- first-flight escape from spheres with  $R^{-2}$  density distribution 4-90085
- fishing trawl net design, hydrodynamic testing facility development 4-115639
- flow field, predictability measures 4-60360
- flows with steady vorticity, reduction theorem 4-91815
- fully developed laminar flow and heat transfer in an arbitrarily shaped triangular duct 4-64911
- galactic disc, hydrodynamic and turbulent motion 4-82536
- galactic discs, influence of bar strength and pattern speed on spiral struct. 4-94958
- galactic discs dynamics, stabilising and destabilising effects of haloes 4-73070
- galactic dynamics, density wave theory, Bessel products summation, closed forms 4-87884
- galactic nonstationary viscous gaseous discs 4-63323
- galaxies, generalised Mestel disc and truncated Toomre discs, exact solns. 4-72865
- galaxy superclusters as nondissipative pancakes, N-body simulations 4-77948
- Garfield Thomas Water Tunnel, hydrodynamics and fluid mechanics research progress 4-65044
- gas-liquid mass transfer in fixed-bed reactors with cocurrent downflow operating in the pulsing flow regime 4-112980
- gas-liquid slug flow in vertical tubes, hydrodynamic model 4-75070
- gasdynamic focusing for sample concentration in ultrasensitive analysis 4-93567
- heat-releasing apparatus inlet, hydromechanics 4-79669
- heated particle cloud, precipitation on horizontal plane 4-71995
- hydraulic jumps, simulation in presence of rot. and mountains 4-62919
- hydraulic jumps in viscous accretion discs, appl. to neutron stars and galaxies 4-90081
- hydrodynamic turbulence, renormalised theory 4-74992
- hydrodynamics, fluctuation effects in 2-D systems 4-112804
- infalling gas deceleration mechanism above magnetized neutron star 4-90172
- interstellar bright rims form. and evolution 4-90213
- interstellar clouds, dynamics of evaporating cloud envelopes 4-90209
- interstellar clouds sweeping from rot. galaxy by intergalactic medium, dynamics 4-94943

**hydrodynamics continued**

- interstellar gas in disturbed galaxies, stability of simplified continuum models 4-63270
- inviscid flow, exponentially derived switching schemes 4-103417
- jets with inhomogeneous viscosity, structure 4-67619
- liquid-solid systems, mixing hydrodynamics 4-69813
- macromolecules, membrane rejection coeffs., conc. and charge effects 4-89333
- mobile bed contactor with low-density packing particles, hydrodynamics 4-60536
- molecular clouds, clump collisions 4-94911
- molecular clouds, spherical, steady-state models 4-77892
- molecular clouds collapse and fragmentation, protostars form. 4-63138
- molten metals, EM vibr. treatment under microgravity, hydrodynamic effects 4-97698
- multi-dimensional flows, radiation boundary conditions 4-82203
- natural gaseous inhomogeneities evolution 4-79619
- nematics, orthorhombic, isothermal hydrodynamics 4-92080
- nonequilibrium hydrodynamic fluctuations, Langevin formalism 4-112805
- petroleum exploration, applied hydrodynamics, book 4-106131
- phenomena and paradoxes 4-113090
- plane and curved flame stability 4-99795
- PMMA colloids, sterically stabilised, shear viscosity, temp. depend. 4-112789
- polyarylates, dil. solns., thermodynamic and hydrodynamic props. (*Russian*) 4-61110
- polymer solutions, hydrodynamic interactions, neutron spin echo obs. 4-84136
- predictability, Lagrangian and Eulerian view 4-62877
- predictability, topological issues 4-58646
- Primakoff blast waves, stability of self-similar flow, correction 4-94573
- protostellar formation in rot. interstellar clouds, nonisothermal collapse 4-94729
- radio sources, extragalactic, struct. of hotspots from time-varying jet 4-101493
- rarefied gases, subsonic flow, particle interaction at low Reynolds number 4-64969
- Rayleigh Taylor instability and high-vel. interstellar clouds accel. 4-110727
- relativistic stellar dynamics 4-77883
- river system, dendritic, water depth, flow simulation, channel hydrodynamic model 4-82100
- rotating self-gravitating gaseous disks, nonlinear disturbances (*Russian*) 4-86061
- self-similar flow stability, Primakoff soln. 4-87668
- sheared suspensions, dynamic simulation 4-74975
- small body motion is perturbed flow formulation 4-113091
- smectic A phase liq. crystals, and 1D solids, hydrodynamic concepts (*French*) 4-98008
- solidification of continuous ingot under conditions of inductive MHD action 4-108138
- spherically symmetric self-similar gasdynamic flows 4-110510
- spiral galaxies, struct. and star form., particle hydrodynamics simulation 4-86050
- spiral patterns excitation in responsive density wave theory 4-63213
- spout-fluid beds, hydrodynamics (*German*) 4-103403
- stars, non-linear pulsations, hydrodynamic models 4-110596
- statistical mechanical development from molecular dynamics 4-78230
- steady state flow of a fluid stream with streamline disturbance around an arbitrary arc (*Russian*) 4-87667
- steering-ducted propeller, hydrodynamic performance (*Chinese*) 4-97636
- stellar atmospheres, nonlinear two-dimens. dynamics 4-77812
- stochastic systems, adiabatic elimination of variables 4-73367
- streamlined surface, curvature discontinuity rel. to flow hydrodynamics (*Russian*) 4-69848
- stress in fluids, theory 4-110828
- submarine depression, sub-sill source fluid dynamical model of brine pools 4-62838
- supernova models, rot. and nonrotating, hydrodynamic collapse calcs. 4-63188
- terephthalic acid aromatic polyesters solns., conformational props. 4-103636
- thermal and hydrodynamic development in square duct 4-60415
- thin accretion discs, nonaxisymmetric baroclinic instability 4-94732
- three phase bubble column, axial mixing hydrodynamics, slurry props. effects 4-87782
- thrust created by vibr. vane, expt. apparatus and method (*Russian*) 4-69835
- transfer function method of modeling systems with frequency-dependent coefficients 4-110879
- two dimensional flow with strong shocks, numerical simulation, review 4-69793
- two-dimensional hydrodynamic systems, nonthermodynamic fluctuations 4-90375
- two-phase planet, stability and free oscils. 4-63092
- viscous fluid flow hydrodynamic params. In convective problems for flow separation in channels 4-79587
- vortex chamber with hyperbolic end covers, hydrodynamics 4-79602
- water-air mixture flow in vertical pipe, hydrodynamic calc. 4-60515
- wave energy devices hydrodynamic props., projecting sidewalls effect 4-112818
- wind-type model for the generation of astrophysical jets 4-101139
- windmills Betz optimum efficiency derivation 4-79617
- H II regions, evolution, mathematical model 4-63245
- H II, thermohydrodynamics eqns. and reduced density matrices 4-84480

**hydroelasticity** *see elasticity***hydroelectric power stations**

- see also dams; tidal power stations; water supply; wave power generation*
- Greenland's future energy plan, role of water power (*Danish*) 4-81520
- Yugoslavian hydropower potential, possibilities of utilisation 4-105094

**hydrogen**

- see also nuclei with .....*
- see also deuterium; hydrogen ions; hydrogen neutral atoms; hydrogen neutral molecules; protons; solid hydrogen; tritium*
- absorption by lanthanide films 4-71984
- absorption in Gd-Pd, effect on mag. and cryst. props. 4-104412
- absorption in rare earth intermetallic compounds, book 4-95076
- absorption in  $YCo_5Fe$ ,  $YCo_5Ni$  and  $Y_0.5Dy_{0.5}Co_5$  (*Russian*) 4-75775
- adsorbed layer on W (111), diffusion, fluctuation method anal. 4-104088
- adsorbed layers on Ni, Pd and Pt vibr. spectra 4-104073

**hydrogen continued**

- adsorbed on Ni (110), dual path surface reconstruction study 4-108716
- adsorbed on Ni (111), phase diagram 4-104083
- adsorbed on Pd-MOS struct., use as  $H_2$  sensor in catalytic reactions 4-93555
- adsorbed on Pt (111), He scattering studies 4-88400
- adsorbed on  $SiO_2$  in optical fibres 4-97079
- adsorbed on W (001), reconstruction domains, finite size effects 4-88379
- adsorbed on W (001), surface reconstruction, LEED and EELS study 4-92492
- adsorbed on W (001), surface reconstruction phase transition, model 4-88380
- adsorbed on Zr, sticking coefficients, binding states, desorption studies 4-113784
- adsorption, on Raney Ni, inelastic neutron scatt. spectrosc. obs. 4-113797
- adsorption and catalytic reaction on Pd (100), EELS and LEED study 4-71969
- adsorption and dissolution by monodisperse Pd catalysts 4-61220
- adsorption isotherms and heats of adsorption on activated charcoal 4-114821
- adsorption location on Pt (111) from corrugation anal. and  $He^+$  diff. 4-65556
- adsorption on activated charcoal at low press. and at 20K 4-99844
- adsorption on Ag and Al (111) surfaces, EHT method studies 4-65544
- adsorption on Al films, electron stimulated desorption study 4-75792
- adsorption on diamond (111), photoemission studies 4-88939
- adsorption on Fe films, surface pot. and thermal desorp. spectra study 4-65555
- adsorption on GaAs (110), EHMO method calc. (*Chinese*) 4-113787
- adsorption on  $Ni_{14}$  cluster, MINDO/SR calc. 4-64647
- adsorption on Ni (110), EELS study 4-65564
- adsorption on Ni (110), kinetics of adsorption and reaction 4-92519
- adsorption on Pt (111), vibr. props., EELS and inelastic neutron scatt. studies 4-113806
- adsorption on S covered Pt (110) (*French*) 4-84504
- adsorption on Si (100)2x1, coverage and temperature-dependent vibr. spectra, EELS and LEED studies 4-80408
- adsorption on W (100), effect on EELS spectrum 4-93159
- adsorption on W (100), surface reconstruction, symm. effects, refl. EELS study 4-80382
- alkali metal halides, interstitial atomic H centers in mixed config., unrelaxed excited states, MCD optical absorpt. 4-70747
- arc plasma, electron density, interferometric and spectrosc. investig. 4-84082
- atomic, three-photon-excited fluoresc. detect. in acetylene/ $O_2$  atm.-press. flame 4-81440
- binary alloys, hydride precipitation, two-level model 4-75688
- bubble form. in 600 MeV proton irradiat., Al 4-108479
- chalcogenide glass,  $H_2O$  and  $H_2$  band reduction 4-107896
- chemisorbed on Al thin film, chemisorption effect an elec. cond. 4-88391
- chemisorbed on Ni surface, quantum motion 4-80385
- chemisorbed on Si (100), surface states, UPS study 4-108709
- chemisorbed overlayer on Fe (110), Monte Carlo studies 4-113816
- chemisorption on a-Si:H 4-108715
- chemisorption on B cluster surfaces, ab initio RHF calc. 4-92555
- chemisorption on Fe (110), ordered struct. form. on metal surface, role of multi-atom interactions 4-80400
- chemisorption on graphite, MINDO/3 cryst. orbital LCAO SCF calc. 4-98430
- chemisorption on liquid Fe-C-Ti system, surface tension meas. (*Japanese*) 4-65517
- chemisorption on Si (100), TDS study (*Chinese*) 4-92510
- chemisorption on Si (100) surface, work function changes 4-70907
- chemisorption on W (100), two-electron bond approach 4-113801
- coadsorption with CO on Mo (100) and  $MoS_2$  (0001) 4-80407
- coadsorption with CO on Ni, ion induced desorption study 4-92547
- coadsorption with  $O_2$  on W (100), temperature-programmed desorp. study 4-84507
- combustion test program in nuclear pressure vessel 4-106927
- compressed, tunable high-power radiation source in 0.72 to 8  $\mu m$  range 4-107738
- concentration in installed optical fibre cables and under accelerated conditions 4-97126
- concentration measurement, by thermocompensated ultrasonic detector 4-112660
- desorption from fusion reactor first wall coatings under electron impact 4-91097
- desorption from Ni (110), influence of magnetisation 4-104081
- determination, in  $Si(SiO_2)$ , by reson. nucl. reactions 4-85347
- diamond- $H_2$ , interstitial muons anal. impurity states 4-80541
- diffusion, in  $\beta$ -Pd-H, Fick's coefficient 4-98334
- diffusion and conc. in metals, electrochem. permeation method (*Japanese*) 4-65467
- diffusion and tunnelling in metals 4-65473
- diffusion coeff. and conc. in metals, electrochemical permeation method (*Japanese*) 4-65468
- diffusion coeff. and conc. in metals (*Japanese*) 4-65466
- diffusion in Al, desorption study 4-65489
- diffusion in metals, trapping model analysis 4-70470
- diffusion in  $WO_3$  thin films 4-70474
- diffusion in ZrH<sub>2</sub> and cold neutron scatt. cross section 4-103611
- diffusion into W (110) field emitter at low temp. 4-92549
- diffusivity in metals meas., by resistance technique 4-68343
- dilute solutions in Pd alloys, thermodynamics 4-70411
- discharge, spatial and temporal current growth; 4-79883
- dissolution in metallic glasses, vol. changes 4-70396
- effect on elec. props. of CdTe films 4-76053
- effusion and penetration in steel, tribologically induced effect 4-109521
- effusion of Fe-Ni-C alloys, martensitic transform., subzero temp. 4-85153
- emission source for line radiation, using hollow cathode arc 4-60129
- evolution from silicone resin primary coatings on optical fibres 4-97124
- evolution in optical cables 4-97125
- flame propagation model in 1-D, pressure transients in reactor vessel 4-106926
- fusion reactor refuelling, pellet acceleration with railgun 4-91099
- galactic  $H_2$  detection in NGC 6240 and ARP 220 merging galaxies 4-115821
- gas, DC breakdown strength, isotope depend. 4-79723

## hydrogen continued

gas, parametric four-wave mixing process in stimulated Raman first order Stokes scatt. (*Chinese*) 4-112512  
 gas, subexcitation electron thermalisation, Monte Carlo simulation 4-83470  
 gas, VUV radiation generation by stimulated Raman scatt. using ArF<sub>19</sub> laser 4-69496  
 gas high-pressure cell, efficient stimulated Raman scatt. of XeCl laser 4-96999  
 graphite+H reactivity, electron bombardment enhanced 4-93529  
 human body N, H and fat, prompt and neutron activation, improved calibration 4-67104  
 implantation of GaAs, range and damage distrib. 4-103774  
 impurities in metals, theoretical studies 4-70706  
 impurity, proton recoil technique for H depth profiling 4-88922  
 Infrared Space Observatory dual liquid H<sub>2</sub>/<sup>3</sup>He superfluid He coding system thermal design 4-73441  
 insertion compounds with V<sub>6</sub>O<sub>13</sub>(V<sub>2</sub>O<sub>5</sub>) 4-70093  
 ion beam phase volume meas., multichannel A/D interface for Elektronika-1001 computer 4-91130  
 light-induced detonation, thermodynamic props. 4-97796  
 liquid, dielectric const., density depend. (*Chinese*) 4-76300  
 liquid, fluid density meas. using microwave open ended cavity tuned oscillator (*Chinese*) 4-73425  
 liquid, target cooled by flowing He 4-59473  
 liquid and gas, viscosity determ. 4-61125  
 liquid bombardment target, circulation, construction, meas. and control (*Chinese*) 4-112001  
 LWR containment, H<sub>2</sub> behaviour during accidents, production, mixing, combustion 4-64221  
 magnetic monopoles, energy loss from elastic collision with H, He atoms 4-68464  
 maser, cryogenically cooled development, for freq. shift and relax. props. meas. 4-69354  
 maser, freq. stability improvement by new state selection 4-96855  
 maser atomic frequency standard (*Japanese*) 4-60006  
 maser frequency standards, limitations due to receiver noise 4-96854  
 maser frequency standards, NR series, microprocessor monitor and control system 4-68202  
 maser time and frequency standards, status and appl. (*Italian*) 4-86389  
 masers, appl. of metal hydrides for gas handling 4-69352  
 masers, compact, performance 4-69353  
 methane, H<sub>2</sub> gas solubility, Henry's constants calc. 4-113640  
 migration process of H isotopes in BCC metals, realistic calc. 4-65465  
 molecular fluid equilb. props. in semiclassical limit 4-103632  
 nonequilibrium positive columns, state transitions, two-temp. model 4-92007  
 nuclear reactor containment building, H<sub>2</sub> combustion and control 4-111666  
 optical effects on optical fibres due to absorpt. spectrum of interstitial H<sub>2</sub> 4-97120  
 optical fibre cable link implementation and reliability, conf., London, England (June 1984) 4-95066  
 optical fibres, H<sub>2</sub> diffusion constant temp. and press. depend. 4-107861  
 Orion Nebula, H<sub>2</sub> infrared emission at 1.064 microns 4-94920  
 pellet injection in tokamak, H<sub>2</sub>-line emission and ablation rate 4-103522  
 perfluoroalkane-H<sub>2</sub> mixtures, RF plasma decomp. during plasma etching or fluoropolymer deposition 4-108230  
 perfluoropropane-H<sub>2</sub> RF discharge, chem. mechanisms 4-108231  
 permeation in oxidised high temp. alloys, thermocycling, acoustic emission 4-76905  
 permeation through CVD SiC fusion reactor first wall material 4-92403  
 plasma, confined by neutral H, time resolved temp. meas. 4-87923  
 plasma, dense, thermodynamic functions calc. 4-83978  
 plasma, edge region H<sub>2</sub> line emission in PDX Tokamak 4-91970  
 plasma, low voltage, interaction with Pd surface 4-113160  
 plasma, oscillator strengths and photoionisation cross sections 4-78804  
 plasma, partially ionised, elec. cond., kinetic theory 4-97758  
 plasma, specific heat, temp. and density meas. behind shock front 4-113116  
 plasma electric fields, low freq., investig. using H line Stark broadening 4-84075  
 plasma etching, appl. to reactive ion etching of organics 4-99620  
 pretreatment affect on CO adsorpt. on NiO-MgO solid solns., reactivity, H<sub>2</sub> pretreatment effects, spectrosc. obs. 4-113796  
 production from alcohol and water photocatalytic reaction on Pt/TiO<sub>2</sub> 4-114820  
 PWR hypothetical core-melt accident, H<sub>2</sub> risks and containment 4-96239  
 quantum crystal, plasticity mechanism (*Russian*) 4-92473  
 recycling constant of TEXTOR liner, in situ meas. 4-108182  
 saturated Si (111) surface, Au deposition, AES and EELS study 4-108742  
 sensor using Pd MOS structure 4-63729  
 a-Si:H film, prep. by reactive sputtering, optical and elec. props. 4-71457  
 solid, adiabatic eqn. of state at 150 kbar 4-113567  
 solid, press. induced rot-libration transition 4-75622  
 solubility in binary Fe melts (*German*) 4-65401  
 solubility in liq. Li-Pb alloy breeder blanket materials, interaction of H isotopes investig. 4-107034  
 solubility in liq. Li-Pb alloy breeder blanket materials, thermodynamic investig. 4-107033  
 sorption, by La alloys, influence on heat pump operation 4-105131  
 sorption by hyperstoichiometric Ce<sub>1-x</sub>Ni<sub>x</sub>Cu<sub>2</sub> alloys 4-61207  
 sorption in TiMn<sub>3</sub> at low press. (*Japanese*) 4-65552  
 spin-polarized film on <sup>3</sup>He substrate, superfluidity detection 4-70527  
 steady state transport in solids exposed to fusion reactor plasmas 4-74041  
 steel, H and D diffusion under fission reactor radiation 4-113503  
 steel, martensitic transformation in alloy 40N25, diffuse-mobile H effects (*Russian*) 4-104780  
 steel, stainless, H transport 4-113722  
 stimulated Raman scatt., spatial and spectral characts. 4-83639  
 stimulated Raman scatt. of XEF\* laser radiation 4-74611  
 storage properties of CeNi<sub>3-x</sub>Al<sub>x</sub> alloys 4-61206  
 surface concentration from methoxylated Mg, TOF direct recoil spectra 4-99827  
 TEXTOR first wall characts. w.r.t. H recycling 4-91968  
 thermal desorption from Pt/TiO<sub>2</sub>, isotope scrambling 4-80377  
 thermal desorption spectra, angle resolved, from Ni 4-70554  
 thytrons, high power plasma switches, atoms and ion prod. 4-65136

## hydrogen continued

thytrons, high power plasma switches, plasma props. 4-65135  
 Titan, atmospheric H<sub>2</sub> density in atomic H cloud 4-67677  
 Tokamak discharge chamber, H interaction 4-103512  
 transition metal compounds, coordination of H at interstitials 4-84288  
 transition metals, H absorpt. kinetics and subsurface bonding 4-75691  
 trapping by Y; in low temp. Li 4-111759  
 trapping of sub-eV H and D atoms in C 4-111761  
 tunnelling in Nb, sp. ht. meas. 4-61103  
 WAK reprocessing plant, H<sub>2</sub> radiolysis in cooling system; H<sub>2</sub> concn safety 4-91065  
 Al-H system, FCC crystal, force consts. between interstitial H atoms and host atoms 4-75629  
 AlH<sub>3</sub>, electronic contrib. to elastic consts. 4-65326  
 Au-Ge(H) interfaces on amorphous Ge, Schottky barrier and cpd. formation 4-84669  
 a-C:H, low emittance coatings for high temperature solar collector 4-114950  
 C:H absorbing films, optical const. unambiguous determ. by reflectance and transmittance meas. 4-65997  
 C:H amorphous coating for IR-optical elements, optical props., thickness, density, laser damage tests 4-76422  
 C:H amorphous film, H<sub>2</sub> gas reactive RF sputtering prep. on low temp. substrates 4-76673  
 C:H amorphous film prep. by H<sub>2</sub> gas reactive RF sputtering of graphite 4-76671  
 a-C:H coating material for passive IR materials 4-74668  
 a-C:H hard thin films, RF plasma deposition 4-76681  
 CaNi<sub>2</sub>H<sub>2</sub>(D<sub>2</sub>), absorption pressure-comp. isotherms, thermodynamic and 4-77032  
 CdTe:H-Au contacts, hydrogenation effects 4-80695  
 Cu/a-Si:H/a-Si:H(n-type)/Cr Schottky diodes, RF magnetron sputtered 4-88557  
 CuH<sub>x</sub>, cryogenic material, heat losses due to H ortho-para conversion (*German*) 4-106326  
 a-Ge:H, bond angle disorder and optical absorption edge 4-99083  
 Ge:H, ion irradi., structural defect study 4-88164  
 a-Ge:H, photoinduced absorption spectra 4-109220  
 a-Ge:H:P, new paramagnetic centres and impurity states 4-109056  
 a-Ge:H films, planar magnetron sputtering, electronic props. 4-88972  
 Ge:H-based impurity complexes, charge state determ. 4-92663  
 H<sub>2</sub> production on poly- and monocrystalline converters in surface-plasma ion source 4-96315  
 H-H oscillations in SU(3)×SU(2)×U(1) theory 4-90777  
 H-H plasma, ion Bernstein wave heating expt. on JIPPT-II-U device 4-60662  
 H-T (H-D)(D-T) mixture equilibria in LaNi alloys 4-108586  
 H<sub>2</sub> distribution in reactor containment following serious accident WAVCO anal. 4-96238  
 n-H<sub>2</sub>, liquid and liquid mixtures, intermolecular free length, acoustic studies 4-88059  
 H<sub>2</sub> production by electrolysis, design and process engineering concepts (*German*) 4-93644  
 H<sub>2</sub>-air mixtures, high-speed turbulent deflagration and transition to detonation 4-103432  
 H<sub>2</sub>-CO mixtures for testing dissociated methanol engine 4-62290  
 H<sub>2</sub>-CO<sub>2</sub> in air, flammability and detonability in radioactive waste processing 4-106741  
 H<sub>2</sub>-HF gasdynamic pure rotational laser based on far IR transition theoretical study 4-79118  
 H<sub>2</sub>-methane flames, ion current calc., temp. depend. 4-89296  
 H<sub>2</sub>-O<sub>2</sub> flames, with excited species mag. quenching of emission intensities 4-78891  
 H<sub>2</sub>-O<sub>2</sub> fuel cell, alkaline low-temp., prep. and characts. of porous gas diffusion electrodes 4-62349  
 H<sub>2</sub>, electron-stimulated field desorption 4-92532  
 He-H Penning ionisation formula 4-91338  
 InSb:H, ionisation energy of magnetodons 4-70714  
 LaNi<sub>2</sub>-NdNi<sub>2</sub>(CeNi<sub>2</sub>), phase diagrams, grain size anisotropy, H absorpt. characts. (*Chinese*) 4-93261  
 LaNi<sub>2</sub>(Ni<sub>4</sub>AlO<sub>3</sub>) and misch metal analogues, H<sub>2</sub> desorption kinetics 4-75787  
 LiF:H, γ-irrad. and mechanically loaded, H atom localisation 4-88179  
 Mo MOS structures, stabilisation using H<sub>2</sub> doping and high temp. forming gas annealing 4-98761  
 N<sub>2</sub>-H<sub>2</sub> glow discharges, emission spectroscopy for metal surface nitriding 4-75222  
 NaCl:H, radiation induced H discharge, optical absorpt. (*Russian*) 4-99139  
 Nb, H permeation, surface effects 4-113723  
 Nb:H, hydrogen embrittlement, electron microscopy study 4-93396  
 Nb:H,N, ultrasonic absorpt. due to H tunnelling 4-70287  
 NbO<sub>2</sub> anodic layer, contamination studies by emission angle dependent XPS with double-pass CMA 4-99282  
 Ne-H<sub>2</sub> pulsed transverse elec. discharge, Ne\* recomb. pumping (*Russian*) 4-112133  
 Ni, thermodynamics, kinetics and props. of gases and C, data tables 4-73173  
 Ni-H sealed batteries, stationary gas cycles 4-81538  
 Ni-H<sub>2</sub> electrode, Raney three layer, for fuel cells (*Japanese*) 4-89396  
 Pd:H, H diffusion, induced Hall voltage 4-70463  
 Pd-Ag-H, struct. and elec. props. (*Russian*) 4-79981  
 SF<sub>6</sub>-Cl<sub>2</sub>(H<sub>2</sub>) gas mixtures, vibr. relax., US absorpt. study 4-75117  
 Si (100) 2×1, pre-exposed to O in submonolayer range, chem. shifts  
 Si-H stretching freqs. 4-80368  
 a-Si:Cl, H films, photocond. spectra (*Chinese*) 4-113989  
 a-Si:H, absorpt. edge, struct. disorder model for amorphous semiconductor 4-80483  
 Si:H, Al-covered, solid-state reaction between film and substrate 4-9245  
 Si:H, amorphous, CVD growth by Si<sub>2</sub>H<sub>6</sub> pyrolysis in hot wall reactor 4-61864  
 Si:H, amorphous, DC triode sputtered, electronic transport 4-61374  
 Si:H, amorphous, electron mobility meas. using 4-terminal FET structure 4-75964  
 Si:H, amorphous, electron-excited Coster-Kronig transitions 4-88908  
 Si:H, amorphous, Fe<sub>2</sub>O<sub>3</sub>-coated semiconductor electrode by solar cell XPS, AES and electrochem. meas. 4-66691  
 Si:H, amorphous, glow discharge chemical vapour deposited, X-ray photoelectron spectroscopy 4-93201  
 Si:H, amorphous, glow-discharge deposition, efficiency of gas usage, for solar cells 4-71602

## hydrogen continued

- Si:H, amorphous, high-rate deposited annealing effects 4-61876  
 Si:H, amorphous, light-induced defects, annealing 4-92762  
 Si:H, amorphous, prepared by photo-CVD, electronic and optical props. 4-70959  
 Si:H, amorphous films, glow discharge decomposition, Hg(Kr) effects 4-76687  
 Si:H, amorphous films, optical storage technique 4-91547  
 Si:H, amorphous solar cells, CVD growth 4-66694  
 Si:H, As, dispersive transport, trap saturation, transient photocurrent meas. 4-76006  
 Si:H, B, P, electron structure and density of states of B-P pairs, cluster calc. 4-65642  
 Si:H, B(P), amorphous CVD layer, impurity doping 4-60941  
 Si:H, broken bonds and electronic density of states, H effects 4-65178  
 Si:H, conductivity, localisation and mobility edge 4-70819  
 Si:H, correlated defects and steady-state photoconductivity 4-61417  
 Si:H, DC elec. cond. Meyer-Neldel rule and Staebler-Wronski effect 4-113948  
 Si:H, deep recombination centres, luminescence and EPR studies 4-104164  
 Si:H, dislocated, impurity exodiffusion 4-103788  
 Si:H, doping and gap states 4-70734  
 Si:H, electronic localisation-delocalisation transitions and H<sup>-</sup>-like states 4-92668  
 Si:H, electronic density of states calcs. (Russian) 4-70740  
 Si:H, electronic struct., theoretical models 4-70638  
 Si:H, electronic struct. study using Auger electron spectroscopy (French) 4-75840  
 Si:H, energy, distrib. of light-induced gap states, photocond. meas. 4-76004  
 Si:H, extended state mobility 4-104208  
 Si:H, F p-n junctions, generation; recombination currents, computer simulation 4-84683  
 Si:H, geminate recombination and mobility 4-104223  
 Si:H, glow discharge decomposition prep., electron drift mobility, photocond. (Chinese) 4-84616  
 Si:H, grown by zone melting, A-centre distrib. study 4-76666  
 Si:H, H<sub>2</sub> chemisorption, AES and EELS meas. 4-108715  
 Si:H, high-rate deposition from SiH<sub>4</sub> using RF discharge technique, elec. and optical props. 4-85119  
 Si:H, high-resolution PMR, high resolution of narrow spectral component 4-104498  
 Si:H, homogeneous CVD growth, review 4-88984  
 Si:H, IR absorpt., gaseous H<sub>2</sub> and Si-H overtone spectra 4-93075  
 Si:H, interstitial muons anal. impurity states 4-80541  
 Si:H, long-time drift mobility, photocurrent study 4-104221  
 Si:H, MIS diode, glow discharge deposited, flat-band capacitance freq. depend. 4-76042  
 Si:H, microcrystalline, IR absorpt. study of Si-H bond formation 4-71416  
 Si:H, microcrystalline, photoinduced free-carrier absorpt. spectra 4-88859  
 Si:H, neutron irradiated, deep levels study (Chinese) 4-92649  
 Si:H, non-substitutional dopant states and carrier density statistics 4-113902  
 Si:H, P(B), dark cond. and photocond., thickness depend. 4-84624  
 Si:H, photoinduced absorption spectra 4-109220  
 Si:H, plasma deposited film, NMR study 4-104502  
 Si:H, plasma deposition, two layer struct., surface contribs. 4-70593  
 Si:H, plasma-enhanced deposition 4-81160  
 Si:H, prep. by glow discharge of Si<sub>2</sub>H<sub>6</sub>, optical and elec. props. 4-114237  
 Si:H, RF sputtered amorphous film, dark cond. and photocond., annealing effects 4-70960  
 Si:H, radiative combination at dangling bonds, quantitative model, expt. study 4-114326  
 Si:H, resolution of DLTS energy scale controversy 4-104166  
 Si:H, structural and vibr. spectra calcs. 4-98017  
 Si:H, study of H-induced defects (Chinese) 4-103736  
 Si:H, TSC meas., density of states behaviour 4-98636  
 Si:H, time-resolved charge transport and photocond. 4-70871  
 Si:H, transient photoinduced absorpt. 4-104634  
 Si:H, undoped, carrier trapping, picosecond. electronic relaxations 4-108892  
 Si:H,B, amorphous, solar cells, deposition from Si<sub>2</sub>H<sub>6</sub> and B doping profiles 4-81540  
 Si:H,B, doping effect on gap states 4-88488  
 Si:H,B amorphous CVD films, optical props., B doping effects 4-99086  
 Si:H,B film, optical props. study 4-76540  
 Si:H,F films, F incorporation, during glow discharge deposition 4-114426  
 Si:H, Li, surface photovolt. and dark conductance, light-induced changes 4-70861  
 Si:H,N film, TSC and photoconductivity 4-104222  
 Si:H,O, grain boundary impurity effect determ. 4-92214  
 Si:H,O(N) alloys, electron trapping states, tight binding formalism calcs. 4-113901  
 Si:H,P, defect states and carrier capture processes 4-104165  
 Si:H,P, new paramagnetic centres and impurity states 4-109056  
 Si:H,P,B film, drift mobility, photoconductivity meas. 4-104259  
 Si:H,P film, acoustoelectric effect, thickness depend. study 4-104273  
 Si:H,P(B), ESR and optical props., thickness depend. 4-84853  
 Si:H (100)(2x1), surface IR studies 4-99116  
 Si:H absorbing films, optical const. unambiguous determ. by reflectance and transmittance meas. 4-65997  
 Si:H amorphous compensated films, xerographic discharge meas. 4-80603  
 Si:H amorphous film 4-85115  
 Si:H amorphous films, glow discharge deposited, electron drift mobility, substrate temp. dependence 4-61393  
 Si:H amorphous films, glow discharge deposition in cascade reactors 4-76680  
 Si:H amorphous films, laser CVD by ArF excimer laser photodissociation of Si<sub>2</sub>H<sub>6</sub> 4-61859  
 Si:H amorphous films, prep., characterisation absorpt. and laser-damage resistance 4-74676  
 Si:H amorphous p-i-n solar cell, design, fabrication and characts. 4-114905  
 Si:H amorphous thin film optical waveguides, propag. characts. 4-107821  
 Si:H film, annealing behaviour of  $\sigma = 2.0026$  ESR line 4-109057  
 Si:H film, complex impedance meas. 4-76055  
 Si:H film, deposition mechanism from plasma 4-114411

## hydrogen continued

- a-Si:H film, drift mobility, xerographic determ. 4-104224  
 a-Si:H film, high rate prep. by reactive evaporation method, photocond. and dark cond. meas. 4-61248  
 a-Si:H film, hole mobility model 4-104220  
 a-Si:H film, hyperfine interaction, ENDOR study 4-65881  
 a-Si:H film, IR quenching of photoluminescence and photoconductivity 4-104656  
 a-Si:H film, low freq. glow discharge prep. (Japanese) 4-76692  
 a-Si:H film, optical props. meas. 4-76539  
 a-Si:H film, produced by magnetron sputtering, ion beam anal. 4-92583  
 a-Si:H film, sputtered, elemental anal., STEM study 4-104105  
 a-Si:H film, Staebler-Wronski effect 4-108852  
 a-Si:H film, time resolved photoluminescence and phonon transport 4-71445  
 a-Si:H film, transient space charge limited cond. study 4-104215  
 a-Si:H film for H passivation of implantation defects in Si-SiO<sub>2</sub> MOS struct. 4-71744  
 a-Si:H films, anodic oxidation, elec. and optical props. of oxidised films 4-109527  
 a-Si:H films, CVD growth, phys. props. 4-92715  
 a-Si:H films, DC planar magnetron reactive sputtering and characterisation 4-93218  
 a-Si:H films, doping effect, RF sputtering and p-n junction form. 4-88973  
 a-Si:H films, electron drift mobility, xerographic determination 4-61377  
 a-Si:H films, low defect grade, prep. by RF magnetron sputtering 4-114397  
 a-Si:H films, luminescence fatigue and ODMR studies 4-85005  
 a-Si:H films, planar magnetron sputtering, electronic props. 4-88972  
 a-Si:H films, pot. barriers and photo-EMF 4-88561  
 a-Si:H films, RF sputtering, substrate temp. calibration (Japanese) 4-76672  
 a-Si:H films, reactive sputtering, elec. and optical props. 4-104203  
 a-Si:H films, thickness effects on electrical and photoelectrical properties 4-98484  
 a-Si:H films, transient photocond. meas. 4-88539  
 a-Si:H glow discharge deposited films, morphology, temp. and substrate depend. 4-61260  
 a-Si:H MIS Schottky barrier struct., dark currents 4-104322  
 a-Si:H nip solar cells, B contamination and photoresponse 4-89407  
 a-Si:H optical confinement type solar cell using milky tin oxide on glass 4-81556  
 a-Si:H p-i-n devices, EBIC decay 4-92796  
 a-Si:H p-i-n solar cells, performance, effect of prep. conditions (Korean) 4-114908  
 a-Si:H photoreceptors, electrophotographic imaging process 4-73544  
 a-Si:H pin devices, excess dark currents and diode quality factor 4-114016  
 a-Si:H pin solar cells, LPCVD growth, transport props. 4-114907  
 a-Si:H reactively sputtered films, H partial press. effects 4-93219  
 a-Si:H Schottky barriers, photocurrent spectral sensitivity 4-65727  
 a-Si:H Schottky barriers, sputtered, freq. depend. capacitance, admittance meas. 4-98693  
 a-Si:H Schottky diodes and nin devices, single and double carrier injection 4-114015  
 a-Si:H Schottky solar cells, gap state density 4-88438  
 Si:H single cryst., defect distrib. and density, X-ray projection topography studies (Chinese) 4-98086  
 a-Si:H solar cells, EBIC microcharacterisation of fabrication defects 4-93629  
 a-Si:H solar cells, photovoltage profiling 4-93617  
 a-Si:H sputtered films, steady-state photocond. and recombination processes 4-108902  
 a-Si:H surface barrier structs., photocurrent, freq. depend. 4-61418  
 a-Si:H thin films, coupled local mode vibrs., IR absorpt. study 4-88259  
 a-Si:H thin films, glow discharge effects on electronic and optical props. 4-75977  
 a-Si:H thin films, O distrib. and modifications induced by heavy ion bombard. 4-70233  
 Si:H wide optical gap binary alloy films, elec. props. 4-113956  
 a-Si:H/Si p-n junction, optoelectronic props. 4-114020  
 Si:H/SiN<sub>x</sub> amorphous semiconductor superlattices, charge transfer doping 4-92219  
 a-Si:H/SiO<sub>2</sub>/Pd diodes, H induced Schottky barrier modulation detect. by photoemission 4-70905  
 a-Si:H/a-Ge/H/a-Si<sub>1-x</sub>C<sub>x</sub> /a-SiN<sub>x</sub>:H superlattices, CVD growth and struct. 4-114416  
 a-Si:H/a-Si<sub>1-x</sub>N<sub>x</sub>/H quantum well struct., luminescence and current transport 4-114024  
 a-Si:H/a-SiN<sub>x</sub>/a-SiO<sub>2</sub> multilayer films, struct., elec. and optical props. 4-114025  
 Si:H-Ag junctions, Schottky barrier form. 4-84694  
 a-Si:H Si<sup>3+</sup>p amorphous-cryst. heterojunctions, elec. characts. 4-84688  
 a-Si:H-a-SiN<sub>x</sub>:H heterojunction, lattice mismatch, electroabsorption study 4-76029  
 a-Si:O:H CVD films, struct. model 4-84827  
 Si/a-Si:H,B/metal junctions, current-volt. characts. 4-114033  
 Si-H-Ag etched junctions, Schottky barrier form. 4-70933  
 p-Si:C,H, amorphous, prepared by photo-CVD, electronic and optical props. 4-70959  
 Si:C,H amorphous film, C diffusion into Si:H 4-80289  
 Si:C,H amorphous films, plasma deposition from SiH<sub>4</sub>+methane (ethylene) 4-114410  
 a-Si:C,H glow-discharge film, electronic and optical props. 4-84623  
 Si<sub>1-x</sub>C<sub>x</sub>H<sub>2</sub> amorphous, CVD prep., XPS and optical studies 4-70600  
 a-Si<sub>1-x</sub>C<sub>x</sub>H<sub>2</sub>, low emittance coatings for high temperature solar collectors 4-114950  
 a-Si<sub>1-x</sub>C<sub>x</sub>H<sub>2</sub>, luminescence from photo-generated carriers, polarisation memory 4-99186  
 a-Si<sub>1-x</sub>C<sub>x</sub>H<sub>2</sub> GD thin film, plasmon behaviour studied by XPS, chem. shifts 4-65627  
 a-Si<sub>1-x</sub>C<sub>x</sub>H<sub>2</sub>/H/a-Si(C:H) heterojunctions, photoemission studies 4-65731  
 Si<sub>1-x</sub>Ge<sub>x</sub>:H, amorphous, gap state distrib., photoconductivity study 4-108820  
 Si<sub>1-x</sub>Ge<sub>x</sub>:H, amorphous, occupied gap state obs. 4-70637  
 Si<sub>1-x</sub>Ge<sub>x</sub>:H amorphous films, planar magnetron sputtered, optical and elec. props. 4-98671  
 Si<sub>1-x</sub>Ge<sub>x</sub>:H amorphous planar magnetron sputtered films, elec. and optical props. (Japanese) 4-99312  
 Si<sub>1-x</sub>Ge<sub>1-x</sub>:H amorphous sputtered films, optical absorpt. 4-93090

## hydrogen continued

- Si<sub>3</sub>H<sub>2n+1</sub> defects, molecular cluster studies 4-84586  
 a-Si<sub>3</sub>N<sub>4</sub> RF sputtered films, internal stress rel. to local H bonding 4-88437  
 SiN<sub>x</sub>:H, amorphous, electronic struct., photoemission 4-108776  
 a-SiN<sub>x</sub>:H layers, prep. by glow discharge decomp. of N<sub>2</sub>/SiH<sub>4</sub> mixtures, optical and photoelectric props., effects of doping 4-114001  
 Si<sub>3</sub>N<sub>4</sub>:H amorphous film, photoinduced ESR study 4-114161  
 Si<sub>3</sub>N<sub>4</sub>:H, amorphous, CVD growth 4-60941  
 SiNi<sub>x</sub>:H, amorphous, localised states at conduction band edge 4-104168  
 SiO<sub>2</sub>:GeO<sub>2</sub> multimode fibres, H<sub>2</sub> effects on IR absorpt. characts. 4-97106  
 SiO<sub>2</sub>:H<sup>+</sup>, amorphous, O<sub>2</sub> vacancy annealing 4-103743  
 SiO<sub>2</sub>-GeO<sub>2</sub>-P<sub>2</sub>O<sub>5</sub> optical fibres, H and D absorption losses, expt. study 4-91589  
 SiSn:H, amorphous sputtered layer, structural props. 4-108739  
 Si<sub>3</sub>N<sub>4</sub>:H, (0 ≤ x ≤ 0.3), amorphous RF sputtered film, struct. and elec. props. 4-70956  
 Si-H, bonds and H-induced defects study 4-66058  
 Ti:H, depth profiling and microanal. 4-81497  
 V:H, hydrogen embrittlement, electron microscopy study 4-93396  
 VO<sub>2</sub>-WO<sub>3</sub>:H, photoinjection of H into the heterostructure, semiconductor-metal transition studies 4-113478  
 Y, H diffusivity, 960 to 1160K 4-113716  
 Y-Nb, H diffusivity, 960 to 1160K 4-113716  
 Y-Nb alloy-H<sub>2</sub> system, isothermal equilib. press. 4-70557  
 Y-Th, H diffusivity, 960 to 1160K 4-113716  
 YIG:H, H diffusion, optical absorption and mag. circular dichroism studies 4-61144  
 Zr-Fe, hydride formation, X-ray diffr., Mossbauer spectra, gas anal. 4-113392  
 Zr-V-Fe alloys, bulk getters, H and D diffusion 4-113719  
 Zr<sub>2</sub>Fe<sub>2</sub>O<sub>6</sub>:H, hydride formation, X-ray diffr., Mossbauer spectra, gas anal. 4-113392

## hydrogen bonds

- acetamide, far IR transmission spectrum, lattice dynamics, temp. 4-104598  
 adenine-water complexes, H bond, ab initio SCF CI STO-3G calcs. 4-64386  
 aggregates, H bonded, resolution by line narrowing transient Raman technique 4-102692  
 alcohol-alkane (1,2-dichloroethane) mixtures, adiabatic compressibilities and viscosities, US meas. 4-92298  
 alcoholic OH vibration bands, intermol. effects 4-59855  
 alkanethiol-tri-n-butylphosphine, H bonding, PMR investig. (German) 4-107369  
 amide complexes, ionic H bonds, intramol. and multiple bonds 4-66568  
 amine-HCl, H bonded complex, matrix isolation IR vibr. spectra 4-96544  
 amino acid derivative complexes, ionic H bonds, intramol. and multiple bonds 4-66568  
 4-aminophenyl N-morpholysulphone, mol. and cryst. struct., X-ray diffr. 4-112293  
 aromatic epds., room temp. phosphoresc., phosphor d solid supports interaction 4-78887  
 N,N'-aryalkyl thioureas, conformation anal. <sup>1</sup>H NMR and IR spectra 4-112178  
 7-azaindole, H-bonded complexes, MPI PES and two-colour MPI threshold spectroscopy 4-91320  
 azole derivatives, H bonded complex form. with nitrophenols, IR and UV investig. 4-66562  
 bacteriorhodopsin, conducting system, ab initio SCF calcs. 4-83288  
 base pairs, H bonding, effect of carcinogenic epoxides 4-76980  
 benzamide molecules, mag. anisotropies, relation to isomerism and H bonding 4-64635  
 p-benzosemiquinone anion radical, powder ENDOR anal. 4-74275  
 2-benzyl-1,7,10,13,19-pentaoxa-4, 16-diazacycloicosane-3,17,21-trione hydrate, cryst. and mol. struct., X-ray diffr. 4-113436  
 betaine hydrate, H bonding, IR spectra 4-87119  
 betaine hydrofluoride, H bonding, IR spectra 4-87119  
 bilirubin, inverse Raman spectroscopy, hydrogen bonding, photoactivation 4-115016  
 bilirubin ditauride, inverse Raman spectroscopy, hydrogen bonding, photoactivation 4-115016  
 binary liq. mixtures, H bonded, lower critical soln. points 4-75641  
 2-bromoethanol, intramolecular H bonds, angle-resolved photoelectron spectra 4-102743  
 calcium meso-tartrate trihydrate, struct. and bonding, X-ray diffr. studies 4-113428  
 carbazole derivatives, 1-substituted, spectrochem. props. 4-64540  
 carboxylic acids, H-bond double-well barrier and H<sup>+</sup> exchange 4-93508  
 chain systems, proton cond. mechanism 4-80285  
 2-chloroethanol, intramolecular H bonds, angle-resolved photoelectron spectra 4-102743  
 choline hydroxide, cryst., H bonding, IR study 4-114263  
 cobalt acetate dihydrate, protiated and deuterated, IR spectra, H-bonds 4-61703  
 p-cyanonitrobenzene anion radical, H bonding, kinetic parameters 4-102713  
 cyclohexanol, H bonds, rot. barriers, INDO and ab initio STO-3G calcs. 4-112115  
 cyclopropane-HCN, H bonded complex, ab initio SCF MO study 4-64343  
 dibenzocarbazoles in solid soln., photoionisation threshold lowering through H bonding with pyridine 4-59861  
 2,6-dichloro-4-nitrophenol, vibr. anal., IR, far-IR and laser Raman spectra 4-91259  
 2,4-dichloro-6-nitrophenol, vibr. anal., IR, far-IR and laser Raman spectra 4-91259  
 dichlorophenols, H-bonded cryst. substituent effects, cryst. struct. 4-113425  
 1,3-diketones, tautomeric equilib., H bonds, NMR spectra 4-59805  
 5,5-dimethyl-2-(dimethylamino)-2-oxo-1,3,2-oxazaphosphorinane, config., X-ray cryst. and PMR and IR spectra in soln. 4-113432  
 2,4-dinitrophenol conformational anal. by nuclear Overhauser effect 4-96581  
 1,3-dioxan-5-ol, H bonds, rot. barriers, INDO and ab initio STO-3G calcs. 4-112115  
 disaccharides, in aprotic solvent, conform. anal., PMR 4-112210  
 dithiorescinols, and derivatives, UPS, ab initio STO-3G calcs. 4-83421

## hydrogen bonds continued

- DNA base components, electrostatic interactions, pot. derived point-charge model study 4-107271  
 epoxide-nucleophile reaction, effect on H bonding involving the nucleophile 4-76980  
 1,2-ethanedithiol, microwave spectrum, dipole moment and conformation 4-96526  
 ethanol, liq., H bonding, X-ray diffr. pattern 4-70015  
 ethanol-tri-n-butylphosphine, H bonding, PMR investig. (German) 4-107369  
 N-ethyl-3-acetylcarbazole, emission props., solvent effects 4-107390  
 excited H-bonding systems, electronic struct., ab initio MO-CI calcs. charge transfer 4-96461  
 α-fluoropropionic acid, microwave spectra rot. absorpt. lines, dipole moments, geometries, internal rot. 4-59723  
 formic acid H-bonded chains, struct. and stability, ab initio calcs. 4-102573  
 gas-phase complexes, H-bonded, transferability test of EPEN/2-type potential functions, SCF calcs. 4-87035  
 D-glucan, mol. cpds., hydroxylated, in aprotic solvent, conform. anal. PMR 4-112210  
 α-D-glucopyranose cryst., H bonds, stretching vibr., IR spectra 4-88824  
 glutaric acid, cryst., bonding, disorder, Raman spectrosc. investigation 4-80936  
 gramicidin S peptide, long range H bond, INEPT chem. shift 4-96568  
 guanidinium salts with interionic H bonds, mol. dynamics, NMR investigation 4-104503  
 guanine-water complexes, H bond, ab initio SCF CI STO-3G calcs. 4-64386  
 heulandite, natural and partially dehydrated, struct., neutron diff. studies 4-103720  
 hydroquinone-N-methylpyrrolidone-(2) adducts, NMR and X-ray diffr. struct. (German) 4-71191  
 3-hydroxyflavone, intramol. excited-state H<sup>+</sup> transfer, H-bonding solvent perturbation 4-107392  
 ice VII, uncoupled O-H stretch, IR freq. and integrated intensity up to 189 kbar 4-104601  
 insulin, α-helix B9-B19, low vibr. freq., Raman spectra, H-bond forces, consts. 4-115017  
 iodates, NQR parameters and internal field symm. (Russian) 4-114181  
 isobutylamine monohydrate, vibr. spectroscopy 4-104611  
 isopropanol, in aqueous soln., in tetrachloroethylene soln., Raman line width, conc. depend. 4-114268  
 lignin/paper composites, temp. depend. of tensile props. 4-109451  
 lithium hydrogen malate, cryst. struct. and hydrogen bonds 4-92192  
 magnesium bis(hydrogen maleate)hexahydrate, cryst. struct., X-ray diff. studies 4-113427  
 malonaldehyde, microwave spectra, vibr. rot. interaction and H<sup>+</sup> tunneling model 4-112160  
 malonic acid, intramol. H-bonding, ab initio study 4-87033  
 malonic acid monoanion, intramol. H-bonding, ab initio study 4-87033  
 methanol, liq., H bonding, X-ray diffr. pattern 4-70015  
 methanol-acetonitrile mixtures, dielec. relax. 4-99013  
 methanol-NH<sub>3</sub>, associated species, D isotope effect, vibr., Raman spectra, normal coordinate anal. 4-66035  
 methylcinitrate, protonation sites, H bonding, IR obs. 4-87118  
 mica surfaces in H-bonding and polar liqs., DLVO theory and solvation forces 4-113840  
 microemulsions extractant anions, FTIR studies on hydration 4-99848  
 molecular complexes, H bonded, stabilisation energies 4-64560  
 molecular conformations, liq. phase, determ. methods 4-65165  
 molecular systems with weak and strong H-bonds, MNDO calcs., core repulsion 4-59642  
 naphthalene-indole soln., IR spectra (Russian) 4-84969  
 nucleic acids and their components, intrinsic luminesc. 4-105178  
 Nylon 5,7 films, dielec. and pyroelec. props., mol. orientation dependent 4-99043  
 organic crystals, H-bond distances and angles 4-84231  
 organic ions, solvation and H bonds, correl. between dissoc. energy and H<sup>+</sup> affinity 4-104973  
 organic onium ions, solvation, H bond, H<sup>+</sup> affinity, enthalpies 4-104974  
 pentachlorophenol in soln., IR dispersion of H-bonded systems, dielectric function for weak complexes 4-102676  
 phenol, H-bonded complexes, MPI PES and two-colour MPI threshold spectroscopy 4-91320  
 1-phenyl-3,5-dimethylpyrazole-oxalic acid adducts, H-bonding in crystals 4-108339  
 1-phenyl-3,5-dimethylpyrazole-perchloric acid adducts, H-bonding in crystals 4-108339  
 α-phenylethyl hydroperoxide, H-bonding investigated by IR spectroscopy methods, thermodynamic props. 4-96542  
 phosphate group interactions, cryst. refined H-bond pots. 4-60879  
 PMMA-Novolac resin mixtures, glass transition temps., H bonding effects 4-103932  
 poly(dG)-poly(dC), DNA: H bond melting, self-consistent microscopical theory 4-89276  
 polyglycine and its model systems, hydrogen bonds theoretical studies 4-59931  
 polypeptides, Potts model for solvent effects on polymer conformation 4-113294  
 polyurethane ionomers, physical bonds (Russian) 4-84203  
 procaine, cryst. struct., X-ray diffr. obs. 4-92190  
 2-propanone, pure and in aq. soln., muonic radical form., μSR studies 4-71950  
 pyridine derivatives, H bonded complex form. with nitrophenols, IR and UV invest. 4-66582  
 pyridine dichromates (IV), synthesis and characterisation 4-104615  
 quinzarin, rot. luminesc. spectra in supersonic expansion 4-97747  
 resorcinol and derivatives, UPS, ab initio STO-3G calcs. 4-83421  
 roseoxin B, secondary struct., X-ray and NMR study 4-115015  
 salicylaldehyde, heteronuclear Overhauser effect 4-109096  
 N-salicylidene-p-dimethylaminoaniline, red modification, cryst. and mol. structures, X-ray diffr. study 4-60911  
 sodium hydrogen maleate trihydrate, cryst. struct., neutron diff. studies 4-113426  
 sodium hydrogen oxalate monohydrate, cryst., electron density, intermolecular interactions, ab initio LCAO-MO-SCF calcs. 4-88160  
 squaric acid, order-disorder transition, <sup>17</sup>O nucl. quadrupole double resonance obs. 4-92977  
 surface (111), H uptake enhancement, deep subsurface bonding with 4-65215

hydrogen bonds continued

2,3,4,5-tetrachloro-6-((diethylamino)methyl)phenol, Mannich base,  $H^+$  transfer equilib., solvent effect 4-81417  
TGS crystals, repeated switching-induced fatigue, struct. props. 4-71300  
thiophenol-N-bond H-bonds, proton polarisability and transfer 4-62226  
thiosemicarbazide hydrobromide, cryst. struct., X-ray diffr. studies 4-113438  
tricyclic nitroxyl biradicals,  $C_{22}H_{36}N_2O_4$ ,  $C_{22}H_{38}N_2O_4$ , cryst. and mol. structures, X-ray diffr. 4-84283  
2,4,6-trimethylphenol in soln., IR dispersion of H-bonded systems, dielec. function for weak complexes 4-102676  
tris-sarcosine calcium chloride, ferroelec. phase transitions, IR and Raman studies 4-71296  
uracil and deuterated uracil in Ar and  $N_2$  mixtures, IR and Raman spectra, vibr. assignment 4-74243  
n-valeric acid, association study from dielec. props. 4-76998  
vibrational spectra of H-bonded crystals, effect of anharmonicity and vibr. reson. interaction 4-61684  
water, liq., H bonded networks, percolation model, computer simulation 4-88056  
water, liquid, H bond conductivity, mol. dynamics calcs. 4-75259  
xanthan solutions, rheology, molecular association and aggregation, liq. cryst. domains 4-112798  
 $Al(NO_3)_3 \cdot Cr^{3+}$ , exchange-coupled  $Cr^{3+} - Cr^{3+}$  pairs, EPR obs. 4-88717  
 $Ca_3KH_7(PO_4)_4 \cdot 2H_2O$ , cryst. struct., X-ray and neutron diffr. studies 4-113405  
 $Ca(NH_4)PO_4 \cdot 7H_2O$ , cryst. struct., H bonds, X-ray diffr. determ. 4-92150  
Co (III) complexes,  $Co(NH_3)_5H_2P_2O_7 \cdot H_2O$ , hydrolysis, NMR 4-109082  
Co complexes, Co-porphyrin complex, linear free energy correl. for reversible dioxygen binding, solvent effect study 4-62178  
 $CsB_3O_7(OH)_4 \cdot 2H_2O$ , twinned cryst. struct. X-ray diffr. determ. 4-92151  
 $CsH_2PO_4$ , Raman OH stretching band shape and H-bonds, transition moment 4-66024  
CuCl complex with acrylamide, cryst. struct., X-ray diffr. 4-113419  
 $Cu_2(NO_3)(OH)_2$ , monoclinic cryst. struct. and H-bonds 4-92166  
 $Cu_4(OH)_4(SO_4)_2 \cdot H_2O$ , langite, cryst. struct. determ. 4-108313  
 $FeNH_4H_2P_2O_7$ , unit cell parameters, anion packing 4-113410  
HBr mol. crystal, lattice dynamical model in phase III, H bond strengths 4-88246  
HCl molecular crystal, lattice dynamical model in phase III, H bond strengths 4-88246  
HCl(Br), lattice dynamics in low temp. phase 4-92328  
HF mol. crystal, lattice dynamical model in phase III, H bond strengths 4-88246  
 $HO_2$ , dimer, cyclic, two-hydrogen-bond form 4-91360  
 $HO_2^+$ , H-O bond energy, rel. to abstraction reactions 4-102574  
 $H_2O$  in liq. crystal, polarised FT-IR spectra 4-64473  
 $H_2O$  molecule orientation on thin film boundaries (Ukrainian) 4-65520  
 $H_2O$  liquid, Raman study of H bonds 4-104612  
 $H_3O^+$ , linear and bifurcated complexation with electron donors, ab initio calc. 4-99752  
 $(H_2O)_n \cdot H_2^{2+}$ , form. from electron impact ionisation, H bonds 4-107480  
 $H_3O^+ \cdot NO_2^-$ ,  $(ClO_4)^-$ , cryst. struct. determ. (French) 4-92147  
 $H_2S \cdot H_2O$  complexes, H bonded, Ar matrix isolated IR spectra 4-112173  
 $H_2S \cdot HCl$ , H bonded complex, rot. consts., Fourier transform microwave obs. 4-59732  
 $K_2Fe(CN)_6 \cdot 3H_2O$ ,  $K^+$  ion conduction, H-bonded aggregates 4-113709  
 $KNaCO_3 \cdot 6H_2O$ , crystal structure 4-103729  
 $La(ClO_4)_3 \cdot 3H_2O$ , cryst. struct. X-ray diffr. determ. 4-92153  
Li complexes,  $Li^+/N$ -methylformamide-water, N-substitution effect on hydrogen bonds, ab initio calcs. 4-96716  
Li complexes,  $Li^+$ /formamide-water, N-substitution effect on hydrogen bonds, ab initio calcs. 4-96716  
 $LiNO_3 \cdot 3H_2O$ , deform. electron density, X-ray and neutron diffr. data 4-65232  
 $NH_3 \cdot HCl$ , H bonded complex, matrix isolated IR vibr. spectra 4-96543  
 $(NH_3)_n \cdot H_2^{2+}$ , form. from electron impact ionisation, H bonds 4-107480  
 $NH_4HCO_3$ , relations between crystallographic characts. and cryst. struct. (Chinese) 4-75378  
 $N_2 \cdot HF(HCl)(HBr)$ , H bonded complexes, ab initio GO SCF MO calcs. 4-64369  
 $Na_2D_2SiO_4 \cdot 8D_2O$ , D atom location and anisotropic refinement, H-bonding, neutron diffr. study 4-75294  
Nb (110), H uptake enhancement, deep subsurface bonding well 4-65215  
 $(Nb_2)_3HPO_4(PO_4H_2)_3Te(OH)_6$ , NMR study of phase transition 4-80877  
 $P_2 \cdot HF(HCl)(HBr)$ , H bonded complexes, ab initio GO SCF MO calcs. 4-64369  
Pd-H, electronic structure, cluster anal. using SW-X $\alpha$  method, relativistic effects 4-65605  
Pt-H, electronic structure, cluster anal. using SW-X $\alpha$  method, relativistic effects 4-65605  
 $Rb_{0.52}(ND_4)_{0.48}D_2PO_4$  cryst., proton glass dielec. behaviour 4-114218  
 $Rb_{1-x}(NH_4)_xH_2PO_4$  glass, H-bonded, NMR relax. study 4-98974  
Re complex, hydrogen cis-diacetyl-tetracarboxylate, single cryst. TOF neutron diffr. obs. 4-80022  
 $\alpha$ -Si-H film, low freq. glow discharge prep. (Japanese) 4-76692  
 $\alpha$ -SiN-H RF sputtered films, internal stress rel. to local H bonding 4-88437  
 $SrCl_2 \cdot 6H_2O$ , cryst. struct., X-ray diffr. 4-65237

hydrogen compounds

see also deuterium compounds; hydroxonium ion; ice; steam; tritium compounds; water  
calcium 2-fluorobenzoate dihydrate, intermolecular H bond, cryst. struct., X-ray diffr. 4-103733  
Group VI hydrides, vibr. self-relax. theory 4-69189  
 $HF + Be \cdot BeF + H$  reaction, classical trajectory study in three dims. 4-99763  
intermetallic compound-H system, two-phase coexistence region, H chemical pot., interface rel. effect 4-104769  
metal hydrides for hydrogen storage in automobiles 4-105130  
polyacetylene- $H_2SO_4$  films, morphology dopant conc. and elec. props. 4-81067  
propyne-HF(DF) microwave spectrum and props. 4-74229  
vapour refractivity meas. using  $CO_2$  laser lines 4-97748  
DF-HF chemical laser atmospheric attenuation meas. (Chinese) 4-62951  
 $H_2$  production by water splitting, using photochemical reaction in concentrated phosphoric acid 4-89470  
 $H_2$ -HF gasdynamic pure rotational laser based, on far IR transitions, theoretical study 4-79118

hydrogen compounds continued

$H_2$ -HF high power pure rotational laser due to vibrational excitation 4-87319  
 $H_2AlP_2O_{10} \cdot 2H_2O$ , electrorheological suspensions, disperse phase, charge transport characteristics 4-103426  
 $HAsO_3$ , iodate oxidation exhibiting bistability, mushrooms and isolas 4-71961  
HB, electric dipole moments calc. using variational cellular method 4-87042  
HBr, cryst., long-wavelength lattice vibrs. 4-113549  
HBr, cryst., two-exciton spectra 4-104586  
HBr in stratosphere 4-115530  
HBr, lattice dynamics in low temp. phase 4-92328  
HBr mol. crystal, lattice dynamical model in phase III, H bond strengths 4-88246  
 $HBr^+ (A^2\Sigma^+ - X^2\Pi)$  fluoresc. investig. 4-83405  
 $HBr + N$ , crossed beam reaction, chemiluminescence study 4-77012  
 $HBr - N_2(P_2)$ , H bonded complexes, ab initio GO SCF MO calcs. 4-64369  
HCF,  $A'A''$  state, mag. props., Zeeman splittings, laser induced fluoresc. 4-69129  
HCL, gaseous,  $H^+$  spin longitudinal relax. time 4-107367  
HCN, (101) level relax. by collisional energy transfer, time-resolved fluoresc. 4-107440  
HCN adsorption on  $SiO_2$  and  $Al_2O_3$  surfaces, far IR Fourier spectroscopy 4-104593  
HCN, excited vibr. states, spacing distrib., role of dynamical symmetry 4-87034  
HCN, form. in ion sources from methane- $N_2O$  mixtures 4-66565  
HCN, ground and excited states, struct., vibr., SCF CI calcs. 4-64391  
HCN, ground and excited states, hyperfine props., dipole moment, mol. beam elec. reson. study 4-69105  
HCN, ground state, geometry, transition state, isomerisation reaction, ab initio calcs. 4-71908  
HCN in Jupiter atmosphere, detectability by mm wave radioastronomy 4-94670  
HCN in Saturn's atmosphere, detectability by radioastronomy method 4-94677  
HCN: interstellar, radio spectra and hyperfine rot.-level splitting, isotopic modifications 4-94925  
HCN  $J=1-0$  88 GHz transition in W3 IRS 4, aperture synthesis map 4-115804  
HCN, K-band studied using microwave Fourier transform spectrometer 4-69055  
HCN, photoelectron branching ratio and asymmetry parameters for two outermost MO 4-59849  
HCN, singlet-triplet transitions by electron impact 4-69230  
HCN, stripping in a packed tower, Henry's law const. meas. 4-62173  
HCN waveguide laser and HCN laser-excited oversized hollow dielec. waveguide submm radiation pattern study 4-107709  
 $HCN^+$ , mobilities in He at 293K 4-79706  
HCN-acetonitrile mixtures in solid Ar, far IR spectra, intramol. vibrs. 4-87112  
HCN-Ar mixtures, thermal decomposition behind incident shock waves 4-89279  
HCN- $NH_3$ , rot., mol. beam elec. reson., microwave spectra 4-64505  
HCN+CN, vibr. energy effect on reaction, laser meas. 4-99769  
HCN+O reaction dynamics, laser fluoresc. spectroscopy 4-114785  
HCN(DCN), vibr. dipole moment function, RF-IR double reson. 4-69122  
HCNH $^+$ ,  $\nu_2$  band, vibro-rot. IR spectra 4-64462  
HCN-cyclopropane, H bonded complex, ab initio SCF MO study 4-64343  
 $HCO^+$ ,  $\nu_3$  fundamental band, IR-obs. 4-96538  
 $HCO^+$ , rot. excitation in interstellar clouds 4-110514  
 $HCO^+/HOC^+$  abundance ratio in dense interstellar clouds 4-94910  
 $HCO^+ + He$ , collision cross sections and rate coeffs. for rot. excitation 4-110514  
 $HCS^+$  rot. excitation in interstellar clouds 4-110514  
 $HCS^+ + He$ , collision cross sections and rate coeffs. for rot. excitation 4-110514  
HCl,  $2B^2\Sigma^+$  state, asymmetric double well pot., reson. enhanced tunnelling 4-91324  
HCl aq. solns., fast  $H^+$ -ion motion, vel. concepts vs. config. description 4-80276  
HCl aq. solns., fast  $H^+$ -ion motion, NMR determ. 4-80277  
HCl aq. solns., fast  $H^+$ -ion motion; neutron scatt. study 4-80278  
HCl chemical laser system, pot. high energy, expt. demonstration 4-69394  
HCl, core electrons, Coulomb and exchange operators, matrix elements, valence electron only SCF calcs. 4-59630  
HCl, cryst., long-wavelength lattice vibrs. 4-113549  
HCl, cryst., two-exciton spectra 4-104586  
HCl detection at sub-parts-per-billion level using tunable diode laser absorpt. 4-115176  
HCl, dissociation, attachment, ang. depend. calcs. 4-107454  
HCl, dissociative electron attachment processes,  $H^-$  ions, ang. distrib. 4-64624  
HCl, electron collisions, correl. polarisation pot., parameter-free model 4-64609  
HCl, ground states, bond function, dissociation energies, CI calcs. 4-74162  
HCl in dil. carbon tetrachloride and trichlorofluoromethane solns., vibr. relax., Raman spectra 4-91331  
HCl in glycol mixtures, cond. meas. 4-65425  
HCl in stratosphere, trace meas. using tunable diode laser absorption 4-89997  
HCl, internal motion, electron density dynamic anal., ab initio MO calcs. 4-87037  
HCl, ionic fragmentation, photoionisation and photoabsorption cross-sections 4-83433  
HCl, ionisation pot. D isotope effect, EELS 4-83467  
HCl, lattice dynamics in low temp. phase 4-92328  
HCl molecular crystal, lattice dynamical model in phase III, H bond strengths 4-88246  
HCl oxides, thermally grown on Si, XPS study of Cl incorporation 4-76640  
HCl pollution from Space Shuttle launches 4-100022  
HCl-amine, H bonded complex, matrix isolation IR vibr. spectra 4-96544  
HCl-Ar, intermolecular forces, HF plus damped dispersion calcs. 4-87039

## hydrogen compounds continued

- HCl-Ar, ps. IR spectroscopy, nearly free induction decay obs. 4-96529  
 HCl-DCI, dipolar correlation times, NQR study 4-80171  
 HCl-H<sub>2</sub>S, H bonded complex, rot. consts., Fourier transform microwave obs. 4-59732  
 HCl-N<sub>2</sub>O liquid mixtures, thermodynamics and densities 4-98311  
 HCl-NH<sub>3</sub>, H bonded complex, matrix isolated IR vibr. spectra 4-96543  
 HCl+chlorodifluoromethyl radical, reaction rate, vibr. excitation influence 4-93507  
 HCl+I<sup>+</sup>, quenching, time resolved IR fluoresc. used to determ. rate const. 4-102730  
 HCl+Xe<sup>+</sup>, supersonic beam-gas conditions, chemiluminescence polarisation meas. 4-89305  
 (HCl)<sub>2</sub>, stretching bands, rot. struct., high resolution IR spectra 4-107343  
 HClO<sub>4</sub> muonium form, spur model 4-71945  
 HCl-N<sub>2</sub>(P<sub>2</sub>), H bonded complexes, ab initio GO SCF MO calcs. 4-64369  
 HCo(CO)<sub>4</sub>, H ligand charges, SCF-X $\alpha$ -scatt. wave MO study 4-96452  
 HD, prod. from H<sub>2</sub>+D<sub>2</sub> reactions on Pt (557), ang. and vel. distrib. 4-99834  
 HD<sup>+</sup>, UV laser photodissoc. 4-69157  
 (HF)<sub>n</sub>, chains with added or inserted H<sub>2</sub>O, energetic behaviour, PCILCO calcs. 4-78780  
 HF 2-dimens. laser beam phase and intensity meas. technique 4-74564  
 HF CW chemical laser, dynamic saturation intensity, depend. on mixing rate of reagents 4-107617  
 HF CW lasers, small signal gain meas. (Chinese) 4-112400  
 HF chemical laser, Blumlein discharge initiated, using SF<sub>6</sub> as F donor 4-69393  
 HF chemical laser, CW supersonic, shock wave effects 4-107615  
 HF chemical laser initiated by fine particle evaporation under IR radiation action 4-60028  
 HF, core electrons, Coulomb and exchange operators, matrix elements, valence electron only SCF calcs. 4-59630  
 HF, dissociation, attachment, ang. depend. calcs. 4-107454  
 HF, dissociative electron attachment processes, H<sup>-</sup> ions, ang. distrib. 4-64624  
 HF, dynamic polarisability, Cauchy moments, coupled HF calc. 4-74147  
 HF, electric dipole moments calc. using variational cellular method 4-87042  
 HF electron beam initiated pulsed chem. laser 4-69391  
 HF electron collisions, correl. polarisation pot., parameter-free model 4-64609  
 HF, internal motion, electron density dynamic anal., ab initio MO calcs. 4-87037  
 HF laser mixtures, electron density of afterglow of pulsed discharge and UV photoionisation, meas. using microwave interferometer (Chinese) 4-87315  
 HF mid-IR waveguide lasers, RF pumped 4-74543  
 HF mol. crystal, lattice dynamical model in phase III, H bond strengths 4-88246  
 HF, mol. electron density, fitting method 4-74143  
 HF, overtone and multiphoton absorpt., classical and quantum mechanics 4-74303  
 HF, pot. curve, energy continuity in multi-reference CI calculations 4-83305  
 HF pulsed H<sub>2</sub>+F<sub>2</sub> chain reaction laser, effect of vibr. and rot. relax. mechanisms 4-91445  
 HF pulsed laser with unstable resonator (Chinese) 4-60026  
 HF pulsed nonchain laser, time-resolved spectral and energy characts. 4-74497  
 HF pulsed-discharge lasers preionised by pulse or CW X-rays 4-69387  
 HF, total energies calc. using electron cloud displacement model (Chinese) 4-74136  
 HF, valence shell dipole excitation spectrum, photoabsorption cross section 4-91345  
 HF, vibr., predissociation using IR laser 4-87172  
 HF<sup>+</sup>, X<sup>II</sup> state, rot. transition, hyperfine splitting, LMR spectra 4-69120  
 HF/DF pulsed optical resonance transfer laser, theoretical simulation 4-79123  
 HF-B series complexes, B=proton acceptor, rot., hyperfine and quadrupole coupling const. 4-112195  
 HF-NF<sub>3</sub>-N<sub>2</sub>(CO)(Ar) mixtures, photolysis, HF multiquantum vibr.-rot. relax. rates 4-102775  
 HF+Ar, finite duration of collisions and vibr. dephasing effect on broadened IR line shapes 4-69177  
 HF+Ar rotationally inelastic cross-sections and fitting laws, energy depend. 4-102772  
 HF+CO, vibr. relax. rate const. determ. using flow IR chemiluminesc. technique 4-89273  
 HF+Ca<sup>+</sup> reactions, crossed laser mol. beam studies and CaF prod. mol. rot. polarisation 4-91364  
 HF+F, vibr. level deactivation 4-96666  
 HF+H nonreactive scatt., quantum mechanical calcs. using localised rot. basis functions 4-59882  
 HF+H<sub>2</sub>(D<sub>2</sub>)(CH<sub>4</sub>)(CD<sub>4</sub>)(CO<sub>2</sub>), HF(v=3, 4, 5) vibr. relax., fluoresc. study 4-69187  
 HF+HF, rotationally inelastic collisions, freq. corrected sudden approx. 4-102777  
 HF+He, collisional roto-vibrational energy transfer, quantum calc. 4-69182  
 HF+He, energy transfer, differential cross sections, pot. energy surfaces 4-76992  
 HF+I<sup>+</sup>, quenching, time resolved IR fluoresc. used to determ. rate const. 4-102730  
 (HF)<sub>n</sub>, in solid Ar matrix, FT IR spectra 4-69066  
 HFPOH struct., bonding and internal rotation 4-68938  
 HFSO<sub>3</sub>, <sup>33</sup>S nucl. mag. shielding, chem. shift 4-102699  
 HF-N<sub>2</sub>(P<sub>2</sub>), H bonded complexes, ab initio GO SCF MO calcs. 4-64369  
 H<sub>2</sub>Fe(CO)<sub>4</sub>, H ligand charges, SCF-X $\alpha$ -scatt. wave MO study 4-96452  
 H<sub>2</sub>FeRu<sub>3</sub>(CO)<sub>13</sub>, cryst. struct. study 4-75390  
 H<sub>2</sub> angle resolved PES of valence shells as a function of photon energy from 13 to 90 eV 4-69141  
 HI catalytic decomposition kinetics in thermochemical H<sub>2</sub> production 4-93647  
 HI complexes, interactions, energy component anal. calcs. 4-59869  
 HI, dissociative electron attachment processes, H<sup>-</sup> ions, ang. distrib. 4-64624

## hydrogen compounds continued

- HI production in high concentration in H<sub>2</sub> production process by thermal decomposition of MgI<sub>2</sub>·8H<sub>2</sub>O-MgO mixture 4-72188  
 HI+F, exchange reaction, pot. surface, I(P<sub>1/2</sub>) two photon laser induced fluoresc. 4-76982  
 HI+I, H and Mu exchange, isotope effects, semiclassical technique 4-71884  
 HI+N, crossed beam reaction, chemiluminescence study 4-77012  
 HMn(CO)<sub>5</sub>, H ligand charges, SCF-X $\alpha$ -scatt. wave MO study 4-96452  
 HN<sub>2</sub><sup>+</sup>, stretching vibr., pot. energy and electric dipole moment depend. ab initio calcs. 4-87105  
 HNC to HCN isomerisation, rate const. calc. using RRKM method 4-66560  
 HNCO adsorbed on Rh (111), effects of preadsorbed O 4-113781  
 HNCSe, IR spectrum, vibr. assignment 4-102675  
 HNCSe, millimeter wave spectrum and struct. 4-102673  
 H<sup>+</sup>(NH<sub>3</sub>)<sub>n-1</sub> clusters, photoionisation in pulsed supersonic nozzle beam by VUV rare-gas reson. lines 4-69258  
 HNO, internal energy distrib. formed in H+NO reaction 4-71871  
 HNO<sub>2</sub>, electronic struct. calc. 4-87032  
 HNO<sub>2</sub>, in atmosphere, for infrared spectra and composition of stratosphere and troposphere 4-72697  
 HNO<sub>2</sub>, in atmosphere of SW United States, conc. and pollution source 4-115527  
 HNO<sub>2</sub>, in stratosphere, spectral obs. for comparison with NIMBUS-LIMS method 4-105666  
 HNO<sub>2</sub>, in stratosphere of Canada in winter, conc. profile observation 4-115529  
 HNO<sub>2</sub>, mm-wave system for remote sensing acidic clouds and precursor gases in troposphere 4-77170  
 HNO<sub>2</sub>, stratosphere conc. monitoring by IR Earth limb scanning from satellite 4-105757  
 HNO<sub>2</sub>, thermal energy electron capture, ECR study 4-91340  
 HNO<sub>2</sub>, tropospheric air trace gas meas. using tunable diode laser absorption spectrometer 4-114998  
 H<sub>2</sub>N<sub>2</sub> free radicals, local spin density theory 4-68933  
 (CHO<sub>2</sub>)<sub>2</sub>, struct., ab initio multicfg. SCF gradient optimisation method 4-83290  
 HO<sub>2</sub>, 265.8 GHz rotational emission lines obs. in stratosphere 4-72667  
 HO<sub>2</sub> dimer, cyclic, two-hydrogen-bond form 4-91360  
 HO<sub>2</sub>, vibr. band strength for  $\nu_3$  band meas. 4-74220  
 HO<sub>2</sub>, H-O bond energy, rel. to abstraction reactions 4-102574  
 HO<sub>2</sub>-He, collisional energy transfer in low-pressure limit unimol. dissociation 4-83451  
 H<sub>2</sub>O and CO<sub>2</sub> laser freq.-mixing expts., beat note S/N ratio characterisation 4-74608  
 H<sub>2</sub>O, condensed gas solids, ion-induced chem. 4-66163  
 H<sub>2</sub>O gas, transport props. prediction at high temps. 4-60576  
 H<sub>2</sub>O<sub>2</sub>, absolute IR intensity calc. of binary overtone, combination and difference bands 4-69074  
 H<sub>2</sub>O<sub>2</sub>, catalytic decomp. investig. using chemiluminesc. oxidation of luminol 4-62188  
 (H<sub>2</sub>O)<sub>2</sub>, electronic struct., semiempirical linear combination of MO method calc. 4-112116  
 H<sub>2</sub>O<sub>2</sub> in Greenland ice core samples 4-115552  
 H<sub>2</sub>O<sub>2</sub>, internal rot. affect on NMR params., ab initio SOS CI calc. 4-91203  
 H<sub>2</sub>O<sub>2</sub> liquid, Raman study of H bonds 4-104612  
 H<sub>2</sub>O<sub>2</sub>, oxidation number, electron distrib., ab initio MO wave function 4-107276  
 H<sub>2</sub>O<sub>2</sub>, photodissociation, nascent fragment rot. state distrib. 4-109674  
 H<sub>2</sub>O<sub>2</sub>+F, vibr. band strength for  $\nu_3$  band meas. 4-74220  
 H<sub>3</sub>O<sup>+</sup> ions in glassy HCl and HBr solns., Raman spectra 4-91267  
 H<sub>3</sub>O<sup>+</sup>, linear and bifurcated complexation with electron donors, ab initio calc. 4-99752  
 H<sub>3</sub>O<sup>+</sup> in crystals, struct. anal., SCF-LCGO calcs. 4-96450  
 HOC<sup>+</sup>, rot. vibr. spectrum, extended ab initio study 4-64395  
 HOCl, isotopic species, atm. monitoring, microwave and nm wave spectroscopy 4-59729  
 HOF, neutral and cationic struct., ab initio calcs. 4-59616  
 HONO, A state, photodissociation, OH fragment charact. 4-77017  
 HONO and NO<sub>3</sub> radicals in atmosphere, implications of simultaneous night-time meas. 4-105660  
 HONO, cluster form. with NO<sub>2</sub><sup>-</sup>, mass spectrosc. investig. 4-69260  
 HONO<sub>2</sub>, photoabsorpt. and photodissoc. in 105-220 nm region 4-102722  
 HOSO<sub>2</sub> radical, Ar matrix isolated, IR spectra 4-78835  
 H<sub>2</sub>O-O<sub>2</sub>, triplet contact charge transfer complexes, pot. energy curves 4-91322  
 H<sub>3</sub>O<sup>+</sup>·NO<sub>2</sub><sup>+</sup>·(ClO<sub>4</sub>)<sub>2</sub>, cryst. struct. determ. (French) 4-92147  
 HPO, H<sub>2</sub>O<sub>2</sub> flames, emission intensity mag. quenching 4-78891  
 H<sub>3</sub>PO, struct., bonding and internal rotation 4-68938  
 H<sub>3</sub>PO, fuel cells, reactions at high temp. and press. rotating disk electrochemical apparatus 4-89398  
 H<sub>3</sub>POH, struct., bonding and internal rotation 4-68938  
 H<sub>2</sub>P(OH)NH<sub>2</sub><sup>+</sup>, conformational energy surfaces, MO STO calc. 4-68954  
 H<sub>2</sub>PP, ab initio SCF and CI study of stability and electronic structure 4-74164  
 HPPH, ab initio SCF and CI study of stability and electronic structure 4-74164  
 H<sub>2</sub>PW<sub>2</sub>(Mo)<sub>12</sub>P<sub>40</sub>·21H<sub>2</sub>O, H<sup>+</sup> motion, AC cond. and <sup>1</sup>H NMR studies 4-108655  
 (H<sub>2</sub>S)<sub>n</sub>, mol. beam photoionisation and fragmentation 4-69154  
 HS+NO+M→HSNO+M, (M=He, Ar, N<sub>2</sub>), rate coeffs. in temperature range 25 to 445K 4-71895  
 H<sub>2</sub>S, <sup>33</sup>S nucl. mag. shielding, chem. shift 4-102699  
 H<sub>2</sub>S (HDS), nucl. hyperfine interactions, elec. dipole moments, mol. beam elec. reson. 4-59803  
 H<sub>2</sub>S as hydrogen source, obtained as waste product from fossil fuel methods of use 4-89471  
 H<sub>2</sub>S determ. in environmental samples, methods review 4-105157  
 H<sub>2</sub>S, diffusion, in NiO, surface and vol. processes 4-98372  
 H<sub>2</sub>S, dipole moment derivatives, coupled HF calc. 4-91361  
 H<sub>2</sub>S, dissociation, attachment, ang. depend. calcs. 4-107454  
 H<sub>2</sub>S, electron collision frequency, resonant determ. method 4-69223  
 H<sub>2</sub>S, mm-wave system for remote sensing acidic clouds and precursor gases in troposphere 4-77170  
 H<sub>2</sub>S, stress enhanced adsorption on annealed Fe, Auger spectra 4-75785  
 H<sub>2</sub>S thermal decomposition with Ni<sub>3</sub>S<sub>2</sub> for H<sub>2</sub> production 4-93648  
 H<sub>2</sub>S<sup>+</sup> in Comet IRAS-Araki-Alcock (1983d), visible spectrum 4-94691  
 H<sub>2</sub>S-H<sub>2</sub>O, mol. beam photoionisation and fragmentation 4-69154

**hydrogen compounds continued**

- H<sub>2</sub>S-H<sub>2</sub>O complexes, H bonded, Ar matrix isolated IR spectra 4-112173  
 H<sub>2</sub>S-HCl, H bonded complex, rot. consts., Fourier transform microwave obs. 4-59732  
 H<sub>2</sub>S-HF, hyperfine coupling consts., rot., pulsed-nozzle Fourier transform microwave spectra 4-107333  
 H<sub>2</sub>S+N reaction, spectrophotometric studies 4-114793  
 H<sub>2</sub>S+NH<sub>3</sub><sup>+</sup> reaction, depend. on translational and internal energy of NH<sub>3</sub><sup>+</sup> 4-71891  
 (H<sub>2</sub>S)<sub>n</sub>, n=2,3, photoionisation, unimolecular decomposition of ions 4-59860  
 (H<sub>2</sub>S)<sub>n</sub><sup>+</sup>, n=2,3, unimolecular decomposition study 4-59860  
 H<sub>2</sub>SO, Ar low temp. matrix, photoinduced isomerisation, IR spectra 4-89249  
 H<sub>2</sub>SO<sub>4</sub>, ambient aerosol, S losses, PIXE anal. 4-99876  
 H<sub>2</sub>SO<sub>4</sub> generation, standardisation and dispensing 4-89285  
 H<sub>2</sub>SO<sub>4</sub>, vapour condensation in cooled tube, mathematical model 4-80199  
 H<sub>2</sub>SiCl, vibr., rovibr., force consts., IR obs. 4-59738  
 H<sub>2</sub>UO<sub>3</sub>, H-insertion cpd., unit cell consts., IR spectra and X-ray diff. studies 4-84267  
 H(UO<sub>2</sub>)(AsO<sub>4</sub>).4H<sub>2</sub>O, phase transition temps. and ferroelec. domain struct. 4-76400  
 HUO<sub>2</sub>P<sub>4</sub>.4H<sub>2</sub>O, solid proton electrolyte, use in T gettering from air 4-86966  
 HUO<sub>2</sub>PO<sub>4</sub>.4H<sub>2</sub>O, bulk proton conductivity (French) 4-98336  
 H<sub>2</sub>S<sub>2</sub>O<sub>3</sub>, cryst. struct., inelastic neutron scatt. study 4-108326  
 H<sub>2</sub>V<sub>2</sub>O<sub>5</sub>, cryst. struct., inelastic neutron scatt. study 4-108326  
 H<sub>2</sub>WO<sub>3</sub>, electrochromic materials for controlled radiant energy transfer in buildings 4-112536  
 HX-cyclopropane complex, (X=F, Cl, Br, I, CN), matrix isolation IR investig. 4-107349  
 HZr<sub>2</sub>P<sub>2</sub>O<sub>12</sub>, and related cpds., prep. and props. 4-104745  
 Hf-Ar, intermolecular forces, HF plus damped dispersion calcs. 4-87039  
 I<sub>2</sub>:H<sub>2</sub>, proton cond. meas. 4-92413  
 Li<sub>2</sub>-H<sub>2</sub>NbO<sub>3</sub>, struct. changes, X-ray diff. studies 4-84272  
 NH<sub>4</sub>HSeO<sub>4</sub>, high temp. phase transition, ionic motion 4-108651  
 OC-HCN, weakly bound complex, rot. spectrum investig. by pulsed nozzle, FT microwave spectroscopy 4-74228  
 O(<sup>1</sup>D<sub>2</sub>)+HCl-<sup>+</sup>OH+Cl reaction on a fitted ab initio surface 4-81414  
 OH<sup>+</sup>, vibr. fine struct. in collisionally induced charge reversal and fragmentation 4-81785  
 Pb/acid cells, rotating ring-disc electrode study of impurity effects on lead corrosion in sulphuric acid 4-81533  
 RbHSO<sub>4</sub>, ferroelectric phase transitions, piezoelectric coeffs., electrostrictive coeffs., temp. depend., resonance studies 4-114217  
 RbHSeO<sub>4</sub>, high temp. phase transition, ionic motion 4-108651  
 SiO<sub>2</sub>:HCl film on Si, impurity distrib., SIMS study 4-113485

**hydrogen distribution** see *hydrogen economy***hydrogen economy**

- aerobic photoelectrochemical converter of regenerative type, water decomposition to produce H<sub>2</sub> 4-93633  
 alternative energy sources, 6th International Conference, Miami Beach, FL, USA (Dec. 1983) 4-63395  
 applications, use of hydriding reactions 4-81599  
 automotive engine, H<sub>2</sub>-fueled, design database 4-62403  
 Canadian trends in hydrogen energy, review of work at Institut de Recherche d'Hydro-Quebec 4-62401  
 cyclic water splitting process, evolved H<sub>2</sub> and O<sub>2</sub> measurement by electrochemical method 4-62209  
 cyclohexane as a liquid phase carrier in hydrogen storage and transport 4-66811  
 diesel-cycle engine, H<sub>2</sub>-fueled, two-stroke, performance improvements 4-62404  
 electrolytic H<sub>2</sub>, economics and potential applications in the future 4-114961  
 electrolytic H<sub>2</sub>, industrial applications, technology and economics 4-89474  
 electrolytic H<sub>2</sub> production status in USA and abroad 4-62400  
 electrolytic hydrogen production market potential in United States northeastern utility service areas 4-105133  
 electrolytic production by modern methods 4-62408  
 electrolytic water splitting, HTR heat source, possibilities of improving power generation efficiency 4-93532  
 energy conversion engineering conference, Orlando, Florida, USA, August, 1983 4-67861  
 hydrocarbons, H<sub>2</sub> synthesis and purification (German) 4-81597  
 hydrogen centres in metals 4-92652  
 metal hydride heat pump operation, effects of dynamic hydrogen sorption 4-105131  
 metal hydride hydrogen storage beds 'In-Out' and 'Out-In' hydrogen reaction alternatives using RET 1 computer code 4-66812  
 metal hydride hydrogen storage in automobiles, technio-economic aspects 4-105130  
 metal hydride storage bed, mass and heat transfer dynamic analysis program 4-66816  
 metal hydride/hydrogen compressor, four-stage, design, fabrication and testing 4-66818  
 mischmetal-Ni based alloys, H storage props. 4-77153  
 natural gas/hydrogen compressed storage, comparison as vehicle fuels 4-89375  
 nonfossil energy sources, impact of hydrogen 4-66819  
 nuclear fusion powered H<sub>2</sub> production 4-62407  
 p-n junction GaAs photovoltaic electrolyser for hydrogen production by water electrolysis 4-89451  
 photocatalytic prod. with CdS<sub>2</sub>-Se<sub>2</sub> solid soln. particles 4-100008  
 photovoltaic solar hydrogen plant material and energy requirements 4-72189  
 pressurised gas, storage and transport, safety (German) 4-109754  
 semiconductor particle, electron energy levels, photocatalytic activity, irradiation effect 4-77029  
 solar thermal H<sub>2</sub> production by direct flux chemical reactor 4-66813  
 storage economy, technoeconomic comparisons 4-66817  
 synthesis from hydrocarbons, purification (German) 4-81597  
 thermomechanical hydrogen production, Co-Br hybrid water-splitting process (Japanese) 4-66806  
 thin-film high temperature water electrolysis cells, for H<sub>2</sub> production, development advances 4-105126  
 USA hydrogen fuel industry 4-66815

**hydrogen economy continued**

- water photoelectrolysis, electrodes and dopants for solar energy conversion 4-72127  
 water splitting by Jeewanu photocell, environmental chemicals effects 4-114964  
 CaNi<sub>5</sub>, stability of rechargeable hydriding alloys during extended cycling 4-72190  
 CeNi<sub>5</sub>-Al alloys, H<sub>2</sub> storage props. 4-61206  
 Ce<sub>1-x</sub>Ni<sub>2-x</sub>Cu<sub>2-x</sub> alloys, hyperstoichiometric, H<sub>2</sub> sorption 4-61207  
 α-Fe<sub>2</sub>O<sub>3</sub> CVD coating on alumina high temp. stable catalyst for SO<sub>2</sub> conversion to SO<sub>2</sub> in hydrogen production process 4-66807  
 Fe<sub>2</sub>O<sub>4</sub> thermal dissociation in solar furnace for H<sub>2</sub> production, 1000 kW concentrator production eval. from 2 kW concentrator 4-62402  
 H masers, appl. of metal hydrides for gas handling 4-69352  
 H production using nonconventional energy resources 4-81598  
 H-evolving solar cells, free energy conversion efficiency 4-72111  
 H<sub>2</sub> evolution reaction, in alkaline media on Ni-Fe codeposits 4-93533  
 H<sub>2</sub> fuel comparison with synthetic fossil fuels, economic and environmental aspects 4-66648  
 H<sub>2</sub> fueled engine for underground mining vehicle, with ultra-low emissions 4-62406  
 H<sub>2</sub> prod. from alcohol photocatalytic reaction on Pt/TiO<sub>2</sub> 4-114820  
 H<sub>2</sub> produced from NH<sub>3</sub>, cost comparisons of various processes 4-105128  
 H<sub>2</sub> production, p-Si cathode surface treatment effects on photoelectrochemical kinetics 4-93649  
 H<sub>2</sub> production, by high temp. high pressure water electrolysis 4-105127  
 H<sub>2</sub> production, by photoelectrochemical decomposition of water (Hungarian) 4-100009  
 H<sub>2</sub> production, from water vapour and CO<sub>2</sub>, thermoradiation processes 4-93651  
 H<sub>2</sub> production, thermochemical processes, coupling with HTGR 4-66808  
 H<sub>2</sub> production and technologies, today, tomorrow and beyond 4-93645  
 H<sub>2</sub> production and use for rural Alaskan community, programme design and planning 4-89473  
 H<sub>2</sub> production by catalytic thermal decomposition of water 4-93646  
 H<sub>2</sub> production by direct decomposition of water in solar furnace 4-62405  
 H<sub>2</sub> production by dye-sensitized photolysis of water 4-93650  
 H<sub>2</sub> production by electrochemical gasification of coal 4-66814  
 H<sub>2</sub> production by electrolysis, design and process engineering concepts (German) 4-93644  
 H<sub>2</sub> production by HV light irradiation of H<sub>2</sub>SO<sub>4</sub> solution containing K<sub>2</sub>Cr<sub>2</sub>O<sub>7</sub>.3H<sub>2</sub>O and FeSO<sub>4</sub> 4-66810  
 H<sub>2</sub> production by photoelectrocatalysis on p-MoS<sub>2</sub> 4-114963  
 H<sub>2</sub> production by solar powered water decomposition, coproduction of iron 4-105129  
 H<sub>2</sub> production by water splitting, using photochemical reaction in concentrated phosphoric acid 4-89470  
 H<sub>2</sub> production from aliphatic alcohols over UV-illuminated powder Ni/TiO<sub>2</sub> catalysts, at room temperature 4-66809  
 H<sub>2</sub> production in autothermal fluidized gasifier 4-72187  
 H<sub>2</sub> thermochemical production by V/Cl<sub>2</sub> cycle, energy and exergy anal. 4-72185  
 H<sub>2</sub> thermochemical production by Y/Cl<sub>2</sub> cycle, chemical engineering aspects 4-72186  
 H<sub>2</sub> thermochemical production using nuclear process heat, developments in West Germany 4-114962  
 H<sub>2</sub>/electrical power simultaneous production, using carbonaceous fuels and high-temperature nuclear process heat, thermodynamic anal. 4-89472  
 H<sub>2</sub>/O<sub>2</sub> evolution photoelectrocatalysis 4-105112  
 H<sub>2</sub> catalytic decomposition kinetics in thermochemical H<sub>2</sub> production 4-93647  
 H<sub>2</sub>S as hydrogen source, obtained as waste product from fossil fuels, methods of use 4-89471  
 H<sub>2</sub>S thermal decomposition with Ni<sub>3</sub>S<sub>2</sub> for H<sub>2</sub> production 4-93648  
 LaNi<sub>5</sub>, stability of rechargeable hydriding alloys during extended cycling 4-72190  
 LaNi<sub>4.7</sub>Al<sub>0.3</sub>, stability of rechargeable hydriding alloys during extended cycling 4-72190  
 Mg long-term hydrogenation-dehydrogenation, effects on hydrogen storage capacity 4-105132  
 Mg<sub>1.8</sub>H<sub>2</sub>O-MgO mixture thermal decomposition for high concentration H<sub>2</sub> production in H<sub>2</sub> production cycle 4-72188  
 NiFe<sub>2</sub>O<sub>4</sub> high temp. stable catalyst for SO<sub>2</sub> conversion to SO<sub>2</sub> in hydrogen production process 4-66807  
 TaH<sub>x</sub>, tracer and chem. diffusion of H, Gorsky effect, neutron spectra meas. 4-75724  
 TiFe, H uptake activation, Auger electron spectroscopy 4-70558  
 ZnFe<sub>2</sub>O<sub>4</sub> high temp. stable catalyst for SO<sub>2</sub> conversion to SO<sub>2</sub> in hydrogen production process 4-66807  
 Zr-based Friauf-Laves phases, lattice consts. and H absorption capacities 4-84234

**hydrogen embrittlement**

- cracking in weldments (Chinese) 4-99478  
 high-tension steel, corrosion fatigue crack growth in NaCl soln. 4-114711  
 metal hydride solubility, elastic and plastic accommodation effects 4-108620  
 pressurised gas, storage and transport, safety (German) 4-109754  
 spallation neutron source materials, H embrittlement, thermal fatigue, irradiation, creep 4-108464  
 steel, austenitic and ferritic stainless, fusion reactor material, crack growth modelling 4-104851  
 steel, austenitic stainless, H attack, TEM study 4-114657  
 steel, austenitic stainless, H induced slow crack growth rel. to α' martensite form. 4-66428  
 steel, austenitic stainless, SCC under compressive stress 4-99636  
 steel, austenitic stainless, stress corrosion in boiling Na<sub>2</sub>S soln. 4-109539  
 steel, C, cast and wrought, H induced ductility losses, annealing effects 4-85193  
 steel, cathodic polarisation curves, S content influence (French) 4-71792  
 steel, Cr-Mo, intergranular H stress cracking rel. to grain boundary segregation of P 4-62112  
 steel, Cr-Mo-V, ultrahigh strength, H-induced delayed cracking of smooth torsional specimens 4-85203  
 steel, CrMn, acoustic emission in H origin defects form. 4-99534  
 steel, H attack, invest. of models 4-104847  
 steel, H corrosion, theory of void growth limited by C diffusion 4-81338  
 steel, H embrittlement by cathodic charging 4-66420  
 steel, high strength, H cracking parameters for predicting safe welding conditions 4-66404

**hydrogen embrittlement continued**

- steel, high strength, H embrittlement fracture morphology (*Japanese*) 4-99511
- steel, HSLA, small fatigue crack initiation and growth, in various environments (*Japanese*) 4-89124
- steel, low alloy, fatigue crack propag. in viscous environment 4-99579
- steel, low alloy, sulphide stress cracking, role of H 4-89168
- steel, maraging, H embrittlement, notch tensile strength rel. to ion plated Al coating 4-114671
- steel, maraging, ultrahigh strength, delayed failure 4-93402
- steel, martensitic stainless, Mo, H embrittlement, effect of surface condition 4-85202
- steel, mech. props., influence of pressurised  $H_2$  4-109494
- steel, medium C, H-assisted cracking after exposure to  $H_2S$ -saturated salt soln., role of MnS inclusions 4-71732
- steel, microalloyed, rel. between microstruct. and H embrittlement 4-99605
- steel, Ni-Co-Mo, ultrahigh strength maraging, H embrittlement enhancement by Ni or Cu coatings (*Japanese*) 4-89114
- steel, Ni-Co-Mo maraging, H embrittlement rel. to coating and heat treatment (*Japanese*) 4-89113
- steel, Ni-Cr-Mo, crack paths and H assisted crack growth in  $H_2$  and  $H_2S$ , temp. and press. depend. 4-66429
- steel, Ni-Cr-Mo, H embrittlement susceptibility, delayed failure time, effect of specimen geometry 4-85204
- steel, Ni-Mo, A533B, fatigue crack growth in simulated PWR loop 4-104834
- steel, spheroidized 1090, dislocation density distrib. in tensile specimens, H effect 4-84298
- steel, stainless,  $TiO_2$  sputter coated, H embrittlement prevention 4-62033 (Fe, Co, Ni) $_3$ V, ductile ordered alloys, phys. metallurgy and mech. props. 4-114612
- Fe, apparent H diffusivity, effect of cathodic charging current density 4-104005
- Fe-Cu, H permeation in  $H_2SO_4$  with and without  $H_2S$ , electrochem. and surface anal. studies 4-104893
- $\alpha$ -Fe-(C), H-induced grain boundary fracture, effect of C 4-93403
- Mg, H embrittlement and environmentally-induced cracking 4-71718
- Nb, Pd- and Ni-coated, hardening and fracture initiation, resulting from  $H_2$  adsorpt.-desorpt. cycling 4-81282
- Nb; H, hydrogen embrittlement, electron microscopy study 4-93396
- Ni, deformed, dislocation struct. and fracture behaviour, effect of  $H_2$  and He 4-62043
- Ni, H embrittlement, influence of plastic deform. 4-71729
- Ni, O assisted intergranular H embrittlement, effects of B, P, Sn and Sb additions 4-62030
- Ni-Pd alloy plating method for H embrittlement in high-strength steel (*Japanese*) 4-104861
- Ti-Al-Sn-Zr-Mo-Si, H-enhanced fatigue crack growth 4-114640
- V and V-Cr-Ti alloy, fusion reactor blanket use, analysis of attack by O and water vapour 4-107019
- V-H, hydrogen embrittlement, electron microscopy study 4-93396

**hydrogen energy** see *hydrogen economy*

**hydrogen ion activity** see *pH*

**hydrogen ion concentration** see *pH*

**hydrogen ions**

- accelerated cluster ions, interaction with  $H_2O$  gas target 4-74378
- charge exchange of heavy ions in matter, radiation calc. 4-76548
- cluster ion formation in free jet expansion processes at low temperatures 4-74381
- conference, polarised proton ion sources, Vancouver, BC, Canada (May 1983) 4-106092
- differential cross sections 4-85295
- excited  $H^+$  transfer in para-N,N-dimethylaminosalicylic acid, excitation wavelength depend. 4-62171
- extraction of  $H^+$  beams 4-78414
- formyl ion(-d), dissociative recombination coeffs. 4-112285
- heavy targets, 1 subshell X-ray production by 1 to 3 MeV protons and  $He^+$  ions 4-96651
- K X-ray prod. cross sections using fluoresc. yield 4-96483
- level population in H II regions 4-101136
- light elements, thick targets,  $H^+$  bombardment, continuous X-ray spectra 4-99214
- methane, protonated, dissociative recombination coeffs. 4-112285
- multicharged ions in alternating field, fine struct., two level approx. (*Russian*) 4-91207
- negative ion production via dissociative attachment to  $H_2$  4-73561
- nonbijective canonical transformations, use in chemical physics 4-71868
- plasma, spectral line wing broadening theory (*Russian*) 4-69015
- plasma recombination coeff. for TFR vacuum vessel 4-97869
- recombination rate coeff. in ISX-B tokamak 4-97868
- spiral galaxies, face-on, H II mass and electron density 4-110749
- tetrafluoromethane+ $H^+$ , mol. very high overtone vibr. levels obs. 4-96672
- three particle system with Coulomb interaction, elastic scatt. 4-102763
- vacuum UV radiation prod. cross sections for  $H^+$  in gases 4-78931
- volume generation of negative ions in high density hydrogen discharges 4-73559
- volume  $H^-$  ion production experiments at LBL 4-73564
- Al, continuum X-rays produced by a few MeV proton bombardment 4-99215
- C, continuum X-rays produced by a few MeV proton bombardment 4-99215
- C foil,  $H^+$ ,  $H_2^+$  and  $H_3^+$  ion bombardments, continuum optical radiation emission 4-81007
- foil,  $H_2^+$  and  $H_3^+$  ion bombardment, mol. enhancement of n-state populations 4-81064
- H arc discharge with bulk cathodes 4-111870
- H ions+alkali metal vapour, spin-depend. charge transfer 4-59890
- $H^-$ , 758.1 nm predicted diffuse  $H^-$  interstellar line, obs. 4-90212
- H autoionisation states, single configuration approx., orthogonality conditions 4-107318
- $H^-$  beam line, IKVT-KFK research 4-73567
- $H^-$ , binding limit in Hartree approx. 4-102569
- H, charge exchange with protons in Na, K, Rb-vapour 4-74324
- H, density in a tandem multicusp discharge 4-73568
- H formation by charge transfer in alkaline earth vapours 4-73572
- H formation by  $H^+$ ,  $H_2^+$  scatt. from W-Cs surfaces 4-73574
- H, generation of intense flux 4-69925
- hydrogen ions continued**
- $H^+$ , generation on composite surfaces rel. to surface/plasma ion source systems 4-93165
- $H^+$ , honeycomb surface-plasma source 4-101975
- $H^-$  ion source, design and fabrication for tokamak 4-112002
- $H^-$  ion source development, sheet plasma 4-78415
- $H^-$  Lamb shift polarised ion source, intensity limitations 4-107241
- $H^-$  Lamb-shift polarised ion sources 4-107239
- $H^-$  polarised ion source, charge transfer processes 4-107246
- $H^-$  polarised ion source, electron polarisation meas. of optically pumped Na atoms 4-64258
- $H^-$  polarised ion source, status at AGS 4-107235
- $H^-$  polarised ion source at Munich 4-107240
- $H^-$  polarised ion source at KEK, optically pumped 4-107244
- $H^-$  polarised ion sources using ring magnetron ioniser 4-107236
- $H^-$  production and destruction mechanisms in low press. discharge 4-73560
- $H^-$  production from Cs-transition metal composite surfaces 4-73573
- $H^-$  production from partially caesiated surfaces in presence of H plasma 4-93166
- $H^-$  production in low press. plasma 4-73569
- $H^-$  production in mag. multipole source 4-73562
- $H^-$  rare gas collisions, electron detachment 4-102766
- $H^-$  sputtering yields from Mo polycryst. target by  $Cs^+$  bombardment 4-73575
- $H^-$  surface conversion sources, sputter yield correl. with work function 4-93167
- $H^-$ , very-low-energy electron detachment 4-91336
- $H^+$  + Al K $\alpha$  vacancy production cross sections, projectile depend. 4-96676
- $H^+$ , atomic beam source for ion production 4-107234
- $H^+$  fraction in RF in source RIG 10 4-91958
- $H^+$ ,  $H_2^+$  and  $H_3^+$  swift beams, convoy electron emission 4-81060
- $H^+$  in softwater lakes, conc. determ., use of  $CO_2$  equilibria 4-77169
- $H^+$  injector/buncher with grounded ion source 4-107252
- $H^+$  permeation through precipitation membranes, rel. to  $OH^-$  4-11482
- $H^+$  transfer reactions, kinetic isotope effect, solvent depend. 4-104968
- $H^+$ , reson. energy levels, vibr. modes, semiclassical calcs. 4-87235
- H-like ions, reson. doublet spectrum in intense elec. field, laser plasma diagnostics appl. 4-84074
- $H^-$  ion mobility in HCl aq. soln., vel. concepts vs. config. description 4-80276
- $H^-$  ion mobility in HCl aq. solns., NMR determ. 4-80277
- $H^-$  ion mobility in HCl aq. soln., neutron scatt. study 4-80278
- $H^+$ , charge exchange and cross sections, symmetric orthogonalization of travelling molecular orbitals 4-64581
- $H^+$  + Ar(He), electron detachment, energy spectra, Born approx. 4-83459
- $H^+$  + Ar(He)(Ne), electron detachment cross sections 4-78952
- $H^+$  +  $H^+$ , mutual neutralisation, 5-2000 eV 4-64591
- $H^+$  + He, electron detachment in slow collisions 4-69198
- $H^+$  + He(Ar)(H $_2$ )(N $_2$ )(O $_2$ )(CO $_2$ ), electron detachment and charge exchange to shape reson. 4-69203
- $H^+$  + methyl fluoride, activation barriers, fourth order MB RSPT calc. 4-62167
- $H^+$  + O, electron capture, electron loss, excitation 4-64590
- $H^+$  + atom collisions, L-shell X-ray prod. and ionisation cross sections 4-67883
- $H^+$  + Au(O)(W), K-shell ionisation cross sections 4-78953
- $H^+$  + C foil, 2p and 3p population, beam-foil excitation 4-64584
- $H^+$  + C(Al) foil, ion energy loss ang. depend. 4-65313
- $H^+$  + C(Ne), charge transfer at large scattering angles in the strong potential Born approximation 4-87210
- $H^+$  + Cs, spin-depend. charge transfer 4-59890
- $H^+$  + Cu(Mo)(Ag) collisions; K-shell ionisation, angular depend. 4-7432
- $H^+$  + F, two state-collision problems for exponential coupling 4-74315
- $H^+$  + H, elastic scatt., intermediate energies, model calcs. 4-107430
- $H^+$  + H collisions, reson. electron transfer from Rydberg atom 4-74329
- $H^+$  + H collisions, triple-centre treatment of ionisation 4-78956
- $H^+$  + H $_2$ , proton interchange process rel. to ortho- $H_2$ /para- $H_2$  ratio interstellar mol. clouds 4-94927
- $H^+$  + H $_2$  collisions, two state charge transfer calc. 4-91341
- $H^+$  + H $^+$ , mutual neutralisation, 5-2000 eV 4-64591
- $H^+$  + H(He), electron capture, symmetries eikonal-type approx. 4-83464
- $H^+$  + H(He) Thomas peak in electron capture 4-96692
- $H^+$  + H(is) reson. electron capture, T-matrix element calcs. 4-102792
- $H^+$  + He, autoionising reson. excited at small ejection angles 4-78956
- $H^+$  + He, elastic scatt., Glauber approx. 4-83447
- $H^+$  + He, electron capture, coherent excitation, multiple scatt. approach 4-87212
- $H^+$  + He, electron capture, differential and total cross-sections calc. 4-107447
- $H^+$  + He, proton impact line widths 4-102638
- $H^+$  + He autoionising state excitation cross section 4-59886
- $H^+$  + He(is), electron capture cross sections 4-69200
- $H^+$  + heavy atom, inelastic scatt. relativistic effects, Born approx. 4-83449
- $H^+$  + inert gas atom, multiply ionising collisions,  $\delta$ -electron spectrum 4-83458
- $H^+$  + inert gas atoms, charge transfer and direct ionisation channels, electron prod. 4-87191
- $H^+$  + Li collisions, single electron capture 4-74327
- $H^+$  + Li $^+$ (C $^+$ )(N $^+$ ), ionisation cross section, PWBA 4-83461
- $H^+$  + Na(K), electron transfer collisions, at. basis calcs. 4-102793
- $H^+$  + O, electron capture, electron loss, excitation 4-64590
- $H_2$  cluster ions-solid surface impact, surface roughness influence obs. 4-71507
- $H_2^-$  existence investig., rel. to form. by electron capture 4-74331
- $H_2^-$ , metastable on production search 4-73566
- $H_2^-$  production from vibrationally excited states 4-73570
- $H_2^-$ ,  $1s\sigma^-$ - $2p\sigma_g^-$  transitions, dipole-length and dipole vel. matrix element modification 4-64348
- $H_2^+$ , Dirac eqn., two dims. numerical soln. 4-112093
- $H_2^+$ , dissociative electron capture, velocity dist., vibrational excitation 4-85307
- $H_2^+$ , electron impact dissociation 4-102812
- $H_2^+$ , ground state binding energy in intense mag. field 4-74354
- $H_2^+$  in magnetic field of neutron star, two-dimensional potential energy surface 4-67612
- $H_2^+$ , kinetic and potential energy fluctuations (*French*) 4-112247
- $H_2^+$ , low-lying energy levels, nonadiabatic calcs. 4-102613

## hydrogen ions continued

- $H_2^+$  momentum distribns., nodal struct. 4-78766  
 $H_2^+$ , muonic; low-lying energy levels, nonadiabatic calcs. 4-102613  
 $H_2^+$  or  $D_2^+$  ion beams, high conc., prod. using short multicusp ion source, use in heating 4-60673  
 $H_2^+$ , pot. energy functions calc. in a strong mag. field 4-107427  
 $H_2^+$ , UV laser photodissoc. 4-69157  
 $H_2^+$  + C foil, 2p and 3p population, beam-foil excitation 4-64584  
 $H_2^+$  + H, excitation to  $n=2$  level, ang. differential and total cross sections 4-102782  
 $H_2^+$  +  $H_2^+$  symm. electron transfer reactors of state-selected ions 4-107446  
 $H_2^+$  +  $H_2^+$  collisions at low energies,  $H^+$  prod. 4-91867  
 $H_2^+$  + He, exchange reaction, ab initio pot. energy surface, quasiclassical trajectory study 4-76996  
 $H_2^+$  existence investig., rel. to form. by electron capture 4-74331  
 $H_2^+$ , metastable ion production search 4-73566  
 $H_2^+$ , dissociative recombination coeffs. laboratory expts. 4-82408  
 $H_2^+$ , dissociative recombination coeffs. 4-112285  
 $H_2^+$ , G-function, generalised diatomics in mols. theory 4-68964  
 $H_2^+$ , ground state, susceptibility and moments, CI variational calcs. 4-107285  
 $H_2^+$ , vibr.-rot. levels, IR predissociation spectra 4-107344  
 $H_2^+$  + C foil, 2p and 3p population, beam-foil excitation 4-64584  
 $H_2^+$  + e, dissociative recombination, reaction product channel anal. 4-74344  
 $H_2^+$  + He, three body dissoc. absolute cross section meas. 4-104984  
 $H_2^+$ , form. from collisionally dissociated  $H_2^+$  4-66555  
 $H_2^+$ , dissociative recombination coeffs. laboratory expts. 4-82408  
 $H_2^+$  + He, collisional dissoc., form. of  $H_4^+$  4-66555  
 $HD^+$ , low-lying energy levels, nonadiabatic calcs. 4-102613  
 $HD^+$  + He, three body dissoc. absolute cross section meas. 4-104984  
 $H_2D^+$ ,  $10^{-11}$  submillimeter line meas. 4-112157  
 $H_2D^+$ ,  $10^{-11}$  submillimeter wave transition 4-112162  
 $HT^+$ , low-lying energy levels, nonadiabatic calcs. 4-102613  
 $H166\alpha$  emission from galactic plane, southern survey 4-63298

## hydrogen neutral atoms

- absorption in centre of galaxy M82, VLA obs 4-110740  
 adsorbed on GaAs (110), temp. programmed desorption study 4-92528  
 adsorption on Al (100) surface, CNDO/BW calcs. 4-61222  
 afterglow plasma, central struct. of  $H_\beta$  line at low electron densities 4-59674  
 atom + isoformyl ion, metastability and isomerisation, interstellar appl. 4-91327  
 atomic beam polarized proton source 4-107464  
 atomic beam source for ion production 4-107234  
 atomic spectroscopy and holography, laboratory expt. 4-67927  
 atoms in He, collisional hyperfine line shifts calc. using exchange perturbation theories 4-64401  
 atoms in superstrong mag. fields 4-74148  
 Balmer  $\alpha$  production rate in corona of Comet Austin 4-94681  
 Balmer lines broadened by plasma turbulence, Stark profiles 4-105871  
 beam-foil excited atoms, Stark quantum beats, use of density matrix neutral expansion 4-83327  
 bound-state energies calc. using variational functional method 4-78765  
 charge exchange with protons in Na, K, Rb-vapour 4-74324  
 chemisorption on BCC Fe, ab initio/effective core pot. cluster calc. 4-108722  
 conference, polarised proton ion sources, Vancouver, BC, Canada (May 1983) 4-106092  
 Cooper-type minima in multipole photoionisation cross section 4-91241  
 diamagnetic Hamiltonian derivation, group theory appl. 4-78924  
 diffusion coeff. in He, interaction pot. 4-103456  
 diffusion cross sections in He gas, interatomic pot. 4-103454  
 diffusion of H-atoms on surface of liquid  $He$  4-88357  
 disc galaxies, distance moduli from H I 21 cm line widths 4-101198  
 distribution and motions in NGC 7013 lenticular galaxy 4-67787  
 dynamic response in elec. field, Born-Oppenheimer and Feynman-Hellmann approx. 4-102589  
 eigenvalues obtained using algebraic technique 4-63444  
 elastic electron and positron scatt. in intermediate energy range 4-78968  
 elastic electron scatt. in intense laser field, cross sections 4-83474  
 elastic scatt., two-electron wave functions, combined hyperspherical and close-coupling description 4-64566  
 electromagnetic transitions, wavelengths, dipole strengths, oscillator strengths and transition probabilities 4-59676  
 electron capture by fully stripped ions, intrashell mixing and Stark effect 4-59888  
 electron impact excitation, distorted wave approx. 4-91353  
 electron impact excitation, linear algebraic separable pot. approach appl. 4-59897  
 electron impact ionisation, cross sections DWBA and DWIA 4-102803  
 electron scattering, pseudostate expansions convergence 4-102805  
 electron scattering total and ionisation cross sections, simplified model 4-74337  
 emission line shapes in hollow-cathode discharge 4-102645  
 evolution in liq. He chamber, recombination and burial 4-77003  
 exact path integral treatment 4-59627  
 excited state, prod. by electron impact on methanol 4-112286  
 extended classical charged particle in mag. field, self-torque, radiation reaction, H atom appl. 4-90394  
 fine-struct. intervals, Breit-Pauli approx., relativistic calcs., relevance to mol. calcs. 4-96467  
 fluoromethane + H, vibr. excitation, IR emission study 4-69186  
 ground state, multipole moments, time derivative fields 4-69021  
 ground state energy, quadratic Zeeman effect, Rayleigh-Schrodinger perturbation theory 4-102639  
 Grw +  $70^\circ 8247$ , H identification, spectra and mag. field effects 4-110609  
 hydrogenic ion, electron capture by fully stripped ion, relativistic second Born approx. 4-87209  
 hydrogenic Zeeman levels, second-order perturbative calc. 4-64365  
 intergalactic H I, spin temp. anal. and implications for X-ray and EUV flux 4-110743  
 interstellar distrib. rel. to  $\gamma$ -ray distrib. 4-63301  
 interstellar H and He in heliosphere, ionisation by 'core' and 'halo' solar wind electrons 4-105863  
 interstellar H I beyond solar circle, 21 cm surveys 4-63305  
 interstellar H I distrib., correl. with  $\gamma$ -ray emission intensity and energy spectra anal. 4-101486  
 interstellar H I distrib. and galactic spiral struct. 4-63306

## hydrogen neutral atoms continued

- interstellar H I high-vel. inflow towards galactic centre 4-86006  
 interstellar H I in outer Galaxy rel. to  $\gamma$ -rays and cosmic rays 4-86049  
 interstellar H I in Sc I galaxies, props. 4-90220  
 interstellar H I survey of southern galactic plane 4-63299  
 interstellar H I towards supernova remnant 3C 58, distance determ. 4-73045  
 interstellar ionised H, interaction with neutron star mag. field, hard radiation emission 4-77863  
 interstellar kinematics used to determine outer Galaxy gamma rays distrib. 4-63303  
 interstellar resonance radiation pressure effects 4-63251  
 kaonic hydrogen, atomic ground state interaction, model-independent formalism 4-96726  
 in Large Magellanic Cloud, vels. and rotation from 21 cm line survey 4-110741  
 lifetime of 2p state and Lamb shift 4-69014  
 Lyman alpha radiation transfer in filamentary prominences (Russian) 4-101283  
 M31, H I structures and holes 4-63317  
 M31, high resolution H I survey 4-63316  
 meso-atoms, quadrupole moment in the excited  $2P_{1/2}$  state 4-59906  
 metallic, ground state energy in Wigner-Seitz approx. 4-80469  
 multiphoton transitions above-threshold, Coulomb Green function calc. 4-112151  
 muonic, excited state, isotope exchange process influence on fusion 4-106653  
 muonic, scattering cross sections 4-107475  
 muonic, weak interactions contrib. to hyperfine level splitting 4-83494  
 muonic H, K-line intensity ratios, pressure depend. of  $(\mu p)_{2S}$  population 4-102831  
 NGC 1510, H I accretion from companion galaxy NGC 1512 and star form. bursts 4-63278  
 nonbijective canonical transformations, use in chemical physics 4-71868  
 one-dimens.,  $\delta$  function interaction, polarisability 4-106149  
 optical spectra in strong mag. fields (Japanese) 4-107307  
 Orion Nebula, Stark broadening in radio recomb. lines 4-90215  
 parity nonconservation, Zeeman and Stark effect, reson. line shapes 4-96489  
 phase-space formulation, nonrelativistic quantum mechanics 4-102590  
 photoionisation in elec. field, overlapping resons. and interference effects 4-69029  
 photoionisation in elec. field, reson. and interference effects 4-69028  
 plasma, ion temps., spectral line broadening (Chinese) 4-87840  
 plasma limiter, H recycling and impurity release by laser induced fluorescence 4-97867  
 plasma recycling model calcs. in JT-60 for Mo, Inconel 625 and TiC walls 4-97870  
 plasma time evolution of transport processes; computer codes 4-87848  
 positron elastic scatt. and positronium form. cross sections 4-83471  
 positron elastic scatt. mechanism, field-theoretic optical pit. calcs. 4-69211  
 potential, approx. continuum wave functions, appl. to photoionisation 4-112252  
 quadrupole moment in the excited  $2P_{1/2}$  state 4-59906  
 radiative decay, final-state interferences 4-83333  
 radiative lifetimes of excited levels 4-107312  
 Rayleigh scatt. from  $n=3$  resonance states, one-pole approx. 4-78824  
 relativistic H atom, WKB semiclassical approx. 4-90407  
 second-order perturbation theory in crossed elec. and mag. fields 4-83329  
 solvation by  $H_2O$  mols. 4-62175  
 spectra and struct. in strong mag. field, spherical basis (French) 4-68927  
 spectrum, resolution of tunable dye lasers 4-64412  
 spectrum transformation in crossed electric and mag. fields 4-59672  
 spherical quadratic Zeeman problem, factorised wavefunction approach 4-64425  
 spin polarised, atomic, condensation on superfluid  $He$  4-104037  
 spin polarised, on liquid  $He$ , polaronic aspects 4-104034  
 spin polarized, collective spin oscillations 4-70525  
 spin polarized, three-body recombination rates 4-70526  
 spin-polarized, nucl. spin waves, NMR study 4-70524  
 Stark effect level crossings, relativistically enhanced ionisation rates 4-69010  
 Stark effect shape resonances in fields up to 3 MV/cm 4-102641  
 Stark-mixed  $n=2$  states, excitation and decay obs. in electron-photon coincidence expt. 4-87073  
 state and behaviour in Si lattice 4-61095  
 three-atom systems, exchange interactions, asymptotic anal. 4-74144  
 three-dimensional, excited state, Zeeman effect 4-102640  
 three-dimensional, rel. to harmonic oscillator, zero-energy case 4-74132  
 two-photon 3s-1s and 3d-1s transitions 4-83357  
 UGC 7576, spindle-like galaxy, mapping in H I, UHF obs. 4-73076  
 Virgo cluster and field galaxies, H I and optical diameters 4-77939  
 VUV laser spectroscopy, two-photon spectra 4-83383  
 wave function, analytic structure 4-83284  
 W Zw 73, spindle-like galaxy, mapping in H I, UHF obs. 4-73076  
 D-H isotope separation between hydrogen and liq. methanols 4-59904  
 H I distrib. and vel. field in nearly face-on spiral galaxy NGC 1058, obs. 4-94946  
 H I distrib. in spiral galaxy NGC 6946, correl. with star form. characts. 4-90227  
 H I in Galaxy, distrib. rel. to gamma ray emission and cosmic rays distrib. 4-90237  
 H I in isolated galaxies, UHF obs. 4-110736  
 H I radial velocity in SMC and Magellanic Stream, characts. 4-106064  
 H I recombination lines obs. and IR extinction towards G333.6-0.2, obs. 4-94917  
 H I-cosmic ray interactions, diffuse galactic gamma-ray emission 4-100890  
 H local vibr. spectra in metal hydrides using TOF spectrometer 4-74088  
 H, muonic,  $e^-$  scattering amplitude estimated below  $\mu^-$  excitation threshold 4-64611  
 H polarised atomic beam source, feasibility study 4-107468  
 H-like atoms, Dirac eqn. soln. within algebraic approx. 4-59621  
 H-2-chloroethyl radical, ab initio MO studies, rot. barrier, dissoc. energy 4-99773  
 H +  $Be^{++}$ , charge transfer cross sections calc. using close coupling calc. 4-78959  
 H +  $Be^{++}(B^3+)(C^6+)(N^7+)(O^8+)$ , electron capture cross-sections calcs. 4-102791

**hydrogen neutral atoms continued**

- H + C<sup>2+</sup> (C<sup>3+</sup>) ions, state-selective electron capture, translational energy spectroscopy 4-59891  
 H + C<sup>4+</sup> electron transfer into C<sup>3+</sup> (nl) orbitals, at. basis calcs. 4-107450  
 H + C<sup>4+</sup> (N<sup>3+</sup>) (O<sup>6+</sup>) electron capture, 0.25-25 keV amu<sup>-1</sup>, 4-69205  
 H + C<sup>9+</sup> (N<sup>8+</sup>) (O<sup>9+</sup>) ions, electron removal cross section 4-83460  
 H + CO, collisional excitation, cross sections, quasiclassical trajectory study 4-78950  
 H + Cl<sub>2</sub>, oriented-averaged rot.-decoupled vibr. 4-99753  
 H + Cl<sub>2</sub>, quantum classical reaction path model 4-114764  
 H + D<sub>2</sub>, nascent HD prod. quantum state distrib., pulsed-laser photolysis, Raman spectra 4-104977  
 H + D<sub>2</sub>, opacity analysis of steric requirements in elementary chemical reactions 4-62159  
 H + D<sub>2</sub>, vibr. and rot. energy disposal reaction at 1.3 eV, surprisal anal. 4-76973  
 H + D<sub>2</sub>, reaction dynamics, product state distrib. determ. at collision energy of 1.3 eV 4-71896  
 H + D<sub>2</sub> → HD + D reaction, coupled state quantum calc. at E<sub>rel</sub>(ν=0, j=0)=0.55 eV 4-99750  
 H + D<sub>2</sub> → HD + D reaction, distorted wave calcs. at E<sub>trans</sub>(ν=0, j=0)=0.55 and 1.3 eV 4-99749  
 H + FH reactive reson., partial widths and isotope effects calc. by reaction path Hamiltonian model 4-71890  
 H + formyl ion (acetyl ion), different activation energies 4-62161  
 H + fully stripped ion, final-states mixing following slow collision, electron capture 4-107451  
 H + H<sub>2</sub>, quantum mechanical coplanar scatt., action angle variables 4-69176  
 H + H<sub>2</sub>, reactive differential cross sections in rot. linear model, ang. distrib. 4-99775  
 H + H<sub>2</sub>, reagent rot. effect, classical trajectory calcs. 4-93506  
 H + H<sub>2</sub> (inert gas atoms), laser excitation, electron loss from H(3p) atoms, H(3p) beam prod. 4-87200  
 H + H<sub>2</sub>, reaction, three dimens., coupled channel distorted wave calcs. 4-99761  
 H + H<sub>2</sub>, reactions, semiclassical adiabatic theory 4-114786  
 H + H<sub>2</sub>, rearrangement collisions, reson. and dynamics calcs. 4-71901  
 H + H<sub>2</sub><sup>+</sup>, excitation to n=2 level, ang. differential and total cross sections 4-102782  
 H + H<sub>2</sub>O reaction dynamics, state distrib. for OH product 4-71873  
 H + H<sub>2</sub>(MuH), H and Mu exchange, isotope effects, semiclassical techniques 4-71884  
 H + H<sub>2</sub> → H<sub>3</sub><sup>2+</sup> → H<sub>2</sub> + H, H<sub>3</sub><sup>2+</sup> absorpt., transition state spectroscopy 4-69194  
 H + H<sup>+</sup>, charge exchange and cross sections, symmetric orthogonalization of travelling molecular orbitals 4-64581  
 H + H<sup>+</sup>, electron capture, symmetries eikonal-type approx. 4-83464  
 H + H<sup>+</sup>, Thomas peak in electron capture 4-96692  
 H + H<sup>+</sup> collisions, reson. electron transfer from Rydberg atom 4-74329  
 H + H<sup>+</sup> reson., electron capture, T-matrix element calcs. 4-102792  
 H + HD → H<sub>2</sub> + D collinear reaction, competition between dissoci. and exchange processes, exact quantum results 4-81409  
 H + HF, nonreactive scatt., quantum mechanical calcs. using localised rot. basis functions 4-59882  
 H + He, H(D) 2s and 2p excitation, integral cross sections 4-102786  
 H + He, rate const. meas. for orientation transfer 4-107435  
 H + He<sup>+</sup>, excitation cross sections calc. using Vainshtein Presnyakov-Sobel'man approx. 4-64586  
 H + He<sup>2+</sup>, charge transfer, laser assisted, coupled dressed quasimolecular states approach 4-96684  
 H + He<sup>2+</sup> (Be<sup>+</sup>) (B<sup>5+</sup>) (C<sup>6+</sup>) (N<sup>7+</sup>) (O<sup>8+</sup>) collisions, electron transfer, at. orbital expansion description 4-78962  
 H + Li<sup>+</sup> (Li<sup>2+</sup>) (Li<sup>3+</sup>), electron capture by fast ions 4-91343  
 H + Li<sup>3+</sup> charge exchange cross-sections, low-energy calcs. 4-64592  
 H + methane → H<sub>2</sub> + methyl, D isotope effect, ab initio pot. surface, transition state theory 4-81416  
 H + N<sup>3+</sup> charge transfer cross sections, extreme UV radiation emission 4-64596  
 H + NO chemiluminescence reactions, HNO(<sup>2</sup>A<sup>+</sup>) internal energy distrib. 4-71871  
 H + O, electron capture, electron loss, excitation 4-64590  
 H + O collisions, energy transfer rate coeff. 4-110517  
 H + O<sub>2</sub> (Δ<sub>g</sub>) → OH(<sup>2</sup>π) + O(<sup>3</sup>P) reaction, primary processes, fluoresc. investig. (German) 4-99785  
 H + O<sup>+</sup> (CO<sup>+</sup>) (CH<sup>+</sup>), reaction rate coeffs. 4-81427  
 H + positron, elastic scatt. and positronium form. cross sections 4-78964  
 H + X<sup>2+</sup> charge transfer collisions, long-range secondary couplings 4-102790  
 H + XY and X + HY where X and Y are Cl, Br or I, 3D DIM-3C pot. energy surfaces 4-66572  
 H<sup>+</sup> + H collisions, triple-centre treatment of ionisation 4-78956  
 H<sub>2</sub> + Mg reactions, MgH nascent internal energy distrib. 4-71872  
 H<sub>2</sub> metastable mols., intense beam prod. 4-87057  
 H<sup>+</sup> electron impact dissoci. of H<sub>2</sub>O, emission cross section 4-107462  
 Hα line Stark broadening at low densities, quantal and semiclassical calcs. 4-64424  
 Si:B,H, neutralisation of shallow acceptor levels by atomic H 4-104153

**hydrogen neutral molecules**

- adsorbed, electron-stimulated field desorption 4-92532  
 adsorbed on GaAs (110), temp. programmed desorption study 4-92528  
 band transition moments between excited singlet states, spontaneous emission 4-95074  
 coadsorption with C<sub>2</sub>N<sub>2</sub> on Pt (111), surface chem. 4-81478  
 correlation energies with explicitly correlated Gaussian geminals 4-91204  
 density in dark clouds and continuum sources 4-110723  
 dipole moment, 2D fully numerical MC SCF calcs. 4-59614  
 dissociative adsorp. on Ni(001), London-Eyring-Polanyi-Sato model 4-62231  
 dynamic polarisability, Cauchy moments, coupled HF calc. 4-74147  
 electron and positron impact, rot. excitation cross sections 4-64630  
 electron collisions, correl. polarisation pot., parameter-free model 4-64609  
 electron correlation calcs. 4-87054  
 electron elastic scatt. and rot. excitation at 10 to 100 eV, optical pot. model 4-96697  
 electron impact, extreme UV emission spectra, appl. to wavelength calibration of UV spectrometers 4-83386  
 electron impact excitation, differential cross sections, independent atom model 4-91356

**hydrogen neutral molecules continued**

- electron impact excitation of high-n states 4-96702  
 electron impact rot. excitation, adiabatic approx. for nuclear excitation 4-74348  
 electron scatt., Eikonal amplitude with effective complex pot. 4-96643  
 electron scattering, ab initio nonadiabatic polarisation pots. 4-74347  
 electron-polarised-photon coincidence excitation of C II<sub>g</sub> state 4-83483  
 electronic motion-mol. vibr. dynamic coupling 4-64446  
 gamma-ray double photoionis., electron correl. 4-64548  
 ground state, FT IR spectra, rot. consts. 4-59741  
 ground state, multireference functions, cluster expansion theory, CI calcs. 4-74161  
 ground state, photoionisation cross sections, linear algebraic method 4-64549  
 interaction energy calc. using Gaussian model 4-91193  
 interatomic force, second energy gradient, momentum density approach 4-112250  
 internal motion, electron density dynamic anal., ab initio MO calcs. 4-87037  
 interstellar gas distribution from γ-ray emission anal. 4-63304  
 interstellar H<sub>2</sub>, ortho-H<sub>2</sub>/para-H<sub>2</sub> ratio in mol. clouds 4-94927  
 interstellar H<sub>2</sub> density in galactic mol. ring, γ-ray flux anal. 4-63302  
 interstellar H<sub>2</sub> distrib., correl. with γ-ray emission intensity and energy spectra anal. 4-101486  
 interstellar H<sub>2</sub> mass and γ-ray emission anal. 4-86049  
 interstellar mass in W3 mol. clouds 4-73003  
 isotopic molecules adsorbed in NaCa zeolites, induced IR overtone and fundamental bands 4-102678  
 magnetic field effects 4-74277  
 molecular consts., high resol. VUV emission spectra 4-83388  
 multipole props., time depend. CHF method 4-87040  
 nonadiabatic quasiclassical local model, intramol. evolution 4-102588  
 nonlinear optical props., ab initio calcs., freq. depend. dipole polarisabilities, susceptibilities 4-102608  
 nonlinear phenomena in laser spectroscopy, wave function calcs. 4-102827  
 ortho-para conversion on mag. surfaces, dynamical aspects 4-70555  
 polarisability and quadrupole moment of the mol. in a 'spheroidal' box 4-59914  
 positron scatt., coupled-state method calcs. 4-64616  
 positron scatt., low energy, cross section calc. using Kohn variational method 4-78975  
 radiative excited level lifetimes, time resolved fluoresc. meas. 4-87160  
 radiative lifetime, in nonadiabatically coupled J=1 state, ab initio calcs. 4-68976  
 radiative lifetimes and collisional quenching cross sections of selectively excited rovibronic states 4-83422  
 relativistic SCF calc. with squared Dirac operator 4-78790  
 scattering on Li<sub>n</sub> cluster, Raman enhancement mechanism assoc. with Raman scatterer interaction 4-61675  
 spectroscopy, high-resolution, at 83 nm 4-64490  
 spherically averaged molecular-electron momentum density, Compton profile 4-83489  
 state and behaviour in Si lattice 4-61095  
 surface collisions, de-excitation and equipartition 4-76576  
 T Tauri stars, circumstellar H<sub>2</sub> prod. due to ice grain-energetic particle interactions 4-94781  
 three photon reson. ionisation 4-83437  
 time-domain CARS in Dicke narrowing region 4-69090  
 total energies calc. using electron cloud displacement model (Chinese) 4-74136  
 transition probabilities for D and B vibr. levels to X vibr. levels and continuum 4-95075  
 van der Waals pot. model 4-69166  
 vibrationally excited generation by H<sub>2</sub><sup>+</sup> wall collisions 4-76574  
 VUV laser spectroscopy, two-photon spectra 4-83383  
 X<sup>1</sup>Σ<sub>g</sub> state, anisotropic electronic intracule densities calcs. 4-96422  
 Be<sub>2</sub> H<sub>2</sub> pot. surface walking and reaction paths 4-114790  
 H + H<sub>2</sub>, quantum mechanical coplanar scatt., action angle variables 4-69176  
 H + H<sub>2</sub> reaction, three dimens., coupled channel distorted wave calcs. 4-99761  
 H + H<sub>2</sub> → H<sub>3</sub><sup>2+</sup> → H<sub>2</sub> + H, H<sub>3</sub><sup>2+</sup> absorpt., transition state spectroscopy 4-69194  
 H + HD → H<sub>2</sub> + D collinear reaction, competition between dissoci. and exchange processes, exact quantum results 4-81409  
 H<sup>+</sup> + H<sub>2</sub> collisions, two state charge transfer calc. 4-91341  
 H<sub>2</sub> 1-0 S(1) emission from distributed galaxies, IR obs. 4-101474  
 H<sub>2</sub> distrib. in spiral galaxy NGC 6946, correl. with star form. characteristics 4-90227  
 H<sub>2</sub> optical quenching and energy extraction involving metastable and dissociative states 4-79112  
 H<sub>2</sub>, positron scatt., polarisation pots. 4-87225  
 H<sub>2</sub>/He ratios in Jupiter and Saturn atm., implications for solar nebula 4-77757  
 H<sub>2</sub>-F<sub>2</sub> pulsed laser, photolysis and electron beam method initiation efficiency 4-74499  
 H<sub>2</sub> + B<sup>+</sup>, pot. energy surfaces, diatomics-in-mols. correl. diagram 4-62166  
 H<sub>2</sub> + Be → BeH<sub>2</sub>, multireference CI gradients and MCSCF second derivatives 4-93522  
 H<sub>2</sub> + C<sub>6</sub>H<sub>6</sub><sup>+</sup> reactions, kinetic energy release distrib., rate constants PIPECO studies 4-82959  
 H<sub>2</sub> + C<sup>+</sup> reaction product rovibr. distrib., surprisal functions 4-114776  
 H<sub>2</sub> + C<sup>4+</sup>, charge transfer, polarised light emission 4-83463  
 H<sub>2</sub> + CN, vibr. energy effect on reaction, laser meas. 4-99769  
 H<sub>2</sub> + CO, Co(ν=1) vibr. deactivation, influence of higher order multipole moments 4-112259  
 H<sub>2</sub> + CO collisions, rigid-rotor pot. energy surface from ab initio calcs. and rot. inelastic scatt. data 4-78940  
 H<sub>2</sub> + C(D), CH radical prod. energetics, laser induced fluorescence 4-114777  
 H<sub>2</sub> + Cr, intramultiplet mixing collisions, fluoresc. 4-64588  
 H<sub>2</sub> + D, initial and state to state cross sections, quantum chemical study, rate consts. 4-62160  
 H<sub>2</sub> + D<sub>2</sub>, exchange reaction on Pt (557) surface, HD ang. and vel. distrib. 4-99834  
 H<sub>2</sub> + D<sub>3</sub><sup>+</sup> collisional dissoci., correl. between channel probabilities 4-78933  
 H<sub>2</sub> + DCl, vibr. energy transfer probabilities, temp. depend. 4-91332

- hydrogen molecular molecules continued**
- H<sub>2</sub>+D(F), BKLT eqn. for reactive scatt. of collinear nonsymm. systems 4-114787
- H<sub>2</sub>+F, collinear exchange reactions, probability densities, stabilisation calcs. 4-81415
- H<sub>2</sub>+F, reactive scatt. resonances 4-99780
- H<sub>2</sub>+F reaction, quantum dynamics, energy partitioning and entropy anal. of collision complex 4-114782
- H<sub>2</sub>+F reaction, quantum dynamics, scatt. wave function density and flux analysis 4-114783
- H<sub>2</sub>+F reactions, reson. periodic orbits, semiclassical theory 4-114788
- H<sub>2</sub>+H, H and Mu exchange, isotope effects, semiclassical techniques 4-71884
- H<sub>2</sub>+H, laser excitation, electron loss from H(3p) atoms, H(3p) beam prod. 4-87200
- H<sub>2</sub>+H, reagent rot. effect, classical trajectory calcs. 4-93506
- H<sub>2</sub>+H rearrangement collisions, reson. and dynamics calcs. 4-71901
- H<sub>2</sub>+H<sub>2</sub>, rot. struct., IR absorpt. and Raman scatt. 4-69174
- H<sub>2</sub>+H<sub>2</sub>, vibr.-vibr. energy transfer rate const. 4-64574
- H<sub>2</sub>+H<sub>2</sub><sup>+</sup>, symm. electron transfer reactors of state-selected ions 4-107446
- H<sub>2</sub>+H<sup>+</sup>, electron detachment and charge exchange to shape reson. 4-69203
- H<sub>2</sub>+H<sup>+</sup>, proton interchange process rel. to ortho-H<sub>2</sub>/para-H<sub>2</sub> ratio in interstellar mol. clouds 4-94927
- H<sub>2</sub>+HF(v=3, 4, 5), HF vibr. relax., fluoresc. study 4-69187
- H<sub>2</sub>+H(D), reactive differential cross sections in rot. linear model, ang. distrib. 4-99775
- H<sub>2</sub>+H(F) reactions, semiclassical adiabatic theory 4-114786
- H<sub>2</sub>+He energy sudden scaling relations, off-energy-shell effects incorporation method 4-69161
- H<sub>2</sub>+hydrocarbon ions, association reaction rates, endothermic reactivity correl. 4-99767
- H<sub>2</sub>+I<sub>2</sub>, state-to-state rot. transfer rates, induced fluoresc. 4-91333
- H<sub>2</sub>+methyl-H+methane, D isotope effect, ab initio pot. surface, transition state theory 4-84116
- H<sub>2</sub>+N<sup>6+</sup>, electron capture in autoionising configurations N<sup>4+</sup> studied by electron spectrometry 4-59889
- H<sub>2</sub>+Ne, bimol. and three body quenching 4-112139
- H<sub>2</sub>+O reaction dynamics, reduced dimensionality quantum and quasiclassical rate consts. 4-114784
- H<sub>2</sub>+O<sub>2</sub>, in Ar shock tube, O<sub>2</sub> vibr. relax. study 4-96668
- H<sub>2</sub>+O<sub>2</sub>H<sup>+</sup>, forward and reverse rate coeff., enthalpy and entropy changes 4-62165
- H<sub>2</sub>+O<sup>+</sup>, ab initio pot. energy surface, CI calcs. 4-96470
- H<sub>2</sub>+OH, electronic quenching, rot. level depend., fluoresc. 4-74281
- H<sub>2</sub>+OH, A doublet population pump mechanism, astronomical maser 4-96652
- H<sub>2</sub>+O(P), exchange reactions, quasiclassical trajectory calcs. 4-71894
- H<sub>2</sub>+O(F) reactions, MRD-CI pot. surfaces using balanced basis sets 4-93521
- H<sub>2</sub>+Si, C<sub>2v</sub> surfaces, MC SCF calcs. 4-91192
- H<sub>2</sub><sup>+</sup>+Ar, charge transfer reactions 4-89272
- (H<sub>2</sub>)<sub>2</sub>, van der Waals dimers, Jupiter and Saturn atm., Voyager far-IR spectra 4-105901
- (H<sub>2</sub>)<sub>n</sub>, (n=2, 3, 5), bound excited state form., CI calcs. 4-96740
- H<sub>2</sub>, field promoted, surface catalyzed formation on transition metals 4-66616
- H<sub>2</sub>, G-function, generalised diatomics in mol. theory 4-68964
- H<sub>2</sub>, linear, Hartree-Fock eqns., numerical solns. 4-74142
- HD, high-resolution spectroscopy at 83 nm 4-64490
- HD, internal motion, electron density dynamic anal., ab initio MO calcs. 4-87037
- HD+F, collinear exchange reactions, probability densities, stabilisation calcs. 4-81415
- HD+HD(D<sub>2</sub>)<sup>+</sup>(He), vibr. relax., mechanisms and rate consts. 4-96669
- HD+O(P), exchange reactions, quasiclassical trajectory calcs. 4-71894
- HT, internal motion, electron density dynamic anal., ab initio MO calcs. 4-87037
- I-H, laser, electron-beam-controlled 4-74498
- LiH, pair correl. eqns., numerical soln. method 4-96423
- hydrogen power** see *hydrogen economy*
- hydrogen production** see *hydrogen economy*
- hydrogen storage** see *hydrogen economy*
- hydrogen transmission** see *hydrogen economy*
- hydrological techniques**
- Antarctic glaciology remote sensing using Landsat 3 RBV images 4-82312
- aquifer pollution protection measures necessary around borehole 4-85723
- colour display and analysis system for hydrographic surveying 4-67452
- differential pulse anodic stripping voltammetry anal. for trace metals in seawater and snow 4-82315
- Doppler satellite meas. of glacier movements in Antarctica (*German*) 4-72731
- Doppler satellite obs. of glacier movements (*German*) 4-72623
- dynamic models, fitting to time series 4-82309
- groundwater movement meas. (*Slovak*) 4-85760
- groundwater prospecting in Nigeria using Landsat images 4-77562
- hydrogeology, inverse coefficient problems formulation 4-105606
- ice covers, combination radiophysical studies 4-100645
- ice shelves meltwater, isotopic tracers and salinity used for shelf characts. determ. 4-67440
- ice-depth radio echo-sounding techniques, appl. on Hispar and Ghulkin glaciers 4-63002
- impulse radar ice-depth sounding system, use on Vatnajökull ice-cap (1977), performance 4-62998
- induced fission track method, quantitative determ. of U in natural waters (*Rumanian*) 4-100822
- information volume content on combining time series differing in length with homogeneous dispersion 4-67448
- inversion voltammetry for metal content in river water, seawater and bottom sediments 4-100816
- log-normal quantiles in hydrology, estimation, Monte Carlo results and first order approx. 4-100771
- micropipeller for measurement of water speed fluctuations 4-67446
- palaeoclimate precipitation rate determ. by glacier ice core method 4-110306
- suspended particulate monitoring instrument using optical sensor 4-115627
- regression parameters change at unknown times, detect. 4-82308
- hydrological techniques continued**
- remote sensing of ice by satellite SAR radar imagery 4-72745
- river flow rates, linear model for data transformation 4-72620
- rivers, nonstationary flows calc. using modified difference scheme (*Bulgarian*) 4-67451
- sediments in glacial meltwater, anal. methods 4-62869
- snow, microwave emission properties of snowpack and passive remote sensing, review 4-110184
- snow mechanical characteristics measurement method and apparatus 4-105764
- snow-cover variations anal. in mountain environments, graphical and statistical techniques 4-110177
- snow-melt run-off studies using remote sensing data 4-110182
- soil microwave remote sensing, for water content and matrix pot. 4-100795
- soil moisture content remote sensing and rainfall estimation method 4-100796
- soil moisture determination from geosynchronous orbit infrared data, feasibility 4-115593
- soil moisture measurement, in-situ instrument for ground truth of radar remote sensing 4-100794
- soil water content and elec. cond. meas. technique 4-110307
- soil wet density meas. using ND-A densimeter (*Chinese*) 4-72715
- time series, freq. and time domain anal., approaches for use in hydrology 4-82307
- time series methods use, conf. at Burlington, Canada (October 1981) 4-78041
- turbidity monitoring, evaluation of airborne spectroradiometer 4-77653
- Vatnajökull ice depth sounding expedition 1977, survey and anal. systems 4-62997
- Walsh solutions in hydrosphere 4-82311
- CO<sub>2</sub> equilibria use for softwater lakes H<sup>+</sup> conc. determ. 4-77169
- Cd, Cu, Pb determ. in water by AAS and ICP-AES spectrochem. methods 4-62430
- <sup>210</sup>Pb, activities and conc. factors in estuarine sediments of rivers in Gujarat, India 4-82103
- <sup>222</sup>Ra, activities and conc. factors in estuarine sediments of rivers in Gujarat, India 4-82103
- Rn measurement in spring waters, appl. of portable continuously working meas. system 4-93671
- hydrology**
- see also *groundwater; lakes; rivers*
- advection-dispersion processes in open channels, dynamic-stochastic approach 4-82118
- aquifer pollution protection measures necessary around borehole 4-85723
- arid lands and droughts 4-82222
- change-point problem for sequence of binomial random variables 4-82113
- chemistry of natural waters, book 4-106139
- climatology and water supply, book 4-90326
- coal mining in Great Britain, groundwater control methods 4-77566
- conference, Hamburg, W Germany (1983) 4-106108
- Coso Range, California, ground mag. survey rel. to faulting and hydrothermal alteration 4-85618
- cryosphere, effect on climate 4-82223
- dam capacity, appl. of partial sums distrib. 4-82111
- dambo features in Zimbabwe, morphological characts. 4-100576
- dynamics of meltwater discharge from ice sheets during deglaciation 4-105613
- equilibria, nonequilibria and natural waters (book) 4-106133
- evaporation from land surface, Turc and Ivanov formulae applicability (*German*) 4-77559
- evapotranspiration calculations 4-77617
- evapotranspiration from trees, implications of gradient distributions and flux profile relations above rough forest 4-82204
- evapotranspiration from vegetation, uncoupled multi-layer model for latent heat flux density 4-105618
- evapotranspiration in Sierras de Cordoba, Argentina, rel. to energy balance of atmospheric surface boundary layer 4-105671
- evapotranspiration potential in Belgium, estimation procedure 4-115476
- Eye-Dashwa pluton, Ontario, Canada, geology of radioactive waste disposal site 4-81919
- flash floods, conf. at Atlanta, United States (March 1980) 4-78032
- flood forecast response systems, concept 4-110181
- flood series, anal. with stochastic models 4-82122
- floodings anal., use of extreme value partial time series model 4-82114
- flow induced by heated vertical wall in a porous medium 4-69821
- forecasting under linear partial information 4-82140
- general description of hydrologic cycle 4-110180
- geochemistry of natural waters (book) 4-95093
- geophysical predictions (book) 4-90308
- N Greece, agriculture influences upon erosion and runoff processes 4-115460
- Hudson Bay, heat budget and freshwater content, runoff and ice cover effects 4-94139
- India, bistable phasing of 18.6 year nodal induced flood 4-94175
- India, drought in north central region during 1979 SW monsoon 4-67292
- India, flood and drought occurrence rel. to double sunspot cycle 4-72686
- India, groundwater, irrigation and water supply, book 4-95090
- James Bay, heat budget and freshwater content, runoff and ice cover effects 4-94139
- central Kansas, USA, flash floods of 1981 June, synoptics and hydrological characts. 4-67287
- Larissa plain, Greece, aquifer pollution protection measures necessary around borehole 4-85723
- Leninabad Region, Tadzhikistan, groundwater level meas. rel. to hydrodynamic earthquake precursors 4-100471
- linear reservoir with seasonal gamma-distributed Markovian inflows 4-82132
- mountain hydrometeorology, conf., Bogota, Columbia (Aug. 1979) 4-86120
- central Nigeria, geological interpretation of Landsat images 4-77478
- SE Nigeria, hydrology and chemistry of water resources of Agwata area 4-115466
- non-stationary behaviour and modelling 4-82115
- nonlinear surface runoff system identification 4-110178
- nonlinear vectorial models, identification parameters (*French*) 4-62858
- W North America, 18.6-yr lunar nodal drought in past millennium 4-72665
- palaeohydrology (book) 4-101585

**hydrology continued**

- peristence estimation from time series containing occasional missing data, water quality data appl. 4-82116
- radioactive waste disposal, site evaluation, geotechnical research 4-83171
- regression model with stationary error process, point of change 4-82112
- reservoir without dam from lowland river (*Russian*) 4-89953
- reservoirs operation, optimal ARMA models for statistical anal. 4-82134
- rock permeability pore space model 4-82106
- runoff simulation with random walk model 4-100647
- saline formation water of US Gulf Coast region, Ra occurrence and behaviour 4-110179
- Sede Zin, Negev, Quaternary geology and hydrology of alluvial plain 4-94133
- slopes on opposite sides of road cutting, erosion and runoff influenced by rain direction 4-77563
- snow and ice covered ground, heat and moisture vertical fluxes 4-77618
- snowmelt infiltration into frozen soil of prairies 4-115464
- snowpack melting in New Zealand alpine basin 4-82101
- soil, seepage water flow, finite element calculation 4-100642
- soil hydrology, two-layer model 4-115463
- bare soil surface, vertical flux of heat and moisture 4-77567
- statistical models, estimation theory and errors 4-82128
- storage sizes-demand-reliability relationship 4-82133
- N Tanzania, high fluoride content of rivers, lakes, springs 4-115467
- time series methods use, conf. at Burlington, Canada (October 1981) 4-78041
- transpiration and evaporation from weather moorland, meas. 4-105619
- urban runoff, linear model phosphorus loading, predictive accuracy determination 4-82097
- water resources, world wide 4-100633
- water resources forecasting, effect of runoff var. due to human activity 4-66826
- water supply from groundwater, book 4-95089
- C cycle adversely affected by man's activities 4-115474
- Rn in spring waters, appl. of portable continuously working meas. system 4-93671

**hydromagnetic waves** see *magnetohydrodynamic waves*

**hydromagnetics** see *magnetohydrodynamics*

**hydrometers**

see also *density measurement*

No entries

**hydrophones**

see also *sonar*

- acoustic power/intensity under water, measurement using dual-hydrophone system (*Chinese*) 4-103091
- acoustic telemetry of video information 4-115624
- arrays, collinear, hybrid time-delay/phase-shift digital beamforming 4-83777
- glass ceramics, polar, for sonar transducers 4-69651
- maximum entropy beamformer, shallow water line array data anal. 4-103082
- ocean internal wave acoustic tomography principles 4-105777
- piezoelectric composites, periodic, dynamic behaviour, generalised Floquet theory 4-99037
- piezoelectric transducers using piezoelectric ceramic composites 4-65951
- polyvinylidene fluoride, transducer appls. 4-97249
- PVDF polymer hydrophones in biomedical ultrasonics 4-100283
- submarine object coordinate determination accuracy, using hydroacoustic methods (*Russian*) 4-107934
- three-dimensional seismic survey positioning 4-72722
- Pb(Zr,Ti)O<sub>3</sub> porous ceramic, appl. to HF underwater transducer 4-97258

**hydrophotometers** see *photometers*

**hydrostatics**

- gravitational interaction of bodies immersed in fluids, theory 4-101124
- weighing method for 1 kg mass comparator 4-63724

**hydrothermal crystal growth** see *crystal growth from solution*

**hydroxonium ion**

No entries

**hydroxyl group** see *oxygen compounds*

**hygiene**

see also *medicine*

No entries

**hygrometers**

see also *humidity measurement*

- capacitive humidity metering circuit with digital displays of the relative humidity and limiting value transducers (*German*) 4-101856
- compact, using thermosensitive capacitor, DIY design (*German*) 4-68235
- direct insertion type zirconia oxygen analyzer hygrometer, Fuji Electric 4-111142
- gravimetric hygrometer, calibration (*Japanese*) 4-101857
- high frequency digital granules hygrometer (*German*) 4-86425

**hyperfine field interactions (condensed matter)**

see also *crystal hyperfine field interactions*; *nuclear screening*

- acetonitrile, liq., solvation of <sup>23</sup>Na<sup>+</sup>, <sup>87</sup>Rb<sup>+</sup> and <sup>14</sup>N, local symm. demonstration, NMR study 4-78870
- bis(pentadienyl)iron cpds., bonding, hyperfine interaction, Mossbauer effect 4-104512
- cyclohexadienyl radicals, muonium substituted, isomer distrib., radiolytical processes, muon spin rot. 4-92984
- di-tertbutylnitroxide, spin label for EPR studies in liq. crystals, proton hyperfine tensor 4-84855
- fluorophosphate and phosphate glasses,  $\gamma$ -ray irradi., colour centres, EPR studies 4-103747
- 4-hydroxy-2,2,6,6-tetramethylpiperidine-1-oxyl, (TANOL), nitroxide radical, ESR 4-71182
- hyperfine interactions of radioactive nuclei, condensed matter studies, book 4-67877
- isomeric nuclei and  $\mu$  emitters as probes in condensed matter, review, book contrib. 4-71197
- Mossbauer spectroscopy appl., using internal standard 4-114185
- polyacetylene:FeCl<sub>3</sub> (FeBr<sub>3</sub>) intercalation cpds., hyperfine interaction, Mossbauer and EPR studies 4-65887
- polyacetylene, soliton wave-functions 4-75878
- polyethylene fibres, X-ray irradi., hyperfine interactions, EPR studies 4-114164
- radioactive nuclei, hyperfine interactions, condensed matter studies, book 4-67877
- TANOL, nitroxide spin probes, line widths and shifts, ESR 4-71181

**hyperfine field interactions (condensed matter) continued**

- transition metal-metalloid amorphous ferromagnets, mag. moment distrib. and temp. depend. of reduced hyperfine fields 4-92899
- transition metals in solution, NMR data for first series. (Sc to Zn) 4-98963
- Fe-B amorphous alloys, mag. anisotropy, thermal treatment effects 4-65805
- Fe-Cr-Co-Si-B amorphous alloys, mag. props. and hyperfine interactions (*Russian*) 4-108994
- Fe-Hf based amorphous alloys, crystallisation and hyperfine fields 4-71030
- Fe-Mo-B amorphous, hyperfine fields mag. props. 4-92933
- Fe<sub>81</sub>B<sub>13</sub>Si<sub>3</sub>C<sub>2</sub>, Metglas 3605SC, mag. and hyperfine interactions 4-71223
- (Fe,Cr<sub>100-x</sub>)B<sub>y</sub> metallic glasses, onset of magnetism, Mossbauer spectra 4-71217
- FeF<sub>3</sub>, amorphous, Mossbauer-Zeeman spectrum study 4-76294
- (Fe,Ni<sub>1-x</sub>)M, M=P, B, Si or Al, metallic glass, Mossbauer study of high press. 4-84880
- Fe<sub>81</sub>B<sub>10-x</sub>Si<sub>10</sub>B<sub>10</sub>, metallic glass, correlated hyperfine interactions 4-70761
- Fe<sub>2</sub>O<sub>3</sub> particles of mag. fluid, superparamagnetic behaviour, Mossbauer spectra 4-104466
- Fe<sub>2</sub>Zr<sub>76</sub> amorphous alloy, <sup>57</sup>Fe quadrupole splitting sign determ., Mossbauer spectra 4-76291
- Rb, liquid, elec. field gradient fluctuations spectrum 4-108826
- Rh<sub>2</sub>MnGe<sub>2</sub>Sn<sub>1-x</sub>, Sn hyperfine fields, Mossbauer study 4-71215
- Si:F, hyperfine and cryst., ion implanted, elec. quadrupole hyperfine interaction at impurity sites 4-92675
- a-Si:H film, hyperfine interaction, ENDOR study 4-65881
- SiO<sub>2</sub>, amorphous, X- and  $\gamma$ -irradi., E'-centre variants, EPR obs. 4-70207
- SiO<sub>2</sub> powder, muonium hyperfine splitting, two freq. method anal. 4-65652
- V<sub>2</sub>O<sub>5</sub>:SeO<sub>2</sub> (TeO<sub>2</sub>)(GeO<sub>2</sub>) glass, ESR and photoacoustic spectra 4-104491

**hyperfine field interactions in crystals** see *crystal hyperfine field interactions*

**hyperfine structure, atomic** see *atomic hyperfine structure*

**hyperfine structure, molecular** see *molecular hyperfine structure*

**hyperfragments** see *hypernuclei*

**hypernuclei**

- nonmesonic decay of heavy  $\Lambda$  hypernuclei 4-95951
- $\Lambda$  hypernuclei, stopped K<sup>-</sup> method, spin-orbit doublets, deep-lying orbital 4-111518
- $\Lambda$ N effective interaction, spin-state dependence, p-shell hypernuclei 4-95950
- $\Sigma$  hypernuclei, stopped K<sup>-</sup> method, spin-orbit doublets, deep-lying orbital 4-111518
- $\Sigma$  optical potential in nuclear matter, mean free path, absorptive pot. 4-68643
- <sup>9</sup>Be  $\Lambda$  and  $\Lambda_c$  hypernuclei binding energies,  $\Lambda_c$ N interaction, HF clac. (*Chinese*) 4-73848
- <sup>9</sup>Be $\Lambda$ , microscopic cluster model wave functions for <sup>9</sup>Be(K<sup>-</sup> $\pi^-$ ) cross section calc. 4-68738
- <sup>9</sup>Be $\Sigma$  hypernuclei and  $\Sigma$ -N forces 4-73849
- <sup>12</sup>C $\Lambda$ , binding energies and  $\Lambda\Lambda$  interaction, in  $2\alpha$ - $2\Lambda$  model 4-90968
- <sup>12</sup>C $\Sigma$ , isospin mixing angle, good quantum number 4-64089
- <sup>4</sup>He $\Lambda$ ,  $\Lambda$ -separation and excitation energies using realistic NN and  $\Lambda$ N interactions 4-83022
- <sup>4</sup>He $\Lambda$  interaction, off-shell behaviour, hypernuclear few-body problem, appl. 4-106588
- <sup>5</sup>He  $\Lambda$  and  $\Lambda_c$  hypernuclei binding energies,  $\Lambda_c$ N interaction, HF clac. (*Chinese*) 4-73848
- <sup>5</sup>He $\Lambda$ , binding energy, quark model anal. Pauli principle consequences 4-102218
- <sup>5</sup>He $\Lambda$ ,  $\Lambda$ - $\alpha$  interaction with hard core  $\Lambda$ -N pot., central repulsion 4-83022
- <sup>5</sup>He $\Lambda$ , overbinding problem, five body problem in strongly coupled channels method 4-86789
- <sup>6</sup>He $\Lambda$ , binding energies and  $\Lambda\Lambda$  interaction in  $\alpha$ - $2\Lambda$  model 4-90968
- <sup>6</sup>He $\Lambda$ ,  $\Lambda$ =4,5,  $\Lambda$ -separation and excitation energies using realistic NN and  $\Lambda$ N interactions 4-83022
- <sup>7</sup>Li $\Lambda$ , microscopic cluster model wave functions for <sup>7</sup>Li(K<sup>-</sup> $\pi^-$ ) cross section calc. 4-68738

**hyperon absorption**

No entries

**hyperon capture**

see also *hypernuclei*

No entries

**hyperon decay**

- $\Delta$ I=1/2 non-leptonic hyperon decays, S- and P-wave amplitudes 4-73751
- charm and charm particles, prod. in strong interactions, decays, review 4-90931
- nonleptonic s-wave amplitudes, negative parity excited baryons 4-86704
- nonmesonic decay of heavy  $\Lambda$  hypernuclei 4-95951
- semiclassical approximation of decays and magnetic moments 4-86708
- soft pion S-wave nonleptonic hyperon decay amplitudes, evidence for corrections 4-95793
- $\Delta$ -N $\pi$ ,  $\Delta$ T=3/2 amplitudes, effective weak Hamiltonian, QCD short distance corrections 4-111449
- $\Delta$  nonleptonic decays, chiral bag model and weak interactions, s- and p-wave amplitudes 4-102119
- $\Delta$ -pe $\pi$ , model independent order and radiative correction 4-86705
- $\Delta_c$ ,  $\Lambda_b$  inclusive nonleptonic decays, bag model, W-exchange contributions 4-106529
- $\Lambda_c^+$ , weak decays of charmed particles 4-95791
- $\Lambda_c^+$ , K<sup>0</sup> $\pi^+$  $\pi^-$ , decay probabilities 4-64149
- $\Lambda_c^+$ , K<sup>0</sup> $\pi^0$  $\pi^+$  ( $\Lambda^0\pi^+\pi^+$ ), branching ratios, mass 4-95830
- $\Lambda_c^+$  lifetime from  $\gamma$ N expt. 4-73749
- $\Lambda_c^+$ ,  $\Lambda^0\pi^+\pi^+$ , decay probabilities 4-64149
- $\Lambda_c^+$ , nonleptonic decay matrix elements in variable press. bag model 4-114148
- $\Omega^-$  hadronic and radiative decays, lifetime, branching ratios and decay asymmetry 4-86702
- $\Sigma^-$ -N $\pi$ ,  $\Delta$ T=3/2 amplitudes, effective weak Hamiltonian, QCD short distance corrections 4-111449
- $\Sigma^-$ -strange particles,  $\chi$  distributions, cross-sections 4-111478
- $\Sigma^-$ -Ac $\pi$ , model independent order and radiative correction 4-86705
- $\Sigma^-$ -ne $\nu$ , electron energy spectrum and asymmetry meas. 4-90877
- $\Sigma^-$ -ne $\nu$ , model independent order and radiative correction 4-86705

- hyperon decay continued**  
 $\Sigma^+(1385) \rightarrow \Lambda \pi^+$ , indirect  $\Lambda$  prod., inclusive cross sections from pp interactions 4-111485  
 $\Sigma \rightarrow \Lambda \pi$ ,  $\Delta T = 3/2$  amplitudes, effective weak Hamiltonian, QCD short distance corrections 4-111449  
 $\Sigma$ —strange particles,  $x_T$  distributions, cross-sections 4-111478  
 $\Sigma \rightarrow \Lambda e \bar{\nu}$ , model independent order and radiative correction 4-86705
- hyperon detection and measurement**  
 No entries
- hyperon-deuteron interactions**  
*see also hyperon-deuteron scattering*  
 No entries
- hyperon-deuteron scattering**  
*see also hyperon-deuteron interactions*  
 No entries
- hyperon effects**  
 No entries
- hyperon interactions** *see hyperon-nucleon interactions; hyperon-nucleus reactions; kaon-hyperon interactions; lepton-hadron interactions; photon-hadron interactions; pion-hyperon interactions*
- hyperon magnetic moment**  
 quark models, sum rules, isovector contributions 4-90881  
 semiclassical approximation of decays and magnetic moments 4-86708
- hyperon mass**  
 ground-state baryon mass splittings from unitarity in SU(6) 4-68556  
 $\Lambda_c^+$  mass, decay in diffraction model 4-64149  
 $\Lambda_c^+ \rightarrow K^0 \pi^+ \pi^- (\Lambda \pi^+ \pi^-)$ , branching ratios, mass 4-95830  
 $N^*$ , 1237.83 MeV mass calc. 4-68554  
 $\Omega$  Faddeev eqns., mass calcs. of  $J^P = 3/2$  systems 4-90832  
 $\Omega^-$  rest mass from Friedmann-Lee bag states 4-63978  
 $\Sigma^*$ , 1395.95 MeV mass calc. 4-68554  
 $\Sigma^*$ , 1512.40 MeV mass calc. 4-68554
- hyperon-nucleon interactions**  
*see also hyperon-nucleon scattering*  
 cross sections, additive props. tested in framework of additive constituent quark models 4-95769  
 p-shell hypernuclei,  $\Lambda N$  effective interaction, spin-state dependence 4-95950  
 $N\Sigma(\Lambda) \rightarrow NNK$ , contribution to kaon production in relativistic heavy-ion collisions 4-83101
- hyperon-nucleon scattering**  
*see also hyperon-nucleon interactions*  
 No entries
- hyperon-nucleus reactions**  
*for inelastic hyperon-nucleus scattering, see "hyperon-nucleus scattering"*  
*see also hyperon capture; hyperon-nucleon interactions*  
 light nuclei, hyperon induced complete breakup, expt. and theoretical review 4-86821
- hyperon-nucleus scattering**  
*see also hyperon-nucleon scattering*  
 $^4\text{He}(\Lambda, \Lambda)$ , low energy, five body problem in strongly coupled channels method 4-86789
- hyperon production**  
 charmed baryon quasielastic production in neutrino-nucleon interactions 4-68563  
 $e^+e^-$  in Upsilon region,  $\Xi$  and  $\Lambda$  prod. from  $T$  decay, gluon and quark fragmentation 4-90900  
 $\gamma\gamma \rightarrow p\bar{p}\pi^+\pi^-$ , 16.95 GeV, cross section and resonance prod. limit 4-95868  
 $\gamma p \rightarrow D^+ \Sigma^+$ , cross section threshold enhancement 4-106534  
 $K^- n \rightarrow \Lambda_c^-$ , hypernuclear spectroscopy using stopped  $K^-$  spin-orbit doublets, deep orbitals 4-111518  
 $K^- n \rightarrow \Sigma^+ \pi^- (\Sigma^- \pi^0)$ , hypernuclear spectroscopy using stopped  $K^-$  spin-orbit doublets, deep orbitals 4-111518  
 $K^- NN \rightarrow \Sigma N$ , hypernuclear spectroscopy using stopped  $K^-$  spin-orbit doublets, deep orbitals 4-111518  
 $K^- p \rightarrow \Lambda_c^0$ , polarisation, differential and integrated cross sections 4-68585  
 $K^- p \rightarrow \Lambda_c^+ \pi^-$ , hypernuclear spectroscopy using stopped  $K^-$  spin-orbit doublets, deep orbitals 4-111518  
 $K^- p \rightarrow \pi^- \Sigma^+ (1385)$ , 8.25 GeV, amplitude anal., spin density matrix 4-86730  
 $K^- p \rightarrow \Sigma^+ \pi^-$ , hypernuclear spectroscopy using stopped  $K^-$  spin-orbit doublets, deep orbitals 4-111518  
 $K^+ p$ , 32 GeV/c,  $K_S^0$ ,  $\Lambda$  and  $\bar{\Lambda}$  prod., total and semi-inclusive cross sections 4-95829  
 $nN \rightarrow \Lambda_c^+ X$ , 40-70 GeV,  $\Lambda_c^+$  mass, decays and cross section 4-95830  
 $pA \rightarrow \Lambda_c^+ K^- X$ , doubly strange  $p$  annihilation channels in complex nuclei 4-106614  
 $pA \rightarrow \Lambda_c^0 X$ , doubly strange  $p$  annihilation channels in complex nuclei 4-106614  
 $pN \rightarrow \Sigma^0(\Lambda)$  inclusive production, cross-section ratios 4-102139  
 $pp \rightarrow \Lambda_c^0(\Lambda) X$ ,  $E = 70$  GeV/c, differential and production cross sections 4-102141  
 $pp \rightarrow \Lambda(\bar{\Lambda}) X$ , inclusive cross sections, indirect  $\Lambda$  prod. from resonance decay 4-111485  
 $\pi^- N \rightarrow N(\Sigma)(\Xi)$ ,  $x_T$  distributions, cross-sections 4-111478  
 $\pi^- p \rightarrow \Sigma^+(1385) X$ , 40 GeV, production cross sections 4-78571  
 $\pi^- p \rightarrow K^+ \Sigma^+$ , threshold-2.35 GeV, energy depend. partial wave anal., SU(3) breaking 4-82971  
 $^{12}\text{C}(n, \Lambda_c^+)$ , 58 GeV, production cross section 4-64149  
 $^{12}\text{C}(n, \Lambda_c^+)$ , 40 GeV, polarisation meas. 4-64150  
 $C(p, x)$ , low energy annihilations,  $\Lambda^0$  prod. 4-64145  
 $Pb(p, x)$ , low energy annihilations,  $\Lambda^0$  prod. 4-64145  
 $Ta(p, x)$ , low energy annihilations,  $\Lambda^0$  prod. 4-64145  
 $Ti(p, x)$ , low energy annihilations,  $\Lambda^0$  prod. 4-64145
- hyperon resonances**  
 beauty and charm particles, prod. in strong interactions, decays, review 4-90931  
 $\Lambda(1405)$  reson., QCD sum rules appl. 4-59041  
 $N^*$ , 1237.83 MeV mass calc. 4-68554  
 $\pi^- p \rightarrow K^+ \Sigma^+$ , threshold-2.35 GeV, energy depend. partial wave anal., SU(3) breaking 4-82971  
 $\Sigma^*$ , 1395.95 MeV mass calc. 4-68554  
 $\Sigma^*$ , 1512.40 MeV mass calc. 4-68554
- hyperon scattering** *see hyperon-nucleon scattering; hyperon-nucleus scattering; kaon-hyperon scattering; lepton-hadron scattering; photon-hadron scattering; pion-hyperon scattering*
- hyperon spin and parity**  
 $\Omega$  Faddeev eqns., mass calcs. of  $J^P = 3/2$  systems 4-90832
- hyperons**  
*see also hyperon resonances*  
 $\Sigma^0$  inclusive production, cross-section ratios 4-102139  
 decays and magnetic moments in semiclassical approx. 4-86708  
 $\Lambda_c^+$  mass, decay in diffraction model 4-64149  
 $\Omega$ , 1670.52 MeV mass calc. 4-68554  
 $\Lambda^0$  inclusive production, cross-section ratios 4-102139
- hypersonic flow**  
 boundary layer, turbulent, three-dimens., on sharp cone at angle of attack, heat transfer interactions 4-79621  
 delta wing, viscous interaction, 3D boundary layer 4-69786  
 dusty hypersonic flow past thick wedges 4-97605  
 finite triangular wing, hypersonic boundary layer flow 4-97606  
 flat body, intense radiative heat transfer 4-112944  
 gas jet exhausting into medium at rest or into supersonic stream 4-69787  
 jets, adjacent pair interaction 4-91830  
 lift airfoil, hypersonic flow, Navier-Stokes eqn. soln. 4-108088  
 radiant heat transfer in the shock layer in volumetric flow around blunt bodies (Russian) 4-83923  
 star-like body flight in rarefied hypersonic flow, aerodynamic and thermal characts. (Russian) 4-60458  
 stationary hypersonic multishocked flow around blunt body with breaks (Russian) 4-112946  
 surface mass transfer in steady flow 4-97600  
 surface mass transfer in unsteady flow 4-97601  
 two-phase mixture flow past blunt-ended bodies, wave surfaces analysis (Russian) 4-91834  
 unsteady three dimens. boundary layer interaction 4-112943  
 viscous gas flow, boundary layer perturbation propag., entropy layer effect 4-60457
- hypersorption** *see sorption*
- hyperthermia** *see biothermics*
- hypertritons** *see hypernuclei; tritons*
- hypervirial theorem** *see quantum theory*
- hypochromism** *see light absorption*
- hypothesis formation** *see heuristic programming*
- hypothetical particles**  
*see also charm particles; heavy leptons; intermediate bosons; magnetic monopoles; quarks; tachyons*  
 axion cosmology 4-90274  
 big bang - supersymmetric relics, neutral gauge/Higgs fermion mass 4-77988  
 boson creation in a subquantum lattice 4-73711  
 boson-fermion duality, neutrino and photon construction from new mass-less boson 4-95777  
 bradyons and tachyons in expansion of spherical wave  $\exp[i(\omega/c)(r-ct)]/r$  into cylindrical waves 4-68375  
 composite scalars in  $e^+e^-$  collisions and radiative Z decays 4-86694  
 DESY storage ring expts. 4-96302  
 $g$  and  $t$  states, decay and spectroscopy, possible detection of supersymmetric particles 4-58987  
 gluino mass generating mechanisms 4-68462  
 gluino production signature, pp collider, lower limit on gluino mass 4-86740  
 goldstinos in broken supersymmetric theories, role in cosmology 4-77705  
 gravitino and photino masses in supersymmetric cosmology, galaxy form. 4-67845  
 gravitino mass generation in locally supersymmetric grand unified theories 4-73703  
 gravitinos, decay and lifetimes, X-ray emission, appl. to galaxy clusters and background radiation 4-101154  
 inflationary model with correct density fluctuations and CP problem soln., SU(5) field 4-73110  
 inos rest mass, lower limit from Galaxy halo data 4-82409  
 leptonic Z decays interpreted as cascade decays through new particle 4-102147  
 light-cone gauge, Feynman integrals,  $N=4$  supersymmetry, gluon self-energy 4-90711  
 mirror particles,  $N=2$  supersymmetric models, low energy constraints 4-102068  
 PETRA  $e^+e^-$  storage ring, review of experimental investigations 1978-83 4-90851  
 photino—photon+gravitino, supersymm. light-inos in primeval plasma recombination 4-110794  
 photino mass and  $\gamma\gamma$  prod. in  $e^+e^-$  annihilation 4-68558  
 photino mass generating mechanisms 4-68462  
 photino-dominated Universe, cosmic-ray antiprotons 4-105818  
 photinos, decay and lifetimes, X-ray emission, appl. to galaxy clusters and background radiation 4-101154  
 photinos in broken supersymmetric theories, role in cosmology 4-77705  
 same-sign dilepton production, possible origin from new class of neutral particles 4-95787  
 squark/gluino mass ratio, lower bound, low energy supergravity 4-86625  
 SU(1,1) supergravity models, gravitino and gaugino masses, Yukawa couplings 4-90473  
 supersymmetric particles, experimental searches for squarks, sleptons and SUSY gauge bosons, mass limits 4-59019  
 two-gluino bound states 4-86670  
 uncoupled fluids, gauge invariant cosmological fluctuations, early Universe axions 4-76819  
 unstable photino mass bound from cosmology 4-78505  
 $e^+e^-$  new particle searches, electroweak interference effects 4-86722  
 QQ— $gg$ , gluino production, decay rates 4-86752  
 $\chi$  hadron from  $\gamma\gamma$  events 4-111391  
 $@ Z^0$  anomalous radiative decay, possible new pseudoscalar particle 4-68577
- hysteresis**  
*see also coercive force; dielectric hysteresis; elastic hysteresis; magnetic hysteresis; remanence*  
 contact angle, equilib. and hysteresis, smooth uniform surfaces, disjoining pressure isotherm 4-80332  
 dynamometers criteria comparison 4-111124  
 Josephson junction, subharmonic steps, fractal struct., analogue computer calc. 4-92869

**hysteresis continued**

- metal hydride solubility, elastic and plastic accommodation effects 4-108620
- photographic zenith tube, timing mechanisms hysteresis (*Japanese*) 4-94618
- porosimetry, Hg, hysteresis theory 4-73418
- porous materials, hysteresis in Hg porosimetry 4-73420
- pressure-generating system, MASS OB-8 mechanism 4-78341
- in film, supercond., surface heat transfer from self-heating hotspots 4-104361
- NH<sub>3</sub> mol. gas, optical hysteresis obs. in all-optical, passive ring cavity 4-64730
- Ni alloy based thermocouples, hysteresis and short-term instabilities up to 1200°C 4-82793
- Pb film, supercond., surface heat transfer from self-heating hotspots 4-104361
- Si MOSFET, hysteresis phenomena in charging in quantising mag. field 4-104319
- Sn film, supercond., surface heat transfer from self-heating hotspots 4-104361

**I-centres** *see colour centres***I-II-VI<sub>2</sub> semiconductors** *see ternary semiconductors***I-III-VI<sub>2</sub> semiconductors** *see ternary semiconductors***IC** *see integrated circuits***ICE engines** *see internal combustion engines***ice***see also glaciology; sea ice; snow*

- 19 GHz space-Earth path, cross-polarisation isolation and discrimination for rain and ice 4-89973
- amorphous, nonexistent glass transition 4-88098
- amorphous phase of ice I formed at 77K and 10 kbar 4-98016
- amorphous solid, vap. deposited, polymorphism study 4-60833
- E Antarctica, perennially frozen lakes at glacier/rock margins 4-82144
- atmosphere, ice nuclei rel. to cloud and microphysical struct. of mesoscale convective bands behind cold fronts 4-82199
- atmosphere, props. of ice in anvil of winter maritime cumulonimbus cloud 4-62916
- atmosphere ice clouds, effects of crystals. horizontal orientation on radiative props. (*Chinese*) 4-67397
- atmosphere ice nuclei concn. in urban and rural environments 4-94223
- atmospheric, ice nucleus meas. using continuous flow chamber 4-62980
- canal with ice on surface, streamflow estimation 4-77561
- clathrate, normal and deuterated, O-H and O-D stretching and vibr., Raman studies 4-61001
- columnar grained, ductile deform., yield function coeffs. 4-89954
- cosmic radiation fossil record by <sup>10</sup>Be accelerator mass spectrometry 4-90047
- crystals, vapour grown, morphological instability, SEM obs. 4-88125
- cubic, H<sup>+</sup> transfer and Bjerrum defect migration 4-70434
- cubic crystals, surface energy, entropy and stability 4-98309
- density evolution in solar system ices 4-101147
- depolarisation on low-angle 11 GHz satellite downlinks (*French, English*) 4-67378
- dielectric properties meas. with large-size coaxial waveguide time domain reflectometry unit 4-110294
- Earth-space links, digital, effect of ice-induced cross polarisation 4-62904
- electronically excited by fast light ions, nonlinear erosion yield 4-61804
- enthalpy of fusion and heat capacity, calorimeter studies 4-95425
- epitaxial freezing of supercooled droplets on ice surfaces 4-98052
- films, enhanced erosion by high energy <sup>19</sup>F ion sputtering 4-80123
- formation in water flow between two horizontal parallel plates, transition phenomenon 4-64834
- formation on flat surfaces, convective boundary layers 4-112811
- fracture mechanics 4-62866
- freezing process, ice nucleation is supercooled water sample, laboratory expts. 4-115545
- glacier ice, fracture toughness 4-62999
- Greece, hail occurrence freq. 4-100718
- grounded ice sheets, plane steady flow, nonuniform temp. distrib. influence 4-60407
- growth of ice sheets 4-115469
- halo phenomena, Monte Carlo simulation, sun ray path tracing through ice crystals 4-72699
- heat and moisture vertical fluxes to atmosphere from snow and ice covered surfaces 4-77618
- hexagonal, translational lattice vibrs. and permittivity, temp. and press. 4-76309
- hoar frost on cylinder, specific mass var. rel. to ang. position 4-94222
- I<sub>h</sub> to I<sub>x</sub> transition, press. effect on Raman spectrum at low temp. 4-61692
- ice:muonium single cryst. hyperfine interaction and spin relax. 4-65924
- ice cover in tailwaters of hydroelectric power plants, release waves effect on breakup 4-64960
- ice X, high press. form occurring at 44 GPa, Brillouin scatt. 4-61057
- ice-forming nuclei in continental-maritime air 4-89971
- I<sub>h</sub> crystals, oscil. freqs. calcs. 4-80174
- I<sub>h</sub> phase, multiphase and nonadditive energy components 4-69263
- III-IX order-disorder transition, high press. Raman spectra 4-61689
- interstellar medium, obs. of 3 μm ice band in Taurus mol. clouds rel. to interstellar chemistry 4-101457
- Lake Baikal, ice thawing (1961-80) 4-72621
- lake ice, ancient ice islands in salt lakes of Central Andes 4-94178
- Lake Saroma, Hokkaido, snow cover on sea ice and snow ice form. (*Japanese*) 4-105612
- latitude of ice edge, sensitivity to finite amplitude baroclinic heat flux divergence 4-72691
- low temp. electronic sputtering by light ions and electrons 4-71502
- Marion Island, Quaternary glaciation of island near Antarctic convergence 4-82142
- Mars, evidence for volcano-ground ice interactions in Elysium Planitia 4-101223
- Mars, Viking IR obs. of north polar hazes and surface ice 4-94665
- melted layer, vertical, with variable viscosity, onset of convection 4-79592
- melting of crystalline solids, US study 4-70351
- melting rates in turbulent recirculating flow systems 4-97297
- melting spherical ice particles greater than 500 μm radius, expt. and theory 4-82178
- melting spherical ice particles less than 500 μm radius, theory 4-82177
- ice continued
- meteorite craters formation, effect of strain-rate dependent yield strength on crater scaling relations 4-94658
- Monte Carlo calcs. for ice-rule model 4-103973
- mountain site in Czechoslovakia, ice accretion rel. to air temperature 4-89960
- New Quebec, Canada, ice lenses in peat bogs, geochemistry, isotope content and genesis 4-100637
- nucleation on surfaces, predictions 4-94221
- OH 32.8-0.3, OH-IR star with absorpt. features of pure water ice, IR spectrum 4-110764
- optical constants from UV to microwave region 4-65998
- orientational correlational tensor in ice I, III, IV, V and VI 4-98053
- permafrost, research, building and transport problems 4-105614
- permafrost marine sediments of N Alaska coast, thawing and brine transport 4-67290
- polar ice-trapped air age difference at Siple Station 4-115475
- polycrystalline, cumulative damage estimation 4-64894
- polymorphs, electrostatic field and mol. dipole moments 4-70051
- positronium form., computer model 4-114341
- proton ordered ices II, VII and IX, lattice mode spectra, water-water pairs 4-70296
- pure and mixed, NH<sub>3</sub> and H<sub>2</sub>O surface mol. photodetachment and photodissociation 4-66604
- remote sensing of ice by satellite SAR radar imagery 4-72745
- rivers and canals, ice cover, breakup mechanism 4-67288
- sheets, indentation, limit anal. 4-94179
- single crystal, vapour growth mechanisms, morphological stability 4-60868
- snow crystal, vapour growth kinetics, morphology, review 4-60867
- solar haloes, ripple struct. due to sound waves from meteors 4-105715
- spectral properties of ice-mineral mixtures and remote sensing implications 4-115682
- stress-strain state estimation by acoustic probe pulse 4-115428
- stretching vibrations of O-H and O-D, Raman spectrum, press. and temp. depend. 4-98218
- sublimation rates in cryoultramicrotome, freeze-dried specimen prep. 4-62647
- superheated, optical homogeneity, elastic light scatt. 4-113578
- surface quasi-liqu. film, evidence from and implications for contact charging 4-70911
- theoretical glaciology, book 4-58591
- thermal patterns obs. under dynamic loading 4-106320
- VII, uncoupled O-H stretch, IR freq. and integrated intensity up to 18 kbar 4-104601
- D<sub>2</sub>O ice, hexagonal, translational lattice vibrs. and permittivity, temp. and press. 4-76309
- D<sub>2</sub>O ice, vap. press. below 273K 4-113595
- H<sub>2</sub>O<sub>2</sub> in Greenland ice core samples 4-115552
- iconoscopes *see television camera tubes*
- identification
  - see also correlation methods; frequency response; modelling; parameter estimation; simulation; state estimation*
  - evoked potential processing, system identification techniques for noise reduction 4-105357
  - hydrology, nonlinear surface runoff system identification 4-110178
  - nonlinear autoregression/stochastic processes, exptl. results and identification features (*Russian*) 4-63485
- IETS *see tunnelling spectra; tunnelling spectroscopy*
- IXE *see ion microprobe analysis; X-ray chemical analysis*
- ig.f.e.t. *see insulated gate field effect transistors*
- ignition
  - see also electric ignition*
  - acetaldehyde-air mixture, two-stage ignition during rapid compression 4-71930
  - acetylene, oxidation reaction mechanism, shock tube and modelling studies 4-85299
  - cylindrical stretched flame, ignition-extinction behaviour 4-109650
  - gun exhaust plumes, ignition 4-81438
  - light-initiated system, times to ignition calcs. 4-105003
  - metal thin plate, heating and ignition by axisymmetric heat source 4-99794
  - methane-propane mixtures, shock-initiated ignition 4-89294
  - propagation and sooting at rich limit of flammability, plasma jet ignition effect 4-89299
  - solid propellant, composite, catalyst role in ignition mechanism 4-77011
  - solid propellant, thermal behaviour obs. using shock tube, ignition delay 4-77010
  - spark-ignition engine, combustion, flame photographs 4-87811
  - thermal ignition, stability of bifurcation branches 4-93499
  - thermal self-ignition of system of hot foci, 4-97301
- II-III-V<sub>2</sub> semiconductors *see ternary semiconductors*
- II-IV-V<sub>2</sub> semiconductors *see ternary semiconductors*
- II-VI semiconductors
  - carrier mobility characs., displaced Maxwellian model 4-75968
  - CdS/Cu<sub>2</sub>S heterojunction, high resolution electron microscopy characterization 4-104294
  - crystal growth, optical and surface props. (*Japanese*) 4-88957
  - crystallite, thin, plastic deform., in situ TEM obs. method 4-62148
  - diamagnetism and Van Vleck paramagnetism 4-71019
  - dislocation loops, irradiation-produced, HVEM study 4-75529
  - HgCdTe infrared focal plane arrays for imaging spectrometer application 4-100758
  - iodide prep. method in flow reactor 4-76660
  - lattice dynamics, local Heine-Abarenkov model pot. 4-98222
  - MBE, technology and appl. (*Japanese*) 4-85104
  - microscopic Ag impurity quantity determ., kinetic method (*Russian*) 4-65287
  - optoelectronic switching, laser controlled, photoconductivity meas. (*German*) 4-84646
  - photovoltaic material bulk single cryst. and epitaxial multilayer growth 4-71548
  - tetrahedrally bonded cpds., press. induced phase transition to NaCl-phase 4-61073
  - wurtzite-type compounds and alloys, cluster-Bethe-lattice approach to electronic struct. 4-70625
  - (Cd,Zn)S-CuInSe<sub>2</sub> Boeing solar cells, current transport 4-81546
  - (Cd,Zn)S-CuInSe<sub>2</sub> solar cells, light-induced junction modification 4-77092

## VI semiconductor continued

- p-Cd<sub>0.9</sub>Hg<sub>0.1</sub>Te, hopping cond. between intrinsic defects 4-104210  
 Cd<sub>0.23</sub>Hg<sub>0.77</sub>Te etalon, low-power nonlinear Fabry-Perot reflection at 10  $\mu\text{m}$  4-96981  
 Cd<sub>1-x</sub>Hg<sub>x</sub>Te:Mn, EPR study 4-71168  
 Cd<sub>0.9</sub>Hg<sub>0.1</sub>Te, ellipsometric studies of interband transitions 4-92999  
 Cd<sub>0.9</sub>Hg<sub>0.1</sub>Te, epitaxial film growth by chem. transport reactions, elec. props. 4-70965  
 Cd<sub>0.9</sub>Hg<sub>0.1</sub>Te, galvanomagnetic effects in quantising mag. field (*Russian*) 4-70843  
 Cd<sub>0.9</sub>Hg<sub>0.1</sub>Te graded energy-gap structures, interf. photoelectromag. effect 4-113992  
 Cd<sub>0.9</sub>Hg<sub>0.1</sub>Te, ion transport and anodic oxidation (*Russian*) 4-70440  
 Cd<sub>0.9</sub>Hg<sub>0.1</sub>Te, metal-organic VPE growth 4-85107  
 n-Cd<sub>0.9</sub>Hg<sub>0.1</sub>Te, minority carrier mobility, Haynes-Shockley method 4-92714  
 Cd<sub>0.9</sub>Hg<sub>0.1</sub>Te, obs. of negative luminescence 4-99190  
 Cd<sub>0.9</sub>Hg<sub>0.1</sub>Te, phonon states, far IR absorpt. spectra study (*Chinese*) 4-92312  
 p-Cd<sub>0.9</sub>Hg<sub>0.1</sub>Te, photoconductivity and photomagnetic effect 4-104268  
 n-Cd<sub>0.9</sub>Hg<sub>0.1</sub>Te single crystals, hot electrons at strong elec. fields (*Russian*) 4-98628  
 Cd<sub>0.9</sub>Hg<sub>0.1</sub>Te solid solutions, homogeneity, carrier conc., magnetic circular dichroism, temp. depend. 4-93061  
 Cd<sub>0.9</sub>Hg<sub>0.1</sub>Te, transport and pyrolysis in MOVPE growth 4-71577  
 Cd<sub>0.9</sub>Hg<sub>0.1</sub>Te under uniaxial deform., photoelec. props. 4-70864  
 Cd<sub>0.9</sub>Hg<sub>0.1</sub>Te, undoped and In-doped, impurity migration 4-70468  
 Cd<sub>0.9</sub>Hg<sub>0.1</sub>Te/In system, current noise in contact regions, defect influences 4-88595  
 Cd<sub>0.9</sub>Hg<sub>0.1</sub>Te-CdTe heterostruct. interfaces, SIMS anal. of impurities 4-108727  
 CdMnS(Se), donor-bound mag. polarons, mag. fluctuations, spin-flip Raman scatt. 4-80759  
 Cd<sub>1-x</sub>Mn<sub>x</sub>Se, semimagnetic semiconductor with metallic conduction, anomalous magnetoconductivity 4-65692  
 Cd<sub>1-x</sub>Mn<sub>x</sub>Te-CdTe multilayers grown by MBE 4-88976  
 CdS, absorptive optical bistability due to band gap shrinkage 4-69482  
 CdS amorphous films, optical absorption coeff. and gap state density 4-66088  
 CdS based polycrystalline thin film solar cells, future trends 4-89446  
 CdS binder layers, electrophotographic props. after heat and light treatment 4-79258  
 CdS, cavityless optical bistability due to light-induced absorpt. 4-102971  
 CdS, colloidal crystallites, excited electronic states, size effects, optical props., Raman spectra 4-71334  
 CdS coupled mode band-pass optical filters, characteristics 4-87438  
 CdS crystal laser beam annealing 4-75508  
 CdS, crystallisation kinetics, growth from CdS+CdCl<sub>2</sub> melt 4-114380  
 CdS, dark current and photocurrent in strong elec. field, temp. dependence 4-113998  
 CdS dispersion best fit, Sellmeier eqn., with various resonances, nonlinear regression anal. 4-93030  
 CdS, edge luminesc. series emitted in elec. field 4-66068  
 CdS, effect of US waves, acoustoluminescence (*Russian*) 4-71454  
 CdS, electron beam annealing, defects diffusion 4-103801  
 CdS, electron irradi., photoluminescence study 4-99189  
 CdS, exciton diffusion and exciton momentum scatt. 4-65616  
 CdS, exciton-polaritons, resonant Brillouin scatt. studies 4-108789  
 CdS, excitons in high mag. fields, gauge-invariant energy variational calc. 4-80508  
 CdS film, deposited by hot wall technique, characterisation of doped and undoped films 4-114405  
 CdS film, photoluminescence method of determ. minority carrier kinetics 4-61748  
 CdS films grown by spray pyrolysis in an N<sub>2</sub> ambient 4-61843  
 CdS, frequency tuning of far-IR radiation on hot excitons 4-69415  
 CdS, graphoepitaxy, two-stage artificial epitaxy 4-66229  
 CdS, ground state energies of shallow donors 4-92654  
 CdS,  $\gamma$ -irrad., photoelectron spectra and photoconductivity (*Russian*) 4-71521  
 CdS, HF holographic diff. grating recording on surface 4-69339  
 CdS, in Nafion film, struct., luminesc. lifetime quantum yield and quenching 4-85000  
 CdS, irradiation-produced dislocation loops, HVEM study 4-75529  
 CdS laser, electron-beam-pumped, excitation density distrib. 4-79162  
 CdS, laser induced gratings 4-104630  
 CdS, luminescence study of polaritons 4-61300  
 CdS monocrystals and films, luminesc. spectra during high levels of excitation (*Russian*) 4-80999  
 CdS, nonlinear exciton transmission, Maxwell's eqn. anal. 4-98535  
 CdS, optically pumped, tunable CW mode locked laser action 4-107699  
 CdS, particle suspensions, electronic processes, microwave probing 4-99852  
 CdS, piezoelec. semicond., stimulated Brillouin scatt. of electromagnetic wave, acoustic amplification 4-114291  
 CdS polycrystalline films, photocorrosion in aq. soln., capacitance and action spectra meas. 4-92818  
 CdS, radiative and nonradiative recomb., plastic deform. depend. 4-61658  
 CdS, radiative recomb. mechanisms for high density excitons 4-88458  
 CdS, resonant Brillouin scatt. study 4-61721  
 CdS, resonant Brillouin spectra calcs. 4-61722  
 CdS Schottky barrier MIS solar cells 4-62350  
 CdS, shock loaded, struct. studies 4-92293  
 CdS single, photoluminescence studies 4-109240  
 CdS single cryst., photoacoustic spectra from unilluminated surface 4-109206  
 CdS sintered layers for solar cells, prep. and annealing effects on characts. 4-62369  
 CdS, small particles, photoluminesc. 4-85004  
 CdS, spectral-time characts. of nonlinear emission (*Russian*) 4-104620  
 CdS, spin relax. of free carriers, Raman scatt. 4-104619  
 CdS, spontaneous oscils. in presence of temp.-electric instability 4-104266  
 CdS surface, clean and Au covered, surface recombination vel., photoluminescence studies 4-80600  
 CdS, thermally stimulated brightening of cryst. boundary in exciton absorption region 4-114234  
 CdS thin crystals, refr. index dispersion curve, thickness depend. (*Ukrainian*) 4-65999

## II-VI semiconductors continued

- CdS thin film, RF-sputtered, elec. props., effect of temp. and bias 4-80699  
 CdS thin films, electrodeposited in fused salt solns., struct. and morphology rel. to substrate 4-66250  
 CdS thin films prep. by spray deposition, vacuum annealing effect on elec., structural and optical props. 4-70966  
 CdS, thin plate, reflection spectrum, interference struct. anal. 4-76402  
 CdS, three-photon absorpt. with subsequent absorpt. by photogenerated carriers 4-79226  
 CdS, uniaxially deformed, current saturation and oscill. (*Russian*) 4-70818  
 CdS, wurtzite-type, hole-phonon interaction, phonon cond. calc. 4-70487  
 CdS:Cu, photoconductivity and luminescence (*Russian*) 4-84658  
 CdS:Cu,In sprayed films, topotaxial growth of Cu<sub>2</sub>S thin films, optical and structural behaviour 4-114433  
 CdS:Cu thin films, photocurrent, field quenching 4-84718  
 CdS:Cu(Cl) films, defect diffusion, luminescence study (*Russian*) 4-88875  
 CdS:In film, elec. props. meas. 4-104329  
 CdS:O, highly photocond. films, spray pyrolysis prep. 4-88533  
 CdS:Sb films, vacuum deposited, struct., elec. and optical props., impurity conc. effect 4-98607  
 CdS/CdTe solar cell, annealing, admittance spectroscopy 4-77101  
 CdS/Cu<sub>2</sub>-S heterostruct., misfit accommodation and growth 4-108730  
 CdS/CuInSe<sub>2</sub>, solar cell interface chem. reaction, thermodynamics 4-85367  
 CdS/CuInSe<sub>2</sub> heterojunction solar cells, conduction band-lineup 4-72105  
 CdS/CuInSe<sub>2</sub> solar cells, thin film, diffusion length determ. using EBIC method 4-72110  
 n-CdS/electrolyte interface, photoelectrochem. characterisation 4-84689  
 n-CdS/n-CdSe heterojunction photoresponse, surface state effects 4-84866  
 n-CdS/S<sup>2-</sup>, S<sup>2-</sup> photoelectrochemical solar cells, quantum efficiency, theoretical model anal. 4-114913  
 CdS/Te thin film Schottky barrier diodes 4-70909  
 CdS-CdTe screen-printed solar cell fabrication with 12.8% efficiency and 0.78 cm<sup>2</sup> active area 4-77107  
 CdS-CdTe thin film solar cells, photocapacitance and current collection 4-81548  
 CdS-CdTe thin films, photoluminescence study 4-80987  
 CdS:Cu,S photoelects formed by electroplating, prep. and props. 4-72115  
 CdS:CuInSe<sub>2</sub> thin film heterojunction solar cells, photoresponse characts. 4-77099  
 CdS:CuInSe<sub>2</sub> photovoltaic devices, short-circuit current meas. 4-88971  
 CdS-electrolyte, SAW characterisation of surface and interface states 4-98681  
 CdS-Ga<sub>2</sub>S<sub>3</sub>, phase diagram, crystallographic study, DTA, X-ray diff. 4-109387  
 CdS-InP heterojunctions, elec. and photoelec. props., solar cell appl. (*Russian*) 4-98713  
 n-CdS/n-CdSe heterojunction, photo-EMF study 4-104307  
 CdS-Se binder layer, photo and dark conductivity, modification by corona charging, expt. 4-98672  
 CdS(Bi) films, in photoelectrochemical cells, photovoltaic characteristics 4-93634  
 CdS(In) films chemical bath-deposited, electrical and optical props. 4-92832  
 CdSse, optically pumped, tunable CW mode locked laser action 4-107699  
 CdS<sub>0.9</sub>Se<sub>0.1</sub> laser optical pumping by CdS streamer laser radiation 4-60050  
 n-CdS<sub>0.9</sub>Se<sub>0.1</sub> electrode, liquid junction photoelectrochemical cells, props. (*Chinese*) 4-81565  
 CdS<sub>1-x</sub>Se<sub>x</sub> particles for photocatalytic production, valence bands 4-100008  
 CdSb:In(Te) dopant distrib. coeffs. (*Japanese*) 4-84313  
 CdSe films, cell form. prior to laser induced synthesis 4-65582  
 CdSe, free exciton dynamics study 4-98788  
 CdSe, hot excitons and electron-hole pairs and Raman spectra 4-114285  
 CdSe, interface states studied by electrochemical photocapacitance spectroscopy 4-98750  
 CdSe, magnetopolaritons, dipole forbidden transmission 4-98544  
 CdSe, optically pumped, tunable CW mode locked laser action 4-107699  
 CdSe, particle desorp. under laser irradi., mass and energy distrib. meas. (*Russian*) 4-113815  
 CdSe photoelectrochemical cells, surface modification using CuS 4-81566  
 CdSe photoelectrochemical solar cells, lifetime improvements 4-99969  
 CdSe, picosecond energy-relax. processes of excitons, luminesc. study 4-109244  
 CdSe, picosecond spectroscopy at high excitation densities 4-81003  
 CdSe, reaction with Pb and S containing reactive gas phase 4-105016  
 CdSe, thin films, noise power spectra meas. 4-80638  
 CdSe/ferro-ferricyanide photoelectrochemical system, I-V behaviour 4-88580  
 CdSe/polysulphide photoelectrochemical cells, performance and stability, pronounced cation effect 4-89453  
 CdSe/sulphide-polysulphide photoelectrochemical system, I-V behaviour 4-88580  
 CdSe-CdTe heterophase films, nonreciprocal photoelec. props. 4-108907  
 CdSe-type uniaxial cryst., excitonic absorpt. band formation (*Russian*) 4-71409  
 CdSe-VO, contact, barrier to antibarrier transition during metal-semiconductor phase transition 4-65738  
 CdSe<sub>1-x</sub>Te<sub>x</sub> thin films, vac. evaporated, for electrochemical photovoltaic cells 4-77115  
 CdSe<sub>1-x</sub>Te<sub>x</sub> hetero-photoconverters, spectral characts. (*Russian*) 4-66692  
 CdTe, atomic layer epitaxy on CdTe substrates, high structural perfection 4-114415  
 CdTe, cooperative processes: spontaneous and stimulated emission 4-104662  
 n-CdTe, deep levels, plastic deform. effects, DLTS studies 4-84591  
 CdTe, dislocations and subboundaries, etching studies 4-75451  
 CdTe doped with mag. ions, anomalous optical effects (*Russian*) 4-99103  
 n-CdTe, electron traps, DLTS study 4-80533  
 CdTe epitaxial films, MOCVD on InSb and GaAs substrates 4-81146  
 CdTe epitaxial films, OMCD grown on sapphire, growth rates, mobilities, X-ray diff. 4-80444  
 CdTe film, composition and elec. props. 4-80696  
 CdTe films, atomic layer epitaxy and electronic struct. 4-81135  
 CdTe films, electrochem. deposited, optical props. 4-85022

## II-VI semiconductors continued

- CdTe films, MBE growth on (001) GaAs and (001) InSb, charact. 4-98471  
 CdTe films, MBE growth and elec. and optical props. 4-81136  
 CdTe films, MBE growth and microstruct. characterisation 4-92578  
 CdTe films on InSb, MBE growth, charact. 4-98470  
 CdTe, growth from vapour phase, on substrate out of contact with vapour walls 4-109315  
 CdTe, heteroepitaxial, on (001) InSb, TEM studies 4-104107  
 CdTe initial growth stages on (001) GaAs, AES and RHEED obs. 4-70580  
 CdTe, ion implanted with  $^1\text{H}$ ,  $^2\text{H}$ ,  $^4\text{He}$ , depth distributions, SIMS study 4-88182  
 CdTe, irradiation-produced dislocation loops, HVEM study 4-75529  
 CdTe large single crystals, grown from vapour phase, polarity 4-70048  
 CdTe MBE films on InSb, impurity doping and photoluminesc. props. 4-88980  
 CdTe MBE growth 4-98473  
 CdTe metal-semicond.-metal struct., pot. barriers 4-84708  
 CdTe, p-type, undoped, thin dielectric films deposition as protection against decomposition during annealing 4-92755  
 CdTe photoelectrodes, photoelectrochemical props., XPS and AES studies 4-88578  
 CdTe, plastically deformed at room temp., dislocations, TEM study 4-98104  
 CdTe polycryst. film, gradient recryst. grown, photolum. 4-76522  
 CdTe, Raman characterisation 4-99106  
 CdTe, solubility in GeTe, effects of temp. 4-108622  
 CdTe, tetrahedrally bonded, anisotropy of Compton profile 4-99217  
 CdTe thin films, DC cond. rel. to  $\text{H}_2$  exposure 4-76053  
 CdTe thin films, electroless deposition 4-88992  
 CdTe, thin films, noise power spectra meas. 4-80638  
 CdTe thin films for solar cell appls., deposition and elec. props. 4-76054  
 CdTe thin layers, crystal and energy structures for photoelectric transducers 4-98298  
 CdTe, two-photon absorpt. with subsequent absorpt. by photogenerated carriers 4-79226  
 p-CdTe, undoped, in situ prep. by cathodic electrochem. deposition 4-61880  
 CdTe, X-ray diffraction study, cryst. struct. (Russian) 4-84280  
 CdTe:Ag(Cu), deep levels, pulsed admittance spectroscopy and capture cross sections 4-92653  
 CdTe:Cl, native acceptor defects, Hall effect study 4-75899  
 CdTe:Co, optical absorpt. spectrum (Russian) 4-84983  
 CdTe:H-Au contacts, hydrogenation effects 4-80695  
 CdTe:In, electroconductivity at high temp. 4-61373  
 n-CdTe:In, electron traps, DLTS study 4-80533  
 CdTe:In, Li, defect complex, IR absorption studies 4-80031  
 CdTe: $\text{In}_2\text{O}_3$ -y structures electrophysical charact., for photoconvertors 4-92795  
 CdTe: $\text{In}_2\text{O}_3$ -x $\text{SnO}_3$ -y, photoconvertors, current transfer mechanism 4-93616  
 CdTe: $\text{In}_2\text{O}_3$  structures electrophysical charact., for photoconvertors 4-92795  
 CdTe/ $\text{In}_2\text{O}_3$  photoconvertors, current transfer mechanism 4-93616  
 CdTe/ $\text{SnO}_2$  structures electrophysical charact., for photoconvertors 4-92795  
 CdTe-based thin film solar cells, elec. and spectral props. 4-93621  
 CdTe-InSb MIS struct., electronic props. 4-98778  
 n-CdTe-p-Cu<sub>2</sub>Te(p-Au<sub>2</sub>Te) heterojunctions, deep levels, photocapacitance spectra 4-61410  
 CdTe-ZnTe heterojunction, interface trap depths 4-61442  
 CdZnS-CuInSe<sub>2</sub> polycryst. thin film solar cells 4-77088  
 Cd<sub>1-x</sub>Zn<sub>x</sub>S films, prep. at various CdZnS ion ratios, use in electrochem. photovoltaic cells 4-85099  
 Cd<sub>1-x</sub>Zn<sub>x</sub>S sprayed film, photoelectrochem. cells, Zn composition effects 4-114912  
 Cd<sub>1-x</sub>Zn<sub>x</sub>Te alloys, growth, elec. props., photoluminesc. 4-66207  
 Cu<sub>2</sub>S-CdS solar cells, elementary degradation mechanisms (Russian) 4-89402  
 Cu<sub>2</sub>S-CdS thin film solar cells development and transfer to industrial production 4-89429  
 (CuZn)S-CuInSe<sub>2</sub> heterojunction solar cell, interface props. 4-89401  
 GaAs (110)-ZnSe interface, LEED and AES characterisation 4-84517  
 GaAs, crystallisation from melt, rate, elec. current effects 4-71551  
 (Hg,Cd)Te photovoltaic detector, near-room-temp., thermoelec. current (Chinese) 4-106382  
 (Hg,Cd)Te/Au overlayer system, deposition, interactions and diffusion, UPS study 4-80439  
 Hg-CdTe phase diagram, thermodynamic data, associated soln. model, book contrib. 4-89031  
 HgCdTe 0.1 eV photoconductive detector, optimum thickness 4-111204  
 HgCdTe detector technology status 4-95515  
 HgCdTe epitaxial films, MOCVD on InSb and GaAs substrates 4-81146  
 HgCdTe, growth, props. and appls. 4-66217  
 n-HgCdTe, Haynes-Shockley expt. 4-104204  
 HgCdTe heterojunction contact photoconductor 4-88528  
 HgCdTe, IR airborne imaging spectrometer appl. 4-115585  
 HgCdTe, IR detector arrays, state-of-the-art review 4-111202  
 HgCdTe IR sensor for fading memory focal plane processor 4-107871  
 HgCdTe, ion implanted with  $^1\text{H}$ ,  $^2\text{H}$ ,  $^4\text{He}$ , depth distributions, SIMS study 4-88182  
 HgCdTe, optically pumped, tunable CW mode locked laser action 4-107699  
 HgCdTe photodiode obs. by electron-beam induced voltage technique (Chinese) 4-108929  
 HgCdTe, pressure-induced epitaxial growth from soln. 4-88993  
 HgCdTe, Raman characterisation 4-99106  
 HgCdTe, thin films, noise power spectra meas. 4-80638  
 HgCdTe wide-bandwidth photodiode photomixers, 28  $\mu\text{m}$  4-68283  
 Hg<sub>0.3</sub>Cd<sub>0.7</sub>Te, LPE grown, photoluminescence study 4-80986  
 Hg<sub>0.3</sub>Cd<sub>0.7</sub>Te, (110), Raman scatt. study 4-80942  
 Hg<sub>0.3</sub>Cd<sub>0.7</sub>Te-CdTe heterojunctions, elect. charact. 4-76036  
 Hg<sub>1-x</sub>Cd<sub>x</sub>Te, annealing of radiation defects, electron irradiation 4-108442  
 Hg<sub>1-x</sub>Cd<sub>x</sub>Te, CPA calcs., Green's function calcs., simplification through analytic continuation 4-61274  
 Hg<sub>1-x</sub>Cd<sub>x</sub>Te, characterisation using transverse acoustoelectric volt. meas. 4-104275  
 Hg<sub>1-x</sub>Cd<sub>x</sub>Te, deep impurity and defect states 4-88474

## II-VI semiconductors continued

- Hg<sub>1-x</sub>Cd<sub>x</sub>Te, deep level anal. using temp. depend. of capacitance (Chinese) 4-113888  
 Hg<sub>1-x</sub>Cd<sub>x</sub>Te, dry oxidation in gas phase, predominance area phase diagrams 4-71748  
 p-Hg<sub>1-x</sub>Cd<sub>x</sub>Te, elec. resist. and Hall coeffs., low-temp. anomalies 4-108885  
 Hg<sub>1-x</sub>Cd<sub>x</sub>Te, electric subbands in the limit  $E_{\text{G}}=0$ , for IR reson. study 4-104286  
 Hg<sub>1-x</sub>Cd<sub>x</sub>Te, electron irradi., elec. props., heat treatment effects 4-65713  
 Hg<sub>1-x</sub>Cd<sub>x</sub>Te epitaxial layers, organometallic growth and elec. props. 4-71566  
 Hg<sub>1-x</sub>Cd<sub>x</sub>Te,  $\Gamma_6$ - $\Gamma_8$  band crossover under press., phase transform., thermoelec. power meas. 4-88524  
 Hg<sub>1-x</sub>Cd<sub>x</sub>Te, Hg diffusion profile meas. by heavy ion backscatt. 4-75730  
 Hg<sub>1-x</sub>Cd<sub>x</sub>Te IR detectors, 100-300  $\mu\text{m}$ , mag.-field effects 4-68281  
 Hg<sub>1-x</sub>Cd<sub>x</sub>Te LPE layers, below band gap photoluminescence 4-71423  
 Hg<sub>1-x</sub>Cd<sub>x</sub>Te large area epitaxial layers, LPE growth 4-61879  
 Hg<sub>1-x</sub>Cd<sub>x</sub>Te layers, CVT growth and characterisation 4-71576  
 Hg<sub>1-x</sub>Cd<sub>x</sub>Te MBE growth 4-98473  
 Hg<sub>1-x</sub>Cd<sub>x</sub>Te, native oxides and interfaces; spectroscopic ellipsometry studies 4-80426  
 Hg<sub>1-x</sub>Cd<sub>x</sub>Te, photogenerated carrier lifetime meas. by optical modulation of IR absorpt. (Chinese) 4-84953  
 Hg<sub>1-x</sub>Cd<sub>x</sub>Te submillimeter mixing, theoretical and expt. study 4-74622  
 Hg<sub>1-x</sub>Cd<sub>x</sub>Te surface accumulation layer, cyclotron resonance studies 4-98507  
 Hg<sub>1-x</sub>Cd<sub>x</sub>Te zero gap MIS struct., size quantisation in accumulation layers 4-65753  
 $\alpha$ -HgS, conductivity anisotropy and Hall coeffs. 4-92719  
 HgS, hydrothermal crystal growth 4-104726  
 HgS mixed films, elec. and optical props. (French) 4-84715  
 HgTe,  $\Gamma_6$ - $\Gamma_8$  band crossover under press., phase transform., thermoelec. power meas. 4-88524  
 n-HgTe MBE growth 4-98473  
 n-HgTe zero gap semicond., effective electron mass, mag. quantisation effects 4-88442  
 HgTe, zero-gap, intrinsic cond. theory 4-70813  
 HgTe-CdTe superlattices, electronic props. 4-84680  
 HgTe-CdTe superlattice, far IR magneto-optics, band structure 4-99101  
 In<sub>0.5</sub>O<sub>0.5</sub>-based transparent film temp. sensors, performance under high-density solar fluxes 4-90585  
 n-InSb-p-CdTe heterojunction, elec. props. 4-108928  
 LiNbO<sub>3</sub>-ZnO piezoelectric interface, Stoneley wave propagation 4-104059  
 LiTaO<sub>3</sub>-ZnO piezoelectric interface, Stoneley wave propagation 4-104059  
 NiO, interaction with O<sub>2</sub>, H<sub>2</sub>S and SO<sub>2</sub>, surface and vol. processes 4-98372  
 Pb chalcogenides, carrier heating mechanisms 4-92738  
 PbTe/ZnS IR filter durability assessment, Space Shuttle 1st LDEF appl. 4-74688  
 Zn chalcogenides, CVD using elemental source materials, struct. props. 4-98481  
 Zn chalcogenides, MOCVD growth 4-93227  
 Zn piezoelectric membranes, SAW charact. and transducers 4-104058  
 Zn<sub>1-x</sub>Cd<sub>x</sub>-S, excitation migration between localised excitons, photoluminescence, absorpt. spectra 4-88456  
 Zn<sub>1-x</sub>Cd<sub>x</sub>-S solid soln., localised exciton migration, pumping intensity effects 4-92618  
 Zn<sub>1-x</sub>Cd<sub>x</sub>-S, structural disorder and solid state transformations 4-103924  
 Zn<sub>1-x</sub>Cd<sub>x</sub>-S/Si, p-n heterojunction photovoltaic solar cell 4-85366  
 Zn<sub>1-x</sub>Cd<sub>x</sub>-S-Cu<sub>2</sub>S heterojunction, energy band diagrams 4-104296  
 Zn<sub>1-x</sub>Cd<sub>x</sub>-S-Cu<sub>2</sub>S reverse-biased p-n heterojunctions, elec. props. and photodiode appls. (Russian) 4-108926  
 Zn<sub>1-x</sub>Cd<sub>x</sub>-S, laser screens, crystals grown from vapour phase, receiving colour image blue component (Russian) 4-96917  
 Zn<sub>1-x</sub>Cd<sub>x</sub>-S, scanning laser emitting in the blue region 4-79163  
 Zn<sub>1-x</sub>Cd<sub>x</sub>-Te, solid soln., sound attenuation study 4-98208  
 Zn<sub>1-x</sub>Cd<sub>x</sub>-Te, Raman scatt. and phonon spectra 4-88835  
 Zn<sub>1-x</sub>Mn<sub>x</sub>-S single crystals, vapour phase grown, stacking faults, structural transform. 4-88278  
 ZnO, 3d impurity excitation spectra, separation of one- and many-electron effects 4-75900  
 ZnO (0001), interaction with methanol at low temp., XPS and UPS study 4-92542  
 ZnO, adsorpt. of NO on (10 $\bar{1}$ 0) surface, thermal desorpt. and photoelectron spectrosc. obs. 4-108705  
 ZnO, adsorption sensitive elements, thermal charact. (Russian) 4-65549  
 ZnO channel waveguide formation on Si substrates 4-103012  
 ZnO electroluminescence, brightness waves, grain size effects 4-104675  
 ZnO electroluminescence, brightness, volt. and freq. depend. 4-104676  
 ZnO film, laser evaporated growth and transducers 4-104537  
 ZnO film on Al<sub>2</sub>O<sub>3</sub> substrate, SAW study 4-104053  
 ZnO films, surface excitation polaritons, ATR mode 4-65618  
 ZnO, irradiation-produced dislocation loops, HVEM study 4-75529  
 ZnO, non-stoichiometric, diffusion processes 4-98352  
 ZnO, nonlinear light absorpt., two-photon absorpt. spectra 4-96992  
 ZnO, organometallic CVD, use of heterocyclic source compounds 4-61870  
 ZnO oriented crystal, cryst. violet dye adsorpt., press. effect 4-98442  
 ZnO, percolation nonohmic conductivity of polycrystalline semiconductors 4-108871  
 ZnO, powdered, freq. dispersion of elec. cond. 4-70802  
 ZnO RF sputtered film on Au/quartz, crystalline props., X-ray diff. studies 4-104101  
 ZnO sputter deposited films for shear mode transducers, effect of RF bias 4-97247  
 ZnO surfaces, work function, electron affinity, and band bending, angle-resolved UPS study 4-92792  
 ZnO textured films for SAW devices, X-ray struct. study 4-75815  
 ZnO transparent conductive films, prep. by RF diode sputtering (Japanese) 4-113831  
 ZnO triode sputtered films, stress relax. study 4-104109  
 ZnO UV laser with longitudinal electron beam pumping 4-79164  
 ZnO varistor, high-field fine-grained, fabrication by sol-gel processing 4-66282  
 ZnO varistor, polycrystalline, elec. props. 4-104199  
 ZnO varistor ceramics, SEM EBIC studies 4-75981  
 ZnO weak accumulation layers, electron transport and Hall effect 4-98686

## I semiconductors continued

- ZnO: transition metal, impurity electron states calcs. 4-70711  
 ZnO:Al films, RF magnetron sputtering, elec. and optical props. 4-85100  
 ZnO:Gd(Pr), thermoluminesc. under UV,  $\beta$ - and  $\gamma$ -ray irradiations 4-93119  
 ZnO:Nd(Yb), electrolum. brightness, voltage and freq. depend. at liq.  $N_2$  temp. 4-93113  
 ZnO:Ni, photoionisation band edge fine struct., electroabsorption studies 4-109162  
 ZnO/CuO:Li junctions I-V characteristics, humidity effects, humidity sensor appl. 4-63750  
 ZnO(S)(Se), RF sputter deposition 4-109323  
 ZnS, 3d impurity excitation spectra, separation of one- and many-electron effects 4-75900  
 ZnS (Se)(Te), chemoeptaxy, reactive diffusion, struct. and growth kinetics 4-80442  
 ZnS (100) surface, relations between surface states and struct. 4-80639  
 ZnS (110), surface structure, atomic geometries, R-factor minimization 4-84494  
 ZnS, CVD, vacancy-hydride complex, optical absorpt., photoluminesc. 4-60916  
 ZnS, charge states of S vacancy, tight-binding approx. 4-61331  
 ZnS conductive film, MBE prep. with single effusion source, luminesc. and elec. props. 4-99323  
 ZnS crystals, anomalous photovoltaic effect and disorder 4-88531  
 ZnS crystals, pure and Mn doped, optically detected ESR 4-80843  
 ZnS disordered cubic cryst., stacking faults, X-ray diffr. study 4-103771  
 ZnS, double-polymorph region form. 4-79991  
 ZnS film on Au substrate, zero reflection at oblique angles of incidence 4-91398  
 ZnS films, RF sputtering prep. and microstruct. props. 4-88417  
 ZnS, hydrothermal crystal growth 4-104726  
 ZnS, irradiation-produced dislocation loops, HVEM study 4-75529  
 ZnS, lattice thermal cond. 4-70484  
 ZnS, multispectral chemically vapour-deposited, initial characterisation 4-76418  
 ZnS, nonthermalised carrier mobility rel. to bulk photovoltaic effect 4-92727  
 ZnS, organometallic CVD, use of heterocyclic source compounds 4-61870  
 ZnS, polycryst. 4-70483  
 ZnS, polymorphism, descriptive symbolism 4-98061  
 ZnS, refr. index, wavelength and temp. derivatives 4-99077  
 ZnS, solution growth and photoluminesc. props. 4-88958  
 ZnS, surface morphology after thermal etching 4-80346  
 ZnS thin film, laser modulation by free carrier absorption, film thickness and temperature influences (Japanese) 4-114339  
 ZnS: transition metal, impurity electron states calcs. 4-70711  
 ZnS:Ag phosphor, phase composition effect on luminescence parameters and EPR spectrum (Polish) 4-85014  
 ZnS:Cu, Er phosphor, electroluminescence and photoluminescence emission spectra 4-76512  
 ZnS:Cu film, cathodoluminescence study of annealing 4-81008  
 ZnS:Cu<sup>2+</sup>, Jahn-Teller coupling forces, self consistent LCAO calc. 4-98577  
 ZnS:Fe<sup>2+</sup>, impurity states, EPR meas. 4-84588  
 ZnS:I with adsorbed O<sub>2</sub>, surface states and LED props. 4-80643  
 ZnS:Mn ACTFEL electroluminescent devices 4-88882  
 ZnS:Mn electroluminesc. thin layers, doping and cryst. struct. 4-75810  
 ZnS:Mn thin films, electrolum., diffusion and trapping 4-104677  
 ZnS:Ni<sup>2+</sup>, ESR, optical absorption and luminescence studies 4-92955  
 ZnS:Ni<sup>2+</sup>, photolum. band arising from  $T_1(P) \rightarrow T_1(F)$  transition 4-104664  
 ZnS:Sm,(Cu) electroluminescent phosphors, Alfrey-Taylor relation 4-114331  
 ZnS-CdS system, solid solns. and phase transform. under hydrothermal conditions 4-98264  
 ZnS,Se<sub>1-x</sub> deep impurity, trap embedding, luminesc. spectra 4-61321  
 ZnS,Se<sub>1-x</sub>Cu, photoluminescence study 4-93095  
 ZnS-Cu<sub>2-x</sub>S n-p heterojunctions, elec. and photoelec. props., UV detector appls. (Russian) 4-108927  
 ZnSe, 3d impurity excitation spectra, separation of one- and many-electron effects 4-75900  
 ZnSe (110) surface atomic geometry, photoemission spectroscopy determ. 4-108684  
 ZnSe (110)-Ge interface, ordered and disordered, electronic struct. 4-84666  
 ZnSe, crystal growth by resublimation, hole mobility meas. 4-109316  
 ZnSe crystal with irregular struct., Raman intensity 4-109184  
 ZnSe crystals, etch pits and polarity identification 4-99621  
 ZnSe cubic crystal, natural birefringence meas. 4-109153  
 ZnSe, deformation pot. consts. determ. by reson. Brillouin scatt. 4-71398  
 ZnSe, epitaxial short wavelength visible laser diodes 4-107628  
 ZnSe films, low press. MOCVD growth and elec. and optical props. 4-93230  
 ZnSe films, MBE growth, elec. cond., Hall effect and photoluminescence studies 4-99344  
 ZnSe films, MOCVD growth using diethylselenide 4-61872  
 ZnSe heteroepitaxial layers, VPE, photoluminesc. 4-61741  
 ZnSe, IR transparent polycrystal, deposited by low purity reagent, props. (Chinese) 4-107767  
 ZnSe, irradiation-produced dislocation loops, HVEM study 4-75529  
 ZnSe, lattice thermal cond. 4-70484  
 ZnSe, localised vacancies, electronic struct. and stability 4-80539  
 ZnSe, luminescence spectra, pulsed irradiation with electrons 4-109230  
 ZnSe, mechanically polished, oxidation on heating in air 4-62076  
 ZnSe, millimeter and submillimeter cyclotron resonance study 4-92963  
 n-ZnSe, OMVPE undoped films, elec. and optical props. 4-93226  
 ZnSe, optical phonon lifetimes, temp. dependence, optical meas. 4-61016  
 ZnSe, organometallic CVD, use of heterocyclic source compounds 4-61870  
 ZnSe, photoelectrochemical etching and nonuniform charge flow in Schottky barriers 4-80672  
 ZnSe photoelectrochemical cells, radiative recombination 4-89456  
 ZnSe, refr. index, wavelength and temp. derivatives 4-99077  
 ZnSe, solution growth and photoluminesc. props. 4-88958  
 ZnSe, tetrahedrally bonded, anisotropy of Compton profile 4-99217  
 ZnSe, thin film, optical properties in the wavelength-range 400 to 1500 nm 4-114336  
 ZnSe, three-photon absorpt. with subsequent absorpt. by photogenerated carriers 4-79226

## II-VI semiconductors continued

- ZnSe, uncoated, surface-to-bulk optical absorpt. using photoacoustic chopping freq. studies 4-76419  
 ZnSe, VPE growth, photoluminesc. props. 4-61858  
 ZnSe, visual grading method, new surface and bulk absorpt. values 4-83732  
 ZnSe, XANES spectra, K-edge region 4-109278  
 ZnSe:I, vacancy-I complex hyperfine interactions, ESR study 4-70150  
 ZnSe:In<sup>+</sup>, ion implanted, high electron mobility obs. 4-108863  
 ZnSe:N, acceptor levels, optically excited DLTS study 4-61322  
 ZnSe-Ge heterojunction, valence-band discontinuities 4-84676  
 ZnTe crystals, etch pits and polarity identification 4-99621  
 ZnTe, donor bound exciton states, Zeeman spectra 4-88452  
 ZnTe films, memory switching in MSM structures 4-70883  
 ZnTe, growth forms, chem. transport reactions 4-109314  
 ZnTe, lattice thermal cond. 4-70484  
 ZnTe polycryst. films, resonant light scatt. spectra 4-99207  
 ZnTe single cryst., nonlinear laser radiation transmission at He temps. 4-64748  
 ZnTe, solubility in GeTe, effects of temp. 4-108622  
 ZnTe, surface phonon polaritons, Raman intense increase on rough surfaces 4-98427  
 ZnTe:Ni, absorpt. spectra, impurity states (Russian) 4-113898  
 ZnTe-CdTe, epitaxial film, degree of perfection and struct. 4-61250  
 Zns refractive indices in 0.405-13  $\mu$ m wavelength range 4-88794

## III-V semiconductors

- ab initio band struct. calc. 4-75832  
 alloy growth by MBE, book contrib. 4-61856  
 AlSb/InAs/AlSb quantum wells, magneto-transport meas. 4-98745  
 antistite defect energy levels 4-80548  
 band struct., APW calc. method appl. 4-92608  
 band struct., semi-empirical tight binding calc. 4-70631  
 contact resistance profiling 4-75499  
 contact technology and modification of metal-semicond. contact interfaces 4-70936  
 covalent crystals, equation of state, bulk modulus press. derivative 4-98236  
 deposited dielectric for III-V semiconductor devices 4-84702  
 diamagnetism and Van Vleck paramagnetism 4-71019  
 doped with 3d transition metals, impurity states 4-75895  
 electrical and electronic props., book 4-86124  
 electrochemical oxidation, surface states (French) 4-76044  
 ellipsometry application in measuring refractive indices and layer thickness of semiconductor materials 4-95495  
 GaAs fast supercomputer circuits (Swedish) 4-65282  
 GaInAs-InP heterojunction, interface 2-D electron gas props., MOCVD growth and characterisation (French) 4-76685  
 heterocomposition-based devices, degradation and thermodynamic instability 4-88312  
 heterostructures, photoacoustic spectroscopy by piezoelec. transducers 4-95527  
 hot carrier transient response, vel. overshoot 4-92736  
 InP:Zn epitaxial layers, MOCVD grown, doping, Hall effect, SIMS, electrochemical profiling 4-80077  
 n-InSb, photoconductivity and hole trapping centre capture coeff., press. studies 4-98668  
 integrated optoelectronic devices for high-speed IC interconnects 4-97139  
 ion implantation, maskless, using Pd-Ni-Si-Be-B liquid metal ion source 4-58913  
 lasers, threshold current, temp. dependence 4-79132  
 lattice dynamics, local Heine-Abarenkov model pot. 4-98222  
 MBE, technology and appl. (Japanese) 4-85104  
 MBE, thermodynamics of O incorporation 4-61253  
 MBE apparatus, source nozzle 4-104734  
 MBE growth for optoelectronic appl. 4-81134  
 MBE growth on Si (100), optical props. 4-88975  
 metal/AlGaAs/GaAs modulation-doped structs., physical correspondence with MOS struct. 4-76041  
 MOS struct., surface electron states and struct. (Russian) 4-65745  
 MOVPE, adduct techniques 4-71575  
 n-p-i doping superlattices, electronic props. 4-104300  
 nonlinear absorpt., coherent radiation-exciton interaction model 4-99078  
 optical sources, dislocations climbing degradation, experimental anal. 4-83654  
 photovoltaic material bulk single cryst. and epitaxial multilayer growth 4-71548  
 physical data, compilation, book 4-63420  
 quantum well struct., free carrier absorption for polar optical phonon scatt. 4-104551  
 quaternary semiconductors, immiscibility and spinodal decomp. rel. to epitaxial layer quality 4-70590  
 quaternary solid solutions, immiscibility anal. 4-65407  
 review of device physics and technology 4-80580  
 semi-insulating, surface, photoexcited 2D electron system, reson. Raman spectra 4-109190  
 solar cells, anisotropically etched, design and anal. using ray-tracing models 4-72114  
 solid solutions, quaternary III-V cpd. system, optical and elec. props. 4-84929  
 solid-state devices and materials, conf., Tokyo, Japan (Aug.-Sept. 1983) 4-82595  
 stratified media technology, conf., Los Angeles, CA, USA (Jan. 1983) 4-82585  
 substrates and epitaxial materials, crystal growth, optical communication requirements, review 4-61833  
 superlattices, optical props. 4-104665  
 ternary antimonides, material prep., cryst. and epitaxial growth, review 4-98045  
 tetrahedrally bonded cpds., press. induced phase transition to NaCl-phase 4-61073  
 thermochemistry study of deep level defects 4-75894  
 wide band-gap, deep levels, review, book contrib. 4-88484  
 (Al,Ga)As heterojunctions, laser-induced defects, photochem. etching 4-113439  
 (Al,Ga)As, interrupted MBE growth, epitaxial InAs protection layer 4-114400  
 (Al,Ga)As, proton-bombarded, thermal annealing, elec. cond. recovery 4-98146  
 n-(Al,Ga)As/GaAs heterojunctions, hot-electron mobility study at moderate elec. fields 4-84678

## III-V semiconductors continued

- (Al,Ga)As/GaAs/Ge/Ga polar semicond. quantum well system, growth and optical props. 4-114314  
 (Al,Ga)As-GaAs double heterostructure laser technology 4-74539  
 Al/n<sup>+</sup>GaAs/n-GaAs Schottky contacts, MBE grown, field-enhanced tunnelling and barrier lowering study 4-114037  
 Al-GaAs Schottky diodes, barrier height modification using MBE 4-70937  
 AlAs, MOCVD growth 4-99329  
 AlAs/GaAs heterojunctions, interface struct., TEM and STEM studies 4-108728  
 AlAs-GaAs heterojunction barriers, inelastic tunnelling characts. 4-98710  
 AlAs-GaAs superlattice, MBE growth and luminescence 4-114403  
 AlGaAs CSP high-power laser diodes under modulation, freq. stabilisation using short guides 4-79190  
 AlGaAs CSP semiconductor laser, negative feedback stabilised for coherent FSK transmitter 4-107875  
 AlGaAs CSP-type lasers, linewidth enhancement estimation method 4-83577  
 AlGaAs, crystal growth by MOCVD (*Japanese*) 4-76684  
 AlGaAs DH diode lasers fabricated on monolithic GaAs/Si substrate 4-112408  
 AlGaAs DH semiconductor diode laser, passive mode locking, subpicosec. coherent pulse generation (*Japanese*) 4-60060  
 AlGaAs, epitaxial short wavelength visible laser diodes 4-107628  
 AlGaAs GaAs modulation doped heterostruct., persistent photocond. studies 4-98705  
 (AlGa)As heterolasers with distrib. feedback, polarisation effects 4-64708  
 AlGaAs heterostructure laser with distributed feedback 4-74538  
 AlGaAs heterostructure, photoelectroluminescence study 4-99193  
 (AlGa)As heterostructure laser diodes, psec. pulse generation 4-107632  
 AlGaAs high power TJS laser diodes, mech. stress compensation 4-96914  
 AlGaAs injection laser with external dispersion resonator using returning mirror 4-107641  
 AlGaAs injection laser, dispersion of linewidth enhancement factor 4-112425  
 AlGaAs, LED, radiative and nonradiative, recombination rates, meas. 4-112434  
 AlGaAs laser, 0.8  $\mu$ m, spectral width with 1/f noise 4-96892  
 AlGaAs laser, modulation freq. characts. for FM direct modulation 4-69463  
 AlGaAs laser amplifiers for fibre transmission, device characts. 4-69578  
 n-AlGaAs, MBE grown, deep electron traps 4-98570  
 AlGaAs, MBE growth of high purity layers, photolum. charact. 4-98474  
 AlGaAs mode locked laser, subpicosecond pulse generation 4-107697  
 AlGaAs nonabsorbing mirror constricted DH large-optical cavity diode lasers 4-83579  
 AlGaAs p/n graded band-gap solar cells grown by organometallic VPE 4-99961  
 AlGaAs phase-locked injection laser arrays with nonuniform stripe spacing 4-107672  
 AlGaAs quantum well lasers, threshold currents 4-79136  
 AlGaAs single- and multiple-stripe quantum-well heterostruct. laser diodes in external grating cavity 4-96902  
 AlGaAs TJS external cavity laser for fibre optic laser Doppler velocimeter 4-97096  
 AlGaAs:Si MBE layers, donor levels anal. 4-61316  
 AlGaAs/GaAs, single quantum well heterostruct. on Al<sub>0.30</sub>Ga<sub>0.70</sub>As buffers, MBE grown, electron mobility study 4-114029  
 AlGaAs/GaAs concentrator solar cells under high temp. and humidity conditions 4-66708  
 AlGaAs/GaAs heterostruct., 2D magnetotransport, electron heating effects 4-98736  
 (AlGa)As/GaAs modulation-doped heterostruct., optimisation for TEG-FET operation at room temp. 4-92804  
 AlGaAs/GaAs modulation-doped heterostructures, anomalous photomagnetoresist. 4-98702  
 AlGaAs/GaAs quantum wells, photoluminescence studies 4-93105  
 n-AlGaAs/GaAs selectively doped heterojunctions, high mobility electron gas 4-80657  
 AlGaAs/GaAs single quantum well structs., MBE grown, photoluminesc. props. 4-61863  
 AlGaAs/GaAs/AlGaAs single quantum well transistor with 2-D electron gas, logic device appl. 4-61443  
 p-AlGaAs/p-GaAs/n-GaAs solar cells, high efficiency 4-114910  
 AlGaAs/Si cascade solar cells, sensitivity and efficiency 4-85375  
 AlGaAs-GaAs heterojunction interfaces, deep levels, forward I-V and DLTS meas. 4-70915  
 AlGaAs-GaAs CW DH long-lifetime laser operated at room temp. 4-69474  
 AlGaAs-GaAs DH, photoluminescence efficiency 4-85006  
 AlGaAs-GaAs DH LED, efficiency for optical communications (*Spanish*) 4-69586  
 AlGaAs-GaAs heterojunction, two-dimens. electron gas gate control characts., optimum doping (*Chinese*) 4-114021  
 AlGaAs-GaAs laser with external dispersive cavity multimode rate-eqn. soln. of mode selection and tuning props. (*Chinese*) 4-91462  
 AlGaAs-GaAs modulation doped layers, 2-D electron gas, room temp. mobility, parallel conduction effects 4-76027  
 AlGaAs-GaAs short-cavity laser and its monolithic integration using microcleaved facets process 4-60064  
 AlGaAs-GaAs solar cells for space appls. 4-81543  
 AlGaAs-GaAs superlattice optical cavity multiple-quantum-well lasers, MBE grown, struct. and fabrication 4-64719  
 AlGaAs-GaAs superlattices, magnetisation meas., de Haas-van Alphen oscils. 4-98734  
 Al<sub>0.2</sub>Ga<sub>0.8</sub>As:Si MBE layers, electron trap conc., DLTS study 4-61317  
 Al<sub>0.3</sub>Ga<sub>0.7</sub>As, encapsulated with Si<sub>3</sub>N<sub>4</sub> films, disorder-activated modes, Raman spectra 4-80916  
 Al<sub>0.3</sub>Ga<sub>0.7</sub>As-GaAs distributed feedback surface emitting laser diode 4-112424  
 Al<sub>0.3</sub>Ga<sub>0.7</sub>As-GaAs heterojunction, selectively doped, persistent photocond. effect 4-98717  
 Al<sub>0.89</sub>Ga<sub>0.12</sub>As/GaAs:Zn diffused superlattice, X-ray rocking curve and backscatt. studies 4-113818  
 AlGa<sub>1-x</sub>As avalanche diodes, heat-and radiation-resistant, elec. props. 4-65728  
 AlGa<sub>1-x</sub>As, cathodoluminescence study 4-71449

## III-V semiconductors continued

- AlGa<sub>1-x</sub>As, correlation of photoluminescence and deep trapping 4-80537  
 n-AlGa<sub>1-x</sub>As epilayers, photoluminescence study 4-114316  
 AlGa<sub>1-x</sub>As epitaxial film, XPS study 4-93189  
 AlGa<sub>1-x</sub>As, Fourier anal. of optical spectra 4-99131  
 AlGa<sub>1-x</sub>As, graded-gap, effective resistance, temp. dependence 4-113961  
 AlGa<sub>1-x</sub>As heteroepitaxial struct. photoluminescence study 4-104673  
 AlGa<sub>1-x</sub>As layers, Rutherford backscatt. using 30 MeV <sup>16</sup>O ions 4-93170  
 AlGa<sub>1-x</sub>As, line broadening in photoluminescence spectra 4-109241  
 n-AlGa<sub>1-x</sub>As, MBE grown, deep electron traps, growth conditions and alloy composition influence 4-98558  
 AlGa<sub>1-x</sub>As MBE growth, Ga desorpt., AES and photoluminesc. studies 4-93220  
 AlGa<sub>1-x</sub>As MBE layers, free carrier conc., Raman scatt. study 4-84977  
 AlGa<sub>1-x</sub>As MBE layers, persistent photocond. centre (*Chinese*) 4-88525  
 AlGa<sub>1-x</sub>As p-n junctions, organometallic VPE, anomalous light sensitivity 4-92817  
 AlGa<sub>1-x</sub>As pulsed DH laser, emission characts., influence of longit. mode carrier-depend. shifts and gain profile 4-87335  
 AlGa<sub>1-x</sub>As, Si donor behaviour, effect of Al comp. 4-98709  
 AlGa<sub>1-x</sub>As solar cell structs., photoluminescence and spectral response 4-89404  
 AlGa<sub>1-x</sub>As:Be, conference, Charlotte, NC, USA (Nov. 1983) 4-73146  
 AlGa<sub>1-x</sub>As:Be, radiative recombinations 4-76515  
 AlGa<sub>1-x</sub>As:Si, grown by MBE, photoluminesc. composition depend. 4-84996  
 AlGa<sub>1-x</sub>As:Si, grown by MBE, photoluminesc. spectra, defect-related emissions 4-84997  
 AlGa<sub>1-x</sub>As:Si MOCVD layers, transport props. 4-92834  
 AlGa<sub>1-x</sub>As:Te(Sn) epitaxial films, carrier density changes due to band struct. modifications 4-61381  
 AlGa<sub>1-x</sub>As:Zn, CVD deposited, luminescence study 4-80985  
 AlGa<sub>1-x</sub>As/GaAs heterostructure, selectively doped, transient photocond. obs. 4-70862  
 AlGa<sub>1-x</sub>As/GaAs heterojunction FET, 2D electrons, cyclotron resonance studies 4-98743  
 AlGa<sub>1-x</sub>As/GaAs heterojunction, subband struct. at low temp. 4-104298  
 AlGa<sub>1-x</sub>As/GaAs single quantum well, exciton transport 4-88451  
 AlGa<sub>1-x</sub>As-GaAs concentrator solar cells, efficient circular contact grid design 4-72113  
 AlGa<sub>1-x</sub>As-GaAs double heterostructure optically pumped laser 4-96888  
 AlGa<sub>1-x</sub>As-GaAs heterostructures, 1/3 and 2/3 fractional quantum Hall effect, activation energies 4-92811  
 AlGa<sub>1-x</sub>As-GaAs heterostruct., anal. of quantised Hall resist. at finite temps. 4-98727  
 AlGa<sub>1-x</sub>As-GaAs heterojunction, EMF due to dynamic deform. 4-98746  
 AlGa<sub>1-x</sub>As-GaAs injection lasers, longitudinal mode selection obs. 4-79153  
 AlGa<sub>1-x</sub>As-GaAs injection laser self-modulation associated with external optical feedback 4-112440  
 AlGa<sub>1-x</sub>As-GaAs multiple well quantum well lasers, wavelength modification 4-64705  
 AlGa<sub>1-x</sub>As-GaAs multiple quantum well laser structures, MBE growth conditions 4-91465  
 AlGa<sub>1-x</sub>As-GaAs twin-channel substrate mesa guide laser with antirefl. coatings, single longit. mode operation 4-83619  
 AlGa<sub>1-x</sub>As layer waveguides, light absorpt. 4-103011  
 AlGa<sub>1-x</sub>AsSb<sub>1-y</sub>/GaSb heterostruct., conditions for LPE growth 4-114429  
 AlGa<sub>1-x</sub>As<sub>1-y</sub>Sb<sub>y</sub> heterojunction photocells, LPE fabrication 4-81559  
 AlGaInP/GaInP DH visible light lasers, MOCVD grown, room temp. pulsed operation 4-69445  
 AlGaInPAs lattice matched to GaAs, LPE growth, photolum. obs. 4-70581  
 AlGaIn<sub>1-x-y</sub>Sb<sub>y</sub> epitaxial layers, luminescence studies 4-76505  
 AlGaSb, LPE, substrate treatment optimisation, carrier conc., Raman spectra, photoluminesc. 4-93235  
 Al<sub>0.17</sub>Ga<sub>0.83</sub>Sb/GaSb multi-quantum well lasers, room-temp. operation, MBE growth 4-60033  
 AlGa<sub>1-x</sub>Sb multilayer heterostructures, coherent light polarisation props. 4-71460  
 AlGa<sub>1-x</sub>Sb-InAs<sub>1-y</sub>Sb<sub>y</sub> heterostructures, LPE growth 4-104097  
 AlInAs/GaInAs avalanche photodiodes and AlInAs electroabsorption p-n photodiodes grown by MBE 4-69591  
 AlInAs/GaInAs heterojunctions and superlattices, 2-D magnetophonon resonance 4-98740  
 Al<sub>0.48</sub>In<sub>0.52</sub>As/Ga<sub>0.47</sub>In<sub>0.53</sub>As avalanche photodiode for long wavelength fibre optic communication, MBE growth 4-79337  
 Al<sub>0.48</sub>In<sub>0.52</sub>As/n<sup>+</sup>Ga<sub>0.47</sub>In<sub>0.53</sub>As, low resist. alloyed ohmic contacts 4-84692  
 Al<sub>1-x</sub>In<sub>x</sub>As, epitaxial growth on InP 4-104735  
 Al<sub>1-x</sub>In<sub>x</sub>As, nominally undoped, MBE growth and charact. 4-98472  
 AlN, sputter deposited, electron binding energy Auger and XPS study 4-75820  
 AlSb-GaSb superlattice, MBE growth and luminescence 4-114403  
 Au-InP junction 4-84625  
 BN RF sputter deposited films, struct. and optical props. rel. to sputtering conditions 4-88415  
 CaAs:Cr LEC wafer, Cr<sup>2+</sup> distribution, EPR studies 4-98124  
 CdS-InP heterojunctions, elec. and photoelec. props., solar cell appl. (*Russian*) 4-98713  
 CdTe-InSb MIS struct., electronic props. 4-98778  
 crystallisation by nonequilibrium electroliq. epitaxy, molten soln. parameter determ. 4-75817  
 (Ga,Al)As/GaAs double heterostructures, LPE, struct. and lasing characts. rel. to As vapour press. 4-66249  
 (Ga,In)(As,P), adducts in MOVPE 4-71575  
 (Ga,In)As, adducts in MOVPE 4-71575  
 Ga-Al-As, luminescence lineshapes of electron-hole plasma 4-109242  
 Ga-Al-As system, MOVPE, current status for optoelectronic appls. 4-104737  
 Ga-Al-As/GaAs, liq. epitaxy capillary effect 4-98408  
 Ga-As crystal dielectric constant meas. in 100 GHz range (*Japanese*) 4-106330  
 Ga-In-As-P system, VPE of mixed III-V compounds 4-71578  
 Ga-In-P-As system, LPE, growth kinetics 4-88426

## III-V semiconductors continued

- Ga-In-P-As system, MOVPE, current status, for optoelectronic appls. 4-104737
- Ga-In-Sb phase diagram, thermodynamic data, associated soln. model, book contrib. 4-89031
- Ga-P solution-melt system, diffusion coeff. determ. by X-ray microanalysis 4-88320
- GaAs, plasma-enhanced epitaxy, low temp. 4-99330
- GaAs:Cr, semi-insulating, Four-wave mixing using photorefractive effect, optical processing appl. 4-74585
- GaAs/Ni reactive interface, soft X-ray photoemission spectra studies 4-113820
- GaAlAs BH 100 Mbit/s laser diode terminal with optical gain, for fibre-optic LANs 4-112586
- GaAlAs BH window lasers, 11 GHz direct modulation bandwidth 4-112410
- GaAlAs bright visible-range injection laser development 4-69441
- GaAlAs buried multi-quantum-well laser fabricated by diffusion induced disordering 4-74547
- GaAlAs buried multi-quantum well lasers fabricated by diffusion-induced disordering 4-91452
- (GaAl)As cleaved coupled-cavity laser anal. 4-96900
- (GaAl)As cleaved-coupled-cavity lasers, coupling strength study 4-91459
- GaAlAs diode laser, picosecond gain meas. 4-107638
- (GaAl)As diode lasers, spectral characteristics at 1.7K 4-112411
- GaAlAs electroabsorption modulators, monolithically integrated array 4-103006
- (GaAl)As heterojunction laser, optically controlled two-component 4-107640
- GaAlAs laser, MESFET and photodiode, monolithic optoelectronic integration 4-74747
- GaAlAs laser, picosecond pulse generation by optoelectronic feedback 4-96885
- GaAlAs laser, simultaneous wavelength and power stabilisation using single detector scheme 4-91456
- GaAlAs laser, wavelength stabilisation using integrated optic Fabry-Perot interferometer 4-91457
- GaAlAs laser diode coupled to an external cavity intensity noise suppression and modulation characts. 4-79144
- GaAlAs laser diode optical switches, isolation characteristics 4-107680
- GaAlAs laser oscillating in single longit. mode, LF feedback noise 4-96909
- GaAlAs laser picosecond pulse temporal coherence props., directly modulated and freq. stabilised optical communication system appls. 4-74509
- GaAlAs lasers, catastrophic and latent damage due to elec. transients 4-79146
- GaAlAs lasers, transverse-mode stabilised MOCVD grown, with embedded confining layer on optical waveguide 4-69443
- GaAlAs light sources, radiative coeffs., carrier dependence 4-64703
- GaAlAs material epitaxial growth, devices for optical communications 4-74746
- GaAlAs, optical communication through low-visibility atmosphere using a CW diode laser 4-112589
- GaAlAs, proton energy loss straggling meas. for nucl. profiling appl. 4-70246
- GaAlAs semiconductor laser fabrication, integration with fibre V-groove alignment struct. 4-96948
- GaAlAs single quantum well size effect modulation light sources 4-97014
- (GaAl)As transverse-mode stabilised laser diodes, MOCVD growth 4-96912
- GaAlAs V-groove lasers, 4 ps light pulses generation 4-69407
- GaAlAs very high speed lasers and detectors for integrated optoelectronic devices 4-96889
- GaAlAs/GaAs quantum-well lasers, organometallic VPE and MBE grown, developments and exp. study 4-69442
- GaAlAs/GaAs selectively doped heterojunction, electron conc., FET appl. 4-98703
- GaAlAs/GaAs surface-emitting injection laser, pulsed oscill. 4-79175
- GaAlAs/GaAs surface emitting injection laser, room-temp. pulsed operation 4-112416
- GaAlAs/GaAs twin channel laser with high CW power and low beam divergence 4-74548
- (GaAl)As-GaAs DH lasers,  $D_2^+$  bombardment isolated stripe geometry (Chinese) 4-112431
- GaAlAs-GaAs DH lasers, narrow-channelled substrate stripe-type, characts. meas. and anal. (Chinese) 4-112433
- GaAlAs-GaAs heterostructure, nuclear profiling of Al 4-98123
- GaAlAs-GaAs integrated optical repeater 4-97143
- GaAlAs-GaAs modulation dopd heterostruct., self-consistent variational calcs. and alloy scatt. 4-98733
- GaAlAs-GaAs-GaAlAs single quantum well struct., resonant tunnelling to 2.5 THz 4-70926
- Ga<sub>0.4</sub>Al<sub>0.6</sub>As-GaAs heterostructures, LPE growth, layer height profiles rel. to convection and cooling rates 4-66248
- Ga<sub>1-x</sub>Al<sub>x</sub>As:(Se), dopant incorporation during MBE growth 4-99320
- Ga<sub>1-x</sub>Al<sub>x</sub>As, carrier transport under impurity radiative recombination conditions 4-104211
- Ga<sub>1-x</sub>Al<sub>x</sub>As, crystalline struct., two-phonon Raman spectra study 4-71385
- Ga<sub>1-x</sub>Al<sub>x</sub>As, spatial dielec. functions, site and comp. depend. 4-104136
- Ga<sub>1-x</sub>Al<sub>x</sub>As superlattices, acoustic modes, Brillouin and Raman scatt. study 4-80928
- p-Ga<sub>1-x</sub>Al<sub>x</sub>As:Be-p-GaAs:Be-n-GaAs:Si heterojunction LPE growth for solar cells 4-109334
- Ga<sub>1-x</sub>Al<sub>x</sub>As:Zn, (Se), doping in MOCVD growth, carrier conc. and cond. 4-88982
- Ga<sub>1-x</sub>Al<sub>x</sub>As/GaAs solar cell with antiref. coating, LPE grown, design, fabrication and characts. (Polish) 4-114904
- Ga<sub>1-x</sub>Al<sub>x</sub>As-GaAs, Raman scatt. theory 4-76460
- Ga<sub>1-x</sub>Al<sub>x</sub>As-GaAs heterostructure, LPE grown, dislocation extension and density distrib. (Chinese) 4-113449
- Ga<sub>1-x</sub>Al<sub>x</sub>As-GaAs interface, fractional quantum Hall effect in a two-dimensional hole system 4-108930
- Ga<sub>1-x</sub>Al<sub>x</sub>As-GaAs/GaAs (001) superlattices, structural parameters, X-ray diff. 4-84257
- Ga<sub>2</sub>Al<sub>1-x</sub>As and Si solar cells, beam splitting concentrator, optical characterisation 4-66665
- Ga<sub>2</sub>Al<sub>1-x</sub>As/GaAs system, elastic surface waves, Green's function anal. 4-108695
- Ga<sub>1-x</sub>Al<sub>x</sub>P, epitaxial structs., luminesc. study 4-85011

## III-V semiconductors continued

- Ga<sub>1-x</sub>Al<sub>x</sub>P p-n structures, epitaxially grown, plastically and elastically deformed, quantum efficiency spectra 4-84651
- Ga<sub>1-x</sub>Al<sub>x</sub>Sb, phonon dispersion calcs. 4-88252
- GaAlSbAs-GaSb injection laser, operation and luminescence study 4-74508
- Ga<sub>1-x</sub>Al<sub>x</sub>Sb<sub>1-x</sub>As<sub>x</sub>/GaSb epitaxial films As segregation coeff. and distrib. over thickness 4-75692
- Ga<sub>1-x</sub>Al<sub>x</sub>Sb<sub>1-x</sub>As<sub>x</sub>/GaSb, LPE, phase equilib. rel. to lattice mismatch strain 4-93236
- GaAs (100), CVD, low press., in Ga-HCl-AsH<sub>3</sub>-H<sub>2</sub>-H<sub>2</sub>S system, modelling of S doping 4-99333
- GaAs (100), chemical etching and annealing 4-65722
- GaAs (100), clean surface prep. using Ar<sup>+</sup> ion bombard. 4-104886
- GaAs (100), laser irradi., photoemission of electrons 4-81116
- GaAs (100), reconstructed, electron microscopy and diff. studies 4-108690
- GaAs (100) 4-70546
- GaAs (100) etch pits and cryst. defects, ellipsometry and reflectivity studies 4-84492
- GaAs (100) surfaces, XPS anal. after technology-etchant appl. 4-93196
- GaAs (110), <sup>20</sup>Ne<sup>+</sup> ion yield and neutralisation, 300-1200 eV 4-76581
- GaAs (110), adsorption of H, EHMO method calc. (Chinese) 4-113787
- GaAs (110), cleaved, surface steps and dislocations, reflection electron microscopy study 4-65529
- GaAs (110), H<sub>2</sub>O adsorption, TDS and LEED studies 4-65568
- GaAs (110), H<sub>2</sub>O chemisorption and Ga and As species-specific densities of states 4-80373
- GaAs (110), initial oxidation, core-level photoemission study 4-93195
- GaAs (110), O<sub>2</sub> chemisorption, photon-simulation, AES and EELS studies 4-113804
- GaAs (110), surface atomic geometry, photoemission spectroscopy determ. 4-108684
- GaAs (110) and GaAs/Au(Pd) interfaces, high energy ion channelling studies 4-65318
- GaAs (110) surface, randomly stepped, ordering kinetics, LEED study 4-84495
- GaAs (110) with adsorbed H, H<sub>2</sub>, temp. programmed desorption study 4-92528
- GaAs (110)-Al interface form. at low temp., electronic and struct. props. 4-84695
- GaAs (110)-ZnSe interface, LEED and AES characterisation 4-84517
- GaAs (111), adsorption of O, XPS study (Chinese) 4-85077
- GaAs (111), direct electron beam writing of oxide layer 4-92235
- GaAs (111), relaxation effects (Chinese) 4-70887
- GaAs (111) A surface, contact with In-Ga-As-P saturated liq., Auger anal. 4-104046
- GaAs (111) surface, vacancy-induced 2×2 reconstruction 4-75764
- GaAs (111)×2 surface, multilayer reconstruction model 4-84497
- GaAs (111)(2×2) surface, struct., vacancy buckling model, LEED study 4-70533
- GaAs, acceptor level, 78 meV, luminescence and Raman scatt. studies 4-70704
- GaAs, amorphous, high-defect-density, subpicosecond carrier trapping 4-80621
- GaAs, amorphous, MBE grown, local struct., EPR and NMR studies 4-104492
- GaAs amorphous thin films, transient annealing, Raman scatt. study 4-80926
- n-GaAs, anodic oxidation, surface treatment effects 4-114702
- GaAs, ballistic large-wavevector phonon propag., direct obs. 4-61013
- GaAs, ballistic photocurrents, mag. field influence 4-70866
- GaAs, Bridgman ingots, photocond., 80-300K, CR and O impurity effects 4-65705
- GaAs, carrier vel. fluctuations in steady-state and transient regimes, Monte Carlo study 4-80637
- GaAs, cleaved, work function var. rel. to cooling 4-88556
- GaAs, compensation resulting from N ion implantation 4-104150
- GaAs, conduction band splitting for k along [110] 4-108777
- n-GaAs, conduction band struct. in 2 and 3 valley band models 4-70649
- GaAs, conduction bands, strain-induced splitting 4-75854
- GaAs, contour maps of EL2 deep level, dislocations 4-80530
- GaAs crystal, numerical simulation of horizontal Bridgman growth 4-66212
- GaAs, crystal and amorphous, pulsed laser irradi. under O<sub>2</sub> and silane atmospheres, O incorporation and losses 4-80091
- GaAs crystal sensor in fibre-optic thermometer, temp. meas. by photoluminescence (Danish) 4-78315
- GaAs, deep acceptor, Hall effect obs. and photoluminescence 4-80532
- GaAs, deep centre point defect introduction 4-108819
- GaAs, deep centres, electron probe method anal. 4-104158
- GaAs, deep impurity levels, ENDOR and ESR spectra 4-84594
- GaAs, deep level wavefunctions, behaviour in shallow energy region (Chinese) 4-92650
- GaAs, deep levels associated with vacancy-impurity pairs 4-92662
- GaAs, deep-level wavefunctions with energies near band edges 4-92656
- GaAs, defect anisotropy following electron irradiation 4-75534
- GaAs, defect visualisation by oxidation in water 4-92194
- GaAs, dislocations and point-defect complex formations, thermal stability 4-103758
- GaAs, doped, cond. electron spin relax. times, precession mechanism, spin splitting 4-98948
- GaAs doping superlattices, bipolar cond., tunability 4-70914
- GaAs doping superlattices, weak localisation and magnetoresist. 4-98720
- GaAs double heterojunction injection laser, constructional details (Dutch) 4-83609
- GaAs, dry etching induced damage 4-81312
- GaAs, ductile brittle transition in (001) surface layers in single crystals, effect of medium 4-70266
- GaAs, E<sub>1</sub> and E<sub>2</sub>, appl. of DLTS and deep level optical spectroscopy 4-108815
- GaAs, EL2 and EL0 midgap levels, electron emission in strong elec. fields 4-88510
- GaAs, EL2 defect, technological and physical aspects 4-75891
- GaAs, electrical properties and impurity states 4-75963
- GaAs, electroluminescence and photoluminescence in aq. redox electrolyte 4-88584
- GaAs, electroluminescence spectra of free excitons, optical resonances 4-88883
- n-GaAs, electron energy relax. due to 2TA phonons 4-92324
- n-GaAs, electron irradi., dislocation glide, TEM studies 4-92207

## III-V semiconductors continued

- GaAs, electron irradi., electronic struct. of E3-defects 4-70720  
 GaAs, electron irradi., surface electron energy spectrum, photoemission studies 4-88554  
 GaAs, electron irradiated, carrier-capture cross sections meas. technique 4-61394  
 n-GaAs, electron irradiated, As anti-site defects, IR spectra and EPR 4-84317  
 GaAs, electron traps, midgap, and multimetastable states, photoquenching studies 4-88466  
 GaAs, electron traps, props. and nature 4-75890  
 GaAs, electron- and proton-irradiated, elec. props. 4-75975  
 GaAs, electron-hole plasma-density meas. 4-61408  
 GaAs, electronic density of states, recursion coeffs., linear prediction theory 4-98502  
 GaAs, electronic structure of (100) and (111) faces, angle resolved photoemission 4-84559  
 n-GaAs, emission band at 1.35 eV, doping and temp. variations 4-76519  
 GaAs, encapsulated annealing in AsH<sub>3</sub>, surface protection 4-88378  
 GaAs epitaxial diode struct., nonequilibrium carrier lifetimes 4-70920  
 GaAs epitaxial film, MBE grown, capture of accidental impurities, influence of growth conditions 4-108743  
 GaAs epitaxial films, 1/f noise under conditions of strong geometric magnetoresist. 4-61427  
 GaAs epitaxial films, line impurity photocond. spectra, fine-struct. splitting 4-65761  
 GaAs epitaxial high-purity layers, low-pressure MOCVD growth 4-61861  
 GaAs epitaxial layer, homogeneity and thickness meas. by IR flaw detection method 4-109609  
 GaAs epitaxial layer, processing technology and characts. (Polish) 4-113827  
 GaAs, epitaxial layer growth in multiwafer VPE system, IMPATT device fabrication 4-104738  
 GaAs epitaxial layers, MOCVD, surface morphology and elec. props. 4-84493  
 GaAs epitaxial selective regions in Si substrate windows, struct. perfection 4-75812  
 GaAs, epitaxial short wavelength visible laser diodes 4-107628  
 GaAs epitaxial structs., photomemory effect, influence of deep levels 4-104261  
 GaAs, excitonic polaritons in elec. fields at surfaces 4-92633  
 GaAs, excitons, self-energy, many particle system calculations 4-98536  
 GaAs, existence of B<sub>As</sub> impurity antisite centres, IR absorption lines study 4-71413  
 GaAs FET microwave refractometer for tropospheric studies (French, English) 4-63778  
 GaAs, far IR optical props. at 6, 300K, amplitude and phase refl. spectra 4-104594  
 GaAs, film growth on insulators by artificial epitaxy 4-61873  
 GaAs flash annealing of Mg implants using incoherent radiation 4-84306  
 GaAs, free carrier lifetime from photoluminescence studies 4-80988  
 n-type GaAs free-carrier absorption, quantum mechanical perturbation theory 4-80893  
 GaAs, gas phase epitaxy, doping and impurity trapping 4-108745  
 GaAs glass-bonded NEA transmission photocathode, XPS study 4-104716  
 GaAs, growth from melt and elec. props. 4-99300  
 GaAs growth using OMVPE, electronic and optical props. 4-114402  
 GaAs, H ion implanted, range and damage distrib. 4-103774  
 GaAs, heteroepitaxial growth on (0001) mica by ionised vapour evaporation under elec. field 4-104100  
 GaAs heterojunctions and homojunctions, deep levels, tunnel spectra meas. 4-84685  
 GaAs heterolayer, low temp. two-dimens. mobility 4-108933  
 GaAs, high field transport of holes 4-80598  
 GaAs high-field transport, model 4-88512  
 GaAs, high-purity, in mag. fields, donor. transition anomalous line broadening 4-109214  
 GaAs, homo- and single heterostructure injection lasers, time delay characts. 4-107633  
 n-GaAs, hopping cond. freq. depend. 4-70806  
 GaAs, hot carrier transient response, vel. overshoot 4-92736  
 GaAs, hot photoluminescence polarisation and spectrum 4-61743  
 GaAs, IR props. of heavily implanted semiconductors 4-104587  
 GaAs impact-ionized plasma instability, delay time estimation, Monte Carlo technique 4-70853  
 GaAs, implanted layers, elec. props., Si<sub>3</sub>N<sub>4</sub> encapsulation effects 4-98609  
 GaAs, impurities identification by magneto-optical photoluminescent spectroscopy 4-60945  
 GaAs, impurity photocurrent and deep level spectroscopy 4-70865  
 GaAs injection laser pulse duration meas. 4-64728  
 GaAs injection lasers, short pulse excitation, threshold current temp. dependence 4-74506  
 GaAs integrated optical device fabrication, Cl<sub>2</sub>-Ar reactive ion etching technique 4-87483  
 GaAs, interrupted MBE growth, epitaxial InAs protection layer 4-114400  
 GaAs, inverse dielectric matrix, direct calc. 4-92645  
 GaAs, ion beam assisted etching using focused ion beam 4-93431  
 GaAs, ion bombarded heated specimens, surface comp., AES and SIMS anal. 4-113510  
 GaAs, ion implanted, ion implanted, diffusion of Be and Mn during damage recovery 4-104002  
 GaAs, ion implanted, photolum. after laser annealing 4-76525  
 GaAs, ion implanted, transient capless annealing, appl. to IC fabrication 4-103779  
 GaAs, irradi., E3 centre accumulation, effect of defect charge state 4-60966  
 GaAs, isotope scatt. of large wave vector phonons 4-108564  
 GaAs JFET low-noise high-speed optical receiver for optical fibre systems 4-74743  
 GaAs, k.p interaction and effective mass, band gap depend. 4-113850  
 GaAs, LEC crystal growth in mag. field (Japanese) 4-88960  
 GaAs, LEC grown, EPR identification of As<sub>Ga</sub> antisite defects 4-71178  
 GaAs, LEC grown, improved elec. uniformity by high temp. annealing 4-65684  
 GaAs, LEC growth in vertical mag. field, homogeneity anal. 4-76661  
 GaAs LEC substrate, characterisation of impurities and microdefects (Japanese) 4-103778  
 GaAs LEC wafers, undoped, defect characterisation by electron-beam-induced charge collection microscopy 4-60932

## III-V semiconductors continued

- GaAs, LPE growth, deep intrinsic centers, anisotropic capture 4-113897  
 GaAs, LPE growth and nonequilib. deep centre trapping 4-108744  
 GaAs, LPE growth rates 4-93237  
 GaAs LPE layers, residual impurities, growth soln. baking effects 4-92226  
 GaAs LPE layers, space-charge scatt. and mobility killers 4-84714  
 GaAs LPE layers, surface morphology, effect of substrate misorientation (Chinese) 4-84521  
 GaAs LSI, Si<sub>3</sub>N<sub>4</sub> film deposition by plasma-enhanced CVD 4-71569  
 GaAs laser, electron-beam-pumped, excitation density distrib. 4-79162  
 GaAs, laser alloyed Sn layers, elec. props., surface damage 4-99622  
 GaAs laser diode and LED, coaxial transverse junction struct., design and characts. 4-87357  
 p-GaAs, laser material, intervalence band absorpt. and Auger recomb. 4-80885  
 GaAs, laser-enhanced reactive ion etching in CCl<sub>4</sub>-H<sub>2</sub> mixture 4-71747  
 GaAs, laser-induced Si diffusion from deposited Si<sub>3</sub>N<sub>4</sub> film 4-60958  
 GaAs, laser-induced sputtering and damage 4-71485  
 GaAs, lateral growth over W gratings by CVD, application to FET transistors 4-81148  
 GaAs layers, MBE grown on Ge islands on insulator, zone melting recrystallisation; grain boundaries, photoluminescence obs. 4-84524  
 GaAs, light scatt., nonequilibrium electron-hole plasma 4-104616  
 GaAs, liquid encapsulated Czochralski growth, deep level study 4-98569  
 GaAs, long-lived short wavelength TA phonons propag., Monte Carlo simulation 4-61015  
 GaAs, MBE, extrinsic effects in RHEED 4-98476  
 GaAs MBE films, growth and elec. props. (Chinese) 4-84523  
 GaAs, MBE grown, surface defects obs. 4-61246  
 GaAs, MBE growth, As source 4-99321  
 GaAs, MBE growth, dynamic RHEED obs. 4-92572  
 GaAs MBE growth, free of oval defects 4-98475  
 GaAs, MBE growth, role of As and As<sub>2</sub> in controlling quality, theoretical studies 4-98477  
 GaAs, MBE growth in diffusion pumped systems 4-85105  
 GaAs MBE growth of high purity layers, photolum. charact. 4-98474  
 GaAs, MBE growth on Si (100), optical props. 4-88975  
 GaAs, MBE growth using trimethylgallium as a Ga source 4-81138  
 GaAs MBE layers, elec. props. of oval defects, FET appl. 4-92574  
 GaAs, MBE layers, spatially-resolved luminescence at oval defects 4-75803  
 GaAs MBE-grown (001) surface, band bending, photoemission studies 4-99276  
 GaAs MIS solar cells, I-V characts. under illum., ideality factor and barrier height 4-93625  
 GaAs, MOCVD grown, deep electron traps, DLTS obs. 4-84585  
 GaAs, MOCVD growth, doping profiles, H<sub>2</sub>Se memory effects 4-81152  
 GaAs, MOCVD growth 4-99329  
 GaAs MOS structures with anodic oxides, defect states, DLTS study 4-114043  
 GaAs, magnetic circular dichroism-ODMR study of EL2 defect 4-104151  
 GaAs, material and devices, thermal wave imaging 4-75711  
 GaAs, melting in Au contacts, in situ X-ray diff. study 4-88593  
 GaAs, midgap level surface density, heat treatment and capping effects 4-114011  
 GaAs, muonium states, positive muon depolarisation 4-71243  
 GaAs n<sup>+</sup>-p-n<sup>+</sup> ballistic struct., I-V charact. calc. (Chinese) 4-80659  
 GaAs, n-p-i crystals, doping to alter electronic and optical props. (German) 4-98590  
 GaAs, n-type, thin films, field-assisted photomagneto-ec. effect 4-80626  
 GaAs n<sup>+</sup>-n-n<sup>+</sup> structures, high field reson. magnetotransport meas. 4-104295  
 GaAs, negative differential cond. at transit reson. frequencies 4-84638  
 GaAs, negative magnetoresist. associated with quantum localisation correction to cond. 4-61400  
 GaAs, neutral impurity scatt., far-IR cyclotron resonance study 4-71185  
 GaAs, neutral impurity scatt., far-IR cyclotron reson. study 4-92964  
 GaAs, neutron irradi., antisite defects, associated defect model, ESR studies 4-88166  
 GaAs, neutron irradi., defect form., EPR obs., comparison with Cu halides 4-70224  
 GaAs, neutron irradi., optical absorption coeff., spectral depend. 4-99137  
 GaAs, ohmic contact brazing using apparatus for pulsed light heat treatment 4-81313  
 GaAs ohmic contacts formation obs., high-temperature substage for a scanning electron microscope 4-101989  
 GaAs, optical bistability, physics and apps. (Italian) 4-107729  
 GaAs optical bistable device, all-optical data switching in optical fibre link 4-91529  
 GaAs, optical guided-wave monolithic interferometer 4-112561  
 GaAs, optical spin orientation of  $\Gamma^{15}_2$  conduction band-electrons, photoemission study 4-66188  
 GaAs optical waveguide modulator with low loss and high speed, fabrication by RIE 4-60148  
 GaAs, optoelectronic switching, laser controlled, photoconductivity meas. (German) 4-84646  
 GaAs, p-n junctions, spectral distrib. of avalanche breakdown radiation (Russian) 4-98715  
 GaAs, p-n-p doped submicron structures, LPE grown, n-channel conductivity modulation 4-61447  
 GaAs p-n-p-n superlattices, LPE growth 4-80665  
 GaAs, phonon frequencies 4-75626  
 GaAs, photoacoustic absorpt. meas. by laser heterodyning (Chinese) 4-58893  
 GaAs, photoacoustic signal meas. by laser heterodyne at high temps. 4-106388  
 GaAs photodetectors, high speed, carrier dynamics, luminesc. study 4-111201  
 GaAs photoemission, monochromatic electron intense source 4-71510  
 GaAs, photoenhanced oxidation, AES and work function meas. 4-81302  
 GaAs, photoexcited, heat pulse propag., large k-vector phonons obs. 4-61014  
 GaAs, photoexcited, phonon transport 4-92322  
 GaAs photoexcited carriers, femtosecond orientational relax. 4-98634  
 GaAs, photoexcited cond. electron spin polarisation precession in band-bending region 4-88945  
 GaAs, photoluminescence characterisation of impurities and defects 4-88876

## IV semiconductors continued

- GaAs, photoluminescence intensities, computer-controlled mapping 4-104650  
 GaAs, photon-assisted dry etching using ArF laser 4-114689  
 GaAs, picosecond photoconductors, circuit limits to time resolution 4-98661  
 GaAs planar structure Schottky barrier photodiode, ultrahigh speed 4-111200  
 GaAs, plasma-assisted epitaxial growth in  $H_2$  plasma, elec. props. 4-104740  
 GaAs, plastic deform., yield stress, photoluminescence, effect of impurity-vacancy complexes 4-70261  
 GaAs pnp quantum well structs., reson. tunnelling 4-104299  
 n-GaAs, power broadening and nonlinear far IR magnetophotocond. 4-108897  
 GaAs, proton-bombarded, thermal annealing, elec. cond. recovery 4-98146  
 GaAs, pulsed laser-assisted MBE technique 4-104733  
 GaAs quantum well lasers, visible, grown by MBE 4-91454  
 GaAs, Raman probe of Brillouin zone for nonequilib. phonons 4-66045  
 GaAs, Raman scatt. and two-phonon density of states 4-66046  
 GaAs, Raman scatt. study of phonon-surface polarizations 4-80931  
 GaAs, reactive ion etching in  $CCl_4/H_2$  and  $CCl_4/O_2$ , AES, Raman spectra 4-81306  
 GaAs, reactive ion etching, H mixing effects in Cl-containing gases 4-89148  
 GaAs, relaxation of hot electron energy, surface plasmons 4-98631  
 n-GaAs, ring structure, self-excited oscillations, microwave generation 4-70948  
 GaAs, SAW characterisation of surface and interface states 4-98681  
 GaAs, scanning DLTS investig. 4-75892  
 GaAs Schottky barrier photodetectors for microwave fibre optic links 4-92793  
 GaAs Schottky barrier photodetectors for microwave fiber optic links 4-101918  
 GaAs Schottky barrier struct., defects and elec. props. 4-108924  
 GaAs Schottky diodes, deep levels, photocapacitance spectra 4-61410  
 GaAs Schottky diodes, transport mechanism, deep centre effects 4-88558  
 GaAs, selectively excited luminesc. 4-104639  
 GaAs, semi-insulating, 0.635 eV photoluminescence band, EL2 level 4-114315  
 GaAs, semi-insulating, deep donor conc., dislocations and elec. resist. 4-103781  
 GaAs, semi-insulating, elec. and photoelectronic props., book contrib. 4-88544  
 GaAs, semi-insulating, elec. props. for microwave electronics 4-108846  
 GaAs, semi-insulating, surface cond. mechanism, space-charge-limited current leakage 4-70901  
 GaAs, semi-insulating, undoped and low Cr doped, LEC grown, photoluminescence props., whole ingot annealing effects 4-84994  
 GaAs, semi-insulating LEC grown, impurity distribution, cathodoluminesc. study 4-88885  
 GaAs, semi-insulating optical photogenerated traps 4-108875  
 GaAs semi-insulating single crystal growth by LEC method, IC appls. (Japanese) 4-104728  
 GaAs semi-insulating substrate monolithically integrated laser diode, photo monitor and electric ccts. 4-60179  
 GaAs semi-insulating substrate, inhomogeneity characterisation, expt. study 4-65759  
 GaAs, shallow acceptors, ground state calc., allowing for valence band corrugations 4-108817  
 n-GaAs, shallow impurity photoexcitation line narrowing in an elec. field 4-80970  
 GaAs, short  $n^{++}nn^{++}$  section, hot electron effects 4-61385  
 GaAs, single cryst. growth of large size, vertical mag. field appl. LEC apparatus 4-85094  
 GaAs, single cryst. growth by liquid encapsulated Czochralski method 4-114377  
 GaAs single domain growth on Ge (100) by MOCVD 4-99342  
 GaAs single quantum wells, low temp. exciton trapping on interface defects, photolum. 4-93111  
 GaAs solar cells, equivalent electron fluence for space qualification 4-77097  
 GaAs solar cells, fabrication using plasma-deposited  $Si_3N_4$  as oxidation mask 4-89409  
 GaAs solar cells, improved performance design for space appl. 4-81552  
 GaAs solar cells, short-circuit current red. caused by proton irradi. damage 4-72108  
 GaAs solar cells, state-of-the-art review 4-81543  
 GaAs solar cells for power supplies to artificial satellites 4-99972  
 GaAs, spectra of quantum yields and photoemission (Polish) 4-93190  
 GaAs, spectroscopy conf., Cambridge, MA, USA (Nov. 1983) 4-95025  
 GaAs, spin doublet, mag. field depend., photocond. obs. 4-104255  
 GaAs, spin polarised photoemission 4-88929  
 GaAs, sputter etch induced electrically active defects, H passivation 4-108918  
 GaAs, stoichiometry, X-ray intensity meas. of quasi-forbidden reflections 4-84416  
 GaAs substrate, annealing as gettering technique prior to MBE growth 4-99615  
 GaAs substrate, organo-metal CVD growth of Fe and  $FeAs_2$  films, AES study 4-61868  
 GaAs substrate for Ge:Sb(Ga) films, doping and elec. props. study (Russian) 4-70182  
 GaAs substrate for  $SrF_2$  single cryst., electron beam resist. and dielec. for insulator/semicond. struct. 4-98758  
 GaAs, substrate for Zn piezoelectric membranes, SAW characts. and transducers 4-104058  
 GaAs substrates for GaAs ICs, growth processes 4-99299  
 GaAs Surface, (110), Fermi level pinning, elec. field induced Raman scatt. 4-88845  
 GaAs surface, phase conjugation, reflecting grating recording by plasma refl. 4-97003  
 GaAs, surface cleaning by ion bombardment 4-88213  
 GaAs, surface disordering by picosecond laser pulses 4-92233  
 GaAs, surface electronic structure, angle resolved photoemission spectra 4-91183  
 GaAs surface preparation, chemical etchants, comparative study 4-114701  
 GaAs surface structure (110), mech. destruction and electron bombardment effects, XPS obs. (Russian) 4-113772

## III-V semiconductors continued

- GaAs, tetrahedrally bonded, anisotropy of Compton profile 4-99217  
 GaAs, thermal cond., hydrostatic press. depend. 4-61157  
 GaAs, thick-film silk-screen deposition technique 4-109320  
 GaAs thin-film semiconductor structure with negative differential conductivity, EM wave propag. anal. 4-79017  
 GaAs, transient hole transport, Monte Carlo study 4-80602  
 GaAs transistors and ICs, advantages and characts. (German) 4-98678  
 GaAs, trap parameters meas. by photo-excited DLTS (Japanese) 4-80544  
 GaAs, US attenuation and nonlinearity const., temp. dependence 4-108552  
 GaAs, undoped, beam coupling at 1.06  $\mu m$  using photorefractive effect 4-96987  
 GaAs, undoped and Cr doped, exciton region, impurity and illumination effect on photoconductivity 4-61411  
 GaAs, VPE, Cl desorption by  $H_2$ , quantum chemistry 4-70553  
 GaAs, vacancy energy levels, impurity state pinning, tight-binding calcs., local density theory 4-88470  
 GaAs wafer, (100) surface, orientation determ. by etching technique 4-99619  
 GaAs wafer production, crystal fabrication device using supercond. mag. field 4-114379  
 GaAs, XANES spectra, K-edge region 4-109278  
 GaAs: Mn, spin-depend. recombination, optical pumping studies 4-99183  
 GaAs: B, interaction between B and defects 4-80082  
 GaAs: B, interstitial centre, radiation induced, cluster-Bethe lattice treatment 4-98090  
 GaAs: Be, ion implanted, reduced damage generation 4-113474  
 GaAs: Be, ion implanted, annealing behaviour, spectroscopic ellipsometry and Raman scatt. 4-113482  
 GaAs: C(Si), impurity and defect anal. by IR absorpt. spectra 4-75893  
 GaAs: Cr, Cr-related complex, photoluminesc. studies 4-88467  
 GaAs: Cr, epitaxial layers, Cr doping and elec. parameters 4-76683  
 GaAs: Cr, eval. of Cr conc. by optical absorpt. 4-104635  
 GaAs: Cr, impurities, optical and transport studies 4-71444  
 GaAs: Cr, impurity photocond., internal quantum efficiency 4-88540  
 GaAs: Cr, ion implanted, Cr redistrib. 4-88194  
 GaAs: Cr, ion irradi. effect on defect thermal annealing 4-98156  
 GaAs: Cr, ionisation processes by upper conduction band electrons, mag. field effects 4-65640  
 GaAs: Cr, LEC growth, mag. field effect on impurity conc. 4-114378  
 GaAs: Cr, photoluminescence excitation spectra,  $Cr^{2+}$  internal luminesc. 4-81004  
 GaAs: Cr, semi-insulating, inhomogeneities, optical obs. 4-60944  
 GaAs: Cr, US attenuation and vel. meas. 4-98212  
 GaAs: Cr picosecond optoelectronic switches, pulse modulation of GaAs-(GaAl)As DH diode laser 4-107701  
 GaAs: Cr-GaAs epitaxial junction, IR characterisation 4-109170  
 n-GaAs:  $Cr^{2+}$ , acoustic paramagnetic resonance study 4-71171  
 GaAs:  $Cr^{2+}$ , comparison of static and dynamic Jahn-Teller models 4-61345  
 GaAs:  $Cr^{2+}$ , trigonal 'symmetry' sites, photoluminescence spectra anal. 4-108391  
 GaAs: Cr(Ni), deep impurity charact., photoluminescence study 4-98557  
 GaAs: Cr(O), electrical properties and impurity states 4-75963  
 GaAs: Fe, Cu, epilayers, deep states, DLTS study 4-108802  
 GaAs: Ge(Si), LEC grown, dislocation structure etching rel. to dopant conc. 4-113451  
 GaAs: Ge(001), MBE grown, TEM image contrast from antiphase domains 4-104098  
 GaAs: In, isoelectric doping, X-ray and electron microprobe. anal. 4-75491  
 GaAs: Mn, charge state of Mn impurities, mag. susceptibility ESR and Hall effect meas. 4-108982  
 GaAs: Mn, Mn redistribution, interstitial-substitutional model anal. 4-92433  
 GaAs: Mn, phonon scatt. at acceptor ground state 4-70729  
 GaAs: Mn, thermal cond. resonances of acceptor states 4-104011  
 GaAs: N, isoelectronic traps study by photoluminesc. (Chinese) 4-93098  
 GaAs: O p-n structs., magnetically sensitive, elec. characts. (Russian) 4-65729  
 GaAs: S(Si), implant sublattice site determ., PIXE studies 4-98119  
 GaAs: Se, deep acceptor, photoluminescence study 4-80534  
 n-GaAs: Se, free electron optical absorpt. theory 4-104637  
 GaAs: Se<sup>+</sup>, implanted, amorphous-cryst. interface, high resolution struct. charact. 4-70171  
 GaAs: Si, (100), vacuum annealed, free carrier reduction 4-98610  
 GaAs: Si, Al p-n structures, radiative recomb., electrolum. characts. (Russian) 4-109249  
 n-GaAs: Si,  $\alpha$ -irrad., positron annihilation study 4-104696  
 GaAs: Si, crystal growth by horizontal gradient freeze technique, carrier and dislocation density 4-66216  
 GaAs: Si, implanted, elec. props., pulse laser annealing effects 4-60953  
 GaAs: Si, implanted, radiation annealing with CW Xe arc lamp 4-75486  
 GaAs: Si, ion implantation, ion beam purity and mass spectra 4-99864  
 GaAs: Si, ion implanted, and semi-insulating GaAs, deep levels, photoconductivity study 4-88469  
 GaAs: Si, LEC and horizontal Bridgman growth, elec. uniformity 4-65683  
 GaAs: Si, local vibr. modes and elec. activation, Raman study 4-84357  
 GaAs: Si, localised vibr. mode IR absorpt. meas. 4-104599  
 GaAs: Si, planar channelling of Si implants 4-75483  
 GaAs: Si, Si diffusion using rapid thermal processing, encapsulant effects 4-65464  
 GaAs: Si, Si doping from  $Si_2H_6$  in MOCVD growth 4-75459  
 GaAs: Si MOCVD films, free carrier profile synthesis by atomic plane doping 4-92221  
 GaAs: Si p-n structures, degree of compensation, photoluminesc. study 4-65736  
 GaAs: Si/AlGaAs DH TJS lasers grown by MBE 4-107671  
 GaAs: Sn, Te, dual implanted damage and annealing, challenging studies 4-80116  
 GaAs: Sn with  $SiO_2$  cap, thermal diffusion, doping mechanism 4-104006  
 GaAs: Sn/GaAs: Cr interface, electron and hole traps, photovoltaic studies 4-104283  
 GaAs: Te, deformed, precip., defect struct., electron microscopy obs. 4-103752  
 GaAs: Te, H ion bombarded, free carrier density, EELS studies 4-98632  
 GaAs: transition metals, electronic struct. of bulk centres 4-108818  
 GaAs: V, semi-insulating, V redistribution during heat treatment 4-80070

## III-V semiconductors continued

- GaAs:Zn, monolayer surface doping from plated Zn source 4-70172  
 p-GaAs:Zn, emission band, electron irradiation and annealing effects 4-88881  
 GaAs:Zn, reproducible leaky tube, Zn diffusion with submicron junction depths 4-98361  
 GaAs:Zn, thermal pulse diffusion of Zn from elemental source 4-98360  
 GaAs/(AlGa)As selectively doped heterostructure, transport props. 4-70913  
 GaAs/(GaAl)As two-dimens. electron gas, cyclotron reson. study 4-104297  
 GaAs/Al interface, electronic struct. and bonding 4-84700  
 GaAs/Al interface, low temp. form. and structure, LEED, AES and work function meas. 4-80425  
 GaAs/Al<sub>1-x</sub>Ga<sub>x</sub>As superlattices and heterojunctions, elec. props., numerical solns. 4-70924  
 GaAs/Al<sub>1-x</sub>Ga<sub>x</sub>As heterostructures, 2D electron localisation 4-98718  
 GaAs/Al<sub>1-x</sub>Ga<sub>x</sub>As heterostructure, photocond. studies 4-98744  
 GaAs/Al<sub>1-x</sub>Ga<sub>x</sub>As quantum well struct., low temp. electron mobility, alloy disorder scatt. contrib. 4-92808  
 GaAs/Al<sub>1-x</sub>Ga<sub>x</sub>As quantum wells, struct. and optical props. 4-99151  
 GaAs/Al<sub>1-x</sub>Ga<sub>x</sub>As quantum wells, Be doped, photoluminescence studies 4-104653  
 GaAs/AlAs multiple quantum well struct., electron-hole plasma, picosecond dynamics 4-92803  
 GaAs/AlAs-GaAs superlattice/GaAs superlattice barrier capacitor: a structure for the investigation of heterojunction interfaces 4-84679  
 GaAs/AlGaAs, MOCVD growth and homogeneous nucleation 4-99340  
 GaAs/AlGaAs DH laser, LPE fabricated, design optimisation for entertainment electronics (*German*) 4-102948  
 GaAs/AlGaAs heterointerfaces, struct. evaluation, TEM studies 4-84516  
 GaAs/AlGaAs heterojunction, 2D electron gas, cyclotron resonance studies 4-76032  
 GaAs/AlGaAs heterostructures, 2D electron plasma, optical processes 4-76523  
 GaAs/AlGaAs heterostructures, carrier density, hydrostatic press. control 4-98735  
 GaAs/AlGaAs heterostructure, screening and polaron effects, cyclotron resonance studies 4-98741  
 GaAs/AlGaAs heterostructure, organometallic VPE growth and characterisation 4-99341  
 GaAs/AlGaAs inverted heterojunctions, photoluminescence studies 4-98460  
 GaAs/AlGaAs MQW heterostructure current-injection lasers, carrier-induced energy-gap shrinkage 4-112423  
 GaAs/AlGaAs multi-quantum-well lasers, polarization-dependent gain 4-112412  
 GaAs/AlGaAs multiple quantum well structures, room temp. excitonic nonlinear absorpt. and refract. 4-74590  
 GaAs/AlGaAs multiple quantum well structs., photoexcited carriers intraband relax., femtosecond studies 4-88565  
 GaAs/AlGaAs single quantum well struct., enhanced luminescence 4-99150  
 GaAs/AlGaAs three-dimensional optical waveguides, anal. of characts. (*Chinese*) 4-83689  
 GaAs/AlGaAs/GaAs heterojunction barrier, MOCVD grown, electron transport 4-80661  
 GaAs/Au contacts, Schottky barrier photosensitivity spectra in strong absorption region (*Russian*) 4-65741  
 GaAs/Au interface struct., XPS, RHEED and ion scatt./channelling studies 4-80421  
 n-GaAs/Au Schottky contacts, elec. props. and interface chem., sputtering effects 4-80674  
 n-GaAs/Au-Ge Ohmic contact fabrication by IR lamp alloying 4-84690  
 GaAs/Au-Ge-Ni ohmic contacts, CO<sub>2</sub> laser alloying 4-76038  
 GaAs/Au-Ti(Au) Schottky contacts, damage-induced degradation 4-84699  
 GaAs/AuGe ohmic contact, Ge and Au profiles, SIMS studies 4-103782  
 GaAs/Ca<sub>1-x</sub>Sr<sub>x</sub>F<sub>2</sub>/GaAs (100) lattice-matched MBE structures 4-88562  
 GaAs/Ga<sub>1-x</sub>Al<sub>x</sub>As quantum well wires, hydrogenic impurity states 4-92815  
 GaAs/GaAlAs, antireflect. coated twin DH diode external cavity ring laser, optical bistability study 4-91460  
 GaAs/GaAlAs DH stripe geometry lasers, Be-implanted, MOCVD growth 4-107635  
 GaAs/GaAlAs integrated optoelectronics for optical interconnect applications 4-97140  
 GaAs/GaAlAs lasers, synchronous mode locking by picosecond-optoelectronic switch 4-96965  
 GaAs/GaAlAs monolithically Peltier-cooled laser diodes 4-74540  
 GaAs/GaAlAs multiple-quantum-well semicond., optical bistability due to increasing absorpt. 4-74598  
 GaAs/GaAlAs quantum well self-electro-optic effect device as hybrid optically bistable switch 4-91522  
 GaAs/GaAlAs quantum well structs., oscillatory magnetoresist. studies 4-98738  
 GaAs/GaAlAs single mode laser diodes, free space optical: communication, design and system requirements 4-79176  
 GaAs/GaAlAs subthreshold DH twin stripe laser, interstripe coupling and current spreading 4-79139  
 GaAs/GaAlAs twin stripe lasers, current rise time effect on beam stability, expt. study 4-91510  
 GaAs/GaAlAs waveguide phase modulator, MBE grown heterostructure, design for PSK optical fibre systems 4-83685  
 GaAs/Ge single crystal layers, MBE growth and patterning on Si substrates 4-99315  
 GaAs/Ge(AlAs) heterojunctions, interface struct., TEM and STEM studies 4-108728  
 GaAs/metal contacts, interface struct., TEM and STEM studies 4-108728  
 GaAs/metal interface, Schottky barrier heights meas. 4-76018  
 GaAs/N-AlGaAs heterostructures, selectively doped, MBE grown, tungsten-halogen lamp annealing effects 4-61444  
 GaAs/native oxide interfaces, density of states, C-V meas. 4-88604  
 GaAs/Ni film system, interfacial reactions, TEM and X-ray diffraction studies 4-108729  
 GaAs/Ni-Ta interfacial reactions, metallisation appl. 4-98367  
 GaAs/Pt, ion beam mixing and ohmic contact form. 4-92244  
 p-GaAs/Ti-Pt ohmic contact (*Chinese*) 4-88589  
 GaAs-(AlGa)As superlattices, MBE grown, growth temp. influence 4-81139  
 GaAs-(AlGa)As large optical cavity lasers 4-107631

## III-V semiconductors continued

- GaAs-(AlGa)As lasers, passive waveguide coupled, mode behaviour 4-91499  
 GaAs-(AlGa)As modulation-doped heterostructures, reson. inelastic light scatt. studies 4-84973  
 GaAs-(AlGa)As strip geometry laser diodes, dynamical thermal props. 4-79206  
 GaAs-(AlGa)As twisted DH laser, composite cavity config., design and longit./transverse mode operation 4-69456  
 GaAs-(AlGa)As two-dimens. electron plasma, optical emission and excitation processes 4-104666  
 GaAs-(GaAl)As DH diode laser, pulse modulation by picosecond optoelectronic GaAs:Cr switches 4-107701  
 GaAs-Ag, high resolution EELS study 4-99248  
 GaAs-Al contact, semicond. electron field emission props., metal adsorption effect 4-99289  
 GaAs-Al interface, IR surface second harmonic generation and characts. (*Chinese*) 4-74606  
 GaAs-Al<sub>0.3</sub>Ga<sub>0.7</sub>As, quantised Hall resistance and 2D electron gas behaviour 4-98724  
 GaAs-Al<sub>0.3</sub>Ga<sub>0.7</sub>As quantum wells, photoluminesc. from spike doped hydrogenic donors 4-104668  
 GaAs-Al<sub>0.3</sub>Ga<sub>0.7</sub>As DH laser with two sections in a common cavity (*Chinese*) 4-112466  
 GaAs-Al<sub>0.3</sub>Ga<sub>0.7</sub>As abrupt heterojunctions grown by MBE, Auger composition profiles 4-80429  
 GaAs-Al<sub>1-x</sub>Ga<sub>x</sub>As quantum well structs., Raman scatt. study 4-93079  
 GaAs-Al<sub>1-x</sub>Ga<sub>x</sub>As heterostructures, 2D electron gas, disorder, fractional quantum Hall effect 4-76033  
 GaAs-Al<sub>1-x</sub>Ga<sub>x</sub>As heterostructures, electron mobility, temp. depend. from 1-10K 4-80669  
 GaAs-Al<sub>1-x</sub>Ga<sub>x</sub>As heterostructure, low temp. fractional quantum Hall effect 4-98722  
 GaAs-Al<sub>1-x</sub>Ga<sub>x</sub>As heterostructure, thermopower meas. on 2D electron gas 4-98729  
 GaAs-Al<sub>1-x</sub>Ga<sub>x</sub>As heterostructure, quantum Hall resistance, temp. depend. 4-114028  
 GaAs-Al<sub>1-x</sub>Ga<sub>x</sub>As multiple quantum well struct., magneto-Raman characterisation 4-104577  
 GaAs-Al<sub>1-x</sub>Ga<sub>x</sub>As quantum well struct., exciton binding energy 4-75868  
 GaAs-Al<sub>1-x</sub>Ga<sub>x</sub>As quantum wells, energy-gap discontinuities and effective masses 4-92623  
 GaAs-Al<sub>1-x</sub>Ga<sub>x</sub>As superlattices, Raman probing of phonons and interfaces 4-80927  
 GaAs-Al<sub>1-x</sub>Ga<sub>x</sub>As stripe geometry lasers, spectral behaviour, lateral hole-burning effects, numerical investigation 4-87334  
 GaAs-Al<sub>1-x</sub>Ga<sub>x</sub>As tunnel junctions, sequential single-phonon emission obs. in electron transport 4-80667  
 GaAs-AlAs heterostructures, photoacoustic spectroscopy by piezoelec. transducers 4-61448  
 GaAs-AlAs multiple quantum well struct., Raman scatt. and luminescence study 4-99105  
 GaAs-AlAs semiconductor superlattices, MOCVD prep., interface struct. study 4-108726  
 GaAs-AlAs:Zn superlattice, Zn impurity diffusion, X-ray study 4-75729  
 GaAs-AlGaAs, optical activity of plasma oscills. 4-84930  
 GaAs-AlGaAs GRIN-SCH lasers, MBE grown for optoelectronic integrated circuit appl. 4-96894  
 GaAs-AlGaAs heterojunction, phonon emission and electron heating 4-70927  
 GaAs-AlGaAs injection lasers (*Dutch*) 4-87329  
 GaAs-AlGaAs monolithically integrated optical circuit fabrication 4-69597  
 GaAs-AlGaAs multiple quantum well heterostructure, delocalised exciton state 4-92621  
 GaAs-AlGaAs superlattice and interface, acoustic props. 4-80366  
 GaAs-AlGaAs superlattices, MBE grown, direct obs. of lattice arrangement 4-84528  
 GaAs-AlGaAs superlattice grown by MBE, struct. and optical props. 4-84538  
 GaAs-AlGaAs transverse junction stripe laser, Si doped, MBE fabrication 4-96893  
 GaAs-AlGaAs window-stripe multi-quantum well heterostructure, laser fabrication 4-69436  
 GaAs-Al(Au) Schottky barrier contacts, LEC grown, electron traps, DLTS signals, effect of metal 4-84691  
 GaAs-Au tunnel structs., differential cond. characts. 4-61455  
 GaAs-Ga<sub>1-x</sub>Al<sub>x</sub>As, lateral superlattice struct. 4-92816  
 GaAs-Ga<sub>1-x</sub>Al<sub>x</sub>As, binding energy of exciton in GaAs-quantum well, magneto-optical determination 4-114027  
 GaAs-Ga<sub>1-x</sub>Al<sub>x</sub>As heterojunction, electron energy level calcs. 4-108915  
 GaAs-Ga<sub>1-x</sub>Al<sub>x</sub>As multilayer struct. masked and selective and thermal oxidation, technology for stripe-geometry DH lasers and integrated optics 4-69610  
 GaAs-Ga<sub>1-x</sub>Al<sub>x</sub>As multiple quantum well structs., Hall mobility, electron conc. and buffer width depend. 4-80668  
 GaAs-GaAlAs channelled-substrate lasers, single longit. mode, grown by MBE 4-69403  
 GaAs-GaAlAs double heterostructure, quantisation of excitonic polaritons 4-92634  
 GaAs-GaAlAs heterojunction, freq. enhanced fractional quantisation, quantum Hall effect 4-80664  
 GaAs-GaAlAs heterostructures, hot photoluminescence polarisation and spectrum 4-61743  
 GaAs-GaAlAs heterostructure, electron mobility limits 4-76030  
 GaAs-GaAlAs heterostructures, 2D electron gas, electron mobility, temp. dependence 4-98704  
 GaAs-GaAlAs heterostructures, interband scatt. in mobility 4-98732  
 GaAs-GaAlAs interface, 2D electron gas, cyclotron reson. 4-109077  
 GaAs-GaAlAs multiple-quantum-well structures, sharp line photolum. spectra 4-93110  
 GaAs-GaAlAs pnpn negative-resistance laser with low threshold current density 4-69448  
 GaAs-GaAlAs quantum well lasers tunable by long wavelength radiation 4-69404  
 GaAs-GaAlAs quantum well struct., optical props., review 4-104146  
 GaAs-GaAlAs quantum wells, coupled, photoluminesc. and excitation spectroscopy 4-104667  
 GaAs-GaAlAs quantum wells, reflectance of two-dimensional excitations 4-109211

## V semiconductors continued

- GaAs-GaAlAs superlattices, third order nonlinear optical susceptibility 4-74586  
 GaAs-GaAlAs superlattice, Raman study of folded modes 4-80929  
 GaAs-GaAlAs system, superlattices, quantum wells, and heterostructs., review 4-80666  
 GaAs-Ge interface, electronic struct. 4-84665  
 GaAs-Ge(100) interfaces, Fermi level position and valence-band edge discontinuity study 4-61450  
 GaAs-HCl-H<sub>2</sub> system, phase equilib., dominant reactions for VPE, etching obs. 4-71579  
 GaAs-Hg Schottky barrier, crystal damage during CV profiling 4-98753  
 GaAs-In<sub>0.53</sub>Ga<sub>0.47</sub>As MOCVD strained-layer superlattices, lattice distortion, TEM study 4-88406  
 p-GaAs-KCl electrolyte interface, photoemission rate law 4-71513  
 GaAs-metallic glass contacts, TEM obs. 4-104094  
 GaAs-n-AlGaAs structures, modulation doped, elec. props., effect of IR flash lamp annealing 4-98712  
 GaAs-NiSi thermal stability ohmic contact 4-88590  
 n-GaAs-p-GaAs-Si-p-Al<sub>0.3</sub>Ga<sub>0.7</sub>As, solar heterophotocells with increased p-n junction depth 4-71703  
 n-GaAs-polysiloxane-metal struct., elec. props. (French) 4-61460  
 GaAs-Si interface, nonlinear surface EM waves 4-80892  
 GaAs-thin Au/Cr bilayer structure, interfacial chemical reactions and drive-out diffusion, AES study 4-80313  
 GaAsP p-n junctions, avalanche multiplication and ionisation rates, SEM studies 4-65733  
 GaAsP strained-layer superlattice structures and their buffer layers, comparison of trapping levels 4-113885  
 n-GaAs<sub>1-x</sub>P<sub>x</sub> anodes in aq. Se<sup>2-</sup>/Se<sub>2</sub><sup>2-</sup> solns., characts. 4-104310  
 GaAs<sub>1-x</sub>P<sub>x</sub>, EL2 metastable state, photocapacitance quenching study 4-70717  
 GaAs<sub>1-x</sub>P<sub>x</sub>, Fourier anal. of optical spectra 4-99311  
 GaAs<sub>1-x</sub>P<sub>x</sub>, internal elec. field-enhanced impurity diffusion and p-n junction form. 4-84469  
 GaAs<sub>1-x</sub>P<sub>x</sub>, localised excitons, luminescence study 4-61291  
 GaAs<sub>1-x</sub>P<sub>x</sub>, n, exciton tunnelling inhibited by disorder 4-92622  
 GaAs<sub>1-x</sub>P<sub>x</sub>, n, excitons and excitonic mols. bound to impurity, calcs. 4-108785  
 GaAs<sub>1-x</sub>P<sub>x</sub>, P<sup>+</sup>, Zn<sup>2+</sup>, implanted, photoluminescence spectra, impurity conc. depend. (Chinese) 4-93099  
 GaAs<sub>1-x</sub>P<sub>x</sub>-GaAs<sub>1-x</sub>P<sub>y</sub> isotype heterojunction electrodes in photoelectrochem. cells, photoluminescent and electroluminescent props. 4-99140  
 GaAs<sub>1-x</sub>P<sub>x</sub> mixed cryst., long-wavelength optical phonons (Chinese) 4-108559  
 GaAs<sub>1-x</sub>P<sub>x</sub>, phonon modes, Raman scatt. study 4-108563  
 GaAs<sub>1-x</sub>P<sub>x</sub>:Cu, LEDs, Cu impurities, thermal redistribution 4-80080  
 GaAs<sub>1-x</sub>P<sub>x</sub>/GaP strained-layer superlattices, Be-implantation doping 4-80057  
 GaAs<sub>1-x</sub>P<sub>x</sub>/GaP superlattices, strain depth profiles, misfit dislocations obs. 4-104095  
 GaAs<sub>1-x</sub>P<sub>x</sub>, fundamental absorpt., optical absorpt. coeff. 4-76408  
 GaAs(001)-Au interface, formation by MBE and thermal stability 4-99328  
 GaAs(1110)-In interface, photoemission study 4-85079  
 GaInAs/AlInAs heterojunctions, cyclotron resonance and polaron effects 4-98742  
 GaInAs/InP heterojunctions and superlattices, cyclotron resonance and polaron effects 4-98742  
 GaInAs/InP(AlInAs) heterojunctions and superlattices, 2-D magnetophonon resonance 4-98740  
 GaInAs-InP double heterostructure, epitaxial low press. MO-CVD growth for device appl., book contrib. 4-61875  
 GaInAs-InP heterostructure emitters, 1.3-1.55  $\mu$ m 4-104308  
 GaInAs-InP IR detectors, applications of electron microscope techniques to semiconductors 4-103622  
 GaInAs-InP quantum-well lasers, gain and intervalence band absorpt. 4-96899  
 Ga<sub>0.47</sub>In<sub>0.53</sub>As, hot electron velocity overshoot 4-70823  
 Ga<sub>0.47</sub>In<sub>0.53</sub>As, ion implanted, annealing, TEM obs. 4-70228  
 Ga<sub>0.47</sub>In<sub>0.53</sub>As layers, MOCVD growth and characterisation (French) 4-76685  
 Ga<sub>0.47</sub>In<sub>0.53</sub>As, MBE planar doped barriers in InP, elec. characts. 4-98708  
 Ga<sub>0.47</sub>In<sub>0.53</sub>As photoconductive detector prepared by VPE 4-86478  
 Ga<sub>0.47</sub>In<sub>0.53</sub>As-InP, Raman scatt. theory 4-76460  
 Ga<sub>1-x</sub>In<sub>x</sub>As based materials, recrystallisation in temp. gradient 4-114390  
 Ga<sub>1-x</sub>In<sub>x</sub>As, bond lengths, virtual crystal approx. 4-75385  
 GaInAsP 1.5  $\mu$ m laser diode, Raman amplification in low fiber loss region 4-96955  
 GaInAsP alloy semiconductors, book 4-58588  
 GaInAsP BH laser, low-threshold, multiple-cavity, longit.-mode stabilised 4-91468  
 GaInAsP cleaved coupled-cavity laser, tunable design, FM operation for communication appl. 4-69451  
 GaInAsP, defect motion and growth of extended non-radiative defect structs., book contrib. 4-60914  
 GaInAsP epitaxial layers, thickness and uniformity by automated scanning double axis X-ray diffr. 4-65589  
 GaInAsP heterostructure laser with distributed feedback 4-74538  
 (GaIn)(AsP) heterostructure laser diodes, psec. pulse generation 4-107632  
 GaInAsP, high field transport meas., review, book contrib. 4-61389  
 GaInAsP, high purity, charact., growth, back contrib. 4-61334  
 GaInAsP inner stripe laser diodes on p-InP substrate 4-96886  
 GaInAsP, ion implantation, book contrib. 4-60943  
 GaInAsP, LPE growth on InP, review, book contrib. 4-61882  
 GaInAsP lattice matched to InP, electronic struct., book contrib. 4-61284  
 GaInAsP, low field carrier mobility, book contrib. 4-61383  
 GaInAsP, low field transport calcs., book contrib. 4-61384  
 GaInAsP, n-type, lattice matched to InP, hot electron transport, book contrib. 4-61388  
 GaInAsP, nonlinear carrier dynamics, optical bleaching study 4-74625  
 GaInAsP, photolum. and optical gain spectra, book contrib. 4-61752  
 GaInAsP picosecond optical absorption saturation 4-91541  
 GaInAsP, VPE growth, review, book contrib. 4-61874  
 GaInAsP/InP 1.3  $\mu$ m distributed feedback lasers, LPE growth 4-96913  
 GaInAsP/InP BH laser diodes, fabrication technique 4-74507  
 GaInAsP/InP BH laser with chemically etched and mass-transported mirror 4-74537

## III-V semiconductors continued

- GaInAsP/InP BH injection lasers, network modelling and modulation characts. 4-96890  
 GaInAsP/InP DFB laser, 1.5  $\mu$ m range, longitudinal mode behaviour 4-74512  
 GaInAsP/InP DFB lasers, 1.3  $\mu$ m, monolithic integrated struct., WDM optical communication appl. 4-83618  
 GaInAsP/InP heterostructure lasers, gas source MBE growth 4-69401  
 GaInAsP/InP hetero-multilayers, LPE, fabrication and reflectivity 4-99357  
 GaInAsP/InP laser, single-mode, low-temp. single-step LPE growth 4-112407  
 GaInAsP/InP phase adjusted active distributed reflector laser, 1.5  $\mu$ m, for dynamic single mode operation 4-69437  
 GaInAsP-InP BH but-jointed built-in integrated, lasers, 1.5-1.6  $\mu$ m operation, static characts. 4-60065  
 GaInAsP-InP DH lasers, review, book contrib. 4-60037  
 GaInAsP-InP DH lasers, temp. depend. of laser threshold current, book contrib. 4-60038  
 GaInAsP-InP DH lasers, carrier leakage current estimation using high mag. fields 4-91453  
 GaInAsP-InP double heterostructure, epitaxial low press. MO-CVD growth for device appl., book contrib. 4-61875  
 GaInAsP-InP lasers, applications of electron microscope techniques to semiconductors 4-103622  
 GaInAsP-InP mass-transported BH lasers, fabrication, characterization and analysis 4-112473  
 Ga<sub>0.33</sub>In<sub>0.67</sub>As<sub>0.70</sub>P<sub>0.30</sub> (100) oriented, electron and hole ionisation coeffs. 4-98662  
 Ga<sub>1-x</sub>In<sub>x</sub>As<sub>1-y</sub>Sb<sub>y</sub> solid solutions, LPE, conc. profiles 4-93233  
 Ga<sub>1-x</sub>In<sub>x</sub>As<sub>1-y</sub>Sb<sub>y</sub> layer on InP:Sn substrate, linear thermal expansion coeff. meas. 4-75709  
 Ga<sub>1-x</sub>In<sub>x</sub>As<sub>1-y</sub>Sb<sub>y</sub>, epitaxial layers, reflection spectra analysis 4-114340  
 GaInP/AlGaAs double heterostructures, LPE, lasing, 77-230K 4-71606  
 Ga<sub>0.5</sub>In<sub>0.5</sub>P, photolum. dynamics of high density electron-hole plasma under psec. laser excitation 4-109228  
 Ga<sub>1-x</sub>In<sub>x</sub>P, phonon modes, Raman scatt. study 4-108563  
 Ga<sub>1-x</sub>In<sub>x</sub>P, photochem. behaviour in aq. and nonaqueous media, common anion rule 4-70928  
 Ga<sub>1-x</sub>In<sub>x</sub>P, LPE growth on GaAs substrates, cathodoluminesc. and photoluminesc. spectra (Chinese) 4-113825  
 Ga<sub>1-x</sub>In<sub>x</sub>P monocryst. layers, LPE on GaAs (Chinese) 4-114427  
 Ga<sub>1-x</sub>In<sub>x</sub>PyAs<sub>1-y</sub> gas source MBE growth 4-81140  
 Ga<sub>1-x</sub>In<sub>x</sub>(Sb,As)<sub>1-y</sub>, short-range clustering, thermodynamic anal. 4-61093  
 GaN crystal growth, vapor-liquid-solid mechanism, NH<sub>3</sub> reaction with Ga 4-61823  
 GaN, crystals, high pressure soln. growth, equilib. N<sub>2</sub> press. over Ga-GaN mixtures 4-61822  
 GaN, polarised luminescence transitions and electroluminescence quenching 4-104670  
 GaN:Zn, cathodoluminesc. anomalous kinetics 4-85015  
 GaP, 3d impurity excitation spectra, separation of one- and many-electron effects 4-75900  
 GaP (110), intrinsic unoccupied surface states and valence band minimum 4-80641  
 GaP (110), surface structure, atomic geometries, R-factor minimization 4-84494  
 GaP amorphous film, local order study and electronic props. 4-70591  
 GaP, crystal growth under microgravity in SALYUT-6 space station 4-98035  
 GaP crystal quality in soln. growth P press. effects 4-103685  
 GaP crystals, Raman light scatt. from polaritons using reflection scheme 4-66042  
 GaP, deep impurity levels, ENDOR and ESR spectra 4-84594  
 GaP, defect electronic struct. calcs. 4-61326  
 GaP diode struct., electroluminescence polarisation study (Russian) 4-88884  
 GaP, donor wave functions and band struct. 4-98519  
 GaP, electron irradi., defect creation, luminescence and elec. studies (Chinese) 4-108441  
 n-GaP, electron irradi., defects, positron annihilation studies 4-109273  
 GaP epitaxial layer, processing technology and characts. (Polish) 4-113827  
 GaP, Hall meas. anal., influence of thermal impurity activation energy temp. depend. 4-104238  
 GaP, large single crystals, LEC growth, LEDs 4-99301  
 GaP, laser-induced sputtering and damage 4-71485  
 GaP, localised vacancies, electronic struct. and stability 4-80539  
 GaP, molecular beam epitaxial growth on Si 4-70587  
 GaP, optical phonon lifetimes, temp. dependence, optical meas. 4-61016  
 GaP p-n junctions, avalanche multiplication and ionisation rates, SEM studies 4-65733  
 GaP, phase transformations at ultrahigh press., X-ray diffr. obs. 4-98273  
 p-GaP photoelectrochem. cells, absorpt. coeff. and diffusion lengths, differential photocurrent determ. 4-89455  
 GaP powders, surface phonons, Raman scatt. 4-109193  
 GaP, press. depend. of bound excitons 4-61293  
 GaP prism couplers, optical characts. (Chinese) 4-60134  
 GaP, Raman scatt. by surface EM waves 4-80930  
 GaP, Raman scatt. efficiency, press. effect 4-76462  
 GaP, Raman scatt. study of phonon-surface polaritons 4-80931  
 GaP, scanning DLTS investig. 4-75892  
 GaP, spinodal decomp., <sup>31</sup>P NMR spectra, chem. shifts 4-76279  
 GaP substrate for a-Si film, epitaxial crystallisation 4-80452  
 GaP, symm. deep level wavefunction for defect pairs (Chinese) 4-104144  
 GaP, thermal oxidation, surface topography and oxide interface struct. 4-80342  
 GaP, thick sample, optical absorpt. coeff. determ. using photoacoustic spectroscopy 4-106402  
 GaP, volume plasmon dispersion, transmission electron energy loss studies 4-88465  
 n-GaP with adsorbed organics, monolayer influence on Schottky barrier height 4-104290  
 GaP: N epitaxial films, n-type, local cathodolum. kinetics 4-109251  
 GaP: transition metal, impurity electron states calcs. 4-70711  
 GaP:Cr, EPR study of Cr<sup>2+</sup> centre 4-104487  
 GaP: N, electron-hole plasma under resonant free exciton excitation 4-71430  
 GaP:N, exciton transfer, NN<sub>2</sub>-pair luminesc. enhancement, stochastic model 4-104660  
 GaP:N, photothermal capacitance meas. 4-84647

## III-V semiconductors continued

- GaP:N, Te VPE layers, minority carrier lifetime, photoluminesc. decay study 4-76520
- GaP:N,Te,Zn, photolum. under high press. (*Chinese*) 4-93097
- GaP:Ni, state of impurity centres, EPR, spin-lattice relax. time, spin Hamiltonian parameters 4-88476
- GaP:Ni<sup>2+</sup>, Jahn-Teller coupling forces, self consistent LCAO calc. 4-98577
- GaP:O, electronic impurity states calcs. 4-80547
- GaP:O, electronic struct. of single neutral ideal P vacancy 4-92657
- GaP:O(Zn), size effects and impurity electronic struct. 4-70723
- GaP:Te(N)(As), impurity influence on electron-hole plasma 4-75862
- GaP:Zn, O LEDs, centre responsible for capacitance slow relax. 4-65735
- GaP:Zn,O, LPE layers, cleaved surfaces photoluminesc., macrosteps and grooves 4-65588
- GaP/GaAs,P<sub>1-x</sub>, strained layer superlattices, minority carrier diffusion lengths 4-76025
- GaP-Si heterojunction band discontinuities, synchrotron radiation photoemission 4-81111
- GaP<sub>1-x</sub>As<sub>x</sub>, crystalline struct., two-phonon Raman spectra study 4-71385
- GaP<sub>1-x</sub>As<sub>x</sub>N<sub>1-x</sub>, covalent, localised states of negative ions stabilised by enhanced correl. effects 4-104157
- GaP<sub>1-x</sub>As<sub>x</sub>Sb<sub>1-x-y</sub>, epitaxial layers, luminescence studies 4-76505
- GaSb (110) surface, ion beam crystallography 4-80343
- GaSb amorphous film, local order study and electronic props. 4-70591
- GaSb, conduction bands, strain-induced splitting 4-75854
- GaSb cryst., facet regions and Czochralski growth 4-75348
- GaSb epitaxial films, photoluminescence spectra 4-88896
- p-GaSb, heavily doped, low temp. thermal cond. 4-70300
- GaSb, oxidation and interfacial chem. reactions, XPS study 4-85226
- GaSb, phonon-phonon interactions, lattice thermal cond. 4-80320
- GaSb, plasma-assisted epitaxial growth in H<sub>2</sub> plasma, elec. props. 4-104740
- GaSb, press. depend. of E<sub>g</sub> gap, reson. Raman technique study 4-76469
- GaSb, Raman freq. depend. on press. 4-109188
- GaSb,Se, quantum localisation of electrons in metal-insulator transition region 4-70654
- GaSb:Zn epitaxial films, photoluminescence spectra 4-88896
- GaSb-AlSb, superlattices, light and heavy valence subband reversal, lattice mismatch 4-114013
- GaSb-GaAlAsSb injection heterolaser, emitted radiation characts. 4-79152
- GaSb-InAs heterojunction, quantum Hall effect study 4-98726
- GaSb-InAs<sub>1-x</sub>Sb<sub>x</sub> heterostructures, LPE growth 4-104097
- GaSb-InSb, behaviour of Sn in solid solns., elec. props. 4-75967
- GaSb(110) surface atomic geometry and dynamics 4-70537
- GaSe-Ge 'Schottky-like' heterojunction 4-108931
- (In,Ga)As/InP n-p-n heterojunction bipolar transistors grown by LPE with high gain 4-85097
- InAs, electroliquid epitaxial growth, carrier density 4-93243
- InAs evaporated films, Hall mobility and carrier conc. 4-70961
- InAs high-field transport, model 4-88512
- n-InAs, hybrid quantum oscils., temp. depend. 4-70839
- InAs, lattice dynamics, phonon dispersion curves 4-61019
- InAs, MBE growth conditions and reconstruction 4-93223
- InAs MIS diodes with N-shaped V-I characteristics in inversion voltage region 4-114044
- InAs, nonlinear refr. at absorpt. edge 4-96988
- InAs, Raman freq. depend. on press. 4-109188
- InAs, struct. and electrical cond. behaviour under deposition conditions 4-98787
- InAs:Si(Te), VPE growth, morphology and elec. props. 4-109326
- InAs/GaSb superlattices, Landau levels and magneto-optical props. 4-98737
- InAs/GaSb superlattices, electronic collective modes 4-104134
- InAs-AlSb quantum wells, electron densities 4-98711
- InAs-GaSb system, superlattices, quantum wells, and heterostructs., review 4-80666
- InAs<sub>1-x</sub>Sb<sub>x</sub> epilayers, impact ionisation coeffs. 4-104333
- InAsP, high mobility, vapour phase heteroepitaxial growth 4-71601
- InAs,P<sub>1-x</sub>As<sub>x</sub> epitaxial layer, bright 300K luminescence 4-70584
- InAs,P<sub>1-x</sub>As<sub>x</sub> LEC growth and characterisation 4-99302
- InAsSb strained layer superlattices for long wavelength detector appls. 4-98706
- InAs<sub>1-x</sub>Sb<sub>x</sub>-Al<sub>1-x</sub>Ga<sub>x</sub>Sb heterostructures, LPE growth 4-104097
- InAs<sub>1-x</sub>Sb<sub>x</sub>GaSb heterostructures, LPE growth 4-104097
- InGaAs, 1.6 μm, radiative and nonradiative minority carrier lifetimes 4-70826
- InGaAs avalanche photodiodes for long-wavelength optical communication appls. 4-97135
- InGaAs epilayers, optical studies of carrier dynamics 4-98788
- InGaAs epitaxial layer, LPE growth and carrier mobility, dopant effects 4-84717
- InGaAs, high-parity, conventional LPE growth, carrier conc. and mobility 4-99353
- InGaAs, LPE using novel graphite boat 4-88994
- InGaAs planar photodiodes, reliability 4-91635
- InGaAs:Mg on INP, LPE-grown, MgO-free surface 4-76699
- InGaAs/GaAs strained layers superlattices, molecular beam growth conditions and characterisation 4-70585
- InGaAs/GaAs strained layer superlattices, high quality p-n junctions 4-98707
- InGaAs/InGaAlAs/InAlAs/InP separate confinement heterostruct. multi-quantum-well laser diodes, MBE grown 4-83617
- InGaAs-InP injection laser, operation and luminescence study 4-74508
- InGaAs-InP modulation doped heterostruct., self-consistent variational calcs. and alloy scatt. 4-98733
- InGaAs-InP superlattices, chloride VPE growth, struct. and optical props. 4-81158
- In<sub>0.53</sub>Ga<sub>0.47</sub>As/GaAs strained-layer superlattice, ion implanted, struct. integrity 4-113821
- In<sub>0.53</sub>Ga<sub>0.47</sub>As 1.6-μm lasers, temp. sensitive operation 4-96903
- In<sub>0.53</sub>Ga<sub>0.47</sub>As, 2D electron gas, alloy scatt. limited mobility 4-98620
- In<sub>0.53</sub>Ga<sub>0.47</sub>As, carrier energy relax., picosecond luminesc. studies 4-114312
- In<sub>0.53</sub>Ga<sub>0.47</sub>As, electron mobility, rel. to two-mode lattice vibrs. 4-80582
- In<sub>0.53</sub>Ga<sub>0.47</sub>As, epilayer thickness meas. from etched steps 4-62074
- In<sub>0.53</sub>Ga<sub>0.47</sub>As, epitaxially grown by LPE, VPE, MBE, band gap energy spatial var., photoluminescence spectra 4-104125
- In<sub>0.53</sub>Ga<sub>0.47</sub>As, LPE growth on InP (100) substrate (*Chinese*) 4-85121

## III-V semiconductors continued

- In<sub>0.53</sub>Ga<sub>0.47</sub>As LPE layers, high purity, photoluminescence processes 4-99187
- In<sub>0.53</sub>Ga<sub>0.47</sub>As, laser operation, thermal behaviour 4-87331
- In<sub>0.53</sub>Ga<sub>0.47</sub>As, MIS diode anodic oxidation, interface characteristics 4-104324
- In<sub>0.53</sub>Ga<sub>0.47</sub>As planar diodes, fabrication using open tube method for Zn diffusion 4-95519
- In<sub>0.53</sub>Ga<sub>0.47</sub>As, shallow donors, submillimeter wave photocond. 4-104256
- In<sub>1-x</sub>Ga<sub>x</sub>As, indirect conduction band minima determ. 4-98517
- In<sub>1-x</sub>Ga<sub>x</sub>As multi quantum well structs., strained, optical props. 4-104669
- In<sub>1-x</sub>Ga<sub>x</sub>As/GaAs strained layer superlattice, MBE growth, strain and layer thickness effects 4-99319
- In<sub>1-x</sub>Ga<sub>1-x</sub>As/InP quantum well struct., low temp. electron mobility, alloy disorder scatt. contrib. 4-92808
- In<sub>1-x</sub>Ga<sub>1-x</sub>As-GaAs strained-layer superlattices, phonon frequencies, Raman scatt. meas. 4-99121
- In<sub>1-x</sub>Ga<sub>1-x</sub>As-InP heterojunction, quantum Hall effect and hopping cond. 4-98723
- InGaAsP, 1.3 μm bandgap, photoexcited carrier lifetime and Auger recomb. 4-108893
- InGaAsP 1.3 μm optical amplifier-modulator integrated with a fibre-resonator mode-locked laser 4-91491
- InGaAsP 1.3 μm real-index-guided lasers, leakage current anal. 4-96895
- InGaAsP 1.53 μm DFB lasers made by mass transport 4-102947
- InGaAsP (InGaP), LPE layers on GaAs (001), composition modulated structures 4-76698
- InGaAsP and InGaP LPE layers, dislocation loops, TEM studies 4-92206
- InGaAsP and InP epitaxial layers, MOVPE at atmospheric press. 4-81154
- InGaAsP BH 1.3 μm lasers, anomalous polarisation characts. 4-69402
- InGaAsP crescent mesa substrate BH lasers at 1.55 μm 4-112429
- InGaAsP double-channel BH lasers, short-cavity, HF small-signal modulation characts. 4-69462
- InGaAsP double-channel buried-hetero structure lasers, 1.55 μm, high-temp. operation, LPE 4-79174
- InGaAsP epilayers, optical studies of carrier dynamics 4-98788
- InGaAsP etched mesa BH lasers, 1.3 μm, threshold current, active layer placement effects 4-112414
- InGaAsP film laser, optically pumped, chirp, passive pulse compression in optical fibres 4-107700
- (InGa)(AsP) heterolasers with distrib. feedback, polarisation effects 4-64708
- InGaAsP heterostructure laser with distributed feedback 4-74538
- InGaAsP injection lasers, short pulse excitation, threshold current temp. dependence 4-74506
- InGaAsP LPE layers on InP, refractive index in transparent wavelength region 4-71333
- InGaAsP, LPE-grown, high-uniformity, λ=1.3 μm 4-76700
- InGaAsP, laser, radiative and nonradiative, recombination rates, meas. 4-112434
- InGaAsP laser diode optical switches, isolation characteristics 4-107680
- InGaAsP laser diode switch, BH type, 1.3 μm operation; design and fibre optic communication appl. 4-112461
- InGaAsP laser-diode optical switch module 4-83616
- InGaAsP lasers, gain- and index-guided, spectral linewidth 4-112417
- InGaAsP lasers for 1.52 operation, linewidth and FM-noise spectrum meas. 4-83580
- InGaAsP, lattice matched to GaAs, lattice dynamics, Raman scatt. study 4-61673
- InGaAsP light sources, radiative coeffs., carrier dependence 4-64703
- InGaAsP, linear electro-optic effects and nonlinear optical coeffs., device design appls. 4-88809
- InGaAsP long-wavelength 1.0-1.6-μm detectors 4-91634
- InGaAsP, MBE growth IR reflectivity, diode laser source/detector 4-71391
- InGaAsP material epitaxial growth, devices for optical communications 4-74746
- InGaAsP, optically pumped, tunable CW mode locked laser action 4-107699
- InGaAsP, quadratic electro-optic Kerr effects, dispersion 4-109159
- InGaAsP ridge lasers, λ≈1.5 μm, grown by gas source MBE 4-112413
- InGaAsP separate confinement heterostructure lasers, 1.5 μm, electron leakage 4-96904
- InGaAsP, theoretical design of single-layer antireflection coatings on laser facets 4-69409
- InGaAsP three-channel buried crescent lasers, 1.51 μm, high-speed analog and digital modulation 4-112409
- InGaAsP tunable DFB laser pumped by heterostructure injection laser 4-96907
- InGaAsP:Zn highly reliable 1.3 μm surface emitting LEDs for high speed optical communication systems 4-97137
- InGaAsP/InGaP lasers, low threshold, 810 nm, LPE growth 4-69435
- InGaAsP/InGaP lasers, LPE growth on GaAs, room temp. CW lasing at 727 nm 4-79133
- InGaAsP/InGaP/GaAs DH lasers, low threshold pulsed and CW operation 4-87336
- InGaAsP/InP 1.3 μm buried crescent lasers using short external optical cavity, single-mode operation 4-74511
- InGaAsP/InP 1.3 μm buried crescent lasers, single transverse-mode conditions 4-96897
- InGaAsP/InP 1.3 μm buried crescent laser diode, degradation mechanism 4-96915
- InGaAsP/InP amplifier-modulator integrated with a cleaved-coupled-cavity injection laser 4-91505
- InGaAsP/InP buried crescent lasers, 1.3 μm, high temp. and long life operation 4-69444
- InGaAsP/InP buried crescent laser, dynamic characts., computer simulation method (*Chinese*) 4-96887
- InGaAsP/InP buried crescent laser diode emitting at 1.3 μm, high temp. CW operation 4-112427
- InGaAsP/InP channelled-substrate BH lasers, VPE base struct. and LPE regrowth 4-96905
- InGaAsP/InP DFB laser diodes, cleaved facet, grating phase effects 4-60063
- InGaAsP/InP DFB laser diodes lasing characts. at 1.5 μm, effect of mirror facets 4-74513
- InGaAsP/InP DFB ridge-waveguide laser, 1.2 Gbit/s optical fibre transmission over 113.7 km 4-107847

## V semiconductors continued

- InGaAsP/InP DH, luminescence and laser threshold characts. 4-85008  
 InGaAsP/InP DH stripe lasers fabricated by O ion implantation 4-96906  
 InGaAsP/InP GRIN rod external coupled-cavity BH lasers, single longit. mode operation 4-91473  
 InGaAsP/InP gigahertz-bandwidth optical modulators/switches with DH waveguides 4-112585  
 InGaAsP/InP heterostructure waveguides integrated with optical devices 4-97146  
 InGaAsP/InP injection lasers, LPE grown, three-layer-waveguide DH design 4-91490  
 InGaAsP/InP laser diode, monolithic integration with heterojunction bipolar transistors 4-102927  
 InGaAsP/InP lasers, failure modes due to adhesives 4-107678  
 InGaAsP/InP lateral p-n-p transistor fabrication using open diffusion technique 4-104003  
 InGaAsP/oxidised films interface, Auger/ion sputtering anal. 4-104884  
 InGaAsP-Au contacts, X-ray study of Au interactions 4-80675  
 InGaAsP-InGaP rapidly degraded DH laser grown by LPE, dark-line defects 4-69406  
 InGaAsP-InP 1.3  $\mu\text{m}$  BH lasers, improved linearity criterion, high-bit-rate fibre communication system appls. 4-74510  
 InGaAsP-InP 1.55  $\mu\text{m}$  DH ridge waveguide laser, optimum design 4-102955  
 InGaAsP-InP BC laser diode emitting at 1.3  $\mu\text{m}$ , fabrication, design, characteristics 4-112474  
 InGaAsP-InP DH, photoluminescence efficiency 4-85006  
 InGaAsP-InP DH modulators, electroabsorption, polarisation depend. 4-93054  
 InGaAsP-InP planar buried DH, LPE growth, melt-carry-over effect 4-99352  
 InGaAsP-InP single-longitudinal-mode 1.3  $\mu\text{m}$  DFB-DC-PBH diodes 4-91467  
 In<sub>0.75</sub>Ga<sub>0.25</sub>As<sub>0.56</sub>P<sub>0.44</sub>, electroreflectance spectrum, on InP substrate 4-109158  
 In<sub>0.76</sub>Ga<sub>0.24</sub>As<sub>0.44</sub>P<sub>0.56</sub>, luminescence study of binding energy variation 4-71435  
 In<sub>1-x</sub>Ga<sub>x</sub>As<sub>1-y</sub>P<sub>y</sub>, composition depend. of microhardness anisotropy 4-108506  
 In<sub>1-x</sub>Ga<sub>x</sub>As<sub>1-y</sub>P<sub>y</sub>, indirect conduction band minima determ. 4-98517  
 In<sub>1-x</sub>Ga<sub>x</sub>As<sub>1-y</sub>P<sub>y</sub> laser material, intervalence band absorpt. and Auger recomb. 4-80885  
 InGaP LED/optical fibre system for optical remote detection of propane gas 4-105155  
 InGaP/InAlP quantum well structures for visible region, MBE growth 4-99314  
 In<sub>0.9</sub>Ga<sub>0.1</sub>P, spinodal decomp., phase segregation, <sup>31</sup>P NMR spectra, chem. shifts 4-76279  
 In<sub>1-x</sub>Ga<sub>x</sub>P<sub>1-x</sub>As<sub>x</sub>, solid solution, LPE, crystn. and optical props. 4-108736  
 In<sub>1-x</sub>Ga<sub>x</sub>Sb, indirect conduction band minima determ. 4-98517  
 InP (001), substrate for MBE growth of Ba<sub>2</sub>Sr<sub>1-x</sub>F<sub>2</sub> films 4-70582  
 InP (100), laser irradi., photoemission of electrons 4-81116  
 InP (100), optical surface phonons obs. using high res. electron energy loss spectroscopy 4-70546  
 InP (100) and (111) surfaces, EELS study, bulk and surface plasmons (Chinese) 4-85047  
 InP (100) surfaces, atomic conc. ratio by X-ray photoelectron spectroscopy 4-66185  
 InP (110)-Cu(Ag)(Au) interface, soft X-ray photoemission study 4-85080  
 InP, absence of core exciton induced resonant photoemission 4-114360  
 InP acceptor impurity incorporation during organometallic VPE, photolum. obs. 4-98122  
 InP amorphous film, local order study and electronic props. 4-70591  
 InP based integrated optics 4-64796  
 n-InP, cyclotron resonance, impurity conc. and compensation effects (Russian) 4-98952  
 n-InP, electron energy relax. due to 2TA phonons 4-92324  
 InP, electron irradi., antisite defects, EPR study 4-80816  
 InP, electron irradi. induced deep traps, deep level optical spectroscopy 4-104156  
 InP, electron irradiation induced defects, energy and orientation depend. 4-108810  
 InP epilayers, cathodoluminescence study 4-104678  
 InP epitaxial, deep and shallow levels due to ion irradi. 4-80531  
 InP epitaxial layer, LPE growth and carrier mobility, dopant effects 4-84717  
 InP epitaxial layers, MOCVD growth 4-61862  
 InP, excitons bound to neutral acceptors, stress effects, photoluminesc. study 4-61294  
 InP, far IR optical props. at 6 and 300K 4-109174  
 InP films, excimer laser induced CVD 4-76679  
 InP, freq. depend. of negative cond., Gunn effect (Russian) 4-70825  
 InP growth mechanism by MOCVD, pyrolyses of group III metal-organics 4-99334  
 InP, high field transport of holes 4-80598  
 InP high-field transport, model 4-88512  
 InP, high-purity, in mag. fields, donor transition anomalous line broadening 4-109214  
 InP, hydride VPE growth, thermodynamic effects of using inert gas 4-99331  
 InP, implant depth profiles 4-65289  
 InP, InP:Zn, adducts in MOVPE, p-type doping 4-71575  
 InP, ion bombardment-enhanced etching 4-99618  
 InP, ion implanted, elec. activation by CW laser annealing 4-80088  
 InP, k.p. interaction and effective mass, band gap depend. 4-113850  
 InP, LEC grown, photoluminesc. study, 1.8 to 40K (Chinese) 4-84993  
 InP, LPE, numerical model of selective meltback morphology 4-65587  
 InP laser optically pumped by injection laser 4-107645  
 InP layers, MOCVD growth and characterisation (French) 4-76685  
 InP layers, prep. by chloride-hydride reaction 4-93232  
 InP, linear electro-optic coeff., Raman scatt. meas. 4-61659  
 InP, localisation of inversion electrons, Fourier transform spectra studies 4-98555  
 InP MOSFET structures, carrier channel mobility correl. with interface state meas. 4-88600  
 InP, mag. field induced metal-insulator transition 4-84566  
 n-InP, mag. field induced metal-insulator transitions 4-92614  
 InP, near IR cathodoluminescence in a TEM 4-81011

## III-V semiconductors continued

- InP, open diffusion technique using Zn<sub>3</sub>P<sub>2</sub>, appl. to lateral p-n-p transistor 4-104003  
 InP p<sup>+</sup>-n junctions,  $\gamma$ -ray irradi., electron trap annealing 4-98748  
 n-InP photoelectrodes, subbandgap response, effect of surface modification 4-88582  
 InP photoelectrodes, surface states, photocapacitance spectra studies 4-114010  
 InP picosecond photoconductors, circuit limits to time resolution 4-98661  
 InP planar diodes, fabrication using open tube method for Zn diffusion 4-95519  
 InP, Rama spectra, optically excited carriers 4-71368  
 InP, residual impurities determ. by charged particle activation anal. 4-85346  
 InP, SAW characterisation of surface and interface states 4-98681  
 n-InP, self-trapping and metastable M-centre 4-108809  
 InP, semi-insulating, simulation of anomalous Be diffusion 4-88193  
 InP single cryst., low temp. thermal cond. and phonons 4-88356  
 InP single crystals and solar cells,  $\gamma$ -irrad. damage 4-62356  
 InP solar cells, radiation resistant, electron irradi. damage 4-62351  
 InP, spinodal decomp., <sup>31</sup>P NMR spectra, chem. shifts 4-76279  
 InP substrate for BN:P film, CVD growth and elec. props. 4-99336  
 InP substrate for MBE grown Al<sub>1-x</sub>In<sub>x</sub>As 4-104735  
 InP substrates, applications of electron microscope techniques to semiconductors 4-103622  
 InP, surface and interface states 4-92782  
 InP surface decomp. rel. to In<sub>0.45</sub>N<sub>0.55</sub> Auger spectrum fine struct. 4-81046  
 InP, transition metal diffusion, photoluminesc. study 4-70461  
 InP, VPE, from In-PH<sub>3</sub>-HCl-H<sub>2</sub> system, growth parameters 4-61871  
 InP, volume plasmon dispersion, transmission electron energy loss studies 4-88465  
 InP Z 4-99619  
 InP:Be(C), acceptor levels, photoluminesc. study 4-80543  
 InP:Cd crystals, bulk and surface effects of heat treatment 4-84625  
 InP:Co, impurities, optical and transport studies 4-71444  
 InP:Cr, thermal conductivity, phonon scattering (French) 4-61155  
 InP:Fe, <sup>3</sup>He<sup>+</sup> bombarded, psec. photocond., very short free carrier lifetimes 4-108894  
 InP:Fe, semi-insulating, Four-wave mixing using photorefractive effect, optical processing appl. 4-74585  
 InP:Fe, semi-insulating, with phosphosilicate glass encapsulation: heat treatment, photoluminesc. and Raman scatt. characterisation 4-84995  
 InP:Fe, thermally annealed, Fe redistribution and diffusion coeff. 4-70460  
 InP:Fe photoconductor for synchrotron radiation research 4-91177  
 InP:Fe photoconductors, pulsed soft X-ray response 4-80620  
 n-InP:Fe-Au diode struct., photocurrent amplification 4-70934  
 InP:Ga,Sb crystals, dislocation density reduction by isoelectronic double doping 4-60940  
 InP:Gd(Yb) epitaxial films, doping effects on low-temp. edge photoluminescence 4-85028  
 InP:Ge(Sn), donor identification, photolum. and far IR photocond. in high mag. fields 4-70705  
 InP:He, ion implanted, elec. cond. study 4-80586  
 InP:Mg(Ca,Zn) crystals grown by synthesis solute diffusion, electrical and optical props. 4-85093  
 InP:Mg(Fe,Mg), implanted, effect on photoluminescence props. 4-85007  
 InP:Mn, hopping cond. between deep impurity states 4-104209  
 InP:Mn, solubility, coeff. of Mn distrib. 4-108621  
 InP:Sn(Sn)(Ge), (100), vacuum annealed, free carrier reduction 4-98610  
 InP:Sn(Sn)(Zn)(Fe) single crystals, LEC growth, perfection, carrier conc., TEM obs. 4-71550  
 InP:Se, ion implanted, annealing and transport props. 4-108397  
 InP:Si, electron irradi.-induced deep traps, impurity conc. effects 4-88468  
 InP:Si MISFETs, post-implantation capless annealing 4-113472  
 n<sup>+</sup>-InP:Si-p InP homojunction, implanted, photoelec. props., minority carrier diffusion length 4-76034  
 InP:Sn films, LPE grown, carrier saturation, Hall meas. 4-98789  
 InP:V(Cr), impurity excited states, optical absorpt. spectra 4-88863  
 InP:Yb p-n junctions; photoluminescence studies 4-66079  
 InP:Zn, electron irradi. damage, carrier conc. effects, minority carrier diffusion length 4-80107  
 InP:Zn, grown-in defects, annealing effects, DLTS studies 4-84287  
 InP:Zn, temp-dependent Zn diffusion mechanism using semiclosed diffusion method 4-80301  
 InP:Zn crystals, bulk and surface effects of heat treatment 4-84625  
 InP:Zn(S) single crystal growth, LEC technique, perfection, preferential etching, SEM and X-ray analysis 4-71549  
 n-InP/Ag Schottky barrier, improvement by Ru surface treatment 4-114035  
 n-InP/Au Schottky diodes with intermediate layer, longitudinal photoelec. effect 4-65743  
 InP/fluoride/InP double heterostructs., MBE growth 4-88420  
 InP/GaInAs heterojunctions and superlattices, 2-D magnetophonon resonance 4-98740  
 InP/InGaAs avalanche photodiode detectors for long-wavelength optical fibre communication systems 4-97134  
 InP/InGaAsP 1.5  $\mu\text{m}$  BH laser with etched cavity 4-83575  
 InP/InGaAsP DFB double-channel PBH laser diode, 1.55  $\mu\text{m}$ , single longit. mode operation 4-87358  
 InP/InGaAsP DH, LPE grown, misfit dislocations, TEM study 4-113826  
 InP/InGaAsP optoelectronic integrated device with optical bistability, design, fabrication and characts. study 4-83726  
 InP/InGaAsP p-type substrate and mass transported doubly BH laser 4-112428  
 InP/InGaAsP stripe geometry lasers, design and fabrication using D<sup>+</sup> bombardment 4-83622  
 InP/InGaAsP/InGaAs high-speed avalanche photodiodes 4-69590  
 InP/metal interfaces, chem. reactions, photoemission study 4-80310  
 InP/Pd interface, In segregation and Pd form., XPS study 4-80422  
 InP/Ta-Si sputtered film contacts, rectifying behaviour and barrier heights 4-70932  
 p-InP/Ti-Pt ohmic contact (Chinese) 4-88589  
 InP-Ag interface, reactions and Schottky barrier form., XPS studies 4-92821  
 InP-Al<sub>2</sub>O<sub>3</sub>, MIS struct. CVD growth and elec. props. 4-80680  
 InP-Au contacts, X-ray study of Au interactions 4-80675  
 InP-Au Schottky barriers, semicond. LEC growth, deep level defects (Chinese) 4-61320  
 InP-BN, density of interface states 4-80443

## III-V semiconductor continued

- InP-fluoride-InP (001) DH, growth by MBE, RHEED and elec. props. 4-98700
- InP-GaInAs IR detectors, applications of electron microscope techniques to semiconductor devices 4-103622
- InP-GaInAsP lasers, applications of electron microscope techniques to semiconductor devices 4-103622
- InP-In<sub>0.53</sub>Ga<sub>0.47</sub>As-InP DH wafers, LPE grown, misfit dislocations, X-ray and photoluminescence topography 4-80042
- InP-InGaAsP-InP DH, photoluminescence intensity 4-61738
- InP-MOS using indirect plasma-enhanced CVD technique for Al<sub>2</sub>O<sub>3</sub> gate dielec. 4-104529
- InP-metal interface, chem. reactivity 4-71973
- InP-n-AlInAs heterostructure, magnetotransport study 4-88570
- (InP)<sub>1-x</sub>Ge<sub>x</sub>, energy gap and phase transition 4-80494
- InSb 52-element imaging array for IR astronomical spectrometers 4-94625
- InSb (110), surface quenching of surface plasmon, exptl. evidence 4-61310
- InSb, anodic oxide film, surface relief and struct. 4-109531
- n-InSb, Auger recombination of holes via deep donors 4-104229
- InSb, band struct., angular resolved photoemission studies 4-84554
- InSb bicrystal, grain boundary barrier height and elec. cond. 4-92216
- InSb, carrier lifetime depend. on electron density 4-104228
- InSb, compensated, magnetooptic activity meas. using long-wave IR magnetopolarimeter 4-73484
- n-InSb, current-induced anisotropy of refractive index 4-104564
- InSb, Czochralski growth, Peltier coeff. at crystal/melt interfaces 4-70845
- InSb, degenerate four-wave mixing with surface guided waves 4-96982
- InSb detectors for ground-based astronomy 4-95517
- InSb dielectric constant calc. using Kane's band model (*Spanish*) 4-70648
- InSb, effective electron mass in inversion layers, surface elec. field effect 4-104280
- p-InSb, elec. current which is even in elec. field obs. 4-113952
- InSb etalon, controlled by guided wave, optical bistability on reflection 4-74597
- n-InSb film, amplification of total reflection mode surface phonons 4-70547
- InSb films, MBE growth and microstruct. characterisation 4-92578
- InSb, four-wave mixing, near-reson., nondegenerate 4-69486
- InSb, high temp. plasticity, anal. of expt. data 4-98186
- InSb, IR detector arrays, state-of-the-art review 4-111202
- InSb IR detectors for European Southern Observatory IR photometer/spectrophotometer 4-94624
- InSb inversion layer narrow gap systems, resonant polaron theory 4-98548
- InSb, ion implanted layers, IR reflection spectra studies 4-61717
- InSb, ion implanted single cryst., damage study by characteristic X-ray emission 4-88214
- InSb, isotope scatt. of large wave vector phonons 4-108564
- InSb, light amplification due to the magnetoelectric-photo effect 4-104578
- InSb MIS diodes with N-shaped V-I characteristics in inversion voltage region 4-114044
- InSb MIS struct., surface irregularity enhanced subband resonance 4-61459
- InSb, magnetised plasma, parametric excitation of electron-acoustic waves 4-88545
- n-InSb magnetised plasma, high-power helicon wave parametric decay 4-98657
- n-InSb, magnetoactive piezoelec. semiconductor, helicon waves, modulational instability 4-61407
- InSb, magnetoconcentration effect, transient processes 4-84628
- InSb, narrow-gap semiconductor, internal photoeffect, quantum efficiency calc. 4-61415
- n-InSb, negative magnetoresistance, upper Hubbard band conduction 4-65693
- n-InSb nonlinear optical props. photoelectronic investigation 4-96986
- InSb, optical bistability, physics and appls. (*Italian*) 4-107729
- InSb, phonon-phonon interactions, lattice thermal cond. 4-80320
- InSb, photo-EMF prod. by photon pulse accompanying optical transitions between Landau levels 4-70858
- InSb, photoconductivity under picosecond illumination (*Russian*) 4-88543
- InSb, photomagnetic effect and photocond. in mag. field, diamag. exciton discrete struct. 4-108903
- InSb, photoresistance on electron heating in mag. field, two-phonon oscills. 4-84650
- InSb photovoltaic IR detector array with quasi-plane struct. (*Chinese*) 4-106383
- InSb, polycrystalline, thermomagnetic and galvanic props. (*German*) 4-75987
- InSb, Raman freq. depend. on press. 4-109188
- InSb, Raman scatt. at high temp., diminishing energy gap near melting point 4-114274
- n-InSb, refractive index, influence of electron drift and heating 4-104561
- InSb, refractive index at 1.5K in near mm wavelength region 4-104554
- InSb, shallow donors in high mag. fields and hydrostatic press. 4-80540
- InSb, spin reson. of magnetoresist. and photo-EMF under stimulated Raman scatt. conditions 4-92962
- n-InSb, strongly compensated, electron mobility meas. 4-70834
- InSb surface, Auger inverse sensitivity factors of In and Sb 4-81048
- InSb surface, chem. etch effect (*Chinese*) 4-109528
- InSb surface, phase conjugation, reflecting grating recording by plasma refl. 4-97003
- InSb, surface magnetoplasma waves, waveguide propagation 4-114100
- InSb, surface periodic structures on intense laser bombardment 4-70202
- InSb, surface polarization dispersion under intense irradiation 4-113877
- InSb, tetrahedrally bonded, anisotropy of Compton profile 4-99217
- InSb, thermal oxidation method, XPS study, resistivity 4-114690
- InSb, tunable far-IR emission from uniaxial stress-enhanced spin-flip transitions 4-69416
- InSb, two photon interband magnetoabsorption, level transitions, photoconductivity meas. 4-71350
- InSb, two-photon reson. photo-Hall effect 4-70863
- InSb, US absorpt., elec. resist., mag. field effects 4-88243
- p-InSb, ultrasonic attenuation and elec. resistivity at low temps. and high mag. fields 4-80165
- InSb, X-ray diffraction study, cryst. struct. (*Russian*) 4-84280
- InSb:Be p<sup>+</sup>-n junction, ion implanted, insulated gate effects 4-61445

## III-V semiconductors continued

- n-InSb:Cr, Mn, impact ions. in 2-mm microwave field 4-70824
- InSb:Ge(Si), impurity solubility, role of acceptor and donor states 4-60949
- InSb:H, ionisation energy of magnetodons 4-70714
- p-InSb:Se, p-n junctions, doping and elec. props. 4-70919
- InSb/Al<sub>2</sub>O<sub>3</sub>-SiO<sub>2</sub> system, slow states, field effect studies 4-65752
- p-InSb/i-GaAs, heteroepitaxial struct., quasi-2D electrons, nonequilibrium galvanomagnetic effects 4-70916
- InSb-based magnetosensitive elements, operating principles at high and low temps., survey (*Russian*) 4-65691
- InSb-InTe, spreading of droplets of eutectic melt 4-113752
- InSe, lamellar, n- and p-type, in aqueous soln., photoelectrochemistry 4-88579
- InSe:Sn(Zn)(Ga)(S), dopant segregation and distrib. study 4-103940
- In<sub>1-x</sub>Sn<sub>x</sub>O<sub>3</sub>/In<sub>2</sub>O<sub>3</sub> solar cells, RF sputtering prep. and device performance 4-99967
- Si-BP-Si double heterojunction, current-voltage characteristics 4-80658
- Si<sub>3</sub>Ge<sub>1-x</sub>Ga<sub>x</sub>As heterojunction, interface carrier recombination velocity determ. 4-104304

## III-VI semiconductors

- electronic and vibrational spectra of III-VI layered semiconductors, review 4-71390
- nontrahedrally bonded binary and ternary cpds., collection of physical data 4-58587
- CdS single cryst., lasing action when illuminated by flashlamp 4-74520
- CdS<sub>1-x</sub>Se<sub>x</sub> single cryst., elec. cond. and Hall effect studies 4-113974
- Ga<sub>1-x</sub>In<sub>x</sub>Se single crystals, energy gap, temp. dependence 4-92610
- Ga<sub>1-x</sub>In<sub>x</sub>-Se, optical phonons, far-IR reflectivity spectra 4-104583
- Ga<sub>1-x</sub>In<sub>x</sub>-Se system, magneto-optical props. near fundamental band gap 4-109166
- GaSe, amorphous, short range order (*Russian*) 4-98015
- GaSe, EXAFS spectra and near edge struct. 4-66128
- GaSe<sub>1-x</sub>Se<sub>x</sub> layer solid solns., Raman scatt. spectra, effect of substitution-type disorder 4-99115
- GaSe, EXAFS spectra and near edge struct. 4-66128
- GaSe, excitons in high mag. fields, gauge-invariant energy variational calc. 4-80508
- GaSe, ground state energies of shallow donors 4-92654
- GaSe, layer crystals, Jahn-Teller effect 4-108824
- GaSe, optical orientation of carriers, optically detected EPR 4-88746
- GaSe, phonon inelastic scatt. from He atom impact 4-98426
- GaSe, Raman scatt. study of phonon-surface polaritons 4-80931
- GaSe single cryst., luminescence spectra, isothermal annealing effects 4-81001
- p-GaSe, space charge limited current behaviour 4-80597
- GaSe, surface pot., Ar<sup>+</sup> sputtering effects, XPS obs. 4-81103
- GaSe, uncooled, optical bistability rel. to excitons 4-74592
- GaSe:Co, injection and thermodepolarisation currents 4-70833
- GaSe:Fe, elec. cond. and impurity states 4-113957
- GaSe:Yb single cryst., photocond. and photoluminescence studies 4-84649
- p-GaSe/n-Cu<sub>3</sub>In<sub>2</sub>Se<sub>3</sub> heterojunctions, elec. and photoelec. props. 4-88573
- GaSe/SnO<sub>2</sub> heterojunctions, energy struct., reflectivity studies 4-66053
- GaSe-metal interface, chem. reactivity 4-71973
- Ga<sub>2</sub>Te<sub>3</sub>, electrical and optical props. meas. 4-61380
- InSb MIS structures, photoresponse enhancement in strong elec. field 4-65751
- InSe Bridgman grown crystals, growth parameters, improvement rel. to defects 4-98043
- InSe, EXAFS spectra and near edge struct. 4-66128
- InSe, elec. props., thickness depend. 4-88507
- InSe, electric field gradients, nuclear quadrupole freqs., anomalous temp. behaviour 4-71221
- n-InSe, electron scatt. mechanisms, Hall effect and magnetoresist. meas. 4-80614
- InSe, lamellar p-type, photointercalation and photodeposition of Cu 4-93539
- InSe, layered monocrystals, photoluminescence spectra, pol. plane orientation change effects 4-66069
- InSe, oxidation, XPS study 4-62075
- n-InSe, photoluminescence and free exciton emission 4-99176
- p-InSe, photomagnetolectric effect, minority carrier transport parameters 4-88530
- InSe, polytypism in the exciton absorpt. spectrum (*Russian*) 4-114304
- InSe, surface pot., Ar<sup>+</sup> sputtering effects, XPS obs. 4-81103
- n-InSe/p-CdTe heterojunction, elec. props. 4-108928
- InSe-Li intercalation cpd., photoelectric props. meas. (*Russian*) 4-104272
- In<sub>2</sub>Te<sub>3</sub>, electrical and optical props. meas. 4-61380
- Sm-GaSe barrier structures, elec. and photoelec. props. 4-84698

## IIR filters see digital filters

## illumination see lighting

## image amplifiers see image intensifiers

## image converters

see also fluorescent screens; image intensifiers

biocular magnifiers for electro-optic displays, visual comfort assessment

4-97024

high-speed photography, taking pictures a hundred million times a second

4-78399

IR flaw detection of semicond. epitaxial layers, homogeneity and thickness

meas. 4-109609

semiconductor technology, book 4-86123

streak image converter camera, linear scan, direct detect. of injection laser

psec pulses 4-74573

two-photon-resonant image upconverters using type I optical system, thick-

ness aberrations (*Japanese*) 4-79336

X-ray electron-optic image converters, temporal characts. 4-73607

## image iconoscopes see television camera tubes

## image intensifiers

air pulsed RF corona, ns. image intensifier investigation 4-84105

alpha particle, microchannel plate detector 4-74111

biocular magnifiers for electro-optic displays, visual comfort assessment

4-97024

cascaed image-intensifier tubes, temp., influence on MTF 4-91627

digital fluoroscopy imaging system, performance evaluation and quality

assurance 4-89706

electro-optical systems, moire phenomena appl. to modulation transfer

function 4-79334

electron-optical converters in flaw detection with ionizing radiation

4-71854

- image intensifiers continued**  
 Fabry-Perot interferometry using an image-intensified rotating-mirror streak camera 4-111190  
 fluoroscopic image quality requirements for coronary angioplasty, high definition video system performance 4-89707  
 focon use combined with luminance amplifiers 4-69579  
 gated X-ray intensifier with 50 picosec. resolution laser produced plasma expt. appls. 4-106441  
 high speed photography, videography and photonics, conf., San Diego, CA, USA (Aug. 1983) 4-106102  
 large-entry-window detector consisting of a microchannel plate and a channel-type electron multiplier 4-87013  
 MCP, direct fast gating study 4-59522  
 MCP in windowless EUV photon detectors, lifetime testing results 4-64297  
 MCP output current saturation and lifetime problems 4-64296  
 MCP photomultiplier tubes, timing props., computer anal. 4-64298  
 MCPs, characts. and appls. 4-95412  
 MEPSICRON photon counter for high dispersion spectrophotometry 4-94621  
 microchannel plate characts. and appls. in high energy physics expts. 4-64305  
 microchannel plate detector with CsI coated photocathode 4-73509  
 microchannel plate gain characts., reflection mode 4-78423  
 microchannel spatial light modulator, materials limitations 4-74697  
 nanosecond gated image intensifier with high gain and resolution 4-64762  
 nanosecond image shuttering studies at Los Alamos National Laboratory 4-69536  
 obliquely incident soft X-ray meas., using microchannel plate 4-86517  
 optical shutters using microchannel plate intensifier tubes 4-107806  
 radiological video imaging, system temporal response effect 4-89700  
 single stage VARO 4215 tube testing for astronomical appls. 4-72889  
 two-dimensional photon counting system, appl. in astronomy (*Japanese*) 4-94627  
 ultrafast gated intensifier design for laser fusion X-ray framing applications 4-68812  
 weak-contrast electron microscopic image restoration (*Russian*) 4-58918  
 X-ray image intensifier combined with high-speed videography for dynamic radiography 4-101991  
 N<sub>2</sub> pulsed RF corona, ns. image intensifier investigation 4-84105
- image orthicons** *see television camera tubes*
- image processing** *see picture processing*
- image sensors**  
*see also television camera tubes*  
 advanced IR sensor technology, conf., Geneva, Switzerland (April 1983) 4-95018  
 astronomical applications, CCD/transit instrument, progress report 4-72886  
 astronomical telescope pointing system using IR multiplex encoding imager 4-94613  
 atmospheric limitations on imaging systems 4-105708  
 balloon altitude mosaic meas., radiometer 4-115584  
 CCD astronomical light detector characts. and future developments (*Japanese*) 4-115690  
 CCD detector for astronomical spectrometer, comparison of two CCDs 4-110534  
 CCD device in cinematographic mode for enhanced resolution of telescope 4-94622  
 CCD image acquisition for digital phase meas. interferometry 4-106374  
 CCD scanning imagers, first-order performance prediction techniques 4-97131  
 CCD sun tracking sensors for sunlight concentrators 4-66667  
 CCDs, X-ray imaging and spectroscopy, performance 4-68340  
 coherent IR radar systems and appls., conf., Arlington, VA, USA (Apr. 1983) 4-95019  
 conference, San Diego, CA, USA (Aug. 1983) 4-95022  
 digital processing of dynamic imagery for photogrammetric applications 4-58902  
 FDL 60 film scanning system, development 4-63797  
 HgCdTe infrared focal plane arrays for imaging spectrometer applications 4-100758  
 infrared (2.6-5  $\mu$ m) mosaic detector mounted on a balloon, design of optical subsystem 4-77652  
 IR, short wavelength, linear imaging array for high resolution spaceborne camera 4-100761  
 IR astronomy, two-dimensional imaging, CCD or CID arrays 4-101159  
 IRAS infrared astronomical telescope in orbit, design and performance 4-77712  
 IRCCD sensors, Schottky barrier, Earth resources features appls. 4-100759  
 line/edge position determ. for optically effective design, CCD line appl. (*German*) 4-86385  
 low light level imaging system field performance estimation, spectral matching considerations 4-73506  
 MEIS II multidetector electrooptical imaging scanner, airborne pushbroom imager 4-100760  
 microwave imaging system, 94 GHz, tapered, slot antenna array design, tracking appl. 4-78375  
 moire topography, sampling theory and charge-coupled devices 4-73496  
 multisensor images for Earth science appls. 4-77659  
 multispectral imaging systems, summary 4-77660  
 nanosecond image shuttering studies at Los Alamos National Laboratory 4-69536  
 near-MM wave IC imaging polarimeter antenna arrays 4-82827  
 optical infrared remote sensors 4-111206  
 photon-imaging detector, variable threshold discrimination 4-68278  
 plasma, MHD unstable, image sensing using multichannel plate detector 4-84072  
 radars, overview 4-77694  
 sampled image systems, MTF anal. 4-107529  
 scanning matrix system for grey-scale picture technique (*German*) 4-64681  
 sensors, for fading memory focal plane processor 4-107871  
 Shuttle spectrometer experiment for late 1980s 4-77695  
 space IR sensors parametric studies 4-94249  
 space-borne optical imagers for Earth observation, large IR detector arrays 4-94248  
 thematic mapper in LANDSAT 4 Earth resources satellite, oscillating scan mirror assembly 4-115667
- image sensors continued**  
 InSb 52-element imaging array for IR astronomical spectrometers 4-94625  
 PtiSi Schottky IR CCD evaluation for astron. appls. 4-64789  
 SiO<sub>2</sub> low-loss high-resolution image fibre fabrication, imaging optics method 4-97095
- image storage tubes**  
 No entries
- imagers** *see image sensors*
- images, optical** *see optical images*
- imaging, acoustic** *see acoustic imaging*
- imaging, infrared** *see infrared imaging*
- imaging, NMR** *see magnetic resonance spectroscopy; nuclear magnetic resonance*
- IMMA** *see ion microprobe analysis*
- immiscibility** *see solubility*
- impact (mechanical)**  
*see also ballistics; impact strength*  
 aerospace biodynamic test devices and methods, AGARD report 4-78058  
 bar, finite length, variable cross-section, elastic wave propag., impact loading effects 4-112750  
 bar, longit. impact, plastic wave propag., strain plateau, Malvern's theory 4-74969  
 brass, erosion in single particle impacts, significance of erosion parameter 4-81295  
 cervical spine, human, 3D model for impact simulation 4-105281  
 circular discs, with central hole, impact loading, crack initiation and propag. 4-97439  
 composite plates, delamination growth during impact, fracture mechanics analysis 4-79526  
 concrete, impact testing, meas. device effect on curve shape (*German*) 4-66535  
 dynamic behaviour of oblique edge-crack under impact loading 4-91770  
 dynamic contact law, expt. determ. method 4-69714  
 dynamic impact of an elastically supported beam-large area contact 4-79527  
 elastic bodies, similarity in contact problem 4-108050  
 elastic impact problems, lumped parameter method 4-97393  
 epoxy polymers, elastic constants under impact loading, plasticiser content effect 4-66364  
 external circular crack form. by normal impact or sudden twisting, dynamic stress intensity factors 4-87622  
 fatigue wear testing method 4-89216  
 fragments from hypervel. impact expts. rel. to asteroid shapes 4-72906  
 glass cloth reinforced polyester panels, elastic props. under low velocity impact 4-89079  
 glass fibre reinforced epoxy resin, fracture initiation under impact compression 4-76863  
 glass fibre reinforced polyester, panels, surface damage due to projectile impact 4-76865  
 half space, elastic, nonhomogeneous, indentation of a system of stamps, press. anal. 4-108051  
 head and neck, human, in vitro response to impact 4-105280  
 hexanitrostilbene, impact initiation, photographic investig. 4-109648  
 layered composite, penny-shaped interface crack, torsional impact response 4-79498  
 long rod impact onto large target, numerical study 4-91778  
 membrane, circular, impact response to blunt projectile 4-87634  
 metal bar, impacted, meas. transient vibration by high speed laser interferometry 4-111189  
 metal-metal collision sticking behaviour and relevance to solar nebula 4-67649  
 metals, impact strength testing, notches appl. 4-99678  
 missile, rigid-plastic, impact force 4-101645  
 multiyear ice floe impact estimation for offshore structures 4-115434  
 orthotropic medium, cracked, impact response 4-74967  
 oscillator, periodically forced impact, with large dissipation 4-95157  
 penetration theory appl. for multilayered targets 4-87637  
 planar collisions, particle and rigid body, friction, restitution and energy loss 4-101646  
 plastic flyer plate, impact spalled, streak photographic anal. 4-111228  
 polymer particles, charge build-up by repeated impact 4-80655  
 polymethylmethacrylate, axially symmetric impacts, stress time history determ. 4-108053  
 quasi-isentropic compression wave generation method 4-108539  
 rocks RF emissions during hypervel. impact expts. 4-72581  
 rod, shock-laden, stress pulseform anal. 4-64878  
 single crystals, dislocation struct. formed under indentation (*Russian*) 4-88168  
 steel, dynamic flow curve, symmetric rod impact test 4-109486  
 steel, ferritic, impact testing, classification of absorbed energy-temperature curves 4-89230  
 steel, hardness testing, with impact action standard-fee instruments 4-99675  
 steel panels, surface damage due to projectile impact 4-76865  
 steel plate, long rod penetration, stress/strain studies 4-108512  
 strain determ. in dynamic compression test 4-112780  
 vibrating circular cylinder, elastic rod collision appl. to nuclear reactor 4-97372  
 Al alloy panels, surface damage due to projectile impact 4-76865  
 Al, damage simulation in high velocity impact 4-108529  
 Al, impact by steel spheres, velocity propagation 4-108532  
 Al impulsively loaded long rod expts., use of manganin stress transducers 4-97448  
 Al rods impactation on PMMA target, radial displacement meas. method 4-106280  
 Au target, impact craters due to glass pellets 4-108689  
 Cu, dynamic tensile fracture due to impact 4-108510  
 Cu, target, impact craters due to glass pellets 4-108689  
 Ti-Al-V (6, 4 wt.%), fatigue strength, influence of adiabatic shear bands 4-99485  
 Ti-Al-V (6, 4 wt.%), erosion by spherical particles at 90° impact angles, effect of microstruct. 4-76876  
 W-Ni-Fe, dynamic strength calcs. based on grain deform. 4-108511
- impact avalanche transit-time diodes** *see IMPATT diodes*
- impact ionisation**  
 dielectric material, transparent, failure mechanism using focused laser single pulse, role of nonlinear refraction and absorpt. 4-91515

**impact ionisation continued**

- p-n junction, reverse-biased; switching to high cond. state, computer simulation 4-61452  
 p-n junctions, avalanche breakdown temp. parameters 4-88568  
 p-n junctions, avalanching, impact ionisation induced minority carrier injection 4-92807  
 semiconductors, Auger and impact ionisation processes, calc. of commonly neglected terms in matrix element 4-99237  
 transparent solid, laser-induced intrinsic damage, seed electron deterrent lack effect in avalanche ionisation 4-81045  
 GaAlAs lasers, catastrophic and latent damage due to elec. transients 4-79146  
 GaAs, high field transport of holes 4-80598  
 GaAs, high-field transport, model 4-88512  
 GaAs impact-ionized plasma instability, delay time estimation, Monte Carlo technique 4-70853  
 GaAs:Cr, ionisation processes by upper conduction band electrons, mag. field effects 4-65640  
 GaAsP p-n junctions, avalanche multiplication and ionisation rates, SEM studies 4-65733  
 Ga<sub>0.33</sub>In<sub>0.67</sub>As<sub>0.70</sub>P<sub>0.30</sub>, (100) oriented, electron and hole ionisation coeffs. 4-98662  
 GaP p-n junctions, avalanche multiplication and ionisation rates, SEM studies 4-65733  
 Ge, impurity breakdown kinetics, small-signal anal. 4-113965  
 n-Ge, low temp. breakdown characts. 4-92737  
 GeSb, photoexcited, impurity breakdown and impact ionisation 4-92739  
 InAs high field transport, model 4-88512  
 InAs<sub>1-x</sub>Sb<sub>x</sub> epilayers, impact ionisation coeffs. 4-104333  
 InP, high field transport of holes 4-80598  
 InP high-field transport, model 4-88512  
 n-InSb:Cr, Mn, impact ions in 2-mm microwave field 4-70824  
 Si p-n junctions, electron irradi., differential resist. in avalanche breakdown region, temp. depend. 4-88571  
 Si solar cells, local area generation characts., elec. field stimulation (*Russian*) 4-109740  
 Si/SiO<sub>2</sub>/Al capacitors, interface trap generation and H electromigration 4-70940  
 SiC p-n junction, ambipolar avalanche multiplication 4-84684  
 SiO<sub>2</sub> gate oxide breakdown, expt. study 4-114207  
 Ta, anodic oxidation, electron injection and avalanche breakdown 4-89183

**impact phenomena** *see collision processes***impact strength**

- see also fracture toughness; notch strength*  
 ABS polymers, craze formation and texture 4-104889  
 bar, notched, impact work method (*German*) 4-99696  
 composites, cement-based, modified instrumented Charpy test 4-89204  
 critical brittleness temperatures determined on specimens with different stress raisers 4-104937  
 epoxide composite, alumina particle filled, fractography (*Japanese*) 4-99512  
 epoxy resin, filler reinforced, impact tensile fatigue strength, statistical analysis (*Japanese*) 4-99504  
 fibre reinforced Al alloy, prep. by explosion technique, mech. props. at low temp. 4-114634  
 glass cloth reinforced polyester panels, elastic props. under low velocity impact 4-89079  
 glass fibre reinforced plastic, sheet moulding cpd., impact damage 4-76829  
 glass fibre reinforced thermoplastic alloy, mech. props. at elevated temps. 4-76855  
 graphite, polycrystalline rods, single impact stress calc. 4-76840  
 impact-tension compression test using split-Hopkinson bar 4-87639  
 metal plate, spalling fracture under shock loading 4-89112  
 metals, spalling microdamage initiation, critical loading conditions 4-89111  
 PMMA, dynamic fracture toughness, determ. by impact bending test (*Japanese*) 4-93488  
 polyamide 6-rubber blends, morphology and mech. props. 4-93344  
 polyamide-6, blending with copolymers, effect on props. (*Polish*) 4-66433  
 polycarbonate blends with ABS and SAN, tensile and impact tests, energy absorpt. 4-66389  
 polyethylene fibrillated tape reinforced cement, mech. props. 4-109493  
 polypropylene fibre reinforced mortar, thin slabs, fracture toughness under flexural or impact loading 4-99576  
 steel, alloy, mech. props. and precip. hardening response 4-89107  
 steel, alloy type, Ca treated resulphurised, mech. props. and machinability, S and sulphide shape effect, report 4-62048  
 steel, C, crack growth and closure under impact fatigue 4-114630  
 steel, C, impact bending test, specimen shape and dimensions effect (*Japanese*) 4-99689  
 steel, C, laser glazed hot rolled Charpy samples, impact testing 4-81377  
 steel, C, plate, projectile impact strength critical fracture energy 4-99477  
 steel, C, yield stress rel. to C content and pearlite morphology, tensile and Charpy obs. 4-81248  
 steel, C-Mn, hot-rolled, ductility and anisotropy of sulphide inclusion spacings, effect of inclusion shape 4-99437  
 steel, carburisation, sintering, mech. props. rel. to Cu and P alloying 4-89069  
 steel, Charpy V notch impact testing with laser glazing pre-cracking 4-99681  
 steel, Co eutectoid, mech. props. 4-114629  
 steel, constructional, fracture resist., method of stress raiser appl. influence 4-62037  
 steel, constructional, strengthening using thermomech. treatment and deform. in intercrit. temp. range 4-114585  
 steel, Cr, fracture toughness and mech. props., effect of tempering 4-76854  
 steel, Cr-Mo, fracture toughness degradation after long-term service in petroleum refining (*Japanese*) 4-89126  
 steel, Cr-Mo-V, hot work, powder metallurgically produced by hot isostatic pressing 4-93248  
 steel, Cr-Mo-V-W, ferritic, impact props., effect of specimen size and Ni content 4-104848  
 steel, Cr-Mo-V-W, ferritic-martensitic, reduction of ductile-brittle transition temp. 4-104849  
 steel, die, mech. props. after low-temp. mech. treatment 4-61962  
 steel, effect on wear resist. in abrasive friction 4-93425  
 steel, eutectoid, mech. props., effect of Si additions 4-93365

**impact strength continued**

- steel, fracture toughness, quasi-state and impact, effect of different thermal treatments 4-99599  
 steel, heat treated, retempering effect on strength props. 4-114587  
 steel, impact fracture toughness rel. to anti-tuffriding coating (*Japanese*) 4-99515  
 steel, low C, ductile-brittle transition temp., effect of tensile prestrain (*Japanese*) 4-114650  
 steel, mechanical props. rel. to US detectable discontinuities 4-71713  
 steel, mild, C-Mn, Charpy V transition temp. rel. to various material parameters 4-66431  
 steel, Mn, 13 to 19 wt.%, sinter-forged, mech. props. 4-81283  
 steel, Nb, strengthening mechanisms, influence of rolling variables 4-71666  
 steel, Ni type, phase comp. effect on low-cycle impact fatigue resist. 4-93389  
 steel, nuclear structural, A-203D, low temp. deform., effect of microstruc. 4-66386  
 steel, powder metallurgy, prod. by dynamic hot pressing, design strength 4-89011  
 steel, roll type 9Kh, small N and B additions effect on struct. and mech. props. 4-93342  
 steel, rolled, impact toughness and transition temp., effect of delamination (*Korean*) 4-76848  
 steel fibre reinforced mortar, thin slabs, fracture toughness under flexural or impact loading 4-99576  
 steels, tool, hot isostatic pressing powder metallurgy fabrication method 4-89004  
 styrene-butadiene block copolymers, deform. rel. to pretreatment, impact strength 4-93331  
 thermoplastics, cellulosic filler efficiency, processing characts. and mech. props. 4-61913  
 thermoplastics, recovery-induced thermal deform. 4-99469  
 thermoplastics testing using computerised machine 4-104934  
 Al and alloys, shear strength under torsional impact, strain rate depend. (*Japanese*) 4-99432  
 Al-glass composite, produced by powder metallurgy route, mech. props. 4-66275  
 Al-Si, silumins, permanent modification with Sr and Sb (*Polish*) 4-85145  
 C fibre reinforced plastic, impact stability evaluation 4-89129  
 Cu-Al-Zn system, high damping  $\beta$  alloys, effect of aging in martensite condition on mech. props. 4-114588  
 Cu-Sn-Al<sub>2</sub>O<sub>3</sub>, abrasive composite, physicomech. props., effect of premoulding press. in elec. discharge sintering 4-89020  
 Fe-base alloys, dynamic fracture toughness, results from instrumented impact machine 4-81373  
 Fe-Ni austenitic alloys, crack growth and plasticity, influence of mag. ordering (*Russian*) 4-93368  
 Mo, purification by arc melting, mech. props. (*Japanese*) 4-89116  
 Mo-base alloy, dynamic fracture toughness, results from instrumented impact machine 4-81373  
 Mo-base alloys, welded joints, long-term strength characts. effect of alloying with N 4-109513  
 Ni-base alloys, dynamic fracture toughness, results from instrumented impact machine 4-81373  
 SiC fibre reinforced Al alloy, fabrication and mech. props. (*Korean*) 4-104755  
 Ti-Al-Nb-Ta-Mo, welds and castings, impact roughness, segregation and influence of B 4-114658  
 WC-Co-P, wear resist., P addition influence 4-66458
- IMPATT diodes**  
 GaAs, epitaxial layer growth in multiwafer VPE system, IMPATT device fabrication 4-104738
- impedance, acoustic** *see acoustic impedance*  
**impedance, electric** *see electric impedance*  
**impedance, electric, measurement** *see electric impedance measurement*  
**impedance, measurement, electric** *see electric impedance measurement*  
**impedance matching**  
 ArF excimer laser, doubly preionised 4-112398
- imperfections, crystal** *see crystal defects*  
**impermeability** *see permeability*  
**implosions** *see explosions*  
**impulse amplifiers** *see pulse amplifiers*  
**impulse generators** *see pulse generators*  
**impulse voltages** *see transients*  
**impulse welding** *see resistance welding*
- impurities**  
 for impurity vibrations *see "lattice localised modes" or "molecular vibrations in solids"*  
*see also chemical analysis; crystal inclusions; crystal purification; diffusion in solids; impurity-defect interactions; impurity distribution; impurity electron states; interstitials; magnetic impurity interactions; phonon-impurity interactions; segregation; semiconductor doping*  
 alkali halide crystals, etch pit studies of dislocations, dissolution kinetics and impurity effects 4-70158  
 alkali metal halides: Mg<sup>2+</sup>(Ca<sup>2+</sup>)(Sr<sup>2+</sup>), impurity complex binding energies 4-60912  
 alloy solid soln., partial impurity volume and lattice deform. 4-108390  
 alloys, impurity atoms solubility, impurity-atom complexes formation (*Russian*) 4-103937  
 alloys, virtual bound state, proximity effect tunnelling 4-114074  
 anharmonic crystals, local vibr., local instability, self-consistent harmonic approx. 4-88258  
 anisotropic superconductor with Kondo impurities, transition temp. 4-104352  
 antiferromagnetic Ising model, anisotropic, long-range order, quenched impurity effects 4-98848  
 Baxter model, impure, universal behaviour, Monte Carlo studies 4-104388  
 benzimidazobenzophenanthrolin type ladder polymers, conducting props. and doping 4-63663  
 biphenyl cryst. reson. excited defect emission 4-109231  
 brittle fracture, impurity effects: Auger electron and scanning electron spectroscopy (*French*) 4-70268  
 calcium oxalate monohydrate, crystallisation kinetics 4-103684  
 CDW cond. with strong impurity pinning, permitt. threshold elec. field 4-98597  
 centres in two-well adiabatic pots., relax. process effect on luminesc. spectra and burnup 4-109223

purities continued  
 cholesteryl benzoate, liq. cryst., impurity effect, UV absorpt. spectra 4-61128  
 complex dielectric cryst. with impurities, acoustic wave absorption 4-80167  
 condensed media, reson. nonradiative electron-excitation energy transfer between impurity ions 4-109226  
 conference, Alanya, France (June-July 1982) 4-95052  
 crystal growth from melt, rapid solidification, computer simulation 4-114383  
 Czochralski process, contamination reduction method 4-66210  
 damage profile in crystals, meas. by channelling technique 4-103840  
 electron gas, 2D, quasi-particle Coulomb inelastic lifetime 4-98554  
 electron probe analysis, detection limit, vol. and surface impurity diffusion effects 4-99918  
 erbium hexa antipyrine tri-iodide:Gd<sup>3+</sup>, soft mode dynamics, phase transition, EPR 4-109068  
 ferroelectric solid soln., 'supersonic' phase transition in disordered sublattice 4-84919  
 ferroelectric symmetrical phase, forbidden Raman lines 4-66026  
 ferromagnetic components quality control by coercive field strength meas. 4-93475  
 fluoride deposits, Gd, Ce and Eu impurities study by EPR and neutron activation anal. 4-80815  
 glass: rare earth ions, low temp. optical dephasing rate 4-88789  
 glass/liquid interface, laser beam induced holographic bubble grating form. 4-83683  
 glycine, radiothermoluminesc., ESR induced 4-61758  
 grain boundary model, impurity effects, cluster variation method calcs. 4-113465  
 ionic crystals, diatomic mol. impurities at cubic sites, rotronic Jahn-Teller effect 4-98578  
 kinetics of impurities in low temp. matrices 4-92434  
 luminescence spectra 4-76506  
 magnetic material with one-component order parameter, phase transition 4-88674  
 many-valley semicond., shallow donor polarisabilities 4-92666  
 measurement of lattice defects in semiconductor diode structures, by capacitance method 4-90611  
 metallic solids, Debye-Waller factor for substitutional Mossbauer impurity 4-75633  
 metallic solids with small conc. of impurities, Mossbauer oscillator strengths, Debye-Waller factor 4-75634  
 metals, BCC and FCC, H and He impurities, self-trapping phenomena 4-80056  
 metals, diffusion of C, N and O, review, 4-65474  
 metals, interatomic forces near a defect, impurity-susceptibility method 4-113490  
 metals, muon states, recent progress 4-65902  
 metals, noncubic, elec. quadrupole interaction studies, review, book contrib. 4-70764  
 metals, pure, impurity diffusion, models, review 4-65471  
 metals, surfaces, impurities and defects, embedded atom method 4-92590  
 metals, thermodynamic scaling theory for impurities 4-113678  
 metals with impurities, solubility and lattice sites, pseudopotential theory (Russian) 4-103938  
 minerals containing water, IR spectral studies 4-93071  
 molecular luminescence and its applications, conf., Kharkov, USSR (1982) 4-106094  
 muonium, anomalous, struct. in crystals 4-65278  
 naphthalene cryst., excitons, defects and intramolecular phonon interactions (Russian) 4-98532  
 narrow band gap semicond., impurity recomb. accompanied by local phonon excitation 4-88516  
 negative Hubbard energy, BCS theory 4-70981  
 nonmagnetic metal with mag. impurity, density of states, sp. ht., triagonalisation 4-92665  
 one-dimensional CDW system, pinning by impurities, dynamics 4-75879  
 oxides, defect energetics and nonstoichiometry 4-92201  
 oxides and carbides, segregation at surface and grain boundaries 4-92377  
 p-n junctions, charge transport, influence of impurity clusters, electron-positron pair annihilation study 4-108934  
 phenothiazine type ladder polymers, conducting props. and doping 4-65663  
 phthalocyaninato stacked bridge macrocyclic metal complexes, synthesis and conduction props. 4-65662  
 poly(2,5-seleniénylene), elec. cond., synthesis 4-70886  
 poly(p-phenylene sulfide), oriented, acceptor doping, struct. changes on annealing 4-75325  
 poly(N-alkyl-3,3'-carbazolyl)-I<sub>2</sub> complexes, highly conducting, synthesis and I<sub>2</sub> doping 4-65664  
 poly(thiophene), chemically coupled, synthesis and elec. props., AsF<sub>5</sub> doping 4-75952  
 poly(vinylidene fluoride), solution growth, ionic impurity effects 4-98037  
 poly-para-phenylene, conducting oriented fibres, synthesis, struct. and AsF<sub>5</sub> doping 4-65666  
 polyacetylene:I<sub>2</sub>, I<sub>2</sub> doping, synchrotron scatt. study 4-65286  
 polyacetylene:I, IR refl. spectra, effect of sample densification 4-99120  
 polyacetylene:I, vibr. props., Raman study 4-75632  
 polyacetylene, donor- and acceptor-doped, structure and props. 4-75323  
 polyacetylene, electrochem. doping with InCl<sub>3</sub>-LiCl in nitromethane soln. 4-75465  
 polyacetylene, electrochemical doping, reduction potentials meas. 4-65284  
 polyacetylene, electrochemistry and aqueous chemistry, p-type doping 4-77013  
 trans-polyacetylene films, thermally isomerised and doped/dedoped 4-65196  
 polyacetylene-polyacetylene-d<sub>2</sub> transcopolymers, I<sub>2</sub> doped, Raman and IR spectra and vibr. freq. dispersion 4-60857  
 polyacetylene/elastomer blends, electrically conductive, doping 4-75940  
 polyacetylenes and polydiacetylenes, solid state reactivity and props. and SbF<sub>6</sub>(Cl<sub>4</sub>) doping 4-75318  
 polycrystalline film, impurity diffusion, Monte Carlo calcs. 4-108660  
 polyethylene terephthalate, crystallisation rate, effect of silicon nucleants 4-88117  
 polymer-polymer diffusion couples, intrinsic and interdiffusion coeff. 4-80312  
 polymers, electrical cond. and carrier traps, review 4-108854  
 polymers, linear chain, localised excitations, resonant energy transfer 4-80505

## impurities continued

polyphenylquinoxaline, conducting polymer, caesium electride doping 4-65285  
 polypropylene, reversible secondary crystallisation during cooling, UV microscopy obs. 4-113374  
 polythiophene:BF<sub>4</sub><sup>-</sup>(Bu<sub>4</sub>N<sup>+</sup>), electrochemical n-type and p-type doping, elec. and optical props. 4-61363  
 polythiophene, conducting polymer, electron beam irradi. in SF<sub>6</sub> gas, elec. and optical props., radiation induced doping obs. 4-75531  
 Potts model, p-component, with correlated impurities, crit. behaviour 4-101780  
 proximity effect sandwiches, local spin fluctuations, renormalisation group anal. 4-114073  
 pure, cold worked, annealing characts. rel. to trace element additions 4-109438  
 pyrrone, conducting polymer, caesium electride doping 4-65285  
 quantum crit. behaviour, quenched impurity influence 4-63656  
 quantum plasma, charged impurity static shielding in mag. field 4-80520  
 quantum systems with long-range correlated impurities, dynamical critical exponent 4-68168  
 quartz:Ag(Cu), X-ray irradi. induced optical absorpt., impurity electrolysis effect 4-70208  
 quartz, hardness properties influenced by high-temp. and impurities 4-94107  
 quartz, hydrolytically weakened, plasticity and rheology 4-92286  
 quartz, natural, struct. defects and impurities diffusion 4-80055  
 quartz, seed treatment effect on dislocations 4-61827  
 quartz containing water, IR spectral studies 4-93071  
 quartz crystals, electrical conductivity and dielectric loss, effect of alkali ions 4-71271  
 quasi-one dimensional superconducting state, impurity induced soliton form. 4-76067  
 radical reactions magnetic and spin effects, paramagnetic impurities influence 4-89252  
 randomly diluted lattices, self-avoiding walks, impurity effects 4-73380  
 rare earth impurity ions in crystals, phonon-assisted energy transfer, conc. depend. 4-92311  
 ruby, negative nonlinearity of refractive index 4-79223  
 ruby, X-ray irradi., phonon decay and lifetimes 4-65358  
 semiconductor purity, Hall effect measurements 4-75986  
 semiconductor thin films, dielec., function calc., screening effect 4-70693  
 semiconductors, defect formation as a result of isovalent doping 4-70181  
 semiconductors, impurity atom diffusion, two-dimensional numerical anal. 4-92432  
 semiconductors, impurity photoabsorption theory 4-99138  
 semiconductors, microkinetics of two-component diffusion 4-88350  
 semiconductors, momentum relax. time of Wannier-Mott excitons scatt. by charged impurities 4-61296  
 semiconductors, multivalley polar with impurities, optical absorption by electron plasmas 4-114230  
 semiconductors, self-diffusion, vacancy mechanism 4-70466  
 semiconductors, undoped, Thomas-Fermi-Dirac statistics of dielectric screening 4-61314  
 n-Si, radiation defect formation, annealing, defect interactions 4-113499  
 solid surface, chemical and electrochemical treatment, low energy electron induced X-ray spectra 4-76572  
 solids, lyoluminescence, effect of transition metal ion impurities 4-76527  
 spin systems with impurities, static and dynamic crit. props., two-loop approx. 4-61541  
 steel, austenitic and ferritic stainless, fusion reactor material, crack growth modelling 4-104851  
 steel, austenitic stainless, heat-resistant, high Si content, oxidation resist. 4-114724  
 steel, Cr, martensitic, impurity level rel. to fusion reactor first wall appl. 4-107013  
 steel, low C, nitrocarburising, annealing, positron annihilation, vacancy-impurity clusters in surface layer 4-66094  
 steel, pressure vessel, A 508 2 and A 533 B, comparison of stress-relief cracking 4-109510  
 steel, steam turbine casing and rotor, mech. props. rel. to service life (Japanese) 4-89119  
 steel, tool, brittle fracture, dopants and impurities effects, AES study 4-62063  
 strong-coupling supercond. with Shiba-Rusinov impurities, free energy formula 4-104358  
 SU(N) Anderson impurity model, thermodynamic Bethe-ansatz eqns. 4-104110  
 substitutional impurities, indirect interaction in linear at. chain 4-61318  
 superconductors, phase transition, influence of correlated impurities 4-88625  
 superlattices, thermopower as probe of density of states distrib. 4-98714  
 surface impurities, low-energy ion beams anal. appl. 4-99893  
 TGS, stabilisation of polar states with impurities 4-75468  
 thiourea, memory effect, defect density waves in modulated systems 4-88163  
 three component solid soln., equilib. competitive segregation 4-66338  
 transition metal carbide and carbonitride solid solns., mag., elec. transport, supercond. props. review 4-80590  
 triplet pairing supercond., possible diminution of impurity pair breaking in weakly localised 2D nearly mag. systems 4-104357  
 two-dimensional random electron system under strong mag. fields, dynamical diffusion coeff., self-consistent treatment 4-98640  
 type II supercond., elemental-flux pinning pot. 4-76093  
 water, high purity, resistivity meas., temp. depend. 4-113940  
 ytterbium hexa antipyrine tri-iodide:Gd<sup>3+</sup>, soft mode dynamics, phase transition, EPR 4-109068  
 Zircaloy-4, microstruct. after air cooling from high temp.  $\beta$ -phase, effect of P impurity content 4-89071  
 Ag, impurity diffusion, isotope effect meas. 4-65476  
 Ag-Gd(Er), dil., impurity-induced muon depolarisation, mag. field depend. 4-71228  
 Al, corrosion resistance of oxide layers rel. to impurity content 4-62102  
 Al, doped, trapping of muons and protons, effect of substitutional impurities 4-65631  
 Al, positive muon pot., self-consistent cluster calc. 4-71236  
 Al, secondary ion emission, O effects 4-76609  
 Al-Cu-Mg wrought alloy 1163, props. 4-62038  
 Al-In, dil., He localised diffusion around In impurities, PAC obs. 4-65470  
 Al-Mg(Ga)(In)(Si)(Ge)(Sn), distribution of electric field gradients around impurities, conduction electron screening lattice strain 4-113910

## impurities continued

- Al(NO<sub>3</sub>)<sub>3</sub>:Cr<sup>3+</sup>, exchange-coupled Cr<sup>3+</sup>-Cr<sup>2+</sup> pairs, EPR obs. 4-88717  
 Al<sub>2</sub>O<sub>3</sub>:Ti, sintering and densification, defect models 4-109364  
 Al<sub>2</sub>O<sub>3</sub>:Zr, sintering and densification, defect models 4-109364  
 Au (110) and (111), adsorption of O<sub>2</sub>, substrate impurity effects, EELS, AES, and XPS study 4-93160  
 Au, adsorption of O<sub>2</sub>, AES, XPS, and thermal desorption study 4-92556  
 Au impurity contaminations, PIXE anal. 4-99874  
 Au, impurity diffusion, isotope effect meas. 4-65476  
 Au-Gd, dil., impurity-induced muon depolarisation, mag. field depend. 4-71228  
 B impurity diffusion in amorphous alloys, SIMS study 4-92435  
 Ba<sub>0.5</sub>Sr<sub>0.5</sub>Nb<sub>2</sub>O<sub>6</sub>, pure and La(Ce) doped, thermally stimulated electron emission, dielectric characs., impurity effects (Russian) 4-114356  
 Ba<sub>0.5</sub>Sr<sub>0.5</sub>TiO<sub>3</sub>, soft mode behaviour, ferroelec. transition and IR reflectometry 4-80872  
 BaTiO<sub>3</sub>:Fe, soft mode behaviour, ferroelec. transition and IR reflectometry 4-80872  
 Bi<sub>2</sub>SiO<sub>5</sub>, deep impurities, photoelectric phenomena 4-113996  
 Bi<sub>2</sub>Si(Ti)<sub>2</sub>O<sub>7</sub>, gyrotropic crystals, electro-optical and optical props. (Russian) 4-93058  
 Bi<sub>2</sub>Te<sub>3</sub> cryst., external shape, impurity complex effects 4-75347  
 CO<sub>2</sub> laser, gaseous medium temp., influence of high-mol. compound impurities 4-79103  
 CaF<sub>2</sub>:La(Er), impurity local structural environments, EXAFS determ. 4-66129  
 CaF<sub>2</sub>:Sr<sup>2+</sup>(Y<sup>3+</sup>), lattice relax. around impurities, EXAFS study 4-93140  
 CaZn<sub>12</sub>Mn<sup>2+</sup> cryst. struct., axial field splitting calc., EPR, optical spectra 4-92159  
 Cd:Bi, crystal growth from vapour, Bi impurities effect 4-113368  
 Cd<sub>0.95</sub>Te-CdTe heterostruct. interfaces, SIMS anal. of impurities 4-108727  
 CdS films grown by spray pyrolysis in an N<sub>2</sub> ambient 4-61843  
 CdS/Sb films, vacuum deposited, struct., elec. and optical props., impurity conc. effect 4-98607  
 CsCaCl<sub>3</sub>:Mn<sup>2+</sup>(Ni<sup>2+</sup>Co<sup>2+</sup>), fluoresc. emission, excitation, IR absorpt. spectra studies 4-99153  
 CsMn<sub>1-x</sub>Co<sub>x</sub>Cl<sub>2</sub>·2H<sub>2</sub>O, random mixture with competing anisotropies, PMR meas. 4-88647  
 Cu, doped, trapping of muons and protons, effect of substitutional impurities 4-65631  
 Cu, impurity diffusion, isotope effect meas. 4-65476  
 Cu, positive muon pot., self-consistent cluster calc. 4-71236  
 Cu-H, electron irradi., elec. resist. meas., annealing behaviour 4-92240  
 CuAg alloys, conc. form. during Ar<sup>+</sup> ion sputtering 4-75552  
 CuGa<sub>1-x</sub>In<sub>x</sub>Se<sub>2</sub> chalcopyritic semicond., ESR studies 4-109070  
 CuH<sub>2</sub>, cryogenic material, heat losses due to H ortho-para conversion (German) 4-106326  
 EuMo<sub>6</sub>S<sub>8</sub>, divalent Chevrel-phase supercond., effect of press. and O defects 4-80711  
 Fe, grain boundary with impurity segregation, atomic and electronic structs., 4-113463  
 Fe, impurity hyperfine fields and adiabatic pot., self-consistent calc. 4-65632  
 α-Fe-C, martensitic, lattice deformation by C impurities (Russian) 4-103773  
 Fe-Cr, surface segregation of S, annealing and O<sub>2</sub> adsorption effect (Japanese) 4-61932  
 Fe-Nb-C-P alloys, grain boundary segregation of P rel. to C content 4-85156  
 Fe-Ni-C, fracture toughness rel. to transform. induced plasticity and grain boundary segregation 4-99585  
 Fe-P-W(Mo)(Mn), grain boundary embrittlement, impurity-induced, influence of alloying elements 4-114654  
 FeF<sub>3</sub> thin film, impurity cond. along least resistance paths 4-80705  
 FeOOH, halogen impurity location, water content, neutron activation anal., Mossbauer spectra, TGA 4-81505  
 Ga<sub>1-x</sub>Al<sub>x</sub>As:Zn, (Se), doping in MOCVD growth, carrier conc. and cond. 4-88982  
 GaAs epitaxial film, MBE grown, capture of accidental impurities, influence of growth conditions 4-108743  
 GaAs, impurities identification by magneto-optical photoluminescent spectroscopy 4-60945  
 GaAs LPE layers, residual impurities, growth soln. baking effects 4-92226  
 GaAs, negative differential cond. at transit reson. frequencies 4-84638  
 GaAs, photoluminescence characterisation of impurities and defects 4-88876  
 GaAs, semi-insulating, elec. props. for microwave electronics 4-108846  
 GaAs substrate, annealing as gettering technique prior to MBE growth 4-99615  
 GaAs:Cr, impurities, optical and transport studies 4-71444  
 GaAs<sub>1-x</sub>P<sub>x</sub>:N<sup>3+</sup>, Zn<sup>2+</sup>, implanted, photoluminescence spectra, impurity conc. depend. (Chinese) 4-93099  
 GaSb:Zn epitaxial films, photoluminescence spectra 4-88896  
 Gd with s-p impurities, hyperfine field systematics 4-70758  
 Ge, electronically neutral impurities on muonium, low temp. meas. 4-65279  
 Ge:Cu, impurity contamination reduction by heat treatments above 700°C 4-71535  
 Ge:H-based impurity complexes, charge state determ. 4-92663  
 Ge:Si(Sn)(Al), thermal cond. meas., impurity conc. effect, temp. depend. 4-80318  
 Ge<sub>2</sub>S<sub>3</sub> glass, undoped and metal doped, impurity surroundings, nature of defects, positron annihilation study 4-79943  
 Ge<sub>2</sub>Se<sub>7</sub>:Ag layers, amorphous, photodoped impurity lateral diffusion 4-70464  
 He solid isotropic mixture, configurational relax. and quantum diffusion (Russian) 4-70516  
 InGaAs epitaxial layer, LPE growth and carrier mobility, dopant effects 4-84717  
 n-InP, cyclotron resonance, impurity conc. and compensation effects (Russian) 4-98952  
 InP epitaxial layer, LPE growth and carrier mobility, dopant effects 4-84717  
 InP, residual impurities determ. by charged particle activation anal. 4-85346  
 InP:Co, impurities, optical and transport studies 4-71444  
 InP:Gd(Yb) epitaxial films, doping effects on low-temp. edge photoluminescence 4-85028  
 InP:Mg(Fe,Mg), implanted, effect on photoluminescence props. 4-85007

## impurities continued

- Ir, electron and neutron irradi., elec. resist. studies 4-108447  
 KBr:In(Tl) polycrystalline films, luminescent, epitaxial growth (Russian) 4-113833  
 KBr:No<sub>2</sub>, Ca<sup>2+</sup>, struct. of luminesc. and absorpt. centres (Ukrainian) 4-66059  
 K<sup>15</sup>N<sub>2</sub><sup>14</sup>N<sub>2</sub>O<sub>2</sub>, disordered linear chain, excitation transfer, polarisability effect 4-70662  
 K<sub>2</sub>SO<sub>4</sub>, impurity anion intermol. vibr., static perturbations 4-61002  
 KTa<sub>1-x</sub>Nb<sub>x</sub>O<sub>3</sub>, glasslike behaviour and press. effects 4-99058  
 KTaO<sub>3</sub>:Li, impurity ion quasi-reorientational dynamics, NMR spectrum 4-98973  
 KTaO<sub>3</sub>:Li, incipient ferroelec., off-centre impurity induced phase transition 4-76383  
 KTaO<sub>3</sub>:Li(Nb)(Na), random site at substituted, NMR 4-65864  
 La compounds, impurity determination by neutron activation anal. (Russian) 4-99911  
 LaMo<sub>6</sub>S<sub>8</sub> films, supercond. props. and normal state resist. 4-92876  
 Li, muon interactions with lattice defects, mol. cluster calcs. 4-65255  
 LiF:Ni<sup>2+</sup>, Ni<sup>2+</sup>-F<sup>-</sup> distance for square planar and linear Ni<sup>2+</sup>-centres from isotropic superhyperfine const. 4-98581  
 LiNbO<sub>3</sub>:Cr<sup>3+</sup>(Mn<sup>2+</sup>), axial cryst. field parameters, EPR spectra 4-98379  
 LiNbO<sub>3</sub>:Ti, impurity diffusion as a function of stoichiometry 4-80304  
 MgAl<sub>2</sub>O<sub>4</sub> spinel, cathodoluminescence induced by impurities 4-85017  
 MgO, pitch-bonded refractories, oxidation and Mg diffusion 4-114698  
 MgO single crystals, thermolum. kinetics rel. to Cr<sup>3+</sup> and Fe<sup>3+</sup> impurity conc. (Japanese) 4-99202  
 Mn<sup>2+</sup> ion in crystalline environment with C<sub>3</sub> symm., relativistic crystal field model 4-113911  
 Mo, purification by arc melting, mech. props. (Japanese) 4-89116  
 Mo, sintered sheet, tensile props., improvement by reducing O impurity levels 4-89132  
 MoO<sub>3</sub>, impurities, defect form. and charge compensation, EPR studies 4-80054  
 NaCl, doped, point defect, pulsed DNMR obs. 4-71211  
 NaCl single crystals, etching, solvent impurity effects 4-65264  
 NaCl:CaCl<sub>2</sub> doped cryst., dissolution at dislocation sites 4-60931  
 NaCl:Ca(Pb), plastic deform. parameters, impurity conc. effect, low temp. anomaly 4-88229  
 NaCl:Gd, microhardness, influence of Gd impurity 4-103868  
 NaCl:Mn<sup>2+</sup>, Suzuki phase, impurity exchange coupling, mag. susceptibility, EPR meas. 4-65788  
 NaCl:Ti, quenched, microhardness meas., impurities effect 4-98190  
 NaF:Ni<sup>2+</sup>, Ni<sup>2+</sup>-F<sup>-</sup> distance for square planar and linear Ni<sup>2+</sup>-centres from isotropic superhyperfine const. 4-98581  
 Na<sub>2</sub>Mo<sub>6</sub>O<sub>21</sub>, impurities, defect form. and charge compensation, EPR studies 4-80054  
 Na<sub>2</sub>O-B<sub>2</sub>O<sub>3</sub> glass, prep., mech., thermal and optical props. rel. to N content 4-60845  
 Na<sub>2</sub>SO<sub>4</sub>, impurity anion intermol. vibr., static perturbations 4-61002  
 Nb, muon depolarisation, impurities trapping of muons 4-65904  
 Nb<sub>2</sub>O<sub>5</sub>, radiation hardening by 14 MeV neutrons rel. to O content. 4-104852  
 Nd<sup>3+</sup> impurity ions in crystals, phonon-assisted energy transfer, conc. depend. 4-92311  
 Ni, monocrystals, volume diffusion of simple and transition metal impurities 4-65478  
 Ni, O assisted intergranular H embrittlement, effects of B, P, Sn and Sb additions 4-62030  
 Ni O embrittlement, prevention and reversal 4-71733  
 Ni, surface segregation of S, annealing and O<sub>2</sub> adsorption effect (Japanese) 4-61932  
 Ni-Yb films, ion beam mixing; radiation enhanced diffusion by Kr<sup>+</sup> and O<sup>+</sup> bombard. 4-103832  
 NiO, cationic self-diffusion and oxidation 4-92419  
 Ni<sub>2</sub>O ceramic, grain boundaries, TEM studies 4-108382  
 POCl<sub>3</sub>, purification by low temp. sublimation and distillation 4-66255  
 PbF<sub>2</sub>(Cn)<sub>2</sub>·2H<sub>2</sub>O, with interstitial water impurity mol., electronic cond. activation 4-75972  
 Pb<sub>2</sub>Ge<sub>2</sub>O<sub>11</sub>, hydrothermally grown crystals, dielec., pyroelectric props., X-ray diff. 4-84915  
 Pb<sub>2</sub>-Ge<sub>2</sub>In, elec. props., band edge struct., impurity effects 4-108880  
 PbMo<sub>6</sub>S<sub>8</sub>, divalent Chevrel-phase supercond., effect of press. and O defects 4-80711  
 Pb<sub>1-x</sub>Sn<sub>x</sub>Te:In, Gunn effect, threshold field rel. to cond. band struct. 4-88513  
 Pb<sub>1-x</sub>Sn<sub>x</sub>Te:In epitaxial layers, photocond. kinetics 4-88538  
 PbTe cryst., external shape, impurity complex effects 4-75347  
 Pr<sub>2</sub>La<sub>1-x</sub>P<sub>2</sub>O<sub>14</sub>, luminesc. theory, oscillator strength, impurity conc. effect (Chinese) 4-93100  
 Pt electrodeposits, incorporation of organic matter, mass spectra 4-88997  
 RbMgF<sub>3</sub>:Mn<sup>2+</sup>, electron irradi., vacancy-interstitial pair and F-centre-impurity ion pair form. 4-70215  
 RbMgF<sub>3</sub>:Ni<sup>2+</sup> (6H), cryst. struct., EPR spectra 4-109063  
 Si, C and O content determ. by IR spectroscopy 4-113484  
 Si, Czochralski growth, impurity clouds, microdefects, scatt. light intensity and etch pit density after annealing 4-84312  
 Si, defect and carrier lifetime; back-surface damage gettering technique 4-113972  
 Si, diffusion of group V impurities 4-108662  
 Si, electronic and solar grade, anal. using atomic emission spectroscopy from inductively coupled plasma 4-60948  
 Si, epitaxial growth from SiCl<sub>4</sub>, C contamination, thermodynamic anal. (Chinese) 4-113824  
 a-Si film, RF sputtered, optical absorpt., elec. cond., effect of thermal annealing 4-80583  
 Si hazed polycryst. layers, STEM microanal. studies 4-108692  
 Si, heavy ion and particle induced X-ray emission anal. 4-62275  
 Si, impurities, activation anal. using charged particle accelerators 4-60946  
 Si, impurity characterisation using neutron activation anal. 4-60947  
 Si, impurity migration, effect of elastic stresses 4-88349  
 Si, impurity photoabsorption, quantum defect method anal. 4-88858  
 Si, ion implanted, amorphous surface layer recrystallisation by epitaxial annealing, effect of foreign atoms 4-71553  
 Si, ion implanted, laser or electron beam annealing, electronically active defects, DLTS 4-80527  
 Si, noncrystalline thin films, struct. props. and impurity content 4-88434  
 Si, photoluminescence characterisation of impurities and defects 4-88876  
 Si, solar grade, spark source mass spectrometry anal. 4-62276

## impurities continued

- Si wafers, impurity characterisation using IR spectra: meas. 4-113486  
 Si:As(Sb)(In), ion implanted, pulsed electron beam annealing, impurity diffusion 4-103984  
 Si:B, implanted, elec. activation and damage annealing by flash lamp irradi. 4-70196  
 Si:B(P)(As), dopant diffusion, numerical soln. by solving, impurity, vacancy and self-interstitial continuity eqns. 4-80303  
 Si:D, anomalous muonium atom site determination 4-65277  
 a-Si:H, DC elec. cond. Meyer-Neldel rule and Staebler-Wronski effect 4-113948  
 a-Si:H, TSC meas., density of states behaviour 4-98636  
 Si:H<sub>2</sub>O, grain boundary impurity effect determ. 4-92214  
 a-Si:H films, thickness effects on electrical and photoelectrical properties 4-98484  
 a-Si:H/Si p-n junction, optoelectronic props. 4-114020  
 Si:Li p-n junction solar cells, electron induced degradation, recovery under space conditions 4-105110  
 Si:N(O), microdefect formation during single crystal growth, influence of impurities on nucleation 4-114386  
 Si:O, Czochralski grown, annealed, impurity precipitates, induced defects, TEM obs. (Chinese) 4-92368  
 Si:O Czochralski crystals, O precipitation and microdefects 4-84411  
 n-Si:P polycrystalline CVD films, elec. props., grain size and impurity conc. effects 4-70963  
 Si:P(As)(Sb), many-valley semicond., shallow donor polarisabilities 4-92666  
 Si:S, deep levels, DLTS meas. 4-84592  
 Si:Sb, ion implanted, supersaturation, vitreous C strip heater annealing, Rutherford backscattering, elec. meas. 4-92375  
 Si:Sn, implanted, subthreshold energy electron beam annealing, Mossbauer effect 4-88205  
 Si-SiO<sub>2</sub> interface, negative elec. effects produced by Gd and La impurities 4-108940  
 a-SiN<sub>x</sub>H layers, prep. by glow discharge decomp. of N<sub>2</sub>/SiH<sub>4</sub> mixtures, optical and photoelectronic props., effects of doping 4-114001  
 Si<sub>3</sub>N<sub>4</sub>, polyphase, cation diffusion through intergranular phase, appl. to environmental reactions 4-76889  
 SiO<sub>2</sub>, synthetic, props. under high-temp. treatment 4-81172  
 SiO<sub>2</sub>/OH, fused silica multimode fibres, UV stimulated Raman scattering 4-112518  
 SnMo<sub>6</sub>S<sub>8</sub>, divalent Chevrel-phase supercond., effect of press. and O defects 4-80711  
 SrTiO<sub>3</sub>, compensated, defects and colour centres, optical study 4-92200  
 TaSi<sub>2</sub>, cosputtered, props., effect of O contamination 4-114046  
 ThBr<sub>3</sub>Gd<sup>3+</sup>, incommensurate, phase fluctuations near transition temp., phase pinning, EPR meas. 4-92956  
 Ti diffusion process in LiNbO<sub>3</sub> 4-64804  
 Ti-V solid solutions, creep, microstruct. 4-109464  
 TiB<sub>2</sub>, powder, pressureless sintered, mech. props. in liq. Al environment, impurity segregation 4-114700  
 TiO<sub>6</sub> octahedral structs., phonon state density 4-70305  
 Ti halides, gas-forming admixtures content meas. 4-64798  
 TiGaSe<sub>3</sub> ternary layered cryst., photoluminescence studies 4-66064  
 UO<sub>2</sub> fuel pellets, sintering, grain growth rel. to S content 4-85134  
 W bicrystals, oriented, brittle-ductile transition temp. rel. to O and C content, AFS 4-104859  
 W hard metals, sintered, mech. props. rel. to O content (German) 4-61909  
 W, plasma growth of single crystals, removal of interstitial impurities 4-66209  
 W-Fe, dil., segregation of Fe to grain boundaries, elec. resist., thermopower, AES meas. 4-103943  
 WC-Co cemented carbide, liq. phase sintering, origins of discontinuous grain growth 4-104759  
 Y<sub>1-x</sub>Sm<sub>x</sub>Lu<sub>1-x</sub>Fe<sub>2</sub>O<sub>7</sub> thin film, rare earth site occupation 4-108392  
 Zr compounds, impurity determination by neutron activation anal. (Russian) 4-99911  
 Zr-Co, fast diffusion of Co atoms, quasielastic neutron scatt. meas. 4-113725

## impurity and defect absorption spectra of inorganic solids

- alkali borate mixed glasses containing Ni, induced optical absorpt. rel. to  $\gamma$ -ray exposure 4-76502  
 alkali chloride: Cu<sup>2+</sup>(Ag<sup>+</sup>), two-photon spectra, impurity states 4-109215  
 alkali halides, K band of F<sub>2</sub> centre 4-60923  
 alkali halides, stability and optical props. of self-trapped exciton 4-104129  
 alkali metal halides, F-centres, photoacoustic signals 4-80964  
 alkali metal halides, interstitial atomic H centers in mixed config., unrelaxed excited states, MCD optical absorpt. 4-70747  
 cubic crystals, polarised Raman spectra of defects 4-80937  
 deep charged impurity centres, multiphonon light absorpt. 4-71417  
 diamond, type Ia, defect-induced one-phonon absorption 4-84981  
 fluorides, perovskite-type, wide band gap expts., excitation of thermally stimulated luminesc. and conductivity 4-85018  
 glass:Cr, dominant visible absorpt. rel. to  $\gamma$ -ray irradi. 4-75503  
 glass:Yb<sup>3+</sup>, statistical modelling, luminescence and absorpt. spectra 4-109247  
 non-metallic cryst., Eu ion impurity optical props. 4-61733  
 polar media, bound two-electron quasi-mol. autolocalised impurity centres, energy states and optical props. 4-84590  
 quartz:Ag(Cu), X-ray irradi. induced optical absorpt., impurity electrolysis effect 4-70208  
 quartz, cultured, random elec. twinning, non-destructive obs., resonator appl. 4-70170  
 quartz, E-centre prod. by ionising radiation, ESR and optical studies 4-70145  
 quartz, natural, defects induced by vac. UV, X-ray and beta-ray irradi. 4-70191  
 quartz, natural, wide band gap expts., excitation of thermally stimulated luminesc. and conductivity 4-85018  
 quartz, neutron irradi., point defects, EPR and optical absorpt. study 4-103742  
 quartz, surface and vol. centres, optical and paramag. props. 4-66057  
 quartz, synthetic, irradi. induced coloration (Turkish) 4-114307  
 quartz, vacuum swept, Al and OH<sup>-</sup> defect centres 4-61335  
 sapphire, synthetic, wide band gap expts., excitation of thermally stimulated luminesc. and conductivity 4-85018  
 semiconductors, deep impurities, final state effects 4-84982  
 semiconductors, impurity photoabsorption theory 4-99138

## impurity and defect absorption spectra of inorganic solids continued

- Ag halide microcrystals, spectroscopic identification of localised electrons and holes 4-114308  
 Ag-Pd disordered single crystals, angle resolved UV photoemission 4-85072  
 Al<sub>2</sub>O<sub>3-x</sub> anodic oxide films, paramagnetic centres and optical absorpt. spectra studies 4-104494  
 AsSi, glassy, optical props. meas. (Russian) 4-71340  
 BaF<sub>2</sub>:Y<sup>3+</sup>(Pb<sup>2+</sup>) crystals, electronic excitation decay, impurity effect 4-109209  
 BaFCl, flux-grown crystals, thermoluminesc., effect of flux 4-104680  
 BaSO<sub>3</sub>:MnO<sub>2</sub>, absorpt. spectra, comparison with other host lattices 4-109217  
 Bi<sub>2</sub>GeO<sub>20</sub>, circular dichroism in region of states prod. due to vacancies 4-71345  
 Bi<sub>2</sub>SiO<sub>20</sub>, circular dichroism in region of states prod. due to vacancies 4-71345  
 Bi<sub>2</sub>SiO<sub>20</sub>, deep impurities, photoelectric phenomena 4-113996  
 Bi<sub>2</sub>SiO<sub>20</sub>:Al(Ga)(Mn)(Cr), optical absorpt. spectra, photochromism (Russian) 4-114311  
 Bi<sub>2</sub>TiO<sub>20</sub>, circular dichroism in region of states prod. due to vacancies 4-71345  
 CaCO<sub>3</sub>, natural calcites, X-irradiated, thermolum., absorption and Mn<sup>2+</sup> EPR spectra 4-71453  
 CaF<sub>2</sub>:Eu, phononless impurity-centre line, inhomogeneous broadening under plastic deform. conditions 4-88864  
 CaF<sub>2</sub>:Na, photochemical conversion of M<sub>A</sub>-centres, identification of M<sub>A</sub><sup>+</sup> centre, absorpt. and fluoresc. spectra 4-76501  
 CaF<sub>2</sub>:Sm crystal, gamma-irradiated, optical study 4-81015  
 CaF<sub>2</sub>:Y<sup>3+</sup>(Pb<sup>2+</sup>) crystals, electronic excitation decay, impurity effect 4-109209  
 Ca<sub>10</sub>(PO<sub>4</sub>)<sub>6</sub>F<sub>2</sub>, fluorapatite, radiation damage and annealing, optical studies 4-70192  
 CaZnF<sub>6</sub>:Mn<sup>2+</sup>, cryst. struct., axial field splitting calc., EPR, optical spectra 4-92159  
 CdBr<sub>2</sub>I<sub>2</sub>, absorpt. spectra and electron localisation (Russian) 4-104161  
 CdP<sub>2</sub>, absorpt. spectra and defect states (Russian) 4-71419  
 CdTe films, electrochem. deposited, optical props. 4-85022  
 CdTe:Co, optical absorpt. spectrum (Russian) 4-84983  
 CdTe:In, Li, defect complex, IR absorption studies 4-80031  
 Cr<sup>3+</sup> impurity absorpt. spectra, crystal field, ground and excited state 4-109218  
 CsCaCl<sub>3</sub>:Mn<sup>2+</sup>(Ni<sup>2+</sup>)(Co<sup>2+</sup>), fluoresc. emission, excitation, IR absorpt. spectra studies 4-99153  
 Cs<sub>1-x</sub>Xe<sub>x</sub>, optical absorpt. by Xe monomers and dimers, solvable one electron model 4-71404  
 CuIn(S<sub>2</sub>Se<sub>2</sub>Te<sub>1-x-y</sub>)<sub>2</sub>, solid solubility, optical energy gap values 4-70074  
 EuVO<sub>4</sub>, stoichiometric, nucl. quadrupole optical hole-burning 4-80969  
 n-GaAs, electron irradiated, As anti-site defects, IR spectra and EPR 4-84317  
 GaAs, existence of B<sub>As</sub> impurity antisite centres, IR absorption lines study 4-71413  
 GaAs, high-purity, in mag. fields, donor transition anomalous line broadening 4-109214  
 GaAs LEC substrate, characterisation of impurities and microdefects (Japanese) 4-103778  
 GaAs neutral impurity scatt., far-IR cyclotron reson. study 4-92964  
 GaAs, neutron irradi., optical absorption coeff., spectral depend. 4-99137  
 n-GaAs, shallow impurity photoexcitation line narrowing in an elec. field 4-80970  
 GaAs:C(Si), impurity and defect anal. by IR absorpt. spectra 4-75893  
 GaAs:Cr, eval. of Cr conc. by optical absorpt. 4-104635  
 GaAs:Cr, impurities, optical and transport studies 4-71444  
 GaAs:Cr, semi-insulating, inhomogeneities, optical obs. 4-60944  
 n-GaAs:Se, free electron optical absorpt. theory 4-104637  
 Ga<sub>2</sub>Te<sub>3</sub>, electrical and optical props. meas. 4-61380  
 Ge:Be, site distortion of Be acceptor, IR spectra 4-92667  
 a-Ge:H, photoinduced absorption spectra 4-109220  
 Ge:Zn, Sb, degree of compensation from optical absorption meas. 4-109221  
 GeS<sub>2</sub>:Cu(Ag), glassy, doping effect on elec. and optical props. (Russian) 4-98625  
 InP, electron irradi. induced deep traps, deep level optical spectroscopy 4-104156  
 InP, high-purity, in mag. fields, donor transition anomalous line broadening 4-109214  
 InP:Co, impurities, optical and transport studies 4-71444  
 InP:V(Cr), impurity excited states, optical absorpt. spectra 4-88863  
 In<sub>2</sub>Te<sub>3</sub>, electrical and optical props. meas. 4-61380  
 K halides, Ba-doped, impurity colour centres, absorpt. spectra 4-88865  
 KBr, Ag atoms behaviour (Russian) 4-76245  
 KBr, F-aggregate centres, refr. index change as function of temp. 4-93037  
 KBr, H centres, low temp. pair associates 4-70149  
 KBr:NCO<sup>-</sup>, absorption band width of impurities ions, IR spectra anal. 4-61737  
 KBr:No<sub>3</sub><sup>-</sup>, Ca<sup>2+</sup>, struct. of luminesc. and absorpt. centres (Ukrainian) 4-60394  
 KCl:Ag, Ca, X-irrad., electron centre form., luminesc., optical absorpt. studies 4-60920  
 KCl:Ag, X-irrad., electron centre form., luminesc., optical absorpt. studies 4-60920  
 KCl:I, impurity-localised excitons, luminesc. and absorpt. spectroscopy study 4-92625  
 KCl:In, optical props. study 4-88860  
 KCl:Li colour centre laser material prep., absorpt. spectra after X-irrad. (Chinese) 4-61829  
 KCl:NCO<sup>-</sup>, absorption band width of impurities ions, IR spectra anal. 4-61737  
 KCl:NO<sub>2</sub>, phonon propag. and impurity absorption spectra 4-65360  
 KCl:Na, electron irradi., F-centre generation, absorption spectra studies 4-113444  
 KCl:Sr, X-irradiated, struct. of (Cl<sub>3</sub>)<sub>2</sub>-centres, optical study (Russian) 4-80968  
 KCl(Br)(I):Ag, surface-enhanced Raman scatt. from Ag colloids, optical absorpt. spectra 4-99117  
 KI:Ag<sup>+</sup>, two elastic configurations at point defect, far IR spectra study 4-61029  
 KI(Br):Ti<sup>2+</sup>, magnetic dichroism study of Ti<sup>2+</sup> centre symm. 4-70719  
 KZnF<sub>3</sub>:Fe<sup>2+</sup> crystal, EPR and far IR study on (FeF<sub>6</sub>)<sup>4-</sup> complex 4-80814

**impurity and defect absorption spectra of inorganic solids continued**

- LaF<sub>3</sub>:Pr<sup>3+</sup>, two-photon transition from <sup>1</sup>H<sub>4</sub> to <sup>1</sup>S<sub>0</sub> 4-104636  
 LiH, electron-phonon interactions in luminescence spectra 4-71439  
 LiH(D), radiation induced defect form. 4-60952  
 LiH(D):Na, radiation induced defect form. 4-60952  
 LiNH<sub>2</sub>SO<sub>4</sub>:Mn<sup>2+</sup>, impurity electronic absorpt. spectrum 4-66055  
 LiNbO<sub>3</sub>:Cu<sup>2+</sup>, EPR and optical absorption spectra, Jahn-Teller effects 4-71166  
 LiNbO<sub>3</sub>:Cu<sup>2+</sup>, single crystal, Jahn-Teller effect 4-108825  
 LiNbO<sub>3</sub>:Eu<sup>3+</sup>, impurity optical absorpt. 4-66056  
 MgO containing metal precipitates, optical and mech. props. 4-70161  
 MgO, F<sup>+</sup> centre, electronic point defects with self consistent lattice polarisation 4-93091  
 MgO, quenched, defect struct., plastic deform., SEM, cathodoluminescence, optical absorpt. spectra 4-71448  
 MgO, thermoluminescence charge transfer mechanism 4-71450  
 MgO, vacancies and multiphonon IR-absorpt. spectra (Russian) 4-71420  
 MgO:Na<sup>+</sup>(Rb<sup>+</sup>), annealed and reimplanted, atomic mixing processes 4-70231  
 MgO:NaAl<sub>2</sub>O<sub>3</sub>:Cr(Mn), impurity ion distrib. in spinel lattice 4-84311  
 NH<sub>4</sub>Cl:Co<sup>2+</sup>(Ni<sup>2+</sup>), X-irrad. effects, optical absorpt. spectra, EPR 4-70206  
 NaCl, electron irrad., appl. to radioactive waste repositories 4-75532  
 NaCl F<sub>2</sub><sup>+</sup> centres, persistent spectral hole detection using ultrasonic modulation 4-83650  
 NaCl, F-centre form., excitonic pot. surface, absorpt. spectra 4-71415  
 NaCl:Ag, surface-enhanced Raman scatt. from Ag colloids, optical absorpt. spectra 4-99117  
 NaCl:Ag<sup>+</sup>, Ag<sup>+</sup> ion dimer centres, optical props. 4-66076  
 NaCl:Br, impurity-localised excitons, luminesc. and absorpt. spectroscopy study 4-92625  
 NaCl:CaCl<sub>2</sub>, decay props. of perturbed and unperturbed M-centres 4-92204  
 NaCl:H, radiation induced H discharge, optical absorpt. (Russian) 4-99139  
 NaF polycrystalline thin films, neutron and X-irrad., photochemical hole burning 4-76518  
 NaF:Cu<sup>2+</sup>, excited state dynamics 4-108803  
 Na<sup>+</sup>, Mg, Al, I<sub>2</sub>, O<sub>2</sub>:Nd<sup>3+</sup> platelet laser absorpt. spectra, fluoresc. life-time, laser-pulse shape and peak emission wavelength 4-60044  
 Na<sub>2</sub>O-B<sub>2</sub>O<sub>3</sub> glass, undoped and Co<sup>2+</sup> doped, acoustic loss and optical absorpt. spectra, matrix analysis 4-84193  
 Na<sub>2</sub>O-SiO<sub>2</sub> glass, nature of dissolved water, effect on phys. props. 4-109180  
 NaPO<sub>3</sub> glass, alpha-particle induced damage, vibr. Raman spectra 4-70237  
 Na<sub>2</sub>Zn(SO<sub>4</sub>)<sub>2</sub>·4H<sub>2</sub>O:Cr<sup>3+</sup>, optical absorption spectrum of Cr<sup>3+</sup> 4-71418  
 PbTe:B, absorpt. spectra and impurity states 4-104638  
 PbTe:Ga, elec. and optical meas. (Russian) 4-84636  
 Rb halides, Ba-doped, impurity colour centres, absorpt. spectra 4-88865  
 RbAg<sub>2</sub>I<sub>3</sub>, I<sub>2</sub> coloured, light absorption studies 4-88854  
 RbBr:Eu, optical study of Eu precipitation 4-80233  
 RbCl:Eu, optical study of Eu precipitation 4-80233  
 RbMgF<sub>3</sub>:Mn<sup>2+</sup>, electron irrad., vacancy-interstitial pair and F-centre-impurity ion pair form. 4-70215  
 Rb<sub>2</sub>ZnCl<sub>4</sub>, colour centre production by additive colouring and X-ray irrad. 4-70144  
 Se-Te amorphous alloys, photogeneration and optical absorption 4-108900  
 Si (111) face, thermally agitated electrons, IR reflection obs. 4-93082  
 Si crystals, Czochralski pulled, O precipitation, diffusion mechanism, etching optical and neutron scatt. obs. 4-65209  
 a-Si film, elastic and inelastic props. 4-88225  
 Si, heavily doped, band-gap narrowing study 4-80490  
 Si, IR spectroscopy characterisation 4-99136  
 Si, impurity photoabsorption, quantum defect method anal. 4-88858  
 Si, laser doping by dissociation of metal alkyls 4-80069  
 Si:C, electron irrad., optical absorpt. spectra 4-88861  
 Si:Ga, neutron irrad., acceptor level, IR absorpt. spectrum 4-93089  
 a-Si:H, absorpt. edge, struct. disorder model for amorphous semiconductor 4-80483  
 a-Si:H, IR absorpt., gaseous H<sub>2</sub> and Si-H overtone spectra 4-93075  
 Si:H, microcrystalline, IR absorpt. study of Si-H bond formation 4-71416  
 Si:H, microcrystalline, photoinduced free-carrier absorpt. spectra 4-88859  
 n-Si:H, neutron irradiated, deep levels study (Chinese) 4-92649  
 a-Si:H, photoinduced absorption spectra 4-109220  
 a-Si:H, transient photoinduced absorpt. 4-104634  
 a-Si:H(P), ESR and optical props., thickness depend. 4-84853  
 a-Si:H(D) thin films, coupled local mode vibrs., IR absorpt. study 4-88259  
 Si:Li and Si:Li, C, electron irrad., luminesc. decay time, absorpt., isotope splitting, and Zeeman meas. 4-71434  
 Si:N, ion implanted, optical props. (Chinese) 4-114306  
 Si(N,O), microdefect formation during single crystal growth, influence of impurities on nucleation 4-114386  
 Si:O, P, thermal donors, optical absorption spectra studies 4-65637  
 Si:P, heavily doped, optical reflectivity spectra 4-61735  
 Si:P, IR absorption spectrum 4-71414  
 Si, Ge<sub>1-x</sub>H amorphous sputtered films, optical absorpt. 4-93090  
 Si<sub>3</sub>N<sub>4</sub> films, amorphous, hydrogenated and deuterated, prepared from plasma-enhanced CVD, IR absorpt. spectra 4-81021  
 SiO, amorphous, optical study of defects 4-88862  
 SiO<sub>2</sub>, amorphous, luminescence and absorption centres, vacuum UV generation 4-71433  
 SiO<sub>2</sub>, electron irrad., IR absorpt. from OH<sup>-</sup> related defects 4-104633  
 SiO<sub>2</sub> glass, alpha-particle induced damage, vibr. Raman spectra 4-70237  
 SiO<sub>2</sub>, vitreous, defects of broken-bond type 4-92097  
 SiO<sub>2</sub>:OH, fused flame prod., for windows, D<sub>2</sub> treatment effect on optical props. 4-74636  
 Si-H, bonds and H-induced defects study 4-66058  
 SrF<sub>2</sub>, interstitial atom: hopping by electronic excitation of Frenkel pairs 4-70140  
 SrF<sub>2</sub>, photo-induced transform. of close Frenkel pairs, absorption and luminesc. props. 4-76500  
 SrF<sub>2</sub>:Y<sup>3+</sup>(Pb<sup>2+</sup>) crystals, electronic excitation decay, impurity effect 4-109209  
 SrTiO<sub>3</sub>, compensated, defects and colour centres, optical study 4-92200  
 Te, neutron irrad. induced defects, optical props. near fundamental energy gap 4-84318

**impurity and defect absorption spectra of inorganic solids continued**

- ThBr<sub>3</sub>:Pa<sup>4+</sup>, incommensurate phase, single cryst., Pa<sup>4+</sup> optical spectroscopy 4-71422  
 TiO<sub>2</sub>, vacancies and multiphonon IR-absorpt. spectra (Russian) 4-71420  
 Y<sub>3</sub>Al<sub>5</sub>O<sub>12</sub>:Nd<sup>3+</sup> garnets, γ-ray irrad., colour centres and optical props. 4-114310  
 YIG:H, H diffusion, optical absorption and mag. circular dichroism studies 4-61144  
 Y(PO<sub>3</sub>)<sub>3</sub> glass, alpha-particle induced damage, vibr. Raman spectra 4-70237  
 ZnO, nonlinear light absorpt., two-photon absorpt. spectra 4-96992  
 Zn<sub>2</sub>P<sub>2</sub>Ge<sub>2</sub> induced absorpt. and transmission (Russian) 4-96984  
 ZnS:Fe<sup>2+</sup>, impurity states, EPR meas. 4-84588  
 ZnTe:Ni, absorpt. spectra, impurity states (Russian) 4-113898
- impurity and defect absorption spectra of solids**  
*see also impurity and defect absorption spectra of inorganic solids*  
 acetate complexes:Er<sup>3+</sup>, UV-visible and IR spectra, radiative transition probabilities for fluoresc. level 4-114309  
 3-acetyl-9-vinyl carbazole oligomers, doped with electron acceptor, impurity, absorpt. and luminesc. spectra (Russian) 4-80975  
 defect-boson systems, photon echo spectrosc. 4-83651  
 di(methyl ammonium)Sb<sub>2</sub>Sn<sub>1-x</sub>Cl<sub>6</sub>, SbCl<sub>6</sub><sup>3-</sup> intervalence absorpt. band 4-61734  
 distortive phase transitions, effect of soft acoustic phonons on spectral parameters 4-75635  
 minerals containing water, IR spectral studies 4-93071  
 naphthalene, absorpt. spectra study of bound exciton states 4-108782  
 poly(thiophene) doped films, charge storage, optical study 4-109219  
 polyacetylene:I, IR refl. spectra, effect of sample densification 4-99120  
 polyacetylene, charge carrier photogeneration 4-108901  
 polyacetylene, thin films, NH<sub>3</sub> doped, optical absorpt., photothermal deflection spectra 4-93092  
 polythiophene films, absorpt. spectra induced by photoexcitation and electrochemical doping 4-99208  
 quartz containing water, IR spectral studies 4-93071  
 semiconductors, polarised light absorpt. in donor-valence band optical transitions 4-61736  
 p-terphenyl, cryst., UV absorpt. and fluoresc. obs. 4-61744  
 p-terphenyl, electron and I<sup>-</sup> irrad., absorpt. spectra (Russian) 4-71421  
 zero-phonon impurity lines, thermal broadening in absorpt. and fluoresc. spectra 4-109216  
 Na<sub>2</sub>O-CaO-SiO<sub>2</sub>, γ radiation colouring in 600-1000 nm region 4-80948  
 SbCl<sub>6</sub><sup>3-</sup>, in cryst. lattice, intervalence absorpt., IR study 4-61734
- impurity clustering see segregation**
- impurity-defect interactions**  
*see also impurity-dislocation interactions; impurity-vacancy interactions*  
 alkali halide cryst., Frenkel defect accumulation, temp. and impurity conc. depend. 4-98093  
 inorganic insulators, cryst., heavy ion bombard., struct. changes and chem. effects 4-75549  
 intergranular embrittlement, impurity interactions within grain boundary, MO calcs. 4-80147  
 metals, diffusion of H, trapping model analysis 4-70470  
 metals, interatomic forces near a defect, impurity-susceptibility method 4-113490  
 semiconductors, defect formation as a result of isovalent doping 4-70181  
 solid solution, supersaturated, radiative swelling problem, intensified recomb. of unlike defects 4-70188  
 solid solution, supersaturated, radiative swelling problem, inclusion growth and impurity pump mechanisms 4-70197  
 transition metal oxides, impurity diffusion and impurity-defect interactions 4-92436  
 Al-Mg, dil., neutron irrad., internal friction, elastic modulus, recovery stages studied by elec. resist. meas. 4-103876  
 Cr, neutron irrad., internal friction, elastic modulus, recovery stages studied by elec. resist. meas. 4-103875  
 Cu-H, electron irrad., elec. resist. meas., annealing behaviour 4-92240  
 Fe dilute alloys, vacancy-impurity interaction, μSR study 4-84886  
 Fe-Ni-V(Mo) alloys, martensite ageing, positron annihilation studies (Russian) 4-104695  
 GaAs:B, interaction between B and defects 4-80082  
 Ge:D, plasma treated, D diffusion and interaction with point defects 4-60951  
 Ge:Si, ultrapure and doped, muonium state, positive muon spin precession signals 4-71242  
 InP:Zn, electron irrad. damage, carrier conc. effects, minority carrier diffusion length 4-80107  
 LiF:Na<sup>+</sup>(Rb<sup>+</sup>), annealed and reimplanted, atomic mixing processes 4-70231  
 MgF<sub>2</sub>:Li, electron irrad., holelike defects, ESR study 4-60964  
 MgO, dipolar defect ordering due to dissolved CO<sub>2</sub> 4-71287  
 MgO, preirradiation defects associated with trace impurities 4-70186  
 MgO:Na<sup>+</sup>(Rb<sup>+</sup>), annealed and reimplanted, atomic mixing processes 4-70231  
 Nb, electronically induced trapping of H by impurities 4-108410  
 NbO<sub>2</sub>(H<sub>2</sub>O), H and D tunnelling, sp. ht. meas. 4-61103  
 n-Si, gamma and neutron irrad., radiation defect interactions 4-92227  
 Si, impurity diffusion, impurity conc. doping effects 4-113728  
 TiO<sub>2</sub>:V<sup>4+</sup>, extended defects, EPR and TEM study 4-75457  
 Zr:D, ion implantation, lattice defect trapping, binding enthalpy, migration 4-108400
- impurity-dislocation interactions**  
*see also dislocation locking; dislocation pinning*  
 Cottrell atmospheres of impurities, dislocation interactions, internal friction and US meas. 4-65486  
 dynamic dragging of dislocations, effect of impurities 4-98127  
 metals, BCC, impurity-dislocation interactions, influence of elastic anisotropy 4-98126  
 steel, carbon, strain ageing, influence of high press. (Russian) 4-85168  
 steel, low C, abnormal grain growth, decarburization treatment 4-71663  
 Udmet 700, metalloid strengthening mechanism 4-61974  
 weld metal, globular silicates effect on ductility and microstruct. 4-114607  
 Fe, BCC crystal, irradiation creep, stress induced edge dislocation-interstitial atom interaction 4-104814  
 GaAs semi-insulating substrate, inhomogeneity characterisation, expt. study 4-65759  
 LiF:OH<sup>-</sup>, mechanical props., dislocation motion anal. 4-70257  
 NaCl:CaCl<sub>2</sub> doped cryst., dissolution at dislocation sites 4-60931  
 NaCl:OH<sup>-</sup>, mechanical props., dislocation motion anal. 4-70257

**purity-dislocation interactions continued**

- NaI(Tl) deformed cryst., relationships among stresses, microstruct. and photolum. 4-71441  
 Nb single crystal, neutron and electron irradi., dislocation sweeping of defects 4-103810  
 Nb-H, internal friction, hydride precip. peak, cooling rate and freq. depend. 4-66360  
 Ni, crack propag., plastic zone, dislocation struct. 4-99488  
 Ni-Cr, conc. FCC alloys, heterogeneous deform. mechanisms 4-81236  
 Pb-In superconductor, with dislocations surrounded by impurity atoms, internal friction (*Russian*) 4-98807  
 Si, dislocation behaviour, review 4-88169  
 Si, gettering efficiency of different dislocation types, EBIC, TEM obs. 4-103787  
 Si-Cu, impurity effect on dislocation motion 4-70187  
 Si-H, dislocated, impurity codiffusion 4-103788  
 Ta-H, internal friction, hydride precip. peak, cooling rate and freq. depend. 4-66360  
 V-H, internal friction, hydride precip. peak, cooling rate and freq. depend. 4-66360

**purity distribution**

- see also doping profiles; segregation  
 analytical electron microscopy, imaging, chem. anal. and microdiff. 4-108255  
 boronised alloys, types VK6, TSK10, T1SK6, distrib. of B, W, Ti and Co (*Russian*) 4-80071  
 crystal grown from melt with variable crystallisation rate, impurity distrib. 4-75492  
 crystal growth from melt, impurity distribution and inclusions (*Russian*) 4-113483  
 Czochralski growth, historical review of technique, impurity conc. and distrib. 4-66213  
 diffusion of interstitial impurities in crystals under action of shock waves 4-65342  
 II-VI semiconductor:Ag, microscopic Ag impurity quantity determ., kinetic method (*Russian*) 4-65287  
 II-VI semiconductors, carrier mobility characts., displaced Maxwellian model 4-75968  
 interstitial solid solutions, impurity solute atoms distribution, interactive interaction effects (*Russian*) 4-108405  
 ion implantation, dose control, annealing and gettering 4-84309  
 materials research, nuclear physical anal. methods (*German*) 4-72030  
 metal overlayer/metal structures, sputtering, AES and EELS studies 4-76617  
 multicomponent systems, surface adsorption 4-98457  
 multicomponent targets, sputtering, implanted ion range and profiles, TRI-DYN TRIM 4-80076  
 multilayered thin film structs., depth profiling and sputtering yields 4-81090  
 oxides, diffusion and association of defects 4-98363  
 cis-polyacetylene, Li doping, diffusion EPR and Raman study 4-88345  
 proton recoil technique for H depth profiling 4-88922  
 semiconducting films, impurity distrib. studied by computer simulation 4-75806  
 semiconductor, diffusion coefficient, rel. to conc. (*Rumanian*) 4-70467  
 semiconductor, near surface layer, role in diffusion studies 4-98333  
 semiconductor impurity diffusion simulation, adaptation of stiff methods 4-75734  
 semiconductors, compensated, spatial distrib. of impurities 4-103784  
 semiconductors, surface diffusion impurity profiles, consecutive diffusion 4-70184  
 semiconductors, surface diffusion impurity profiles, mutual diffusion 4-70185  
 single crystals, impurity atom localisation, Rutherford backscatt. yield in planar channelling 4-75489  
 solidification, rapid, impurity trapping models 4-89038  
 steel, austenitization, component redistribution in intercritical temp. range (*Russian*) 4-109436  
 steel, C-Mn, grain boundary segregation of Cu, Sb and Sn at 900°C 4-93300  
 steel, high Cr, impurity redistrib. and mech. props. during 475°C ageing (*Russian*) 4-93317  
 steel, stainless, N ion implanted, lattice location, nuclear reaction, channelling and RBS studies 4-75463  
 superconducting-normal-superconducting sandwiches with nonmagnetic impurities near critical temp. 4-65775  
 Zircaloy-4, SAM determ. of O gradients, deform. modelling 4-88191  
 Al alloys, Type 6063, surface characterisation, for vacuum chamber materials 4-88386  
 Al-Ti-(B), impurity distrib. 4-114538  
 Al<sub>2</sub>O<sub>3</sub>, translucent sintered tubes, thermophysical stability rel. to impurities and dopants 4-61937  
 Au, implanted <sup>3</sup>He depth profiles, <sup>4</sup>He post-bombardment effects 4-80073  
 B, diffusion coefficient determ. for drive-in in oxidising atmosphere (*Hungarian*) 4-113715  
 Ba<sub>2</sub>Sr<sub>1-x</sub>Nb<sub>2</sub>O<sub>6</sub>, pyroelectric effect, ferroelectric transition 4-114214  
 Bi<sub>2</sub>Ge<sub>2</sub>O<sub>7</sub>Nd<sub>2</sub>, hexagonal crystal, growth and luminesc. 4-76510  
 Bi<sub>2</sub>SiO<sub>5</sub>, single crystal, effect of doping with Al, Ga and Cr on props. 4-76407  
 Bi<sub>2</sub>(Te,Se)<sub>3</sub>, crystal growth under microgravity in SALYUT-6 space station 4-98035  
 C foil, implanted with T, prep. and analysis w.r.t. fusion reactor safety 4-91100  
 CaCO<sub>3</sub>, calcite, growth rate from soln., influence of impurities 4-92116  
 CaWO<sub>4</sub>, structural imperfection, vacancy disordering, diffusive mass transfer 4-75438  
 CdSb:In(Te) dopant distrib. coeffs. (*Japanese*) 4-84313  
 Cd<sub>1-x</sub>Zn<sub>x</sub>Te alloys, growth, elec. props., photoluminesc. 4-66207  
 Cu, low energy N atom implantation, profiles, ranges and straggling 4-80062  
 Fe and alloys, N implanted, SIMS, Auger and nucl. reaction analysis 4-88185  
 FeOOH, halogen impurity location, water content, neutron activation anal., Mossbauer spectra, TGA 4-81505  
 GaAlAs-GaAs heterostructure, nuclear profiling of Al 4-98123  
 GaAs, crystal and amorphous, pulsed laser irradi. under O<sub>2</sub> and silane atmospheres, O incorporation and losses 4-80091  
 GaAs LEC substrate, characterisation of impurities and microdefects (*Japanese*) 4-103778

**impurity distribution continued**

- GaAs, semi-insulating, elec. and photoelectric props., book contrib. 4-88544  
 GaAs, semi-insulating LEC grown, impurity distribution, cathodoluminesc. study 4-88885  
 GaAs:Be, ion implanted, reduced damage generation 4-113474  
 GaAs:Cr, eval. of Cr conc. by optical absorpt. 4-104635  
 GaAs:Cr, LEC growth, mag. field effect on impurity conc. 4-114378  
 GaAs:Sn:Te, dual implanted damage and annealing, challenging studies 4-80116  
 GaAs/AuGe ohmic contact, Ge and Au profiles, SIMS studies 4-103782  
 GaAsP p-n junctions, avalanche multiplication and ionisation rates, SEM studies 4-65733  
 GaAs<sub>1-x</sub>P<sub>x</sub>, internal elec. field-enhanced impurity diffusion and p-n junction form. 4-84469  
 GaAsP<sub>1-x</sub>As<sub>x</sub>, Cu, LEDs, Cu impurities, thermal redistribution 4-80080  
 GaP, crystal growth under microgravity in SALYUT-6 space station 4-98035  
 GaP p-n junctions, avalanche multiplication and ionisation rates, SEM studies 4-65733  
 GaSb cryst., facet regions and Czochralski growth 4-75348  
 Ge, impurities microinhomogeneities, capture channels, time-amplitude anal. 4-108876  
 p-Ge, nuclear doped, elec. cond., 0.06 to 300K, impurity conc. depend. 4-61382  
 Ge:Al, implanted ion projected range distrib. 4-80079  
 Ge:Ga, migration of molten inclusion 4-108659  
<sup>76</sup>Ge, neutron doped, low-temp. elec. cond. 4-80594  
 H<sub>2</sub> in D<sub>2</sub>, solid soln., H and D behaviour at lig. He temp. 4-70517  
 HgCdTe and CdTe, ion implanted with <sup>1</sup>H, <sup>2</sup>H, <sup>3</sup>He, depth distributions, SIMS study 4-88182  
 InP:Mg(Ca,Zn) crystals grown by synthesis solute diffusion, electrical and optical props. 4-85093  
 InP:Mn, solubility, coeff. of Mn distrib. 4-108621  
 InSb:Ge(Si), impurity solubility, role of acceptor and donor states 4-60949  
 InSe:Sn(Zn)(Ga)(S), dopant segregation and distrib. study 4-103940  
 Li-Al, T release on heating or NaOH dissolving rel. to Li conc. 4-75733  
 Mo<sub>2</sub>NiAl<sub>2</sub>O<sub>3</sub>:Cr(Mn), impurity ion distrib. in spinel lattice 4-84311  
 Mo:O films, O depth profiles under high temp. annealing 4-98490  
 Mo-Co dilute alloy, lattice location studies by PIXE and ion channelling 4-99894  
 Na<sub>2</sub>O-SiO<sub>2</sub>, glass, ion implanted impurities, range and spatial distrib. 4-108287  
 Nb, implanted <sup>3</sup>He depth profiles, <sup>4</sup>He post-bombardment effects 4-80073  
 Nb-N, ion implanted, N diffusion, ion beam studies 4-70431  
 Nb-Zr (1.5 at.%), oxidation, O distrib., field ion microscopy, mass spectrometry 4-66483  
 Nd:YAG crystals, Czochralski, vertical distrib. conc. determ. of Nd ion (*Chinese*) 4-84310  
 PbS, nonstoichiometry, voltammetry using paste electrode 4-108407  
 Pd-Si film, ion implanted, amorphisation, channelling anal. 4-92247  
 Pd<sub>3</sub>FeH<sub>3</sub>, Mossbauer study of hyperfine interactions 4-88756  
 Si (100) inversion layer, electron mobility, neutral scatt. effects 4-76040  
 Si, clusters of electrically active centres and impurity states 4-70183  
 Si crystals, interface shape and radial distribution of impurities 4-113371  
 Si, Czochralski growth, O segregation control by combining mag. field and cryst. rot. 4-104729  
 Si epitaxial layers, thickness meas. by IR reflectance studies 4-111105  
 Si, impurity diffusion, impurity conc. doping effects 4-113728  
 Si, impurity incorporation during Czochralski growth 4-114385  
 Si multiply implanted targets, range distrib., Rutherford scatt. studies 4-92268  
 Si:As, implanted under channelling conditions, impurity spatial distrib., localisation, defect form. characts. 4-84321  
 Si:As, ion implanted, carrier density profiles, elec. meas., annealing behaviour 4-70179  
 Si:As, shallow implants, depth profiling using SIMS 4-108408  
 Si:As(Sb)(In), ion implanted, pulsed electron beam annealing, impurity diffusion 4-103984  
 Si:Au, solid solution, nuclear-spin lattice relaxation 4-76282  
 Si:B, (100), shallow junction implants through surface oxide, theoretical and expt. study 4-113476  
 Si:B, ion implanted, flash-lamp annealing study 4-108395  
 Si:B(As), ion implant in-depth error anal., mass interference effects in ion microprobe studies (*Chinese*) 4-111248  
 Si:F, amorphous and cryst., ion implanted, elec. quadrupole hyperfine interaction at impurity sites 4-92675  
 Si:F, As, ion implanted, defect struct. detection 4-103776  
 Si:Ge, Ge diffusion and conc. profiles, SIMS studies 4-65490  
 a-Si:H nip solar cells, B contamination and photoresponse 4-89407  
 a-Si:H thin films, O distrib. and modifications induced by heavy ion bombard. 4-70233  
 Si<sub>3</sub>N<sub>4</sub>, low energy implant depth profiles, surface peak, Auger studies 4-80074  
 Si:O, impurity conc. meas. using IR spectra, multiple reflection effects 4-113487  
 Si:O, impurity conc., IR absorption studies 4-113488  
 Si:P, proton and neutron irradi., impurity composition and defect clustering 4-65291  
 Si:P(Sb), ion implanted, flash lamp annealing 4-108735  
 Si:S, implanted, depth distrib. as function of ion energy, fluence and anneal temp., SIMS meas. 4-80078  
 Si:Sb, implanted laser irradi., crystn. annealing, time-resolved reflectivity, TEM, Rutherford backscattering anal. 4-80093  
 Si:Xe, implanted Xe reemission by He<sup>+</sup> ion bombardment 4-75462  
 Si-on-insulator films, zone-melting recrystallized, O distribution and sub-boundary formation 4-80433  
 Si:C:Al, B(Be),<sup>9</sup> interstitial diffusion studies 4-80302  
 p-Si:C:B, diffusion, track autoradiography studies 4-84466  
 SiO<sub>2</sub>:As, shallow implants, depth profiling using SIMS 4-108408  
 SiO<sub>2</sub>:HCl(Cl<sub>2</sub>) film on Si, impurity distrib., SIMS study 4-113485  
 SnO<sub>2</sub>, film, impurity phases, hydrolysis of SnCl<sub>4</sub> 4-113829  
 Ta<sub>2</sub>O<sub>5</sub>, altered layer prod. by He ion sputtering, depth profiling 4-80075  
 Ti:H, depth profiling and microanal. 4-81497  
 TiO<sub>2</sub>:O<sub>2</sub>, O diffusion coeff. and conc. profile, SIMS studies 4-92438  
 V-Cr-Ti(Fe-Zr), mech. props. rel. to O contamination, fusion appls. 4-109499  
 V-N, ion implanted, N diffusion, ion beam studies 4-70431

**impurity distribution continued**

- $V_{2/3}Ge_{1/3}Ga_{2/3}$  A-15 superconductor; impurity location using EXAFS 4-88190  
 W-<sup>3</sup>He, ion implanted, diffusivity study 4-104004  
 W-Ni-Fe, fracture behaviour, effect of substitutional impurity elements 4-89134  
 YAG cryst., impurity distrib. and Bridgman-Stockbarger growth 4-60950  
<sup>64</sup>Zn distrib. in zinc during zone recrystallisation, gravitational force effects 4-76667  
 Zr-D, ion implantation, lattice defect trapping, binding enthalpy, migration 4-108400

**impurity electron states**

- see also A-centres; Anderson model; charge compensation; deep levels; electron traps; heavily doped semiconductors; impurity scattering; OH<sup>-</sup> centres; U-centres; Z-centres  
 activated crystals, impurity centres, nonradiative transitions, vibr. relax. 4-99145  
 alkali halide phosphors, S<sup>2</sup> ion impurity centres with O<sub>h</sub>, D<sub>4h</sub>, C<sub>4v</sub> and C<sub>2v</sub> symm., cryst. field theory 4-61346  
 alkali metal halides, activator light sum photorelease, photoluminescence (Russian) 4-114321  
 alkali metal halides, interstitial atomic H centers in mixed config., unrelaxed excited states, MCD optical absorpt. 4-70747  
 amorphous hosts, optical impurity dephasing, homogeneous linewidths 4-71328  
 Anderson model, degenerate, with strong correl., mag. susceptibility 4-92659  
 band model for the understanding of divergences in perturbation theory 4-92586  
 bielectron-impurity complexes, energy spectrum and optical props. 4-92660  
 CDW ground state, effects of impurities, mean field calc. 4-70687  
 Coulombic impurity states in a deep quantum well (Chinese) 4-113899  
 covalent semiconductors, spectroscopy of 3d impurities 4-70712  
 crystal with impurity, LCAO calc. of excess orbitals 4-98568  
 CWD superconductors, nonmagnetic impurity effects 4-70683  
 deep charged impurity centres, multiphonon light absorpt. 4-71417  
 delocalised surface exciton-impurity states with low binding energy (Russian) 4-70900  
 depletion regions, carrier capture from free-carrier tails 4-92746  
 diamond:Fe, electronic struct. calcs. 4-113894  
 diamond:H, interstitial muons anal. impurity states 4-80541  
 dicalcium lead propionate, ferroelec.-paraelec. transition, dopant conc. depend. 4-99048  
 dynamic quantum Hall effect in 2-d electron impurity system 4-113975  
 europium ethylsulphate, Ce<sup>3+</sup>, Ce<sup>3+</sup> EPR spin-lattice relax. rate, press. effects 4-65855  
 excited electronic-vibr. levels, low-temp. Arrhenius decay 4-88480  
 ferroelectrics, dipole-dipole mechanism of energy transfer 4-88482  
 glass: rare earth ions, low temp. optical dephasing rate 4-88789  
 hydrogen centres in metals 4-92652  
 III-V semiconductors doped with 3d transition metals, impurity states 4-75895  
 impurity complexes, excites state deactivation, correlated electron tunnelling 4-98559  
 InP:Zn epitaxial layers, MOCVD grown, doping, Hall effect, SIMS, electrochemical profiling 4-80077  
 inversion layers, bound electron states of Coulombic impurities and effect on mobility 4-98770  
 layered cpds., many-particle impurity complexes in strong mag. fields 4-88481  
 metals, impurity states, positron states and chemisorption, theoretical studies 4-70706  
 mixed valence impurities in metallic host, static and dynamic susceptibility 4-70749  
 multiwell one-dimensional struct., tunnelling theory 4-70912  
 naphthalene, mol. cryst. triplet excited states, spin-lattice relax. 4-98556  
 naphthalene cryst., excitons, defects and intramolecular phonon interactions (Russian) 4-98532  
 non-metallic cryst., Eu ion impurity optical props. 4-61733  
 nonmagnetic metal with mag. impurity, density of states, sp. ht., tridiagonalisation 4-92665  
 nonmetallic crystals, optically stimulated electron jumps between local electron centres 4-65641  
 one-impurity level model and carrier density temp. depend. (Russian) 4-98560  
 oxide cations, emission mechanism, semiconductor model 4-61812  
 p-n junctions, tunnel capture influence on impurity-level recombination of charge carriers (Russian) 4-70923  
 paramagnetic cryst., electron impurity centres (Russian) 4-88483  
 PbTe:Bi, Hall study of self-compensation of donor effect 4-104242  
 phononless lines in luminesc. spectra 4-99144  
 point impurities, generalised Green's function anal. 4-98566  
 polar media, bound two-electron quasi-mol. autocatalysed impurity centres, energy states and optical props. 4-84590  
 polar semicond., donor-acceptor pair capture cross section highly excited electrons 4-61330  
 quantum well wire, hydrogenic impurity states 4-70708  
 quantum-well struct., resonant impurity states 4-61327  
 rare earth impurity ions in crystals, phonon-assisted energy transfer, conc. depend. 4-92311  
 rare earth orthoaluminate, AlO<sub>3</sub>, paramag., mag. field-induced localisation of electron excitations 4-61348  
 ruby:Cr<sup>3+</sup>, cryst. fields superposition model, appl. to non-S-state impurity ions 4-98574  
 semiconductor, anisotropic, shallow donors, appl. of energy variational principle and gauge invariance 4-92654  
 semiconductor, doped, excitation spectrum in nonmetallic regime, concentration-fluctuation model 4-61328  
 semiconductor, electronic struct. and hyperfine interaction of muonium 4-65633  
 semiconductor, lightly doped compensated, Coulomb gaps and Hubbard gaps 4-80542  
 semiconductor doping superlattice, hydrogenic donor, binding energy and wavefunction in effective pot. 4-75902  
 semiconductor inversion layer, two-dimens. electrons, bound impurity states, ionisation prob. in strong mag. field 4-65750  
 semiconductor quantum wells, screened Coulombic impurity-bound states 4-108917

**impurity electron states continued**

- semiconductor superlattices, quantum wells, and heterostructs., elec. and optical props. 4-80666  
 semiconductors, compensated, spatial distrib. of impurities 4-103784  
 semiconductors, conf., Cambridge, MA, USA (Nov. 1983) 4-95025  
 semiconductors, covalent, localised states of negative ions stabilised by enhanced correl. effects, appl. to GaP, As<sub>2</sub>S<sub>3</sub>, N 4-104157  
 semiconductors, deep levels, expt. and theoretical studies, review 4-84593  
 semiconductors, disordered, spatially extended quasiparticles, disorder effects 4-98499  
 semiconductors, impurity centres, nonlinear polarisability 4-84589  
 semiconductors, impurity level electron statistics (German) 4-84587  
 semiconductors, magnetically mixed, spin-flip Raman scatt. by shallow donors, polarisation and linewidth 4-66038  
 semiconductors, multi-valley, Auger processes with energy transfer to bound charge carriers 4-80607  
 semiconductors, multiple binding energies in hydrogenic impurity centres, variational calc. 4-61329  
 semiconductors, nonradiative transitions in deep impurities 4-80989  
 semiconductors, polarised light absorpt. in donor-valence band optical transitions 4-61736  
 semiconductors, positive magnetoresistance in the variable-range hopping region 4-65695  
 semiconductors, shallow donors, self-oscill. and flip-flop effect 4-108848  
 semiconductors, surface barrier variations with temp., complex surface state distrib. 4-88551  
 solid solutions, self-quenching of electron excitations 4-70727  
 SOS, ion implanted, elec. props., effect of heat treatment 4-98759  
 substitutional impurities, indirect interaction in linear at. chain 4-61318  
 p-terphenyl, cryst., UV absorpt. and fluoresc. obs. 4-61744  
 transition metal based alloys, dipole force tensor, cryst. field effect 4-84597  
 transition metal oxides: Co, electronic struct. and cryst. field transitions 4-113891  
 weakly compensated classical impurity band, neutral donor energies 4-92658  
 yttrium ethylsulphate, Ce<sup>3+</sup>, Ce<sup>3+</sup> EPR spin-lattice relax. rate, press. effects 4-65855  
 zero-gap semiconductors, impurity states in mag. field 4-61332  
 zinc-blende semiconductors, localised lattice instability, microscopic model for large lattice relax. and high temp. anomalous diamagnetism 4-70718  
 AgBr:I, multiphonon emission, excitons, photoluminescence 4-99159  
 Al, doped, trapping of muons and protons, effect of substitutional impurities 4-65631  
 AlGaAs:Si MBE layers, donor levels anal. 4-61316  
 Al<sub>0.9</sub>Ga<sub>0.1</sub>As:Si MOCVD layers, transport props. 4-92834  
 Al<sub>0.9</sub>Ga<sub>0.1</sub>As:Te(Sn) epitaxial films, carrier density changes due to band struct. modifications 4-61381  
 Al<sub>0.9</sub>Ga<sub>0.1</sub>As/GaAs heterojunction, subband struct. at low temp. 4-104298  
 Al<sub>2</sub>O<sub>3</sub>, doped, mixed cond. and impurity electron states 4-92773  
 Au(Ni/Co), impurity lineshapes in dilute alloys, UPS study 4-113893  
 BaClF:Sm<sup>2+</sup>, impurity states in mag. field, fluoresc. study 4-108805  
 BaClF:Sm<sup>2+</sup>, low-lying energy levels under mag. field 4-98564  
 BaFCl:Gd flux grown cryst., thermoluminescence studies 4-66081  
 BaSO<sub>4</sub>:MnO<sub>4</sub><sup>2-</sup> absorpt. spectra, comparison with other host lattices 4-109217  
 BaTiO<sub>3</sub>, pure and Nb-doped, elec. cond. 600-800°C, defect struct. 4-98604  
 BaTiO<sub>3</sub>:Ca, impurity site occupancy, channelling enhanced microanal. studies 4-108394  
 BaTiO<sub>3</sub>:Co, impurity valence states, EPR 4-75901  
 Bi<sub>2</sub>SiO<sub>5</sub>, deep impurities, photoelectric phenomena 4-113996  
 Bi<sub>2</sub>Te<sub>3</sub>:Pb(Ge), doping props., elec. cond. and Seebeck measurements 4-75467  
 CaF<sub>2</sub>:Eu, phononless impurity-centre line, inhomogeneous broadening under plastic deform. conditions 4-88864  
 CaF<sub>2</sub>:Eu<sup>2+</sup>, phononless line profile under random deformations, luminesc. bands 4-70726  
 CaF<sub>2</sub>:La<sup>2+</sup>, intermediate Jahn-Teller coupling, vibronic Raman and EPR spectra 4-88491  
 CaSO<sub>4</sub>:Dy, photo-transfer thermoluminescence 4-104683  
 CaWO<sub>4</sub>, tunnel-processes and assoc. of donor and acceptor centres 4-109258  
 CdBr<sub>2</sub>:I<sub>2</sub>, absorpt. spectra and electron localisation (Russian) 4-104161  
 CdBr<sub>2</sub>:Mn<sup>2+</sup>, phononless luminescence spectrum (Russian) 4-114328  
 CdF<sub>2</sub>:Eu, deep centre characterisation by thermally controlled EPR 4-71174  
 Cd<sub>1-x</sub>Hg<sub>x</sub>Te:Mn, EPR study 4-71168  
 Cd<sub>2</sub>Nb<sub>2</sub>O<sub>7</sub>:Gd<sup>3+</sup>, ferroelec. transitions, EPR spectra 4-98945  
 CdS, edge luminesc. series emitted in elec. field 4-66068  
 CdS, ground state energies of shallow donors 4-92654  
 n-CdS/electrolyte interface, photoelectrochem. characterisation 4-84689  
 CdS-CdTe thin films, photoluminescence study 4-80987  
 CdS:Se<sub>1-x</sub> single cryst., elec. cond. and Hall effect studies 4-113974  
 CdSiAs<sub>2</sub>, impurity photoluminescence polarisation 4-88873  
 CdTe, cooperative processes, spontaneous and stimulated emission 4-104662  
 CdTe thin layers, crystal and energy structures for photoelectric transducers 4-98298  
 CdTe:Ag(Cu), deep levels, pulsed admittance spectroscopy and capture cross sections 4-92653  
 CdTe:Cl, native acceptor defects, Hall effect study 4-75899  
 n-CdTe:In, electron traps, DLTS study 4-80533  
 n-CdTe-p-Cu<sub>2</sub>Te(p-Au,Te) heterojunctions, deep levels, photocapacitance spectra 4-61410  
 Co-Ag-Pd, transient fields, g-factor, gyromagnetic ratios 4-113914  
 CoO, 3d impurity excitation spectra, separation of one- and many-electron effects 4-75900  
 Cr<sup>3+</sup> impurity absorpt. spectra, crystal field, ground and excited state 4-109218  
 Cr-Co alloys, local electron states, elec. resist. and magnetoresist. studies 4-80550  
 CsCaCl<sub>2</sub>:Mn<sup>2+</sup>(Ni<sup>2+</sup>)(Co<sup>2+</sup>), fluoresc. emission, excitation, IR absorpt. spectra studies 4-99153  
 Cu, doped, trapping of muons and protons, effect of substitutional impurities 4-65631  
 Cu, electronic props. of 4d transition metal and sp impurities 4-70731  
 Cu-Ti glasses, surface composition, composition profiles, Auger electron spectroscopy 4-113758

## purity electron states continued

- CuInS<sub>2</sub>, defect chemistry, elec. and Mossbauer studies 4-70730  
 n-CuInSe<sub>2</sub>, elec. and thermal conductivity, donor levels 4-75974  
 CuNi impurity lineshapes in dilute alloys, UPS study 4-113893  
 CuRh, valence band photoelectron spectra 4-88941  
 Eu (III) in silica gel glass, fluoresc., cation binding and cage symm. 4-114835  
 Fe, impurity hyperfine fields and adiabatic pot., self-consistent calc. 4-65632  
 Fe-Ag-Pd, transient fields, g-factor, gyromagnetic ratios 4-113914  
 Fe-based 3d-metal alloys, impurity charge screening 4-98562  
 GaAs, acceptor level, 78 meV, luminescence and Raman scatt. studies 4-70704  
 GaAs, compensation resulting from N ion implantation 4-104150  
 GaAs, deep impurity levels, ENDOR and ESR spectra 4-84594  
 GaAs, deep levels associated with vacancy-impurity pairs 4-92662  
 GaAs, doped, cond. electron spin relax. times, precession mechanism, spin splitting 4-98948  
 n-GaAs, emission band at 1.35 eV, doping and temp. variations 4-76519  
 GaAs epitaxial film, MBE growth, capture of accidental impurities, influence of growth conditions 4-108743  
 GaAs epitaxial films, line impurity photocond. spectra, fine-struct. splitting 4-65761  
 GaAs, existence of B<sub>As</sub> impurity antisite centres, IR absorption lines study 4-71413  
 GaAs, high-purity, in mag. fields, donor transition anomalous line broadening 4-109214  
 GaAs, MOCVD grown, deep electron traps, DLTS obs. 4-84585  
 GaAs, photoluminescence characterisation of impurities and defects 4-88876  
 GaAs Schottky diodes, deep levels, photocapacitance spectra 4-61410  
 GaAs, semi-insulating, deep donor conc., dislocations and elec. resist. 4-103781  
 GaAs, shallow acceptors, ground state calc., allowing for valence band corrugations 4-108817  
 n-GaAs, shallow impurity photoexcitation line narrowing in an elec. field 4-80970  
 GaAs, vacancy energy levels, impurity state pinning, tight-binding calcs., local density theory 4-88470  
 GaAs: Mn, spin-depend. recombination, optical pumping studies 4-99183  
 GaAs:B, interaction between B and defects 4-80082  
 GaAs:Cr, Cr-related complex, photoluminesc. studies 4-88467  
 GaAs:Cr, impurity photocond., internal quantum efficiency 4-88540  
 GaAs:Cr, ionisation processes by upper conduction band electrons, mag. field effects 4-65640  
 GaAs:Cr, photoluminescence excitation spectra, C<sup>2+</sup> internal luminesc. 4-81004  
 GaAs:Cr<sup>2+</sup>, comparison of static and dynamic Jahn-Teller models 4-61345  
 GaAs:Cr<sup>2+</sup>, trigonal symmetry sites, photoluminescence spectra anal. 4-108391  
 GaAs:Cr(Ni), deep impurity charact., photoluminescence study 4-98557  
 GaAs:Cr(O), electrical properties and impurity states 4-75963  
 GaAs:Mn, charge state of Mn impurities, mag. susceptibility ESR and Hall effect meas. 4-108982  
 GaAs:Mn, phonon scatt. at acceptor ground state 4-70729  
 GaAs:Mn, thermal cond. resonances of acceptor states 4-104011  
 GaAs:N, isoelectronic traps study by photoluminesc. (Chinese) 4-93098  
 GaAs:Se, deep acceptor, photoluminescence study 4-80534  
 GaAs:Si, ion implanted, and semi-insulating GaAs, deep levels, photoconductivity study 4-88469  
 GaAs:Sn/GaAs:Cr interface, electron and hole traps, photovoltaic studies 4-104283  
 GaAs:transition metals, electronic struct. of bulk centres 4-108818  
 GaAs/AlGaAs heterostructures, carrier density, hydrostatic press. control 4-98735  
 GaAs/Ga<sub>1-x</sub>Al<sub>x</sub>As quantum well wires, hydrogenic impurity states 4-92815  
 GaAs-Al<sub>0.3</sub>Ga<sub>0.7</sub>As quantum wells, photoluminesc. from spike doped hydrogenic donors 4-104668  
 GaAs-Al<sub>0.3</sub>Ga<sub>0.7</sub>As quantum well structs., Raman scatt. study 4-93079  
 GaAs-GaAlAs quantum well struct., optical props., review 4-104146  
 GaAs<sub>1-x</sub>P<sub>x</sub>N, excitons and excitonic mols. bound to impurity, calcs. 4-108785  
 GaAs<sub>1-x</sub>P<sub>x</sub>N<sup>+</sup>, Zn<sup>2+</sup> implanted, photoluminescence spectra, impurity conc. depend. (Chinese) 4-93099  
 GaInAsP, high purity, charact., growth, back contrib. 4-61334  
 GaP, 3d impurity excitation spectra, separation of one- and many-electron effects 4-75900  
 GaP, deep impurity levels, ENDOR and ESR spectra 4-84594  
 GaP, donor wave functions and band struct. 4-98519  
 GaP, Hall meas. anal., influence of thermal impurity activation energy temp. depend. 4-104238  
 GaP: transition metal, impurity electron states calcs. 4-70711  
 GaP:N, exciton transfer, NN<sub>2</sub>-pair luminesc. enhancement, stochastic model 4-104660  
 GaP:N, photothermal capacitance meas. 4-84647  
 GaP:Ni, state of impurity centres, EPR, spin-lattice relax. time, spin Hamiltonian parameters 4-88476  
 GaP:Ni<sup>2+</sup>, Jahn-Teller coupling forces, self consistent LCAO calc. 4-98577  
 GaP:O, electronic impurity states calcs. 4-80547  
 GaP:O(Zn), size effects and impurity electronic struct. 4-70723  
 GaP:As<sub>1-x</sub>N<sub>x</sub>, covalent, localised states of negative ions stabilised by enhanced correl. effects 4-104157  
 GaSe, ground state energies of shallow donors 4-92654  
 GaSe:Co, injection and thermopolarisation currents 4-70833  
 GaSe:Fe, elec. cond. and impurity states 4-113957  
 GdTaO<sub>5</sub>Tb<sup>3+</sup>, energy transfer phenomena, photoluminescence 4-109234  
 Ge (111), shallow donor impurities, variational soln. 4-70893  
 Ge, deep impurity conc., elec. resist. and Hall coeff. meas. 4-65638  
 Ge, impurity breakdown kinetics, small-signal anal. 4-113965  
 a-Ge, localised impurity states 4-104163  
 p-Ge, nuclear doped, elec. cond., 0.06 to 300K, impurity conc. depend. 4-61382  
 Ge, shallow acceptors, ground state calc., allowing for valence band corrugations 4-108817  
 n-Ge:Au, deform. influence on deep level position of impurity 4-104160  
 Ge:Be, site distortion of Be acceptor, IR spectra 4-92667  
 Ge:Cu, impurity states, annealing effects 4-104148  
 Ge:Cu, quenched-in deep acceptors 4-70713

## impurity electron states continued

- a-Ge:H:P, new paramagnetic centres and impurity states 4-109056  
 Ge:H-based impurity complexes, charge state determ. 4-92663  
 Ge:Hg<sup>+</sup>, hole capture cross section 4-98567  
 Ge:Sb, photoexcited, impurity breakdown and impact ionisation 4-92739  
 n-Ge:Sb, US attenuation, mag. field effects, impurity conc. depend. 4-75618  
 Ge:Sb(As), impurity state breakdown under uniaxial compression 4-70715  
 Ge:Se, impurity levels, Hall effect study 4-108804  
 Ge:Zn, far-IR magnetooptical absorption of bound excitons 4-114247  
 Ge:Zn, nonohmic hopping cond. in strong elec. fields 4-88515  
 GeS film, crystalline and amorphous, photoconductivity study (Russian) 4-70870  
 GeS, hole drift mobility anisotropy 4-70814  
 He+Cu surface, time-depend. wavepacket scatt. calcs., isolated impurities effect 4-61794  
 Hg<sub>1-x</sub>Cd<sub>x</sub>Te, deep impurity and defect states 4-88474  
 InP, excitons bound to neutral acceptors, stress effects, photoluminesc. study 4-61294  
 InP, high-purity, in mag. fields, donor transition anomalous line broadening 4-109214  
 InP, LEC grown, photoluminesc. study, 1.8 to 40K (Chinese) 4-84993  
 InP, mag. field induced metal-insulator transition 4-84566  
 InP, transition metal diffusion, photoluminesc. study, deep acceptor levels obs. 4-70461  
 InP:Be(C), acceptor levels, photoluminesc. study 4-80543  
 InP:Gd(Yb) epitaxial films, doping effects on low-temp. edge photoluminescence 4-85028  
 InP:Ge(Sn), donor identification, photolum. and far IR photocond. in high mag. fields 4-70705  
 InP:Mg(Fe,Mg), implanted, effect on photoluminescence props. 4-85007  
 InP:Mn, hopping cond. between deep impurity states 4-104209  
 InP:V(Cr), impurity excited states, optical absorpt. spectra 4-88863  
 n-InSb, Auger recombination of holes via deep donors 4-104229  
 n-InSb nonlinear optical props. photoelectronic investigation 4-96986  
 InSb, shallow donors in high mag. fields and hydrostatic press. 4-80540  
 InSb, two-photon reson. photo-Hall effect 4-70863  
 InSb:Ge(Si), impurity solubility, role of acceptor and donor states 4-60949  
 InSb:H, ionisation energy of magnetodons 4-70714  
 InSb/Al<sub>0.3</sub>SiO<sub>2</sub>-SiO<sub>2</sub> system, slow states, field effect studies 4-65752  
 K halides, Ba-doped, impurity colour centres, absorpt. spectra 4-88865  
 KBr:In, A<sup>2+</sup>, F-centres formed by low-energy excitons, photoluminescence spectra (Russian) 4-113874  
 KBr:In, radiation storage of activator light sums, role of surface effect, photoluminescence (Russian) 4-114322  
 KBr:In(Tl), light sum slow component charact. in presence of fast component, photoluminescence (Russian) 4-114320  
 KCl:I, impurity-localised excitons, luminesc. and absorpt. spectroscopy study 4-92625  
 KCl:O<sub>2</sub><sup>-</sup>, fluoresc. time depend. study 4-109239  
 KCl:Ti<sup>3+</sup>, impurity level ground and excited states, Green's function calc. 4-98563  
 KI(Br):Ti<sup>2+</sup>, magnetic dichroism study of Ti<sup>3+</sup> centre symm. 4-70719  
 KTaO<sub>3</sub>, spin-flip Raman scatt. in mag. fields, obs. of donor states 4-71384  
 KTaO<sub>3</sub>:Fe<sup>3+</sup>, EPR spectra, superhyperfine struct., spin Hamiltonian parameters 4-98942  
 LaCl<sub>3</sub>:Nd<sup>3+</sup>, isotope shifts, laser-induced fluoresc. 4-71428  
 LaF<sub>3</sub>:Eu<sup>2+</sup>, fine struct. parameters, hyperfine splittings, X-band EPR meas. 4-71176  
 LaF<sub>3</sub>:Pr<sup>3+</sup>, cooperative energy transfer among Pr<sup>3+</sup> ions, photoluminescence spectra 4-92664  
 LiF:LiO, impurity centres, visible spectra studies 4-80546  
 LiNH<sub>2</sub>SO<sub>4</sub>:Mn<sup>2+</sup>, impurity electronic absorpt. spectrum 4-66055  
 LiNbO<sub>3</sub>:Co, Fe<sup>3+</sup>, electron capture, non-equilibrium population, Mossbauer spectra studies 4-108807  
 LiNbO<sub>3</sub>:Eu<sup>3+</sup>, impurity optical absorpt. 4-66056  
 LiNbO<sub>3</sub>:Ni<sup>2+</sup>, cryst. field splitting of impurity levels 4-65647  
 LiTaO<sub>3</sub>:Co, Fe<sup>3+</sup>, electron capture, non-equilibrium population, Mossbauer spectra studies 4-108807  
 LiYF<sub>4</sub>:Pr<sup>3+</sup>, crystal-field energy levels, splitting chain calc. (Chinese) 4-113908  
 MgO phosphor, thermolum. and trapping kinetics 4-88887  
 MgO, surface γ-conductivity, kinetics and decay, F<sub>2</sub>-centres 4-65726  
 MnO, 3d impurity excitation spectra, separation of one- and many-electron effects 4-75900  
 MnO, stabilised and Mn<sub>1-x</sub>Zn<sub>x</sub>O solid solns., elec. props. 4-98605  
 n-MoTe<sub>2</sub>, carrier mobility, thermoelec. power and elec. resist., one-band model anal. 4-98612  
 NaCl:Br, impurity-localised excitons, luminesc. and absorpt. spectroscopy study 4-92625  
 NaF:Cu<sup>2+</sup>, excited state dynamics 4-108803  
 NaH<sub>2</sub>(SeO<sub>3</sub>)<sub>2</sub>:Cr<sup>3+</sup>, EPR spectra, temp. and external elec. field effects 4-88715  
 Nb, electronically induced trapping of H by impurities 4-108410  
 Nd<sup>3+</sup> impurity ions in crystals, phonon-assisted energy transfer, conc. depend. 4-92311  
 NiO, 3d impurity excitation spectra, separation of one- and many-electron effects 4-75900  
 Pb<sub>1-x</sub>Hg<sub>x</sub>Se flash-evaporated films, optical and elec. props. 4-114335  
 PbI<sub>2</sub>, binding energies of exciton-ionised donor complex and exciton line n=1 4-70666  
 PbS polycryst. samples, current and photocurrent flow mechanisms 4-104196  
 PbSe<sub>1-x</sub>Te<sub>x</sub>:Ti, energy spectra and elec. cond 4-70724  
 Pb<sub>1-x</sub>Sn<sub>x</sub>Te:In, photoconductivity and impurity states 4-113993  
 PbTe:B, absorpt. spectra and impurity states 4-104638  
 PdH<sub>2</sub>, electronic props. of dilute H 4-88472  
 Pr<sub>2</sub>La<sub>1-x</sub>P<sub>2</sub>O<sub>7</sub>, luminesc. theory, oscillator strength, impurity conc. effect (Chinese) 4-93100  
 Rb halides, Ba-doped, impurity colour centres, absorpt. spectra 4-88865  
 RbAl<sub>2</sub>Si<sub>2</sub>(S)(Se)(Te), electron level struct., photoluminescence spectra 4-99192  
 Sb<sub>2</sub>Te<sub>3</sub>:Pb(Ge), doping props., elec. cond. and Seebeck measurements 4-75467  
 Si (001), shallow donor impurities, variational soln. 4-70893  
 Si, A-centre and thermal donor levels, Hall effect, DLTS meas., press. depend. 4-80529  
 Si, acceptor pairs, hydrogenic, first ionisation energies calc. 4-70710

## impurity electron states continued

- Si, carrier lifetime, elec. resist. meas. by contactless method 4-61392  
 Si, clusters of electrically active centres and impurity states 4-70183  
 Si, Czochralski grown compensated thermodonors, EPR and Hall studies 4-75898  
 Si, deep impurity levels, ENDOR and ESR spectra 4-84594  
 Si, defects and high press. steam oxidation, stacking faults 4-114706  
 Si, ESR meas. of chalcogen pairs, theory 4-104493  
 n-Si, electron capture coeff. of quenching centres 4-104159  
 Si, impurity conduction effect of uniaxial compression on p-type Si 4-98617  
 Si MOS structures, donor-like defects 4-61457  
 Si, magnetic energy states of shallow acceptors, spin depend. luminesc. study 4-104655  
 n-Si, many-valley semicond., impurity states, clustering model 4-80549  
 Si, photoconductive asymmetries of donor and acceptor impurities 4-70857  
 Si, photoluminescence characterisation of impurities and defects 4-88876  
 n-Si, proton irradiated, electrophysical props. 4-108861  
 Si, substitutional and interstitial donors, many electron effect 4-113895  
 Si surface, excess carriers, light-induced recombination 4-76005  
 Si, vacancy energy levels, impurity state pinning, tight-binding calcs., local density theory 4-88470  
 Si:Al, electronically simulated defect migration 4-113730  
 Si:Au, donor and acceptor levels, DLTS meas. 4-88473  
 Si:Au, donor level, entropy factor, resist. and DLTS meas. 4-70707  
 Si:Au, photocurrent deep level transient spectra 4-80535  
 Si:Au, transient capacitance of Au acceptor energy level under uniaxial stress (Chinese) 4-75888  
 Si:B, deep level impurities at bond centered interstitial site 4-108814  
 Si:B, Fe, excitation photoluminescence study 4-109243  
 Si:B, impurity electronic struct. cluster  $X\alpha$  calc. 4-65639  
 Si:B, thermal cond. resonances of acceptor states 4-104011  
 Si:B,H, neutralisation of shallow acceptor levels by atomic H 4-104153  
 Si:B(In), point defects influence on acceptor ground state splittings 4-70728  
 Si:B( $\mu^+$ ), tetrahedral interstitial impurities, electronic struct. 4-65636  
 n-Si:Fe, impurity bands of Fe clusters, ESR and elec. props. 4-109067  
 Si:Ga, neutron irradiat., acceptor level, IR absorpt. spectrum 4-93089  
 a-Si:H, As, dispersive transport, trap saturation, transient photocurrent meas. 4-76006  
 a-Si:H, B, P, electron structure and density of states of B-P pairs, cluster calc. 4-65642  
 a-Si:H, deep recombination centres, luminescence and EPR studies 4-104164  
 a-Si:H, doping and gap states 4-70734  
 Si:H, electron localisation-delocalisation transitions and H<sup>-</sup>-like states 4-92668  
 Si:H, interstitial muons anal. impurity states 4-80541  
 Si:H, microcrystalline, photoinduced free-carrier absorpt. spectra 4-88859  
 a-Si:H, non-substitutional dopant states and carrier density statistics 4-113902  
 a-Si:H, radiative combination at dangling bonds, quantitative model, expt. study 4-114326  
 a-Si:H,B, doping effect on gap states 4-88488  
 a-Si:H,O(N) alloys, electron trapping states, tight binding formalism calcs. 4-113901  
 a-Si:H,P, new paramagnetic centres and impurity states 4-109056  
 a-Si:H film, IR quenching of photoluminescence and photoconductivity 4-104656  
 Si:In(B), phonon scatt. at acceptor ground state 4-70729  
 Si:Mg(Al)(S), third-period interstitials, electronic struct. calcs. 4-108808  
 Si:Mn, Cu, impurity energy levels, DLTS and capacitance studies 4-88471  
 Si:muon, spin polarised electron struct. of positive muon, LCAO-Green's function anal. 4-65634  
 Si:N, ion implanted, optical props. (Chinese) 4-114306  
 Si:O, nonequilibrium cond. and thermal donors 4-104212  
 Si:O, O thermal donor, symmetry and electronic props., DLTS studies 4-113886  
 Si:O, P, thermal donors, optical absorption spectra studies 4-65637  
 Si:O, piezocalvanomagnetic effects in presence of thermal donor levels 4-104239  
 Si:O, rare earth atoms, impurity interaction and donor accumulation 4-103783  
 Si:O, recombination centres induced by heat treatment at 600 to 800°C 4-104154  
 Si:O<sub>2</sub>, precipitation at various impurity levels 4-113654  
 p-Si:P, elec. activity of P in diffusion zone (Russian) 4-70817  
 Si:P, motional narrowing of ESR line 4-104484  
 Si:P IR detector field enhanced photoresponse up to 43  $\mu$ m 4-90656  
 Si:S, charge states, electronic struct. 4-104152  
 Si:Se, photocapacitance, photocond. and donor levels 4-65714  
 Si:Sn, amorphous vacuum deposited films, impurity states 4-84595  
 Si:Te, donor states, Hall effect and cond. meas. 4-104145  
 Si:Ti, recombination props., capture rates 4-104149  
 Si:SiO<sub>2</sub> interface, shallow donor impurities, variational soln. 4-70893  
 Si<sub>1-x</sub>Ge<sub>x</sub>:H, amorphous, gap state distrib., photoconductivity study 4-108820  
 Si<sub>3</sub>Ge<sub>1-x</sub> alloys, substitutionally sp<sup>3</sup>-bonded defects, deep energy levels 4-108813  
 Si<sub>3</sub>Ge<sub>1-x</sub>P<sub>x</sub>(As)(Sb), paired donor impurities energy levels 4-61315  
 SiO<sub>2</sub>+B<sub>2</sub>O<sub>3</sub> phase stabilisation, quantum-chem. calc. 4-61325  
 SrCl<sub>2</sub>:Sm<sup>3+</sup>, low-lying energy levels under mag. field 4-98564  
 SrF<sub>2</sub>:Gd<sup>3+</sup>, phosphors, thermostimulable center-center transitions, luminesc. 4-80996  
 SrS:Pb<sup>2+</sup>, phosphors, impurity dimer centres, luminesc. obs. 4-99158  
 SrSe:Pb<sup>2+</sup>, phosphors, impurity dimer centres, luminesc. obs. 4-99158  
 Ti<sub>0.97</sub>Ru<sub>0.03</sub>O<sub>2</sub>, biphasic cryst. in aq. soln., photoelec. props. 4-84648  
 Zn, impurity lineshapes in dilute alloys, UPS study 4-113893  
 ZnO, 3d impurity excitation spectra, separation of one- and many-electron effects 4-75900  
 ZnO: transition metal, impurity electron states calcs. 4-70711  
 ZnS, 3d impurity excitation spectra, separation of one- and many-electron effects 4-75900  
 ZnS, CVD, vacancy-hydride complex, optical absorpt., photoluminesc. 4-60916  
 ZnS: transition metal, impurity electron states calcs. 4-70711  
 ZnS:Cu<sup>2+</sup>, Jahn-Teller coupling forces, self consistent LCAO calc. 4-98577  
 ZnS:Fe<sup>2+</sup>, impurity states, EPR meas. 4-84588
- impurity electron states continued**  
 ZnS:I, with adsorbed O<sub>2</sub>, surface states and LED props. 4-80643  
 ZnS:Mn thin films, electrolum., diffusion and trapping 4-104677  
 ZnSe, Se<sub>1-x</sub>, deep impurity, trap embedding, luminesc. spectra 4-61321  
 ZnSe, 5d impurity excitation spectra, separation of one- and many-electron effects 4-75900  
 ZnSe:N, acceptor levels, optically excited DLTS study 4-61322  
 ZnSe:Na, donor-acceptor-pair line luminesc. 4-104659  
 ZnTe, donor bound exciton states, Zeeman spectra 4-88452  
 ZnTe:Ni, absorpt. spectra, impurity states (Russian) 4-113898
- impurity scattering**  
 used for carrier scattering by impurities  
 see also Kondo effect  
 alloys, anisotropic superconducting, time depend. Ginzburg-Landau eqns. 4-88630  
 CWD superconductors, nonmagnetic impurity effects 4-70683  
 graphite intercalation compounds, c-axis cond. and thermoelec. power 4-80561  
 II-VI semiconductors, carrier mobility characts., displaced Maxwellian model 4-75968  
 inversion layer, impurity band cond. in mag. fields, theory 4-98768  
 inversion layers, bound electron states of Coulombic impurities and effect on mobility 4-98770  
 ion scattering near interfaces, energy loss method anal. 4-65655  
 metal, surface impedance temp. depend., effect of impurity dynamic disorder, rel. to anomalous skin effect 4-92788  
 metals, electrical conductivity of impurity-containing metals, field effects 4-65670  
 quasi-one-dimensional metal, mutual influence of phase transitions, scatt. and localisation of electrons 4-70796  
 RPA quasiparticle energies, low density approach 4-80526  
 semiconductors, charge carrier transfer and diffusion in strong mag. field (Russian) 4-88520  
 semiconductors, ionised-impurity scatt., coherent multi-ion interference effects 4-98601  
 semiconductors, quasi-one-dimensional, low-field electron transport 4-80605  
 single metals elec. resistivity and scatt. theory 4-92694  
 transport eqn. for isotropic electron distrib. function and electron relax. (Russian) 4-65654  
 n-Bi<sub>1-x</sub>Sb<sub>x</sub>, electron scatt., low temp. 4-108835  
 Bi<sub>2</sub>Te<sub>3</sub>(Se<sub>2</sub>), weak-field transport, thermoelec., galvanic- and thermo-mag. coefficients 4-98613  
 n-Cd<sub>3</sub>As<sub>2</sub>, degenerate, Debye screening length under influence of arbitrary mag. quantisation 4-70836  
 Cd<sub>3</sub>P<sub>2</sub>(As<sub>2</sub>)(Sb<sub>2</sub>), disordered, Mott transitions and impurity scattering (Russian) 4-88450  
 Cu, electronic props. of 4d transition metal and sp impurities 4-70731  
 n-CuInSe<sub>2</sub>, elec. and thermal conductivity 4-75974  
 GaAs, Bridgman ingots, photocond., 80-300K, CR and O impurity effects 4-65705  
 GaAs, neutral impurity scatt., far-IR cyclotron resonance study 4-71185  
 GaAs neutral impurity scatt., far-IR cyclotron reson. study 4-92964  
 GaAs/(AlGa)As selectively doped heterostruct., transport props. 4-70913  
 GaAs/Ga<sub>1-x</sub>Al<sub>x</sub>As quantum well wires, hydrogenic impurity states 4-92815  
 GaAs-AlGa<sub>1-x</sub>As heterostructures, electron mobility, temp. depend. from 1-10K 4-80669  
 GaAs-GaAlAs heterostructure, electron mobility limits 4-76030  
 GaP:Te(N)(As), impurity influence on electron-hole plasma 4-75862  
 n-Ge, hot electron capture by dipoles at low temps., field depend. 4-75979  
 Ge:Sb, intervalley neutral impurity scatt. (Russian) 4-104197  
 InAsP, high mobility, vapour phase heteroepitaxial growth 4-71601  
 In<sub>0.53</sub>Ga<sub>0.47</sub>As, 2D electron gas, alloy scatt. limited mobility 4-98620  
 n-InSb, strongly compensated, electron mobility meas. 4-70834  
 In<sub>2-x</sub>Sn<sub>x</sub>O<sub>3-y</sub> films, transparent and heat-reflecting, elec. and optical props., ionised impurity scatt. 4-66087  
 La<sub>100-x</sub>Al<sub>x</sub>, amorphous, supercond., thermodynamic and transport props. 4-70986  
 Pb chalcogenides, carrier heating mechanisms 4-92738  
 Pb<sub>1-x</sub>Ge<sub>x</sub>Te, undoped and In-doped, anomalous scatt. of carriers by defects and impurities near ferroelec. phase transition 4-98622  
 PdH, thin films, weak localisation, electron-electron interactions 4-84713  
 Sb<sub>2</sub>Te<sub>3</sub> single cryst., weak field charge transport 4-108887  
 Sb<sub>2</sub>Te<sub>3</sub>, weak-field transport, thermoelec., galvanic- and thermo-mag. coefficients 4-98613  
 Si (100) inversion layer, electron mobility, neutral scatt. effects 4-76040  
 Si, impurity conduction effect of uniaxial compression on p-type Si 4-98617  
 Si inversion layers, 2D Na impurity band cond. in activated regions, mag. field depend. 4-98769  
 Si-MOSFET inversion layer, warm electron coeff. calc. for two-dimens. electron gas 4-65748  
 Ta, electron-electron scatt., elec. resist. meas. 4-113935  
 Zn<sub>3</sub>P<sub>2</sub>(As<sub>2</sub>)(Sb<sub>2</sub>), disordered, Mott transitions and impurity scattering (Russian) 4-88450
- impurity-vacancy interactions**  
 alkali halides:Eu<sup>2+</sup>(Pb<sup>2+</sup>)(Ca<sup>2+</sup>)(Sr<sup>2+</sup>), X-irrad. effect on impurity vacancy dipoles and aggregation precipitation state, F-centre production 4-70209  
 alloys, dilute, free enthalpy of impurity-vacancy binding, solvent diffusion meas. 4-84465  
 fluorite struct. oxides, O ion cond., dopant size effects 4-70446  
 n-Si, radiation defect formation, annealing, defect interactions 4-113499  
 Ag-Sn(In) dilute alloys, correlated impurity diffusion jump processes, isotope effect 4-84446  
 Al-In, dil., He localised diffusion around In impurities, PAC obs. 4-65470  
 Au-Fe, positron lifetimes in vacancies and vacancy-Fe clusters 4-109274  
 BaTiO<sub>3</sub>:Nb(Al), donor doped, defect chem. 4-84307  
 Co<sub>1-x</sub>O<sub>x</sub>:Ni single cryst., Ni impurity diffusion and interaction with vacancies 4-92437  
 Cu, irradi., stored energy, calorimetric determ. 4-103829  
 Cu-In (0.1 at.%), vacancy trapping, PAC and ion channelling study 4-84876  
 Fe alloys, dil., electron irradiat., muon spin rot. obs. 4-65913  
 Fe, electron irradiat., internal friction (Polish) 4-92234  
 $\alpha$ -Fe, positron annihilation expts. in thermal equil., one-interstitial model confirmation 4-109271

- impurity-vacancy interactions continued**  
 Fe, pure and doped, muon trapping at vacancies 4-65901  
 Fe-Ta(Mn), neutron irradiat. at 325K, defect annealing stages (*Russian*) 4-92242  
 GaAs, deep levels associated with vacancy-impurity pairs 4-92662  
 GaAs, plastic deform., yield stress, photoluminescence, effect of impurity-vacancy complexes 4-70261  
 He-vacancy clusters, stability during irradiat. 4-108415  
 He, BCC phase, spin lattice relax. 4-104035  
 InP, LEC grown, photoluminesc. study, 1.8 to 40K (*Chinese*) 4-84993  
 KBr:Si<sup>2+</sup>, impurity-vacancy dipoles, dielec. relaxation 4-99019  
 KBr:Si<sup>2+</sup>,  $\gamma$ -irrad., thermally stimulated depolarisation currents 4-71263  
 MgO, containing dissolved traces of water, surface charges and subsurface space charge distrib. 4-80650  
 NaCl crystals, doped, solution hardening due to fixed and rotating impurity-vacancy dipoles 4-75502  
 NaCl-type crystals, doped, impurity-vacancy pairs, computer simulation of induced Snoek effect 4-75501  
 Ni, ion implanted D trapping by vacancies, channelling studies 4-108409  
 PbF<sub>2</sub>:Na(K)(Rb), ionic cond., dielec. relax. and activation vol. 4-113701  
 Si, electron and  $\gamma$  irradiat., influence on defect annihilation 4-98094  
 Si, impurity diffusion, impurity conc. doping effects 4-113728  
 Si, impurity migration, effect of elastic stresses 4-88349  
 Si, vacancy capture cross section by impurity atoms 4-103789  
 Si:As, P, ion implanted, diffusion modelling 4-113729  
 Si:P, diffusion study, influence of internal electric field 4-108662  
 SrTiO<sub>3</sub>:Fe<sup>2+</sup>-V<sub>O</sub> pairs, electronic struct. calcs. 4-113890  
 TiCl<sub>3</sub>, doped with divalent cation and anion impurities, point-defect mobility 4-84448  
 W, noble gas atom implanted, cascade annealing, computer simulation studies 4-75556  
 ZnS, CVD, vacancy-hydride complex, optical absorpt., photoluminesc. 4-60916  
 ZnSe-I, vacancy-I complex hyperfine interactions, ESR study 4-70150  
 ZrO<sub>2</sub>-Y<sub>2</sub>O<sub>3</sub> single cryst., elec. cond., 400 to 1100K, temp. and freq. depend. 4-70451
- incandescent lamps** *see filament lamps*
- inclusions in crystalline material** *see crystal inclusions*
- inclusive reactions, elementary particle** *see elementary particle inclusive interactions*
- incoloy** *see chromium alloys; iron alloys; nickel alloys*
- incommensurate-commensurate transformations** *see commensurate-incommensurate transformations*
- inconel** *see chromium alloys; nickel alloys*
- independent particle model** *see nuclear optical model; nuclear shell model*
- indeterminacy**  
 beam chopping, quantum mech. effects 4-68013  
 Einstein-Podolsky-Rosen paradox, non-localities 4-90423  
 entropic uncertainty relations for angle-ang. momentum and position momentum 4-90421  
 four-dimensional symmetry, uncertainty relations, R-inherent quantum mechanics 4-95226  
 Franck-Condon principle, erroneous formulation, violation of Heisenberg uncertainty principle 4-96625  
 Heisenberg's microscope and Compton scatt. 4-67919  
 neutron wavepackets and longit. coherence 4-68014  
 partially coherent light, new class of uncertainty relations 4-87273  
 photon absorption, Mandel'shtam-Tamm uncertainty relation 4-90440  
 position meas., minorant of indefiniteness 4-82703  
 quantum frames of reference, finite mass objects, principle of equivalence 4-90434  
 quantum meas., additional uncertainties 4-110905  
 quantum mech., arrival and departure time 4-68005
- index terms** *see vocabulary*
- indexing**  
*see also vocabulary*  
 No entries
- indicating devices** *see indicators*
- indicating instruments** *see indicators*
- indicators**  
*see also alarm systems*  
 friction coefficient measurement, mech. sensor/indicator device 4-86411  
 liquid crystal temperature indicator films as highly sensitive IR visualiser 4-90584  
 magnification-indicating unit for the REM-200 scanning electron microscope 4-101982  
 min-max indicator 4-106304  
 miniature readout devices for metal-cutting lathes 4-58844  
 semiconductor majority carrier type indicator, portable instrument 4-86404
- indium**  
*see also nuclei with .....*  
 adsorbed on Si (100), superlattice structures, RHEED study 4-113802  
 anti-Stokes Raman laser 4-79110  
 anti-Stokes Raman laser up-converter of excimer lasers using stimulated anti-Stokes Raman scatt. 4-74486  
 atom, 410 nm line, perturbation by foreign gases, press. broadening and shift. 4-102634  
 atom, 5s<sup>2</sup>5p<sup>2</sup>(P<sub>1/2</sub>), static elec. dipole polarisability 4-78979  
 atomic ions in laser-prod. plasma, for UV spectra 4-68997  
 deformed, low-temp., recovery activation enthalpy, positron annihilation meas. 4-76556  
 diffusion in Cu, Ag and Au, isotope effect meas. 4-65476  
 diffusion of W, Ta, Re, Os, and Ir in single crystals of W 4-65479  
 diffusivity in Cu along stationary and migrating grain boundaries 4-65484  
 electron-dislocation interaction during plastic deform. at supercond. transitions 4-98178  
 electron-phonon mass-enhancement parameter anisotropy and cyclotron mass 4-84544  
 electronic lifetime anisotropy, pseudopotential model calc. 4-113928  
 Fermi surface, topological transitions under stress (*Russian*) 4-108761  
 film, supercond., surface heat transfer from self-heating hotspots 4-104361  
 films, electromigration 4-61152  
 films on mica substrates, surface plasmon modes and energy loss function 4-85024  
 impurity diffusion in solid Na 4-65475
- indium continued**  
 interaction with Si surface in Si MBE, use as surface cleaning agent 4-99616  
 ion beam generation by selective multistage laser photoionisation of atoms 4-74207  
 L-edge absorpt. systematics, EXAFS obs. 4-66121  
 liquid, solubility and diffusivity of oxygen 4-92373  
 liquid film, substrate for CuInSe<sub>2</sub> rheotaxial growth 4-61877  
 local-field enhancement of rough surface 4-104047  
 metastable isomer prod. for analytical work using isotopic neutron sources, Sr, Cd, In, Ba detection 4-77037  
 O-ring seals design 4-78327  
 oxide film thickness and composition, AES decomposition 4-61193  
 photodissociation lasers using metal hydrides 4-107616  
 photoionic laser epitaxy, purity and nucleation conditions of cryst. films 4-76694  
 resistance thermometer for low temps. 4-101843  
 solid and liq., ultrasonic vel., temp. depend., elastic moduli, vol. depend. 4-60989  
 stopping power for 6.5 MeV protons and mean excitation energies 4-92271  
 superconducting film, polycryst., US attenuation of bulk shear waves below 4K 4-98811  
 superconducting thin film, resistive transition in mag. field, symmetry breakdown 4-65779  
 surface (111), CO oxidation kinetics, lattice gas model 4-66613  
 thin film, surface plasmons detection by attenuated total refl. 4-93123  
 thin films, photoabsorption in 4d excitation energy range, absorpt. coeff., transmission meas. 4-104691  
 triple point, appl. to Pt resistance thermometer calibration 4-111135  
 type I superconducting microbridge, flux flow voltage, time dependent, high resolution recording 4-76084  
 vacuum condensates, adhesion to glass, effect of surface prep. of glass 4-81397  
 whiskers, charge imbalance relax. in phase slip centre, effect of supercurrent 4-92863  
 Ag-In, electronic structure and surface comp., ion etching, X-ray photoelectron spectra 4-66187  
 AgBr:Ir<sup>3+</sup>, I<sup>3+</sup> site geom. by Raman vib. spectroscopy 4-80921  
 CdCr<sub>2</sub>Se<sub>4</sub>, static I-V characs. 4-70815  
 Cd,Hg<sub>1-x</sub>, Te:In, impurity migration 4-70468  
 CdS:Cu:In sprayed films, topoaxial growth of Cu<sub>2</sub>S thin films, optical and structural behaviour 4-114433  
 CdS:In film, elec. props. meas. 4-104329  
 CdS(In) films chemical bath-deposited, electrical and optical props. 4-92832  
 CdSb:In dopant distrib. coeffs. (*Japanese*) 4-84313  
 CdTe:In, electroconductivity at high temp. 4-61373  
 n-CdTe:In, electron traps, DLTS study 4-80533  
 CdTe:In, Li, defect complex, IR absorption studies 4-80031  
 GaAs:In, isoelectronic doping, X-ray and electron microprobe anal. 4-75491  
 GaAs(1110)-In interface, photoemission study 4-85079  
 In I, autoionising levels studied by photoionisation expts. 4-78810  
 In/InO<sub>3</sub>(N<sub>2</sub>) composites, reactive ion beam sputter deposited, optical recording appl. 4-79249  
 In-Al system, mixing behaviour study by Ar ion beam irradiation 4-65402  
 In-Au, excess enthalpies meas. using heat flow calorimeter 4-80237  
 In-pyrrole-N-methylpyrrole contact, XPS study of Schottky barrier 4-104289  
 In-Si (111) interface, charge transfer and surface electromigration 4-108667  
 In-SrTiO<sub>3-x</sub> contact, tunnelling electron-phonon interaction strength 4-98754  
 In+CO(O<sub>2</sub>)(NH<sub>3</sub>)(methane)(ethane)(ethane), intramultiplet mixing collisions 4-107393  
 In labelling of human lymphocytes, detrimental effects 4-72419  
 In radiopharmaceutical prep. and quality control 4-77387  
 In-generator, INER sterile, prep. and medical appls. 4-77388  
 In, international fluence-rate intercomparison for 2.5 MeV and 5.0 MeV neutrons 4-102561  
 KBr:In, A<sup>2+</sup>, F-centres formed by low-energy excitons, photoluminescence spectra (*Russian*) 4-113874  
 KBr:In, radiation storage of activator light sums, role of surface effect, photoluminescence (*Russian*) 4-114322  
 KBr:In(Tl), light sum slow component characs. in presence of fast component, photoluminescence (*Russian*) 4-114320  
 KBr:In(Tl) polycrystalline films, luminescent, epitaxial growth (*Russian*) 4-113833  
 KCl:In, optical props. study 4-88860  
 KI:In(Tl), fast luminescence processes 4-99167  
 2H-NbSe<sub>2</sub>:In, in thermal diffusion 4-88347  
 Pb<sub>1-x</sub>Ge<sub>x</sub>Te:In, elec. props., band edge struct., impurity effects 4-108880  
 Pb<sub>1-x</sub>Ge<sub>x</sub>Te:In, solid solns., impurity photocond., spectra and kinetics 4-113994  
 Pb<sub>1-x</sub>Ge<sub>x</sub>Te:In, anomalous scatt. of carriers by defects and impurities near ferroelec. phase transition 4-98622  
 Pb<sub>1-x</sub>Sn<sub>x</sub>Te:In, elec. transport props. 4-61371  
 Pb<sub>1-x</sub>Sn<sub>x</sub>Te:In, Gunn effect, threshold field rel. to cond. band struct. 4-88513  
 Pb<sub>1-x</sub>Sn<sub>x</sub>Te:In, photoconductivity and impurity states 4-113993  
 Pb<sub>1-x</sub>Sn<sub>x</sub>Te:In epitaxial films, optical absorption spectra and photoconductivity 4-65711  
 Pb<sub>1-x</sub>Sn<sub>x</sub>Te:In epitaxial layers, optical absorption studies 4-71456  
 Pb<sub>1-x</sub>Sn<sub>x</sub>Te:In epitaxial layers, photocond. kinetics 4-88538  
 Si (111)-In abrupt interfaces, electronic props. 4-84696  
 Si:As(Sb)(In), ion implanted, pulsed electron beam annealing, impurity diffusion 4-103984  
 Si:B, thermal cond. resonances of acceptor states 4-104011  
 Si:In, isoelectronic bound excitons, transient photoluminesc. study 4-80507  
 Si:In, phonon scatt. at acceptor ground state 4-70729  
 Si:In, point defects influence on acceptor ground state splittings 4-70728  
 W impregnated cathodes, Ir coated, surface anal. by AES 4-76630  
 ZnSe:In<sup>+</sup>, ion implanted, high electron mobility obs. 4-108863
- indium alloys**  
*see also indium compounds*  
 liquid, mag. props. of transition metal solutes 4-76109

**indium alloys continued**

- Ag-Cd-In alloys, X-ray determ. of mean Debye-Waller factors, vibr. amp. and Debye temp. 4-84358  
 Ag-In dilute alloys, correlated impurity diffusion jump processes, isotope effect 4-84446  
 Ag-Pt-In dilute alloys, In migration, PAC studies 4-65460  
 Al-In, dil., He localised diffusion around In impurities, PAC obs. 4-65470  
 Al-In, distribution of electric field gradients around impurities, conduction electron screening lattice strain 4-113910  
 Al-In, ion irradi., vacancy-solute atom complexes, channelling study 4-103836  
 Al-In (17.5 wt.%), monotectic alloy, unidirectional solidification struct. 4-109391  
 Al-In (17.5 wt.%), unidirectional solidification, monotectic struct. 4-109392  
 Al-In-Sn, irregular monotectic struct., effects of temp. gradient and growth vel. 4-66321  
 Au-In, dil., channelling effect of conversion electrons emitted from radioactive impurities 4-75569  
 Bi-Cd-In system, eutectic alloys, microstruct. 4-93263  
 Bi-In, liq., activities of components 4-71635  
 Bi-In, liq., activity coeff. of O 4-80242  
 Bi-In system, phase diagram and eutectic struct. 4-93264  
 CeIn<sub>3</sub>, mixed-valence system, muon Knight shift meas. 4-80852  
 Ce(In<sub>1-x</sub>Sn<sub>x</sub>)<sub>3</sub>, intermediate valence study 4-61340  
 Co-Ir sputtered films, mag. props. 4-71141  
 Cu-In, dil., channelling effect of conversion electrons emitted from radioactive impurities 4-75569  
 Cu-In, free enthalpy of impurity-vacancy binding, solvent diffusion meas. 4-84465  
 Cu-In, interdiffusion, thermodynamic factor and vacancy flow term 4-70479  
 Cu-In, precip. of  $\delta$ -phase on ageing 4-81201  
 Cu-In (0.1 at.%), vacancy trapping, PAC and ion channelling study 4-84876  
 Cu-In system, volume In diffusion, SIMS studies 4-65457  
 EuI<sub>2</sub>, Mossbauer isomer shift, trivalent <sup>151</sup>Eu 4-114191  
 Gd<sub>2</sub>In, magnetic and electrical props., metamagnetic-ferromagnetic transition, magnetic struct. 4-114138  
 GdIn, Sn<sub>1-x</sub>, elec. resist. below Neel temp. 4-75924  
 In-Bi alloys, phase diagram and metallography 4-114483  
 In-Bi-Pb, liquid, thermodynamic props., EMF meas., 673 to 873K 4-98310  
 In-Ga-Sb alloys, liq., phase diagram calc., Krupkowski's eqn. (Polish) 4-85139  
 In-Ga-Sn, natural convection, mag. field orientation influence (Russian) 4-113061  
 In-Ga-Sn liq. alloy in pipe, degenerate turbulence behind grid in mag. field (Russian) 4-113040  
 In-Hg/Si ohmic contacts, differential resistance and capacitance characts. 4-92819  
 In-Hg/insulator contacts, differential resistance and capacitance characts. 4-92819  
 In-Mn, polyvalent films, elec. cond. anomaly 4-80688  
 In-Mn, superconducting transition temp. determ., using SQUID magnetometer combined with ion implantation 4-58877  
 In-Pb alloys, transition from slip to twinning (Russian) 4-103760  
 In-Pb single crystal, superelastic, irreversible twinning transition 4-85174  
 In-Sb system, high press. intermediate phases, form., struct., stability, supercond. props. 4-89029  
 In-Sn and In-Bi-Sn eutectic alloy solders for Josephson packaging, mech. props. 4-71687  
 In-Tl, elec. resist. studies, average phonon energy 4-113920  
 In-Tl, premartensitic phenomena, role of Fermi surface 4-84384  
 InSb film, condensed at low temp., conductance, transition temp. meas. 4-61482  
 (In<sub>1-x</sub>Te<sub>x</sub>)<sub>2</sub>Sn<sub>1-x</sub>, obtained by splat cooling, Mossbauer study 4-109101  
 LaIn<sub>3</sub>, mixed-valence system, muon Knight shift meas. 4-80852  
 Li-In, cryst. struct. determ. 4-79986  
 Mo-In, dil., channelling effect of conversion electrons emitted from radioactive impurities 4-75569  
 Ni<sub>2</sub>MnIn Heusler alloy, elec. resist. and magnetisation 4-92695  
 Pb-In, electron-dislocation interaction during plastic deform. at supercond. transitions 4-98178  
 Pb-In, thermo-EMF determ. in temp. range 25-400°C, temp. and conc. depend. 4-80569  
 Pb-In alloy films, nonequilibrium superconductivity, Pb-In/Pb-In/Pb double tunnelling junctions appls. 4-98815  
 Pb-In superconducting tunnel junctions, fabrication and cycling stability (Chinese) 4-104370  
 Pb-In superconductor, with dislocations surrounded by impurity atoms, internal friction (Russian) 4-89807  
 PdIn, constitutional and thermally created lattice defects, TDPAC study 4-103745  
 PrIn<sub>3</sub>, mixed-valence system, muon Knight shift meas. 4-80852  
 Sb-InSb, eutectic alloys, melting mechanism 4-114507  
 Se<sub>2</sub>In weak itinerant electron ferromag., negative magnetoresistance 4-75931  
 Sn-In (8.0 to 9.5 at.%), phase transform. 4-109395  
 Ti-In, plastic deformation, induced polymorphic transform., positron annihilation obs. 4-66093  
 Zn-In, diffusion and hyperfine interactions 4-61134  
 Zr<sub>10</sub>Ir<sub>30</sub>, superconducting amorphous alloy, elec. resist. meas. 4-65768

**indium antimonide**

- band struct., angular resolved photoemission studies 4-84554  
 bicrystal, grain boundary barrier height and elec. cond. 4-92216  
 carrier lifetime depend. on electron density 4-104228  
 Czochralski growth, Peltier coeff. at crystal/melt interfaces 4-70845  
 Czochralski pulling, numerical modelling of elec. current induced growth layers 4-88121  
 degenerate four-wave mixing with surface guided waves 4-96982  
 dielectric constant calc. using Kane's band model (Spanish) 4-70648  
 effective electron mass in inversion layers, surface elec. field effect 4-104280  
 electrical properties, two stage nonmagnetic high press. equipment appl. (Chinese) 4-90607  
 equation of state, bulk modulus press. derivative 4-98236  
 films, MBE growth and microstruct. characterisation 4-92578  
 four-wave mixing, near-reson., nondegenerate 4-69486  
 inversion layer narrow gap systems, resonant polaron theory 4-98548

**indium antimonide continued**

- ion implanted layers, IR reflection spectra studies 4-61717  
 ion implanted single cryst., damage study by characteristic X-ray emission 4-88214  
 IR detector arrays, state-of-the-art review 4-111202  
 IR detectors for ground-based astronomy 4-95517  
 isotope scatt. of large wave vector phonons 4-108564  
 lattice dynamics, local Heine-Abarenkov model pot. 4-98222  
 light amplification due to the magnetoelectric photo effect 4-104578  
 magnetised plasma, high-power helicon wave parametric decay 4-98657  
 magnetised plasma, parametric excitation of electron-acoustic waves 4-88545  
 magnetotransport effect, transient processes 4-84628  
 magnetotopic activity measurement using long-wave IR magnetopolarimeter 4-73484  
 magnetosensitive elements, operating principles at high and low temps. survey (Russian) 4-65691  
 MIS diodes with N-shaped V-I characteristics in inversion voltage region 4-114044  
 MIS struct., surface irregularity enhanced subband resonance 4-61459  
 MIS structures, photoreponse enhancement in strong elec. field 4-65751  
 n-type, Auger recombination of holes via deep donors 4-104229  
 n-type, current-induced anisotropy of refractive index 4-104564  
 n-type, magnetoactive piezoelec. semiconductor, helicon waves, modulational instability 4-61407  
 n-type, nonlinear optical props. photoelectronic investigation 4-96986  
 n-type, refractive index, influence of electron drift and heating 4-104561  
 n-type, strongly compensated, electron mobility meas. 4-70834  
 n-type films, amplification of total reflection mode surface phonons 4-70547  
 narrow-gap semiconductor, internal photoeffect, quantum efficiency calc. 4-61415  
 negative magnetoresistance, upper Hubbard band conduction 4-65693  
 optical bistability, physics and appls. (Italian) 4-107729  
 optical bistability on reflection in InSb etalon controlled by guided waves 4-74597  
 p-type, elec. current which is even in elec. field obs. 4-113952  
 p-type, ultrasonic attenuation and elec. resistivity at low temps. and high mag. fields 4-80165  
 phonon-phonon interactions, lattice thermal cond. 4-80320  
 photo-EMF prod. by photon pulse accompanying optical transitions between Landau levels 4-70858  
 photoconductivity and hole trapping centre capture coeff., press. studies 4-98668  
 photoconductivity under picosecond illumination (Russian) 4-88543  
 photomagnetic effect and photocond. in mag. field, diamag. exciton discrete struct. 4-108903  
 photoreistance on electron heating in mag. field, two-phonon oscillations 4-84650  
 photovoltaic IR detector array with quasi-plane struct. (Chinese) 4-106383  
 physical data, compilation, book 4-63420  
 polycrystalline, thermomagnetic and galvanic props. (German) 4-75987  
 Raman freq. depend. on press. 4-109188  
 Raman scatt. at high temp., diminishing energy gap near melting point 4-114274  
 shallow donors in high mag. fields and hydrostatic press. 4-80540  
 spin reson. of magnetoresist. and photo-EMF under stimulated Raman scatt. conditions 4-92962  
 surface, (110), surface quenching of surface plasmon, exptl. evidence 4-61310  
 surface, Auger inverse sensitivity factors of In and Sb 4-81048  
 surface, chem. etch effect (Chinese) 4-109528  
 surface, phase conjugation, reflecting grating recording by plasma reflection 4-97003  
 surface magnetoplasma waves, waveguide propagation 4-114100  
 surface periodic structures on intense laser bombardment 4-70202  
 surface polariton dispersion under intense irradiation 4-113877  
 tetrahedrally bonded, anisotropy of Compton profile 4-99217  
 thermal oxidation method, XPS study, resistivity 4-114690  
 tunable far-IR emission from uniaxial stress-enhanced spin-flip transition 4-69416  
 two photon interband magnetoabsorption, level transitions, photoconductivity meas. 4-71350  
 two-photon reson. photo-Hall effect 4-70863  
 US absorpt., elec. resist., mag. field effects 4-88243  
 X-ray diffraction study, cryst. struct. (Russian) 4-84280  
 Al<sub>2</sub>Ga<sub>1-x</sub>In<sub>x</sub>-Sb epitaxial layers, luminescence studies 4-76505  
 CdTe-InSb MIS struct., electronic props. 4-98778  
 Ga<sub>1-x</sub>(Sb,As)<sub>x</sub>P, short-range clustering, thermodynamic anal. 4-61093  
 GaSb-InSb, behaviour of Sn in solid solns., elec. props. 4-75967  
 In-Sb system, high press. intermediate phases, form., struct., stability, supercond. props. 4-89029  
 InAs<sub>1-x</sub>Sb<sub>x</sub> epilayers, impact ionisation coeffs. 4-104333  
 InAs<sub>1-x</sub>Sb<sub>x</sub>-Al<sub>1-x</sub>Ga<sub>x</sub>Sb heterostructures, LPE growth 4-104097  
 InAs<sub>1-x</sub>Sb<sub>x</sub>-GaSb heterostructures, LPE growth 4-104097  
 InSb, anodic oxide film, surface relief and struct. 4-109531  
 InSb:Be p<sup>+</sup>-n junction, ion implanted, insulated gate effects 4-61445  
 n-InSb:Cr, Mn, impact ions. in 2-mm microwave field 4-70824  
 InSb:Ge(Si), impurity solubility, role of acceptor and donor states 4-60949  
 InSb:H, ionisation energy of magnetodons 4-70714  
 InSb:H, p-n junctions, doping and elec. props. 4-70919  
 InSb/Al<sub>2</sub>O<sub>3</sub>-SiO<sub>2</sub> system, slow states, field effect studies 4-65752  
 p-InSb-i-GaAs, heteroepitaxial struct., quasi-2D electrons, nonequilibrium galvanomagnetic effects 4-70916  
 InSb-InTe, spreading of droplets of eutectic melt 4-113752  
 refractive index at 1.5K in near mm wavelength region 4-104554

**indium compounds**

see also indium alloys; indium antimonide

- $\alpha$ - and  $\gamma$ -phases, Raman and IR spectra 4-109185  
 AlSb/InAs/AlSb quantum wells, magneto-transport meas. 4-98745  
 GaInAs-InP heterojunction, interface 2-D electron gas props., MOCVD growth and characterisation (French) 4-76685  
 III-V semiconductors, phys. data, compilation, book 4-63420  
 InP:Zn epitaxial layers, MOCVD grown, doping, Hall effect, SIMS, electrochemical profiling 4-80077  
 AlGaInP/GaInP DH visible light lasers, MOCVD grown, room temp. pulsed operation 4-69445

## II-VI compounds continued

- AlGaInPAs lattice matched to GaAs, LPE growth, photolum. obs. 4-70581
- AlInAs/GaInAs avalanche photodiodes and AlInAs electroabsorption p-i-n photodiodes grown by MBE 4-69591
- AlInAs/GaInAs heterojunctions and superlattices, 2-D magnetophonon resonance 4-98740
- Al<sub>0.48</sub>In<sub>0.52</sub>As/Ga<sub>0.47</sub>In<sub>0.53</sub>As avalanche photodiode for long wavelength fibre optic communication, MBE growth 4-79337
- Al<sub>0.48</sub>In<sub>0.52</sub>As/n<sup>+</sup>-Ga<sub>0.47</sub>In<sub>0.53</sub>As, low resist. alloyed ohmic contacts 4-84692
- Al<sub>1-x</sub>In<sub>x</sub>As, epitaxial growth on InP 4-104735
- Al<sub>1-x</sub>In<sub>x</sub>As, nominally undoped, MBE growth and charact. 4-98472
- Au-InP junction 4-84625
- CdIn<sub>2</sub>S<sub>4</sub> luminescence kinetics study 4-104671
- n-CdIn<sub>2</sub>Se<sub>4</sub> single cryst. electrodes in polysulphide electrolytes, photoelectrochemical behaviour 4-77117
- CdS-CuInSe<sub>2</sub> photovoltaic devices, short-circuit current meas. 4-88971
- CdS-InP heterojunctions, elec. and photoelec. props., solar cell appl. (*Russian*) 4-98713
- (Cu<sub>1-x</sub>Ag<sub>x</sub>)(Ga<sub>1-y</sub>In<sub>y</sub>)(Se<sub>1-z</sub>Te<sub>z</sub>)<sub>2</sub>, lattice parameter and energy gap 4-75847
- (CuCr<sub>2</sub>Se<sub>4</sub>)(Cu<sub>0.5</sub>In<sub>0.5</sub>Cr<sub>2</sub>Se<sub>4</sub>)<sub>1-x</sub>, semiconducting spin glasses, resistance, magnetoresistance, studies 4-108862
- CuGa<sub>1-x</sub>In<sub>x</sub>Se<sub>2</sub> chalcopyritic semicond., ESR studies 4-109070
- Cu<sub>1/2</sub>In<sub>1/2</sub>Cr<sub>2</sub>Se<sub>4</sub> solid solutions, radiographic study of struct. 4-108317
- CuInS<sub>2</sub> single crystal growth by travelling heater method 4-71539
- CuIn(S<sub>2</sub>Se<sub>2</sub>Te<sub>2</sub>)<sub>1-x</sub>, solid solubility, optical energy gap values 4-70074
- n-CuInSe<sub>2</sub>, optical absorption edge, influence of carrier conc. 4-80943
- CuInSe<sub>2</sub>, radiative recombination and shallow centres 4-109250
- CuInSe<sub>2</sub>, reactive sputtering for photovoltaic applications 4-88971
- CuInSe<sub>2</sub> single cryst. electrode, solar cell performance, surface chemistry 4-66696
- CuInSe<sub>2</sub>, sintered, grain size, SEM obs., resist., Hall obs. 4-66284
- CuInSe<sub>2</sub> sputtered surface characterisation using AES, O<sub>2</sub> adsorpt. 4-93147
- CuInSe<sub>2</sub> thin films, flash evaporated, photocond. 4-104264
- CuInSe<sub>2</sub>(Cd,Zn)S solar cells, light-induced junction modification 4-77092
- CuInSe<sub>2</sub>(Cd,Zn)S Boeing solar cells, current transport 4-81546
- CuInSe<sub>2</sub>-CdS thin film heterojunction solar cells, photoresponse charact. 4-77099
- CuInSe<sub>2</sub>-CdZnS polycryst. thin film solar cells 4-77088
- p-CuInSe<sub>2</sub>-metal contacts, elec. props., solar cell appls. 4-70935
- CuInTe<sub>2</sub> MIS struct., field effect studies 4-80679
- (CuZn)S-CuInSe<sub>2</sub> heterojunction solar cell, interface props. 4-89401
- (Ga<sub>1-x</sub>Al<sub>x</sub>)(AsP)<sub>3</sub>, adducts in MOVPE 4-71575
- (Ga<sub>1-x</sub>In<sub>x</sub>)As, adducts in MOVPE 4-71575
- Ga-In-AsP system, VPE of mixed III-V compounds 4-71578
- Ga-In-P system, phase diagram calcs. near growth temp. and comp., Ga<sub>1-x</sub>In<sub>x</sub>-P LPE (*Chinese*) 4-114427
- Ga-In-P-As system, LPE, growth kinetics 4-88426
- Ga-In-P-As system, MOVPE, current status for optoelectronic appls. 4-104737
- Ga-In-Sb phase diagram, thermodynamic data, associated soln. model, book contrib. 4-89031
- GaInAs-InGa<sub>1-x</sub>As MOCVD strained-layer superlattices, lattice distortion, TEM study 4-88406
- GaInAs epitaxial layers, thickness and uniformity by automated scanning double axis X-ray diff. 4-65589
- GaInAs, MBE, thermodynamics of O incorporation 4-61253
- GaInAs/AlInAs heterojunctions, cyclotron resonance and polaron effects 4-98742
- GaInAs/InP heterojunctions and superlattices, cyclotron resonance and polaron effects 4-98742
- GaInAs/InP(AlInAs) heterojunctions and superlattices, 2-D magnetophonon resonance 4-98740
- GaInAs-InP double heterostructure, epitaxial low press. MO-CVD growth for device appl., book contrib. 4-61875
- GaInAs-InP heterostructure emitters, 1.3-1.55 μm 4-104308
- GaInAs-InP IR detectors, applications of electron microscope techniques to semiconductors 4-103622
- GaInAs-InP quantum-well lasers, gain and intervalence band absorpt. 4-96899
- Ga<sub>0.47</sub>In<sub>0.53</sub>As, hot electron velocity overshoot 4-70823
- Ga<sub>0.47</sub>In<sub>0.53</sub>As, ion implanted, annealing, TEM obs. 4-70228
- Ga<sub>0.47</sub>In<sub>0.53</sub>As layers, MOCVD growth and characterisation (*French*) 4-76685
- Ga<sub>0.47</sub>In<sub>0.53</sub>As, MBE planar doped barriers in InP, elec. charact. 4-98708
- Ga<sub>0.47</sub>In<sub>0.53</sub>As photoconductive detector prepared by VPE 4-86478
- Ga<sub>0.47</sub>In<sub>0.53</sub>As/Al<sub>0.48</sub>In<sub>0.52</sub>As heterojunction, conduction band discontinuity, photoluminescence study 4-76028
- Ga<sub>0.47</sub>In<sub>0.53</sub>As-InP, Raman scatt. theory 4-76460
- Ga<sub>1-x</sub>In<sub>x</sub>As based materials, recrystallisation in temp. gradient 4-114390
- Ga<sub>1-x</sub>In<sub>x</sub>As, bond lengths, virtual crystal approx. 4-75385
- GaInAsP 1.5 μm laser diode, Raman amplification in low fiber loss region 4-96955
- GaInAsP alloy semiconductors, book 4-58588
- GaInAsP BH laser, low-threshold, multiple-cavity, longit.-mode stabilised 4-91468
- GaInAsP cleaved coupled-cavity laser, tunable design, FM operation for communication appl. 4-69451
- GaInAsP, defect motion and growth of extended non-radiative defect structs., book contrib. 4-60914
- (GaIn)(AsP) epilayers, growth, optical communication requirements, review 4-61833
- GaInAsP epitaxial layers, thickness and uniformity by automated scanning double axis X-ray diff. 4-65589
- GaInAsP heterostructure laser with distributed feedback 4-74538
- (GaIn)(AsP) heterostructure laser diodes, psc. pulse generation 4-107632
- GaInAsP, high field transport meas., review, book contrib. 4-61389
- GaInAsP, high purity, charact., growth, back contrib. 4-61334
- GaInAsP inner stripe laser diodes on p-InP substrate 4-96886
- GaInAsP, ion implantation, book contrib. 4-60943
- GaInAsP, LPE growth on InP, review, book contrib. 4-61882
- GaInAsP lattice matched to InP, electronic struct., book contrib. 4-61284
- GaInAsP, low field carrier mobility, book contrib. 4-61383
- GaInAsP, low field transport calcs., book contrib. 4-61384

## indium compounds continued

- GaInAsP, n-type, lattice matched to InP, hot electron transport, book contrib. 4-61388
- GaInAsP, nonlinear carrier dynamics, optical bleaching study 4-74625
- GaInAsP, photolum. and optical gain spectra, book contrib. 4-61752
- GaInAsP picosecond optical absorption saturation 4-91541
- GaInAsP, VPE growth, review, book contrib. 4-61874
- GaInAsP/InP 1.3 μm distributed feedback lasers, LPE growth 4-96913
- GaInAsP/InP BH laser diodes, fabrication technique 4-74507
- GaInAsP/InP BH laser with chemically etched and mass-transported mirror 4-74537
- GaInAsP/InP BH injection lasers, network modelling and modulation charact. 4-96890
- GaInAsP/InP DFB laser, 1.5 μm range, longitudinal mode behaviour 4-74512
- GaInAsP/InP DFB lasers, 1.3 μm, monolithic integrated struct., WDM optical communication appl. 4-83618
- GaInAsP/InP heterostructure lasers, gas source MBE growth 4-69401
- GaInAsP/InP hetero-multilayers, LPE fabrication and reflectivity 4-99357
- GaInAsP/InP laser, single-mode, low-temp. single-step LPE growth 4-112407
- GaInAsP/InP phase adjusted active distributed reflector laser, 1.5 μm, for dynamic single mode operation 4-69437
- GaInAsP-InP BH but-jointed built-in integrated, lasers, 1.5-1.6 μm operation, static charact. 4-60065
- GaInAsP-InP DH lasers, review, book contrib. 4-60037
- GaInAsP-InP DH lasers, temp. depend. of laser threshold current, book contrib. 4-60038
- GaInAsP-InP DH lasers, carrier leakage current estimation using high mag. fields 4-91453
- GaInAsP-InP double heterostructure, epitaxial low press. MO-CVD growth for device appl., book contrib. 4-61875
- GaInAsP-InP lasers, applications of electron microscope techniques to semiconductors 4-103622
- GaInAsP-InP mass-transported BH lasers, fabrication, characterization and analysis 4-112473
- Ga<sub>0.33</sub>In<sub>0.47</sub>As<sub>0.70</sub>P<sub>0.30</sub>, (100) oriented, electron and hole ionisation coeffs. 4-98662
- Ga<sub>1-x</sub>In<sub>x</sub>AsP<sub>1-y</sub>, solid solutions, LPE, conc. profiles 4-93233
- Ga<sub>1-x</sub>In<sub>x</sub>AsP<sub>1-y</sub> layer on InP:Sn substrate, linear thermal expansion coeff. meas. 4-75709
- Ga<sub>1-x</sub>In<sub>x</sub>AsSb<sub>1-y</sub>, epitaxial layers, reflection spectra analysis 4-114340
- GaInP/AlGaAs double heterostructures, LPE, lasing, 77-230K 4-71606
- Ga<sub>3</sub>In<sub>3</sub>P<sub>3</sub>, photolum. dynamics of high density electron-hole plasma under psc. laser excitation 4-109228
- Ga<sub>1-x</sub>In<sub>x</sub>P, phonon modes, Raman scatt. study 4-108563
- Ga<sub>1-x</sub>In<sub>x</sub>P, electrochem. behaviour in aq. and nonaqueous media, common anion rule 4-70928
- Ga<sub>1-x</sub>In<sub>x</sub>P, LPE growth on GaAs substrates, cathodoluminesc. and photoluminesc. spectra (*Chinese*) 4-113825
- Ga<sub>1-x</sub>In<sub>x</sub>PyAs<sub>1-y</sub>, gas source MBE growth 4-81140
- Ga<sub>1-x</sub>In<sub>x</sub>(Sb,As,P)<sub>3</sub>, short-range clustering, thermodynamic anal. 4-61093
- Ga<sub>1-x</sub>In<sub>x</sub>Se single crystals, energy gap, temp. dependence 4-92610
- Ga<sub>1-x</sub>In<sub>x</sub>Se, optical phonons, far-IR reflectivity spectra 4-104583
- Ga<sub>1-x</sub>In<sub>x</sub>Se system, magneto-optical props. near fundamental band gap 4-109166
- GaSb-InAs heterojunction, quantum Hall effect study 4-98726
- GeTe-InTe, phase transformations, 300-900K 4-108602
- HfO<sub>2</sub>-In<sub>2</sub>O<sub>3</sub> fluoride solid soln., elect. cond. study 4-80297
- HgIn<sub>2</sub>□Te<sub>4</sub>, pressure-induced phase transitions, elec. resistivity meas. 4-80497
- (In,Ga)As/InP n-p-n heterojunction bipolar transistors grown by LPE with high gain 4-85097
- In complex with valine, polarographic investig. 4-72032
- In/InO<sub>2</sub>(N<sub>2</sub>) composites, reactive ion beam sputter deposited, optical recording appl. 4-79249
- In-Sb-As, phase equilibria, supercooling phenomenon 4-61051
- InAs, electroliquid epitaxial growth, carrier density 4-93243
- InAs, equation of state, bulk modulus press. derivative 4-98236
- InAs evaporated films, Hall mobility and carrier conc. 4-70961
- InAs high-field transport, model 4-88512
- n-InAs, hybrid quantum oscills., temp. depend. 4-70839
- InAs, lattice dynamics, phonon dispersion curves 4-61019
- InAs, lattice dynamics, local Heine-Abarenkov model pot. 4-98222
- InAs, MBE growth conditions and reconstruction 4-93223
- InAs MIS diodes with N-shaped V-I characteristics in inversion voltage region 4-114044
- InAs, nonlinear refr. at absorpt. edge 4-96988
- InAs, Raman freq. depend. on press. 4-109188
- InAs, struct. and electrical cond. behaviour under deposition conditions 4-98787
- InAs:Si(Te), VPE growth, morphology and elec. props. 4-109326
- InAs/GaSb superlattices, Landau levels and magneto-optical props. 4-98737
- InAs/GaSb superlattices, electronic collective modes 4-104134
- InAs-AlSb quantum wells, electron densities 4-98711
- InAs-GaSb system, superlattices, quantum wells, and heterostructs., review 4-80666
- InAsP, high mobility, vapour phase heteroepitaxial growth 4-71601
- InAsP<sub>1-x</sub>, epitaxial layer, bright 300K luminescence 4-70584
- InAsP<sub>1-x</sub>, LEC growth and characterisation 4-99302
- InAsSb strained layer superlattices for long wavelength detector appls. 4-98706
- InAs<sub>1-y</sub>Sb<sub>y</sub>-AlGa<sub>1-x</sub>Sb heterostructures, LPE growth 4-104097
- InAs<sub>1-y</sub>Sb<sub>y</sub>-GaSb heterostructures, LPE growth 4-104097
- InBO<sub>3</sub>, cryst. growth 4-61817
- InBr, magneto-reflectance of excitons 4-76439
- InCr<sub>2</sub>S<sub>4</sub>, cation deficient chalcogenide spinels, electron microscope study 4-113443
- InGaAs, 1.6 μm, radiative and nonradiative minority carrier lifetimes 4-70826
- InGaAs epilayers, optical studies of carrier dynamics 4-98788
- InGaAs epitaxial layer, LPE growth and carrier mobility, dopant effects 4-84717
- InGaAs, high-purity, conventional LPE growth, carrier conc. and mobility 4-99353
- InGaAs, LPE using novel graphite boat 4-88994
- InGaAs planar photodiodes, reliability 4-91635
- InGaAs:Mg on InP, LPE-grown, MgO-free surface 4-76699

## indium compounds continued

- InGaAs/GaAs strained layers superlattices, molecular beam growth conditions and characterisation 4-70585  
 InGaAs/GaAs strained layer superlattices, high quality p-n junctions 4-98707  
 InGaAs/InGaAlAs/InAlAs/InP separate confinement heterostruct. multi-quantum-well laser diodes, MBE grown 4-83617  
 InGaAs-InP injection laser, operation and luminescence study 4-74508  
 InGaAs-InP modulation doped heterostruct., self-consistent variational calcs. and alloy scatt. 4-98733  
 InGaAs-InP superlattices, chloride VPE growth, struct. and optical props. 4-81158  
 In<sub>0.53</sub>Ga<sub>0.47</sub>As/GaAs strained-layer superlattice, ion implanted, struct. integrity 4-113821  
 In<sub>0.53</sub>Ga<sub>0.47</sub>As 1.6-μm lasers, temp. sensitive operation 4-96903  
 In<sub>0.53</sub>Ga<sub>0.47</sub>As, 2D electron gas, alloy scatt. limited mobility 4-98620  
 In<sub>0.53</sub>Ga<sub>0.47</sub>As, carrier energy relax., picosecond luminesc. studies 4-114312  
 In<sub>0.53</sub>Ga<sub>0.47</sub>As, electron mobility, rel. to two-mode lattice vibrs. 4-80582  
 In<sub>0.53</sub>Ga<sub>0.47</sub>As, epilayer thickness meas. from etched steps 4-62074  
 In<sub>0.53</sub>Ga<sub>0.47</sub>As, epitaxially grown by LPE, VPE, MBE, band gap energy spatial var., photoluminescence spectra 4-104125  
 In<sub>0.53</sub>Ga<sub>0.47</sub>As, LPE growth on InP (100) substrate (Chinese) 4-85121  
 In<sub>0.53</sub>Ga<sub>0.47</sub>As LPE layers, high purity, photoluminescence processes 4-99187  
 In<sub>0.53</sub>Ga<sub>0.47</sub>As, laser operation, thermal behaviour 4-87331  
 In<sub>0.53</sub>Ga<sub>0.47</sub>As, MIS diode anodic oxidation, interface characteristics 4-104324  
 In<sub>0.53</sub>Ga<sub>0.47</sub>As planar diodes, fabrication using open tube method for Zn diffusion 4-95519  
 In<sub>0.53</sub>Ga<sub>0.47</sub>As, shallow donors, submillimeter wave photocond. 4-104256  
 In<sub>1-x</sub>Ga<sub>x</sub>As, indirect conduction band minima determ. 4-98517  
 In<sub>1-x</sub>Ga<sub>x</sub>As multi quantum well structs., strained, optical props. 4-104669  
 In<sub>1-x</sub>Ga<sub>x</sub>As/GaAs strained layer superlattice, MBE growth, strain and layer thickness effects 4-99319  
 In<sub>1-x</sub>Ga<sub>x</sub>As/InP quantum well struct., low temp. electron mobility, alloy disorder scatt. contrib. 4-92808  
 In<sub>1-x</sub>Ga<sub>x</sub>As-GaAs strained-layer superlattices, phonon frequencies, Raman scatt. meas. 4-99121  
 In<sub>1-x</sub>Ga<sub>x</sub>As-InP heterojunction, quantum Hall effect and hopping cond. 4-98723  
 InGaAsP, 1.3 μm bandgap, photoexcited carrier lifetime and Auger recomb. 4-108893  
 InGaAsP 1.3 μm optical amplifier-modulator integrated with a fibre-resonator mode-locked laser 4-91491  
 InGaAsP 1.3 μm real-index-guided lasers, leakage current anal. 4-96895  
 InGaAsP 1.53 μm DFB lasers made by mass transport 4-102947  
 InGaAsP (InGaP), LPE layers on GaAs (001), composition modulated structures 4-76698  
 InGaAsP and InGaP LPE layers, dislocation loops, TEM studies 4-92206  
 InGaAsP BH 1.3 μm lasers, anomalous polarisation characs. 4-69402  
 InGaAsP crescent mesa substrate BH lasers at 1.55 μm 4-112429  
 InGaAsP double-channel BH lasers, short-cavity, HF small-signal modulation characs. 4-69462  
 InGaAsP double-channel buried-hetero structure lasers, 1.55 μm, high-temp. operation, LPE 4-79174  
 InGaAsP epilayers, optical studies of carrier dynamics 4-98788  
 InGaAsP epitaxial layers, MOVPE at atmospheric press. 4-81154  
 InGaAsP etched mesa BH lasers, 1.3 μm, threshold current, active layer placement effects 4-112414  
 InGaAsP film laser, optically pumped, chirp, passive pulse compression in optical fibres 4-107700  
 (InGa)(AsP) heterolasers with distrib. feedback, polarisation effects 4-64708  
 InGaAsP heterostructure laser with distributed feedback 4-74538  
 InGaAsP injection lasers, short pulse excitation, threshold current temp. dependence 4-74506  
 InGaAsP LPE layers on InP, refractive index in transparent wavelength region 4-71333  
 InGaAsP, LPE-grown, high-uniformity, λ=1.3 μm 4-76700  
 InGaAsP, laser, radiative and nonradiative, recombination rates, meas. 4-112434  
 InGaAsP laser diode optical switches, isolation characteristics 4-107680  
 InGaAsP laser diode switch, BH type, 1.3 μm operation; design and fibre optic communication appl. 4-112461  
 InGaAsP lasers, gain- and index-guided, spectral linewidth 4-112417  
 InGaAsP lasers for 1.52 operation, linewidth and FM-noise spectrum meas. 4-83580  
 InGaAsP, lattice matched to GaAs, lattice dynamics, Raman scatt. study 4-61673  
 InGaAsP light sources, radiative coeffs., carrier dependence 4-64703  
 InGaAsP, linear electro-optic effects and nonlinear optical coeffs., device design appls. 4-88809  
 InGaAsP long-wavelength 1.0-1.6-μm detectors 4-91634  
 InGaAsP, MBE growth IR reflectivity, diode laser source/detector 4-71391  
 InGaAsP material epitaxial growth, devices for optical communications 4-74746  
 InGaAsP, optically pumped, tunable CW mode locked laser action 4-107699  
 InGaAsP, quadratic electro-optic Kerr effects, dispersion 4-109159  
 InGaAsP ridge lasers, λ≈1.5 μm, grown by gas source MBE 4-112413  
 InGaAsP separate confinement heterostructure lasers, 1.5 μm, electron leakage 4-96904  
 InGaAsP, theoretical design of single-layer antireflection coatings on laser facets 4-69409  
 InGaAsP three-channel buried crescent lasers, 1.51 μm, high-speed analog and digital modulation 4-112409  
 InGaAsP tunable DFB laser pumped by heterostructure injection laser 4-96907  
 InGaAsP/Zn highly reliable 1.3 μm surface emitting LEDs for high speed optical communication systems 4-97137  
 InGaAsP/GaAs, double heterojunctions, photoluminesc. studies 4-76504  
 InGaAsP/GaAs, LPE growth, defects, TEM and STEM studies 4-108387  
 InGaAsP/InGaP lasers, low threshold, 810 nm, LPE growth 4-69435  
 InGaAsP/InGaP lasers, LPE growth on GaAs, room temp. CW lasing at 727 nm 4-79133  
 InGaAsP/InGaP/GaAs DH lasers, low threshold pulsed and CW operation 4-87336

## indium compounds continued

- InGaAsP/InP 1.3 μm buried crescent lasers using short external optical cavity, single-mode operation 4-74511  
 InGaAsP/InP 1.3 μm buried crescent lasers, single transverse-mode conditions 4-96897  
 InGaAsP/InP 1.3 μm buried crescent laser diode, degradation mechanism 4-96915  
 InGaAsP/InP amplifier-modulator integrated with a cleaved-coupled-cavity injection laser 4-91505  
 InGaAsP/InP buried crescent lasers, 1.3 μm, high temp. and long life operation 4-69444  
 InGaAsP/InP buried crescent laser, dynamic characs., computer simulation method (Chinese) 4-96887  
 InGaAsP/InP buried crescent laser diode emitting at 1.3 μm, high temp. CW operation 4-112427  
 InGaAsP/InP channelled-substrate BH lasers, VPE base struct. and LPE regrowth 4-96905  
 InGaAsP/InP DFB laser diodes, cleaved facet, grating phase effect 4-60063  
 InGaAsP/InP DFB laser diodes lasing characs., at 1.5 μm, effect of mirror facets 4-74513  
 InGaAsP/InP DFB ridge-waveguide laser, 1.2 Gbit/s optical fibre transmission over 113.7 km 4-107847  
 InGaAsP/InP DH, luminescence and laser threshold characs. 4-85008  
 InGaAsP/InP DH stripe lasers fabricated by O ion implantation 4-96906  
 InGaAsP/InP double heterojunctions, photoluminesc. studies 4-76504  
 InGaAsP/InP GRIN rod external coupled-cavity BH lasers, single longitudinal mode operation 4-91473  
 InGaAsP/InP gigahertz-bandwidth optical modulators/switches with DH waveguides 4-112585  
 InGaAsP/InP heterostructure waveguides integrated with optical devices 4-97146  
 InGaAsP/InP injection lasers, LPE grown, three-layer-waveguide DH design 4-91490  
 InGaAsP/InP lasers, 4-5 μm emissions and excitations in split-off valence band 4-96916  
 InGaAsP/InP laser diode, monolithic integration with heterojunction bipolar transistors 4-102927  
 InGaAsP/InP lasers, failure modes due to adhesives 4-107678  
 InGaAsP/InP lateral p-n-p transistor fabrication using open diffusion technique 4-104003  
 InGaAsP/oxidised films interface, Auger/ion sputtering anal. 4-104884  
 InGaAsP-Au contacts, X-ray study of Au interactions 4-80675  
 InGaAsP-InGaP rapidly degraded DH laser grown by LPE, dark-line defects 4-69406  
 InGaAsP-InP 1.3 μm BH lasers, improved linearity criterion, high-bit-rate fibre communication system appls. 4-74510  
 InGaAsP-InP 1.55 μm DH ridge waveguide laser, optimum design 4-102955  
 InGaAsP-InP BC laser diode emitting at 1.3 μm, fabrication, design, characteristics 4-112474  
 InGaAsP-InP DH, photoluminescence efficiency 4-85006  
 InGaAsP-InP DH modulators, electroabsorption, polarisation dependence 4-93054  
 InGaAsP-InP planar buried DH, LPE growth, melt-carry-over effect 4-99352  
 InGaAsP-InP single-longitudinal-mode 1.3 μm DFB-DC-PBH diodes 4-91467  
 In<sub>0.75</sub>Ga<sub>0.25</sub>As<sub>0.56</sub>P<sub>0.44</sub>, electroreflectance spectrum, on InP substrate 4-109158  
 In<sub>0.75</sub>Ga<sub>0.25</sub>As<sub>0.44</sub>P<sub>0.56</sub>, luminescence study of binding energy variation 4-71435  
 In<sub>1-x</sub>Ga<sub>x</sub>AsP<sub>1-y</sub>, composition depend. of microhardness anisotropy 4-108506  
 In<sub>1-x</sub>Ga<sub>x</sub>AsP<sub>1-y</sub>, indirect conduction band minima determ. 4-98517  
 In<sub>1-x</sub>Ga<sub>x</sub>AsP<sub>1-y</sub>, laser material, intervalence band absorpt. and Auger recomb. 4-80885  
 InGaP LED/optical fibre system for optical remote detection of propane gas 4-105155  
 InGaP/GaAs, LPE grown, defects, TEM and STEM studies 4-108387  
 InGaP/InAlP quantum well structures for visible region, MBE growth 4-99314  
 In<sub>0.9</sub>Ga<sub>0.1</sub>P, spinodal decomp., phase segregation, <sup>31</sup>P NMR spectra, chem. shifts 4-76279  
 In<sub>1-x</sub>Ga<sub>x</sub>P<sub>1-x</sub>As<sub>2x</sub>, solid solution, LPE, crystn. and optical props. 4-108736  
 In<sub>1-x</sub>Ga<sub>x</sub>Sb, indirect conduction band minima determ. 4-98517  
 InI, magneto-reflectance of excitons 4-76439  
 In<sub>2</sub>MoS<sub>2</sub> (0≤x≤1) intercalation compound, synthesis and characs. 4-104200  
 In<sub>2</sub>O<sub>3</sub>/CdTe photoconvertors, current transfer mechanism 4-93616  
 In<sub>2</sub>O<sub>3</sub>, amorphous, electron mobility, cond., and supercond. near metal-insulator transition 4-80710  
 In<sub>2</sub>O<sub>3</sub>, UPS, DV-Xα method 4-83413  
 In<sub>2</sub>O<sub>3</sub> film, transparent and electrically conductive, props. and appl. 4-107802  
 In<sub>2</sub>O<sub>3</sub> films, excimer laser induced CVD 4-76679  
 In<sub>2</sub>O<sub>3</sub>, In<sub>2</sub>-Sn<sub>2</sub>O<sub>3-y</sub>, selective optical coating prod. on plastic sheet as heat reflecting films 4-112555  
 In<sub>2</sub>O<sub>3</sub>, ion plated, IR and optical study 4-62085  
 In<sub>2</sub>O<sub>3</sub> transparent conducting film prep. by reactive magnetron sputtering, optical props. control 4-76536  
 In<sub>2</sub>O<sub>3</sub>/Sn, DC reactive magnetron sputtering technique for thin film production (Polish) 4-93217  
 In<sub>2</sub>O<sub>3</sub>/CdTe structures: electrophysical characs., for photoconvertors 4-92795  
 In<sub>2</sub>O<sub>3</sub>-based transparent film temp. sensors, performance under high-density solar fluxes 4-90585  
 In<sub>2</sub>O<sub>3</sub>-Fe<sub>2</sub>O<sub>3</sub>-CuO(CoO), phase relations and cryst. structures 4-98242  
 In<sub>2</sub>O<sub>3</sub>-Ga<sub>2</sub>O<sub>3</sub>-CuO(CoO), phase relations and cryst. structures 4-98242  
 In<sub>2</sub>O<sub>3</sub> films, reactive ion sputtering in magnetron system, phenomenological model 4-114396  
 InP (001), substrate for MBE growth of Ba<sub>2</sub>Sr<sub>1-x</sub>F<sub>2</sub> films 4-70582  
 InP (100), laser irradi., photoemission of electrons 4-81116  
 InP (100), optical surface phonons obs. using high res. electron energy loss spectroscopy 4-70546  
 InP (100) and (111) surfaces, EELS study, bulk and surface plasmons (Chinese) 4-85047  
 InP (100) surfaces, atomic conc. ratio by X-ray photoelectron spectroscopy 4-66185

## Ilium compounds continued

- InP (110)-Cu(Ag)(Au) interface, soft X-ray photoemission study 4-85080  
 InP, absence of core exciton induced resonant photoemission 4-114360  
 InP acceptor impurity incorporation during organometallic VPE, photolum. obs. 4-98122  
 InP amorphous film, local order study and electronic props. 4-70591  
 InP based integrated optics 4-64796  
 n-InP, cyclotron resonance, impurity conc. and compensation effects (*Russian*) 4-98952  
 n-InP, electron energy relax. due to 2TA phonons 4-92324  
 InP, electron irradi. antisite defects, EPR study 4-80816  
 InP, electron irradi. induced deep traps, deep level optical spectroscopy 4-104156  
 InP, electron irradiation induced defects, energy and orientation depend. 4-108810  
 InP epilayers, cathodoluminescence study 4-104678  
 InP epitaxial, deep and shallow levels due to ion irradi. 4-80531  
 InP epitaxial layer, LPE growth and carrier mobility, dopant effects 4-84717  
 InP epitaxial layers, MOCVD growth 4-61862  
 InP epitaxial layers, MOVPE at atmospheric press. 4-81154  
 InP, excitons bound to neutral acceptors, stress effects, photoluminesc. study 4-61294  
 InP, far IR optical props. at 6 and 300K 4-109174  
 InP films, excimer laser induced CVD 4-76679  
 InP, freq. depend. of negative cond., Gunn effect (*Russian*) 4-70825  
 InP growth mechanism by MOCVD, pyrolyses of group III metal-organics 4-99334  
 InP, high field transport of holes 4-80598  
 InP high-field transport, model 4-88512  
 InP, high-purity, in mag. fields, donor transition anomalous line broadening 4-109214  
 InP, hydride VPE growth, thermodynamic effects of using inert gas 4-99331  
 InP, implant depth profiles 4-65289  
 InP, InP:Zn, adducts in MOVPE, p-type doping 4-71575  
 InP, ion bombardment-enhanced etching 4-99618  
 InP, ion implanted, elec. activation by CW laser annealing 4-80088  
 InP, k,p interaction and effective mass, band gap depend. 4-113850  
 InP, LEC grown, photoluminesc. study, 1.8 to 40K (*Chinese*) 4-84993  
 InP, LPE, numerical model of selective meltback morphology 4-65587  
 InP laser optically pumped by injection laser 4-107645  
 InP, lattice dynamics, local Heine-Abarenkov model pot. 4-98222  
 InP layers, MOCVD growth and characterisation (*French*) 4-76685  
 InP layers, prep. by chloride-hydride reaction 4-92322  
 InP, linear electro-optic coeff., Raman scatt. meas. 4-61659  
 InP, localisation of inversion electrons, Fourier transform spectra studies 4-98555  
 InP, MBE, thermodynamics of O incorporation 4-61253  
 InP MOSFET structures, carrier channel mobility correl. with interface state meas. 4-88600  
 InP, mag. field induced metal-insulator transition 4-84566  
 n-InP, mag. field induced metal-insulator transitions 4-92614  
 InP, near IR cathodoluminescence in a TEM 4-81011  
 InP, open diffusion technique using  $\text{Zn}_2\text{P}_2$ , appl. to lateral p-n-p transistor 4-104003  
 InP p<sup>+</sup>-n junctions,  $\gamma$ -ray irradi., electron trap annealing 4-98748  
 n-InP photoelectrodes, subbandgap response, effect of surface modification 4-88582  
 InP photoelectrodes, surface states, photocapacitance spectra studies 4-114010  
 InP picosecond photoconductors, circuit limits to time resolution 4-98661  
 InP planar diodes, fabrication using open tube method for Zn diffusion 4-95519  
 InP, Rama spectra, optically excited carriers 4-71368  
 InP, residual impurities determ. by charged particle activation anal. 4-85346  
 InP, SAW characterisation of surface and interface states 4-98681  
 n-InP, self-trapping and metastable M-centre 4-108809  
 InP, semi-insulating, simulation of anomalous Be diffusion 4-88193  
 InP single cryst., low temp. thermal cond. and phonons 4-88356  
 InP single crystals and solar cells,  $\gamma$ -irrad. damage 4-62356  
 InP solar cells, radiation resistant, electron irradi. damage 4-62351  
 InP, spinodal decomp.,  $^{31}\text{P}$  NMR spectra, chem. shifts 4-76279  
 InP substrate for BN:P film, CVD growth and elec. props. 4-99336  
 InP substrate for MBE grown  $\text{Al}_{1-x}\text{In}_x\text{As}$  4-104735  
 InP substrates, applications of electron microscope techniques to semiconductors 4-103622  
 InP substrates, LEC growth, optical communication requirements, review 4-61833  
 InP, surface and interface states 4-92782  
 InP surface decomp. rel. to  $\text{In M}_{4.5}\text{N}_{4.5}\text{As}_5$  Auger spectrum fine struct. 4-81046  
 InP, transition metal diffusion, photoluminesc. study 4-70461  
 InP, VPE, from  $\text{In-PH}_3\text{-HCl-H}_2$  system, growth parameters 4-61871  
 InP, volume plasmon dispersion, transmission electron energy loss studies 4-88465  
 InP Z 4-99619  
 InP:Be(C), acceptor levels, photoluminesc. study 4-80543  
 InP:Cd crystals, bulk and surface effects of heat treatment 4-84625  
 InP:Co, impurities, optical and transport studies 4-71444  
 InP:Cr, thermal conductivity, phonon scattering (*French*) 4-61155  
 InP:Fe,  $^3\text{He}^+$  bombarded, psec. photocond., very short free carrier lifetimes 4-108894  
 InP:Fe, semi-insulating, Four-wave mixing using photorefractive effect, optical processing appl. 4-74585  
 InP:Fe, semi-insulating, with phosphosilicate glass encapsulation heat treatment, photoluminesc. and Raman scatt. characterisation 4-84995  
 InP:Fe, thermally annealed; Fe redistribution and diffusion coeff. 4-70460  
 InP:Fe photoconductor for synchrotron radiation research 4-91177  
 InP:Fe photoconductors, pulsed soft X-ray response 4-80620  
 n-InP:Fe-Au diode struct., photocurrent amplification 4-70934  
 InP:GaSb crystals, dislocation density reduction by isoelectronic double doping 4-60940  
 InP:Gd(Yb) epitaxial films, doping effects on low-temp. edge photoluminescence 4-85028  
 InP:Ge(Sn), donor identification, photolum. and far IR photocond. in high mag. fields 4-70705  
 InP:He, ion implanted, elec. cond. study 4-80586

## Indium compounds continued

- InP:Mg(Ca,Zn) crystals grown by synthesis solute diffusion, electrical and optical props. 4-85093  
 InP:Mg(Fe,Mg), implanted, effect on photoluminescence props. 4-85007  
 InP:Mn, hopping cond. between deep impurity states 4-104209  
 InP:Mn, solubility, coeff. of Mn distrib. 4-108621  
 InP:S(Sn)(Ge), (100), vacuum annealed, free carrier reduction 4-98610  
 InP:S(Sn)(Zn)(Fe) single crystals, LEC growth, perfection, carrier conc., TEM obs. 4-71550  
 InP:Se, ion implanted, annealing and transport props. 4-108397  
 InP:Si, electron irradi.-induced deep traps, impurity conc. effects 4-88468  
 InP:Si MISFETs, post-implantation capless annealing 4-113472  
 n<sup>+</sup>-InP:Si-p-InP homojunction, implanted, photoelec. props., minority carrier diffusion length 4-76034  
 InP:Sn films, LPE growth, carrier saturation, Hall meas. 4-98789  
 InP:V(Cr), impurity excited states, optical absorpt. spectra 4-88863  
 InP:Yb p-n junctions, electroluminescence studies 4-66079  
 InP:Zn, electron irradi. damage, carrier conc. effects, minority carrier diffusion length 4-80107  
 InP:Zn, grown-in defects, annealing effects, DLTS studies 4-84287  
 InP:Zn, temp-dependent Zn diffusion mechanism using semiclosed diffusion method 4-80301  
 InP:Zn crystals, bulk and surface effects of heat treatment 4-84625  
 InP:Zn(S) single crystal growth, LEC technique, perfection, preferential etching, SEM and X-ray analysis 4-71549  
 n-InP/Ag Schottky barrier, improvement by Ru surface treatment 4-114035  
 n-InP/Au Schottky diodes with intermediate layer, longitudinal photoelec. effect 4-65743  
 InP/fluoride/InP double heterostructs., MBE growth 4-88420  
 InP/GaInAs heterojunctions and superlattices, 2-D magnetophonon resonance 4-98740  
 InP/InGaAsP 1.5  $\mu\text{m}$  BH laser with etched cavity 4-83575  
 InP/InGaAsP DBF double-channel PBH laser diode, 1.55  $\mu\text{m}$ , single longit. mode operation 4-87358  
 InP/InGaAsP DH, LPE grown, misfit dislocations, TEM study 4-113826  
 InP/InGaAsP optoelectronic integrated device with optical bistability, design, fabrication and characts. study 4-83726  
 InP/InGaAsP p-type substrate and mass transported doubly BH laser 4-112428  
 InP/InGaAsP stripe geometry lasers, design and fabrication using D<sup>+</sup> bombardment 4-83622  
 InP/InGaAsP/InGaAs high-speed avalanche photodiodes 4-69590  
 InP/metal interfaces, chem. reactions, photoemission study 4-80310  
 InP/Pd interface, In segregation and Pd form., XPS study 4-80422  
 InP/Ta-Si sputtered film contacts, rectifying behaviour and barrier heights 4-70932  
 p-InP/Ti-Pt ohmic contact (*Chinese*) 4-88589  
 InP-Ag interface, reactions and Schottky barrier form., XPS studies 4-92821  
 InP-Al<sub>2</sub>O<sub>3</sub> MIS struct. CVD growth and elec. props. 4-80680  
 InP-Au contacts, X-ray study of Au interactions 4-80675  
 InP-Au Schottky barriers, semicond. LEC growth, deep level defects (*Chinese*) 4-61320  
 InP-BN, density of interface states 4-80443  
 InP-fluoride-InP (001) DH, growth by MBE, RHEED and elec. props. 4-98700  
 InP-GaInAs IR detectors, applications of electron microscope techniques to semiconductor devices 4-103622  
 InP-GaInAsP lasers, applications of electron microscope techniques to semiconductor devices 4-103622  
 InP-In<sub>0.35</sub>Ga<sub>0.65</sub>As-InP DH wafers, LPE grown, misfit dislocations, X-ray and photoluminescence topography 4-80042  
 InP-InGaAsP-InP DH, photoluminescence intensity 4-61738  
 InP-MOS using indirect plasma-enhanced CVD technique for Al<sub>2</sub>O<sub>3</sub> gate dielec. 4-104529  
 InP-metal interface, chem. reactivity 4-71973  
 InP-n-AlInAs heterostructure, magnetotransport study 4-88570  
 (InP)<sub>1-x</sub>Ge<sub>x</sub>, energy gap and phase transition 4-80494  
 InP<sub>2</sub>, Brillouin scatt. meas. of elastic constants 4-84334  
 InSb, high temp. plasticity, anal. of expt. data 4-98186  
 InSb-InTe, spreading of droplets of eutectic melt 4-113752  
 InSe Bridgman grown crystals, growth parameters, improvement rel. to defects 4-98043  
 InSe, EXAFS spectra and near edge struct. 4-66128  
 InSe, elec. props., thickness depend. 4-88507  
 InSe, electric field gradients, nuclear quadrupole freqs., anomalous temp. behaviour 4-71221  
 n-InSe, electron scatt. mechanisms, Hall effect and magnetoresist. meas. 4-80614  
 InSe, lamellar, n- and p-type, in aqueous soln., photoelectrochemistry 4-88579  
 InSe, lamellar p-type, photointercalation and photodeposition of Cu 4-93539  
 InSe, layered monocrystals, photoluminescence spectra, pol. plane orientation change effects 4-66069  
 InSe, oxidation, XPS study 4-62075  
 n-InSe, photoluminescence and free exciton emission 4-99176  
 p-InSe, photomagnetolectric effect, minority carrier transport parameters 4-88530  
 InSe, polytropism in the exciton absorpt. spectrum (*Russian*) 4-114304  
 InSe, surface pot., Ar<sup>+</sup> sputtering effects, XPS obs. 4-81103  
 InSe:Sn(Zn)(Ga)(S), dopant segregation and distrib. study 4-103940  
 n-InSe/p-CdTe heterojunction, elec. props. 4-108928  
 InSe-Li intercalation cpd., photoelectric props. meas. (*Russian*) 4-104272  
 InSe<sub>3</sub> films, flash and thermal evaporation growth, struct. and elec. characterisation 4-114409  
 In<sub>0.9</sub>Se<sub>0.1</sub> films, optical absorption, heat treatment effects 4-85027  
 In<sub>0.9</sub>Se<sub>0.1</sub> annealing in Se vapour, physical props. 4-61414  
 In<sub>1-x</sub>Sn<sub>x</sub>O<sub>3-y</sub>/InP solar cells, RF sputtering prep. and device performance 4-99967  
 In<sub>2-x</sub>Sn<sub>x</sub>O<sub>3-y</sub>, 1D linear refr. index. profiles from angular refl. meas. at one wavelength 4-68268  
 In<sub>2-x</sub>Sn<sub>x</sub>O<sub>3-y</sub> coating deposition, three-step process, low sheet resist. 4-81139  
 In<sub>2-x</sub>Sn<sub>x</sub>O<sub>3-y</sub> films, transparent and heat-reflecting, elec. and optical props., ionised impurity scatt. 4-66087  
 In<sub>2-x</sub>Sn<sub>x</sub>O<sub>3-y</sub>, optimised transparent and heat refl. films 4-112532  
 In<sub>2-x</sub>Sn<sub>x</sub>O<sub>3-y</sub> structures electrophysical characts., for photoconvertors 4-92795

**indium compounds continued**

- $\text{In}_{2-x}\text{Sn}_x\text{O}_{3-y}$  thin films, deposition by reactive ion plating, elec. resist., visible transmittance meas. 4-99348  
 $\text{In}_{2-x}\text{Sn}_x\text{O}_{3-y}$  transparent conducting films, DC reactive sputtering deposition, optical and elec. props. 4-112533  
 $\text{In}_{2-x}\text{Sn}_x\text{O}_{3-y}$  transparent and heat-reflecting films, optical props. 4-114334  
 $\text{In}_{2-x}\text{Sn}_x\text{O}_{3-y}/\text{CdTe}$  photoconvertors, current transfer mechanism 4-93616  
 $\text{In}_2\text{Sn}_{0.5}\text{S}_7$ , cryst. struct., X-ray diffr. (French) 4-84255  
 $\text{InTe}_3$  amorphous films, elec. breakdown in pulsed fields 4-114209  
 $\text{InTe}_3$ , electrical and optical props. meas. 4-61380  
 $\text{InY}_2\text{Cl}_7$ , crystallographic characterisation and phase transitions 4-70077  
 $\text{InCl}_2$  complexes, excited states, emission, solvent effects 4-107291  
 $\text{KIn}(\text{MoO}_4)_2$ , ferroelastic domain switching 4-92343  
 $\text{MgIn}_2\text{Se}_4$ , layered cpd., cryst. growth 4-93205  
 $\text{Pb}_2\text{InNbO}_6$ , order-disorder transitions and dielec. props. 4-65980  
 $\text{Pb}_2\text{InNbO}_6$ , single crystal, perovskite and pyrochlore modifications, prep. and props. 4-76662  
 $\text{Pd}_{1-x}\text{In}_x$ , optical props. in VUV region, ( $E=5-43$  eV) 4-109210  
 $\text{RbIn}(\text{MoO}_4)_2\cdot\text{Cr}$ , ferroelastic, structural phase transitions, EPR study 4-70372  
 $\text{TlInS}$ , crystal, incommensurate phase transition 4-113601  
 $\text{TlInSe}_2$ , reflection spectrum and band struct. calcs. 4-104562  
 $\text{ZnIn}_2\text{S}_4$ , optical consts., ellipsometric determ. 4-76414

**INDO calculations**

- acetamides,  $\beta$ -halo substituted radical anions in X-irrad. crystals, INDO calcs., EPR obs. 4-102714  
 alkali halides, polarisation energy by point defects, INDO cluster calc. 4-80861  
 benzonitrile, and derivatives, spin-spin coupling consts., FPT INDO calcs. 4-64498  
 (biphenyl)methyl/lithium, charge densities, struct., INDO calcs.,  $^{13}\text{C}$  NMR 4-102702  
 bis(pentadienyl)iron, INDO calcs. photoelectron spectra 4-68960  
 bisglyoximate nickel(II), solid phase transitions and band struct. 4-88282  
 bromoacetamide, cryst. struct. and radical anion stability 4-70130  
 carbonium ions, cryst. bonding dipole moments, SINDO calcs. 4-87049  
 chloroacetamide, cryst. struct. and radical anion stability 4-70130  
 cyclohexanol, H bonds, rot. barriers, INDO and ab initio STO-3G calcs. 4-112115  
 cyclopentadienylmanganese(II), mixed valence state stabilisation, cryst. orbital formalism anal. 4-104172  
 1,3-dioxan-5-ol, H bonds, rot. barriers, INDO and ab initio STO-3G calcs. 4-112115  
 1,3-dithianyllithium, 2-substituted, charge densities, struct., INDO calcs.,  $^{13}\text{C}$  NMR 4-102702  
 electronic struct. geometry, energetics, INDO calcs. 4-96454  
 [1,1]ferrocenophane carbocation, electronic struct. geometry, energetics, INDO calcs. 4-96454  
 fluorenyllithium, 9-substituted, charge densities, struct., INDO calcs.,  $^{13}\text{C}$  NMR 4-102702  
 fluoracetamide, cryst. struct. and radical anion stability 4-70130  
 cis-fluoropropene, polarisation propagation anal. of through-space transmission of non-contact terms of F-F coupling consts. 4-96566  
 formhydroxamic acid, equilib. geometry and electronic props. 4-96453  
 iodoacetamide, X-irrad.,  $\sigma^*$  radical anion struct., EPR and INDO calc. 4-69119  
 1-methyl-7-azaindole, struct. and props., ab initio MO calcs. 4-78782  
 7-methyl-7H-pyrrolo(2,3-b)pyridine, 1-methyl-7-azaindole, struct. and props., ab initio MO calcs. 4-78782  
 naphthaldehydes, picosecond time resolved absorpt. spectra and intersystem crossing kinetics 4-64484  
 polyatomic mols., IR vibr. freqs. and intensities, semiempirical NDO calcs. 4-64387  
 polymer donor-acceptor systems, one-dimens., band struct., INDO calcs. 4-113847  
 porphyrinatonicel(II) polymer, band struct., semiempirical INDO crystal-orbital approach 4-75829  
 porphyrinatonicel(II) system, one dimens. tetrahedrally distorted, electronic struct. 4-75851  
 tetracyanatonicelate(II), mixed valence state stabilisation, cryst. orbital formalism anal. 4-104172  
 tetrathiosquarato nickel(II), one dimens. crystal orbital calcs., neighbour-strand interactions 4-113853  
 tetraza porphin nickel(II), one-dimensional, electronic struct., solid state props., SCF HF crystal-orbital approach based on semiempirical Hamiltonian 4-70627  
 transition metal complexes, orbital relax. and correl. in photoelectron spectra, INDO calcs. 4-102740  
 1,1,2-trichloroethane, catalytic dehydrochlorination, CNDO/2, INDO and MINDO/3 calcs. 4-91202  
 KCl, cryst., point defects, INDO calcs. 4-108359  
 LiCl, substitutional defects, molecular cluster-INDO calcs. 4-108806  
 LiF, substitutional defects, molecular cluster-INDO calcs. 4-108806  
 $^{13}\text{N}$ ,  $^{13}\text{C}$  spin-spin coupling consts., dihedral angle depend., INDO calcs. (German) 4-83298  
 NaCl, substitutional defects, molecular cluster-INDO calcs. 4-108806  
 NaF, substitutional defects, molecular cluster-INDO calcs. 4-108806  
 Ni complex, porphyrinatonicel(II), band struct., tight binding semiempirical cryst. orbital calcs. 4-75846  
 $\text{Ni}_4$  cluster, 14-atom, H atom interaction, MINDO/SR calc. 4-64647  
 $\text{Ni}(\text{CN})_4^{2-}$  system, symm. isolations in partially oxidised one dimens. transition metal polymers 4-98524

**INDOR**

- see also nuclear Overhauser effect  
 No entries

**induced anisotropy (magnetic)**

- ferromagnet, cubic, with induced uniaxiality, mag. phase diagrams and domain struct. 4-65809  
 metallic glasses, mag. aftereffects, induced anisotropy and role of two-level systems 4-84821  
 thin ferromagnetic film, mag. bubble domain stretching (Russian) 4-65844  
 Co-P electrodeposited amorphous alloys, reorientation kinetics of induced mag. anisotropy 4-84783  
 $\text{Co}_{65}\text{Fe}_{35}(\text{MO}, \text{Si}, \text{B})_{30}$  alloys, amorphous, mag. props., influence of induced anisotropy 4-84782  
 $\text{Co}_{55}\text{Ni}_{10}\text{Fe}_{35}\text{Si}_{10}\text{B}_{10}$  amorphous, mag. hysteresis loops after heat treatment below Curie point 4-80781

**induced anisotropy (magnetic) continued**

- $\text{Fe}_{60}\text{B}_{40}$ , amorphous, mag. hysteresis loops after heat treatment below Curie point 4-80781  
 $\text{Fe}_2\text{Co}_2\text{Si}_2\text{B}_{12}$ , zero magnetostrictive amorphous alloy, permeability and field-induced anisotropy 4-71056  
 $\text{Fe}_{60}\text{Ni}_{40}\text{B}_{20}$ , amorphous, mag. hysteresis loops after heat treatment below Curie point 4-80781  
 $\text{YSmLuCaFeGe}$  garnet film, mag. anisotropy study 4-88704
- inductance**  
 magnetic field problems, nonlinear transient, comparison of lumped and distributed solns. 4-59959
- inductance measurement**  
 LC oscillator technique for inductance meas. to investigate mag. aftereffects 4-68243  
 metrological research in Czechoslovakia, by TESLA, Brno 4-90614
- induction, electromagnetic** see *electromagnetic induction*
- induction heating**  
 see also electric furnaces; ovens  
 electromagnetic heating techniques for the in situ recovery of heavy oils 4-72039  
 optical glassmelting in Pt container system, induction heater power control 4-69608  
 tool steel, inductive rapid tempering 4-114580
- inductor microphones** see *microphones*
- inductors**  
 see also coils; transformers  
 induction-dynamic systems optimal inductor thickness selection 4-112319  
 watt-hour efficiency of system loop inductor-ferromagnetic plate 4-102851
- industrial atmospheres** see *air pollution*
- industrial control**  
 see also process control  
 electro-optical instrumentation for industrial applcs., conf., Arlington, USA (Apr. 1983) 4-90286
- industrial economics** see *economics*
- industrial plants**  
 waste heat recovery in industry with turbomachines using organic fluids (Rumanian) 4-66738  
 waste heat utilisation, high-temperature salt/ceramic thermal storage phase-change media app. 4-66797
- industrial research management** see *research and development management*
- industrial robots**  
 optical precision instrument mounting appl. (German) 4-112595  
 stereoscopic television equipment for biotechnical robots in nuclear technology 4-107172
- industrial standards** see *standards*
- industries**  
 this heading is restricted to those industries which are not covered by other specific headings  
 see also automobile industry; brewing industry; chemical industry; construction industry; electricity supply industry; food processing industry; glass industry; metallurgical industries; mineral processing industry; paper industry; petroleum industry; plastics industry; textile industry  
 absorption heat pump, for upgrading industrial waste heat to process steam temperatures 4-72163  
 fossil fuel industries and energy policy, 1973-83 4-77050  
 high temp. gas engine driven heat pumps, industrial appls. 4-89463  
 Japanese industries, energy anal., time series methods 4-72191  
 microelectronics, optical techniques, industrial appl. 4-97117  
 optical data transmission, industrial appl. 4-97118  
 organic Rankine bottoming cycles waste heat recovery 4-66748  
 solar industrial process heat, prospects reexamination 4-62306
- inelastic electron tunnelling spectra** see *tunnelling spectra*
- inelastic electron tunnelling spectroscopy** see *tunnelling spectroscopy*
- inert anodes** see *anodes*
- inert gas compounds**  
 see also argon compounds; helium compounds; krypton compounds; neon compounds; radon compounds; xenon compounds  
 chlorides, spectroscopic and kinetic study with VUV synchrotron radiation excitation 4-85289  
 fluoride dimers and trimers dissolved in liq. rare gases 4-96608  
 halide lasers, high repetition rate 4-69383  
 halide lasers, X-ray preionisation 4-74488  
 inert gas halogen excimer lasers, VUV and EUV generation 4-96863
- inert gases**  
 see also argon; helium; krypton; neon; radon; xenon  
 adsorbed atoms on alkali halides 4-80390  
 adsorbed films on graphite, incomplete wetting 4-92530  
 adsorbed on graphite, lateral variation of physisorption potential 4-92529  
 adsorbed on Li, conduction electron spin scatt. cross-sections 4-84663  
 adsorbed on smooth solid substrates, wetting characts. at zero temp. 4-80388  
 afterglow,  $\text{I}_2^+ \text{A}^2\P_{3/2}$  emission 4-112190  
 atmospheric environment, Xe and noble gases in shales, plastic bag expt. 4-94220  
 atom +  $\text{H}^+$ , multiply ionising collisions,  $\delta$ -electron spectra 4-83458  
 atom +  $\text{H}^+$  collisions, electron detachment 4-102766  
 atom + He collision, single and double electron loss cross sections of He metastable and ground states 4-59884  
 atom + ion electron capture collisions, recoil charge distrib. 4-59892  
 atoms, electron scatt., optical model pot., investig. of the shape of the imaginary part 4-78966  
 atoms, metastable state, low energy electron inelastic scatt. 4-112279  
 atoms, metastable states, quenching by Cu atoms 4-96485  
 atoms, nuclear spin polarisation by spin exchange with optically pumped alkali metal atoms 4-78932  
 atoms +  $\text{Cl}^+$ , positive ion prod., double electron detachment cross sections 4-87187  
 atoms +  $\text{H}^+$  ( $\text{He}^+$ ), charge transfer and direct ionisation channels, electron prod. 4-87191  
 atoms + NO, mol. beam expt. for rot. excitation, fluoresc., cross sections meas. (German) 4-78957  
 biological uptake, regulation and pulmonary elimination of inert vapours and gases 4-115003  
 clusters, ionisation effect on magic numbers 4-96735  
 crystal, excitation processes study, synchrotron radiation appl. (Russian) 4-98530  
 crystal, ideal, vibr. thermodynamic props., anharmonic contrib. 4-98307

- ri gases continued  
 crystal binding energies, many-body pots. construction 4-70057  
 crystals, local optical centres and exciton states 4-98561  
 crystals, surface energy, entropy and stability 4-98309  
 crystals, vacancy interactions, statistical mechanical theory (*Russian*) 4-84285  
 electrical discharge, externally maintained, preionised, IR radiation generation, laser efficiency 4-64695  
 electron swarm parameters calc. 4-65145  
 equilibrium and transport props. at low density 4-97744  
 flowing, in hollow cathode discharge, vac. UV radiation investig. 4-91988  
 geochemistry, book 4-82611  
 glow discharge, doubly ionised metal ions, mass spectroscopic anal. 4-97923  
 glow-discharge plasmas, noise 4-113254  
 hollow cathode filled with dense inert gas plasma, arc discharges, temp. and density 4-65148  
 inert gas-benzene van der Waals complexes, vibr. relax./predissociation dynamics 4-102753  
 inert gas-CO<sub>2</sub>(O<sub>2</sub>) binary system, diffusion coeffs. and thermal diffusion coeffs 4-103458  
 ion + atom, collisions, integral cross section meas. 4-78929  
 ion laser, hollow cathode, excitation mechanism (*Russian*) 4-69368  
 ionisation coeff. and total excitation cross section 4-92011  
 ionisation in plasma ion source, use of Penning effect 4-86502  
 ionisation yield of low-energy electrons, statistical fluctuations 4-59899  
 ions, electron-impact double ionisation 4-64618  
 isotope enrichment using quadrupole mass spectrometer 4-83486  
 isotopic analysis of Antarctic shergottite EETA 79001, possible Martian origin 4-110575  
 liquid, interatomic core forces deduced from struct. factors 4-92044  
 liquid, thermodynamically consistent theory, pair pot. extraction 4-92043  
 magnetic birefr. meas. 4-103465  
 magnetic properties, local exchange correl. pot. calcs. (*German*) 4-108156  
 mixtures, equilibrium and transport props. at low density 4-97744  
 multiphoton ionisation, electron energy spectra, statistical model 4-78819  
 nonequilibrium pulsed discharge plasma, ionisation relax. 4-60765  
 nuclear facility unplanned release, in situ noble gas radionuclide spectroscopic meas. 4-106889  
 PES satellite intensities, incident photon energy effect 4-78815  
 Rydberg at. states fine struct. 4-107290  
 shock wave structures 4-103365  
 solid, model, thermodynamic props. and dynamic compression 4-70409  
 solid, optical consts., self-consistent anal. 4-71332  
 solidified, contact charging expts. 4-76022  
 solids, cathodoluminescence excitation spectra 4-85013  
 solids, conduction band states, excitons, photoemission 4-85057  
 solids, self-trapped holes calcs. 4-84582  
 solids, time resolved VUV luminesc. under synchrotron radiation selective excitation 4-84985  
 stack effluent monitoring for an operating four reactor unit CANDU nuclear station 4-59450  
 atom+H(H<sub>2</sub>), laser excitation, electron loss from H(3p) atoms, H(3p) beam prod. 4-87200  
 Cl<sub>2</sub> + inert gases, spectroscopic and kinetic study with VUV synchrotron radiation excitation 4-85289  
 Li-inert gas mols., near-UV emission bands meas., collision induced bands, quenching rate coeff. 4-83385  
 Na+inert gases, collisional relax., two-photon absorpt. spectra 4-78930  
<sup>18</sup>O<sub>2</sub>, thermal electron attachment mechanism, isotope effect studies in inert gases and hydrocarbons 4-102795  
 Si, ion implanted with noble gases, optical defects, photoluminesc. study 4-71429  
 TI-inert gases, adiabatic pots. and oscillator strengths, improved pseudopot. calc. 4-91228
- inertial navigation**  
 geodetic datum development and positional errors 4-72484
- infinite impulse response filters** *see digital filters*
- infinite series** *see series (mathematics)*
- inflammability** *see combustion*
- information analysis**  
*see also cataloguing; classification; indexing*  
 radiobiology publications growth, computer analysis (*Russian*) 4-109884
- information retrieval**  
 holography, multiple embossment for hologram recording, holographic memory for information retrieval (*Japanese*) 4-107580  
 National Ocean Service automated tides archival and retrieval system 4-67505  
 organised documentation for information retrieval at nuclear power stations 4-86958
- information retrieval systems**  
 Cambridge Database of molecular structures 4-64327  
 CEDAG, clusters of galaxies data centre 4-94974  
 data-base, computer-searchable form., for matching unknown mass spectra 4-89357  
 IAEA's Safeguards Information System, 3 years of experience 4-111724  
 Lawrence Livermore nuclear data libraries used for fusion reactor calcs. 4-111773  
 Los Alamos nuclear data libraries for fusion neutronics calcs. 4-111774  
 marine pollution data archiving, user preferences 4-115455  
 mass spectrometry-mass spectrometry, instrument database system 4-114853  
 National Ocean Service automated tides archival and retrieval system 4-67505  
 SIMBAD data base, astronomical contents 4-94901  
 SIMBAD data base at CDS, 1984 software capabilities for stellar astronomy 4-94900  
 VITAMIN-E cross-section library for fusion neutronics calcs. 4-111775  
 WIS computerized information system for a waste processing facility, nuclear safeguards 4-111731  
 T breeding in He cooled fusion blankets, nuclear data library comparison 4-111779
- information services**  
 acid rain information 4-90279  
 Canadian Marine Environment Data Service, achievements of first decade 4-115578  
 Nuclear Criticality Information System, status, plans and capabilities 4-106911  
 radioactive materials packaging, RAMPAC database 4-106757
- information services continued**  
 scientific journals in Mexico 4-110842  
 UK Meteorological Office archive for marine enquiries 4-115556  
 UKCND data libraries, evaluated decay data 4-102335
- information storage systems** *see information retrieval systems*
- information theory**  
*see also channel capacity; codes; correlation theory; decision theory and analysis; estimation theory; filtering and prediction theory; modulation; signal detection; signal processing; speech intelligibility*  
 free energy, linear relationships, information theoretic view (*German*) 4-78287  
 homodyne and heterodyne detection, noise 4-79069  
 information entropy and Thomas-Fermi theory 4-91201  
 nervous transmission systems 4-100122  
 quantal friction, nonlinear Hamiltonian and information theory 4-73889  
 redundancy reducing processes in single neurons 4-105222  
 trimethylchlorosilane, liq., orientational distrib. function calcs. from Raman band shapes (*German*) 4-109197
- information use**  
 NOAA satellite data utilisation by oceanographers 4-115621
- infrared astronomical observations**  
 3K background in far-IR (900-2000 microns) 4-77981  
 3K background radiation in 400-1100 microns range, large scale anisotropy 4-77982  
 1983 SN, IRAS semiaccurate positions of Apollo object 4-82439  
 1984 N 1, size and planetary distance from SAO 186001 event 4-101257  
 Abell 2151, Hercules Cluster, IRAS obs. 4-86068  
 AGK3-0°965, central star to PN NGC 2346, IR light curves and circumstellar shell characts. 4-115755  
 Nova Aquilae 1982, IR photometry and spectrometry 4-63178  
 ARP 220, H<sub>2</sub> detection in IR luminous merging galaxies 4-115821  
 Arp 220, H<sub>2</sub> emission from distributed galaxy, IR obs. 4-101474  
 asteroids, IRAS fast mover program 4-101227  
 E Aurigae, eclipsing binary B V R I J H K photometric obs. 4-94866  
 e Aurigae; IR obs. during eclipse 4-72980  
 background radiation in near IR and early Universe obs. (*Japanese*) 4-115837  
 Barnard 5, IRAS obs. of dark cloud, solar type star formation 4-86014  
 BD+30°3639, planetary nebula, far IR spatial anal. and optical obs. 4-90203  
 Becklin-Neugebauer objects, catalogue of extremely young, massive and compact IR sources 4-94643  
 blue compact galaxies, near-IR photometry rel. to nature, stellar populations, and age 4-94957  
 blue stragglers of M67, IR photometry and echelle spectroscopy 4-94757  
 44-i Bootis, contact binary, period change, IR photometric anal. 4-115781  
 3C 109, broad-line radiogalaxy, dust characts. from visible and IR obs. 4-90223  
 3C 371, N galaxy with BL Lac nucleus, multifrequency obs. 4-90222  
 3C 390.3, 25  $\mu$ m component from IRAS obs. of radiogalaxy 4-86055  
 OY Carinae, eclipsing dwarf nova, light curves and accretion disc characts. 4-110632  
 $\mu$  Cassiopeiae, astrometric binary, speckle interferometry and mass meas. 4-72977  
 Cepheus A-GGD 37 complex, visible and IR obs. 4-115798  
 o Ceti, infalling matter characts. from inverse P Cyg profiles 4-72946  
 Chamaeleon I dark cloud, IRAS obs. 4-86016  
 Circinus galaxy, infrared activity of galaxy containing luminous H<sub>2</sub>O masers 4-94990  
 classical Cepheids, JHK photometry 4-94799  
 P/Comet Austin (1982 VI), spectropolarimetric observations 4-115714  
 Comet Austin (1984i), IR magnitudes and ephemeris (1984 August 28 to October 15) 4-101272  
 Comet Cernis (1983i), coma icy grains detect. in IR 4-101258  
 P/Comet Churyumov-Gerasimenko (1982 VIII), spectropolarimetric observations 4-115714  
 Comet IRAS-Araki-Alcock (1983d), IRAS 12-100  $\mu$ m obs. 4-85893  
 comets, IRAS fast mover program 4-101227  
 compact H II regions, He I 10830 Å line obs. 4-72998  
 Corona Austrina dark cloud, far-IR obs. of star-forming region 4-86001  
 R Coronae Borealis, IR photometry of irregular variable supergiant 4-77842  
 Coronet, obscured young cluster adjacent to R Coronae Austrinae, IR obs. 4-94905  
 CPD-48°1577, cataclysmic variable, spectroscopy and optical-IR photometry 4-82483  
 Crab Nebula, far IR obs. by IRAS 4-86012  
 Crab Nebula filaments, visible and IR spectrophotometry 4-90200  
 CH Cygni, spectrophotometric obs. red giant with hot spot and dust shell 4-94796  
 dark clouds, young embedded stars in dense cores, 2.2  $\mu$ m obs. 4-90216  
 DDM 1, halo planetary nebula, chem. comp. 4-90198  
 diffuse galactic and extragalactic radiation in far-IR, balloon meas. 4-86091  
 diffuse IR background, IRAS obs. 4-86092  
 dust cloud structure in young R associations NGC 1333, S68 and NGC 7129, IR obs. 4-85993  
 early-type stars, IR obs. of mass loss 4-94756  
 early-type strong emission line supergiants in Magellanic Clouds, spectral types and characts. 4-105983  
 faint blue radiogalaxies, IR photometry 4-77930  
 G333.6-0.2, line-of-sight IR extinction, spectral obs. 4-94917  
 G-type stars in Orion LC association, incidence of IR excesses 4-72934  
 galactic centre, IRAS images 4-86051  
 Galactic Centre, near IR imaging and polarimetry 4-77924  
 galactic disc, large-scale struct. from far-IR survey in southern hemisphere 4-115833  
 galactic plane, 2.2  $\mu$ m star counts and stellar distrib. 4-77917  
 galaxies, interacting, evidence from JHKL photometry for recent star form. 4-94959  
 galaxies in IRAS minisurvey 4-86054  
 GL 961, high resolution maps of IR double source 4-110774  
 globular clusters, UBVRI half-light integrated photometry of 72 southern clusters 4-110703  
 globular clusters in NGC 5128, stellar content and metallicity from IR photometry 4-86032  
 H 2215-086, intermediate polar, IR and optical obs. anal. 4-110686  
 HD 193793, high-resolution IR spectrum and composition of W-R star 4-67744

**infrared astronomical observations continued**

- HD 218393, spectrophotometry of peculiar shell star revealing binary star nature 4-82491  
 HD 97048 and 97300 in Cha I assoc., IRAS obs. of pre-main-sequence stars 4-85928  
 Herbig Ae stars CD-44°3318 and UX Ori, shell and atm. anal. 4-94792  
 Herbig Ae-Be stars, IR spectroscopy 4-77830  
 Herbig-Haro objects, nebulae and exciting stars 4-110714  
 Herbig-Haro objects and exciting stars, far-IR studies 4-94907  
 AM Herculis, IR and optical photometry 4-63204  
 HH 46-47, young object with bipolar outflow, IRAS obs. 4-86015  
 IC 5146 molecular cloud, high resolution IR obs. 4-82533  
 Infrared Astronomical Satellite (IRAS), early results 4-101501  
 interstellar extinction towards dusty WC8/9 Wolf-Rayet stars 4-77897  
 Io, Loki volcano eruption, far IR obs. 4-101238  
 IR cirrus, IRAO obs. 4-85892  
 IR sources, 1-millimetre continuum obs. of galactic and extragalactic sources 4-115834  
 IRAS minisurvey, unidentified point sources 4-86086  
 IRAS minisurvey 4-86087  
 IRAS preliminary scientific results from the first six months 4-77692  
 IRC+10216 (CW Leo), C star, circumstellar SiH<sub>4</sub> detect. 4-82490  
 Jupiter, periodic intensity var. in [S III] 9531 Å emission from hot plasma torus 4-94671  
 Kleinmann-Low nebula, IR cavity model and obs. 4-110708  
 L1455 FIR and L1551 IRS 5, low-luminosity protostars, far IR obs. 4-63150  
 BL Lacertae objects, JHK photometry and polarimetry 4-94961  
 late-type pre-main-sequence stars, UBVR photometry 4-115750  
 late-type stellar spectra, 2400-2778 cm<sup>-1</sup>, atlas 4-94735  
 LDN 1551, young object with bipolar outflow, IRAS obs. 4-86015  
 LHS 1126, peculiar white dwarf, narrow-band IR photometry 4-85929  
 long-period variables in Baade's Window, 1-12 µm photometry 4-115757  
 α Lyrae, IRAS discovery of shell 4-85927  
 M1-7, planetary nebula, plasma characts., element abundances and central star nature 4-115797  
 M31, IR emission, IRAS obs. 4-86052  
 M82, far IR forbidden O I and III emission from galactic nucleus 4-90241  
 M8E region, radio interferometry and IR obs. rel. to star form. 4-85994  
 M-type giant stars in Baade's Window, spectral classifications, positions and apparent I magnitudes 4-101325  
 Markarian 231, IR spectra, effects of silicate interstellar features 4-110744  
 Mars, Viking IR obs. of north polar hazes and surface ice 4-94665  
 Mars atmosphere, 10 micron heterodyne spectroscopy 4-105896  
 Miranda, IR spectra of H<sub>2</sub>O ice surface, albedo, diameter 4-101252  
 Moon, geological units identified by Skylab multi-MS spectral scanner 4-67652  
 MXB 1730-335, Rapid Burster, no IR burst during type I X-ray burst 4-90190  
 NGC 1068, Seyfert 2 galaxy, IR spectropolarimetry 4-106068  
 NGC 1275, nucleus radio and IR emission anal. 4-94963  
 NGC 1333, NGC 7129, young R associations, IR obs. of dust cloud struct. 4-85993  
 NGC 2024 IRS 2, interstellar CO absorpt. lines in IR spectrum 4-86000  
 NGC 2024 No.2, IR speckle interferometry of B star with shell 4-94734  
 NGC 2024 No.2, IR speckle obs. of foreground molecular cloud 4-94734  
 NGC 2264, mol. cloud assoc. with galactic cluster, far IR emission sources 4-94923  
 NGC 2782, starburst galaxy obs. at radio, IR, optical, UV and X-ray freqs. 4-110754  
 NGC 3256, far IR obs. of peculiar galaxy indicating starburst 4-94969  
 NGC 3783, Seyfert galaxy, reddening and high-excitation emission lines 4-63286  
 NGC 4945, infrared activity of galaxy containing luminous H<sub>2</sub>O masers 4-94990  
 NGC 6240, H<sub>2</sub> detection in IR luminous merging galaxies 4-115821  
 NGC 6240 (= IRAS 1650+024P04), ultraluminous interacting galaxy, 10 µm and 20 µm photometry 4-77925  
 NGC 6240 H<sub>2</sub> emission from distributed galaxy, IR obs. 4-101474  
 NGC 6302, central IR disk of bipolar planetary nebula, photometry and maps 4-115803  
 NGC 6543, planetary nebula, Ne III forbidden line at 36 µm, detect. and abundance determ. 4-110718  
 NGC 7023, 2023 and 2068, refl. nebulae, near-IR continuum emission 4-86009  
 NGC 7027, cold dust halo, 370 µm obs. of planetary nebula 4-77898  
 NGC 7027, Mg IV and V line obs. of planetary nebula 4-63242  
 NGC 7027, planetary nebula, high spatial resolution obs. with 10-micron array camera 4-86002  
 NGC 7172, obscured edge-on disc galaxy, nucleus activity obs. 4-73074  
 NGC 7538 molecular cloud, near-IR and radio spectroscopy rel. to star form. 4-85998  
 Nova Aquilae 1982, nature of 10 microns emission feature 4-110612  
 Nova Muscae 1983, multispectral obs. during early decline 4-110616  
 Nova Vulpeculae 1984, spectral and visual magnitude observations 4-115762  
 Nova Vulpeculae 1984, spectral var. (1984 July 27 to August 18) 4-110626  
 OH 32.8-0.3, OH-IR star with absorpt. features of pure water ice, IR spectrum 4-110764  
 one millimetre wavelength sources, nebula, galaxies and unidentified sources 4-94989  
 Orion Nebula, H<sub>2</sub> infrared emission at 1.064 microns 4-94920  
 SZ Piscium RS CVn star, IR light curve, JHK photometry 4-90186  
 planetary nebulae, IRAS spectra of five objects 4-86013  
 planetary nebulae, near-IR sources 4-73001  
 planets, millimetre-wave continuum photometry at Italian IR Telescope on Gornergrat 4-72888  
 pre-main sequence stars detect. in dark clouds dense cores 4-101340  
 pre-main-sequence stars in young R associations NGC 1333, S68 and NGC 7129, IR photometry 4-85993  
 RX Puppis, symbiotic system with Mira component, visible and IR emission 4-72955  
 ζ Puppis, wind-corona models comparison, IR spectral obs. anal. and flux distrib. 4-94790  
 quasars, IRAS obs. of radio-quiet and radio-loud objects 4-86084  
 quasars at high redshift, continuum energy distrib. and absorpt. by intervening material 4-110765

**infrared astronomical observations continued**

- V348 Sagittarii, peculiar variable star, struct. model anal. and spectral obs. 4-85945  
 Sagittarius spiral arm at  $l=305^\circ$  near-IR study 4-63277  
 Saturn's satellites, near IR spectra of leading and trailing edges and composition 4-101249  
 Sc I galaxies, distances and props., visible and IR anal. 4-90220  
 Shapley-Ames galaxies, IRAS obs. 4-86053  
 Sharpless 106, bipolar nebula and central star, radio, visible and IR obs. 4-94922  
 Sharpless 68, young R association, IR obs. of dust cloud struct. 4-85993  
 spiral galaxies, obs. of IR H I recomb. line emission 4-86039  
 star formation in Horsehead Nebula optical and IR obs. 4-115740  
 star formation regions, IR and SHF obs. 4-110712  
 stars photometric parallaxes of colour class m stars in NLTT catalogue 4-110594  
 stellar IR photometry, comparison of SAAO, AAO and CTIO systems 4-77726  
 Sun, chromospheric sunspot oscills., propag. characts., spectral obs. 4-94701  
 Sun, corona, emission line struct., polarisation and mag. field 4-105932  
 Sun, facular contrast near limb 4-94702  
 Sun, far infrared imaging observations 4-77810  
 Sun, far IR imaging from balloon-borne platform 4-110589  
 Sun, flare of 1982 September 4, nature, IR and X-ray emission 4-101299  
 Sun, limb brightening obs. at 820 microns 4-63119  
 Sun, sunspot temperature variations throughout solar cycle from umbra-photosphere intensity ratios anal. 4-85905  
 Sun, sunspot umbrae, temp. struct. models from IR spectra 4-105926  
 sunspot umbra/photosphere contrast, high spectral resolution obs. 4-63126  
 supergiant stars in Magellanic Clouds, 10-micron obs. 4-101334  
 supergiants in Magellanic Clouds and Galaxy, photometry of late type cluster members 4-63140  
 supernova in NGC 4419, IR behaviour of Type I object 4-67753  
 supernova in NGC 4419, IR magnitudes (29 February 1984) 4-67755  
 supernova remnants in Galaxy and Magellanic Clouds, spectra 4-73032  
 Triton, methane identified by IR spectra 4-101254  
 Triton, nitrogen identified in near IR spectra 4-101253  
 V2-45, WC9 star, IR dust shell model 4-85946  
 Venus, IR spectrometry by Venera 15 and 16, first results (Russian) 4-85884  
 W28 region, sources photometry; mapping and star form. evidence 4-73004  
 W28 SNR-mol. cloud complex, far-IR sources characts. 4-86008  
 W49, interstellar mol. cloud, millimetre-wave continuum photometry at Italian IR Telescope on Gornergrat 4-72888  
 W5, giant H II region, massive star formation along ionization front 4-94908  
 young southern compact IR sources, Brackett-alpha emission obs. 4-77904  
 H II regions in external galaxies, near-IR photometry and comparison with blue compact galaxies 4-94957  
 OH masers, Type II, radio and IR obs. of optically invisible sources 4-73089  
 OH/IR stars, IRAS obs. 4-85948
- infrared astronomy**  
*see also infrared sources (astronomical)*  
 bolometer system, He-3 cooled, 1 mm continuum obs. appl. 4-105882  
 cometary origins, constraints from deep far-IR meas. 4-101273  
 conference on IR technology and appl., San Diego, CA, USA (Aug. 1983) 4-110800  
 contrast-mode radiometer for AMOS 1.6 m telescope 4-115691  
 cryogenic IR radiance instrument for shuttle CIRRIS telescope 4-94614  
 cryogenic metal mesh bandpass filters for submm astronomy 4-110532  
 cryogenic telescope on IRAS 4-110525  
 deployable optical systems, conf., Los Angeles, CA, USA (Jan. 1983) 4-73138  
 deployable reflector configurations 4-77707  
 deployable reflector segmented mirror system point spread function generation 4-74433  
 detector arrays for telescopes, using CCD and CID arrays 4-101159  
 detectors using InSb arrays, used at European Southern Observatory 4-94624  
 detectors using Si:P or Ge:Be for low photon background work 4-101160  
 diffuse galactic and extragalactic radiation in far-IR, balloon meas. 4-86091  
 extrasolar planets, IR detect. and cosmic ray, Cherenkov radiation 4-77725  
 fluoromethane line profile meas. using heterodyne spectroscopy 4-94637  
 focal plane optics in far IR and submm astronomy 4-101173  
 Fourier transform spectrometers, absolute radiometry 4-101944  
 galactic disc, large-scale struct. from /far-IR survey in southern hemisphere 4-115833  
 galaxies, IR photometry rel. to optimal means of comparative H I anal. 4-90233  
 galaxy clusters, radial velocities, determ., using submm spectrophotometry (Russian) 4-86071  
 graphite, interstellar and circumstellar, spectroscopic method for detect. 4-101187  
 Infrared Astronomical Satellite, computerised data processing 4-82421  
 Infrared Astronomical Satellite (IRAS), early results 4-101501  
 Infrared Telescope in Space (IRTS), optical system and mirror physical characts. (Japanese) 4-94619  
 interstellar dust, far-IR pros. of metallic grains 4-67779  
 interstellar dust, identification of 'unidentified' IR emission features 4-115790  
 interstellar grains, spectroscopic identification 4-67780  
 IR detectors, conf., San Diego, CA, USA (Aug. 1983) 4-95022  
 far IR Michelson interferometer for GIRL telescope on Spacelab 4-77716  
 IR telescopes, purging flow protection 4-101158  
 IRAS fast mover program 4-101227  
 IRAS fast-moving object search 4-77691  
 IRAS infrared astronomical telescope in orbit, design and performance 4-77712  
 IRAS minisurvey 4-86087  
 IRAS mission, Monte Carlo simulation and proposed catalogue completeness 4-94559

**infrared astronomy continued**

- IRAS mission 4-85857  
 IRAS mission operations experience at RAL 4-101116  
 IRAS observations of stars, preliminary results 4-86088  
 IRAS preliminary scientific results from the first six months 4-77692  
 ISO and PIROG, new IR space experiments 4-63069  
 Michelson spatial interferometer, use in far IR astronomy 4-106367  
 millimeter-wave continuum photometry, using Italian IR Telescope on Gornegrat 4-72888  
 Multiple Mirror Telescope use as a phased array 4-110523  
 NASA development of large deployable reflector astronomical facility, modular approach, feasibility study 4-115669  
 NASA space programs in IR astronomy 4-110490  
 novae, prediction of hydrocarbon features in IR spectrum from grain growth and destruction theory 4-101372  
 one-channel photometer for 0.9 to 2.5  $\mu\text{m}$  spectral region; design and construction (Russian) 4-101174  
 photometer for submm continuum obs. 4-115692  
 reflector antenna structure design concepts 4-77709  
 review (Japanese) 4-115832  
 Shuttle IR telescope facility, system design parameter study 4-110489  
 Shuttle IR Telescope Facility, thermal modelling 4-110488  
 stellar IR photometry, comparison of SAAO, AAO and CTIO systems 4-77726  
 Sun, 12 micron unidentified emission lines, possible origins 4-94720  
 Taurus molecular clouds, implications of 3  $\mu\text{m}$  ice band for interstellar chemistry 4-101457  
 telescope design, fused-SiO<sub>2</sub> mirror cryogenic test implications 4-105878  
 telescope pointing system using IR multiplex encoding imager 4-94613  
 InSb 52-element array for spectroscopic application 4-94625  
 InSb detectors for ground-based astronomy 4-95517  
 PbSi Schottky IR CCD evaluation for astron. appls. 4-64789  
 Si 1, meas. of <sup>3</sup>P<sub>0-3</sub> <sup>3</sup>P<sub>1</sub> fine-struct. interval and g<sub>J</sub>-factor by laser mag. reson. 4-85866

**infrared communication** see optical communication**infrared detectors**

see also bolometers; photodetectors

- advanced IR sensor technology, conf., Geneva, Switzerland (April 1983) 4-95018  
 balloon altitude mosaic meas. radiometer 4-115584  
 bolometers operated at 0.1K and 0.2K-cooled by adiabatic demagnetisation 4-111205  
 broadband detector, using pyroelectric materials 4-95514  
 complex mixture charact., IR and photoionisation detector eval. 4-85349  
 conference, San Diego, CA, USA (Aug. 1983) 4-95022  
 conference on IR technology and appl., San Diego, CA, USA (Aug. 1983) 4-110800  
 coupling efficiency to IR fibre optics in focal plane, radiometric analysis 4-106380  
 cryogenic telescope on IRAS 4-110525  
 detection by depletion of trapped charge 4-73514  
 electro-optical instrumentation for industrial appls., conf., Arlington, USA (Apr. 1983) 4-90286  
 European Southern Observatory IR photometer/spectrophotometer detectors 4-94624  
 fatigue test, IR monitoring 4-109585  
 fibre sensors, polarisation, press. sensitivity 4-78371  
 flaw detector for semiconductors free-carrier conc. determ. 4-89211  
 image sensors for fading memory focal plane processor 4-107871  
 integrating IR detector, interface to A/D converter, readout electronics 4-90653  
 international conference on thermal infrared sensing for diagnostics and control, Oak Brook, Illinois, USA, (1983) 4-95012  
 IR laser radiation detection using antenna-coupled point contact Schottky diode, responsiveness study (Japanese) 4-78374  
 medical application of IR sensors 4-93837  
 microbolometers, far-IR 4-86481  
 MOM detector for optical of submillimetre regions, developments 4-73516  
 mosaic detector mounted on high-altitude balloon, optical subsystem design 4-77652  
 motion detection for burglar and false alarm signals, developments in ultrasonic and IR detectors 4-64816  
 optical infrared remote sensors 4-111206  
 optothermal transient emission radiometry 4-86465  
 photoacoustic spectra of solids, normalisation, use of IR detector 4-63791  
 photographic recording of IR light signals 4-111207  
 point-contact diodes for IR heterodyne detection 4-68282  
 point-contact Schottky diode detector and laser/microwave diagnostic system for far IR 4-73517  
 proximity/interruption/reflection detection, IR optoelectronic systems with optical fibres (French) 4-111208  
 pyroelectric detectors, operation theory, phys. model and resulting operation modes 4-86480  
 pyroelectric radiometer, null detecting system for IR radiation absolute meas. 4-106387  
 radiation temperature meas. method based on temp. depend. of radiation noise (Chinese) 4-111203  
 radiation thermometers, industrial, design concepts for running in hostile environments 4-106323  
 semiconductor detector arrays, state-of-the-art review 4-111202  
 space IR sensors parametric studies 4-94249  
 suspended particulate monitoring optical sensor 4-115627  
 technological developments and appls. 4-68279  
 TGS cryst. and preamplifier IR detection system 4-73510  
 threshold sensitivity determ. 4-86415  
 ultrawide wave band optical materials and systems, multi-sensor appl. 4-112552  
 uncooled, pyroelectric ceramic material appls. 4-90654  
 window manufacturing technology 4-106381  
 BaPb<sub>1-x</sub>Bi<sub>x</sub>O<sub>3</sub> supercond. thin films for highly sensitive optical detector fabrication 4-82825  
 Bi far-IR microbolometer, design, fabrication and characts. 4-73515  
 Cd<sub>2</sub>Hg<sub>1-x</sub>Te graded energy-gap structures, interf. photoelectromag. effect 4-113992  
 Ge:Au photocells, spectral characts. obs. 4-101919  
 Ge:Be IR detectors for low-photon-background IR astronomy 4-101160  
 Ge:Be photoconductor, 30 to 50  $\mu\text{m}$  detector performance and material aspects 4-108899

**infrared detectors continued**

- (Hg,Cd)Te photovoltaic detector, near-room-temp., thermoelec. current (Chinese) 4-106382  
 HgCdTe 0.1 eV photoconductive detector, optimum thickness 4-111204  
 HgCdTe airborne imaging spectrometer 4-115585  
 HgCdTe detector technology status 4-95515  
 HgCdTe wide-bandwidth photodiode photomixers, 28  $\mu\text{m}$  4-68283  
 Hg<sub>1-x</sub>Cd<sub>x</sub>Te IR detectors, 100-300  $\mu\text{m}$ , mag.-field effects 4-68281  
 InGaAsP, MBE growth, IR reflectivity, diode laser source/detector 4-71391  
 InP-GaInAs IR detectors, applications of electron microscope techniques to semiconductors 4-103622  
 InSb detectors for ground-based astronomy 4-95517  
 InSb photovoltaic IR detector array with quasi-plane struct. (Chinese) 4-106383  
 Na<sub>1/2</sub>Bi<sub>1/2</sub>TiO<sub>3</sub> ceramics, pyroelectric props., perspective appl. in pyroelectric radiation detectors 4-88776  
 Pb<sub>3</sub>Ge<sub>2-3</sub>Si<sub>1-x</sub>O<sub>11</sub> pyroelec. detector chips, printing fabrication 4-104541  
 Pb<sub>1-x</sub>Hg<sub>x</sub>S, photocond. cells, hot body detection 4-90655  
 PbS and PbSe detectors and arrays, review 4-95518  
 PbS polycrystalline films, chemical deposition, for use as infrared detector (Spanish) 4-114392  
 PbSe and PbS detectors and arrays, review 4-95518  
 PbSi IR CCD detector array used in digital heterodyne interferometer 4-111193  
 Si extrinsic IR detectors, development status 4-95516  
 Si, photoconductive asymmetries of donor and acceptor impurities, IR detectors appl. 4-70857  
 Si:As contrast-mode radiometer for AMOS 1.6 m telescope 4-115691  
 Si:P IR detector field enhanced photoresponse up to 43  $\mu\text{m}$  4-90656  
 Si:P IR detectors for low-photon-background IR astronomy 4-101160

**infrared imaging**

- advanced IR sensor technology, conf., Geneva, Switzerland (April 1983) 4-95018  
 airborne imaging spectrometer using HgCdTe detector array 4-115585  
 airborne IR sensing systems, modelled and empirical atmospheric propagation data comparison 4-115567  
 along-track scanning radiometer development 4-82816  
 astronomical telescope pointing system using IR multiplex encoding imager 4-94613  
 colour imaging thermal video system 4-58839  
 conference, San Diego, CA, USA (Aug. 1983) 4-95022  
 conference on IR technology and appl., San Diego, CA, USA (Aug. 1983) 4-110800  
 development and 1980s state of art, AGA Thermovision DISCON system 4-58847  
 eye movement anal. system using IR fundus images (Japanese) 4-85486  
 fading memory focal plane processor 4-107871  
 far-IR interferometric phase imaging of Tokamak plasma 4-75211  
 fatigue test, IR monitoring 4-109585  
 HgCdTe infrared focal plane arrays for imaging spectrometer applications 4-100758  
 high-altitude sensor systems development, using IR cloud, radiance model 4-115566  
 ice, thermal patterns obs. under dynamic loading 4-106320  
 international conference on thermal infrared sensing for diagnostics and control, Oak Brook, Illinois, USA, (1983) 4-95012  
 IRCCD sensors, Schottky barrier, Earth resources features appls. 4-100759  
 laser infrared imaging with CO<sub>2</sub> laser, field tests 4-107870  
 lenses for thermal imaging, transmittance meas. 4-103035  
 linear imaging array for high resolution spaceborne camera 4-100761  
 liquid crystal temperature indicator films as highly sensitive IR visualiser 4-90584  
 locomotor diseases, clinical appl. of advanced IR thermography 4-93839  
 medical aperture synthesis thermography—a new approach to passive microwave temperature measurements in the body 4-115158  
 medical application of IR sensors 4-93837  
 medical imaging techniques and appls., tracers, IR imaging, NMR, X-rays, ultrasonics 4-77417  
 medical optoelectronics: laser appls., fibre-optic instrumentation and IR thermography (Japanese) 4-89678  
 medical thermography, development and criteria for use 4-93838  
 medical thermography, methodological errors rel. to diagnostic conclusions accuracy (Russian) 4-115155  
 MEIS II multidetector electrooptical imaging scanner, airborne pushbroom imager 4-100760  
 microwave applicators, contact-type tissue cooling effects on brightness temp. 4-72217  
 moving vehicles detection 4-97130  
 nematic-chiral thermochromic mixtures for thermography appls. 4-75276  
 nonlinear filtering of thermographic images 4-85491  
 optical infrared remote sensors 4-111206  
 optics for non-visible photography 4-111237  
 orbital mosaic IR image simulation and processing 4-97129  
 photographic recording of IR light signals 4-111207  
 photothermal imaging of subsurface struct., definition and resolution 4-101841  
 radiometer input circuit requirements for microwave thermography, comments and reply 4-85480  
 satellite-ocean remote sensing systems and their prospects 4-110164  
 scanning thermography for cavity detection in plane slab and rectangular prism 4-114731  
 smectic A-nematic phase transition for thermal imaging 4-111131  
 space IR sensors parametric studies 4-94249  
 space-borne optical imagers for Earth observation, large IR detector arrays 4-94248  
 speckle phenomena at 10  $\mu\text{m}$  wavelength 4-69317  
 spectral emissivity meas. of human skin for potential early cancer detect. 4-105320  
 spectrum bands for infrared thermography (French) 4-60171  
 thermal photography, surface tension forces, thermally conc. capillary flows (Russian) 4-68227  
 thermal wave imaging anal. of defects in semiconductors 4-86414  
 thermal wave imaging of subsurface structure with IR detection 4-86413  
 thermographic tomography problem, soln. by direct substitution eqn. error technique 4-77199  
 Thermosense VI conference scope 4-95487  
 AI radiators, quality assurance by IR thermography 4-66531

**infrared imaging continued**

- C fibre reinforced plastic, thermal NDT method for inspecting large parts 4-71838
- CO<sub>2</sub> imaging laser radar field tests 4-107870
- GaAs, material and devices, thermal wave imaging 4-75711
- HgCdTe detector technology status 4-95515
- InSb 52-element imaging array for IR astronomical spectrometers 4-94625
- PbS and PbSe detectors and arrays, review 4-95518
- PbSe and PbS detectors and arrays, review 4-95518
- PtSi Schottky IR CCD evaluation for astron. appls. 4-64789
- Si:P(B), thermal wave contrast, dopant conc. depend. 4-103978
- Y<sub>2</sub>O<sub>3</sub> sputtered films as protective overcoats for Al mirrors in forward looking IR imaging systems 4-79269

**infrared-infrared double resonance** *see optical double resonance***infrared radiometers** *see radiometers***infrared sources**

- combined source-detector response characteristics 4-90637
- continuum IR radiation pulsed source for time resolved absorption spectroscopy in laser prod. plasmas 4-69871
- far-IR radiation of UCSB free electron laser 4-74529
- fluoromethane tunable FIR laser, frequency trimming (*Chinese*) 4-69374
- semiconductors, direct-gap, coherent far IR radiation sources on hot excitons 4-109213
- synchrotron radiation as IR source, dipole magnets 4-74641
- CdS, frequency tuning of far-IR radiation on hot excitons 4-69415
- H<sub>2</sub>, compressed, tunable high-power radiation source in 0.72 to 8  $\mu$ m range 4-107738
- InSb, tunable far-IR emission from uniaxial stress-enhanced spin-flip transitions 4-69416
- KH<sub>2</sub>PO<sub>4</sub> cavity optical parametric oscillator, subpicosecond continuously freq. tunable IR pulse generation 4-74620
- LiF pulsed F<sub>2</sub> colour centre laser, room temp. operation in near IR 4-64710
- W, spectral emissivity, analytic expressions for 340 nm to 2.6  $\mu$ m spectral region 4-60127

**infrared sources (astronomical)**

- 1-millimetre continuum observations of galactic and extragalactic sources 4-115834
- Abell 2151, Hercules Cluster, IRAS obs. 4-86068
- AFGL 2688, bipolar nebula, visible spectra and spectrophotometry obs. 4-106054
- AGK3-0°965, central star to PN NGC 2346, IR light curves and circumstellar shell characts. 4-115755
- ARP 220, H<sub>2</sub> detection in IR luminous merging galaxies 4-115821
- $\epsilon$  Aurigae, IR obs. during eclipse 4-72980
- B335, isolated dark globule, relation between far-IR source and NH<sub>3</sub> emission peak 4-115794
- Barnard 5, IRAS obs. of dark cloud, solar type star formation 4-86014
- BD+30°3639, planetary nebula, far IR spatial anal. and optical obs. 4-90203
- Becklin-Neugebauer objects, catalogue of extremely young, massive and compact IR sources 4-94643
- 3C 390.3, 25  $\mu$ m component from IRAS obs. of radiogalaxy 4-86055
- $\gamma$  Carinae, spectroscopy of shell episode (1981 to 1983) 4-115760
- PV Cephei, bipolar flow and cometary nebula GM 29, EHF obs. 4-85922
- VW Cephei, W UMa star, HK photometry anal. 4-94863
- Cepheus A-GGD 37 complex, visible and IR obs. 4-115798
- Chamaeleon I association Infrared Nebula, IR source nature and disc characts. 4-63339
- Chamaeleon I dark cloud, IRAS obs. 4-86016
- Circinus galaxy, infrared activity of galaxy containing luminous H<sub>2</sub>O masers 4-94990
- circumstellar composite dust shell heated by supernova, IR emission 4-105971
- circumstellar shells, obs. and anal. of cyanoacetylene (HC<sub>3</sub>N) 4-85907
- Cn 1-1, possible planetary nebula and F5 III-IV star as binary components, obs. 4-90196
- comet clouds surrounding nearby stars, constraints from isotropy of cosmic microwave background 4-101273
- compact H II regions, He I 10830 Å line obs. 4-72998
- Corona Austrina dark cloud, far-IR obs. of star-forming region 4-86001
- Coronet, obscured young cluster adjacent to R Coronae Austrinae, IR obs. 4-94905
- Crab Nebula, far IR obs. by IRAS 4-86012
- V1016 Cygni, emission lines, geometric implications for eruptive symbiotic 4-67727
- dust clouds in young R associations NGC 1333, S68 and NGC 7129, IR photometry 4-85993
- early-type stars with mass loss, curve of growth method for IR and radio spectrum 4-101312
- EIC-1 sources in AFGL catalogue, optical identification 4-82560
- G-type stars in Orion IC association, incidence of IR excesses 4-72934
- galactic centre, IRAS images 4-86051
- Galactic Centre, near IR imaging and polarimetry 4-77924
- galactic disc, large-scale struct. from far-IR survey in southern hemisphere 4-115833
- galactic sources, dust emission features near 10  $\mu$ m, extinction estimation 4-86018
- galaxies in IRAS minisurvey 4-86054
- GC-IRS 7, IR spectrum rel. to identification of interstellar grains 4-67780
- GGD 37, Herbig-Haro object, obs. and assoc. with Cepheus A 4-115798
- GL 437, multiple IR source, CO obs. of assoc. mol. cloud 4-85999
- GL 961, high resolution maps of IR double source 4-110774
- H 2215-086, intermediate polar, IR and optical obs. anal. 4-110686
- HD 35155, S-type star, emission lines interpretation 4-85971
- HD 97048 and 97300 in Cha I assoc., IRAS obs. of pre-main-sequence stars 4-85928
- Herbig Ae-Be stars, IR spectroscopy 4-77830
- Herbig-Haro objects, exciting stars bolometric luminosities 4-110714
- Herbig-Haro objects and exciting stars, far-IR studies 4-94907
- HH 46-47, young object with bipolar outflow, IRAS obs. 4-86015
- Hubble-Sandage variables in M31 and M33, mass loss rates determ. from IR excesses 4-85941
- IC 5146 molecular cloud, high resolution IR obs. 4-82533
- Infrared Astronomical Satellite (IRAS), early results 4-101501
- interstellar dust, identification of 'unidentified' IR emission features 4-115790
- infrared sources (astronomical) continued**
- interstellar dust clouds, far-IR props. of metallic grains 4-67779
- IRAS 1650+024P04, identification with ultraluminous interacting galaxy (NGC 6240) 4-77925
- IRAS minisurvey, unidentified point sources 4-86086
- IRAS minisurvey 4-86087
- IRAS point sources, unidentified, optical counterparts are IR luminous galaxies 4-77970
- IRAS preliminary scientific results from the first six months 4-77692
- IRC+10216, C star, C<sub>2</sub>H detect. in shell 4-77834
- IRC+10216, CN and C<sub>2</sub>H in C star 4-94787
- IRC+10216 (CW Leo), C star, circumstellar SiH<sub>4</sub> detect., IR obs. 4-82490
- IRC+10420, VLA UHF obs. of OH masers assoc. with F8 supergiant 4-94759
- IRc 9, wind effect on high vel. gas struct. in Orion Molecular Cloud 4-110710
- Kleinmann Low Nebula, H<sub>2</sub>O maser outburst region, rot. meas. (*Russian*) 4-67785
- Kleinmann-Low H<sub>2</sub>O maser outburst characts. (*Russian*) 4-94933
- Kleinmann-Low Nebula, HDO mapping 4-77891
- Kleinmann-Low nebula, IR cavity model and obs. 4-110708
- L1455 FIR and L1551 IRS 5, low-luminosity protostars, far IR obs. 4-63150
- BL Lacertae objects, continuum spectral energy distrib. of X-ray observed sample 4-82546
- LDN 1551, young object with bipolar outflow, IRAS obs. 4-86015
- LDN 1551 IRS 5, bipolar CO gas-flow, vel. gradients 4-115796
- LDN 1551 IRS-5, rot. disc nature and possible planetary system form., EHF obs. 4-77890
- $\alpha$  Lyrae, IRAS discovery of shell 4-85927
- $\alpha$  Lyrae, IRAS obs. of circumstellar dust, possible pre-planetary system 4-86088
- M17, high resolution study at 1.3, 2, 6 and 21 cm wavelength 4-101451
- M2-9, bipolar nebula, polarisation, nebula struct. and grains characts. 4-94918
- M31, IR emission, IRAS obs. 4-86052
- M8E region, radio interferometry and IR obs. rel. to star form. 4-85994
- Markarian 231, IR spectra, effects of silicate interstellar features 4-110744
- MXB 1730-335, Rapid Burster, no IR burst during type I X-ray burst 4-90190
- NGC 1068, Seyfert 2 galaxy, IR spectropolarimetry 4-106068
- NGC 1275, nucleus radio and IR emission anal. 4-94963
- NGC 2024 IRS 2, interstellar CO absorpt. lines in IR spectrum 4-86000
- NGC 2071 molecular cloud, obs. of high-vel. HCO<sup>+</sup> flow assoc. with cluster of IR sources 4-85997
- NGC 2264, mol. cloud assoc. with galactic cluster, far IR emission sources 4-94923
- NGC 3079, water maser discovery in infrared emitting galaxy 4-115805
- NGC 3256, far IR obs. of peculiar galaxy indicating starburst 4-94969
- NGC 4945, infrared activity of galaxy containing luminous H<sub>2</sub>O masers 4-94990
- NGC 6240, H<sub>2</sub> detection in IR luminous merging galaxies 4-115821
- NGC 6302, central IR disk of bipolar planetary nebula, IR obs. 4-115803
- NGC 7023, 2023 and 2068, refl. nebulae, near-IR continuum emission 4-86009
- NGC 7027, planetary nebula, high spatial resolution obs. with 10-micron array camera 4-86002
- NGC 7172, obscured edge-on disc galaxy, nucleus activity obs. 4-73074
- NGC 7538 molecular cloud, near-IR and radio spectroscopy rel. to star form. 4-85998
- novae, prediction of hydrocarbon features in IR spectrum from grain growth and destruction theory 4-101372
- NSV 2229, new variable star in Orion Nebula, visual and photographic magnitude estimates (October 1983 to March 1984) 4-72952
- OH 32.8-0.3, OH-IR star with absorpt. features of pure water ice, IR spectrum 4-10764
- OH-IR stars distrib. and kinematics in Galaxy centre region 4-63312
- one millimetre wavelength sources, nebula, galaxies and unidentified sources 4-94989
- Orion IRC 2, SiO maser emission from rotating, expanding disk 4-94912
- Orion Nebula, H<sub>2</sub> infrared emission at 1.064 microns 4-94920
- planetary nebulae, IRAS spectra of five objects 4-86013
- planetary nebulae, near-IR sources 4-73001
- pre-main sequence stars, IRAS obs. 4-86088
- pre-main sequence stars detect. in dark clouds dense cores, IR obs. 4-101340
- pre-main-sequence stars, far-IR studies of exciting stars of Herbig-Haro objects 4-94907
- pre-main-sequence stars in Horsehead Nebula, obs. of collimated interstellar flow 4-115740
- pre-main-sequence stars in young R associations NGC 1333, S68 and NGC 7129, IR photometry 4-85993
- RX Puppis, symbiotic system with Mira component, visible and IR emission 4-72955
- quasars, IRAS obs. of radio-quiet and radio-loud objects 4-86084
- review (*Japanese*) 4-115832
- HM Sagittae, circumstellar shell struct. and wind interactions, SHF/UHF obs. 4-85910
- Shapley-Ames galaxies, IRAS obs. 4-86053
- Sharpless 106, bipolar nebula and central star, radio, visible and IR obs. 4-94922
- solar companion star, possible observability in IR 4-72593
- spiral galaxies, obs. of IR H I recomb. line emission 4-86039
- star formation regions, IR and SHF obs. 4-110712
- supergiant stars in Magellanic Clouds, 10-micron obs. 4-101334
- supernova in NGC 4419, IR magnitudes (29 February 1984) 4-67755
- supernovae, silicate grains in dust shells, IR emission 4-115769
- symbiotic stars; spectral characts. 4-101373
- T Tauri, primary and infrared secondary nature (*French*) 4-82473
- Taurus molecular clouds, implications of 3  $\mu$ m ice band for interstellar chemistry 4-101457
- W Ursae Majoris, JHK photometry and circumstellar shell evidence 4-94863
- Ve2-45, WC9 star, IR dust shell model and obs. 4-85946
- Vega ( $\alpha$  Lyrae), circumstellar shell of asteroids or comets 4-110602
- W28 region, sources photometry; mapping and star form. evidence 4-73004
- W28 SNR-mol. cloud complex, far-IR sources characts. 4-86008

- rared sources (astronomical) continued  
W3 IRS 4, aperture synthesis map of HCN emission 4-115804  
W49, interstellar mol. cloud, millimetre-wave continuum photometry at Italian IR Telescope on Gornegrat 4-72888  
W51, H II region-mol. cloud complex, core continuum emission mapping and complex characts., THF obs. 4-82542  
young southern compact IR sources, Brackett-alpha emission obs. 4-77904  
H<sub>2</sub>O masers assoc. with stellar mass outflow regions, VLA positions 4-85913  
OH masers, Type II, radio and IR obs. of optically invisible sources 4-73089  
OH/IR stars, IRAS obs. 4-85948  
OH/IR stars, VLBI obs. of circumstellar shells 4-77849  
OH-IR stars, circumstellar shell struct. from OH maser emission anal. 4-85970  
OH-IR stars, IR counterparts detect. by IRAS 4-86088
- Infrared spectra** see *infrared spectra of diatomic inorganic molecules; infrared spectra of inorganic solids; infrared spectra of organic molecules d substances; infrared spectra of polyatomic inorganic molecules; spectra inorganic liquids and solutions*
- Infrared spectra of diatomic inorganic molecules**  
diatomic mols., in dil. van der Waals solns., IR and Raman spectra, product approx. calcs. 4-104613  
linear dipole molecules in inert solvents, dielec. susceptibility dispersion, model 4-83316  
liquid phases, IR spectra, dielectric shift, mol. model, vapour press. isotope effects 4-64460  
molecular spectroscopy, high resolution, in submillimeter wavelength region 4-90669  
CO, 2.45  $\mu$ m spectral meas. using IR high-resolution cooled-optics grating spectrometer 4-95532  
CO adsorbed on (Ru,Si<sub>3</sub>)<sub>2</sub>O<sub>2</sub> surface, FT-IR study of surface acid sites 4-113783  
CO, adsorbed on LaMO<sub>3</sub> (M=Cr,Mn,Fe,Co), IR spectra 4-104071  
CO, adsorpt. on Pd electrode, IR refl. spectrosc. obs. 4-107348  
CO chemisorbed layer on Ni (100), vibr. spectroscopy by IR emission 4-98439  
CO, collision widths of IR lines broadened by H<sub>2</sub>O vapour at elevated temps. 4-69149  
CO, IR absorpt. line shape and width across supersonic free jets 4-83374  
CO, liq., IR spectra, solvent-induced shift, Monte Carlo simulation 4-61698  
CO, prod. from formaldehyde photodissociation, collisions, IR fluoresc. study 4-78900  
CO<sup>+</sup>, isolated ions, IR spectra quantitative prediction 4-69075  
CO<sub>2</sub>, vibr.-rot. pot. energy curves, IR spectra 4-59754  
Cs<sub>2</sub>, first two excited <sup>3</sup> $\Sigma_g^-$  states, IR fluoresc. study 4-64525  
H<sub>2</sub>, I-O S(1) emission from distributed galaxies 4-101474  
H<sub>2</sub>, ground state, FT IR spectra, rot. consts. 4-59741  
H<sub>2</sub> isotopic molecules adsorbed in NaCaA zeolites, induced IR overtone and fundamental bands 4-102678  
H<sub>2</sub>+H<sub>2</sub>, rot. struct., IR absorpt. and Raman scatt. 4-69174  
HCl-Ar, ps. IR spectroscopy, nearly free induction decay obs. 4-96529  
HF+Ar, finite duration of collisions and vibr. dephasing effect on broadened IR line shapes 4-69177  
HX-cyclopropane complex, (X=F, Cl, Br, I, CN), matrix isolation IR investig. 4-107349  
K<sub>2</sub>, triplet transitions, laser induced fluoresc. 4-74287  
LiF, high temp. IR tunable diode laser spectra, no-vibr. meas. and Dunham consts. calcs. 4-59743  
N<sub>2</sub>, adsorbed on Co-Al<sub>2</sub>O<sub>3</sub>, FT-IR studies 4-113786  
N<sub>2</sub>, adsorpt. on Al<sub>2</sub>O<sub>3</sub>, IR spectra 4-77030  
N<sub>2</sub>, far-IR collision-induced absorpt. spectrum, lineshape, information theory 4-74232  
N<sub>2</sub>, temp. depend. collision induced IR absorpt. 4-69058  
NO, stratospheric, in situ meas. using balloon-borne tunable diode laser spectrometer 4-72706  
NO, vibr. overtone band, colour centre laser spectroscopy of small free radicals 4-64479  
NS radical, far IR LMR spectroscopy 4-91286  
Na<sub>2</sub>, double minimum state, IR fluoresc. spectra 4-91305  
Ni<sub>2</sub>, dimer, jet-cooled, IR gas-phase electronic spectrum 4-78839  
O<sub>2</sub>, symmetric vibr., collision-induced IR absorpt. 4-87107  
OH (D), IR and microwave lines, difference freq. laser spectra 4-59756  
OH, fundamental vibr. spectrum, colour centre laser spectroscopy of small free radicals 4-64479  
OH gas-phase radical, vibration-rotation line strength meas. using tunable IR diode-laser 4-112331  
PH, 4.4 micron band characts. from 341 nm band in solar photosphere 4-77797  
PH(D), X<sup>2</sup> $\Sigma^-$  vibronic state, far-IR laser mag. reson. 4-59814
- Infrared spectra of inorganic solids**  
alkali halide:BF<sub>4</sub><sup>-</sup>, IR and Raman spectra, Fermi resonances isotope shift 4-61695  
alkali halides, IR modulation spectroscopy 4-63790  
alkali metal pyrophosphates, M<sup>II</sup>M<sup>III</sup>P<sub>2</sub>O<sub>7</sub>, vibr. spectra and crystal struct. 4-65247  
alkaline earth fluorides, IR modulation spectroscopy 4-63790  
alkaline earth-ferrite glasses, glass forming region and Fe<sup>3+</sup> coordination (Japanese) 4-113348  
 $\gamma$ -alumina, coatings from plasma spraying process, IR study 4-61681  
amorphous, doped, IR and reson. Raman spectrosc. obs. 4-61707  
borates, carbonates and nitrates, intermolecular vibrational coupling, IR spectra 4-65350  
borosilicate glasses, M<sub>2</sub>O-B<sub>2</sub>O<sub>3</sub>-SiO<sub>2</sub>, M=Li, Na, K, OH extinction coeff. determ., IR spectra 4-84958  
copper (I) complexes with some disubstituted acetylenes and dimethylsulphoxide, <sup>1</sup>H NMR, UV and IR spectra 4-76467  
diamond, type Ia, defect-induced one-phonon absorption 4-84981  
diamond powders, synthetic, adsorpt. of organic compounds, IR spectroscopy (Russian) 4-75791  
granitic rocks, near IR spectrochemical analysis method and obs. 4-72719  
graphite epoxy laminates, pulsed photothermal evaluation 4-88818  
halide glasses, thermal and elastic props., molecular dynamics calc. 4-109455  
high-temperature analysis techniques, surface characteristics 4-99927  
ice VII, uncoupled O-H stretch, IR freq. and integrated intensity up to 189 kbar 4-104601
- Infrared spectra of inorganic solids continued**  
ice-mineral mixtures, spectra and remote sensing implications 4-115682  
inorganic thin coatings on metals, Fourier transform IR spectra 4-104688  
ionic crystals, integral intensity of IR absorpt. (Russian) 4-99125  
metal particles, IR radiation, anomalous absorpt. theory 4-66041  
metal particles, small, in composite material, far-IR absorption 4-61708  
microcline, potash feldspar, single crystal, IR reflection spectra 4-76452  
microelectronic device and packaging manuf., opt. microanalytical techniques 4-93574  
minerals containing water, IR spectral studies 4-93071  
MIS struct., surface irregularity enhanced subband resonance 4-61459  
MOS device, IR FT spectroscopy of two dims. space charge layers 4-99109  
oxide glass, structure, vibr. spectroscopy 4-79945  
phosphate glasses, containing fluorides of Group I-IV elements, optical and spectral props. rel. to struct. 4-92098  
phosphosilicate glass film, void formation and IR absorpt. after heat treatment in H<sub>2</sub> atmosphere 4-60840  
polyatomic mol., condensed phase, intramolecular dephasing, single-particle time correlation function theory 4-71359  
pyrochlore families, force fields, vibr. spectra and cryst. defects 4-98055  
quartz, crystalline, refl. spectrum variation on fast neutron irradi. 4-88829  
quartz, cultured, Q capability recalibration from IR meas. 4-61626  
quartz, cultured, random elec. twinning, non-destructive obs., resonator appl. 4-70170  
quartz, electrical and optical props., neutron,  $\gamma$ , and electron irradi. effects 4-60968  
quartz, hydrothermally grown, Q determ., IR meas. and etch channel meas. 4-61627  
quartz, natural, defects induced by vac. UV, X-ray and beta-ray irradi. 4-70191  
quartz, vacuum swept, Al<sup>3+</sup> and OH<sup>-</sup> defect centres 4-61335  
quartz containing water, IR spectral studies 4-93071  
refractory compound powders, optical props., refl. spectrum 0.2 to 25  $\mu$ m 4-61730  
semiconductor superlattices, optical props. 4-104665  
semiconductor superlattices, quantum wells, and heterostructs., elec. and optical props. 4-80666  
semiconductors, impurity distribution anal. by IR spectroscopy 4-76478  
Si-H film, prep. by reactive sputtering, optical and elec. props. 4-71457  
silicate glasses containing TiO<sub>2</sub>, refractive index, density, thermal expansion and IR spectra 4-84199  
skolecite natural zeolite, IR vibr. spectra studies 4-76445  
soda-lime-silica glass, complex refl. spectra determ. using switched-field-of-view interferometer 4-101912  
sodalite, natural, IR spectra 4-104602  
solid surfaces, FT-IR, diffuse reflectance and photoacoustic spectrum 4-61706  
spectral material high refl. precision meas. in IR range using JF-1 type reflectometer (Chinese) 4-11185  
steel, stainless, Ni and Pd filled coloured 4-114949  
3Y<sub>2</sub>O<sub>3</sub>-Fe<sub>2</sub>O<sub>3</sub>, solid state reaction study, IR and mag. props. 4-85301  
Ag (I) complexes, bis(N-methyl)-dithioformamidinium, IR spectra 4-66032  
Ag halide microcrystals, spectroscopic identification of localised electrons and holes 4-114308  
AgBr:Li<sup>+</sup>, Ir<sup>3+</sup> site geom. by Raman vibr. spectroscopy 4-80921  
Ag<sub>2</sub>CdI<sub>4</sub>, superionic conductor, Raman and far IR studies 4-109195  
Ag<sub>2</sub>HgI<sub>4</sub>, Raman and IR spectra, ionic cond. studies 4-99119  
AgI, chaotic attractors,  $\beta$ - $\alpha$  transition phenomena 4-61140  
AgSm(PO<sub>3</sub>)<sub>4</sub>, cryst. struct. and IR spectra 4-98249  
AlF<sub>3</sub> fluoride glass, optical props. 4-65189  
AlN sputtered films, polycryst. and amorphous, optical phonons, Raman studies 4-80179  
Al<sub>2</sub>O<sub>3</sub> films on Au, Al, and Si, vibr. props., IR refl. absorpt. spectroscopy study 4-71459  
Al<sub>2</sub>O<sub>3</sub> surface with adsorbed HCN, far IR Fourier spectroscopy 4-104593  
Al<sub>2</sub>O<sub>3</sub> thin film deposition by UV laser photolysis 4-99337  
Al<sub>2</sub>O<sub>3</sub>:Cr<sup>3+</sup>(V<sup>4+</sup>), phonons, far IR vol. generation and detection 4-61005  
Al<sub>2</sub>O<sub>3</sub>:nH<sub>2</sub>O thin films, ageing, elec. struct. and moisture response characts., sensor appls. 4-86393  
As, amorphous, optic vibr. modes, Raman, IR and inelastic neutron spectra 4-76461  
As-S amorphous system, vibr. props. and network topology 4-109178  
As<sub>4</sub>, low temp. phase states, IR spectra 4-61683  
(As<sub>2</sub>S<sub>3</sub>)<sub>x</sub>(AsI<sub>3</sub>)<sub>1-x</sub> glasses, Raman scatt., IR and depolarisation spectra 4-109182  
Au (I) complexes, bis(N-methyl)-dithioformamidinium, IR spectra 4-66032  
BN, films, interaction with Ni at high temps. 4-70583  
BaFCl(FBr)(OCl), far IR spectra 4-66047  
Ba(PO<sub>3</sub>)<sub>2</sub>-AlF<sub>3</sub>-LiF, elec. cond. rel. to struct., IR spectra studies 4-92771  
Ba<sub>0.9</sub>Sr<sub>0.1</sub>TiO<sub>3</sub>, soft mode behaviour, ferroelec. transition and IR reflectometry 4-80872  
BaTiO<sub>3</sub>, dispersive/order-disorder crossover, soft mode temp. depend., contrib. to low freq. permittivity 4-65369  
BaTiO<sub>3</sub> form by thermal decomposition of oxalate (Japanese) 4-76718  
BaTiO<sub>3</sub>:Fe, soft mode behaviour, ferroelec. transition and IR reflectometry 4-80872  
Bi oxides, sillenite phase form, mag., EPR and IR studies 4-88137  
Bi-Te system, struct. and band gap, X-ray and IR absorpt. obs. 4-104124  
Bi<sub>2</sub>Fe<sub>2</sub>O<sub>9</sub>, amorphous, mag., optical and resonant props. 4-104424  
Bi<sub>2</sub>Fe<sub>2</sub>O<sub>9</sub> glass, IR study 4-70381  
Bi<sub>2</sub>GeO<sub>9</sub> thin films, IR spectra and lattice phonons 4-88893  
Bi<sub>2</sub>SiO<sub>5</sub> thin films, IR spectra and lattice phonons 4-88893  
Bi<sub>2</sub>SiO<sub>5</sub>:Al, photocond., absorption spectra and TSC studies 4-65710  
Bi<sub>2</sub>Si<sub>2</sub>-Ti<sub>2</sub>O<sub>10</sub>, optical spectra, dispersion of optical rot. 4-104627  
C plasma deposited films, struct., IR spectra studies 4-98465  
C:H amorphous film prep. by H<sub>2</sub> gas reactive RF sputtering of graphite 4-76671  
CN adsorbed on Ag electrode, Fourier transform IR spectra studies 4-93067  
CO chemisorbed layer on Ni (100), vibr. spectroscopy by IR emission 4-98439  
CO, high coverage struct. on metal FCC (111) and HCP (0001) surfaces, LEED, HREELS and IR spectra study 4-65573

## infrared spectra of inorganic solids continued

- CO, solid, adsorption of multilayers on Cu (100), epitaxial growth of new  
cryst. struct., LEED, IR spectra 4-113373  
Ca<sub>2</sub>Cr<sub>2</sub>Si<sub>2</sub>O<sub>7</sub>, synthetic garnets, Cr coordination and vibr. props., IR  
study 4-65249  
CaF<sub>2</sub>, IR excitation of high-freq. phonons by multiphonon absorpt.  
4-61027  
CaF<sub>2</sub>-Sm crystal, gamma-irradiated, optical study 4-81015  
Ca<sub>3</sub>La<sub>2</sub>W<sub>2</sub>O<sub>12</sub>, rare earth, luminescence and sensitised emission 4-88871  
CaO-B<sub>2</sub>O<sub>3</sub>-Al<sub>2</sub>O<sub>3</sub>-Fe<sub>2</sub>O<sub>3</sub> glass system, photoacoustic spectra of Fe  
4-99130  
Ca<sub>2</sub>P<sub>2</sub>O<sub>7</sub>·2H<sub>2</sub>O, solid state, vibr., IR and Raman spectra 4-80922  
CaSeO<sub>4</sub>·2H<sub>2</sub>O, IR spectra, vibr. anal. 4-61702  
CdGa<sub>2</sub>S<sub>4</sub>, vibr. props., polarisation depend. IR reflectivity studies  
4-75624  
Cd<sub>2</sub>Hg<sub>1-x</sub>Te, phonon states, far IR absorpt. spectra study (Chinese)  
4-92312  
Cd(OH)<sub>2</sub>, brucite-like, struct. and IR relations 4-79996  
n-Cd<sub>3</sub>P<sub>2</sub> degenerate semicond. intrinsic phonon parameters 4-92317  
CdS, spectral-time characts. of nonlinear emission (Russian) 4-104620  
CdTe:In, Li, defect complex, IR absorption studies 4-80031  
Co complexes containing 2,2,3,4,4-pentamethylphosphonic acid, IR,  
Raman, UV and NMR spectra 4-79989  
Co II complexes, IR spectra, mag. susceptibility meas., antiferromag. inter-  
actions 4-80918  
Co-based heat resisting alloys, radiative and optical props. 4-74847  
Co<sub>2</sub>AlO<sub>4</sub> spinel, cryst. struct. and IR absorption bands 4-88145  
CoAs<sub>2</sub>, CoSb<sub>3</sub>, skutterudites, far IR refl. spectra, temp. depend.  
4-104595  
Co(II) complex with 1-phenyl-3,5-dimethylpyrazole, cond., electronic and  
IR spectra, mag. susceptibility meas. 4-76104  
Co(NH<sub>4</sub>)<sub>2</sub>(BeF<sub>4</sub>)<sub>2</sub>·6H<sub>2</sub>O, optical absorption spectrum 4-104588  
CoNbO<sub>5</sub>·6H<sub>2</sub>O, optical spectra obs. 4-71402  
Co<sub>2</sub>O<sub>3</sub>-based selective surfaces prep. by dip-coating process for solar  
absorber-converters 4-72172  
Co(OH)<sub>2</sub>, brucite-like, struct. and IR relations 4-79996  
Cr<sub>2</sub>O<sub>3</sub> plasma-sprayed deposits, IR Fourier transform specular reflection  
spectroscopy of surfaces 4-101942  
Cr<sub>2</sub>O<sub>3</sub>, mixed valence cpds., mag. and struct. studies 4-98071  
CrS<sub>2</sub>, optical props. and electronic struct. 4-80935  
CsCaCl<sub>3</sub>:Mn<sup>2+</sup>(N<sup>3+</sup>)(Co<sup>3+</sup>), fluoresc. emission, excitation, IR absorpt.  
spectra studies 4-99153  
Cs<sub>2</sub>NaSeCl<sub>6</sub>:Cr<sup>3+</sup> cryst., dopant fluoresc. props. 4-61745  
Cs<sub>2</sub>O-Na<sub>2</sub>O-5SiO<sub>2</sub> glass, vibr. spectra 4-109179  
Cu (I) complexes, bis(N-methyl)-dithioformamidine, IR spectra  
4-66032  
Cu II complexes, IR spectra, mag. susceptibility meas., antiferromag. inter-  
actions 4-80918  
Cu oxidised surface solar absorbers, thermal stability, AES and refl. meas.  
4-114951  
Cu-L-isoleucine complex, polycryst., IR absorpt. spectra, vibr. mode  
assignment 4-109173  
Cu-L-tryptophan complex, polycryst., IR absorpt. spectra, vibr. mode  
assignment 4-109173  
Cu<sub>1-x</sub>Cd<sub>x</sub>Fe<sub>2</sub>O<sub>4</sub>, IR absorption spectra and stretching bond interatomic  
vibrs. 4-80933  
Cu<sub>2</sub>Cd<sub>1-x</sub>, superionic conductor, Raman and far IR studies 4-109195  
CuCl, excitonic absorpt. edge, IR laser radiation induced electroabsorpt.  
4-61287  
p-CuGe<sub>2</sub>P<sub>3</sub>, optical lattice modes and IR reflectivity 4-88834  
Cu<sub>2</sub>Hg<sub>1-x</sub>, Raman and IR spectra, ionic cond. studies 4-99119  
Cu(II) complex with 1-phenyl-3,5-dimethylpyrazole, cond., electronic and  
IR spectra, mag. susceptibility meas. 4-76104  
Cu(II) complex with 1-phenyl-3,5-dimethylpyrazole, cond., electronic and  
IR spectra, mag. susceptibility meas. 4-76104  
n-CuInSe<sub>2</sub>, optical absorption edge, influence of carrier conc. 4-80943  
CuO-CaO-P<sub>2</sub>O<sub>5</sub> glass, IR spectra 4-76446  
Cu<sub>2</sub>O/CuO, selective surface optical props. and surface composition  
4-72170  
D<sub>2</sub>, solid, proton irradi., electron trapping, IR absorption studies 4-75751  
EuS, FIR dielec. energy loss function 4-84895  
Eu<sub>2</sub>TaO<sub>7</sub>, IR and Raman vibr. spectra 4-61679  
Fe catalyst for NH<sub>3</sub> synthesis, surface struct. and reactivity study  
4-80355  
Fe ferromagnetic, magneto-optic effect on thermal IR spectra, expt. study  
4-76442  
Fe spinels, Fe-M-O (M=Al, Cr, Zn, Co, Mn), vacancy substituted,  
order-disorder, IR absorpt. spectra (French) 4-76447  
Fe-based heat resisting alloys, radiative and optical props. 4-74847  
FeAs<sub>2</sub> films, organo-metal CVD growth from (CO)<sub>2</sub>Fe+AsH<sub>3</sub> on GaAs,  
optical gap and IR transmission 4-61868  
Fe<sub>2</sub>O<sub>3</sub>-NiO mixed oxides, phase anal., IR, mag. and X-ray diff. studies  
4-98243  
Fe(OH)<sub>2</sub>, brucite-like, struct. and IR relations 4-79996  
n-GaAs, electron irradiated, As anti-site defects, IR spectra and EPR  
4-84317  
GaAs, existence of B<sub>As</sub> impurity antisite centres, IR absorption lines study  
4-71413  
GaAs, far IR optical props. at 6, 300K, amplitude and phase refl. spectra  
4-104594  
GaAs, heavily implanted 4-104587  
GaAs, phonon frequencies 4-75626  
GaAs, semi-insulating, deep donor conc., dislocations and elec. resist.  
4-103781  
GaAs:C(Si), impurity and defect anal. by IR absorpt. spectra 4-75893  
GaAs:Cr, eval. of Cr conc. by optical absorpt. 4-104635  
GaAs:Cr, semi-insulating, inhomogeneities, optical obs. 4-60944  
GaAs:Cr-GaAs epitaxial junction, IR characterisation 4-109170  
GaAs:Si, localised vibr. mode IR absorpt. meas. 4-104599  
GaCrSe<sub>3</sub>, antiferromag. semicond., mag. susceptibility, cond., EPR, IR  
reflection spectrum, Neel temp., energy gap meas. 4-61522  
Ga<sub>2</sub>In<sub>1-x</sub>As<sub>2</sub>Sb<sub>1-x</sub>, epitaxial layers, reflection spectra analysis 4-114340  
Ga<sub>2</sub>In<sub>1-x</sub>Se, optical phonons, far-IR reflectivity spectra 4-104583  
Ga<sub>2</sub>O<sub>3</sub>-CaO glass, form. density, refr. index, crystn. temp., hardness, IR  
spectra 4-113635  
GaP, electron irradi., defect creation, luminescence and elec. studies  
(Chinese) 4-108441  
Ge, heavily implanted 4-104587  
Ge, hot hole submillimetre emission in transverse mag. field 4-71412  
Ge MIS struct., surface irregularity enhanced subband resonance  
4-61459

## infrared spectra of inorganic solids continued

- Ge:Be, site distortion of Be acceptor, IR spectra 4-92667  
a-Ge:H, photoinduced absorption spectra 4-109220  
GeS single crystal, reflectance and thermoreflectance studies 4-71356  
Ge<sub>2</sub>S<sub>3</sub>:Cu(Ag), glassy, doping effect on elec. and optical props. (Russian)  
4-98625  
Ge<sub>2</sub>S<sub>3-x</sub> glasses, short range order model, optical gap calc., IR band  
intensity 4-75310  
Ge(111)2X1, polarisation depend. of surface-state absorption, photother-  
mal displacement spectroscopy 4-92488  
H-bonded crystals, vibr. spectra, anharmonicity and reson. interaction  
effects 4-61684  
HBr, cryst., two-exciton spectra 4-104586  
HCl, cryst., two-exciton spectra 4-104586  
H<sub>2</sub>O, matrix isolated in D<sub>2</sub>O cubic ice, vibr. data 4-69045  
H<sub>2</sub>UO<sub>3</sub>:H-insertion cpd., unit cell const., IR spectra and X-ray diff.  
studies 4-84267  
HfS<sub>3</sub>, IR, Raman, and reson. Raman spectra, valence force field  
4-93077  
Hg<sub>2</sub>Br<sub>2</sub> single crystals, IR refl. spectra, optical const. and phonon  
parameters 4-88830  
Hg<sub>1-x</sub>Cd<sub>x</sub>Te, electric subbands in the limit E<sub>G</sub>→0, for IR reson. study  
4-104286  
Hg<sub>1-x</sub>Cd<sub>x</sub>Te, photogenerated carrier lifetime meas. by optical modulation  
of IR absorpt. (Chinese) 4-84953  
HgS mixed films, elec. and optical props. (French) 4-84715  
HoP<sub>2</sub>O<sub>7</sub> crystal, spectra and struct. (Chinese) 4-60887  
InGaAsP, MBE growth IR reflectivity, diode laser source/detector  
4-71391  
In<sub>2</sub>O<sub>3</sub>, ion plated, IR and optical study 4-62085  
InP, far IR optical props. at 6 and 300K 4-109174  
InSb, ion implanted layers, IR reflection spectra studies 4-61717  
InSb MIS struct., surface irregularity enhanced subband resonance  
4-61459  
InSb, refractive index at 1.5K in near mm wavelength region 4-104554  
In<sub>2</sub>Se<sub>3</sub> α- and γ-phases, Raman and IR spectra 4-109185  
In<sub>2</sub>-Sn<sub>2</sub>O<sub>3-y</sub> films, transparent and heat-reflecting, elec. and optical  
props., ionised impurity scatt. 4-66087  
In<sub>2</sub>-Sn<sub>2</sub>O<sub>3-y</sub> transparent and heat-reflecting films, optical props.  
4-114334  
K-Na alloys, Fermi edge singularity reduction 4-76415  
KBr, IR spectra, elec. field influence 4-99122  
KBr:Cr(CN)<sub>3</sub>, ESR, IR, Raman and emission spectra, radiative and  
nonradiative transition 4-65850  
KBr:NCO<sup>+</sup>, absorption band width of impurities ions, IR spectra anal.  
4-61737  
KCl:NCO<sup>+</sup>, absorption band width of impurities ions, IR spectra anal.  
4-61737  
KCl/Sn granular supercond., far IR absorption spectrum 4-76076  
K<sub>2</sub>Co<sub>2</sub>F<sub>6</sub>, F<sub>4</sub> spin waves, obs. in planar and oblique antiferromag.  
phases, Raman and far IR absorpt. spectra 4-98869  
K<sub>4</sub>Fe(CN)<sub>6</sub>·3H<sub>2</sub>O cryst., IR second-order spectrum of H<sub>2</sub>O 4-61680  
K<sub>4</sub>Fe(CN)<sub>6</sub>·3H<sub>2</sub>O, cryst. vibr., second order IR spectrum 4-65348  
KH<sub>2</sub>PO<sub>4</sub>, far IR reflectivity in 10 to 420K temp. range 4-76477  
KH<sub>2</sub>PO<sub>4</sub> single crystal, far IR reflectivity spectra 4-114257  
K<sup>+</sup>:Ag<sup>+</sup>, two elastic configurations at point defect, far IR spectra study  
4-61029  
KIO<sub>3</sub>:HIO<sub>3</sub> polymorphs, NQR, IR absorpt. spectra and thermograms rel.  
to cryst. struct. 4-60897  
K<sub>1-x</sub>Li<sub>x</sub>TaO<sub>4</sub>, IR reflectivity, two mode behaviour 4-71363  
K<sub>1-x</sub>Na<sub>x</sub>TaO<sub>4</sub>, IR reflectivity, two mode behaviour 4-71363  
KNbO<sub>3</sub>, dispersive/disorder-disorder crossover, soft mode temp. depend., con-  
trib. to low freq. permittivity 4-65369  
KNbO<sub>3</sub>, ferroelec. domain struct., IR spectra anal. 4-71323  
K<sub>2</sub>SeO<sub>4</sub>, Raman and far IR spectra, rel. to selenate radical movement at  
orthorhombic sites 4-76448  
K<sub>2</sub>ZnCl<sub>4</sub>, commensurate ferroelec. phase, phonon freq., permitt., IR refl.  
spectra 4-71387  
KZn<sub>1-x</sub>Co<sub>x</sub>F<sub>3</sub>, Fourier transform IR spectroscopy of Co<sup>2+</sup> excitations  
4-104596  
KZnF<sub>3</sub>:Fe<sup>3+</sup> crystal, EPR and far IR study on (FeF<sub>6</sub>)<sup>4-</sup> complex  
4-80814  
La<sub>2</sub>TaO<sub>7</sub>, IR and Raman vibr. spectra 4-61679  
Li/SO<sub>2</sub> cell, Li<sub>2</sub>S<sub>2</sub>O<sub>4</sub> discharge product, spectroscopic studies 4-89387  
Li/SO<sub>2</sub> cells, discharge capacity at high current and temp., chem. reac-  
tions 4-66679  
LiF, single cryst., IR transmission spectra at 300K, effect of stepped creep  
on exhaustion of dislocations 4-65271  
Li<sub>2</sub>GeO<sub>3</sub> pyroelec. material, vibr. spectra and polariton dispersion  
4-71362  
β-LiIO<sub>3</sub>, IR absorption and Raman spectra at low temps. 4-71361  
LiIO<sub>3</sub>-HIO<sub>3</sub> system, influence of growth conditions on optical props.  
4-76430  
LiNbO<sub>3</sub>, electron irradi., point defects, ESR and IR spectra studies  
4-70139  
LiNbO<sub>3</sub>, ferroelec., band struct. and optical props. in fundamental absorp-  
tion region 4-75845  
LiNbO<sub>3</sub>, Li<sup>+</sup> ionic cond., activation energy and IR spectra 4-84453  
LiNbO<sub>3</sub>, single cryst., near-normal reflectivity and absorpt. spectra  
4-93083  
LiNbO<sub>3</sub>:Cu<sup>2+</sup>, EPR and optical absorption spectra, Jahn-Teller effects  
4-71166  
Li<sub>2</sub>O, optical mode frequencies, IR reflectivity, Raman spectra 4-104617  
LiSM(PO<sub>3</sub>)<sub>2</sub>, cryst. struct. and IR spectra 4-98249  
LiTaO<sub>3</sub>, ferroelec., band struct. and optical props. in fundamental absorp-  
tion region 4-75845  
LiTaO<sub>3</sub>, single cryst., near-normal reflectivity and absorpt. spectra  
4-93083  
MgCaSiO<sub>4</sub>, vibr., force const., isotope shift, IR and Raman obs.  
4-61705  
MgO (001), IR optical const., EELS meas. 4-71337  
MgO microcrystals, electromagnetic surface modes, optical response  
4-98543  
MgO, vacancies and multiphonon IR-absorpt. spectra (Russian) 4-71420  
Mg(OH)<sub>2</sub>, brucite-like, struct. and IR relations 4-79996  
Mn dihalides, d-excitons, vibr. struct., IR and Raman spectra studies  
4-113873  
Mn(OH)<sub>2</sub>, brucite-like, struct. and IR relations 4-79996  
Mo catalysts supported on Al<sub>2</sub>O<sub>3</sub> or SiO<sub>2</sub>, Fourier transform IR spectro-  
scopy of sulphidation 4-105014  
Mo complexes, solid state IR and Raman spectra, vibr. anal. 4-76468

# ared spectra of inorganic solids continued

- MoPO<sub>3</sub>, vibr. spectra, IR and Raman spectra 4-76457  
 MoS<sub>3</sub>, prep. by solid state reaction, characts. 4-61838  
 Mo(V) hydroxides, IR study 4-61678  
 Ni, solid, NH<sub>3</sub> rotation, FTIR study 4-79964  
 Ni(D<sub>2</sub>H<sub>1-2</sub>)(D<sub>2</sub>H<sub>1-2</sub>)<sub>2</sub>PO<sub>4</sub>, dielectric and electro-optical props. meas. 4-76313  
 (ND<sub>2</sub>)<sub>2</sub>D<sub>2</sub>O, IR spectra and phase transitions between 100 and 15K 4-114258  
 (ND<sub>2</sub>)<sub>2</sub>H<sub>2</sub>O, IR spectra and phase transitions between 100 and 15K 4-114258  
 (NH<sub>4</sub>HCO<sub>3</sub>), relations between crystallographic characts. and cryst. struct. (Chinese) 4-75378  
 (NH<sub>4</sub>)<sub>2</sub>D<sub>2</sub>O, IR spectra and phase transitions between 100 and 15K 4-114258  
 (NH<sub>4</sub>)<sub>2</sub>H<sub>2</sub>O, IR spectra and phase transitions between 100 and 15K 4-114258  
 NH<sub>3</sub>·2H<sub>2</sub>O, X-ray diffr., IR spectra 4-109175  
 Na<sub>2</sub>CO<sub>3</sub>, incommensurate struct., Raman and far IR spectroscopy study 4-76449  
 NaCl, two-beam interferometer for dispersive refl. spectroscopy of solids in far IR 4-106405  
 NaClO<sub>3</sub>, radiative surface phonon-polariton dispersion, ATR studies 4-80514  
 Na<sub>2</sub>O-CaO-SiO<sub>2</sub>, γ radiation colouring in 600-1000 nm region 4-80948  
 Na<sub>2</sub>O-CaO-SiO<sub>2</sub>, interaction with chloride melts, including MgCl<sub>2</sub> or ZnCl<sub>2</sub>, IR spectroscopic study 4-80949  
 Na<sub>2</sub>O-CaO-SiO<sub>2</sub>-Si<sub>3</sub>N<sub>4</sub> glass, prep., Fourier transform IR spectra, XPS 4-84192  
 Na<sub>2</sub>O-MgO-SiO<sub>2</sub>, interaction with chloride melts, including MgCl<sub>2</sub> or ZnCl<sub>2</sub>, IR spectroscopic study 4-80949  
 Na<sub>2</sub>O-SiO<sub>2</sub>, interaction with chloride melts, including MgCl<sub>2</sub> or ZnCl<sub>2</sub>, IR spectroscopic study 4-80949  
 Na<sub>2</sub>O-SiO<sub>2</sub>, glass, nature of dissolved water, effect on phys. props. 4-109180  
 NaSm(PO<sub>3</sub>)<sub>3</sub>, cryst. struct. and IR spectra 4-98249  
 Na<sub>2</sub>WO<sub>4</sub>, films, optical absorption spectra, electrochromic cell appls. 4-76544  
 Nb-S<sub>2</sub> (2H), superconducting energy gap, far-IR transmission spectra 4-104340  
 β-NbPO<sub>5</sub>, IR and Raman spectra, cryst. struct. 4-61669  
 NbPO<sub>5</sub>, vibr. spectra, IR and Raman spectra 4-76457  
 NbSe<sub>2</sub> (2H) superconducting energy gap, far-IR transmission spectra 4-104340  
 Nd<sub>2</sub>Si<sub>2</sub>O<sub>7</sub>N<sub>4</sub>, IR and neutron diffr. study 4-61682  
 Nd<sub>2</sub>Si<sub>2</sub>O<sub>7</sub>N<sub>4</sub>, IR and neutron diffr. study 4-61682  
 Nd<sub>2</sub>TaO<sub>7</sub>, IR and Raman vibr. spectra 4-61679  
 Ni-based heat resisting alloys, radiative and optical props. 4-74847  
 Ni-P amorphous electrodeposits, IR reflectivity spectra 4-93078  
 Ni(II) complex with 1-phenyl-3,5-dimethylpyrazole, cond., electronic and IR spectra, mag. susceptibility meas. 4-76104  
 Ni<sub>2</sub>NbBO<sub>6</sub>, polarised absorpt. spectra of Ni<sup>2+</sup> ion 4-93085  
 Ni(OH)<sub>2</sub>, brucite-like, struct. and IR relations 4-79996  
 NiTeMoO<sub>6</sub>, mag. props. and electronic reflectance spectra 4-76106  
 Np(BH<sub>4</sub>)<sub>3</sub>, in Zr(BD<sub>4</sub>)<sub>3</sub>, D isotope effects, mag. props., optical and EPR spectra 4-88718  
 O<sub>2</sub>, solid α-phase, far IR spectra in high mag. fields, magnons 4-114260  
 PD electrode of CO, IR refl. spectrosc. obs. 4-107348  
 PLZT ceramics, ion implanted, optical absorption 4-114233  
 P<sub>2</sub>Se<sub>3-x</sub> glasses, struct., conc. depend. of short- and intermediate-range order 4-113342  
 PbF<sub>2</sub>-MnF<sub>2</sub>-GaF<sub>3</sub>, fluoride glasses, vibrational spectroscopy 4-114261  
 Pb<sub>1-x</sub>Hg<sub>x</sub>Se flash-evaporated films, optical and elec. props. 4-114335  
 Pb<sub>1-x</sub>Hg<sub>x</sub>Te films, optical energy gap, composition dependence 4-76541  
 Pb<sub>0.67</sub>Nb<sub>1.77</sub>Zn<sub>0.23</sub>O<sub>6.66</sub>, crystal structure 4-103727  
 nPbO-Nb<sub>2</sub>O<sub>5</sub> (Ta<sub>2</sub>O<sub>5</sub>), (1.5 ≤ x ≤ 2.5), vibr., IR and Raman study (French) 4-66034  
 Pb<sub>1-x</sub>Sn<sub>x</sub>Te system, plasma oscill. freq., temp. depend. 4-88836  
 Pb<sub>1-x</sub>Sn<sub>x</sub>Te in epitaxial films, optical absorption spectra and photoconductivity 4-65711  
 Pb<sub>1-x</sub>Sn<sub>x</sub>Te in epitaxial layers, optical absorption studies 4-71456  
 Pt II complexes, bis(acetonitrile)dichloroplatinum II, mol. and cryst. struct., vibr., IR and Raman study 4-103708  
 β-PtO<sub>2</sub>, new high-pressure form 4-70081  
 R<sub>2</sub>BO<sub>4</sub> (R=La, Pr, Nd, Sm, Gd; B=Fe, Al, Co, Cu), vibr., IR spectra 4-84964  
 R<sub>2</sub>BO<sub>4</sub> (R=La, Pr, Nd, Sm, Gd; B=Fe, Al, Co, Cu), vibr., IR spectra 4-84964  
 Rb<sub>2</sub>MnCl<sub>4</sub>, two-dimensional antiferromagnet, IR absorpt., Raman spectra, MCD studies 4-61713  
 Rb<sub>2</sub>Mn<sub>2</sub>Cl<sub>7</sub>, two-dimensional antiferromagnet, IR absorpt., Raman spectra, MCD studies 4-61713  
 Ru catalyst for NH<sub>3</sub> synthesis, surface struct. and reactivity study 4-80355  
 SbCl<sub>3</sub><sup>n</sup>, in cryst. lattice, intervalence absorpt., IR study 4-61734  
 Sb<sub>2</sub>Te<sub>3</sub> single cryst., band struct. and scatt. mechanisms, IR transmission studies 4-80934  
 Se, orthorhombic mol. crystal, IR and Raman studies 4-98062  
 Si (100) 2×1, dissociative adsorption of water, IR spectra obs. 4-93557  
 Si (110), electron subband reson., IR reson. absorpt. 4-61431  
 Si (111) face, thermally agitated electrons, IR reflection obs. 4-93082  
 Si, amorphous, from ion implantation, refractive index, thermal annealing effect 4-76417  
 Si, chemisorption of water on (100), water mol. dissoci., IR spectra study 4-62233  
 Si crystals, Czochralski pulled, O precipitation, diffusion mechanism, etching optical and neutron scatt. obs. 4-65209  
 Si, far IR transmission spectrum, two-phonon difference band obs. 4-104597  
 a-Si film, elastic and inelastic props. 4-88225  
 Si, heavily implanted 4-104587  
 Si, IR radiation absorption from CO<sub>2</sub> laser 4-71367  
 Si, IR spectroscopy characterisation 4-99136  
 Si, implantation doped, elec. and struct. characterisation by IR refl. 4-76476  
 Si, implanted oxides, annealing, activation energy 4-75490  
 n-Si, inversion layers in MOSFET, phonon limited hot-electron temp. 4-70945  
 a-Si, ion implantation form. and optical state characterisation 4-88186  
 Si, low energy implantation of N<sub>2</sub> and NH<sub>3</sub>, Si<sub>3</sub>N<sub>4</sub> formation study 4-75484

# infrared spectra of inorganic solids continued

- Si MIS struct., surface irregularity enhanced subband resonance 4-61459  
 Si MOS structures, intersubband hole reson. and interaction with two-dimens. plasmons 4-104320  
 Si microcrystalline films, structure changes on deposition 4-61247  
 Si on insulators, CVD single crystal characterisation, heteroepitaxy and epitaxial lateral overgrowth 4-70589  
 n<sup>+</sup>-Si, surface plasmon polaritons, IR studies 4-108788  
 Si wafers, impurity characterisation using IR spectra meas. 4-113486  
 Si:Ga, neutron irradi., acceptor level, IR absorpt. spectrum 4-93089  
 Si:H, amorphous, high-rate deposited annealing effects 4-61876  
 a-Si:H, IR absorpt., gaseous H<sub>2</sub> and Si-H overtone spectra 4-93075  
 Si:H, lattice state and behaviour of H impurity 4-61095  
 Si:H, microcrystalline, IR absorpt. study of Si-H bond formation 4-71416  
 n-Si:H, neutron irradiated, deep levels study (Chinese) 4-92649  
 a-Si:H, photoinduced absorption spectra 4-109220  
 a-Si:H, prep. by glow discharge of Si<sub>2</sub>H<sub>6</sub>, optical and elec. props. 4-114237  
 a-Si:H,Cl films glow discharge deposition from SiCl<sub>4</sub>-SiH<sub>4</sub> mixtures, elec. and optical characts. 4-71580  
 a-Si:H,P(B), ESR and optical props., thickness depend. 4-84853  
 Si:H (100)2×1, surface IR studies 4-99116  
 a-Si:H films, reactive sputtering, elec. and optical props. 4-104203  
 a-Si:H thin films, glow discharge effects on electronic and optical props. 4-75977  
 a-Si:H(D) thin films, coupled local mode vibr., IR absorpt. study 4-88259  
 Si:Li and Si:Li, C, electron irradi., luminesc. decay time, absorpt., isotope splitting, and Zeeman meas. 4-71434  
 Si:N, ion implanted, optical props. (Chinese) 4-114306  
 Si(N/O), microdefect formation during single crystal growth, influence of impurities on nucleation 4-114386  
 SiO, impurity conc. meas. using IR spectra, multiple reflection effects 4-113487  
 SiO, P, thermal donors, optical absorption spectra studies 4-65637  
 SiO, rare earth atoms, impurity interaction and donor accumulation 4-103783  
 a-SiO<sub>2</sub>H CVD films, struct. model 4-88427  
 SiO<sub>2</sub> cryst., minority carrier lifetime, O precipitation effects, IR studies 4-113971  
 SiO<sub>2</sub> impurity conc., IR absorption studies 4-113488  
 Si:P, IR absorption spectrum 4-71414  
 Si-electrolyte interface, elec. field modulated IR internal reflection studies 4-98749  
 SiC:H amorphous films, plasma deposition from SiH<sub>4</sub>+methane (ethylene), IR anal. 4-114410  
 Si<sub>1-x</sub>Ge<sub>x</sub>:H amorphous films, planar magnetron sputtered, optical and elec. props. 4-98671  
 Si<sub>1-x</sub>Ge<sub>x</sub>:H amorphous planar magnetron sputtered films, elec. and optical props. (Japanese) 4-99312  
 (SiH<sub>2</sub>)<sub>n</sub> films, thermal dehydrogenation, IR spectra study 4-99781  
 Si<sub>3</sub>N<sub>4</sub> amorphous films, impurities, IR investig. 4-80913  
 Si<sub>3</sub>N<sub>4</sub> films, amorphous, hydrogenated and deuterated, prepared from plasma-enhanced CVD, IR absorpt. spectra 4-81021  
 Si<sub>3</sub>N<sub>4</sub> thin film deposition by UV laser photolysis 4-99337  
 SiO<sub>2</sub> amorphous thin films, optical absorpt. edge 4-81023  
 SiO<sub>2</sub> film, low temp. photochemical deposition 4-99339  
 SiO<sub>2</sub> film, O<sub>2</sub> plasma anodised, IR absorpt. bands (Chinese) 4-109263  
 SiO<sub>2</sub> film, photo-induced CVD using direct excitation by D<sub>2</sub> lamp 4-61860  
 SiO<sub>2</sub> films, IR transmission spectra, nitridation effects 4-81022  
 SiO<sub>2</sub>, fused, subsurface Al films, ion beam mixing, IR reflection study 4-88189  
 SiO<sub>2</sub>, pyrogenic, chemisorpt. of Cr<sub>2</sub>OCl<sub>2</sub>, IR spectrosc. investig. 4-109196  
 SiO<sub>2</sub> surface with adsorbed HCN, far IR Fourier spectroscopy 4-104593  
 SiO<sub>2</sub> thin film deposition by UV laser photolysis 4-99337  
 SiO<sub>2</sub>, vitreous, defects of broken-bond type 4-92097  
 SiO<sub>2</sub>:GeO<sub>2</sub> multimode fibres, H<sub>2</sub> effects on IR absorpt. characts. 4-97106  
 SiO<sub>2</sub>:OH, fused flame prod., for windows, D<sub>2</sub> treatment effect on optical props. 4-74636  
 SiO<sub>2</sub>-B<sub>2</sub>O<sub>3</sub> glasses, sol-gel-processing, vibrations, optical study 4-70038  
 5SiO<sub>2</sub>-M<sub>2</sub>O glass, (M=Li, Na, K, Rb, Cs), vibr. spectra 4-109179  
 SiO<sub>2</sub>-Na<sub>2</sub>O-Fe<sub>2</sub>O<sub>3</sub> glasses, radiation damage, EPR spectra 4-84200  
 SiO<sub>2</sub> films, IR absorpt. spectra meas. 4-88895  
 SiSe<sub>2</sub>, cryst. and glassy, vibr. studies 4-109191  
 Si-H bonds and H-induced defects study 4-66058  
 Sn complexes, solid state configurations, cond. behaviour in nonaqueous solvents 4-76466  
 SnO<sub>2</sub> adsorpt. of CO<sub>2</sub>, IR investigation 4-104603  
 SnO<sub>2</sub>-PdO, adsorpt. of CO<sub>2</sub>, IR investigation 4-104603  
 SnO<sub>2</sub>-SiO<sub>2</sub>, adsorpt. of CO<sub>2</sub>, IR investigation 4-104603  
 Sn<sub>2</sub>P<sub>2</sub>S<sub>6</sub>, low freq. lattice vibr. in IR spectra 4-71389  
 Sn<sub>2</sub>P<sub>2</sub>S<sub>6</sub>(Se<sub>2</sub>), IR spectra of ferroelectric transition splitting 4-84966  
 β-TaPO<sub>4</sub>, IR and Raman spectra, cryst. struct. 4-61669  
 Te, neutron irradi. induced defects, optical props. near fundamental energy gap 4-84318  
 Te<sub>2</sub>O<sub>3</sub> film, stoichiometry changes, IR study 4-113836  
 ThBr<sub>4</sub>·Pa<sup>4+</sup>, incommensurate phase, single cryst., Pa<sup>4+</sup> optical spectroscopy 4-71422  
 Ti complexes, solid state configurations, cond. behaviour in nonaqueous solvents 4-76466  
 βTiCl<sub>3</sub>, IR and Raman spectra, vibr., normal coordinate anal. 4-114276  
 TiO<sub>2</sub>, polymorphic transform. by mech. grinding 4-66328  
 TiO<sub>2</sub>, vacancies and multiphonon IR-absorpt. spectra (Russian) 4-71420  
 Ti ternary chalcogenides, cryst. struct., X-ray, IR and photoacoustic studies 4-84273  
 Ti-based quaternary chalcogenide 4-84270  
 TiBiTe<sub>2</sub>, growth, elec. and optical props. 4-65676  
 TiBiTe<sub>2</sub> single cryst., IR reflectivity plasma spectra 4-99118  
 TiCl(Br), phonons, far IR vol. generation and detection 4-61005  
 TmAsO<sub>4</sub>, optical and mag. studies of lowest levels 4-88831  
 U(BD<sub>4</sub>)<sub>3</sub>, in Hf(BD<sub>4</sub>)<sub>3</sub>, host cryst., mag. susceptibility, visible and IR obs. 4-88820  
 UO<sub>2</sub>, charact. of oxides formed by reaction with water IR and sorption anal. 4-74012  
 V fluorooxoperoxo complexes, elemental anal., IR and Raman spectra and X-ray powder patterns 4-79988  
 VMOO<sub>3</sub>, vibr. spectra and normal coord. anal. 4-104618

## infrared spectra of inorganic solids continued

- VO<sub>2</sub> thin films, optical props. and preparation 4-88891  
 V<sub>2</sub>O<sub>5</sub> amorphous thin films, props., influence of quenching rate 4-108956  
 V<sub>2</sub>O<sub>5</sub>-B<sub>2</sub>O<sub>3</sub> glass, struct., IR spectra and elec. cond. 4-88107  
 V<sub>2</sub>O<sub>5</sub>-B<sub>2</sub>O<sub>3</sub> glasses, struct. study, IR spectra anal. 4-84961  
 V<sub>2</sub>O<sub>5</sub>-P<sub>2</sub>O<sub>5</sub> and V<sub>2</sub>O<sub>5</sub>-P<sub>2</sub>O<sub>5</sub>-TeO<sub>2</sub> glasses, IR absorpt. and struct. investig. 4-61670  
 V<sub>2</sub>O<sub>5</sub>-As<sub>2</sub>O<sub>3</sub> glasses, IR study 4-104614  
 VPO, vibr. spectra and normal coord. anal. 4-104618  
 VSO, vibr. spectra and normal coord. anal. 4-104618  
 W interaction with Al<sub>2</sub>O<sub>3</sub> and Cr<sub>2</sub>O<sub>3</sub> thin films 4-70576  
 YIG:Bi epitaxial films, refr. index and optical absorption spectra at UV to near IR wavelengths 4-104553  
 YPO<sub>2</sub>·2H<sub>2</sub>O, IR spectra, vibr. anal. 4-61702  
 Yb(C<sub>2</sub>H<sub>3</sub>SO<sub>4</sub>)<sub>9</sub>H<sub>2</sub>O, cooperative absorpt. lines existence for Yb-(OH, OD) pairs, absolute oscil. strengths 4-71370  
 YbCl<sub>6</sub>·6H<sub>2</sub>O, cooperative absorpt. lines existence for Yb-(OH, OD) pairs, absolute oscil. strengths 4-71370  
 Yb(OH<sub>2</sub>), cooperative absorpt. lines existence for Yb-(OH, OD) pairs, absolute oscil. strengths 4-71370  
 Yb(OOH), cooperative absorpt. lines existence for Yb-(OH, OD) pairs, absolute oscil. strengths 4-71370  
 Zn<sub>3</sub>As<sub>2</sub>, optical constants and band transitions 4-80898  
 ZnF<sub>2</sub> fluoride glass, optical props. 4-65189  
 ZnF<sub>2</sub> two-photon absorpt. spectral depend. 4-99123  
 ZnF<sub>2</sub> optical constants and band transitions 4-80898  
 ZnS, CVD, vacancy-hydride complex, optical absorpt., photoluminesc. 4-60916  
 ZnSe, mechanically polished, oxidation on heating in air 4-62076  
 ZnSe, thin film, optical properties in the wavelength range 400 to 1500 nm 4-114336  
 ZrF-BaF<sub>2</sub> multispectral glass development and characteristics 4-74639  
 ZrF<sub>4</sub> fluoride glass, optical props. 4-65189  
 Zr(MoO<sub>4</sub>)<sub>2</sub>, polymorphism, X-ray diffr. and vibr. spectroscopy study 4-70053  
 ZrO<sub>2</sub> thin layers, struct., IR spectrosc. obs. 4-76459  
 ZrO<sub>2</sub>-P<sub>2</sub>O<sub>5</sub> system, re-examination of crystalline phases 4-84258

## infrared spectra of organic molecules and substances

- see also molecular rotation  
 acetamide, far IR transmission spectrum, lattice dynamics, temp. 4-104598  
 acetanilide, IR and Raman spectrum, vibr. assignments 4-91260  
 acetone, IR spectra, temp. and press. effects 4-61699  
 acetone adsorbed on (Ru<sub>3</sub>Si<sub>11</sub>)O<sub>2</sub> surface, FT-IR study of surface acid sites 4-113783  
 acetonitrile, IR spectra, temp. and press. effects 4-61699  
 acetonitrile, liq., ultra-fine far IR struct., barrier crossing theory 4-109187  
 acetonitrile-HCN mixtures in solid Ar, far IR spectra, intramol. vibrs. 4-87112  
 acetylene,  $\nu_4 + \nu_5$  band high-resolution line-intensity meas. using diode-laser spectrometer 4-111221  
 acetylene dimer, predissoc. lifetime, sub-Doppler resolution IR spectroscopy study 4-78919  
 acetylene-1(I<sub>2</sub>), Ar matrix isolated, fine struct., IR and UV spectra 4-74231  
 4-acyl-3-methyl-1-phenylpyrazol-5-ones in chloroform, IR, <sup>1</sup>H and <sup>13</sup>C NMR spectra 4-74242  
 1-adamantanamine hemiperchlorate, IR spectra, (NHN)<sup>+</sup> bridges, temp. and isotope effects 4-61701  
 adsorbed layers on metal surfaces, survey of vibr. spectroscopic methods 4-104065  
 adsorption of organic compounds on synthetic diamond powders, IR spectroscopy (Russian) 4-75791  
 alcohol dehydrogenase, horse liver, CoII substituted, complexes, active sites PMR study 4-102836  
 alcohols, aliphatic, OH oscillators, fourth overtone IR spectra 4-112166  
 aliphatic N bases, far IR continua caused by large polarisabilities of intramol. NLi<sup>+</sup>...N=...Li<sup>+</sup>N bonds 4-107346  
 allene-d<sub>6</sub>, C=C stretching band  $\nu_6$  4-64468  
 amine-HCl, H bonded complex, matrix isolation IR vibr. spectra 4-96544  
 L-amino acids and related mols., FIR FT spectra 4-96531  
 2-amino-4,6-dichloropyrimidine, vibr., IR absorpt. spectra 4-87109  
 p-aminoacetanilide, IR and Raman spectrum, vibr. assignments 4-91260  
 5-aminoindole, vibr. fundamentals, IR and UV absorpt. spectra 4-102679  
 aromatic cpds., room temp. phosphoresc., phosphor d solid supports interaction 4-78887  
 aromatic N bases, far IR continua caused by large polarisabilities of intramol. NLi<sup>+</sup>...N=...Li<sup>+</sup>N bonds 4-107346  
 N,N'-aryllalkyl thioureas, conformation anal. <sup>1</sup>H-NMR and IR spectra 4-112178  
 azidomethane in N<sub>2</sub> matrices, UV photolysis, IR spectra 4-59758  
 3-azidopropene in N<sub>2</sub> matrices, UV photolysis, IR spectra 4-59758  
 azole derivatives, H bonded complex form. with nitrophenols, IR and UV investig. 4-66562  
 azulene, vibr. excited in its electronic ground state, energy transfer study 4-59880  
 azulene, vibrationally excited, temp. depend. energy transfer, IR fluoresc. 4-83453  
 bacterial cells, intact and living ultrastructural information from FTIR 4-100094  
 benzanilide, vibr. spectra, amide and thioamide bands 4-59772  
 benzene, CH overtones, low temp. IR spectra 4-74239  
 benzene, frozen, ion implantation, polymer films production, IR spectra study 4-65281  
 benzene-d<sub>6</sub>(d<sub>6</sub>), highly excited overtones, classical dynamics 4-102664  
 benzene-d<sub>6</sub>(d<sub>6</sub>), intramolecular vibr. relax., IR overtone spectra 4-102663  
 3,1-benzoxazines, substituted, tautomerism, UV, IR and mass spectrosc. obs. 4-64487  
 benzoyl peroxides, substituent effect on spectral structural charact., IR vibr. spectra 4-78848  
 betaine hydrate, H bonding, IR spectra 4-87119  
 betaine hydrofluoride, H bonding, IR spectra 4-87119  
 2,3'-bipyridyl-I charge transfer complex, vibr., IR spectra 4-64476  
 2,4-[2-bisbenzoxazolyl]pyridine, solvent effects, IR absorpt. spectra 4-59736  
 block copolymers of styrene and vinyltrimethyl silane, optical and mech. props. (Russian) 4-81227  
 p-bromoacetanilide, IR and Raman spectrum, vibr. assignments 4-91260  
 infrared spectra of organic molecules and substances continued  
 bromobenzene ion, IR fluoresc. relax., two-pulse photodissoc. 4-102734  
 5-bromindole, IR vibr. spectra 4-96536  
 bromotrifluoromethane, collision-free IR multiphoton absorpt., thermal effects 4-74234  
 bromotrifluoromethane, IR and Raman spectra, cryst. struct. 4-104690  
 1,3-butadiene, adsorbed on silica surface, Fourier transform IR spectra 4-78843  
 t-butanol, cryst., torsion band, IR obs. 4-61691  
 t-butyl cyanide, IR spectra, temp. and press. effects 4-61699  
 calcium oxalate, pyrolysis, rate const., IR spectra 4-114794  
 carbazole:trinitrobenzene, piezoelec. charge transfer complex, phase transition obs. 4-70364  
 carbazole derivatives, 1-substituted, spectrochem. props. 4-64540  
 3-(carboethoxy)carbazole, spectrochem. props. 4-112227  
 carboxydrates, aq. solns., mutarotation FT IR spectrosc. investig. 4-78833  
 carbon tetrachloride, in Kr matrix, orientational ordering, site struct., IR spectra 4-64459  
 carbon tetrachloride, IR laser stimulated desorpt. from Ge substrate, time of flight distrib. 4-61203  
 cellulose, struct. low freq. vibr. Raman and IR study 4-80924  
 cellulose acetates, struct. low freq. vibr. Raman and IR study 4-80924  
 4-chloro-2,6-diaminopyrimidine, vibr., IR absorpt. spectra 4-87109  
 5-chloro-2-oxo-1,3,2-dioxathianes, twist conformations, IR, PMR and X-ray diffr. 4-83377  
 chlorobenzene, optical const., IR transmission and ATR spectra (German) 4-84965  
 chloroform, C-H stretching, IR intensity, solvent effect 4-69077  
 5-chloroindole, vibr. fundamentals, IR and UV absorpt. spectra 4-102679  
 N-chloroisocyanid dichloride, gas, liq. and solid, vib. force const., IR and Raman obs. 4-59739  
 chlorotrifluoromethane, IR diode laser spectra of  $\nu_1$  band 4-64464  
 cholesteric solutions circular dichroism in IR spectra 4-88806  
 choline hydroxide, cryst., H bonding, IR study 4-114263  
 coal, IR microspectroscopy, specimen prep. technique, computer-controlled microspectrophotometer 4-93572  
 cobalt acetate dihydrate, protiated and deuterated, IR spectra, H-bonds 4-61703  
 coronene, IR spectrum rel. to identification of 'unidentified' IR emission features 4-115790  
 crotonates, mol. dynamics using IR band shapes 4-65159  
 cubane, force const., vibr., IR and Raman spectra, HF level calcs. 4-59694  
 (cyano)phthalocyaninatometal bridged macrocyclic metal complexes, synthesis and conductivity 4-75948  
 3-cyanobenzaldehyde, IR and electronic absorpt. spectra 4-107340  
 3-cyanocarbazole, spectrochem. props. 4-112227  
 (cyanomethyl)cyclopropane, vibr. spectra and conformational behaviour 4-104610  
 cyclobutane, mol. struct., electron diffr. and spectrosc. obs. 4-59893  
 cyclohexane, liq., dielec. loss in millimetre and submillimetre wavelength region 4-99015  
 cyclohexane, shock wave diagnostics by Raman and IR meas. 4-109712  
 cyclohexane-1-d<sub>1</sub> isomers, IR and Raman spectra, vibr. anal., ab initio HF calcs. 4-59770  
 cyclohexanol, cryst., torsion band, IR obs. 4-61691  
 cyclohexadienyl thorium(IV) and uranium(IV) chlorides and uranium(IV) N-thiocyanates, complexes with neutral donor ligands 4-76454  
 cyclopentanol, cryst., torsion band, IR obs. 4-61691  
 2-cyclopenten-1-one, liq. and solid state, ring puckering, IR and Raman spectra, vibr. study 4-59747  
 cyclopentyl silanes and germanes, IR spectra, isolated SiH and GeH stretching freq., bond strength 4-112179  
 cyclopropane, jet-cooled, IR laser spectrosc. 4-83373  
 cyclopropane-1,1-d<sub>2</sub> and cyclopropane-1,1,2,2-d<sub>4</sub> IR and Raman spectra, splitting patterns, vibr. modes 4-66029  
 cyclopropane-d<sub>3</sub>(d<sub>3</sub>), lattice vibr. spectra and intermol. forces 4-71371  
 cyclopropyl silanes and germanes, IR spectra, isolated SiH and GeH stretching freq., bond strength 4-112179  
 cyclopropylmethyl ketone, IR and Raman spectra, vibr. anal. and conformational stability 4-69079  
 cyclopropylsilane, silyl group internal rot. barrier, combination band spectra obs. 4-59744  
 cytosine and derivatives, matrix isolation, IR spectra 4-87104  
 cytosine and isocytosine methyl derivatives isolated in N<sub>2</sub> matrix, IR spectra 4-62442  
 cytosine in Ar matrix, IR spectra, mol. struct., force const. 4-69080  
 di(methyl ammonium)Sb<sub>2</sub>Sn<sub>1-x</sub>Cl<sub>6</sub>, SbCl<sub>6</sub><sup>3-</sup> intervalence absorpt. band 4-61734  
 diacyl phosphatidylcholines, ice melting induced phase transition 4-61676  
 1,4-diaminoanthraquinone, electronic spectrum, anal. of vibr. struct. 4-83368  
 diazine,  $\nu_7$  fundamental, rovibrational anal., mid IR spectra 4-59753  
 2,4-dibromomethylenecyclopropane, B=C double bond, ab initio SCF calcs. 4-112094  
 dibutyl tin-semicarbazole (thiosemicarbazole) complex, struct., spectrosc. investig. 4-96714  
 2,6-dichloro-4-nitrophenol, vibr. anal., IR, far-IR and laser Raman spectra 4-91259  
 2,4-dichloro-6-nitrophenol, vibr. anal., IR, far-IR and laser Raman spectra 4-91259  
 1,2-dichloroethane, internal rot. angle, IR study, press. effects on conformations 4-107347  
 trans-dichloroethylene-d<sub>2</sub>(d<sub>2</sub>), IR gas-phase vibr. intensity meas., polar tensors and effective charges 4-69073  
 $\alpha,\alpha$ -dicyclohexyl-cyclohexanemethanol, infrared and Raman investigations 4-93074  
 diethyl ether, energy partitioning to product translation in IR multiphoton dissociation 4-62214  
 diethylamine, gaseous, overtone absorpt. spectra, conformationally non-equivalent C-H and N-H local mode oscillators 4-96528  
 4,4'-difluorobiphenyl, vibrational spectra, IR and Raman studies 4-112624  
 difluorocarbene,  $\nu_3$  band, IR diode laser spectroscopy 4-59740  
 trans-difluoroethylene-d<sub>2</sub>(d<sub>2</sub>), IR gas-phase vibr. intensity meas., polar tensors and effective charges 4-69073  
 p-dihalogenobenzenes, S<sub>1</sub> state, vibr. freq., spin-orbit coupling 4-102682  
 dihalogenolutes, liq. and vapour, IR, Raman and near UV spectra, thermodynamic functions 4-11277

## infrared spectra of organic molecules and substances continued.

4-dihydroxyanthraquinone, in glasses, ground state tunnelling, photochemical hole burning 4-71952  
 4-hydroxypyrimidines, electronic absorpt. and vibr. spectra 4-96564  
 diketopiperazine, cryst., vibr. anal., Raman and IR spectra 4-84962  
 dimethyl ether, intramol. vibr. relax., IR laser induced fluoresc. spectra 4-78936  
 dimethyl silane, stretching anharmonicity, dissociation energies, IR spectra 4-107336  
 dimethyl siloxanes, liq., monomer to polymer, relax. study by FIR absorpt. 4-99110  
 5,5-dimethyl-2-(dimethylamino)-2-oxo-1,3,2-oxazaphosphorinane config., X-ray cryst. and PMR and IR spectra in soln. 4-113432  
 dimethylamine, gaseous, overtone absorpt. spectra, conformationally non-equivalent C-H and N-H local mode oscillators 4-96528  
 1,2-dimethylindole, liq. and solid phase, vibr., IR spectra 4-88817  
 1,2-dimethylnaphthalene, n-hexane matrix, vibr. struct., IR and fluoresc. obs. 4-78903  
 1,4-dinitrobenzene- $d_6$  ( $d_6$ ), vibr. normal coordinate anal., IR and Raman spectra 4-59765  
 1,4-dioxane, intramol. vibr. energy transfer, IR laser induced fluoresc. spectra 4-78937  
 1,1-diphenylethylene,  $S_0$  state IR spectral components, quantum chem. calcs. (German) 4-59775  
 diphenylhalostannates, Raman and far IR spectra 4-114256  
 DMSO- $d_6$  ( $d_6$ ) solns., vibr. band shape, freq. shift, IR obs. 4-59766  
 ethane,  $\nu_5$ ,  $\nu_7$ , and  $\nu_8 + \nu_{11}$  band intensities, IR spectral study (French) 4-78911  
 ethanol vapour,  $CO_2$  laser optoacoustic absorpt. spectra (Chinese) 4-112169  
 ethenes, substituted, IR predissoc. spectra and vibr. relax. 4-96630  
 ethyl acetate, IR and Raman spectra, vibr. anal. 4-59771  
 ethyl monohaloacetates, IR and Raman spectra, vibr. anal. 4-59771  
 ethyl thiocyanate, gas and solid, conform. investig. and vibr. anal. 4-69044  
 ethylamines, trans and gauche forms, vibr., force const., ab initio MO calcs. 4-59622  
 ethylene, ethylene oxide, radiative cooling with selectively IR emitting gases 4-87834  
 ethylene, high press. polymerisation, IR and near IR region spectra 4-71917  
 ethylene 4-69059  
 ethylene adsorbed on Pt or Pd, EELS and IR spectra studies 4-104065  
 ethylene complexes with metal cations on surface of heterogeneous catalysts, IR spectra, struct. 4-64471  
 ethylene crystal, vibr. spectrum calc. 4-108557  
 ethylene-Ar(Ne), van der Waals mol., hindered internal rotors, IR photodissociation spectra 4-74238  
 ethylisothiocyanate- $d_0$  ( $d_0$ ), IR and Raman spectra, vibr. assignments, normal coordinate anal. 4-112177  
 fatty acid esters, stereoisomers, laser spectrochromatographic identification 4-62269  
 flames, oxy-fuel, H and OH radicals distrib. determ. 4-99798  
 fluorinated ethylamines, in inert gas matrices, IR and Raman spectra, conformational behaviour 4-59759  
 fluoro-2-ethanol, trans conformer, FT IR and Raman spectra, vibr. anal. 4-64481  
 fluorobenzene, optical consts., IR transmission and ATR spectra (German) 4-84965  
 fluorochloroacetonitriles, mol. dynamics., racemic modification, for IR spectra 4-104591  
 2-fluoroethylamine in solid Xe, thermal and IR-induced conformer inter-conversion processes 4-62170  
 fluoroform, Raman and IR spectra, crystal field splitting, conformer 4-61671  
 fluoromethane+H, vibr. excitation, IR emission study 4-69186  
 fluoromethane line profile meas. using heterodyne spectroscopy, astrophysical appls. 4-94637  
 fluoromethane- $d_4$ , far IR laser lines, energy-level structure 4-112394  
 formaldehyde,  $\tilde{X}A_1$  state, vibr. consts., stimulated emission spectra 4-87111  
 formaldehyde- $Cl_2$ ,  $N_2$  matrices, photolysis form. of  $CO(HCl)_2$ , IR spectra 4-89315  
 formyl chloride,  $N_2$  matrices, photolysis form. of  $CO(HCl)_2$ , IR spectra 4-89315  
 formyl fluoride, IR: multiple-photon decomp., time-resolved IR emission obs. 4-107413  
 formyl ion, IR laser spectroscopy of  $\nu_3$  fundamental 4-107345  
 Freon-123, T separation by laser (Chinese) 4-64631  
 fulminic acid, IR spectrum in  $\nu_4$  fundamental region 4-64469  
 $\alpha$ -D-glucopyranose cryst., H bonds, stretching vibr., IR spectra 4-88824  
 L-glutamine, IR spectra, band assignments 4-107339  
 halomethane sulphonyl halides, IR and Raman spectra, vibr. anal., rot. isomerism 4-64470  
 halomethanes, in MBBA matrix, local field anisotropy meas. 4-83375  
 1-halopropanes, far IR and Raman spectra, conformational stability 4-87113  
 n-heptane, liq., dielec. loss in millimetre and submillimetre wavelength region 4-99015  
 hexahydro-1,3,5-trinitro-s-triazine, mol. struct. in vapour, soln. and solid phases, IR obs. 4-69064  
 1,1,1,3,3,3-hexamethyltrisilane, IR and Raman spectra, vibr. anal., H/D isotopic shift data 4-112180  
 n-hexane, liq., dielec. loss in millimetre and submillimetre wavelength region 4-99015  
 L-histidine, IR spectra, band assignments 4-107339  
 HMX, melt-phase characterisation by rapid-scan FT-IR spectrosc. 4-109701  
 5-hydroxyindole, IR vibr. spectra 4-96536  
 8-hydroxyquinoline, visible, UV and IR spectra 4-96546  
 immersion liquids for interf.-polarisation filters, physical and chem. props. 4-64761  
 indan, far IR spectra, puckering vibr., pot. consts. and barriers 4-96541  
 indandione-1,3 derivatives, substituent effects, chem. struct., IR, UV and fluoresc. study 4-78905  
 indole-3-aldehyde, IR vibr. spectra 4-96536  
 indoline, far IR spectra, puckering vibr., pot. consts. and barriers 4-96541  
 indoline, IR and UV absorpt. spectra 4-96535  
 infrared spectra of organic compounds, automated structure analysis 4-91258  
 inositols, IR and Raman vibr. spectra 4-69071

## infrared spectra of organic molecules and substances continued

intensely absorbing liqs., far-IR spectra 4-104592  
 iodobenzene, optical consts., IR transmission and ATR spectra (German) 4-84965  
 isobutylamine monohydrate, vibr. spectroscopy 4-104611  
 isoprene, struct. and conformations by vibr. spectroscopy and gas phase electron diff. 4-64606  
 isopropylisothiocyanate, conformational stability, vibr., low resol. microwave IR and Raman obs. 4-112164  
 ketones, chemisorpt. on  $SnO_2$ , IR investig. 4-102681  
 lactic acids, mol. dynamics., racemic modification, for IR spectra 4-104591  
 linear dichroism using polarisation modulation FT-IR technique 4-104566  
 liquid crystals, IR birefringence meas. 4-80901  
 liquid phases, IR spectra, dielectric shift, mol. model, vapour press. isotope effects 4-64460  
 L-lysine, IR spectra, band assignments 4-107339  
 magnesium nickel oxalate dihydrate powders, coprecipitation from aq. soln. 4-75683  
 Maoming oil shale kerogen, extraction by supercritical gas process, chemical structure determ. 4-78837  
 metal carboxylates, hydrates, IR spectra, water-anion vibr. coupling 4-61704  
 methane, 7.6  $\mu m$  spectral meas. using IR high-resolution cooled-optics grating spectrometer 4-95532  
 methane, absorpt. spectrum obtained using intracavity spectroscopy utilising LiF  $F_2$  colour centre lasers 4-59774  
 methane, E line freq. meas. of He-Ne/methane laser 4-96868  
 methane, IR transition moments, isotopic depend. 4-69146  
 methane low-level gas, remote absorpt. meas. in near-IR using optical-fibre-based gas sensor 4-99865  
 methane- $^{12}C$ , vibr. polyads, rot. anal., IR spectrum, line parameters 4-59781  
 methane- $d_3$ ,  $\nu_3$  fundamental, IR spectral line intensities 4-59751  
 methane- $d_3$ , CH chromophore spectrosc. and dynamics 4-112167  
 methane- $d_3$ , IR anal. of  $\nu_3$  band 4-64467  
 methanol, cryst., torsion band, IR obs. 4-61691  
 methanol, high-resolution FIR and IR spectroscopy 4-96533  
 methanol, OH group vibr. freqs., intermol. interactions and matrix effects 4-102665  
 methanol, torsionally excited stretch states, anal. 4-59746  
 methanol absorption around  $CO_2$  waveguide laser lines 4-78852  
 methanol C-O stretch band, IR obs. 4-78853  
 methanol dimers, stretching vibr., IR photodissociation spectrum 4-78841  
 methanol FIR laser lines obs. using fine-tuned high power  $CO_2$ TEA laser 4-102918  
 methanol laser line assignments, IR spectra study 4-79119  
 methanol laser optically pumped, far IR transition lines, triple resonance study 4-79121  
 methanol vapour,  $CO_2$  laser optoacoustic absorpt. spectra (Chinese) 4-112169  
 methanol- $d_3$  laser lines, optically pumped, assignment and correction anal. 4-79120  
 2-methoxy-pyridine- $d_0$  ( $d_3$ ), combination bands, vibr. 4-87108  
 methyl 3 $\beta$ -nonanoyloxycholesterol-5-en-24-oate, cholesteric pitch, temp. depend. 4-84150  
 methyl acetate, IR laser line absorpt. and emission at elevated temps. 4-112171  
 methyl fluoride,  $CO_2$  pumped far IR laser line assignment using IR diode laser spectroscopy 4-107610  
 methyl germanes, deuterated, IR spectra, geometries 4-69078  
 methyl phenyl selenide, IR spectrosc. investig. 4-102683  
 methyl radical, IR laser line absorpt. and emission at elevated temps. 4-112171  
 methyl thionitrite, light induced reversible isomerisation in Ar matrix, IR spectra 4-112170  
 3-methyl-1,5-diphenyl-1,4-pentadien-3-ol, soln. and solid, dielectric props., IR study 4-99017  
 methylamine, gaseous, overtone absorpt. spectra, conformationally non-equivalent C-H and N-H local mode oscillators 4-96528  
 methylamine, intensity and electro-optical parameters, CNDO calc. 4-83397  
 methylcyclopentadiene, positional isomers, laser spectrochromatographic identification 4-62269  
 methyldimethylphosphinate, and isotopically substituted derivatives, vibr., config., IR obs. 4-87116  
 methyldimethylphosphinate, isotope derivatives, vibr., IR and Raman spectra 4-83378  
 methylene, singlet,  $\nu_1$  and  $\nu_3$  spectra, IR flash kinetic method obs. 4-59737  
 methylene ( $CH_2$ ), Einstein A-coefficients for rot. transitions 4-67613  
 methylenimine,  $\nu_8$  band, high-resolution IR spectra in 10  $\mu m$  region 4-96534  
 methylethers, conformation, vibr., IR, Raman  $^{13}C$  and  $^1H$  NMR study 4-87136  
 5-methylindole, IR and UV spectra 4-91262  
 N-methylindole, liq. and solid phase, vibr., IR spectra 4-88817  
 methylnicotinate, protonation sites, H bonding, IR obs. 4-87118  
 methylnitrate, gas phase struct., rigid asymmetric rotor theory, IR transitions 4-112172  
 methylsilanes, in MBBA matrix, local field anisotropy meas. 4-83375  
 cis-N-methylthioacetamide, IR spectra in low temp. matrices 4-69070  
 methylthiocarbamate, O and S isomers, mol. and cryst. struct., IR and Raman spectra 4-80923  
 methylthiocyanate, vibr. conformations, IR and Raman spectra 4-59767  
 3-methylthiophene polymer films, in situ Fourier transform IR spectra, vibronic coupling 4-87115  
 microemulsions extractant anions, FTIR studies on hydration 4-99848  
 monobromonitrobenzenes, valence force field, pot. energy distrib. and IR vibr. spectra, normal coord. anal. 4-83492  
 monohalogenobenzenes,  $S_1$  state, vibr. freq., spin-orbit coupling 4-102682  
 naphthalene, internal and external phonon interactions, intermolecular pot. 4-113557  
 naphthalene-indole soln., IR spectra (Russian) 4-84969  
 naphthazarin, rare gas matrices, vibr. energy redistribution, IR and fluoresc. spectra 4-74286  
 neptunium tetrakis-methylborohydride, mag. props., optical and EPR spectra 4-88718  
 S-nitrosocysteine, vibr. spectra, assignments and valence force field, isotope effects 4-78834

**infrared spectra of organic molecules and substances continued**

- octamethyltrisilane, IR and Raman spectra, vibr. anal., H/D isotopic shift data 4-112180  
 n-octane, liq., dielec. loss in millimetre and submillimetre wavelength region 4-99015  
 oligobutadiene urethane, intermol. interactions studied by IR spectra, thermodynamic props. (*Russian*) 4-102761  
 organic cpds., substructure recognition, artificial intelligence method, IR spectra 4-59762  
 organic sulphides(selenides)-I charge transfer complexes, vibr., IR and Raman obs. 4-64474  
 pentachlorophenol in soln., IR dispersion of H-bonded systems, dielec. function for weak complexes 4-102676  
 pentaerythritoltrinitrate, shock wave diagnostics by Raman and IR meas. 4-109712  
 pentafluoroethyl free radical, matrix isolation IR spectrum 4-69069  
 perfluoromethyl oxalate, rotational isomerism, vibr. props., Raman, IR, F NMR spectra studies 4-114267  
 PET films, drawn, molecular orientation, polarized IR spectra and birefringence obs. 4-84215  
 petroleum asphaltenes structure anal. by infrared spectroscopy 4-78836  
 3-phenacylidene 2,3,5,6-tetrahydroimidazo(2,1-b)thiazole, IR and PMR spectra struct. 4-112176  
 phenanthrene, oriented single crystals, far-IR spectra, temp. depend. 4-114262  
 phenols, screened, vibr. spectra and struct.; reduction, oxidation and H<sup>+</sup> transfer 4-59806  
 phenoxy radicals and ions, vibr. spectra and struct., reduction, oxidation and H<sup>+</sup> transfer 4-59806  
 phenylacetylene, vibr. line intensity distrib. in IR absorpt. spectra 4-107350  
 $\alpha$ -phenylethyl hydroperoxide, H-bonding investigated by IR spectroscopic methods, thermodynamic props. 4-96542  
 1-phosphapropyne (CH<sub>3</sub>CP), gaseous and solid, IR spectra 4-69063  
 2-phospholene-d<sub>4</sub>(-d<sub>5</sub>) low-freq. vibr. spectra and ring-puckering pot. energy function 4-102680  
 phthalan, far IR spectra, puckering vibr., pot. consts. and barriers 4-96541  
 o-phthalic acid, vibr. anal., Raman and IR spectra 4-114269  
 phthalocyanine films, structural info. from reflection absorption IR spectroscopy 4-71369  
 piperazine-bis(dithiocarbamate) complexes, mag., thermogravimetric and spectral studies 4-66033  
 pivalone, IR spectra, temp. and press. effects 4-61699  
 plasma membranes, rat liver, radiation effects, IR spectroscopy obs. (*Russian*) 4-77321  
 PMMA, syndiotactic, ordered struct. in soln. solid state 4-65166  
 PMMA-Novolac resin mixtures, glass transition temps., H bonding effects 4-103932  
 poly(2,6-dimethyl 1,4-phenylene oxide)-atactic polystyrene blends, orientation and relax. 4-79955  
 poly( $\gamma$ -benzyl glutamate),  $\alpha$ -helical conformation, Fourier transform IR photoacoustic spectra 4-95533  
 poly(N-alkyl-3,3'-carbazoyle)-I<sub>2</sub> complexes, highly conducting, synthesis and I<sub>2</sub> doping, FTIR study 4-65664  
 poly(thiophene), photoexcitations, photoinduced IR absorption and photoinduced ESR 4-114275  
 poly(vinylidene fluoride) film, dipolar orientation study 4-65946  
 polyacetylene-I<sub>2</sub>, highly oriented, IR spectra 4-59925  
 polyacetylene-I, IR refl. spectra, effect of sample densification 4-99120  
 trans-polyacetylene, deuterated, photoinduced absorption, isotope energy shifts 4-80945  
 polyacetylene, polymerisation and oxidation using Luttinger's catalyst, Raman and IR study 4-66590  
 polyacetylene, vibr. spectra calcs. 4-61709  
 polyacetylene-polyacetylene-d<sub>2</sub> transcopolymers, I<sub>2</sub> doped, Raman and IR spectra and vibr. freq. dispersion 4-60857  
 polyacetylene/elastomer blends, electrically conductive 4-75940  
 polyacetylenes, highly oriented, polarised IR spectra 4-80946  
 polyacrylonitrile, pyrolysed, optical and IR absorpt. spectra, TGA 4-92106  
 polyamides, aliphatic, chem. conversion under  $\gamma$ -irrad.; spectrosc. investig. 4-85320  
 polyamides obtained from 1,2-bis(4'-carboxy-phenoxy)ethane, synthesis, charact., mesogenic and phys. props. 4-113304  
 polyatomic mol., condensed phase, intramolecular dephasing, single-particle time correl. function theory 4-71359  
 polyatomic mols., IR vibr. freqs. and intensities, semiempirical NDO calcs. 4-64387  
 polyatomic mols. in soln., IR absorpt. band width and shape, temp. effects 4-78847  
 polybutadiene-polystyrene, graded block and randomised copolymers, comp. and microstruct. investig. 4-113362  
 polycarbazole-I<sub>2</sub> complexes, elec. conduction mechanism 4-75938  
 polycarbonate, oriented, Young's modulus, temp. depend., IR spectra, Gruneisen parameter (*Russian*) 4-109445  
 polyesters, with mesogenic groups and flexible spacers, conform. states investig. (*Russian*) 4-59936  
 polyesters obtained from 1,2-bis(4'-carboxy-phenoxy)ethane, synthesis, charact., mesogenic and phys. props. 4-113304  
 polyethylene, FT-IR study of soln. grown crystals 4-108343  
 polyethylene, high density, cryst. axes orientation and state of order during elongation FTIR study 4-99111  
 polyethylene, IR and Raman spectra, chemistry, crystallinity and texture 4-72015  
 polyethylene mixed crystals, infrared CD<sub>2</sub> bending vibration, Fourier self-deconvolution 4-93069  
 polyethylene oxide-PMMA blends, crystallisation, microstruct., phase separation, IR spectra, calorimetry 4-92107  
 polyimide, oriented, Young's modulus, temp. depend., IR spectra, Gruneisen parameter (*Russian*) 4-109445  
 polymer degradation on refl. metal films, Fourier transform IR refl. absorpt. obs. 4-112539  
 polymer film, electropolymerised, spectroscopic studies of electronic props., effect of prep. parameters (*French*) 4-66192  
 polymeric residues of astrophysical interest, IR spectra 4-72859  
 polymeric thermotropic liquid crystals, synthesis and characterisation 4-75283  
 polymers, comb shaped, liq. cryst. transitions, IR spectra and dilatometry obs. (*Russian*) 4-84388  
 polymers, Fourier transform IR spectroscopy, theory and appl. 4-76458

**infrared spectra of organic molecules and substances continued**

- polymers, semiconducting, synthesis from aromatic and heterocyclic nuclei, I<sub>2</sub> doping 4-80578  
 polyphenylacetylene-I, reson. Raman, Raman polaris. and far IR spectrosc. 4-80915  
 polypropylene, mech. deform., Fourier transform IR obs. 4-66363  
 polypropylene films, uniaxially and biaxially oriented, IR internal reflection spectroscopy 4-93073  
 polypropylene films, uniaxially extended, surface orientation, IR internal reflection spectroscopy 4-93072  
 polypropylene-copolymer laminates, biaxial orientation, refractometry, IR spectra 4-84959  
 polypropylenes, isotactic quenched melts, cooling rate effect on morphology 4-108291  
 polypyrrole, band struct., polarons, and optical spectrum 4-98546  
 polystyrene, chain scission and mech. degradation 4-93395  
 polystyrene, IR spectra, temp. effects 4-80914  
 polystyrene, isotactic, vibr. spectrum, mass defects effect 4-80912  
 polystyrene(divinylbenzene), plasma oxidised, photoacoustic IR spectroscopy 4-102832  
 polystyrene-d<sub>8</sub>, isotactic, vibr. spectrum, normal coord. calcs. 4-80911  
 polytetrafluoroethylene films, chain orientation param. from IR-dichroism and X-ray data (*Russian*) 4-84536  
 polythiophene:BF<sub>4</sub><sup>-</sup>(Bu<sub>4</sub>N<sup>+</sup>), electrochemical n-type and p-type doping, elec. and optical props. 4-61363  
 polyvinylalcohol-chitosan blends, intermolecular interactions, mech. props., Fourier transform IR spectra 4-84409  
 polyvinylidene fluoride films, piezoelec. effect at high temp., Fourier transform IR spectra 4-76334  
 polyvinylidene fluoride films, poled semicrystalline, FIR Fourier spectra, X-ray obs. 4-60858  
 polyvinylpyridine-FeCl<sub>3</sub>(Fe(NO<sub>3</sub>)<sub>3</sub>) polymers, Mossbauer and IR spectra 4-59821  
 propanal, struct. studied by electron diff., microwave and IR spectra, force field 4-64603  
 propane-propylene fuel, C particle effect on radiation spectrum in test furnace 4-96530  
 1-propanol in low temp. matrices, IR-induced rotamerisation, ab initio, calcs. 4-64634  
 propylene complexes with metal cations on surface of heterogeneous catalysts, IR spectra, struct. 4-64471  
 PVC-ethylacrylate 4-vinylpyridine copolymers blends, miscibility, interactions, mech. props. 4-103670  
 pyridine, adsorbed on LaMO<sub>3</sub> (M=Cr, Mn, Fe, Co), IR spectra 4-104071  
 pyridine adsorbed on (Ru<sub>3</sub>Si<sub>1-x</sub>)O<sub>2</sub> surface, FT-IR study of surface acid sites 4-113783  
 pyridine derivatives, H bonded complex form. with nitrophenols, IR and UV investig. 4-66562  
 pyridine dichromates (IV), synthesis and characterisation 4-104615  
 pyridine-2-thione, S-methylated and N-deuterated, Raman and polarised IR spectra 4-114278  
 pyridine-3-aldehyde-aromatic 1,3-diamine linear condensation polymers, form., spectrosc. investig. 4-104987  
 pyridines, disubstituted, IR, Raman and near UV spectra, thermodynamic functions, internal rot. 4-91271  
 pyrimidine in Ar matrix, IR spectra, mol. struct., force consts. 4-69080  
 quinaldines, substituted, IR and near UV absorpt. spectra 4-91261  
 RDX, melt-phase characterisation by rapid-scan FT-IR spectrosc. 4-109701  
 13-cis-retinal, prerezon. Raman and IR spectra, vibr. anal., isomerisation 4-89502  
 saccharides, mono- and di-, FIR FT absorpt. spectra 4-96532  
 Schiff base derivatives of 5-nitro-2-furaldehyde, UV, IR and <sup>1</sup>H NMR spectra 4-96527  
 1-silacyclopent-3-ene-d<sub>0</sub>(1-d<sub>1</sub>)(1,1-d<sub>2</sub>), two dimens. pot. energy surface for ring puckering and ring twisting 4-78840  
 sodium dodecyl sulphate-water system, phase transitions, FT IR obs. 4-84389  
 TCNQ salt, DTT-TCNQ, optical props., cond. and cryst. struct. 4-113435  
 TCNQ salt, tetraethylammonium-(TCNQ)<sub>2</sub>, IR reflectivity spectra anisotropy 4-61693  
 TCNQ salts, C<sub>52</sub> (TCNQ)<sub>3</sub>(II), synthesis, anal., novel isomeric struct. 4-114376  
 TCNQ salts with 8-hydroxyquinolylenes, elec. and optical props. 4-75951  
 p-terphenyl, in CS<sub>2</sub> soln., vibr. modes, mol. struct., IR absolute band intensities 4-64475  
 2,3,4,5-tetrachloro-6-((diethylamino)methyl)phenol, Mannich base, H<sup>+</sup> transfer equilib., solvent effect 4-81417  
 tetracyclohexane, struct., complete harmonic force field, vibr. spectra and IR intensities 4-87233  
 tetrafluoromethane, F IR intensities, charge flux param. and transferability 4-69072  
 tetramethylammonium uranyl tetrafluoride, luminesc. and vibr. spectra 4-69138  
 tetramethyldioxetane, vibr. freq. Fourier transform IR and Raman spectra 4-64478  
 meso-tetraphenylporphine, stretching bands, isotope effects, IR spectra 4-74240  
 tetraphenylsilane, IR dichroism and Raman meas., vibr. anal. 4-61653  
 tetraphenylsilane, vibr., Raman spectra, IR dichroism 4-84963  
 thioacetamide, <sup>13</sup>C and <sup>15</sup>N substituted species, Raman spectrum, struct. 4-66030  
 thiobenzanilide, polymorphism, IR obs. 4-61686  
 thiobenzanilide, vibr. spectra, amide and thioamide bands 4-59772  
 thiopivalic acid, solns., self-assoc., IR and PMR spectrosc. obs. 4-74241  
 thioureas, substituted, IR spectra, conformation 4-59769  
 thorium (1-phenyl-4,4,4-trifluoro-1,3-butanedione):U (IV), polarised high resolution spectra, struct. 4-108341  
 thorium tetrakis- $\beta$  diacetate:U (IV), polarised high resolution spectra, struct. 4-108341  
 TMTSeF, and radical cation, superconductors, vibr. IR and Raman obs. 4-88821  
 (TMTSF)<sub>2</sub>ClO<sub>4</sub> organic supercond., polarised far IR reflectivity meas. 4-114279  
 TMTTF, and radical cation 4-88821  
 tobacco samples, FT-NIR diffuse reflectance spectroscopy anal. 4-105034  
 toluene and its deuterium derivatives, IR spectra, charge distrib. determ. 4-112181

rared spectra of organic molecules and substances continued  
 transition metal formate dihydrates, Evans holes, IR spectra 4-66019  
 tribromoacetonitrile and  $^{15}\text{N}$  isotopic derivative, IR and Raman vibr. spectra 4-69081  
 tribromomethane, polycryst., IR spectrum 4-114255  
 trichloroacetic acid vapour, IR absorpt. spectrum 4-78849  
 triethanolammonium oleate, lyotropic liq. cryst., IR spectra and X-ray diff. 4-84144  
 triethylamine-DCN system,  $\text{CN}^-$  rot., IR study 4-64463  
 trifluoroethene, multiphoton excitation, allene prod., via difluorovinylidene 4-109671  
 trifluoroethylamine in 1:1 complexes with bases, anharmonic force consts. determ. for amino group 4-96547  
 trifluoromethane- $\text{d}_3(\text{d}_1)$ , isotopically selective IR multiphoton dissociation 4-112240  
 trifluoromethane- $\text{d}_1$ , sub-MM wave and IR heterodyne spectra 4-74245  
 trimethyl silane, stretching anharmonicity, dissociation energies, IR spectra 4-107336  
 trimethylaluminium, Ar matrix isolation, IR spectra 4-78842  
 trimethylammonium manganese copper trichloride, polarised cryst. spectra and cryst. struct. 4-88825  
 trimethylchlorosilane polymorphism, FIR study 4-61685  
 trimethylene oxide and its deuterated analogs, CARS, ring puckering, vibr. 4-64482  
 2,3,4-trimethylhexane, vibr., force consts., IR spectra, normal coordinate calcs. 4-112174  
 2,3,4-trimethylpentane, vibr., force consts., IR spectra, normal coordinate calcs. 4-112174  
 2,4,6-trimethylphenol in soln., IR dispersion of H-bonded systems, dielectric function for weak complexes 4-102676  
 trioxane-dioxolane copolymer, conform., press. and mech. treatment effect, IR spectra 4-70043  
 triphenylhalostannates, Raman and far IR spectra 4-114256  
 tris-sarcosine calcium chloride, ferroelec. phase transitions, IR and Raman studies 4-71296  
 tris-sarcosine calcium chloride (bromide), ferroelec. phase transition, IR and Raman studies 4-93023  
 tris-sarcosine calcium chloride-bromide, soft modes, IR, and Raman spectra studies 4-71290  
 TTF-FeOCl intercalation cpd., struct., IR spectra and mag. susceptibility 4-70128  
 TTT-FeOCl intercalation cpd., struct., IR spectra and mag. susceptibility 4-70128  
 uracil, monomeric, trapped in Ar and  $\text{N}_2$  cryogenic matrices, IR spectra 4-64472  
 uracil and deuterated uracil in Ar and  $\text{N}_2$  mixtures, IR and Raman spectra, vibr. assignment 4-74243  
 uracil- $\text{d}_6(\text{d}_2)$ , vibr., force consts. CNDO/2 calcs., IR spectra 4-59699  
 uranium tetrakisethylborohydride, mag. susceptibility, visible and IR obs. 4-88820  
 UV-visible and IR spectra, radiative transition probabilities for fluoresc. level 4-114309  
 vinyl acetate-ethyl  $\alpha$ -cyanocinnamate copolymers, IR,  $^1\text{H}$  and  $^{13}\text{C}$  NMR spectra 4-84208  
 vinylidene cyanide-vinyl acetate copolymer, piezoelectricity and remanent polarisation 4-99028  
 vinylidene fluoride-trifluoroethylene copolymers, ferroelec. transition, struct. studies 4-99054  
 xylene isomers, IR absorpt. spectra, component spectral curve estimation from unknown mixture spectra 4-90659  
 Dy compounds in nonaq. soln., absorpt. and luminesc. spectra, f-f absorpt. bands, oscillator strengths, luminesc. 4-59768  
 GeH<sub>4</sub>, IR spectra, geometries 4-69078  
 $(\text{HCl})_2$ , stretching bands rot. spect., high resolution IR spectra 4-107343  
 HX-cyclopropane complex, (X=F, Cl, Br, I, CN), matrix isolation IR investigation 4-107349  
 $\text{Li}_{0.82}(\text{Pt}(\text{S}_2\text{C}_2(\text{CN})_2)_2) \cdot 2\text{M}_2\text{O}$ , Peierls instability study 4-70791  
 $\text{SiO}_2$ , electron irradiation, IR absorpt. from OH-related defects 4-104633  
 TCNQ, IR reflectivity spectrum, soft modes 4-88816  
 TGS, surface layer far IR spectra 4-88828

#### infrared spectra of polyatomic inorganic molecules

bromotrifluoromethane clusters, IR predissoc. in mol. beam expts. 4-69259  
 ferric neurosporin, cryst., chem. and mol. struct., spectral charact. 4-102720  
 IR active modes, electronic struct. and vibr. anal. 4-87106  
 liquid phases, IR spectra, dielectric shift, mol. model, vapour press. isotope effects 4-64460  
 molecular spectroscopy, high resolution, in submillimeter wavelength region 4-90669  
 rare earth hexacyano complexes,  $\text{RK}(\text{Fe}(\text{CN})_6) \cdot 4\text{H}_2\text{O}$ , IR and Mossbauer spectra 4-59757  
 solns. in dipolar aprotic, IR spectra and struct. 4-112175  
 water-vapour absorption in 8-14  $\mu\text{m}$  atmospheric window, temp. dependence 4-77613  
 $\text{AlBr}_3$  in vapour phase, IR spectra, valence force fields 4-74244  
 $\text{AlI}_3$  in vapour phase, IR spectra, valence force fields 4-74244  
 $\text{ArHCl}$ , IR spectrum, thermodynamic props. 4-74236  
 $\text{AsH}_3$ , ground state, far IR spectrum, spectrosc. consts. 4-59742  
 $\text{BF}_3$ , F IR intensities, charge flux param. and transferability 4-69072  
 $\text{BF}_3 \cdot \text{CO}(\text{N}_2)$ , weakly bound complexes, Fourier transform IR spectra 4-87125  
 $\text{Ba}(\text{Fe}(\text{CN})_6) \cdot \text{NO} \cdot 2\text{H}_2\text{O}$ , IR spectra, vibr. dipole-dipole coupling between nitrosyl groups, fine struct., force consts. 4-96540  
 $\text{CO}_2$ , adsorbed on  $\text{LaMO}_3$  ( $\text{M}=\text{Cr}, \text{Mn}, \text{Fe}, \text{Co}$ ), IR spectra 4-104071  
 $\text{CO}_2$ , high resolution IR spectra atlas 4-91257  
 $\text{CO}_2$ , laser bands, freq. tables, rovibr. consts. 4-60015  
 $\text{CO}_2$ , photofragment product, vibr. energy distrib., IR diode laser probes 4-107325  
 $\text{CO}_2$ , spectral band contour in 4.3  $\mu\text{m}$  region (Chinese) 4-107337  
 $\text{CO}_2$ , symmetric vibr., collision-induced IR absorpt. 4-87107  
 $\text{CO}_2$ , vibr. rot. bands in 540 to 890  $\text{cm}^{-1}$  region 4-64466  
 $\text{CO}_2$ , vibrationally nonequilibrium 12-19  $\mu\text{m}$  radiation calcs. 4-96545  
 $\text{CO}_2$ , isolated ions, IR spectra quantitative prediction 4-69075  
 $^{12}\text{C}^{16}\text{O}_2$ , 2 and  $\Pi$  Fermi dyads in 4.5  $\mu\text{m}$  region, wavenumbers, spectrosc. consts. 4-59745  
 $\text{CO}_2$ -methanol gas mixture, molecular IR transitions, saturated absorption obs. 4-69150  
 $\text{CS}_2$ , IR spectra of isotopic species 4-69065  
 $\text{CS}_2$ ,  $\nu_3$ - $\nu_1$  band IR spectra, S isotope affects 4-87102

#### infrared spectra of polyatomic inorganic molecules continued

$\text{CS}_2^+$ , isolated ions, IR spectra quantitative prediction 4-69075  
 $\text{Ca}(\text{NCS})_2$  solns. in dipolar aprotic, IR spectra and struct. 4-112175  
 $\text{Cd}(\text{II})$  complex, xanthinium cadmium tetrachloride, thermal props. investigation 4-78846  
 $\text{ClONO}_2$  in  $\text{N}_2$  and Ar matrices, high resolution FTIR spectra 4-74233  
 Cr complexes,  $\pi$ -electron delocalisation NMR, IR and XPS study 4-87117  
 $\text{Cr}(^{13}\text{CO})_6$  in Ar matrix, FT-IR spectra, isotropic substitution effects 4-112183  
 $\text{Cr}(^{12}\text{CO})_5(^{13}\text{CO})$  in Ar matrix, FT-IR spectra, isotropic substitution effects 4-112183  
 $\text{Cs}_2\text{XO}_4$  where X=S, Cr, Mo, W, matrix isolated, IR and Raman spectra, isotope shifts, bond angles evaluation 4-96539  
 Cu (II) cyanates, polymeric, far IR spectra, Cu-OCN bonding, stretching and deformation bands 4-69076  
 Cu-L-glutamine complex, IR spectra, band assignments 4-107339  
 Cu-L-histidine complex, IR spectra, band assignments 4-107339  
 Cu-L-lysine complex, IR spectra, band assignments 4-107339  
 $\text{D}^{14}\text{N}_3$ ,  $\nu_2$  band, Raman and IR rot. vibr. spectra 4-69087  
 $\text{D}_2\text{O}$ , OD group vibr. freqs., intermol. interactions and matrix effects 4-102665  
 $\text{F}_2 + \text{O}_2$ , chemical reactions in red spectral range, excitation spectrum, low-energy pathways 4-85318  
 $\text{FHF}^-$  ( $\text{FDF}^-$ ) isolated in alkali halides crystals, IR and Raman spectra, temp. depend. 4-59760  
 $\text{FNO}$ ,  $\nu_2$  and  $\nu_3$  fundamentals, high resolution Fourier transform spectroscopy 4-59749  
 $\text{FO}_2$ , FIR laser mag. reson. detection from  $\text{F} + \text{O}_2(\text{O}_3)$  reactions 4-59811  
 $\text{FO}_2$ , radical,  $\nu_2$  band, IR diode laser spectra 4-74237  
 $\text{FONO}_2$ , gas phase struct., rigid asymmetric rotor theory, IR transitions 4-112172  
 Fe complex form. in 1,3-butanediol matrix, IR spectra 4-64477  
 Fe(II) porphyrins, dioxygen adducts, matrix isolation IR spectra 4-69068  
 $\text{GaCl}_3$  in vapour phase, IR spectra, valence force fields 4-74244  
 $(\text{H}_2)_2$ , van der Waals dimers, Jupiter and Saturn atm., Voyager far-IR spectra 4-105901  
 $\text{H}_2^+$ , vibr.-rot. levels, IR predissociation spectra 4-107344  
 HCN-acetonitrile mixtures, in solid Ar, far IR spectra, intramol. vibr. 4-87112  
 $\text{HCNH}^+$ ,  $\nu_2$  band, vibr.-rot. IR spectra 4-64462  
 $\text{HCO}^+$ ,  $\nu_3$  fundamental band, IR obs. 4-96538  
 $(\text{HF})_n$  in solid Ar matrix, FT IR spectra 4-69066  
 $\text{HNH}_2$ , stretching vibr., pot. energy and electric dipole moment depend., ab initio calcs. 4-87105  
 HNCSe, IR spectrum, vibr. assignment 4-102675  
 $\text{H}_2\text{O}$  in Ar and Kr matrices, rot. translation, high resolution spectra, linewidths 4-59733  
 $\text{H}_2\text{O}$  in liq. crystal, polarised FT-IR spectra 4-64473  
 $\text{H}_2\text{O}$  isolated in solid gas matrices, far IR Fourier spectroscopy 4-102677  
 $\text{H}_2\text{O}$ , matrix isolated in  $\text{D}_2\text{O}$  cubic ice, vibr. data 4-69045  
 $\text{H}_2\text{O}$ , molecule, absorpt. lines, accurate wavelength meas. by 0.8  $\mu\text{m}$  AlGaAs laser 4-59735  
 $\text{H}_2\text{O}$ , pure rot. spectrum, mm, sub-mm and far IR analysis 4-107341  
 $\text{H}_2\text{O}$  resonance absorption spectrum, expl. study using line-tunable CO laser (Chinese) 4-67398  
 $\text{H}_2\text{O}$  vapour, absorpt. spectrum obtained using intracavity spectroscopy utilising  $\text{LiF F}_2$  colour centre lasers 4-59774  
 $\text{H}_2\text{O}$  vapour, IR absorption temp. depend. 4-96537  
 $\text{H}_2\text{O}_2$ , absolute IR intensity calc. of binary overtone, combination and difference bands 4-69074  
 $(\text{H}_2\text{O}_2)$ , IR predissoc. spectra in supersonic mol. beam 4-69060  
 $\text{HOSO}_2$  radical, Ar matrix isolated, IR spectra 4-78835  
 $\text{H}_2\text{S-H}_2\text{O}$  complexes, H bonded, Ar matrix isolated IR spectra 4-112173  
 $\text{HSNO}$ , Ar low temp. matrix, photoinduced isomerisation, IR spectra 4-89249  
 $\text{H}_2\text{SiCl}_2$ , vibr., rovibr., force consts., IR obs. 4-59738  
 $\text{HgCl}_2$ , triarylphosphine complexes,  $^{31}\text{P}$  and  $^{199}\text{Hg}$  NMR and vibr. spectrosc. obs. 4-83391  
 $\text{Hg}(\text{ClO}_4)_2$ , phosphine complexes,  $^{31}\text{P}$  and  $^{199}\text{Hg}$  and vibr. spectrosc. obs. 4-83392  
 $\text{Hg}(\text{II})$  complex, xanthinium mercury tetrachloride, thermal props. investigation 4-78846  
 $\text{KBrO}_3$ , vibr., normal coordinate anal., IR and laser Raman spectra 4-74235  
 KCN, ab initio dipole surfaces, vibr. averaged dipole moments and IR transition intensities 4-64461  
 KNCS, IR and Raman spectra, vibr. anal., normal coord. treatment 4-107338  
 KNCS solns. in dipolar aprotic, IR spectra and struct. 4-112175  
 $\text{K}_2\text{O}_2$ , IR active modes, electronic struct. and vibr. anal. 4-87106  
 LiCN, ab initio dipole surfaces, vibr. averaged dipole moments and IR transition intensities 4-64461  
 Mg complex form. in 1,3-butanediol matrix, IR spectra 4-64477  
 $\text{N}_2$ , symmetric vibr., collision-induced IR absorpt. 4-87107  
 NANCs solns. in dipolar aprotic, IR spectra and struct. 4-112175  
 $\text{NF}_3$ , F IR intensities, charge flux param. and transferability 4-69072  
 $\text{NF}_3(\text{X}^2\text{B}_1)$ ,  $\nu_2$  band, IR laser spectroscopy 4-69082  
 $\text{NH}_3$ , absorpt. spectrum obtained using intracavity spectroscopy utilising  $\text{LiF F}_2$  colour centre lasers 4-59774  
 $\text{NH}_3$ , expanding jet, rotational temp. and mol. density determ. by IR absorpt. 4-83490  
 $\text{NH}_3$  gas IR absorpt. spectroscopic data spectral slit width and blind deconvolution estimation by homomorphic filtering 4-73533  
 $\text{NH}_3$ , IR laser optogalvanic spectroscopy, Doppler free and double reson. effects 4-74230  
 $\text{NH}_3$ , IR multiple photon absorpt. spectra, optothermal detection 4-69059  
 $\text{NH}_3$  isolated in solid gas matrices, far IR Fourier spectroscopy 4-102677  
 $\text{NH}_3$ , Q branch transition, diode laser IR spectra 4-59750  
 $\text{NH}_3$ , radiative cooling with selectively IR emitting gases 4-87834  
 $\text{NH}_3$ , rot. struct. of spectra, inversion effect, anomalous behaviour of spectroscopic parameters 4-83370  
 $\text{NH}_3$ , sub-Doppler double reson. spectroscopy using tunable diode laser 4-112220  
 $\text{NH}_3$ , tunable diode laser optogalvanic spectroscopy 4-112168  
 $\text{NH}_3 \cdot \text{HCl}$ , H bonded complex, matrix isolated IR vibr. spectra 4-96543  
 $\text{NH}_4^+$ ,  $\nu_2$  band, vel. modulation IR laser spectra 4-69062  
 $\text{N}_2\text{H}_4$ , gaseous, overtone absorpt. spectra, conformationally non-equivalent C-H and N-H local mode oscillators 4-96528

**infrared spectra of polyatomic inorganic molecules continued**

- NH<sub>2</sub>OH, OH stretching fundamental, IR absorpt. and Stark spectra 4-59752  
 NH<sub>2</sub>(X<sup>2</sup>B<sub>1</sub>) free radical detect. by CARS spectroscopy 4-62262  
 (NO)<sub>2</sub> dimer heat of form., low temp. near IR study (French) 4-69057  
 NO<sub>2</sub> IR laser line absorpt. and emission at elevated temps. 4-112171  
 NO<sub>2</sub> IR spectra, rot. anal. 4-59773  
 NO<sub>2</sub> tunable diode laser optogalvanic spectroscopy 4-112168  
 NO<sub>2</sub><sup>+</sup> ion isolated in Rb halides, external and internal vibr. modes, Raman and IR study 4-112188  
 NO<sub>2</sub><sup>+</sup> isolated in alkali halide systems, IR and Raman spectra 4-59761  
 N<sub>2</sub>O and rare isotopic derivatives, line strengths in 1120 to 1440 cm<sup>-1</sup> region 4-87103  
 N<sub>2</sub>O IR transmittance band model 4-115568  
 N<sub>2</sub>O IR vibr. rot. spectrum in lowest fundamental  $\nu_2$  region 4-64465  
 N<sub>2</sub>O line strengths meas. from high resolution Fourier transform spectra 4-59748  
 N<sub>2</sub>O  $\nu_3$  IR band, vibr.-rot. line interf., strong-collision approx. 4-83367  
 N<sub>2</sub>O+Ar, mol. <sup>6</sup> mean square torques and rot. correl. functions of  $\nu_3$  vibr. perturbed by Ar 4-78838  
 NOF, cubic force field determ. by vibr.-rot.  $\alpha$  consts. 4-83491  
<sup>14</sup>N<sup>16</sup>O<sub>2</sub>  $\nu_1$  band, line positions and intensities, Fourier transform IR spectra 4-59755  
 NbOX<sub>3</sub> X=Cl, Br, I, matrix isolated, stretch vibr., IR spectra 4-83379  
 NbX<sub>5</sub> (X=Cl, Br, I), and with Nb<sub>2</sub>O<sub>5</sub>, matrix isolated, stretch vibr., IR spectra 4-83379  
 Ni complex form. in 1,3-butadiene matrix, IR spectra 4-64477  
<sup>18</sup>O<sub>2</sub>+dichloroethylene, O-atom prod. via. dissoc. of primary Criegee intermediate 4-89281  
 OCS, vibr. rot. bands in 540 to 890 cm<sup>-1</sup> region 4-64466  
 OCS+OCS(He)(Ar), IR linewidth meas., rot. levels, intermol. pot. 4-59764  
 PF<sub>3</sub>NH<sub>3</sub>, N<sub>2</sub> matrix isolated, intramolecular rearrangement, vibr., IR obs. 4-78845  
 Pb<sub>3</sub>P<sub>2</sub>S<sub>8</sub>, far IR, IR and Raman spectra, crystal struct. and vibr. spectra (German) 4-70073  
 Pd complex form. in 1,3-butadiene matrix, IR spectra 4-64477  
 Pd complexes, Pd(0,1,IV) states, synthesis, mol. spectrosc. obs. 4-64458  
 Pt complexes, electronic effects, PMR, IR and UV spectra 4-78866  
 SF<sub>6</sub>, collision-free IR multiphoton absorpt., thermal effects 4-74234  
 SF<sub>6</sub> IR multiple photon absorpt. spectra, optothermal detection 4-69059  
 SF<sub>6</sub> multiphoton absorption of broad-band CO<sub>2</sub> laser radiation 4-107420  
 SO<sub>2</sub> Fourier transform absorption spectrum, analysis 4-112165  
 SO<sub>2</sub> pure rotational spectroscopy using fixed line far IR lasers 4-74246  
 SO<sub>2</sub>(NH<sub>3</sub>)<sub>n</sub> complexes, matrix isolated IR spectrosc. obs. 4-69067  
 SO<sub>2</sub>amine complexes, matrix isolated IR spectrosc. obs. 4-69067  
 SiF<sub>4</sub> clusters, IR predissoc. in mol. beam expts. 4-69259  
 SiH<sub>4</sub>, D isotope substituted, polar tensors, effective charges, IR intensities 4-107342  
 SiH<sub>4</sub>, stretching anharmonicity, dissoc. energies, IR spectra 4-107336  
 SiH<sub>4</sub>, vibr. overtones, visible and near IR spectra 4-87110  
 Sr(Fe(CN)<sub>5</sub>NO)<sub>4</sub>·4H<sub>2</sub>O, IR spectra, vibr. dipole-dipole coupling between nitrosyl groups, fine struct., force consts. 4-96540  
 T<sub>2</sub>O, absorpt. spectrum at 0.04 cm<sup>-1</sup>, rot. and distortion consts., fundamental bending mode obs. 4-59722  
 UF<sub>6</sub> molecule, IR absorpt. spectra,  $\nu_3$  band, pulsed supersonic jet study 4-59734  
 WF<sub>6</sub>, cold jet IR absorpt. spectra,  $\nu_3$  band at low rot. and vibr. temp., isotope shift 4-87114  
 XeH<sup>+</sup> and XeD<sup>+</sup>, IR transition probabilities, calc., equilib. pot. energy and dipole moment functions 4-69061  
 Zn(II) complex, xanthinium zinc tetrachloride, thermal props. investig. 4-78846

infrared telescopes *see telescopes*infrared transmitters *see infrared sources*infrasonic waves *see acoustic waves***initial value problems**

- compressible fluid, with weak diffusion, Rayleigh problem (Russian) 4-112672  
 fluids, US field propag. calc. using finite difference techniques 4-98205  
 high resolution total variation stable finite difference schemes 4-58620  
 ordinary differential equations numerical integration, global error estimation, stochastic approach, celestial mechanics appl. 4-82401  
 plates, thin, viscoelastic, finite element anal. 4-112721  
 Poiseuille flow, stationary perturbation, eigenvalues, initial value method calcs. 4-97683  
 thermoelastic oscillations, initial boundary value problems (German) 4-82681  
 time-asymmetric initial data for N black hole problem in general relativity 4-72974  
 wave equation with piecewise smooth coefficients, numerical soln. 4-86230

injection lasers *see semiconductor junction lasers*injury by radiation *see biological effects of radiation*inorganic insulators *see insulating materials***inorganic molecule configurations***see also isomerism*

- ferric neurosporin, cryst., chem. and mol. struct., spectral charact. 4-102720  
 hydrides, first- and second-row, sp hybridisation, ab initio MO study 4-102575  
 ice, stretching vibrs. of O-H and O-D, Raman spectrum, press. and temp. depend. 4-98218  
 point group symmetry 4-64326  
 tetracoordinate C cpds., geometries calcs. 4-64346  
 water clusters, neutral and protonated, struct. calc. with mol. graphics 4-96734  
 AlBr<sub>3</sub> in vapour phase, IR spectra, valence force fields 4-74244  
 AlI<sub>3</sub> in vapour phase, IR spectra, valence force fields 4-74244  
 AsH<sub>3</sub>, ground state, far IR spectrum, spectrosc. consts. 4-59742  
 B cage cpds., polyhedral struct., 2-dimens. <sup>11</sup>B-NMR spectrosc. investig. 4-64503  
 BCN, ground state, geometry, transition state, isomerisation reaction, ab initio calcs. 4-71908  
 B<sub>2</sub>O<sub>2</sub> vapour, struct., photoelectron spectra, ab initio STO calcs. 4-83414  
 Be<sub>18</sub> clusters, energy optimised configs., ab initio STO-3G SCF calcs. 4-69261  
 Be<sub>20</sub> clusters, energy optimised configs., ab initio STO-3G SCF calcs. 4-69261

**inorganic molecule configurations continued**

- Be<sub>2</sub>F<sub>2</sub><sup>+</sup>, geometric struct., force field and vibr. spectrum, MO-LCAO-SCF calcs. 4-59629  
 Be<sub>2</sub>H<sub>2</sub><sup>+</sup>, geometric struct., force field and vibr. spectrum, MO-LCAO-SCF calcs. 4-59629  
 C, linear polytypes, struct. aspects and conformation 4-92139  
 CO, chemisorption on Pd (111), angle-resolved photoelectron spectra 4-81114  
 CO-H<sup>+</sup>(Li<sup>+</sup>)(Na<sup>+</sup>)(K<sup>+</sup>) struct., binding energies, ab initio HF calcs. 4-112096  
 CO<sub>2</sub>, liq., thermodynamic state, struct., neutron diff. study 4-70017  
 CO<sub>2</sub><sup>+</sup> low-lying electronic states, linear and bent configs. 4-68980  
 C<sub>2</sub>O<sub>2</sub>, struct. and harmonic vibr. freqs., analytic derivative methods 4-96431  
 Co II complex, ethyl  $\alpha$ -ketocyclopentylcarboxylate, V-UV spectrosc. investig. 4-112191  
 Cr binuclear complexes, triple metal bond HF-Slater transition state method 4-59619  
 Cu (II) complexes, five-coord., distortion, optical absorpt. and ESR obs. 4-78872  
 Cu (II) cyanates, polymeric, far IR spectra, Cu-OCN bonding, stretching and deformation bands 4-69076  
 CuAg<sub>4</sub> matrix isolated, ESR spectra 4-107371  
 Cu<sub>2</sub>Ag<sub>4</sub> matrix isolated, ESR spectra 4-107371  
 Cu(NO<sub>2</sub>)<sub>2</sub>, gas phase, mol. struct., electron diff. 4-78965  
 CuO<sub>2</sub> photochem. and struct. in inert gas matrices 4-109672  
 FONO<sub>2</sub>, gas phase struct., rigid asymmetric rotor theory, IR transitions 4-112172  
 Fe<sup>2+</sup> complex, A23187 antibiotic, cryst. and mol. struct., X-ray diff. 4-109775  
 GaCl<sub>3</sub> in vapour phase, IR spectra, valence force fields 4-74244  
 H<sub>2</sub><sup>+</sup> momentum distrib., nodal struct. 4-78766  
 HCN, ground and excited states, struct., vibr., SCF CI calcs. 4-64391  
 HCN, ground state, geometry, transition state, isomerisation reaction, ab initio calcs. 4-71908  
 HFPOH struct., bonding and internal rotation 4-68938  
 HNCSe, millimeter wave spectrum and struct. 4-102673  
 (CHO<sub>2</sub>)<sub>2</sub> struct., ab initio multiconfig. SCF gradient optimisation method 4-83290  
 H<sub>2</sub>O, equilib. struct. calcs. using isotopic differences in  $r_e$  struct. 4-68984  
 H<sub>2</sub>O<sub>2</sub><sup>+</sup> in crystals, struct. anal., SCF-LCGO calcs. 4-96450  
 H<sub>2</sub>O<sub>2</sub> struct., bonding and internal rotation 4-68938  
 H<sub>2</sub>POH struct., bonding and internal rotation 4-68938  
 H<sub>2</sub>S-HF, hyperfine coupling consts., rot., pulsed-nozzle Fourier transform microwave spectra 4-107333  
 HSNO, Ar low temp. matrix, photoinduced isomerisation, IR spectra 4-89249  
 HgCl<sub>2</sub> triarylphosphine complexes, <sup>31</sup>P and <sup>199</sup>Hg NMR and vibr. spectrosc. obs. 4-83391  
 Hg(ClO<sub>4</sub>)<sub>2</sub> phosphine complexes, <sup>31</sup>P and <sup>199</sup>Hg NMR and vibr. spectrosc. obs. 4-83392  
 LiBF<sub>4</sub> solid, mol. reorientation, diffusion NMR study 4-88734  
 Mo binuclear complexes, triple metal bond HF-Slater transition state method 4-59619  
 Mo complex, MoCl<sub>3</sub>(OC(NH<sub>2</sub>)<sub>2</sub>)<sub>2</sub>, crystal and molecular structure 4-70089  
 N<sub>2</sub>-H<sup>+</sup>(Li<sup>+</sup>)(Na<sup>+</sup>)(K<sup>+</sup>) struct., binding energies, ab initio HF calcs. 4-112096  
 NO<sup>+</sup>, stepwise hydration, struct., ab initio calcs. 4-81402  
 NO<sub>3</sub><sup>+</sup> isolated in alkali halide systems, IR and Raman spectra 4-59761  
 NSCl, geometry, ab initio SCF force field calcs. 4-64344  
 N<sub>2</sub>-HF(HCl)(HBr), H bonded complexes, ab initio GO SCF MO calcs. 4-64369  
 Na<sub>n</sub> (n $\leq$ 7), cluster geom. calc. by Hellmann-Feynman forces 4-74372  
 Na<sub>n</sub> clusters, electronic structs., equilib. geometry self-consistent LSD calcs. 4-102843  
 NaCN and Na<sup>13</sup>CN, mol. beam electric reson. in microwave region, hyperfine transitions, quadrupole cou. 4-64501  
 Ni II complex, ethyl  $\alpha$ -ketocyclopentylcarboxylate, V-UV spectrosc. investig. 4-112191  
 Ni(CO)<sub>4</sub>, geometry optimisation, relativistic corrections, HF approx. 4-78762  
 OH<sup>+</sup>(CO)<sub>2</sub> clusters, (n=1, 2), ab initio investig. 4-96737  
 OH<sup>+</sup>(H<sub>2</sub>O)<sub>n</sub> clusters, (n=0, 2, 3, 4), ab initio investig. 4-96736  
 P<sub>n</sub> allotropes, bond energetics and mol. struct., MNDO calcs. 4-64374  
 P<sub>n</sub>H<sub>n</sub>, bond energetics and mol. struct., MNDO calcs. 4-64374  
 PH(D), X<sup>2</sup> $\Sigma^+$  vibronic state, far-IR laser mag. reson. 4-59814  
 P<sub>2</sub>O<sub>5</sub> bond energetics and mol. struct., MNDO calcs. 4-64374  
 P<sub>2</sub>-HF(HCl)(HBr), H bonded complexes, ab initio GO SCF MO calcs. 4-64369  
 Pt II complexes, bis(acetonitrile)dichloroplatinum II, mol. and cryst. struct., vibr. IR and Raman study 4-103708  
 Re complex, [( $\eta^5$ -C<sub>5</sub>H<sub>5</sub>)<sub>2</sub>Re(H)Cu]<sub>2</sub>, cryst. and mol. struct., Cu(I)-Cu(I) bond 4-96715  
 Rn monohalides, laser amplification 4-83567  
 S<sub>n</sub> mol. and ions, n=3 to 8, geometry, MNDO calcs. 4-68961  
 Se<sub>8</sub> struct., charge redistribution model, electron diff. study 4-112275  
 SiH<sub>4</sub>, uniform decomp., Si chem. vapour deposition 4-71900  
 Si<sub>2</sub>H<sub>2</sub> conformers, relative stabilities, ab initio and CI calcs. 4-74145  
 SiH<sub>3</sub>NCO, skeletal bending pot. function, microwave spectra 4-59872  
 SiH<sub>3</sub> protonated ions, ab initio calcs. appl. to interstellar detect. possibility 4-87051  
 SiS protonated ions, ab initio calcs. appl. to interstellar detect. possibility 4-87051  
 W binuclear complexes, triple metal bond HF-Slater transition state method 4-59619

inorganic molecule electronic structure *see molecular electronic states*insolubility *see solubility***inspection***see also quality control; reliability; testing*

- accuracy estimation using probability methods 4-109618  
 accuracy rel. to geometrical testpiece dimensions fluctuation 4-81387  
 acoustic emission, multichannel inspection device 4-109599  
 acoustic emission for materials processing, reviews 4-99692  
 adhesive bonded joint, strength tests using acoustic emission method 4-109614  
 bar, magnetised, vibration displacement compensation for residual field meas. 4-71831  
 burns revealing using opt. differential structurescope 4-109616

**inspection continued**

cable inspection using electro-optical technique and microprocessing technology 4-106347  
 capillary and bubble methods for detection of through-defects 4-76956  
 capillary flow inspection, appl. of aq. soln. of detergents 4-76955  
 CEGB, US NDT systems, recent developments, review 4-93483  
 conference on safeguards and nuclear materials management, Venice, Italy, (May 84) 4-106114  
 Doppler effect in ultrasonic inspection 4-71847  
 dye penetrant inspection, brightness-colour coeff. of visibility of indications 4-109610  
 eddy current equipment for aircraft maintenance 4-76943  
 eddy current inspection, mag. field intensity vector direction 4-71844  
 eddy current test lines, integration of microcomputers, review 4-62137  
 EM field of defect in form of cylindrical cavity 4-76952  
 fatigue damage inspection in stainless steel VNS-25, by positron annihilation method 4-81390  
 ferromagnetic material inspection; harmonic analysis of hysteresis loops 4-71127  
 ferrosone flow detector, appl. to welded joints 4-71835  
 fuel cycle facilities, inspection goals for safeguards 4-106955  
 ground surfaces, inspection of quality by X-ray sliding beam method 4-71813  
 high-strength EM field visualisation method, model defects investig. 4-109607  
 impedance inspection unit, split-combined transducer, elec. simulation method 4-76945  
 impedance inspection unit, split-combined transducer, elec. simulation method 4-76946  
 industrial piezoelectric transducers for US flaw detection, quality evaluation parameters 4-79413  
 interference-holographic inspection of resonators of frequency pressure transducers 4-78369  
 international nuclear safeguards, optimal allocation of inspection resources 4-106961  
 light materials, X-ray inspection, radiation contrast rel. to scatter 4-71846  
 magnetic, design parameter of local magnetizers 4-109606  
 magnetic inspection method, mag. leakage flux as function of orientation between direction of defect and mag. field direction 4-81392  
 metal rods, US inspection, EM excitation, contactless registration of normal flexural waves 4-71848  
 MOX fuel fabrication plant, observed MUF as function of throughput 4-106964  
 naval structures, underwater NDT methods 4-114759  
 neutron radiometric instruments and installation for nondestructive absorpt. inspection 4-109608  
 nondestructive, spark erosion, reference defects (*German*) 4-114746  
 nonuniformly magnetised long rod moving through scanning coil, EMF 4-76953  
 nuclear installation inspection for safeguards, in-field computer support 4-111727  
 nuclear material large bulk handling facilities, tag inventory, physical inventory verification 4-106966  
 nuclear safeguards, IAEA inspection effort allocation and distrib. in 1982 4-106960  
 optical fibre links fault detection method 4-112573  
 optical filling line inspection system for breweries 4-112558  
 photonutron inspection, scattered radiation effect 4-99706  
 piezoelectric transducers, nondestructive inspection characts. 4-99709  
 pulsed self-excited oscillator for electromagnetic flaw inspection devices 4-109604  
 PWR primary coolant pumps, long-term inspection requirements 4-96187  
 radiographic inspection, pocket computer appl. to exposure parameters 4-71805  
 radiography, TV fluoroscopy, automated inspection system 4-93476  
 reactor pressure vessels, thick walled components, US inspection, time of flight data evaluation, ALOK system 4-71804  
 rod, conducting, AC inspection, contactless method 4-71832  
 rolled sheet, automated contactless US quality control 4-71841  
 SEM image, pattern inspection techniques 4-96828  
 semiconductor wafer surface defects, automated detection by laser scanning 4-113773  
 steam pipe bends flaws, ultrasonic inspection 4-66545  
 steam turbine-generator, acceptance test demonstration and verification 4-87826  
 steel, annealing, monitoring, pulse magnetisation and demagnetisation 4-76954  
 steel, austenitic stainless, radiographic crack detection in thick sections using linear accelerator source 4-89224  
 steel, grading by combined eddy current and thermoelec. methods 4-99705  
 steel, stainless, ferritic-austenitic, embrittlement, mag. inspection 4-99704  
 steel, stainless, US inspection, flaw visibility, split spectrum processing, grain size effect 4-89226  
 steel, tool alloy, magnetographic inspection, flaw image rel. to heat treatment 4-71834  
 steel pipe barrier, radiographic inspection, dose build up factors of isotropic point source 4-99707  
 steel plate, crack type defects, US inspection with inclined transducers 4-71850  
 subsurface hole location and size, Rayleigh surface wave scatt. 4-62135  
 surfaces, quality control, automated interference meas. 4-81391  
 transmission pipelines, electromag. field distrib. in flaw detector 4-81389  
 turbine-generator disc-type LP rotors, stress corrosion control, design, operating and inspection considerations 4-88237  
 US inspection by oblique transducer, elastic vibration wavelength determ. by interference method 4-71849  
 US inspection tool, acoustic emission, techniques and appls. 4-93482  
 US reflection from natural defects propagating from surface, echo signal amplitude 4-109615  
 US testing of polyethylene tube welded joint (*French*) 4-114756  
 welded joint with backing ring, US inspection 4-81388  
 welded joints, radiation inspection, sensitivity evaluation 4-71845  
 welded joints, radiographic inspection in welding-in cylindrical components 4-76951  
 welded joints in pipes, automatic ultrasonic inspection apparatus characts. 4-66510  
 welds, flaw characterisation, nondestructive inspection, international codes and standards 4-89225

**inspection continued**

Al alloy sheet, flaw inspection, fatigue crack parameter selection in setting specimens 4-109605  
 Al welds, miniature, in composite structures, nondestructive inspection 4-66529  
 C fibre reinforced plastic, thermal NDT method for inspecting large parts 4-71838  
 Pu determination in MOX fuel fabrication plant wastes by passive neutron assay 4-111710  
**instability** *see stability*  
**installation**  
 solar power plant heliostat facets installation and adjustment costs anal. 4-93593  
**instrumentation**  
*see also aerospace instrumentation; computerised instrumentation; digital instrumentation; digital readout; display instrumentation; nuclear instrumentation; physical instrumentation control; signal generators*  
 advances in instrumentation, conf. Houston, Texas, USA (Oct. 1983) 4-106121  
 domestic solar system instrumentation, long-term stability and performance 4-99989  
 electronic meas. and laboratory practice, book 4-58585  
 IR and MM waves, conf., Miami Beach, FL, USA (Dec. 1983) 4-73154  
 measurement facilities maintenance planning 4-101805  
 physical instruments, microvibr. protection by burying in ground (*Russian*) 4-106294  
 test equipment for ambient stressed products (*Italian*) 4-69716

**instruments**

*see also individual types of instruments, e.g. astronomical instruments, bridge instruments, optical instruments*  
 electrical measurement types, review (*German*) 4-82807  
 measurement instrument renovation, to reduce costs 4-106308  
 measurement instrument yard and metrology laboratory, administrative and technical management 4-106307  
 measurement instruments with two types of failure, check-interval determ. 4-90548  
 measuring instruments, purchase and rental considerations (*German*) 4-106316  
 measuring instruments calibration using automatic calling software system 4-106261  
 surface crack depth meas., alternating potential method and measuring instrument appl. (*Chinese*) 4-81366

**insulated gate field effect transistors**

FET humidity sensor incorporates temperature sensor 4-73443  
 ISFET, membranes fabrication by ion-beam technique 4-95402  
 MIS thin gate oxide structures, direct and Fowler-Nordheim tunnelling 4-61464  
 MOS buried-channel transistor, cutoff voltage (*Russian*) 4-108943  
 MOSFET, anal. of quantised Hall resist. at finite temps. 4-98727  
 MOSFET, applications of electron microscope techniques to semiconductors 4-103622  
 MOSFET, energy relax. of warm electrons under substrate bias 4-104318  
 MOSFET, hysteresis phenomena in charging in quantising mag. field 4-104319  
 MOSFET, interface carrier mobility transport theory anal. 4-70944  
 Al<sub>2</sub>O<sub>3</sub>-SiO<sub>2</sub> gate dielectric ISFET ph sensor, surface and buried channel, characterisation 4-72033  
 GaAs, lateral growth over W gratings by CVD, application to FET transistors 4-81148  
 GaAs:Se, deep acceptor, photoluminescence study 4-80534  
 InP MOSFET structures, carrier channel mobility correl. with interface state meas. 4-88600  
 InP:Si MISFETs, post-implantation capless annealing 4-113472  
 InP-MOS using indirect plasma-enhanced CVD technique for Al<sub>2</sub>O<sub>3</sub> gate dielec. 4-104529  
 Mo-Ti/Si interface, metallisation for self-aligned TiSi<sub>2</sub> process 4-89145  
 n-Si inversion layers, two-dimensional plasmons and far infrared emission 4-104140  
 n-Si, inversion layers in MOSFET, phonon limited hot-electron temp. 4-70945  
 Si laser recrystallised MOSTs, current cond. mechanism 4-76057  
 Si, polycrystalline SOI structures, RF zone melting recrystn. for MOSFET fabrication 4-88965  
 Si, thick isolated layers, growth, characterisation and MOSFET props. 4-99309  
 Si/SiO<sub>2</sub> MOSFET, elec. props. and atomic struct. 4-80677  
 Si-MOSFET inversion layer, warm electron coeff. calc. for two-dimens. electron gas 4-65748  
 Si-SiO<sub>2</sub> laser recrystn. of Si films with heat sink struct., MOSFET fabrication 4-60954  
 n-Si-tunnel oxide-metal struct. with MOSFET for meas. elec. cond. of SiO<sub>2</sub> films 4-61476  
 SiO<sub>2</sub> films, plasma enhanced MOCVD, MOSFET fabrication 4-81153

**insulating coatings**

*see also varnish; waxes*  
 Al<sub>2</sub>O<sub>3</sub> sputtered coating, improved adhesion to Cu substrate 4-76967

**insulating materials**

*see also asbestos; ceramics; composite insulating materials; dielectric materials; gaseous insulation; glass; insulating thin films; mica; organic insulating materials; thermal insulating materials*  
 attapulgite, temp. and freq. variations of elec. props. 4-61616  
 dielectric materials, measurements anal. appls., conf., Lancaster, England (Sept. 1984) 4-106120  
 electrical insulation degradation for chem. sprays in loss of coolant accidents 4-68799  
 electrokinetic streaming current, induction sensing 4-65033  
 glass insulation, self heating and surface resist. 4-70903  
 liquids, semi-insulating, tube flow, flow-induced charge accumulation and field generation 4-65032  
 LV thermoplastic/thermosetting insulating materials for industrial use, laboratory tests (*Italian*) 4-99410  
 measurement of tan  $\delta$  and  $\epsilon$  4-101874  
 polyethylene films, treed and crosslinked, anal. of water 4-71281  
 porcelain, high-alumina, for HV insulators, strength under dynamic and cyclic loads (*German, English*) 4-76836  
 porcelain, low-voltage elec., prod. using perlite 4-81173  
 SIMS analysis using fast atom beams 4-93576

insulating materials, acoustic *see noise abatement*

insulating materials, thermal *see thermal insulating materials*

### insulating oils

electrohydrodynamic behaviour of viscous dielectric fluid and current response to voltage changes 4-97702

transformer insulating oil dissolved gases chromatographic anal. (Portuguese) 4-114860

### insulating thin films

*see also dielectric thin films; electronic conduction in insulating thin films*

anodic oxide films, diffusion and transport numbers 4-104001

Auger electron spectra, electron and ion beam effects 4-109283

breakdown rel. to recording mech. in thin-film breakdown counters 4-102525

2-bromonaphthalene glassy films, spectral diffusion and triplet exciton localisation 4-98538

bromotrifluoromethane, IR and Raman spectra, cryst. struct. 4-104690

cadmium arachidate:perylene, probing phonon processes 4-70303

compositional anal. using null or fixed wavelength ellipsometry 4-90645

deposited dielectric for III-V semiconducting devices 4-84702

fluorinated hydrocarbon films, electron-stimulated desorption 4-98451

gate oxides, dual two step trichloroethylene oxidation growth 4-81151

glass thin films, phonon dispersion meas. 4-70326

homogeneous, effective spin-pinning, critical angles, surface modes 4-98896

hydrocarbon polymer dielectric films, hot-electron transport 4-92837

integrated UHV system for thin film deposition 4-90601

Kapton-H polymer thin film, space charge and dipolar relax. 4-76328

laser CVD using CW and pulsed lasers 4-109330

metal oxides, defect processes 4-81358

metal/insulating thin film system, surface polariton refraction 4-92631

nitride insulating films, CVD using  $\text{NF}_3$  4-85108

organic translucent thin films, optical microscopy, visibility enhancement using fibre-optic cables 4-106378

pentacene layers, dispersive charge carrier transport 4-80703

polyacetylene, highly oriented, struct. and cond. (Japanese) 4-92111

polyethylene films, treed and crosslinked, anal. of water 4-71281

polypropylene evaporated thin films in MIM struct., electroforming 4-80686

polystyrene thin layers, dielec. breakdown, definition and characts. 4-109122

polysulphone films, corona charged, surface potential decay characts. determ., expt. 4-92836

rate earth sesquioxide thin films, fine struct., EELS investig. 4-70247

small molecules condensed films, shape reson. in photoemission 4-83061

spinel films, epitaxial growth by solid state reactions 4-61252

transition metal oxide films, deconvolution of EELS 4-81053

$\text{Ag}_2\text{Te}$ ,  $\text{Cu}_2\text{Te}$ , high and low temp. modifications 4-75800

$\text{Al}(\text{SnO}_2 + \text{Sb}_2\text{O}_3)$ -Al mixed thin films, dielec. studies 4-84719

AlN films, ion beam deposition technique 4-85114

$\alpha\text{-Al}_2\text{O}_3$ , electronic energy levels from Al L-edge photoabsorption, small-cluster CNDO calcs. 4-81038

$\text{Al}_2\text{O}_3$ , thin film and powder,  $\gamma$  to  $\alpha$  transformation, TEM studies 4-108613

$\text{Al}_2\text{O}_3$  thin layers, dielec. breakdown, definition and characts. 4-109122

$\text{Al}_2\text{O}_3$  thin microporous layers, prep. and characterisation 4-70601

Ar films, structural order effects in low-energy electron transmission spectra 4-98520

BN films, glow discharge prep., insulator for semicond. device passivation 4-85120

BN, films, interaction with Ni at high temps. 4-70583

BN:P film in InP, grown by CVD, elec. props. 4-99336

$\text{BaF}_2$  epitaxial films, vacuum deposition on PbSe 4-99316

$\text{BaTiO}_3$  amorphous film, elec. and struct. props. 4-80701

$\text{Bi}_2\text{TeO}_{20}$  thin films, IR spectra and lattice phonons 4-88893

$\text{Bi}_2\text{SiO}_{20}$  thin films, IR spectra and lattice phonons 4-88893

C film growth on Ir by vacuum sputtering, initial stages 4-61257

C thin films, plasma induced chem. transport prep. 4-71603

a-C:H hard thin films, RF plasma deposition 4-76681

CO films, structural order effects in low-energy electron transmission spectra 4-98520

$\text{C}_2\text{Si}_{1-x}$ , amorphous film, elec. and optical props. 4-113962

$\text{CeF}_3$  doped optical films, tensile stress cracks and stress modification 4-76543

CoO film, on metallic substrate, solar thermal absorbing props. 4-89465

$\text{Cr/SiO}_2$  thin films, elec. transport props. 4-92830

$\text{Cr}_2\text{O}_3$  film thickness meas. using Raman scatt. 4-104689

$\text{CsBi}(\text{MoO}_4)_2$  layer cryst., structural phase transitions 4-88286

Cu-In-S layers, electrodeposition, photoelectrochemical characterisation 4-99355

Cu-SiO/GeO<sub>2</sub>-Cu sandwich structures, elec. props. time, temp. press. depend. 4-108949

$\text{Cu}_2\text{O}$  thin films on Cu, defect luminesc. 4-66062

$\text{Dy}_2\text{O}_3$  thin films, high resolution CTEM images, effect of slight disorientation on image aspect 4-70602

$\text{ErF}_3$  amorphous thin films, AC cond. meas. 4-76059

$\text{FeF}_3$  granular thin films, localised electronic state spatial distrib., polarisation study 4-104334

$\text{FeF}_3$  thin film, impurity cond. along least resistance paths 4-80705

Ge with adsorbed  $\text{CaF}_2$ , layer thickness meas. by RBS (Chinese) 4-70968

$\text{GeO}_2$  films, amorphous, elec. characterisation in MIS and MIM structures. 4-70816

$\text{GeO}_2$  films, optical const., random bonding model 4-85025

$\text{KBr:In(Tl)}$  polycrystalline films, luminescent, epitaxial growth (Russian) 4-113833

KI thin films, high-field elec. cond. study 4-80702

Kr films, structural order effects in low-energy electron transmission spectra 4-98520

Kr layer on graphite in one-to-two layer regime, phase diagram, freezing transitions 4-103910

$\text{LaMo}_2\text{S}_9$  films, supercond. props. and normal state resist. 4-92876

$\text{LiF-AlF}_3$  thin film, ionic cond. meas. 4-84450

$\text{LiF-CaF}_2$  thin film, ionic cond. meas. 4-84450

$\text{LiF-CeF}_3$  thin film, ionic cond. meas. 4-84450

$\text{LiF-CrF}_3$  thin film, ionic cond. meas. 4-84450

$\text{LiF-MgF}_2$  thin film, ionic cond. meas. 4-84450

$\text{LiF-NiF}_2$  thin film, ionic cond. meas. 4-84450

$\text{MgF}_2$  films, evaporated, internal stress, struct., substrate temp. depend., electron microscopy obs. 4-98495

### insulating thin films continued

$\text{N}_2$  films, structural order effects in low-energy electron transmission spectra 4-98520

NO dimeric thin films, vibr. excitation via shape reson. in electron scatt. 4-99250

NaF polycrystalline thin films, neutron and X-irrad., photochemical hole burning 4-76518

$\text{Na}_2\text{WO}_3$  films, optical absorption spectra, electrochromic cell appls. 4-76544

$\text{Nb}_2\text{O}_5$  amorphous film, elec. behaviour study (Russian) 4-84722

$\text{Nb}_2\text{O}_5$ , XPS and optical spectra, low-valence cations and electron props. 4-98623

Ni oxides on Ni, transpassive thin films, sputter profiling, AES, XPS studies 4-113823

Ni-P thin film, selective absorber, for photothermal conversion of solar radiation 4-81589

NiO film, on metallic substrate, solar thermal absorbing props. 4-89465

NiSi thin film form. in  $\text{Ni}_2\text{Si/Si}$  system, diffusion mechanisms 4-92446

$\text{O}_2$  films, structural order effects in low-energy electron transmission spectra 4-98520

Pb- $\text{PbF}_2$  films, TSC and space charge 4-84903

PbO layers, microscopic appearance, preferred orientation, and platelet thickness, X-ray diffr. and SEM obs. (Chinese) 4-88411

PbO<sub>2</sub> vacuum evaporated films, electron emission and I-V characts. (Japanese) 4-76643

phosphosilicate glass films on Si wafers, quantitative anal. for calibration of X-ray fluorescence spectrometry standards 4-105046

RhSi on polycrystalline and amorphous Si, struct. and growth kinetics 4-80446

Si oxide films, elec. props. and oxidation characts. 4-65762

$\text{Si}_3\text{N}_4$ -H amorphous film, photoinduced ESR study 4-114161

$\text{Si}_3\text{N}_4$  amorphous films, impurities, IR investig. 4-80913

$\text{Si}_3\text{N}_4$  dielectric film; electron conduction; expt. study 4-114053

$\text{Si}_3\text{N}_4$  film deposition by plasma-enhanced CVD, appl. to GaAs LSI 4-71569

$\text{Si}_3\text{N}_4$  film deposition on Si (Rumanian) 4-81155

$\text{Si}_3\text{N}_4$  film deposition processes and plasma assisted deposition, book contrib. 4-85111

$\text{Si}_3\text{N}_4$  film on GaAs, laser-induced Si diffusion 4-60958

$\text{Si}_3\text{N}_4$  films, amorphous, hydrogenated and deuterated; prepared from plasma-enhanced CVD, IR absorpt. spectra 4-81021

$\text{Si}_3\text{N}_4$  films, electron beam assisted CVD, conformal step coverage 4-61689

$\text{Si}_3\text{N}_4$  films, encapsulation of  $\text{Al}_0.3\text{Ga}_{0.7}\text{As}$ , disorder-activated modes, Raman spectra 4-80916

$\text{Si}_3\text{N}_4$  films, plasma enhanced CVD, transient phenomena 4-93225

$\text{Si}_3\text{N}_4$  films, plasma-deposited, prep. and characterisation 4-88986

$\text{Si}_3\text{N}_4$  on Si, film thicknesses determined by X-ray photoelectron spectroscopy 4-88946

$\text{Si}_3\text{N}_4$  surface oxide film growth by CVD, XPS anal. (Chinese) 4-61805

$\text{Si}_3\text{N}_4/\text{F}$  films, plasma enhanced CVD, insulating props. 4-61865

$\text{Si}_3\text{N}_4$  films, photo-CVD, props. study 4-99338

$\text{SiO}/\text{V}_2\text{O}_5$  thin film sandwich assemblies, co-evaporation, electroforming, insulator in MIM struct., voltage-memory effects 4-65757

$\text{SiO}_2$  defect density, influence of halogens in thermal oxidation of Si (Russian) 4-99624

$\text{SiO}_2$  film, ion implanted, electron beam recrystallisation 4-98137

$\text{SiO}_2$  film, low temp. photochemical deposition 4-99339

$\text{SiO}_2$  film, photo-induced CVD using direct excitation by  $\text{D}_2$  lamp 4-61860

$\text{SiO}_2$  film, thickness meas. using automatic ellipsometer (Japanese) 4-86471

$\text{SiO}_2$  film deposition processes and plasma assisted deposition, book contrib. 4-85111

$\text{SiO}_2$  film growth from Al-Cu-Si solid soln. 4-71783

$\text{SiO}_2$  film traps, microcomputer-based avalanche injection system, area density anal. 4-101870

$\text{SiO}_2$  films, C ion implantation, CO and  $\text{CO}_2$  form. 4-77016

$\text{SiO}_2$  films, current-temp. characts. in metal-insulator-metal struct. 4-84721

$\text{SiO}_2$  films, electron beam assisted CVD, conformal step coverage 4-61869

$\text{SiO}_2$  films, IR transmission spectra, nitridation effects 4-81022

$\text{SiO}_2$  films, photo-CVD, props. study 4-99338

$\text{SiO}_2$  films, plasma enhanced MOCVD, MOSFET fabrication 4-81153

$\text{SiO}_2$  films, space charges study with pulsed electron beam 4-88622

$\text{SiO}_2$  films, thermally nitrided, elec. characts. study 4-88620

$\text{SiO}_2$  films, thermally nitrided, Si LW and N KLL Auger signals 4-88911

$\text{SiO}_2$  films grown on oxidised Si 4-98485

$\text{SiO}_2$  gate oxide breakdown, expt. study 4-114207

$\text{SiO}_2$  glass film, crack tip geometry, water ageing, high resolution electron microscopy 4-71724

$\text{SiO}_2$  growth from laser oxidation of Si surface 4-81324

$\text{SiO}_2$  halogen containing layers, cathodoluminescence spectra (Russian) 4-99198

$\text{SiO}_2$  in  $^{\circ}\text{Cr-SiO}_2\text{-pSi}$  capacitor, conduction and charge storage 4-61474

$\text{SiO}_2$  layers on Si, film thicknesses determined by X-ray photoelectron spectroscopy 4-88946

$\text{SiO}_2$  low temp. CVD, etching kinetics 4-99614

$\text{SiO}_2$  MOS struct., tunnelling current in high field regime 4-88598

$\text{SiO}_2$  surface films, refr. index determ. by polarisation method of PEM investigation 4-93124

$\text{SiO}_2$  thermal film, defect creation by ion implantation 4-65343

$\text{SiO}_2$  thin film, annealing in  $\text{NH}_3 + \text{CF}_4$  plasma, nitride layer form. 4-93433

$\text{SiO}_2$  thin film, elec. cond. meas. using MIS struct. with MOSFET 4-61476

$\text{SiO}_2$  thin film thickness measurement by SEM or AES, appl. of low angle beveling 4-95380

$\text{SiO}_2$  thin films, chemical sputtering by  $\text{Ar}^+$  ions and  $\text{XeF}_4$  4-93177

$\text{SiO}_2$  thin films, nitridation and elec. props. 4-61435

$\text{SiO}_2$  thin films, photon-induced O loss, ESR and Auger electron spectroscopy 4-80092

$\text{SiO}_2$  thin layers, dielec. breakdown, definition and characts. 4-109122

$\text{SiO}_2\text{-Cr}$  thin films, cathodoluminescence and G-V characts. (Russian) 4-99173

$\text{SiO}_2\text{-Cu}$  films, elec. breakdown strength, Cu precipitates effect 4-99022

$\text{SiO}_2\text{-poly-Si/SiO}_2$  composite filter, reaction ion etching process in single reactor 4-85236

$\text{SiO}_2$  films IR absorpt. spectra meas. 4-88895

**insulating thin films continued**

- SiO<sub>2</sub>, reactive film deposition, surface processes, planar magnetron sputtering 4-113798  
 SiO<sub>2</sub>N<sub>x</sub>, thermally nitrided, chem. structure, XPS study 4-75797  
 SmF<sub>3</sub>, amorphous thin films, DC elec. cond. 4-113949  
 SrF<sub>2</sub>Gd<sup>3+</sup>, phosphors, thermostimulable center-center transitions, luminesc. 4-80996  
 TaO<sub>2</sub>, amorphous film, electret state relax. 4-88765  
 Ta<sub>2</sub>O<sub>5</sub>, anodically growth on Ta, ultra-high resolution depth profiling 4-81098  
 Ta<sub>2</sub>O<sub>5</sub>, XPS and optical spectra, low-valence cations and electron props. 4-89623  
 Te<sub>2</sub>O<sub>3</sub> film, stoichiometry changes, IR study 4-113836  
 TiN non-diffusing and mech. hard IR refl. thin film coatings, characts. 4-113828  
 TiSi<sub>2</sub> films, sputter deposition at high substrate temps., elec. and struct. props. 4-114393  
 WO<sub>3</sub> amorphous films, electrochromic colour centres, Raman scatt. studies 4-113445  
 WO<sub>3</sub> film, electrochromic props. 4-81027  
 WO<sub>3</sub> thin films, diffusion of H 4-70474  
 Xe films, structural order effects in low-energy electron transmission spectra 4-98520  
 Y<sub>3-x</sub>Gd<sub>x</sub>Fe<sub>2</sub>O<sub>7</sub>, noncrystalline garnet films, electron transport and thermopower 4-108958  
 Yb<sub>2</sub>O<sub>3</sub> thin films, trap levels, thermally stimulated method anal. 4-65763  
 ZrN non-diffusing and mech. hard IR refl. thin film coatings, characts. 4-113828  
 ZrO<sub>2</sub>, short-range struct., radial distrib. curve of atomic density 4-75801

**insulation**

- see also cable insulation; electric breakdown; insulating coatings; insulating materials; insulators; transformer insulation*  
 dielectric materials, measurements anal appls., conf., Lancaster, England (Sept. 1984) 4-106120  
 monitoring of insulation of a series of rechargeable cells (Russian) 4-105100  
 SF<sub>6</sub>, corona discharge under switching impulse, insulator in gap effects 4-79888

**insulation, thermal *see* thermal insulation****insulation testing**

- nuclear power station cables, gamma radiation and thermal ageing of polyethylene insulation 4-75526

**insulator-metal boundaries *see* metal-insulator boundaries****insulator-semiconductor boundaries *see* semiconductor-insulator boundaries****insulators**

- i.e. insulating devices. For materials *see* insulating materials*  
*see also insulation*  
 air pollution hazards, evaluation using sedimentation methods (Polish) 4-105139  
 exchange-correlation potential determ. 4-61279  
 high tension, failure prediction, NDT methods comparison 4-62154  
 surface discharge in vacuum in presence of charged particles 4-79870  
 thermal props. meas., using transient hot-strip method 4-68242

**integral equations**

- see also integro-differential equations*  
 3D fracture mechanics, boundary integral equation-boundary element method appls. (Chinese) 4-79398  
 acoustic scattering, boundary element methods and their asymptotic convergence 4-83751  
 acoustic waves, time harmonic, inverse scattering problem 4-103054  
 acoustics, integral equations, numerical methods 4-83748  
 astronomical image sharpening techniques, maximum entropy method (German) 4-67640  
 boundary integral eqn. axisymmetric stress analysis, interior point solns. 4-63510  
 Carleman integral eqn., spectral relationships, appl. to contact problems 4-60345  
 collision estimates, dispersion minimisation in variable sign element problems, Monte Carlo soln. (Russian) 4-63489  
 composite annular plates, vibr. anal. by integral eqn. technique 4-112756  
 conducting cylinders embedded in lossy medium, EM scatt. 4-112324  
 continuum mechanical problems reduction to second-order integral eqns. (Ukrainian) 4-67976  
 convective heat transfer in laminar flow over flat plate, approx. integral methods improvement 4-75020  
 convolution and deconvolution methods in nuclear medicine 4-115201  
 crack thermoelastic boundary integro-differential eqn. formulation 4-64882  
 degenerate functional integral, functional delta-functions and Fourier transforms 4-58619  
 dynamic elastic problems, boundary integral eqn. method 4-95175  
 dynamic impact of an elastically supported beam-large area contact 4-79527  
 elastic system small vibrs., Hilbert-Schmidt theorem extension to problems with unsymmetric kernels 4-110865  
 elasticity, asymmetric theory, axial-symmetric contact problem 4-91776  
 elasticity, weighted residuals based general soln. method 4-73235  
 elasticity problems, appl. of weak formulation of boundary integral equations 4-78137  
 elasticity theory, boundary integral eqn. method for external boundary value problem soln. 4-106188  
 elastodynamic boundary-value problems, integral eqn. method appls. 4-60283  
 electromagnetic E-polarised wave diffraction on plane ship, dual integral eqns. (Russian) 4-96758  
 electron lenses, open, computation by coupled finite element and boundary integral methods 4-91392  
 EM scattering by homogeneous dielectric bodies, integral eqn. 4-64656  
 EM wave scattering, semiinfinite dielectric layer imbedded in perfectly conducting half space 4-69287  
 EM wave scattering and transmission by dielectric body, integral eqns. 4-64655  
 evaluation of integral involving associated Legendre polynomials and inverse powers of (1-X<sup>2</sup>) 4-63472  
 Feynman path integrals, transformations for curvilinear coordinates 4-58618  
 finite plane domain fracture problem anal. using surface integral finite element hybrid method 4-79501  
 Fredholm eqns. solns. through nonlinear iterative processes 4-67960

**integral equations continued**

- Frenkel-Kontorova systems in high temp. regions, comparison of thermodynamics with Schneider-Stoll exact solns. 4-106253  
 frictional contact under moving loads, approach to slip steady state 4-97442  
 hybrid finite element boundary element solutions using half-space Green's functions 4-59951  
 infinite solid with thin foreign inclusion, integral eqns. for stress determ. (Ukrainian) 4-69680  
 inverse heat conduction problem, descriptive soln. in B-spline basis 4-97272  
 isotropic medium with curvilinear sections, second dynamic problem soln. in elasticity theory (Ukrainian) 4-69694  
 laser resonator modes, coherence theory 4-69454  
 layered composite, penny-shaped interface crack; torsional impact response 4-79498  
 lifting surfaces in unsteady flow, aerodynamic press., integral eqns. 4-64922  
 linear elastic cracked body, transient elastodynamic second boundary-value problem 4-64881  
 liquid theory, linear integral equations and renormalization group 4-103634  
 magnetic field in cavity of perfect diamagnetic material, integral eqn. method 4-105811  
 magnetic fields, secondary source method of computation (Russian) 4-83515  
 magnetic recording, reciprocity integral, convolution or correlation 4-79002  
 membranes, elastic, circular, large axisymm. deforms. 4-112703  
 momentum integrals in 2-D 4-78128  
 multiple crack problem solns. using Fredholm integral eqns. 4-79509  
 Navier-Stokes eqns., steady, anal. based on Green's function approach 4-79541  
 Navier-Stokes eqns., unsteady, anal. based on Green's function approach 4-79542  
 nonlinear Volterra equation, bifurcation theory of the time-dependent von Karman equations 4-112720  
 optical waveguide junctions analysis using integral eqn. method 4-107819  
 penny-shaped crack, symmetric indentation by embedded rigid circular disc inclusion 4-79506  
 penny-shaped interface crack with heat flow, imperfect contact 4-97425  
 perfectly conducting strip on planar interface between semiinfinite half-spaces, induced current determ. 4-69275  
 planar crack of arbitrary shape at interface of two anisotropic elastic half spaces 4-79508  
 plane elastic media, curvilinear cracks tip stress intensity factors 4-64886  
 plate containing circular hole, Fredholm integral eqn. 4-103251  
 polynomial Hamiltonians, quantum mech. path integrals with Wiener measures 4-58680  
 potential integrals for uniform and linear source distributions on polygonal and polyhedral domains 4-69268  
 radiative transfer problems in spherical media, soln. using integral eqns. 4-94601  
 radiative transfer theory, nonuniqueness of soln. for nonlinear integral eqns. 4-72864  
 scalar wave scattering from rough surfaces, anal. 4-79009  
 shell, cylindrical, eddy current problem, integral eqn. approach 4-102850  
 simple layer potential method for domains having external corners 4-63511  
 singular integral problem in surfaces, comments and reply 4-87251  
 square aperture reflector, implementation of stationary phase method (French) 4-83518  
 stamp, vibrating, wave excitation in medium with inhomogeneous initial stresses 4-108032  
 stress intensity factors of crack between two nonhomogeneous materials with antiplane shear loading 4-79516  
 thermoelasticity, nonstationary, appl. of boundary element problem 4-112711  
 thin-walled cylindrical screens, Fredholm eqn. soln. for two-dimensional EM field, screening efficiency (Russian) 4-102856  
 three-dimensional electric field calculation by means of surface charges and surface currents 4-102849  
 transformation in Lobachevsky space 4-63867  
 two-wave X-ray field, calc. by integral eqn. methods 4-75235  
 viscous Stokes flows past collection of particles in circular cylinder, boundary integral eqns. 4-65026  
 Voigt spectral line profile, mathematical props. 4-63043  
 Volterra-Runge-Kutta methods stability 4-58621  
 watt-hour efficiency of system loop inductor-ferromagnetic plate 4-102851  
<sup>6</sup>Li ground state discrete generator coordinates method, for solution of many-particle Schrodinger equation 4-86774

**integral transforms *see* transforms****integrated circuit manufacture**

- Used for commercial manufacture only*  
*see also masks; photolithography*  
 optical microanalysis in microelectronic device and packaging manufacture 4-93574  
 photomasks, absolute measurements of structure widths in micrometer range with the optical microscope 4-95386  
 surface preparation for high quality interface formation for IC technology 4-89170  
 wafer flatness tester, automatic, using Fizeau interferometer, VLSI circuit wafer appls. 4-106270  
 Si, conference, San Jose, CA, USA (Jan. 1982) 4-110812

**integrated circuit technology**

- See also under specific integrated circuit headings*  
*see also semiconductor technology*  
 CMOS active lateral diffusion and linewidth test struct. 4-108665  
 DC monolithic accelerometer design and fabrication 4-111122  
 dry etching processes, topography modeling 4-80344  
 FET humidity sensor incorporates temperature sensor 4-73443  
 Langmuir-Blodgett films, prep. charact. and appls. 4-61245  
 moire topography of substrates 4-101811  
 multielectrode microprobe for extracellular biopotential recording 4-115320  
 multilayer ceramic substrates, selective Cu plating Mo structs. 4-66242  
 photomasks, absolute measurements of structure widths in micrometer range with the optical microscope 4-95386  
 plasma etching device for microelectronic circuit processing 4-79850

**integrated circuit technology continued**

- semiconductor technology, book 4-86123
- SOI three-dimensional ICs fabrication by laser recrystn. of Si islands 4-75798
- solid-state devices and materials, conf., Tokyo, Japan (Aug.-Sept. 1983) 4-82595
- stratified media technology, conf., Los Angeles, CA, USA (Jan. 1983) 4-82585
- submicron features replication using PVC 4-68222
- surface preparation for high quality interface formation for IC technology 4-89170
- synchrotron radiation X-ray lithography 4-90704
- VLSI, selective plasma etching of polycryst. Si 4-81311
- VLSI by selective epitaxy, local loading effect 4-93228
- VLSI circuit processing, Si material phenomena 4-103738
- X-ray lithography, demagnified projection printing using no thin-film masks 4-90697
- X-ray lithography with synchrotron radiation for LSI micropatterning (Japanese) 4-86516
- Al, electromigration at high current density, phenomenological obs. 4-84470
- Al-Si/ $n^+$ -Si system, metallisation by fast heat pulse alloying, hillock elimination 4-114034
- Au-a-SiO<sub>2</sub>, metallisation technology comparative study of Nb and TiW barrier layers 4-88969
- CoSi<sub>2</sub> films, solid-phase epitaxial growth, patterning effects 4-84537
- GaAs integrated optical device fabrication, Cl<sub>2</sub>-Ar reactive ion etching technique 4-87483
- GaAs, ion implanted, transient capless annealing appl. to IC fabrication 4-103779
- GaAs LSI, Si<sub>3</sub>N<sub>4</sub> film deposition by plasma-enhanced CVD 4-71569
- GaAs substrates for GaAs ICs, growth processes 4-99299
- Mo films, taper dry etching, LSI interconnections appl. 4-89184
- Mo-Ti/Si interface, metallisation for self-aligned TiSi<sub>2</sub> process 4-89145
- Si, C and O content determ. by IR spectroscopy 4-113484
- Si, conference, San Jose, CA, USA (Jan. 1982) 4-110812
- Si films, monocrystalline and polycrystalline, simultaneous epitaxial growth, struct., elec. props. 4-98488
- Si integrated circuits, cross sectioning for SEM, TEM and optical microscopy 4-95400
- Si wafer, mechanical properties, effects of laser back-side damage 4-98132
- Si:B, deep implanted layers, for IC appl. 4-75482
- SiO<sub>2</sub> gate dielects., charge build-up and breakdown 4-109124
- TiSi<sub>2</sub>/ $n^+$  poly-Si, co-sputter-deposited, rapid lamp heating, MOS device fabrication appl. 4-99311
- WSi<sub>2</sub>-poly-Si-SiO<sub>2</sub>-Si MOS struct., interface reaction and resistivity 4-114040

**integrated circuit testing**

- semiconductor device manufacture, Raman microprobe appl. 4-93573
- submicron features replication using PVC 4-68222

**integrated circuits**

- see also *digital integrated circuits; hybrid integrated circuits; large scale integration; linear integrated circuits; masks; microwave integrated circuits; monolithic integrated circuits; substrates; thick film circuits; thin film circuits*
- biomedical electronics applications, development from idea to finished product (Danish) 4-81810
- electrical and electronic phenomena and devices, book 4-67952
- MM waves and IR, conf., Miami Beach, FL, USA (Dec. 1983) 4-73154
- optical techniques, industrial appl. 4-97117
- polymers, conductive materials, microelectronics appls. 4-70794
- SEM image, pattern inspection techniques 4-96828

**integrated logic circuits**

- flip-flops based logic system design for RISK spectrometer, using event preselector 4-86998
- interfacing 15VSM5 minicomputer and Elektronika D3-28 to expt. equipment, using TTL ICs 4-90569
- semiconductor laser diode modulators triggered by logical IC 4-60082

**integrated optics**

- see also *fibre optics; optical films; optical modulation; optical waveguides; semiconductor junction lasers*
- acousto-optics, integrated, technology and competition 4-64674
- anisotropic waveguide, acoustooptic and electrooptic guided wave conversion to leaky waves 4-91583
- applications in industrial process control 4-107891
- asymmetrical dielectric slab waveguide, power loss at step discontinuity 4-87449
- beam splitter and focuser in LiNbO<sub>3</sub>:Ti planar waveguide 4-74680
- bistable optical devices, fundamental performance limits 4-64738
- book, optical waves in crystals, laser radiation propag. and control 4-86135
- coupling length calc. for optical waveguides in a semiconductor heterostructure 4-91584
- device patterns, quadrupole electron-beam exposure technology 4-107889
- DFB laser, quarter-wave shifted grating type, wavelength selectivity analysis 4-64716
- DFB lasers with strong modulation, threshold gains and resonance freqs. calc. 4-79095
- dielectric thin films with bounding media, guided nonlinear waves, dispersion relations 4-69483
- diffraction optical-heterodyning schemes, dynamic operating mode 4-69543
- diffused thin films, realisation and meas. 4-103025
- diffused waveguides containing Ag<sup>+</sup> optical breakdown, laser colouring 4-107712
- diffused waveguides on glass substrates, optical props., fabrication process 4-74706
- diode lasers, chirped arrays for supermode control 4-102942
- diode lasers, phase-locked arrays, supermodes obs. 4-102943
- directional-coupler powder divider by two-step K<sup>+</sup>-ion exchange 4-107822
- division-of-wavefront polarising beam splitter and half-shade device using dielectric thin film on dielectric substrate 4-74679
- electrooptic leaky anisotropic waveguides using nematic liquid crystal overlays 4-97063
- EM wave field distrib. at open end of microstrip waveguide 4-107825
- Fabry Perot waveguide resonators, parametric oscillation investigation 4-64741
- Fabry-Perot cavity, bistable system, switching times 4-112500

**integrated optics continued**

- fibre and integrated optics in Germany, national review 4-64788
- film lenses analysis, with complex source point method 4-64792
- functional waveguide device physical realisation, analytic conditions 4-87482
- general planar guiding struct. at 10.6  $\mu$ m 4-91639
- geodesic optics 4-64756
- guided wave control technology 4-107817
- gyro chip, experimental and theoretical data 4-91613
- intensity-dependent guided wave obs. 4-79220
- interfaces for digital ccts. and systems, conf., Los Angeles, CA, USA (Jan. 1984) 4-95026
- isolator and circulator using nonreciprocal phase shifters 4-87481
- Langmuir-Blodgett films, prep. charact. and appls. 4-61245
- matching methods for integrated-optics devices and fibre-optic communication lines, review 4-60184
- metal-dielectric heterostructures, singularities in guided TM mode absorption spectrum 4-74749
- 3-methyl-4-nitropyridine-1-oxide optically nonlinear thin films, definition and bulk performance 4-74589
- methyl-(2,4-dinitrophenyl)-aminopropanoate optically nonlinear thin films, definition and bulk performance 4-74589
- mode conversion of acoustooptic interaction in crossed channel waveguide 4-104568
- monolithic laser/multiplexer optoelectronic integrated circuit, operation 4-97141
- multilayered thin film optical separators, tunable wavelength selection characts. 4-79275
- multimode Y-coupler for heterodyne detection 4-112566
- nonlinear integrated optics 4-64739
- open dielectric strip waveguides, leakage and resonance effects, expt. study (Japanese) 4-60168
- optical communication device research, epitaxial growth, lasers and integrated optics 4-74746
- optical vector matrix multiplier, high data rate 4-97145
- optical Y-junctions, behaviour 4-69548
- optoelectronic devices for high-speed interconnects 4-97139
- optoelectronic logic ccts. 4-97144
- organic thin films in integrated optics, Langmuir-Blodgett film fabrication 4-69593
- parallel digital optical adder construction method 4-60001
- phase-locked injection laser arrays with integrated phase shifters, design and operation 4-64723
- planar gradient-index glass waveguide, appl. to 4-port branched circuit and star coupler 4-87442
- planar monolithic fiber optic receiver chip on a GaAs semi-insulating substrate 4-97142
- planar multilayer waveguide, thin-films field-transfer matrix theory, refl. from prism-loaded waveguides 4-87448
- planar waveguide optical channel multiplexers and demultiplexers, spectral and aberration characts. 4-107823
- PMMA doped films, optical recording of refr. index patterns 4-107772
- polariser, metal-clad tapered optical waveguide 4-83690
- polymer thin films, structure and morphology, investig. by integrated optical techniques 4-113835
- semiconductor integrated etalon interference lasers, stable longit.-mode operation, tuning temp. depend. study 4-69455
- semiconductor phase-locked laser arrays, supermode anal. 4-60097
- signal processing using fibre and integrated optical devices 4-64794
- single-mode integrated optical strip waveguides on glass substrates by Na<sup>+</sup>-K<sup>+</sup> ion exchange (Chinese) 4-112591
- single-mode integrated-optical polarisers in LiNbO<sub>3</sub> and glass waveguides, low loss 4-112568
- single-mode optical Y junctions, formed by Ag ion exchange in glass, radiation losses 4-60181
- slanted anisotropic gratings, scatt. and waveguiding props. analysis 4-69539
- stationary reference grating based optical detection method for SAW detect. 4-60180
- stratified media technology, conf., Los Angeles, CA, USA (Jan. 1983) 4-82585
- strip waveguide fabrication of predictable cross section by diffusion in elec. field 4-91641
- thin film complex reflectivity and refr. index profiles from reflectivity magnitude meas. 4-73487
- thin film guided-wave optical spectroscopy 4-63787
- thin film optics, appl. of ion implantation 4-74757
- thin film technologies, conf., Geneva, Switzerland (Apr. 1983) 4-73137
- trapped molecules in oriented polymer films, optical anisotropy, waveguide Raman spectrosc. obs. 4-78377
- travelling wave switch/modulators vel.-matching techniques 4-74748
- travelling-wave optical modulator for  $\lambda = 1.32 \mu$ m 4-69595
- United States fiber optics market overview 4-107879
- video-bandwidth ADC using optical techniques for extended precision 4-69594
- voltage probe, design and testing 4-106295
- waveguide materials and fabrication techniques for integrated optics 4-83728
- YIG:Ga(La) magneto-optical waveguide, TE to TM mode conversion by alternating-coupling coeff. 4-69545
- YIG film Y-branch interferometer grown by liq. phase epitaxy 4-97138
- AlGaAs DH diode lasers fabricated on monolithic GaAs/Si substrate 4-112408
- AlGaAs-GaAs short-cavity laser and its monolithic integration using microcleaved facets process 4-60064
- As<sub>2</sub>S<sub>3</sub> planar waveguide, hologram recording and readout 4-83553
- CO<sub>2</sub> IR laser, freq. synthesized and continuously tunable in 9-11  $\mu$ m range 4-96947
- GaAlAs electroabsorption modulators, monolithically integrated array 4-103006
- GaAlAs laser, MESFET and photodiode, monolithic optoelectronic integration 4-74747
- GaAlAs lasers, transverse-mode stabilised MOCVD grown, with embedded confining layer on optical waveguide 4-69443
- GaAlAs very high speed lasers and detectors for integrated optoelectronic devices 4-96889
- GaAlAs-GaAs integrated optical repeater 4-97143
- GaAs integrated optical device fabrication, Cl<sub>2</sub>-Ar reactive ion etching technique 4-87483
- GaAs, optical guided-wave monolithic interferometer 4-112561

**grated optics continued**

GaAs semi-insulating substrate monolithically integrated laser diode, photo monitor and electric ccts. 4-60179  
 GaAs:Si/AlGaAs DH TJS lasers grown by MBE 4-107671  
 GaAs/GaAlAs integrated optoelectronics for optical interconnect applications 4-97140  
 GaAs/GaAlAs monolithically Peltier-cooled laser diodes 4-74540  
 GaAs/GaAlAs twin stripe lasers, current rise-time effect on beam stability, expt. study 4-91510  
 GaAs/GaAlAs waveguide phase modulator, MBE grown heterostruct., design for PSK optical fibre systems 4-83685  
 GaAs-(AlGa)As twisted DH laser, composite cavity config., design and longit./transverse mode operation 4-69456  
 GaAs-AlGaAs monolithically integrated optical circuit fabrication 4-69597  
 GaAs-Ga<sub>1-x</sub>Al<sub>x</sub>As multilayer struct. masked and selective and thermal oxidation, technology for stripe-geometry DH lasers and integrated optics 4-69610  
 GaInAsP/InP DFB lasers, 1.3  $\mu$ m, monolithic integrated struct., WDM optical communication appl. 4-83618  
 GaInAsP-InP DH lasers, review, book contrib. 4-60037  
 InGaAsP/InP gigahertz-bandwidth optical modulators/switches with DH waveguides 4-112585  
 InGaAsP/InP heterostructure waveguides integrated with optical devices 4-97146  
 InGaAsP/InP injection lasers, LPE grown, three-layer-waveguide DH design 4-91490  
 InGaAsP/InP laser diode, monolithic integration with heterojunction bipolar transistors 4-102927  
 InP based integrated optics 4-64796  
 InP/InGaAsP optoelectronic integrated device with optical bistability, design, fabrication and characs. study 4-83726  
 InP/InGaAsP stripe geometry lasers, design and fabrication using D<sup>+</sup> bombardment 4-83622  
 LiNbO<sub>3</sub> broad-band guided-wave electrooptic modulators 4-97057  
 LiNbO<sub>3</sub> different cuts, photorefractive effect in optical waveguides, holographic grating form. 4-74708  
 LiNbO<sub>3</sub> electro-optic modulator for diode laser, design and 600 Mbit/s operation (German) 4-79199  
 LiNbO<sub>3</sub> Fabry-Perot interferometer for GaAlAs laser wavelength stabilisation 4-91457  
 LiNbO<sub>3</sub> grating, annealing effect on surface relief 4-107812  
 LiNbO<sub>3</sub> integrated optical waveguides, fabrication using ion implantation 4-79347  
 LiNbO<sub>3</sub> intersecting channel waveguides, light switching at an electrooptic mirror 4-79348  
 LiNbO<sub>3</sub> optical waveguide surface, rippled grating coupling efficiency 4-107824  
 LiNbO<sub>3</sub> optical-optical guided-wave modulator 4-103004  
 LiNbO<sub>3</sub> planar ion implanted optical waveguides, computer simulation 4-69347  
 LiNbO<sub>3</sub> planar slab waveguide anal. using hypothetical boundaries (Japanese) 4-60155  
 LiNbO<sub>3</sub> planar waveguide prep. with dip coating method and embossing technique, grating coupler fabrication 4-69602  
 LiNbO<sub>3</sub> Ti diffused optical waveguide, effects of lossy thin plasma film 4-107818  
 LiNbO<sub>3</sub> Ti diffused waveguide interferometric modulator (Chinese) 4-112564  
 LiNbO<sub>3</sub> waveguide bistable devices, blocking oscill., theoretical and expt. study (Japanese) 4-87484  
 LiNbO<sub>3</sub> waveguide electro-optic prism beam deflector, bistability obs. 4-103005  
 LiNbO<sub>3</sub>:Ti acousto-optic bistable device 4-107890  
 LiNbO<sub>3</sub>:Ti based waveguide devices 4-69555  
 LiNbO<sub>3</sub>:Ti channel waveguides and directional couplers, 3-D anal. 4-79286  
 LiNbO<sub>3</sub>:Ti channel waveguide low-loss multiple-branching circuit 4-79346  
 LiNbO<sub>3</sub>:Ti coupled channel waveguides and  $\Delta\beta$  electrodes for electrooptical modulator 4-74699  
 LiNbO<sub>3</sub>:Ti directional coupler based low-crossstalk waveguide polarisation multiplexer/demultiplexer for 1.32  $\mu$ m 4-60183  
 LiNbO<sub>3</sub>:Ti directional coupler travelling wave optical modulator, high-speed pulse generation 4-69596  
 LiNbO<sub>3</sub>:Ti integrated oscillators and multivibrators 4-64795  
 LiNbO<sub>3</sub>:Ti monomode channel waveguides, optical parametric amplification investigation 4-64741  
 LiNbO<sub>3</sub>:Ti planar optical waveguide anal. 4-60150  
 LiNbO<sub>3</sub>:Ti planar waveguide based beam splitter and focuser 4-74680  
 LiNbO<sub>3</sub>:Ti stripe waveguide modulators, polarisation insensitive 4-79281  
 LiNbO<sub>3</sub>:Ti stripe waveguide integrated optical freq. translator 4-112562  
 LiNbO<sub>3</sub>:Ti travelling wave microwave optical modulator 4-112563  
 LiNbO<sub>3</sub>:Ti waveguide Mach-Zehnder modulator, low drive voltage, fibre-optic sensing appl. 4-91575  
 LiNbO<sub>3</sub>:Ti waveguide integrated optics processing, uses of EDTA etch soln. 4-112590  
 LiNbO<sub>3</sub>:Ti waveguides, nonlinear interactions, SHG experiments 4-64742  
 LiNbO<sub>3</sub>:Ti waveguides with low loss, fabrication and performance 4-69554  
 LiNbO<sub>3</sub>:Ti waveguides, polarisation plane rot., photogalvanic mechanism 4-74709  
 LiNbO<sub>3</sub>:Ti X-cut waveguide to fibre coupling, design and characs. for 1.32  $\mu$ m region 4-83725  
 LiNbO<sub>3</sub>+Ti waveguide, acousto-optical conversion study 4-107827  
 LiTaO<sub>3</sub>:Ag waveguide based electro-optic Bragg modulator with apodised electrode struct. 4-74700  
 PLZT thin-film waveguides, electrooptic Kerr coeffs. 4-91578  
 Si optical I/O IC, technology description 4-107888  
 Si:H amorphous film optical waveguides, propag. characs. 4-107821  
 SiO<sub>2</sub>-TiO<sub>2</sub> multimode channel waveguide/optical fibre coupling technique with fibre-guiding grooves 4-64793  
 SiO<sub>2</sub>-TiO<sub>2</sub> planar waveguide based switches and gas sensors using grating couplers and Bragg reflector grating 4-60182  
 SiO<sub>2</sub>-TiO<sub>2</sub> planar waveguide prep. with dip coating method and embossing technique, grating coupler fabrication 4-69602  
 Si<sub>3</sub>N<sub>4</sub> thin-film waveguides, low temp. plasma CVD 4-107887  
 Ti diffusion process in LiNbO<sub>3</sub> 4-64804  
 Y<sub>2</sub>Ga<sub>2</sub>O<sub>7</sub>:Nd thin film waveguide, RF sputtering growth, fluoresc. spectrum, optical amplifier appl. 4-60146  
 ZnO channel waveguide formation on Si substrates 4-103012

**integrated services digital network** *see communication networks; digital communication systems*

**integrating circuits**

fast-response radiation-identifying instrument with separate integration of the signal components 4-102559  
 high speed stabilised gated integrator for NaI(Tl) scintillation pulses 4-64311  
 T gas monitoring system using digital integrating circuit (Japanese) 4-77043

**integrating spheres** *see photometry*

**integration**

celestial mechanics, Lie series use as numerical integration method 4-82400  
 Fokker-Planck eqn., functional integrals for degenerate diffusion matrix 4-101627  
 Gauss definite integration using GISP program 4-95141  
 Gottlieb-Turkel time filter for Chebyshev spectral methods 4-101633  
 inverse scattering problem, integration of differential eqn. linear hyperbolic system (Ukrainian) 4-63574  
 Ito's theorem and stochastic simulation 4-58741  
 Killing spinors, integrability conditions in supergravity 4-68102  
 nonlinear Dirac equations, integrability from soliton theory 4-95656  
 numerical procedure for Galilean satellites long-term motion determ. 4-82402  
 numerical time integration in dynamics 4-87557  
 ordinary differential equations numerical integration, global error estimation, stochastic approach, celestial mechanics appl. 4-82401  
 piezoceramic shell theory, symbolic integration method appl. 4-60280  
 plates, thin, viscoelastic, finite element anal. 4-112721  
 quantum generalisation of stochastic integration, Ito-Doob theory 4-67992  
 semidiscretisation and time integration in solid and struct. mech., book contrib. 4-60266  
 shells, cylindrical, component type, vibr. anal. by dynamic stiffness method 4-74942  
 sine-Gordon eqn. in one space-one time dimens., complete and partial integrability 4-86229  
 square aperture reflector, implementation of stationary phase method (French) 4-83518  
 SU(2) Yang-Mills fields, integrability props., infinitesimal part 4-95655  
 surface integration, 2-D numerical square mesh method 4-78106  
 transient structural responses, implicit finite element methods, time integration, book contrib. 4-60276

**integro-differential equations**

*see also Boltzmann equation; Fokker-Planck equation; Liouville equation; master equation; Vlasov equation*  
 Benjamin-Ono eqn., solvable integrodifferential eqns., rel. to Painleve conjecture 4-90389  
 conductor, complex cross section, skin effect under pulsed current flow (Russian) 4-98655  
 crack thermoelastic boundary integro-differential eqn. formulation 4-64882  
 dynamic light scatt. in model suspension, memory function moment anal. 4-96802  
 EM wave diffraction by nonclosed surfaces of revolution 4-87253  
 fluid-solid heat exchange, transient single-blow responses, numerical prediction 4-97662  
 glass, fictive temp., calc. algorithm 4-84395  
 gyrostat integrodifferential equations of motions, soln. (Russian) 4-90356  
 harmonic oscillator, path integration, with two-time quadratic action 4-95231  
 intermediate long wave eqn., limit to Benjamin-Ono eqn. 4-63522  
 intermediate long wave eqn., solvable integrodifferential eqns., rel. to Painleve conjecture 4-90389  
 Landau density and distribution functions, asymptotic expansions 4-98157  
 liquids, virial eqn. conformity condition and compressibility (Russian) 4-70332  
 modified intermediate long wave eqn., Backlund transformation and scatt. problem 4-63523  
 molecular crystals, solitary wave excitation by coherent EM field 4-98534  
 moving medium with thermal nonlinearity, wave beam propag. 4-74632  
 non-equilibrium states, heat fluctuation distrib. 4-90544  
 nonlinear integro-differential wave system, Galerkin method 4-101657  
 nonlinear viscoelasticity, nonstrictly hyperbolic problem soln. existence 4-69687  
 plate with thin-walled inclusion, stress state along arc of circle 4-60279  
 viscoelastic crack analysis by boundary integral eqn. 4-112766

**intelligence, artificial** *see artificial intelligence*

**intelligibility, speech** *see speech intelligibility*

**intensification** *see amplification*

**intensity measurement**

*see also acoustic intensity measurement*

No entries

**interacting binary stars** *see binary stars; cataclysmic binary stars; eclipsing binary stars; X-ray binary stars*

**interacting boson model** *see nuclear collective model*

**interacting control systems** *see multivariable control systems*

**interactive systems**

*see also interactive terminals; online operation*  
 chemistry, interactive graphics 4-95109  
 INSAT meteorological imagery, data processing 4-100764  
 marine pollution data archiving, user preferences 4-115455  
 modules for controlling expt. on-line hardware with ES computer 4-58836  
 organic photochem. synthesis, microcomputer interactive program appls. 4-114813  
 photogrammetry, digitization of aerial stereo photos using interactive computer graphics system 4-62659  
 seismic data interpretation, interactive system use 4-100774  
 weather analysis, based on interactive cooperation between forecaster and computers 4-105672

**interactive terminals**

*see also interactive systems; remote consoles*

3-D graphic display devices for X-ray crystal structural analysis reproduction 4-97943  
 eye scanning behaviour 4-81706

**interactive terminals continued**

HIPAS, interactive image processing in geophysical analysis 4-77674  
video display terminal lighting 4-109790

**interatomic potentials** *see potential energy functions***intercalation compounds**

diffuse X-ray scatt., review (*Japanese*) 4-114343  
electrochemical intercalation of fluorides into pyrographite, for high energy density battery cathodes 4-81444  
graphite, domain walls, elastic plates model anal. 4-113660  
graphite, intercalated, stage depend. of mag. susceptibility 4-104400  
graphite, modification of material props. 4-60890  
graphite fibres, intercalated, for electrical power transmission appl. 4-80562  
graphite intercalated with Li, electron momentum distrib., Compton profile 4-109268  
graphite intercalation compound, low stage, Shubnikov-de Haas oscils. (*Russian*) 4-98592  
graphite intercalation compound with FeCl<sub>3</sub>, thermal anal. 4-80223  
graphite intercalation compound with K, liq.-solid transitions, in-plane liq. K density 4-70348  
graphite intercalation compound with Li, LiC<sub>6</sub>, optical spectra, ab initio calc., origins of plasmons 4-88802  
graphite intercalation compounds, c-axis cond. and thermoelec. power 4-80561  
graphite intercalation compounds, theory of press-induced staging transitions 4-75696  
graphite intercalation compounds, ultramicrostruct. 4-84417  
graphite intercalation compounds containing AsF<sub>6</sub><sup>-</sup> and AsF<sub>6</sub><sup>-</sup>-AsF<sub>3</sub>, NMR 4-114160  
graphite intercalation compounds with CuCl<sub>2</sub>(CoCl<sub>2</sub>), sp. ht. and thermal expansion 4-80260  
graphite intercalation cpd. with ICl, C<sub>16</sub>I, press. induced change in intercalation step 4-61397  
graphite intercalation cpds., K<sub>1-x</sub>Rb<sub>x</sub>C<sub>8</sub>, phonon softening, inelastic neutron scatt. 4-92319  
graphite intercalation cpds. with K and SbCl<sub>3</sub>, absolute spin susceptibility, orbital paramagnetism 4-76105  
graphite ternary compound, KHgC<sub>4</sub>, compressibility and phonon spectra 4-80183  
graphite-alkali metal intercalation cpds. stage-one, Thomas-Fermi density functional theory 4-92131  
graphite-AsF<sub>3</sub>, foils and compacted flakes, elec. resist. studies 4-92683  
graphite-AsF<sub>3</sub>, X-ray absorpt. near edge struct. meas. 4-66115  
graphite-CoCl<sub>3</sub>, mag. order, neutron diff. studies 4-61511  
graphite-FeCl<sub>3</sub>, mag. order, neutron diff. studies 4-61511  
graphite-K(NH<sub>4</sub>)<sub>3</sub>, intercalation cpd., K(NH<sub>4</sub>)<sub>3</sub>C<sub>24</sub>, tuneable sandwich thickness, cryst. struct. 4-70101  
graphite-Li, LiC<sub>6</sub>, Compton profile, X-ray scatt. meas. 4-61765  
graphite-MnCl<sub>2</sub> intercalation cpds., first and second stage, mag. props. 4-109058  
graphite-NiCl<sub>2</sub>, two-dimensional ferromagnet, EPR meas. 4-109069  
graphite-SbCl<sub>3</sub>, lattice expansion, phase transition effects, X-ray diff. studies 4-98076  
graphite-SbCl<sub>3</sub>, ultrasonic velocity meas. 4-70284  
graphite-SbCl<sub>3</sub>-C<sub>12</sub>SbCl<sub>3</sub>, resistivity and Hall effect (*Russian*) 4-113917  
layer metals, electronic spectrum and structural transition 4-92605  
layer semiconductors, electron spectrum and structural transition 4-92605  
layered materials, collective excitations, continuum model 4-98551  
phase transformations in solids, Crete, Greece (June-July 1983) 4-110811  
polyacetylene:FeCl<sub>3</sub> (FeBr<sub>3</sub>) intercalation cpds., hyperfine interaction, Mossbauer and EPR studies 4-65887  
review (*Japanese*) 4-88158  
transition metal dichalcogenides, Ag intercalated, ionic cond. studies 4-70444  
TTF-FeOCl, struct., IR spectra and mag. susceptibility 4-70128  
TTF-FeOCl, struct. and EXAFS studies 4-70129  
TTF-FeOCl, struct. and EXAFS studies 4-70129  
TTF-FeOCl, struct., IR spectra and mag. susceptibility 4-70128  
TTF-FeOCl, struct. and EXAFS studies 4-70129  
Ag, TaS<sub>2</sub>, Ag intercalation, electron diffraction studies 4-80068  
C<sub>54</sub>SnCl<sub>6</sub> layer cpd., <sup>35</sup>Cl NQR spectra 4-114180  
Ca<sup>2+</sup>-exchanged montmorillonite, intercalated mol. dynamics, quasielastic neutron scatt. 4-65154  
CoCl<sub>2</sub>-FeCl<sub>3</sub>-graphite, mag. phase transitions, susceptibility meas. 4-98881  
FeOCl, intercalated with  $\alpha$ -picoline, Mossbauer study 4-71226  
FeOCl, Lewis base intercalation compounds, charge transfer model, Mossbauer spectra, X-ray diff. 4-70746  
Fe<sub>2</sub>TiSe<sub>2</sub>, cryst. struct., mag. ordering, susceptibility meas., X-ray diff. 4-76119  
In<sub>2</sub>MoS<sub>4</sub> (0 ≤ x ≤ 1) intercalation compound, synthesis and characts. 4-104200  
InSe, lamellar p-type, photointercalation and photodeposition of Cu 4-93539  
InSe-Li intercalation cpd., photoelectric props. meas. (*Russian*) 4-104272  
KHg<sub>2</sub>-graphite, electronic struct., Shubnikov-de Haas effect 4-92596  
Li<sub>2</sub>FeO<sub>3</sub>, struct. characts. 4-70120  
Li<sub>2</sub>FeO<sub>4</sub>, struct. characts. 4-70120  
Li<sub>2</sub>Mn<sub>2</sub>O<sub>4</sub>, struct. characts. 4-70120  
Li<sub>2</sub>MoO<sub>4</sub>, Li<sup>+</sup> transport, pulse NMR relax. time meas. 4-75727  
Li<sub>2</sub>MoSe<sub>4</sub>, Li intercalation model, mean-field lattice gas 4-70098  
Li<sub>2</sub>Na<sub>0.1</sub>CrS<sub>3</sub>, cathode for secondary Li cells, props. and cyclic performance 4-93605  
Li<sub>2</sub>Ta<sub>2</sub> (1T<sub>2</sub>HB), elec. resist. meas., metallic and supercond. states 4-84726  
Li<sub>2</sub>TiS<sub>2</sub>, intercalation study by TEM 4-103953  
Li<sub>2</sub>V<sub>2</sub>O<sub>7</sub>, intercalation study by TEM 4-103953  
Li<sub>2</sub>ZrX<sub>2</sub> (X=S, Se) intercalates, phase transitions, mag. studies 4-70657  
MnPS<sub>2</sub>, layered cpd., disorder effects by cation intercalation, EXAFS studies 4-61773  
Na<sub>2</sub>CoO<sub>2</sub>, electrode material, electronic processes during intercalation 4-76012  
Na<sub>2</sub>CoO<sub>2</sub>, intercalation cpd., transport props. 4-92734  
Na<sub>2</sub>(H<sub>2</sub>O)<sub>2</sub> TaS<sub>2</sub> Hendricks-Teller disordered layer lattice, X-ray diff. studies 4-98075  
2H-NbSe<sub>2</sub>-In, in thermal diffusion 4-88347  
NbSe<sub>2</sub>-H<sub>2</sub>, supercond., crit. parameters, and resist. temp. depend. (*Russian*) 4-92873  
SbCl<sub>3</sub>-graphite, de Haas-van Alphen effect meas. 4-88440

**intercalation compounds continued**

TaS<sub>2</sub>-3R intercalation cpd. with NH<sub>3</sub>, proton NMR meas. 4-61598  
TiS<sub>2</sub>, formation by deintercalation of Na<sub>2</sub>TiS<sub>2</sub>, cryst. struct. and mag. susceptibility 4-75425  
TiS<sub>2</sub>, intercalation cpd. with Mn, chemical vapor growth and EPR studies 4-66201  
Ti<sub>2</sub>V<sub>2</sub>(V<sub>2</sub>)<sub>2</sub>Se<sub>2</sub>, self-intercalated, angle resolved XPS study 4-71512

**interconnected systems** *see large-scale systems*

**interdiffusion** *see diffusion*

**interface electron states**  
dynamics, conf., Lille, France (Sept. 1983) 4-78030  
elemental semiconductors, electrochemical oxidation, surface states (*French*) 4-76044  
III-V semiconductors, electrochemical oxidation, surface states (*French*) 4-76044  
III-V semiconductors, surface electron states and struct. (*Russian*) 4-65745  
metal semiconductor interface, electronic props., contrib. of defects 4-84697  
metal-semiconductor interface, atomic and electronic struct., soft X-ray photoemission characterisation 4-93187  
metal/metal interfaces, electronic struct. and interface energy 4-114019  
MIS struct., surface irregularity enhanced subband resonance calcs. 4-61458  
MIS struct., surface irregularity enhanced subband resonance 4-61459  
MIS structure, interface electron state calc. 4-108912  
MIS structures, current DLTS spectra due to dielec. polarisation of the insulator 4-76043  
MIS structures, hole traps, trivalent Si centres, EPR meas. 4-80817  
MIS structures hysteresis effects reduction method in meas. 4-88602  
MOS capacitors, field controlled charge trapping in tunnel oxides 4-70939  
polyimide, cured, interfacial reaction during metallisation, XPS obs., chem. bond form. 4-88932  
polystyrene-metal interfaces, injected charge carrier props. 4-108937  
relativistic, in one-dimens. solid 4-65730  
rough interface between media, local EM oscils. 4-70899  
Schottky-barrier 4-88559  
semiconductor interfaces, dispersion and instability of localised polaritons 4-80511  
semiconductor superlattice, plasmon and intersubband modes, classical and quantum limits 4-104141  
semiconductor superlattices, disordered, electronic props. and phonon states 4-84682  
semiconductor superlattices, narrow, breakdown of three dimens. effective mass approx. 4-84681  
semiconductor superlattices, optical absorpt. and luminesc. expts. 4-84977  
semiconductor superlattices, quantum wells, and heterostructs., elec. and optical props. 4-80666  
semiconductor-insulator interface, electrophysical props., general theory 4-76045  
semiconductors, deep levels and interface states, electrochem. photocapacitance spectroscopy method 4-65635  
solid/solid interfaces, computer simulations, conf., Philadelphia, USA (Oct. 1983) 4-110806  
Ag-Fe interface, electronic struct. and mag. props. 4-80645  
Ag-Fe (100) interface, growth, structural and electronic props. 4-104093  
Ag-Pd disordered single crystals, angle resolved UV photoemission 4-85072  
Al-SiO<sub>2</sub>-Si MOS structure, X-ray induced interface traps, stress relax. effects 4-98755  
Al-SiO<sub>2</sub>-Si struct., X-ray irradi., interface traps 4-104281  
AlGaAs-GaAs heterojunction interfaces, deep levels, forward I-V and DLTS meas. 4-70915  
Al<sub>0.5</sub>Ga<sub>0.5</sub>As/GaAs heterojunction, subband struct. at low temp. 4-104298  
BN-P film in InP, grown by CVD, elec. props. 4-99336  
BN-InP, density of interface states 4-80443  
C-Ag junctions, Schottky barrier form. 4-84694  
CO-Ni interaction in presence of K, site pot. effect 4-81477  
(Cd,Zn)S-CuInSe<sub>2</sub> solar cells, light-induced junction modification 4-77092  
n-CdS/electrolyte interface, photoelectrochem. characterisation 4-84689  
CdS-electrolyte, SAW characterisation of surface and interface states 4-98681  
CdSe, interface states studied by electrochemical photocapacitance spectroscopy 4-98750  
Cu-Ni interface, electronic struct. and mag. props. 4-80645  
GaAs/Ni reactive interface, soft X-ray photoemission spectra studies 4-113820  
GaAs MOS structures with anodic oxides, defect states, DLTS study 4-114043  
GaAs, SAW characterisation of surface and interface states 4-98681  
GaAs Schottky diodes, transport mechanism, deep centre effects 4-88558  
GaAs:Sn/GaAs:Cr interface, electron and hole traps, photovoltaic studies 4-104283  
GaAs/(GaAl)As two-dimens. electron gas, cyclotron reson. study 4-104297  
GaAs/native oxide interfaces, density of states, C-V meas. 4-88604  
GaAs/(AlGa)As modulation-doped heterostructs., reson. inelastic light scatt. studies 4-84973  
GaAs-Ga<sub>1-x</sub>Al<sub>x</sub>As heterojunction, electron energy level calcs. 4-108915  
GaAs-Ge(100) interfaces, Fermi level position and valence-band edge discontinuity study 4-61450  
n-GaAs-polyisiloxane-metal struct., elec. props. (*French*) 4-61460  
Ge (111) with chemisorbed Sm, photoemission spectra 4-80392  
Ge/Al interface, chemisorption and metallisation, electronic struct. 4-92527  
Ge-GaAs interface, electronic struct. 4-84665  
HgTe-CdTe superlattices, electronic props. 4-84680  
In-pyrrole-N-methylpyrrole contact, XPS study of Schottky barrier 4-104289  
In<sub>0.5</sub>Ga<sub>0.5</sub>As, MIS diode anodic oxidation, interface characteristics 4-104324  
InP MOSFET structures, carrier channel mobility correl. with interface state meas. 4-88600  
InP photoelectrodes, surface states, photocapacitance spectra studies 4-114010  
InP, SAW characterisation of surface and interface states 4-98681

# interface electron states continued

- InP, surface and interface states 4-92782  
 InP-Ag interface, reactions and Schottky barrier form., XPS studies 4-92821  
 KI-KI colloid interface, Raman scatt., Rayleigh line broadening 4-80925  
 MIS structures, lateral variation determ. of interface states by scanned light pulse technique 4-61434  
 Nb (110)-Pd interface, electronic struct. 4-84674  
 Nb-Ti layered ultrathin coherent structures, elec. conduction (*Chinese*) 4-76023  
 Ni/Cu (001) interface, electronic struct., magnetism, muon spin relax. 4-70888  
 PbSe-Si heterojunctions, solution-grown, elec. and photoelec. props. 4-114023  
 Pd-Au interface, electronic struct. and mag. props. 4-80645  
 Si(111) interface, atomic intermixing and electronic interaction 4-70478  
 Pt-SiO<sub>2</sub>-Si MIS struct., flat-band voltage shift 4-108944  
 Si (001) wafers, thermally oxidised, P<sub>b</sub> interface centres, ESR study, effect of As<sup>+</sup> ion implantation 4-92960  
 Si (111) slab, interface, electron-phonon interaction and broken symm. 4-80517  
 Si (111) with chemisorbed Sm, photoemission spectra 4-80392  
 Si (111)-Al(Ga)(In) abrupt interfaces, electronic props. 4-84696  
 Si (111)-Mo interfaces, electronic struct., XPS and X-ray excited AES study 4-85085  
 a-Si, AC field effect and density of gap states 4-92670  
 Si MIS struct., amorphous C covered, tunnelling to insulator gap states 4-92824  
 Si MIS struct., X-ray irradi., interface traps, DLTS studies 4-104282  
 Si overlayer on GaP, heterojunction band discontinuities, synchrotron radiation photoemission 4-81111  
 Si, solar cell, H passivation of electrically active defects (*French*) 4-62359  
 Si:B-SiO<sub>2</sub> MIS struct., ion bombarded, defect annealing study 4-80685  
 Si:P, trap spectrum of O donor, DLTS study 4-92651  
 SiP(As), ion implanted film, elec. props. 4-61473  
 Si/SiO<sub>2</sub> interface with gradual chem. transition, electronic density of states 4-108756  
 Si/SiO<sub>2</sub> MOS capacitors, donor state generation rate, anode field depend. 4-92826  
 Si/SiO<sub>2</sub> MOS struct., interface state density and atomic roughness 4-98684  
 Si/SiO<sub>2</sub> MOSFET, elec. props. and atomic struct. 4-80677  
 Si/SiO<sub>2</sub>/Al capacitor struct., ion beam fluorination and interface state density 4-70176  
 Si/SiO<sub>2</sub>/Al capacitors, interface trap generation and H electromigration 4-70940  
 Si/SiO<sub>2</sub>/Si<sub>3</sub>N<sub>4</sub>/Al capacitors, ion/atom beam milling, damage effects 4-70941  
 Si/ZnO-B<sub>2</sub>O<sub>3</sub>-SiO<sub>2</sub> glass system, surface charges, C-V characteristic meas. 4-65747  
 Si-Ag and Si-H-Ag junctions, Schottky barrier form. 4-84694  
 Si-electrolyte interface, elec. field modulated IR internal reflection studies 4-98749  
 Si-Pd/Si interface, electronic struct. 4-84665  
 Si-SiO<sub>2</sub> interface cyclotron resonance lineshape distortion (*Chinese*) 4-84701  
 Si-SiO<sub>2</sub> interface traps in diode struct., small signal admittances 4-80678  
 Si-SiO<sub>2</sub>, XPS study of interface states 4-98682  
 Si-SiO<sub>2</sub> interface, electronic struct. 4-84665  
 Si-SiO<sub>2</sub> interface, shallow donor impurities, variational soln. 4-70893  
 Si-SiO<sub>2</sub> interface states, degeneracy and capture cross sections, DLTS studies 4-76039  
 Si-SiO<sub>2</sub> MOS struct., C-V charact. different oxidation process effect 4-92823  
 Si-SiO<sub>2</sub> MOS struct., H passivation of implantation defects using a-Si:H film 4-71744  
 Si-SiO<sub>2</sub> MOS struct., microstructural variations in oxides, electron spin reson. obs. 4-61590  
 Si-SiO<sub>2</sub>-Mo MOS diodes, carrier trapping centres and interface states induced by RF sputtering of Mo 4-88603  
 Si-SiO<sub>2</sub>-Na, Na<sup>+</sup>-induced surface states, DLTS study 4-61463  
 Si-Ti(Hf) 4-70906  
 a-Si, C<sub>1s</sub>/H<sub>1s</sub>-Si(H) heterojunctions, photoemission studies 4-65731  
 Si<sub>3</sub>N<sub>4</sub> film MNOS struct., trapped charge profile and relax. currents 4-65749  
 Si<sub>3</sub>N<sub>4</sub> MNOS structures using atmospheric press. and plasma enhanced CVD coatings 4-98760  
 SiO<sub>2</sub> thin films, nitridation and elec. props. 4-61435  
 SiO<sub>2</sub>-Si interface, oxidation, chem. bonding in transition layer, photoemission spectra using synchrotron radiation 4-85062  
 SnO<sub>2</sub>/GaSe heterojunctions, energy struct., reflectivity studies 4-66053  
 Zn<sub>0.99</sub>Cd<sub>0.01</sub>S-Cu<sub>2</sub>S heterojunction, energy band diagrams 4-104296  
 ZnSe (110)-Ge interface, ordered and disordered, electronic struct. 4-84666

## interface phenomena

- see also adsorption; crystal surface and interface vibrations; interface structure; Kapitza resistance; semiconductor-electrolyte boundaries; surface phenomena  
 acoustic and EM wave scattering anal. 4-83754  
 acoustic pseudo-Rayleigh waves at fluid/solid interface, Green's function anal. 4-60189  
 air-water interface, static and dynamic response to shear, meas. instrument 4-113751  
 alloys, binary, cellular solidification theory 4-76764  
 austenite, cementite dissol., computer simulation 4-71653  
 automation of surface cleaning and sample addition for surface balances 4-63853  
 blood, interfacial film, with vitreous body, struct., physicochemical props., in case of haemophthalmia 4-81610  
 capillary gravitational waves at homogeneous liq.-liq. interface 4-112925  
 cellular solidification front, model for evaluation of shape parameters 4-93275  
 characteristics modelling using finite element method 4-79521  
 contact-line problems in fluid mechanics 4-98409  
 crack stopped by elastic inclusion, model problem (*Russian*) 4-74959  
 crack tip singularity powers, finite element anal. for cracks terminating at finite width interfaces 4-87621

# interface phenomena continued

- critical phenomena and scalar order parameters 4-58802  
 crystal growth, molecular mechanisms, review 4-60869  
 crystal growth from solution, top seeded method, hydrodynamics in high temp. solns., simulation 4-65208  
 crystal-melt interfaces, coupled convective instabilities 4-88120  
 dendritic structures, Ostwald ripening and relaxation 4-93283  
 diffusion bonding, development of theoretical model 4-114762  
 dislocation-particle elastic interactions, diffusionaly-modified 4-98125  
 double layer dipole orientation at electrodes, polarisation catastrophes anal. 4-98690  
 drop in partial contact with solid support, free vibrations 4-75757  
 droplet spreading, liquid-air interface (*French*) 4-75753  
 dynamic interactions between approaching surfaces of biological interest, review 4-77204  
 edge defined film fed crystal growth, lateral solute segregation 4-88119  
 electric double layer, interface potential between diffuse and dense parts 4-81443  
 electron current modulation in light wave field at interface between two media 4-74409  
 EM wave focusing through dielectric interface 4-112323  
 epoxy coated mild steel, polymer-metal adhesion, appl. of X-ray photoelectron spectroscopy 4-93485  
 FCC crystals, mechanisms and shapes of cryst. growth 4-75340  
 fibre reinforced composite, anisotropic layered, singularities at tip of crack normal to interface 4-74952  
 fibre reinforced composites, fibre-matrix bond form. kinetics during rolling 4-71674  
 fibre reinforced composites, short fibres, stress distrib., effect of fibre-end geometry 4-74869  
 fibre reinforced composites, stiffness reduction due to fibre breakage 4-80136  
 fibre reinforced composites model, acoustic emission evaluation 4-81380  
 fluctuation spectroscopy, expt. technique and capillary ripple theory, comments 4-78389  
 fluid interfaces, mech. theory and Maxwell's rule 4-61185  
 fluid-solid interface, loaded and stiffened, finite acoustic beam reflection 4-74780  
 foam flooding process for heavy oil recovery, interfacial phenomena 4-61097  
 free dendritic growth 4-89041  
 GaInAs-InP heterojunction, interface 2-D electron gas props., MOCVD growth and characterisation (*French*) 4-76685  
 gaseous heat transfer between solid surfaces, photoacoustic expts. 4-83801  
 germination, of solid on powdery solid, statistical model (*French*) 4-114816  
 glass fibre reinforced epoxy, thin-walled tubes, deform. and failure after transverse indentation 4-99573  
 glass fibre reinforced epoxy, unidirectional, fracture toughness in mode II 4-93366  
 glass fibre reinforced PET, strength, effect of temp. and strain rate 4-93375  
 glass fibre reinforced plastic, roving cloth reinforced, strength in flatwise direction, temp. depend. (*Japanese*) 4-89087  
 glass fibre reinforced plastic laminates, interlaminar shear strength 4-99575  
 glass-bentonite nuclear waste interfaces after one year burial in STRIPA 4-111605  
 glass-glass nuclear waste interfaces after one year burial in STRIPA 4-111604  
 glass/liquid interface, laser beam induced holographic bubble grating form. 4-83683  
 graphite fibre reinforced Al, interfacial strength meas. 4-99370  
 graphite fibre reinforced epoxy, delamination and transverse fracture 4-99577  
 graphite fibre reinforced epoxy laminates, tensile failure, delamination fracture surfaces, SM obs. 4-66418  
 H-guide structure containing, semicond., magnetoplasma surface wave anal. 4-108890  
 hydrophilic solid, adsorp. of nonionic surfactant, fluoresc. decay obs. 4-108679  
 hydroxypropyl methylcellulose, aq. soln., interfacial tension, structural interpretation 4-80338  
 insulator wetted by liq. dielec., surface cond. and losses 4-108920  
 interface delocalization transitions in finite systems 4-70343  
 interphase layer, mass, momentum and energy conservation law, surface parameters 4-112692  
 ion scattering near interfaces, energy loss method anal. 4-65655  
 ions localised near interface, low temp. mobility (*Russian*) 4-92452  
 jellium/hard sphere electrolyte interphase, model for electric double layer 4-70908  
 Kevlar 29 braid, bending fatigue life rel. to resin impregnation 4-93394  
 Kevlar fibre-reinforced epoxy resin composites, fracture toughness rel. to controlled interfacial bonding 4-66423  
 kinetic depinning transitions 4-70338  
 lateral waves, weak optical absorption meas. at surfaces 4-88790  
 linear molecular fluid, in contact with solid, density profile, HNC eqns. 4-79917  
 liquid drops, spherical fluid-vapour interfaces, surface tension, curvature corrections 4-88372  
 liquid surface and interface waves 4-79613  
 liquid-solid interface, press., density functional, integral eqns. 4-108258  
 liquid-solid interface, US beam back reflection, beam profile effects 4-113542  
 liquid-solid interface, US beam backscatt., role of backward waves 4-113541  
 liquid-solid transition, absolute kinetic coeffs., mol. theory 4-65374  
 liquid-vapour interface, anisotropic van der Waals model 4-70530  
 liquid-vapour interface, scaling relations 4-80337  
 magnetised medium/magnetically inactive medium interface, US transmission 4-92307  
 mass transfer, kinetics, across interface, effect of surface processes 4-94864  
 metal-molten salt interface, capacitance depend. on local density profiles near electrode 4-92797  
 metal-oxide interface, transpassive thin films 4-113823  
 metal/Si<sub>3</sub>N<sub>4</sub>/SiO<sub>2</sub>/Si capacitors, interfacial charging 4-104292  
 metals, bulk and interfaces, pair pots. for atomistic simulations 4-113885  
 metals, FCC, interfacial free energy between dislocation core and bulk material 4-65262

**interface phenomena continued**

- methylcellulose, aq. soln., interfacial tension, structural interpretation 4-80338  
 microsegregation, influence of mutual interaction of alloying elements 4-66340  
 microstructure formation, investigation using transparent model systems (*German*) 4-81183  
 MOSFET, interface carrier mobility transport theory anal. 4-70944  
 multi-state models, interfacial adsorption, Monte Carlo studies 4-113812  
 nematic liquid crystals, interfacial props., induced orientational order and wetting transitions 4-88069  
 nematic liquid crystals, interfacial props. of nematic-isotropic and nematic-vapour interfaces 4-88068  
 nematic/isotropic interfacial energy, determ. from Frenkel relation for droplet coalescence 4-75758  
 one-component plasma, impermeable surface separation, interface exactly solvable model 4-65051  
 oxidation nonprotective, alloys depletion profiles 4-62101  
 phase changes, statistical mech. anal. 4-108581  
 phosphatidylcholine head groups in vesicles, short-range order in interfacial water 4-113287  
 planar crack of arbitrary shape at interface of two anisotropic elastic half spaces 4-79508  
 plastically deforming matrix, stress and strain fields around inclusions 4-97360  
 Plexiglas-steel interface, US transmission at subcrit. angles 4-69641  
 polyethylene terephthalate substrate surface condition, influence of adhesion layer components (*Russian*) 4-82850  
 polyimide, cured, interfacial reaction during metallisation, XPS obs., chem. bond form. 4-88932  
 polymer interfaces and interphases 4-84490  
 polymeric alloys, theory, recent advances 4-84221  
 polystyrene, glass bead filled, craze form., microscopic in situ obs., interfacial adhesion 4-62073  
 polystyrene films, underwater, interfacial polaris. in bilamellar struct., dielec. anal. 4-84901  
 porous layers, fluid saturated, US pulse propag. 4-98215  
 protective surface film, continuous, criterion for compressive failure 4-99612  
 PVC, particle filled, fracture mechanism rel. to fatigue crack growth (*Japanese*) 4-89120  
 quiescent gas-liquid absorption, interfacial resistance effect 4-80329  
 salol, solid-liq. interface props., dynamic light scatt., thermal diffusivity, lattice const. 4-109203  
 semi-infinite composite with long reinforced phase, edge crack analysis 4-97400  
 semi-transparent flat plate, thermal stresses, effect of interface reflections and angle of incidence of radiation 4-60277  
 semiconductor-metal boundary, radiation and voltage effects on interlayer props. (*Russian*) 4-104316  
 simple liquids, surface tension, liq.-vapour phase interface, statistical mechs. 4-113755  
 solid-liquid interface, convective coupling in internally heated vertical cylinder 4-97562  
 solid-liquid interface, wetting by gas, free energy functional 4-88373  
 solid-liquid metal interaction, phase layer formation, effect of gravity 4-70386  
 solid/liq. and solid/vacuum interfaces, surface acoustic waves 4-84501  
 solid/liquid interface, US beam displacement and attenuation coeff. 4-92505  
 solidification, pattern selection 4-93279  
 solidification, steady-state cellular and dendritic growth, numerical finite difference model 4-93282  
 solidification mechanisms, microsegregation-free 4-89039  
 solutions, strictly regular, conc. profile of boundary, cluster approach 4-80333  
 steel, austenitic stainless, butt joint, friction welded, fatigue strength and fractographic features (*Japanese*) 4-114648  
 steel, austenitic stainless, H attack, TEM study 4-114657  
 steel, austenitic stainless, swelling and precip. behaviour during irradi., effect of P 4-103818  
 steel, Cr-Mn, diffusion reaction with Al coating, Si content effect 4-114723  
 steel, dual-phase, C-Mn, mech. props. and fracture mechanism, influence of martensite morphology 4-99530  
 steel, dual-phase, Mn-C, tensile behaviour and fracture characteristics 4-99598  
 steel, ferritic, D and He trapping at TiC particles 4-98152  
 steel, low C, Al clad, reaction diffusion, intermetallic layer growth kinetics 4-114722  
 steel, medium C, H-assisted cracking after exposure to H<sub>2</sub>S-saturated salt soln., role of MnS inclusions 4-71732  
 steel, oxide-scale cracking and spallation, initiation conditions 4-62100  
 steel, pressure vessel, plated with anticorrosive claddings, fracture behaviour 4-99595  
 steel, stainless, Nb-stabilized, Cr-depleted, oxidation, Cr conc. for healing layer form. 4-81326  
 steel fibre reinforced cement, fibre debonding and pullout, adhesional interfacial shear strength 4-66388  
 steel fibre reinforced cement, free shrinkage, theoretical model 4-93255  
 steel fibre reinforced mortar, polystyrene impregnated, interfacial failure 4-99571  
 stratified media technology, conf., Los Angeles, CA, USA (Jan. 1983) 4-82585  
 stress-deformation behaviour, nonlinear, meas. with interfacial viscometers 4-61177  
 surface fluctuation spectroscopy, liquid interface characterisation 4-78388  
 surface tension of non-critical interfaces near crit. end points 4-88371  
 testosterone-aq. electrolyte interface, electroosmosis, electrophoresis and streaming 4-99838  
 thermal stresses in crystals grown by Stockbarger method, generated by different thermal expansion coeffs. 4-70046  
 total internal reflection fluorescence in biophysics, book contrib. 4-93987  
 two-phase interface, planar, free energy study 4-92478  
 vapour condensation, waves in interphase surface, calc. 4-108597  
 water, interfacial, in electrolytes, surface enhanced Raman scatt., metal cation effect 4-91268  
 wear, oxidation, origins and development at low ambient temps. 4-81293  
 wetting film on solid surface, vertical ascension (*French*) 4-80327

**interface phenomena continued**

- Ag electrodes, interfacial OH and OD, surface enhanced Raman scatt. 4-93570  
 Ag epitaxial film on Cu (111), interfacial effects in electron transmission 4-114050  
 Al/Mo thin films, reactions 4-61148  
 Al-In-Sn, irregular monotectic struct., effects of temp. gradient and growth vel. 4-66321  
 Al-Si (12.4 wt.%), near-eutectic, solid-liq. interface (*German*) 4-81184  
 Al<sub>2</sub>O<sub>3</sub> fibre reinforced Mg, tensile and fatigue behaviour, fibre fraction and orientation 4-114652  
 Al<sub>2</sub>O<sub>3</sub> fibre reinforced Mg alloys, tensile and fatigue behaviour, matrix alloying effects 4-114653  
 Au-Si-SiO<sub>2</sub> interface, Au surface-state energy level determ. 4-80640  
 B fibre reinforced Al, fibre-matrix bond form. kinetics during rolling 4-71674  
 B fibre reinforced Al composite, fracture mode and shear strength rel. to interface strength 4-62022  
 B<sub>2</sub>C/B fibre reinforced Ti-Al-V, fatigue crack growth behaviour 4-93374  
 C fibre/glass fibre reinforced polyester, hybrid composites, interlaminar shear strength (*Japanese*) 4-99430  
 Cu-Ni-Zn system, diffusion at 775°C, zero-flux planes and flux reversals 4-65496  
 Cu-Pb, irregular monotectic struct., effects of temp. gradient and growth vel. 4-66321  
 Fe/Zn system,  $\delta$  phase form. and growth 4-80314  
 Fe-C, high purity, forced vel. pearlite, expt. 4-93294  
 Fe-C, high purity, forced velocity pearlite, theoretical 4-93295  
 Fe-C(Cr), austenite, cementite dissol., computer simulation 4-71653  
 Fe-Mg multilayered films with superlattice, mag. props. study 4-80791  
 GaAs layers, MBE grown on Ge islands on insulator, zone melting recrystallisation, grain boundaries, photoluminescence obs. 4-84524  
<sup>4</sup>He, equilibrium crystallisation, interface problem 4-108670  
<sup>4</sup>He superfluid-crystal interface, quantum effects in faceting transition 4-80321  
 InSb, Czochralski growth, Peltier coeff. at crystal/melt interfaces 4-70845  
 Na/S cell, electrode-electrolyte interface obs., using SEM 4-78421  
 NaCl, anisotropic interface diffusion and precipitation morphology 4-61088  
 Nb<sub>3</sub>Sn phase formation, influence of thermal regime of multifilamentary wire prep. 4-76063  
 Ni-Al-Mo alloy, unidirectional solidification 4-76765  
 Ni<sub>3</sub>Si, Ni<sub>2</sub>Si, thin films, metal silicide form., AES and SIMS study 4-75795  
 PtSi, Pt<sub>2</sub>Si, thin films, metal silicide form., AES and SIMS study 4-75795  
 Si and sapphire ribbons, produced by EFG, comparison of growth characteristics 4-66222  
 Si, excess interstitial distribution during thermal oxidation, two-dimensional model 4-84286  
 poly-Si interface phenomena at Si grain boundaries 4-70925  
 Si-H, Al-covered, solid-state reaction between film and substrate 4-92498  
 Si-metal interface, dislocation mediated melting 4-103912  
 Si-polyacetylene interface, Auger spectra obs. of Si-C binding, peak shift depend. on adsorpt. level (*French*) 4-66141  
 Si-SiO<sub>2</sub> structure, transparent layer ellipsometric study in layer-substrate structs. with indistinct transition region 4-86469  
 SiC fibre reinforced Ti-Al-V, fatigue crack growth behaviour 4-93374  
 SiC filament reinforced Ti, model composite, fibre-matrix chem. reaction at high temps. 4-104754  
 SiC-Al, sintered composite interfacial reactions, joint bending strength rel. to microstruct. 4-66295  
 Ta<sub>2</sub>O<sub>5</sub> films on Si, electrical props. 4-84720  
 TiC-TiB<sub>2</sub> eutectics, directional solidification 4-76767  
 UO<sub>2</sub>/Zircaloy 4 reaction layer sequence, total interfacial energy 4-83142  
 UO<sub>2</sub>/Zircaloy-4 chemical interaction 4-83140  
 W fibre reinforced Ni, mech. props. at elevated temps., diffusion barriers to improve struct. stability 4-93423  
<sup>65</sup>Zn diffusion coeff. determ. in Zn-Sn alloy from conc. distrib. near diffusion interface, conc. effect 4-88330  
 ZrC-TiB<sub>2</sub> eutectics, directional solidification 4-76767  
 ZrC-ZrB<sub>2</sub> eutectics, directional solidification 4-76767

**interface structure**

- alkali halide bicrystals, high-angle (001) twist grain boundaries 4-103768  
 ceramics, grain and phase boundary structs. 4-108381  
 chalcogenide glasses, electron microscopy of reactions with metals and electron beam induced crystn. 4-80315  
 constrained dendritic growth and spacing 4-89043  
 cracks, atomistic versus continuum models 4-113532  
 crystal surface, layered structures 4-61194  
 4-cyano-4'-n-heptylbiphenyl nematic/isotropic interface, mol. orientation and anchoring energy 4-60821  
 detonation-deposited coatings on metals, contact zone structural characteristics 4-66502  
 dislocation structures, characterisation using TEM 4-108371  
 dislocations and coherency, interpretation of discrete atomic positions 4-113447  
 electron microscopy, conference, Boston, USA (Nov. 1983) 4-106124  
 eutectics, irregular, theoretical basis of grain growth (*Polish*) 4-93258  
 FCC/BCC interfaces, semicoherent and incoherent, electron diffr. obs. of dislocation arrays 4-70160  
 III-V semiconductors, surface electron states and struct. (*Russian*) 4-65745  
 interphase boundary migration, dislocations and steps 4-108372  
 lattice models, correlation function 4-98461  
 low-energy electron induced X-ray spectrometry 4-113767  
 metal overlayer/metal structures, sputtering, AES and EELS studies 4-76617  
 metal-semiconductor heterostructures, transition regions, exam. using electron microscopy and Auger spectroscopy 4-65579  
 metal-semiconductor interface, atomic and electronic struct., soft X-ray photoemission characterisation 4-93187  
 metal/insulator/metal structure formation, upper electrode effects 4-61466  
 metallic superlattices, artificial, struct. and electronic props. 4-84532  
 multilayer solid adsorption and the roughening transition 4-113817  
 multilayered thin film structs., depth profiling and sputtering yields 4-81090

**surface structure continued**

- nanocrystalline structure, proposed new material struct. (*German*) 4-70045
- $\alpha$ -quartz with adsorbed  $\text{SnO}_2$ , interface struct., RHEED study 4-104043
- refractory metal silicides, AES, principal component anal. 4-77041
- selected area stationary beam cratering for high sensitivity depth profiling with computerised Auger microprobe 4-99711
- semiconductor interfaces, Rutherford, scatt.-channelling anal. 4-99255
- solid liquid interface, freezing solutions, motion of interface 4-108592
- solid on solid interface model, free energies of surface steps 4-113780
- solidification, directional, interdendritic spacing, comparison of theory and expt. 4-93281
- solidification, directional, interdendritic spacing, expt. 4-93280
- solidification, microstruct. and phase spacings 4-93284
- solidification, rapid, impurity trapping models 4-89038
- steel, dual-phase, metallography and partitioning of alloying elements 4-93301
- steel, dual-phase, tempered, fracture behaviour 4-89127
- succinonitrile-acetone system, solidification, directional, interdendritic spacing, expt. 4-93280
- Zircaloy-4/ $\text{UO}_2$  chemical interaction 4-83140
- Zircaloy-4/ $\text{UO}_2$  diffusion couple, interfacial energy and work of adhesion 4-83141
- Ag epitaxial layers, quantum size effects, surface and interface roughness influence, LEED study 4-84526
- Ag-Ge (100) interface, growth, structural and electronic props. 4-104093
- Ag-Pd-Ag multilayered films, microstructure changes rel. to layer spacing, TEM obs. 4-80432
- Al-Al<sub>3</sub>Cu eutectic thin films, directionally solidified, interlamellar spacing 4-93285
- Al-Al<sub>3</sub>Ni eutectics, directionally solidified, interfacial microstructures, TEM obs. 4-81187
- Al-Au(Cu) thin film bilayers, ion beam bombarded, interfacial phase formation 4-70241
- Al-Si/ $n^+$ -Si system, metallisation, by fast heat pulse alloying, hillock elimination 4-114034
- Al-SiO<sub>2</sub>-Si MOS structure, X-ray induced interface traps, stress relax. effects 4-98755
- Al-Ti-C-Si contact system, thermal stability 4-84703
- Al<sub>0.85</sub>Ga<sub>0.15</sub>As/GaAs:Zn diffused superlattice, X-ray rocking curve and backscatt. studies 4-113818
- Al<sub>0.5</sub>Ga<sub>0.5</sub>As/Sb<sub>0.5</sub>-y/GaSb heterostruct., conditions for LPE growth 4-114429
- Au/Al contacts, intermetallic bonds and contact resist. (*Russian*) 4-113819
- Au/Cu bilayers, ion-induced solid solutions and ordered cpd. form. 4-108470
- Au/Ga thin film couples, room temp. interdiffusion 4-61149
- Au-Ag-Au multilayered films, microstructure changes rel. to layer spacing, TEM obs. 4-80432
- Au-Ge bilayers, ion beam mixing, amorphous and metastable phases formation 4-80113
- Au-Ge(H) interfaces on amorphous Ge, Schottky barrier and cpd. formation 4-84669
- B fibre reinforced Al-Mg, interaction between B and matrix 4-70577
- BN, films, interaction with Ni at high temps. 4-70583
- CdTiO<sub>3</sub>, polycryst., viscous creep deform. at elevated temps. 4-103863
- Cd-Pb eutectic thin films, directionally solidified, interlamellar spacing 4-93285
- Cd<sub>1-x</sub>Mn<sub>x</sub>Te mag. semicond. superlattices, MBE growth and optical props. 4-114399
- Cr/Ni/Cu multilayer film system, laser mixed, AES and Rutherford backscatt. studies 4-98458
- Cr/Si (100) interface, silicide growth kinetics, cross-sectional TEM 4-61146
- CrSi<sub>2</sub>, form. by ion beam mixing 4-80121
- Cu epitaxial layers, quantum size effects, surface and interface roughness influence, LEED study 4-84526
- Cu oxidised surface solar absorbers, thermal stability, AES and refl. meas. 4-114951
- Cu/Al thin film interface reactions, X-ray diffr. and Rutherford backscatt. studies 4-88409
- Cu/ $\gamma$ -Fe/Cu epitaxial sandwich layers, struct. and Mossbauer studies 4-84531
- Cu<sub>2</sub>-S/CdS heterostruct., misfit accommodation and growth 4-108730
- Fe-C-Si, irregular eutectic, theoretical basis of grain growth. (*Polish*) 4-93258
- Fe-Cr-C (10, 0.2 wt.%), austenite form., TEM and optical microscopy study 4-66331
- Fe<sub>2</sub>Si/Zn diffusion couples, periodic struts. and two phase band form. 4-65499
- GaAs/Ni reactive interface, soft X-ray photoemission spectra studies 4-113820
- GaAs-Au(Pd) interface, high energy ion channelling studies 4-65318
- Ga<sub>1-x</sub>Al<sub>x</sub>As-GaAs heterostructure, LPE grown, dislocation extension and density distrib. (*Chinese*) 4-113449
- Ga<sub>1-x</sub>Al<sub>x</sub>As-GaAs(GaAs) (001), structural parameters, X-ray diffr. 4-84257
- GaAs (110)-Al interface form. at low temp., electronic and struct. props. 4-84695
- GaAs/Al interface, low temp. form. and structure, LEED, AES and work function meas. 4-80425
- GaAs/Al<sub>0.5</sub>Ga<sub>0.5</sub>As quantum wells, struct. and optical props. 4-99151
- GaAs/AlGaAs heterostructures, struct. evaluation, TEM studies 4-84516
- GaAs/AlGaAs heterostruct., organometallic VPE growth and characterisation 4-99341
- GaAs/AlGaAs inverted heterojunctions, photoluminescence studies 4-98460
- GaAs/Au interface struct., XPS, RHEED and ion scatt./channelling studies 4-80421
- n-GaAs/Au Schottky contacts, elec. props. and interface chem., sputtering effects 4-80674
- GaAs/Ge(AlAs) heterojunctions, interface struct., TEM and STEM studies 4-108728
- GaAs/metal contacts, interface struct., TEM and STEM studies 4-108728
- GaAs/Ni film system, interfacial reactions, TEM and X-ray diffr. studies 4-108729
- GaAs/Ni-Ta interfacial reactions, metallisation appl. 4-98367
- GaAs/Pt, ion beam mixing and ohmic contact form. 4-92244

**interface structure continued**

- GaAs-AlAs semiconductor superlattices, MOCVD prep., interface struct. study 4-108726
- GaAs-Al(Au) Schottky barrier contacts, LEC grown, electron traps, DLTS signals, effect of metal 4-84691
- GaAs(110)-In interface, photoemission study 4-85079
- GaP, thermal oxidation, surface topography and oxide interface struct. 4-80342
- GaSb, oxidation and interfacial chem. reactions, XPS study 4-85226
- GaSe-metal interface, chem. reactivity 4-71973
- Ge (111)-Pb interface form. dynamics and oxidation 4-84518
- Ge<sub>2</sub>Si<sub>3</sub>/Si strained layer superlattice, MBE growth 4-92576
- Hf-Ni films, amorphisation by thin film solid state reaction 4-80428
- Hg<sub>1-x</sub>Cd<sub>x</sub>Te, native oxides and interfaces, spectroscopic ellipsometry studies 4-80426
- InGaAsP/oxidised films interface, Auger/ion sputtering anal. 4-104884
- InP (110)-Cu(Ag)(Au) interface, soft X-ray photoemission study 4-85080
- InP/InGaAsP DH, LPE grown, misfit dislocations, TEM study 4-113826
- InP/metal interfaces, chem. reactions, photoemission study 4-80310
- InP-metal interface, chem. reactivity 4-71973
- Mg<sub>2</sub>Si form., thin film reaction kinetics, AES and SIMS 4-81131
- Mo-Si interface, silicide form. kinetics induced by ion bombard. 4-61243
- Na, liquid-vapour interface struct., Monte Carlo simulation 4-88062
- Na-Cs liquid-vapour interface struct., Monte Carlo simulation 4-88062
- Nb/Si, metal-semiconductor heterostructures, exam. using electron microscopy and Auger spectroscopy 4-65579
- Nb-Si interface, silicide form. kinetics induced by ion bombard. 4-61243
- Nb<sub>2</sub>Al, low temp. diffusion, supercond. and struct. props. 4-65498
- Ni/Si interfaces, silicide form., atom-probe study 4-70475
- Ni/SiC mixed layers, ion and laser irradi., microstruct. anal. 4-84415
- Ni-base superalloy, single cryst., CMSX2, long-range order and phase comp. in  $\gamma$  phase, atom probe study 4-66337
- Ni-Si (111) interface, Ni<sub>2</sub>Si islands growth, ion scatt. study 4-92444
- NiO-Y<sub>2</sub>O<sub>3</sub> system, composite microstruct. and interface struct. 4-70578
- NiSi<sub>2</sub> nucleation on Si (111), direct struct. determ., SEXAFS meas. 4-99227
- Pb-Sn eutectic thin films, directionally solidified, interlamellar spacing 4-93285
- PbSnTe-PbTe lasers with high efficiencies, lattice-matching to reduce misfit dislocations 4-112420
- PbTe/Pb<sub>1-x</sub>Sn<sub>x</sub>Te superlattices, struct. and electronic props. 4-98463
- Pd/Si Schottky contacts, XPS study (*Chinese*) 4-114358
- Pd-Si(111) interface, atomic intermixing and electronic interaction 4-70478
- Pt/Si Schottky contacts, XPS study (*Chinese*) 4-114358
- Si crystals, interface shape and radial distribution of impurities 4-113371
- Si reconstructed surface reordering on room temperature Ge deposition 4-98411
- Si:As/Al interface, sintering and diffusion, As dopant effect 4-80427
- Si:As/Ti interface, As implantation, As out-diffusion during TiSi<sub>2</sub> formation 4-65493
- a-Si:H/a-Ge:H/a-Si<sub>1-x</sub>C<sub>x</sub>/a-Si<sub>1-x</sub>N<sub>x</sub>H superlattices, CVD growth and struct. 4-114416
- a-Si:H/a-SiN<sub>x</sub>/a-SiO<sub>2</sub> multilayer films, struct., elec. and optical props. 4-114025
- Si/Ag system, atomic mixing using 45 keV Ar<sup>+</sup> ion beam 4-80119
- Si/Al interface, atomic redistributions, XPS studies 4-80311
- Si/Au interface, atomic redistributions, XPS studies 4-80311
- Si/Au(Ag) interfaces, reactivity, MeV ion scatt. studies 4-80424
- Si/Pt interface, silicide form., Raman spectra studies 4-80423
- Si/SiO<sub>2</sub> interface, amorphous Si/cryst. Si facet form. during solid phase epitaxy 4-88423
- Si/SiO<sub>2</sub> interface, atomic struct. and elec. props. 4-80677
- Si/SiO<sub>2</sub> MOS struct., interface state density and atomic roughness 4-98684
- Si/SiO<sub>2</sub>/Si<sub>3</sub>N<sub>4</sub>, N and O distrib. profiles, Auger studies (*Russian*) 4-65578
- Si-Er interface, ErSi<sub>3</sub> formation using electron beam heating 4-65494
- Si-SiO<sub>2</sub> interface, As<sup>+</sup> implanted, defects, ESR study 4-61591
- Si-SiO<sub>2</sub> interface, Cl incorporation during Si oxidation in HCl/O<sub>2</sub> ambient 4-62079
- Si-SiO<sub>2</sub> MOS struct., H passivation of implantation defects using a-Si:H film 4-71744
- Si-Ti interface, TiSi<sub>2</sub> formation by fast radiative processing 4-113731
- SiC cubic single cryst., CVD prep. and elec. props. 4-99345
- SiC/Al(Pd) interface form., annealing and oxidation, AES studies 4-80420
- SiO<sub>2</sub>/Si interface, XPS and electron escape depth variation 4-81104
- SiO<sub>2</sub>-Si interface, oxidation, chem. bonding in transition layer, photoemission spectra using synchrotron radiation 4-85062
- Ta<sub>2</sub>O<sub>5</sub>, anodically growth on Ta, ultra-high resolution depth profiling 4-81098
- Te/metal binary thin film systems, Te cpd. formation 4-98371
- Ti/Ni bilayered thin films, amorphisation and ion beam mixing 4-88408
- Ti-Si interface, Ti-Si<sub>2</sub> formation by wide-area electron beam irradi. 4-92236
- TiC-stainless steel interface, reaction zone struct. produced by vacuum-annealing 4-104918
- UO<sub>2</sub>/Zircaloy-4, diffusion couple, interfacial energy and work of adhesion 4-83141
- V/Fe compositionally-modulated struct., mag. props. and superconductivity 4-61561
- V<sub>2</sub>Ga composite superconductors, in situ, prep. by external diffusion, microstruct. and supercond. props. 4-92844
- V<sub>2</sub>O<sub>5</sub>/Cr, metallic phase-insulating phase interface, misfit dislocations 4-108373
- VSi<sub>2</sub> form., thin film reaction kinetics, AES and SIMS 4-81131
- W interaction with Al<sub>2</sub>O<sub>3</sub> and Cr<sub>2</sub>O<sub>3</sub> thin films 4-70576

**interface tension** see *surface tension*

**interface vibrations** see *crystal surface and interface vibrations*

**interfaces, computer** see *computer interfaces*

**interfaces, mechanical** see *mechanical contact*

**interfacial energy** see *surface energy*

interfacial tension *see surface tension*

interfacial waves *see surface waves (fluid)*

## interference

*see also interference (signal)*

biprism interferences with 1 MeV electrons from monofile Van de Graaff generator 4-107503

frequency domain description of interferogram analysis 4-107516

## interference (signal)

*see also crosslink; electromagnetic interference*

ECG, 50 Hz interference subtraction 4-85545

evoked potential processing, system identification techniques for noise reduction 4-105357

homodyne and heterodyne detection, noise 4-79069

seismic optimum data editing technique for noise reduction in multi-channel data 4-110278

semiconductor lasers, direct FM and FM noise 4-69463

## interference spectrometers

automated interferometer for Fourier transform spectroscopy at near-mm wavelengths 4-101914

cryogenic IR radiance instrument for shuttle CIRRIS telescope 4-94614

double cat's eye small interferometer for rapid-scanning Fourier transform spectroscopy 4-101913

far IR, microcomputer expt. control and data analysis 4-106406

Fourier spectrometer, theory and use for astronomical obs. (Japanese) 4-94628

Fourier spectrometer for visible light using Michelson interferometer 4-101936

Fourier transform spectrometers, absolute radiometry 4-101944

interference microscope in electron microprobe, specimen exact focusing 4-82864

polarising interferometer, high efficiency, for far IR Fourier transform spectroscopy 4-106407

rocket-borne pure interferometric high resolution spectrometer (Japanese) 4-115687

two-beam interferometer for dispersive refl. spectroscopy of solids in far IR 4-106405

## interference spectroscopy

*see also Fourier transform spectroscopy*

extreme UV absorption spectroscopy using two laser-produced plasmas 4-60728

rapid-scanning Fourier transform spectroscopy, source of problem 4-73536

## interference suppression

3-D digital images, noise reduction techniques 4-107544

acoustic background noise immunity, multisensor speech input 4-103131

acoustic noise suppression using two-point receiving signals (Japanese) 4-91695

audio signal enhancement, digital techniques appl. 4-103109

building attenuation enhancement, conductive paint appl. 4-107496

cinematography, video/sound tracks, time-advanced noise reduction system (Russian) 4-90679

double-integrating DVM, A/D convertor interf. suppression and error considerations (Bulgarian) 4-86398

fighter cockpit environment, adaptive noise cancellation 4-103132

interferometer with automatic fringe counting, vibration amplitudes of diffusely reflecting surfaces meas. 4-95509

LMS spatial cancellation, interference extent effects 4-103081

NMR pickup coil design, noise current meas. and S/N improvement, low-temp. expts. 4-68252

noisy speech, optimal estimators for spectral restoration 4-103130

rusty-bolt intermodulation, chemical suppression 4-109574

sea surface reverberation rejection 4-103119

speech, harmonic magnitude suppression for intelligibility enhancement 4-103133

Weibull-distributed weather clutter, frequency domain anal. 4-100688

## interferometers

*see also acoustic wave interferometers; electromagnetic wave interferometers; interferometry*

two cryst. neutron interferometer, rot. motion, phase shift 4-68342

## interferometry

*see also acoustic wave interferometry; electromagnetic wave interferometry; holographic interferometry; interferometers*

IR and MM waves, conf., Miami Beach, FL, USA (Dec. 1983) 4-73154

neutron interferometry, static and time-depend. absorpt. 4-103610

neutron interferometry, symmetry violations and Schwinger scatt. in neutron interferometry 4-68450

neutron interferometry and its relation to fundamental phys. 4-68011

neutron single crystal interferometry, energy conservation and complementarity 4-113271

neutron wavepackets and longit. coherence 4-68014

quaternions, in quantum theory 4-63566

spinel voids, electron interferometry using TEM 4-97983

superfluid interferometer for Earth rot. detection using Josephson effect 4-58728

time dependent neutron interferometry, de Broglie waves evidence 4-110916

time-dependent neutron interferometry, Aharonov-Bohm and Wheeler-type delayed choice expts. 4-68012

violations of quantum mechanics, upper bounds, modified hamiltonian equation of motion 4-90404

viscous gas flowing from slit or cylindrical channels into region of lower press., interferometric study 4-113021

wave optics expts. with cold neutrons 4-68744

wave-particle dualism, testing using time-dependent neutron interferometry 4-78186

## intergalactic matter

*see also clusters of galaxies; galaxies*

Abell 1367 galaxy cluster, intracluster medium-UGC 6697 interaction 4-115818

Abell 2634, interaction of ambient cluster gas with radio galaxy 3C 465 (NGC 7720) 4-86072

accretion onto elliptical galaxies, nucl. activity and supernova occurrence 4-82548

3C 411, distant radio galaxy, mag. field struct. from VLA obs. 4-73064

clouds and their evolution, prod. of quasar absorpt. lines 4-77964

Coma cluster, centimetre-wavelength obs. of extended radio source near Coma A 4-73091

cosmological molecular clouds, identification via correl. procedure 4-67790

## intergalactic matter continued

dark matter, galaxies, superclusters and voids, review 4-63379

density rel. to radiogalaxies and quasars 4-73101

energisation through action of zero-point field accel. 4-100887

galaxy clusters, compact groups dominated by dark matter, N-body simulation 4-86070

galaxy clusters, dark matter, evidence for non-baryonic nature 4-67795

in galaxy superclusters, contrib. of dark matter to gravit. imagin. 4-86069

gas affected by collisions between clusters of galaxies 4-77945

gas content of galaxy clusters, ram pressure stripping 4-77944

heavy element enrichment 4-73083

hot intercluster gas, effects on X-ray emission from clusters of galaxies 4-63266

infall onto galactic disc and galactic chem. evolution 4-63293

interstellar clouds sweeping from rot. galaxy by intergalactic medium dynamics 4-94943

intracluster gas, cooling flows leading to star form. and central galaxy growth 4-110759

intracluster gas in Coma and Abell 1367, rel. to radial gradients in props. of spiral galaxies 4-82553

intracluster gas-active galaxies interactions, radio-trail galaxies form. 4-94968

intracluster hypothetical particles, decay, UV and X-ray emission 4-101154

magnetic field strengths in galaxy clusters, lower limits from hard X-ray emission obs. 4-86065

missing mass problem 4-90268

multiphase evolution in early Universe 4-73128

NGC 1275, Seyfert galaxy, Lyman  $\alpha$  emission and intracluster gas infall 4-73077

obscuration of cosmologically distant objects by dust, test using quasar 4-86025

PKS 2155-304, BL Lacertae object, X-ray absorpt. by hot intergalactic medium 4-86056

protogalactic eddies, structure 4-63290

protogalactic gas thermochemical evolution in galaxy formation adiabatic theory 4-63291

Q1101-264, red shift systems anal., intervening galaxies or intergalactic clouds 4-90250

QSOs intervening clouds, mag. fields and column densities from rot. meas. distrib. anal. 4-86082

quantum theory of EM interactions, particle acceleration and zero-point field 4-63044

radio jet sidedness, magnetic field config., and collimation 4-115809

rich galaxy clusters, He gravit. separation from D (Russian) 4-94971

H I, spin temp. anal. 4-110743

H I radial velocity in Magellanic Stream 4-106064

## intermediate bosons

axion and mag. monopole theories 4-59010

book on nucleus comp., elementary particles and fields 4-82617

boson creation in a subquantum lattice 4-73711

CERN UA1 collaboration, physics results 4-95835

CERN-collider, obs. interpreted as Higgs boson prod. SU(3) $\times$ SU(2) $\times$ U(1) model 4-106468

CERN-collider Z<sup>0</sup> anomalous decays, conjectured second strong force or heavy quarks 4-106508

charged Higgs bosons, phenomenological predictions from extended Weinberg-Salam electroweak model 4-73712

composite Higgs mass, confining ultracolour group SU(N), N $\geq 3$  4-106467

composite model of quarks and leptons, fermion and weak boson masses 4-90826

composite W bosons,  $\rho$ -parameter in weak interactions 4-73731

conference, particles and fields, Blacksburg, VA, USA (Sept. 1983) 4-73135

conference on particles and fields, Banff, Canada (Aug. 1981) 4-63404

cosmological Bose-Einstein condensate due to light bosons and heavy photons 4-86099

covariant polarisation bases for spin  $1/2$ , 1 and  $3/2$  particles, vector boson decay and prod. 4-64025

decay properties in SU(3) $\times$ SU(2) $\times$ U(1) model 4-68485

dispersive medium, weak force/long range interaction, Z<sub>0</sub> mixing 4-68498

effective field theory and weak non-leptonic interactions 4-90804

electroweak theory, intermediate bosons, currents, CP violation 4-95736

flavour changing suppression in technicolour, pseudo-Goldstone bosons Cabibbo mixing 4-102075

flavour non-conservation induced by Higgs particle exchange in SU(2) $\times$ SU(2) $\times$ U(1) model 4-73702

gauge boson/Higgs boson unification: the Higgs bosons as superpartners of massive gauge bosons 4-63904

gauge-boson masses and mixings in left-right-symmetric models 4-73692

GUTs; minimal SU(5) Higgs scalar effects and supersymmetry, p decay 4-90763

GUTs in curved space-time, renormalisation group anal., coupling constants 4-68091

Higgs boson, neutral and charged mass upper bounds from radiative corrections 4-102021

Higgs boson decay following prod. in lepton+lepton and hadron+hadron collisions 4-106503

Higgs bosons, mass sum rule in SU(2) $\times$ U(1) 4-63915

Higgs masses, renormalisation, effective potential in SU(5) to one loop 4-73704

Higgs models, custodial SU(2) theory, SU(2) $\times$ U(1) and U(1) gauge interactions 4-111424

Higgs particles, lightest mass upper limit in supersymmetric theories 4-86620

interacting boson model and Dyson mapping, microscopic anal. 4-59179

invisible axion detection, properties, P- and CP-conservation 4-90767

locally supersymmetric GUTs coupled to N=1 supergravity, weak symmetry breaking 4-78503

low mass second neutral vector boson in SO(10) 4-68475

magnetic monopole bound states of gauge boson, SU(2) theory, Prasad-Sommerfield limit 4-106466

masses, weak mixing angle effects 4-68484

particle properties review, masses, decays and lifetimes 4-67885

particles and interactions, supersymmetric theories, quarks, leptons, W, Z, Winos, Zinos and Higgs 4-73674

pp-Z<sup>0</sup>X, high p<sub>T</sub> studies 4-73776

## intermediate bosons continued

- pseudo-Goldstone boson masses in technicolour model with massive techniquarks 4-73691  
 scalar neutrino mass, effect on intermediate boson, tau lepton and kaon decays 4-90744  
 SL(N,C) gauge interactions, linear descript., cosmological implications, hadrons formed from vector bosons 4-111284  
 SO(10) GUT with low mass  $W_R$  boson, baryon generation mechanism 4-95721  
 SO(10) model with  $54+126+10$  Higgs, scalar particle spectrum 4-106482  
 soft quantum-chromodynamics radiation and the weak-boson transverse momentum 4-73717  
 spinless boson radiative decay, possible source of anomalous  $l^+l^-\gamma$  in Z searches 4-102148  
 standard electroweak model, lepton triplets, neutrino masses,  $W^+Z$  mass ratio 4-106498  
 strong CP soln. in UT, small  $\theta$  and invisible axion 4-63946  
 strong CP violation and axion mechanism 4-95714  
 SU(3)×SU(2)×U(1) gauge group, baryon number non-conservation, low mass scale 4-111363  
 SU(8) theory of multigenerational grand unification 4-59000  
 substructure effects, composite leptons, quarks and W bosons, W couplings 4-111422  
 Summer School, Chilton, Didcot, England (Sept. 1983) 4-58542  
 theory and CERN discovery, review (French) 4-59117  
 vector particles, renorminvariant mass, vacuum struct. in mag. field 4-82900  
 W boson mass constraints in SU(2)<sub>L</sub>×SU(2)<sub>R</sub>×U(1)<sub>Y</sub> gauge theories 4-111310  
 wave functions, internal structure in composite model 4-90830  
 $e^+e^-$ , nonstandard Higgs bosons prod. 4-59066  
 $e^+e^-$  colliders, tests for substructure of leptons, quarks,  $W^\pm$ , Z bosons 4-111428  
 $e^+e^-$  collisions, resonance production and decay estimates from radiative Z decays 4-90903  
 $e^+e^- \rightarrow e^+e^-(\gamma\gamma)(\mu^+\mu^-)(\tau^+\tau^-)$ , 39.8-45.2 GeV, spin-0 boson partial width limits 4-73737  
 $e^+e^- \rightarrow \mu^+\mu^-$ , charge asymmetry, weak single loop corrections,  $\gamma Z$  box 4-59063  
 $e^+e^- \rightarrow \mu^+\mu^-H$ , Higgs mass calcs. in QED 4-86695  
 $e^+e^-$  results from PETRA, QED and electroweak tests, lepton searches, jets, Higgs 4-64010  
 $e^+e^- \rightarrow W^+e^- \nu$ , single W prod. cross section 4-59064  
 $e^+e^- \rightarrow W^+W^-(Z\gamma)(ZZ)(ZH)$ , muon spectra from W and Z decays 4-73738  
 $\gamma d \rightarrow He$  differential cross-section, backward scatt., Higgs production in Weinberg-Salam model (Chinese) 4-90847  
 $\gamma e \rightarrow W$  differential cross-section, ang. dist. 4-111433  
 $H \rightarrow W^\pm W$  Higgs branching ratio 4-90938  
 $hh \rightarrow W^\pm(Z^0)$  in Weinberg model with QCD bremsstrahlung, Monte Carlo program WIZJET 4-95825  
 $K^+ \rightarrow \pi^+ X^0$ , neutral exotics search, axions 4-102115  
 $K^+ \rightarrow \pi^+ \alpha$  ( $\alpha$ =Goldstone boson) in SU(5)×SU(3) theory 4-68480  
 $ll \rightarrow$  pseudoscalar, numerical formula for total cross-section calcs. 4-95784  
 $\mu \rightarrow e\alpha$  ( $\alpha$ =Goldstone boson) in SU(5)×SU(3) theory 4-68480  
 $\mu^+N \rightarrow \mu^+X$ , muon interference expts.,  $Z^0$  existence, unification and electroweak reviews (Russian) 4-78557  
 p decay theory in SU(5) GUT, lifetime uncertainties, Higgs scalar effects 4-59013  
 pp, 540 GeV, very high energy density events at CERN SPS, quark-gluon plasma relevance 4-68592  
 pp,  $\sqrt{s}=540$  GeV, electron and hard jet prod., large missing  $p_T$ ,  $W^\pm$  prod., QCD processes 4-68595  
 pp, neutrino species counting, Z and W production ratios 4-73726  
 pp collider at CERN, supersymmetric partners, of gluons, quarks, W-bosons 4-90749  
 pp  $\rightarrow l^+l^-X$ , lepton pair production with  $M(l^+l^-) < M_Z$  4-86739  
 pp  $\rightarrow W^\pm$ , masses cross-sections widths 4-73775  
 pp  $\rightarrow W^\pm X$ , 540 GeV, production cross-section 4-78570  
 pp  $\rightarrow W^\pm X$ , high  $p_T$  studies 4-73776  
 pp  $\rightarrow W^\pm(Z^0)X$  review of COLLIDER project 4-102134  
 pp  $\rightarrow Z^0$ , masses, cross-sections, widths 4-73775  
 pp  $\rightarrow Z^0(\rightarrow e^+e^-)X$ , neutrino species determ. 4-90930  
 pp  $\rightarrow Z^0 X$ , scaling violations in intermediate boson prod., QCD deviations 4-95828  
 pp  $W^\pm(Zh)$ , hadronic remnants in W and Z prod. 4-59108  
 T decay, W couplings 4-90893  
 W and Z multiple prod. as strong interaction signal for electroweak symmetry breaking 4-95722  
 W decay, new composite bound state 4-68602  
 W decay, weak spectral functions and applications 4-64026  
 W decay in QCD and Weinberg model, constraint on  $N_c$  species 4-68467  
 W-heavy lepton-electron decay signature study 4-73788  
 W- $\nu$ , heavy unstable neutrinos from weak boson decays 4-86751  
 W- $L\tau$ , heavy lepton detection in pp collider 4-68604  
 W- $tb$ , top particle weak production, mass  $\approx 35$  GeV 4-111482  
 W- $tb$ , top quark, QCD radiation effects, lepton signatures 4-95827  
 W- $tb$ , top quark, QCD radiation effects, lepton signatures 4-95827  
 W $^\pm$  decay, experimental searches for squarks, sleptons and SUSY gauge bosons, mass limits 4-59019  
 W $^\pm \rightarrow e^+e^-(e^+\bar{\nu})$ , decay props., comparison with electroweak theory 4-95832  
 W $^\pm \rightarrow e^+e^-\nu$ , invariant mass 4-73776  
 W $^\pm \rightarrow e^+e^-\nu$ , parity violation, spin 4-73775  
 W $^\pm \rightarrow l^+l^+X$ , same-sign dilepton production, possible physical origin 4-95787  
 W $^\pm$ -neutral scalar, electroweak theory 4-73686  
 W $^\pm Z^0$  mass relation, electroweak higher order effects test, leading log corrections 4-82929  
 $W_R^\pm \rightarrow Z_l H^\pm$ , search for Higgs in left-right symmetric models 4-95865  
 Z decay in QCD and Weinberg model, constraint on  $N_c$  species 4-68467  
 Z- $e^+e^-\gamma$ , composite scalars in  $e^+e^-$  collisions and radiative Z decays 4-86694  
 Z- $e^+e^-\gamma$ , interpretations and other tests 4-78578  
 Z- $e^+e^-\gamma$ , proton theories of particle struct., compositeness scale lower bound 4-106522  
 Z- $e^+e^-\gamma$ , test of standard model 4-68603  
 Z- $eE(eE) \rightarrow e\bar{e}\gamma$ , cascade decays through new particle, electron mag. moment, coupling constraint 4-102147

## intermediate bosons continued

- Z- $ll\gamma\gamma$ , Z mixing with degenerate bound colour quarkonium 4-111486  
 Z neutral current flavour changing decay induced by radiative corrections 4-95751  
 Z- $\nu\mu\mu$ , heavy neutrino explanation for anomalous  $l^+l^-\gamma$  events 4-102149  
 Z-boson decay, effective flavour-changing neutral current 4-82979  
 Z $^0$  anomalous radiative decay 4-78579  
 Z $^0$  composite nature, experimental test, pp collisions 4-86682  
 Z $^0 \rightarrow e^+e^-(2)$ , invariant mass 4-73776  
 Z $^0 \rightarrow e^+e^-(e^+e^-\gamma)$ , decay props., comparison with electroweak theory 4-95832  
 Z $^0 \rightarrow e^+e^-\gamma$ , composite boson coloured constituents, hypercolour binding 4-111425  
 Z $^0 \rightarrow e^+e^-\gamma$ , scalar/pseudoscalar boson contributions to:  $e^+e^-$  interactions, masses, decay 4-111436  
 Z $^0$  four body decay, heavy flavours 4-68605  
 Z $^0 \rightarrow \gamma$ - $\gamma$  squarkonium, production of  $^1S_0$  squarkonium states, gluon jets 4-111487  
 Z $^0 \rightarrow l^+l^-\gamma$ , anomalous lepton magnetic moments, constraints 4-86750  
 Z $^0 \rightarrow l^+l^-\gamma$ , collinear radiation and lepton universality 4-78577  
 Z $^0 \rightarrow \nu\nu$ , heavy unstable neutrinos from weak boson decays 4-86751  
 Z $^0 \rightarrow \nu\nu$ , neutrino generation counting 4-86754  
 Z $^0 \rightarrow q\bar{q}l^+l^-$ , Monte Carlo calcs. 4-90936  
 Z $^0$  radiative decays, parity violation, spin 4-73775  
 Z $^0 \rightarrow \tau^+\tau^-$  limits on composite structure, CP violation 4-90937  
 Z $^0$  width, neutrino flavors, cosmological constraints 4-95009  
 Z $^0 \rightarrow Z_l H^0$ , search for Higgs in left-right symmetric models 4-95865  
 @ W- $\nu\gamma$ , collinear radiation and lepton universality 4-78577  
 @ Z $^0$  anomalous radiative decay, possible new pseudoscalar particle 4-68577  
 $^{162}\text{Er}$ , g-boson study 4-59181  
 W-heavy fermion-light fermion cascade decay covariant formalism 4-73788  
 $^{184}\text{W}$ , g-boson study 4-59181  
 Z boson, second mass in SU(2)<sub>L</sub> electroweak gauge theories 4-90779  
 Z- $l^+l^-\gamma$ , excited lepton states 4-78580  
 $\zeta$  (8.3 GeV), from upsilon decay, interpreted as Higgs boson 4-111447
- intermediate state**  
 thin films, optically driven, picosecond pulse generation capability 4-92861
- intermediate valence compounds** see *mixed valence compounds*
- intermetallic compounds** see *alloys*
- intermodulation**  
 rusty-bolt intermodulation interference, chemical suppression 4-109574
- intermodulation measurement**  
 No entries
- intermolecular forces**  
 see also *Van der Waals forces*  
 alkali halide, crack edge contact restoration phenomena 4-98191  
 n-alkanes, free vol. temp. depend. and intermol. forces study using energy of vaporisation 4-84374  
 bicyclo (2.2.2) octane, solid, rotator phase, mol. dynamics calcs. 4-75331  
 electrostatic interaction energy anal., separated electronic groups theory (German) 4-78927  
 fluids, orthobaric props. of spherical and linear mols., intermol. pot. effect 4-74310  
 higher order contributions in perturbation treatment of long-range forces 4-69163  
 inositols, IR and Raman vibr. spectra 4-69071  
 interaction energies calc. using pseudopot. Hartree-Fock-Slater-LCAO method 4-96639  
 interaction energy calc., first order, basis set development 4-64561  
 liquid metal mixtures, intermolecular forces, excess Gibbs energy 4-65418  
 long range forces, interaction energy minimisation (Spanish) 4-87178  
 metals disordered interaction, macroscopic theory 4-80466  
 methyl iodide(d-j), liq. vibr. relax. studies, vibr. coupling contrib. to  $\nu_2$  mode 4-74224  
 molecular pairs of arbitrary symmetry, electrostatic energy, forces and torques 4-87185  
 nematic liquid crystals, spatial correls., mol. pot. model 4-84177  
 perfluorochemicals as O<sub>2</sub> carriers, interaction forces 4-59875  
 potentials that are functions of thermodynamic variables 4-87184  
 simple fluids and electrolytes, statistical mechs. aspects 4-108261  
 solutions, strictly regular, conc. profile of boundary, cluster approach 4-80333  
 trapped molecules in oriented polymer films, optical anisotropy, waveguide Raman spectrosc. obs. 4-78377  
 Ar-HCl(HF), intermolecular forces, HF plus damped dispersion calcs. 4-87039  
 CO<sub>2</sub> absorption coefficient temp. depend. beyond edge of vibr.-rot. bands 4-83366  
 Cu complexes, diacetyl-bis(thiosemicarbazone)Cu(II), electronic struct. and intermol. interactions 4-61586  
 Cu complexes, methylglyoxal-bis(thiosemicarbazone)Cu(II), electronic struct. and intermol. interactions 4-61586  
 HF+Ar, finite duration of collisions and vibr. dephasing effect on broadened IR line shapes 4-69177  
 N<sub>2</sub>O+Ar collisions, intermol. pot., electron gas model, comparison with mean square torques meas. 4-78923  
 Na+N<sub>2</sub>, electronic to vibr. energy transfer collision, Na(3p) fluoresc. 4-74320  
 O<sub>2</sub>,  $^3\Sigma_g^-$  ground state, electrostatic and exchange interactions 4-112249
- intermolecular mechanics**  
 see also *association; intermolecular forces; kinetic theory of gases; liquid structure; liquid theory; Morse potential; potential energy functions*  
 acetone, carbon disulphide soln., Monte Carlo simulation using quantum mech. intermol. pot. 4-65160  
 acetone-water binary liq. mixtures, intermol. interactions and viscosity 4-113687  
 alcoholic  $^{\circ}\text{OH}$  vibration bands, intermol. effects 4-59855  
 alkanols-water systems, thermodynamic props. 4-92388  
 aniline, low temp. cage effect and phosphorescence 4-96690  
 benzene dimer, interaction and dispersion effects, ab initio HF calcs. 4-102579  
 benzene-carbon tetrachloride binary liq. mixtures, intermol. interactions and viscosity 4-113687  
 benzene-cyclohexane binary liq. mixtures, intermol. interactions and viscosity 4-113687

**intermolecular mechanics continued**

- benzene-s-tetrazine mixed dimer, interaction and dispersion effects, ab initio HF calcs. 4-102579  
 chlorobenzene-carbon tetrachloride, binary liq. mixtures, intermol. interactions and viscosity 4-113687  
 2,3-dibromo-1-propene, mol. struct. mechanics, electron diffraction study 4-112272  
 N,N-dimethylaniline, low temp. cage effect and phosphorescence 4-96690  
 DNA, interaction with mols., steric surface, electrostatic contours 4-72206  
 DNA-ethidium, binding consts., elec. pots. 4-109774  
 B-DNA-polyglycine, interaction energies, complex struct. and stability 4-77181  
 doublet mols., ensemble averaged spin pair dynamics 4-69234  
 ethene dimer+Na<sup>+</sup> interaction, PCIL0 investig. (German) 4-107429  
 fluorinated methanes, <sup>19</sup>F nuclear shielding, intermol. interactions, rovibr. motion 4-102706  
 guanidinium-carboxylate interaction, ab initio SCF HF calcs. 4-96436  
 interacting mols., dipole induced dipole model, polarisability tensor 4-69165  
 liquids, vibr. line shapes, role of resonant intermol. coupling 4-96521  
 local electron pair model, test calcs. (German) 4-107428  
 local electron pair models for intra- and inter-molecular exchange interactions (German) 4-78774  
 $\alpha,\omega$ -lors(methyl)dodeca-1,12-diylammonio)hexane, dibromide, conformation, X-ray struct. 4-98083  
 methane, halo substituted, rovibr. motion, mag. shielding, <sup>19</sup>F NMR 4-107366  
 methanol, OH group vibr. freqs., intermol. interactions and matrix effects 4-102665  
 methanol-aqueous soln., hydrophobic interaction, Monte Carlo calc. 4-97994  
 molecular complexes, H bonded, stabilisation energies 4-64560  
 myoglobin, native sperm whale, orientation influence on affinity 4-107477  
 non-Condon intermolecular electron transitions (Ukrainian) 4-87182  
 nonelectrolyte mixtures, thermodynamic excess functions, mol. interactions 4-71964  
 nucleic acid-base interactions, solvent effects, Monte Carlo simulation 4-64559  
 oligobutadiene urethane, intermol. interactions studied by IR spectra, thermodynamic props. (Russian) 4-102761  
 cis-pent-2-ene, vibr., mol. mechanics, electron diffraction 4-112277  
 penta-1,4-diene, vibr. mol. mechs., electron diffraction 4-112278  
 pleochroic dyes, intermol. guest-host interactions and optical order parameter 4-88085  
 polyethylene-acrylic acid graft copolymers, intermol. interaction energies and mech. props. 4-75603  
 proteins, ligand binding to receptor sites 4-69171  
 pyridine solns., ion-H<sub>2</sub>O interactions, PMR obs. 4-112207  
 tetraazacyclododecane, ring conformation calc., mol. mechanical method (Japanese) 4-11246  
 1,2,3,4-tetrahydroquinoline, excited state, fluoresc. charact. and mol. interaction in soln. 4-112130  
 s-tetrazine dimer, interaction and dispersion effects, ab initio HF calcs. 4-102579  
 thermophysical props. of material and its rel. to intermol. interaction parameters 4-61105  
 tricyclo[4.2.2.2<sup>0,3</sup>]dodeca-1,5-diene, struct. bonding, intermolecular interactions 4-96636  
 triplet mols., ensemble averaged spin pair dynamics 4-69234  
 Ar and Kr, clathrate hydrate formation in struct. II modification 4-112251  
 Ba(Fe(CN)<sub>5</sub>NO)<sub>2</sub>·2H<sub>2</sub>O, IR spectra, vibr. dipole-dipole coupling between nitrosyl groups, fine struct., force consts. 4-96540  
 CO<sub>2</sub>, microwave spectra, intermol. interaction mechs. 4-59731  
 Co complex, Co(ethylenediamine)<sub>3</sub><sup>3+</sup>, rot. motion and ion interactions, NMR obs. 4-59802  
 Cu complex, bis(di-ethanol-dithiocarbamate) Cu(II), intermol. interactions, EPR obs. 4-64516  
 D<sub>2</sub>O, OD group vibr. freqs., intermol. interactions and matrix effects 4-102665  
 HI complexes, interactions, energy component anal. calcs. 4-59869  
 (H<sub>2</sub>O)<sub>n</sub> clusters, multiplicity and total nonadditive energy components 4-69263  
 HeSF<sub>6</sub>, multiproperty empirical anisotropic intermol. pots. 4-74308  
 I<sub>2</sub> complexes, interactions, energy component anal. calcs. 4-59869  
 Mg(H<sub>2</sub>PO<sub>4</sub>)<sub>2</sub> soln., complex form. and phosphate-H<sub>2</sub>O interactions 4-89256  
 NH<sub>2</sub>-electrolyte solns., NH stretching and bending vibrs., intermol. coupling, polarised Raman scatt. 4-61700  
 NeSF<sub>6</sub>, multiproperty empirical anisotropic intermol. pots. 4-74308  
 Sr(Fe(CN)<sub>5</sub>NO)<sub>2</sub>·4H<sub>2</sub>O, IR spectra, vibr. dipole-dipole coupling between nitrosyl groups, fine struct., force consts. 4-96540

**intermolecular vibrations** see molecular rotational-vibrational energy transfer

**intermolecular vibrations (molecular crystals)** see lattice dynamics of molecular crystals

**internal combustion engines**

- alcohol-fueled engine cold starting 4-62292  
 automotive engine, H<sub>2</sub>-fueled, design database 4-62403  
 automotive Stirling engine development program—overview and status report 4-66777  
 carburetors, activation anal. of corrosion by alcohol 4-93442  
 closed-cycle diesel engines, use of Ar, He and CO<sub>2</sub> as working fluids instead of N<sub>2</sub>, effects on performance 4-66743  
 cyclic heat transfer phenomena in closed spaces, simplistic model 4-64820  
 diesel engine fuel displacement by biomass producer gas 4-66652  
 diesel-cycle engine, H<sub>2</sub>-fueled, two-stroke, performance improvements 4-62404  
 dissociated methanol engine testing results using H<sub>2</sub>-CO mixtures 4-62290  
 electrohydraulic gas sampling valve 4-78305  
 flame temperature in intermittent-combustion chamber 4-85312  
 HCLB engine, air pollution remedy (Dutch) 4-114989  
 MOD I automotive Stirling engine development 4-66776  
 petrol engine, homogeneous combustion parameters and emissions control, computer simulation 4-77171

**internal combustion engines continued**

- reciprocating gas-handling machinery, heat transfer, during compression and expansion 4-64821  
 reformed methanol vehicle system considerations 4-62291  
 Ringbom-Stirling air engine design aspects 4-66769  
 H<sub>2</sub> fueled engine for underground mining vehicle, with ultra-low emissions 4-62406

**internal conversion**

- see also conversion electron spectra  
 interdisciplinary appls. and HF calcs. 4-78607  
 Wigner-Seitz boundary conditions effect on internal conversion coeffs. 4-73854  
<sup>244</sup>Am nucl. structure study with (n, $\gamma$ ) reaction 4-68651  
<sup>40</sup>Ca, A=106, 108, levels study from  $\beta^+$ /EC decay of <sup>106</sup>In<sup>m+8</sup> and <sup>108</sup>In<sup>m+8</sup> 4-68645  
<sup>134</sup>Ce level structure study using  $\gamma$  and  $\alpha$  spectroscopic methods 4-59127  
<sup>188</sup>Ir levels, J<sup>π</sup>, T<sub>1/2</sub>, transitions and ICC from <sup>187</sup>Re( $\alpha$ ,n) 4-111490  
<sup>4</sup>Th, A=228, 230, rotational levels from ( $\alpha$ , $\alpha'$ n) reactions 4-68609  
<sup>128</sup>Xe, low-lying states, internal conversion study from <sup>128</sup>Cs decay 4-95962  
<sup>172</sup>Yb multipole mixing ratios, energy levels, from <sup>172</sup>Lu decay 4-95955

**internal conversion in atoms** see Auger effect

**internal conversion in molecules** see nonradiative transitions

**internal fields, crystal** see crystal field interactions

**internal friction**

- see also Bordoni effect; damping; Snoek effect; Zener relaxation  
 Al-Fe, cold worked, damping capacity, mech. props. rel. to heat treatment and comp. (Japanese) 4-61968  
 anisotropic BCC metal, mobile interstitial internal friction and viscosity 4-70271  
 Cottrell atmospheres of impurities; dislocation interactions, internal friction and US meas. 4-65486  
 Gorsky relaxation of light interstitials, linear response anal. 4-75613  
 low-frequency resonance curves associated with non-linear internal friction 4-110869  
 metals, anelastic interaction between moving kink and point defect pairs (Chinese) 4-103785  
 metals, peaking effect due to electron or  $\gamma$ -ray irradiation 4-103873  
 phonon-dislocation interaction, frictional force, fluttering mechanism 4-103750  
 $\alpha$ -quartz, natural, twinning dynamics, internal friction study 4-103766  
 rock, internal friction and wave attenuation in water containing rock 4-94106  
 steel, structural, deform. mechanisms using high temp. tests 4-109481  
 steel 40 Kh, damping capacity and residual life, preliminary cyclic loading influence 4-99544  
 superconductors, dislocation phonon interactions, viscosity effects in plastic flow and internal friction 4-103861  
 time measurement technique with torsion pendulum 4-112778  
 Al, dislocation internal friction hysteresis 4-70165  
 Al, high purity, polygonised, TEM, internal friction peak 4-113534  
 Al, internal friction, time measurement technique with torsion pendulum 4-112778  
 Al, internal friction originated by grain boundaries 4-103872  
 Al-Mg, dil., neutron irradiation, internal friction, elastic modulus, recovery stages studied by elec. resist. meas. 4-103876  
 Al-Mg class I high temp. creep alloys, internal and friction stresses 4-85185  
 Al-Si, cold worked, damping capacity, mech. props. rel. to heat treatment 4-61967  
 Al<sub>2</sub>O<sub>3</sub>, internal friction and Young's modulus under thermal shock conditions 4-62009  
 Al<sub>2</sub>O<sub>3</sub>, Young's modulus and internal friction, temp. depend. 4-61965  
 Ar crystals, low temp. internal friction 4-60987  
 B fibres, elastic energy absorpt. mechanism 4-66366  
 BaO-P<sub>2</sub>O<sub>5</sub> glass, internal friction, temp. depend. 4-61966  
 CaO-P<sub>2</sub>O<sub>5</sub> glass, internal friction, temp. depend. 4-61966  
 Co-Si-B metallic glasses, Young's modulus, internal friction, magnetomechanical effects, permeability meas. 4-76216  
 Cr, neutron irradiation, internal friction, elastic modulus, recovery stages studied by elec. resist. meas. 4-103875  
 Cu and Cu-Al alloys, strain hardening in microdeform., dislocation density, internal friction obs. 4-66397  
 Cu-based shape-memory alloy, mech. and elec. props., sonic studies 4-76773  
 Cu-Be alloy, struct. transform. mechanisms during ageing, internal friction and resist. obs. 4-114536  
 Cu-Ni-Fe, internal friction and precipitation morphology (Russian) 4-99416  
 Cu-Ni-Sn (8, 6 wt.%), ageing, internal friction, Young's modulus, modulated structure 4-66362  
 Cu-Ti, internal friction and precipitation morphology (Russian) 4-99416  
 Cu-Ti-Cr, internal friction and precipitation morphology (Russian) 4-99416  
 Cu-Ti-Cr (4, 0.5 wt.%), ageing, internal friction, Young's modulus, modulated structure 4-66362  
 Fe, electron irradiation, internal friction (Polish) 4-92234  
 Fe; stress relaxation and static strain aging, short range heavy interstitials reordering 4-85172  
 $\alpha$ -Fe-N solid solns., N diffusion activation energies and nitrides precipitation study 4-65452  
 Fe-Ni, H<sub>2</sub> charged, internal friction 4-104802  
 Fe<sub>1-x</sub>Nb<sub>x</sub>-Se<sub>0</sub> elastic props. and Mossbauer effect 4-84881  
 Fe<sub>2</sub>Si<sub>2</sub>B<sub>2</sub> metallic glass, Young's modulus, internal friction, mag. hysteresis loop 4-76215  
 KH<sub>2</sub>(SeO<sub>3</sub>)<sub>2</sub>, ferroelastic domain struct. dynamics, internal friction meas. 4-80158  
 K<sub>2</sub>ZnCl<sub>4</sub>, low temperature phase transition, torsion pendulum method 4-113610  
 LiKSO<sub>4</sub> crystals, ferroelasticity and internal friction 4-75612  
 MgFe<sub>2</sub>O<sub>4</sub>, polycryst., elastic behaviour and internal friction in mag. field 4-71143  
 Mn-Cu, high-damping-capacity alloy, martensitic and mag. transitions after powder metallurgical prep. (Russian) 4-109403  
 Mo, diffusion of N at low temps., internal friction meas. 4-65487  
 NaCl,  $\gamma$  and laser irradiation, internal friction and dislocation damping 4-80153  
 Nb, stress relaxation and static strain aging, short range heavy interstitials reordering 4-85172

**internal friction continued**

- Nb-H, internal friction, hydride precip. peak, cooling rate and freq. depend. 4-66360  
 Ni-base creep-resisting alloys, cast, grain boundary relax., effect of struct. of boundary vol. 4-71677  
 Ni-Co-Nb, damping capacity, mag. and mech. props. 4-61564  
 $\text{Ni}_{0.968}\text{Co}_{0.012}\text{Mn}_{0.02}\text{Fe}_2\text{O}_4$ , magnetostrictive, magnetomechanical props., hysteresis loop, elastic moduli, internal friction, influence of mag. history 4-76212  
 Pb-In semiconductor, with dislocations surrounded by impurity atoms, internal friction (*Russian*) 4-98807  
 Si, crystal whiskers, cyclically deformed, relaxation spectrum 4-61264  
 Si, neutron irradi., radiation defects and electrophys. parameters 4-84319  
 Si, plastically deformed crystal, low freq. internal friction 4-60979  
 $\text{Si}_3\text{N}_4$ , hot pressed, fracture toughness, mech. props. rel. to comp. and microstruct. 4-76870  
 $\text{Si}_3\text{N}_4$ , Young's modulus and internal friction, temp. depend. 4-61965  
 SrO-P<sub>2</sub>O<sub>5</sub> glass, internal friction, temp. depend. 4-61966  
 Ta, stress relaxation and static strain aging, short range heavy interstitials reordering 4-85172  
 Ta-H, internal friction, hydride precip. peak, cooling rate and freq. depend. 4-66360  
 Ta<sub>2</sub>S<sub>3</sub>, elec. field depend. of elastic props. 4-103855  
 Ti-Ni-Cu system, dissipative props. and struct., martensitic transform. 4-66361  
 V-H, internal friction, hydride precip. peak, cooling rate and freq. depend. 4-66360  
 V-H alloy, hydride precip., automodulation 4-85157  
 ZrO<sub>2</sub>, partially stabilised, Young's modulus and internal friction, temp. depend. 4-61965

**internal friction of liquids** *see viscosity of liquids***internal mechanics, molecular** *see molecular vibration***internal mechanics of atoms** *see atomic structure***internal modes** *see molecular vibration in solids***internal stresses**

- acoustic microscopy, phase information, appls. 4-97229  
 alkali halides, elastic consts. and force const., bond deform.-model 4-61034  
 alkali halides, space charge elec. field form. during cleaving 4-76021  
 alkaline earth oxides, elastic consts. and force const., bond deform.-model 4-61034  
 alloys, amorphous, stress relief annealing, mag. props. 4-104797  
 amorphous systems, spinodal decomp., internal stress effect due to coherency strain 4-113646  
 binary crystal, displacement domains caused by defects (*Chinese*) 4-70254  
 brittle materials, compressive surface strengthening 4-93307  
 ceramics, surface damage, strength degradation, erosion and wear, acoustic NDT 4-76872  
 coating, modified X-ray method for macrostress determ. 4-99700  
 coating for tools and sliding elements, acoustic microscopy studies 4-104957  
 coatings on steel substrate, phys. and mech. props. after pulse shock loading 4-66489  
 composite materials, viscoelastic, thick-wall cylindrical shell, optimal non-steady cooling process 4-87589  
 composites, antisymmetrically laminated, thermal residual stresses, finite element anal. 4-97306  
 composites, damaged, affine equivalence of local stress and displacement distrib. 4-79448  
 composites, polymeric, thick-wall cylinders, allowance for rheology 4-87590  
 critical-resolved shear stress and dislocation glide obstacles 4-80049  
 crystal lattice internal strain, contrib. to elastic consts. and piezoelec. coeffs. 4-80135  
 crystals in external stress field, phase form. thermodynamics 4-84386  
 cubic materials with orthorhombic or monoclinic symm., residual stresses, texture effects, X-ray diff. obs. 4-79896  
 cubic one-phase materials with orthorhombic or monoclinic symm., residual macrostresses, texture effects, X-ray diff. obs. 4-79897  
 cylinder, two-layer, long, with nonsteady cooling, residual stresses problem soln. 4-64864  
 cylindrical components and elements, three-dimens. and plane residual stressed states under radial stress gradient 4-97315  
 electrodeposits, internal stress calc. 4-80464  
 embedded strain gaging of plastic models 4-91780  
 epoxide resin coatings, internal stress, network struct., glass transition temp., rel. to curing process (*Japanese*) 4-88966  
 epoxy beam, residual stresses and warp generated by one-sided quench 4-71672  
 ethylene-vinyl alcohol copolymer, struct., mech. and dielec. props., temp. depend. (*German*) 4-71261  
 fatigue crack propagation, residual stress distrib., X-ray meas. (*Japanese*) 4-99685  
 ferrites, polycrystalline, model of initial mag. permeability (*Russian*) 4-98921  
 ferroelectric ceramics, internal mechanical stresses 4-113530  
 ferromagnetic components quality control by coercive field strength meas. 4-93475  
 fibre reinforced composites, residual stresses during thermal cycling 4-71634  
 fibre reinforced porous metallic matrix, stresses at fibre/matrix boundaries 4-93335  
 films, compressed, delamination and spalling mechanics 4-79500  
 fusion reactor components, dynamic deform. due to EM forces, finite element anal. 4-74050  
 glass, toughened, thin thermally polished, strength asymmetry 4-89103  
 glass and glass ceramic, brittle, disturbed surface layer parameters effect on struct. strength 4-99541  
 glass fibre filled polypropylene, injection molded bars, residual stress distrib., distortion, annealing temp. gradient 4-81256  
 glass fibre reinforced epoxy, thick laminates thermoelastic behaviour 4-75706  
 glass fibre reinforced epoxy resin laminates, transverse cracking rel. to mech. props. of matrix 4-99489  
 glass fibre reinforced phenolformaldehyde, laminate. plates, shrinkage strains 4-61915  
 glass grinding damage, single- and multi-point comparison 4-85206  
 grain boundary interaction stress meas. using neutron diff., texture effects 4-85282

**internal stresses continued**

- grain boundary interaction stress meas. using time of flight neutron diff., texture effects 4-85281  
 graphite fibre reinforced epoxy, angle-ply laminates, long-term moisture absorpt. 4-76882  
 hardness measurement, influence of residual stress 4-99691  
 hollow cylinder, residual stress meas. by X-ray diff. 4-113518  
 hollow cylinder, residual stress meas. by X-ray diff. method 4-74971  
 imperfect crystal, laser irradi., thermoelastic stresses, optical polarisation study 4-61114  
 infection lasers, stimulated emission polarisation, stress effects 4-87333  
 long-range, determ. by controlled unloading technique 4-85280  
 measurement methods development (*German*) 4-103274  
 metal plates, residual deform. stress, US meas. using SAW 4-99731  
 metallic components, residual stress meas. by portable X-ray diff. instrument, displacement errors 4-62146  
 metals, acoustoelastic response, plastic deform. effect 4-74903  
 metals, anelastic interaction between moving kink and point defect pairs (*Chinese*) 4-103785  
 metals, dislocation interactions and deform. theory 4-113489  
 metals, high-speed deform., residual stresses 4-65330  
 metals, mechanical instability of cellular dislocation structure 4-65268  
 metals, polycrystalline, elastic deform., X-ray strain analysis (*Japanese*) 4-114598  
 metals, polycrystalline, finite elastic-plastic deformation 4-89093  
 metals, stresses and elastic const. with classical ion motion 4-98181  
 optical glass, thermostructural component of residual stresses, birefr. 4-69520  
 optical monomode fibres, linear birefr. meas. using thermic method 4-107829  
 Permalloy evaporated films, coercive force and mag. domains (*Japanese*) 4-104474  
 Permalloy films, mag. anisotropy and domain struct. patterning effects 4-88707  
 pipes, welded, residual stress meas., back computation 4-104952  
 plastic disc subjected to circular heat source, stresses 4-83841  
 plate, transversely isotropic, circular, thick, initially stressed, vibr. 4-83849  
 plate having rectangular notches with rounded corners, under tension, stress conc. 4-97311  
 Plexiglas with deposited Al, macrocrack opening, residual compressive stress study 4-64885  
 polyethylene, low density, blow extended annealed films, relax. characts. (*Russian*) 4-109446  
 polymer glasses, press. effects, densification and dielectric losses 4-65190  
 polystyrene, injection molded bars, residual stress distrib., distortion, annealing temp. gradient 4-81256  
 powder compacts, bimodal, sintering behaviour 4-99359  
 redistribution in normally incident shock wave 4-64874  
 residual stress evaluation with X-rays in steels having preferred orientation 4-114749  
 ribbons with negative magnetoelastic const., induced mag. anisotropy 4-104475  
 rod, shock-laden, stress pulseform anal. 4-64878  
 semiconductor structures, multilayer, thermal stresses 4-113682  
 shell, cylindrical, coiled, loaded by internal press., elastoplastic deform. analysis 4-97335  
 single crystals, plasticity, effects of dislocation collective behaviour 4-98101  
 sintered compacts, grain size, internal strain, photoluminesc. spectra 4-99160  
 SOI films, laser recrystallisation, Raman microprobe study 4-80462  
 solid solution, supersaturated, radiative swelling problem, intensified recomb. of unlike defects 4-70188  
 solid-liquid interface under residual stresses, plane waves reflection and refraction 4-87618  
 steel, alloy and stainless, acoustoelastic coeffs. of Rayleigh waves 4-114733  
 steel, austenitic, explosion hardened high Mn, residual stress distribution (*Japanese*) 4-114645  
 steel, austenitic stainless, annealed, load relax. near 563K, thermally activated dislocation motion 4-99413  
 steel, austenitic stainless, high temp. creep, biaxial expts., constitutive laws 4-93352  
 steel, austenitic stainless, SCC under compressive stress 4-99636  
 steel, austenitic stainless, stress relax. in bending at 773K 4-81229  
 steel, C, US props., higher-order, influence of C content, rel. to residual stress determ. 4-99730  
 steel, C, wires, stress relax., influence of work hardening (*French*) 4-81230  
 steel, Cr, tempered, residual stress meas. in near surface layers (*German*) 4-71818  
 steel, dual-phase, work hardening at small plastic strains 4-114568  
 steel, fatigue strength of butt welded joints with different plate thickness, stress relief effect 4-62011  
 steel, ferrite-martensite, dual phase, Bauschinger effect, coercivity meas. (*Chinese*) 4-93330  
 steel, high strength structural, stress relief cracking susceptibility 4-109509  
 steel, high temp. bolting, reloading stress relax. behaviour with specified reloading time interval 4-81234  
 steel, low alloys heat treated, grinding residual stress, hardness (*Japanese*) 4-89117  
 steel, low C, notched fatigue strength rel. to pre-straining and nitriding 4-109489  
 steel, martensitic transformation in alloy 40N25, diffuse-mobile H effects (*Russian*) 4-104780  
 steel, Ni-Co-Mo, ultrahigh strength maraging, H embrittlement enhancement by Ni or Cu coatings (*Japanese*) 4-89114  
 steel, pressure vessel, A 508 2 and A 533 B, comparison of stress relief cracking 4-109510  
 steel, stainless, pipe weldments, inside surface residual stress meas. using X-rays 4-89206  
 steel, structural, fatigue fractured surfaces, residual stress, X-ray diff. (*Japanese*) 4-99513  
 steel 45, plastically deformed, oriented microstresses and cold brittleness (*Russian*) 4-93334  
 steel 45 and U10, laser treatment, residual stress distrib., optimum surface hardening conditions (*Russian*) 4-71774  
 steel cylinders, circular, residual stress determ. by US vel. meas. 4-99733

## internal stresses continued

- steel plate, explosively bonded stainless clad pressure vessel, fatigue crack growth (*Japanese*) 4-114643
- steel plate, laser melted surface, microstruct., hardness, residual stress 4-71794
- steel plate, long rod penetration, stress/strain studies 4-108512
- steel rails, mixed fatigue-tensile surface crack growth 4-89100
- steels, plastically deformed, oriented microstresses depend. on external load direction (*Russian*) 4-93332
- strain softening, materials model with appl. in modelling strain localisation 4-99407
- stress measurement methods; for cyclic internal and effective stresses 4-71817
- surface residual-stress evaluation using horizontally polarized shear waves 4-81379
- thermo-piezoelectric continua, moving dislocations and disclinations, mechanical electrical and thermal fields 4-98102
- transparent materials, meas. of residual strain and stress 4-97443
- welding residual stress fields, crack problems, linear elastic fracture mechanics 4-104878
- X-ray stress analysis, influence of surface profile (*German*) 4-81394
- zircon-structure crystals, internal strain, orbit-lattice coupling and phase transitions 4-80220
- Ag-based thin films, ultramicrohardness and internal stresses 4-92582
- Ag-Sn alloys, rapidly quenched, TEM study of struct. defects, depend. on internal residual stresses 4-88172
- Al plate, acoustoelastic stress meas., suppression of microstruct. influences 4-99729
- Al, polycrystalline aggregates with transverse isotropy, US acoustoelastic response 4-62129
- Al, transverse thermal vibrations and strength 4-80178
- Al-Al<sub>3</sub>Ni eutectic composites, work hardening in stage II, 293-673K (*Japanese*) 4-89067
- Al-Mg (1.74 at.%), creep, strain transients in stress drop tests 4-85196
- Al-Mg alloys, steady-state creep, stress components 4-85181
- Al-Mg class I high temp. creep alloys, internal and friction stresses 4-85185
- Al-Si-Fe, AL-4, stress relax. resist., effect of plastic surface strain methods 4-109453
- Al-SiO<sub>2</sub>-Si MOS structure, X-ray induced interface traps, stress relax. effects 4-98755
- AlGaAs high power TJS laser diodes, mech. stress compensation 4-96914
- Al<sub>0.85</sub>Ga<sub>0.15</sub>As/GaAs:Zn diffused superlattice, X-ray rocking curve and backscatt. studies 4-113818
- Au-based thin films, ultramicrohardness and internal stresses 4-92582
- BaF<sub>2</sub>, fluorite struct., inner displacement, internal strain tensor, lattice dynamic models 4-92315
- BaTiO<sub>3</sub>, ferroelec., permittivity, effect of grain size 4-76306
- CaF<sub>2</sub>, fluorite struct., inner displacement, internal strain tensor, lattice dynamic models 4-92315
- CeF<sub>3</sub> doped optical films, tensile stress cracks and stress modification 4-76343
- Co electrolytic films, mag. props. and struct. (*Russian*) 4-80797
- Co(Cr,Ni)-TaC, eutectic, thermal cycling, calc. of residual stresses and strains 4-66380
- Cr films, evaporated, internal stress, struct., substrate temp. depend., electron microscopy obs. 4-98495
- Cr films, evaporated, mechanical stresses 4-75819
- Cr foil, influence of heat treatment on struct. and props. (*Russian*) 4-65412
- Cu, cyclic internal and effective stress meas. 4-71817
- Cu, fracture stresses time depend. during spall 4-99499
- Cu halides, deformation pots., relativistic LMO calc. 4-80473
- Cu, tough-pitch, drawn and extruded, stress/strain props. 4-104824
- Cu-Al, sliding wear induced residual stresses, X-ray diff. analysis methods 4-76927
- Cu-based shape-memory alloy, mech. and elec. props., sonic studies 4-76773
- Cu-Fe, elastic distortion of  $\alpha$ -Fe particles by Orowan loops, moiré fringes, TEM obs. 4-66358
- Cu-Ni (25 wt.%), sintered and pressed coinage alloy, tensile props., SEM and X-ray obs. 4-71697
- Cu-Ni-Cr (30.5 wt.%), quenching, ageing, spinodal decomp., hardness, X-ray diff. obs. 4-114526
- Cu-Ni-Sn spinodal alloys, deformation behaviour, ageing treatment effects 4-114628
- Fe, cast, malleable, laser treatment, residual stress distrib., optimum surface hardening conditions (*Russian*) 4-71774
- $\alpha$ -Fe, nitriding, heterogeneous, dislocation production and oriented precip. 4-66498
- Fe, pure, orthogonally planed surface layer, X-ray lattice strains rel. to texture (*Japanese*) 4-114567
- Fe-C martensite, incommensurate direction of modulated struct., strain energy, lattice distortion 4-109454
- Fe-Co based amorphous alloys, struct. relax. processes, dilatometric anal. (*Russian*) 4-92394
- Fe-Co electrodeposited films, field induced mag. anisotropy 4-92943
- Fe-Mo (6.3 at.%), high temp. creep, stress exponent and substruct. 4-76821
- Fe<sub>41</sub>B<sub>13</sub>Si<sub>4</sub>C<sub>2</sub>, amorphous, mag. anisotropy meas. (*Russian*) 4-65804
- Fe<sub>40</sub>Ni<sub>40</sub>B<sub>20</sub> amorphous alloy, ferromag. resonance and antiresonance studies 4-76256
- Fe<sub>40</sub>Ni<sub>40</sub>B<sub>20</sub> metallic glass, strength and plasticity, temp. depend. (*Russian*) 4-71692
- Ga<sub>1-x</sub>Al<sub>x</sub>Sb<sub>1-y</sub>As<sub>y</sub>/GaSb, LPE, phase equil. rel. to lattice mismatch strain 4-93236
- p-Ge, anisotropic internal stresses, electroreflectance and photovoltaic effect meas. 4-84947
- Ge island films on insulator, single crystalline, residual strain 4-92573
- Ge surface, electroreflectance and photo EMF (*Russian*) 4-104576
- In<sub>0.2</sub>Ga<sub>0.8</sub>As/GaAs strained-layer superlattice, ion implanted, struct. integrity 4-113821
- LiTaO<sub>3</sub>:Ti, changes in refractive index due to diffusion 4-99085
- MgF<sub>2</sub> films, evaporated, internal stress, struct., substrate temp. depend., electron microscopy obs. 4-98495
- Mo films, DC magnetron sputtering with RF substrate bias 4-81126
- MoSi<sub>2</sub> sputtered films, tensile stresses and stress relax. 4-98494
- NaI(Tl) deformed cryst., relationships among stresses, microstruct. and photolum. 4-71441
- Ni, crack propag., plastic zone, dislocation struct. 4-99488

## internal stresses continued

- Ni, electrodeposition, hardness, microstruct. 4-66252
- Ni electrodeposits, struct., X-ray diff. and Mossbauer studies 4-104102
- Ni electroplating bath control using saccharin additive (*German*) 4-66241
- Ni, fracture stresses time depend. during spall 4-99499
- Ni, H embrittlement, influence of plastic deform. 4-71729
- Ni-Cu alloy, domain wall-dislocation interaction behaviour, role of Cu atoms 4-104457
- Ni-Ni<sub>3</sub>Al-NbC, eutectic, thermal cycling, calc. of residual stresses and strains 4-66380
- Ni-TiO<sub>2</sub>, dispersion hardened, work hardening 4-66349
- Ni<sub>72</sub>Si<sub>18</sub>B<sub>10</sub> metallic glass, strength and plasticity, temp. depend. (*Russian*) 4-71692
- (Pb,Ln)(Zr,Ti)O<sub>3</sub> ceramics, stress anisotropy induced by polarisation 4-104536
- PbTe/ZnS IR filter durability assessment, Space Shuttle 1st LDEF appt. 4-74688
- Si dislocation stress distrib., effects on pendulum fringes 4-60783
- Si, impurity migration, effect of elastic stresses 4-88039
- Si SOS patterned structures, residual stresses, Raman microprobe study 4-92575
- Si SOS structures, pulse laser irradiat., internal stresses, Raman scatt. studies 4-99108
- Si SOS structures, residual stresses, Raman scatt. studies 4-99107
- Si single cryst., elastically deformed, Pendellosung fringes 4-88035
- Si vapour deposited, cryst. and amorphous films, stresses, X-ray diff., studies 4-75824
- Si:C layers, CVD growth, microstruct. and resist. 4-70599
- a-Si:H reactively sputtered films, H partial press. effects 4-93219
- Si/CaF<sub>2</sub> heterostructure interface, MBE grown, Raman spectra studies 4-98462
- a-Si:H RF sputtered films, internal stress rel. to local H bonding 4-88437
- SiO<sub>2</sub>, vitreous, electron bombarded, stress relaxation 4-70218
- SrF<sub>2</sub>, fluorite struct., inner displacement, internal strain tensor, lattice dynamic models 4-92315
- steel, low alloy, cyclic strength, effect of laser irradi. 4-71723
- TaSi<sub>3</sub>, cosputtered, props., effect of O contamination 4-114046
- TaSi<sub>3</sub> sputtered film on polycryst. Si, stress 4-70606
- Ti, fracture stresses time depend. during spall 4-99499
- Ti-Al-Si (5, 2.5 wt.%), internal stress, deform. at 300K 4-71700
- Ti-Al-V plate, residual stresses after localised heat treatment, US eval. 4-99728
- Ti-V, fatigue crack propag. rel. to overload cycling 4-62029
- TiC, low Z films, correl. of residual stress with microstruct. 4-114695
- TiC, low Z films, PVD coated, residual stresses 4-114696
- TiC, low Z films, residual stress measurement by X-ray diffractometry 4-114694
- TiN, low Z films, correl. of residual stress with microstruct. 4-114695
- TiN, low Z films, PVD coated, residual stresses 4-114696
- TiN, low Z films, residual stress measurement by X-ray diffractometry 4-114694
- W fibre reinforced stainless steel, residual stresses during thermal cycling 4-71634
- W films, DC magnetron sputtering with RF substrate bias 4-81126
- Y<sub>3</sub>Fe<sub>5</sub>O<sub>4</sub> garnet epitaxial layers, ion implantation-induced strain and damage profiles 4-75558

internuclear double resonance *see* INDR

## interplanetary magnetic fields

- see also* interplanetary matter
- angular momentum of IMF and solar wind particles 4-110482
- B<sub>z</sub> component, obs. during intense mag. storms rel. to dynamic variations of auroral oval 4-72776
- B<sub>z</sub>-component, positive jumps rel. to induced onset of explosive phase of magnetospheric substorm 4-110374
- B-component polarity, relation to struct. of magnetosphere polar cusps 4-110373
- cosmic ray fluctuations, interplanetary magnetic field effects 4-100980
- cosmic ray flux decreases, heliosphere cold plasma effects 4-101069
- cosmic ray interplanetary pitch angle scattering, absolute value, functional depend. 4-100936
- cosmic ray kinetics in anisotropic mag. field 4-94374
- cosmic ray muon north-south anisotropy, high rigidities, 27-day recurrence 4-94459
- cosmic ray propagation, effect of convection on charged particle transport in random mag. fields 4-94569
- cosmic ray sidereal variations, interplanetary mag. field direction effects 4-101015
- cosmic ray sidereal variations, interplanetary mag. field effect 4-101011
- cosmic ray solar diurnal variation, long term changes 4-100983
- cosmic ray solar diurnal variation, relation to interplanetary mag. field 4-100982
- delayed energetic particle event of June 6, 1979 interplanetary shock effect 4-100952
- Earth magnetosphere, identification of flux erosion events with flux transfer events 4-72828
- Earth magnetosphere interaction, scale size and interior struct. of flux transfer events 4-94313
- electrons, acceleration in interplanetary space 4-94376
- Forbush decrease, pitch angle anisotropy, spectrographic global survey 4-94458
- galactic cosmic rays, Forbush decreases, variations in IMF and solar wind velocity 4-94456
- galactic cosmic rays, intensity depression, effect of solar wind disturbances 4-94451
- geomagnetic field variation interplanetary magnetic field sector structure influence 4-100449
- geomagnetic storms, main phase, solar wind and interplanetary mag. field effects 4-100884
- heliomagnetic cycle of geomag. and ionospheric disturbances and interplanetary activity 4-110369
- heliosphere current sheet shape and location, from pot. field model and corona obs. 4-110481
- high-frequency fluctuations, comparison with whistler turbulence spectrum in interplanetary plasma 4-110478
- kinky heliospheric current sheet, cause of CDAW-6 substorms 4-101109
- long term changes and radial gradients at 1 AU 4-101108
- low energy ions, mean free path in front of interplanetary shock waves 4-100933

**interplanetary magnetic fields continued**

- magnetosphere interaction, correl. with spectrum of Pc 3-4 mag. pulsations 4-85835
- magnetosphere interaction, influence on electric fields and potential patterns in high latit. ionosphere 4-110365
- magnetosphere interaction, rel. to north-south asymmetries of solar particle events in stratospheric O<sub>3</sub> 4-110229
- magnetosphere of Earth, IMF field merging sites on dayside magnetopause 4-67563
- MHD disturbances due to solar flares, determ. of cross-sectional configurations 4-110479
- northward component and assoc. terrestrial polar cap vertical currents 4-94296
- orientation of interplanetary mag. field, effects on ionosphere dayside high-latitude correction 4-85811
- particle acceleration, turbulent dynamo  $\alpha$ -effect 4-94379
- random magnetic field component, effect of anisotropy on cosmic ray density distrib. 4-110393
- rotational and tangential discontinuities of solar wind 4-110483
- sector boundaries, energetic ion enhancements 4-94540
- sector structure and cosmic ray intensity second harmonic 4-100998
- shock event Nov. 11-12, 1978, test of acceleration theory 4-94543
- shock wave, upstream plasma and energetic particle struct. 4-110485
- solar wind, current sheet, phenomenological model 4-105861
- solar wind, effect on polar cap 4-72791
- solar wind, field var. and primary cosmic rays zonal modulation 4-94396
- solar wind, field var. over solar cycle 20, periodicity 4-94539
- solar wind, flux transfer events at dayside magnetopause 4-72810
- solar wind, hydromagnetic model of corotating conductive streams 4-67587
- solar wind clouds, correl with coronal mass ejections 4-101110
- solar wind field, effect on polar cap convection 4-94305
- solar wind-Mars interaction and mag. field characs. 4-85885
- sudden storm commencement and Forbush decreases, correlation to solar wind and IMF 4-94447
- three-dimensional diffusion of high-energy solar cosmic rays 4-100932

**interplanetary matter**

- see also comets; cosmic dust; interplanetary magnetic fields*
- acceleration between approaching shock fronts 4-94380
- anisotropy distributions associated with interplanetary shocks 4-94387
- cosmic ray acceleration and drift in latitude at the solar-wind termination shock 4-94383
- cosmic ray acceleration in interplanetary medium, associated solar wind disturbances 4-94378
- cosmic ray density distribution effect of anisotropy of random component of mag. field 4-110393
- cosmic ray propagation, effect of convection on charged particle transport in random mag. fields 4-94569
- cosmic ray protons, estimate of heliolatit. gradient (1981-1982) 4-85849
- diffuse ions production by EM ion beam instabilities, computer simulation 4-85855
- dust distrib. in Solar System 4-90115
- dust grains, origin, size distrib., and evolution (*Japanese*) 4-110563
- dust particle size and solar coronal IR polarization 4-63121
- energetic storm particle events, shock wave anisotropies 4-94390
- Fermi acceleration at interplanetary shocks 4-94381
- grains, reson. orbits trapping time with Poynting-Robertson drag 4-90112
- grains from comets, heterogeneous destruction near Sun 4-77765
- hydrocarbon generation from frozen methane-keV proton irradiation 4-115711
- interstellar wind atoms ionisation, role of 'core' and 'halo' solar wind electrons 4-105863
- ion acceleration at interplanetary shocks, hydromagnetic wave excitations 4-94384
- ion anisotropies associated with interplanetary shocks 4-94385
- ion-acoustic turbulence in interplanetary plasma, meas. via radio backscatter method 4-110480
- IR cirrus, IRAO obs. 4-85892
- IR diffuse background, IRAS obs. 4-86092
- kinky heliospheric current sheet, cause of CDAW-6 substorms 4-10109
- LOW CA hydrated particle, transmission electron microscopy 4-110564
- magnetosphere-ionosphere interaction heliomag. cycle of geo-effective parameters of interplanetary medium 4-110369
- MHD disturbances due to solar flares, determ. of cross-sectional configurations 4-110479
- micro-meteoroids, capture-cell expt. on Long Duration Exposure Facility (LDEF) mission 4-105876
- neutron modulation, shock related diffusion-acceleration models 4-94392
- neutrons, solar flare flux from interplanetary charged particle meas. 4-100942
- particle acceleration by flare-induced interplanetary shocks 4-94377
- planetary Mach cones, theory and obs. 4-85856
- proton acceleration mechanisms, associated interplanetary shocks 4-94386
- proton energetic spectra, associated planetary shock waves 4-94389
- proton spectra, propagation and acceleration 4-94391
- scintillation observations of interplanetary medium near Sun 4-110477
- shock acceleration events, association with interplanetary proton events 4-105864
- shock wave acceleration of cosmic ray particles, contribs. of Fermi accel. and turbulent accel. 4-110392
- shock wave interaction with magnetosphere, obs. of resonant Alfvén waves excited by sudden impulse 4-85834
- solar wind, hydromagnetic model of corotating conductive streams 4-67587
- solar wind electric field, contrib. to field-aligned currents in a magnetosphere polar cap 4-110372
- solar wind speed variations, rel. to latit. distance from solar mag. neutral line 4-72844
- storm particle events, effects of adiabatic deceleration and shock lifetime 4-94382
- upstream protons, energy spectra 4-94393
- whistler turbulence spectrum in interplanetary plasma, comparison with mag. field fluctuations 4-110478
- Bi in interplanetary dust collected from stratosphere 4-115712
- He of interstellar origin, flow in Solar System, obs. at 58.4 nm (by Prognoz) 4-77767
- He-rich solar particle events, ionic charge state meas. 4-110587
- He-rich solar particle events, ionic charge distrib., ISEE 3 meas. 4-110586

**interplanetary medium *see interplanetary matter*****interpolation**

- see also function approximation*
- aqueatic velocity field interpolation from boundary and regional data 4-63518
- background determ. in quantitative gamma-resonance spectroscopy 4-74094
- band-limited discrete-time signals, out-of-band energy minimisation 4-103110
- bat's sonar signal, wideband ambiguity function computation and numerical anal. 4-109845
- CT images, restoring spline interpolation 4-62562
- dynamometers criteria comparison 4-111124
- holograms, computer-generated, interpolation approach 4-107558
- interferogram analysis, frequency domain description 4-112343
- Kriging interpolation procedure for acid rain spatial variability anal. 4-82251
- road traffic noise, time series prediction by adaptive functions, Newton's interpolation formulae (*Japanese*) 4-62425
- seismology, time-shift estimation and alignment of discrete time signals, frequency domain method 4-105772
- spectral ratio peak intensity meter convertor, transformation function table dimension reduction (*Russian*) 4-101846
- rotation splines for vertical interpolation of data 4-94267
- thin plate flexure, Kirchhoff boundary-element theory 4-64847
- transition metals, 3d, band struct. interpolation (*Rumanian*) 4-98513

**interstellar dust *see cosmic dust*****interstellar magnetic fields**

- see also interstellar matter*
- clouds struct. and evolution 4-77913
- Corona Austrina dark cloud complex, mag. fields rel. to Kelvin-Helmholtz interface instability 4-82535
- coupled hydromagnetic wave excitation and cosmic ray acceleration at interstellar shocks 4-94351
- flux decrease in interstellar clouds, effect of intercloud medium 4-73005
- G127.1+0.5, SNR, mag. field anal. from polarisation data 4-72997
- galactic secondary/primary ratio and energy-dependent truncation of the pathlength distribution 4-94346
- Galaxy, Gemini region, mag. fields determ. from extragalactic radio source obs. 4-77893
- local interstellar magnetic bubbles, implications for Galaxy global magnetic field determination 4-106052
- massive gas cloud, star form. and mag. field interactions 4-101452
- Monogem X-ray ring, mag. field struct. from polarisation obs. anal. 4-94993
- NGC 650-651, planetary nebula, kinematics and morphology 4-110725
- origin mechanism 4-101138
- planetary nebulae 4-82541
- perions, pulsar dominated evolution, mag. field, relativistic particles and luminosity 4-90201
- QSOs intervening clouds, mag. fields and column densities from rot. meas. distrib. anal. 4-86082
- quasars, hotspots and radiolobes, occurrence, mag. fields and struct., SHF obs. 4-86075
- special relativistic effects in rapidly moving plasmoids 4-94983
- in spiral galaxies, configuration and origin of mag. fields 4-101475
- spiral galaxies, face-on, mag. field and cosmic ray electrons distrib. 4-110749
- spiral galaxies and companions, mag. fields anal. 4-106052
- supernova remnants, radio emission rel. to mag. field strength 4-73025
- supernova remnants, radioemission evolution, role of relativistic electrons accel. by MHD turbulence 4-73026
- C II regions, upper limits to mag. fields from C166 $\alpha$  lines obs. 4-86003
- H I shells and supershells, mag. fields and energetics, effects of artificial boundaries in sky 4-63259

**interstellar matter**

- see also cosmic dust; H-I regions; H-II regions; interstellar magnetic fields; nebulae*
- 280 nm absorption feature 4-82539
- 280 nm absorption feature as artifact of IUE SEC vidicon detectors 4-82538
- 758.1 nm predicted diffuse H<sup>+</sup> interstellar line, obs. 4-90212
- absorption line spectroscopy 4-63253
- abundances, effect on spiral galaxies spectra 4-110745
- acceleration mechanisms for high-vel. clouds and QSO emission line clouds 4-110727
- active galaxies nuclei, accretion and X-ray emission 4-67812
- ARP 220, H<sub>2</sub> detection in IR luminous merging galaxies 4-115821
- atomic and molecular abundances towards Pleiades cluster, determ. from obs. of five stars 4-94904
- atomic particles, resonance radiation pressure 4-63251
- $\alpha$  Aurigae, He II 30.4 nm line search, interstellar medium implications 4-85924
- B335, isolated dark globule, obs. of NH<sub>3</sub> (1, 1) and (2, 2) lines 4-115794
- bacteria, UV absorption and mass-density constraints 4-101458
- binary spiral galaxies, mass-light distrib. and massive haloes 4-73075
- biological grains, evidence against 4-106055
- black hole thick discs as energy sources 4-90175
- Bok globules, struct., comp. and star form. 4-106053
- bright rims form. and evolution 4-90213
- bullets generation due to shock wave-mol. cloud interaction 4-115801
- 3C 109, broad-line radiogalaxy, dust characts. from visible and IR obs. 4-90223
- 3C 293, radio galaxy, radio jets propag. through gaseous disc rel. to extended optical line emission 4-63267
- 3C 380, quasar, interstellar medium rel. to peculiar radio struct. 4-63338
- Carina Nebula giant molecular cloud, CO mapping 4-63264
- Cepheus A-GGD 37 complex, visible and IR obs. 4-115798
- Cepheus OB3 molecular cloud, UV obs. of interstellar extinction 4-94909
- chemical composition in external galaxies from supernova remnants spectrophotometry 4-77905
- circumstellar medium, effect on evolution of young Type II SNR 4-77900
- cloud accretion and evaporation, implication for cosmic rays and  $\gamma$ -ray emission 4-100892
- clouds, formation, evolution and contraction, to form stars 4-77913
- clouds in intervening galaxy towards QSO 2345+007A, B 4-110769
- Coalsack, CO distrib. 4-63261

## interstellar matter continued

compact H II regions, extinction curves from He I 10830 Å obs. 4-72998  
 composition from anomalous cosmic ray component meas. 4-101185  
 conference at Cargèse, France (September 1982) 4-58564  
 conference on Southern Galaxy Surveys at Leiden, Netherlands (August 1982) 4-58565  
 Corona Austrina dark cloud, far-IR obs. of star-forming region 4-86001  
 Corona Austrina dark cloud complex, evidence for Kelvin-Helmholtz interface instability 4-82535  
 Coronae Austrina dust complex, discovery of obscured young star cluster (Coronet) 4-94905  
 cosmic ray acceleration by collapsing molecular clouds 4-100904  
 cosmic ray interactions and diffuse  $\gamma$ -ray background origin 4-77975  
 cosmic ray interactions and gamma ray emission 4-101525  
 cosmic ray interactions and nucleosynthesis 4-63293  
 cosmic ray interactions and obs. anal. 4-94362  
 Cygnus A, nucleus struct. and dust distrib. 4-82551  
 Cygnus Loop, evidence for evaporation around filamentary struct. 4-73000  
 Cygnus Superbubble, nature and characts. 4-63134  
 dark clouds, 1-millimetre continuum obs. 4-115834  
 dark clouds, formaldehyde 4.8 GHz and 14.5 GHz transition obs. 4-110723  
 dark clouds, mass distrib. 4-94929  
 dark clouds dense cores, assoc. young stars detect. in IR 4-101340  
 dark clouds in Southern Hemisphere,  $^{12}\text{CO}$  (J=2-1) survey 4-101455  
 dark mass in dwarf irregular galaxies, cosmological implications 4-90243  
 dense clouds,  $\text{C}^{18}\text{O}$  ratio role of low vel. shocks 4-110726  
 diffuse 578.0 and 579.6 nm bands towards NGC 7027, nature 4-106054  
 diffuse cloud chemistry, obs. tests for surface chemistry on grains 4-94928  
 diffuse component, radio obs. anal. 4-63252  
 diffuse component atomic processes 4-63258  
 dissipative structures form. in galaxies 4-86042  
 distribution around Sun 4-115789  
 distribution rel. to incidence of open clusters with structural peculiarities (Russian) 4-63220  
 dust, meas. of diffuse galactic radiation in far-IR 4-86091  
 dust cloud structure in young R associations NGC 1333, S68 and NGC 7129, IR obs. 4-85993  
 dynamics and energetics 4-63256  
 electron density var. and pulsars fading 4-94919  
 electrons, acceleration in interplanetary space 4-94376  
 element abundances in interstellar medium, implications for chemical evolution of galaxies 4-101459  
 emission lines, IR and visible 4-63257  
 ESO 210-6A, dark globule in Gum Nebula, star form. anal. 4-63262  
 evaporating cloud envelopes, dynamics 4-90209  
 extinction towards dusty WC8/9 Wolf-Rayet stars 4-77897  
 extinction towards IR sources, use of 10  $\mu\text{m}$  dust emission features 4-86018  
 first galactic quadrant, mapping in  $^{12}\text{CO}$  and  $^{13}\text{CO}$  4-63315  
 formaldehyde in Orion molecular flow, evidence for gentle acceleration 4-63239  
 G109.1-1.0, SNR, relation to neighbouring mol. cloud 4-73055  
 G35.2-0.74, molecular cloud, assoc. H II regions characts. 4-110728  
 G35.2-0.74, mol. cloud with bipolar and monopolar outflow, EHF obs. 4-106050  
 galactic centre, radioemission from large scale structures 4-106066  
 galactic centre region, CO struct. with strong positional and kinematic gradients 4-63310  
 galactic CO and H I distrib. rel. to  $\gamma$ -ray distrib. 4-63301  
 galactic corona, soft X-ray emission evidence 4-73103  
 galactic corona supported by cosmic rays, model 4-82550  
 galactic disc, hydrodynamic and turbulent motion 4-82536  
 galactic dust, effect on meas. of 3K background radiation in 400-1100 microns range 4-77982  
 galactic H I and CO distrib. and spiral struct. 4-63306  
 galactic halo, inos rest mass, lower limit 4-82409  
 galactic halo, obs. of gas inflow from direction of galactic North Pole 4-101450  
 galactic halo formation, mathematical soln. of MHD equations 4-101468  
 galactic haloes, dark matter, evidence for non-baryonic nature 4-67795  
 galactic haloes, hypothetical particles, decay, UV and X-ray emission 4-101154  
 galactic needle-shaped grains and thermalisation of microwave background 4-78001  
 galactic nonstationary viscous gaseous discs 4-63323  
 galactic radiosources,  $^{13}\text{CN}$  detect., EHF obs. 4-106072  
 galactic spiral struct. form. with accreted matter flowing in corotating reson. region (Russian) 4-94972  
 galactic X-ray emissivity due to cosmic ray-interstellar matter interactions 4-100886  
 in galaxies, influence of bar strength and pattern speed on spiral struct. 4-94958  
 galaxies in Coma cluster, gas stripping, constraints on galaxy vel. dispersion 4-90246  
 galaxies massive halos and neutrinos (Japanese) 4-110790  
 gamma-ray intensity rel. to column density of H and  $^{12}\text{CO}$  4-110409  
 gas, ion composition and chem. reactions 4-101460  
 gas cloud particles in spiral galaxies, hydrodynamics simulation 4-86050  
 gas distribution correlation with galactic  $\gamma$ -ray emission 4-63300  
 gas in disturbed galaxies, stability of simplified continuum models 4-63270  
 in giant elliptical galaxy in front of BAL QSO, cold clouds 4-63332  
 giant molecular clouds causing globular cluster disruption, role in X-ray binaries form. in cores 4-110674  
 giant molecular clouds in galaxies, contrib. to heating of stellar discs 4-67803  
 global radio continuum of nearby galaxies 4-94334  
 grains, evolution and structure 4-94935  
 grains as bacteria, discussion meeting, London, England (November 1983) 4-95046  
 graphite detection, spectroscopic method 4-101187  
 heating by supernova remnants 4-73049  
 hierarchical cloud fragmentation and star form., initial mass function and ang. momentum 4-110724  
 high-velocity molecular gas assoc. with Herbig-Haro objects 4-110713  
 Horsehead Nebula, obs. of collimated flow assoc. with low-mass star form. 4-115740

## interstellar matter continued

hot component, X-ray large scale features 4-73047  
 IC 443, SNR, interstellar medium interaction, X-ray obs. 4-73040  
 IC 5146 molecular cloud, high resolution IR obs. 4-82533  
 ice, implications for interstellar chemistry of 3  $\mu\text{m}$  ice band in Taurus mol. clouds 4-101457  
 ice, pure and mixed,  $\text{NH}_3$  and  $\text{H}_2\text{O}$ , surface mol. photodetachment and photodissociation 4-66604  
 in dwarf irregular galaxies, fraction gas mass rel. to stochastic star form. model 4-67806  
 in galaxies, test of obscuration of cosmologically distant objects by dust 4-86025  
 interaction with stellar winds and supernovae 4-63254  
 intercloud medium effect on interstellar cloud mag. flux decreases 4-73005  
 interstellar grains, spectroscopic identification 4-67780  
 ionisation characts. in young galaxies 4-82557  
 ionised gas discs in early-type galaxies NGC 5266 and NGC 3108, struct. and kinematics 4-86030  
 ionised H, interaction with neutron star mag. field, hard radiation emission 4-77863  
 IR cirrus, IRAO obs. 4-85892  
 IR diffuse background, IRAS obs. 4-86092  
 IR extinction towards G333.6-0.2 H II region 4-94917  
 far-IR sources in southern galactic disc, large-scale space distrib. 4-115833  
 isoformyl ions, metastability in collisions with H and He 4-91327  
 isolated elliptical galaxies, X-ray cooling flows 4-73078  
 isotope fractionation of C and O in dense interstellar clouds, time dependent model 4-90208  
 kinematics in E and S0 galaxies NGC 1052, 2749, 3998 and 4125, comparison with stellar kinematics 4-73066  
 l=333° giant molecular cloud, CO mapping 4-63264  
 large-scale bubble structure, origin, role of stellar winds (Russian) 4-67784  
 LDN 1551 IRS-5, rot. disc nature and possible planetary system form. EHF obs. 4-77890  
 light extinction in and near OB associations 4-94903  
 LMC, gas-cosmic ray interactions and expected  $\gamma$ -ray and radio emission 4-101485  
 LMC ring shaped nebulae, optical obs. 4-77908  
 local abundances, implications for solar nebula characts. 4-77733  
 local gas distribution correl. with galactic  $\gamma$ -ray emission 4-63304  
 local interstellar magnetic bubbles, implications for Galaxy global magnetic field determination 4-106052  
 M17, high resolution radio study of H II region and mol. clouds 4-101451  
 M17 SW, giant mol. cloud, CO emission obs. 4-73002  
 M31, high resolution H I survey 4-63316  
 M51, spiral galaxy SHF radio maps 4-94979  
 M71, globular cluster, photometric anal. of foreground interstellar reddening 4-101441  
 in M82, distrib. and kinematics of interstellar CO 4-101471  
 M87, mass profile and gas content anal. 4-90224  
 Markarian 348 (NGC 262), core dominated Seyfert, sub-arcsecond radio struct. 4-94966  
 masers,  $\text{H}_2\text{O}$  and OH, distrib. in Galaxy 4-63296  
 Massachusetts-Stony Brook CO survey of the galactic plane 4-63307  
 massive black holes accretion, cosmic rays prod., radiowave and  $\gamma$ -ray emission 4-100929  
 massive galactic haloes, baryonic nature 4-67794  
 massive gas cloud, star form. and mag. field interactions 4-101452  
 massive gas clouds, effect on stellar vel. dispersions in galactic discs 4-77882  
 massive neutrinos in galactic halo, decay, photon emission, UV background origin 4-77912  
 metal abundances, correl. with halo stars abundances 4-90137  
 metallic dust grains, far-IR props. 4-67779  
 methanol, interstellar maser detect. of 23.121 GHz 4-77889  
 methanol, OH stretch fourth overtone, oscillator strength, visible spectra 4-59788  
 methyl formate, MM wave spectra 4-59720  
 methylene ( $\text{CH}_2$ ), Einstein A-coefficients for rot. transitions 4-67613  
 methyleneimine,  $\nu_8$  band, high-resolution IR spectra in 10  $\mu\text{m}$  region 4-96534  
 missing mass problem 4-90268  
 molecular cloud assoc. with multiple IR source (GL 437), CO obs. 4-85999  
 molecular cloud collapse to protostar 4-101322  
 molecular clouds, age determ., use of cyanopolynes 4-110541  
 molecular clouds, discussion meeting, London, England (October 1983) 4-95045  
 molecular clouds, fluctuation spectrum 4-115795  
 molecular clouds, formaldehyde ortho-para ratio 4-115799  
 molecular clouds, gamma-ray line emission and cosmic ray interaction 4-101463  
 molecular clouds, meas spectrum and mean lifetime from  $^{13}\text{CO}$  obs. (Chinese) 4-82543  
 molecular clouds, prod. mechanism for  $\text{CH}_3\text{CN}$  and  $\text{CH}_3\text{OH}$  4-94192  
 molecular clouds, protostars form. and birthline concept on HR diagram 4-101345  
 molecular clouds, review 4-82544  
 molecular clouds, size and mass distrib. 4-110729  
 molecular clouds, spherical, steady-state models 4-77892  
 molecular clouds, star formation and galactic structure 4-90219  
 molecular clouds and formation of stellar systems 4-110601  
 molecular clouds and OB assoc. form. 4-63234  
 molecular clouds collapse and fragmentation, protostars form. 4-63138  
 molecular clouds in intervening galaxies as origin for QSOs absorpt. lines 4-77965  
 molecular clouds in solar neighbourhood, kinematics 4-106051  
 molecular clouds in spiral galaxies and star form., CO obs. 4-63318  
 molecular clouds near Monoceros OB1 and OB2, OH emission anal. 4-94916  
 molecular clouds sweeping from rot. galaxy by intergalactic medium dynamics 4-94943  
 molecular outflows assoc. with peculiar nebulosities and star formation 4-86022  
 molecule spectra, effective straight-line trajectory approach to collisional excitation 4-101129

## interstellar matter continued

- Monogem Ring, extended galactic X-ray source, theory of X-ray emission 4-94992
- Monogem X-ray ring, mag. field struct. from polarisation obs. anal. 4-94993
- MR 2251-178, nearby quasar, struct. of [O III] emitting gas 4-101496
- MR 2251-178, QSO, variable X-ray absorpt., cloud ionisation model 4-110766
- multiple supernova remnants, evolution in non-uniform medium 4-73051
- neutral atoms in heliosphere, ionisation by 'core' and 'halo' solar wind electrons 4-105863
- neutron stars, interstellar matter accretion and thermonuclear runaway, gamma ray bursts 4-101520
- NGC 1510, H I accretion from companion galaxy NGC 1512 and star form. bursts 4-63271
- NGC 2024 IRS 2, interstellar CO absorpt. lines in IR spectrum 4-86000
- NGC 2024 No.2, IR speckle obs. of foreground molecular cloud 4-94734
- NGC 2264, mol. cloud assoc. with galactic cluster, far IR emission sources 4-94923
- NGC 3201, globular cluster, age, reddening and comp., RR Lyr stars anal. 4-63216
- NGC 6240, H<sub>2</sub> detection in IR luminous merging galaxies 4-115821
- in NGC 7013, H I distrib. and motions in lenticular galaxy 4-67787
- NGC 7538 molecular cloud, near-IR and radio spectroscopy rel. to star form. 4-85998
- Nordic Optical Telescope observing plans 4-63265
- OB associations, environment dynamical evolution 4-63230
- $\rho$  Ophiuchi cloud core, turbulent velocity structure determ. from C<sup>18</sup>O obs. 4-90204
- $\rho$  Ophiuchi dark cloud, high-resolution radio obs. of nonthermal sources 4-72995
- Ophiuchus complex, OH obs. 4-90211
- Orion A, mol. cloud temp. from methyl cyanide obs. 4-106049
- Orion Molecular Cloud, high vel. gas struct., role of IRc 9 wind 4-110710
- Orion Nebula, large-scale internal motions 4-115800
- PKS 0634-20, radiogalaxy, O III forbidden line emission along radio axis 4-86059
- plasma, comp. near stellar X-ray sources 4-101512
- plasmas, X-ray emission spectra 4-67617
- Pleiades cluster, polarisation and reddening of brighter stars 4-115787
- polar rings, orbital characts. 4-115808
- polarization, wavelength depend. towards stars 4-77896
- polycyclic aromatic hydrocarbons, rel. to identification of 'unidentified' IR emission features of cosmic dust 4-115790
- polymeric residues of astrophysical interest, IR spectra 4-72859
- propynol cation, potential interstellar molecule, geometry 4-102602
- proteins and 280 nm feature 4-82537
- protons, intensity increases, associated planetary shocks 4-94388
- protosolar nebula, contributing nucleosynthesis, duration and rate 4-77735
- protostellar formation in rot. interstellar clouds, nonisothermal collapse 4-94729
- PSR 1937+214, millisecond pulsar, pulse timings and interstellar dispersion and scatt. determ. 4-101387
- pulsar long-term intensity variations due to interstellar radiowave propag. effects 4-101386
- Puppis A, SNR, interstellar medium interaction, X-ray obs. 4-73040
- QSO's narrow-line absorpt. systems, ionisation spectra 4-82557
- QSOs intervening clouds, mag. fields and column densities from rot. meas. distrib. anal. 4-86082
- quasar pairs, absorpt. lines origin in haloes 4-106081
- radio scintillation, rel. to metre-wave outburst from QSO (1055+018) 4-94987
- radio scintillation pattern, linear scale determ. from obs. of binary pulsar (PSR 0655+64) 4-101389
- radioemission from interstellar medium, polarisation between 408 and 1411 MHz 4-94921
- radiosource interstellar broadening of low galactic latitudes 4-94949
- reddening towards open cluster NGC 4755 and distance determ. 4-101444
- reflection nebulae in Southern Hemisphere, <sup>12</sup>CO (J=2-1) survey 4-101455
- regulation by SNRs and star formation bursts 4-63248
- rotating isothermal clouds, criteria for collapse and fragmentation 4-85908
- rotation measure of BL Lacertae, Galactic contrib. 4-73062
- Sagittarius B2, mol. cloud, NH<sub>3</sub> (5,2) transition detect. 4-94915
- second galactic quadrant, <sup>13</sup>CO mapping 4-63314
- CV Serpentis, binary Wolf-Rayet star, double shell discovery, nature 4-94791
- in Seyfert and radio galaxies, catapult model for narrow-line region 4-101477
- in Seyfert galaxies, dynamics of narrow line regions 4-86034
- in Seyfert galaxies, H I survey 4-63268
- Seyfert galaxies, nuclei extinction, colours and axial ratios anal. 4-106061
- Seyfert nuclei, envelopes cloud form. and line emission 4-101480
- shock waves with energy supply and release 4-115825
- silicate feature in Markarian 231, IR obs. 4-110744
- small dark clouds, evidence from magnitude discrepancies in Almagest star catalogue 4-110691
- SMC, UV extinction curve from stellar spectra obs. 4-63281
- SNRs in cloudy medium, X-ray emission 4-73013
- SO(3-2)<sub>v</sub> mapping of the Orion KL cloud components 4-63244
- southern galactic hemisphere line surveys 4-63297
- spiral galaxies, face-on, H II mass and electron density 4-110749
- spiral galaxies, mass to light ratios and haloes nature 4-67796
- in spiral galaxies in clusters, H I radial gradients in Coma and (Abell 1367) 4-82553
- star formation and emergence from surrounding cloud 4-105977
- star formation regions, IR and SHF obs. 4-110712
- star-forming regions, winds from low-mass stars rel. to self-regulated star formation in Taurus, Ophiuchus, NGC 226 and Orion 4-115741
- stellar wind bubbles, photoionised, in cloudy medium, evolution 4-86017
- stellar wind interactions 4-63134
- stellar winds interaction with surrounding interstellar medium, similarity soln. 4-67712
- superbubble model of local interstellar medium, appl. to soft X-ray and EUV background 4-94926

## interstellar matter continued

- supernova ejecta, interaction with ambient interstellar medium and circumstellar shell 4-72963
- supernova remnant interactions, effect on radio emission evolution 4-73026
- supernova remnants, interactions with ambient medium 4-73029
- supernova remnants in non-uniform media, theoretical thermal X-ray maps 4-73050
- Taurus dark cloud complex, NH<sub>3</sub> obs. and star counts 4-115791
- The Galaxy, radio lobe above galactic centre 4-106067
- TMC-1, dark dust cloud, methylidyne detect., SHF obs. 4-94915
- turbulent velocity structure in interstellar clouds, autocorrel. and struct. functions determ. 4-90204
- Tycho's SNR, shocked interstellar material emission 4-73007
- Tycho's supernova remnant, distance determ. from distrib. of foreground interstellar matter 4-72994
- UGC 7576, spindle-like galaxy, mapping in H I, UHF obs. 4-73076
- UV extinction and diffuse band strength correlations 4-63241
- UV extinction curves, vars. from mean galactic extinction law 4-86004
- UV extinction in 30 Doradus nebula, results from IUE obs. of stars 4-85996
- UV extinction in field in Cygnus, effects on S201 far-UV imaging survey 4-94762
- Virgo cluster and field galaxies, H I and optical diameters 4-77939
- in Virgo cluster spiral galaxies, evidence for low dust content 4-101464
- W28, SNR, optical features and interactions with interstellar medium 4-73037
- W28 SNR-mol. cloud complex, far-IR sources characts. 4-86008
- W3(OH), formaldehyde SHF obs. 4-90214
- W3 molecular clouds, formaldehyde mapping at 60 mm 4-73003
- W49, interstellar mol. cloud, millimetre-wave continuum photometry at Italian IR Telescope on Gornegrat 4-72888
- W 51 M, HDO mapping 4-77891
- warm H I medium, ionisation rates from radio recomb. line obs. towards radio source (3C 123) 4-101448
- wind-type model for the generation of astrophysical jets, appl. to active galactic nuclei 4-101139
- II Zw 73, spindle-like galaxy, mapping in H I, UHF obs. 4-73076
- C II regions, heavy elements radio recomb. lines obs. 4-90197
- C II regions, upper limits to mag. fields from C166 $\alpha$  lines obs. 4-86003
- C<sup>+</sup>, branching ratios of 2s<sup>2</sup>3p <sup>2</sup>P<sup>o</sup> term, Fourier transform and VUV spectroscopy 4-87066
- C<sub>2</sub>H, distrib. and abundance in mol. clouds 4-72999
- CO distribution along southern galactic plane, Galaxy spiral struct. 4-63294
- CO distribution in southern galactic hemisphere (fourth quadrant) 4-63295
- CO emission from M82, mol. halo obs. 4-86047
- CO emission from outer Galaxy mol. clouds, distrib. 4-63309
- CO in southern sources 4-63261
- CO J=2-1 obs. towards southern H II regions 4-63260
- CO latitude distribution in southern galactic hemisphere 4-63308
- CO observations in southern galactic hemisphere H II regions 4-63263
- CO photoabsorpt. and photodissoc. in 900 to 1200 angstrom region 4-83441
- CO survey of Southern Hemisphere dark clouds, refl. nebulae and Herbig-Haro objects 4-101455
- C<sub>2</sub>O J=2-1 19 GHz transition detection 4-94932
- CO(J=2-1) survey of fourth galactic quadrant 4-94948
- <sup>13</sup>CO emission from galactic disc in  $\lambda$ =40°-60° range 4-63313
- <sup>13</sup>CO in interstellar molecular clouds, J=1-0 EHF obs. 4-67782
- CI, abundance and chem. in Galaxy 4-86020
- H I beyond solar circle, 21 cm surveys 4-63305
- H I cloud in Pleiades, line profile obs. rel. to cloud-cluster collision 4-101449
- H I clouds sweeping from rot. galaxy by intergalactic medium, dynamics 4-94943
- H I distrib., correl. with  $\gamma$ -ray emission intensity and energy spectra anal. 4-101486
- H I distrib. and vel. field in nearly face-on spiral galaxy NGC 1058, obs. 4-94946
- H I distrib. in spiral galaxy NGC 6946, correl. with star form. characts. 4-90227
- H I high-vel. inflow towards galactic centre 4-86006
- H I in Galaxy, distrib. rel. to gamma ray emission and cosmic rays distrib. 4-90237
- H I in isolated galaxies, UHF obs. 4-110736
- H I in outer Galaxy rel. to  $\gamma$ -rays and cosmic rays 4-86049
- H I in Sc I galaxies, props. 4-90220
- H I kinematics used to determine outer Galaxy gamma rays distrib. 4-63303
- H I radial velocity in SMC, characts. 4-106064
- H I structures and holes in M31, anal. 4-63317
- H I survey of southern galactic plane 4-63299
- H I towards supernova remnant 3C 58, distance determ. 4-73045
- H I-cosmic ray interactions, diffuse galactic gamma-ray emission 4-100890
- H+O<sup>+</sup> (CO<sup>+</sup>)(CH<sup>+</sup>), reaction rate coeffs. 4-81427
- H<sub>2</sub> density in galactic mol. ring,  $\gamma$ -ray flux anal. 4-63302
- H<sub>2</sub> distrib. in spiral galaxy NGC 6946, correl. with star form. characts. 4-90227
- H<sub>2</sub> distribution, correl. with  $\gamma$ -ray emission intensity and energy spectra anal. 4-101486
- H<sub>2</sub> in interstellar mol. clouds, ortho-H<sub>2</sub>/para-H<sub>2</sub> ratio 4-94927
- H<sub>2</sub> mass and  $\gamma$ -ray emission anal. 4-86049
- H<sub>3</sub><sup>+</sup> and H<sub>3</sub><sup>+</sup>, dissociative recombination coeffs. laboratory expts. 4-82408
- HCN, ground and excited states, struct., vibr., SCF CI calcs. 4-64391
- HCN, radio spectra and hyperfine rot.-level splitting, isotopic modifications 4-94925
- HCO<sup>+</sup> high velocity flow in star-bearing mol. cloud NGC 2071, J=1-0 and J=3-2 lines obs. 4-85997
- HCO<sup>+</sup>, rot. excitation in interstellar clouds 4-110514
- HCO<sup>+</sup>/HOC<sup>+</sup> abundance ratio in dense clouds 4-94910
- HCS<sup>+</sup> rot. excitation in interstellar clouds 4-110514
- H<sub>2</sub>O maser emission from galactic nuclei, 22.235 GHz obs. 4-101478
- H<sub>2</sub>O maser in Centaurus, discovery, intensity, and radial vels. 4-77955
- H<sub>2</sub>O maser sources, obs. with acousto-optical 1008 channel radio spectrometer (Russian) 4-94934
- H<sub>2</sub>O<sup>+</sup> in diffuse interstellar clouds, search towards four stars 4-63240

## interstellar matter continued

- H<sub>2</sub>O + methyl cation (protonated formic acid), ternary association reaction in He buffer 4-93525  
 H166 $\alpha$  emission from galactic plane, southern survey 4-63298  
 He and D observations 4-63255  
 He charac'ts., flow in Solar System, obs. of 58.4 nm (by Prognoz 6) 4-77761  
 N/O versus O/H relationship and galactic chemical evolution 4-86063  
 NH<sub>3</sub> icy solids, surface mol. photodetachment and photodissociation 4-66604  
 NH<sub>3</sub> towards SNR Cassiopeia A, vel., temp. and densities 4-101453  
 Na/Ca<sup>+</sup> ratios in spectra of high velocity clouds 4-110730  
 O II forbidden emission in elliptical galaxies, spectroscopic survey 4-77927  
 O<sub>2</sub>, abundance, excitation, and prospects for radio detect. of <sup>16</sup>O<sup>18</sup>O 4-90205  
 O<sub>2</sub>, vacuum-UV oscillator strengths of Schumann-Runge lines rel. to prospects for Space Telescope obs. 4-90206  
 OH large-scale survey in galactic centre region 4-63311  
 OH maser, explained by H<sub>2</sub>O photodissociation at 157 nm 4-83439  
 OH megamaser in peculiar galaxy IC 4553, VLA-A obs. 4-86036  
 OH, photodissociation in interstellar clouds 4-90207  
 OH/H<sub>2</sub>O masers, obs. of Brackett-alpha emission from assoc. compact IR sources 4-77904  
 SiN, upper limits, EHF obs. 4-110711  
 SiO protonated ions, ab initio calcs. appl. to interstellar detect. possibility 4-87051  
 SiS protonated ions, ab initio calcs. appl. to interstellar detect. possibility 4-87051

## interstitials

- see also Cottrell atmospheres; crowlons; Snoek effect  
 alloy solid soln., partial impurity volume and lattice deform. 4-108390  
 alloy system, irradi., constrained equilb. thermodynamics 4-103793  
 alloys, concentrated, radiation-induced instability calc. 4-75505  
 alloys, interstitial, phase transitions of interstitial atoms in voids (Russian) 4-103741  
 alloys, interstitial atom ordering transition in variable volume model (Russian) 4-92124  
 alloys, interstitial distrib., variable-volume model (Russian) 4-84289  
 alloys, irradi., solute enhanced diffusion due to interstitials 4-88334  
 anisotropic BCC metal, mobile interstitial internal friction and viscosity 4-70271  
 anisotropic diffusion of point defects to edge dislocations 4-104007  
 binary substitutional alloy, FCC struct., interstitial impurity effect on atomic ordering 4-60919  
 cavity growth mechanisms, thermal and athermal processes 4-108349  
 damage profile in crystals, meas. by channelling technique 4-103840  
 damage structures, evolution under 14 MeV neutron, 4 MeV ion and 1.25 MeV electron irradi. 4-108418  
 diamond:Fe, electronic struct. calcs. 4-113894  
 diamond:H, interstitial muons anal. impurity states 4-80541  
 diffusion in metals and alloys, conf., Tihany, Hungary (Aug.-Sept. 1982) 4-63405  
 diffusion of interstitial impurities in crystals under action of shock waves 4-65342  
 fusion reactor materials, D-T neutron radiation damage, defect struct. 4-103812  
 Gorsky relaxation of light interstitials, linear response anal. 4-75613  
 grain boundary diffusion, struct. props. and point defect mobility, mol. dynamics simulations 4-80305  
 II-VI compounds, irradiation-produced dislocation loops, HVEM study 4-75529  
 interstitial alloys, thermal expansion study (Russian) 4-103976  
 ion implantation, damaged layer formation and growth, three-dimensional Monte Carlo simulation 4-75565  
 irradiation-produced point defects, chem. rate equations, global asymptotic stability 4-105004  
 lanthanide films, hydridisation and catalysis 4-71984  
 metals, BCC and FCC, H and He impurities, self-trapping phenomena 4-80056  
 metals, diffusion of C, N and O, review 4-65474  
 metals, dislocation loop punching by He bubbles 4-103748  
 metals, FCC, irradi., solute enhanced diffusion due to interstitials 4-88334  
 metals, light atom diffusion and tunnelling 4-65473  
 metals, point defects obs. and dynamics, perturbed  $\gamma\gamma$  angular correl. method 4-88757  
 metals, pure, two-phase oxide growth 4-98047  
 metals, vacancy-twin boundary interactions, computer simulation studies 4-113491  
 metals and alloys, book contrib. 4-108357  
 polymer-metal adhesion compounds; spontaneous increase in strength 4-81396  
 quartz, neutron irradi., point defects, EPR and optical absorpt. study 4-103742  
 radiation defect clusters, annealing of divacancies 4-108351  
 n-Si, radiation defect formation, annealing, defect interactions 4-113499  
 silions,  $\alpha$ - $\beta$  relationship 4-70125  
 solid solution, supersaturated, radiative swelling problem, intensified recomb. of unlike defects 4-70188  
 solid solution, supersaturated, radiative swelling problem, inclusion growth and impurity pump mechanisms 4-70197  
 solid solutions, impurity solute atoms distribution, interactive interaction effects (Russian) 4-108405  
 soliton state of an interstitial atom (Ukrainian) 4-88351  
 steel, austenitic stainless, gamma-ray induced short-range ordering, point defect influence 4-92123  
 steel, austenitic stainless, Ti- and Si-modified, microstruct. evolution, effects of pulsed and/or dual ion irradi. 4-98154  
 steel, austenitic stainless, Ti-modified, irradi. response in specimens prep. by rapid solidification processing 4-103816  
 steel, austenitic stainless, type 0Kh16N15M3B, ion irradi., pore formation (Russian) 4-65308  
 steel sheet, continuous annealed cold-rolled, overaging treatment and ductility, interstitial atom supersaturation (French) 4-89096  
 transition metal compounds, coordination of H at interstitials 4-84288  
 transition metals, interstitial migration anomaly, vel. to band electron energy 4-98364  
 urea-ammoniumchloride: Mn<sup>2+</sup>, zero-field splittings and site distortions, EPR studies 4-98580

## interstitials continued

- vacancy-interstitial pair formation in solids, phonon model 4-103895  
 void formation during ion bombardment, conditions for suppression 4-108477  
 void nucleation suppression by injected interstitials during heavy ion bombardment 4-75561  
 Ag halides, halide ion and Ag<sup>+</sup> adsorption, interaction pot. 4-75785  
 Ag-Cu dilute alloys, defect production and annealing 4-75442  
 Ag-Cu dilute alloys, electron irradi., defect prod. and annealing 4-75441  
 Ag-Zn, conc., electron irradi., elec. resist., recovery 4-104182  
 AgBr, role of Frenkel defects in radiation stimulated processes 4-98095  
 Al, cyclic irradi., void growth and swelling at low temp. 4-103795  
 Al FCC crystal, force const. between interstitial H atoms and host atom 4-75629  
 Al, FCC tilt boundary, vacancy migration, computer simulation studies 4-113694  
 Al-Mg, dil., neutron irradi., internal friction, elastic modulus, recovery stages studied by elec. resist. meas. 4-103876  
 B, diffusion coefficient determ. for drive-in in oxidising atmosphere (Hungarian) 4-113715  
 BaF:He, interstitial diffusion, solubility of He, dissolution energy 4-113727  
 Be-HfO, H<sup>+</sup> implanted, O gettering 4-92218  
 Bi<sub>2</sub>WO<sub>3</sub> bronze, microstructure and X-ray emission spectra 4-84419  
 CaF:He, interstitial diffusion, solubility of He, dissolution energy 4-113727  
 CaF<sub>2</sub>, electron irradi., anion voidage and void superlattice 4-108350  
 CaF<sub>2</sub>, thermally induced anion disorder, neutron struct. meas. 4-98338  
 CaF<sub>2</sub>:Ce<sup>3+</sup>, O<sup>2-</sup>, thermoluminescence spectra, irradi. effects 4-109259  
 CdF<sub>2</sub>:Er<sup>3+</sup>, insulator to semiconductor transition, site selective laser spectroscopy 4-99155  
 CdTe:In, Li, defect complex, IR absorption studies 4-80031  
 CeO<sub>2</sub>:La<sup>3+</sup>, Nb<sup>5+</sup>, dielectric relaxation, orientation of dipole complexes 4-114020  
 CoF<sub>2</sub>, antiferromagnets, hyperfine fields, muon spin relax. 4-71253  
 Co<sub>2</sub>-O<sub>2</sub>, chem. diffusion, creep meas. 4-92418  
 Cr, neutron irradi., internal friction, elastic modulus, recovery stages studied by elec. resist. meas. 4-103875  
 Cu, irradi., stored energy, calorimetric determ. 4-103829  
 Cu, neutron cross sections for defect prod. by high energy displacement cascades 4-108462  
 Cu, small-angle X-ray scatt. by small clusters of intrinsic point defects, intensity calc. 4-98129  
 Cu, vacancies and interstitials, energy and vol. charac'ts. (Russian) 4-92199  
 Cu-H, electron irradi., elec. resist. meas., annealing behaviour 4-92240  
 Cu-In, dil., channelling effect of conversion electrons emitted from radiatively impurities 4-75569  
 Cu-Zn, high energy electron irradi., radiation enhanced diffusion, interstitialcy mechanism, elec. resist. meas. 4-92239  
 Cu<sub>2</sub>-O, elec. cond. meas. 4-98624  
 Fe, BCC, electron or neutron irradi. induced defects, model 4-65300  
 Fe, BCC crystal, irradiation creep, stress induced edge dislocation interstitial atom interaction 4-104814  
 $\alpha$ -Fe, electron and neutron irradiated, low-temp., mag. relax. spectra 4-84831  
 Fe, ferromagnetic, high purity, magnetomechanical damping, influence on struct. defects 4-76226  
 Fe, grain boundary with impurity segregation, atomic and electronic struct., 4-113463  
 Fe, hyperfine interactions of interstitial <sup>125</sup>I<sup>2</sup>B, asymmetric  $\beta$  decay studies 4-65651  
 $\alpha$ -Fe, positron annihilation expts. in thermal equil., one-interstitial model confirmation 4-109271  
 Fe, pure, irradi. in HVEM, void form. onset temp. 4-103804  
 Fe, pure and C doped, electron irradi., resistivity recovery 4-108834  
 Fe, stress relaxation and static strain aging, short range heavy interstitial reordering 4-85172  
 Fe-Ni dilute alloys, electron and neutron irradiated, low-temp., mag. relax. spectra 4-84831  
 Fe-P (0.1 wt.%), single crystals, deform. behaviour, effect of orientation and temp. 4-71702  
 Fe-P-Ti (0.1, 0.16 wt.%) 4-71702  
 Fe-Si-C substitutional solns., interstitial diffusivity, solvation shell analysis 4-113696  
 Fe<sub>73</sub>B<sub>12</sub>Si<sub>10</sub>, amorphous, isothermal crystallisation and mag. props. (Russian) 4-65384  
 Fe<sub>3</sub>C, diffusion coeff. meas. 4-98345  
 Fe<sub>40</sub>Ni<sub>35</sub>B<sub>18</sub>Mo<sub>7</sub>, Metglas 2826 MB 5 keV He implantation, bubble growth, free vol. relax. model 4-103822  
 GaAs:B, interstitial centre, radiation induced, cluster-Bethe lattice treatment 4-98090  
 GaAs:Mn, Mn redistribution, interstitial-substitutional model analysis 4-92433  
 GaAs:Te, H ion bombarded, free carrier density, EELS studies 4-98632  
 Ge, quenching centre form., host interstitial injection by oxidising surface 4-65258  
 Ge:Cu, impurity states, annealing effects 4-104148  
 Ge:H(He), ion irradi., structural defect study 4-88164  
 InP:Zn, grown-in defects, annealing effects, DLTS studies 4-84287  
 KBr, H centres, low temp. pair associates 4-70149  
 KCl:Ag, Ca, X-irradi., electron centre form., luminesc., optical absorption studies 4-60920  
 KCl:Ag, X-irradi., electron centre form., luminesc., optical absorption studies 4-60920  
 KCl:I<sup>-</sup>, polarised Raman spectra and interstitials 4-80938  
 K<sub>2</sub>O-SiO<sub>2</sub> glass, gamma-irradi., defect centre struct., EPR obs. 4-70211  
 La<sub>0.827</sub>Al<sub>1.9</sub>O<sub>1.05</sub>, cryst. struct., single cryst. X-ray diff. studies 4-103723  
 LiF:OH<sup>-</sup>, gamma-ray irradi., lattice defects, EPR studies 4-75437  
 MgF<sub>2</sub>:Li, electron irradi., holelike defects, ESR study 4-60964  
 MgO, electron irradi., point defect kinetics, HVEM study 4-70214  
 MgO, preirradiation defects associated with trace impurities 4-70186  
 MnF<sub>2</sub>, antiferromagnets, hyperfine fields, muon spin relax. 4-71253  
 MnO, self-diffusion studies 4-98344  
 Mo, cyclic irradi., void growth and swelling at low temp. 4-103795  
 Mo, irradiation by fast neutrons, annealing, interstitial clusters; X-ray scatt. obs. 4-75538  
 Mo, low energy heavy ion bombardment, self-interstitial generation 4-80117

## Interstitials continued

- Mo, void shrinkage rel. to irradi. temp., two-dimensional self-interstitial diffusion 4-75563  
 Mo-Co dilute alloy, Co impurity location, PIXE and ion channelling studies 4-80072  
 Mo-Co dilute alloy, lattice location studies by PIXE and ion channelling 4-99894  
 Na, martensitic nucleation and growth, mol. dynamics simulation studies 4-114520  
 NaCl,  $\gamma$ -irrad., interstitial dislocation loops (*Russian*) 4-113455  
 NaCl:H, radiation induced H discharge, optical absorb. (*Russian*) 4-99139  
 Nb, electron irradi., isochronal recovery spectrum, metastable self-interstitial config. 4-70212  
 Nb, electronically induced trapping of H by impurities 4-108410  
 Nb, stress relaxation and static strain aging, short range heavy interstitials reordering 4-85172  
 Nb, void shrinkage rel. to irradi. temp., two-dimensional self-interstitial diffusion 4-75563  
 Nb-N, ion implanted, N diffusion, ion beam studies 4-70431  
 NbO<sub>2</sub>(H<sub>2</sub>O), H and D tunnelling, sp. ht. meas. 4-61103  
 Ni foils, He injected, self-ion irradi., annealing, voids, TEM obs. 4-103827  
 Ni, low energy heavy ion bombardment, self-interstitial generation 4-80117  
 Ni:He, preimplanted, electron irradi., 1 MeV, He bubble growth 4-103803  
 Ni-based alloys, HVEM irradi., void form. rel. to  $\gamma'$  precipitation 4-108446  
 Ni-Fe-C substitutional solns., interstitial diffusivity, solvation shell anal. 4-113696  
 Ni-Ge dilute alloys, defect reactions, diffuse X-ray scatt. studies 4-75440  
 Ni-Si dilute alloys, defect reactions, diffuse X-ray scatt. studies 4-75439  
 NiO, influence of O<sub>2</sub> press. on self-diffusion 4-98341  
 Pb-Al<sub>2</sub>O<sub>3</sub>-Al junctions, ion irradi., defect vibrs., supercond. tunnelling meas. 4-98826  
 PbF<sub>2</sub>, thermally induced anion disorder, neutron scatt. meas. 4-98338  
 PbF<sub>2</sub>:Na(K)(Rb), ionic cond., dielec. relax. and activation vol. 4-113701  
 Pd-Fe, ion implanted, ferromagnetism study 4-71137  
 Pd-Si(111) interface, atomic intermixing and electronic interaction 4-70478  
 Pd<sub>2</sub>FeH<sub>3</sub>, Mossbauer study of hyperfine interactions 4-88756  
 RbCl:L, polarised Raman spectra and interstitials 4-80938  
 RbMgF<sub>2</sub>:Mn<sup>2+</sup>, electron irradi., vacancy-interstitial pair and F-centre-impurity ion pair form. 4-70215  
 Si, atomic diffusion mechanisms theory 4-70430  
 Si, electron and  $\gamma$  irradi., influence on defect annihilation 4-98094  
 Si, electron and  $\gamma$ -ray irradiated, efficiency of radiation defect formation 4-92237  
 Si, excess interstitial distribution during thermal oxidation, two-dimensional model 4-84286  
 n-Si, gamma and neutron irradi., radiation defect interactions 4-92227  
 Si, IR spectroscopy characterisation 4-99136  
 Si, impurity diffusion, fraction of interstitial mechanism 4-80308  
 Si, impurity diffusion, impurity conc. doping effects 4-113728  
 Si, intrinsic point defects and diffusion processes 4-108358  
 Si, neutron irradi., radiation defects and electrophys. parameters 4-84319  
 Si, proton irradi., induced defects interaction with surface 4-75564  
 n-Si, proton irradiated, electrophysical props. 4-108861  
 Si, self-interstitials, electronic struct. and total energy migration barriers 4-108811  
 Si, self-interstitial scatt. and imaging 4-80033  
 Si, substitutional and interstitial donors, many electron effect 4-113895  
 Si wafer, mechanical properties, effects of laser back-side damage 4-98132  
 Si:Al, electronically simulated defect migration 4-113730  
 Si:B, deep level impurities at bond centered interstitial site 4-108814  
 Si:B solar cell, electron irradi., photon effects 4-93618  
 Si:B(P)(As), dopant diffusion, numerical soln. by solving impurity, vacancy and self-interstitial continuity eqns. 4-80303  
 Si:C, self-interstitial enhanced C diffusion 4-98358  
 Si:Cr(Mn)(Fe)(Co)(Ni), breathing mode relax around tetrahedral interstitial 3d impurities 4-108567  
 Si:H, interstitial muons anal. impurity states 4-80541  
 Si:Mg, implanted, doping behaviour, elec. props. 4-75485  
 Si:Mg(Al)(S), third-period interstitials, electronic struct. calcs. 4-108808  
 Si:muon, spin polarised electron struct. of positive muon, LCAO-Green's function anal. 4-65634  
 Si:muonium, interstitial atom mobility, radiation defect effects 4-65256  
 Si:N single, cryst., ion implanted, photoluminescence studies 4-114313  
 Si:O, Czochralski grown, thermally-induced microdefects, high resolution TEM studies 4-108626  
 Si:O Czochralski crystals, O precipitation and microdefects 4-84411  
 Si:P, Sb, P diffusion, self-interstitial supersaturation and vacancy undersaturation 4-70457  
 Si:S, deep levels, DLTS meas. 4-84592  
 Si:Ca:Al, B(Be),  $\alpha$  interstitial diffusion studies 4-80302  
 Si:N<sub>4</sub>,  $\alpha$ - $\beta$  relationship 4-70125  
 SiO<sub>2</sub>, ion implanted, E' defects, isothermal annealing studies 4-70146  
 SrCl<sub>2</sub>, thermally induced anion disorder, neutron scatt. meas. 4-98338  
 Sr:Fe, interstitial diffusion, solubility of He, dissolution energy 4-113727  
 SrF<sub>2</sub>, interstitial atom hopping by electronic excitation of Frenkel pairs 4-70140  
 Ta, hyperfine interactions of interstitial <sup>12</sup>B, asymmetric  $\beta$  decay studies 4-65651  
 Ta, stress relaxation and static strain aging, short range heavy interstitials reordering 4-85172  
 Ti, plastic flow and fracture at low temps. 4-76803  
 Ti-V solid solutions, creep, microstruct. 4-109464  
 TiN, nonstoichiometric and hydrogenated, cluster calcs. of electronic states and chem. binding 4-70623  
 TiO<sub>2</sub>, rutile, threshold radiation damage, computer simulation 4-108420  
 TiO<sub>2-x</sub>, interaction of small and extended defects 4-75443  
 TiO<sub>2-x</sub>, isothermal chem. diffusion 4-92421  
 TiO<sub>2-x</sub>, isothermal electromigration 4-92448  
 TiO<sub>2-x</sub>, nonstoichiometric, small defect contrast in electron microscopy 4-97982  
 (u,Pu)<sub>2</sub>O<sub>7</sub>, nuclear fuel oxide, diffusion processes, surface effects 4-98353  
 UO<sub>2</sub>/(U,Pu)<sub>2</sub>O<sub>7</sub>, chem. interdiffusion coeff., O pot. depend. 4-92447

## Interstitials continued

- UO<sub>2-x</sub>, nuclear fuel oxide, diffusion processes, surface effects 4-98353  
 V, hyperfine interactions of interstitial <sup>12</sup>B, asymmetric  $\beta$  decay studies 4-65651  
 V, T charged, <sup>3</sup>He bubble formation, TEM obs. 4-103825  
 V-Cr-Ti(Fe-Zr), mech. props. rel. to O contamination, fusion appls. 4-109499  
 V-N, ion implanted, N diffusion, ion beam studies 4-70431  
 V<sub>2</sub>N, crystal struct. from 1 MV electron microscopy 4-92161  
 W, interstitial atom interaction with grain boundaries (*Russian*) 4-65293  
 W, low energy heavy ion bombardment, self-interstitial generation 4-80117  
 W surface, interstitial atom interactions, field-ion microscopy studies 4-61798  
 W-Re (10 at.%), neutron irradi., homogeneous rad.-induced precip., atomic resoln. study 4-108449  
 WO<sub>3-x</sub>, interaction of small and extended defects 4-75443  
 ZnSe:Na, donor-acceptor-pair line luminesc. 4-104659  
 Zr, electron irradi., disloc. loops, electron microscopy studies 4-84296  
 Zr tritides, ageing, TEM study 4-75503  
 Zr-Sn (0.1-1.5 wt.%), neutron irradi., effect of tin on growth of polycryst. Zr 4-75537  
 ZrF<sub>2</sub>, O<sub>0.67</sub>, cryst. struct. determ. (*French*) 4-84264  
 Zr<sub>0.74</sub>O<sub>0.26</sub>, slow-neutron inelastic scatt. spectra 4-84127  
 Zr(Y)<sub>0.862</sub>, cryst. struct. determ. 4-103715
- intersystem crossing** see nonradiative transitions  
**intramolecular forces** see atomic forces  
**intramolecular mechanics** see atomic forces  
**intramolecular potentials** see potential energy functions  
**intramolecular vibrations** see molecular vibration; molecular vibration in solids  
**intrinsic magnetisation** see spontaneous magnetisation
- Invar**  
 atomic short range order, neutron scatt. study 4-113337  
 Perminvar, mag. domain struct., complex permeability meas. 4-76164  
 pin-tool steel couple, crit. thickness of protective films 4-109519  
 Fe-Ni Invar alloys, Mossbauer spectra 4-88748  
 Fe-Ni Invar alloys, phase transforms. 4-70373  
 Fe<sub>0.66</sub>Ni<sub>0.34</sub>, Curie point at ultrahigh press. 4-88676
- invariance**  
 see also conservation laws  
 shells, thin elastic spherical, free vibrations, rederivation of differential eqns. in invariant form 4-112753
- inversion layers**  
 bound electron states of Coulombic impurities and effect on mobility 4-98770  
 electron gas, 2-dimens., quantized Hall conductance in a two dimensional periodic potential 4-70770  
 impurity band cond. in mag. fields, theory 4-98768  
 narrow band gap semicond., effective electron mass in inversion layers, surface elec. field effect, appl. to InSb 4-104280  
 narrowband semiconductors with inverting band bending at surface, photoconductor theory 4-65715  
 quantum Hall regime critical non-dissipative current 4-98762  
 quasi-2D electron systems: electron-phonon interaction and screening effects 4-98547  
 semiconductor inversion layer, two-dimens. electrons, bound impurity states, ionisation prob. in strong mag. field 4-65750  
 semiconductors, low-conductivity, carrier mobility using the travelling wave technique 4-92752  
 solar cell, collection mechanisms anal. 4-89412  
 two dimensional electronic systems, cond. near mobility edge 4-80682  
 two-dimensional electron gas, disordered, resist. in mag. field 4-84634  
 two-dimensional electron systems, magnetothermal effect 4-80684  
 two-dimensional systems, electronic props., conf., Oxford, England (Sept. 1983) 4-95050  
 width, electron-electron interactions, fractional quantum Hall effect 4-75880  
 Ge bicrystal p-type inversion layers, anomalous magneto-transport props. 4-98719  
 Ge bicrystals, anomalous magneto-transport props. of p-type inversion layers (*Japanese*) 4-70842  
 HgMnTe semimagnetic MIS inversion layers, quantum transport 4-98775  
 InAs MIS diodes with N-shaped V-I characteristics in inversion voltage region 4-114044  
 InP, localisation of inversion electrons, Fourier transform spectra studies 4-98555  
 InSb inversion layer narrow gap systems, resonant polaron theory 4-98548  
 InSb MIS diodes with N-shaped V-I characteristics in inversion voltage region 4-114044  
 Si, 2D Na impurity band cond. in activated regions, mag. field depend. 4-98769  
 Si (100) inversion layer, electron mobility, neutral scatt. effects 4-76040  
 Si (111), adsorbed Cs, inversion layers, positive and negative magnetoresistance 4-98645  
 Si, electron inversion layer, scatt. and adsorption of ballistic phonons, theory and expt. 4-98767  
 Si inversion layer, 2D, weak localisation and interaction effects 4-98766  
 Si inversion layer, ballistic phonon scatt. and absorption 4-65756  
 Si inversion layers, de Hass-van Alphen effect obs. 4-98771  
 Si, inversion layers, freq.-induced electron delocalisation and fractional quantisation 4-80681  
 Si inversion layers, impurity band cond. in mag. fields, theory 4-98768  
 Si inversion layers, magnetoelectronic and quantised confinement 4-98764  
 Si inversion layers, multiple connected quantised resistance regions 4-98725  
 Si inversion layers, submicron width, quasi 1D effects 4-98765  
 n-Si inversion layers, two-dimensional plasmons and far infrared emission 4-104140  
 n-Si, inversion layers in MOSFET, phonon limited hot-electron temp. 4-70945  
 Si, MIS inversion channel, quantum Hall effect studies 4-104321  
 Si MIS struct., magnetoresist. of inversion and accumulation layers 4-61461  
 Si MOS inversion layers, complex capacitance in quantised resist. regime 4-98773

## inversion layers continued

- Si quantised Hall resistor, two-terminal conductance meas. 4-70942  
 Si, thermal oxidation in HCl and trichloroethylene, MOS capacitors fabrication 4-62078  
 Si:Na<sup>+</sup>, two-dimensional hopping cond. in mag. field 4-98687  
 Si/SiO<sub>2</sub>/metal struct., electron inversion layers, tunnelling spectra of Landau levels 4-98772  
 Si-MOSFET, warm electron coeff. calc. for two-dimens. electron gas 4-65748  
 Si-SiO<sub>2</sub> phase boundary, surface hole mobility 4-104323

## iodine

see also nuclei with .....

- <sup>127</sup>I, A=123, 131 phys., charact. rel. to differentiating relative activity in the kidneys 4-72369  
 acetylene-I<sub>2</sub>, Ar matrix isolated, fine struct., IR and UV spectra 4-74231  
 adsorbed on Pt (111), core electron binding energies 4-104085  
 anti-Stokes Raman laser up-converter of excimer lasers using stimulated anti-Stokes Raman scatt. 4-74486  
 atom, two photon induced VUV fluoresc. 4-83325  
 atomic laser, degenerate transition, self-induced transparency, coherent pulse propag. 4-96882  
 atomic vapour, pulse reshaping in coherent interaction with resonant absorber, homogeneous relax. time meas. 4-69511  
 atoms, photoemission in soft X-ray range 4-83341  
 BWR, FNR program for core, Xe and I monitoring, safety measures 4-86964  
 complexes, interactions, energy component anal. calcs. 4-59869  
 contrast media, levels in human body, determ. via X-ray fluoresc. (*German*) 4-89724  
 laser, degenerate mag. dipole transitions self-induced transparency 4-83653  
 laser, near IR high power, pulse duration and beam flux density 4-69395  
 laser, photodissociation, flashlamp-pumped, gasdynamic shock wave influence on lasing kinetics 4-60027  
 laser using photolytic O<sub>2</sub> <sup>1</sup>Δ generation, kinetic model 4-112401  
 molecular photodissociation in liqs., picosecond transient spectra 4-89313  
 molecular supersonic beam, photodissoc. in nozzle expansion region, cluster spectra effect 4-69156  
 molecule, 2880 Å emission spectrum, ion-pair states near 47000 cm<sup>-1</sup> 4-64489  
 molecule, absorption lines as wavelength references for solar spectra Doppler shift meas. 4-77790  
 molecule, angle- and spin-resolved photoelectron spectroscopy 4-83417  
 molecule, B-X fluoresc. system, vibr. intensity distrib., population distrib., transition moments 4-78827  
 molecule, Cordes bands, gas phase UV MCD spectra 4-83399  
 molecule, E<sub>0</sub>+...+B<sub>0</sub><sup>+</sup> system hyperfine struct., CW optical-optical double reson. 4-112213  
 molecule, electron impact, emission cross section for I<sup>+</sup> laser lines 4-112288  
 molecule, electronic spectra from mol. dynamics, simple approach 4-68940  
 molecule, geminate recombination, role of A and A' states 4-69092  
 molecule, photolytic cage effect and atom recombination in compressed gases and liqs. 4-99807  
 molecule, photon-catalysed bound-continuum process, post saturation fluorescence, quenching and fragments 4-62219  
 molecule electron excited, laser irradi., vibr. relax. rates determ. (*Russian*) 4-83455  
 molecules, collisions with solid surface, dissociation, centrifugal mechanism 4-81404  
 molecules, photolysis, MTGLE classical stochastic trajectory calc., absorpt. spectra, quantum yields 4-8317  
 nickel phthalocyanine: I, struct. change by I doping 4-84305  
 optically pumped laser, kinetics in optically thick medium 4-64702  
 poly(3-methylthienylene) films, I<sub>2</sub> doped, electrochemical prep. 4-80577  
 poly(N-alkyl-3,3'-carbazolyl)-I<sub>2</sub> complexes, highly conducting, synthesis and I<sub>2</sub> doping 4-65664  
 polyacetylene:I<sub>2</sub>, cis and trans, DC and microwave cond. 4-92716  
 polyacetylene:I<sub>2</sub>, highly oriented, IR spectra 4-59925  
 polyacetylene:I<sub>2</sub>, I<sub>2</sub> doping, synchrotron scatt. study 4-65286  
 cis-polyacetylene:I<sub>2</sub>, lightly doped, freq. dependent conductivity 4-75953  
 polyacetylene:I<sub>2</sub>, stability after encapsulation, microwave meas. 4-109112  
 polyacetylene:I<sub>2</sub>, X-ray diff. studies 4-60860  
 polyacetylene:I<sub>2</sub> films, fibrillar, morphology-props. correlations 4-80306  
 polyacetylene:I<sub>2</sub>, IR refl. spectra, effect of sample densification 4-99120  
 polyacetylene:I<sub>2</sub>, material for neutron activation anal. of I 4-62260  
 polyacetylene morphology upon I<sub>2</sub> doping, SEM 4-60861  
 polyethylene:I<sub>2</sub>, elec. conduction 4-88511  
 polyphenylacetylene:I<sub>2</sub>, reson. Raman, Raman polaris. and far IR spectrosc. 4-80915  
 pulsed gas lasers, high power 4-96865  
 radionuclide (*Chinese*) 4-71934  
 stack effluent monitoring for an operating four reactor unit CANDU nuclear station 4-59450  
 vapour, saturation holes, frequency-modulation-polarisation spectroscopy 4-111218  
 vapour density mapping by optical tomography, noise theory expt. verification 4-91414  
 vapour density mapping using optical fan beam tomography 4-108157  
 AgBr:I<sub>2</sub>, multiphonon emission, excitons, photoluminescence 4-99159  
 Al-I-Au(Cu)(Ag) tunnel junction, fast light emission, plasmon polaritons (*French*) 4-80998  
 atoms in solns., geminate recombination, generalized Langevin treatment, inelastic transitions effect 4-62162  
 n-Bi<sub>2</sub>Te<sub>3</sub>, I, free carrier mobility, Hall and Seebeck coeffs., temp. depend. 4-61369  
 CdBr<sub>2</sub>:I<sub>2</sub>, absorpt. spectra and electron localisation (*Russian*) 4-104161  
<sup>127</sup>I, neutron activation anal. in environmental samples 4-105135  
 I, H<sup>+</sup> impact, X-ray prod. cross sections 4-96648  
 I-CsI-Cs solns., electron localisation, NMR obs. 4-98965  
 I-H<sub>2</sub> laser, electron-beam-controlled 4-74498  
 I-O<sub>2</sub> laser, nuclear-generation of O<sub>2</sub> by photolysis of O<sub>3</sub> 4-62222  
 I+HI(Mul), H and Mu exchange, isotope effects, semiclassical techniques 4-71884  
 I+Pb collisions, δ-electron spectra study 4-74321  
 I+Cl<sub>2</sub> charge transfer and electron detachment, absolute total cross-sections meas. 4-69202

## iodine continued

- I<sup>+</sup>+He, kinetic energy loss, double-focussing mass spectrometer me. 4-64567  
 I<sub>2</sub> absorpt. spectra recorded using frequency-modulation spectroscopy with pulsed dye laser 4-73520  
 I<sub>2</sub> in chloroform, reson. Raman excitation profiles interpretation 4-9654  
 I<sub>2</sub> molecular beam subjected to separated fields, saturated absorpt. res. obs. 4-74255  
 I<sub>2</sub> photodissoc., picosecond transient spectra, chemical reactions in sol. mol. dynamics 4-85316  
 I<sub>2</sub>, resonance Raman scatt. and vibronic states 4-102691  
 I<sub>2</sub>, in rare gas afterglows, A<sup>2</sup>Π<sub>g</sub>-X<sup>2</sup>Π<sub>g</sub> emission 4-112190  
 I<sub>2</sub>, photodissoc. spectra, predissoc. mechanism, vibr. levels 4-87171  
 I<sub>2</sub>:HI, proton cond. meas. 4-92413  
 I<sub>2</sub>-doped polyacetylene, millimeter-wave and far IR cond. 4-70850  
 I<sub>2</sub>-O<sub>2</sub> chemical laser, ICl fueled 4-91446  
 I<sub>2</sub>+butyrophene (and related cpds.) assoc., dielectric study 4-10497  
 I<sub>2</sub>+ethylene, electrophilic addition reaction, ab initio MO calcs. 4-6656  
 I<sub>2</sub>+F, exchange reaction, pot. surface, I(P<sub>1/2</sub>) two photon laser induced fluoresc. 4-76982  
 I<sub>2</sub>+I<sub>2</sub>, state-to-state rot. transfer rates, induced fluoresc. 4-91333  
 I<sub>2</sub>+He(He)(Ne)(Ar)(H<sub>2</sub>)(I<sub>2</sub>)(D<sub>2</sub>), state-to-state: rot. transfer rates induced fluoresc. 4-91333  
 I<sub>2</sub>(P<sub>1/2</sub>), fluoresc. study as product of F+HI(I<sub>2</sub>)(ICN) reactions 4-7691  
 I<sub>2</sub> dosimetry using LiF 4-72432  
 I<sub>2</sub> insulin absorpt. meas. during subcutaneous infusion, portable detector 4-67157  
 I<sub>2</sub>, testicular uptake and dominant lethal induction in mice 4-67019  
 I<sub>2</sub>, activity levels for low level radioactive waste 4-106731  
 I<sub>2</sub>, global environmental transport model review 4-83253  
 I<sub>2</sub>, in human thyroid tissues of Utah populations, 1947-54 4-109888  
 I<sub>2</sub>, in waterfowl muscle, collection from radioactive leaching pond, S. Idaho 4-115231  
 I<sub>2</sub>, management from fuel reprocessing plants, air and water discharge 4-91115  
 I<sub>2</sub>, Mossbauer spectroscopy, high quality sources 4-86513  
 I<sub>2</sub>, nuclear fuel reprocessing gaseous wastes management 4-59438  
 I<sub>2</sub>, volatile radionuclides from nuclear fuel reprocessing, treatment and disposal (*German*) 4-59318  
 I<sub>2</sub> applied with <sup>90</sup>Sr, <sup>45</sup>Ca, tumour induction in rats (*Russian*) 4-67011  
 I<sub>2</sub> release from defective LWR fuel rods at temps. up to 1100°C, LOEC appl. 4-96233  
 I<sub>2</sub>, thyroid uptake blocking by RI, nuclear accidental appl., review 4-115232  
 I<sub>2</sub>, various forms, therapeutic, dose calibrator assays discrepancy 4-89760  
 I<sub>2</sub>, gas adsorption on rocks 4-96147  
 I<sup>+</sup>+DF(HF)(HCl), quenching, time resolved IR fluoresc. used to determine const. 4-102730  
 KCl:I<sub>2</sub>, impurity-localised excitons, luminesc. and absorpt. spectroscopy study 4-92625  
 KCl:I<sub>2</sub>, luminescence of localised excitons at low temp. 4-80990  
 KCl:I<sub>2</sub>, polarised Raman spectra and interstitials 4-80938  
 N<sub>2</sub>O, coolant reactor loop, radioiodine behaviour, decontamination (*Russian*) 4-74035  
 O<sub>2</sub>:I<sub>2</sub> laser, use of O<sub>2</sub> generated by nuclear pumping in flowing Ar-CO<sub>2</sub> mixture 4-60025  
 Pb-I-NbN tunnelling junction, resist., supercond. fluctuations effect, existence of ultrathin layer in NbN films 4-88827  
 RbCl:I<sub>2</sub>, polarised Raman spectra and interstitials 4-80938  
 ZnS:I<sub>2</sub> with adsorbed O<sub>2</sub>, surface states and LED props. 4-80643  
 ZnSe:I<sub>2</sub>, vacancy-I complex hyperfine interactions, ESR study 4-70150
- iodine compounds**
- intercalation cpd. with graphite, C<sub>16</sub>I<sub>2</sub>, press. induced change in intercalation step 4-61397  
 iodate-arsenite systems, bistability and chemical waves form. 4-85303  
 Cu,Rb,Cu<sub>16</sub>I<sub>2</sub>Cl<sub>13</sub>/Rb,Cu<sub>16</sub>I<sub>2</sub>Cl<sub>13</sub>/Cu<sub>2</sub>Se solid electrolyte cells, single and multilayer, performances 4-99956  
 IBr, ion-pair state, absolute quenching rate, fluoresc. lifetime 4-107384  
 IBr photodissoc. Br laser, solar-powered, theory and operation 4-87322  
 IBr+Ba, chemiluminescence broad emission study 4-114801  
 ICN, photodissociation, spin-aligned CN(X<sup>2</sup>Σ<sup>+</sup>) 4-114802  
 ICN, photofragmentation, parent mol. bending and rot. effects, trajectory method 4-89312  
 ICN+F, exchange reaction, pot. surface, I(P<sub>1/2</sub>) two photon laser induced fluoresc. 4-76982  
 ICl, A' state characterisation by optical three-photon reson. 4-96632  
 ICl, bound valence states D'-A' transition, visible obs. 4-112189  
 ICl+Ba, chemiluminescence broad emission study 4-114801  
 IF laser, short wavelength 4-96883  
 IO radical, A<sup>2</sup>Π<sub>3/2</sub>-X<sup>2</sup>Π<sub>3/2</sub> system, laser-RF spectrosc. obs. 4-59819
- ion-atom collisions** see atom-ion collisions
- ion beam effects**
- see also ion-surface impact; ionoluminescence; plasma-beam interactions
- alkali silicate glasses, ion bombard., alkali depletion, ion beam mixing 4-70239  
 alkali silicate glasses, ion irradi., glass comp. modification by alkali ion migration 4-70238  
 alloys, preferred sputtering, segregation effects 4-81203  
 amorphous alloys, crystn., effect of irradi. particle mass 4-79936  
 atomic mixing induced by ion beams, atomic collisions 4-80118  
 austenitic alloys, He bubbles at grain boundaries 4-108471  
 binary alloy surfaces, irradiated, conc. profiles calc. 4-113509  
 biological action of low-energy heavy ions using photonuclear reaction (*Russian*) 4-67016  
 biological molcs., mol. size effects in fast heavy ion induced desorption 4-66880  
 bombardment induced cascade mixing and importance of post-cascade relaxation 4-65403  
 borosilicate waste glasses, ion bombard., fracture toughness and leaching behaviour 4-75545  
 cellulose triacetate, ion irradi., damage study 4-88211  
 cellulose triacetate, ion irradi., track model 4-88212  
 charge exchange of heavy ions in matter, radiation calc. 4-76548  
 damage profile in crystals, meas. by channelling technique 4-103840  
 damage structures, evolution under 14 MeV neutron, 4 MeV ion and 1.2 MeV electron irradi. 4-108418  
 diamond, vacancy formation energy, crystallisation studies 4-108354  
 effective stopping power charge of ions in condensed matter 4-92255

- beam effects continued
- electron loss by multiply-charged ion moving at small angle to cryst. planes 4-84328
- electron-stripping cross-sections for fast hydrogenic ions penetrating solids 4-78947
- electronic stopping cross sections and projected ion-range distribution moments (*Chinese*) 4-113512
- equilibrium charge distrib. for B, C, N ions passing through matter 4-75586
- eye lens, accelerated heavy particle irradi., cataractogenic pot. 4-67036
- fast ions in solids, excited state populations and charge-exchange 4-80126
- film preparation and etching, vacuum or plasma technology, conf., Brighton, UK (March, 1983) 4-78031
- fluorescent lamps, lumen depreciation due to ion bombardment 4-99157
- fusion reactor materials, radiation damage, pulse ion irradi. microstruct. 4-103821
- graphite, ion damaged, annealed, 2-D ordering, Raman study 4-70535
- graphite, pyrolytic, 1s binding energy shift under deuterium ion bombardment 4-91103
- heavy ion beam fusion, target study 4-102388
- high energy density ion cascades, surface damage, computer simulation studies 4-75553
- ice films, enhanced erosion by high energy  $^{19}\text{F}$  ion sputtering 4-80123
- ICF targets, ion beam interactions 4-107148
- inorganic insulators, cryst., heavy ion bombard., struct. changes and chem. effects 4-75549
- insulating thin films, Auger electron spectra, electron and ion beam effects 4-109283
- insulators, track damage and erosion by ion-induced electronic interactions 4-75551
- insulin, bovine, fast heavy ion-induced desorption, damage cross sections 4-77188
- ion gun for surface studies, beam profile and scanning characts. 4-64252
- ionized cluster beam deposition, wafer processing appls. 4-99317
- IV-VI semiconductors, ion implantation, review 4-92220
- L-shell populations of ions penetrating solids 4-78946
- Maskrol Polycarbonate plastic track detector, calibration using heavy ions 4-64307
- masking film deposition by ion induced polymerisation 4-75566
- membranes fabrication for ISFETs 4-95402
- metal films on  $\text{SiO}_2$ , ion beam mixing 4-108732
- metallic, glasses, ion irradi., damage, He and Ar, bubble form., blistering, exfoliation 4-108481
- metallic bilayers, ion mixing, chemically enhanced diffusion 4-92445
- metallic foils, ion stopping power and effective charge theorem 4-92254
- metallic novel surfaces, directed energy production 4-74775
- metals, implanted  $\text{N}_2^+$  mol. ion range, nuclear reaction anal. 4-92250
- metals, light ion implantation, amorphisation, statistical aspect 4-80114
- metals, wear reduction and analysis, surface modification by ion beams 4-81290
- mica, muscovite, ion implanted, defect struct. thermal annealing 4-70177
- mica, oriented U ion nuclear tracks, small angle X-ray and neutron scatt. studies 4-75554
- minerals, nuclear track formation models, etching and annealing, review 4-70235
- negatively charged GeV particles, axial channelling, kinetic approach 4-75573
- nonmetallic solids, amorphisability under heavy ion bombard., covalent-ionic transition 4-80122
- nuclear track technique using heavy ion beams, potential appls. 4-59607
- n-octacosane crystal faces, ion bombardment effects 4-103815
- optical devices, effects of ion implantation on props. 4-80067
- optical thin films, ion-assisted deposition, prep. and appls. 4-87402
- organic solids, ion form., conf., Munster, Germany (Sept. 1982) 4-86114
- phosphor depreciation by ion bombardment 4-99157
- PMMA, ion beam modifications, electronic stopping power 4-84322
- PMMA films, ion beam induced decomp. and diffusion 4-70234
- polycrystalline foils, multiply peaked energy loss spectra of heavy ions 4-92272
- polymer films, elec. cond. changes induced by pyrolysis and high energy ion irradi. 4-75966
- polymer films, ion beam irradi., secondary electron, ion, and photon emission 4-76577
- quartz, E-centre prod. by ionising radiation, ESR and optical studies 4-70145
- $\alpha$ -quartz, ion bombard. damage, 50 to 295K 4-70230
- radioactive waste glass, simulated, density changes under ion, electron, and gamma irradi. 4-73974
- random solids, sputtering by keV light-ion bombard. 4-71498
- range distrib. calc. using Boltzmann transport eqn. 4-92249
- rare earth metal, thin films, struct., effect of ion irradi. 4-70240
- reactive ion beam etching, for semiconductor production, review 4-81322
- SAW devices, Ar and reactive ion beam etching 4-81318
- selected area stationary beam cratering for high sensitivity depth profiling with computerised Auger microprobe 4-99711
- semiconductors, amorphisation by ion implantation, modification to defect accumulation models 4-88210
- semiconductors, Raman characterisation 4-99106
- silicates, high energy U ion tracks, struct. and annealing 4-70236
- single crystals, bent, with slowly varying curvature, GeV charged particle channelling 4-75568
- solar system, charged particle channelling radiation 4-77762
- solid, soliton state in wake interaction following ion or positron motion 4-75550
- solids, at. collisions, conf., Bad Iburg, Germany (July 1983) 4-73144
- solids, heavy ion charge states and charge transfer 4-76589
- spore radiobiology, conf., Amsterdam, Netherlands (July 1983) 4-63388
- sputtering, with AES and XPS surface and thin film analysis 4-81506
- steel, aluminised, irradi. with He ions, erosion resist. 4-66488
- steel, austenitic stainless, C or N ion irradi., double peak of voidage depth profile 4-98147
- steel, austenitic stainless, D permeation, plasma-driven, effect of surface comp. 4-113718
- steel, austenitic stainless, dual-ion and/or electron irradi. in HVEM, in-situ obs. of cavity growth process 4-98134
- steel, austenitic stainless, dual-ion irradi., microstruct. evolution under various He injection schedules 4-98150
- steel, austenitic stainless, fracture modes under He ion and neutron irradi., temp. depend. 4-104853
- ion beam effects continued
- steel, austenitic stainless, ion-irradiated, depth-dependent microstruct. 4-98151
- steel, austenitic stainless, irradiation creep, light ion simulation 4-104815
- steel, austenitic stainless, microstructural evolution in PCA, dual ion irradi., effect of He 4-103819
- steel, austenitic stainless, pressurised tube, ion bombardment, fatigue life, simulated fusion first wall environment 4-104850
- steel, austenitic stainless, swelling and precip. behaviour during irradi., effect of P 4-103818
- steel, austenitic stainless, Ti modified, prep. by rapid solidification processing, dual-ion irradi. 4-98155
- steel, austenitic stainless, Ti- and Si-modified, microstruct. evolution, effects of pulsed and/or dual ion irradi. 4-98154
- steel, austenitic stainless, Ti-modified, irradi. response in specimens prep. by rapid solidification processing 4-103816
- steel, austenitic stainless, type 06Kh16N15M3B, ion irradi., pore formation (*Russian*) 4-65308
- steel, ferritic, D and He trapping at TiC particles 4-98152
- steel, stainless,  $^{12}\text{C}^+$  ion beam effects, microstructure (*Chinese*) 4-70226
- steel, stainless, ferritic and austenitic, P segregation, radiation-induced 4-98148
- steel, stainless, radiation erosion by  $\text{H}^+$  and  $\text{He}^+$  simultaneous bombardment 4-107066
- stopping power effective charge of energetic ions in metals 4-65321
- submicron structures, dry etching techniques 4-89146
- surfaces, ion bombardment excitation of molecules 4-76584
- TEM specimen thinning, ion sources (*German*) 4-82870
- TEM specimens preparation, ion thinning apparatus using cold cathode ion gun 4-68338
- thin film analysis by low energy proton induced X-ray emission 4-109705
- thin film formation under effect of electron and ion bombardment 4-84529
- thin foils, shock wave generation using lasers and light ion beams 4-103877
- valine, amino acid, fast heavy ion-induced desorption, damage cross sections 4-77188
- void formation during ion bombardment, conditions for suppression 4-108477
- void nucleation suppression by injected interstitials during heavy ion bombardment 4-75561
- Al-Sn(In), ion irradi., vacancy-solute atom complexes, channelling study 4-103836
- Ag-Si, ion beam induced at. mixing, in-situ Rutherford backscattering meas. 4-65404
- Al creep velocity, high-energy ion irradi. effects 4-70243
- Al foil, inelastic ion energy loss and scatt. angle in transmission expts. 4-92265
- Al, He blistering effect of stress state 4-60969
- Al, low energy heavy ion range parameters,  $Z_1$  dependence 4-92248
- Al, proton stopping power, energy loss straggling, effective-charge fractions and straggling of heavy ions 4-103843
- Al, self-ion damage and comparison of ion damage rates with neutron damage rates 4-113506
- Al-Ag(In) $\text{Sn}$  systems, mixing behaviour study by Ar ion beam irradiation 4-65402
- Al-Au(Cu) thin film bilayers, ion beam bombarded, interfacial phase formation 4-70241
- Al-Cu, implanted, disorder studied by ion channelling and Rutherford backscattering 4-98145
- Al-Mg-Sc, He blistering effect of stress state 4-60969
- $\text{Al}_2\text{O}_3$ , ion implantation, ion beam mixing, and annealing of metals 4-70229
- Ar films, ion beam irradi., secondary electron, ion, and photon emission 4-76577
- Au, ion channelling, energy stopping power depend., interatomic interaction potentials at high projectile velocities 4-80125
- Au, proton stopping power, energy loss straggling, effective-charge fractions and straggling of heavy ions 4-103843
- Au/Cu bilayers, ion-induced solid solutions and ordered cpd. form. 4-108470
- Au-Ge bilayers, ion beam mixing, amorphous and metastable phases formation 4-80113
- $\text{AuGa}_2$  (001), surface net characterisation and electronic struct. 4-80642
- Be:D, retention and thermal release of implanted D 4-113477
- Bi $^{\text{L}}$ -shell X-ray prod. cross sections,  $\text{H}^+$  induced, ratios 4-66131
- $\text{Br}_2$  gas, proton and  $^4\text{He}$  stopping cross sections 4-92259
- C film, elec. cond. changes induced by pyrolysis and high energy ion irradi. 4-75966
- C foil, heavy ion irradiated, charge distribution meas. 4-78945
- C foil, specific energy loss of  $^{16}\text{O}$  ions, thickness depend. 4-92261
- C, proton stopping power, energy loss straggling, effective-charge fractions and straggling of heavy ions 4-103843
- C thin foil, pre-equilibrium stopping for  $^1\text{H}$  and  $^4\text{He}$  ions 4-92253
- C thin targets, stopping power for He, Li and C ions, charge state depend. 4-92252
- C very thin foils, energy loss of  $\text{He}^+$  beams, nonequilibrium effects 4-103837
- C-graphite materials, He ion irradi., surface erosion 4-80120
- $\text{CO}_2$  solid, range meas. of keV H ions 4-92263
- $\text{CO}_2$ , condensed gas solids, ion-induced chem. 4-66163
- $\text{CaAl}_2\text{O}_6$ , Ar $^+$  ion irradi., damage cross sections 4-104844
- $\text{Cl}_2$  gas, proton and  $^4\text{He}$  stopping cross sections 4-92259
- Co-Nb amorphous films, electron beam deposited, ion mixed, FMR, magnetisation meas. 4-71138
- $\text{CoSi}_2$ , single cryst. films,  $^4\text{He}$  irradi., elec. cond. studies 4-98782
- CrSi $_2$ , form. by ion beam mixing 4-80121
- $\text{CsAlSi}_2\text{O}_6$ , pollicite, Ar $^+$  ion irradi., damage cross sections 4-104844
- Cu alloys, dil., chem. redistrib. under simulation irradi. 4-108478
- Cu film, epitaxial growth, effects of low energy ion bombardment 4-98478
- Cu, ion bombard., temp. effects in fast recoil ejection 4-65309
- Cu single-crystal films,  $\text{Na}^+(\text{K}^+)(\text{Rb}^+)$  ion beams transmission, angular and energy distrib. 4-98159
- Cu surface, target adatom form. during quenching of energetic Ar ion induced cascade 4-88209
- Cu targets, fast ionised recoils, directional effects 4-109297
- Cu-Be (1.35 at.%), undersaturated, irradiated, formation of precipitates 4-104791

## ion beam effects continued

- Cu-In, dil., channelling effect of conversion electrons emitted from radioactive impurities 4-75569  
 Cu-In (0.1 at.%), vacancy trapping, PAC and ion channelling study 4-84876  
 Cu-Ti glasses, surface composition, composition profiles, Auger electron spectroscopy 4-113758  
 CuAg alloys, cone form. during Ar<sup>+</sup> ion sputtering 4-75552  
 Cu<sub>2</sub>Au, displacement cascade collapse at low temps. 4-103835  
 D<sub>2</sub>O, condensed gas solids, ion-induced chem. 4-66163  
 (Fe,Ca,Mg)<sub>1</sub>Si<sub>2</sub>O<sub>6</sub> glass, ion bombard. effect, XPS 4-84320  
 Fe, dislocation loop form. by self-ion irradi. at 40K, electron microscopy obs. 4-70242  
 Fe-Al (40 at.%), ion implantation, phase changes, TEM studies 4-108403  
 Fe-Cr-Ni-Mo, austenitic alloy, void swelling, effect of pulsed irradi. 4-108474  
 Fe-Cr-Ni-Mo, austenitic alloy, pulsed ion irradi., temp. aspects 4-108476  
 Fe-Cr-Si(Ti), electron and ion-irradi., void and precip. struct. 4-103802  
 Fe-Ni-Cr (16, 15 wt.%), void swelling, effect of C and Nb additions 4-103817  
 Fe<sub>90</sub>B<sub>10</sub>, amorphous alloy, He ion irradi., blister and bubble form., TEM obs. 4-108434  
 Fe<sub>40</sub>Ni<sub>38</sub>B<sub>18</sub>Mo<sub>4</sub>, Metglas 2826 MB 5 keV He implantation, bubble growth, free vol. relax. model 4-103822  
 (Fe<sub>40</sub>Ni<sub>50</sub>)<sub>3</sub>V, ordered alloys, microstruct. and creep rel. to implanted He 4-108399  
 α-Fe<sub>2</sub>O<sub>3</sub> electrode for H<sub>2</sub>O photodecomposition, surface studies log Ar<sup>+</sup> bombardment 4-108936  
 (GaAl)As-GaAs DH lasers, D<sub>2</sub><sup>+</sup> bombardment isolated stripe geometry (Chinese) 4-112431  
 GaAs, ion bombarded heated specimens, surface comp., AES and SIMS anal. 4-113510  
 GaAs, reactive ion etching, H mixing effects in Cl-containing gases 4-89148  
 GaAs, surface cleaning by ion bombardment 4-88213  
 GaAs:Be, ion implanted, reduced damage generation 4-113474  
 GaAs:Cr, ion irradi. effect on defect thermal annealing 4-98156  
 GaAs:Te, H ion bombarded, free carrier density, EELS studies 4-98632  
 n-GaAs/Au Schottky contacts, elec. props. and interface chem., sputtering effects 4-80674  
 GaAs/Pt, ion beam mixing and ohmic contact form. 4-92244  
 Ga<sub>0.97</sub>In<sub>0.03</sub>As, ion implanted, annealing, TEM obs. 4-70228  
 Ge, ion channelling, interaction pot., stopping power, ion scatt. spectra 4-75570  
 Ge, irradiated with high-energy heavy ion, induced radioactivities 4-59560  
 Ge:H(He), ion irradi., structural defect study 4-88164  
 H<sub>2</sub>O, condensed gas solids, ion-induced chem. 4-66163  
 He ion impacts, target ionisation, dissociation, excitation 4-96682  
 Ho, L-shell X-ray prod. cross sections, H<sup>+</sup> induced, ratios 4-66131  
 InP epitaxial, deep and shallow levels due to ion irradi. 4-80531  
 InP:Mg(Fe,Mg), implanted, effect on photoluminescence props. 4-85007  
 LiF, R<sup>+</sup>-centre aggregate, spectral linewidths, depend. on irradi. method 4-70193  
 LiF:U, pure and doped, preferential sputtering and ion induced comp. changes 4-71501  
 LiNbO<sub>3</sub> cryst. surface layer props. after low-energy ion bombardment (Chinese) 4-70532  
 MgAl<sub>2</sub>O<sub>4</sub>, spinel, Ar<sup>+</sup> ion irradi., damage cross sections 4-108484  
 Mo, BCC superlattice with and without dislocations, ion-lattice interaction potentials 4-92246  
 Mo, He trapping at low-angle tilt boundary 4-113505  
 Mo, low energy heavy ion bombardment, self-interstitial generation 4-80117  
 Mo, pulse ion irradi., void nucleation 4-103826  
 Mo, pulsed irradiation, theory of depleted zone annealing 4-108417  
 Mo, pure, electron and He ion irradi., vacancy loop form. 4-108480  
 Mo-Co dilute alloy, lattice location studies by PIXE and ion channelling 4-99894  
 Mo-Si interface, silicidation, kinetics induced by ion bombard. 4-61243  
 Nb, void shrinkage rel. to irradi. temp., two-dimensional self-interstitial diffusion 4-75563  
 Nb-Si interface, silicidation, kinetics induced by ion bombard. 4-61243  
 Ni, <sup>12</sup>C<sup>+</sup> ion beam effects, microstructure (Chinese) 4-70226  
 Ni (100), He ion irradiation, He precipitate nucleation at point defects 4-103823  
 Ni foils, He injected, self-ion irradi., annealing, voids, TEM obs. 4-103827  
 Ni, He<sup>+</sup> ion irradiated, bubble growth, microstruct. contrib. 4-108472  
 Ni, low energy heavy ion bombardment, self-interstitial generation 4-80117  
 Ni, pure, heavy ion irradi. damage, in situ electron microscopy 4-103828  
 Ni, void formation during ion bombardment, conditions for suppression 4-108477  
 Ni/SiC mixed layers, ion and laser irradi., microstruct. anal. 4-84415  
 Ni-Al thin film, ion irradi., EELS study 4-88916  
 Ni-Au films, ion-induced comp. change, role of grain boundary diffusion at elevated temps. 4-108475  
 Ni-Si (12.7 at.%), solute redistrib. under irradi., TEM invest. 4-108416  
 Ni-Yb films, ion beam mixing, radiation enhanced diffusion by Kr<sup>+</sup> and O<sub>2</sub><sup>+</sup> bombard. 4-103832  
 NiSi<sub>2</sub> single cryst. films, <sup>4</sup>He irradi., elec. cond. studies 4-98782  
 O<sub>2</sub>, solid, range meas. of keV H ions 4-92263  
 Pb-Al<sub>2</sub>O<sub>3</sub>-Al junctions, ion irradi., defect vibrs., supercond. tunnelling meas. 4-84826  
 Pd-Si film, ion implanted, amorphisation, channelling anal. 4-92247  
 Pd<sub>80</sub>Si<sub>20</sub>, amorphous, prep. by ion implantation, proton irradi. damage, elec. resist. meas. 4-103833  
 Pt, L-shell X-ray prod. cross sections, H<sup>+</sup> induced, ratios 4-66131  
 Pt layer on graphite and RuO<sub>2</sub> substrates, ion bombard., electrocatalytic props. 4-71968  
 Ru, ion irradi., vacancy loops, electron microscopy obs. 4-80046  
 S, sputtering by He<sup>+</sup> and Ar<sup>+</sup> ions 4-71500  
 SO<sub>2</sub>, condensed gas solids, ion-induced chem. 4-66163  
 Sb, L-shell X-ray prod. cross sections, H<sup>+</sup> induced, ratios 4-66131  
 Se, sputtering by He<sup>+</sup> and Li<sup>+</sup> ions 4-71500  
 Si, disorder profiles at high sputtering dose by oxide growth rate profiling 4-66470  
 Si, elastically bent crystals, dechannelling of planar channelled protons 4-75575

## ion beam effects continued

- Si, heavy-ion induced damage and annealing TEM and channelling studies 4-80115  
 Si, ion bombarded, 14 MeV O ions, non-registered Si produced at metal-Si interface 4-114351  
 Si, ion bombardment, sputtered particles and cascade recoils 4-76621  
 Si, ion etching, effect of ion species on bombardment induced topography 4-81320  
 Si, ion implanted, pyrometric temp. meas. during laser annealing 4-70203  
 Si, irradiated with high-energy heavy ion, induced radioactivities 4-59560  
 Si, low energy heavy ion range parameters, Z<sub>i</sub> dependence 4-92248  
 Si, low Z shielding materials, implanted H effects at high co. 4-111760  
 Si, oxidation induced stacking faults, dislocations, effects of Cl<sup>+</sup> and implantation, X-ray topography 4-80053  
 Si single crystals, bent, high energy channelled proton deflection 4-75575  
 Si substrate, ion implanted and processed, interface characterisation 4-84304  
 Si, surface cleaning by ion bombardment 4-88213  
 Si:As, implanted under channelling conditions, impurity spatial distribution, localisation, defect form. charact. 4-84321  
 Si:As(Sb)(In), ion implanted, pulsed electron beam annealing, impurity diffusion 4-103984  
 a-Si:H thin films, O distrib. and modifications induced by heavy ion bombard. 4-70233  
 Si:P<sup>+</sup>, implanted, dislocation struct. development, effect of cryst. orientation, TEM obs. 4-80040  
 Si:Sb, ion implanted, dopant site location and profiles, channelling studies 4-103893  
 Si:Xe, implanted Xe reemission by He<sup>+</sup> ion bombardment 4-75462  
 Si/Ag system, atomic mixing using 45 keV Ar<sup>+</sup> ion beam 4-80119  
 Si/PtSi<sub>3</sub>, ion beam mixing and amorphous Pt<sub>2</sub>Si<sub>3</sub> form. 4-108750  
 Si/SiO<sub>2</sub>/Si<sub>3</sub>N<sub>4</sub>, N and O distrib. profiles, Auger studies (Russian) 4-65578  
 Si/SiO<sub>2</sub>/Si<sub>3</sub>N<sub>4</sub>/Al capacitors, ion/atom beam milling, damage effects 4-70941  
 SiC, fusion reactor first wall material, radiation erosion 4-80120  
 SiC, ion implantation, ion beam mixing, and annealing of metal contacts 4-70229  
 Si<sub>3</sub>N<sub>4</sub>, Ar<sup>+</sup> ion bombarded, electron irradiation effect on surface composition 4-80109  
 Si<sub>3</sub>N<sub>4</sub>, ion implantation, ion beam mixing, and annealing of metal contacts 4-70229  
 SiO<sub>2</sub>, charge neutralisation by electron bombardment 4-98694  
 SiO<sub>2</sub>, fused, subsurface Al films, ion beam mixing 4-88189  
 SiO<sub>2</sub>, radial energy distrib. around ionising particle tracks 4-108487  
 SiO<sub>2</sub>N<sub>2</sub>, Ar<sup>+</sup> ion bombarded, electron irradiation effect on surface composition 4-80109  
 Ta film, first wall in ICF chamber, chem. reactions with pellet debris 4-107057  
 Ta, L-shell X-ray prod. cross sections, H<sup>+</sup> induced, ratios 4-66131  
 Ta-C system, He bombardment, sputtering, TRIDYN TRIM simulation 4-80076  
 Ta<sub>2</sub>O<sub>5</sub> targets, transmitted MeV <sup>4</sup>He ions, multiple scatt. angular distribution 4-92269  
 Te, L-shell X-ray prod. cross sections, H<sup>+</sup> induced, ratios 4-66131  
 Te, sputtering by He<sup>+</sup> and Li<sup>+</sup> ions 4-71500  
 Ti, proton irradi., positron annihilation study (Russian) 4-85033  
 Ti/Ni bilayered thin films, amorphisation and ion beam mixing 4-88400  
 Ti-Au, amorphisation, pulsed ion beam annealing study 4-103831  
 Ti-Sn, proton irradi., positron annihilation study (Russian) 4-85033  
 TiC-graphite, thermal cycling tests, surface damage study 4-111756  
 TiNi-based alloy, radiation-induced amorphisation 4-103830  
 TiO<sub>2</sub> (110), surface defects, XPS, X-ray induced AES, EELS studies 4-80351  
 V, T charged, <sup>3</sup>He bubble formation, TEM obs. 4-103825  
 VO<sub>2</sub> films, ion irradi. and thermal annealing 4-70244  
 W, L-shell X-ray prod. cross sections, H<sup>+</sup> induced, ratios 4-66131  
 W, low energy heavy ion bombardment, self-interstitial generation 4-80117  
 W, molecular ion collision cascades, spatial configurations, computer simulation studies 4-75557  
 W, range distrib. of Xe ions, expt. and computer simulation studies 4-92256  
 Xe, lateral multiple scatt. of 15-60 keV ions 4-92266  
 Zr-D, ion implantation, lattice defect trapping, binding enthalpy, migration 4-108400
- ion beam lithography**  
 film preparation and etching, vacuum or plasma technology, conf., Brighton, UK (March, 1983) 4-78031  
 high-brightness duoplasmatron ion source for ion beam lithography 4-73587  
 liquid metal ion sources for microscopy and lithography 4-78416  
 masking film deposition by ion induced polymerisation 4-75566  
 nuclear track technique using heavy ion beams, potential appls. 4-59607  
 reactive ion beam etching, for semiconductor production, review 4-8132  
 SAW devices, Ar and reactive ion beam etching 4-81318  
 Si, ion etching, effect of ion species on bombardment induced topography 4-81320
- ion beams**  
 see also beam-foil spectra; beam-foil spectroscopy; energy loss particles; ion beam effects; ion optics; ion-surface impact; mass spectrometers; particle accelerators; sputtering  
<sup>23</sup>Na beam prod., cold cathode PIG source for use with cyclotron 4-74072  
 A=2-17, neg. ion beam form. by charge transfer in metal vapour 4-107197  
 acceleration by multiple electrostatic quadrupole array linear accelerator 4-107179  
 acceleration column, laminar flow quadrupole-focused, design 4-107212  
 air flowmeter based on constant deflection of ions 4-87824  
 alkali closed shell ions, repulsive interactions with Ar, Kr and Xe, beam transport meas. comparison 4-96653  
 annular magnetically insulated ion diode operated in long pulse mode, diode, mechanism study 4-112016  
 applications of ion beam technology 4-76887  
 atoms, highly ionised, lifetime meas. using fast ion beam excitation method, review 4-80709  
 B<sub>2</sub> diode floating anode experiments at Sandia National Labs 4-60756

- beams continued
- beam cross-section tilt angle monitoring 4-92223
- bunch propagation in neutral medium, compensating electron effect 4-74411
- charged particles, RF bunching technique 4-73581
- collective ion acceleration using slow space charge waves 4-60754
- conference, polarised proton ion sources, Vancouver, BC, Canada (May 1983) 4-106092
- current amplification in ion beam, numerical soln. (*Russian*) 4-83538
- deuteron beams prod. in plasma focus 4-68856
- diode research overview 4-112009
- extraction electrode opening effect 4-82861
- fast ion beam velocity meas., Doppler-shift technique 4-86988
- halogen closed shell ions, repulsive interactions with Ar, Kr and Xe, beam and transport meas. comparison 4-96653
- heavy-ion beams for biomedical studies, online characterisation with semiconductor detectors 4-85501
- hollow cathode ion source, beam emittance determ. 4-60649
- identification by their masses, in multichannel energy analysers 4-87929
- intense ion beam, high brightness point-like source 4-112014
- intense pulsed ion beams for fusion reactors, generation and transportation (*Japanese*) 4-74078
- light ion beam prod. by applied Br magnetically insulated annular diode for ICF appl. 4-112013
- light ion beams, rot. and propag., stabilisation by self-induced mag. field 4-101967
- linac, effect of drift spaces on longitudinal motion 4-91128
- low energy continuous ion beams, parameter meas. technique 4-73596
- magnetic insulation time for coaxial diodes 4-73580
- magnetically insulated intense ion beam diodes, studies of conditions 4-112010
- microchannel plate gain characts., reflection mode 4-78423
- MID with cryogenic anode, performance tests 4-112017
- negative fraction of  $^2\text{H}$  and  $^3\text{He}$  scattered from Na surface 4-107194
- negative ion beam sources for field-reversed fusion devices 4-107223
- negative ion clusters, collimated beam from plasma focus source 4-107210
- negative ion neutralisation by plasma targets 4-107217
- neutral beam injector system for MARS tandem mirror reactor 4-107221
- neutral beam line of neg. ions stripped in photoneutraliser 4-107216
- neutral beam system, negative-ion based, design considerations 4-107220
- neutral beam systems, negative-ion-based, tokamak and mirror confinement device requirements 4-107219
- neutralisation of intense ion beam in vacuum, theory 4-74410
- nonlinear theory of the instability of an electron-ion two-beam system 4-87266
- photodetachment neutraliser with laser resonator technology 4-107218
- pinching electron-ion beam, quasi-equilib. states 4-69941
- polarised ion source, atomic beam, optimisation method 4-107238
- polarised ion sources, spin exchange optical pumping 4-107243
- polarised ion sources at RCNP status and performance 4-107237
- polarised neg. ion beam production by collisional pumping 4-107231
- precise high-intensity atomic and ionic beam production 4-73579
- production and neutralisation of negative ions and beams, conf. Brookhaven, NY, USA (Nov. 1983) 4-73134
- self-magnetically B<sub>0</sub>-insulated ion diode performance study 4-112015
- SITEX neg. ion source, short-pulse D<sup>-</sup> operation 4-107200
- SNOW ion beam extraction simulation program, computers for design and testing 4-73590
- sputter-type negative ion source, emittance calc. and meas. 4-64256
- strip and axisymmetrical ion beams, mutual transformation (*Chinese*) 4-74081
- thick gas targets, proton small angle multiple scatt. 4-107431
- transmission by equipotential electrostatic lens (*Czech*) 4-83262
- C<sup>2+</sup> intense ion beam diode, anode heating with CO<sub>2</sub> laser 4-112011
- Cs vapour, plasma channels for ion beam transport initiated by XeCl laser 4-103533
- D<sup>-</sup> Lamb-shift polarised ion sources 4-107239
- D<sup>-</sup> ribbon beams, focusing by transverse electric fields 4-107211
- D<sup>+</sup> polarised ion source, ECR technique 4-107242
- H<sup>-</sup> phase volume meas., multichannel A/D interface for Elektronika-1001 computer 4-91130
- H<sup>-</sup> beam line, IKVT-KFK research 4-73567
- H<sup>-</sup> beams, high brightness, production in surface-plasma sources 4-107202
- H<sup>-</sup> density in a tandem multicusp discharge 4-73568
- H<sup>-</sup> extraction and acceleration from mag. multipole source 4-107206
- H<sup>-</sup> generation of intense flux 4-69925
- H<sup>-</sup> injector for radio-frequency quadrupole accelerator 4-107188
- H<sup>-</sup> intense beam production by Penning surface-plasma source with circular emitter 4-107209
- H<sup>-</sup> Lamb shift polarised ion source, intensity limitations 4-107241
- H<sup>-</sup> Lamb-shift polarised ion sources 4-107239
- H<sup>-</sup> multiampere source, extrapolation of double-electron-capture source 4-107207
- H<sup>-</sup> multicusp ion source, development for accelerator appl. 4-107204
- H<sup>-</sup> multicusp source for KEK proton synchrotron injector 4-107213
- H<sup>-</sup> polarised, production by laser optical pumping 4-107226
- H<sup>-</sup> polarised intense beams, production by double charge exchange in alkali vapours 4-107227
- H<sup>-</sup> polarised ion source, charge transfer processes 4-107246
- H<sup>-</sup> polarised ion source, status at AGS 4-107235
- H<sup>-</sup> polarised ion source at Munich 4-107240
- H<sup>-</sup> polarised ion source at KEK, optically pumped 4-107244
- H<sup>-</sup> polarised ions, production methods from ground-state polarised atoms 4-107230
- H<sup>-</sup> production by plasma-surface interaction 4-107191
- H<sup>-</sup> production from polycryst. and monocryst. W and Mo surfaces 4-107192
- H<sup>-</sup> production from various metallic converter surfaces 4-107193
- H<sup>-</sup> pulsed multiampere surface-plasma source 4-107201
- H<sup>-</sup> spontaneous emission by surface chemi-ionisation on W(110) 4-107195
- H<sup>-</sup> surface production in plasma, work function depend. 4-107190
- H<sup>-</sup> volume produced, extraction from multicusp plasma generator 4-107205
- H<sup>+</sup>, atomic beam source for ion production 4-107234
- In ion beam generation by selective multistage laser photoionisation of atoms 4-74207
- Li<sup>+</sup> volume production by dissociative attachment 4-107196
- ion beams continued
- <sup>15</sup>N beam accelerating facility using 7 MV Van de Graaff, H depth profiling 4-64249
- <sup>20</sup>Ne ion beam, depth dose relations in water 4-109935
- PbO-containing glass, XPS study of angular dependence of preferential sputtering 4-88926
- Si, etching using Ar-ion assisted Cl<sub>2</sub> 4-85054
- ion chambers see ionisation chambers
- ion counters see counters
- ion cyclotron resonance heating see plasma heating
- ion cyclotron resonance spectra see mass spectra
- ion cyclotron resonance spectroscopy see mass spectroscopy
- ion density
- see also plasma density
- EBT, birth of new folds and competing point attractors 4-65122
- fusion plasmas, inertially confined, ion density correlations, thermonuclear reaction rate 4-91974
- hollow cathode ion source, plasma investig. (*German*) 4-84102
- low pressure plasma, probe characts. plotting and electron vel. distrib. measuring equipment (*German*) 4-84060
- mid-latitude ionospheric trough and ion densities, electron precipitation and 630 nm emission 4-100845
- plasma thermal barriers, ion trapping rate 4-65120
- plasma with negative ions, ion wave modulational instability 4-97778
- ion emission
- see also field ion emission; secondary ion emission; thermionic ion emission
- charged particle emission in failure of solids 4-99291
- charged particle emission in failure of solids 4-99292
- cyclotrimethylenetrinitramine (RDX) explosive single crystals, fractoemission 4-81120
- photon stimulated desorption, surface characterization, instrumentation 4-90703
- polybutadiene, fracto-emission, effect of cross-linking 4-66419
- polymers, fracture and emission of electrons, ions and photons 4-98189
- styrene-butadiene copolymer, fracto-emission, effect of cross-linking 4-66419
- sucrose, fracture, electron and positive ion emission, triboluminescence 4-104686
- sucrose, fracture and emission of electrons, ions and photons 4-98189
- Wint-o-green Lifesavers, fracture, electron and positive ion emission, triboluminescence 4-104686
- SiO<sub>2</sub>, fracture and emission of electrons, ions and photons 4-98189
- ion engines
- see also aerospace propulsion; rockets
- discharge plasma in an inert gas ion thruster (*Japanese*) 4-103589
- ion etching see sputter etching
- ion exchange
- benzoic acid, H<sup>+</sup> transfer 4-93510
- bipolar ion-exchange membranes, electrolytic dissoc. of water 4-62211
- carboxylic acids, H-bond double-well barrier and H<sup>+</sup> exchange 4-93508
- carboxylic acids, solid, H<sup>+</sup> dynamic 4-93509
- cyanocetylene, H<sup>+</sup> affinity, selected ion flow tube study 4-71881
- electrodeposited Zn and Cd coatings, automatic regeneration by ion exchange (*German*) 4-104970
- formamide+glyoxals charge transfer, ab initio calcs., appl. electronic theory of cancer 4-87205
- free radicals in ion-exchange materials, spin-lattice relax. via excited vibr. states 4-59815
- glass waveguides, single mode, fabrication by electrolytic Ag<sup>+</sup> ion exchange process 4-91580
- high-dose radiation dosimeter appls. 4-74119
- inorganic materials, selective action, simulation of solvation interactions 4-62185
- integrated optical strip waveguides, single-mode, Na<sup>+</sup>-K<sup>+</sup> ion exchange (*Chinese*) 4-112591
- lysozyme solns., nucl. mag. relax. dispersion, H<sup>+</sup> exchange coupling 4-102707
- membranes, valency-induced counterion selectivity, conc. polarisation effect 4-71975
- metal-ion exchange layer structures, EXAFS studies 4-62196
- micellar aqueous soln., aromatic hydrocarbon fluoresc. quenching by counterions, ion exchange relationship 4-62248
- optical waveguide, planar, by ion exchange on glass substrates 4-79288
- pH-metering control in unit-type water preparation plants for thermal power stations 4-93583
- phenolsulphonic acid ion exchange membrane, Donnan conc., self-diffusion coeff. and mobility of SO<sub>4</sub><sup>2-</sup> co-ion 4-81457
- photosensitive glass, discontinuous/continuous metal films growth by ion exchange 4-87404
- polyglycine and its model systems, hydrogen bonds theoretical study 4-59931
- raw water treatment-using stratified-bed cation-exchange filter systems 4-71915
- redox-flow battery, voltage drop and elec. resist. for ion exchange membranes 4-109681
- single-mode optical Y junctions, formed by Ag ion exchange in glass, radiation losses 4-60181
- soda-lime silicate glass, stress relax. and ion exchange 4-108284
- solid state chemistry, struct. aspects 4-70062
- sorbents for radiiodide based on finely divided Ag in porous materials 4-77023
- volume reduction system, ion exchange resin, nuclear reactors 4-106750
- water solution, PIXE anal. using ion exchange filter 4-99857
- C fibres, electrodeposition of metals after cation-exchange, catalysts appl. 4-76701
- C<sub>2</sub>N<sub>2</sub>, H<sup>+</sup> affinity, selected ion flow tube study 4-71881
- K<sup>+</sup>, directional-coupler powder divider by two-step K<sup>+</sup> ion exchange 4-107822
- LiNbO<sub>3</sub> and LiTaO<sub>3</sub>, waveguide fabrication by proton diffusion from benzoic acid soln. 4-69553
- Li<sub>2</sub>O-Al<sub>2</sub>O<sub>3</sub>-SiO<sub>2</sub>, structural features, for gradient optical elements 4-79947
- NaNbO<sub>3</sub>, ilmenite-type allotropic, proton exchange 4-70092
- Na<sub>2</sub>O-Al<sub>2</sub>O<sub>3</sub>-SiO<sub>2</sub>, structural features, for gradient optical elements 4-79947
- <sup>96</sup>TcO<sub>4</sub><sup>-</sup>, carrier-free, prep. method 4-77385

ion exchanging *see* ion exchange

ion excited X-ray emission *see* ion microprobe analysis

## ion implantation

*see also semiconductor doping*  
 400 keV Research Implanters at Surrey Univ. 4-73583  
 alkali silicate glasses, ion bombard., alkali depletion, ion beam mixing 4-70239  
 alkali silicate glasses, ion irradiat., glass comp. modification by alkali ion migration 4-70238  
 alloys, ternary, ion implantation prep., surface binding energy 4-79972  
 applications of ion beam technology 4-76887  
 applied surface anal., conf., Dayton, USA (June 1983) 4-95016  
 beam cross-section tilt angle monitoring 4-92223  
 beam purity and mass spectroscopy 4-99864  
 beam scanning systems comparison 4-73593  
 benzene, frozen, ion implantation, polymer films production 4-65281  
 bubble garnet implantation, review 4-80064  
 damage profile in crystals, meas. by channelling technique 4-103840  
 damaged layer formation and growth, three-dimensional Monte Carlo simulation 4-75565  
 diffusion studies, implantation as tool to introduce tracer 4-65432  
 dopant implantation distribution technique 4-75473  
 dose control, annealing and gettering 4-84309  
 dosimetry and beam quality 4-73595  
 electron-beam-induced recoil implantation in semiconductors at 300K 4-75475  
 electrostatic switch used for 600 kV ion implanter 4-73594  
 equipment and techniques, conf., Berchtesgaden, Germany (Sept. 1982) 4-73155  
 GaAs fast supercomputer circuits (*Swedish*) 4-65282  
 garnet films, ion implanted, induced mag. anisotropy 4-76205  
 garnet ion implanted film, strain distrib. (*Japanese*) 4-108753  
 garnet multilayer bubble films, domain wall dynamics and interface pinning 4-92946  
 glass, ion implanted; SAW propagation velocity 4-113776  
 graphite:Fe, ion implanted, mag. props. 4-61562  
 graphite,  $D_2^+$  trapping and reflection coeffs. at oblique incidence 4-61793  
 graphite, ion damaged, annealed, 2-D ordering, Raman study 4-70535  
 implanted samples, applicability of van der Pauw-Hall meas. technique 4-88521  
 inorganic insulators, cryst., heavy ion bombard., struct. changes and chem. effects 4-75549  
 ion implanter, 200 keV (*Chinese*) 4-95558  
 IV-VI semiconductors, ion implantation, review 4-92220  
 materials processing, book 4-73184  
 membranes fabrication for ISFETs 4-95402  
 metals, implanted  $N_2^+$  mol. ion range, nuclear reaction anal. 4-92250  
 metals, light ion implantation, amorphisation, statistical aspect 4-80114  
 metals, oxidation, metal oxide thin films influence 4-81358  
 metals, wear reduction and analysis, surface modification by ion beams 4-81290  
 metals modification, ion beam anal. appl. 4-76914  
 mica, muscovite, ion implanted, defect struct. thermal annealing 4-70177  
 mica, muscovite, nuclear track detector, ion stimulated desorption 4-68900  
 molecular ion implantation in monocrystals, ion channeling prevention 4-65283  
 multicomponent targets, sputtering, implanted ion range and profiles, TRIDYN TRIM 4-80076  
 multipole ion source for ion implantation and isotope separation 4-73591  
 Mylar, crit. dose of blistering during ion implantation, in situ obs. 4-75548  
 optical aspheric surface generation methods 4-87489  
 optical devices, effects of ion implantation on props. 4-80067  
 optoelectronic materials fabrication using MBE and ion implantation 4-109325  
 PET films, ion implantation with F ions, elec. cond. 4-92717  
 physical limitation on implantation equipment 4-75471  
 PMMA:Si ion implanted film, struct. anal. using differential etching 4-79951  
 polyacetylene films, ion implantation doping and p-n junction form. 4-113471  
 polymers, ion implantation effects 4-75547  
 powders, high temp. implantation by horizontal ion beam 4-75472  
 radio frequency ion accelerator for ion implantation studies 4-73584  
 radioactive waste materials, ion implantation effects on dissolution props., simulation of internal irradiat. due to  $\alpha$ -decay 4-75544  
 rotating attenuator for concentration profiling of implanted helium ions 4-75477  
 semiconductor, sputtered ions during ion implantation, SIMS system anal. 4-111244  
 semiconductor doping processes, two-dimensional numerical anal., appl. to MOS processing 4-75470  
 semiconductor implantation source 4-73592  
 semiconductors, amorphisation by ion implantation, modification to defect accumulation models 4-88210  
 SIMOX films, Hall mobility and electrical conductivity, temp. dependence 4-80700  
 single slit multipole ion sources for ion implantation 4-86992  
 SNOW ion beam extraction simulation program, computers for design and testing 4-73590  
 soft X-ray laser investigations using ion-implanted target 4-97819  
 solar cell fabrication using new ion implanter 4-77114  
 SOS films, material improvement, process by solid phase epitaxial growth 4-81124  
 SOS heteroepitaxial film, surface photovoltage characterisation 4-80697  
 sputtered ions during ion implantation, SIMS system anal. 4-111244  
 sputtering by particle bombardment, book 4-95080  
 SQUID magnetometer combined with ion implantation 4-58877  
 steady-state, migration current and implant densities 4-75469  
 steel, austenitic stainless, cavity formation during electron irradiat., effect of pre-implanted He 4-108444  
 steel, high C and stainless, intermetallic phases formed by Sn ion implantation 4-92225  
 steel, ion-nitrided structure, electron microscopic studies (*Bulgarian*) 4-81354  
 steel, low C, corrosion, effect of P ion implantation 4-9637  
 steel, nitriding, ion implantation and conventional processes 4-76918

## ion implantation continued

steel, stainless, N ion implanted, lattice location, nuclear reaction, channelling and RBS studies 4-75463  
 steel, stainless and bearing, surface analysis, ion implantation and tribological processes 4-99607  
 steel, Ti ion implanted, corrosion resist. of amorphous Fe-Ti-C surface 4-76917  
 stratified media technology, conf., Los Angeles, CA, USA (Jan. 1984) 4-82585  
 superconducting transition temperature, implanted ions influence (*Chinese*) 4-92838  
 surface treatment to reduce tool bit wear 4-76915  
 SURIM, Westinghouse surface ion implantation machine 4-73582  
 target heating control methods 4-75480  
 techniques and equipment for implantation into metals 4-75479  
 thin film deposition, ion-surface interactions 4-80437  
 thin film optics, appl. of ion implantation 4-74757  
 Van de Graaff vacuum system improvement for clean ion implantation 4-74063  
 VLSI technology, textbook 4-82610  
 wafer cooling and photoresist masking problems in ion implantation 4-75474  
 wafer cooling in ion implantation 4-75476  
 Si, ion implantation and laser annealing (*Japanese*) 4-108404  
 Ag, radiation damage, O decoration and  $^{111}\text{In}$  TDPAC studies 4-75555  
 Ag wear behaviour, ion mixing effects 4-76877  
 Al superconducting thin film, N ion implanted, critical temp. 4-61483  
 AlSb, ion implanted, hardness, friction and wear props. 4-66451  
 Al-Cu, ion implanted, disorder studied by ion channelling and Rutherford backscattering 4-98145  
 Al-Mo alloys, ion implanted, corrosion resist., AES studies 4-99626  
 Al-Si-Ge,  $\text{Si}^{+}$  ion implantation effects on supercond. temp. (*Chinese*) 4-76062  
 $\text{Al}_x\text{Ga}_{1-x}\text{As}$ :Be, radiative recombinations 4-76515  
 $\text{Al}_2\text{O}_3$ , ion implantation, ion beam mixing, and annealing of metal 4-70229  
 $\text{Al}_2\text{O}_3$ , synthesis by  $\text{O}_2^+$  ion implantation into Al 4-70174  
 Au film, deposited on Si, dynamic recoil mixing, parameter optimisation 4-70180  
 Au, implanted  $^3\text{He}$  depth profiles,  $^4\text{He}$  post-bombardment effects 4-80073  
 Be-D, retention and thermal release of implanted D 4-113477  
 Be-Hf-O,  $\text{H}^+$  implanted, O gettering 4-92218  
 C foil, implanted with T, prep. and analysis w.r.t. fusion reactor safety 4-91100  
 $\text{CdIn}_2\text{S}_4$  single cryst., photocond., photoluminescence and non-equilibrium carrier recombination 4-65706  
 Co-Cr-Al(-Y),  $\text{Si}^{+}$  implanted, 1050°C oxidation behaviour 4-62124  
 Cu, ion implantation of Au and Ta at non-normal incidence, sputter yields 4-76619  
 Cu, low energy N atom implantation, profiles, ranges and straggles 4-80062  
 Fe and alloys, N implanted, SIMS, Auger and nucl. reaction analysis 4-88185  
 Fe, intermetallic phases formed by Sn ion implantation 4-92225  
 Fe, of Al, use in reduction of T permeation 4-88184  
 Fe, pure, carbonitride precipitation by successive ion implantation and N, XPS and Mossbauer obs. 4-76906  
 Fe-Al (40 at.%), ion implantation, phase changes, TEM studies 4-108753  
 Fe-Cr-Ni (15, 15 wt.%), He bubble form. during dual beam irradiation 4-75562  
 Fe-Ti alloys, ion implanted,  $\text{C}^+$  implantation effects on surface morphology 4-114707  
 $\text{Fe}_{0.9}\text{Ni}_{0.1}\text{B}_{18}\text{Mo}_{80}$ , Metglas 2826 MB 5 keV He implantation, bubble growth, free vol. relax. model 4-103822  
 ( $\text{Fe}_{0.9}\text{Ni}_{0.1}\text{B}_{18}\text{Mo}_{80}$ ) $\text{V}$ , ordered alloys, microstruct. and creep rel. to implantation 4-108399  
 GaAs, compensation resulting from N ion implantation 4-104150  
 GaAs flash annealing of Mg implants using incoherent radiation 4-84316  
 GaAs, H ion implanted, range and damage distrib. 4-103774  
 GaAs, implanted layers, elec. props.,  $\text{Si}_3\text{N}_4$  encapsulation effects 4-98145  
 GaAs, ion implanted, diffusion of Be and Mn during damage recovery 4-104002  
 GaAs, ion implanted, photolum. after laser annealing 4-76525  
 GaAs, ion implanted, transient capless annealing appl. to IC fabrication 4-103779  
 GaAs, semi-insulating, elec. props. for microwave electronics 4-10884  
 GaAs:Be, ion implanted, reduced damage generation 4-113474  
 GaAs:Be, ion implanted, annealing behaviour, spectroscopic ellipsometry and Raman scatt. 4-113482  
 GaAs:Cr, ion implanted, Cr redistribution 4-88194  
 GaAs:S(Si), implant sublattice site determ., PIXE studies 4-98119  
 GaAs:Se $^{+}$ , implanted, amorphous-cryst. interface, high resolution spectroscopy 4-70171  
 GaAs:Si, implanted, radiation annealing with CW Xe arc lamp 4-75470  
 GaAs:Si, ion implanted, and semi-insulating GaAs, deep levels, photoconductivity study 4-88469  
 GaAs:Si, planar channelling of Si implants 4-75483  
 GaAs:Sn,Te, dual implanted damage and annealing, challenging studies 4-80116  
 GaAs:V, semi-insulating, V redistribution during heat treatment 4-80116  
 GaAs/GaAlAs DH stripe geometry lasers, Be-implanted, MOCVD grown 4-107635  
 GaAs, $\text{P}_{1-x}\text{N}_x$ /GaP strained-layer superlattices, Be-implantation dose 4-80057  
 $\text{Ga}_{0.4}\text{In}_{0.53}\text{As}$ , ion implanted, annealing, TEM obs. 4-70228  
 GaInAsP, ion implantation, book contrib. 4-60943  
 Ge, book, deposition, growth and technology 4-58579  
 Ge, submicron layers produced by ion implantation and laser annealing 4-84316  
 Ge:Al, implanted ion projected range distrib. 4-80079  
 Ge:He, ion irradiat., structural defect study 4-88164  
 Ge:Te, ion implanted, amorphisation phenomena, electron microscope studies, electron diff. studies 4-103656  
 HgCdTe and CdTe, ion implanted with  $^1\text{H}$ ,  $^2\text{H}$ ,  $^4\text{He}$ , depth distribution, SIMS study 4-88182  
 (In,Ga)As:Be/InP n-p-n heterojunction bipolar transistors grown by metalorganic chemical vapour deposition with high gain 4-85097  
 $\text{In}_2\text{Ga}_{0.9}\text{As}$ /GaAs strained-layer superlattice, ion implanted, structural analysis 4-113821

## implantation continued

- nGaAsP/InP DH stripe lasers fabricated by O<sup>+</sup> ion implantation 4-96906  
 p, ion implanted, elec. activation by CW laser annealing 4-80088  
 p,He, ion implanted, elec. cond. study 4-80586  
 p,Mg(Fe,Mg), implanted, effect on photoluminescence props. 4-85007  
 p,Se, ion implanted, annealing and transport props. 4-108397  
 p,Si MISFETs, post-implantation capless annealing 4-113472  
 p-Si:p-InP homojunction, implanted, photoelec. props., minority carrier diffusion length 4-76034  
 p/InGaAsP stripe geometry lasers, design and fabrication using D<sup>+</sup> bombardment 4-83622  
 nSb, ion implanted layers, IR reflection spectra studies 4-61717  
 nSb, ion implanted single cryst., damage study by characteristic X-ray emission 4-88214  
 nSb:Be p<sup>+</sup>-n junction, ion implanted, insulated gate effects 4-61445  
 n-Sb:Si, p-n junctions, doping and elec. props. 4-70919  
 p,Na<sup>+</sup>(Rb<sup>+</sup>), annealed and reimplanted, atomic mixing processes 4-70231  
 nNbO<sub>3</sub> integrated optical waveguides, fabrication using ion implantation 4-79347  
 nNbO<sub>3</sub> planar ion implanted optical waveguides, computer simulation 4-69547  
 MgO:Na<sup>+</sup>(Rb<sup>+</sup>), annealed and reimplanted, atomic mixing processes 4-70231  
 Mo, pure, electron and He ion irradi., vacancy loop form. 4-108480  
 MoO films, reactively sputtered, for MOS gate appl., ion implantation stopping props. 4-61850  
 Mo-Co dilute alloy, Co impurity location, PIXE and ion channelling studies 4-80072  
 Mo-N ion implanted single cryst., computer simulation anal. 4-108402  
 Na<sub>2</sub>O-CaO glass, antireflection effects induced by Ar<sup>+</sup> implantation 4-60125  
 Na<sub>2</sub>O-CaO-SiO<sub>2</sub> glasses, ion implanted, mech. props. 4-75542  
 Na<sub>2</sub>O-SiO<sub>2</sub> glass, ion implanted impurities, range and spatial distrib. 4-108287  
 Nb, implanted <sup>3</sup>He depth profiles, <sup>4</sup>He post-bombardment effects 4-80073  
 Nb-N, ion implanted, N diffusion, ion beam studies 4-70431  
 Nb<sub>2</sub>Ge:Mg<sup>+</sup>, supercond. film, implantation effect on resistance anomaly (Chinese) 4-92872  
 Ni, ion implanted D trapping by vacancies, channelling studies 4-108409  
 Ni, laser irradiation, defect struct. and surface alloys 4-75509  
 Ni:He, preimplanted, electron irradi., 1 MeV, He bubble growth 4-103803  
 Ni-La single crystals; implanted, pulsed laser treatment studied by the <sup>4</sup>He<sup>+</sup> channelling 4-84315  
 (Pb,Sn)Te-Pb(Te,Se) DH laser diodes, ion-implantation confined shallow mesa stripe, single mode tuning 4-112459  
 Pd-Fe, ion implanted, ferromagnetism study 4-71137  
 Pd-Ni-Si-Be-B liquid metal, ion source for maskless ion implantation 4-58913  
 Pd-Si film, ion implanted, amorphisation, channelling anal. 4-92247  
 Pd<sub>2</sub>Si<sub>2</sub>, amorphous, prep. by ion implantation, proton irradi. damage, elec. resist. meas. 4-103833  
 Si (001) wafers, thermally oxidised, P<sub>i</sub> interface centres, ESR study, effect of As<sup>+</sup> ion implantation 4-92960  
 Si, amorphous, from ion implantation, refractive index, thermal annealing effect 4-76417  
 Si, amorphous, ion implanted, crystn. growth velocities, charged dangling bonds 4-88093  
 Si, book, deposition, growth and technology 4-58579  
 Si, damage profiles, comparison of angle lapping/staining and cross-sectional TEM 4-103775  
 Si, disorder profiles at high sputtering dose by oxide growth rate profiling 4-66470  
 Si EFG ribbon solar cells, ion implantation and pulsed electron beam annealing fabrication 4-62364  
 Si, electron beam annealing, pulsed, thermal model 4-60963  
 Si, electron structure change during amorphisation, electrorefl. spectra (Russian) 4-98509  
 Si film, ion implanted, electron beam recrystallisation 4-98137  
 Si film, polycryst., ion implanted, dopant diffusion (Russian) 4-108657  
 Si, implantation doped, elec. and struct. characterisation by IR refl. 4-76476  
 Si, implanted O profiles, model 4-80065  
 Si, implanted oxides, annealing, activation energy 4-75490  
 a-Si, inert gas implantation and sputtering yield enhancement 4-76600  
 a-Si, ion implantation form. and optical state characterisation 4-88186  
 Si, ion implantation synthesis of SiO<sub>2</sub> 4-70175  
 Si, ion implanted, amorphous surface layer recrystallisation by epitaxial annealing, effect of foreign atoms 4-71553  
 Si, ion implanted, beam annealing 4-75510  
 Si, ion implanted, CO<sub>2</sub> laser annealing, relax. characts. of metastable concentrations 4-75512  
 Si, ion implanted, characterisation by Rutherford backscatt. spectrometry and ellipsometry 4-85043  
 a-Si, ion implanted, etching in HF soln. and annealing effects 4-80063  
 Si, ion implanted, explosive liq. phase crystallisation by double pulse laser irradi. 4-84188  
 Si, ion implanted, halogen lamp rapid annealing, p-n junction formation 4-88195  
 Si, ion implanted, pulse-laser-induced epitaxial regrowth 4-75511  
 Si, ion implanted, pulsed laser and thermal processing, defect anal. 4-70133  
 Si, ion implanted, pyrometric temp. meas. during laser annealing 4-70203  
 Si, ion implanted, rapid thermal arc lamp and pulsed laser annealing, photoluminesc. study 4-93094  
 Si ion implanted film, photogacoustic response study 4-84955  
 n-Si, ion implanted with He<sup>+</sup>, deep donor levels 4-61323  
 Si, ion implanted with noble gases, optical defects, photoluminesc. study 4-71429  
 Si, ion-implanted, pulsed laser annealing, transient reflectivity studies 4-80086  
 Si, ion-implanted, pulsed laser annealing, reflectivity studies 4-80087  
 Si, low energy implantation of N<sub>2</sub> and NH<sub>3</sub>, Si<sub>3</sub>N<sub>4</sub> formations 4-75484  
 Si, low Z shielding materials, implanted H effects at high conc. 4-111760  
 Si MOS struct., implantation-induced defects, RF annealing using H plasma 4-84308

## ion implantation continued

- Si multiply implanted targets, range distrib., Rutherford scatt. studies 4-92268  
 Si, negative secondary ion emission, influence of alkali metal implantation 4-104710  
 Si on insulator form. by O ion implantation 4-80061  
 Si, oxidation induced stacking faults, dislocations, effects of Cl<sup>+</sup> and F<sup>+</sup> implantation, X-ray topography 4-80053  
 Si p<sup>+</sup>-n-n<sup>+</sup> solar cells, all-implanted, characts. 4-62355  
 Si, passivated ion-implanted X-ray detectors performance and appl. 4-59564  
 Si, photocurrent carrier lifetime study during ion implantation 4-75984  
 Si photovoltaic devices, P implanted, Ar ion implantation gettering influence on props. 4-66703  
 Si, polycrystalline, implantation under thermal and laser annealing, sheet resist. and doping profiles 4-75487  
 Si, polycrystalline films amorphised by ion implantation, solid phase epitaxial growth 4-108731  
 Si processing for device fabrication, ion implantation appl. 4-75481  
 Si, recrystallized on SiO<sub>2</sub>, laterally seeded, implantation and annealing studies 4-98121  
 Si, shallow npn bipolar transistors fabrication by triple ion implantation 4-75460  
 Si solar cell, ion implanted, laser annealed 4-72121  
 Si solar cell fabrication by ion implantation and thermal annealing 4-77089  
 Si solar cell junction profiles in ion-implanted texture-etched surfaces 4-93620  
 Si solar cells, ion implantation and pulsing annealing processes 4-81563  
 Si solar cells, low-dose ion implanted, optimum flashlamp annealing conditions for fabrication 4-85368  
 Si solar cells, P ion implantation emitter tailoring and annealing 4-62366  
 Si substrate, ion implanted and processed, interface characterisation 4-84304  
 p-Si surface, <sup>14</sup>N<sub>2</sub><sup>+</sup> (H<sub>2</sub><sup>+</sup>) bombardment, Raman scatt. obs. 4-114283  
 Si surface, D<sub>2</sub><sup>+</sup> bombarded, Raman spectrum investig. 4-114284  
 Si, thick isolated layers, growth, characterisation and MOSFET props. 4-99309  
 Si wafer, implantation quality monitoring by amorphisation contrast 4-75478  
 Si:<sup>31</sup>P<sup>+</sup>, implanted, optical refl. changes as function of implantation energy 4-71330  
 Si:Ar, carrier lifetime reduction by Ar ion implantation 4-80604  
 Si:Ar Schottky barrier, ion implantation effects on elec. characts. 4-114014  
 Si:As, high current density implantation, dynamic self-annealing mechanism 4-65280  
 Si:As, high dose ion implanted, As clustering, TEM and SIMS studies 4-70384  
 Si:As, implanted (111), twin formation, effect of heating rate and annealing temp. 4-103765  
 Si:As, implanted under channelling conditions, impurity spatial distrib., localisation, defect form. characts. 4-84321  
 Si:As, ion implantation doses, ellipsometry and spectral reflectance meas. 4-113480  
 Si:As, ion implanted, carrier density profiles, elec. meas., annealing behaviour 4-70179  
 Si:As, ion implanted, IR radiation annealing of extended defects 4-92228  
 Si:As, ion implanted and laser annealed, struct. changes, X-ray diffr. study 4-75461  
 Si:As, ion implanted channelling Rutherford back-scatt. study (Chinese) 4-84324  
 Si:As, ion implanted regions, 2-D shape, etching and EBIC studies 4-88187  
 Si:As, ion implanted through screen oxide, residual disorder after high temp. anneal 4-113511  
 Si:As, low energy implanted, laser-annealed, channeling and high-resolution backscatt. studies 4-75493  
 Si:As, low-energy ion implantation 4-75466  
 Si:As, P, B, ion implanted, fast isothermal annealing and elec. props. 4-92224  
 Si:As, P, ion implanted, diffusion modelling 4-113729  
 Si:As implanted layers, struct., total external reflection spectra studies 4-108330  
 Si:As/Al interface, sintering and diffusion, As dopant effect 4-80427  
 Si:As/Ti interface, As implantation, As out-diffusion during TiSi<sub>2</sub> formation 4-65493  
 Si:As<sup>+</sup>(BF<sub>3</sub>), implanted, rapid thermal annealing 4-88181  
 Si:As<sup>+</sup>(Sb<sup>+</sup>), ion implanted and laser annealed, defects, photoluminescence studies 4-75433  
 Si:As(B), ion implanted and electron beam annealed, TEM and HREM studies 4-80058  
 Si:As(Sb), shallow dopant profile production by low-angle ion implantation 4-108396  
 Si:As(Sb)(In), ion implanted, pulsed electron beam annealing, impurity diffusion 4-103984  
 Si:B, (100), shallow junction implants through surface oxide, theoretical and expt. study 4-113476  
 Si:B, deep implanted layers, for IC appl. 4-75482  
 Si:B, focused ion beam B<sup>+</sup> implantation 4-92222  
 Si:B, implanted, elec. activation and damage annealing by flash lamp irradi. 4-70196  
 p-Si:B, ion implanted, electron beam annealing 4-60960  
 Si:B, ion implanted, flash-lamp annealing study 4-108395  
 Si:B, ion implanted shallow layers, electron beam annealing, expt. study using SIMS 4-98133  
 a-Si:B, pure and doped, ion implanted, recrystallisation studies 4-88422  
 Si-B-SiO<sub>2</sub> MIS struct., ion bombarded, defect annealing study 4-80685  
 Si:B(As), ion implant in-depth error anal., mass interference effects, in ion microprobe studies (Chinese) 4-111248  
 Si:B(As), low resistance ion implanted films 4-108398  
 Si:F, amorphous and cryst., ion implanted, elec. quadrupole hyperfine interaction at impurity sites 4-92675  
 Si:F, As, ion implanted, defect struct. detection 4-103776  
 Si:Ge, implantation, pre-amorphisation/rapid thermal annealing procedure for shallow junction formation 4-88188  
 Si:Mg, implanted, doping behaviour, elec. props. 4-75485  
 Si:Mo doping by recoil implantation, RBS anal; (Chinese) 4-70173  
 Si:N, ion implanted, optical props. (Chinese) 4-114306  
 Si:N, low energy implant depth profiles, surface peak, Auger studies 4-80074

## ion implantation continued

- Si:N single cryst., ion implanted, photoluminescence studies 4-114313  
 Si:O, buried oxide layers formation by O<sup>+</sup> implantation 4-88180  
 Si:P, heavily doped, optical reflectivity spectra 4-61735  
 Si:P, ion implanted, diffusion during rapid thermal annealing 4-113713  
 a-Si:P, ion implanted, phonon scatt. study 4-70325  
 Si:P, ion implanted, Xe flash lamp annealing, Rutherford backscatt. study 4-88196  
 Si:P, Cl<sup>+</sup> implantation effects on oxidation enhanced P diffusion 4-92429  
 Si:P,N, pulsed laser annealing, substitutional N impurities, EPR studies 4-98120  
 Si:P<sup>+</sup>, implanted, dislocation struct. development, effect of cryst. orientation, TEM obs. 4-80040  
 Si:P(As), ion implanted film, elec. props. 4-61473  
 Si:P(B), heavy doping effect on band struct. and optical props. 4-92998  
 Si:S, implanted, depth distrib. as function of ion energy, fluence and anneal temp., SIMS meas. 4-80078  
 Si:Sb, implanted laser irr., crystn. annealing, time-resolved reflectivity, TEM, Rutherford backscattering anal. 4-80093  
 Si:Sb, ion implanted, dopant site location and profiles, channelling studies 4-108393  
 Si:Sb, ion implanted, supersaturation, vitreous C strip heater annealing, Rutherford backscattering, elec. meas. 4-92375  
 Si:Sn, implanted, subthreshold energy electron beam annealing, Mossbauer effect 4-88205  
 Si:Xe, implanted Xe reemission by He<sup>+</sup> ion bombardment 4-75462  
 Si/SiO<sub>2</sub>/Al capacitor struct., ion beam fluorination and interface state density 4-70176  
 Si/Ti:P<sup>+</sup>(B<sup>+</sup>)(As<sup>+</sup>), ion implanted, doping effects on TiSi<sub>2</sub> formation 4-88183  
 Si-on-insulator films, ion implanted, annealing-using scanned graphite strip heater 4-80066  
 Si-SiO<sub>2</sub> interface, As<sup>+</sup> implanted, defects, ESR study 4-61591  
 Si-SiO<sub>2</sub> MOS struct., H passivation of implantation defects using a-Si:H film 4-71744  
 Si-SiO<sub>2</sub>/Ar<sup>+</sup>(As<sup>+</sup>), ion implanted layers, EPR study 4-84849  
 SiB, implanted, impurity depth profiles,  $\alpha$ -particle spectra, Monte Carlo calc 4-80081  
 SiC, book, deposition, growth and technology 4-58579  
 SiC, ion implantation, ion beam mixing, and annealing of metals 4-70229  
 Si<sub>3</sub>N<sub>4</sub>, ion implantation, ion beam mixing, and annealing of metals 4-70229  
 SiO<sub>2</sub> films, C ion implantation, CO and CO<sub>2</sub> form. 4-77016  
 SiO<sub>2</sub>, fused, subsurface Al films, ion beam mixing 4-88189  
 SiO<sub>2</sub>, ion implanted, damage recovery, EPR studies 4-92245  
 SiO<sub>2</sub>, ion implanted, E<sub>f</sub> defects, isothermal annealing studies 4-70146  
 SiO<sub>2</sub> thermal film, defect creation by ion implantation 4-65343  
 SiO<sub>2</sub>:B, implanted, impurity depth profiles,  $\alpha$ -particle spectra 4-80081  
 SiO<sub>2</sub>:H<sup>+</sup>, amorphous, O<sub>2</sub> vacancy annealing 4-103743  
 Ti-Al-V, ion implantation effect on fretting fatigue 4-76916  
 TiB<sub>2</sub>, implanted with 1 MeV Ni<sup>+</sup> ions, microstruct. and surface mech. props. 4-70232  
 V:As, ion implanted, plastic deformation, channelling studies 4-70178  
 V-N, ion implanted, N diffusion, ion beam studies 4-70431  
 W, noble gas atom implanted, cascade annealing, computer simulation studies 4-75556  
 W:He, ion implanted, diffusivity study 4-104004  
 Xe<sup>+</sup> implantation in Al, depth distribution obs. by Rutherford backscattering (*Japanese*) 4-104707  
 YAG:Nd<sup>3+</sup>, planar optical waveguide fabrication by ion implantation 4-69552  
 Y:Fe<sub>2</sub>O<sub>3</sub>, garnet epitaxial layers, ion implantation-induced strain and damage profiles 4-75558  
 YIG, Me<sup>+</sup> implanted, mag. props., annealing effects 4-71057  
 (YSmCa)<sub>2</sub>(FeGe)<sub>2</sub>O<sub>7</sub>, garnet films, Ne<sup>+</sup> implanted, cylindrical mag. domains obs. 4-114148  
 Zn:Se, ion implanted, high electron mobility obs. 4-108863  
 Zr:D, ion implantation, lattice defect trapping, binding enthalpy, migration 4-108400

## ion lasers

- compact sputtering device, high conc. metal vapour beam for lasers 4-79177  
 construction operating modes, and characts. (*Italian*) 4-107596  
 inert gas mixture hollow cathode, excitation mechanism (*Russian*) 4-69368  
 metal vapour ion lasers, hollow cathode, with lateral HF discharge (*Russian*) 4-69370  
 plasma recombination lasers in CO<sub>2</sub> laser vaporized target 4-87316  
 recombination lasers, ionization/recombination kinetics 4-64613  
 review of solid-state and gas laser characts. 4-60008  
 UV ion laser, continuous, DC electron beam excited (*Russian*) 4-69367  
 Ar, high-strobe-rate lasers for high-speed holographic testing 4-102903  
 Ar ion laser, air cooled, design and appl. 4-64722  
 Ar ion laser, cavity dumped freq. doubled, sine-wave modulated UV radiation 4-69459  
 Ar, ion laser, injection locking for high-power single-freq. emission 4-102960  
 Ar laser therapy using fibre optics transmission 4-85474  
 Ar<sup>+</sup> ion lasers, acousto-optic mode locking, subnanosecond transient spectroscopy appl. (*Japanese*) 4-101923  
 Ar<sup>+</sup> pulsed hollow cathode discharge laser, operational characteristics 4-83565  
 Be II recombining plasma, lasing transitions 4-96878  
 Be isoelectronic sequence, optical pumped quasi-CW UV plasma lasers 4-102922  
 Cu II slotted hollow cathode discharge laser, Cu at. diffusion meas. 4-83569  
 He-Cd<sup>+</sup> hollow cathode laser, population inversion mechanism 4-83570  
 He-Cd<sup>+</sup>(Zn<sup>+</sup>)(Ne) lasers, excitation mechanisms anal. (*Japanese*) 4-79116  
 He-Kr<sup>+</sup> hollow cathode discharge laser, electron energy distrib. function 4-84117  
 He-Zn-Cd, hollow cathode laser, simultaneous laser oscillation by Cd II and Zn II lines (*French*) 4-112399  
 He<sup>+</sup>+neutral ats., charge transfer in low-energy collisions 4-74326  
 Li<sup>+</sup>+neutral ats., charge transfer in low-energy collisions 4-74326  
 N<sub>2</sub><sup>+</sup>, laser action using transverse discharge pumping scheme 4-69382  
 Ne like ions, UV radiation amplification in laser plasma 4-74493

## ion lasers continued

- Xe ion-pumped pump for subpicosecond dye laser 4-96937  
 Xe ion-pumped open dye stream laser time resolved spectrum 4-10763  
 Zn<sup>+</sup> vapor, high-gain soft X-ray pumped photoionization laser 4-11232
- ion lenses see lenses
- ion lithography see ion beam lithography
- ion microanalysis  
 see also ion microprobe analysis  
 Si:B,C,O, impurity profiling and analysis by recoil atoms in heavy beams 4-108406  
 Si-SiO<sub>2</sub>-Mo MOS diodes, carrier trapping centres and interface states induced by RF sputtering of Mo 4-88603
- ion microprobe analysers see ion microprobe analysis
- ion microprobe analysis  
 see also ion microanalysis  
 aerosol deposition in human respiratory tract, PIXE investigation 4-105066  
 aerosol sampling and samples matched to PIXE analysis 4-99901  
 aerosol trace element analysis, large scale intercomparison of different analytical methods 4-99897  
 alloys, soldering, PIXE anal. 4-99898  
 alloys, ternary, ion implantation prep., surface binding energy 4-7997  
 ambient aerosol composition determ. by PIXE anal. 4-100031  
 apatite; Durango, nucl. microprobe PIXE anal. 4-100787  
 applied surface anal., conf., Dayton, USA (June 1983) 4-95016  
 archaeological potsherds from West Africa, PIXE anal. and provenance study 4-100571  
 automobile studded tyres, environmental investigation using PIXE 4-105146  
 Beijing, China, aerosol composition during summer, vertical, temporal particle size distrib. 4-100041  
 biological materials, sample and target prep. for PIXE anal. 4-100386  
 biological samples, target prep. on PIXE anal. 4-100381  
 biological target preparation, rel. to element distrib. deviation 4-1053  
 blastocysts, mouse, heavy metal incorporation and distrib., micro-PIXE anal. 4-100389  
 blood, human, from addicted and non-addicted persons, PIXE anal. 4-105365  
 blood cells, elemental profiles, PIXE anal. 4-100387  
 blood serum proteins, PIXE anal. using gel filtration 4-105367  
 cancer diagnosis, PIXE appls. 4-105369  
 cascade impactor samples collected over Pacific Ocean, PIXE analysis 4-100029  
 cerebral atherosclerosis, PIXE investigation 4-105370  
 coal fly ash, elemental particle size distrib. in thick samples, PIXE analysis 4-105069  
 dental cementum, human teeth; elemental composition, PIXE analysis 4-100390  
 elemental anal. of PIXE, FAST, LIPM and mass study 4-99896  
 environmental samples, trace element anal. by PIXE 4-99902  
 external PIXE milliprobe at Davis cyclotron, laser alignment, calibration and quality assurance 4-105076  
 Faeroe Islands, marine and nonmarine transported aerosols anal. by PIXE 4-100034  
 forward alpha scattering techniques (FAST) for elements H to He 4-99890  
 fusion materials, impurity elements in JIPP T-II fusion device, PIXE analysis 4-105073  
 Göteborg, Sweden, airborne particles distrib. determ. using EDXRF and PIXE methods 4-100033  
 Gutenberg Bible, PIXE anal. 4-99906  
 hair, human, elemental concs., PIXE anal. 4-105364  
 hair, human, PIXE meas. normalisation by nucl. reaction 4-105065  
 hair, human, trace element incorporation, micro PIXE anal. 4-10039  
 hair strands, longit. scanning PIXE anal. 4-105363  
 heavy-ion induced satellite X-ray emission, fine struct. 4-99231  
 Heidelberg proton microprobe, secondary electron imaging 4-101973  
 human skin, proton and electron microprobe analysis 4-105390  
 in-plant aerosols, PIXE anal. 4-105071  
 ion implant in-depth error anal., mass interference effects (*Chinese*) 4-111248  
 Karlsruhe proton microprobe appl. to medical samples 4-105389  
 kidney, elemental conc. meas. in mouse arteries, micro-PIXE analysis 4-100385  
 Lake Constance, settling materials precipitation, PIXE study of environmental catalysis 4-105603  
 lanthanide mixed crystals, elemental analysis using PIXE 4-89358  
 lateral trace element distrib. determ. with Bochum proton microprobe 4-105075  
 lenses, normal and cataractous, PIXE and microprobe anal. in rats 4-100386  
 leukemia manifestation in blood cell microelement profile, nuclear microprobe determ. 4-100388  
 light elements, thick targets, H<sup>+</sup> bombardment, continuous X-ray spectroscopy 4-99214  
 liver, medical diagnostic appl. of Oxford scanning proton microprobe 4-105332  
 liver tissue, global element composition comparison with different fractions composition PIXE study 4-105391  
 lunar rocks, trace element determ., PIXE anal. 4-101210  
 Mediterranean and Atlantic ocean, atmospheric aerosol particles transport, determ. by PIXE 4-100035  
 metals, ion implantation modification, ion beam anal. appl. 4-76914  
 metals, self-ion sputtering yields, PIXE and Rutherford backscattering 4-76628  
 meteoritic minerals, rare earth element fractionation, PIXE analysis 4-101276  
 Milan aerosol monitoring by means of PIXE analysis 4-100040  
 multielement depth analysis by Rutherford forward scattering and detection of projectiles and recoils in a time-of-flight experiment 4-99892  
 nails, human, elemental concs., PIXE anal. 4-105364  
 New Zealand obsidian anal., provenance studies, PIXE and PIGE methods 4-100573  
 nuclear microprobe anal., appl. to (d,p) reactions 4-72014  
 Oxford proton microprobe, wide area scanning system 4-101972  
 oyster shells, element distrib., environmental and chronological effects, PIXE investigation 4-105067  
 particle and photon excited X-ray charact. spectra; appl. to trace element anal. of hair 4-99887

- microprobe analysis continued**  
 article elastic scattering anal. of thin samples, calibration procedure 4-99891  
 article-induced X-ray spectra, anal. using NANOLEX Fortran program 4-101976  
 PIXE, anals. of biological and medical samples 4-105063  
 PIXE, appl. in neurological diseases investigation 4-105368  
 PIXE, appls. and results 4-99868  
 PIXE, computer program for background and multiple peak fitting 4-101977  
 PIXE, conjunction with inertial spectrometer aerosol sampler, use in particle size meas. 4-99903  
 PIXE, multielement anal., advantages and difficulties 4-114873  
 PIXE's analytic appls., conference, Heidelberg, Germany (July 1983) 4-95034  
 PIXE anal., preconcentration method low temp. ashing evaluation 4-100382  
 PIXE anal., sample inhomogeneity influence on precision 4-99875  
 PIXE anal., sample uniformity and surface contamination, Al X-ray yield ratio 4-109704  
 PIXE anal. bombardment chamber 4-95567  
 PIXE anal. laboratory based on 4 MV Van der Graff accelerator 4-95566  
 PIXE anal. of biomedical samples using external piston beam 4-105362  
 PIXE anal. using thin film standards 4-99879  
 PIXE analysis, appl. of microprobes 4-105074  
 PIXE analysis of intermediate and thick targets via line intensity ratios 4-99880  
 PIXE analysis of Pt group elements preconcentrated from geological samples 4-100784  
 PIXE analysis with external beams: systems and applications 4-99882  
 PIXE and neutron activation methods in human hair material analysis 4-99895  
 PIXE detection limits for some aerosol collection substrates by excitation with protons and  $^4\text{He}^{2+}$  ions from a 3 MV tandem accelerator 4-99904  
 PIXE determ. of Se in biological samples with preconcentration technique 4-100384  
 PIXE for elemental analysis of thick target metal alloys 4-89359  
 PIXE peak doublet separation, effects of statistical quality of data 4-101978  
 PIXE semi-microprobe analysis, proton CT as means of density normalisation 4-105077  
 PIXE spectra, least-squares fitting with digital filter 4-105062  
 PIXE system, expt. arrangement design 4-95565  
 PIXE system calibration, linearity precision and accuracy 4-95568  
 PIXE technique for environmental and biomedical anal. 4-99873  
 PIXE trace anal. of biological materials, using single multielement standard 4-105385  
 PIXE trace element anal., biological appls. 4-105064  
 PIXE trace element anal., biomedical appls. 4-105361  
 PIXE-induced XRF for analysis of steels and biological samples, comparison with tube-excited XRF 4-99888  
 PIXE-PIGE thick-target anal., accuracy and precision determ. with geological standards 4-99881  
 positive mass identification on an ion microprobe mass analyser by use of a digital squarer module 4-114867  
 pottery and glasses, 18th and 19th century, PIXE and PIPPS anal. 4-100572  
 pottery samples, powdered bound in organic matrix, quantitative PIXE anal. 4-99899  
 power station particulate emissions, elemental and size anal. using PIXE 4-105163  
 proton-induced X-ray fluorescent anal. for trace element anal. in hair 4-89360  
 quartz, O diffusion between quartz and surrounding water, laboratory expts. 4-94093  
 radioactivity registration stations, aerosol samples, elemental composition by PIXE 4-100030  
 review of surface analytical techniques, book contrib. 4-85053  
 Sao Paul PIXE system and its use on a national monitoring air quality program 4-100032  
 scanned micro-PIXE by  $\text{H}^+$  backscatt. for local matrix thickness determ. in organic tissues 4-99889  
 scanning Auger microprobe and ion scattering spectrometry combination 4-93116  
 sea water, trace metal determ., PIXE anal. 4-100783  
 surface analysis by resonance ionisation of sputtered atoms 4-105080  
 surface analysis facility 4-73605  
 surface impurities, low-energy ion beams anal. appl. 4-99893  
 Sweden, south, long range aerosol transport, multivariate statistical technique appl. to PIXE data 4-100037  
 synchrotron radiation application to elemental anal. 4-99884  
 synchrotron radiation trace element analysis, comparison with other modes of excitation of X-rays 4-99885  
 teeth, enamel layer, trace element distrib., PIXE and PIGE anal. 4-100391  
 teeth, human, enamel pre-carious lesions, trace element surface distrib., PIXE anal. 4-100392  
 telecommunication exchange buildings, indoor and outdoor air, fine particle aerosols characterisation 4-100038  
 thick target PIXE anal. review 4-99878  
 thin film analysis by low energy proton induced X-ray emission 4-109705  
 three-dimensional nondestructive material testing using nuclear microprobe 4-99862  
 tip growing plant cells, intracellular Ca distrib., PIXE meas. 4-100394  
 toxic effect of Al in grape vines, PIXE, anal. 4-105388  
 trace element quantitative analysis, relativistic electrons to induce X-ray emission (REIXE) appl. 4-100786  
 tree-ring analysis by PIXE for a historical record of soil chemistry response to acidic air pollution 4-105068  
 urine, ion exchange, selective preconcentration method, PIXE anal. 4-100383  
 water, heavy metal detection, calibration and errors in PIXE technique 4-99877  
 water, nonselective preconcentration, PIXE anal. 4-100054  
 water solution, PIXE anal. using ion exchange filter 4-99857  
 western United States, anthropogenic pollutants, long range transport and transformation obs. by PIXE 4-100036  
 work environment aerosols, PIXE anal. 4-105070
- ion microprobe analysis continued**  
 working environment aerosols in lead battery factory, toxicity monitoring by PIXE and AAS 4-105072  
 X-ray microprobe design at SRS Daresbury (UK) 4-99886  
 Zurich, ambient air, particulate matter sampling and anal. 4-100039  
 Ag Celtic coins, surface compositions determ. by PIXE 4-99900  
 Al, angular distribution of particle-induced X-ray emission 4-99213  
 Al, continuum X-rays produced by a few MeV proton bombardment 4-99215  
 Au (110)-(1 $\times$ 2), atomic displacements,  $\text{He}^+$  backscatt. study 4-65533  
 Au impurity contaminations, PIXE anal. 4-99874  
 Ba, L-shell X-ray prod. cross sections for protons of energy 1-2 MeV 4-96656  
 Bi layer struct. depth profiling, PIXE anal. 4-99874  
 C: continuum X-rays produced by a few MeV proton bombardment 4-99215  
 Cr determ. in blood plasma, rel. to coronary heart disease, cineangiographic meas. 4-105366  
 Cs, L-shell X-ray prod. cross sections for protons of energy 1-2 MeV 4-96656  
 GaAs:S(Si), implant sublattice site determ., PIXE studies 4-98119  
 Gd, L-shell X-ray prod. cross sections for protons of energy 1-2 MeV 4-96656  
 $\text{H}^+$ , K X-ray prod. cross sections using fluoresc. yield 4-96483  
 $\text{H}_2\text{SO}_4$ , ambient aerosol, S losses, PIXE anal. 4-99876  
 $\text{H}^+$  induced  $\gamma$ -ray emission (PIGE) analysis, external beam technique 4-99883  
 La, L-shell X-ray prod. cross sections for protons of energy 1-2 MeV 4-96656  
 Mo cpds. and alloys, chemical effects in  $\text{C}^{19+}$  induced L X-ray emission satellites 4-99872  
 Mo-Co dilute alloy, Co impurity location, PIXE and ion channelling studies 4-80072  
 Mo-Co dilute alloy, lattice location studies by PIXE and ion channelling 4-99894  
 $\text{NH}_4\text{HSO}_4$ , ambient aerosol, S losses, PIXE anal. 4-99876  
 $(\text{NH}_4)_2\text{SO}_4$ , ambient aerosol, S losses, PIXE anal. 4-99876  
 NiO films grown by sputter oxidation 4-99658  
 $\text{NiO-MoO}_3/\gamma\text{-Al}_2\text{O}_3$  catalysts, atomic distrib. studied by ion scatt. spectroscopy 4-71972  
 Pt, layer struct. depth profiling, PIXE anal. 4-99874  
 Si wafers covered with layers of Pb and Ge, PIXE anal. signal enhancement, matrix effects 4-99869  
 n-TiO<sub>2</sub> anodes in photoelectrolytic cells, struct. and electronic props. 4-114031  
 W surface layers formed by chem. reactions, PIXE anal. 4-99874  
 Y, localisation behaviour and tumours in nude mice, PIXE investigation 4-105386
- ion microscopes**  
 see also field emission ion microscopes; ion microscopy  
 No entries
- ion microscopy**  
 see also field emission ion microscopy; ion microscopes  
 liquid metal ion sources for microscopy and lithography 4-78416  
 long trace elements distrib., imaging by ion microscopy 4-115316  
 W (100) stepped surfaces, adsorbed K, desorption kinetics and directional depend. of surface diffusion 4-92545
- ion mobility**  
 see also electrolytic ion mobility; ionic conduction in solids  
 ion, ionised, ionic cond. determ. using reson. cavity 4-60579  
 alkali closed shell ions, repulsive interactions with Ar, Kr and Xe, beam and transport meas. comparison 4-96653  
 aromatic hydrocarbons, polynuclear, polyatomic ion mobility calc., ionic size estimate 4-113107  
 electrostatic, precipitator rods, DC corona discharge and ion flow distribution characts. 4-97933  
 glow discharge plasma,  $\text{ArH}^+$  Doppler shift ion mobility meas. using diode laser spectroscopy 4-113217  
 halogen closed shell ions, repulsive interactions with Ar, Kr and Xe, beam and transport meas. comparison 4-96653  
 low temperature mobility of ions localised near interfaces (Russian) 4-92452  
 methylimine cation, mobilities in He at 293K 4-79706  
 molten salts, assoc. and mobility isotherms 4-75247  
 nonstoichiometric compounds, transport processes, conf., Cracow, Poland (Aug. 1980) 4-95060  
 toxic substance detector alarm using ion mobility spectrometry, developments 4-99907  
 Ar afterglows, conversion reaction rate coeff. and ambipolar diffusion coeff. meas. 4-79877  
 $\text{C}_2\text{H}_3\text{N}^+$ , mobilities in He at 293K 4-79706  
 $\text{C}_2\text{N}^+$ , mobilities in He at 293K 4-79706  
 $\text{C}_2\text{N}_2^+$ , mobilities in He at 293K 4-79706  
 $\text{Fe}_3\text{-O}_4$ , magnetite, diffusion of cations and point defects 4-99378  
 $\text{HCN}^+$ , mobilities in He at 293K 4-79706  
 Na atoms and ions, diffusion coeff. in inert gases 4-75111  
 $(\text{u,Pu})\text{O}_{2+x}$ , nuclear fuel oxide, diffusion processes, surface effects 4-98353  
 $\text{UO}_{2+x}$ , nuclear fuel oxide, diffusion processes, surface effects 4-98353
- ion-molecule collisions**  
 see also charge exchange; ion-molecule reactions  
 charge exchange processes 4-96694  
 low-frequency vibrations, geometries and energetics calcs. 4-107432  
 methylimine cation, mobilities in He at 293K 4-79706  
 multiply charge ion-gas target collision, charge transfer cross sections 4-102789  
 tetrafluoromethane- $\text{H}^+$ , mol. very high overtone vibr. levels obs. 4-96672  
 thick gas targets, proton small angle multiple scatt. 4-107431  
 $\text{Ar}^+ + \text{CS(PN)}$  radicals, emission spectra prod. from thermal energy charge transfer reactions 4-74325  
 $\text{Ar}^+ + \text{N}_2$ , energy depend. of reactions 4-69193  
 $\text{Ar}^+ + \text{CO(N}_2)$  collisions, integral cross section meas. 4-78929  
 $\text{B}^+ + \text{H}_2$ , pot. energy surfaces, diatomics-in-mols. correl. diagrams 4-62166  
 $\text{C}_2\text{H}_3\text{N}^+$ , mobilities in He at 293K 4-79706  
 $\text{C}_2\text{N}^+$ , mobilities in He at 293K 4-79706  
 $\text{C}_2\text{N}_2^+$ , mobilities in He at 293K 4-79706  
 $\text{Cl}_2 + \text{Cl}^- (\text{Br}^-) (\text{I}^-)$  charge transfer and electron detachment, absolute total cross-sections meas. 4-69202

## ion-molecule collisions continued

- $D_2^+ + H_2$ , collisional dissociation, correl. between channel probabilities 4-78933  
 H accelerated cluster ions, interaction with  $H_2O$  gas target 4-74378  
 $H + CO^+$  ( $CH^+$ ), reaction rate coeffs. 4-81427  
 $H^+ + He(Ar)(H_2)(N_2)(O_2)(CO_2)$ , electron detachment and charge exchange to shape resonances, 4-69203  
 $H^+ + H_2$  collisions, two-state charge transfer calc. 4-91341  
 $H_2 + C^+$ , charge transfer, polarised light emission 4-83463  
 $HCN^+$ , mobilities in He at 293K 4-79706  
 $HCO$ , low-energy  $H^+$  stopping power, modified local plasma model 4-83485  
 $H_2O + Ca^{2+}(Cl^-)$ , intramol. vibr. freq., single ion effect 4-69036  
 He ion impacts, target ionisation, dissociation, excitation 4-96682  
 $He^+ + N_2$ ,  $N^+$  ions prod. in dissociation double ionisation, ang. correl. 4-102779  
 $He^+ + N_2$  thermal charge transfer reaction,  $N_2^+$  predissoc. channel 4-91317  
 $N II + He^+(N_2)$  collisions,  $N II$  reson. line excitation in VUV region in cathode sheath of hollow cathode discharge 4-87203  
 $N^+ + CO$  chemisorbed on Ni (100) and Cu (100) 4-80380  
 $N^{6+} + H_2$ , electron capture in autoionising configurations  $N^{4+}$  studied by electron spectrometry 4-59889  
 $N_2$ , low-energy  $H^+$  stopping power, modified local plasma model 4-83485  
 $N_2 + B^+$  fast beam excitation study 4-107294  
 $N_2 + Ar$ , state-selected charge transfer cross sections 4-87206  
 $N_2^+ + N_2$ , charge transfer reaction dynamics, crossed mol. beam study at low and intermediate energies 4-96683  
 $NO^+$  ( $X, v > 0$ ), collisional quenching by neutrals at low energies 4-87196  
 $O_2$ , low-energy  $H^+$  stopping power, modified local plasma model 4-83485  
 $SF_6$  ion lifetime in RF quadrupole trap 4-96644

## ion-molecule reactions

- acetylene mol. affinity for  $Li^+$ , STO calc. 4-62182  
 allene, ion-molecule reactions, photoionisation mass spectra 4-93517  
 association reaction rates, endothermic reactivity correl. 4-99767  
 carbon tetrachloride, solids containing acetals, gamma-irrad.,  $CCl_3$  radical prod. 4-93504  
 methane-keV proton irradiation interplanetary hydrocarbon generation 4-115711  
 methyl fluoride +  $F^-(H^-)$ , activation barriers, fourth order MB RSPT calcs. 4-62167  
 2-phenylallyl anions, gas phase structs., investig. using abstraction reactions 4-81413  
 1-phenylcyclopropyl anions, gas phase structs., investig. using abstraction reactions 4-81413  
 polyatomic ion-neutral target collisions over 10 to 6000 eV, collision energy effect 4-93520  
 porphyrin dianions +  $H^+$  donors (alkyl halides), reaction products electron density distrib. 4-107284  
 ter-molecular ion-molecule association reaction, rates and energy randomisation time 4-99765  
 tetrachlorosilane reactions in Ar- $H_2$  microwave plasma 4-89268  
 three-body ion+molecule association reaction rate consts., temp. variation constraints 4-85292  
 $Ar + H_2^+(O_2^+)(NO^+)$ , charge transfer reactions 4-89272  
 $B^+ + H_2$ , pot. energy surfaces, diatomics-in-mols. correl. diagrams 4-62166  
 $C^+ + H_2$ , reaction product rovibr. distrib., surprisal functions 4-114776  
 $C^+ + NO$ , temp. depend. of reaction from 90-450K 4-76987  
 $C_2H_3^+$  ions, form., kinetics and deactivation, mass spectrosc. obs. 4-102751  
 $(C_2H_3)^+$  ions, form., kinetics and deactivation, mass spectrosc. obs. 4-102751  
 $CO^+ + CS_2$ , in flowing afterglow, charge-transfer excitation, energy reson. and Franck-Condon criteria 4-93500  
 $H^+ + H_2$ , proton interchange process rel. to ortho- $H_2$ /para- $H_2$  ratio in interstellar mol. clouds 4-94927  
 $H^+ +$  methane ( $NH_3$ )( $H_2O$ ), differential cross sections 4-85295  
 $H_2 + H^+$  proton interchange process rel. to ortho- $H_2$ /para- $H_2$  ratio in interstellar mol. clouds 4-94927  
 $H_2^+ + H_2^+$  collisions at low energies,  $H^+$  prod. 4-91867  
 $H_2O$ , interaction with ion at intermediate separation 4-85296  
 $H_2O^+$  methyl cation (protonated formic acid), ternary association reaction in He buffer 4-93525  
 $(H_2S)_n^+$ ,  $n=2,3$ , unimolecular decomposition study 4-59860  
 $N^+ + CO$ , temp. depend. of reaction from 90-450K 4-76987  
 $N^+ + CO$ , thermal and near-thermal energy charge exchange, energy disposal 4-76984  
 $N^+ + CO$  chemisorbed on Ni (100) and Cu (100) 4-80380  
 $N_2 + O_2$  Townsend discharge, ion-molecule reaction prediction 4-88034  
 $N_2 + O_2^+(NO^+)$ , vibr. energy transfer reactions, rate coeff. at 300K 4-89271  
 $N_2^+ + 2N_2$ , association reaction rate const. determ. in temp. range 20 to 160K by CRESU technique 4-76986  
 $N_2^+ + Ar$ , state-selected charge transfer cross sections 4-87206  
 $N_2^+ + N_2 + M \rightarrow N_2^+ + M$ , ion-molecule association reaction for  $M=N_2$ , Ne and He 4-99764  
 $NH_3^+ + H_2S$  reaction, depend. on translational and internal energy of  $NH_3^+$  4-71891  
 $O^+ + H_2$ , ab initio pot. energy surface, CI calcs. 4-96470  
 $O_2 + C^+(CO^+)(CO_2^+)$ , temp. depend. of reaction from 90-450K 4-76987  
 $O_2^+ + 2O_2$ , association reaction rate const. determ. in temp. range 20 to 160K by CRESU technique 4-76986  
 $O_4^+ + N_2$ , three-body reactions,  $O_4^+(N_2)$  formation with  $n \leq 4$  4-89291  
 $O_2 D^+ + D_2$ , forward and reverse rate coeff., enthalpy and entropy changes 4-62165  
 $O_2 H^+ + H_2$ , forward and reverse rate coeff., enthalpy and entropy changes 4-62165  
 $OH^-(H_2O)_n + CO_2(SO_2)$ , reaction cross sections, translational energy depend. 4-76983  
 $SiF_4$  ion-molecule reactions, FT mass spectra 4-93518  
 $Sm^+ + O_2$ , exothermic reaction, cross-section, thermal rate const. 4-89261

## ion optics

see also ion beams; ion microscopes; mass spectrometers  
 air flowmeter based on constant deflection of ions 4-87824

## ion optics continued

- bunch propagation in neutral medium, compensating electron effect 4-74411  
 Doublet III neutral injector ion sources, linear optics theory ap. 4-59458  
 EGP-10-1 tandem generator, heavy-ion accel., ion optical investigation 4-59456  
 electrode and pole piece reconstruction from optimized axial field distrib. 4-112337  
 electron microscopy and anal., conference, Guildford, England (Aug.-Sep. 1983) 4-78034  
 fringing integrals of arbitrary field distrib., FRIC computer program 4-112339  
 heavy ion beam source, probe appls., mag. field effect on accelerating field 4-78413  
 Heidelberg proton microprobe, secondary electron imaging 4-101973  
 mass spectrometer design, ion optics calc. using program in BASIC 4-78410  
 microchannel plate gain characts., reflection mode 4-78423  
 Oxford proton microprobe, wide area scanning system 4-101972  
 SITES neg. ion source, short-pulse  $D^-$  operation 4-107200  
 SNOW ion beam extraction simulation program, computers for design and testing 4-73590  
 trapped ion, laser cooled, steady state in Lamb-Dicke limit 4-69020
- ion plating**  
 DC ion-plating systems, substrate temp. prediction 4-99349  
 discharge plasma flow, bending method (Japanese) 4-76693  
 field emission deposition, high adherence coatings 4-81161  
 front/back thickness ratio of ion-plated films 4-85118  
 fusion reactor deposited and redeposited materials, review 4-107065  
 glow discharge electron beam technique for reactive ion plating 4-114  
 organometallic films, ion beam assisted deposition using focused beams, AES 4-85112  
 plasma diagnostics, in ion-assisted physical vapour deposition systems 4-79853  
 yield estimates at low bombarding energies 4-99346  
 Al film, using inexpensive rotating barrel 4-66494  
 Al, ion plated on maraging steel, H embrittlement 4-114671  
 Al- $Al_2O_3$  film, using inexpensive rotating barrel 4-66494  
 Al-Zn film, using inexpensive rotating barrel 4-66494  
 C diamond-like coatings for optical component protection 4-74677  
 $In_2O_3$  ion plated, IR and optical study 4-62085  
 $In_2O_3-Sn_2O_3$  thin films, deposition by reactive ion plating, elec. resist. visible transmittance meas. 4-99348  
 Mo single crystals, low temp. bend props., surface effect 4-99561
- ion probe analysers** see ion microprobe analysis
- ion probe microanalysis** see ion microprobe analysis
- ion pumps**  
 sputter ion pumps, evaluation by discharge intensity meas. 4-78333  
 sputter ion vacuum pump, principles of operation and advantages (Japanese) 4-73446  
 Zr-Al composite-cathode sputter-ion pump 4-78332
- ion recombination**  
 air, ionised, ionic cond. determ. using reson. cavity 4-60579  
 air, microwave discharge with preexcitation of neutral mols. 4-103597  
 alkylbenzenes, liq., excited by UV and  $\beta$  radiation, fluoresc. quench 4-59831  
 complex mols., population inversion of electronic-vibr. states during adiabatic thermal explosion 4-102746  
 dielectronic recombination, complex-pot. model 4-96695  
 discharges, electron beam ionised, with added attaching gases, charact. 4-84118  
 formyl ion ( $d^-$ ), dissociative recombination coeffs. 4-112285  
 interstellar matter, diffuse component atomic processes 4-63258  
 ionosphere depletion expts., snowplough effects or plasma recomb. mechanism for depletion core form 4-100851  
 ionosphere F-region, recombination dynamics 4-110352  
 ions in dense plasmas, excitation-deexcitation and ionisation-recombination 4-69863  
 laser optogalvanic effect for atms. and mols. in recomb.-limited plasmas 4-87091  
 methane, protonated, dissociative recombination coeffs. 4-112285  
 molecules, electron resonant scattering, model calcs. on dissociative attachment and vibr. excitation 4-112287  
 radioactive flow, electric fields from ion recombination effects 4-1034  
 three-body electron-ion recombination, reson. mechanism (Russian) 4-112257  
 Ar ion, Na-like, dielectronic recombination rates 4-96696  
 Ar, liq., geminate recombination 4-69207  
 Ar $^{16+}$  excited states in D Tokamak plasma, recombination population 4-87936  
 C ions, effective dielectric recomb. coeffs., astrophysical appl. 4-96477  
 CO- $O_2$  mixtures, population inversion of electronic-vibr. states during adiabatic thermal explosion 4-102746  
 Ca II, reson. electron capture to high Rydberg states 4-112268  
 Ca XIX, effective excitation and recomb. rate coeffs., appl. to stars 4-87218  
 $D_3^+$ , dissociative recombination coeffs. 4-112285  
 Fe ion, Na-like, dielectronic recombination rates 4-96696  
 H-like ions, fine struct., spectral intensities, collisional-radiative calculations 4-102643  
 $H + H_2 \rightarrow H_3^+ + H_2 + H$ ,  $H_3^+$  absorpt., transition state spectroscopy 4-69194  
 $H_2$  vibrationally excited generation by  $H_2^+$  wall collisions 4-76574  
 $H_2^+$  mol. ion beam bombard. of solid and gaseous targets 4-76579  
 $H_3^+$ , dissociative recombination coeffs. laboratory expts. 4-82408  
 $H_3^+$ , dissociative recombination coeffs. 4-112285  
 $H_3^+$ , dissociative recombination coeffs. laboratory expts. 4-82408  
 $H_2O$  vapour, electron-ion recombination, Monte Carlo simulation 4-69232  
 He ion, dielectronic recombination study 4-107459  
 He- $CO_2-N_2$  electron-ion recombination 4-102794  
 $He_2^+$  afterglow, Rydberg dissociative recombination 4-81421  
 $I_2$  geminate recombination, role of A and A' states 4-69092  
 Mg XI, effective excitation and recomb. rate coeffs., appl. to stars 4-87218  
 Mo ion, Na-like, dielectronic recombination rates 4-96696  
 N ions, effective dielectric recomb. coeffs., astrophysical appl. 4-96477  
 $N_4^+$  recombination rate vs. electron temp. in  $H^+$  beam created plasmas 4-11115

## recombination continued

- $D^+$ , dissociative recombination coeffs. 4-112285
- $H^+$ , dissociative recombination coeffs. 4-112285
- $He^+$  recombination pumping, in  $Ne-H_2$  pulsed transverse elec. discharge (Russian) 4-112133
- ions effective dielectric recomb. coeffs., astrophysical appl. 4-96477
- molecular formation in nonselfsustained discharge in air 4-87839

## scattering see collision processes; ion mobility; ion-surface impact

## solvation see solvation

## sources

## see also ion emission

- $Na$  beam prod., cold cathode PIG source for use with cyclotron 4-74072
- $\alpha$ -2-17, neg. ion beam form. by charge transfer in metal vapours 4-107197
- annular magnetically insulated ion diode operated in long pulse mode, diode, mechanism study 4-112016
- arc, with heated gas discharge chamber, multiply charged ions generation 4-73578
- Bethge-Baumann source performance with RF operation 4-73585
- collective acceleration, Thomson spectrometer anal. 4-107180
- conference, polarised proton ion sources, Vancouver, BC, Canada (May 1983) 4-106092
- cryogenic magnetically insulated diode for pulsed ion beams generation 4-91126
- $(Cs)_2(Sc)_2^+$  cluster ions, generation and detection ranging up to  $m/z=90000$  4-69262
- Doublet III neutral injector ion sources, linear optics theory appl. 4-59458
- dual purpose, pulsed or continuous mode 4-86994
- duopigatron ion sources, use in accelerating high Z and intermediate Z atoms 4-59476
- duoplasmatron for multiple charged ions (Chinese) 4-83260
- EBIS, electron beam ion source test-stand construction and operation 4-64257
- electrical discharges and combustion, colloquium, London, England (April 1984) 4-67870
- electron feed assembly for ORNL/MFTF-B 30-s ion sources, arc behaviour 4-58917
- extraction electrode opening effect 4-82861
- fast atom beams generation for SIMS analysis of polymers and insulators 4-93576
- fusion reactor, gas-feed system for ion sources 4-111869
- fusion reactor ion source components, fabrication 4-111867
- GeV ion production from laser prod. plasmas 4-108229
- $H^-$  polarised source at Brookhaven National Lab., status and future 4-107229
- heavy ion beam source, probe appls., mag. field effect on accelerating lens 4-78413
- heavy ion beams from GSI-UNILAC using acceleration-stripping deceleration method 4-87207
- heavy ion source, indirectly heated, emittance measurements 4-73586
- high current source for nonvolatile elements 4-73589
- high current sources, single aperture extraction system optimisation 4-73588
- high-brightness duoplasmatron ion source for ion beam lithography 4-73587
- hollow anode ion-electron source 4-103528
- hollow cathode in magnetised arc, ion source props. meas. 4-88007
- hollow cathode ion source, beam emittance determ. 4-60649
- hollow cathode ion source, plasma investig. (German) 4-84102
- hollow cathode source with mag. multipole semicylindrical arc chamber 4-101974
- hybrid electron-ion gun, structural design electron optics and appl. 4-63807
- inert gases ionisation in plasma ion source, use of Penning effect 4-86502
- intense ion beam, high brightness point-like source 4-112014
- intense pulsed ion beams for fusion reactors, generation and transportation (Japanese) 4-74078
- interference effects in negative ion formation 4-73571
- inverse pinch ion diode characts. for ICF appl. 4-112019
- ion beam extraction by over-acceleration method 4-60654
- ion cyclotron reson. mass spectrometer, HCN form. in methane/ $N_2O$  mixtures 4-66565
- ion diode research overviews 4-112009
- ion extraction from plasma, three dims. Poisson Vlasov algorithm 4-58916
- ion gun for surface studies, beam profile and scanning characts. 4-64252
- ion implantation equipment and techniques, conf., Berchtesgaden, Germany (Sept. 1982) 4-73155
- ion implanter, 200 keV (Chinese) 4-95558
- ions in flames, origin and props. 4-71932
- laser-produced plasma ion source for heavy ion inertial fusion 4-102389
- light atom beams of neutralised neg. ions, fusion applications 4-107224
- light ion beam prod. by applied Br magnetically insulated annular diode for ICF appl. 4-112013
- liquid metal ion source, shape dynamic model 4-81117
- liquid metal ion sources for microscopy and lithography 4-78416
- low pressure plasma, probe characts. plotting and electron vel. distrib. measuring equipment (German) 4-84060
- low-temperature attachment to the field ionization source in the MI-1201 mass spectrometer 4-101963
- magnetically insulated diode, ion beam divergence and deflections anal. and electron flux study 4-60752
- magnetically insulated intense ion beam diodes, studies of conditions 4-112010
- magnetically insulated ion diodes, ion production efficiency 4-78743
- mass reflection for studying laser light-molecules interaction in supersonic gas jet 4-90686
- mass spectrometer attachment, for secondary ions analysis 4-101962
- microwave, extraction-type, using permanent magnet 4-68321
- MID with cryogenic anode, performance tests 4-112017
- multicharge and negative ion generation and accel. by collective effects 4-111985
- multiply charged ion production from ECR plasmas 4-107245
- multipole ion source for ion implantation and isotope separation 4-73591
- nanosecond accelerator for generating ion and electron beams 4-74076
- negative corona discharges, negative ion extraction 4-84106
- negative ion beam sources for field-reversed fusion devices 4-107223

## ion sources continued

- negative ion clusters, collimated beam from plasma focus source 4-107210
- negative ion formation and extraction in Cs-H discharge 4-58915
- negative ion production from low work function surfaces 4-73577
- negative ion production via dissociative attachment to  $H_2$  4-73561
- negative ion source, open electron orbits in cross-field direction 4-63806
- neutral and ionized alkaline metal bombardment type heavy negative-ion source (NIABNIS) 4-86987
- neutral beam developments for MFTF  $\alpha$ +T system 4-91947
- neutral beam heating of Tokamaks, past performance and future appls. 4-91946
- OLION code for ion beam diode simulation 4-102399
- ORNL positive ion source designed for high power, long pulse neutral beam injection 4-60655
- Penning surface-plasma source with circular emitter, intense  $H^-$  beam production 4-107209
- Penning trap, highly charged ion prod. and storage at room temp. 4-82860
- permanent magnet system, peripheral mag. field for cylindrical ion source (Russian) 4-74075
- pinch reflex diode operation for light ion prod., generator struct. effect 4-60750
- plasma focus discharge, deuteron, X-ray and neutron emission 4-60601
- polar dissociation as a source of negative ions 4-73563
- polarised ion source, atomic beam, optimisation method 4-107238
- polarised ion sources, spin exchange optical pumping 4-107243
- polarised ion sources at RCNP status and performance 4-107237
- polarised neg. ion beam production by collisional pumping 4-107231
- precise high-intensity atomic and ionic beam production 4-73579
- primary ion sources for fast atom bombardment MS 4-101960
- production and neutralisation of negative ions and beams, conf. Brookhaven, NY, USA (Nov. 1983) 4-73134
- pulsed arc discharge ion source with pulsed gas feed 4-90688
- pulsed ion source with cryogenically refrigerated anode cooled by liq. He 4-112018
- quadrupole mass spectrometer,  $O_2$  contamination on ion source (Chinese) 4-105045
- reactive ion beam etching, for semiconductor production, review 4-81322
- RF ion source, gas pressure regularisation 4-90687
- RF ion source development for neutral beam appls. 4-91949
- RF ion source fabrication 4-59477
- RF ion sources, breakdown behaviour 4-78417
- self-magnetically  $B_0$ -insulated ion diode performance study 4-112015
- semiconductor implantation source 4-73592
- series-field-coil ion beam diode 4-96314
- sheet plasma, extraction of  $H^-$  and  $D^-$  ions 4-78415
- single slit multiple ion sources for ion implantation 4-86992
- single-ring magnetic cusp ion source 4-60709
- SITEX neg. ion source, 2D accelerator design 4-107214
- SITEX neg. ion source, end effects in slot extraction 4-107215
- SITEX neg. ion source, short-pulse  $D^-$  operation 4-107200
- SITEX negative ion source, normalised emittance 4-107208
- sputter-type negative ion source, emittance calc. and meas. 4-64256
- surface conversion  $H^-$  source, Cs in plasma effects 4-73576
- surface-plasma sources, high-brightness  $H^-$  beam production 4-107202
- surface/plasma ion source systems, generation of  $H^-$  and  $D^-$  ions on composite surfaces 4-93165
- TAMS technique for radiocarbon dating, graphite target prep. 4-86989
- TEM specimen thinning, ion sources (German) 4-82870
- total beam magnetic species analyzer for  $13 \times 43 \text{ cm}^2$ , 50 A ion source 4-58921
- TRISTAN mass separator thermal ion source, rare-earth ions,  $^{235}U$  fission products 4-102414
- unipolar ion generator for indoor Rn progeny conc. control, cost effectiveness 4-115229
- volume generation of negative ions in high density hydrogen discharges 4-73559
- volume  $H^-$  ion production experiments at LBL 4-73564
- $C^{2+}$  intense ion beam diode, anode heating with  $CO_2$  laser 4-112011
- D beam species meas. by D-D fusion product anal. 4-107247
- $D^-$  Lamb-shift polarised ion sources 4-107239
- $D^+$  polarised ion source, ECR technique 4-107242
- Ga, liquid, ion source, construction and technology (Chinese) 4-82858
- H arc discharge with bulk cathodes 4-111870
- $H^-$  beam extraction 4-78414
- $H^-$  beam line, IKVT-KFK research 4-73567
- $H^-$  charge exchange injection method for 500 MeV booster to KEK 12 GeV PS 4-102408
- $H^-$ , charge exchange with protons in Na, K, Rb-vapour 4-74324
- $H^-$  density in a tandem multicusp discharge 4-73568
- $H^-$  extraction and acceleration from mag. multipole source 4-107206
- $H^-$  formation by charge transfer in alkaline earth vapours 4-73572
- $H^-$  formation by  $H^+$ ,  $H_2^+$  scatt. from W/Cs surfaces 4-73574
- $H^-$  generation of intense flux 4-69925
- $H^-$  honeycomb surface-plasma source 4-101975
- $H^-$  injector for radio-frequency quadrupole accelerator 4-107188
- $H^-$  ion source, design and fabrication for tokamak 4-112002
- $H^-$  ion source development at Brookhaven National Lab. 4-107198
- $H^-$  Lamb shift polarised ion source, intensity limitations 4-107241
- $H^-$  Lamb-shift polarised ion source 4-107239
- $H^-$  magnetron source at BNL linac, operational experience 4-107203
- $H^-$  multiampere source, extrapolation of double-electron-capture source 4-107207
- $H^-$  multicusp ion source, development for accelerator appl. 4-107204
- $H^-$  multicusp source for KEK proton synchrotron injector 4-107213
- $H^-$  polarised, production by laser optical pumping 4-107226
- $H^-$  polarised intense beams, production by double charge exchange in alkali vapours 4-107227
- $H^-$  polarised ion source, charge transfer processes 4-107246
- $H^-$  polarised ion source, electron polarisation meas. of optically pumped Na atoms 4-64258
- $H^-$  polarised ion source, status at AGS 4-107235
- $H^-$  polarised ion source at Munich 4-107240
- $H^-$  polarised ion source at KEK, optically pumped 4-107244
- $H^-$  polarised ion sources, basic design principles 4-107225
- $H^-$  polarised ion sources using ring magnetron ioniser 4-107236
- $H^-$  polarised ions, production methods from ground-state polarised atoms 4-107230
- $H^-$  polarised source, optically pumped, for KEK proton synchrotron 4-107233

## ion sources continued

- H<sup>+</sup> production and destruction mechanisms in low press. discharges 4-73560
- H<sup>+</sup> production by plasma-surface interaction 4-107191
- H<sup>+</sup> production from Cs-transition metal composite surfaces 4-73573
- H<sup>+</sup> production from partially caesiased surfaces in presence of H plasma 4-93166
- H<sup>+</sup> production from polycryst. and monocryst. W and Mo surfaces 4-107192
- H<sup>+</sup> production from various metallic converter surfaces 4-107193
- H<sup>+</sup> production in low press. plasma 4-73569
- H<sup>+</sup> production in mag. multipole source 4-73562
- H<sup>+</sup> production on poly- and monocrystalline converters in surface-plasma ion source 4-96315
- H<sup>+</sup> pulsed multiampere surface-plasma source 4-107201
- H<sup>+</sup> source, focusing of spin-polarised H atomic beam 4-107228
- H<sup>+</sup> spontaneous emission by surface chemi-ionisation on W(110) 4-107195
- H<sup>+</sup> sputtering yields from Mo polycryst. target by Cs<sup>+</sup> bombardment 4-73575
- H<sup>+</sup> surface conversion sources, sputter yield correl. with work function 4-93167
- H<sup>+</sup> surface production in plasma, work function depend. 4-107190
- H<sup>+</sup> surface-production ion source,  $\geq 1$  A, status 4-107199
- H<sup>+</sup> volume produced, extraction from multicusp plasma generator 4-107205
- H<sup>+</sup> atomic beam source for ion production 4-107234
- H<sup>+</sup> fraction in RF in source RIG 10 4-91958
- H<sup>+</sup> injector/buncher with grounded ion source 4-107252
- H<sub>2</sub><sup>+</sup> metastable on production search 4-73566
- H<sub>2</sub><sup>+</sup> production from vibrationally excited states 4-73570
- H<sub>2</sub><sup>+</sup> metastable ion production search 4-73566
- H<sub>2</sub><sup>+</sup> scattered from Na surface, neg. fraction determ. 4-107194
- He scattered from Na surface, neg. fraction determ. 4-107194
- He<sup>+</sup> direct production from He(2<sup>3</sup>S<sub>1</sub>) metastable state 4-96316
- Li<sup>+</sup> formation by Li<sup>+</sup> scatt. from W/Cs surfaces 4-73574
- Li<sup>+</sup> volume production by dissociative attachment 4-107196
- P<sup>+</sup> liq. metal ion source development 4-83261
- Pd-Ni-Si-Be liquid metal ion source for maskless ion implantation 4-58913
- SiH<sub>4</sub> multipole discharges, positive and negative extraction, mass spectra study 4-79857
- SiH<sub>4</sub> multipole discharges, positive and negative extraction, mass spectra study 4-79857

## ion-surface impact

- see also particle backscattering; sputtering
- alloys, binary 4-76606
- amorphous solids, Rutherford backscatt. enhancement, two-atom scatt. model anal. 4-66180
- amorphous target, anomalous backscattering of fast light ions 4-81091
- amorphous target, ion beam bombardment, SASAMAL computer code using liquid model (*Japanese*) 4-109295
- atomic and molecular ions emerging from thin solid targets, non-equilibrated charge and excitation states 4-81065
- atomic collisions in solids, conf., Strasbourg, France (July 1981) 4-63398
- atomic row with correlated thermal vibrs., surface backscattering yield 4-81075
- beam-foil convoy electron distributions, energy and angular dependence 4-81059
- bombardment induced cascade mixing and importance of post-cascade relaxation 4-65403
- brass, preferential sputtering studies by AES and XPS 4-93215
- charge exchange in HF approx. of time depend. Anderson model 4-107448
- circumstellar dust grains in nova ejecta, surface reactions rel. to grain destruction 4-101372
- composite surface, H<sup>+</sup> and D<sup>+</sup> ion generation rel. to surface/plasma ion source systems 4-93165
- composite surface, partially caesiased, H<sup>+</sup> prod. in presence of H plasma 4-93166
- condensed gas solids, electronically excited by fast light ions, nonlinear erosion yield 4-61804
- condensed gases, desorption by electronic processes 4-61238
- convoy electron production from swift H<sup>0</sup>, H<sup>+</sup> and H<sub>2</sub><sup>+</sup> beams 4-81060
- convoy electron velocity and ion velocity correlation 4-81061
- desorption induced by electronic transitions, workshop, Williamsburg, VA, USA (May 1982) 4-58556
- desorption mechanisms, substrate role, fusion device relevance 4-93164
- desorption processes, effect of image interaction 4-92557
- desorption stimulated by ion impact 4-61237
- dielectric materials, erosion by high-energy ions 4-61802
- dynamical interactions, surface potential determ. 4-66181
- electron ejection, ion induced, projectile vel. depend. oscills. 4-76578
- elements, medium Z, H<sup>+</sup> impact, X-ray prod. cross sections 4-96648
- fast ion-surface interactions at grazing incidence, review 4-81067
- glass, H depth profiling using <sup>15</sup>N beam 4-64249
- graphite, D<sub>2</sub><sup>+</sup> trapping and reflection coeffs. at oblique incidence 4-61793
- heavy target elements bombarded with protons in energy range 0.5 MeV to MeV, K-shell ionisation 4-96507
- heavy-ion backscatt. by thin single crystals, quantum calc. 4-66182
- impact-collision ion scattering spectroscopy and appl. to TiC 4-93163
- incidence angles associated with quasi-stable intersections during ion erosion 4-93171
- inelastic scattering at surfaces 4-81066
- inner shell ionisation by light ions, conf., Linz, Austria (Aug. 1983) 4-95035
- inner-shell ionisation, nonperturbative effects 4-99260
- inner-shell ionization and the Z<sub>1</sub><sup>3</sup> and Barkas effects in stopping power 4-99259
- ion gun for surface studies, beam profile and scanning characs. 4-64252
- ion-induced KL<sup>V</sup> and K<sup>L</sup><sub>V</sub> multiple vacancy production 4-99262
- jellium, scattered and re-emitted H<sub>2</sub> charged fractions, trajectory depend. 4-76597
- K shell X-ray cross section ratios for <sup>1</sup>H, <sup>4</sup>He and <sup>6</sup>Li projectiles 4-99261
- K-fluorescence yield in K and L shells, multiple ionisation effects 4-99232
- layered target, backscattering 4-76575
- ion-surface impact continued
- light elements, thick targets, H<sup>+</sup> bombardment, continuous X-ray spectroscopy 4-99214
- light ion impact, K-shell ionisation cross sections 4-99258
- light ion sputtering, angular depend. 4-76601
- light-ion and heavy-ion sputtering, threshold energies, incidence angle depend. 4-76612
- low energy ion scatt., neutralisation contribs. 4-81085
- low energy ion scatt. using alkalis 4-81074
- low energy ion scattering, charge states anal. 4-88923
- low temperature solid soln., low energy He atom scatt. 4-76627
- metal catalysts, dispersed, ISS anal., H<sub>2</sub> effects 4-99269
- metal heated spikes, evaporation and heat loss 4-107993
- metal overlayer/metal structures, sputtering, AES and EELS studies 4-76617
- metal surfaces, low energy He<sup>+</sup> ion scatt., inelastic loss energy 4-81081
- metallic crystal, shadowing effects obs. in slow ions backscatt. 4-66169
- metals, elastic collision spikes in sputtering at normal and oblique incidence 4-76602
- metals, K and L X-rays prod. by ion impact 4-99216
- metals, L-subshell ionisation cross section, projectile atomic number depend. 4-99267
- metals, L-subshell ionisation cross sections by protons 4-99266
- metals, single cryst. FCC, sputter-induced pits and pyramids 4-76615
- metals, sputtered particle energy distrib. at low bombarding energy 4-109290
- metastable atoms and ions for surface studies 4-85050
- mica, muscovite, nuclear track detector, ion stimulated desorption 4-68900
- molecular ion sputtering consequences 4-88974
- molecular targets, proton and  $\alpha$ -particle irradiated,  $\delta$ -ray emission 4-81058
- molecule transmission and convoy electron production by fast projectiles in thin solids 4-81063
- momentum transfer by H<sub>2</sub> cluster ions, surface roughness influence 4-71507
- multiple-vacancy production in the independent-Fermi-particle model 4-81093
- near-resonant and off-resonant charge exchange in ion-surface collisions 4-114354
- negative secondary ion emission from oxidized surfaces 4-66178
- nonideal system, poorly conducting, beam techniques for surface analysis 4-93575
- organic molecules, desorption by electronic processes 4-61238
- polycrystalline monatomic solids, sputtering yield at normal incidence 4-76603
- positive ion-surface scatt., negative ion form., Anderson correl. energy 4-66577
- proton recoil technique for H depth profiling 4-88922
- proton-surface collisions, charged fractions for low energy protons 4-81084
- review of surface analytical techniques, book contrib. 4-85053
- solid state Compton profiles by inelastic ion-electron scattering 4-81077
- solids, at. collisions, conf., Bad Iburg, Germany (July 1983) 4-73144
- solids, ion energy loss ang. depend. 4-65313
- spatiotemporally heterogeneous sputtering, surface topography development 4-76614
- stopping power effective charge of energetic ions in metals 4-65321
- surface anal., background subtraction techniques 4-93577
- surface anal., determ. of intensities of known spectral components 4-93578
- surface structure anal. by low-energy ion scatt. 4-81077
- thin film deposition, ion-surface interactions 4-80437
- UHV system for channelling/blocking analysis of surfaces and interfaces 4-88219
- Ag, backscattering of N<sub>2</sub><sup>+</sup> ions at 180°, enhanced surface yield 4-81070
- Ag, differential sputtering yields using collector method and electron backscatt. 4-76616
- Ag, ion-induced kinetic electron emission; Z<sub>1</sub> oscills. 4-76595
- Al, Auger spectra induced by Ne<sup>+</sup> and Ar<sup>+</sup> impact 4-109292
- Al, continuum X-rays produced by a few MeV proton bombardment 4-99215
- Al, ion-excited Auger electron emission, angular distribts. 4-76592
- Al, ion-induced Auger electron spectra, O<sub>2</sub> adsorp. effects 4-61795
- Al, proton small angle scatt. at grazing incidence 4-71499
- Al surface, ion bombarded, Auger emission anisotropies anal. 4-114355
- Al, surface-A<sup>+</sup> collisions, L<sub>23</sub>Al Auger electrons, polar angular distribts. 4-76585
- Al<sup>+</sup> secondary ion emission, ionisation probability following Ar<sup>+</sup> bombardment 4-66177
- Al-Fe(Cu), Ar<sup>+</sup> ions impact in ultrahigh vacuum, secondary ion electron Auger emission (*French*) 4-66170
- Al<sub>2</sub>O<sub>3</sub>, ion implantation, ion beam mixing, and annealing of metal 4-70229
- Au, backscattering of N<sub>2</sub><sup>+</sup> ions at 180°, enhanced surface yield 4-81070
- Au films, reactive ion beam etching, mol. ion dissociation upon impact 4-71772
- Au, ion impact L-shell ionisation, higher order processes 4-99265
- Au, ion-induced secondary electrons, energy spectra, mol. effects 4-76596
- Au, ion-induced secondary electron emission projectile incident angle depend. 4-76596
- Au, L-shell ionisation by Si and S ions, cross sections and alignment 4-99263
- Au, L-substrate ionisation cross sections, projectile depend. 4-99264
- B, ion-induced secondary electron emission projectile incident angle depend. 4-76596
- Be, ion-induced secondary electron emission projectile incident angle depend. 4-76596
- C, continuum X-rays produced by a few MeV proton bombardment 4-99215
- C foil, excitation by fast B<sup>+</sup> beam 4-107294
- C foil, H<sup>+</sup>, H<sub>2</sub><sup>+</sup> and H<sub>3</sub><sup>+</sup> ion bombardments, continuum optical radiation emission 4-81007
- CO adsorbed on Rh (001), photoemission, ion scatt. and secondary electron studies 4-75777
- CO, solid, low temp. electronic sputtering by light ions and electrons 4-71502
- CsBr, scatt. primary and recoiled surface neutrals and ions, TOF spectroscopy 4-63800

## surface impact continued

- Cu (001), surface semichannelling effect on energy distrib. of refl. ions 4-81056  
 Cu (001) and (011), small-angle ion refl. 4-81095  
 Cu (100), ion scattering spectrometry, shadowing effects 4-81088  
 Cu (100), keV Ne<sup>+</sup> and H<sub>2</sub>O<sup>+</sup> ion scatt., neutralisation study 4-81082  
 Cu (100), N<sub>2</sub><sup>+</sup> ions reflection, surface semichannelling obs. 4-81099  
 Cu (110), adsorption of O<sub>2</sub>, influence of Ne<sup>+</sup> ion bombard. 4-108723  
 Cu (110), He ion reson. neutralisation into reson. states 4-76588  
 Cu (110), low-energy ion scatt., 100 to 600K, temp. effects 4-81089  
 Cu (110), surface reconstruction determ. with impact-collision alkali ion scatt. 4-81100  
 Cu, excited H reflection at grazing incidence, light emission 4-76587  
 Cu, ion implantation of Au and Ta at non-normal incidence, sputtering yields 4-76619  
 Cu single cryst., sputtering yields, weight loss method study 4-76620  
 Cu<sub>2</sub>Au (100), keV Ne scatt., atom layer effects 4-76580  
 CuInSe<sub>2</sub>, sputtered surface characterisation using AES, O<sub>2</sub> adsorpt. 4-93147  
 F ion bombardment of ferromagnetic surface, polarization pick-up detection 4-81062  
 F<sup>+</sup>+C(X) foils, equilib. charge state, particle vel. depend. 4-64594  
 Fe (001) clean surface, surface struct. anal. using low energy ion scatt. 4-92496  
 foil, H<sub>2</sub><sup>+</sup> and H<sub>3</sub><sup>+</sup> ion bombardment, mol. enhancement of n-state populations 4-81064  
 GaAs (100), clean surface prep. using Ar<sup>+</sup> ion bombard. 4-104866  
 GaAs (110), <sup>6</sup>Ne<sup>+</sup> ion yield and neutralisation, 300-1200 eV 4-76581  
 GaAs/Au interface struct., XPS, RHEED and ion scatt./channelling studies 4-80421  
 GaSb (110) surface, ion beam crystallography 4-80343  
 Ge, clean and H<sub>2</sub>O adsorbed, scatt. primary and recoiled surface neutrals and ions, TOF spectra 4-63800  
 GeO<sub>2</sub>, scatt. primary and recoiled surface neutrals and ions, TOF spectra 4-63800  
 H<sup>+</sup> sputtering yields from Mo polycryst. target by Cs<sup>+</sup> bombardment 4-73575  
 H<sup>+</sup> surface conversion sources, sputter yield correl. with work function 4-93167  
 H<sup>+</sup>+C foil, 2p and 3p population, beam-foil excitation 4-64584  
 H<sup>+</sup>+C(AI) foil, ion energy loss ang. depend. 4-65313  
 H<sub>2</sub><sup>+</sup> mol. ion beam bombard. of solid and gaseous targets 4-76579  
 H<sub>2</sub><sup>+</sup> wall collisions, H<sub>2</sub> vibrationally excited generation 4-76574  
 H<sub>2</sub><sup>+</sup>+C foil, 2p and 3p population, beam-foil excitation 4-64584  
 H<sub>2</sub><sup>+</sup>+C foil, 2p and 3p population, beam-foil excitation 4-64584  
 H<sub>2</sub>O, solid, low temp. electronic sputtering by light ions and electrons 4-71502  
 InP (100) surfaces, atomic conc. ratio by X-ray photoelectron spectroscopy 4-66185  
 InP, surface and interface states 4-92782  
 La, scatt. primary and recoiled surface neutrals and ions, TOF spectra 4-63800  
 LJF surfaces, F<sup>+</sup> ejection by ion bombardment 4-61800  
 Li<sup>0</sup> formation by Li<sup>+</sup> scatt. from cesiated W (110) surface 4-76624  
 Mg, Auger spectra induced by Ne<sup>+</sup> and Ar<sup>+</sup> impact 4-109292  
 Mg, ion-excited Auger electron emission, angular distrib. 4-76592  
 Mg, ion-induced Auger electron spectra, O<sub>2</sub> adsorpt. effects 4-61795  
 Mg, ion-induced secondary electron emission projectile incident angle depend. 4-76596  
 Mo (001), C, N, O overlayers, adsorbate ordering, low energy K<sup>+</sup>-ion scatt. 4-98448  
 Mo (001), clean and adsorbate covered, low energy alkali ion scatt. 4-76582  
 Mo (001), dissociative adsorption of O<sub>2</sub>, low energy ion scatt. study, adsorbate induced neutralisation effects 4-81078  
 Mo, atom sputtering at grazing incidence, spherical angular distrib. 4-76613  
 Mo surface, kinetics of N<sub>2</sub><sup>+</sup> and N<sup>+</sup> reactions, 7.5-100 eV impact energies 4-93560  
 N<sup>+</sup> beam-surface interaction at grazing incidence, N ground term selective population 4-59885  
 N<sup>+</sup> ion beam surface interaction, fluorescence, Stark effect obs. 4-78948  
 Na, negative charge-state fraction of reflected <sup>3</sup>He and <sup>4</sup>He, trajectory effects 4-76594  
 NaBr mols. impinging on Re surface, Na<sup>+</sup> ions prod., temp. depend. 4-105015  
 Nb, H permeation, surface effects 4-113723  
 Ni (110), adsorption of N<sub>2</sub> at low coverage, ion scatt. spectroscopy study 4-81080  
 Ni (110), clean and CO covered, medium energy ion scatt. studies 4-88381  
 Ni (110), He ion reson. neutralisation into reson. states 4-76588  
 Ni (110), molecular N<sub>2</sub> adsorpt., phase transitions obs. by ISS 4-88395  
 Ni (110), surface analysis by surface channelling using ion induced Auger electron emission 4-81068  
 Ni (110) and (111), adsorbed D site location, surface channelling study 4-80375  
 Ni (111), H<sub>2</sub><sup>+</sup> and N<sub>2</sub><sup>+</sup> mol. ion scatt. at grazing incidence, dissociation products 4-76583  
 Ni, atom sputtering at grazing incidence, spherical angular distrib. 4-76613  
 Ni, ion bombardment-induced O<sup>-</sup> desorption, energy distrib. 4-75781  
 Ni, ion desorption spectrometry for surface anal. 4-66609  
 Ni passivity breakdown by fluoride, surface anal. 4-89177  
 Ni surface, polycryst., clean and S covered, low energy ion and neutral scatt. 4-81083  
 Ni/Ni<sub>2</sub>C two layered films, Ni sputtering yield, temp. and flux depend. 4-76605  
 Ni-Si (111) interface, Ni-Si islands growth, ion scatt. study 4-92444  
 PbO-containing glass, XPS study of angular dependence of preferential sputtering 4-88926  
 Pt (100), catalytic oxidation of CO, MeV ion scatt. study 4-81069  
 Pt (111), H<sub>2</sub> adsorption location from corrugation anal. and He<sup>+</sup> diff. 4-65556  
 SO<sub>2</sub>, solid, sputtering by MeV and keV ions 4-71504  
 Si (100), clean and Cs covered, neutralisation of scattered He ions 4-109294  
 Si (100), energetic He ion scatt., neutralisation, channelling studies 4-76591  
 Si (111)2×1 surface, MeV ion backscattering/channelling studies 4-85051

## ion-surface impact continued

- Si, Auger spectra induced by Ne<sup>+</sup> and Ar<sup>+</sup> impact 4-109292  
 Si, inert gas ion bombardment, secondary ion emission, angular depend. 4-76618  
 Si, ion-excited Auger electron emission, angular distrib. 4-76592  
 Si, low energy proton scatt. 4-81087  
 Si, sputtering by SO<sup>+</sup>, yield data 4-88974  
 p-Si surface, <sup>14</sup>N<sub>2</sub><sup>+</sup> (H<sub>2</sub><sup>+</sup>) bombardment, Raman scatt. obs. 4-114283  
 Si surface, D<sub>2</sub><sup>+</sup> bombarded, Raman spectrum investig. 4-114284  
 Si surface, interaction with tetrafluoromethane, evidence for parallel etching mechanisms 4-71496  
 Si/Au(Ag) interfaces, reactivity, MeV ion scatt. studies 4-80424  
 SiC, ion implantation, ion beam mixing, and annealing of metals 4-70229  
 Si<sub>3</sub>N<sub>4</sub>, ion implantation, ion beam mixing, and annealing of metals 4-70229  
 Ta, backscattering of N<sub>2</sub><sup>+</sup> ions at 180°, enhanced surface yield 4-81073  
 TiC, ion surface scatt. near 180° scatt. angle, thermal vibrs. effect, two-atom scatt. model 4-81072  
 TiC, surface studies by impact-collision ion scattering spectroscopy 4-93163  
 Ti<sub>2</sub>O<sub>3</sub> (047) surface, preparation by ion bombardment and annealing, XPS and UPS studies 4-65528  
 W, clean and O covered, noble gas ion impact, adsorbate depend. ion neutralisation 4-81079  
 W:Cs surface, H<sup>+</sup>, H<sub>2</sub><sup>+</sup>, Li<sup>+</sup> scatt. for H<sup>-</sup>, Li<sup>-</sup> formation 4-73574  
 W(110)+K<sup>+</sup> ion impact, angle and energy resolved, rainbows 4-81092  
 Xe atom implantation in Al, depth distribution obs. by Rutherford backscattering (Japanese) 4-104707  
 Xe, frozen, sputtering by keV heavy ions 4-71503  
 (YBiPb)<sub>3</sub>(FeAlPt)<sub>5</sub>O<sub>12</sub> LPE layers, lattice site determ. by channelling 4-80440  
 Zr, collision cascade anisotropy by light-ion irr., fluorescence studies 4-76607

ion thrusters *see* ion enginesionic conduction in liquids *see* electrical conductivity of electrolytic liquids; electrical conductivity of liquids

## ionic conduction in solids

*see also* superionic conducting materials

- alkali glasses, ionic elec. cond., temp. depend. 4-113703  
 alkali halide mixed crystals, growth and characterisation, microhardness, colour centres, radiation hardening 4-70152  
 alkali metal fluorides, M<sub>1-x</sub>BiF<sub>1+2x</sub> (M=Na, K, Rb), elec. props. and struct. characts. 4-70452  
 binary systems, ionic cond., path probability method of irreversible statistical mechanics 4-61131  
 chain systems, H-bonded, proton cond. mechanism 4-80285  
 conference, Alanya, France (June-July 1982) 4-95052  
 dielectric films, ionic transport, transient current calc. 4-70433  
 doped fluorite oxides, ionic transport and point defects 4-98340  
 electrode-dielectric interface investigation using superimposed AC and DC voltages 4-108939  
 fast ionic conductors, review 4-70439  
 fluorite struct. oxides, O ion cond., dopant size effects 4-70446  
 fluorite-type solid solutions, theory 4-92428  
 glassy materials, temp. coeffs. of transport props. 4-92409  
 ice, cubic, H<sup>+</sup> transfer and Bjerrum defect migration 4-70434  
 nonstoichiometric compounds, transport processes, conf., Cracow, Poland (Aug. 1980) 4-95060  
 Nylon 5,7 films, dielec. and pyroelec. props., mol. orientation depend. 4-99043  
 oxide, exchange of O between gas and solid, electrochemical study 4-98357  
 poly(ethylene oxide) complex electrolyte, PEO(LiCF<sub>3</sub>SO<sub>3</sub>)<sub>n</sub>, DSC, NMR studies 4-61047  
 poly(ethylene oxide)-ammonium trifluoromethylsulphate, complex, amorphous and cryst., form., stoichiometry and cond. response 4-88303  
 poly(ethylene oxide)-NH<sub>4</sub>SCN complex, amorphous and cryst., form., stoichiometry and cond. response 4-88303  
 poly(ethylene succinate)-LiBF<sub>4</sub> solid electrolyte complex, ion transport 4-75721  
 polyester polymer matrix, ion transport and injection 4-108653  
 polyethylene oxide-NaSCN ionic cond., elec. props., complex reactions (Chinese) 4-92407  
 α-quartz, electrodiffusion of charge-compensating ions 4-61153  
 quartz crystals, electrical conductivity and dielectric loss, effect of alkali ions 4-71271  
 quasi-DC ionic conduction in dielec. materials 4-108656  
 rare earth compounds, R<sub>0.8</sub>Co<sub>0.2</sub>CrO<sub>3</sub>, R=Ce, Pr, Nd, Sm, Eu, Gd, Tb, Dy, Ho, Er, Tm, Yb, Lu, ionic cond. and thermal expansion 4-84461  
 rare earth cpds., R<sub>x</sub>Zr<sub>1-x</sub>O<sub>2-0.5x</sub> solid solns., struct. and ionic cond. 4-70445  
 rare earth fluorite cryst., ionic thermocurrents and ionic cond. 4-70443  
 rare earth ionic conductors, K<sub>8-x</sub>R<sub>3</sub>(Si<sub>6</sub>O<sub>16</sub>)<sub>2</sub>(OH)<sub>1-x</sub>, R=Gd, Ho, Yb, cryst. struct. and chem., X-ray diff., study 4-60895  
 silicate glass, E-glass fabric and high-silica glass, vol. resist. depend. on temp. and leaching parameters 4-70880  
 solid state chemistry, conf., Veldhoven, Netherlands (June 1982) 4-67863  
 three dimensional skeleton phosphates, ionic cond., phase transitions and struct. 4-70448  
 transition metal dichalcogenides, Ag intercalated, ionic cond. studies 4-70444  
 two-phase system, ionic cond. enhancement and space charge region defects 4-80286  
 tysonite-type solid solutions, theory 4-92428  
 Ag halide emulsion microcrystals, dielec. loss obs. of ionic cond. (Japanese) 4-113699  
 Ag<sub>2</sub>As<sub>2</sub>S<sub>3</sub>, proustite, Raman spectra and Ag ion conduction 4-71365  
 Ag<sub>1-x</sub>Bi<sub>x</sub>F<sub>1+2x</sub>, elec. props. and struct. characts. 4-70452  
 Ag<sub>2</sub>HgI<sub>4</sub>, phase transitions, ionic cond. study 4-88287  
 AgI, phase transitions, ionic cond. study 4-88287  
 AgI-AgBr, ionic conductivity and phase transformations, homovalent ion substitution effects 4-92426  
 AgPO<sub>3</sub>, low temp. ionic cond., rel. to struct. 4-113712  
 α-Ag<sub>2</sub>Rb<sub>1-x</sub>Cs<sub>x</sub>I<sub>3</sub>, ionic elec. cond. and phase transitions 4-84455  
 Ag<sub>2</sub>S, chem. prepared films, mixed conductivity study 4-104277  
 α-Al<sub>2</sub>O<sub>3</sub>:Cr<sub>2</sub>O<sub>3</sub>(Y<sub>2</sub>O<sub>3</sub>), ionic cond., doping effects 4-92417  
 β-Al<sub>2</sub>O<sub>3</sub>:Li<sup>+</sup>, vibr. dynamics of Li ions 4-70441

## ionic conduction in solids continued

- $\beta''$ - $\text{Al}_2\text{O}_3$ - $\text{Na}_2\text{O}$  electrolyte ceramic tubes, sintering, radial DC resist. 4-103994  
 $\beta''$ - $\text{Al}_2\text{O}_3$ - $\text{ZrO}_2$  slip cast transform. toughened composites, mech. props., ionic cond. 4-103995  
 $\text{Al}(\text{PO}_3)_3$ - $\text{Li}_2\text{O}$ - $\text{K}_2\text{O}$  glasses, mixed-alkali effect 4-80296  
 $\text{B}_2\text{O}_3$ - $\text{Li}_2\text{O}$  glass, ionic cond. meas. 4-84457  
 $\text{Ba}(\text{NO}_3)_2$ -K, d.c. ionic cond. meas. 4-84456  
 $\text{BaSr}_{1/3}\text{Nb}_{2/3}\text{O}_3$ , defect struct., elec. and ionic cond. 4-98676  
 $\text{Ba}_{1-x}\text{U}_x\text{F}_{2+2x}$ , high temp. ionic cond. study 4-70450  
 $\text{Ba}_{1-x}\text{U}_x\text{F}_{2+2x}$ , ionic conductivity, crit. temp. 4-92423  
 $\text{Bi}_2\text{O}_3$ - $\text{Y}_2\text{O}_3$ , ionic and elec. cond. meas. 4-88547  
 $\text{Bi}_2\text{O}_3$ - $\text{Y}_2\text{O}_3$  system high ionic conductor, ionic cond. and electronic cond. (Chinese) 4-70879  
 $\text{Ca}(\text{OH})_2$ , proton dynamics,  $^1\text{H}$  NMR relax. meas. 4-104505  
 $\text{CaS}$ , ionic cond., Schottky defect model 4-70456  
 $\text{CdF}_2$ , alkali metal doped, association and bound motion 4-80294  
 $\text{Cd}_2\text{Hg}_{1-x}\text{Te}$ , ion transport and anodic oxidation (Russian) 4-70440  
 $\text{Ce}_{1-x}\text{Ca}_x\text{O}_{2-x}$ , vacancy binding energy, polarisation contrib. 4-88165  
 $\text{Ce}_{1-x}\text{Gd}_x\text{O}_{2-x}$ , vacancy binding energy, polarisation contrib. 4-88165  
 $\text{CeO}_2$ - $\text{CaO}$  solid solutions, elec. cond., temp. depend., 400-1200°C 4-61142  
 $\text{CeO}_2$ - $\text{Ln}_2\text{O}_3$  (Ln=La, Nd, Sm, Gd, Er, Y) solid solutions, elec. cond., temp. depend., 400-1200°C 4-61142  
 $(\text{CeO}_3)_{0.99}(\text{CaO})_{0.11}$  solid solution, bulk cond. and grain boundary resist., effect of  $\text{SiO}_2$  (French) 4-80295  
 $\text{Ce}_{1-x}\text{Y}_x\text{O}_{2-x}$ , vacancy binding energy, polarisation contrib. 4-88165  
 $\text{Cu}_2\text{MgI}_4$ , phase transitions, ionic cond. study 4-88287  
 $\text{Cu}_2\text{S}(\text{Se})$ , ionic thermoelectromotive force, rel. to temp. and mobile ion conc. 4-75719  
 $\text{Cu}_2$ -Se, mixed conductor, DC ionic cond. meas. 4-88340  
 $\text{CuTeBr}$ , phase transitions, ionic cond. study 4-88287  
 $\text{EuF}_2$ , permitt., dielec. loss tangent, cond. meas. 4-104523  
 $\text{H}(\text{NH}_3)_2\text{SbO}_3$ , proton cond. and cryst. struct. (French) 4-84451  
 $\text{H}_3\text{PW}_{12}(\text{Mo})_{12}\text{P}_{40}\cdot 21\text{H}_2\text{O}$ ,  $\text{H}^+$  motion, AC cond. and  $^1\text{H}$  NMR studies 4-108655  
 $\text{I}_2$ -HI, proton cond. meas. 4-92413  
 $\text{K}_1\text{Al}_3\text{Si}_6\text{O}_{16}$ , hollandite, one-dimens. ionic cond., three-dimens. long range order, diffuse X-ray scatt. 4-98067  
 $\text{KI-KBr}$ , ionic conductivity and phase transformations, homovalent ion substitution effects 4-92426  
 $\text{KSbF}_4$ , structural phase transitions, NQR, specific heat, X-ray powder anal., permitt., elec. cond. 4-113605  
 $\text{La}_{1-x}\text{Ba}_x\text{F}_{3-x}$  solid solns., elec. props., small-signal AC response and TSDC meas. 4-70449  
 $\text{La}_{1-x}\text{Ba}_x\text{F}_{3-x}$  solid solutions, small signal AC response 4-92424  
 $(\text{LiNa})_2\text{O}\cdot\text{B}_2\text{O}_3$  glasses, mixed alkali effect 4-84449  
 $\gamma$ - $\text{LiAlO}_2$ , polycrystalline, elec. cond., AC meas. 4-108645  
 $\text{LiBiO}_2$ , ionic cond., cryst. struct., and sp. ht. studies 4-70455  
 $\text{Li}_2\text{BiO}_3$ , ionic conductivity 4-70437  
 $\text{Li}_2$ - $\text{Cd}_{1-x}\text{Cl}_x$  spinel, ionic cond. and phase transition 4-75720  
 $\text{LiF-AlF}_3$  thin film, ionic cond. meas. 4-84450  
 $\text{LiF-CaF}_2$  thin film, ionic cond. meas. 4-84450  
 $\text{LiF-CeF}_3$  thin film, ionic cond. meas. 4-84450  
 $\text{LiF-CrF}_3$  thin film, ionic cond. meas. 4-84450  
 $\text{LiF-MgF}_2$  thin film, ionic cond. meas. 4-84450  
 $\text{LiF-NiF}_2$  thin film, ionic cond. meas. 4-84450  
 $\alpha$ - $\text{LiIO}_3$ , ion transport and relax., polarising microscopy studies (Chinese) 4-98335  
 $\alpha$ - $\text{LiIO}_3$ , quasi-one-dimensional ionic conductor, light diff. due to space charge fluctuations 4-109156  
 $\alpha$ - $\text{LiIO}_3$ , quasi-one-dimensional ionic conductor, light diff. due to space charge fluctuations 4-109157  
 $\text{Li}_{1-x}\text{Mg}_x\text{Cl}_4$  spinel, ionic cond. and phase transition 4-75720  
 $\text{Li}_{1-x}\text{Mn}_x\text{Cl}_4$  spinel, ionic cond. and phase transition 4-75720  
 $\text{Li}_2\text{MoO}_4$ ,  $\text{Li}^+$  transport, pulse NMR relax. time meas. 4-75727  
 $\text{LiNbO}_3$ ,  $\text{Li}^+$  ionic cond., activation energy and IR spectra 4-84453  
 $\text{Li}_2\text{O}$ - $\text{ZnO}$ , ceramics system, ionic and mixed cond. rel. to comp. and humidity 4-98339  
 $\text{LiPO}_3$ - $\text{LiCl}$  glass, ionic cond. meas. 4-84457  
 $\text{Li}_2\text{SiO}_3$ , polycrystalline, elec. cond., AC meas. 4-108645  
 $\text{Li}_2\text{Si}_2\text{O}_5$ - $\text{Li}_2\text{SO}_4$  glass, ionic cond. meas. 4-84457  
 $\text{Li}_2\text{SiO}_3$ - $\text{Li}_2\text{VO}_4$  solid solns.,  $\text{Li}^+$  ion conductivity 4-108647  
 $\text{Li}_2\text{ThF}_6$ , ionic transport props., AC cond. and pulsed NMR study 4-70453  
 $\text{Li}_2\text{WO}_4$  amorphous film, electrochromism colouring/bleaching processes,  $\text{Li}^+$  ion transport 4-114244  
 $\text{Li}_{1-x}\text{Zn}_x(\text{GeO}_3)_2$ , LISICON ceramic, synthesis and elec. props. 4-75728  
 $\text{Li}$  ion conductors of polyanion complexes dispersed with  $\text{LiClO}_4$ , appl. to solid state batteries 4-92414  
 $\text{Mg}_2\text{SiO}_4$ , forsterite,  $\text{SiO}_2$  solubility, solid state EMF measurements 4-61092  
 $\text{NH}_4\text{HSO}_4$ , high temp. phase transition, ionic motion 4-108651  
 $\text{Na}_{1-x}\text{Hf}_x\text{Si}_{1-x}\text{P}_{1-x}\text{O}_{13}$ ,  $\text{Na}^+$  ion cond. and crystallographic cell characterisation 4-113706  
 $\text{Na}_2\text{O-B}_2\text{O}_3\text{-Al}_2\text{O}_3$ , aluminoborate glass, cond. max. 4-113702  
 $\text{Na}_2\text{O-CuO-GeO}_2$  glass, elec. cond., chem. content depend. 4-98673  
 $\text{Na}_{3-4x}\text{Zr}_x\text{PO}_4$ , ionic cond. meas. 4-108650  
 $\text{Nd}_2\text{Zr}_2\text{O}_7$ , anionic disorder, neutron diff. and ionic cond. study 4-70108  
 $\text{Nd}_2\text{Zr}_2\text{O}_7$ - $\text{Nd}_2\text{Ce}_2\text{O}_7$  system, anion cond., order/disorder effects 4-70447  
 $\beta''$ - $\text{Nb}_2\text{O}_5$ - $\text{Al}_2\text{O}_3$ - $\text{ZnO}$  ceramics, ionic cond. and activation energy 4-113708  
 $\text{P}_2\text{S}_5$ - $\text{Li}_2\text{S}$  glass, ionic cond. meas. 4-84457  
 $\text{PbF}_2$ - $\text{Na}(\text{K})(\text{Rb})$ , ionic cond., dielec. relax. and activation vol. 4-113701  
 $\text{Pb}_{1-x}\text{U}_x\text{F}_{2+2x}$ , high temp. ionic cond. study 4-70450  
 $\text{Pb}_{1-x}\text{U}_x\text{F}_{2+2x}$ , ionic conductivity, crit. temp. 4-92423  
 $\alpha$ - $\text{RbAg}_4\text{I}_5$ , ionic cond. up to far IR freqs. 4-108654  
 $\text{RbHSO}_4$ , high temp. phase transition, ionic motion 4-108651  
 $\text{Sb}_2\text{O}_3\cdot\text{nH}_2\text{O}$ , d.c. proton cond. and Nernst effect meas. 4-84462  
 $\text{SiO}_2$ , vitreous,  $\text{Al}_2\text{O}_3$  substruct. and elec. cond. 4-113341  
 $\text{SrCa}_{1/3}\text{Nb}_{2/3}\text{O}_3$ , defect struct., elec. and ionic cond. 4-98676  
 $\text{Sr}(\text{NO}_3)_2$ , d.c. ionic cond. meas. 4-84456  
 $\text{Sr}(\text{NO}_3)_2$ - $\text{Na}(\text{Al})$ , d.c. ionic cond. meas. 4-84456  
 $\text{Ta}_2\text{O}_5$ , stabilised with  $\text{TiO}_2$ ,  $\text{HfO}_2$  and  $\text{Cr}_2\text{O}_3$ , ionic cond. studies 4-70435  
 $\text{H-Ta}_2\text{O}_5\text{-TiO}_2(\text{HfO}_2)(\text{Cr}_2\text{O}_3)$ , ionic conductivity 4-75722  
 $\text{Ti}_{1-x}\text{Bi}_x\text{F}_{2+2x}$ , elec. props. and struct. characts. 4-70452  
 $\text{TiCl}_4$  doped with divalent cation and anion impurities, point-defect mobility 4-84448  
 $\text{U}_{0.7}\text{Ce}_{0.3}\text{O}_{2-x}$ , transport props. 4-104245  
 $\text{WO}_3$ , nonstoichiometric, point defect to shear plane evolution 4-92202

## ionic conduction in solids continued

$\alpha$ - $\text{Zr}(\text{HPO}_4)_2\cdot\text{H}_2\text{O}$ , d.c. proton cond. and Nernst effect meas. 4-84462  
 $\text{ZrO}_2$ - $\text{Y}_2\text{O}_3$ , polycryst. and single cryst. elec. cond. 4-80290

## ionic conductivity in solids see ionic conduction in solids

## ionic thermocurrents see thermally stimulated currents

## ionisation

see also associative ionisation; autoionisation; charge exchange; electron attachment; electron capture; field ionisation; ion recombination; ionisation of atoms; ionisation of gases; ionisation of liquids; ionisation of molecules; ionisation of solids; ionisation potential; Penning ionisation; photoionisation; surface ionisation

microparticles volatilisation and ionisation, laser-induced, mass spectroscopic analysis 4-105088

plasma ionisation processes, time dependent, four stage approx. 4-87922  
 reactive components, fluctuation thermodynamic props., species correlation function integrals 4-71965

solar wind, ionisation temps. inferred from charge state comp. of diff. particle events 4-85854

## ionisation chambers

absolute ionisation image chamber 4-112044

collection efficiency in a pulsed and mag. swept electron beam 4-10993

CT dosimetry system using ionisation chambers 4-89764

design methods for shockproofed ionisation chambers 4-64290

DIogene pictorial drift chamber 4-59503

double ionisation chamber for fission fragment detection 4-64284

Fuji Electric's ionization chamber type monitoring post 4-112036

gridded ion chambers, particle counting method 4-102429

gridded ionisation chamber for alpha-particle spectroscopy 4-102427

heavy ion gas detectors, developments at LNL, avalanche counter 4-87022

indoor exposure meas. system 4-93894

jet chamber of JADE expt. 4-59502

large area Frisch grid chambers for low level alpha spectrometry 4-102428

large solid angle ionisation chamber with ring counter geometry 4-64282

limited streamer mode characteristics 4-59549

multielectrode particle detectors, cross talk 4-59592

multistep avalanche chambers, low press. operation 4-64278

multistep parallel plate chamber, development as time projection chamber 4-59544

parallel plate avalanche chamber as endcap detector for TPC 4-59506

position-sensitive counter telescope for light and heavy ions 4-64281

position-sensitive ionization chamber for a flight-time spectrometer 4-74108

position-sensitive multistep gaseous detector for very low energy heavy ions 4-68893

pulse shapes 4-63446

range sensitive telescope detector using ionisation chamber and solid state detector 4-102518

spherical ionisation chamber for neutron spectroscopy 4-91166

SQS  $\mu$ -counter model, working gas conc. meas. by chromatograph (Chinese) 4-74116

tetramethylsilane for liquid ionisation chamber 4-91163

wire chamber particle detectors 4-96409

wire chambers, streamer mode, dead times and dead zones 4-59537

n- $\gamma$  dose rate, NDK 601 instrument dosimetric characts. 4-59454

Ar, liq., calorimeter read-out scheme 4-68891

Ar-C<sub>2</sub>H<sub>6</sub>-CH<sub>3</sub>CH<sub>2</sub>OH, wire chamber gas mixture, breakdown processes 4-59539

Ar-methane fission fragment energy loss meas. 4-87024

$^{60}\text{Co}$   $\gamma$ -rays exposure, calc. response and wall correction factors 4-64304

$^{235}\text{U}(\text{ZrU})$  fission counter assembly detection efficiency calc. and meas. 4-68897

Xe liquid in ionisation chamber, spectrometry of 1 MeV electrons 4-107263

## ionisation gauges

additional electrodes for transducers, for improving performance 4-101864

axial-emission self-modulating ion gauge 4-86435

Bayard-Alpert ionisation gauges, unstable and nonreproducible sensitivities 4-78337

high-pressure ionisation head, limitations of meas. range (Polish) 4-111147

modulated emission, remote UV pressure meas. 4-86436

stable and reproducible sensitivities using new geometries 4-78338

vacuum measurement, and control, Joint European Torus project 4-86970

## ionisation of atoms

see also atomic electron impact ionisation

adiabatic ang. wave functions in atomic ionisation problem (Russian) 4-112289

alkali metal atoms, excited states, photoionisation, initial wave function 4-83438

alkali-like atoms and ions, quasi-metastable quartet levels 4-74201

alpha-particle-induced, inner-shell ionization measurements for the underground laboratory 4-82625

at. and solid state effects, photoionisation processes 4-83346

atom-ion collisions, ionisation probabilities, charge scaling calculations 4-107343

atomic spectra and oscillators, conf., Lund, Sweden, 17-19 Aug. (1983) 4-86109

distributed source corona photoionization calculations applicable to finite element computer models 4-96506

doubly alignment parameter  $A_2$  for  $L_3$  subshell ionisation by light-ion impact 4-96510

electron atom shell influence on effective neutron charge value (Russian) 4-96505

electron density energy in external potential, ionisation dependence 4-78776

electron tunnelling, from potential well, in electric field 4-86247

Electronic relativistic effect in inner-shell ionization cross section and electron momentum distribution 4-96509

elemental electronegativities, electron affinities, ionis. pots. and hardnesses, calcs. 4-112099

flames, laser-enhanced ionisation, theory 4-64638

fluorocarbon hydrocarbon systems in atoms+ion collisions, elec. field ionisation 4-102784

heavy atoms, ionisation pot., universal asymptotic limit in non-relativistic theory 4-112084

## sation of atoms continued

heavy targets, 1 subshell X-ray production by 1 to 3 MeV protons and He<sup>+</sup> ions 4-96651  
 high excited atoms, nonlinear ionisation 4-107319  
 high-Z elements, 5d and 4f subshells photoionisation 4-96504  
 highly charge ion prod. and storage at room temp. appl. to electron transfer and photoionisation meas. 4-82860  
 highly charged ions, ionis. from 5l and 6l sublevels 4-107292  
 highly-excited atoms in the electromagnetic field, bound-bound and bound-free transitions 4-83311  
 inert gases, multiphoton ionisation, electron energy spectra, statistical model 4-78819  
 inner shell ionisation; wave function effects 4-99235  
 inner shell ionisation by light ions, conf., Linz, Austria (Aug. 1983) 4-95035  
 inner shell photoeffect, screened Coulomb continuum wave functions 4-83345  
 inner shell vacancy production in ion-atom collisions, review 4-69199  
 inner-shell ionization and the Z<sub>1</sub><sup>3</sup> and Barkas effects in stopping power 4-99259  
 inner-shell ionization by light ions 4-64582  
 interstellar wind atoms ionisation, role of 'core' and 'halo' solar wind electrons 4-105863  
 ion-atom asymmetric collisions, inner shell ionisation, binding effects 4-96674  
 ion-atom collisions, ionisation cross sections, numerical calcs. 4-96675  
 ion-induced, inner-shell ionisation, nonperturbative effects 4-99260  
 ionised atoms, ionisation effects in inner electron shells, review 4-87068  
 ions in dense plasmas, excitation-deexcitation and ionisation-recombination 4-69863  
 isotopic cataphoresis in a crossed-field plasma centrifuge 4-75212  
 K-fluorescence yield in K and L shells, multiple ionisation effects 4-99232  
 K-shell electrons, ionisation probability as function of impact parameter 4-96680  
 K-shell ionisation, 2-parameter representation in binary collision approx. 4-102659  
 laser optogalvanic effect for ats. and mols. in recomb.-limited plasmas 4-87091  
 light ion impact, K-shell ionisation cross sections 4-99258  
 maximum negative ionisation bound 4-78773  
 metals, H<sup>+</sup> induced L shell X-ray production cross sections 4-96649  
 metals, L-subshell ionisation cross section, projectile atomic number depend. 4-99267  
 metals, L-subshell ionisation cross sections by protons 4-99266  
 multiphoton absorption, recoil charge distrib., Fermi-Dirac distrib. 4-59892  
 multiphoton ionisation, electron spectra, strong-field effects 4-102654  
 multiphoton ionisation, nonHermitian quantum theory 4-102657  
 multiphoton ionisation and third-harmonic generation, quantum theory 4-64442  
 multiphoton ionisation process, final-state interactions 4-96503  
 multiply charge ion-gas target collision, charge transfer cross sections 4-102789  
 N-electron atomic core, adiabatic polarisation pot. experienced by single valence electron 4-96444  
 negative ions, electron detachment in slow collisions with atoms 4-69198  
 nonexponential decay in autoionization near threshold 4-91315  
 nova ejecta, effects of C and H ionisation on grain growth and destruction 4-101372  
 PES satellite intensities, incident photon energy effect 4-78815  
 photoionisation in strong laser fields (*Dutch*) 4-64436  
 proton impact K-shell ionisation, binary encounter approx. 4-59887  
 rarefied gas, effect of charge-exchange reactions on ionisation equilib. 4-94577  
 reactive sputtering plasmas, preferential ionisation, glow discharge mass spectrometry anal. 4-99313  
 Rydberg series, autoionisation, multichannel quantum defect theory 4-64439  
 shock-heated Ar plasma, collisional and radiative mechanism simulations 4-91965  
 three-electron atomic systems, autoionisation states, correl. and relativistic effects 4-102614  
 three-particle system, Coulomb break-up, Wannier threshold theory 4-83475  
 two-photon ionisation: interference and population trapping 4-74203  
 vacuum polarisation and tunnel transition, potential well in electric field 4-86635  
 VUV photoionisation, recent progress and problems 4-87088  
 VUV radiation physics, conf., Jerusalem, Israel, 8-12 Aug. (1983) 4-82583  
 A+ 2p shell, photoionisation, excited electron wave functions 4-83350  
 Ar, alignment prod. in ionisation of 2p shell by specific momentum transfer 4-96701  
 Ar clusters, Penning, photo and electron impact ionisation 4-74366  
 Ar, laser induced cascade ionisation, secondary ionisation processes 4-83355  
 Ar, photoionisation, electron source, collision processes 4-83338  
 Ar, positive column, low press., stepwise ionisation effects modelling 4-92013  
 Ar+H<sup>+</sup>(Li<sup>+</sup>)(Na<sup>+</sup>)(K<sup>+</sup>), electron detachment cross sections 4-78952  
 Ar+Kr atoms, ionisation processes for highly excited Ar atoms 4-87201  
 Ar+Xe, corals. between charge-changing interactions and projectile K-alpha X-ray emission 4-64595  
 Au, ion impact L-shell ionisation, higher order processes 4-99265  
 Au, L X-ray emission probabilities by 70 MeV Ar ion impact 4-78949  
 Au, L-shell ionisation by Si and S ions, cross sections and alignment 4-99263  
 Au, L-substrate ionisation cross sections, projectile depend. 4-99264  
 Au<sup>q+</sup>+He, electron capture, ionisation and transfer ionisation cross sections 4-78960  
 Ba, 7s<sub>n</sub>d autoionisation states, two-photon spectroscopy 4-78822  
 Ba, autoionisation rate enhancement of two-photon excited states near Ba<sup>+</sup>6d<sub>3/2</sub> limit 4-91239  
 Ba, excited states, inner and outer shell photoionisation 4-83340  
 Ba, multistep excitation of autoionizing Rydberg states 4-74202  
 Ba, nonlinear ionisation, influence of self-ionisation states 4-107324  
 Ba, nonlinear ionisation by 0.53 mkm wavelength laser radiation 4-83354  
 Ba, three- and five-photon ionis. probabilities meas. 4-69031  
 Ba<sup>2+</sup> formation via reson. nonlinear process 4-107320

## ionisation of atoms continued

Ba<sup>2+</sup> ions, 4d photoabsorption spectrum, potential-barrier effects, photoionization 4-112138  
 Be II autoionis. widths, optical emission spectrosc. investig. 4-69025  
 Be<sup>+</sup> doubly excited states, autoionisation widths calcs. 4-64403  
 Be<sup>2+</sup>, photoionisation and double excitation spectrum 4-87089  
 Be+C(N)(O)(Ne) ions, single and double K-shell ionization cross-sections meas. 4-64583  
 Br, relative photoionis. cross-section, autoionis. Rydberg series 4-64435  
 Br<sup>+</sup>+Ne-Br<sup>+</sup>+Ne<sup>+</sup>, contribution of K-capture to Ne<sup>q+</sup> production 4-83466  
 CA XVIII/CA XIX ionisation balance in solar flares, derivation from XRP solar X-ray data 4-72916  
 Ca, hypersatellite X-ray spectra, H<sup>+</sup> induced 4-107301  
 Cd I, d<sup>8</sup>s<sup>2</sup>p electron configs., empirical Slater-Condon parameters 4-68943  
 Cd ions in laser-prod. plasma, for UV spectra 4-68997  
 Cl, photoionisation, reson. struct. 4-112149  
 Cl, reson. struct., autoionisation, photoionisation spectra 4-83339  
 Cr, half-filled shells, photoionisation cross section 4-83353  
 Cs, excited 7S state, photoionisation cross section absolute meas. 4-78816  
 Cs, isoelectronic series, ionis. pots., relativistic effects, core polaris. and relax. 4-68985  
 Cs, nonreson. multiphoton ionisation in strong fields, angular distrib. and above threshold ionisation 4-74206  
 Fe I, ionisation potential by multistep laser spectroscopy 4-74353  
 Fe sputtered neutrals, ionisation length near wall in ISX-B using laser-induced fluoresc. 4-91971  
 Ga, photoionisation saturation by reson. ionisation 4-64434  
 Ga single atoms detection in atomic beams 4-107321  
 Gd, heavy charged particle impact, K-shell ionis. 4-69195  
 H, Cooper-type minima in multipole photoionisation cross section 4-91241  
 H photoionisation in elec. field, reson. and interference effects 4-69028  
 H photoionisation in elec. field, overlapping reson. and interference effects 4-69029  
 H, potential, approx. continuum wave functions, appl. to photoionisation 4-112252  
 H, Stark effect level crossings, relativistically enhanced ionisation rates 4-69010  
 H, Stark effect shape resonances in fields up to 3 MV/cm 4-102641  
 H<sup>+</sup>, autoionisation states, single configuration approx., orthogonality conditions 4-107318  
 H-like ions, fine struct., spectral intensities, collisional-radiative calcs. 4-102643  
 H+C<sup>q+</sup>(N<sup>q+</sup>)(O<sup>q+</sup>) ions, electron removal cross section 4-83460  
 H<sup>+</sup>+He, electron detachment in slow collisions 4-69198  
 H<sup>+</sup>+Au(U)(W), K-shell ionisation cross sections 4-78953  
 H<sup>+</sup>+inert gas atom, multiply ionising collisions,  $\delta$ -electron spectra 4-83458  
 H<sup>+</sup>+Li<sup>+</sup>(C<sup>+</sup>)(N<sup>+</sup>), ionisation cross section, PWBA 4-83461  
 He, autoionisation states, single configuration approx., orthogonality conditions 4-107318  
 He I autoionisation rate determ. by optical emission spectroscopy 4-87087  
 He, interchannel reson. coupling, photo- and Auger emission 4-83356  
 He ion impacts, target ionisation, dissociation, excitation 4-96682  
 He isoelectronic series, autoionis. states and widths 4-69024  
 He, laser induced cascade ionisation, secondary ionisation processes 4-83355  
 He, photoionisation above N=2 threshold 4-69027  
 He photoionisation cross sections, oscillator strengths, polarised orbital method 4-64438  
 He<sup>+</sup>, autoionisation states, single configuration approx., orthogonality conditions 4-107318  
 He<sup>+</sup>(n=0, 1, 2), electron loss and capture in various media 4-69206  
 He+C<sup>q+</sup>(N<sup>q+</sup>)(O<sup>q+</sup>) ions, electron removal cross section 4-83460  
 He+H<sup>+</sup>(Li<sup>+</sup>)(Na<sup>+</sup>)(K<sup>+</sup>), electron detachment cross sections 4-78952  
 He+inert gas atom, single and double electron loss cross sections of He metastable and ground states 4-59884  
 He I 1s<sub>n</sub>l energy levels, ionisation energies and Lamb shift 4-64427  
 He<sup>+</sup>(S), electron beam excited, transient absorpt. in UV and VUV 4-78796  
 Hg, reson. multiphoton ionisation, polarisation depend. 4-78813  
 I, photoemission in soft X-ray range 4-83341  
 In ion beam generation by selective multistage laser photoionisation of atoms 4-74207  
 In ions in laser-prod. plasma, for UV spectra 4-68997  
 In photoion laser epitaxy, purity and nucleation conditions of cryst. films 4-76694  
 K, excited states, inner and outer shell photoionisation 4-83340  
 K<sup>+</sup>+K<sup>+</sup> collisional ionis., spectral variation 4-69197  
 Kr, 4s photoelectron ang. distrib. relativistic RPA approx. 4-83342  
 La, photoionisation, local density-based random phase approx. calc. 4-102656  
 Li, autoionisation states, single configuration approx., orthogonality conditions 4-107318  
 Li I, autoionisation rate determ. by optical emission spectroscopy 4-87087  
 Li, photoionisation, excited metastable state prod. laser-produced plasma soft X-rays 4-112131  
 Li<sup>+</sup>, photoionisation cross sections, oscillator strengths, polarised orbital method 4-64438  
 Li-like ions principal series, oscillator strengths, photoionisation cross section calc. 4-83332  
 Li<sup>+</sup>+Li<sup>+</sup> collision, charge transfer and ionis. cross-sections determ. 4-64593  
 Mg-like positive ions, oscillator strengths and photoionisation cross sections 4-91240  
 Mn, half-filled shells, photoionisation 4-83353  
 Na, ion formation in vapour containing Rydberg atoms 4-91242  
 Na<sup>+</sup> isoelectronic series, oscil. strengths and photoionis. cross-sections 4-69030  
 Na+Ba, two-photon radiative collision, Ba<sup>+</sup> prod. 4-64587  
 Na+He<sup>+</sup>, laser and ion beam excitation, autoionisation 4-69196  
 Na+Na, associative ionisation reaction, rate consts. 4-89283  
 Ne, 1s ionis. energy calcs., rel. to electron spectrosc. 4-78984  
 Ne, high Rydberg states and autoionising reson., centrifugal 4-68989  
 Ne, lowest 'two particles-two holes' reson. calc., diagonalisation approx. 4-83310  
 Ne+H<sup>+</sup>(Li<sup>+</sup>)(Na<sup>+</sup>)(K<sup>+</sup>), electron detachment cross sections 4-78952

## ionisation of atoms continued

- Pd I, Rydberg series in photoionisation spectrum 4-83351  
 Rb, isoelectronic series, ionis. pots., relativistic effects, core polaris. and relax. 4-68985  
 $\text{Rb} + \text{Rb}(\text{Se}) \rightarrow \text{Rb}^+ + \text{Rb}^-$  collisional reaction investig. 4-102769  
 Sr, two- and three-photon autoionisation under strong laser radiation 4-78812  
 Tc, half-filled shells, photoionisation 4-83353  
 Th, photoionisation, local density-based random phase approx. calc. 4-102656  
<sup>90</sup>Th heavy charged particle impact, K-shell ionis. 4-69195  
 Ti, hypersatellite X-ray spectra,  $\text{H}^+$  induced 4-107301  
 U 7s shell, photoionisation parameters 4-83344  
 U, Penning ionisation in hollow cathode discharge 4-88006  
 U, photoionisation, local density-based random phase approx. calc. 4-102656  
<sup>238</sup>W, heavy charged particle impact, K-shell ionis. 4-69195  
 Xe, 5s photoelectron ang. distrib. relativistic RPA approx. 4-83342  
 Xe, interchannel reson. coupling, photo- and Auger emission 4-83356  
 Xe, isoelectronic series, 3d photoabsorpt. in near-threshold region, HF approx. 4-83349  
 Xe, photoelectron satellite spectrum in 5s and 5p shells at low photon energy 4-112150  
 Xe, VUV radiation, reson. enhanced tunable source 4-83661  
 $\text{Xe}^{q+}$ , electron impact, single-ionisation cross sections 4-59900  
 $\text{Xe}^{q+}$  ions, electron impact multiple ionisation 4-59901  
 Yb, selective photoionisation for laser isotope separation, three-stage scheme 4-64440  
 Zn<sup>+</sup> vapor, high-gain soft X-ray pumped photoionisation laser 4-112383

## ionisation of gases

- see also atmospheric ionisation; electron avalanches; Townsend discharge  
 air, avalanche breakdown, water vapour effects 4-65144  
 air, ionised, ionic cond. determ. using reson. cavity 4-60579  
 bounded RF discharge, stimulated ionisational scatt. dynamics 4-103502  
 critical ionisation velocity phenomenon, theory 4-108154  
 CW arc pluming at high-power aerials, pulsed RF plasmas obs. 4-69970  
 electrical discharges and combustion, colloquium, London, England (April 1984) 4-67870  
 electrical fields application to combustion systems 4-69985  
 electrodeless discharge, stability in EM wave 4-103600  
 electron beam form. and propag. at elevated press. 4-84035  
 gases/solids ignition by electrical discharges 4-69986  
 ionizing additive, physico-chemical transformation simulation (French) 4-81567  
 ions in flames, origin and props. 4-71932  
 nanosecond volume discharge form. with UV radiation preionisation 4-79732  
 net ionisation rates, meas. by transient techniques 4-79728  
 non-self-sustained discharge with a plasma cathode 4-84114  
 PES satellite intensities, incident photon energy effect 4-78815  
 plasmas, effects of non-equilib. ionisation on X-ray emission spectra 4-67617  
 quasimonochromatic light beam, spectral broadening by focusing 4-91400  
 rarefied gas, effect of charge-exchange reactions on ionisation equilib. 4-94577  
 semiconductors, photovoltaic effects and parity nonconservation 4-80624  
 shock wave ionisation, irreversible processes, heterogeneity and stochastic phenomena 4-63696  
 ArF excimer laser, doubly preionised 4-112398  
 CO cryogenic electroionisation laser, energy characts. 4-69379  
 F<sub>2</sub> electron swarm parameters, Boltzmann eqn. calcs. 4-79713  
 He filled spark chamber, ionisation meas. and time depend. discharge characts. study 4-59570  
 He, spark discharge formation time, discharge gap ionisation depend. 4-69974  
 Kr, ionisation growth measurements 4-79733  
 Kr-Hg mixture, ionisation coeff. meas. 4-79707  
 N<sub>2</sub> discharge, volume-dominated, UV preionisation effect 4-84112  
 N<sub>2</sub> prebreakdown ionis., quenching mechanisms investigation 4-79722  
 NO density quantitative meas. by reson. three-photon ionisation 4-75108  
 Ne gas, weakly ionised, laser-induced perturbation spectrosc. investig. 4-83319

## ionisation of liquids

- ionizing additive, physico-chemical transformation simulation (French) 4-81567  
 molecular liquids, anion form., correl. with mol. shape 4-92059  
 nicotinamide adenine dinucleotide in aq. soln., formation kinetics and quantum yield of electron ejection 4-93535  
 optical electron transfer, dispersion spectroscopy 4-80854  
 pyridine lasers in water,  $\text{H}^+$  ionisation, volumetric investig. 4-78934  
 stochastic ionization of surface-state electrons: classical theory 4-92459

## ionisation of molecules

- see also molecular electron impact ionisation  
 alkylbenzenes, liq., excited by UV and  $\beta$  radiation, fluoresc. quenching 4-59831  
 allene, ion-molecule reactions, photoionisation mass spectra 4-93517  
 aniline, multiphoton ionisation, time resolved two colour photoacoustic spectra 4-74297  
 7-azaindole, H-bonded complexes, MPI PES and two-colour MPI threshold spectroscopy 4-91320  
 benzene cation- $\text{d}_0(\text{d}_0)$ , excited states, intramolecular relax., fluoresc. study 4-83400  
 benzene dimers, isotope effects in seeded supersonic jet 4-59651  
 benzoic acid, electronic spectra in supersonic free jet 4-107394  
 benzophenone, UV induced thermoluminescence studies 4-99201  
 bound and scatt. states, Schrodinger spectra 4-59608  
 bromomethane, photoelectron spin polarisation, VUV spectra 4-83418  
 carbon tetrachloride, photoionis.,  $\text{CCl}_3^+$  ion form. and kinetic energy meas. 4-59862  
 chemical ionisation mass spectrometry, electron impact mass spectra simulation by charge exchange 4-111241  
 citraconic acid in methanol-water mixtures, ionis. const. meas. 4-71911  
 Coulomb explosion and mol. decomposition study methods 4-62223  
 cyclooctatetraene cation, unimolecular dissociation, time resolved photoionisation mass spectrometry 4-83434  
 diatomic molecules, electrons angular distrib. from reson. two-photon ionisation 4-69155  
 diazabicyclooctane, two-colour spectrosc. and excited state dynamics in free jet expansion 4-107412

## ionisation of molecules continued

- dibenzocarbazoles in solid soln., photoionisation threshold lowering through H bonding with pyridine 4-59861  
 dienes, conjugated, electronic excited state, multiphoton ionisation and electron impact spectra 4-83428  
 dipole oscillator strengths for mol. photoabsorpt., photoionis. and ion fragmentation 4-78915  
 ethylene, valence and Rydberg excitations and ionisations, wave function cluster expansion 4-68931  
 flames, laser-enhanced ionisation, theory 4-64638  
 fluorescein in boric acid glass, thermoluminesc. study of biphoton systems sensitivity to light fluctuations 4-114810  
 fluorobenzene van der Waals complexes, two-colour photoionis. in supersonic free jet 4-83436  
 formaldehyde metastable cations, unimol. decay 4-68988  
 fumaric acid in methanol-water mixtures, ionis. const. meas. 4-71911  
 gas-phase cpds., photon and electron-impact excitation and ionisation 4-83481  
 2,4-hexadiyne, laser multiphoton ionisation dissociation mass spectroscopy 4-78920  
 trans-1,3,5-hexatriene, ionis. spectra, LND/S PERTCI calcs. 4-68966  
 homonuclear molecules, ionisation pot., universal asymptotic limit and non-relativistic theory 4-112084  
 hydrocarbons, aliphatic and aromatic, near K-edge C 1s absorpt. spectra rel. to ionic fragmentation 4-96565  
 inert gas clusters, ionisation effect on magic numbers 4-96735  
 ionisation energies, Rydberg term values, correl. algorithm, 1-electron model 4-83279  
 ionisation energies, Rydberg term values, correl. algorithms, 1-electron model 4-83278  
 ionisation spectra, outer and inner valence region, Green's function method 4-59706  
 isobutene, photoionisation in nonpolar gas mixtures, mass spectrosc. investigation 4-102751  
 K-shell photoionisation, relax. effects 4-112238  
 laser optogalvanic effect for at. and mol. in recomb.-limited plasmas 4-87091  
 maleic acid in methanol-water mixtures, ionis. const. meas. 4-71911  
 maximum negative ionisation bound 4-78773  
 mesoanionic acid in methanol-water mixtures, ionis. const. meas. 4-71911  
 methanes, halogenated, fragmentation, photoionisation efficiency curves 4-83429  
 methyl butyl ether, field ionisation mass spectra 4-59902  
 methyl butyl ketone, field ionisation mass spectra 4-59902  
 methyl propyl ether, field ionisation mass spectra 4-59902  
 methyl propyl ketone, field ionisation mass spectra 4-59902  
 methylacetylene, relative partial photoionis. cross-section,  $\text{X}^2\text{E}$  ion state 4-78918  
 micellar systems photoionisation yields, interfacial elect. charge effects 4-62249  
 molecular photoion production processes induced by surface laser irradiation 4-81043  
 multidimensional optimization of structural changes of molecules upon ionization in Franck-Condon factor calculations 4-59853  
 muon spin rot., chem. aspects 4-71947  
 nicotinamide adenine dinucleotide in aq. soln., formation kinetics and quantum yield of electron ejection 4-93535  
 nitrobenzene( $\text{d}_3$ ), metastable ions, dissociation, ionisation, heat of formation 4-71878  
 nonexponential decay in autoionization near threshold 4-91315  
 trans-1,3,5,7-octatetraene, ionis. spectra, LND/S PERTCI calcs. 4-68966  
 organic free complex molecules, picosecond spectroscopy 4-102819  
 phenol, H-bonded complexes, MPI PES and two-colour MPI threshold spectroscopy 4-91320  
 phenol solvated complexes, supersonic jet spectroscopy 4-62177  
 polyatomic cations, recent approaches to spectroscopic studies, and related studies by means of ionisation techniques 4-91251  
 polymer macromol. degradation in elec. fields and under mech. loading (Russian) 4-104869  
 polyuridylic acid interaction with adenosine, complexing and deprotonisation, UV spectra 4-66853  
 pyridine lasers in water,  $\text{H}^+$  ionisation, volumetric investig. 4-78934  
 reactive sputtering plasmas, preferential ionisation, glow discharge mass spectrometry anal. 4-99313  
 resonant ionisation experiments on molecular beams, Cu vapour laser pumped dye laser for spectroscopic appl. 4-107666  
 small molecules condensed films, shape reson. in photoemission 4-85061  
 cis-stilbene, time-resolved multiphoton ionis., picosec. conform. dynamics 4-69153  
 tetraphenylethylene, time-resolved multiphoton ionis., picosec. conform. dynamics 4-69153  
 time resolved photoionisation mass spectrometry 4-83434  
 toluene, supersonic free jet, torsional motion, fluoresc. and multiphoton ionisation spectra 4-102735  
 VUV radiation physics, conf., Jerusalem, Israel, 8-12 Aug. (1983) 4-82583  
 water, privacy photoprocesses under two-quantum laser UV photolysis, picosecond spectroscopy 4-62221  
 o-xylene, UV PES, low energy non-Koopmans (shake-up) ionisation 4-96612  
 Ar-NO van der Waals complex, resonant multiphoton ionisation spectroscopy 4-107421  
 Ba cpds., at. and solid state effects, photoionisation processes 4-83346  
 CO cryogenic electroionisation laser, energy characts. 4-69379  
 CO<sub>2</sub>, autoionisation, fluoresc. polarisation study 4-83402  
 CO<sub>2</sub>, electronic excited state, multiphoton ionisation and electron impact spectra 4-83428  
 CO<sub>2</sub>, ground state, photoionisation cross-sections, linear algebraic method 4-64549  
 CO<sub>2</sub><sup>+</sup>, C<sup>2</sup> $\Sigma_g^-$  state, photoionis. shape reson., electron spectrosc. obs. 4-112236  
 CS<sub>2</sub>, autoionisation, fluoresc. polarisation study 4-83402  
 CS<sub>2</sub>, multiphoton excitation, ionisation and photofragment fluorescence 4-112241  
 Co, near K-edge C 1s absorpt. spectra rel. to ionic fragmentation 4-96565  
 Cu halide clusters, ionisation, fragmentation, mass spectra 4-69264  
 H<sup>+</sup>D<sub>2</sub> reaction dynamics, product state distrib. determ. at collision energy of 1.3 eV 4-71896

# ionisation of molecules continued

- $H+H_2 \rightarrow H_2^+ + H$ ,  $H_3^{2+}$  absorpt., transition state spectroscopy 4-69194  
 $H^+$  + methane ( $NH_3$ )( $H_2O$ ), differential cross sections 4-85295  
 $H_2$ , gamma-ray double photoion., electron correls. 4-64548  
 $H_2$ , ground state, photoionisation cross sections, linear algebraic method 4-64549  
 $H_2$ , three photon reson. ionisation 4-83437  
HCl, ionic fragmentation, photoionisation and photoabsorption cross-sections 4-83433  
 $H^+(NH_3)_n$  clusters, photoionisation in pulsed supersonic nozzle beam by VUV rare-gas reson. lines 4-69258  
 $H_2S-H_2O$  mol. beam photoionisation and fragmentation 4-69154  
 $(H_2S)_n$ ,  $n=2,3$ , photoionisation, unimolecular decomposition of ions 4-59860  
 $(H_2S)_n$  and  $(D_2S)_n$ , mol. beam photoionisation and fragmentation 4-69154  
 $He_2^+(a)$ , electron beam excited, transient absorpt. in UV and VUV 4-78796  
 $K_2$ ,  $B^1\Pi_u-X^1\Sigma_g^+$  band, crossed laser-mol. beam two-photon ionisation spectra 4-74296  
 $Li_2$ , isotope separation, sequential two-photon ionisation 4-87167  
 $Li_2$ , isotope separation using different laser wavelengths for excitation and ionisation processes 4-69235  
LiNa singlet states, reson. two-photon ionis. 4-83435  
N heteroaromatics, chem. ionis. mass spectra 4-78985  
 $N_2$ , dissociative photoionisation caused by autoionisation 4-83431  
 $N_2$ , ground state, photoionisation cross sections, linear algebraic method 4-64549  
 $N_2$ , Hopfield series, electronic autoionisation, multichannel quantum defect calcs. 4-83427  
 $N_2$ , photoionisation in external elec. fields, fluoresc. study 4-83401  
 $N_2$  radiolysis,  $N_2^+/N_2^+$  prod. ratio meas. 4-71941  
 $ND_3$ ,  $C^1A_1$  state, predissoc. dynamics, multiphoton ionis. spectrosc. investig. 4-102752  
 $NH_3$ ,  $C^1A_1$  state, predissoc. dynamics, multiphoton ionis. spectrosc. investig. 4-102752  
 $NH_3$  chemisorbed on Ni (111), surface Penning ionisation study 4-65575  
 $NH_3+Re$  surface, single-colour energy transfer and catalytic decomposition at high temps. 4-71971  
 $(NH_3)_n$  clusters, multiphoton ionisation with tunable laser 4-74368  
 $(NH_3)_n$  clusters, photochemistry computationally based speculations 4-96741  
 $(NH_3)_n^+$  clusters, ( $n=2, 3, 4$ ), photoionisation in pulsed supersonic nozzle beam by VUV rare-gas reson. lines 4-69258  
NO density quantitative meas. by reson. three-photon ionisation 4-75108  
NO, ground state, photoionisation cross sections, linear algebraic method 4-64549  
NO, partial photoionisation cross section excited by synchrotron radiation 4-87163  
NO photoionisation, multiplet-specific spectral shapes of  $(5\sigma^{-1})b^1\Pi$  and  $(5\sigma^{-1})A^1\Pi$  partial cross sections 4-102748  
NO, struct. and decay of highly excited states 4-87162  
NO, supersonic free jets, high Rydberg states, two-colour excitation, autoionisation 4-107411  
 $N_2O$ , dissoci. electroionisation studied by ion kinetic energy and mass anal. 4-89265  
 $N_2O$ , dissociative photoionisation study 4-83432  
 $Na_2$ , three-photon ionisation spectrum 4-96633  
 $Ni_2$ , dimer, jet-cooled, IR gas-phase electronic spectrum 4-78839  
 $O_2$ , dissociative photoionisation caused by autoionisation 4-83431  
 $O_2$ , partial photoionisation cross section excited by synchrotron radiation 4-87163  
OH, anomalous photodetachment thresholds from electron dipole interactions, rot. doubling effects 4-74298  
OH, photoionisation cross sections UV spectra 4-112237  
 $SF_6$  negative ions, electron detachment and its importance in elec. breakdown 4-91337  
 $SO_2$ , double photoionis. and fragmentation spectrosc., PIPICO method obs. 4-102749  
 $SO_2^+$ , double photoionis. and fragmentation spectrosc., PIPICO method obs. 4-102749  
 $UF_6$ , electronic struct., ESCA shake-up, X $\alpha$  and EHT calcs. 4-107401  
 $Xe_2^*$  excimers, photoionisation processes 4-83430  
 $Xe_2^*$ , photoionisation absolute cross section in the UV region 4-74299

# ionisation of solids

- at. and solid state effects, photoionisation processes 4-83346  
dibenzocarbazoles in solid soln., photoionisation threshold lowering through H bonding with pyridine 4-59861  
electron loss by multiply-charged ion moving at small angle to cryst. planes 4-84328  
epoxide polymers, breakdown, ionisation processes role, mechanoemission mechanism 4-88952  
gases/solids ignition by electrical discharges 4-69986  
light nonlinear absorption dynamics in solids 4-69514  
rare earth compounds, photoemission, intershell coupling phenomena 4-93181  
rare earth metals, photoemission, intershell coupling phenomena 4-93181  
small molecules condensed films, shape reson. in photoemission 4-85061  
transition metal compounds, photoemission, intershell coupling phenomena 4-93181  
transition metals, photoemission, intershell coupling phenomena 4-93181  
 $Al^+$  secondary ion emission, ionisation probability following  $Ar^+$  bombardment 4-66177  
Ba cpds., at. and solid state effects, photoionisation processes 4-83346  
Cd-CdO solid solns.,  $^{113}C$  NMR investig. 4-98977  
 $SiO_2$  polymorphs, relationship between refr. index and density 4-66001

# ionisation potential

- see also work function  
absolute hardness, companion parameter to absolute electronegativity 4-59659  
alkali metal atoms, core polarisation pot., intershell correl. effects, ab initio SCF CI calcs. 4-68970  
alkali metal clusters thermodynamic props., ionis. pots. and binding energies 4-69266  
alkaline earth metal atoms, core polarisation pot., intershell correl. effects, ab initio SCF CI calcs. 4-68970  
alkyl radicals, ionisation pot., oscillator strength, UV spectra 4-96561  
alkyl radicals, UV spectra, ab initio SCF and CI calcs. 4-96560

# ionisation potential continued

- allyl cation, photoionisation mass spectrometry, ionisation and appearance energies determ. 4-89319  
2-aminobenzoxazoles substituted in benzene nucleus, UV spectra and ionisation consts. 4-74256  
aniline  $^2B_1$  radical cation, jet cooled, two colour photoionisation spectra, vibr. 4-64547  
anions, adsorpt. on metal, adsorpt. props. rel. to ionis. pot. 4-61221  
anthracene, fluoresc. excitation spectrum beyond first ionisation pot., photoelectron spectra 4-84989  
atom, kinematics of multiphoton ionization in a steady laser beam 4-64443  
atom in resonant laser field, ionisation pot., intensity depend. 4-78982  
atomic energy differences, electron correl. coeffs. approximate method 4-83304  
atomic ions, electrostatic pot. at nucleus, rel. to chem. pot. 4-68916  
atomic ions, solvation shifts of core electron binding energies, statistical model 4-91359  
atoms, ionisation and excitation energies, HF and HF-Slater calcs. 4-107273  
atoms, Stark width and shift depend. on ionisation pot. 4-91221  
atoms and ions, electron densities, ionisation pots., X-ray scatt. 4-96441  
7-azindole, H-bonded complexes, MPI PES and two-colour MPI threshold spectroscopy 4-91320  
benzene, polycyano derivatives, electron affinity and ionisation pot., MNDO calcs. 4-68958  
benzene-( $d_6$ ), first ionisation pot. determ. 4-91366  
N-benzylquinolinium chloride-diphenylamine hemihydrate 1:1 complex, cryst. and mol. struct. 4-60908  
carbazole-containing compounds, ionisation potentials (Russian) 4-83508  
conjugated-bond molecules, UV spectra. CNDO/S and PPP calcs. 4-59705  
cyanamide, ionisation pot., valence ionisation spectra, MO model 4-69140  
diazabicyclooctane, two-colour spectrosc. and excited state dynamics in free jet expansion 4-107412  
diazirine, ionisation pot., valence ionisation spectra, MO model 4-69140  
diazomethane, ionisation pot., valence ionisation spectra, MO model 4-69140  
dimethyl ketene, He I photoelectron spectra and vertical ionisation pots. by using Koopmans' theorem 4-112229  
dimethyl phosphine, ionisation pot., mol. props., photoelectron spectra 4-69143  
electron density energy in external potential, ionisation dependence 4-78776  
elemental electronegativities, electron affinities, ionis. pots. and hardnesses calcs. 4-112099  
elements, electronegativities, density functional theory HF Slater theory 4-96442  
fluorobenzene van der Waals complexes, two-colour photoionis. in supersonic free jet 4-83436  
hydrocarbons, doubly charged ions, appearance energies, mass spectra 4-64637  
iodobenzene, appearance energies and kinetic energy releases, mass spectra and electron impact ionisation 4-87222  
ionic masses and appearance energies, using pulsed-laser time-of-flight atom probe 4-111256  
ions and molecules gas-liquid correlation of ionization energies 4-91365  
isocyanamide, ionisation pot., valence ionisation spectra, MO model 4-69140  
lanthanide atoms and ions, average energy of config. and valence orbital ionis. pots. (Chinese) 4-78785  
metal clusters, small, ionisation pot., effect of electron statistics 4-108923  
metallic atomic clusters, electronic props., photoionization and TOF mass spectroscopy studies 4-83509  
metallic clusters, preparation and props., theory 4-74369  
methane ( $-d_4$ ), electron impact spectra 4-83482  
methanes, halogenated, fragmentation, photoionisation efficiency curves 4-83429  
methyl ketene, He I photoelectron spectra and vertical ionisation pots. by using Koopmans' theorem 4-112229  
molecules, ionisation energies, Rydberg term values, correl. algorithms, 1-electron model 4-83278  
molecules, ionisation energies, Rydberg term values, correl. algorithm, 1-electron model 4-83279  
molecules, ionization pots. dipole moments geometries and binding energies calc. extended Huckel theories (German) 4-83299  
open-shells, cluster expansion techniques appl., ionisation pot., electron affinity and excitation energy calcs. 4-74129  
organic radicals, heat of form. from appearance energies 4-89318  
phenol, H-bonded complexes, MPI PES and two-colour MPI threshold spectroscopy 4-91320  
rare earth metal trihalides, UPS, DV-X $\alpha$  calcs. 4-83415  
reactions having large kinetic shift and energy partitioning, appearance energies 4-89257  
solar photosphere spectroscopy, accurate at. data, review 4-90135  
spin adapting many-body theory, use of spin graphs 4-78758  
transition metal complexes, orbital relax. and correl. in photoelectron spectra, INDO calcs. 4-102740  
unsaturated hydrocarbon, polycyano derivatives, electron affinity and ionisation pot., MNDO calcs. 4-68958  
4-vinylcyclohexene cation radical, retro-Diels-Alder reaction mechanism 4-81408  
virial and the independent particle models of the atom 4-74133  
 $Ag_2$ , relativistic electronic struct. calc. using SCF X $\alpha$  Dirac scatt. wave programs 4-59636  
AlF, vibr. struct., ionisation pot., PNO/CEPA calcs., photoelectron spectra 4-96613  
AlF $_3$ , vibr. struct., ionisation pot., PNO/CEPA calcs., photoelectron spectra 4-96613  
Ar-NO van der Waals complex, resonant multiphoton ionisation spectroscopy 4-107421  
Au $_2$ , relativistic electronic struct. calc. using SCF X $\alpha$  Dirac scatt. wave programs 4-59636  
BF $_3$ , electron and thermal dissoci. 4-96700  
Br containing compounds, ground states, MNDO calcs. 4-64378  
C neutral bases,  $H^+$  and methyl- and ethyl-cation affinities, MNDO calcs. 4-64381  
C $_3$ , vertical electron affinity and ionisation potentials 4-112295  
Cs, isoelectronic series, ionis. pots., relativistic effects, core polaris. and relax. 4-68985

## ionisation potential continued

- Fe I, ionisation potential by multistep laser spectroscopy 4-74353  
 Fe transition series atoms, s-d interconfig. energies, s-spin flip energies and ionisation pots. 4-83303  
 Ga<sub>2</sub>O, UPS, DV-X $\alpha$  method 4-83413  
 HCl, ionisation pot. D isotope effect, EELS 4-83467  
 H<sub>2</sub>S-H<sub>2</sub>O, mol. beam photoionisation and fragmentation 4-69154  
 (H<sub>2</sub>S)<sub>n</sub> and (D<sub>2</sub>S)<sub>n</sub>, mol. beam photoionisation and fragmentation 4-69154  
 In<sub>2</sub>O, UPS, DV-X $\alpha$  method 4-83413  
 Li<sup>+</sup> 1p<sup>0</sup> levels, beam-foil spectral line identification 4-74188  
 Li-H systems, thermodynamic props., ionis. pots. and binding energies 4-69266  
 Li-O systems, thermodynamic props., ionis. pots. and binding energies 4-69266  
 LiNa singlet states, reson. two-photon ionis. 4-83435  
 Mg II, 3p<sup>2</sup> P level, electron impact excitation cross section, reson. struct. 4-91351  
 (N<sub>2</sub>)<sub>2</sub>, electron impact ionisation, appearance energies of N<sub>3</sub><sup>+</sup> and N<sub>4</sub><sup>+</sup>, mass spectra 4-64627  
 N neutral bases, H<sup>+</sup> and methyl- and ethyl-cation affinities, MNDO calcs. 4-64381  
 N<sub>2</sub>, excitation and ionisation, general-model-space perturbation theory 4-112126  
 N<sub>2</sub>, valence ionisation energies, correl. effects, generalised-valence bond interpretation 4-64385  
 N<sub>2</sub><sup>+</sup>, excitation and ionisation, general-model-space perturbation theory 4-112126  
 Na<sub>n</sub>, (n $\leq$ 7), cluster geom. calc. by Hellmann-Feynman forces 4-74372  
 Ne, is ionis. energy calcs., rel. to electron spectrosc. 4-78984  
 Ne, high Rydberg states and autoionising reson., centrifugal 4-68989  
 O neutral bases, H<sup>+</sup> and methyl- and ethyl-cation affinities, MNDO calcs. 4-64381  
 OH<sup>+</sup>, shape reson., photofragment spectroscopy 4-107417  
 PCI<sub>3</sub> molecule, X-ray spectra and electronic struct. 4-112194  
 Rb, isoelectronic series, ionis. pots., relativistic effects, core polaris. and relax. 4-68985  
 Si, negative secondary ion emission, influence of alkali metal implantation 4-104710  
 SiC<sub>2</sub>, jet cooled, geom. and electronic struct., visible spectroscopy 4-69091  
 Sr I, principal series, photoabsorpt. spectrum 4-68996  
 TiO, UPS, DV-X $\alpha$  method 4-83413  
 W(CO)<sub>6</sub>, electronic struct., relativistic effects, SCF X $\alpha$  Dirac scatt. wave calcs. 4-78775  
 Zn IV, ionisation pot., UV spectra 4-59666

## ionisation time see ionisation

## ionogen see electrolytes

## ionoluminescence

- ion milling, end point detection by sputter-induced optical emission spectroscopy 4-93432  
 polymer films, ion beam irradi., secondary electron, ion, and photon emission 4-76577  
 Ar films, ion beam irradi., secondary electron, ion, and photon emission 4-76577  
 Ar, solid, electronically excited, sputtering and luminesc. 4-104708  
 C foil, H<sup>+</sup>, H<sub>2</sub><sup>+</sup> and H<sub>3</sub><sup>+</sup> ion bombardments, continuum optical radiation emission 4-81007

## ionosondes see ionospheric measuring apparatus

## ionosphere

- see also D-region; E-region; F-region; ionospheric electromagnetic wave propagation; ionospheric techniques; sporadic-E layer  
 accelerated ions on auroral lines of force to magnetosphere 4-94292  
 afternoon auroral oval, field-aligned currents, electron beams and density enhancements 4-82338  
 anisotropic ionisation (French) 4-77681  
 antenna in ionospheric plasma, expts. on VLF multibeam loop antenna 4-85858  
 aurora and electrojet configuration in early morning sector, ground-based and satellite obs. 4-72789  
 aurora excitation and energy dissipation processes, general description 4-72798  
 aurora pulsations correl. with micropulsations 4-67518  
 auroral double layers and ion conics production 4-67522  
 auroral electrojet irregularities studied using STARE radar 4-67523  
 auroral electrojets, evolution during geomag. disturbances, correl. with polar cap currents devel. 4-77682  
 auroral electron density vars., power spectra rel. to electron drift vel. in eastward electrojet 4-72777  
 auroral F-region, expt. evidence of non-isotropic ion temp. distrib. 4-105793  
 auroral ionosphere, current convective instability in long wavelength limit 4-85816  
 auroral ionosphere, effects of oblique double layers on upgoing ion pitch angle and gyrophase 4-85841  
 auroral ionosphere, onset time interval of geomag. disturbances in conjugate areas 4-110386  
 auroral ionosphere, quantitative parameters from photometry by Atmosphere Explorer C satellite 4-72778  
 auroral ionosphere, thermal electrons field-aligned drift vel. 4-72792  
 auroral oval, dynamic var. during intense mag. storms 4-72776  
 auroral oval diameter, ring coupling model and implications for ground state of magnetosphere 4-72809  
 auroral plasma formation by magnetospheric convection and injection 4-110356  
 auroral rays, mechanism involving plasma drift instabilities 4-94286  
 auroral roar, characts. 4-90025  
 auroral zone, decay of electrostatic ion cyclotron waves 4-94294  
 beam plasma discharges causing optical emissions, laboratory expts. 4-67526  
 bubble, radiowave propag. and pulse distortion 4-90032  
 characteristics and interactions (book) 4-90309  
 chemical modification expt. using rocket exhaust; incoherent scatter obs. 4-67533  
 conductivity variations assoc. with periodic VLF emissions; contrib. to short-period mag. pulsations 4-85836  
 conductivity variations in auroral ionosphere, rel. to correl. between optical and mag. pulsations 4-105789  
 conference, Boston, USA (Aug. 1982) 4-67862

## ionosphere continued

- conference on beacon satellite studies of ionosphere, at New Delhi, India (February 1983) 4-86110  
 convection electric field as manifestation of magnetosphere convection 4-72790  
 coupling to lower atmosphere planetary waves, radioabsorpt. study (Chinese) 4-63006  
 dayside high-latitude correction, influence of interplanetary mag. field orientation 4-85811  
 double layer-like and soliton-like structures, rocket obs. 4-105791  
 double layer-like structures at rocket altitudes 4-105792  
 dynamics and electrodynamics of thermosphere 4-72773  
 dynamo currents, anal. of variability 4-90021  
 dynamo currents representing geomag. L variation 4-82341  
 EXB plasma instability in inhomogeneous elec. field, theory 4-94298  
 earthquake induced ionospheric motions in Japan area 4-105801  
 effective electron collision rate, empirical altitude depend. 4-94288  
 EISCAT meas. of ion temps., non-isotropic ion vel. distrib. 4-105799  
 EISCAT workshop on first year's operation, Aussois, France (Sept. 1983) 4-95040  
 electric current global distrib. during substorm disturbances 4-67534  
 electric current system, rel. to induced mag. field at Peruvian dip equator 4-62668  
 electric currents, coupling with MHD generator in solar wind energy transfer regions inside dayside magnetopause 4-105814  
 electric field potential, distrib. near electron-injecting satellite during active expts. 4-110353  
 electric field spike effect on thermosphere model 4-85807  
 electric fields and potential patterns in high-latitude ionosphere, for different situations in interplanetary space 4-110365  
 electric potential, response to vars. of atmospheric cond. profiles 4-89970  
 electrical conductance mapping technique using auroral spectroscopic method 4-67438  
 electrical conductivities, spatial distrib. rel. to control of magnetospheric convection 4-72807  
 electrical conductivity of thermosphere and low and middle atmosphere, solar activity effects 4-85826  
 equatorial electrojet in radiowave heating expt. 4-115654  
 electron beam antenna expt. for satellites, EM wave excitation study 4-94281  
 electron beam injected into ionosphere, wave-particle interactions, simulation 4-87888  
 electron content at low latitudes, day-to-day var. 4-90036  
 electron content at low-latitude during solar minimum, semi-empirical model 4-105796  
 electron content determ., use of geodetic Doppler receivers 4-90009  
 electron content irregularities and UHF/SHF scintillation at Ascension Island 4-90030  
 electron content var. during mag. storms, effect on VHF equatorial scintillation 4-90034  
 electron content var. throughout solar eclipses, satellite beacon obs. 4-90038  
 electron densities at high-latitudes, determ. from convection elec. fields 4-85828  
 electron density depletion at high latitude, EISCAT meas. 4-100858  
 electron density irregularities produced by HF radio waves, evidence from UHF scintillations 4-105794  
 electron precipitation induced by ground-based VLF signal sources, spatial distrib. 4-85813  
 electron precipitation patterns and visual aurora characts. during geomag. quiescence 4-85810  
 electrons, low energy, in E and F-regions, nonthermal components obs. 4-63008  
 electrostatic drift instability, theory 4-113142  
 electrostatic hydrogen-cyclotron wave emission below EHC freq. in auroral accel. region 4-67537  
 electrostatic ion cyclotron waves in diffuse aurora 4-67536  
 ELF waves generated during radiowave heating of auroral electrojet 4-67538  
 energy exchange processes, role of magnetosphere large scale convection 4-100844  
 equatorial electrojet, local time depend. of response to DP2 and SI disturbances 4-105802  
 equatorial electrojet meas. from daily geomag. var., coastal effect in Peruvian and Nigerian zones 4-110044  
 equatorial enhancement of geomagnetic sudden commencement 4-82349  
 equatorial ionosphere, depend. of seasonal var. of radio wave absorpt. on solar activity 4-90022  
 field-aligned current intensity in auroral zone, dependence on Kp 4-67540  
 field-aligned currents as diagnostic tool 4-72806  
 field-aligned irregularities, contrib. to direct multiple path magnetospheric propag. for VLF waves 4-85839  
 gradient drift and collisional Rayleigh-Taylor instabilities 4-72799  
 heating, soliton vs. parametric instabilities params. 4-82334  
 heating by corpuscular fluxes 4-105790  
 heliomagnetic cycle of geomag. and ionospheric disturbances and interplanetary activity 4-110369  
 hemispherical Joule heating as function of AE indices; linear regression anal. 4-72788  
 HF radiowave modification expt., ELF excitation by modulated HF source 4-82324  
 HF-induced plasma line below threshold 4-90028  
 high-latitude electrodynamics, energy principle 4-85812  
 International Reference Ionosphere, test using single-freq. Al absorpt. data 4-90020  
 ion acceleration parallel and perpendicular to mag. field 4-94297  
 ion beams driving electrostatic H cyclotron waves on auroral field lines 4-72826  
 ion chemistry of E- and D-regions, photochemical aspects 4-72774  
 ion cloud release expts. and elec. fields during spread-F onset 4-82328  
 ion cyclotron wave propagation 4-67532  
 ion energization by broadband plasma waves and ion transport to magnetosphere 4-110357  
 ionization patches in polar cap nighttime F-layer 4-67539  
 auroral ionosphere electrodynamic parameters; radar sound study 4-100850  
 irregularities generated by thermal source, effect of electron-ion collisions 4-82343  
 Jaeger's formula, ionospheric absorpt. and transionospheric propagation calcs. 4-115645

# ionosphere continued

- Joule heating due to auroral electrojets, latit. vars. 4-72784
- L equivalent current systems, seasonal vars. 4-72785
- large-scale waves in thermosphere at approx. 260 km altitude 4-100838
- magnetoplasmodynamic source in upper atmosphere, mass spectrometer probe meas. 4-85795
- magnetosphere convection electric field at ionospheric altitudes, latit. profile 4-72787
- magnetosphere coupling, role of ion beams 4-72780
- magnetosphere-ionosphere coupling and auroral particle beams, review 4-82352
- magnetostatic fluctuations excited by filamentation instability of whistlers 4-67544
- micropulsations (ULF) causing ionosphere Joule heating 4-100883
- micropulsations observed at ground ionospheric damping effects 4-82351
- MITHRAS project description 4-90027
- modelling of mid-latitude region 4-100846
- modulation pattern for the EISCAT incoherent scatter radar 4-100861
- morning sector convection reversal, SABRE obs. during mag. storm 4-110364
- negative ion zone at 88 km altitude 4-115647
- neutral air winds influence on mid-latitude electron content in winter 4-82336
- nonuniform elec. fields and currents assoc. with auroral arcs, generation by Alfvén disturbances 4-110370
- orbiting vehicle induced luminosities, obs. on Space Shuttle STS-8 mission 4-105866
- order-statistics anal. and props. depend. on solar activity 4-94290
- outflowing energetic ions, magnitude and comp., mag. activity depend. 4-72779
- parallel electric field above auroral ionosphere, causes and consequences 4-72834
- plasma, interaction with STS-3 DC and modulated electron beams, wave emissions 4-90023
- plasma, ion phase-space vortices form. behind electrostatic ion acoustic shocks 4-60606
- plasma, struct. and inside specific energy from dielectric chamber 4-91888
- plasma, whistler scatt. from density fluctuations 4-79792
- plasma (book) 4-67900
- plasma characts. var. due to acoustic wave interactions 4-90026
- plasma convection at high latitudes, EISCAT obs. 4-100865
- plasma density drift instabilities and wave-particle transport 4-83992
- plasma depletion expts., snowplough effects or plasma recomb. model for depletion core form 4-100851
- plasma dynamics model for parameter sequential estimation algorithms (Russian) 4-82346
- plasma flow rel. to thermospheric circulation over N Scandinavia 4-100859
- plasma instabilities in auroral F-region 4-65074
- plasma irregularities anal. from scintillation obs. 4-90029
- plasma jet of rocket expt. exciting lower oblique resonance 4-67529
- plasma turbulence, interaction with VLF waves 4-100852
- plasma-electron beam interaction simulations for SEPAC/Spacelab 1 mission 4-87887
- plasma-pulsed electron beam interaction, EM wave emission 4-87886
- plasmasphere-ionosphere coupling model 4-82339
- plasmosphere-ionosphere transition level, depend. on geomag. latitude and longitude 4-94287
- polar cap electric field and current distrib., Fourier anal. 4-72791
- polar cap vertical currents associated with northward interplanetary magnetic field 4-94296
- proton precipitation stimulated by artificial low-freq. radiation 4-115653
- pulsating luminescence of lower ionosphere, synchronous with powerful radio wave pulsed action 4-82332
- radial plasma drifts deduced from VLF whistler mode signal propagation 4-82335
- radio aurora at medium latitude, diurnal, seasonal, solar cycle variations 4-115649
- radiowave heating, initial stage of interaction of intense radio waves with upper ionosphere plasma 4-110354
- radiowave heating experiments, electrostatic wave generation process 4-94299
- radiowave heating expt. using 430 MHz radar, obs. of enhanced plasma lines 4-85825
- relativistic electron precipitation, X-ray bremsstrahlung and ELF emission 4-67530
- research carried out in Poland in the period 1978 to 1982 AD 4-72486
- resonant auroral radar echoes due to ion cyclotron waves 4-67531
- riometer absorption day-to-day variability and prediction 4-115650
- solar eclipse effects on ionosphere, for Chinese eclipses (Chinese) 4-85809
- solar wind electric field penetration 4-94305
- Space Shuttle glow, N<sub>2</sub> spectral emission mechanism 4-110492
- Space Shuttle glow, plasma effects 4-90052
- Space Shuttle Orbiter, interaction with ionosphere 4-110495
- spikelike electric field obs. at poleward edge of auroral zone 4-67535
- Sq current loop positions over Africa 4-82323
- storm-time disturbance of mid-latitude ionosphere 4-100849
- stratification events at night-time due to polar mag. storms (Chinese) 4-63007
- theoretical description of ionosphere, review 4-72797
- thermal electron heating rate due to precipitation and photoelectrons 4-72793
- thermosphere O and N<sub>2</sub> changes rel. to topside ionisation depletion event 4-67514
- tidal fluctuations, correl. with troposphere, perturbation effects 4-89967
- topside, light ions winter nighttime abundances 4-85815
- topside ion depletion in evening sector during equinoctial periods 4-110359
- topside ionosphere, thermospheric control of auroral source of O<sup>+</sup> ions for magnetosphere 4-72786
- total electron content, NAVSTAR L band ionospheric calibration rel. to Faraday rot. meas. 4-90010
- total electron content of modified Chapman layer (Spanish) 4-115656
- total electron content over E Mediterranean, spatial var., Faraday rot. obs. 4-90037
- travelling ionospheric disturbances, dispersion relations rel. to determ. of thermospheric wind vectors 4-90015
- travelling ionospheric disturbances effect on radio interferometry 4-90095
- turbulence generated by artificial Xe ion beam 4-67525
- ULF hydromagnetic waves, propagation at mid-latitude 4-82327

# ionosphere continued

- upflowing ions in auroral ionosphere 4-110382
  - upward ion injection into magnetosphere and subsequent precipitation 4-67564
  - solar UV flux and photoelectron fluxes showing inconsistency 4-110362
  - velocities, EISCAT data errors 4-100860
  - Venus and Mars ionospheres compared to Earth 4-72901
  - VHF/UHF fast Faraday polarisation var. and amplitude scintillation in ionosphere 4-90033
  - virtual height variation, correction for effect on time lag of short-wave propag. (Chinese) 4-82321
  - westward travelling surge, mechanism involving magnetosphere. Hall current blockage and ionosphere charge buildup 4-72781
  - whistlers generation due to STS-3 Space Shuttle electron beam interaction with ambient plasma 4-90024
  - X-ray and electron absorpt. in nighttime middle atmosphere 4-110361
  - X-ray images of auroral arcs, satellite observations 4-100842
  - e, N<sub>2</sub> collision, rotational excitation, mean fractional energy loss, atmospheric gas 4-113105
  - Ba release experiment, study of plasma column density fluctuations 4-110355
  - He<sup>+</sup> distrib. in equatorial ionosphere, neutral wind effects 4-82337
  - He<sup>+</sup> dominance regions in high-latit. topside ionosphere, role of plasma convection 4-110363
  - He<sup>+</sup> plasmasphere distrib. by diffusive equilibrium model 4-82340
  - NO<sup>+</sup> ionospheric chemistry 4-67528
  - O, at low ionosphere altitudes, calc. of auroral zone concs. 4-100835
  - O<sup>+</sup> density depressions in topside nighttime ionosphere, ISS-b satellite obs. 4-63009
- ionospheric electromagnetic wave propagation**  
*see also atmospherics*
- A1 absorption data, single-freq., appl. to test of International Reference Ionosphere 4-90020
  - A1 absorption data reduction, validity of George's method 4-90019
  - atmospheric radio noise, global distrib. study using satellite obs. of thunderstorm activity (Japanese) 4-63015
  - auroral absorption, day/night absorpt. ratio in auroral and subauroral zone riometer meas. 4-90018
  - Bragg resonator excitation in ionospheric plasma containing artificial periodic array 4-115658
  - conference on beacon satellite studies of ionosphere, at New Delhi, India (February 1983) 4-86110
  - correction to radioastronomy interferometry observations (French, English) 4-67643
  - D-region radioabsorpt. seasonal variations at mid-latitude (Chinese) 4-63006
  - E<sub>s</sub>-layer, reflection of VHF television signals and E<sub>s</sub>-layer struct. 4-115652
  - electrical breakdown due to radiowaves, artificial ionized layer characts. 4-90017
  - equatorial electrojet in radiowave heating expt. 4-115654
  - electron content var. throughout solar eclipses 4-90038
  - ELF waves excited in Earth-ionosphere waveguide by ELF modulated powerful HF wave 4-82324
  - f<sub>o</sub>F<sub>2</sub> dependence on solar activity 4-94290
  - F<sub>2</sub>-layer, statistical model of critical freq. 4-110350
  - F<sub>2</sub>-layer critical frequencies, correl. relations between cyclical increments 4-110351
  - F<sub>2</sub>-layer ionospheric electron content of Wuchang, China, VHF obs. 4-115659
  - F layer, parametric plasma heating, turbulent expansion 4-72795
  - F-region, EISCAT obs. of plasma convection in high-latitude winter 4-100856
  - F-region, plasma flows during prolonged northward IMF, EISCAT obs. 4-100855
  - heating, soliton vs. parametric instabilities params. 4-82334
  - HF band, real-time update of two well-known models of the maximum usable frequency 4-63018
  - HF band radiowaves, ionospheric heating experiments (Japanese) 4-63011
  - HF path between Japan and Germany, geomagnetic disturb. effects on usable freq. bands 4-82331
  - HF propagation predictability, comparison of IONCAP predictions with AN/TRQ-35 (V) oblique-incidence sounder meas. 4-63017
  - HF radio noise spectrum, satellite obs. above ionosphere (Japanese) 4-63014
  - HF radiowave heating expt. using 430 MHz radar, obs., of enhanced plasma lines 4-85825
  - HF ray tracing at high-latitudes using observed meridional electron density distrib. 4-85823
  - HF-induced plasma line below threshold 4-90028
  - HF-produced electron density irregularities in polar ionosphere, evidence from UHF scintillations 4-105794
  - HF/VHF propagation conditions on Nikolayev-Havana path, multifrequency anal. 4-94291
  - high latitude ionospheric scintillations 4-82322
  - Jaeger's formula, ionospheric absorpt. and transionospheric propagation calcs. 4-115645
  - JJY (Tokyo) time service, SW standard radio appl. (Japanese) 4-58831
  - lighting generated ELF and VLF transverse reson. in Earth-ionosphere cavity 4-82345
  - meteor burst communications systems 4-63016
  - meteor scatter channel for TV signals, multipath spread study 4-85824
  - micropulsations observed at ground ionospheric damping effects 4-82351
  - microwave transmission effects (Japanese) 4-63010
  - nocturnal sporadic-E activity, f<sub>o</sub>E<sub>s</sub> and f<sub>h</sub>E<sub>s</sub> meas. at southern hemisphere station 4-63005
  - nonducted VLF waves, direct multiple path propag. in ionosphere and magnetosphere 4-85839
  - Omega navigational waves, EW nonreciprocal propagation at low latitude and equator (Japanese) 4-63013
  - Omega VLF waves, anomalous propagation near geomagnetic equator (Japanese) 4-63012
  - pulsed radio wave, obs. of synchronous pulsating luminesc. of lower ionosphere 4-82332
  - QL mode radio wave reflection in ionosphere, crit. angle effect 4-100854
  - radar in auroral ionosphere, incoherent scattering and vel. distrib. 4-100862
  - radio wave absorpt. in equatorial ionosphere, depend. of seasonal var. on solar activity 4-90022

**ionospheric electromagnetic wave propagation continued**

- radio wave frequency Doppler shift due to ground weak explosion (*Russian*) 4-115641  
 radiowave heating, initial stage of interaction of intense radio waves with upper ionospheric plasma 4-110354  
 radiowave heating experiments, electrostatic wave generation process 4-94299  
 radiowave propagation, frequency dependence of parameters for the ionospheric channels (*Chinese*) 4-110349  
 radiowave pulse distortion after propag. through ionospheric bubble 4-90032  
 radiowave ray tracing in cold stratified loss free plasma 4-77683  
 radiowave sounding of inhomogeneities, phase fluctuations of signals 4-72725  
 radiowaves, interferometry, effects of travelling ionospheric disturbances 4-90095  
 radiowaves propagation through F-region equatorial bubbles 4-90035  
 resonant auroral radar echoes due to ion cyclotron waves 4-67531  
 RF propagation, results of PLACES ionospheric plasma test series 4-62954  
 riometer absorption day-to-day variability and prediction 4-115650  
 scintillation and ionospheric plasma irregularities anal. 4-90029  
 scintillation of radiowaves by power law phase screen model 4-94302  
 scintillation of transionospheric VHF signals received at Luning 4-100866  
 scintillation of UHF and SHF, at Ascension Island 4-90030  
 solar activity influence on 2.3 and 2.5 MHz absorpt. at Udaipur, India 4-105797  
 sporadic-E layers, HF Doppler sounding rel. to refl. mechanism 4-100867  
 sporadic-E propagation at frequencies around 70 MHz 4-82344  
 sudden ionospheric disturbances in VLF atmospheric noise, rel. to solar flares 4-77680  
 transequatorial VHF propagation due to scatt. from F-region 4-115646  
 transionospheric propagation, wide bandwidth signals in random media 4-85821  
 transionospheric scintillation at 4 and 6 GHz, meas. by Asian ground stations 4-85822  
 UHF propagation and total electron content determ. 4-90010  
 ULF hydromagnetic waves, propagation at mid-latitude 4-82327  
 VHF equatorial scintillations, effect of 1981 April mag. storm and assoc. elec. fields 4-90034  
 VHF Faraday rot. over E Mediterranean and ionosphere total electron content var. 4-90037  
 VHF intensity scintillation of transionospheric signals, due to F- and E-regions 4-115648  
 VHF nighttime scintillations, control by equatorial spread-F irregularities 4-90031  
 VHF-UHF radar instrumentation, plasma disturbance investigation (*Japanese*) 4-62983  
 VHF/UHF fast Faraday polarisation var. and amplitude scintillation in ionosphere 4-90033  
 VLF in auroral D-region, effect of heated patch 4-85820  
 VLF Omega signals, anomalous interference on E to W equatorial paths 4-115651  
 VLF reflection, electron density profile estimation, improved technique (*Japanese*) 4-85827  
 VLF waves, interaction with turbulent ionosphere 4-100852  
 VLF whistlers, reln. between propag. distance and polarisation chars. 4-110348  
 whistler mode signals used to study radial plasma drifts 4-82335  
 whistler nonlinear excitation by plasma waves, theory 4-115655  
 whistler thermal filamentation instability exciting magnetostatic fluctuations 4-67544  
 wide bandwidth signal propagation through random media 4-85821

**ionospheric measuring apparatus**

- automatic DC measurement instrument 4-77641  
 Doppler radar multifrequency sounding equipment 4-94279  
 EISCAT facility 4-100806  
 magnetoplasma dynamic source in upper atmosphere, mass spectrometer probe meas. 4-85795  
 solid plasma probe in ionospheric or magnetospheric plasma, ion acoustic wave radiation props. 4-85859  
 HF radar used for ionospheric research at Bribie Island, Australia, calibration procedure 4-85790

**ionospheric measuring instruments** *see ionospheric measuring apparatus***ionospheric propagation** *see ionospheric electromagnetic wave propagation***ionospheric techniques**

- see also electron density; ion density*  
 AI absorption data reduction, validity of George's method 4-90019  
 antenna in ionospheric plasma, expts. on VLF multiturn loop antenna 4-85858  
 auroral arc X-ray imaging by satellite 4-100842  
 chemical modification expt. using rocket exhaust, incoherent scatter obs. 4-67533  
 D-region, electron density profile estimation with VLF refl. coeffs., improved technique (*Japanese*) 4-85827  
 Doppler radar multifrequency sounding technique 4-94279  
 electric currents meas. from daily geomag. var., coastal effect at equatorial latits. 4-110044  
 electrical conductance mapping technique using auroral spectroscopic method 4-67438  
 electron beam antenna expt. for satellites, EM wave excitation study 4-94281  
 electron beam injection form stellite, elec. field pot. distrib. near satellite at beginning of expt. 4-110353  
 electron densities at high-latitudes, determ. from convection elec. fields 4-85828  
 electron density profile meas. at night by rocket radio expt. 4-94280  
 geodetic Doppler receivers use for electron content var. determ. 4-90009  
 HF band radiowaves, ionospheric heating experiments (*Japanese*) 4-63011  
 HF Doppler array sounding of TID's, appl. to thermospheric wind vel. vectors determ. 4-90015  
 incoherent scatter radar meas. spectral estimation, nonlinear MEM 4-100808  
 Langmuir probe for ion parameters determ., errors 4-105731  
 magnetometer with nonconducting sensor enclosure in conducting fluid, calc. of instrumental corrections 4-100789

**ionospheric techniques continued**

- NAVSTAR L band ionospheric calibration for electron content rel. to Faraday rot. method 4-90010  
 PLACES ionospheric plasma testing, rocket vehicle targeting 4-62954  
 solid plasma probe in ionospheric or magnetospheric plasma, ion acoustic wave radiation props. 4-85859  
 plasma vel. meas. method using EISCAT 4-100807  
 radar probing technique at HF freqs. using pulse compression techniques 4-94278  
 radar sounding at high-latitude, problem of achieving orthogonality to field-aligned irregularities 4-85823  
 HF radar used for ionospheric research at Bribie Island, Australia, calibration procedure 4-85790  
 radiowave heating experiments, electrostatic wave generation process 4-94299  
 radiowave sounding of inhomogeneities, phase fluctuations of signals 4-72725  
 satellite charged particle beam expts., changes in satellite elec. pot. 4-72851  
 sudden ionospheric disturbance monitoring using sweep freq. method (*Chinese*) 4-82245  
 VLF sounding, signal spectrum broadening as diagnostic of turbulence 4-100852  
 SF<sub>6</sub> release experiments, calc. of chemistry, spectral emissions and plasma instabilities 4-94300

**ionotophoresis** *see electrophoresis***ions**

- see also atoms; electrolytic ions; hydrogen ions; negative ions*  
 d-dimensional heavy positive ions, energy relations in density functional theory 4-90545  
 solar wind energetic ion enhancements near magnetic sector boundaries 4-94540

**I.R. astronomy** *see infrared astronomy***I.R. detectors** *see infrared detectors***IR drop** *see electric potential***IR focal plane arrays** *see image sensors; infrared imaging***I.R. imaging** *see infrared imaging***I.R. sources** *see infrared sources***I.R. spectra** *see infrared spectra of diatomic inorganic molecules; infrared spectra of inorganic solids; infrared spectra of organic molecules and substances; infrared spectra of polyatomic inorganic molecules; spectra of inorganic liquids and solutions***irasers** *see lasers***iridium**

- see also nuclei with .....*  
 catalyst, for <sup>3</sup>H<sub>2</sub> production by catalytic thermal decomposition of water 4-93646  
 Cretaceous-Tertiary boundary impact, Ir anomaly in nonmarine sequence of Raton Basin 4-72588  
 Late Devonian mass extinction horizon, no Ir anomaly 4-62811  
 electrode, activated, potentiometric behaviour in acrylamide and H<sub>2</sub>SO<sub>4</sub> (*French*) 4-62247  
 electrodeposited coatings from molten alkali metal cyanide baths 4-93244  
 electron and neutron irradi., elec. resist. studies 4-108447  
 enrichment in Cretaceous/Tertiary boundary clays, Bidart section, France 4-105554  
 nuclear spin-lattice relaxation rates, relativistic APW calc. 4-71204  
 powder metallurgy production of refractory metals and alloys 4-66264  
 refractory, thermal expansion meas. 4-75710  
 surface, CO<sub>2</sub> desorption ang. distrib. from CO oxidation 4-80378  
 transcrystalline SCC mechanism, cleavage-like fracture surfaces 4-71793  
 Ir electrodes, electrochemical form. of oxide films, SEM and TEM studies 4-104908  
 Ir<sup>2+</sup>, in alkali halide matrix, lifetimes, fluoresce. spectra 4-102631  
 Ir<sub>2</sub> clusters, electronic struct., X<sub>α</sub>-SW and EHT calcs. 4-92603  
<sup>192</sup>Ir, low-cost hot facility for high-CI gamma-source processing 4-74084  
<sup>192</sup>Ir wire, standard planar implants, dosimetry tables 4-85516  
<sup>192</sup>Ir wire used in interstitial radiation therapy, activity meas. intercomparison 4-81759

**iridium alloys***see also iridium compounds*

- Cr-Ir, active dissoln. in H<sub>2</sub>SO<sub>4</sub>, effect of Pt group element additions 4-71770  
 Cr-Ir, Debye characteristic temps. 4-70330  
 Mo-Ir, refractory, thermal expansion meas. 4-75710  
 Nb-Ir, refractory, thermal expansion meas. 4-75710  
 Pd-Ir (18 wt.%), field ion imaging of surface atoms 4-88384  
 Pd-Ir-Pt(Rh), phase equilib. of Pt metals at 1400°C 4-71637  
 Pt-Pd-Rh-Ir, phase equilib. of Pt metals at 1400°C 4-71637  
 Pt-Rh-Pd(Ir), phase equilib. of Pt metals at 1400°C 4-71637  
 Rh-Ru-Pd(Ir), phase equilib. of Pt metals at 1400°C 4-71637  
 TmIr<sub>2</sub>, Mossbauer study and quadrupole splitting 4-114188

**iridium compounds***see also iridium alloys*

- polyacetylene: IrCl<sub>6</sub>, giant dielectric const. 4-92997  
 BaRu<sub>1-x</sub>Ir<sub>x</sub>O<sub>3-y</sub>, cryst. struct. and elec. cond. (*German*) 4-84265  
 Ir<sub>4</sub>(CO)<sub>12</sub>, adsorbed mol. clusters, electronic struct., UPS, XPS studies 4-78995  
 IrO<sub>x</sub>, reactively sputtered coatings, electrochromism (*Japanese*) 4-99095

**irru***see also nuclei with .....*

- (100) with chemisorbed S, electronic struct. study 4-92779  
 (110), spin-dependent bremsstrahlung 4-88898  
 (110) with chemisorbed Br, LEED and ARUPS study 4-92518  
 ab initio hyperfine struct. parameter calcs. 4-78981  
 abundance in corona 4-105932  
 adsorption and growth on Ni (100), LEED and EELS studies 4-113808  
 amorphous, local density of states via recursion and equation of motion methods, comparative study 4-98505  
 amorphous, struct., computer simulation by Markov chain method 4-75301  
 annealed, stress enhanced H<sub>2</sub>S adsorption, Auger spectra 4-75789  
 Armc, coating with W by electrolytic plasma process (*Russian*) 4-71775  
 Armc, formability, max. uniform strain, effect of matrix and second phase 4-99465  
 Armc, oxide scaling in technical flue gases 4-93438  
 Armc, strain hardening exponent 4-99406  
 atoms, s-d interconfig. energies, s-spin flip energies and ionisation pots. 4-83303

- iron continued
- atoms, two-electron, one-photon transitions 4-74340
- automobiles using Ni-Fe accumulators, operating characts. and dimens. (French) 4-93604
- axisymmetric conductor, current-carrying, magnetostatic field calcs. using eigenfunction expansion, effects of Fe 4-59948
- BCC, electron or neutron irradi. induced defects, model 4-65300
- BCC, Fermi surface and energy bands under press., APW calc. 4-80478
- BCC, grain boundary diffusion, mol. dynamics simulation studies 4-80287
- BCC, interaction with H, ab initio/effective core pot. cluster calc. 4-108722
- BCC, local densities of states, work functions and surface stabilities 4-88443
- BCC, local density of states via recursion and equation of motion methods, comparative study 4-98505
- BCC, migration process of H isotopes calc. 4-65465
- BCC, screw dislocation core struct. and plastic deformation 4-70154
- BCC crystal, irradiation creep, stress induced edge dislocation-interstitial atom interaction 4-104814
- BCC-HCP transition, neutron diff. expts. using diamond anvils at ultrahigh pressures 4-88038
- catalyst for NH<sub>3</sub> synthesis, surface struct. and reactivity study 4-80355
- chemical bonding, mag. susceptibility 4-114090
- chemisorption of H on (110), ordered struct. form. on metal surface, role of multi-atom interactions 4-80400
- coated by Sb layer, oxidation, Mossbauer spectra obs. 4-61609
- cold rolled, defect annealing, alloying element effects, positron studies 4-76550
- cold-rolled and recrystallised, metallographic methods for studying crystallographic orientation 4-114576
- corrosion in molten carbonate, electrochem. studies 4-104917
- corrosion in molten chloride, electrochem. studies 4-104915
- corrosion in molten sulphate, electrochem. studies 4-104916
- corrosion of pure Fe, Ni and Cr in formic acid soln., comparison with austenitic stainless steel 4-71763
- corrosion pit growth, early stages, meas. of shape change 4-104897
- corrosion scales, high temp., TEM studies 4-104927
- crack tip under mixed mode loading, atomic model 4-62013
- cylindrical sample,  $\gamma$ -ray self-absorption, correction factors 4-109267
- damage structures, evolution under 14 MeV neutron, 4 MeV ion and 1.25 MeV electron irradi. 4-108418
- diamond:Fe, electronic struct. calcs. 4-113894
- diffusion of C in  $\alpha$ -Fe, review 4-65474
- diffusion of Co in  $\alpha$ -Fe, effect of mag. transition 4-65481
- diffusion of N in  $\alpha$ -Fe during precipitation 4-65452
- diffusion of positive muons and other light particles in metals 4-65893
- dislocation loop form. by self-ion irradi. at 40K, electron microscopy obs. 4-70242
- electrochemical behaviour, effect of Br<sup>-</sup> 4-89165
- electrode material in vacuum spark discharge, electron temp. scaling 4-103592
- electrolytic, thermal conductivity meas., compact apparatus for good conductors, performance testing 4-11129
- electron and neutron irradiated, low-temp., mag. relax. spectra in  $\alpha$ -phase 4-84831
- electron irradiated, internal friction (Polish) 4-92234
- electron transport in sub-MeV region, Monte Carlo anal. (Chinese) 4-80560
- electronic struct., exchange splitting, spin- and angle-resolved photoemission spectra 4-88944
- electronic struct., magnetism and Curie temps. 4-75843
- electronic struct., XPS studies 4-75838
- element analysis using charged-particle induced prompt  $\gamma$  rays 4-89362
- epitaxial films, electronic and mag. states 4-80646
- equation of state and melting curve at very high press. 4-108576
- EXAFS, multiple scattering effects 4-66108
- EXAFS contributions and near neighbour components 4-61774
- fatigue crack initiation, Coffin-Manson relations 4-85212
- fatigue threshold, effect of strength and surface asperities on closure 4-76852
- fatigue threshold, thermally activated behaviour of effective stress intensity 4-76853
- ferromagnetic, even magneto-optical effect, spectral thermal emission linear polarisation 4-99096
- ferromagnetic, exchange interactions and spin-wave stiffness 4-84776
- ferromagnetic, high purity, magnetomechanical damping, influence of struct. defects 4-76226
- ferromagnetic, magneto-optic effect on thermal IR spectra, expt. study 4-76442
- ferromagnetic, spin polarised positron annihilation and enhancement effects 4-93126
- ferromagnetic, wave-vector depend. temp. behaviour of empty bands 4-104123
- ferromagnetic thin films, high rate magnetron sputtering 4-66232
- ferromagnetic-paramagnetic phase transformations and collective phenomenon (German) 4-71068
- ferrous laminated composites, steel/Fe, superplasticity 4-81235
- fibre texture, quantitative representation (Korean) 4-104946
- film, epitaxially grown on GaAs, surface magnons, Brillouin scatt. study 4-88852
- film and single cryst., microwave generation of 9.4 GHz phonons 4-61422
- films, H<sub>2</sub> adsorption, surface pot. and thermal desorpt. spectra study 4-65555
- films, organo-metal CVD growth from (CO)<sub>2</sub>Fe+AsH<sub>3</sub> on GaAs 4-61868
- fine particles, prep. from goethite microcrysts., morphology and mag. props. 4-65835
- foil, magnetic hyperfine fields determ. by Mossbauer spectroscopy, using internal standard 4-114185
- foil melting by laser-guided discharges 4-75219
- fully relativistic band struct. calcs. 4-113855
- Gilbert damping, critical fluctuation effects, ferromag. resonance study 4-61539
- Goa mineral deposits, India, remote sensing using Landsat multispectral scanner 4-67427
- grain boundary fracture, H-induced, effect of C 4-93403
- grain boundary with impurity segregation, atomic and electronic structs., 4-113463
- graphite:Fe, ion implanted, mag. props. 4-61562
- iron continued
- hyperfine interactions of interstitial <sup>12</sup>B, asymmetric  $\beta$  decay studies 4-65651
- impact-tension compression test using split-Hopkinson bar 4-87639
- impurity hyperfine fields and adiabatic pot., self-consistent calc. 4-65632
- intermetallic phases formed by Sn ion implantation 4-92225
- ion, Na-like, dielectronic recombination rates 4-96696
- ion implanted with N, SIMS, Auger and nuel. reaction analysis 4-88185
- ion source, multiply charged, using heated gas discharge chamber 4-73578
- K $\alpha$  emission from solar flares, excitation source 4-90128
- K-absorption edge, X-ray absorpt. near edge struct. obs. 4-66123
- Kevlar 49:Fe<sup>2+</sup>(Fe<sup>3+</sup>), EPR study of stress induced free radicals 4-109076
- laser irradi., surface structural and electronic props. 4-60956
- laser microprobe mass analysis detection limits and lateral resolution 4-72016
- liquid, local density of states via recursion and equation of motion methods, comparative study 4-98505
- local-field enhancement of rough surface 4-104047
- magnetic anisotropic constants, Mossbauer spectroscopy determ. 4-109100
- magnetic Compton profile meas. using circularly polarised  $\gamma$ -rays from oriented <sup>191</sup>Ir nuclei 4-71462
- mechanisms and kinetics of dissolution in liquid Cu 4-114530
- melting influence on shocked free surface behaviour 4-108541
- metal-metal collision sticking behaviour and relevance to solar nebula 4-67649
- meteorites, group IIIE resolution from IIIAB, Cu as taxonomic parameter and elemental comp. 4-77787
- muon, uniaxially stress-induced freq. shifts 4-65918
- muon precession, var. with magnetisation angle 4-65920
- muon trapping at vacancies in pure and doped Fe 4-65901
- nitriding kinetics under electrolytic heating conditions of commercial grade Fe (Russian) 4-85253
- overionisation in Am star 15 Vul 4-101355
- oxidation, high temp, cation diffusing scale form., SEM obs. 4-71791
- particle filled epoxy composite, dynamic mech. props. 4-76794
- particle interaction and clumping in an electrically conducting magnetic liquid 4-108623
- passive film, duplex struct., photoacoustic spectra studies 4-66492
- passive film form. in borate solns., electrochem. and ellipsometric studies 4-66490
- passive films, in borate solns., electrochemical and ellipsometric studies, film growth 4-89178
- passive films on Fe, mech. of breakdown in chloride containing solns. 4-93450
- permeation of T<sub>2</sub>, reduction by Al implantation 4-88184
- photon backscattering, angle albedo meas. 4-61782
- pigments, mag. props. rel. to specific surface area 4-65836
- polycrystalline, ferromagnetic, density of unoccupied states, SXAPS study 4-85039
- positive muon quantum diffusion in  $\alpha$ -Fe 4-104516
- positron annihilation expts. in thermal equil. on  $\alpha$ -Fe, one-interstitial model confirmation 4-109271
- potential at at. boundaries in Thomas-Fermi model and eqns. of states (Chinese) 4-70333
- powder, electrodeposition of Cu, coating props. 4-89188
- powder, Ni-coated, compacted, phase identification by colour etching 4-114755
- powder, porous, type PZ-2-MZ high-voltage breakdown 4-80867
- powder, shock wave effects, thermoelectric emission 4-99272
- powder compacts, rearrangement phenomenon, theoretical model expressing assoc. shrinkage 4-104747
- powders, chem. instability and corrosion, mag. tape appls. (Chinese) 4-98982
- powders, rotating electrode process atomisation mechanisms 4-89001
- pure, annealed, fatigue crack nucleation sites under reversed bending stress (Japanese) 4-99516
- pure, anodic behaviour in high temp. and high press. aq. soln., straining electrode technique 4-109571
- pure, carbonitride precipitation by successive ion implantation of C and N, XPS and Mossbauer obs. 4-76906
- pure, irradi. in HVEM, void form. onset temp. 4-103804
- pure, orthogonally planed surface layer, X-ray lattice strains rel. to texture (Japanese) 4-114567
- pure and C doped, electron irradi., resistivity recovery 4-108834
- pure and siliconised, corrosion and oxidation kinetics in SO<sub>2</sub> atm. 4-109554
- radiation damage calc., nuclear model codes 4-107045
- radiation damage calc. by NJOY nuclear data processing system 4-107044
- radiation shielding geometry, dose factors of  $\gamma$ -ray build up 4-102406
- radiative properties at high temp. 4-84952
- rainwater of Bermuda, trace metals content 4-67320
- scratch scars generated in aq. soln., repassivation kinetics 4-71766
- Sea of Japan, Fe, Mn, Zn, Cu in seawater of USSR coast 4-94171
- seawater of Kattegat and Skagerrak, trace metal concentrations 4-85714
- seawater trace metal content meas. technique using isotope dilution mass spectrometry 4-85797
- single crystals, spin polarised Auger electrons 4-85044
- sintered, apparent diffusion coeff. of C during gas carburising process 4-103989
- sintered, crack propag. and processes near crack tip 4-66435
- sintered, mag. suscep. and porosity, semi-empirical rel. 4-84774
- sintered compacts, alloying element effect on carburising response 4-99642
- sintered materials, coercive force, influence of microstruct. 4-66461
- slip line patterns during work hardening stages 4-99419
- small clusters, electronic struct., spin density functional theory anal. 4-113859
- solar cosmic ray events, FE ionic charge dist. 4-105960
- specimens with flat ends, region of appl. of method of upsetting 4-109597
- spheres, neutron leakage spectra, meas. and calc. 4-68837
- sputtered atom vel. and electronic state distrib. by laser-induced fluoresc. spectroscopy 4-93168
- sputtered atoms, laser-induced fluoresc. investig. (German) 4-69008
- sputtered film, filamentous C growth, surface morphology effects 4-92114

## iron continued

- sputtered neutrals, ionisation length near wall in ISX-B using laser-induced fluoresc. 4-91971  
 strain hardening behaviour, statistical anal. 4-99403  
 stress relaxation and static strain aging, short range heavy interstitials reordering 4-85172  
 substrate for Nb film, laser treatment, Mossbauer study (*Russian*) 4-70204  
 sulphidation, microstruct. and growth rates of FES 4-88304  
 supernova remnants, coronal [Fe] lines for nonequilibrium ionisation models 4-94913  
 surface, (001), clean, surface struct. anal. using low energy ion scatt. 4-92496  
 surface, (001), magnetic domains obs. by SEM using spin polarised secondary electrons 4-61549  
 surface, (100), c(2x2) Si overlayer, ang., resolved photoemission study 4-93199  
 surface, (110), exchange split empty energy bands inverse photoemission studies 4-84551  
 surface, (110), ferromag., spin-polarised low-energy electron diff., temp. effects 4-104456  
 surface, (110), H chemisorbed overlayer, Monte Carlo studies 4-113816  
 surface, (111), CO interaction, thermal desorpt. and LEED studies 4-65566  
 surface, (111), N<sub>2</sub> chemisorbed,  $\pi$ -bonded complex, the precursor for dissociation 4-105029  
 surface, adsorption and thermal decomposition of tricresylphosphate, XPS studies 4-98428  
 surface (001), electronic struct., magnetism, muon spin relax. 4-70888  
 surface (310), struct., parallel and perpendicular multilayer relax., LEED study 4-80349  
 surface alloying using continuous laser rad. 4-93443  
 surface layer at nonmag. material interfaces, magnetisation, temp. depend. 4-61575  
 surface treatment with SULF BT, XPS study (*Chinese*) 4-62091  
 surface with oxide, silicate and phosphate coatings, Fourier transform IR spectra 4-104688  
 surface with very thin oxide layer, Mossbauer spectra obs. 4-61609  
 texture, fine structure anisotropy, X-ray method 4-93480  
 thick foil, mag. domain wall obs. 4-80780  
 thin film, electron transmission, electron NGR spectroscopy study 4-60971  
 thin films, Brillouin light scatt. study of magnon branch crossover 4-80959  
 thin foils, STEM energy dispersive X-ray microanalysis 4-69999  
 transformation superplastic deformation 4-114610  
 uniaxially strained, muon states calc. 4-65939  
 vertical distribution in Arctic Ocean rel. to Cd and Al profiles and hydrography 4-82089  
 whisker, Barkhausen jump field distrib., temp. depend. 4-76182  
 wires, Barkhausen jumps, deform. effects 4-76187  
 work hardening charact., plastic behaviour depend. on temp., strain rate, cryst. orientation 4-99418  
 X-ray spectra of Fe<sup>2+</sup> and Fe<sup>3+</sup> inner-shell transitions in solar flares 4-94707  
 yielding and plastic flow, model, rel. to thermal activation 4-103860  
 zone-refined, oxidation at 1200°C, scale morphology and growth rate 4-62118  
 $\alpha$ -Al<sub>2</sub>O<sub>3</sub>/Fe, defect structure, electron emission meas. 4-93145  
 Al<sub>2</sub>O<sub>3</sub>-Fe cermets, metal to ceramic bonding, Mossbauer studies 4-109622  
 $\beta$ -Al<sub>2</sub>O<sub>3</sub>-Na<sub>2</sub>O/Fe, decomposition processes, microscopic mechanisms 4-109415  
 As<sub>2</sub>Se<sub>3</sub>/Fe, extrinsic cond. and optical const. meas. 4-75971  
 Au/Fe interface boundary, interdiffusion 4-65497  
 Au/Fe, creep-induced dislocation subgrain arrangement in ferrite, effect of stress changes 4-76799  
 $\alpha$ -Fe, nitriding, heterogeneous, dislocation production and oriented precip. 4-66498  
 BaTiO<sub>3</sub>/Fe, dielectric relax. meas. 4-80864  
 BaTiO<sub>3</sub>/Fe, electrolum., elec. field depend. 4-66077  
 BaTiO<sub>3</sub>/Fe, soft mode behaviour, ferroelec. transition and IR reflectometry 4-80872  
 Cd<sub>2</sub>Nb<sub>2</sub>O<sub>7</sub>/Fe, narrow phase transitions, elec. field and impurity effects 4-71316  
 Cu $\gamma$ -Fe/Cu epitaxial sandwich layers, struct. and Mossbauer studies 4-84531  
 CuInS<sub>2</sub>, defect chemistry, elec. and Mossbauer studies 4-70730  
 Fe (II)-ferene complexation study 4-109626  
 Fe (001) ferromagnetic, spin- and angle-resolved photoemission spectra 4-85063  
 Fe (110)p(2x2)-S, surface ferromagnetism, chemisorption, absorbate-induced substrate reconstruction effect, spin-polarised LEED calcs. 4-80395  
 Fe complex form. in 1,3-butadiene matrix, IR spectra 4-64477  
 Fe group atoms, 3d<sup>4</sup>4p configs., effective electrostatic interactions 4-83317  
 Fe I, II and III, atomic partition functions 4-107270  
 Fe I, ionisation potential by multistep laser spectroscopy 4-74353  
 Fe I 557.61 nm line changes rel. to solar oscills. 4-63127  
 Fe I oscillator strengths meas. 4-87080  
 Fe I solar lines anal. and determ. of atm. turbulence and damping const. (*Russian*) 4-101282  
 Fe II emission and excitation in stellar atm. and laboratory anal. 4-110516  
 Fe II fluorescence in stellar atmospheres, UV triplet lines 4-63154  
 Fe II oxidation expts. in Ag and Ag<sub>2</sub>S electrodes (*Russian*) 4-68306  
 Fe II spectrum, comparison between observed and predicted emission lines in different plasmas 4-87061  
 $\alpha$ -Fe, positive muon quantum diffusion and location 4-84890  
 Fe, SCC in NaH<sub>2</sub>PO<sub>4</sub> soln., effect of heat treatment and C 4-89167  
 Fe XI, electron collisional excitation rate coeffs. 4-91862  
 Fe XV, energy levels, oscillator strengths 4-102617  
 Fe XV, lifetimes of low lying levels 4-107313  
 Fe XVII, Ne-like, laser-produced plasmas, 2p<sup>3</sup>3s, 3p and 3d configurations 4-102620  
 Fe XVII transitions identification in solar flares 4-72922  
 Fe XVIII-XXIII 8-14 nm lines, plasma electron density meas. 4-87927  
 Fe XXIV, spectral line strengths in laser plasma 4-107314  
 Fe<sup>+</sup> electron impact ionis. cross-section meas. 4-69222  
 Fe<sup>2+</sup>, oscillator strengths, photoionisation cross section calc. 4-83332

## iron continued

- Fe<sup>2+</sup>, high precision X-ray spectra 4-78797  
 Fe<sup>2+</sup> region in active galactic nuclei 4-77919  
 $\alpha$ -Fe-C, martensitic, lattice deformation by C impurities (*Russian*) 4-103773  
 Fe/Al cylinders, diffusion under high mech. stress and accelerations, AES studies (*German*) 4-103993  
 Fe/Cr redox battery; mathematical model 4-89469  
 Fe/Fe<sub>2</sub>O<sub>3</sub>, high magnetisation material with alternate layer struct., HF mag. core appl. 4-104470  
 Fe/Ni system, interdiffusion, activation energy and freq. factor 4-65495  
 Fe/Zn system,  $\delta$  phase form. and growth 4-80314  
 Fe<sup>2+</sup>/thionine photogalvanic cell, effect of Triton X-100 micelles 4-105113  
 Fe-Ag, interface magnetism, self-consistent spin-polarised localised spin density calcs. using APW method 4-98863  
 Fe-Ag composite sheets, anisotropy of phys. and mech. props. 4-99368  
 Fe-Ag interface, electronic struct. and mag. props. 4-80645  
 Fe-Ag(MnF<sub>2</sub>) interface, magnetisation study 4-80789  
 Fe-Cr (9.75 wt.%), protective oxidation in CO<sub>2</sub>, TEM obs. 4-62094  
 Fe-LiClO<sub>4</sub>, shock compression, physicochemical transformations 4-70273  
 Fe-Mg multilayered films with superlattice, mag. props. study 4-80791  
 Fe-Ni codeposits, H<sub>2</sub> evolution reaction, in alkaline media 4-93533  
 Fe-Ni layered films, ferromagnetic, appl. of phase resolved photoacoustic microscopy 4-79406  
 Fe-V interface, mag. props. study 4-80790  
 Fe-V multilayered films with artificial superstructures, mag. props. 4-109045  
 Fe<sup>2+</sup>+Ar(Kr)(Zr)(Ag)(Sn) near-symmetric collisions, K-K transfer cross-sections 4-64571  
 Fe, clusters Ar, Kr and Xe matrices, mag. circular dichroism study 4-78799  
<sup>57</sup>Fe film, spectral analysis of spin-echo signals 4-104510  
<sup>57</sup>Fe/<sup>56</sup>Fe thin film system, surface and interface magnetism, Mossbauer spectra studies 4-104468  
 Fe<sup>+</sup> production from electron impact on Fe(CO)<sub>5</sub>, at. fluoresc. study 4-96709  
 GaSe/Fe, elec. cond. and impurity states 4-113957  
 Ga<sub>2</sub>Se<sub>3</sub>/<sup>57</sup>Fe single cryst., Mossbauer effect and mag. susceptibility 4-104513  
 $\alpha$ -Ge/Fe(Ni) films, cond. and localised states 4-104163  
 $\gamma$ -Fe, high purity, thermotransport, isotope effect 4-108664  
 H diffusivity, apparent 4-104005  
 H electrochemical penetration, effect of As additions to electrolyte 4-66497  
 H isotope permeation in structural alloys 4-113720  
 H<sub>2</sub> production by water splitting, using photochemical reaction in concentrated phosphoric acid 4-89470  
 InP/Fe, <sup>76</sup>He<sup>+</sup> bombarded, psec. photocond., very short free carrier lifetimes 4-108894  
 InP/Fe, semi-insulating, Four-wave mixing using photorefractive effect, optical processing appl. 4-74585  
 InP/Fe, semi-insulating, with phosphosilicate glass encapsulation heat treatment, photoluminesc. and Raman spect. characterisation 4-84995  
 InP/Fe, thermally annealed, Fe redistribution and diffusion coeff. 4-70460  
 InP/Fe/Mg, implanted, effect on photoluminescence props. 4-85007  
 InP/Fe photoconductor for synchrotron-radiation research 4-91177  
 InP/Fe photoconductors, pulsed soft X-ray response 4-80620  
 InP/Fe single crystals, LEC growth, perfection, carrier conc., TEM obs. 4-71550  
 n-InP/Fe-Au diode struct., photocurrent amplification 4-70934  
 KTaO<sub>3</sub>/Fe, photocurrent, optical quenching 4-113990  
 KTaO<sub>3</sub>/Fe<sup>2+</sup>, EPR spectra, superhyperfine struct., spin Hamiltonian parameters 4-98942  
 KZnF<sub>6</sub>/Fe<sup>2+</sup> crystal, EPR and far IR study on (FeF<sub>6</sub>)<sup>4-</sup> complex 4-80814  
 LiNbO<sub>3</sub>/<sup>57</sup>Co, Fe<sup>3+</sup>, electron capture, non-equilibrium population, Mossbauer spectra studies 4-108807  
 LiNbO<sub>3</sub>/Fe, photocurrent jumps due to domain struct. (*Russian*) 4-75996  
 LiNbO<sub>3</sub>/Fe, polarisation-anisotropic light-induced light scatt. 4-87395  
 LiNbO<sub>3</sub>/Fe, Rayleigh scatt., effect of photorefr. 4-80957  
 LiNbO<sub>3</sub>/Fe (III) ferroelec., Mossbauer spectra and EPR studies 4-65960  
 LiNbO<sub>3</sub>/Fe crystals, photoelec. and photorefr. prop. control during growth by elec. current 4-80904  
 LiTaO<sub>3</sub>/<sup>57</sup>Co, Fe<sup>3+</sup>, electron capture, non-equilibrium population, Mossbauer spectra studies 4-108807  
 LiTaO<sub>3</sub>/Fe, photorefractive, photovoltaic effect, photocond., depend. on light intensity (*Russian*) 4-114226  
 MgCO<sub>3</sub>/<sup>57</sup>Fe (II), orbit-lattice interaction effect on Mossbauer studies 4-71222  
 MgCO<sub>3</sub>/Fe<sup>2+</sup>, Mossbauer lineshapes, ion-phonon process effects 4-114186  
 MgO/Fe, self-diffusion meas., vacancies 4-98346  
 NaAl(SO<sub>4</sub>)<sub>2</sub>.12H<sub>2</sub>O/Fe<sup>2+</sup>, single crystal EPR, resonance linewidths, crystal field splittings 4-84851  
 Ni/Fe accumulators, new generation, for industrial manufacturing (*French*) 4-62331  
 Pb(Zr<sub>0.1</sub>Ti<sub>0.9</sub>)O<sub>3</sub>/Fe, doping ion lattice site, X-ray anal. 4-75488  
 Si/B, Fe, exciton photoluminescence study 4-109243  
 Si/Fe, breathing mode relax around tetrahedral interstitial 3d impurities 4-108567  
 p-Si/Fe, conductance along grain boundaries 4-80585  
 n-Si/Fe, impurity bands of Fe clusters, ESR and elec. props. 4-109067  
 SrTiO<sub>3</sub>/Fe<sup>2+</sup>-V<sub>0</sub> pairs, electronic struct. calcs. 4-113890  
 Ti/Fe redox flow battery discharge performance 4-81534  
 V/Fe compositionally-modulated struct., mag. props. and superconductivity 4-61561  
 ZnCO<sub>3</sub>/Fe<sup>2+</sup>, Mossbauer lineshapes, ion-phonon process effects 4-114186  
 ZnS/Fe<sup>2+</sup>, impurity states, EPR meas. 4-84588

## iron alloys

- see also Elinvar; Invar; iron compounds; Permalloy; steel  
 Al-Fe, cold worked, damping capacity, mech. props. rel. to heat treatment and comp. (*Japanese*) 4-61968  
 Alloy 800, fatigue, high temp., damage mechanics 4-93422  
 Alloy 800H, creep of tubular components, influence of multiaxiality of stress and environmental induced degradation 4-93360  
 Alnico magnets, microstruct., comp., atom probe field ion microscopy 4-71828  
 amorphous alloys, structural relaxation (*Russian*) 4-104801

## iron alloys continued

- amorphous ribbon, as-cast, crystal and heat treatment effect (*Chinese*) 4-84190  
 BCC, nitrogenation kinetics, mechanisms, thermodynamics 4-71988  
 binary Fe melts, H solubility prediction (*German*) 4-65401  
 bulk martensite nucleation study (*Russian*) 4-81198  
 cast, metallographic differences between compacted and vermicular graphite 4-114753  
 cast, nodular, fatigue crack growth obs. using bonded-resistance gauges 4-93477  
 cast Fe, and nodular, laser surface hardening, erosion resist., near surface microstructure 4-66453  
 cast Fe, atomised powder, reduction-decarburisation in H stream 4-66269  
 cast Fe, ductile, fracture toughness, X-ray diffr. obs. of fracture surface 4-99581  
 cast Fe, flake graphite, fracture toughness 4-104872  
 cast Fe, graphite morphology, appl. of secondary ion mass spectrometry 4-66343  
 cast Fe, grey, profilometric characterisation of microstruct. (*French*) 4-71820  
 cast Fe, hardened high-strength, with nodular graphite cryst. struct. changes during tempering 4-93260  
 cast Fe, high-strength, mech. props. after prior heat treatment and isothermal hardening 4-93321  
 cast Fe, laser treatment, residual stress distrib., optimum surface hardening conditions (*Russian*) 4-71774  
 cast Fe, Mg treated, graphite nodularisation and graphitisation during solidification under 145 atm. Ar pressure 4-66325  
 cast Fe, microstruct. and phase comp. after irradi. by pulsed or continuous rad. of optical quantum generator 4-66485  
 cast Fe, obtained at superhigh quenching rates, struct. investig., 20 to 1150°C 4-93286  
 cast Fe, SG, fracture mechanics, cracks, elasticity anal., microtension tests (*Chinese*) 4-62027  
 cast Fe, spheroidal graphite, cavity initiation criteria at inclusions 4-104874  
 cast Fe, surface modification of materials by laser treatment 4-109547  
 cast Fe, tribological behaviour in inert and reducing gas media 4-71742  
 cast Fe, white, 4-104790  
 cast Fe, white, annealing, Fermi energy, thermoEMF obs. rel. to crystallisation in acoustic vibration field 4-76768  
 cast Fe, white, high Cr, abrasion by quartz particles, carbide removal mechanism rel. to particle shape 4-85220  
 cast Fe, with vermicular graphite, struct. and heat treatment 4-114471  
 cast Fe powder, laser deposition on steel surface for hard-facing (*Russian*) 4-85251  
 cast iron, white, wear resist. meas. using abrasive wear testing machine (*Japanese*) 4-76874  
 diffusion carburising, growth of carbide fibres 4-93454  
 dilute, magnetic anisotropic constants, Mossbauer spectroscopy determ. 4-109100  
 dilute alloys, vacancy-impurity interaction,  $\mu$ SR study 4-84886  
 eutectic coatings, boride and carbide strengthened, laser irradi. treated, wear resist. (*Russian*) 4-85250  
 FeCrAlloy, Fe-Cr-Al, D permeation 4-111754  
 Hastelloy X, oxidation, thermal cycling, H permeation, acoustic emission 4-76905  
 Hastelloy XR for HTGR, H<sub>2</sub> permeation in simulated reactor environment 4-75732  
 Incoloy, Fe-base superalloys, oxide dispersion strengthened, developments in prod. 4-114452  
 Incoloy 800, compatibility with flowing Li 4-107062  
 Incoloy 800, dynamic fracture toughness, results from instrumented impact machine 4-81373  
 Incoloy 800, oxidation in moist air containing HCl at 800°C 4-81327  
 Incoloy 802, H<sub>2</sub> permeation inhibition by corrosion oxide layers (*German*) 4-66506  
 Inconel 600, low temp. SCC effect of thermal stabilisation 4-99633  
 Inconel 718, fatigue and creep-fatigue crack propag., influence of neutron irradi. 4-99496  
 Inconel 718, vacuum brazed Ni-Cr-Si joint, struct. 4-66548  
 Inconel X750, in BWR primary system, corrosion products release rates meas. using radiotracer technique 4-91040  
 Inconel X-750, Ni-base superalloy, creep and fracture, prior deform. effects 4-114656  
 ion implanted with N, SIMS, Auger and nucl. reaction analysis 4-88185  
 neutron irradiated to high fluence, swelling resist. 4-98142  
 Nimonic PE-16, irradi. in HFIR at 430°C, fatigue performance 4-109497  
 physical metallurgy, book contrib. 4-109379  
 rare earth alloy, RFe<sub>2</sub>Si<sub>2</sub>, R=Ce, Eu, valence change, X-ray absorpt. study 4-85037  
 rare earth alloys, R<sub>2</sub>Fe<sub>23</sub> intermetallic cpds., magnetisation, mol. field anal. 4-71031  
 rare earth alloys, R-Fe-based metallic glasses, anomalous mag. hysteresis and coercive force 4-114140  
 rare earth intermetallics, RFe<sub>2</sub>H<sub>2</sub> (R=Gd, Ho, Er, Tm, Lu), mag. props. and cryst. struct., absorbed H<sub>2</sub> effects (*Russian*) 4-104458  
 siliconising, thermodynamic calcs. 4-89191  
 surface in acid media, H<sub>2</sub> evolution kinetics, metallurgical and electrochem. factors 4-85335  
 transition metal alloys, Fe-M, M=Nb, Ti, Zr, coercive field rel. to solid solubilities and nucleation behaviour 4-76185  
 transition metal alloys, Fe-M-N, M=Ti, Zr, mag. after effect spectrum 4-76185  
 transition metal-Fe-B amorphous alloys, magnetisation reversal, mech. stress effects 4-76171  
 transition metal-Fe-B metallic glasses, electronic struct., XPS study 4-75837  
 Al-Co-Fe, Alcofer 122, magnetostrictive, piezomagnetic coeffs., annealing, mag. field depend. 4-76214  
 Al-Fe alloys, Fe precipitation and dissolution, thermoelec. study 4-61938  
 Al-Fe-Mg-Cu, periodic load serrations in tensile curve, occurrence conditions 4-85194  
 Al-Fe-Mn system, Al-rich corner, phase equilib. and crystn. studies 4-114480  
 Al-Fe-Ni-Co, prep. from atomised powder, prod. struct. and props. 4-114446  
 Al-Fe-Si (0.31, 0.11 wt.%), recovery and recrystn., DSC study 4-85167  
 Al-Fe-misch metal, rapidly solidified, microstruct. characterisation 4-114442

## iron alloys continued

- Al-Mg-Si-Fe alloy, effect of Fe on precipitation 4-104783  
 Al-Si-Fe, AL-4, stress relax. resist., effect of plastic surface strain methods 4-109453  
 Al-Si-Fe, Luders band deform., stress relax., load suppression effect 4-76801  
 Al-Si-Fe-Mn, cast, quaternary Fe-containing phases 4-81204  
 AlMnFeSi particles in Al alloys, STEM study 4-76920  
 Au-Fe, positron lifetimes in vacancies and vacancy-Fe clusters 4-109274  
 Au-Fe alloys, chemical interdiffusion at interface with Au 4-65497  
 Au-Fe alloys, evidence against metastable phase separation 4-80239  
 Au-Fe alloys, metastable phase separation 4-80238  
 Au-Fe dilute alloy, exchange-circulation electron current between Fe atoms (*Chinese*) 4-114102  
 AuFe alloys, spin glass freezing, PAC study 4-71216  
 AuFe, dilute alloy spin glass, susceptibility, neutron scatt. and muon spin rot. 4-71249  
 AuFe, spin glass dynamics, muon spin relax., neutron spin echo meas. 4-71080  
 Co-(Fe, Mn)-Nb system, amorphous sputtered films, magnetostriction and HF permeability 4-71147  
 Co-Fe-Mn-B-Si, metallic glass, fatigue crack propag. and overload effect 4-109511  
 Co-Fe-Mo-B-Si, metallic glass, fatigue crack propag. and overload effect 4-109511  
 Co-Fe-Mo-Ni, phase equilib., Gibbs energy and activity coeff., SOLGAS-MIX program 4-84369  
 Co-Fe-Si-B metallic glasses, mag. props., annealing effects 4-109039  
 Co-Fe-V, Wiegand wire sensor characts. (*German*) 4-101830  
 Co<sub>8</sub>Fe<sub>4</sub>(MO, Si, B)<sub>30</sub> alloys, amorphous, mag. props., influence of induced anisotropy 4-84782  
 CoNiFe-SiB amorphous zero magnetostrictive alloy, compositional short-range order and ordering kinetics 4-70035  
 Co<sub>5</sub>Ni<sub>4</sub>Fe<sub>2</sub>B<sub>10</sub>Si<sub>16</sub> foil, thermal expansion coeff. and isothermal compressibility (*Russian*) 4-65421  
 Co<sub>5</sub>Ni<sub>4</sub>Fe<sub>2</sub>B<sub>10</sub>Si<sub>16</sub>, amorphous, mag. aftereffects after field annealing 4-84823  
 Co<sub>5</sub>Ni<sub>4</sub>Fe<sub>2</sub>Si<sub>16</sub>B<sub>16</sub>, amorphous, mag. hysteresis loops after heat treatment below Curie point 4-80781  
 Co<sub>3</sub>Si<sub>8</sub>Fe<sub>2</sub>B<sub>2</sub>S<sub>5</sub>, amorphous alloy, crystn. study using DTA and elec. resist. meas. 4-65181  
 Cr-Fe, antiferromagnetic spin glass, HF characts. (*Russian*) 4-71105  
 Cu-Al-Fe (10, 1 wt.%), corrosion and mech. props., effect of solidification struct. 4-85243  
 Cu-Al-Fe alloys, laser surface melted, microstruct., X-ray diffr. study 4-108628  
 Cu-Fe, elastic distortion of  $\alpha$ -Fe particles by Orowan loops, moiré fringes, TEM obs. 4-66358  
 Cu-Fe (1.59 wt.%),  $\alpha$ - $\gamma$  martensitic transform. of Fe particles, magnetisation obs. 4-66335  
 Cu-Fe (2 wt.%), precipitation strengthened, high temp. creep 4-61990  
 Cu-Fe dilute alloy, exchange-circulation electron current between Fe atoms (*Chinese*) 4-114102  
 Cu-Ni-Fe, coarsening of extremely small particles 4-113588  
 Cu-Ni-Fe, internal friction and precipitation morphology (*Russian*) 4-99416  
 Cu-Ni-Fe (9.4, 1.7 wt.%), corrosion behaviour in air-saturated aqueous NaCl soln. 4-93447  
 Cu-Ni-Fe (9.4, 1.7 wt.%), corrosion in aqueous NaCl soln., effect of sulphide 4-93448  
 Cu-Ni-Fe alloys, decomposition neutron scatt. studies 4-114539  
 Cu-Ni-Fe alloys, electron irradi., clustering and decomposition, neutron scatt. studies 4-114555  
 Cu-Ni-Fe alloys, short-range clustering and decomposition, dynamic scaling props. 4-114554  
 dilute, electron irradi., muon spin rot. obs. 4-65913  
 Dy-Tb-Fe, elastic props. nonlinearity and magnetostriction (*Russian*) 4-80133  
 DyFe<sub>2</sub> intermetallics, SXAPS studies 4-81039  
 DyFe<sub>2</sub>Al<sub>2-x</sub>, Fe L<sub>III</sub> X-ray emission spectra, electron microprobe anal. 4-76563  
 Dy<sub>2</sub>(Fe<sub>1-x</sub>Al<sub>x</sub>)<sub>17</sub>, pseudobinary intermetallic cpd., mag. props. 4-71032  
 (Dy<sub>0.7</sub>Tb<sub>0.3</sub>)Fe<sub>23</sub>, magnetostrictive strain as a function of magnetic field and mechanical elastic stresses 4-113523  
 ErFe<sub>2</sub> intermetallics, SXAPS studies 4-81039  
 Er<sub>2</sub>Fe<sub>23</sub>, mag. struct. study 4-108987  
 EuFe<sub>2</sub>Al<sub>8</sub>, X-ray absorpt. near edge struct. study 4-61769  
 (Fe, Co, Ni)<sub>3</sub>V, ductile ordered alloys, phys. metallurgy and mech. props. 4-114612  
 (Fe, Co)<sub>3</sub>V single crystals, flow stress, temp. and orientation depend. 4-71699  
 (Fe,Ni)V, ordered alloy, irradi. in HFIR, microstruct. and bend ductility 4-108454  
 (Fe,Ni)<sub>3</sub>V, long-range ordered, strain rate and ageing effect on mech. props. 4-109501  
 Fe base alloys, inoculation particles dissolution, carbide precipitation 4-89057  
 Fe base metallic glasses, ion irradi., damage, He and Ar, bubble form., blistering, exfoliation 4-108481  
 $\alpha$ -Fe binary alloys, BCC, fatigue, effect of alloying elements 4-66426  
 Fe-<sup>175</sup>Ta, mag. hyperfine splitting frequencies, mag. moments, NMR-ON obs. 4-109083  
 Fe-Ag-Pd, transient fields, g-factor, gyromagnetic ratios 4-113914  
 Fe-Al, anodic polarisation characteristics in 1N H<sub>2</sub>SO<sub>4</sub> 4-85247  
 Fe-Al, Ar<sup>+</sup> ions impact in ultrahigh vacuum, secondary ion and Auger electron emission (*French*) 4-66170  
 Fe-Al, at correlations, Mossbauer spectra 4-61613  
 Fe-Al, coercive field rel. to solid solubilities and nucleation behaviour 4-76185  
 Fe-Al (10 to 50 at.%), quenched, shrinkage during annealing 4-89074  
 Fe-Al (40 at.%), ion implantation, phase changes, TEM studies 4-108403  
 Fe-Al (48 at.%), mag. props. rel. to heat treatment 4-109003  
 Fe-Al alloys, Ar<sup>+</sup>-ion-sputtered, secondary ion and Auger electron emission 4-81101  
 Fe-Al alloys, nitrated, interaction of Al and N atoms, mag. aftereffect study 4-84829  
 Fe-Al alloys, segregation to static and migrating diffuse antiphase boundaries 4-114541  
 Fe-Al rapidly quenched cryst. ribbons, mag., elec. and mech. props. 4-76174

## iron alloys continued

- Fe-Al-Cr (Ni)(Mn), oxidation, effect of ternary alloying additions 4-85242
- Fe-Al-Mo, Mossbauer study of atomic struct. and mag. polarisation 4-80848
- Fe-Al-Ni-Mo (5.7, 2.5, 2.0 at.%), containing coherent precipitates, effect of plastic deform. on elevated temp. Ostwald ripening 4-85159
- Fe-Al-Si, anodic polarisation characteristics in 1N H<sub>2</sub>SO<sub>4</sub> 4-85247
- Fe-Al-Si, Sndust, brittleness, effect of solidification and heat treatment 4-81281
- Fe-Al-Si (20.5 at.%), DO<sub>3</sub>-ordered alloys, tensile behaviour 4-93337
- Fe-Al-Si (6, 9 at.%), ordering with phase separation, annealing, TEM, X-ray diffr. study 4-114472
- Fe-B, amorphous alloys, mag. anisotropy, plastic deform., annealing, Mossbauer obs. 4-65803
- Fe-B, crystalline and amorphous, cryst. struct., NMR study (Russian) 4-79982
- Fe-B alloys,  $\alpha$ - $\gamma$  transition lines and activity coeffs., conductometric studies 4-103926
- Fe-B amorphous alloys, cryst., and press., elec. resist. study 4-60837
- Fe-B amorphous alloys, mag. anisotropy, thermal treatment effects 4-65805
- Fe-B metallic glass, transition elements effect on thermal stability, crystn. activation energy 4-108283
- Fe-base alloy, gaseous corrosion in H<sub>2</sub>O-HCl environment 4-89164
- Fe-base austenitic alloys, high strength evaluation for generator retaining rings 4-99448
- Fe-base metallic glasses, thermal embrittlement model 4-89098
- Fe-base superalloy,  $\sigma$ -phase, planar faults, domain structures, high resolution electron microscopy obs. 4-104793
- Fe-base superalloys, creep-rupture of candidate Stirling engine, alloys 4-99553
- Fe-based 3d-metal alloys, impurity charge screening 4-98562
- Fe-based amorphous alloys, magnetoelastic props., X-ray diffr. studies 4-76209
- Fe-based heat resisting alloys, radiative and optical props. 4-74847
- Fe-based powders, shock wave consolidation theory 4-109337
- Fe-Be and Fe-Bi amorphous alloys, Mossbauer obs. of short-range order 4-92981
- Fe-Be system, B32 metastable precip., identification by APFIM and TEM 4-61922
- Fe-C, dissolv. in molten pure Al under forced flow 4-92378
- Fe-C, high purity, forced vel. pearlite, expt. 4-93294
- Fe-C, high purity, forced velocity pearlite, theoretical 4-93295
- Fe-C, induced mag. moment by tetragonally elongated lattice expansion, magnetisation, Mossbauer spectra meas. 4-98930
- Fe-C, martensitic transform., amplitude distrib. of acoustic emission 4-71651
- Fe-C, pearlite growth, by combined vol. and phase boundary diffusion 4-114470
- Fe-C, proeutectoid ferrite reaction, thermodynamics 4-99376
- Fe-C, SCC in NaH<sub>2</sub>PO<sub>4</sub> soln., effect of heat treatment and C 4-89167
- Fe-C alloy series, US attenuation meas. 4-65347
- Fe-C base alloys, equil., paraequil. and no-partition phase diagrams 4-104764
- Fe-C eutectic solidification, equil., partition coeff. of third element rel. to graphitization 4-99380
- Fe-C martensite, incommensurate direction of modulated struct., strain energy, lattice distortion 4-109454
- Fe-C powder compacts, sintered and carburised, graphite growth 4-93306
- Fe-C-Si, irregular eutectic, theoretical basis of grain-growth (Polish) 4-93258
- Fe-C-Si alloys, positron lifetime, trapping and diffusion 4-88901
- Fe-C-Sn system, phase comp. and metallography of Fe-corner 4-114475
- Fe-C-Ti, liquid system, surface tension under H<sub>2</sub> atm. (Japanese) 4-65517
- Fe-C-(Cr), austenite, cementite dissolv., computer simulation 4-71653
- Fe-Ce liq. alloy, Ce valence state determ. 4-61357
- Fe-Co, mech. polishing, surface film thickness and comp., XPS obs. 4-62093
- Fe-Co alloys, magnetostriction, recrystn., heat treatment, and strain texture effects (Russian) 4-104476
- Fe-Co based metallic glasses, nearly magnetostrictive, disaccommodation 4-84828
- Fe-Co disordered alloys, magnetisation, tight-binding calc. 4-98924
- Fe-Co electrodeposited films, field induced mag. anisotropy 4-92943
- Fe-Co-C, ternary systems, phase equilib. 4-76750
- Fe-Co-Cr mag. disc., Lorentz microscopy and read/write characs. 4-80746
- Fe-Co-Ni-Al, Alnico 5, hot workability, microstruct. 4-114626
- Fe-Cr, accelerated oxidation in atmosphere containing water vapour 4-81356
- Fe-Cr, cast, surface layer alloying using laser treatment 4-109548
- Fe-Cr, corrosion and passivation, in Cl-containing H<sub>2</sub>SO<sub>4</sub> 4-85241
- Fe-Cr, mech. polishing, surface film thickness and comp., XPS obs. 4-62093
- Fe-Cr, passive film form. and props. 4-81332
- Fe-Cr, spinodal decomposition, small angle neutron scatt. studies 4-114552
- Fe-Cr, surface segregation of Si, annealing and O<sub>2</sub> adsorption effect (Japanese) 4-61932
- Fe-Cr, thermal expansion coeff., mag. contrib. 4-84843
- Fe-Cr (26.6 at.%), sulphidation props. in H<sub>2</sub>S-H<sub>2</sub> atmospheres at temps. 973 to 1173K and S press. 10<sup>-2</sup> to 10<sup>-4</sup> Pa 4-93459
- Fe-Cr (26.6 at.%), sulphidation mechanism in H<sub>2</sub>S-H<sub>2</sub> atmospheres at temps. of 973 to 1173K and S press. 10<sup>-2</sup> to 10<sup>-4</sup> Pa 4-93460
- Fe-Cr (30 wt.%), high temp. corrosion mechanism, XPS and AES studies 4-62098
- Fe-Cr (8 wt.%), ferrite-austenite, isothermal transform. kinetics, grain boundary nucleation 4-109396
- Fe-Cr (9.75 wt.%), cold worked, ion beam thinned, protective oxidation in CO<sub>2</sub> 4-62095
- Fe-Cr alloys, BCC self-diffusion of Fe 4-65449
- Fe-Cr alloys, inhomogeneous, X-ray fluoresc. intensities, Monte Carlo simulation 4-109246
- Fe-Cr alloys, pit initiation, current fluctuations obs. 4-89181
- Fe-Cr  $\alpha$  and  $\sigma$  phase alloys, sp. ht. and entropy of formation 4-103959
- Fe-Cr system, irradi., constrained equil., thermodynamics 4-103793
- Fe-Cr-Al, oxide dispersion strengthened MA 956, fatigue crack growth 4-62031

## iron alloys continued

- Fe-Cr-Al, oxide films, characterisation by soft X-ray spectroscopy and microanal. 4-76909
- Fe-Cr-Al, sulphidation in H<sub>2</sub>S, multilayered corrosion scales 4-71801
- Fe-Cr-Al alloys, sulphidation protection by Al<sub>2</sub>O<sub>3</sub> scales 4-93468
- Fe-Cr-Al-Ti alloy, Y<sub>2</sub>O<sub>3</sub> dispersed, characs. of Al<sub>2</sub>O<sub>3</sub> scales 4-89180
- Fe-Cr-Al-X, X=Cu, Ti, Ni, anodic polarisation in H<sub>2</sub>SO<sub>4</sub> 4-114719
- Fe-Cr-Al-Y plasma sprayed coatings, post-treated, mech. props. 4-93471
- Fe-Cr-Al-(Y), precip., small-angle neutron scatt. study 4-93304
- Fe-Cr-B, metallic glass, mag. props. and density 4-84773
- Fe-Cr-B, Mossbauer study of packing fraction 4-84877
- Fe-Cr-C, hypereutectic alloys unidirectionally solidified, hot hardness of primary carbides 4-99492
- Fe-Cr-C (10, 0.2 wt.%), austenite form., TEM and optical microscopy study 4-66331
- Fe-Cr-C, phase separation and coarsening 4-109407
- Fe-Cr-C, Ti effect on rate of high-coercivity transform. 4-93296
- Fe-Cr-C (12 wt.%) permanent magnet alloys, mag. props., effect of alloying 4-84771
- Fe-Cr-C alloys, spinodal decomposition, atom probe field ion microscopy studies 4-114553
- Fe-Cr-Co-Si-B amorphous alloys, mag. props. and hyperfine interactions (Russian) 4-108994
- Fe-Cr-Mo-Ti heat-resisting alloy, Chi phase strengthened 4-71800
- Fe-Cr-Ni, austenitic alloy, He bubbles at grain boundaries 4-108471
- Fe-Cr-Ni, martensitic transition and cryst. geometry (Russian) 4-66332
- Fe-Cr-Ni (15, 15 wt.%), He bubble form. during dual beam irradi. 4-75562
- Fe-Cr-Ni (15, 15 wt.%), weak beam imaging of He bubbles 4-103618
- Fe-Cr-Ni (20, 10 wt.%), oxidation, TEM microstructural study 4-104926
- Fe-Cr-Ni-Mo, austenitic alloy, void swelling, effect of pulsed irradi. 4-108474
- Fe-Cr-Ni-Mo, austenitic alloy, pulsed ion irradi., temp. aspects 4-108476
- Fe-Cr-Ni-W, amorphous, crystn., effect of irradi. particle mass 4-79936
- Fe-Cr-Ni(Si), acoustic emission and resist. variation during cyclic heating 4-81296
- Fe-Cr-Si(Ti), electron and ion-irrad., void and precip. struct. 4-103802
- Fe-Cr(Mn), binding energy, CPA calcs. (Russian) 4-98060
- Fe-Cr(Si), dissolv. in molten pure Al under forced flow 4-92378
- Fe-Cu, Cu role in radiation damage 4-108423
- Fe-Cu, H permeation in H<sub>2</sub>SO<sub>4</sub> with and without H<sub>2</sub>S, electrochem. and surface anal. studies 4-104898
- Fe-Cu, liq. phase sintering, Ostwald ripening, effect of vol. fraction on coarsening kinetics 4-99362
- Fe-Cu, strengthening effect of Cu 4-89062
- Fe-Cu (10 wt.%), powder compacts, liq. phase sintering, dimens. changes 4-66267
- Fe-Cu (2 wt.%), needle-precip. growth directions, invariant line strain 4-66336
- Fe-Cu powders, liquid phase sintering, pore-filling process 4-99361
- Fe-Cu-C, ternary systems, phase equilib. 4-76750
- Fe-Cu-Ni, sintered, fracture mechanics behaviour, influence of specimen size 4-81372
- Fe-Fe-C phase diagram, mathematical model 4-114484
- Fe-Ge eutectics, X-ray spectral investigation (Russian) 4-76564
- Fe-graphite, sintering, C absorpt. by Fe 4-11437
- Fe-graphite, sintering, mechanism of C absorpt. by Fe 4-114438
- Fe-Hf based amorphous alloys, crystallisation and hyperfine fields 4-71030
- Fe-Ho-B, metallic glass, mag. props. and crystallisation 4-84793
- Fe-Mn, binary liquid alloys, thermodynamic props., formalism appls. 4-114478
- Fe-Mn, neutron irradi. at 325K, defect annealing stages (Russian) 4-92242
- Fe-Mn (13 wt.%), tetragonality in antiferromag. ordering and mech. props. 4-65808
- Fe-Mn alloys,  $\gamma$ - $\epsilon$ - $\gamma$  martensitic transformations, recrystn. (Russian) 4-109398
- Fe-Mn-Al, high temp. oxidation, scale struct., metallography, SEM obs. 4-109562
- Fe-Mn-Al-C (15, 8, 2 wt.%), rapidly solidified, phase struct. and morphology 4-114504
- Fe-Mn-Al-Si, high-temp. oxidation resistant alloys 4-93461
- Fe-Mn-Al-Si, high-temp. oxidation, in situ SEM study 4-93462
- Fe-Mn-Al-Si system alloys, phase comp., Al and Si additions effect 4-114481
- Fe-Mn-Ni-Al-Si, high-temp. oxidation resistant alloys 4-93461
- Fe-Mn-Si (19, 1.2 wt.%), stretched, anomaly of  $\alpha/\epsilon$  orientation ratio (Russian) 4-93289
- Fe-Mo, lattice imaging of solute atom clusters, electron microscopy obs. 4-81362
- Fe-Mo (6.3 at.%), high temp. creep, stress exponent and substruct. 4-76821
- Fe-Mo alloys, BCC self-diffusion of Fe 4-65449
- Fe-Mo-B, amorphous, hyperfine fields mag. props. 4-92933
- Fe-Mo-C, secondary hardening mechanisms 4-99396
- Fe-Mo-Ni, magnetisation reversal study (Russian) 4-80783
- Fe-Mo-W-C, phase equilib. and diagrams 4-85140
- Fe-N, induced mag. moment by tetragonally elongated lattice expansion, magnetisation, Mossbauer spectra meas. 4-98930
- Fe-Nb, lattice imaging of solute atom clusters, electron microscopy obs. 4-81362
- Fe-Nb, nitrided, void form., mech. props., optical microscopy, SEM, TEM obs. 4-81361
- Fe-Nb, solubility product of NbC<sub>0.87</sub> in austenite, 950-1250°C 4-61933
- Fe-Nb-C-P alloys, grain boundary segregation of P rel. to C content 4-85156
- Fe-Nb-C-(B), isothermally transformed, microstruct. 4-114510
- Fe-Nb-Si-B amorphous alloys, mag. props. 4-71145
- Fe-Nd-B alloy permanent magnets, domain walls, Lorentz electron-microscopy study 4-92934
- Fe-Nd-B permanent magnet system, metallurgy 4-109381
- Fe-Nd-Ti films with perpendicular mag. anisotropy, RF sputtering 4-61570
- Fe-Ni, H<sub>2</sub> charged, internal friction 4-104802
- Fe-Ni, mech. polishing, surface film thickness and comp., XPS obs. 4-62093
- Fe-Ni, phase equilibrium diagram modification 4-114492
- Fe-Ni, positron lifetime after annealing and cooling (Russian) 4-109270
- Fe-Ni, single particle martensitic growth, computer simulation studies 4-114521

## Iron alloys continued

- Fe-Ni, thermal expansion coeff., mag. contrib. 4-84843  
 Fe-Ni alloy,  $\alpha$ - $\gamma$  transformation, austenite grain growth (*Russian*) 4-109402  
 Fe-Ni alloys, martensite to austenite transformations by laser irradiation (*Russian*) 4-109399  
 Fe-Ni alloys, Ni redistribution by diffusion precipitation (*Russian*) 4-104785  
 Fe-Ni amorphous alloys, flame spray quenching, coating on metal substrates 4-71797  
 Fe-Ni austenitic alloys, crack growth and plasticity, influence of mag. ordering (*Russian*) 4-93368  
 Fe-Ni binary alloy, massive transform. study using DTA (*Korean*) 4-104778  
 Fe-Ni dilute alloys, electron and neutron irradiated, low-temp., mag. relax. spectra 4-84831  
 Fe-Ni films, reverse  $\alpha$ - $\gamma$  transformation (*Russian*) 4-109401  
 Fe-Ni system, irradiated, constrained equilib. thermodynamics 4-103793  
 Fe-Ni wires, Barkhausen jumps, deform. effects 4-76187  
 Fe-Ni-Al-Mn-Si, high-temp. oxidation resistant alloys 4-93461  
 Fe-Ni-C, fracture toughness rel. to transform. induced plasticity and grain boundary segregation 4-99585  
 Fe-Ni-C, induced mag. moment by tetragonally elongated lattice expansion, magnetisation, Mossbauer spectra meas. 4-89930  
 Fe-Ni-C, martensitic transform., H effusion in subzero temp. 4-85153  
 Fe-Ni-C, shock induced martensitic transform. 4-109406  
 Fe-Ni-C, ternary systems, phase equilib. 4-76750  
 Fe-Ni-C alloys, martensitic transformations and primary struct. parameters (*French*) 4-104781  
 Fe-Ni-C(7.6, 0.48 wt.%) alloys, bainite formation kinetics, effect of step quenching 4-114514  
 Fe-Ni-Co film, mag. domain walls, dynamic props. 4-88705  
 Fe-Ni-Cr, austenitic, neutron irradiated, swelling and creep 4-108452  
 Fe-Ni-Cr,  $\gamma$  precip., influence on elastic limit (*French*) 4-81200  
 Fe-Ni-Cr (16, 15 wt.%), void swelling, effect of C and Nb additions 4-103817  
 Fe-Ni-Cr ferritic alloy, soft mag. props. and mech. strength 4-61555  
 Fe-Ni-Cr-Al-(Y)(Zr)(Ti), high temp. oxidation resist. influence of Y, Zr or Ti additions 4-104899  
 Fe-Ni-Cr-B-C, swelling behaviour, influence of Li shell effect on microscopy determ. 4-109580  
 Fe-Ni-Cr-C, butterfly martensite, TEM study 4-108363  
 Fe-Ni-Cr-C, Ti-modified, void swelling, pre-irrad. ageing effects 4-104798  
 Fe-Ni-Cr-C(3.6, 1.45, 0.5 wt.%) alloys, bainite formation kinetics, effect of step quenching 4-114514  
 Fe-Ni-Cr-Mo-N, weld metal, annealing, precipitation, metallographic analysis 4-109417  
 Fe-Ni-Cr-W amorphous alloys, corrosion resist. 4-99632  
 Fe-Ni-Mn (21, 4 wt.%), isothermal lath martensite growth at -80°C, cinemicrophotography 4-81193  
 Fe-Ni-Mn (21.1, 4.0 wt.%), athermal martensitic transform. with isothermal component 4-89052  
 Fe-Ni-Mn-C alloys, martensitic transform. studies 4-99383  
 Fe-Ni-Mn(Cr) alloys with mixed exchange interactions, mag. phase transitions, sp. ht. study 4-65820  
 Fe-Ni-P alloys, growth of intragranular ferrite 4-76777  
 Fe-Ni-P alloys, nucleation of intragranular ferrite 4-76776  
 Fe-Ni-P spin glass alloys, ESR study 4-71153  
 Fe-Ni-P-B amorphous alloys, mag. props., proton implantation effects 4-104416  
 Fe-Ni-P-B-C eutectic, surface morphology, crack section morphology and metallographic struct. after laser irradi., SEM study (*Chinese*) 4-62106  
 Fe-Ni-P-B-(Si) metallic glasses, magnetoelastic effects in ferromag. resonance 4-61581  
 Fe-Ni-P-C, amorphous, compaction process, stability, DSC obs. 4-114448  
 Fe-Ni-Ti(Cr)(Al), nitrided layer, Mossbauer studies (*Russian*) 4-109555  
 Fe-Ni-V-(Mo) alloys, martensite ageing, positron annihilation studies (*Russian*) 4-104695  
 Fe-Ni-based metallic glasses, fracture and annealing, ferromag. resonance studies 4-109078  
 Fe-Ni-(C), martensitic transform., amplitude distrib. of acoustic emission 4-71651  
 Fe-P, segregated grain boundaries crack propag. mol. dynamics calcs. 4-114663  
 Fe-P (0.1 wt.%), single crystals, deform. behaviour, effect of orientation and temp. 4-71702  
 Fe-P (0.8 wt.%), sintered, mag. props., influence of processing parameters 4-66266  
 Fe-P alloys, intergranular fracture planes, chemical states, Auger and electron energy loss spectra 4-93385  
 Fe-P amorphous electrodeposited layers, Barkhausen effect, torsion effects 4-76198  
 Fe-P amorphous electrodeposits, elastic props. and struct. relax. 4-92282  
 Fe-P-C amorphous alloys, B impurity diffusion, SIMS studies 4-92435  
 $\alpha$ -Fe-P-C solid solns., grain boundary brittleness, low-temp. reversibility (*Russian*) 4-104835  
 Fe-P-Cu, mech. props. and microstructure rel. to sintering atmosphere 4-109354  
 Fe-P-Cu(Ni)(Mo), powder compacts, anisotropic shrinkage during liq. phase sintering 4-104752  
 Fe-P-Ti (0.1, 0.16 wt.%) 4-71702  
 Fe-P-W(Mo)(Mn), grain boundary embrittlement, impurity-induced, influence of alloying elements 4-114654  
 Fe-Sb-Ce alloys, Ce state at cryst. boundaries, electron diff. studies (*Chinese*) 4-98114  
 Fe-Si, anodic polarisation characteristics in 1N H<sub>2</sub>SO<sub>4</sub> 4-85247  
 Fe-Si, coercive field rel. to solid solubilities and nucleation behaviour 4-76185  
 Fe-Si, compression test, ordering heat treatment 4-89095  
 Fe-Si, fatigue threshold, thermally activated behaviour of effective stress intensity 4-76653  
 Fe-Si, reaction with liq. Zn, immersion time depend., galvanising appl. 4-109570  
 Fe-Si, saturation magnetisation, mag. anisotropy, g-factor determ., FMR, ferromagnetic antiresonance obs. 4-76258  
 Fe-Si (10 at.%) solid soln., corrosion and oxidation kinetics in SO<sub>2</sub> atm. 4-109554  
 Fe-Si (3.4 wt.%), cold workability, effect of struct. and texture (*Chinese*) 4-61950

## Iron alloys continued

- Fe-Si (3 wt.%), coarse-grained anisotropic elec. engineering steel, mag. losses and induction (*Russian*) 4-109036  
 Fe-Si (3 wt.%), deformation and heat treatment, C content effects (*Russian*) 4-109437  
 Fe-Si (3 wt.%), electrical engineering steel, anisotropic, mag. losses, annealing and elongation effects (*Russian*) 4-104459  
 Fe-Si (3 wt.%), hot rolled, texture formation (*Russian*) 4-109435  
 Fe-Si (3 wt.%), reversible magnetisation curve at any angle to rolling direction 4-61558  
 Fe-Si (3 wt.%), single cryst., fatigue crack propag. and crystallographic path, effect of single peak overload 4-99475  
 Fe-Si (3 wt.%), surface segregation kinetics, Auger spectroscopic obs. (*French*) 4-66142  
 Fe-Si (3 wt.%), texture development and final mag. props., effect of secondary cold-reduction ratios (*Korean*) 4-81215  
 Fe-Si (3 wt.%), thin sheets, development of (110)[001] texture, effect of S content in coating 4-114575  
 Fe-Si (3 wt.%) (100) surfaces, interaction with O<sub>2</sub> and electron stimulated desorption 4-92560  
 Fe-Si (3 wt.%) pin-tool steel couple, crit. thickness of protective films 4-109519  
 Fe-Si (3.25 wt.%), mechanisms of crack origin and twins role in dynamic loading, 77-573K 4-99539  
 Fe-Si (3.5 wt.%), dynamic obs. of slip band evolution using synchrotron white radiation topography 4-62152  
 Fe-Si (3.5 wt.%), single crystals, high strain rate deform. and positron annihilation 4-99434  
 Fe-Si (6.5 wt.%), rapidly quenched, grain growth and texture form. by annealing 4-81214  
 Fe-Si (6.5 wt.%) rapidly quenched ribbons, mag. props. and preparation 4-84819  
 Fe-Si (6.5 wt.%) rapidly quenched ribbon, texture and mag. props. 4-104455  
 Fe-Si alloys, BCC self-diffusion of Fe 4-65449  
 Fe-Si alloys, mag. domains, stroboscopic study using SEM 4-68323  
 Fe-Si fatigue threshold, effect of strength and surface asperities on closure 4-76852  
 Fe-Si laser scribed grain oriented steel, stacked transformer core appls. 4-61552  
 Fe-Si multilayered films, mag. props. and domain struct. 4-61574  
 Fe-Si sheets, Bitter patterns, ferrofluid birefringence studies 4-76202  
 Fe-Si sheets, high temp. mag. aftereffect 4-84830  
 Fe-Si sheets, magnetisation processes, grain boundary effects 4-76180  
 Fe-Si single crystals, non-equilibrium Si surface segregation 4-65522  
 Fe-Si steel, magnetisation, thermodynamic pot. model 4-61557  
 Fe-Si steel, magnetostriction and magnetocrystalline energy anisotropy, texture effects 4-61532  
 Fe-Si transformer steel, decarburisation in anodic process of elec. heating (*Russian*) 4-71776  
 Fe-Si-Al, Sendust, hot rolling rel. to alloy comp. and mag. props. 4-93322  
 Fe-Si-Al, Sendust, hot workability, microstruct. 4-114626  
 Fe-Si-B metallic glass ribbons, mag. props., surface feature effects 4-76173  
 Fe-Si-C, cast, fracture micromechanism 4-62036  
 Fe-Si-C substitutional solns., interstitial diffusivity, solvation shell anal. 4-113696  
 Fe-Si-Sn, segregation of Si and Sn to Fe (100) surface 4-92485  
 Fe-Si(B) amorphous film, ion mixing and mag. props. 4-104471  
 Fe-Sn dil. alloys, tracer diffusion coeffs. meas. 4-65450  
 Fe-Ta, neutron irradi. at 325K, defect annealing stages (*Russian*) 4-92242  
 Fe-Ti alloys, ion implanted, C<sup>+</sup> implantation effects on surface mech. props. 4-114707  
 Fe-V, solubility of N 4-114524  
 Fe-V alloys, BCC self-diffusion of Fe 4-65449  
 Fe-V-C, secondary hardening mechanisms 4-99396  
 Fe-V-C system, C activity and solubility, metallography, thermal analysis 4-114523  
 Fe-V(Cr), sigma phase, pair-wise interaction model 4-84422  
 Fe-W alloys, BCC self-diffusion of Fe 4-65449  
 Fe-W dilute alloy wires, diffusion coefficients, resistometric methods 4-65427  
 Fe-W-B, metallic glass, mag. props. and density 4-84773  
 Fe-W-B, Mossbauer study of packing fraction 4-84877  
 Fe-W-B glasses, mag. aftereffect, effect of W 4-84827  
 Fe-Zn system, formation and growth of  $\delta$  phase, cracks 4-89026  
 Fe-Zr amorphous films, corrosion props. in 1N H<sub>2</sub>SO<sub>4</sub> 4-76904  
 Fe-Zr amorphous films, elec. and mag. props. 4-75923  
 FeAl, ordered, LMTO approach to optical props. 4-71342  
 FeAl-CoAl, length changes rel. to heat treatment, phase transform., vacancy annihilation 4-109442  
 Fe<sub>2</sub>Al, neutron irradi., at. ordering, Mossbauer spectra, X-ray diff. 4-65306  
 FeB BCC alloys, electronic struct., APW calcs. 4-108769  
 Fe<sub>1-x</sub>B<sub>x</sub> amorphous alloys, electronic struct., XPS studies 4-75838  
 Fe<sub>1-x</sub>B<sub>x</sub> amorphous films, crystallisation kinetics and mag. props. 4-75807  
 Fe<sub>1-x</sub>B<sub>x</sub> amorphous films, magnetostriction, strain-modulated FMR study 4-76217  
 Fe<sub>1-x</sub>B<sub>x</sub> glass, crystallisation, elec. cond. study 4-88109  
 Fe<sub>100-x</sub>B<sub>x</sub> amorphous alloys, mag. anisotropy, mag. annealing effects 4-76131  
 Fe<sub>100-x</sub>B<sub>x</sub> metallic glass, mag. props. meas. 4-84814  
 Fe<sub>100-x</sub>B<sub>x</sub> metallic glass, mag. and mechanical props. 4-84841  
 Fe<sub>72</sub>B<sub>28</sub>-based metallic glasses, struct., small angle X-ray scatt. studies 4-113346  
 Fe<sub>90-x</sub>B<sub>10+x</sub> metallic glasses, struct., radial distrib. function calc. from X-ray diff. 4-103657  
 Fe<sub>90</sub>B<sub>10</sub> amorphous, extended freq. anal. of permeability aftereffect 4-84822  
 Fe<sub>90</sub>B<sub>10</sub> amorphous, mag. hysteresis loops after heat treatment below Curie point 4-80781  
 Fe<sub>90</sub>B<sub>10</sub> amorphous alloy, He ion irradi., blister and bubble form., TEM obs. 4-108434  
 Fe<sub>90</sub>B<sub>10</sub> amorphous foil, sputtered ductile, mag. and structural study 4-80782  
 Fe<sub>80</sub>B<sub>20</sub>, Fe<sub>70</sub>Cr<sub>10</sub>B<sub>20</sub> and Fe<sub>70</sub>Cr<sub>5</sub>Ni<sub>5</sub>B<sub>20</sub> amorphous alloys, elastic characts. and microplastic deform 4-93325

## iron alloys continued

- Fe<sub>80</sub>B<sub>20</sub> metallic glass, radial distrib. function asymmetry by EXAFS 4-93133  
 Fe<sub>2</sub>B<sub>1.7</sub>-Al<sub>2</sub>O<sub>3</sub> granular system, XPS anal., surface composition study 4-81113  
 Fe<sub>3</sub>B<sub>1.7</sub>, ferromag., spin polarised L<sub>23</sub>M<sub>23</sub>M<sub>23</sub> AES 4-104703  
 Fe<sub>3</sub>B<sub>1.7</sub> metallic glasses, struct., neutron diff. studies (*Chinese*) 4-98020  
 Fe<sub>84</sub>B<sub>16</sub>, amorphous, microcrystalline domain obs. 4-113333  
 Fe<sub>86</sub>B<sub>14</sub>, amorphous, thermoelectric power and elec. cond. (*Russian*) 4-65660  
 Fe<sub>86</sub>B<sub>14</sub>, amorphous layer form. on surface using elec. spark 4-65180  
 Fe<sub>2</sub>B<sub>1.7</sub>, itinerant magnetism in metallic glasses 4-104438  
 (Fe<sub>0.82</sub>B<sub>0.18</sub>)<sub>90</sub>La<sub>0.05</sub>Ru<sub>0.05</sub> amorphous metal alloys, ferromag. reson. and g-factor 4-71188  
 Fe<sub>78</sub>B<sub>1.7</sub>Si<sub>10</sub>, amorphous, isothermal crystallisation and mag. props. (*Russian*) 4-65384  
 Fe<sub>2</sub>B<sub>1.7</sub>Si<sub>6</sub>, amorphous and crystallised, UPS, XPS and EELS 4-104122  
 Fe<sub>2</sub>B<sub>1.7</sub>Si<sub>6</sub> ferromagnet, spin-flip Stoner excitations, EELS studies 4-104410  
 Fe<sub>40</sub>B<sub>1.7</sub>Si<sub>8</sub>-Al<sub>1</sub>, crystallisation and mag. props. study 4-114137  
 Fe<sub>81</sub>B<sub>1.7</sub>Si<sub>2</sub>C<sub>2</sub>, amorphous, mag. anisotropy meas. (*Russian*) 4-65804  
 Fe<sub>81</sub>B<sub>1.7</sub>Si<sub>2</sub>C<sub>2</sub> glass, primary crystallisation and  $\alpha$ -Fe dendrites, EELS studies 4-84202  
 Fe<sub>81</sub>B<sub>1.7</sub>Si<sub>2</sub>C<sub>2</sub>, Metglas 3605SC, mag. and hyperfine interactions 4-71223  
 FeCo alloy, brittleness, purity and impurity segregation effects (*Russian*) 4-109496  
 FeCo based alloys, strength and mag. props. rel. to cold rolling and heat treatment 4-98918  
 FeCo, self-diffusion, influence of order-disorder transition 4-113695  
 Fe<sub>67</sub>Co<sub>33</sub>B<sub>20</sub>, amorphous, mag. aftereffects after field annealing 4-84823  
 Fe<sub>67</sub>Co<sub>33</sub>B<sub>14</sub>Si<sub>1</sub>, amorphous, extended freq. anal. of permeability aftereffect 4-84822  
 FeCo(Mn)(V), coupling between chemical and mag. interactions, NMR study 4-114173  
 Fe<sub>2</sub>Co<sub>31</sub>Ni<sub>20</sub>-Cr<sub>2</sub>B<sub>1</sub>Si<sub>8</sub> metallic glass, mag. props. study 4-84790  
 (FeCoNi)SiB nonmagnetostriuctive amorphous ribbons for magnetic cores, DC and AC magnetic characs. 4-92939  
 Fe<sub>2</sub>Co<sub>38</sub>Ni<sub>10</sub>Si<sub>11</sub>B<sub>16</sub>, amorphous, struct. relax. processes, dilatometric anal. (*Russian*) 4-92394  
 (Fe<sub>100-x</sub>Co<sub>x</sub>)<sub>90</sub>Pr<sub>10</sub>O<sub>0.1</sub> thermal effects of Co moderate substitutions 4-71124  
 (FeCo)SiB nonmagnetostriuctive amorphous ribbons for magnetic cores, DC and AC magnetic characs. 4-92939  
 Fe<sub>2</sub>Co<sub>70</sub>Si<sub>15</sub>B<sub>10</sub> amorphous, mag. noise study (*Russian*) 4-65846  
 Fe<sub>2</sub>Co<sub>70</sub>Si<sub>15</sub>B<sub>10</sub>, amorphous, struct. relax. processes, dilatometric anal. (*Russian*) 4-92394  
 Fe<sub>2</sub>Co<sub>70</sub>Si<sub>15</sub>B<sub>10</sub>, amorphous, mag. permeability, annealing in transverse mag. field (*Russian*) 4-104467  
 Fe<sub>2</sub>Co<sub>70</sub>Si<sub>15</sub>B<sub>10</sub>, magnetic annealing kinetics 4-80795  
 Fe<sub>2</sub>Co<sub>70</sub>Si<sub>15</sub>B<sub>10</sub>, zero magnetostriuctive amorphous alloy, permeability and field-induced anisotropy 4-71056  
 Fe<sub>67</sub>Co<sub>38</sub>Si<sub>11</sub>B<sub>16</sub>, metallic glass, crystn. kinetics 4-65187  
 Fe<sub>2</sub>Co<sub>90-x</sub>Si<sub>10</sub>B<sub>15</sub>, magnetostriuctive amorphous alloys, stress-induced anisotropy and permeability 4-71055  
 (Fe<sub>1-x</sub>Co<sub>x</sub>)<sub>90</sub>Zr<sub>10</sub> amorphous alloy, elec. resist. minima and mag. props. 4-75922  
 (Fe<sub>22</sub>Co<sub>78</sub>)<sub>2</sub>V, tensile deforms, 20-1000°C, fracture mode and ductility rel. to order-disorder transform. 4-66427  
 Fe<sub>1-x</sub>Cr<sub>x</sub>, short range order inversion, alloy conc. depend. 4-103690  
 (Fe<sub>2</sub>Cr<sub>100-x</sub>)<sub>2</sub>B<sub>2</sub> metallic glasses, onset of magnetism, Mossbauer spectra 4-71217  
 (Fe<sub>1-x</sub>Cr<sub>x</sub>), Mn<sub>1-x-y</sub>, <sup>55</sup>Mn and <sup>57</sup>Fe NMR, comp. depend. 4-98960  
 (Fe<sub>1-x</sub>Cr<sub>x</sub>), Mn<sub>1-x-y</sub>, impurity mag. state, <sup>55</sup>Mn and <sup>57</sup>Fe NMR study 4-98961  
 Fe<sub>80</sub>M<sub>2</sub>B<sub>1.7</sub> (M=transition metal) metallic glass, elec. resist., transition metal effects 4-108832  
 Fe<sub>80</sub>M<sub>2</sub>B<sub>1.7</sub> based glassy alloys, ferromag. exchange and Curie temp. 4-76129  
 (FeMn)CP alloys, amorphous, ferromag. reson. and mag. ordering 4-71187  
 (Fe<sub>0.64</sub>Mn<sub>0.36</sub>)<sub>75</sub>P<sub>16</sub>B<sub>9</sub>Al<sub>3</sub>, spin glass transition calcs. 4-88667  
 (Fe<sub>1-x</sub>Mn<sub>x</sub>)<sub>75</sub>P<sub>16</sub>C<sub>10</sub> amorphous alloy, transport and mag. props. 4-88498  
 Fe<sub>78</sub>Mo<sub>20</sub>B<sub>2</sub>, metallic glass, elec. resist., crystallisation and thermoelec. power, annealing effects 4-108831  
 Fe<sub>100</sub>N<sub>25</sub>, hexagonal to FCC transformation, Mossbauer study (*French*) 4-99382  
 FeNi, neutron irradiat. effect on mag. props. 4-92907  
 FeNi(Si,Cr,Mo), neutron irradiat. effect on mag. props. 4-92907  
 Fe<sub>66</sub>Ni<sub>34</sub>, Curie point at ultrahigh press. 4-88676  
 (Fe<sub>0.3</sub>Ni<sub>0.5</sub>)<sub>1-x</sub>B<sub>x</sub> amorphous alloys, mag. moments, temp. variation 4-76122  
 (Fe<sub>0.3</sub>Ni<sub>0.5</sub>)<sub>1-x</sub>B<sub>x</sub> amorphous alloys, elec. cond. and struct. stability 4-92693  
 (Fe<sub>0.3</sub>Ni<sub>0.5</sub>)<sub>1-x</sub>B<sub>x</sub> metallic glass, Mossbauer and soft X-ray appearance pot. spectra studies 4-76292  
 Fe<sub>39</sub>Ni<sub>39</sub>B<sub>22</sub> metallic glass ribbon, pull-out tests in different matrices 4-71717  
 Fe<sub>40</sub>Ni<sub>40</sub>B<sub>20</sub>, amorphous, mag. hysteresis loops after heat treatment below Curie point 4-80781  
 Fe<sub>40</sub>Ni<sub>40</sub>B<sub>20</sub>, amorphous, structural relax., contraction and creep meas. 4-85195  
 Fe<sub>40</sub>Ni<sub>40</sub>B<sub>20</sub>, amorphous alloys, neutron irradiat., mag. props. isotope effects 4-75541  
 Fe<sub>40</sub>Ni<sub>40</sub>B<sub>20</sub> amorphous alloy, ferromag. resonance and antiresonance studies 4-76256  
 Fe<sub>40</sub>Ni<sub>40</sub>B<sub>20</sub>, amorphous alloys, as-quenched, mag. aftereffect 4-84826  
 Fe<sub>40</sub>Ni<sub>40</sub>B<sub>20</sub> foil, thermal expansion coeff. and isothermal compressibility (*Russian*) 4-65421  
 Fe<sub>40</sub>Ni<sub>40</sub>B<sub>20</sub>, metallic glass, melt surface tension and embrittlement, effects of elemental additions and superheat 4-65184  
 Fe<sub>40</sub>Ni<sub>40</sub>B<sub>20</sub> metallic glass, amorphous-cryst. transition kinetics, elec. resist. meas. 4-70039  
 Fe<sub>40</sub>Ni<sub>40</sub>B<sub>20</sub> metallic glass, strength and plasticity, temp. depend. (*Russian*) 4-71692  
 Fe<sub>40</sub>Ni<sub>40</sub>B<sub>20</sub>, metallic glass, field ion microscopic study at liq. H temp. 4-75311  
 Fe<sub>40</sub>Ni<sub>40</sub>B<sub>20</sub>, sliding friction and struct. relax. 4-99606  
 Fe<sub>80-x</sub>Ni<sub>x</sub>B<sub>20</sub> amorphous sputtered films, ferromag. saturation 4-61520  
 Fe<sub>80-x</sub>Ni<sub>x</sub>B<sub>20</sub>, amorphous, mag. props. study 4-84840

## iron alloys continued

- Fe<sub>40</sub>Ni<sub>40</sub>B<sub>14</sub>B<sub>6</sub> foil, amorphous-cryst. transition, elec. resist. variations 4-65182  
 Fe<sub>40</sub>Ni<sub>38</sub>B<sub>18</sub>Mo<sub>4</sub>, Metglas 2826 MB 5 keV He implantation, bubble growth, free vol. relax. model 4-103822  
 Fe<sub>78-x</sub>Ni<sub>x</sub>B<sub>18</sub>Mo<sub>4</sub> metallic glasses, short range order, EXAFS studies 4-60856  
 Fe<sub>25</sub>Ni<sub>5</sub>B<sub>10</sub>Si<sub>10</sub>, metallic glass, Curie point relax. study 4-84791  
 Fe<sub>40</sub>Ni<sub>40</sub>B<sub>13</sub>Si<sub>7</sub> glassy ribbon, elec. and mag. props. 4-84604  
 Fe<sub>2</sub>Ni<sub>80-x</sub>B<sub>19</sub>Si<sub>1</sub> metallic glasses, absolute thermoelec. power meas. 4-92701  
 FeNiCo thin film, multiple spin echo study 4-84870  
 Fe<sub>25</sub>Ni<sub>35-x</sub>Cr<sub>x</sub> magnetoresist., and ferromag-spin glass transitions 4-113924  
 Fe<sub>40-x</sub>Ni<sub>x</sub>Cr<sub>20</sub>, mag. phase diagram, neutron diff. study 4-71069  
 FeNiCrMoBSi amorphous ribbons, magnetostriction, capacitance studies 4-61580  
 (Fe<sub>1-x</sub>Ni<sub>x</sub>)<sub>2</sub>Ge, magnetisation, Curie temp., mag. moments, X-ray diff. studies 4-98862  
 (Fe<sub>1-x</sub>Ni<sub>x</sub>)<sub>2</sub>Ge, magnetisation, Curie temp., mag. moments, X-ray diff. studies 4-98862  
 (Fe<sub>2</sub>Ni<sub>1-x</sub>)<sub>2</sub>M, M=P, B, Si or Al, metallic glass, Mossbauer study of high press. 4-84880  
 Fe<sub>25</sub>Ni<sub>35</sub>Mn<sub>20</sub> spin glass, static mag. props. (*Russian*) 4-92915  
 Fe<sub>25</sub>Ni<sub>35</sub>Mn<sub>20</sub> spin glass, freezing point freq. depend. 4-109016  
 Fe<sub>70</sub>Ni<sub>30</sub>-Mn<sub>x</sub>, paramagnet-spin glass state transition, AC susceptibility, Mossbauer effect, small angle neutron scatt. meas. 4-104437  
 Fe<sub>2</sub>Ni<sub>80-x</sub>Mn<sub>x</sub>, specific heat determ. (*Russian*) 4-65414  
 Fe<sub>40</sub>Ni<sub>40</sub>Mo<sub>18</sub>B<sub>2</sub>, metallic glass, cavitation erosion resistance 4-104880  
 Fe<sub>40</sub>Ni<sub>40</sub>Mo<sub>18</sub>B<sub>2</sub>, metallic glass, elec. resist., crystallisation and thermoelec. power, annealing effects 4-108831  
 Fe<sub>39</sub>Ni<sub>39</sub>Mo<sub>10</sub>Si<sub>6</sub>B<sub>12</sub> metallic glass, mag. props., Mossbauer studies 4-109012  
 Fe<sub>39</sub>Ni<sub>39</sub>Mo<sub>10</sub>Si<sub>6</sub>B<sub>12</sub> metallic glass, elec. resist., crystallisation and thermoelec. power, annealing effects 4-108831  
 Fe<sub>10</sub>Ni<sub>70</sub>P<sub>20</sub> amorphous spin glass, weak transverse freezing region 4-114117  
 Fe<sub>40</sub>Ni<sub>40</sub>P<sub>20</sub> metallic glasses, accuracy of expt. radial distrib. functions, X-ray diff. study 4-60843  
 Fe<sub>40</sub>Ni<sub>40</sub>P<sub>12</sub>B<sub>8</sub>, amorphous, rotational mag. field annealing effect on anisotropy 4-109041  
 Fe<sub>40</sub>Ni<sub>40</sub>P<sub>14</sub>B<sub>6</sub>, amorphous isotropic ferromag., mag. excitations 4-71043  
 Fe<sub>40</sub>Ni<sub>40</sub>P<sub>14</sub>B<sub>6</sub>, amorphous ribbons, mag. props. and struct., influence of laser annealing 4-88663  
 Fe<sub>40</sub>Ni<sub>40</sub>P<sub>14</sub>B<sub>6</sub>, glass transition of thin film on substrate 4-92367  
 Fe<sub>40</sub>Ni<sub>40</sub>P<sub>14</sub>B<sub>6</sub> metallic glass, dynamical power loss annealing effects 4-76175  
 Fe<sub>40</sub>Ni<sub>40</sub>P<sub>14</sub>B<sub>6</sub> metallic glass, mag. permeability with AC and DC currents 4-76176  
 Fe<sub>40</sub>Ni<sub>40</sub>P<sub>14</sub>B<sub>6</sub> metallic glass, mag. props., cold rolling effects 4-104472  
 Fe<sub>40</sub>Ni<sub>40</sub>P<sub>14</sub>B<sub>6</sub>, Metglas 2826, struct. factor, influence of cold rolling 4-61954  
 Fe<sub>40</sub>Ni<sub>40</sub>P<sub>14</sub>B<sub>6</sub>, proton irradiat., crystallisation study 4-88099  
 Fe<sub>40</sub>Ni<sub>40</sub>P<sub>14</sub>B<sub>6</sub>, amorphous, explosive loading of powder, three-dimens. parts prod. 4-114443  
 Fe<sub>2</sub>Ni<sub>80-x</sub>P<sub>14</sub>B<sub>6</sub>, amorphous, spin glass alloys, EPR meas. and mag. props. 4-84847  
 Fe<sub>2</sub>Ni<sub>80-x</sub>P<sub>14</sub>B<sub>6</sub>, amorphous ferromag. and reentrant alloys, ferromag. reson. study 4-84856  
 Fe<sub>2</sub>Ni<sub>80-x</sub>Ru<sub>x</sub>, thermal expansion coeff., mag. contrib. 4-84843  
 Fe<sub>2</sub>Ni<sub>80-x</sub>Si<sub>10</sub>B<sub>10</sub>, metallic glass, Curie temp. press. depend. 4-84792  
 (Fe<sub>2</sub>Ni<sub>1-x-y</sub>Si<sub>10</sub>B<sub>10</sub>)<sub>2</sub> metallic glass, short range ordering study 4-88108  
 Fe<sub>2</sub>Ni<sub>80-x</sub>Si<sub>10</sub>B<sub>10</sub>, metallic glass, correlated hyperfine interactions 4-70761  
 (Fe<sub>0.49</sub>Ni<sub>0.51</sub>)<sub>2</sub>V, ordered alloys, microstruct. and creep rel. to implanted He 4-108399  
 (Fe<sub>1-x</sub>Ni<sub>x</sub>)<sub>90</sub>Zr<sub>10</sub> amorphous alloy, elec. resist. minima and mag. props. 4-75922  
 Fe<sub>1-x</sub>P<sub>x</sub>, amorphous and liquid, struct. determ. (*Russian*) 4-65177  
 Fe<sub>78</sub>P<sub>22</sub> amorphous alloys, EXAFS contributions and near neighbour components 4-61774  
 FePCr(Cr), structural and mag. coherence lengths 4-88100  
 Fe<sub>2</sub>P<sub>1-x</sub>Si<sub>2</sub>, hexagonal-orthorhombic transition, Mossbauer studies 4-109102  
 Fe<sub>2</sub>Pd<sub>80-x</sub>Si<sub>10</sub>B<sub>10</sub> metallic glasses, mag. props. and chemical short-range order 4-114109  
 Fe<sub>2</sub>Pt, mag. transition temp., influence of plastic deform. 4-84785  
 FeRh, ordered, LMTO approach to optical props. 4-71342  
 FeSi grain oriented laminations, local correl. effects between Bloch walls 4-76167  
 FeSi tape wound cores, specific Bloch wall area 4-76165  
 FeSi-Fe<sub>2</sub>Si eutectic alloy, sintered, annealing, FeSi<sub>2</sub> form., elec. props. 4-109414  
 Fe<sub>2</sub>Si, DO<sub>2</sub> ordered alloys, tensile behaviour 4-93337  
 Fe<sub>2</sub>Si/Zn diffusion couples, periodic structs. and two phase band form. 4-65499  
 Fe<sub>3</sub>Si<sub>4</sub>B<sub>15</sub> metallic glass, Young's modulus, internal friction, mag. hysteresis loop 4-76215  
 Fe<sub>81.5</sub>Si<sub>18.5</sub> metallic glass, stress pattern mag. domains 4-76161  
 Fe<sub>88-x</sub>Si<sub>12</sub>B<sub>2</sub> amorphous alloy, crystallisation behaviour 4-75309  
 Fe<sub>2</sub>Si<sub>90-x</sub>B<sub>10</sub> metallic glasses, mag. props., chem. composition depend. 4-76135  
 (Fe<sub>1-x</sub>V<sub>x</sub>)<sub>84</sub>B<sub>16</sub> amorphous alloys, mag. and elec. props. (*Chinese*) 4-114094  
 Fe<sub>24</sub>Zr<sub>76</sub> amorphous alloy, <sup>57</sup>Fe quadrupole splitting sign determ., Mossbauer spectra 4-76291  
 Fe<sub>90</sub>Zr<sub>10</sub> amorphous alloy, struct. and mech. props. rel. to heat treatment 4-75305  
 Fe<sub>90</sub>Zr<sub>10</sub> glass, H induced mag. phase transform., Mossbauer spectroscopy study 4-61536  
 Fe:Si strips, mag. props. and domain struct., laser scribing effects 4-61550  
 Gd-Fe amorphous alloy films, crystallisation and ferromag. reson. behaviour 4-71189  
 Gd-Fe amorphous films, vacuum deposited, Kerr hysteresis meas. 4-66014  
 Gd-Fe composition-graded thin films, mag. meas. device appl. 4-88710  
 Gd-Fe evaporated films, crystn. behaviour 4-80445  
 Gd-Fe-Co amorphous film, struct. and mag. props. 4-80434  
 Gd-Fe-Ni amorphous film, struct. and mag. props. 4-80434  
 GdFe film, oxidation by overlaid SiO<sub>2</sub> film, Kerr enhancement 4-84949

## iron alloys continued

- GdFe/TbFe amorphous double-layer films, magneto-optical characts. 4-61665  
 GdFe<sub>2</sub>Ge<sub>2</sub> charge transfer, X-ray absorpt. spectra study 4-81037  
 GdTbFe amorphous sputtered films, mag. props. 4-65843  
 La(Fe,Al)<sub>1-x</sub>, metamagnetic transitions and struct. aspects 4-92910  
 Li-Fe film, conduction electron surface mag. relax. (Russian) 4-65862  
 Mn<sub>12</sub>Al<sub>2</sub>-Fe<sub>x</sub> thermal expansion, atomic order effects (Russian) 4-103971  
 Nd<sub>2</sub>Fe<sub>14</sub>B, cryst. struct., mag. props. 4-65828  
 Nd<sub>2</sub>Fe<sub>14</sub>B, permanent magnet, cryst. struct. 4-70069  
 Nd<sub>2</sub>Fe<sub>14</sub>B, single crystal, mag. props. study 4-114143  
 Ni-Cr-Fe, alloy X-750, SCC resist. in deaerated high temp. water rel. to solution heat treatment (Japanese) 4-62110  
 Ni-Cr-Fe, Inconel X-750, HVEM irradi., void form. rel. to  $\gamma'$  precipitation 4-108446  
 Ni-Fe, dissoln. and passivation, influence of S adsorpt. 4-71756  
 Ni-Fe, dissoln. and passivation, influence of S adsorpt. 4-71757  
 Ni-Fe, low temp. lattice parameters 4-108306  
 Ni-Fe electroplating, US agitation effect on mech. props. and comp. 4-114430  
 Ni-Fe-C substitutional solns., interstitial diffusivity, solvation shell anal. 4-113696  
 Ni-Fe-Co-Ti, Incalloy, domain struct. study by differential phase contrast Lorentz microscopy, max. specimen thickness 4-65825  
 Ni-Fe-Co-Ti, STEM study of mag. domain walls 4-80779  
 Ni-Fe-Cr alloys, extraordinary Hall coeff. sign reversal and DC resist. 4-113922  
 Ni-Fe-S, friction and wear modification by sulphide form. 4-66460  
 Ni-Fe-V, thin sheets, effective mag. permeability and its stress sensitivity, effect of heat treatment and comp. 4-104883  
 Ni-Fe-V alloys, extraordinary Hall coeff. sign reversal and DC resist. 4-113922  
 Ni-Mo-Fe ternary alloys, mag. props. and ferromag. shielding at cryogenic temps. 4-109038  
 NiFe-Ge amorphous and cryst. films, planar Hall effect and magnetisation reversal 4-75930  
 Ni<sub>0.76</sub>Fe<sub>0.23</sub>, short range order parameter determ. 4-113339  
 Ni<sub>3</sub>Fe, short range ordering, atomic configurations 4-113338  
 Ni<sub>60</sub>Fe<sub>40</sub> (100), O<sub>2</sub> and S<sub>2</sub> coadsorption, surface phases, LEED study 4-84506  
 Ni<sub>3</sub>Fe<sub>9</sub>-Ni<sub>100-x</sub>Co<sub>x</sub> mag. films, exchange-coupled; mag. reversal characts. 4-76200  
 Ni<sub>3</sub>Fe<sub>3</sub>Cr<sub>14</sub>Pt<sub>16</sub>B<sub>6</sub> metallic glass, surface oxidation in crystalline and amorphous states 4-89187  
 Ni<sub>80-x</sub>Fe<sub>20</sub> amorphous alloy, onset of magnetism, magnetisation studies 4-76172  
 Ni<sub>80-x</sub>Fe<sub>20</sub> amorphous film, composition study 4-76633  
 Ni<sub>80-x</sub>Fe<sub>20</sub> amorphous, surface characterisation study 4-76634  
 Ni<sub>40</sub>Fe<sub>60</sub>P<sub>14</sub>B<sub>6</sub>, electronic struct. extreme UV photoemission 4-85066  
 Ni<sub>40</sub>Fe<sub>60</sub>P<sub>14</sub>B<sub>6</sub>, glassy metal, UPS study 4-76632  
 Ni<sub>78-x</sub>Fe<sub>22</sub>Si<sub>2</sub>B<sub>10</sub> amorphous alloys, mag. props. 4-84794  
 Ni<sub>46.5</sub>Ti<sub>50</sub>Fe<sub>23.5</sub> phonon softening study 4-84354  
 Pb-Fe, polyvalent films, elec. cond. anomaly 4-80688  
 Pd-Fe, ferromagnetic transition temp. determ., using SQUID magnetometer combined with ion implantation 4-58877  
 Pd-Fe, ion implanted, ferromagnetism study 4-71137  
 (Pd<sub>1-x</sub>Au<sub>x</sub>)<sub>2</sub>Fe, hyperfine mag. field study 4-88493  
 PdCuSiAl<sub>5</sub> alloys, spin glasses, exptl. evidence for mag. two level systems 4-71082  
 Pd<sub>67-x</sub>Cu<sub>33-x</sub>Si<sub>16</sub>M<sub>10</sub> (M=Fe or Mn), glasses, ferro- and antiferromagnetism study 4-71063  
 Pd(Fe,Co) dilute, Mossbauer study of relax., spin glass props. 4-104514  
 PdFe, dil. solns of H<sub>2</sub>(D<sub>2</sub>), thermodynamics 4-70411  
 PdFeCd dilute alloys, hyperfine field at Cd, PAC spectroscopy studies 4-92681  
 Pd,FeH<sub>x</sub>, Mossbauer study of hyperfine interactions 4-88756  
 Pd<sub>2</sub>(Fe<sub>1-x</sub>Mn<sub>x</sub>) alloys, ordered and disordered, average mag. moments (Russian) 4-104406  
 Pd<sub>0.83-x</sub>Fe<sub>0.17</sub>Si<sub>0.17</sub> metallic glasses, form., crystallisation and elec. props. 4-92685  
 Pr-Fe-Co alloy sheets, rapid quenching, magnetic properties (Japanese) 4-114141  
 Pr<sub>2</sub>Sm<sub>1-x</sub>Fe<sub>2</sub>, Laue phase, spin-reorientation temp., mag. anisotropy, Mossbauer spectra (Japanese) 4-61533  
 Pt-Fe alloys, mag. props. 4-84842  
 Pt<sub>3</sub>Fe, mag. transition temp., influence of plastic deform. 4-84785  
 Pt<sub>3</sub>FeMn<sub>1-x</sub>, elec. cond. and mag. props. 4-104180  
 Rh-Fe resistance thermometer, ceramic encapsulated, props. and stability below 80K 4-111134  
 ribbon, 6.5%, rapidly quenched, mag. props. stability (Japanese) 4-76196  
 Sc<sub>1-x</sub>Ti<sub>x</sub>Fe<sub>2</sub>, itinerant electron system, coexistence of ferro- and antiferromagnetism 4-98857  
 Se-<sup>57</sup>Fe, Mossbauer study of electric field gradient 4-88754  
 Si-Fe, Bloch wall motion, surface EMF meas. 4-76168  
 Si-Fe grain oriented sheets, transformer building factor, cryst. texture effects 4-61554  
 Si-Fe nonoriented semiprocessed steel, core loss and permeability, elec. resist. effects 4-61556  
 Si-Fe oriented sheets, mag. interactions and domain struct., Mossbauer study 4-76163  
 Si-Fe sheets, quenching destabilisation of domain struct., effect on mag. props. 4-76166  
 Si-Fe-Sn(Cu) high permeability grain oriented steel, recrystallisation and grain sizes 4-61953  
 SiFe, polycrystalline, approach to saturation at intermediate fields, role of internal demagnetising fields 4-76183  
 Sm-Fe-Co alloy sheets, rapid quenching, mag. props. (Japanese) 4-114141  
 Sm(Co,Fe,Cu,Zr)<sub>7.5</sub> magnets, high resolution electron microscopy study 4-61098  
 SmFe<sub>2</sub>, elastic props. nonlinearity and magnetostriction (Russian) 4-80133  
 SmFe<sub>2</sub>, magnetostrictive strain as a function of magnetic field and mechanical elastic stresses 4-113523  
 Sm<sub>2</sub>Fe<sub>17-x</sub>Co<sub>x</sub>, magnetic cooling near Curie temperatures above 300K 4-88677  
 SmFe<sub>2</sub>(Co<sub>2</sub>)(Ni<sub>2</sub>) cpds., bonding, X-ray emission study 4-85042  
 Sn-Fe, electrodeposition, effect of amino acid surfactants 4-93242  
 TbFe thin films, amorphous, ageing phenomena, hysteresis cycles 4-71134

## iron alloys continued

- TbFe<sub>2</sub>, elastic props. nonlinearity and magnetostriction (Russian) 4-80133  
 TbFe<sub>2</sub>, mag. and magnetomech. hysteresis 4-76219  
 TbFe<sub>2</sub>, magnetostrictive strain as a function of magnetic field and mechanical elastic stresses 4-113523  
 Ti-Al-Fe, Mossbauer study of <sup>57</sup>Fe atom vibr. 4-84882  
 Ti-Fe, influence of ageing on incommensurate struct. (Russian) 4-65218  
 Ti-Fe-Ni, sintering processes, Ni effect 4-61889  
 Ti-V-Fe-Al (40, 2, 3 wt%), technique for revealing deformed and recrystallised structs. 4-114571  
 TiC-Fe-Cr-Mo, bonded carbides, wear-resistant, produced by powder metallurgy techniques 4-66455  
 TiFe, bulk and surface two-particle spectra 4-84550  
 TiFe, EXAFS, multiple scattering effects 4-66108  
 TiFe, H uptake activation, Auger electron spectroscopy 4-70558  
 Ti(Fe,Al)<sub>1-x</sub>, paramagnetic props. study (Russian) 4-71020  
 Ti<sub>0.5</sub>Ni<sub>0.5</sub>Fe<sub>x</sub>, martensitic transform., X-ray anal., shear modulus meas. 4-61077  
 TiNi<sub>1-x</sub>M<sub>1-x</sub> (M=Cu, Fe, Co), multiphase diffusion 4-61136  
 Ti<sub>2</sub>Fe<sub>2</sub>Te, segregation of Fe to grain boundaries, first order phase transitions 4-84796  
 V-Cr-Fe-Zr, candidate materials for fusion appl., weldability 4-99494  
 V-Cr-Fe-Zr, mech. props. rel. to O contamination, fusion appls. 4-109499  
 V<sub>3-x</sub>Fe<sub>x</sub>Ga, NMR Knight shift and paramagnetism 4-65873  
 W-Fe, dil., segregation of Fe to grain boundaries, elec. resist., thermopower, AES meas. 4-103943  
 W-Ni-Fe, dynamic strength calcs. based on grain deform. 4-108511  
 W-Ni-Fe, fracture behaviour, effect of substitutional impurity elements 4-89134  
 W-Ni-Fe, liq. phase sintered, interphase boundary precip. 4-99364  
 W-Ni-Fe (5.5 wt%) heavy alloy, precipitation hardening 4-114564  
 W-Ni-Fe alloys, dual-phase, work hardening and microstruct. (Chinese) 4-61951  
 Y-Cu-Fe metallic glasses, XPS study of electronic struct. 4-104121  
 Y-Fe alloys, exchange interactions, coordination props. studies 4-114104  
 Y<sub>2</sub>(Co, Fe, Cu)<sub>17</sub>, single cryst. cpds., growth conditions and characterisation 4-66220  
 Y<sub>2</sub>(Co, Fe)<sub>17</sub>, single cryst. cpds., growth conditions and characterisation 4-66220  
 YCo<sub>2</sub>Fe, H absorption in 0-40°C temp. range (Russian) 4-75775  
 YFe, interionic distance effect on local fields, NMR study 4-84869  
 YFe<sub>2</sub>, electronic struct. and mag. props. 4-92602  
 Y(Fe,Al)<sub>1-x</sub>, alloys, mag. behaviour 4-76116  
 Y<sub>2</sub>Fe<sub>14</sub>B, single crystal, mag. props. study 4-114143  
 Y<sub>2</sub>Fe<sub>17-x</sub>Co<sub>x</sub>, magnetic cooling near Curie temperatures above 300K 4-88677  
 Zr-Fe, hydride formation, X-ray diffr., Mossbauer spectra, gas anal. 4-113392  
 Zr-V-Fe alloys, bulk getters, H and D diffusion 4-113719  
 ZrCrFe-based hyperstoichiometric alloys and hydrides, mag. props. 4-109025
- iron compounds**  
 see also ferrites; iron alloys  
 corrosion products solubility in O<sub>2</sub> containing aq. solns. under extreme conditions 4-113642  
 ferric complexes, quantum mixed-spin, EPR param. 4-92951  
 ferric nosporin, cryst., chem. and mol. struct., spectral charact. 4-102720  
 flashed brine geothermal system scale control 4-62298  
 garnet magneto-optic spatial light modulator in optical image processor or display system 4-74696  
 graphite-FeCl<sub>3</sub> interstitial cpds., isobaric thermal anal. 4-81425  
 halides, ionicity, XPS studies 4-66193  
 ilvaite, cryst. and mag. struct., neutron powder diffr. study 4-113412  
 intercalation cpd. with graphite, graphite-FeCl<sub>3</sub>, mag. order, neutron diffr. studies 4-61511  
 iron (III) benzoate thermal decomposition, Fe<sub>2</sub>O<sub>3</sub> particles prod., Mossbauer study 4-114868  
 ore concentrates, X-ray fluoreno. anal. 4-99925  
 oxides, six coordinated high spin Fe(IV) and Fe(V) oxidation states 4-70753  
 oxides, X-ray spectra, K-absorpt. edge 4-66130  
 oxides and sulphides, local symm. effects, X-ray absorpt. near edge struct. spectra 4-66116  
 phthalocyanine film electrodes, anodic dissolution in H<sub>2</sub>SO<sub>4</sub> 4-61453  
 polyacetylene-FeCl<sub>3</sub> (FeBr<sub>3</sub>) intercalation cpds., hyperfine interaction, Mossbauer and EPR studies 4-65887  
 polyvinylpyridine-FeCl<sub>3</sub>(Fe(NO<sub>3</sub>))<sub>3</sub> polymers, Mossbauer and IR spectra 4-59821  
 rare earth iron borides, RFe<sub>2</sub>B, with struct. of CeCo<sub>4</sub>B type, unit cell parameters determ. 4-65243  
 spinels, Fe-M-O (M=Al, Cr, Zn, Co, Mn), vacancy substituted, order-disorder, IR absorpt. spectra (French) 4-76447  
 spinels, valence states, X-ray absorption and emission spectra studies 4-61341  
 titanates, Fe doped, point defects and semicond. behaviour 4-70137  
 Al<sub>2</sub>O<sub>3</sub>-Fe<sub>2</sub>O<sub>3</sub>-MnO-SiO<sub>2</sub> glass, crystallisation and mag. props. 4-65188  
 Ba<sub>2</sub>MCrF<sub>6</sub> and Ba<sub>2</sub>MFeF<sub>6</sub> (M=Ni, Co, Fe), crystal structure and mag. props. 4-71040  
 BaO-B<sub>2</sub>O<sub>3</sub>-Fe<sub>2</sub>O<sub>3</sub> glasses, splat cooled, mag. props. 4-71107  
 BaO-B<sub>2</sub>O<sub>3</sub>-Fe<sub>2</sub>O<sub>3</sub> system, magnetic vitroceraics, prep. and props. 4-93256  
 BaRu<sub>1-x</sub>Fe<sub>x</sub>O<sub>3-y</sub>, cryst. struct. and elec. cond. (German) 4-84265  
 Ca<sub>2</sub>Fe<sub>1-x</sub>Mn<sub>x</sub>O<sub>8+y</sub>, O defect perovskite struct., X-ray diffr. and HREM study 4-92382  
 Ca<sub>3</sub>Mn<sub>1.35</sub>Fe<sub>1.65</sub>O<sub>8.02</sub>, struct. and frustrated antiferromag. props. 4-108998  
 CaO-B<sub>2</sub>O<sub>3</sub>-Al<sub>2</sub>O<sub>3</sub>-Fe<sub>2</sub>O<sub>3</sub> glass system, photoacoustic spectra of Fe 4-99130  
 CaO-Fe<sub>2</sub>O<sub>3</sub>-SiO<sub>2</sub> glass formation and props. 4-79946  
 (Co,Fe)<sub>1-x</sub>O, defects; thermodynamic calcs. 4-98087  
 Co<sub>9</sub>Fe<sub>16</sub>Fe<sub>24</sub>O<sub>4</sub> ferrite, mag. anisotropy, torque meas. 4-114105  
 CuFe<sub>2-x</sub>Al<sub>x</sub>O<sub>4</sub>, orthorhombic distortions due to doping 4-70103  
 Cu,Fe<sub>1-x</sub>Cr<sub>x</sub>S<sub>4</sub> films, elec. and galvanomagnetic props. 4-76056  
 Cu,Fe<sub>2-x</sub>O<sub>4</sub>, oxidation states, <sup>57</sup>Fe Mossbauer study 4-71225  
 Cu,Fe<sub>2-x</sub>O<sub>4</sub>, X-ray spectra, K-absorpt. edge 4-66130  
 (Fe,Ca,Mg)<sub>1-x</sub>Si<sub>2</sub>O<sub>6</sub> glass, ion bombard. effect, XPS 4-84320

## iron compounds continued

- (Fe,Nb)Nb<sub>5</sub>Se<sub>10</sub>, (Fe,V,Nb)Nb<sub>5</sub>Se<sub>10</sub> and (Fe,Ta,Nb)(Nb,Ta)Se<sub>10</sub>, one-dimensional systems, resistivity, structure and mag. props. 4-61364  
 Fe (III) solutions, magnetisation meas. for oligomer formation detection 4-98917  
 Fe (II)-bipyridine complex, resonance Raman spectra study 4-104609  
 Fe complex, Fe(phen)<sub>2</sub>(N<sup>13</sup>CS), spin-lattice relax., <sup>13</sup>C NMR 4-80837  
 Fe complex, halobis(diethyldiselenocarbamate)iron(III); mag. props. 4-76124  
 Fe complex, high spin-low spin equilib., particle size-effect, Mossbauer spectra 4-76288  
 Fe complex,  $\mu$ -oxo Fe (III) porphyrin dimers, antiferromag. coupling, <sup>13</sup>C NMR spectra 4-64508  
 Fe complex, tris(dithiocarbamate)iron(III), vibr. motion study 4-103891  
 Fe complexes, 2,2'-bipyridine-d<sub>8</sub>-Fe(II) 4-71379  
 Fe complexes, Fe hexacyanides, local structures, X-ray absorpt. near edge struct. spectra 4-66112  
 Fe<sup>2+</sup> complex, A23187 antibiotic; cryst. and mol. struct., X-ray diffr. 4-109775  
 Fe/Fe<sub>2</sub>O<sub>3</sub>, high magnetisation material with alternate layer struct., HF mag. core appl. 4-104470  
 Fe-Co complexes, high spin to low spin transition, thermally induced, metal dilution effect 4-65815  
 Fe-graphite system, carbide form. high press. and temp., mag. props. 4-99371  
 Fe-N films, reactively RF sputtered, microstructure and bombardment effects 4-71559  
 Fe-Na-O system, phase relationships, DTA and X-ray obs. 4-93268  
 Fe-O, work function, determination of phase transitions 4-98698  
 Fe<sup>3+</sup>-containing layer silicates, Mossbauer spectra quadrupole splitting lines, relative intensities and EFG calcs. 4-115397  
 $\alpha$ -(Fe<sub>1-x</sub>Al<sub>x</sub>)<sub>2</sub>O<sub>3</sub>, substituted hematite, Morin transition, <sup>57</sup>Fe Mossbauer study 4-71072  
 FeAs<sub>2</sub> and related minerals, reinterpretation of electronic struct. 4-113866  
 FeAs films, organo-metal CVD growth from (CO)<sub>2</sub>Fe+AsH<sub>3</sub> on GaAs 4-61868  
 FeBO<sub>3</sub>, accelerated decay of nuclear excitation during resonant  $\gamma$ -scatt. 4-92980  
 FeBO<sub>3</sub>, Mossbauer transmission spectra at pure nucl. dynamical diffr. in Bragg geometry 4-71218  
 FeBO<sub>3</sub>, nonlinear optical effects due to influence of optical fields on mag. props. 4-69513  
 FeBO<sub>3</sub>, nuclear resonance diffraction in Bragg geometry, anomalous high reflectivity obs. 4-69995  
 FeBO<sub>3</sub>, photoinduced optical and magnetic anisotropy 4-61534  
 FeBO<sub>3</sub>, single crystal, magneto-optic effects 4-114248  
 Fe<sub>2</sub>BO<sub>6</sub>, antiferromag., Raman scatt. from phonons and magnons 4-76471  
 FeBr<sub>2</sub>, high freq. dielec. const. 4-61646  
 FeBr<sub>2</sub>, metamagnet, one- and two-magnon excitations, Raman spectra 4-61527  
 FeBr<sub>2</sub> metamagnet, phase boundary depend. on hydrostatic press. 4-76137  
 Fe<sub>2</sub>C, diffusion coeff. meas. 4-98345  
 Fe(CN)<sub>6</sub><sup>3-</sup> ion, aq. soln., positronium quenching and inhibiting props. 4-103805  
 Fe(CN)<sub>6</sub><sup>4-</sup> ion, aq. soln., positronium quenching and inhibiting props. 4-103805  
 Fe(CN)<sub>6</sub><sup>4-</sup> (n=3,4), Fe-C bond lengths, EXAFS spectroelectrochemistry 4-107364  
 Fe(CO)<sub>4</sub> IR laser-induced isomerisation and Jahn-Teller effect 4-66567  
 Fe(CO)<sub>5</sub>, electron impact dissociation, Fe<sup>+</sup> prod. at fluoresc. anal. 4-96709  
 FeCl<sub>2</sub>, high freq. dielec. const. 4-61646  
 FeCl<sub>3</sub>, intercalation compound with graphite, thermal anal. 4-80223  
 FeCl<sub>3</sub>-CoCl<sub>2</sub>-graphite intercalation cpds. mag. phase transitions, susceptibility meas. 4-98881  
 Fe(CIO<sub>4</sub>)<sub>2</sub>-HClO<sub>4</sub>, etching kinetics of low C-steel 4-76969  
 Fe<sub>1-x</sub>Co<sub>x</sub>Br<sub>2</sub>, antiferromag., random mixture with competing spin anisotropies, uniform and localised mag. modes 4-109066  
 Fe<sub>1-x</sub>Co<sub>x</sub>Br<sub>2</sub>, randomly mixed antiferromag. with competing Ising and XY spin anisotropies, mag. transitions 4-104446  
 Fe<sub>0.725</sub>Co<sub>0.275</sub>Cl<sub>2</sub>, disordered spin-flop phase obs. 4-104420  
 Fe<sub>1-x</sub>Co<sub>x</sub>Cl<sub>2</sub>, competing anisotropy system, Fe<sup>2+</sup> spin orientation, Mossbauer spectra 4-92906  
 Fe<sub>1-x</sub>Co<sub>x</sub>Cl<sub>2</sub>, nondiluted random-field Ising system, neutron diffr. study 4-108992  
 Fe<sub>1-x</sub>Co<sub>x</sub>Cl<sub>2</sub>, random mixture with competing spin anisotropies, AFMR, FMR obs. 4-76259  
 Fe<sub>3</sub>Co<sub>1-x</sub>Cr<sub>2</sub>S<sub>4</sub>, magnetisation and Curie point meas. 4-104461  
 Fe<sub>1-x</sub>Co<sub>x</sub>S, single cryst. solid solutions, homogeneity studies 4-75693  
 $\alpha$ -Fe<sub>1-x</sub>Co<sub>x</sub>/Si<sub>3</sub>N<sub>4</sub>O<sub>2</sub>, hematite, resonant and static mag. props., Co<sup>2+</sup> doping effects 4-92938  
 Fe<sub>3</sub>Co<sub>1-x</sub> complex, hexa(pyridine-N-oxide) (ClO<sub>4</sub>)<sub>2</sub>, decoupled mag. sub-systems 4-98895  
 Fe(Cr<sub>1-x</sub>Al<sub>x</sub>)<sub>2</sub>O<sub>4</sub> spinels, next-nearest neighbour effects, Mossbauer studies 4-98987  
 Fe<sub>2-x</sub>Cr<sub>x</sub>O<sub>3</sub>, chem. transport of haematite with TeCl<sub>4</sub> as transporting agent 4-61824  
 Fe<sub>1-x</sub>Cu<sub>x</sub>C<sub>4</sub>S<sub>4</sub>, ferrimagnetic to ferromagnetic order transition, ion valence states, NMR 4-88670  
 FeF<sub>3</sub>, antiferromagnet, mag. polaritons, photothermal detection 4-61526  
 FeF<sub>3</sub>, amorphous, Mossbauer-Zeeman spectrum study 4-76294  
 FeF<sub>3</sub>, granular thin films, localised electronic state spatial distrib., polarisation study 4-104334  
 FeF<sub>3</sub>, thin film, impurity cond. along least resistance paths 4-80705  
 FeF<sub>3</sub>-based fluoride glasses, Mossbauer studies 4-114192  
 FeF<sub>3</sub>·0.33 H<sub>2</sub>O, normal and anhydrous, mag. ordering, Mossbauer studies 4-109103  
 Fe<sup>11</sup>Fe<sup>13</sup>F<sub>8</sub>(H<sub>2</sub>O)<sub>2</sub>, cryst. struct. and idle spin behaviour 4-108321  
 Fe<sub>3</sub>Fe<sub>0.9</sub>Sn<sub>0.1</sub>N<sub>0.7</sub>C<sub>0.3</sub>, ferromag. material for magnetic recording 4-104464  
 Fe<sub>3-x</sub>Ga<sub>x</sub>BO<sub>3</sub>, boroferrite, hyperfine interactions, Mossbauer studies 4-109099  
 Fe<sub>2</sub>Ge<sub>2</sub>O<sub>7</sub>, mixed valent, prep. struct., mag. props. (French) 4-88148  
 FeH<sub>2</sub>, low and high spin pot. energy surface, CI calcs. 4-96459  
 Fe(H<sub>2</sub>O)<sub>6</sub><sup>3+</sup>, etching kinetics of low C-steel 4-76969  
 Fe<sub>2</sub>, d-excitations, vibr. struct., IR and Raman spectra studies 4-113873  
 Fe<sub>1</sub>, single crystal, permittivity, electronic states, UV reflectivity 4-84975  
 Fe(II) porphyrins, dioxygen adducts, matrix isolation IR spectra 4-69068  
 FeMoO<sub>4</sub>S<sub>2</sub> Chevrel-phase cpd., struct. and mag. transitions 4-76139

## iron compounds continued

- Fe<sub>2</sub>Mg<sub>1-x</sub>Cl<sub>2</sub>, phase diagram, mag. susceptibility meas. 4-61535  
 Fe<sub>2.96</sub>Me<sub>0.04</sub>O<sub>4</sub>, magnetite, annealing and cryst. struct., X-ray diffr. studies 4-113402  
 Fe<sub>1-x</sub>Mn<sub>x</sub>F<sub>2</sub>, light scatt. by mag. excitons 4-71388  
 Fe<sub>2</sub>Mn<sub>1-x</sub>S, metal-insulator transition study 4-98527  
 Fe<sub>2</sub>(MoO<sub>4</sub>)<sub>3</sub>, antiferromagnetic, magnetic and Mossbauer studies 4-71034  
 Fe<sub>2</sub>(MoO<sub>4</sub>)<sub>3</sub>, polycrystalline, elec. cond., 370-900K, O partial press. depend. 4-75965  
 Fe<sub>2</sub>Mo<sub>2</sub>O<sub>8</sub>, crystal growth, mag. and elec. props. 4-71537  
 Fe<sub>2</sub>N, dissociation, CAS SCF and contracted CI calcs. 4-81407  
 Fe<sub>2</sub>N pigments, mag. props. rel. to specific surface area 4-65836  
 $\epsilon$ -Fe<sub>2</sub>N, (x=2/3), mag. props., Mossbauer obs. 4-61611  
 Fe(NH<sub>3</sub>)<sub>2</sub>(ClO<sub>4</sub>)<sub>2</sub> and Fe(NH<sub>3</sub>)<sub>6</sub>(BF<sub>4</sub>)<sub>2</sub>, phase transitions, microscopic theory 4-61071  
 FeNH<sub>4</sub>HP<sub>2</sub>O<sub>10</sub>, unit cell parameters, anion packing 4-113410  
 Fe(NH<sub>4</sub>)<sub>2</sub>(SO<sub>4</sub>)<sub>2</sub>·6H<sub>2</sub>O·VO<sup>2+</sup>, paramag. Tutton salts, EPR studies 4-71167  
 Fe(NH<sub>4</sub>)<sub>2</sub>(SO<sub>4</sub>)<sub>2</sub>·6H<sub>2</sub>O·Ni(NH<sub>4</sub>)<sub>2</sub>(SO<sub>4</sub>)<sub>2</sub>, co-precipitated, thermal decomp. Mossbauer invest. 4-65883  
 Fe<sub>1-x</sub>Nb<sub>x</sub>-Se<sub>10</sub>, cryst. struct., metal-insulator transition, resist., mag. susceptibility meas. 4-88448  
 Fe<sub>1-x</sub>Nb<sub>x</sub>-Se<sub>10</sub>, elastic props. and Mossbauer effect 4-84881  
 Fe<sub>2</sub>NbSe<sub>4</sub>, charge density waves, magnetoresistance elec. field depend. 4-70788  
 Fe<sub>40</sub>Ni<sub>40</sub>Co<sub>20</sub>S<sub>8</sub>, cryst. struct. determ. 4-103714  
 Fe<sub>1-x</sub>Ni<sub>x</sub>S, single cryst. solid solutions, homogeneity studies 4-75693  
 Fe<sub>1-x</sub>Ni<sub>x</sub>Mo<sub>2</sub>S<sub>8</sub>, cryst. struct. determ. 4-103714  
 (Fe<sub>1-x</sub>Ni<sub>x</sub>)<sub>2</sub>Sb, antiferromag., mag. props. 4-104422  
 FeO, band or Mott insulators and magnetism 4-70699  
 FeO, eqn. of state and Gruneisen parameters 4-92331  
 FeO, high temp. corrosion scales, TEM studies 4-104927  
 FeO, laboratory millimetre-wave spectrum meas. 4-85867  
 FeO, orange system subband rot. anal., fluoresc. spectra 4-59839  
 FeO, temp.-press. stability fields at high press., thermodynamic calc. 4-103965  
 FeO, wustite, struct. props., cluster component method anal. 4-70109  
 FeO-Fe<sub>2</sub>O<sub>3</sub>, magnetite, magnetostriiction isotherms at low temps. 4-61582  
 Fe<sub>1-x</sub>O, electrochemical kinetic studies 4-99803  
 Fe<sub>1-x</sub>O, chem. and self diffusion coeff. calc. 4-98356  
 Fe<sub>1-x</sub>O, oxidation and reduction influences on grain morphology 4-93436  
 Fe<sub>1-x</sub>O, self-diffusion and defects 4-98343  
 $\gamma$ -Fe<sub>2</sub>O<sub>3</sub> (maghemite), stability to change to  $\alpha$ -phase for heating up to 600°C 4-100539  
 $\alpha$ -Fe<sub>2</sub>O<sub>3</sub>, anisotropy of elec. props., mag. order depend. 4-108853  
 $\alpha$ -Fe<sub>2</sub>O<sub>3</sub> CVD coating on alumina high temp. stable catalyst for SO<sub>2</sub> conversion to SO<sub>3</sub> in hydrogen production process 4-66807  
 $\alpha$ -Fe<sub>2</sub>O<sub>3</sub> colloidal particles, Mossbauer parameters, size effects 4-65886  
 Fe<sub>2</sub>O<sub>3</sub>, doped, p-n assembly, water, catalytic photodissoc. 4-62207  
 $\alpha$ -Fe<sub>2</sub>O<sub>3</sub>, ESCA and Auger spectroscopy determ. of binding energy (French) 4-66638  
 $\alpha$ -Fe<sub>2</sub>O<sub>3</sub>, electrode for H<sub>2</sub>O photodecomposition, surface studies 4-108936  
 Fe<sub>2</sub>O<sub>3</sub>, external forces influence on sound velocity 4-70277  
 $\gamma$ -Fe<sub>2</sub>O<sub>3</sub>, fine particles, surface effect on saturation magnetisation, empirical formula 4-65829  
 Fe<sub>2</sub>O<sub>3</sub>, hematite, quadrupole shifts, temp. depend.,  $\gamma$ -ray spectra anal. 4-65888  
 $\gamma$ -Fe<sub>2</sub>O<sub>3</sub>, magnetic powder, perpendicular orientation, Mossbauer study 4-65838  
 Fe<sub>2</sub>O<sub>3</sub>, magnetic tape, scatt. and absorption corrections in X-ray fluorescence anal. (Chinese) 4-72001  
 Fe<sub>2</sub>O<sub>3</sub>, metastable transformation, simultaneous thermomag. and dilatometric meas. 4-113602  
 $\gamma$ -Fe<sub>2</sub>O<sub>3</sub>, microparticle materials, mag. and Mossbauer studies 4-104542  
 $\gamma$ -Fe<sub>2</sub>O<sub>3</sub>, particle product from iron (III) benzoate thermal decomposition, Mossbauer study 4-114868  
 Fe<sub>2</sub>O<sub>3</sub> photoelectrodes, photocurrent, thickness depend. 4-92764  
 Fe<sub>2</sub>O<sub>3</sub>, porous, thermal diffusivity, unsteady state method 4-80316  
 Fe<sub>2</sub>O<sub>3</sub> powders, shear strength up to 600°C and 4 GPa 4-104811  
 Fe<sub>2</sub>O<sub>3</sub>, pure and doped semicond., elec. cond. and Seebeck voltage 4-92759  
 Fe<sub>2</sub>O<sub>3</sub> stacked thin-film photoelectrode 4-98665  
 $\alpha$ -Fe<sub>2</sub>O<sub>3</sub>, surface and interface magnetism, Mossbauer spectra studies 4-104468  
 $\alpha$ -Fe<sub>2</sub>O<sub>3</sub>, surface electronic structure with O<sub>2</sub> (H<sub>2</sub>O) adsorpt. 4-84664  
 Fe<sub>2</sub>O<sub>3</sub> thin film photoanodes, carrier conc. determ. in MIS struct. 4-88505  
 $\alpha$ -Fe<sub>2</sub>O<sub>3</sub>, topochemical conversion of  $\gamma$ -FeOOH and comparative transform. methods of iron oxide in mag. spinels 4-109632  
 $\gamma$ -Fe<sub>2</sub>O<sub>3</sub>-Co, textural and surface props. rel. to mag. recording appls. 4-65833  
 $\gamma$ -Fe<sub>2</sub>O<sub>3</sub>-Co magnetic powder, perpendicular orientation, Mossbauer study 4-65838  
 $\gamma$ -Fe<sub>2</sub>O<sub>3</sub>-Cr particles for audio recording, high orientation effect 4-65832  
 Fe<sub>2</sub>O<sub>3</sub>-B<sub>2</sub>O<sub>3</sub>-PbO glasses, ferric ion distrib., EPR studies 4-109064  
 Fe<sub>2</sub>O<sub>3</sub>-CaO-SiO<sub>2</sub> glasses, DC cond., Mossbauer and ESR spectra 4-70807  
 $\gamma$ -Fe<sub>2</sub>O<sub>3</sub>-Fe<sub>2</sub>O<sub>3</sub>-Co thin films, coercivity study 4-114145  
 Fe<sub>2</sub>O<sub>3</sub>-NiO mixed oxides, phase anal., IR, mag. and X-ray diffr. studies 4-98243  
 Fe<sub>2</sub>O<sub>3</sub>-TiO<sub>2</sub>-K<sub>2</sub>O solid soln. with K<sup>+</sup> electrolyte, elec. cond. 4-61129  
 $\alpha$ -Fe<sub>2</sub>O<sub>3</sub>-ZrO<sub>2</sub>, elec. cond. rel. to stoichiometry depend. Zr solubility 4-70820  
 Fe<sub>3</sub>-O<sub>4</sub>, magnetite, diffusion of cations and point defects 4-99378  
 Fe<sub>3</sub>-O<sub>4</sub>, self-diffusion and defects 4-98343  
 Fe<sub>2</sub>O<sub>4</sub> and Zn<sub>2</sub>Fe<sub>2</sub>O<sub>4</sub>, partially oxidised spinels, defect phase  $\gamma$ , diffusion coeff. and vacancy conc. 4-92422  
 Fe<sub>3</sub>O<sub>4</sub>, bacterial magnetite, struct., morphology and cryst. growth 4-100069  
 Fe<sub>3</sub>O<sub>4</sub>, ceramic ferrite, mag. props. (Spanish) 4-88649  
 Fe<sub>3</sub>O<sub>4</sub>, ESCA and Auger spectroscopy determ. of binding energy (French) 4-66638  
 Fe<sub>3</sub>O<sub>4</sub>, heat capacity at Verwey transition 4-70405  
 Fe<sub>3</sub>O<sub>4</sub>, magnetite, elec. cond. below Verwey temperature 4-70809  
 Fe<sub>3</sub>O<sub>4</sub>, magnetite, elec. cond. below mech. and rel. to mag. after-effects 4-76195  
 Fe<sub>3</sub>O<sub>4</sub>, magnetite, Verwey transition 4-88447  
 Fe<sub>3</sub>O<sub>4</sub>, magnetite particles in ferromagnetic colloids, size distrib. anal. 4-109043  
 Fe<sub>3</sub>O<sub>4</sub>, point defects and transport props. 4-98366

iron compounds continued

- Fe<sub>3</sub>O<sub>4</sub>, precip. in magnetotactic bacteria, mag. guidance of organisms, book contrib. 4-93769  
 Fe<sub>3</sub>O<sub>4</sub>, thermal dissociation in solar furnace for H<sub>2</sub> production, 1000 kW concentrator production eval. from 2 kW concentrator 4-62402  
 Fe<sub>3</sub>O<sub>4</sub>/Ni, self-diffusion, SIMS study 4-98342  
 Fe<sub>3</sub>O<sub>4</sub>/MgFe<sub>2</sub>O<sub>4</sub> system, cation distrib., thermoelec. coeff., 600-1300°C 4-61402  
 Fe<sub>3</sub>O<sub>4</sub>, magnetite, annealing and cryst. struct., X-ray diffr. studies 4-113402  
 Fe<sub>3</sub>O<sub>4</sub>, wustite, Fe-rich phase boundary, press. and temp. var. effects 4-66318  
 (Fe<sub>2</sub>O<sub>3</sub>)<sub>2</sub>(B<sub>2</sub>O<sub>3</sub>.PbO)<sub>1-x</sub> glass, mag. props. study 4-88654  
 FeOCl, intercalated with  $\alpha$ -picoline, Mossbauer study 4-71226  
 FeOCl intercalation cpd. with TTF and TTT, struct., IR spectra and mag. susceptibility 4-70128  
 FeOCl, intercalation cpd. with TTF, TTN and TTT, struct. and EXAFS studies 4-70129  
 FeOCl, Lewis base intercalation compounds, charge transfer model, Mossbauer spectra, X-ray diffr. 4-70746  
 Fe(OH)<sub>2</sub>, brucite-like, struct. and IR relations 4-79996  
 Fe(OH)<sub>3</sub>, ESCA and Auger spectroscopy determ. of binding energy (French) 4-66638  
 Fe(OH)<sub>3</sub> in freshwater sediments, interaction with Ra 4-80376  
 Fe(OH)<sub>3</sub> membrane, transport phenomena, permeability 4-71987  
 FeOHSO<sub>4</sub> superparamagnetic particles, EPR linewidth 4-84820  
 $\gamma$ -FeOOH, ESCA and Auger spectroscopy determ. of binding energy (French) 4-66638  
 FeOOH, halogen impurity location, water content, neutron activation anal., Mossbauer spectra, TGA 4-81505  
 $\beta$ -FeOOH, Neel temp., struct. depend. 4-88665  
 $\gamma$ -FeOOH powder, grinding, lepidocrocite to hematite transform., morphology and mag. props., Mossbauer obs. 4-66329  
 $\beta$ -FeOOH, thermal decomposition into hematite, struct. props. 4-109636  
 $\gamma$ -FeOOH, topotactic conversions and comparative transform. methods of iron oxides in mag. spinels 4-109632  
 (Fe<sub>2</sub>O<sub>3</sub>(RCOO)<sub>2</sub>)<sub>n</sub><sup>+</sup> clusters, magnetic behaviour, isotropic dynamic distortion model 4-92905  
 Fe<sub>2</sub>O<sub>3</sub>.H<sub>2</sub>O, coprecipitated hydrated oxides, sorption props. 4-109679  
 $\gamma$ -(Fe<sub>1-x</sub>O<sub>3-x</sub>)<sub>2</sub>O<sub>3</sub> thin films, perpendicular mag. anisotropy 4-84833  
 Fe<sub>2</sub>P, EXAFS contributions and near neighbour components 4-61774  
 Fe<sub>2</sub>P, metamagnetic transitions, magnetisation studies 4-98883  
 Fe<sub>2</sub>P, metamagnetic transitions, PT diagram studies 4-114111  
 Fe<sub>2</sub>(PO<sub>4</sub>)<sub>3</sub>, mixed valent, prep., cryst. struct., mag. props., Mossbauer spectra (French) 4-88146  
 FePS<sub>3</sub>, electronic struct., partial-yield synchrotron-radiation photoelectron spectra 4-61810  
 FePS<sub>3</sub>, soft X-ray absorption 4-109279  
 FeS high temp. corrosion scales, TEM studies 4-104927  
 FeS, (Fe<sub>2</sub>S<sub>3</sub>)(FeS) surfaces, AES and EELS studies 4-114349  
 FeS<sub>2</sub>, band struct. calcs., Mossbauer spectra 4-92611  
 FeS<sub>2</sub>, electronic struct., reflectivity spectra, optical consts., meas. between 0.2-4.4 eV 4-80963  
 FeS<sub>2</sub>, Mossbauer study 4-61612  
 FeS<sub>2</sub>, pyrite, Mossbauer study of lattice dynamics 4-61000  
 Fe<sub>9</sub>S<sub>8</sub> (pyrrhotite), eqn. of state at Earth core conditions 4-115395  
 Fe<sub>1-x</sub>S, plasma chem. prep. 4-99335  
 Fe<sub>1-x</sub>S, self-diffusion coeffs., Mossbauer spectroscopy 4-98351  
 Fe<sub>1-x</sub>S, chem. and self diffusion coeff. calc. 4-98356  
 Fe<sub>1-x</sub> $\gamma$ -Fe<sub>2</sub>S<sub>3</sub> mixture, cryst. struct. and defect struct. 4-75422  
 Fe<sub>2</sub>S<sub>4</sub> (pyrrhotite), mag. hysteresis of sized dispersed monoclinic grains 4-100541  
 Fe<sub>2</sub>S<sub>4</sub> pyrrhotite type nonstoichiometric cpds., with different vacancy concs., magnetisation 4-61523  
 Fe<sub>2</sub>S<sub>10</sub>, defect struct., high resolution transmission electron microscopy studies 4-108388  
 FeSO<sub>4</sub>.7H<sub>2</sub>O dosimeter,  $\epsilon$ (Fe<sup>3+</sup>) determ. (Chinese) 4-68833  
 FeSO<sub>4</sub>.7H<sub>2</sub>O, K-absorption edge, X-ray absorpt. near edge struct. obs. 4-66123  
 FeSb<sub>2</sub>S<sub>4</sub>, berthierite, antiferromag. phase transition 4-65813  
 FeSi<sub>3</sub>, electronic density of states, XPS study 4-61272  
 FeSiF<sub>6</sub>.6H<sub>2</sub>O, phase transition and cryst. field effects, Mossbauer study 4-75668  
 Fe<sub>2</sub>SiO<sub>4</sub>, Fayalite sinter, segregates or precipitates anal. by electron probe microanal. (Japanese) 4-99698  
 FeSn, pyrrhotite, elec. cond. meas. 4-80587  
 Fe<sub>2</sub>SnMo<sub>2</sub>S<sub>8</sub>, Chevrel phase, supercond. crit. temp. meas. 4-84729  
 FeTiO<sub>3</sub>-Fe<sub>2</sub>O<sub>3</sub> cluster spin glasses, neutron scattering and muon spin rotation collaborations 4-65890  
 FeTiO<sub>3</sub>-Fe<sub>2</sub>O<sub>3</sub> solid solutions, remanent magnetization of paramagnetic composition 4-100547  
 Fe<sub>2</sub>TiO<sub>4</sub> and Fe<sub>2</sub>Ti<sub>6</sub>O<sub>4</sub>, neutron diffraction study of cryst. struct. and mag. props. 4-100540  
 Fe<sub>2</sub>TiO<sub>3</sub>, cryst. struct., TEM, electron diffr., X-ray powder diffr. studies 4-103726  
 Fe<sub>2</sub>TiO<sub>3</sub>, spin glass, irreversible phenomena, effect of cryst. field anisotropy 4-104432  
 Fe<sub>2</sub>TiSe<sub>2</sub> intercalation cpd., cryst. struct., mag. ordering, susceptibility studies, X-ray diffr. 4-76119  
 FeVNbO<sub>6</sub>, semicond., elec. resist., mag. susceptibility meas. 4-109000  
 FeV<sub>2</sub>Se<sub>4</sub>, Mossbauer spectra, 4.8 to 700K 4-80849  
 Fe<sub>2</sub>Zn<sub>1-x</sub> complex, hexa(pyridine-N-oxide) (ClO<sub>4</sub>)<sub>2</sub>, randomly diluted mag., sp. ht. studies 4-98903  
 (Fe(bipy)<sub>2</sub>(NCS)<sub>2</sub>), high spin (<sup>2</sup>T<sub>2</sub>)=low spin (<sup>1</sup>A<sub>1</sub>) transition 4-92970  
 Fe<sub>0.003</sub>Co<sub>0.997</sub>Cl<sub>2</sub> magnetoelastic coupling at Fe<sup>2+</sup> ions Mossbauer spectrum 4-92948  
 GdFe<sub>2</sub>Hf<sub>3</sub> films, ferromag. resonance and mag. props. 4-61594  
 Ge<sub>2</sub>Fe<sub>2-x</sub>O<sub>4</sub> mixed valent, prep., struct., mag. props. (French) 4-88148  
 H<sub>2</sub>FeRu<sub>2</sub>(CO)<sub>13</sub>, cryst. struct. study 4-75390  
 Hg<sub>1-x</sub>Fe<sub>x</sub>Te, crystal, negative magnetoresist. and Hall effect 4-65696  
 In<sub>2</sub>O<sub>3</sub>-Fe<sub>2</sub>O<sub>3</sub>-CuO(CoO), phase relations and cryst. structures 4-98242  
 K<sub>2</sub>Co<sub>0.77</sub>Fe<sub>0.23</sub>F<sub>4</sub>, magnetic ordering, elastic neutron study 4-104404  
 KFe(MoO<sub>4</sub>)<sub>2</sub>, ferroelectric domain switching 4-92343  
 Li-Al/FeS cell, FeS positive electrode effective conductivities in LiCl-KCl eutectic electrolyte 4-99958  
 LiCl-KCl eutectic melts, Fe<sub>2</sub>S and FeS equilibrium concentrations 4-88300  
 Life phengite, mica, cryst. struct. of di-trioctahedral 1M polymorphic modification, electron diffr. study 4-60894  
 Li<sub>2</sub>O-B<sub>2</sub>O<sub>3</sub>-Fe<sub>2</sub>O<sub>3</sub> system, magnetic vitroceraamics, prep. and props. 4-93256

iron compounds continued

- (Mg,Fe)<sub>2</sub>Al<sub>2</sub>Si<sub>2</sub>O<sub>8</sub> cordierites, heating and radiation effects on optical absorpt. and Mossbauer spectra 4-89911  
 (Mg,Fe)<sub>2</sub>S ningerite solid solns., Mossbauer studies 4-98992  
 Mn<sub>1-x</sub>Fe<sub>x</sub>CO<sub>3</sub>, mixed antiferromag. system, competing anisotropy and random field effects 4-109019  
 MnFe<sub>2</sub>F<sub>8</sub>(H<sub>2</sub>O)<sub>2</sub>, cryst. struct. and idle spin behaviour 4-108321  
 Mn<sub>0.90</sub>Fe<sub>0.10</sub>P, mag. phases, Mossbauer spectroscopy study 4-88753  
 Mn<sub>1-x</sub>Fe<sub>x</sub>Si<sub>2</sub>, Mossbauer effect, magnetisation meas., in external mag. fields 4-98879  
 NaFe<sub>2</sub>O<sub>7</sub>, crystallographic, mag. and Mossbauer studies 4-108323  
 Ni<sub>1-x</sub>Fe<sub>x</sub>O<sub>4</sub>, cation-site occupancy, effect of Ni content 4-98079  
 PbFe<sub>2</sub>M<sup>II</sup>F<sub>2</sub>M<sup>III</sup>F<sub>3</sub> (M<sup>II</sup>=Mn, Zn; M<sup>III</sup>=Fe, Ga), fluoride glasses, local order, EXAFS studies 4-70036  
 PbFe<sub>2-x</sub>Ga<sub>x</sub>O<sub>9</sub>, optical props. 4-93086  
 PbO-B<sub>2</sub>O<sub>3</sub>-Bi<sub>2</sub>O<sub>3</sub>-Y<sub>2</sub>O<sub>3</sub>-Ga<sub>2</sub>O<sub>3</sub>-Fe<sub>2</sub>O<sub>3</sub>, phase diagram invest. 4-93208  
 RbFeF<sub>4</sub>, structural phase transitions, Mossbauer study 4-61064  
 SiO<sub>2</sub>-B<sub>2</sub>O<sub>3</sub>-Na<sub>2</sub>CO<sub>3</sub>-Fe<sub>2</sub>O<sub>3</sub> glasses, coordination of Fe ions 4-88110  
 SiO<sub>2</sub>-Na<sub>2</sub>O-CaO-Fe<sub>2</sub>O<sub>3</sub> glasses, EPR study of behaviour and effect of Fe 4-88111  
 SiO<sub>2</sub>-Na<sub>2</sub>O-Fe<sub>2</sub>O<sub>3</sub> glasses, radiation damage, EPR spectra 4-84200  
 (SnO<sub>2</sub>)<sub>1-x</sub>(Fe<sub>2</sub>O<sub>3</sub>)<sub>x</sub>, Mossbauer study 4-114187  
 TiO<sub>2</sub>-FeNb<sub>2</sub>O<sub>6</sub>-NbO<sub>2</sub> system, rutiles, struct., mag. and electron transport props. 4-84238  
 Ti<sub>2</sub>Fe<sub>2</sub>S<sub>4</sub>, phase relationships 4-104772  
 V<sub>1-x</sub>Fe<sub>x</sub>S<sub>2</sub>, crystallographic and spin rotation transitions, Mossbauer studies 4-98270  
 (YBi)<sub>2</sub>(FeGa<sub>2</sub>O<sub>12</sub>)<sub>2</sub> garnet, cryst. growth from flux and LPE 4-93208  
 Y<sub>3-x</sub>Ca<sub>x</sub>Fe<sub>2-x</sub>Ti<sub>x</sub>O<sub>12</sub> garnets, hyperfine fields and Mossbauer spectra 4-109098  
 YIG, crystal growth by floating zone method 4-76665  
 YIG, influence of pre-sintering on mag. props. 4-84789  
 YIG, seed and unseeded, growth from high temp. solns., studied by growth striations 4-76656  
 YIG single crystal spheres, dissoln. forms in H<sub>3</sub>PO<sub>4</sub> and HBr 4-75687  
 YIG, solubility and growth kinetics on (111) substrates, influence of excess iron oxide 4-75802  
 Y<sub>2</sub>O<sub>3</sub>-Fe<sub>2</sub>O<sub>3</sub>, solid state reaction for garnet formation by sintering 4-85302  
 (Zn<sub>0.70</sub>Fe<sub>0.30</sub>)(PO<sub>4</sub>)<sub>2</sub>, farringtonite struct., cation distrib., neutron powder diffr., Rietveld technique 4-60889  
 Zr<sub>4</sub>Fe<sub>2</sub>O<sub>16</sub>, hydride formation, X-ray diffr., Mossbauer spectra, gas anal. 4-113392

iron phosphate semiconductor glasses see amorphous semiconductors

irradiation effects see radiation effects

irradiation induced creep

- fusion blankets, stress distrib., influence of irradiation and thermal creep 4-91111  
 nuclear reactor materials neutron irradiation effects 4-103806  
 rock salt, gamma irradiation, thermomech. props., rel. to radioactive waste disposal 4-75527  
 spallation neutron source materials, He embrittlement, thermal fatigue, irradiation creep 4-108464  
 steel, austenitic stainless, dislocation struct. during radiation creep (Russian) 4-80041  
 steel, austenitic stainless, first wall lifetime, impact of swelling 4-96269  
 steel, austenitic stainless, irradiation creep, light ion simulation 4-104815  
 steel, austenitic stainless, proton irradiation creep of thin foil specimens, thickness effects on mech. props. 4-103820  
 steel, austenitic stainless, radiation damage, fusion reactor candidate material 4-98140  
 steel, austenitic stainless, stress rupture in-reactor creep cavity form. model 4-104854  
 Fe, BCC crystal, irradiation creep, stress induced edge dislocation-interstitial atom interaction 4-104814  
 Fe-Ni-Cr, austenitic, neutron irradiated, swelling and creep 4-108452  
 (Fe<sub>0.49</sub>Ni<sub>0.51</sub>)<sub>3</sub>V, ordered alloys, microstruct. and creep rel. to implanted He 4-108399  
 Ni, dislocation/obstacle interaction during low dose D. irradiation creep 4-104813  
 (U,Pu)C fuel, swelling, densification and creep under irradiation 4-83144  
 UO<sub>2</sub>, indentation creep before and after irradiation, sintered pellets 4-61977  
 Zr proton irradiation and thermal creep at elevated temps. under stress 4-75559

ISDN see communication networks; digital communication systems

Ising lattices

- see also Ising model  
 cluster expansions in (2+1)D, high-temp. series 4-78254  
 critical exponent universality, renormalisation group theory 4-95326  
 disorder induced phase transitions 4-58780  
 Euclidean lattice field theory, Ising model, particle masses, perturbation theory 4-106473  
 extended  $\phi^4$  model, square lattice, critical behaviour 4-86535  
 fractal lattices, dilute Ising models, phase diagram and critical exponents 4-90516  
 frustrated Ising zigzag chains, dilution and boundary condition effects, 2 spin correl. 4-71109  
 fully frustrated Ising model on 2-dimens. lattice, Kosterlitz-Thouless phase transition 4-76152  
 gauge theory, successive screw approx. 4-68170  
 linear lattice systems, direct correl. function decay 4-73392  
 microcanonical simulation, convergence and ergodicity criteria 4-82756  
 Monte Carlo method, stochastic models and renormalization group procedures 4-111033  
 multicomponent Ising model, Mayer expansions for gas at low temp. 4-101783  
 nucleation and metastability in 3-D, Monte Carlo calcs. 4-111057  
 quantum chains, leading order corrections to the energy gap 4-86345  
 random external fields, physical realisations 4-86359  
 random interfaces, dynamics in phase transitions 4-86363  
 random walkers, phase transition in 1-D 4-86335  
 structure factor and magnetization, simple cubic Ising model 4-95334  
 surface free energy in (1+1)D, metastability 4-78260  
 two-dimensional model, detailed balance and the dynamical crit. exponent 4-73382  
 two-dimensional spin-polarised fermion lattice gas, Monte Carlo study 4-68177

## Ising model

see also Ising lattices  
 1d quantum ground state, Monte Carlo renormalisation group simulation 4-58762  
 adsorbed monolayers, spin-one Ising model 4-92534  
 adsorbed solid film, multilayer, layering critical points, renormalisation group anal. 4-104082  
 anisotropic Ising model in complex temp. plane, zeros location, Lee-Yang theorem absence 4-61500  
 ANNNI model, low temp. anal. in external mag. field 4-58774  
 antiferromagnet, FCC, hysteresis and free energy, computer simulation 4-114127  
 antiferromagnetic Ising model, anisotropic, long-range order, quenched impurity effects 4-98848  
 antiferromagnetic partially frustrated systems 4-104387  
 Baxter model, impure, universal behaviour, Monte Carlo studies 4-104388  
 BCC binary alloys, with first, second, third and fifth neighbour interactions, ordered structures 4-113577  
 betaine arsenate, dielec. props. near ferroelec. transition 4-71307  
 Blume-Capel model, two spin cluster approx., expansion of free energy, tricritical point 4-95343  
 bond-moving and variational methods in real-space renormalization, book contrib. 4-63685  
 boundary magnetization and spin correlations in inhomogeneous two-dimensional Ising systems 4-104449  
 cellular automata, equivalence to Ising models and directed percolation 4-95340  
 closed Cayley tree, zeros of the partition function 4-111062  
 cluster free energy, interfacial contribs., Ising model Monte Carlo method calc. 4-111073  
 commensurate-incommensurate transitions, two-dimensional ANNNI type models, Monte Carlo studies 4-113608  
 complex zeroes, finite-size scaling, critical amplitudes 4-68152  
 critical wetting in systems with long-range forces 4-88374  
 crystal growth from melt, rapid solidification, computer simulation 4-114383  
 d-dimensional Ising model, global and local Markov props. 4-90533  
 decorated hypercubic lattice with multiple transitions, transition point location 4-109034  
 dedecoration transformation for linear Ising chain 4-104390  
 dilute Ising system, dipolar field direction changes 4-92884  
 dilute magnets, phase transitions, critical behaviour, percolation, random fields 4-88690  
 diluted ANNNI models, modulated phases, conc. depend., spin configs., percolation 4-80770  
 diluted quantum transverse Ising model in two dimensions 4-63681  
 disordered alloy, magnetisation, susceptibility in cluster-variational method 4-92900  
 disordered Hubbard alloys, spin glass behaviour 4-92928  
 domain growth, temp. depend., Ising model Monte Carlo simulation 4-58761  
 domain wall renormalisation-group study of 2D random Ising model 4-71113  
 domain-wall renormalization-group study of the three-dimensional random Ising model 4-104444  
 extrapolation techniques, perturbation expansions, series acceleration procedures 4-90547  
 fermionic degrees of freedom on a lattice; particles and strings 4-58948  
 ferroelectric materials, surface modes 4-61632  
 ferroelectric transitions, Ising models 4-65821  
 ferroelectrics, surface modes, dispersion curves and soft mode temp., Ising model anal. 4-65538  
 ferromagnet, 2-D, universality, Monte Carlo renormalisation group studies 4-114085  
 ferromagnet, amorphisation, high-field magnetisation 4-84762  
 ferromagnet, bond-diluted, bond percolation on the pentagon lattice 4-114083  
 ferromagnet, correl. functions in two-dimens. narrow strips at phase coexistence, Monte-Carlo calcs. 4-104439  
 ferromagnet, cubic, critical behaviour, Potts model anal. 4-61546  
 ferromagnet, diluted, amorphisation, effective field theory with correl. 4-80771  
 ferromagnet, finite-size scaling at first-order phase transitions 4-104448  
 ferromagnet, polar states and charge ordering 4-71117  
 ferromagnet, pure and dil. Ising, reaction fields 4-114082  
 ferromagnetic, Ising model, anisotropic, thermodynamical props., correlated-effective-field treatment 4-98910  
 ferromagnetic Ising model, dilute crystalline, amorphisation and high-field magnetisation 4-98911  
 ferromagnetic Ising model, triangular lattice, renormalisation group study 4-104450  
 ferromagnetic spin-1/2 model, appl. to Li-Mg short range order 4-113664  
 ferromagnetic transitions, Ising-models 4-65821  
 ferromagnets, classical, with complex external field 4-61502  
 ferromagnets, Ising model of surfaces, phase separation, critical temp. 4-88636  
 ferromagnets, three-dimensional, phase transitions in classical vector models 4-61548  
 Fisher droplet model, modified and Monte Carlo equilb. cluster distrib. 4-111074  
 fractal lattices, dilute Ising models, phase diagram and critical exponents 4-90516  
 frustrated Ising zigzag chains, dilution and boundary condition effects, 2 spin corrs. 4-71109  
 frustrated spin systems 4-98904  
 fully frustrated Ising model on 2-dimens. lattice, Kosterlitz-Thouless phase transition 4-76152  
 functional integral method in solid-state statistics (Russian) 4-95339  
 graphite with adsorbed methane, orientational transition calcs. 4-70573  
 Green function ansatz for K-space pair correl. function 4-58763  
 Heisenberg-Ising spin 1/2 chain, quantum domain walls 4-104442  
 hexagonal lattice, simple, with competing interactions, modulated phases 4-92925  
 high temp. d-dimensional, inverse correlation length, analyticity 4-76097  
 homogeneously random Ising antiferromagnet, Monte Carlo study 4-61501  
 honeycomb and diced lattices, Ising and classical n-vector spins 4-109033  
 interfacial tension for lattice models, Monte Carlo calc. 4-92481  
 Ising spin glass, mag. field depend. of magnetisation 4-104460

## Ising model continued

lattice gauge theory, successive screw approx. 4-68170  
 linear Ising ferromagnet with antiferromagnetic impurities ground state 4-71118  
 linear Ising model, crystal field effect, ferromag. and antiferromag. susceptibilities 4-98845  
 long-period superstructure models, ANNNI model 4-113366  
 low temp. d-dimensional, inverse correlation length, analyticity 4-76098  
 low-dimensional phase transition, droplet theory 4-78283  
 magnetic thin films and semi-infinite model, local autocorrelation time, nearest-neighbour Ising model 4-76201  
 Monte Carlo processor results 4-58784  
 Monte Carlo renormalised group methods for critical points and flow diagrams determ. 4-68406  
 Monte Carlo simulation results 4-58785  
 nearest neighbour model, with uniaxial incommensurate phase and Lifshitz point 4-71115  
 next-nearest neighbour, soliton pinning and annealing 4-82764  
 non-equilibrium effects in random field, Monte Carlo evidence 4-98841  
 one-dimensional spin models, random fields, Glauber dynamics 4-98907  
 one-dimensional spin system,  $S=1/2$ , mag. scatt. of neutrons 4-88640  
 one-dimensional systems, Ising model, fluctuation study 4-98849  
 ordering under quenched random mag. fields 4-71103  
 pair correlation functions at critical temp. 4-111061  
 paramagnetic system, two-dimens., nonlinear response theory for nearest-neighbour Ising model 4-80740  
 perturbation expansions and series acceleration procedures 4-71011  
 phase transitions,  $C^*$  algebra methods, review 4-71108  
 phase transitions from Grassmann path integrals 4-92911  
 planar Ising ferromagnets, magnetisation and phase transitions 4-71067  
 positive symmetry matrices, renormalisation group transformation, spin 1/2 Ising model 4-106235  
 Potts model of magnetism, critical dimensionalities and props. 4-61499  
 quantum lattice models, ground state props., real-space renormalisation group method 4-111069  
 quasi-one-dimensional Ising magnet, magnetisation (Russian) 4-98842  
 random field, domain growth and self-similar scaling breakdown 4-82763  
 random field Ising model in dimens. 2, possible line of crit. points 4-88691  
 random field model, nonequilibrium crit. exponents 4-71111  
 random field model, nonequilibrium props. and interface motion 4-71112  
 random field model on Bethe lattice, spin-flip ferromag. transitions 4-98909  
 random field on Bethe lattice, critical behaviour 4-98844  
 random model, magnetisation, critical temp. and percolation thresholds 4-58759  
 random-field, equilibration 4-78275  
 random-field, spin-glass order parameter 4-114128  
 random-field Ising model, domain wall width, lower bounds 4-78269  
 real space dynamic renormalization group, book contrib. 4-63686  
 regular Ising model on Cayley tree, effective field behaviour, spin glass 4-104440  
 roughening transitions, geometric interpretation 4-111051  
 semi-infinite Ising spin system with transverse field, surface phase diagrams 4-88687  
 simple cubic, critical behaviour, Monte Carlo renormalisation group calcs. 4-71114  
 simple-cubic, fully and partially frustrated, Landau-Ginzburg-Wilson theory 4-104389  
 six-state Potts model, 2D, phase transitions and critical props. 4-58760  
 smectic C ordered phases, cooperative dynamical behaviour 4-79932  
 smectic liq. crystals, phase transition between monolayer and bilayer phases 4-65399  
 spin 1/2, in external field, thermodynamic props., correl. effects 4-88639  
 spin glass, bidimensional, 1/f noise, disorder and dimensionality 4-58740  
 spin glass, Sompolinsky and Parisi solutions equivalence 4-88683  
 spin glass behaviour, correlation-induced reentrant, Ising model with random interactions 4-104445  
 spin glass models, recursive algorithm for ground state calcs. 4-98901  
 spin glasses, infinite range, dynamic susceptibility field and temp. depend. 4-114115  
 spin glasses, irreversible and reversible behaviour, broken ergodicity 4-114125  
 spin glasses, lower crit. dimens. 4-88684  
 spin glasses, scaling theory 4-88685  
 spin glasses, short range three-dimensional nearest-neighbour Ising model, Monte Carlo simulations 4-92926  
 spin glasses, sp. ht., time-dependent, two-dimensional  $\pm J$ -Ising model 4-65822  
 spin Hamiltonians, anisotropic infinite range, thermodynamic props., XY and Ising-type states 4-114081  
 spin models, percolation, clusters, and phase transitions 4-78270  
 spin system on a Cayley tree,  $i$ - $\delta$  relations 4-84811  
 spin systems with random fields, crit. dynamics 4-98893  
 spin-1 antiferromagnetic chain, ground-state props. calcs. 4-71102  
 spin-1 antiferromagnetic Heisenberg-Ising chain 4-71101  
 spin-1 in 2-D, magnetisation, specific heat and susceptibility 4-98843  
 spin-1/2 chain with Ising/Heisenberg/XY exchange, multiple bound states 4-88689  
 spin-glass near de Almeida-Thouless line 4-98902  
 spin-lattice coupling in an Ising chain with nearest neighbour and next-nearest neighbour exchange interactions 4-76153  
 spontaneous magnetisation calcs. of 2-D lattice 4-65782  
 spontaneous magnetisation in weak random field 4-88637  
 square-lattice Ising model, two-parameter modified Kadanoff var. method 4-111040  
 squaric acid, Ising model, Monte Carlo calc. 4-71306  
 squaric acid, layered antiferroelectric, Ising spin chain models 4-71285  
 stacked frustrated antiferromagnetic triangular Ising system, ordering study 4-71116  
 statistical mechanics of a triple Ising chain (Russian) 4-92924  
 structure factor and magnetization, simple cubic Ising model 4-95334  
 SU(N) lattice QCD, non-zero baryon density, antiferromag. Ising model 4-102062  
 susceptibility using exponents far from  $T_c$  4-88635  
 TGS group ferroelectrics; mean field to critical behaviour crossover (Japanese) 4-93012  
 three dimensional, cell distribution functions, Monte Carlo study 4-76155  
 three-dimensional Onsager problem 4-58787  
 transfer matrix method study, Suzuki-Trotter formula 4-101772  
 transfer matrix solution on Koch curve 4-80733

## ing model continued

- transverse, (1+1)-dimensional, crit. behaviour for spin  $S \geq 1/2$  4-104447  
 transverse, dilution, effective field treatment 4-88638  
 transverse, longitudinal relaxation spectra 4-84365  
 transverse field dynamics, interaction effects 4-106246  
 transverse Ising model with disordered surface, surface magnetism 4-88688  
 triangular lattice, percolation, scaling of order parameter, comparison to Ising model 4-111064  
 two component spin model on lattice, star-triangle relation, classification conditions 4-58768  
 two component spin model on lattice, star-triangle relation, appl. and generalisation 4-58769  
 two dimensional, local mag. field distrib. and thermodynamic quantities 4-98908  
 two-dimensional, diagonal spin-spin correl. functions, series expansions calc. 4-98905  
 two-dimensional, quantum, time correlations and X-ray absorption problem 4-71012  
 two-dimensional, renormalisation group and high-temp. series 4-68145  
 two-dimensional, tricritical behaviour, finite size scaling anal. 4-61547  
 two-dimensional generalised arbitrary spin model, effective Hamiltonian derivation 4-98847  
 two-dimensional Ising ferromagnet, energy variable, scaling limit 4-111041  
 two-dimensional random field, crossover scaling test 4-68175  
 two-dimensional random Ising model, cluster-quench simulation 4-88686  
 two-dimensional square, cluster variation method calcs. of crit. temp. (Turkish) 4-114126  
 two-step renormalisation group 4-101761  
 uniaxial crystals, with defects, crit. fluctuations and phase transitions 4-71308  
 universal combinations between thermodynamic crit. amplitudes for Ising-like systems 4-102023  
 $\text{CsH}_2\text{PO}_4$  ( $\text{CsD}_2\text{PO}_4$ ) ferroelectric phase transitions in transverse Ising model 4-93025  
 $\text{CsH}_2\text{PO}_4$ , thermal expansion, quasi-one-dimensional Ising model 4-80268  
 $\text{FeBr}_2$  metamagnet, phase boundary depend. on hydrostatic press. 4-76137  
 $\text{Fe}_{1-x}\text{Co}_x\text{Br}_2$ , randomly mixed antiferromagnet, with competing Ising and XY spin anisotropies, mag. transitions 4-104446  
 $\text{Fe}_{1-x}\text{Co}_x\text{Cl}_2$ , nondiluted random-field Ising system, neutron diff. study 4-108992  
 $\text{Fe}_2\text{Zn}_{1-p}$  complex, hexa(pyridine-N-oxide) ( $\text{ClO}_4$ )<sub>2</sub>, randomly diluted mag., sp. ht. studies 4-98903  
 $\text{K}_2\text{CoF}_4$  2D Ising model, critical fluctuations, neutron scatt. meas. 4-92927  
 $\text{KD}_2\text{PO}_4$ -type ferroelectrics, static and dynamic props., applicability of mean-field approx. 4-93022  
 $\text{NH}_4\text{AlF}_6$ , clusters and critical slowing down near  $T_c$ , EPR study 4-65982  
 $\text{Pb}_{1-x}\text{Ge}_x\text{Te}$ , ferroelec. phase transition, high press. investigation, DC resist., capacitance meas. 4-71312  
 $\text{Rb}_2\text{Co}_{0.85}\text{Mg}_{0.15}\text{F}_4$ , crossover scaling and specific heat 4-68175  
 island-like metallic thin films *see discontinuous metallic thin films*  
 sheet-like metallic thin films *see discontinuous metallic thin films*

## isobaric analogue resonances

- see also nuclear collective states and giant resonances*  
 near magic nuclei, isobaric analogue resonance, partial proton widths, optical shell model 4-95988  
 peripheral heavy-ion collisions, pion prod. via isobar giant reson. formation and decay 4-64159  
<sup>24</sup>Al levels, transitions, giant dipole resonance analogue, DWA anal. of (<sup>3</sup>He,t) 4-86758  
<sup>40</sup>Ca(<sup>3</sup>He,<sup>3</sup>He), 197 MeV, levels, transitions, giant dipole resonance analogue, DWA anal. 4-86758  
<sup>37</sup>Cl resonances, bound states excitation energies and  $\gamma$ -branchings from <sup>36</sup>S(p, $\gamma$ ) 4-90991  
<sup>51</sup>Mn  $g_{9/2}$  isobaric analogue resonances, spins and spectroscopic factors from <sup>50</sup>Cr(p, $\gamma$ ) and <sup>50</sup>Cr(p, $\gamma$ ) 4-106602  
<sup>12</sup>N levels, transitions, giant dipole resonance analogue, DWA anal. of (<sup>3</sup>He,t) 4-86758  
<sup>28</sup>P levels, transitions, giant dipole resonance analogue, DWA anal. of (<sup>3</sup>He,t) 4-86758  
<sup>40</sup>Sc levels, transitions, giant dipole resonance analogue, DWA anal. of (<sup>3</sup>He,t) 4-86758  
<sup>74</sup>Se(p,p), (p,p'), excitation function meas. to study IAR in <sup>75</sup>Br 4-59233  
<sup>130</sup>Te(p,p), (in)elastic scatt. ang. distrib. of cross section and analyzing power 4-96033

## isobaric analogue states

- see also isobaric analogue resonances*  
<sup>13</sup>C( $\gamma,\pi$ )<sup>13</sup>N<sub>gs</sub>,  $E_\pi=48$  MeV, differential cross section,  $J_i=J_f=1/2^-$  4-102252  
 fine-structure of isobaric analogous states (Hungarian) 4-90955  
<sup>14</sup>C, transfer reaction studies, level population 4-102292  
<sup>24</sup>He(e,e'p)n,  $P_\pi=295$ -500 MeV/c, cross section, isobar configuration influence 4-90996  
<sup>14</sup>N, transfer reaction studies, state population 4-102292  
<sup>28</sup>Si proton resonances, diff. cross sections, analogue states, spectroscopic factors from <sup>27</sup>Al+p 4-73880  
<sup>90</sup>Zr(p,n), 200 MeV, microscopic background calcs. 4-59235  
<sup>90</sup>Zr(p,n), relativistic description to analogue state 4-96038

isobars *see atmospheric pressure and density*

## isoelectronic series

- <sup>35</sup>3p<sup>1</sup> ground configurations, (ionised Cu to Mo), magnetic-dipole transition predicted wavelengths and transition rates 4-68969  
 atomic energy level distributions, HF calc. 4-64333  
 atomic isoelectronic series, second differences in total electronic energies (German) 4-78761  
 atomic positive ions, chem. pot., density functional theory 4-96437  
 electrostatic pot., total energy Z expansion 4-96637  
 hydrogenic fine struct. spectrum in space of const. negative curvature 4-102591  
 hydrogenic ion, electron capture by fully stripped ion, relativistic second Born approx. 4-87209  
 multicharged ions in alternating field, fine struct., two level approx. (Russian) 4-91207  
 noble gases, oscillator strengths, isoelectronic atoms (Spanish) 4-87074  
 nonbijective canonical transformations, use in chemical physics 4-71868  
 P sequence from Cu to Mo, ground config. 4-74140

## isoelectronic series continued

- three electron systems, (2p2p2p) <sup>4</sup>S<sup>o</sup> states, optical emission 4-87175  
 Al isoelectronic sequence, struct. calc. using multiconfig. optimised pot. model, oscillator strengths 4-102592  
 Be II, (2p2p2p) <sup>4</sup>S<sup>o</sup> states, optical emission 4-87175  
 Be isoelectronic series, oscil. strengths and at. wavefunctions accuracy 4-87084  
 Be, transition energy calc. using multiconfig. Dirac Fock and RPA calcs. 4-64364  
 Be-like, oscillator strengths, transition, wavelengths, HF relativistic calcs. 4-106127  
 Be-like atoms, two-electron correl. calcs. 4-64392  
 Be-like ions, fine struct. transitions between 2s<sub>1/2</sub> and 2l<sub>1/2</sub>3l<sub>1/2</sub> configurations, collision and line strengths 4-95072  
 Be-like ions, oscillator strengths, wavelengths, energy levels, O V to Ni XXV 4-67881  
 Be-like ions in solar transition region diagnostics, electron vel. distrib. effects 4-101288  
 C-like ions, optically allowed transitions, oscillator strengths, CI calcs. 4-74196  
 Cl, H-like, is Lamb shift determ. by X-ray transitions meas. using beam-foil excitation 4-74195  
 Cs, isoelectronic series, ionis. pots., relativistic effects, core polaris. and relax. 4-68985  
 Cu-like ions,  $\text{Ge}^{2+}$ - $\text{Mo}^{3+}$ , 3d-4p transitions, anal. 4-69001  
 Fe XV, energy levels, oscillator strengths 4-102617  
 Fe XVII, Ne-like, laser-produced plasmas, 2p<sup>2</sup>3s, 3p and 3d configurations 4-102620  
 Ga isoelectronic sequence from  $\text{Rb}^{6+}$  to  $\text{In}^{18+}$ , 4s<sup>2</sup>4p<sup>2</sup> intervals, fine struct. splitting meas. 4-64400  
 H I like ions, electron impact polarisation of Lyman- $\alpha$  radiation 4-67609  
 H-like atomic orbitals, bound-states 4-64366  
 H-like atoms, Dirac eqn. soln. within algebraic approx. 4-59621  
 H-like heavy ions, energies calc. of 1s, 2s and 2p states 4-83307  
 H-like ions, reson. doublet spectrum in intense elec. field, laser plasma diagnostics appl. 4-84074  
 He isoelectronic sequence, two-electron ions, QED, radiative corrections of order  $\alpha(\alpha Z)^2 mc^2$  4-96466  
 He isoelectronic series, autoionis. states and widths 4-69024  
 He isoelectronic series, poorly convergent perturbation expansions via shifted origin series: atomic 1/Z expansions 4-112089  
 He-like ions, 1s<sub>2s</sub><sup>2</sup>-<sup>3</sup>S<sub>1</sub>-1s<sub>2p</sub><sup>2</sup> <sup>3</sup>P<sub>1</sub> transition freq., two-electron Lamb shifts 4-59675  
 He-like ions, asymptotic eigenvalues and wave functions for restricted quantum-mechanical three-body problems 4-101132  
 He-like ions, electronic density of the nucleus, bounds calcs. 4-68935  
 He-like ions, laser produced B<sup>3+</sup>, Be<sup>2+</sup> and C<sup>4+</sup> plasmas, EUV spectra 4-83320  
 He-like ions, X-ray spectra excited in low-inductance spark plasma 4-74181  
 Li I, (2p2p2p) <sup>4</sup>S<sup>o</sup> states, optical emission 4-87175  
 Li isoelectronic series, radiative decay following charge exchange on neutral gas targets 4-87069  
 Li isoelectronic series, Rydberg energy levels determ. by relativistic quantum defect interpretation 4-102778  
 Li to Ar, core electrons, Coulomb and exchange operators, matrix elements, valence electron only SCF calcs. 4-59630  
 Li-like ion plasma, kinetics excitation spectral line intensities 4-91989  
 Li-like ions, (2p2p2p) <sup>4</sup>S<sup>o</sup> states, optical emission 4-87175  
 Li-like ions, laser produced Be<sup>2+</sup>, B<sup>2+</sup> and C<sup>3+</sup> plasmas, EUV spectra 4-83320  
 Li-like ions principal series, oscillator strengths, photoionisation cross section calc. 4-83332  
 Mg-like positive ions, oscillator strengths and photoionisation cross sections 4-91240  
 Na<sup>+</sup> isoelectronic series, oscil. strengths and photoionis. cross-sections 4-69030  
 Na-like ions, dielectric recombination rates 4-96696  
 Ne-like ions, transitions identification in solar flares 4-72922  
 P-like ions, energy levels, transition probabilities, multiconfiguration DF study 4-106126  
 Rb, isoelectronic series, ionis. pots., relativistic effects, core polaris. and relax. 4-68985  
 Ti X, energy levels, oscillator strengths 3s-3p, 3p-3d transition arrays 4-68955  
 Ti XIII, Ne-like, laser-produced plasmas, 2p<sup>2</sup>3s, 3p and 3d configurations 4-102620  
 Xe, isoelectronic series, 3d photoabsorpt. in near-threshold region, HF approx. 4-83349  
 Zn-like ions from  $\text{Ru}^{14+}$  to  $\text{Dy}^{36+}$ , 4s<sup>2</sup>1S-4s4p<sup>1</sup>P<sub>1</sub> transitions 4-102626

isolators, microwave *see microwave isolators*

## isomer shift

- martensite, elec. cond., thermoelectric power and electronic struct. (Russian) 4-65657  
 Al<sub>2</sub>O<sub>3</sub>-Fe cermets, metal to ceramic bonding, Mossbauer studies 4-109622  
 BaBiO<sub>3</sub>-BaPbO<sub>3</sub>, dielec. and supercond. transitions, Mossbauer line isomer shift 4-65973  
 Ba(Pb<sub>1-x</sub>Bi<sub>x</sub>)O<sub>3</sub>, supercond. transition temp. and Mossbauer line isomeric shift 4-61486  
 BaSnF<sub>6</sub>, fluoride ionic cond. with  $\alpha$ -PbSnF<sub>6</sub> struct., ionic cond. and Mossbauer study 4-92411  
 BaTiO<sub>3</sub>, lattice deformation induced cryst. field variations, Mossbauer and EPR studies 4-71159  
<sup>209</sup>Bi, muonic, magnetic hyperfine structure 4-91368  
 CaFe<sub>2</sub><sup>2+</sup>Fe<sup>3+</sup>(Si<sub>2</sub>O<sub>7</sub>(OH)<sub>2</sub>), ilvaite, electron delocalisation and Mossbauer spectra 4-98993  
 Cd<sub>2</sub>Cu<sub>1-x</sub>Fe<sub>x</sub>O<sub>4</sub>, hyperfine field interactions, Mossbauer spectra 4-65885  
 Cu<sub>2</sub>TaSe<sub>4</sub>(Se<sub>4</sub>)(Te<sub>4</sub>), isomer shifts of 6.2 keV ncl. transition, Mossbauer spectra 4-109104  
 Eu compounds, mixed valence phenomena, phenomenological thermodynamics 4-113906  
 Eu-Hg, Mossbauer spectra and X-ray diff. study 4-76290  
 EuCu<sub>2</sub>Si<sub>2</sub>, mixed valent, isomer shift, mag. susceptibility 4-98573  
 EuIr<sub>2</sub>, Mossbauer isomer shift, trivalent <sup>151</sup>Eu 4-114191  
 EuNi<sub>5</sub>, Mossbauer isomer shift, trivalent <sup>151</sup>Eu 4-114191  
 Eu<sub>2</sub>Ni<sub>17</sub>, Mossbauer isomer shift, trivalent <sup>151</sup>Eu 4-114191  
 EuPd<sub>3</sub>, Mossbauer isomer shift, trivalent <sup>151</sup>Eu 4-114191  
 EuPd<sub>2</sub>P<sub>2</sub>, valence state of Eu and unit-cell vol. anomaly, Mossbauer isomer shift meas. 4-104174

## isomer shift continued

- EuPt<sub>3</sub>, Mossbauer isomer shift, trivalent <sup>151</sup>Eu 4-114191  
 EuRh<sub>2</sub>, Mossbauer isomer shift, trivalent <sup>151</sup>Eu 4-114191  
 Fe-based 3d-metal alloys, impurity charge screening 4-98562  
 Fe-Be and Fe-B-Si amorphous alloys, Mossbauer obs. of short-range order 4-92981  
 Fe-Cr-B, Mossbauer study of packing fraction 4-84877  
 Fe-W-B, Mossbauer study of packing fraction 4-84877  
 FeF<sub>3</sub>, amorphous, Mossbauer-Zeeman spectrum study 4-76294  
 (Fe,Ni<sub>1-x</sub>)M, M=P, B, Si or Al, metallic glass, Mossbauer study of high press. 4-84880  
 Fe<sub>2</sub>Ni<sub>80</sub>Si<sub>10</sub>B<sub>10</sub>, metallic glass, correlated hyperfine interactions 4-70761  
 α-Fe<sub>2</sub>O<sub>3</sub> colloidal particles, Mossbauer parameters, size effects 4-65886  
 (Mg,Fe)S niningite solid solns., Mossbauer studies 4-98992  
 Sb(III) complexes, struct., <sup>121</sup>Sb Mossbauer spectral obs. 4-96583  
 Sn isotope and isomer shift in IBM 4-90961  
 Sn thin film, struct. and transformations during vacuum heating, RHEED and Mossbauer studies 4-75818  
 SnMo<sub>6</sub>S<sub>4</sub>O<sub>4</sub>, O point defects, <sup>119</sup>Sn Mossbauer spectra studies 4-103746  
 U<sub>1-x</sub>Np<sub>x</sub>O<sub>2</sub> solid solns., <sup>237</sup>Np Mossbauer effect and magnetisation 4-76125  
 Zr<sub>0.25</sub>Ni<sub>0.75+x</sub>Ti<sub>x</sub>Fe<sub>2-2x</sub>O<sub>4</sub>, hyperfine field meas., Mossbauer effect study 4-71224

## isomerisation

- acetone/enol ion, non-ergodic dissoc. 4-93519  
 alkali halide dimers, electric dipole polarisabilities 4-69239  
 allene, ion-molecule reactions, photoionisation mass spectra 4-93517  
 allyl cations, phenyl substituted, gas phase isomerisation, mass spectra investig. 4-11882  
 1,4-anthraquinone, aryloxy derivatives, photochem. migration of acetyl group 4-109640  
 9,10-anthraquinone, aryloxy derivatives, photochem. migration of acetyl group 4-109640  
 benzene, excited to 4.7 eV above ground state, red fluoresc. 4-87147  
 benzene, nonradiative processes, photoacoustic spectra, photochemical isomerisation obs. 4-91302  
 benzene cation radical, unimol. and bimol. reactions, kinetic energy release distrib., rate consts., PIPECO studies 4-89259  
 benzene cation-d<sub>0</sub>(d<sub>6</sub>), excited states, intramolecular relax., fluoresc. study 4-83400  
 bilirubin, inverse Raman spectroscopy, hydrogen bonding, photoactivation 4-115016  
 butadiene, one-end pyramidalised, sudden charact. of sudden polarisation effect 4-99751  
 butene isomers, isomerisation, rate consts. for proton transfer, dipole moment 4-89262  
 butyl radical cation+acetylene, reactions, kinetic energy release distrib., rate consts., PIPECO studies 4-89259  
 carboxyl positive and negative ions, collisionally induced dissoc. 4-71879  
 2-chloroallyl alcohol in low temp. matrices, thermal and IR-induced conformer interconversion processes 4-104967  
 cyclobutene/butadiene, thermally allowed electrocyclic interconversion, substituent effects, MNDO calcs. 4-85306  
 cyclobutyl cation radical+acetylene, reactions, kinetic energy release distrib., rate consts., PIPECO studies 4-89259  
 1,2-di-(1-naphthyl)ethylenes, cis-trans-photoisomerisation, luminesc. and X-ray studies 4-93540  
 diphenyl butadiene, solns. and jets, isomerisation, nonradiative decay 4-71902  
 1,4-dithiane, conformational change from chair to boat upon ionisation, optical spectra, MO calcs. 4-89246  
 enamino aldehydes (ketones) (amides), UV spectra, CNDO/S CI calcs. 4-78789  
 energies, lower and upper bounds calcs. 4-114771  
 ethylene, one-end pyramidalised, sudden charact. of sudden polarisation effect 4-99751  
 fluoro-2-ethanol, trans conformer, FT IR and Raman spectra, vibr. anal. 4-64481  
 2-fluoroethylamine in solid Xe, thermal and IR-induced conformer interconversion processes 4-62170  
 formate positive and negative ions, collisionally induced dissoc. 4-71879  
 free radical liq. phase chem., radical struct. and reaction rates using positive muon probes 4-71885  
 hexadienes, laser-induced IR multiphoton isomerisation reactions 4-81420  
 hexafluorobenzene, excited to 4.7 eV above ground state, red fluoresc. 4-87147  
 2-hydroxypyridine to 2-pyridone tautomeric equil., proton transfer mechanism 4-76977  
 ideal gas, mol. beam, isomerisation reaction rate 4-81403  
 indolizine and azaindolizines struct. relationship and their ability to undergo rearrangement 4-59907  
 isoformyl ion+H (He), metastability and isomerisation, interstellar appl. 4-91327  
 isopropyl formate and acetate, rearrangement and fragmentation, 4K matrix ESR study 4-59810  
 methyl formate radical cation, matrix ESR study, rearrangement 4-59809  
 methylenebis(oxy), H at migration reaction channel, formed in formaldehyde oxidation 4-71897  
 molecular gases, nonequilibrium chem. kinetics, linear mixture rule deviations 4-99747  
 octahedral complexes XY<sub>6</sub>, isomerisation, chem. graph symmetry props. 4-99758  
 cis,trans-1,3,5,7-octatetraene in n-alkane matrices, one-photon fluoresc. spectra, vibr. resolved 4-64529  
 polyacetylene: NaCl<sub>2</sub> film, Mossbauer, EPR and Raman studies 4-114193  
 polyacetylene:Li, vibr. props., Raman study, cis-trans isomerisation 4-75632  
 trans-polyacetylene, absorb. and resonant Raman scatt. spectra 4-109189  
 polyacetylene, electrochemical doping, in situ Raman scatt. 4-76465  
 polyacetylene, electrochemical doping, transient effects, EPR obs. 4-84846  
 cis-polyacetylene, Li doping, diffusion EPR and Raman study 4-88345  
 polyacetylene, polymerisation and oxidation using Luttinger's catalyst 4-66590  
 trans-polyacetylene films, thermally isomerised and doped/dedoped 4-65196

## isomerisation continued

- polyphenylacetylene and poly(pentadeuterophenylacetylene), microstructure and cis-trans isomerisation 4-75322  
 propene, sigmoidal shifts, MC-SCF STO calcs. 4-104972  
 propylene, one-end pyramidalised, sudden charact. of sudden polarisation effect 4-99751  
 propynal, photodissoc., pot. energy surfaces, ab initio and CI calcs. 4-66601  
 1-(1-pyrene)-3-(dimethylaminophenyl)propane, conformational dynamics viscosity and temp. depend. 4-62168  
 pyridine, excited to 4.7 eV above ground state, red fluoresc. 4-87147  
 13-cis-retinal, prereson. Raman and IR spectra, vibr. anal., isomerisation 4-89502  
 retinal chromophores, photoisomerization, adiabatic potential surfaces 4-109807  
 retinals, isomeric, transient Raman spectra, lowest excited triplet state, cis-trans isomerisation 4-91265  
 rhodopsin chromophore, photoisomerisation, role of bond lengths change 4-99814  
 trans-stilbene, in n-alkohols, isomerisation dynamics, UV ps. absorpt. recovery obs. 4-114775  
 stilbene, triplet state, benzophenone-sensitised photoisomerisation 4-62174  
 meso-tetraphenylporphyrine, soln., low temp. dynamic NMR 4-78869  
 trans-thioindigo, photoisomerisation studied by picosecond and nanosecond laser photolysis method 4-99772  
 triatomic mol., bending vibr., energy level pattern studied using semirigid-bender model 4-78232  
 vinyl cations, phenyl substituted, gas phase isomerisation, mass spectra investig. 4-71882  
 Ag<sub>2</sub>Mo<sub>4</sub>O<sub>33</sub>, interlayer reactions with n-alkylammonium ions 4-89284  
 BCN, ground state, geometry, transition state, isomerisation reaction, ab initio calcs. 4-71908  
 C<sub>6</sub>H<sub>5</sub><sup>+</sup>+H<sub>2</sub>, reactions, kinetic energy release distrib., rate consts., PIPECO studies 4-89259  
 [C<sub>6</sub>H<sub>5</sub>O]<sup>+</sup>, isomerisation, ab initio SCF calc. in gas phase (French) 4-71880  
 Fe(CO), IR laser-induced isomerisation and Jahn-Teller effect 4-66567  
 H<sub>2</sub>, ortho-para conversion on mag. surfaces, dynamical aspects 4-70555  
 HCN, ground state, geometry, transition state, isomerisation reaction, ab initio calcs. 4-71908  
 HNC to HCN isomerisation, rate consts. calc. using RRKM model 4-66560  
 H<sub>2</sub>PP, ab initio SCF and CI study of stability and electronic struct. 4-74164  
 HPPH, ab initio SCF and CI study of stability and electronic struct. 4-74164  
 HSNO, Ar low temp. matrix, photoinduced isomerisation, IR spectra 4-89249  
 N<sub>2</sub>H<sub>2</sub> and its fluoro derivatives, energy difference between geometrical isomers bond orbital calcs. 4-87036  
 ZnO oriented crystal, cryst. violet dye adsorpt., press. effect 4-98442

## isomerism

- see also isomerisation; nuclear isomerism; rotational isomerism*  
 acetaldehyde, ionised, keto-enol tautomerism mechanism and dissociation, ab initio MO study 4-91196  
 4-acyl-3-methyl-1-phenylpyrazol-5-ones in chloroform, IR, <sup>1</sup>H and <sup>13</sup>C NMR spectra 4-74242  
 alcohols, aliphatic, OH oscillators, fourth overtone IR spectra 4-112166  
 benzamide molecules, mag. anisotropies, relation to isomerism and H-bonding 4-64635  
 3,1-benzoxazines, substituted, tautomerism, UV, IR and mass spectrosc. obs. 4-64487  
 diazoles, N,N-linked and their quaternary salts, MNDO calc. on conformation 4-107282  
 2-bromo-3-chloro-1-propene, gas phase mol. struct. and conformational composition determ. by electron diff. 4-69212  
 1-bromo-bipropargyl, gas phase electron diff., conformation and mol. struct. 4-69216  
 1,3-butadiene, adsorbed on silica surface, Fourier transform IR spectra 4-78843  
 butanal, conformational anal. and mol. struct., ab initio calcs. 4-102581  
 butanes, isomer yield following γ-ray radiation degradation of polyolefins 4-77015  
 butenes, isomer yield following γ-ray radiation degradation of polyolefins 4-77015  
 carbene-type cation radicals, gas-phase chem. 4-114791  
 cis-1-chloro-3-fluoropropene, electron diff., mol. struct. and conformation 4-69213  
 cyclohexane+triethylamine mixtures, keto-enol tautomerism 4-113589  
 cyclohexane-1-d, isomers, IR and Raman spectra, vibr. anal., ab initio HF calcs. 4-59770  
 cytosine, tautomerism, ab initio calcs. 4-112100  
 cytosine and derivatives, matrix isolation, IR spectra 4-87104  
 cytosine and isocytosine methyl derivatives isolated in N<sub>2</sub> matrix, IR spectra 4-62442  
 dialkylphosphate ions, conform., micellisation effects, <sup>13</sup>C NMR chem. shift and <sup>31</sup>P/<sup>13</sup>C coupling 4-107365  
 2,3-dibromo-1-propene, mol. struct. mechanics, electron diff. study 4-112272  
 1,3-diketones, tautomeric equil., H bonds, NMR spectra 4-59805  
 dimethylcyclohexane, ring decomp., skeletal conform. conservation 4-114806  
 ethylamines, trans and gauche forms, vibr., force const., ab initio MO calcs. 4-59622  
 fatty acid esters, stereoisomers, laser spectrochromatographic identification 4-62269  
 fluorinated ethylamines, in inert gas matrices, IR and Raman spectra, conformational behaviour 4-59759  
 fluorochloroacetanitriles, mol. dynamics, racemic modification, for IR spectra 4-104591  
 fluoropentanes, isomerie, multiphoton dissoc. selectivity and energetics 4-99805  
 5-fluorouracil, tautomerism, ab initio calcs. 4-112100  
 gangliosides, fast atom bombardment mass spectrometry analysis and identification 4-7180  
 1-halopropanes, far IR and Raman spectra, conformational stability 4-87113  
 1,5-hexadiene-3-yne, gas phase electron diff. and mol. mechanics calcs., conformation and struct. 4-64605

- erism continued
- xydroxy styrylquinolinium dyes, acid-base tautomeric equilib., electronic struct. (*German*) 4-59645
- 2-hydroxy-born-2-yl)phenylacetic acids, diastereoisomeric, circular dichroism curves, configurations 4-64524
- iodo-2-methylbutane, force consts., vibr. assignment, normal coordinate calcs. 4-112154
- isobutylamine monohydrate, vibr. spectroscopy 4-104611
- isoprene, struct. and conformations by vibr. spectroscopy and gas phase electron diff. 4-64606
- isoprene-propylene copolymer, regularly alternating, thermodynamic props., stereoisomerism effects (*Russian*) 4-103970
- lactic acids, mol. dynamics., racemic modification, for IR spectra 4-104591
- methyl dichlorophosphite, PES and electronic struct., orbital model of conformational isomerism 4-112118
- methyl dichlorothiophosphite, PES and electronic struct., orbital model of conformational isomerism 4-112118
- methylcyclopentadiene, positional isomers, laser spectrochromatographic identification 4-62269
- methylethers, conformation, vibr., IR, Raman  $^{13}\text{C}$  and  $^1\text{H}$  NMR study 4-87136
- methylsilanone and isomers, stabilities, SCF calcs. 4-74146
- monoalkylphosphate ions, conform., micellisation effects,  $^{13}\text{C}$  NMR chem. shift and  $^{31}\text{PO}_4^{3-}$  coupling 4-107365
- naphthalene-tetracyanoethylene system, electron donor-acceptor orbital corrs. 4-74163
- 2-nitraminopyridine, and methyl derivatives, electronic struct., UV spectra, PPP calcs. 4-64486
- organophosphorus compounds, PES and electronic struct., orbital model of conformational isomerism 4-112118
- perchloro-1,5-hexadiene-3-yne, gas phase electron diff. and mol. mechanics calc., conformation and struct. 4-64605
- 2-phenyl-(4'-hydroxycoumarinyl-3')-methylindane-1,3-dione derivatives, ring-chain tautomerism phenomena 4-59912
- poly(tetrafluoroethylene-alt-trifluoronitrosomethane) isomerism,  $^{19}\text{F}$  NMR spectroscopy 4-102833
- polyacetylenes, ab initio Hartree-Fock calcs. 4-96728
- polyesters, with mesogenic groups and flexible spacers, conform. states investig. (*Russian*) 4-59936
- polyolefins,  $\gamma$ -ray radiation degradation, isomer yields for butanes and butenes 4-77015
- porphyrin dimers, covalently linked, isocycle-containing, NH tautomerism, spectrosc. investig. 4-107355
- porphyrin dimers, covalently linked, isocycle-containing NH tautomerism, spectrosc. investig. 4-107355
- porphyrins, isocycle-containing, NH tautomerism, spectrosc. investig. 4-107355
- propanal, conformational anal. and mol. struct., ab initio calcs. 4-102581
- propionyl chloride, struct. and conformation determ. by electron diff., microwave spectra, force const. 4-69214
- carbosine derivatives, cis-trans isomerism around urethane and amide bond 4-96577
- tetraselenafulvalenes, substituted, cis/trans assignments, coupling consts.,  $^{77}\text{Se}$  NMR 4-102701
- thioureas, substituted, IR spectra, conformation 4-59769
- thymine, tautomerism, ab initio calcs. 4-112100
- uracil, tautomerism, ab initio calcs. 4-112100
- vibrational circular dichroism meas. of single enantiomer on FT-IR spectrometers 4-102816
- zinc porphyrins, ODMR, triplet-state zero-field splitting parameters 4-64519
- $\text{C}_2\text{NH}_2^+$  isomers, struct., relative energies ab initio MO STO calcs. 4-102572
- $\text{C}_2\text{NH}_2^+$  isomers, struct., relative energies ab initio MO STO calcs. 4-102572
- $\text{CSiF}_2$  isomers, lowest singlet and triplet surfaces, ab initio calcs. 4-107424
- Co (III) complex, bis(ethylenediamine)-Co (III)  $^{13}\text{C}$  NMR signals, assignment 4-91278
- Cu ( $\pi$ ) complexes, crystal struct., EPR and optical study, stereochemistry (*French*) 4-70075
- $(\text{H}_2\text{CN})^+$ , generation, heat of form. and dissoc. characts. 4-109633
- $(\text{H}_2\text{CN})^+$ , generation, heat of form. and dissoc. characts. 4-109633
- HO $\cdot$ , neutral and cationic struct., ab initio calcs. 4-59616
- $\text{PF}_3\text{NH}_2$ ,  $\text{N}_2$  matrix isolated, intramolecular rearrangement, vibr., IR obs. 4-78845
- Rh complexes, stereochemical rigidity, NMR spectra 4-78861
- $\text{SiC}_2$ , energetically low-lying silacyclopolyne isomer, SCF and CI calc. 4-68972
- morphism**
- $\text{KH}_2\text{PO}_4$ -type transition, struct. studies, review 4-76351
- $\text{Rb}_2\text{ZnBr}_4$ , isomorphs, EFG tensor modulation, model calc. 4-75904
- thermal transformations**
- pearlite interlamellar spacing, review of data 4-93293
- steel, martensitic transformations in 18kNVA steel, residual austenite (*Russian*) 4-104779
- steel, microalloyed, hot-rolled, isothermal decomp. of austenite 4-99409
- Fe-Cr-Co alloy, Ti effect on rate of high-coercivity transform. 4-93296
- Fe-Nb-C(-B), isothermally transformed, microstruct. 4-114510
- isotope detection**
- see also mass spectra
- mass spectrometer upgrading for trace amounts analysis 4-105081
- stable isotope ratios determ. with dual sample inlet comparison method, ref. line selection, background correction (*Chinese*) 4-112301
- $^{10}\text{Be}$  detection and conc. meas. using tandem accelerator at 3 MV 4-64632
- Rn mapping using LR-115 particle track detector film 4-59584
- isotope effects**
- see also isotope shifts
- acetone, soln., partial molal and molar vols., D isotope effect 4-65322
- acetone cation,  $\gamma$ -irrad.,  $^{13}\text{C}$  ESR and ENDOR investig. 4-69114
- acetonitrile, soln., partial molal and molar vols., D isotope effect 4-65322
- 1-adamantanamine hemiperchlorate, IR spectra, (NHN) $^+$  bridges, temp. and isotope effects 4-61701
- alkane eliminations from radical cations through ion-radical complexes 4-114778
- all-trans-n-alkanes, cryst. struct. and C-H stretching modes 4-70126
- anharmonic crystals, local vibrs., local instability, self-consistent harmonic approx. 4-88258
- isotope effects continued
- benzene, mol. dynamics simulations of self-diffusion coeffs. in binary Lennard-Jones solns., isotope effects 4-75253
- benzene dimers, isotope effects in seeded supersonic jet 4-59651
- benzene- $\text{d}_0$ (- $\text{d}_6$ ), vibr. anal., force const. 4-91246
- benzene- $\text{d}_0$ ( $\text{d}_6$ ), solns. and mixtures, isotope effects, isothermal compressibility 4-84330
- borates, carbonates and nitrates, intermolecular vibrational coupling, IR spectra 4-65350
- carbocations, normal mode vibr. freq. calc., appl. to secondary deuterium isotope effects 4-64454
- chemical reactions, vibrational intensities, G sum rule formulation 4-89277
- chloroacetylene cations, supersonically cooled, spin-orbit components, vibr. freq., UV emission spectra 4-69225
- N-chloroisocyanide dichloride, gas, liq. and solid, vib. force consts., IR and Raman obs. 4-59739
- chlorophosphathene, microwave spectra, quadrupole and dipole moments, struct. parameters 4-59726
- choline hydroxide, cryst., H bonding, IR study 4-114263
- cubane, force consts., vibr., IR and Raman spectra, HF level calcs. 4-59694
- cyclohexadienyl radical, muonium substituted +2, 3-dimethyl-1,3-butadiene, rate const. 4-71887
- cyclohexane, soln., partial molal and molar vols., D isotope effect 4-65322
- cyclohexane- $\text{d}_0$ ( $\text{d}_{12}$ ), solns. and mixtures, isotope effects, isothermal compressibility 4-84330
- cyclopentene ozonide, synthesis, microwave spectra, elec. dipole moment and mol. struct. 4-59716
- diacyl phosphatidylcholines, ice melting induced phase transition 4-61676
- dichloromethane- $\text{d}_0$ ( $\text{d}_2$ ), force consts. thermodynamic props., vibr. anal. 4-64448
- m-dinitrobenzene- $\text{d}_0$ ( $\text{d}_4$ ), vibr. normal coordinate anal., IR and Raman spectra 4-59765
- ethane- $\text{d}_0$ (- $\text{d}_4$ ), Raman intensities determ. 4-74249
- N-ethyl-3-acetylcarbazole, emission props., solvent effects 4-107390
- ethylamines, trans and gauche forms, vibr., force const., ab initio MO calcs. 4-59622
- FCC lattice, tracer correl. factors for diffusion via bound vacancies, Monte Carlo simulation 4-75715
- fluoromethane, photoinduced drift separation of nuclear modifications 4-107407
- fluoromethyl- $\text{d}_0$ (- $\text{d}_1$ ) cations, ground states, photoelectron spectrosc. obs. 4-107403
- formaldehyde, equilib. struct. calcs. using isotopic differences in  $r_2$  struct. 4-68984
- formaldehyde metastable cations, unimol. decay 4-68988
- formaldehyde- $\text{d}_0$ (- $\text{d}_2$ ) lower vibr. energy levels, var. calcs. 4-74219
- formyl radical +  $\text{NO}(\text{O}_2)$  reaction, collision complex form. 4-71899
- formyl radicals, vibr. excited, reactions and relax. 4-71898
- hard sphere liq. mixtures, diffusion coeff., mol. dynamics simulation 4-92399
- ice, hexagonal, translational lattice vibrs. and permittivity, temp. and press. 4-76309
- ice  $\text{I}_h$  to IX transition, press. effect on Raman spectrum at low temp. 4-61692
- IR and microwave lines, difference freq. laser spectra 4-59756
- lanthanide (III)-Ag (I) NMR shift reagents, secondary D isotope effects 4-102710
- liquid phases, IR spectra, dielectric shift, mol. model, vapour press. isotope effects 4-64460
- metal, superconducting state parameters pseudopotential approach 4-61478
- metals, BCC and FCC, H and He impurities, self-trapping phenomena 4-80056
- metals, BCC migration process of H isotopes calc. 4-65465
- metals, moon states, recent progress 4-65902
- methane- $\text{d}_0$ (- $\text{d}_4$ ) gas, DC breakdown strength, isotope depend. 4-79723
- methane- $\text{d}_0$ ( $\text{d}_4$ ), matrix isolated, vibr. modes, Raman study 4-87122
- methanol, electron impact, H excited atom prod. 4-112286
- (+)-(3R)-methylcyclohexanone, skeletal motion, chiral mixing, Raman optical activity 4-102687
- methylidimethylphosphinate, and isotopically substituted derivatives, vibr., config., IR obs. 4-87116
- methylidimethylphosphinate, isotope derivatives, vibr., IR and Raman spectra 4-83378
- neptunium tetrakis(methylborohydride), mag. props., optical and EPR spectra 4-88718
- organic cpds., deuteration effects,  $^{13}\text{C}$  NMR spin-echo investig. 4-64502
- phenoxyl radical- $\text{d}_0$ (- $\text{d}_3$ )(- $\text{d}_5$ ), aq. solns., vibr. modes, reson. Raman obs. 4-107352
- 1-phenylethanol,  $^{13}\text{C}\{^1\text{H}\}$  polarisation transfer, isotopic labeling NMR 4-59800
- phonon focusing in highly dispersive and isotopically impure crystals, theory 4-61011
- 2-phenylene- $\text{d}_0$ (- $\text{d}_2$ ) low-freq. vibr. spectra and ring-puckering potential function 4-102680
- polyacetylene, photoinduced absorption, nonlinear dynamics and breathers 4-75877
- cis-polyacetylene films, luminesc., D effects, reson. Raman spectra 4-109264
- propyne-HF(DF) microwave spectrum and props. 4-74229
- pyramidal symmetrical  $\text{XY}_3$  mols., Coriolis coupling consts., geometry parameters, isotopic invariants 4-64636
- quinizarin, glass matrix, photochemical hole burning, visible spectra 4-77014
- meso-tetraphenylporphine, stretching bands, isotope effects, IR spectra 4-74240
- TGSe, phase transition rel. to deuteration 4-76387
- thietene, dipole moment, substitution struct., microwave struct. 4-78832
- thiobenzenide, polymorphism, IR obs. 4-61686
- thioformaldehyde, equilib. struct. calcs. using isotopic differences in  $r_2$  struct. 4-68984
- trifluoromethane- $\text{d}_0$ ( $\text{d}_3$ ), isotopically selective IR multiphoton dissoc. 4-112240
- 2,4,5-trimethylbenzaldehyde- $\text{d}_0$ ( $\text{d}_1$ ), cryst. isolated, dipole moments, isotope effect, Stark and phosphoresc. study 4-69128
- 1,2,4-triolane, microwave spectrum, struct. and elec. dipole moment 4-78829
- uracil- $\text{d}_0$ ( $\text{d}_2$ ), vibr., force consts. CNDO/2 calcs., IR spectra 4-59699

## isotope effects continued

- water, liq. struct. at room temp., time of flight neutron diffr. study 4-92053  
 Ag, impurity diffusion, isotope effect meas. 4-65476  
 Ag-Sn(In) dilute alloys, correlated impurity diffusion jump processes, isotope effect 4-84446  
 Au, impurity diffusion, isotope effect meas. 4-65476  
 CO+H(D), collisional excitation, cross sections, quasiclassical trajectory study 4-78950  
 CO<sub>2</sub>, laser bands, freq. tables, rovibr. consts. 4-60015  
 Ca<sub>3</sub>Cr<sub>2</sub>Si<sub>2</sub>O<sub>12</sub>, synthetic garnets, Cr coordination and vibr. props., IR study 4-65249  
<sup>111,113</sup>Cd<sup>+</sup> matrix isolated, fast atom bombardment, ESR investig. 4-74218  
<sup>111,113</sup>CdOH matrix isolated, fast atom bombardment, ESR investig. 4-74218  
 Cl+ethyl chloride-d<sub>3</sub> (-d<sub>4</sub>) (-d<sub>5</sub>), D abstraction from methyl-d<sub>3</sub> group 4-62163  
 Cr, permeation of H and D, diffusion, permeability, and solubility (*German*) 4-103992  
 Cr(<sup>12</sup>CO)<sub>6</sub>, in Ar matrix, FT-IR spectra, isotropic substitution effects 4-12183  
 Cr(<sup>12</sup>CO)<sub>5</sub>(<sup>13</sup>CO), in Ar matrix, FT-IR spectra, isotropic substitution effects 4-12183  
 CsH<sub>2(1-3)</sub>D<sub>2</sub>PO<sub>4</sub>, ferroelectric, dielec. relaxation, activation energy, isotope effects 4-65989  
 CsND<sub>2</sub>, molar heat capacity, X-ray and neutron diffr. study (*German*) 4-60997  
 CsNH<sub>2</sub>, molar heat capacity, X-ray and neutron diffr. study (*German*) 4-60997  
 Cu, impurity diffusion, isotope effect meas. 4-65476  
 β-CuZn, self-diffusion, influence of order-disorder transition 4-113695  
 D+FD reactive reson., partial widths and isotope effects calc. by reaction path Hamiltonian model 4-71890  
 D<sub>2</sub>O, electron impact dissoci., D\* emission cross section 4-107462  
 D<sub>2</sub>O ice, hexagonal, translational lattice vibrs. and permittivity, temp. and press. 4-76309  
 D<sub>2</sub>S, nucl. hyperfine interactions, elec. dipole moments, mol. beam elec. reson. 4-59803  
 F+H<sub>2</sub>(HD)(D<sub>2</sub>), collinear exchange reactions, probability densities, stabilisation calcs. 4-81415  
 γ-Fe, high purity, thermotransport, isotope effect 4-108664  
 FeCo, self-diffusion, influence of order-disorder transition 4-113695  
 Fe<sub>40</sub>Ni<sub>60</sub>, amorphous alloys, neutron irradi., mag. props. isotope effects 4-75541  
 Fe<sub>3</sub>O<sub>4</sub>, magnetite, Verwey transition 4-88447  
 Fr hyperfine struct. intervals, relativistic many-body calcs. 4-68986  
 Ge, isotopically enriched, low-field anomalous muonium depolarisation 4-71241  
 Ge surface, nonequilibrium charge carrier recombination, isotopic effects 4-92750  
 GeS, hyperfine and isotopically invariant parameters, microwave spectra 4-59728  
 H and D atoms, can X-ray cryst. struct. anal. distinguish between them 4-75233  
 H bonded cryst., isotope effect on critical temp. 4-70341  
 H<sup>+</sup> transfer reactions, kinetic isotope effect, solvent depend. 4-104968  
 H+FH reactive reson., partial widths and isotope effects calc. by reaction path Hamiltonian model 4-71890  
 H+H<sub>2</sub>(MuH), H and Mu exchange, isotope effects, semiclassical techniques 4-71884  
 H<sub>2</sub><sup>+</sup> low-lying energy levels, nonadiabatic calcs. 4-102613  
 H<sub>2</sub><sup>+</sup>, muonic, low-lying energy levels, nonadiabatic calcs. 4-102613  
 H<sub>2</sub>+hydrocarbon ions, association reaction rates, endothermic reactivity correl. 4-99767  
 H<sub>2</sub>+methyl-H+methane, D isotope effect, ab initio pot. surface, transition state theory 4-81416  
 H<sub>2</sub><sup>+</sup>, vibr.-rot. levels, IR predissociation spectra 4-107344  
 H<sub>2</sub><sup>+</sup>+He, collisional dissoci., form. of H<sub>2</sub><sup>+</sup> 4-66555  
 HCN(DCN), vibr. dipole moment function, RF-IR double reson. 4-69122  
 HCl, ionisation pot. D isotope effect, EELS 4-83467  
 (HCl)<sub>2</sub>, stretching bands rot. struct., high resolution IR spectra 4-107343  
 H<sub>2</sub>(D<sub>2</sub>) gas, DC breakdown strength, isotope depend. 4-79723  
 (HF)<sub>2</sub>, in solid Ar matrix, FT IR spectra 4-69066  
 HNCSe, IR spectrum, vibr. assignment 4-102675  
 HNCSe, millimeter wave spectrum and struct. 4-102673  
 H<sub>2</sub>O electron impact dissoci., H\* emission cross section 4-107462  
 H<sub>2</sub>O, equilib. struct. calcs. using isotopic differences in r<sub>e</sub> struct. 4-68984  
 H<sub>2</sub>O gas, including D(T) isotope, transport props. prediction at high temps. 4-60576  
 HOCl, isotopic species, atm. monitoring, microwave and nm wave spectra 4-59729  
 H<sub>2</sub>S (HDS), nucl. hyperfine interactions, elec. dipole moments, mol. beam elec. reson. 4-59803  
 H<sub>2</sub>S-HCl, H bonded complex, rot. consts., Fourier transform microwave obs. 4-59732  
 H<sub>2</sub>S-HF, hyperfine coupling consts., rot., pulsed-nozzle Fourier transform microwave spectra 4-107333  
 (H<sub>2</sub>S)<sub>n</sub> and (D<sub>2</sub>S)<sub>n</sub>, mol. beam photoionisation and fragmentation 4-69154  
 HSNO, Ar low temp. matrix, photoinduced isomerisation, IR spectra 4-89249  
 He+H(D), H(D) 2s and 2p excitation, integral cross sections 4-102786  
 I+HI(MuI), H and Mu exchange, isotope effects, semiclassical techniques 4-71884  
 α-N<sub>2</sub>, librational motion, anharmonic effects 4-103892  
 NH<sub>3</sub>, collisional relax., steady-state IR-IR double reson. 4-69188  
 NH<sub>4</sub>HSeO<sub>4</sub>, ferroelec., with varying D content, phase transitions, dielec. anomalies 4-99061  
 (NH<sub>4</sub>)<sub>2</sub>H(SeO<sub>4</sub>)<sub>2</sub>, thermal and dielec. studies, 90 to 357K, isotope effects 4-70365  
 NH<sub>3</sub>(ND<sub>3</sub>) gas, DC breakdown strength, isotope depend. 4-79723  
 NbH<sub>2</sub>, dynamic muon-H correlations, positive muon as a tracer 4-65431  
 NbH<sub>2</sub>(D<sub>2</sub>), acoustic phonon assisted H diffusion 4-61139  
 Ni<sup>2+</sup> complexes in aq. soln., muonium addition reactions and spin conversion reactions, muon spin rot. study 4-71957  
 Np(BH<sub>4</sub>)<sub>4</sub>, in Zr(BD<sub>4</sub>)<sub>4</sub>, D isotope effects, mag. props., optical and EPR spectra 4-88718  
 O+H<sub>2</sub>(D<sub>2</sub>) reaction dynamics, reduced dimensionality quantum and quasiclassical rate consts. 4-114784

## isotope effects continued

- O+H<sub>2</sub>(HD)(D<sub>2</sub>) exchange reactions, quasiclassical trajectory calcs. 4-71894  
<sup>18</sup>O<sub>2</sub>, thermal electron attachment mechanism, isotope effect studies inert gases and hydrocarbons 4-102795  
 PH(D), X<sup>2Σ</sup> vibronic state, far-IR laser mag. reson. 4-59814  
 PdH(D), supercond. transition temp., effect of zero-point motion 4-709  
 PdH(D)<sub>x</sub>, vibr. spectra, neutron inelastic scatt. meas., isotope depend. supercond. transition temp. 4-98229  
 PdH<sub>2</sub>(D<sub>2</sub>), acoustic phonon assisted H diffusion 4-61139  
 PdT<sub>2</sub>, T solubility, partial molar enthalpy and nonconfigurational entropy 4-92372  
 Ru catalysts, adsorbed N<sub>2</sub>, temp. programmed desorption and isotope study 4-93558  
 Si:Ge, Ge diffusion, isotope effects, SIMS studies 4-65491  
 Si:Li and Si:Li, C, electron irradi., luminesc. decay time, absorpt., isotope splitting, and Zeeman meas. 4-71434  
 Si:O, isotope effects and photoluminescence spectra 4-104661  
 SiH<sub>4</sub>, D isotope substituted, polar tensors, effective charges, IR intensities 4-107342  
 Si<sub>3</sub>N<sub>4</sub> films, amorphous, hydrogenated and deuterated, prepared from plasma-enhanced CVD, IR absorpt. spectra 4-81021  
 W (111), H and D diffusion, fluctuation method anal. 4-104088  
 YbO, laser fluoresc. spectroscopy, 0<sup>0</sup>→1<sup>2</sup> transitions obs. and anal. 4-64535
- isotope exchanges**  
 fluoroform+HOD, equilib. D distrib., temp. depend., isotope exchange 4-81419  
 isotope enrichment by high press. ion exchange displacement chromatography 4-59905  
 Tokamak discharge chamber, H interaction 4-103512  
 CO self-exchange reaction mechanism studied using mercury photosensitisation technique 4-89270  
 Pt/TiO<sub>2</sub>, H<sub>2</sub> and D<sub>2</sub> isotope scrambling, thermal desorption 4-80377  
 Rh surface, isotope exchange-reaction of CO 4-81479
- isotope relative abundance**  
*see also element relative abundance*  
 Allende meteorite, presolar age indicated by Ar isotopes 4-105906  
 atmospheric H<sub>2</sub>O vapour at Palisades, New York, USA 4-115539  
 Bishop Tuff, California, USA, Nd, Sr, O isotope study of zoned volcanic rocks 4-89891  
 BWR spent fuel, <sup>137</sup>Cs γ-spectrometry for burn-up verification and isotope comp., safeguards 4-106983  
 cosmic ray detector, high charge and energy resolution for isotope measurements 4-102502  
 Cretaceous-Tertiary boundary geochem. at York-Canyon, New Mexico 4-89892  
 diamonds from Mbuji Mayi kimberlite district, Zaire, C. N., isotopic 4-89893  
 Earth crust, Nd and Hf isotopes rel. to mean life of continents 4-94047  
 Earth mantle, large-scale SR and Pb isotope anomaly in Southern Hemisphere 4-89899  
 FIDES automated U-enrichment meter for nuclear safeguards inspection 4-106992  
 galactic cosmic ray nuclei, age and source characts., isotopic comp. and analysis 4-94357  
 geochemistry, Pb isotope ratios throughout geological time 4-89898  
 HEU detection in UF<sub>6</sub> centrifuge process piping, γ-meas., safeguards applications 4-106994  
 ice shelves meltwater, isotopic tracers and salinity used for shelf characteristics 4-67440  
 in meteorites, conference, London, England (1984 May 24) 4-95036  
 inert gases in Antarctic shergottite EETA 79001, possible Martian origin 4-110575  
 interstellar abundances 4-82544  
 isotopic cataphoresis in a crossed-field plasma centrifuge 4-75212  
 isotopic ratio estimation using pulse counting mass spectrometric data 4-114866  
 LEU fuel, non-destructive assay using photoneutron interrogation, safeguards appl. 4-106990  
 LEU samples, active well coincidence counter meas. for safeguards applications 4-106991  
 measurements in deep-sea sediments 4-110128  
 meteorite isotopic anomalies and solar nebula characts. 4-77736  
 meteorites, isotope anomalies, role of grain physics and chem. 4-77706  
 meteorites, isotopic anomalies, implications for solar nebula characteristics 4-77733  
 methane, IR transition moments, isotopic depend. 4-69146  
 Mount Ontake volcano, Japan, <sup>3</sup>He emissions rel. to volcanic activity 4-89902  
 Mount St. Helens, Washington, USA, radioactive <sup>210</sup>Pb, <sup>210</sup>Po in volcanic ash 4-115367  
 New Quebec, Canada, ice lenses in peat bogs, geochemistry, isotope content and genesis 4-100637  
 S Peru, Pb isotope study of magma-tracer interaction in Andes 4-10547  
 petroleum and gas prospecting in Oklahoma, USA, by soil gas radioactivity method 4-110104  
 protosolar nebula, contributing nucleosynthesis, duration and rate 4-77735  
 Queriguit, France, granite-granodiorite complex genesis, recycling processes, Nd-Sr isotopic systematics 4-110096  
 radioactive dating, appl. to rocks for solar nebula characteristics 4-77734  
 rare isotopic atoms, highly selective detect. by means of reson. laser light press. 4-59903  
 Siberia, lead ore deposits, Pb isotope study 4-105499  
 snow O isotope composition prediction model for glacier core climate studies 4-115522  
 spectral analysis, choice of scanning freq. for recording spectra (*Russian*) 4-112290  
 Trinity peridotite, California, USA, Nd-Sr isotope study and mantle evolution 4-89890  
 U enrichment mechanically driven ultracentrifuge flow field 4-74350  
<sup>222</sup>Rn excess in deep Pacific Ocean water 4-100627  
<sup>40</sup>Ar/<sup>39</sup>Ar ages of L-chondrites 4-110578  
<sup>40</sup>Ar/<sup>39</sup>Ar dating of basalt containing incompletely degassed xenoliths 4-85764  
<sup>10</sup>B/<sup>11</sup>B ratio in saline lakes of Qinghai-Xizang Plateau, <sup>11</sup>B(n,α)<sup>7</sup>Li influence 4-110401

- isotope relative abundance continued  
 Be in soil, concentrations and possible  $^{10}\text{Be}$  radioactive dating method 4-81880  
 isotope record in pinyon pine tree rings, variability within and between trees 4-115607  
 isotopic anomalies in carbonate minerals due to suboxic diagenesis 4-77514  
 $\text{O}_2$  in aqs. soln., diffusion, isotope fractionation meas. 4-87226  
 $\text{O}_2$  in atmosphere, of Pacific, concentration variations and isotopic composition 4-115520  
 $\text{CN}/^{13}\text{C}$  ratio in galactic radiosources; EHF obs. 4-106072  
 $^{12}\text{C}$  isotope fractionation in dense interstellar clouds, time-dependent model 4-90208  
 a, isotopic analysis of refractory inclusions 4-110577  
 J, isotopic variations in nature, determ. method 4-77651  
 $\text{H}$  ratio in solar neighbourhood, implications for solar nebula characts. 4-77733  
 $\text{H}$  ratio in upper atmosphere, meas. from optical detect. by Spacelab. I mission 4-90016  
 $\text{He}$  and  $^4\text{He}$ , relative abundance in cosmic radiation 4-101072  
 $^{129}\text{I}$ , neutron activation anal. in environmental samples 4-105135  
 $\text{Li}/^{7}\text{Li}$ , isotope ratio determ. in FG-type dwarf stars 4-101327  
 $\text{Li}/^{7}\text{Li}$ , ratio in saline lakes of Qinghai-Xizang Plateau,  $^6\text{Li}(\text{n},\alpha)^3\text{H}$  influence 4-110401  
 $\text{Li}/^{7}\text{Li}$  in metal-deficient stars 4-63147  
 $\text{Li}/^{6}\text{Li}$ , chemical evolution of cosmic isotope ratio rel. to Big Bang nucleosynthesis 4-67843  
 $^{25}\text{Mg}$ , isotopic composition in solar flares 4-105953  
 $\text{Mg}$ , isotope composition meas., MI-1201 mass spectrometer upgrading 4-105081  
 N comp. in Antarctic shergottite EETA 79001, possible Martian origin 4-110575  
 $\text{NH}_3$ , light induced drift 4-74349  
 $\text{N}$  abundance in lunar highlands breccias, presence of recent isotopic signature 4-67650  
 $\text{Nd}$ , composition of Zacatecas mid-Tertiary felsic volcanic rocks, Mexico 4-110113  
 $\text{Nd}$  isotope anal. of coexisting alkali magma series from Cantal, France 4-110098  
 $\text{Nd}$ , isotopic composition of Seychelles granites and xenoliths 4-110102  
 $\text{Nd}$  isotopic ratios in Archaean igneous rocks, implications for mantle fractionation 4-100499  
 $^{142}\text{Nd}/^{144}\text{Nd}$  in NE Africa, model  $\text{Nd}$  ages rel. to Proterozoic crustal evolution 4-89900  
 $\text{Ne}$  isotopic variation in Mid-Atlantic Ridge basalt, mantle component 4-110095  
 $^{20}\text{Ne}/^{22}\text{Ne}$ , isotope composition in solar flares 4-105953  
 $^{20}\text{Ne}/^{22}\text{Ne}$  ratio, isotopic studies in solar flare 4-105952  
 $^{20}\text{Ne}/^{22}\text{Ne}$  isotope abundance in solar flares 4-105954  
 $\text{O}$  in conodonts, use for palaeoclimate and palaeoceanography anal. 4-110283  
 $^{18}\text{O}/^{16}\text{O}$  in foraminiferal rel. to Sea of Japan, palaeogeography 4-105598  
 $^{18}\text{O}/^{16}\text{O}$  in K-rich volcanic rocks, mantle implications 4-110094  
 $^{18}\text{O}/^{16}\text{O}$  in oceans, rel. to dynamics of meltwater discharge from ice sheets during deglaciation 4-105613  
 $^{18}\text{O}/^{16}\text{O}$  rel. to fluid regimes in deep fault zones 4-94072  
 $^{18}\text{O}/^{16}\text{O}$  isotope fractionation in dense interstellar clouds, time-dependent model 4-90208  
 $^{18}\text{O}/^{16}\text{O}$  ratio, validity of local approx. for s-process nucleosynthesis and implications for  $^{187}\text{Re}$ - $^{187}\text{Os}$  cosmochronology 4-115680  
 $\text{Pb}$  geochronological dating method, calc. of isotope growth curves 4-90004  
 $\text{Pb}$  isotope composition of Seychelles granites and xenoliths, dating 4-110102  
 $\text{Pb}$  isotope ratio meas. using the Isomass 54E in fully automatic mode 4-96711  
 $\text{Pb}$  isotopic composition of Xigaze ophiolite, Tibet, relation between magmatites and tectonites 4-110139  
 $\text{Pb}$  isotopic composition of minerals and U-Pb dating 4-110285  
 $\text{Pb}$  ore deposits in Siberia, isotope geochemistry study 4-105499  
 $\text{Pu}$ , isotopic composition, gamma-spectrometric determ., safeguards appl. 4-106978  
 $\text{Pu}$  isotopic composition determ. by high res.  $\gamma$ -ray spectrometry, safeguard appl., PLUTO code 4-106979  
 $\text{Pu}$ , A=238-241, simultaneous determ. in low activity environmental samples 4-102443  
 $^{239}\text{Pu}/^{240}\text{Pu}$  isotope ratio, high resolution alpha spectrometric determ. 4-102439  
 $^{240}\text{Pu}/^{239}\text{Pu}$  radio in environmental samples, Lx/ $\alpha$ -ray activity ratio meas. 4-115238  
 $\text{Pu}$  in early Solar System (book) 4-78049  
 $^{87}\text{Rb}/^{87}\text{Sr}$  isobaric pair, appl. to cosmochronology of s- and r-process nucleosynthesis 4-101133  
 $\text{Ru}$ , isotope composition meas., MI-1201 mass spectrometer upgrading 4-105081  
 $\text{Si}$  isotopes use in geochemistry 4-81905  
 $\text{Sn}$ , minor isotopes abundances and p-process nucleosynthesis 4-90082  
 $\text{Sr}$ , composition of Zacatecas mid-Tertiary felsic volcanic rocks, Mexico 4-110113  
 $\text{Sr}$  isotope diversity in oceanic basalts, inverse relation to volcanic eruption rate 4-77490  
 $\text{Sr}$  isotopic anal. of coexisting alkali magma series from Cantal, France 4-110098  
 $^{87}\text{Sr}/^{86}\text{Sr}$  in gneisses, scale of  $\text{Sr}$  isotopic diffusion during post-metamorphic cooling 4-67216  
 $^{235}\text{Th}$  in Atlantic ocean sediments, glacial to interglacial changes in carbonate and clay sedimentation 4-110129  
 $\text{U}$ , isotopic composition, gamma-spectrometric determ., safeguards appl. 4-106978  
 $\text{Zr}$ , isotopic abundances in S-type stars rel. to s-process nucleosynthesis 4-72926

## isotope separation

- see also isotope exchanges; laser isotope separation; radiochemistry  
 DC discharge, isotope separation in longit. mag. field 4-88011  
 end wall effects on separation in magnetised rot. plasma 4-102814  
 ICRH antenna designs for plasma isotope selective excitation 4-60670  
 inert gases, isotope enrichment using quadrupole mass spectrometer 4-83486  
 isotopic cataphoresis in a crossed-field plasma centrifuge 4-75212

## isotope separation continued

- Laval nozzles, curved, two-phase flow, quasi-one dimens. method anal. 4-60476  
 metallic ion magnetised plasma source 4-60672  
 metallic plasma, selective heating and separation of isotopes 4-60668  
 metallic plasmas, isotope separation using selective ICR heating 4-60669  
 multipole ion source for ion implantation and isotope separation 4-73591  
 nozzles, flow and diffusion processes, appls. 4-75068  
 nuclear chemistry and radiochemistry, conf., Tunxi, China (Sept. 1983) (Chinese) 4-110798  
 plasma centrifuge, vacuum-arc, element and isotope separation 4-108223  
 in positive column of DC discharge 4-88010  
 refractory compounds for on-line mass separator targets, nucl. reaction products release 4-68851  
 sputter-produced metallic plasma source 4-60671  
 systematic errors in isotope anal., fringe mag. field influence 4-95371  
 $\text{U}$  enrichment mechanically driven ultracentrifuge flow field 4-74350  
 $\text{CO}_2$  in aqs. soln., diffusion, isotope fractionation meas. 4-87226  
 $\text{D-H}$  isotope separation between hydrogen and liq. methanols 4-59904  
 $^{111}\text{In}$ , simultaneous prod. with  $^{96}\text{Tc}$  by  $\alpha$ -particle irradi. of stacked foils, carrier-free separation 4-77385  
 $\text{Li}$  isotope separation by cryopand ( $2g,2,1$ ) polymer 4-74039  
 $\text{NH}_3$ , light induced drift 4-74349  
 $^{232}\text{Pa}$ , production from Th, isolation 4-78978  
 $\text{T}$  extraction by gettering with Y for impure Li blanket case 4-107027  
 $\text{T}$  isotopic enrichment using host-guest chemistry 4-59414  
 $^{96}\text{Tc}$ , simultaneous prod. with  $^{111}\text{In}$  by  $\alpha$ -particle irradi. of stacked foils, carrier-free separation 4-77385  
 $^{235}\text{U}$ , isomeric level excitation by positrons (Russian) 4-71474

## isotope shifts

- see also atomic spectra  
 acetaldehyde- $\text{d}_0$  ( $-\text{d}_4$ ), time-resolved phosphoresc. spectra 4-107391  
 alkali halide:  $\text{BH}_4^-$ , IR and Raman spectra, Fermi resonances isotope shift 4-61695  
 appl. to laser spectroscopy of Sr isotopes 4-83646  
 atomic spectroscopy, symposium, Berkeley, CA, USA (Sept. 1983) 4-67852  
 cumene, long range spin-spin coupling const., isotope shift,  $^{13}\text{C}$  NMR 4-64497  
 cyclopropane- $\text{d}_0$  ( $-\text{d}_8$ ), lattice vibr. spectra and intermol. forces 4-71371  
 1,1-dichloroethylene, microwave spectrum, harmonic force field and ground state mol. struct. 4-59721  
 $\text{DMSO-d}_6$  ( $\text{d}_8$ ) solns., vibr. band shape, freq. shift, IR obs. 4-59766  
 ethylbenzene, long range spin-spin coupling const., isotope shift,  $^{13}\text{C}$  NMR 4-64497  
 even-even nuclei, isotope shifts and zero-point motion of nucl. surface 4-68618  
 1,1,1,3,3,3-hexamethyltrisilane, IR and Raman spectra, vibr. anal., H/D isotopic shift data 4-112180  
 lanthanides, isotope shift, parametric description appl. 4-74191  
 measurement of radioactive Au isotope, high-temp. resonance cell for laser spectroscopy 4-102648  
 methanol- $\text{d}_0$  ( $-\text{d}_4$ ) vibr. overtones, photoacoustic spectrosc. obs. 4-69097  
 cis-N-methylthioacetamide, IR spectra in low temp. matrices 4-69070  
 naphthalene, isotopically mixed crystals, triplet states, high resolution optical spectroscopy 4-75863  
 S-nitrosocysteine, vibr. spectra, assignments and valence force field, isotope effects 4-78834  
 octamethyltrisilane, IR and Raman spectra, vibr. anal., H/D isotopic shift data 4-112180  
 trans-polyacetylene, deuterated, photoinduced absorption, isotope energy shifts 4-80945  
 polystyrene, isotopic, vibr. spectrum, mass defects effect 4-80912  
 polystyrene- $\text{d}_4$ , isotactic, vibr. spectrum, normal coord. calcs. 4-80911  
 spherical top mols., props., vibr. effects rot. corrections 4-59702  
 three level atom, isotopically selective two-photon excitation 4-74211  
 (TMTSF) $\text{ClO}_4$  organic superconductor, isotope effect on  $T_c$  4-70972  
 toluene, long range spin-spin coupling const., isotope shift,  $^{13}\text{C}$  NMR 4-64497  
 tribromoacetone and  $^{15}\text{N}$  isotopic derivative, IR and Raman vibr. spectra 4-69081  
 Au I, low-lying transitions, vol. isotope shifts 4-64409  
 Ba I, II, energy levels in optical spectrum, isotope shifts, specific mass effect 4-74200  
 BaI, highly excited states, Stark effect, hyperfine struct., isotope shifts 4-64405  
 $\text{CO}_2$ , vibr. levels, spectrosc. const., isotope effects 4-59711  
 $\text{CS}_2$ , IR spectra of isotopic species 4-69065  
 $\text{CS}_2$ ,  $\nu_2$ - $\nu_1$  band IR spectra, S isotope affects 4-87102  
 Ca, HFS, field isotope shift, multiconfigurational HF method 4-102594  
 Ca isotope shifts meas. using laser spectroscopy 4-78806  
 CaI, highly excited states, Stark effect, hyperfine struct., isotope shifts 4-64405  
 $\text{Cs}_2\text{XO}_4$  where X=S, Cr, Mo, V, matrix isolated, IR and Raman spectra, isotope shifts, bond angles evaluation 4-96539  
 Dy, isotope shift, parametric description appl. 4-74191  
 Eu I spectrum,  $4f^6 6s^2$  configuration, isotope shift, parametric anal. 4-59678  
 Eu II, hyperfine structure and isotope shifts 4-87085  
 Eu, isotope shift, parametric description appl. 4-74191  
 FeO, orange system subband rot. anal., fluoresc. spectra 4-59839  
 $\text{H}_2\text{SiCl}_2$ , vibr., rovibr., force const., IR obs. 4-59738  
 He,  $\text{Is}_{2p}$  states, isotope shifts and energies 4-74199  
 HgI mol., UV emission spectrum 4-69098  
 $\text{LaCl}_3\text{Nd}^{3+}$ , isotope shifts, laser-induced fluoresc. 4-71428  
 LiF, high temp. IR tunable diode laser spectra, no-vibr. meas. and Dunham const. calcs. 4-59743  
 $\text{MgCaSiO}_4$ , vibr., force const., isotope shift, IR and Raman obs. 4-61705  
 $\text{N}_2$ ,  $\text{C}^{12}\text{H}_2$ - $\text{B}^{12}\text{H}_2$ , second positive system, isotope shifts 4-91252  
 $(\text{NH}_3)_n$  clusters, multiphoton ionisation with tunable laser 4-74368  
 $\text{N}_2\text{O}_2$  and its isotopic species, Raman spectra and force const. 4-87123  
 Na, anomalous isotopes search, binding energies, D2 transition 4-95890  
 $\text{NaNO}_2$ , zero-phonon transition, isotope shifts, UV absorpt. spectra 4-88853  
 $\text{P}^{19}\text{N}$ ,  $\text{E}^{\Sigma^+}-\text{X}^{\Sigma^+}$  transition 4-112193  
 Pb, muonic even-A isotopes, L and M transition energies 4-107469  
 Si, Czochralski, C in radiation damage centres, luminesc. study 4-93107  
 $^{29}\text{SiH}_4$ , silane, mol. transitions, stimulated Raman scatt. studies (French) 4-59785

## isotope shifts continued

- Sm, isotope shift, parametric description appl. 4-74191  
 Sr levels, config. mixing and isotope shifts 4-68978  
 $UF_6$  molecule, IR absorpt. spectra,  $\nu_3$  band, pulsed supersonic jet study 4-59734  
 $VC_2(Br_2)(I_2)$ , triangular Heisenberg antiferromagnet in paramag. state, hyperfine field,  $^{51}V$  nucl. relax., NMR 4-92973  
 $WF_6$ , cold jet IR absorpt. spectra,  $\nu_3$  band at low rot. and vibr. temp., isotope shift 4-87114  
 W1, isotope and hyperfine splittings for two UV transitions, saturation and polarisation spectroscopy 4-87064  
 $Zn^{+}$  vapor, high-gain soft X-ray pumped photoionization laser 4-112383

## isotopes

- see also radioisotopes  
 $^{114}Cd/^{113}Cd$ , neutron fluence determ. for isotopic variation meas. 4-91186  
 $^{158}Gd/^{157}Gd$ , neutron fluence determ. for isotopic variation meas. 4-91186  
 $^{87}Sr$  A=87, 86, high precision mass meas. using spectrometer 4-68317

## isotopic generators see radioactive sources

## isotopic spin (elementary particles)

- see also baryon spin and parity; lepton spin and parity  
 non-relativistic quark cluster model of the isospin-violating two-nucleon interaction 4-86641  
 nucleon internal structure, spin-isospin excitation, sum rules 4-78594  
 $\pi^- \rightarrow 3\pi^0$ , isospin violating, branching ratio 4-78551  
 $(KK\pi)$  isoscalar resonances,  $J^{PC}$  assignments 4-73727  
 $\pi N \rightarrow \pi\pi N$ , reaction cross sections, isospin analysis, chiral-symm. breaking 4-106541

## iteration methods see iterative methods

## iterative methods

- acoustic propagation, ground effect, meteorology (French) 4-60196  
 asymmetric clock model on Cayley tree 4-68158  
 atoms, Slater-type basis functions, iteration procedure 4-68920  
 attenuative subsurface layered media parameter estimation, frequency-domain approach 4-107941  
 beam, thermally restrained, nonlinear anal. 4-112732  
 bearings-only tracking, recursive vs. batch processing algorithms 4-107942  
 composite materials, thermal conductivity, nonlinear inverse problem, accuracy of soln. anal. 4-97277  
 composites, fibre-reinforced multilayer, delamination stress determ., iterative approach 4-112702  
 computerised tomography, iterative correction algorithm of incomplete projections 4-93857  
 conference on transport theory, Blacksburg, VA, USA (March 1983) 4-95053  
 digital image processing, statistically weighted non-local method 4-100309  
 Dirichlet problem of Laplace eqn., integral difference soln. method (Russian) 4-63517  
 discrete ordinates problems, diffusion synthetic acceleration methods, review 4-95361  
 drop, curvature parameter, theory of nucleation on charged nuclei 4-80331  
 duct flow, near sonic, sound propagation, finite difference soln. 4-60197  
 Einstein's field eqns., iterative solution for radiative gravitational fields (French) 4-78201  
 electron micrographs, 3D image reconstruction, iterative algorithm 4-85597  
 Ericksen's problem of elasticity, iterative soln. method 4-110874  
 evolution patterns and iterative maps 4-73360  
 feature extraction of machine parts, multi-level thresholding appl. 4-102898  
 ferromagnetic cylindrical conductor with weak nonlinearity in harmonic quasistationary regime, weak skin effect (French) 4-65698  
 few group two-dimens. HEXAB-II-30K, outer iteration convergence acceleration (Russian) 4-78660  
 frames with Timoshenko members, second order analysis 4-112712  
 Fredholm eqns. solns., through nonlinear iterative processes 4-67960  
 frictional contact, finite-element stress anal., iterative procedure 4-87632  
 FT-IR absorbance subtraction from mixtures, automated procedure 4-105036  
 gapless supercond. in strong exchange fields, Eliashberg theory (Chinese) 4-70977  
 heat conduction, inverse boundary-value problem, soln. by iteration algorithm 4-97275  
 heat exchanger performance simulation using programmable calculator 4-111127  
 infinite strip confocal resonator filled with a saturable-absorpt. gas, lowest-order eigenvalue evaluation 4-87400  
 inverse black-body radiation, closed form approximations 4-86419  
 inverse heat conduction problem, convergence of iteration methods 4-97274  
 linear systems, extrapolated iterative methods 4-58639  
 lossy dielectric bodies, EM wave specific absorption rate distrib., calc. using FFT method 4-85459  
 LPC voiced-speech synthesis, improved algorithm using iterative method 4-74817  
 m-particle n-hole fermion level densities, iteration scheme, semiclassical approx. 4-102154  
 magnetic field computation using Delaunay triangulation and complementary finite element methods 4-59946  
 man-made quantum well, heterostructs. and superlattices 4-67920  
 metals, potential at a boundaries in Thomas-Fermi model and eqns. of states (Chinese) 4-70333  
 modal equations, linear structural dynamics 4-86185  
 multidimensional optimization of structural changes of molecules upon ionization in Franck-Condon factor calculations 4-59853  
 Navier-Stokes eqn., full implicit iteration method for soln. 4-91789  
 Navier-Stokes eqns., steady, anal. based on Green's function approach 4-79541  
 noise-induced phases of iterated functions 4-58750  
 noisy images, adaptive estimation procedure comparison 4-102902  
 nonlinear, high-resolution spectral estimation 4-69649  
 nonlinear analysis, stiffness matrix extrapolation strategy 4-79451  
 nonlinear filtration, difference schemes 4-87789  
 nonlinear particle transport theory, iterative schemes, rigorous results, review 4-96097  
 iterative methods continued  
 nonlinear suspensions under random excitation, identification proced. (French) 4-58637  
 nonmultiplying half-space, reflection matrix, monotone iterative procedure convergence 4-96101  
 nonquadratic one-dimensional maps, iterative props. 4-67965  
 ocean acoustic tomography, iterative perturbation approach 4-74799  
 physico-mathematical model for thermal storage useful for high temp. 4-81595  
 polymer conformation statistics, iterative convolution approach 4-90521  
 porous body, internal heat transfer coeffs., inverse problem cal. 4-107980  
 porous layers, fluid saturated, US pulse propag. 4-98215  
 PWR steam generator transient analysis computer code 4-59310  
 seepage and membrane contact problems 4-65016  
 smoothing methods as preprocessing for iterative deconvolution (Japanese) 4-95396  
 sound propagation, ray theory, two-variable Taylor series 4-74798  
 spin glass model, mapping iterations 4-98891  
 supersonic flow, potential theory, finite difference numerical method 4-97604  
 Thomas-Fermi eqns. soln. using imaginary time step method 4-68627  
 two-dimensional magnetostatics, nonlinear boundary element method 4-59950  
 unsteady free convection flow of a visco-elastic fluid past a vertical porous flat plate 4-69763  
 vacuum systems with adsorbing surfaces, adsorbed gas flows, iterative calc. 4-82801  
 X-ray CT image reconstruction method from projection data with quantum noise (Japanese) 4-67116  
 $Ge_2H_4$ , charge iterative relativistic extended Huckel theory and its appl. 4-59643  
 Mo (100), surface states, appl. of quick iterative scheme for transition matrix calc. 4-76013  
 $Pb_2H_4$ , charge iterative relativistic extended Huckel theory and its appl. 4-59643  
 Si solar cells, I-V characts. and performance between low- and high-level injection 4-81551  
 $Sn_2H_4$ , charge iterative relativistic extended Huckel theory and its appl. 4-59643  
 itinerant model of magnetism see band model of magnetism  
 IV-VI semiconductors  
 dynamical properties, book 4-58590  
 electronic and dynamical props., book contrib. 4-61003  
 iodine prep. method in flow reactor 4-76660  
 ion implantation, review 4-92220  
 n-p-i doping superlattices, electronic props. 4-104300  
 $PbTe:Bi$ , Hall study of self-compensation of donor effect 4-104242  
 $Cd_{1-x}Hg_xTe$ , narrow-gap semiconductor, internal photoeffect, quantum efficiency calc. 4-61415  
 CdTe films, MBE growth on InSb 4-85103  
 GeS film, crystalline and amorphous, photoconductivity study (Russian) 4-70870  
 GeS, hole drift mobility anisotropy 4-70814  
 GeS layered monocystals, photoluminescence spectra, pol. plane orientation change effects 4-66069  
 GeS single crystal, reflectance and thermoreflectance studies 4-71356  
 GeSe, crystal growth from GeSe-I vapour, complex equilibria and phase diagrams 4-81122  
 GeSe, thin film, laser-induced synthesis 4-80095  
 GeTe, heats of polymorphic transitions 4-61065  
 GeTe-Ag<sub>2</sub>Sb<sub>2</sub>Te<sub>3</sub> system, solid soln., fabrication technology 4-75682  
 GeTe-InTe, phase transformations, 300-900K 4-108602  
 (Pb, Sn)Te, crystal growth by Bridgman method and by travelling heat method 4-103678  
 (Pb,Sn)Te-Pb(Te,Se) DH laser diodes, ion-implantation confined shallow mesa stripe, single mode tuning 4-112459  
 Pb chalcogenides, carrier diffusion length and lifetime, EBIC measurements 4-92748  
 Pb chalcogenides, electron scatt. interaction and elementary excitations 4-70694  
 Pb chalcogenides, resonance absorpt. in indirect transitions (Russian) 4-88855  
 Pb salt, tunable diode lasers for 3 to 30  $\mu m$  IR operation 4-112456  
 Pb salt tunable diode lasers for heterodyne appls. 4-96940  
 Pb salt tunable diode lasers, Cd diffused, multicomponent gas analysis, appl. 4-112457  
 $Pb_{1-x}Eu_xTe$ , MBE growth and elec. and optical props. 4-81142  
 $Pb_{1-x}Ge_xTe$ , ferroelec. phase transition, high press. investigation, D.C. resist., capacitance meas. 4-71312  
 $Pb_{1-x}Ge_xTe$ , rhombohedral phase, energy surfaces and domain structures 4-76010  
 $Pb_{1-x}Ge_xTe$ , undoped and In-doped, anomalous scatt. of carriers by defects and impurities near ferroelec. phase transition 4-98622  
 $Pb_{1-x}Ge_xTe:In$ , elec. props., band edge struct., impurity effects 4-10888  
 $Pb_{1-x}Ge_xTe:In$ , solid solns., impurity photocond., spectra and kinetics 4-113994  
 PbS and PbSe detectors and arrays, review 4-95518  
 PbS, at. vibr. amplitudes, Debye-Waller factor 4-98232  
 PbS film, photosensitivity and luminescence studies 4-104679  
 PbS, nonstoichiometry, voltammetry using paste electrode 4-108407  
 PbS polycryst. samples, current and photocurrent flow mechanisms 4-104196  
 PbS, single crystal, localised spin scatt. magnetoresistivity 4-61396  
 PbS theoretical refractive index determ. 4-93032  
 PbS thin films, laser and thermal annealing effects on elec. properties 4-65298  
 PbS, thin films, noise power spectra meas. 4-80638  
 PbS(Se), IR detector arrays, state-of-the-art review 4-111202  
 $PbSe_0.9Se_{0.1}$  small gap semicond., second order Auger recombination 4-80606  
 $PbS_{1-x}Se_x$  DH diode lasers fabricated by compositional interdiffusion 4-102952  
 $PbS_{1-x}Se_x$ , n<sup>+</sup>-p-p<sup>+</sup> injection laser, performance characts. 4-79154  
 PbSe and PbS detectors and arrays, review 4-95518  
 PbSe, anisotropy of Fermi surface of holes 4-104117  
 PbSe epitaxial film, photoconductivity relax. study 4-104270  
 PbSe epitaxial narrow-gap semicond. films, optical four-wave mixing 4-83640  
 PbSe film, photoelectric props. meas. 4-104267

## I semiconductors continued

- bSe theoretical refractive index determ. 4-93032  
 bSe/BaF<sub>2</sub> epitaxial MIS structures 4-99316  
 bSe-Si heterojunctions, solution-grown, elec. and photoelec. props. 4-114023  
 bSe<sub>1-x</sub>Te<sub>x</sub> solid solution, p-n heterojunction form. by LPE 4-88996  
 bSe<sub>1-x</sub>Te<sub>x</sub>Tl<sub>x</sub> energy spectra and elec. cond. 4-70724  
 b<sub>2</sub>Sn<sub>2</sub>S multilayer single crystal. semiconductor, X-ray effects, Mossbauer investig. 4-109106  
 b<sub>1-x</sub>Sn<sub>x</sub>Se, thin film, unit cell parameters, phase composition 4-61249  
 bSnTe cleaved-coupled cavity lasers 4-87327  
 bSnTe, crystal growth under microgravity, segregation obs. 4-98036  
 bSnTe, negative differential mobility in high elec. fields 4-104216  
 bSnTe tunable diode laser, wide-range amplification using optically pumped high-pressure NH<sub>3</sub> 4-91466  
 bSnTe-PbSeTe DBR diode lasers grown by LPE 4-112460  
 bSnTe-PbSeTe lattice-matched DH laser diodes, lasing characts. 4-112421  
 bSnTe-PbTeSe lasers with high efficiencies, lattice-matching to reduce misfit dislocations 4-112420  
 Pb<sub>0.9</sub>Sn<sub>0.1</sub>Te/p-PbSe<sub>1-x</sub>Te<sub>x</sub> heterojunction photodiodes, LPE and elec. props. 4-88575  
 Pb<sub>0.9</sub>Sn<sub>0.1</sub>Te, absorption edge, free carrier Fermi-liq. interaction effects 4-114236  
 Pb<sub>0.9</sub>Sn<sub>0.1</sub>Te epitaxial films, heating by short laser pulses 4-88203  
 b<sub>1-x</sub>Sn<sub>x</sub>Te, band struct. changes during struct. and band inversion transitions 4-63607  
 Pb<sub>1-x</sub>Sn<sub>x</sub>Te, defect states, impurity photoconductivity transient studies 4-80545  
 Pb<sub>1-x</sub>Sn<sub>x</sub>Te diodes, excess noise rel. to I-V characts. 4-61426  
 Pb<sub>1-x</sub>Sn<sub>x</sub>Te, ferroelec. phase transition close to band inversion 4-76364  
 Pb<sub>1-x</sub>Sn<sub>x</sub>Te large homogeneous single crystals, growth by vapour-melt-solid mechanism 4-71547  
 Pb<sub>1-x</sub>Sn<sub>x</sub>Te, longitudinal magneto-resist., magnetophonon oscils. 4-65694  
 Pb<sub>1-x</sub>Sn<sub>x</sub>Te, refractive index dispersion meas. 4-99074  
 Pb<sub>1-x</sub>Sn<sub>x</sub>Te, Shubnikov-de Haas effect, temp. depend. scatt. parameter 4-113978  
 Pb<sub>1-x</sub>Sn<sub>x</sub>Te, solid solution, vapour phase growth of epitaxial films 4-76689  
 Pb<sub>1-x</sub>Sn<sub>x</sub>Te system, plasma oscill. freq., temp. depend. 4-88836  
 Pb<sub>1-x</sub>Sn<sub>x</sub>Te tunable diode laser fabricated by horizontal unseeded vapour growth (Chinese) 4-60035  
 Pb<sub>1-x</sub>Sn<sub>x</sub>Te, valence band struct. near phase transition 4-84564  
 Pb<sub>1-x</sub>Sn<sub>x</sub>Te, elec. transport props. 4-61371  
 Pb<sub>1-x</sub>Sn<sub>x</sub>Te, In, Gunn effect, threshold field rel. to cond. band struct. 4-88513  
 Pb<sub>1-x</sub>Sn<sub>x</sub>Te, In, photoconductivity and impurity states 4-113993  
 Pb<sub>1-x</sub>Sn<sub>x</sub>Te, In epitaxial films, optical absorption spectra and photoconductivity 4-65711  
 Pb<sub>1-x</sub>Sn<sub>x</sub>Te, In epitaxial layers, optical absorption studies 4-71456  
 Pb<sub>1-x</sub>Sn<sub>x</sub>Te, In epitaxial layers, photocond. kinetics 4-88538  
 Pb<sub>1-x</sub>Sn<sub>x</sub>Te, ferroelectric transition temp. and saturation effect (Russian) 4-71318  
 PbTe cryst., external shape, impurity complex effects 4-75347  
 PbTe, crystal growth by Bridgman method and by travelling heater method 4-103678  
 PbTe epitaxial films, photoluminescence characts. 4-66067  
 PbTe epitaxial narrow-gap semicond. films, optical four-wave mixing 4-83640  
 PbTe films, hot wall epitaxy, elec. characts., SEM and X-ray obs. 4-71564  
 PbTe films grown by hot wall epitaxy technique, AC field effect study 4-92835  
 PbTe, iodide prep. method in flow reactor 4-76660  
 PbTe, negative differential mobility in high elec. fields 4-104216  
 PbTe Schottky barriers, resonant magneto-optical transitions from a deep level 4-76440  
 PbTe, sintered, elec. cond. and thermoelec. power, annealing effects 4-84621  
 PbTe, size quantised films, p-polarised optical properties 4-114338  
 PbTe theoretical refractive index determ. 4-93032  
 PbTe thin film, electrophys. props., degradation and recovery 4-88619  
 PbTe thin films, elec. props., effect of boundary layers 4-88618  
 PbTe:B, absorpt. spectra and impurity states 4-104638  
 PbTe:Ga, elec. and optical meas. (Russian) 4-84636  
 PbTe:Tl, pure and doped, defect struct., X-ray double cryst. studies 4-75383  
 PbTe/Pb<sub>1-x</sub>Sn<sub>x</sub>Te superlattices, struct. and electronic props. 4-98463  
 PbTe/Pb<sub>1-x</sub>Sn<sub>x</sub>Te superlattices, optical and elec. props. 4-99209  
 PbTe/ZnS IR filter durability assessment, Space Shuttle 1st LDEF appl. 4-74688  
 PbTe-Bi system, anomalous transport props. 4-88588  
 PbTe(Se) polar multivalley semicond. with impurities, optical absorption by electron plasmas 4-114230  
 PbTe<sub>1-x</sub>Se<sub>x</sub>/PbTe heterojunctions, epitaxially grown, misfit dislocations 4-88431  
 PbTe(Se)(S), lattice thermal cond. meas. 4-98598  
 SnSe, electroreflectance and thermoelectr. 4-71348  
 SnSe thin films, UPS and reflectivity meas. 4-84976  
 SnTe, low carrier conc., Fermi surface, Shubnikov-de Haas studies 4-98506  
 p-SnTe, struct. and ferroelec. transitions, review 4-65390  
 SnTe thin films, elec. cond. and Hall effect 4-84716  
 ZnS(Se) phosphor DC electroluminescent cells, self-activated centers, low field recombination 4-99196

od testing see dynamic testing

particles see psi mesons

## Jahn-Teller effect

- [X] Jahn-Teller matrix elements, evaluation by group theory method 4-92678  
 alkali chloride: Cu<sup>+</sup>(Ag<sup>+</sup>), two-photon spectra, impurity states 4-109215  
 alkali halide:Tl<sup>+</sup> cryst., optical props. and Jahn-Teller effects 4-61643  
 benzene, mol. Rydberg states, vibronic coupling, Franck-Condon spectrum, Jahn-Teller ion core 4-87096  
 cerium ethyl sulphate, US vel. and attenuation near cooperative Jahn-Teller dilation 4-70292  
 cooperative Jahn-Teller E-b<sub>1</sub>b<sub>2</sub> systems, thermal cond. 4-70486  
 Dicke-like models, fluctuations and phase transitions 4-92923  
 Ham factors for Jahn-Teller T×(r<sub>2</sub>+e) system at strong coupling 4-98575

## Jahn-Teller effect continued

- Ham reduction factors for excited states of the E<sub>g</sub> Jahn-Teller system 4-92677  
 hexaimidazolecadmium-(II) nitrate: Cu (II), Jahn-Teller distortion, EPR 4-71165  
 ionic crystals, diatomic mol. impurities at cubic sites, rotronic Jahn-Teller effect 4-98578  
 Jahn-Teller crystals, antiferrodistortive ordering in external mag. field 4-108608  
 local distortion correlation influence on mag. props. of Jahn-Teller centre pair 4-88646  
 metal complexes, tetrahedral symmetry, Jahn-Teller effect, absorpt. and EPR spectra 4-114153  
 methane, lowest triplets and single-triplet splittings, excitation energies calc. using perturbation theory 4-78770  
 mixed valence d<sup>1</sup>-d<sup>2</sup> clusters, vibronic reduction effects 4-88490  
 nickelocenium cation, electronic struct., Jahn-Teller effect, EPR study 4-64517  
 nuclear eff. transition to deformed states 4-83007  
 octupole ang. momentum in octahedra exhibiting E<sub>g</sub> Jahn-Teller effect 4-98576  
 palladium phthalocyanine, reson. Raman, fluoresc., and phosphorescence spectra in Shpol'skiy matrices 4-71426  
 porphyrins, central protons, pseudo-Jahn-Teller dynamics 4-64398  
 semiconductors, deep levels, expt. and theoretical studies, review 4-84593  
 symmetric and spherical top molecules, rot. energy levels, Jahn-Teller and L-uncoupling effects 4-59690  
 transition metal compounds, Jahn-Teller distortions, NDDO calcs. 4-87050  
 sym-triazine, jet isolated, vibronic struct., UV two-photon absorpt. spectra 4-96559  
 vibronic interactions and Jahn-Teller effect 4-67899  
 zircon-structure crystals, internal strain, orbit-lattice coupling and phase transitions 4-80220  
 Al<sub>2</sub>O<sub>3</sub>, strongly coupled mag. ions, obs. by low temp. thermal expansion meas. 4-70419  
 Al<sub>2</sub>O<sub>3</sub>:V(Mn), low-temp. thermal expansion meas. 4-61112  
 CaF<sub>2</sub>:La<sup>3+</sup>, intermediate Jahn-Teller coupling, vibronic Raman and EPR spectra 4-88491  
 Cs<sub>2</sub>CrF<sub>6</sub>, cryst. struct. and Jahn-Teller effect 4-70095  
 Cs<sub>2</sub>Cl<sub>2</sub>, Jahn-Teller induced phase transition, hydrostatic press. effects 4-65392  
 Cs<sub>2</sub>FeF<sub>6</sub>, cryst. struct. and Jahn-Teller effect 4-70095  
 Cs<sub>2</sub>VF<sub>6</sub>, cryst. struct. and Jahn-Teller effect 4-70095  
 Cu tetrahedra, adiabatic opt., mag. props., Jahn-Teller effect 4-108823  
 CuFe<sub>2</sub>Al<sub>2</sub>O<sub>4</sub>, orthorhombic distortions due to doping 4-70103  
 Cu<sub>2</sub>Ge<sub>2</sub>Fe<sub>2</sub>O<sub>4</sub>, orthorhombic distortions due to doping 4-70103  
 Fe(CO)<sub>4</sub> IR laser-induced isomerisation and Jahn-Teller effect 4-66567  
 GaAs, EL2 defect, technological and physical aspects 4-75891  
 GaAs:Cr, photoluminescence excitation spectra, Cr<sup>2+</sup> internal luminesc. 4-81004  
 GaAs:Cr, US attenuation and vel. meas. 4-98212  
 n-GaAs:Cr<sup>2+</sup>, acoustic paramagnetic resonance study 4-71171  
 GaAs:Cr<sup>2+</sup>, comparison of static and dynamic Jahn-Teller models 4-61345  
 GaAs:Mn, phonon scatt. at acceptor ground state 4-70729  
 GaAs:Mn, thermal cond. resonances of acceptor states 4-104011  
 GaP, localised vacancies, electronic struct. and stability 4-80539  
 GaP:Ni<sup>2+</sup>, Jahn-Teller coupling forces, self consistent LCAO calc. 4-98577  
 GaP:O, electronic impurity states calcs. 4-80547  
 GaP:O, electronic struct. of single neutral ideal P vacancy 4-92657  
 GaSe, layer crystals 4-108824  
 K<sub>2</sub>CrF<sub>6</sub>, cryst. struct. and Jahn-Teller effect 4-70095  
 K<sub>2</sub>FeF<sub>6</sub>, cryst. struct. and Jahn-Teller effect 4-70095  
 K<sub>2</sub>VF<sub>6</sub>, cryst. struct. and Jahn-Teller effect 4-70095  
 KZnF<sub>3</sub>:Fe<sup>2+</sup> crystal, EPR and far IR study on (FeF<sub>6</sub>)<sup>4-</sup> complex 4-80814  
 Li in inert gas matrices, mag. circular dichroism study of <sup>2</sup>S-<sup>2</sup>P transition 4-59670  
 LiNbO<sub>3</sub>:Cu<sup>2+</sup>, EPR and optical absorption spectra, Jahn-Teller effects 4-71166  
 LiNbO<sub>3</sub>:Cu<sup>2+</sup>, single crystal 4-108825  
 MgO:Co, electronic Raman spectrum and perturbation calcs. 4-114281  
 MgO:Co<sup>2+</sup>, g value, Jahn-Teller effect 4-88492  
 ND<sub>4</sub>, rot. energy levels, Jahn-Teller and L-uncoupling effects 4-59690  
 NaCa<sub>2</sub>Cu<sub>2</sub>V<sub>2</sub>O<sub>12</sub> garnet, mag. props. study 4-61563  
 NaF:Cu<sup>2+</sup>, excited state dynamics 4-108803  
 PbCl<sub>2</sub>-<sub>2</sub>Br<sub>2</sub>, self-trapped excitons, luminesc. (Russian) 4-80982  
 Pb<sub>1-x</sub>Sn<sub>x</sub>Te, In epitaxial layers, photocond. kinetics 4-88538  
 Rb<sub>2</sub>CrF<sub>6</sub>, cryst. struct. and Jahn-Teller effect 4-70095  
 Rb<sub>2</sub>FeF<sub>6</sub>, cryst. struct. and Jahn-Teller effect 4-70095  
 Rb<sub>2</sub>VF<sub>6</sub>, cryst. struct. and Jahn-Teller effect 4-70095  
 Si (111), electron correlation effects at vacancies 4-98092  
 Si, localised vacancies, electronic struct. and stability 4-80539  
 Si:B, thermal cond. resonances of acceptor states 4-104011  
 Si:In(B), phonon scatt. at acceptor ground state 4-70729  
 TmAsO<sub>4</sub>, crystal-field parameters, Mossbauer meas. 4-61350  
 TmAsO<sub>4</sub>, optical and mag. studies of lowest levels 4-88831  
 TmVO<sub>4</sub>, cooperative Jahn-Teller system, US attenuation at megahertz freq. 4-70282  
 TmVO<sub>4</sub>, cooperative vibronic system, thermal cond. 4-70485  
 W (001), surface instability and reconstruction, pseudo Jahn-Teller approach 4-80347  
 ZnS:Cu<sup>2+</sup>, Jahn-Teller coupling forces, self consistent LCAO calc. 4-98577  
 ZnSe, localised vacancies, electronic struct. and stability 4-80539  
 ZnSiF<sub>6</sub>·6H<sub>2</sub>O:Cu<sup>2+</sup>, EPR, dynamical peculiarities of Jahn-Teller effect (Russian) 4-98938  
 ZrH<sub>2</sub>, electronic struct., tetragonal distortion, X-ray diff. and PMR study 4-84858

jellies see gels

## jellium

- binary ionic mixtures and a solvable model 4-103631  
 Bogoljubov coupled-cluster formalism, electron correlation in jellium model 4-108799  
 insulators, exchange-correlation potential determ. 4-61279  
 jellium/hard sphere electrolyte interphase, model for electric double layer 4-70908

## jellium continued

- metal, positron annihilation characteristics for positron in divacancies and vacancy clusters 4-70742  
 metal, small particles, dynamical polarisability, self-consistent spherical jellium background model 4-75883  
 metal clusters, small, ionisation pot., effect of electron statistics 4-108923  
 metal surface, attractive pots. for He atom near surface 4-80707  
 metallic, cooperative magnetism and transitions 4-76149  
 metals, interatomic forces near a defect, impurity-susceptibility method 4-113490  
 scattered and re-emitted H charged fractions, trajectory depend. 4-76597  
 semiconductors, exchange-correlation potential determ. 4-61279  
 solids, planar, spherical and cylindrical, dynamical screening and surface excitations 4-78234  
 superconducting critical temperature, electron-electron interaction 4-88626  
 surface, Coulomb pot. acting on charge 4-84667  
 two-dimensional, translational invariance, symmetry breakdown 4-61266  
 Ag, core level binding energies, density functional calcs. 4-113861  
 Cu (100), long-range electron-phonon coupling at metal surfaces, EELS meas. 4-80647  
 Cu (100), surface dynamic processes, excitation of electron-hole pairs 4-70902  
 Mg, core level binding energies, density functional calcs. 4-113861  
 Ni (100), long-range electron-phonon coupling at metal surfaces, EELS meas. 4-80647  
 Ni (100), surface dynamic processes, excitation of electron-hole pairs 4-70902

## jet stream see atmospheric movements

## jets

## see also plasma jets; sprays

- 8th Australasian Fluid Mechanics Conference, Newcastle, NSW, Australia (Nov.-Dec. 1983) 4-67858  
 aerodynamically generated sound by turbulent jets 4-69748  
 air, jet impinging on inclined adjacent wall, flow characts. 4-87770  
 air, supersonic jet, apparent mass calc. 4-79634  
 air jets from rectangular slits, noise meas. 4-60470  
 air quality improvement in open jet windtunnel 4-85393  
 annular jets interacting with ambient medium, length 4-112973  
 V1343 Aquilae (SS 433), jet instabilities rel. to nonthermal emission 4-72948  
 V1343 Aquilae (SS 433), radio emission knots obs. rel. to twin-jet models 4-101371  
 axis-symmetrical jet, symmetrically surrounded by jet system, anal. (Bulgarian) 4-97632  
 axisymmetric flow, press. distrib. on plate (Russian) 4-64996  
 axisymmetric jet, turbulence struct., vel. and temp. fluctuations, azimuthal correl. 4-64998  
 axisymmetric jet flows, spontaneous rot. (Russian) 4-112911  
 beam charge conc. spreading, electrohydrodynamics 4-96773  
 benzaldehyde, sensitised phosphoresc. excitation spectra in supersonic jets 4-107380  
 benzene,  $B_{2u}$  state, jet-cooled, radiationless processes, vibr. state depend. 4-102727  
 benzene,  $B_{2u}$  state, jet-cooled vibronic level fluoresc. 4-102726  
 benzoic acid, electronic spectra in supersonic free jet 4-107394  
 benzophenone, sensitised phosphoresc. excitation spectra in supersonic jets 4-107380  
 biacetyl, sensitised phosphoresc. excitation spectra in supersonic jets 4-107380  
 body of revolution in liq. with jet separation, unsteady weakly perturbed motion 4-112896  
 boundary layer control by means of strong injection, wall jet problem 4-97710  
 bubbles rising in a tube and jets falling from a nozzle 4-75066  
 BWR jet discharge experiment, DRIX-2D code anal. 4-86881  
 BWR LOCA, jet discharge test results 4-86880  
 3C 293, radio galaxy, radio jets propag. through gaseous disc rel. to extended optical line emission 4-63267  
 cavities, nonlinear self-excited acoustic oscillations 4-91678  
 chemically reactive flow, holographic interferometry method study 4-69833  
 chlorodifluoronitrosomethane, jet-cooled, visible spectra, dispersed fluoresc. 4-64528  
 choked jet noise, screech spectra (Chinese) 4-83762  
 clustering in free jets-aggregation by dispersion 4-74375  
 coflowing jets and wakes, 3D vortex motions, flow visualisation meas. 4-75038  
 combined flow field of moving wall with parallel wall jet 4-60472  
 combustion of low-calorific value gas jet in cross-flow, flame stability problem 4-75096  
 confined spaces jet 4-83935  
 construction of liquid metal screens in high-temperature MHD apparatus (Russian) 4-113056  
 convective heat transfer, physical and computational aspects, book 4-86128  
 cosmic phenomena (Japanese) 4-115679  
 cyclopropane, jet-cooled, IR laser spectrosc. 4-83373  
 cylindrical laminar jet, formation of vorticity fronts in shear flow 4-64959  
 diazabicyclooctane, two-colour spectrosc. and excited state dynamics in free jet expansion 4-107412  
 9,10-dichloroanthracene- $Ar_n$ , van der Waals complexes, UV absorpt. and fluoresc. spectra meas. 4-96594  
 diphenyl butadiene, solns. and jets, isomerisation, nonradiative decay 4-71902  
 dispersed liquid jet mixing with drifting gas flow 4-60475  
 double concentric jet, initial region characts. 4-64990  
 EHD jets theory, self-similar solutions 4-108137  
 electrically cond. liquids, free jets, reson. breakdown, EM forces, drop form. phases (Russian) 4-113057  
 electrically conducting liquid, turbulent jet in strong longit. mag. field 4-108120  
 ethylene mol. jets, cw CO<sub>2</sub> laser excited, Raman anal. 4-112182  
 fast jet furnace with top-mounted burners, heat exchange 4-97629  
 flat turbulent jets, in restricted volume, distribution determ. by numerical method (Bulgarian) 4-97630  
 flow in weakly cond. dielectric liquids produced by nonuniform electric field 4-108136  
 fluid jet stream of high optical quality, wire guided 4-112969  
 jets continued  
 fluorobenzene van der Waals complexes, two-colour photoionis. in supersonic free jet 4-83436  
 forced oscillation experiments in supercritical diffuser flows 4-97626  
 free jets from shaper-edged orifices, vel. coeff. 4-103382  
 gas jet propag. in liquid, discharge from submerged nozzle with different degree of gas assimilation 4-103380  
 geometrically thick discs, jets, appl. to extragalactic radio jets 4-72867  
 half-limited flat turbulent jet, interaction with satellite homogeneous flow in mixer boxes (Bulgarian) 4-97631  
 heat transfer from a gas jet impinging onto a liq. surface 4-83890  
 heated turbulent place jet, temp. and vel. spectra 4-64992  
 high press. jet vacuum pumps theory, simulation and design 4-58861  
 high-pressure fluid and gas jets, starting valve for laboratory apparatus 4-7817  
 HV electrohydrodynamic generator, liquid flow study 4-97705  
 hydrodynamical jets with inhomogeneous viscosity, structure 4-6761  
 hypersonic jets, adjacent pair interaction 4-91830  
 impingement heat transfer, entrainment temp. effect 4-112867  
 incipient round, visual obs., of evolution 4-75067  
 incompressible fluid jet flow past a wedge 4-91829  
 industrial air jet, quiet and efficient, design and performance evaluation technique 4-77165  
 industrial flow circuits, jet system appls. for heat transfer 4-83936  
 jet-aerodynamic surface interference effects, theoretical model 4-112973  
 jet-flap thrust recovery theory 4-75058  
 laminar and turbulent jet flow over a moving wall 4-64994  
 laminar mixing of parallel flows of a conducting liquid in a transverse magnetic field (Russian) 4-113060  
 laminar swirling jet with allowance for buoyancy forces 4-69807  
 line momentum source in shallow inviscid fluid 4-112974  
 liquid atomising jets, spray angle meas. 4-97657  
 liquid gas two phase flow theory of jet pump 4-60532  
 liquid jet issuance from channel 4-60547  
 liquid-fuel spray in jet-type burner 4-104991  
 liquid-liquid jet breakup, drops size, mass transfer and solute adsorption effects 4-64993  
 liquid-metal jet, hollow, stabilisation of Rayleigh instability by mag. field 4-108132  
 low press. bubble with jet attachment, transient response 4-87780  
 M87, optical spectrophotometry of jet and environs 4-86037  
 mass reflection for studying laser light-molecules interaction in supersonic gas jet 4-90686  
 measurement of complex flow fields, directional pressure probe design, calibration and testing 4-69843  
 methane free jet expansion, picosec. coherent anti-Stokes Raman spectroscopy 4-74251  
 N<sub>2</sub>, spatially and spectrally resolved multipoint CARS 4-112516  
 Newtonian fluid jet, swelling and shrinking study 4-79633  
 Newtonian jet swell, plane stick-slip problem soln. 4-97467  
 NGC 6251, radio galaxy, high-resolution VLA obs. of radio jet 4-949  
 NGC 7385, radio galaxy, obs. of optical knots assoc. with radio 4-90231  
 O<sub>2</sub>, spatially and spectrally resolved multipoint CARS 4-112516  
 oceanic jets in California current 4-105583  
 oppositely directed jets of different density, spontaneous oscils. 4-108  
 particle velocity and size distrib. meas. by laser Doppler velocimetry 4-84076  
 perylene, jet-cooled, excess vibr. energy relax., fluoresc. study 4-69132  
 plane and axisymmetric viscous-gravity jets, eqns. governing flow 4-103384  
 plane jet as a limit case of the radial jet 4-69809  
 plane jets, Newtonian and non-Newtonian, Navier-Stokes anal. 4-103384  
 plume in supersonic crossflow, viscosity and surface tension effects 4-97625  
 polymer jet, extruded from capillary die, elasticity, stretching and swelling 4-69722  
 premixed jet flame, flow field struct. meas. 4-97628  
 pulsation velocities correl. of disperse phase in jet flows 4-69808  
 quasars, effect of dissipative jets on separation ratio of outer radio components 4-110771  
 radial jet in rotating outer flow incompressible laminar flow 4-87769  
 radio sources, extragalactic, struct. of hotspots from time-varying 4-101493  
 ramjet combustion efficiencies comparison (German) 4-99797  
 rarefied gas, supersonic flow, interaction of jet exhausting from body 4-69799  
 rhodamine 6G continuous high-power dye laser exptl. design (Russian) 4-69432  
 round jet in cross flow, initial conditions, Reynolds no. effects and flow field characteristics (German) 4-97517  
 round jets, heat and momentum transport calc. 4-69806  
 shear flow turbulence modelling, buoyancy effects 4-79575  
 similarity solution of turbulent free jet 4-87681  
 slot jet flowing along curved surface, momentum losses 4-64995  
 soot particles formation, growth and oxidation, sonic sampling technique and flat flames 4-104990  
 soot particles formation, growth and oxidation 4-104989  
 sound propagation in nonuniform and nonstationary flows (French) 4-112842  
 star formation, mini-QSO model for mass outflow from newly-forming stars 4-67719  
 submerged of nonNewtonian fluid, laminar length meas. by flow visualisation technique 4-64997  
 subsonic, near field, two-dimens. acoustic intensity probe measurements (French) 4-60227  
 subsonic jets, high-speed, acoustic meas. 4-112649  
 subsonic whistler nozzle jet, noise characteristics 4-79632  
 supersonic fluid jets, surface waves propag. and growth 4-63039  
 supersonic jet expansion, gas condensation, mol. beam study 4-60561  
 symmetric impact of compressible fluid streams, jet form. and penetration in steady flow 4-91821  
 thin liquid jets in air, dynamics, instability condition 4-60473  
 throttling valve noise, aerodynamic sound level calc. 4-74807  
 toluene-He (methane) clusters, supersonic mol. jet, fluoresc., time of flight mass spectra 4-107387  
 transient three dimens. turbulent flowfields press.-vel. finite difference code 4-87682  
 transitory gaseous film study (French) 4-62206  
 triple free jet, mixing process, coherent struct., laser meas. 4-87771

continued  
 turbulence and combustion studies, laser scatt. for conc. and temp. determ. 4-68289  
 turbulence flow with heat transfer in plane and curved wall jets 4-112862  
 turbulent, thermal and vel. boundary layers 4-103306  
 turbulent, through cavity, attenuation of self-sustained oscillations 4-103381  
 turbulent 4-60471  
 turbulent jets, mixing process, noise, coherent struct. 4-64991  
 turbulent plane free jets, oblique impingement study 4-112972  
 turbulent shear flow, conf., St. Louis, Missouri, USA, June 1982 4-86119  
 two dimens. circular jet impingement with crossflow, heat transfer characs. 4-112868  
 two dimens. plane jet issuing in porous medium Brinkman eqn. soln. 4-97633  
 two-dimensional impinging jet; heat transfer augmentation technique (Japanese) 4-103379  
 two-dimensional inviscid jets, calculations 4-112971  
 two-phase turbulent round jet, laser Doppler anemometer meas. 4-97627  
 underwater explosion of ring charge near a free surface 4-87759  
 velocity distrib. meas. by laser beam, appls., aerosol introduction into fluid 4-97718  
 vertical annular liquid jets dynamics, flow characteristics 4-103383  
 viscous gas flowing from slit or cylindrical channels into region of lower press., interferometric study 4-113021  
 viscous liquids, laminar mixing of parallel flows of cond. liq. in transverse mag. fields (Russian) 4-113060  
 viscous swirling jets, heat and mass transfer, excess temp. distrib. 4-75065  
 vortex chamber aerodynamics, flow pattern investigation 4-79601  
 wall cooling, protective layer, temp. distrib., boundary conditions effect 4-60405  
 water, evaporation under an obliquely impinging laminar ducted slot jet—a numerical model 4-108100  
 wave tank flow region, US images of jets and wakes, oceanographic appls. 4-113085  
 weakly-conducting fluid, isothermal flow in nonuniform elec. field (Russian) 4-83958  
 wing aerodynamics in supersonic shear flow 4-97602  
 Al-plexiglass target, high speed water jet penetration simulation 4-108533  
 CO<sub>2</sub> IR absorpt. line shape and width across supersonic free jets 4-83374  
 CO supersonic expansion, coherent extreme UV and vacuum UV radiation generation using pulsed nozzles 4-107745  
 CO<sub>2</sub>, expanding supersonic jets, condensation processes similarity 4-60474  
 Cs plasma jet flowing into He, diagnostics 4-91993  
 He gas, 35 nm coherent radiation generation using KrF laser 4-107744  
 He II, fluid mechanics, nonlinear interactions 4-92461  
 N<sub>2</sub> low-pressure gas jet, multipass dark-ground photography 4-91851  
 N<sub>2</sub> superheated liq., explosive flashing in discharge through short nozzles 4-112936  
 NH<sub>3</sub> expanding jet, rotational temp. and mol. density determ. by IR absorpt. 4-83490  
 NO, supersonic free jets, high Rydberg states, two-colour excitation, autoionisation 4-107411  
 Na/Na<sub>2</sub> free jet, laser-induced fluoresc. study, effective relax. cross sections to off-axis dimmer distrib. 4-112223  
 O<sub>2</sub> superheated liq., explosive flashing in discharge through short nozzles 4-112936  
 Pb, electrically cond. liquids, free jets, reson. breakdown, EM forces, drop form. phases (Russian) 4-113057  
 S<sub>2</sub>, supersonic free jet, B<sup>2</sup>Π<sub>g</sub>-X<sup>3</sup>Σ<sub>g</sub><sup>-</sup> transition, laser induced fluoresc. 4-102728  
 SF<sub>6</sub>, laser pumped mols., electron diff. study 4-96626  
 SF<sub>6</sub> molecule, IR absorpt. spectra, ν<sub>3</sub> band, pulsed supersonic jet study 4-59734  
 Xe supersonic expansion, coherent extreme UV and vacuum UV radiation generation using pulsed nozzles 4-107745  
**i.e.t. see junction gate field effect transistors**  
**Jensen-Rahbek effect see adhesion; electrostatics**  
**Johnson noise see thermal noise**  
**Joining processes**  
 see also brazing; cable jointing; soldering; welding  
 steel, diffusion bonding below A<sub>1</sub> transform. point, heat treatment effect on tensile strength (Japanese) 4-66547  
 SiC, reaction bonded, and liq. Al, cast bonding, exchange diffusion phenomenon involving free Si 4-99741  
**Jointing, cable see cable jointing**  
**Jordan-Thiry field see cosmology; general relativity**  
**Josephson effect**  
 array, microscopic formulation using Feynman diagrams 4-92868  
 chaos, onset, in Josephson junctions, influence of nonlinear conductance and cosφ term 4-104375  
 DC Josephson current, step structures within one flux quantum period (Chinese) 4-114070  
 DC Josephson current within one flux quantum period, step struct., oscill. effect (Chinese) 4-70990  
 driven junctions, statistical props. of intermittent diffusion in chaotic systems 4-90490  
 Josephson junction chain, quantum fluctuations 4-98812  
 Josephson oscillator, nonlinear dynamics model 4-98823  
 Josephson tunnel junctions, current density distrib. (German) 4-84750  
 junction, current-driven, microwave induced steps 4-65772  
 junction, subharmonic steps, fractal struct., analogue computer calc. 4-92869  
 junction analogue, transition from quasiperiodicity to chaos 4-98820  
 junction series array, microwave-induced constant-volt. steps at 1 V 4-114069  
 junctions, circle maps and chaotic transitions 4-98825  
 linear chain compounds, moving CDW, Josephson-type oscillations 4-92644  
 localised magnetic impurities, effect on steady-state Josephson effect (Russian) 4-98817  
 magnetic insulators, dynamics probe by supercond. pair tunnelling 4-61544  
 microwave irradiation effects, Green's function calc. (Chinese) 4-104369  
 MM-wave spectrometer comprising Josephson junction 4-82829

## Josephson effect continued

one-dimensional Josephson tunnel junctions, focused laser beam irradi., nonlocal response 4-92864  
 period doubling in Josephson circuit, calcs. 4-65773  
 phonon source, tunable, for high resolution spectroscopy 4-61495  
 planar junction in mag. field, charge fractionalisation 4-104373  
 point contacts, freq. locking 4-80727  
 quantum oscillations of the nonequilibrium chemical potential in Josephson junctions 4-92870  
 quasi-2D weak coupled Josephson junctions on a semicond. surface (Russian) 4-70992  
 sine-Gordon equation, perturbed, exact numerical solutions 4-104377  
 students introduction to supercond. microelectronics 4-58610  
 sub-MM wave response in tunnel-type and bridge-type Josephson junction 4-76087  
 superconducting films, Josephson junction oscills. (Russian) 4-70991  
 superconducting point contact fabrication 4-76086  
 superconducting rings containing Josephson junctions, static and dynamic behaviour 4-108977  
 superconducting weak link constriction ring, solns. of Schrödinger equation 4-114075  
 superconductor/semicond./supercond. structs., carrier coherence length 4-65774  
 superfluid interferometer for Earth rot. detection using Josephson effect 4-58728  
 superradiance and superfluorescence in Josephson junction arrays 4-61732  
 thermodynamic limit of a Josephson junction at non-zero temperature 4-76082  
 tunnel junction, overdamped, I-V characs., capacitance effects 4-108976  
 tunnel junctions, chaotic noise in presence of DC current and MM radiation 4-104376  
 tunnel junctions, fabrication of planarised structure 4-84761  
 tunnel junctions, soliton excitations 4-80728  
 voltage standard utilisation (Czech) 4-82805  
 Al-Al<sub>2</sub>O<sub>3</sub>-Pb junction, effects of patterned laser illumination 4-70998  
 Al<sub>2</sub>O<sub>3</sub>/V<sup>2+</sup>, zero-field hyperfine splitting by Josephson phonon spectroscopy 4-61353  
 BaPb<sub>0.7</sub>Bi<sub>0.3</sub> superconducting films, current-voltage curves, discrete current behaviour 4-61492  
 BaPb<sub>0.7</sub>Bi<sub>0.3</sub>O<sub>3</sub> films, two-dimensional Josephson tunnel junction arrays, EM coupling effects 4-61493  
 BaPb<sub>0.7</sub>Bi<sub>0.3</sub>O<sub>3</sub> superconducting photodetector 4-71002  
 BaPb<sub>0.7</sub>Bi<sub>0.3</sub>O<sub>3</sub> supercond. thin films for highly sensitive optical detector fabrication 4-82825  
 Mo<sub>6</sub>C<sub>37</sub> superconducting film, RF-induced DC voltage obs. 4-88628  
 Nb Josephson junction, thin film point-contact, Stewart-McCumber model 4-114072  
 Nb Josephson junction characs., effect of substrate bias 4-84751  
 Nb Josephson junctions, point contact, Riedel singularity, damping factor meas. 4-70994  
 Nb nm bridge type Josephson junction on edge junction, props. 4-84752  
 Nb thin film point contact Josephson junctions, fabrication by magnetron sputtering and electron beam lithography 4-80721  
 Nb/Au/Nb Josephson tunnel junction, ESR study 4-92871  
 Nb-Nb oxide-Pb well-damped Josephson transmission line, fluxon propagation 4-65771  
 Nb-NbO<sub>x</sub>-Pb Josephson tunnel junctions fabricated by CF<sub>4</sub> plasma cleaning process 4-80720  
 Nb-NbO<sub>x</sub>-Pb alloy Josephson tunnel junctions, resist. at cryogenic and ambient temps. 4-98819  
 Nb<sub>2</sub>Ge<sub>4</sub>-Si-Pb Josephson tunnel junction 4-104374  
 NbN electrodes for Josephson tunnel junction fabrication process 4-98813  
 NbN granular Josephson microbridges, noise props., freq. mixer appl. 4-70995  
 NbN/Nb double-layered electrodes, mag. props. anal., Josephson tunnel junctions 4-98814  
 NbN/Pb Josephson tunnel junctions with plasma oxidized barriers, annealing stability 4-84746  
 NbN-Nb junction with plasma oxidised barrier, growth and props. 4-84747  
 Nb<sub>3</sub>Sn-Pb Josephson junctions using Nb<sub>3</sub>Sn formed by reaction of Nb/Sn dual-layer films 4-61491  
 Pb alloys, Josephson junctions, electrode surfaces, characteristics and failures (Chinese) 4-92866  
 Pb Josephson junctions, electrode surfaces, characteristics and failures (Chinese) 4-92866  
 Pb/Nb oxide/Nb resistively coupled Josephson transmission line, fluxon threshold props. 4-70989  
 Pb-alloy Josephson junctions, size effects 4-84748  
 Pb-Zn-Pb SNS junctions, DC Josephson effect 4-80722  
 Pb<sub>2</sub>Bi superconducting films for Josephson junctions, microstruct. control 4-114071  
 Si:B neck for Josephson bridges 4-98828  
 V-V<sub>2</sub>O<sub>5</sub>-Pb Josephson junctions self-field effects aspects 4-61494  
**Joshi effect see glow discharges**  
**Joule-Thomson effect**  
 aerosols, gas-solid, Joule-Thomson effect statistical thermodynamics 4-65048  
 coolers at very low powers 4-101855  
 microminiature Joule-Thomson refrigerators, fine channel heat exchangers, gas flow anal. 4-101851  
 minicooler based on Joule-Thomson expansion 4-95440  
**junction gate field effect transistors**  
 GaAs fast supercomputer circuits (Swedish) 4-65282  
 GaAs JFET low-noise high-speed optical receiver for optical fibre systems 4-74743  
**junction lasers see semiconductor junction lasers**  
**Jupiter**  
 Adrastea (1979J1), orbital parameters of Jupiter satellite 4-101231  
 approach orbit determ. for Galileo mission 4-110494  
 atmosphere, geostrophic regimes, intermediate solitary vortices and eddies 4-94672  
 atmosphere, H<sub>2</sub>/He ratio, implications for solar nebula 4-77757  
 atmosphere, voyager far-IR spectra 4-105901  
 auroral emission, longitudinal and temporal vars., IUE obs. 4-90107  
 capture of Periodic Comet Boethin 4-90119  
 chorus radioemissions 4-94675  
 chorus related electrostatic bursts, Voyager obs. 4-67679

## Jupiter continued

- comet orbits and minimum planetary distances (*Russian*) 4-101259  
 P/Comet Russel 3 (1982 IX), orbit, encounters with Jupiter 4-77771  
 P/Comet Wild 3, orbital perturbations due to close encounter with Jupiter (May 1977) 4-94683  
 cosmic ray contribution 4-94394  
 differential rotation in a solar-driven quasi-axisymmetric circulation 4-101215  
 electron events, interplanetary transport, modulation in Earth's orbit 4-94434  
 Galilean satellite eclipse timings (1975-82), ALPO report 4-110558  
 Galilean satellite eclipses (1652-1982) manuscripts anal. 4-90109  
 Galilean satellite spin rates 4-101233  
 Galilean satellites, 1975-1982 eclipse timings 4-63096  
 Galilean satellites, ephemerides comparison with obs. and mutual phenomena 4-82440  
 Galilean satellites, long-term motion determ. via numerical integration procedure 4-82402  
 Galilean satellites, motion, analytic theory first approx. and ephemerides 4-82443  
 Galilean satellites, mutual phenomena in 1973 and 1979/80, astrometric obs. 4-63098  
 Galilean satellites, obs., ephemerides and residuals anal. 4-82441  
 Galilean satellites, orbital evolution 4-82442  
 Galileo mission, CCD TV camera for spacecraft 4-94615  
 Galileo Mission, near IR mapping spectrometer 4-94612  
 Great Red Spot, temporal evolution of Taylor columns over topography 4-62843  
 icy satellite cratering by impacts, effects of viscosity 4-82427  
 icy satellites, interior struts. 4-63097  
 icy satellites, internal differentiation 4-67653  
 Io, eclipse observations collected by Delambre (1775 to 1802) 4-101229  
 Io, Loki volcano eruption, far IR obs 4-101238  
 Io, S and O escape by charged particle sputtering mechanism 4-94676  
 Io, volcanic flows not consisting of sulphur 4-101234  
 Io decametric emission cone 4-90108  
 Io plasma torus, aperiodic ion temp. vars. 4-67673  
 Io plasma torus, evidence for ion-cyclotron instability 4-101230  
 Io plasma torus, longitudinal asymmetry 4-85891  
 ionosphere and upper atmos. of outer planets, comparison 4-72909  
 magnetodisc, pitch angle diffusion theory 4-85890  
 magnetosphere, 3-D ray tracing in 2-35 MHz range 4-67672  
 magnetosphere energetic particle acceleration mechanisms 4-94674  
 magnetosphere gamma ray prod. and process involving trapped protons and electrons 4-101239  
 magnetosphere upstream region, energetic particle transport 4-94673  
 magnetosphere-rings interaction, theory of channelling radiation by charged particles 4-77762  
 magnetospheres with rapid rotation, adiabatic theory 4-110551  
 magnetotail current sheet fine-scale struct. 4-67591  
 magnetotail plasma densities at large distances from Jupiter 4-67671  
 methane IR spectra and  $^{12}\text{C}/^{13}\text{C}$  ratio in atmosphere 4-69146  
 Metis (1979J13), orbital parameters of Jupiter satellite 4-101231  
 millisecond radio bursts, Voyager obs. 4-85889  
 nonthermal radio radiation, VLA obs. 4-77756  
 perturbation of meteor stream density (*Russian*) 4-85899  
 photographic positional observations of Jupiter and Galilean satellites, results (*Russian*) 4-101237  
 resonance locking with Uranus 4-110506  
 satellite drag due to plasmasphere Alfvén wave effect 4-101232  
 outer satellites, multicolour photometry obs. 4-101236  
 satellites, naked eye obs. 4-72907  
 Thebe (1979J12), orbital parameters of Jupiter satellite 4-101231  
 whistler mode instability in presence of parallel electric field, unified theory 4-79789  
 $\text{H}_2$ , ortho-para conversion in atmosphere and atmosphere dynamics 4-67670  
 HCN detectability by mm wave radioastronomy method 4-94670  
 Io, spectral reflectivity and props. of powdered S 4-101235  
 $\text{PH}_4$ , photolysis mechanism, rel. to Jovian atm. photochem. 4-66603  
 S III 9531 Å forbidden line emission from hot plasma torus, periodic intensity var. 4-94671

**K-capture** see nuclear electron capture

**K mesons** see kaons

**K-N interactions** see kaon-nucleon interactions

## Kalman filters

- artificial satellites, synchronous orbits, appl. of extended semianalytical Kalman filter 4-90057  
 global Positioning System (GPS) appl. to geodesy, estimation and large-scale multiple hypothesis testing 4-77656  
 in-pile LMFBR accident simulations anal. by Kalman filter methods 4-86936  
 optically implemented multiple-stage Kalman filter algorithm 4-97044  
 time series data editing method using Kalman filter 4-100736

## kaon-baryon interactions

see also kaon-baryon scattering; kaon-hyperon interactions; kaon-nucleon interactions

No entries

## kaon-baryon scattering

see also kaon-baryon interactions; kaon-hyperon scattering; kaon-nucleon scattering

No entries

## kaon decay

- see also kaon hadronic decay; kaon leptonic decay  
 $K \rightarrow \pi \nu$ ,  $K_{12}$  form factors in bag model 4-82954  
 $K \rightarrow \pi \mu \nu$ , symmetry violation studies at Brookhaven 4-102051  
 $K \rightarrow \pi \pi \nu$ , discrepancies due to departure from chiral symmetry, unitarity and analyticity 4-102116  
 $K^+ \rightarrow \pi^+ \nu \bar{\nu}$ , rare decays, universality test, generation puzzle, search status, review 4-102112

## kaon hadronic decay

see also kaon regeneration

- four-fermion operators, matrix elements, nonleptonic decays 4-86665  
 $K \rightarrow 3\pi$ , matrix element quadratic terms, chiral Lagrangians, current-algebra analysis 4-106527  
 $K \rightarrow \pi \pi$ ,  $\Delta I = 1/2$  rule in chiral quark model, one-loop renormalisation group eqns. 4-111444  
 $K^0 \rightarrow 3\pi^0$ , CPT symmetry, Bell-Steinberger unitarity relation 4-73748  
 $K_L^0 \rightarrow \pi^+ \pi^-$  ( $\pi^0 \pi^0$ ), symmetry violation studies at Brookhaven 4-102051

## kaon hadronic decay continued

- $K^+ \rightarrow \pi^+ X^0$ , neutral exotics search, axions 4-102115  
 $K^+ \rightarrow \pi^+ \alpha$  ( $\alpha \equiv \text{Goldstone boson}$ ) in  $\text{SU}(5) \times \text{SU}(3)$  theory 4-68480

## kaon-hyperon interactions

see also kaon-hyperon scattering

No entries

## kaon-hyperon scattering

see also kaon-hyperon interactions

No entries

**kaon interactions** see kaon-baryon interactions; kaon-nucleon reactions; ion-hadron interactions; meson-meson interactions; photon-hadron interactions

## kaon leptonic decay

- review of recent results, electroweak theory, lepton number violation 4-73685  
 $K \rightarrow e^+ \mu^-$ , flavour changing suppression in technicolour, pseudo-Goldstone bosons, Cabibbo mixing 4-102075  
 $K^0 \rightarrow \mu e$  ( $e e$ ), symmetry violation studies at Brookhaven 4-102051  
 $K^+ \rightarrow \mu^+ \nu$ , heavy neutrino search and muon longitudinal polarisation 4-102115  
 $K^+ \rightarrow \mu^+ \nu$ , longitudinal polarisation meas. 4-63989  
 $K_L^0 \rightarrow \mu^+ \mu^-$ , six-quark scheme tests, CP violation, top-quark 4-111389

## kaon-nucleon interactions

see also kaon-nucleon scattering; kaon-proton interactions

- g-particle multiplicity in p, p,  $\pi$  and K collisions with emulsion 4-102092  
 KN interaction, quark compound bag model 4-102092  
 $K^- N \rightarrow \bar{K}^0 (890) X$ ,  $E = 175$  GeV, integrated cross-sections, quark counting rules 4-102142  
 $K^- N \rightarrow \bar{K}^{*0} (890) X$ ,  $E = 175$  GeV, integrated cross-sections, quark counting rules 4-102142  
 $K^- n \rightarrow \Lambda \pi^-$ , hypernuclear spectroscopy using stopped  $K^-$  spin-orbit doublets, deep orbitals 4-111518  
 $K^- n \rightarrow \Sigma^0 \pi^-$  ( $\Sigma^- \pi^0$ ), hypernuclear spectroscopy using stopped  $K^-$  spin-orbit doublets, deep orbitals 4-111518  
 $K^+ N$ , 600-1500 MeV/c, phase-shift anal. 4-64019  
 $K^- N N \rightarrow \Sigma N$ , hypernuclear spectroscopy using stopped  $K^-$  spin-orbit doublets, deep orbitals 4-111518  
 $K^+ N \rightarrow K^+ n$ , coherent dissociation study 4-111469

## kaon-nucleon scattering

see also kaon-nucleon interactions; kaon-proton scattering

- KN inverse scatt. problem, interaction form factor 4-111471  
 KN low energy scatt. in cloudy bag model,  $\text{SU}(3)$  chiral generalisation 4-59106  
 $K^+ N$ , 600-1500 MeV/c, phase-shift anal. 4-64019

## kaon-nucleus reactions

for inelastic kaon-nucleus scattering, see "kaon-nucleus scattering"

see also kaon-nucleon interactions

- analytic distorted wave approximation for kaon-nucleus interactions  
 optical potentials 4-73862  
 $(K, X)$ , in emulsion, g-particle mean multiplicity 4-102132  
 $\text{Be}(K, \pi^-)^7\text{Be}$ , ang. distrib. and excitation spectra using three-chamber model wave functions 4-68738  
 $^1\text{H}(K^+, X)$ , 600-1500 MeV/c, phase-shift anal. 4-64019  
 $^2\text{H}(K^+, X)$ ,  $X = \Sigma^+$  or  $\Delta$ , disintegration with two-body final states, sections, form factors 4-102321  
 $^7\text{Li}(K^+, \pi^-)^7\text{Li}$ , ang. distrib. and excitation spectra using three-chamber model wave functions 4-68738

## kaon-nucleus scattering

see also kaon-nucleon scattering

( $K^0, K^0$ ), inelastic kaon regeneration cross section, DWIA calcs. 4-9101

## kaon production

- heavy ion reactions, subthreshold  $K^-$  production, final state interaction effect 4-64106  
 $D(1285) \rightarrow K^+ K^- \pi^0$ ,  $\delta$ -dominance model,  $K^+ K^-$  effective mass spectrum 4-111445  
 $D(1285) \rightarrow K^+ K^- \pi^0$ , invariant mass distrib. and differential spectra 4-90867  
 $K^+$  production, cascade model, nucleus-nucleus collisions 4-91012  
 $K^- p \rightarrow K^+ \pi^- p$ , 100 and 175 GeV,  $K^+$  (890) and (1430) production 4-86731  
 $K^+ p$ , 32 GeV/c,  $K_s^0$ ,  $\Lambda$  and  $\bar{\Lambda}$  prod., total and semi-inclusive cross sections 4-95829  
 $n \rightarrow \bar{p} K^0$ , lifetimes and branching ratios 4-73684  
 $n \rightarrow \bar{p} K^0$  GUT predictions for strangeness yield 4-86624  
 $N_2(\Lambda) \rightarrow \text{NNK}$ , contribution to kaon production in relativistic heavy ion collisions 4-83101  
 $\bar{p} N$ , neutral current interaction, neutral strange particle prod.,  $K^0$  multiplicity 4-73740  
 $n \rightarrow K^+ X$ , neutral current production of strange particles 4-111437  
 $(p, K^+ X)$ , low energy annihilation,  $K^+$  prod. in intranuclear cascade model 4-78633  
 $p \rightarrow e^+ \pi^0$  ( $e^+ K^0$ ) lifetimes and branching ratios 4-73684  
 $p \rightarrow \mu^+ \pi^0$  4-73684  
 $p \rightarrow \mu^+ K^0 (\bar{p} K^+)$  GUT predictions for strangeness yield 4-86624  
 $p \rightarrow \mu^+ + K^0$ , Higgs mediated in  $\text{SU}(5)$  theory, 5-D interactions, fermion masses 4-86703  
 $p \Lambda \rightarrow K^+ K^+ X$ , doubly strange  $\bar{p}$  annihilation channels in complex nucleus 4-106614  
 $p \Lambda \rightarrow \Lambda^0 K^+ X$ , doubly strange  $\bar{p}$  annihilation channels in complex nucleus 4-106614  
 $pd \rightarrow hX$ , 70 GeV,  $h = \pi^+$ ,  $K^+$ ,  $p$ ,  $\bar{p}$ , invariant cross sections for large hadron prod. 4-90923  
 $pp$ , 3.0-4.5 GeV/c,  $K_s^0$ , ( $K_s^0 K_s^0$ ) and  $K^{*+}(892)$  inclusive prod., cross sections 4-95809  
 $pp \rightarrow hX$ , effect of strange particles on cosmic ray processes and energy dist. 4-95839  
 $pp \rightarrow K_s^0 X$ ,  $E = 70$  GeV/c, differential and production cross sections 4-102141  
 $pp \rightarrow K^+ X$ , in nuclei, low energy annihilation,  $K^+$  prod. in intranuclear cascade model 4-78633  
 $pp \rightarrow K^+ X$ , parton fragmentation model with diffractive resonance production 4-111483  
 $pp \rightarrow \Lambda^0 K^+ p$ , partial wave anal., deck model, double Regge exchange 4-78564  
 $pp \rightarrow pK^+ K^- \pi^0$  ( $p \eta \pi^+ \pi^-$ ) resonances in glueball-glueball collisions 4-95818  
 $pp \rightarrow pp \pi^+ \pi^-$  ( $pp K^+ K^-$ ), exclusive central collisions,  $f(1270)$  prod., resonance gluon content 4-59109  
 $\pi^- N \rightarrow K_S^0 K_S^0 \pi^- \pi^-$ , 200 GeV, diffractive production 4-73773

- production continued**  
 $N-K^0K^0X$ , charge multiplicity, mass distrib., differential cross-sections 4-111479  
 $\pi^+K^0K^0$ , 63 GeV, evidence for non- $q\bar{q}$  tensor meson at 1410 MeV 4-95819  
 $\pi^+K^0K^0$  p, 50, 100 and 175 GeV,  $A_2(1320)$  and  $(2040)$  production 4-86731  
 $\pi^+p-K^+(892)X$ , 40 GeV, production cross sections 4-78571  
 $\pi^+p-K^+\Sigma^+$ , threshold-2.35 GeV, energy depend. partial wave anal.,  $SU(3)$  breaking 4-82971  
 $F(Ne, K^+X)$ , 2.1 GeV/N,  $K^+$  inclusive diff. cross section in rel. collisions from transport theory 4-102290  
 $Na(Ne, K^+X)$ , 2.1 GeV/N,  $K^+$  inclusive diff. cross section in rel. collisions from transport theory 4-102290  
 $Na(Ne, X)$  on NaF, 2.1 GeV/A,  $K^+$  cross section, cascade model 4-102300  
 $Pb(Pb, K^+X)$ ,  $K^+$  inclusive diff. cross section in rel. collisions from transport theory 4-102290
- n-proton interactions**  
 see also kaon-proton scattering  
 $Kp$ , secondary inclusive spectra using additive quark model and quark statistics rule 4-82978  
 $Kp$ , kaonic hydrogen ground state, model-independent formalism 4-96726  
 $Kp-\eta A$ , polarisation, differential and integrated cross sections 4-68585  
 $Kp-hX$ , effect of strange particles on cosmic ray processes and energy dist. 4-95839  
 $Kp-K^0n$ , up to 40 GeV, integrated and differential cross sections 4-106542  
 $Kp-K^0\pi^+p$ , 100 and 175 GeV,  $K^+(890)$  and  $(1430)$  production 4-86731  
 $Kp-\Delta\pi^+$ , hypernuclear spectroscopy using stopped  $K^-$  spin-orbit doublets, deep orbitals 4-111518  
 $(Kp-\pi^+\Sigma^+(1385), 8.25$  GeV, amplitude anal., spin density matrix 4-86730  
 $Kp-\pi^+$ , string fragmentation model predictions at 110 GeV 4-59111  
 $Kp-\Sigma\pi$ , hypernuclear spectroscopy using stopped  $K^-$  spin-orbit doublets, deep orbitals 4-111518  
 $Kp$ , 32 GeV/c,  $K_s^0$ ,  $\Lambda$  and  $\bar{\Lambda}$  prod., total and semi-inclusive cross sections 4-95829  
 $(K^+p-\gamma)$ s, inclusive production cross-section 4-86738  
 $K^+p-(R-A^{++})X$ , production of gluonic long-lived state 4-111481  
 $K^+p$ -jets, planar events, structures, momentum flows 4-95833  
 $K^+p-K^+p3\pi^+3\pi^-$  ( $4\pi^+4\pi^-$ ), 32 GeV, multiparticle production spectra 4-64020  
 $K^+p-K^+\pi^+\pi^-$ , 32 GeV/c, diffraction peaks cross sections, diffraction excitation 4-86732  
 $K^+p$ ,  $\leq 20$  GeV/c, charged particle average multiplicities, energy depend. 4-111475
- non-proton scattering**  
 see also kaon-proton interactions  
 No entries
- kaon regeneration**  
 $(K^0K^0)$ , inelastic kaon regeneration cross section, DWIA calcs. 4-91025
- meson resonances** see meson resonances
- on scattering** see kaon-baryon scattering; kaon-nucleus scattering; lepton hadron scattering; meson-meson scattering; photon-hadron scattering
- ons**  
 see also kaon regeneration  
 $K_L-K_S$  mass difference and CP-violation in supersymmetric models 4-111331  
 $K^0\bar{K}^0$  mixing, CP violation, dispersive contributions 4-68536  
 $K_L-K_S$  mass diff., left-right symmetric model, Higgs induced flavour changing neutral currents 4-90778  
 $K_L-K_S$  mass matrix and top quark mass 4-63990  
 $K_L-K_S$  mass difference,  $N=2$  supersymmetric models, low energy constraints 4-102068  
 $K^{*2}-K^+\gamma$  Coulomb dissociation, decay widths 4-90885
- kapitza-Dirac effect**  
 see also Schwarz-Hora effect  
 No entries
- kapitza resistance**  
 solid/solid interfaces, thermal phonons, critical cone channelling 4-65541  
 Ag powders, sintered, appl. in mK heat exchangers 4-111139  
 $Cd_{Mg_{1-x}}(NO_3)_2\cdot He$ -He liquid boundary, thermal resistance study 4-84484  
 $Ce_2Mg_3(NO_3)_{12}\cdot^3He$  system, anomalous low temp. Kapitza resistance 4-65542  
 $^4He$  liquid small particle thermal boundary resistance, review 4-65510  
 $^4He$  powder system, Kapitza resist., shaking box model 4-65513  
 $^4He$ -He dilute mixtures, Kapitza resist. in Cu powder, size effect 4-65514  
 $^4He$ , liquid and gaseous, Kapitza resistance, spectral depend. between 0.5 and 2.3K 4-65512  
 $^4He$ , solid-liq. interface, phonon, transmission and Kapitza resist. 4-70501  
 $^4He$ , superfluid, Kapitza resistance effect on standing surface waves 4-84478  
 $^4He$ -Si interface, Kapitza resistance of laser-annealed surfaces 4-70500
- DP** see potassium compounds
- elvin-Helmholtz instability** see flow instability
- ennelly-Heaviside layer** see E-region; ionosphere
- eratin** see proteins
- erma** see dosimetry
- kerr effect (optical)** see optical Kerr effect
- kerr electro-optical effect**  
 see also optical Kerr effect  
 benzene, in cyclohexane, Kerr const., mol. anisotropic polarisabilities, dielectric study 4-102721  
 t-butylbenzenes, in cyclohexane, Kerr const., mol. anisotropic polarisabilities, dielectric study 4-102721  
 liquid crystals, cubic, birefringence and Fredericks effect 4-60817  
 methylbenzenes, in cyclohexane, Kerr const., mol. anisotropic polarisabilities, dielectric study 4-102721  
 poly N-vinylcarbazole soln., dipole moment, Kerr const., stereoregularity 4-93053  
 transient Kerr effect student apparatus 4-95103  
 water, dielec. props., charge injection and transport anal. 4-99023
- Kerr electro-optical effect continued**  
 InGaAsP, quadratic electro-optic Kerr effects, dispersion 4-109159  
 $KD_2PO_4$ , electrooptic Kerr effect, electronic contrib. 4-109164  
 $NH_2H_2PO_4$ , electrooptic Kerr effect, electronic contrib. 4-109164  
 PLZT thin-film waveguides, electrooptic Kerr coeffs. 4-91578
- Kerr magneto-optical effect**  
 amorphous ribbons, electropolishing, power loss and domain struct. 4-76158  
 Permalloy evaporated films, coercive force and mag. domains (Japanese) 4-104474  
 steel, Fe-Si (3 wt.%), power loss and flux density of neighbouring grains 4-80776  
 $CoFe_2O_4$  thin films, interference enhanced magneto-optic Kerr rotation, storage appls. 4-93059  
 Gd-Fe amorphous films, vacuum deposited, Kerr hysteresis meas. 4-66014  
 GdCo amorphous cosputtered film, surface versus bulk magnetisation curves, longit. Kerr rot. meas. 4-71131  
 GdFe film, oxidation by overlaid  $SiO_2$  film, Kerr enhancement 4-84949  
 GdFe/TbFe amorphous double-layer films, magneto-optical characts. 4-61665  
 MnZn ferrite, (100) surface, mag. surface props., influence of sputter etching 4-88813  
 PtMnSb, magneto-optical props. and electronic struct. 4-61662  
 TmS(Se), exchange-induced plasma edge splitting, magneto-optical study 4-61663  
 $UAs_2Se_{1-x}$ , electronic and mag. struct. determ. 4-61281  
 $Y_{3-x-y}Bi_xPb_yFe_{10-x-y}$ - $Pt_{10}$  garnet films, magneto-optic prop. meas. using piezobirefr. modulation 4-66013
- kicksorters** see counting circuits
- kidney**  
 artificial kidneys, review (Japanese) 4-109998  
 artificial organs and their materials, review (Japanese) 4-89831  
 collagen and fluid contents of mouse kidney, increases after X-irrad. 4-105298  
 elemental conc. meas. in mouse arteries, micro-PIXE anal. 4-100385  
 glomerular filtration rate, determ. using  $^{99m}Tc$ -DTPA, in-house computer program 4-89730  
 glomerular filtration rate, meas. without blood sample, validation in renal transplant patients 4-62555  
 haemodialysis unit, microprocessor-controlled, for terminal renal patients 4-93963  
 imaging techniques comparison for abdominal, pelvic and thyroid disease 4-115215  
 magnetic relaxation times in vitro of ischemic and reperfused rabbit kidney 4-81721  
 multifraction X-irrad. dose response of mouse kidney 4-77344  
 neutron activation and PIXE anal. 4-100380  
 pig tissue,  $^{23}Na$  NMR study 4-100081  
 PIXE anal., target prep. influence in rate organs 4-100381  
 relative activity in the kidneys, differentiation rel. to phys. characts. of  $^{125}I$  and  $^{131}I$  4-72369  
 spinal cord thermal stimulation in rabbit, ear-skin and renal blood flow changes 4-81725  
 volume, in vivo estimation using a rot.  $\alpha$  camera and  $^{99m}Tc$ -dimercaptosuccinic acid 4-81764
- Kikuchi lines** see electron diffraction crystallography
- killed steel** see alloy steel
- kinematic viscosity** see viscosity
- kinematics**  
 see also acceleration; ballistics  
 Arp 91, interacting galaxy pair, dynamical model rel. to optical morphology and kinematics 4-90230  
 compact planetary nebulae, expansion vels. from high dispersion spectra 4-101456  
 Cygnus A, hotspots velocity from multi-freq. radio study 4-101492  
 E and S0 galaxies (NGC 1052, 2749, 3998 and 4125), stellar and gaseous kinematics 4-73066  
 elliptical galaxies, vel. dispersion of stellar dynamical models 4-115813  
 interstellar clouds, turbulent velocity structure determ. 4-90204  
 interstellar molecular cloud assoc. with multiple IR source (GL 437), vel. field from CO obs. 4-85999  
 M82, distrib. and kinematics of interstellar CO 4-101471  
 mixtures, Lagrangian time rates, volume fractions 4-90369  
 NGC 5266, NGC 3108, early-type galaxies with ionised gas discs, struct. and kinematics 4-86030  
 planetary nebulae, expansion vels. rel. to evolution and formation rate 4-115793  
 radio sources, extragalactic, relativistic plasmon model for apparent superluminal motion (Chinese) 4-82555  
 radiogalaxies, kinematic models rel. to statistics of extended components 4-94942  
 rigid-body kinematics, ang. vel. theory 4-110831  
 stellar clusters and associations, rigorous formulae for proper motions calc. (German) 4-67715  
 superkinematics, SUSY groups with one Majorana bispinor generator 4-102050
- kinematography** see cinematography
- kinerecording** see video recording
- kinetic theory**  
 see also Boltzmann equation; collision processes; intermolecular mechanics; kinetic theory of gases  
 aggregation, diffusion limited, position space renormalisation group 4-78278  
 book, kinetic theory of electromagnetic process 4-82601  
 cerebellar cortex simulation using kinetic theory of neural systems 4-100119  
 charged test particle dynamics in hard rod fluid 4-111014  
 collisionless plasma, statistical mech. of relativistic charges and radiation 4-75165  
 fluids, neutron spectra width and heat mode, kinetic theory 4-60802  
 granular materials, Couette flow, inelastic and slightly inelastic particles, collisional distrib. function 4-60362  
 irreversible kinetic aggregation, diffusive cluster size distrib., Smoluchowski's eqn. 4-111043  
 liquids, Brownian limits for tagged particle motion 4-113285  
 neutrinos transport properties during stellar core collapse, relativistic kinetic theory 4-101313

## kinetic theory continued

- noncollisional plasma, one-dimensional Vlasov-Poisson eqn., particle methods 4-60591
- particle traps, kinetics of diffusion controlled reaction 4-78228
- polymer solns., non-Newtonian shear viscosity, normal stress coeffs., corresponding states in rheology 4-64899
- polymer solutions, equilibration in momentum space in kinetic theory 4-64989
- randomly kicked quantum rotator, energy growth, expectation value 4-82704
- regression law and renormalisation of transport coeff. 4-58744
- relativistic kinetic eqns. for inelastically interacting particles in gravit. 4-73311
- self-gravitating system, random fluctuations in general relativity 4-110945
- sintering processes estimation and regulation (Russian) 4-76705
- transport equation in plane-parallel geometry (Russian) 4-90537
- ultra-relativistic heavy-ion collision, thermal equilibration 4-59265

## kinetic theory of gases

- see also Brownian motion; collision processes; equations of state; intermolecular mechanics; Joule-Thomson effect
- Boltzmann constitutive equations invariance 4-103455
- dense gases, second virial coeffs., phase space subdivision 4-97736
- electron energy distribution in gases 4-79702
- gas discharge in electric field, kinetic theory 4-79876
- gas in electric field, Boltzmann eqn. for electrons, multi-term soln. 4-69860
- gaseous state at low temp., thermodynamics (Russian) 4-113096
- ideal gas with most general power sources, gas dynamic eqns. self-similar solns. (Ukrainian) 4-65047
- mass ratio dependence of the mixed species collision integral 4-79701
- moderately dense gas, long-range boundary effects 4-60575
- momentum change in molecule-wall collision, determ. of gas pressure 4-113094
- multidimensional inverse problems for kinetic equations (Russian) 4-113093
- muons charge exchange in gases, kinetic eqns. appl. to muon spin reson. signals 4-74330
- nonequilibrium gas flow, nonlinear Boltzmann eqn. soln. 4-91849
- open Bose gas, time evolution, exact kinetic equation 4-90481
- polytropic gas spheres, boundary conditions 4-79697
- relaxation times calc. using kinetic cooling data 4-64577
- sound propagation, boundary value problems 4-91860
- stress in fluids, theory 4-110828
- transport processes, kinetic processes in inertial reference frame 4-69858
- CsCl, vap. press., viscosity coeff. and interdiffusion coeff. in Ar and He, Ruff-MKW-boiling point method 4-97743
- K vapour, electron charact. energy and momentum transfer cross-section (Korean) 4-79705
- Kr dense gas, dynamic struct. 4-91859
- Kr, dynamic struct. factor determ. 4-83968
- N<sub>2</sub>, electron distrib. function, analytical model 4-79703
- N<sub>2</sub>, rot. relax., depolarised Rayleigh spectral line width, viscosity, self-diffusion and thermal cond. 4-97739
- SF<sub>6</sub>, Monte Carlo simulation of electron swarm motion 4-79700

## kinetic theory of liquids see kinetic theory; liquid theory

## kinetics of chemical reactions see reaction kinetics

## kink bands

- Mo, deformation mechanism and dislocation struct., HVEM study 4-71682

## kinoforms see computer-generated holography

## Kirkendall effect see diffusion in solids

## kitchen appliances see domestic appliances

## KKR calculations

- Au,Pt<sub>1-x</sub>(Ni<sub>1-x</sub>), substitutionally disordered, electronic struct. calcs. 4-70644
- Cu, electronic props. of 4d transition metal and sp impurities 4-70731
- Cu<sub>3</sub>Au, substitutionally disordered, electronic struct. calcs. 4-70644
- Fe fully relativistic band struct. calcs. 4-113855
- Fe, impurity hyperfine fields and adiabatic pot., self-consistent calc. 4-65632
- Ni fully relativistic band struct. calcs. 4-113855
- Ni,Pt<sub>1-x</sub>, substitutionally disordered, electronic struct. calcs. 4-70644
- TiC, Fermi surface, const. energy KKR-GF calc. 4-84545
- TiN, Fermi surface, const. energy KKR-GF calc. 4-84545

## klystrons

## see also reflex klystrons

- 50 MV klystron for Stanford Linear Collider 4-68842
- optical klystron experiments for the ACO storage ring free electron laser 4-96920
- optical klystron harmonic generator with electron microbunches induced and frozen by lasers, intense coherent soft X-ray source 4-97001
- plasma heating in lower hybrid resonance (French) 4-91950
- CO<sub>2</sub> and H<sub>2</sub>O laser freq.-mixing expts., beat note S/N ratio characts. 4-74608

## Knight shift

## see also nuclear magnetic resonance

- Grafoil, positive muon Knight shifts and relax. rates 4-71234
- graphite, positive muon Knight shifts and relax. rates 4-71234
- metals, muon states, recent progress 4-65902
- rare earth alloys, RCo<sub>2</sub>B<sub>2</sub>, R=Gd-Tm, antiferromag. and paramag. states, NMR spectra 4-109089
- TCNQ salt, TTF-TCNQ, <sup>13</sup>C NMR studies and spin susceptibility 4-92975
- Be, muon Knight shift, spin rot. meas. 4-65916
- Bi, muon Knight shift and relaxation 4-84888
- Cd, Lifshitz phase transition, muon Knight shift study 4-71230
- Cd, muon Knight shift, spin rot. meas. 4-65916
- Cd-Mg, local electron density of states, Van Hove singularities,  $\mu^+$  Knight shift 4-84887
- CeSn<sub>3</sub>(Pd<sub>3</sub>(In<sub>3</sub>), mixed-valence system, muon Knight shift meas. 4-80852
- GdAl<sub>2</sub>,  $\mu$ SR spectroscopy 4-84894
- GdZn, ferromagnetically saturated single crystal, high-field NMR Knight shift, magnetisation studies 4-114176
- LaSn<sub>3</sub>(Pd<sub>3</sub>(In<sub>3</sub>), mixed-valence system, muon Knight shift meas. 4-80852
- Mo<sub>5</sub>Sn<sub>3</sub>, Knight shift of <sup>119</sup>Sn 4-92969
- NbH<sub>2</sub>, electronic struct., NMR study 4-76280

## Knight shift continued

- Pb, muon Knight shift, 20 to 785K 4-71233
- $\beta$ -PdH<sub>1.5</sub>, muon Knight shift, 20 to 785K 4-71233
- PrSn<sub>3</sub>(In<sub>3</sub>), mixed-valence system, muon Knight shift meas. 4-80852
- Pt small particles, <sup>195</sup>Pt NMR and Knight shift 4-84861
- Sb-Bi, muon spin rot. and muon Knight shift meas. 4-71235
- SeCo<sub>2</sub>, exchange enhanced Pauli paramagnet, mag. susceptibility, Knight shift meas. 4-108983
- V<sub>3-x</sub>Fe<sub>x</sub>Ga, NMR Knight shift and paramagnetism 4-65873
- V<sub>6</sub>O<sub>13</sub>, NMR study of mag. props. 4-80835
- Zn, muon Knight shift, spin rot. meas. 4-65916
- Zn, muon Knight shift at struct. defect 4-71231

## Knudsen flow

- binary gas mixture, nonisothermal motion through plane channel, kinetic phenomena 4-103368
- Boltzmann eqn. with small Knudsen number, singular perturbation method, (Chinese) 4-97610
- dynamic Knudsen vacuum gauge 4-86434
- gas motion in front of a completely absorbing wall 4-60463
- homogeneous condensation, droplet growth study 4-60506
- steady behaviour, around group of bodies at rest with various temp. tribs. 4-112958
- surface, evaporation and condensation, mass and heat transfer, kinetic anal. 4-88270
- Ar, gas, effective viscosity oscillatory depend. on Knudsen number 4-64983
- N<sub>2</sub>, gas, effective viscosity oscillatory depend. on Knudsen number 4-64983

## Knudsen number see Knudsen flow

## Kohn effect see lattice dynamics

## Kondo effect

- alloy, Kondo problem soln. for orbital singlet 4-75960
- Anderson Hamiltonian with cryst. field splitting and spin-orbit interactions, ground state props. 4-108821
- Anderson lattice in Kondo regime, one particle excitation spectra 4-61270
- conduction electron polarisation, absence 4-71021
- Cogblin-Schrieffer model, Wilson number derivation 4-61519
- heavy fermion superconductivity, renormalised perturbation theory 4-104354
- magnetic amorphous metals, absolute thermoelec. power at low temp. (Chinese) 4-104186
- magnetoresistance and Kondo effect in weakly localised regime 4-108186
- metals, thermodynamic scaling theory for impurities 4-113678
- strong coupling superconductors, effects of Kondo impurities 4-92845
- transition metal superconductor, Anderson impurities and Kondo effect 4-84734
- Ce ion in cubic environment, ground state, effects of cryst. field 4-104403
- Ce metal, alloys and compounds, dense Kondo state, spin-orbit coupling, crystal field splitting 4-84613
- Ce systems, valence fluctuation dynamics, appl. of self consistent perturbation theory 4-70743
- CeAl<sub>3</sub>, low-temp. specific heat meas. 4-75702
- CeAl<sub>10-x</sub>, amorphous, transport and mag. props. 4-108985
- CeCu<sub>2</sub> Kondo lattice intermetallic compound, anisotropic negative magnetoresistance 4-76111
- CeCu<sub>2</sub>Si<sub>2</sub>, Kondo lattice substance superconductivity 4-98797
- CeCu<sub>2</sub>Si<sub>2</sub>, low-temp. specific heat meas. 4-75702
- Ce<sub>2</sub>La<sub>1-x</sub>Al<sub>2</sub>, dense Kondo state, elec. resist., mag. susceptibility measurements 4-108984
- Ce<sub>0.8</sub>La<sub>0.2</sub>Cu<sub>2</sub>Si<sub>2</sub>, disordered, low-temp. specific heat meas. 4-75702
- Ce<sub>2</sub>La<sub>1-x</sub>Cu<sub>2</sub>Si<sub>2</sub>, mag. props. during Kondo impurity-Kondo lattice transition 4-61509
- Ce<sub>0.9</sub>Y<sub>0.1</sub>Cu<sub>2</sub>Si<sub>2</sub>, disordered, low-temp. specific heat meas. 4-75702
- Cu-Mn, elec. resist. max. and thermo-EMF, short-range antiferromagnetism (Russian) 4-84608
- Ge bicrystal p-type inversion layers, anomalous magneto-transport properties 4-98719
- PbS, single crystal, localised spin scatt. magnetoresistivity 4-61396
- Tb<sub>2</sub>Gd<sub>25</sub>, Hall effect and elec. resist. near Curie point 4-61361
- Korringa-Kohn-Rostoker calculations see KKR calculations
- Koster effect see dislocation damping
- k.p. calculations
  - GaAs, conduction band splitting for  $k$  along [110] 4-108777
  - GaAs, conduction bands, strain-induced splitting 4-75854
  - GaAs, k.p. interaction and effective mass, band gap depend. 4-113850
  - GaSb, conduction bands, strain-induced splitting 4-75854
  - InP, k.p. interaction and effective mass, band gap depend. 4-113850
- Kramers-Kronig relations
  - chalcogenide glasses, dispersion of dielectric constant, freq. dependence 4-80858
  - dielectric permittivity, Kramers-Kronig relations isolation 4-84899
  - inert gas solids, optical constants, self-consistent anal. 4-71332
  - metallic samples, paramagnetic reson. lineshape anal., appl. to Gd alloys 4-88714
  - photographic film with dye substituted Ag, phase hologram recording 4-79083
  - ray tracing in absorbing media 4-74423
  - scolecite natural zeolite, IR vibr. spectra studies 4-76445
  - squarylium dye, polymorphs, cryst. field influence on UV spectra 4-104626
  - TCNQ salts, quasi-one-dimensional metals and semiconds., mol. exciton optical props. 4-76494
  - (TMTSF)<sub>2</sub>ClO<sub>4</sub> organic supercond., polarised far IR reflectivity measurements 4-114279
  - Ag-KCl random composite materials, EM propag. 4-71331
  - Al<sub>2</sub>Ga<sub>1-x</sub>As, Fourier anal. of optical spectra 4-99131
  - Al<sub>2</sub>O<sub>3</sub>, sintered, microstructure and optical props. 4-61649
  - (As<sub>2</sub>S<sub>3</sub>)<sub>x</sub>(As<sub>2</sub>I<sub>3</sub>)<sub>1-x</sub> glasses, Raman scatt., IR and depolarisation spectra 4-109182
  - BaFCl(FBr)(OCl), far IR spectra 4-66047
  - Co Kramers-Kronig relation of measured atomic scatt. factors 4-9806
  - CoCl<sub>2</sub>(Br<sub>2</sub>), high freq. dielec. const. 4-61646
  - CoS<sub>2</sub>, electronic struct., reflectivity spectra, optical constants, meas. between 0.2-4.4 eV 4-80963
  - Cu Kramers-Kronig relation of measured atomic scatt. factors 4-9806
  - Cu, X-ray anomalous scattering factors from X-ray absorption data, Kramers-Kronig analysis 4-61768

mers-Kronig relations continued  
 $\text{FeCl}_2(\text{Br}_2)$ , high freq. dielec. const. 4-61646  
 $\text{FeS}_2$ , electronic struct., reflectivity spectra, optical const., meas. between 0.2-4 eV 4-80963  
 $\text{GaAs}_{1-x}\text{P}_x$ , Fourier anal. of optical spectra 4-99131  
 $\text{GaIn}_{1-x}\text{Se}_x$ , optical phonons, far-IR reflectivity spectra 4-104583  
 $\text{Ge}$ , single crystal and amorphous, optical props. meas. 4-95496  
 $\text{GeS}$  single crystal, reflectance and thermoreflectance studies 4-71356  
 $\text{Hg}_2\text{Br}_2$  single crystals, IR refl. spectra; optical const. and phonon parameters 4-88830  
 $\text{n-InSb}$ , refractive index, influence of electron drift and heating 4-104561  
 $\text{K}_2\text{MoO}_3$ , 1D, CDW modes, far IR reflectivity studies 4-108798  
 $\text{LiNbO}_3$ , single cryst., near-normal reflectivity and absorpt. spectra 4-93083  
 $\text{LiTaO}_3$ , single cryst., near-normal reflectivity and absorpt. spectra 4-93083  
 $\text{Ni}$  Kramers-Kronig relation of measured atomic scatt. factors 4-98063  
 $\text{NiBr}_2$ , high freq. dielec. const. 4-61646  
 $\text{NiCl}_2(\text{Br}_2)(\text{I}_2)$ , UV reflectance and electronic states 4-71406  
 $\text{NiS}_2$ , electronic struct., reflectivity spectra, optical const., meas. between 0.2-4 eV 4-80963  
 $\text{PbFe}_{1-x}\text{Ga}_x\text{O}_9$ , optical props. 4-93086  
 $\text{PnSe}$  thin films, UPS and reflectivity meas. 4-84976  
 $\text{TlCl}(\text{N}_2)$ , optical props., EELS study 4-99082  
 $\text{VC}(\text{Nx})$ , optical props., EELS study 4-99082  
 $\text{VSe}_2$  (1T), reflectivity, CDW band struct., Kramers-Kronig anal. 4-71401  
 $\text{Zn}_3\text{As}_2$ , optical constants and band transitions 4-80898  
 $\text{Zn}_3\text{P}_2$ , optical constants and band transitions 4-80898  
**amers systems** *see determinants*  
**omayer lamps** *see mercury vapour lamps*  
**onig-Penney model**  
 one-dimensional disordered system, extended states 4-80484  
 $\text{GaAs-GaAlAs}$  superlattices, third order nonlinear optical susceptibility 4-74586  
**rypton**  
*see also nuclei with* .....  
 adsorbed layer on Mg and Al, optical spectra, configurational effects 4-80391  
 adsorbed on graphite domain growth, Monte Carlo simulations 4-98444  
 adsorbed on  $\text{MgO}$  substrate preparation 4-104067  
 adsorption after separation from nuclear installation waste gases 4-100047  
 atom, 4s photoelectron ang. distrib. relativistic RPA approx. 4-83342  
 atom, electron elastic scattering calcs. 4-107456  
 atom, low energy elastic electron scatt. cross section calcs. 4-83472  
 atom, near-threshold electron impact excitation functions 4-96702  
 atom, outer shells, photoionisation cross sections cal. using relativistic local-density approx. 4-83352  
 atoms, highly ionised, unresolved transition arrays 4-87062  
 atoms, low energy positron scatt., critical points 4-74313  
 atoms, Rydberg states, multiphoton ionisation, photoelectron kinetic energy and ang. distrib. meas. 4-83348  
 atoms, single and multiple ionisation by low energy electron impact using crossed beam apparatus 4-69217  
 clathrate hydrate formation in struct. II modification 4-112251  
 coaxial high-freq. electrodeless lamp, Kr filled, spectral distrib. of radiation 4-78385  
 dense gas, density fluctuation calcs. 4-83967  
 dense gas, dynamic struct. 4-91859  
 dense gas, struct. factor, bridge contribs. and many-body effects 4-75263  
 dimers, model pot. method, SCF and dispersion energy calcs. 4-107426  
 dynamic struct. factor determ. 4-83968  
 excimer radiation in VUV, build-up and decay frequencies, excited by  $\alpha$ -particles 4-91437  
 excimers, electronic struct., ab initio CI calc. (French) 4-78788  
 films, structural order effects in low-energy electron transmission spectra 4-98520  
 fission product, beneficial uses 4-109930  
 fluid, electron energy bands 4-84645  
 gas, ionisation growth measurements 4-79733  
 gas, mag. birefr. meas. 4-103465  
 ion, H- and He-like, time of flight X-ray emission spectra 4-102629  
 ion etching, of Si, effect of ion species on bombardment induced topography 4-81320  
 layer on graphite in one-to-two layer regime, phase diagram, freezing transitions 4-103910  
 liquid, compressional viscosity, US absorpt.; modified hole theory 4-103884  
 LX spectrum interpretation in terms of vacancies distrib. 4-99225  
 matrix isolated in solid Kr, Ar and  $\text{N}_2$ , EXAFS studies 4-64416  
 methane-Kr mixtures, solid and liq., spin-lattice relax. 4-80831  
 monolayer, on graphite, commensurate-incommensurate transition; X-ray scatt. study 4-61215  
 monolayer, physisorbed on graphite, modulation of at. positions, anharmonicity 4-92531  
 plasma, dense, absorpt. coeff. and thermodynamic props. meas. 4-84017  
 radioactive gaseous wastes from nuclear plants, treatment methods 4-106786  
 solid, sputtering by keV heavy ions 4-88920  
 $\text{Ar-Xe}$ , fluid, extrinsic photocond., Wannier-Mott impurity exciton, binding energy and effective mass 4-63701  
 $\text{Ar/Kr}$  system, mutual diffusion coeff.  $D_{12}$  det. by mol. dynamics method 4-103628  
 $\text{Ar+Kr}$  atoms, ionisation processes for highly excited Ar atoms 4-87201  
 $\text{He-Kr}^+$  hollow cathode discharge laser, electron energy distrib. function 4-84117  
 $\text{Kr II}$ , Stark broadening params. 4-91225  
 $\text{Kr IV } 4s^2 4p^2$  and  $4s4p^3$  configs., VUV spectrosc. 4-69003  
 $\text{Kr}^+$  closed shell ions repulsive interaction, beam and transport meas. comparison 4-96653  
 $\text{Kr-F}_2$ -He atmospheric discharge, electron density, streak interferometric method 4-84092  
 $\text{Kr-Hg}$  interaction pots. calcs. from temp.-depehd. absorpt. spectra 4-69170  
 $\text{Kr-Hg}$  mixture, ionisation coeff. meas. 4-79707  
 $\text{Kr-N}_2$  solid mixtures, phase diagrams, X-ray study (Russian) 4-84372  
 $\text{Kr-Ne}$  systems, interaction second initial coeffs. at low temps. 4-98234  
 $\text{Kr-SF}_6$  mixture, collisional relaxation as function of vel. using photon-echo method 4-69152

## krypton continued

$\text{Kr+CsF}(\text{CsBr})$ , collision-induced dissoci., cross sections 4-76993  
 $\text{Kr+Fe}^{26+}$  near-symmetric collisions, K-K transfer cross-sections 4-64571  
 $\text{Kr+Kr}$ , metastable interaction,  $^3\text{P}_2$  state 4-91335  
 $\text{Kr+Kr}(\text{Xe})$ ,  $4f\sigma$  excitation; L-shell vacancy prod. 4-59883  
 $\text{Kr+Ne}^{2+}$ , low energy electron transfer collisions 4-87213  
 $\text{Kr+X}_2$  ( $\text{X=halogen}$ ) metastable atom quenching cross-section calcs. 4-107304  
 $\text{Kr+Xe}_2(\text{Ne}_2)(\text{NeAr})$ , three-body exchange reactions, tunnelling process, WKB calcs. 4-64589  
 $\text{Kr}^+ + \text{He}$ , one-electron capture at low energies, Landau-Zener model calcs. 4-96685  
 $\text{Kr}^{2+} + \text{Li}$  collisions,  $q=2$  to 10; electron capture cross sections from slow projectiles 4-74328  
 $\text{Kr}_2$ , electron impact dissociation 4-102812  
 $^{83}\text{Kr}$ , 5p levels, hyperfine struct. const. meas. (French) 4-78980  
 $^{85}\text{Kr}$ , global environmental transport model review 4-83253  
 $^{85}\text{Kr}$ , nuclear fuel reprocessing gaseous wastes management 4-59438  
 $^{85}\text{Kr}$  off-gas  $\beta$  monitor, for nuclear reprocessing plants 4-59447  
 $^{85}\text{Kr}$ , volatile radionuclides from nuclear fuel reprocessing, treatment and disposal (German) 4-59318  
 $^{86}\text{Kr}$  afterglow plasma, Kr  $^3\text{P}_2$  state at. binary collision ionisation rate const. determ. 4-91335  
 $\text{Kr}(5s^3\text{P}_{3,0})$  beam, intracavity state selection using CW dye laser 4-60095  
 $\text{N}_2\text{-Kr}(\text{Xe})$ , phase diagrams and solid-liquid equilibria 4-113638

## krypton compounds

$\text{Bi}_x\text{Kr}_{1-x}$  mixtures, amorphous, metal-insulator transition, elec. cond., supercond. transition temp. meas., scaling theories 4-75860  
 $\text{KrCl}$ , laser action using transverse discharge pumping scheme 4-69382  
 $\text{KrF}$  excimer laser, electron beam excited, high efficiency operation 4-74491  
 $\text{KrF}$  fast discharge excimer laser with symmetric geometry (Chinese) 4-83610  
 $\text{KrF}$  injection locking excimer lasers in the UV 4-83608  
 $\text{KrF}$  laser, electron beam pumped, high energy, multi atm. 4-60066  
 $\text{KrF}$  laser, electron beam pumped, for laser fusion appl. 4-79113  
 $\text{KrF}$  laser, electron-beam pumped 4-69388  
 $\text{KrF}$  laser, electron-beam pumped, optimisation with Ne buffer gas 4-112384  
 $\text{KrF}$  laser, process kinetics meas., radiative lifetimes and quenching rate const. 4-64701  
 $\text{KrF}$ , laser action using transverse discharge pumping scheme 4-69382  
 $\text{KrF}$  laser based ultrashort laser pulse generation method 4-96934  
 $\text{KrF}$  laser radiation, stimulated Brillouin scatt., in  $\text{SF}_6$  4-107752  
 $\text{KrF}$  laser system pulse compression, laser drivers for inertial-fusion reactors 4-69464  
 $\text{KrF}$  laser with automatic preionisation, construction and design 4-96945  
 $\text{KrF}$  lasers, electron beam controlled discharge pumping 4-60018  
 $\text{KrF}$  lasers, electron-beam-excited, using Ar-free mixtures at 1 atm. 4-112382  
 $\text{KrF}$  pulsed gas lasers, high power 4-96865  
 $\text{Kr}_2\text{F}$  photochemical laser, active medium bleaching wave optical inhomogeneities, interferometric study 4-60022  
 $\text{KrF}^*$  electrodischarge, excimer laser plasmas, runaway electron current and form. of spatial struct. 4-97929  
 $\text{KrF}^*$  excimer laser picosecond gain dynamics 4-60056  
 $\text{KrHCl}$ , rot. Zeeman effect and Coriolis coupling, spin-rot. const. 4-59823  
 $\text{KrXe}^+$ , form. and decay in electron beam excited inert gas mixtures 4-83479

Kuhn-Thomas sum rule *see molecular energy levels*Kurie plots *see beta-decay theory*kymography *see radiography*Kypoupolous method *see crystal growth from melt*labelled atoms *see radioactive tracers*labelled compounds *see radioactive tracers*labelled molecules *see radioactive tracers*

## laboratories

*see also acoustical laboratories*  
 biomechanics laboratory, automated, appl. to rehabilitation 4-81806  
 HV laboratory, EMI investigation 4-106165  
 mobile test laboratory, operation modes optimisation 4-95399  
 National Physics Laboratory, current work 4-95013  
 neurofunction laboratory for movement disorder evaluation 4-81804  
 NPL, a brief history 4-90342  
 PERLA Laboratory at Ispra for nuclear safeguards performance, calibration and training 4-111697  
 synchrotron radiation facilities, worldwide census 4-95110  
 underground lab. for radioactive waste disposal in clay 4-83170  
 undersea laboratory system HYDROLAB 4-110318  
 United States Naval Academy alternative energy conversion demonstration laboratory 4-63464

## laboratory apparatus and techniques

*see also specific instruments and techniques, e.g. balances, plasma probes, vacuum techniques*  
*see also instrumentation; instruments; measurement; student laboratory apparatus; test equipment; test facilities; testing*  
 cart pushing and pulling, human motion anal.; specialised laboratory 4-89645  
 cryogenic storage device, simple and inexpensive, for microscopy specimens 4-95572  
 electronic meas. and laboratory practice, book 4-58585  
 excitation-, radio-, photo- and thermoluminescence spectra, experimental arrangement for in situ meas. 4-90663  
 gases in liquid streams, relative solubility determ. 4-99909  
 high-pressure fluid and gas jets, starting valve for laboratory apparatus 4-87817  
 image analyser, Olympus-Cambridge Quantimet 10 4-106293  
 impedance audiometers, laboratory and commercial, clinical comparison 4-115261  
 knee capsule deform., microprocessor-based tissue displacement monitor 4-89864  
 laboratory, EMI investigation 4-106165  
 magnetic screening appls. of amorphous soft mag. materials 4-82783  
 measurement instrument yard and metrology laboratory, administrative and technical management 4-106307  
 microtome, instrumented for improved histological sections and fracture toughness meas. 4-62637

**laboratory apparatus and techniques continued**

- plasma waves self-focusing, demonstration apparatus 4-101613  
 robots appl. prospects 4-86407  
 semiconductor pressure strain gauge for precision heating expts. (*Russian*) 4-101831  
 single mode fibres, industrialised meas. system development 4-107836  
 small sample storage under liq. N<sub>2</sub>, rapid-access system 4-73428  
 solar collector simulator and actual performance comparison 4-66788  
 stratified flow channel with microcomputer monitoring and control 4-103448  
 suspended particulate monitoring optical sensor 4-115627  
 thermal wave imaging system, low cost, lab. appls. 4-89221  
 throttling in capillary tubes, laboratory equipment (*Bulgarian*) 4-97682  
<sup>3</sup>H gas, small scale experimental system, design, construction, performance tests (*Japanese*) 4-64246  
 Rn, exhalation and diffusion from building materials 4-93908  
 Ti microelectrodes, simple method for shaping 4-89856

**labyrinth speakers** see *loudspeakers***Lacertids** see *BL Lacertae-type objects***ladder filters** see *filters***lakes**see also *rivers*

- acid Adirondack lake, New York, short-term changes in base neutralising capacity 4-100643  
 acoustic wave generation by low freq. gravity modes 4-82109  
 Central Andes, ancient ice islands in salt lakes 4-94178  
 E Antarctica, perennially frozen lakes at glacier/rock margins 4-82144  
 Baikal, ice thawing (1961-80) 4-72621  
 Benmore, New Zealand, delta changes caused by lake level lowering 4-62855  
 Big Quill Lake, Saskatchewan, saline lake, effect of groundwater inflow on evaporation 4-100632  
 Big Soda Lake, Nevada, hydrogeochemistry 4-77564  
 Burullus, in Nile delta, Egypt, sediment mineralogy and sources 4-115468  
 cosmic radiation fossil record by <sup>10</sup>Be accelerator mass spectrometry 4-90047  
 Dead Sea surface water; trace element determ. by neutron activation 4-105604  
 Eliza, Australia, marginal sediments, significance for oil shale genesis 4-94172  
 Erie, N America, wind speed overlake calc. from overland wind speed 4-67305  
 Erie, wave prediction by numerical model 4-85726  
 evidence for enhanced atmospheric circulation 4-100712  
 Flood Lake, Canada, glacier outburst and sudden discharge of 1979 August 4-94174  
 Great Lakes of N America, pollution studies, book 4-95091  
 Idukki reservoir catchment, Kerala, India, valley slumping, sedimentation and reservoir capacity 4-100628  
 Lake Constance, settling materials precipitation, PIXE study of endogenous catalysis 4-105603  
 limnology (book) 4-73193  
 El Limonero dam site, Malaga, Spain, seismic risk and expected strong motion (*Spanish*) 4-115342  
 Lonar, India, possible meteorite crater origin, palaeomagnetic and geomag. data anal. 4-77517  
 Louisiana, USA, freshwater sediment heavy metal pollution 4-93654  
 Malawi, Africa, structural evolution 4-62732  
 Mediterranean Sea site in Messinian, lakes characts., river flow directions and erosion 4-100625  
 Mount St. Helens, 1980 eruptions effect on surface and groundwater quality 4-105616  
 Nero, Canada, <sup>234</sup>Th determ., effect of contaminants 4-109757  
 Onondaga, United States, flow release to Oswego River and chloride dynamics 4-100014  
 Ontario, Canada, radioactive and thermal plume from nuclear. power station 4-66823  
 Ontario, octachlorostyrene in sediments 4-100012  
 playa lakes of W. Canada and northern USA, sedimentation processes 4-62856  
 Rock Mountains, remote lakes, anthropogenic pollutants in sediments, deposition evidence 4-77155  
 Saroma, Hokkaido, snow cover on sea ice and snow ice form. (*Japanese*) 4-105612  
 sediment core anal. and change-point problem for sequence of binomial random variables 4-82113  
 sedimentology (book) 4-86136  
 sediments as historical record of heavy metals air pollution 4-100046  
 softwater lakes, H<sup>+</sup> conc. determ., use of CO<sub>2</sub> equilibria 4-77169  
 stratified lake, wind induced circulation, time var. 4-62834  
 N Tanzania, high fluoride content of rivers, lakes, springs 4-115467  
 turbidity currents in glacial lake, occurrence and movement monitoring with three-dimensional sensor network 4-100644  
 underwater irradiance meas. using IOZ-1 miniature instrument 4-72729  
 Yli-Jitka, Finland, mapping from satellites 4-100430  
<sup>10</sup>B/<sup>11</sup>B ratio in saline lakes of Qinghai-Xizang Plateau, <sup>11</sup>B(n,α)<sup>7</sup>Li influence 4-110401  
 C cycle adversely affected by man's activities 4-115474  
<sup>6</sup>Li/<sup>7</sup>Li, ratio in saline lakes of Qinghai-Xizang Plateau, <sup>6</sup>Li(n,α)<sup>3</sup>H influence 4-110401  
 Pb pollution in Belgium, record held in pond sediments 4-114983

**Lamb shift**

- conference, polarised proton ion sources, Vancouver, BC, Canada (May 1983) 4-106092  
 methane gas-laser beam interaction 4-107405  
 methanol, Stark modulated Lamb dip signal, CO<sub>2</sub> laser freq. stabilisation appls. (*Japanese*) 4-74485  
 QED, finite temperature effects, bound electrons, hydrogen Lamb shift 4-95750  
 two frequency lasers, Zeeman effect and mode-competition effect 4-69364  
 Cl, H-like, is Lamb shift determ. by X-ray transitions meas. using beam-foil excitation 4-74195  
 D<sup>-</sup> Lamb-shift polarised ion sources 4-107239  
 H atom, lifetime of 2p state and Lamb shift 4-69014  
 H<sup>-</sup> Lamb shift polarised ion source, intensity limitations 4-107241  
 H<sup>-</sup> Lamb-shift polarised ion sources 4-107239  
 H<sup>-</sup> polarised ion source at Munich 4-107240

**Lamb shift continued**

- HCF, <sup>1</sup>A<sup>1</sup> state, mag. props., Zeeman splittings, laser induced fluorescence 4-69129  
 He, Schrodinger eqn. soln. 4-112112  
 He-like ions, 1s2s <sup>3</sup>S<sub>1</sub>-1s2p <sup>3</sup>P<sub>1</sub> transition freq., two-electron Lamb shift 4-59675  
 He-Ne sensitive gas laser, line shapes 4-91435  
<sup>4</sup>He 1s<sub>nl</sub> energy levels, ionisation energies and Lamb shift 4-64427  
 OCS, polarisability anisotropy, dipole moment, laser microwave double reson. 4-87146  
 P-like ions, energy levels, transition probabilities, multiconfiguration study 4-106126  
 S<sup>15+</sup>, H-like, metastable 2S<sub>1/2</sub> state, Lamb-shift meas. 4-102649

**Lamb waves** see *surface acoustic waves***lambda point** see *liquid helium-4; superfluidity***laminar flow**see also *laminar to turbulent transitions*

- aquatic animals, actively-moving, boundary layer stability (*Russian*) 4-72280  
 asymmetric flowfield development on slender body, laminar boundary layer separation 4-64951  
 axially symmetric incompressible viscous flow, with perturbations, numerical stability anal. 4-83874  
 axisymmetric thermal plume linear stability eqns. 4-79549  
 axisymmetric wake behind slender body in exterior irrotational flow, reaction, asymptotic struct. 4-69734  
 Benard convection by energy integral method 4-97533  
 boundary layer, multifold series expansion anal. appl. 4-112808  
 boundary layer flow induced by an airfoil (*German*) 4-64916  
 boundary layer flow on a rotating sphere, numerical prediction 4-64916  
 boundary layers, Dorodnitsyn finite element formulation 4-112809  
 boundary-layer interaction theory 4-97479  
 boundary-layer transition on heated underwater body 4-103286  
 buoyancy-driven laminar and turbulent natural convection in an enclosure cavity 4-87660  
 n-butanol-N<sub>2</sub>, heat and mass transfer in a laminar boundary layer under mist formation (*Japanese*) 4-97477  
 capillary Poiseuille flow, shear dispersion, residence time 4-79668  
 cavitation phenomena within regions of flow separation 4-60468  
 channel expansion, laminar flow, spectral element method 4-87797  
 coating flow theory by finite element and asymptotic analysis of Navier-Stokes system 4-79545  
 compliant coatings interactions with boundary-layer flows 4-60366  
 compressible flow, time-split finite element method 4-112932  
 compressible laminar boundary layer flow, numerical soln. 4-87666  
 compressible laminar boundary layers along curved walls, suction, control instability 4-64912  
 contaminant dispersion in time depend. laminar flows 4-79548  
 convective heat transfer, physical and computational aspects, 4-86128  
 convective heat transfer over flat plate, approx. integral methods improvement 4-75020  
 counterflowing fluids separated by heat conducting plate, heat transfer 4-97522  
 curved duct flow, secondary motion, turbulent and laminar flow, meas. 4-87805  
 curved duct of rectangular cross section, rot., laminar flow 4-103347  
 cylindrical laminar jet, formation of vorticity fronts in shear 4-64959  
 diffusion laminar flames, spatially resolved soot-absorpt. meas. using vapourisation of particle 4-79211  
 dislocation kinetics and viscosity of liquids, laminar flow, nonequilibrium dynamics 4-84437  
 Doppler velocimeter signal spectral broadening in presence of flow gradient 4-75104  
 duct, elliptical, entrance region, laminar flow 4-103422  
 duct flow, fully developed, discrete singularity formulation 4-87795  
 duct flow development with external radiation and convection 4-97466  
 duct flow problems, effective vorticity, numerical solution 4-87662  
 ducts with const. wall temp., heat transfer coeff. 4-60421  
 effusion-cooling, fouling rate advantages, particulate thermophoresis effects 4-65011  
 elastic fluid flow over circular cylinder, complex variables anal. 4-87666  
 enclosed concentric vertical cylinders natural convection, laminar flow, term visualisation 4-97531  
 exponential law fluid, flow rate calc. in rectangular channel, form invariance 4-75063  
 falling liquid films, entrance region lengths 4-64910  
 film boiling in laminar boundary-layer flow along a horizontal surface 4-97473  
 film condensation in nonuniform gravity, approximate method 4-69734  
 finite element method to solve the Navier-Stokes equations using method of characteristics 4-79546  
 flame fronts, visualisation via planar laser-induced fluorescence 4-97492  
 flame stability inside refractory tube 4-103430  
 flames, thickness, definition 4-108141  
 flow inversion, coiled configuration and effect on residence time distribution 4-112806  
 fluid convection between concentric and eccentric heated rot. cylinders 4-79550  
 fluid dynamics, numerical methods, book 4-110817  
 fluid velocity measurement, two-dimens., case of digital-speckle correlation techniques 4-87815  
 forced convection heat transfer through self-similar thermal boundary layers on plane and axisymmetric bodies 4-64914  
 forced convection systems, correl. of thermophoretically modified particle diffusion deposition rates 4-87703  
 free convection between concentric spheres, Navier Stokes and energy eqns. 4-79588  
 free convection from vertical flat plate 4-75007  
 frozen plasma boundary-layer flows over isothermal flat plates, parametric study 4-65063  
 fully developed laminar flow and heat transfer in an arbitrarily shaped triangular duct 4-64911  
 gas flow near retardation point, critical conditions for inertial particle deposition 4-60361  
 gas pressure within semi-infinite capillary tubes, similar solns. 4-97686  
 gaseous detonation, dynamic parameters 4-91822  
 heat flux gauge calibration for skin friction meas. 4-97723  
 heat transfer from rot. cylinder with external longitudinal fins 4-60414

laminar flow continued  
 heat transfer in periodically converging-diverging tube 4-60412  
 heat transfer of air in in-line tube bank 4-79551  
 horizontal line heat source, laminar natural convection flow, stability characteristics 4-75013  
 hydrodynamic and thermal development in square duct 4-60415  
 hypersonic flow past a lift airfoil, Navier-Stokes eqn. soln. 4-108088  
 ice, formation on flat surfaces, convective boundary layers 4-112811  
 immiscible fluids flow through homogeneous porous material 4-97674  
 incompressible flow, instream recirculation regions with single vorticity component, stagnation 4-79544  
 incompressible flow, reference press. location, finite element anal. 4-64909  
 incompressible flow past a semi-infinite flat plate in a stream with uniform shear 4-97478  
 incompressible fluid flow over rotating disk with applied mag. field 4-75033  
 incompressible permanent flow through circular pipe with axial cond. and viscosity, temp. calc. 4-103284  
 incompressible viscous fluid stabilised laminar flow through rotating radial channel 4-112813  
 interacting boundary layers and heat transfer 4-87665  
 internal heat generation in vertical triangular channel, combined free and forced convection 4-103327  
 inviscid and viscous flow computations, multiple-grid convergence acceleration 4-60455  
 jet flow over a moving wall 4-64994  
 jets, submerged of non-Newtonian fluid, laminar length meas. by flow visualisation technique 4-64997  
 laminar falling film, effective areas and mass transfer coeffs. in packed columns 4-87661  
 laminar-turbulent boundary layer transition, thermal imaging system 4-112814  
 liquid film, vaporising, laminar and turbulent boundary layers, momentum, heat and mass transfer 4-60414  
 liquid film falling laminarily down vertical plate, film thickness 4-88377  
 liquid film flow over reducer surface model 4-91790  
 liquid films, asymmetrical thinning beneath liq. drop 4-79694  
 liquid flow falling over horizontal cylinders, heat transfer 4-97545  
 liquid metals, flow through channel with transverse mag. field, in elect. insulated channel 4-75093  
 MHD, conference, Riga, Latvian SSR 4-106123  
 MHD flow and heat transfer in channel with porous walls 4-87808  
 mixing of parallel flows of cond. liq. in transverse mag. fields (*Russian*) 4-113060  
 natural convection along isothermal vertical surface 4-112859  
 natural convection heat transfer from slender cone to power-law fluid 4-60399  
 natural convection in density-stratified layers in rectangular vessel, flow patterns 4-97528  
 Newtonian fluid steady laminar flows, between a ball and a spherical cavity 4-97470  
 non-Newtonian fluid laminar flow in tube of arbitrary cross-section (*Russian*) 4-79626  
 non-Newtonian fluids, turbulent pipe flow, comparison of methods for predicting head loss 4-83929  
 non-Newtonian fluid, laminar radial flow between parallel discs in axial elec. field, inertia effects 4-83930  
 nonselfsimilar unsteady boundary-layer eqn. soln. 4-60368  
 nonsimilar stratified flow over vertical flat plate unsteady incompressible laminar free convection boundary layer 4-97639  
 nonspherical objects at high Rayleigh number, natural convection mass transfer 4-79577  
 nonuniform approach flow, laminar boundary layer eqns., uniform suction effect 4-87664  
 Oldroyd fluid, boundary layer flow along vertical wall 4-74987  
 parallel plates, natural convection cooled, thermally optimum spacing 4-112875  
 particle deposition by diffusion and interception from boundary layer flows 4-97472  
 particle deposition from laminar boundary layer, wall suction and thermophoresis effect 4-97474  
 particle-capture coefficient at channel wall 4-113014  
 physical modelling of multi-phase flow, conference, Coventry, England (April 1983) 4-58559  
 plane wing shaped grids, viscous laminar flow (*German*) 4-83875  
 polymer melts, laminar, three-dimensional flow, temp. profiles and heat transfer rates, matched asymptotic solns. 4-75001  
 porous pipe with variable suction, laminar flow 4-103411  
 protein precipitate, shear induced break-up during exposure to laminar Couette flow 4-79547  
 pushing aileron in supersonic flow, laminar interaction processes (*German*) 4-83924  
 radial jet in rotating outer flow incompressible laminar flow 4-87769  
 recirculating flow, two and three dimens. numerical methods 4-103453  
 rotating compressible laminar boundary layer, similar solns. and integral quantities 4-112888  
 rotating cylindrical cavity, laminar source-sink flow 4-87736  
 rotating electrically conducting fluid, spinup or spindown in mag. field 4-103342  
 rotating non-aligned straight pipe 4-103418  
 rotation symmetric vortex in laminar flow, stability and break-up location (*German*) 4-83915  
 second order fluid, unsteady laminar flow due to flat plate movement 4-97484  
 separated forced convection in cavities, finite difference anal. 4-112812  
 sliding bearing hydrodynamics model for laminar flow 4-74985  
 spherical particles, lateral migration in porous flow channel, appl. to membrane filtration 4-65020  
 square cylinder, natural convection heat transfer in laminar and turbulent regions 4-87696  
 stability in cylindrical channel, transversal vel. effect 4-103288  
 steady state flow of a fluid stream with streamline disturbance around an arbitrary arc (*Russian*) 4-87667  
 Stirling engine performance predictions, effects of pressure-drop correlations 4-66752  
 Stokeslet arrays in a pipe and their application to ciliary transport 4-87731  
 stratified fluid, simulation of shear (*Russian*) 4-112977  
 streamlines calc. from wall press. on fusiform body 4-91793  
 streamwise corner, laminar boundary layer stability 4-60374

## laminar flow continued

structure of flow past wing body junctions 4-103287  
 subsonic laminar separation from discontinuity edge of profile 4-108063  
 supercritical airfoil, self-sustained oscills. of a shock wave 4-103359  
 supersonic boundary layers, laminar to turbulent transitions, stability 4-79554  
 supersonic flow past flat plate, boundary layer separation 4-97603  
 supersonic flow past oscillating cone, boundary layer, blowing influence 4-69784  
 suspension, plane laminar two-phase jet flow (*German*) 4-97659  
 swirling core flow, similarity soln. 4-97566  
 swirling flow in closed vessels, flame development 4-75029  
 swirling jet under influence buoyancy forces 4-69807  
 thermal boundary layer along semi-infinite plate with variable surface temp., similar solns. 4-75021  
 thermopolar fluid, elec. cond., laminar free convection flow from vertical plate 4-97475  
 thin liquid jets in air, dynamics, instability condition 4-60473  
 thin wavy film, vertical flow, simulation by finite element method 4-74984  
 three-dimensional flow, temp. profiles and heat transfer rates, matched asymptotic solns. 4-75001  
 transient laminar convective heat transfer inside circular duct 4-60427  
 tube bundles, laminar flow, vortices separation, heat transfer, vel. fluctuations 4-97542  
 turbomachine cascade profile, friction and heat transfer calcs. 4-112833  
 turbulent boundary layer, viscous laminar sublayer 4-60390  
 two phase flow through capillary tube with variable square cross-section 4-60548  
 unsteady flow through channel with permeable walls, solute dispersion, vel. distrib. 4-113020  
 unsteady laminar and turbulent boundary layers characteristics 4-60365  
 unsteady laminar natural convection, MAC scheme in boundary-fitted curvilinear coordinates 4-60409  
 velocity determ. using photon correlator, systematic errors (*Russian*) 4-108142  
 viscous flow over circular cylinder, turbulence effect on heat transfer coeff. 4-97537  
 viscous flow through sinusoidal channels 4-87798  
 viscous fluid, subsonic and supersonic laminar flow past forward-facing small step 4-60363  
 viscous liquids, laminar mixing of parallel flows of cond. liq. in transverse mag. fields (*Russian*) 4-113060  
 viscous three-dimensional flow with large secondary vel. 4-103354  
 viscous-inviscid interactions on axisymmetric bodies of revolution in supersonic flow 4-60367  
 water, evaporation under an obliquely impinging laminar ducted slot jet—a numerical model 4-108100  
 water in inclined square cavity density inversion, natural convection 4-79584  
 CO<sub>2</sub> gasdynamic 16  $\mu$ m laser, boundary layer effects on laser gain 4-87314  
 H<sub>2</sub>O-N<sub>2</sub>, heat and mass transfer in a laminar boundary layer under mist formation (*Japanese*) 4-97477

## laminar to turbulent transitions

axisymmetric rotary shear flow in homogeneous axial mag. field, fluctuations 4-108123  
 Blasius boundary layer, three dimens. instability calcs. 4-64917  
 boundary layer transition, thermal imaging system 4-112814  
 boundary-layer transition on heated underwater body 4-103286  
 circular pipe flow complexities arising from sudden expansion and coiling 4-69830  
 cross-flow around roughened circular cylinders universal wake numbers 4-97565  
 film condensation on horizontal circular cylinder 4-69744  
 flame fronts, visualisation via planar laser-induced fluoresc. 4-97492  
 flat plate, boundary layer flow stability for small disturbances (*German*) 4-83883  
 heat transfer and friction effect on cylinder in longitudinal turbulent air flow with variable physical props. 4-83891  
 jet, incipient round, visual obs. of evolution 4-75067  
 liquid film, free surface wave propag., laminar-turbulent transition (*French*) 4-60370  
 liquid metals, flow through channel with transverse mag. field, in elect. insulated channel 4-75093  
 low Prandtl number convection, transition to turbulence, numerical anal. 4-69765  
 periodic series entropies and complexities, appl. to turbulent transition in logistic map 4-111034  
 Poiseuille flow, laminar to shear turbulent transition, stability study 4-60546  
 porous slab, single-period oscillatory convection (*French*) 4-112998  
 preturbulence, generation and mutual transformations 4-90496  
 profiles, boundary layer calc. with laminar transition and turbulent flow zones 4-74999  
 pulsatile flowfield in the vicinity of an abrupt circular channel expansion 4-103421  
 recirculating flow, three dimens., shear driven, visualisation study 4-87829  
 reorganization of a fluid flow downstream from a curved pipe (*French*) 4-69825  
 supersonic boundary layers, laminar to turbulent transitions, stability 4-79554  
 Taylor wavy vortex flow, transition sequency 4-83913  
 Tollmien-Schlichting wave, excitation in boundary layer by acoustic and vortex disturbance scatt. 4-91792  
 turbomachine cascade profile, friction and heat transfer calcs. 4-112833  
 vibrating surface, boundary layer transition, unstable wave excitation 4-91791  
 NH<sub>4</sub>H<sub>2</sub>PO<sub>4</sub>, cryst. perfection, flow visualisation expts. 4-65042

## laminates

beam structure, multilayer, dynamics under moving conc. load 4-108002  
 composite plates, delamination growth during impact, fracture mechanics analysis 4-79526  
 composites, antisymmetrically laminated, thermal residual stresses, finite element anal. 4-97306  
 composites, fatigue failure, probabilistic modelling employing Markov process 4-74961  
 composites, matrix crack growth, stochastic simulation model 4-74960

## laminates continued

- composites, physically nonlinear, effective dependence relationship derivation (*Russian*) 4-60275  
 composites, unidirectional, matrix cracking 4-74962  
 composites 4-76864  
 cylinders, multilaminate finite, nonaxisymmetric loading, stress state algorithm 4-108011  
 delamination, fracture mechanics 4-97431  
 elasticity problems with singularities, hybrid finite element approach 4-97324  
 fatigue under spectrum loading 4-62021  
 ferrous laminated composites, steel/Fe, superplasticity 4-81235  
 fibre reinforced composite, anisotropic layered, singularities at tip of crack normal to interface 4-74952  
 fibre reinforced composite, initial failure and ultimate strength theory (*Japanese*) 4-97417  
 fibre reinforced composite laminates, onset of delamination, expt. and analytical study 4-76847  
 fibre reinforced composites, fracture toughness meas., using three-point bend and compact-tension specimen 4-99735  
 fibre reinforced composites, laminated plates, optimum design 4-97367  
 fibre reinforced composites, material design with required flexural stiffness 4-99391  
 fibre reinforced composites, thermal expansion, effect of microcracks 4-80270  
 fibre reinforced composites, with circular holes, interlaminar stresses, effect of geometry 4-79447  
 fibre reinforced laminated plates, design for max. stiffness 4-75599  
 fibre reinforced plastic, plates, stresses around partial contact pin-loaded holes 4-79520  
 fibre-reinforced multilayer composites, delamination stress determ., iterative approach 4-112702  
 free edge stress analysis, superposition method 4-60287  
 glass fibre reinforced epoxy laminates, orthotropic, birefringent, prep. and photoelasticity 4-89022  
 glass fibre reinforced epoxy resin laminates, transverse cracking rel. to mech. props. of matrix 4-99489  
 glass fibre reinforced phenolformaldehyde, laminate plates, shrinkage strains 4-61915  
 glass fibre reinforced plastic, interlaminar shear strength 4-99575  
 glass fibre reinforced polyester, creep behaviour of reinforced and non-reinforced resins 4-99456  
 glass fibre reinforced polyester, laminated hybrid, crack growth resist., flexural strength 4-62012  
 glass fibre reinforced polyester laminate, residual strength degradation prediction model (*Japanese*) 4-99503  
 glass fibre reinforced polyester laminates, elastic consts. rel. to fibre orientation and matrix microcracking 4-109447  
 glass fibre-reinforced epoxy, vibr. damping parameters, prediction and meas. 4-80155  
 graphite fibre reinforced epoxy, angle-ply laminates, long-term moisture absorpt. 4-76882  
 graphite fibre reinforced epoxy, thermal expansion, effect of microcracks 4-80270  
 graphite fibre reinforced epoxy, with circular holes, interlaminar stresses, effect of geometry 4-79447  
 graphite fibre reinforced epoxy laminate, elastoplastic response, finite element micromechanical analysis 4-87581  
 graphite fibre reinforced epoxy laminates, damage accumulation, final fracture rel. to ply thickness 4-81288  
 graphite fibre reinforced epoxy laminates, matrix crack growth, stochastic model 4-109506  
 graphite fibre reinforced epoxy laminates, pin loaded holes, sizing methods, failure load 4-109507  
 graphite fibre reinforced epoxy laminates, rail shear-strength, characteristic lengths 4-109478  
 graphite fibre reinforced epoxy laminates, tensile failure, delamination fracture surfaces, SM obs. 4-66418  
 graphite fibre reinforced epoxy laminates, thermal expansion behaviour, surface anisotropy 4-80269  
 graphite fibre reinforced epoxy laminates, three dimensional thermal stress distrib. 4-61943  
 graphite fibre reinforced epoxy laminates containing pin loaded holes, failure prediction 4-109583  
 graphite fibre reinforced polyimide, fracture and elastic props., influence of 4-99572  
 half-plane, laminated, with elastic-plastic layer deform., surface buckling 4-97363  
 inelastic response, appl. of theory of plasticity without yield surface (*Russian*) 4-64851  
 interlaminar stresses around a circular hole (*Chinese*) 4-69678  
 layered composite, penny-shaped interface crack, torsional impact response 4-79498  
 layered plates, delamination buckling and growth 4-79480  
 mechanical behaviour, appl. of stress and strain polarization 4-112726  
 membrane theory for layered ellipsoidal shells 4-74882  
 metal-polymer two-layer plate, circular 4-108010  
 metallic composite materials, generalised classif., book contrib. 4-109357  
 organic materials for fusion reactor applications 4-111757  
 orthotropic structures, adhesive bonded, with part through crack, stress intensity factors analysis 4-79494  
 plates, anisotropic laminated, compressive and shear loading, postbuckling anal. 4-64866  
 plates, elastic, laminated, isotropic and anisotropic, mixed variational theorem and appls. 4-90374  
 plates, inelastic, fibre-reinforced, laminated, constitutive relations 4-103200  
 plates, laminated, anal. using mixed shear flexible finite element 4-103193  
 plates, laminated, anisotropic, natural vibr., finite element model 4-74930  
 plates, laminated, composite, shear-flexible triangular finite element model 4-64840  
 plates, laminated, with free edge in edgewise bending and compression, buckling 4-79474  
 plates, laminated composite, mixed finite element anal. 4-74904  
 plates, natural freq. prediction by higher order shear deform. theory 4-79491  
 plates, viscoelastic, multilaminate, piezoelectric, geometrically nonlinear theory 4-79470  
 plates and beams, fibre vol. fraction, dynamic mech. props. 4-89078

## laminates continued

- polypropylene-copolymer laminates, biaxial orientation, refractometry, spectra 4-84959  
 random laminates, heat diffusion 4-69670  
 sandwiched solid-metal flat gasket between two discs, contact stress 4-112774  
 semiconductor structures, multilayer, thermal stresses 4-113682  
 shear testing, pinned-end fixture for off-axis testing 4-114738  
 shell, three-layered, cylindrical, infinitely long, free wave propagation 4-74941  
 shells, cylindrical, contact rigidity 4-87635  
 shells, triple-layer, anisotropic, cylindrical, stability anal. 4-74906  
 shells, triple-layer, with delaminations, stability problems, filler third dimens., model appl. 4-87603  
 shells, viscoelastic, multilaminate, piezoelectric, geometrically nonlinear theory 4-79470  
 shells of revolution, laminated, vibration, numerical analysis 4-108036  
 shells operating on stability, optimisation problems 4-87602  
 SPALRAD-S laminate for fusion reactor appls., irradiation and mech. props. 4-111768  
 specially orthotropic, stacking combination stiffness matrices 4-60288  
 strength and elastic props., macroscopic description 4-97399  
 viscoelastic, attenuation of stresses in uniform harmonic loading 4-64871  
 C fibre reinforced epoxy, unnotched laminates, fatigue and reliability evaluation 4-76846  
 C fibre reinforced epoxy, angle-ply laminates, notch sensitivity 4-93386  
 C fibre reinforced epoxy laminates, fatigue failure behaviour with edge notch 4-114669  
 C fibre reinforced plastic laminates, compression fatigue rel. to angle buckling guides 4-89099  
 C fibre reinforced plastic laminate, uniaxial tension, stress-strain diagram (*Japanese*) 4-97417  
 C fibre reinforced plastic laminates, rigidity and strength (*Japanese*) 4-99431  
 C fibre reinforced plastic laminates, fault detection by X-ray NDT (*German*) 4-99693  
 C fibre/glass fibre reinforced polyester, hybrid composites, flexural and fracture props. (*Japanese*) 4-99429  
 C fibre-reinforced epoxy, vibr. damping parameters, prediction and meas. 4-80155  
 C-fibre reinforced plastics, under uniaxial tension, failure behaviour stress-strain diagram (*Japanese*) 4-99550  
 Ni/Cu/(001)Ni triple layer films, tensile props. 4-99324  
 Ti-Al-V (6.4 wt.%), laminated plate, damage tolerance life 4-104862
- laminations**  
 magnetic laminations, location of Barkhausen jumps and moving domain walls 4-88700  
 Fe-Si multilayered films, mag. props. and domain struct. 4-61574
- lamps**  
 see also discharge lamps; filament lamps; light sources  
 goniophotometer, 7.5 m moving arm, performance for spatial distrib. of luminaires light 4-111181  
 mirrors with diffuse reflection coatings, heat-resistant, for concentrating high-intensity sources radiation onto receiving surface 4-91566  
 D<sub>2</sub> lamps, time depend. of spectral radiance with MgF<sub>2</sub> window 4-83662
- Landau levels**  
 anomalous quantum Hall effect, particle-hole symm. 4-75881  
 Bloch-Wannier transform, in mag. fields from Landau funcs. 4-65602  
 density of states in lowest Landau band in uniform mag. field and white noise potential 4-70620  
 dynamic quantum Hall effect in 2-d electron impurity system 4-113975  
 electron gas, 2-D, magnetisation and mag. susceptibility 4-113881  
 electron gas, 2D, crystallisation of incompressible quantum fluid state in strong mag. field 4-108792  
 fractional quantum Hall effect, role of reversed spins in correlated ground state 4-92758  
 fractional quantum Hall effect and mag. symm. 4-108881  
 graphite, charge density wave and magnetoresistance anomaly 4-92639  
 graphite, far IR magneto-reflection and dielec. const. under high mag. field 4-66016  
 Hall effect, fractional quantum, and liq-solid transition 4-104240  
 multiquantum well heterostructures, magneto-optical studies of two dimens. electrons 4-104580  
 narrow band gap semiconductor, magnetabsorption of weak light wave in presence of strong wave 4-84951  
 plasma, semi-infinite, degenerate, linear response function in external mag. field 4-92643  
 quantised Hall effect and ground state of 2D electrons in strong mag. field 4-98647  
 quantum Hall effect, anomalous ground state degeneracy and fractionally charged excitations 4-108882  
 quantum Hall effect, sum rule 4-98649  
 quantum Hall effect formalism, Hilbert space of analytic functions 4-81011  
 quantum plasma, charged impurity static shielding in mag. field 4-80520  
 semiconductor superlattice two-dimensional electron gas, sp. ht., magnetothermal oscils. in quantising mag. field 4-70688  
 semiconductors, 2D 4-98548  
 semiconductors, photoelectromagnetic effect and photocond. in quantising mag. fields 4-70860  
 semiconductors subjected to quantising mag. fields, photoelectrons inverted distrib. and negative cond. 4-88514  
 two-dimensional disordered system in strong mag. field, N-orbital model 4-98641  
 two-dimensional electron system, broadening effect on magnetothermal oscils. 4-61537  
 two-dimensional lattice, transverse Hall cond. in Landau subbands 4-104233  
 two-dimensional random electron system under strong mag. fields, dynamical diffusion coeff., self-consistent treatment 4-98640  
 two-dimensional strip, quantized Hall cond. and edge states 4-92591  
 two-dimensional system, fractional quantum Hall effect 4-92757  
 two-dimensional systems, quantum Hall effect and density of states 4-98650  
 zero-gap semiconductors, impurity states in mag. field 4-61332  
 AlGaAs-GaAs superlattices, magnetisation meas., de Haas-van Alphen oscils. 4-98734  
 Al<sub>1-x</sub>Ga<sub>x</sub>As-GaAs heterostructures, 1/3 and 2/3 fractional quantum Hall effect, activation energies 4-92811  
 CdSb, mag. band struct. in valence band 4-75849

- lanthanum levels continued
- LaAs  $n+n$  structures, high field reson. magnetotransport meas. 4-104295
- GaAs, power broadening and nonlinear far IR magnetophotocond. 4-108897
- LaAs/(GaAl)As two-dimens. electron gas, cyclotron reson. study 4-104297
- LaAs- $\text{Al}_x\text{Ga}_{1-x}\text{As}$ , quantised Hall resistance and 2D electron gas behaviour 4-98724
- LaAs- $\text{Al}_x\text{Ga}_{1-x}\text{As}$  heterostructures, 2D electron gas, disorder, fractional quantum Hall effect 4-76033
- LaAs- $\text{Al}_x\text{Ga}_{1-x}\text{As}$  heterostructure, low temp. fractional quantum Hall effect 4-98722
- LaAs- $\text{Al}_x\text{Ga}_{1-x}\text{As}$  heterostructure, thermopower meas. on 2D electron gas 4-98729
- LaAs- $\text{Al}_x\text{Ga}_{1-x}\text{As}$  multiple quantum well struct., magneto-Raman characterisation 4-104577
- LaAs-GaAlAs heterojunction, freq. enhanced fractional quantisation, quantum Hall effect 4-80664
- La, In, Se system, magneto-optical props. near fundamental band gap 4-109166
- GaSb-InAs heterojunction, quantum Hall effect study 4-98726
- Ge, hot hole submillimetre emission in transverse mag. field 4-71412
- He liquid, fully spin polarised, ground state energy and Landau parameters 4-75750
- Hg<sub>1-x</sub>Fe<sub>x</sub>Te, negative magnetoresist. and Hall effect 4-65696
- InAs/GaAs superlattices, Landau levels and magneto-optical props. 4-98737
- In, Ga<sub>1-x</sub>As-InP heterojunction, quantum Hall effect and hopping cond. 4-98723
- InSb, photo-EMF prod. by photon pulse accompanying optical transitions between Landau levels 4-70858
- InSb, photomagnetic effect and photocond. in mag. field, diamag. exciton discrete struct. 4-108903
- InSb, two photon interband magnetoabsorption, level transitions, photoconductivity meas. 4-71350
- Pb<sub>1-x</sub>Sn<sub>x</sub>Te, longitudinal magnetoresist., magnetophonon oscils. 4-65694
- PbTe Schottky barriers, resonant magneto-optical transitions from a deep level 4-76440
- Si inversion layers, multiple connected, quantised resistance regions 4-98725
- Si MIS structure, fractional quantum Hall effect 4-108947
- Si quantised Hall resistor, two-terminal conductance meas. 4-70942
- Si/SiO<sub>2</sub>/metal struct., electron inversion layers, tunnelling spectra of Landau levels 4-98772
- Landé g-factor** see *g-factor*
- Landé splitting factor** see *g-factor*
- Landé fields** see *airports*
- Langmuir films**
- alternating multilayer film, prep. method 4-81164
- azo dye Langmuir multimolecular layers, optical anisotropy, visible absorpt. spectra 4-109208
- barium stearate, Langmuir films, structure 4-108734
- cadmium arachidate, Langmuir-Blodgett film, technique for charact. 4-113834
- dyes adsorbed in Langmuir-Blodgett films, selectively laser excited, persistent spectral hole burning 4-88878
- integrated optics, Langmuir-Blodgett film fabrication 4-69593
- manganese stearate Langmuir-Blodgett film, 2-D mag. props. 4-98926
- organic and polymer crystals, nonlinear molecular optics, review 4-74594
- polydiacetylene, Langmuir-Blodgett multilayers, linear optical props. 4-76411
- preparation, charact. and appls. 4-61245
- w-tricosenoic acid, Langmuir-Blodgett film, technique for charact. 4-113834
- on Ag film, surface plasmon enhanced Raman scatt. 4-76453
- n-GaP with adsorbed organics, monolayer influence on Schottky barrier height 4-104290
- Langmuir probes**
- see also *plasma diagnostics*
- characteristics in various mag. field configs. 4-106156
- divertor discharges in D-III Langmuir probe meas. 4-97839
- double layers in linear turbulent-heating device, space resolved obs. 4-91943
- double plasma device, fast ion generation, wave excitation 4-65096
- electrostatic probes for dense flowing plasma 4-87935
- hollow cathode ion source, plasma investig. (German) 4-84102
- instabilities feedback control in tandem-mirror fusion device 4-87866
- instabilities feedback control in Tokamak 4-87866
- ion parameters determ., errors, appl. to ionosphere 4-105731
- low pressure plasma, probe characts. plotting and electron vel. distrib. measuring equipment (German) 4-84060
- metal atom condensation coeff. determ. by spectral probe 4-60731
- neutral beam-heated limiter discharges in D-III tokamak, power flow 4-98777
- particle and heat flux measurements in PDX edge plasmas 4-97900
- Q-machine plasma column, convective cell evolution 4-91879
- scrape-off layer, impurity flux meas. in TCA tokamak 4-97840
- size and limiter shadow effects, obs. on DITE scrape-off plasmas 4-91984
- turbulence, Tokamak edge plasma, space-time stats. 4-87869
- Ar plasma, sheath motion and related wave phenomena 4-91941
- Ne hollow cathode discharge, optogalvanic effect, Langmuir probe meas. 4-84063
- languages, programming** see *programming languages*
- lanthanides** see *rare earth metals*
- lanthanons** see *rare earth metals*
- lanthanum**
- see also *nuclei with ....*
- atom, L-shell X-ray prod. cross sections for protons of energy 1-2 MeV 4-96656
- clean and adsorbate covered, scatt. primary and recoiled surface neutrals and ions, TOF spectra 4-63800
- lattice dynamics, depend. of <sup>140</sup>Ce recoil motion on phonon spectrum, nucl. reson. fluorescence study 4-98216
- photoionisation, local density-based random phase approx. calc. 4-102656
- pressure effects, on band structure, Fermi surface and superconductivity 4-84553
- relaxation effects in inner-shell photoemission and absorption 4-64441
- lanthanum continued
- superconducting transition temp. under high press., vol. depend. 4-84728
- threshold electron excitation of Auger electron and X-ray emissions 4-93142
- valence band photoemission study 4-81108
- X-ray anomalous scattering and specular reflection in M, photoabsorption regions 4-93129
- YIG:Ga(La) magneto-optical waveguide, TE to TM mode conversion by alternating-coupling coeff. 4-69545
- BaCeO<sub>3</sub>:La, mixed elec. cond., dopant effects 4-108910
- Ba<sub>0.5</sub>Sr<sub>0.5</sub>Nb<sub>2</sub>O<sub>6</sub>:La, thermally stimulated electron emission, dielec. characts., impurity effects (Russian) 4-114356
- CaF<sub>2</sub>:La<sup>2+</sup>, intermediate Jahn-Teller coupling, vibronic Raman and EPR spectra 4-88491
- CaF<sub>2</sub>:La(Er), impurity local structural environments, EXAFS determ. 4-66129
- CaTiSiO<sub>5</sub>:La sphene-based glass-ceramics, La partitioning, Auger studies 4-88112
- CeO<sub>2</sub>:La<sup>3+</sup>Nb<sup>5+</sup>, dielectric relaxation, orientation of dipole complexes 4-114202
- Ge<sub>2</sub>Se<sub>3</sub>:La glass, impurity surroundings, nature of defects, positron annihilation study 4-79943
- La, H<sup>+</sup> impact, X-ray prod. cross sections 4-96648
- Si:La-SiO<sub>2</sub> interface, negative elec. effects produced by La impurities 4-108940
- SrTiO<sub>3</sub>:La, oxidation-reduction behaviour 4-103739
- lanthanum alloys**
- see also *lanthanum compounds*
- sorption of H, influence on heat pump operation 4-105131
- transition to nonmagnetic f states, bremsstrahlung isochromat spectra studies 4-113884
- Al-La, solid solubility, metastable extension (Chinese) 4-61918
- Al-Mg-La system, Al-rich corner, liquidus invest. (Chinese) 4-61917
- Ce<sub>1-x</sub>Al<sub>x</sub>:La, dense Kondo state, elec. resist., mag. susceptibility meas. 4-108984
- Ce<sub>0.8</sub>La<sub>0.2</sub>Cu<sub>2</sub>Si<sub>2</sub>, disordered, low-temp. specific heat meas. 4-75702
- Ce<sub>1-x</sub>La<sub>x</sub>Cu<sub>2</sub>Si<sub>2</sub>, mag. props. during Kondo impurity-Kondo lattice transition 4-61509
- Ce<sub>1-x</sub>La<sub>x</sub>Ni<sub>2</sub>, mixed valence, thermopower and band struct. 4-113927
- Ce<sub>0.9-x</sub>La<sub>0.1+x</sub>Th<sub>0.1</sub>,  $\gamma$ - $\alpha$  transition, x-P-T phase diagrams 4-76755
- Cu-La, liquid alloys, enthalpies of mixing, intermetallic compound form. 4-92374
- (Fe<sub>0.82</sub>B<sub>0.18</sub>)<sub>0.90</sub>La<sub>0.05</sub>Ru<sub>0.05</sub> amorphous metal alloys, ferromag. reson. and g-factor 4-71188
- Gd<sub>1-x</sub>La<sub>x</sub>Al<sub>2</sub>, loss of ferromagnetism 4-98885
- La-Ga metallic glasses, elec. cond. meas. 4-98588
- La-Ni, scanning Auger surface study 4-80356
- La-Rh-Si system, superconducting study 4-80713
- La<sub>100-x</sub>Al<sub>x</sub>, amorphous, supercond., thermodynamic and transport props. 4-70986
- La<sub>80</sub>Al<sub>20</sub> metallic glass, elastic props. and thermal expansion 4-84335
- LaCo<sub>5</sub>-H system, two-phase coexistence region, H chemical pot., interface rel. effect 4-104769
- La(Fe<sub>2</sub>Al<sub>1-x</sub>)<sub>13</sub>, metamagnetic transitions and struct. aspects 4-92910
- La<sub>2</sub>Ga, amorphous, superconductivity obs. (Chinese) 4-104338
- LaIn<sub>3</sub>, mixed-valence system, muon Knight shift meas. 4-80852
- LaNi<sub>5</sub>, H<sub>2</sub> storage, appl. in H masers 4-69352
- LaNi<sub>5</sub> hydrides, H-T, H-D, D-T mixtures isotope equilibria 4-108586
- LaNi<sub>5</sub>, stability of rechargeable hydriding alloys during extended cycling 4-72190
- LaNi<sub>5</sub>-NdNi<sub>5</sub>(CeNi<sub>5</sub>), phase diagrams, grain size anisotropy, H absorpt. characts. (Chinese) 4-93261
- LaNi<sub>4</sub>Al<sub>3</sub>, H<sub>2</sub> storage, appl. in H masers 4-69352
- LaNi<sub>4</sub>Al<sub>3</sub>, stability of rechargeable hydriding alloys during extended cycling 4-72190
- LaNi<sub>4</sub>Cr hydrides, H-T, H-D, D-T mixtures isotope equilibria 4-108586
- LaNi<sub>3</sub>Cu<sub>2</sub> hydrides, H-T, H-D, D-T mixtures isotope equilibria 4-108586
- LaNi<sub>4</sub>Cu hydrides, H-T, H-D, D-T mixtures isotope equilibria 4-108586
- LaNi<sub>5</sub>H<sub>6</sub>, muon trapping and jump mode 4-84889
- LaNi<sub>5</sub>(Ni<sub>4</sub>Al<sub>3</sub>) and misch metal. analogues, H<sub>2</sub> desorption kinetics 4-75787
- LaNi<sub>5</sub>Sb<sub>2</sub>, cryst. struct. determ. 4-79985
- LaPd<sub>3</sub>, mixed-valence system, muon Knight shift meas. 4-80852
- LaPtSi(Ge), supraconductivity and superconducting T<sub>c</sub> 4-61484
- La<sub>80</sub>Ru<sub>20</sub> (R=Nd, Pr), universal response of EM, acoustic, and mech. influences 4-92851
- LaSn<sub>3</sub>, mixed-valence system, muon Knight shift meas. 4-80852
- LaZn, comparison of conduction-electron susceptibility with GdZn and Zn 4-114176
- Ni-La single crystals, implanted, pulsed laser treatment studied by the <sup>4</sup>He<sup>+</sup> channelling 4-84315
- Ni-LaNi<sub>2</sub>-Zr<sub>2</sub>Ni<sub>7</sub>, peritectic equilibrium studies 4-76749
- Ti-La, rapidly solidified dispersion strengthened, struct. and props. 4-114561
- lanthanum compounds**
- see also *lanthanum alloys*
- acetates, <sup>13</sup>C chemical shielding anisotropies 4-65871
- complexes, relaxation effects in inner-shell photoemission and absorption 4-64441
- dilanthanum carbides, thermodynamic study by high temp. mass spectrometry 4-69859
- ethylsulphate:Ce<sup>3+</sup>, energy level shift under hydrostatic press. (Russian) 4-84598
- impurity determination by neutron activation anal. (Russian) 4-99911
- lanthanum ethyl sulphate:Gd<sup>3+</sup>, zero field splitting of Gd<sup>3+</sup> 4-96713
- PLZT, ferroelec. films, reactive sputtering prep. and dielec. props. 4-104731
- PLZT ceramics, polarisation switching characts 4-99006
- PLZT epitaxial thin films, ferroelec. and electrooptical props. 4-104530
- $\beta$ -Al<sub>2</sub>O<sub>3</sub>-La<sub>2</sub>O<sub>3</sub>:Eu<sup>3+</sup>, structure, laser excited fluorescence study 4-66071
- BaF<sub>2</sub>-LaF<sub>3</sub>-ZrF<sub>4</sub>-AlF<sub>3</sub> glass, crystallisation, devitrification on reheating 4-84194
- Ca<sub>2</sub>LaFeO<sub>8+x</sub>, cryst. struct. determ. 4-80014
- Ca<sub>1-x</sub>La<sub>x</sub>Ti<sub>1-x</sub>Fe<sub>x</sub>O<sub>3</sub>, perovskite solid soln. systems, prep. and charact. 4-70123
- CeO<sub>2</sub>-La<sub>2</sub>O<sub>3</sub> solid solutions, elec. cond., temp. depend., 400-1200°C 4-61142
- EuLa-S<sub>8</sub>, band gap width, rel. to short-range environment of S atom 4-80493
- 0.69Ga<sub>2</sub>S<sub>3</sub>0.31.La<sub>2</sub>O<sub>3</sub>:Nd<sup>3+</sup>, glass spectral luminesc. props. 4-76511

## lanthanum compounds continued

- $\text{HfF}_2\text{-BaF}_2\text{-LaF}_3\text{-AlF}_3$  glass, IR transparent, stability in humid air, AES study 4-109534  
 $\text{K}_2\text{La}_2\text{Ce}_2\text{Th}_2(\text{PO}_4)_2$  luminophors, instrumental neutron activation anal. 4-85345  
 $\text{KLa}(\text{MoO}_4)_2\cdot\text{Er}^{3+}(\text{H}_2\text{O})^{3+}$ , stimulated emission studies 4-84980  
 $\text{KLa}(\text{WO}_4)_2$ , lattice thermal expansion coeffs., 30 to 500°C 4-70415  
 $\text{La}_{0.72}\text{Pr}_{0.28}\text{Nd}_{0.03}\text{F}_3$ , fluorescence decay characts. 4-74436  
 $\text{LaAlO}_3$ , multicrystalline points 4-65385  
 $\text{La}_{0.827}\text{Al}_{1.19}\text{O}_{10.09}$ , cryst. struct., single cryst. X-ray diffr. studies 4-103723  
 $\text{LaB}_6$ , directly heated filaments, physical props. 4-104712  
 $\text{LaB}_6$ , long-life emitter for electron beam generation 4-86501  
 $\text{LaB}_6$ , X-ray reflections intensity, nonstoichiometry effect 4-61099  
 $\text{LaB}_6\text{-ZrB}_2$  system, interaction, phase diagram study 4-89030  
 $\text{La}_2\text{Ba}_2\text{Cu}_6\text{O}_{14+x}$ , struct., electron transport and mag. props. 4-70110  
 $\text{La}_{1-x}\text{Ba}_x\text{F}_3$ , solid solns., elec. props., small-signal AC response and TSDC meas. 4-70449  
 $\text{La}_{1-x}\text{Ba}_x\text{F}_3$ , solid solutions, small signal AC response 4-92424  
 $\text{La}_{1-x}\text{Ba}_x\text{F}_3$ , tysonite-type solid solns., ionic cond. 4-92410  
 $\text{La}_{1-x}\text{Ca}_x\text{FeO}_{3-y}$  ferrites, mixed valence and electrochem. props. 4-70752  
 $\text{La}_{1-x}\text{Ca}_x\text{FeO}_{3-y}$ , high temp. order-disorder transition 4-113618  
 $\text{LaCl}_3\cdot\text{Nd}^{3+}$ , isotope shifts, laser-induced fluoresc. 4-71428  
 $\text{LaCl}_3\cdot\text{Pr}^{3+}$ , crystal field levels, coord. geometry depend. 4-70755  
 $\text{LaCl}_3\text{-KCl}(\text{NaCl})(\text{CaCl}_2)$  mixtures, refr. index, goniometric meas. 4-109147  
 $\text{La}(\text{ClO}_4)_3\cdot 3\text{H}_2\text{O}$ , cryst. struct., X-ray diffr. determ. 4-92153  
 $\text{LaCoO}_3$  single cryst., tracer diffusion coeff. of oxide ions 4-103999  
 $\text{LaCoO}_3$ , spin-state transitions at low temp., near-neighbour impurity effect 4-88643  
 $\text{La}_2\text{CoO}_4$ ,  $\text{La}_2\text{CoO}_3$ , synthesis and high-temperature study (French) 4-85095  
 $\text{La}_2\text{CoO}_4$ , standard Gibbs energy of form. and high temp. thermodynamic stability 4-71958  
 $\text{LaCo}_2\text{P}_2$ , cryst. struct. determ. 4-80011  
 $\text{LaCo}_2\text{P}_2$ , flux growth and cryst. struct. 4-108335  
 $\text{LaCrO}_3$ , perovskite-type oxide, kinetics of CO adsorption 4-61208  
 $\text{LaCrO}_3\cdot\text{Mg}$ , defect struct., model and thermogravimetric meas. 4-75434  
 $\text{LaCrO}_3\text{-Cr}$  cermet, high-temp. creep 4-71693  
 $\text{La}_2\text{CuO}_4$ , with  $\text{K}_2\text{NiF}_4$  struct., at displacements, mag. and transport props., anisotropic bonding effects 4-75358  
 $\text{La}_{1-x}\text{Eu}_x\text{FeO}_3$ , perovskite solid soln. systems, prep. and charact. 4-70123  
 $\text{LaF}_3$ , NMR study, relax. time 4-71203  
 $\text{LaF}_3$  potentiometric sensor for  $\text{O}_2$  (Japanese) 4-86395  
 $\text{LaF}_3\cdot\text{Er}^{3+}$ , high freq. phonon dynamics, optical detection methods 4-65357  
 $\text{LaF}_3\cdot\text{Eu}^{3+}$ , fine struct. parameters, hyperfine splittings, X-band EPR meas. 4-71176  
 $\text{LaF}_3\cdot\text{Pr}^{3+}$ , coherently driven, optical line narrowing, Bloch eqns. 4-97007  
 $\text{LaF}_3\cdot\text{Pr}^{3+}$ , cooperative energy transfer among  $\text{Pr}^{3+}$  ions, photoluminescence spectra 4-92664  
 $\text{LaF}_3\cdot\text{Pr}^{3+}$ , optical free induction decay, magic-angle line narrowing in spectroscopy 4-64749  
 $\text{LaF}_3\cdot\text{Pr}^{3+}$ , two-photon transition from  $^1\text{H}_4$  to  $^1\text{S}_0$  4-104636  
 $\text{LaF}_3\text{-BaF}_2\text{-ZrF}_4$ , fluoride glass, surface crystals formed by reaction with water 4-81298  
 $\text{LaF}_3\text{-PbF}_2\text{-Nd}$ , NMR study, relax. time 4-71203  
 $\text{LaF}_3\text{-PrF}_3$ , NMR study, relax. time 4-71203  
 $\text{LaGaOSe}_2$ , cryst. struct., X-ray diffr. study (French) 4-65234  
 $\text{LaH}_2$ , electron-phonon interaction and supercond. destruction by H absorption 4-65622  
 $\text{LaH}_2$ , normal and deuterated, cubic-tetragonal transition, X-ray diffr. studies 4-80222  
 $\text{LaHO}$ , cryst. struct., X-ray and neutron diffr. (French) 4-88149  
 $\text{LaM}_2\text{Al}_2\text{O}_{10+x}$  ( $\text{M}=\text{Mn}, \text{Co}, \text{Cu}$ ), struct., substitution effects, X-ray diffr. studies 4-103722  
 $\text{LaMO}_3$  ( $\text{M}=\text{Cr}, \text{Mn}, \text{Fe}, \text{Co}$ ), adsorbed pyridine, CO and  $\text{CO}_2$ , IR spectra 4-104071  
 $\text{LaMgAl}_2\text{O}_9$ , thermally stimulated phenomena 4-113967  
 $\text{La}_2\text{Mg}_3(\text{NO}_3)_{12}\cdot\text{Ce}^{3+}\cdot\text{Co}^{2+}\cdot 24\text{H}_2\text{O}$ , paramagnetic, maser effect due to thermal excitation by pulsed mag. field 4-64692  
 $\text{La}_2\text{Mg}_3(\text{NO}_3)_{12}\cdot 24\text{H}_2\text{O}\cdot\text{Ni}^{2+}$ , spin system excitation, ESR study 4-98943  
 $\text{La}_2(\text{MoO}_4)_3\cdot x\text{H}_2\text{O}$ , solubility, Liesegang ring form., adsorpt. and salt effect 4-65410  
 $\text{LaMo}_6\text{S}_8$ , Chevrel phase, resistivity meas. 4-84619  
 $\text{LaMo}_6\text{S}_8$  films, supercond. props. and normal state resist. 4-92876  
 $\text{LaMo}_6\text{Se}_8$ , Chevrel phase, resistivity meas. 4-84619  
 $\text{LaNbO}_4$ , ferroelastic, spontaneous birefringence obs. 4-93045  
 $\text{LaNbO}_4$ , photochromic coloration enhancement by doping 4-61639  
 $\text{La}_{0.9}\text{Nd}_{0.1}\text{MgAl}_2\text{O}_9$  grown by Czochralski method, continuous laser effect obs. (French) 4-79155  
 $\text{LaNi}_{1-x}\text{Co}_x\text{O}_3$ , ferrimagnetic interactions, mag. susceptibility meas. 4-88662  
 $\text{LaNi}_{1-x}\text{Cr}_x\text{O}_3$ , ferrimagnetic interactions, mag. susceptibility meas. 4-88662  
 $\text{LaNi}_{1-x}\text{Fe}_x\text{O}_3$ , antiferromagnetic interactions, mag. susceptibility meas. 4-88662  
 $\text{LaNi}_2\text{H}_6$ , muon diffusion, spin rot. meas. 4-65914  
 $\text{LaNi}_{1-x}\text{Mn}_x\text{O}_3$ , valence states and mag. props. 4-84772  
 $\text{LaNiO}_2$ , reduced phases, Ni oxidation states, XANES and EXAFS studies 4-61343  
 $\text{LaNiO}_2$ , struct. and  $\text{Ni}^{2+}$  local environment, X-ray diffr. and EXAFS studies 4-60901  
 $\text{La}_2\text{NiO}_4$ , with  $\text{K}_2\text{NiF}_4$  struct., at displacements, mag. and transport props., anisotropic bonding effects 4-75358  
 $\text{La}_2\text{O}_3\text{-P}_2\text{O}_5$  system, phase equilib. and transform. 4-61923  
 $\text{LaOCl}$  single cryst., Raman spectra 4-71380  
 $\text{LaO}_{1-x}\text{F}_{1+2x}$ ,  $^{19}\text{F}$  NMR study of anion mobility 4-114168  
 $\text{LaPd}_2\text{Al}_{1-x}\text{O}_3$ , stabilisation conditions of trivalent Pd 4-71616  
 $\text{LaS}$ , energy band struct., X-ray study 4-84565  
 $\text{LaS}_2$ , non-stoichiometric, thermoelectric props. 4-75992  
 $\text{LaS}_2$ , stoichiometry determination using wet analytical method 4-75697  
 $\text{La}_2\text{S}_3$ , prep. in high purity powder form from elements 4-108298  
 $\text{La}_{1-x}\text{Sr}_x\text{CrO}_{3-y}$ , defect struct. and thermodynamic props. 4-98099  
 $\text{La}_{1-x}\text{Sr}_x\text{FeO}_{3-y}$  ferrites, mixed valence and electrochem. props. 4-70752  
 $\text{La}_{1-x}\text{Sr}_x\text{VO}_3$ , metal-insulator transition, photoemission study 4-84567  
 $\text{La}_2\text{TaO}_7$ , IR and Raman vibr. spectra 4-61679  
 $\text{LaTi}_2\text{Al}_2\text{O}_9$ , difficult-to-form crystal structures, preparation 4-70094  
 $\text{La}_2\text{Ti}_2\text{O}_7\cdot\text{Cr}^{3+}$  and  $\text{La}_2\text{Ti}_2\text{O}_7\cdot\text{Cr}^{3+}$ , photoelectrochem. props. 4-70874

## lanthanum compounds continued

- $\text{La}_2\text{Ti}_2\text{O}_7\cdot\text{CaTiO}_3$ , ferroelectric, crystallochemical props. 4-71288  
 $\text{LaVO}_3\text{-LaVO}_4$ , O chemical pot., solid solubility, EMF obs. 4-113669  
 $\text{LaVO}_3\cdot\text{Nd}^{3+}$ , hypersensitive vibronic transition obs. (French) 4-99132  
 $\text{La}_{1-x}\text{Ba}_x\text{F}_3$  crystals, fluoride ion cond., electronic cond. meas. 4-92772  
 $\text{NaCl-LaCl}_3$  binary melt, density (Korean) 4-80131  
 $(\text{Nd}, \text{La})\text{P}_2\text{O}_{14}$ , large good-quality laser crystals, growth method 4-71543  
 $\text{Nd}, \text{La}_{1-x}\text{P}_2\text{O}_{14}$ , four wave mixing and exciton dynamics 4-83638  
 $\text{PLZT}$ , ageing and space charge arising in hot poling 4-76327  
 $\text{PLZT}$  ceramic, coarse-grain light scatt. and elec. hysteresis 4-76399  
 $\text{PLZT}$  ceramic for recording of volume amplitude-phase holograms 4-107579  
 $\text{PLZT}$  ceramics, ferroelec. and electrooptic props. 4-76353  
 $\text{PLZT}$  ceramics, hot pressed polarisation and depolarisation behaviour 4-76318  
 $\text{PLZT}$  ceramics, ion implanted, optical absorption 4-114233  
 $\text{PLZT}$  ceramics, poling strategy 4-76319  
 $\text{PLZT}$ , chemically prepared, charact. and props. 4-76712  
 $\text{PLZT}$ , ferroelec. ceramic, hot poling, polarisation, ageing rel. to space charge 4-99045  
 $\text{PLZT}$ , ferroelec. diffuse phase transition, exponent  $\gamma$  determ. 4-76384  
 $\text{PLZT}$ , microscopic characterisation 4-61903  
 $\text{PLZT}$  piezoelectric ceramic, fabricated by atmospheric sintering, electric characts. and optical transmittance (Korean) 4-114211  
 $\text{PLZT}$  retardation plates, nonhomogeneity of light modulation 4-61660  
 $\text{PLZT}$ , tetragonal ceramic, 90° domains under poling, XRD study 4-76398  
 $\text{PLZT}$  thin-film waveguides, electrooptic Kerr coeffs. 4-91578  
 $(\text{Pb}, \text{La})(\text{Zr}, \text{Ti})\text{O}_3$  ceramics, stress anisotropy induced by polarisation 4-104536  
 $\text{Pb}_{0.91}\text{La}_{0.09}(\text{Zr}_{0.65}\text{Ti}_{0.35})_{0.98}\text{O}_3$ , microscopic characterisation 4-61903  
 $\text{Pr}, \text{La}_{1-x}\text{P}_2\text{O}_{14}$ , luminesc. theory, oscillator strength, impurity conc. effect (Chinese) 4-93100  
 $\text{Sr}_{1-x}\text{La}_x\text{FeO}_3$ ,  $\text{Fe}^{4+}$  ion electronic state, Mossbauer spectra study 4-104171  
 $\text{Sr}_2\text{La}_2\text{W}_2\text{O}_{12}$ , rare earth, luminescence and sensitised emission 4-104657  
 $\text{Zr-Ba-La-Al-F}$  glass, crystn. kinetics 4-70037  
 $\text{ZrF}_4\text{-BaF}_2\text{-LaF}_3\text{-AlF}_3$  glass, IR transparent, stability in humid air, AES study 4-109534  
 $\text{ZrO}_2\text{-La}_2\text{O}_3\text{-B}_2\text{O}_3\text{-SiO}_2$ , radioactive waste disposal, long term leaching 4-111607

## Laplace transforms

- Dirichlet problem of Laplace eqn., integral difference soln. method (Russian) 4-63517  
 linear elastic cracked body, transient elastodynamic second boundary-value problem 4-64881  
 metals, sputtered particle energy distrib. at low bombarding energy 4-109290  
 neuronal response to stochastic stimulation 4-115045  
 piezoelectric transducers, thickness-mode, three-port model 4-97255  
 pionic atom, relativistically corrected Schrodinger eqn. with Coulomb interaction 4-69250  
 plasma, semi-infinite, degenerate, linear response function in external mag. field 4-92643  
 wing aerodynamics in supersonic shear flow 4-97602

## Large Magellanic Cloud

- 0525-66.0 SNR progenitor as Type III supernova 4-77973  
 bar population struct., red giants colour-magnitude diagram anal. and construction 4-90229  
 Cepheids, period-luminosity-colour relations and UBVR photometry 4-77835  
 classical Cepheid variables, coeff. of colour term in P-L-C relation 4-94804  
 cosmic rays origin, models and expected radio and  $\gamma$ -ray emission 4-101485  
 30 Doradus, IUE obs. of stars rel. to UV extinction and stellar continua 4-85996  
 30 Doradus Nebula, low density envelope, radio obs. 4-67781  
 early type supergiants, luminosity -  $\text{H}\alpha$  and  $\text{H}\beta$  equivalent widths relation 4-110603  
 early-type supergiants, spectral line features 4-110751  
 field stars, ages and colour-magnitude diagrams 4-110746  
 Hodge 11 globular cluster, electronographic stellar photometry 4-94623  
 intermediate age star clusters, ages from red giants luminosities anal. in evolution models 4-90193  
 LMC X-3, soft X-ray spectrum, HEAO 1 A-2 and Einstein SSS obs. 4-110653  
 M and S stars in LMC globular clusters, spectroscopic obs. 4-77886  
 N44, H II region, obs. of high-vel. component within small shell 4-115815  
 N49 supernova remnant as site of 1979 March 5  $\gamma$ -ray burst 4-77909  
 R136, nature and spectrum 4-106011  
 R136a, supermassive star and visual binary, position angle and separation 4-85949  
 ring-shaped nebulae, optical obs. 4-77908  
 SNR 0540-69.3 X-ray pulsar, Einstein IPC obs. 4-67771  
 supernova remnants, kinematics 4-73041  
 supernova remnants, number-diameter distrib. 4-110717  
 supernova remnants, optical obs. 4-77908  
 far UV emission by nebulae and starfields, S201 camera obs. by Apollo 16 4-110531  
 X-ray Balmer-dominated supernova remnants, optical obs. and radio emission 4-77907  
 X-ray sources, Einstein Observatory obs. 4-101510  
 H I 21 cm line survey, velocities and rotation 4-110741

## large scale integration

- acoustic arrays, digital signal processor module architecture, implementation using VLSIs 4-103122  
 audio signal processing, digital, CMOS-VLSI rate conversion digital filter appl. 4-103121  
 central nervous system quantisation for VLSI implementation of robotic neural systems 4-77231  
 CMOS LSI circuit for an implantable cardiac pacemaker 4-77428  
 GaAs fast supercomputer circuits (Swedish) 4-65282  
 I<sup>2</sup>L device circuit model with layout patterns 4-104192  
 portable test instrumentation development, using CMOS LSI technology, flat displays and microprocessors 4-73429

## laser scale integration continued

- resist pattern reformation by reactive ion etching using Ar-methane gas mixture 4-81301
- submicron structures, dry etching techniques 4-89146
- VLSI, selective plasma etching of polycryst. Si 4-81311
- VLSI by selective epitaxy, local loading effect 4-93228
- VLSI technology, textbook 4-82610
- wafer flatness tester, automatic, using Fizeau interferometer, VLSI circuit wafer appls. 4-106270
- X-ray lithography alignment system 4-95596
- Al films, prep. by low press. MOCVD 4-81156
- Al-Si interconnects, DC magnetron-sputtered, influence of residual gas composition on lifetime 4-71560
- Au-SiO<sub>2</sub>, metallisation technology comparative study of Nb and TiW barrier layers 4-88969
- GaAs LSI, Si<sub>3</sub>N<sub>4</sub> film deposition by plasma-enhanced CVD 4-71569
- Mo-Ti/Si interface, metallisation for self-aligned TiSi<sub>2</sub> process 4-89145
- Si, conference, San Jose, CA, USA (Jan. 1982) 4-110812
- Si material phenomena in VLSI circuit processing 4-103738
- WSi<sub>2</sub>-poly-Si-SiO<sub>2</sub>-Si MOS struct., interface reaction and resistivity 4-114040

## laser-scale systems

- deployable optical systems, conf., Los Angeles, CA, USA (Jan. 1983) 4-73138

## laser accessories

- 1.3  $\mu$ m window material effective absorpt. coeff. data survey 4-74638
- accelerator technology for high power short wavelength free electron laser 4-83255
- achromatic prism beam expanders 4-107800
- acousto-optic output coupler for free electron lasers 4-83601
- acoustooptical mode locking of a CW Nd:YAG laser 4-69473
- angular interferometers for laser scanners 4-82821
- automated beam expander device 4-83629
- calibrating equipment for laser power 4-96969
- calibration of power deposition in nuclear pumped lasers, using ozone dosimetry 4-112454
- calibrator for high power and high energy laser power meters and calorimeters (Chinese) 4-112492
- calorimeter with rapidly moving thin fluid technique, intense laser radiation meas. appls. 4-58889
- catalyst evaluation for closed cycle operation of high energy pulsed CO<sub>2</sub> laser 4-96939
- chalcogenides, vitreous, multilayer reflecting systems for IR lasers 4-69532
- coated window and mirror components, pulsed DF chain laser damage 4-74582
- collimation, principal optical systems of afocal adapters (Russian) 4-91516
- composite optical multichannel analyzer for laser parameter measurement (Chinese) 4-112453
- continuously tunable He replenisher for long lifetime He-Cd laser (Chinese) 4-60089
- current-limited capacitor charging power supply for spark-gap-driven high repetition rate laser pulser 4-79172
- dielectric film degradation by XeF excimer laser intermediates 4-74534
- dye no.5 for fast laser mode locking, excited state absorpt. dynamics, fluoresc. lifetime 4-107760
- dye ring-lasers, femtosecond, multilayer dielec. mirror generated chirp 4-83573
- electro-optic modulator for diode laser, design and 600 Mbit/s operation (German) 4-79199
- electro-optical modulators on the basis of KDP and DKDP crystals 4-112489
- electrooptic switch for unpolarised radiation in Nd<sup>3+</sup>:YAG laser with intracavity SHG in crystals exhibiting aperture effect 4-74574
- electrostatic technology for dust and hydrocarbon vapour control in high power laser systems 4-74533
- energy and power meas. device, receiving element (Russian) 4-83606
- feedback circuit for stable single-wavelength operation of two-section coupled cavity laser under modulation 4-91470
- flash lamp, high power vortex gas flow, for dye laser pumping 4-64718
- fluid jet stream of high optical quality, wire guided 4-112969
- free electron generators of coherent radiation, conf., Orcas Island, WA, USA (June 1983) 4-82588
- frequency measurement chain to 30 THz using FIR Schottky diodes and submm. backward wave oscillator 4-73414
- glow discharge laser amplifier, rel. to effect of quantum modulation of electron beams by lasers 4-96864
- gradient-index lens for laser-diode beam, focusing props. 4-87411
- grazing-incidence grating cavities with Brewster-prism beam preexpander for pulsed dye lasers (Chinese) 4-112481
- heterodyne Mach-Zehnder interferometer system for testing laser diode wavefront quality 4-106363
- high energy laser optical elements, cooled finite element modelling 4-87416
- hollow-cathode cell for a pulsed vapor laser 4-102939
- in-laser interferometer using anisotropic mirrors, linear polarization production (Russian) 4-69465
- intensity profile measurement apparatus, materials processing environment appls. 4-106344
- interferometric liquid gate plate positioner, design and appl. 4-102941
- intracavity plasma shutter for transversely excited CO<sub>2</sub> lasers 4-103584
- IR laser radiation detection using antenna-coupled point contact Schottky diode, responsivity study (Japanese) 4-78374
- Lambdascope, used for measuring laser beam wavelengths (French) 4-86459
- large aperture optical switching devices for inertial confinement fusion lasers 4-96944
- metallic optics of technological laser apparatus 4-107687
- microcomputer-controlled scanning of a laser beam at constant speed 4-64717
- miniature optical cryostat for a semiconductor laser with temperature stabilization 4-91486
- mirror, cooled, coating defects rel. to limiting flux density 4-79208
- mirror, cooled, multiple defects effect on performance, predictive evaluation 4-79173
- mirror operation at cryogenic temps. 4-74657
- mirrors, cooled, thermoelastic stability 4-102940
- mirrors, high intensity laser, heat carrier use in powder and felt porous structs. 4-74659

## laser accessories continued

- mirrors, high reflectivity development using cavity attenuated phase shift method 4-74774
- mirrors, water-cooled, ultrasonic nondestructive testing and meas. 4-103032
- mode corrugated pipe design for CO<sub>2</sub> grating selecting freq. laser (Chinese) 4-87360
- multielement matrix measurement facilities for laser radiation energy meas., errors 4-101893
- nanosecond light flash source for multichannel system calibration 4-74096
- nanosecond pulse generator using TGI-2000/35 thyratron for Cu vapour lasers 4-60058
- narrowband dye laser with a large scan range 4-91489
- optical component specification, overview 4-83600
- optical specifications, components and systems, conf., Arlington, VA, USA (Apr. 1983) 4-82586
- optical surfaces, laser desorption analysis of H<sub>2</sub>O and other contaminants 4-74777
- oxide films used in lasers, refr. index (Chinese) 4-109262
- permanent magnetic wiggler design and simulation device with a few periods (Chinese) 4-112462
- phase measurement interferometer for wavefront evaluation on laser diodes 4-106364
- phased array beam expander simulation to predict far-field performance 4-106342
- phased array telescopes, image-plane phase sensing 4-97020
- photorefractive laser beamsteering using thick diffr. gratings, configurations 4-96968
- plasma focus, Mather-type dense, as optical pump for lasers 4-64720
- point-contact Schottky diode detector and laser/microwave diagnostic system for far IR 4-73517
- precision photometer for measuring low levels of maximum power of a pulsed laser 4-101891
- prismatic pulsed dye lasers, multi-pass dispersion theory 4-69398
- quartz mirrors, Zerodur and ULE, dimens. stability under thermal cycling 4-74658
- resonators with non-uniform mirrors, producing uniform laser beam (Russian) 4-69449
- rhodamine 6G CW dye ring laser with a Mach-Zehnder interferometer, efficient single mode operation 4-91496
- saturable absorber, CN-1, Q-switch of Nd:glass laser (Rumanian) 4-96918
- secondary emission electron gun, appl. to gas lasers and plasma chem. reactor 4-90689
- semiconductor laser diode modulators triggered by logical IC 4-60082
- shutters using microchannel plate intensifier tubes 4-107806
- single pulse selector for high repetition rate mode-locked lasers (Chinese) 4-87355
- solid laser pumping, HV pulse generator, 20 kV, design and operation (Bulgarian) 4-87352
- spark gap switch for repetitive excimer lasers (Chinese) 4-107659
- stabilisation system for optically pumped CO<sub>2</sub> CW far IR lasers 4-102954
- structural mechanics of optical systems, conf., Cambridge, MA, USA (Nov. 1983) 4-86104
- subharmonic buncher for Los Alamos free electron laser oscillator expt. 4-83603
- submillimetre laser couple, strip grating type, design, photolithographic fabrication and transmission meas. 4-74693
- super-smooth surface damage effect identification by scatter evaluation 4-83729
- switching of N<sub>2</sub> TEA laser 4-64721
- synchronisation scheme using streak camera system for picosec. mode-locked dye laser oscillator-amplifier 4-112475
- synthetic aperture beam control system 4-96967
- synthetic aperture phase meas. system using metering rod bridge with corner cubes 4-97016
- thyratron switch pulse generator for laser Q-switching 4-91506
- total integrated scattering meas. of laser films (Chinese) 4-111166
- transmission elements for technological CO<sub>2</sub> lasers, materials for windows and lenses 4-107658
- transmissive optics for high power CO<sub>2</sub> lasers, failure phenomena (Japanese) 4-74530
- transparent materials, absorpt. of laser rad. by metallized microinclusions 4-69468
- two-wavelength antireflection coating at 1.06 and 0.53  $\mu$ m (Chinese) 4-91485
- ultra-smooth laser mirror coating and substrate surface roughness assessment 4-74755
- variable emittance filter for electron laser facility 4-82859
- window materials, 1.3  $\mu$ m, thermo-optic coeff. 4-76443
- YAG high repetition rate laser power supply, pre-control protection (Chinese) 4-112493
- AlGaAs injection laser with external dispersion resonator using returning mirror 4-107641
- Ar mode synchronised laser amplifier system, high-power pulse prod. at high repetition freq. (Russian) 4-69369
- CO<sub>2</sub> high power laser optics 4-102937
- CO<sub>2</sub> laser polarimeter 4-78363
- GaAs diode lasers, variable-resolution data collection 4-69428
- GaAs:Cr picosecond optoelectronic switches, pulse modulation of GaAs-(Ga)AlAs DH diode laser 4-107701
- GaAs/GaAlAs monolithically Peltier-cooled laser diodes 4-74540
- GaInAsP/InP BH laser with chemically etched and mass-transported mirror 4-74537
- HF 2-dimens. laser beam phase and intensity meas. technique using acousto-optic modulator, heterodyne detector and raster-scanning mirrors 4-74564
- HF CW lasers, small signal gain meas. (Chinese) 4-112400
- He-Ne laser emission power stabilisation, using gas-discharge lens 4-102938
- KH<sub>2</sub>PO<sub>4</sub> with plasma electrodes, electro-optic harmonic conversion switch for large-aperture multipass laser systems 4-97000
- N<sub>2</sub> compact capacitively coupled laser with new electrode design 4-60067
- Nd<sup>3+</sup>:YAG pulse-periodic laser with wavefront reversal in stimulated-Brillouin-scatt. mirror and with freq. doubling 4-74522
- Si switch development for optical pulse generation in Nova, Novette fusion lasers 4-107702
- Si<sub>1-x</sub>H<sub>x</sub> coatings for high power IR lasers 4-74675

## laser accessories continued

- SiO<sub>2</sub> porous antireflection coating for use at 248, 266 nm 4-79268  
 SiO<sub>2</sub>/TiO<sub>2</sub> multilayer films, reactively evaporated, laser mirrors appl. 4-99327

laser annealing *see laser beam annealing*laser applications *see laser beam applications*

## laser beam annealing

- industrial applications of high power lasers, conf., Linz, Austria (Sept. 1983) 4-101561  
 laser surface modification 4-104892  
 semiconductor processing, laser annealing, advantages over thermal annealing 4-113497  
 semiconductors, laser annealing mechanisms 4-88202  
 semiconductors, laser treatment, scattered radiation intensity variation 4-70200  
 semiconductors, Raman characterisation 4-99106  
 SOI films, laser recrystallisation, Raman microprobe study 4-80462  
 SOI structures, laser annealing equipment for recrystn. (Japanese) 4-88200  
 SOI technology, laser recrystallisation technique 4-80458  
 solar cells, laser processing techniques, future developments 4-89434  
 steels, corrosion-resistant, surface strengthening by laser irradiation (Russian) 4-81340  
 time resolved TEM studies 4-65297  
 Si, ion implantation and laser annealing (Japanese) 4-108404  
 Au-Ge-Ni ohmic contacts on GaAs, CO<sub>2</sub> laser alloying 4-76038  
 CdS crystal laser beam annealing 4-75508  
 Fe<sub>40</sub>Ni<sub>40</sub>P<sub>10</sub>B<sub>6</sub> amorphous ribbons, mag. props. and struct., influence of laser annealing 4-88663  
 GaAs amorphous thin films, transient annealing, Raman scatt. study 4-80926  
 GaAs, ion implanted, photolum. after laser annealing 4-76525  
 GaAs:Si, implanted, elec. props., pulse laser annealing effects 4-60953  
 GaAs/AuGe ohmic contact, Ge and Au profiles, SIMS studies 4-103782  
 Ge amorphous film, laser enhanced crystallisation, nucleation, growth velocity, recombination enhanced diffusion 4-65295  
 Ge, picosecond-pulse laser annealing, phenomenological model 4-88198  
 Ge, pulsed laser irradiated, time resolved temp. meas. by thin film thermocouple 4-113494  
 Ge, submicron layers produced by ion implantation and laser annealing 4-84316  
 Ge surface, periodic struct. form. due to action of intense UV excimer laser light 4-81042  
 InP, ion implanted, elec. activation by CW laser annealing 4-80088  
 InP:Zn, grown-in defects, annealing effects, DLTS studies 4-84287  
 KH<sub>2</sub>PO<sub>4</sub> crystals, bulk laser-damage resistance improvement by baking and pulsed laser irradi. 4-75517  
 PbS thin films, laser and thermal annealing effects on elec. props. 4-65298  
 Si amorphous film, laser enhanced crystallisation, nucleation, growth velocity, recombination enhanced diffusion 4-65295  
 a-Si film, epitaxial crystallisation on GaP substrate 4-80452  
 Si, ion implanted, beam annealing 4-75510  
 Si, ion implanted, CO<sub>2</sub> laser annealing, relax. characts. of metastable concentrations 4-75512  
 Si, ion implanted, laser or electron beam annealing, electronically active defects, DLTS 4-80527  
 Si, ion implanted, laser or electron beam annealing, minority carrier recomb., EBIC, photoluminescence meas. 4-80601  
 Si, ion implanted, pulsed-laser-induced epitaxial regrowth 4-75511  
 Si, ion implanted, pulsed laser and thermal processing, defect anal. 4-70133  
 Si, ion implanted, pyrometric temp. meas. during laser annealing 4-70203  
 Si, ion implanted, rapid thermal arc lamp and pulsed laser annealing, photoluminesc. study 4-93094  
 Si, ion-implanted, pulsed laser annealing, transient reflectivity studies 4-80086  
 Si, ion-implanted, pulsed laser annealing, reflectivity studies 4-80087  
 Si laser recrystallised MOSTs, current cond. mechanism 4-76057  
 Si, laser-annealed surface, Kapitza resist. at liq. He interface 4-70500  
 Si laser-irradiated, instability at melting threshold 4-80094  
 Si optical I/O IC, technology description 4-107888  
 Si, oxidation stacking fault elimination by CW CO<sub>2</sub> laser annealing (Chinese) 4-113496  
 Si, picosecond-pulse laser annealing, phenomenological model 4-88198  
 Si, point defects due to laser annealing, DLTS study (Chinese) 4-84584  
 Si, polarisation sensitive Raman microprobe studies of local cryst. quality 4-101925  
 Si, polycryst., laser annealed, diffr. studies 4-104106  
 Si, polycrystalline, implantation under thermal and laser annealing, sheet resist. and doping profiles 4-75487  
 Si, polycrystalline, recrystallisation by combined CW laser and furnace heating 4-88199  
 a-Si, pulsed laser irradiation, melting temp. and explosive crystallisation 4-88201  
 Si, rapid melting and regrowth velocities by UV ps laser pulse heating 4-92232  
 Si solar cell, ion implanted, laser annealed 4-72121  
 Si substrate, ion implanted and processed, interface characterisation 4-84304  
 Si:As, implanted under channelling conditions, impurity spatial distrib., localisation, defect form. characts. 4-84321  
 Si:As, ion implanted and laser annealed, struct. changes, X-ray diffr. study 4-75461  
 Si:As, low energy implanted, laser-annealed, channeling and high-resolution backscatt. studies 4-75493  
 Si:As<sup>+</sup>(Sb<sup>+</sup>), ion implanted and laser annealed, defects, photoluminescence studies 4-75433  
 Si:P, heavily doped, optical reflectivity spectra 4-61735  
 Si:P,N, pulsed laser annealing, substitutional N impurities, EPR studies 4-98120  
 Si:P(B), heavy doping effect on band struct. and optical props. 4-92998  
 Si:Sb, implanted laser irradi., crystn. annealing, time-resolved reflectivity, TEM, Rutherford backscattering anal. 4-80093  
 Si-on-insulator, Si stripes in SiO<sub>2</sub> grooves, double laser recrystn., orientation control 4-75506

## laser beam applications

*see also holography; integrated optics; laser beam annealing; laser beam machining; laser beam welding; laser isotope separation; matrix isolation*

## laser beam applications continued

- spectroscopy; measurement by laser beam; modulation spectroscopy; optical communication; optical radar; patient treatment; plasma production and heating by laser beam; Raman spectra; Raman spectroscopy; remote sensing by laser beam; spectroscopy; surgery; two-photon spectroscopy*  
 70 mm laser flying spot telecine projector for HDTV (Russian) 4-73557  
 absolute distance interferometer using dye laser heterodyne interferometer and spatial separation of beams 4-106366  
 accelerometer of aviation gravimetric system (Russian) 4-96976  
 air pollution detection with multicomponent gas analyser based on He-Ne laser (Russian) 4-89485  
 astrometry, linking of reference systems from space 4-72856  
 atmospheric remote sensing by tunable diode laser heterodyne spectroscopy, progress review 4-115590  
 atmospheric trace gas measurements using airborne tunable diode laser system 4-115588  
 atom slowing down and pumping using very long cavity laser 4-96723  
 atomic spectroscopy, symposium, Berkeley, CA, USA (Sept. 1983) 4-67852  
 atomic vapour density meas. by least-squares fit to spectra 4-102825  
 biological objects, N isotope composition, lasing methods 4-81825  
 biomedical optical fibres, conf., Paris, France (May 1983) 4-82587  
 broadly tunable mid-IR radiation by difference freq. mixing in LiNbO<sub>3</sub> and AgGaS<sub>2</sub> 4-107742  
 bubbles in water, critical angle laser light scatt., meas., models, appls. to bubble sizing 4-69311  
 calorimetric apparatus for low optical absorption meas. 4-86422  
 cancer treatment by laser beam (Swedish) 4-109897  
 catheter, fibre optic laser tunnelling device, for thromboembolic disease therapy 4-72343  
 cavity power increases caused by reflections from workpiece surfaces 4-91519  
 chemistry, appl. to analysis, vibr. relax. and mol.-surface interaction 4-66641  
 chirp effect on optical systems, wavelength shift 4-91521  
 circular-scan photochron streak camera, spaceborne ranging appls. 4-107725  
 coherent IR radar systems and appls., conf., Arlington, VA; USA (Apr. 1983) 4-95019  
 communication systems design and development, component solution (German) 4-60173  
 compression and interaction investigs. 4-96977  
 computer generated holographic laser scanner for 2D graphics 4-69332  
 conference, lasers in mechanical engineering, Zvenigorod, USSR (Oct. 1982) 4-106095  
 conference on lasers, Beijing, China (May 1980) 4-63396  
 CVD using CW and pulsed lasers 4-109330  
 CW laser diodes, appl. for space communications 4-102931  
 dermatology, current laser instrumentation 4-72336  
 developments in China 4-69481  
 diagnostic medicine, spectroscopic techniques 4-72340  
 digital heterodyne interferometer using phase modulation of Ar ion laser polarisation 4-111194  
 directed energy weapons, development (Dutch) 4-112495  
 double annular aperture method for laser speckle interference photography (Chinese) 4-86494  
 dye oriented film, laser marking process based on microcrystallite photothermal transform. 4-107773  
 electron acceleration, laser-driven 4-107185  
 electron acceleration by laser, dynamics of synchronisation 4-69479  
 endoscopic fibre optic surgery and therapy, appls. in USA 4-85473  
 endoscopic photocoagulation for upper gastrointestinal bleeding, Nd:YAG laser appl. 4-72334  
 endoscopic resections in bronchology, technical problems 4-85475  
 entertainment electronics, design optimisation of GaAs lasers (German) 4-102948  
 excimer lasers, laser processing, semiconductor surface processing, materials purification and formation (Japanese) 4-74474  
 flames, spatially resolved soot-absorpt. meas. using laser vapourisation of particle 4-79211  
 framing high-speed shearing interferography with pulsed He-Ne lasers, frequency, shock, combustion and explosion problem appls. 4-68275  
 frequency-modulation spectroscopy with pulsed dye laser, sensitivity, signal-to-noise ratio 4-73520  
 fusion and isotope separation research and development at Lawrence Livermore National Lab., review 4-90324  
 fusion research at ILE Osaka 4-68824  
 gas analysis using Pb salt laser technology 4-107719  
 glass, optical, surface treatment resulting in min. surface roughness and max. beam surface penetration 4-79351  
 gynecology, laser appls. 4-72335  
 gyro performance, quantisation: reduction using moving average filter 4-102970  
 gyroscope beat freq. correction (Chinese) 4-86399  
 HDTV laser beam recording on 35 mm colour film, electrocinematography appl. 4-106418  
 heterogeneous materials, large-grained, step-heating technique for thermal diffusivity meas. 4-75738  
 high energy laser techniques in industrial measurements 4-102967  
 high-power laser system development for laser-fusion research in China 4-68825  
 holographic memory units using laser diodes, binary images (Russian) 4-107553  
 holographic testing, high-speed, high strobe-rate lasers 4-102903  
 holography, multiple embossment for hologram recording, holographic memory for information retrieval (Japanese) 4-107580  
 induced rapid etching of surface relief in solids 4-60100  
 industrial applications of high power gas lasers 4-102966  
 industrial applications of high power lasers, conf., Linz, Austria (Sept. 1983) 4-101561  
 industrial material processing applications 4-107661  
 inertial fusion research using short-pulse high-energy CO<sub>2</sub> laser system at Los Alamos scientific laboratory 4-68823  
 inertial-confinement-fusion implosion experiment status at LLL 4-68822  
 interstellar optical communication, technologies 4-107722  
 interstellar travel using laser-pushed lightsails 4-82364  
 intracavity laser spectroscopy, combustion diagnostics appls. 4-73519  
 ion beam diode, anode heating with CO<sub>2</sub> laser 4-111976  
 isocentric machines, improved optical backpointer using 2 laser beams 4-109900

laser beam applications continued  
 kinoform optical element fabrication 4-83742  
 laser gas cutting, physical models and technological aspects 4-107718  
 laser induced chemical vapor deposition 4-81157  
 laser measurement interferometry microscope for emulsion telescope in high energy physics 4-96391  
 laser probe mass spectrometer, for quantitative anal. 4-114874  
 laser probe-molecular beam sampling plasma diagnostic technique 4-84071  
 laser source technology, recent developments 4-87356  
 laser weapons, fiction and reality, teaching approach 4-110835  
 living organs metabolism, in situ monitoring with laser fluorimeter system 4-85586  
 LLL laser-fusion-programme overview and future directions in laser fusion systems 4-68821  
 LP100 Ex laser-light barrier in pressure-resistant housing (German) 4-69478  
 magnetic resonance spectrometer for far IR freqs., meas. on  $\text{LiErF}_4$  4-90623  
 magnetic resonance spectroscopy, review 4-95485  
 mass reflection for studying laser light-molecules interaction in supersonic gas jet 4-90686  
 materials processing, basic elements 4-107717  
 medical aspects, laser injurious effects and clinical appls. 4-72341  
 medical optoelectronics: laser appls., fibre-optic instrumentation and IR thermography (Japanese) 4-89678  
 medical therapy (Chinese) 4-115157  
 medicine, hazards and safety rules 4-85524  
 metal, laser-heated, eddy current monitoring and pot. process control use 4-71808  
 metal films, discontinuous, for optical storage, laser induced coalescence writing mechanism 4-97010  
 metals, surface alloying using continuous laser rad. 4-93443  
 microfluorimeter, pulsed laser, automatic, with high spatial and temporal resolution 4-89859  
 micro lenses terminated optical fibres, fabrication, biomedical appls. 4-83737  
 microscope, design (Japanese) 4-82824  
 microscopic fluorescence measurement method, for cancer cells (Japanese) 4-115315  
 mirrors, dielectric, high reflectance, laser damage meas. at 492 nm using flashlamp-pumped dye laser 4-74549  
 modular laser graphics projection system, animated laser show appls. 4-111165  
 multichannel systems with photographic recording calibration using laser light pulse source 4-74096  
 multiple-glint targets under laser illumination, statistical properties 4-112342  
 NDT, noncontact crack detection method (French) 4-93478  
 nephelometry: development, clinical appl. and future prospects 4-81756  
 Newtonian fluid steady laminar flows between ball and spherical cavity, expt. anal. using laser Doppler anemometry 4-97470  
 NRL Optical Sciences Division research and development program 4-107849  
 ophthalmology appls. of red Kr laser and green Ar laser (French) 4-89676  
 optical communication through low-visibility atmosphere using a CW diode laser 4-112589  
 optical disk-memory pregroove inspection system 4-106338  
 optical fibre manufacture, laser modification of thermophoretic deposition of aerosol 4-60186  
 optical fibres, enlarged taper ended, for laser radiation delivery systems, construction, surgical appls. 4-85472  
 optical heterodyne profilometer 4-106346  
 optical klystron harmonic generator with electron microbunches induced and frozen by lasers, intense coherent soft X-ray source 4-97001  
 optical position modulation systems time synchronisation anal. 4-60178  
 optical switching and routing system using freq. tunable  $\text{C}^3$  semicond. laser 4-79345  
 optical waveguiding devices, thin film components 4-79289  
 optically controlled discharges, recent advances 4-113256  
 optically transparent medium laser probing with aid of high speed photography (Russian) 4-83630  
 optics in entertainment, conf., Los Angeles, CA, USA (Jan. 1984) 4-110802  
 optometer for low-luminance myopia meas. 4-100132  
 particle acceleration, high energy, by laser beatwave 4-107186  
 particles, suspended, detection by laser-induced electron emission 4-90705  
 PCB direct imaging 4-87383  
 phase measurement algorithm anal. utilising two-beam interference 4-106359  
 phased array laser transmitter concept 4-106340  
 photo radiation therapy involving hematoporphyrin derivative, laser-fibre optic system appl. 4-85478  
 photochemical hole burning and its appls. (Japanese) 4-66598  
 photoelectron sources of high apparent brightness, electron beam lithography appls. 4-58914  
 photothermal laser probe, acoustic wave detection by collinear Bragg scatt. 4-86412  
 photothermal laser spectrometer, autoranging and synchronous demodulator circuitry 4-106401  
 polarization sensitive laser calorimetry 4-74584  
 polymer-metal bilayer deform. recording process, optical storage appls. 4-79251  
 positron acceleration, laser-driven 4-107185  
 progress in optics, book, vol. XXI 4-106130  
 projectile motion measurement using laser interferometric techniques 4-111192  
 pulsed laser generation of acoustic pulses, US thickness meas. appl. 4-112648  
 pulsed laser-assisted MBE technique 4-104733  
 ranging, use in geodesy 4-72765  
 rare isotopic atoms, highly selective detect. by means of reson. laser light press. 4-59903  
 rhinopharyngeal infection treatment by He-Ne laser acupuncture 4-85479  
 scanner, scan lens design w.r.t. performance and cost 4-107783  
 scanners, diffraction-limited resolution 4-96834  
 scanners using angular interferometers 4-82821  
 scatterometer, variable angle, instrumentation 4-74773

laser beam applications continued  
 semiconductor injection lasers, near IR, appls. 4-69480  
 semiconductor laser fluorimetry, near IR region, anal. appl. region 4-114852  
 semiconductor wafer surface defects, automated detection by laser scanning 4-113773  
 signal processing using laser light and SAW interaction 4-74565  
 single-mode fibre transmission systems, active and passive optical devices use 4-64790  
 soft X-ray production, progress in high peak and average power lasers 4-97913  
 solar cells, laser processing techniques, future developments 4-89434  
 solid diode lasers, applications (German) 4-83620  
 solids, laser spectroscopy as a physical and chem. tool 4-68290  
 space laser applications in geophysics 4-110319  
 space laser appls. and technology, conf., Les Diablerets, Switzerland (March 1984) 4-106122  
 space laser communications, prospects 4-107880  
 space operations and navigation, appl. 4-110496  
 spacecraft, laser communication links accommodation 4-107886  
 spectroscopy, maximum resolving power using freq. reson. 4-68288  
 spectroscopy and detection, conf., San Diego, CA, USA Aug. 1983 4-101562  
 steel, quenching with  $\text{CO}_2$  laser radiation, parameters optimisation 4-93318  
 steel, surface hardening by laser, technological control of surface condition parameters 4-71779  
 steel hardening, laser heat treatment, hardening 4-76792  
 streak camera, operating at high repetition rates 4-101956  
 surface alloying during laser melting 4-109552  
 surface layer alloying using laser treatment 4-109548  
 surface modification of materials by laser treatment 4-109547  
 surgery, microscopic and endoscopic, review 4-72333  
 surgery, plastic and general 4-72337  
 surgery and medical problems, treating cancer by laser 4-81757  
 surgery and medicine, review 4-89680  
 surgical applications with  $\text{CO}_2$  laser 4-72342  
 switching, laser-triggered, recent advances 4-69471  
 synchronization of a picosecond mode-locked dye laser oscillator-amplifier with a streak camera system 4-112475  
 technological laser development and appl. at Physics Institute, AS USSR 4-107657  
 TGS, lateral struct. of domains, obs. using laser probe technique with high pyroelectric signal 4-88786  
 therapeutic applications of lasers, review 4-85471  
 therapy, low-level laser, CW He-Ne laser use 4-77369  
 therapy and surgery appl., review 4-72330  
 therapy in tissue contact using quartz fibres 4-85476  
 thermochemical laser-induced image recording 4-102969  
 thoracic and cardiovascular surgery, review 4-72331  
 tunable diode laser development and spectroscopy appls., conf., San Diego, CA, USA (Aug. 1983) 4-110801  
 tunable UV laser excitation source for Raman spectrosc. 4-78381  
 turbulent flame fronts, visualisation via planar laser-induced fluorescence 4-97492  
 urologic laser surgery instrumentation 4-72332  
 UV pulse light source, using noble gas halide excimer laser (German) 4-112544  
 video camera tubes, laser-formed fiducials and reticles 4-96933  
 video recording, bright visible-range injection laser development 4-69441  
 X-radiation from laser-heated plasmas, characts. and uses 4-97817  
 X-ray lithography and appls. of soft X-rays to technology, conf., Upton, NY, USA (Oct. 1983) 4-95023  
 YAG laser appls. in ophthalmology 4-105313  
 Al plate, UV waveforms using laser generation and interferometric detection 4-97265  
 Ar laser therapy using fibre optics transmission 4-85474  
 BeO films, laser evaporated, thermally and optically stimulated electroelectron emission 4-88949  
 $\text{Br}_2$  gas diffusion through capillaries, laser control, energy efficiency 4-75113  
 $\text{CO}_2$  coherent laser radar performance study 4-96974  
 $\text{CO}_2$  coherent transversely excited atm. laser radar, field meas. 4-96973  
 $\text{CO}_2$  commercial technological laser prod. of power 1 to 10 kW 4-107663  
 $\text{CO}_2$  high power laser technology overview 4-107668  
 $\text{CO}_2$  laser industrial processing facility, Rayleigh range for Hermite-Gaussian modes 4-91508  
 Cr film, laser induced thermochemical image recording 4-102969  
 Cr films, laser induced metal deposition from organometallic solution 4-66239  
 $\text{Cr}^{3+}$ : $\text{BeAl}_2\text{O}_4$  laser technology for chem. appls. 4-107669  
 Cu, oxidation early stages by CW  $\text{CO}_2$  laser irradi. 4-99653  
 $\text{H}^+$ , polarised, production by laser optical pumping 4-107226  
 $\text{H}^+$  polarised source, optically pumped, for KEK proton synchrotron 4-107233  
 He-Ne laser needle clinical appls. (Chinese) 4-93840  
 $\text{In}_2\text{O}_3$  films, excimer laser induced CVD 4-76679  
 InP films, excimer laser induced CVD 4-76679  
 Mo films, laser induced metal deposition from organometallic solution 4-66239  
 Nd:YAG laser-fibre optic system, surgical coagulation appls. 4-85477  
 Ni ferromagnetic film, FMR imaging using photothermal deflection 4-88725  
 Pb salt tunable diode laser technology overview 4-107667  
 $\text{SF}_6$  puffer circuit breaker hot circulation, laser Schlieren visualisation following fault interruption 4-113078  
 Si films and wafers, structural perfection testing using optical scanner 4-96975  
 Si, laser doping by dissociation of metal alkyls 4-80069  
 Si, laser-controlled plasma etching 4-85232  
 Si, laser-induced oxidation for patterned  $\text{SiO}_2$  formation 4-99613  
 Si, MBE growth, use of laser processing 4-114406  
 n-Si: Au, doping by laser (Chinese) 4-113473  
 $\text{SiO}_2$  amorphous rods, laser-induced deposition, optical studies 4-66235  
 $\text{TiO}_2$ - $\text{Al}_2\text{O}_3$ - $\text{SiO}_2$  glass system preparation using  $\text{CO}_2$  laser melting (Chinese) 4-114466  
 $\text{ZrO}_2$ - $\text{Y}_2\text{O}_3$ - $\text{HfO}_2$  ceramic powders, laser sintering 4-88998  
 $\text{ZrO}_2$ - $\text{Al}_2\text{O}_3$ - $\text{SiO}_2$  glass system preparation using  $\text{CO}_2$  laser melting (Chinese) 4-114466

## laser beam effects

see also laser beam annealing; plasma-beam interactions; plasma production and heating by laser beam

aerosol medium optical breakdown, low-threshold; comprehensive diagnostics 4-65109

air, laser increased breakdown thresholds by admixing electronegative gas 4-79708

air, laser-produced breakdown interferograms, high-speed recording 4-75120

alkali halide crystals, laser-produced damage in UV region and in crossed UV-IR beams 4-75514

antireflection-coated  $\text{LiNbO}_3$  surfaces, laser induced failure 4-75524

aqueous aerosols, weakly absorbing, disruption and optical breakdown in intense light field 4-65108

atom, autoionising, finite interaction times and laser-bandwidth effects on photoemission 4-102652

atom, kinematics of multiphoton ionization in a steady laser beam 4-64443

atom in resonant laser field, ionisation pot., intensity depend. 4-78982

atom slowing down and pumping using very long cavity laser 4-96723

atom-atom collisions, laser-assisted 4-96646

atom-ion collisions charge transfer, laser assisted, coupled dressed quasi-molecular states approach 4-96684

atomic electron scatt. in strong laser field 4-69209

atomic gases, laser breakdown near metal surfaces 4-113111

atomic resonance fluorescence in strong monochromatic laser fields, book contrib. 4-64422

atomic spectroscopy, symposium, Berkeley, CA, USA (Sept. 1983) 4-67852

beta decay of nuclei, laser field effect 4-83035

biological mechanisms of laser damage, laser radiation hazards 4-77396

n-butane, slow oxidation induced by  $\text{CO}_2$  laser (French) 4-71905

capillary porous bodies, transport processes, laser monitoring 4-112999

capillary waves in nonuniformly heated liquid, instability under effect of lower radiation 4-64961

cell damage, Ar laser microbeam irradi. (Chinese) 4-109876

coated electrodes, current generation efficiency increase by laser light 4-76007

coated window and mirror components, pulsed DF chain laser damage 4-74582

coulomb effects in atomic reactions in the presence of a low-frequency laser field 4-66578

crystal growth, laser driven explosive, front propag. 4-103686

CW on-resonance 'self-focusing' obs. in Na vapour 4-79244

damage induced in optical materials, conf., Boulder, CO, USA (Nov. 1981) 4-73169

damage to optical materials, nature of the cumulative effect 4-108438

dielectric material, transparent, failure mechanism using focused laser single pulse, role of nonlinear refraction and absorpt. 4-91515

diffused waveguides containing  $\text{Ag}^+$  optical breakdown, laser colouring 4-107712

diffusion instability in a laser radiation field 4-75112

dissipative systems in quantum optics, reson. fluoresc. optical bistability superfluoresc., book 4-63410

DNA in proliferating and resting HeLa cells, replications and transcription, UV laser pulse effect (Russian) 4-66999

eggs, mouse, effect of laser microbeam irradi. of nucleus on cleavage in culture 4-93799

elastic wave in surface tracked by laser beam 4-75768

electron current modulation in light wave field at interface between two media 4-74409

electron shell effect on gamma ray emission by nuclei in laser irradi. crystals 4-88755

EM field generation in course of electron emission from metal target surfaces subjected to laser radiation 4-81041

ferroelectric, permittivity in the field of a strong EM wave 4-92988

fibre optic element radiation strength meas. 4-74572

field statistics effects on coherent anti-Stokes Raman spectroscopy intensities 4-78392

fluorination by  $\text{XeF}_2$  etching, photoeffects 4-77031

fluorophosphate laser glasses, causes of light scatt. and laser damage (Chinese) 4-60124

fovea, 20 ns ruby laser exposure, bioeffects evaluation by grating visual evoked pots. 4-62476

free-free scattering processes, inhomogeneous radiation fields effects 4-107455

gas mixture, laser radiation-collision generation of sound 4-91709

glass, electron irradiation, discharge form. 4-71275

glass, laser induced crystallisation kinetics, Raman scatt. studies 4-108288

glass/liquid interface, laser beam induced holographic bubble grating form. 4-83683

glasses, laser-induced damage 4-102962

glasses, nonlinear refractive coeff. and self-focusing damage 4-79247

graded-index surfaces and film, review 4-83672

graphite, thermodynamic props., pulse laser melting, ion channelling 4-98315

heat transfer processes in phase conversions under the action of intense energy fluxes 4-103191

hexadienes, laser-induced IR multiphoton isomerisation reactions 4-81420

hexamethyl aluminium, surface adsorbed, laser photochemical reactions 4-81451

imperfect cryst., laser irradi., thermoelastic stresses, optical polarisation study 4-61114

Josephson tunnel junctions, one-dimensional, focused laser beam irradi., nonlocal response 4-92864

Kapton films,  $\text{CO}_2$  laser assisted UV ablative photoetching 4-93429

light induced detonation of gas, lateral expansion, optical discharge 4-113252

liquid dielectric, radiation force and momentum of light 4-102965

liquid metal surface instability under intense IR laser irradi. 4-80340

liquid-filled photoacoustic cells, laser pulse excited, electrostriction effects 4-104538

liquids, laser-induced acoustic waves, diff. characts. 4-88239

liquids, laser-induced breakdown, shock wave production 4-61624

liquids, self-focusing use for laser-induced damage prevention 4-79246

magnetic field generation by powerful laser beams 4-79749

metal, laser beam deep penetration, physical processes 4-108432

metal, laser-heated, eddy current monitoring and pot. process control use 4-71808

metal 'dagger' melting model by high-power laser beam, max. depth of penetration 4-75507

## laser beam effects continued

metal mirror short-pulse  $\text{CO}_2$  laser radiation damage thresholds 4-74578

metal surface, laser induced electron-phonon processes 4-75873

metal surface, relativistic photoelectrons generation by excimer laser irradi. 4-114357

metal surfaces, Nd: glass laser irradiation damage, surface roughness effects 4-69469

metal-dielectric-semiconductor struct. 4-84704

metallic coatings on glass substrates, laser damage study 4-108433

metallic novel surfaces, directed energy production 4-74775

metallic surface, laser destruction products, phase comp. analysis (Russian) 4-70199

metals, heating by laser rad. in oxidising atmos., calc. 4-65503

metals, laser glazing, mass transfer, role of diffusion in liq. state 4-71790

metals, laser interaction, evaporation influence on melt behaviour 4-76566

metals, surface phenomena induced by intense laser irradi. 4-81044

methane gas-laser beam interaction 4-107405

mica, fine-pore, toluene diffusion under resonant laser beam irradi. 4-91840

microparticles volatilisation and ionisation, laser-induced, mass spectroscopic analysis 4-105088

microsome bound bromothymol blue, binding rel. to protein conformation, laser radiation effect 4-89498

mirror, cooled, coating defects rel. to limiting flux density 4-79208

mirrors, dielectric, high reflectance, laser damage meas. at 492 nm using flashlamp-pumped dye laser 4-74549

molecular desorption by reson. laser-mol. vibr. coupling, time-of-flight spectra calcs. 4-93556

molecular photoion production processes induced by surface laser irradi. 4-81043

molecule-laser field interaction problem, Floquet theory, energy shifts induced by radiation 4-107408

molecules, interaction studied by recursive-residue generation method 4-107409

multilayer 3.8  $\mu\text{m}$  coatings, pulsed damage and optical characts., influence of cleaning solvents, sunlight, humidity and HF gas 4-75523

multilayer nonquarterwave reflector designs, multiple-shot UV laser damage resist. at 248 nm 4-74581

multilayer planar targets, anomalous laser penetration depths obs. 4-65104

multilayer UV reflectors, laser damage results under multiple-shot irradi. 4-74580

nematic liq. crystals, light-induced threshold reorientation under nonadiabatic deformations. 4-108274

noise modelling by jump processes in strong laser-atom interactions 4-69019

nonlinear absorption dynamics in solids 4-69514

nonlinear ring cavity, laser-driven, fluctuations, instabilities and chaos, book contrib. 4-107737

ocular hazard from GaAs lasers and near IR radiation 4-93797

optical coatings, laser induced damage, physical aspects 4-74566

optical coatings, laser induced damage, spot size scaling 4-79209

optical fibres in adverse environments, conf., Paris, France (May 1983) 4-78025

optical glass, type K-8, bulk damage by single and multiple periodic laser pulses of nanosec. duration 4-74577

optical surfaces, laser desorption analysis of  $\text{H}_2\text{O}$  and other contaminants 4-74777

optical thin films, laser-induced damage 4-69472

optically absorbing coatings, laser generation of SAW 4-104056

organometallic molecules, Raman reson. spectrum and its appls. (Dutch) 4-64483

oxides, laser-induced sputtering and damage 4-71485

4-n-pentyl-4-cyanobiphenyl, nematic liq. cryst., mol. reorientation, laser heating 4-113327

periodic structure form. in absorbing condensed media under action of radiation 4-76567

periodic structures on solid surfaces, laser irradi., temporal and spatial evolution 4-104702

Permalloy, surface layer, light irradi., magnetoelectric phenomena 4-76218

photochemical hole burning and its appls. (Japanese) 4-66598

photodesorption of weakly bound molecules 4-92553

photon-assisted dry etching using ArF laser 4-114689

piezoelectric semicond. magnetised plasma, high-power helicon wave parametric decay 4-98657

plasma waves, excitation in laser beat wave accelerator 4-113137

poly(vinylidene fluoride) films, piezoelectric studies 4-65952

polyimide films, excimer laser etching, emission spectra 4-89142

polymer film, ablative photodecomposition by far UV radiation, microscopic model 4-71483

pre-Gaussian noise in strong laser-atom interactions 4-83335

proteins, radical formation under pulsed picosec. laser radiation action 4-109777

pulsed IR laser interaction with material surfaces, appls., visible luminesc. (Chinese) 4-92231

quartz, fused, laser-produced damage in UV region and in crossed UV-IR beams 4-75514

quartz, nonequilibrium phonons, direct generation by IR radiation, X-ray evidence 4-108558

quartz microporous glass, optical breakdown 4-107713

radiation wavelength influence on laser excited elastic pulses 4-108437

refractory metals, groups IV-VI, laser erosion, gas atmosphere effect 4-93146

resonance light scattering, intensity depend., stationary homogeneously broadened atom driven by incident field, book contrib. 4-64430

resonant molecules flow through metal capillary, laser control 4-69800

retinal nerve fibres in primate optic nervehead, axons degeneration obs., glaucoma causes 4-77241

all-trans-N-retinylidene-n-butylamine soln., resonance Raman and UV absorpt. 4-104604

rhodamine-590 physisorbed thin films, surface photoacoustic wave spectra 4-104693

ripple structure associated with ordered surface defects in dielectrics 4-80090

RNA, synthetic, selective nonlinear laser cutting 4-77191

ruby, electric domains due to laser irradi., hysteresis 4-114224

ruby, electric domains due to laser irradi. 4-114223

sapphire, laser-produced damage in UV region and in crossed UV-IR beams 4-75514

- laser beam effects continued
- sapphire with surface adsorbed  $\text{Na}_2$  laser irradi., photostimulated desorption 4-113793
- semiconductors, laser-induced sputtering and damage 4-71485
- SHG with high power short pulses from an IR FEL 4-83643
- shock wave effects, conf., Santa Fe, USA (July 1983) 4-106116
- shock wave generation in solid laser targets 4-84345
- skin, wounded, of white mice, regenerative process, He-Ne laser irradi. effects 4-72301
- small molecules, laser pulse-induced field desorption 4-80418
- solid surface, thermoelectric action of powerful high repetition rate laser radiation 4-75522
- solid transparent insulators, optothermochem. instability development, initial stage 4-62183
- solids, laser induced shock struct. simulation 4-113540
- solids, nonlinear absorption, laser multimode effects 4-102978
- steel, C, laser glazed hot rolled Charpy samples, impact testing 4-81377
- steel, C, laser hardening, struct. and property study (Chinese) 4-62105
- steel, C, laser hardening, using transversely-excited flowing  $\text{CO}_2$  laser (Chinese) 4-62104
- steel, C, surface hardening by laser treatment 4-81337
- steel, Charpy V notch impact testing with laser glazing pre-cracking 4-99681
- steel, mech. props., effect of laser quenching 4-66356
- steel, Nb-microalloyed and medium C, laser hardening 4-114563
- steel 45 and U10, laser treatment, residual stress distrib., optimum surface hardening conditions (Russian) 4-71774
- steel plate, laser melted surface, microstruct., hardness, residual stress 4-71794
- superconductor films, optically driven, picosecond pulse generation capability 4-92861
- superconductors, nonequilibrium, inhomogeneous gap distrib., laser beam scanning probe method 4-71001
- surface desorption, light induced, threshold laser intensity 4-81481
- surface diffusion, Brownian motion model 4-70607
- surface grating formation under action of laser radiation on metal, semiconductor, and insulator surfaces 4-107813
- surface layer alloying using laser treatment 4-109548
- surface melting, rapid solidification microstructures 4-89046
- surface modification of materials by laser treatment 4-109547
- surface studies with lasers, conf., Mauterndorf, Austria (March 1983) 4-86118
- surface thermoelectric deformations caused by a laser 4-103798
- temporal coherence effects in multiphoton transitions, model depend. 4-60094
- thin absorbing layer, refr. index thermal variation in strong laser field 4-74593
- thin amorphous layer of metal, produced by laser radiation 4-80089
- thin foils, shock wave generation using lasers and light ion beams 4-103877
- thin-film optical coatings, laser damage thresholds meas. at 248 nm 4-74579
- three-level atom dynamics in resonant light field 4-83361
- transient orientational grating technique for fast mol., relax. process investigation 4-83625
- transition probabilities for laser photon absorpt. by free electrons 4-69349
- transmissive optics for high power  $\text{CO}_2$  lasers, failure phenomena (Japanese) 4-74530
- transparent materials, absorpt. of laser rad. by metallised microinclusions 4-69468
- transparent polymers as new class of optical materials for lasers, laser damage resistance 4-74576
- transparent solid, laser-induced intrinsic damage, seed electron deterrent lack effect in avalanche ionisation 4-81045
- trapped ion, laser cooled, steady state in Lamb-Dicke limit 4-69020
- trapped two-level particle system, laser cooling, master eqn. 4-107315
- two-atom coherence, laser-induced 4-64572
- two-level atom, laser induced deflection, light-induced force statistical mech. 4-102964
- two-photon absorption from a phase-diffusing laser field 4-96514
- undercoats and overcoats, effects on damage thresholds of 248 nm coatings 4-74671
- UV laser radiation, max. permissible exposure estimates 4-62526
- vapour, optically pumped relax. signal, influence of optical factor 4-102963
- weakly absorbing dielectrics and semiconductors, convective instability and self-focusing in laser-induced breakdown 4-97009
- Ag electrodes, laser damage, surface-enhanced Raman scatt. and Auger emission-spectrosc. obs. 4-60955
- Ag film on piezoceramic surface physical mechanism of laser generated shock waves (Chinese) 4-113535
- (Al,Ga)As heterojunctions, laser-induced defects, photochem. etching 4-113439
- Al alloy, laser treatment, strengthening and microstruct. (Russian) 4-71665
- Al, behaviour under microsecond pulsed TEA  $\text{CO}_2$  laser radiation 4-79815
- Al, foil, laser shock press. and energy loss at 1.05  $\mu\text{m}$  wavelength 4-80159
- Al foil irradiated with Nd:YAG laser pulses particle vel. meas. of laser-induced shock waves using ORVIS 4-113495
- Al mirrors, laser irradiated in air, damage study by electron microscopy 4-79203
- Al mirrors, thin film deposited and dielectric overcoated, UV laser damage studies 4-74567
- Al, picosecond laser induced shock wave press. meas. 4-113259
- Al target, laser interaction, time resolved X $\alpha$  spectra 4-66133
- Al target, laser-driven shock wave evolution 4-113258
- Al target for laser pulses, press. meas. 4-111097
- Al thin film, laser induced melting, time resolved picosecond electron diff. study 4-88269
- Al-Al $_2\text{O}_3$ -Pb junction, effects of patterned laser illumination 4-70998
- Al-Si eutectic, surface morphology, crack section morphology and metallographic struct. after laser irradi., SEM study (Chinese) 4-62106
- Al-Si-Cu-Mg, strengthening with continuous  $\text{CO}_2$  laser 4-62117
- Al-Si-Mg-Mn eutectic, surface morphology, crack section morphology and metallographic struct. after laser irradi., SEM study (Chinese) 4-62106
- Al-SiO $_2$ -Si $_3\text{N}_4$ -Si struct. circuit, nonlinear reson. curve illuminated by light 4-84704
- Al $_2\text{O}_3$ , laser sputtering mechanism, SEM study 4-71484
- laser beam effects continued
- C target, collision of laser accelerated discs, high press. shock production 4-113257
- C:H amorphous coating for IR-optical elements, optical props., thickness, density, laser damage tests 4-76422
- C-Si, picosecond laser induced shock wave press. meas. 4-113259
- $\text{CO}_2$  lasers, pulsed, damage thresholds for large irradiated spots 4-107595
- CdSe films, cell form, prior to laser induced synthesis 4-65582
- CdSe, particle desorp. under laser irradi., mass and energy distrib. meas. (Russian) 4-113815
- Cl, electronic Raman spectra, ion laser excitation 4-102621
- Cr/Ni/Cu multilayer film system, laser mixed, AES and Rutherford backscatt. studies 4-98458
- Cu (100), time of flight mass spectra study on IR laser photodesorption of  $\text{NH}_3$  4-80384
- Cu alloy, laser treatment, strengthening and microstruct. (Russian) 4-71665
- Cu based alloys, laser melted, microstruct. and props. 4-109553
- Cu mirrors, diamond machined, laser damage at nonnormal incidence 4-75520
- Cu mirrors, diamond turned and mechanically polished, intensity depend. absorpt. and laser induced catastrophic damage at 1.06  $\mu\text{m}$  4-75519
- Cu, surface struct. generation by laser pulses 4-80358
- Cu-Al-Fe alloys, laser surface melted, microstruct., X-ray diff. study 4-108628
- Fe, cast, malleable, laser treatment, residual stress distrib., optimum surface hardening conditions (Russian) 4-71774
- Fe, cast, microstruct. and phase comp. after irradi. by pulsed or continuous rad. of optical quantum generator 4-66485
- Fe eutectic alloy coatings, boride and carbide strengthened, laser irradi. treated, wear resist. (Russian) 4-85250
- Fe, gray and nodular cast, laser surface hardening, erosion resist., near surface microstructure 4-66453
- Fe, laser irradi., surface structural and electronic props. 4-60956
- Fe-Ni alloys, martensite to austenite transformations by laser irradiation (Russian) 4-109399
- Fe-Ni-P-B-C eutectic, surface morphology, crack section morphology and metallographic struct. after laser irradi., SEM study (Chinese) 4-62106
- Fe-Si laser scribed gain oriented steel, stacked transformer core appls. 4-61552
- Fe/Si strips, mag. props. and domain struct., laser scribing effects 4-61550
- GaAs (100), laser irradi., photoemission of electrons 4-81116
- GaAs, crystal and amorphous, pulsed laser irradi. under  $\text{O}_2$  and silane atmospheres, O incorporation and losses 4-80091
- GaAs, laser alloyed Sn layers, elec. props., surface damage 4-99622
- GaAs, laser-enhanced reactive ion etching in  $\text{CCl}_4\text{-H}_2$  mixture 4-71747
- GaAs, laser-induced Si diffusion from deposited  $\text{Si}_3\text{N}_4$  film 4-60958
- GaAs, light scatt. nonequilibrium electron-hole plasma 4-104616
- GaAs, picosecond laser induced shock wave press. meas. 4-113259
- GaAs, surface disordering by picosecond laser pulses 4-92233
- GaAs-AlAs multiple quantum well struct., Raman scatt. and luminescence study 4-99105
- Ge exciton studies, laser heating effects at liquid He temps. 4-70672
- Ge, IR laser radiation nonlinear absorpt. and self-defocusing due to free carrier generation 4-79248
- Ge, laser pulse irradi., plasma and melting kinetics, IR reflectivity studies 4-108594
- Ge, laser-induced periodic surface struct., fluence regimes, feedback and topography 4-108436
- Ge, surface periodic structures on intense laser bombardment 4-70201
- GeSe, thin film, laser-induced synthesis 4-80095
- GeSe $_2$ , thin film, laser-induced synthesis 4-80095
- $\text{H}_2$  gas, VUV radiation generation by stimulated Raman scatt. using ArF\* laser 4-69496
- $\text{H}_2\text{O}^+$ , laser generated shock waves, reflective probing 4-114800
- $\text{He}^{++} + \text{H}$ , charge transfer, laser assisted, coupled dressed quasimolecular states approach 4-96684
- $\text{I}_2$  electron excited, laser irradi., vibr. relax. rates determ. (Russian) 4-83455
- InP (100), laser irradi., photoemission of electrons 4-81116
- n-InSb, current-induced anisotropy of refractive index 4-104564
- InSb, magnetised plasma, parametric excitation of electron-acoustic waves 4-88545
- InSb, surface periodic structures on intense laser bombardment 4-70202
- KCl absorption, reversible and irreversible changes during multiple pulse 10.6  $\mu\text{m}$  irradi. 4-75518
- KCl crystals, optical breakdown thresholds due to action of  $\text{CO}_2$  laser pulses 4-60957
- KCl single-crystal, technique for increasing optical strength through temp. cycling 4-75516
- KCl surface breakdown threshold, effect of treatment and ageing 4-75521
- $\text{KH}_2\text{PO}_4$  crystals, bulk laser-damage resistance improvement by baking and pulsed laser irradi. 4-75517
- $\text{KH}_2\text{PO}_4$  crystals, laser induced damage, X-ray topography 4-65296
- $\text{LiIO}_3$  single crystals, optical damage, nonlinear transmission and doubling efficiency 4-75513
- $\text{LiIO}_3$  single crystal, laser induced damage, nonlinear absorpt. and doubling efficiency 4-79205
- $\text{LiNbO}_3$ , bulk acoustophotorefractive effects 4-93050
- $\text{LiNbO}_3$ , laser irradi., polariton Raman scatt. 4-61715
- $\text{LiNbO}_3$ , laser irradi., photovoltaic effects 4-70868
- $\text{LiNbO}_3\text{:Fe}$ , Rayleigh scatt., effect of photorefr. 4-80957
- $\text{LiNbO}_3\text{:MgO}$ , increased optical damage resist., holographic diff. meas. of photorefr. 4-69521
- Mg, laser vaporisation, energy distrib. meas. 4-66135
- Mo, surface struct. generation by laser pulses 4-80358
- Na beam laser cooling by AC Stark effect 4-69017
- Na compression by laser beam, semipermeable optical piston demonstration 4-87092
- Na D, line, laser-induced fluorescence line narrowing 4-69012
- Na, vapour, laser initiated discharge channels 4-113255
- Na+Ba, two-photon radiative collision, Ba $^+$  prod. 4-64587
- Na+He $^+$ , laser and ion beam excitation, autoionisation 4-69196
- NaCl absorption, reversible and irreversible changes during multiple pulse 10.6  $\mu\text{m}$  irradi. 4-75518
- NaCl, cryst., X-irrad., F-centre decay during photoannealing 4-80036
- NaCl crystals, optical breakdown thresholds due to action of  $\text{CO}_2$  laser pulses 4-60957

**laser beam effects continued**

- NaCl,  $\gamma$  and laser irradi., internal friction and dislocation damping 4-80153  
 NaCl single-crystal, technique for increasing optical strength through temp. cycling 4-75516  
 NaCl with adsorbed methyl fluoride, IR laser induced desorption, momentum distrib. study 4-80419  
 Na<sub>2</sub>O-B<sub>2</sub>O<sub>3</sub>-SiO<sub>2</sub> graded-index antiref. coatings deposited by sol-gel process, laser damage thresholds, high power laser appls. 4-74673  
 Nb film on Fe substrate, laser treatment, Mossbauer study (*Russian*) 4-70204  
 Ni, laser irradiation, defect struct. and surface alloys 4-75509  
 Ni/SiC mixed layers, ion and laser irradi., microstruct. anal. 4-84415  
 Ni-La single crystals, implanted, pulsed laser treatment studied by the <sup>4</sup>He<sup>+</sup> channelling 4-84315  
 Pb(N<sub>3</sub>)<sub>2</sub> laser radiation effect on thermal decomposition (explosions) 4-71927  
 Pb<sub>0.9</sub>Sn<sub>0.1</sub>Te epitaxial films, heating by short laser pulses 4-88203  
 Pt-electrolyte interface, laser induced processes 4-81452  
 Si (111), laser irradi., photoemission of electrons 4-81116  
 Si (111), surface, far UV laser induced oxidation by bond rearrangement 4-81310  
 Si, clean and SiO<sub>2</sub> covered, picosecond laser heating and evaporation 4-70198  
 Si, crystalline, laser damage by multiple 1.06  $\mu$ m picosec. pulses 4-75515  
 Si, crystalline and amorphous, energy transfer during laser irradi. 4-76412  
 Si, electron structure change during amorphisation, electrorefl. spectra (*Russian*) 4-98509  
 Si film, solid, laser heated, Raman scatt. at melting temp. 4-76464  
 Si, high purity, intercarrier scatt. effects, laser and electron beam excitation 4-92725  
 Si, highly undercooled, molten, nucleation and amorphous phase form. 4-70346  
 Si, IR laser radiation nonlinear absorpt. and self-defocusing due to free carrier generation 4-79248  
 Si, IR radiation absorption from CO<sub>2</sub> laser 4-71367  
 Si, ion implanted, explosive liq. phase crystallisation by double pulse laser irradi. 4-84188  
 Si, ion implanted, laser or electron beam annealing, minority carrier recomb., EBIC, photoluminescence meas. 4-80601  
 Si islands, single crystalline, laser recrystn., SOI IC fabrication 4-75798  
 Si, laser heating, thermal radiation, pyrometric temp. measurements 4-92230  
 p-Si, laser induced changes in surface states 4-104288  
 Si, laser irradi., influence of electron-hole density profile on reflectivity 4-104559  
 Si, laser pulse irradi., plasma and melting kinetics, IR reflectivity studies 4-108594  
 Si, pulse laser irradiated, surface morphology and phase transitions 4-88197  
 Si, pulsed laser induced recombination centres 4-108873  
 Si SOS structures, pulse laser irradi., internal stresses, Raman scatt. studies 4-99108  
 Si, surface disordering by picosecond laser pulses 4-92233  
 Si, surface struct. generation by laser pulses 4-80358  
 Si wafer, mechanical properties, effects of laser back-side damage 4-98132  
 Si wafer props., influence of laser marking 4-113498  
 Si-SiO<sub>2</sub>, laser recrystn. of Si films with heat sink struct. 4-60954  
 SiO<sub>2</sub> fibers, irradi. and photobleaching at low temps. 4-80099  
 SiO<sub>2</sub> growth from laser oxidation of Si surface 4-81324  
 SiO<sub>2</sub> thin films, photon-induced O loss, ESR and Auger electron spectroscopy 4-80092  
 SrF<sub>2</sub>, photo-induced transform. of close Frenkel pairs, absorption and luminesc. props. 4-76500  
 steel, low alloy, cyclic strength, effect of laser irradi. 4-71723  
 Ta<sub>2</sub>O<sub>5</sub>/SiO<sub>2</sub> antireflection coatings, electron-beam deposited, 1064-nm damage tests, review 4-75525  
 Te film optical recording media, writing and degradation charact., subbing layer surface energy effects 4-91552  
 Te thin films for optical data storage, optical props. and stability 4-91553  
 Te-Bi thin films for optical data storage, optical props. and stability 4-91553  
 Te-Ge film optical recording media, writing and degradation charact., subbing layer surface energy effects 4-91552  
 Te-Ge thin films for optical data storage, optical props. and stability 4-91553  
 TeSi thin films for optical data storage, optical props. and stability 4-91553  
 Ti, laser ignition and combustion, optical props. and scale growth kinetics 4-77009  
 Ti target, laser interaction, time resolved K $\alpha$  spectra 4-66133  
 TiO<sub>2</sub>-Al<sub>2</sub>O<sub>3</sub>-SiO<sub>2</sub> glass system preparation using CO<sub>2</sub> laser melting (*Chinese*) 4-114466  
 U, resonant pulsed laser excitation 4-102650  
 Zr surface, laser irradi., at. beam prod., fluoresc. investig. 4-108435  
 ZrO<sub>2</sub>-Al<sub>2</sub>O<sub>3</sub>-SiO<sub>2</sub> glass system preparation using CO<sub>2</sub> laser melting (*Chinese*) 4-114466

**laser beam machining**

- conference, lasers in mechanical engineering, Zvenigorod, USSR (Oct. 1982) 4-106095  
 industrial applications of high power lasers, conf., Linz, Austria (Sept. 1983) 4-101561  
 laser surface modification 4-104892  
 materials processing, basic elements 4-107717  
 metal, laser beam deep penetration, physical processes 4-108432  
 multilayer PCBs laser drilling 4-87384  
 piacril cutting by laser beam (*German*) 4-112596  
 steel, laser beam machining, worked surface props. (*Italian*) 4-91518  
 textured optical storage media, threshold laser writing powers 4-107769  
 worked surface properties (*Italian*) 4-91518  
 CO<sub>2</sub> commercial technological laser prod. of power 1 to 10 kW 4-107663

**laser beam modulation** *see optical modulation***laser beam properties** *see laser beams***laser beam welding**

- conference, lasers in mechanical engineering, Zvenigorod, USSR (Oct. 1982) 4-106095

**laser beam welding continued**

- joint, NDT, plume spectra, statistical analysis 4-104955  
 metal, laser beam deep penetration, physical processes 4-108432  
 CO<sub>2</sub> commercial technological laser prod. of power 1 to 10 kW 4-107663  
 CO<sub>2</sub> laser processing induced plasma, optical absorption prop. development 4-108189  
 CO<sub>2</sub> pulse periodic lasers, appl. to industrial welding 4-107660

**laser beams**

- see also holography; laser frequency stability; Schwarz-Hora effect*  
 adaptive transmission, two-wavelength, diffractive and refractive effects comparison 4-87280  
 automated beam expander device 4-83629  
 bleaching capacity of continuous laser beam in atmosphere 4-79243  
 book, optical waves in crystals, laser radiation propag. and control 4-86135  
 calibrating equipment for laser power 4-96969  
 coherent anti-Stokes Raman spectra, accurate convolutions 4-79236  
 coherent detection using interferometric and filtering technique (*Chinese*) 4-87380  
 coherent light scattering by particles, moving in two crossed light beams 4-96803  
 collimation and divergence determ. using retroreflectors 4-107705  
 coupling to optical fibres using anamorphic gradient-index lenses 4-87407  
 CW Gaussian laser beam, harmonic-like and efficient AM by mech. chopper 4-69461  
 double-proton bombarded laser, emission properties, kinks and self-sustained oscils. 4-112437  
 dye DFB laser pulses, directional and wavelength sweep 4-69466  
 dye laser, excimer pumped, picosec. pulse amplification (*Japanese*) 4-83574  
 dye laser, synchronously pumped, picosecond pulse amplification 4-60032  
 energy measurement using current integrator with bipolar transfer function 4-91517  
 equivalent optical resonators, g-parameter, mode struct. and beam divergence 4-79188  
 excimer laser based ultrashort laser pulse generation method 4-96934  
 extremely short pulse form. 4-60059  
 far IR radiation subnanosecond optical switching using method laser irradiation of Si and GaAs 4-74575  
 far IR waveguide laser, optically pumped, wavefront curvature 4-107708  
 femtosecond optical pulses and technology, self-phase modulation and grating compression 4-107696  
 fibres, single-mode, highly twisted, Gaussian pulse splitting and nonsplitting condition 4-97078  
 field profiles, one dimens. meas. by CCD (*Chinese*) 4-87381  
 FIR laser active medium refr. index variations induced by interacting microwave field 4-79109  
 free electron laser gain optimisation for gaussian beam 4-87342  
 free electron laser unstable resonators beam quality and small mode area 4-87370  
 Gaussian beam parameter measurement 4-87378  
 Gaussian laser beam intensity modification by acousto-optic effect (*Chinese*) 4-112491  
 heterodyne detection phase and amplitude uncertainties 4-96851  
 holographic interference fringes recorded from diffusely illuminated objects, amplitude-phase charact., fluctuations effect 4-91425  
 holographic interferograms, image enhancement for fringe patterns tracing 4-96821  
 image relaying through saturated amplifiers 4-60096  
 industrial applications of high power lasers, conf., Linz, Austria (Sept. 1983) 4-101561  
 injection laser with active mode locking, psec pulse direct detect. 4-74573  
 intensity perturbation transverse distribution investigation by probing gaseous lens-like media with He-Ne laser radiation 4-79207  
 intensity uniformisation by mirror folding 4-74570  
 IR pulsed laser radiation field photographic recording 1-10  $\mu$ m spectral region 4-78400  
 linear polarisation production by in-laser interferometer using anisotropic mirrors (*Russian*) 4-69465  
 linewidths meas. using optical spectrum analyser 4-60093  
 microcomputer-controlled scanning of a laser beam at constant speed 4-64717  
 misaligned resonator with lenslike medium, emitted radiation directivity 4-83624  
 modulation using chalcogenide glasses (*Russian*) 4-79252  
 multipulse illumination system, controllable synchronised, for electronic speckle pattern interferometry and holography 4-101909  
 Nova, Novette fusion lasers, Si switch development for optical pulse generation 4-107702  
 off-axis Gaussian beam propag. for unstable resonator alignment 4-91500  
 phase perturbations and laser resonator beam quality 4-87367  
 phased array telescopes, image-plane phase sensing 4-97020  
 photorefractive laser beamsteering using thick diffr. gratings, configurations 4-96968  
 picosecond frequency shifted pulse generation with low temporal jitter 4-83645  
 picosecond light pulses, energy and duration determ. by bleaching of dyes 4-69512  
 picosecond rotating-mirror autocorrelator, optimisation study, measurement of laser pulse duration 4-107793  
 polarisation degree measurement apparatus using TP801 microcomputer (*Chinese*) 4-91514  
 power limiting with nonlinear media 4-60102  
 power measurement, applic. of integrating sphere technology 4-82814  
 power measurement of high-power lasers, calorimeter development (*Japanese*) 4-64715  
 profiling by optoacoustic induced US waves meas. 4-64814  
 propagation, fundamental mode, optically inhomogeneous electrochem. media with electrochem. species conc. gradients 4-112341  
 pulse reshaping in coherent interaction with resonant I absorber, appl. to homogeneous relax. time meas. 4-69511  
 pulse shortening using negative dispersion produced by pairs of prisms 4-74416  
 pulsed laser energy automatic monitoring (*Chinese*) 4-60086  
 pulses as short as 16 fs, generation and meas. 4-69460  
 pump-probe meas. with collinear copropag. beams, coherent coupling effects 4-96989

# er beams continued

- quasingle-mode laser radiation, second harmonic duration under strong energy exchange conditions 4-74616
- radiation coupling into fibre waveguides of elliptic cross section 4-107826
- radiation directivity pattern axis instability meas. 4-74571
- Raman-type free-electron laser, two-dimensional hollow beam, optimum thickness (*Japanese*) 4-107714
- semiconductor diode laser picosecond pulse generation 4-107632
- semiconductor film picosecond laser, chirp, passive pulse compression in optical fibres 4-107700
- semiconductor lasers, optically pumped, mode locked psec pulses from 490 nm to 2  $\mu$ m 4-107699
- single pulse selection in amplifiers 4-69470
- single-mode fibre tapers, beam spot size radius 4-91594
- SIR heterodyning using Ag halide fibres, CO<sub>2</sub> lasers 4-107854
- solid-state Fourier-transform ring laser, good-quality beam 4-69453
- Stanford superconducting 3.2  $\mu$ m FEL optical beam quality meas. 4-83626
- strong-field region volume of Gaussian beam 4-107711
- subnanosecond-pulse generation at 308 and 450 nm by truncated stimulated Brillouin scattering 4-107753
- subpicosecond laser pulse shape distortions due to photochronographic camera imprecise focusing 4-64729
- synthetic aperture beam control system 4-96967
- synthetic aperture phase meas. system using metering rod bridge with corner cubes 4-97016
- ultrashort laser pulses passing through saturable absorbers, freq. chirp form. 4-60118
- ultrashort pulse generation using excimer laser based system 4-96934
- ultrashort pulse TPF pattern meas. and anal. using closed circuit TV with memory system (*Chinese*) 4-60057
- waist location and Rayleigh range for higher-order mode laser beams 4-91508
- zoom system for Gaussian beam, general paraxial theory 4-91562
- AlGaAs mode locked laser, subpicosecond pulse generation 4-107697
- Ar ion laser, cavity dumped freq. doubled, sine-wave modulated UV radiation 4-69459
- CO<sub>2</sub> and H<sub>2</sub>O laser freq.-mixing expts., beat note S/N ratio characts. 4-74608
- CO<sub>2</sub> CW laser, appl. of IR sensitization photography 4-112229
- CO<sub>2</sub> laser pulse shapes determ. using methyl-methacrylate plate 4-91509
- CO<sub>2</sub> laser with variable output pulse duration 4-60070
- GaAs/GaAlAs twin stripe lasers, current rise time effect on beam stability, expt. study 4-91510
- H<sub>2</sub>O monomode CW 119  $\mu$ m laser, output beam polarisation improvement 4-112471
- InGaAsP BH 1.3  $\mu$ m lasers, anomalous polarisation characts. 4-69402
- KrF laser radiation, stimulated Brillouin scatt. in SF<sub>6</sub> 4-107752
- KrF laser system pulse compression, laser drivers for inertial-fusion reactors 4-69464
- LiIO<sub>3</sub>, crystal, laser beam pulses duration meas. using noncollinear SHG 4-107707

# laser cavity resonators

- active resonators, acousto-optic interaction, theory 4-79196
- adaptive optics basis functions for obscured aperture, phase aberration correction 4-74427
- anisotropic superregenerative laser amplifier, linear mode, polarised signal amplification 4-79191
- beam alignment and mode-matching to stable optical resonator 4-112480
- cascade pumped picosecond dye laser system 4-91448
- cleaved coupled cavity lasers, optimum gap width for mode discrimination, theoretical study 4-87330
- cleaved coupled-cavity lasers, single freq. operation stabilisation 4-96898
- cleaved coupled-cavity lasers, verification of coupling gap dependence 4-91469
- cleaved-coupled-cavity lasers, threshold anal. 4-112415
- cleaved-coupled-cavity lasers with large cavity length ratios 4-91498
- coherence theory of laser resonator modes 4-69454
- cooperative transient for atoms driven by a weak coherent field 4-83557
- coupled cavity semiconductor lasers, detuned loading and quantum noise 4-112418
- coupled cavity semiconductor lasers, optoelectronic props. 4-64704
- coupled lasers, semiclassical theory 4-79092
- coupled resonator beam combining 4-107688
- coupled resonators employing phase-conjugating and ordinary mirrors 4-107795
- coupled-cavity 1.5  $\mu$ m injection lasers, freq. stability and temp. characts. 4-79140
- coupled-cavity laser rate eqn. model 4-60010
- coupled-cavity lasers, three-terminal type, const. power curve generation technique 4-64724
- coupled-cavity lasers, threshold gain anal. and design guidelines 4-91463
- coupled-cavity lasers, transient anal. 4-91464
- coupled-cavity lasers, two-section, stable single wavelength operation under modulation using feedback control 4-91470
- coupled-cavity-semiconductor lasers, reduced chirping 4-91455
- critical length, ABCD matrix formalism (*French*) 4-60074
- CW high-power sum-freq. generation near 243 nm using two intersecting enhancement cavities 4-79235
- degenerate parametric amplifier in a Fabry-Perot cavity, multimode quantum theory 4-83644
- detuned laser optical turbulence with compound cavity 4-112484
- DFB lasers with strong modulation, threshold gains and resonance freqs. calc. 4-79095
- diffraction loss investigation using diffracted light, picked-off with knife-edge mirror 4-60075
- diode laser, feedback of light interacting coherently, incoherently with laser cavity field, influence on oscill. spectrum 4-91451
- diode single-mode lasers of large-optical-cavity type, lateral mode discrimination and control 4-112436
- dispersive free electron laser, a hybrid optical-klystron-free electron laser 4-96927
- dispersive small-aperture resonators exhibiting angular dispersion, selective props. 4-79198
- dye CW laser single longit. mode oscill. with tilted intracavity Fabry-Perot etalons (*Korean*) 4-112483
- dye CW laser with self pumped phase-conjugating resonator cavity, self scanning 4-107692
- dye CW laser with standing wave and travelling wave cavities, single freq. output (*Chinese*) 4-107621

# laser cavity resonators continued

- dye CW mode-locked lasers, role of cavity dispersion 4-79124
- dye laser, cavity configuration for dispersion on two output beams 4-74554
- dye laser, CW, for intracavity state selection of atomic and molecular gases 4-60095
- dye laser, double-wavelength pulsed tunable (*Chinese*) 4-112465
- dye laser, pulsed single-mode, cavity of prism-grating-mirror combination, spectral linewidth 4-112477
- dye laser, synchronously pumped, picosecond pulse amplification 4-60032
- dye laser, synchronously pumped, rate eqn. simulation 4-74503
- dye laser design, short-cavity, piezoelec. tuned 4-69434
- dye laser femtosecond cavity, quarter-wave dielec. mirror dispersion analysis 4-102957
- dye laser with intracavity absorpt. cell, radiation conc. in spectrum 4-74505
- dye lasers, cavity length detuning properties in synchronous mode locking 4-96964
- dye lasers, prismatic, pulsed, multi-pass dispersion theory 4-69398
- dye pulsed laser, Xe ion laser pumped, time-resolved spectrum 4-107625
- dye ring lasers, CW, injection locking 4-74501
- dye two freq. tunable laser with high efficiency intracavity radiation divider 4-79192
- dyes in polymer matrices as active media, passive and generation characts. 4-107618
- eigenstate flipping effects (*French*) 4-74553
- EM behaviour of far-IR waveguides laser 4-87374
- equivalent optical resonators, g-parameter, mode struct. and beam divergence 4-79188
- Fabry-Perot cavity, bistable system, switching times 4-112500
- far IR waveguide laser, discrete and continuous modes study 4-79094
- fluoromethane, CW far IR optically pumped open-cavity laser (*Chinese*) 4-112392
- fluoromethane grazing-incidence far-IR laser 4-96949
- formic acid, CW far IR optically pumped open-cavity laser (*Chinese*) 4-112392
- free electron generators of coherent radiation, conf., Orcas Island, WA, USA (June 1983) 4-82588
- free electron IR laser, broadband optical cavities 4-112479
- free electron laser, Frascati-ADONE, gain meas. and energy extraction optimisation from electrons 4-87341
- free electron laser, gain mechanism calc. 4-79169
- free electron laser, low-gain, low-voltage, mode struct. 4-96942
- free electron laser, two-stage, low loss quasioptical cavity 4-87369
- free electron laser gain optimisation for gaussian beam 4-87342
- free electron laser oscillator, storage ring, operation at 6500 Å 4-87340
- free electron laser oscillator mirror alignment tolerance scaling laws 4-83602
- free electron laser power output performance, superradiation generation (*Chinese*) 4-107654
- free electron laser rectangular waveguide resonator, cylindrical Gaussian eigenmodes, gain per mode 3D calc. 4-87368
- free electron laser unstable resonators beam quality and small mode area 4-87370
- free electron tapered wiggler laser, long pulse evolution 4-83584
- free electron tapered wiggler laser gain displacement effects 4-83595
- free electron two-stage laser programme at KMS Fusion Inc., review 4-83615
- free-electron laser, gain enhancement by external laser 4-83597
- gas laser, steady state synchronisation of lateral modes (*Russian*) 4-60079
- gas ring laser with circularly anisotropic resonator, nonreciprocal effects, transverse mag. field 4-79195
- graded-index lens external cavity semiconductor laser with optical feedback, spectral props. study 4-87371
- grazing-incidence dye lasers with and without intracavity lenses, comparative study 4-91447
- grazing-incidence grating cavities with Brewster-prism beam preexpander for pulsed dye lasers (*Chinese*) 4-112481
- half-symmetric unstable resonator with internal axicon, reflexicon deforms effect on geom. parameters 4-69524
- in-resonator laser spectroscopy, generation intensity, kinetic processes 4-82831
- industrial applications of high power lasers, conf., Linz, Austria (Sept. 1983) 4-101561
- infinite strip confocal resonator filled with a saturable-absorpt. gas, lowest-order eigenvalue evaluation 4-87400
- inhomogeneous optical resonator, modal analysis 4-91502
- injection laser, multimode homogeneously broadened, output in terms of resonator reflectivities and saturation 4-112439
- injection laser, single-mode, line narrowing due to external optical feedback 4-79142
- injection laser noise properties due to optical feedback 4-79143
- injection laser with external dispersive resonator, psec pulse direct detect. 4-74573
- injection lasers, mode interaction and single-freq. emission self-stabilisation 4-60036
- interacting collective modes in an optical cavity 4-79197
- interferometric semiconductor laser (*Japanese*) 4-79150
- intracavity adaptive optics, theory and expt. comparison 4-74552
- intracavity laser pumping of selectively absorbing media, raising efficiency 4-83582
- media free electron lasers for VUV and X-ray radiation production 4-96925
- metallic optics of technological laser apparatus 4-107687
- methanol, CW far IR optically pumped open-cavity laser (*Chinese*) 4-112392
- methanol laser, high-power 119  $\mu$ m operation, water-cooled cavity design, electron density meas. appl. 4-79185
- methanol-methyl bromide-methyl iodide optically-pumped multigas far-IR laser 4-102924
- misaligned resonator with lenslike medium, emitted radiation directivity 4-83624
- non-uniform mirrors, producing uniform laser beam (*Russian*) 4-69449
- nonabsorbing mirror constricted DH large-optical cavity diode lasers 4-83579
- nonimaging concentrators as pump cavities for laser rods 4-96960
- nonlinear ring cavity, laser-driven, fluctuations, instabilities and chaos, book contrib. 4-107737
- nonlinear ring resonator, bistability and solitons 4-74599
- nonuniform magnification resonators 4-87373

## laser cavity resonators continued

- one-dimensional laser with output coupling, phase noise above threshold 4-83561
- one-dimensional laser with output coupling, quantum theory, linear approx. 4-112372
- optical instabilities in a nonlinear Kerr medium 4-102974
- optical resonance cavity oscillation freq., unified expression (Chinese) 4-91504
- oscillation characteristics of laser resonators (Chinese) 4-87372
- phase noise in a laser with output coupling 4-96860
- phase perturbations and laser resonator beam quality 4-87367
- power increases caused by reflections from workpiece surfaces 4-91519
- progress in optics, book, vol.XXI 4-106130
- pulse compression, high-efficiency, with intracavity Raman amplifiers 4-96935
- pulse compression in phase conjugated Brillouin cavity 4-91539
- quantum well heterostructure lasers, multiple-stripe, in external grating cavity, far-field supermode patterns 4-112455
- radiation directivity pattern axis instability meas. 4-74571
- rhodamine 590 dye laser oscillators, narrow linewidth, high PRF Cu laser pumped 4-74535
- rhodamine 6G CW dye laser radiation freq. doubling with an external auxiliary active cavity (Chinese) 4-60107
- rhodamine 6G CW dye ring laser with a Mach-Zehnder interferometer, efficient single mode operation 4-91496
- rhodamine 6G dye laser, multimode, pulsed, single-shot spectral meas. and mode correl. 4-69467
- rhodamine 6G dye ring laser saturable amplification, picosec. pulse intracavity degenerate four-wave mixing 4-91524
- rhodamine 6G femtosecond dye laser, expt. and theoretical study 4-107627
- rhodamine 6G homogeneously broadened laser, higher order dynamical states 4-69399
- rhodamine 6G thin layer two-frequency tunable laser 4-107626
- rhodamine 6G tunable dye jet laser pumped synchronously by second harmonic of Nd:YAG laser 4-60031
- rhodamine 6G tunable dye laser, single-mode picosec., with ultra-short cavity (Chinese) 4-112468
- rhodamine B DFB dye laser, amplified spontaneous emission 4-83572
- ring cavity optical bistability, semiclassical and quantum-statistical treatment, book contrib. 4-64736
- ring laser, beat frequency, effect of low-freq. periodic perturbations 4-79194
- ring laser subjected to transverse mag. field, nonreciprocal effect theory 4-107693
- ring lasers, unidirectional traveling-wave, mode locking by continuous resonator-length variation, computer simulation 4-60080
- ring resonator with negative dispersion 4-74555
- ruby laser with stimulated Brillouin scatt.-stimulated thermal scatt. mirrors 4-96962
- ruby laser with thin absorbing layer in resonator, lasing parameters 4-79159
- self-excitation of resonators with four-wave hypersonic reversing mirrors 4-60078
- self-focusing-induced optical turbulence 4-102991
- semiconductor cleaved-coupled-cavity laser, single mode, spectral props., external optical feedback effect 4-69405
- semiconductor cleaved-coupled-cavity laser with large cavity length ratios for enhanced stability 4-69450
- semiconductor film picosecond laser, ultrashort cavity, chirp, passive pulse compression in optical fibres 4-107700
- semiconductor integrated etalon interference lasers, stable longit.-mode operation, tuning temp. depend. study 4-69455
- semiconductor laser, external cavity, stable linewidth reduction with automatic linewidth control loop 4-91503
- semiconductor laser diodes, longitudinal mode stabilisation by extremely short optical waveguides 4-91474
- semiconductor laser oscillation freq. shift suppression for coupling to external cavity 4-79134
- semiconductor lasers, ultrashort cavity, optically pumped by injection laser 4-107645
- semiconductor single-mode lasers, noise theory in presence of optical feedback 4-79137
- semiconductor two-section coupled cavity lasers, longitudinal mode behaviour, anal. and simulation studies 4-79141
- sensitivity to misadjustment 4-60077
- single longitudinal mode semicond. laser model with internal-refl. optical coupling (Chinese) 4-60034
- single-frequency cleaved-coupled cavity and DFB laser, direct modulation transient chirping study 4-83627
- source flow chemical laser cavity performance 4-74551
- spherical optical resonator, incident wave coupling coeffs. and modes, in case of mismatching and misalignment 4-74550
- spherical surface high reflectance meas. using cavity phase shift method 4-74772
- square-waveguide resonator coupling losses 4-69458
- stimulated Raman radiation pulse generation within a laser resonator (Russian) 4-79193
- submillimetre laser, optical pump absorpt. efficiency (Chinese) 4-107606
- TE<sub>M</sub> thermosensitive cavity with several thermoperturbing centres, design 4-69457
- temperature compensated coupled cavity diode lasers 4-107691
- temporal and spatial spectrum broadening in nonlinear optical medium double mode oscillator design (French) 4-60109
- tetrafluoromethane laser, 16  $\mu$ m, high repetition rate 4-87362
- theoretical development in 1960s, Doppler effects 4-91432
- toric unstable resonators, geometrical, diffractive and asymptotic theory 4-91501
- tunnel generation and locking stimulated Raman radiation components 4-112515
- two-segment cavity theory for mode selection in semicond. lasers 4-60073
- two-stage free electron laser, cavity design 4-69424
- unstable cavity and short inversion time lasers, kinetics 4-96877
- unstable phase-conjugate resonator 4-79189
- unstable resonator alignment using off-axis Gaussian beam propagation 4-91500
- unstable resonator with field rotation, wave approx. calc. 4-107694
- waveguide laser resonators formed by flat mirrors, coupling efficiency 4-112482
- wide-aperture optical resonators formed by plane reflectors, eigenwaves 4-74556

## laser cavity resonators continued

- AlGaAs DH semiconductor diode laser, passive mode locking, subpicosec. coherent pulse generation (Japanese) 4-60060
- AlGaAs injection laser with external dispersion resonator using returning mirror 4-107641
- AlGaAs mode locked laser, subpicosecond pulse generation 4-107697
- AlGaAs single- and multiple-stripe quantum-well heterostruct. laser diodes in external grating cavity 4-96902
- AlGaAs TJS external cavity laser for fibre optic laser Doppler velocimeter 4-97096
- AlGaAs-GaAs laser with external dispersive cavity multimode rate-eqn. soln. of mode selection and tuning props. (Chinese) 4-91462
- AlGaAs-GaAs short-cavity laser and its monolithic integration using microcleaved facets process 4-60064
- AlGaAs-GaAs superlattice optical cavity multiple-quantum-well lasers, MBE grown, struct. and fabrication 4-64719
- Al<sub>0.5</sub>Ga<sub>0.5</sub>As-GaAs injection lasers, longitudinal mode selection obs. 4-79153
- Ar ion laser, air cooled, design and appl. 4-64722
- Ar ion laser, cavity dumped freq. doubled, sine-wave modulated UV radiation 4-69459
- Ar<sup>+</sup> passively mode-locked laser, output light energy characts. 4-64696
- CO chem. laser, Cs<sub>2</sub>N<sub>2</sub>O-O<sub>2</sub> type with 2-m long active region output characts. 4-74496
- CO waveguide laser with selective resonator, emission freq. wide tuning range 4-60069
- CO<sub>2</sub> CW far IR lasers, optically pumped, using new stabilisation system 4-102954
- CO<sub>2</sub> cascade laser, 4.4 micron, resonator design 4-87313
- CO<sub>2</sub> fast axial flow laser with 1000 watt output power 4-102945
- CO<sub>2</sub> gasdynamic laser, Fabry-Perot resonator, mode struct. 4-60072
- CO<sub>2</sub> high power laser plasma investigation 4-102917
- CO<sub>2</sub> high power laser with folded resonator, computer simulation 4-102916
- CO<sub>2</sub> injection-locked TEA laser, tunable single-mode design for D<sub>2</sub>O laser pumping 4-79184
- CO<sub>2</sub> laser, hybrid TE-TEA sealed-off with corona preionisation 4-69430
- CO<sub>2</sub> single-mode etalon-tuned TEA laser, optimised design for NH<sub>3</sub> laser pumping 4-79182
- CO<sub>2</sub> TEA laser, beam expanding grating plane cavity (Chinese) 4-107689
- CO<sub>2</sub> TEA laser, injection locking studies for stable high-power operation 4-60014
- CO<sub>2</sub> TEA lasers, miniature type, self modulation props. study 4-79202
- CO<sub>2</sub> TEA lasers, multipass-prism interferometer for fine-freq.-turning, single-mode operation 4-107683
- CO<sub>2</sub> thermally excited cascade laser, resonator length selection 4-107594
- CO<sub>2</sub> tunable high-power CW laser using compound cavity, individual transition selection 4-69366
- CO<sub>2</sub>-TEA laser, injection locking, effect of unstable resonator 4-87375
- CS<sub>2</sub>, stimulated Raman scatt. ps pulse generation in an external cavity 4-83566
- Co:MgF<sub>2</sub> CW tunable mode-locked lasers, 1.65-2.01  $\mu$ m range 4-60043
- Cr<sup>3+</sup>:Be<sub>2</sub>Al<sub>2</sub>(SiO<sub>3</sub>)<sub>6</sub> laser, CW Kr laser pumped, 728.8 to 809.0 nm tuning range 4-60041
- DCN CW waveguide laser operating at 195, 190  $\mu$ m, quartz tube cavity (Chinese) 4-107604
- D<sub>2</sub>O optically pumped laser with unstable resonator, high-energy design for plasma diagnostics 4-79183
- D<sub>2</sub>O submm laser for single shot ion temp. meas. by Thomson scatt. 4-103569
- (GaAl)As cleaved-coupled-cavity lasers, coupling strength study 4-91459
- GaAlAs laser diode coupled to an external cavity intensity noise suppression and modulation characts. 4-79144
- GaAlAs very high speed lasers and detectors for integrated optoelectronic devices 4-96889
- GaAs/GaAlAs, antirefl. coated twin DH diode external cavity ring laser, optical bistability study 4-91460
- GaAs-(AlGa)As large optical cavity lasers 4-107631
- GaAs-(AlGa)As twisted DH laser, composite cavity config., design and longit./traverse mode operation 4-69456
- GaAs-Al<sub>0.3</sub>Ga<sub>0.7</sub>As DH laser with two sections in a common cavity (Chinese) 4-112466
- GaInAsP BH laser, low-threshold, multiple-cavity, longit.-mode stabilised 4-91468
- GaInAsP cleaved coupled-cavity laser, tunable design, FM operation for communication appl. 4-69451
- HF pulsed laser with unstable resonator (Chinese) 4-60026
- H<sub>2</sub>O monomode CW 119  $\mu$ m laser, output beam polarisation improvement 4-112471
- He-Ne and Ar<sup>+</sup> laser low-freq. beat noise (Chinese) 4-91511
- He-Ne highly stable laser at 1.15  $\mu$ m (Chinese) 4-112469
- He-Ne intracavity laser, magnetic field induced beat noise (Chinese) 4-60017
- He-Ne intracavity laser, polarisation behaviour at 632.8 nm (Chinese) 4-107597
- He-Ne laser, mode struct. optical spectrum analyser study, undergraduate expt. 4-106152
- He-Ne laser appl. to intracavity dispersion meas. 4-112478
- He-Ne laser excitation using lateral discharge VHF pumping resonators (Russian) 4-69431
- He-Ne ring laser with selective losses, counter-propag. wave competition and emission spectrum produced by reson. phase-polarisation method 4-79107
- He-Ne/methane laser, freq.-modulated resonances (Russian) 4-102961
- InGaAsP 1.3  $\mu$ m optical amplifier-modulator integrated with a fibre-resonator mode-locked laser 4-91491
- InGaAsP/InP 1.3  $\mu$ m buried crescent lasers using short external optical cavity, single-mode operation 4-74511
- InGaAsP/InP GRIN rod external coupled-cavity BH lasers, single longit. mode operation 4-91473
- InP/InGaAsP 1.5  $\mu$ m BH laser with etched cavity 4-83575
- Ind:glass laser, glass vitrification boundary optical inhomogeneity effect on laser emission characts. 4-107710
- Nd:YAG AM mode-locked laser stability (Chinese) 4-60088
- Nd:YAG CW laser with passive stabilisation of self-mode locking 4-107649
- Nd:YAG high repetition rate mode-locked laser, thermally stable resonator anal. (Chinese) 4-60040
- Nd:YAG picosecond regenerative ring amplifier, multiple pulse injection 4-64725

- laser cavity resonators continued
- Nd:YAG Q-switched oscillator, single axial mode operation by injection seeding 4-60042
- Nd<sup>3+</sup>:YAG laser with intracavity SHG in crystals exhibiting aperture effect, unpolarised radiation electrooptic switch 4-74574
- Nd<sup>3+</sup>:YAG single-frequency periodic-pulse laser 4-74546
- Ni:MgF<sub>2</sub> CW tunable mode-locked lasers, 1.61-1.73  $\mu$ m range 4-60043
- PbSnTe cleaved-coupled cavity lasers 4-87327
- XeCl excimer laser, aerodynamic device and elec. excitation system description (*French*) 4-102949
- XeF laser low-magnification positive-branch unstable resonator, transverse mode form. 4-73521
- XeF laser using grating-interferometer-based cavity, single-mode tunable operation 4-102956
- XeF\* laser radiation stimulated Raman scatt. in H<sub>2</sub> 4-74611
- laser damage *see laser beam effects*
- laser effects *see laser beam effects*
- laser frequency stability
- cleaved coupled-cavity lasers, single freq. operation stabilisation 4-96898
- coupled-cavity 1.5  $\mu$ m injection lasers, freq. stability and temp. characts. 4-79140
- coupled-cavity lasers, two-section, stable single wavelength operation under modulation using feedback control 4-91470
- difluoromethane 889  $\mu$ m laser, optically pumped, absolute two photon light shift heterodyne meas. 4-91442
- difluoromethane far-IR laser, optically pumped, self-pulsing instability 4-91444
- digital fibre transmission using optical homodyne detection 4-60172
- dye laser, Rhodamine 6G, <sup>12</sup>I<sub>2</sub>-stabilized design, 576 nm, characts. 4-87324
- formic acid laser freq. determ. by mixing expts. between submillimeter lasers using heterodyne system with Schottky barrier diode 4-102923
- free electron laser collective instabilities and high-gain regime 4-91483
- free electron laser instabilities and quantum initiation 4-87351
- injection laser emission freq. stabilisation by an external confocal interferometer 4-60098
- injection lasers, mode interaction and single-freq. emission self-stabilisation 4-60036
- methanol laser freq. determ. by mixing expts. between submillimeter lasers using heterodyne system with Schottky barrier diode 4-102923
- narrowband dye laser with a large scan range 4-91489
- perylene-3,4,9,10-tetracarboxylic acid-bis-N,N'(2,6'-xylylidyl)diimide laser dye, high stability and broad band lasing action pot. 4-107623
- rhodamine 6G homogeneously broadened laser, higher order dynamical states 4-69399
- ring laser, freq. fluctuation meas. 4-87382
- semiconductor integrated etalon interference lasers, stable longit.-mode operation, tuning temp. depend. study 4-69455
- semiconductor laser, external cavity, stable linewidth reduction with automatic linewidth control loop 4-91503
- semiconductor laser diodes, longitudinal mode stabilisation by extremely short optical waveguides 4-91474
- semiconductor laser frequency stabilisation, intensity-independent, using fibre optic Fabry-Perot resonator 4-91458
- semiconductor laser oscillation freq. shift suppression for coupling to external cavity 4-79134
- semiconductor lasers, transverse switching due to Hopf bifurcation 4-74514
- single-frequency cleaved-coupled cavity and DFB laser, direct modulation transient chirping study 4-83627
- single-frequency long-wavelength lasers for broadband fibre communication 4-91497
- single-frequency stabilised lasers beat frequency meas., autocorrel. functions and Allen dispersion (*Russian*) 4-60085
- submillimetre lasers, power level stabilisation with optical excitation (*Russian*) 4-79088
- tunable laser stabilisation techniques for ultrahigh-resolution spectroscopy 4-63789
- two-photon laser and optical-bistability sidemode instabilities 4-74477
- AlGaAs CSP high-power laser diodes under modulation, freq. stabilisation using short guides 4-79190
- AlGaAs, frequency stabilization by thermal and current feedback control 4-60071
- CO CW laser two-mode multiline stabilisation using Fabry-Perot filter under analog and digital computer control 4-60092
- CO<sub>2</sub> compact hybrid single mode TEA laser, stabilisation 4-91495
- CO<sub>2</sub> laser bands, freq. tables, rovibr. consts. 4-60015
- CO<sub>2</sub> laser frequency stabilisation for sub-MM laser pumping by Stark modulated Lamb dip signal in methanol (*Japanese*) 4-74485
- CO<sub>2</sub> laser heterodyne bias freq.-locking (*Chinese*) 4-91512
- CO<sub>2</sub> pulsed and CW laser, heterodyne freq. offset locking technique 4-96951
- CO<sub>2</sub> pump laser freq. controlling method 4-96950
- CO<sub>2</sub> TEA laser, injection locking studies for stable high-power operation 4-60014
- CO<sub>2</sub> waveguide laser, freq. sweep stabilisation using inverted Lamb dip in NH<sub>2</sub>D 4-79098
- CO<sub>2</sub> waveguide laser, RF discharge excited, freq. depend. 4-79099
- CO<sub>2</sub>/OsO<sub>4</sub> waveguide laser with freq. stability of 10<sup>-13</sup> 4-79102
- CO<sub>2</sub> TEA laser, injection locking, effect of unstable resonator 4-87375
- Er:glass laser, 1.545  $\mu$ m, Q-switched, output-stabilised, high-repetition rate 4-74545
- GaAlAs laser, simultaneous wavelength and power stabilisation using single detector scheme 4-91456
- GaAlAs laser, wavelength stabilisation using integrated optic Fabry-Perot interferometer 4-91457
- GaAlAs lasers, transverse-mode stabilised MOCVD grown, with embedded confining layer on optical waveguide 4-69443
- (GaAl)As transverse-mode stabilised laser diodes, MOCVD growth 4-96912
- GaAs/GaAlAs single mode laser diodes, free space optical. communication, design and system requirements 4-79176
- H-Ne 633 nm laser, I<sub>2</sub> stabilised, freq. stability and reproducibility 4-91436
- He-Ne laser, freq. stabilisation with modular electronic system 4-112476
- He-Ne laser, internal mirror, output-and frequency-stabilisation by discharge current control 4-79105
- He-Ne laser, stabilisation on absorpt. saturation in <sup>127</sup>I 4-79106
- He-Ne laser locked to methane E-line, accurate freq. meas. 4-96868
- He-Ne lasers, active element striation freq. shifts 4-107598
- laser frequency stability continued
- LiF F<sub>2</sub> centre laser, relationship between F<sub>2</sub> centre density and laser stability (*Chinese*) 4-91477
- N<sub>2</sub> laser, TEA, thyatron-switched 4-64721
- Nd:YAG AM mode-locked laser stability (*Chinese*) 4-60088
- Nd:YAG CW laser with passive stabilisation of self-mode locking 4-107649
- Nd:YAG laser, electro-optically Q-switched design, freq. stability 4-87364
- Nd:YAG simple high power nanosec. laser 4-87366
- laser hardening *see laser beam effects; radiation hardening; surface hardening*
- laser induced breakdown *see laser beam effects*
- laser induced damage *see laser beam effects*
- laser isotope separation
- free-electron laser theory and applications 4-64714
- Freon-123, T separation by laser (*Chinese*) 4-64631
- fusion and isotope separation research and development at Lawrence Livermore National Lab, review 4-90324
- gasdynamic jet, selective laser excitation 4-60561
- Thirteenth international quantum electronics conf., Anaheim, CA, USA (Jun. 1984) 4-86105
- three level atom, isotopically selective two-photon excitation 4-74211
- I<sub>2</sub>, isotope separation, sequential two-photon ionisation 4-87167
- Li<sub>2</sub>, isotope separation using different laser wavelengths for excitation and ionisation processes 4-69235
- T laser isotope separation in Freon-123 (*Chinese*) 4-64631
- Yb, selective photoionisation for laser isotope separation, three-stage scheme 4-64440
- laser magnetic resonance
- double modulation spectrometer, differential gated integrator 4-73467
- free radicals, spectral line detect. using double modulation laser mag. reson. spectrometer 4-73467
- radical-radical reactions, products, vel. consts., far IR LMR study (*German*) 4-71913
- Far-IR laser mag. reson. detection from F+O<sub>2</sub>(O<sub>3</sub>) reactions 4-59811
- HF, X<sup>2</sup> $\Sigma^+$  state, rot. transition, hyperfine splitting, LMR spectra 4-69120
- HO<sub>2</sub>, vibr. band strength for  $\nu_3$  band meas. 4-74220
- NH<sub>2</sub>O radical, gas phase, far-IR LMR study 4-87128
- NS radical, far IR LMR spectroscopy 4-91286
- PH(D), X<sup>2</sup> $\Sigma^+$  vibronic state, far-IR laser mag. reson. 4-59814
- Si I, meas. of <sup>3</sup>Po-<sup>3</sup>P<sub>1</sub> fine-struct. interval and g-factor by laser mag. reson. 4-85866
- laser mirrors *see laser accessories; mirrors*
- laser mode locking
- colliding pulse mode locking expt. and theoretical study 4-96884
- DH laser, multiple twisted separately pumped, longitudinal mode behaviour 4-112486
- dye CW mode-locked lasers, role of cavity dispersion 4-79124
- dye laser, excimer pumped, picosec. pulse amplification (*Japanese*) 4-83574
- dye laser, narrow radiation spectrum locked to compound atomic absorption lines (*Russian*) 4-69396
- dye laser femtosecond cavity, quarter-wave dielec. mirror dispersion analysis 4-102957
- dye lasers, cavity length detuning properties in synchronous mode locking 4-96964
- dye lasers, femtosecond pulse generation by mode locking (*Japanese*) 4-74560
- dye ring lasers, CW, injection locking 4-74501
- dye saturable absorpt. recovery time rel. to laser mode locking, sample length effects (*Chinese*) 4-60117
- femtosecond duration pulse generation with a passively mode locked dye laser 4-79130
- femtosecond light pulses using colliding pulse mode locking (*Japanese*) 4-73529
- fibre Raman laser, mode-locked and Nd-YAG laser pumped, design and appl. (*Korean*) 4-83623
- free electron laser injection locking by BeAl<sub>2</sub>O<sub>4</sub>: Cr<sup>3+</sup> (Alexandrite) laser 4-83587
- gas laser, stability of self-locking of two modes 4-74561
- gas lasers, picosecond pulse generation using acoustooptic modulator (*Japanese*) 4-74558
- homogeneous gain laser, mode locking through temporally modulated phase-conjugate reflectivity 4-79201
- injection laser with active mode locking, psec pulse direct detect. 4-74573
- passively mode-locked laser theory including self-phase modulation and group-vel. dispersion 4-74479
- passively mode-locked lasers, calc. of light pulses with chirp inc. absorber and amplifier phase memory 4-107695
- phase-locked injection laser arrays, coupled mode anal. 4-91487
- phosphate glass laser, mode-locked, high repetition rate (*Chinese*) 4-112442
- phosphate glass oscillator, Q-switched and actively mode locked 4-112487
- picosecond optoelectronics, conf., San Diego, CA, USA (Aug. 1983) 4-106106
- rhodamine 6G CW tunable ring dye laser, passively mode-locked, picosec. pulse SHG correl. meas. (*Chinese*) 4-87354
- rhodamine 6G femtosecond dye laser, expt. and theoretical study 4-107627
- rhodamine 6G subpicosecond dye laser pumped by Xe ion laser, passively mode locked 4-96937
- rhodamine 700 dye laser, flashlamp-pumped, passive mode locking in near IR 4-60030
- ring lasers, unidirectional traveling-wave, mode locking by continuous resonator-length variation, computer simulation 4-60080
- self-consistent profile approach to mode-locking, problems 4-79090
- semiconductor laser picosecond mode-locking and X-band modulation 4-107698
- semiconductor lasers, injection locking characts. 4-64707
- semiconductor lasers, optically pumped, mode locked psec pulses from 490 nm to 2  $\mu$ m 4-107699
- semiconductor lasers, synchronous mode locking by picosecond optoelectronic switch 4-96965
- single pulse selector for high repetition rate mode-locked lasers (*Chinese*) 4-87355
- solid-state lasers with passive mode locking, steady-state pulses 4-107650

**laser mode locking continued**

- spaceborne laser ranging transmitter, ultra-short pulses generation 4-107724  
 stimulated Raman radiation components, tunnel generation and locking 4-112515  
 styryl 9 dye laser, subpicosecond generation via hybrid mode locking in near IR 4-60083  
 YAG crystal, specially doped growth and multi-function props. (*Chinese*) 4-114364  
 YAG laser appls. in ophthalmology 4-105313  
 AlGaAs DH semiconductor diode laser, passive mode locking, subpicosec. coherent pulse generation (*Japanese*) 4-60060  
 AlGaAs mode locked laser, subpicosecond pulse generation 4-107697  
 Ar, ion laser, injection locking for high-power single-freq. emission 4-102960  
 Ar<sup>+</sup> ion lasers, acousto-optic mode locking, subnanosecond transient spectroscopy appl. (*Japanese*) 4-101923  
 Ar<sup>+</sup> passively mode-locked laser, output light energy characts. 4-64696  
 CO<sub>2</sub> laser heterodyne bias freq.-locking (*Chinese*) 4-91512  
 CO<sub>2</sub> pulsed and CW laser, heterodyne freq. offset locking technique 4-96951  
 CO<sub>2</sub> TEA laser, injection locking studies for stable high-power operation 4-60014  
 CO<sub>2</sub> TEA lasers, injection locked, transient freq. shift induced by electron density 4-102915  
 CO<sub>2</sub>-TEA laser, injection locking, effect of unstable resonator 4-87375  
 Co:MgF<sub>2</sub> CW tunable mode-locked lasers, 1.65-2.01  $\mu$ m range 4-60043  
 GaAs/GaAlAs, antirefl. coated twin DH diode external cavity ring laser, optical bistability study 4-91460  
 H-Ne 633 nm laser, I<sub>2</sub> stabilised, freq. stability and reproducibility 4-91436  
 HgBr laser system, narrow-band injection locking, B-X transition 4-79111  
 InGaAsP 1.3  $\mu$ m optical amplifier-modulator integrated with a fibre-resonator mode-locked laser 4-91491  
 Nd:glass laser with plasma mirror 4-107704  
 Nd:glass lasers, fast mode-locking, with dye no.5, excited state absorption dynamics 4-107760  
 Nd:glass picosecond laser, passively mode-locked temporal pulse development anal. 4-83598  
 Nd:phosphate glass laser, active-passive mode locking using Eastman 5 saturable dye 4-91478  
 Nd:YAG AM mode-locked laser stability (*Chinese*) 4-60088  
 Nd:YAG CW laser, acoustooptical mode locking 4-69473  
 Nd:YAG CW laser with passive stabilisation of self-mode locking 4-107649  
 Nd:YAG high repetition rate mode-locked laser, thermally stable resonator anal. (*Chinese*) 4-60040  
 Nd:YAG high-power oscillator, stable single-axial-mode operation by injection locking 4-69417  
 Nd:YAG laser, continuously pumped, Q-switching and double mode-locking 4-91475  
 Nd:YAG lasers, feedback to maintain injection locking 4-79157  
 Ni:MgF<sub>2</sub> CW tunable mode-locked lasers, 1.61-1.73  $\mu$ m range 4-60043  
 XeCl laser, long pulse, generation of 300 psec pulse by direct mode locking using acousto-optic modulator and saturable absorber 4-112490  
 XeCl laser, microwave-pumped, active mode locking 4-74487  
 XeCl laser, passive mode locking using dye saturable absorbers 4-112485  
 XeF<sub>2</sub> injection-locked, quenching of backward stimulated Raman scatt. by broadband forward Raman rad. 4-91535  
 YAG lasers, pulse generation using US made locker (*Japanese*) 4-74559

**laser modes**

- see also laser mode locking  
 beam intensity profile measurement apparatus, materials processing environment appls. 4-106344  
 cleaved coupled cavity lasers, optimum gap width for mode discrimination, theoretical study 4-87330  
 cleaved coupled-cavity lasers, single freq. operation stabilisation 4-96898  
 cleaved coupled-cavity lasers, verification of coupling gap dependence 4-91469  
 coherence theory of laser resonator modes 4-69454  
 coupled cavity semiconductor lasers, optoelectronic props. 4-64704  
 coupled lasers, semiclassical theory 4-79092  
 coupled-cavity 1.5  $\mu$ m injection lasers, freq. stability and temp. characts. 4-79140  
 coupled-cavity laser rate eqn. model 4-60010  
 coupled-cavity lasers, threshold gain anal. and design guidelines 4-91463  
 coupled-cavity lasers, transient anal. 4-91464  
 coupled-cavity lasers, two-section, stable single wavelength operation under modulation using feedback control 4-91470  
 coupled-cavity-semiconductor lasers, reduced chirping 4-91455  
 degenerate parametric amplifier in a Fabry-Perot cavity, multimode quantum theory 4-83644  
 detuned laser optical turbulence with compound cavity 4-112484  
 DFB helical far IR laser, theory, realisation and mode characts. 4-79186  
 DH laser, multiple twisted separately pumped, longitudinal mode behaviour 4-112486  
 DH lasers, carrier-induced index depressions effect on transverse-mode characts. 4-74516  
 difluoromethane far-IR laser, optically pumped, self-pulsing instability 4-91444  
 diode laser, feedback of light interacting coherently, incoherently with laser cavity field, influence on oscill. spectrum 4-91451  
 diode lasers, chirped arrays for supermode control 4-102942  
 diode lasers, phase-locked arrays, supermodes obs. 4-102943  
 diode single-mode lasers of large-optical-cavity type, lateral mode discrimination and control 4-112436  
 double-channel planar BH C<sup>3</sup> lasers, 1.5  $\mu$ m, single longit. mode operation at 2 Gbit/s 4-69438  
 equivalent optical resonators, g-parameter, mode struct. and beam divergence 4-79188  
 evanescent-wave-coupled multistripe lasers, modal gain 4-79138  
 far IR laser, optically-pumped, multimode phenomena 4-79096  
 far IR waveguide laser, discrete and continuous modes study 4-79094  
 far IR waveguide laser, optically pumped, wavefront curvature 4-107708  
 FIR lasers, slab and cylindrical, waveguide continuous modes 4-87310  
 free electron generators of coherent radiation, conf., Orcas Island, WA, USA (June 1983) 4-82588  
 free electron laser, chaotic optical modes 4-87343

**laser modes continued**

- free electron laser, long pulse, driven by linear induction accelerator 4-87348  
 free electron laser, low-gain, low-voltage, mode struct. 4-96942  
 free electron laser, two-stage, low loss quasi-optical cavity 4-87369  
 free electron laser linear gain and stable pulse propag. 4-83586  
 free electron laser rectangular waveguide resonator, cylindrical Gaussian eigenmodes, gain per mode 3D calc. 4-87368  
 free electron laser transverse modes evolution, appl. to Orsay expt. 4-87339  
 free electron laser unstable resonators beam quality and small mode area 4-87370  
 free electron lasers, Lawson-Penner limit and single passage laser performance, supermode theory 4-91482  
 free electron tapered wiggler laser gain displacement effects 4-83595  
 gain saturation mode-free description in laser rods 4-79093  
 gas laser, steady state synchronisation of lateral modes (*Russian*) 4-60079  
 graded-index lens external cavity semicond. laser with optical feedback, spectral props. study 4-87371  
 inhomogeneous optical resonator; modal analysis 4-91502  
 injection laser, multimode homogeneously broadened, analytic description 4-112439  
 injection laser, single-mode, line narrowing due to external optical feedback 4-79142  
 injection laser noise properties due to optical feedback 4-79143  
 injection lasers, mode interaction and single-freq. emission self-stabilisation 4-60036  
 injection lasers, single mode, space-time characts. 4-107639  
 interferometric semiconductor laser (*Japanese*) 4-79150  
 ion lasers, construction operating modes, and characts. (*Italian*) 4-107596  
 magnetised free electron lasers and auto resonance cyclotron masers, nonlinear efficiency 4-96921  
 multimode laser field, spatial coherence (*Russian*) 4-96862  
 nearly single-longitudinal-mode lasers, partition fluctuations 4-96896  
 one-dimensional laser with output coupling, phase noise above threshold 4-83561  
 order parameter fluctuations of a laser with polarization symmetry 4-91433  
 orthogonality relations of modes obtained by the effective-index method 4-69359  
 phase perturbations and laser resonator beam quality 4-87367  
 planar injection lasers, gain and current profiles, carrier diffusion and recombination 4-107634  
 quasisingle-mode laser radiation, second harmonic duration under strong energy exchange conditions 4-74616  
 Raman free electron laser, three-dimens. theory 4-96924  
 reflectivity calculations, 2D, for modes reflected by laser end facet, effective-index method 4-69360  
 resonant optical cavities, alignment and mode-matching 4-112480  
 resonators with nonuniform magnification 4-87373  
 rhodamine 6G CW dye laser radiation freq. doubling with an external auxiliary active cavity (*Chinese*) 4-60107  
 rhodamine 6G CW dye ring laser with a Mach-Zehnder interferometer efficient single mode operation 4-91496  
 rhodamine 6G dye laser, CW, single longitudinal mode oscill. (*Korean*) 4-112483  
 rhodamine 6G dye laser, multimode, pulsed, single-shot spectral meas. and mode correls. 4-69467  
 rhodamine 6G tunable dye laser, single-mode picosec., with ultra-short cavity (*Chinese*) 4-112468  
 ring laser subjected to transverse mag. field, nonreciprocal effect theory 4-107693  
 ring lasers, single and two-mode statistical props. 4-102958  
 semiconductor, longitudinal modes, modulated power distrib. 4-79145  
 semiconductor, modal noise reduction of laser diodes with specific thickness coating 4-79135  
 semiconductor BH laser, transverse mode selection and lateral carrier leakage 4-107642  
 semiconductor cleaved-coupled-cavity laser, single mode, spectral props., external optical feedback effect 4-69405  
 semiconductor cleaved-coupled-cavity laser with large cavity length ratios, single longit. mode operation 4-69450  
 semiconductor gain-guided lasers, spontaneous emission factor, heuristic approach 4-83581  
 semiconductor integrated etalon interference lasers, stable longit.-mode operation, tuning temp. depend. study 4-69455  
 semiconductor laser arrays, phase-locked, rate eqn. analysis 4-112435  
 semiconductor laser diodes, longitudinal mode stabilisation by extremely short optical waveguides 4-91474  
 semiconductor laser mode selection, two-segment cavity theory 4-60073  
 semiconductor lasers, spectral linewidth enhancement, power dependence 4-87328  
 semiconductor lasers, stationary characts., numerical anal. (*Chinese*) 4-112419  
 semiconductor lasers, transient, temp. variation under pulsed current excitation obs. (*Japanese*) 4-102930  
 semiconductor phase-locked laser arrays, supermode anal. 4-60097  
 semiconductor phased arrays, longitudinal modes control by phase velocity matching 4-91471  
 semiconductor single-mode lasers, noise theory in presence of optical feedback 4-79137  
 semiconductor two-section coupled cavity lasers, longitudinal mode behaviour, anal. and simulation studies 4-79141  
 single longitudinal mode semicond. laser model with internal-refl. optical coupling (*Chinese*) 4-60034  
 single-frequency long-wavelength lasers for broadband fibre communication 4-91497  
 source flow chemical laser cavity performance 4-74551  
 spherical optical resonator, incident wave coupling coeffs. and modes, in case of mismatching and misalignment 4-74550  
 square-waveguide laser resonator coupling losses 4-69458  
 stimulated Compton free electron lasers, expt., theoretical and design concepts 4-96943  
 stripe geometry lasers, spectral behaviour, lateral hplburning effects, numerical investigation 4-87334  
 TEM<sub>00</sub>-thermoinsensitive cavity with several thermoperturbing centres, mode aberration compensation 4-69457  
 theoretical development in 1960s, Doppler effects 4-91432  
 three-mode laser, quantum theory 4-87311

## lasers continued

toric unstable resonators, geometrical, diffractive and asymptotic theory 4-91501  
 transverse-magnetic-like modes, 2D refl. calc. formulation 4-87309  
 two-frequency lasers, Zeeman effect and mode-competition effect 4-69364  
 two-mode optical pumping of a laser 4-79089  
 two-photon laser and optical-bistability sidemode instabilities 4-74477  
 unguided wave Cherenkov amplifier 4-102913  
 waist location and Rayleigh range for higher-order mode laser beams 4-91508  
 waveguide laser resonators formed by flat mirrors, coupling efficiency 4-112482  
 waveguide with graded index and gain, mode behaviour anal. 4-97066  
 YAG crystal, specially doped growth and multi-function props. (Chinese) 4-113464  
 AlGaAs-GaAs laser with external dispersive cavity multimode rate-eqn. soln. of mode selection and tuning props. (Chinese) 4-91462  
 AlGaAs-GaAs short-cavity laser and its monolithic integration using microcleaved facets process 4-60064  
 Al<sub>0.5</sub>Ga<sub>0.5</sub>As pulsed DH laser, emission characts., influence of longit. mode carrier-depend. shifts and gain profile 4-87335  
 Al<sub>0.5</sub>Ga<sub>0.5</sub>As-GaAs injection lasers, longitudinal mode selection obs. 4-79153  
 Al<sub>0.5</sub>Ga<sub>0.5</sub>As-GaAs injection laser self-modulation associated with external optical feedback 4-112440  
 Al<sub>0.5</sub>Ga<sub>0.5</sub>As-GaAs twin-channel substrate mesa guide laser with antiref. coatings, single longit. mode operation 4-83619  
 AlGaInP/GaInP DH visible light lasers, MOCVD grown, room temp. pulsed operation 4-69445  
 Ar mode synchronised laser amplifier system, high-power pulse prod. at high repetition freq. (Russian) 4-69369  
 CO<sub>2</sub> CW laser two-mode multiline stabilisation using Fabry-Perot filter under analog and digital computer control 4-60092  
 CO<sub>2</sub> compact hybrid single mode TEA laser, stabilisation 4-91495  
 CO<sub>2</sub> gasdynamic laser, Fabry-Perot resonator, mode struct. 4-60072  
 CO<sub>2</sub> grating selected freq. laser, mode corrugated pipe design (Chinese) 4-87360  
 CO<sub>2</sub> laser, quasi-CW, tunable, 1-sec pulse, optical pumping appls. 4-74536  
 CO<sub>2</sub> TEA lasers, multipass-prism interferometer for fine-freq.-turning, single-mode operation 4-107683  
 Cu halide, burst-mode, interdependence of buffer gas press. and optimum interpulse delay 4-112396  
 GaAlAs buried multi-quantum-well laser fabricated by diffusion induced disordering 4-74547  
 (GaAl)As cleaved coupled-cavity laser anal. 4-96900  
 GaAlAs laser oscillating in single longit. mode, LF feedback noise 4-96909  
 GaAlAs lasers, transverse-mode stabilised MOCVD grown, with embedded confining layer on optical waveguide 4-69443  
 (GaAl)As transverse-mode stabilised laser diodes, MOCVD growth 4-96912  
 GaAlAs-GaAs DH lasers, narrow-channelled substrate stripe-type, characts. meas. and anal. (Chinese) 4-112433  
 GaAs/GaAlAs single mode laser diodes, free space optical. communication, design and system requirements 4-79176  
 GaAs-(AlGa)As twisted DH laser, composite cavity config., design and longit./transverse mode operation 4-69456  
 GaAs-GaAlAs channelled-substrate lasers, single longit. mode, grown by MBE 4-69403  
 GaInAsP BH laser, low-threshold, multiple-cavity, longit.-mode stabilised 4-91468  
 GaInAsP/InP DFB laser, 1.5  $\mu$ m range, longitudinal mode behaviour 4-74512  
 GaInAsP/InP phase adjusted active distributed reflector laser, 1.5  $\mu$ m, for dynamic single mode operation 4-69437  
 GaInAsP-InP BH but-jointed built-in integrated, lasers, 1.5-1.6  $\mu$ m operation, static characts. 4-60065  
 HCN CW laser, RF excited, capacitive coupling (Japanese) 4-96879  
 HCN waveguide laser and HCN laser-excited oversized hollow dielec. waveguide submm radiation pattern study 4-107709  
 H<sub>2</sub>O monomode CW 119  $\mu$ m laser, output beam polarisation improvement 4-112471  
 He-Ne and Ar<sup>+</sup> laser low-freq. beat noise (Chinese) 4-91511  
 He-Ne laser, 0.63  $\mu$ m, effect of an external modulation signal 4-79108  
 He-Ne laser, mode struct. optical spectrum analyser study, undergraduate expt. 4-106152  
 InGaAsP BH 1.3  $\mu$ m lasers, anomalous polarisation characts. 4-69402  
 InGaAsP tunable DFB laser pumped by heterostructure injection laser 4-96907  
 InGaAsP/InP 1.3  $\mu$ m buried crescent lasers using short external optical cavity, single-mode operation 4-74511  
 InGaAsP/InP 1.3  $\mu$ m buried crescent lasers, single transverse-mode conditions 4-96897  
 InGaAsP/InP DFB laser diodes lasing characts., at 1.5  $\mu$ m, effect of mirror facets 4-74513  
 InGaAsP/InP GRIN rod external coupled-cavity BH lasers, single longit. mode operation 4-91473  
 InGaAsP-InP 1.3  $\mu$ m BH lasers, improved linearity criterion, high-bit-rate fibre communication system appls. 4-74510  
 InGaAsP-InP single-longitudinal-mode 1.3  $\mu$ m DFB-DC-PBH diodes 4-91467  
 InP/InGaAsP DFB double-channel PBH laser diode, 1.55  $\mu$ m, single longit. mode operation 4-87358  
 Nd:phosphate glass laser, active-passive mode locking using Eastman 5 saturable dye 4-91478  
 Nd:YAG CW laser with passive stabilisation of self-mode locking 4-107649  
 Nd:YAG high-power oscillator, stable single-axial-mode operation by injection locking 4-69417  
 Nd:YAG Q-switched oscillator, single axial mode operation by injection seeding 4-60042  
 (Pb,Sn)Te-Pb(Te,Se) DH laser diodes, ion-implantation confined shallow mesa stripe, single mode tuning 4-112459  
 Pb salt laser technology advances and implications for gas analysis 4-107719  
 Pb salt tunable diode lasers, single mode, for 3 to 30  $\mu$ m IR operation 4-112456  
 Pb<sub>1-x</sub>Eu<sub>x</sub>Se<sub>1-y</sub>Te<sub>y</sub> heterojunction stripe geometry lasers grown by MBE, single longit. mode emission 4-112458

## laser modes continued

Pb<sub>1-x</sub>Eu<sub>x</sub>Se<sub>1-y</sub>Te<sub>y</sub> long-wavelength laser diodes, fabrication and props. 4-96954  
 Pb<sub>1-x</sub>Mn<sub>x</sub>Se IR laser diode emission in high mag. fields 4-69412  
 PbSnTe-PbSeTe DBR diode lasers, single longit. mode operation 4-112460  
 XeCl laser, single longitudinal mode operation 4-112386  
 XeF laser low-magnification positive-branch unstable resonator, transverse mode form. 4-73521  
 XeF laser using grating-interferometer-based cavity, single-mode tunable operation 4-102956  
 laser Q-switching *see* Q-switching  
 laser radar *see* optical radar  
 laser theory  
*see also* laser transitions; population inversion; stimulated emission bandwidth, phase diffusion and random telegraph signal models 4-69361  
 beam attenuation method 4-74568  
 cavities, critical length, ABCD matrix formalism (French) 4-60074  
 Cherenkov lasers in the Compton regime 4-96856  
 chaos in simple laser systems 4-79097  
 chemical CW lasers, dynamic saturation intensity, depend. on mixing rate of reagents 4-107617  
 chemical laser, CW flow, generalised kinetic model 4-69392  
 cleaved coupled cavity lasers, optimum gap width for mode discrimination, theoretical study 4-87330  
 cleaved-coupled-cavity lasers, threshold anal. 4-112415  
 coherence theory of laser resonator modes 4-69454  
 Compton laser, non-collinear, effects of saturation and inhomogeneous broadening 4-60052  
 condensed active media laser, linear anisotropy induced by polarised pumping radiation 4-79126  
 coupled lasers, semiclassical theory 4-79092  
 coupled-cavity laser rate eqn. model 4-60010  
 CW laser oscillation anal. via optical Bloch equations (Chinese) 4-60009  
 detuned lasers with injected signals, period-doubling bifurcations 4-74481  
 development in 1960s, Doppler effects 4-91432  
 DFB helical far IR laser, theory, realisation and mode characts. 4-79186  
 DFB laser, quarter-wave shifted grating type, wavelength selectivity analysis 4-64716  
 DFB laser with strong modulations, resonance frequencies and threshold gains calc. 4-107589  
 DFB lasers with strong modulation, threshold gains and resonance freqs. calc. 4-79095  
 DH lasers, carrier-induced index depressions effect on transverse-mode characts. 4-74516  
 Dicke model systems, single mode laser radiation 4-102914  
 Dicke type model systems, radiation, asymptotically exact eqns., laser radiation app. 4-73335  
 diode laser, feedback of light interacting coherently, incoherently with laser cavity field, influence on oscil. spectrum 4-91451  
 diode single-mode lasers of large-optical-cavity type, lateral mode discrimination and control 4-112436  
 dye CW mode-locked lasers, role of cavity dispersion 4-79124  
 dye laser, synchronously pumped, rate eqn. simulation 4-74503  
 extended system superradiance dynamics, radiation field and active medium transverse inhomogeneity influence 4-74471  
 far IR laser, optically-pumped, multimode phenomena 4-79096  
 far IR waveguide laser, discrete and continuous modes study 4-79094  
 far IR waveguide laser, optically pumped, wavefront curvature 4-107708  
 far IR waveguide laser, oscillation conditions 4-107588  
 fast-flow lasers, current flow mechanism in glow discharge positive column 4-113249  
 FIR lasers, slab and cylindrical, waveguide continuous modes 4-87310  
 free electron laser, coherence and fluctuations, fully quantum mech. approach 4-87345  
 free electron laser, finite-length, gain, velocity spread effect 4-107655  
 free electron laser, gain mechanism calc. 4-79169  
 free electron laser, small signal gain simplified calcs. 4-107656  
 free electron laser, wiggler periodic length choice and freq. variations (Chinese) 4-112446  
 free electron laser amplifier, theoretical analysis 4-107652  
 free electron laser amplifier performance in Compton regime 4-87338  
 free electron laser instabilities and quantum initiation 4-87351  
 free electron laser multiphoton transitions 4-69422  
 free electron laser oscillator, noise to coherence, photon noise and electron shot noise theory 4-87344  
 free electron laser pulse propagation, model for noise introduction into computer simulations 4-87346  
 free electron laser quantum theory, Glauber coherence, antibunching and squeezing 4-83596  
 free electron laser rectangular waveguide resonator, cylindrical Gaussian eigenmodes, gain per mode 3D calc. 4-87368  
 free electron laser transverse modes evolution, appl. to Orsay expt. 4-87339  
 free electron laser unstable resonators beam quality and small mode area 4-87370  
 free electron lasers, computer simulation of lasers with variable Wigglers 4-102935  
 free electron lasers, nonlinear orbits with linear mag. wiggler and strong axial mag. guide field 4-74527  
 free electron lasers, oscillation stability of electron near quasipotential minimum 4-91484  
 free electron lasers, particle motion stochastic instability 4-74525  
 free electron lasers, single particle dynamics and gain, Lorentz force eqn. 4-79167  
 free electron lasers, theory and expt., review 4-112448  
 gain saturation mode-free description in laser rods 4-79093  
 gas laser, stability of self-locking of two modes 4-74561  
 gas ring laser, medium, excitation spatial-temporal coherence effect on statistical characts. 4-107590  
 Gaussian laser lineshape in resonance fluorescence 4-69363  
 generalized formula for absorption and stimulated emission of light 4-60011  
 I laser using photolytic O<sub>2</sub><sup>1</sup> $\Delta$  generation, kinetic model 4-112401  
 induced interaction of electron beam with superstrong EM radiation at boundary of two media 4-107706  
 inhomogeneous optical resonator, modal analysis 4-91502  
 injection laser, homogeneously broadened, differential quantum efficiency, analytic approx. 4-112406

## laser theory continued

- injection laser, multimode homogeneously broadened, analytic description 4-112439
- interacting collective modes in an optical cavity 4-79197
- kinetics of lasers with unstable cavities and short inversion times 4-96877
- Lorenz strange attractor, quantum fluctuations, master eqns. 4-60012
- macroscopic two-level system, conversion time, resonator free superradiative laser appl. 4-74484
- magnetic crystal, channelled particle radiation, appl. to laser gain 4-113513
- Maxwell-Bloch equation, statistical props. in chaotic regime 4-74478
- microscopic, numerical calcs. 4-96861
- mode-locking, self-consistent profile approach 4-79090
- monochromatic laser with freq. tuning 4-79091
- multimode laser field, spatial coherence (Russian) 4-96862
- Non-equilibrium open system model, laser and biological systems (Japanese) 4-74476
- nondegenerate two photon amplifier theory 4-69362
- nonlinear laser model with multiplicative coloured noise, distrib. function 4-87312
- Novette short wavelength laser-target interaction system 4-96956
- one-dimensional laser with output coupling, phase noise above threshold 4-83561
- one-dimensional laser with output coupling, quantum theory, linear approx. 4-112372
- optically pumped far IR lasers, efficiency improvement 4-107611
- order parameter fluctuations of a laser with polarization symmetry 4-91433
- organic compound based lasers, active medium stimulated emission charact. calc. 4-74482
- orthogonality relations of modes obtained by the effective-index method 4-69359
- passive and active optical systems, instabilities, Gaussian transverse intensity profile 4-112502
- passively mode-locked laser theory including self-phase modulation and group-vel. dispersion 4-74479
- phase noise in a laser with output coupling 4-96860
- photon recyclers, optically pumped NMMW lasers 4-87317
- photon statistical distribution evolution in laser radiation field 4-107592
- planar injection lasers, gain and current profiles, carrier diffusion and recombination 4-107634
- quasiperiodicity in lasers with saturable absorbers 4-74480
- radiative plasma in lasers for exciting thermonuclear fusion reactions (Russian) 4-97770
- recombination lasers, ionization/recombination kinetics 4-64613
- reflectivity calculations, 2D, for modes reflected by laser end facet, effective-index method 4-69360
- ring laser subjected to transverse mag. field, nonreciprocal effect theory 4-107693
- semiconductor laser arrays, phase-locked, rate eqn. analysis 4-112435
- semiconductor lasers, spectral linewidth enhancement, power dependence 4-87328
- semiconductor lasers, stationary characts., numerical anal. (Chinese) 4-112419
- semiconductor lasers, transverse switching due to Hopf bifurcation 4-74514
- single-frequency cleaved-coupled cavity and DFB laser, direct modulation transient chirping study 4-83627
- slab geometry laser, theory 4-74517
- solid-state lasers, optically pumped, energy parameters, self-consistent calc. method 4-60046
- squeezed state generation, critical discussion 4-87386
- stimulated undulator radiation of electrons in waveguide and free electron lasers 4-79022
- strip geometry laser diodes, dynamical thermal props. 4-79206
- stripe geometry lasers, self-consistent model based on beam propagation method 4-112438
- sub- $T_c$  optical pulse generation appl. to optically pumped far-IR lasers 4-79171
- three-mode laser, quantum theory 4-87311
- toric unstable resonators, geometrical, diffractive and asymptotic theory 4-91501
- transverse-magnetic-like modes, 2D refl. calc. formulation 4-87309
- two frequency lasers, Zeeman effect and mode-competition effect 4-69364
- two-mode laser with coupled transitions, atomic coherence effects 4-107591
- two-mode optical pumping of a laser 4-79089
- two-photon laser and optical-bistability sidemode instabilities 4-74477
- two-photon laser with injected signal, theory 4-91431
- two-photon lasers, semiclassical theory 4-96859
- two-photon lasers, theory, Fokker-Planck eqn. treatment 4-91430
- unguided wave Cherenkov amplifier 4-102913
- UV and soft X-ray radiation amplification possibility on multiply charged ion transitions in a recombining plasma 4-74475
- wide-band laser spectrum depend. on selective loss profile 4-74483
- Zeeman laser, transverse, theoretical anal. (Chinese) 4-91429
- Ar mode synchronised laser amplifier system, high-power pulse prod. at high repetition freq. (Russian) 4-69369
- CO<sub>2</sub> CW steady-state laser model 4-112373
- CO<sub>2</sub> gasdynamic laser, radiation intensification in boundary layer on Laval nozzle cooled walls (Russian) 4-96867
- Cu vapour laser, self-heating, numerical anal. of parameters 4-112393
- (GaAl)As cleaved-coupled-cavity lasers, coupling strength study 4-91459
- H<sub>2</sub>-HF gasdynamic pure rotational laser based on far IR transitions, theoretical study 4-79118
- HF pulsed H<sub>2</sub>+F<sub>2</sub> chain reaction laser, effect of vibr. and rot. relax. mechanisms 4-91445
- He-Kr<sup>+</sup> hollow cathode discharge laser, electron energy distrib. function 4-84117
- He-Ne positive column, laser gain distrib. determ. 4-84111
- I optically pumped laser, kinetics in optically thick medium 4-64702
- KrF lasers, electron-beam-excited, using Ar-free mixtures at 1 atm. 4-112382
- N<sub>2</sub> discharge laser, model calc. and expts. 4-83568
- Nc like ions, UV radiation amplification in laser plasma 4-74493
- XeCl laser, self-sustained discharge pumped, theory 4-96875

## laser transitions

- see also laser theory
- alkali-like atoms and ions, quasi-metastable quartet levels 4-74201

## laser transitions continued

- chlorofluoromethane, optically pumped far IR laser action 4-112395
- Cl<sub>2</sub> (D<sup>3</sup>  $\Pi_g$ -A<sup>2</sup>  $\Pi_g$ ) transition, improved gain at 258 nm by halogen donor mixing 4-107601
- diatomic molecule light amplification coeff. calc. at electron transitions (Russian) 4-79115
- dichlorofluoromethane far IR CW lasing lines, optically pumped, freq. meas. 4-102925
- 1,1-difluoroethane new far IR laser lines, CO<sub>2</sub> laser pumping 4-91440
- dye laser, radiation 605 to 725 nm region pumped by 544 nm fluorescein dye laser 4-112402
- far IR laser, optically-pumped, multimode phenomena 4-79096
- fluoromethane, CW far IR optically pumped open-cavity laser (Chinese) 4-112392
- fluoromethane 1.60 THz (187  $\mu$ m) optically pumped laser emission freq. meas. 4-96873
- fluoromethane laser, optically pumped 496  $\mu$ m, linear DFB, helical DFB and grazing-incidence types (Chinese) 4-107677
- fluoromethane-d<sub>3</sub> far IR laser lines, energy-level structure 4-112394
- formic acid, CW far IR optically pumped open-cavity laser (Chinese) 4-112392
- free electron laser oscillator, storage ring, operation at 6500 Å 4-87340
- methanol, CW far IR optically pumped open-cavity laser (Chinese) 4-112392
- methanol absorption around CO<sub>2</sub> waveguide laser lines 4-78852
- methanol laser, high-power 119  $\mu$ m operation, water-cooled cavity design, electron density meas. appl. 4-79185
- methanol laser, optically pumped, far IR, emission, torsional transition obs. and assignment 4-107607
- methanol laser, optically pumped, new laser lines in 27.7 to 61.7  $\mu$ m wavelength range 4-91438
- methanol laser line assignments, IR spectra study 4-79119
- methanol laser optically pumped, far IR transition lines, triple resonance study 4-79121
- methanol pumped by <sup>13</sup>C<sup>18</sup>O<sub>2</sub> pump laser, sub-MM laser line obs. and assignments 4-69375
- methanol-d<sub>3</sub> laser, optically pumped, far IR line assignments 4-107608
- methanol-d<sub>3</sub> laser, optically pumped, new laser lines in 27.7 to 61.7  $\mu$ m wavelength range 4-91438
- methanol-d<sub>3</sub> laser lines, optically pumped, assignment and correction anal. 4-79120
- methyl fluoride, CO<sub>2</sub> pumped far IR laser line assignment using IR diode laser spectroscopy 4-107610
- one-dimensional laser with output coupling, phase noise above threshold 4-83561
- perylene-3,4,9,10-tetracarboxylic acid-bis-N,N'(2,6'-xylylidyl)diimide laser dye, high stability and broad band lasing action pot. 4-107623
- tetrafluoromethane tunable laser, 16  $\mu$ m, optically pumped (Chinese) 4-87359
- two-photon laser and optical-bistability sidemode instabilities 4-74477
- vinyl bromide, CO<sub>2</sub> laser pumped, 47 CW far IR laser lines 453 to 2356  $\mu$ m 4-96869
- vinyl bromide far-IR laser action, optically pumped by CW N<sub>2</sub>O laser 4-112397
- vinyl chloride far-IR laser action, optically pumped by CW N<sub>2</sub>O laser 4-112397
- vinyl fluoride far-IR laser action, optically pumped by CW N<sub>2</sub>O laser 4-112397
- Be II recombining plasma, lasing transitions 4-96878
- Be isoelectronic sequence, optical pumped quasi-CW UV plasma lasers 4-102922
- Br<sub>2</sub> recombination gas dynamic laser, electron transitions (Russian) 4-96881
- CO<sub>2</sub> 00<sup>0</sup>1 upper laser level spectroscopy based on 4.3  $\mu$ m spontaneous emission intensity modulation meas. 4-78851
- CO<sub>2</sub> cascade laser, 4.4 micron, resonator design 4-87313
- CO<sub>2</sub> laser, gaseous medium temp., influence of high-mol. compound impurities 4-79103
- CO<sub>2</sub> laser frequency stabilisation for sub-MM laser pumping by Stark modulated Lamb dip signal in methanol (Japanese) 4-74485
- CO<sub>2</sub> transverse-flow laser vibrational and translational temp. determ. (Chinese) 4-112378
- CO<sub>2</sub> tunable high-power CW laser using compound cavity, individual transition selection 4-69366
- CO<sub>2</sub> waveguide laser, continuously tunable, RF excited, high-pressure 4-74542
- CO<sub>2</sub>/OsO<sub>4</sub> waveguide laser with freq. stability of 10<sup>-13</sup> 4-79102
- Ca(NbO<sub>3</sub>)<sub>2</sub>:Pr<sup>3+</sup> (Er<sup>3+</sup>), stimulated emission and laser channels 4-91480
- CaWO<sub>4</sub>:Pr<sup>3+</sup>, stimulated emission and laser channels 4-91480
- DCN CW waveguide laser operating at 195, 190  $\mu$ m, quartz tube cavity (Chinese) 4-107604
- Er<sup>3+</sup>:YAG cross-relaxation laser emitting at 2.94  $\mu$ m, <sup>4</sup>I<sub>11/2</sub>-<sup>4</sup>I<sub>13/2</sub> transition 4-60048
- F CW laser action 4-91439
- GaAs/AlGaAs multi-quantum-well lasers, polarization-dependent gain 4-112412
- H-Ne 633 nm laser, I<sub>2</sub> stabilised, freq. stability and reproducibility 4-91436
- H<sub>2</sub>-HF gasdynamic pure rotational laser based on far IR transitions, theoretical study 4-79118
- HF CW lasers, small signal gain meas. (Chinese) 4-112400
- HF/DF pulsed optical resonance transfer laser, theoretical simulation 4-79123
- H<sub>2</sub>O monomode CW 119  $\mu$ m laser, output beam polarisation improvement 4-112471
- He-Cd<sup>+</sup> hollow cathode laser, population inversion mechanism, red, green and blue emission 4-83570
- He-Ne intracavity laser, polarisation behaviour at 632.8 nm (Chinese) 4-107597
- He-Ne laser appl. to intracavity dispersion meas., 3.39  $\mu$ m transition 4-112478
- He-Zn-Cd hollow cathode laser, simultaneous laser oscillation by Cd II and Zn II lines (French) 4-112399
- HgBr laser system, narrow-band injection locking, B-X transition 4-79111
- HoP<sub>2</sub>O<sub>4</sub> crystal <sup>1</sup>I<sub>7</sub>-<sup>3</sup>I<sub>8</sub> transition determ. (Chinese) 4-60887
- I laser, degenerate transition, self-induced transparency, coherent pulse propag. 4-96882
- I laser using photolytic O<sub>2</sub> <sup>1</sup>Δ generation, transition I\* (<sup>2</sup>P<sub>1/2</sub>) to I (<sup>2</sup>P<sub>3/2</sub>) at 1.31  $\mu$ m 4-112401
- InGaAsP BH 1.3  $\mu$ m lasers, anomalous polarisation characts. 4-69402

## laser transitions continued

- InGaAsP-InP BC laser diode emitting at 1.3  $\mu\text{m}$ , fabrication, design, characteristics 4-112474  
 K vapour laser, optically pumped, tunable far-IR radiation from Rydberg transitions 4-87318  
 LiF, tunable room temp. laser operation of colour centres, red and near IR emission 4-91479  
 Mn vapour laser,  $\text{MnCl}_2$  lasant, 7 green laser lines (*Chinese*) 4-107602  
 $\text{NH}_3$  laser, TEA  $\text{CO}_2$  laser pumped, high-power pulsed operation at 257/281  $\mu\text{m}$  transitions 4-79182  
 $\text{NH}_3$ , pure MW Raman laser emission in superradiant mode,  $\text{CO}_2$  laser line pumping 4-69376  
 $\text{NH}_3$ , two-photon optical pumping in multipass cell, lasing lines 16 to 35  $\mu\text{m}$  4-74495  
 $\text{NaYGeO}_4\text{Nd}^{3+}$ , luminescence and stimulated emission, laser channels 4-93109  
 $\text{Nd}^{3+}$ , phosphate glass laser amplification characts. 4-91476  
 $\text{Nd}^{3+}$ , silicate glass laser amplification characts. 4-91476  
 $\text{NdP}_2\text{O}_7$  crystals, stimulated emission cross section estimate from super-radiance decay kinetics 4-60047  
 $\text{O}_2$  laser, optically pumped, CW obs. and assignment of 7 lines 4-107609  
 $\text{Pr}^{3+}$ :LiYF $_4$ , visible lasing on five intermultiplet transitions 4-74519  
 Rn monohalides, laser amplification 4-83567  
 $\text{S}_2$  recombination gas dynamic laser, electron transitions (*Russian*) 4-96881  
 $\text{SrWO}_4\text{Nd}^{3+}$ , stimulated emission and laser channels 4-91480  
 XeCl excimer laser, IR laser emission 4-96876  
 XeCl laser, spectral composition of radiation (*Russian*) 4-69380  
 XeF laser output spectrum, XeF(B) to XeF(X) transition, photolytic pumping of XeF $_2$  4-79117  
 Zn $^{2+}$  vapor, high-gain soft X-ray pumped photoionization laser 4-112383  
 Zn,Cd $_{1-x}$ Se scanning laser emitting in the blue region 4-79163

laser trimming see laser beam machining

## laser tuning

- beam attenuation method 4-74568  
 cavity configuration in dye laser for dispersion on two output beams 4-74554  
 cleaved coupled-cavity lasers, verification of coupling gap dependence 4-91469  
 cleaved-coupled-cavity freq. tunable laser based optical switching and routing system 4-79345  
 cleaved-coupled-cavity lasers, threshold anal. 4-112415  
 coumarin 1-acriflavine-uranine-rhodamine 6G dye mixture systems, continuously tunable energy transfer laser generation 4-107619  
 detuned lasers with injected signals, period-doubling bifurcations 4-74481  
 DH laser, multiple twisted separately pumped, longitudinal mode behaviour 4-112486  
 dimer lasers, review 4-96870  
 diode laser development and spectroscopy appls., conf., San Diego, CA, USA (Aug. 1983) 4-110801  
 dye laser, distributed feedback, picosecond pulses generation using grating hologram 4-112405  
 dye laser, double-wavelength pulsed tunable (*Chinese*) 4-112465  
 dye laser, radiation 605 to 725 nm region pumped by 544 nm fluorescein dye laser 4-112402  
 dye laser, two-wavelength narrow-band, independently tunable (*Chinese*) 4-112464  
 dye laser, white light operation (*Chinese*) 4-112403  
 dye laser design, short-cavity, piezoelec. tuned 4-69434  
 dye lasers, cavity length detuning properties in synchronous mode locking 4-96964  
 dye tunable laser resolution for laser spectroscopy of H 4-64412  
 dye two freq. tunable laser with high efficiency intracavity radiation divider 4-79192  
 fluoromethane tunable far IR laser pumped by  $\text{CO}_2$  TE laser 4-112472  
 fluoromethane tunable FIR laser, frequency trimming (*Chinese*) 4-69374  
 fluoromethane- $^{13}\text{C}$  tunable Raman FIR laser, optically pumped, tunability study 4-79122  
 free electron high-gain lasers, small signal gain spectrum 4-83593  
 free electron IR laser, broadband optical cavities, appl. tunable FELs 4-112479  
 free electron laser injection locking by  $\text{BeAl}_2\text{O}_4$ :  $\text{Cr}^{3+}$  (Alexandrite) laser 4-83587  
 free electron lasers, broadly tunable, capabilities 4-107653  
 free electron lasers, continuous tunability 4-69427  
 IR dye laser,  $\text{N}_2$  laser pumped, efficiency improvement by energy transfer excitation 4-107620  
 IR picosecond pulses, narrow-band, tunable between 1.2-1.4  $\mu\text{m}$ , generated by travelling-wave dye laser 4-74569  
 mm-wave free electron laser operating in collective regime radiation growth and emission spectrum 4-96922  
 monochromatic laser with freq. tuning 4-79091  
 Raman free electron laser, tunable, spectral meas. 4-96929  
 rhodamine 560, 6G tunable picosec. dye laser oscillator-amplifier system, spatial and temporal props. 4-91488  
 rhodamine 590 dye laser oscillators, narrow linewidth, high PRF Cu laser pumped 4-74535  
 rhodamine 6G CW dye ring laser with a Mach-Zehnder interferometer, efficient single mode operation 4-91496  
 rhodamine 6G CW tunable ring dye laser, passively mode-locked, picosec. pulse SHG correl. meas. (*Chinese*) 4-87354  
 rhodamine 6G double wavelength dye laser,  $\text{N}_2$  laser pumped (*Chinese*) 4-91492  
 rhodamine 6G femtosecond dye laser, expt. and theoretical study 4-107627  
 rhodamine 6G tunable dye jet laser pumped synchronously by second harmonic of Nd:YAG laser 4-60031  
 rhodamine 6G tunable dye laser, single-mode picosec., with ultra-short cavity (*Chinese*) 4-112468  
 rhodamine 6G-saffron T-cresyl violet-Nile blue dye mixture systems, continuously tunable energy transfer laser generation 4-107619  
 ring laser, beat frequency, effect of low-freq. periodic perturbations 4-79194  
 ring lasers, single and two-mode statistical props. 4-102958  
 semiconductor integrated etalon interference lasers, stable longit.-mode operation, tuning temp. depend. study 4-69455  
 semiconductor lasers, optically pumped, mode locked psec pulses from 490 nm to 2  $\mu\text{m}$  4-107699  
 semiconductor lasers, ultrashort cavity, optically pumped by injection laser 4-107645

## laser tuning continued

- semiconductor two-section coupled cavity lasers, longitudinal mode behaviour, anal. and simulation studies 4-79141  
 spectroscopy in solids using tunable laser techniques 4-63786  
 stabilisation techniques for tunable lasers, for ultrahigh-resolution spectroscopy 4-63789  
 stimulated undulator radiation of electrons in waveguide and free electron lasers 4-79022  
 tetrafluoromethane tunable laser, 16  $\mu\text{m}$ , optically pumped (*Chinese*) 4-87359  
 tunable diode lasers, heterodyne freq. meas. and freq. calibration standards 4-112422  
 two-photon laser and optical-bistability sidemode instabilities 4-74477  
 AlGaAs injection laser with external dispersion resonator using returning mirror 4-107641  
 AlGaAs single- and multiple-stripe quantum-well heterostruct. laser-diodes in external grating cavity 4-96902  
 AlGaAs-GaAs laser with external dispersive cavity multimode rate-eqn. soln. of mode selection and tuning props. (*Chinese*) 4-91462  
 CO waveguide laser with selective resonator, emission freq. wide tuning range 4-60069  
 $\text{CO}_2$  IR laser, freq. synthesized and continuously tunable in 9-11  $\mu\text{m}$  range 4-96947  
 $\text{CO}_2$  injection-locked TEA laser, tunable single-mode design for  $\text{D}_2\text{O}$  laser pumping 4-79184  
 $\text{CO}_2$  laser, quasi-CW, tunable, 1-sec pulse, optical pumping appls. 4-74536  
 $\text{CO}_2$  laser heterodyne bias freq.-locking (*Chinese*) 4-91512  
 $\text{CO}_2$  single-mode etalon-tuned TEA laser, optimised design for  $\text{NH}_3$  laser pumping 4-79182  
 $\text{CO}_2$ , TEA lasers, multipass-prism interferometer for fine-freq.-turning, single-mode operation 4-107683  
 $\text{CO}_2$ , TEA repetitive tunable laser, long lifetime, without He (*Chinese*) 4-112377  
 $\text{CO}_2$ , tunable double wavelength laser study (*Chinese*) 4-91513  
 $\text{CO}_2$ , tunable high pressure RF excited laser 4-96938  
 $\text{CO}_2$ , tunable high-power CW laser using compound cavity, individual transition selection 4-69366  
 $\text{CO}_2$  waveguide laser, continuously tunable, RF excited, high-press. 4-74542  
 $\text{CO}_2$  waveguide laser design for max. output power at specified freq. offset 4-107679  
 $\text{CO}_2$ -TEA laser, injection locking, effect of unstable resonator 4-87375  
 CdS, frequency tuning of far-IR radiation on hot excitons 4-69415  
 $\text{Co:MgF}_2$  CW tunable mode-locked lasers, 1.65-2.01  $\mu\text{m}$  range 4-60043  
 $\text{Cr}^{3+}$  doped tunable vibronic lasers, overview 4-107644  
 $\text{Cr}^{3+}:\text{Be}_2\text{Al}_2(\text{SiO}_3)_4$  laser, CW Kr laser pumped, 728.8 to 809.0 nm tuning range 4-60041  
 $\text{Cr}^{3+}:\text{GdSO}_4$  garnet, tunable room temp. CW laser action 4-74518  
 GaAs-GaAlAs quantum well lasers tunable by long wavelength radiation 4-69404  
 GaInAsP BH laser, low-threshold, multiple-cavity, longit.-mode stabilised 4-91468  
 GaInAsP cleaved coupled-cavity laser, tunable design, FM operation for communication appl. 4-69451  
 $(\text{Gd}_{1-x}\text{Er}_x)\text{Al}_2\text{O}_3$  garnet, 3  $\mu\text{m}$  stimulated emission, concentrational tuning 4-76498  
 He-Cd long lifetime laser using continuously tunable He replenisher (*Chinese*) 4-60089  
 In anti-Stokes Raman laser 4-79110  
 InGaAsP heterostructure laser with distributed feedback 4-74538  
 InGaAsP tunable DFB laser pumped by heterostructure injection laser 4-96907  
 InSb, tunable far-IR emission from uniaxial stress-enhanced spin-flip transitions 4-69416  
 K vapour laser, optically pumped, tunable far-IR radiation from Rydberg transitions 4-87318  
 LiF  $\text{F}_2$  centre tunable laser with distributed feedback 4-107651  
 LiF pulsed  $\text{F}_2^+$  colour centre laser, room temp. operation in near IR 4-64710  
 LiF tunable pulsed  $\text{F}_2^+$  colour centre laser, 0.69-1.0  $\mu\text{m}$  4-69413  
 LiF, tunable room temp. laser operation of colour centres, red and near IR emission 4-91479  
 $\text{NH}_3$  laser, 16-21  $\mu\text{m}$  line tunable, two-step optical pumping 4-112381  
 $\text{NH}_3$ - $\text{N}_2$  laser amplifier in 800-870  $\text{cm}^{-1}$  range 4-69440  
 Na $_2$  optically pumped laser, freq. control 4-87321  
 Nd:YAG lasers, feedback to maintain injection locking 4-79157  
 Ni:MgF $_2$  CW tunable mode-locked lasers, 1.61-1.73  $\mu\text{m}$  range 4-60043  
 (Pb,Sn)Te-Pb(Te,Se) DH laser diodes, ion-implantation confined shallow mesa stripe, single mode tuning 4-112459  
 Pb salt, tunable diode lasers for 3 to 30  $\mu\text{m}$  IR operation 4-112456  
 Pb salt heterojunction stripe geometry lasers grown by MBE 4-112458  
 Pb salt laser technology advances and implications for gas analysis 4-107719  
 Pb salt tunable diode lasers for heterodyne appls. 4-96940  
 Pb salt tunable diode lasers, Cd diffused, multicomponent gas analysis appl. 4-112457  
 $\text{Pb}_{1-x}\text{Mn}_x\text{S}$  IR laser diode emission in high mag. fields 4-69412  
 PbSnTe-PbSeTe DBR diode lasers, continuous tuning range 4-112460  
 KCl laser, single longitudinal mode operation 4-112386  
 XeCl tunable UV excimer laser system (*Chinese*) 4-112467  
 XeCl, tunable electron-beam-pumped excimer lasers 4-69384  
 XeF laser using grating-interferometer-based cavity, single-mode tunable operation 4-102956  
 XeF, tunable electron-beam-pumped excimer lasers 4-69384

## laser velocimeters

- acousto-optic modulators for  $\text{CO}_2$  chirp-modulated CW heterodyne laser rangefinder/velocimeter 4-96963  
 anemometer gas streak vel. meas., electro-optical converter and photoelectric controller appl. (*Russian*) 4-60564  
 angular windowing system for rotating equipment tests 4-86392  
 backscatter-modulated Doppler velocimeter, S/N ratio 4-91850  
 blood Doppler velocimeter, temporal resolution estimation with optical fiber 4-66989  
 blood flow monitor, diode laser source and detection in probe 4-115154  
 bloodstream, local velocity meas., laser method based on two or three light guides (*Russian*) 4-72323  
 combustion studying using optical techniques (*Italian*) 4-66591  
 differential laser Doppler anemometer with semiconductor laser (*Russian*) 4-69476

**laser velocimeters continued**

- differential-type laser Doppler velocimetry, particle size effect on photodetector signal 4-68220  
 Doppler, multicomponent, for vel. meas. of gas and liq., currents in strong elec. fields (*Russian*) 4-69837  
 Doppler and time-of-flight velocimeters for atm. crosswind measurement using photon-burst correl. techniques 4-62966  
 doppler anemometry, Mie scattering functions for milk fat globules 4-79682  
 Doppler anemometry signal processing, using processor-operated correlator 4-78299  
 Doppler differential-type velocimetry particle density effect on photodetector signal 4-87823  
 Doppler velocimeter, variable-fringe-spacing, homogeneous monodisperse particle number density meas. appls. 4-108143  
 Doppler velocimeter signal spectral broadening in presence of flow vel. gradient 4-75104  
 Doppler velocimeters using polarisation-maintaining optical fibres for simultaneous meas. of two velocity components 4-83961  
 Doppler velocimetry, quadrature demodulation 4-83960  
 Doppler velocity meter signal processing using automatically controlled filter (*Russian*) 4-106277  
 Fabry-Perot velocimetry techniques, Doppler shift rel. to surface normal direction 4-101904  
 fibre optic laser Doppler velocimeter using external-cavity semiconductor laser 4-97096  
 flow, on-axis velocity measurement by laser Doppler anemometry 4-87818  
 flow meas., CCD chirp-Z FFT Doppler signal processor, laser velocimetry, oceanographic appl. 4-87819  
 flow velocity using laser Doppler velocimeter using electro-optic modulator 4-103443  
 flowing media, velocity distrib. meas. by laser beam; appls., aerosol introduction into fluid 4-97718  
 grating laser microscope for microvessel blood flow vel. meas. 4-115281  
 interferometry for time-resolved high-velocity meas. 4-101903  
 laser diagnostics, techniques and appls. 4-65039  
 length meas. appl. of Doppler anemometry, signal processing requirements (*German*) 4-78294  
 Mitsubishi fiber-optic laser Doppler velocimeter 4-106279  
 monomode fibre optic vortex shedding flowmeter 4-97711  
 moving phase plate velocimetry using laser speckle patterns 4-95394  
 Newtonian fluid steady laminar flows between ball and spherical cavity, expt. anal. using laser Doppler anemometry 4-97470  
 nonpremixed turbulent flame, vel. and scalars, laser Doppler velocimetry and Raman scatt. 4-75101  
 particle velocity meas., in hypersonic flame spraying of WC-Co 4-81353  
 particle velocity meas. using optical fibre device (*Japanese*) 4-78297  
 plasma jet particle velocity and size distrib. meas. by laser Doppler velocimetry 4-84076  
 pulsed laser measurement of fluid flow, scatt. particle characts., speckle velocimetry vs. particle image velocimetry 4-83963  
 pulsed laser velocimetry, 2-D particle displacement meas. using orthogonal compression and 1-D anal. techniques 4-83962  
 reorganization of a fluid flow downstream from a curved pipe (*French*) 4-69825  
 review (book contrib.) 4-79687  
 shear flow, laser velocimeter sampling bias and its correction, expt. verification 4-103444  
 speckle photography and particle image velocimetry, photographic film noise 4-113076  
 swirl combustor flow meas. with and without combustion 4-103436  
 time-of-flight velocimeter, turbulence effect on focused laser beam propag. 4-89994  
 turbulent combustion, in premixed flame, theory and expt. 4-103429  
 unsteady reacting muzzle exhaust flow, flow field and vel. meas. 4-60563  
 wind meas. with coherent laser radar at 10 micron 4-107685

**laser windows** see *laser accessories; optical elements***lasers**

- see also *chemical lasers; distributed Bragg reflector lasers; distributed feedback lasers; dye lasers; excimer lasers; free electron lasers; gas lasers; laser beams; laser frequency stability; laser tuning; liquid lasers; nuclear pumped lasers; Raman lasers; ring lasers; solid lasers; X-ray lasers*  
 accomplishments at Hughes Aircraft Company, review 4-90322  
 conference on lasers, Beijing, China (May 1980) 4-63396  
 development and applications at AT&T Bell Labs., review 4-90321  
 development and applications at MIT Lincoln Lab. 4-90325  
 developments made by IBM, 1960 to present, review 4-90323  
 electron beams for electron-beam lasers 4-74532  
 FIR lasers, slab and cylindrical, waveguide continuous modes 4-87310  
 historical perspective 4-90340  
 IR and MM waves, conf., Miami Beach, FL, USA (Dec. 1983) 4-73154  
 material research in China 4-69429  
 phase conjugate lasers, config. and operation 4-74624  
 quantum electronics, ideas and stumbling blocks 4-91427  
 standard photoelectric measurement facility, for pulsed laser emission meas. 4-101890  
 sub-T<sub>1</sub> optical pulse generation appl. to optically pumped far-IR lasers 4-79171  
 Thirteenth international quantum electronics conf., Anaheim, CA, USA (Jun. 1984) 4-86105  
 types, industrial material processing applications 4-107661
- latent heat**  
 see also *heat of fusion; heat of sublimation; heat of vaporisation*  
 heat storage equipment for solar energy, transient heat transfer anal. 4-66792  
 hybrid desiccant air conditioning systems for commercial buildings, performance influencing factors 4-72166  
 solar desiccant air-conditioner using heat exchangers and humidifiers 4-72164  
 space heating using latent heat thermal storage heat pumps 4-62386
- latent heat of adsorption** see *heat of adsorption*  
**latent heat of combustion** see *heat of combustion*  
**latent heat of crystallisation** see *heat of crystallisation*  
**latent heat of dissociation** see *heat of dissociation*  
**latent heat of formation** see *heat of formation*  
**latent heat of fusion** see *heat of fusion*  
**latent heat of mixing** see *heat of mixing*

**latent heat of reaction** see *heat of reaction***latent heat of solution** see *heat of solution***latent heat of sublimation** see *heat of sublimation***latent heat of transformation** see *heat of transformation***latent heat of vaporisation** see *heat of vaporisation***latent image** see *photographic process***lattice constants**

- see also *crystal atomic structure*  
 alkali metals, lattice props., Heisenberg Hamiltonian studies 4-108501  
 benzyldiene-amino-4'-cyanobiphenyls, smectic C<sub>2</sub> struct. and solid polymorphism 4-60825  
 betaine borate, ferroelastic phase transition 4-61072  
 binary solid solutions, high conc., lattice dilatation 4-75410  
 blue phase liq. cryst. mixtures, lattice parameters, Bragg refl. obs. 4-88089  
 chalcopyrite type E1, phases, lattice constns. and Pearson plots 4-75352  
 cholesteric blue phase 1, cryst. habit 4-103735  
 close-packed ordered alloys lattice constns., Pauling-Simon law 4-75365  
 commensurate lattices, higher-order, orientational stability 4-103947  
 convergent beam diffr., lattice parameter and cryst. symmetry appls. (*French*) 4-88041  
 convergent beam electron diffraction, recent developments 4-88042  
 cyclotrimethylene-trinitramine single cryst., density and thermal expansion 4-88222  
 diamond, cohesive and struct. props. ab initio LCAO calc. 4-60881  
 fluorite struct. oxides, O ion conc., dopant size effects 4-70446  
 fractal lattices, connectivity dimension for square and triangular lattices 4-86349  
 graphite-alkali metal intercalation cpds. stage-one, Thomas-Fermi density functional theory 4-92131  
 heulandite, natural and partially dehydrated, struct., neutron diffr. studies 4-103720  
 IN-738LC, Ni-base superalloy, precip. of  $\beta$  phase in  $\gamma$  particles 4-114559  
 ionic solids, spin-orbit fine struct. of vacancy-trapped electrons, host-lattice effects 4-70147  
 linked cluster expansions, free multiplicities and weak lattice constants 4-114080  
 measurement, X-ray interferometry applications (*Japanese*) 4-86515  
 measurement using X-ray double cryst. method 4-103606  
 metals, self-diffusion and melting, thermodynamic relations 4-70432  
 metals, surfaces, impurities and defects, embedded atom method 4-92590  
 noble metals, lattice props., Heisenberg Hamiltonian studies 4-108501  
 phosphate group interactions, cryst. refined H-bond pots. 4-60879  
 pTS, lattice props. as function of polymer content 4-75321  
 rare earth aluminates, solid state reaction prep. and struct. 4-92186  
 rare earth mixed valence cpds., struct. props. 4-70751  
 refinement from two-circle diffractometer meas. 4-108251  
 rigid ion lattice models anal. and lower mantle elastic props. 4-72551  
 salol, solid-liq. interface props., dynamic light scatt., thermal diffusivity, lattice const. 4-109203  
 sodium cadmium formate, thermal expansion, X-ray powder diffr. study 4-103975  
 soft X-ray absolute wavelength values from intrinsic cryst. props. 4-84124  
 spinels, cations interaction on octahedral and tetrahedral sites 4-79975  
 steel, high speed, powders, morphology and struct. of splat caps (*German, English*) 4-71615  
 steel, Mn-Al, austenitic precipitation, fine structure after annealing (*Russian*) 4-104787  
 structure factor and magnetization, simple cubic Ising model 4-95334  
 synchrotron topography of growth defects 4-65212  
 TCNQ salts, elec. mag. and struct. characterisation 4-88162  
 transition metals, multi-ion interaction using empirical N-body pot. 4-103695  
 tricosane-tetracosane, binary paraffin, X-ray diffr. and calorimetric study 4-88161  
 zinc phthalocyanine film, charge transfer complex with piperidine, unit cell constns., crystal habit 4-88425  
 Ag, soft surface vibr. of fine particles 4-61201  
 Ag-Cd-In alloys, X-ray determ. of mean Debye-Waller factors, vibr. amp. and Debye temp. 4-84358  
 Ag-La(Ce) (Pr) (Nd) (Gd), solid solubility, metastable extension (*Chinese*) 4-61918  
 AgCl(Br), interaction pots. and van der Waals forces 4-98058  
 AgCl(Br), ion polarisability, lattice const. and exciton energies 4-113387  
 Ag<sub>2</sub>PbNb<sub>10</sub>O<sub>30</sub>, ferroelec. struct. and piezoelec. props. 4-65963  
 Al, crystallographic transitions and equilb. props., Gaussian-orbitals calcs. 4-92353  
 Al-Zr-Mg-Cu-Mn, supersaturation of Mn solid soln. 4-61935  
 Al<sub>6</sub>F<sub>3</sub>O<sub>15</sub>, Jeremejevitze, cryst. struct. refinement 4-92173  
 $\alpha$ -Al<sub>2</sub>O<sub>3</sub>, high-temperature thermal expansion standard, neutron diffr. meas. 4-103972  
 AlP(As)(Sb), high-pres. phase transition 4-88283  
 Al<sub>2</sub>SiC<sub>4</sub> mixed carbide, prep. and struct. studies 4-88144  
 Au small particles, crystalline struct., STEM microdiffraction studies 4-108305  
 Au, soft surface vibr. of fine particles 4-61201  
 B<sub>2</sub>C, hardness and fracture toughness rel. to stoichiometry 4-62019  
 BaPb<sub>1-x</sub>Bi<sub>x</sub>O<sub>3</sub> perovskite supercond., transition temp., substitution effects 4-104341  
 Ba<sub>2</sub>Sr<sub>1-x</sub>F<sub>2</sub> lattice-matched single cryst. film growth on InP (001) by MBE 4-70582  
 BeO, structural and electronic props., phase transform., pseudopotential calcs. 4-70100  
 Bi-Se-Te system, struct. and band gap, X-ray and IR absorpt. obs. 4-104124  
 Bi<sub>100-x</sub>Sb<sub>x</sub> mould grown cryst., component distrib., X-ray study 4-75694  
 C, BC-8 crystal phase, struct. props., phase stability and phase transistors 4-113389  
 Ca(OH)<sub>2</sub>, brucite-like, struct. and IR relations 4-79996  
 Cd<sub>1-x</sub>Mn<sub>x</sub>Te-CdTe multilayers grown by MBE 4-88976  
 Cd(OH)<sub>2</sub>, brucite-like, struct. and IR relations 4-79996  
 CdTe thin layers, crystal and energy structures for photoelectric transducers 4-98298  
 Ce(In<sub>1-x</sub>Sn<sub>x</sub>)<sub>3</sub>, intermediate valence study 4-61340  
 CeO<sub>2</sub>-CaO solid solutions, elec. cond., temp. depend., 400-1200°C 4-61142  
 CeO<sub>2</sub>-Ln<sub>2</sub>O<sub>3</sub> (Ln=La, Nd, Sm, Gd, Er, Y) solid solutions, elec. cond., temp. depend., 400-1200°C 4-61142

## lattice constants continued

- Co,MnAl(Si), spin echo study of hyperfine interactions 4-71209  
 Co(OH)<sub>2</sub>, brucite-like, struct. and IR relations 4-79996  
 CoRh<sub>2</sub>Ga<sub>2</sub>O<sub>4</sub>, oxide spinel solid soln., cation distrib. study 4-80016  
 Co,Zn<sub>1-x</sub>Al<sub>2</sub>O<sub>4</sub>, oxide spinel solid soln., cation distrib. study 4-80016  
 Cs<sub>2</sub>Ca(Nb<sub>2</sub>)<sub>2</sub>H<sub>2</sub>O<sub>4</sub>, cryst. struct., X-ray diff. studies 4-92164  
 CsO-Al<sub>2</sub>O<sub>3</sub>-TiO<sub>2</sub> system, phase stability, TGA and DTA obs. 4-71642  
 Cu clusters on graphite, valence bands and core levels, XPS, Auger and EELS studies 4-113860  
 Cu powder, nonequilibrium vacancy formation during plastic flow (*Russian*) 4-80030  
 Cu, soft surface vibr. of fine particles 4-61201  
 Cu ternary sulphides and selenides, symmetry and dislocations, electron microscopy studies 4-95580  
 Cu-Ag isovalent solid soln., elastic core effects, EXAFS studies 4-60886  
 Cu-In, precip. of  $\delta$ -phase on ageing 4-81201  
 Cu-Ni-Si, cellular precip., effect of B and P additions 4-66342  
 Cu, Mg<sub>1-x</sub>Al<sub>2</sub>O<sub>4</sub>, oxide spinel solid soln., cation distrib. study 4-80016  
 Dy<sub>2</sub>(Fe<sub>1-x</sub>Al<sub>x</sub>)<sub>2</sub>, pseudobinary intermetallic cpd., mag. props. 4-71032  
 Dy<sub>2</sub>Si<sub>3</sub>, low-temp. phase transitions and mag. ordering 4-71071  
 Eu-Pd-P<sub>2</sub>, valence state of Eu and unit-cell vol. anomaly 4-104174  
 Eu<sub>2</sub>Ni<sub>10</sub>B<sub>4</sub>B<sub>6</sub> foil, amorphous-cryst. transition, elec. resist. variations 4-65182  
 Fe(OH)<sub>2</sub>, brucite-like, struct. and IR relations 4-79996  
 Ga-Al-As system, MOVPE, current status for optoelectronic appls. 4-104737  
 GaAs<sub>1-x</sub>P<sub>x</sub>/GaP superlattices, strain depth profiles, misfit dislocations obs 4-104095  
 Ga<sub>2</sub>In<sub>1-x</sub>As<sub>2x</sub>P<sub>1-2x</sub> layer on InP:Sn substrate, linear thermal expansion coeff. meas. 4-75709  
 GaS<sub>3</sub>, charge density wave depinning and nonlinear transport 4-70790  
 (GaSb)<sub>1-x</sub>(Ge<sub>2</sub>)<sub>x</sub> semicond. alloys, phase transforms. 4-92347  
 Gd<sub>2</sub>Si<sub>3</sub>, low-temp. phase transitions and mag. ordering 4-71071  
 Ge, electronic and structural props., non-local density functional theory 4-108760  
 Ge<sub>20</sub>Te<sub>80</sub> glass, elec. cond. transition, press. and temp. depend. 4-98619  
 H<sub>2</sub>UO<sub>3</sub> H-insertion cpd., unit cell const., IR spectra and X-ray diff. studies 4-84267  
 HZr<sub>2</sub>P<sub>2</sub>O<sub>7</sub>, and related cpds., prep. and props. 4-104745  
 HfO<sub>2</sub>-Yb<sub>2</sub>O<sub>3</sub> system, phase equilibria and ordering, X-ray diff. and thermal expansion obs. 4-66317  
 HoC<sub>2</sub>, tetragonal cryst. struct., neutron diff. studies 4-108322  
 InAs<sub>1-x</sub>P<sub>x</sub>, LEC growth and characterisation 4-99302  
 KBr<sub>1-x</sub>(CN)<sub>x</sub>, dipole glass phase, dielec., thermal, elastic, and struct. props. (*Japanese*) 4-104525  
 KCdF<sub>3</sub>, phase transitions and cryst. struct. 4-84379  
 KH<sub>2</sub>PO<sub>4</sub>, ferroelectric, phase transition at T=110°C 4-76389  
 K<sub>1-x</sub>Li<sub>x</sub>TaO<sub>3</sub>, dipole glass phase, dielec., thermal, elastic, and struct. props. (*Japanese*) 4-104525  
 KMg<sub>2</sub>Si<sub>3</sub>AlO<sub>10</sub>F<sub>2</sub>-BaO<sub>2</sub>Mg<sub>2</sub>Si<sub>3</sub>AlO<sub>10</sub>F<sub>2</sub> system, solid solns., lattice const., melting temp. 4-109384  
 (K<sub>1-x</sub>Na<sub>x</sub>)<sub>0.8</sub>(Sr<sub>1-x</sub>Ba<sub>x</sub>)<sub>0.8</sub>Nb<sub>2</sub>O<sub>6</sub>, single cryst. growth and phys. props. 4-76352  
 K<sub>2</sub>Pb<sub>2</sub>Nb<sub>10</sub>O<sub>30</sub>, ferroelec. struct. and piezoelec. props. 4-65963  
 K<sub>2</sub>V<sub>8</sub>S<sub>8</sub>, prep., cryst. struct., and props. 4-84269  
 LaB<sub>6</sub>, X-ray reflections intensity, nonstoichiometry effect 4-61099  
 LaH<sub>3</sub>, normal and deuterated, cubic-tetragonal transition, X-ray diff. studies 4-80222  
 LaNiO<sub>2</sub>, struct. and Ni<sup>+</sup> local environment, X-ray diff. and EXAFS studies 4-69091  
 Li, muon interactions with lattice defects, mol. cluster calcs. 4-65255  
 LiH, ground-state props., LCAO HF study using polarisable basis set 4-60882  
 Li<sub>2</sub>Mo<sub>2</sub>Se<sub>8</sub>, Li intercalation model, mean-field lattice gas 4-70098  
 Li<sub>2</sub>NiP<sub>2</sub>Se<sub>6</sub>, prep. and structural studies, powder X-ray diff. studies 4-113421  
 $\beta$ -Li<sub>2</sub>O-Na<sub>2</sub>O-Al<sub>2</sub>O<sub>3</sub>, water absorpt., TG, DSC and X-ray meas. 4-113794  
 Mg-Zn isovalent solid soln., elastic core effects, EXAFS studies 4-60886  
 MgAl<sub>2</sub>Fe<sub>2-x</sub>O<sub>4</sub>, Mossbauer study of spin struct. 4-84875  
 MgAl<sub>2</sub>O<sub>4</sub> spinel, order-disorder transition at high temp. 4-92125  
 Mg(OH)<sub>2</sub>, brucite-like, struct. and IR relations 4-79996  
 Mn-Ge, Invar type, antiferromag., transition metal influence on props. (*Japanese*) 4-65826  
 Mn<sub>11</sub>Ge<sub>8</sub>, cryst. struct. and lattice const. temp. depend. 4-103702  
 MnO-ZnO solid solutions, diffuse reflectance spectra, struct. 4-76488  
 Mn(OH)<sub>2</sub>, brucite-like, struct. and IR relations 4-79996  
 MnRhAs, antiferromagnetic-ferromagnetic transition, mag. props., elec. resist. meas. 4-104417  
 Mo, FCC needle crystals, Auger and electron diff. studies 4-92584  
 Mo-V solid solutions, molecular beam deposition in vacuum, phase form, lattice parameters 4-93222  
 N<sub>2</sub>-Kr solid mixtures, phase diagrams, X-ray study (*Russian*) 4-84372  
 (NH<sub>4</sub>)<sub>2</sub>CoCl<sub>4</sub>, commensurate-commensurate phase transitions 4-75667  
 NaFeP<sub>2</sub>O<sub>7</sub>, crystallographic, mag. and Mossbauer studies 4-108323  
 Na<sub>1-x</sub>Hf<sub>2</sub>Si<sub>2</sub>P<sub>2</sub>O<sub>13</sub>, Na<sup>+</sup> ion cond. and crystallographic cell characterisation 4-113706  
 NaMoO<sub>3</sub>F, single cryst., new oxyfluoromolybdate, synthesis and growth 4-76663  
 Na<sub>2</sub>WO<sub>3</sub>, compressibilities and high-press. phase transitions 4-88276  
 Nb-Sn A15 alloys, struct. and supercond. props. 4-104344  
 Nb<sub>2</sub>Al-based ternary supercond. A-15 phases, vol. depend. of T<sub>c</sub> 4-92846  
 Nb<sub>2</sub>SnH<sub>3</sub> ternary supercond. A-15 phases, vol. depend. of T<sub>c</sub> 4-92846  
 NbZr multilayers, struct. and superconductivity 4-70594  
 Ni powder, nonequilibrium vacancy formation during plastic flow (*Russian*) 4-80030  
 Ni-base superalloys, struct. and space groups by convergent beam electron diff. 4-88132  
 Ni-based superalloys, precipitate/matrix lattice mismatch, temp. depend. 4-80430  
 Ni-Cr-Co-Al-Ti-Nb-W-Mo-V-Hf, cryst. lattice periods mismatch determ. 4-65219  
 Ni-Fe, low temp. lattice parameters 4-108306  
 Ni-Mo-B system, phase relationships at 1223K 4-104767  
 Ni-P amorphous, hexagonal metastable phase formed during crystallisation (*Chinese*) 4-103698  
 Ni-W-B system, phase relationships at 1223K 4-104767  
 NiGa<sub>4</sub> vacancy controlled  $\gamma$ -brass phase, struct. determ. 4-60885  
 Ni<sub>2</sub>MnIn Heusler alloy, elec. resist. and magnetisation 4-92695  
 Ni<sub>2-x</sub>MnSb, chemical order and mag. props. 4-88666  
 Ni(OH)<sub>2</sub>, brucite-like, struct. and IR relations 4-79996

## lattice constants continued

- Ni<sub>3</sub>(PO<sub>4</sub>)<sub>2</sub>-based solid solns., crystallographic studies, X-ray and neutron diff. studies 4-92178  
 NiS:transition metals, first-order mag. and elec. transition, impurity effects 4-92909  
 Ni<sub>1-x</sub>Zn<sub>x</sub>Fe<sub>2</sub>O<sub>4</sub> ferrite, mag. props., Fe<sup>2+</sup> ion effects 4-109035  
 $\alpha$ -O<sub>2</sub>, solid, high press. props. 4-61066  
 PZT, lattice site of Zn, Sc, Fe ions, X-ray anal. 4-75488  
 Pb, soft surface vibr. of fine particles 4-61201  
 Pb-Au dil. solutions, bulk equilib. lattice parameters, neutron diff. meas. 4-75372  
 Pb-Au dilute solutions, single, cryst., struct. in quenched state, X-ray and neutron diff. studies 4-75371  
 (Pb<sub>0.75</sub>Ca<sub>0.25</sub>)(Mg<sub>1/3</sub>Nb<sub>2/3</sub>)<sub>0.0625</sub>Ti<sub>0.9375</sub>O<sub>3</sub>:Mn ceramics, US, elastic and dielec. props. 4-104543  
 Pb<sub>2</sub>CrO<sub>3</sub>, cryst. struct. determ. 4-65245  
 Pb<sub>1-x</sub>Eu<sub>x</sub>Te, MBE growth and elec. and optical props. 4-81142  
 Pb<sub>2</sub>P<sub>2</sub>Se<sub>6</sub>, far IR, IR and Raman spectra, crystal struct. and vibr. spectra (*German*) 4-70073  
 PbSO<sub>4</sub>-PbO, high temp.  $\beta$  phase, struct. study (*French*) 4-98065  
 Pb<sub>1-x</sub>Sn<sub>x</sub>Se, thin film, unit cell parameters, phase composition 4-61249  
 p-Pb<sub>0.8</sub>Sn<sub>0.2</sub>Te/n-PbSe<sub>1-x</sub>Te<sub>x</sub> heterojunction photodiodes, LPE and elec. props. 4-88575  
 PbTe-Ga, elec. and optical meas. (*Russian*) 4-84636  
 Pd-ir-Pt(Rh), phase equilib. of Pt metals at 1400°C 4-71637  
 Pd<sub>7</sub>Au<sub>3</sub>Si<sub>13</sub>, amorphous alloy, cryst., SAXS study 4-65186  
 PrAlO<sub>3</sub>Gd<sup>3+</sup>, order parameter behaviour, EPR study 4-70076  
 Pt-Pd-Rh-ir, phase equilib. of Pt metals at 1400°C 4-71637  
 Pt-Rh-Pd(Ir), phase equilib. of Pt metals at 1400°C 4-71637  
 Pu alloys, lattice correspondence of  $\delta$ - $\alpha$  displacive transform. 4-75351  
 Rb<sub>1-x</sub>(NH<sub>4</sub>)<sub>x</sub>H<sub>2</sub>PO<sub>4</sub>, dipole glass phase, dielec., thermal, elastic, and struct. props. (*Japanese*) 4-104525  
 Rb<sub>2</sub>Pb<sub>2</sub>Nb<sub>10</sub>O<sub>30</sub>, ferroelec. struct. and piezoelec. props. 4-65963  
 Rb<sub>2</sub>ZnBr<sub>4</sub>, modulated-cell parameters, morphological determ. 4-92122  
 Re-Al alloys, phase relations and cryst. struct., X-ray diff. studies 4-70066  
 Re<sub>2</sub>P, cryst. struct. determ. 4-80009  
 Rh-Ru-Pd(Ir), phase equilib. of Pt metals at 1400°C 4-71637  
 Ru-Rh system, constitution, solid solubility and lattice const. 4-70390  
 SbCl<sub>3</sub>-graphite intercalation cpd., lattice expansion, phase transition effects, X-ray diff. studies 4-98076  
 Sb<sub>2</sub>MoO<sub>6</sub>, cryst. struct., X-ray and powder neutron diff. studies 4-108334  
 Sb<sub>2</sub>O<sub>3</sub>Cl<sub>2</sub>, onoratoite, pure and hydrated, cryst. structs. and twin planes 4-113407  
 SbTeI, cryst. struct., full matrix least squares refinement 4-92168  
 Sc<sub>2</sub>OC, prep. and struct. props., powder diff. studies 4-71608  
 Se, MBE growth on cleaved Te, RHEED, AES and LEELS characterisation 4-99343  
 Si, BC-8 crystal phase, struct. props., phase stability and phase transistors 4-113389  
 Si, electronic and structural props., non-local density functional theory 4-108760  
 Si, lattice parameter and thermal expansion coeff. between 300 and 1500K 4-88316  
 Si single crystal, unit cell parameters determ. (*German*) 4-79980  
 SiAs, ion implanted and laser annealed, struct. changes, X-ray diff. study 4-75461  
 Si/CaF<sub>2</sub> heterostructure interface, MBE growth, Raman spectra studies 4-98462  
 SiC cubic single cryst., CVD prep. and elec. props. 4-99345  
 SiC, lattice imaging of 201R polytype 4-75384  
 SiC powders, prep. from glass and C black, lattice constants 4-109365  
 SiC-AlN solid solution, Si<sub>3</sub>Al<sub>2</sub>N<sub>3</sub>C<sub>2</sub> and Si<sub>3</sub>Al<sub>2</sub>C<sub>3</sub> cpds. 4-66316  
 SiP<sub>2</sub>, struct. parameters and valence electron density distrib. 4-108331  
 Sn thin film, struct. and transformations during vacuum heating, RHEED and Mossbauer studies 4-75818  
 Sn-In (8.0 to 9.5 at.%), phase transform. 4-109395  
 Sr<sub>2</sub>Al<sub>2</sub>Sb<sub>6</sub>, Zintl phases with complex anions (*German*) 4-70067  
 Sr<sub>2</sub>Al<sub>2</sub>SiO<sub>7</sub>, synthetic Sr-gehlenite, cryst. struct. 4-108333  
 SrZn<sub>2-x</sub>Co<sub>x</sub>Fe<sub>16</sub>O<sub>27</sub> hexaferrite, mag. and crystallographic studies 4-88697  
 Tb<sub>2</sub>Si<sub>3</sub>, low-temp. phase transitions and mag. ordering 4-71071  
 Te phosphides, crystal struct. determ. 4-80010  
 Ti<sub>2</sub>Nb<sub>2</sub>Mo<sub>2</sub>Si<sub>4</sub>, melt spinning and phase transforms 4-114450  
 TiO<sub>2</sub>, polymorphic transition. by mech. grinding 4-66328  
 Ti ternary chalcogenides, cryst. struct., X-ray, IR and photoacoustic studies 4-84273  
 Ti-based quaternary chalcogenide 4-84270  
 TiNO<sub>2</sub>, dipole glass phase, dielec., thermal, elastic, and struct. props. (*Japanese*) 4-104525  
 Ti(SbAs)<sub>2</sub>Si<sub>16</sub>, pierrotite, cryst. struct., least squares determ. 4-92171  
 Ti<sub>2</sub>SeO<sub>4</sub>, phase transition and lattice const., X-ray diff. study 4-71294  
 UGaCo, mag. props., temp. depend. 4-71033  
 UPT<sub>3</sub> whiskers, unusual form. and morphology, screw dislocation growth mechanism 4-98496  
 U<sub>2</sub>Th<sub>1-x</sub>Se solid solns., mag. props. and lattice parameters meas. 4-104419  
 V<sub>2</sub> Si-based ternary supercond. A-15 phases, vol. depend. of T<sub>c</sub> 4-92846  
 $\delta$ -VN<sub>2</sub>, N<sub>2</sub> partial press.-temp.-comp. relations 4-70401  
 V<sub>1-x</sub>Te<sub>x</sub>, cryst. struct., X-ray diff. studies 4-108324  
 W, total energy full potential linearised APW method 4-104143  
 W-Mo solid solutions, molecular beam deposition in vacuum, phase form, lattice parameters 4-93222  
 YC<sub>2</sub>, tetragonal cryst. struct., neutron diff. studies 4-108322  
 Y<sub>2</sub>Ho<sub>1-x</sub>C<sub>2</sub>, tetragonal cryst. struct., neutron diff. studies 4-108322  
 YIG:Ca films, charge compensation mechanism, annealing effects, behaviour on treatment with oxidising and reducing solns. 4-80799  
 YIG:Ca films, surface layer contraction, X-ray diff. and magneto-optical studies 4-61262  
 Y<sub>2</sub>O<sub>3</sub>-Nb<sub>2</sub>O<sub>5</sub> system, cubic solid soln. region 4-76772  
 $\beta$ -ZnP<sub>2</sub>, X-ray study of phase transitions 4-84835  
 ZnP<sub>2</sub> single crystals grown by recrystallisation, morphological and structural properties 4-113369  
 ZnS-CdS system, solid solns. and phase transforms. under hydrothermal conditions 4-98264  
 Zr-based Friauf-Laves phases, lattice const. and H absorption capacities 4-84234  
 Zr<sub>2</sub>Be<sub>7</sub>, cryst. struct., X-ray diff. studies 4-113404  
 ZrH<sub>2</sub>, electronic struct., tetragonal distortion, X-ray diff. and PMR study 4-84858

**lattice constants continued**

ZrN powder, prep. from  $\text{ZrCl}_4\text{-N}_2$  system using reducing agents (Japanese) 4-76720  
 $\text{Zr}_2\text{Nb}_3\text{Ge}_4$ , crystal struct., X-ray diffr. studies 4-113393

**lattice defects** *see crystal defects***lattice diffusion** *see diffusion in solids***lattice dynamics**

*see also crystal surface and interface vibrations; displacive transformations; Gruneisen coefficient; lattice dynamics of covalent crystals; lattice dynamics of ferroelectric crystals; lattice dynamics of ionic crystals; lattice dynamics of metallic crystals; lattice dynamics of molecular crystals; lattice localised modes; lattice phonons; soft modes; vibrational states in disordered systems*

alkali metal pyrophosphates,  $\text{M}^{\text{I}}\text{M}^{\text{II}}\text{P}_2\text{O}_7$ , vibr. spectra and crystal struct. 4-65247

correlated Einstein model for the equilibrium properties of solids 4-70293  
 crystal Green's functions in complex energy plane, analytical tetrahedron method 4-60996

dislocation-point defect interaction, lattice dynamics model 4-103786  
 elastic and ferroelectric properties, lattice and spin dynamical theories 4-76357

excitation spectrum for vibr. on percolating network, effective medium approx. 4-70294

homogeneous solid, lattice dynamics and elastic wave propagation 4-80175

instability phenomena in crystal under external force, continuum approx. of self-consistent Einstein model 4-88247

iodates, NQR parameters and internal field symm. (Russian) 4-114181  
 methanol- $\text{NH}_3$ , associated species, D isotope effect, vibr., Raman spectra, normal coordinate anal. 4-66035

molecular-crystal model, adiabatic limit and phonon dispersion influence 4-113553

nonlocal piezoelectricity, point charge, IR dispersion and cond. 4-80870  
 piezoelectric powders, electroacoustic echoes 4-76342

rare earth antimonates,  $\text{R}_2\text{SbO}_7$ , structural studies by vibrational spectroscopy 4-65248

surface structural phase transition, effective 2-D lattice dynamical hamiltonian 4-92484

transition metal dichalcogenides, CDW transitions and lattice vibr. (Japanese) 4-92641

two dimensional lattice, virial theorem, lattice dynamics and struct. instability (Russian) 4-68154

two-dimensional electron solids, static and dynamic props., effects of anharmonicities and broken time-reversed invariance 4-70689

X-ray and Mossbauer radiation scatt., effect of forced vibr. 4-76558  
 $\text{BaFCl}(\text{FBr})(\text{OCl})$ , far IR spectra 4-66047

$\text{Ca}_3\text{Cr}_2\text{Si}_2\text{O}_{12}$ , synthetic garnets, Cr coordination and vibr. props., IR study 4-65249

$\text{CdGa}_2\text{S}_4$ , vibr. props., polarisation depend. IR reflectivity studies 4-75624

$\text{FeS}_2$ , pyrite, Mossbauer study of lattice dynamics 4-61000  
 GaAs, isotope scatt. of large wave vector phonons 4-108564

GaAs-GaAlAs superlattices, Raman study of folded modes 4-80929  
 GaGeTe, Raman spectrum and lattice dynamics 4-80941

Ge-Si, vibrational modes and phase transition 4-88253  
 $\text{HfS}_3$ , IR, Raman, and reson. Raman spectra, valence force field 4-93077

$\text{HfTe}_5$ , lattice dynamics calc., Raman data 4-75623  
 InGaAsP, lattice matched to GaAs, lattice dynamics, Raman scatt. study 4-61673

InSb, isotope scatt. of large wave vector phonons 4-108564  
 $\text{KAlF}_4$ , structural phase transitions and lattice dynamics 4-65352

$\text{K}_4\text{UO}_2(\text{CO}_3)_3$ , photoluminescence and mol. vibr. modes 4-99164  
 $\text{MgAl}_2\text{O}_4$  spinel, anharmonic thermal vibr. of atoms up to 1933K, struct. refinement 4-65225

$\text{MgCaSiO}_4$ , vibr., force const., isotope shift, IR and Raman obs. 4-61705  
 $\text{MoS}_2\text{-2H}$ , interlayer potential and vibr. freq. 4-70298

$\text{Na}_2\text{CO}_3$ , incommensurate struct., Raman and far IR spectroscopy study 4-76449

$2\text{H-NbSe}_2$ , lattice dynamics, lattice instabilities and phonon anomalies, theoretical study 4-65353

NiTi premartensitic alloys, acoustic phonon branches, inelastic neutron scatt. studies 4-92316

$\text{RbAlF}_4$ , structural phase transitions and lattice dynamics 4-65352  
 a-Si:H, IR absorpt., gaseous  $\text{H}_2$  and Si-H overtone spectra 4-93075

$\text{SiSe}_2$ , cryst. and glassy, vibr. studies 4-109191  
 $2\text{H-TaSe}_2$ , lattice dynamics, lattice instabilities and phonon anomalies, theoretical study 4-65353

$\text{TeO}_2$  crystal, vibr. spectra, group theoretical anal. (Russian) 4-80176  
 $\text{Ti}_3\text{Al}$  and  $\text{TiAl}$ , Young's modulus and Debye temp., 300 to 1300K (Russian) 4-92281

$\text{TiO}_{0.99}$ , electron transfer and thermal vibr. parameters, X-ray diffr. study 4-92329

$\text{TiAlF}_4$ , structural phase transitions and lattice dynamics 4-65352  
 $\text{Zr}(\text{MoO}_4)_2$ , polymorphism, X-ray diffr. and vibr. spectroscopy study 4-70053

$\text{ZrTe}_3$ , lattice dynamics calc., Raman data 4-75623

**lattice dynamics of covalent crystals**

bis(pentadienyl)iron cpds., bonding, hyperfine interaction, Mossbauer effect 4-104512

diamond, cohesive and struct. props., ab initio LCAO calc. 4-60881  
 inert gas crystal, ideal, vibr. thermodynamic props., anharmonic contrib. 4-98307

ionic-covalent cryst. pot. function struct., force const. method 4-92130  
 $\text{Ge, Si-x}$  solid solutions, local and band mode freqs. 4-70307

**lattice dynamics of ferroelectric crystals**

*see also displacive transformations; soft modes*

acoustic-phonon dispersion at incommensurate phase transitions, Brillouin scatt. obs. 4-61724

ferroelectrics, lattice dynamics and phase transitions 4-80169  
 IV-VI compounds, electronic and dynamical props., book contrib. 4-61003

optical phonons, contribution to electronic transitions 4-65371  
 perovskite ferroelectrics, existence of ferroelectric phases of different symmetries 4-114221

phonon anomalies in ferroelectrics and supercond. 4-65351  
 thiourea, incommensurate phase transitions, phase mode dynamics, neutron and Raman scatt. studies 4-65966

**lattice dynamics of ferroelectric crystals continued**

tris-sarcosine calcium chloride (bromide), ferroelec. phase transition, IR and Raman studies 4-93023

$\text{Cd}_2\text{Nb}_2\text{O}_7$ , anharmonicity of thermal vibr., X-ray diffr. 4-65367  
 $\text{HCl-DCl}$ , dipolar correlation times, NQR study 4-80171

(K-Na) $\text{TaO}_3$ , dynamics of random-site interacting dipoles 4-80170  
 KCN antiferroelectric phase III, lattice dynamic calcs. 4-103890

$\text{KH}_2\text{PO}_4$ , single crystal, far IR reflectivity spectra 4-114257  
 $\text{KH}_2\text{PO}_4$ -type transition, struct. studies, review 4-76351

$\text{KNO}_3$ , lattice dynamics and anomalous Raman spectrum 4-71360  
 $\text{K}_2\text{SeO}_4$ , incommensurate phase transitions, phase mode dynamics, neutron and Raman scatt. studies, review 4-65966

$\text{KTAO}_3$ , anharmonicity of thermal vibr., X-ray diffr. 4-65367  
 $\text{KTAO}_3\text{-Li}$ , heat capacity and random field sources 4-80253

$\text{K}_2\text{ZnCl}_4$ , commensurate ferroelec. phase, phonon freq., permitt., IR refl. spectra 4-11387

$\text{K}_2\text{ZnCl}_4$ , incommensurate ferroelec., phase transitions, lattice dynamics, Raman effect 4-84922

$\text{K}_2\text{ZnCl}_4$ , noncommensurate ferroelec., lattice dynamics and transitions, Raman studies 4-92313

$\text{LiNbO}_3$ , stimulated Raman scatt. by transverse and longit. lattice vibr. 4-60115

$\text{LiTaO}_3$ , stimulated Raman scatt. by transverse and longit. lattice vibr. 4-60115

$\text{NH}_4\text{HSeO}_4$ , ferroelec. transitions, Raman scatt. and vibr. props. 4-93066  
 $\text{NaCN}$ , antiferroelectric phase III, lattice dynamic calcs. 4-103890

$\text{NaNbO}_3$ , orientationally disordered paraelec. phase, phonon-orientational coupling 4-70295

(Pb, Sn, Ge)Te, semicond., dielec. props. and soft modes, review, book contrib. 4-61622

$(\text{Pb}_{0.22}\text{Ba}_{0.78})\text{Ti}_3$ , ferroelec., phase-transition, high press. Raman study 4-76451

$\text{Pb}(\text{Fe}_{0.5}\text{Nb}_{0.5})\text{O}_3$ , anharmonicity of thermal vibr., X-ray diffr. 4-65367  
 $\text{Pb}(\text{Fe}_{0.5}\text{Ta}_{0.5})\text{O}_3$ , anharmonicity of thermal vibr., X-ray diffr. 4-65367

$\text{Pb}_2\text{GeO}_7$ , crystals, Raman scatt. near phase transition, isofrequency temp. depends. 4-66043

$\text{Pb}_2\text{GeO}_7$ , lattice dynamics near Curie point (Russian) 4-98221  
 $\text{Pb}(\text{Ti}_{0.9}\text{Sn}_{0.1})\text{O}_3$ , ferroelec., phase-transition, high press. Raman study 4-76451

$\text{Rb}_2\text{ZnCl}_4$ , incommensurate ferroelec., phase transitions, lattice dynamics, Raman effect 4-84922

$\text{Rb}_2\text{ZnCl}_4$ , noncommensurate ferroelec., lattice dynamics and transitions, Raman studies 4-92313

$\text{Sn}_2\text{P}_{25}$ , influence of hydrostatic pressure on vibrational spectra 4-109192

$\text{Sn}_2\text{Te}_6$ , low freq. lattice vibr. in IR spectra 4-71389

**lattice dynamics of ionic crystals**

alkali halides, elastic const. and force const., bond deform. model 4-61034

alkaline earth oxides, elastic const. and force const., bond deform. model 4-61034

Coulomb coeffs. matrix for electrostatic interactions 4-92321  
 covalent-ionic cryst. pot. function struct., force const. method 4-92130

effective ionic charge, press. depend. 4-103692  
 Faraday effect due to mag. moments of optical phonons 4-66017

lanthanide oxyhalides, Matlockite-type struct., lattice dynamics calcs. 4-108560

lattice and thermodynamic props., overlap repulsion pot. 4-92327  
 AgI, chaotic attractors,  $\beta\text{-}\alpha$  transition phenomena 4-61140

AgI, disorder-induced Raman scatt., vibr. dynamics 4-71392  
 $\text{BaF}_2$ , fluorite struct., inner displacement, internal strain tensor, lattice dynamic models 4-92315

$\text{BaFBr}$ , Matlockite-type struct., lattice dynamics calcs. 4-108560  
 $\text{BaFCl}$ , Matlockite-type struct., lattice dynamics calcs. 4-108560

$\text{CaF}_2$ , fluorite struct., inner displacement, internal strain tensor, lattice dynamic models 4-92315

KCl:Li, optically excited colour centres, relaxation dynamics 4-113896  
 LiKSO<sub>4</sub>, phonon dispersion relation calcs. 4-70308

$\text{NH}_4\text{Br}$ , model calcs. for phonons 4-84353  
 $\text{NH}_4\text{Cl}$ , model calcs. for phonons 4-84353

$\text{NH}_4\text{F}$ , model calcs. for phonons 4-84353  
 $\text{NH}_4\text{I}$ , model calcs. for phonons 4-84353

NaF, lattice dynamics, perturbation-theoretical-model calc. in Watson pot. approx. 4-61020

$\beta\text{-PbF}_2$ , point defect stability, computer simulation 4-103744  
 RbBr, acoustic-mode Gruneisen parameters, inelastic neutron scatt. study 4-80187

RbCl, first-order Raman scatt. due to F-centres 4-93076  
 RbF, lattice dynamics, perturbation-theoretical-model calc. in Watson pot. approx. 4-61020

$\text{SrF}_2$ , fluorite struct., inner displacement, internal strain tensor, lattice dynamic models 4-92315

**lattice dynamics of metallic crystals**

A15 compound, phonon dispersion curves and electron-phonon interaction calcs. 4-70313

cubic alloy, vibr. entropy due to order-disorder transition 4-113668  
 metals, amorphous non-transition, superconductivity and phonon spectra (Chinese) 4-98793

phonon states of metallic compounds, disordered alloys, data compilation 4-73178

thermal diffuse scattering and Fourier analysis of charge and spin density 4-76113

transition metals, BCC, lattice dynamics local field correction, soft mode shapes 4-80180

Ag thin film, interference fringes intensity of X-ray diffr. line profiles 4-75799

Al FCC crystal, force const. between interstitial H atoms and host atoms 4-75629

Al, FCC metal lattice dynamics, nine-parameter model, specific heats 4-75625

Al, lattice dynamics, second-order perturbation theory 4-92320  
 Al, melting curve study at high press. 4-103911

Al, transverse thermal vibrations and strength 4-80178  
 Ca, lattice dynamics, model-potential approach 4-61022

Cd, X-ray diffr. data, anharmonic parameters 4-84233  
 CeMg, antiferromag. cpd., magnons and phonons 4-84777

Co, FCC cryst., phonon dispersion, multipole interactions 4-61018  
 Co Kramers-Kronig relation of measured atomic scatt. factors 4-98063

Cs, phonon frequencies, Debye temp., Gruneisen parameter, transport props., lattice dynamical model 4-108561

- lattice dynamics of metallic crystals continued**
- As, solid and liq., Grueneisen parameter at high press., nature of isostructural electronic transition 4-61035
  - Cs-K(Rb), volume effect, pure constituent, phonon dispersion relations, local and band modes, calcs. 4-98224
  - Du, FCC metal lattice dynamics, nine-parameter model, specific heats 4-75625
  - Du, Kramers-Kronig relation of measured atomic scatt. factors 4-98063
  - Du, phonon anomalies on Fermi surface maps 4-70312
  - Du-Zn-Al alloys, softened phonons, calorimetry, susceptibility and inelastic neutron scatt. study 4-75636
  - Hf, phonon density of states determ. from sp. ht. (*Russian*) 4-92314
  - Mo-Ru alloy, lattice dynamics, inelastic neutron scatt. 4-84350
  - NbH<sub>3</sub>, soft modes, X-ray Bragg intensity meas. 4-70319
  - Nb<sub>3</sub>Sn and Nb<sub>3</sub>Sb, phonon dispersion curves and electron-phonon interaction calcs. 4-70313
  - Ni, FCC metal lattice dynamics, nine-parameter model, specific heats 4-75625
  - Ni, Kramers-Kronig relation of measured atomic scatt. factors 4-98063
  - Pt, FCC cryst., phonon dispersion, multiple interactions 4-61018
  - Rb, solid and liq., Grueneisen parameter at high press., nature of isostructural electronic transition 4-61035
  - Rb<sub>1-x</sub>K<sub>x</sub>, lattice dynamics and local mode behaviour 4-84356
  - Ti, phonon density of states determ. from sp. ht. (*Russian*) 4-92314
  - VD<sub>2</sub>, soft modes, X-ray Bragg intensity meas. 4-70319
  - Yb, lattice dynamics, model-potential approach 4-61022
  - Zn, X-ray diff. data, anharmonic parameters 4-84233
  - Zr, phonon density of states determ. from sp. ht. (*Russian*) 4-92314
- lattice dynamics of molecular crystals**
- acetamide, far IR transmission spectrum, lattice dynamics, temp. 4-104598
  - antiferroelectric phase III, lattice dynamic calcs. 4-103890
  - biphenyl, solid, phonon density of states near struct. transition 4-88251
  - borates, carbonates and nitrates, intermolecular vibrational coupling, IR spectra 4-65350
  - m-chloronitrobenzene, phonon spectra lattice vibr. Raman scatt. 4-109181
  - coupled phonon vibr. and dipole plasma quanta (*Russian*) 4-104131
  - cyanogen, lattice dynamics, pot. model and zone-centre phonons 4-92310
  - cyclopropane-d<sub>0</sub>(-d<sub>2</sub>), lattice vibr. spectra and intermol. forces 4-71371
  - diiketopiperazine, cryst. vibr., normal mode. calcs. 4-84352
  - ethylene, neutron inelastic scatt. 4-70314
  - ethylene crystal, vibr. spectrum calc. 4-108557
  - ferrocene-d<sub>10</sub> cryst., thermodynamic props. 4-88307
  - glutaric acid, cryst., bonding, disorder, Raman spectrosc. investig. 4-80936
  - ices II, VIII and IX, proton ordered, lattice mode spectra, water-water pots. 4-70296
  - naphthalene, internal and external phonon interactions, intermolecular pot. 4-113557
  - naphthalene, lattice vibr., Raman intensities 4-113550
  - naphthalene, phonon harmonic dynamics, block method 4-88254
  - squaric acid, rigid layer model, Brillouin and Raman scatt., temp. and uniaxial stress depend. 4-98220
  - $\alpha$ -CO, librational motion, anharmonic effects 4-103892
  - CO, translation rot. coupling and lattice dynamics 4-98219
  - CO<sub>2</sub>, librational motion, anharmonic effects 4-103892
  - HBr, cryst., long-wavelength lattice vibr. 4-113549
  - HBr mol. crystal, lattice dynamical model in phase III, H bond strengths 4-88246
  - HCl, cryst., long-wavelength lattice vibr. 4-113549
  - HCl molecular crystal, lattice dynamical model in phase III, H bond strengths 4-88246
  - HCl(Br), lattice dynamics in low temp. phase 4-92328
  - HF mol. crystal, lattice dynamical model in phase III, H bond strengths 4-88246
  - KCN antiferroelectric phase III, lattice dynamic calcs. 4-103890
  - $\alpha$ -N<sub>2</sub>, librational motion, anharmonic effects 4-103892
  - N<sub>2</sub>O, librational motion, anharmonic effects 4-103892
  - $\alpha$ -O<sub>2</sub>, solid, high press. props. 4-61066
  - S<sub>2</sub>, orthorhombic crystal, lattice dynamical calcs., non-rigid mol. model 4-98217
- lattice energy**
- see also binding energy
  - actinide metals, light, cohesive energies calc. 4-75354
  - alkali halides, Born-Mayer parameters for next nearest neighbours 4-92127
  - alkali halides, lattice energies calc. from elastic constants 4-79971
  - alkali metal alloys, MAu (M=Li, Na, K, Rb, Cs), electronic props., self-consistent relativistic band struct. calcs. 4-92604
  - alkali metal fluorides and chlorides, solution enthalpies of divalent defects 4-98316
  - alkali metals, anharmonic effects and thermodynamic props., theory 4-61033
  - copper phthalocyanine, chlorinated, mol. energetics of epitaxial growth on KCl 4-98480
  - cubic crystals, fourth-order elastic consts. and uniaxial stresses 4-80137
  - cyanogen, lattice dynamics, pot. model and zone-centre phonons 4-92310
  - delafossite type compounds, deform. of octahedral layers (*Japanese*) 4-75606
  - graphite-alkali metal intercalation cpds. stage-one, Thomas-Fermi density functional theory 4-92131
  - ionic cryst., lattice and thermodynamic props., overlap repulsion pot. 4-92327
  - ionic solids, electron momentum densities, refinement 4-113381
  - layer cpds., Madelung consts. 4-70056
  - many-electron systems, ground state energy and X-ray scatt. cross sections 4-114344
  - metals, bulk and interfaces, pair pots. for atomistic simulations 4-113385
  - metals, surfaces, impurities and defects, embedded atom method 4-92590
  - 7-methoxycoumarin, topochem. dimerisation in solid state 4-109628
  - multimolecular systems, force field simulation of moving ions 4-79977
  - oxides, defect energetics and nonstoichiometry 4-92201
  - phosphate group interactions, cryst. refined H-bond pots. 4-60879
  - refractory compounds, phys. props. depend. on electronic struct. (*Russian*) 4-75423
  - silicate minerals, structure prediction using energy-minimisation techniques 4-84244
  - superlattice alloys, one-dimensional long-period, stability due to Madelung energy 4-60880
- lattice energy continued**
- TCNQ salts, heterofulvalene-TCNQ, cryst. struct., Madelung energy calcs. 4-70131
  - transition metal oxides, struct. prediction using energy-minimisation techniques 4-84243
  - AgCl(Br), interaction pots. and van der Waals forces 4-98058
  - Al, crystallographic transitions and equilib. props., Gaussian-orbitals calcs. 4-92353
  - Be, temp. and press. induced phase transitions 4-70369
  - C, BC-8 crystal phase, struct. props., phase stability and phase transistors 4-113389
  - Ca, FCC, phonon freqs. and binding energies, pseudopot. calc. 4-80181
  - KCl, electron momentum densities, refinement 4-113381
  - KF, electron momentum densities, refinement 4-113381
  - LaH<sub>3</sub>, cryst. struct., X-ray and neutron diff. (*French*) 4-88149
  - LiCl, electron momentum densities, refinement 4-113381
  - LiF, electron momentum densities, refinement 4-113381
  - MgO, electron momentum densities, refinement 4-113381
  - Mg<sub>2</sub>SiO<sub>4</sub>, olivine and spinel polymorphs, structural and phys. props., computer simulations 4-89912
  - Mg<sub>2</sub>SiO<sub>4</sub>, olivine and spinel forms, struct. and elastic consts., computer modelling 4-113411
  - NH<sub>3</sub> halides, struct. stability and static props. 4-98059
  - NaBr.2H<sub>2</sub>O, total lattice pot. energy calc. 4-103696
  - NaCl, electron momentum densities, refinement 4-113381
  - NaF, electron momentum densities, refinement 4-113381
  - Na<sub>2</sub>Ti<sub>2</sub>O<sub>9</sub>, electron microscopic study, struct. refinement by lattice energy minimization 4-69996
  - Ne, FCC, high press. eqn. of state, Gaussian orbital techniques 4-92332
  - Ne, low temp. eqn. of state under megabar press. 4-61042
  - Ni<sub>3</sub>Fe<sub>3-x</sub>O<sub>4</sub>, cation-site occupancy, effect of Ni content 4-98079
  - PdH<sub>x</sub>, non-stoichiometric, heat of form., cluster-Bethe lattice approx. 4-75355
  - PrO<sub>2</sub>, vacancy struct., lattice energy calcs. 4-70058
  - Pr<sub>2</sub>O<sub>3</sub>, vacancy struct., lattice energy calcs. 4-70058
  - Pr<sub>2</sub>O<sub>6</sub>, vacancy struct., lattice energy calcs. 4-70058
  - Si, BC-8 crystal phase, struct. props., phase stability and phase transistors 4-113389
  - Ta<sub>2</sub>S<sub>5</sub>, Madelung consts. 4-70056
  - TiC refractories, electronic struct., CNDO/2 calc. 4-75848
  - WC refractories, electronic struct., CNDO/2 calc. 4-75848
  - Yb-Es dilute alloys, thermodynamics, Henry's Law vaporisation studies 4-92390
- lattice gas** see lattice theory and statistics
- lattice gauge theory** see axiomatic field theory: gauge field theory
- lattice localised modes**
- see also phonon-defect interactions; phonon-impurity interactions
  - alkali halide:CN<sup>-</sup>, vibrational fluoresc., nonradiative luminesc. quenching 4-81005
  - alkali halide crystals, localised phonon mode associated with dislocations 4-70321
  - anharmonic crystals, local vibr., local instability, self-consistent harmonic approx. 4-88258
  - defect solids, free energy, lattice spectrum contrib. 4-75630
  - ice, melting of crystalline solids, US study 4-70351
  - metallic compounds and disordered alloys, phonon states, data compilation 4-73178
  - metallic solids, Debye-Waller factor for substitutional Mossbauer impurity 4-75633
  - mismatched overlayers, collective modes and dislocation ordering, mol. dynamics study 4-108555
  - molecular dynamics simulation of localised soft mode systems 4-70320
  - narrow band gap semicond., impurity recomb. accompanied by local phonon excitation 4-88516
  - polystyrene, isotactic, vibr. spectrum, mass defects effect 4-80912
  - polystyrene-d<sub>4</sub>, isotactic, vibr. spectrum, normal coord. calcs. 4-80911
  - semiconductor, electronic struct. and hyperfine interaction of muonium 4-65633
  - $\beta$ -Ag<sub>2</sub>S, Ag diffusion, inelastic neutron scatt. studies 4-75726
  - Al FCC crystal, force consts. between interstitial H atoms and host atoms 4-75629
  - CdGa<sub>2</sub>(S<sub>2</sub>Se<sub>1-x</sub>)<sub>4</sub>, mixed defect cryst., Raman scatt. 4-61688
  - CdTe:In, Li, defect complex, IR absorption studies 4-80031
  - Cs-K(Rb), volume effect, pure constituent, phonon dispersion relations, local and band modes, calcs. 4-98224
  - FeMO<sub>2</sub>S<sub>2</sub>, Chevrel-phase cpd., struct. and mag. transitions 4-76139
  - GaAs:Si, local vibr. modes and elec. activation, Raman study 4-84357
  - GaAs:Si, localised vibr. mode IR absorpt. meas. 4-104599
  - Ga<sub>2</sub>Se<sub>3</sub>, Se, layer solid solns., Raman scatt. spectra, effect of substitution-type disorder 4-99115
  - Ge<sub>2</sub>Si<sub>2-x</sub>, solid solutions, local and band mode freqs. 4-70307
  - H local vibr. spectra in metal hydrides using TOF spectrometer 4-74088
  - KCl:Ti, lattice defects creation and corrosion during annihilation of electronic excitations (*Russian*) 4-80035
  - KI:Ag<sup>+</sup>, two elastic configurations at point defect, far IR spectra study 4-61029
  - LiF, localised phonon mode associated with dislocations, thermal props. 4-70321
  - MgO:Co<sup>2+</sup>, g value, Jahn-Teller effect 4-88492
  - Mn<sub>2</sub>Zn<sub>1-x</sub>Te solid solns., weak dipole vibr., Raman scatt. studies 4-65354
  - N<sub>2</sub>, solid, exciton resonances in VUV spectra (*Russian*) 4-99134
  - NbH<sub>3</sub>, soft modes, X-ray Bragg intensity meas. 4-70319
  - Pb-Al<sub>2</sub>O<sub>3</sub>-Al junctions, ion irradi., defect vibr., supercond. tunnelling meas. 4-98826
  - PdH(D), supercond. transition temp., effect of zero-point motion 4-70973
  - PdH(D)<sub>2</sub>, vibr. spectra, neutron inelastic scatt. meas. 4-98229
  - Rb<sub>1-x</sub>K<sub>x</sub>, lattice dynamics and local mode behaviour 4-84356
  - Si, Czochralski, C in radiation damage centres, luminesc. study 4-93107
  - Si, irradiated, excitation spectroscopy on 0.79 eV (C) line defect 4-93112
  - Si:Cr(Mn)(Fe)(Co)(Ni), breathing mode relax around tetrahedral interstitial 3d impurities 4-108567
  - SiO<sub>2</sub>, isotope effects and photoluminescence spectra 4-104661
  - Si-H, bonds and H-induced defects study 4-66058
  - VD<sub>2</sub>, soft modes, X-ray Bragg intensity meas. 4-70319
  - Zn<sub>2</sub>Cd<sub>1-x</sub>Ga<sub>2</sub>S<sub>4</sub>, mixed defect cryst., Raman scatt. 4-61688

lattice mechanics *see* lattice dynamics

lattice parameters *see* lattice constants

## lattice phonons

*see also* electron-phonon interactions; lattice dynamics of covalent crystals; lattice dynamics of ferroelectric crystals; lattice dynamics of ionic crystals; lattice dynamics of metallic crystals; lattice dynamics of molecular crystals; lattice localised modes; phonon-defect interactions; phonon dispersion relations; phonon drag; phonon-exciton interactions; phonon-impurity interactions; phonon-magnon interactions; phonon-phonon interactions; phonon-plasmon interactions; polaritons; soft modes; spin-phonon interactions; tunnelling spectra; tunnelling spectroscopy

A<sup>1</sup>B<sup>VI</sup> cpds., cubic cryst., vibronic const. calcs. 4-61025

anharmonic cryst., statistical mechanics of phonons and phonon linewidths 4-70309

anharmonic temperature factors of atoms with 4 mm and 42 m site symmetries 4-113377

anthracene, density of phonon states, inelastic noncoherent neutron scatt. spectra 4-61023

anthracene crystals, reson. Raman scatt. and low temp. luminesc. formation 4-104644

anthracene-TCNB, charge transfer complexes, order-disorder and displacive transitions 4-70367

ballistic phonon transport from amplitude modulated heat pulses 4-61160

bilayer systems, p-polarised guided wave phonon-polaritons and guided wave surface phonon-polaritons 4-92629

bottleneck effects, lowering of the mag. bistability threshold 4-114151

calcium tartrate, Raman spectrum, mode assignments, permitt. meas. 4-93011

cerium ethyl sulphate, US vel. and attenuation near cooperative Jahn-Teller dilation 4-70292

m-chlorinitrobenzene, phonon spectra lattice vibrs. Raman scatt. 4-109181

complex layer struct., normal mode dispersion and spectral density, band struct. 4-113554

condensed explosives, shock-induced mol. excitation 4-80160

crystal surface, diffuse surface scatt. of thermal phonons 4-65540

crystals, neutron scatt. involving energy transfer to lattice 4-88907

crystals, nondecaying TA phonon propag. 4-92323

diamond, cohesive and struct. props., ab initio LCAO calc. 4-60881

diamond, type Ia, defect-induced one-phonon absorption 4-84981

dilaton model of thermal fluctuation crack nucleation 4-88236

direct gap semicond., stochastic self-oscillations in two-temp. electron-hole plasma 4-98656

dislocation-point defect interaction, lattice dynamics model 4-103786

distorted cryst., three wave X-ray images, numerical simulation 4-60780

excitation spectrum for vibrs. on percolating network, effective medium approx. 4-70294

ferroelectrics, optical phonons, contribution to electronic transitions 4-65371

ferroelectrics, phonon anomalies 4-65351

focusing in highly dispersive and isotopically impure crystals, theory 4-61011

freezing, density wave theory with crystal symmetry 4-70350

heavily doped p-type semiconductors, phonon attenuation 4-84349

heavily doped semiconductors, electron relax. effect on phonon damping 4-70317

heavy fermion superconductivity, renormalised perturbation theory anal. 4-104354

Heisenberg antiferromagnetic linear chain, spin-Peierls instabilities, antiferromag. transitions and phonon dynamics 4-65824

highly excited phonon mode decay, master eqn. anal. 4-65362

ice III-IX order-disorder transition, high press. Raman spectra 4-61689

ideal interfaces, phonon transitions, reciprocity theorem with acoustic mismatch model 4-65539

II-VI semiconductors, carrier mobility charact., displaced Maxwellian model 4-75968

III-VI layered semiconductors, electronic and vibrational spectra 4-71390

indirect gap semiconductor, recombination in electron-hole droplets 4-70832

inhomogeneous materials, thermal conductivity, phonon distribution 4-61161

ionic crystals, Faraday effect due to mag. moments of optical phonons 4-66017

ionic semiconductors, hydrodynamic instability at transverse optical phonon freq. (Russian) 4-71329

Jahn-Teller T $\times$ ( $\tau_2$ +e) system at strong coupling, Ham factors 4-98575

large wavenumber phonons, ballistic transport and Raman scatt. (Japanese) 4-92451

magnetic materials, magneto-optical figure of merit, light scatt. meas. 4-61666

magnetic materials near phase transition, relax. process 4-88671

marble, thermal cond. and phonon scatt. by twin planes 4-65507

metallic compounds and disordered alloys, phonon states, data compilation 4-73178

metals, electron relax. effect on phonon damping 4-70317

metals, muon motion, limitations of diffusion approx. 4-65897

microcline, potash feldspar, single crystal, IR reflection spectra 4-76452

mixed valence compounds, phonon-induced virtual states 4-70750

molecular crystals, additive conservation law for phonon collision operator 4-70310

naphthalene, phonon harmonic dynamics, block method 4-88254

naphthalene ( $d_8$ ) phonons at low temp., Raman band profiles, vibr. relax. 4-66023

naphthalene cryst., excitons, defects and intramolecular phonon interactions (Russian) 4-98532

naphthalene crystal, multiphonon inelastic incoherent neutron scatt. 4-65361

nitromethane, condensed explosive, shock-induced mol. excitation 4-80160

nonequilibrium phonon distribution in quantising mag. field, phonon generator appl. 4-61008

nonequilibrium phonons in solids, review 4-61017

nonequilibrium superconductors, new instability toward inhomogeneous states 4-70979

nonlinear phonon focusing, theory 4-61010

nonlocal phonon heat transfer calcs. 4-61156

ODIC crystal, two-dimensional, mol. dynamics simulation 4-113551

one-dimensional anharmonic chain, soliton struct. of lattice vibrs. 4-80172

## lattice phonons continued

p-n junctions, tunnel capture influence on impurity-level recombination of charge carriers (Russian) 4-70923

phonon-dislocation scatt. and thermal cond. review 4-70189

piezoelectric semicond. magnetised plasma, high-power helicon wave parametric decay 4-98657

quantum Hall regime critical non-dissipative current 4-98762

quartz, Brillouin scattering study of sound velocity at  $\alpha$ - $\beta$  transition 4-71400

quartz, cryst. and vitreous, LO-TO phonon mode splitting, many-particle effects 4-98223

quartz, lattice vibrs., dielec. function, ellipsometry 4-75627

quartz, nonequilibrium phonons, direct generation by IR radiation, X-ray evidence 4-108558

quartz, phonon echo generation, enhancement by defects 4-70304

quartz, sp. ht., time depend., meas. between 0.1 and 1 K 4-70407

rare earth impurity ions in crystals, phonon-assisted energy transfer, conc. depend. 4-92311

resonant scattering, crossing effects 4-61004

Rochelle salt, Raman spectrum, mode assignments, permitt. meas. 4-93011

ruby, Raman spin-lattice relax. induced by optically generated zone boundary phonons 4-66044

ruby, X-ray irradi., phonon decay and lifetimes 4-65358

ruby, Zeeman states, stimulated emission and decay of phonons 4-65359

sapphire, specularly reflected phonons from cryst. boundary, imaging 4-65508

scattering in condensed matter, conf., Stuttgart, Germany (Aug. 1983) 4-58557

semiconductor, optical phonons, carrier-assisted laser pumping under strong mag. fields 4-80182

semiconductor superlattices, disordered, electronic props. and phonon states 4-84682

semiconductor superlattices, Stark cyclotron-phonon oscillations of sound absorption 4-70276

semiconductors, inelastic light scattering for structural/electronic props. characterisation (French) 4-84956

semiconductors, mobility fluctuation 1/f noise parameter and phonons 4-114005

semiconductors, nonequilibrium electrons, optical phonons and acoustic phonons, transport eqns. 4-108851

semiconductors, nonradiative multiphonon capture of carriers by deep traps 4-75889

semiconductors, p-type, phonon attenuation 4-70300

semiconductors, wurtzite-type, hole-phonon interaction, phonon cond. calc. 4-70487

sodalite, natural, IR spectra 4-104602

solid solutions, quaternary III-V cpd. system, optical and elec. props. 4-84929

solid-phase charge transfer rate, intermol. vibrs. 4-81429

solid/solid interfaces, thermal phonons, critical cone channelling 4-65541

solids, dilaton mechanism for strength 4-88235

solids, nucl. stopping power, binding force effect 4-65316

stearic acid B form, polytypism and LF Raman spectra 4-61674

strong-coupling superconductors, theory comprehensive study of renormalisation 4-108967

superconducting pairing condensates, exciton mediated, phonon effect on T<sub>c</sub> 4-70974

superconducting T<sub>c</sub>, Eliashberg eqn. soln. for small  $\lambda$  (Chinese) 4-104335

superconducting thin films in resistive state, heating of electrons due to EM radiation 4-61487

superconductivity, phonon and nonphonon mechanisms, coexistence and separation method 4-108966

superconductor, phonon generation during HF EM field absorpt. (Russian) 4-84743

superconductor films, optically driven, picosecond pulse generation capability 4-92861

superconductors, phonon anomalies 4-65351

superionics, 2-D, chaotic dynamics and low freq. Raman lines 4-113710

Toda lattice, Bethe ansatz, ground state and excitations 4-95314

transport eqn. for isotropic electron distrib. function and electron relax. (Russian) 4-65654

two dimensional lattice, virial theorem, lattice dynamics and struct. instability (Russian) 4-68154

two-level systems, interconversion valence-alternation pair originated, anomalous interaction with phonons 4-92309

vacancy-interstitial pair formation in solids, phonon model 4-103895

vibron solitons in one-dimensional molecular crystals 4-80177

VUV radiation physics, conf., Jerusalem, Israel, 8-12 Aug. (1983) 4-82583

AgBr:I, multiphonon emission, excitons, photoluminescence 4-99159

Ag<sub>2</sub>CdI<sub>4</sub>, superionic conductor, Raman and far IR studies 4-109195

AgCl(Br), interaction pots. and van der Waals forces 4-89058

AgI, disorder-induced Raman scatt., vibr. dynamics 4-71392

Ag<sub>2</sub>TaS<sub>4</sub>, phonon modes, Raman spectra, valence force field model 4-104584

Al, electron irradi., incoherent tunnelling of positive muons and trapping by vacancies, muon spin relax. meas. 4-65909

Al, melting curve study at high press. 4-103911

AlN sputtered films, polycryst. and amorphous, optical phonons, Raman studies 4-80179

Al<sub>2</sub>O<sub>3</sub>:Cr<sup>3+</sup>(V<sup>4+</sup>), phonons, far IR vol. generation and detection 4-61005

Al<sub>2</sub>O<sub>3</sub>:V, quasi-diffusive phonon propag. obs. 4-61012

Al<sub>2</sub>O<sub>3</sub>:Y<sup>3+</sup>, zero-field hyperfine splitting by Josephson phonon spectroscopy 4-61353

Au point contacts for high freq. phonon generation 4-61007

BaClF ionic conductor, anharmonic thermal vibrs., X-ray diffr. study 4-113560

BaF<sub>2</sub>, fluorite struct., inner displacement, internal strain tensor, lattice dynamic models 4-92315

Be, temp. and press. induced phase transitions 4-70369

BeAl<sub>2</sub>O<sub>4</sub>:Cr<sup>3+</sup>, alexandrite, resonant 40 cm<sup>-1</sup> phonons, lifetime and linewidth 4-65356

Bi whiskers, longit. magnetoresist. meas. 4-88500

Bi<sub>2</sub>GeO<sub>20</sub>, phonon echo generation, enhancement by defects 4-70304

Bi<sub>2</sub>GeO<sub>20</sub> thin films, IR spectra and lattice phonons 4-88893

Bi<sub>2</sub>SiO<sub>20</sub> thin films, IR spectra and lattice phonons 4-88893

Bi<sub>2</sub>TiO<sub>20</sub> single cryst., Raman spectra and phonons 4-88833

C, BC-8 crystal phase, struct. props., phase stability and phase transitions 4-113889

CO, translation rot. coupling and lattice dynamics 4-98219

- ce phonons continued
- Ca, FCC, phonon freqs. and binding energies, pseudopot. calc. 4-80181
- CaCO<sub>3</sub>, calcite, thermal cond. and phonon scatt. by twin planes 4-65507
- CaF<sub>2</sub>, fluorite struct., inner displacement, internal strain tensor, lattice dynamic models 4-92315
- CaF<sub>2</sub>, IR excitation of high-freq. phonons by multiphonon absorpt. 4-61027
- Ca<sub>1-x</sub>Y<sub>x</sub>Mn<sub>2</sub>Ge<sub>2</sub>O<sub>12</sub>, thermopower and elec. cond., -30 to 1000°C 4-70847
- CdGa<sub>2</sub>S<sub>4</sub>, effective ionic charges, optic phonon spectra 4-103894
- CdGa<sub>2</sub>Se<sub>4</sub>, effective ionic charges, optic phonon spectra 4-103894
- Cd<sub>1-x</sub>Hg<sub>x</sub>Te, phonon states, far IR absorpt. spectra study (Chinese) 4-92312
- Cd<sub>1-x</sub>, Raman spectra meas. 4-80944
- n-Cd<sub>3</sub>P<sub>2</sub>, degenerate semicond. intrinsic phonon parameters 4-92317
- CdS, resonant Brillouin scatt. study 4-61721
- CdS, resonant Brillouin spectra calcs. 4-61722
- CdSb, vibr. modes symm. and Raman scatt. (Russian) 4-99124
- CdSe, picosecond energy-relax. processes of excitons, luminesc. study 4-109244
- CdTe:Co, optical absorpt. spectrum (Russian) 4-84983
- CaF<sub>2</sub>, bound state between phonons and crystalline electric field states 4-104175
- Ce<sub>2</sub>Mg<sub>3</sub>(NO<sub>3</sub>)<sub>12</sub>/He system, anomalous low temp. Kapitza resistance 4-65542
- CoAs<sub>3</sub>, CoSb<sub>3</sub>, skutterudites, far IR refl. spectra, temp. depend. of phonon freqs. 4-104595
- Cs, phonon frequencies, Debye temp., Gruisenen parameter, transport props., lattice dynamical model 4-108561
- CsCaF<sub>3</sub>, parameter free eqn. of state calcs. 4-70336
- CsH<sub>2</sub>PO<sub>4</sub>, antiferroelec. fluctuations, Raman spectroscopy studies 4-71297
- CsH<sub>2</sub>PO<sub>4</sub>, normal and deuterated, ferroelec. phase transition, Raman studies 4-71295
- Cs<sub>2</sub>NaBiCl<sub>6</sub>, cryst. struct. and phase transitions 4-80015
- Cu halides, superionic, phase transition and soft mode behaviour 4-92330
- Cu<sub>2</sub>Cd<sub>4</sub>, superionic conductor, Raman and far IR studies 4-109195
- CuCl, resonant Raman scatt. in region of edge excitons 4-76472
- CuCl/CuBr piezoelectric composition-modulated structures 4-99040
- p-CuGe<sub>2</sub>P<sub>3</sub>, optical lattice modes and IR reflectivity 4-88834
- CuInS<sub>2</sub>, Raman study of optical phonons 4-80917
- CuInTe<sub>2</sub>, thermal expansion coeffs., 30 to 300K 4-103974
- Cu<sub>2</sub>O, ortho-exciton states, time-resolved hot luminesc., reson. Raman scatt. 4-71438
- EuS, ferromagnetic semicond., thermal cond., phonon and magnon contributions 4-71050
- EuSr<sub>1-x</sub>S spin glass, cryst., phonon scatt. by mag. two-level systems 4-71106
- Fe<sub>2</sub>BO<sub>6</sub>, antiferromag., Raman scatt. from phonons and magnons 4-76471
- Ga-Al-As, luminescence lineshapes of electron-hole plasma 4-109242
- Ga<sub>1-x</sub>Al<sub>x</sub>As, crystalline struct., two-phonon Raman spectra study 4-71385
- Ga<sub>1-x</sub>Al<sub>x</sub>As superlattices, acoustic modes, Brillouin and Raman scatt. study 4-80928
- Ga<sub>1-x</sub>Al<sub>x</sub>As-GaAs, Raman scatt. theory 4-76460
- GaAs (100) 4-70546
- GaAs, ballistic large-wavevector phonon propag., direct obs. 4-61013
- GaAs, isotope scatt. of large wave vector phonons 4-108564
- GaAs, long-lived short wavelength FA phonons propag., Monte Carlo simulation 4-61015
- GaAs, phonon frequencies 4-75626
- GaAs, photoexcited, heat pulse propag., large k-vector phonons obs. 4-61014
- GaAs, photoexcited, phonon transport 4-92322
- GaAs, Raman probe of Brillouin zone for nonequilib. phonons 4-66045
- GaAs, Raman scatt. and two-phonon density of states 4-66046
- GaAs:Mn, thermal cond. resonances of acceptor states 4-104011
- GaAs-Al<sub>1-x</sub>Ga<sub>x</sub>As superlattices, Raman probing of phonons and interfaces 4-80927
- GaAs-AlAs multiple quantum well struct., Raman scatt. and luminescence study 4-99105
- GaAs-AlGaAs superlattice and interface, acoustic props. 4-80366
- GaAs-Ga<sub>1-x</sub>Al<sub>x</sub>As, lateral superlattice struct. 4-92816
- GaAs<sub>1-x</sub>P<sub>x</sub>, localised excitons, luminescence study 4-61291
- GaAs<sub>1-x</sub>P<sub>x</sub>, mixed cryst., long-wavelength optical phonons (Chinese) 4-108559
- GaAs<sub>1-x</sub>P<sub>x</sub>, phonon modes, Raman scatt. study 4-108563
- Ga<sub>0.47</sub>In<sub>0.53</sub>As-InP, Raman scatt. theory 4-76460
- Ga<sub>1-x</sub>In<sub>x</sub>P, phonon modes, Raman scatt. study 4-108563
- GaP, optical phonon lifetimes, temp. dependence, optical meas. 4-61016
- GaP, Raman scatt. efficiency, press. effect 4-76462
- GaP:Te(N)(As), impurity influence on electron-hole plasma 4-75862
- GaP<sub>1-x</sub>As<sub>x</sub>, crystalline struct., two-phonon Raman spectra study 4-71385
- p-GaSb, heavily doped, low temp. thermal cond. 4-70300
- Ge, elastic props., ultrasonic meas. 4-98170
- Ge, electron-hole liquid, phonon-absorpt. imaging 4-61292
- Ge, high energy LA phonons, anharmonic decay 4-65355
- Ge, phonon focusing, imaging by electron-beam scanning 4-61009
- Ge, phonon pulses detection by fluorescence of deposited YF<sub>3</sub>Tb<sup>3+</sup> film 4-113555
- Ge:Cu(Au), nonradiative multiphonon capture of carriers by deep traps 4-75889
- Ge:P, ballistic phonon transport under mag. field 4-70301
- Ge-Si, lattice vibr. props., Raman spectra, alloying and press. depend. 4-108562
- HCl(Br), lattice dynamics in low temp. phase 4-92328
- He phonon induced desorption, thermodynamic and perturbation theory anal. 4-65577
- He, solid, HCP, near zone boundary acoustic phonons propag. 4-61170
- Hf, lattice vibr., seven parameter model anal. 4-70306
- Hf, phonon density of states determ. from sp. ht. (Russian) 4-92314
- Hg<sub>2</sub>Br<sub>2</sub>, single crystals, IR refl. spectra, optical consts. and phonon parameters 4-88830
- Hg<sub>0.8</sub>Cd<sub>0.2</sub>Te, (110), Raman scatt. study 4-80942
- HgCr<sub>2</sub>Se<sub>4</sub>, mag. semicond., resist, and magnetisation changes and relax. 4-65682
- Hg<sub>1-x</sub>, polariton energy relax., thermal barrier effect 4-84573
- In-Tl, elec. resist. studies, average phonon energy 4-113920
- InP, LEC grown, photoluminesc. study, 1.8 to 40K (Chinese) 4-84993
- InP single cryst., low temp. thermal cond. and phonons 4-88356
- lattice phonons continued
- n-InSb film, amplification of total reflection mode surface phonons 4-70547
- InSb, isotope scatt. of large wave vector phonons 4-108564
- KBr, Landau-Placzek ratio, light scatt. study 4-104623
- KCl:Na<sub>2</sub>O, phonon propag. and impurity absorption spectra 4-65360
- KCl(Br)(I):Ag, surface-enhanced Raman scatt. from Ag colloids, optical absorpt. spectra 4-99117
- KH<sub>2</sub>PO<sub>4</sub>, type crystals, low freq. E mode Raman spectra 4-71364
- K<sub>1-x</sub>Li<sub>x</sub>TaO<sub>3</sub>, IR reflectivity, two mode behaviour 4-71363
- K<sub>0.3</sub>MoO<sub>3</sub>, 1D, CDW modes, far IR reflectivity studies 4-108798
- K<sub>1-x</sub>Na<sub>x</sub>TaO<sub>3</sub>, IR reflectivity, two mode behaviour 4-71363
- K<sub>2</sub>SeO<sub>4</sub>, acoustic phonon wavevector depend. near commensurate-incommensurate transition, Brillouin spectra 4-71313
- K<sub>2</sub>SeO<sub>4</sub>, Brillouin spectra, scatt. angle and press. depend. 4-76481
- K<sub>2</sub>SeO<sub>4</sub>, phonon-soliton interaction, discommensurations at lock-in transition 4-70299
- KZn<sub>1-x</sub>Co<sub>x</sub>F<sub>3</sub>, Fourier transform IR spectroscopy of Co<sup>2+</sup> excitations 4-104596
- La, depend. of <sup>140</sup>Ce recoil motion on phonon spectrum, nucl. reson. fluorescence study 4-98216
- LaF<sub>3</sub>, depend. of <sup>140</sup>Ce recoil motion on phonon spectrum, nucl. reson. fluorescence study 4-98216
- LaF<sub>3</sub>Er<sup>3+</sup>, high freq. phonon dynamics, optical detection methods 4-65357
- Li<sub>2</sub>GeO<sub>3</sub>, pyroelec. material, vibr. spectra and polariton dispersion 4-71362
- β-LiIO<sub>3</sub>, IR absorption and Raman spectra at low temps. 4-71361
- LiNbO<sub>3</sub>, ballistic heat pulse propag., effect of piezoelec. 4-76335
- LiNbO<sub>3</sub>, laser irradi., polariton Raman scatt. 4-61715
- LiNbO<sub>3</sub>, type ferroelectrics, dielec. thermal and soft mode behaviour 4-71298
- Li<sub>2</sub>O, optical mode frequencies, IR reflectivity, Raman spectra 4-104617
- MgO, apparent, lattice and radiative thermal cond., 300-1500K, up to 5.6 GPa 4-78322
- MgO:Co, electronic Raman spectrum and perturbation calcs. 4-114281
- MgO:Co<sup>2+</sup>, g value, Jahn-Teller effect 4-88492
- Mn dihalides, d-excitons, vibr. struct., IR and Raman spectra studies 4-113873
- Mn<sub>2</sub>Zn<sub>1-x</sub>Te solid solns., weak dipole vibr., Raman scatt. studies 4-65354
- Mo chalcogenides, binary and ternary, Chevrel type, supercond., heat capacity anal. 4-92858
- NH<sub>4</sub>Cl, hypersound attenuation and dispersion, back and forward Brillouin scatt. 4-76487
- Na, martensitic BCC:HCP transformation, pretransitional phenomena 4-114519
- NaCl, apparent, lattice and radiative thermal cond., 300-1500K, up to 5.6 GPa 4-78322
- NaCl:Ag, surface-enhanced Raman scatt. from Ag colloids, optical absorpt. spectra 4-99117
- Na<sub>2</sub>O-Al<sub>2</sub>O<sub>3</sub>-SiO<sub>2</sub>-xS<sub>2</sub> cluster cryst., Raman, ESR spectra and dielec. permittivity 4-61714
- Nb, Raman scatt. theory and optical phonons 4-71386
- Nb<sub>2</sub>H<sub>2</sub>N, ultrasonic absorpt. due to H tunnelling 4-70287
- Nb<sub>3</sub>Al(Ge)(Sn), thermodynamic props. calc. 4-84741
- NbH<sub>2</sub>(D<sub>2</sub>), acoustic phonon assisted H diffusion 4-61139
- NbS<sub>2</sub> (2H), phonon modes, Raman spectra, valence force field model 4-104584
- Nb<sub>3</sub>Sn, Raman scatt. theory and optical phonons 4-71386
- Nd<sup>3+</sup> impurity ions in crystals, phonon-assisted energy transfer, conc. depend. 4-92311
- Nd<sub>2</sub>La<sub>1-x</sub>P<sub>2</sub>O<sub>7</sub>, four wave mixing and exciton dynamics 4-83638
- Ni with surface adsorbed S, O and CO, anharmonicity and adsorbate vibr. lifetimes 4-104084
- NiH<sub>2</sub>, optical phonon density of states determ., incoherent inelastic neutron scatt. 4-61021
- Pb chalcogenides, electron scatt. interaction and elementary excitations 4-70694
- Pb/Ag superlattice, superconductivity 4-92839
- Pb-Cu films, localisation and superconducting fluctuations 4-80719
- PbCl<sub>2</sub>, Raman-active modes, anharmonic effects 4-71381
- Pb<sub>1-x</sub>Ge<sub>x</sub>Te, undoped and In-doped, anomalous scatt. of carriers by defects and impurities near ferroelec. phase transition 4-98622
- PbTe(Sn)(S), lattice thermal cond. meas. 4-98598
- PdH<sub>2</sub>(D<sub>2</sub>), acoustic phonon assisted H diffusion 4-61139
- PdMn, thermoelectric power, phonon drag effect 4-104187
- ReO<sub>4</sub>, molecules in alkali halides, anharmonic vibr. relax. dynamics 4-91311
- Si (100) surface electronic excitations, EELS study 4-108914
- Si, BC-8 crystal phase, struct. props., phase stability and phase transitions 4-113389
- Si classical periodic structs., light absorption edge 4-66002
- Si, elastic props., ultrasonic meas. 4-98170
- Si, far IR transmission spectrum, two-phonon difference band obs. 4-104597
- p-Si, heavily doped, low temp. thermal cond. 4-70300
- Si on sapphire, phonon boundary scatt. at interface 4-104050
- Si, phonon pulses detection by fluorescence of deposited YF<sub>3</sub>Tb<sup>3+</sup> film 4-113555
- Si:B, Fe, exciton photoluminescence study 4-109243
- Si:B, magnetothermal cond. study 4-71076
- Si:B, thermal cond. resonances of acceptor states 4-104011
- Si:B(In), point defects influence on acceptor ground state splittings 4-70728
- a-Si:H film, time resolved photoluminescence and phonon transport 4-71445
- Si:Li, phonon scatt., acoustic paramagnetic resonance study 4-71157
- Si:O, isotope effects and photoluminescence spectra 4-104661
- Si:P, IR absorption spectrum 4-71414
- β-SiC, polymorphic struct., additional phonon spectra 4-61024
- (SnO<sub>2</sub>)<sub>1-x</sub>(Fe<sub>2</sub>O<sub>3</sub>)<sub>x</sub>, Mossbauer study 4-114187
- SrF<sub>2</sub>, fluorite struct., inner displacement, internal strain tensor, lattice dynamic models 4-92315
- SrF<sub>2</sub>:Eu<sup>2+</sup>, phonon diffusion and decay, impurity luminesc. study 4-61006
- Ta<sub>2</sub>S<sub>5</sub> (2H), phonon modes, Raman spectra, valence force field model 4-104584
- Ti, phonon density of states determ. from sp. ht. (Russian) 4-92314
- TiO<sub>6</sub> octahedral structs., phonon state density 4-70305
- TiCl(Br), phonons, far IR vol. generation and detection 4-61005

## lattice phonons continued

- $\text{IrVO}_3$ , cooperative Jahn-Teller system, US attenuation at megahertz freq. 4-70282  
 $\text{V}_2\text{Ga}$ , thermodynamic props. calc. 4-84741  
 $\text{V}_2\text{Si}$ , Raman scatt. theory and optical phonons 4-71386  
 $\text{W}$  (110), inelastic scatt. of He and Ne, semiclassical perturbation approx. 4-85052  
 $\text{W}_{1-x}\text{Mo}_x\text{Se}_2$ ,  $x=0-1$  fundamental absorpt. edges, optical indirect band gaps 4-99076  
 $\text{Zn}_x\text{Cd}_{1-x}\text{S}$ , excitation migration between localised excitons, photoluminescence, absorpt. spectra 4-88456  
 $\text{Zn}_x\text{Cd}_{1-x}\text{Te}$ , Raman scatt. and phonon spectra 4-88835  
 $\text{ZnSe}$ , deformation pot. consts. determ. by reson. Brillouin scatt. 4-71398  
 $\text{ZnSe}$ , optical phonon lifetimes, temp. dependence, optical meas. 4-61016  
 $\text{Zr}$ , phonon density of states determ. from sp. ht. (Russian) 4-92314

## lattice structure, crystals see crystal atomic structure

## lattice theory and statistics

see also Ising lattices; percolation; renormalisation; X-Y model

- (1+1)-dimensional Ashkin-Teller model, phase diagram and critical props. 4-68162  
 1d quantum ground state, Monte Carlo renormalisation group simulation 4-58762  
 $\phi^4$  field theories, random walk appls., survey 4-68391  
 $n$ -step random walker on lattice, trapping in two- and three-dimens. 4-95341  
 adsorption phenomena, Monte Carlo studies 4-113816  
 aggregates, diffusion limited, dynamical scaling and growth 4-113644  
 aggregates, fractal dimension of random walk, possible breakdown of Alexander-Orbach rule 4-86368  
 aggregation, ballistic model 4-73388  
 aggregation, diffusion-controlled, continuum approx. calcs. 4-65408  
 aggregation fractals, homogeneity and spectral dimension 4-86348  
 Anderson localisation, mathematical theory 4-75828  
 anharmonic chains with higher neighbour interactions and long range forces, quasi-solitons 4-82762  
 ANNNI model, low temp. anal. in external mag. field 4-58774  
 antiferromagnetic hierarchical Dyson models, ground states, devil's staircase functions 4-95367  
 antiferromagnetic Ising model, anisotropic, long-range order, quenched impurity effects 4-98848  
 antiferromagnetic lattice gases, generalised Bragg-Williams method 4-86369  
 antiferromagnetic plane rotator model on triangular lattice, spin wave anal., symm. breaking in mag. field 4-109004  
 Ashkin-Teller model, 1+1 dimens., critical props., phase diagram 4-58789  
 Ashkin-Teller model, time-continuous Hamiltonian, finite size studies 4-111046  
 asymmetric clock model on Cayley tree 4-68158  
 asymptotically exact solution of the one-dimensional trapping problem 4-73361  
 atomic ordering study including conduction electron gas effects 4-58786  
 automodel regimes in circular shear flows and in circular MHD flows with coherent vortex structures (Russian) 4-113033  
 baker's transformation, folding paper and thermodynamics, chaos 4-58754  
 Baxter model, generalised, diagram technique 4-111065  
 Bethe lattice, Coulomb potential problem, random walk Green's function 4-86365  
 Bethe lattice, mathematical props. 4-90513  
 Bethe lattice, site-bond percolation problems 4-111053  
 Bethe lattice, statistical mech. 4-76151  
 Bethe lattice, validity of use as substitute for actual lattice 4-90536  
 Bethe lattices, exactly solvable irreversible processes 4-101765  
 Bethe-Ansatz methods for vertex systems 4-68165  
 biased correlated walks, long-time asymptotic probability distrib. 4-68142  
 bifurcations in parameter space of 16-vertex model 4-78263  
 binary alloys, kinetics of first order phase transition 4-75642  
 binary substitutional alloy, FCC struct., interstitial impurity effect on atomic ordering 4-60919  
 bivalent nearest available neighbour distrib. in  $n$  dimensions 4-90535  
 block spin renormalization group, non-Gaussian scaling limits, hierarchical model approx. 4-101767  
 Blume-Capel model, linked-cluster series anal. 4-78272  
 bond percolation critical probability determ. based on star-triangle transformation 4-68161  
 bond-percolation problems for short-range and infinite-range bonds 4-78268  
 bootstrap percolation, renormalisation group approach 4-78262  
 branched polymers, Smoluchowski's eqn. and  $\theta$ -exponent 4-90523  
 cellular automata, reversible, time invariant quantity for subclass 4-78251  
 chemically limited cluster-cluster aggregation, hierarchical model, fractal dimension, active sites 4-111044  
 classical diffusion in random environments, numerical method 4-111076  
 classical  $n$ -vector model with free surface, high-temp. series anal. 4-90528  
 classical Toda lattice, finite-temp. excitation spectrum, soliton-phonon phenomenology 4-111067  
 cluster aggregation, diffusion-limited, dynamic scaling relation 4-68173  
 cluster free energy, interfacial contribs., Ising model Monte Carlo method calc. 4-111073  
 cluster growth on the Cayley tree, diffusion controlled processes 4-95347  
 cluster variation method, consistent relations in method of reducibility 4-58776  
 cluster-cluster aggregation model, universality props. 4-90525  
 commensurate phase, physisorbed on substrate of triangular lattice symm., melting transition 4-80386  
 commensurate-soliton structures, phase diagram in 2-D 4-86357  
 commensurate-incommensurate phase transitions, Percival variational principle for invariant meas. 4-101795  
 compliant coatings interactions with boundary-layer flows 4-60366  
 conference, common trends in particle and condensed matter physics, Les Houches, France (Feb., 1983) 4-58554  
 conference on mathematical physics, Boulder, CO, USA (Aug. 1983) 4-67856  
 Coniglio's lemma 4-68163  
 connectivity transitions 4-90532  
 conserved multicomponent systems, quenching kinetics 4-95344  
 constants definition, free multiplicities, occurrence factors 4-95327
- lattice theory and statistics continued**  
 continuum percolation, discs with distrib. of radii, Monte Carlo simulation 4-111045  
 coordination number of percolating clusters on simple and cubic lattice 4-111063  
 Coulomb gas, spin models in 2-D, charge asymmetry, critical behaviour 4-86356  
 d-dimensional bond-percolating network, effective-medium approx. 4-90534  
 d-dimensional classical lattice models, exact variational methods and cluster-variation approx. 4-101768  
 d-dimensional lattice, critical exponents for long-range interaction 4-68169  
 defect space,  $\epsilon$  expansion, critical phenomena and renormalisability 4-82761  
 dense random packings of hard spheres, radial distrib. functions a microgeometry 4-68143  
 devil's staircase in a one-dimensional mapping 4-111059  
 diffusion processes and random walks, localised partial traps 4-58793  
 diluted quantum transverse Ising model in two dimensions 4-63681  
 dimensional crossover in directed percolation position space renormalisation group 4-111047  
 directed bond percolation on square lattice 4-86351  
 directed compact animals model 4-95338  
 directed diffusion-controlled aggregation versus directed animals 4-95346  
 directed systems, real-space renormalisation group, lattice animals and self-avoiding walks 4-58770  
 disorder induced phase transitions 4-58780  
 disorder induced walk as strange fractal phenomenon 4-90491  
 disordered lattice, 1-dimens., diffusion, renormalisation-group calcs. 4-63683  
 disordered transport, high and low density expansions, Green's function 4-73393  
 domain growth kinetics, universality of kinetic exponents, Potts model 4-58779  
 double sine-Gordon chain, damped, uniformly moving domain wall 4-90391  
 duality and Potts critical amplitudes on a class of hierarchical lattice 4-101776  
 eight-vertex SOS model and generalized Rogers-Ramanujan-type identities 4-101766  
 electron-phonon interactions, discrete lattice model, asymptotic behaviour Maslov's method 4-95349  
 electrostatic potential of square ionic lattice 4-78267  
 ethyl alcohol vertical layer with thermogravitational convections, temp. fluctuations spectra 4-79580  
 excitation trapping of random walker on fractal and regular lattice 4-86347  
 Feigenbaum attractors, universal exponents and fractal dimension 4-101775  
 ferromagnet, cubic, critical behaviour, Potts model anal. 4-61546  
 ferromagnet, cubic, with fourth- and sixth-order anisotropy, crit. behavior Potts models 4-98897  
 ferromagnetic  $q$ -state Potts model on BCC and FCC lattice, critical point 4-80734  
 finite chain with arbitrary conc. of pure absorbers, random walk problem exact soln. 4-73365  
 finite chains with chaotically distributed pure absorbers, random walks appl. of cluster length distrib. 4-58748  
 finite-size scaling, conformal invariance and universality 4-68157  
 finitely ramified fractals, self-avoiding walks, renormalisation group technique 4-63684  
 Fisher droplet model, modified and Monte Carlo equilb. cluster distrib. 4-111074  
 flat square lattice, multiphase behaviour of large interacting molecules Percus-Yevick approx. 4-73396  
 Flory-Stockmayer theory, polymerisation model  $A_1RB_2$  4-95330  
 flow transition under action of acoustic oscillations 4-103289  
 formal diagrams derived from prototypes of eight or less points 4-78250  
 fractal and directed percolation clusters, spreading dimens., lattice animal analogy 4-58767  
 fractal dimensionality for kinetic gelation with conserved initiator 4-81434  
 fractal lattices, connectivity dimension for square and triangular lattice 4-86349  
 fractal lattices, infinitely ramified, phase transitions 4-58771  
 fractal model of percolation clusters 4-73362  
 fractal spaces, harmonic anal., random walk statistics, Schrodinger eqn. spectrum 4-58783  
 fractal structures, transport processes 4-86353  
 fractals, percolation and anomalous diffusion 4-86361  
 fractals, squig clusters, diffusion, dimensionality 4-86360  
 free random surface simulation using Monte Carlo techniques 4-68403  
 frustrated spin systems 4-98904  
 gas, tricritical point from low temp. series expansions 4-95322  
 gas interface, field dependence of eigenvalues of correlation function matrices 4-78253  
 gas model, alternate site, phase diagram 4-111058  
 gas model, cluster free energy existence 4-111056  
 gas model, critical behaviour 4-78266  
 gas-solid coexistence curve in three and four dimensions, low temp. expansions 4-68174  
 gauge Potts model, phase transitions, Monte Carlo calcs. 4-73381  
 Gaussian model, discrete, equivalence with generalised sine-Gordon theory on lattice 4-101777  
 geminate recombination on a lattice 4-111042  
 glissile dislocation loops ensemble, thermodynamics 4-60930  
 hard hexagon model, generalised, deviations from critical densit. 4-90518  
 hard particle lattice gases, universality of nonphase transition singularity 4-101770  
 hard-triangle lattice gas, mag. exponent, renormalisation 4-86366  
 heat transfer through turbulent and transitional boundary layers on convexly curved wall 4-60417  
 hexagonal lattice, simple, with competing interactions, modulated phases Ising model 4-92925  
 hexagonal lattice with boundary, dimer problem soln. 4-68159  
 hierarchical lattice spin systems, phase transition phenomena 4-95364  
 hopping conduction, DC conductivity tensor in mag. field 4-80558  
 hypercubic lattice in  $d$ -dimensions, percolation thresholds 4-78259

## lattice theory and statistics continued

- hypercubic lattices, bond percolation, extended mean cluster size series anal. 4-111071
- ICL DAP parallel processor, Monte Carlo simulations in solid-state and elementary particle physics 4-59029
- incommensurate harmonic chain, 1-D, dynamics 4-95348
- incommensurate structures, twist map trajectories 4-58782
- indistinguishable dumbbells on rectangular lattice space, occupation statistics 4-101762
- interacting random walk models, comparative study 4-90520
- interface zone, lattice models, correlation function 4-98461
- ionic conductors, nonequilibrium steady states of stochastic lattice gas 4-73385
- irreversible kinetic aggregation, diffusive cluster size distrib., Smoluchowski's eqn. 4-111043
- irreversible processes in 1-D, exact solution 4-101764
- Ising ferromagnet, amorphisation, high-field magnetisation 4-84762
- Ising ferromagnet, bond-diluted, bond percolation on the pentagon lattice 4-114083
- Ising ferromagnet, correl. functions in two-dimens. narrow strips at phase coexistence, Monte-Carlo calcs. 4-104439
- Ising model, functional integral method in solid-state statistics (*Russian*) 4-95339
- Ising model, Green function ansatz for K-space pair correl. function 4-58763
- Ising model, simple cubic, critical behaviour, Monte Carlo renormalisation group calcs. 4-71114
- Ising nearest neighbour model, with uniaxial incommensurate phase and Lifshitz point 4-71115
- Ising spin system on a Cayley tree, i- $\delta$  relations 4-84811
- Ising systems, two-step renormalisation group 4-101761
- isotropic-nematic transitions, helix-coil induced reentrant, lattice theory 4-113626
- jellium, two-dimensional classical translational invariance, symmetry breakdown 4-61266
- kinetic spin models, dynamical renormalisation through classical equations of motion 4-58765
- kink, uniformly driven, in damped  $\phi^4$ -chain 4-68148
- Kosterlitz-Thouless transitions, 2D XY and Coulomb gas models, Mayer expansion 4-90511
- lattice gases, phase transitions, G-condition satisfaction 4-90526
- lattice gases with 2nd nearest neighbour interactions, cluster sums on 1-dimens. lattice 4-73384
- lattice k-packings density, Schrodinger operator spectral struct. (*Russian*) 4-90512
- lattice tubes for pair correlation in uniaxial ferromagnet 4-111308
- linear lattice systems, direct correl. function decay 4-73392
- linear polymers, failure of Flory approx. 4-95320
- linear polymers, kinetic growth walk model for irreversible growth 4-58778
- local and global Markov random fields 4-63677
- Lorentz model with fractal distribution of impurities, long time-tails 4-101773
- magnetic lattice gas of molecules with internal structure, phase diagrams 4-111060
- mean field bound for magnetisation, single-component spin system, GHS inequality 4-95335
- mean-field method with four-body interactions 4-68164
- Mellin transforms associated with Julia sets and phys. appls. 4-58775
- metastability and analyticity in drop-like model 4-58805
- Monte Carlo method, appls. in condensed-matter physics, statistical mechanics and related fields, book 4-101584
- multichain athermal lattice systems, entropy 4-113675
- multiparticle diffusive-fractal aggregation, computer simulation studies 4-95345
- n-vector model, pair correlation function eqn. 4-90527
- nonequilibrium statistical mech., projection operator techniques, book 4-67897
- nonlinear resonant interaction of acoustic fields with Tollmien-Schlichting waves in flat channel 4-69826
- O(N) lattice spin models, 1/D expansion, two-loop effective action 4-102041
- one dimensional lattice, random walks with traps, exact enumeration 4-58766
- one-dimensional classical planar model with competing interactions 4-80767
- one-dimensional lattice, motion and capture in presence of cooperative trap interactions 4-111055
- one-dimensional lattice, random, dilute, one-particle Green function 4-90524
- one-dimensional randomly hopping lattice gases, two-point spatial correlations 4-111068
- one-dimensional self-avoiding walk 4-68176
- one-dimensional system, localisation in limit of strong random pots. 4-70702
- order-disorder transitions, layering, and multicritical phenomena, lattice gas model 4-101779
- p-state chiral clock model, low temp. phase diagram, mean-field approx. 4-92917
- Pariser-Parr-Pople and linear Hubbard models, valence bond theory 4-78273
- Pearls chain, transition by analyticity breaking 4-58781
- percolation, critical probabilities, branching processes 4-95332
- percolation and self-avoiding walks, Gaussian-cluster models 4-68160
- percolation cluster hulls, fractal dimens. 4-68155
- percolation clusters, fractal-to-Euclidean crossover and scaling for random walkers 4-95317
- percolation clusters, segment distribution in self-similar patterns 4-86350
- percolation conductivity, critical exponents rel. to static exponents 4-95323
- percolation lattices, acoustic wave absorpt. enhancement near a percolation threshold 4-69614
- percolation lattices, mobility and linear response theory, particle motion 4-58777
- percolation through finite layer, Markov model for percolation probability, asymptotic behaviour 4-95350
- period doubling bifurcations, renormalisation group computer-assisted proofs in analysis 4-73387
- periodic ground states, one-dimension, Lennard-Jones-type potentials 4-95336
- perturbed Liouville/Toda systems, Newtonian eqn. 4-90529

## lattice theory and statistics continued

- phase equilibrium and lattice models in statistical mechanics 4-63689
- Pirogov-Sinai theory of phase transitions on lattices 4-78248
- plane quadratic lattice gas, extended cluster variation calcs., phase diagram 4-90519
- plates, random array, percolation threshold criterion 4-86370
- polymer chain statistics and universality, random to self-avoiding walk crossover 4-63680
- polymer conformation statistics, iterative convolution approach 4-90522
- polymer melt with rigid and flexible, chain elements, liq. cryst. ordering (*Russian*) 4-75294
- polymer statistics and universality, cluster renormalisation 4-59922
- polymeric fractals, statics and dynamics 4-111032
- polymers, branched, corrections to cluster-radius scaling and percolation 4-68144
- polymers, branched, growth method, and large percolation clusters below  $p_c$  4-103638
- polymers, irreversible kinetic gelation, fractal nature 4-95319
- polymers, long, lattice models, generalised Bethe approx. 4-68146
- polymers in solution, instantonic conformation 4-95321
- Potts lattice gauge theory, n-depend. topological anomalies 4-68358
- Potts lattice-gas, multicritical behaviour in q-state 4-78257
- Potts model, asymmetric three-state, phase struct. 4-111075
- Potts model, p-component, with correlated impurities, crit. behaviour 4-101780
- Potts model, plaquette percolation, Fortuin-Kasteleyn result extension 4-68149
- Potts model, q-state, free energy critical amplitude 4-73394
- Potts model, q-states, oscillatory critical amplitudes 4-78249
- Potts model, three-component ferromagnetic, Yang-Lee zeros 4-101769
- Potts model of magnetism, critical dimensionalities and props. 4-61499
- Potts model on a closed Cayley tree 4-61497
- Potts model partition function, location of the phase transition 4-86346
- Potts model quantum, many-component limit 4-78265
- Potts model with quadratic symmetry breaking, crossover exponents 4-111070
- Potts models, ferromag. and antiferromag., phase transition, Bethe approx. 4-92918
- Potts models, pseudodimensional var. and tricriticality by hierarchical breaking of translational invariance 4-101804
- Potts models on triangular and checkerboard lattices, inversion rels. and disorder solns. 4-90517
- purely diffusive systems, mode-coupling theory, 1D lattice gas appl. 4-101790
- quantum chains, leading order corrections to the energy gap 4-86345
- quantum few-body problem, Monte Carlo calc. 4-95293
- quantum integrable systems,  $d > 2$ , Baxter model 4-86563
- quantum lattice models, ground state props., real-space renormalisation group method 4-111069
- quantum models, local Hamiltonians 4-106248
- quantum percolation, real-space renormalisation-group anal. 4-101781
- quantum systems with long-range correlated impurities, dynamical critical exponent 4-68168
- quasi-one-dimensional mol. chains, solitons 4-86227
- rando lattices, statistics of self-avoiding walks 4-68147
- random anisotropy model, spin glass phase gaussian fluctuations, 1/N expansion, instability 4-104426
- random chain with correlated hopping rates, diffusion const. 4-101793
- random geometry and the statistics of two-dimensional cells 4-68150
- random interfaces, dynamics in phase transitions 4-86363
- random percolating systems, classical diffusion, drift and trapping 4-101778
- random percolation, 2D and 3D, large-cell Monte Carlo renormalisation study 4-82765
- random walk, large cell renormalisation of systems with dimensionality larger than upper marginal dimes. 4-58764
- random walks on Vicsek fractals 4-101757
- randomly diluted lattices, self-avoiding walks, impurity effects 4-73380
- randomly distributed particles of percolation topology, optical props. 4-93039
- randomly substituted lattice, long range and nearest neighbour interactions, hopping transport 4-84600
- real-space renormalisation appl. to adsorbed systems, book contrib. 4-63687
- recursion method basic vectors for periodic Hamiltonians, asymptotic form 4-111049
- renormalisation group, asymptotic freedom and nongaussian fixed points 4-73631
- renormalisation groups, Monte Carlo simulation, critical phenomena 4-86362
- renormalisation-group decimation technique for spectra, wave functions and density of states 4-104114
- resistive susceptibility of 3-D random diode-insulator network 4-78261
- rotating disk, boundary layer transition, spiral vortices 4-83910
- Schrodinger operator with point interactions and short range expansions, mesic atoms, crystals, quantum fields 4-68022
- self avoiding random walks, resistance and related scaling props. 4-90514
- self-avoiding path walks on lattice, universality class 4-95328
- self-avoiding random chain field theory 4-86364
- self-avoiding random surfaces, field theory 4-82760
- self-avoiding random surfaces, scaling behaviour, renormalisation group calcs. 4-90531
- self-avoiding random walks on 2-D and 3D lattices, new exponent 4-101749
- self-avoiding walk, critical exponents in two- and three-dimensional lattices 4-86343
- self-avoiding walk, homotopy parameter expansion appl., critical phenomena 4-106247
- self-avoiding walk, universality on square lattice 4-95329
- self-avoiding walks, asymptotic expansion for square lattice 4-86344
- self-avoiding walks, winding angle on planar lattice 4-95318
- self-avoiding walks in four dimensions, logarithmic corrections to scaling 4-111072
- self-avoiding walks on percolation clusters 4-68156
- self-avoiding walks on percolation clusters at criticality and lattice animals 4-101760
- shear flow at high Reynolds no., wavelike disturbances propag. 4-64918
- Sierpinski gasket in mag. field, spectrum study 4-78274
- Sierpinski gaskets, random walker motion on fractally structured object 4-73391
- Sierpinski-type fractals, renormalisation, random walks and mappings 4-90515

**lattice theory and statistics continued**

- site-bond-correlated percolation and a sublattice dilute Potts model at finite temperatures 4-78271  
 six-state Potts model, 2D, phase transitions and critical props. 4-58760  
 sixteen vertex model, diagrammatic construction of algebraic invariants 4-78264  
 space correlated quenched defects critical behaviour 4-111048  
 spectral functions, calc. procedure based on moment expansions 4-82757  
 spin  $1/2$  anisotropic Heisenberg model in infinite lattice dims., time depend. behaviour 4-68172  
 spin glass, Shpolinsky and Parisi solutions equivalence 4-88683  
 spin glass model, mapping iterations 4-98891  
 spin models, percolation, clusters, and phase transitions 4-78270  
 spin systems, monte Carlo calculation of renormalized coupling parameters 4-58941  
 spin systems with impurities, static and dynamic crit. props., two-loop approx. 4-61541  
 spinless fermion model, order-disorder transition 4-78258  
 square lattice, 2-dimens., simple XY model, continuous to 1st order transition 4-90530  
 square lattice, average self-avoiding random walk 4-95316  
 square-lattice Ising model, two-parameter modified Kadanoff var. method 4-111040  
 steady state flow of a fluid stream with streamline disturbance around an arbitrary arc (*Russian*) 4-87667  
 stochastic crystal growth, order and disorder lines 4-76099  
 strange attractors in disordered systems 4-58788  
 SU(N) Toda lattice, 2-dimens., Liouville-Bäcklund transformation 4-86355  
 surfaces, roughening transition 4-113569  
 symmetric one-dimensional random walk, span distrib. moments 4-82755  
 tensor product for physical interpretation 4-82758  
 tetrahedron integration scheme 4-73395  
 thermogravitational convection, struct. in flat variously oriented layers of liq. and on vertical wall 4-112815  
 third-rank-tensor Hamiltonian, phase transitions, appl. to systems with tetrahedral symm. 4-101782  
 three-dimensional lattice model with directional bonding, renormalization group study 4-111052  
 three-state Potts model, dynamical exponent, Monte Carlo renormalisation group calc. 4-111050  
 Toda chain  $A_1^{(1)}$ , two-dimens., elliptic solns. parametrised by arbitrary function 4-73389  
 Toda lattice, Bethe ansatz, ground state and excitations 4-95314  
 Toda lattice type Hamiltonian systems, classical flow solutions, Lie groups 4-95315  
 Toda systems with unequal masses, integrals of motion 4-86354  
 tracer diffusion, continued fraction expansion, exact soln. 4-88331  
 transition control by periodic suction blowing 4-83876  
 transverse Ising model with disordered surface, surface magnetism 4-88688  
 trial problem on square and cubic lattices, direct renormalisation group approach 4-68166  
 triangular lattice, percolation, scaling of order parameter, comparison to Ising model 4-111064  
 triangular percolation lattice, diffusion, renormalisation study 4-101771  
 true self-avoiding walk, series study 4-86352  
 tunnelling resistivity, one-dimens. random lattice, Petersburg problem 4-95337  
 two component spin model on lattice, star-triangle relation, classification conditions 4-58768  
 two component spin model on lattice, star-triangle relation, appl. and generalisation 4-58769  
 two dimensional lattice, virial theorem, lattice dynamics and struct. instability (*Russian*) 4-68154  
 two dimensional random lattice hopping model, diffusion and conduction 4-90492  
 two-dimensional and 3D flow, laminar instability theory 4-97480  
 two-dimensional model, coexistence of atomic and mol. phases, Monte Carlo study 4-73390  
 two-dimensional ordered struct., formation dynamics in lattice gas models 4-111054  
 two-loop corrections to the  $\Lambda$  parameters of one-plaquette actions 4-68360  
 Voronoi and regular networks, 3D, percolation and cond., topological disorder theory 4-90539  
 Voronoi and triangular networks, percolation and cond. 4-58773  
 water, Bell lattice model, Monte Carlo investigation 4-78255  
 $Z_3$  Potts model, critical behaviour, conformal algebra 4-68151  
 $Z_3$  Potts model, critical behaviour and associated conformal algebra 4-86358  
 Z(4) model, phase diagrams for square lattice in whole parameter space 4-90521  
 Z(N) invariant spin models on triangular lattice, exact solution 4-95325  
 Ge(111), lattice gas model of  $(7 \times 7)$ ,  $(5 \times 5)$  and  $(2 \times 8)$  structures 4-75767  
 Li<sub>2</sub>MoSe<sub>4</sub>, Li intercalation model, mean-field lattice gas 4-70098  
 SiO<sub>2</sub> small particles, colloidal aggregates, fractal geometry 4-89352  
 Si(111), lattice gas model of  $(7 \times 7)$ ,  $(5 \times 5)$  and  $(2 \times 8)$  structures 4-75767

**lattice vibrations see lattice dynamics****Laves phases see alloys****lawrencium**

No entries

**lawrencium compounds**

No entries

**laying, cable see cable laying****LCAO calculations**

- azulotropones, isomeric, mag. circular dichroism and MO studies 4-96584  
 benzoic acid, substituent effects, ab initio LCAO STO calcs. 4-96435  
 beryllium hydride polymer, LCAO band struct. calcs. 4-70628  
 chloromethane, Cl quadrupole coupling consts., nonempirical calcs. 4-107281  
 conjugated hydrocarbons, enthalpy of formation calc.,  $\pi$ -electron approx. of MO LCAO SCF method 4-62229  
 crystal with impurity, LCAO calc. of excess orbitals 4-98568  
 diamond, cohesive and struct. props., ab initio LCAO calc. 4-60881  
 diamond (111) surfaces, total energy minimisation, support for undimerised  $\pi$ -bonded chain reconstruction 4-92489

**LCAO calculations continued**

- 10,10-dichloro-10-germa-9-oxa-9,10-dihydroanthracene, conjugation effects calcs. 4-59648  
 10,10-dimethyl-10-germa-9-thia-9,10 dihydroanthracene, conjugation effects calcs. 4-59648  
 glycine, eq. soln., conformational energy; ab initio LCAC-MO-SCF calcs. 4-96449  
 graphite surface, H chemisorpt., MINDO/3 cryst. orbital LCAO SCF calc. 4-98430  
 inorganic ion-exchange materials, selective action, simulation of solvation interactions 4-62185  
 molecular interaction energies calc. using pseudopot. Hartree-Fock-Slater-LCAO method 4-96639  
 molecules, electric field depend. basis functions for elec. polarisability and moment calcs. 4-68956  
 Mulliken's population anal., bond order and valence 4-96438  
 polyatomic molecules, electronic-vibr. spectra calcs., program package 4-74221  
 $[N+1]\pi$ -polymethines, closed shell mol. geometry, MO LCAO calcs. 4-87048  
 pseudosymmetry, LCAO type perturbation expansions, derivation method 4-68914  
 retinal Schiff-base, protonated, with torsion about bonds in polyene chain, optical absorption 4-77190  
 sodium hydrogen oxalate monohydrate, cryst. electron density, intermolecular interactions, ab initio LCAO-MO-SCF calcs. 4-88160  
 state correlation diagrams, plotting using SCF MO LCAO method 4-107280  
 $[N+1]\pi$ -streptopolymethines, closed and open shell ground and excited state geometries, MO-LCAO calc. 4-87047  
 transition metal compounds, band struct. calcs.; Mossbauer spectra 4-92611  
 trichloromethane, Cl quadrupole coupling consts., nonempirical calcs. 4-107281  
 urea, aq. soln., hydration, mol. dynamics calcs. 4-75249  
 Al(111), O chemisorption LCAO-X $\alpha$  method anal. 4-113799  
 $\alpha$ -B, electronic energy levels of icosaederan calcs. 4-113862  
 Be<sub>2</sub>F<sub>3</sub><sup>+</sup>, geometric struct., force field and vibr. spectrum, MO-LCAO-SCF calcs. 4-59629  
 Be<sub>2</sub>H<sub>3</sub><sup>+</sup>, geometric struct., force field and vibr. spectrum, MO-LCAO-SCF calcs. 4-59629  
 Cr<sub>3</sub>, LCAO local spin density, X $\alpha$  calcs. 4-87046  
 Cu<sub>2</sub>Zn<sub>2</sub>, metallic glass, electronic struct. calcs. 4-104120  
 Eu oxide and chalcogenides, exchange interactions, LCAO calculations 4-109009  
 2-Fe ferredoxin model, electronic struct., mag. props., ESR and optical spectral, LCAO-X $\alpha$  VB theory 4-112312  
 Fe small clusters, electronic struct., spin density functional theory anal. 4-113859  
 GaP: Ni<sup>2+</sup> Jahn-Teller coupling forces, self consistent LCAO calc. 4-98577  
 LiCl crystal, electronic energy bands, density functional calcs., self-interaction-correction theory 4-70651  
 LiD, D elec. field gradient, LCAO MO SCF calcs. 4-112103  
 LiH, ground-state props., LCAO HF study using polarisable basis set 4-60882  
 Mg (0001), O chemisorption, LCAO-X $\alpha$  calcs. 4-113799  
 MnO, self-consistent Hartree energy band calcs. 4-92612  
 Mo complexes, bis carbene tetracarbonyl systems, rot. isomerism, LCAO-MO-SCF calcs. 4-68949  
 Mo<sub>2</sub>, LCAO local spin density, X $\alpha$  calcs. 4-87046  
 N<sub>2</sub>, symmetry restricted and unrestricted HF calc. ab initio LCAO-MO-SCF level 4-87043  
 N<sub>2</sub><sup>+</sup>, valence hole state, ab initio LCAO-MO-SCF level HF calcs. 4-68957  
 Ne, FCC, high press. eqn. of state, Gaussian orbital techniques 4-92332  
 PH<sub>3</sub>, oxidation catalysed by Cu(II) and Fe(II) halides, intermediate form., MO LCAO calcs. 4-62236  
 SbCl<sub>3</sub>-graphite intercalation cpd., de Haas-van Alphen effect meas. 4-88440  
 Si:B( $\mu^+$ ), tetrahedral interstitial impurities, electronic struct., LCAO-Green's function calc. 4-65636  
 Simuon, spin polarised electron struct. of positive muon, LCAO-Green's function anal. 4-65634  
 SiH<sub>2</sub>, defects, molecular cluster studies 4-84586  
 SiHCl<sub>2</sub>, Cl quadrupole coupling consts., nonempirical calcs. 4-107281  
 SiH<sub>2</sub>Cl<sub>2</sub>, Cl quadrupole coupling consts., nonempirical calcs. 4-107281  
 ZnS (100) surface, relations between surface states and struct. 4-80639  
 ZnS:Cu<sup>2+</sup>, Jahn-Teller coupling forces, self consistent LCAO calc. 4-98577

**LCD see liquid crystal displays****lead***see also nuclei with .....*

- 24.8 MeV electrons backscattering, energy spectra 4-88912  
 absorptivity of 10.6  $\mu$ m, temp. depend., computed from Drude theory 4-76405  
 acid battery active mass, microstruct. model anal. 4-105103  
 aerosol conc. in Norwegian Arctic, sources 4-105140  
 air pollution in Belgium record held in pond sediments 4-114983  
 alkali halides: Pb<sup>2+</sup>, X-irrad. effect on impurity vacancy dipoles and aggregation precipitation state, F-centre production 4-70209  
 anomalous fast diffusion in metals 4-65440  
 atom, L<sub>2</sub>-L<sub>3</sub> Coster-Kronig transition probability meas. 4-96493  
 atom, photoionisation processes in 5d, 6s- and 6p shells, electron correl. and relativistic effects 4-96502  
 atoms, Compton scatt. differential cross sections 4-112146  
 atoms, metastable, relax. in decaying plasma 4-108236  
 average M-shell fluorescence yield meas. 4-87071  
 backscattering of He<sup>+</sup> ions, excitations, optical spectrometry study 4-78944  
 battery, lead-acid, maintenance-free sealed miniature, objectives and requisites 4-62346  
 battery, Pb-acid, research developments and trends 4-62343  
 battery, Pb-acid, sealed and semisealed, development trends 4-62344  
 battery, Pb-acid, technological developments and challenges 4-62342  
 clusters, multiply charged, observability 4-96742  
 coadsorption with O<sub>2</sub> on Ti 4-92568  
 concentration at roadside, effects on human and animal health 4-100044  
 Congost River, Catalonia, Spain, Cd, Cu, Pb, conc. obs. 4-62430  
 corrosion in tap water and aq. solns. 4-109573

continued  
crystal growth rate of pure metals nucleated from undercooled melt 4-98042  
cylindrical sample,  $\gamma$ -ray self-absorption, correction factors 4-109267  
discontinuous thin film, mass fluctuations meas. 4-82759  
doubly charged cluster obs. by time of flight mass spectra 4-112316  
electrically cond. liquids, free jets, reson. breakdown, EM forces, drop form. phases (*Russian*) 4-113057  
electron backscattering from thick layers 4-99249  
electron-dislocation interaction during plastic deform. at supercond. transitions 4-98178  
electrothermal atomic absorpt. spectrometry using external sampling tube atomiser 4-99913  
element analysis using charged-particle induced prompt  $\gamma$  rays 4-89362  
film, supercond., surface heat transfer from self-heating hotspots 4-104361  
fluorite:  $\text{Pb}^{3+}$  crystals, hyperfine interactions 4-88494  
gas phase temperatures in Massmann furnaces equipped with L'vov plat-forms 4-105038  
geochemistry, Pb isotope ratios throughout geological time 4-89898  
geochronological dating method, calc. of Pb isotope growth curves 4-90004  
granular films, SAW attenuation in normal and supercond. states 4-98422  
inversion voltammetry for metal content in river water, seawater and bot-tom sediments 4-100816  
isotope ratio meas. using the Isomass 54E in fully automatic mode 4-96711  
isotopic composition of minerals and U-Pb dating 4-110285  
isotopic composition of Seychelles granites and xenoliths, dating 4-110102  
isotopic composition of Xigaze ophiolite, Tibet, relation between magmat-ites and tectonics 4-110139  
Josephson junctions, electrode surfaces, characteristics and failures (*Chinese*) 4-92866  
Li shell X production cross sections,  $\text{H}^+$  induced 4-96649  
Li-shell X-ray prod. cross sections,  $\text{H}^+$  induced, ratios 4-66131  
laser microprobe mass analysis detection limits and lateral resolution 4-72016  
liquid metal for D-T, D-D and T-T fusion sources, energy deposition 4-68810  
local-field enhancement of rough surface 4-104047  
Loihi Seamount, Hawaii, Pb, Nd, Sr isotope ratios of basalts 4-105508  
Louisiana, USA, freshwater sediment heavy metal pollution 4-93654  
Manchester Ship Canal, Pb pollution distrib. 4-85391  
melting curve calcs. using model potential 4-113582  
Mersey Estuary, England, Pb pollution distrib. 4-85391  
metal-metal collision sticking behaviour and relevance to solar nebula 4-67649  
Mount St. Helens, Washington, USA, radioactive  $^{210}\text{Pb}$ ,  $^{210}\text{Po}$  in volcanic ash 4-115367  
ocean surface waters of N Atlantic and N Pacific, Cu, Ni, Cd, Pb concs. 4-85710  
output voltage, discharge and temperature characts. of Pb batteries (*French*) 4-85364  
oxidation, XPS and EELS obs. 4-88913  
particulate emission and dispersion from roadway, line-source models 4-66832  
S Peru, Pb isotope study of magma-crust interaction in Andes 4-105475  
photon backscattering, energy albedo meas. 4-61782  
potential at at. boundaries in Thomas-Fermi model and eqns. of states (*Chinese*) 4-70333  
rainwater of Bermuda, trace metals content 4-67320  
Sargasso Sea, Pb depth profile perturbed by industrial input 4-85716  
N Saskatchewan, Canada, Pb isotope composition in U deposits 4-115348  
seawater of Kattegat and Skagerrak, trace metal concentrations 4-85714  
seawater trace metal content meas. technique using isotope dilution mass spectrometry 4-85797  
Siberia, lead ore deposits, Pb isotope study 4-105499  
single cryst., boundary and dislocation phonon scatt. 4-65365  
soft surface vibr. of fine particles 4-61201  
solid and liq., ultrasonic vel., temp. depend., elastic moduli, vol. depend. 4-60989  
stopping power for 6.5 MeV protons and mean excitation energies 4-92271  
storage battery, negative electrode porous struct., porosimetric investig. 4-62341  
superconducting film, spatial inhomogeneous states under strong quasipar-ticle injection (*Chinese*) 4-76081  
surface (111), electronic energy bands, angle resolved photoemission and self-consistent field calcs. 4-113858  
thick layers, penetration of 24.8 MeV electrons, energy spectra 4-66148  
thin films on Si, strain relaxation mechanisms 4-80463  
vapour long-lived sealed-off lasers, operating characts. and projected life-times 4-69386  
working environment aerosols in lead battery factory, toxicity monitoring by PIXE and AAS 4-105072  
Ag-Pb (111) solid solns., Pb surface segregation and vapour deposition on Ag (111), LEED-AES study 4-113837  
Al-Al<sub>2</sub>O<sub>3</sub>-Pb junction, effects of patterned laser illumination 4-70998  
Al-Al<sub>2</sub>O<sub>3</sub>-Pb tunnelling junctions, interaction with 3-(trimethyloxysilyl)propanethiol, IETS study 4-92827  
Al-insulator-Pb junctions, doped with aromatic aldehydes, ring sub-stituent effects, elastic tunnelling study 4-92828  
Al-Mg-Si:Pb, Sn, Mossbauer and X-ray diff. obs. 4-65882  
BaF<sub>2</sub>:Pb<sup>2+</sup> crystals, electronic excitation decay, impurity effect 4-109209  
Bi<sub>2</sub>SiO<sub>20</sub>:Pb PRIZ modulator, increased photosensitivity (*Russian*) 4-69544  
Bi<sub>2</sub>Te<sub>3</sub>:Pb(Ge), doping props., elec. cond. and Seebeck measurements 4-75467  
CaF<sub>2</sub>:Pb<sup>2+</sup> crystals, electronic excitation decay, impurity effect 4-109209  
Cu-Pb thin proximity layers, electron localisation and superconductivity 4-76083  
Ge (111)-Pb interface form. dynamics and oxidation 4-84518  
NaCl:Pb, plastic deform. parameters, impurity conc. effect, low temp. anomaly 4-88229  
NaCl:Pb<sup>2+</sup>, luminescence, effect of additional M<sup>2+</sup> doping 4-109245  
NaI:Pb, photoluminescence decay, temp. and aggregation depend. 4-99177  
Nb (110)-Pd interface, electronic struct. 4-84674

## lead continued

Nb-Nb oxide-Pb well-damped Josephson transmission line, fluxon prop-agation 4-65771  
Nb-NbO<sub>x</sub>-Pb Josephson tunnel junctions fabricated by CF<sub>4</sub> plasma clean-ing process 4-80720  
Nb<sub>2</sub>Ge-a-Si-Pb Josephson tunnel junction 4-104374  
NbN/Pb Josephson tunnel junctions with plasma oxidized barriers, annealing stability 4-84746  
Nb<sub>2</sub>Sn-Pb Josephson junctions using Nb<sub>2</sub>Sn formed by reaction of Nb/Sn dual-layer films 4-61491  
Pb/acid batteries, catalyst plug deterioration prevention 4-93613  
Pb/acid batteries, future outlook in Japan 4-62340  
Pb/acid batteries, influence on capacity of pulsed discharge, importance for electric vehicles 4-66683  
Pb/acid batteries, performance study using diffraction techniques 4-62326  
Pb/acid batteries for UPS and telephone system back-up power, acid age-ing behaviour of polycarbonates 4-93612  
Pb/acid battery, new ideas 4-62329  
Pb/acid battery lifetime prediction, computerised pattern recognition application to life-cycling test data 4-81530  
Pb/acid cells, immobilized electrolyte, design limitations 4-81532  
Pb/acid cells, rotating ring-disc electrode study of impurity effects on lead corrosion in sulphuric acid 4-81533  
Pb/acid cells for electric vehicles, comparison with alternate cells 4-62335  
Pb/acid SLI batteries, high power 4-62328  
Pb/acid sealed battery, mechanism and characts., production in Japan 4-93611  
Pb/acid sealed recombination cells for standby power 4-93610  
Pb/acid stationary battery, reliability 4-93609  
Pb/Ag superlattice, superconductivity 4-92839  
Pb/Ag ultrathin layered structs., electron tunnelling spectra 4-76024  
Pb/graphite accumulator using aqueous HF acid, advantages and disad-vantages 4-66682  
Pb/Nb oxide/Nb resistively coupled Josephson transmission line, fluxon threshold props. 4-70989  
Pb/PbO/Pb supercond. junctions, I-V characts. and self-induced step struct. 4-104372  
Pb-acid accumulators and atmospheric pollution (*German*) 4-81537  
Pb-acid automotive battery, 'precharged' positive plate, incorporation of PbO<sub>2</sub> 4-77070  
Pb-acid automotive-battery, PbO<sub>2</sub> incorporation into 'precharged' positive plate 4-77069  
Pb-acid batteries, positive plates cryst. and amorphous components, quan-titative phase anal., elec. vehicle appl. 4-77068  
Pb-acid battery cathodes incorporating chemically prepared PbO<sub>2</sub> 4-77073  
Pb-Ag<sub>1-x-y</sub>Mn<sub>x</sub>Al<sub>y</sub>-Pb, S-N-S junction, pair-breaking mechanism 4-98824  
Pb-Al<sub>2</sub>O<sub>3</sub>-Al junctions, ion irradi., defect vibrs., supercond. tunnelling meas. 4-98826  
Pb-AlO<sub>x</sub>-Al, barrier height and electric field induced barrier shifts 4-70946  
Pb-Ge sandwich targets on Si matrix, PIXE anal. signal enhancement, matrix effects 4-99869  
Pb-I-NbN tunnelling junction, resist., supercond. fluctuations effect, exis-tence of ultrathin layer in NbN films 4-98827  
Pb-NbO<sub>2</sub>-Nb Josephson tunnel junctions, current density distrib. (*German*) 4-84750  
Pb-PbS, melt, metallographic anal. 4-61052  
Pb-Zn host granular supercond., frustration and disorder 4-98799  
Pb-Zn-Pb SNS junctions, DC Josephson effect 4-80722  
Pb+Br collisions,  $\delta$ -electron spectra study 4-74321  
Pb+I collisions,  $\delta$ -electron spectra study 4-74321  
Pb+O collisions, K-shell ionisation, angular depend. 4-74322  
Pb+O<sub>2</sub> reaction, chemiluminesc. characterisation 4-99799  
 $^{210}\text{Pb}$ , determ. in seawater and marine particulate matter 4-105059  
 $^{210}\text{Pb}$ , activities and conc. factors in estuarine sediments of rivers in Gujarat, India 4-82103  
 $^{210}\text{Pb}$  and heavy metal content in Finnish peat, alpha spectrometric meas. 4-102445  
 $^{210}\text{Pb}$  distribution in environmental samples by CR-39  $\alpha$ -detector 4-100053  
 $^{210}\text{Pb}$  in liver and lung of Lapps, comparison with southern Finns 4-62590  
 $^{210}\text{Pb}$ , precipitation exchange separation and detection technique 4-109951  
Sb<sub>2</sub>Te<sub>3</sub>:Pb(Ge), doping props., elec. cond. and Seebeck measurements 4-75467  
SrF<sub>2</sub>:Pb<sup>2+</sup> crystals, electronic excitation decay, impurity effect 4-109209  
SrS:Pb<sup>2+</sup> phosphors, impurity dimer centres, luminesc. obs. 4-99158  
SrSe:Pb<sup>2+</sup> phosphors, impurity dimer centres, luminesc. obs. 4-99158  
V-V<sub>2</sub>O<sub>5</sub>-Pb Josephson junctions self-field effects aspects 4-61494  
Y<sub>3</sub>Fe<sub>5</sub>O<sub>12</sub>:Pb, epitaxial films, Pb effect on optical props. 4-99210

## lead alloys

## see also lead compounds

brass, Cu-Zn-Pb, precipitation and coarsening of Pb particles 4-109413  
dilute, anomalous fast diffusion 4-65440  
Josephson junctions, electrode surfaces, characteristics and failures (*Chinese*) 4-92866  
Josephson junctions, size effects 4-84748  
KPb, compound forming liquid alloys, hard sphere system, entropy of mixing calcs. 4-113650  
MARS, liquid Li<sub>2</sub>Pb<sub>3</sub> cooled fusion reactor blanket, corrosion product cleanup system 4-111785  
thin films on Si, strain relaxation mechanisms 4-80463  
Ag-Pb, liq., thermodynamic study of dissolved O 4-92379  
AuSn-Pb quasibinary section of phase diagram, thermal anal. 4-93265  
Bi-Cd-Sn-Pb, Wood's metal, melting and solidification, US study 4-60991  
Bi-Pb, strain gauge fabrication by vacuum evaporation 4-95410  
Bi-Pb alloys, amorphous, supercond., upper critical fields 4-76089  
Bi-Pb-Sn-Cd, Wood's metal model, inclined simulated cracks, eddy current detect. 4-66516  
Cd-Pb, eutectic alloy thin films, growth 4-88995  
Cd-Pb, thermodynamic props. at 900°C 4-80263  
Cd-Pb composite amalgam cathode for standard cells (*Japanese*) 4-86439  
Cd-Pb eutectic thin films, directionally solidified, interlamellar spacing 4-93285

## lead alloys continued

- Cu-O-Pb system, thermodynamics of O, miscibility gap, 1200°C 4-108631  
 Cu-Pb, irregular monotectic struct., effects of temp. gradient and growth vel. 4-66321  
 Cu-Pb engine bearings, multilayer diffusion barriers 4-98331  
 In-Bi-Pb, liquid, thermodynamic props., EMF meas., 673 to 873K 4-98310  
 In-Pb alloys, transition from slip to twinning (*Russian*) 4-103760  
 Li-Pb single crystal, superelastic, irreversible twinning transition 4-85174  
 Li-Pb, liq., breeder blanket materials, thermodynamic investig. of dil. solns. of H 4-107033  
 Li-Pb, liq., breeder blanket materials, interaction of H isotopes investig. 4-107034  
 Li-Pb liq. alloys, model, chemical short-range order, heat and entropy of formation 4-75266  
 Li<sub>17</sub>Pb<sub>83</sub> alloy blanket concept for tritium breeding in INTOR-NET 4-111747  
 Li<sub>17</sub>Pb<sub>83</sub> liquid alloy, physical and chemical props. for fusion reactors 4-111748  
 Nb/Nb<sub>2</sub>O<sub>5</sub>/Pb-In-Au junctions, RF oxidised, tunnel barrier shape 4-80724  
 Nb-NbO<sub>2</sub>-Pb alloy Josephson tunnel junctions, resist. at cryogenic and ambient temps. 4-98819  
 Ni/Sn-Pb metallisation process, improved reproducibility for crystalline Si solar cells 4-93626  
 Pb-Au dil. solutions, bulk equilib. lattice parameters, neutron diff. meas. 4-75372  
 Pb-Au dilute solutions, single cryst., struct. in quenched state, X-ray and neutron diff. studies 4-75371  
 Pb-Cu films, localisation and superconducting fluctuations 4-80719  
 Pb-In, electron-dislocation interaction during plastic deform. at supercond. transitions 4-98178  
 Pb-In alloy films, nonequilibrium superconductivity, Pb-In/Pb-In/Pb double tunnelling junctions appls. 4-98815  
 Pb-In superconducting tunnel junctions, fabrication and cycling stability (*Chinese*) 4-104370  
 Pb-In superconductor, with dislocations surrounded by impurity atoms, internal friction (*Russian*) 4-98807  
 Pb-In(Tl), thermo-EMF determ. in temp. range 25-400°C, temp. and conc. depend. 4-80569  
 Pb-Li, liq., fusion reactor blankets, compatibility of steels, review 4-107054  
 Pb-Li, molten static, corrosion reactions of ferritic and type 316 steels 4-107064  
 Pb-Li eutectic in fusion reactor, corrosion behaviour of steels 4-107056  
 Pb-Mn(Fe), polyvalent films, elec. cond. anomaly 4-80688  
 Pb-Sb ingot casting, equiaxed zone form., dendritic solidification front 4-99379  
 Pb-Sn, eutectic alloy thin films, growth 4-88995  
 Pb-Sn, superplastic eutectic alloy, stress/strain in biaxial tensile system 4-71698  
 Pb-Sn (7.6 wt.%) role of excess vacancies in discontinuous precipitation (*Russian*) 4-81199  
 Pb-Sn eutectic thin films, directionally solidified, interlamellar spacing 4-93285  
 Pb-Sn freezing, periodic growth rate effect on morphological stability 4-98039  
 Pb-Zn system, complex model, appl. to systems with asymmetric miscibility gap 4-70397  
 Pb<sub>3</sub>Bi superconducting films for Josephson junctions, microstruct. control 4-114071  
 Pb<sub>30</sub>Bi<sub>20</sub> superconducting filament, high transition temp., produced by glass-coated melt spinning 4-80712  
 Sn-Pb, binary liq., compressibility, conc. depend., expt. and theoretical invest. 4-70250  
 Sn-Pb (38.1 wt.%), eutectic, fine-grained, accelerated coarsening of microstruct. during superplastic deformation 4-61997  
 Sn-Pb droplets, highly undercooled, solidification 4-114502  
 Sn-Pb sputtering alloy, effect of ion mass and energy on the surface composition 4-98493  
 SnPb, contact materials with reduced noble metal content, corrosion behaviour (*German*) 4-99640  
 SnPb molten alloys, ultrasonic velocity, compressibility effects 4-92303  
 Sr<sub>2</sub>Pb<sub>3</sub>, cryst. struct., X-ray diff. 4-75373  
 Sr<sub>3</sub>Pb<sub>5</sub>, cryst. struct., X-ray diff. 4-75373  
 Zn-Pb-Cd, cast ingots and sheets, microstructure rel. to cooling rate 4-109390

## lead compounds

see also lead alloys

- chalcogenides, carrier diffusion length and lifetime, EBIC meas. 4-92748  
 chalcogenides, carrier heating mechanisms 4-92738  
 chalcogenides, electron scatt. interaction and elementary excitations 4-70694  
 chalcogenides, resonance absorpt. in indirect transitions (*Russian*) 4-88855  
 dicalcium lead propionate, ferroelec. press. induced II-III transition, polarising microscope obs., permitt. meas. 4-80879  
 dicalcium lead propionate, ferroelec.-paraelec. transition, dopant conc. depend. 4-99048  
 diode laser, tunable, for heterodyne appls. 4-96940  
 laser technology using Pb salts, advances and implications for gas analysis 4-107719  
 oxides, PbM<sub>2</sub>O<sub>4</sub>, M=Al, Ga, luminesc. props. 4-76514  
 PbTe-Bi, Hall study of self-compensation of donor effect 4-104242  
 perovskite oxides, ferroelec. transition effects on absorption edges 4-93020  
 phosphate glasses for high level nuclear waste immobilisation and disposal 4-83132  
 phthalocyanine, vapour press. determ. (*German*) 4-80209  
 PLZT, ferroelec. films, reactive sputtering prep. and dielec. props. 4-104731  
 PLZT ceramics, polarisation switching chars. 4-99006  
 PLZT epitaxial thin films, ferroelec. and electrooptic props. 4-104530  
 PZT, electrically excitable mechanical reson. 4-114225  
 PZT piezoelectric ceramic transverse acoustoelectric wave refl. 4-83796  
 tunable diode laser technology overview 4-107667  
 Ag<sub>2</sub>Pb<sub>3</sub>Nb<sub>10</sub>O<sub>30</sub>, ferroelec. struct. and piezoelec. props. 4-65963  
 BaO-PbO-Nd<sub>2</sub>O<sub>3</sub>-TiO<sub>2</sub>, dielec. resonators, microwave chars. 4-84908  
 BaPb<sub>0.7</sub>Bi<sub>0.3</sub>O<sub>3</sub> superconducting photodetector 4-71002

## lead compounds continued

- Bi<sub>2</sub>Pb<sub>3</sub>Bi<sub>3</sub>Ti<sub>4</sub>W<sub>2</sub>O<sub>30</sub>, perovskite ferroelec., dielec. props. 4-88783  
 Cu-Pb<sub>2</sub>, antiferrelectric cermet, photodecomposition, optical charact. 4-101949  
 Fe<sub>2</sub>O<sub>3</sub>-B<sub>2</sub>O<sub>3</sub>-PbO glasses, ferric ion distrib., EPR studies 4-109064  
 (Fe<sub>2</sub>O<sub>3</sub>)(B<sub>2</sub>O<sub>3</sub>PbO)<sub>1-x</sub> glass, mag. props. study 4-88654  
 K<sub>2</sub>O-MgO-PbO-SiO<sub>2</sub> glass, Rayleigh scatt. loss coeffs. 4-114289  
 K<sub>2</sub>PbNb<sub>10</sub>O<sub>30</sub>, ferroelec. struct. and piezoelec. props. 4-65963  
 LaF<sub>3</sub>-PbF<sub>2</sub>-Nd, NMR study, relax. time 4-71203  
 PLZT, ageing and space charge arising in hot poling 4-76327  
 PLZT ceramic, coarse-grain light scatt. and elec. hysteresis 4-76399  
 PLZT ceramic for recording of volume amplitude-phase holograms 4-107579  
 PLZT ceramics, ferroelec. and electrooptic props. 4-76353  
 PLZT ceramics, hot pressed polarisation and depolarisation behaviour 4-76318  
 PLZT ceramics, ion implanted, optical absorption 4-114233  
 PLZT ceramics, poling strategy 4-76319  
 PLZT, chemically prepared, charact. and props. 4-76712  
 PLZT, ferroelec. ceramic, hot poling, polarisation, ageing rel. to space charge 4-99045  
 PLZT, ferroelec. diffuse phase transition, exponent  $\gamma$  determ. 4-76384  
 PLZT ferroelec. films, prep., props. and appls. 4-66230  
 PLZT, microscopic characterisation 4-61903  
 PLZT piezoelectric ceramic, fabricated by atmospheric sintering, electrical charact. and optical transmittance (*Korean*) 4-114211  
 PLZT retardation plates, nonhomogeneity of light modulation 4-61660  
 PLZT, tetragonal ceramic, 90° domains under poling, XRD study 4-76398  
 PLZT thin-film waveguides, electrooptic Kerr coeffs. 4-91578  
 PZT, amorphous, ferroelec. phase transition 4-61637  
 PZT cylindrical phase shifter and modulator in single-mode fibre interferometer 4-97090  
 PZT, dielec. props. at high press., p-T phase diagrams 4-99062  
 PZT, doped, diffuse phase transition, ultrasound meas. 4-76385  
 PZT films prepared by reactive cosputtering 4-71558  
 PZT, lattice site of Zn, Se, Fe ions, X-ray anal. 4-75488  
 PZT material, high density, prep. by coprecipitation technique 4-76711  
 PZT microparticle materials, amorphous state ferroelectricity 4-104542  
 PZT, piezoelectric ceramics, microstruct., props. and phase relations 4-61629  
 PZT, prep. using cupferron 4-61904  
 PZT, sintered, densification by hot isostatic pressing 4-66286  
 PZT/semi-crystalline polymer composite piezoelectrics 4-71283  
 PZT-polymer composites, piezoelec., with two dimensional periodicity reson. modes of vibr. 4-76331  
 (Pb, Ca)TiO<sub>3</sub> piezoelectric ceramic, modified, low mech. quality factor 4-76330  
 (Pb,La)(Zr,Ti)O<sub>3</sub> ceramics, stress anisotropy induced by polarisation 4-104536  
 (Pb, Sn, Ge)Te, semicond., dielec. props. and soft modes, review, book contrib. 4-61622  
 (Pb, Sn)Te, crystal growth by Bridgman method and by travelling heater method 4-103678  
 (Pb,Sn)Te-Pb(Te,Se) DH laser diodes, ion-implantation confined shallow mesa stripe, single mode tuning 4-112459  
 (Pb,Zr)TiO<sub>3</sub> thin films, magnetron RF sputtering and dielectric props. 4-88970  
 Pb glass shower counters, pulse height, energy resolution 4-59535  
 Pb/acid secondary cells, kinetics of PbO<sub>2</sub> growth on electrode 4-109732  
 Pb/PbO/Pb supercond. junctions, I-V charact. and self-induced step struct. 4-104372  
 Pb-glass drift collection calorimeter, design 4-59532  
 Pb-PbS, melt, metallographic anal. 4-61052  
 Pb<sub>3</sub>Ba<sub>2</sub>O<sub>13</sub>, single cryst., phase transitions and phys. props. 4-75656  
 (Pb<sub>1-x</sub>Bi<sub>x</sub>)<sub>1-y</sub>La<sub>y</sub>Nb<sub>2</sub>O<sub>6</sub> ceramic, dielectric, piezoelectric and optical props. 4-98999  
 Pb<sub>1-x</sub>Ba<sub>x</sub>Nb<sub>2</sub>O<sub>6</sub> ceramics, hot pressed, dielec. and piezoelec. props. 4-104533  
 Pb<sub>1-x</sub>Ba<sub>x</sub>Nb<sub>2</sub>O<sub>6</sub>, ferroelec. props., dielec. const., piezoelec. and electromechanical coupling coeffs. 4-65958  
 (Pb<sub>0.25</sub>Ba<sub>0.75</sub>)Ti<sub>3</sub>, ferroelec., phase-transition, high press. Raman study 4-76451  
 (Pb<sub>0.7</sub>Ca<sub>0.25</sub>)(Co<sub>1/2</sub>W<sub>1/2</sub>)<sub>0.04</sub>Ti<sub>0.96</sub>O<sub>3</sub> ceramics, piezoelec. props. MnO addition effects 4-104532  
 (Pb<sub>0.75</sub>Ca<sub>0.25</sub>)(Mg<sub>0.15</sub>Nb<sub>0.85</sub>Ti<sub>0.0625</sub>Ti<sub>0.9375</sub>)O<sub>3</sub>:Mn ceramics, US, elastic and dielec. props. 4-104543  
 PbCdS tunable diode lasers, Cd diffused, multicomponent gas analysis, appl. 4-112457  
 Pb<sub>1-x</sub>Cd<sub>x</sub>S tunable diode lasers for 3 to 30  $\mu$ m IR operation 4-112456  
 PbCl<sub>2</sub>, PbBr<sub>2</sub>, melting, solid-solid transitions at high pressures 4-80195  
 PbCl<sub>2</sub>, Raman-active modes, anharmonic effects 4-71381  
 PbCl<sub>2</sub>-Br<sub>2</sub>, self-trapped excitons, luminesc. (*Russian*) 4-80982  
 Pb<sub>2</sub>CrO<sub>5</sub> ceramic disk, photoconductivity with surface electrodes 4-61405  
 Pb<sub>2</sub>CrO<sub>5</sub>, cryst. struct. determ. 4-65245  
 Pb<sub>1-x</sub>Eu<sub>x</sub>Se<sub>1-y</sub>Te<sub>y</sub> diode lasers, wavelength coverage 4-102928  
 Pb<sub>1-x</sub>Eu<sub>x</sub>Se<sub>1-y</sub>Te<sub>y</sub> heterojunction stripe geometry lasers grown by MBE 4-112458  
 Pb<sub>1-x</sub>Eu<sub>x</sub>Se<sub>1-y</sub>Te<sub>y</sub> long-wavelength laser diodes, fabrication and props. 4-96954  
 Pb<sub>1-x</sub>Eu<sub>x</sub>Te, MBE growth and elec. and optical props. 4-81142  
 PbF<sub>2</sub>, cubic, electron-coupled nuclear spin-spin interactions and <sup>19</sup>F chem. shift 4-80827  
 PbF<sub>2</sub>, dielectric constant, temp. depend., polarisability 4-92995  
 $\beta$ -PbF<sub>2</sub> films, TSC and space charge 4-84903  
 $\beta$ -PbF<sub>2</sub>, point defect stability, computer simulation 4-103744  
 PbF<sub>2</sub>, thermally induced anion disorder, neutron scatt. meas. 4-98338  
 PbF<sub>2</sub>:Na(K)(Rb), ionic cond., dielec. relax. and activation vol. 4-113701  
 PbF<sub>2</sub>-R, R= rare earth, dielec. spectrum study, 5.5 to 380K 4-71272  
 PbF<sub>2</sub>-GaF<sub>3</sub>-Al(PO<sub>3</sub>)<sub>3</sub>-ErF<sub>3</sub>-based fluoride glasses, fluorescence studies 4-99170  
 PbF<sub>2</sub>-LiF pellets, thermal neutron irradiated, T release behaviour, fusion reactor appl. 4-74040  
 PbF<sub>2</sub>-M<sup>I</sup>F<sub>2</sub>-M<sup>III</sup>F<sub>3</sub> (M<sup>I</sup>=Mn, Zn; M<sup>III</sup>=Fe, Ga), fluoride glasses, local order, EXAFS studies 4-70036  
 PbF<sub>2</sub>-MF<sub>2</sub>-MF<sub>3</sub> glass, struct. and props. 4-79948  
 PbF<sub>2</sub>-MnF<sub>2</sub>-GaF<sub>3</sub>, fluoride glasses, vibrational spectroscopy 4-114261  
 PbF<sub>2</sub>-RF<sub>3</sub>, R=La, Nd, Gd, Ho, Yb and Y, synthesis, cryst. struct., electron diff. obs. (*French*) 4-75405  
 PbF<sub>2</sub>-ZnF<sub>2</sub> system, amorphous phase form. by roller splat cooling 4-85122

## ad compounds continued

- Pb<sub>2</sub>Fe(Cn)<sub>6</sub>·2H<sub>2</sub>O, with interstitial water impurity mols., electronic cond. activation 4-75972
- PbFe<sub>1/2</sub>-Ga<sub>2</sub>O<sub>9</sub>, optical props. 4-93086
- Pb(FeNb)<sub>0.5</sub>O<sub>3</sub> ceramics and single crystals, prep., struct., X-ray diffr., neutron powder diffr., dielec. and elec. meas., SEM 4-75412
- Pb(Fe<sub>0.5</sub>Nb<sub>0.5</sub>)O<sub>3</sub>, anharmonicity of thermal vibrs., X-ray diffr. 4-65367
- Pb(Fe<sub>0.5</sub>Nb<sub>0.5</sub>)O<sub>3</sub> ferroelec., mag. and magnetoelec. props. 4-65847
- Pb(Fe<sub>1/2</sub>Nb<sub>1/2</sub>)O<sub>3</sub>-Pb(Ni<sub>1/3</sub>Nb<sub>2/3</sub>)O<sub>3</sub> solid soln. system, dielec. props. 4-104517
- Pb(Fe<sub>0.5</sub>Ta<sub>0.5</sub>)O<sub>3</sub>, anharmonicity of thermal vibrs., X-ray diffr. 4-65367
- PbFe<sub>0.5</sub>Ta<sub>0.5</sub>O<sub>3</sub> single cryst., ferroelec./antiferromag., spontaneous birefringence 4-71344
- PbGe<sub>2</sub>O<sub>7</sub>, luminesc. props. 4-76514
- Pb<sub>2</sub>Ge<sub>2</sub>O<sub>7</sub> crystals, Raman scatt. near phase transition, isofrequency temp. depends. 4-66043
- Pb<sub>2</sub>Ge<sub>2</sub>O<sub>7</sub> crystals, spatial modulation of light 4-84941
- Pb<sub>2</sub>Ge<sub>2</sub>O<sub>7</sub>, ferroelec., surface states role in polarisation reversal 4-71325
- Pb<sub>2</sub>Ge<sub>2</sub>O<sub>7</sub> ferroelec. thin film, reactive sputtering prep. and props. 4-65961
- Pb<sub>2</sub>Ge<sub>2</sub>O<sub>7</sub>, hydrothermally grown, crystals, dielec., pyroelectric props., X-ray diffr. 4-84915
- Pb<sub>2</sub>Ge<sub>2</sub>O<sub>7</sub>, lattice dynamics near Curie point (*Russian*) 4-98221
- Pb<sub>2</sub>Ge<sub>2</sub>O<sub>7</sub>, metastable form, hydrolysis, X-ray diffr. studies 4-65220
- Pb<sub>2</sub>Ge<sub>2</sub>O<sub>7</sub>, pyroelectric coeff., Q-factor, determ. by absolute dynamic method 4-84914
- Pb<sub>2</sub>Ge<sub>2</sub>O<sub>7</sub>, soft modes rel. to crit. fluctuations, neutron and Raman scatt. meas. 4-65370
- Pb<sub>2</sub>Ge<sub>2</sub>O<sub>7</sub> type crystals., electrogyration, dispersive and temp. depend. 4-76433
- Pb<sub>2</sub>Ge<sub>2</sub>O<sub>7</sub>:Gd<sup>3+</sup>, superhyperfine interaction, ESR and ENDOR studies 4-14159
- Pb<sub>2</sub>Ge<sub>2</sub>O<sub>7</sub>-BaTiO<sub>3</sub> composite ceramic, dielec. props. and sintering prep. 4-104746
- Pb<sub>2</sub>Ge<sub>2</sub>-Si<sub>2</sub>O<sub>7</sub> thick films, printing technique prep. and pyroelec. props. 4-104541
- Pb<sub>1-x</sub>Ge<sub>x</sub>Te, ferroelec. phase transition, high press. investigation, DC resist., capacitance meas. 4-71312
- n-Pb<sub>1-x</sub>Ge<sub>x</sub>Te, free carrier mobility, ferroelectric phase transition 4-71317
- Pb<sub>1-x</sub>Ge<sub>x</sub>Te, rhombohedral phase, energy surfaces and domain struct. 4-76010
- Pb<sub>1-x</sub>Ge<sub>x</sub>Te, synthesis and cryst. struct. 4-84261
- Pb<sub>1-x</sub>Ge<sub>x</sub>Te, undoped and In-doped, anomalous scatt. of carriers by defects and impurities near ferroelec. phase transition 4-98622
- Pb<sub>1-x</sub>Ge<sub>x</sub>Te:In, elec. props., band edge struct., impurity effects 4-108880
- Pb<sub>1-x</sub>Ge<sub>x</sub>Te:In, solid solns., impurity photocond., spectra and kinetics 4-113994
- PbH, low-lying electronic states, relativistic quantum and CI calcs., spin-orbit interaction 4-96462
- Pb<sub>2</sub>H<sub>2</sub>, charge iterative relativistic extended Huckel theory and its appl. 4-59643
- PbHfO<sub>3</sub>, ferroelec. transition effects on absorption edges 4-93020
- Pb<sub>1-x</sub>Hg<sub>x</sub>S, photocond. cells, hot body detection 4-90655
- Pb<sub>1-x</sub>Hg<sub>x</sub>Se flash-evaporated films, optical and elec. props. 4-114335
- Pb<sub>1-x</sub>Hg<sub>x</sub>Te films, optical energy gap, composition dependence 4-76541
- Pb<sub>2</sub>, binding energies of exciton-ionised donor complex and exciton line n=1 4-70666
- Pb<sub>2</sub>, photoelectronic props. study using lasers 4-88532
- Pb<sub>2</sub> polar cryst. plate, exciton state and binding energy 4-70673
- Pb<sub>2</sub>, thermally stimulated currents at low elec. fields 4-65689
- Pb<sub>2</sub>-PbO system, condensed phase diagram 4-98245
- Pb<sub>2</sub>:Ag, exciton spectrum, photodoping effects (*Russian*) 4-92626
- Pb<sub>2</sub>InNbO<sub>6</sub>, order-disorder transitions and dielec. props. 4-65980
- Pb<sub>2</sub>InNbO<sub>6</sub>, single crystal, perovskite and pyrochlore modifications, prep. and props. 4-76662
- Pb<sub>0.91</sub>La<sub>0.09</sub>(Zr<sub>0.65</sub>Ti<sub>0.35</sub>)<sub>0.98</sub>O<sub>3</sub>, microscopic characterisation 4-61903
- Pb<sub>2</sub>(MF<sub>6</sub>)<sub>2</sub> (M=Ti, V, Cr, Fe, Ga), ferroelectric phase transitions 4-71311
- PbMg<sub>1/3</sub>Nb<sub>2/3</sub>O<sub>3</sub> ceramics, dielec. props., microstruct. rel. to sintering temp. and comp. 4-84897
- PbMg<sub>1/3</sub>Nb<sub>2/3</sub>O<sub>3</sub>, diffuse phase transition 4-65967
- PbMg<sub>1/3</sub>Nb<sub>2/3</sub>O<sub>3</sub>, mean square displacements, thermal expansion coeff. in diffuse ferroelec. transition region, X-ray diffr. meas. 4-65971
- PbMg<sub>1/3</sub>Nb<sub>2/3</sub>O<sub>3</sub>, single cryst., growth by mass crystallisation method, elec. relax. study 4-76315
- Pb(Mg<sub>1/3</sub>Nb<sub>2/3</sub>)O<sub>3</sub>-Pb(Zn<sub>1/3</sub>Nb<sub>2/3</sub>)O<sub>3</sub> solid solns., ceramic, dielec. characts. 4-76354
- Pb<sub>1-x</sub>Mn<sub>x</sub>S, IR laser diode emission in high mag. fields 4-69412
- Pb<sub>1-x</sub>Mn<sub>x</sub>Te, band struct., cyclotron reson. obs. 4-84546
- n-Pb<sub>1-x</sub>Mn<sub>x</sub>Te, intraband magneto-optical transitions in epitaxial film 4-71355
- Pb<sub>1-x</sub>Mn<sub>x</sub>Te spin-glass semicond., mag. and transport props. 4-88681
- PbMoO<sub>4</sub>, electrical cond. and optical absorpt. study 4-104205
- PbMoO<sub>4</sub>, stoichiometry deviation, electron transfer, elec. cond. meas. 4-80591
- PbMoO<sub>4</sub>S<sub>8</sub>, Chevrel phase, resistivity meas. 4-84619
- PbMoO<sub>4</sub>S<sub>8</sub>, divalent Chevrel-phase supercond., effect of press. and O defects 4-80711
- PbMoO<sub>4</sub>S<sub>8</sub> tapes, superconducting props. study (*Chinese*) 4-104336
- PbMoO<sub>4</sub>S<sub>8</sub>, Chevrel phase, resistivity meas. 4-84619
- Pb(Ni<sub>1/2</sub>)<sub>2</sub>, laser radiation effect on thermal decomposition (explosions) 4-71927
- Pb(NO<sub>3</sub>)<sub>2</sub>, cohesive energy, elastic const. and Grüneisen coeff. calcs. 4-84230
- Pb<sub>2</sub>NaNb<sub>2</sub>O<sub>15</sub>, tetragonal bronze-like struct., modulated phases and domain struct. 4-113616
- Pb<sub>0.67</sub>Nb<sub>1.77</sub>Zn<sub>0.23</sub>O<sub>6.66</sub>, crystal structure 4-103727
- PbO layers, microscopic appearance, preferred orientation, and platelet thickness, X-ray diffr. and SEM obs. (*Chinese*) 4-88411
- α-PbO, low temp. phase obs. by X-ray diffr., ferroelastic transitions (*French*) 4-80211
- PbO, standard molar Gibbs free energy of form., O conc. cell meas. 4-105010
- PbO, tetragonal and rhombohedral, Mossbauer effect on <sup>119</sup>Sb impurity atoms 4-65884
- PbO-B<sub>2</sub>O<sub>3</sub> glass, photoelastic consts., compositional trends 4-84945
- PbO-B<sub>2</sub>O<sub>3</sub>-BaO-Y<sub>2</sub>O<sub>3</sub>-Ga<sub>2</sub>O<sub>3</sub>-Fe<sub>2</sub>O<sub>3</sub>, phase diagram invest. 4-93208
- PbO-BaO-TiO<sub>2</sub>-B<sub>2</sub>O<sub>3</sub> glass ceramic system, crystal clamping, X-ray diffr., dilatometry 4-109386

## lead compounds continued

- PbO-Bi<sub>2</sub>O<sub>3</sub> system, crystallographic parameters, Mossbauer studies 4-61614
- PbO-CO<sub>2</sub>-H<sub>2</sub>O solid systems, stability and solubility rels. 4-84399
- PbO-containing glass, XPS study of angular dependence of preferential sputtering 4-88926
- PbO-K<sub>2</sub>O-Na<sub>2</sub>O-As<sub>2</sub>O<sub>3</sub>-SiO<sub>2</sub>, optical glass, effects of salt additions on specific surface and polishing 4-79257
- nPbO-Nb<sub>2</sub>O<sub>5</sub> (Ta<sub>2</sub>O<sub>5</sub>), (1.5≤n≤2.5), vibr., IR and Raman study (*French*) 4-66034
- PbO-PbCl<sub>2</sub> glasses, coordination of divalent Pb studied by EXAFS 4-84198
- PbO-PbX<sub>4</sub> (X=S, Cr, Mo) cryst. struct., neutron powder diffr. studies 4-84268
- PbO-SiO<sub>2</sub>, <sup>29</sup>Si NMR study of struct. 4-76269
- PbO<sub>2</sub>, α and β, proton localisation, X-ray and neutron diffr. studies. (*French*) 4-88142
- PbO<sub>2</sub>, chemically prepared, incorporation in Pb-acid battery cathodes 4-77073
- PbO<sub>2</sub>, incorporation into 'precharged' positive plate for Pb-acid automotive battery 4-77069
- PbO<sub>2</sub>, incorporation into 'precharged' positive plate for Pb-acid automotive battery 4-77070
- β-PbO<sub>2</sub>, struct. parameters and Pb-acid battery failure 4-103718
- PbO<sub>2</sub> vacuum evaporated films, electron emission and I-V characts. (*Japanese*) 4-76643
- PbO, exciton luminescence under powerful laser excitation 4-109235
- Pb<sub>2</sub>P<sub>2</sub>S<sub>6</sub>, far IR, IR and Raman spectra, crystal struct. and vibr. spectra (*German*) 4-70073
- PbS (100), low energy electron double reflection 4-103616
- PbS and PbSe detectors and arrays, review 4-95518
- PbS, at. vibr. amplitudes, Debye-Waller factor 4-98232
- PbS film, photosensitivity and luminescence studies 4-104679
- PbS, lattice thermal cond. meas. 4-98598
- PbS, nonstoichiometry, voltammetry using paste electrode 4-108407
- PbS polycryst. samples, current and photoconcurrent flow mechanisms 4-104196
- PbS polycrystalline films, chemical deposition, for use as infrared detector (*Spanish*) 4-114392
- PbS, single cryst., localised spin scatt. magnetoresistivity 4-61396
- PbS theoretical refractive index determ. 4-93032
- PbS thin films, laser and thermal annealing effects on elec. props. 4-65298
- PbS, thin films, noise power spectra meas. 4-80638
- mPbS-nBi<sub>2</sub>S<sub>3</sub>, long period modulated struct. with continuously variable periodicity 4-113469
- PbSO<sub>4</sub>-PbO, high temp. β phase, struct. study (*French*) 4-98065
- Pb(Se), IR detector arrays, state-of-the-art review 4-111202
- PbSe tunable diode lasers, Cd diffused, multicomponent gas analysis appl. 4-112457
- PbSe<sub>0.9</sub>Se<sub>0.9</sub> small gap semicond., second order Auger recombination 4-80606
- PbSe<sub>1-x</sub>Se<sub>x</sub> DH diode lasers fabricated by compositional interdiffusion 4-102952
- PbSe<sub>1-x</sub>Se<sub>x</sub>, n<sup>+</sup>-p<sup>+</sup> injection laser, performance characts. 4-79154
- PbSe<sub>1-x</sub>Se<sub>x</sub>, tunable diode lasers for 3 to 30 μm IR operation 4-112456
- Pb<sub>2</sub>ScNbO<sub>6</sub>, order-disorder transitions and dielec. props. 4-65980
- Pb(Sc<sub>0.5</sub>Ta<sub>0.5</sub>)O<sub>3</sub> single cryst., ordered domains, TEM obs. 4-65411
- PbSe and PbS detectors and arrays, review 4-95518
- PbSe, anisotropy of Fermi surface of holes 4-104117
- PbSe epitaxial film, photoconductivity relax. study 4-104270
- PbSe epitaxial narrow-gap semicond. films, optical four-wave mixing 4-83640
- PbSe film, photoelectric props. meas. 4-104267
- PbSe, lattice thermal cond. meas. 4-98598
- PbSe theoretical refractive index determ. 4-93032
- PbSe/BaF<sub>2</sub> epitaxial MIS structures 4-99316
- PbSe-Si heterojunctions, solution-grown, elec. and photoelec. props. 4-114023
- PbSe<sub>1-x</sub>Te<sub>x</sub> solid solution, p-n heterojunction form. by LPE 4-88996
- PbSe<sub>1-x</sub>Te<sub>x</sub>, IR, Raman spectra and elec. cond. 4-70724
- (Pb<sub>1-x/2</sub>Sm<sub>x/2</sub>)(Ti<sub>1-x/2</sub>Mn<sub>x/2</sub>)O<sub>3</sub> ceramic ultrasonic probe 4-100341
- Pb<sub>2</sub>SnO<sub>4</sub> single crystals, flux growth, X-ray charact. 4-76651
- Pb<sub>2</sub>SnO<sub>4</sub>S multilayer single crystal, semiconductor, X-ray effects, Mossbauer invest. 4-109106
- PbSnSe tunable diode lasers, Cd diffused, multicomponent gas analysis appl. 4-112457
- Pb<sub>1-x</sub>Sn<sub>x</sub>Se, thin film, unit cell parameters, phase composition 4-61249
- Pb<sub>1-x</sub>Sn<sub>x</sub>Se tunable diode lasers for 3 to 30 μm IR operation 4-112456
- PbSnTe cleaved-coupled cavity lasers 4-87327
- PbSnTe, crystal growth under microgravity, segregation obs. 4-98036
- PbSnTe, negative differential mobility in high elec. fields 4-104216
- PbSnTe tunable diode laser, wide-range amplification using optically pumped high-pressure NH<sub>3</sub> 4-91466
- PbSnTe-PbSeTe DBR diode lasers grown by LPE 4-112460
- PbSnTe-PbSeTe lattice-matched DH laser diodes, lasing characts. 4-112421
- PbSnTe-PbTeSe lasers with high efficiencies, lattice-matching to reduce misfit dislocations 4-112420
- p-Pb<sub>0.8</sub>Sn<sub>0.2</sub>Te/n-PbSe<sub>1-x</sub>Te<sub>x</sub> heterojunction photodiodes, LPE and elec. props. 4-88575
- Pb<sub>0.81</sub>Sn<sub>0.19</sub>Te, absorption edge, free carrier Fermi-liq. interaction effects 4-114236
- Pb<sub>0.9</sub>Sn<sub>0.1</sub>Te epitaxial films, heating by short laser pulses 4-88203
- Pb<sub>1-x</sub>Sn<sub>x</sub>Te, band struct. changes during struct. and band inversion transitions 4-65607
- Pb<sub>1-x</sub>Sn<sub>x</sub>Te, defect states, impurity photoconductivity transient studies 4-80545
- Pb<sub>1-x</sub>Sn<sub>x</sub>Te diodes, excess noise rel. to I-V characts. 4-61426
- Pb<sub>1-x</sub>Sn<sub>x</sub>Te, ferroelec. phase transition close to band inversion 4-76364
- Pb<sub>1-x</sub>Sn<sub>x</sub>Te large homogeneous single crystals, growth by vapour-melt-solid mechanism 4-71547
- Pb<sub>1-x</sub>Sn<sub>x</sub>Te, longitudinal magnetoresist., magnetophonon oscils. 4-65694
- Pb<sub>1-x</sub>Sn<sub>x</sub>Te, refractive index dispersion meas. 4-99074
- Pb<sub>1-x</sub>Sn<sub>x</sub>Te, Shubnikov-de Haas effect, temp. depend. scatt. parameter 4-113978
- Pb<sub>1-x</sub>Sn<sub>x</sub>Te, solid solution, vapour phase growth of epitaxial films 4-76689
- Pb<sub>1-x</sub>Sn<sub>x</sub>Te system, plasma oscil. freq., temp. depend. 4-88836
- Pb<sub>1-x</sub>Sn<sub>x</sub>Te tunable diode laser fabricated by horizontal unseeded vapour growth (*Chinese*) 4-60035

## lead compounds continued

- Pb<sub>1-x</sub>Sn<sub>x</sub>Te, valence band struct. near phase transition 4-84564  
 Pb<sub>1-x</sub>Sn<sub>x</sub>Te:In, elec. transport props. 4-61371  
 Pb<sub>1-x</sub>Sn<sub>x</sub>Te:In, Gunn effect, threshold field rel. to cond. band struct. 4-88513  
 Pb<sub>1-x</sub>Sn<sub>x</sub>Te:In, photoconductivity and impurity states 4-113993  
 Pb<sub>1-x</sub>Sn<sub>x</sub>Te:In epitaxial films, optical absorption spectra and photoconductivity 4-65711  
 Pb<sub>1-x</sub>Sn<sub>x</sub>Te:In epitaxial layers, optical absorption studies 4-71456  
 Pb<sub>1-x</sub>Sn<sub>x</sub>Te:In epitaxial layers, photocond. kinetics 4-88538  
 Pb<sub>1-x</sub>Sn<sub>x</sub>Te, ferroelectric transition temp. and saturation effect (*Russian*) 4-71318  
 Pb<sub>1-x</sub>Sn<sub>x</sub>Te(Se), synthesis and cryst. struct. 4-84261  
 (Pb<sub>1-x</sub>Sn<sub>x</sub>)<sub>1-y</sub>Yb<sub>y</sub>Te-Pb<sub>1-x</sub>Sn<sub>x</sub>Te heterojunction stripe geometry lasers grown by MBE 4-112458  
 PbTaO<sub>3</sub>, piezoelectric interface, Stoneley wave propagation 4-104059  
 PbTe cryst., external shape, impurity complex effects 4-75347  
 PbTe, crystal growth by Bridgman method and by travelling heater method 4-103678  
 PbTe epitaxial films, photoluminescence characs. 4-66067  
 PbTe epitaxial narrow-gap semicond. films, optical four-wave mixing 4-83640  
 PbTe films, hot wall epitaxy, elec. characs., SEM and X-ray obs. 4-71564  
 PbTe films grown by hot wall epitaxy technique, AC field effect study 4-92835  
 PbTe, iodide prep. method in flow reactor 4-76660  
 PbTe, lattice thermal cond. meas. 4-98598  
 PbTe, negative differential mobility in high elec. fields 4-104216  
 PbTe Schottky barriers, resonant magneto-optical transitions from a deep level 4-76440  
 PbTe, sintered, elec. cond. and thermoelec. power, annealing effects 4-84621  
 PbTe, size quantised films, p-polarised optical properties 4-114338  
 PbTe theoretical refractive index determ. 4-93032  
 PbTe thin film, electrophys. props., degradation and recovery 4-88619  
 PbTe thin films, elec. props., effect of boundary layers 4-88618  
 PbTe:B, absorpt. spectra and impurity states 4-104638  
 PbTe:Ga, elec. and optical meas. (*Russian*) 4-84636  
 PbTe:Ti, pure and doped, defect struct., X-ray double cryst. studies 4-75383  
 PbTe/Pb<sub>1-x</sub>Sn<sub>x</sub>Te superlattices, struct. and electronic props. 4-98463  
 PbTe/Pb<sub>1-x</sub>Sn<sub>x</sub>Te superlattices, optical and elec. props. 4-99209  
 PbTe/ZnS IR filter durability assessment, Space Shuttle 1st LDEF appl. 4-74688  
 PbTe-Bi system, anomalous transport props. 4-88588  
 PbTe(Se) polar multivalley semicond. with impurities, optical absorption by electron plasmas 4-114230  
 PbTe<sub>1-x</sub>Se<sub>x</sub>, synthesis and cryst. struct. 4-84261  
 PbTe<sub>1-x</sub>Se<sub>x</sub>/PbTe heterojunctions, epitaxially grown, misfit dislocations 4-88431  
 (PbTe)<sub>1-x</sub>(SnSe)<sub>x</sub>, solid solns., single cryst., phys. props. 4-65673  
 Pb<sub>2-x</sub>K<sub>x</sub>Ta<sub>2</sub>O<sub>15</sub>, crystallographic and dielec. props. (*French*) 4-79987  
 Pb<sub>2-x</sub>Ta<sub>x</sub>O<sub>15</sub>, crystallographic and dielec. props. (*French*) 4-79987  
 PbTiO<sub>3</sub>, amorphous, Raman spectra, low wave-number response 4-104590  
 PbTiO<sub>3</sub>, amorphous and cryst., bond lengths, annealing effect, Raman spectra, EXAFS study 4-79935  
 PbTiO<sub>3</sub> amorphous films, dielec. and elec. props. 4-104531  
 PbTiO<sub>3</sub>, delayed phenomena in transient pyroelectric response derived from cylindrical shaped domains 4-61630  
 PbTiO<sub>3</sub>, electron energy struct. of cond. band, X-ray photoemission yield spectra 4-61282  
 PbTiO<sub>3</sub>, ferroelec. phase transitions, stress effects 4-71315  
 PbTiO<sub>3</sub> heteroepitaxial ferroelec. films, domain struct. 4-65993  
 PbTiO<sub>3</sub>, single crystal, dislocation and domain struct. 4-75452  
 PbTiO<sub>3</sub>, six sites model for successive transitions 4-80873  
 PbTiO<sub>3</sub>, substituted, ferroelec. phase transitions and phase diagrams 4-65978  
 PbTiO<sub>3</sub> thin films, CVD prep. and dielec. props. 4-104736  
 PbTiO<sub>3</sub> type crystals, electrogyration, dispersive and temp. depend. 4-76433  
 PbTiO<sub>3</sub>/synthetic rubber composites, piezoelec. and dielec. props. 4-104535  
 PbTiO<sub>3</sub>-PbZrO<sub>3</sub>, high-temp. reactions, EPMA and SEM investig. 4-80292  
 (PbTiO<sub>3</sub>)<sub>0.9</sub>[Pb(Mg<sub>1/2</sub>W<sub>1/2</sub>)O<sub>3</sub>]<sub>0.1</sub>, photovoltaic effect and beam intensity sensor 4-98664  
 Pb(Ti<sub>0.81</sub>Sn<sub>0.19</sub>)O<sub>3</sub>, ferroelec., phase-transition, high press. Raman study 4-76451  
 Pb(Ti<sub>1-x</sub>Zr<sub>x</sub>)O<sub>3</sub>, ferroelec. phase transitions and phase diagrams 4-65978  
 PbTiAs<sub>2</sub>S<sub>6</sub>, cryst. struct. and coordination polyhedra 4-92174  
 Pb<sub>2</sub>TiO<sub>4</sub> electrodeposit, cryst. structure (*Japanese*) 4-88138  
 Pb<sub>1-x</sub>U<sub>x</sub>F<sub>2+2x</sub>, high temp. ionic cond. study 4-70450  
 Pb<sub>1-x</sub>U<sub>x</sub>F<sub>2+2x</sub>, ionic conductivity, crit. temp. 4-92423  
 Pb<sub>2</sub>O<sub>7</sub>, crystn. in Pt crucible, DTA study 4-109317  
 Pb<sub>2</sub>V<sub>2</sub>O<sub>8</sub>, cryst. struct. of ferroelectric  $\alpha$  phase (*French*) 4-84259  
 Pb<sub>8</sub>V<sub>2</sub>O<sub>13</sub> and Pb<sub>8</sub>V<sub>2</sub>(1-x)P<sub>2</sub>O<sub>13</sub>, ferroelastic props. and crystal struct. 4-70264  
 Pb<sub>8</sub>V<sub>2</sub>(1-x)P<sub>2</sub>O<sub>8</sub>, ferroelectric transition and acousto-optic props. 4-75660  
 Pb(Zr,Ti)O<sub>3</sub> ceramic, fracture mechanics evaluation of acoustic fatigue 4-95416  
 Pb(Zr,Ti)O<sub>3</sub> ceramics, ageing and ferroelec. props., heterovalent substitution effects 4-99046  
 Pb(Zr,Ti)O<sub>3</sub> ceramics, spray dried, piezoelec. props. 4-109130  
 Pb(Zr,Ti)O<sub>3</sub> ferroelec. films, reactive sputtering prep. and dielec. props. 4-104731  
 Pb(Zr,Ti)O<sub>3</sub>, high-freq. transducer 4-97241  
 Pb(Zr,Ti)O<sub>3</sub>, piezoceramic substrate, vacuum arc-plasma deposition of Ni-Cu 4-76691  
 Pb(Zr,Ti)O<sub>3</sub> porous ceramic, appl. to HF underwater transducer 4-97258  
 Pb(Zr,Ti)O<sub>3</sub> ring transducer, vibr. mode anal. 4-97240  
 Pb(Zr,Ti)O<sub>3</sub>/synthetic rubber composites, piezoelec. and dielec. props. 4-104535  
 Pb(Zr,Ti)O<sub>3</sub>-polyethylene composite, pyroelectric effect study 4-99044  
 Pb<sub>2</sub>ZrF<sub>10</sub>, F diffusion mechanism, NMR studies 4-108646  
 PbZrO<sub>3</sub>, soft mode in ferroelectric transition 4-99063  
 PbZrO<sub>3</sub>, with O vacancies, phase transitions, dielec. props. 4-76391  
 PbZrO<sub>3</sub>, with vacancies, para, ferro and antiferroelectric phase transitions, influence of hydrostatic press. 4-76390

## lead compounds continued

- Pb(Zr<sub>0.53</sub>Ti<sub>0.47</sub>)O<sub>3</sub> ceramics, piezoelec. props., porous struct. effects 4-104534  
 Pb(Zr<sub>1-x</sub>Ti<sub>x</sub>)O<sub>3</sub> ceramic strips, width and thickness strain meas. 4-80869  
 PbZr<sub>1-x</sub>Ti<sub>x</sub>O<sub>3</sub> cryst., T, x, E phase diagram anal. 4-76359  
 PbZr<sub>1-x</sub>Ti<sub>x</sub>O<sub>3</sub> ceramics, electrostrictive coeff., time resolved X-ray diffraction studies 4-71282  
 Pb<sub>(1-y/2)</sub>Zr<sub>(1-x+y)</sub>Ti<sub>x</sub>Nb<sub>y</sub>O<sub>3</sub> ceramic transducers, pyroelec. and mechano-dielec. characs. 4-109136  
 R<sub>2-x-y</sub>Bi<sub>1-x</sub>Pb<sub>y</sub>Fe<sub>1-x-y</sub>M<sub>2</sub>O<sub>12</sub> garnet films, mag. and magneto-optical props. 4-80802  
 Rb<sub>2</sub>Pb<sub>2</sub>Nb<sub>10</sub>O<sub>30</sub>, ferroelec. struct. and piezoelec. props. 4-65963  
 Sn-Ge-Pb, nonequilibrium crystn., rel. to cooling rate 4-61054  
 (Sr<sub>0.50</sub>Pb<sub>0.25</sub>Cd<sub>0.25</sub>TiO<sub>3</sub>)<sub>100-x</sub>(Bi<sub>2</sub>O<sub>3</sub>·3TiO<sub>2</sub>)<sub>x</sub> dielectric props., HV capacitor application 4-98997  
 Te-Ge-Pb alloys, glass stability, cryst. struct. effect 4-60836  
 W bronze tetragonal struct. non-stoichiometric phases, dielec., ferroelastic and nonlinear optical props. 4-65972

## leak detection

- air mass spectrometer leak detection using the SALT cart 4-90598  
 borehole monitoring by US echography (*French*) 4-67444  
 capillary and bubble methods for detection of through-defects 4-76956  
 channels, long and narrow, internally cooled superconducting coil 4-86428  
 chemical sensor research at the laboratory of applied physics in Linköping 4-111116  
 colliding beam accelerator, first string full cell vacuum system 4-91125  
 common problems and solutions 4-90597  
 design considerations for achieving high vacuum integrity in fusion devices 4-91101  
 nuclear reactor containments, integrated leakage rate test duration criteria 4-59393  
 vacuum system, leak detection using unidirectional vac. gauge (*Japanese*) 4-63755  
 Westinghouse LCP coil, He leak testing, test sensitivity 4-111886  
 He leak detection using closed loop system 4-95449

## leakage, magnetic see magnetic leakage

## leakage currents

- GaAs semi-insulating substrate, inhomogeneity characterisation, expt. study 4-65759

## least squares approximations

- advection-diffusion equations, space-time least-square finite element scheme 4-64903  
 atomic vapour density meas. by least-squares fit to spectra 4-102825  
 Auger effect, elemental intensity determination by pre-filtered least squares fitting 4-96512  
 beta-ray spectra, data anal. using response function 4-59481  
 boundary function approximation, Lagrangian, spline and weighted finite difference methods 4-64848  
 boundary problems in generalised analytical functions, variational-difference method (*Russian*) 4-63490  
 composites, orthotropic, elastic and photoelastic calibration, appl. of least squares method 4-69717  
 computational methods in linear algebra 4-67957  
 cubic spline techniques for curve fitting X-ray photoelectron cross sections 4-59682  
 curve fitting, least squares and utmost correl. methods comparison 4-67967  
 cyclohexanol, plastic and glassy crystalline phases, structure, X-ray diffraction 4-60866  
 data smoothing, matrix formulation, least-squares principle 4-102557  
 dihydronolizines photochromic systems, photokinetic examinations 4-99093  
 ENDOR and EPR, g-tensors and A-tensors, anisotropic and non-coincident, least squares fitting 4-61607  
 frequency meas., mean square relative random frequency variation calc. 4-95393  
 FT-IR absorbance subtraction from mixtures, automated procedure 4-105036  
 geometrical approach 4-110830  
 image restoration using Hunt's method, inverse filter effects 4-91411  
 interferogram analysis, freq. domain description 4-107516  
 interferogram analysis, frequency domain description, global least squares fit 4-112343  
 inversion of geophysical data by least-squares techniques 4-67423  
 monobromonitrobenzenes, valence force field, pot. energy distrib. and IR vibr. spectra, normal coord. anal. 4-83492  
 nuclear power plant failure detection and isolation under steady-state conditions by constrained least-squares method 4-86934  
 output parameter estimation technique, stability anal. (*French*) 4-58624  
 photoelastic solutions at stress concentrations 4-112710  
 positron annihilation lifetime spectrum anal. using multiple-exponential function model (*Chinese*) 4-71466  
 radioactive decay constants, least squares fit 4-90980  
 spectral analysis of short-time biomedical data using adaptive filters 4-72453  
 tensor structure approach to least-squares method 4-72474  
 US imaging through an inhomogeneous layer by least-mean-square error fitting 4-60234  
 US measurement of grain size, estimation of scatterer spacing using non-linear least-squares technique 4-99726  
 wavelength dispersive spectrometer, deconvolution method for overlapping spectral peaks 4-82872  
 X-ray anomalous dispersion meas. by X-ray interferometry 4-61767  
 ClO<sub>2</sub>, absolute absorpt. cross sections at high resolution in A<sup>2</sup>Π<sub>1/2</sub>-X<sup>2</sup>Π<sub>1/2</sub> band system 4-78857  
 GAP, Hall meas. anal., influence of thermal impurity activation energy temp. depend. 4-104238  
 Se IX, UV spectrum 100 to 140 Å, least squares fit 4-59667

## leather see materials

## LEC growth see crystal growth from melt

## LED see light emitting diodes

## ledeburitic steel see alloy steel

## Lee model

- coupled Nπ-Nππ system, three-particle eqns., nucleon propagator 4-106578  
 three-particle eqns. for model field theory 4-68658

- ED** see low energy electron diffraction
- al: research (computing applications)** see government data processing; al and behavioural sciences computing
- isolation**
- diving operations, regulation and safety organisation 4-106169
- fission reactor safety legislation, Nuclear Technical Committee work review (German) 4-111669
- Law of the Sea, problems for marine science 4-106168
- radioactive waste, disposal regulations for geological repositories 4-83163
- United States national programmes promoting renewable energy business development 4-93589
- gth measurement**
- see also micrometry
- automation, based on interference patterns analysis 4-101812
- laser Doppler anemometry, appl. signal processing requirements (German) 4-78294
- laser gravimetric measurement accuracy, effect of Gaussian struct. of beam (Russian) 4-60099
- laser interferometer calibration at NPL 4-95508
- metre, new definition 4-86381
- metre definition documents 4-63718
- optical length determ. in diamond-anvil cell 4-68237
- optical length measurement with CCD-array (German) 4-90565
- sarcomere length determ. using laser diff., effect of beam and fibre diameter 4-89849
- synthetic MM-wave signal generation for long length meas. 4-58812
- C material, dimensional changes, under compressive stress at high temp. 4-85182
- gth standards** see measurement standards
- Lennard-Jones and Devonshire theory** see liquid theory
- Lennard-Jones potential**
- adatom dimer diffusion on (111) surface of Lennard-Jones face-centred crystal, molecular dynamics simulation 4-65557
- atomic clusters, melting behaviour Metropolis Monte Carlo simulations 4-113579
- atomic system, quenched condensation, computer simulation 4-75295
- benzene, liq., Lennard-Jones interactions, Monte Carlo study 4-70014
- benzene, mol. dynamics simulations of self-diffusion coeffs. in binary Lennard-Jones solns., isotope effects 4-75253
- bicrystal, grain boundary phase equilb., computer mol. dynamics simulation 4-113461
- binary liq. model mixtures, Lennard-Jones pot., diffusion coeff., mol. dynamics calcs. 4-70010
- binary liquid mixt., local composition with differing sizes of components 4-88046
- binary mixtures, mol. dynamic studies with different component sizes 4-88045
- Bose liquid, one-dimensional, many-body props. 4-84475
- curved interfaces in simple fluids, generalised van der Waals theory 4-113753
- cyanogen, lattice dynamics, pot. model and zone-centre phonons 4-92310
- dense fluids, transport processes, projection operator methods, kinetic eqns. 4-65162
- dense gases, mol. dynamics simulations, continuous pots. effects 4-63648
- dense monatomic and molecular fluids and their mixtures, shear viscosity, thermal cond., anal. 4-113688
- diametric fluid, perturbation theory, thermodynamic and quasithermodynamic props. 4-97990
- dipolar two centre Lennard-Jones mol. liqs., dielec. behaviour and multi-body orientational correl. 4-97988
- enamino aldehydes (ketones) (amides), UV spectra, CNDO/S CI calcs. 4-78789
- FCC solid surfaces, memory function parameterisation in generalized Langevin eqn.-ghost atom function 4-92493
- fluids, liquid-vapour coexistence line 4-113592
- fluids, orthobaric props. of spherical and linear mols., intermol. pot. effect 4-74310
- hard spheres and discs, melting, density functional theory 4-70347
- hard-disk and Lennard-Jones systems, 2-D melting, Monte Carlo studies 4-113286
- Lennard-Jones solid, second-order elastic const. calcs. 4-70252
- light induced drift theory, derivation of combination rules 4-107410
- liquid drops, Lennard-Jones pot. surface tension, mol. dynamics study 4-97987
- liquid state, vapour condensation, canonical partition function, virial expansion 4-97991
- Lorentz-Berthelot mixtures, mutual diffusion coeff.  $D_{12}$  det. by mol. dynamics method 4-103628
- molecules obeying Lennard-Jones pot., basis functions for quantum mechanical treatment 4-87029
- periodic ground states, one dimension, Lennard-Jones-type potentials 4-95336
- polymer glasses, press. effects, densification and dielectric losses 4-65190
- stearic acid, intermolecular potential and surface energies of crystalline polymorph 4-113379
- supercooled liquid homogeneous nucleation, periodic boundary conditions, computer simulation 4-98247
- surface self-diffusion, transition state theory 4-84499
- thermodynamic props. calc. of fluids in mol. dynamics expts. 4-113666
- two dims. eqn. of state, mol. dynamics study 4-84361
- two-dimensional aqueous solution-like system, conc. fluctuations, Monte Carlo study 4-70008
- two-dimensional lattice, dynamics uniaxial strain, Monte Carlo simulation 4-113522
- two-dimensional lattice, struct. transition, mol. dynamics studies 4-108603
- Ar/Kr system, mutual diffusion coeff.  $D_{12}$  det. by mol. dynamics method 4-103628
- Cd vapour, interatomic pots., UV absorpt. spectra 4-107297
- H<sub>2</sub> evolution in liq. He chamber, recombination and burial 4-77003
- <sup>3</sup>He and <sup>4</sup>He, Lennard-Jones pot., effective-range expansion parameters calc. 4-108671
- <sup>3</sup>He, liquid, effective-range expansion parameters for central potentials 4-70497
- <sup>4</sup>He-<sup>3</sup>He mixture, triplet correlations in boson-boson mixtures 4-98397
- <sup>4</sup>He, liquid, effective-range expansion parameters for central potentials 4-70497
- Hg vapour, interatomic pots., UV absorpt. spectra 4-107297
- In, 410 nm line, perturbation by foreign gases, press. broadening and shift. 4-102634
- Lennard-Jones potential continued**
- N<sub>2</sub>, adsorption on graphite, mol. dynamics simulation, herringbone orientational ordering 4-61211
- N<sub>2</sub> gas, structural second virial coeff., neutron scat., meas. 4-69854
- NH<sub>4</sub>Cl, librational motion of NH<sub>4</sub><sup>+</sup> 4-60865
- Rh (100) and (111), surface self-diffusion, transition state theory 4-84499
- W (110) and (211), surface self-diffusion, transition state theory 4-84499
- Zn vapour, interatomic pots., UV absorpt. spectra 4-107297
- lens antennas**
- EHF aplanatic zoned dielectric lens antenna, anal. 4-102998
- millimeter wave imaging lens antenna 4-91560
- lenses**
- see also aberrations; aspherical lenses; contact lenses; electron lenses; electrostatic lenses; focusing; magnetic lenses; photographic lenses
- aberration polynomials for computer anal. of interferograms 4-97148
- acoustic lens design using geometrical theory of diffraction 4-74833
- acoustic microscopy, miniature lens scanner 4-97230
- adaptive spherical lens performance via elec. modulation of refr. index in tandem liq. cryst. cell arrangement 4-107782
- anamorphic gradient-index lenses for laser diode to fibre coupling 4-87407
- Angenieux's high technology product range 4-107786
- apochromatic two-element objectives for astronomy appl. 4-102994
- aspheric surface generation methods 4-87489
- aspheric surface testing with interference type, computer-generated holograms (Chinese) 4-87427
- asymmetric spline surfaces, design of high-quality general optical systems 4-107780
- audio acoustic, vane-type and acoustic wavefront visualisation device (Korean) 4-112657
- ball lens demultiplexer (German) 4-87430
- birefringence, permissible, in lenses of optical instruments, calc. method 4-91563
- book, aberration and optical design theory 4-95086
- Bragg-grating optical-waveguide lenses, out-of-phase props. 4-87444
- CAD, intelligent program 4-102996
- Canon lenses, design experience 4-107787
- catadioptric magnifiers, aberration corrected, for microfiche readers 4-69525
- chirped grating lens on BeO glass waveguide using ion beam etching 4-62071
- chromatic aberration coefficient computation, power series weighted truncation 4-59993
- chromatic aberration coefficients, weighted over doubling in computation in systems composed of homogeneous lenses and mirrors 4-112352
- cinematographic projector 5-element objective lens parameters, tolerances 4-90670
- compensation plate, plane-parallel, aberration props. 4-60136
- computer-generated holographic tandem component with optimum light efficiency, combination of lens and phase filters 4-79077
- conical lens for azimuthal integration of scat. light intensity 4-101895
- cover sheet aberrations in optical recording 4-91408
- crystalline lens, intact, nondestructive method for refr. index meas. 4-67161
- cylindrical optics, defining and testing methods 4-79349
- EHF aplanatic zoned dielectric lens antenna, anal. 4-102998
- electro-optical focusing devices, optimisation 4-74644
- equivalent optical resonators, g-parameter, mode struct. and beam divergence 4-79188
- eye, fast B-scan diagnostics in severe trauma situations (Italian) 4-81749
- eye lens, theoretical optical power rel. to refr. index (Italian) 4-81667
- eye lens alterations after chronic professional exposure to low LET ionising radiation (Italian) 4-81741
- far-IR lens optical quality assessment using 300 mm aperture high precision scanning interferometer 4-74765
- film camera eye-piece lenses, optical characteristics (Russian) 4-90677
- film lenses analysis, with complex source point method 4-64792
- Fujinon lenses, technological advances 4-107788
- Gaussian lens equations extension 4-74650
- glass constants, nondestructive collimation meas. technique using Ronchi grating shearing interferometer 4-73495
- graded-index (GRIN) rod-lens directional couplers, design 4-74742
- gradient-index conical rod, transmittance function and modal propag. 4-69546
- gradient-index lens array, reduction/enlargement type 4-83665
- gradient-index lens for laser-diode beam, focusing props. 4-87411
- gradient-index lenses, coupling characts. for light source to fibre systems 4-83664
- gradient-index light-focusing plastic rod form, by photocopolymerisation of multiple monomer systems 4-87485
- gradient-index optical imaging systems, conf., Monterey, CA, USA (April 1984) 4-95057
- gradient-index optical systems in holographic endoscopy 4-83549
- gradient-rod single radial lens, spherical aberration model 4-83545
- grating lenses, linearly chirped, of medium Q in dielec. waveguides, perturbation and iterative perturbation anal. 4-79262
- grazing-incidence dye lasers with and without intracavity lenses, comparative study 4-91447
- GRIN light-focusing plastic rod lens prepared by photocopolymerisation of ternary monomer system 4-87486
- half-symmetric unstable resonator with internal axicon, reflexicon deforms effect on geom. parameters 4-69524
- high precision optical assembly tolerances and techniques 4-83736
- holographic lens, aberration-containing design for post-objective holographic deflector 4-102907
- holographic lens for an optical correlator 4-107576
- holographic lens imaging quality evaluation, use of classical OTF (Chinese) 4-87301
- holographic microscope objective, small spherical aberration and coma 4-106379
- holotens, multifocus, for optical matrix-matrix multiplication method 4-102896
- IR optics elements design, materials, coatings and fabrication, update 4-79250
- kinoform optical element fabrication 4-87342
- laser scanner, scan lens design w.r.t. performance and cost 4-107783
- microlens terminated optical fibres, fabrication, biomedical appls. 4-87337

## lenses continued

- microlenses, two-dimens., propagating-beam-method anal. 4-87447  
microobjective, low power, design 4-107781  
multichannel optical fire control sight, channel interaction 4-91564  
multifacet holographic field lens for diffraction pattern sampling 4-96844  
multifacet holographic lens with parallel axes (*Chinese*) 4-112359  
nonsymmetrical optical systems, matrix theory 4-74645  
optical manufacturing and testing, conf., San Diego, CA, USA (Aug. 1983) 4-106104  
optical radiation coupling into fibre waveguides of elliptic cross section 4-107826  
optical system design (*German*) 4-74656  
optical system performance criteria simplification 4-97025  
optical waveguide, multiple waveguide lens 4-91579  
Optics in Australia conference, Sydney, Australia (May 1983) 4-95047  
pancratic sights for hunting guns 4-64755  
photographic information difference detect using simple optical information-processing method 4-69331  
planar microlens array, design (*Japanese*) 4-83669  
plasma lens, oscillations effect on focused ion beams 4-113229  
polarisation, definitions and nomenclature, instrument polarisation 4-82604  
polyhedral lens array fabrication, photolithographic appls. 4-74770  
radial gradient lenses compared to homogeneous lenses, first-order props. 4-107778  
radial-shear interferometers, thick lens, survey 4-68273  
reading performance and eye-movements through Varilux 2 and ST-25 lenses 4-62488  
refractive index determ. using moire deflectometry 4-87488  
relay for electron cyclotron emission transportation in plasma diagnosis, microwave and visible radiation 4-75204  
Schneider-Kreuznach TV camera lenses, review 4-107789  
Selfoc lenses, radiation effects at low dose rates in communication systems 4-91626  
semiconductor laser/single mode fibre coupler development 4-91632  
simple lens holder for introductory optics laboratories, design and development 4-110836  
single mode fibre microlenses, self-centering using optical levitation 4-112571  
single-mode fibre lens coupling to laser diodes, effect of aberrations 4-97064  
size calculations of optical systems, use of Gaussian brackets 4-64753  
solar energy concentrators, adjustable, for seasonal and daily changes accommodation without requiring tracking equipment 4-72047  
space power system using Fresnel lenses for solar power utilisation, thermal energy storage 4-72176  
spherical and orthogonal cylindrical lenses, mixed systems, matrix optical analysis of skew rays 4-107779  
spherocylinder lenses, decentrations, Prentice's rule appl. 4-100351  
stereograms, intermediate aspects synthesis 4-91415  
telecentric large-aperture wide-range objective 4-74654  
telescope lens distortion effect reduction on ang. meas. error 4-79265  
test signal image appl. for computation of focal length and aberration (*Russian*) 4-107776  
testing in transmission using Twyman-Green lateral-shearing heterodyne interferometer 4-106372  
thermal imaging lenses, transmittance meas. 4-103035  
transmission elements for technological CO<sub>2</sub> lasers, materials for windows and lenses 4-107658  
triplet lenses, achromatisation in 3 to 5  $\mu$ m spectral region with visible light transmitting materials 4-69523  
TV camera lenses, servicing requirements 4-107790  
TV cameras appl., technological development 4-107785  
two-lens achromat, chromatic longit. aberration convection, optical material struct. 4-97028  
two-lens cemented objective calc. using a computer 4-74653  
ultrawide wave band optical materials and systems, multi-sensor appl. 4-112552  
ultrawide waveband lens system design for 0.4 to 12  $\mu$ m waveband 4-74647  
vignetting effect in one-lens and two-lens optical systems for rainbow holography 4-69336  
wavefront reconstruction in a two-lens system 4-74613  
waveguide grating lenses for optical couplers 4-87443  
zoom system for Gaussian beam, general paraxial theory 4-91562  
Ge lenses, surface struct., veiling glare and image quality in 3 to 10  $\mu$ m spectral region 4-74648

## lepton decay

- see also *muon decay*  
electron lifetime, decay process 4-90879  
lepton conservation in weak interaction processes 4-90756  
massive neutrinos, masses and decay times rel. to neutrino-dominated Universe 4-106085  
massive neutrinos in galactic halo, decay, photon emission, UV background origin 4-77912  
neutrinos, UV emission; appl. to galaxy clusters and background radiation 4-101154  
scalar neutrino mass, effect on intermediate boson, tau lepton and kaon decays 4-90744  
standard electroweak model, neutrino masses, lepton triplets, decay lifetimes 4-106498  
tau lepton, lifetimes, review 4-73751  
tripositronium decay, yield at electron accelerators (*Russian*) 4-95795  
 $L \rightarrow \nu_l + \nu_{\bar{l}}$  leptonic decay, massless spin 3/2 neutrinos with nonmaximal helicity states 4-95794  
 $\nu \rightarrow J$ , invisible decay modes, lepton number as spontaneously broken symmetry 4-90880  
 $\tau \rightarrow 3\pi^0 \nu_{\tau}$ ,  $m_{\mu}$  upper limit determ. 4-73754  
 $\tau \rightarrow e \nu_{\tau} (\mu \nu_{\tau})$ ,  $g$ -value test, radiation zeros 4-86707  
 $\tau \rightarrow K_{\nu} (K_{\nu} \pi^0)$ , Cabibbo suppressed decay, branching fractions 4-73755  
 $\tau \rightarrow \rho + \pi$  pions, branching ratios for  $x \geq 2$  4-73756  
 $\tau$  lepton, leptonic decays, finite  $\nu$  mass and effects of mass mixing 4-59078  
 $\tau \rightarrow h\nu$ , hadronic decays in virtino-quark model 4-111450

## lepton-deuteron interactions

- see also *lepton-deuteron scattering*  
deep inelastic scatt., QCD parametrizations; nucleon structure functions 4-95801  
deuteron six-quark component from struct. functions 4-59047

## lepton-deuteron interactions continued

- ed, electrodisintegration, d quark struct. and relativistic quark dynamics 4-95800  
ed  $\rightarrow eX$ , high energy inclusive cross section polarisation depend 4-78574  
ed  $\rightarrow e p n$ ,  $P_{\beta} = 295$ -300 MeV/c, cross section, isobar configuration influence 4-90996  
 $\mu d \rightarrow 2n\gamma$ , neutron yield, capture rate meas. 4-83049  
 $\nu d$  and other low energy interactions 4-90861

## lepton-deuteron scattering

- see also *lepton-deuteron interactions*  
ed elastic scatt., degrees of freedom, pol. effects, rel. approach, review 4-95799  
ed scatt., d quark struct. and relativistic quark dynamics 4-95800

## lepton-hadron interactions

- see also *lepton-hadron scattering*; *lepton-nucleon interactions*  
dilepton production phenomena in high energy hadronic collisions 4-68590  
nonrelativistic deep inelastic scatt.,  $x$ - versus  $y$ -scaling 4-78558  
QCD, hadronic wavefunctions, large momentum transfer interactions, deep inelastic lepton scatt. 4-63975  
eh  $\rightarrow eX$ , deep inelastic scatt., parton distrib. function, evol. eqns. for higher twist operators 4-82964

## lepton-hadron scattering

- see also *lepton-hadron interactions*; *lepton-nucleon scattering*  
No entries

lepton interactions see *lepton-deuteron interactions*; *lepton-lepton interactions*; *photon-lepton interactions*

## lepton-lepton interactions

- see also *electron-electron interactions*; *electron-positron interactions*; *lepton-lepton scattering*; *neutrino-electron interactions*; *neutrino-neutrino interactions*  
Higgs boson production, collisional, effect of decay 4-106503  
 $\Pi \rightarrow$  pseudoscalar, numerical formula for total cross-section calc. 4-95784

## lepton-lepton scattering

- see also *electron-electron scattering*; *electron-positron scattering*; *lepton-lepton interactions*; *neutrino-electron scattering*; *neutrino-neutrino scattering*  
 $e\mu \rightarrow e\mu$ , covariant formulation for cross-sections 4-64006

## lepton mass

- <sup>76</sup>Ge double beta decay, Battelle-Carolina expt. status 4-90976  
dileptonic system, mass bounds from cosmology, cosmic mass density 4-67625  
extended survival hypothesis and fermion masses 4-73670  
fermion-fermion condensation in superconductivity model,  $n\bar{n}$  oscillation and  $\nu$  mass 4-82927  
flavour mixing and masses of leptons and quarks 4-63981  
intermediate mass scales and electron-muon-tau-lepton universality 4-86627  
massive neutrinos, masses and decay times rel. to neutrino-dominated Universe 4-106085  
neutrino mass calcs. from <sup>158</sup>Tb electron capture, Q-value difference 4-83033  
neutrino mass determ., model independent lower bound from tritium  $\beta$  spectrum 4-111527  
neutrino mass eigenstates, CP properties 4-86605  
neutrino mass from oscillations and double beta-decay expts. 4-73683  
neutrino mass spectrum, lepton charge conservation, massless and massive nondegenerate Majorana neutrinos 4-106490  
neutrino mass upper limit astrophysical consequences 4-72874  
neutrino mass upper limit from <sup>76</sup>Ge double beta decay 4-59208  
neutrino masses, mixing and oscillations in  $S_2$  model 4-90781  
neutrino mass mass, role in galaxy formation 4-115826  
neutrino oscillation parameters, experimental sensitivity for cosmic rays 4-110427  
neutrino oscillations, rest mass, weak interaction mixing 4-63929  
neutrino role in cosmology 4-77999  
neutrinoless double  $\beta$ -decay, interference between light and heavy Majorana neutrinos 4-90973  
neutrinos, effect on galaxy formation in neutrino dominated universes 4-78006  
neutrinos, massive, cosmological bounds 4-95008  
QED, one-loop corrections, temperature effect on electron charge, mass wave function 4-86636  
quark and lepton mass hierarchy in  $N=1$  supergravity GUTs 4-78224  
scalar neutrino mass, effect on intermediate boson, tau lepton and kaon decays 4-90744  
SO(10) fermion mass matrix model, Majorana  $\nu$  masses and lepton mixing angle limits 4-68470  
standard electroweak model,  $Y=0$  lepton triplets, neutrino masses 4-106498  
SU<sub>L</sub>(2)  $\times$  SU<sub>R</sub>(3) model, scalar field set addition fermion mass generation radiative corrections 4-73637  
SU<sub>L</sub>(2)  $\times$  U(1) model, pseudo-Dirac neutrino, mass splitting 4-106531  
three-fermion model for quarks and leptons with three families 4-63983  
 $e^-$  mass, magnetic moment and vacuum energy from field theory finite temp. corrections 4-68346  
 $K^+ \rightarrow \mu^+ \nu_{\mu}$ , heavy neutrino search and muon longitudinal polarisation 4-102115  
 $\nu$  mass from double  $\beta$ -decay, recent developments 4-59210  
 $\nu$  mass from spectroscopic meas. and oscillations,  $\beta$ -decay, solar neutrinos 4-59016  
 $\nu$  mass in left-right symmetric electroweak model, leptonic charged weak interactions 4-86615  
 $\nu$  mass matrix, oscillations and double beta-decay, review 4-90766  
 $\bar{\nu}_e$  mass bounds from <sup>3</sup>H-<sup>3</sup>He  $\beta$  decay 4-90987  
 $\nu$  mass, upper limit from  $\tau \rightarrow 3\pi^0 \nu_{\tau}$  4-73754  
 $\nu$  mass and effects of mass mixing;  $\tau$  lepton decays 4-59078  
<sup>76</sup>Ge double  $\beta$ -decay, Guelph expt., preliminary tests using Ge crystal 4-90979  
<sup>76</sup>Ge neutrinoless double  $\beta$ -decay, Mont Blanc expt.,  $\nu$  mass effects 4-90974  
<sup>76</sup>Ge neutrinoless double  $\beta$ -decay, CIT results, lepton number conservation,  $\nu$  mass 4-90975  
<sup>3</sup>H, atomic and molecular,  $\beta$ -decay expt., apparatus,  $\nu$  mass 4-90977  
<sup>3</sup>H, beta decay, neutrino rest mass calcs. 4-95973  
<sup>3</sup>H  $\beta$ -decay, neutrino mass and end-point energy 4-90978  
 $\pi^+ \rightarrow \mu^+ \nu_{\mu}$  at rest, neutrino mass and  $\pi^+$  rest mass 4-102111

**on-nucleon interactions**

- see also *electron-nucleon interactions; lepton-nucleon scattering; muon-nucleon interactions; neutrino-nucleon interactions*  
 deep inelastic lepton interactions QCD anal. 4-90887  
 deep inelastic scatt., in Fe, C, QCD parametrizations, nucleon structure function 4-95801  
 deep inelastic singlet struct. functions and scaling violation (*Chinese*) 4-68573  
 IN deep inelastic scatt., struct. function, nuclear effects 4-111460  
 IN-IX, electroweak structure functions, deep inelastic scatt., quark-parton model 4-102103  
 IN- $\nu$ X, electroweak structure functions, deep inelastic scatt., quark-parton model 4-102103  
 $\nu$  deep inelastic scatt., QCD parametrizations, nucleon structure functions 4-95801

**on-nucleon scattering**

- see also *electron-nucleon scattering; lepton-nucleon interactions; muon-nucleon scattering; neutrino-nucleon scattering*  
 IN-IX, polarisation in high energy scatt., charge current interactions, EM interference 4-90886

**on-nucleus reactions**

- see also *electron-nucleus reactions; lepton-nucleon interactions; muon-nucleus reactions; neutrino-nucleus reactions*  
 conference, intermediate energy nuclear physics, San Miniato, Italy (Aug. 1983) 4-101570  
 deep inelastic lepton scatt., quark-proton distrib. 4-64120  
 deep inelastic lepton scattering, clustering and quark distributions in nuclei 4-64077  
 nuclear excitation by various probes 4-102263  
 (IX) inclusive reaction, multiple scatt. expansion 4-90995  
 Fe(IX), deep inelastic scatt., quark-parton distrib., quark-cluster model 4-68674  
 H(IX), deep inelastic scatt., quark-parton distrib., quark-cluster model 4-68674  
 He(IX), deep inelastic scatt., quark-parton distrib., quark-cluster model 4-68674

**on-nucleus scattering**

- see also *electron-nucleus scattering; lepton-nucleon scattering; muon-nucleus scattering; neutrino-nucleus scattering*  
 $^{16}\text{O}$ , longitudinal and transverse nucl. responses to isovector spin probes 4-96010

**on production**

- see also *electron pair production; muon production; neutrino production*  
 asymmetric production, control of black hole accretion discs 4-82500  
 dilepton production phenomena in high energy hadronic collisions 4-68590  
 Drell-Yan cross section high-moment corrections with alternate parton density 4-86743  
 Drell-Yan process, lepton pair  $P_T$  distrib. is asymptotically free scalar field theory 4-59043  
 Drell-Yan processes in nuclear targets, cross section corrections 4-95974  
 hard scattering processes, transverse hadronic energy emission, high-mass lepton pair prod. 4-102099  
 initial state interactions, factorization, and the Drell-Yan process 4-63967  
 same-sign dilepton production, possible origin from new class of neutral particles 4-95787  
 spinless boson radiative decay, anomalous  $\gamma\ell$  events 4-111440  
 $e^+e^- \rightarrow l^+l^-$ , electroweak model dependence of electromagnetic corrections 4-73705  
 hh-sleptons, production cross-section limits in cosmic rays 4-101079  
 hN-IX, in nuclei, soft and hard quark processes role in dilepton prod., A depend. 4-95820  
 $p\bar{p} \rightarrow n\bar{e}^+$ , expts. at Mount Blanc tunnel 4-96410  
 $p \rightarrow l^+l^-$  pseudoscalar-meson decay amplitudes, model insensitive relations 4-90865  
 $p\bar{p} \rightarrow b\bar{b}$  mixing, dilepton signals from heavy quark pair decay 4-102096  
 $p\bar{p} \rightarrow l^+l^-X$ , lepton pair production with  $M(l^+l^-) < M_X$  4-86739  
 $p\bar{p} \rightarrow lX$ , Drell-Yan parton-quark model relation, two gluon radiation modification 4-111476  
 $\tau$  lifetime determ. from  $e^+e^- \rightarrow \tau^+\tau^-X$  4-86696  
 W decay, new composite bound state 4-86802  
 $Z^0 \rightarrow q\bar{q}l^+l^-$ , Monte Carlo calcs. 4-90936  
 $Z^0 \rightarrow \tau^+\tau^-$  limits on composite structure, CP violation 4-90937

- on scattering see *lepton-deuteron scattering; lepton-hadron scattering; pion-lepton scattering; photon-lepton scattering*

**on spin and parity**

- neutrinos, massless, spin 3/2, with nonmaximal helicity states and leptonic decays 4-95794  
 QED 8th order contributions to electron anomaly from vacuum polarization graphs 4-95749

**on decays**

- see also *baryon leptonic decay; meson leptonic decay; muon decay*  
 conference, particles and fields, Blacksburg, VA, USA (Sept. 1983) 4-73135  
 scalar neutrino mass, effect on intermediate boson, tau lepton and kaon decays 4-90744  
 spinless boson radiative decay, possible source of anomalous  $l^+l^-\gamma$  in Z searches 4-102148  
 $\mu \rightarrow e^+e^-e^-$ , search using SINDRUM mag. spectrometer 4-59480  
 $\tau \rightarrow \nu\gamma(\nu\nu\gamma)$ , g-value test, radiation zeros 4-86707  
 $\tau$  lepton, leptonic decays, finite  $\nu_\tau$  mass and effects of mass mixing 4-59078  
 W- $\nu$ , heavy unstable neutrinos from weak boson decays 4-86751  
 W $^- \rightarrow e^+\nu$ , invariant mass 4-73776  
 W $^- \rightarrow e^+\nu$ , parity violation, spin 4-73775  
 W $^- \rightarrow l^+\nu$ , scaling violations, intermediate boson prod. by  $p\bar{p}$  4-95828  
 W $^-$ -neutral scalar, electroweak theory 4-73686  
 Z $^0 \rightarrow e^+\nu$ , composite scalars in  $e^+e^-$  collisions and radiative Z decays 4-86694  
 Z $^0 \rightarrow e^+\nu$ , interpretations and other tests 4-78578  
 Z $^0 \rightarrow e^+\nu$ , test of standard model 4-68603  
 Z $^0 \rightarrow e^+e^-e^+$ , cascade decays through new particle, electron mag. moment, coupling constraint 4-102147  
 Z $^0 \rightarrow e^+e^-$  (2), invariant mass 4-73776  
 $Z^0 \rightarrow l^+l^-\gamma$ , anomalous lepton magnetic moments, constraints 4-86750  
 $Z^0 \rightarrow l^+l^-\gamma$ , collinear radiation and lepton universality 4-78577  
 $Z^0 \rightarrow \nu\nu$ , heavy unstable neutrinos from weak boson decays 4-86751  
 $Z^0 \rightarrow \nu\nu$ , neutrino generation counting 4-86754

**leptonic decays continued**

- $Z^0$  radiative decays, parity violation, spin 4-73775  
 $Z^0 \rightarrow \tau^+\tau^-$  limits on composite structure, CP violation 4-90937  
 $Z^0 \rightarrow l^+l^-$ , scaling violations, intermediate boson prod. by  $p\bar{p}$  collision 4-95828  
 @ W- $\nu$ , collinear radiation and lepton universality 4-78577  
 Z $^0 \rightarrow l^+l^-\gamma$ , excited lepton states 4-78580

**leptons**

- see also *electrons; heavy leptons; lepton spin and parity; muons; neutrinos; positrons*  
 (4/3)e charged lepton search in cosmic rays 4-101071  
 anomalous moments, constraints on  $Z^0 \rightarrow l^+l^-\gamma$  4-86750  
 composite models, motivation, hopes and difficulties, review 4-68546  
 composite quarks and leptons, lower and upper bounds on radius 4-63984  
 composite quarks and leptons, SU(3)XSU(2)XU(1) to rishon model 4-63985  
 conference on higher energy physics, Austin, TX, USA (Nov. 1982) 4-67857  
 cosmic ray leptons, search for 4/3e charge 4-101078  
 fermionic gauge fields, common origin of leptons and quarks 4-86521  
 flavour mixing and masses of leptons and quarks 4-63981  
 generation puzzle, lepton universality and conservation, double  $\beta$ -decay 4-63944  
 horizontal interactions as the source of family mixing 4-95742  
 intermediate mass scales and electron-muon-tau-lepton universality 4-86627  
 left-right symmetric composite model, fermion mass relation and t-quark mass 4-73730  
 mass relations in SO(10)XU(1)<sub>PC</sub> model 4-59002  
 massless composite fermion struct., large N limit of SU(N) gauge theory 4-90836  
 multilepton signals from production and cascade decay of top quarks in  $p\bar{p}$  colliders 4-68564  
 particle properties review, masses, decays and lifetimes 4-67885  
 particles and interactions, supersymmetric theories, quarks, leptons, W, Z, Winos, Zinos and Higgs 4-73674  
 S<sub>4</sub> permutation symmetry, CP nonconservation, rare decays and quark/lepton electric moments 4-86600  
 SO(10) fermion mass matrix model, Majorana  $\nu$  masses and lepton mixing angle limits 4-68470  
 SU(2)XU(1)XU(1) unified models, rel. to electroweak interactions of leptons 4-95716  
 substructure effects, composite leptons, quarks and W bosons, W couplings 4-111422  
 supersymmetric composite models, 't Hooft anomaly constraints-Nambu-Goldstone mech. interplay 4-63982  
 three-fermion model for quarks and leptons with three families 4-63983  
 $e^+e^-$  colliders, tests for substructure of leptons, quarks, W $^\pm$ , Z bosons 4-111428  
 $e^+e^-$  results from PETRA, QED and electroweak tests, lepton searches, jets, Higgs 4-64010

**leucocytes see blood; cellular biophysics****level control**

- automatic liquid N<sub>2</sub> filler controller 4-86402  
 liquid nitrogen autofill unit and level controller (*Chinese*) 4-82798  
 optical short-range radar, level control meas. 4-79210

**level crossing (energy) see energy level crossing****level measurement**

- cryogenic level indicator using voltage controlled oscillator 4-68208  
 flat-plate collectors with phase-changing fluids, testing 4-114940  
 image instability analysis using low cost moire pattern sheet 4-111195  
 lecture notes and study guide on basic instrumentation, book 4-106137  
 liquid He level indicator, appl. of amorphous supercond. alloys 4-86403  
 optical level based on moire effect with ambient light 4-95502  
 optical short-range radar, level control meas. 4-79210  
 He level sensor using superconducting wire 4-101808  
 He, liquid, level detector based on vapour press. meas. 4-101813  
 SrTiO<sub>3</sub> detector of liquid  $^3\text{He}$  level 4-101833

**levels, energy see energy states****levitation, magnetic see magnetic levitation****library mechanisation**

- optical discs systems and applications, conf., Arlington, VA, USA (June 1983) 4-90287

**LIDAR see optical radar****Lie groups**

- see also *elementary particle symmetry*  
 accidental degeneracies, Zeeman effect, symmetry groups 4-90785  
 algebras, cohomology theory 4-102019  
 algebras, Kostant partition function 4-95134  
 Bhabha fields, half-integer spin, hermitianizing matrix 4-95668  
 boson mapping in seniority scheme, commutators method 4-111512  
 celestial mechanics, Lie series use as numerical integration method 4-82400  
 charge-monopole duality, Coulomb phase of gauge theories 4-111298  
 charged particles with EM interactions, Hamiltonian and Lagrangian formalisms 4-86566  
 classifying space of classical Lie groups, 4-connective fibre space, cohomology mode p 4-90753  
 Clifford algebras, exponential mapping 4-95131  
 collective states, oscillator shell model, analogy with Zeeman effect 4-95878  
 combined symmetries in curved space-times 4-102081  
 complex SU(2), matrix elements for indecomposable representations 4-63908  
 composition of interactions in relativistic quantum theory 4-90411  
 connected nilpotent, nonlinear reps. 4-67958  
 connected Poincare group, nonlinear massive representations, formal linearisation 4-63909  
 current algebra, Lie algebra over physical space 4-58990  
 extended Lie superalgebras Clifford algebras 4-102055  
 F<sub>4</sub> type Lie algebras over fields of characteristic 2, nilpotent classes 4-82913  
 fixed symmetry and fixed class generating functions for compact Lie group 4-86598  
 gas flow, 1-D, infinite Lie group of symmetry, entropy distributions 4-103358  
 gauge field introduction by Lie-isotopic lifting of Hilbert space 4-90723  
 generalised supermanifolds, p-supermanifolds 4-63913

**Lie groups continued**

- generalised supermanifolds, anal. on superspaces 4-63912  
 generalised supermanifolds, superspaces and linear operators 4-63911  
 grand unified models,  $E_6$ ,  $SU(5)$ ,  $SO(10)$  maximal subalgebras 4-90458  
 gravity, exterior forms, geometrical structure 4-90448  
 $Gsl(2)$ , unified description of irreducible representations 4-78105  
 Hamiltonian transformation in quadratic Lie transforms 4-67600  
 Harry-Dym eqns., elliptic solns., recursion operators and Lie-Backlund symm. 4-67985  
 Hermitian operators, unitarily invariant decomposition, Lie algebra 4-63475  
 Higgs-Landau system, Lie symmetry breaking patterns, extended Morse theory, GUTs 4-58985  
 Hirota-Satsuma system, prolongation algebra 4-63478  
 integrable field theory models, Hamiltonian structs. Lie algebra 4-73651  
 irreducible representations of the  $SU(1/N)$  Lie superalgebras 4-63918  
 isotropic or admissible approach in field theory 4-68448  
 Kac-Moody algebra struct. in Lax representation (*Chinese*) 4-68441  
 Kac-Moody algebras and exact solvability in hadronic physics, review 4-111339  
 KdV equation, general prolongations and  $(x,t)$ -depend. pseudopot., Lie algebra 4-86228  
 KdV equation, infinitesimal transforms. about solns. through Lie product 4-90382  
 Konno-Wadati formalism, rel. to Backlund transformations 4-67984  
 linear ordinary differential equations, Lie-Backlund symmetry 4-86596  
 maximally embedded self-dual monopoles, Lie group soln., Higgs field behaviour 4-68422  
 $n+1$  photon, Poisson reduction and quantisation, Lie groups 4-86248  
 non-Abelian tensor gauge fields, geometry in  $SU(N)$  Lie algebra 4-58943  
 noncompact sigma model, dynamical mass generation, composite gauge bosons, supergravity theories 4-111299  
 nonlinear Dirac equations, integrability from soliton theory 4-95656  
 nonsymmetric gravity, Lie admissible algebra 4-68447  
 Olshanetsky-Perelomov many-body system in an external field 4-86778  
 one-dimensional gas dynamics, infinite dims. noncommutative Lie-Backlund algebra 4-75059  
 orbit spaces of simple compact connected Lie groups, group invariant scalar potential extrema 4-102007  
 $OSp(M/N)$ , finite-dimensional graded tensor representations, Young diagrams, weight space techniques 4-111323  
 planar incompressible Yang-Mills magnetohydrodynamics for quark soup, Lie algebras 4-78458  
 potential scattering, Lie algebras for Pöschl-Teller potential 4-68038  
 QCD, noncompact with stochastic gauge fixing, Monte Carlo simulation 4-78451  
 quantum mech. and geometrical dynamics deformations, book contrib. 4-58687  
 quantum mechanics, Lie isotopic lifting and noncanonical commutation relations 4-58677  
 representation spaces and Wigner-Racah calculus interrelation 4-95710  
 $SO_0(3,2)$  linear and unitary irreducible representation, book contrib. 4-58689  
 semisimple subalgebras, generators 4-78104  
 sine-Gordon equation, infinitesimal transforms. about solns. through Lie product 4-90382  
 $SL(3,R)$  realisations, damped harmonic oscillator 4-86595  
 $SO(3) \otimes SO(3)$  bases and structural zeros of 6 j-symbol, realisation of  $F_4$  4-63907  
 $SO(3)$  tensor operators, Lie algebras generation 4-63910  
 $SO(4)$  Lie algebra, integrable Euler equations and appls. 4-68444  
 $Sp(p+q)$  and  $Sp(p,q)$  in  $Sp(p) \times Sp(q)$  basis, structure of most degenerate representations 4-63906  
 spinorial relativistic rotator, transformation from quasi-Newtonian to Minkowski coordinates 4-90735  
 structure constants in root space 4-78103  
 $SU_N$  symmetries, Lie isotopic lifting, Lie isotopic  $SU_N$  algebra 4-73666  
 $SU(2)_R$  theory, commuting subgroup scalar operators 4-78491  
 $SU(n|1)$ , mixed super tableaux 4-102052  
 $SU(p,q)$  finite representation signatures 4-86597  
 superalgebras  $osp(1,2n)$ , Micu-type invariants for Casimir operators 4-78101  
 superfibre bundles, math. global theory, supermanifolds and super Lie groups 4-68105  
 superluminal Lorentz transformations, maps between manifolds, fibre bundles, Lie group bundle manifold 4-63505  
 Thompson eqn., hereditary operator, Lax pair, Lie-Backlund symmetry 4-90752  
 three-wave resonant interaction, eigenvalue problem via prolongation Lie algebra 4-90383  
 time-dependent mechanical symmetries and extended Hamiltonian systems 4-58989  
 Toda lattice, generalized, translationally noninvariant quantisation, cyclic space coordinate 4-86557  
 Toda lattice type Hamiltonian systems, classical flow solutions, Lie groups 4-95315  
 $U(1)$  gauge theory, Hamiltonian and Lagrangian formalisms 4-86566  
 unstable state decay, Lie-admissible lifting of the Schrödinger eqn. 4-90416  
 vector field Lie algebra, subalgebra classification, nonlinear coupled 1st-order diff. eqns. 4-86599  
 vector fields on straight line, Lie algebra, general position homologs (*Russian*) 4-68446  
 Verma submodules of Verma modules, extremal vectors 4-101618  
 Yang-Baxter eqn., solutions for simple superalgebras 4-102063  
 Yang-Mills fields, group-invariant measure as by-product of path integration 4-68373

**life testing**

- combustible gas sensors, development of poison resistant type 4-95414  
 injection lasers and transmitter modules, accelerated service life tests 4-74531  
 MCP in windowless EUV photon detectors, lifetime testing results 4-64297  
 optical fibres, double mandrel, technique for studying static fatigue 4-60161  
 polymers, thermal ageing kinetics, thermogravimetric testing 4-71859  
 secondary cells,  $Li/LiClO_4$  in polypropylene carbonate/ $V_2O_5$ , evolution of AC impedance 4-99954

**life testing continued**

- $CO_2$  sealed TEA lasers, high peak power and sustained long life operation 4-87365  
 CdSe photoelectrochemical solar cells, lifetime improvements 4-99969  
 $GaAs_P_{1-x}Cu$  LEDs, Cu impurities, thermal redistribution 4-80080  
 $InGaAsP/InP$  buried crescent lasers, 1.3  $\mu m$ , high temp. and long life operation 4-69444  
 $InGaAsP/InP$  buried crescent laser diode emitting at 1.3  $\mu m$ , high temp. CW operation 4-112427  
 Li-metal sulphide cell development for satellite batteries 4-72075  
 $LiSO_4$  cell capacity degradation, effect of low drain rates, obs. 4-72079  
 $LiSOCl_4$  cylindrical primary cells, design for safety, testing 4-66677  
 Na-S cells for high power satellite/spacecraft appls. 4-72076  
 Ni-Cd battery, life test with simulation of orbital thermal flux 4-72081  
 Ni-Cd cells, degradation study using impedance measurements 4-72068  
 Ni-H<sub>2</sub> battery, bipolar, prototype, test results 4-72090  
 Ni-H<sub>2</sub> cell, long-life Ni electrodes, initial performance test 4-72088  
 Ni-H<sub>2</sub> cells, cycle life test and failure model 4-72087
- ligand field theory** see bonds (chemical); crystal field interactions; molecular energy levels
- light**  
 see also airglow; optics; sunlight; zodiacal light  
 antibunched and sub-Poisson light generation, role of primary excitation statistics 4-87306
- light absorption**  
 see also atmospheric optics; densitometry; light transmission; optical constants; optical films; optical filters; optical saturable absorption; pleochroism; spectra  
 1.3  $\mu m$  window material effective absorpt. coeff. data survey 4-74638  
 absorptive bistability in three-level system interacting with two fields 4-79214  
 3-acetyl-9-vinyl carbazole oligomers, doped with electron acceptor, impurity, absorpt. and luminesc. spectra (*Russian*) 4-80975  
 aerosols, blackness (light absorbing ability) rel. to filter blackening 4-62252  
 agarose gels, mol. wt., rheological props. 4-60357  
 alkali halide:  $Tl^+$  cryst., optical props. and Jahn-Teller effects 4-61643  
 alkali halide mixed crystals, growth and characterisation, microhardness, colour centres, radiation hardening 4-70152  
 anthraquinone dichroic dyes, liq. cryst. characterisation and synthesis 4-84156  
 apparent optical figure error meas. caused by coating nonuniformity, ellipsometric meas. technique 4-74778  
 Arctic haze, radiation absorption by combustion-generated C particles 4-105143  
 Arctic haze season, solar radiation absorption 4-105711  
 aromatic polyamide film, luminophor addition, absorpt. spectra, TGA (*Russian*) 4-109222  
 atmosphere, water vapour reson. absorpt. study using line-tunable  $CO_2$  laser (*Chinese*) 4-67398  
 atmospheric precipitation water, extinction coeff. in 200 to 1100 nm region (*Russian*) 4-66836  
 atom, electric dipole moment light absorpt., semiclassical radiation theory 4-102651  
 beam thermal self-interaction in a moving medium, numerical study 4-74631  
 biexciton-impurity complexes, energy spectrum and optical props. 4-92660  
 black coatings in high alloy stainless steels produced by chem. methods 4-69606  
 circular metallic dielectric-coated waveguides for IR transmission, design theory 4-74704  
 CW on-resonance 'self-focusing' obs. in Na vapour 4-79244  
 deep charged impurity centres, multiphonon light absorpt. 4-71417  
 dielectric film on metal substrate zero reflection at oblique angles of incidence 4-91398  
 direct gap semiconductor, stochastic self-oscillations in two-temp. electron-hole plasma 4-86566  
 direct-gap semiconductor, nondegenerate, interband luminesc. and absorpt. coeff. 4-61749  
 dye laser radiation polarisation, steady-state approx. theory 4-79131  
 elements and compounds, photon cross-section meas. 30 to 660 keV 4-59680  
 fibre, sharply bent, radiation interaction with absorbing medium 4-79326  
 fibre optic absorption cell with variable path length for meas. of extinction in liquids 4-63765  
 fibres, graded-index, comparative spectral attenuation meas., final report by members of COST 208 4-87466  
 fibres, single-mode, higher-order mode attenuation meas., effective cutoff wavelength 4-79322  
 films, thickness measurement by optical absorption 4-63712  
 Fresnel's drag coeff., photon theory 4-86161  
 gas, spatially inhomogeneous, containing macroscopic particles, emission line shape 4-69315  
 generalized formula for absorption and stimulated emission of light 4-60011  
 graphite epoxy laminates, pulsed photothermal evaluation 4-88818  
 high order optical susceptibilities, obs. via angularly resolved multiwave mixing, anharmonic absorption grating 4-107731  
 III-V semiconductor quantum well struct., free carrier absorption for polar optical phonon scatt. 4-104551  
 III-V semiconductors, nonlinear absorpt., coherent radiation-exciton interaction model 4-99078  
 inert gas solids, optical consts., self-consistent anal. 4-71332  
 interstellar dust, far-IR pros. of metallic grains 4-67779  
 isotropic absorbing and intensifying medium, light refr. 4-74419  
 laser calorimetric apparatus for low optical absorption meas. 4-86422  
 laser calorimetry, polarisation sensitive 4-74584  
 laser fusion pellet, absorpt. rate and uniformity 4-78735  
 metal gratings,  $CO_2$  laser radiation absorption 4-114232  
 metal-dielectric heterostructures, singularities in guided TM mode absorpt. spectrum 4-74749  
 metallic particles, IR absorption coeff., nonlocal theory anal. 4-93042  
 microspectrophotometer for absorptometric and reflectometric analysis of crystals 4-95492  
 MOS solar cells, perform. calcs. at various temps. 4-72117  
 multimode resonance Raman scatt. and optical absorpt., linear non-Condon terms exact treatment 4-109176  
 multiple SHG, light fluctuation filtering in two-photon absorpt. process 4-107751

## light absorption continued

- nematogenic cpds, orientational order parameters 4-84149  
 nonimaging concentrators as unwanted radiation absorbers, curved conical horns 4-96793  
 nonlinear absorption dynamics in solids 4-69514  
 opaque materials, optothermal transient emission radiometry 4-86465  
 optical fibre,  $\text{OH}$ -absorption in fluoride glass IR fibres 4-91592  
 optical fibres in adverse environments, conf., Paris, France (May 1983) 4-78025  
 optical thin films and surfaces, selected characterisation techniques 4-83667  
 perylene dichroic dyes, liq. cryst. characterisation and synthesis 4-84156  
 photolayer radiation field optical characts. (Russian) 4-82852  
 photometric spherical integrator, coeff. of reflectivity of diffusive samples meas. 4-101889  
 plastic, dyed, transient interference gratings and holograms 4-91419  
 polar semiconductors, dielectric materials, phase transitions, absorption edge anomalies 4-109146  
 pollutant monitoring using  $\text{CO}_2$ -laser long-path absorption system 4-62426  
 polydiacetylene in dil. toluene soln., rod-to-coil transition theory, optical absorpt. spectra 4-75261  
 polydiethylene-glycol bis allyl carbonate, layered optical struct., photoacoustic spectra, interference effects 4-109143  
 polyester fibre insulation, optical props. and radiative heat transfer 4-80896  
 proton transfer reactions, rate consts., extinction coeffs. 4-99779  
 quarter-wave multilayers, high-reflectance, evaluation through secondary struct. anal., limits of validity 4-74672  
 quartz, electrical and optical props., neutron,  $\gamma$ , and electron irradi. effects 4-60968  
 quartz microporous glass laser active elements, optical characts. 4-79253  
 quasi-1D solids, band struct. shapes 4-92592  
 radiation pulses nonlinear coupling to absorbing anharmonic molecular media 4-78917  
 random light beams subject to thermal self-interaction, spatial coherence 4-60122  
 retinal rods outer segment, Monte Carlo simulation of light absorpt., rhodopsin conc. 4-81680  
 retinal Schiff-base, protonated, with torsion about bonds in polyene chain, optical absorption 4-77190  
 rhodamine-590 physisorbed thin films, surface photoacoustic wave spectra 4-104693  
 ruby,  $\gamma$ -irradiated, X-ray and optical spectra of Cr ions 4-114345  
 sapphire, uncoated, surface-to-bulk optical absorpt. using photoacoustic chopping freq. studies 4-76419  
 semiconductor, transient photoconductivity spectrum, surface recombination effects 4-65712  
 semiconductor superlattices, np-layered, optical absorption, time depend. 4-93034  
 semiconductor superlattices, optical props. 4-104665  
 semiconductor superlattices, quantum wells, and heterostructs., elec. and optical props. 4-80666  
 semiconductor thin films, intersubband absorption, depolarisation field effects 4-81025  
 semiconductors, absorption edge, free carrier Fermi-liq. interaction effects 4-114236  
 semiconductors, absorptive optical bistability due to band gap shrinkage 4-69482  
 semiconductors, direct gap alloys, free exciton optical absorption, disorder effects 4-65996  
 semiconductors, multivalley polar with impurities, optical absorption by electron plasmas 4-114230  
 semiconductors, polarised light absorpt. in donor-valence band optical transitions 4-61736  
 semiconductors, resonant absorpt. of high-intensity light 4-71408  
 semiconductors, thermal contraction of energy gap effect on optical breakdown 4-80910  
 single-polarisation single-mode optical fibres, absorption reducing, structure design 4-64784  
 solar cells, amorphous, optical loss mechanisms 4-77108  
 solids, nonlinear absorption, laser multimode effects 4-102978  
 solids, polarisation depend. of three-photon absorpt. 4-109145  
 surfaces, weak optical absorption meas. using lateral waves 4-88790  
 Taurus dark cloud complex, star counts and visual extinction rel. to  $\text{NH}_3$  obs. 4-115791  
 tetracene-anthracene chemically mixed mol. cryst., optical props. 4-76410  
 thin absorbing layer, refr. index thermal variation in strong laser field 4-74593  
 thin film, on Lambertian reflector substrate, optical absorpt. 4-81020  
 thin film absorption coefficients, calc. from laser calorimetric data 4-114333  
 thin-film laser calorimetry for optical absorpt. meas. 4-90591  
 three-level system probe absorpt. spectroscopy four-wave mixing effects with standing-wave laser beams 4-79218  
 three-level systems, dispersion and absorption anomalies 4-99072  
 transition metal dichalcogenides, optical anisotropy, photoelectrochem. determ. 4-71335  
 transparent film coating on absorbing substrate, inverting ratio of complex parallel and perpendicular refl. coeffs. 4-87271  
 transparent materials, absorpt. of laser rad. by metallised microinclusions 4-69468  
 visual pigments, dense samples, method for peak absorbance meas. 4-81828  
 water, pure, absorption coefficients in the wavelength range 400 to 580 nm 4-114231  
 weakly absorbing dielectrics and semiconductors, convective instability and self-focusing 4-97009  
 Ag absorptivity of  $10.6 \mu\text{m}$ , temp. depend., computed from Drude theory 4-76405  
 Ag microcrystallites, optical props., size depend. and matrix effects 4-109168  
 Ag surface light absorpt., effects of roughness 4-88797  
 AgBr emulsion microcrystals, spectral transmittance reflectance and absorpt. coeff. 4-104556  
 AgS films on Ag, spectrally selective props., for solar absorber converters 4-99211  
 Al absorptivity of  $10.6 \mu\text{m}$ , temp. depend., computed from Drude theory 4-76405  
 Al, optical const. meas. above melting point 4-88798  
 $\text{Al}_x\text{Ga}_{1-x}\text{As}$  layer waveguides, light absorpt. 4-103011

## light absorption continued

- $\text{Al}_2\text{O}_3$ , sintered, microstructure and optical props. 4-61649  
 $\text{As}_2\text{S}_3$  chalcogenide glass films, photostruct. changes 4-104560  
 $\text{AsSe}$  chalcogenide glass films, photostruct. changes 4-104560  
 $\text{AsSe}_{1-x}$  thin films, photoinduced optical absorption, storage appls. 4-85026  
 Au absorptivity of  $10.6 \mu\text{m}$ , temp. depend., computed from Drude theory 4-76405  
 Au submonolayer film, optical absorption,  $\epsilon_{\text{bound}}$  size depend. in small island particles 4-66089  
 $\text{BaSO}_4$  barytes single crystals,  $\gamma$  irradi., optical absorpt., thermolum. 4-66080  
 $\text{BaTiO}_3$  band struct. and ferroelec. transition, two-photon spectra studies 4-93016  
 $\text{BeO}$  ceramics, dielec. props. in near-mm wavelength range 4-99075  
 Bi size-quantised film, optical absorpt. coeff. calc. 4-109265  
 $\text{BiFeO}_3$  single cryst., ferroelec. domains, birefringence, and light absorption 4-71324  
 $\text{C:H}$  amorphous coating for IR-optical elements, optical props., thickness, density, laser damage tests 4-76422  
 $\text{CO}_2$  laser processing induced plasma, optical absorption prop. development 4-108189  
 $\text{CaCO}_3$  light absorpt. coeff. anisotropy in  $0.4\text{--}2.0 \mu\text{m}$  region 4-76416  
 $\text{CdS}$  amorphous films, optical absorpt. coeff. and gap state density 4-66088  
 $\text{CdS}$ , radiative and nonradiative recomb., plastic deform. depend. 4-61658  
 $\text{CdS}$  single cryst., photoacoustic spectra from unilluminated surface 4-109206  
 $\text{CdSe}$ -type uniaxial cryst., excitonic absorpt. band formation (Russian) 4-71409  
 $\text{CdTe}$  thin films, DC cond. rel. to  $\text{H}_2$  exposure 4-76053  
 Co base alloys, wear resistant, optical consts. of carbides and borides, interference microscopy 4-104949  
 $\text{CsI}$  fibre lightguide material, designed to operate in visible and IR spectral regions 4-74634  
 $\text{CsI}$ , optical transmittancy, xenon high pressure transmitting, band closing 4-114299  
 $\text{CsI:TI}^+$ , optical absorption and mag. circular dichroism spectra 4-99098  
 $\text{CsPbCl}_3$  ( $\text{Br}_3$ ), optical props. in region of self-absorption edge (Russian) 4-93044  
 $\text{Cs}_{1-x}\text{Xe}_x$ , optical absorpt. by Xe monomers and dimers, solvable one electron model 4-71404  
 Cu absorptivity of  $10.6 \mu\text{m}$ , temp. depend., computed from Drude theory 4-76405  
 Cu mirrors, diamond turned and mechanically polished, intensity depend. absorpt. and laser induced catastrophic damage at  $1.06 \mu\text{m}$  4-75519  
 Cu, surface light absorpt., effects of roughness 4-88797  
 Cu, temperature dependent absorpt., calorimetric meas. 4-76420  
 DF-HF chemical laser atmospheric attenuation meas. (Chinese) 4-62951  
 $\text{Fe}_{1-x}\text{Co}_x\text{S}$ , single cryst. solid solutions, homogeneity studies 4-75693  
 $\text{Fe}_{1-x}\text{Ni}_x\text{S}$ , single cryst. solid solutions, homogeneity studies 4-75693  
 n-type  $\text{GaAs}$  free-carrier absorption, quantum mechanical perturbation theory 4-80893  
 $\text{GaAs}$ , neutron irradi., optical absorpt. coeff., spectral depend. 4-99137  
 $\text{GaAs/AlGaAs}$  heterostructures, 2D electron plasma, optical processes 4-76523  
 $\text{GaAs/AlGaAs}$  multiple quantum well structures, room temp. excitonic nonlinear absorpt. and refract. 4-74590  
 $\text{GaAs/GaAlAs}$  multiple-quantum-well semicond., optical bistability due to increasing absorpt. 4-74598  
 $\text{GaAs}_{1-x}\text{Px}$ , fundamental absorpt., optical absorpt. coeff. 4-76408  
 $\text{GaP}$ , thick sample, optical absorpt. coeff. determ. using photoacoustic spectroscopy 4-106402  
 $\text{Gd-Ga}$  garnet, absorpt. coeff. and refractive index determ. 4-80895  
 $\text{a-Ge:H}$ , bond angle disorder and optical absorption edge 4-90983  
 $\text{GeO}_2\text{-V}_2\text{O}_5\text{-VCl}_3$  glass, optical absorpt., DC cond. rel. to  $\text{VCl}_3$  content 4-65675  
 $\text{GeO}$  films, optical consts., random bonding model 4-85025  
 $\text{H}_2\text{O}$  vapour absorption in visible and near IR, field meas. 4-89992  
 $\text{HgI}_2$ , optically excited electronic processes 4-104254  
 $\text{In}_2\text{Se}_3$  films, flash and thermal evaporation growth, struct. and elec. characterisation 4-114409  
 $\text{In}_{0.9}\text{Se}_{10}$  films, optical absorption, heat treatment effects 4-85027  
 $\text{K-Na}$  alloys, Fermi edge singularity reduction 4-76415  
 $\text{KCl}$  absorption, reversible and irreversible changes during multiple pulse  $10.6 \mu\text{m}$  irradi. 4-75518  
 $\text{KCl}$  crystals, optical breakdown thresholds due to action of  $\text{CO}_2$  laser pulses 4-60957  
 $\text{KCl}$  single crystal, X-ray irradi., F-band absorpt., mag. field effects 4-71352  
 $\text{LaF}_3\text{:Er}^{3+}$ , high freq. phonon dynamics, optical detection methods 4-65357  
 $\text{Mn}$  dihalides, d-excitons, vibr. struct., IR and Raman spectra studies 4-113873  
 $\text{Mn}_2\text{Zn}_{1-x}\text{Te}$ , optical absorption edge and spectra 4-99079  
 $\text{NaCl}$  absorption, reversible and irreversible changes during multiple pulse  $10.6 \mu\text{m}$  irradi. 4-75518  
 $\text{NaCl}$  crystals, optical breakdown thresholds due to action of  $\text{CO}_2$  laser pulses 4-60957  
 $\text{NaCl}$  single cryst., X-ray irradi., F-band absorpt., mag. field effects 4-71352  
 Ni base alloys, wear resistant, optical consts. of carbides and borides, interference microscopy 4-104949  
 $\text{NiCl}_2$ , valence-band photoemission and optical absorption 4-99279  
 $\text{NiO}$ , valence-band photoemission and optical absorption 4-99279  
 Pb absorptivity of  $10.6 \mu\text{m}$ , temp. depend., computed from Drude theory 4-76405  
 Pb perovskite oxides, ferroelec. transition effects on absorption edges 4-93020  
 $\text{PbF}_2\text{-ZnF}_2$  system, amorphous phase form. by roller splat cooling 4-85122  
 $\text{PbHfO}_3$ , ferroelec. transition effects on absorption edges 4-93020  
 $\text{PbI}_2\text{:Ag}$ , exciton spectrum, photodoping effects (Russian) 4-92626  
 $\text{Pb}_{1-x}\text{Sn}_x\text{Te}$  in epitaxial films, optical absorption spectra and photoconductivity 4-65711  
 $\text{Pb}_{1-x}\text{Sn}_x\text{Te}$  in epitaxial films, optical absorption studies 4-71456  
 $\text{PbTe}$ , size quantised films, p-polarised optical properties 4-114338  
 $\text{PbTe/Pb}_{1-x}\text{Sn}_x\text{Te}$  superlattices, optical and elec. props. 4-99209  
 Pd small particle composites, far IR absorption studies 4-99073

**light absorption continued**

- SbSI, para-ferroelec. phase transition, photoacoustic spectra studies 4-65975  
 Si classical periodic structs., light absorption edge 4-66002  
 a-Si, ion implantation form. and optical state characterisation 4-88186  
 Si solar cells, limiting efficiency, extended detailed balance method 4-81554  
 Si:Ga sputtered amorphous alloys, thermopower and elec. cond. 4-61403  
 a-Si:H, high-rate deposition from SiH<sub>4</sub> using RF discharge technique, elec. and optical props. 4-85119  
 a-Si:H,P(B), ESR and optical props., thickness depend. 4-84853  
 Si:H amorphous films, prep., characterisation absorpt. and laser-damage resistance 4-74676  
 a-Si:H film, optical props. meas. 4-76539  
 a-Si:H films, CVD growth, phys. props. 4-92715  
 a-Si:H films, DC planar magnetron reactive sputtering and characterisation 4-93218  
 a-Si:H Schottky solar cells, gap state density 4-88438  
 Si:O, impurity conc., IR absorption studies 4-113488  
 a-SiC:H glow-discharge film, electronic and optical props. 4-84623  
 a-SiH<sub>3</sub> solar cell, on Lambertian reflector substrate, optical absorpt. 4-81020  
 Si<sub>1-x</sub>H<sub>x</sub> coatings for high power IR lasers 4-74675  
 SiO amorphous films, optical absorpt. edge, temp. depend. 100 to 474K 4-93122  
 SiO<sub>2</sub> fibres, induced absorpt. due to drawing and irradi., Raman study 4-80919  
 SiO<sub>2</sub>N<sub>x</sub> reactively sputtered films for antireflection coatings, for a-Si solar absorber converters 4-99998  
 Sr I, principal series, photoabsorpt. spectrum 4-68996  
 Sr<sub>2</sub>Ta<sub>2</sub>O<sub>7</sub>, ferroelec. transition temp. and optical absorption edge, press. depend. 4-93018  
 SrTiO<sub>3</sub>, band struct. and ferroelec. transition, two-photon spectra studies 4-93016  
 Ta<sub>2</sub>O<sub>5</sub>/SiO<sub>2</sub> antireflection coatings, electron-beam deposited, 1064-nm damage tests, review 4-75525  
 ThF-BaF<sub>2</sub> multispectral glass development and characts. 4-74639  
 TiCl<sub>3</sub> polarisation depend. of three-photon absorpt. 4-109145  
 Ti<sub>1-x</sub>Ta<sub>x</sub> exponential optical absorption edge tail, Urbach rule verification 4-109149  
 Ti<sub>1-x</sub>VS<sub>x</sub> exponential optical absorption edge tail, Urbach rule verification 4-109149  
 W absorptivity of 10.6 μm, temp. depend., computed from Drude theory 4-76405  
 WO<sub>3</sub> amorphous films, electrochromic colour centres, Raman scatt. studies 4-113445  
 Zn<sub>1-x</sub>Co<sub>x</sub>S, single cryst. solid solutions, homogeneity studies 4-75693  
 ZnIn<sub>2</sub>S<sub>4</sub> layered cpd., energy gap, temp. depend., optical meas. 4-88803  
 ZnS film on Au substrate, zero reflection at oblique angles of incidence 4-91398  
 ZnS, multispectral chemically vapour-deposited, initial characterisation 4-76418  
 ZnS thin film, laser modulation by free carrier absorption, film thickness and temperature influences (*Japanese*) 4-114339  
 ZnSe, uncoated, surface-to-bulk optical absorpt. using photoacoustic chopping freq. studies 4-76419  
 ZnSe, visual grading method, new surface and bulk absorpt. values 4-83732  
 ZrF-BaF<sub>2</sub> multispectral glass development and characteristics 4-74639  
 ZrF<sub>4</sub>-based optical fibres, transmission losses, humidity effects 4-83712

**light absorption spectra** *see spectra***light amplifiers** *see image intensifiers***light attenuation** *see light absorption; light scattering; light transmission; optical dispersion***light coherence**

- see also laser beams; lasers*  
 antibunched and sub-Poisson light generation, role of primary excitation statistics 4-87306  
 apodised system using triangular and assoc. filters, two-point resolution in partially coherent light 4-64680  
 centro-symmetry and partial coherence 4-102881  
 coherent reception of images 4-74465  
 convex face irradiated with coherent light, reflected light interference 4-96782  
 dissipative systems in quantum optics, reson. fluoresc. optical bistability superfluoresc., book 4-63410  
 fibre mode-power fluctuations between polarisation states, source coherence time influence 4-97085  
 fields generated by homogeneous and by quasi-homogeneous planar secondary sources 4-83517  
 finite-aperture effects in the measurement of the degree of coherence 4-87270  
 Foucault target image contrast, effect of small defocusing for partially coherent illum. 4-79065  
 free electron generators of coherent radiation, conf., Orcas Island, WA, USA (June 1983) 4-82588  
 free electron laser, coherence and fluctuations, fully quantum mech. approach 4-87345  
 free electron laser oscillator, noise to coherence, photon noise and electron shot noise theory 4-87344  
 Fresnel images of periodic objects, lateral shift under coherent plane wave illum. 4-96831  
 gas ring laser, medium, excitation spatial-temporal coherence effect on statistical characts. 4-107590  
 Gaussian Schell-model fields, propag. characteristics through first-order optical systems 4-83541  
 high-power coherent radiation sources at mm to UV wavelengths 4-60053  
 holographic image quality, influence of spatial and temporal coherence 4-74457  
 homogeneous gain laser, mode locking through temporally modulated phase-conjugate reflectivity 4-79201  
 image formation by optical systems, energy model 4-64683  
 isotropic planar sources, complex degree of spectral coherence 4-87274  
 laser resonator modes, coherence theory 4-69454  
 laser temporal coherence effects in multiphoton transitions, model depend. 4-60094  
 multimode laser field, spatial coherence (*Russian*) 4-96862  
 multimode step-index fibre, light spatial coherence retention 4-107864

**light coherence continued**

- nonlinear media, optical field statistics, investigation using Monte Carlo method 4-107728  
 partially coherent light, new class of uncertainty relations 4-87273  
 partially coherent sources, radiometric definitions 4-68258  
 phase gratings hidden by diffusers detect. using intensity interferometry 4-59980  
 picosecond sampling experiments, coherence peaks 4-79227  
 pump-probe meas. with collinear copropag. beams, coherent coupling effects 4-96989  
 random light beams subject to thermal self-interaction, spatial coherence 4-60122  
 randomly distributed nonspherical particle vector radiative-transfer theory matrix representations 4-59979  
 restricting the radiation directivity during transmission of an image 4-74442  
 rhodamine 560, 6G tunable picosec. dye laser oscillator-amplifier system spatial and temporal props. 4-91488  
 Schell-model sources, coherent-mode eigenfunctions, completeness 4-107517  
 spatial and temporal coherence control, and incoherent methods, for optical processing 4-74434  
 spatial coherence, acousto-optical diffr. effect 4-74421  
 spatially periodic wavefield propag. 4-96796  
 squeezed state generation, critical discussion 4-87386  
 Strehl ratio symmetries and periodicities 4-96832  
 strong scattering, intensity fluctuations, two-scale solns. 4-87277  
 turbulent atmosphere, light beam intensity fluctuations, effect of initial degree of spatial coherence 4-107522  
 two-level atom, randomly modulated, coherent light scatt. 4-64689  
 two-level atoms, superfluorescence initiation, three dims. theory 4-112369  
 US wave modulation of light wave, mutual coherence function (*French*) 4-107518  
 Walsh transform by the coherent optical method 4-69330  
 white-light signal processor, noise performance, temporally partially coherent illum. 4-69320  
 Wigner distribution function and optical geometrical transformation 4-79028  
 GaAlAs laser picosecond pulse temporal coherence props., directly modulated and freq. stabilised optical communication system apps. 4-74509  
 LiNbO<sub>3</sub> crystals with polysynthetic domains, SHG enhancement 4-69508

**light communication** *see optical communication***light cones**

- see also current algebra*  
 causality, antiparticles, spin-statistics connection, annihilation and creation operators 4-106464  
 Euclidean space, algebraic, field description, spinor field, Minkowski double light cones 4-106462  
 Feynmann integrals, N=4 supergravity, gluon self-energy 4-90711  
 integral transformation in Lobachevsky space 4-63867  
 N=1 light-front supergravity, Ogievetsky-Sokatchev superspace, Yang Mills theory 4-111005  
 nonlinear  $\langle \chi \rangle$ - $\sigma$  model, symmetry relations, dual transformation and Noether symmetry 4-95660  
 quark-quark-gluon vertex in light-cone gauge, self-energy and Ward identity 4-86554  
 hh at extreme energies, light-cone QCD with axial-vector anomaly current 4-59039

**light diffraction**

- see also holography; optical zone plates*  
 acousto-optical light diffraction by profiled ultrasound 4-79027  
 acoustooptic deflector, bichromatic nondispersive 4-91569  
 adaptive transmission, two-wavelength, diffractive and refractive effects comparison 4-87280  
 anisotropic media, light diffr. by ultrasound 4-83542  
 anisotropic media, propag. and interaction of transversely-confined beams (*Russian*) 4-96794  
 anisotropic medium, light diffr. from US wave, acousto-optic interaction 4-96798  
 apodisation for maximum central irradi. and specified large Rayleigh limit of resolution 4-59972  
 auto-stereoscopic holographic display devices 4-74459  
 beam-splitters, ideal, Babinet's principle for submm waves 4-97039  
 Blue Phase I liquid crystal, order parameter optical meas. 4-103645  
 Bragg double diffraction of two laser beams by ultrasound 4-69308  
 bubbles in water, critical angle laser light scatt., meas., models, apps. to bubble sizing 4-69311  
 centro-symmetry and partial coherence 4-102881  
 chiral liquid-crystal mixture, electric-field-induced helix uncoiling 4-75292  
 cholesteric blue phase, struct. anal. by optical Bragg diffraction 4-88090  
 coherence peaks in picosecond sampling experiments 4-79227  
 coherent optical spectrum analysers, assembly and alignment errors 4-74651  
 complex rays and diffraction by smooth object 4-102882  
 concentration limits in physical optics and wave mechanics 4-96788  
 concentration limits in physical optics and wave mechanics 4-96795  
 convergent beam electron diffr. and optical reconstruction, conf., Liege, Belgium (May 1983) 4-86107  
 CW on-resonance 'self-focusing' obs. in Na vapour 4-79244  
 dielectric layer with sinusoidally corrugated boundary, light diffr. 4-107511  
 diffraction coupler diffracted field anal. using coarse grating made from cylindrical elements 4-79280  
 diffraction transducers, freq. props. and SAW emission 4-74834  
 DOBAMBC, ferroelec. smectic liq. cryst., phase diagram in external mag. field, laser light diffr. meas. 4-65170  
 Elasser-related approximation to the Airy function, comments 4-90660  
 fibre diameter measurement using diffraction method (*Russian*) 4-107851  
 fraunhofer diffraction patterns of microparticles 4-82628  
 frequency correlation of optical radiations propagating in a medium with large-scale random inhomogeneities 4-96805  
 Fresnel diffr. fields, television technique study 4-86157  
 Fresnel diffraction and white-light processing based system for real-time depth meas. and display 4-73412  
 Fresnel diffraction by two-dimensional periodic structures 4-107514  
 Fresnel-Kirchhoff diffraction in optical systems, approx. computational algorithm 4-96781

**light diffraction** continued  
 grating efficiencies, differential methods for mag. field parallel to grooves 4-69541  
 grazing incidence spectrometer designs based on conical diff., comparison 4-95522  
 half-plane, diff. of plane-wave, elementary derivation 4-96786  
 Hartmann test, diff. struct. of Hartmann-pattern images 4-63076  
 p-n-heptyloxybenzoic acid smectic C liq. cryst., electrohydrodynamic transient instability 4-75270  
 high order optical susceptibilities, obs. via angularly resolved multiwave mixing, higher Bragg diffraction orders: 4-107731  
 image formation by optical systems, energy model 4-64683  
 imaging quality limitations (*German*) 4-112346  
 isotropic solid dielec., light diff. from shear waves, theory 4-74417  
 kinoform quartz axicons, fabrication diff. props., appls. 4-83670  
 laser resonator diffraction loss investigation using diffracted light, picked-off with knife-edge mirror 4-60075  
 Malvern particle size calibration 4-95372  
 materials science appls., microdiff. techniques and cryst. struct. determ. 4-88043  
 methoxybenzylidenetoluidine nematic liq. cryst., acousto-optical phenomena 4-114243  
 micro-Fresnel high-performance lens fabricated by UV lithography 4-87408  
 mode conversion of acoustooptic interaction in crossed channel waveguide 4-104568  
 muscle fibres, single glycerinated frog semitendinosus, light diff. patterns rel. to fibre rotation 4-89647  
 nematic liq. cryst., longitudinal domain struct., laser diff. studies 4-60829  
 nonlinear optics, energy balance criterion for diff. 4-79221  
 nonspherical aerosol particles, light scatt. props. 4-96801  
 optical array, large curvature radius, pseudo-phase-conjugation, props. (*Chinese*) 4-97002  
 Optics in Australia conference, Sydney, Australia (May 1983) 4-95047  
 partially apodised systems, diffracted field characs. 4-96785  
 phase and amplitude of diff. field 4-74420  
 phase grating diffraction, coupled wave method determ. 4-91573  
 point diffraction interferometry, optical system focusing appl. 4-58887  
 polarisation holographic recording, diff. efficiency and selectivity 4-96845  
 polygonal apertures, Fraunhofer diff. formula derivation from Maggi-Rubinowicz transform. 4-69304  
 polystyrene monodisperse colloids, light diff. and cryst. struct. 4-103661  
 ripple measurement using Talbot diffraction imaging of gratings 4-63707  
 ripple tank, optical caustics and diff. study 4-95102  
 rippled interface, intense light wave diff. 4-74422  
 sarcomere length determ. using laser diff., effect of beam and fibre diameter 4-89849  
 sonine's Bessel identity applied to apodization 4-94605  
 spatial coherence, acousto-optical diff. effect 4-74421  
 speckle photography, diffraction halo 4-87268  
 speckle statistics with small no. of scatterers 4-107524  
 spider diffraction, curved and straight leg comparison 4-91397  
 superposed converging spherical wave focus, three-dimens. intensity distrib. 4-59973  
 Talbot and Lau effects, a parametrical approach 4-69322  
 three-dimensional intensity distribution near the focus in systems of different Fresnel numbers 4-102878  
 TM-component suppression during polarised-light diffraction by volumetric phase lattices (*Russian*) 4-59974  
 transmission hologram N gratings, diff. efficiency changes induced by coupling effects 4-91422  
 transversely stratified sinusoidal dielectric grating, diffraction anal. using modal expansion theory (*Japanese*) 4-83684  
 two photon resonant image upconvertors, diffraction integral representations (*Japanese*) 4-87396  
 two-stage spatial filtering for diff. pattern anal., processor digital simulation using cytogenetic data 4-59986  
 US wave modulation of light wave, mutual coherence function (*French*) 4-107518  
 US waves, amplitude-time-modulation of diffracted laser beam 4-102876  
 visual perception of apparent world form, by humans, diff. effect (*Italian*) 4-72253  
 BaTiO<sub>3</sub>, anisotropic self diffraction 4-107762  
 Bi<sub>12</sub>Si(Ti)O<sub>20</sub>, gyrotropic crystals, electro-optical and optical props. (*Russian*) 4-93058  
 GaAs, surface disordering by picosecond laser pulses 4-92233  
 Ge, laser-induced periodic surface struct., fluence regimes, feedback and topography 4-108436  
 $\alpha$ -LiIO<sub>3</sub>, ionic transport and relax., polarising microscopy studies (*Chinese*) 4-98335  
 $\alpha$ -LiIO<sub>3</sub>, phase-type gratings induced by electro-optical effect, space charge fluctuation 4-66012  
 $\alpha$ -LiIO<sub>3</sub>, quasi-one-dimensional ionic conductor, light diff. due to space charge fluctuations 4-109156  
 $\alpha$ -LiIO<sub>3</sub>, quasi-one-dimensional ionic conductor, light diff. due to space charge fluctuations 4-109157  
 LiKSO<sub>4</sub> single cryst., light diff. from vol. phase gratings (*Chinese*) 4-96784  
 Si, surface disordering by picosecond laser pulses 4-92233  
 XeF laser low-magnification positive-branch unstable resonator, transverse mode form. 4-73521

**light diffusion** see *light scattering*

**light dispersion** see *optical dispersion*

**light emitting devices**  
 see also *light emitting diodes; light sources; luminescent devices*  
 No entries

**light emitting diodes**  
 see also *semiconductor junction lasers*  
 communication systems design and development, component solution (*German*) 4-60173  
 fibres, single mode, chromatic dispersion meas., using phase-shift technique 4-83695  
 high-speed efficient light sources, semiconductor lasers and LEDs, reviews 4-96908  
 optical communication system semiconductor devices, recent progress (*Korean*) 4-91628  
 photoreceiver characteristic determ. using LED 4-73511

**light emitting diodes** continued  
 self-detecting light-emitting diode optical sensor for object proximity meas. 4-95411  
 AlGaAs, radiative and nonradiative, recombination rates, meas. 4-112434  
 AlGaAs-GaAs DH LED, efficiency for optical communications (*Spanish*) 4-69586  
 GaAlAs single quantum well size effect modulation light sources 4-97014  
 GaAs LED, coaxial transverse junction struct., design and characs. 4-87357  
 GaAs, P<sub>1-2</sub>-Cu, LEDs, Cu impurities, thermal redistribution 4-80080  
 GaP diode struct., electroluminescence polarisation study (*Russian*) 4-88884  
 GaP, large single crystals, LEC growth, LEDs 4-99301  
 GaP, scanning DLTS investig. 4-75892  
 GaP:Zn, O LEDs, centre responsible for capacitance slow relax. 4-65735  
 InGaAsP:Zn highly reliable 1.3  $\mu$ m surface emitting LEDs for high speed optical communication systems 4-97137  
 InGaAsP-InP planar buried DH, LPE growth, melt-carry-over effect 4-99352  
 InGaP LED/optical fibre system for optical remote detection of propane gas 4-105155  
 InP/InGaAsP optoelectronic integrated device with optical bistability, design, fabrication and characs. study 4-83726

**light filters** see *optical filters*

**light intensifiers** see *image intensifiers*

**light interference**  
 see also *light interferometers; light interferometry; Moiré fringes*  
 coherence peaks in picosecond sampling experiments 4-79227  
 concentration limits in physical optics and wave mechanics 4-96788  
 concentration limits in physical optics and wave mechanics 4-96795  
 convex face irradiated with coherent light, reflected light interference 4-96782  
 cytoskeletal components visualisation using surface refl. interference microscopy 4-62646  
 double-exposure specklegram whole-field filtering and upper meas. limit, statistical anal. 4-102886  
 fibre gyroscope, drift stability improvement by ratio recording 4-106306  
 finite-aperture effects in the measurement of the degree of coherence 4-87270  
 group and phase velocity difference demonstration using interf. effects between light waves 4-106157  
 hybrid bistable optical device using a TE-TM mode interference waveguide modulator (*Chinese*) 4-112496  
 imaging quality limitations (*German*) 4-112346  
 immersion liquids for interf.-polarisation filters, physical and chem. props. 4-64761  
 laser speckle interference photography using double annular aperture method (*Chinese*) 4-86494  
 MBBA on Ga liq. surface, director orientation (*French*) 4-75273  
 multiple interaction bandstop filters based on the Talbot effect 4-74687  
 multiple spherical waves, interf. profiles, general case 4-69303  
 Nomarski differential interference contrast microscopy technique for refr. index meas. of isotropic particles 4-63781  
 PAA on Ga liq. surface director orientation (*French*) 4-75273  
 pentylicyanobiphenyl on Ga liq. surface, director orientation (*French*) 4-75273  
 phase measurement algorithm anal. utilising two-beam interference 4-106359  
 phase unwrapping in two contexts 4-79055  
 prisms, right-angle, use in total internal reflection and interference meas. 4-63458  
 projected interference fringes applied to nonoptical surface microscopic topography 4-111099  
 spatial fringe scanning for optical phase measurement 4-106369  
 spatially periodic wavefield propag. 4-96796  
 superposed converging spherical wave focus, three-dimens. intensity distrib. 4-59973  
 surface grating formation under action of laser radiation on metal, semiconductor, and insulator surfaces 4-107813  
 temperature compensated coupled cavity diode lasers, interference effect 4-107691  
 thermoplastic films, interf. colour creation using diff. gratings for embossing 4-69538  
 BaTiO<sub>3</sub>, self-pumped phase conjugation, optical feedback, wavelength response and interf. effects 4-97004  
 CdS, thin plate, reflection spectrum, interference struct. anal. 4-76402  
 PLZT radiation plates, nonhomogeneity of light modulation 4-61660  
 YAlO<sub>3</sub>:Pr<sup>3+</sup>, Raman heterodyne interference of inequivalent nuclear sites 4-71212

**light interferometers**  
 see also *light interferometry*  
 absolute distance interferometer using dye laser heterodyne interferometer and spatial separation of beams 4-106366  
 angular interferometers for laser scanners 4-82821  
 astronomical instrumentation and assoc. Fourier spectrometer (*Japanese*) 4-94628  
 automated interferometer for Fourier transform spectroscopy at near-mm wavelengths 4-101914  
 birefringent-fibre polarisation coupler, output coupler of Mach-Zehnder interferometer 4-112582  
 book 4-95081  
 conference on astronomical instrumentation, at London, England (September 1983) 4-106099  
 diffraction element interferometer, for attenuated wave phase meas. 4-90648  
 digital heterodyne, for use in meas. wavefront figure error 4-111193  
 digital heterodyne interferometer for analysis and control of adaptive optics 4-111194  
 digital Talbot interferometer for lateral aberration meas. 4-87409  
 distributed nonlinear Fabry-Perot interferometer, switching waves 4-96991  
 double cat's eye small interferometer for rapid-scanning Fourier transform spectroscopy 4-101913  
 Fabry-Perot, ellipsometer appl. 4-86468  
 Fabry-Perot, measurement optimisation, generalized error anal. (*Russian*) 4-58892  
 Fabry-Perot camera and digitized interferogram reduction 4-67631  
 Fabry-Perot cavity, nonlinear, with nematic liquid crystal, dynamics 4-83635

## light interferometers continued

- Fabry-Perot etalon, spectral characts. meas. of branch selected CO laser at room temp. (*Chinese*) 4-112389
- Fabry-Perot etalon, use as RF freq. channeliser 4-95507
- Fabry-Perot etalons, tilted intra-cavity, use in CW dye laser (*Korean*) 4-112483
- Fabry-Perot interferometer, multiple-beam, adjustable, for comparing laser wavelengths 4-90647
- Fabry-Perot interferometer fringe broadening 4-96783
- Fabry-Perot interferometer mirror confinement and control through radiation press. 4-78368
- Fabry-Perot interferometers for solar prominence characts. determ. 4-101165
- Fabry-Perot spectrally agile filter, dual tunable 4-69535
- Fabry-Perot type interferometer theory for surface polaritons 4-75870
- Fabry-Perot ultrathin solid etalon fabrication, high precision digital interferometry appl. 4-90650
- fibre Fizeau interferometer for minute biological displacements meas., tympanic membrane appl. 4-89853
- fibre interferometers, polarisation fading elimination, passive technique 4-64778
- fibre optic Doppler velocimeter, mixed-fibre interferometric sensor with microretroreflectors 4-91618
- fibre optic gyroscope with passive quadrature detection 4-69570
- fibre optic interferometer demonstration of gravitationally induced phase shift of optical waves (*Japanese*) 4-101739
- fibre optic interferometry for vibration and velocity measurements (*Japanese*) 4-87462
- fibre optic Michelson high resolution thermometer 4-97105
- fibre optic ring interferometer with a multimode waveguide 4-73498
- fibre optic sensor readout, output linearisation 4-91595
- fibre optical interferometer as a temperature sensor 4-107852
- fibre ring interferometer with a monochromatic-light depolariser 4-78370
- glass fibre sensors, technology and appls. (*German*) 4-95409
- heterodyne Mach-Zehnder interferometer system for testing laser diode wavefront quality 4-106363
- holographic interferometer, common-path, for simple heterodyne interferometry 4-79073
- holographic interferometry system, microprocessor control/data acquisition, real-time signal processing, NDT appl. 4-73501
- in-laser interferometer using anisotropic mirrors, linear polarization production (*Russian*) 4-69465
- instantaneous phase measuring interferometer, displacement meas. appls. 4-106373
- internally modulated Michelson interferometers for Fourier transform spectroscopy, thermal radiation problem 4-95520
- far IR Michelson interferometer for GIRL telescope on Spacelab 4-77716
- IR phase-shifting interferometer design, aspheric component testing appls. 4-101910
- large-aperture interferometer with local reference beam 4-78365
- laser Doppler velocity interferometer, appl. to mech. vibrs. meas. (*Korean*) 4-112785
- laser Doppler vibration amplitude meas. with optical fibre probe (*Japanese*) 4-112781
- laser gravimetric measurement accuracy, effect of Gaussian struct. of beam (*Russian*) 4-60099
- laser illuminated multibeam interferometers, thermal limitations on sensitivity 4-73497
- laser interferometer calibration at NPL 4-95508
- laser type, appl. 4-95504
- mechanical surface scanning with external force and passive feeler at a laser interferometer displacement comparator 4-95510
- metallic glass, magnetostrictive props. meas. using fibre optic interferometer 4-90618
- Michelson, laser beam, displacement monitor for use in characterization of single mode fibres 4-107830
- Michelson interferometer, spectral emissivity meas. of human skin for potential early cancer detect. 4-105320
- Michelson interferometer for dispersive Fourier transform spectroscopy, optical const. determ. of solids in visible 4-101934
- Michelson interferometer in a gravitational Lense-Thirring field (*Russian*) 4-68120
- Michelson interferometer used as Fourier spectrometer for visible light 4-101936
- Michelson spatial interferometer, use in far IR astronomy 4-106367
- multifunctional laser displacement-measuring instruments 4-63721
- multiple-beam grating interferometer for coating thickness meas. 4-111188
- multiplex with a spherical interferometer 4-90649
- nonlinear bistable interferometer, field transverse struct., beam profile depend. on Fresnel no. 4-73499
- optical fibre sensor telemetry, branch couplers construction (*Japanese*) 4-87461
- optoelectronic correlator based on modified Michelson interferometer with computer control (*Russian*) 4-107527
- phase measurement interferometer for wavefront evaluation on laser diodes 4-106364
- picosecond rotating-mirror autocorrelator, optimisation study 4-107793
- plasma, pulsed discharge, diagnostics using multicolour laser interferometer 4-60727
- polarising interferometer, high efficiency, for far IR Fourier transform spectroscopy 4-106407
- polystable semiconductor Fabry-Perot interferometer with thermal load, instability and spontaneous oscils. of temp. 4-73500
- precision surface metrology, conf., San Diego, CA, USA (Aug. 1983) 4-106103
- radial-shear interferometers, thick lens, survey 4-68273
- Raman-fluorescence discrimination, time resolved picosecond interferometry 4-111215
- refractive index meas. using double arm converging beam interferometer 4-84939
- rhodamine 6G CW dye ring laser with a Mach-Zehnder interferometer, efficient single mode operation 4-91496
- rocket-borne pure interferometric high resolution spectrometer (*Japanese*) 4-115687
- rule corrector arm, design using circularly ruled gratings for surface metrology 4-112559
- scanning Fabry Perot interferometer using piezoelectric transducer tube and photodiode, construction 4-111198

## light interferometers continued

- scatter plate interferometer, scatter plate aperture effect on fringe contrast 4-82822
- speckle shearing interferometer, three-aperture, slope and curvature simultaneous meas. 4-73411
- stabilised fibre-end retroreflecting interferometer 4-106357
- stellar interferometer with fibre optic synthetic aperture 4-110524
- subaperture interferometer system for testing large aspheric mirrors for mid-frequency figure control 4-112549
- surface microprofiling instrument 4-106262
- switched-field-of-view interferometer for complex refl. spectra determ. of heavily-absorbing solids 4-101912
- synthetic aperture phase meas. system using metering rod bridge with corner cubes 4-97016
- synthetic apertures, multiline, performance and phasing 4-97019
- television speckle interferometer with real-time digital image processing, 4-63072
- TFTR tokamak diagnostic system using Fourier spectrometer 4-75201
- translation insensitive heterodyne interferometers 4-95505
- translation insensitive interferometers for multimirror telescope alignment systems 4-101162
- triple-frequency highly sensitive laser interferometer, plasma diagnostics appl. 4-103567
- two-beam interferometer for dispersive refl. spectroscopy of solids in far IR 4-106405
- Twyman-Green interferometer system for measuring He-Ne laser wavelength (*Polish*) 4-86477
- Twyman-Green lateral-shearing heterodyne interferometer stability, lens testing appls. 4-106372
- underwater sound detection using optical interference in optical fibres (*Japanese*) 4-112621
- US fields measurement in transparent media using scanning diff. interferometer 4-97186
- velocity interferometer obs. of rain burning behaviour in HMX explosive 4-101908
- velocity interferometer system for any reflector, VISAR, wave growth obs. in granular explosives 4-101907
- velocity interferometer system for any reflector, VISAR performance improvement 4-101906
- vibration amplitudes of diffusely reflecting surfaces meas., automatic fringe counting 4-95509
- YIG film Y-branch interferometer grown by liq. phase epitaxy 4-97138
- CO<sub>2</sub>, TEA lasers, multipass-prism interferometer for fine-freq.-turning, single-mode operation 4-107683
- Cd<sub>0.23</sub>Hg<sub>0.77</sub>Te etalon, low-power nonlinear Fabry-Perot reflection at 10  $\mu$ m 4-96981
- GaAs, optical guided-wave monolithic interferometer 4-112561
- HCN laser interferometer of ASDEX tokamak plasma 4-86475
- H<sub>2</sub>O laser interferometer, 28  $\mu$ m, for plasma diagnostics 4-108213
- He-Ne laser, mode struct. optical spectrum analyser study, undergraduate expt. 4-106152
- InSb etalon, controlled by guided wave, optical bistability on reflection 4-74597
- LiNbO<sub>3</sub> broad-band guided-wave electrooptic modulators 4-97057
- LiNbO<sub>3</sub> integrated optic Fabry-Perot interferometer for GaAlAs laser wavelength stabilisation 4-91457
- LiNbO<sub>3</sub>:Ti diffused waveguide interferometric modulator (*Chinese*) 4-112564
- LiNbO<sub>3</sub>:Ti integrated oscillators and multivibrators 4-64795
- LiNbO<sub>3</sub>:Ti travelling wave microwave optical modulator 4-112563
- PZT cylindrical phase shifter and modulator in single-mode fibre interferometer 4-97090
- XeF laser using grating-interferometer-based cavity, single-mode tunable operation 4-102956

## light interferometry

- see also *holographic interferometry*; *Moiré fringes*
- 30 MHz standard attenuator, design 4-73408
- AC phase measurement technique for moiré interferograms 4-106365
- air, laser-produced breakdown interferograms, high-speed recording 4-75120
- alteration of interferometer for discontinuous coplanar surfaces 4-82779
- applied mechanical experimental methods 4-97451
- aspherical surface testing with shearing interferometer using fringe scanning detection method 4-107909
- aspherical surface testing with shearing interferometer using fringe scanning detection method 4-112592
- astronomy, meas. of stellar diameters by combining light issuing from two telescopes (*French*) 4-105888
- atoms, oscillator strengths meas. using double-layer interferometer technique 4-59679
- binary stars, speckle interferometric measurements during (1981) 4-94862
- boundary optical-polarisation measurement checking 4-74974
- Cassegrain type null-corrector for surface tests of parabolic microwave reflectors 4-111196
- cathode glow, sputtered atom light emission, interferometry 4-87981
- cement testing for interferometric appls. 4-64751
- coating thickness meas. with multiple-beam grating interferometer, 4-111188
- conference on solid state optical control devices, Los Angeles, USA (Jan. 1984) 4-95024
- cosinusoidal transforms in white light 4-59987
- coupled resonators employing phase-conjugating and ordinary mirrors, appl. to interferometry 4-107795
- cracked specimens, elastic and plastic anal., use of speckle interferometry (*Chinese*) 4-83854
- diffraction halo in speckle photography 4-87268
- digital interferometry, high precision, appl. to ultrathin solid Fabry-Perot etalon prod. 4-90650
- digital phase measurement interferometry using CCD image acquisition 4-106374
- diode laser spectra calibration using a confocal etalon 4-74562
- dual beam interferometry and double chopping for scintillation free measurements 4-106368
- Elsasser-related approximation to the Airy function, comments 4-90660
- Fabry-Perot coatings characts., in vacuum UV range, optical constants influence 4-58886
- Fabry-Perot interferometer, multiple-beam, adjustable, for comparing laser wavelengths 4-90647

## light interferometry continued

- Fabry-Perot interferometry using an image-intensified rotating-mirror streak camera 4-111190
- Fabry-Perot velocimetry techniques, Doppler shift rel. to surface normal direction 4-101904
- far-IR interferometric phase imaging of Tokamak plasma 4-75211
- fibre connector, surface testing method using optical interf. technique (Japanese) 4-83743
- fibre optic interferometers, thermal phase compensation 4-73494
- fibre-optic interferometric detection of slow temperature change using unlimited phase compensation 4-107862
- fibre-optic magnetic-field sensor detect. scheme free from ambiguity due to material mag. hysteresis 4-78303
- fibres, single-mode, cutoff wavelength determination by equalisation wavelength meas. 4-107845
- fibres, single-mode, dispersion-spectra variations, interferometric meas. 4-74718
- flat optical surface, absolute calibration 4-107910
- Fourier spectroscopy in high background noise 4-90661
- Fourier transform spectroscopy, phase error correction 4-101930
- framing high-speed shearing interferography with pulsed He-Ne lasers, flow, shock, combustion and explosion problem appls. 4-68275
- frequency domain description of interferogram analysis 4-107516
- frequency domain description of interferogram analysis 4-112343
- frequency shifter for heterodyne interferometry using counterrotating wave plates 4-101916
- gauge-length meas. interferometer for classroom demonstrations 4-82642
- glass constants, nondestructive collimation meas. technique using Ronchi grating shearing interferometer 4-73495
- glass fibre reinforced plastic fatigue crack growth meas. using compliance and moire techniques 4-89200
- grating-based interferometric processor for real-time optical Fourier transformation 4-95500
- heterodyne interferometry, generalised data reduction 4-106371
- heterodyne speckle interferometry 4-106370
- high speed photography, videography and photonics, conf., San Diego, CA, USA (Aug. 1983) 4-106102
- high-speed laser interferometry, transient vibration meas. of impacted metal bar 4-111189
- hybrid optical-digital image processing method (French) 4-68270
- hydrogel materials, refr. indices meas. by interferometry 4-62542
- injection laser emission freq. stabilisation by an external confocal interferometer 4-60098
- instantaneous phase measuring interferometry 4-106362
- IR MTF measurements, effect of surface textures on reliability 4-79027
- IR system optical quality assessment using 300 mm aperture high precision scanning interferometer 4-74765
- J-integral for arbitrary geometry and loading, laser moire determ. 4-60348
- kinofom quartz axicons, fabrication diff. props., appls. 4-83670
- laser interferometric techniques for wide-range high-resolution meas. of projectile motion 4-111192
- laser interferometry appls. in chemistry 4-68274
- laser interferometry for time-resolved high-velocity meas. 4-101903
- laser interferometry in space, future prospects 4-110323
- laser light coherent detection using interferometric and filtering technique (Chinese) 4-87380
- laser speckle photography with cross-slit aperture (Chinese) 4-107520
- laser-based strain gaugemeter for accurate meas. of small deform. (Spanish) 4-88433
- lateral extensometer long-term accuracy assessment using optical technique 4-78296
- length meas. automation, based on interference patterns analysis 4-101812
- length measurement using synthetic MM wave signal generation 4-58812
- liquid crystals, distortions and director distrib., coherent light interferometry 4-92086
- liquids, refr. indices determ. at submm. wavelengths, phase and amplitude modulation techniques 4-111186
- long-baseline Michelson interferometry with large ground-based telescopes operating at optical wavelengths, general formalism 4-90094
- Mach-Zehnder, natural convection from an isothermal downward facing horizontal plate obs. 4-69755
- magnetic confinement fusion plasmas, appl. of lasers 4-108218
- magnetic media, surface characts. by optical profilometer 4-86382
- mechanical guidance adjustment parallel to optic axis by speckle interferometry 4-68272
- mirror testing methods, astron. appl. (Japanese) 4-91642
- moire fringe techniques in engineering metrology 4-78366
- moire fringes, vector representation 4-64673
- moire interferometry with  $\pm 45$  deg. gratings 4-69540
- moire shearing interferometry, whole-field strain determ. 4-97444
- moire topography, sampling theory and charge-coupled devices 4-73496
- moire topography of substrates, IC production appl. 4-101811
- moving sample surface profile, interferometric meas. 4-78291
- multiaperture speckle shearing arrangements for stress analysis 4-58888
- multiple spherical waves; interf. profiles, general case 4-69303
- multipulse illumination system, controllable synchronised, for electronic speckle pattern interferometry and holography 4-101909
- NDT, noncontact crack detection method (French) 4-93478
- nematic liquid crystals, Fredericksz transition, static distortion, interferometric study 4-60816
- nonNewtonian fluid, free convection motion studied by interferograms 4-103326
- object repositioning using hybrid moire system 4-86476
- object spatial spectrum phase reconstruction from speckle interferograms 4-107548
- optical coordinate transform filter production by computer controlled scanning interferometric pattern system 4-107801
- optical fibre sensors, interference reactions (Polish) 4-112578
- optical flat, absolute calibration 4-103029
- optical gyroscopes 4-68276
- optical level based on moire effect with ambient light 4-95502
- optical testing interferograms, separating misalignment from misfigure on off-axis aspheres 4-112593
- optical-black coating specular reflectance in the far-IR 4-97030
- paint coatings, laser interferometric meas. of flatness (German) 4-82823
- particle dynamic transverse velocity meas. using interferometric techniques 4-101905
- particles in two-phase flows velocity and size meas. using laser interferometer technique 4-79679

## light interferometry continued

- Petula B Tokamak density fluctuation meas. by fast FIR laser interferometry 4-75206
- phase conjugate techniques 4-74624
- phase Fresnel lens realisation by multiple beam interferometry 4-87429
- phase grating use in moire interferometry 4-73492
- phase gratings hidden by diffusers detect. using intensity interferometry 4-59980
- phase measurement algorithm anal. utilising two-beam interference 4-106359
- phase measurement using spatial synchronous detect. 4-106361
- phase measurement using spatial synchronous detection 4-106375
- phase object measurement using Talbot effect and moire techniques 4-95501
- phase-conjugate interferometry 4-95506
- phased array experiment overview 4-106343
- photographic glass plate positioner, liquid gate, design and appl. 4-102941
- plasma, refractive fringe diagnostic method, simulation 4-84083
- plates, flexed, image-shearing Moire method to record partial slopes 4-64898
- PMMA, fatigue loaded, crack propag., craze zone, optical interference obs. 4-66422
- point diffraction interferometry, optical system focusing appl. 4-58887
- polyethylene, high density, high press. injection molded, birefringence at 70.5 microns, tensile modulus, press. depend. 4-61655
- polymer deformation studies by time-resolved FT-IR spectroscopy 4-103851
- polystyrene, shock loaded, shock wave study using Fabry-Perot velocimeter 4-112949
- precision surface metrology, conf., San Diego, CA, USA (Aug. 1983) 4-106103
- projected interference fringes applied to nonoptical surface microscopic topography 4-111099
- PVC, fatigue loaded, crack propag., craze zone, optical interference obs. 4-66422
- quality control of surfaces, automated interference meas. 4-81391
- Raman-fluorescence discrimination, time resolved picosecond interferometry 4-111215
- range measurement using Talbot diffraction imaging of gratings 4-63707
- real time image difference by cosinusoidal modulation 4-74446
- real-time interferometry using optically controlled liq. cryst. spatial light modulators 4-83687
- rectangular acoustic array elements, normal surface displacements, optical interferometry studies 4-112655
- reversed field pinch device ZT-40M, fluctuating signals from multichord interferometer 4-97835
- rhodamine 6G dye laser, multimode, pulsed, single-shot spectral meas. and mode correls. 4-69467
- scanning piezoelectric ceramics, displacement, linearity measurement using scanning interferometry method (Chinese) 4-111101
- segmented primary mirror tilt and phase alignment using multiple-order radial-grating shearing interferometer 4-74642
- semiconductor bistable Fabry-Perot devices, performance characts. 4-87387
- pseudo-shear interferometry 4-106360
- shear strain meas., diff. beam interferometry 4-87638
- single-mode fibre, dispersion spectra, axial uniformity meas. 4-107837
- skin friction meas. by laser interferometer in three dims. flows 4-97505
- spatial frequency pseudocolouring by interference, texture appl. 4-74432
- spatial fringe scanning for optical phase measurement 4-106369
- speckle photographs distortion of deformed objects 4-90651
- speckle shear interferometry, multiplexing 4-101915
- stellar interferometric obs. review 4-77821
- subaperture testing data anal. 4-107894
- submilliarcsecond speckle displacement meas. using cross spectrum anal. 4-94631
- surface-generated second-harmonic radiation; interferometric enhancement 4-74609
- testing, optical, by lateral shearing interferogram analysis 4-112594
- thermal expansion coeff. meas., double-path laser interferometer system 4-95382
- thickness measurement of very thin air gaps or films 4-68271
- thin film channel spectra, fringe order determ. 4-63779
- tilt measurement with speckle-shear interferometry 4-68211
- time-resolved FTS of molecular and atomic IR emission 4-96473
- tomography by iterative convolution, empirical study and appl. to interferometry 4-95503
- transducers for pulsed pressures 4-101827
- transparent materials, dynamic optical and mech. props., evaluation by interferometry 4-79529
- UCLA Microtor plasma, simultaneous FIR interferometry/polarimetry meas. 4-75205
- ultra-thin air film thickness meas. in 100 nm range, white light interferometry 4-63711
- unidirectional solidification and related fluid parameters in microgravity optical obs. 4-80194
- vibration analyser, low-freq., using fibre-optic interferometer (French) 4-78293
- vibration isolation for broadband gravitational wave antennas 4-111012
- vibration measurement, small amplitude, by He-Ne laser interferometry (Rumanian) 4-68212
- vibrational circular dichroism meas. of single enantiomer on FT-IR spectrometers 4-102816
- VISAR, data reduction method 4-111191
- wafer flatness tester, automatic, using Fizeau interferometer, VLSI circuit wafer appls. 4-106270
- Zerodur, interferometric test setup for low thermal expansion coeffs. meas. 4-107770
- Al alloys, D-16 sample, particle vel. distrib. in elastic precursor of compression wave 4-92296
- Al foil irradiated with Nd:YAG laser pulses particle vel. meas. of laser-induced shock waves using ORVIS 4-113495
- Al plate, US waveforms using laser generation and interferometric detection 4-97265
- CO CW laser two-mode multiline stabilisation using Fabry-Perot filter under analog and digital computer control 4-60092
- CO<sub>2</sub> coherent laser radar performance study 4-96974
- DCN laser interferometer for plasma electron density meas. 4-113220

**light interferometry continued**

- Kr<sup>2</sup>F photochemical laser, active medium bleaching wave optical inhomogeneities, interferometric study 4-60022  
 LiNbO<sub>3</sub> mirror-type optical switch and appls. 4-97043  
 NH<sub>4</sub>Cl metal-model unidirectional solidification in microgravity optical obs. 4-80194  
 PLZT thin-film waveguides, electrooptic Kerr coeffs., Mach-Zehnder interferometric meas. 4-91578  
 Si wafers, impurity characterisation using IR spectra meas. 4-113486  
 UO<sub>2</sub>, U-H<sub>2</sub>O vapour reaction, kinetics and mechanisms 4-74011  
 Zr, oxide film growth kinetics, interferometry, ellipsometry, X-ray photoelectron spectra obs. 4-66482

**light meters** *see photometers***light microscopes** *see optical microscopes***light microscopy** *see optical microscopy***light modulation** *see optical modulation***light polarisation**

- see also birefringence; optical rotation; photoelasticity; polarimetry*  
 A 0538-66, neutron star and Be star model from light polarisation anal. 4-94858  
 absolute retardation fringe separation using polarisation holography 4-69343  
 absorbent optically active crystals of the orthorhombic system, light transmission 4-61650  
 angle-resolved scattering, comparison of theory and expt. 4-74412  
 anisotropic superregenerative laser amplifier, linear mode, polarised signal amplification 4-79191  
 anthracene crystals, reson. Raman scatt. and low temp. luminesc. formation 4-104644  
 Ap stars, mag. fields meas. via polarimetry of 5200 Å depression (*German*) 4-67738  
 aspherical optically anisotropic particles, microstruct. determ. by optical shift spectrosc. 4-79032  
 atomic system orientation under linearly polarized nonreson. light irradi., classical-oscillator model 4-83336  
 beam splitting due to finite size of medium in total reflection conditions 4-91402  
 bilayer systems, p-polarised guided wave phonon-polaritons and guided wave surface phonon-polaritons 4-92629  
 birefringent fibre active polarisation coupler 4-79287  
 birefringent fibres, single-polarisation operation 4-107828  
 birefringent-fibre polarisation coupler, output coupler of Mach-Zehnder interferometer 4-112582  
 blazars, radio morphology rel. to optical polarisation and normal radiogalaxies 4-86083  
 book, optical waves in crystals, laser radiation propag. and control 4-86135  
 boundary optical-polarisation measurement checking 4-74974  
 Brewster's law, simplistic explanation 4-86162  
 3C 109, broad-line radiogalaxy, dust characts. from visible and IR obs. 4-90223  
 3C 273, quasar, vars. in linearly polarised component rel. to radio flux density vars. 4-106074  
 cataclysmic variables, optical polarisation and white dwarfs mag. fields 4-110633  
 cholesteric liquid crystal, optical eigen mode ellipticity calcs. 4-114229  
 chromatophores and chromatophore fractions of *Rhodospirillum rubrum*, cell fluoresc. polarisation spectra 4-77187  
 $\alpha$ -chymotrypsin-dyes assoc., fluoresc. circular polarisation, Cotton effect 4-102838  
 circulator, polarisation independ., design and expt. results (*Chinese*) 4-107820  
 classroom demonstration 4-95115  
 coherent communication systems, based on polarisation-preserving fibres, bandwidth-limiting effects 4-69587  
 coiled-birefringent-fibre polarisers 4-91599  
 complex Fourier spectrum phase meas. method 4-79061  
 computer-generated polarization holography 4-107564  
 concentration limits in physical optics and wave mechanics 4-96795  
 conference on solid state optical control devices, Los Angeles, USA (Jan. 1984) 4-95024  
 definitions and nomenclature, instrument polarisation 4-82604  
 dichroic polarisers, high efficiency for visible region 4-97038  
 dielectric-coated metallic mirrors as 3-refl. polarisers 4-97035  
 digital heterodyne interferometer using phase modulation of Ar ion laser polarisation 4-111194  
 division-of-wavefront polarising beam splitter and half-shade device using dielectric thin film on dielectric substrate 4-74679  
 DQCl, polarisation spectrum, electronic and thermal contrbs. 4-69093  
 dye laser radiation polarisation, steady-state approx. theory 4-79131  
 dye oriented film, laser marking process based on microcrystallite photo-thermal transform. 4-107773  
 dynamic scattering of light by optically anisotropic particles in external fields 4-87282  
 electrical signals of controllable waveform generation, polarised-light techniques 4-97036  
 elementary spatial filtering with magneto-optic light modulators 4-79273  
 ethane-d<sub>0</sub> (-d<sub>1</sub>), Raman intensities determ. 4-74249  
 Fabry-Perot resonator, optical bistability, semiclassical approach, coupled amplitude eqns. 4-79222  
 fiber depolarizer for monochromatic light 4-79330  
 fibre, low crosstalk polarisation-maintaining optical fibre with an 11 km length 4-112574  
 fibre, single mode, anisotropic, degree and state of polarisation 4-60165  
 fibre gyroscopes with high-birefringent fibre and broadband sources, polarizer requirements 4-91612  
 fibre interferometers, polarisation fading elimination, passive technique 4-64778  
 fibre mode-power fluctuations between polarisation states 4-97085  
 fibre optic gyroscope with passive quadrature detection 4-69570  
 fibre optic taper-polarisers, highly birefringent, finite cladding effects 4-69569  
 fibre polariser, in-line birefr. 4-91606  
 fibre ring interferometer with a monochromatic-light depolariser 4-78370  
 fibre waveguide couplers, polarisation behaviour 4-87463  
 fibre-optic gyroscopes with imperfect polariser/depolariser phase error bounds study 4-63732  
 fibre-optic polarising directional coupler 4-74726  
 fibres, polarisation maintaining, update 4-91605

**light polarisation continued**

- fibres, polarisation-preserving high birefringence, characterisation and performance 4-91604  
 fibres, single-mode, highly twisted, Gaussian pulse splitting and nonsplitting condition 4-97078  
 flare stars, optical photometry and polarisation characts. 4-94822  
 frequency domain storage, polarisation gated writing of photochem. holes for FM polarisation detection 4-87292  
 frequency-modulation-polarisation spectroscopy, I<sub>2</sub> vapour saturation holes 4-111218  
 Galactic Centre, near IR imaging and polarimetry 4-77924  
 gas laser, stability of self-locking of two modes 4-74561  
 glass polarisers containing Ag 4-97037  
 grazing incidence spectrometer designs based on conical diffraction, comparison 4-95522  
 heterolasers with distrib. feedback, polarisation effects 4-64708  
 holographic correction of light polarisation at exit of fibre light guides (*Russian*) 4-87480  
 holographic recording, polarisation type, diffraction efficiency and selectivity 4-96845  
 horizontal solar telescope, instrumental polarisation assoc. with refl. from flat mirror (*Russian*) 4-101167  
 RV Hydrae, red variable star, polarimetric obs. 4-85950  
 immersion liquids for inter-polarisation filters, physical and chem. props. 4-64761  
 imperfect cryst., laser irradi., thermoelastic stresses, optical polarisation study 4-61114  
 in-laser interferometer using anisotropic mirrors, linear polarization production (*Russian*) 4-69465  
 in-line fibre-polarisation-rotating rotator and filter 4-91597  
 infection lasers, stimulated emission polarisation, stress effects 4-87333  
 interferometer, high efficiency polarising, for far IR Fourier transform spectroscopy 4-106407  
 internal reflection phase retarder design, graphical method 4-64758  
 interstellar polarization, wavelength depend. towards stars 4-77896  
 isotropic media, degenerate four-wave mixing (*Chinese*) 4-96978  
 BL Lacertae objects, radio morphology and optical polarisation 4-86083  
 laser calorimetry, polarisation sensitive 4-74584  
 laser Doppler velocimeters using polarisation-maintaining optical fibres for simultaneous meas. of two velocity components 4-83961  
 layered structure in situ ellipsometry, inverse problem soln. 4-107513  
 long period variables, intrinsic polarisation var. due to flare effects on circumstellar material 4-94779  
 Lyman- $\alpha$  radiation, from H I like ions, electron impact polarisation 4-67609  
 M2-9, bipolar nebula, polarisation, nebula struct. and grains characts. 4-94918  
 magnetic circular polarisation by induced atomic orientation 4-94570  
 Mars, dust storms (1973), polarimetric anal. 4-94664  
 materials used as optical components in submm and mm region, polarisation properties 4-107768  
 metal-clad tapered optical waveguide polariser 4-83690  
 methane collisions, narrow nonlinear magneto-optical resonances 4-78882  
 monomode fibres, polarisation meas. of cut-off wavelength 4-60159  
 monomode optical fibres, low birefr., polarisation rot. due to geometric effects 4-107859  
 Moon, polarimetric mapping via electronic analogue transform. of polarisation pictures 4-105893  
 multiple light-scattering near the critical point, critical opalescence 4-84938  
 N-galaxies optical spectropolarimetry and radio struct. correl. 4-90221  
 nematic liq. cryst., longitudinal domain struct., laser diffraction studies 4-60829  
 NGC 1068, Seyfert 2 galaxy, IR spectropolarimetry 4-106068  
 NGC 2068, refl. nebula, optical polarisation anal. 4-86019  
 NGC 6334/6357, H II region, polarimetric and new photometric obs. 4-115792  
 nonlinear optical media, electro-optic shock radiation theory 4-112498  
 optical fibres, linear polarisation preserving single-mode, birefr. meas. (*French*) 4-87471  
 $\alpha$  Orionis, linear polarisation var. due to photospheric effects 4-110620  
 $\alpha$  Orionis, lower atm. var. from linear polarisation obs. 4-85968  
 $\alpha$  Orionis, semi-regular star, multi-band photoelectric photometry 4-85966  
 $\alpha$  Orionis, visible polarisation, photospheric hotspot model, broadband obs. anal. 4-63166  
 $\alpha$  Orionis, visible polarisation, photospheric hotspot model, narrowband obs. anal. 4-63167  
 orthogonal polarization and colour states for information processing 4-102892  
 partially coherent radiation depolarisation by doubly refracting elements (*Russian*) 4-79029  
 periodically variable linear optical polarisation, Fourier components and description method 4-94588  
 p-phenylenes, homologous, liq. cryst. transitions, orientation-dependent interactions and optical anisotropies 4-113622  
 photoanisotropic medium reaction, polarisation-holographic recording 4-74467  
 photoelastic modulator, low freq., for photoacoustic and photothermal polarisation spectroscopy 4-91574  
 PJ 287, BL Lacertae object, vars. in linearly polarised component rel. to radio flux density vars. 4-106074  
 PKS 0219-164, BL Lac. object, rapid optical variability and polarisation 4-82549  
 PKS 0735-17, BL Lacertae object vars. in linearly polarised component rel. to radio flux density vars. 4-106074  
 Pleiades cluster, polarisation and reddening of brighter stars 4-115787  
 polyacetylenes, highly oriented, polarised IR spectra 4-80946  
 polyphenylacetylene:1, reson. Raman, Raman polaris. and far IR spectrosc. 4-80915  
 polyphenylmethyl siloxane, relax. processes, polarised photon correlation spectra under high press. 4-104624  
 quasars, comparison of props. of high-polarisation and low-polarisation QSOs 4-86080  
 quasars, optical polarisation props. 4-86081  
 quasars, optical spectropolarimetry and radio struct. correl. 4-90221  
 radiogalaxies, optical spectropolarimetry and radio struct. correl. 4-90221  
 radiogalaxies, SHF maps and polarisation spectra 4-110733  
 Raman cell, polarisation scrambling by glass window, up to 18 kbar 4-112187

# light polarisation continued

- Raman microspectroscopy, polarisation meas. anal. of isotropic and single cryst. samples 4-71378
- red giant stars in globular clusters, discovery of intrinsic polarisation 4-82470
- resonance fluorescence flame atomic detection, polarisation rejection of scatt. laser light 4-109707
- ring laser, bidirectional homogeneously broadened, stability analysis, adiabatic elimination of polarisation 4-107690
- ring laser subjected to transverse mag. field, nonreciprocal effect theory 4-107693
- rough surfaces, polarisation of scatt. light, appl. to planet surfaces 4-110515
- Saturn B-ring, particles surface microstructure, polarimetric model appl. 4-94680
- semiconductors, magnetically mixed, spin-flip Raman scatt. by shallow donors, polarisation and linewidth 4-66038
- Seyfert galaxies, optical spectropolarimetry and radio struct. correl. 4-90221
- single mode fibres, high-birefringence, polarisation quality meas. 4-69573
- single polarisation fibres, stress anal. 4-64783
- single-mode fibres, polarisation-maintaining type with vacuum circular pits across core-clad interface, anal. (Japanese) 4-60167
- single-mode fibres, scatt. loss versus polarisation holding ability 4-69561
- single-mode integrated-optical polarisers in LiNbO<sub>3</sub> and glass waveguides, low loss 4-112568
- single-mode polarisation-preserving fibre coupling to single-mode semicond. lasers 4-69558
- single-mode twisted fibre as polarisation-maintaining fibre 4-64782
- single-polarisation single-mode fibres, absorption reducing, fabrication 4-64801
- single-polarisation single-mode optical fibres, absorption reducing, structure design 4-64784
- sky background polarisation, meas. with European Southern Observatory polarimeter 4-101172
- solar corona, IR polarization and interplanetary dust particle size 4-63121
- solar corona, polarimetric investigations during total eclipse (1970 March 7) (German) 4-67708
- states and operators, representation by quaternions (French) 4-69306
- stimulated Brillouin scattering depolarisation, noise component angular distrib. 4-74615
- stratosphere, UV polarization inversion, O<sub>3</sub> and aerosol profiling 4-62960
- stratospheric dust from El Chichon, optical sky polarimetry and photometry at Mauna Loa 4-62950
- Sun, unipolar sunspots, mag. fields from polarisation anal. 4-72923
- surface polarizations at interfaces, transmission and reflection coefficients for s and p polarisation 4-113876
- symmetric layered struct., p-polarised nonlinear surface waves 4-61301
- synthetic aperture optical telescope array design considerations 4-106341
- T Tauri stars, intrinsic polarisation var. due to flare effects on circumstellar material 4-94779
- tetracene-anthracene chemically mixed mol. cryst., optical props. 4-76410
- three-dimensional projection with circular polarizers 4-112344
- TM-component suppression during polarised-light diffraction by volumetric phase lattices (Russian) 4-59974
- transparent film coating on absorbing substrate, inverting ratio of complex parallel and perpendicular refl. coeffs. 4-87271
- trimethylammonium manganese copper trichloride, polarised cryst. spectra and cryst. struct. 4-88825
- turbulent atmosphere, light polarisation change 4-107525
- AN Ursae Majoris, polar. polarimetric obs. 4-106038
- Venus atmosphere, polarization features, morphology and movements from OCPP data 4-82430
- volume phase gratings, optical anisotropy, phase shift between S, P polarisation components 4-91571
- weakly ferromagnetic rhombohedral antiferromagnets, magneto-optic effects 4-112428
- X-ray binaries, periodically variable linear optical polarisation 4-94588
- YAG crystal, specially doped growth and multi-function props. (Chinese) 4-114364
- Ag high index faces, surface plasmon excitation, photoemission-intoelectrolyte study 4-109308
- AgCl emulsion, polarisation holographic study (Chinese) 4-112361
- (AlGa)As heterolasers with distrib. feedback, polarisation effects 4-64708
- Al<sub>0.5</sub>Ga<sub>0.5</sub>Sb multilayer heterostructures, coherent light polarisation props. 4-71460
- Bi<sub>2</sub>Si(Ti)O<sub>10</sub> gyrotropic crystals, electro-optical and optical props. (Russian) 4-93058
- CO<sub>2</sub>, light multiple scatt. contributions to depolarisation in critical region 4-112186
- CaCO<sub>3</sub>, light absorpt. coeff. anisotropy in 0.4-2.0  $\mu$ m region 4-76416
- CdGa<sub>2</sub>S<sub>4</sub>, vibr. props., polarisation depend. IR reflectivity studies 4-75624
- Cd<sub>1-x</sub>Mn<sub>x</sub>S, s-d exchange interaction sign, spin flip Raman scatt. studies 4-71052
- Cr<sub>2</sub>B<sub>2</sub>O<sub>7</sub>Cl, ferroelec. orthorhombic to monoclinic transition 4-71301
- Cs, electron impact excitation, light emission, Stokes' parameter 4-96703
- Cu complexes, Cu-phthalocyanine single cryst., visible absorpt. band, temp. depend. 4-76489
- GaAs:Cr, photolum. at 0.839 eV, polarisation of Zeeman spectra 4-71427
- GeS layered monocrystals, photoluminescence spectra, pol. plane orientation change effects 4-66069
- H<sub>2</sub>O monomode CW 119  $\mu$ m laser, output beam polarisation improvement 4-112471
- He-Ne intracavity laser, polarisation behaviour at 632.8 nm (Chinese) 4-107597
- He-Ne ring laser with gain greatly exceeding losses, counterpropag. circularly polarised wave interaction 4-74557
- InGaAsP BH 1.3  $\mu$ m lasers, anomalous polarisation characs. 4-69402
- (InGa)(AsP) heterolasers with distrib. feedback, polarisation effects 4-64708
- InGaAsP-InP DH modulators, electroabsorption, polarisation depend. 4-93054
- InSe, layered monocrystals, photoluminescence spectra, pol. plane orientation change effects 4-66069
- KI, F-centre luminesc., mag. circular polarisation, anomalous effect 4-93062

# light polarisation continued

- $\alpha$ -LiIO<sub>3</sub>, ionic transport and relax., polarising microscopy studies (Chinese) 4-98335
- LiNbO<sub>3</sub>:Fe, polarisation-anisotropic light-induced light scatt. 4-87395
- LiNbO<sub>3</sub>:Ti directional coupler based low-crossstalk waveguide polarisation multiplexer/demultiplexer for 1.32  $\mu$ m 4-60183
- LiNbO<sub>3</sub>:Ti waveguides, polarisation plane rot., photogalvanic mechanism 4-74709
- NO<sub>2</sub>, excited state, fluoresc. light polarisation inversion, light-induced stabilisation 4-96605
- <sup>23</sup>Na atomic beam, polarisation by laser optical pumping 4-107467
- Nd<sup>3+</sup>:YAG laser with intracavity SHG in crystals exhibiting aperture effect, unpolarised radiation electrooptic switch 4-74574
- Ni<sub>2</sub>Nb<sub>2</sub>O<sub>6</sub>, polarised absorpt. spectra of Ni<sup>2+</sup> ion 4-93085
- Pb<sub>2</sub>GeO<sub>4</sub>, crystals, spatial modulation of light 4-84941
- PbTe, size quantised films, p-polarised optical properties 4-114338
- a-Si<sub>3</sub>C<sub>4-x</sub>H<sub>x</sub>, luminescence from photo-generated carriers, polarisation memory 4-99186
- SiO<sub>2</sub> surface films, refr. index determ. by polarisation method of PEM investigation 4-93124
- TiBr-TiTi polycrystalline fibre, optical props. at individual CO<sub>2</sub> laser lines, magneto-optic effects 4-109165
- TiN<sub>2</sub>, single cryst., edge photoluminescence under laser excitation 4-66066
- Xe, light multiple scatt. contributions to depolarisation in critical region 4-112186

# light propagation

- see also atmospheric light propagation; guided light propagation
- anisotropic media, propag. and interaction of transversely-confined beams (Russian) 4-96794
- beam thermal self-interaction in a moving medium, numerical study 4-74631
- book, optical waves in crystals, laser radiation propag. and control 4-86135
- cholesteric liquid crystal, optical eigen mode ellipticity calcs. 4-114229
- elements based on screen for light beam mode transformation, design and development (Chinese) 4-60133
- Fokker-Planck equation for ray dispersion in gyrotropic stratified media 4-107521
- Gaussian beam optical system anal. and synthesis 4-87275
- Gaussian Schell-model fields, propag. characteristics through first-order optical systems 4-83541
- gravitational light deflection in the solar system 4-94585
- group and phase velocity difference demonstration using interf. effects between light waves 4-106157
- images, adaptive correction 4-107549
- inhomogeneous media, exptl. problems 4-59984
- isotropic media subjected to DC electric field, nonlinear refr. index phenomena 4-64750
- laser-beam propagation fundamental mode, optically inhomogeneous electrochrom. media with electrochem. species conc. gradients 4-112341
- layered media synthesis, a priori estimates 4-83674
- Maxwell's eqns., in free space, spinor solns. 4-91401
- negative group velocity restoration (French) 4-59977
- nonlinear media, optical field statistics, investigation using Monte Carlo method 4-107728
- nonspherical scatterer cloud, randomly oriented macroscopic optical consts. 4-91403
- packellike solutions of the homogeneous-wave equation 4-87249
- photographic density RMS granularity calc. in three-dimens. plane parallel layer, Monte Carlo method (Russian) 4-68304
- standing wave, Lorentz transformation (French) 4-96787
- symmetric layered struct., p-polarised nonlinear surface waves 4-61301
- synthetic aperture propag., point spread function, computer model 4-96813
- turbulent atmosphere, light beam intensity fluctuations, effect of initial degree of spatial coherence 4-107522
- vapour, optically pumped relax. signal, influence of optical factor 4-102963
- waveguides, active coupled, light propag., wave eqn. soln. 4-97070
- waveguides, rectangular active, light propag. and waveguide modes 4-91585
- weakly biaxial crystals, props. of light-wave propag. 4-107512
- Na vapour, CW off-reson. rings and CW on-reson. enhancement 4-102973

# light propagation in plasma

- conductivity change at hollow cathode illuminated by ns. laser pulses 4-75227
- continuum IR radiation pulsed source for time resolved absorption spectroscopy in laser prod. plasma 4-69871
- electron plasma wave excitation by laser, nonlinear eqn. 4-65070
- far forward scattering from fluctuations, volume effects 4-84019
- laser beam self focusing, wave optical theory 4-65088
- laser driven pellet, microwave simulation, parametric instabilities 4-103562
- laser fusion pellet, absorpt. rate and uniformity 4-78735
- laser irradi. targets, suprathermal electron generation transport and deposition 4-103538
- laser plasma interaction research in Australia at ultra-high intensity 4-103507
- laser-plasma interaction scaling with laser wavelength and plasma size 4-103509
- laser-plasma interactions, double layers, absorpt. and dynamics 4-103514
- laser-plasma research at Soreq review 4-103537
- long scalelength laser plasma, parametric instability obs. 4-103510
- low density plasma, macroscopic self-focusing effects 4-113192
- resonance particles, nonhomogeneous laser radiation field effect 4-84018
- stimulated scattering and harmonic generation in homogeneous and inhomogeneous laser plasma 4-69915
- transparency of a laser plasma during afterglow 4-75166
- two-plasmon decay and three-halves harmonic generation in filaments in a laser-produced plasma 4-69887
- underdense plasma, hot electron prod., Raman scatt. 4-103508
- underdense plasma, laser press. effects, Lagrangian code study 4-65087
- underdense plasma, laser prod., HF instabilities 4-103503
- Be on Al target, laser irradi., lateral and axial transport charact. 4-79819
- CO<sub>2</sub> laser produced plasma, harmonic generation study 4-102920
- Ne hollow cathode discharge, optogalvanic effect, Langmuir probe meas. 4-84063

## light reflection

- see also *mirrors; optical films*  
 atmosphere, reflected solar radiance from broken cloud scenes 4-72663  
 atmospheric haze, spectral luminance calc. 4-82240  
 beam splitting due to finite size of medium in total reflection conditions 4-91402  
 beam-splitters, ideal, Babinet's principle for submm waves 4-97039  
 blue phase liq. cryst., lattice spacing fluctuations, refl. microscopy obs. 4-103649  
 blue phase liq. cryst. mixtures, lattice parameters, Bragg refl. obs. 4-88089  
 Brewster's law, simplistic explanation 4-86162  
 cholesteric liquid crystal, optical eigen mode ellipticity calcs. 4-114229  
 cholesteric liquid crystals, blue phase, optical props. 4-88791  
 cholesteric N-alkanoates, ternary system press. induced reentrant cholesteric phase 4-98002  
 coated optical components, meas. of scatter and residual reflectance in visible region 4-102999  
 coatings, transparent and heat reflecting, planar magnetron sputtering 4-74666  
 colour reflection hologram recording, modulation mechanisms 4-74450  
 colours of reflecting specimens 4-90644  
 convex face irradiated with coherent light, reflected light interference 4-96782  
 corneal markers and reflections, translation invariance 4-85421  
 cubic crystals, surface EM local-field effects 4-80889  
 curved cylinder, light beam eqns. anal., specular reflection (*Russian*) 4-83543  
 degenerate four-wave mixing, amplified reflection 4-112524  
 delocalised surface exciton-impurity states with low binding energy (*Russian*) 4-70900  
 dielectric coated metallic mirrors for three-refl. halfwave and quarterwave retarders 4-107796  
 diffuse reflection problem, effective depth of line form in planetary atmospheres 4-101213  
 diffusion reflection, scattering factor, particle size effect 4-59978  
 electro-optical spatial light modulator, linear array total internal refl., for optical information processing 4-74695  
 ellipsometric determination of complex reflection coeffs. 4-86470  
 Fabry-Perot coatings characs., in vacuum UV range 4-58886  
 Gaussian beam incident on parabolic inhomogeneous slab, transmission and reflection characs. (*Japanese*) 4-96806  
 glass, types LAK9 and SF1, scatter meas. at 0.915  $\mu\text{m}$  4-107508  
 ground surfaces, optical props., refl. matrices appls. 4-84935  
 halo phenomena, Monte Carlo simulation, sun ray path tracing through ice crystals 4-72699  
 Helmholtz coupled amplitude eqns., soln., nondepleted-pump approx. 4-112506  
 horizontal solar telescope, instrumental polarisation assoc. with refl. from flat mirror (*Russian*) 4-101167  
 ice clouds, effects of horizontal orientation of crystals on radiative props. (*Chinese*) 4-67397  
 images, on curved surfaces with rotational symmetry, determ. using graphic method 4-107538  
 injection laser noise properties due to optical feedback 4-79143  
 internal reflection phase retarder design, graphical method 4-64758  
 IR Earth/atmosphere background meas. during sunrise, using radiometer and interferometer 4-115569  
 laser cavity power increases caused by reflections from workpiece surfaces 4-91519  
 lateral beam displacements in transmitting layered structures 4-74415  
 layered structure in situ ellipsometry, inverse problem soln. 4-107513  
 low temperature spectra, empirical method for eliminating background prod. by diffuse reflection 4-96482  
 metal layer, adsorbed mols., surface polaritons, internal reflection spectrum 4-109150  
 metal/insulating thin film system, surface polariton refraction 4-92631  
 microspectrophotometer for absorptiometric and reflectometric analysis of crystals 4-95492  
 multilayer dielectric coatings of unequal thickness 4-87432  
 multiple-glint targets under laser illumination, statistical properties 4-112342  
 nonspherical aerosol particles, light scatt. props. 4-96801  
 oceanic whitecaps, effective reflectance 4-89916  
 optical activity, phenomenological description, other crystal optics problems (*French*) 4-74414  
 optical schemes for display and demonstration 4-112557  
 Optics in Australia conference, Sydney, Australia (May 1983) 4-95047  
 phase transmission grating, diffraction reflection (*Russian*) 4-69307  
 photolayer radiation field optical characs. (*Russian*) 4-82852  
 planar multilayer waveguide, thin-films field-transfer matrix theory, refl. from prism-loaded waveguides 4-87448  
 plates, flexed, image-shearing Moire method to record partial slopes 4-64898  
 polytetrafluoroethylene films, chain orientation param. from IR-dichroism and X-ray data (*Russian*) 4-84536  
 prisms, right-angle, use in total internal reflection and interference meas. 4-63458  
 randomly inhomogeneous medium, ray description of waves reflected with wave front reversal 4-96804  
 Saturn ring system, theoretical optical thickness profile for bimodal gravitating system 4-101243  
 single longitudinal mode semicond. laser model with internal-refl. optical coupling (*Chinese*) 4-60034  
 spectrophotometer attachment for semiconductor structures testing 4-90641  
 specular reflection in turbulent atmosphere, intensity fluctuations 4-72702  
 spherical particles, dense distrib., retroreflectance 4-102883  
 stratified dielectric layer permittivity profile numerical reconstruction 4-96797  
 surface polaritons at interfaces, transmission and reflection coefficients 4-113876  
 surface profile characs., coupling with light refl. coeff. 4-76409  
 three-layer medium, light reflection, electrodynamic Green's functions 4-109150  
 tracking accuracy of moving targets, angular coordinates appl. 4-64760  
 transmission hologram reflection mounts, format compatibility issues 4-112354  
 vegetated randomly located vertical protrusion field, reflection 4-93795

## light reflection continued

- water surface, statistical theory of aureole phenomenon (*Russian*) 4-67220  
 zero reflection from a dielectric film on metal substrate at oblique angles of incidence 4-91398  
 Ar, solid and liq., excitons, reflection spectra study 4-84570  
 BaTiO<sub>3</sub> photorefractive crystal, asymmetric transmission studies 4-84927  
 Bi<sub>2</sub>GeO<sub>20</sub> photorefractive crystals, beam coupling and decoupling in degenerate two-wave mixing in refl. geometry 4-107732  
 Ge ground surfaces, optical props., refl. matrices appls. 4-84935  
 KH<sub>2</sub>(SeO<sub>3</sub>)<sub>2</sub> ferroelastic, light deflection by domain walls 4-104550  
 Na<sub>2</sub>O-CaO glass, antireflection effects induced by Ar<sup>+</sup> implantation 4-60125  
 RbHSeO<sub>4</sub> ferroelec. ferroelastic, light deflection 4-80883  
 ZnS film on Au substrate, zero reflection at oblique angles of incidence 4-91398

light reflection spectra see reflectivity; spectra

light reflectometry see reflectometry

## light refraction

- see also *birefringence*  
 adaptive transmission, two-wavelength, diffractive and refractive effects comparison 4-87280  
 antireflection coatings, two-film, stable optical props., CAD method (*Russian*) 4-109261  
 Brewster's law, simplistic explanation 4-86162  
 curved cylinder, light beam eqns. anal., specular reflection (*Russian*) 4-83543  
 eye, comparison of Dioptron Nova data with conventional data 4-109795  
 eye, contrast sensitivity and ocular refr. of rabbits, VECP obs. 4-62472  
 eye, refractive error development theories, review, and evaluation 4-100128  
 fluid mixture, binary, diffusion coeff. meas. using an optical method 4-75712  
 halo phenomena, Monte Carlo simulation, sun ray path tracing through ice crystals 4-72699  
 isotropic absorbing and intensifying medium, light refr. 4-74419  
 magneto-opt. effects, isotropic and anisotropic, in crystals, review 4-61668  
 metal/insulating thin film system, surface polariton refraction 4-92631  
 nematic cells, twisted, average tilt angle determ. 4-73488  
 nonspherical aerosol particles, light scatt. props. 4-96801  
 objective refraction: comparison of retinoscopy and automated techniques 4-62543  
 ocular component anal. by vergence contrib. 4-109794  
 optical activity, phenomenological description, other crystal optics problems (*French*) 4-74414  
 optical schemes for display and demonstration 4-112557  
 photolayer radiation field optical characs. (*Russian*) 4-82852  
 plasma, refractive fringe diagnostic method, simulation 4-84083  
 ripple tank, optical caustics and diffraction study 4-95102  
 semiconductor struts., vaporisation deposited, light refraction mechanism 4-76542  
 spherical refracting surfaces, spherical aberration function singularities 4-112350  
 stigmatic mapping of small surface element orthogonal to axis, sine condition as sufficient condition 4-107510  
 Ba(PO<sub>3</sub>)<sub>2</sub>-CdF<sub>2</sub> high refractive index glass, optical constants, density and atomic refraction rel. to struct. 4-93043  
 KH<sub>2</sub>(SeO<sub>3</sub>)<sub>2</sub> ferroelastic, light deflection by domain walls 4-104550  
 RbHSeO<sub>4</sub> ferroelec. ferroelastic, light deflection 4-80883

## light scattering

- see also *Brillouin spectra; opalescence; Raman spectra; Rayleigh scattering; stimulated scattering*  
 acetonitrile-pentyl acetate (n-butanol) (n-propanol) (carbon tetrachloride), excess Gibbs function determ. 4-80262  
 aerosol size distrib. determ. from aureole around point source, theory 4-62961  
 aerosols, atmospheric, wavelength depend. spectral extinction 4-72696  
 agarose, gel saturated with binary liq. mixtures, critical behaviour 4-93565  
 alkyltrimethylammonium bromide colloids, viscosity, light scatt. studies 4-89344  
 angle-resolved scattering, comparison of theory and expt. 4-74412  
 anisotropic two dimens. scatt., finite depth and refractive index effects 4-96800  
 anisotropically scatt. infinite uniform medium, point source 4-96799  
 anisylidene-p-aminophenylacetate, nematic, viscoelastic props. study 4-103845  
 antireflection coatings, five-layer achromatic, for multicomponent movie camera lens 4-79271  
 aromatic polyester-chlorinated polymer blends, miscibility, morphology, small angle light scatt. 4-84412  
 arterial O<sub>2</sub> saturation, meas. with pulse-type oximeter, multiple scatt. and peripheral circulation effects 4-115166  
 aspherical optically anisotropic particles, microstruct. determ. by optical shift spectrosc. 4-79032  
 atmosphere, scatt. characs. of aerosol media with anisotropic particles, homogeneous spheres models use (*Russian*) 4-82235  
 upper atmosphere, Spacelab 1 detect. of D Lyman- $\alpha$  reson. scatt. 4-90016  
 atmospheric aerosol backscatter and attenuation meas. using CO<sub>2</sub> tunable coherent lidar 4-100763  
 atmospheric aerosol backscatter determ. at 10.6  $\mu\text{m}$  4-100728  
 atmospheric crosswind measurement using photon-burst correl. techniques 4-62966  
 atmospheric light scattering, computing aspects 4-67391  
 azimuthal integration of scattered light intensity using a conical lens 4-101895  
 binary fluid mixture, anisotropic spinodal decomposition under shear flow 4-69738  
 biological macromolecules, rheologically active, studies by quasilastic light scatt. 4-115292  
 bipolar reflection nebulae, contrib. of multiple scatt. to optical appearance 4-85995  
 book, scattering theory for diffraction gratings 4-86125  
 Brownian doublets, scattered light intensity cross-correl. function meas. 4-79033  
 calibration of optical system for light scattering and resonance fluorescence meas. 4-101887  
 $\kappa$ -carrageenan, aq. soln., light scatt. investig. 4-104622

## light scattering continued

- m-chloronitrobenzene, phonon spectra lattice vibrs. Raman scatt. 4-109181
- cholesteric blue mesophases, circular intensity differential scattering 4-109200
- cholesteric blue phase, struct. anal. by optical Bragg diffraction 4-88090
- clouds, droplet scatt. rel. to optical device for liq. water content meas. 4-62978
- coated optical components, meas. of scatter and residual reflectance in visible region 4-102999
- coherent light scattering by particles, moving in two crossed light beams 4-96803
- colloidal dispersion in nonpolar solvents, light scatt. 4-114837
- cooling tower drift-measuring devices compared 4-62432
- copolyester of lactic and glycolic acid, strain induced crystallisation, optical and X-ray scatt. obs. 4-85186
- copolymers of vinyl chloride and vinylidene chloride, hydrodynamics and conformation in soln. (*Russian*) 4-78989
- coupled-cavity lasers, threshold gain anal. and design guidelines 4-91463
- critical angle laser light scatt. from bubbles in water, meas., models, appls. to bubble sizing 4-69311
- $\beta$ -crystallin accumulation in chicken embryo lens, laser light scatt. spectroscopy 4-72229
- crystals near phase transition points, light scatt. from point defects 4-88850
- cubic crystal: rare earth ion crystals, forbidden two-photon transitions 4-84972
- cylindrical particles, radiation pressure 4-83540
- dense particles, circularly polarised light differential scatt. 4-74361
- depolarised light scatt. R parameter, kinetic theory 4-80886
- depolarised light scatt. R parameter, kinetic theory 4-80887
- detection optics design for light scattering expts. 4-79263
- di-2-ethylhexyl sebacate monodisperse optically absorbing spherical particles, IR radiation emission 4-69309
- diffraction coupler diffracted field anal. using coarse grating made from cylindrical elements 4-79280
- diffusion reflection, scattering factor, particle size effect 4-59978
- discrete random media; comparison of diffusion theories for optical pulse waves 4-69312
- discrete random media, difference between Ishimaru and Furutsu theories on pulse propag. 4-69313
- discrete scatterers, random distrib., backscattering enhancement 4-102884
- dissipative systems in quantum optics, reson. fluoresc. optical bistability superfluoresc., book 4-63410
- dynamic light scatt. in model suspension, memory function moment anal. 4-96802
- elastic light scattering near phase transitions 4-71394
- ester mixture, dynamic scatt. and conductivity anisotropy 4-109161
- ferroelectric, polarised defects, effects near Curie point 4-70134
- ferroelectric liquid crystals, microsecond electro-optic switching using transient light scatt. 4-93052
- fibre backscatter channel, point process estimation 4-79333
- fibre multiple scattering effects, backscattering meas. method (*Japanese*) 4-60169
- fibre optic materials, scattering losses at minimum dispersion wavelength 4-79316
- fibres, dual-mode, with zero intermodal dispersion 4-87465
- fibres, graded-index, comparative spectral attenuation meas., final report by members of COST 208 4-87466
- fibres, multimode, graded-index, with differential mode attenuation, backscatt. signatures 4-74715
- fibres, single-mode, backscattering theory 4-74711
- fibres, single-mode, higher-order mode attenuation meas., effective cutoff wavelength 4-79322
- fibres, single-mode, microdeform. losses 4-69556
- fluorophosphate laser glasses, causes of light scatt. and laser damage (*Chinese*) 4-60124
- fluorotoluene liquid, far wings of the mol. light scatt. spectra 4-109202
- fog monitoring using variable angular field-of-view transmissometer 4-100813
- gas, spatially inhomogeneous, containing macroscopic particles, emission line shape 4-69315
- gelation of chains, gamma-radiation induced, exptl. study 4-77033
- geometrical optics in Ellis geometry, light scatt. cross section 4-63600
- glass, reflecting light-diffusing, scatt. indicatrices 4-79255
- glass, types LAK9 and SF1, scatter meas. at 0.915  $\mu$ m 4-107508
- glass and cryst. materials, scatt. losses, numerical estimates 4-83709
- gratings hidden by diffusers, detect. using photon-correlation techniques 4-112560
- p-heptyl-p'-cyanobiphenyl, phase transition meas. in bulk and boundary 4-92361
- holographic interference fringes recorded from diffusely illuminated objects, amplitude-phase characts. fluctuations effect 4-91425
- homogeneous isotropic turbulent medium light scatt. spectrum 4-59975
- Huang light scatt. near struct. phase transition temp., theory 4-109199
- o-hydroxy-p-methoxybenzylidene-p'-butylaniline nematic, viscoelastic props. study 4-103845
- ice, superheated, optical homogeneity, elastic light scatt. 4-113578
- ice clouds, effects of horizontal orientation of crystals on radiative props. (*Chinese*) 4-67397
- illuminator for dark field microscopy 4-106376
- image formation by optical systems, energy model 4-64683
- immunological reactions study by reson. light scatter method 4-66867
- incommensurate crystal phases, X-ray and light scatt. 4-76480
- inhomogeneous, cryst., local phase transition points, fluctuation enhancement 4-65373
- intensity fluctuations in strong scattering, two-scale solns. 4-87277
- interfacial, light scattering spectrosc. (*Japanese*) 4-99127
- interstellar grains, scatt. props. rel. to OH photodissociation in interstellar clouds 4-90207
- intraocular light scatter 4-93734
- Kevlar in conc.  $H_2SO_4$ , laser light scatt. characterisation of rod-like polymers in corrosive solvents 4-114861
- laser Doppler anemometry, Mie scattering functions for milk fat globules 4-79682
- lidar, quantitative 532 nm data for vertical extinction profiles, relative humidity effect 4-100755
- liquid suspensions, small electrophoretic mobilities by light scatt. and phase struct. function anal. 4-114844

## light scattering continued

- macromolecules, spherical, in binary mixtures, radii and conc. ratio determ. from second-order factorial moment meas. 4-91369
- Malvern particle size calibration 4-95372
- MBBA, light induced decrease in light scatt. (*Russian*) 4-114293
- metal particles, elastic light scatt., quantum size effects 4-64672
- methanol-cyclohexane mixtures, turbidity near critical point 4-66052
- methyl methacrylate-styrene block copolymers, characterisation of light scatt. 4-89366
- methylphenol liquid, far wings of the mol. light scatt. spectra 4-109202
- microemulsion system, critical, apparent field variable, exptl. evidence 4-75646
- mirror, superpolished, surface scatt. theory and meas. comparison 4-87428
- multilayer filter coating light scatt. 4-74413
- multiple light-scattering near the critical point, critical opalescence 4-84938
- multiple scattering during particle diffusion, Pade approximant calcs. 4-101126
- multiple-glint targets under laser illumination, statistical properties 4-112342
- multiply quasi-elastically scattered light spectrum 4-107523
- multiply scattering medium intensity distrib. 4-59983
- near-resonance scattering of collision-perturbed atoms with double excited states 4-69022
- nematics, fluctuations, mean fields and order parameters 4-88070
- n-nonane, vapour, homogeneous nucleation rates, two-piston expansion chamber meas. 4-75649
- non-spherical aerosol particles, light scatt. props. 4-96801
- non-spherical scatterer cloud, randomly oriented macroscopic optical const. 4-91403
- optical couplers, inverse scattering, Marchenko eqns., exact solns. 4-103010
- optical fibres, mode degeneration anal. 4-83696
- optical thin films and surfaces, selected characterisation techniques 4-83667
- particle ensemble, large size-distrib. spherical, asymptotic extinction 4-69314
- particles, spherical, two-layer, integral light scatt. function calc. 4-79035
- PET, molecular orientation, mol. wt., birefringence, density, light scatt. 4-84219
- phase retrieval, essential role of prior knowledge 4-69323
- phase separating  $^4He$ - $^3He$  mixtures, dynamic light scattering obs. 4-104032
- phase transitions, light scatt. studies, book 4-101581
- photographic density RMS granularity calc. in three-dimens. plane parallel layer, Monte Carlo method (*Russian*) 4-68304
- photographic undeveloped monodispersed layers, unit vol. parameters (*Russian*) 4-82853
- photolayer radiation field optical characts. (*Russian*) 4-82852
- photon statistics of light scatt. by a small no. of particles 4-96850
- planetary atmospheres, effective depth of line form for isotropic scatt. theory 4-101213
- plasma, for forward light scatt. from fluctuations, volume effects 4-84019
- polarized scattering of light by optically anisotropic particles in external fields 4-87282
- poly- $\gamma$ -benzyl-L-glutamate, semidilute solns., diffusion coeffs., dynamic light scatt. study 4-76486
- polyacrylamide gel saturated with binary liq. mixtures, critical behaviour 4-93565
- polydiacetylene solns., rod-to-coil transition and gelation, light scatt. study 4-64645
- polydisperse scatterer number fluctuations, single-interval statistics and expt. errors 4-102888
- polyester fibre insulation, optical props. and radiative heat transfer 4-80896
- polymer solutions, dilute, dynamical-scatt. factor, initial decay rate 4-108268
- polymer solutions, light scatt. asymmetry at high dil. (*Russian*) 4-80950
- polymers dilute solutions, light scatt., degree of interpenetration of macromolecules (*Russian*) 4-104625
- polymethylmethacrylate, evolution of fractures, prolonged action of electric field 4-108507
- polyoxyethylene, micelle soln., cloud point transition, light scatt. 4-81486
- polyphenylmethyl siloxane, relax. processes, polarised photon correlation spectra under high press. 4-104624
- polypropylene, supermol. struct. and mech. props., cooling rate influence (*German*) 4-98032
- polystyrene, evolution of fractures, prolonged action of electric field 4-108507
- polystyrene, semidilute theta solns., dynamic light scatt. 4-88848
- polystyrene charged spheres in dilute soln., fluorescence labeled, electrolyte friction meas. 4-98323
- polystyrene latex, aq. solns., diffusion temp. depend., light scatt. 4-80275
- polystyrene latex, liq. like ordered suspension, struct. factor temp. depend. 4-114845
- polystyrene monodisperse colloids, light diffr. and cryst. struct. 4-103661
- polystyrene solns., expansion coeff. light scatt. (*Japanese*) 4-97999
- polystyrene spheres, size and refractive index determ. 4-63715
- polystyrene suspensions, self-diffusion coeff., light scatt. meas. 4-98324
- polyurethane-polyvinyl interstitial composites, microphase structure, X-ray and light scatt. obs. 4-84216
- polyvinylidene fluoride-PMMA blends, melting pt., crystalline morphology, light scatt. obs. 4-84217
- PVC polyacrylonitrile-co-butadiene blends, two-phase struct., optical, thermal and X-ray obs. 4-84207
- quartz microporous glass laser active elements, optical characts. 4-79253
- random Gaussian-correlated surface, light scatt. calcs., surface electronic struct. 4-69316
- randomly distributed non-spherical particle vector radiative-transfer theory, matrix representations 4-59979
- rare earth molybdates, ferroelec., soft mode temp. depend., light scatt. anal. 4-71299
- resonance fluorescence flame atomic detection, polarisation rejection of scatt. laser light 4-109707
- resonance light scattering, intensity depend., stationary homogeneously broadened atom driven by incident field, book contrib. 4-64430
- resonance lines, photon escape and scattering 4-94592
- retinal rod photoreceptor membranes, enzymatic processes, light scatt. probe 4-72224

## light scattering continued

- rough surface evaluation, light scatt. method appl. condition (French) 4-59982
- rough surfaces, polarisation of scatt. light, appl. to planet surfaces 4-110515
- salol, solid-liq. interface props., dynamic light scatt., thermal diffusivity, lattice const. 4-109203
- scattering particle characteristics and their effect on pulsed laser meas. of fluid flow, speckle velocimetry vs. particle image velocity 4-83963
- schlieren measurements in weakly inhomogeneous media, multiple scatt. allowance 4-79034
- self-pulsing at stimulated scattering processes 4-107747
- semi-dilute, diffusion, conc. depend. 4-88849
- semiconductor wafer surface defects, automated detection by laser scanning 4-113773
- semiconductors, Raman characterisation 4-99106
- serum albumin soln., bovine, osmotic susceptibility, mutual diffusion coeff. 4-72205
- silica gel saturated with binary liq. mixtures, critical behaviour 4-93565
- single-mode fibres, scatt. loss versus polarisation holding ability 4-69561
- skeletal muscle, polysarcomeric unit of activation, microdifferential holography 4-66998
- slanted anisotropic gratings, scatt. and waveguiding props. analysis 4-69539
- small angle, by large spheroids, rel. to erythrocytes under shear 4-115116
- small dielectric clusters, resonance optical response 4-74388
- soil particles and spheroids, light scatt. by size/shape distrib. 4-69310
- solutions, concentration fluctuations, acoustic wave propag. and light scatt. 4-92302
- spherical particles, dense distrib., retroreflectance 4-102883
- spherical small particle embedded in nonabsorbing medium, near-field scatt. 4-102885
- spiral magnetic struts, one-magnon light scatt. 4-93081
- stratified dielectric layer permittivity profile numerical reconstruction 4-96797
- stratus clouds, lidar determ. of extinction 4-94239
- structured particle, homogeneous sphere with holes, light scatt. soln. 4-87267
- styrene-ethylene oxide block copolymers, characterisation of light scatt. 4-89366
- supersmooth surface damage effect identification by scatter evaluation 4-83729
- surface, light scatt. near phase transition point 4-99128
- surface, light scattering spectrosc. (Japanese) 4-99127
- surface fluctuation spectroscopy, expt. technique and capillary ripple theory, comments 4-78389
- surface fluctuation spectroscopy, liquid interface characterisation 4-78388
- surface quality standards 4-82777
- surface roughness autocorrelation function meas. using stray light scatt. 4-99126
- surface statistics calculation from light scatter 4-107912
- surface statistics calculations from light scatter 4-106266
- surfaces, light scatt. near phase transition points 4-66049
- surfaces, weak optical absorption meas. using lateral waves 4-88790
- thin film technologies, conf., Geneva, Switzerland (Apr. 1983) 4-73137
- thin films, light scatt. by acoustic surface phonons, asymmetric lineshape 4-80954
- thin-films on optical elements, physical and chem. aspects 4-74664
- Thomson scatt. of CW  $Ar^+$  laser beam in wall-stabilised cascade arc 4-84078
- total integrated scattering meas. of laser films (Chinese) 4-111166
- transparent fibres, weakly anisotropic, sizing using light scatt., correction factors 4-63714
- transparent single layers on glass substrates, light scatt. 4-99205
- trifluoromethane, thermal diffusivity meas. using dynamic light scatt. (German) 4-65502
- tropospheric and stratospheric parameter meas. using ground-based coherent lidar 4-100662
- turbulence and combustion studies, laser scatt. for conc. and temp. determ. 4-68289
- two-level atom, randomly modulated, coherent light scatt. 4-64689
- ultrasmooth laser mirror coating and substrate surface roughness assessment 4-74755
- variable angle scatterometer, instrumentation 4-74773
- vegetation canopies, complete homogeneous, with various leaf-orientation distrib., directional refl. modelling 4-89649
- velocimeter, backscatter-modulated Doppler, S/N ratio 4-91850
- vinyl chloride-vinyl acetate copolymer solutions, hydrodynamic and thermodynamic props. (Russian) 4-75264
- vinylidene fluoride-3-oxa-perfluorohexene-1 copolymers, mol. mass distrib. (Russian) 4-85309
- xanthan biopolymer in semi-dil. solns., dynamics studied by photon correl. spectroscopy viscosity 4-115006
- Ag film, surface plasmon excitation and light scatt. 4-108794
- Ag surface periodic gratings, light scattering, field enhancement and SERS 4-114292
- As-Se chalcogenide glass films, thermally-induced light scatt. (Russian) 4-109167
- As<sub>2</sub>S<sub>3</sub> chalcogenide glass films, thermally-induced light scatt. (Russian) 4-109167
- Au surface periodic gratings, light scattering, field enhancement and SERS 4-114292
- Au thin films, agglomerated, phys. and optical props. 4-76545
- Bi<sub>2</sub>Ge<sub>2</sub>O<sub>7</sub>, crystal, light scatt. from substructure 4-66050
- CO<sub>2</sub>, light multiple scatt. contributions to depolarisation in critical region 4-112186
- CO<sub>2</sub>, thermal diffusivity meas. using dynamic light scatt. (German) 4-65502
- CO<sub>2</sub>-SF<sub>6</sub>, thermal diffusivity meas. using dynamic light scatt. (German) 4-65502
- Cu surface periodic gratings, light scattering, field enhancement and SERS 4-114292
- DF-HF chemical laser atmospheric attenuation meas. (Chinese) 4-62951
- GaAs-(AlGa)As modulation-doped heterostructs., reson. inelastic light scatt. studies 4-84973
- <sup>3</sup>He, liq., critical fluctuations near gas-liq. critical point, decay rates 4-92468
- <sup>3</sup>He-He liq. mixtures, critical fluctuations near gas-liq. critical point, decay rates 4-92468
- LiNbO<sub>3</sub>, inelastic light scatt. and dielec. anomalies connection 4-84923

## light scattering continued

- Na+Ar, emitted monochromatic light reson. scatt. 4-69022
- Na+He, emitted monochromatic light reson. scatt. 4-69022
- PLZT ceramic, coarse-grain light scatt. and elec. hysteresis 4-76399
- SF<sub>6</sub>, thermal diffusivity meas. using dynamic light scatt. (German) 4-65502
- Si crystals, Czochralski pulled, O precipitation, diffusion mechanism, etching optical and neutron scatt. obs. 4-65209
- Si, Czochralski growth, impurity clouds, microdefects, scatt. light intensity and etch pit density after annealing 4-84312
- Si, low pressure CVD growth and phys. props. 4-81150
- Si, surface sub-band calcs. and light scatt. meas. 4-61430
- SiO<sub>2</sub>, colloidal dispersion in nonpolar solvents, light scatt. 4-114837
- SiO<sub>2</sub>, small particles, colloidal aggregates, fractal geometry 4-89352
- SiO<sub>2</sub>-B<sub>2</sub>O<sub>3</sub>-Na<sub>2</sub>O gel-derived glasses, microhomogeneity light scatt. meas. 4-114290
- TiO<sub>2</sub> films, sputtered, on glass substrates, light scatt. meas. 4-99205
- Xe, light multiple scatt. contributions to depolarisation in critical region 4-112186
- ZnTe polycryst. films, resonant light scatt. spectra 4-99207
- ZrF<sub>4</sub>-based optical fibres, transmission losses, humidity effects 4-83712

**light sensitive materials** *see optical materials; photographic material sensitivity; photographic materials*

## light sources

- see also infrared sources; light emitting devices; photometric light sources; spectroscopic light sources*
- acousto-optical generation of light, comparison of phased-array Bragg cells in second order 4-112556
- antibunched and sub-Poisson light generation, role of primary excitation statistics 4-87306
- artificial lighting for greenhouses, for optimised plants production 4-114917
- colour characteristics, international standards and determ. using spectrometer/computer program (Bulgarian) 4-87406
- cumulative plasmadynamic reactor for laser and photochemical studies 4-60746
- fiber depolarizer for monochromatic light 4-79330
- fields generated by homogeneous and by quasi-homogeneous planar secondary sources 4-83517
- gradient-index lenses, coupling characts. for light source to fibre systems 4-83664
- ICP, near-IR spectral emission characts. 4-78390
- III-V optical sources, dislocations climbing degradation, expt. anal. 4-83654
- Illuminating Engineering Society Annual Conf., Los Angeles, USA (Aug. 1983) 4-90291
- illumination source with grid structure, use in visualisation of three dimensional shape of objects 4-107538
- illuminator for dark field microscopy 4-106376
- incoherent IR light nonthermal effect on gas diffusion through a capillary 4-79671
- inert gas halogen excimer lasers, VUV and EUV generation 4-96863
- IR pulsed intense broadband source at National Synchrotron light source 4-112545
- isotropic planar sources, complex degree of spectral coherence 4-87274
- klystron harmonic generator with electron microbunches induced and frozen by lasers, intense coherent soft X-ray source 4-97001
- laser source technology, recent developments 4-87356
- laser-light barrier in press-resistant housing, explosion-risk environment sensing appls. (German) 4-69478
- metal halide projection lamp 4-91555
- mirrors with diffuse reflection coatings, heat-resistant, for concentrating high-intensity sources radiation onto receiving surface 4-91566
- multicolour periodic stimulated-Raman-scatt. laser, appl. as source for colour holographic motion pictures 4-107682
- multipulse illumination system, controllable synchronised, for electronic speckle pattern interferometry and holography 4-101909
- partially coherent sources, radiometric definitions 4-68258
- polarisation, definitions and nomenclature, instrument polarisation 4-82604
- Schell-model sources, coherent-mode eigenfunctions, completeness 4-107517
- semiconductor source, local radiance measurement, near-field method possible limits (French) 4-68262
- sources and detectors, optical communication appl. 4-91633
- spatially incoherent source tunable spectral filtering using acousto-optic deflector 4-60137
- undulator use in atomic, molecular and solid state physics 4-91554
- UV pulse light source, using noble gas halide excimer laser (German) 4-112544
- vacuum-ultraviolet Cerenkov radiation source 4-107498
- VUV coherent tunable radiation generation 4-87405
- VUV radiation, reson. enhanced tunable source 4-83661
- VUV radiation emission of laser prod. plasmas, radiometric transfer standards 4-83988
- VUV radiation physics, conf., Jerusalem, Israel, 8-12 Aug. (1983) 4-82583
- VUV source from VHF plasma device 4-83663
- D<sub>2</sub> lamps, time depend. of spectral radiance with MgF<sub>2</sub> window 4-83662
- KrF<sub>2</sub> injection locking excimer lasers in the UV 4-83608
- LiF tunable pulsed F<sub>2</sub><sup>+</sup> colour centre laser, 0.69-1.0  $\mu$ m 4-69413
- Na light sources for laboratory expts. 4-106162
- W halogen tubular lamps, TiO<sub>2</sub>-SiO<sub>2</sub> multilayer IR reflective filters 4-112534
- W, spectral emissivity, analytic expressions for 340 nm to 2.6  $\mu$ m spectral region 4-60127
- XeF<sub>2</sub> injection locking excimer lasers in the UV 4-83608

## light transmission

- see also light absorption; optical filters*
- absorbent optically active crystals of the orthorhombic system, light transmission 4-61650
- absorbing condensed media, refr. index meas. by refl. and transmission 4-73486
- acousto-optic bistability with fluctuations, nonlinear Fokker-Planck eqn. 4-83636
- adaptive transmission, two-wavelength, diffractive and refractive effects comparison 4-87280
- antireflection coatings, five-layer achromatic, for multicomponent movie camera lens 4-79271

**light transmission continued**

- asymptotic medium concept and averaged Green function, optical consts. and electronic density of states 4-80472  
 atmospheric band transmittance, approx. of product error during calc. 4-72701  
 beam-splitters, ideal, Babinet's principle for submm waves 4-97039  
 BMBOA-isooctane mixture, extinction, optical props. of highly opalescent systems 4-84936  
 circular metallic dielectric-coated waveguides for IR transmission, design theory 4-74704  
 curved fibre light pipe, optical losses, heating effects 4-69580  
 dyes, bleaching by picosecond light pulses, energy and duration determ. 4-69512  
 electrochromic materials for controlled radiant energy transfer in buildings 4-112536  
 evaporated film, optical props. influence substrate temp. 4-76546  
 Fabry-Perot coatings characts., in vacuum UV range 4-58886  
 fibre braids, light transmission coeff. meas. using goniometer 4-87458  
 fibres, single-mode, higher-order mode attenuation meas., effective cutoff wavelength 4-79322  
 fibres, single-mode, mode field result meas. method consistency 4-74719  
 fibres, single-mode, transmission losses in the 1.3  $\mu\text{m}$  wavelength region 4-97077  
 fibres, single-mode graded and step-index with zero-dispersion near 1.55  $\mu\text{m}$ , fundamental mode size and bend sensitivity 4-97076  
 fibres single-mode, transmission charact. evaluation using time domain reflectometry 4-63777  
 film camera eye-piece lenses, optical characteristics (*Russian*) 4-90677  
 film coating deposition monitoring with wide-band scanning monochromator, layer microstruct. 4-69600  
 Fresnel images of periodic objects, lateral shift under coherent plane wave illum. 4-96831  
 Gaussian beam incident on parabolic inhomogeneous slab, transmission and reflection characts. (*Japanese*) 4-96806  
 glass, types LAK9 and SF1, scatter meas. at 0.915  $\mu\text{m}$  4-107508  
 gradient-index antireflection layer props. on phase-separable glass 4-69533  
 gradient-index conical rod, transmittance function and modal propag. 4-69546  
 halo phenomena, Monte Carlo simulation, sun ray path tracing through ice crystals 4-72699  
 holograms, thin amplitude, film nonlinearities variations rel. to reconstruction wavelength 4-69337  
 intensity-dependent guided wave obs. 4-79220  
 lateral beam displacements in transmitting layered structures 4-74415  
 layered media synthesis, a priori estimates 4-83674  
 material transmission of room-temp. radiation at cryogenic temp. 4-106325  
 measurement using spectrophotometer with computer response correction 4-68264  
 metal/insulating thin film system, surface polariton refraction 4-92631  
 monoclinic crystals, optical parameters 4-61648  
 multilayer dielectric coatings of unequal thickness 4-87432  
 nematic liq. cryst., nonlinear thin film, optical transverse intensity bistability 4-74602  
 Optics in Australia conference, Sydney, Australia (May 1983) 4-95047  
 oxide-metal-oxide low-emittance films on glass, industrial realisation 4-112531  
 plane-parallel plate transmittance, system of eqns. solubility 4-107515  
 polyester fibre insulation, optical props. and radiative heat transfer 4-80896  
 porous layers, electrophysical and optical props. 4-65680  
 quartz microporous glass laser active elements, optical characts. 4-79253  
 retinal rod photoreceptor membranes, enzymatic processes, light scatt. probe 4-72224  
 in seawater, long baseline meas. in Pacific 4-62828  
 seawater off S California coast, chlorophyll a rel. to light transmission 4-62850  
 single-mode integrated-optical polarisers in LiNbO<sub>3</sub> and glass waveguides, low loss 4-112568  
 solar cells, amorphous, optical loss mechanisms 4-77108  
 stratified dielectric layer permittivity profile numerical reconstruction 4-96797  
 surface polaritons at interfaces, transmission and reflection coefficients 4-113876  
 thin films, optical props. on rough surfaces 4-79030  
 transmissibility calc. (*Chinese*) 4-102877  
 vapour, optically pumped relax. signal, influence of optical factor 4-102963  
 Ag halide fibres, transmission meas. in 1-11  $\mu\text{m}$  wavelength region 4-69575  
 Ag thin films on InP and glass substrates, elec. conductivity and optical transmittance 4-88612  
 AgBr, emulsion microcrystals, spectral transmittance reflectance and absorpt. coeff. 4-104556  
 Al<sub>2</sub>O<sub>3</sub> ceramic, strength rel. to microstructure 4-62060  
 Al<sub>2</sub>O<sub>3</sub>/MgO/CaO, translucent, fracture, influence of temp. and CaO 4-92290  
 As<sub>2</sub>S<sub>3</sub>/Ge<sub>2</sub>S<sub>3</sub> glassy semicond., photostructural transformations 4-61076  
 Au thin films, agglomerated, phys. and optical props. 4-76545  
 Au-polymer, film, prep. by plasma polymerisation 4-81162  
 BaTiO<sub>3</sub> photorefractive crystal, asymmetric transmission studies 4-84927  
 Bi<sub>2</sub>GeO<sub>20</sub> thin films, IR spectra and lattice phonons 4-88893  
 Bi<sub>2</sub>SiO<sub>20</sub> thin films, IR spectra and lattice phonons 4-88893  
 C diamond-like coatings for optical component protection 4-74677  
 C:H absorbing films, optical const. unambiguous determ. by reflectance and transmittance meas. 4-65997  
 CdS coupled mode band-pass optical filters, characteristics 4-87438  
 CdS, nonlinear exciton transmission, Maxwell's eqn. anal. 4-98535  
 CdS thin films prep. by spray deposition, vacuum annealing effect on elec., structural and optical props. 4-70966  
 CdTe thin films, DC const. rel. to H<sub>2</sub> exposure 4-76053  
 Cr obliquely deposited films, spectral and angular selectivity 4-112535  
 CsI fibre lightguide material, designed to operate in visible and IR spectral regions 4-74634  
 CsI, optical transmittancy, xenon high pressure transmitting, band closing 4-114299  
 GaP prism couplers, optical characts. (*Chinese*) 4-60134  
 p-Ge, 3.39  $\mu\text{m}$  transmission modulation by tunable CW CO<sub>2</sub> laser, excitation spectrum 4-79240  
 Ge obliquely deposited films, spectral and angular selectivity 4-112535

**light transmission continued**

- GeSe<sub>2</sub>, amorphous thin film, light induced transmittance oscillation 4-76538  
 In<sub>2</sub>-Sn<sub>2</sub>O<sub>3</sub> transparent conducting films, DC reactive sputtering deposition, optical and elec. props. 4-112533  
 LiIO<sub>3</sub> single crystals, optical damage, nonlinear transmission and doubling efficiency 4-75513  
 LiNbO<sub>3</sub> cryst. growth, melt composition effect on props. 4-84227  
 MgF<sub>2</sub> windows, spectral transmission change caused by prolonged UV irradi. 4-64752  
 (Pb,Ba<sub>1-x</sub>)<sub>1-3y</sub>/La<sub>2</sub>Nb<sub>2</sub>O<sub>6</sub> ceramic, dielectric, piezoelectric and optical props. 4-98999  
 PbTe, size quantised films, p-polarised optical properties 4-114338  
 PbTe/Pb<sub>1-x</sub>Sn<sub>x</sub>Te superlattices, optical and elec. props. 4-99209  
 Rb<sub>2</sub>ZnBr<sub>4</sub>, incommensurate cryst. energy levels, optical transmission study 4-98518  
 $\alpha$ -Si absorbing films, optical const. unambiguous determ. by reflectance and transmittance meas. 4-65997  
 Si:H absorbing films, optical const. unambiguous determ. by reflectance and transmittance meas. 4-65997  
 SnO<sub>2</sub>/Sb film deposition by sol-gel technique, optical and elec. characts. 4-71604  
 TiN reactively sputtered films, solar selective props. 4-77148  
 Y<sub>2</sub>O<sub>3</sub> films, struct. and phys. props. 4-65585  
 ZnO:Al films, RF magnetron sputtering, elec. and optical props. 4-85100  
 Zn<sub>3</sub>P<sub>2</sub> polycryst. and single cryst., optical and photoelec. props. 4-84937  
 ZnS, multispectral chemically vapour-deposited, initial characterisation 4-76418  
 ZnSe-CaF<sub>2</sub> deposited by laser-assisted evaporation, as broadband gradient-index antiref. coating 4-107765  
 ZnTe single cryst., nonlinear laser radiation transmission at He temps. 4-64748  
 ZrO<sub>2</sub> amorphous coatings, prep. from metal-organic solns. 4-76696
- light velocity**  
 light-in-flight recording, compensation for limited speed of light used for obs. 4-79075
- light velocity measurement**  
 No entries
- light water** *see water*
- lighting**  
*see also street lighting*  
 artificial lighting for greenhouses, for optimised plants production 4-114917  
 building retrofit, optimal strategies identification 4-72048  
 experimental solar house providing 960 W peak power in Saudi Arabia 4-77064  
 film and video, equipment requirements 4-73543  
 film shooting use of special lighting equipment (*Russian*) 4-58905  
 flexible desk luminaire, behavioural responses 4-93733  
 goniophotometer for measuring luminous intensity at small distances (*Russian*) 4-68265  
 HID lamps design and evaluation for colour photographic purposes 4-90673  
 illuminance distribution produced by fibre bundle 4-112570  
 Illuminating Engineering Society Annual Conf., Los Angeles, USA (Aug. 1983) 4-90291  
 motion photometry 4-111177  
 motion picture film, lighting, use of discharge lamps 4-111240  
 motion picture lighting compensation filters (*Russian*) 4-73552  
 motion picture network, film projection equipment, advanced series (*Russian*) 4-78404  
 organic translucent thin films, optical microscopy, visibility enhancement using fibre-optic cables 4-106378  
 triggered, expts. in France and New Mexico 4-110196  
 video display terminal lighting 4-109790
- lightning**  
 ball lightning and related phenomena (book) 4-78060  
 electrical breakdown in soil, arc initiation characteristics, effect of ambient gas 4-62799  
 ELF and VLF transverse resonances in Earth-ionosphere cavity due to lightning 4-82345  
 flash density rel. to altitude and storm structure, radar obs. 4-94186  
 Gaighata tornado of 12 April 1983, case study 4-100686  
 Gulf of Mexico, underwater sound from lightning strikes to water 4-105567  
 HV laboratory, EMI investigation 4-106165  
 Mount St. Helens 1980 May 18 eruption, fine particles generation and electrification 4-105693  
 neutron detection from lightning bolts using Pb-free monitors 4-100832  
 optical and elec. field signals from return strokes 4-115536  
 soil, elec. breakdown, high resolution studies 4-62797  
 soil, elec. breakdown initiation by water vapourisation 4-62798  
 stroke occurrence and interstroke characts. for Florida, USA 4-115537  
 triggered lightning flash parameters 4-67317  
 triggered lightning in New Mexico 4-77597  
 VHF radiation near to lightning return strokes 4-67318  
 VHF sources, space-time mapping rel. to severe storm struct. 4-105657  
 N<sub>2</sub>O production by lightning channel corona discharge 4-67319
- lightning conductors** *see lightning protection*
- lightning protection**  
*see also surge protection*  
 indirect lightning surges at subscriber line ends 4-77609  
 Cu, lightning conductor plates, corrosion in soil, over 50 years 4-109543
- lightning rods** *see lightning protection*
- limited space charge accumulation**  
*see also Gunn effect; negative resistance effects; space-charge limited devices*  
 No entries
- linear accelerators**  
*see also collective accelerators; electrostatic accelerators*  
 Advanced Test Accelerator, beam dynamics 4-112026  
 asymmetric alternating phase focusing, smooth approx. (*Russian*) 4-83257  
 beam-breakup calculations for Los Alamos free-electron laser linac 4-83256  
 Beijing Proton Linac, 10 MeV accelerating cavity, mean axial electric field adjustment (*Chinese*) 4-74060  
 colliding  $\gamma$  e and  $\gamma\gamma$  beams from single-pass e<sup>+</sup> e<sup>-</sup> accelerators 4-86984  
 diaphragmed electron beams, stability 4-96301

**linear accelerators continued**

- Dynaray-CH 20 linear accelerators, features and performance 4-115175
- Dynaray-CH 6 linear accelerator, for radiotherapy treatment, service experience 4-115173
- electron accelerators, standing wave accelerating struts. 4-107182
- electron beams for electron-beam lasers 4-74532
- free electron generators of coherent radiation, conf., Orcas Island, WA, USA (June 1983) 4-82588
- free electron laser, high power, short wavelength, accelerator technology 4-83255
- free electron laser, long pulse, driven by linear induction accelerator 4-87348
- free electron tapered-wiggler laser, large electron-beam energy extraction 4-83588
- frequency ratio, injector linac and electron-position storage ring (*Chinese*) 4-102407
- giant particle accelerators, circular and straight, beam focusing and accelerating, parameters 4-68841
- heavy ion linear induction accelerators 4-59459
- high gradient linear accelerators, wake field transformation 4-74061
- imploding linear driven ring accelerators, stability 4-111980
- induction accelerators, dynamic props. of ferromagnetic soft core 4-107181
- induction proton accelerators, beam generation and control 4-111981
- ion linac, effect of drift spaces on longitudinal motion 4-91128
- IR laser particle accelerators, linear and helical DFB struts, theory and feasibility 4-74062
- LAMPF irradiation facility for fusion materials, radiation environment characteris. 4-107041
- LAMPF Users Group Meeting, Los Alamos, NM, USA (Nov. 1983) 4-86101
- Lawrence Berkeley Laboratory and Lawrence Livermore National Laboratory free electron laser status 4-83611
- linear accelerator, 20 MeV, modified neutron shield, neutron leakage meas. 4-62569
- Los Alamos free electron laser oscillator expt. using subharmonic buncher 4-83603
- medical accelerator neutron survey, remmeter sensitivity to leakage X-rays 4-62568
- medical linac electron applicator assembly, radiation leakage 4-115181
- microwave powered electron linear accelerator, radiotherapy appls. 4-72401
- neutron leakage measurements from a medical linear accelerator 4-109914
- neutrons from high-energy X-ray medical accelerators, risk to radiotherapy patient 4-85498
- PBFA-I Applied-B diode, ion beam diagnostics 4-112031
- pilot CW superconducting electron accelerator design, fabrication and test 4-102409
- pulsed high-frequency single resonator electron accelerator, design 4-74058
- radiation therapy system, microwave interference effects 4-89737
- radio frequency ion accelerator for ion implantation studies 4-73584
- radiotherapy application, advances in linear accelerator design 4-67095
- RIKEN heavy ion linear accelerator, variable freq., cavity mech. and thermal characts. (*Japanese*) 4-91122
- sealed-off linear waveguide electron accelerator development 4-86982
- silica aerogel threshold Cherenkov counters, pion detection, intermediate energies 4-102496
- standing-wave electron accelerators, RF electronics 4-107183
- standing-wave linear electron accelerators, multiperiodic struct. adjustment 4-64248
- Stanford Linear Collider, 50 MW klystron 4-68842
- superconducting linear accelerator cryostat 4-111977
- H<sup>-</sup> magnetron source at BNL linac, operational experience 4-107203
- H<sup>+</sup> injector/buncher with grounded ion source 4-107252

**linear algebra**

- see also determinants; eigenvalues and eigenfunctions; matrix algebra; tensors; vectors*
- algebraic equations, direct and indirect optical solutions, error source modelling 4-96816
- computational methods in linear algebra 4-67957
- pattern recognition, feature extraction, linear algebra techniques 4-96819
- transformations in optical signal processing, conf., Seattle, WA, USA (Feb. 1981) 4-78023

**linear-beam tubes** *see microwave tubes***linear combination of atomic orbitals calculations** *see LCAO calculations***linear differential equations**

- engineering problems, numerical soln. based on finite elements 4-110857
- quasilinear wave eqn., effect of boundary damping 4-86225

**linear integrated circuits**

- Fahrenheit temperature sensor, monolithic IC implementation with internal offsetting function 4-95423

**linear programming**

- reverberation characts. improvement of enclosed space, with aid of computer (*Slovak*) 4-60213
- scattering response of object to excitation waveform, deconvolution methods 4-69280
- InGaAsP crescent mesa substrate BH lasers at 1.55  $\mu\text{m}$  4-112429

**linear rectification** *see rectification***linear systems**

- failure detection in dynamical systems, hierarchical diagnosis based on linear modelling (*Japanese*) 4-76957
- nonconservative system, mass distrib. effect on stability (*Russian*) 4-64836
- PWR linear-time-invariant systems monitoring and sensor placement, output uniformity index 4-86937

**linear vibrations** *see vibrations***linearisation techniques**

- bearings-only tracking, recursive vs. batch processing algorithms 4-107942
- resistance thermometers linearisation 4-63745

**lines (telephone)** *see telephone lines***linewidths (spectral)** *see spectral line breadth***linguistics**

- phonological processor for Italian 4-69633

**linguistics, computational** *see computational linguistics***linguistics, language** *see linguistics***linking** *see joining processes***Liouville equation***see also Vlasov equation*

- Backlund transformations, infinitesimal, gauge symmetries and conserved currents 4-82890
- Bloch electrons transport in const. elec. or mag. field 4-70768
- electron-phonon interactions, solitons, generalised master eqns. and polar propag. 4-104133
- four-dimensional statistical mechanics, Poincare invariant Hamiltonian dynamics. 4-95169
- general relativity, canonical formalism and invariant single-particle distrib. function 4-73310
- molecular crystals and aggregates, exciton dynamics calcs. 4-78064
- nearly free molecular flow, drag force on moving disc 4-83926
- nonequilibrium dynamics of infinite particle systems 4-73212
- Polyakov model for closed string 4-68551
- quantum Liouville field theory, nonperturbative weak-coupling anal. 4-58931
- quantum Liouville theory, random surfaces 4-58757
- relativistic string, Backlund transformation for Liouville eqn. and gauge conditions 4-63894
- string field theory, triangle relation, absence of tachyons 4-68356
- strings, classical Liouville theory, soln. sectors and minimal energies 4-86686
- superfield N=4 superextension of Liouville eqn., gauge SU(2)×SU(2) symm. 4-111322
- supersymmetric Liouville equation in quantum case, coupling constants 4-82920
- temperature and heat flux from nonequilib. state, coupled fluctuations 4-112681
- Yang-Mills equations, external sources, kink, sine-Gordon and Liouville equations 4-95657

**lip microphones** *see microphones***lipid bilayers**

- aqueous codispersions, phase transition props. rel. to those of covalent analogues 4-85408
- artificial lipid-coated membrane, electrokinetic effects 4-72221
- cancer cells, latent, phys. models of lipid membranes, ordering effects of petroleum hydrocarbons 4-85412
- cation-anion selectivity and conductivity of venom formed channels 4-66891
- cholesterol containing, reversible elec. breakdown 4-66890
- dimyristoylphosphatidylcholine bilayers, lateral diffusion and phase separation in 2D solns. 4-66898
- dipalmitoylphosphatidylcholine, oriented, vibr., polarised Raman spectra. 4-107351
- (dodecylammonium)<sub>2</sub>Cl<sub>4</sub> where M=Mn<sup>2+</sup>, Cd<sup>2+</sup> or Cu<sup>2+</sup>, phase transitions, DSC and X-ray studies 4-89515
- DPPC lipid bilayers, <sup>1</sup>H, <sup>2</sup>H and <sup>13</sup>C spin-lattice relax. 4-62448
- dynamic interactions between approaching surfaces of biological interest review 4-77204
- electroelastic effects in cell membranes 4-77206
- energy-transducing protein complexes, mol. aspects, review 4-66901
- giant planar lipid bilayer, conductance and interfacial effect of inhalation anaesthetics 4-62451
- giant planar lipid bilayer capacitance and its biphasic response to inhalation anaesthetics 4-62450
- gramicidin channels, elec. potential difference effect 4-89527
- hexane, in dimyristoylphosphatidyl bilayers; NMR and thermal. anal. investig. 4-80823
- image potential of ion-pore system, symmetrical channel 4-89528
- immuno potential of ion-pore system, unsymmetrical channels 4-89529
- immunoglobulins G, normal and myeloma, in monomolecular layers, orientation at interfaces, comparison 4-66887
- ion interaction in amphotericin channels 4-66918
- ionic channels formed by haemocyanin in planar lipid bilayers, elec. props. 4-93699
- ionic channels in bilayer lipid membranes formed by polymyxin B 4-66895
- ionising radiation effect on biomembrane structure and function 4-77335
- lamellar lyotropic mesophases, mol. dynamics, <sup>2</sup>H NMR spectra 4-76271
- lamellar lyotropic mesophases, mol. dynamics, <sup>2</sup>H nuclear mag. relax. times 4-76272
- lipid bilayer vesicles, giant neutral, free energy pot. for aggregation by Van der Waals attraction 4-115026
- lipid-protein complexes in mollusc slime and human bile ordering, optical morphological characts. 4-66856
- lipid-protein interactions in membranes, thermodynamic model 4-105171
- liposomes containing various carotenoids and chlorophyll, temp.-induced changes in spectral props. 4-115022
- lysozyme interaction with phospholipid bilayer, molecular conformation, M obs. 4-66888
- micelles and vesicles, partition and binding constants. from fluoresc. quenching data 4-99845
- microsomal membrane structure, enzymatic crosslink influence 4-66896
- monoglyceride bilayer membrane conductance, thickness dependence 4-105196
- nuclear spin-lattice relax. theory, dipolar relax. 4-62447
- orientation ordering of chains at water interface 4-66889
- orientational ordering of carotenoids, resonance Raman spectroscopy 4-89514
- osmotic control of bilayer fusion 4-105198
- phase transitions, DSC and X-ray studies 4-89515
- phase transitions, self-consistent chain model 4-115024
- phosphatidylcholine head groups in vesicles, short-range order in interfacial water 4-113287
- phospholipid bilayer solns. at ordered-fluid phase transition, microwave dielectric spectrum 4-91255
- phospholipid bilayers, latent heat meas. by adiabatic compression 4-85407
- phospholipid dispersions, thermotropic and high-pres. phases, Raman spectroscopy, book contrib. 4-93701
- phospholipid head groups, perturbation by membrane proteins, <sup>31</sup>P NMR spin lattice relax 4-89513
- phospholipid membrane vesicles, cylindrical, thermal fluctuations 4-81643
- phospholipid vesicle membrane, main phase transition, n-alkanols biphasic effect 4-89516

bilayers continued  
phospholipid-water system, myelin figure form. pH and ion effects 4-77202  
photosensitised electron transfer, quantum yield, chemical models 4-81645  
protein correlation functions, lipid ordering 4-81642  
quadrupolar spectrum of spin  $I=1$ , NMR study 4-81615  
ripple phase theory and simulation 4-77201  
rod outer segment disc membranes, bovine, attached to lecithin bilayer, photoelec. signals generation 4-105237  
vesicles, highly charged, nonlinear Poisson-Boltzmann eqn. soln. 4-105200

**liquefaction of gases**  
magnetic liquefaction, total, field strength determ., nomogram and formulae (Russian) 4-70352

**liquid alloys**  
see also liquid metals  
average atomic order effect, bulk and surface props. 4-65518  
binary, compressibility, conc. depend., expt. and theoretical invest. 4-70250  
DTA using cassette-type installation 4-66522  
entropy, expansion coeff., sp. ht. and Debye temp. 4-103963  
KPB, compound forming liquid alloys, hard sphere system, entropy of mixing calcs. 4-113650  
mixing enthalpies, interchange energies, equilib. const., association model 4-88301  
mixing enthalpies, interchange energies, equilib. const., association model 4-89060  
partially ionic, screening role in electronic and atomic struct. 4-70635  
phase diagram calculations, Krupkowski's eqn. (Polish) 4-85139  
solidifying, 4-98276  
structure and thermodynamics, model, chemical short-range order 4-75266  
ultrasonic velocity, compressibility effects 4-92303  
Ag-Au, elec. resist., conc. depend., role of pseudopot. refinements 4-84605  
Ag-Pb, thermodynamic study of dissolved O 4-92379  
Ag-TiTe system, molten, elec. and mag. props. 4-104179  
Al alloys, solidification, grain refinement, pseudosurface nucleation mechanisms 4-114497  
Al alloys, thermodynamics and struct., solvent-solute interaction 4-113670  
Al, liquid, struct. factor, influence of electron-gas response junction 4-75265  
Al-Cu, liq., structural props., elec. resist., X-ray diff. 4-79925  
Al-Cu-Cd, strengthening mechanism of Cd additions 4-61985  
Al-Mg, incorporates of  $Al_2O_3$  particles by stirring in melt 4-93252  
Al-Si melt, wetting of graphitised C strip 4-92476  
Al-Si system, enthalpies of form. of liq. alloys 4-113679  
Au-Zn, liquid alloy, mixing thermodynamics 4-109420  
 $Au_{1-x}Si_x$  liq. and amorphous, elec. resist., Ziman theory anal. 4-70774  
Bi-In, activities of components 4-71635  
Bi-In, liq., activity coeff. of O 4-80242  
Bi-Sb, liq. alloys, activities and free energy of form., EMF obs. (Japanese) 4-61920  
BiMg molten alloys, ultrasonic velocity, compressibility effects 4-92303  
BiSn molten alloys, ultrasonic velocity, compressibility effects 4-92303  
Co-Ce liq. alloy, Ce valence state determ. 4-61358  
Cu base liquid alloys, enthalpies of mixing, intermetallic compound form. 4-92374  
Cu-Au, elec. resist., conc. depend., role of pseudopot. refinements 4-84605  
Cu-Ni-Sn melts, thermodynamics analysis by associated solution model 4-109380  
Cu-O-Pb system, thermodynamics of O, miscibility gap, 1200°C 4-108631  
Fe binary melts, H solubility prediction (German) 4-65401  
Fe-C-Ti, liquid system, surface tension under  $H_2$  atm. (Japanese) 4-65517  
Fe-Ce liq. alloy, Ce valence state determ. 4-61357  
Fe-V, solubility of N 4-114524  
 $Fe_{60}Ni_{40}B_{20}$ , metallic glass, melt surface tension and embrittlement, effects of elemental additions and superheat 4-65184  
 $Fe_{1-x}P_x$ , struct. determ. (Russian) 4-65177  
Ga-Te, molten, at. arrangement of  $Ga_2Te_3$  associates, metallic-like bonding, neutron scatt. obs. 4-103639  
In-Bi-Pb, thermodynamic props., EMF meas., 673 to 873K 4-98310  
In-Ga-Sb alloys, liq., phase diagram calc., Krupkowski's eqn. (Polish) 4-85139  
In-Ga-Sn, natural convection, mag. field orientation influence (Russian) 4-113061  
In-transition metal, liquid, mag. props. of transition metal solutes 4-76109  
KTI, compound forming liquid alloys, hard sphere system, entropy of mixing calcs. 4-113650  
Li-Pb, breeder blanket materials, thermodynamic investig. of dil. solns. of H 4-107033  
Li-Pb, breeder blanket materials, interaction of H isotopes investig. 4-107034  
Li-Pb(Ag) (Mg) liq. alloys, model, chemical short-range order, heat and entropy of formation 4-75266  
Li-Sn, liquid structure, neutron diff., cpd. form. 4-113295  
Mn, binary liquid alloys, thermodynamic props., formalism appls. 4-114478  
Mn-Ge, liquid, struct. determ. (Russian) 4-103640  
Na-Cs liquid alloys, conc. fluctuations 4-92063  
Na-Sn liq. alloys, mag. susceptibilities 4-76108  
NaGa, compound forming liquid alloys, hard sphere system, entropy of mixing calcs. 4-113650  
NaHg liquid alloys, entropy of mixing, hard-sphere system calcs. 4-92371  
Ni, powder production by centrifugal atomisation 4-89006  
Pb-Li, fusion reactor blankets, compatibility of steels, review 4-107054  
Pb-Li, molten static, corrosion reactions of ferritic and type 316 steels 4-107064  
Pb-Li eutectic in fusion reactor, corrosion behaviour of steels 4-107056  
Pd-Ni-Si-Be-B liquid metal ion source for maskless ion implantation 4-58913  
 $Pd_{1-x}Si_x$  liq. alloy, mag. susceptibility, diamagnetism and paramagnetism 4-76107

**liquid alloys continued**

$Pd_{1-x}Si_x$ , struct. determ. (Russian) 4-65177  
SbZn liquid alloys, entropy of mixing, hard-sphere system calcs. 4-92371  
Se-Te liquid alloys, positron lifetimes, temp. and conc. depend. 4-76553  
Sn-Bi, binary liq., compressibility, conc. depend., expt. and theoretical invest. 4-70250  
Sn-Pb, binary liq., compressibility, conc. depend., expt. and theoretical invest. 4-70250  
Sn-Se liq. alloy, thermoelec. power, semicond.-semimetal transition 4-108909  
Sn-transition metal, liquid, mag. props. of transition metal solutes 4-76109  
SnPb molten alloys, ultrasonic velocity, compressibility effects 4-92303  
 $Te_0Se_{10}$ , role of temp. in struct., Raman study 4-88063  
 $Te_{1-x}Se_x$  liquid alloy, Raman study of structural transitions 4-80210  
TiAl-Al, molten system, peritectic equilb., EM phase separation 4-89027  
Zn-Ag liq. alloys,  $^{110}Ag$  diffusion coeff., radiometric absorption method anal. 4-65458

**liquid crystal devices**

see also liquid crystal displays  
adaptive spherical lens performance via elec. modulation of refr. index in tandem liq. cryst. cell arrangement 4-107782  
bistable optical device, regenerative oscill. and monostable pulse generation 4-74694  
critical-fusion frequency equipment using high-speed liq. cryst., trial prod. (Japanese) 4-93841  
Fabry-Perot cavity, nonlinear, with nematic liquid crystal, dynamics 4-83635  
heat switch, elec. field controlled 4-108272  
IR detectors, threshold sensitivity determ. 4-86415  
IR flaw detection of semicond. epitaxial layers, homogeneity and thickness meas. 4-109609  
IR flaw detector for semiconductors free-carrier conc. determ., cholesteric liq. cryst. use 4-89211  
local heat transfer coeff. estimation using liq. crystals 4-97286  
nematic liquid crystals, 90° twisted, optical rotatory power, use in IR light valves 4-71343  
smectic A cells, ferroelectric, preparation for electrooptical microsecond switches appl. 4-75272  
spatial light modulators, optically controlled developments and appls. 4-83687  
temperature indicator films as highly sensitive IR visualiser 4-90584  
twisted-wedge nematic structures, domain type, electrooptical behaviour 4-93051  
variable grating mode device for optical processing and computing functions, physical characterisation 4-74690

**liquid crystal displays**

cholesteric texture change electro-optical effect, two-freq. addressing 4-71347  
dual-frequency addressable liq. cryst. displays 4-88763  
electro-optic display devices, liq. cryst. props. 4-103651  
ferroelectric liquid crystals, microsecond electro-optic switching using transient light scatt. 4-93052  
high technology electronics exhibition and conference, Detroit, MI, USA, (June, 1983) 4-95014  
microwave hologram recording in liquid crystal screen 4-102908  
nematogens, monoester and diester, dielec. obs. 4-88764  
overhead projectors, use of LCD devices 4-67931  
Smectic liquid crystals, in colour image displays 4-75676

**liquid crystal phase transformations**

50.7, modulated crystal smectic B phase, mol. dynamics, neutron scatt. study 4-79929  
p-n-alkoxybenzylidene-p-aminobenzoic acids, liq. cryst., phase transitions, thermal studies 4-113629  
4-alkyl-4'-trans-4-alkylcyclohexyl-biphenyls, nematic transition temps. 4-88082  
4-(trans-4'-n-alkylcyclohexyl) benzoates, mesomorphic, thermodynamic and dielec. props. 4-84390  
trans-4-[ $\beta$ -(trans-4'-n-alkylcyclohexyl)-1'-ethylcyclohexane-1-carboxylates, nematic phase, physical props. 4-92359  
4,4'-bis(trans-4-alkylcyclohexyl)-biphenyls, nematic transition temps. 4-88082  
1-trans-4-n-alkylcyclohexyl-2-(4-hydroxyphenyl)ethane, ether and ester derivatives, nematic liq. cryst. props. 4-113625  
4-trans-4-alkylcyclohexyl-alkylbenzenes, nematic transition temps. 4-88082  
amphiphilic liquid crystals, ionic cond. anisotropy 4-84435  
amphiphilic monolayers at LE-LC transition, equilb. and nonequilb. behaviour, broken symmetry model 4-80231  
anisylidene-p-aminophenylacetate, nematic, viscoelastic props. study 4-103845  
benzene-hexa-n-alkanoate discotic nematogen, phase diagrams, regular soln. theory 4-84393  
bilayer smectic-A liq. crystals, crit. behaviour of smectic elastic const. 4-75288  
biphenyl mesogens, heterocyclic analogues, mesophase thermal stability 4-88083  
bis-(4-(4'-n-heptyloxybenzylidene)-1,4-phenylenediamine, liq. cryst., phase behaviour under press. 4-113627  
blue phase liq. cryst. mixtures, lattice parameters, Bragg refl. obs. 4-88089  
butyloxy phenylnonyl oxybenzoate, ferroelastic smectic A-smectic C transition 4-80229  
caesium perfluoro-octanoate-water lyotropic liq. cryst., lamellar-nematic tricrit. behaviour 4-98278  
chiral mixture, electric-field-induced helix uncoiling 4-75292  
chiral triphenyl esters, columnar mesophases, structure and ferroelectric-antiferroelectric transition 4-60815  
cholesteric liq. cryst., pretransitional effects near blue phases 4-70379  
cholesteric liq. cryst.-KNO<sub>3</sub> mixtures, ferroelec. behaviour 4-109134  
cholesteric liquid crystals, blue phase, optical props. 4-88791  
cholesteric mesophases, photopolymerisation 4-113305  
cholesteric  $\omega$ -arylalkanoates, liq. cryst., cholesteric-isotropic transitions, thermal props. 4-108615  
cholesteric myristate (propionate) mixed liq. crystals, compressibility and thermal expansion anomalies 4-80227  
cholesteric myristate-azobenzene derivative mixed liq. cryst. state, smectic A=Blue Phase transition 4-98279

## liquid crystal phase transformations continued

- cholesteryl N-alkanoates, ternary system press. induced reentrant cholesteric phase 4-98002  
cholesteryl pelargonate and chloride, charge carrier mobility meas. 4-92709  
cholesterylpelargonate, thermally stimulated currents and phase transitions (*Russian*) 4-88519  
columnar-crystalline phase transition, elastic degrees of freedom 4-80230  
cyano end group binary mixtures, smectic C phase induction 4-75671  
4-cyano-4'-pentylbiphenyl, nematic liq. cryst., orientation distrib., two-photon dichroism 4-113326  
cyano- or nitro- polar compounds, bilayered fluid smectic phases 4-60818  
cyanobiphenyl liq. cryst. mixtures, alignment near smectic A-nematic transition 4-88087  
cyanobiphenyl liq. crystals, alignment on substrate surface by collective interactions 4-88086  
decylammonium chloride-H<sub>2</sub>O-NH<sub>4</sub>Cl, lyotropic liquid crystal, smectic-nematic transition 4-88289  
4,4'-di-n, n'-alkoxyazoxybenzenes, liq. crystals, binary mixtures, nematic-isotropic coexistence lines 4-108617  
1,1'-diacetylferrocene in cold smectic C liq. crystal, Mossbauer temp. study 4-109105  
1,1-dialkyl-4,4'-bipyridinium salts, ionomeric liq. crystals, mesophase transition temps. and electrochromism 4-88078  
dimyristoyl phosphatidylcholine-water system, phase transitions, high press. study 4-113624  
disc-like phases, extension of McMillan's model 4-84166  
discotic liquid crystals, phase transitions, ordering phenomena, Landau theory 4-61082  
DOBAMBC, ferroelec. smectic liq. cryst. structural phase transition, energy-dispersive X-ray diff. 4-75674  
DOBAMBC, ferroelec. smectic liq. cryst., phase diagram in external mag. field, laser light diff. meas. 4-65170  
dye dissolved in liq. cryst. soln., wavefront reversal in superluminesc. 4-107755  
enthalpy and birefringence in liquid crystals phase transition 4-98277  
EPPCB, smectic B-nematic phase transition, X-ray scatt. studies 4-75675  
eutectic liquid crystalline systems, phase diagrams 4-108618  
2-fluorenylmethylidene-4'-n-alkylanilines, mesomorphic behaviour 4-113306  
3-fluoro-4-cyanophenyl 4'-n alkylbenzoates, synthesis, mesomorphic and phys. props. 4-113318  
Fredericksz transition near nematic-smectic A phase transition 4-103648  
p-heptyl-p'-cyanobiphenyl, phase transition meas. in bulk and boundary 4-92361  
4-heptylphenyl-4-(4-nitrobenzyloxy)benzoate, smectic A<sub>1</sub>-smectic A transition, calorimetric studies 4-108619  
N-(p-hexyloxybenzylidene)-p-toluidine, liq. cryst. phase transitions, thermodielect. effects 4-61085  
p-n-hexyloxybenzylidene-p'-butylaniline, smectic liq. cryst., glass transition 4-84392  
high pressure studies 4-88288  
HOAB, density meas. across liq. cryst. phase transformations 4-108496  
hydrocarbons with trans-4-alkylcyclohexyl group, nematogenicity 4-88082  
o-hydroxy-p-methoxybenzylidene-p'-butylaniline nematic, viscoelastic props. study 4-103845  
infinitely thin hard platelets, isotropic-nematic transition, Monte Carlo study 4-108616  
isotropic-cholesteric liq. cryst. phase transition, orientational ordering 4-70380  
isotropic-nematic liq. cryst. phase transition, tricritical phenomena (*Russian*) 4-113632  
isotropic-nematic transitions, helix-coil induced reentrant, lattice theory 4-113626  
lamellar systems, B-phases, restacking phase transitions, dislocation model 4-98283  
light scattering near phase transitions, book 4-101581  
linear flexible macromolecules, thermotropic mesophases and mesophase transitions 4-98011  
lipid bilayers, mixed, phase transition props. rel. to those of covalent analogues 4-85408  
liquid crystal homologous series with bent linkages, thermal props. 4-75275  
liquid crystalline polymers with amphiphilic and nonamphiphilic side chains, phase behaviour 4-88080  
low molecular wt. cpds. with rigid group-flexible spacer struct., liq. cryst. behaviour 4-75282  
macromolecules, rodlike, in conc. soln., rot. relax., free energy, external flow effect, isotropic-nematic transition 4-69251  
MBBA, liq. cryst., pretranslational behaviour, time resolved degenerate four wave mixing (*Chinese*) 4-92355  
MBBA, nematic liq. cryst. structural phase transitions, energy-dispersive X-ray diff. 4-75673  
MBRA8 liquid crystal, smectic A-chiral-smectic C transition, Landau free energy 4-92358  
(+)-2-methylbutyl-p-(p-methoxy benzylidene)amino cinnamate, liq. cryst., transitions and texture, enthalpy and entropy 4-113628  
micellar additions, interaction with thermotropic liq. crystals 4-113623  
micellar systems of mixed composition, nematic states 4-113320  
monolayer smectic-A liq. crystals, crit. behaviour of smectic elastic const. 4-75288  
monosaccharides, liq. cryst. phases 4-113308  
nematic cell, multistable orientation induced by external field and interfacial interaction 4-70023  
nematic liq. cryst. mixtures, nematic-isotropic transition, phase diagrams 4-88290  
nematic liq. crystals, helical twisting power of terpenes, mol. conform. effects 4-88092  
nematic liquid cryst. binary mixtures, orientational order and nematic-isotropic transition, mol. field theory 4-84176  
nematic liquid cryst. tilt angles on SiO<sub>2</sub>, temp. depend. 4-88064  
nematic liquid crystals, critical dynamics near uniaxial-to-biaxial phase transition 4-113631  
nematic liquid crystals, high pressure props., perturbation theory for axially symmetric mols. 4-92084  
nematic liquid crystals, interfacial props., induced orientational order and wetting transitions 4-88069  
nematic liquid crystals, interfacial props. of nematic-isotropic and nematic-vapour interfaces 4-88068  
nematic liquid crystals, molecular theory 4-92089

## liquid crystal phase transformations continued

- nematic liquid crystals, pressure effects, reentrant phenomena, tricritical point 4-70033  
nematic-isotropic phase transition, interaction model using Corner-type potential 4-113630  
nematic-smectic A transition, gauge-invariant de Gennes model 4-92362  
nematic-smectic A transition, spin probe mol. dynamics, ESR obs. 4-108614  
nematic-substrate interaction, rel. to boundary layer phase transition 4-88088  
nematics, variational approach to theory and phase transitions (*Russian*) 4-88074  
4,4'-nitrobenzyloxybenzylidene-4'-alkoxyaniline, polar cpd., liq. cryst., inverted sequence S<sub>A</sub> N S<sub>C</sub> 4-75672  
4-octyl-4'-cyano-biphenyl, phase transitions, photoacoustic detection (*French*) 4-80228  
p-octyloxyazoxybenzene, liq. cryst. phase transition, positron lifetime temp. depend. 4-76557  
PAA, liq. cryst. phase transition, positron lifetime temp. depend. 4-76557  
PEBAB, phase transition studies 4-98280  
4-pentyl-4'-cyanobiphenyl, liq. cryst. isotropic phase, pretranslational behaviour in elec. fields, NMR 4-88071  
phenyl benzyloxybenzoates, reentrant nematic phase, effect of lateral substituent 4-113312  
phenyl cinnamoyloxybenzoates, reentrant nematic phase, effect of lateral substituent 4-113312  
3-phenyl-4-hydroxybenzoic acid liq. cryst. esters, thermodynamic props. 4-84391  
phenylbenzoates, liq. cryst. phase transitions, thermodielect. effects 4-61085  
p-phenylenes, homologous, liq. cryst. transitions, expts. 4-113620  
p-phenylenes, homologous, liq. cryst. transitions, orientation-dependent interactions and optical anisotropies 4-113622  
p-phenylenes, homologous, liq. cryst. transitions, theory 4-113621  
p-phenylenes, homologous, mixtures, liq. cryst. transitions, expts. 4-113620  
p-phenylenes, homologous, mixtures, liq. cryst. transitions, theory 4-113621  
phenylhydroquinone, liq. cryst. esters, thermodynamic props. 4-84391  
phospholipid dispersions, thermotropic and high-pressure phases, Raman spectroscopy, book contrib. 4-93701  
PMBA, phase transition studies 4-98280  
polar thermotropic liq. cryst. binary mixture, smectic A<sub>1</sub>-A<sub>2</sub> transition, X-ray diff. study 4-88293  
polyamides obtained from 1,2-bis(4'-carboxy-phenoxy)ethane, synthesis, charact., mesogenic and phys. props. 4-113304  
polyesteramides, linear thermotropic, transitions study 4-61083  
polyesters, liq. cryst. props. rel. to chem. struct., DSC, miscibility, and X-ray diff. studies 4-84170  
polyesters, main chain, thermotropic liq. cryst. props., effect of mesogenic unit and spacer structs. 4-84168  
polyesters, thermotropic liq. cryst., combined with low mol. wt. mesogens, phase behaviour 4-113300  
polyesters obtained from 1,2-bis(4'-carboxy-phenoxy)ethane, synthesis, charact., mesogenic and phys. props. 4-113304  
polymer melt with rigid and flexible, chain elements, liq. cryst. ordering (*Russian*) 4-75294  
polymer side chain liquid crystals, struct., optical and phase transition props. 4-98013  
polymeric system, rheological props. (*Russian*) 4-75293  
polymeric thermotropic liquid crystals, synthesis and characterisation 4-75283  
polymers, comb shaped, liq. cryst. transitions, IR spectra and dilatometry obs. (*Russian*) 4-84388  
polymers, flexible nematic, stiffening near clearing point 4-92087  
polymers, mesomorphic, three-component struct. and thermodynamic model 4-88091  
polymers, natural, liq. crystalline and crystalline phase equilibria, phase diagrams, morphology (*Russian*) 4-103913  
polymers, properties and appls. book 4-95088  
polymethylene- $\alpha$ ,  $\omega$ -bis(p-oxybenzylidene aniline) homologous series, thermotropic cpds., mesomorphic props. 4-113311  
potassium laurate-1-decanol-D<sub>2</sub>O nematic mixture, uniaxial-biaxial phase transform. 4-103931  
4-n-propoxybiphenyl-4-ethyl carboxylate, smectic A-smectic B transition optical effects 4-61086  
smectic A binary mixtures with enhanced nematic phase 4-88291  
smectic A-nematic phase transition for thermal imaging 4-111131  
smectic A-nematic transition temp., from twist deformation 4-88292  
smectic A-smectic C transition, heat capacity behaviour, effect of tricrit. region 4-84394  
smectic C ordered phases, cooperative dynamical behaviour 4-79932  
smectic liq. cryst., light-induced Fredericksz transition and optical non-linearity 4-61084  
smectic liq. crystals, phase transition between monolayer and bilayer phases 4-65399  
Smectic liquid crystals, in colour image displays 4-75676  
smectic phases, order parameter symmetries for phase transitions 4-75670  
smectic-A and -C phases, glassy behaviour 4-98007  
smectic-A-smectic-C (chiral smectic-C) transitions in liq. crystals, possible general behaviour 4-92363  
smectic-nematic binary mesophases nonlinear behaviour and polymesomorphism 4-75281  
sodium dodecyl sulphate-water system, phase transitions, FT-IR obs. 4-84389  
supermolecular liquid-crystalline structures in solutions of amphiphilic molecules, review 4-98010  
TBAA liquid crystals, phase behaviour at high press., DTA studies 4-98282  
TBPrA, smectic-G phase, PMR study 4-98956  
terephthalylidene-bis-(4-n-decylaniline), liq. cryst., phase behaviour under press. 4-113627  
terminally substituted cyano-nitro binary mixtures, liq. cryst. A-A transition 4-92360  
thermotropic, thin films, transform. of banded struct. on annealing 4-92357  
thermotropic discogens, phase diagrams and texture 4-84157  
thermotropic liquid crystals, polymorphism, book contrib. 4-92090  
transition temperature depression by a mag. field 4-98281

**id crystal phase transformations continued**

Cu complex, organometallic disc-like cpd., hexagonal columnar mesophase obs. 4-70025  
 4-octyloxy-4'-cyanobiphenyl, liq. crystals, crystallisation kinetics, Raman spectrosc. obs. 4-88846

**mid crystals**

see also *cholesteric liquid crystals; liquid crystal phase transformations; nematic liquid crystals; smectic liquid crystals*  
 alkyl and acyl glycosides, carbohydrate liq. crystals, mesogenic props. 4-113309

alkyl carboxylate-alkyltrimethylammonium mixed amphiphilic system, alkali metal and halide ion binding 4-84143  
 bis[3-(p-n-alkylanilino)-2-butenoyl] benzenes, liq. crystals, mesomorphic and thermal props. 4-88079

4-(trans-4-n-alkylcyclohexyl) benzoates, mesomorphic, thermodynamic and dielec. props. 4-84390  
 amphiphilic, ionic cond. anisotropy 4-84435  
 anthraquinone dye liq. crystal, display appls. 4-103651

azoxyarylethanes, mesomorphic props., potential stationary phases in gas chromatography 4-113316  
 binaphthyl-based liq. crystals, monomeric and polymeric, mesophase props. 4-88077

binary mixtures, obs. of liq.-liq. immiscibility 4-75689  
 bistable cell, Clausius eqn. and thermodynamics 4-88065  
 blue phase liq. crystal, lattice spacing fluctuations, refl. microscopy obs. 4-103649

BMBOA-isocotane mixture, extinction, optical props. of highly opalescent systems 4-84936  
 caesium perfluoro-octanoate-water lyotropic liq. crystal, lamellar-nematic tricrit. behaviour 4-98278

cesium alkanolates, temp. and enthalpy changes meas. by thermal anal., liq. crystal region 4-70022  
 chiral mixture, electric-field-induced helix uncoiling 4-75292  
 cholesterol myristate shear elasticity in region of solid-liq. crystal transition 4-61060

columnar discotic liq. crystals, Saint-Venant principle 4-60823  
 condensed matter physics, Iberian Symposium, Lisbon, Portugal (Sept. 1983) 4-78036

conference, Charlotte, NC, USA (Nov. 1983) 4-73146  
 conference, Las Vegas (USA), (March-April 1982) 4-82596  
 copolymers, aromatic, liq. crystal props., role of sequence distrib. 4-84169  
 copolymers of 4-hydroxybenzoic and 2-hydroxy-6-naphthoic acids, liquid crystalline, X-ray diff. 4-92075

copper dodecanoate, discotic mesophase, X-ray diff. study 4-92076  
 4-cyano-4'-alkoxybiphenyls, liq. crystal, energy transfer and migration 4-76516  
 cyanobiphenyls, current flow, relax. processes 4-88770

cyclohexane, plastic, nonplastic and liq. crystals, muonium temp. depend. 4-71245  
 1,1-dialkyl-4,4'-bipyridinium salts, ioneneomeric liq. crystals, mesophase transition temps. and electrochromism 4-88078

difluorinated Siamese Twin mesogens, mol. struct. and mesomorphism 4-84179  
 1,3-dioxanes, liq. crystals, synthesis and props. 4-84158  
 disc-like mesogen polymorphism 4-75280

disc-like phases, extension of McMillan's model 4-84166  
 discotic mesophases, complementary review 4-82620  
 discotic phases, partially frustrated systems 4-104387  
 disodium cromoglycate lyomesophases,  $^{23}\text{Na}$  NMR 4-92082

distortions and director distrib., coherent light interferometry 4-92086  
 1,3-dithianes, liq. crystals, synthesis and props. 4-84158  
 DPPC lipid bilayers,  $^1\text{H}$  and  $^{13}\text{C}$  spin-lattice relax. 4-62448  
 dual-frequency with dielec. anisotropy, torque distrib. 4-92079

dye dissolved in liq. crystal soln., wavefront reversal in superluminescence 4-107755  
 electronographic images, spatial charge determ., bulk elec. props. anal., appls. 4-89850

ethyl cellulose in chloroform soln., mesomorphic, viscosity, conc. and temp. depend. 4-65428  
 ferroelectric liquid crystals, mol. orientation dynamic response 4-98005  
 ferroelectric liquid crystals, permittivity 4-76307

fluorescence depolarisation intensity deconvolution 4-93103  
 Frank elastic consts., mol. struct. 4-103641  
 heteroaromatic azo dyes exhibiting negative dichroism 4-93046  
 hexa-n-octyloxtriphenylene, discotic liq. crystal, column buckling instability 4-113325

n-hexadecane- $d_{34}$  solubilised in lamellar liq. crystal,  $^2\text{H}$  NMR spectra 4-88066  
 n-hexane, plastic, nonplastic and liq. crystals, muonium temp. depend. 4-71245

homologous series, mol. struct. and ordering 4-88076  
 homologous series with bent linkages, thermal props. 4-75275  
 p-hydroxybenzoic acid, aromatic polyester PHBA, ordering and topotactic transitions 4-65197

IR birefringence meas. 4-80901  
 isotropic liq. crystal phase separation in rodlike particle soln. 4-70388  
 lamellar lyotropic mesophase, neutron scatt. study of structural defects 4-103646

lamellar lyotropic mesophases, mol. dynamics,  $^2\text{H}$  NMR spectra 4-76271  
 lamellar lyotropic mesophases, mol. dynamics,  $^2\text{H}$  nuclear mag. relax. times 4-76272  
 linear flexible macromolecules, thermotropic mesophases and mesophase transitions 4-98011

living tissue, liquid crystal components, book contrib. 4-93685  
 magnetic and polar cluster cpds., behaviour in elec. and mag. fields 4-98003  
 MBBA, four-wave mixing and its relax. effect 4-69490

p-methoxybutyl oxyazobenzene, four-wave mixing and its relax. effect 4-69490  
 mixed, opposite diamagnetic anisotropies, NMR spectra 4-109090  
 molecular alignment on surfaces, review 4-88084

molecules, oriented in liq. crystal, NMR spectroscopy, book contrib. 4-92968  
 naphthoquinone dyes in liquid crystalline media 4-92085  
 nematogens, monoester and diester, dielec. obs. 4-88764

neopentane, plastic, nonplastic and liq. crystals, muonium temp. depend. 4-71245  
 4-octyl-4'-cyanobiphenyl thermotropic liq. crystals, mol. motion, D relax. and spectral densities of spin probe 4-79927

organic and polymer crystals, nonlinear molecular optics, review 4-74594

**liquid crystals continued**

PEBAB, phase transition studies 4-98280  
 4-pentyl-4'-cyanobiphenyl, liq. crystal, isotropic phase, pretransitional behaviour in elec. fields, NMR 4-88071  
 PET-p-acetoxybenzoic acid copolymer, thermotropic liq. crystal, mol. orientation meas. 4-60824

3-phenyl-4-hydroxybenzoic acid liq. crystal esters, thermodynamic props. 4-84391  
 p-phenylenes, homologous, liq. crystal transitions, expts. 4-113620  
 p-phenylenes, homologous, liq. crystal transitions, orientation-dependent interactions and optical anisotropies 4-113622

p-phenylenes, homologous, liq. crystal transitions, theory 4-113621  
 p-phenylenes, homologous, mixtures, liq. crystal transitions, expts. 4-113620  
 p-phenylenes, homologous, mixtures, liq. crystal transitions, theory 4-113621

phenylhydroquinone, liq. crystal esters, thermodynamic props. 4-84391  
 phospholipid dispersions, thermotropic and high-pressure phases, Raman spectroscopy, book contrib. 4-93701  
 piperazines, liq. crystals, synthesis and props. 4-84158

PMBAB, phase transition studies 4-98280  
 poly(bisphenol E isophthalate-co-naphthalate), thermotropic liq. crystal, rheology and props. 4-113686  
 poly  $\gamma$ -benzyl glutamate, racemic liq. crystals, reformation of struct., rheo-optics 4-84946

polyamides obtained from 1,2-bis(4'-carboxy-phenoxy)ethane, synthesis, charact., mesogenic and phys. props. 4-113304  
 polyesteramides, linear thermotropic transitions study 4-61083  
 polyesters, liq. crystal props. rel. to chem. struct., DSC, miscibility, and X-ray diff. studies 4-84170

polyesters, main chain, thermotropic liq. crystal props., effect of mesogenic unit and spacer structs. 4-84168  
 polyesters, rigid-flexible struct., thermotropic liq. crystal props. 4-84161  
 polyesters, thermotropic liq. crystal, combined with low mol. wt. mesogens, phase behaviour 4-113300

polyesters obtained from 1,2-bis(4'-carboxy-phenoxy)ethane, synthesis, charact., mesogenic and phys. props. 4-113304  
 polyesters with mesogenic elements, conformational energy calcs. 4-113301  
 polymer melt with rigid and flexible, chain elements, liq. crystal ordering (Russian) 4-75294

polymer rheo-optics, conf., Seattle, WA, USA (Mar. 1983) 4-82590  
 polymer solution, splay and bend elastic consts., mol. wt. depend. 4-84332  
 polymeric system, rheological props. (Russian) 4-75293

polymeric thermotropic liquid crystals, synthesis and characterisation 4-75283  
 polymers, comb shaped, liq. crystal transitions, IR spectra and dilatometry obs. (Russian) 4-84388  
 polymers, deform. studies 4-113303

polymers, mesomorphic, three-component struct. and thermodynamic model 4-88091  
 polymers, properties and appls., book 4-95088  
 polymers, rigid chain conc. solns., state diagrams study (Russian) 4-84155

polymers, thermotropic liq. crystal, shear induced optical texture 4-75277  
 polymers with amphiphilic and nonamphiphilic side chains, phase behaviour 4-88080  
 polymethylene- $\alpha$ ,  $\omega$ -bis(p-oxybenzylidene aniline) homologous series, thermotropic cpds., mesomorphic props. 4-113311

polymorphism, NMR, dielec. props. and presence in living tissue, book 4-90313  
 principles, props., cell configs., and appls. (Spanish) 4-108273  
 pyrene carbonaceous mesophases, thermal behavior 4-92068  
 relaxation current increase study 4-75291

sodium dibutylphosphate-water lamellar liq. crystal, phase, orientation and mol. dynamics (French) 4-113298  
 sodium dodecyl sulphate-water system, phase transitions, FT IR obs. 4-84389  
 sodium methylpentanoates, thermotropic liq. crystal, struct., NMR study 4-84862

solution of rodlike molecules, rheological props. 4-103279  
 solutions, broadband decoupling sequences evaluation 4-88728  
 spiropyran-merocyanine organization, quasi-liq. crystals, optical props. 4-88072

stress, thermal and EM effects, entropy, constitutive theory 4-75271  
 supermolecular liquid-crystalline structures in solutions of amphiphilic molecules, review 4-88010  
 symposium on liquid crystals and ordered fluids, St. Louis, Missouri, USA (April 1984) 4-110805

ternary mixtures, eutectic compositions, determ. methods 4-113317  
 thermotropic disc-like mesogens, phase sequences 4-84181  
 thermotropic discogens, phase diagrams and texture 4-84157

thermotropic liquid crystalline polymers, domains and walls 4-79933  
 thermotropic liquid-crystalline polymers with mesogenic groups and flexible spacers in the main chain 4-84167  
 thermotropic mixed liq. crystals, oriented mols., NMR studies 4-84860

three-dimensional disordered structs. with variable short-range order, power spectrum and scatt. props. 4-92092  
 tobacco mosaic virus liquid crystals, twist and splay Frederiks transitions 4-75285

triethanolammonium oleate, lyotropic liq. crystal, IR spectra and X-ray diff. 4-84144  
 trioxethylene glycol monohexadecyl ether- $\text{D}_2\text{O}$  system, gel. and liq. crystal phase structs. 4-84145

xanthan solutions, rheology, molecular association and aggregation, liq. crystal domains 4-112798  
 Cu complex, organometallic disc-like cpd., hexagonal columnar mesophase obs. 4-70025

$\text{D}_2$  in mixtures of nematic liq. crystals, D NMR spectra, quadrupole moment, orientational ordering 4-91276  
 4-octyloxy-4'-cyanobiphenyl, liq. crystals, crystallisation kinetics, Raman spectrosc. obs. 4-88846

liquid drop model (nuclear) see *nuclear liquid drop model*  
 liquid encapsulated Czochralski method see *crystal growth from melt*  
 liquid films

see also *adsorbed layers; helium films; liquid helium; superfluidity; surface tension*  
 annular flow in tubes, crit. heat flux, rel. to crit. liq. film thickness 4-75085

**liquid films continued**

- annular mist flow in pipe, water film behaviour in nonequilib. region 4-60480
- asymmetrical thinning beneath liq. drop 4-79694
- condensation in vertical tube with closed top 4-75009
- cooling process of hot steel plate by laminar water bar, prediction modelling 4-93315
- critical heat flux in flowing liquid films 4-112696
- critical thickness, rupture and black spot 4-61191
- EHD squeeze films between spherical planes under periodic motion 4-97699
- falling, mass transfer kinetics, nonlinear effects influence, gas absorpt., chemical reaction 4-103433
- falling film flow in a co-current gas flow, wave characts. 4-69828
- falling laminarily down vertical plate, film thickness 4-88377
- falling liquid films with surfactants, thermocapillary breakdown 4-60545
- falling thin liquid film, flows, wave instability (*Rumanian*) 4-69778
- flow over reducer surface model 4-91790
- free falling, dynamic surface tension 4-61190
- free liquid films, disjoining pressure calc. 4-61192
- free surface wave propag., laminar-turbulent transition (*French*) 4-60370
- gas-liquid flow, horizontally and vertically separated, large disturbance wave initiation 4-60494
- Gibbs elasticity of multicomponent solutions 4-108681
- glycerol films, falling, CO<sub>2</sub> desorption, mass transfer enhancement 4-65551
- ice, surface, quasi-liq. film, evidence from and implications for contact charging 4-70911
- insoluble monolayers, static and dynamic response to shear, meas. instrument 4-113751
- interfaces, acoustic impedance and Konstantinov effect 4-108550
- laminar falling film, effective areas and mass transfer coeffs. in packed columns 4-87661
- laminar falling films, entrance region lengths 4-64910
- liquid film, vaporising, laminar and turbulent boundary layers, momentum, heat and mass transfer 4-60414
- nematic liq. cryst., nonlinear thin film, optical transverse intensity bistability 4-74602
- rewetting of a hot surface by a falling liquid film—effects of liquid sub-cooling 4-98403
- soap film, liquid drop suspension, simplified model 4-88376
- soap films, liquid drop suspension, general formulation 4-88375
- spreading and van der Waals forces (*French*) 4-80328
- stretching of plane fluid film 4-97453
- surface film motion in rot. cylinder 4-112981
- swirling annular-mist two-phase flow, liq. film characts. 4-97571
- swirling annular-mist two-phase flow, liq. film flowrate along tube 4-97570
- swirling annular-mist two-phase flow, torque and swirler efficiency 4-97569
- thin films, disjoining press. oscils. 4-75759
- thin liquid films, flow, stabilisation length 4-69737
- thin wavy film, vertical flow, simulation by finite element method 4-74984
- two-dimensional grid turbulence obs. 4-69742
- upflow laminar liq. films, flooding, multiple stable states modelling 4-60364
- viscous film flow with free boundaries, one-dimensional approx. 4-87831
- viscous films flowing down vertical wall, solutions 4-69777
- viscous fluid, thin films, weakly nonlinear stationary waves 4-103353
- viscous incompressible liq. down dry wall, flow regimes 4-69801
- viscous incompressible liq., spreading over horizontal surface 4-92479
- viscous liq. flowing on inclined plane, steady travelling wave problem soln. 4-112915
- viscous thin liq. film, wave flow with reduced gravitation 4-79612
- water, subcooled, falling liq. turbulent films, critical heat fluxes 4-97544
- water film, photon and electron-stimulated desorption, mech. of ion formation and desorption 4-61241
- wetting film on solid surface, vertical ascension (*French*) 4-80327
- on Ag film, surface plasmon enhanced Raman scatt. 4-76453
- H<sub>2</sub>O molecule orientation on thin film boundaries (*Ukrainian*) 4-65520
- <sup>2</sup>He adsorbed layer, spin-diffusion coeffs. 4-113742
- LiBr film, water vapour absorpt., heat and mass transfer 4-64937
- LiBr film flowing down adiabatic wall, mass transfer in absorpt. of water 4-64831

**liquid flow coaxial cables** see coaxial cables

**liquid He** see liquid helium

**liquid helium**

- see also helium films; liquid helium-3; liquid helium-4; liquid helium sound propagation; ripples; vortices
- 2D electron solid, low wavelength phonons 4-65509
- charged surface stability in a condenser (*Russian*) 4-70489
- cryostat, He transfer gas-liquid separator 4-73440
- cryostat, interfacing to closed-cycle refrigerators 4-58858
- heat flux density emission by metal film 4-70491
- level detector based on vapour press. meas. 4-101813
- level sensor using superconducting wire 4-101808
- microwave acoustics, high resolution microscopy and phonon dispersion meas. 4-61165
- pool boiling, crit. heat flux, heater thermophys. props. effects 4-69667
- pool cryopump 4-68236
- supercritical, mixed convection heat transfer to upflow in vertical tube 4-69750
- superheated, soil interface, light induced nucleation of vapour bubbles, photoemission model 4-61163
- surface, two-dimens. electron cryst., liq.-solid transition, coupled electron-ripple vibrs., RF absorpt. spectra 4-88358
- surface, two-dimens. electron solid, electron-ripple resons. (*Russian*) 4-84486
- surface wave velocity, capacitive technique anal. (*Japanese*) 4-92453
- transport vessel, cryostat for use at 1.5-300K 4-101853
- two-dimensional electron solid on liquid He, propag. of shear 4-104018

**liquid helium-3**

- see also fermion systems; superfluid helium-3
- acoustic excitations spectrum 4-75748
- adsorbed layer, spin-diffusion coeffs. 4-113742
- adsorbed on fluorocarbon microspheres, dynamic polarisation effects, EPR study 4-80324
- cooling heat exchangers, comparison of Cu, Ag and Pd 4-95433
- critical fluctuations near gas-liq. critical point, decay rates 4-92468

**liquid helium-3 continued**

- dimers and trimers, unified framework anal. 4-104013
- effective quasiparticle potential model, Landau parameters 4-70504
- effective-range expansion parameters for central potentials 4-70497
- exchange scatt. of quasiparticles by positive ion 4-104029
- ferromagnetism, surface-induced, review (*Japanese*) 4-70512
- fully spin polarised, ground state energy and Landau parameters 4-7575
- ground state, spin depend. correlations, variational Monte Carlo stud 4-104027
- Lennard-Jones pot., effective-range expansion parameters calc. 4-108671
- localised electron energy spectrum, surface thermal fluctuations effect 4-70499
- normal phase, spin waves-zero sound coupling 4-92466
- nuclear magnetisation relax. in confined geometries 4-61166
- particle-hole excitations, RPA calcs. 4-70509
- polarisation potentials, differences and continuity 4-113743
- positronium bubbles in <sup>3</sup>He and <sup>4</sup>He fluids and solids 4-108672
- restricted geometry and bulk liq., spin diffusion coeff. 4-113744
- rotating, NMR of textures 4-84483
- small pores, superfluid density and transition temp. 4-92463
- solidification in porous glass, NMR relax. meas. 4-84485
- thermal cond. and specific heat meas. 4-70510
- vapour pressure equations 4-98381
- viscoelasticity and zero sound 4-98395
- Vycor glass with liquid <sup>3</sup>He and superfluid <sup>4</sup>He, effects on two-level systems 4-75745
- <sup>3</sup>He liquid small particle thermal boundary resistance, review 4-65510
- <sup>3</sup>He/Ce<sub>2</sub>Mg<sub>3</sub>(NO<sub>3</sub>)<sub>12</sub> system, anomalous low temp. Kapitza resistance 4-65542
- <sup>3</sup>He/powder system, Kapitza resist., shaking box model 4-65513
- <sup>3</sup>He-CO<sub>2</sub> mixture, coexisting phases near liquid-vapour transition (*Russian*) 4-88364

**liquid helium 3-4 mixtures**

- convection onset near λ line, effect of parametric modulation 4-104031
- critical fluctuations near gas-liq. critical point, decay rates 4-92468
- dielectric formalism for <sup>3</sup>He-<sup>4</sup>He mixtures 4-92470
- dilute, surface superfluidity 4-61167
- dilute mixtures, Kapitza resist. in Cu powder, size effect 4-65514
- excess thermodynamic functions of <sup>3</sup>He-<sup>4</sup>He liquid solutions (*Russian*) 4-92467
- film, ions localised near interface, low temp. mobility (*Russian*) 4-92452
- film, third sound studied 4-92469
- films, superfluid onset temp., third sound vel. 4-88365
- phase separating <sup>3</sup>He-<sup>4</sup>He mixtures, dynamic light scattering obs. 4-104032
- polarised, spin rotation effect obs. 4-70513
- sound attenuation, <sup>3</sup>He-<sup>4</sup>He interaction determ. 4-70515
- superfluid ordering near a wall 4-88363
- surface trapped two-dimensional electrons 4-98387
- thin films, phase separation study 4-104030
- triplet correlations in boson-boson mixtures 4-98397
- Cd<sub>2</sub>Mg<sub>1-x</sub>(NO<sub>3</sub>)<sub>2</sub>·<sup>3</sup>He-<sup>4</sup>He liquid boundary, thermal resistance study 4-84484
- <sup>4</sup>He films with <sup>3</sup>He, binding energy calcs. 4-70514

**liquid helium-4**

- see also boson systems; superfluid helium-4
- adsorbed layer on Y-zeolite, semiquantum liquid and ordered phases obs. 4-65515
- binding energy, hypernetted chain method 4-61162
- Bose-Einstein condensation problem (*Russian*) 4-104023
- caloric eqn. of state near crit. point (*Russian*) 4-84360
- coherent excitation of surface waves by neutrons 4-104021
- convection in rot. cell, stability and heat transfer study 4-113736
- dielectric breakdown delay time, superconductivity effect 4-109125
- dimers and trimers, unified framework anal. 4-104013
- dislocation mediated melting of 2-d electron lattice 4-98386
- effective-range expansion parameters for central potentials 4-70497
- electrokinetic phenomena with no mass transport 4-92457
- electron mobility and surface states 4-70498
- equilibrium crystallisation, interface problem 4-108670
- film, electron mobility, polaronic transition 4-98399
- film, polaronic state of surface two-dimensional electrons 4-98390
- film, strongly-coupled ripplonic polarons in high magnetic fields 4-98388
- film adsorbed on solid Ne, electron density 4-98683
- film adsorbed on solid Ne, surface trapped two-dimensional electrons 4-98387
- hard sphere fluid, correlation functions, struct. factor 4-98380
- isotherms analysis, density and dielectric virial coeffs., NPL-75 temp. scale accuracy 4-63746
- Kapitza resistance, spectral depend. between 0.5 and 2.3K 4-65512
- Kapitza resistance between liq. and solid <sup>4</sup>He, and phonon transmission 4-70501
- Kapitza resistance of laser-annealed surfaces 4-70500
- Lennard-Jones pot., effective-range expansion parameters calc. 4-108671
- level detector using SrTiO<sub>3</sub> crystals 4-101833
- linear response functions, density-wave instability 4-113740
- liquid-solid interface, evidence for new quantum state, crystallisation waves 4-70520
- localised electron energy spectrum, surface thermal fluctuations effect 4-70499
- momentum distrib. for Bose systems with mixture formalism, hypernetted-chain theory 4-98384
- phase change and heat flow near λ point 4-92455
- phonon and roton-induced evaporation 4-65511
- positronium bubbles in <sup>3</sup>He and <sup>4</sup>He fluids and solids 4-108672
- quantum evaporation by rotors and phonons 4-70492
- solid-liquid interface, sound transmission 4-70502
- solidification and growth on Grafoil 4-104033
- sound velocity temp. variation calcs. 4-70496
- static structure factor below T<sub>λ</sub>, temp. depend. 4-70493
- stochastic ionization of surface-state electrons: classical theory 4-92459
- surface, diffusion of H atoms 4-88357
- surface, natural oscils. of charged dimples 4-104022
- surface critical electron density 4-98385
- surface multielectron dipole formation 4-113741
- surface Wigner solid, topological defects and melting 4-98389
- thin film on sapphire, desorption studies 4-98398
- two-particle pot. function from scatt. data 4-113738
- vapour pressure equations 4-98381

- solid helium sound propagation**  
 see also second sound; zero sound  
 microwave acoustics, high resolution microscopy and phonon dispersion meas. 4-61165  
 small pores, superfluid density and transition temp. 4-92463  
 Vycor glass with liquid  $^3\text{He}$  and superfluid  $^4\text{He}$ , effects on two-level systems 4-75745  
 $\text{Cd}_3\text{Mg}_{1-x}(\text{NO}_3)_2 \cdot x\text{He}$  liquid boundary, thermal resistance study 4-84484  
 $^3\text{He}$ , liq., acoustic excitations spectrum 4-75748  
 $^3\text{He}$ , superfluid, B-phase, US oscills. 4-98392  
 $^4\text{He}$ , superfluid A and B phases, collective excitations in electric field 4-108673  
 $^3\text{He}$ - $^4\text{He}$  liquid mixtures, sound attenuation,  $^3\text{He}$ - $^4\text{He}$  interaction determ. 4-70515  
 $^4\text{He}$ - $^4\text{He}$  mixture film, third sound studied 4-92469  
 $^4\text{He}$ - $^4\text{He}$  mixture films, superfluid onset temp., third sound vel. 4-88365  
 $^4\text{He}$  film, sound velocity temp. variation calcs. 4-70496  
 $^4\text{He}$  liquid film adsorbed on packed powders, Kosterlitz-Thouless superfluid transition 4-104019  
 $^4\text{He}$ , solid-liquid interface, sound transmission 4-70502  
 $^4\text{He}$ , sound velocity temp. variation calcs. 4-70496  
 $^4\text{He}$ , superfluid, acoustic properties of superleaks partially saturated with superfluid 4-70490  
 $^4\text{He}$ , superfluid, fourth sound, probe of multilayer adsorption of solid  $^4\text{He}$  on graphite 4-88366  
 $^4\text{He}$ , superfluid, fourth sound refraction by superleak grains (Chinese) 4-113735  
 $^4\text{He}$ , superfluid, nonanalytic hydrodynamic dispersion relations, mode-coupling theory 4-75746  
 $^4\text{He}$ , superfluid, temperature oscills., electroacoustic meas. by reciprocity method 4-98391  
 $^4\text{He}$ , superfluid, third sound, healing, relax. thermal cond. and viscosity effect 4-88359  
 $^4\text{He}$ , superfluid, transverse acoustic impedance under press. 4-92456  
 $^4\text{He}$ , superfluid film, US third sound scatt. from substrate surface defects 4-104017  
 $^4\text{He}$ , superfluid films, third-sound phenomena studied by thin-film oscillator 4-61168  
 $^4\text{He}$  superfluid surface, condensation of spin polarised atomic H 4-104037  
 $^4\text{He}$  superfluid waveguide with superleak, acoustic props. 4-84479
- liquid lasers**  
 see also dye lasers  
 No entries
- liquid metal embrittlement**  
 FCC metals, transcrystalline SCC mechanism, cleavage-like fracture surfaces 4-71793  
 steel, austenitic and ferritic, corrosion behaviour in eutectic Pb-Li environment 4-107056  
 steel, austenitic and ferritic, for use in fusion reactor liq. metal blankets, compatibility, review 4-107054  
 steel, Cr-Mo-V martensitic, liq. metal induced embrittlement, dislocation emission from crack tips 4-85210  
 steel, HSLA, Cu-bearing, hot shortness 4-89104  
 steel, stainless, austenitic, type 316, flowing Li environment effect on fatigue and tensile props. 4-107055  
 Zircaloy, fracture, influence of environment on form. of fluting microstruct. 4-104911  
 Zircaloy cladding, chemical model for cadmium liquid-metal embrittlement 4-106770  
 Ni and alloys, fatigue lifetimes and fractography in air and liq. Hg 4-99557  
 Ni and alloys, tensile fracture characts. in liq. Hg 4-99558  
 TiB<sub>2</sub> powder, pressureless sintered, mech. props. in liq. Al environment, impurity segregation 4-114700
- liquid metals**  
 see also electron energy states of liquid metals; liquid alloys; mercury (metal)  
 acoustic nonlinearity parameter calc. 4-84346  
 alkali, acoustic wave velocity, influence of many-body interactions 4-98204  
 alkali, liquid structure factor near freezing point, calcs. 4-113296  
 alkali metals, liq., longitudinal viscosity, classical one-component plasma model 4-61126  
 alkali metals, liquid, thermodynamic props. using classical plasma reference system 4-60810  
 alkali metals, molten, O<sub>2</sub> solubility study 4-113641  
 conductors in mag. fields, bifurcation figures for equilib. (Russian) 4-113059  
 construction of liquid metal screens in high-temperature MHD apparatus (Russian) 4-113056  
 dense matter in liq. metal phase, low-temp. quantum corrections to elec. and thermal conds. 4-63040  
 effective interactive forces, general formulation and effective medium approx. 4-60809  
 electrical cond. and thermoelectric power computation 4-92686  
 electrical conductivity, effective medium approx. 4-92690  
 electron-ion plasma, struct. factor 4-84577  
 energy spectrum and density of states calcs. (Russian) 4-113854  
 entropy, expansion coeff., sp. ht. and Debye temp. 4-103963  
 films, electromag. induced breakdown during free flow on surface (Russian) 4-114210  
 flow in narrow gap perpendicular to mag. field (Russian) 4-113043  
 flow in pipe in longit. mag. field of solenoid, heat exchange 4-108117  
 flow through channel with transverse mag. field, in elect. insulated channel 4-75093  
 fusion reaction chamber, for inertial fusion energy conversion, magnetically guided flow obs. (Japanese) 4-102397  
 fusion reactor blankets, liquid metal corrosion product transfer, MHD effects, safety 4-111786  
 Hall effect theory, mass renormalisation corrections 4-113921  
 interatomic core forces deduced from observed liquid structure factors 4-92044  
 intrastructural distribution of additions in liquid metals 4-113297  
 ion source, shape, dynamic model 4-81117  
 ion sources for microscopy and lithography 4-78416  
 isomeric nuclei and  $\mu$  emitters as probes in condensed matter, review, book contrib. 4-71197  
 laser interaction, evaporation influence on melt behaviour 4-76566
- liquid metals continued**  
 liquid metal cooling system, mass transfer in presence of strong mag. field (Russian) 4-113035  
 mechanisms and kinetics of dissolution 4-114530  
 metal-nonmetal melts, thermodynamic props. (Russian) 4-70413  
 MHD, conference, Riga, Latvian SSR 4-106123  
 MHD, equilib. bifurcations, automatic control influence 4-113024  
 MHD convection in two-layer systems heated from below 4-108135  
 mixtures, intermolecular forces, excess Gibbs energy 4-65418  
 molten metals, EM vibr. treatment under microgravity, hydrodynamic effects 4-97698  
 planar metal jet, Rayleigh instability, stabilisation by mag. field and by heat flow (Russian) 4-112820  
 polyvalent metals model pots. and trends in liq. struct. 4-84141  
 quantum liqs., inhomogeneous, direct correl. function, appl. to liq. metals 4-60796  
 rare earth metals, liquid, density, surface tension, periodic depend. 4-113517  
 short-wave capillary struct. parametric excitation at liq. metal surface contiguous to unstable plasma 4-84013  
 solid-liquid metal interaction, phase layer formation, effect of gravity 4-70386  
 solidifying, temp. meas. 4-99740  
 surface in contact with dense plasma, nonlinear capillary waves excitation 4-84540  
 surface instability under intense IR laser irradi. 4-80340  
 surface motion detection, using masked aperture technique 4-113084  
 surface tension, theory 4-84487  
 thermal expansion 4-84425  
 thermodynamically consistent theory, pair pot. extraction 4-92043  
 transition metals, Muffin-tin model, local density of states, calcs. 4-108755  
 ultrasound absorpt. 4-84347  
 US atomisation of melts, metal powder prod. 4-89007  
 Al, and reaction bonded SiC, cast bonding, exchange diffusion phenomenon involving free Si 4-99741  
 Al, band energies, elec. resist., thermoelec. power, pseudopotential parameters determ. 4-98512  
 Al, chem. reaction with B fibres 4-61891  
 Al, liq., structural props., elec. resist., X-ray diffr. 4-79925  
 Al, liq., thermal expansion 4-84425  
 Al, liquid, computer simulation of dynamic behaviour 4-60811  
 Al, liquid, pair pots., Monte Carlo simulation 4-92047  
 Al, liquid, struct. factor, influence of electron-gas response junction 4-75265  
 Al melt, wetting of graphitised C strip 4-92476  
 Al, radial distrib. functions calc. using Percus-Yevick and mean spherical model approx. 4-70020  
 Bi, liquid, propagating collective excitations; neutron scatt. study 4-65167  
 Bi, liquid struct. determ. 4-98000  
 Cd, self-diffusion coeffs., temp. depend. 4-65426  
 Cs, enhanced mag. susceptibility 4-92891  
 Cs, eqn. of state and pVT data up to 2000K and 600 bar 4-103898  
 Cs, liquid, density calcs. using model-potential approach 4-92065  
 Cs, molten, O<sub>2</sub> solubility study 4-113641  
 Cs, solid and liq., Grueneisen parameter at high press., nature of isostructural electronic transition 4-61035  
 Cs-CsCl(CsI) liq. solns., mag. susceptibility 4-80741  
 Cu, liq., structural props., elec. resist., X-ray diffr. 4-79925  
 Cu, liq., thermal expansion 4-84425  
 Cu, liquid, pair pots., Monte Carlo simulation 4-92047  
 Fe, local density of states via recursion and equation of motion methods, comparative study 4-98505  
 Ga, ion source, construction and technology (Chinese) 4-82858  
 Ga, liq. and amorphous, radial distrib. function and struct. factor, quasi-cryst. model 4-84186  
 Ga, liquid, explosive emission study 4-109311  
 Ga, liquid struct. determ. 4-98000  
 Ga, supercooled and normal, elec. resist., temp. depend. 4-75921  
 Ga-glass interface, phonons, Brillouin-scatt. study 4-80955  
 Hg, liquid struct. determ. 4-98000  
 In, liquid, solubility and diffusivity of oxygen 4-92373  
 K, liquid, density calcs. using model-potential approach 4-92065  
 K-KCl liq. solns., mag. susceptibility 4-80741  
 Li, blanket materials, candidate, for fusion reactor appl. 4-91107  
 Li, compatibility of fusion reactor materials 4-107062  
 Li, corrosion and phase stability of Cr-Mn austenitic steel 4-107061  
 Li, corrosion behaviour of stainless steel using LIL0-7 thermoconvection loop 4-107059  
 Li, fusion reactor blankets, compatibility of steels, review 4-107054  
 Li, fusion reactor blankets, effect on fatigue and tensile props. of steel 4-107055  
 Li, in fusion reactor, chem. behaviour of dissolved Si 4-107058  
 Li, liquid, effect of Born-Mayer potential on props. 4-92064  
 Li, mass transfer behaviour of modified PCA austenitic stainless steel 4-107063  
 Mg, molten, melting and self-diffusion coeffs., pressure effects (Russian) 4-107405  
 Mn, viscosity meas. (German) 4-79681  
 Mo, liq., thermal expansion 4-84425  
 Na circuit with supercond. magnet, local MHD resistances (Russian) 4-113050  
 Na, dil. soln. in low-melting Bi-Cd-In system, activity 4-61109  
 Na, dynamic struct. factor, inelastic neutron scatt. 4-92066  
 Na, liquid, density calcs. using model-potential approach 4-92065  
 Na, liquid, effect of Born-Mayer potential on props. 4-92064  
 Na, liquid-vapour interface struct., Monte Carlo simulation 4-88062  
 Na, radial distrib. functions calc. using Percus-Yevick and mean spherical model approx. 4-70020  
 Na-Cs liquid-vapour interface struct., Monte Carlo simulation 4-88062  
 Na-NaBr(NaCl) liq. solns., mag. susceptibility 4-80741  
 Nd, solid and liq., elec. resist. studies 4-92691  
 P<sup>+</sup> liq. metal ion source development 4-83261  
 Pb, electrically cond. liquids, free jets, reson. breakdown, EM forces, drop form. phases (Russian) 4-113057  
 Pr, solid and liq., elec. resist. studies 4-92691  
 Rb, liq., struct. factors calc. using optimised random-phase approx. 4-84142  
 Rb, liquid, density calcs. using model-potential approach 4-92065  
 Rb, liquid, elec. field gradient fluctuations spectrum 4-108826  
 Rb, liquid, microscopic dynamics 4-75267

**liquid metals continued**

- Rb, radial distrib. functions calc. using Percus-Yevick and mean spherical model approx. 4-70020  
 Rb, solid and liq., Gruenisen parameter at high press., nature of isostructural electronic transition 4-61035  
 Sb, liquid, thermodynamics, pseudopotential theory 4-79924  
 Sc, density, surface tension studies 4-113517  
 Sm, solid and liq., elec. resist. studies 4-92691  
 Sn, liquid, solubility and diffusivity of oxygen 4-92373  
 Sn, liquid struct. determ. 4-98000  
 Ta, liq., thermal expansion 4-84425  
 Tl, self-diffusion coeffs., temp. depend. 4-65426  
 W, enthalpy of solid and liquid, heat capacity, levitation calorimetry 4-108632  
 W, liq., thermal expansion 4-84425  
 Y, density, surface tension studies 4-113517  
 Zn, molten, melting and self-diffusion coeffs., pressure effects (Russian) 4-103908  
 Zn, reaction with Fe-Si alloys, immersion time depend. 4-109570

**liquid oscillations**

see also liquid waves

- acoustic relaxation oscillations in supersonic flow past pipe diameter increase (German) 4-83955  
 cavities of revolution, liq. oscills. characts. soln. 4-112895  
 centrifugal pump piping systems, press. pulsations in liq. columns 4-60444  
 continuous spectrum in differentially rotating perfect fluids, model with analytic soln. 4-94581  
 duet, circular, abrupt expansion, self-excited flow oscillation 4-103412  
 flow past infinite porous vertical plate, suction and free convection effects 4-75081  
 ideal stratification flow in vessel, free oscillations (Russian) 4-64965  
 MHD free-convection flow near vertical oscillating plate, theory 4-67618  
 MHD free-convection oscillatory flow past porous limiting surface; effects of Joule heating and viscous dissipation 4-67616  
 MHD free-convective oscillatory flow past porous limiting surface, effects of Joule heating and viscous dissipation 4-67615  
 paraboloid containers, forced liq. oscils. 4-64966  
 paradoxical phenomena in vibrating fluids and solid bodies 4-101635  
 spherical shell, oscillations in microgravity, nodal circles obs. 4-97586

**liquid permeability** see permeability**liquid phase epitaxial growth**

- apparatus using two-way movable melt slider and visual observation device 4-99351  
 crystal growth, conference, Stuttgart, Germany (Sept. 1983) 4-58552  
 diamond, natural, metastable epitaxial crystallisation 4-70592  
 garnet film structural props. 4-80805  
 garnet monocrystalline cathodoluminesc. layers 4-81010  
 hexaferrite films, prep. and device appls. 4-61883  
 III-V quaternary semiconductors, immiscibility and spinodal decomp. rel. to epitaxial layer quality 4-70590  
 materials for optical communications, review 4-61833  
 newberyite, heterogeneous nucleation and epitaxy 4-92115  
 optical communication device research, epitaxial growth, lasers and integrated optics 4-74746  
 production of multilayer type solid diode lasers (German) 4-83620  
 reactor, modelling and numerical simulation 4-109335  
 semiconductor photovoltaic material bulk single cryst. and epitaxial multilayer growth 4-71548  
 uric acid crystals, heterogeneous nucleation and epitaxy 4-92115  
 YIG film Y-branch interferometer grown by liq. phase epitaxy 4-97138  
 (Al,Ga)As-GaAs double heterostructure laser technology 4-74539  
 AlGaAs/GaAs concentrator solar cells under high temp. and humidity conditions 4-66708  
 Al<sub>0.1</sub>Ga<sub>0.9</sub>As heteroepitaxial struct. photoluminescence study 4-104673  
 Al<sub>0.1</sub>Ga<sub>0.9</sub>As<sub>0.1</sub>Sb<sub>0.9</sub> heterostruct., conditions for LPE growth 4-114429  
 Al<sub>0.1</sub>Ga<sub>0.9</sub>As<sub>0.1</sub>Sb<sub>0.9</sub> heterojunction photocells, LPE fabrication 4-81559  
 AlGaInPAs lattice matched to GaAs, LPE growth, photolum. obs. 4-70581  
 Al<sub>0.1</sub>Ga<sub>0.9</sub>In<sub>0.1</sub>P<sub>0.9</sub>Sb<sub>0.9</sub> epitaxial layers, luminescence studies 4-76505  
 AlGaSb, LPE, substrate treatment optimisation, carrier conc., Raman spectra, photoluminesc. 4-93235  
 Au thin films 4-75814  
 Bi<sub>0.5</sub>Fe<sub>0.5</sub>Ga<sub>0.5</sub>O<sub>1.5</sub> garnet layer growth by LPE, review 4-80453  
 (Bi,Tm)<sub>0.5</sub>(Fe,Ga)<sub>0.5</sub>O<sub>1.5</sub> epitaxial film, mag. bubbles study 4-109049  
 CuGa<sub>1-x</sub>In<sub>x</sub>S<sub>2</sub> LPE growth on ZnSe substrate 4-80436  
 (Ga,Al)As/GaAs double heterostructures, LPE, struct. and lasing characts. rel. to As vapour press. 4-66249  
 Ga-Al-As/GaAs, liq. epitaxy capillary effect 4-98408  
 Ga-As-Sn system, phase diagram and LPE growth rates 4-93237  
 Ga-In-P-As system, LPE, growth kinetics 4-88426  
 Ga<sub>0.4</sub>Al<sub>0.6</sub>As-GaAs heterostructures, LPE growth, layer height profiles rel. to convection and cooling rates 4-66248  
 p-Ga<sub>1-x</sub>Al<sub>x</sub>As:Be-p-GaAs:Be-n-GaAs:Si heterojunction LPE growth for solar cells 4-109334  
 Ga<sub>1-x</sub>Al<sub>x</sub>As/GaAs solar cell with antiref. coating, LPE grown, design, fabrication and characts. (Polish) 4-114904  
 Ga<sub>1-x</sub>Al<sub>x</sub>As-GaAs, Raman scatt. theory 4-76460  
 Ga<sub>1-x</sub>Al<sub>x</sub>As-GaAs heterostructure, LPE grown, dislocation extension and density distrib. (Chinese) 4-113449  
 Ga<sub>1-x</sub>Al<sub>x</sub>Sb<sub>1-x</sub>As<sub>0.5</sub>Ga<sub>0.5</sub>Sb, LPE, phase equilib. rel. to lattice mismatch strain 4-93236  
 GaAs crystallisation by nonequilibrium electroliq. epitaxy, molten soln. parameter determ. 4-75817  
 GaAs, excitonic polaritons in elec. fields at surfaces 4-92633  
 GaAs, LPE growth, deep intrinsic centers, anisotropic capture 4-113897  
 GaAs, LPE growth and nonequilibrium, deep centre trapping 4-108744  
 GaAs, LPE growth rates 4-93237  
 GaAs LPE layers, residual impurities, growth soln. baking effects 4-92226  
 GaAs LPE layers, surface morphology, effect of substrate misorientation (Chinese) 4-84521  
 GaAs, p-n-p doped submicron structures, LPE grown, n-channel conductivity modulation 4-61447  
 GaAs p-n-p-n superlattices, LPE growth 4-80665  
 GaAs substrates for GaAs ICs, growth processes 4-99299  
 GaAs/AlGaAs DH laser, LPE fabricated, design optimisation for entertainment electronics (German) 4-102948  
 GaAs-(AlGa)As large optical cavity lasers 4-107631

**liquid phase epitaxial growth continued**

- Ga<sub>0.47</sub>In<sub>0.53</sub>As-InP, Raman scatt. theory 4-76460  
 GaInAsP, LPE growth on InP, review, book contrib. 4-61882  
 GaInAsP/InP 1.3 μm distributed feedback lasers, LPE growth 4-96913  
 GaInAsP/InP hetero-multilayers, LPE fabrication and reflectivity 4-99357  
 GaInAsP/InP laser, single-mode, low-temp. single-step LPE growth 4-112407  
 Ga<sub>1-x</sub>In<sub>x</sub>As<sub>0.5</sub>P<sub>0.5</sub> solid solutions, LPE, conc. profiles 4-93233  
 Ga<sub>1-x</sub>In<sub>x</sub>As<sub>0.5</sub>P<sub>0.5</sub>, epitaxial layers, reflection spectra analysis 4-114340  
 GaInP/AlGaAs double heterostructures, LPE, lasing, 77-230K 4-71606  
 Ga<sub>1-x</sub>In<sub>x</sub>P, LPE growth on GaAs substrates, cathodoluminesc. and photoluminesc. spectra (Chinese) 4-113825  
 Ga<sub>1-x</sub>In<sub>x</sub>P monocryst. layers, LPE on GaAs (Chinese) 4-114427  
 GaN, crystals, high pressure soln. growth, equilib. N<sub>2</sub> press. over Ga-GaN mixtures 4-61822  
 GaP:ZnO, LPE layers, cleaved surfaces photoluminesc., macrosteps and grooves 4-65588  
 GaP:As<sub>0.1</sub>Sb<sub>0.9</sub> epitaxial layers, luminescence studies 4-76505  
 Ge, book, deposition, growth and technology 4-58579  
 Ge single cryst. film growth on SiO<sub>2</sub> by laterally seeded heteroepitaxy 4-93234  
 HgCdTe, growth, props. and appls. 4-66217  
 HgCdTe, pressure-induced epitaxial growth from soln. 4-88993  
 Hg<sub>0.3</sub>Cd<sub>0.7</sub>Te, LPE grown, photoluminescence study 4-80986  
 Hg<sub>1-x</sub>Cd<sub>x</sub>Te large area epitaxial layers, LPE growth 4-61879  
 (In,Ga)As/InP n-p-n heterojunction bipolar transistors grown by LPE with high gain 4-85097  
 InAs, electroliq. epitaxial growth, carrier density 4-93243  
 InAs<sub>1-x</sub>Sb<sub>x</sub> epilayers, impact ionisation coeffs. 4-104333  
 InAs<sub>1-x</sub>Sb<sub>x</sub>Al<sub>0.1</sub>Ga<sub>0.9</sub>Sb heterostructures, LPE growth 4-104097  
 InAs<sub>1-x</sub>Sb<sub>x</sub>Ga<sub>0.1</sub>Sb heterostructures, LPE growth 4-104097  
 InGaAs epitaxial layer, LPE growth and carrier mobility, dopant effects 4-84717  
 InGaAs, high-parity, conventional LPE growth, carrier conc. and mobility 4-99353  
 InGaAs, LPE using novel graphite boat 4-88994  
 InGaAs:Mg on InP, LPE-grown, MgO-free surface 4-76699  
 In<sub>0.53</sub>Ga<sub>0.47</sub>As, LPE growth on InP (100) substrate (Chinese) 4-85121  
 InGaAsP 1.53 μm DFB lasers made by mass transport 4-102947  
 InGaAsP (InGaP), LPE layers on GaAs (001), composition modulated structures 4-76698  
 InGaAsP and InGaP LPE layers, dislocation loops, TEM studies 4-92206  
 InGaAsP double-channel buried-hetero structure lasers, 1.55 μm, high-temp. operation, LPE 4-79174  
 InGaAsP, LPE-grown, high-uniformity, λ=1.3 μm 4-76700  
 InGaAsP separate confinement heterostructure lasers, 1.5 μm, electron leakage 4-96904  
 InGaAsP tunable DFB laser pumped by heterostructure injection laser 4-96907  
 InGaAsP/InGaP lasers, low threshold, 810 nm, LPE growth 4-69435  
 InGaAsP/InGaP lasers, LPE growth on GaAs, room temp. CW lasing at 727 nm 4-79133  
 InGaAsP/InP channelled-substrate BH lasers, VPE base struct. and LPE regrowth 4-96905  
 InGaAsP/InP injection lasers, LPE grown, three-layer-waveguide DH design 4-91490  
 InGaAsP-InGaP rapidly degraded DH laser grown by LPE, dark-line defects 4-69406  
 InGaAsP-InP planar buried DH, LPE growth, melt-carry-over effect 4-99352  
 In<sub>1-x</sub>Ga<sub>x</sub>P<sub>1-x</sub>As<sub>0.5</sub> solid solution, LPE, crystn. and optical props. 4-108736  
 InP epitaxial layer, LPE growth and carrier mobility, dopant effects 4-84717  
 InP, LPE, numerical model of selective meltback morphology 4-65587  
 InP:Sn films, LPE grown, carrier saturation, Hall meas. 4-98789  
 InP-In<sub>0.35</sub>Ga<sub>0.65</sub>As-InP DH wafers, LPE grown, misfit dislocations, X-ray and photoluminescence topography 4-80042  
 InP-n-AlInAs heterostructure, magnetotransport study 4-88570  
 KNbO<sub>3</sub> ferroelec. films, liquid phase epitaxy growth 4-76695  
 PbSe<sub>1-x</sub>Te<sub>x</sub> solid solution, p-n heterojunction form. by LPE 4-88996  
 PbSnTe-PbSeTe DBR diode lasers grown by LPE 4-112460  
 p-Pb<sub>0.5</sub>Sn<sub>0.5</sub>Te/n-PbSe<sub>1-x</sub>Te<sub>x</sub> heterojunction photodiodes, LPE and elec. props. 4-88575  
 PbTe films grown by hot wall epitaxy technique, AC field effect study 4-92835  
 Si, book, deposition, growth and technology 4-58579  
 Si homoeptaxial structs., LPE growth, power transistor fabrication (Russian) 4-109333  
 Si, ion implanted, pulse-laser-induced epitaxial regrowth 4-75511  
 SiC, book, deposition, growth and technology 4-58579  
 SiC, epitaxial and chemical vapour growth for optoelectronic devices 4-109331  
 (Y, Lu, Sm, Ca)<sub>3</sub>(Fe, Ge)<sub>2</sub>O<sub>12</sub> garnet system, distrib. coeffs. 4-61881  
 (YBi)<sub>3</sub>(FeGa)<sub>2</sub>O<sub>12</sub> garnet, cryst. growth from flux and LPE 4-93208  
 Y<sub>3-x</sub>Eu<sub>x</sub>Fe<sub>2-x</sub>Ga<sub>2</sub>O<sub>12</sub> mag. bubble films, LPE growth 4-109332  
 YIG, solubility and growth kinetics on (111) substrates, influence of excess iron oxide 4-75802  
 Y<sub>3-x</sub>Sm<sub>x</sub>Fe<sub>2-x</sub>Ga<sub>2</sub>O<sub>12</sub> mag. bubble films, LPE growth 4-109332  
 (YSmLuCa)<sub>3</sub>(GeFe)<sub>2</sub>O<sub>12</sub> epitaxial film, cloudlike charged wall, bubble propagation 4-104473  
 ZnS(Se), solution growth and photoluminesc. props. 4-88958

**liquid semiconductors**

see also electron energy states of liquid semiconductors

- cluster-type struct. defects, review 4-60806  
 polyacetylene, electrochemical doping, in situ Raman scatt. 4-76465  
 thermopower and electrical conductivity, automated meas. using fused quartz cell 4-68241  
 water, protonic semicond., protonic p-n junction props. 4-92398  
 As-Ge-Se, glass, small conc. of Se, elec. cond. rel. to temp. 4-92729  
 As<sub>2</sub>Se<sub>3</sub> glassy and liq., thermally generated defects 4-113335  
 Cu<sub>2</sub>S-Cu<sub>2</sub>Te, molten, thermal cond. meas. 4-104193  
 Ga-In-Sb phase diagram, thermodynamic data, associated soln. model, book contrib. 4-89031  
 Ga-P solution-melt system, diffusion coeff. determ. by X-ray microanalysis 4-88320  
 Ga<sub>2</sub>Te<sub>3</sub>, electrical cond. and Hall coeff. meas. using van der Pauw's method 4-98606

## solid semiconductors continued

- Ga<sub>2</sub>Te<sub>3</sub> liquid semicond. elec. transport activation energies 4-88506  
 Ge liq., structural study by thermal neutron scatt. 4-108266  
 Hg-Cd-Te phase diagram, thermodynamic data, associated soln. model, book contrib. 4-89031  
 Si:As(Sb)(In), ion implanted, pulsed electron beam annealing, impurity diffusion 4-103984  
 Sn-Se liq. alloy, thermoelec. power, semicond.-semimetal transition 4-108909  
 Tl<sub>2</sub>Se<sub>100-21</sub> elec. cond. and thermopower, temp. depend., ionic and electronic transport 4-80592

solid-solid transformations *see solid-liquid transformations*

## fluid structure

- see also classical theories of fluid structure; long-range order; neutron diffraction examination of liquids; quantum theories of fluid structure; short-range order; X-ray diffraction examination of liquids*  
 acetone, carbon disulphide soln., Monte Carlo simulation using quantum mech. intermol. pot. 4-65160  
 alkali-group IV alloys, liq. and solid, electronic struct. and cluster form. 4-92601  
 alkyl carboxylate-alkyltrimethylammonium mixed amphiphilic system, alkali metal and halide ion binding 4-84143  
 alloy, partially ionic, screening role in electronic and atomic struct. 4-70635  
 alloys, liq., model, chemical short-range order, struct. and thermodynamics 4-75266  
 anthraquinone dichroic dyes, liq. cryst. characterisation and synthesis 4-84156  
 benzene, liq., Lennard-Jones interactions, Monte Carlo study 4-70014  
 benzyldiene-amino-4'-cyanobiphenyls, smectic C<sub>2</sub> struct. and solid polymorphism 4-60825  
 binary associating mixtures, zero wavenumber struct. factors 4-92041  
 binary fluid, nonlinear effects in supercritical quenches 4-61043  
 biphenyls, struct. study 4-114264  
 blue phase liq. cryst., lattice spacing fluctuations, refl. microscopy obs. 4-103649  
 blue phase liq. cryst. mixtures, lattice parameters, Bragg refl. obs. 4-88089  
 boson hard sphere fluid, correlation functions, struct. factor 4-98380  
 carbon tetrachloride, liq., radial distrib. functions and struct. factor, Monte Carlo calcs. 4-92051  
 cellulose, N,N-dimethylacetamide-LiCl solns., phase equil. 4-108584  
 cholesteric blue phase, struct. anal. by optical Bragg diffraction 4-88090  
 cholesteric liquid crystals, blue phase, optical props. 4-88791  
 cholesterol nonanoate-chloride mixture, blue phase struct. 4-60820  
 colloidal interacting particles, dynamic struct. correl. study 4-89340  
 computer simulation by Markov chain method 4-75301  
 copolymers, thermotropic liq. cryst., X-ray diff., studies 4-113302  
 copolymers of 4-hydroxybenzoic and 2-hydroxy-6-naphthoic acids, liquid crystalline, X-ray diff. 4-92075  
 crossover integral equation for the structure of simple liquids, thermodynamic functions 4-70006  
 crotonates, mol. dynamics using IR band shapes 4-65159  
 cyano end group binary mixtures, smectic C phase induction 4-75671  
 cyano-ester isomeric homologous series, liq. cryst. props. 4-84159  
 cyano-ester isomeric homologous series, reentrant nematic phase, mol. features 4-84163  
 cyclohexylamine-water mixture, positron annihilation, compressibility, US meas. 4-103635  
 difluorinated Siamese Twin mesogens, mol. struct. and mesomorphism 4-84179  
 dipolar two centre Lennard-Jones mol. liqs., dielec. behaviour and multi-body orientational correl. 4-97988  
 disc-like mesogen polymorphism 4-75280  
 discotic mesophases, complementary review 4-82620  
 double layer dipole orientation at electrodes, polarisation catastrophes anal. 4-98690  
 electrolyte surface struct. near critical point, free energy formalism anal. 4-92038  
 ester nematic mixtures, viscosity, struct. effects 4-84440  
 ethanol, liq., H bonding, X-ray diff. pattern 4-70015  
 trans-4-ethoxy-4'-N-alkanoxyloxazobenzenes, homologous nematogens, order parameters 4-84165  
 fatty acid binary mixtures, struct. correl., 2- and 3-dimens. models (German) 4-60803  
 ferroelectric smectic C\* liq. crystals, helicoidal struct., field induced processes 4-65171  
 fluid thin films, disjoining press. oscils. 4-75759  
 hard rod fluid, triplet correl. function superposition approx. topological reduction 4-65163  
 hard sphere binary mixture, additive parameter, Percus-Yevick results 4-70012  
 hard-sphere fluid, two particle distrib. approx. near hard wall at low densities 4-97989  
 HOAB smectic C phase, layer thickness, temp. depend., X-ray studies 4-84182  
 immiscible rot. simple fluids, interfacial shapes 4-112902  
 inherent pair correlation in simple liquids, mol. dynamics simulation; thermodynamic states 4-70005  
 interatomic core forces deduced from observed liquid structure factors 4-92044  
 intramolecular distribution of additions in liquid metals 4-113297  
 Lennard-Jones binary liquid mixt., local composition with differing sizes of components 4-88046  
 liquid alkali metals near freezing point, calcs. 4-113296  
 liquid crystals, homologous series, mol. struct. and ordering 4-88076  
 metal acetate cpds., conc. aq. solns., NMR, X-ray diff. 4-98957  
 metal-molten salt interface, capacitance depend. on local density profiles near electrode 4-92797  
 metals, electrical conductivity, effective medium approx. 4-92690  
 methane, liquid, self-diffusion and shear viscosity theory 4-88327  
 methane, liquid, self-diffusion and shear viscosity theory 4-88328  
 methanol, liq., H bonding, X-ray diff. pattern 4-70015  
 methanol-aqueous soln., hydrophobic interaction, Monte Carlo calcs. 4-97994  
 methyl 38-nonanoxyxyol-5-en-24-oate, cholesteric pitch, temp. depend. 4-84150  
 methylpyridinium iodides, molten, transport props., <sup>1</sup>H NMR spectra and struct. 4-92966

## liquid structure continued

- mixed aqueous electrolytes, local structure., Raman and EXAFS studies 4-60808  
 molecular conformations, liq. phase, determ. methods 4-65165  
 monatomic liquids, dense, struct. factor, relation between principal peak height, position and width 4-92045  
 monatomic liquids, structure function 4-92050  
 naphthalene, solns. in water-ethanol mixtures, thermodynamic props. 4-80264  
 nematic liq. cryst., high electric field effects and walls 4-84164  
 nematic liquid cryst. tilt angles on SiO<sub>2</sub>, temp. depend. 4-88064  
 4-nitrophenyl-4-p-octyloxybenzoate, bilayer smectic-A struct., X-ray diff. study 4-60826  
 nondegenerate fluids, quantum radial distrib. functions (Russian) 4-88058  
 nondegenerate fluids, quantum radial distrib. functions (Russian) 4-97992  
 one-component liq., transport props., RPA approx. 4-88049  
 perylene dichroic dyes, liq. cryst. characterisation and synthesis 4-84156  
 phosphatidylcholine head groups in vesicles, short-range order in interfacial water 4-113287  
 photoresist soln., AZ1350J, chem. and dielec. props. 4-104519  
 PMMA, syndiotactic, ordered struct. in soln. solid state 4-65166  
 polar rod systems, fluid mesophases 4-88081  
 poly(1,6 hexamethylene adipate), synthesis and characterisation by dilatometry and X-ray diff. 4-79956  
 poly(1,6 hexamethylene sebacate), synthesis and characterisation by dilatometry and X-ray diff. 4-79956  
 poly(2,5 hexamethylene adipate), synthesis and characterisation by dilatometry and X-ray diff. 4-79956  
 poly(pentamethylene pimelate), synthesis and characterisation by dilatometry and X-ray diff. 4-79956  
 polycapromide obtained in anionic polymerisation of caprolactam, chemical and physical props. 4-92056  
 polyesters, rigid-flexible struct., thermotropic liq. cryst. props. 4-84161  
 polyethylene-tetrachlorobenzene mixtures, polydispersity effects 4-108590  
 polymer melt with rigid and flexible, chain elements, liq. cryst. ordering (Russian) 4-75294  
 polymer melts, viscosity and self-diffusion rel. to segment bonding (Russian) 4-108641  
 polymer semidilute soln., unified model of struct. 4-79923  
 polymer solns. conformations, multiparticle correl. functions 4-113284  
 polymer solutions, dilute, dynamical-scatt. factor, initial decay rate 4-108268  
 polymer solutions and blends, long range correlation's, low angle X-ray and neutron scatt. 4-75262  
 polymeric oils, interfacial shapes between two rot. immiscible simple fluids 4-112902  
 polymers, entangled flexible, dynamics, Monte Carlo simulations and their interpretation 4-113289  
 polymers, mesomorphic, three-component struct. and thermodynamic model 4-88091  
 polymers, mesomorphic struct., miscibility studies 4-84178  
 polymers, semi-flexible, anisotropy induced by liq. cryst. solvent 4-84140  
 polymers with amphiphilic and nonamphiphilic side chains, phase behaviour 4-88080  
 polypeptides, Potts model for solvent effects on polymer conformation 4-113294  
 polystyrene in toluene and methyl ethyl ketone soln., conc. fluctuation dynamics 4-103637  
 polystyrene latex, liq. like ordered suspension, struct. factor temp. depend. 4-114845  
 polyvalent metals model pots. and trends in liq. struct. 4-84141  
 pyridines, substituted in benzene soln., mol. dynamics, time depend. correl. function anal. 4-92055  
 quantum liqs., inhomogeneous, direct correl. function, appl. to liq. metals 4-60796  
 random packing densities of mono-sized spheres in two and three dimens., theoretical anal. 4-109312  
 rare earth metals, liquid, density, surface tension, periodic depend. 4-113517  
 semiconductors, molten, cluster-type struct. defects, review 4-60806  
 smectic A liq. cryst., screw dislocation lines, helical instability 4-60822  
 smectic liquid cryst., orientational disorder, struct. aspects 4-84160  
 sodium di-2-ethylsuccinate-D<sub>2</sub>O-decane microemulsions, struct., small angle neutron scatt. 4-114847  
 sodium oleate, supercooled, struct. changes in hydrocarbon, swelling obs. 4-108262  
 solns. in dipolar aprotic, IR spectra and struct. 4-112175  
 solutions, aqueous, structural studies using EXAFS and X-ray diff. 4-60807  
 solvation, geometrical features, pattern recognition anal. 4-114781  
 solvation forces in model fluid mixtures of ions and dipoles 4-65164  
 styrene-butadiene-styrene block copolymer in n-tetradecane, viscoelasticity, temp. and conc. depend. 4-112800  
 swallow-tailed liq. cryst. cpds., smectic and nematic behaviour 4-75269  
 terephthalic acid aromatic polyesters solns., conformational props. 4-103636  
 thermotropic discogens, phase diagrams and texture 4-84157  
 thermotropic liquid crystalline polymers, domains and walls 4-79933  
 thermotropic liquid crystals, polymorphism, book contrib. 4-92090  
 trioxyethylene glycol monohexadecyl ether-D<sub>2</sub>O system, gel. and liq. cryst. phase structs. 4-84145  
 two-dimensional aqueous solution-like system, conc. fluctuations, Monte Carlo study 4-70008  
 viscous liquids, relaxation theory 4-98021  
 water, liq. struct. at room temp., time of flight neutron diff. study 4-92053  
 water, liquid, struct. at extended hydrophobic surface, mol. dynamics simulations 4-70007  
 water, liquid and supercritical, X-ray investig. of struct. of first coord. sphere 4-113290  
 water normal and supercooled, disrupted network model, near IR spectra 4-88822  
 water structure, quasithermodynamic interpretation of hydrated ion effect 4-113291  
 Winsor concentrated microemulsions, X-ray scatt. study 4-79922  
 Al alloys, solidification, grain refinement, pseudosurface nucleation mechanisms 4-11497  
 Al alloys, thermodynamics and struct., solvent-solute interaction 4-113670

## liquid structure continued

- Al, liq., structural props., elec. resist., X-ray diffr. 4-79925  
 Al, liquid, computer simulation of dynamic behaviour 4-60811  
 Al, liquid, pair pots., Monte Carlo simulation 4-92047  
 Al, radial distrib. functions calc. using Percus-Yevick and mean spherical model approx. 4-70020  
 Al-Cu, liq., structural props., elec. resist., X-ray diffr. 4-79925  
 Ar, liquid, pair pots., Monte Carlo simulation 4-92047  
 Ar, liquid, sound nonanalytic dispersion relations 4-103887  
 Ar, short wavelength sound modes, neutron diffr. 4-98231  
 As<sub>2</sub>S<sub>3</sub>-S system, liq. and amorphous, phase diagram and short range order 4-103905  
 As<sub>2</sub>Se<sub>3</sub>, glassy and liq., thermally generated defects 4-113335  
 B<sub>2</sub>O<sub>3</sub>, molten, struct. anal. by X-ray radial distrib. method 4-113293  
 Bi, liquid, propagating collective excitations, neutron scatt. study 4-65167  
 Bi, liquid struct. determ. 4-98000  
 CO<sub>2</sub>, liq., thermodynamic state, struct., neutron diffr. study 4-70017  
 Ca(NCS)<sub>2</sub> solns. in dipolar aprotic, IR spectra and struct. 4-112175  
 Cd(NO<sub>3</sub>)<sub>2</sub> aq. solns., struct. determ. by X-ray diffr. and Raman spectrosc. 4-108265  
 Cl<sub>2</sub>, struct. factor, mol. vibr., neutron diffr. study 4-108263  
 CoCl<sub>2</sub>-LiCl aq. solns. X-ray diffr. study 4-60805  
 Cs-Sl-I solns., electron localisation, NMR obs. 4-98965  
 Cu, liq., structural props., elec. resist., X-ray diffr. 4-79925  
 Cu, liquid, pair pots., Monte Carlo simulation 4-92047  
 Cu(NO<sub>3</sub>)<sub>2</sub> aq. solns., Cu(II) coordination, X-ray diffr. study 4-75260  
 n-D<sub>2</sub>, liquid and liquid mixtures, intermolecular free length, acoustic study 4-88059  
 Fe<sub>1-x</sub>Cr<sub>x</sub>, struct. determ. (Russian) 4-65177  
 Ga, liq. and amorphous, radial distrib. function and struct. factor, quasi-cryst. model 4-84186  
 Ga, liquid struct. determ. 4-98000  
 Ga-Te, molten, at. arrangement of Ga<sub>2</sub>Te<sub>3</sub> associates, metallic-like bonding, neutron scatt. obs. 4-103639  
 Ge liq., structural study by thermal neutron scatt. 4-108266  
 Ge-Se<sub>2</sub>Se system, liq. and amorphous, phase diagram and short range order 4-103905  
 H solvation by H<sub>2</sub>O mols. 4-62175  
 n-H<sub>2</sub>, liquid and liquid mixtures, intermolecular free length, acoustic study 4-88059  
 H<sub>2</sub>O cluster, mol. and dynamic study (Russian) 4-92062  
 H<sub>2</sub>O molecule orientation on thin film boundaries (Ukrainian) 4-65520  
 He, liq., static structure factor below T<sub>λ</sub>, temp. depend. 4-70493  
 Hg, liquid struct. determ. 4-98000  
 K<sub>0.8</sub>-(KCl)<sub>0.2</sub> liquid mixture, struct. study 4-84135  
 KBr, fused, partial structs. and compressibilities of ions 4-92061  
 KNCS solns. in dipolar aprotic, IR spectra and struct. 4-112175  
 Li, liquid, effect of Born-Mayer potential on props. 4-92064  
 Li-Sn, liquid structure, neutron diffr., cpd. form. 4-113295  
 MgCl<sub>2</sub> in methanol soln., X-ray diffr. study 4-75258  
 Mg(ClO<sub>4</sub>)<sub>2</sub>-acetonitrile solns., struct. investig. by neutron diffr. 4-75257  
 Mn-Ge, liquid, struct. determ. (Russian) 4-103640  
 Mn<sub>2</sub>Ca<sub>1-x</sub>(NO<sub>3</sub>)<sub>2</sub>·6H<sub>2</sub>O paramag. solns., conc., muon spin relax. study 4-71244  
 Mn(NO<sub>3</sub>)<sub>2</sub> aq. solns. conc., hydration and ion-pairing; X-ray and Raman spectra 4-93512  
 Mn(NO<sub>3</sub>)<sub>2</sub> paramag. solns., conc., muon spin relax. study 4-71244  
 NANCS solns. in dipolar aprotic, IR spectra and struct. 4-112175  
 Na, dynamic struct. factor, inelastic neutron scatt. 4-92066  
 Na, liquid, effect of Born-Mayer potential on props. 4-92064  
 Na, radial distrib. functions calc. using Percus-Yevick and mean spherical model approx. 4-70020  
 NaCl ion pair interaction in water, computer simulation 4-60795  
 NaI solution, struct. study, neutron and X-ray diffr. 4-108264  
 Ne, liquid and liquid mixtures, intermolecular free length, acoustic study 4-88059  
 Pd<sub>1-x</sub>Si<sub>x</sub>, struct. determ. (Russian) 4-65177  
 Rb, liq., struct. factors calc. using optimised random-phase approx. 4-84142  
 Rb, radial distrib. functions calc. using Percus-Yevick and mean spherical model approx. 4-70020  
 RbBr, molten, rigorous study of partial struct. and allied functions 4-92060  
 RbCl, molten, structure and thermodynamic props. calcs. 4-70016  
 Rb<sub>2</sub>O-SiO<sub>2</sub> glass and melt, structure, Raman spectra meas. (Japanese) 4-113349  
 Rh(ClO<sub>4</sub>)<sub>3</sub>, dil. soln., Rh III coordination, X-ray diffr. 4-92052  
 Sb<sub>2</sub>Se<sub>3</sub>-Se system, liq. and amorphous, phase diagram and short range order 4-103905  
 Se, liquid, density, surface tension studies 4-113517  
 Se-Tl, melt, near-order struct., X-ray diffraction study 4-60804  
 Si, molten, electronic and bonding props. 4-98503  
 Sn, liquid struct. determ. 4-98000  
 Te<sub>0.7</sub>Se<sub>0.3</sub>, role of temp. in struct., Raman study 4-88063  
 Y, liquid, density, surface tension studies 4-113517

## liquid surface waves see surface waves (fluid)

## liquid theory

- see also classical theories of fluid structure; equations of state of liquids; quantum theories of fluid structure  
 acetone-water binary liq. mixtures, intermol. interactions and viscosity 4-113687  
 acetonitrile, liq., ultra-fine far IR struct., barrier crossing theory 4-109187  
 alkali metals, liquid, thermodynamic props. using classical plasma reference system 4-60810  
 aqueous 1:1 electrolytes, pair correl. functions from linearised Poisson-Boltzmann eqn. 4-103627  
 benzene, mol. dynamics simulations of self-diffusion coeffs. in binary Lennard-Jones solns., isotope effects 4-75253  
 benzene-carbon tetrachloride binary liq. mixtures, intermol. interactions and viscosity 4-113687  
 benzene-cyclohexane binary liq. mixtures, intermol. interactions and viscosity 4-113687  
 binary ionic mixtures and a solvable model 4-103631  
 binary liq. model mixtures, Lennard-Jones pot., diffusion coeff., mol. dynamics calcs. 4-70010  
 S-bromochlorofluoromethane, liq., translational motion, external elec. field effect 4-103625  
 Brownian limits for tagged particle motion 4-113285

## liquid theory continued

- sec-butyl chloride, supercooled, rise transient dynamics, computer simulation 4-65161  
 caloric eqn. of state near crit. point (Russian) 4-84360  
 carbon tetrachloride, liq., mean free path temp. depend. determ. using Brillouin scatt. expt. 4-109198  
 charged hard spheres in electrolyte soln., equilb. props., Monte Carlo and integral eqn. results 4-70004  
 chlorobenzene-carbon tetrachloride, binary liq. mixtures, intermol. interactions and viscosity 4-113687  
 classical fluids, triplet correl. function at crit. point 4-75251  
 classical hard sphere solvents, excess electrons, equilb. theory 4-113284  
 classical liquid struct., thermodynamically consistent theory, pair pot. extraction 4-92043  
 colloidal dispersion, conc., one-component macrofluid theory 4-113288  
 crossover integral equation for the structure of simple liquids, thermodynamic functions 4-70006  
 dense fluids, transport processes, projection operator methods, kinetic eqns. 4-65162  
 dense molecular fluids, thermodynamic anal. 4-108633  
 dense monatomic and molecular fluids and their mixtures, shear viscosity, thermal cond., anal. 4-113688  
 dipolar liquids, coexistence curve, orientation correls., effective pair pot. 4-88055  
 dipolar two centre Lennard-Jones mol. liqs., dielec. behaviour and multi-body orientational correl. 4-97988  
 electric double layer, free energy 4-61436  
 electrolyte solution, charged aggregates interaction, Monte Carlo simulation 4-97986  
 electrolytes, aqueous, diffusion const., intermolecular dipolar spin relax., microdynamical models 4-88321  
 ethane in dilute aq. soln., Monte Carlo simulation 4-92036  
 fluid distribution function, Kirkwood coupling parameter expansion calcs. 4-75255  
 fluids, orthobaric props. of spherical and linear mols., intermol. pot. effect 4-74310  
 fluorochloroacetonitrile, racemic mixture, rot. translation coupling obs. 4-92049  
 hard convex bodies and hard body eqn. of state, average correl. function 4-60798  
 hard convex mol. fluids, third and fourth virial coeff. 4-60799  
 hard disk systems, two-dimens., long-range correls., nonequilb. mol. dynamics calcs. 4-103633  
 hard dumbbells at hard wall, density profiles, RAM perturbation theory 4-75246  
 hard heteronuclear diatomic fluids, site-site pair correl. functions, RAM theory 4-88053  
 hard rod fluid, triplet correl. function superposition approx. topological reduction 4-65163  
 hard sphere fluids, classical and quantum, eqns. of state 4-60793  
 hard sphere liq. mixtures, diffusion coeff., mol. dynamics simulation 4-92399  
 hard sphere of eqn. of state, molecular dynamics calcs. 4-103626  
 hard spheres and discs, melting, density functional theory 4-70347  
 hard spheres near soft repulsive wall, thermodynamics, variational approach 4-60800  
 hard-disk and Lennard-Jones systems, 2-D melting, Monte Carlo studies 4-113286  
 hard-sphere fluid, two particle distrib. approx. near hard wall at low densities 4-97989  
 n-heptane-dichloromethane (1,2-dichloroethane) liq. mixtures, excess internal press. and interactions 4-97993  
 n-hexane-dichloromethane (1,2-dichloroethane) liq. mixtures, excess internal press. and interactions 4-97993  
 inherent pair correlation in simple liquids, mol. dynamics simulation, thermodynamic states 4-70005  
 interatomic core forces deduced from observed liquid structure factors 4-92044  
 internal pressure behaviour w.r.t. variations in temp., vol. and cohesive energy density 4-108571  
 Lennard-Jones, supercooled liquid homogeneous nucleation, periodic boundary conditions, computer simulation 4-98247  
 Lennard-Jones binary liquid mixt., local composition with differing sizes of components 4-88046  
 Lennard-Jones diatomic fluid, perturbation theory, thermodynamic and quasithermodynamic props. 4-97990  
 Lennard-Jones fluid binary mixtures, mol. dynamic studies with different component sizes 4-88045  
 Lennard-Jones fluids, liquid-vapour coexistence line 4-113592  
 Lennard-Jones two dimens. eqn. of state, mol. dynamics study 4-84361  
 linear integral equations and renormalization group 4-103634  
 linear molecular fluid, in contact with solid, density profile, HNC eqn. calcs. 4-79917  
 liquid alkali metals near freezing point, structure factor calcs. 4-113296  
 liquid-solid interface, press., density functional, integral eqns. 4-108258  
 local orientational order 4-84225  
 metal-electrolyte boundary, hard core ions at charged surfaces, unrescreened primitive model, HNC/MSA approx. 4-88587  
 metals, effective interactive forces, general formulation and effective medium approx. 4-60809  
 methane, liquid, self-diffusion and shear viscosity theory 4-88328  
 methane, VIM theory of mol. thermodynamics, analytic eqn. of state 4-113282  
 methanol-aqueous soln., hydrophobic interaction, Monte Carlo calc. 4-97994  
 3-methyl-2,4,10-trioxo-adamantan, nonexponential relax., correl. times, microscopic vel. 4-92971  
 molecular fluids, effective spherical pot. 4-108267  
 molecular fluids, equilb. props. in semiclassical limit 4-103632  
 molecular fluids in external field, functional perturbation theory for orientation profile 4-60801  
 molecular hydrodynamic variables, at. and mol. representations 4-88051  
 molecular liquids, anion form., correl. with mol. shape 4-92059  
 molecular liquids, thermodynamic props. of binary mixtures of weakly nonspherical mols. 4-113563  
 molecular simulation calcs., error estimation 4-88050  
 neutron spectra width and heat mode, kinetic theory 4-60802  
 nondegenerate fluids, quantum radial distrib. functions (Russian) 4-88058  
 nondegenerate fluids, quantum radial distrib. functions (Russian) 4-97992

- d theory continued  
nonequilibrium statistical mech., projection operator techniques, book 4-67897  
nonlinear phenomena in physics (*Japanese*) 4-101741  
nonrigid molecular liquids orientational motion, depolarised light scatt. invest. 4-66048  
octamethyl-cyclotetrasiloxane, solvation forces between mica surface, temp. depend. 4-71903  
one-dimensional identical elastic hard rods, hydrodynamics 4-70013  
ordered fluids, orientational correl. functions, short time expansion 4-88052  
Ornstein-Zernike eqn. for two-Yukawa correl. function with core condition 4-103629  
overpopulation phenomena in two-region system, mol. dynamics calcs. 4-75248  
pair correls., square-gradient theory nonlinear extensions 4-70001  
pair pot. with hard core and Yukawa tail, self-consistent approx. 4-103630  
perturbation theory, approximate free energy functional minimisation 4-88054  
perturbed hard-sphere equations of state of real fluids, effective hard-sphere diameters calc. 4-113566  
polar fluids, anisotropic screening, mol. perturbation theory calcs. 4-70003  
polar fluids, dielectric props., static and freq. depend., computer simulation 4-71259  
polar fluids, VIM theory of mol. thermodynamics, analytic eqns. of state 4-113283  
polar liquids, molecular dynamics study of dielectric props. 4-88057  
polar molecular fluids, interaction sites, critical points 4-70011  
polar-polarisable liq. mixtures, induction effects, thermodynamic props., renormalised perturbation theory 4-108259  
polarising liquid, perturbation theory 4-68194  
polydisperse fluids, thermodynamic props., statistical mechs. 4-70410  
polyelectrolyte solns., thermodynamic props., ellipsoidal model 4-84137  
polymer chain soln., excluded vol. interaction, perturbation theory 4-84133  
polymer melt with rigid and flexible, chain elements, liq. cryst. ordering (*Russian*) 4-75294  
polymer soln., coexistence curve universality 4-97997  
polymer solns., conc. nontangled, dynamics model calc. 4-97996  
polymer solns., non-Newtonian shear viscosity, normal stress coeffs., corresponding states in rheology 4-64899  
polymer solutions, equilibration in momentum space in kinetic theory 4-64989  
polymers, entangled flexible, dynamics, Monte Carlo simulations and their interpretation 4-113289  
polymers solns., conc. nontangled, dynamic multiple scatt. approach 4-97995  
pseudomolecular fluid model, exact and approx. struct. props. 4-75250  
pyridines, substituted in benzene soln., mol. dynamics, time depend. correl. function anal. 4-92055  
quadrupolar fluids, polarisable, single particle props. and static dielectric const. 4-61619  
quadrupolar fluids, quantum theory 4-60797  
relaxation processes, nonlinear and nonMarkovian effects 4-92046  
simple fluids, integral equations, thermodynamically consistent 4-108260  
simple fluids, long-range boundary effects 4-60575  
simple fluids and electrolytes, statistical mechs. aspects 4-108261  
solutions, solute mole. coupling by solvent, internal tension enhancement 4-92042  
solvation forces in model fluid mixtures of ions and dipoles 4-65164  
square-triangle well fluid, intermolecular potential function 4-92040  
Stockmayer 3D fluid, permittivity, thermodynamic props., mol. dynamics simulation 4-70002  
thermodynamic props. calc. of fluids in mol. dynamics expts. 4-113666  
three-body effect in gradient theories of fluid interfaces 4-92037  
Tolman's length for surface tension, critical exponent at liquid-gas critical point 4-61172  
triangle well fluid, perturbation calcs. 4-92039  
two state mol. liq., statistical mechs. 4-84132  
van der Waals fluid, periodic thermal perturbation: Malnikov function approach 4-79918  
Van der Waals fluids, saturation and metastable props. 4-61039  
Van der Waals Kac fluid, spinodal phase separation, extended irreversible thermodynamics theory 4-84410  
vapour condensation, canonical partition function, virial expansion 4-97991  
virial eqn., conformity condition and compressibility (*Russian*) 4-70332  
viscous liquids, relaxation theory 4-98021  
water, liquid, struct. at extended hydrophobic surface, mol. dynamics simulations 4-70007  
water, ST2, stochastic boundary conditions for mol. dynamics simulation 4-60794  
Ar like liquid, molecular motion, fractal geometry and Brownian motion 4-70018  
Ar, mol. dynamics simulation method in the canonical ensemble 4-75252  
Ar<sub>2</sub>, VIM theory of mol. thermodynamics, analytic eqn. of state 4-113282  
CS<sub>2</sub>, liq., orientational pair correl. factors with interaction site formalism calc. 4-70009  
D<sub>2</sub> mol. fluid, equil. props. in semiclassical limit 4-103632  
H<sub>2</sub> mol. fluid, equil. props. in semiclassical limit 4-103632  
K<sub>2</sub>O-(KCl)<sub>2</sub> liquid mixture, struct. study 4-84135  
Kr, dense gas, struct. factor, bridge contribs. and many-body effects 4-75263  
Li, liquid, effect of Born-Mayer potential on props. 4-92064  
Na, liquid, effect of Born-Mayer potential on props. 4-92064  
NaCl ion pair interaction in water, computer simulation 4-60795

#### liquid-vapour transformations

- see also boiling; condensation; evaporation; liquefaction of gases  
acetone, aq. solution, vapour-liquid equilibrium at 101.325 kPa 4-113590  
N-alkyl substituted cyclic amides, selective separation, UNIFAC model calcs. (*German*) 4-98250  
binary azeotropic distillation design 4-65379  
charged colloidal dispersions, liq.-gas transitions, perturbation theory anal. 4-62256  
charged nuclei, nucleation, chem. potential of vapour 4-108596  
corresponding states correl. for nucleation from the vapour 4-92340  
crown ether aqueous solns., vapor-liquid equilibrium 4-113591

#### liquid-vapour transformations continued

- cyclohexane+triethylamine mixtures, keto-enol tautomerism and vapour-liquid equilibria 4-113589  
droplet growth kinetics in systems with arbitrary degeneracy 4-65380  
droplets, nucleation on charged nuclei in strong field 4-108595  
equilibrium measurement, high pressure-high temp. chromatographic apparatus 4-70355  
ethane, vapour-liq. critical point, orthopositronium annihilation rates 4-87237  
ethane/propane+ethane/n-butane system, liquid-vapour crit. region 4-70353  
fluid interfaces, phase transforms., use of standard variational thermodynamics 4-113756  
gas-liquid phase transition and singularities, space of undercritical states 4-65381  
Ginzburg-Landau functional, liquid-vapour phase transitions 4-103917  
graphite with surface adsorbed submonolayer Ar, melting transition, specific heat study 4-104077  
hexane, liquid-gaseous coexistence, specific refraction (*Russian*) 4-99087  
hydrocarbon-CO<sub>2</sub> mixture meas., vapour-liquid equilibria and saturated densities determ. 4-103916  
Landau-Ginzburg-Wilson model, renormalisation scheme 4-111091  
lattice gas model, nonequilibrium, mean-field theory 4-103902  
Lennard-Jones fluids, liquid-vapour coexistence line 4-113592  
linear integral equations and renormalization group in liquid theory 4-103634  
liquid-vapour coexistence, mean field integral eqn. theories 4-108599  
liquid-vapour interface, scaling relations 4-80337  
metals, shock-compressed, vapourisation on expansion 4-61063  
methane, adsorbed on graphite, two-dimens. liq.-vapour crit. point exponent, sp. ht. study 4-92341  
methanol-based ternary mixtures, liq.-liq. equilibria at 298.15K 4-103920  
molecular liquids, thermodynamic props. of binary mixtures of weakly nonspherical mols. 4-113563  
multicomponent mixtures, vapour-liquid equilibrium calc. 4-70354  
pentane-benzene soln., coexistence of liquid and vapour (*Russian*) 4-113594  
seawater, critical point and two-phase boundary, 200 to 500°C 4-67219  
spontaneous droplet nucleation in clean saturated moist air at atmospheric press. 4-80200  
tetrachloromethane+ $\alpha,\omega$ -dichloroalkane, vapour pressure, vapour-liquid equil. 4-98256  
tetrahydrofuran-acetonitrile-1,2-dichloroethane mixtures, isothermal vapour-liq. equilibrium 4-98258  
Tolman's length for surface tension, critical exponent at liquid-gas critical point 4-61172  
UNIQUAC parameter, temp. depend. 4-65420  
Van der Waals fluid, dynamic phase transitions 4-88272  
viscosity of fluid meas. in critical region, rotating disc viscometer appl. 4-60568  
CO<sub>2</sub> hydrocarbon mixtures, Peng-Robinson eqn. of state for vapour-liquid equil. calc. 4-70334  
<sup>3</sup>He-CO<sub>2</sub> mixture, <sup>3</sup>He numerical density on liquid-vapour boundary curve 4-70357  
<sup>3</sup>He-CO<sub>2</sub> mixture, coexisting phases near liquid-vapour transition (*Russian*) 4-88364  
Na, liquid-vapour interface struct., Monte Carlo simulation 4-88062  
Na-Cs liquid-vapour interface struct., Monte Carlo simulation 4-88062  
NaF-AlF<sub>3</sub>, melt, vapour phase studies, activity data 4-84423
- liquid waves**  
see also capillary waves; ocean waves; surface waves (fluid)  
arterial pressure wave propagation, theory and model 4-72296  
diffraction of regular waves on two circular cylinders of different cross sections (*Russian*) 4-86222  
edge waves over a shelf, linearised shallow water eqns. soln. 4-82068  
falling thin liquid film, flows, wave instability (*Rumanian*) 4-69778  
linear random gravity wave propag. in variable depth water 4-75051  
metal surface in contact with dense plasma, nonlinear capillary waves excitation 4-84540  
nonlinear water waves, numerical method 4-87741  
stream function solutions for steady water waves 4-94138  
transient pressure waves in liq. transmission line, radial and axial variations 4-97693  
vapour condensation, waves in interphase surface, calc. 4-108597  
viscous liq. flowing on inclined plane, steady travelling wave problem soln. 4-112915  
water, surface wave attenuation, US reflection studies 4-97587  
water solitary waves, capillary effects 4-103349  
water waves propagating in infinite narrow channel, normalised Boussinesq eqn., cusp and usual soliton solns. 4-108083  
wave asymmetry in liquid of variable depth (*Russian*) 4-86223

#### liquids

- for generalities only; for specific aspects see appropriate headings  
see also liquid structure; liquid theory; solutions  
No entries

#### literature reviews see reviews

#### lithium

- see also nuclei with .....  
abundance in M-type giant stars (*Russian*) 4-101331  
adsorbed rare gases, conduction electron spin scatt. cross-sections 4-84663  
anode cells, primary and secondary, review 4-72054  
atom, in high mag. field, spacing between quasi-Landau reson. 4-87058  
atom, orbital relax. in Rydberg series, excited state SCF calc. 4-64361  
atomic levels multiplet component alignment during collisions 4-107445  
atoms, autoionisation states, single configuration approx., orthogonality conditions 4-107318  
atoms, relativistic SCF calc. with squared Dirac operator 4-78790  
atoms in inert gas matrices, mag. circular dichroism study of <sup>2</sup>S<sub>1/2</sub>→<sup>2</sup>P<sub>1/2</sub> transition 4-59670  
batteries, chemistry, energy features, technology (*German*) 4-72053  
batteries, low-temp. performance and Ah capacity, electrolytes (*German*) 4-77067  
batteries 4-105105  
batteries for electric vehicles, new design project, general overview 4-85363  
clusters, unrestricted Hartree-Fock and ab initio configuration interaction calcs. 4-98500  
crystal struct. at 4.2K 4-92140

## lithium continued

- CTR blanket performance parameters, discrepancies between meas. and calcs. 4-59407  
 depletion in solar type stars 4-85933  
 electron dynamic structure factor, inelastic synchrotron X-ray scatt. 4-80524  
 element analysis using charged-particle induced prompt  $\gamma$  rays 4-89362  
 film, O<sub>2</sub> and water adsorption, XPS studies 4-98429  
 fusion reactor breeder blanket, impure, T extraction by Y, thermochem., analysis 4-107027  
 fusion reactor cooling He-Li test loop for two-phase flow (*Japanese*) 4-91102  
 gaseous phase, viscosity and thermal conductivity meas. 4-97742  
 geochemical cycle and basalt hydrothermal alteration 4-67191  
 impurity diffusion in solid Na 4-65475  
 intercalated with InSe, photoelectric props. meas. (*Russian*) 4-104272  
 isoelectronic series, radiative decay following charge exchange on neutral gas targets 4-87069  
 isoelectronic series, Rydberg energy levels determ. by relativistic quantum defect interpretation 4-107278  
 isotope enrichment by high press. ion exchange displacement chromatography 4-59905  
 isotope separation by cryptand (2B<sub>2</sub>L1) polymer 4-74039  
 laser microprobe mass analysis detection limits and lateral resolution 4-72016  
 liquid, blanket materials, candidate, for fusion reactor appl. 4-91107  
 liquid, compatibility of fusion reactor materials 4-107062  
 liquid, corrosion and phase stability of Cr-Mn austenitic steel 4-107061  
 liquid, corrosion behaviour of stainless steel using LiLO-7 thermoconvection loop 4-107059  
 liquid, effect of Born-Mayer potential on props. 4-92064  
 liquid, fusion reactor blankets, compatibility of steels, review 4-107054  
 liquid, fusion reactor blankets, effect on fatigue and tensile props. of steel 4-107055  
 liquid, in fusion reactor, chem. behaviour of dissolved Si 4-107058  
 liquid, mass transfer behaviour of modified PCA austenitic stainless steel 4-107063  
 liquid, struct. factor determ. using plasma reference system 4-113296  
 liquid, tokamak fusion reactor liq. metal blankets, mag. field penetration 4-111824  
 liquid metal for D-T, D-D and T-T fusion sources, energy deposition 4-68810  
 metal, T conc. from neutron irradiation, extraction, facility calibration 4-111811  
 molecule, B<sup>11</sup>L-X<sup>1</sup> $\Sigma^+$  g band system, fluoresc. study 4-59836  
 molecule, isotope separation, sequential two-photon ionisation 4-87167  
 molecule, isotope separation using different laser wavelengths for excitation and ionisation processes 4-69235  
 molecule, pot. curves, spin-extend HF study 4-64383  
 molecule, semiempirical parameters, bond length depend. corrls. effective valence shell Hamiltonian appl. 4-64353  
 molecules, collisions with solid surface, dissc. centrifugal mechanism 4-81404  
 muon interactions with lattice defects, mol. cluster calcs. 4-65255  
 normalised core-valence band Auger spectra 4-61783  
 phonon effects, core-level spectra 4-84581  
 poly(p-phenylene)Li, electron spin echo studies 4-71155  
 polyacetylene/Li, vibr. props., Raman study 4-75632  
 polyacetylene/Li batteries, contacts for current collector 4-89393  
 pool fires in fusion reactor safety anal., comp. with Na and Li-Pb, LIT-FIRE code 4-111787  
 potential at at. boundaries in Thomas-Fermi model and eqns. of states (*Chinese*) 4-70333  
 secondary cells, Li/LiClO<sub>4</sub> in polypropylene carbonate/V<sub>2</sub>O<sub>5</sub>, evolution of AC impedance 4-99954  
 secondary cells, NaCrS<sub>2</sub> cathode, props. and cyclic performance effect of synthesis temp. 4-93605  
 secondary electrochemical cell, electrochemical, thermodynamic and O pot. quantities 4-77072  
 stellar Li abundance determ., effects of chromospheric activity 4-63131  
 surface, interaction with acetylene, electronic and geometric struct. of acetylide C, AES and UPS study 4-92543  
 surface, lattice relax., effect of strong elec. field 4-75766  
 thin film cells, solid electrolytes and cathode materials (*Japanese*) 4-93597  
 vapour, angled-beam photon echoes 4-69510  
 $\beta$ -Al<sub>2</sub>O<sub>3</sub>/Li<sup>+</sup>, vibr. dynamics of Li ions 4-70441  
 CdTe:InLi, defect complex, IR absorption studies 4-80031  
 CoO:Li, pure and doped, elec. cond., carrier mobility and conc. 4-92731  
 Cr<sub>2</sub>O<sub>3</sub>/Li, elec. cond., O activity depend. 4-61376  
 Cr<sub>2</sub>O<sub>3</sub>/Li, hot pressing, annealing, elec. cond., density, grain size 4-113946  
 CuO:Li/ZnO junctions I-V characteristics, humidity effects, humidity sensor appl. 4-63750  
 Ge(Li) detector, time resolution improvements by compensation (*Chinese*) 4-68874  
 H trapping by Y, in low temp. Li 4-111759  
 KBr:Li<sup>+</sup>, paraelec. reson. absorption, decomposition under hydrostatic press. 4-104549  
 KCl:Li, optically excited colour centres, relaxation dynamics 4-113896  
 KCl:Li F<sub>2</sub>(II) colour centre laser, optical pumping improvement 4-107648  
 KCl:Li single crystal growth, colour centre laser appls. (*Chinese*) 4-61829  
 KTaO<sub>3</sub>:Li, heat capacity and random field sources 4-80253  
 KTaO<sub>3</sub>:Li, impurity ion quasi-reorientational dynamics, NMR spectrum 4-98973  
 KTaO<sub>3</sub>:Li, incipient ferroelec., off-centre impurity induced phase transition 4-76383  
 KTaO<sub>3</sub>:Li (single cryst., dielec. dispersion, dielec. spectra studies 4-76322  
 KTaO<sub>3</sub>:Li(Nb)(Na), random site at, substituted, NMR 4-65864  
 Li anode batteries high watt-hour per unit weight, electrolytes 4-93601  
 Li batteries, ambient temperature type, progress and future developments 4-62336  
 Li batteries, current status and future developments 4-62332  
 Li cell, nonaqueous, electrochemistry 4-62333  
 Li I, 1s2sn and 1s2pnl quartet levels, transition wavelengths, radiative lifetimes, fine struct. 4-96491  
 Li I, (2p2p2p) <sup>2</sup>S<sup>o</sup> states, optical emission 4-87175  
 Li I, autoionisation rate determ. by optical emission spectroscopy 4-87087  
 Li I 670.7 nm resonance doublet in Ba stars, Li abundance 4-67746

## lithium continued

- Li to Ar, core electrons, Coulomb and exchange operators, matrix elements, valence electron only SCF calcs. 4-59630  
 Li<sup>+</sup>, doubly excited quintet states, fine and hyperfine struct., many-body calcs. 4-102609  
 Li<sup>+</sup> formation by Li<sup>+</sup> scatt. from W:C surfaces 4-73574  
 Li<sup>+</sup>, <sup>7</sup>P Feshbach reson., line-shape parameters, autoionisation states 4-64433  
 Li<sup>+</sup>, <sup>10</sup>P levels, beam-foil spectral line identification 4-74188  
 Li<sup>+</sup> in aq. soln., mol. dynamic simulation of quadrupole relax. 4-80841  
 Li<sup>+</sup>, photoionisation cross sections, oscillator strengths, polarised orbital method 4-64438  
 Li<sup>+</sup> solvation, geometrical features, pattern recognition anal. 4-114781  
 Li<sup>2+</sup>, H-like, elastic positron scatt., polarised orbital method 4-102798  
 Li/CF battery, electrochemical characs. 4-99955  
 Li/CrO<sub>2</sub> battery, performance characs. and safety tests, for electronic applications 4-93602  
 Li/Cu<sub>2</sub>V<sub>2</sub>O<sub>7</sub> battery with 1-M LiClO<sub>4</sub>-propylene carbonate/1,2-dimethoxyethane electrolyte 4-93607  
 Li/CuMoO<sub>4</sub> voltage compatible battery, performance 4-77074  
 Li/MnO<sub>2</sub> 3 V power module for direct plug-in into circuit boards (*German*) 4-114899  
 Li/SO<sub>2</sub> cell, Li<sub>2</sub>S<sub>2</sub>O<sub>4</sub> discharge product, spectroscopic studies 4-89387  
 Li/SO<sub>2</sub> cells, discharge capacity at high current and temp., chem. reactions 4-66679  
 Li/SO<sub>2</sub>Cl<sub>2</sub> electrochemical cell, development 4-77071  
 Li/SOCl<sub>2</sub> static cell with acid electrolyte, math. model 4-89388  
 Li/SOCl<sub>2</sub> static cell with neutral electrolyte, math. model 4-89389  
 Li/TiS<sub>2</sub> battery, discharge prop., effect of nonstoichiometry and solvent 4-93603  
 Li-Al electrode secondary cell, cycling behaviour in LiClO<sub>4</sub>-propylene carbonate solutions 4-72058  
 Li-Al electrode secondary cell at room temp., Li-Al alloy electrochemical formation kinetics 4-72059  
 Li-Al/FeS cell, FeS positive electrode effective conductivities in LiCl-KCl eutectic electrolyte 4-99958  
 Li-like ions, (2p2p2p) <sup>2</sup>S<sup>o</sup> states, optical emission 4-87175  
 Li-SO<sub>2</sub> batteries in pressure housings, abuse tests and safety features 4-114900  
 Li+Ar<sup>q+</sup> (Ne<sup>q+</sup>)(Kr<sup>q+</sup>)(Xe<sup>q+</sup>) collisions, q=2 to 10, electron capture cross sections from slow projectiles 4-74328  
 Li+C<sup>+</sup>, electron transfer into C<sup>3+</sup>(nl) orbitals, at. basis calcs. 4-107450  
 Li+FH collinear reaction, quasi-classical versus quantum calcs. 4-66556  
 Li+H<sup>+</sup>(He<sup>+</sup>)(He<sup>2+</sup>) collisions, single electron capture 4-74327  
 Li+He, Li(2s-3d) excitation, D state scatt. amplitudes 4-64570  
 Li+Na<sup>+</sup> collisions, semiclassical scatt. theory based on dynamical-state representation 4-78955  
 Li<sup>+</sup>+Ar(He)(Ne), electron detachment cross sections 4-78952  
 Li<sup>+</sup>+H, electron capture by fast ions 4-91343  
 Li<sup>+</sup>+H<sup>+</sup>, ionisation cross section, PWBA 4-83461  
 Li<sup>+</sup>+Li, differential cross sections calc. using mol. bases, quantum effect 4-87211  
 Li<sup>+</sup>+Li<sup>+</sup> collision, charge transfer and ionis. cross-sections determ. 4-64593  
 Li<sup>+</sup>+Na collisions, semiclassical scatt. theory based on dynamical-state representation 4-78955  
 Li<sup>2+</sup>+H, electron capture by fast ions 4-91343  
 Li<sup>2+</sup>+H, charge exchange cross-sections, low-energy calcs. 4-64592  
 Li<sup>2+</sup>+H, electron capture by fast ions 4-91343  
 Li<sup>2+</sup>+neutral ats., charge transfer in low-energy collisions 4-74326  
 Li<sub>2</sub>, <sup>2</sup> $\Sigma^+$ -(<sup>2</sup>p-<sup>2</sup>p) crossing states, pot. energy curves, ab initio calcs. 4-68995  
 Li<sub>2</sub> A<sup>2</sup> $\Sigma^+$  state lifetime and electronic dipole moment, time-resolved spectrosc. obs. 4-83423  
 Li<sub>2</sub>, electron screening function, anal. representation 4-83306  
 Li<sub>2</sub>, X<sup>2</sup> $\Sigma^+$  crossing states, pot. energy curves, ab initio calcs. 4-68995  
 Li<sub>2</sub>+He collision-induced dissc., reaction mechanism, rate const. 4-76976  
 Li<sub>2</sub> clusters, matrix isolated, g-value, HF coupling, EPR spectra 4-74266  
 Li<sub>2</sub> cluster, H<sub>2</sub> capture, Raman enhancement mechanism assoc. with Raman scatterer interaction 4-61675  
 Li<sub>2</sub>C<sup>+</sup>(N<sup>2+</sup>)(N<sup>3+</sup>)(O<sup>4+</sup>) core-conserving electron capture ion excitation metastable fraction meas. 4-83465  
 LiSOCl<sub>2</sub> cylindrical primary cells, design for safety, testing 4-66677  
<sup>6</sup>Li/<sup>7</sup>Li, isotope ratio determ. in FG-type dwarf stars 4-101327  
<sup>6</sup>Li/<sup>7</sup>Li, ratio in saline lakes of Qinghai-Xizang Plateau, <sup>6</sup>Li(n, $\alpha$ )<sup>3</sup>H influence 4-110401  
<sup>6</sup>Li/<sup>7</sup>Li in metal-deficient stars 4-63147  
<sup>7</sup>Li, possible synthesis by pregalactic massive stars 4-67841  
<sup>7</sup>Li, synthesis by Population III remnants 4-67842  
<sup>7</sup>Li/<sup>6</sup>Li, chemical evolution of cosmic isotope ratio rel. to Big Bang nucleosynthesis 4-67843  
<sup>7</sup>Li<sup>3</sup> formation by <sup>7</sup>Li<sup>+</sup> scatt. from cesiated W (110) surface 4-76624  
<sup>7</sup>Li, A=6, <sup>7</sup> antiprotonic atoms, strong interaction effects on X-ray transitions 4-59921  
 Li<sub>2</sub><sup>+</sup>, electron screening function, anal. representation 4-83306  
 Li<sub>2</sub><sup>+</sup>/Ar, rotationally inelastic transfer, scaling of state multipoles 4-87198  
 Li<sub>2</sub><sup>+</sup>/He, rotationally inelastic transfer, scaling of state multipoles 4-87198  
 Li<sub>2</sub><sup>+</sup>+Ar(Ne)(Xe) 4-74319  
 Li<sub>2</sub><sup>+</sup>+Ne(Ar)(Xe), rot. inelastic collisions, vel. depend. 4-102764  
 Li<sup>+</sup>(1s2s), excited metastable state prod. by laser-produced plasma soft X-rays 4-112131  
 Li(2p) excitation by electron transfer in slow metal surface collisions 4-66179  
 MgF<sub>2</sub>/Li, electron irradi., holelike defects, ESR study 4-60964  
 NiO:Li, elec. cond. and high temp. defect struct. 4-80617  
 Se<sub>2</sub>Te<sub>2</sub>O<sub>4</sub>As<sub>2</sub>Li, chemical modification and elec. cond. 4-75970  
 a-Si:H, Li, surface photovolt. and dark conductance, light-induced changes 4-70861  
 Si:Li, phonon scatt., acoustic paramagnetic resonance study 4-71157  
 Si:Li and Si:Li, C, electron irradi., luminesc. decay time, absorpt., isotope splitting, and Zeeman meas. 4-71434  
 Si:Li p-n junction solar cells, electron induced degradation, recovery under space conditions 4-105110  
 Si:Li solar cells, counterdoped, increased radiation resistance to electron irradi. 4-81539

## Lithium continued

- Si(Li)-Si(Li) superconducting magnetic spectrometer, internal pair transitions 4-91145  
 ZnO film, laser evaporated growth and transducers 4-104537
- Lithium alloys**  
 MARS, liquid  $\text{Li}_2\text{Pb}_{83}$  cooled fusion reactor blanket, corrosion product cleanup system 4-111785  
 Al-Cu-Li, recrystallised 2020, mech. props. rel. to soln. heat treatment 4-76781  
 Al-Cu-Li alloys, mech. props., effect of minor alloying additions of Zr, Cd or Fe 4-99526  
 Al-Cu-Li-Cd, 2020, microstruct., fracture toughness and SCC 4-76851  
 Al-Cu-Li-Mg-Zr, splat-quenched, microstruct. and tensile props. 4-114620  
 Al-Cu-Li-Mn-Cd, Al 2020, fatigue crack growth behaviour 4-71728  
 Al-Li, microcrystal evolution, DSC obs. 4-71659  
 Al-Li, nucleation, growth and coarsening of precipitates 4-81202  
 Al-Li, precipitate-matrix interfacial energy 4-85160  
 Al-Li (22 wt.%), dislocation dynamics, mean jump distance and activation length of moving dislocations 4-108364  
 Al-Li-Cu-Mg-Zr, powder metallurgy produced, superplastic behaviour 4-76820  
 Al-Li-Si system, liquidus surface, thermal and microstructural analysis 4-61921  
 Al-Li-Zr (2.34, 1.07 wt.%), composite precipitates 4-85154  
 Al-Mg-Li and Al-Li-Mg low-activation alloy development for fusion device 4-108460  
 $\text{CaSOCl}_2$  cells with anodes made from Ca/Ca-Li alloys, electrochemical studies 4-72080  
 Cu-Li alloy, surface material for fusion devices 4-97888  
 Li-Al, T release on heating or NaOH dissolving rel. to Li conc. 4-75733  
 Li-B/LiNO<sub>3</sub> anode-electrolyte system, potentiostatic studies 4-66676  
 Li-Fe film, conduction electron surface mag. relax. (Russian) 4-65862  
 Li-Mg, short range order, Clapp and Moss high temp. formulation, effects of Tahir-Kheli intermediate temp. terms 4-113664  
 Li-Pb, liq., breeder blanket materials, thermodynamic investig. of dil. solns. of H 4-107033  
 Li-Pb, liq., breeder blanket materials, interaction of H isotopes investig. 4-107034  
 Li-Pb(Ag) (Mg) liq. alloys, model, chemical short-range order, heat and entropy of formation 4-75266  
 Li-Sn, liquid structure, neutron diff., cpd. form. 4-113295  
 Li-Tl(In)(Ga), cryst. struct. determ. 4-79986  
 LiAl, fast Li ion conductor, irreversible behaviour on elec. resist. 4-80634  
 LiAl thin film electrodes for secondary batteries, overpotentials 4-109737  
 LiMg, pair ordering pots., Clapp and Moss approx. inadequacy 4-92129  
 $\text{Li}_2\text{Pb}_{83}$  alloy blanket concept for tritium breeding in INTOR-NET 4-111747  
 $\text{Li}_2\text{Pb}_{83}$  alloy blanket material for fusion reactor, tritium recovery 4-111745  
 $\text{Li}_2\text{Pb}_{83}$  liquid alloy, physical and chemical props. for fusion reactors 4-111748  
 Mg-Li-Al-Mn and Mg-Li-Al-Zn-Mn-Ce systems, mech. props. and corrosion resist. 4-93455  
 Pb-Li, liq., fusion reactor blankets, compatibility of steels, review 4-107054  
 Pb-Li, molten static, corrosion reactions of ferritic and type 316 steels 4-107064  
 Pb-Li eutectic in fusion reactor, corrosion behaviour of steels 4-107056

## Lithium compounds

see also lithium alloys

- acetates,  $^{13}\text{C}$  chemical shielding anisotropies 4-65871  
 anisotropic planar waveguides with bent optical axes, wave propag. anal. 4-83691  
 brazing of bulk graphite/solid T breeder materials to metal substrates 4-111753  
 ethanoate hydrates, thermodynamic props., phase transitions 4-98305  
 ferropinell ordered struct., uniqueness 4-79994  
 formate deuterate, nonlinear susceptibilities by modification of localised bond charges method 4-112507  
 glasses, fast ion conducting, review 4-103997  
 intercalation compound with graphite,  $\text{LiC}_6$ , electron momentum distrib., Compton profile 4-109268  
 intercalation compound with graphite,  $\text{LiC}_6$ , optical spectra, ab initio calc., origins of plasmons 4-88802  
 intercalation cpd. with graphite,  $\text{LiC}_6$ , Compton profile, X-ray scatt. meas. 4-61765  
 intergrowth compounds between members of the bismuth titanate family and structures of the  $\text{LiBi}_2\text{O}_4\text{Cl}_2$  type. An architectural approach 4-92148  
 $\text{LiNbO}_3$  optical waveguides, out-diffused, fabrication at low temps. in molten salts 4-112569  
 $\text{LiNbO}_3$  plate, device structs. based on interdigital-transducer-generated bulk waves 4-97248  
 lithium benzophenone-LiBr complex form., equilb. const. 4-71906  
 polymer/Li salt hybrids as superionic conductors 4-75723  
 secondary cells, Li/ $\text{LiClO}_4$  in polypropylene carbonate/ $\text{V}_2\text{O}_5$ , evolution of AC impedance 4-99954  
 tokamak first wall/blanket/shield programme, e-beam effects, designs, recent progress 4-111800  
 $\text{AgCl}:\text{LiCl}$ , molten, electrolytic cond. 4-108638  
 $\text{Al}(\text{PO}_3)_2\text{-Li}_2\text{O-K}_2\text{O}$  glasses, mixed-alkali effect 4-80296  
 $\text{B}_2\text{O}_3\text{-}0.5\text{Li}_2\text{O-}0.7\text{LiCl}$  glass, pseudospin echoes 4-70291  
 $\text{B}_2\text{O}_3\text{-Li}_2\text{O}$  (Li halides)<sub>2</sub>, fast ion cond., press. effects 4-88336  
 $\text{BaO-Li}_2\text{O-Nb}_2\text{O}_5$ , phase equilibria in crystn. region, tetragonal phase 4-114495  
 $\text{Ba}_2\text{O}_3\text{-(Li}_2\text{O)}_{0.7}\text{-(LiCl)}_{0.7}$ , amorphous, fast ionic cond. meas. (Chinese) 4-103996  
 $\text{Ba}(\text{PO}_3)_2\text{-AlF}_3\text{-LiF}$ , elec. cond. rel. to struct. 4-92771  
 Ca/ $\text{LiCl}$ ,  $\text{LiNO}_3/\text{LiNO}_3$ ,  $\text{AgNO}_3/\text{Ni}$  thermal battery cells, discharge characts. 4-66675  
 $\text{CsLiMoO}_4$ -type crystals, ferroelec. phase transitions 4-65979  
 $(\text{CuO})_x\text{-(}2\text{B}_2\text{O}_3\text{Li}_2\text{O)}_{1-x}$  glass, EPR and mag. susceptibility meas. 4-61587  
 $\text{KLiSO}_4$  cryst. struct. at room temp., neutron diff. study (Chinese) 4-75379  
 $\text{KLiSO}_4$  ferroelastic transition, microscopic model 4-75664  
 $\text{K}_{1-x}\text{Li}_x\text{TaO}_3$ , dipole glass phase, dielec., thermal, elastic, and struct. props. (Japanese) 4-104525
- lithium compounds continued**  
 $\text{K}_{1-x}\text{Li}_x\text{TaO}_3$ , IR reflectivity, two mode behaviour 4-71363  
 $(\text{Li}_2\text{Na})_2\text{O-B}_2\text{O}_3$  glasses, mixed alkali effect 4-84449  
 Li complexes,  $\text{Li}^+/\text{N-methylformamide-water}$ , N-substitution effect on hydrogen bonds, ab initio calcs. 4-96716  
 Li complexes,  $\text{Li}^+/\text{formamide-water}$ , N-substitution effect on hydrogen bonds, ab initio calcs. 4-96716  
 $^{22}\text{Li}$  cryptates, in water, stability consts. 4-114817  
 Li-B/ $\text{LiNO}_3$  anode-electrolyte system, potentiostatic studies 4-66676  
 Li-H systems, thermodynamic props., ionis. pots. and binding energies 4-69266  
 Li-inert gas molcs., near-UV emission bands meas., collision induced bands, quenching rate coeff. 4-83385  
 Li-O systems, thermodynamic props., ionis. pots. and binding energies 4-69266  
 Li-Si disilicate glasses with Nd-U contents, response to  $\gamma$ -rays and neutrons 4-96399  
 $\text{LiAlCl}_4$  solutions conductivity in nitromethane containing  $\text{SO}_2$ , concentration and temp. dependence, applicability assessment for  $\text{Li}/\text{SO}_2$  cells 4-66596  
 $\gamma\text{-LiAlO}_2$  breeder blanket material developments 4-107020  
 $\gamma\text{-LiAlO}_2$  breeder material, TRIO-01 expt. for in-situ T recovery 4-107023  
 $\text{LiAlO}_2$  breeder materials, fast neutron irradiat. expts. 4-107024  
 $\gamma\text{-LiAlO}_2$ , polycrystalline, elec. cond., AC meas. 4-108645  
 $\gamma\text{-LiAlO}_2$  solid breeder, in-situ T recovery and heat transfer performance 4-111817  
 $\text{LiAlSi}_2\text{O}_6$ ,  $\alpha$ -spodumene, microplasticity, dislocation glide and dissoc., TEM obs. 4-65331  
 $\text{LiAsF}_6$  in 2-methyltetrahydrofuran, mol. relax., US absorpt. investig. 4-109108  
 $\text{LiBF}_4$  in 2-methyltetrahydrofuran, mol. relax., US absorpt. investig. 4-109108  
 $\text{LiBF}_4$ , solid, mol. reorientation, diffusion NMR study 4-88734  
 $\text{LiBF}_4$ -poly(ethylene succinate) solid electrolyte complex, ion transport 4-75721  
 $\text{LiBH}_4$ , nonrigid rearrangement barriers, ab initio many-body Rayleigh-Schrodinger perturbation theory calcs. 4-68925  
 $\text{Li}_2\text{B}_2\text{O}_7$ , bulk acoustic wave props., SAW appls. 4-70280  
 $\text{Li}_2\text{B}_2\text{O}_7$ , growth and props. for SAW devices 4-98419  
 $\text{LiBiO}_2$ , ionic cond., cryst. struct. and sp. ht. studies 4-70455  
 $\text{LiBiO}_6$ , ionic conductivity 4-70437  
 LiBr, aq. soln., laminar liquid film falling over horizontal cylinders, heat transfer 4-97545  
 LiBr film, water vapour absorpt., heat and mass transfer 4-64937  
 LiBr film flowing down adiabatic wall, mass transfer in absorpt. of water 4-64831  
 LiBr-water double effect absorption cooling cycle modelling 4-72159  
 $\text{LiC}_6$ , tritium release from irradiated Li compounds obs. (Japanese) 4-102396  
 $\text{Li}_2\text{C}_2$ , tritium release from irradiated Li compounds obs. (Japanese) 4-102396  
 $\text{LiClO}_4$ , in organic solvents, solvation process, IR spectra 4-61697  
 LiCN, ab initio dipole strengths, vibr. averaged dipole moments and IR transition intensities 4-64461  
 $\text{Li}_2\text{CO}_3$ , single cryst., sub-boundaries on (002) cleavages 4-103751  
 $\text{Li}_2\text{CO}_3$ , tritium release from irradiated Li compounds obs. (Japanese) 4-102396  
 $\text{Li}_2\text{-Cd}_{1-x}\text{Cl}_4$ , spinel, ionic cond. and phase transition 4-75720  
 LiCl crystal, electronic energy bands, density functional calcs., self-interaction-correction theory 4-70651  
 LiCl desiccant air-conditioner using heat exchangers and humidifiers 4-72164  
 LiCl, electron momentum densities, refinement 4-113381  
 LiCl, optical const. calcs. 4-99084  
 LiCl, substitutional defects, molecular cluster-INDO calcs. 4-108806  
 $\text{LiCl-CoCl}_2$  aq. solns., X-ray diff. study 4-60805  
 LiCl-KCl eutectic melts,  $\text{FeSe}_2$  and  $\text{FeS}$  equilibrium concentrations 4-88300  
 LiCl-KCl eutectic mixtures,  $\text{Al}_2\text{O}_3$  solubility 4-75686  
 LiCl-KCl molten system, internal contact mobilities determ. at 723K 4-92400  
 LiCl, excited state electronic struct., RHF calcs. 4-74176  
 $(\text{LiCl})_x(\text{H}_2\text{O})_{1-x}$  glass, hypersonic velocity and attenuation, Brillouin scatt. 4-70286  
 $\text{LiClO}_4$  dispersed with polyion complexes,  $\text{Li}^+$  ion conductors, appl. to solid state batteries 4-92414  
 $\text{LiClO}_4$  in 2-methyltetrahydrofuran, mol. relax., US absorpt. investig. 4-109108  
 $\text{LiClO}_4\text{-Mg}(\text{Al})(\text{Fe})(\text{Cr})(\text{Ni})$ , shock compression, physicochemical transformations 4-70273  
 $\text{LiClO}_4$ -propylene carbonate electrolytic props., additive effects of  $\text{Li}^+$  ion solvation compounds 4-65424  
 $\text{LiCrO}_2$ , EPR linewidths and exchange integrals 4-76244  
 $\text{LiCr}_2\text{O}_7\cdot 2\text{H}_2\text{O}$ , struct., neutron diff. investigations 4-60899  
 LiCs recombinant plasma, optimisation of inverse population of Li levels (Russian) 4-69023  
 LiD, D elec. field gradient, LCAO MO SCF calcs. 4-112103  
 $\text{LiErF}_4$  far IR mag. reson. meas. using laser based mag. reson. spectrometer 4-90623  
 LiF (001), inelastic He scatt., eikonal approx., surface dynamics 4-108700  
 LiF (001), NO collisions vibr. energy transfer, stochastic trajectory method 4-69183  
 LiF (100) surface, elastic and inelastic scatt. of slow positrons 4-104704  
 LiF and LiF-PbF<sub>2</sub> pellets, thermal neutron irradiated, T release behaviour, fusion reactor appl. 4-74040  
 LiF,  $\alpha$ -particle ionisation, controlled secondary electron emission 4-76570  
 LiF, ballistic phonon interaction with defects, heat-pulse technique study 4-98228  
 LiF bicrystals, fracture at plastic deform. 4-75609  
 LiF, channelling radiation from relativistic positrons 4-65314  
 LiF, charge transport by moving dislocations, diffusion model 4-75448  
 LiF, crack edge contact restoration phenomena 4-98191  
 LiF cryst., dislocation band interactions with a healed crack 4-113492  
 LiF cryst.,  $\gamma$ -ray irradiat. effects on dislocation damping coeff. 4-65267  
 LiF crystallites, cold-worked, microstrains, X-ray diff. lines anal. (French) 4-79892  
 LiF crystals, annealed and aged, dislocation behaviour 4-103759  
 LiF crystals, fast electron irradiated, space-charge dynamics 4-71279

## lithium compounds continued

- LiF, dislocation mobility at low temps., etch pit obs., Peierls mechanism 4-98105  
 LiF, dislocation strain-field scatt. of fast-transverse acoustic phonons 4-84355  
 LiF, dislocation struct. evolution at premelting temp. (*Russian*) 4-88174  
 LiF, dissoc. energy; HF STO calcs. 4-112092  
 LiF, electric field influence on dynamic yield point 4-75605  
 LiF, electron momentum densities, refinement 4-113381  
 LiF, exoelectron emission during fracture, energy distrib. function depend. on charge struct. 4-88951  
 LiF  $F_2$  centre laser, relationship between  $F_2$  centre density and laser stability (*Chinese*) 4-91477  
 LiF  $F_2$  centre tunable laser with distributed feedback 4-107651  
 LiF  $F_2$  laser pumped by  $Nd^{3+}$  glass laser (*Chinese*) 4-107646  
 LiF for  $^{125}I$  dosimetry 4-72432  
 LiF, fracture-induced luminesc. and crack vel. 4-104685  
 LiF, high temp. IR tunable diode laser spectra, no-vibr. meas. and Dunham consts. calcs. 4-59743  
 LiF, localised phonon mode associated with dislocations, thermal props. 4-70321  
 LiF, optical const. calcs. 4-99084  
 LiF, photon-stimulated desorption study 4-70571  
 LiF, phototransferred thermoluminesc. for high LET radiation dosimetry 4-105339  
 LiF, planar channelling radiation from relativistic positrons and electrons 4-75581  
 LiF powered crystals, photoacoustic spectroscopy for thermoluminescent dosimetry 4-93116  
 LiF pulsed  $F_2^-$  colour centre laser, room temp. operation in near IR 4-64710  
 LiF,  $R'$ -centre aggregate, spectral linewidths, depend. on irradiation method 4-70193  
 LiF, sensitised phosphors, thermolum. readout, photon energy depend. 4-89758  
 LiF, single cryst., IR transmission spectra at 300K, effect of stepped creep on exhaustion of dislocations 4-65271  
 LiF single cryst., lattice const. meas. using X-ray double cryst. method 4-103606  
 LiF single crystal, crack tip deform. 4-84343  
 LiF single crystals, grinding, surface layer, strain hardening, dislocation density, microhardness 4-93312  
 LiF, specular reflection spectra in the Li-K absorpt. region 4-85035  
 LiF, substitutional defects, molecular cluster-INDO calcs. 4-108806  
 LiF surfaces,  $F^+$  ejection by ion bombardment 4-61800  
 LiF TLD, increased thermolum. due to brief preheating 4-62587  
 LiF TLD, reproductive annealing procedure 4-99401  
 LiF TLD 100, order of kinetics 4-88888  
 LiF thermoluminescent detectors, sensitivity for 2-144 keV neutrons 4-96288  
 LiF, transparent melts, thermal conductivity 4-113732  
 LiF, tritium release from irradiated Li compounds obs. (*Japanese*) 4-102396  
 LiF tunable pulsed  $F_2^+$  colour centre laser, 0.69-1.0  $\mu m$  4-69413  
 LiF, tunable room temp. laser operation of colour centres, red and near IR emission 4-91479  
 LiF vapour deposited thin films, TSEE, thermolum. meas. 4-81119  
 LiF, voltage and freq.-selective storage at GaAs laser wavelengths 4-83655  
 LiF, X-irrad., thermolum. spectra at LNT 4-66084  
 LiF, X-ray refractive index meas. 4-104557  
 LiF  $F_2^+$  colour centre laser pumped by Cu vapour and dye laser radiation 4-74523  
 LiF:H,  $\gamma$ -irrad. and mechanically loaded, H atom localisation 4-88179  
 LiF:Li<sub>2</sub>O, impurity centres, visible spectra studies 4-80546  
 LiF:Mg, OH, room temp. laser action using  $F_2$  centres 4-91481  
 LiF:Mg,Cu,P, high sensitivity thermoluminesc. dosimeter, environmental monitoring appl. 4-109934  
 LiF:Na<sup>+</sup>(Rb<sup>+</sup>), annealed and reimplanted, atomic mixing processes 4-70231  
 LiF:Ni<sup>2+</sup>, Ni<sup>2+</sup>-F<sup>-</sup> distance for square planar and linear Ni<sup>2+</sup>-centres from isotropic superhyperfine const. 4-98581  
 LiF:OH<sup>-</sup>, gamma-ray irradi., lattice defects, EPR studies 4-75437  
 LiF:OH<sup>-</sup>, mechanical props., dislocation motion anal. 4-70257  
 LiF:U, pure and doped, preferential sputtering and ion induced comp. changes 4-71501  
 LiF/CaF<sub>2</sub> isotropic interface, TE-surface polaritons 4-75869  
 LiF:AlF<sub>3</sub> cryolite melts, interdiffusion 4-88324  
 LiF:AlF<sub>3</sub> thin film, ionic cond. meas. 4-84450  
 LiF:BaF<sub>2</sub>-LiBO<sub>2</sub> mixture field for BaTiO<sub>3</sub> type oxide fluoride growth at low temp. 4-99296  
 LiF:CaF<sub>2</sub> thin film, ionic cond. meas. 4-84450  
 LiF:CeF<sub>3</sub> thin film, ionic cond. meas. 4-84450  
 LiF:CrF<sub>3</sub> thin film, ionic cond. meas. 4-84450  
 LiF-KF eutectic melt, oxide ion anodic behaviour at glassy C electrode 4-66594  
 LiF:MgF<sub>2</sub> thin film, ionic cond. meas. 4-84450  
 LiF:NiF<sub>2</sub> thin film, ionic cond. meas. 4-84450  
 LiF<sub>2</sub>, excited state electronic struct., RHF calcs. 4-74176  
 LiF phengite, mica, cryst. struct. of di-tri-octahedral 1M polymorphic modification, electron diff. study 4-60894  
 Li<sub>0.5</sub>Fe<sub>1.5</sub>Al<sub>1.5</sub>O<sub>6</sub>, atomically ordered spinel, mag. struct., neutron diff. study 4-61513  
 LiFeO<sub>2</sub>, mag. domain walls interaction with microstruct. features 4-71122  
 LiFeO<sub>2</sub>, magnetic vitroceraamics, prep. and props. 4-93256  
 Li<sub>2</sub>FeO<sub>3</sub>, struct. characts. 4-70120  
 Li<sub>2</sub>FeO<sub>4</sub>, struct. characts. 4-70120  
 LiFePO<sub>4</sub>(OH, F), tavorite, hydrothermally grown, cryst. struct., X-ray diff. study 4-113418  
 Li<sub>2</sub>FeSbO<sub>8</sub>, cryst. struct., X-ray powder diff. 4-108325  
 LiFeSnO<sub>4</sub>, polymorphic transition between hexagonal close-packed struct. and ramsdellite type struct. 4-70055  
 Li<sub>2</sub>GeO<sub>3</sub> pyroelec. material, vibr. spectra and polariton dispersion 4-71362  
 Li<sub>1-x</sub>Ge<sub>x</sub>V<sub>1-x</sub>O<sub>4</sub>, solid electrolytes, prep. props. and appl. 4-103998  
 LiH, core electrons, Coulomb and exchange operators, matrix elements, valence electron only SCF calcs. 4-59630  
 LiH crystals, cleaved, excitonic struct., optical spectra study 4-61746  
 LiH, dipole moment, 2D fully numerical MC SCF calcs. 4-59614

## lithium compounds continued

- LiH, electric dipole moments calc. using variational cellular method 4-87042  
 LiH, electron elastic scatt. cross section 4-83469  
 LiH, electron scatt., R-matrix method, ab initio calcs. 4-83484  
 LiH, electron-phonon interactions in luminescence spectra 4-71439  
 LiH, ground-state props., LCAO HF study using polarisable basis set 4-60882  
 LiH, molecular correlation energies with explicitly correlated Gaussian geminals 4-91204  
 LiH, pair correl. eqns., numerical soln. method 4-96423  
 LiH, pot. curves, spin-extended HF study 4-64383  
 LiH, RHF, NDDO and MOM mol. one-electron expectation values calc. using minimum basis sets 4-102598  
 LiH, relativistic SCF calc. with squared Dirac operator 4-78790  
 LiH, shielding materials for space power reactor appls. 4-107170  
 LiH, Stark effect, polarisabilities and elec. dipole moment in  $\Sigma$  states 4-112217  
 LiH+He rotationally inelastic collisions, quasi-classical dynamics of atom-rigid rotor trajectories 4-112260  
 LiH<sub>2</sub>, binding energy, ab initio calcs. 4-59615  
 LiH(D), radiation induced defect form. 4-60952  
 LiH(D):Na, radiation induced defect form. 4-60952  
 LiHF system, pot. energy surface, ab initio values 4-104963  
 Li<sub>1-x</sub>H<sub>x</sub>NbO<sub>3</sub>, struct. changes, X-ray diff. studies 4-84272  
 LiH<sub>2</sub>(SeO<sub>3</sub>)<sub>2</sub>, ferroelec., single cryst. growth from soln. (*Korean*) 4-114375  
 LiH:  $\Sigma^+$  states, multireference functions, cluster expansion theory, CI calcs. 4-74161  
 LiHg, van der Waals pot. model 4-69166  
 LiI 4-103907  
 LiI, in organic solvents, solvation process, IR spectra 4-61697  
 LiI, predissociation study 4-107415  
 LiIO<sub>3</sub>, broadband piezoelec. transducers for recording press. pulses 4-69658  
 LiIO<sub>3</sub> crystal, laser beam pulses duration meas. using noncollinear SHG 4-107707  
 $\beta$ -LiIO<sub>3</sub>, IR absorption and Raman spectra at low temps. 4-71361  
 $\alpha$ -LiIO<sub>3</sub>, ionic transport and relax., polarising microscopy studies (*Chinese*) 4-98335  
 $\alpha$ -LiIO<sub>3</sub>, Li<sup>+</sup> migration in DC elec. field,  $^6Li(n,\alpha)t$  nucl. reaction anal. (*Chinese*) 4-113698  
 $\alpha$ -LiIO<sub>3</sub>, phase-type gratings induced by electro-optical effect, space charge fluctuation 4-66012  
 $\alpha$ -LiIO<sub>3</sub>, pyroelec. coeff. below room temp. 4-76348  
 $\alpha$ -LiIO<sub>3</sub>, quasi-one-dimensional ionic conductor, light diff. due to space charge fluctuations 4-109156  
 $\alpha$ -LiIO<sub>3</sub>, quasi-one-dimensional ionic conductor, light diff. due to space charge fluctuations 4-109157  
 LiIO<sub>3</sub>, single crystal growth, properties, appls. (*Russian*) 4-75334  
 LiIO<sub>3</sub> single crystals, optical damage, nonlinear transmission and doubling efficiency 4-75513  
 LiIO<sub>3</sub> single crystal, laser induced damage, nonlinear absorpt. and doubling efficiency 4-79205  
 LiIO<sub>3</sub>-HIO<sub>3</sub> system, influence of growth conditions on optical props. 4-76430  
 LiKSO<sub>4</sub>, cryst. and domain struct., neutron diff. studies 4-88159  
 LiKSO<sub>4</sub> crystals, ferroelasticity and internal friction 4-75612  
 LiKSO<sub>4</sub>, incommensurate phase (*Chinese*) 4-70359  
 LiKSO<sub>4</sub>, incommensurate-commensurate phase transitions, superstructure, X-ray diff., neutron diff., thermal anal. 4-103929  
 LiKSO<sub>4</sub>, phase transitions at low temp., domain textures, dielec. meas. 4-75655  
 LiKSO<sub>4</sub>, phonon dispersion relation calcs. 4-70308  
 LiKSO<sub>4</sub>, press. effect on phase transitions 4-104546  
 LiKSO<sub>4</sub> single cryst., unit cell correl. effects, polarised Raman spectra 4-71374  
 LiKSO<sub>4</sub> single cryst., light diff. from vol. phase gratings (*Chinese*) 4-96784  
 Li<sub>2-2x</sub>Mg<sub>1+x</sub>Cl<sub>4</sub> spinel, ionic cond. and phase transition 4-75720  
 Li<sub>2-2x</sub>Mg<sub>1+x</sub>Cl<sub>4</sub> spinel, ionic cond. and phase transition 4-75720  
 LiMnFeF<sub>6</sub>,  $\alpha$ - and  $\beta$ -phases, magnetisation, Mossbauer and neutron studies 4-88752  
 LiMnMF<sub>6</sub> (M=Fe, V, Ti, Cr, Ga), cationic distribution and mag. behaviour 4-71026  
 LiMnO<sub>2</sub>, crystal growth, hydrothermal and flux synthesis 4-71541  
 Li<sub>2</sub>MnO<sub>3</sub>, crystal growth, hydrothermal and flux synthesis 4-71541  
 Li<sub>2</sub>MnO<sub>3</sub>, struct. characts. 4-70120  
 Li<sub>0.4</sub>MoO<sub>4</sub>, Li<sup>+</sup> transport, pulse NMR relax. time meas. 4-75727  
 Li<sub>0.9</sub>Mo<sub>0.1</sub>O<sub>7</sub>, quasi-two-dimensional electronic props. 4-104189  
 LiMo<sub>2</sub>S<sub>2</sub>Br(l), preparation and cryst. struct. 4-70097  
 Li<sub>2</sub>MoSe<sub>4</sub>, Li intercalation model, mean-field lattice gas 4-70098  
 Li<sub>3</sub>N, electronic struct., Hartree-Fock studies 4-98522  
 Li<sub>3</sub>N, superionic cond., Li diffusion const., NMR meas. 4-113704  
 Li<sub>3</sub>N, superionic cond., obs. of solitary-wave cond. in mol. dynamics simulation 4-61138  
 LiNCS solns. in dipolar aprotic, IR spectra and struct. 4-112175  
 LiNH<sub>4</sub>SO<sub>4</sub>, ferroelec. domain struct., SEM studies 4-71321  
 LiNH<sub>4</sub>SO<sub>4</sub>, normal and deuterated, II-III phase transition, elec. field effects 4-65396  
 LiNH<sub>4</sub>SO<sub>4</sub>, phase transitions, X-ray diff. study 4-88277  
 LiNH<sub>4</sub>SO<sub>4</sub>Mn<sup>2+</sup>, impurity electronic absorpt. spectrum 4-66055  
 LiNO<sub>3</sub>, force and vibr. spectrum, ab initio study 4-112110  
 LiNO<sub>3</sub>, ionic crystals growing from melts, morphology and kinetics 4-113370  
 LiNO<sub>3</sub>·3H<sub>2</sub>O, deform. electron density, X-ray and neutron diff. data 4-65232  
 LiNa singlet states, reson. two-photon ions. 4-83435  
 Li<sub>0.5</sub>Na<sub>1-x</sub>NbO<sub>3</sub>, piezoelectric ceramics, microstruct., props. and phase relations 4-61629  
 LiNaSO<sub>4</sub>, single cryst., unit cell correl. effects, polarised Raman spectra 4-71374  
 LiNbO<sub>3</sub> 4-97184  
 LiNbO<sub>3</sub>, (YXl)128°, SAW filters, residual bulk mode levels 4-104049  
 LiNbO<sub>3</sub>, acoustoelec. coeffs. meas., appl. to signal processing devices 4-97214  
 LiNbO<sub>3</sub>, amorphous films, dielec. and elec. props. 4-104531  
 LiNbO<sub>3</sub>, anisotropic effects in spectra of surface polaritons and phonons 4-108699  
 LiNbO<sub>3</sub>, anomalous props. near 75°C, Mossbauer study 4-71219  
 LiNbO<sub>3</sub>, ballistic heat pulse propag., effect of piezoelec. 4-76335

- ium compounds continued
- LiNbO<sub>3</sub>, broad-band guided-wave electrooptic modulators 4-97057
- LiNbO<sub>3</sub>, bulk acoustic wave transducers, testing using laser pyroelec. imaging technique 4-86397
- LiNbO<sub>3</sub>, bulk acoustophotorefractive effects 4-93050
- LiNbO<sub>3</sub>, complex elastoelectric effect 4-80629
- LiNbO<sub>3</sub>, congruently grown, temp.-depend. dispersion eqn., three beam parametric mixing appls. 4-88801
- LiNbO<sub>3</sub> cryst. growth, melt composition effect on props. 4-84227
- LiNbO<sub>3</sub> cryst. surface layer props. after low-energy ion bombardment (Chinese) 4-70532
- LiNbO<sub>3</sub> crystal, conoscopic interference pattern and refractive index (Chinese) 4-114239
- LiNbO<sub>3</sub>, crystalline, Nb<sub>2</sub>O<sub>5</sub> precipitates, TEM studies 4-98290
- LiNbO<sub>3</sub> crystals, polariton Raman scatt., temp. gradient effect 4-84574
- LiNbO<sub>3</sub> crystals with polysynthetic domains, SHG enhancement 4-69508
- LiNbO<sub>3</sub> different cuts, photorefractive effect in optical waveguides, holographic grating form. 4-74708
- LiNbO<sub>3</sub> directional coupler modulation with low insertion loss for 1.3  $\mu$ m 4-64765
- LiNbO<sub>3</sub>, elastic, piezoelectric and dielectric props., 78-800K 4-76332
- LiNbO<sub>3</sub>, elec. field effect on polariton Raman spectra 4-104575
- LiNbO<sub>3</sub> electro-optic modulator for diode laser, design and 600 Mbit/s operation (German) 4-79199
- LiNbO<sub>3</sub>, electron irradi., point defects, ESR and IR spectra studies 4-70139
- LiNbO<sub>3</sub> electrooptic cells,  $\gamma$ -irrad. effect on optical inhomogeneity 4-76438
- LiNbO<sub>3</sub>, ferroelec., band struct. and optical props. in fundamental absorption region 4-75845
- LiNbO<sub>3</sub>, gamma irradi., influence on photovoltaic effects 4-84656
- LiNbO<sub>3</sub> grating, annealing effect on surface relief 4-107812
- LiNbO<sub>3</sub> groove grating, bulk radiation by SAW propag. 4-92501
- LiNbO<sub>3</sub> high-speed directional coupler modulators, design 4-64764
- LiNbO<sub>3</sub>, inelastic light scatt. and dielec. anomalies connection 4-84923
- LiNbO<sub>3</sub>, integrated optic Fabry-Perot interferometer for GaAlAs laser wavelength stabilisation 4-91457
- LiNbO<sub>3</sub> intersecting channel waveguides, light switching at an electrooptic mirror 4-79348
- LiNbO<sub>3</sub>, laser irradi., polariton Raman scatt. 4-61715
- LiNbO<sub>3</sub>, laser irradi., photovoltaic effects 4-70868
- LiNbO<sub>3</sub>, leaky SAW propagation study 4-104055
- LiNbO<sub>3</sub>, Li<sup>+</sup> ionic cond., activation energy and IR spectra 4-84453
- LiNbO<sub>3</sub>, magnetron sputtered film, prep., crazing rel. to tensile stress 4-81130
- LiNbO<sub>3</sub> mirror-type optical switch and appls. 4-97043
- LiNbO<sub>3</sub>, Mossbauer diff., separation of elastically and inelastically scatt.  $\gamma$ -radiation 4-98985
- LiNbO<sub>3</sub>, nonlinear acoustic props. and third-order elastic consts. 4-74793
- LiNbO<sub>3</sub> optical waveguide surface, rippled grating coupling efficiency 4-107824
- LiNbO<sub>3</sub> optical-optical guided-wave modulator 4-103004
- LiNbO<sub>3</sub> piezoelec.-gas system, acoustic excitation of EM emission from gas 4-69621
- LiNbO<sub>3</sub>, piezoelectric, X-ray diff. by SAW 4-75232
- LiNbO<sub>3</sub> planar ion implanted optical waveguides, computer simulation 4-69547
- LiNbO<sub>3</sub> planar lightguides, hologram writing 4-79082
- LiNbO<sub>3</sub> planar slab waveguide anal. using hypothetical boundaries (Japanese) 4-60155
- LiNbO<sub>3</sub> planar waveguide prep. with dip coating method and embossing technique, grating coupler fabrication 4-69602
- LiNbO<sub>3</sub>, Raman scatt. isofrequency temp. depend. 4-76474
- LiNbO<sub>3</sub> rotated Y-cuts, SAW and SSBW propag. (Japanese) 4-61199
- LiNbO<sub>3</sub>, shock induced luminescence studies 4-109260
- LiNbO<sub>3</sub>, single crystal, phys. props. 20-200°C 4-76397
- LiNbO<sub>3</sub>, single crystal, near-normal reflectivity and absorpt. spectra 4-93083
- LiNbO<sub>3</sub> single crystal, cathodoluminescence emission, surface damage 4-93115
- LiNbO<sub>3</sub> single crystal, electroluminescence obs. 4-99197
- LiNbO<sub>3</sub>, single-mode integrated-optical polarisers in LiNbO<sub>3</sub> and glass waveguides, low loss 4-112568
- LiNbO<sub>3</sub>, spontaneous polarisation screening on free surface 4-88767
- LiNbO<sub>3</sub>, stimulated Raman scatt. by transverse and longit. lattice vibrs. 4-60115
- YZ-LiNbO<sub>3</sub> substrate 4-104568
- LiNbO<sub>3</sub> substrate for Al and Mo films, elastic const. study 4-104052
- LiNbO<sub>3</sub>, surface and bulk acoustic wave vel. 4-98425
- LiNbO<sub>3</sub>, thermochemically reduced and electron irradi., positron annihilation, optical absorpt. meas. 4-104697
- LiNbO<sub>3</sub>, Ti diffused optical waveguide, effects of lossy thin plasma film 4-107818
- LiNbO<sub>3</sub>, Ti diffused waveguide interferometric modulator (Chinese) 4-112564
- LiNbO<sub>3</sub> type ferroelectrics, dielec. thermal and soft mode behaviour 4-71298
- LiNbO<sub>3</sub> waveguide bistable devices, blocking oscill., theoretical and expt. study (Japanese) 4-87484
- LiNbO<sub>3</sub> waveguide electro-optic prism beam deflector, bistability obs. 4-103005
- LiNbO<sub>3</sub>, waveguide fabrication by proton diffusing from benzoic acid soln. 4-69553
- LiNbO<sub>3</sub> waveguides, proton exchanged, light propagation anal. 4-64768
- LiNbO<sub>3</sub>, weak periodic surface acoustic shock waves 4-61198
- LiNbO<sub>3</sub> wideband electro-optic modulators 4-97056
- LiNbO<sub>3</sub>, Y-Z type, waveguide, nonlinear interaction of SAWs, theoretical and expt. study (Japanese) 4-79359
- LiNbO<sub>3</sub>, Y-cut, SAW generation, simplified Green's function allowing for leaky surface wave 4-92500
- LiNbO<sub>3</sub>, Y-cut, SAW propag. vel., effect of applied elec. field 4-98424
- LiNbO<sub>3</sub>, YZ cut layered cpd., bulk wave energy reflection coeffs. 4-113545
- LiNbO<sub>3</sub>, YZ-cut, SAW diff. compensation 4-97183
- LiNbO<sub>3</sub>, <sup>57</sup>Co, Fe<sup>3+</sup>, electron capture, non-equilibrium population, Mossbauer spectra studies 4-108807
- LiNbO<sub>3</sub>:Cr<sup>3+</sup>(Mn<sup>2+</sup>), axial cryst. field parameters, EPR spectra 4-98579
- LiNbO<sub>3</sub>:Cu holographic refl. gratings, angular and spectral selectivities 4-74692
- lithium compounds continued
- LiNbO<sub>3</sub>:Cu<sup>2+</sup>, EPR and optical absorption spectra, Jahn-Teller effects 4-71166
- LiNbO<sub>3</sub>:Cu<sup>2+</sup>, single crystal, Jahn-Teller effect 4-108825
- LiNbO<sub>3</sub>:Eu<sup>3+</sup>, impurity optical absorpt. 4-66056
- LiNbO<sub>3</sub>:Fe, photocurrent jumps due to domain struct. (Russian) 4-75996
- LiNbO<sub>3</sub>:Fe, polarisation-anisotropic light-induced light scatt. 4-87395
- LiNbO<sub>3</sub>:Fe, Rayleigh scatt., effect of photorefr. 4-80957
- LiNbO<sub>3</sub>:Fe (III) ferroelec., Mossbauer spectra and EPR studies 4-65960
- LiNbO<sub>3</sub>:Fe crystals, photolec. and photorefr. prop. control during growth by elec. current 4-80904
- LiNbO<sub>3</sub>:MgO, increased optical damage resist., holographic diff. meas. of photorefr. 4-69521
- LiNbO<sub>3</sub>:Mn<sup>2+</sup>(Cr<sup>3+</sup>)(Cu<sup>2+</sup>), spin-lattice relax., EPR studies 4-114157
- LiNbO<sub>3</sub>:Ni<sup>2+</sup>, cryst. field splitting of impurity levels 4-65647
- LiNbO<sub>3</sub>:Ti, impurity diffusion as a function of stoichiometry 4-80304
- LiNbO<sub>3</sub>:Ti, indiffused, planar waveguide modes, water vapour effects 4-103008
- LiNbO<sub>3</sub>:Ti, indiffused, optical waveguides, in-plane scattering 4-112565
- LiNbO<sub>3</sub>:Ti based optical waveguide devices 4-69555
- LiNbO<sub>3</sub>:Ti CW modulator for laser beams, 6 Gbit/s modulation rate (German) 4-60081
- LiNbO<sub>3</sub>:Ti channel waveguides and directional couplers, 3-D anal. 4-79286
- LiNbO<sub>3</sub>:Ti channel waveguide low-loss multiple-branching circuit 4-79346
- LiNbO<sub>3</sub>:Ti coupled channel waveguides and  $\Delta\beta$  electrodes for electrooptical modulator 4-74699
- LiNbO<sub>3</sub>:Ti directional coupler based low-crossstalk waveguide polarisation multiplexer/demultiplexer for 1.32  $\mu$ m 4-60183
- LiNbO<sub>3</sub>:Ti directional coupler travelling wave optical modulator, high-speed pulse generation 4-69596
- LiNbO<sub>3</sub>:Ti indiffused channel waveguides, thermal fixing for reduced photorefractive susceptibility 4-91581
- LiNbO<sub>3</sub>:Ti integrated oscillators and multivibrators 4-64795
- LiNbO<sub>3</sub>:Ti integrated acousto-optic bistable device 4-107890
- LiNbO<sub>3</sub>:Ti monomode channel waveguides, optical parametric amplification investigation 4-64741
- LiNbO<sub>3</sub>:Ti planar optical waveguide anal. 4-60150
- LiNbO<sub>3</sub>:Ti planar waveguide based beam splitter and focuser 4-74680
- LiNbO<sub>3</sub>:Ti single-mode planar waveguide end fire coupling to single-mode optical fibre (Chinese) 4-60149
- LiNbO<sub>3</sub>:Ti strip waveguide modulators, polarisation insensitive 4-79281
- LiNbO<sub>3</sub>:Ti stripe waveguide integrated optical freq. translator 4-112562
- LiNbO<sub>3</sub>:Ti travelling wave microwave optical modulator 4-112563
- LiNbO<sub>3</sub>:Ti waveguide Mach-Zehnder modulator, low drive voltage, fibre-optic sensing appl. 4-91575
- LiNbO<sub>3</sub>:Ti waveguide integrated optics processing, uses of EDTA etch soln. 4-112590
- LiNbO<sub>3</sub>:Ti waveguides, nonlinear interactions, SHG experiments 4-64742
- LiNbO<sub>3</sub>:Ti waveguides with low loss, fabrication and performance 4-69554
- LiNbO<sub>3</sub>:Ti X-cut waveguide to fibre coupling, design and characts. for 1.32  $\mu$ m region 4-83725
- LiNbO<sub>3</sub>:Ti(Mg), single crystal, chemical and microscopical studies 4-103777
- LiNbO<sub>3</sub>:Ge, parametric amplification of SAW 4-108697
- LiNbO<sub>3</sub>:Ge multilayer structure, nonlinear self-contraction of acoustoelectronic fluctuations spectrum 4-70877
- LiNbO<sub>3</sub>:ZnO piezoelectric interface, Stoneley wave propagation 4-104059
- LiNbO<sub>3</sub>+Ti waveguide, acousto-optical conversion study 4-107827
- LiNdP<sub>2</sub>O<sub>12</sub>, detuned lasers with injected signals, period-doubling bifurcations 4-74481
- Li<sub>2</sub>NiP<sub>2</sub>S<sub>6</sub>, prep. and structural studies, powder X-ray diff. studies 4-113421
- LiO, dissoc. energy; HF STO calcs. 4-112092
- Li<sub>2</sub>/2-GeO<sub>2</sub> glass, structure, Raman spectra meas. (Japanese) 4-113347
- Li<sub>2</sub>O, activity coeff. of dissolved LiOH, water press.-temp. regime, breeder material 4-107029
- Li<sub>2</sub>O, blanket materials, candidate, for fusion reactor appl. 4-91107
- Li<sub>2</sub>O, bond length-bond strength correlations 4-103693
- Li<sub>2</sub>O breeder blanket material developments 4-107020
- Li<sub>2</sub>O breeder blanket pellet, water vapour adsorption in He sweep gas stream 4-107032
- Li<sub>2</sub>O breeder material, neutron irradi., T release expts. 4-107030
- Li<sub>2</sub>O breeder material, neutron irradi. behaviour and compatibility testing 4-107031
- Li<sub>2</sub>O breeder materials, fast neutron irradi. expts. 4-107024
- Li<sub>2</sub>O fusion reactor breeder, chem. compatibility with transition metals 4-107060
- Li<sub>2</sub>O, optical mode frequencies, IR reflectivity, Raman spectra 4-104617
- Li<sub>2</sub>O pellet, T recovery, assay techniques 4-107022
- Li<sub>2</sub>O pellet breeder materials, Li<sub>2</sub>T recovery expt. 4-107026
- Li<sub>2</sub>O single crystal, breeder material, D<sub>2</sub> solubility 4-107025
- Li<sub>2</sub>O slab assemblies, angle depend. neutron spectra by time-of-flight method 4-74047
- Li<sub>2</sub>O, thermal neutron irradi. effects, lattice parameter and expansion changes, F<sup>+</sup>-centres 4-107028
- Li<sub>2</sub>O, vapourisation, effect of H<sub>2</sub>O vapour in the carrier gas 4-75650
- Li<sub>2</sub>O-5SiO<sub>2</sub> glass, vibr. spectra 4-109179
- Li<sub>2</sub>O-(LiCl)<sub>2</sub>-B<sub>2</sub>O<sub>3</sub>-Al<sub>2</sub>O<sub>3</sub> system, Raman spectra of glasses (Chinese) 4-93065
- Li<sub>2</sub>O-Al<sub>2</sub>O<sub>3</sub>-B<sub>2</sub>O<sub>3</sub> glass, form. and transition temp. 4-113634
- Li<sub>2</sub>O-Al<sub>2</sub>O<sub>3</sub>-SiO<sub>2</sub>, structural features, for gradient optical elements 4-79947
- Li<sub>2</sub>O-Al<sub>2</sub>O<sub>3</sub>-SiO<sub>2</sub> glass ceramic, effective radiative thermal cond./diffusivity, role of view factor 4-84473
- Li<sub>2</sub>O-Al<sub>2</sub>O<sub>3</sub>-SiO<sub>2</sub> glasses, Young's modulus, effect of vol. and struct. 4-85170
- Li<sub>2</sub>O-Al<sub>2</sub>O<sub>3</sub>-SiO<sub>2</sub> glass-ceramic, superplastic ductility, rel. to hydrostatic press. and humidity 4-109474
- Li<sub>2</sub>O-B<sub>2</sub>O<sub>3</sub> glass, ionic cond. meas. 4-84457
- Li<sub>2</sub>O-B<sub>2</sub>O<sub>3</sub>-Fe<sub>2</sub>O<sub>3</sub> system, magnetic vitrocramics, prep. and props. 4-93256
- Li<sub>2</sub>O-B<sub>2</sub>O<sub>3</sub>-SiO<sub>2</sub>, phase-separated glass, dissoln. rate, influence of pH 4-84403
- Li<sub>2</sub>O-B<sub>2</sub>O<sub>3</sub>-SiO<sub>2</sub> glass, OH extinction coeff. determ., IR spectra 4-84958
- Li<sub>2</sub>O-LiF-B<sub>2</sub>O<sub>3</sub> glasses, fast ionic cond., role of F in struct., Raman spectra 4-98025

## lithium compounds continued

- Li<sub>2</sub>O-LiNbO<sub>3</sub>-B<sub>2</sub>O<sub>3</sub>, new solid electrolyte glass material, electrical conductivity 4-108649
- Li<sub>2</sub>O-M<sub>2</sub>O<sub>3</sub>-M<sub>2</sub>O<sub>4</sub>, M=Nb, Ta, M'=Ti, Zr, non-stoichiometric phases, cryst. chem. and ferroelec. props. 4-65968
- $\beta$ -Li<sub>2</sub>O-Na<sub>2</sub>O-Al<sub>2</sub>O<sub>3</sub>, water absorpt., TG, DSC and X-ray meas. 4-113794
- Li<sub>2</sub>O-Nb<sub>2</sub>O<sub>5</sub>, amorphous dielectrics, crystallisation, elastic and dielec. props. 4-104518
- Li<sub>2</sub>O-Nd<sub>2</sub>O<sub>3</sub>-GeO<sub>2</sub>(SiO<sub>2</sub>) ternary systems, subsolidus phase equilib. and fluorescence activity 4-113596
- Li<sub>2</sub>O-SiO<sub>2</sub> glass and glass-ceramic, hydrothermal corrosion 4-85235
- Li<sub>2</sub>O-SiO<sub>2</sub> glass ceramic systems, density, crystallisation, elec. cond. 4-113937
- Li<sub>2</sub>O-SiO<sub>2</sub> glasses, struct., <sup>29</sup>Si NMR studies 4-98964
- Li<sub>2</sub>O-SiO<sub>2</sub> system, glass forming regions rel. to cooling rate, liquidus viscosity obs. (Japanese) 4-75680
- Li<sub>2</sub>O<sub>3</sub>-ZnO, ceramics system, ionic and mixed cond. rel. to comp. and humidity 4-98339
- LiOH, conc. aq. solns., heat capacities, vols., expansibilities and compressibilities 4-103954
- LiOH, dissoc. energy calc., HF and GTO methods 4-64347
- LiOH dissolved in Li<sub>2</sub>O, activity coeff., water press.-temp. regime 4-107029
- Li<sub>3</sub>P<sub>7</sub>, cryst. struct. and plastic phases 4-80018
- LiPn<sub>2</sub>, crystal structure 4-70114
- LiPO<sub>3</sub>-LiCl glass, ionic cond. meas. 4-84457
- LiPO<sub>3</sub>-Sm(PO<sub>3</sub>)<sub>3</sub>, solid-liq. equilib., DTA and X-ray studies 4-98249
- LiPrP<sub>2</sub>O<sub>12</sub>, absorption and fluoresc. intensity anal. of Pr<sup>3+</sup> 4-104654
- Li<sub>2</sub>S-P<sub>2</sub>S<sub>5</sub> glass, ionic cond. meas. 4-84457
- LiSM(PO<sub>3</sub>)<sub>4</sub>, cryst. struct. and IR spectra 4-98249
- Li<sub>2</sub>SO<sub>4</sub>, superionic cond. phase, neutron struct. factor, simulations 4-98068
- Li<sub>2</sub>SO<sub>4</sub>-Ag<sub>2</sub>SO<sub>4</sub>, ionic cond. meas. 4-88342
- Li<sub>2</sub>SO<sub>4</sub>-K<sub>2</sub>SO<sub>4</sub>, ionic cond. meas. 4-88342
- Li<sub>2</sub>SO<sub>4</sub>-MgSO<sub>4</sub>, ionic cond. meas. 4-88342
- Li<sub>2</sub>SO<sub>4</sub>-Na<sub>2</sub>SO<sub>4</sub>, ionic cond. meas. 4-88342
- Li<sub>2</sub>SO<sub>4</sub>-ZnSO<sub>4</sub>, ionic cond. meas. 4-88342
- Li<sub>2</sub>SeO<sub>4</sub>, cryst. struct., X-ray diff. 4-88153
- Li<sub>2</sub>SiO<sub>3</sub>, coloration of irradiated samples, during isothermal annealing (Russian) 4-98100
- Li<sub>2</sub>SiO<sub>3</sub>, polycrystalline, elec. cond., AC meas. 4-108645
- Li<sub>2</sub>SiO<sub>3</sub>, glass ceramics, grain oriented, hydrostatic piezoelec. props. and appls. 4-84913
- Li<sub>2</sub>SiO<sub>3</sub>-Li<sub>2</sub>SO<sub>4</sub> glass, ionic cond. meas. 4-84457
- Li<sub>2</sub>SiO<sub>4</sub> breeder blanket material developments 4-107020
- Li<sub>2</sub>SiO<sub>4</sub> breeder materials, fast neutron irradiation expts. 4-107024
- Li<sub>2</sub>SiO<sub>4</sub>-Li<sub>2</sub>VO<sub>4</sub> solid solns., Li<sup>+</sup> ion conductivity 4-108647
- Li<sub>3</sub>Si<sub>2</sub>Y<sub>1-x</sub>O<sub>4</sub> solid electrolytes, ion trapping and conductivity 4-108648
- LiTaO<sub>3</sub>, acoustoelec. coeffs. meas., appl. to signal processing devices 4-97214
- LiTaO<sub>3</sub>, complex elastoelectric effect 4-80629
- LiTaO<sub>3</sub> crystal, extraordinary phonons, Raman spectra and directional dispersion 4-104582
- LiTaO<sub>3</sub> crystals, polling using interdigital electrodes, appl. to bulk wave transducers 4-99068
- LiTaO<sub>3</sub>, degenerate four-wave parametric light scatt. (Russian) 4-88851
- LiTaO<sub>3</sub>, electro-optic shock radiation in nonlinear optical media 4-112498
- LiTaO<sub>3</sub>, ferroelec., band struct. and optical props. in fundamental absorption region 4-75845
- LiTaO<sub>3</sub>, ferroelec. crystal, electrostatic pot. at surface 4-76350
- LiTaO<sub>3</sub>, leaky SAW propagation study 4-104055
- LiTaO<sub>3</sub>, Raman scatt. isofrequency temp. depend. 4-76474
- LiTaO<sub>3</sub>, reduced photoelec. props., spectral and temp. depend. 4-84657
- LiTaO<sub>3</sub>, single cryst., near-normal reflectivity and absorpt. spectra 4-93083
- LiTaO<sub>3</sub>, sintering with the aid of MnO 4-61901
- LiTaO<sub>3</sub>, stimulated Raman scatt. by transverse and longit. lattice vibrs. 4-60115
- LiTaO<sub>3</sub>, temp. compensated bulk shear microwave resonators 4-112647
- LiTaO<sub>3</sub>, waveguide fabrication by proton diffusion from benzoic acid soln. 4-69553
- LiTaO<sub>3</sub>:<sup>57</sup>Co, Fe<sup>3+</sup> electron capture, non-equilibrium population, Mossbauer spectra studies 4-108807
- LiTaO<sub>3</sub>:Ag waveguide based electro-optic Bragg modulator with apodised electrode struct. 4-74700
- LiTaO<sub>3</sub>:Fe, photorefractive, photovoltaic effect, photocond., depend. on light intensity (Russian) 4-114226
- LiTaO<sub>3</sub>:Nb waveguides and light modulators using guided-to-radiation mode coupling (Japanese) 4-60143
- LiTaO<sub>3</sub>:Ti, changes in refractive index due to diffusion 4-99085
- LiTaO<sub>3</sub>-ZnO piezoelectric interface, Stoneley wave propagation 4-104059
- Li<sub>2</sub>TaO<sub>6</sub> substituted phases, Li ionic cond. meas. 4-92415
- LiTa<sub>2</sub> intercalation cpds., (1T,4Hb), elec. resist. meas., metallic and supercond. states 4-84726
- Li<sub>2</sub>ThF<sub>6</sub>, ionic transport props., AC cond. and pulsed NMR study 4-70453
- LiTiO<sub>3</sub> ferroelec. cryst., photogalvanic effect anisotropy 4-75995
- LiTi<sub>2</sub>O<sub>4</sub>, cryst. struct., neutron diff. powder profile anal. 4-88151
- Li<sub>2</sub>TiO<sub>3</sub>, cryst. struct., neutron diff. powder profile anal. 4-88151
- Li<sub>1-x</sub>Ti<sub>2-x</sub>O<sub>4</sub> ceramics, elec. and supercond. props. 4-104342
- Li<sub>1-x</sub>Ti<sub>2-x</sub>O<sub>4</sub>, semicond. props., elec. cond., thermopower meas. 4-108858
- Li<sub>2</sub>TiO<sub>4</sub>, cryst. struct., neutron diff. powder profile anal. 4-88151
- Li<sub>2</sub>TiS<sub>2</sub>, intercalation study by TEM 4-103953
- Li<sub>1-x</sub>V<sub>2-x</sub>O<sub>8</sub> solid soln. cathodes for secondary Li batteries 4-109736
- $\beta$ -Li<sub>1-x</sub>V<sub>2-x</sub>O<sub>8</sub>, bipolaron ordering, X-ray scatt. study 4-80519
- Li<sub>1-x</sub>V<sub>2-x</sub>O<sub>8</sub>, intercalation study by TEM 4-103953
- Li<sub>2</sub>WO<sub>3</sub> amorphous film, electrochromism colouring/bleaching processes, Li<sup>+</sup> ion transport 4-114244
- Li(Y,Eu)F<sub>4</sub>:Tm<sup>3+</sup>, lasing channels, stimulated emission 4-112444
- Li(Y,Lu)F<sub>4</sub>:Tm<sup>3+</sup>, lasing channels, stimulated emission 4-112444
- LiYF<sub>4</sub>, crystal growth, thermocapillary effects 4-65206
- LiYF<sub>4</sub>:Er,Pr crystal quasi-continuous lasing at 0.85  $\mu$ m 4-60049
- LiYF<sub>4</sub>:Nd<sup>3+</sup>, electronic Raman scatt. and two-photon fluorescence (Chinese) 4-104581
- LiYF<sub>4</sub>:Pr<sup>3+</sup>, crystal-field energy levels, splitting chain calc. (Chinese) 4-113908
- LiYF<sub>4</sub>:Pr<sup>3+</sup>, visible lasing on five intermultiplet transitions 4-74519
- LiYF<sub>4</sub>:Tm, Ho, Er, laser emission parameters 4-79158

## lithium compounds continued

- Li<sub>0.5-1.0</sub>Zn<sub>0.5-1.0</sub>Fe<sub>2.5-2.0</sub>O<sub>4</sub> ferrites, Curie temp. and mag. moments 4-109013
- Li<sub>1/2</sub>Zn(GeO<sub>4</sub>), thin films, for solid state batteries, preparation and characteristics 4-93224
- Li<sub>16-22</sub>Zn<sub>2</sub>(GeO<sub>4</sub>)<sub>4</sub>, LISICON, solid electrolytes, prep. props. and appl. 4-103998
- Li<sub>16-22</sub>Zn<sub>2</sub>(GeO<sub>4</sub>)<sub>4</sub>, LISICON ceramic, synthesis and elec. props. 4-75728
- Li<sub>12-22</sub>Zn<sub>12</sub>(GeO<sub>4</sub>)<sub>4</sub>, solid electrolytes, ion trapping and conductivity 4-108648
- Li<sub>2</sub>ZrO<sub>3</sub> breeder materials, fast neutron irradiation expts. 4-107024
- Li<sub>2</sub>ZrO<sub>3</sub> breeder blanket material developments 4-107020
- Li<sub>0.8</sub>Zr<sub>0.2</sub>Ta<sub>0.2</sub>(PO<sub>4</sub>)<sub>3</sub>, NASICON superionic conductor thick films 4-80288
- Li<sub>2</sub>ZrX<sub>2</sub> (X=S, Se) intercalates, phase transitions, mag. studies 4-70657
- LiF, EELS in band gap region 4-99254
- (Mg<sub>(x-12/35)</sub>Ca<sub>(4/35)</sub>Si<sub>(x-4/3)</sub>O<sub>8</sub>), enstatite-IV series, superstruct., cryst. struct. study and twinning 4-65229
- Na<sub>3-x</sub>Li<sub>1-x</sub>W<sub>3</sub>O<sub>9</sub>F<sub>3</sub>, Bridgman-Stockbarger growth, ferroelec. and ferroelastic props., permittivity, birefr. meas. 4-65969
- RbLiMoO<sub>4</sub>, cryst. struct. determ. and phase transition 4-79999
- Ti:LiNbO<sub>3</sub> strip-waveguides, electrically induced, electrooptic effect 4-64767
- Ti:LiNbO<sub>3</sub> travelling-wave optical modulator for  $\lambda=1.32 \mu$ m 4-69595
- Ti<sub>1-x</sub>Li<sub>x</sub>M<sub>3</sub>O<sub>6</sub> (M=Nb, Ta, Sb) rutile solid solns., X-ray characterisation 4-84274

## lithography

- see also electron beam lithography; ion beam lithography; photolithography
- micrometrology, conference, Germany (2-3 November 1983) 4-90299
- VLSI technology, textbook 4-82610

## lithospace see Earth crust

## lithosphere see Earth crust

## liver

- alcohol dehydrogenase, horse liver, CoII substituted, complexes, active sites PMR study 4-102836
- animal, consumed by man, fallout nuclides conc. 4-62610
- artificial organs and their materials, review (Japanese) 4-89831
- cells of intact and regenerating rat liver, genome mutations yield after  $\gamma$ -irrad. (Russian) 4-67002
- hepatoma cells, cultured, thermotolerance obs. 4-66913
- hepatoma cells, morphological response and survival during fractionated hyperthermia 4-93706
- hepatomas, rat, tumour-cord parameters 4-89657
- imaging techniques comparison for abdominal, pelvic and thyroid disease 4-115215
- liver, medical diagnostic appl. of Oxford scanning proton microprobe 4-105332
- lymphatic system, roentgenoradiation study (Russian) 4-89686
- mitochondrial membranes of heterothermic bat in summer and winter, thermal response 4-105190
- neutron activation and PIXE anal. 4-100380
- normal and diffuse disease, ultrasound attenuation 4-105301
- pig tissue, <sup>23</sup>Na NMR study 4-100081
- PIXE anal., target prep. influence in rate organs 4-100381
- plasma membranes, rat liver, radiation effects, IR spectroscopy obs. (Russian) 4-77321
- radioisotope liver images, digitised, automatic analysis of diagnostic features 4-115216
- rat liver, cryoprotected, cryosectioning 4-85598
- scintigraphic estimation of arterial and portal blood supplies, online computer system 4-72385
- segmental assessment on ordinary scintigrams and SPECT images 4-81763
- single photon emission CT for estimates of liver and spleen vol. 4-81772
- tissue, frequency-dependent US attenuation coeff. meas. 4-100238
- tissue, global element composition comparison with different cell fractions composition PIXE study 4-105391
- tissue characterisation by US scattering 4-83746
- tumours in dog liver, development at later times following long-term  $\gamma$ -irrad. (Russian) 4-77329
- US attenuation in tissue, frequency dependent, echographic A-lines, time-freq. representation 4-100241
- valyl-tRNA synthetases isolated from chick embryo and brain, difference in radiosensitivity 4-66873
- volume measurement by single photon emission CT 4-93859
- HTO ingestion, effects on mice, hexokinase isozymes in brain, liver and spleen 4-100259
- <sup>239</sup>Pu, A=239, 240, body burden in Lapps, comparison with southern Finns 4-62590
- <sup>239</sup>Pu injected intramuscularly in complexon therapy conditions, behaviour and biological effect (Russian) 4-67015

## livestock see farming

## living systems

- see also biocybernetics; brain models; extraterrestrial life; physiological models
- mechanical stresses as a factor in morphogenesis 4-81606
- mortality, rel. to temporary order amid chaos 4-73370

## LMC see Large Magellanic Cloud

## LME see liquid metal embrittlement

## load (electric)

- see also load regulation
- American Power Conference, Chicago, USA (April 1983) 4-86112
- linearity increase of load cell (Chinese) 4-99953
- residential solar/electric water heater simulation model development and evaluation 4-72050
- Pb/acid batteries, future outlook in Japan 4-62340

## load control see load regulation

## load regulation

- advanced molten carbonate and solid oxide fuel cells for utility load levelling appls. 4-72104
- Na-S battery development and appl., Ford Aerospace program, USA 4-66685
- Pb-acid advanced batteries for utility load levelling appls., performance testing and evaluation 4-72093
- Zn<sub>2</sub>F(CN)<sub>2</sub>-Zn<sub>2</sub>Fe(CN)<sub>4</sub> battery system for utility load levelling and solar photovoltaic/wind appls. 4-72055

lobes (distribution) see antenna radiation patterns

local area networks see communication networks; computer networks

### local moments in dilute systems

- asymmetric single orbital Anderson model, localized magnetic moments, full rotational invariance 4-98856
- local distortion correlation influence on mag. props. of Jahn-Teller centre pair 4-88646
- localised moments, magnetisation, temp. and field depend. 4-76193
- nonmagnetic metal with mag. impurity, density of states, sp. ht., tridiagonalisation 4-92665
- $\text{Al}(\text{NO}_3)_3$ : $\text{Cr}^{3+}$ , exchange-coupled  $\text{Cr}^{3+}$ - $\text{Cr}^{3+}$  pairs, EPR obs. 4-88717
- AuFe alloys, spin glass freezing, PAC study 4-71216
- AuFe, dilute alloy spin glass, susceptibility, neutron scatt. and muon spin rot. 4-71249
- Ce systems, valence fluctuation dynamics, appl. of self consistent perturbation theory 4-70743
- CuMn (1.1 at.%), spin glass, static and dynamic effects, muon spin relax. 4-71250
- CuMn, dilute alloy spin glass, susceptibility, neutron scatt. and muon spin rot. 4-71249
- $\text{La}_{100-x}\text{Al}_x$ , amorphous, supercond., thermodynamic and transport props. 4-70986
- $\text{LaCoO}_3$ , spin-state transitions at low temp., near-neighbour impurity effect 4-88643
- $\text{La}_2\text{CuO}_4$ , with  $\text{K}_2\text{NiF}_6$  struct., at displacements, mag. and transport props., anisotropic bonding effects 4-75358
- $\text{La}_2\text{NiO}_4$ , with  $\text{K}_2\text{NiF}_6$  struct., at displacements, mag. and transport props., anisotropic bonding effects 4-75358
- Mn-Zr amorphous alloys, local Mn moment 4-114091

local networks see communication networks; computer networks

### localised electron states

- see also Anderson model; charge-ordered states; charge transfer states; Wigner crystal
- adsorbed atoms and molcs., adsorbed, core-level binding energy shift anal. 4-61217
- alloy, Auger spectra, core-valence-valence, CPA theory, disorder-induced vertex corrections role 4-71491
- alloys, chem. bonding and heat of form., core level shift calorimetry method 4-104714
- amorphous semiconductor, dispersive transport, multiple trapping model, effect of energy depend. capture cross section 4-70830
- amorphous semiconductors, electron states, multielectron effects 4-98510
- amorphous semiconductors, electronic states, transitions from localised states, rel. to density of states meas. 4-84547
- amorphous semiconductors, transient photocond., effect of repeated carrier trapping 4-61420
- amorphous solids, physics, book 4-90312
- bipolarons in disordered media 4-70680
- core level angle-resolved photoemission extended fine structure 4-93186
- crystals, inhomogeneous electron damping and electron states 4-70615
- density of localised states in long range correl. pot. 4-98571
- diamond, one-electron excitations, exchange-correlation pot. 4-84579
- dielectrics, conduction and breakdown phenomena, role of electrodes 4-108869
- disordered solid, localisation in Lloyd model 4-61338
- disordered systems, 3-D, exponential band tails and localisation 4-113900
- disordered systems, electron-electron interaction in a self-consistent localization theory 4-92673
- disordered systems, hopping cond. and weak localisation in strong elec. field 4-75976
- disordered systems, localised states as bound states in pot. wells 4-113904
- disordered systems, struct. of wavefunction in mag. fields 4-70732
- disordered systems, weak localisation and Coulomb interaction 4-104162
- disordered systems with periodic lattice distortion, electronic structure 4-70733
- dynamic quantum Hall effect in 2-d electron impurity system 4-113975
- electron glass, electronic props. theory 4-70736
- epoxy resin, two-level states, effect on thermal cond. and sp. ht. 4-70488
- extended-state band levitation in strong mag. field 4-84846
- ferroelectric semicond., photoferroelectric phenomena caused by fluctuations and phasons 4-66009
- ferromagnetic slab, power spectra and localised retarded modes 4-80736
- glass, spontaneous two-pulse elec. echo decay 4-70329
- heavy metal azides, radiation physics and radiolytic particle form. (Russian) 4-99815
- incommensurate d-dimensional struct., localisation theory 4-70700
- infinite cluster, percolation, mass fluctuations meas. 4-82759
- localisation with phase correlations and the effect of periodic cycles 4-70735
- metallic glasses, elec. resist. and sp. ht. due to interaction of cond. electrons with two-level systems 4-92689
- metallic glasses, phonon absorpt. due to two-level systems 4-70327
- metallic glasses, quasielastic electron scatt. by two-level systems 4-92688
- metallic layered structs., electron localisation models 4-98701
- metallic long wires, quantum particle kinetics, cond. and localisation 4-92669
- metallic phase, localised and extended electronic states, coexistence 4-104169
- metallic thin films, electron-electron interaction, weak localisation and magnetoconductance 4-114048
- metallic thin films, weak localisation and magnetoconductivity 4-98784
- mixed valence  $d^1$ - $d^2$  clusters, vibronic reduction effects 4-88490
- naphthalene cryst., excitons, defects and intramolecular phonon interactions (Russian) 4-98532
- nonmetallic crystals, optically stimulated electron jumps between local electron centres 4-65641
- one-dimensional system, localisation in limit of strong random pots. 4-70702
- one-dimensional system with incommensurate modulation of hopping integrals, electron localisation 4-70703
- organic materials, soft X-ray spectroscopy 4-95584
- organic molecular crystals, excitonic processes (Russian) 4-98531
- organic polyiodide chain complexes, elec. conduction, press. depend. 4-75962
- organic solids, photogenerated charge relaxation and localisation 4-98550
- polarised X-ray emission spectra, appl. to single crystals, review 4-99233
- quasi-one-dimensional metal, mutual influence of phase transitions, scatt. and localisation of electrons 4-70796
- random systems, exponential band tails 4-104167

### localised electron states continued

- rare earth compounds, photoemission, intershell coupling phenomena 4-93181
- rare earth metals, core level resonances monitored by EELS 4-93156
- rare earth metals, photoemission, intershell coupling phenomena 4-93181
- rare gas crystals, local optical centres and exciton states 4-98561
- rough interface between media, local EM oscils. 4-70899
- self-consistent theory of localisation 4-98501
- semiconductor, amorphous, electron transport, Mott-CFO model anal. 4-113939
- semiconductor crystallites, electron-electron and electron-hole interactions, size depend. of excited electronic state 4-70660
- semiconductor interfaces, dispersion and instability of localised polaritons 4-80511
- semiconductor superlattices, disordered, electronic props. and phonon states 4-84682
- semiconductor superlattices, electronic state localisation, theory 4-88566
- semiconductors, diamond-like, Frenkel exciton self-localisation 4-61295
- semiconductors, disordered, spatially extended quasiparticles, disorder effects 4-98499
- semiconductors, disordered organic and inorganic, non-equilibrium diffusive transport 4-70801
- semiconductors, positive magnetoresistance in the variable-range hopping region 4-65695
- semiconductors, tetrahedral, core electron binding energy, tight-binding theory anal. 4-108800
- size quantised systems with rough boundaries, electron states, cond. 4-75914
- space groups, band representations, localised orbitals in crystals 4-88124
- surface enhanced Raman scatt., adatom model, review 4-66037
- topologically disordered systems, localisation, self consistent theory 4-92672
- transition metal alloy, second-order perturbation treatment of correls. and disorder 4-70645
- transition metal compounds, photoemission, intershell coupling phenomena 4-93181
- transition metal cpds., XPS study of core level splitting 4-109303
- transition metal dichalcogenides, zone-axis patterns for HEED rel. to cryst. pot. 4-103615
- transition metal monoxides 4-70699
- transition metals, core electron binding energies determ. by XPS, AEAPS and EELS 4-85081
- transition metals, photoemission, intershell coupling phenomena 4-93181
- transition metals and their cpds., electronic struct. and muon hyperfine field calcs. 4-65643
- triplet electron spins, dipolar-induced dephasing 4-108778
- two-dimensional strip, quantized Hall cond. and edge states 4-92591
- two-dimensional systems, electronic props., conf., Oxford, England (Sept. 1983) 4-95050
- weak localisation in thin films, review 4-92829
- weakly localised regime, higher order interaction effects, case of repulsive force 4-75908
- wires, localisation in 1-D 4-88487
- Ag (110), CO adsorbed layer, photoemission screening effects 4-66189
- Ag epitaxial films on Ge (001), superconductivity and electron localisation 4-114062
- Al, metallic granular, three-dimensional, magnetoresist., localisation and electron-interaction contribs. 4-113923
- Al-SiO<sub>2</sub>-Si MIS structures, with plasma deposited SiO<sub>2</sub>, alkali ion motion, C-V charact. (Russian) 4-114042
- Am, localisation of 5f electrons, XPS study 4-70892
- As<sub>2</sub>Se<sub>3</sub>Te<sub>x</sub> glasses, DC props., neutron and gamma-ray effects 4-103814
- Be, 1s binding energy, core levels, state-specific many-electron theory 4-75887
- Bi discontinuous thin film, electron localisation and conductivity (Russian) 4-98780
- CaO, triplet electron spins, dipolar-induced dephasing 4-108778
- Cd-Mg, local electron density of states, Van Hove singularities,  $\mu^+$  Knight shift 4-84887
- CdBr<sub>2</sub>·2, absorpt. spectra and electron localisation (Russian) 4-104161
- CdS amorphous films, optical absorption coeff. and gap state density 4-66088
- Ce alloys, transition to nonmagnetic f states, bremsstrahlung isochromat spectra studies 4-113884
- Co<sub>2</sub>, localised and extended f-symmetry states 4-92648
- CoO, band or Mott insulators and magnetism 4-70699
- CoSi<sub>3</sub> single cryst. films,  $^1\text{H}$  irradi., elec. cond. studies 4-98782
- Cr, valence band and 2p core lines, XPS obs. 4-99278
- Cr/SiO<sub>2</sub> thin films, elec. transport props. 4-92830
- Cu (100), 2p core-level binding energy shifts, XPS 4-76016
- Cu clusters on graphite, valence bands and core levels, XPS, Auger and EELS studies 4-113860
- Cu, one-electron states, dispersion and lifetime calcs. 4-70701
- Cu-Pb thin proximity layers, electron localisation and superconductivity 4-76083
- $\text{EuAl}_3(\text{BO}_3)_4$ , UV absorpt., luminesc., circular dichroism spectra, gyrotropic charact. 4-114301
- $\text{Eu}_2\text{Sr}_{1-x}\text{S}$  spin glass, cryst., phonon scatt. by mag. two-level systems 4-71106
- Fe, BCC, local densities of states, work-functions and surface stabilities 4-88443
- Fe, electronic struct., XPS studies 4-75838
- $\text{Fe}_{1-x}\text{B}_x$  amorphous alloys, electronic struct., XPS studies 4-75838
- $\text{FeF}_3$  granular thin films, localised electronic state spatial distrib., polarisation study 4-104334
- $\text{FeO}$ , band or Mott insulators and magnetism 4-70699
- GaAs doping superlattices, weak localisation and magnetoresist. 4-98720
- GaAs, optical spin orientation of  $I^{15}$  conduction band electrons, photoemission study 4-66188
- GaAs/AlGa<sub>1-x</sub>As heterostructures, 2D electron localisation 4-98718
- GaSb:Se, quantum localisation of electrons in metal-insulator transition region 4-70654
- Gd, d-f exchange reson. and j polaron 4-75874
- a-Ge, localised impurity states 4-104163
- n-Ge:As, conductivity and magnetoresistance, effect of localised states 4-113950
- Ge-Sn(Sb)(Al) amorphous thin films, hopping cond. meas., 130 to 300K, localised state variations 4-92713
- He, liq., localised electron energy spectrum, surface thermal fluctuations effect 4-70499

**localised electron states continued**

- InP, localisation of inversion electrons, Fourier transform spectra studies 4-98555  
 La alloys, transition to nonmagnetic f states, bremsstrahlung isochromat spectra studies 4-113884  
 Li phonon effects, core-level spectra 4-84581  
 $\text{LiNbO}_3$ ,  $^{57}\text{Co}$ ,  $\text{Fe}^{3+}$ , electron capture, non-equilibrium population, Mossbauer spectra studies 4-108807  
 $\text{LiTaO}_3$ ,  $^{57}\text{Co}$ ,  $\text{Fe}^{3+}$ , electron capture, non-equilibrium population, Mossbauer spectra studies 4-108807  
 Mg, atom-metal XPS and Auger shifts, excited atom model using  $\Delta\text{SCF}$  HF calcs. 4-93191  
 Mg cylindrical film, resist. oscils. and electron localisation 4-80568  
 Mg honeycomb network, mag. flux quantisation in weak localisation regime 4-104184  
 $\text{MnO}$ , band or Mott insulators and magnetism 4-70699  
 Mo, BCC, local densities of states, work functions and surface stabilities 4-88443  
 $\text{MoS}_2$ , electronic struct. and angle depend. X-ray S K-emission bands 4-98521  
 Na phonon effects, core-level spectra 4-84581  
 Ni particles metallic or insulating matrices, electron distrib. localisation 4-92647  
 $\text{NiO}$ , band or Mott insulators and magnetism 4-70699  
 $\text{NiSi}_2$ , single cryst. films,  $^4\text{He}$  irradi., elec. cond. studies 4-98782  
 $\text{Ni}_2\text{Si}$ ,  $x=3, 2.5, 2, 1.5, 1, 0.5$ , valence band reson. photoelectron spectra 4-88940  
 $\text{Np}^{4+}$ , Stevens factors calc. in intermediate coupling scheme 4-80553  
 P, black, reson. photoemission theory 4-85088  
 Pb, discontinuous thin films, mass fluctuations meas. 4-82759  
 $\text{Pb}_{1-x}\text{Sn}_x$ , Te, defect states, impurity photoconductivity transient studies 4-80545  
 Pd/ $\text{PdSi}$  ultrathin film system, magnetoresist. and spin-orbit scatt. 4-98783  
 $\text{PdH}_x$ , X-ray photoemission study of electronic struct. 4-84561  
 a-Si, AC field effect and density of gap states 4-92670  
 a-Si alloys, photocond., dark Fermi level position depend. 4-113987  
 Si, amorphous CVD films,  $\text{H}_2$  plasma annealing localized state density 4-61337  
 a-Si, electronic and vibr. props., book 4-67878  
 a-Si films, localised density of states, electrophotography studies 4-113844  
 Si inversion layer, 2D, weak localisation and interaction effects 4-98766  
 Si inversion layers, submicron width, quasi 1D effects 4-98765  
 a-Si, ion implantation form. and optical state characterisation 4-88186  
 a-Si, localised electron state spectroscopy 4-70741  
 Si, one-electron excitations, exchange-correlation pot. 4-84579  
 Si, oxidised surface, localised electronic states 4-88553  
 a-Si-H, B, P, electron structure and density of states of B-P pairs, cluster calc. 4-65642  
 a-Si-H, conductivity, localisation and mobility edge 4-70819  
 Si-H, electron localisation-delocalisation transitions and  $\text{H}^+$ -like states 4-92668  
 a-Si-H, extended state mobility 4-104208  
 a-Si-H, non-substitutional dopant states and carrier density statistics 4-113902  
 a-Si-H(O,N) alloys, electron trapping states, tight binding formalism calcs. 4-113901  
 a-Si-H,P(B), ESR and optical props., thickness depend. 4-84853  
 a-Si-H Schottky diodes and nin devices, single and double carrier injection 4-114015  
 a-Si-H sputtered films, steady-state photocond. and recombination processes 4-108902  
 Si-H wide optical gap binary alloy films, elec. props. 4-113956  
 a-Si-based field effect transistors, flat-band volt. and surface states 4-92825  
 a-Si, $\text{C}_{1-x}\text{H}_x$ , luminescence from photo-generated carriers, polarisation memory 4-99186  
 $\text{Si}_{1-x}\text{Ge}_x$ , H, amorphous, occupied gap state obs. 4-70637  
 $\text{SiNi}_x$ , H, amorphous, localised states at conduction band edge 4-104168  
 $\text{SiO}_2$ , amorphous, local electronic density of states, influence of Si-Si bonds 4-92671  
 $\text{SiO}_2$ , charge neutralisation by electron bombardment 4-98694  
 $\text{SiO}_2$  glass, radiation induced charges 4-70217  
 $\text{SiO}_2$  glass, rotary phonon echoes 4-70328  
 $\text{SnS}_2$ , electronic struct. and angle depend. X-ray S K-emission bands 4-98521  
 $\text{Ta}_{0.93}\text{Ti}_{0.07}\text{S}_2$  1T polytype, sp. ht. in Anderson localised states 4-75703  
 Ti cpds., electronic relax. effects, X-ray absorpt. 4-66114  
 $\text{U}^{4+}$ , Stevens factors calc. in intermediate coupling scheme 4-80553  
 W, BCC, local densities of states; work functions and surface stabilities 4-88443  
 $\text{Y}_{3-x}\text{Gd}_x\text{Fe}_2\text{O}_{12}$  noncrystalline garnet films, electron transport and thermopower 4-108958  
 Zr-Cu, amorphous, sputtered; low-energy excitations, thermal cond., sp. ht. meas. 4-70987  
 $\text{Zr}_x\text{Cu}_{1-x}$  metallic glass, sp. ht., thermal cond. props. after structural relax. 4-70406  
 $(\text{ZrF}_4)_{57.5}(\text{BaF}_2)_{33.75}(\text{ThF}_4)_{8.75}$  (V-52) glass, reson. interaction of acoustic waves with two-level systems 4-70290  
 $\text{Zr}_{1-x}\text{Ni}_x$ , amorphous, low-energy excitations, thermal cond., sp. ht. meas. 4-70987

**localised modes in crystals** see lattice localised modes**localised states, electron** see localised electron states**locomotives**

see also railways

rail tractors, external noise reduction 4-74808

**loggers** see data loggers; recorders**logging (recording)** see recording**logic analysers** see display instrumentation; logic testing**logic arrays** see cellular arrays**logic circuit elements** see logic devices**logic circuits**

see also flip-flops; integrated logic circuits; logic devices; threshold logic  
 automatic telemetering rangefinder, electronic logic circuit 4-110299  
 integrated optoelectronic logic ccts. 4-97144

**logic devices**

see also fluidic logic

optical logical processing in parallel with theta modulation 4-112349  
 AlGaAs/GaAs/AlGaAs single quantum well transistor with 2-D electron gas, logic device appl. 4-61443

**logic testing**

portable test instrumentation development, using CMOS LSI technology, flat displays and microprocessors 4-73429

**long-range order**

see also order-disorder transformations

- alkaline earth niobates, electronic cond. rel. to complex perovskite structs. 4-70821  
 alloy, book contrib. 4-109423  
 alloys, Auger spectra, partial long range order effects 4-99238  
 alloys, binary FCC, modelling of mag. and chemical ordering 4-104421  
 alloys, interstitial, phase transitions of interstitial atoms in voids (Russian) 4-103741  
 alloys, interstitial distrib., variable-volume model (Russian) 4-84289  
 antiferromagnetic Ising model, anisotropic, long-range order, quenched impurity effects 4-98848  
 antiferromagnetic model, partially frustrated systems 4-104387  
 binary alloys, order-disorder transitions, electronic theory 4-113572  
 binary substitutional alloys, order-disorder transitions, appl. of grand canonical ensemble 4-113570  
 EXAFS and X-ray scatt., model comparison 4-66109  
 first order mag. phase transitions of the order-disorder type 4-65814  
 graphite intercalation compounds, ultramicrostruct. 4-84417  
 interstitial alloys, thermal expansion study (Russian) 4-103976  
 modulated phases, Ginzburg-Levanyuk criterion for phase transitions 4-98274  
 molecular crystal, one-dimensional electron-phonon system 4-70315  
 order-disorder transformations, order-wave description using continuum model 4-113574  
 ordered alloys, long-range, phys. metallurgy and struct. appl., review 4-114638  
 ordering under quenched random mag. fields 4-71103  
 polar rod systems, fluid mesophases 4-88081  
 solid solution structure, book contrib. 4-108308  
 spin glasses, antiferromagnetic, spin waves and metastability 4-80768  
 superparamagnetism of ferromagnets with thermodynamically unstable long-range mag. order 4-71128  
 Au-Cd liq. and solid alloy, elec. resist. studies 4-88499  
 Co-Al, long range 21R struct. during martensitic transform. (Chinese) 4-103699  
 Cu-Au alloys, (100) surface, order-disorder transitions and segregation 4-98268  
 Cu-Ni vapour deposited composition modulated film, long-range interaction effect on diffusion 4-70476  
 Cu-Ni-Zn,  $\text{Li}_1$  and  $\text{Li}_2$  alloys, order-disorder transitions, microstructure obs. 4-114511  
 $\beta$ -CuZn, disordered, vibr. spectra study (Russian) 4-65366  
 (Fe, Co, Ni) $_3$ V, ductile ordered alloys, phys. metallurgy and mech. props. 4-114612  
 (Fe,Ni)V, ordered alloy, irradi. in HFIR, microstruct. and bend ductility 4-108454  
 (Fe,Ni) $_3$ V alloy, long-range ordered, strain rate and ageing effect on mech. props. 4-109501  
 $\text{K}_3\text{Al}_2\text{Ti}_6\text{O}_{16}$ , hollandite, one-dimens. ionic cond., three-dimens. long range order, diffuse X-ray scatt. 4-98067  
 $\text{Mn}_{1/2}\text{Al}_{1/2}\text{Fe}_x$ , thermal expansion, atomic order effects (Russian) 4-103971  
 Ni base superalloys,  $\text{Li}_2$  type precipitates, long range order study by atom probe field ion microscopy (French) 4-104788  
 Ni particles metallic or insulating matrices, electron distrib. localisation 4-92647  
 Ni-base alloys with high vol. fraction of  $\gamma'$ , flow stress and creep props. 4-114611  
 Ni-base superalloy, single cryst., CMSX2, long-range order and phase comp. in  $\gamma'$  phase, atom probe study 4-66337  
 Ni-Mo, long range ordering to  $\text{Ni}_3\text{Mo}$ ,  $\text{DO}_{22}$  type superlattice form. 4-71650  
 Ni-Mo ordered alloys, phys. metallurgy, microstruct. and props., review 4-114556  
 $\text{Ni}_3\text{Al}$ , ordered alloy, flow stress and creep props. 4-114611  
 $\text{Ni}_3\text{Cr}$ , ordered state, annealing, elec. resist., electron diff. obs. 4-109394  
 Pd-Cu-Ni alloys, elec. resist., atomic ordering effects (Russian) 4-108833  
 $\text{Zr}_3\text{Al}$ , ordered alloy, flow and fracture, review 4-114639  
 ZrCrFe-based hyperstoichiometric alloys and hydrides, mag. props. 4-109025

**loop antennas**

ionosphere multirun loop VLF antenna, impedance measurements 4-85858

**Lorentz transformation**

- action integral in electrodynamics, general expression, Maxwell eqns. derivation 4-69278  
 Bohm-Bub hidden-variable theory, relativistically covariant generalization 4-106200  
 causality, antiparticles, spin-statistics connection, annihilation and creation operators 4-106464  
 classical charged particle with spin in external EM field, projective constrained variational principle 4-64666  
 deduction of the general Lorentz transformations from a set of necessary assumptions 4-63445  
 dimensional reduction of fermions, generalized grav., modification of Riemannian geometry 4-95273  
 Dirac equation and Hestenes' geometric algebra 4-102010  
 electric charge motion under superluminal Lorentz transformations 4-101649  
 Euclidean space, algebraic field description, electromag. field, Lorentz transformations, duality rotations 4-106462  
 first-order relativistic wave eqns. for unique-spin, unique-mass particles 4-68371  
 global conserved charges, Lorentz transform. props. 4-110871  
 half orbital angular momentum and Lorentz invariance in an anisotropic space 4-68449  
 optics, relativistic phase invariance 4-110872  
 revised Robertson's test theory of special relativity 4-101647  
 semileptonic interactions, strong gravity and Lorentz non-invariance 4-90789

# Lorentz transformation continued

- spin-1 fields, Lorentz invariance, helicity and gauge transformations 4-58939
- spin-1 massive particles, associated fields, tachyon-like behaviour of magnetic monopole 4-90724
- standing wave, invariance groups (French) 4-96787
- subluminal and superluminal Lorentz transformations in eight-dimensional space 4-90370
- superluminal frames, extensions of special relativity, interrelations with many-wave hypothesis 4-95170
- superluminal Lorentz transformations, revisitation and generalisation 4-78132
- superluminal transformations, maps between manifolds, fibre bundles, Lie group bundle manifold 4-63505
- tachyon-bradon EM interactions 4-101648
- tachyons, spin-1/2, charge conservation calcs. 4-106186
- timelike and spacelike particles from first principles; Lorentz transformation 4-78135
- unified kinematics in eight dimensions 4-58643
- Wightman localisations, causal transformations 4-68008
- Yang-Mills and spinor-isospinor field interactions, isovector current density 4-95669

# Lorentz number

- metal film, Wiedemann-Franz law expressions 4-108951
- W, high-temperature Lorentz number, thermal and elec. cond. meas. (German) 4-80564

# Loschmidt number see constants

# loss angle

- see also dielectric losses
- disodium sulphosaltate pyroelec. cryst., elec. props. (Chinese) 4-114212

# loss angle, dielectric see dielectric losses

# loss-angle measurement

- dielectric properties of New Brunswick oil shale 4-72043
- MM-wave meas. of loss tangent, quasi-optical methods 4-95463

# loss measurement

- depressed clad single-mode fibre, mass production 4-91654
- fibre optic cables, local area and business premises appl., field trial (Japanese) 4-79311
- optical fibre multiple scattering effects, backscattering meas. method (Japanese) 4-60169
- optical low-loss single-mode fibres, fabrication 4-91652
- optical multi-fibre losses meas. technique 4-97102
- submarine optical fibre, cable, design 4-74728
- submarine optical fibre cable, design 4-74730

# loss tangent, dielectric see dielectric losses

# losses

- see also dielectric losses; eddy current losses; heat losses; loss angle; magnetic leakage
- asymmetrical dielectric slab waveguide, power loss at step discontinuity 4-87449
- birefringent optical fibres, single-polarisation operation 4-107828
- cascade three-dimensional boundary layer approach flow, effect of degree of turbulence 4-69746
- curved fibre light pipe, optical losses, heating effects 4-69580
- dual-coated optical fibres, small dia. type, microbending loss characts. study (Japanese) 4-107868
- fibre optic connectors and joints (Italian) 4-60158
- fibre optic materials, scattering losses at minimum dispersion wavelength 4-79316
- fibre optic taper-polarisers, highly birefringent, finite cladding effects 4-69569
- free electron laser, two-stage, low loss quasioptical cavity 4-87369
- laser resonator diffraction loss investigation using diffracted light, picked-off with knife-edge mirror 4-60075
- losses in multifilament superconducting wire at increasing transport current and magnetic field 4-92879
- microbend fiber optic sensor 4-112584
- multifilamentary superconducting cables, coupling losses calc. 4-70983
- multimode graded-index fibre, hydroxyl group formation 4-60162
- optical fibre cable link implementation and reliability, conf., London, England (June 1984) 4-95066
- optical fibre loss increase for silicone coating containing the Si-D group 4-97072
- optical fibre splice loss distribution, theoretical study (Japanese) 4-83720
- optical fibre V-groove mass splice, loss temp. characts., expt. study, reliability improvement (Japanese) 4-87474
- optical fibres, Al hermetically coated, transmission loss reduction 4-97112
- optical fibres, Al-coated, optical, mechanical and radiation perform. at high temp. 4-97111
- optical fibres, excess loss due to surrounding temp., increment expt study (Japanese) 4-87477
- optical fibres, jacketing structure for loss increase suppression caused by hydraulic pressure (Japanese) 4-83717
- optical fibres, multimode, two, modal noise and distortion caused by intervening longitudinal gap 4-69560
- optical fibres, single mode, axis misalignment and splice loss characts., theoretical and expt. study (Japanese) 4-83718
- optical fibres, single mode, exposed to H<sub>2</sub>, long term loss increase prediction 4-97123
- optical fibres, single mode, H<sub>2</sub> exposure, long-term loss stability, expt. study 4-83704
- optical fibres, single-mode, H<sub>2</sub> and D<sub>2</sub> gas-in-glass effects 4-97121
- optical fibres, single-mode, microdeform. losses 4-69556
- optical fibres, twisted, as strain sensor, tensile strain conversion to optical loss 4-97086
- optical fibres in communication systems, radiation effects at low dose rates 4-91626
- optical fibres with radiation-resistant ethylene-tetrafluoroethylene copolymer protective coatings 4-97110
- optical metallic waveguide, low loss props. 4-69549
- optical single-mode fibres, scatt. loss versus polarisation holding ability 4-69561
- RE 1-11 rotary expander engine testing and analysis 4-66746
- semiconductor laser, lateral field coupling control, modulation characts. anal. (Japanese) 4-60084
- single mode fibre biconical taper couplers, efficient coupling ratio control 4-91625
- single mode fibre effective cutoff wavelength, bending effects 4-97103

# losses continued

- single mode optical fibre specifications 4-97089
- single mode stranded cables, commercially manufactured, low loss, design and preform. 4-97100
- slab optical waveguide bending, radiation losses anal. (Chinese) 4-97059
- solar cells, amorphous, optical loss mechanisms 4-77108
- solar cells, contact resist. meas. and importance rel. to power loss 4-81545
- square-waveguide laser resonator coupling losses 4-69458
- thin-port graded-index waveguide star coupler fabricated by dry ion diffusion process 4-97060
- UV curable silicone-coated fibres, IR transmission loss study 4-64777
- waveguide laser resonators formed by flat mirrors, coupling efficiency 4-112482
- Cr<sup>2+</sup>:Be<sub>2</sub>Al<sub>2</sub>(SiO<sub>3</sub>)<sub>6</sub> laser, CW Kr laser pumped, 728.8 to 809.0 nm tuning range 4-60041
- CsI fibre lightguide material, designed to operate in visible and IR spectral regions 4-74634
- GaAs optical waveguide modulator with low loss and high speed, fabrication by RIE 4-60148
- LiNbO<sub>3</sub>:Ti waveguides with low loss, fabrication and performance 4-69554
- Nb<sub>3</sub>Sn, thick diffusion produced layers, struct. and power losses rel. to electrochemical polishing 4-65781
- SiO<sub>2</sub>:GeO<sub>2</sub> multimode fibres, H<sub>2</sub> effects on IR absorpt. characts. 4-97106
- SiO<sub>2</sub>:GeO<sub>2</sub> core graded index fibres, mode attenuation at 1.39  $\mu$ m, OH absorption study 4-91590
- SiO<sub>2</sub>:GeO<sub>2</sub>:P<sub>2</sub>O<sub>5</sub> optical fibres, H and D absorption losses, expt. study 4-91589
- SiO<sub>2</sub>:GeO<sub>2</sub>:OD 4-64779
- Zn<sub>2</sub>F(CN)<sub>6</sub>:Zn<sub>2</sub>Fe(CN)<sub>4</sub> battery system for utility load levelling and solar photovoltaic/wind apps. 4-72055

# loudness

## see also acoustic intensity measurement

- auditory modality, relative distance discrimination 4-105252
- British Standard 4198-Method A, BASIC computer program for calculations 4-69636
- complex noise consisting of impact sound and steady noise (Japanese) 4-83772
- hearing protection device effectiveness at industrial facility with 107 dB 4-112633
- impact sound loudness measurement by sound level meter, time constant meas. 4-87528
- measurement, BASIC program for execution of International Standard ISO 532 B 4-79403

# loudspeakers

- air-modulated sound source, speech intelligibility in long distance broadcasting (Chinese) 4-87529
- arrays, coverage modelling for any room configuration 4-64809
- ferroelectric polymers, props. and applications 4-65954
- LF sound reproduction system design using Thiele-Small driver parameters 4-87533
- monitoring speakers for control rooms 4-79408
- sound column, resonance freq. and efficiency (Chinese) 4-107916
- sound reinforcement systems, comparison of real-time anal. and time-delay spectrometry 4-87526
- sound reproduction, timbre, meas. and prediction 4-97226
- sound-image quality, physical and psychological factors 4-79373
- sound-pressure responses effect of acoustic field in enclosure 4-64815
- standard control room, proposal 4-79374
- theatre and cinema sound, standards improvement 4-69625

# Love waves

- Canadian Shield area, upper mantle seismic velocity struct. 4-105454
- crystal/overlay system, elastic surface waves, Green's function anal. 4-108695
- inhomogeneous plane waves, apps. 4-86220
- interaction, ray theory and coupling 4-64873
- isotropic layers on isotropic substrate, surface Love waves 4-108701
- laterally and vertically homogeneous half-space seismic wave propagation 4-77454
- W Pacific, surface seismic wave polarization 4-72495
- plate, elastic, under torsional moment and horizontal force, waves generation 4-60315
- dry sandy media, surface wave propagation influenced by gravity field 4-77455
- second-order coupling of two Love waves 4-79485
- two-layer system on a substrate, Love surface waves 4-113775

# low energy electron diffraction

- acetylene adsorbed on oxidised and carbided W (100), C-H bond activation 4-93553
- adsorbed layers, order-disorder phenomena, and surface struct. 4-80414
- adsorbed overlayers, LEED angular profiles calc. for island size distributions meas. 4-88399
- crystal surfaces, electron current image diffraction at low energies 4-92034
- epitaxial growth, atomic pair correlation function during early stages 4-92577
- graphite, physisorbed O<sub>2</sub>, phase transitions, LEED studies 4-88396
- graphite with adsorbed H<sub>2</sub>O, adsorption depend. on substrate struct. 4-92515
- high resolution, electron gun and detector 4-90691
- high-temperature analysis techniques, surface characteristics 4-99927
- II-VI semiconductors, crystal growth, optical and surface props. (Japanese) 4-88957
- LEPD, positron scattering and surface state formation 4-88914
- low-energy electron induced X-ray spectrometry, surface characterisation 4-113767
- metal surfaces, anion and cation hydration, double layer simulation in ultrahigh vacuum 4-108703
- misoriented surfaces with randomly distributed steps, electron diffr. beam intensity ang. distrib. 4-92494
- stepped surfaces, LEED and RHEED intensities calc. 4-84496
- surface analysis by low energy SEM with a field emission gun 4-79915
- surface band bending variation during thermal oxidation 4-70897
- surface defect meas. by LEED 4-104041
- very low energy, excitation map concept, critical anal. 4-97978
- very low energy, threshold effects and excitation map concept 4-97979
- Ag (110), O<sub>2</sub>, CO and CO<sub>2</sub> interactions, AES, XPS, TDS and LEED studies 4-113810

**low energy electron diffraction continued**

- Ag epitaxial film on Cu (111), interfacial effects in electron transmission study 4-114050  
 Ag epitaxial layers, quantum size effects, surface and interface roughness influence, LEED study 4-84526  
 Ag surfaces, (100) and (111), chemical polishing, LEED studies 4-99645  
 Ag-Pb (111) solid solns., Pb surface segregation and vapour deposition on Ag (111), LEED-AES study 4-113837  
 Al (110) surface, truncation-induced multilayer relax. 4-70534  
 Al, surface struct. from low energy electron channelling 4-92482  
 Ar films, structural order effects in low-energy electron transmission spectra 4-98520  
 AuGa<sub>2</sub> (001), surface net characterisation and electronic struct. 4-80642  
 Au(111) surface, adsorpt. of Cu in underpotential region, LEED and RHEED investig. 4-108702  
 Ba, adsorbed on W (001), phase transitions, LEED study 4-92544  
 C, glassy with adsorbed H<sub>2</sub>O, adsorption depend. on substrate struct. 4-92515  
 C segregation to Ni (100) surface in presence of adsorbed S 4-61089  
 CO, adsorbed on Ni (100), stretching vibr., IR emission spectroscopy study 4-92508  
 CO films, structural order effects in low-energy electron transmission spectra 4-98520  
 CO, high coverage struct. on metal FCC (111) and HCP (0001) surfaces, LEED, HREELS and IR spectra study 4-65573  
 CO, solid, adsorption of multilayers on Cu (100), epitaxial growth of new cryst. struct., LEED, IR spectra 4-113373  
 CdTe films, atomic layer epitaxy and electronic struct. 4-81135  
 CoSi<sub>2</sub> epitaxial growth on Si (111) surface 4-61844  
 Cu (001), azimuthal X-ray photoelectron diffr. from Cu<sub>2</sub>p<sub>3/2</sub> core level 4-76639  
 Cu (001) with chemisorbed K monolayers, rotational epitaxy study 4-70566  
 Cu (110), adsorption of O<sub>2</sub>, influence of Ne<sup>+</sup> ion bombard. 4-108723  
 Cu electrodeposition on Pt (111), LEED and AES studies 4-66244  
 Cu epitaxial layers, quantum size effects, surface and interface roughness influence, LEED study 4-84526  
 Cu/γ-Fe<sub>3</sub>O<sub>4</sub> epitaxial sandwich layers, struct. and Mossbauer studies 4-84531  
 Fe (110), ferromag., spin-polarised low-energy electron diffr., temp. effects 4-104456  
 Fe (110) with chemisorbed Br, LEED and ARUPS study 4-92518  
 Fe (110)p(2×2)-S, surface ferromagnetism, chemisorption, adsorbate-induced substrate reconstruction effect, spin-polarised LEED calcs. 4-80395  
 Fe (111), CO interaction, thermal desorpt. and LEED studies 4-65566  
 Fe (310), struct., parallel and perpendicular multilayer relax., LEED study 4-80349  
 Fe-Si (3 wt.%) (100) surfaces, interaction with O<sub>2</sub> and electron stimulated desorption 4-92560  
 GaAs (100), clean surface prep. using Ar<sup>+</sup> ion bombard. 4-104886  
 GaAs (100), laser irradi., photoemission of electrons 4-81116  
 GaAs (110), H<sub>2</sub>O adsorption, TDS and LEED studies 4-65568  
 GaAs (110) and GaAs/Au(Pd) interfaces, high energy ion channelling studies 4-65318  
 GaAs (110) surface, randomly stepped, ordering kinetics, LEED study 4-84495  
 GaAs (110)-Al interface form. at low temp., electronic and struct. props. 4-84695  
 GaAs (110)-ZnSe interface, LEED and AES characterisation 4-84517  
 GaAs (111)(2×2) surface, struct., vacancy buckling model, LEED study 4-70533  
 GaAs/Al interface, low temp. form. and structure, LEED, AES and work function meas. 4-80425  
 GaP (110), surface structure, atomic geometries, R-factor minimization 4-84494  
 Ge (111)-Pb interface form. dynamics and oxidation 4-84518  
 Ge<sub>2</sub>Si<sub>3</sub> (111), (5×5) LEED pattern, growth conditions 4-65596  
 InP (100), laser irradi., photoemission of electrons 4-81116  
 Kr films, structural order effects in low-energy electron transmission spectra 4-98520  
 Mo (100), reversible phase transition, LEED study 4-92345  
 Mo (100) and MoS<sub>2</sub> (0001), CO coadsorption with S<sub>2</sub>, H<sub>2</sub>, and O<sub>2</sub>, LEED, AES and TDS studies 4-80407  
 MoS<sub>2</sub>-2H, layered, low energy electron, reflection intensities, scatt. matrix, calcs. 4-109286  
 N<sub>2</sub> films, structural order effects in low-energy electron transmission spectra 4-98520  
 Ni (001) with chemisorbed pyridine, molecular orientation effects on electronic excitations 4-93551  
 Ni (100), adsorption of residual gases, electron impact effects 4-65543  
 Ni (100), Fe adsorption and growth, LEED and EELS studies 4-113808  
 Ni (100), N<sub>2</sub> adsorption, thermodynamic meas. 4-92563  
 Ni (100), S-covered, adsorption of CO, vibr. spectroscopy study 4-108720  
 Ni (110), chemisorption of D, saturation coverage 4-92550  
 Ni (110), molecular N<sub>2</sub> adsorpt., phase transitions obs. 4-88395  
 Ni (110), multilayer relax., LEED and metric dist. anal. 4-113762  
 Ni (110) surface, adsorbed H, dual path surface reconstruction study 4-108716  
 Ni (111), dissociative adsorption and recomb. of CO, N<sub>2</sub>, SO, and O<sub>2</sub> 4-93559  
 Ni<sub>60</sub>Fe<sub>40</sub> (100), O<sub>2</sub> and S<sub>2</sub> coadsorption, surface phases, LEED study 4-84506  
 NiSi<sub>2</sub> epilayers on Si (001), electronic struct. determ. 4-88549  
 O<sub>2</sub> films, structural order effects in low-energy electron transmission spectra 4-98520  
 O<sub>2</sub>, physisorbed on graphite, † phase struct., LEED determ. 4-108712  
 PbS (100), low energy electron double reflection 4-103616  
 Pd (100), adsorpt. and catalytic reaction of H<sub>2</sub>O, O and H, EELS and LEED study 4-71969  
 Pd-Si (111), study by LEED, RHEED and AES 4-113765  
 Pt (100), electrodeposition of Ag, thermal desorption, Auger effect, LEED 4-80449  
 Pt (100) CO oxidation, kinetic oscils., Rutherford backscattering, LEED study 4-66611  
 Re (0001) and stepped surfaces, adsorption and dissoc. of water, TDS, LEED, AES, ESDIAD studies 4-80401  
 Rh (111), adsorption and decomposition of methanol, EELS and thermal desorption spectroscopy 4-92565  
 Rh (111), Al+O<sub>2</sub> reactions, AES and LEED studies 4-89327

**low energy electron diffraction continued**

- Rh (111), CO and K coadsorption, HREELS, TPD, AES and LEED study 4-84508  
 Rh (111), NO+CO reactions, AES, LEED, XPS, UPS and temp. programmed desorpt. study 4-89326  
 Ru (001), coadsorption of CO and Na, mol. reorientations 4-108717  
 Si (100) surface, H chemisorbed, work function change, LEED expt. 4-70907  
 Si (100)2×1, H adsorpt., coverage and temperature-dependent vibr. spectra, EELS and LEED studies 4-80408  
 Si (100)(2×1) surface, atomic geometry, elastic LEED intensity anal. 4-92490  
 Si (111), laser irradi., photoemission of electrons 4-81116  
 Si (111) (7×7), NO adsorption and reactions, EELS, LEED and AES studies 4-65562  
 Si MBE layer, Sb adsorption, LEED, AES and TDS study 4-65560  
 Si reconstructed surface reordering on room temperature Ge deposition 4-98411  
 a-Si, vacuum deposited, solid-phase epitaxial growth anisotropy 4-75811  
 Si/SiO<sub>2</sub> interface, atomic struct. and elec. props. 4-80677  
 Si/SiO<sub>2</sub> MOS struct., interface state density and atomic roughness 4-98684  
 Si(111)2×1, surface geometry, buckled chain model, LEED calc., work function meas. 4-75765  
 Si(111)2×1 surface, structure analysis 4-113769  
 Sm homogeneous intermediate valence monolayers on Cu (001), LEED and XPS study 4-61807  
 Ti<sub>2</sub>O<sub>3</sub> (047) surface, preparation by ion bombardment and annealing, XPS and UPS studies 4-65528  
 W (001), adsorbed H-induced surface reconstruction, LEED and EELS study 4-92492  
 W (001), reconstruction domains, finite size effects 4-88379  
 W (001) surface, c(2×2) struct. stability, surface reconstruction temp. depend. 4-80348  
 W (100), adsorption of H, surface reconstruction, symm. effects, refl. EELS study 4-80382  
 W (112) with chemisorbed O<sub>2</sub>, kinetics of antiphase domain coarsening 4-98435  
 Xe films, structural order effects in low-energy electron transmission spectra 4-98520  
 ZnS (110), surface structure, atomic geometries, R-factor minimization 4-84494
- low gravity experiments** *see zero gravity experiments*  
**low induction loss** *see loss angle*  
**low-pass filters**  
 RC-filter, active, design, for sharp bands-separation 4-112640  
 X-ray bandpass filter from Ge solid state detector and GeO<sub>2</sub> foil. 4-91176
- low-temperature physics** *see cryogenics*  
**low-temperature production**  
*see also Joule-Thomson effect; magnetic cooling; refrigeration*  
 1.5K using vacuum insulated siphon for a continuously filled cold plate 4-95432  
 atom probe field ion microscopy, microrefrigerators appl. 4-95438  
 closed-cycle refrigerators, interfacing to liquid He cryostats 4-58858  
 cryorefrigerators, thermodynamics cycles 4-95435  
 Joule Thomson coolers at very low powers 4-101855  
 microminiature Joule-Thomson refrigerators, fine channel heat exchangers, gas flow anal. 4-101851  
 minicooler based on Joule-Thomson expansion 4-95440  
 refrigerators for use near high-homogeneity superconducting NMR magnets 4-68233  
 regenerative heat exchangers for low temp. refrigeration, theory 4-111140  
 regenerative refrigeration, generalised ideal reference cycle 4-95429  
 three-stage refrigerator for temperatures down to 4.2K 4-95437  
 Vuilleumier minicyclicrefrigerator 4-101848  
<sup>3</sup>He cooling heat exchangers, comparison of Cu, Ag and Pd 4-95433  
<sup>3</sup>He refrigerator, construction and test for Ge exciton condensation, microwave study 4-68234  
<sup>3</sup>He-<sup>4</sup>He dilution refrigerator with <sup>3</sup>He cryogenic circulation cycle 4-85859
- low-temperature techniques**  
*see also cryostats; refrigeration*  
 capacitive vitroceraic thermometers, vitroceraic sample behaviour 4-65940  
 creep testing, equipment 4-104930  
 cryogenic heat transfer 4-82799  
 cryogenic liquids, calorific props. meas. at low temps. and high press. 4-95428  
 far IR transmission expts., low temp. cryomagnetic set 4-73525  
 freeze-dried cryosection preparation, sublimation rates of ice in cryo-ultramicrotome 4-62647  
 freeze-dried cryosection preparation using section press and low elemental support 4-62645  
 gravitation, torsional type antenna for low temp. expts. 4-68119  
 IR radiance instrument for shuttle CIRRIS telescope 4-94614  
 level indicator using voltage controlled oscillator 4-68208  
 liquid nitrogen autofill unit and level controller (Chinese) 4-82798  
 magnetically simulated diode for pulsed ion beams generation 4-91126  
 mass spectrometer attachment to field ionisation source 4-101963  
 material transmission of room-temp. radiation at cryogenic temp. 4-106325  
 measurement techniques 4-95421  
 Near-IR Mapping Spectrometer; optical subsystem development and testing 4-110526  
 NMR pickup coil design 4-68252  
 NMR probe head, high-pressure, RbAg<sub>2</sub>I<sub>3</sub> superionic conductor phase study appl. 4-111164  
 optical microscope stage for solidification studies in aqueous soln. 4-111199  
 quartz oscillator, design (Japanese) 4-58860  
 rat liver, cryoprotected, cryosectioning 4-85598  
 reciprocating magnetic refrigerator, efficiency, cooling power between 1.8 and 4.2K (Chinese) 4-82797  
 satellite-borne cryogenic limb array etalon spectrometer for upper atmosphere research, performance analysis 4-115668  
 sealing using elastic metallic joints 4-95447  
 SEM, resolution limit due to thermal effects 4-101983  
 Shuttle IR telescope facility, system design parameter study 4-110489

**low-temperature techniques continued**

- Shuttle IR Telescope Facility, thermal modelling 4-110488  
slam freezer, liq. He cooled, for biological specimens 4-115299  
small sample storage under liq. N<sub>2</sub>, rapid-access system 4-73428  
TEM, liquid He stage 4-78438  
tunable pulsed dye laser cryogenic photocalorimeter, for photochemical reactions obs., theory and design 4-105005  
vacuum thermometry in cryogenic industrial environments 4-95439  
X-ray goniometer of meas. in temp. range 10 to 293K 4-69988  
Ag plugs, sintered, for cryogenic heat exchangers 4-101852  
Ag powders, sintered, appl. in mK heat exchangers 4-111139  
D<sub>2</sub>O ice, vap. press. below 273K 4-113595  
Ge exciton studies, laser heating effects at liquid He temps. 4-70672  
He level sensor using superconducting wire 4-101808  
He, liquid, level detector based on vapour press. meas. 4-101813  
In resistance thermometer for low temps. 4-101843  
Pt-Co dilute alloys, resistance thermometers with low magnetoresistive effects 4-111132  
Rh-Fe resistance thermometer, ceramic encapsulated, props. and stability below 80K 4-111134  
Si diode temp. sensors, stability, 4.2 to 273K 4-68229  
<sup>129</sup>Xe isotope, mixture prep. for low conc. standards using liq. He transport agent 4-101807

**LPE** see liquid phase epitaxial growth

**LS coupling** see Russell-Saunders coupling

**LSA** see limited space charge accumulation

**LSI** see large scale integration

**lubrication**

see also friction

- boundary layers at lubricated walls, local nonsimilarity solns. 4-97471  
EHD squeeze films between spherical pins under periodic motion 4-97699  
elastohydrodynamic lubrication of cylinder in line contact, nonlinear complementarity problem 4-97436  
elliptical contact, numerical soln. for thermelastohydrodynamic problem (Chinese) 4-97437  
material squeezed between parallel plates, power law creep, perturbation scheme 4-87586  
nonNewtonian fluid, laminar radial flow between parallel discs in axial elec. field, inertia effects 4-83930  
opthalmic solutions lubrication props. meas., using strain gauge bridge 4-89797  
optical glass, fine diamond grinding, lubricating-cooling liquid role 4-69607  
pressure generator, multiple-anvil sliding system, with X-ray diffraction 4-82804  
Ringbom-Stirling air engine, design and operational experience with water as lubricant 4-66770  
Ringbom-Stirling air engine design aspects 4-66769  
sheared suspensions, dynamic simulation 4-74975  
slide bearing, lubricant flow in deformed curvilinear gap, mag. field effects (German) 4-75094  
thermal elastohydrodynamic problems, lubrication theory 4-91779  
turbomolecular pump, water cooling, lubrication, use with corrosive gases (Japanese) 4-73447  
Fe, cast, tribological behaviour in inert and reducing gas media 4-71742  
He atmosphere effects on machine components, bearings, lubricants, sliding surfaces, contacts, HTGR appl. 4-106838  
Zn-Al-Si (21, 2 at.%), frictional surface charact. under boundary lubrication 4-66452

**Luders' bands**

- bar, elastic in uniaxial tension, bifurcation absence study 4-87570  
deformation instabilities 4-99450  
metal, plastic deform., book contrib. 4-109483  
plastic flow, inhomogeneous, constitutive eqns., appl. to Luders band prop. 4-65329  
steel, ferritic stainless, irradi. embrittlement 4-93392  
steel sheet, plastic bending instability 4-99461  
Al-Fe-Mg-Cu, periodic load serrations in tensile curve, occurrence conditions 4-85194  
Al-Si-Fe, Luders band deform., stress relax., load suppression effect 4-76801  
Cu, neutron irradiated thin flat crystals, slip band growth and dislocation velocities 4-70164  
Cu, single crystal, strain bursts in cyclic creep at ambient temp. 4-66371  
Cu-Zn, neutron irradiated thin flat crystals, slip band growth and dislocation velocities 4-70164

**Ludwig-Soret effect** see diffusion in solids

**luminance** see brightness

**luminescence**

- see also cathodoluminescence; chemiluminescence; electroluminescence; fluorescence; fluorescent screens; ionoluminescence; luminescence of gases; luminescence of liquids and solutions; luminescence of solids; luminescent devices; phosphorescence; phosphors; photoluminescence; sonoluminescence; stimulated emission; superradiance; thermoluminescence; triboluminescence  
aromatic cpds., room temp. phosphoresc., phosphor d solid supports interaction 4-78887  
biology appl. of luminesc. and fluoresc. methods, review 4-115324  
decay data deconvolution, phase plane method, scattered light effects corrections 4-59824  
luminophor plane-parallel, correction for reabsorption 4-85003  
molecules, transient processes, spectrochronography 4-96586  
positive luminescence photographic process, image sensing method optimisation according to signal/noise criterion during luminesc. and absorpt. sensing (Russian) 4-68309  
VUV radiation physics, conf., Jerusalem, Israel, 8-12 Aug. (1983) 4-82583

**luminescence chambers** see scintillation chambers

**luminescence of gases**

- benzaldehyde triplet dynamics as studied by electron impact excitation 4-96706  
breakdown waves, spatiotemporal luminous investigations 4-79729  
diacetyl vapor, triplet state, multiphoton vibr. excitation, luminesc. spectra 4-102738  
organic free complex molecules, picosecond spectroscopy 4-102819  
piezoelectric-gas system, acoustic excitation of EM emission from gas 4-69621  
quinizarin, hot luminesc. spectra in supersonic expansion 4-97747

**luminescence of gases continued**

- BaO\* (A<sup>2</sup>Σ), vibr. relaxation and electronic quenching in Ar and N 4-107442  
Hg-NH<sub>3</sub> complex, excited, laser-induced luminesc. 4-107381  
O<sub>2</sub>, low density discharge, bimolecular processes 4-75225  
Xe, electroluminescence, partial excitation and VUV fluoresc. at normal press. 4-83973  
Xe, electroluminescence and electron resonance trapping 4-108158  
Zn tetraphenylporphyrin, spectral-fluoresc. props., aggregate state and temp. effects 4-78906

**luminescence of inorganic solids**

- alkali halide:CN<sup>-</sup>, vibrational fluoresc., nonradiative luminesc. quenching 4-81005  
alkali halide:Ti<sup>3+</sup> cryst., optical props. and Jahn-Teller effects 4-61643  
alkali halide, γ-irrad., lyoluminescence characts. (Chinese) 4-76526  
alkali halide cryst., image reduction using photo-stimulated luminescence (Russian) 4-68302  
alkali halide crystals, colour centre IR luminesc. and stimulated emission 4-80997  
alkali halide mixed crystals, growth and characterisation, microhardness, colour centres, radiation hardening 4-70152  
alkali halides, fracture-induced luminesc. and crack vel. 4-104685  
alkali halides, stability and optical props. of self-trapped exciton 4-104129  
alkali halides thermoluminesc. 4-109252  
alkali metal halides, activator light sum photorelease, photoluminescence (Russian) 4-114321  
alkali metal rare earth fluorides, MR<sub>3</sub>F<sub>6</sub>:Eu<sup>2+</sup> (M=K, Rb, Cs; R=Y, Gd, Lu), Eu<sup>2+</sup> luminesc. 4-66073  
chalcogenide glasses, two-step optical excitation, rel. to valence band struct. 4-85002  
crystals, mechanoluminescence, microhardness and disloc. density depend. 4-85020  
depreciation by ion bombardment 4-99157  
diamond, natural, type II, cathodoluminescence from dislocations 4-81012  
diamond, type IIb, individual dislocation and cathodoluminescence emission polarisation 4-99199  
double heterostructures, photoluminescence, photocarrier spreading effects 4-93106  
epitaxial high-purity layers, low-pressure MOCVD growth 4-61861  
fluorides, perovskite-type, wide band gap expts., excitation of thermally stimulated luminesc. and conductivity 4-85018  
fluorophosphate glass:Tm<sup>3+</sup>, fluorescence and oscillator strengths 4-99165  
garnet monocrystalline cathodoluminesc. layers 4-81010  
glass:Yb<sup>3+</sup>, statistical modelling, luminescence and absorpt. spectra 4-109247  
glass, anomalous thermal, acoustic and dielec. props. at low temp. 4-60994  
glassy semiconductors, electronic transitions in mobility gap 4-61275  
hydrophilic solid, adsorpt. of nonionic surfactant, fluoresc. decay obs 4-108679  
III-V optical sources, dislocations climbing degradation, expt. anal. 4-83654  
III-VI layered semiconductors, electronic and vibrational spectra 4-71390  
inert gases, solid, cathodoluminescence excitation spectra 4-85013  
ionic crystal, three-channel exciton decay by light emission (Russian) 4-99171  
microelectronic device and packaging manuf., opt. microanalytical techniques 4-93574  
multiquantum well heterostructures, magneto-optical studies of two-dimens. electrons 4-104580  
niobate phosphors, rare earth activated, luminesc. props. 4-88868  
non-metallic cryst., Eu ion impurity optical props. 4-61733  
phosphate glass:Nd<sup>3+</sup>, Yb<sup>3+</sup>, phonon-assisted energy transfer and spectra (Chinese) 4-93096  
phosphors, spectrophotometric measurements of luminophors (Polish) 4-85010  
piezoelectric solids, sonoluminescence mechanisms 4-88890  
polyacetylene, A<sub>g</sub> state, IR photoluminesc. 4-76524  
quartz, defect struct. and thermoluminesc. props., review 4-109256  
quartz, growth sector characts. by cathodoluminesc. 4-61755  
quartz, luminescence, ODMR study 4-85001  
quartz, natural, defects induced by vac. UV, X-ray and beta-ray irradi. 4-70191  
quartz, natural, wide band gap expts., excitation of thermally stimulated luminesc. and conductivity 4-85018  
quartz, pin, thermoluminescent spectra, complex, anal. 4-81014  
quartz, shock induced luminescence studies 4-109260  
quartz, X-ray irradi., thermoluminesc. from different growth sectors 4-61759  
quartz glass, triboluminesc. during frictional sliding 4-105547  
rare earth ions, RE<sup>3+</sup>, anti-Stokes luminescence efficiency, kinetic limitations for IR-visible conversion 4-66070  
rare earth molybdates, Eu<sup>3+</sup> doped, fluorescence studies 4-66072  
rare earth tetracyanoplatinate, R<sub>2</sub>[Pt(CN)<sub>4</sub>]<sub>2</sub>·yH<sub>2</sub>O single crystals, mag. field effect on luminesc. 4-61740  
rare earths in amorphous media and on-high surface area supports, fluorescence and nonradiative relax 4-99156  
ruby, Raman spin-lattice relax. induced by optically generated zone boundary phonons 4-66044  
ruby, resonant energy transfer in mag. field 4-93063  
ruby, Zeeman states, stimulated emission and decay of phonons 4-65359  
sapphire, neutron irradi. and thermochem. treated, colour centres, visible luminescence study 4-81000  
sapphire, synthetic, wide band gap expts., excitation of thermally stimulated luminesc. and conductivity 4-85018  
semiconductor superlattices, optical absorpt. and luminesc. expts. 4-84977  
semiconductor superlattices, optical props. 4-104665  
semiconductor superlattices, quantum wells, and heterostructs., elec. and optical props. 4-80666  
semiconductors, conf., Cambridge, MA, USA (Nov. 1983) 4-95025  
semiconductors, non-radiative capture and emission statistics, self-consistent semi-classical theory 4-71431  
silica, defect struct. and thermoluminesc. props., review 4-109256  
sintered compacts, grain size, internal strain, photoluminesc. spectra 4-99160

## luminescence of inorganic solids continued

- solids, time resolved VUV luminesc. under synchrotron radiation selective excitation 4-84985  
thermoluminescence systems with two or more glow peaks described by anomalous kinetic parameters 4-71451  
TLD, uncommon materials, review 4-109933  
topaz, X-ray irradi., thermoluminescence anal. 4-88889  
tourmaline, pyroelectroluminescence during heating and cooling 4-66078  
Ag halide microcrystals, spectroscopic identification of localised electrons and holes 4-114308  
AgBr:I, multiphonon emission, excitons, photoluminescence 4-99159  
AgBr(I) photographic layers, luminesc. and photo-emf, halogen ion effect 4-88870  
Al(Ga)As/GaAs/Ge:Ga polar semicond. quantum well system, growth and optical props. 4-114314  
Al, mechanoluminescence at low loading rates 4-81019  
Al/Sm<sub>2</sub>O<sub>3</sub>/Al capacitor struct., dielec. props. and thermoluminescence 4-76047  
Al-Al<sub>2</sub>O<sub>3</sub>Ag tunnel junctions, surface plasmons and light emission 4-98553  
Al-I-Au(Cu)(Ag) tunnel junction, fast light emission, plasmon polaritons (French) 4-80998  
AlAs-GaAs superlattice, MBE growth and luminescence 4-114403  
AlGaAs and GaAs, MBE growth on Si (100), optical props. 4-88975  
AlGaAs heterostructure, photoelectroluminescence study 4-99193  
AlGaAs, MBE growth of high purity layers, photolum. charact. 4-98474  
AlGaAs/GaAs quantum wells, photoluminescence studies 4-93105  
AlGaAs/GaAs single quantum well structs., MBE grown, photoluminesc. props. 4-61863  
AlGaAs-GaAs DH, photoluminescence efficiency 4-85006  
AlGa<sub>1-x</sub>As, cathodoluminescence study 4-71449  
Al<sub>1-x</sub>Ga<sub>x</sub>As, correlation of photoluminescence and deep trapping 4-80537  
n-Al<sub>1-x</sub>Ga<sub>x</sub>As epilayers, photoluminescence study 4-114316  
Al<sub>1-x</sub>Ga<sub>x</sub>As heteroepitaxial struct. photoluminescence study 4-104673  
Al<sub>1-x</sub>Ga<sub>x</sub>As, line broadening in photoluminescence spectra 4-109241  
n-Al<sub>1-x</sub>Ga<sub>x</sub>As, MBE grown, deep electron traps, growth conditions and alloy composition influence 4-98558  
Al<sub>1-x</sub>Ga<sub>x</sub>As MBE growth, Ga desorpt., AES and photoluminesc. studies 4-93220  
Al<sub>1-x</sub>Ga<sub>x</sub>As, Si donor behaviour, effect of Al comp. 4-98709  
Al<sub>1-x</sub>Ga<sub>x</sub>As solar cell structs., photoluminescence and spectral response 4-89404  
Al<sub>1-x</sub>Ga<sub>1-x</sub>As:Be, conference, Charlotte, NC, USA (Nov. 1983) 4-73146  
Al<sub>1-x</sub>Ga<sub>1-x</sub>As:Be, radiative recombinations 4-76515  
Al<sub>1-x</sub>Ga<sub>1-x</sub>As:Si, grown by MBE, photoluminesc. composition depend. 4-84996  
Al<sub>1-x</sub>Ga<sub>1-x</sub>As:Si, grown by MBE, photoluminesc. spectra, defect-related emissions 4-84997  
Al<sub>1-x</sub>Ga<sub>1-x</sub>As:Zn, CVD deposited, luminescence study 4-80985  
Al<sub>1-x</sub>Ga<sub>1-x</sub>As/GaAs single quantum well, exciton transport 4-88451  
Al<sub>1-x</sub>Ga<sub>1-x</sub>As-GaAs multiple quantum well laser structures, MBE growth conditions 4-91465  
AlGaInPAs lattice matched to GaAs, LPE growth, photolum. obs. 4-70581  
Al<sub>1-x</sub>Ga<sub>1-x</sub>In<sub>1-x</sub>Sb epitaxial layers, luminescence studies 4-76505  
AlGaSb, LPE, substrate treatment optimisation, carrier conc., Raman spectra, photoluminesc. 4-93235  
Al<sub>1-x</sub>In<sub>1-x</sub>As, nominally undoped, MBE growth and charact. 4-98472  
α-Al<sub>2</sub>O<sub>3</sub>, single cryst., thermoluminesc., review 4-109255  
Al<sub>2</sub>O<sub>3</sub>, X-ray irradiated, F-centre glow peaks spectral emission 4-71452  
Al<sub>2</sub>O<sub>3</sub>:Co, thermoluminescence and trap parameters 4-76532  
α-Al<sub>2</sub>O<sub>3</sub>:Er(Gd)(Tb) crystals, radiative and thermochem. effects 4-76491  
β-Al<sub>2</sub>O<sub>3</sub>:La<sub>2</sub>O<sub>3</sub>:Eu<sup>3+</sup>, structure, laser excited fluorescence study 4-66071  
AlSb-GaSb superlattice, MBE growth and luminescence 4-114403  
Ar, cryocrystals, high-energy excitations, hot luminesc. 4-99194  
Ar films, ion beam irradi., secondary electron, ion, and photon emission 4-76577  
Ar, solid, cathodoluminescence excitation spectra 4-85013  
Ar solid, electron stimulated desorpt., luminesc. and exciton creation 4-80381  
Ar, solid, electronically excited, sputtering and luminesc. 4-104708  
As, Se<sub>3</sub>, cryst. and amorphous, recomb. and excited-state absorption at photolum. centres 4-99182  
As<sub>2</sub>Se<sub>3</sub> glass, photoluminescence fatigue and structural disorder 4-104672  
Au thin film, fluorescence detection of surface EXAFS 4-93136  
B<sub>2</sub>O<sub>3</sub>-Na<sub>2</sub>O-Na<sub>2</sub>O glasses, thermoluminescent props. 4-66086  
BaClF:Sm<sup>2+</sup>, impurity states in mag. field, fluoresc. study 4-108805  
BaFCl, flux-grown crystals, thermoluminesc., effect of flux 4-104680  
BaFCl:Eu<sup>2+</sup> + γ-ray irradi., thermoluminescence glow curves 4-76533  
BaFCl:Gd flux grown cryst., thermoluminescence studies 4-66081  
BaFCl:Na crystals, flux grown thermoluminesc. glow curves, emission spectra 4-99200  
Ba(NO<sub>3</sub>)<sub>2</sub>·H<sub>2</sub>O, pure and doped single crystals, fluoresc. and phosphoresc. study 4-109227  
Ba(PO<sub>3</sub>)<sub>2</sub>:Er<sup>3+</sup>(Yb<sup>3+</sup>)(Nd<sup>3+</sup>), quenching of Er luminesc., effect of Nd<sup>3+</sup> and OH 4-81006  
Ba<sub>2</sub>Pt(H<sub>2</sub>P<sub>2</sub>O<sub>7</sub>)<sub>4</sub>, two-level phosphoresc., magneto-optical effect 4-93102  
BaSR, phosphors, photoluminescence spectra 4-61747  
BaSO<sub>4</sub>, barytes single crystals, γ irradi., optical absorpt., thermolum. 4-66080  
BaSO<sub>4</sub>:Dy, thermoluminesc. detectors response functions to γ-radiation 4-112037  
BaTiO<sub>3</sub>:Fe, electrolum., elec. field depend. 4-66077  
Be, 1s binding energy, core levels, state-specific many-electron theory 4-75887  
BeAl<sub>2</sub>O<sub>4</sub>:Cr<sup>3+</sup>, alexandrite, resonant 40 cm<sup>-1</sup> phonons, lifetime and line-width 4-65356  
BeAl<sub>2</sub>O<sub>4</sub>:Cr<sup>3+</sup>, alexandrite, fluorescence of inversion site Cr<sup>3+</sup> ions 4-107647  
BeO, thermally stimulated spontaneous RF emission 4-99203  
Bi oxides, Bi<sub>2</sub>MO<sub>2</sub>, M=Ge,Ti, luminesc. props. 4-76514  
Bi<sub>2</sub>Al<sub>2</sub>O<sub>7</sub>, luminesc. props. 4-76514  
Bi<sub>2</sub>Ge<sub>2</sub>O<sub>9</sub>, luminesc. props. 4-76514  
Bi<sub>2</sub>Ge<sub>2</sub>O<sub>9</sub>:Nd<sup>3+</sup>, hexagonal crystal, growth and luminesc. 4-76510  
Bi<sub>2</sub>SiO<sub>5</sub>:Nd, luminescence centres, selective excitation 4-114327  
Ca<sub>0.25</sub>Ba<sub>0.75</sub>Tb<sub>0.05</sub>Mg<sub>1.05</sub>B<sub>2</sub>O<sub>5</sub>, Kurchatovite struct., phosphor props. 4-66074  
CaCO<sub>3</sub>, natural, luminesc. 4-80995  
CaCO<sub>3</sub>, natural calcites, X-irradiated, thermolum., absorption and Mn<sup>2+</sup> EPR spectra 4-71453

## luminescence of inorganic solids continued

- CaCO<sub>3</sub>, review of thermoluminesc. 4-109253  
CaF<sub>2</sub>, review of thermoluminesc. 4-109253  
CaF<sub>2</sub> vapour deposited thin-films, TSEE, thermolum. meas. 4-81119  
CaF<sub>2</sub>:Ce<sup>3+</sup>, O<sup>2-</sup> thermoluminescence spectra, irradi. effects 4-109259  
CaF<sub>2</sub>:Dy<sup>3+</sup>, Eu<sup>2+</sup> crystals, electron-excitation relax. kinetics and nonequilibrium acoustic phonons. 4-88256  
CaF<sub>2</sub>:Eu<sup>2+</sup>, phononless line profile under random deformations, luminesc. bands 4-70726  
CaF<sub>2</sub>:Na, photochemical conversion of M<sub>A</sub>-centres, identification of M<sub>A</sub>-centre, absorpt. and fluoresc. spectra 4-76501  
CaF<sub>2</sub>:Sm crystal, gamma-irradiated, optical study 4-81015  
CaF<sub>2</sub>:ScF<sub>3</sub>:Nd<sup>3+</sup> system, stimulated emission channels 4-104632  
Ca<sub>1-x</sub>La<sub>x</sub>W<sub>0.12</sub>: rare earth, luminescence and sensitised emission 4-88871  
CaO, IR-radiated luminesc. due to O vacancies 4-81017  
CaS, single cryst. thermolum. study, 8-275K 4-104684  
CaS:Cu, Er (Sm) electrolumins., radiation controlled enhancement of electroluminescence 4-76520  
CaS:Er phosphor, electrolum. spectrum and Er<sup>3+</sup> ion energy level splitting 4-71446  
CaSO<sub>4</sub> phosphors, thermoluminescence and exoelectron emission, radical effects 4-93120  
CaSO<sub>4</sub>, review of thermoluminesc. 4-109253  
CaSO<sub>4</sub>:Dy, photo-transfer thermoluminescence 4-104683  
CaSO<sub>4</sub>:Dy dosimeters, TLD-900, thermolum. isothermal decay 4-68835  
CaSO<sub>4</sub>:Dy thermoluminesc. detectors response functions to γ-radiation 4-112037  
CaSO<sub>4</sub>:Dy(Tm), Bulgarian synthesis, thermoluminescent and dosimetry props. (Russian) 4-78747  
CaSO<sub>4</sub>:Dy(Tm), synthesis effect on phosphor props. (Russian) 4-78748  
CaSO<sub>4</sub>:Eu(Sm), thermoluminesc. and radiophotoluminesc. 4-93118  
CdBr<sub>2</sub>:Mn<sup>2+</sup>, phononless luminescence spectrum (Russian) 4-114328  
CdF<sub>2</sub>:Er<sup>3+</sup>, energy transfer up-conversion 4-99162  
CdF<sub>2</sub>:Er<sup>3+</sup> insulator to semiconductor transition, site selective laser spectroscopy 4-99155  
CdF<sub>2</sub>:Eu, thermoluminescence processes, photo-ESR studies 4-66085  
Cd,Hg<sub>1-x</sub>Te, obs. of negative luminescence 4-99190  
Cd<sub>1-x</sub>Te, photoluminescence study of polytype layer struct. (Russian) 4-71443  
CdIn<sub>2</sub>S<sub>4</sub>, luminescence kinetics study 4-104671  
CdIn<sub>2</sub>S<sub>4</sub> single cryst., photocond., photoluminescence and non-equilibrium carrier recombination 4-65706  
Cd<sub>1-x</sub>Mn<sub>x</sub>Te mag. semicond. superlattices, MBE growth and optical props. 4-114399  
Cd<sub>1-x</sub>Mn<sub>x</sub>Te-CdTe multilayers grown by MBE 4-88976  
CdS, colloidal crystallites, excited electronic states, size effects, optical props., Raman spectra 4-71334  
CdS, edge luminesc. series emitted in elec. field 4-66068  
CdS, effect of US waves, acoustoluminescence (Russian) 4-71454  
CdS, electron irradi., photoluminescence study 4-99189  
CdS film, photoluminescence method of determ. minority carrier kinetics 4-61748  
CdS, in NaFon film, struct., luminesc. lifetime quantum yield and quenching 4-85000  
CdS, luminescence study of polaritons 4-61300  
CdS monocrystals and films, luminesc. spectra during high levels of excitation (Russian) 4-80999  
CdS, radiative and nonradiative recomb., plastic deform. depend. 4-61658  
CdS, radiative recomb. mechanisms for high density excitons 4-88458  
CdS single, photoluminescence studies 4-109240  
CdS, small particles, photoluminesc. 4-85004  
CdS surface, clean and Au covered, surface recombination vel., photoluminescence studies 4-80600  
CdS:Cu, photoconductivity and luminescence (Russian) 4-84658  
CdS:Cu(Cl) films, defect diffusion, luminescence study (Russian) 4-88875  
CdS-CdTe thin films, photoluminescence study 4-80987  
CdSe, picosecond energy-relax. processes of excitons, luminesc. study 4-109244  
CdSe, picosecond spectroscopy at high excitation densities 4-81003  
CdSiAs<sub>2</sub>, impurity photoluminescence polarisation 4-88873  
CdSnO<sub>3</sub> and Cd<sub>2</sub>SnO<sub>4</sub>, EPR signals due to vacancies, comparison with CdO, yellow fluoresc. phenomenon 4-71179  
CdTe, cooperative processes, spontaneous and stimulated emission 4-104662  
CdTe films, MBE grown on (001) GaAs and (001) InSb, charact. 4-98471  
CdTe films, MBE growth and elec. and optical props. 4-81136  
CdTe films on InSb, MBE growth, charact. 4-98470  
CdTe MBE films on InSb, impurity doping and photoluminesc. props. 4-88980  
CdTe polycryst. film, gradient recryst. grown, photolum. 4-76522  
Cd<sub>1-x</sub>Zn<sub>x</sub>Te alloys, growth, elec. props., photoluminesc. 4-66207  
Cr complex, of tris(acetylacetonato), lowest doublet excited states, optical Zeeman spectra 4-66061  
CsCaCl<sub>2</sub>:Mn<sup>2+</sup>(Ni<sup>2+</sup>)(Co<sup>2+</sup>), fluoresc. emission, excitation, IR absorpt. spectra studies 4-99153  
CsI, irradiated single crystals, intrinsic hole colour centres 4-114332  
CsMnBr<sub>2</sub>:Er<sup>3+</sup>, one-dimensional antiferromagnet, energy migration, luminesc. 4-99149  
CsMnI<sub>2</sub>:Er<sup>3+</sup>, one-dimensional antiferromagnet, energy migration, luminesc. 4-99149  
Cs<sub>2</sub>Na<sub>2</sub>ScCl<sub>6</sub>:Cr<sup>3+</sup> cryst., dopant fluoresc. props. 4-61745  
Cs<sub>2</sub>TaOCl<sub>5</sub>, prep., fluoresc. spectra 4-108299  
Cs<sub>2</sub>TaCl<sub>5</sub>, prep., fluoresc. spectra 4-108299  
Cu complex, bis(2,9-diphenyl-1,10-phenanthroline) copper(I), solid, luminesc. 4-99148  
Cu, luminescence during static loading 4-99204  
Cu, mechanoluminescence at low loading rates 4-81019  
CuI single cryst., band-edge emission 4-80994  
CuInS<sub>2</sub>, radiative recombination and shallow centres 4-109250  
Cu<sub>2</sub>O, ortho-exciton states, time-resolved hot luminesc., reson. Raman scatt. 4-71438  
Cu<sub>2</sub>O, para-exciton luminesc. polarisation in mag. field 4-92624  
Cu<sub>2</sub>O thin films on Cu, defect luminesc. 4-66062  
Cu<sub>2</sub>O, triplet states, photoluminescence ODMR obs. 4-61608  
DyF<sub>3</sub>, optically excited, fluorescent excitation and absorpt. spectra 4-99154  
(Er<sub>1-x</sub>Y<sub>x</sub>)Al<sub>2</sub>O<sub>12</sub> crystals, temp. dependence of phononless f-f transitions 4-71339

# luminescence of inorganic solids continued

- EuAl<sub>3</sub>(BO<sub>3</sub>)<sub>3</sub>, UV absorpt., luminesc., circular dichroism spectra, gyrotropic characts. 4-114301
- Ga-Al-As, luminescence lineshapes of electron-hole plasma 4-109242
- GaAlAs single quantum well size effect modulation light sources 4-97014
- Ga<sub>1-x</sub>Al<sub>x</sub>As, carrier transport under impurity radiative recombination conditions 4-104211
- Ga<sub>1-x</sub>Al<sub>x</sub>As-GaAs heterostructure, LPE grown, dislocation extension and density distrib. (Chinese) 4-113449
- Ga<sub>1-x</sub>Al<sub>x</sub>P, epitaxial struts., luminesc. study 4-85011
- GaInSbAs-GaSb injection laser, operation and luminescence. study 4-74508
- GaAs, acceptor level, 78 meV, luminescence and Raman scatt. studies 4-70704
- GaAs crystal sensor in fibre-optic thermometer, temp. meas. by photoluminescence (Danish) 4-78315
- GaAs, deep acceptor, Hall effect obs. and photoluminescence 4-80532
- GaAs, electroluminescence and photoluminescence in aq. redox electrolyte 4-88584
- GaAs, electroluminescence spectra of free excitons, optical resonances 4-88883
- GaAs, electron-hole plasma density meas. 4-61408
- n-GaAs, emission band at 1.35 eV, doping and temp. variations 4-76519
- GaAs, free carrier lifetime from photoluminescence studies 4-80988
- GaAs growth using OMVPE, electronic and optical props. 4-114402
- GaAs, hot photoluminescence polarisation and spectrum 4-61743
- GaAs, impurities identification by magneto-optical photoluminescent spectroscopy 4-60945
- GaAs, ion implanted, photolum. after laser annealing 4-76525
- GaAs LEC substrate, characterisation of impurities and microdefects (Japanese) 4-103778
- GaAs LPE layers, residual impurities, growth soln. baking effects 4-92226
- GaAs layers, MBE grown on Ge islands on insulator, zone melting recrystallisation, grain boundaries, photoluminescence obs. 4-84524
- GaAs MBE films, growth and elec. props. (Chinese) 4-84523
- GaAs MBE growth of high purity layers, photolum. charact. 4-98474
- GaAs p-n-p-n superlattices, LPE growth 4-80665
- GaAs photodetectors, high speed, carrier dynamics, luminesc. study 4-111201
- GaAs, photoluminescence characterisation of impurities and defects 4-88876
- GaAs, photoluminescence intensities, computer-controlled mapping 4-104650
- GaAs, plastic deform., yield stress, photoluminescence, effect of impurity-vacancy complexes 4-70261
- GaAs, selectively excited luminesc. 4-104639
- GaAs, semi-insulating, 0.635 eV photoluminescence band, EL2 level 4-114315
- GaAs, semi-insulating, undoped and low Cr doped, LEC grown, photoluminescence props., whole ingot annealing effects 4-84994
- GaAs, semi-insulating LEC grown, impurity distribution, cathodoluminesc. study 4-88885
- GaAs semi-insulating substrate, inhomogeneity characterisation, expt. study 4-65759
- GaAs single quantum wells, low temp. exciton trapping on interface defects, photolum. 4-93111
- GaAs substrate, annealing as gettering technique prior to MBE growth 4-99615
- GaAs: Mn, spin-depend. recombination, optical pumping studies 4-99183
- GaAs: Cr, Cr-related complex, photoluminesc. studies 4-88467
- GaAs: Cr, impurities, optical and transport studies 4-71444
- GaAs: Cr, photolum. at 0.839 eV, polarisation of Zeeman spectra 4-71427
- GaAs: Cr, photoluminescence excitation spectra, Cr<sup>2+</sup> internal luminesc. 4-81004
- GaAs: Cr, semi-insulating, inhomogeneities, optical obs. 4-60944
- GaAs: Cr<sup>2+</sup>, trigonal. symmetry sites, photoluminescence spectra anal. 4-108391
- GaAs: Cr(Ni), deep impurity charact., photoluminescence study 4-98557
- GaAs: N, isoelectronic traps study by photoluminesc. (Chinese) 4-93098
- GaAs: Se, deep acceptor; photoluminescence study 4-80534
- GaAs: Si, Al p-n structures, radiative recomb., electrolum. characts. (Russian) 4-109249
- GaAs: Si p-n structures, degree of compensation, photoluminesc. study 4-65736
- p-GaAs: Zn, emission band, electron irradi. and annealing effects 4-88881
- GaAs/Al<sub>0.3</sub>Ga<sub>0.7</sub>As quantum wells, struct. and optical props. 4-99151
- GaAs/Al<sub>0.3</sub>Ga<sub>0.7</sub>As quantum wells, Be doped, photoluminescence studies 4-104653
- GaAs/AlAs multiple quantum well struct., electron-hole plasma, picosecond dynamics 4-92803
- GaAs/AlGaAs heterostructures, 2D electron plasma, optical processes 4-76523
- GaAs/AlGaAs inverted heterojunctions, photoluminescence studies 4-98460
- GaAs/AlGaAs single quantum well struct., enhanced luminescence 4-99150
- GaAs/Ge single crystal layers, MBE growth and patterning on Si substrates 4-99315
- GaAs-(AlGa)As superlattices, MBE grown, growth temp. influence 4-81139
- GaAs-(AlGa)As two-dimens. electron plasma, optical emission and excitation processes 4-104666
- GaAs-Al<sub>0.3</sub>Ga<sub>0.7</sub>As quantum wells, photoluminesc. from spike doped hydrogenic donors 4-104668
- GaAs-Al<sub>0.3</sub>Ga<sub>0.7</sub>As quantum well struts., Raman scatt. study 4-93079
- GaAs-Al<sub>0.3</sub>Ga<sub>0.7</sub>As multiple quantum well struct., magneto-Raman characterisation 4-104577
- GaAs-AlAs multiple quantum well struct., Raman scatt. and luminescence study 4-99105
- GaAs-AlGaAs superlattice grown by MBE, struct. and optical props. 4-84538
- GaAs-Ga<sub>1-x</sub>Al<sub>x</sub>As, binding energy of exciton in GaAs quantum well, magneto-optical determination 4-114027
- GaAs-GaAlAs double heterostructure, quantisation of excitonic polaritons 4-92634
- GaAs-GaAlAs heterostructures, hot photoluminescence polarisation and spectrum 4-61743

# luminescence of inorganic solids continued

- GaAs-GaAlAs multiple-quantum-well structures, sharp line photolum. spectra 4-93110
- GaAs-GaAlAs quantum wells, coupled, photoluminesc. and excitation spectroscopy 4-104667
- GaAs-GaAlAs quantum wells, reflectance of two-dimensional excitations 4-109211
- GaAs<sub>1-x</sub>P<sub>x</sub>, localised excitons, luminescence study 4-61291
- GaAs<sub>1-x</sub>P<sub>x</sub>N, exciton tunnelling inhibited by disorder, luminescence line shape 4-92622
- GaAs<sub>1-x</sub>P<sub>x</sub>N<sub>1-x</sub>Zn<sub>1-x</sub>, implanted, photoluminescence spectra, impurity conc. depend. (Chinese) 4-93099
- GaAs<sub>1-x</sub>P<sub>x</sub>-GaAs<sub>1-y</sub>P<sub>y</sub> isotype heterojunction electrodes in photoelectrochem. cells, photoluminescent and electroluminescent props. 4-99140
- Ga<sub>0.47</sub>In<sub>0.53</sub>As/Al<sub>0.48</sub>In<sub>0.52</sub>As heterojunction, conduction band discontinuity, photoluminescence study 4-76028
- GaInAsP, photolum. and optical gain spectra, book contrib. 4-61752
- Ga<sub>0.5</sub>In<sub>0.5</sub>P, photolum. dynamics of high density electron-hole plasma under psec. laser excitation 4-109228
- Ga<sub>1-x</sub>In<sub>x</sub>P, LPE growth on GaAs substrates, cathodoluminesc. and photoluminesc. spectra (Chinese) 4-113825
- GaN, polarised luminescence transitions and electroluminescence quenching 4-104670
- GaN: Zn, cathodoluminesc. anomalous kinetics 4-85015
- $\beta$ -Ga<sub>2</sub>O<sub>3</sub>: Cr crystals, luminesc. parameters, impurity centre electron capture effects 4-81016
- GaP crystal quality in soln. growth P press. effects, photolum. meas. 4-103685
- GaP diode struct., electroluminescence polarisation study (Russian) 4-88884
- GaP, electron irradi., defect creation, luminescence and elec. studies (Chinese) 4-108441
- GaP: N epitaxial films, n-type, local cathodolum. kinetics 4-109251
- GaP: N, electron-hole plasma under resonant free exciton excitation 4-71430
- GaP: N, exciton transfer, NN<sub>2</sub>-pair luminesc. enhancement, stochastic model 4-104660
- GaP: N, Te VPE layers, minority carrier lifetime, photoluminesc. decay study 4-76520
- GaP: N, Te, Zn, photolum. under high press. (Chinese) 4-93097
- GaP: Zn, O, LPE layers, cleaved surfaces-photoluminesc., macrosteps and grooves 4-65588
- GaP, As, Sb,  $\gamma$ -irradi., epitaxial layers, luminescence studies 4-76505
- 0.69Ga<sub>0.31</sub>S<sub>0.31</sub>La<sub>0.31</sub>Nd<sub>0.31</sub>, glass spectral luminesc. props. 4-76511
- GaSb epitaxial films, photoluminescence spectra 4-88896
- GaSb: Zn epitaxial films, photoluminescence spectra 4-88896
- GaSe single cryst., luminescence spectra, isothermal annealing effects 4-81001
- GaSe: Yb single cryst., photocond. and photoluminescence studies 4-84649
- GdCl<sub>3</sub>: Pr<sup>3+</sup>, crystal field levels, coord. geometry depend. 4-70755
- Gd<sub>2</sub>Ga<sub>2</sub>O<sub>7</sub>, fluorescence radiation due to X-ray standing waves 4-71437
- Gd<sub>2</sub>Se<sub>2</sub>Al<sub>2</sub>O<sub>7</sub>: Cr<sup>3+</sup>, tunable room temp. CW laser action 4-74518
- GdTaO<sub>4</sub>: Tb<sup>3+</sup>, energy transfer phenomena, photoluminescence 4-109234
- Gd<sub>2</sub>Te<sub>2</sub>Li<sub>2</sub>O<sub>7</sub>, photoluminesc. and energy transfer in rare earth activated garnets (German) 4-76508
- Ge, electron-hole liq. droplet destruction in nonuniform deformation field 4-61297
- Ge exciton condensation, microwave breakdown, one- and two-photon carrier excitation luminescence 4-70670
- Ge, luminescence signal of electron-hole plasma 4-104674
- Ge monocrystalline, K-shell fluoresc. yield 4-85041
- Ge, phonon pulses detection by fluorescence of deposited YF<sub>3</sub>: Tb<sup>3+</sup> film 4-113555
- GeS layered monocrystals, photoluminescence spectra, pol. plane orientation change effects 4-66069
- Ge<sub>2</sub>S<sub>3</sub>: Cu(Ag), glassy, doping effect on elec. and optical props. (Russian) 4-98625
- Ge<sub>2</sub>Se<sub>3</sub>, glass, photoluminescence characts. 4-76513
- Hg<sub>0.3</sub>Cd<sub>0.7</sub>Te, LPE grown, photoluminescence study 4-80986
- Hg<sub>1-x</sub>Cd<sub>x</sub>Te LPE layers, below band gap photoluminescence 4-71423
- HgCr<sub>2</sub>Se<sub>4</sub> ferromag. semiconductor, luminesc. study with quantum energy exceeding the forbidden band 4-80992
- Hg<sub>2</sub>In<sub>2</sub>Te<sub>6</sub>, recombination radiation 4-71447
- HoP<sub>0.4</sub>O<sub>1.4</sub> crystal, spectra and struct. (Chinese) 4-60887
- InAs<sub>1-x</sub>P<sub>x</sub>, epitaxial layer, bright 300K luminescence 4-70584
- InGaAs-InP injection laser, operation and luminescence study 4-74508
- InGaAs-InP superlattices, chloride VPE growth, struct. and optical props. 4-81158
- In<sub>0.53</sub>Ga<sub>0.47</sub>As, carrier energy relax., picosecond luminesc. studies 4-114312
- In<sub>0.53</sub>Ga<sub>0.47</sub>As, epitaxially grown by LPE, VPE, MBE, band gap energy spatial var., photoluminescence spectra 4-104125
- In<sub>0.53</sub>Ga<sub>0.47</sub>As LPE layers, high purity, photoluminescence processes 4-99187
- In<sub>0.53</sub>Ga<sub>0.47</sub>As multi quantum well struts., strained, optical props. 4-104669
- InGaAsP/GaAs, double heterojunctions, photoluminesc. studies 4-76504
- InGaAsP/InP DH, luminescence and laser threshold characts. 4-85008
- InGaAsP/InP double heterojunctions, photoluminesc. studies 4-76504
- InGaAsP-InGaP rapidly degraded DH laser grown by LPE, dark-line defects 4-69406
- InGaAsP-InP DH, photoluminescence efficiency 4-85006
- In<sub>0.75</sub>Ga<sub>0.25</sub>As<sub>0.44</sub>P<sub>0.56</sub>, luminescence study of binding energy variation 4-71435
- InGaP/InAlP quantum well structures for visible region, MBE growth 4-99314
- In<sub>1-x</sub>Ga<sub>x</sub>P<sub>1-x</sub>As<sub>2-x</sub>, solid solution, LPE, crystn. and optical props. 4-108736
- InP acceptor impurity incorporation during organometallic VPE, photolum. obs. 4-98122
- InP epilayers, cathodoluminescence study 4-104678
- InP, excitons bound to neutral acceptors, stress effects, photoluminesc. study 4-61294
- InP, LEC grown, photoluminesc. study, 1.8 to 40K (Chinese) 4-84993
- InP, near IR cathodoluminescence in a TEM 4-81011
- InP, transition metal diffusion, photoluminesc. study 4-70461
- InP: Be(C), acceptor levels, photoluminesc. study 4-80543
- InP: Co, impurities, optical and transport studies 4-71444
- InP: Fe, semi-insulating, with phosphosilicate glass encapsulation heat treatment, photoluminesc. and Raman scatt. characterisation 4-84995

## luminescence of inorganic solids continued

- InP:Gd(Yb) epitaxial films, doping effects on low-temp. edge photoluminescence 4-85028  
 InP:Ge(Sn), donor identification, photolum. and far IR photocond. in high mag. fields 4-70705  
 InP:Mg(Ca,Zn) crystals grown by synthesis solute diffusion, electrical and optical props. 4-85093  
 InP:Mg(Fe,Mg), implanted, effect on photoluminescence props. 4-85007  
 InP:Yb p-n junctions; electroluminescence studies 4-66079  
 InP-In<sub>0.3</sub>Ga<sub>0.7</sub>As-InP DH wafers, LPE grown, misfit dislocations, X-ray and photoluminescence topography 4-80042  
 InP-InGaAsP-InP DH, photoluminescence intensity 4-61738  
 InSe, layered monocrystals, photoluminescence spectra, pol. plane orientation change effects 4-66069  
 n-InSe, photoluminescence and free exciton emission 4-99176  
 KBr, excited F-centre emission, effect of CO<sub>2</sub> laser light 4-61742  
 KBr:Cl, undoped crystals, anion Frenkel defect creation, luminesc. study (Russian) 4-80980  
 KBr:Cl, X-irradiated, luminesc. study (Russian) 4-80981  
 KBr:Cr(N)<sub>3</sub><sup>2+</sup>, ESR, IR, Raman and emission spectra, radiative and nonradiative transition 4-65850  
 KBr:In, A<sup>2+</sup>, F-centres formed by low-energy excitons, photoluminescence spectra (Russian) 4-113874  
 KBr:In, radiation storage of activator light sums, role of surface effect, photoluminescence (Russian) 4-114322  
 KBr:In(Tl), light sum slow component characts. in presence of fast component, photoluminescence (Russian) 4-114320  
 KBr:In(Tl) polycrystalline films, luminescent, epitaxial growth (Russian) 4-113833  
 KBr:No<sup>+</sup>, Ca<sup>2+</sup>, struct. of luminesc. and absorpt. centres (Ukrainian) 4-66059  
 KCl crystals, optical breakdown thresholds due to action of CO<sub>2</sub> laser pulses 4-60957  
 KCl, X-irrad., thermolum. spectra 4-90663  
 KCl:Ag, Ca, X-irrad., electron centre form., luminesc., optical absorpt. studies 4-60920  
 KCl:Ag, X-irrad., electron centre form., luminesc., optical absorpt. studies 4-60920  
 KCl:I, impurity-localised excitons, luminesc. and absorpt. spectroscopy study 4-92625  
 KCl:I, luminescence of localised excitons at low temp. 4-80990  
 KCl:Li, optically excited colour centres, relaxation dynamics 4-113896  
 KCl:O<sub>2</sub><sup>+</sup>, fluoresc. time depend. study 4-109239  
 KCl:Sr, X-irradiated, struct. of (Cl<sub>3</sub>)<sub>2</sub>-centres, optical study (Russian) 4-80968  
 KCl:Ti, lattice defects creation and corrosion during annihilation of electronic excitations (Russian) 4-80035  
 KCl:Br<sub>2</sub>, mixed crystals, thermolum. studies 4-104681  
 KI, F-centre luminesc., mag. circular polarisation, anomalous effect 4-93062  
 KI, generation of free excitons by optical excitation of self-trapped excitons, luminesc. emission 4-88453  
 KI, UV irrad., V<sub>K</sub> motion and luminesc. quenching 4-66063  
 KI:In(Tl), fast luminescence processes 4-99167  
 KI:Se<sup>+</sup>, secondary luminesc. formation, phase relax. effect 4-104640  
 KI:Ti<sup>+</sup>, hot luminescence and vibr. relax. 4-85019  
 K<sub>2</sub>La<sub>1-x</sub>Ce<sub>x</sub>Tb<sub>1-x</sub>(PO<sub>4</sub>)<sub>2</sub> luminophors, instrumental neutron activation anal. 4-85345  
 KNdPO<sub>4</sub>, radiative transition probabilities 4-80973  
 KNdPO<sub>4</sub>-based cryst., laser time resolved selective excitation 4-99163  
 KP<sub>15</sub>, crystalline and amorphous, semiconducting props. 4-98603  
 K<sub>4</sub>UO<sub>2</sub>(CO<sub>3</sub>)<sub>3</sub>, photoluminescence and mol. vibr. modes 4-99164  
 La<sub>0.72</sub>Pr<sub>0.28</sub>Nd<sub>0.03</sub>F<sub>3</sub>, fluorescence decay characts. 4-71436  
 LaCl<sub>3</sub>:Nd<sup>3+</sup>, isotope shifts, laser-induced fluoresc. 4-71428  
 LaCl<sub>3</sub>:Pr<sup>3+</sup>, crystal field levels, coord. geometry depend. 4-70755  
 LaF<sub>3</sub>:Pr<sup>3+</sup>, cooperative energy transfer among Pr<sup>3+</sup> ions; photoluminescence spectra 4-92664  
 LiF, phototransferred thermoluminesc. for high LET radiation dosimetry 4-105339  
 LiF powered crystals, photoacoustic spectroscopy for thermoluminescent dosimetry 4-93116  
 LiF, R<sup>+</sup>-centre aggregate, spectral linewidths, depend. on irrad. method 4-70193  
 LiF TLD 100, order of kinetics 4-88888  
 LiF vapour deposited thin films, TSEE, thermolum. meas. 4-81119  
 LiF, X-irrad., thermolum. spectra at LNT 4-66084  
 LiF:Mg,Cu,P, high sensitivity thermoluminesc. dosimeter, environmental monitoring appl. 4-109934  
 LiH crystals, cleaved, excitonic struct., optical spectra study 4-61746  
 LiH, electron-phonon interactions in luminescence spectra 4-71439  
 LiNbO<sub>3</sub>, shock induced luminescence studies 4-109260  
 LiNbO<sub>3</sub> single cryst., cathodoluminescence emission, surface damage 4-93115  
 LiNbO<sub>3</sub> single cryst., electroluminescence obs. 4-99197  
 Li<sub>2</sub>O-Nd<sub>2</sub>O<sub>3</sub>-GeO<sub>2</sub>(SiO<sub>2</sub>) ternary systems, subsolidus phase equilib. and fluorescence activity 4-113596  
 LiPrPO<sub>4</sub>, absorption and fluoresc. intensity anal. of Pr<sup>3+</sup> 4-104654  
 LiYF<sub>4</sub>:Nd<sup>3+</sup>, electronic Raman scatt. and two-photon fluorescence (Chinese) 4-104581  
 MgAl<sub>2</sub>O<sub>4</sub> spinel, cathodoluminescence induced by impurities 4-85017  
 MgO (100), surface dislocation, secondary electron emission study 4-80345  
 MgO, F<sup>+</sup> centre, electronic point defects with self consistent lattice polarisation 4-93091  
 MgO phosphor, thermolum. and trapping kinetics 4-88887  
 MgO, quenched, defect struct., plastic deform., SEM, cathodoluminescence, optical absorpt. spectra 4-71448  
 MgO, quenched, photoluminescence study 4-88872  
 MgO single cryst., high anion vacancy conc., cathodoluminescence obs. 4-88886  
 MgO single crystals, thermolum. kinetics rel. to Cr<sup>3+</sup> and Fe<sup>3+</sup> impurity conc. (Japanese) 4-99202  
 MgO, TL mechanisms and luminesc. characts., review 4-109254  
 MgO, thermoluminescence charge transfer mechanism 4-71450  
 MgO:Ce<sup>3+</sup>, fluoresc., thermoluminesc. and decay 4-93117  
 MgO:Ni, irradiated, thermolum. study 4-81018  
 MgO:Na<sub>2</sub>O<sub>2</sub>:Cr(Mn), impurity ion distrib. in spinel lattice 4-84311  
 Mn II complex, di(aminophenazone)MnCl<sub>4</sub>, cryst., photoexcitation and photoluminesc. study 4-80976  
 Mn II complex, di(phenazone)MnCl<sub>4</sub>, cryst., photoexcitation and photoluminesc. spectra 4-80976

## luminescence of inorganic solids continued

- Mn(H<sub>2</sub>PO<sub>4</sub>)<sub>2</sub>, luminesc. props. 4-80993  
 MnH<sub>2</sub>P<sub>2</sub>O<sub>7</sub>, luminesc. props. 4-80993  
 Mn(H<sub>2</sub>PO<sub>4</sub>)<sub>2</sub>·2H<sub>2</sub>O, luminesc. props. 4-80993  
 Mn<sub>2</sub>P<sub>2</sub>O<sub>7</sub>, luminesc. props. 4-80993  
 Mo, mechanoluminescence at low loading rates 4-81019  
 N<sub>2</sub> crystalline, exciton luminesc. and luminesc. spectrum struct. 4-104641  
 (NH<sub>4</sub>)<sub>2</sub>ZnCl<sub>4</sub>, X-ray irrad., photoluminescence and EPR studies 4-93108  
 NaA and NaX zeolites, luminescent, migration of electronic excitations (Russian) 4-80983  
 Na<sub>3</sub>(AlO<sub>2</sub>)<sub>3</sub>(SiO<sub>2</sub>)<sub>40</sub>·24H<sub>2</sub>O:Eu<sup>2+</sup>, adsorption of O<sub>2</sub>, fluorescence study 4-84511  
 NaCl crystals, optical breakdown thresholds due to action of CO<sub>2</sub> laser pulses 4-60957  
 NaCl, electron irrad., appl. to radioactive waste repositories 4-75532  
 NaCl:Ag<sup>+</sup>, Ag<sup>+</sup> ion dimer centres, optical props. 4-66076  
 NaCl:Ba, post γ-irradiation thermolum., effect of plastic deform. 4-104682  
 NaCl:Ba, thermoluminescence, pre- and post-irrad. deformation effects 4-66083  
 NaCl:Br, impurity-localised excitons, luminesc. and absorpt. spectroscopy study 4-92625  
 NaCl:CaCl<sub>2</sub>, decay props. of perturbed and unperturbed M-centres 4-92204  
 NaCl:Pb<sup>2+</sup>, luminescence, effect of additional M<sup>2+</sup> doping 4-109245  
 Na<sub>2</sub>Eu(MO<sub>4</sub>)<sub>4</sub>, M=Mo, W, cryst. field effect, mag. susceptibility, fluoresc. study 4-88867  
 NaEvTiO<sub>4</sub>, 2D system, luminescence and energy migration 4-99161  
 NaF polycrystalline thin films, neutron and X-irrad., photochemical hole burning 4-76518  
 NaF:O, X-ray irrad., thermoluminescence studies 4-99181  
 NaF:Cu, fluorescence kinetics, three-level model anal. 4-99184  
 NaGdTiO<sub>4</sub>:Eu<sup>3+</sup>, nonradiative relax. by multiphonon emission 4-76507  
 NaI crystals, cleaved, excitonic struct., optical spectra study 4-61746  
 NaI:Pb, photoluminescence decay, temp. and aggregation depend. 4-99177  
 NaI:Ti, excitation fluoresc. intensity in VUV 4-84987  
 NaI(Tl) deformed cryst., relationships among stresses, microstruct. and photolum. 4-71441  
 Na<sub>1-x</sub>Mg<sub>x</sub>Al<sub>1-x-y</sub>O<sub>7</sub>:Nd<sup>3+</sup> platelet laser absorpt. spectra, fluoresc. lifetime, laser-pulse shape and peak emission wavelength 4-60044  
 Na<sub>2</sub>Nd<sub>2</sub>M<sub>2</sub>-xGa<sub>2</sub>S<sub>4</sub> (M=Ca,Sr,Ba), luminescent props. and electron transfer 4-109233  
 NaR(SO<sub>4</sub>)<sub>2</sub>·H<sub>2</sub>O (R=lanthanides), luminescence in host lattice with high energy vibrs. 4-88869  
 NaYF<sub>4</sub>, order of kinetics of thermoluminesc. 4-76535  
 NaYF<sub>4</sub>, polycryst. powder, X-irrad., thermolum. and colour centre obs. 4-61757  
 NaYGeO<sub>4</sub>:Nd<sup>3+</sup>, luminescence and stimulated emission, laser channels 4-93109  
 Na<sub>2-x-y</sub>Ca<sub>2</sub>(1-x-y)Ce<sub>x</sub>Tb<sub>y</sub>(PO<sub>4</sub>)<sub>2</sub> orthophosphates, luminescence and struct. relations 4-99169  
 Nd:SiO<sub>2</sub> glasses prep. by axial injection plasma torch CVD 4-93229  
 Nd<sub>2</sub>O<sub>3</sub>-WO<sub>3</sub>-GeO<sub>2</sub> (MO; M=Ca, Sr, Ba, Mg, Zn), subsolidus phase equilib. and fluorescence activity 4-113597  
 Ne, cryocrystals, high-energy excitations, hot luminesc. 4-99194  
 Ne, solid, Ne<sup>+</sup> centres, vibr. relax. and hot luminescence 4-99178  
 Pb oxides, PbM<sub>2</sub>O<sub>4</sub>, M=Al, Ga, luminesc. props. 4-76514  
 PbCl<sub>2</sub>:Br<sub>2</sub>, self-trapped excitons, luminesc. (Russian) 4-80982  
 PbF<sub>2</sub>-GaF<sub>3</sub>-Al(PO<sub>3</sub>)<sub>3</sub>-ErF<sub>3</sub>-based fluoride glasses, fluorescence studies 4-99170  
 PbGeO<sub>3</sub>, luminesc. props. 4-76514  
 PbO, exciton luminescence under powerful laser excitation 4-109235  
 PbS film, photosensitivity and luminescence studies 4-104679  
 PbTe epitaxial films, photoluminescence characts. 4-66067  
 PrF<sub>3</sub>, cooperative energy transfer among Pr<sup>3+</sup> ions, photoluminescence spectra 4-92664  
 Pr<sub>2</sub>La<sub>1-x</sub>P<sub>2</sub>O<sub>14</sub>, luminesc. theory, oscillator strength, impurity conc. effect (Chinese) 4-93100  
 RbAg<sub>2</sub>I<sub>3</sub>:S(Se)(Te), electron level struct., photoluminescence spectra 4-99192  
 RbBr:Eu, optical study of Eu precipitation 4-80233  
 RbCl:Eu, optical study of Eu precipitation 4-80233  
 RbGd<sub>2</sub>F<sub>10</sub>:Eu<sup>3+</sup>, Eu<sup>3+</sup> fluorescence, Gd<sup>3+</sup> effects 4-104663  
 RbMgF<sub>3</sub>:Eu,Mn, Eu<sup>2+</sup>-sensitised Mn<sup>2+</sup> luminescence 4-76521  
 RbMgF<sub>3</sub>:Mn<sup>2+</sup>, electron irrad., vacancy-interstitial pair and F-centre-impurity ion pair form. 4-70215  
 RbMnBr<sub>3</sub>:Er<sup>3+</sup>, one-dimensional antiferromagnet, energy migration, luminesc. 4-99149  
 RbMnCl<sub>3</sub>, antiferromag. with alternating strong and weak coupling, absorpt. spectra, fluoresc. meas. 4-88659  
 Rb<sub>2</sub>MnCl<sub>4</sub>, 2D antiferromag., optical absorption and luminesc. 4-80991  
 Rb<sub>2</sub>Mn<sub>2</sub>Cl<sub>7</sub>, 2D antiferromag., optical absorption and luminesc. 4-80991  
 Ru complex, tris(bipyridyl) ruthenium (II) surfactant luminesc. activity rel. to monolayer deposition 4-114318  
 SC<sub>2</sub>O<sub>3</sub>, ODMR study of exciton trapping 4-80503  
 Si, amorphous CVD films, H<sub>2</sub> plasma annealing localized state density 4-61337  
 Si, Czochralski, C in radiation damage centres, luminesc. study 4-93107  
 Si, heavily doped, band-gap narrowing study 4-80490  
 p-Si high-purity quenched samples, defect photoluminesc. 4-80979  
 Si, ion implanted, laser or electron beam annealing, minority carrier recomb., EBIC, photoluminescence meas. 4-80601  
 Si, ion implanted, rapid thermal arc lamp and pulsed laser annealing, photoluminesc. study 4-93094  
 Si, ion implanted with noble gases, optical defects, photoluminesc. study 4-71429  
 Si, irradiated, excitation spectroscopy on 0.79 eV (C) line defect 4-93112  
 n-Si, irradiated, Si-Si centre, optical excitation and relaxation, EPR study 4-109075  
 Si, magnetic energy states of shallow acceptors, spin depend. luminesc. study 4-104655  
 Si, phonon pulses detection by fluorescence of deposited YF<sub>3</sub>:Tb<sup>3+</sup> film 4-113555  
 Si, photoluminescence characterisation of impurities and defects 4-88876  
 Si:As<sup>+</sup>(Sb<sup>+</sup>), ion implanted and laser annealed, defects, photoluminescence studies 4-75433  
 Si:B, Fe, exciton photoluminescence study 4-109243  
 Si:H, amorphous, high-rate deposited annealing effects 4-61876

## luminescence of inorganic solids continued

- a-Si:H, deep recombination centres, luminescence and EPR studies 4-104164  
 a-Si:H, geminate recombination and mobility 4-104223  
 a-Si:H, high-rate deposition from SiH<sub>4</sub> using RF discharge technique, elec. and optical props. 4-85119  
 a-Si:H, prep. by glow discharge of Si<sub>2</sub>H<sub>6</sub>, optical and elec. props. 4-114237  
 a-Si:H, radiative combination at dangling bonds, quantitative model, expt. study 4-114326  
 a-Si:H film, IR quenching of photoluminescence and photoconductivity 4-104656  
 a-Si:H film, time resolved photoluminescence and phonon transport 4-71445  
 a-Si:H films, luminescence fatigue and ODMR studies 4-85005  
 Si:H wide optical gap binary alloy films, elec. props. 4-113956  
 a-Si:H/a-Si<sub>1-x</sub>N<sub>x</sub>H quantum well struct., luminescence and current transport 4-114024  
 Si(In,Tl), iso-electronic bound excitons, transient photoluminesc. study 4-80507  
 Si:Li and Si:Li<sub>2</sub>, C, electron irradi., luminesc. decay time, absorpt., isotope splitting, and Zeeman meas. 4-71434  
 Si:N single cryst., ion implanted, photoluminescence studies 4-114313  
 Si:O, C, annealed, photoluminesc. of impurity complexes 4-88866  
 Si:O, isotope effects and photoluminescence spectra 4-104661  
 Si<sub>3</sub>C<sub>1-x</sub>H<sub>x</sub>, amorphous, CVD prep., XPS and optical studies 4-70600  
 a-Si<sub>1-x</sub>C<sub>x</sub>H<sub>x</sub>, luminescence from photo-generated carriers, polarisation memory 4-99186  
 SiO<sub>2</sub>, amorphous, optical study of defects 4-88862  
 SiO<sub>2</sub>, amorphous, luminescence and absorption centres, vacuum UV generation 4-71433  
 SiO<sub>2</sub>, halogen containing layers, cathodoluminescence spectra (Russian) 4-99198  
 SiO<sub>2</sub>, luminescence study of elec. cond. 4-61756  
 SiO<sub>2</sub> MIS struct., electroluminescence emission studies 4-93114  
 SiO<sub>2</sub>:Cr thin films, cathodoluminescence and C-V characts. (Russian) 4-99173  
 Sr<sub>2</sub>Cd<sub>1-x</sub>F<sub>2</sub>:Er<sup>3+</sup>, energy transfer up-conversion 4-99162  
 SrF<sub>2</sub>, interstitial atom hopping by electronic excitation of Frenkel pairs 4-70140  
 SrF<sub>2</sub>, photo-induced transform. of close Frenkel pairs, absorption and luminesc. props. 4-76500  
 SrF<sub>2</sub>:Eu<sup>2+</sup>, phonon diffusion and decay, impurity luminesc. study 4-61006  
 SrF<sub>2</sub>:Gd<sup>3+</sup>, phosphors, thermostimulable center-center transitions, luminesc. 4-80996  
 Sr<sub>2</sub>La<sub>2</sub>W<sub>2</sub>O<sub>12</sub>, rare earth, luminescence and sensitised emission 4-104657  
 Sr<sub>2</sub>, electronic excitations and recomb. luminesc. (Russian) 4-80984  
 Sr<sub>2</sub>:Ce:Sm, luminescence, optical and thermal stimulation 4-99174  
 Sr<sub>2</sub>:Pb<sup>2+</sup> phosphors, impurity dimer centres, luminesc. obs. 4-99158  
 Sr<sub>2</sub>:Pb<sup>2+</sup> phosphors, impurity dimer centres, luminesc. obs. 4-99158  
 SrTiO<sub>3</sub>, compensated, defects and colour centres, optical study 4-92200  
 TbF<sub>3</sub>, fluorescence, exciton diffusion and up conversion mechanisms 4-66075  
 ThBr<sub>3</sub>:Pa<sup>4+</sup>, incommensurate phase, single cryst., Pa<sup>4+</sup> optical spectroscopy 4-71422  
 TiO<sub>2</sub>, multiphoton interactions, laser induced photoluminesc. and photocond. 4-93093  
 TiGaS<sub>2</sub> (Se<sub>2</sub>):Nd semiconducting chalcogenides, photoluminescence studies 4-99180  
 TiGaS<sub>2</sub> ternary layered cryst., photoluminescence studies 4-66064  
 TiGaS<sub>2</sub>-Nd<sub>2</sub>S<sub>3</sub>, TiGaSe<sub>2</sub>-Nd<sub>2</sub>Se<sub>3</sub>, interactions, solubility, optical props. 4-109385  
 TiInS<sub>2</sub>, crystals, free and bound excitons radiative recombination 4-80504  
 TiInS<sub>2</sub> single cryst., edge photoluminescence under laser excitation 4-66066  
 Xe, cryocrystals, high-energy excitations, hot luminesc. 4-99194  
 Xe, solid and liq. excited by synchrotron radiation, luminesc. decay 4-84986  
 YAG:Ce<sup>3+</sup>, defect emission, photoluminesc. decay time measurements 4-80971  
 YAG:Fr, photoluminescence spectra meas. (Russian) 4-71442  
 Y<sub>2</sub>O<sub>3</sub>:Nd thin film waveguide, RF sputtering growth, fluoresc. spectrum, optical amplifier appl. 4-60146  
 (Y<sub>1-x</sub>Gd<sub>x</sub>)<sub>2</sub>O<sub>3</sub>:Ca luminesc. study 4-81013  
 Y<sub>2</sub>O<sub>3</sub>, ODMR study of exciton trapping 4-80503  
 Y<sub>2</sub>(WO<sub>4</sub>)<sub>3</sub>:Eu<sup>3+</sup>, prep. and luminesc. props. 4-81009  
 Y<sub>2</sub>(WO<sub>4</sub>)<sub>3</sub>.nH<sub>2</sub>O:Eu<sup>3+</sup>, luminescent precipitate prep., photolum. brightness 4-114330  
 (Zn,Mn)S mixed cryst. and thin film, photoluminescence studies 4-99179  
 Zn chalcogenides, MOCVD growth 4-93227  
 Zn,Cd<sub>1-x</sub>S, excitation migration between localised excitons, photoluminescence, absorpt. spectra 4-88456  
 Zn,Cd<sub>1-x</sub>S solid soln., localised exciton migration, pumping intensity effects 4-92618  
 ZnO electrolumiphosphor, brightness waves, grain size effects 4-104675  
 ZnO electrolumiphosphors, brightness, volt. and freq. depend. 4-104676  
 ZnO UV laser with longitudinal electron beam pumping 4-79164  
 ZnO:Gd(Pr), thermoluminesc. under UV, β- and γ-ray irradiations 4-93119  
 ZnO:Nd(Yb), electrolum. brightness, voltage and freq. depend. at liq. N<sub>2</sub> temp. 4-93113  
 ZnS, CVD, vacancy-hydride complex, optical absorpt., photoluminesc. 4-60916  
 ZnS conductive film, MBE prep. with single effusion source, luminesc. and elec. props. 4-99323  
 ZnS:Ag phosphor, phase composition effect on luminescence parameters and EPR spectrum (Polish) 4-85014  
 ZnS:Cu, Cl, Er films, electroluminesc., hot electron energy distribution 4-85012  
 ZnS:Cu, Er phosphor, electroluminescence and photoluminescence emission spectra 4-76512  
 ZnS:Cu film, cathodoluminescence study of annealing 4-81008  
 ZnS:Er(Mn,Er) phosphors, electro- and photo-luminescence props. 4-104652  
 ZnS:I with adsorbed O<sub>2</sub>, surface states and LED props. 4-80643  
 ZnS:Mn, coprecipitated phosphors, photo- and electro-luminescence 4-61739  
 ZnS:Mn ACTFEL electroluminescent devices 4-88882  
 ZnS:Mn electroluminesc. thin layers, doping and cryst. struct. 4-75810  
 ZnS:Mn thin films, electrolum., diffusion and trapping 4-104677

## luminescence of inorganic solids continued

- ZnS:NI<sup>2+</sup>, photolum. band arising from <sup>3</sup>T<sub>1</sub>(P)→<sup>3</sup>T<sub>1</sub>(F) transition 4-104664  
 ZnS:Sn(Cu) electroluminescent phosphors, Alfrey-Taylor relation 4-114331  
 ZnS:SmF<sub>3</sub> thin films, red electroluminesc. and crystallinity 4-99195  
 ZnS(Se) phosphor DC electroluminescent cells, self-activated centers, low field recombination 4-99196  
 ZnS(Se), solution growth and photoluminesc. props. 4-88958  
 ZnS,Se<sub>1-x</sub>, deep impurity, trap embedding, luminesc. spectra 4-61321  
 ZnS,Se<sub>1-x</sub>Cu, photoluminescence study 4-93095  
 ZnS films, low press. MOCVD growth and elec. and optical props. 4-93230  
 ZnS films, MBE growth, elec. cond., Hall effect and photoluminescence studies 4-99344  
 ZnSe heteroepitaxial layers, VPE, photoluminesc. 4-61741  
 n-ZnSe, OMVPE undoped films, elec. and optical props. 4-93226  
 ZnSe photoelectrochemical cells, radiative recombination 4-89456  
 ZnSe, pulsed irradiation with electrons 4-109230  
 ZnSe, VPE growth, photoluminesc. props. 4-61858  
 ZnSe:Na, donor-acceptor-pair line luminesc. 4-104659  
 ZnTe:Ni, absorpt. spectra, impurity states (Russian) 4-113898
- luminescence of liquids and solutions**  
 2-acetylthiophene, luminesc. and coplanar conformations, temp. depend. 4-104648  
 aromatic hydrocarbons, polynucly., dil. solns., β-induced fluoresc. spectra 4-88879  
 p-benzoquinone, fluid soln., phosphoresc. and fluoresc. spectrum 4-66065  
 9,9'-bianthryl, intramolecular electron transfer, solvent effects, fluoresc. study 4-96598  
 9,9'-bianthryl, viscous solvents, intramolecular electron transfer luminesc., high press. study 4-80977  
 cholesteric mixture, compensated liquid crystals, fluorescent guests props. 4-65168  
 4-cyano-4'-alkoxybiphenyls, liq. cryst., energy transfer and migration 4-76516  
 p-cyano-N,N-dialkylanilines in nonpolar solns., luminescence studies 4-99168  
 diarylethylenes, conformers (rotamers) proof of existence by luminesc. methods 4-104649  
 1,1'-diethyl-2,4'-carbocyanine, in methanol, S<sub>0</sub>-S<sub>1</sub> absorpt., UV and fluoresc. spectra 4-96597  
 2,5-diphenyloxazole in liq. hexane, energy transfer for excitation energies up to 21.2 eV, fluoresc. 4-84992  
 glycerol-rhodamine 6G soln., photoluminescence conc. depolarisation 4-80974  
 hydantoin derivatives, absorpt. and luminesc. props. 4-59707  
 4-isocyanate-3'-4'-dimethoxy-trans-stilbene, luminesc. intensity distrib., orientation polarisation relax. time 4-76509  
 4-isocyanate-4'-dimethylamino-trans-stilbene, luminesc. intensity distrib., orientation polarisation relax. time 4-76509  
 4-isocyanate-4'-methoxy-trans-stilbene, luminesc. intensity distrib., orientation polarisation relax. time 4-76509  
 liquids and liq. cryst., fluorescence depolarisation intensity deconvolution 4-93103  
 metalloporphyrins in solns., stored vibr. energy effect on fluoresc. and quantum yield 4-109237  
 2-(4-methoxyphenyl)-5-(2-naphthyl)-1,3,4-oxadiazole, liq. scintillator, energy transfer quenching 4-104651  
 methyl retinoate in solns. and films, spectroluminesc. props. 4-109236  
 molecular luminescence and its applications, conf., Kharkov, USSR (1982) 4-106094  
 1,8-naphthoylene-1',2'-benzimidazole-lumiphores liq. mixtures, luminescent defectoscopic composition 4-99143  
 nucleic acids and their components, intrinsic luminesc. 4-105178  
 organic dyes, photovoltaic cells, chem. props. 4-84998  
 organic lumiphosphors, chem. struct. features and directed synthesis 4-104645  
 organic lumiphosphors, luminescent properties formation due to photochem. processes, review 4-104646  
 organolumiphosphors, solns., elec. generated chemiluminesc. 4-104687  
 oxazine dyes, solvent deuteration effects, fluoresc., laser efficiency 4-79127  
 oxazine-1-perchlorate, in ethanol, S<sub>0</sub>-S<sub>1</sub> absorpt., UV and fluoresc. spectra 4-96597  
 2-phenylbenzoxazole, spectral-luminesc. and lasing props. rel. to struct. 4-87155  
 polydiacetylene solns. and glasses, absorpt., fluoresc. and emission spectra 4-71425  
 polymethine dyes, luminesc. studies of absorpt. transitions between excited states 4-83506  
 polynuclear aromatic hydrocarbons, in cyclodextrins, room-temp. phosphoresc. 4-78884  
 polystyrene, head-to-head, intramol. excimer form. and energy migration 4-114325  
 polyvinylcarbazole-vinylbenzocarbazole, fluorescence and host-guest energy transfer 4-99166  
 pyrene-N,N-dimethylaniline complex radical pairs, exciplex luminesc., environment effect on mag. field modulation 4-99147  
 rare gas fluoride dimers and trimers dissolved in liq. rare gases 4-96608  
 retinoic acid in solns. and films, spectroluminesc. props. 4-109236  
 retinyl acetate in solns. and films, spectroluminesc. props. 4-109236  
 riboflavin solns., lifetime meas. using nanosecond laser fluorimeter 4-83406  
 smectic mesophases, rank order parameters, angle resolved fluoresc. depolarised meas. 4-62443  
 solvation, intermolecular relaxation, luminescence spectroscopy study 4-109225  
 thiohydantoin derivatives, absorpt. and luminesc. props. 4-59707  
 vinyl alcohol-vinyl acetate copolymer, water-soluble, chem. and intramol. struct. (Russian) 4-102840  
 vinyl aromatic polymers in soln., phosphorescence study (Russian) 4-114329  
 xanthene dyes, solvent deuteration effects, fluoresc., laser efficiency 4-79127  
 CdBr<sub>2</sub>-NO<sub>2</sub>, aqueous soln., luminescence study (Russian) 4-85009  
 CdCl<sub>2</sub>-NO<sub>2</sub>, aqueous soln., luminescence study (Russian) 4-85009  
 Dy compounds in nonaq. soln., absorpt. and luminesc. spectra, f-f absorpt. bands, oscillator strengths, luminesc. 4-59768

**luminescence of liquids and solutions continued**

- Eu complexes in soln., electronic spectra modelling for struct. study 4-114245  
 EuCl<sub>3</sub> in soln., Eu<sup>3+</sup> vibronic spectra of luminesc. excitation 4-104642  
 Eu(III) complexes, cryptates, luminesc. and UV spectra 4-80978  
 Eu(NO<sub>3</sub>)<sub>3</sub> in soln., Eu<sup>3+</sup> vibronic spectra of luminesc. excitation 4-104642  
 KNO<sub>3</sub>:Tm<sup>3+</sup> soln., optical absorpt. spectra 4-84957  
 MgNO<sub>3</sub>·6H<sub>2</sub>O:Tm<sup>3+</sup> soln., optical absorpt. spectra 4-84957  
 NH<sub>4</sub>NO<sub>3</sub>:Tm<sup>3+</sup> soln., optical absorpt. spectra 4-84957  
 NaCl-γ-irrad., aqualuminesc. in presence of metal ions 4-114317  
 NaNO<sub>3</sub>:Tm<sup>3+</sup> soln., optical absorpt. spectra 4-84957  
 O<sub>2</sub> molecular, luminescence quenching time, effect of solvent deuteration and external heavy atom 4-83411  
 pyrene-diethylaniline exciplexes, in methanol, delayed fluoresc. 4-59845  
 Tm(NO<sub>3</sub>)<sub>3</sub>·5H<sub>2</sub>O soln., optical absorpt. spectra 4-84957  
 Xe, solid and liq. excited by synchrotron radiation, luminesc. decay 4-84986  
 Zn tetraphenylporphyrin, spectral-fluoresc. props., aggregate state and temp. effects 4-78906  
 ZnBr<sub>2</sub>·NO<sub>2</sub> aqueous soln., luminescence study (*Russian*) 4-85009  
 ZnCl<sub>2</sub>·NO<sub>2</sub> aqueous soln., luminescence study (*Russian*) 4-85009

**luminescence of organic solids**

- 3-acetyl-9-vinyl carbazole oligomers, doped with electron acceptor, impurity, absorpt. and luminesc. spectra (*Russian*) 4-80975  
 anthracene, cryst., carrier pairs prod. and recombination by VUV radiation 4-84571  
 anthracene, doped and undoped, exciton-polariton luminesc. (*Russian*) 4-99172  
 anthracene, exciton luminesc., metallic quenching 4-76517  
 anthracene, excitons and diffusion effects 4-92617  
 anthracene, fluoresc. excitation spectra 4-84990  
 anthracene, fluoresc. excitation spectrum beyond first ionisation pot., photoelectron spectra 4-84989  
 anthracene, luminescence of strong exciton transitions 4-104643  
 anthracene cryst., fluoresc. excitation and absorpt. spectra relationship for photon energies up to 10 eV 4-84988  
 anthracene crystals, reson. Raman scatt. and low temp. luminesc. formation 4-104644  
 anthracene-TCND charge transfer cryst. at 1.2K, optical and ESR studies, nπ\* triplet excitation evidence 4-99146  
 aromatic polyamide film, lumiphor addition, absorpt. spectra, TGA (*Russian*) 4-109222  
 benzene, eqn. of state and optical luminosity shocked up to 210 GPa (2.1 Mbar) 4-61041  
 benzophenone, UV induced thermoluminescence studies 4-99201  
 benzo[c]quinoline in n-paraffins, quasilinear phosphorescence spectra 4-91297  
 3,4-benzpyrene, multiplets in the Shpolskii spectra 4-99188  
 betaine 2-N-pyridinium indandione-1,3, single crystals and polycrystalline layers, luminesc. spectra (*Russian*) 4-114319  
 biphenyl cryst. reson. excited defect emission 4-109231  
 biphenyl-naphthalene mixed crystals, delayed fluoresc., role of quadratic terms in kinetics 4-109232  
 bis(2-methylimidazolium) tetrachlorodioxouranate(VI), photoluminesc. spectra at cryogenic temp. 4-99185  
 1,4-bis(6-pyridyl-2-vinyl)benzene, anal. mixed cryst., fluoresc. and lifetime meas. 4-104658  
 bis(imidazolium) tetrachlorodioxouranate(VI), photoluminesc. spectra at cryogenic temp. 4-99185  
 α, ω-biscarbazolyalkanes, doped in polycarbonate, excimer fluoresc. 4-107382  
 2-bromonaphthalene glassy films, spectral diffusion and triplet exciton localisation 4-98538  
 coronene in n-heptane single cryst., phononless line intensity and shift 4-109238  
 di(9-anthryl)-(CH<sub>2</sub>)<sub>2</sub>, systems, intramolecular excited complex, role of ground state conform. and high press. luminesc. 4-114323  
 1,2-di-(1-naphthyl)ethylenes, cis-trans-photoisomerisation, luminesc. and X-ray studies 4-93540  
 p-difluorobenzene-dp(d<sub>8</sub>), solid soln. matrix, low temp. fluoresc. and phosphoresc. study 4-59835  
 diphenyl with fluoranthene impurity, mol. crystals, sensitised and delayed fluoresc. kinetics 4-104647  
 2,5-diphenyloxazole, in liq. mesitylene, far vacuum UV excitation spectrum, fluoresc. 4-84991  
 2,5-distyrylpyrazine, anal. mixed cryst., fluoresc. and lifetime meas. 4-104658  
 DPA-TCNB complexes, triplet-triplet annihilation, reson. microwave field effect 4-76287  
 dye molecule on metallic surface, distance dependence of surface enhanced luminescence 4-88877  
 fluorescein in boric acid glass, thermoluminesc. study of biphotonic systems sensitivity to light fluctuations 4-114810  
 glycine, radiothermoluminesc., ESR investig. 4-61758  
 n-heptane, multiplets in the Shpolskii spectra 4-99188  
 impurity centers, luminescence spectra 4-76506  
 methyl retinoate in solns. and films, spectroluminesc. props. 4-109236  
 3-methylbenzo[fl]quinoline in n-paraffins, quasilinear phosphorescence spectra 4-91297  
 naphthalene, isotopically mixed cryst., delayed fluoresc. study 4-84999  
 naphthalene, isotopically mixed crystals, triplet states, high resolution optical spectroscopy 4-75863  
 naphthalene, mixed cryst., migration kinetics, time resolved luminesc. study 4-66060  
 organic mol. cryst. in strong mag. fields, low temp. phosphoresc. 4-99142  
 palladium phthalocyanine, reson. Raman, fluoresc., and phosphorescence spectra in Shpolskii matrices 4-71426  
 pentacene, in benzoic acid, photosite photon echo study 4-64745  
 β-erylene, self-trapped exciton states, zero-phonon lines 4-108781  
 phenanthrene, fluoresc. excitation spectra 4-84990  
 5-phenyltetrazole and methyl derivatives, phosphorescence spectra 4-93104  
 phthalocyanine, β-metal-free, carrier generation, photoconductivity, delayed fluoresc. study 4-70855  
 cis-polyacetylene films, luminesc., D effects, reson. Raman spectra 4-109264  
 polybutene, eqn. of state and optical luminosity shocked up to 210 GPa (2.1 Mbar) 4-61041

**luminescence of organic solids continued**

- polydiacetylene solns. and glasses, absorpt., fluoresc. and emission spectra 4-71425  
 polyethylene, elec. ageing effects, TSC and electroluminesc. meas. 4-109127  
 polyethylene, eqn. of state and optical luminosity shocked up to 210 GPa (2.1 Mbar) 4-61041  
 polyethylene film, polarisation spectrosc. and phosphoresc. study 4-96610  
 polymer films, ion beam irradi., secondary electron, ion, and photon emission 4-76577  
 polymers, electric breakdown, review 4-114208  
 polystyrene films, doped, α-particles irradi., delayed specific luminesc. 4-61753  
 polystyrene spheres on Ag substrates, structural resonances observed in the fluoresc. emission 4-84984  
 polystyrene-polyvinylmethylether blends, phase separation, fluoresc. emission anal. 4-114324  
 pyrene, fluoresc. excitation spectra 4-84990  
 resorcinol crystals, mechanoluminesc. at low temp. 4-93121  
 retinoic acid in solns. and films, spectroluminesc. props. 4-109236  
 retinyl acetate in solns. and films, spectroluminesc. props. 4-109236  
 tartaric acid crystals, mechanoluminesc. at low temp. 4-93121  
 p-terphenyl, cryst., UV absorpt. and fluoresc. obs. 4-61744  
 p-terphenyl, fluoresc. excitation spectra 4-84990  
 n-terphenyl, pure and impure crystals, exciton, visible absorpt. and fluoresc. spectra 4-99141  
 tetracene, delayed fluoresc., role of charge transfer states in triplet exciton form. 4-99191  
 1,2,4,5-tetrachlorobenzene, triplets, exciton trapping, nonexponential luminesc. intensities 4-93101  
 tetramethylammonium uranyl tetrafluoride, luminesc. and vibr. spectra 4-69138  
 thermoluminescence of organic polymers, review 4-109257  
 2,4,5-trimethylbenzaldehyde in durene phosphoresc. excitation spectrum 4-112221  
 UV-visible and IR spectra, radiative transition probabilities for fluoresc. level 4-114309  
 vinyl chloride-vinyl acetate vapour-swollen polymers, fluoresc. probe for microenvironment, solvent vapour effect 4-81002  
 p-(CH<sub>3</sub>)<sub>2</sub>NC<sub>6</sub>H<sub>4</sub>-CH<sub>2</sub>-(9-anthryl), intramolecular excited complex, role of ground state conform. and high press. luminesc. 4-114323
- luminescence of solids**  
 see also *fluorescence of inorganic solids; luminescence of organic solids*  
 activated crystals, impurity centres, nonradiative transitions, vibr. relax. 4-99145  
 direct-gap semiconductor, nondegenerate, interband luminesc. and absorpt. coeff. 4-61749  
 geminate recombination on a lattice 4-111042  
 impurity centres in two-well adiabatic pots., relax. process effect on luminesc. spectra and burnup 4-109223  
 lyoluminescence, effect of transition metal ion impurities 4-76527  
 molecular crystals, exciton luminesc. 4-109224  
 molecular luminescence and its applications, conf., Kharkov, USSR (1982) 4-106094  
 phononless lines in luminesc. spectra 4-99144  
 polar semicond., donor-acceptor pair capture cross section highly excited electrons 4-61330  
 semiconductor, quantum well structures, photoluminesc. lineshape, interfacial flux influence 4-71424  
 semiconductors, electron-hole droplets, book 4-101582  
 thin scattering films, optical emission and absorpt. spectra 4-104692  
 tunnel junctions, statistically rough, mech. of light emissions 4-76528  
 visible luminescence from surface of some materials irradiated by pulsed IR laser (*Chinese*) 4-92231  
 LiNbO<sub>3</sub> piezoelec.-gas system, acoustic excitation of EM emission from gas 4-69621
- luminescent devices**  
 see also *fluorescent screens; phosphors; scintillation counters*  
 electroluminescent emitters, activated by rare earth elements (*Russian*) 4-109248  
 photovoltaic energy concentrating systems compared 4-66658  
 solar concentrator photon-transport props., anal. and optimisation 4-107799  
 GaInAs-InP heterostructure emitters, 1.3-1.55 μm 4-104308  
 SiO<sub>2</sub> MIS struct., electroluminescence emission studies 4-93114  
 ZnS:Mn ACTFEL electroluminescent devices 4-88882
- lumiphors** see *phosphors*  
**luminors** see *phosphors*  
**lunar atmosphere** see *Moon; planetary satellite atmospheres*  
**lunar geology** see *lunar rocks and minerals*  
**lunar rocks and minerals**  
 cosmic ray tracks anal. 4-101098  
 highlands breccias, N isotopes abundances 4-67650  
 magnetic field between 3.6 Ga and present 4-72895  
 radiation history of meteoritic and lunar material by track data 4-115665  
 soil electrostatic erosion 4-94656  
 surface temp. gradients, SHF/UHF obs. 4-94655  
 trace element determ., PIXE anal. 4-101210  
 Zr/Nb partitioning between coexisting opaque phases, quantitative proton microprobe anal. 4-67651
- lunar seismology**  
 No entries
- lunar structure**  
 see also *lunar rocks and minerals; Moon*  
 internal structure and origin 4-77742
- lung**  
 see also *pneumodynamics*  
 alveolar epithelium, effects of cell swelling on fluid flow 4-89534  
 alveolar macrophages, rat, effects of X-irrad. on cytoskeleton in vitro 4-105290  
 artificial heart and lung machines, review (*Japanese*) 4-110000  
 artificial human respiration biosignals, microprocessor-assisted automatic meas. (*Polish*) 4-7283  
 artificial lungs, review (*Japanese*) 4-109999  
 artificial organs and their materials, review (*Japanese*) 4-89831  
 automatic recording of biological model variables (*German*) 4-77419  
 bronchi, excised, human, bioelec. props. and ion flow 4-100114

**lung** continued

- bronchial mucus, viscoelastometer for rheological props. study in clinical practice 4-115247  
 bronchial mucus transport, model for assessment 4-66925  
 bronchial secretions, human, rheological props. rel. to ciliary beat freq. 4-105276  
 cancer, possible risk from indoor exposure to Rn daughters 4-93813  
 cancer induction by Rn daughters inhalation, dose required 4-93809  
 cancer risk for miners and atomic bomb survivors, rel. to indoor exposure 4-93812  
 computer assisted respiration tests (*German*) 4-77421  
 deposition and clearance analysis, histogram skew, dispersion moment, polar coordinate grid 4-85454  
 diver decompression sickness, heart and lung injury evaluation 4-109871  
 dose, improved calc. using tissue-max. ratios in Batho correction 4-85519  
 extravascular thermal volume, effect of oedema and haemodynamic changes 4-100087  
 ferrimagnetic particles, magnetising process 4-66969  
 ferrimagnetic particles, relax. process 4-66970  
 fibrosis in gamma irradiated lung, D-penicillamine modification 4-77343  
 filtration coefficient obtained by stepwise pressure elevation in isolated dog lung 4-100194  
 fluid mechanics of the pulmonary circulation 4-62509  
 Fourier processed images of dynamic lung function from list mode data 4-89741  
 human,  $\alpha$ -active nuclides microdistrib. using CR-39 SSNTD 4-100370  
 inert vapours and gases, uptake, regulation and pulmonary elimination 4-115003  
 inhalation studies using  $^{81}\text{Kr}$  data from gamma camera 4-100223  
 interstitial fluid press. gradient, excised dog lung, micropuncture obs. 4-93773  
 laser endoscopic resections in bronchology, technical problems 4-85475  
 leukocyte uptake and release by dog lung, effect of pulmonary blood flow 4-100198  
 magnetometry of ingested particles in pulmonary macrophages 4-105264  
 mechanical behaviour of tissue, constitutive eqns. 4-105283  
 mechanical breathing parameters, microcomputer determination (*German*) 4-77280  
 microvascular permeability, assessment in acutely prepared sheep 4-100107  
 model, medical education appls. 4-110827  
 mucociliary transport, unsedated animal models 4-105277  
 neoplasms, induction in rats by fission neutrons and Rn daughters 4-93818  
 nodules, CT images, problems of attenuation and area meas. 4-67074  
 optical mapping, lung function studies 4-62547  
 phonopneumogram, numerical methods for anal. 4-89667  
 pig tissue,  $^{23}\text{Na}$  NMR study 4-100081  
 PIXE anal., target prep. influence in rate organs 4-100381  
 plethysmograph for respiration rate meas. of rats with lung damage 4-105394  
 pleural liquid pressure gradients and intrapleural distribution of injected bolus 4-93786  
 pneumocytes, type II, radiation induced secretion of surfactant 4-81747  
 residual volume, spirogramme anal. (*German*) 4-77281  
 respiratory parameter anal., microprocessor assisted research tool (*German*) 4-77422  
 sheep, fetal, US attenuation and mean backscatter size meas. by digital signal processing 4-100269  
 spirometer turbine transducer, design (*Polish*) 4-77279  
 static mechanics of excised lungs, nonlinearly elastic finite deform. anal. 4-115103  
 tissue, inclusion identification by Raman microprobe 4-105380  
 trace elements distrib., imaging by ion microscopy 4-115316  
 vascular thoracic impedance, meas. after complete obstruction of pulmonary artery (*French*) 4-66984  
 water changes, radiometric technique for meas. 4-85483  
 water content, changes measurement by microwave methods 4-77363  
 water content measurement 4-77410  
 $\text{CO}_2$  volume per breath, evaluation (*German*) 4-77282  
 $\text{PuO}_2$  particles in lungs of hamsters, rats, and dogs, microscopic dose distrib. 4-89767  
 $^{239}\text{Pu}$ , A=239, 240, body burden in Lapps, comparison with southern Finns 4-62590  
 $^{239}\text{Pu}$  submicron dioxide inhalation, haemodynamics and heart mass parameters in dogs (*Russian*) 4-67014  
 $^{239}\text{PuO}_2$  particle in lung,  $\alpha$ -particle microdosimetry 4-62595  
 Rn daughter exposure at low doses, rel. to lung cancer in rats 4-93811  
 Rn daughters, respiratory tract deposition in humans 4-93932  
 Rn daughters rel. to lung tumours occurrence, rat. obs. 4-93810  
 T distrib. and excretion after intratracheal installation of glass microballoon fragments in rats 4-62594  
 $^{99\text{m}}\text{Tc}$  Pseudogas for diagnostic studies in the lung 4-93861  
 $^{99\text{m}}\text{Tc}$  S colloid radioaerosol inhalation, dose to lung calcs. 4-72422

luteum *see lutetium***lutetium**

- see also nuclei with .....*  
 evaporated film, oxidation, photoemission study 4-85073  
 films, hydridisation and catalysis 4-71984  
 L shell X production cross sections,  $\text{H}^+$  induced 4-96649

**lutetium alloys**

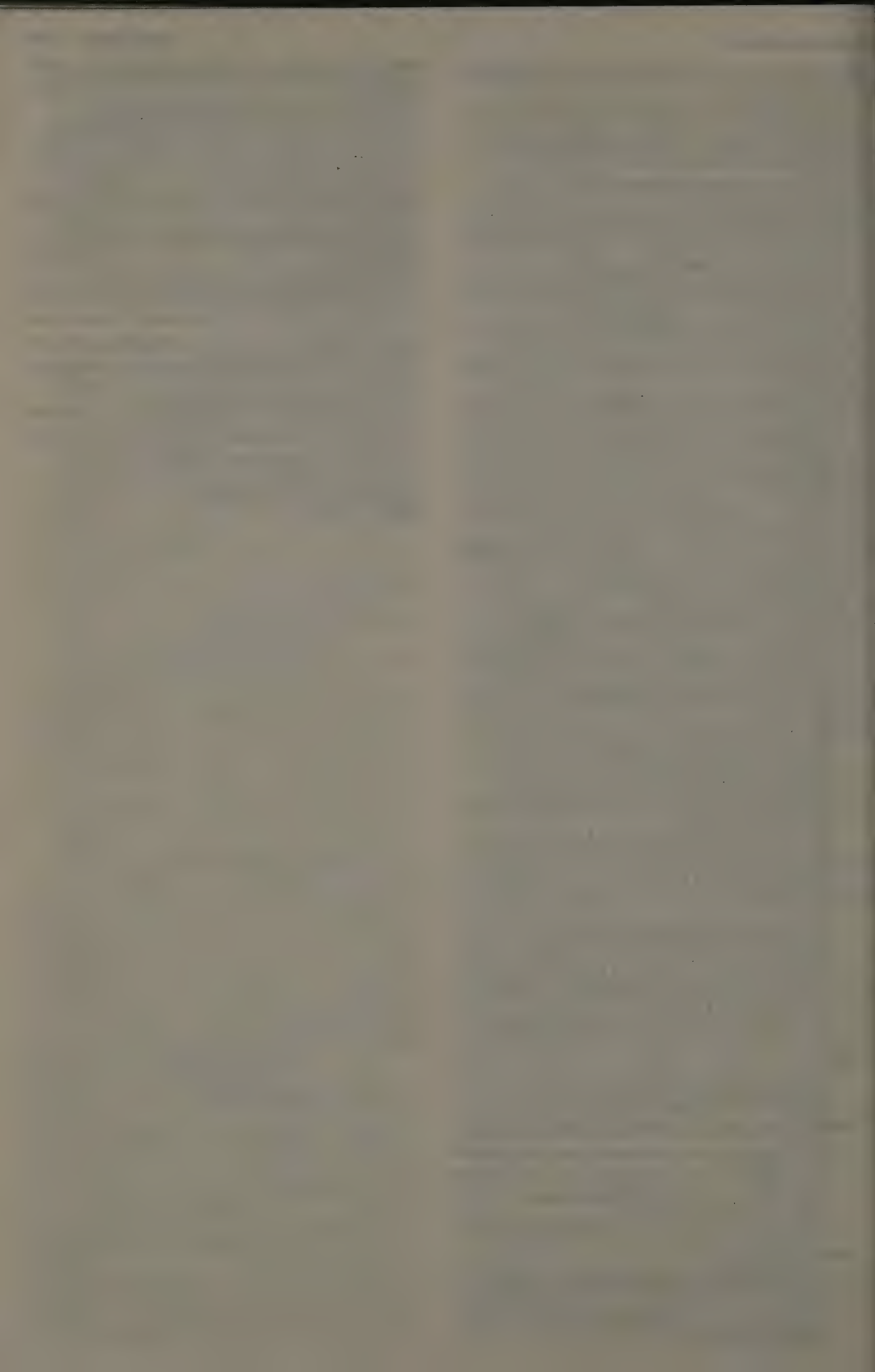
- Cu-Lu, liquid alloys, enthalpies of mixing, intermetallic compound form. 4-92374  
 Gd-Y-Lu single cryst., double ferromagnetism, mag., elec. and thermal studies 4-84817  
 $\text{LuCo}_2$ , quenching of spin fluctuations, heat capacity and magnetisation meas. 4-80744  
 $\text{LuCo}_2\text{Sn}_6$ , cryst. struct. and mag. props. (*Russian*) 4-88135  
 $\text{LuNiSn}_2$ , cryst. struct. determ. 4-75374  
 $\text{LuXGe}$ , X=Ni, Co, cryst. struct., mag. and elec. props. (*Russian*) 4-88134

**lutetium compounds**

- see also lutetium alloys*  
 $\text{K}_2\text{Lu}(\text{OH})_2(\text{Si}_6\text{O}_{20})$ , cryst. struct. determ. 4-75421  
 $\text{Li}(\text{Y,Lu})\text{F}_4\cdot\text{Tm}^{3+}$ , lasing channels, stimulated emission 4-112444  
 Lu-H solid solutions, mag. susceptibility, 2-300K, low temp. heat capacity 4-88653  
 $\text{Lu}_3\text{Al}_5\text{O}_{12}\cdot\text{Cr}^{3+}\cdot\text{Tm}^{3+}$ ,  $\text{Ho}^{3+}$ , stimulated emission of  $\text{Tm}^{3+}$  and  $\text{Ho}^{3+}$ , cross-cascade generation 4-71411  
 $\text{LuB}_{12}$ , XPS study 4-81112

**lutetium compounds continued**

- $\text{Lu}_{0.8}\text{Ca}_{0.2}\text{CrO}_3$ , ionic cond. and thermal expansion 4-84461  
 $\text{LuFe}_4\text{B}_8$ , with struct. of  $\text{CeCo}_4\text{B}$  type, unit cell parameters determ. 4-65243  
 $\text{LuH}_2$ , proton self-diffusion, multipulse  $^1\text{H}$  NMR study 4-75725  
 $\text{Lu}_2\text{O}_3\cdot\text{H}_2\text{O}\cdot\text{CO}_2$  system, hydrothermal phase equilib. 4-84371  
 (Y, Lu, Sm, Ca) $_3(\text{Fe, Ge})_3\text{O}_{12}$  garnet system, distrib. coeffs. 4-61881  
 $(\text{Y}_{1-x}\text{Lu}_x)_3\text{Al}_5\text{O}_{12}$ , anharmonicity const., longit. acoustic wave absorpt. 4-88248  
 $\text{Y}_{1-x}\text{Lu}_x\text{CrO}_3$ , substituted orthochromites with nonmagnetic rare-earth ions, spin flip obs. 4-71066  
 $\text{YSmLuCaFeGe}$  garnet film, mag. anisotropy study 4-88704  
 $(\text{YSmLuCa})_3(\text{GeFe})_3\text{O}_{12}$  epitaxial film, cloudlike charged wall, bubble propagation 4-104473  
 $\text{Y}_{1.7}\text{Sm}_{0.6}\text{Lu}_{0.7}\text{Fe}_5\text{O}_{12}$  thin film, rare earth site occupation 4-108392  
**Luxemburg effect** *see ionospheric electromagnetic wave propagation*  
**Lyapunov methods**  
 asteroids, stability and capture anal., use of the Lyapunov Charact. Numbers 4-82397  
 chaos in 1-D maps, probability dist. function 4-73354  
 critical stability anal. of dynamic systems in equilibrium (*German*) 4-83848  
 discrete dynamic systems with stochastic parameters, Liapunov's direct method 4-73211  
 discrete Schrodinger eqn., Cauchy soln. and positivity of Lyapunov exponent 4-63539  
 equilibrium and Lyapunov exponents of some Brownian flows (*French*) 4-110856  
 gravity waves, rotational, hydrodynamic stability calcs. 4-75049  
 intermittency of periodic regions in 1-D maps 4-63670  
 irradiation-produced point defects, chem. rate equations, global asymptotic stability 4-105004  
 Robinson-Trautman metrics, approach to Schwarzschild metric, Lyapunov method 4-10173  
 solitons, multiple-charged, conditional stability 4-63864  
 thermal model reduction by nodal anal. 4-106251  
**lymphocytes** *see blood; cellular biophysics*  
**lyotropic liquid crystals** *see liquid crystals*  
**lysozyme** *see proteins*



# ABSTRACTS AND CURRENT PAPERS JOURNALS SUBSCRIPTION PRICES 1985

	1984 \$	1985 \$	1986 \$	1987 \$
PHYSICS ABSTRACTS (PA) and associated supplements	1000 145	910 237	920 239	940 500 190 000
ELECTRICAL & ELECTRONICS ABSTRACTS (EEA)	1 350	900	890	340 000
COMPUTER & CONTROL ABSTRACTS (CCA)	700	530	515	187 000
MECHANICAL ENGINEERING ABSTRACTS (and associated supplements)	1010 2300	1000 1000	1000 1000	401 000
BIOMEDICAL ENGINEERING ABSTRACTS	1000	700	680	300 000
TECHNICAL	100	75	70	30 000
CURRENT PAPERS IN PHYSICS (Current in Physics)	90 700	45 110	45 110	20 000
CURRENT PAPERS IN ELECTRICAL & ELECTRONICS ENGINEERING (Current in Electrical & Electronics)	90 700	45 110	45 110	20 000
CURRENT PAPERS IN COMPUTER & CONTROL (Current in Computer & Control)	90 700	45 110	45 110	20 000
MECHANICAL ENGINEERING (Mechanical Engineering)	90 700	45 110	45 110	20 000
BIOMEDICAL ENGINEERING (Biomedical Engineering)	90 700	45 110	45 110	20 000
TECHNICAL (Technical)	90 700	45 110	45 110	20 000

\*The new Abstracts Supplement is available in microfiche or microfilm and 1000 sets.

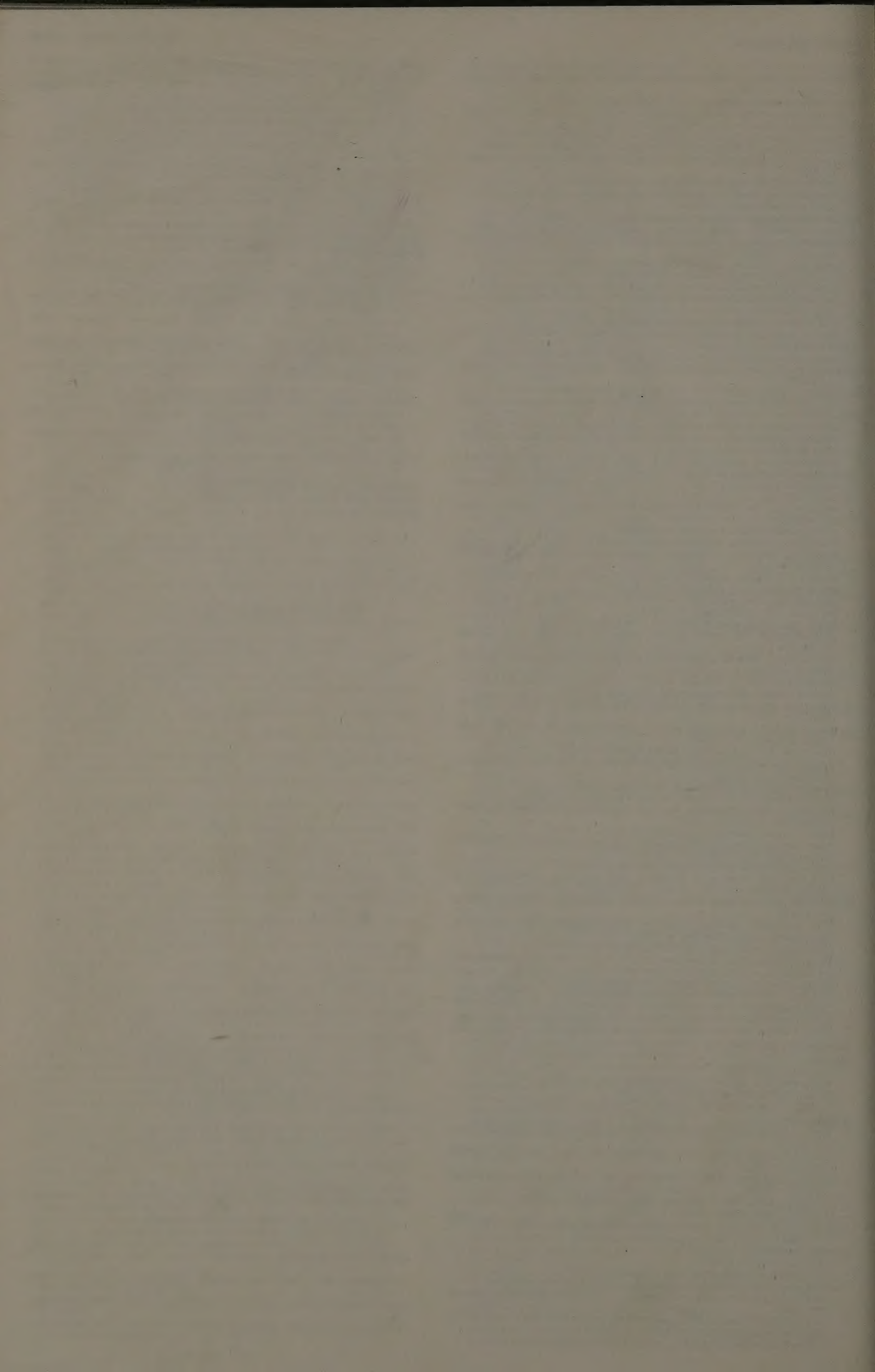
## CUMULATIVE INDEXES

These indexes provide the cumulative index to the Abstracts and Current Papers Journals. They are available in microfiche or microfilm and 1000 sets.

These indexes provide the cumulative index to the Abstracts and Current Papers Journals. They are available in microfiche or microfilm and 1000 sets.

These indexes provide the cumulative index to the Abstracts and Current Papers Journals. They are available in microfiche or microfilm and 1000 sets.

	PHYSICS ABSTRACTS		ELECTRICAL & ELECTRONICS ABSTRACTS		COMPUTER & CONTROL ABSTRACTS	
	Subject	Author	Subject	Author	Subject	Author
1950-59	20	1	11	1	1	1
1960-69	40	12	20	12	1	1
1970-79	60	15	30	15	1	1
1980-84	80	18	40	18	1	1
1985-89	100	20	50	20	1	1
1990-94	120	22	60	22	1	1
1995-99	140	24	70	24	1	1
2000-04	160	26	80	26	1	1
2005-09	180	28	90	28	1	1
2010-14	200	30	100	30	1	1
2015-19	220	32	110	32	1	1
2020-24	240	34	120	34	1	1
2025-29	260	36	130	36	1	1
2030-34	280	38	140	38	1	1
2035-39	300	40	150	40	1	1
2040-44	320	42	160	42	1	1
2045-49	340	44	170	44	1	1
2050-54	360	46	180	46	1	1
2055-59	380	48	190	48	1	1
2060-64	400	50	200	50	1	1
2065-69	420	52	210	52	1	1
2070-74	440	54	220	54	1	1
2075-79	460	56	230	56	1	1
2080-84	480	58	240	58	1	1
2085-89	500	60	250	60	1	1
2090-94	520	62	260	62	1	1
2095-99	540	64	270	64	1	1
2100-04	560	66	280	66	1	1
2105-09	580	68	290	68	1	1
2110-14	600	70	300	70	1	1
2115-19	620	72	310	72	1	1
2120-24	640	74	320	74	1	1
2125-29	660	76	330	76	1	1
2130-34	680	78	340	78	1	1
2135-39	700	80	350	80	1	1
2140-44	720	82	360	82	1	1
2145-49	740	84	370	84	1	1
2150-54	760	86	380	86	1	1
2155-59	780	88	390	88	1	1
2160-64	800	90	400	90	1	1
2165-69	820	92	410	92	1	1
2170-74	840	94	420	94	1	1
2175-79	860	96	430	96	1	1
2180-84	880	98	440	98	1	1
2185-89	900	100	450	100	1	1
2190-94	920	102	460	102	1	1
2195-99	940	104	470	104	1	1
2200-04	960	106	480	106	1	1
2205-09	980	108	490	108	1	1
2210-14	1000	110	500	110	1	1
2215-19	1020	112	510	112	1	1
2220-24	1040	114	520	114	1	1
2225-29	1060	116	530	116	1	1
2230-34	1080	118	540	118	1	1
2235-39	1100	120	550	120	1	1
2240-44	1120	122	560	122	1	1
2245-49	1140	124	570	124	1	1
2250-54	1160	126	580	126	1	1
2255-59	1180	128	590	128	1	1
2260-64	1200	130	600	130	1	1
2265-69	1220	132	610	132	1	1
2270-74	1240	134	620	134	1	1
2275-79	1260	136	630	136	1	1
2280-84	1280	138	640	138	1	1
2285-89	1300	140	650	140	1	1
2290-94	1320	142	660	142	1	1
2295-99	1340	144	670	144	1	1
2300-04	1360	146	680	146	1	1
2305-09	1380	148	690	148	1	1
2310-14	1400	150	700	150	1	1
2315-19	1420	152	710	152	1	1
2320-24	1440	154	720	154	1	1
2325-29	1460	156	730	156	1	1
2330-34	1480	158	740	158	1	1
2335-39	1500	160	750	160	1	1
2340-44	1520	162	760	162	1	1
2345-49	1540	164	770	164	1	1
2350-54	1560	166	780	166	1	1
2355-59	1580	168	790	168	1	1
2360-64	1600	170	800	170	1	1
2365-69	1620	172	810	172	1	1
2370-74	1640	174	820	174	1	1
2375-79	1660	176	830	176	1	1
2380-84	1680	178	840	178	1	1
2385-89	1700	180	850	180	1	1
2390-94	1720	182	860	182	1	1
2395-99	1740	184	870	184	1	1
2400-04	1760	186	880	186	1	1
2405-09	1780	188	890	188	1	1
2410-14	1800	190	900	190	1	1
2415-19	1820	192	910	192	1	1
2420-24	1840	194	920	194	1	1
2425-29	1860	196	930	196	1	1
2430-34	1880	198	940	198	1	1
2435-39	1900	200	950	200	1	1
2440-44	1920	202	960	202	1	1
2445-49	1940	204	970	204	1	1
2450-54	1960	206	980	206	1	1
2455-59	1980	208	990	208	1	1
2460-64	2000	210	1000	210	1	1
2465-69	2020	212	1010	212	1	1
2470-74	2040	214	1020	214	1	1
2475-79	2060	216	1030	216	1	1
2480-84	2080	218	1040	218	1	1
2485-89	2100	220	1050	220	1	1
2490-94	2120	222	1060	222	1	1
2495-99	2140	224	1070	224	1	1
2500-04	2160	226	1080	226	1	1
2505-09	2180	228	1090	228	1	1
2510-14	2200	230	1100	230	1	1
2515-19	2220	232	1110	232	1	1
2520-24	2240	234	1120	234	1	1
2525-29	2260	236	1130	236	1	1
2530-34	2280	238	1140	238	1	1
2535-39	2300	240	1150	240	1	1
2540-44	2320	242	1160	242	1	1
2545-49	2340	244	1170	244	1	1
2550-54	2360	246	1180	246	1	1
2555-59	2380	248	1190	248	1	1
2560-64	2400	250	1200	250	1	1
2565-69	2420	252	1210	252	1	1
2570-74	2440	254	1220	254	1	1
2575-79	2460	256	1230	256	1	1
2580-84	2480	258	1240	258	1	1
2585-89	2500	260	1250	260	1	1
2590-94	2520	262	1260	262	1	1
2595-99	2540	264	1270	264	1	1
2600-04	2560	266	1280	266	1	1
2605-09	2580	268	1290	268	1	1
2610-14	2600	270	1300	270	1	1
2615-19	2620	272	1310	272	1	1
2620-24	2640	274	1320	274	1	1
2625-29	2660	276	1330	276	1	1
2630-34	2680	278	1340	278	1	1
2635-39	2700	280	1350	280	1	1
2640-44	2720	282	1360	282	1	1
2645-49	2740	284	1370	284	1	1
2650-54	2760	286	1380	286	1	1
2655-59	2780	288	1390	288	1	1
2660-64	2800	290	1400	290	1	1
2665-69	2820	292	1410	292	1	1
2670-74	2840	294	1420	294	1	1
2675-79	2860	296	1430	296	1	1
2680-84	2880	298	1440	298	1	1
2685-89	2900	300	1450	300	1	1
2690-94	2920	302	1460	302	1	1
2695-99	2940	304	1470	304	1	1
2700-04	2960	306	1480	306	1	1
2705-09	2980	308	1490	308	1	1
2710-14	3000	310	1500	310	1	1
2715-19	3020	312	1510	312	1	1
2720-24	3040	314	1520	314	1	1
2725-29	3060	316	1530	316	1	1
2730-34	3080	318	1540	318	1	1
2735-39	3100	320	1550	320	1	1
2740-44	3120	322	1560	322	1	1
2745-49	3140	324	1570	324	1	1
2750-54	3160	326	1580	326	1	1
2755-59	3180	328	1590	328	1	1
2760-64	3200	330	1600	330	1	1
2765-69	3220	332	1610	332	1	1
2770-74	3240	334	1620	334	1	1
2775-79	3260	336	1630	336	1	1
2780-84	3280	338	1640	338	1	1
2785-89	3300	340	1650	340	1	1
2790-94	3320	342	1660	342	1	1
2795-99	3340	344	1670	344	1	1
2800-04	3360	346	1680	346	1	1
2805-09	3380	348	1690	348	1	1
2810-14	3400	350	1700	350	1	1
2815-19	3420	352	1710	352	1	1
2820-24	3440	354	1720	354	1	1
2825-29	3460	356	1730	356	1	1
2830-34	3480	358	1740	358	1	1
2835-39	3500	360	1750	360	1	1
2840-44	3520	362	1760	362	1	1
2845-49	3540	364	1770	364	1	1
2850-54	3560	366	1780	366	1	1
2855-59	3580	368	1790	368	1	1
2860-64	3600	370	1800	370	1	1
2865-69	3620	372	1810	372	1	1
2870-74	3640	374	1820	374	1	1
2875-79	3660	376	1830	376	1	1
2880-84	3680	378	1840	378	1	1
2885-89	3700	380	1850	380	1	1
2890-94	3720	382	1860	382	1	1
2895-99	3740	384	1870	384	1	1
2900-04	3760	386	1880	386	1	1
2905-09	3780	388	1890	388	1	1
2910-14	3800	390	1900	390	1	1
2915-19	3820	392	1910	392	1	1
2920-24	3840	394	1920	394	1	1
2925-29	3860	396	1930	396	1	1
2930-34	3880	398	1940	398	1	1
2935-39	3900	400	1950	400	1	1
2940-44	3920	402	1960	402	1	1
2945-49	3940	404	1970	404	1	1
2950-54	3960	406	1980	406	1	1
2955-59	3980	408	1990	408	1	1
2960-64	4000	410	2000	410	1	1
2965-69	4020	412	2010	412	1	1
2970-74	4040	414	2020	414	1	1



# ABSTRACTS AND CURRENT PAPERS JOURNALS SUBSCRIPTION PRICES 1985

	USA \$	UK £	ROW £	JAPAN ¥
<b>PHYSICS ABSTRACTS (PA)</b> .....	1560	625	820	389,500
2nd and subsequent copies .....	645	350	355	168,600
<b>ELECTRICAL &amp; ELECTRONICS ABSTRACTS (EEA)</b> .....	1155	535	670	318,200
<b>COMPUTER &amp; CONTROL ABSTRACTS (CCA)</b> .....	705	330	415	197,100
<b>PA/EEA/CCA COMBINED SUBSCRIPTION</b> .....	3070	1295	1700	807,500
2nd and subsequent copies .....	2260	1080	1285	—
<b>EEA/CCA COMBINED SUBSCRIPTION</b> .....	1690	755	985	467,800
<b>IT FOCUS</b> .....	100	75	82	38,900
<b>CURRENT PAPERS IN PHYSICS</b> .....				
Member rate .....	90	45	45	—
Non-Member rate .....	200	118	118	56,000
<b>CURRENT PAPERS IN ELECTRICAL &amp; ELECTRONICS ENGINEERING</b> .....				
Member rate .....	90	45	45	—
Non-Member rate .....	170	95	95	45,100
<b>CURRENT PAPERS ON COMPUTERS &amp; CONTROL</b> .....				
Member rate .....	90	45	45	—
Non-Member rate .....	170	95	95	45,100
<b>KEY ABSTRACTS</b> .....				
Member rate* .....	45	23	23	—
Non-Member rate .....	95	43	43	20,400
<b>KEY ABSTRACTS</b> .....				
EMI/PMI COMBINED .....	—	72	72	34,200
All Key Abstracts combined .....				
Member rate .....	325	165	165	—
Non-Member rate .....	685	325	325	154,300

\*The Key Abstracts Member rate is available to Members of the IEE and IEEE only.

## CUMULATIVE INDEXES

Cumulative indexes are available for *Physics Abstracts*, *Electrical & Electronics Abstracts* and *Computer & Control Abstracts*, for both

authors and subjects. These cumulations generally cover a period of four years, with the exception of *Computer & Control Abstracts*

where the initial volume covered the period 1966-68. The table below shows the prices and periods for the two types of cumulative index.

PHYSICS ABSTRACTS			ELECTRICAL & ELECTRONICS ABSTRACTS		COMPUTER & CONTROL ABSTRACTS	
Subject	Author		Subject	Author	Subject	Author
1955-59	£ 20	£ —	£ 15	£ 20	£ —	£ —
1960-64	40	17	20	12	—	—
1965-68	60	—	35	20	—	—
1969-72	—	—	72	64	48	30
1973-76	600	300	250	150	150	75
1977-80	770	450	380	250	250	120
*1981-84	1000	600	500	350	345	165
1966-68	—	—	—	—	15	

\* Available in Spring of 1985.

For US\$ and Yen prices please contact the appropriate address below

## ORDERING PROCEDURE

### THE AMERICAS

North (including Canada), Central and South

All orders from the above areas, and orders from members of Institute of Electrical and Electronics Engineers Inc. anywhere in the world, should be sent to Fulfillment Manager, Institute of Electrical & Electronics Engineers Inc., 445 Hoes Lane, Piscataway, N.J. 08854, USA. Telephone (201) 981 0060

### 日本 :

INSPEC 刊行物の購入価格は、すべて円建てとなっており、航空便(ASP扱)で送られます。詳細については、最寄りの洋書取扱店又は、総代理店ユサコ株式会社(昭和58年10月1日より社名変更) 〒105 東京都港区新橋1-13-12 電話(03)502-6471までお問合わせ下さい

### REMAINDER OF THE WORLD

All remaining subscriptions should be sent to INSPEC Marketing Department, P.O. Box 26, Hitchin, Herts SG5 1SA, England. Telephone Hitchin 53331, Telex 825962, Telegrams IEE G.

## OTHER INSPEC SERVICES

### SDI

(Selective Dissemination of Information.)

This is a service individually tailored to the requirements and interests of the engineer or research worker. Details of information relevant to the interest profile of the individual subscriber are selected from the data being processed for the INSPEC Database. Information is dispatched weekly on 150 mm x 100 mm (6" x 4") cards.

### TOPICS

This is an SDI service based on standard profiles. There are over 90 subjects covering

high-activity areas of research and development. This is an inexpensive card service designed to alert engineers and researchers to the availability of literature within their subject area.

### MAGNETIC TAPES

Tapes containing all the information included in the INSPEC publications are issued twice monthly. They enable the larger research and development organisations to produce their

own internal information and current-awareness services.

### JAPAN UPDATE

\* Six high-technology subjects are covered by Japan Update Services. Abstracts are provided for articles selected from over 250 Japanese journals and despatched weekly on conveniently-sized cards. This inexpensive service is designed to help engineers stay abreast of technological developments reported in the Japanese literature.



**Coming  
Soon!**

# **Cumulative Indexes 1981-1984**

to

## **Physics Abstracts**

Order your copies NOW and take  
advantage of the

# **15% Prepublication Discount**

Orders & Enquiries to:

**UK & REST OF WORLD**

INSPEC Publication Sales Dept.  
Institution of Electrical Engineers  
PO Box 26  
Hitchin  
Herts SG5 1SA, ENGLAND  
Tel: (0462) 53331  
Telex: 825962 IEE G

**USA, CANADA & SOUTH AMERICA**

INSPEC  
IEEE Service Center  
445 Hoes Lane  
Piscataway  
NJ 08854, USA  
Tel: (201) 981 0060  
Telex: 833233 IEEE PWAY